Russian Chemical Reviews, Volume 62 (1993)

Contents of Volume

Number 1

Vibrational relaxation and vibrational predissociation as dynamic tunnelling processes 1
E E Nikitin

Thermodynamics of plane-parallel emulsion and foam films 11
V G Babak

The use of correlation equations for the prediction of retention parameters in gas-liquid chromatography 23
V M Nabivach, V P Dmitrikov

Processes amplifying the effects of light on polymer layers 35
A V Vannikov, A D Grishina

Reactions of 4,5-dihydro-5-oxo-1,3-oxazoles with oxygen-containing nucleophiles 51
V O Topuzyan, N S Nesunts

Oxidative degradation of nucleic acids 65
D G Knorre, O S Fedorova, E I Frolova

Number 2

The chemical synthesis of diamond. Aspects of the general theory 87
A P Rudenko, I I Kulakova, V L Skvortsova

Use of IR spectroscopy in studies of catalysts based on molybdenum heteropoly compounds supported on oxides 105
A A Davydov, O I Goncharova

Electrochemistry of diarenechromium complexes 121
L P Yur'eva, L N Nekrasov, S M Peregudova

Regioselective methods of synthesis of asymmetrically substituted diazene oxides 143
S G Zlotin, O A Luk'yanov

The synthesis and properties of unsaturated nitro-compounds of the furan series 169
R A Karakhanov, V I Kelarev, Yu N Polivin

Spirocyclic compounds of the siloxane series 193
M A Sipyagina, E E Stepanova, N M Buzyreva, T V Vasetchenkova, E A Chernyshev

Number 3

Macroscopic kinetics of thermochemical processes on laser heating: current state and prospects 203
N V Karlov, N A Kirichenko, B S Luk'yanchuk

Crystal sensorics 227
I V Melikhov

Synthesis of thin-layer structures by the ionic layer deposition method 237
V P Tolstoi

Phosphorus-containing nucleophiles in reactions with polyfluorinated organic compounds 243
G G Furin

Asymmetric synthesis of fluorine- and phosphorus-containing analogues of aminoacids 261
V P Kukhar', N Yu Svistunova, V A Solodenko, V A Soloshonok

The catalase, peroxidase, and oxidase properties of the coordination compounds of manganese 279
A Ya Sychev, V G Isak

Number 4

Metal-containing liquid-crystal phases 291
A P Polishchuk, T V Timofeeva

Low-frequency IR spectroscopy in the study of the structures of cellulose and cellulose nitrates 323
R M Mukhamadeeva, R G Zhbankov, V F Sopin, G N Marchenko

The chemistry of acetylcyclopropane 337
B A Cheskis, N M Ivanova, A M Moiseenkov, O M Nefedov

Redox potentials and electronic structures of organic complexes of ruthenium and rhodium 359
T V Magdesieva, K P Butin

Imperfectly matched nucleic acid complexes and their biochemical manifestation 387
M A Zenkova, G G Karpova

Number 5

Studies of heterogeneous catalytic systems and of their models by scanning tunnelling microscopy 409
Sh K Shaikhutdinov, D I Kochubey

The fullerenes - new allotropic forms of carbon: molecular and electronic structure, and chemical properties 419
V I Sokolov, I V Stankevich

Inhibitors of the crystallisation of amorphous materials 437
L A Reznitskii, S E Filippova

Carbene reactions of diazoesters with σ-bonds as an effective method for the alkoxycarbonylmethylenation of organic compounds 447
E A Shapiro, A B Dyatkin, O M Nefedov

Fine organic synthesis with the aid of heteropolycompounds 473
I V Kozhevnikov

Radiation-induced inactivation of proteolytic enzymes 493
M A Orlova

Number 6

Relation between molecular and chemical dynamics for elementary radical reactions in viscous media 509
R R Rakhimov, A I Prokof'ev, Ya S Lebedev

The molecular spectra and structure of the oxides of boron and aluminium 527
A V Nemukhin, L V Serebrennikov

Excimers of organic molecules 539
N N Barashkov, T V Sakhno, R N Nurmukhametov, O A Khakhel'

[3,3]-Sigmatropic rearrangements as a method of organofluorine synthesis 553
V G Andreev, A F Kolomiets

Glycals in enantiospecific synthesis 579
A G Tolstikov, G A Tolstikov

New aspects of the problem of the ageing and stabilisation of polymers 603
G E Zaikov, A Ya Polishchuk

Number 7

Influence of the polarity of the medium on the electronic structure and energetics of molecules in solutions 625
I P Gol'dshtein, E S Petrov

Iron-subgroup metal carbonyls in reactions with olefins having functional group substituents 637
L V Rybin, M I Rybinskaya

Derivatives of diphosphonic acids: synthesis and biological activity 647
M M Zolotukhina, V I Krutikov, A N Lavrent'ev

Steroids with a side chain containing a heterocyclic fragment: synthesis and transformations 661
A V Baranovskii, R P Litvinovskaya, V A Khripach

Mechanisms of interaction of pesticides with the lipid bilayer in cell membranes 683
V N Golubev

Gradient barochromatography 693
M S Vigdergauz

Number 8

Thermodynamics of free and of interacting curved interfaces in liquid films 703
V G Babak

New trends in capillary isotachophoresis 729
O V Oshurkova, A I Gorshkov

Niobic acid - a new heterogeneous catalyst for processes in petrochemical and organic syntheses 743
F A Chernyshkova

Methods of synthesis of acrolein and its α-substituted derivatives 751
N A Keiko, M G Voronkov

Thiols as synthons 769
I V Koval'

Immunoassay of alkaloids 787
S K Volkov

Number 9

Catalytic decomposition of diazomethane as a general method for the methylenation of chemical compounds 799
Yu V Tomilov, V A Dokitchev, U M Dzhemilev, O M Nefedov

Ativated cyclopropanes in the synthesis of five-membered carbocycles and heterocycles 839
O G Kulinkovich

Electrical birefringence in solutions of rigid-chain polymers 851
V N Tsvetkov, N V Tsvetkov

New reactions involving the oxidative *O*-, *N*-, and *C*-phosphorylation of organic compounds by phosphorus and phosphides in the presence of metal complexes 877
Ya A Dorfman, M M Aleshkova, G S Polimbetova, L V Levina, T V Petrova, R R Abdreimova, D M Doroshkevich

Aminoacids of the cyclobutane series 897
F M Avotins

Number 10

Bifunctional electrochemical systems 907
N D Ivanova, S V Ivanov

Orbital interactions through space and through σ-bonds 919
E I Brodskaya, G V Ratovskii, M G Voronkov

Reactions of cyclopropene derivatives with electrophiles 935
V R Kartashov, E V Skorobogatova, N S Zefirov

Coordination-radical (co)polymerisation of vinyl monomers in the presence of organic compounds of Group III-V elements 951
D F Grishin

Synthesis of molecular complexes based on porphyrins for the investigation of the energy transfer and primary charge separation in photosynthesis 963
S E Gribkova, R P Evstigneeva, V N Luzgina

The chemistry of volatile β-diketonates and their application in the synthesis of high-temperature superconducting thin films 981
G V Bazuev, L D Kurbatova

Number 11

Electric charge in irradiated dielectrics, and their properties 991
V V Gromov

Naphthacenequinones: synthesis and properties 1005
N T Sokolyuk, V V Romanov, L P Pisulina

The chemistry of cymantrene 1025
A G Ginzburg

Oligosaccharins — a new class of signalling molecules in plants 1047
A I Usov

Number 12

Second generation of magnetic effects in chemical reactions 1073
A L Buchachenko

Relaxation of the surface properties of aqueous solutions of surfactants and the mechanism of adsorption 1083
N N Kochurova, A I Rusanov

Cycloaddition of nitrile oxides to multiple bonds containing a heteroatom 1097
A A Esipenko, L I Samarai

Selenium- and tellurium-centred radicals 1107
E N Deryagina, M G Voronkov, N A Korchevin

Polycarbodiimides 1119
V A Pankratov

© 2008, No Rights Reserved.

Russian Chemical Reviews **62** (1) 1 – 10 (1993)
© 1993 Russian Academy of Sciences and Turpion Ltd

UDC 541.127/.128

Vibrational relaxation and vibrational predissociation as dynamic tunnelling processes

E E Nikitin

Contents

I.	Introduction	1
II.	Vibrational relaxation and vibrational predissociation as classically forbidden processes	2
III.	Correlation functions for the interaction and the rate constants for relaxation and predissociation	3
IV.	Models with a reduced dimensionality for VT and VR processes	4
V.	Energy exchange in three-dimensional collisions	6
VI.	Examples of vibrational relaxation and vibrational predissociation	8
VII.	Conclusion	9

Abstract. The dynamics of vibrational relaxation and vibrational predissociation processes, forbidden by the classical adiabatic Ehrenfest principle, are examined. A general approach to the calculation of rate constants for processes represented by total collision and half-collision models is formulated. Simple models which make it possible to understand the characteristics of the processes discussed are described and are extended to the case of real three-dimensional motion. Examples providing a fairly complete illustration of the present understanding of dynamic tunnelling processes are presented. The bibliography includes 45 references.

I. Introduction

The vibrational relaxation of molecules in gases is an energy exchange process between the vibrational degrees of freedom of a molecule and the translational and rotational degrees of freedom as a result of collisions between molecules and the particles of a heat reservoir. The mechanism of this process is especially simple in the case of diatomic molecules where there is only one vibrational degree of freedom and there is no intramolecular energy exchange in the intervals between successive collisions.

The experimental studies of energy transfer processes involving diatomic molecules have been some of the first investigations which laid the foundations for a new field in chemistry—chemical physics (see, for example, Kondrat'ev[1]). At the present time, these processes continue to be investigated vigorously by methods which permit the measurements not only of thermal rate constants for transitions between specified vibrational states of the molecules $n \to n'$ but of also the state-to-state rate constants for transitions between specific vibrational and rotational states: $n, j \to n', j'$.

We shall confine ourselves to the discussion of the mechanisms of purely vibrational transitions and methods for the calculation of the rate constants $k_{nn'}(T)$. We shall begin with the fact that the distribution of energy among rotational and translational degrees of freedom is canonical, i.e. is described by a Boltzmann distribution with a temperature T. We shall also assume that the heat reservoir consists of a monatomic inert gas A. The elementary collision step

$$\mathrm{A} + \mathrm{BC}(n) \to \mathrm{A} + \mathrm{BC}(n') , \qquad (1)$$

as a result of which the vibrational energy of the molecule changes by an amount $\Delta E_{nn'} = E_{n'} - E_n$, is thus discussed. The energy $\Delta E_{nn'}$ is either converted into the energy of the translational motion of A and BC and into the rotational energy of BC in the case of a deactivating collision ($\Delta E_{nn'} < 0$) or is borrowed from these degrees of freedom in the case of an activating collision ($\Delta E_{nn'} > 0$). We shall designate the rate constant for process (1) by $k^{\mathrm{rel}}_{nn'}(T)$.

Together with vibrational relaxation processes, the processes involving the so-called vibrational predissociation of weakly bound (usually van der Waals) complexes are widely investigated nowadays:

$$\mathrm{A} \cdots \mathrm{BC}(n) \to \mathrm{A} + \mathrm{BC}(n') . \qquad (2)$$

In process (2), a weak bond between the atom A and the molecule BC is ruptured as a result of the conversion of part of the vibrational energy of the molecule BC into the energy of the relative motions of A and BC. We shall designate the rate constant for process (2) by $k^{\mathrm{diss}}_{nn'}(T)$.

Clearly the mechanisms of processes (1) and (2) have much in common. In recognition of this fact, a terminology has been established in modern literature according to which process (1) is referred to as a total collision and process (2) as a half-collision.

We shall consider below the mechanisms of the total collision (1) and the half-collision (2) from a single standpoint within the framework of the so-called method of optimum trajectories. In this method, the dynamics of the collision is characterised by a single trajectory, which describes the relative motion of A and BC and the rotation of BC. The possibility of operating with one trajectory and not with a large set of trajectories, normally employed in the theoretical study of the dynamics of molecular processes,[2-4] is associated with the specific features of the vibrational relaxation and predissociation: processes of both types are forbidden in classical terms. At the same time, the optimum trajectory is not a fully classical object because it requires the introduction of the concept of the evolution of a classical system during an imaginary time interval.

Henceforth we shall consider for simplicity two limiting cases where the molecule BC is homonuclear (or 'almost' homo-

E E Nikitin Laboratory of Elementary Processes,
Institute of Chemical Physics, Russian Academy of Sciences,
117977 Moscow, ul. Kosygina 4, Fax (7-095) 938 21 56
Present address: Technion — Israel Institute of Technology, 32000 Haifa, Israel

Received 1st July 1992
Uspekhi Khimii **62** (1) 3 – 13 (1993); translated by A K Grzybowski

nuclear) or where it is highly asymmetric (for example, the molecule of a hydrogen halide). The preferred VT (vibrational–translational) or RT (rotational–translational) mechanisms can be isolated in this way from the overall mechanism of the so-called VRT process (vibrational–rotational–translational energy exchange). It is found that the vast majority of molecules can be assigned, from the standpoint of the energy exchange mechanism, to one of these groups. The present article does not claim to represent a complete survey of the theoretical questions associated with relaxation and predissociation processes to which a very extensive literature is devoted nowadays. Thus the interpretation of the existing experimental results within the framework of the models described above has been described in recent reviews.[5,6]

This review is constructed as follows. First the characteristic features of the dynamics of processes forbidden by the classical adiabatic Ehrenfest principle are discussed. Next we formulate a general approach to the calculation of the rate constants for processes which represent the total collision and the half-collision, and simple models which make it possible to understand the characteristics of the processes discussed are described and also extended to real three-dimensional collisions. The review ends with examples which illustrate fairly completely the present understanding of the dynamic tunnelling processes.

II. Vibrational relaxation and vibrational predissociation as classically forbidden processes

The transitions between the vibrational levels n and n' of a molecule BC in the region of thermal energies are as a rule forbidden in classical terms. This means that the solution of the classical problem of the vibrational activation or deactivation in process (1) leads to the following result: none of the multidimensional trajectories, beginning at an arbitrary point in the phase space corresponding to the classical vibrational state $N = \hbar(n + \frac{1}{2})$, ever reaches a point in the phase space which would correspond to the final vibrational state $N' = \hbar(n' + \frac{1}{2})$. For process (2), this fact means that any trajectory which describes in the initial state the complex with the vibrational energy corresponding to the classical state $N = \hbar(n + \frac{1}{2})$ in the final state describes dissociation products in which the change in the vibrational energy of BC is less than a single vibrational quantum.

The classical unattainability of the final state n' shows that processes (1) and (2) are in a certain sense tunnel processes. However, this type of tunnelling, referred to in the literature as dynamic tunnelling, differs significantly from the familiar tunnelling through a potential barrier.[7–9] Tunnelling through a potential barrier has no classical analogy, whereas the energy exchange in process (1) and the dissociation in process (2) do have classical analogies. However, these analogies do not permit the determination by the usual quasi-classical method of the probability of the transition from a solution of the classical problem, as was done, for example, within the framework of the classical S-matrix method based on the correspondence principle.[10,11]

At the same time, the classical prohibition of the $n \to n'$ transitions means that the quantum probability of processes (1) and (2) is low and it is therefore possible to employ a particular version of the perturbation theory for its calculation. In principle, this is indeed so. However, the application of this approach in practice is extremely complex, since the wave functions of the initial and final states, taking into account the strong interaction between the relative translational motions A–BC and the rotation of BC are not known with adequate accuracy. In other words, before solving the problem of the vibrational transition, one must solve fully the problem of the energy exchange between the translational and rotational degrees of freeedom at the level of the determination of the wave functions of the rotational inelastic scattering (and not only at the level of the calculation of the probabilities of the translational–rotational transitions which are determined solely by the asymptotic behaviour of the scattering wave functions).

Since the relative motions of A and BC and the rotation of BC under typical conditions satisfy the quasi-classical conditions, it is desirable to formulate a method which would operate with classical trajectories describing the motion in terms of these degrees of freedom. However, the following difficulty arises in this instance. If the classical description is adopted, then, for a very small change δN in the classical initial vibrational action N, the projection of the total exact multidimensional trajectory (for a vibrational non-elastic process) onto the translational–rotational subspace is located very close to the vibrational-elastic trajectory. In a quantum description, the minimum change in the quantum number $\delta n = n' - n$ cannot be less than unity and the corresponding change in the classical action $\delta n \times \hbar$ cannot therefore exceed δN. Under such conditions, the significance of the unperturbed trajectory becomes obscure even when the probability of the transition is very low. One of the possible ways of retaining the classical description of motion in terms of translational and rotational degrees of freedom is provided by the method of optimum trajectories (OT) which is described briefly below. This method has been applied to the description of the dynamics of the vibrational relaxation of molecules in a solid matrix, non-radiative transitions in molecules, and the photodissociation of molecules in a number of studies.[12–14]

For a specified vibrational transition $n \to n'$, the OT method defines the 'classical' trajectory of the translational–rotational motion (i.e. the pathway which satisfies the classical equations of motion) along which the system evolves during a complex time interval; this trajectory need not necessarily be either continuous or real. When the trajectory has been found, the probability of the transition is determined within the framework of perturbation theory. An important property of the OT method is the possibility of a comparatively simple averaging over the initial canonical distribution, since the quantum operator of the evolution and the operator of the Boltzmann distribution have the same (exponential) form. In calculations on the system dynamics, the canonical averaging is carried out with a displacement along the time axis by the imaginary increment $i\hbar/kT$.

The OT method is one of the versions of the so-called semiclassical methods based on the subdivision of all the degrees of freedom of the system under consideration in two subsystems —quantum and classical. The interaction between these subsystems is described within the framework of the non-stationary quantum perturbation theory. The simplifications arising in this instance are evident. Instead of a general consideration of the quantum problem for the entire system, an approach in stages is proposed: one solves initially the dynamic problem only for the classical subsystem, after which the simplified dynamic problem is solved for the quantum subsystem. However, the non-trivial question of the adjustment for self-consistency of the motions of the above two subsystems arises under these conditions. The OT method, discussed below, makes possible such adjustment for consistency.

The idea of the OT method in relation to the calculation of the rate constants for processes (1) and (2) will now be expressed in concrete terms. Other methods for the description of vibrational energy transfer processes have been described in books and reviews.[15–17]

III. Correlation functions for the interaction and the rate constants for relaxation and predissociation

We shall begin the consideration of the computational methods for the first-order time-dependent perturbation theory having assumed that the relative motion of A and BC and the rotation of BC are described in classical terms, while the BC vibrations are described in terms of quantum mechanics. We shall call this approximation semiclassical (SC). The potential energy surface for the system considered depends on three coordinates— the

distance R between the atom A and the centre of gravity of the molecule BC, the distance r between the atoms B and C, and the angle γ between the vectors $\boldsymbol{R}$ and $\boldsymbol{r}$. Instead of the variable r, it is frequently convenient to use another variable $x = r - r_e$, i.e. the deviation of the distance r from its equilibrium value r_e in a free molecule BC.

In the zeroth approximation, we have a five-dimensional trajectory $\boldsymbol{Q}(t)$ which describes the rotational non-elastic collision of A with BC for a fixed vibrational quantum number of BC ($\boldsymbol{Q}$ designates the set of coordinates which specify the relative positions of A and BC in space—three coordinates for translational motion and two coordinates for rotational motion). If $V_{nn'}(\boldsymbol{Q})$ is a matrix element of the interaction which relates the vibrational states n and n', then the probability of the first-order transition is

$$P_{nn'}^{\mathrm{SC}} = \left| \int V_{nn'}[\boldsymbol{Q}(t); \boldsymbol{Q}_i, \boldsymbol{P}_i] \exp(\mathrm{i}\omega_{nn'}t) \frac{\mathrm{d}t}{\hbar} \right|^2 , \tag{3}$$

where the time integral is with respect to the classical five-dimensional trajectory. Here account has been taken explicitly of the fact that the probability $P_{nn'}^{\mathrm{SC}}$ depends on the coordinates $\boldsymbol{Q}_i$ and the momenta $\boldsymbol{P}_i$ of the system before the collision. Eqn. (3) shows that the probability of the transition is proportional to the square of the Fourier component of the matrix element of the interaction energy at the vibrational transition frequency. The rate constant is determined from the probability of the transition by integrating it with respect to the initial collision parameters.

A more convenient representation is obtained after a series of transformations, which express the rate constant for the transition simply as the Fourier component of a bilinear combination of the matrix elements of the interaction at the vibrational transition frequency, i.e. the following relations are valid:

$$k_{nn'}^{\mathrm{SC}}(T) = [F(\beta)]^{-1} W_{nn'}^{\mathrm{SC}}(T) , \tag{4}$$

where F is the partition function for the system in the initial state and $\beta = 1/kT$;

$$W_{nn'}^{\mathrm{SC}}(T) = \int_{-\infty}^{\infty} G_{nn'}^{\mathrm{SC}}(T, t) \exp(\mathrm{i}\omega_{nn'}t)\mathrm{d}t , \tag{5}$$

where $G_{nn'}^{\mathrm{SC}}(T, t)$ is the classical autocorrelation function of the matrix element of the interaction:

$$G_{nn'}^{\mathrm{SC}}(T, t) = \int \mathrm{d}\Gamma_0 (2\pi\hbar)^{-s} \exp[-\beta H(\boldsymbol{P}_0, \boldsymbol{Q}_0)] \times$$
$$\times V_{nn'}\left[\boldsymbol{Q}\left(\frac{t}{2}\right); \boldsymbol{Q}_0, \boldsymbol{P}_0\right] V_{n'n}\left[\boldsymbol{Q}\left(-\frac{t}{2}\right); \boldsymbol{Q}_0, \boldsymbol{P}_0\right] , \tag{6}$$

where $H(\boldsymbol{P}_0, \boldsymbol{Q}_0)$ is the hamiltonian of the A–BC system (excluding the vibrations of BC), which contains the potential energy $U(R, \gamma)$ for the interaction between A and the molecule BC corresponding to the equilibrium internuclear distance. In Eqn. (6), the integration with respect to the phase space of $\mathrm{d}\Gamma_0 = \mathrm{d}^s\boldsymbol{Q}_0\,\mathrm{d}^s\boldsymbol{P}_0$ is extended over the entire phase volume of the reactants (s is the number of degrees of freedom; in our case $s = 5$).

Evidently the translational and rotational degrees of freedom enter symmetrically into Eqn. (6), so that the latter is applicable to the calculation of both $k_{nn'}^{\mathrm{rel}}(T)$ and $k_{nn'}^{\mathrm{diss}}(T)$. In the former case, H represents the hamiltonian of the translational–rotational motion of the collision partners and F designates the products of the translational and rotational partition functions; the corresponding dimensions of $k_{nn'}^{\mathrm{rel}}(T)$ are $\mathrm{s}^{-1}\ \mathrm{cm}^{-3}$. In the second case, H is the hamiltonian of the van der Waals complex and F is the partition function of the complex taking into account its rotation as a whole and the hindered rotation of BC in the complex; $k_{nn'}^{\mathrm{diss}}(T)$ is expressed in s^{-1}.

If the transition $n \to n'$ is forbidden in classical terms, then the rate constant is exponentially small. This means that the overall expression for $k_{nn'}^{\mathrm{SC}}$ (here $k_{nn'}^{\mathrm{SC}}$ denotes both $k_{nn'}^{\mathrm{rel}}$ and $k_{nn'}^{\mathrm{diss}}$ calculated in terms of the semiclassical approximation) assumes the form

$$k_{nn'}^{\mathrm{SC}} = \Phi_{nn'}^{\mathrm{SC}} \exp(-\Psi_{nn'}^{\mathrm{SC}}) , \tag{7}$$

where $\Phi_{nn'}^{\mathrm{SC}}$ is the pre-exponential factor and $\Psi_{nn'}^{\mathrm{SC}}$ is a function which greatly exceeds unity in absolute magnitude and increases with increase in the energy transferred; it depends on the parameters of the interaction potential and temperature. The pre-exponential factor $\Phi_{nn'}^{\mathrm{SC}}$ also depends on these parameters but to a much lesser extent than the exponential part of Eqn. (7). From the symmetry of the probability of the transition, it follows that $\Phi_{nn'}^{\mathrm{SC}} = \Phi_{n'n}^{\mathrm{SC}}$ and $\Psi_{nn'}^{\mathrm{SC}} = \Psi_{n'n}^{\mathrm{SC}}$.

It is seen from Eqn. (7) that the rate constants for the forward ($n \to n'$) and reverse ($n' \to n$) processes are the same, i.e. $k_{nn'}^{\mathrm{SC}}(T)/k_{n'n}^{\mathrm{SC}}(T) = 1$, which conflicts with the principle of detailed balance:

$$\frac{k_{nn'}(T)}{k_{n'n}(T)} = \exp(-\beta E_{n'} + \beta E_n) . \tag{9}$$

Thus the semiclassical approximation is valid subject to the condition that the energy transferred $E_{n'} - E_n$ is small compared with kT, i.e. when the right-hand side of Eqn. (9) is close to unity. This condition does not usually hold for vibrational relaxation at not unduly high temperatures; it is even less likely to hold for vibrational predissociation when the temperature of the van der Waals complex is very low.

The semiclassical approximation (SC) can be refined by going over to the quasiclassical approximation (QC). The latter can also be used in our approach, since the quasiclassical wave functions can be constructed on the basis of an assembly of classical trajectories.[19] The required refinement is achieved by replacing the classical autocorrelation function by its quasi-classical analogue. The corresponding expression for G^{QC} is

$$G_{nn'}^{\mathrm{QC}}(T, t) = \int \mathrm{d}^s\boldsymbol{Q}' \int \mathrm{d}^s\boldsymbol{Q}'' \{V_{nn'}(\boldsymbol{Q}') V_{n'n}(\boldsymbol{Q}'') B(\boldsymbol{Q}', \boldsymbol{Q}'') \times$$
$$\times \exp[\mathrm{i}A_t(\boldsymbol{Q}', \boldsymbol{Q}'') - \mathrm{i}A_{t+\mathrm{i}\beta}(\boldsymbol{Q}', \boldsymbol{Q}'')]\} , \tag{10}$$

where A_t represents the classical action along the rotational–translational trajectory from the space–time point $-t/2$, $\boldsymbol{Q}'$ to the space–time point $t/2$, $\boldsymbol{Q}''$, while $A_{t+\mathrm{i}\beta}$ represents the action along another trajectory, which begins at the point $(t + \mathrm{i}\beta)/2$, $\boldsymbol{Q}'$ and terminates at the point $(t + \mathrm{i}\beta)/2$, $\boldsymbol{Q}''$. The complex quantity added to time ensures the canonical averaging of the transition probability. The multiplier B is expressed in terms of the determinants of the second-derivative matrices:

$$B(\boldsymbol{Q}', \boldsymbol{Q}'') = (2\pi\hbar)^{-s} \mathrm{Det}\left[\frac{\partial^2 A_t}{\partial Q_m \partial Q_k}\right] \mathrm{Det}\left[\frac{\partial^2 A_{t+\mathrm{i}\beta}}{\partial Q_m \partial Q_k}\right] . \tag{11}$$

Thus Eqns. (4) and (5) are replaced by

$$k_{nn'}^{\mathrm{QC}}(T) = F(\beta)^{-1} W_{nn'}^{\mathrm{QC}}(T) , \tag{12}$$

$$W_{nn'}^{\mathrm{QC}}(T) = \int_{-\infty}^{\infty} G_{nn'}^{\mathrm{QC}}(T, t) \exp(\mathrm{i}\omega_{nn'}t)\mathrm{d}t . \tag{13}$$

It follows from Eqns. (12) and (13) that

$$k_{nn'}^{\mathrm{QC}} = \Phi_{nn'}^{\mathrm{QC}} \exp(-\Psi_{nn'}^{\mathrm{QC}}) , \tag{14}$$

where $\Phi_{nn'}^{\mathrm{QC}} \gg 1$, but now $\Phi_{nn'}^{\mathrm{QC}} \neq \Phi_{n'n}^{\mathrm{QC}}$, and $\Psi_{nn'}^{\mathrm{QC}} \neq \Psi_{n'n}^{\mathrm{QC}}$. It can also be shown that the rate constants for the forward and reverse processes satisfy the principle of detailed balance:

$$\frac{k_{nn'}^{\mathrm{QC}}(T)}{k_{n'n}^{\mathrm{QC}}(T)} = \exp(-\beta E_{n'} + \beta E_n) . \tag{15}$$

The calculation of the integral (10) requires the preliminary determination of a large number of trajectories describing the rotational non-elastic processes and subsequent integration with respect to the initial and final states, i.e. the problem of the calculation of the rate constant still remains extremely complex. However, under certain conditions it can be simplified: instead of a large number of trajectories one seeks one trajectory [it is called henceforth the optimum trajectory (OT)] and the probability flux is determined within a comparatively narrow flux tube along the OT. All the properties of this flux are determined by the properties of the OT and also by the additional characteristics of the motion along the optimum trajectory, which are contained in the so-called monodromic matrix.

From the mathematical point of view, the OT method is in fact a generalisation of the stationary phase method for the calculation of quasi-classical matrix elements. Within the famework of this approximation, the optimum trajectory $\mathscr{L}^*$ is sought. It consists of two branches ($\mathscr{L}_i^*$ and $\mathscr{L}_{i+i\beta}^*$), each of which corresponds to the boundary conditions ($-t^*/2$, $\boldsymbol{Q}'^*$; $t^*/2$, $\boldsymbol{Q}''^*$) and ($-t^*/2-i\beta/2$, $\boldsymbol{Q}'^*$; $t^*/2 + i\beta/2$, $\boldsymbol{Q}''^*$) respectively. These conditions ensure a stationary value of the exponent in the exponential function. Next the difference between the actions $A_t - A_{t+i\beta}$ together with the product $V_{nn'}(\boldsymbol{Q}')V_{n'n}(\boldsymbol{Q}'')$ is expanded in series in the vicinity of this trajectory up to second-order terms in the deviations $\delta t = t - t^*$, $\delta\boldsymbol{Q}' = \boldsymbol{Q}' - \boldsymbol{Q}'^*$, and $\delta\boldsymbol{Q}'' = \boldsymbol{Q}'' - \boldsymbol{Q}''^*$, after which the integral with respect to δt, $\delta\boldsymbol{Q}'$, and $\delta\boldsymbol{Q}''$ is calculated.

We obtain as a result the following expression for k:

$$k_{nn'}^{\mathrm{OT}} = \Phi_{nn'}^{\mathrm{OT}} \exp(-\Psi_{nn'}^{\mathrm{OT}}) . \tag{16}$$

It can be shown that it satisfies the detailed balance relation. This expression will be used subsequently to elucidate the dependence of the rate constants on the principal parameters of the interaction between the species involved and temperarture.

IV. Models with a reduced dimensionality for VT and VR processes

In modern molecular dynamics calculations, the so-called models with a reduced dimensionality play a major role. The number of degrees of freedom in these models is reduced to a minimum set for which it is possible to reproduce the principal features of the process considered. The success of such models depends on how simply they can be extended to real cases. We shall describe below two such models: colinear collision of a species A with a harmonic oscillator BC (a model of a VT process) and interaction of a harmonic oscillator BC with a species A, perturbing the rotation of a planar rotator BC (a model of a VR process).

1. Model of a VT Process

The model involving the linear collision of a harmonic oscillator with a structureless species for the description of the vibrational and translational energies was examined by Landau and Teller[20] in 1936. Despite the enormous progress in the description of the dynamics of molecular collisions during the last decade by virtue of the use of computers, this model continues to be of interest because its principal predictions concerning the dependence of the probability of the transition on temperature and the interaction parameters remain in force for a wide range of interactions.

Since the Landau–Teller model is very simple, we shall use it to explain the principal ideas of the OT method and to derive two main relations, referred to in the literature as the law of the energy and momentum gaps. Next we shall supplement the Landau–Teller model by the principal correction for anharmonicity, which is important for the consideration of transitions between not unduly low vibrational states.

We shall consider the colinear collision of a diatomic molecule BC, modelled by a harmonic oscillator with a frequency ω, and a structureless species A (A–BC configuration), which interacts with the species B via an exponential repulsion potential $\exp(-\alpha R_{\mathrm{AB}})$. It is assumed that the vibrational amplitude x is small compared with $1/\alpha$, so that the product αx can be regarded as a small parameter of the perturbation theory.

Within the famework of the semiclassical approximation, one considers initially the motion of a classical subsystem (relative motion), which is described by the simple hamiltonian

$$H_{c1} = \frac{P^2}{2\mu} + A\exp(-\alpha R) , \tag{17}$$

where P is the momentum coupled with R, and μ is the reduced mass of the species involved—A and BC. The transitions in the quantum subsystem (vibrations) are induced by a time-dependent perturbation of the type

$$V(x,t) = \lambda\alpha x A \exp[-\alpha R(t)] , \tag{18}$$

where $\lambda = M_{\mathrm{C}}/(M_{\mathrm{C}} + M_{\mathrm{B}})$, M_{C} and M_{B} being the masses of the atoms C and B respectively. The trajectory $R(t)$ can be found from classical equations of motion by using the hamiltonian (17).

We shall consider initially the probability of the transition $n = 1 \to n' = 0$ averaged with respect to the thermal distribution of the collision energies. Knowing the analytical expression for $\langle P_{10}^{\mathrm{SC}}\rangle$ (see, for example, Nikitin[15]), we obtain the principal corrections to the semiclassical approximation within the framework of the OT method. The application of the stationary phase approximation to the integral (10) makes it possible to determine the points R'^*, R''^*, the optimum kinetic energy in the initial vibrational state E_{t1}^*, and the energy difference $E_{t1}^* - E_{t0}^* = \hbar\omega$. Instead of integrating with respect to the coordinates and time, it is possible to integrate with respect to the coordinates and the energy. The latter is equivalent to the calculation of the matrix element by the Landau method[20] with subsequent canonical averaging of the square of the matrix element. Omitting the intermediate steps, we shall only note that we are seeking a stationary value of the function

$$\begin{aligned}\Psi_{10}(R', R'', E_{t1}) = \alpha R' - \frac{\mathrm{i}}{\hbar}\int_{R_1}^{R'} P(R, E_{t1})\mathrm{d}R + \\ + \frac{\mathrm{i}}{\hbar}\int_{R_0}^{R'} P(R, E_{t0})\mathrm{d}R + \alpha R'' - \frac{\mathrm{i}}{\hbar}\int_{R_1}^{R''} P(R, E_{t1})\mathrm{d}R + \\ + \frac{\mathrm{i}}{\hbar}\int_{R_0}^{R''} P(R, E_{t0})\mathrm{d}R + \beta E_{t1} ,\end{aligned} \tag{19}$$

where R_1 and R_0 are the turning points in classical motion for the translational energies E_{t1} and $E_{t0} = E_{t1} + \hbar\omega$, and the momentum of the relative motion is given by the expression

$$P(R, E_t) = \{2\mu[E_t - A\exp(-\alpha R)]\}^{1/2} . \tag{20}$$

The first three terms in Eqn. (19) arise from the exponent of the first quasiclassical matrix element and the next three terms arise from the exponent of the second element (this yields the square of the matrix element), while the last term arises from the Boltzmann exponential function. The stationary conditions assume the form

$$\left.\begin{aligned} R'^* = R''^* &= R^* , \\ P(R^*, E_{t1}^*) - P(R^*, E_{t0}^*) &= \mathrm{i}\alpha\hbar , \\ t(R^*, E_{t1}^*) - t(R^*, E_{t0}^*) &= \mathrm{i}\beta\hbar , \end{aligned}\right\} \tag{21}$$

where $E_{t0}^* = E_{t1}^* + \hbar\omega$, and $t(R, E_{tk})$ is the classical time required for movement from point R_k to point R:

$$t(R, E_{tk}) = \int_{R_k}^{R} \frac{\mathrm{d}R}{v(R, E_{tk})} .$$

The first Eqn. (21) means that the stationary coordinate points coincide and define the 'transition distance' R^*. The second equation defines the change in momentum between the two parts

of the trajectory at the transition point. The third equation defines the difference between the times required to reach the transition point from the turning points. Hence the optimum energies E^*_{t0} and E^*_{t1} and the optimum turning points R^*_1 and R^*_2 are defined. For the case under consideration, R^* is a real quantity, while the momenta and the time are imaginary quantities. Fig. 1 illustrates the positions of these times in the phase space generated by the real variable R and the complex variable P as well as the two parts of the optimum trajectory (non-elastic transition) and the elastic transition trajectories *00* and *11*.

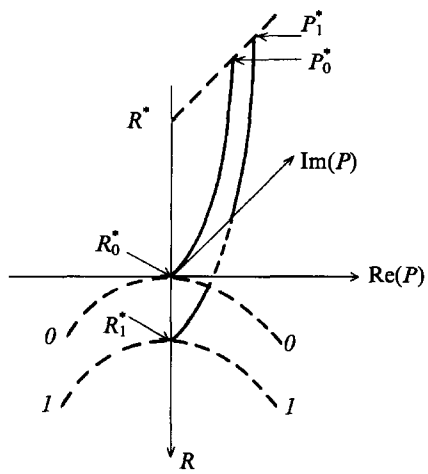


Figure 1. Optimum trajectory for vibrational relaxation in a linear A + BC ($n' = 0$) collision in the 'real coordinate–complex momentum' phase space. R^*_1 and R^*_0 are the turning points for the elastic scattering trajectories in the vibrational states with $n = 1$ and $n = 0$, while R^* is the non-elastic transition point.

In the language of classical trajectories, the vibrational deactivation in process (1) is described as follows. Initially the species approach one another along trajectory *1* from the left and reach the turning point R^*_1; they then 'penetrate' into the classically forbidden region, moving along the complex trajectory $R^*_1 - P^*_1$. At the point P^*_1, there is a sudden change in momentum (from P^*_1 to P^*_0) and the system returns to the turning point R^*_0 at which it 'emerges' from the classical forbidden region. From this point, the particles diverge to the right along the classically allowed trajectory *0*.

The function Ψ^{OT}_{10}, which defines the transition surface, is calculated in terms of R^* and E^*_{t1}, which are found from the second and third Eqns (21) and from the conditions for the conservation of energy, $E_{t0} = E_{t1} + \hbar\omega$:

$$\Psi^{OT}_{10} = \Psi_{10}(R^*, E^*_{t1}). \tag{22}$$

In an explicit form, we have

$$\Psi^{OT}_{10} = \frac{2\pi}{\hbar\alpha}\{[2\mu(E^*_{t1} + \hbar\omega)]^{1/2} - [2\mu E^*_{t1}]^{1/2}\} + \beta E^*_{t1}, \tag{23}$$

where E^*_{t1} is found from the equation

$$\frac{d\Psi^{OT}_{10}(E^*_{t1})}{dE^*_{t1}} = 0. \tag{24}$$

Henceforth we shall be interested in two limits corresponding to high and low temperatures.

In the high-temperature limit, when $\hbar\omega/E^*_{t1} < 1$, the expression for Ψ^{OT}_{10} can be written in the form

$$\Psi^{OT}_{10} \simeq \Psi^{SC}_{10} + \Delta\Psi^{OT}_{10}, \tag{25}$$

where $\Delta\Psi^{OT}_{10} = -\hbar\omega/2kT$ represents a relatively small correction to Ψ^{SC}_{10}:

$$\Psi^{SC}_{10} = 2\frac{\pi\omega}{\alpha v^*} + \beta E^* = 3\left(\frac{\theta^*}{T}\right)^{1/3}, \tag{26}$$

where $v^* = (E^*/2\mu)^{1/2}$ is the optimum relative rate of collision and $\theta^* = \pi^2\mu\omega^2/2\alpha k$ is the characteristic temperature of the model.

In the low temperature limit, when $\hbar\omega/E^* \gg 1$, Eqn. (23) becomes

$$\Psi^{OT}_{10} \simeq \Psi^{(0)}_{10} = \frac{2\pi}{\hbar\alpha}[2\mu\hbar\omega]^{1/2}, \tag{27}$$

where $\Psi^{(0)}_{10}$ denotes Ψ^{OT}_{10} at $T = 0$.

It follows from Eqn. (25) that in the high-temperature limit the exponent for the probability of the transition is proportional to the transferred energy $\hbar\omega$. This relation is called the energy gap law. The high-temperature limit is interesting in connection with vibrational relaxation processes. We may note that the Planck constant does not enter into the expression for Ψ^{SC}_{10}, which makes it possible to attribute the classical significance to this quantity. The correction $\Delta\Psi^{OT}_{10}$ characterises the difference between the quasiclassical and semiclassical descriptions.

In the low-temperature limit, the exponent is proportional to the transferred momentum $(2\mu\hbar\omega)^{1/2}$. This relation is called the momentum gap law. The low-temperature limit is interesting in connection with vibrational predissociation processes.

The application of the Landau–Teller model to predissociation processes requires additional comments. The repulsive potential in the Landau–Teller model cannot of course be used in the literal form for the description of the transition from the bound to the dissociated state. However, it is seen from Eqn. (23) that the probability of the transition between the states of the continuous spectrum is determined mainly by the momentum of the final state subject to the condition that it is appreciably greater than the momentum of the initial state. This factor permits the application of Eqn. (27) also to transitions between the bound state and the state corresponding to the continuous spectrum of the potential with a minimum (subject to the condition that the final energy exceeds appreciably the depth of the potential well: $\hbar\omega \gg \epsilon$). It is also seen that the parameter α in Eqn. (27) should be interpreted as the logarithmic derivative of the potential at the turning point relative to the motion in the final state.

We shall now consider the general case of the transition $n \to n-1$ ($n \geqslant 1$) and at the same time we introduce the most important corrections for the anharmonicity of the vibrations. Clearly the latter arise solely due to the marked dependence of the exponent on the vibration frequency (which in the case of an anharmonic oscillator depends on its energy, i.e. on the number of the level). A linear dependence of the transition frequency ω_n on n is usually employed:

$$\omega_n = \omega(1 - 2x_e n), \tag{28}$$

where x_e is the anharmonicity parameter ($x_e \ll 1$). If the factor $\Phi^{SC}_{nn'}$ is calculated in terms of the harmonic approximation and account is taken of the linear (in terms of n) correction for anharmonicity in the exponent $\Psi^{SC}_{nn'}$, then the overall expression for the probability of the vibrational transition or vibrational predissociation can be written in the form

$$P^{r,d}_{n,n-1} = n\exp(\gamma^{r,d}n)P^{r,d}_{10}, \tag{29}$$

where $P^{r,d}_{10}$ are the probabilities of relaxation and predissociation for the transition $1 \to 0$ and the parameters $\gamma^{r,d}$ have a different significance for vibrational relaxation and vibrational predissociation:

$$\gamma^r = \Psi^{SC}_{10}x_e; \quad \gamma^d = \Psi^{(0)}_{10}x_e.$$

The probability of the $1 \to 0$ transition can be written in its turn as follows:

$$P_{10} = A^{OT}_{10}\exp(-\Psi^{OT}_{10}). \tag{30}$$

Eqns. (29) and (30) make it possible to calculate the probabilities of transitions in the A + BC colinear collision. The task of the theory is now to employ the results obtained in order to calculate the rate constants for three-dimensional collisions and for the interpretation of the dynamics of these processes.

2. Model of a VR process

We shall now proceed to the consideration of a model for VR processes.

Recent studies on the mechanism of the vibrational relaxation on collision between an atom A and a highly asymmetric molecule BC (for example, a hydride molecule) made it possible to formulate a comparatively simple model[22] which is to some extent analogous to the Landau–Teller model. The probability of the loss of a vibrational quantum by the BC molecule not as a result of a single colinear collision with an atom A but during a single period of the rotation BC perturbed by the interaction with an atom A is calculated at the same modelling level. The probability of the transition found in this way is then used to calculate the rate constant for the three-dimensional collision in which the vibrational energy of the molecule BC is converted mainly into its rotational energy.

The semiclassical planar rotator model can be introduced as follows. Initially one considers the motion of the classical subsystem (the rotation of BC), which is described by the hamiltonian

$$H_{cl} = \frac{j^2}{2I} + A\cosh^{-2}\left(\frac{\delta\gamma}{2}\right), \tag{31}$$

where j is the angular momentum of the molecule (for a planar rotator, the variable j is coupled with the angle γ), $I = Mr_e^2$ the moment of inertia of the molecule BC (M is the reduced mass of the molecule BC and r_e its equilibrium internuclear distance). The transitions in the quantum subsystem (vibrations) are induced by a time-dependent perturbation of the type

$$V(x, t) = A\delta x A\cosh^{-2}\left[\frac{\delta\gamma(t)}{2}\right], \tag{32}$$

where the trajectory $\gamma(t)$ is found from the classical equations of motion with the hamiltonian (31).

In contrast to the hamiltonian (17), which describes a comparatively simple form of motion for any relation between the total energy E and the coefficient A (mutual approach of A and BC and their subsequent divergence—elastic one-dimensional scattering of the particle A by the rigid 'rod' BC), the hamiltonian (31) corresponds to a more complex type of motion. Namely, when $E > A$, the rotator BC executes hindered rotation and, when $E < A$, it librates. Accordingly, when $\gamma = 0$, the direction of motion of the rotator either does not change or it is reversed after the attainment of fairly small values of γ.

The semiclassical probability of the transition (again for simplicity one considers the transitions $n = 1 \to n = 0$) is described by the general formula (30), in which the exponent and the pre-exponential factor are expressed in terms of the parameters of the model and temperature. The principal corrections to the semiclassical probability of the transition are obtained by using the optimum trajectory method.

Somewhat more complex steps, but in principle analogous to those presented above, lead to the following expression for Ψ_{10}^{OT}:

$$\Psi_{10}^{OT} = \frac{2\pi r_e}{\hbar\delta}\left\{[2M(E_{r1}^* + \hbar\omega)]^{1/2} - [2ME_{r1}^*]^{1/2}\right\} + \beta E_{r1}^*, \tag{33}$$

where the optimum rotational energy E_{r1}^* is found from the equation

$$\frac{d\Psi_{10}^{OT}(E_{r1}^*)}{dE_{r1}^*} = 0. \tag{34}$$

In the case of VR processes, there exist, as in the case of VT processes, two simple limits in Eqn. (33)—at high and low temperatures. We shall not quote them, since they are fully analogous to Eqns. (26) and (27).

We may note two features of the model of VR processes under consideration.

One of them consists in the fact that Eqn. (33) retains the same form regardless of whether it describes the optimum libration trajectory or hindered rotation. This is extremely important because in the three-dimensional generalisation of the model the sharp difference between the two types of trajectory vanishes as a result of the influence of the centrifugal potential.

Another feature of the model of VR processes consists in the fact that the pre-exponential factor in the expression for the probability of the transition oscillates as a function of the rotational energy. This factor, which also exists for more complex models, hinders the averaging of the probability found in numerical calculations.[13] The oscillatory nature of the transition probability is related to the interference of two tunnel amplitudes: one associated with the initial branch of the optimum trajectory (from the turning point to the transition point) and the other associated with the final OT branch (from the transition point to the other turning point). Oscillations of this kind are absent from the Landau–Teller model, since the phase difference between the two transition amplitudes is extremely small in this model. The oscillations in the transition probability vanish after averaging with respect to energy. Such averaging can be achieved most simply within the famework of the OT method.

V. Energy exchange in three-dimensional collisions

Despite the wide-scale use of virtually exact computer calculations in the dynamics of molecular collisions, including the dynamics of the intermolecular energy exchange, the results obtained hitherto are of limited interest, since each refers to a definite potential energy surface selected on the basis of particular considerations. The use of approximate methods, which make it possible to follow comparatively simply the relation between the final result (the rate constant) and the initial parameters of the problem (the potential energy surface), is therefore of undoubted interest. In this section, we shall consider various approximate methods used in the vibrational relaxation and vibrational predissociation theory. The main task is to determine the relative contributions of the A–BC translational motion (taking into account the radial and relative rotational motions) and of the rotation of BC to the interaction inducing the vibrational transition. Significant progress in this respect has been achieved with the use of the OT method.

As mentioned above, the optimum trajectory is a multidimensional classical trajectory, which begins at the turning point of the relative motion in the initial vibrational state of the molecule and then extends over an imaginary time interval into the classically forbidden region of the potential, reaches the transition point, and, undergoing a discontinuity at this point, returns to the turning point in the final vibrational state of the molecule. The potential energy surface in the classically forbidden region is then constructed as an analytical prolongation of the surface from the classically allowed region. In the case considered this surface depends solely on two coordinates—the distance R between the atom A and the centre of gravity of BC and the angle γ between the axis of the molecule AC and the vector $\boldsymbol{R}$.

We shall consider initially VT processes. The main idea of the OT method in relation to VT energy transfer processes dates back to Takayanagy's 'modified quantum number method'[24] formulated for an isotropic potential. If the length $\mathscr{L}$ of the optimum trajectory (i.e. the distance between the turning points and the transition points) is small compared with the radius of curvature $\mathscr{R}$ of the equipotential line on the potential energy surface at the turning point, then one can carry out a local separation of the variables of motion in order to simplify the description of the collision dynamics. This approximation gives

rise to a one-dimensional 'reaction coordinate' directed at right angles to the constant energy surface; the remaining coordinates behave merely as 'observers'.

Thus the use of one-dimensional models for the description of the dynamics of three-dimensional collisions becomes possible. In particular, the Landau–Teller model is of this kind; its extension to three dimensions within the framework of the method indicated can be called the breathing shells model (the BSH model[15]). This model constitutes in its turn a generalisation of more approximate models: models based on the so called approximation of sudden perturbations relative to rotational transitions (the IOSA method[17]) and the breathing spheres model [the BSP model or the SSH model (after Schwartz, Slawski, and Herzfeld who first formulated it)]. In the last two models, the angle γ is assumed to be the 'observer' and the reaction coordinate is identified with the distance R. The BSH model identifies the reaction coordinate with a linear combination of R and γ. In order to apply the one-dimensional Landau–Teller model to the calculation of the rate constant for a three-dimensional collision, we specify a point with the coordinates R^* and γ^*, which is located on the potential energy surface:

$$U(R^*,\gamma^*) = E^*, \tag{35}$$

where E^* is the optimum energy. The probability of the Landau–Teller transition for the OT which begins at a turning point R^*, γ^*, assumes the form

$$\langle P^* \rangle = A(R^*,\gamma^*)\exp(-\Psi^*), \tag{36}$$

where the multiplier A and the exponent depend on R^* and γ^*. In particular

$$\Psi^* = 3\left(\frac{\theta^*}{T}\right)^{1/3}, \tag{37}$$

where $\theta^* = \omega^2\mu^*/2(\alpha^*)^2k$ is the characteristic temperature of the model. In conformity with the BSH model,

$$\alpha^{\mathrm{BSH}} = \frac{|\mathrm{grad}\,U(R^*,\gamma^*)|}{U(R^*,\gamma^*)},$$

$$\mu^{\mathrm{BSH}} = \mu\left\{1 + \frac{(\mu/M)(R^*)^2(\mathrm{d}R^*/\mathrm{d}\gamma^*)^2}{[(R^*)^2 + (\mathrm{d}R^*/\mathrm{d}\gamma^*)^2]r_e^2}\right\}^{-1} \tag{38}$$

where r_e is the equilibrium internuclear distance in the diatomic molecule BC. The energy E^* is related to Ψ^* by the expression

$$E^* = \frac{\Psi^*}{3}kT, \tag{39}$$

whence follows the condition defining implicitly the optimum surface of the turning points $R^* = R^*(\gamma^*)$.

We now rewrite Eqn. (36) as follows:

$$P^{\mathrm{BSH}}(\gamma^*) = A^{\mathrm{BSH}}(\gamma^*)\exp[-\Psi^{\mathrm{BSH}}(\gamma^*)]. \tag{40}$$

The rate constant k^{BSH} is expressed in terms of $\langle P(\gamma^*)\rangle$ as the probability flux through the optimum surface of turning points:

$$k^{\mathrm{BSH}} = 2\pi\int_0^{\pi}\left(\frac{kT}{2\pi\mu^*}\right)^{1/2}(R^*)^2A^{\mathrm{BSH}}(\gamma^*)\times$$
$$\times\exp[-\Psi^{\mathrm{BSH}}(\gamma^*)]\sin\gamma^*\mathrm{d}\gamma^*. \tag{41}$$

It follows from the analysis[25] of the models mentioned above (BSH, IOSA, BSP) that only the first takes into account the dynamic contribution of the rotation of the BC model to the vibrational relaxation or predissociation process, because in terms of the IOSA and BSP approximations the angle γ is assumed to be constant throughout the period of the collision. The change in the angle γ during the motion of the system along the optimum trajectory does actually imply that the rotation participates dynamically in the energy exchange process between the vibrations and other degrees of freedom. It can be shown intuitively that for an interaction with a low anisotropy (for example, the collision of a homonuclear molecule with an atom), the dynamic contribution of the rotation is small. This is true in the sense that allowance for the rotation alters comparatively little (in relative terms) the exponent in Eqn. (16). However, even a small relative change in Ψ can alter appreciably the rate constant. In this sense, a small anisotropy can alter greatly the rate constant and the dependence of the latter on the principal parameters of the given problem is then the same as for the breathing spheres model or the collinear model. It is found that the contribution of the rotation is determined by the parameter Q, given by

$$Q = \frac{\mu(\Delta R)^2}{Mr_e^2}, \tag{42}$$

where ΔR is the difference between the distances separating the turning points for the collinear and T-shaped configurations and M is the reduced mass of the molecule BC. This parameter enters into the exponent as a relative correction and hence the correction to the rate constant for rotation may be significant even when the parameter Q is very small. We may note that the parameter Q was introduced previously as a characteristic of the efficiency of the purely rotational excitation of molecules on collision with atoms.[26]

Thus the following type of temperature variation may be expected for the vibrational relaxation of homonuclear molecules at fairly high temperatures:

$$k_{10} = B\exp\left[-3\left(\frac{\theta^+}{T}\right)^{1/3}\right], \tag{43}$$

where θ^+ denotes the minimum of all the possible values of θ^* (the corresponding OT and its vicinity make the main contribution to k_{10}). The temperature variation of type (43) is known in the literature as the Landau–Teller law.

For further estimates, we resort to a simple formula for $(\theta^+/T)^{1/3}$:

$$\left(\frac{\theta^+}{T}\right)^{1/3} = 8.1\left[\frac{\omega/\mathrm{cm}^{-1}}{2000}\right]^{2/3}\left[\frac{\alpha/\text{Å}^{-1}}{4}\right]^{-2/3}\times$$
$$\times\left[\frac{\mu/\mathrm{a.e.}}{10}\right]^{1/3}\left[\frac{T/\mathrm{K}}{1000}\right]^{-1/3}. \tag{44}$$

For typical values of ω, μ, and T (ω = 2000 cm^{-1}, μ = 20 a.u., and T = 1000 K) and the values of α in the expected range 3.5 Å^{-1} < α < 4.1 Å^{-1}, the parameter $(\theta^+/T)^{1/3}$ is of the order of 10. As a result, Ψ_{10}^{SC} is in the vicinity of 30, which explains the very low probability of vibrational relaxation in a single collision.

We shall now proceed to the consideration of VR processes. When the planar hindered rotator (HR) model is extended to the three-dimensional case, we shall assume that the angle γ is the reaction coordinate and R is the 'observer'. The parameters A and δ in the hamiltonian (31) are functions of R and the probability of the transition in the model case is averaged with respect to R. In such averaging, account must naturally be taken of the contribution of the isotropic interaction $U_0(R)$.

The general expression for the vibrational relaxation rate constant is

$$k_{10} = \left(\frac{8kT}{\pi I}\right)^{1/2}\pi s\int R^2\,\mathrm{d}R\,P_{01}^{\mathrm{HR}}(T,R)\exp[-\beta U_0(R)], \tag{45}$$

where s is the steric factor arising on passing from the planar rotation model to real three-dimensional rotation (s < 1).[27] The temperature variation of the rate constant defined by Eqn. (45) is described by Eqn. (43), in which θ^+ can be calculated by Eqn. (44), having replaced the reduced mass of the colliding pair by the reduced mass of the molecule and the radial potential gradient by the angular gradient:

$$\alpha \to \frac{\delta}{r_e}, \qquad \mu \to M. \tag{46}$$

The parameter δ, characterising the degree of anisotropy of the potential, varies in the range from 3 to 4 for hydrogen halide molecules.[6]

We may note in conclusion that the VT or VR type of any vibrational relaxation process is determined by the parameter Q: in the former case $Q \ll 1$ and in the latter $Q > 1$. In principle, there is a possibility of a situation where $Q \simeq 1$, i.e. when the relative A–BC motion and the rotation of BC are equally important in inducing the vibrational transition, but in systems of practical interest this is usually not encountered.

VI. Examples of vibrational relaxation and vibrational predissociation

Experimental study of vibrational relaxation under thermal conditions usually makes it possible to obtain information about the kinetics of the population of the lowest vibrational levels, from which it is comparatively difficult to extract the dependence of the relaxation rate constant on the number of the vibrational level. The corresponding data can therefore be used mainly for the elucidation of the dependence of the constants k_{10} on the dynamic and kinematic parameters of the partner species and also on temperature. We present below three examples illustrating the negligibly small, appreciable, and dominant contributions of the rotation of a diatomic molecule to the dynamics of vibrational relaxation.

1. Small contribution of rotation (VT process)

The breathing shells model and even its simplest limiting case—the breathing spheres model—describe comparatively well the experimental results of measurements of the rates of vibrational relaxation of homonuclear diatomic molecules in the heat reservoir of inert gas atoms (see, for example, a recent review[5]). As an example, we shall consider the vibrational relaxation of nitrogen in helium:

$$N_2(n=1, \text{thermal } j) + He \rightarrow N_2(n'=0, \text{all } j') + He. \quad (47)$$

In terms of the combination of masses, this system belongs to the light atom–heavy molecule type of system. For a system of this kind, the average collision time is short compared with the average period of the rotation of the molecule ($\mu/M \simeq 1/2$ and the parameter Q is very small). Fig. 2 illustrates the existing experimental data on the high-temperature and low-temperature vibrational relaxation of N_2 on He[28–30] and also the theoretical temperature dependence of the rate constant. The parameter α was chosen to be 3.8 $Å^{-1}$ in conformity with a non-empirical estimate.[31] The theoretical curve in Fig. 2 corresponds to the expression

$$k_{10}(T) = 1.6 \times 10^{-7}\left[\frac{T/K}{1000}\right]^{1/3} \times \exp\left\{-19.6\left[\frac{1000}{T/K}\right]^{1/3} + \frac{1680}{T/K}\right\} \text{cm}^3\,\text{s}^{-1}. \quad (48)$$

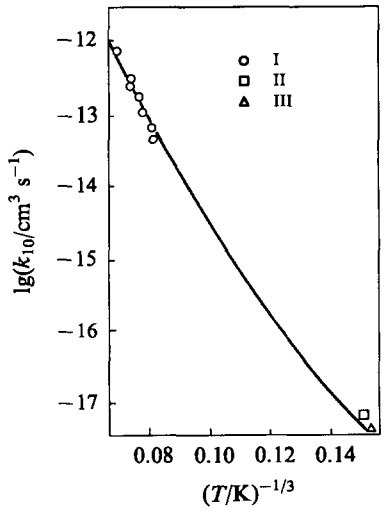


Figure 2. Temperature dependence of the rate constant for the vibrational deactivation of nitrogen by helium. Points I–III represent experimental data obtained in a number of studies.[28–30] Continuous line—results of calculation by Eqn. (48).

We may note the following interesting features of the temperature variation:

(a) The linear high-temperature part of the curve illustrates the Landau–Teller temperature variation [Eqn. (43)], which, as follows from the considerations presented above, permits a semiclassical interpretation.

(b) The low-temperature part of the curve resembles the Arrhenius plot for a chemical reaction rate constant which has been bent by tunnel effects. In this case the above analogy between the two processes is apt, since the curvature of the plot is due to quantum corrections to the semiclassical relation.

(c) The semiclassical approximation with the first quasi-classical correction can describe the variation of the relaxation rate constant over a range of more than six orders of magnitude, the lower limit of the range corresponding to temperatures which are much smaller than the characteristic vibrational temperature of N_2 ($\hbar\omega/k$ = 3360 K). The complete quantum description of the energy transfer process must be used below room temperature.

2. Appreciable contribution of rotation (VT process)

We shall now turn to another example—the vibrational deactivation of H_2 on collision with He. This system belongs to the class of light molecule–heavy atom systems and one may therefore expect an appreciable contribution of the rotation of the molecule to the rate of vibrational relaxation [we have the ratio $\mu/M \simeq 3$ and in this case the parameter Q is appreciably greater than for process (41) but is still less than unity]. However, experimental data for the vibrational relaxation of H_2 on He can be reasonably described within the framework of the IOSA model and even in terms of a rougher approximation—within the framework of the breathing spheres model.[5] The reason for this apparent contradiction is simple. For not unduly anisotropic potentials, a slight variation of the parameter α within the limits of its 'allowed' range of variation makes it possible to reconcile the simple model with experimental data without observing any defects of the model under these conditions. In order to observe the contribution of rotation, it is necessary to carry out a more detailed analysis of the dynamics. Such a problem has been solved and it has been shown[32–34] that an appreciable part of the energy evolved on vibrational deactivation is converted into the rotational energy of the hydrogen molecule. As an illustration of the importance of the rotational transitions accompanying the evolution of vibrational energy, we shall consider the deactivation process not under thermal conditions (equilibrium distribution with respect to translational and rotational energies) but under conditions where the initial energies of all the degrees of freedom are specified:

$$H_2(n = 1, j = 0) + He \rightarrow H_2(n' = 0, \text{all } j') + He. \quad (49)$$

The cross-section of this process is illustrated[35] in Fig. 3 as a function of the collision energy. It is seen from the figure that, when the dynamic contribution of rotation is ignored (the IOSA approximation or the breathing spheres model), then the cross-section is found to be smaller by an order of magnitude than the values obtained in the exact calculation. Analysis of the wave function for relative motion shows[29] that this difference between the cross-sections is induced by very small differences in the interaction potentials corresponding to different rotational states

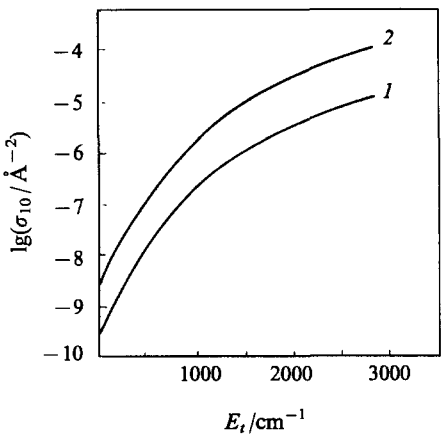


Figure 3. Dependence of the cross-section for the vibrational relaxation of hydrogen by helium on the collision energy:[35] (*1*) theoretical calculation without taking into account the dynamic contribution of the rotation of H_2 to the probability of the transition; (*2*) theoretical calculation taking into account the dynamic contribution of the rotation of H_2.

of H_2. Such a great sensitivity of the cross-section (or rate constant) to small variations in the potential is typical for tunnel processes in general and for dynamic modelling processes in particular.

3. A dominant contribution of rotation (VR process)

The process

$$\text{HF}(n = 1, \text{thermal } j) + \text{Ar} \rightarrow \text{HF}(n' = 0, \text{all } j') + \text{Ar} \quad (50)$$

may serve as an example of vibrational deactivation induced by the rotation of the relaxing molecule.

Experimental data[36–38] together with the theoretical relation,[6] obtained by fitting the hindered rotator model to various potential energy surfaces,[39,40] are presented in Fig. 4. In connection with this figure, we may note two factors. First, any attempt to interpret the experimental data within the framework of the BSP, IOSA, or BSH models would give rise to a discrepancy between the theory and experiment of several orders of magnitude. Second, the use for this system of various potential surfaces described hitherto in the literature leads to a greater scatter of the predicted rate constants compared with the error which is introduced when the planar rotator model potential is fitted to any surface. This illustrates yet again the fact that with the existing uncertainty in the calculations of intermolecular interactions accurate dynamic calculations provide comparatively little information.

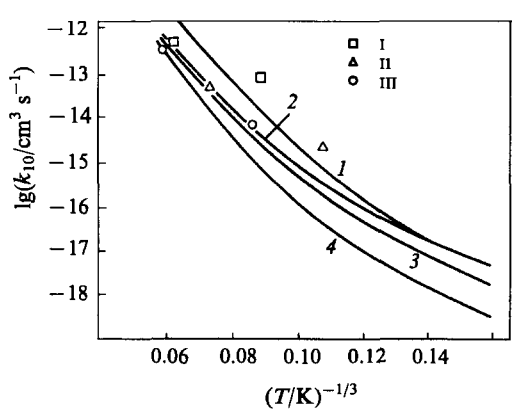


Figure 4. Temperature dependence of the rate constant for the vibrational relaxation of HF by collision with Ar: (I)–(III) experimental data obtained in Refs. 36–38 respectively; (*1*)–(*4*) theoretical calculations with the planar rotator model potential parameters determined for potential energy surfaces calculated in Refs. 39–41.

We shall now proceed to vibrational predissociation processes. In contrast to thermal vibrational relaxation, the study of vibrational predissociation makes it possible to test the dependence of the rate of predissociation on the number of the vibrational level n predicted by the theory, since laser excitation methods make it possible to synthesise the van der Waals complexes BC(n)...A with a wide range of values of n. In this respect, the predissociation of iodine–inert gas complexes, in particular the complex with neon, has been investigated in greatest detail:[42]

$$I_2^*(n)...\text{Ne} \rightarrow I_2^*(n-1) + \text{Ne}\,. \quad (51)$$

Fig. 5 presents the experimental results of the measurement of the rate of vibrational predissociation, which demonstrate a clearly non-linear dependence of the rate on n. This dependence can be fitted very satisfactorily by a function of type (29) and the gradient of the repulsive potentials $\alpha = 4.90\ \text{Å}^{-1}$ can be obtained from the parameters [we may note that this value is twice as high as the value of α quoted by Willberg et al.[42] because the repulsive branch of the Morse potential used in their study is described by the function $\exp(-2\alpha R)$]. The parameter α obtained in this way is only slightly outside the limits of the "expected" range (see above), which is associated simply with the errors of the model that uses a purely repulsive potential for the description of the transition from the bound to the dissociated state.

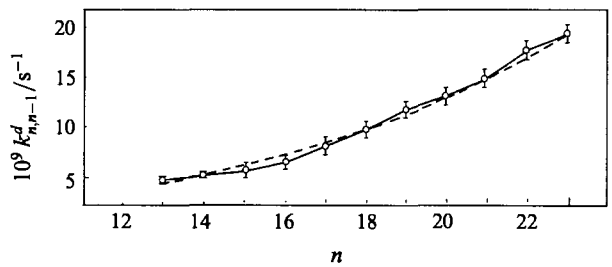


Figure 5. Dependence of the rate constant for the vibrational predissociation of the iodine–neon complex on the vibrational quantum number of the iodine molecule. The continuous curve connects the experimental points,[42] while the dashed curve represents the theoretical relation described by Eqn. (29).

VII. Conclusion

Dynamic tunnelling is a process which is forbidden in classical terms not because the initial and final states are separated by a high potential barrier but because the transition between these states is impossible by virtue of the adiabatic Ehrenfest principle. In the quantum formulation, this principle is expressed in the form of the claim that the probability of the transition betweeen the corresponding states is exponentially small. In many instances, and this applies particularly to vibrational relaxation and predissociation processes, this low probability can be associated with a non-adiabatic transition between two non-intersecting potential energy surfaces. Within the framework of the OT method, such a transition is described as the motion of the system along two trajectories and transition from one to the other takes place in the classically forbidden region of the potential. These trajectories are 'classical' in the sense that they are described by classical equations of motion; at the same time they are not classical in the literal sense because they characterise the motion of the system during an imaginary time. The latter is not a specific feature of dynamic tunnelling, since tunnelling

through a potential barrier can also be described as 'classical' motion in an imaginary time.

The method of optimum trajectories for the calculation of the vibrational relaxation rate constant examined above can be represented as an analogue of the transition state method in relation to the calculation of chemical reaction rate constants. Both methods are based on the same idea: instead of the traditional approach, based on the successive calculation of the probability of the process, its cross-section, and finally its rate constant, in this instance one calculates the average probability flux through the optimum critical surface. In this way, it is possible to avoid the search for the part of the information about the process dynamics which is always contained in the probability and the cross-section but which is lost on averaging with respect to the canonical ensemble in the stage involving the calculation of the rate constant. From this standpoint, the OT method can be regarded as a 'non-reaction' analogue of the so-called theory of reduced dimensionality for the calculation of the rates of 'reaction' events. The latter approach proved extremely fruitful in the theory of chemical reactions.[43-45]

Just as the transition state method makes it possible to calculate the pre-exponential factor for the reaction rate constant in the form proposed by Arrhenius, the optimum trajectories method permits the calculation of pre-exponential factor for the relaxation rate constant in the form proposed by Landau and Teller. At the same time, it is clear that the method of optimum trajectories can be criticised to the same extent as the transition state method: the fundamental question under what conditions the canonical distribution with respect to the degrees of freedom of species before collision can be 'transferred' to the critical surface, which is in the region of their interaction, cannot be regarded as fully solved at the present time.

References

1. V N Kondrat'ev *Kinetika Khimicheskikh Gazovykh Reaktsii* (Kinetics of Chemical Gas-Phase Reactions) (Moscow: Izd. Akad. Nauk SSSR, 1958)
2. E E Nikitin *Kinetika i Kataliz* (*Itogi Nauki i Tekhniki* T.11) [Kinetics and Catalysis (Advances in Science and Engineering, Vol. 11)] (Moscow: Izd. VINITI, 1983) Vol. 11
3. E E Nikitin *Fotokhimiya* (*Itogi Nauki i Tekhniki* T.4) [Photochemistry (Advances in Sciences and Engineering, Vol. 4)] (Moscow: Izd. VINITI, 1985) Vol. 4
4. A L Buchachenko *Rus. Chem. Rev.* **56** 1593 (1987)
5. E E Nikitin, A I Osipov, S Ya Umanskii *Khimiya Plazmy* (The Chemistry of Plasma) (Edited by B M Smirnov) (Moscow: Atomizdat, 1989) Vol. 15, p. 3
6. E E Nikitin, V V Shalashilin, S Ya Umanskii *Khim. Fiz.* **8** 1011 (1989)
7. V I Gol'danskii, L I Trakhtenberg, V N Flerov *Tunnel'nye Yavleniya v Khimicheskoi Fizike* (Tunnel Phenomena in Chemical Physics) (Moscow: Nauka, 1986)
8. V I Gol'danskii, V N Flerov, L I Trakhtenberg *Sov. Sci. Rev. B: Chem.* **9** 59 (1987)
9. A I Voronin, V I Osherov *Dinamika Molekulyarnykh Reaktsii* (Dynamics of Molecular Reactions) (Moscow: Nauka, 1990)
10. W H Miller *Adv. Chem. Phys.* **30** 77 (1976)
11. M S Child in *Semiclassical Methods in Molecular Scattering and Spectroscopy* (Dordrecht: Reidel, 1979) p 127
12. E E Nikitin, M Ya Ovchinnikova *Zh. Eksp. Teor. Fiz.* **78** 1551 (1980)
13. A A Ovchinnikov, M Ya Ovchinnikova *Adv. Quant. Chem.* **16** 161 (1982)
14. E E Nikitin, M Ya Ovchinnikova *Chem. Phys.* **138** 45 (1989)
15. E E Nikitin *Teoriya Elementarnykh Atomno-Molekulyarnykh Protsessov v Gazakh* (Theory of Elementary Atomic-Molecular Processes in Gases) (Moscow: Khimiya, 1974)
16. R C Amme *Adv. Chem. Phys.* **28** 171 (1975)
17. F Gianturco *The Transfer of Molecular Energies by Collisions* (Berlin: Springer, 1979)
18. J A Beswick, J Jortner *Adv. Chem. Phys.* **47** 363 (1981)
19. V P Maslov, M V Fedoryuk *Kvaziklassicheskoe Priblizhenie dlya Uravnenii Kvantovoi Mekhaniki* (Quasiclassical Approximation for Quantum-Mechanical Equations) (Moscow: Nauka, 1976)
20. L Landau, E Teller *Phys. Z. Sow.* **10** 34 (1936)
21. L D Landau, E M Lifshits *Kvantovaya Mekhanika* (Quantum Mechanics) (Moscow: Nauka, 1989)
22. E E Nikitin, M Ya Ovchinnikova *Khim. Fiz.* **5** 291 (1986)
23. M Ya Ovchinnikova *Khim. Fiz.* **4** 867 (1985)
24. K Takayanagy *Adv. Atom. Mol. Phys.* **1** 149 (1965)
25. E E Nikitin *Khim. Fiz.* **7** 867 (1988)
26. F A Gianturco, J P Toennis, M Bernardi *J. Chem. Soc., Faraday Trans.* **87** 31 (1991)
27. E E Nikitin *Khim. Fiz.* **5** 1155 (1986)
28. D R White *J. Chem. Phys.* **48** 525 (1968)
29. R Frey, J Lukasik, J Ducuing *Chem. Phys. Lett.* **14** 514 (1972)
30. M M Maricq, E A Gregory, C T Wickham-Jones et al. *Chem. Phys.* **75** 347 (1983)
31. A J Banks, D C Clary, H J Werner *J. Chem. Phys.* **84** 3788 (1986)
32. H Rabitz, G Zarur *J. Chem. Phys.* **61** 5076 (1974)
33. M H Alexander, P McGuire *J. Chem. Phys.* **64** 452 (1975)
34. A W Raczkowski, W A Lester, W H Miller *J. Chem. Phys.* **69** 2692 (1978)
35. J J Tanner, M M Maricq *Chem. Phys.* **119** 307 (1988)
36. J F Bott, N Cohen *J. Chem. Phys.* **55** 3698 (1971)
37. L S Blair, W D Breashears, G L Scott *J. Chem. Phys.* **59** 1582 (1973)
38. G K Vasil'ev, E F Makarov, V G Papin, V L Tal'roze *Zh. Eksp. Teor. Fiz.* **64** 2046 (1973)
39. G L Berend, R L Thommarson *J. Chem. Phys.* **58** 3454 (1973)
40. J M Douretis, J M Hudson, B J Orr, G Scoles *Mol. Phys.* **52** 763 (1984)
41. T F Eving, J Detrich, R W Conne *J. Chem. Phys.* **69** 4662 (1978)
42. D M Willberg, M Gutman, J J Breen, A H Zeweil *J. Chem. Phys.* **96** 198 (1992)
43. J M Bowman *J. Chem. Phys.* **95** 4960 (1991)
44. M V Bazilevskii, D M Kovtun, V M Ryaboi *Khim. Fiz.* **6** 871 (1987)
45. M V Basilevsky, V M Ryaboy *J. Comput. Chem.* **8** 683 (1987)

Russian Chemical Reviews **62** (1) 11–22 (1993)
© 1993 Russian Academy of Sciences and Turpion Ltd

UDC 541.18 + 532.6

Thermodynamics of plane-parallel emulsion and foam films

V G Babak

Contents

I.	Introduction	11
II.	Thermodynamics of planar free interfaces	12
III.	Thermodynamics of plane-parallel thin liquid films	16
IV.	Conclusion	21

Abstract. Studies on the thermodynamics of plane-parallel thin liquid films (emulsion and foam films) are surveyed. Various approaches to the thermodynamics of planar non-interacting interfaces in thick liquid films (Gibbs dividing surface method, Rusanov's method based on a layer with a finite thickness, Hansen's method) as well as the thermodynamics of plane-parallel thin liquid films based on different models [membrane of zero thickness, membrane of finite thickness, two interacting dividing (as defined by Gibbs) surfaces] are examined. The bibliography includes 56 references.

I. Introduction

The interaction between the particles of a disperse phase in emulsions and foams takes place through thin layers—microscopic liquid films (MLF) of the dispersion medium. This interaction determines the stability and the structural-mechanical properties of disperse systems.

Despite the strikingly non-equilibrium character of processes involved in the formation and breakdown of MLF under real emulsification and foam-formation conditions, equilibrium thermodynamics can serve as a first approximation in the description of the properties of such films, which is more accurate the lower the rate of change of the external perturbing influences compared with the rates of internal relaxation processes (hydrodynamic and adsorption processes, surfactant reconformation processes on interfaces, etc.) in such films. The effects associated with the non-equilibrium nature of the physicochemical processes can be described under such conditions as excess effects compared with standard effects in equilibrium thermodynamics. This guarantees that they are unambiguous.

The difficulty of the thermodynamic description of MLF consists in the lack of a generally recognised definition of the concept of interfacial interaction in the so-called transition region in the film. The forces of the interaction between the surfaces of the film in the transition region vary in magnitude and sign (Figs. 1*a* and 1*b*), vanishing on emerging from the film into the bulk phase α of the Plato region of the film meniscus, where the wedging pressure is zero (Fig. 1*c*). No problems arise in describing the interaction with the central part of the plane-parallel film because thermodynamic methods for plane-parallel liquid films have been developed.[1–10] But the thermodynamics of the transition region of the film have as yet been inadequately developed. In particular, there is no generally recognised way of determining and describing the disjoining pressure in the transition region of the film, which leads to ambiguous and inconsistent estimates of the interaction energy in this region of the film.

If the area corresponding to the transition region of the film constitutes a small fraction of the plane-parallel region, then one can neglect the contribution by the energy of the interaction of the transition region to the overall interaction energy in such a film. However, with decrease in the size of the MLF, the contribution to the interaction energy in the transition region is appreciable and cannot be disregarded. In the latter case, the thermodynamic description of the interaction in the MLF is based on idealised models. For example, the real film, having a complex profile in the transition region, is replaced by a plane-parallel film with a thickness H_f and a radius r_f and two lateral surfaces having a constant average curvature and a constant interfacial tension. The excess amounts of the thermodynamic quantities are then referred to the contact (dividing according to Gibbs[11]) line separating the plane-parallel region of the film from the bulk phase α. For example, the concept of the linear tension, which represents the excess free energy of the film referred to a unit length of the contact line, has thus arisen.[12–14]

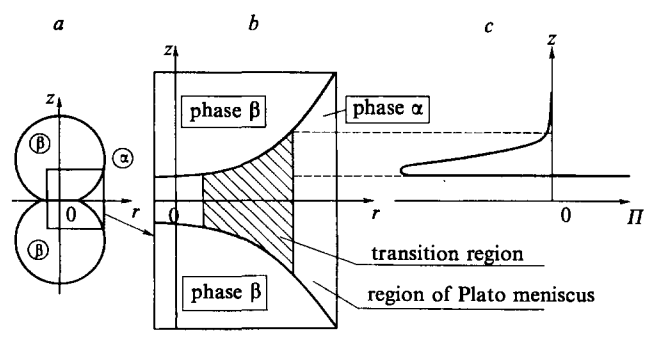


Figure 1. Thermodynamics of liquid films (see text): (*a*) a symmetrical microscopic liquid (emulsion or foam) film arises between two identical flowing (liquid or gaseous) particles of a phase β in a liquid phase α; (*b*) in a symmetrical liquid film one can distinguish a central plane-parallel region, the transition region, and the region of the bulk-phase meniscus of the phase α; (*c*) the disjoining pressure $\Pi(H)$ isotherm in the transition region ($H = 2z$ is the local thickness of the film in the transition region).

V G Babak Department of Physical and Colloid Chemistry, All-Russian Correspondence Institute of the Food Industry, 109803 Moscow, Zemlyanoi val 73, Tel. (7-095) 2974324

Received 1st July 1992
Uspekhi Khimii **62** (1) 14–26 (1993); translated by A K Grzybowski

represents the excess free energy of the film referred to a unit length of the contact line, has thus arisen.[12-14]

At the same time, it is evident that the use of idealised (reference according to Gibbs[11]) thermodynamic models, which is undoubtedly convenient in a formal thermodynamic description of thin liquid films, does not solve the problem of calculating the excess quantities arising under these conditions (for example, the linear tension) in the films. It is therefore necessary to devise the thermodynamics of the transition region of thin liquid films. Such thermodynamics can be defined as a self-consistent and closed system of concepts and relations between parameters characterising the interfacial interaction in the transition region of the film (for example, the disjoining pressure) and other thermodynamic parameters and functions.[13-15] The thermodynamics of the transition region of the film reduces to the thermodynamics of plane-parallel films and the thermodynamics of free interfaces in the appropriate regions where determinations are carried out.[16]

Problems of the thermodynamics of plane-parallel liquid films, which constitute the basis for the construction of the thermodynamics of the transition region of the liquid films,[13,16,17] are discussed in this review.

II. Thermodynamics of planar free interfaces

We shall consider briefly the principal definitions and postulates of the thermodynamics of planar free interfaces, which in fact constitute the thermodynamics of thick plane-parallel liquid films where the interfaces bounding them do not interact by definition. The thermodynamics of such surfaces, developed by Gibbs,[11] has been described in detail in a number of publications.[8,18-23]

1. Description of the thermodynamic system

We shall consider, with reference to Fig. 2, a multicomponent two-phase thermodynamic system with a volume V containing two liquid phases, α and β (or a liquid phase β and a gaseous phase α) and a planar interface dividing them, whose area $A = Ll$, where L is the length and l the width. Under equilibrium conditions, the temperature T as well as the chemical potentials μ_i of the ith components ($i = 1, 2, ..., N$; N is the number of components) are equal in all parts of the system under consideration. We shall neglect the effect of the force of gravity, i.e. we shall assume that the hydrostatic pressures P_α and P_β in the macroscopic phases α and β are the same and equal to P.

We shall postulate that the right-hand wall of the cell is mobile and that it is acted upon by an external force f_e, which balances the forces of the interfacial tension σ_0 of the planar surface. If necessary, the chemical potentials μ_i of the ith components can be varied or kept constant with the aid of a material source v_i.

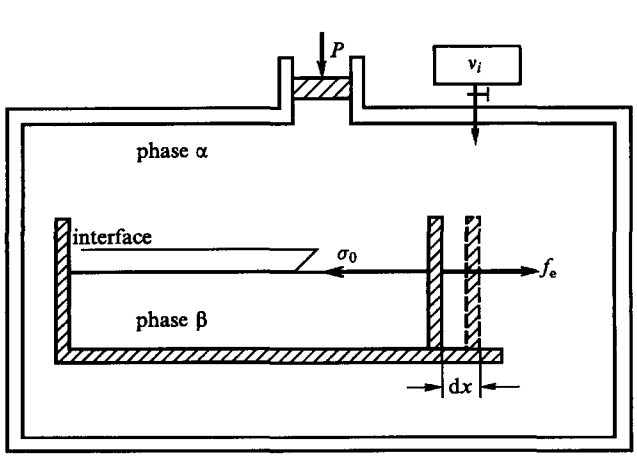


Figure 2. Thermodynamic system containing a flowing (liquid or gaseous) phase β, a liquid phase α, and the interface.

2. Hydrostatic description of the interface

Within the framework of local thermodynamics (which is also known as quasi-thermodynamics or microscopic thermodynamics[21]), one uses a hydrostatic description of the interface, in which the latter is represented as an anisotropic continuous medium in each microscopic volume for which the principal thermodynamic relations hold.[15,19,21-27]

Despite the artificiality of the concept of the interface as a continuous medium with a thickness of ~ 1 nm, such representation is internally consistent, i.e. it constitutes a non-contradictory system of concepts and equations and, furthermore, is extremely clear. In order to formulate the thermodynamic equations, it is necessary to define the concept of the hydrostatic pressure in the medium.

The components of the intermolecular interaction due to the thermal motion of the molecules, short-range forces (Born repulsion, hydrogen bonds), and long-range forces (van der Waals attraction, electrostatic interaction between the electrical double layers) are usually included in the pressure tensor.[28,29] The mechanical equilibrium in the mixture is then fully determined by this generalised hydrostatic pressure tensor and external (for example, gravitational) forces. Sometimes only the short-range intermolecular forces and thermal motion are included in the pressure tensor, with the assumption that the long-range forces are external with respect to the volume elements of the medium.[30-32]

The condition for mechanical equilibrium in the medium is formulated as follows within the framework of local thermodynamics:[8,19,21,22,27,33]

$$\operatorname{div} \boldsymbol{P} = 0, \tag{1}$$

where $\boldsymbol{P}$ is the generalised hydrostatic pressure tensor. In an isotropic medium, the tangential components of the pressure tensor are zero. The normal components of the tensor are equal to one another (Fig. 3*a*):

$$P_{xx} = P_{yy} = P_{zz} = P.$$

In a continuous anisotropic medium, with the aid of which the transition region of the interface is modelled, the tangential components of the pressure tensor are also zero, and the normal components are

$$P_{zz} = P_N(z), \quad P_{xx} = P_{yy} = P_T(z).$$

The qualitative dependence of the components of the pressure tensor $P_N(z)$ and $P_T(z)$ on the coordinate z in the case of a planar interface is presented in Figs. 3*b* and 3*c*. In the region of the bulk phases α and β, these components are equal: $P_N = P_T = P$. In the transition layer with a thickness δ, the component P_N does not change and remains equal to P, while $P_T(z)$ becomes negative and greatly exceeds the compressive pressure P in absolute magnitude. We may note that, in the case of a curved interface, the component

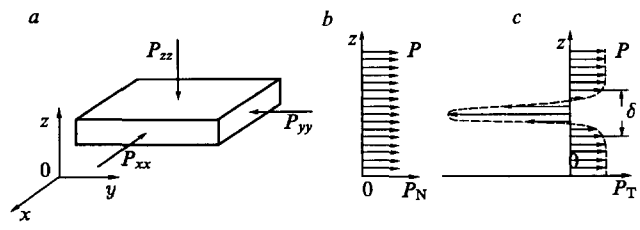


Figure 3. Description of the interface in terms of local thermodynamics: (*a*) different components of the hydrostatic pressure tensor in a system containing an interface; (*b*) and (*c*) dependence of the components P_N and P_T of the hydrostatic pressure tensor on the coordinate z.

P_N does vary in the transition layer with a thickness δ but remains positive (i.e. the pressure P_N remains compressive).

3. Fundamental equation of a system containing a planar free interface

When the mobile lateral wall of the cell (see Fig. 2) moves by dx, the area of the interface increases by $dA = l\,dx$, and the external force f_e executes an amount of work

$$dW_\sigma = \sigma_0\,dA. \tag{2}$$

The volume of the system V may then change by dV and the work performed by forces external to the system is

$$dW_P = -P\,dV. \tag{3}$$

Furthermore, as a result of adsorption on the newly formed surface, the number of moles N_i of the ith components changes by dN_i and the amount of work then performed is

$$dW_\mu = \sum_i \mu_i\,dN_i. \tag{4}$$

Thus the Helmholtz free energy of the system changes by

$$dF = -S\,dT + \sum_i \mu_i\,dN_i - P\,dV + \sigma_0\,dA, \tag{5}$$

where S is the entropy of the system. Eqn. (5) is called the fundamental equation of a system containing a planar free interface.

In the study of the mechanical equilibrium in the energy properties of liquid films, it is convenient to operate with the intensive variables T and μ_i instead of T and N_i. Instead of the Helmholtz free energy F, one therefore uses the grand thermodynamic potential

$$\Omega = F - \sum_i \mu_i N_i,$$

whose differentiation and combination of the resulting expression with Eqn. (5) yields the fundamental equation of the system under consideration in the form

$$d\Omega = -S\,dT - \sum_i N_i\,d\mu_i - P\,dV + \sigma_0\,dA. \tag{6}$$

The following definitions of the interfacial tension σ_0 for a planar free interface follow from Eqns. (5) and (6):

$$\sigma_0 = \left.\frac{\partial F}{\partial A}\right|_{T,V,N_i} = \left.\frac{\partial \Omega}{\partial A}\right|_{T,V,\mu_i}. \tag{7}$$

4. Thermodynamic description of the interface

The interface is described on the basis of different thermodynamic models. The Gibbs method of excess quantities, based on the modelling of the interface by the so-called dividing surface, i.e. an imaginary surface which has a zero thickness but is characterised by a finite surface energy, entropy, mass, etc. has come to be most widely used. This method is convenient also for thin liquid films.

The method based on a layer with a finite thickness, developed by Rusanov[18, 19] and Hansen,[34] and subsequently developed in the studies of Motomura,[35] Markin, Volkov,[36] and others, is convenient for the description of the physicochemical properties of adsorbed surfactant layers. On the other hand, this method is not used for interacting interfaces in thin liquid films.

Brief characteristics of these methods are given below from the standpoint of their possible extension to thin liquid films.

a. The dividing surface method

In this method, a real system with a volume V, containing an interface with a thickness δ (Fig. 4*a*), is replaced by an idealised model consisting of two reference phases α and β separated by a dividing surface of zero thickness and we have

$$V = V_\alpha + V_\beta, \tag{8}$$

where $V_\alpha = Al_\alpha$ and $V_\beta = Al_\beta$ are the volumes of the reference phases. The extensive parameters, the local densities of which change sharply in the transition region, are represented by the sum of the bulk-phase components and surface excess amounts:

$$S = S_\alpha + S_\beta + S_s, \tag{9}$$

$$N_i = N_{i\alpha} + N_{i\beta} + N_{is}, \tag{10}$$

$$\Omega = \Omega_\alpha + \Omega_\beta + \Omega_s, \tag{11}$$

where S_α and S_β, $N_{i\alpha}$ and $N_{i\beta}$, and Ω_α and Ω_β are respectively the bulk-phase entropies, numbers of moles of the ith components, and grand thermodynamic potentials of the reference phases α and β, while S_s, N_{is}, and Ω_s are the excess values of these quantities for the reference phases referred to the dividing surface.

Fundamental equation for a planar free dividing surface. Having substituted Eqns. (8)–(11) in the fundamental equation for system (6), we obtain

$$d\Omega = d\Omega_\alpha + d\Omega_\beta + d\Omega_s, \tag{12}$$

where

$$d\Omega_\alpha = -S_\alpha\,dT - \sum_i N_{i\alpha}\,d\mu_i - P\,dV_\alpha, \tag{13}$$

$$d\Omega_\beta = -S_\beta\,dT - \sum_i N_{i\beta}\,d\mu_i - P\,dV_\beta, \tag{14}$$

$$d\Omega_s = -S_s\,dT - \sum_i N_{is}\,d\mu_i + \sigma_0\,dA. \tag{15}$$

Eqns. (13)–(15) are fundamental for the reference phases α and β and the planar dividing surface respectively. The Gibbs method of excess quantities described here makes it possible to extract from the fundamental equation for a system containing a planar interface the so-called surface component, i.e. Eqn. (15), which describes the thermodynamic properties of the dividing surface. However, one should bear in mind that the excess amounts S_s and N_{is} depend on the location of the dividing surface. The method of establishing this location must be specially stipulated for an unambiguous thermodynamic description of the dividing surface. On the other hand, for constant T and μ_i, the interfacial tension σ_0, defined by the relation

$$\sigma_0 = \left.\frac{\partial \Omega_s}{\partial A}\right|_{T,\mu_i}, \tag{16}$$

is independent of the location of the interface, like the excess grand thermodynamic potential Ω_s. Indeed, bearing in mind that Ω_s is a homogeneous first-order function relative to the extensive parameter A for constant intensive parameters T and μ_i and applying Euler's theorem to Eqn. (15), we obtain

$$\Omega_s = \sigma_0 A. \tag{17}$$

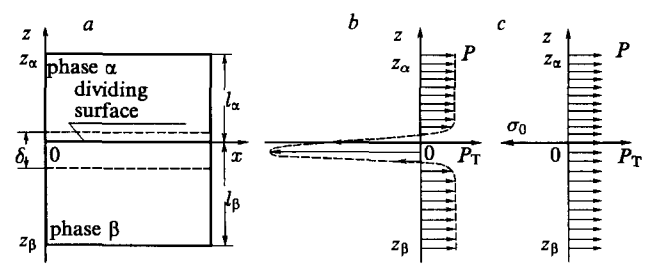


Figure 4. Illustration of the dividing surface (as defined by Gibbs) method in the thermodynamics of a planar free interface: (*a*) open system-containing an interface; (*b*) dependence of the component P_T of the hydrostatic pressure tensor on z; (*c*) result of the replacement of the interface by a dividing surface.

In this connection we may note that, by virtue of the invariance of the function Ω_s as regards the choice of the dividing surface, its use for the thermodynamic description of the interface is preferable to the use of the Helmholtz free energy, whose excess amount

$$F_s = \sigma_0 A + N_i \mu_i, \tag{18}$$

depends on the position of the dividing surface.

The Gibbs–Duhem equation. On differentiating Eqn. (17) and combining it with Eqn. (15), we obtain the familiar Gibbs–Duhem equation for a planar free dividing surface:

$$d\sigma_0 = -S_s dT - \sum_i \Gamma_i d\mu_i, \tag{19}$$

where $S_s = S_s/A$ and $\Gamma_i = N_{is}/A$ are the specific excess entropy and excess number of moles (adsorption) of the ith component referred to the dividing surface. If the procedure used to derive the Gibbs–Duhem equation is applied to the grand thermodynamic potential Ω of a system containing a planar free interface [see Eqn. (6)], we obtain the following expression:[35]

$$A\, d\sigma_0 = -S dT - \sum_i N_i d\mu_i + V dP. \tag{20}$$

Hydrostatic representation of the interfacial tension. Within the framework of the ideas of local thermodynamics it is possible to express the force f with which the system acts on a surface area element $\Delta A = z_\alpha z_\beta l$ (where $l = 1$) of a mobile wall (see Fig. 4*a*) by the component $P_T(z)$ of the pressure tensor in terms of the relation (Fig. 4*b*):

$$f = \int_{z_\beta}^{z_\alpha} P_T(z)\, dz. \tag{21}$$

When the real system is replaced by an idealised system containing two reference phases α and β and the dividing surface, the corresponding force f^{id} (Fig. 4*c*) is

$$f^{id} = \int_{z_\beta}^{z_\alpha} P dz - \sigma_0. \tag{22}$$

The minus sign of σ_0 reflects the direction of the action of the interfacial tension.

The familiar Bakker formula[37] for the interfacial tension of a planar free dividing surface can be obtained from the condition for the mechanical equivalence of the real and idealised systems, i.e. from the conditions $f = f^{id}$:

$$\sigma_0 = \int_{-\infty}^{+\infty} [P - P_T(z)] dz, \tag{23}$$

where the integration limits have been replaced by infinity, bearing in mind that outside the transition region with thickness δ we have the equality $P_T(z) = P$.

The influence of pressure on the interfacial tension. According to Gibbs,[11] the derivative $(\partial\sigma_0/\partial P)_T$ represents a volume decrement associated with the specific expansion of the interface. Such interpretation of the $\sigma_0(P)$ relation apparently follows from the Gibbs–Duhem equation [Eqn. (20)], which can be transformed into

$$d\sigma_0 = -\frac{S}{A} dT - \left(\frac{\Gamma_1}{n_{1\alpha}} \frac{1-\varphi_2}{1-\varphi_1\varphi_2} + \frac{\Gamma_2}{n_{2\beta}} \frac{1-\varphi_1}{1-\varphi_1\varphi_2} \right) dP + \sum_{i=3}^{N} \left(\frac{\Gamma_1}{n_{1\alpha}} \frac{n_{i\alpha} - \varphi_2 n_{2\beta}}{1-\varphi_1\varphi_2} + \frac{\Gamma_2}{n_{2\beta}} \frac{n_{i\beta} - \varphi_1 n_{i\alpha}}{1-\varphi_1\varphi_2} - \Gamma_i \right) d\mu_i, \tag{24}$$

by eliminating the intensive parameters μ_1 and μ_2 (it is assumed that the components $i = 1$ and $i = 2$ correspond to water and oil molecules), where $n_{i\alpha} = N_{i\alpha}/V_\alpha$ and $n_{i\beta} = N_{i\beta}/V_\beta$, $\varphi_1 = n_{1\beta}/n_{1\alpha}$, and $\varphi_2 = n_{2\alpha}/n_{2\beta}$. If one considers a two-component system in which the two components are immiscible, for example with $n_{1\beta} = 0$ and $n_{2\alpha} = 0$, then we obtain from Eqn. (24):[38]

$$\left.\frac{\partial\sigma_0}{\partial P}\right|_T = -\left(\frac{\Gamma_1}{n_{1\alpha}} + \frac{\Gamma_2}{n_{2\beta}} \right). \tag{25}$$

If the dividing surface has been chosen in such a way that either $\Gamma_1 = 0$ or $\Gamma_2 = 0$, we obtain from Eqn. (25)

$$\left.\frac{\partial\sigma_0}{\partial P}\right|_T = -\frac{\Gamma_2}{n_{2\beta}} = -\frac{\Gamma_1}{n_{1\alpha}}. \tag{26}$$

Since $v_1 = 1/n_{1\alpha}$ and $v_2 = 1/n_{2\beta}$ are the molar volumes of components 1 and 2 respectively and the quantities Γ_1 and Γ_2 have the dimensions mol m^{-2}, the right-hand side of Eqn. (26) has the dimensions $m^3\, m^{-2}$ and has therefore been interpreted by Gibbs[11] as a decrease in volume associated with the specific expansion of the interface.

At the same time, one should note that, since the signs of Γ_1 and Γ_2 are not known beforehand, one cannot say whether the interfacial tension σ_0 will increase or decrease with increase in P. This applies also to the specific change in the volume of the interface.

The experimental results obtained from measurements of the $\sigma_0(P)$ relation are contradictory: a negative value $(\partial\sigma_0/\partial P)_T = -0.07$ Å has been obtained[39] for the benzene–water systems; a positive value $(\partial\sigma_0/\partial P)_T \simeq +0.025$ Å has been found[38,40–42] for the hexane–water system, and this decreased to +0.01 Å after the addition of tetradecanol to the system.[35] It follows from Eqn. (23) that, with increase in pressure, the interfacial tension should not change if the interfacial layer is liquid-like. In this case, an increase in hydrostatic pressure is transmitted in all directions without change, i.e. P and $P_T(z)$ increase by the same amount, and the integral (23) does not change.

On the other hand, if the structure of the layer is such that it exhibits 'solid-like' properties, the increase in σ_0 with increase in the pressure P is induced by the 'shielding' effect. Indeed, if it is assumed that the increase in pressure dP is not transmitted at all to the narrow transitional interfacial layer (Fig. 4), then the depth of the minimum in the $P_T(z)$ curve does not change and the external force acting on the mobile wall from the right increases. In this case, the derivative $(\partial\sigma_0/\partial P)_T$ has the physical significance of the thickness of the interfacial layer. If the interfacial layer is structured but not so much that it can be regarded as 'solid-like', then its effective thickness

$$h_f = \left(\frac{\partial\sigma_0}{\partial P} \right)_T, \tag{27}$$

is less than δ.

In connection with the proposed interpretation of the influence of hydrostatic pressure P on the interfacial tension σ_0 we may note that the results of Motomura and coworkers[35,40–42] agree with the conclusion that σ_0 should increase with increase in P for a two-component system. It has been shown[42] that in the water–hexane–octadecanol system the interfacial tension σ_0 decreases with increase in P and the decrease is fairly considerable $[(\partial\sigma_0/\partial P)_T = -2$ Å] in the phase transition from extended octadecanol monolayers to condensed (i.e. 'solid-like') monolayers. This result conflicts with the proposed interpretation of the influence of P on σ_0.

b. The method based on a layer with a finite thickness

This method[6,18,19] is based on the replacement of a real system with a volume V, containing a planar interface, by an idealised system incorporating two phases, α and β, with volumes $V_\alpha^f = l_\alpha A$ and $V_\beta^f = l_\beta A$ respectively (Fig. 5*a*) and a layer with a thickness h_f and a volume $V_f = h_f A$ dividing them, i.e.

$$V = V_\alpha + V_\beta + V_f. \tag{28}$$

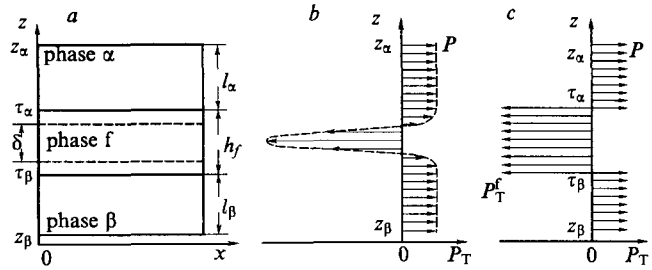


Figure 5. Illustration of the method of the finite thickness layer method in the thermodynamics of a planar free interface: (*a*) open system containing an interface; (*b*) dependence of the component P_T of the hydrostatic pressure tensor on z; (*c*) result of the replacement of the interface by a layer of finite thickness.

The extensive parameters S, N_i, and Ω are also represented by sums of the corresponding bulk-phase components referring to the reference phases α and β and of the excess amounts S_f, N_{if}, and Ω_f referring to the volume V_f of a layer having a finite thickness, i.e.

$$S = S_\alpha + S_\beta + S_f, \tag{29}$$

$$N_i = N_{i\alpha} + N_{i\beta} + N_{if}, \tag{30}$$

$$\Omega = \Omega_\alpha + \Omega_\beta + \Omega_f. \tag{31}$$

Fundamental equation of a layer with a finite thickness. Having substituted Eqns. (28)–(31) in the fundamental equation for the system [Eqn. (6)], we obtain

$$d\Omega = d\Omega_\alpha + d\Omega_\beta + d\Omega_f, \tag{32}$$

where

$$d\Omega_\alpha = -S_\alpha dT - \sum_i N_{i\alpha} d\mu_i - P dV_\alpha, \tag{33}$$

$$d\Omega_\beta = -S_\beta dT - \sum_i N_{i\beta} d\mu_i - P dV_\beta, \tag{34}$$

$$d\Omega_f = -S_f dT - \sum_i N_{if} d\mu_i - P dV_f + \sigma_0 dA. \tag{35}$$

Eqns. (33)–(35) are fundamental for the reference phases α and β and the layer with a finite thickness, respectively.

Hydrostatic description of the layer with a finite thickness. The force f with which the real system acts on the mobile wall is described by Eqn. (21). For the description of the force f^{id} with which the idealised system, containing a layer with a finite thickness h_f, acts on the same surface element of the wall, one has to refine the concept of the layer. If the layer is assumed to be a formation uniform along its thickness and characterised by constant volume densities of the thermodynamic quantities, for example, the entropy

$$s_f = \frac{S_f}{V_f}, \tag{36}$$

and the number of moles of the ith component

$$n_i = \frac{N_{if}}{V_f}, \tag{37}$$

but anisotropic as regards mechanical properties [for example, the layer is extended by the operation of the pressure $P_T^f = P_{xx} = P_{yy}$ (Fig. 5*c*)], then the force f^{id} can be formulated thus:

$$f^{id} = \int_{z_\beta}^{\tau_\beta} P dz + \int_{\tau_\beta}^{\tau_\alpha} P_T^f dz + \int_{\tau_\alpha}^{z_\alpha} P dz, \tag{38}$$

where τ_α and τ_β are the coordinates of the upper and lower surfaces of the layer with $h_f = \tau_\alpha - \tau_\beta$. Taking into account Eqn. (23), we obtain from the condition for the mechanical equivalence of the systems $f = f^{id}$

$$P_T^f h_f = P h_f - \sigma_0. \tag{39}$$

Having substituted Eqn. (39) in Eqn. (35), we find the fundamental equation for a layer of finite thickness:

$$d\Omega_f = -S_f dT - \sum_i N_{if} d\mu_i - PA\, dh_f - P_T^f h_f dA. \tag{40}$$

If it is assumed that a layer uniform with respect to its thickness and having a volume V_f is a liquid phase, then the hypothesis that its properties are anisotropic is unjustified (an isotropic pressure P operates in the liquid phase). In this case, we are forced to consider two dividing surfaces[43] to which the excess pressure P_T^f is referred, assuming that the pressure in the layer is isotropic and equal to P. We may note that the excess amounts of the other thermodynamic quantities are referred to a layer with a thickness h_f, i.e. only the excess pressure, which we shall call the interfacial tension σ_0, is referred to two dividing surfaces.

For this representation of a layer of finite thickness, the force acting on a surface element of the mobile wall is

$$f^{id} = \int_{z_\alpha}^{z_\beta} P dz - \sigma_0. \tag{41}$$

From the condition for the mechanical equivalence of the systems $f = f^{id}$, we obtain an expression for σ_0 which agrees in form with Eqn. (23). However, in this case it is implied that both dividing surfaces are equivalent as regards mechanical properties (unless the difference between them is specially stipulated), i.e. it is assumed that

$$\sigma_0 = \sigma_{0\alpha} + \sigma_{0\beta}, \tag{42}$$

where $\sigma_{0\alpha}$ and $\sigma_{0\beta}$ are the interfacial tensions of the dividing surfaces of finite thickness.

Hansen's method. Hansen[34] proposed a modified finite thickness layer method for the description of systems with a planar interface. He used the model of a layer containing a liquid phase and two dividing surfaces which are placed in such a way that the degrees of adsorption Γ_1 and Γ_2 of the components, which are solvents for phases α and β respectively, are zero. The distance between such dividing surfaces with the coordinates τ_α^H and τ_β^H is

$$\tau^H = \tau_\alpha^H - \tau_\beta^H. \tag{43}$$

By applying to Eqns. (33)–(35) the procedure used to obtain equations of the Gibbs–Duhem type, we obtain

$$s_\alpha dT + n_{1\alpha} d\mu_1 + n_{2\alpha} d\mu_2 + \sum_{i=3}^{N} n_{i\alpha} d\mu_i = dP, \tag{44}$$

$$s_\beta dT + n_{1\beta} d\mu_1 + n_{2\beta} d\mu_2 + \sum_{i=3}^{N} n_{i\beta} d\mu_i = dP, \tag{45}$$

$$-d\sigma_0 = \frac{S_f}{A} dT + \tau^H n_{1f} d\mu_1 + \tau^H n_{2f} d\mu_2 + \sum_{i=3}^{N} \frac{N_{if}}{A} d\mu_i - \tau^H dP, \tag{46}$$

where $n_{1\alpha} = N_{i\alpha}/V_\alpha$, $n_{i\beta} = N_{i\beta}/V_\beta$, $n_{if} = N_{if}/V_f$, $V_f = A\tau^H$, and $s_{\alpha,\beta} = S_{\alpha,\beta}/V_{\alpha,\beta}$.

Assuming that $n_{1f} = n_{1\beta}$ and $n_{2f} = n_{2\alpha}$, which is equivalent to the conditions $\Gamma_1 = 0$, $\Gamma_2 = 0$, and $\varphi_1 = n_{1\beta}/n_{1\alpha}$, $\varphi_2 = n_{2\alpha}/n_{2\beta}$, we obtain from Eqns. (44)–(46)

$$d\sigma_0 = -s_f dT + \frac{(1-\varphi_1)(1-\varphi_2)}{1-\varphi_1\varphi_2}\tau^H dP - \sum_{i=3}^{N}\left[\Gamma_i - \frac{\varphi_1(n_{i\alpha}-\varphi_2 n_{i\beta}) + \varphi_2(n_{i\beta}-\varphi_1 n_{i\alpha})}{1-\varphi_1\varphi_2}\right]d\mu_i, \quad (47)$$

where $\Gamma_i = N_{if}/A$, and $s_f = S_f/A$.

In the case of a two-component system, the following relation follows from Eqn. (47):

$$d\sigma_0 = -s_f dT + \frac{(1-\varphi_1)(1-\varphi_2)}{1-\varphi_1\varphi_2}\tau^H dP, \quad (48)$$

For immiscible components (for example, for component 1, forming phase α, and component 2, forming phase β) and when account is taken of the conditions $\varphi_1 = \varphi_2 = 0$, Eqn. (48) is converted into

$$d\sigma_0 = -s_f dT + \tau^H dP. \quad (49)$$

In this case,[34,35] the distance between the dividing surfaces, for which $\Gamma_1 = 0$ and $\Gamma_2 = 0$, is

$$\tau^H = \left.\frac{\partial\sigma_0}{\partial P}\right|_T, \quad (50)$$

which agrees with the result obtained by Good and Buff.[38] The expression obtained agrees with the conclusion reached by Gibbs,[11] who noted that the derivative $(\partial\sigma_0/\partial P)_T$ characterises the distance between the two equimolecular surfaces. Having compared Eqn. (50) with Eqn. (26), we obtain

$$\tau^H = -\left.\frac{\Gamma_2}{n_{2\beta}}\right|_{\Gamma_1=0} = -\left.\frac{\Gamma_1}{n_{1\alpha}}\right|_{\Gamma_2=0}. \quad (51)$$

In the case of a three-component system (for example, water–oil–surfactant) subject to the additional condition that the oil and water are immiscible, Eqn. (47) gives rise to the following relation:[34,35]

$$d\sigma_0 = -s_f dT - \Gamma_3 d\mu_3 + \tau^H dP. \quad (52)$$

In this representation, a layer with a thickness τ^H is filled solely with component 3 (i.e. the surfactant) and can be regarded as a phase. Attention must be drawn to the fact that the quantity τ^H, defined by Eqn. (43), may be negative (even in the absence of a surfactant or for a constant μ_3), whereupon the concept of a layer with a finite thickness τ^H and filled with the surfactant is not quite so clear. In particular, it has been found[42] for the water–hexane–octadecanol system that σ_0 diminishes from 35 to 25 mJ m^{-2} with increase in P from 0.1 to 50 MPa for a constant mole fraction of the surfactant in the oil $x_3 = 2.21 \times 10^{-3}$. Since the chemical potential μ_3 changes with increase in pressure, Motomura[35] suggested that one goes over to the variables T, P, and x_3 (the mole fraction of component 3 in one of the phases) by replacing μ_3 in Eqn. (52) by x_3 in accordance with the relation

$$d\mu_3 = \frac{\partial\mu_3}{\partial T}dT + \frac{\partial\mu_3}{\partial P}dP + \frac{\partial\mu_3}{\partial x_3}dx_3. \quad (53)$$

Then instead of Eqn. (52), we obtain at a constant temperature T

$$d\sigma_0 = \left(\tau^H - \Gamma_3\frac{\partial\mu_3}{\partial P}\right)dP - \Gamma_3\frac{\partial\mu_3}{\partial x_3}dx_3. \quad (54)$$

If the solvent is ideal in relation to the surfactant, one can write[35]

$$\mu_3 = \mu_3^0(T,P) + RT\ln x_3, \quad (55)$$

and instead of Eqn. (54) we have

$$d\sigma_0 = \left(\tau^H - \Gamma_3\frac{\partial\mu_3^0}{\partial P}\right)dP - RT\Gamma_3 d\ln x_3, \quad (56)$$

where μ_3^0 is the standard value of the chemical potential μ_3, i.e. its value at $x_3 = 1$. Since $\partial\mu_3^0/\partial P$ can be interpreted as the volume of one surfactant molecule $v_3 \simeq 10^{-29}$ m^3 and the adsorption Γ_3 is $\sim 10^{-6}$ mol m^{-2}, the product $\Gamma_3(\partial\mu_3^0/\partial P)$ in Eqn. (56) increases from 0 to ~ 1 Å with increase in x_3 from 0 to the value corresponding to a surfactant monolayer on the interface.

If the thickness of the layer τ^H does not change as x_3 increases, then the quantity

$$\tau_*^H = \tau^H - \Gamma_3\frac{\partial\mu_3}{\partial P} = \left.\frac{\partial\sigma_0}{\partial P}\right|_{T,x_3} \quad (57)$$

should diminish with increase in x_3, which was observed by Motomura and coworkers[35,40–42] for tetradecanol and octadecanol. However, for a water-soluble surfactant (NaDDS) τ_*^H does not vary with increase in x_3,[41] which may indicate the simultaneous increase in τ^H in Eqn. (57). Furthermore, an abrupt decrease in τ_*^H from positive ($\sim +0.2$) to negative (~ -0.2) values at a certain critical pressure P has been observed for octadecanol, which has been attributed[35–41] to a phase transition within the surfactant adsorption layer.

Thus the finite thickness layer method, in particular Hansen's method improved by Motomura,[35] permits certain definite conclusions concerning the structure of interfacial (adsorption) layers. On the other hand, the mechanism of the influence of hydrostatic pressure P on the interfacial tension σ_0 is not entirely clear. For example, it follows from Eqn. (49) that a layer with a thickness τ^H is 'solid-like' (if one uses the ideas of local thermodynamics), i.e. an increase in pressure in the bulk phase is not transmitted to the mobile wall in contact with this layer (Fig. 2). The interfacial layer with a thickness τ^H as it were shields the wall from the external pressure and an increase in pressure dP leads to an increase in interfacial tension by $d\sigma_0 = \tau^H dP$. The decrease in σ_0 with increase in P proves to be difficult to express in terms of local thermodynamics, since it is not clear why an increase in pressure leads in this instance to a marked decrease in the depth of the minimum on the $P_T(z)$ curve (Fig. 3), which is greater than the increase in P in the system.

III. Thermodynamics of plane-parallel thin liquid films

1. Definition of a thermodynamic system incorporating a thin liquid film

We shall consider a system (Fig. 6) incorporating a plane-parallel liquid film with an area A fixed on a rigid frame which can be moved without friction by an external force f_e.[10,13,44] The film is in mechanical equilibrium with the flowing (liquid or gaseous) phase β surrounding it and the liquid phase α from which it is formed. The chemical potentials μ_i of the ith components are equal in all the phases of the system and in the film. The external force f_e is balanced by the tension of the film γ. A force f_α is applied to the left-hand piston. With its aid, the pressure P_α within phase α in this piston is controlled. The chemical potentials (the numbers of moles of the components) can be varied with the aid of a material source ν_i.

An open subsystem with a volume V (Fig. 6) (containing phase β and the film element) in thermal, material, and mechanical equilibrium with the system considered above is examined simultaneously.

2. Fundamental equation of a system containing a thin liquid film

If the variable parameters of the system are the temperature T, the volume of the system V, the area of the film A, and the number of moles N_i of the ith component, then the fundamental equation for such a system can be written in the form[4,9,10,13,45]

$$dF = -S dT - P_\beta dV + \sum_i \mu_i dN_i + \gamma dA.$$

In terms of the variables T, V, μ_i, and A, the fundamental equation for the system becomes[13, 16, 46, 47]

$$d\Omega = -S\,dT - P_\beta\,dV - \sum_i N_i\,d\mu_i + \gamma\,dA, \tag{58}$$

where $\Omega = F - \sum \mu_i N_i$ is the grand thermodynamic potential and F is the Helmholtz free energy of the system.

3. Membrane model of a thin liquid film

By analogy with Gibb's approach[11] to the thermodynamic description of free interfaces, Deryagin and coworkers[1,2] developed the thermodynamics of thin liquid films using a membrane of zero thickness as the reference thermodynamic model of the film. They determined the excess thermodynamic quantities relative to this membrane.

Within the framework of this model, the volume of the system V is equal to the volume of the reference phase β, i.e. $V_\beta = V$, and one assumes arbitrarily that

$$N_i = N_{i\beta} + \tilde{N}_{if}, \tag{59}$$

$$S = S_\beta + \tilde{S}_f, \tag{60}$$

where $N_{i\beta}$ and S_β are the number of moles of the ith component and the entropy of the reference phase β, and $\tilde{N}_{if}$ and $\tilde{S}_f$ are the corresponding excess values of these quantities for the reference phase referred to the membrane. The free energy of the system Ω is also expressed by the sum

$$\Omega = \Omega_\beta + \tilde{\Omega}_f, \tag{61}$$

where Ω_β and $\tilde{\Omega}_f$ are the free energy of the reference phase β and the excess free energy referred to the membrane, respectively.

The fundamental equation (58) for the system is written in the form

$$d\Omega = d\Omega_\beta + d\tilde{\Omega}_f, \tag{62}$$

where

$$d\Omega_\beta = -S_\beta\,dT - P_\beta\,dV_\beta - \sum_i N_{i\beta}\,d\mu_i \tag{63}$$

is the fundamental equation of the reference phase β and

$$d\tilde{\Omega}_f = -\tilde{S}_f\,dT - \sum_i \tilde{N}_{if}\,d\mu_i + \gamma\,dA \tag{64}$$

is the fundamental equation for the membrane.

a. Hydrostatic pressure in a thin liquid film

A thin liquid film cannot be regarded as a phase because, as within the transition region of the interface, intensive thermodynamic parameters (such as the pressure and the densities of matter, internal energy, entropy, etc.) change sharply within it perpendicular to its plane. Within the framework of local thermodynamics,[26–29, 47, 48] thin liquid films are represented as an anisotropic medium in each microscopic volume of which the fulfillment of the principal thermodynamic relations is postulated. In particular, the fulfillment of the condition for mechanical equilibrium [condition (1)] is postulated, whereas in an isotropic medium the tangential components of the hydrostatic pressure tensor $\boldsymbol{P}$ are zero, while the normal components P_{xx}, P_{yy}, and P_{zz} are equal to the hydrostatic pressure P in the isotropic medium. As in interfaces (Fig. 3), the tangential components within the liquid film are zero, while the normal components (Fig. 7*a*) are

$$P_{xx} = P_{yy} = P_T(z), \tag{65}$$

$$P_{zz} = P_N = P. \tag{66}$$

In the case of a plane-parallel thin liquid film, the pressure tensor component P_N is independent of the coordinate z. Within curved thin liquid films of constant thickness, the pressure P_N varies, remaining nevertheless compressive (positive).

b. Film tension

In the membrane approach, the film tension γ is understood as the specific excess pressure $P_T(z)$ (per unit length) relative to the isotropic hydrostatic pressure P_β in the reference phase β acting in the direction tending to reduce the film area:[7, 9, 26–29, 45, 47, 48]

$$\gamma = -\int_{-\infty}^{+\infty} [P_T(z) - P_\beta]dz = -\int_{-\infty}^{+\infty} [P_T(z) - P_N]dz, \tag{67}$$

where the integration with respect to z is carried out in the region of the inhomogeneity of the film and the minus sign before the integral is selected in conformity with the definition of the film tension as the force tending to reduce the length of the film.

Fig. 7*b* shows that in the membrane approach the plane bounding the system on the right is acted upon by the pressure P_β directed to the right and the film tension γ directed to the left. These forces are balanced by the force of the pressure P_β acting on the plane from the right and by the external force f_e directed to the right. Thus the specific force (per unit length of the film) is equal in magnitude to the film tension γ.

The following definition of the film tension follows from the fundamental equation (64):

$$\gamma = \left.\frac{\partial \tilde{\Omega}_f}{\partial A}\right|_{\mu_i, T}, \tag{68}$$

$$\gamma = \left.\frac{\partial \Omega}{\partial A}\right|_{\mu_i, T, V_\beta}. \tag{69}$$

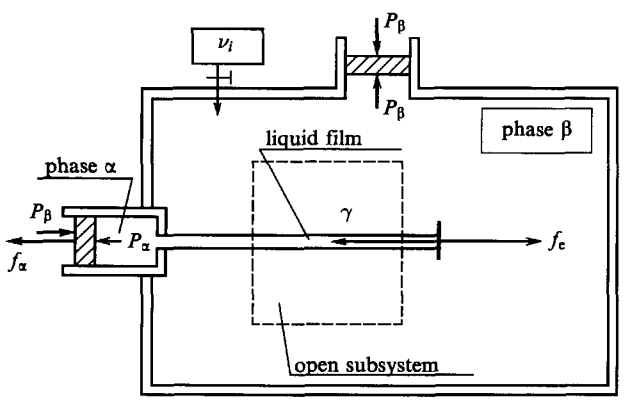


Figure 6. A closed system incorporating a flowing (liquid or gaseous) phase β and a plane-parallel liquid film formed from the liquid phase α.

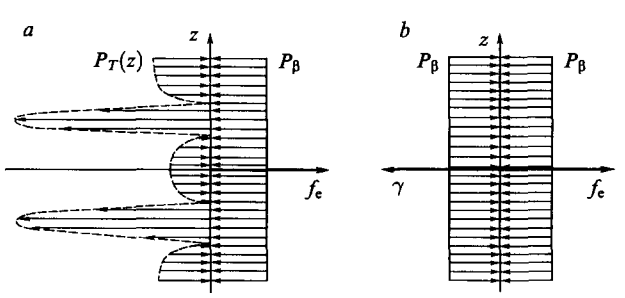


Figure 7. The membrane model of a liquid film: (*a*) equilibrium in a section of the vertical plane of the film holder acted upon by an external force f_e and the hydrostatic pressure P_β from the right and by the local pressure $P_T(z)$ from the direction of the film on the left; (*b*) result of the replacement of the film by a membrane of zero thickness.

This actually means that the film is stretched when the piston comprising the cylinder containing phase α is stationary (the volume of phase β is then also kept constant).

4. The model of the film based on the concept of two dividing surfaces

The thermodynamics of thin liquid films, based on this idea, was first worked out by Rusanov[3-5,8] and was subsequently developed in a number of other studies.[6,7,9,16,17,44-47]

In this model, the thin liquid film is represented by a thin layer of the reference phase α with a finite thickness H, separated from the external reference phase β by the dividing surfaces (as defined by Gibbs) (Fig. 8). The volume of the open subsystem V is equal to the sum of the volumes of the reference phase β and phase α from which the film has been obtained:

$$V = V_\beta + V_\alpha. \tag{70}$$

Under these conditions, $V_\alpha = V_f$, and $dV_\alpha = -dV_\beta$ (if V = const.) and the following relation also holds:

$$dV_f = dV_\alpha = A\,dH + H\,dA. \tag{71}$$

The grand thermodynamic potential of the system Ω is now formulated as the sum

$$\Omega = \Omega_\beta + \Omega_\alpha + \tilde{\Omega}_s, \tag{72}$$

where Ω_β and Ω_α are the free energies of the reference phases β and α respectively and $\tilde{\Omega}_s$ is the excess grand thermodynamic potential for the reference phases β and α referred to the two dividing surfaces.

The fundamental equation for the system is written in the form

$$d\Omega = d\Omega_\beta + d\Omega_\alpha + d\tilde{\Omega}_\sigma, \tag{73}$$

where the fundamental equations for phases β and α are respectively

$$d\Omega_\beta = -S_\beta\,dT - \sum_i N_{i\beta}\,d\mu_i - P_\beta\,dV_\beta, \tag{74}$$

$$d\Omega_\alpha = -S_\alpha\,dT - \sum_i N_{i\alpha}\,d\mu_i - P_\alpha\,dV_\alpha, \tag{75}$$

where P_α is the pressure in phase α, which is the reference phase for the film:

$$S = S_\beta + S_\alpha + \tilde{S}_s, \tag{76}$$

$$N_i = N_{i\beta} + N_{i\alpha} + \tilde{N}_{is}. \tag{77}$$

Here $\tilde{S}_s$ and $\tilde{N}_{is}$ are the excess entropy and the excess number of moles of the ith component respectively for the reference phases β and α relative to the two dividing surfaces.

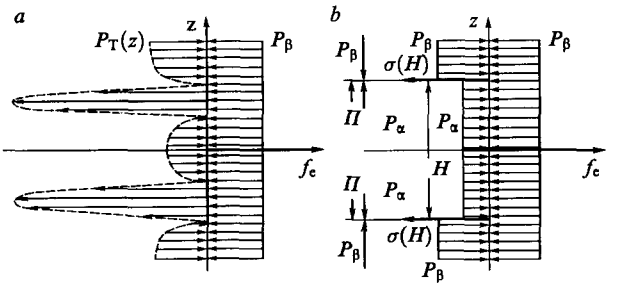


Figure 8. Illustration of the model of the liquid film based on the concept of two dividing surfaces in the film: (*a*) equilibrium in the film holder acted upon by $P_T(z)$, P_β, and f_e; (*b*) result of the replacement of the film by an idealised model comprising two interacting dividing surfaces and a layer of phase α having a thickness H.

The fundamental equations for two interacting dividing film surfaces is obtained from Eqns (58), (70), and (73)–(77):[13,16,47]

$$d\tilde{\Omega}_s = -\tilde{S}_s\,dT - \sum_i \tilde{N}_{is}\,d\mu_i - (P_\beta - P_\alpha)\,dV_\alpha + \gamma\,dA. \tag{78}$$

Taking into account Eqn. (71) as well as the definition of the disjoining pressure[28,29]

$$\Pi = P_\beta - P_\alpha, \tag{79}$$

and the definition[5,8,17,44] of the interfacial tension $\sigma(H)$ in a film with a thickness H, i.e.

$$\gamma = 2\sigma + \Pi H, \tag{80}$$

the fundamental equation for interacting dividing surfaces was obtained:[16]

$$d\tilde{\Omega}_s = -\tilde{S}_s\,dT - \sum_i \tilde{N}_{is}\,d\mu_i - \Pi A\,dH + 2\sigma\,dA. \tag{81}$$

a. The disjoining pressure in a liquid film

According to the formal definition, the disjoining pressure Π in a film[28,29] is equal to the difference between the hydrostatic pressures in the two reference phases β and α under the conditions of the equilibrium between the film and these phases. Since, as shown above [see Eqn. (66)], the normal component of the pressure $P_{zz} = P_N$ in the film is equal to the pressure P_β in phase β, Eqn. (79) can be rewritten in the following form:

$$\Pi = P_N - P_\alpha, \tag{82}$$

which corresponds best, according to a number of workers,[6,7,8,20,28,29] to the physical significance of the disjoining pressure.

There exist two points of view on the interpretation of the physical significance of the disjoining pressure Π. One group of workers[9,28,29,45,49,50] understand the disjoining pressure as the manifestation of forces of the 'second kind',[28,29,51] which arise in the region of the mutual overlap of the "surface forces of the first kind", i.e. two interfacial discontinuity surfaces (dividing surfaces according to Gibbs). The disjoining pressure is then represented as a pressure acting within the bulk of the film and existing, as it were, independently of the dividing surfaces of the film. The dividing surfaces are assumed not to interact with one another, so that the interfacial tension remains constant in magnitude as the film thickness diminishes and is equal to σ_0 (i.e. to the interfacial tension of the boundary of the bulk phases). The reference pressure in the film (the Gibbs reference pressure) chosen in some investigations[9,45,50] is not the hydrostatic pressure P_α but the hydrostatic pressure P_β. It has been shown[16] that this choice of reference pressure leads to the appearance of a pressure gradient in the transition region of the film and to difficulties in the determination of the disjoining pressure in this region.

The second group of workers[10,13,14,16,17,44,52-54] use the concept of the disjoining pressure as a specific force (per unit area) of the interaction between the dividing surfaces in the film. The chosen reference phase and pressure in the film are α and P_α respectively, so that a pressure gradient does not arise in the transition region of the film.[16]

The interfacial tension $\sigma(H)$ corresponding to this concept of the pressure is a function of the film thickness H. The following expression for the disjoining pressure arises from the fundamental Eqn. (81):

$$\Pi = -\frac{1}{A}\left.\frac{\partial\tilde{\Omega}_s}{\partial H}\right|_{T,\mu_i,A}, \tag{83}$$

where $\tilde{\Omega}_s$ has the significance of the excess free energy of the interacting dividing surfaces in a film with a thickness H. The function $\Pi(H)$ is called the isotherm of the disjoining pressure in the film. Despite the fact that the film thickness was chosen arbitrarily, the disjoining pressure is independent of the choice of the parameter H, i.e. is invariant for a fixed physical state of the film (is determined by the parameters T, μ_i, P_α, and P_β).

b. The interfacial tension in a thin liquid film

According to the definition, the interfacial tension σ [Eqn. (80)] depends on the choice of the positions of the dividing surfaces in the film (i.e. on the parameter H) for a fixed physical state of the film. If the film tension γ and the disjoining pressure Π are invariant and independent of the parameter H for the constant T, μ_i, P_α, and P_β, then σ depends linearly on H:

$$2\{\sigma\} = \gamma - \Pi\{H\}, \tag{84}$$

(the braces denote that the parameter H varies virtually for a fixed physical state of the system).

The interfacial tension σ is by definition the specific (referred to unit length) excess pressure $P_T(z)$ from the reference phases β and α compared with the isotropic pressures P_β and P_α in the reference phases relative to the dividing surfaces[6,9,10,16] (Fig. 8):

$$2\sigma(H) = -\int_{-\infty}^{-H/2} [P_T(z) - P_\beta]\,dz - \int_{-H/2}^{+H/2} [P_T(z) - P_\alpha]\,dz - \int_{+H/2}^{+\infty} [P_T(z) - P_\beta]\,dz. \tag{85}$$

If the film thickness really increases, which may be indicated by a decrease in the difference between the hydrostatic pressures $\Pi = P_\beta - P_\alpha$ (for $P_\beta \geqslant P_\alpha$), then it follows from Eqn. (67) that the film tension γ also varies and tends to γ_0, corresponding to the condition $\Pi = 0$. Then, according to Eqn. (80), the interfacial tension also tends to its limiting value σ_0 corresponding to the absence of interaction between the dividing surfaces and we have $\gamma_0 = 2\sigma_0$. As was to be expected, under these conditions the interfacial tension in such a thick liquid film is independent of the position of the dividing surfaces.

c. The specific free energy of the interaction in the film

For a real increase in film thickness from a certain value H to infinity for constant parameters T, μ_i, and A, the disjoining pressure executes an amount of work which is given by the following expression according to the fundamental Eqn. (81):

$$\tilde{\Omega}_s(\infty) - \tilde{\Omega}_s(H) = -A\int_H^\infty \Pi(H)\,dH. \tag{86}$$

Having put

$$\Delta\Omega(H) = \frac{\tilde{\Omega}_s(H) - \tilde{\Omega}_s(\infty)}{A}, \tag{87}$$

where $\Delta\Omega(H)$ is the specific (referred to unit surface area) free energy (grand thermodynamic potential) of the interaction between the dividing surfaces in a film with a thickness H, we obtain a relation which is valid for constant T, μ_i, and A:

$$\Delta\Omega(H) = \int_H^\infty \Pi(H)\,dH. \tag{88}$$

By putting

$$\tilde{S}_s = 2As_s, \tag{89}$$

$$\tilde{N}_{is} = 2A\Gamma_i, \tag{90}$$

we can rewrite the fundamental Eqn. (81) in the form

$$d\tilde{\Omega}_s = -2As_s\,dT - 2A\sum_i \Gamma_i\,d\mu_i - \Pi A\,dH + 2\sigma\,dA, \tag{91}$$

where s_s and Γ_i are the specific (referred to one of the dividing surfaces of a film with a thickness H) excess entropy and number of moles of the ith component respectively and Γ_i is referred to as the adsorption of the ith component on the film surface.

When the surfaces in the film are really moved apart an infinitely great distance, the disjoining pressure Π tends to zero and we obtain the following expression for free non-interacting surfaces in a plane-parallel film when account is taken of Eqn. (91):

$$d\Omega_s^0 = -2As_s^0\,dT - 2A\sum_i \Gamma_i^0\,d\mu_i + 2\sigma_o\,dA, \tag{92}$$

where the superscript 0 means that the corresponding quantity refers to a free planar surface.

By integrating the fundamental Eqn. (91) with respect to the film area A for constant T, μ_i, and H, we obtain[16]

$$\tilde{\Omega}_s(H) = 2\sigma(H)A. \tag{93}$$

If the film thickness is infinte in such integration (the case of non-interacting planar dividing surfaces), we have from Eqn. (92)

$$\tilde{\Omega}_s(\infty) = 2\sigma_o A. \tag{94}$$

An important relation of the thermodynamics of plane-parallel thin liquid films arises from Eqns. (86)–(88), (92)–(94):[16]

$$\Delta\Omega(H) = 2\Delta\sigma = 2\sigma(H) - 2\sigma_0 = \int_H^\infty \Pi(H)\,dH. \tag{95}$$

We recall that the definition (95) is valid for constant parameters T, μ_i, and A. Taking into account the relation between the grand thermodynamic potential Ω and the Helmholtz free energy F, i.e. $\Omega = F - \sum N_i\mu_i$, we obtain the following relation for the constant parameters indicated above:

$$\Delta F(H) = \Delta\sigma(H) - 2\sum_i \Delta\Gamma_i(H)\mu_i, \tag{96}$$

where

$$\Delta F(H) = \frac{F_s(H) - F_s(\infty)}{A}, \tag{97}$$

and

$$\Delta\Gamma_i(H) = \Gamma_i(H) - \Gamma_i(\infty), \tag{98}$$

Here $\Gamma_i(\infty)$ and $F_s(\infty)$ are the adsorption and the Helmholtz free energy of the non-interacting surfaces. Furthermore, the following relation holds:[16]

$$\Delta F(H) = \int_H^\infty \Pi(H)\,dA - 2\sum_i \Delta\Gamma_i(H)\mu_i. \tag{99}$$

d. The Gibbs–Duhem equation for a plane-parallel thin liquid film

On differentiating Eqn. (93) and combining the result with Eqn. (91), we obtain[13,16] the Gibbs–Duhem equation for interacting dividing surfaces in a thin liquid film with a thickness H:

$$2d\sigma = -2s_s\,dT - 2\sum_i \Gamma_i\,d\mu_i - \Pi\,dH, \tag{100}$$

which is converted into the familiar Gibbs–Duhem equation for free (non-interacting) planar surfaces:[11,23]

$$d\sigma_0 = -s_s^0\,dT - \sum_i \Gamma_i^0\,d\mu_i. \tag{101}$$

Evidently the disjoining pressure $\Pi(H)$ and the interfacial tension $\sigma(H)$ are linked by the relation

$$\Pi(H) = -2\frac{\partial\sigma(H)}{\partial H}\bigg|_{T,\mu_i}, \tag{102}$$

which follows from Eqn. (100) and is also known as the Gibbs–Duhem equation for a plane-parallel film.

In thermodynamics based on the membrane approach, the Gibbs–Duhem equation

$$d\gamma = -s_f\,dT - \sum_i \Gamma_{if}\,d\mu_i, \tag{103}$$

is obtained from the fundamental Eqn. (64) in the same way as Eqn. (100), i.e. by integrating Eqn. (64) with respect to A for constant T and μ_i as well as P_α and P_β and subsequent differentiation and simultaneous solution with Eqn. (64). Here

$$s_f = \frac{\tilde{S}_f}{A}; \quad \Gamma_{if} = \frac{\tilde{N}_{if}}{A}, \tag{104}$$

are the specific (referred to unit area of a membrane of zero thickness) excess entropy and number of moles of the ith component.

We may note that s_f and Γ_{if} differ from the corresponding excess amounts s_s and Γ_i defined by Eqns. (89) and (90).

5. The film model based on the concept of a membrane of finite thickness

In the approach based on the concept of the film as a membrane of zero thickness, the film thickness naturally cannot be regarded as a thermodynamic parameter of the system. This approach can be used for the description of those experiments in which the film thickness H is not measured and the pressure in the reference phase α is also unknown.

If the change in the volume of the system dV can be measured experimentally with adequate accuracy (Fig. 6), then, for a known film area A, it is possible to determine the effective film thickness H^*. When the temperature T and the chemical potential μ_i of the ith components are kept constant, it is of interest to examine two situations.

1. If the hydrostatic pressure in phase β as well as the external force f_α are kept constant then, following an increase in the film area A by dA when the film is acted upon by f_e, the volume of the system increases by dV, while the effective film thickness can be determined from the relation

$$H^* = dV\,dA \quad .$$

The volume of the system then changes largely as regards the volume of phase α from which the film has been formed.

2. If the force f_α is constant (i.e. the pressure in phase α is constant although unknown) and the film area is likewise constant, then an increase in the pressure in phase β can lead to a measurable decrease in the volume of the system by an amount dV. This makes it possible to determine the change in the effective film thickness dH^* from the relation $dH^* = dV/A$. Furthermore, in the latter case it is possible to determine the change in the film tension γ, which is interpreted as the influence of the external pressure on the mechanical (energy) properties of the film.

We may note that in both cases it is assumed that the composition of phase α within the film and the constant pressure P_α are assumed to be unknown and the variable parameters are the pressure P_β, the temperature T, the chemical potentials μ_i of the ith components, and the film tension γ which is equal to the force f_e.

The film thermodynamics, based on the model of a membrane with a finite thickness, is constructed on the basis of the fundamental Eqn. (58) and the volume V of the open subsystem is represented by the sum

$$V = V_\beta + V_f, \tag{105}$$

where V_β is the volume of the reference phase β and V_f is the volume of the film which can be found by varying the volume of the reference phase β during the formation of a film having an area A for constant parameters T, μ_i, P_β, and P_α.

a. Fundamental equation for a membrane with a finite thickness

Having put the fundamental Eqn. (58) for an open subsystem containing a plane-parallel thin liquid film in the form

$$d\Omega = d\Omega_\beta + d\tilde{\Omega}_f^*,$$

having retained the previous form of the fundamental equation [Eqn. (63)] for the reference phase β, and using for the membrane the expression

$$d\tilde{\Omega}_f^* = -\tilde{S}_f^*\,dT - \sum_i \tilde{N}_{if}^*\,d\mu_i - P_\beta\,dV_f + \gamma\,dA, \tag{106}$$

($\tilde{S}_f^*$ and $\tilde{N}_{if}^*$ are the excess entropy and the number of moles of the ith component of the reference phase β on a membrane of finite thickness), we obtain the following equation defining the tension of a film of finite thickness:

$$\gamma = \left.\frac{\partial \tilde{\Omega}_f^*}{\partial A}\right|_{T,\mu_i,V_f}. \tag{107}$$

We may note that the excess entropy and the excess numbers of moles of components in Eqn. (106) differ from the corresponding excess amounts which enter into Eqn. (64) because the volumes of the reference phases β are different in the two cases.

b. The Gibbs–Duhem equation for a membrane of finite thickness

Having integrated the fundamental equation for a membrane of finite thickness [Eqn. (106)] with respect to the extensive parameters V_f and A for constant intensive parameters T and μ_i, we obtain

$$\tilde{\Omega}_f^* = -P_f V_f + \gamma A.$$

After differentiating the resulting equation and combining the result with Eqn. (106), we have

$$A\,d\gamma = -\tilde{S}_f^*\,dT - \sum_i \tilde{N}_{if}^*\,d\mu_i + V_f\,dP_\beta. \tag{108}$$

Introducing the effective film thickness

$$H^* = \frac{V_f}{A}, \tag{109}$$

and also the effective specific surface excess entropy and excess number of moles of the ith component, i.e.

$$s_f^* = \frac{\tilde{S}_f^*}{A} \qquad \Gamma_i^* = \frac{\tilde{N}_{if}^*}{A}, \tag{110}$$

which differ from the corresponding values defined by Eqn. (104), we obtain the Gibbs–Duhem equation for this case in the form

$$d\gamma = -s_f^*\,dT - \sum_i \Gamma_i^*\,d\mu_i + H^*\,dP_\beta. \tag{111}$$

c. Frumkin's equation

We may note that the effective film thickness H^*, defined by Eqn. (109), can be obtained from Eqn. (111):

$$H^* = \left.\frac{\partial \gamma}{\partial P_\beta}\right|_{T,\mu_i}. \tag{112}$$

It differs from the film thickness defined as the distance between two equimolecular (as defined by Gibbs) surfaces for which $\Gamma_1 = 0$ (Γ_1 is the adsorption of the solvent on the film interface) or in other ways (for example, as the distance between two tension surfaces, etc.).

Using the definitions of the disjoining pressure [see Eqns. (79) and (82)] and taking into account the fact that for a constant pressure P_α the relation $dP_\beta = d\Pi$ holds, one can rewrite Eqn. (112) as follows:[55]

$$H^* = \left.\frac{\partial \gamma}{\partial \Pi}\right|_{T,\mu_i}. \tag{113}$$

The relation obtained is known as Frumkin's equation in a differential form.[10, 45]

Integrating Eqn. (111) with respect to Π for constant T and μ_i, we find (in terms of our notation)

$$\gamma = \gamma^0 + H^*\Pi + \int_{H^*}^{\infty} \Pi \, dH. \tag{114}$$

Assuming that γ^0, the film tension at $\Pi = 0$ (i.e. in the case of an infinitely large H^*), can be replaced by $2\sigma_0$ (where σ_0 is the interfacial tension of a free planar surface), Eqn. (114) can be rewritten thus:[45, 55]

$$\gamma = 2\sigma_0 + H^*\Pi + \int_{H^*}^{\infty} \Pi \, dH. \tag{115}$$

This expression is known as the integral form of Frumkin's equation.

We may note that Eqn. (115) was derived for the special case corresponding to the special selection of the film thickness defined by Eqn. (190). In contrast to this, on taking into account Eqn. (95), Eqn. (80) can be written in the form

$$\gamma = 2\sigma_0 + H\Pi + \int_{H}^{\infty} \Pi \, dH, \tag{116}$$

and is valid for any choice of the positions of the dividing surfaces in the film and it is therefore more general than Eqn. (115).

The introduction into consideration of the disjoining pressure Π in the approach based on the concept of the film as a membrane of finite thickness is equivalent to the formal replacement of the pressure P_β by Π in the fundamental Eqn. (106) for the membrane. Such replacement was natural in the approach based on the concept of two dividing surfaces in the film [see Eqn. (78)], because the reference phase α with a pressure P_α was introduced into consideration in order to calculate the excess thermodynamic parameters relative to the dividing surfaces. On the other hand, in the case of a membrane of finite thickness, where the excess thermodynamic parameters are calculated relative to the entire membrane, the pressure P_α is assumed to be unknown (although it is kept constant with the aid of an external force f_α—see Fig. 6). The disjoining pressure Π in Eqn. (115) is also unknown because it was determined with an accuracy to within a constant quantity.

Thus the replacement of P_β by the disjoining pressure Π in Eqn. (106)[9, 45] is, strictly speaking, illegitimate. On the other hand, the Gibbs–Duhem equation, derived on the basis of a weaker condition, namely that $dP_\beta = d\Pi$, is more rigorous, like Frumkin's equation in the differential form (113), which follows from Eqn. (111) written in the form[45]

$$d\gamma = -s_f^* \, dT - \sum_i \Gamma_i^* \, d\mu_i + H^* \, d\Pi. \tag{117}$$

The discussion concerning the definition of the disjoining pressure in thermodynamics, based on the concept of a film as a membrane of finite thickness, was taken up by a number of workers.[9, 31, 44, 45] One of the considerations was the problem of the choice of the reference pressure for the film: de Feijter et al.[44] used P_α as the reference pressure, Toshev and Ivanov[6, 45] chose P_β. Whereas for plane-parallel films the choice of the reference pressure is insignificant, since it leads formally to the same Gibbs–Duhem equation for the film, it has been shown[16] that in the case of the transition region the second approach leads to difficulties associated with the need to take into account the hydrostatic pressure gradient in this region of the film.

IV. Conclusion

The above analysis of studies in the thermodynamics of plane-parallel liquid thick and thin films showed that three main approaches to the construction of such thermodynamics have now been developed.

The first approach, based on the thermodynamic film model as a membrane of zero thickness, developed by Deryagin and coworkers,[1,2] relates the excess free energy (grand thermodynamic potential) of the system $\tilde{\Omega}_f$, referred to the membrane, to variable thermodynamic parameters: the temperature T, the chemical potentials μ_i of the ith components, and the film area A:

$$d\tilde{\Omega}_f = -\tilde{S}_f \, dT - \sum_i \tilde{N}_{if} \, d\mu_i + \gamma \, dA,$$

where $\tilde{S}_f$ and $\tilde{N}_{if}$ are the excess entropy and the excess number of moles of the ith component of the reference phase β (Fig. 7), referred to the membrane, and γ is the film tension.

The Gibbs–Duhem equation for constant T, μ_i, and P_β assumes the form

$$d\gamma = -s_f \, dT - \sum_i \Gamma_{if} \, d\mu_i,$$

where s_f and Γ_{if} are the specific (referred to unit area of the membrane) excess entropy and excess numbers of moles of the ith components.

The membrane approach is convenient when a description of the mechanical and energy behaviour of thin liquid films, whose thickness is not measured experimentally, is required.

The second approach is based on the concept of the film as a membrane of finite thickness[6, 7, 9, 45, 56] and relates the excess free energy $\tilde{\Omega}_f^*$ to the variable parameters T, μ_i, and A and also to the film volume V_f, which is assumed equal to the apparent change in the volume of the system (Fig. 7) on formation of a film with an area A for constant T, μ_i, P_β, and P_α [see Eqn. (106)]:

$$d\tilde{\Omega}_f^* = -\tilde{S}_f^* \, dT - \sum_i \tilde{N}_{if}^* \, d\mu_i + H^* \, dP_\beta,$$

where the excess amounts $\tilde{S}_f^*$ and $\tilde{N}_{if}^*$ differ from the corresponding excess amounts in Eqn. (64).

The Gibbs–Duhem equation is written in this case in the form

$$d\gamma = -s_f^* \, dT - \sum_i \Gamma_{if}^* \, d\mu_i + H^* \, dP_\beta,$$

or, if $P_\alpha = \text{const.}$, then, taking into account that $dP_\beta = d\Pi$, it is formulated as follows:

$$d\gamma = -s_f^* \, dT - \sum_i \Gamma_{if}^* \, d\mu_i + H^* \, d\Pi,$$

where $H^* = V_f/A$ is the effective film thickness.

This approach is convenient when the experimental determination of the mechanical properties of a liquid film is accompanied by the measurement of the volume of the system containing the given film.

The third approach is based on the concept of two dividing surfaces in the film[3–5, 6] and relates the excess grand thermodynamic potential of the film $\tilde{\Omega}_s$ to the variable parameters T, μ_i, A, and the film thickness by the equation

$$d\tilde{\Omega}_s = -\tilde{S}_s \, dT - \sum_i \tilde{N}_{is} \, d\mu_i - \Pi A \, dH + 2\sigma \, dA,$$

in which the interfacial tension σ in a film having a thickness H is related to the tension γ by the expression

$$2\sigma = \gamma - \Pi H.$$

The corresponding Gibbs–Duhem equation is

$$2d\sigma = -2s_s \, dT - 2\sum_i \Gamma_i \, d\mu_i - \Pi \, dH.$$

The specific excess amounts s_s and Γ_i are referred to one of the dividing surfaces of the film.

This approach is convenient when the experimental measurement of the mechanical properties of the film is accompanied by the simultaneous measurement of its thickness at a known pressure P_α in phase α.

Thus the use of a specific approach to the description of the thermodynamic and mechanical behaviour of plane-parallel liquid (emulsion and foam) films is determined and limited by the possibility of the experimental measurement of the liquid film thickness and the pressure in the reference phase α from which the film has been formed. The approach based on the concept of two dividing surfaces in the film is optimum when it is extended to the transition region in liquid films within the limits of which the disjoining pressure varies sharply both in magnitude and in sign.

References

1. B V Deryagin, G A Martynov, Yu V Gutop *Kolloidn. Zh.* 27 367 (1965)
2. B V Derjaguin, G A Martynov, Yu V Gutop, in *Research in Surface Forces* Vol. 1 (New York: Consultants Bureau, 1966) p. 9
3. A I Rusanov *Kolloidn. Zh.* 28 718 (1966)
4. A I Russanov, in *Research in Surface Forces* Vol. 3 (New York: Consultants Bureau 1971) p. 103
5. A I Russanov *J. Colloid Interface Sci.* **53** 20 (1975)
6. B V Toshev, I B Ivanov *Colloid Polym. Sci.* **253** 558 (1975)
7. I B Ivanov, B V Toshev *Colloid Polym. Sci.* **253** 593 (1975)
8. A I Russanov *Phasengleichgewichte und Grenzflächenerscheinungen* (Berlin: Akademie Verlag, 1978)
9. J C Eriksson, B V Toshev *Colloids Surf.* **5** 241 (1982)
10. J A de Feijter, in *Thin Liquid Films. Fundamentals and Applications* (New York: Marcel Dekker, 1988) p. 1
11. J W Gibbs *Thermodynamic Papers* (Translated into Russian) (Moscow–Leningrad: Gostekhteorizdat, 1955)
12. A Scheludko, V Chakarov, B Toshev *J. Colloid Interface Sci.* **82** 83 (1981)
13. V G Babak *Fizikokhimiya Mikroskopicheskikh Zhidkikh Plenok Stabilizirovannykh Polimerami. I. Termodinamika Kontaktnykh Vzaimodeistvii v Zhidkikh Sredakh* (Physical Chemistry of Microscopic Liquid Films Stabilised by Polymers. I. Thermodynamics of Contact Interactions in Liquid Media) (Sverdlovsk: Ural Univ., 1988)
14. V G Babak *Colloids Surf.* **25** 205 (1987)
15. I B Ivanov, P A Kralchevsky, in *Thin Liquid Films. Fundamentals and Applications* (New York: Marcel Dekker, 1988) p. 49
16. V G Babak *Voprosy Termodinamiki Geterogennykh Protsessov i Teorii Poverkhnostnykh Yavlenii* (Problems of the Thermodynamics of Heterogeneous Processes and the Theory of Surface Phenomena) (St. Petersburg: Izd. Petersburg. Univ., 1992) p. 82
17. V G Babak *Colloids Surf.* **25** 1 (1985)
18. A I Rusanov *Termodinamika Poverkhnostnykh Yavlenii* (Thermodynamics of Surface Phenomena) (Leningrad: Izd. Leningrad. Gos. Univ., 1960)
19. A I Rusanov *Fazovye Ravnovesiya i Poverkhnostnye Yavleniya* (Phase Equilibria and Surface Phenomena) (Leningrad: Khimiya, 1967)
20. A I Rusanov *Sovremennaya Teoriya Kapillyarnosti* (Modern Theory of Capillarity) (Leningrad: Khimiya, 1980) p. 13
21. S Ono, S Kondo, in *Handbuch der Physik* Band 10 (Berlin: Springer Verlag, 1960) S. 134
22. F P Buff, in *Handbuch der Physik* Band 10 (Berlin: Springer Verlag, 1960) S. 281
23. J S Rowlinson, B Widom *Molecular Theory of Capillarity* (Oxford: Oxford University Press, 1982)
24. F C Godrich *Surface and Colloid Science* (New York: Wiley, 1969)
25. V S Markin, M M Kozlov, S L Leikin *J. Chem. Soc., Faraday Trans. 2* **84** 1149 (1988)
26. P Kralchevsky, A Dimitrov, T Gurkov *J. Colloid Interface Sci.* **137** 217 (1990)
27. P Kralchevsky, I B Ivanov *J. Colloid Interface Sci.* **137** 234 (1990)
28. B V Deryagin, N V Churaev *Kolloidn. Zh.* 38 438 (1976)
29. B V Derjaguin, N V Churaev *J. Colloid Interface Sci.* **66** 389 (1978)
30. B U Felderhof *J. Chem. Phys.* **49** 44 (1968)
31. P M Bish, H Wendel *J. Colloid Interface Sci.* **96** 555 (1983)
32. G Rickayzen, P Richmond, in *Thin Liquid Films. Fundamentals and Applications* (New York: Marcel Dekker, 1988) p. 131
33. J C Melrose *Ind. Eng. Chem.* **60** 53 (1968)
34. R S Hansen *J. Phys. Chem.* **66** 410 (1962)
35. K Motomura *Adv. Colloid Interface Sci.* **12** 1 (1980)
36. V S Markin, A G Volkov *J. Colloid Interface Sci.* **135** 553 (1990)
37. C Bakker *Kapilläritat und Oberflächenspannung. Handbuch der experimentallen Physik* Band 6 (Leipzig: Wien-Harms,1928)
38. R J Good, F P Buff *Sovremennaya Teoriya Kapillyarnosti* (Modern Theory of Capillarity, translated into Russian) (Leningrad: Khimiya, 1980) p. 63
39. H Y Jennings *J. Colloid Interface Sci.* **24** 323 (1967)
40. K Motomura, N Matabayasi, M Aratono, R Matuura *J. Colloid Interface Sci.* **64** 356 (1978)
41. K Motomura, M Aratono, N Matabayasi, R Matuura *J. Colloid Interface Sci.* **67** 247 (1978)
42. N Matabayasi, K Motomura, M Aratono, R Matuura *Bull. Chem. Soc. Jpn.* **51** 2800 (1978)
43. J C Eriksson *Ark. Kemi* **25** 331 (1965)
44. J A de Feijter, J B Rijnbout, A Vrij *J. Colloid Interface Sci.* **64** 258 (1978)
45. B V Toshev *Colloids Surf.* **2** 243 (1981)
46. B V Babak, in *Proceedings of the 8th Conference on Surface and Colloid Chemistry* (Liblice, 1989) p. 5
47. V G Babak, in *Proceedings of the International Symposium on Calorimetry and Chemical Thermodynamics 1991* p.121
48. B V Derjaguin, Yu V Gutop, in *Research in Surface Forces* Vol. 3 (New York: Consultants Bureau, 1971) p. 122
49. N V Churaev, V M Starov, B V Derjaguin *J. Colloid Interface Sci.* **89** 16 (1982)
50. J C Eriksson, B V Toshev *Colloids Polym. Sci.* **264** 807 (1986)
51. B V Deryagin, N V Churaev, V M Muller *Poverkhnostnye Sily* (Surface Forces) (Moscow: Nauka, 1985)
52. J A de Feijter, A Vrij *J. Electroanal. Chem.* **37** 9 (1972)
53. V G Babak *Colloids Surf.* **25** 25 (1987)
54. P A Kralchevsky, I B Ivanov *Chem. Phys. Lett.* **121** 116 (1985)
55. A N Frumkin *Zh. Fiz. Khim.* **12** 337 (**1938**)
56. G A Martynov, I B Ivanov, B V Toshev *Kolloidn. Zh.* 38 474 (1976)

Russian Chemical Reviews **62** (1) 23–33 (1993) ©Russian Academy of Sciences and Turpion Ltd

UDC 543.544.45+541.6

The use of correlation equations for the prediction of retention parameters in gas–liquid chromatography

V M Nabivach, V P Dmitrikov

Contents

I.	Introduction	23
II.	Dependence of retention parameters on the number of carbon atoms and the molecular mass	23
III.	Correlation between retention, the vapour pressure, and the boiling point	25
IV.	Dependence of the retention on the molecular refraction and the dipole moment	26
V.	Relation between the retention and the molar volume of the sorbate	27
VI.	The retention parameters and the principle of linear free energy relations	27
VII.	The use of the principle of the additivity of properties for the prediction of retention parameters	28
VIII.	Calculation of retention parameters with the aid of structural and topological parameters	29

Abstract. The correlations between the retention parameters and the physicochemical properties of sorbates are examined and the possibility of their use for the identification of compounds in gas–liquid chromatography is discussed. It is shown that the chromatographic retention can be most accurately fitted by multifactorial equations based on structural and topological parameters. The bibliography includes 256 references.

I. Introduction

A number of reviews and monographs have been devoted to the problem of the preliminary calculation of retention parameters and the identification of substances in gas–liquid chromatography (GLC).[1–4] At the present time, this topic continues to interest investigators, particularly in connection with the universal chemical analysis system being developed.[5, 6] The methodology underlying such a system involves using a computerised standard reference data bank to derive individual retention parameters and functional relations between the retention parameters and the physicochemical properties of the substances analysed.

Considerable advances have been achieved in qualitative analysis with the aid of so called standard-free identification methods[7, 8] based on the correlations between retention parameters and various physicochemical characteristics of the substances being separated. An advantage of these methods is that they do not require the availability of the postulated components of the test mixture.

The interaction in the sorbate–sorbent system, which determines the chromatographic retention of a substance, is a result of the structural units of the molecule being brought into contact. The mathematical modelling of the retention, which reflects the characteristics of such interactions, gives rise to the possibility of not only identifying the compound but also of predicting the chromatographic behaviour of its molecule as a whole, i.e. of achieving a predictive calculation of retention parameters on the basis of the postulated structural formula.[9–12]

V M Nabivach, V P Dmitrikov Chemical Engineering Institute, prosp. Gagarina 8, 320640 Dnepropetrovsk 5, Ukraine; Industrial Institute, ul. Dneprostroevskaya 2, 322618 Dneprodzerzhinsk, Ukraine

Received 15th August 1992
Uspekhi Khimii **62** (1) 27–38 (1993); translated by A K Grzybowski

The correlations between the structure of substances and chromatographic parameters frequently assume the form of linear equations, although other types of functions are also possible: fractional-linear, third degree, etc.[13, 14] The retention parameters used in correlation equations are proportional to the free energy change associated with the chromatographic distribution process. The relations between the structures of the substances separated and their chromatographic parameters can be regarded as an example of the linear free energy relations (LFER).[15]

The correlations between the physicochemical properties of sorbates, obtained mainly on non-polar and weakly polar stationary phases, for which adsorption effects do not exert a significant influence on the retention parameters, are analysed in this review.

II. Dependence of retention parameters on the number of carbon atoms and the molecular mass

A relation of the following type is frequently used in practice for chromatographic identification:

$$R = an + b, \qquad (1)$$

where R are logarithms of the corrected retention time or volume, the specific or relative retention volume, or the retention index, a is a constant characterising the contribution of the interaction energy of a CH_2 group with the stationary phase, b is a constant reflecting the contribution of the interaction of the functional groups with the sorbent to the retention energy, and n is the number of carbon atoms. The validity of Eqn. (1) for homologous series of different compounds has been confirmed in both early[7, 16–18] and later[19–23] studies. A relation of type (1) is characteristic of a wide range of organic substances (Table 1).

A linear relation holds more accurately for non-polar stationary phases, the retention on which is determined by dispersion forces. However, it has been noted[2] that the first members of a homologous series do not obey a linear correlation. This effect is apparently due to the fact that the properties of the methyl (or methylene) group located close to a functional group change under the influence of the latter. It has come to be assumed that the linear relation (1) holds rigorously starting from the third or fourth member of a homologous series, but there have been frequent instances of the breakdown of the linear relation up to the fifth to eighth members[40] and above.[41] Rohrschneider[42] noted the breakdown of linearity in the series of n-alkanes up to C_9,

Table 1. Homologous series of compounds for which the linear relation (1) has been established.

Homologous series	R	Stationary phase	Refs.
C_9-C_{19} *n*-alkanes	$\lg t'_R$	Squalane, phases with cyano-groups	24
C_5-C_8 *n*-alkanes, alkenes	$\lg V_R$	Porapak Q, Polysorbate-2, Polysorb	25
C_1-C_{12} *n*-alkanes	$\lg t'_R$	SE-30, OV-25, Silar 7CP	26
C_6-C_{14} *n*-alkenes	I	PEG 4000, poly(phenyl ether), OV-101, 1,2,3-tris-(2-cyanoethoxy)propane	27–29
n-Alkanes, cycloalkanes, C_4-C_{12} cycloalkenes	I	SE-30	30
C_6-C_{12} aromatic hydrocarbons	I	Squalane, OV-101	31, 32
C_6-C_9 alkylphenols and alkylanilines	I	Apiezon M	8
C_6-C_{10} alkyl- and alkenylpyridines	$\lg V_R$	PEG 1000	33
C_4-C_{10} aldehydes	I	Carbowax 1540	34
C_1-C_{12} aliphatic alcohols and amines	I	Apiezon L, PEG 2000	8, 35
C_1-C_{15} aliphatic amines	I	Apiezon L, Triton X-305, PEG 1000	36
C_2-C_{20} aliphatic amines	I	SE-30	30
Methyl esters of $C_{12}-C_{24}$ aliphatic acids	I	SE-30, OV-225, Silar 5CP	37
Methyl ethers of C_7-C_{17} phenols	$\lg V_g$	Apiezon L, poly(ethylene glycol succinate)	38
C_5-C_{14} esters	I	Squalane, Carbowax 1540	39

while Grigor'eva and Golovnya[43] showed that Eqn. (1) does not hold for any sequence of homologues containing more than 7–8 members. As regards the prediction of retention parameters, the above limitations extend over the interpolation range, the expansion of which leads to an increase in the error of the determination.[44]

The distortion of the linear relation is influenced by the parity of the number of carbon atoms: the free energy of solution increment for the methylene group in n-alkanes with an even number of carbon atoms is greater than in those with an odd number.[3]

The inaccurate determination of the 'dead' volume, the use of methane as the non-sorbable component, and the assumption that its retention volume is zero may also cause deviations from linearity. Reviews[45,46] have been devoted to these questions and to comparing the characteristics of the computational methods for the determination of the 'dead' volume.

In order to take into account the non-linear variation of retention parameters as a function of the number of carbon atoms, various equations have been proposed (Table 2). The majority of them describe the gas-chromatographic parameters of *n*-alkanes. Comparison of the retention parameters calculated by Eqns. (2)–(9) and determined experimentally showed that the highest accuracy of the calculation is achieved on the basis of Eqns. (4) and (8).[53] At the same time the error of the determination of retention indices by Eqn. (8), which is 3–6 units, restricts its application in identification with the use of a computer.[43]

The universal equation (10), describing the gas-chromatographic behaviour of all the members of any homologous series R_nX on stationary liquid phases of different polarity with an accuracy sufficient for the identification of homologues, including the first members, is free from this disadvantage.

It is easy to show that the change in the length of the hydrocarbon chain of the molecule by one CH_2 group (or another group or atom) leads to the corresponding change in the molecular weight of the compound, so that

$$R = aM_S + b, \tag{11}$$

where M_S is the molecular weight of the sorbate.

Eqn. (11), which was already noted by James,[56] has been confirmed in relation to various classes of compounds.[8,21,35,57] It is based on the enhancement of the dispersion interaction with increase in the volume and mass of the molecule and holds most rigorously for homologous series.[58,59] For non-polar systems, this relation is linear[60] and standard deviations of the calculated retention indices are 4–7 units[59] but can be also higher. They can be reduced with the aid of multifactorial equations. Thus the retention indices of 1-haloalkanes calculated by the equation $I = f(n, M_S)$ differ from the experimental values by 1–2 units.[61]

In polar systems, the correlation coefficient for Eqn. (11) is appreciably smaller[62] or this relation does not hold at all.[63]

Table 2. Non-linear equations for the calculation of the retention parameters in GLC as a function of the number of carbon atoms.

Homologous series	Equation	No. of equation	Refs.
n-Alkanes, *n*-alkenes	$\lg V_g = an - n/2 - b$	(2)	47
	$\lg t'_R = an + b\lg(n-4) + c$	(3)	48
n-Alkanes	$\lg V_g = an + b/(n-c) + d$	(4)	49
	$\lg t'_R = an + b\lg n + c\lg(\lg n) + d$	(5)	50
	$\lg V^{rel} = an + bn^2 + cn^3 + d + D\varphi$	(6)	51
n-Alkanes, *n*-alkenes, *n*-alkynes	$\lg t'_R = an + bn^2 + c$	(7)	29
n-Alkenes, amines, sulphides, aliphatic acids, alhehydes, ketones	$I = an + b/n + c$	(8)	36, 37
n-Alkenes, alkyl trichloroacetates	$\lg t'_R = an + bn^2 + cn^3 + d$	(9)	52
n-Alkanes,, amines, alcohols, aldehydes, ketones, sulphides, carbamates, alkylbenzenes	$I = an + b(\lg n)/n + c/[(n-2)^2 + 0.1] + d$	(10)	43, 53–55

III. Correlation between the retention, the vapour pressure, and the boiling point

A linear relation between the retention and the vapour pressure of the sorbate is valid for homologous series:

$$\lg V_g = a \lg p^0 + b. \quad (12)$$

It can be obtained from the fundamental Herington equation and the dependences of the vapour pressure and the activity coefficient on the number of carbon atoms in the molecule.[64]

Eqn. (12) holds over a wide temperature range up to a pressure of several atmospheres and can be used for identification.[3] The correlation improves if a term incorporating the activity coefficients of substances analysed is introduced into Eqn. (12).[4,64]

Dimov and Shopov[11] proposed a more accurate equation for the calculation of the retention indices of hydrocarbons on non-polar phases:

$$I_{p^0,v^0} = 100\frac{\lg(p_n^0 v_n^0/p_x^0 v_x^0)}{\lg(p_n^0 v_n^0/p_{n+1}^0 v_{n+1}^0)} + 100n, \quad (13)$$

where v_x^0, v_n^0, v_{n+1}^0 are the molar volumes of substances x and of n-hydrocarbons containing n and $n+1$ carbon atoms. Since the retention indices calculated by Eqn. (3) differ from the experimental Kovats indices, corrections must be applied in order to convert I_{p^0}, v^0 into I. The error of the calculation for isoalkanes in squalane is then reduced to 1.4 units, but the number of empirical corrections becomes as much as five, which renders the calculation extremely complex and cumbersome.

Relations similar to Eqn. (12) have been found for isoalkanes and cycloalkanes,[65] aromatic hydrocarbons,[32] and the hydrocarbons in petrol [gasoline] fractions.[66]

The linear dependence of retention parameters on the vapour pressure on non-polar phases has been widely used for the solution of the converse problem: the determination of the vapour pressure from GLC data.[13] The boiling points of compounds are most often used for the determination of correlations with chromatographic retention parameters. The simultaneous solution of Eqn. (12) and

$$\lg p^0 = b - aT_b$$

yields

$$R = aT_b + b. \quad (14)$$

Eqn. (14) does not hold rigorously even for homologous series, since the dependence of the boiling point on the number of carbon atoms is non-linear.[3] In homologous series, an increase in the boiling point per methylene group is approximately constant. However, in reality this difference between the boiling points diminishes with increase in the number of carbon atoms, i.e. it depends on the type of homologous series and M_S. Thus the difference between the boiling points for successive C_9-C_{16} n-alkanes decreases from 23.5 to 17.0 °C.[67]

Over a wide range of boiling points, deviations from linearity are observed even for hydrocarbons, especially for the lower members of this series.[3,68] These deviations are most notable in series of polar compounds such as phenols,[69] pyridines, quinolines,[60,70] etc.[71] Table 3 presents a list of homologous series for which Eqn. (14) is valid.

When a two-parameter relation $I = f(T_b, n)$ is used, the linear correlation improves and the predictive power of the computational method for the determination of retention indices increases.[34,84] A similar equation for esters may include the numbers of carbon atoms in the acid and alcohol fragments.[19]

The generalised dimensionless parameter φ, called the retention number, is used for the identification of related compounds:[3,13]

$$\varphi = \frac{\lg V_{g_x} - \lg V_{g_1}}{\lg V_{g_2} - \lg V_{g_1}} = \frac{T_{b(x)} - T_{b(1)}}{T_{b(2)} - T_{b(1)}},$$

where V_{g_x}, V_{g_1}, V_{g_2}, $T_{b(x)}$, $T_{b(1)}$, and $T_{b(2)}$ are respectively the retention volumes and boiling points of the related substances: the unknown substance x and the known substances 1 and 2. In the calculation of φ, it is essential to use standard compounds belonging to the same homologous series as the test substance. When n-alkanes are used as reference substances, the parameter φ acquires the functions of the temperature retention index, which is unambiguously related to the Kovats index. The index φ is independent of the temperature of the analysis and the stationary phase.

Table 3. Homologous series of compounds for which the linear relation (14) has been established.

Homologous series	R	Stationary phase	Refs.
n-Alkanes, n-alkenes, cycloalkanes	I	Squalane	72
C_6-C_{12} n-alkenes	$\lg t_R^{rel}$	SKTFT-100, penta(phenyl ether)	73
n-Alkanes, isoalkanes, cycloalkanes	I	Squalane, dinonyl phthalate	66
C_8-C_{10} isoalkanes	I	Squalane	3, 68
C_5-C_8 cycloalkenes, cycloalkadienes	I	Squalane	74
Aromatic hydrocarbons			
C_6-C_{12}	$\lg t_R^{rel}$	Squalane	75
C_6-C_{11}	I	Squalane, UCON LB-550X, 50HB-280X, tributyl acetylcitrate, PEG-2CM	76
C_6-C_9	I	Dinonyl phthalate, PEG-4000	77
C_6-C_{10}	I	Squalane	78
Chlorobenzenes	I	Apiezon M, OV-210	79
Methyl ethers of phenols	I	Apiezon L	38
C_5-C_8 alkylpyridines	I	n-Tetracosane, squalane, n-dotriacontane, Apiezon L	60
C_9-C_{11} alkylquinolines	I	OV-101, UKON LB-550X	80
Aliphatic amines			
C_1-C_{15}	I	Liquid paraffin, tristearin, PEG-1000, Twin-80, Triton X-305	7
C_1-C_{14}	I	Apiezon M, PEG 2000	8, 35, 81
C_2-C_{12} n-alkyl sulphides, n-alkyl disulphides	I	SE-30, DC-550, diphenylamine, Apiezon M	82
C_3-C_7 aliphatic n-aldehydes, C_2-C_9 ketones, C_2-C_6 esters, C_3-C_9 aliphatic alcohols	I	Squalane, PEG 1540, 29 different stationary liquid phases	19
Aliphatic n-alcohols	I	OV-101, PEG 20M	83

It has been established[85] that the relation between the retention indices and boiling points is most accurately described by an expression similar to the Antoine equation:

$$T_b = A - \frac{B}{I + C}$$

The standard deviations of the boiling points calculated from the retention indices of polar compounds are 3.3 °C on polar stationary phases, 2.3 °C on non-polar phases, and less than 1.1 °C for hydrocarbons.

Using the principle of linear free energy relations, Sojak[86] obtained a modified Hammett equation for the relation between the retention indices of alkylbenzenes and their boiling points:

$$\lg T_{b(a)} = \lg T_{b(t)} - \frac{1}{\rho}\left(\lg \frac{I_t}{I_a} - b\right), \quad (15)$$

where $T_{b(a)}$ and $T_{b(t)}$ are respectively the boiling points of the alkylbenzene and toluene (adopted as the standard), I_a and I_t are the retention indices of the alkylbenzene and toluene respectively, and ρ and b are constants. The maximum deviations of the boiling points calculated by Eqn. (15) do not exceed 0.6 °C and those of the retention index do not exceed 0.6 unit.

The use of the universal equation (10) made it possible to achieve the predictive calculation of the boiling points of members of homologous series of polar organic compounds (such as amines, alcohols, carboxylic acids, and their nitriles) with a high accuracy: the standard deviation of the calculated boiling points T_b did not exceed 2 °C.[87]

The widely used second Kovats rule,[88] based on the similarity of properties, reflects a linear correlation between I and T_b for isomeric compounds on non-polar stationary phases:

$$\delta I = k\,\delta T_b,$$

where δI and δT_b are respectively the differences between the retention indices and boiling points for two isomers and $k = 5$ is a proportionality coefficient.

Further studies showed that k differs from 5 for certain isoalkanes and isoalkenes.[3] Wide ranges of values of k have been found for alkylbenzenes (1.7–8.2)[31, 89] and alkylpyridines (0.8–6.4).[60] For isomeric C_{10}–C_{11} alkylquinolines, k = 3.9–4.2 on OV-101 and increases with increasing polarity of the stationary phases.[57, 90]

An important characteristic is the temperature coefficient of the retention indices dI/dT, which is frequently used for the identification of components.[91] The identification is based on the dependence of the temperature coefficients on the molecular structures of the substances analysed: on the degree of saturation and branching,[92] on the number of carbon atoms,[93] and on the position of the multiple bond.[27, 28] Sojak and coworkers have shown[86, 94] that the temperature coefficients for alkylbenzene vary within comparatively wide limits and reflect the fine structure differences between the hydrocarbons: they are directly proportional to the polarity of the stationary phases and inversely proportional to the symmetry of the molecules and the number of their alkyl substituents.

Relations have been established between the quantities dI/dT and the molecular structures of amines,[8, 35] alkylpyridines,[60] alkylquinolines,[57, 90] alkylphenols,[38] alcohols and ethers,[34] and hydrocarbons.[31, 32, 89, 95]

IV. Dependence of the retention on the molecular refraction and the dipole moment

In systems formed by polar and weakly polar phases, the chromatographic retention is determined by the strength of the dispersion forces, which is proportional to the polarisability of the substances interacting, i.e. to their refractions. It has been shown[96] that the dependence of the logarithms of the retention volumes of substances in a homologous series on the molar refraction is expressed by a linear function:

$$\lg V_g = aR_M + b. \quad (16)$$

Numerous publications indicate that Eqn. (16) is valid for different homologous series of organic substances.[60, 97–99] Thus the correlation coefficient for the equation

$$I = aR_M + b$$

reaches 0.999–1.000 for the homologous series of hydrocarbons on non-polar and weakly polar phases with a standard deviation of 0.5–2.0 units. For cycloalkanes, the analogous data are 0.990–0.997 and 3.4–4.4 units respectively.[98] The impairment of linearity for cycloalkanes is apparently associated with the manifestation of the effect of intramolecular shielding.

In order to improve the correlation, the specific and molar refractions are frequently used in two-parameter equations in combination with T_b,[76, 77, 99, 100] the dipole moment,[101] or the Hammet constant.[102]

Multiple correlation equations including the molar refraction and the refractive index as independent variables are used for the description of various mechanisms of the intermolecular interaction.[74, 76, 103]

Equations of type (16) make it possible to determine the molar refractions from GLC data with a high accuracy.[104, 105] Thus the average value of R_M for *n*-pentylbenzene, calculated from five equations for different polyester phases, is 50.00, while the value found from familiar formulae using the experimental densities and refractive indices is 49.96.[98]

According to the theory of intermolecular interactions, the dipole moments of substances exert a direct influence on their retention in GLC.[56] The retention indices of alkyl halides are related to the dipole moments as follows:[106]

$$\Delta I_{130} = 6\Delta R_M + 50\mu_{C-X},$$

where ΔI_{130} is the difference between the retention indices on polar and non-polar stationary phases at 130 °C, ΔR_M is the difference between the refractions of the C–X and C–H bonds (X = halogen), and μ is the dipole moment of the C–X bonds.

Franc[107] established a linear relation between the relative retention times and the dipole moments of isomeric alkylphenols, aromatic amines, and nitro-compounds:

$$\lg V^{rel} = a\mu + b. \quad (17)$$

It is noteworthy that the dipole moment enters into Eqn. (17) with an exponent of unity. This conflicts with the equation for the orientation interaction energy.[108] At the same time, the majority of compounds are characterised by having a quadrupole moment as well as the dipole moment.[109] The factors listed are the cause of the appreciable deviations from linearity when Eqn. (17) is used.[62, 109, 110] Therefore Eqn. (17) holds only for a limited number of compounds belonging to separate homologous series.[71, 78] The replacement of μ by μ^2 in Eqn. (17) makes this relation valid for the estimation of the orientation and inductive interaction energies.

Sakharov[111] suggested that the difference between the retention parameters of two substances having equal molar refractions be determined as follows:

$$RT\Delta \lg V_g = \frac{2}{9}\frac{\Delta\mu^2}{r^3}\left(1 - \frac{1}{\varepsilon}\right), \quad (18)$$

where $\Delta\mu^2$ is the difference between the squares of the dipole moments of the sorbates, r is the molecular radius, and ε the dielectric constant of the solvent. The requirement that the molar refractions are equal is stipulated to eliminate the effect of the electronic polarisability.

Eqn. (18) makes it possible to estimate the dipole moments of substances from GLC data with a greater accuracy than Eqn. (17). In the derivation of Eqn. (18), a simplified model of the interaction of the sorbates and the stationary phase, which does not take into

account the mutual polarisation of two molecules, was used. According to Onsager,[112] when account is taken of such polarisation, the following relation should hold:[113]

$$RT \lg V_g = \frac{\Delta\mu^2}{r^3} \frac{\varepsilon - 1}{2\varepsilon + 1}. \quad (19)$$

It is widely used to characterise the intermolecular interaction in various systems.[113-115]

In the multiple regression equations employed, the dipole moment functions as a descriptor of the polarity of the solute.[35,62] Apart from the dipole moment, such equations include the molecular weight, the sum of the steric factors,[62] the molar refraction,[116] the number of carbon atoms, the ionisation potential, the sum of the steric factors,[35] the molecular connectivity index,[117,118] and topological, electronic, and quantum-chemical parameters.[119,120] the correlation coefficients for the proposed equations are fairly high, amounting to 0.740–0.975 on polar phases and to 0.940–0.999 on non-polar phases.

At the same time, the use of the dipole moment of the molecule for the description of the intermolecular interaction does not correspond to the real nature of the orientation interaction.[121] It is known that specific interactions between the molecules of sorbates and the stationary phase depend to a greater extent on the local polarity of these molecules than on the overall dipole moment.[119-122] The electronic topological index (ETI) has been proposed for the quantitative description of the differences between the polar properties of sorbates.[123] It is calculated by the summation of the absolute differences between the excess charges on all the atomic pairs of the given molecule divided by the squares of the corresponding interatomic distances. The correlation equations based on the ETI have a high level of statistical significance for chromatographic parameters obtained on both non-polar and polar stationary phases.

Among other parameters associated with the energy characteristics of sorbates and used in correlations, mention should be made of the electronic polarisability,[13,124] the ionisation potential,[60,98,125,126] the diamagnetic susceptibility,[98] the electron density in molecules,[127] and the resonance energy of the π-electron system.[128]

V. Relation between the retention and the molar volume of the sorbate

The dependence of the retention indices on the molar volume follows from Eqn. (13), which has been used to predict the retention indices of different hydrocarbons.[129] It has been shown[64,131] in relation to alkylsilanes,[130] alcohols, hydrocarbons, and their derivatives that the relation between the retention parameters and the molar volumes of sorbates is linear:

$$I \text{ (or } \lg V_g) = aV_M + b. \quad (20)$$

The validity of Eqn. (20) has been confirmed for short homologous series of aromatic hydrocarbons (r = 0.999 and above) but for the series of C_6–C_{11} alkylbenzenes the correlation coefficient was found to be only 0.88 on squalane and 0.77 on PEG-20M.[99] The correlations considered can be improved with the aid of two- and three-parameter equations including the boiling point and the specific refraction together with V_M as independent parameters.[76,77] The correlation coefficient for such an equation reaches 0.998 on polar stationary phases and more than 0.999 on non-polar ones.

Other physical properties of sorbates which have found applications in correlations include the heat and energy of formation,[13] surface tension,[64] density,[64,68,97,132] viscosity,[133] and heats of crystallisation, evaporation, and combustion.[134,135] Since such characteristics have been determined for a small number of compounds, the possibility of predicting the retention parameters on their basis is extremely limited.

VI. The retention parameters and the principle of linear free energy relations

The interaction of a substance with the stationary phase, determined by the free energy change, can be described by the Hammett equation:[136]

$$\lg \frac{R}{R_0} = \rho\sigma, \quad (21)$$

where R and R_0 are the retention parameters of the given and standard compounds, their ratio being a measure of the free energy change on passing from the standard component to the given component within the limits of the homologous series investigated, σ is the inductive constant of the substituent which serves as a quantitative characteristic of the effect of the substituent on the electron density at the given centre, and ρ is a constant characterising the stationary phase.

The linear relation between the retention parameters of aromatic hydrocarbons and the Hammett constants of stationary phases was first noted by Araki and coworkers and by Nabivach and coworkers[137-140] and was then discovered for a whole series of similar systems.[141,142] This relation was subsequently used to characterise the selectivity of solvents—with the aid of the ratio of the activity coefficients of the sorbates.[143]

The application of the Hammett constants proved to be extremely useful when there is a significant contribution by the specific interaction forces (for example, by the donor–acceptor bond) to the overall intermolecular interaction energy. The series of correlations

$$\lg \frac{R}{R_0} = a\sigma + b$$

(σ is the Hammett constant for the corresponding substituent in the sorbate molecules) have been established for derivatives of phenol, aniline,[144-147] methyl benzoates,[145] alkylbenzenes,[148,149] and nitrobenzenes.[150]

The Taft equation has come to be widely used for the description of the characteristics of intermolecular interactions:[151]

$$\lg \frac{R}{R_0} = \rho^*\sigma^*, \quad (22)$$

in which the parameters R_0, ρ^*, and σ^* are analogous to the corresponding quantities in Eqn. (21). It is assumed that the constant σ^* characterises the purely inductive polar effect of substituents. The linear relation based on Eqn. (22) has been demonstrated for series of alkylbenzenes,[98,149] haloalkanes, halo-derivatives of epoxy-compounds, ethers,[115,152] ethoxyalkanes, amines, alcohols,[153] and alkylquinolines.[57,90]

A method has been proposed for the determination of the induction constant of the methyl group (arbitrarily assumed to be zero) for which the principle of the additivity of the change in the quantity σ^* corresponding to a change in the length of the alkyl group of alkylbenzenes per methylene group holds under GLC conditions.[98] An experimental test confirmed the legitimacy of such calculation of σ^* for the methyl group based on the correlation with the retention indices for different series of alkylbenzenes.

A complex equation has been proposed for the calculation of the retention indices of aniline, phenol, and pyridine derivatives:[154]

$$\Delta \lg V_N = \rho_I\sigma_I + \rho_R\sigma_R + \rho_E\sigma_E,$$

where σ_I, σ_R, and σ_E were derived from literature data with the aid of factorial analysis and were found to be close to the corresponding Taft induction and resonance constants.

The Taft equation for the estimation of the steric effect of substituents[151]

$$\lg \frac{R}{R_0} = \delta E_S, \quad (23)$$

where E_S are the steric constants of the substituents, can be used to characterise the quantitative measures of the steric effects of individual groups in the vicinity of the reaction centres of molecules, in the separation of polar compounds on polar stationary phases. Experimental data have shown that the Taft[57,90,149] and Palm[57,90,155] steric constants as well as their sum[62,102] can be used with equal success in equations of type (23).

In order to increase the correlation coefficient for Eqn. (23) for a series of aromatic hydrocarbons containing branched substituents (for example, butylbenzene isomers), a corrected Palm constant has been proposed:[98]

$$E^0_{S_{cor}} = E^0_S - \varphi,$$

where E^0_S is the Palm steric constant and φ is the contribution of the φ-interaction arising between the groups of the substituent linked directly.[15] The use of $E^0_{S_{cor}}$ instead of E^0_S increases the correlation coefficient of Eqn. (23) for butylbenzene isomers from 0.87 to 0.99.

By combining Eqns (22) and (23), we obtain the Hammett–Taft equation, which makes it possible to describe more complex types of intermolecular interaction[156,157] and to estimate quantitatively the role of each effect.

The Hammett–Taft equation has been improved by French investigators,[153,158] who proposed the following relation:

$$\lg t'_R = \rho^*\delta^* + \delta E_S + h(n_H - 3),$$

where n_H is the number of hydrogen atoms at the carbon atom in the α-position relative to oxygen. Assessment of the resulting coefficients showed that the contribution of E_S is much smaller than the contributions of the remaining terms of the equation, which can be rewritten in the form

$$\lg t'_R = \rho^*\delta^* + h(n_H - 3).$$

The application of this equation to a series of oxygen-containing compounds yielded satisfactory results.

VII. The use of the principle of the additivity of properties for the prediction of retention parameters

A general relation for the calculation of the chromatographic retention, based on the additivity of the contributions by structural fragments, has been proposed by Berezkin and coworkers:[159,160]

$$R = \sum_{ij}^{K} n_{ij}C_{ij} + C_0, \qquad (24)$$

where C_{ij} is the contribution of a particular structural fragment (atoms, a group of atoms, bonds) to R, and n_{ij} is the number of structural fragments in the molecule. Bonds were selected as the computational structural fragments taking into account the immediate environment. If more distant environment is also taken into account, it is possible to obtain more accurate results.

The simplest expression for the additivity rule—Eqn. (1)—is a special case of Eqn. (24). Eqns (11), (14), and (20) are also special cases of this kind.

The principles formulated by Berezkin have found applications in the predictive calculation of retention parameters in accordance with an additive scheme by the summation of increments corresponding to subtypes of bonds between carbon atoms[3,161] or functional groups.[162]

The additivity of the retention characteristics considered logically presupposes also the additivity of the retention indices,[162] whose calculation is based on the principle of the additivity of the intermolecular interaction energies for individual groups of molecules.[106]

The increments in the differences between the retention indices, measured on stationary phases of different polarity and reflecting the specific interaction between the test molecules and the stationary phase, are also additive.[163–166]

The functional retention index proposed by Swoboda[167] reflects the dispersion and specific interactions of the functional group of the sorbate with the sorbent:

$$H_X = I_{R-X} - I_{R-H},$$

where X is the functional group and R–H the homomorphic n-alkane with the same number of carbon atoms. The functional group is understood not only as a group containing a heteroatom but also as any structural group differing in its multiple or aromatic bond or in the arrangement of carbon atoms in space.

Schomburg[9] proposed that the quantity H be called the homomorphy factor and showed that it is extremely sensitive to the characteristics of the fine structure of the molecule.[168]

Andersons and coworkers[8,35] introduced the concept of two homomorphy factors: H_H describes the effect of the substitution of a hydrogen atom by a functional group and H_C describes the effect of the substitution of a carbon atom by a heteroatom or a group of atoms.

Among compounds for which the values of H have been determined and the corresponding correlations with the structure have been established, mention should be made of cycloalkanes, cycloalkenes, cycloalkadienes,[93] alkylbenzenes,[20,89,169] alkylnaphthalenes,[170] alkylpyridines,[60] amines, alcohols, and ethers.[8,35]

Extensive experimental data on the increments for various functional groups or individual fragments, used in accordance with Eqn. (24) for the predictive calculation of retention indices and for the identification of components of complex mixtures, are available in the literature.[171–173]

The principle of additivity breaks down when the structural fragments of the molecule are close to one another, on passing from unbranched to branched compounds, and with increase in the polarity of stationary phase and in the capacity of the functional group for specific interactions.

The non-additivity of the retention indices and their increments in homologous series is also indicated by data in numerous publications.[174,175] Correction coefficients are usually introduced in such cases or one calculates second-order increments, taking into account the positions and interaction of functional groups, the nature of the bonds in the molecule, steric factors, and other effects of substitution and the environment.

The causes of non-additivity and procedures for the reliable prediction of retention indices based on allowance for the non-identity of the energy contributions of identical alkyl groups have been described in detail.[179–185]

One of the causes of the breakdown of additivity is the presence in the molecule of a heteroatom or a functional group, the degree of shielding of which by neighbouring alkyl groups affects appreciably the specific forces of the interaction of the test substance with the stationary phase. Linear relations for such compounds (alkylphenols, alkylpyridines, alkylquinolines, alkylanilines, etc.) are therefore characterised by a low correlation coefficient. In order to take into account the shielding effect, the entire set of compounds (for example, alkylpyridines) can be usefully divided into three groups: alkylpyridines with a non-shielded nitrogen atom, i.e. with alkyl groups in the 3-, 4-, and 5-positions, alkylpyridines with one alkyl group in the *o*-position relative to the nitrogen atom, and alkylpyridines with two alkyl groups in the 2- and 6-positions.[165] Such subdivision is based on the change in the π-electronic charges on the reaction centre under the influence of the alkyl groups introduced into the molecule. This factor is responsible for the linear variation of the basicity of alkylpyridines as a function of the groups indicated, which makes it possible to represent the dependence of the retention indices on the dissociation constants of alkylpyridines by three equations, whose correlation coefficient is 0.995.

The system for the predictive calculation of retention indices developed by Takacs and coworkers[186-188] provides for the use of not only the properties of the pure sorbates but also of the characteristics of their interaction with the stationary phase:

$$I = I_a + I_b + I_i,$$

where I_a is the contribution of atoms, I_b the contribution of bonds, and I_i the contribution of the interaction in the sorbate and the stationary phase.

The Takacs system is based on the separate determination of all the factors responsible for the chromatographic retention of the test substance; its undoubted advantage is the use of molecular constants instead of empirical characteristics or sorbates such as the boiling point, the vapour pressure, and the molar refraction. At the same time, the semiempirical nature of the determination of the components of the index and the need to calculate a large number of empirical parameters give rise to considerable difficulties in the practical application of this system.[189]

VIII. Calculation of retention parameters with the aid of structural and topological parameters

The effect of molecular size on chromatographic retention was first noted by Hively and Hinton,[92] who concluded that the quantity dI/dT increases with increase in the cross-sectional area of the isoalkane molecule.

Similar results were obtained by Littlewood[190] for *n*-alkanes and their derivatives, whose retention is proportional to the surface area of the molecules calculated with the aid of a computer.

Altenburg[3,191] developed a method for the determination of the retention indices of hydrocarbons and their derivatives based on the correlation with the square of the molecular radius:

$$I = I_0 + bM_S d + \frac{c\overline{R^2}}{a_1^2},$$

where d is the density of the hydrocarbon, I_0 a constant which depends on M_S, $\overline{R^2}$ the mean square molecular radius, a_1 the length of a carbon–carbon single bond, and b and c are constants of the equation.

More accurate results were obtained by using equations including, together with $\overline{R^2}/a_1^2$, the boiling point:[3,68]

$$I = a + b(T_b - 273.15) + \frac{c\overline{R^2}}{a_1^2},$$

$$I = a + b(T_b - 273.15) + C(T_b - 273.15)^2 + \frac{D\overline{R^2}}{a_1^2} + E\left(\frac{\overline{R^2}}{a_1^2}\right) + Fd + Gd^2.$$

The error of the calculated retention indices of isoalkanes varies in the range 0.3–5.5 units. For example, equations of the following type are valid for the homologous series of alkylbenzenes:

$$I = f\left(\frac{\overline{R^2}}{a_1^2}\right)$$

with a correlation coefficient of 0.994 and above.[192,193]

Correlation equations relating the retention index to the shape parameters of the molecules, which have been calculated on the basis of the van der Waals radii of the hydrogen atom for polycyclic aromatic hydrocarbons[194] or the van der Waals surface areas for polychlorinated dibenzofurans,[195] have been proposed.

Correlations based on the van der Waals volumes of sorbate molecules V_W have come to be widely used. Hammers and De Ligny[196] already showed that the thermodynamic functions of solution in squalane, calculated from the retention volumes, are linearly related to V_W for hydrocarbons in different homologous series.

Linear relations between retention indices and the van der Waals volume have been observed for the homologous series of alcohols, ketones, aldehydes, ethers,[197] *n*-alkanes and isoalkanes,[198] ketone derivatives,[21] alkylbenzenes[99,105,199] and alkylphenols.[200] The correlation coefficients of such equations are 0.999–1.000 for hydrocarbons on non-polar phases and 0.994–1.00 for other compounds. When the above relation is applied not to short homologous series but to the entire set of isomeric compounds (for example, alkylbenzenes), the correlation coefficient falls as a function of the polarity of the stationary phases to 0.88–0.98. The level of correlation can be improved by combining V_W with characteristics of sorbate such as the boiling point, the refractive index, and the specific refaction within the framework of three- and five parameter equations.[76,79,99,197]

When correlations in the structure–retention system are considered, various methods for the conversion of molecular structures into unique characteristic structural descriptions, expressed by numerical indices, are very promising. For this purpose, one uses chemical graph theory, according to which the chemical structural formula of a compound is expressed by a mathematical graph. The mathematical graph describes abstract vertices connected by faces. Each molecular graph can be represented either by a matrix, or by a polynomial, or by numerical index (topological index).[201] The topological index contains information about the size and shape of the molecule, about the connections between atoms and structural groups, and about their mutual disposition.[202]

More than 40 different topological indices are known at the present time. An approximate classification, the characteristic principles of the derivation of topological indices, and their realistic possibilities as a means of describing chemical structures when correlations of the structure–property type are considered have been described in detail in a number of reviews.[201-208a]

The topological index W proposed by Wiener[209] for the comparison of carbon skeletons is defined as the sum of the C–C bonds between all the pairs of carbon atoms in the molecular graph:

$$W = \frac{1}{2}\sum_{ij} D_{ij}.$$

The smaller this number, the more compact the corresponding structure.

Correlations between the Wiener index and the chromatographic retention parameters of various hydrocarbons have been described.[105,199,210-212] A disadvantage of the Wiener index is the fact that part of the information contained in the distances matrix is lost during the summation of its elements. This explains the finding that the values of W referring to different isomers frequently overlap. It has been established that, compared with W, a higher level of correlation is ensured by the molecular connectivity index.[105,199,212]

The concept of the connectivity index, which is one of the most popular topological indices in theoretical chemistry, was introduced by Randic.[213] Later this method of topological analysis was used as a basis of the molecular connectivity system.[214]

Molecular connectivity constitutes a topological description of the molecular structure and represents mathematically coded information about the size of the molecule, the degree of its branching, cyclisation, and unsaturation, and about its content of heteroatoms. The first-order connectivity index is most common:[214]

$$^1\chi = \sum_{q=1}^{K} (\delta_i \delta_j)^{-1/2}, \qquad (25)$$

where δ is the difference between the numer of valence electrons and the number of hydrogen atoms connected to the given atom, i and j are the atoms of the molecule formally connected by the bond under consideration, δ_i and δ_j are the values of δ for two

atoms involved in a bond q, and K is the total number of bonds in the molecule.

The second-order to fourth-order and higher-order connectivity indices are calculated similarly. These take into account the numbers of two, three, four, and more of neighbouring bonds respectively. In Eqn. (25), the first-order connectivity index takes into account the pair interactions of neighbouring atoms in the molecule. A disadvantage is that it does not distinguish the *m*- and *p*-isomers of aromatic compounds. Higher-order connectivity indices, taking into account not only the nearest pair interactions but also remote interactions between atoms in the molecule, ensure a more complete description of the structural features of the test compounds.

Thus molecular connectivity is a fundamental parameter and expresses structural information in the form of a weighted sum of all the types of bonds in the molecule. Compared with other indices, the molecular connectivity model is more flexible, since it makes it possible to relate both general and local structural properties of molecules.

The application of connectivity indices in GLC in order to establish the sorption-structural correlations for different compounds has proved especially fruitful.[77,100,215–221] Table 4 presents data on the correlations based on connectivity indices. A significant advantage of this index compared with the Wiener index is the possibility of describing a compound with polar functional groups. Although a high level of correlation is observed mainly on non-polar phases, it does not reduce the practical value of the proposed equations.[76,239–242]

The application of multiparameter equations, including, apart from the connectivity indices of different orders, also other physicochemical constants of sorbates (the number of carbon atoms, the boiling point, the molar refraction, the dipole moment) makes it possible to increase the correlation coefficient of the equations and to reduce the standard deviation.[241,243] It has been concluded that satisfactory results for compounds of different classes are obtained when a multiparameter equation of the following type is used:[105,199,200]

$$I = f(V_w, {}^1\chi \ldots {}^n\chi_m), \qquad (26)$$

where n is the order of the connectivity index and m the designation of the chain or branching index. In Eqn. (26) the van der Waals volume describes the size of the solute and the connectivity indices of different orders characterise the fine structure features of its form. A close relation has been noted[244] between the indices obtained in accordance with graph theory and by quantum-chemical methods.

Eqn. (26) has been successfully tested for alkylbenzenes and alkylarylcarbamates,[105,199,245] alkylphenols,[200,246] alkylquinolines,[247] aliphatic alcohols,[248] and alkylanilines.[249] The correlation coefficients of the above equations are 0.996–1.000 and the standard deviations are 0.5–8.0 units.

The program packs developed for the calculation of connectivity indices[250–252] and also the combined program for the determination of sorption–structure correlations on the basis of topological indices[253] greatly facilitate chromatographic identification and permit its automation using computers.[2,254]

Another topological system (DARC)[255] involves the arbitrary specification in each molecule of a focus (the given functional group) and its environment—the first, second, third, and subsequent spheres. The reliability and accuracy of the calculations increase with increase in the number of surrounding spheres taken into account. This leads to an increase of the prespecified empirical parameters for the calculation, whose number can reach 2000 and more.[256]

Despite the complexity of the calculations and the large amount of the information used, the accuracy attained in the determination of the retention indices varies within wide limits (3–48 units). Comparison with other computational methods showed that the DARC system has no special advantages and its use for the prediction of the retention parameters involves considerable difficulties.[2]

Analysis of the studies examined shows that the simplest correlations between chromatographic retention and the physicochemical properties of sorbates can be used for a homologous series of compounds in order to characterise their retention on non-polar stationary phases. However, the prediction of the retention parameters is then rather difficult, since physicochemical properties have been determined for a limited number of substances.

Table 4. Characteristics of the correlation equations based on connectivity indices.

Compound	Equation	Stationary phase	Correlation coefficient	Standard deviation	Refs.
n-Alkanes, isoalkanes	$I = a^1\chi + b$	Squalane	0.994	17.3	198
	$\lg t_R^{rel} = a^1\chi + b$	Dimethylsulpholan	0.996	0.1	222
Alkylbenzenes	$I = a^1\chi + b$	Squalane, SE-30	0.999–1.000	–	223
Alkylnaphthalenes	$I = f({}^1\chi \ldots {}^5\chi_p)$	Hepta(phenyl ether)	0.998	4.8	224
Polycyclic aromatic	$I = a^1\chi + b$	SE-52	0.996	8.8	225
hydrocarbons (PAC)	$I = a^1\chi + b$	0V-101	0.998	36.9	226
Nitro-derivatives of PAC	$I = f({}^0\chi \ldots {}^5\chi_p)$	SE-52	0.999	2.3	227
Chloroalkanes	$I = f({}^1\chi, {}^5\chi_p, {}^5\chi_{pc}, {}^6\chi_p)$	PEG-20M	1.000	–	228
Chlorobenzenes	$I = f({}^1\chi, {}^4\chi_{pc})$	SE-30	0.988	–	229
Chlorobiphenyls	$\lg t_R^{rel} = f({}^1\chi, {}^4\chi_{pc}, {}^5\chi_p)$	SE-54	0.999	0.006	230
Alkylpyridines	$I = f({}^0\chi \ldots {}^5\chi_{pc})$	0V-1	0.996–0.999	3.6–8.4	231
Nitrogen-containing heterocycles	$I = f({}^1\chi, {}^4\chi_{pc}, {}^5\chi_p, {}^6\chi_p, {}^6\chi_{pc})$	0V-1	0.960	54.0	232
Alkylpyrimidinone derivatives	$I = a^1\chi + b$	0V-1	0.970	–	233
Cyclic methyl esters and alcohols	$I = a^1\chi + b$	SE-30	0.952	32.2	234
Aliphatic alcohols	$I = a^1\chi + b$	Squalane	0.950	–	235
	$I = a^0\chi + b^1\chi + c$	Squalane	0.994	–	236
Esters	$I = a^1\chi + b^4\chi_p + c$	Squalane	0.996–0.998	–	237
Ethers	$I = a^1\chi + b$	Squalane	0.968	–	236
5,5-Disubstituted barbiturates	$I = a^1\chi_N + b$	SE-30	0.996	–	238

Correlation equations taking into account the deviations from additivity in the intermolecular interaction energy [in particular the universal equation (10)] as well as equations based on the structural and topological parameters of compounds (for example, the van der Waals volume and the connectivity indices) are more reliable and promising. Such sorption–structure correlations can be used in schemes for the automatic identification of complex mixtures with the aid of computers.

References

1. A N Korol' *Usp. Khim.* **51** 1225 (1982) [*Russ. Chem. Rev.* **51** 698 (1982)]
2. D N Grigor'eva, R V Golovnya *Zh. Anal. Khim.* **40** 1733 (1985)
3. M S Vigdergauz, L V Semenchenko, V A Ezrets, et al. *Kachestvennyi Gazokhromatograficheskii Analiz* (Qualitative Gas-Chromatographic Analysis) (Moscow: Nauka, 1976)
4. A A Anderson, M V Shimanskaya *Usp. Khim.* **48** 1337 (1979) [*Russ. Chem. Rev.* **48** 714 (1979)]
5. L A Gribov, Yu A Zolotov, V I Kalmanovskii, et al. *Zh. Anal. Khim.* **37** 1104 (1982)
6. N F Belyaev, M S Vigdergauz, *Zh. Anal. Khim.* **41** 1882 (1986)
7. R V Golovnya, G A Mironov, I L Zhuravleva *Dokl. Akad. Nauk SSSR* **163** 369 (1965)
8. A Andersons, S Jurels, M V Shimanskaya *Izv. Akad. Nauk Latv. SSR, Ser. Khim.* **677** 723 (1973)
9. G Schomburg *J. Chromatogr.* **23** 1 (1966)
10. V Pacakova, E Smolkova *Chem. Listy* **60** 1130 (1966)
11. N Dimov, D Shopov *J. Chromatogr.* **44** 170 (1969)
12. J K Haken *J. Chromatogr. Sci.* **11** 144 (1973)
13. A V Kiselev, A V Iogansen, K I Sakodynskii, et al. *Fizikokhimicheskoe Primenenie Gazovoi Khromatografii* (Physicochemical Applications of Gas Chromatography) (Moscow: Nauka, 1973)
14. R V Golovnya, D N Grigor'eva, I L Zhuravleva *Izv. Akad. Nauk SSSR, Ser. Khim.* 1825 (1981)
15. V Palm *Osnovy Kolichestvennoi Teorii Organicheskikh Reaktsii* (Fundamentals of a Quantitative Theory of Organic Reactions) (Leningrad: Khimiya, 1977)
16. V I Yakerson, L I Lafer *Izv. Akad. Nauk SSSR, Ser. Khim.* 611 (1965)
17. J R Ashes, J K Haken *J. Chromatogr.* **62** 39 (1971)
18. A Radecki, J Grzybowski *J. Chromatogr.* **152** 211 (1978)
19. F Saura-Calixto, A Garcia-Raso, P M Deya *J. Chromatogr. Sci.* **20** 7 (1982)
20. E Matisova, F Kovačičova, Ha Pham Thi, et al. *J. Chromatogr.* **475** 113 (1989)
21. L F R Cafferata, A I Canizo, G N Eyler *J. High Resolut. Chromatogr.* **12** 423 (1989)
22. V A Terent'ev *Zh. Anal. Khim.* **42** 1870 (1987)
23. S V Gribanova, Yu Ya Kharitonov, D N Dzhabarov, et al. *Zh. Anal. Khim.* **45** 1009 (1990)
24. N S Zakirov *Zh. Anal. Khim.* **35** 725 (1980)
25. K I Sakodynskii, L I Panina *Polimernye Sorbenty dlya Molekulyarnoi Khromatografii* (Polymeric Sorbents for Molecular Chromatography) (Moscow: Nauka, 1977)
26. M S Wainwright, J K Haken, D Srisukh *J. Chromatogr.* **188** 246 (1980)
27. S Rang, K Kuningas, A Orav, et al. *Chromatographia* **10** 55 (1977)
28. A Orav, K Kuningas, S Rang, et al. *Izv. Akad. Nauk Est. SSR, Khimiya* **29** 18 (1980)
29. S Rang, K Kuningas, T Strenze, et al. *J. Chromatogr.* **406** 75 (1987)
30. C T Peng, S F Ding, R Hua, et al. *J. Chromatogr.* **436** 137 (1988)
31. V M Nabivach, P Bur'yan, J Macak *Zh. Anal. Khim.* **33** 1416 (1978)
32. V A Gerasimenko, V M Nabivach *Zh. Anal. Khim.* **37** 110 (1982)
33. L G Sednevets, A G Pankov *Zh. Anal. Khim.* **32** 1039 (1977)
34. F Saura-Calixto, A Garcia-Raso *J. Chromatogr.* **216** 326 (1981)
35. A Andersons *Gazovaya Khromatografiya Aminosoedinenii* (Gas Chromatography of Amino-compounds) (Riga: Zinatne, 1982)
36. R V Golovnya, I L Zhuravleva, Yu P Kapustin *Zh. Anal. Khim.* **30** 2241 (1975)
37. R V Golovnya, V P Uralets, T E Kuz'menko *Zh. Anal. Khim.* **32** 340 (1977)
38. U Lille, H Kundel, N Kaidas, et al. *Izv. Akad. Nauk Est. SSR, Khimiya, Geologiya* **25** 101 (1976)
39. F Saura-Calixto, A Garcia-Raso *Chromatographia* **14** 143 (1981)
40. J K Haken, D K M Ho, M Wainwright *J. Chromatogr.* **106** 327 (1975)
41. P Buryan, J Macak, J Hrivňak *J. Chromatogr.* (1977) **137** 425
42. L Rohrschneider *Chromatographia* **2** 437 (1969)
43. D N Grigor'eva, R V Golovnya *Zh. Anal. Khim.* **40** 1733 (1985)
44. A F Shlyakhov, M S Telkova *Zavod. Lab.* **30** 9 (1973)
45. M S Wainwright, J K Haken *J. Chromatogr.* **184** 1 (1980)
46. V S Vigdergauz, E I Petrova *Chromatographia* **25** 589 (1988)
47. A Grobler *A kőolaj és földgáz kémiaja és kemiai feldolgozása konferencia Budapest, 1965* p. 1
48. R Luft, C Pin *C.R. Acad. Sci.* **266** 537 (1968)
49. V M Sakharov, Yu N Bogoslovsky, K I Sakodynsky *J. Chromatogr.* **58** 103 (1971)
50. V G Arakelyan, Candidate's Thesis in Chemical Sciences, State Institute for the Nitrogen Industry, Moscow, 1969
51. M S Vigdergauz, V I Semkin *Zh. Fiz. Khim.* **46** 948 (1972)
52. F J Heeg, R Zinburg, H J Neu, et al. *Chromatographia* **12** 790 (1979)
53. R V Golovnya, D N Grigor'eva, I L Zhuravleva *Izv. Akad. Nauk SSSR, Ser. Khim.* 1825 (1981)
54. R V Golovnya, D N Grigor'eva *Zh. Anal. Khim.* **40** 316 (1985)
55. A M Makogon, I V Bubentsova, V L Trostyanetskaya, et al. *Zh. Anal. Khim.* **39** 353 (1984)
56. A T James *Anal. Chem.* **28** 1564 (1956)
57. P Buryan, J Macak, J Tříska, et al. *J. Chromatogr.* **391** 89 (1987)
58. B A Markov, T I Rybkina, V A Kochetov, et al. *Zh. Anal. Khim.* **35** 1347 (1980)
59. T I Rybkina, E A Kirichenko, V A Kochetov, et al. *Zh. Anal. Khim.* **44** 105 (1989)
60. V M Nabivach, V P Dmitrikov *Zh. Anal. Khim.* **34** 2412 (1979)
61. N Dimov, R Milina *J. Chromatogr.* **463** 159 (1989)
62. V Satcs, A Avots, V A Belikov *Zh. Anal. Khim.* **32** 797 (1977)
63. C A Streuli, M Orloff *J. Chromatogr.* **101** 23 (1974)
64. G Castello, G D'Amato *J. Chromatogr.* **107** 1 (1975)
65. N C Saha, G D Mitra *Technology* **8** 3 (1971)
66. M Kh Lunskii, I L Paizanskaya *Zh. Anal. Khim.* **43** 127 (1988)
67. R Kremann, M Pestemer *Physikalische Eigenschaften und Chemische Konstitution* (Translated into Russian). (Moscow–Leningrad: ONTI, 1939)
68. A A Martynov, M S Vigdergauz *Neftekhimiya* **10** 763 (1970)
69. A Kreyenbuhl, H Weiss *Bull. Soc. Chim. France* 1880 (1959)
70. A W Decora, G U Dinneen *Anal. Chem.* **32** 164 (1960)
71. C M White, A Robbat, R M Hoes *Chromatographia* **17** 605 (1983)
72. L Sojak, J Krupčik, J Rijks *Chromatographia* **7** 26 (1974)
73. E I Petrova, E Yu Gerasimova, M V Sosnina, et al. *Izv. Vyssh. Uchebn. Zaved., Khim. Khim. Tekhnol.* **31** 81 (1988)
74. J Bermejo, C G Blanco, M A Diez, et al. *Chromatographia* **23** 33 (1987)
75. V I Kulikov, M E Sorokin *Zh. Anal. Khim.* **30** 1594 (1975)
76. J Bermejo, M D Guillen *Chromatographia* **17** 664 (1983)
77. K Heberger *Chromatographia* **25** 725 (1988)
78. P P Alikhanov, K I Sakodynskii, G N Kuznetsov *Zh. Anal. Khim.* **47** 712 (1987)
79. J Bermejo, C G Blanco, M D Guillen *J. Chromatogr.* **31** 237 (1985)
80. P Buryan, J Macak, Yu S Berlizov, et al. *Chem. Prùm.* **36** 88 (1986)
81. A Andersons, P Mekss, M V Shimanskaya *Izv. Akad. Nauk Latv. SSR, Ser. Khim.* 515 (1982)
82. R V Golovnya, Yu R Arsen'ev *Izv. Akad. Nauk SSSR, Ser. Khim.* 1402 (1972)
83. S Boneva *Chromatographia* **23** 50 (1987)
84. L V Semenchenko, F I Lapteva *Zh. Fiz. Khim.* **52** 2319 (1978)
85. R V Golovnya, V G Garbuzov, T A Misharina *Izv. Akad. Nauk SSSR, Ser. Khim.* 103 (1976)
86. L Sojak *Ropa a Uhlie* **27** 356 (1985)
87. D N Grigor'eva, R V Golovnya, T E Kuz'menko *Zh. Anal. Khim.* **42** 1104 (1987)
88. E Kovats, in *Advances in Chromatography* (Edited by J C Giddings) (New York: Marcel Dekker, 1965) Vol. 1, p. 229

89. J Macak, V M Nabivach, P Buryan, et al. *J. Chromatogr.* **234** 285 (1982)
90. Yu S Berlizov, V M Nabivach, V P Dmitrikov *Zh. Anal. Khim.* **42** 1119 (1987)
91. E Matisova *J. Chromatogr.* **438** 131 (1988)
92. R A Hively, R E Hinton *J. Gas Chromatogr.* **6** 203 (1968)
93. W Engewald, U Billing, T Welsch, et al. *Chromatographia* **23** 590 (1987)
94. L Sojak, J Janak, J A Rijks *J. Chromatogr.* **138** 119 (1977)
95. V A Gerasimenko, A V Kirilenko, V M Nabivach *J. Chromatogr.* **208** 9 (1981)
96. L N Vorob'ev *Collect. Czech. Chem. Commun.* **27** 1045 (1962)
97. M Ts Yanotovskii *Zh. Fiz. Khim.* **44** 2451 (1970)
98. V M Nabivach, A V Kirilenko *Chromatographia* **13** 93 (1980)
99. J Bermejo, J S Canga, O M Gayol, et al. *J. Chromatogr. Sci.* **24** 252 (1984)
100. K Heberger *Anal. Chim. Acta* **223** 161 (1989)
101. M Luo, X Yan, S Xu, et al. *J. Wuhan. Univ.* (3) 72 (1987)
102. A Radecki, J Grzybowski, H Lamparczyk, et al. *J. High Resolut. Chromatogr.* **2** 581 (1979)
103. J Bermejo, M Guillen *Anal. Chem.* **59** 94 (1987)
104. O Papp, M Jozan, Gy Szasz, et al. *J. Chromatogr.* **403** 11 (1987)
105. V M Nabivach, V E Vasil'ev *Izv. Vys. Ucheb. Zaved., Khim. Khim. Tekhnol.* **30** (10) 72 (1987)
106. A Wehrli, E Kovats *Helv. Chim. Acta.* **42** 2709 (1958)
107. J Franc *Collect. Czech. Chem. Commun.* **25** 1573 (1960)
108. W H Keeson *Physik. Z.* **22** 129 (1921)
109. E Kovats, P Weisz *Ber. Bunsenges. Phys. Chem.* **69** 812 (1965)
110. A Avots, V Satcs *Izv. Akad. Nauk Latv. SSR, Ser. Khim.* 475 (1971)
111. V M Sakharov *Gazovaya Khromatografiya. Trudy 2 Vsesoyuznoi Konferentsii* (Gas Chromatography. Proceedings of the 2nd All-Union Conference) (Moscow: Nauka, 1964) p. 346
112. L Onsager *J. Amer. Chem. Soc.* **58** 1486 (1936)
113. V A Granzhan, I M Shevchuk *Neftekhimiya* **8** 908 (1968)
114. B I Anvaer, A A Zhukhovitskii, I I Litovtseva, et al. *Zh. Anal. Khim.* **19** 178 (1964)
115. V V Keiko, B V Prokop'ev, L P Kuz'menko, et al. *Izv. Akad. Nauk SSSR, Ser. Khim.* 2697 (1972)
116. R Kaliszan, H-D Höltje *J. Chromatogr.* **234** 303 (1982)
117. M Gassiot-Matas, G Firpo-Pamies *J. Chromatogr.* **187** 1 (1980)
118. A Voelkel *Chromatographia* **25** 655 (1988)
119. L Buydens, D L Massart, P Geerlings *Anal. Chem.* **53** 738 (1983)
120. A I Ermakov, E A Zharikova, E A Kirichenko *Zh. Fiz. Khim.* **62** 1260 (1988)
121. A N Korol' *Nepodvizhnye Fazy v Gazozhidkostnoi Khromatografii* (Stationary Phases in Gas–Liquid Chromatography) (Moscow: Khimiya, 1985)
122. K Osmialowski, J Halkiewicz, A Radecki, et al. *J. Chromatogr.* **346** 53 (1985)
123. K Osmialowski, J Halkiewicz, R Kaliszan, et al. *J. Chromatogr.* **361** 63 (1986)
124. A V Kiselev *Mezhmolekulyarnye Vzaimodeistviya v Adsorbtsii i Khromatografii* (Intermolecular Interactions in Adsorption and Chromatography) (Moscow: Vysshaya Shkola, 1986)
125. R I Sidorov, A N Denisenko, M P Ivanova, et al. *Teor. Eksp. Khim.* **5** 697 (1969)
126. A Voelkel *Chromatographia* **23** 195 (1987)
127. A E Ermoshkin, V A Kuznetsov, A N Egorochkin, et al. *Dokl. Akad. Nauk SSSR* **227** 366 (1976)
128. W Ecknig *Z. Chem.* **25** 240 (1985)
129. D Papazova, N Dimov *J. Chromatogr.* **216** 321 (1981)
130. M Wurst, J Churaček *J. Chromatogr.* **70** 1 (1972)
131. G Castello, G D'Amato *J. Chromatogr.* **76** 293 (1973)
132. I I Bardyshev, V I Kulikov *Dokl. Bolg. Akad. Nauk* **11** 342 (1967)
133. A E Habboush, N M Said *Separ. Sci. Techn.* **14** 345 (1979)
134. V I Kulikov, V V Trostyanskaya *Zh. Fiz. Khim.* **59** 1300 (1985)
135. F Wang, Y Ma *Anal. Chem. (Jpn.)* **15** 839 (1987)
136. L P Hammett *Fundamentals of Physical Organic Chemistry* (Translated into Russian) (Moscow: Mir, 1972)
137. T Araki, R Goto, A Ono *Nippon Kagaku Zasshi* **82** 1081 (1961)
138. T Araki *Bull. Chem. Soc. Jpn.* **36** 879 (1963)
139. V M Nabivach *Neftepererabotka i Neftekhimiya* (12) 25 (1963)
140. V M Nabivach, V I Dal' *Gazovaya Khromatografiya Koksokhimicheskikh Produktov* (Gas Chromatography of Coke-Chemical Products) (Kiev: Tekhnika, 1967)
141. V M Nabivach *Collect. Czech. Chem. Commun.* **42** 259 (1977)
142. A Ono *Nippon Kagaku Zasshi* **92** 242, 433 (1971)
143. A A Gaile, Ya I Leitman *Zh. Fiz. Khim.* **41** 2886 (1967)
144. B L Karger, Y Elmehrik, R L Stern *Anal. Chem.* **40** 1227 (1968)
145. B L Karger, Y Elmehrik, W Andrade *J. Chromatogr. Sci.* **7** 209 (1969)
146. M Kremser, M Jernejčič, L Premru *J. Chromatogr.* **65** 129 (1972)
147. A V Kiselev, D P Poshkus, Y A Yashin *Molekulyarnye Osnovy Adsorbtsionnoi Khromatografii* (Molecular Foundations of Adsorption Chromatography) (Moscow: Khimiya, 1986)
148. J Krupčik, O Liška, L Sojak *J. Chromatogr.* **51** 119 (1970)
149. A Ono *Nippon Kagaku Zasshi* **92** 429, 986 (1971)
150. Yu N Arsen'ev, R V Golovnya *Izv. Akad. Nauk SSSR, Ser. Khim.* 851 (1980)
151. R W Taft *J. Am. Chem. Soc.* **74** 3120 (1952)
152. V V Keiko, B V Prokop'ev, L P Kuz'menko, et al. *Izv. Akad. Nauk SSSR, Ser. Khim.* 111 (1972)
153. R Fellous, L Lizzani-Cuvelier, R Luft, et al. *J. Chromatogr.* **110** 13 (1975)
154. G H E Nieuwdorp, C L De Ligny *J. Chromatogr.* **154** 133 (1978)
155. V A Dektyarev, K I Sakodynskii *Novye Sorbenty dlya Molekulyarnoi Khromatografii: Sbornik Nauchnykh Trudov po Gazovoi Khromatografii* (New Sorbents for Molecular Chromatography: Collected Reports on Gas Chromatography) (Moscow: Izd. NIFKhI im Karpova, 1973) Nos. 20–21
156. S V Vitt, E A Paskonova, M G Bezrukov, et al. *Izv. Akad. Nauk SSSR, Ser. Khim.* 1712 (1971)
157. S Hillers, A V Eremeev, V G Andrianov *Zh. Fiz. Khim.* **52** 2330 (1978)
158. R Fellous, L Lizzani-Cuvelier, R Luft, et al. *Bull. Soc. Chim. France* 2482 (1974)
159. V G Berezkin, V S Kruglikova *Neftekhimiya* **2** 845 (1962)
160. G L Gromova, O E Grikina, V G Berezkin, et al. *Neftekhimiya* **13** 767 (1973)
161. V G Berezkin, V S Kruglikova *Izv. Akad. Nauk SSSR, Ser. Khim.* 1505 (1964)
162. V N Kobzar' *Zavod. Lab.* **37** 543 (1971)
163. M S Vigdergauz *Usp. Khim.* **36** 1810 (1967) [*Russ. Chem. Rev.* **36** 777 (1967)]
164. R V Golovnya, I L Zhuravleva, N I Svetlova *Zh. Anal. Khim.* **36** 742 (1981)
165. V N Nabivach *Zh. Anal. Khim.* **35** 952 (1980)
166. I O O Korhonen *J. Chromatogr.* **315** 185 (1984)
167. P A T Swoboda *Gas Chromatography* (London: Butterworths, 1962)
168. G Schomburg *Anal. Chim. Acta* **38** 45 (1967)
169. W Engewald, L Wennrich *Chromatographia* **9** 540 (1976)
170. W Engewald, L Wennrich, E Ritter *J. Chromatogr.* **174** 315 (1979)
171. V A Gerasimenko, V V Voskoboinikov *Zh. Anal. Khim.* **42** 2043 (1987)
172. N P Dimov, A L Tsoutsoulova *Izv. Khim. Nauki Blg. Akad. Nauk* **17** 700 (1989)
173. G J Price, M R Dent *J. Chromatogr.* **483** 1 (1989)
174. R V Golovnya, D N Grigoryeva *Chromatographia* **17** 613 (1983)
175. R V Golovnya, D N Grigoryeva, A V Vasilyev *J. High Resolut. Chromatogr.* **13** 47 (1990)
176. W Engewald, U Billing, I Topalova, et al. *J. Chromatogr.* **446** 71 (1988)
177. N Dimov, O Mekenyan *J. Chromatogr.* **471** 227 (1989)
178. D T Stanton, P C Jurs *Anal. Chem.* **61** 1328 (1989)
179. R V Golovnya, D N Grigor'eva *Izv. Akad. Nauk SSSR, Ser. Khim.* 596 (1987)
180. R V Golovnya, A L Samusenko. L B Dmitriev *Zh. Anal. Khim.* **42** 699 (1987)
181. R V Golovnya, V V Shenderyuk, I L Zhuravleva *Zh. Anal. Khim.* **44** 2037 (1987)
182. I L Zhuravleva, M B Terenina, V V Shenderyuk, et al. *Zh. Anal. Khim.* **45** 722 (1990)
183. I L Zhuravleva, V V Shenderyuk, E V Yakush, et al. *Izv. Akad. Nauk SSSR, Ser. Khim.* 1338 (1990)
184. R V Golovnya *J. Chromatogr.* **346** 193 (1986)

185. R V Golovnya, I L Zhuravleva, E V Yakush *Chromatographia* **23** 595 (1987)
186. J Takacs, C Szita, G Tarjan *J. Chromatogr.* **56** 1 (1971)
187. J Takacs, Zs Talas, I Bernath, et al. *J. Chromatogr.* **67** 203 (1972)
188. J Taks, E Kocsi, E Garamvolgyi *J. Chromatogr.* **81** 1 (1973)
189. G Tarjan *J. Chem. Sci.* **14** 309 (1976)
190. A B Littlewood *Wiss. Z. Karl-Marx-Univ.* **26** 361 (1977)
191. K Altenburg *J. Chromatogr.* **44** 167 (1969)
192. W Engewald, L Wennrich, J Pörschmann *Chromatographia* **11** 434 (1978)
193. V A Gerasimenko, V M Nabivach *Zh. Anal. Khim.* **43** 109 (1988)
194. A Radecki, H Lamparczyk, R Kaliszan *Chromatographia* **12** 595 (1979)
195. W J Dunn, M Kochler, D Stalling, et al. *Anal. Chem.* **58** 1835 (1986)
196. W E Hammers, C L De Ligny *Rec. Trav. Chem.* **90** 175 (1971)
197. F Saura-Calixto, A Garcia-Raso *Chromatographia* **14** 596 (1981); **15** 771 (1982)
198. F Saura-Calixto, A Garcia-Raso *Chromatographia* **15** 521 (1982)
199. V M Nabivach, V E Vasil'ev *Zh. Fiz. Khim.* **62** 1873 (1988)
200. V M Nabivach, P Buryan, J Macak *Zh. Anal. Khim.* **43** 1288 (1988)
201. R Kaliszan *CRC Crit. Rev. Anal. Chem.***16** 323 (1986)
202. N Trinajstić *Kem. Ind.* **33** 311 (1984)
203. T Görnerová *Petrochemia* **23** 172 (1983)
204. A T Balaban *J. Chem. Inf. Comp. Sci.* **25** 334 (1985)
205. L Ekiert, J Bojarski, J L Mokrosz *Wiad. Chem.* **40** 65 (1986)
206. M Šingliar *Petrochemia* **27** 4 (1987)
207. S Hala *Sb. Prazhskogo Khim-Tekhnol. Inst., Tekhnologiya Topliv* **46** 229 (1982)
208. M I Stankevich, I V Stankevich, N S Zefirov *Usp. Khim.* **57** 337 (1988) [*Russ. Chem. Rev.* **57** 191 (1988)]
208a. *Chemical Applications of Topology and the Theory of Graphs* (Translated into Russian), (Moscow: Mir, 1988)
209. H Wiener *J. Am. Chem. Soc.* **69** 17 (1947)
210. D Bonchev, G Protić, O Mekenyan, et al. *J. Chromatogr.* **176** 149 (1979)
211. N Trinajstić, G Protić, V Švob, et al. *Kem. Ind.* **28** 527 (1979)
212. L Buydens, D L Massart *Anal. Chem.* **53** 1990 (1981)
213. M Randić *J. Am. Chem. Soc.* **97** 6609 (1975)
214. L B Kier, L H Hall *Molecular Connectivity in Chemistry and Drug Research* (New York: Academic Press, 1976)
215. Z Yu Bulycheva, B A Rudenko *Zh. Anal. Khim.* **44** 197 (1989)
216. W Chen, X Chen, Y Wang *Fenxi Huaxue* **12** 688 (1984)
217. Z Suprynowicz, W M Buda, M Mardarowicz, et al. *J. Chromatogr.* **333** 11 (1985)
218. H Lamparczyk, R J Ochocka *Chromatographia* **21** 409 (1986)
219. H Masuda, S Mihara *J. Chromatogr.* **366** 373 (1986)
220. S Zhang, G Zhao, G Wang *J. Dalian Inst. Technol.* 133 (1988)
221. F Khorosheh, M R Gray, M L Selucky *J. Chromatogr.* **481** 1 (1989)
222. J S Millership, A D Woolfson *J. Pharm. Pharmacol.* **30** 483 (1978)
223. J Bermejo, J S Canga, O M Gayol *Intern. J. Environ. Anal. Chem.* **11** 271 (1982)
224. V M Nabivach, V E Vasil'ev, V A Gerasimenko *Zh. Fiz. Khim.* **61** 3354 (1987)
225. P J Doherty, R M Hoes, A Robbat *Anal. Chem.* **56** 2697 (1984)
226. B A Rudenko, Z Yu Bulycheva, L V Dylevskaya *Zh. Anal. Khim.* **39** 344 (1984)
227. A Robbat, N P Corso, P J Doherty, et al. *Anal. Chem.* **58** 2072 (1986)
228. A Sabljić *J. Chromatogr.* **314** 1 (1984)
229. A Sabljić *J. Chromatogr.* **319** 1 (1985)
230. A Robbat, G Xyrafas, D Marshall *Anal. Chem.* **60** 982 (1988)
231. V M Nabivach *Zh. Anal. Khim.* **44** 1615 (1989)
232. O Papp, G Szasz, M Farkaš, et al. *J. Chromatogr.* **403** 19 (1987)
233. G Szasz, K Valko, O Papp, et al. *J. Chromatogr.* **243** 347 (1982)
234. P Kaliszan *Chromatographia* **10** 529 (1977)
235. Y Michiotte, D L Massart *J. Pharm. Sci.* **66** 1630 (1977)
236. L B Kier, L H Hall *J. Pharm. Sci.* **68** 120 (1979)
237. R Carbo, A J Farre *Afinidad* **37** 491 (1980)
238. A H Stead, R Gill, A T Evans, et al. *J. Chromatogr.* **234** 277 (1982)
239. R Kaliszan, H Lamparczyk *J. Chromatogr. Sci.* **16** 246 (1978)
240. J S Millership, A D Woolfson *J. Pharm. Pharmacol.* **32** 610 (1980)
241. Z Yu Bulycheva, B A Rudenko, L V Dylevskaya, et al. *Zh. Anal. Khim.* **40** 330 (1985)
242. N P Dimov *J. Chromatogr.* **360** 25 (1986)
243. R H Rohrbaugh, P S Jurs *Anal. Chem.* **58** 1210 (1986)
244. L Benedetti, G B Gavioll, C Fontanesi *J. Chem. Soc., Faraday Trans. 2* 329 (1990)
245. V A Gerasimenko, V M Nabivach *J. Chromatogr.* **498** 357 (1990)
246. P Buryan, V M Nabivach, V P Dmitrikov *J. Chromatogr.* **509** 3 (1990)
247. V M Nabivach *Zh. Fiz. Khim.* **62** 2152 (1988)
248. A V Volkov, V M Nabivach *Zh. Anal. Khim.* **45** 812 (1990)
249. V M Nabivach, S A Dyachenko *Zh. Anal. Khim.* **45** 1107 (1990)
250. I V Peredunova, V E Kuz'min, Yu P Konovorotskii *Zh. Strukt. Khim.* **24** (4) 145 (1983)
251. L M Shtain, A S Kabankin, M A Landau *Zh. Strukt. Khim.* **26** (6) 129 (1985)
252. I V Peredunova, Yu A Kruglyak *Zh. Strukt. Khim.* **29** (1) 174 (1988)
253. I I Baskin, M I Stankevich, R O Devdariani, et al. *Zh. Strukt. Khim.* **30** (6) 145 (1989)
254. D N Grigor'eva, R V Golovnya, I L Zhuravleva, et al. *Zh. Anal. Khim.* **34** 2434 (1979)
255. J E Dubois, D Laurent, H Viellard *C.R. Acad. Sci.* **263** 764 (1966)
256. V G Berezkin, G L Gromova, O E Grikina, et al. *Neftekhimiya* **10** 754 (1970)

Russian Chemical Reviews **62** (1) 35 – 49 (1993)
© 1993 Russian Academy of Sciences and Turpion Ltd

UDC 541.14 + 771.53

Processes amplifying the effects of light on polymer layers

A V Vannikov, A D Grishina

Contents

I. Introduction 35
II. The influence of spin – orbit and hyperfine interactions on the efficiency and mode of the photochemical reaction 36
III. Processes amplifying the latent image 39
IV. Photochemical etching of bismuth films 47

Abstract. Processes bringing about amplification of the primary photoeffect in polymer layers through complex formation, autocatalysis, autosensitisation, and acid catalysis are discussed and their practical applications are considered. Attention is concentrated on highly sensitive photoresists for the photolithographic process used in advanced technologies. The bibliography includes 114 references.

I. Introduction

The problem of the amplification of the primary photoeffects on polymer systems is of cardinal importance because it is based on fundamental phenomena such as spectral and chemical sensitisation, complex formation, and electronic excitation energy and charge transfer. Furthermore, the use of amplification processes makes it possible to create highly sensitive polymer layers for the optical recording of information and highly sensitive photoresists and electronic resists and also to achieve directed far-reaching modification of polymer layers.

Systems in which the amplification processes occur with participation of components present in the polymer layers and do not require additional treatment of these layers in liquid or gaseous media, in contrast to, for example, well known photographic materials with chemical or physical development of the latent image in developer solutions, are considered below. The amplification coefficient of the primary photoeffect is equal to the ratio η_{ef}/η_0, where η_0 is the quantum yield of the formation (consumption) of the products of the primary action of light and η_{ef} is the effective quantum yield measured after the amplification of the primary effect.

These systems can be used in fields such as highly sensitive optical recording of information, detection of weak optical signals, photomodification of spectral and physicochemical properties of polymer layers, and selective photosynthesis of a series of chemical compounds in polymer matrices.

In the present communication, attention is concentrated on processes involving the amplification of the primary photoeffects in polymer layers in order to create on their basis highly sensitive photoresists for use in photolithography. In the first stage of the photolithographic process, photochemical reactions in polymer layers result in a change in the physicochemical properties of the exposed sections such as solubility, thermal stability, light transmittance, etc. On subsequent heating, treatment in solvents, or plasmachemical etching, the exposed (positive) or unexposed (negative) sections are fully removed from the support. The next stage of the photolithographic process is the treatment of the support (a plate made of silicon, a metal, or another material) through apertures obtained in the polymer layer (resistor) by etching or in some other way.[1–3] We emphasise that photolithography based on the use of photoresists has in fact made it possible to achieve a qualitative major advance in electronics—the introduction of the manufacture of integrated circuits.

The high sensitivity of polymer compositions to the action of light, X-rays, and electron irradiation is ensured by the electron donor – acceptor (EDA) interactions, the formation of aggregates from chromophoric groups, as well as autocatalytic,[4] chemical,[5,6] and optical[4,7] processes amplifying the primary photoeffects. In the systems considered below, catalysts are formed directly during the photochemical reaction or in the reaction of photoproduct with a compound introduced additionally—a chemical sensitiser. The mechanism of the optical amplification in the resist-free photoetching of metallic films by halogen-containing radicals, formed and deposited on these films of polymeric EDA compositions as a result of the dissociative addition of an electron to the halogen-containing acceptor, is also discussed.

A photoinitiated autocatalytic free-radical process is characteristic of the well known class of photoresists based on aromatic azides.[8] In order to create highly sensitive photoresists for use in microelectronics, detailed studies have been made in recent years, in connection with the manufacture and copying of optical [compact] discs, of the photoinitiated cross-linking of polyfunctional oligomeric acrylates in which $10^4 - 10^5$ cross-links arise as a result of a single photochemical act.[9]

The primary chemical stage of the photoprocess in polymeric EDA systems is electron transfer from the donor (D) to the acceptor (A). Compounds which dissociate into free radicals when acted upon by light, for example, ketones [R – C(O) – R'], are used as photoinitiators of the cross-linking of acrylates. This results in the formation of radical-ion pairs $[D^{\cdot+}...A^{\cdot-}]$ or radical pairs $[\dot{R}-\dot{C}(O)...\dot{R}']$. The spin – orbit and hyperfine interactions of the unpaired electrons determine the efficiency and mode of the subsequent reactions. Examples of reactions in which magnetic interactions exert an appreciable influence on the characteristics of the photoprocess are examined below.

A V Vannikov, A D Grishina Division of Electrochemistry of Polymer Systems and Radiation Chemistry, Frumkin Institute of Electrochemistry, Russian Academy of Sciences, Leninskii prosp. 31, 117071 Moscow, Fax (7-095)135 87 41

Received 10 September 1992
Uspekhi Khimii **62** (1) 39 – 54 (1993); translated by A K Grzybowski

II. The influence of spin–orbit and hyperfine interactions on the efficiency and mode of the photochemical reaction

The efficiency and mode of the photochemical reaction depend on the multiplicity of the radical-ion or radical pair formed as a result of the action of light. Indeed, the reverse electron transfer or recombination of radicals are allowed only for the singlet orientation of the radical-ion spins in the geminal pair $[D^{\cdot+}...A^{\cdot-}]$ or the radicals in the pair $[R-\dot{X}...\dot{R}']$ respectively:

$$\begin{array}{c} D+A \rightleftharpoons D\cdot A \\ D\cdot A \xrightarrow{h\nu} {}^1(D\cdot A)_1 \longrightarrow {}^1[D^{\cdot+}\ldots A^{\cdot-}] \longrightarrow [D\ldots A] \\ \downarrow \qquad\qquad \Updownarrow \\ {}^3(D\cdot A)_1 \longrightarrow {}^3[D^{\cdot+}\ldots A^{\cdot-}] \longrightarrow (D^{\cdot+}+A^{\cdot-}) \end{array} \tag{1}$$

$$\begin{array}{c} R-X-R' \xrightarrow{h\nu} {}^1[R-\dot{X}-R']_1 \longrightarrow {}^1[R-\dot{X}\ldots\dot{R}'] \longrightarrow R-X-R' \\ \downarrow \qquad\qquad \Updownarrow \\ {}^3[R-\dot{X}-R']_1 \longrightarrow {}^3[R-\dot{X}\ldots\dot{R}'] \xrightarrow{RH} R-XH+ \\ +R-R'. \end{array}$$

The spin forbiddenness of these reactions in triplet pairs increases the probability of the liberation of radical-ions from the pair and is also responsible for the preferential interaction of radicals with the compounds (RH) present in the composition. For this reason, the quantum yield of the free radical-ions or the mode of the photochemical reaction depend on the rate of intersystem crossing in the pair (i.e. on the rate of change of the spin of the unpaired electron in one of the radicals as a consequence of either spin–orbit interaction (SOI)[10] or hyperfine interaction (HFI)[11]. These interactions ensure an admixture of the singlet (triplet) configuration in the triplet (singlet) state of the pair:

$$\varphi^T[D^{\cdot+}\ldots A^{\cdot-}] = \varphi^3[D^{\cdot+}\ldots A^{\cdot-}] + \alpha\varphi^1[D^{\cdot+}\ldots A^{\cdot-}],$$

or

$$\varphi^S[D^{\cdot+}\ldots A^{\cdot-}] = \varphi^1[D^{\cdot+}\ldots A^{\cdot-}] + \alpha\varphi^3[D^{\cdot+}\ldots A^{\cdot-}].$$

The probability of intersystem crossing in the radical-ion pair is determined by the contribution of the singlet (triplet) state α^2, where

$$\alpha = \frac{1}{{}^1E - {}^3E}\int \varphi^1[D^{\cdot+}\ldots A^{\cdot-}]H_n\varphi^3[D^{\cdot+}\ldots A^{\cdot-}]. \tag{2}$$

Here ${}^1E-{}^3E$ is the distance between the the energy levels of the 'pure' S and T states in the radical-ion pair and $H_n = H_{SOI}$ and H_{HFI}, where H_{SOI} and H_{HFI} are the operators of the spin–orbit and hyperfine interactions respectively:

$$H_{SOI} = \sum_i \xi_i\rho_i\bar{l}_i\bar{S}_i\ ,$$

$$H_{HFI} = \sum_i a_i\bar{S}_i\bar{I}_i\ ,$$

where ξ_i is the SOI constant for the ith atom, $\bar{l}_i$ is the azimuthal quantum number of the atom, $\bar{\rho}_i$ and $\bar{S}_i$ are the density and spin of the unpaired electron on the ith atom, a_i is the HFI constant, and I_i is the spin of the ith nucleus. According to Buchachenko et al.,[11]

$${}^1E - {}^3E = 2J_0\exp[-(R-R_0)],$$

where $J_0\exp(-R_0) \simeq 1.5$ eV is the energy of the exchange interaction between the radical-ions separated by the van der Waals distance R_0. R is the distance between the radical-ions in the pair (Å).

It follows from Eqn. (2) that intersystem crossing occurs for distances between the radical-ions such that the following relation holds:

$${}^1E - {}^3E \leq \int \varphi^1[D^{\cdot+}\ldots A^{\cdot-}]H_n\varphi^3[D^{\cdot+}\ldots A^{\cdot-}].$$

Thus for SOI and HFI, intersystem crossing takes place with the greatest probability under the following conditions:

$$\begin{aligned} 2J_0\exp[-(R-R_0)] &\simeq \sum_i \xi_i\rho_i\ , \\ 2J_0\exp[-(R-R_0)] &\simeq \sum_i \alpha_i\ . \end{aligned} \tag{3}$$

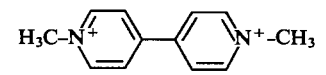
In polymeric media, where the separation of the radical-ion components may be difficult, the probability of the S → T or T → S conversion increases with increase in ξ_i and α_i.

1. Spin–orbit interaction

The spin–orbit interaction constant ξ_i increases with increase in the charge on the nucleus (Z_i) with which the unpaired electron interacts:

$$\xi_i = \sum_i \frac{Z_i^4}{n_i^3}\ ,$$

where n_i is the principal quantum number of the ith atom. In liquid-phase donor–acceptor–sensitiser systems, where the donor is an amine (Am), the acceptor is Methyl Viologen (MV^{2+})



and the sensitisers are the organometallic complexes $M(L)_3^{2+}[M^{2+} = Ru^{2+}, Os^{2+}$; L = bipyridyl (bipy) or other ligands], electron transfer takes place with participation of the triplet-excited sensitiser. The equilibrium reduction potential of MV^{2+} is $E_{1/2}(MV^+/MV^{2+}) = -0.44$ V relative to the potential of the normal hydrogen electrode (n.h.e.).[12] Depending on the oxidation potential of the donor $E_{1/2}(Am/Am^{\cdot+})$, two types of electron transfer are possible. In one of them, the primary reaction is

$$\begin{array}{c} Am + {}^3[M(L)_3^{2+}]_1 \longrightarrow {}^3[Am^{\cdot+}\ldots M(L)_3^{1+}] \longrightarrow \\ \longrightarrow Am^{\cdot+} + M(L)_3^{1+}, \end{array} \tag{4}$$

while the second reaction is

$$M(L)_3^{1+} + MV^{2+} \longrightarrow M(L)_3^{2+} + M^{\cdot+}. \tag{5}$$

In the other type of electron transfer, the primary reaction is

$${}^3[M(L)_3^{2+}]_1 + MV^{2+} \longrightarrow {}^3[M(L)_3^{3+}\ldots MV^{\cdot+}] \longrightarrow M(L)_3^{3+} + MV^{\cdot+} \tag{6}$$

while the second reaction is

$$M(L)_3^{3+} + Am \longrightarrow M(L)_3^{2+} + Am^{\cdot+}. \tag{7}$$

The free energies of reactions (4)–(7) can be calculated from the following formulae respectively:

$$\Delta G(4) = eE_{1/2}\left(\frac{Am}{Am^{\cdot+}}\right) - eE_{1/2}\left(\frac{M(L)_3^{1+}}{{}^3[M(L)_3^{2+}]_1}\right),$$

$$\Delta G(5) = eE_{1/2}\left(\frac{M(L)_3^{1+}}{M(L)_3^{2+}}\right) - eE_{1/2}\left(\frac{MV^{\cdot+}}{MV^{2+}}\right),$$

$$\Delta G(6) = eE_{1/2}\left(\frac{{}^3[M(L)_3^{2+}]_1}{M(L)_3^{3+}}\right) - eE_{1/2}\left(\frac{MV^{\cdot+}}{MV^{2+}}\right),$$

$$\Delta G(7) = eE_{1/2}\left(\frac{Am}{Am^{\cdot+}}\right) - eE_{1/2}\left(\frac{M(L)_3^{2+}}{M(L)_3^{3+}}\right).$$

We shall consider as an example a system where the sensitiser is a bipyridyl complex of ruthenium. The corresponding reduction and oxidation potentials of the triplet-excited ruthenium complex $^3[Ru(bipy)_3^{2+}]_1$ are

$$E_{1/2}\left(\frac{Ru(bipy)_3^{1+}}{^3[Ru(bipy)_3^{2+}]_1}\right) = E_{1/2}\left(\frac{Ru(bipy)_3^{1+}}{Ru(bipy)_3^{2+}}\right) + \frac{E(^3[Ru(bipy)_3^{2+}]_1)}{e} = -1.27 + 2.1 = 0.83 \text{ V (n.h.e.)} \quad (8a)$$

and

$$E_{1/2}\left(\frac{^3[Ru(bipy)_3^{2+}]_1}{Ru(bipy)_3^{3+}}\right) = E_{1/2}\left(\frac{Ru(bipy)_3^{2+}}{Ru(bipy)_3^{3+}}\right) - \frac{E(^3[Ru(bipy)_3^{2+}]_1)}{e} = 1.27 - 2.1 = -0.83 \text{ V (n.h.e.)}; \quad (8b)$$

$E_{1/2}[Ru(bipy)_3^{1+}/Ru(bipy)_3^{2+}]$ and $E_{1/2}[Ru(bipy)_3^{2+}/Ru(bipy)_3^{3+}]$ are the equilibrium reduction and oxidation potentials of $Ru(bipy)_3^{2+}$ in the ground state respectively and $E(^3[Ru(bipy)_3^{2+}]_1)$ is the distance from the ground to the excited triplet level of the sensitiser.

Reactions (4) and (5) are more favourable on energy grounds only in the case where one uses as the donors compounds with equilibrium oxidation potentials $E_{1/2}(D/D^{\cdot+}) < 0.83$ (n.h.e.) [see Eqn. (8a)] for which the free energies $\Delta G(4)$ and $\Delta G(5)$ are negative. The aromatic amines tetramethyl-*p*-phenylenediamine [$E_{1/2}(Am/Am^{\cdot+}) = 0.16$ V], diphenyl-*p*-phenylenediamine (0.36 V), tetramethylbenzidine (0.49 V), phenothiazine (0.53 V), β-naphthylamine (0.64 V),[13] as well as anthracene, 9-methylanthracene, and 9-bromoanthracene are classified as donors of this kind.[12] If compounds such as ethylenediaminetetraacetic acid (EDTA) or triethanolamine (TEOA), having $E_{1/2}(D/D^{\cdot+}) = 1.0$ or 0.9 V (n.h.e.), are used as the donors, then reaction (4) has a positive free energy: $\Delta G(4) = +0.16$ and $+0.06$ eV respectively. In this case, reactions (6) and (7) are energetically more favourable, because in both of them ΔG is negative [see Eqn. (8b)]:

$$\Delta G(6) = -0.83 - eE_{1/2}\left(\frac{MV^{\cdot+}}{MV^{2+}}\right) = -0.83 + 0.44 = -0.39 \text{ eV}$$

and

$$\Delta G(7) = eE_{1/2}\left(\frac{D}{D^{\cdot+}}\right) - 1.27 = \begin{cases} 1.0 - 1.27 = -0.27 \text{ eV (for EDTA)}, \\ 0.9 - 1.27 = -0.37 \text{ eV (for TEOA)}. \end{cases}$$

The quantum yield of the free radical-cations $D^{\cdot+}$, which avoided recombination in pairs, depends on a number of factors: the reaction pathway and the chemical structures of the sensitiser and donor. A number of systems can be quoted as examples.

(1) In systems comprising the donors Am sensitising $M(L)_3^{2+}$ (where $M^{2+} = Ru^{2+}$ or Os^{2+}) and the acceptor MV^{2+}, the quantum yield reaches 1, if the primary reaction (4) takes place, and is 0.2 ± 0.07 for the primary reaction (6).[12,13] According to the concepts developed, such decrease in the quantum yield is caused by the increase in the probability of the T → S intersystem crossing in the radical-ion pair and hence by the increase in the rate of the reverse reaction in the transition from the $^3[Am^{\cdot+}...M(L)_3^{1+}]$ pairs [see reaction (4)], where the electron transferred from Am to the metal complex is concentrated on the ligands and the spin–orbit interaction constant does not exceed $\xi = 76$ cm^{-1}, to the $^3[M(L)_3^{3+}...MV^{\cdot+}]$ pairs. In the latter case, the unpaired electron interacts with the orbitals of the central heavy atom, which has a spin–orbit constant $\xi = 1100-1350$ cm^{-1} (Ru^{2+}) or 3000 cm^{-1} (Os^{2+}).[14]

(2) The T → S intersystem crossing in the radical-ion pairs is responsible for the low quantum yield (~0.01) of the free radical-cations $MV^{\cdot+}$ and $D^{\cdot+}$ in systems containing a set of xanthen dyes, incorporating heavy iodine atoms ($\xi = 5060$ cm^{-1}) as sensitiser.[15,16]

(3) The quantum yield of the free radical-cations $D^{\cdot+}$ and $MV^{\cdot+}$ in reactions (4) and (5) is reduced from 1 to 0.74 when donors such as anthracene or 9-methylanthracene are replaced by 9-bromoanthracene and to 0.3 on subsequent addition of CH_3I to the solvent (a mixture of CH_3CN and CH_2Cl_2).[12] The authors explained this decrease by the effect of the heavy bromine ($\xi = 2640$ cm^{-1}) and iodine ($\xi = 5060$ cm^{-1}) atoms.

(4) In systems containing EDTA or TEOA as donors, Methyl Viologen as the acceptor, and Ru^{2+}, Os^{2+}, and Cu^+ complexes or the set of xanthen dyes as sensitisers,[15,16] an increase in the quantum yield of the radical-ion $D^{\cdot+}$ (which avoided recombination within the pairs) by a factor of 3–80 was attained by introducing species such as the anthracene-9-carboxylate anion (AA^-) or 9-methyl-anthracene.[12,15–17] These species are effective acceptors of the triplet energy of the photoexcited sensitiser and participate in the excited triplet state in the subsequent redox reactions (6) and (7) with formation of the triplet pairs $^3[AA^{\cdot}...MV^{\cdot+}]$, which do not contain heavy atoms.

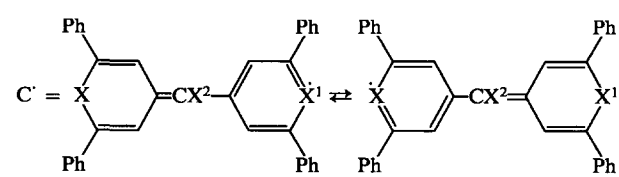
(5) In the photosensitive EDA composition consisting of a poly(vinyl ethylal) (PVE) matrix, in which are dissolved diphenylbenzylamine (DPBA) [$E_{1/2}(DPBA/DPBA^{\cdot+}) = 0.98$ V relative to the saturated calomel electrode (s.c.e.) or 0.74 V (n.h.e.)] as the donor and di(tribromomethyl) sulphone (DTBMS) as the acceptor, the dye (S^+)-sensitised formation of the coloured product (CP^+) takes place in accordance with the reaction[18]

$$S^+ \xrightarrow{h\nu, S\to T} {}^3(S^+)_1 \xrightarrow{DPBA} {}^3(DPBA^{\cdot+}...S^{\cdot-})_1 \longrightarrow$$

$$\longrightarrow {}^3[DPBA^{\cdot+}...S^{\cdot}] \xrightarrow{DTBMS} S^+ + {}^3[DPBA^{\cdot+}...DTBMS^{\cdot-}] \longrightarrow$$

$$\longrightarrow CP^+Br^- + HR \text{ (or } CP^+R^- + HBr). \quad (9)$$

Here $Cp^+Br^- = N,N$-diphenyl(phenylmethyleneiminium) bromide $(C_6H_5)_2N^+=CH-C_6H_5Br^-$ with $\lambda_{max} = 665$ and $HR = H[CBr_2=S(O_2)-CBr_3]$.[19] In the case of the dyes listed in Table 1, the pair $^3[DPBA^{\cdot+}...S^{\cdot}]$ is formed during reaction (9), the unpaired electron in the radical $S^{\cdot}$ being concentrated on the X^1 and X atoms. The decrease in the quantum yield in the formation of CP^+ via reaction (19) on passing from oxygen- to sulphur-containing dyes, indicated in Table 1, was explained[20] by the corresponding increase in the rate of the reverse reaction owing to the acceleration of T → S intersystem crossing in the pair $^3[DPBA^{\cdot+}...S^{\cdot}]$ with increase in the spin–orbit interaction constant from 113–130 cm^{-1} for the O atom to 382 cm^{-1} for the S atom. The unpaired electron interacts weakly under these conditions with a H atom or the heavy bromine atom in the central methine group of the dye:



2. Hyperfine interaction

Those S → T and T → S transitions in which the overall magnetic quantum number M_z of the electronic-nuclear system does not change become allowed as a result of hyperfine interaction:

$$M_z = M_s(1) + M_s(2) + \sum_i m_i(1) + \sum_k m_k(2),$$

Table 1. Equilibrium redox potentials $E_{1/2}$(Ox) and $E_{1/2}$(Red) (measured relative to the saturated calomel electrode) and the maxima positions in the optical spectra (λ_{max}) of the sensitising dyes (S^+), the quantum yield η_0 of *N,N*-diphenyl(phenylmethyleneiminium) bromide [formed by reaction (9)] in the composition consisting of PVE, DPBA, DTBMS, and S^+.

Dye (S^+)	$E_{1/2}$(Ox)/ V	$E_{1/2}$(Red)/ V	λ_{max}/ nm	η_0
2,2',6,6'-Tetraphenylpyrylomethinecyanine-perchlorate (X = X¹ = O, X² = H)	1.2 *	–0.65 *	571	0.12
2,2',6,6'-Tetraphenylthiopyrylo-methinecyanine perchlorate (X = O, X¹ = S, X² = H)	1.15 *	–0.55 *	596	0.02
2,2',6,6'-Tetraphenylpyrylobromo-methinecyanine perchlorate (X = X¹ = O, X² = Br)	1.7	~0	620	0.09
2,2',6,6'-Tetraphenyldithiopyrylo-methinecyanine perchlorate (X = X¹ = S, X² = H)	1.08 *	–0.46 *	630	0.00

* The redox potentials of the dyes were taken from Mikheeva et al.[21]

where $M_s(1)$ and $M_s(2)$ are the magnetic quantum numbers of the unpaired electrons 1 and 2 in the pair, and $m_i(1)$ and $m_k(2)$ are the magnetic quantum numbers of the nuclei over which the electron densities of the unpaired electrons 1 and 2 extend.

We shall consider how hyperfine interaction affects the rate of recombination of the components of the triplet pair in relation to dibenzyl ketone (DBK).[11] This influence is manifested by the photochemical enrichment of dibenzyl ketone in the ^{13}C isotope. The process is due to the fact that dibenzyl ketone dissociates in the excited triplet state into radicals, which form the radical pair $^3[R-\dot{C}(O)...\dot{R}]$, where $\dot{R} = \dot{C}H_2C_6H_5$. The triplet pairs decompose preferentially with formation of the dibenzyl ketone cleavage product if they contain the ^{12}C isotope in the $R-\dot{C}(O)$ group, but recombine with reformation of the initial ketone if the group contains the ^{13}C isotope. The effect is caused by the fact that, in contrast to the ^{12}C isotope, the ^{13}C isotope (the natural abundance of which is 1.1%) has a magnetic moment ($I = 1/2$) and the T → S transitions become allowed as a consequence of the hyperfine interaction:

$$-\overset{O}{\overset{\|}{C}}\cdot^{\uparrow}(m_i = -1/2)\ldots R\cdot^{\uparrow} \xrightarrow{T_{+1}\to S} -\overset{O}{\overset{\|}{C}}\cdot^{\downarrow}(m_i = +1/2)\ldots R\cdot^{\uparrow}$$

$$-\overset{O}{\overset{\|}{C}}\cdot^{\downarrow}(m_i = +1/2)\ldots R\cdot^{\downarrow} \xrightarrow{T_{-1}\to S} -\overset{O}{\overset{\|}{C}}\cdot^{\uparrow}(m_i = -1/2)\ldots R\cdot^{\downarrow}$$

$$-\overset{O}{\overset{\|}{C}}\cdot^{-}(m_i = \pm 1/2)\ldots R\cdot^{-} \xrightarrow{T_0\to S} -\overset{O}{\overset{\|}{C}}\cdot^{\downarrow}(m_i = \pm 1/2)\ldots R\cdot^{\uparrow}\ .$$

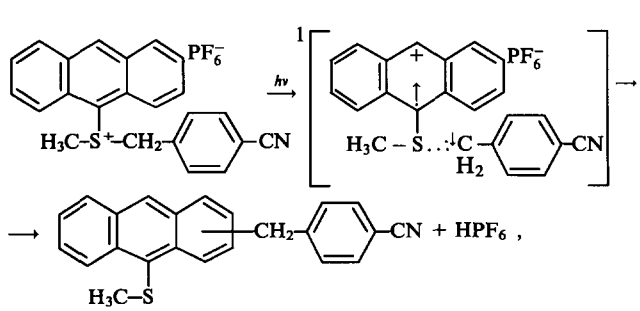
This permits the recombination of the radical pair. (The direction of the electron spin is indicated in the above formulae by arrows.)

In the general case the probability of the T → S transitions is determined by the sum of the hyperfine interaction constants:[11]

$$a^2 = \left[\sum_i a_i^2(1) + \sum_k a_k^2(2)\right] t\ ,$$

where t is the hyperfine interaction time.

In order to devise photoresists whose operation is based on acid photocatalysis, a large number of onium salts, such as arenediazonium salts ($ArN_2^+\ MX_n^-$), aryliodonium salts ($Ar_2I^+\ MX_n^-$), arylsulphonium salts ($Ar_3S^+\ MX_n^-$), and arylammonium salts, arylphosphonium salts, and arylarsonium salts ($Ar_4M'^+\ MX_n^-$; M' = N, P, and As respectively) were synthesised; $MX_n^- = PF_6^-$, AsF_6^-, BF_4^-, etc. On photoexcitation of the onium salt, the spectral sensitiser, or the charge-transfer complex between the additional organic donor (RH) and acceptor (onium salt), a reaction accompanied by the appearance of a Lewis (MX_{n-1}) or Brønsted (HMX_n) acid takes place. The acids induce the degradation of the chains or the cross-linking of the polyesters. The mode of such photochemical reactions is determined by the hyperfine interaction,[22,23] because S → T intersystem crossing in the singlet radical pair formed in the primary step competes with the reaction between the radicals. Thus the photolysis of sulphonium, arsonium, and phosphonium salts proceeds in different ways,[22] which is associated with the increase in the hyperfine interaction constant on passing from sulphonium [$a(^{32}S) = 0$ Oe] to arsonium [$a(^{75}As) = 4.65$ Oe], and further to phosphonium [$a(^{31}P) = 306$ Oe]. Whereas the products of the photolysis of sulphonium salts are formed as a result of an intramolecular rearrangement via the singlet state of the pair,[22,23] the photolysis of arsonium salts takes place both via the singlet and triplet states of the pair,[22] while the ammonium and phosphonium salts are photolysed solely via the triplet state, because in this case S → T intersystem crossing predominates and results in the formation of a triplet radical pair. In this case, the intramolecular rearrangement becomes spin-forbidden and the formation of HMX_n requires the involvement of a molecule of the solvent. For example, in the case of the salt 9-anthrylmethyl-*p*-cyano-benzylsulphonium hexafluorophosphate the photoexcitation of the 9-anthryl chromophore entails charge transfer from the sulphonium fragment and subsequent rearrangement within the pair[23]



whereas in arsonium salts the following reactions takes place.

$$(C_6H_5)_3As^+ - CH_2 - C_6H_4 - CN \xrightarrow{h\nu}$$
$$\rightarrow\ {}^1[(C_6H_5)_3As^{\cdot+}\ldots\dot{C}H_2C_6H_4 - CN\ MX_n^-] \rightarrow (C_6H_5)_2As - C_6H_4 - CH_2 - C_6H_4CN + HMX_n\ ,$$
$$\rightarrow\ {}^3[(C_6H_5)_3As^{\cdot+}\ldots\dot{C}H_2C_6H_4 - CN\ MX_n^-] \xrightarrow{H_2O} (C_6H_5)_3AsO + (CH_3 - C_6H_4CN) + HMX_n\ . \qquad (10)$$

A high rate of S → T intersystem crossing is to be expected in the radical pairs of iodonium salts via both spin–orbit and hyperfine interaction mechanisms as well as the predominance of reaction (10), because high spin–orbit and hyperfine interaction constants are characteristic of the iodine atom.

III. Processes amplifying the latent image

1. Highly sensitive photoresists based on [2 + 2] photoaddition

In the familiar photoresists consisting of poly(vinyl cinnamates) (PVCI) and related compounds $-CH_2-CHR-$, the chromophore R incorporates the $-CH=CH-$ group, which is responsible for the photoinduced cross-linking of the polymer chain via the [2 + 2] photocycloaddition mechanism:[2]

$$2(-CH=CH-) \xrightarrow{h\nu} \begin{matrix} -CH-CH- \\ | \quad | \\ -CH-CH- \end{matrix} \qquad (11)$$

As a result of this reaction, the exposed polymer film is not removed from the support throughout the period of the dissolution of the unexposed sections in organic solvents.

[2 + 2] Photocycloaddition involving PVCI proceeds via the excited singlet and triplet states of the chromophores R when the latter are themselves photoexcited. The process proceeds with a much higher efficiency under the conditions of triplet energy transfer to R from the photoexcited spectral sensitiser. For a random relative distribution of the chromophores in neighbouring PVCI chains ($R = -OCO-C=CH-C_6H_5$), the quantum yield of the cyclobutane rings formed via reaction (11) is $\eta_0 \simeq 0.045$ and the exposure corresponding to the onset of gel formation is $H_g \simeq 700$ mJ cm^{-2}. In order to increase the photosensitivity of photoresists, much attention has been devoted in recent years to the synthesis of new polymers with an increased triplet energy migration distance[24] and also the synthesis of compounds in which the cinnamoyl groups form aggregates.[7,25,26]

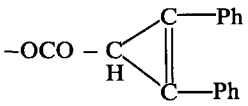
The lifetimes of the triplet excitation (τ), the quantum yield of the cyclobutane ring (η_0), and the photosensitivities $S = 1/H_g$ (estimated relative to S for PVCI) have been compared[24] for PVCI and the polymers **1–3**

$$(-CHR-CH_2-)_{0.9}-(-CHOH-CH_2-)_{0.1};$$

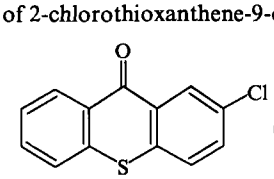
1–3

1: R = $-OCO-CH=CH-C_6H_4-COOC_2H_5$;

2: R = $-OCO-CH=CH-C_{10}H_8$

3: R = 

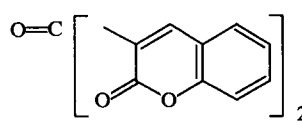
in the presence of 2-chlorothioxanthene-9-one **4**



(E_T = 65 kcal mol^{-1})

4

or 3,3′-carbonylbiscoumarin **5**



(E_T = 56.2 kcal mol^{-1})

5

as the sensitiser (Table 2). The table shows that, on passing from PVCI to the polymer **3**, the lifetime of the triplet excitation increases by more than four orders of magnitude. This is responsible for the increase in S by a factor of 17.5, i.e. a decrease in H_g to 40 mJ cm^{-2}.

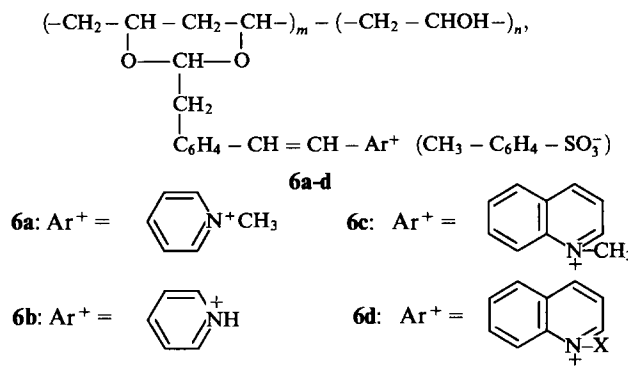
In order to obtain intermolecularly bound chromophoric groups, poly(vinyl cinnamates) $-CH_2-CH(RX)-$ were synthesised with chromophoric groups (RX) containing a fragment X with electron-donating (PVCI–D) or electron-accepting (PVCI–A) properties:[25,26]

$$-CH_2-\underset{|}{CH}-O-CO-CH=CH-C_6H_4-D \quad \text{(PVCI-D)}$$

$$-CH_2-\underset{|}{CH}-O-CO-CH=CH-C_6H_4-A \quad \text{(PVCI-A)}$$

Table 3 presents the quantum yields of the overall consumption of the double bonds (η') and the intermolecular cross-links (η'') and the values of H_g for different combinations of PVCI-D and PVCI-A in the absence of a sensitiser and on photoexcitation of 3,3-carbonylbiscoumarin as the sensitiser.[25,26] Table 3 shows that the relative efficiency of the gel formation, which can be estimated from the ratio η''/η', increases with enhancement of the donor–acceptor interaction from 0.18 for pure PVCI to 0.82 for the PVCI–OCH_3/PVCI–Cl (50 : 50) pairs. As a consequence of this, on passing from the homopolymer PVCI to the equimolar mixture of polymers PVCI–OCH_3/PVCI–Cl, there is also a decrease in H_g from 700 to 152 and 62 mJ cm^{-2} in the non-sensitised and sensitised systems respectively.

The highly sensitive water-soluble photoresists



6a-d

6a: Ar^+ = **6c**: Ar^+ =

6b: Ar^+ = **6d**: Ar^+ =

whose operation is based on [2 + 2] photocycloaddition, have been proposed.[27,28] The capacity of these photoresists to form aggregates is responsible for their high sensitivity even at a low concentration of chromophoric groups:

Polymer	(m/n)/%	H_g/ mJ cm^{-2}
6a	2.2	~12
6b	2.5	~10

It has been shown in relation to the polymer **6c** [27,28] that the deprotonation of the quinoline group by treatment in an organic solvent containing amines, i.e. its transformation from an electron-accepting into an electron-donating group, leads to a 100-fold increase in H_g and also to a shift of the long-wavelength optical absorption maximum from 420 nm to 360 nm. It was therefore suggested that a polymer with a low sensitivity be employed and that it be sensitised directly before exposure by treatment in acid-containing solvents. The photosensitivity obtained under these conditions depends on the nature of

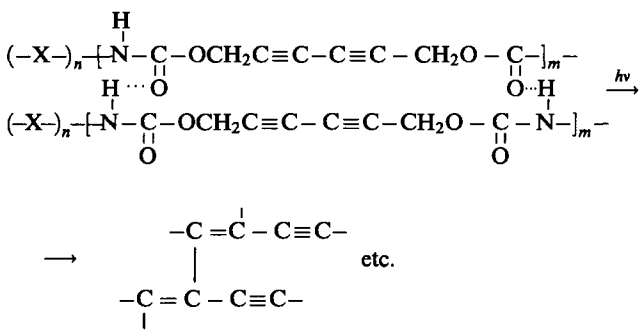
Table 2. The lifetimes of the triplet excitation (τ), the quantum yield in the formation of the cyclobutane ring (η_0), and the photosensitivity ($S = 1/H_g$) relative to S for PVCI) of PVCI and the polymers **1–3**.[24]

Polymer	τ/ μs	η_0	S/ cm^2 mJ^{-1}
PVCI	0.01	0.045	1
1	6.9	0.073	2.5
2	10	0.12	3.3
3	360	0.53	17.5

the acid[28] and increases in the sequence corresponding to the ratios HCl : HPO_3 : $HClO_4$: H_2SO_4 : p-$CH_3C_6H_4SO_3H$ = = 1 : 21 : 71 : 100 : 101.

The intermolecular interactions in the linear polyesters $-CO-C(CN)=CH-CH=CHC_6H_4CH=C(CN)-CO-O-[(-CH_2-)_2-O-]_3-$ in the ground state ensure their high photosensitivity[29] with H_g = 1.6 mJ m^{-2}.

It has been suggested[30,31] that the hydrogen bonds in the block-copolymers of diacetylene with polyurethanes, polyesters, and polyamides are responsible for the formation of stacks of chains containing diacetylene fragments. Light at the wavelength corresponding to the absorption bands of diacetylene ($\leqslant$400 nm) initiates the chain reaction involving the cross-linking of neighbouring acetylene groups with formation of a branched system of conjugate bonds. This reaction proceeds effectively when an exposed film is heated (80 °C, 10 min):



The highest sensitivity (H_g = 0.5 mJ cm^{-2} when the content of diacetylene groups is 30 wt%) is shown by copolymers based on aliphatic polyurethanes, which is associated with the flexibility of the chains promoting the formation of stacks of rigid diacetylene fragments and also with the absence of groups which absorb light in the same region as the diacetylene chromophore.

2. Autocatalysis

A typical example of compositions in which the catalyst is formed as a result of a photochemical reaction directly from the photosensitive components is the system incorporating a polymer matrix and an electron donor [$(C_5H_5)_2Fe$] and acceptor (CBr_4) dissolved in it. The donor–acceptor complex $(C_5H_5)_2Fe \cdot CBr_4$, the optical absorption maximum of which is in the range 370–400 nm, is responsible for the photosensitivity of the composition. Photoexcitation of the complex leads to its dissociative decomposition:[5,32,33]

$$(C_5H_5)_2Fe \cdot CBr_4 \xrightarrow{h\nu}$$
$$\longrightarrow (C_5H_5)_2Fe^+ \ldots Br^- \ldots \dot{C}Br_3 \text{ (or } Br^{\cdot} \ldots CBr_3^-) \longrightarrow$$
$$\longrightarrow [Fe^{3+}Br_4]^- + \text{products} \qquad (12)$$

with formation of the ferrocenium cation $(C_5H_5)_2Fe^+$, which is converted by interaction with the free radical $\dot{C}Br_3$ into the tetrabromoferrate(III) anion $[Fe^{3+}Br_4]^-$ with characteristic optical absorption bands at λ_{max} = 397 and 472 nm, which are responsible for the brown colour.

It has been noted[34] that heating of the exposed layer at 70–100 °C ensures the development of the latent image. It has been established[5,34,35] that the key factor in this process is the formation of trivalent iron which enters into the thermal reaction[36]

$$Fe^{3+} + (C_5H_5)_2Fe \longrightarrow Fe^{2+} + (C_5H_5)_2Fe^+.$$

This is followed by charge transfer:

$$Fe^{2+} + CBr_4 \longrightarrow Fe^{3+} + Br^- \ldots CBr_3^{\cdot} \text{ (or } Br^{\cdot} \ldots CBr_3^-).$$

Thus the Fe^{3+}/Fe^{2+} pair, arising as a result of illumination, catalyses the thermal electron transfer between the donor and acceptor components. The overall process can be formulated as follows:

$$(C_5H_5)_2Fe + CBr_4 \xrightarrow{Fe^{3+}/Fe^{2+}}$$
$$\longrightarrow (C_5H_5)_2Fe^+ + Br^- \ldots CBr_3^{\cdot} \text{ (or } Br^{\cdot} \ldots CBr_3^-). \qquad (13)$$

The thermal stages of the photochemical reaction (12) are then repeated.

The factors limiting the amplification coefficient as a consequence of the parallel occurrence of the photoinitiated autocatalytic reaction (13) and the dark thermal electron transfer in the complex $(C_5H_5)_2Fe \cdot A$, where A = CBr_4 or halo-derivatives of organic compounds of different structure, have been analysed.[37] It was established that the principal stages of the autocatalytic process (13) include diffusion-controlled reactions, so that the decisive factors are the size of the acceptor and the segmental mobility of the polymer chains at elevated temperatures. The primary quantum yield of the coloured product [formed via reaction (12)] is η_0 = 0.05–0.1 regardless of the nature of the acceptor. It has been shown that, when a polystyrene matrix is used, the highest

Table 3. The influence of the donor–acceptor interaction on the principal characteristics of PVCI-based photoresists.

Polymer	η'	η''	H_g/ mJ cm^{-1}
	Without sensitiser, λ = 300 nm		
PCVI	0.28	0.05	700
PVCI–CO–OCH_3/ PVCI–Cl	0.28	0.03	~1160
PVCI–CH_3/ PVCI	0.245	0.085	410
PVCI/PVCI–Cl	0.1265	0.1	350
PVCI–OCH_3/ PVCI	0.32	0.13	270
PVCI–CH_3/ PVCI–CO–OCH_3	0.27	0.125	280
PVCI–OCH_3/ PVCI–Cl			
100 : 0	–	0.06	–
50 : 50	0.28	0.23	152
0 : 100	–	0.02	–
	6 wt% of sensitiser, λ = 400 nm		
PVCI–OCH_3/PVCI–Cl			
100 : 0	–	0.08	–
50 : 50	–	0.58	62
0 : 100	–	0.02	–

amplification coefficient (~6000) is attained in the case of CBr_4. When CBr_4 is replaced by $O_2N-C_6H_4-SO_2-CBr_3$, the amplification coefficient is reduced to 450.

Compositions containing, in addition to the ferrocene donor, also aromatic amines (Am), namely diphenylamine (DPA), DPBA, and dibenzylaniline (DBA), have been investigated.[38-41] It was established that the photoexcitation of the complex $(C_5H_5)_2Fe \cdot CBr_4$ and subsequent heating of the composition to 60–100 °C results in the autocatalytic accumulation not only of the ferrocene decomposition products but also of the triphenylmethane dye (TPM D) derived from the aromatic amine, the dye being responsible for the absorption at λ_{max} = 605 nm. It has been suggested[40,41] that the charge transfer

$$(C_5H_5)_2Fe^+ + Am \longrightarrow (C_5H_5)_2Fe + Am^{\cdot+} \qquad (14)$$

and subsequent thermal reactions of the radical cation $Am^{\cdot+}$ and of $Br^-...CBr_3^{\cdot}$, i.e.

$$Am^{\cdot+}...Br^- \ ...CBr_3^{\cdot} \xrightarrow[HBr]{2Am}$$

$$\longrightarrow R^1R^2N^+ = C_6H_4 = C(C_6H_4NR^1R^2)_2Br^- \qquad (15)$$

(TPM D)

take place.

Under the conditions of the photoexcitation of the complex $(C_5H_5)_2Fe \cdot CBr_4$ in the presence of amines it was established[38] that DPA inhibits the autocatalytic accumulation of $[Fe^{3+}Br_4]^-$ to a much greater extent than do DPBA and DBA. It is most likely that the inhibition is due to the charge-transfer process (14), the rate of which is determined by the nature of the aromatic amine. Indeed, the ionisation potentials of ferrocene (I_D = 6.88 eV[42]), DPA (7.2 eV[43]), DPBA (~7.5 eV[20]), and DBA (7.55 eV[20]) correspond to the following free energies of activation for reaction (14): ΔG_1 = 7.2–6.88 = 0.32 eV for DPA, ΔG_2 = = 7.5–6.88 = 0.62 eV for DBA. Hence it follows that the rate constants for reaction (14) with participation of the tertiary amines DPBA and DBA are smaller by the factor $\exp[(\Delta G_2 - \Delta G_1)/kT]$, i.e. by approximately five orders of magnitude, than in the case of DPA. However, it has been established experimentally that the rate of formation of the coloured products from the tertiary amines DPBA and DBA is the same as the rate measured for the secondary amine DPA. It is most likely that the coloured products derived from the tertiary amines DPBA and DBA and the secondary amine DPA are formed via different pathways.

It is known that the photoexcitation of complexes between DPA and CBr_4 involves electron transfer from the donor to the acceptor component with formation of the radical-ions $CBr_3^{\cdot}...Br^-$ and $DPA^{\cdot+}$ and the products of their interaction:[44]

$$DPA^{\cdot+} + + CBr_3^{\cdot} \ ...(Br^-) \longrightarrow p\text{-DPA} - CBr_3 + HBr\,.$$

It has been suggested[45,46] that the free radical chain process

$$\begin{array}{l} DPA + \dot{C}Br_3\ (Br^{\cdot}) \longrightarrow DPA^{\cdot} + CHBr_3\ (HBr) \\ \quad\uparrow\qquad\qquad\qquad\qquad\quad\downarrow \\ DPA^{\cdot} + CBr_4 \longrightarrow p\text{-DPA}-CBr_3 + Br^{\cdot} \end{array} \qquad (16)$$

takes place and leads to the amplification of the latent image. The interaction of DPA – CBr_3 with DPA ensures the formation of the triphenylmethane dye.

The interaction of tertiary amines with $\dot{C}Br_3$ radicals involves the abstraction of a hydrogen atom from the α-position relative to the nitrogen atom:[47]

$$C_6H_5(R)N - CH_2 - C_6H_5 + CBr_3^{\cdot} \longrightarrow$$

$$\longrightarrow C_6H_5(R)N - \dot{C}H - C_6H_5 + HCBr_3\,. \qquad (17)$$

The α-radicals $R_2N-\dot{C}H-R$ exhibit powerful electron-donating properties and transfer an electron to the acceptor in dark reactions.[46,49] On this basis, one may postulate the occurrence of a chain process involving the formation of the coloured products CP^+Br^- [see Eqn. (9)]:

$$C_6H_5(R)N - \dot{C}H - C_6H_5 + CBr_4 \longrightarrow$$

$$\longrightarrow C_6H_5(R)N^+ = CH - C_6H_5\ Br^- ...\dot{C}Br_3 \qquad (18)$$

and its subsequent accumulation via reactions (17) and (18). On heating, the product CP^+Br^- reacts with the amine and other components of the layer with formation of compounds of the type of triphenylmethane dyes.[19,50,51]

Molecular oxygen lowers the rate of autocatalytic accumulation of the coloured species $[Fe^{3+}Br_4]^-$ due to its consumption via the reaction

$$Fe^{3+} \xrightarrow{O_2} Fe_2O_3 + Fe(OH)_3\ \text{, etc.}$$

It has been shown[40,41] that the autocatalytic amplification of the latent image occurs also at room temperature when the content of molecular oxygen has been reduced appreciably in the polymeric photosensitive layer by placing it between two protecting films of poly(vinyl alcohol) (PVA). It is known[52,53] that PVA prevents the penetration of O_2 from the atmosphere and also adsorbs the oxygen dissolved in the polymer layer. The autocatalytic formation of coloured products ceases completely when the upper protective PVA film is removed from the photosensitive layer. The high amplification coefficients (~10^4 in the absence of oxygen), characteristic of these compositions, are responsible for their maximum photosensitivity (~0.01 $lx^{-1}\ s^{-1}$) among non-silver photographic systems.

Exposure to laser radiation at 441 or 488 nm, acting in the region corresponding to absorption by the complex $(C_5H_5)_2Fe \cdot CBr_4$, and subsequent heating at 70–90 °C results in the formation of ester bonds in the copolymer of vinyl acetate and crotonic acid $[-CH_2-C(COOH)H-]_n-[-CH_2-C(OCOCH_3)H-]_m$ containing $(C_5H_5)_2Fe$ and CBr_4, which leads to an appreciable decrease in the solubility of the polymer composition in aqueous alkaline solution.[54] It has been shown[54,55] that the divalent iron formed via reactions (12) and (13) catalyses the processes:

$$Fe(II) + (-CH_2 - \underset{\displaystyle O - COCH_3}{\underset{|}{CH}}-) \longrightarrow - CH_2 - \underset{\displaystyle O^- ...\dot{C}OCH_3}{\underset{|}{CH}} - + Fe(III) \xrightarrow{H_2O}$$

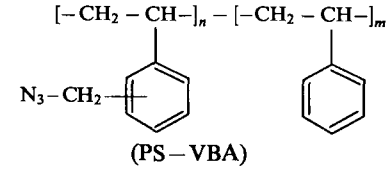
$$\longrightarrow - CH_2 - \underset{\displaystyle OH}{\underset{|}{CH}} - + CH_3COOH + Fe(II)$$

and further

$$- CH_2 - \underset{\displaystyle COOH}{\underset{|}{CH}} - + - CH_2 - \underset{\displaystyle OH}{\underset{|}{CH}} - \longrightarrow \underset{\displaystyle HC-CO-O-CH}{\underset{|}{H_2C}} \quad \underset{|}{CH_2} + H_2O.$$

After the exposed film has been placed in a 2.5% aqueous solution of $(CH_3)_4NOH$ for 5 min, the non-exposed sections are fully dissolved, while the thickness of the sections which receives an exposure $H_g \geqslant 10$ mJ cm^{-2} (λ = 488 nm) remains unchanged.

Photoinitiated autocatalytic decomposition is characteristic also of aromatic azides, a very familiar class of photoresists. The branched chain decomposition has been investigated in relation to low-molecular-weight azides[8,56-59] as well as layers made up the styrene–vinylbenzyl azide (PS–VBA) copolymer:[60-62]



(PS–VBA)

The chain mechanism of the decomposition of phenyl azide in liquid media has been established:[8,56]

(a) chain initiation

$$C_6H_5-N_3 \xrightarrow{\lambda=254\ nm} C_6H_5-N: + N_2,$$

(b) chain propagation

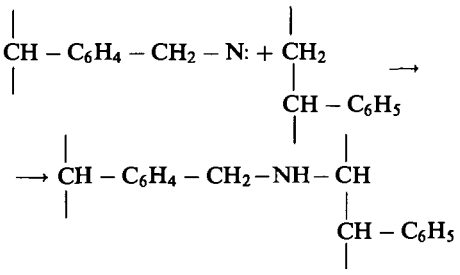
$$C_6H_5-N: + C_6H_5-N_3 \longrightarrow 2C_6H_5-N: + N_2,$$

(c) chain termination

$$C_6H_5-N: + C_6H_5-N_3 \longrightarrow C_6H_5-N=N-C_6H_5+N_2,$$

$$2C_6H_5-N: \longrightarrow C_6H_5-N=N-C_6H_5.$$

The initial quantum yield of $C_6H_5-N:$, measured either in diluted (to 10^{-4} M) solutions at room temperature or in organic glasses frozen at 77 K, is ~0.58. At high $C_6H_5-N_3$ concentrations (~0.08–0.72 M) at room temperature, the amplification coefficient reaches 10^3-10^4.[8] The efficiency of the chain decomposition of PS–VBA layers increases under the conditions of the photoexcitation of additional triplet energy donors (thioxanthone, anthracene, and their derivatives).[60,61] The azide-containing compositions are negative photoresists, their reduced solubility in organic media being caused by the cross-linking of the



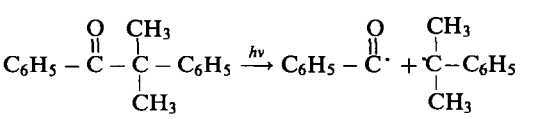
polymer chains with participation of the nitrene formed under the inluence of light:

In compositions comprising PS–VBA (m/n = 14.9%) and 2,4-diisopentylthioxanthone (sensitiser), the onset of gel formation corresponds to the exposure H_g = 45 mJ cm^{-2}.[62]

3. Photochemically induced cross-linking of polyfunctional acrylates

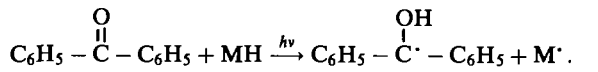
In recent years, much attention has been devoted to the photoinitiated cross-linking of polyfunctional oligomeric acrylates (compounds containing two and more $-O-CO-CH=CH_2$ groups). Studies on this subject have been recently discussed in detail in review publications[63–66] and only compositions proposed as highly sensitive photoresists for use in micro-electronics, in the manufacture and copying of compact discs,[9,67–69] and also in the manufacture of microencapsulated photographic material[70] will therefore be considered below.

Diacrylates of aliphatic polyurethanes, the diacrylates of polyepoxybisphenol A, and the triacrylate of trimethylpropane [trimethylpropanetriol?] have been used as polyfunctional acrylates. The photoinitiators (I) were ketones of different structure: dimethylphenylacetophenone, isobutyl ether of benzoin or benzophenone, phenanthrenequinone, etc. Depending on the structure of the initiator, either direct photodissociation



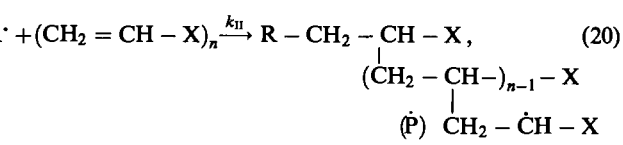
(19)

or (in the presence of added MH) a photoredox process with the transfer of an electron and a proton)



(19a)

Free radicals formed in sections (19) and (19a) give rise to polymerisation



(20)

and chain termination

$$P^{\cdot} + P^{\cdot} \xrightarrow{k_0} 2P, \quad (21)$$

$$P^{\cdot} + R^{\cdot} \longrightarrow PR. \quad (21a)$$

The influence of hyperfine interaction on the rate of recombination of radicals in the pair formed via reactions (19) and (19a) was discussed above (see sub-section II.2).

The quantum yield of radicals formed by reactions (19) and (19a) is ~0.1 both in dilute liquid solutions and in viscous media.[67] The chain termination corresponds to the second-order reaction (21) in the polymerisation of monofunctional acrylates in any condensed media. The chain termination in the polymerisation of monomers in microcapsules has been shown to be a first-order process,[70] where the consumption of radicals mainly as a result of their preferential reaction with the walls of the capsule predominates. The first-order process of destruction of the radical $\dot{P}$ has also been observed on exposure to intense pulsed laser radiation.[9] On the basis of the analysis of the kinetics of photopolymerisation with the use of photoinitiators of different kinds, it has been suggested[77] that, in the photoredox reaction (19a), the radicals formed serve simultaneously as initiators and inhibitors of polymerisation and are responsible for the first order of the consumption of $\dot{P}$ via reaction (21a).

The polymerisation of a polyfunctional molecule involves simultaneously several groups and the polymer network is formed already in the early stages of the reactions. The mutual approach of the radicals grafted to the network is sterically hindered. In the case of the diacrylate of polyepoxybisphenol A, the kinetic chain of reaction (20) included 10^4-10^5 links,[9,69] which is the reason for the high photosensitivity of the system[9] corresponding to $H_g \simeq 3$ mJ cm^{-2}. Molecular oxygen greatly reduces the rate of polymerisation and the length of the kinetic chain when low-intensity light sources are used.[69]

4. Chemical amplification of the latent image

Nowadays much attention is devoted to photoresists whose action is based on the photochemical formation of acids and subsequent occurrence of chain processes (chemical amplification) involving the polymerisation of vinyl monomers or epoxides,[6,7,72–74] cationic polycondensation and cross-linking of polymer chains (for example novolac resin and hexamethoxymethylenemelamine),[75,76] and cationic depolymerisation [degradation of poly(phthalic aldehyde) to gaseous products].[77–79] The creation of photoresists based on polymers with protecting groups, which are abstracted by a photochemically generated acid, thus altering the polarity and hence the solubility of the polymers, has found wide application.[80–84] Specific photoresist systems of this type have been discussed in detail in recent years in the review literature[6,7,55] and only fundamental questions referring to chemical amplification will therefore be considered below.

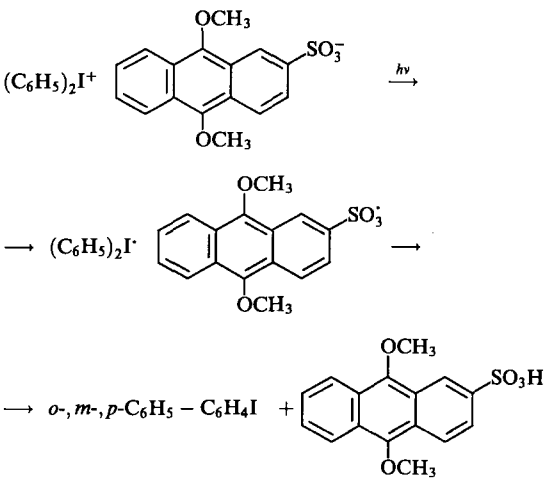
As stated above (see sub-section II.2), acids are generated photochemically from onium salts via reaction (10). Iodonium

Table 4. The free energies $^{S}\Delta G$ and $^{T}\Delta G$ of electron transfer from singlet-excited and triplet-excited dye respectively to the onium salt.

Dye	$\Delta G(22)$	ΔG/eV			
		$C_6H_5N_2^+$ BF_4^- [0.3 V][a]	$(C_6H_5)_2I^+$ BF_4^- [−0.16 V][a]	$(C_6H_5)_3S^+$ BF_4^- [−1.06 V][a]	$Bz(C_6H_5)_3P^+$ BF_4^- [−1.83 V][a]
Xanthone					
$E_{1/2}(Ox) = 1.41$ V					
$^1E_{00} = 3.41$ eV	$^{S}\Delta G$	−1.91	−1.45	−0.55	0.22
$^3E_{00} = 3.2$ eV	$^{T}\Delta G$	−1.7	−1.24	−0.35	0.43
Thioxanthone					
$E_{1/2}(Ox) = 1.67$ V					
$^1E_{00} = 3.14$ eV	$^{S}\Delta G$	−1.77	−1.31	−0.41	0.36
$^3E_{00} = 2.8$ eV	$^{T}\Delta G$	−1.43	−0.97	−0.07	0.7
Acridone					
$E_{1/2}(Ox) = 1.5$ V					
$^1E_{00} = 2.5$ eV	$^{S}\Delta G$	−1.75	−1.29	−0.39	0.38
$^3E_{00} = 2.6$ eV	$^{T}\Delta G$	−1.4	−0.94	−0.04	0.73
10-Methylacridone					
$E_{1/2}(Ox) = 1.46$ V					
$^1E_{00} = 2.92$ eV	$^{S}\Delta G$	−1.76	−1.3	−0.4	0.37
$^3E_{00} = 2.6$ eV	$^{T}\Delta G$	−1.44	−0.98	−0.08	0.69

[a] Equilibrium potentials of the reduction the ionium salts are shown in brackets.

salts have been synthesised in which the photosensitivity is due to the optical absorption of the counteranion.[85] The acid is formed as a result of the electron phototransfer via the reaction



The decomposition of ionium salts under the conditions of the photoexcitation of organic sensitisers (dyes or aromatic hydrocarbons ArH) has been investigated in detail.[86–90] Electron transfer takes place via a stage involving the formation of an exciplex, for example, we have for a diphenyliodonium salt

$$\mathrm{ArH} \xrightarrow{h\nu} {}^{1,3}(\mathrm{ArH})_1 \xrightarrow{(C_6H_5)_2I^+X^-} {}^{1,3}(\mathrm{ArH})_1\cdot(C_6H_5)_2I^+X^- \longrightarrow$$

$$\longrightarrow {}^{1,3}[\mathrm{ArH}^{\cdot+}\ldots(C_6H_5)_2I^{\cdot}\,X^-] \longrightarrow$$

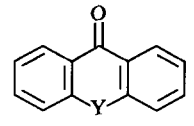
$$\longrightarrow \mathrm{Ar}-C_6H_5 + C_6H_5I + HX. \qquad (22)$$

It has been established experimentally that for onium salts the reaction proceeds effectively only when the free energy change on electron transfer is $\Delta G(22) \leqslant -0.43$ eV:[86–89]

$$\Delta G(22) = e\left[E_{1/2}\left(\frac{^{1,3}(\mathrm{ArH})_1}{\mathrm{ArH}^{\cdot+}}\right) - E_{1/2}\left(\frac{\mathrm{On}^{\cdot}\mathrm{X}^-}{\mathrm{On}^+\mathrm{X}^-}\right)\right]\mathrm{eV}\ ,$$

where $E_{1/2}[^{1,3}(\mathrm{ArH})_1/\mathrm{ArH}^{\cdot+}] = E_{1/2}(\mathrm{ArH}/\mathrm{ArH}^{\cdot+}) - {}^{1,3}E_{00}$ and $E_{1/2}(\mathrm{ArH}/\mathrm{ArH}^{\cdot+})$ are equilibrium potentials of the oxidation of the sensitiser in the excited singlet and triplet ground states respectively [via the reactions $^{1,3}(\mathrm{ArH})_1 \rightleftarrows \mathrm{ArH}^{\cdot+} + e$ and $\mathrm{ArH} \rightleftarrows \mathrm{ArH}^{\cdot+} + e$], $^{1,3}E_{00}$ is the distance from the ground to the reactive singlet or triplet level of the sensitiser, and $E_{1/2}(\mathrm{On}^{\cdot}\mathrm{X}^-/\mathrm{On}^+\mathrm{X}^-)$ are the equilibrium potentials of the reduction of the onium salts by the reaction $\mathrm{On}^{\cdot}\mathrm{X}^- = \mathrm{On}^+\mathrm{X}^- + e$ (listed in brackets in Table 4).

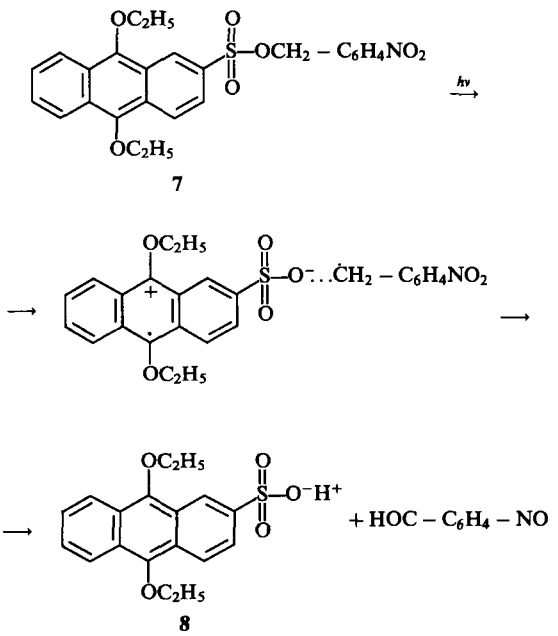
Table 4 also includes the values of ΔG_{22} ($^{S}\Delta G$ and $^{T}\Delta G$, the free energies of electron transfer to the onium salt from the acridine dye in the excited singlet and triplet states respectively).[87,89]



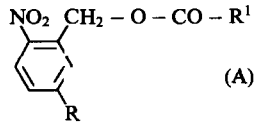
Y = O	xanthone
S	thioxanthone
NH	acridone
NCH_3	10-methylacridone

It follows from the tabulated data that the diazonium and iodonium salts can be sensitised by any of the dyes considered in the excited singlet or triplet state. The effective electron phototransfer to the sulphonium salt is possible only from the singlet-excited xanthone. As a rule, the sensitisers used for sulphonium salts are aromatic hydrocarbons, for example, perylene (Pe),[87,91] the equilibrium oxidation potential of which in the excited singlet state is $E_{1/2}(^1\mathrm{Pe}_1/\mathrm{Pe}^{\cdot+}) = -1.86$ V, since $E_{1/2}(^1\mathrm{Pe}_1/\mathrm{Pe}^{\cdot+}) = 1$ V and $^1E_{00} = 2.86$ eV. Owing to the high reduction potentials, it has not been possible to sensitise phosphonium and ammonium salts.

Special interest attaches to organic acid-forming compounds such as *p*-nitrobenzyl 9,10-diethoxyanthracene-2-sulphonate **7**,[91–93] in which dissociative intramolecular electron transfer takes place under the influence of light (250–300 nm) with the subsequent formation of the strong 9,10-diethoxyanthracene-2-sulphonic acid **8**:

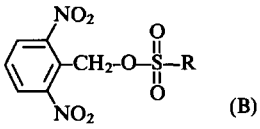


Esters having the structures (A),[94] (B),[80,84,95] and (C),[81,96] also belong to the acid-forming class:



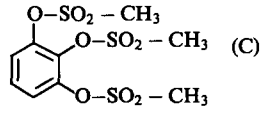
where R = H, NO_2; $R^1 = CH_3$, C_2H_5;

(A)



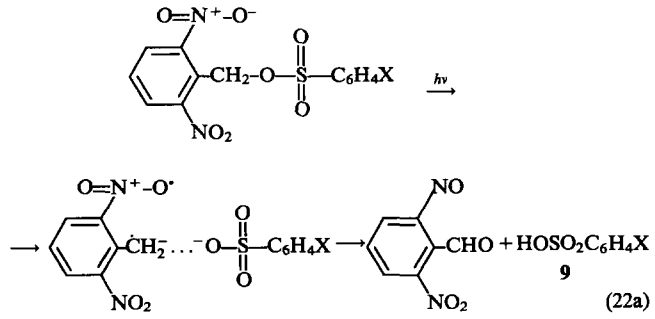
where R = CH_3, *p*-C_6H_4–CH_3, C_6H_5, *p*-C_6H_4–NO_2 etc.

(B)



(C)

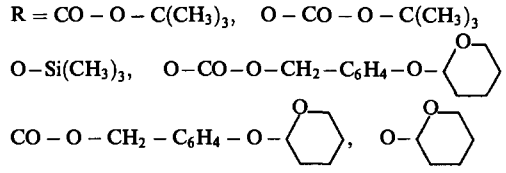
Acids are formed from these esters as a result of the dissociative intramolecular electron phototransfer, for example by the reaction



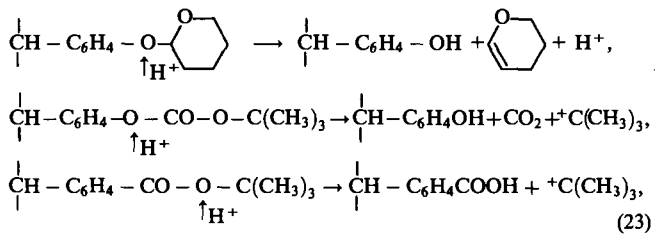
(22a)

The quantum yield of the acid **9** diminishes when the electron-donating substituent X is replaced by an electron-accepting one and its values are 0.16 (X = CH_3), 0.14 (X = H), and 0.1 (X = NO_2).

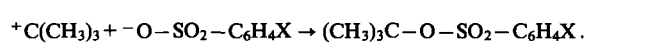
Photochemically generated acids deblock polymers which contain protecting groups[6,7,82,84,91,96,97] such as $-C(p\text{-}C_6H_4R)H-CH_2-$, $-C(p\text{-}C_6H_4R)(CH_3)-CH_2-$, and $-C(p\text{-}C_6H_4R)H-CH_2-)_2-SO_2-$, where

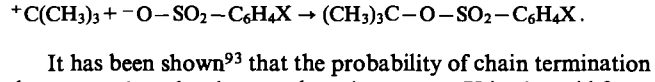


i.e. they transform them in accordance with the schemes presented below[6,82,93,96,97] into polymers which readily dissolve in 1–2% aqueous solution of $(CH_3)_4NOH$:



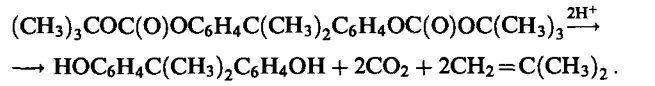
(23)





It has been shown[93] that the probability of chain termination decreases when the electron-donating groups X in the acid **9** are replaced by electron-accepting groups which withdraw the negative charge from the oxygen atom in the direction of the phenyl fragment. As a result, following the replacement of CH_3 by NO_2, the chain length, i.e. the chemical amplification coefficient (holding at 120 °C for 4 min), increases from 200 to 800.

Processes based on the inhibition of the dissolution of the novolak resin $[-C_6H_2(OH)(CH_3)-CH_2-]_n$ following the addition to the solvent of compounds with protecting groups have been widely investigated in recent years.[7] As an example, one may quote the composition of the novolak resin, the acid-forming ester, and an inhibitor—bisphenol A with *tert*-butoxycarbonyl groups.[81] As a result of the formation of acids on photoexcitation of the acid-forming ester, the inhibitor is transformed into bisphenol A via the reaction



It has been shown[81] that the initial quantum yield of the acid is 0.205 and the kinetic length of this chain, i.e. the amplification coefficient, is 76–123.

The working exposures in photoresists with chemical amplification are in the range $H = 2-10$ mJ cm^{-2}.

5. Chemical sensitisation of photosensitive systems

Chemical sensitisation is understood as the increase in the effectiveness of the chemical amplification by the introduction of an additional compound—a chemical sensitiser.

The mechanisms of the chemical sensitisation have been examined[55,98–100] as a function of the nature of the donor in photoresists based on charge-transfer complexes. Systems consisting of a poly(vinyl ethylal) matrix containing DTBS as the acceptor and tertiary amines—diphenylbenzylamine and triphenylamine (TPA)—as the donor have been investigated.

Dimethylaminobenzaldehyde (DMABA) was used as the chemical sensitiser. Under the influence of light at the wavelength corresponding to absorption by the complex Am · DTBMS, the latter dissociates into radical-ions with subsequent formation of coloured products and an acid, for example:

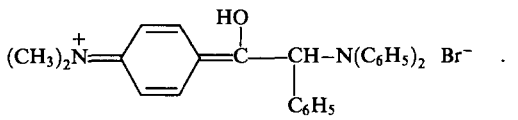
$$\text{DPBA}\cdot\text{DTBMS} \xrightarrow{h\nu} \text{DPBA}^{\cdot+} + \text{Br}^- \ldots \text{R}^\cdot \text{ (or } \text{R}^- \ldots \text{Br}^\cdot) \longrightarrow$$

$$\longrightarrow \text{CP}^+\text{Br}^- + \text{HR} \text{ (or } \text{CP}^+\text{R}^- + \text{HBr}) , \quad (24)$$

$$\text{DPBA}^{\cdot+} = (\text{C}_6\text{H}_5)_2\text{N}^{\cdot+} - \text{CH}_2 - \text{C}_6\text{H}_5,$$

$$\text{R}^\cdot = [\text{CBr}_2 - \text{SO}_2 - \text{CBr}_3]^\cdot .$$

The structures of CP^+Br^- and HR are given in Scheme (9). The quantum yield of CP^+Br^- and hence of the acids HR and HBr is ~0.05. The coloured product reacts with DMABA and forms a compound whose absorption has a maximum at 450 nm:[99,100]



(CP'^+Br^-)

It has been established[98–100] that the main chemical sensitisation reaction involves the protonation of DMABA by the acids HR and HBr, formed by the photochemical reaction (24), and the conversion of part of the keto-form $(CH_3)_2N^+H-C_6H_4-CHO\ R^-$ (and Br^-) into the enolic tautomer $(CH_3)_2N^+=C_6H_4=CHOH\ R^-$, the low oxidation potential of which $E_{1/2}$ = 0.49 V (s.c.e.) is responsible for the thermal electron transfer to DTBMS:

$$(\text{CH}_3)_2\text{N} - \text{C}_6\text{H}_4 - \text{CHO} \xrightarrow{\text{HR}} (\text{CH}_3)_2\text{N}^+\text{H} - \text{C}_6\text{H}_4 - \text{CHO} \rightleftarrows$$

$$\rightleftarrows (\text{CH}_3)_2\text{N}^+ = \text{C}_6\text{H}_4 = \text{CH(OH)R}^- \xrightarrow{\text{DTBMS}}$$

$$\longrightarrow (\text{CH}_3)_2\text{N}^+ = \text{C}_6\text{H}_4 = \text{C}^\cdot\text{OH} \ldots \text{Br}^- \ldots \text{R}^\cdot + \text{HR} . \quad (25)$$

$$(\text{DMABA}^+)$$

As shown in Scheme (25), the electron transfer from the enolic tautomer is followed by the abstraction of a proton, which leads to the formation of the radical-cation $DMABA^{\cdot+}$, the equilibrium reduction potential of which (via the reaction $DMABA \rightleftarrows DMABA^{\cdot-} + e$) is 1.1 (s.c.e.).[101] The mechanisms of the subsequent reactions depend on the ionisation potential of the tertiary amine.

In the case of compositions containing donors with high ionisation potentials $I_D \geqslant 7.3$ eV, such as DPBA (I_D = 7.5 eV) and DMABA itself (I_D = 7.36 eV),[102] new coloured products are formed via the reactions[99]

$$\text{DMABA}^{\cdot+} + \text{Br}^- \ldots \text{R}^\cdot \longrightarrow$$

$$\xrightarrow[-\text{HR}]{\text{DPBA}} (\text{CH}_3)_2\text{N}^+ = \text{C}_6\text{H}_4 = \text{C(OH)HC}(\text{C}_6\text{H}_5)\text{N}(\text{C}_6\text{H}_5)_2\text{Br}^- \quad (\text{CP}'^+\text{Br}^-)$$

$$\xrightarrow[-\text{HR}]{\text{DMABA}} (\text{CH}_3)_2\text{N}^+ = \text{C}_6\text{H}_4 = \text{C(OH)C(O)C}_6\text{H}_4\text{N}(\text{CH}_3)_2\text{Br}^- \quad (\lambda_{max} = 430 \text{ nm})$$

$$\xrightarrow[-\text{HR}]{} (\text{CH}_3)_2\text{N}^+ = \text{C}_6\text{H}_4 = \text{C} = \text{O}\ \text{Br}^- \quad (26)$$

The acid HR (or HBr) formed in addition enters into reaction (25) and ensures the further occurrence of reaction (26). The chemical amplification coefficient in the formation of the product CP'^+Br^- and hence of the acid HR via the upper pathway of reaction (26) is $\eta_{ef}/\eta_0 \simeq 50$.

In layers containing donors with low ionisation potentials, for example TPA (I_D = 6.8 eV),[102] the nature of the coloured product does not change during the chemical amplification process. In contrast to DPBA, a cyclic process takes place in these layers, where the photochemical formation of the acid, i.e.

$$\text{TPA}\cdot\text{DTBMS} \xrightarrow{h\nu} \text{TPA}^{\cdot-} \ldots \text{Br}^- \ldots \text{R}^\cdot$$

$$\text{TPA}^{\cdot+} \ldots \text{Br}^- \ldots \text{R}^\cdot \begin{cases} \longrightarrow \text{BPDPA} + \text{HR}^\cdot \\ \longrightarrow \text{CP}''^+\text{Br}^- + \text{HR} \end{cases} \quad (27)$$

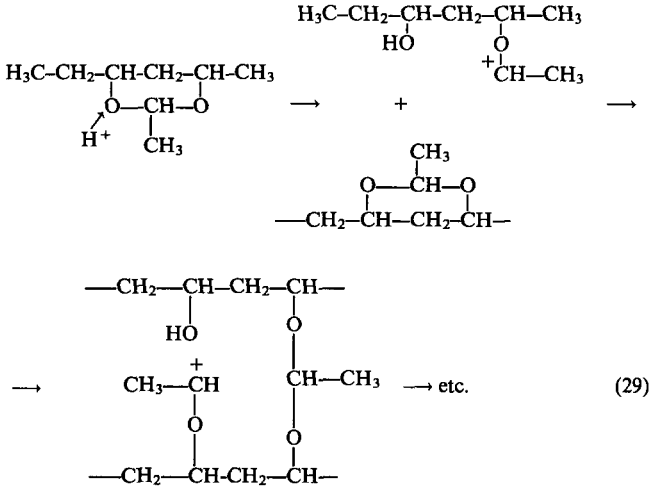
[BPDPA = 4-bromophenyl(diphenyl)amine] is followed by reaction (25) and charge transfer:

$$\text{TPA} \xrightarrow{\text{DMABA}^+ \ldots \text{Br}^- \ldots \text{R}^\cdot} \text{TPA}^+ \ldots \text{Br}^- \ldots \text{R}^\cdot + \text{DMABA} . \quad (28)$$

where CP''^+Br^- is the coloured product obtained from TPA (with λ_{max} = 610 nm).

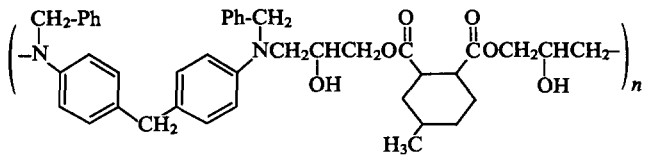
The formation of BPDPA as a result of the reaction between $TPA^{\cdot+}$ and Br^- in the presence of the anthracene radical has been established.[103] Reaction (27) is then repeated. The chemical amplification coefficient, determined from the product CP''^+Br^-, reaches ~600.

The acid ensures the effective cross-linking of the PVE chains by the reaction[55,97,99]
and a decrease in the solubility of the exposed section of the layer in the developer—a mixture of water and alcohol.



It is seen from the schemes presented above that, under the conditions of the chemical sensitisation of compositions based on tertiary aromatic amines, the photochemical formation of coloured products and the acids HR and HBr [reactions (24) and (27)] is followed by the thermal stages (25), (26), and (28) involving the additional formation of coloured products and the acids HR and HBr, in contrast to the systems based on onium salts and other compounds in which the acid is formed only under the influence of light [see reaction (23)].

Polymers containing electron-donating groups in the main chain, for example polyhydroxyaminoester (PHAE)[104]

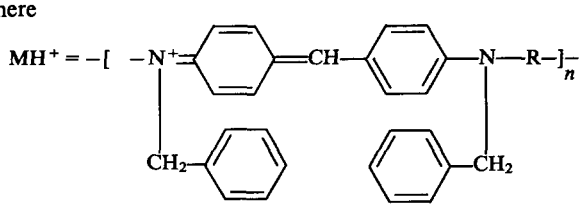


are especially interesting. Polymers of this type are photosemiconductors[105] and, after the addition of halogen-containing acceptors (for example DTBMS) acquire the properties of photoresists. In principle, this makes it possible to use photolithography for the manufacture of microcircuits based on organic photosemiconductors. The photosensitivity is due to the formation of a charge-transfer complex between the donor fragment of the macromolecule and the acceptor. The complex has its intrinsic optical absorption in the visible region (300–550 nm) and its ionic photodissociation leads to the formation of coloured polycationic products of the type of Michler's hydrol (MH^+) (λ_{max} = 630 nm) and the acids HR:

$$PHAE \cdot DTBMS \xrightarrow{h\nu} PHAE^{\cdot+} \ldots Br^- \ldots R^{\cdot} \longrightarrow$$

$$\longrightarrow MH^+Br^- + HR \ , \qquad (30)$$

where



The polyhydroxyaminoester has a low ionisaion potential ($I_D \simeq 7.0$ eV). The addition of DMABA to the layer does not alter the nature of the coloured product but increases its quantum yield from η_0 = 0.12 to 1.2.[106] Thus, as in the case of TPA, in layers based on PHAE the photochemical formation of the acid via reaction (30) is followed by a cyclic process involving reaction (25), charge transfer with formation of $PHAE^{\cdot+}...Br^-...R^{\cdot}$ [a reaction of type (28)], and the repetition of the thermal stage of reaction (30). The different solubilities of the polycationic products and of the initial PHAE in polar and non-polar solvents are used in development.

In contrast to tertiary amines and PHAE, in compositions containing the secondary amine DPA as the donor, the Mannich reaction between $(CH_3)_2N^+H-C_6H_4-CHO$ and DPA takes place effectively in the presence of DMABA without the participation of DTBMS and with retention of the concentration of the acid formed on photolysis. The quantum yield of the triphenylmethane dye is 0.07 in the primary photochemical reaction. The ratio $\eta_{ef}/\eta_0 \simeq 35$ and 54 after the films have been maintained at 22 °C and 70 °C respectively.[99] The preferential occurrence of the Mannich reaction restricts the involvement of the acid in the cross-linking of the polymer chains via reaction (29).

6. Optical amplification of the latent image

Processes leading to the optical amplification of the latent image in non-silver photographic layers have been frequently discussed in the review literature.[5,20,43,107–110] Optical amplification (autosensitisation) was first established by Fotland.[107] In this process, the entire film carrying the latent image is acted upon by light in the spectral range where only the coloured products of the photochemical reaction [the auto-sensitiser, for example the product CP^+ formed by reactions (9) and (24)] absorbs, while the remaining components of the layer do not. In polymer systems containing donors such as the leuco-form of the triphenylmethane dye (LTD),[107] styryl derivatives,[108] heterocyclic aromatic compounds,[109] and the CBr_4 acceptor, the photoexcited coloured product transmits the energy absorbed to the complex via a triplet–triplet mechanism, ensuring the additional formation of the coloured product via a reaction of type (24). It has been demonstrated for LTD·CBr_4 that such transfer is possible by virtue of the low position of the triplet level of the complex.[107] In this complex, the triplet level ($E_T \simeq 1.8$ eV) lies appreciably below the excited singlet level ($E_S \simeq 3.2$ eV) and is close to the triplet level formed as a result of the action of light on the triphenylmethane dye (E_T = 1.7 eV).[107]

In compositions containing benzylanilines (DPBA and DBA) as donors and CBr_4 or DTBMS as acceptors, optical amplification occurs as a result of the transfer of triplet energy to the complex from the two-quantum-excited (with light at $\lambda \geqslant 650$ nm) coloured product CP^+. The subsequent ionic dissociation of the excited triplet complex via reaction (24) is responsible for the additional formation of CP^+ on the exposed sections.[5,110,111] This two-quantum process requires the use of powerful light sources. It has been established[19,97,112] that, when a pyrylium dye (Table 1, 2,2′,6,6′-tetraphenylpyrylomethinecyanine perchlorate) is introduced into the system consisting of PVE, DPBA, and DTBMS, the optical amplification changes from a two-quantum process to a low-energy one-quantum process. It has been shown that the above dye does not quench the fluorescence of the CP^+ but it does quench its phosphorescence. The unfavourable relative positions of the oxidation-reduction potentials of the reacting components are responsible for the low probability of quenching via electron transfer.[19] The coincidence of the upper limit of the spectral range corresponding to the emission of the triplet energy of CP^+ (1.77–1.41 eV) with the position of the triplet level of the pyrylium dye (1.77 eV) ensures that the autosensitisation reaction takes place via the triplet energy transfer mechanism:

$$CP^+ \xrightarrow{h\nu,\ S-T} {}^3(CP^+)_1 + Dy \longrightarrow CP^+ + {}^3(Dy)_1. \qquad (31)$$

Next $^3(Dy)_1$ induces the additional formation of CP^+ via reaction (9), as in the direct photoexcitation. Thus the pyrylium dye fulfills two functions in the photosensitive composition: it is a

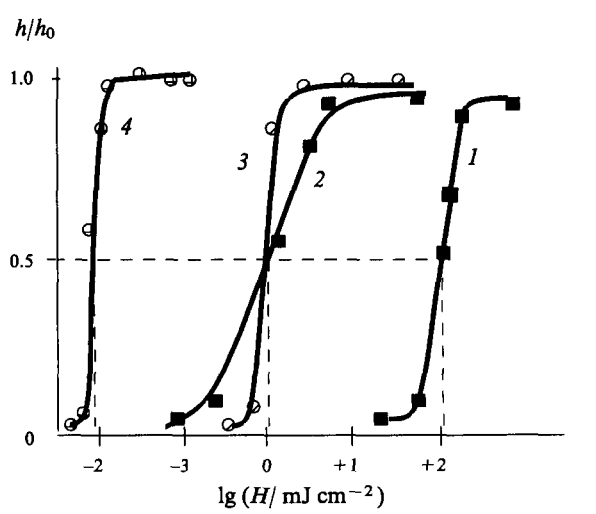


Fig.1 Dependence of the relative height of the relief h/h_0 on the exposure at λ = 576 ± 5 nm: (*1*) and (*3*) without amplification; (*2*) and (*4*) with optical amplification, the energy of the amplifying light being 0.1 J cm^{-2} (λ = 690–720 nm). h is the thickness of the layer retained on the exposed sections after the complete removal of the unexposed sections by dissolution in a mixture of water and alcohol; h_0 is the thickness of the initial layers. Concentrations employed (mol dm^{-3}): [DPA] = [DTBMS] = 0.8; [DMABA] = 0 (curves *1* and *2*) and 0.8 (curves *3* and *4*). The optical density of the dye at λ_{max} is 0.08. After exposure and optical amplification, the layers were maintained for 2.5 min at 100 °C.

Table 5. The photolithographic sensitivities ($H_{0.5}$ and H_{20}) and the photosensitivities ($S_{0.2}$) of layers comprising PHAE and DTBMS.

Optical amplification	$H_{0.5}$/ mJ cm^{-2}	H_{20}/mJ cm^{-2}	$S_{0.2}$/cm^2 J^{-1}
	Layer without DMABA		
Absent	180	180	16.3
Present	–	–	270
	DMABA introduced into layer		
Absent	28	12	163
Present	~0.4	~0.2	2.5×10^4

spectral sensitiser (S^+) in reaction (9) and ensures the formation of CP^+ on photoexcitation with a quantum yield $\eta_0 = 0.12$ (Table 1). Furthermore, it alters the mechanism of the optical amplification of the latent image by entering into reaction (31).

The transformation of the two-quantum process into a one-quantum process in these compositions is also achieved by adding indole. On interaction with the intermediate products of the photochemical reaction (24), the latter forms a new indole-containing coloured compound (ICC, λ_{max} = 550 nm, long-wavelength limit 700 nm), which is an autosensitiser of the oxidation–reduction type and ensures (in the photoexcited state) the occurrence of the one-quantum reaction (9) (in this case S^+ = ICC).[18] It is noteworthy that in compositions based on the DPA donor and the DTBS or CBr_4 acceptor the primary coloured product (λ_{max} = 665 nm) formed on photoexcitation is not an autosensitiser and the optical amplification becomes possible solely by virtue of the addition of indole.[18]

In photoresist systems, optical amplification has been achieved in layers based on charge-transfer complexes between the DPBA or PHAE donor and the DTBMS acceptor.[55,98,99,106] Fig. 1 illustrates the characteristic curves for the photoresists consisting of PVE, DPBA, DTBMS, and the dye 2,2',6,6'-tetraphenylpyrylomethinecyanine perchlorate (Table 1) in the absence or presence of DMABA on photoexcitation of the dye by light at a wavelength of ~576 nm. Fig. 1 shows that, in the absence of DMABA, the exposure giving the relative height of the relief is $h/h_0 = 0.5$, $H_{0.5}$ = 100 mJ cm^{-2}. Optical amplification makes it possible to increase $H_{0.5}$ to ~1 mJ cm^{-2}. Fig. 1 shows that this value of $H_{0.5}$ can be obtained also without optical amplification as a result of the addition of DMABA to the layer. Evidently, under the conditions of chemical and optical amplification of the latent image, a working exposure $H_{0.5}$ = 0.01 mJ cm^{-2} is attained.[98,99] Such low working exposures (high sensitivities) had not been obtained previously.

In layers based on PHAE, Michler's hydrol [formed via reaction (30) on exposure] is an autosensitiser of the oxidation–reduction type and ensures the optical amplification of the latent image [via a reaction of type (9), where $S^+ = MH^+$] on illumination of the entire layer with red light, which acts solely on MH^+, since the remaining components do not absorb in this region. The quantum yield of the additionally formed MH^+ under the conditions of its intrinsic photoexcitation is 0.9×10^{-2} and 0.24 in the absence and with addition of DMABA respectively. Analysis led to the conclusion[106] that in the presence of DMABA optical amplification proceeds in accordance with the mechanism

$$MH^+ \xrightarrow{h\nu,\ S-T} {}^3(MH^+)_1 + DMABA \longrightarrow MH^\cdot + DMABA^{\cdot+},$$

$$MH^\cdot + DTBMS \longrightarrow MH^+ + Br^- \ldots R^\cdot \ (\text{or } R^- \ldots Br^\cdot),$$

which is followed by the charge-transfer process

$$DMABA^{\cdot+} + PHAE \longrightarrow DMABA + PHAE^{\cdot+}$$

and the additional formation of MH^+ as a result of the occurrence of the thermal stages of reaction (30).

Table 5 presents the principal characteristics of the layers based on PHAE and DTBMS, namely $H_{0.5}$ and H_{20}, where H_{20} is the exposure for which the selectivity of the development is $U = t_e/t_u = 20$, where t_e and t_u are the times required for the dissolution of the exposed and unexposed sections, as well as $S_{0.2} = 1/H_{0.2}$, where $H_{0.2}$ is the exposure for which the optical density at the MH^+ absorption maximum (at 630 nm) reaches 0.2. Table 5 shows that the use of chemical and optical amplification of the latent image makes it possible to increase by approximately three orders of magnitude the photosensitivity of the recording layers based on polyhydroxyaminoesters and to obtain $H_{0.5} \simeq 0.4$ and $H_{20} \simeq 0.2$ mJ cm^{-2}, and $S_{0.2} = 2.5 \times \times 10^4$ cm^2 J^{-1}.

IV. Photochemical etching of bismuth films

The processes amplifying the primary effects of light in recording layers and in the photoresists examined above are universal and can be used for the sharp increase of the efficiency of any photochemical processes occurring in polymer systems. As an example, the non-resist photoetching of metallic films with the aid of polymer layers is examined below.

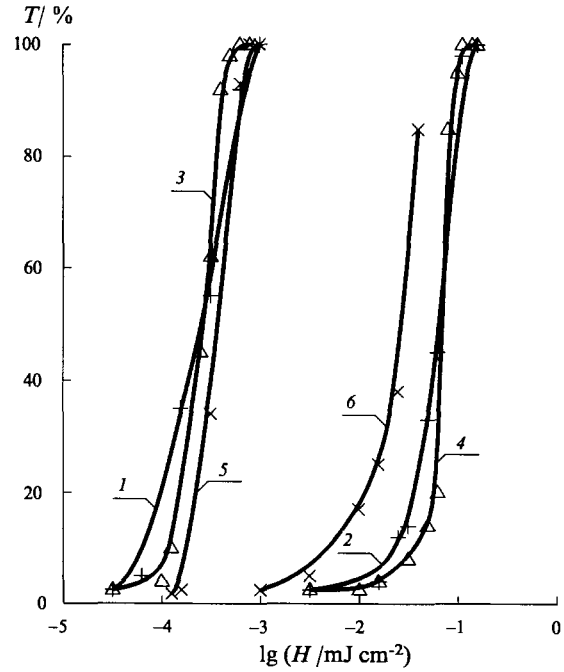


Fig. 2. Dependence of the transmittance of light (T) by a Bi film on the exposure: (*1*), (*3*), (*5*), and (*6*) with optical amplification; (*2*) and (*4*) without amplification; energy of amplifying light 0.06 J cm^{-2}; λ = 650–700 nm. Exposure: λ = 436 nm (curves *1*–*5*) and 633 nm (curve *6*). Composition of the photosensitive layer:
(*1*) and (*2*) PVC–DPA–indole–DTBMS;
(*3*) and (*4*) PVC–DPBA–indole–DTBMS;
(*5*) and (*6*) PVC–DBA–indole–DTBMS.

A new highly sensitive non-resist process for the photoetching of metallic bismuth films has been developed on the basis of polymer compositions incorporating DPBA, DPA, or DBA donors, the DTBMS acceptor, and indole.[113,114] The photosensitive polymer composition was deposited on a bismuth film (film thickness 0.2 μm) sputtered onto a support. It was established that metallic bismuth dissolves in the exposed sections of the polymer layer as a result of a two-stage reaction. In the first stage, bismuth reacts with the radical product Br$^{\cdot}$ (or R$^{\cdot}$) formed on illumination by reaction (24):

$$Bi \xrightarrow{Br^{\cdot}(R^{\cdot})} BiBr_{3-n}R_n ,$$

where $n = 0, 1, 2, 3$. In the second stage, after prolonged storage or on heating to 80–105 °C, the compound $BiBr_{3-n}R_n$ dissolves in the polymer composition as a result of the reaction with the photochemically generated acid HR(HBr). The degree of photoetching was inferred from the transmittance (T) in the range 750–800 nm, where only the metallic film absorbs and the polymer layer does not, or from the transmittance in the range 560–600 nm after the removal of the entire polymer layer by dissolution, for example, in acetone. Fig. 2 illustrates the dependence of the transmittance by the bismuth film on the exposure obtained under conditions with optical amplification of the latent image and without such intensification. Evidently the increase in transmittance from 1.56 to 50% under the influence of light at $\lambda = 436$ nm is attained for exposures $H_{50} \simeq 0.07$ J cm^{-2} in the absence of amplification, but the etching process is characterised by a high photosensitivity: $H_{50} \simeq 3 \times 10^{-4}$ J cm^{-2} for optical amplification of the latent image. For exposure in the region of the long-wavelength absorption limit of the complex DBA · DTBMS at $\lambda = 633$ nm, the photosensitivity is $H_{50} \simeq 2 \times 10^{-2}$ J cm^{-2}, as shown in Fig. 2.

***

Thus, a common feature of all the methods of amplifying the primary effects of light is the formation of photoproducts whose physicochemical properties differ significantly from those of the initial components and the accumulation of these photoproducts as a result of the subsequent occurrence of autocatalytic reactions with their participation, the selective action of light on them, etc.

A distinctive property of the systems considered is the fact that only components present in polymer layers participate in the amplification process and there is therefore no need for their additional treatment in liquid or gaseous media.

The fields where these systems are used, determined by the characteristic features of their functioning, are, in particular, the highly sensitive optical recording of information, the detection of weak optical signals, the photomodification of spectroscopic and physicochemical properties of polymer layers, and the selective photosynthesis of a number of chemical compounds in polymer matrices.

References

1. O D Parfenov *Tekhnologiya Mikroskhem* (Technology of Microcircuits) (Moscow: Vys. Shkola, 1986)
2. B Bednar, A V El'tsov, J Zachoval, et al. *Svetochuvstvitel'nye Polimernye Materialy* (Photosensitive Polymeric Materials (Leningrad: Khimiya, 1985)
3. U Moro *Microlithography* (Translated into Russian) (Moscow: Mir, 1990) Parts 1 and 2
4. A A Lin, A Reiser *Macromolecules* **22** 3898 (1989)
5. A V Vannikov in *Neserebryanye Fotograficheskie Protsessy* (Non-Silver Photographic Processes) [Edited by A L Kartuzhanskii (Leningrad: Khimiya, 1984) Chapter 6
6. M J Bowden, S R Turner (Eds) *Polymers for High Technology. Electronics and Photonics*. Am. Chem. Soc. Symp. Ser. 346 (Washington, DC: ACS, 1987) Chapters 12, 14, 17, 29
7. E Reichmanis, L F Thompson *Chem. Rev.* **89** 1273 (1989)
8. J P Castantino, H W Richter, C H Lee Go, W H Waddell *J. Am. Chem. Soc.* **107** 1744 (1985)
9. C Carre, C Decker, J P Fouassier, D J Lougnot *Laser Chem.* **10** 349 (1990)
10. S M McGlynn, T Azumi, M Kinoshita *Molecular Spectroscopy of the Triplet State* (Translated into Russian) (Moscow: Mir, 1972)
11. A L Buchachenko, R Z Sagdeev, K M Salikhov *Magnitnye i Spinovye Effekty v Khimicheskikh Reaktsiyakh* (Magnetic and Spin Effects in Chemical Reactions) (Novosibirsk: Nauka, 1978)
12. J Olmsted, T J Meyer *J. Phys. Chem.* **91** 1649 (1987)
13. H Shioyama, H Masuhara, N Mataga *Chem. Phys. Lett.* **88** 161 (1982)
14. E M Kober, T J Meyer *Inorg. Chem.* **28** 3877 (1984)
15. O Johansen, A W-H Mau, W H F Sasse *Chem. Phys. Lett.* **94** 503 (1983)
16. A Edel, P A Marton, J P Sauvage *Nouv. J. Chim.* **8** 495 (1984)
17. A W-H Mau, O Johansen, W H F Sasse *Photochem. Photobiol.* **41** 503 (1985)
18. A D Grishina, A V Vannikov, Z P Gol'dman, et al. *Khim. Fiz.* **6** 960 (1987)
19. A D Grishina, M G Tedoradze, A V Vannikov *Mendeleev Commun.* (2) 44 (1992)
20. A V Vannikov, A D Grishina in *Uspekhi Nauchnoi Fotografii* (Advances in Scientific Photography) (Moscow: Nauka, 1989) Vol. 25, p. 74
21. L I Mikheeva, A I Tolmachev, B I Shapiro *Zh. Nauchn. Prikl. Fotogr. Kinematogr.* **30** 426 (1985)
22. D T Breslin, F D Saeva *J. Org. Chem.* **53** 713 (1988)
23. F D Saeva, D T Breslin, H R Luss *J. Am. Chem. Soc.* **113** 5333 (1991)
24. S Farid, R C Daly, R E Moody, et al. *Macromolecules* **24** 4041 (1991)
25. A A Lin, C-F Chu, A Reiser *Macromolecules* **23** 3611 (1990)
26. W-Y Huang, A A Lin, A Reiser *Macromolecules* **24** 4600 (1991)
27. K Ichimura, T Kamatsu *J. Polymer Sci. Polymer Chem.* **25** 1475 (1987)
28. K Ichimura , N Oohara *J. Polymer Sci. Polymer Chem.* **25** 3063 (1987)
29. P L Egerton, J Trigg, E M Hyde, A Reiser *Macromolecules* **14** 95 (1981)
30. R-C Liang, A Reiser *J. Imaging Sci.* **30** 69 (1986)
31. R-C Liang, A Reiser *J. Polymer Sci. Polymer Chem.* **25** 451 (1987)
32. D M Allen *J. Photogr. Sci.* **24** 61 (1976)
33. A N Nesmeyanov, A V Vannikov, V A Zver'kov, et al. *Dokl. Akad. Nauk SSSR* **240** 121 (1978); **252** 143 (1980)
34. V A Zver'kov, A Yu Kryukov, A V Vannikov *Zh. Nauchn. Prikl. Fotogr. Kinematogr.* **28** 429 (1983)
35. V A Zver'kov, A N Tsura, B Lozhkin, A E Kryukov *Zh. Nauchn. Prikl. Fotogr. Kinematogr.* **30** 352 (1985)
36. L J Wilputte-Steinert *Mol. Catal.* **4** 11 (1978)
37. A A Petrova, S V Novikov, A N Tsura, et al. *Zh. Nauchn. Prikl. Fotogr. Kinematogr.* **34** 180 (1989)
38. V A Zver'kov, A Yu Kryukov, A N Tsura, B T Lozhkin in *V Vsesoyuznoe Soveshchanie po Fotokhimii: Tezisy Dokladov* (The Vth All-Union Conference on Photochemistry: Abstracts of Reports) (Moscow, 1985) p. 380
39. V A Zver'kov, A A Petrova, A V Vannikov *Zh. Nauchn. Prikl. Fotogr. Kinematogr.* **34** 365 (1990)
40. A A Petrova, V A Zver'kov, A N Tsura, et al. *Izv. Akad. Nauk SSSR, Ser. Khim.* (2) 346 (1991)
41. V A Zver'kov, A A Petrova, A V Vannikov *J. Inform. Rec. Mater.* **19** 127 (1991)
42. S Evans, M L H Green, B Jewitt, et al. *J. Chem. Soc. Faraday Trans. 2* **68** 1847 (1972)
43. L V Koshkin, P Filippova *Izv. Vyssh. Uchebn. Zaved., Khim. Khim. Tekhnol.* **33** 33 (1990)
44. M F Budyka, M G Stunjas, O D Lauhina, M V Alfimov *J. Photogr. Sci.* **38** 44 (1990)
45. R H Sprague, H L Fichter, E Wainer *Photogr. Sci. Eng.* **5** 98 (1961)
46. L H G Leenders *J. Photogr. Sci.* **26** 234 (1978)
47. T. Latowski, B Zelent *Rocz. Chem.* **48** 831 (1974)
48. K Kalyanasundaram, J Kiwi, M Gratzel *Helv. Chim. Acta* **61** 2720 (1978)
49. K Kalyanasundaram *Nouv. J. Chim.* **3** 511 (1979)

50. A D Grishina, M G Tedoradze, A V Vannikov *Zh. Nauchn. Prikl. Fotogr. Kinematogr.* **37** 237 (1992)
51. A D Grishina, G M Chernov *Zh. Nauchn. Prikl. Fotogr. Kinematogr.* **28** 251 (1983)
52. K Okada, T Ohfuji, J Matsui *Jpn. J. Appl. Phys. Pt. 2* **24** L545 (1985)
53. A D Grishina, A V Vannikov *Zh. Nauchn. Prikl. Fotogr. Kinematogr.* **31** 276 (1986)
54. I V Ivanin, A L Karasev, V A Zver'kov, et al. *Khim. Vys. Energ.* **26** 333 (1992)
55. A V Vannikov, A D Grishina *Zh. Nauchn. Prikl. Fotogr. Kinematogr.* **36** 197 (1991)
56. W H Waddell, C H Lee Go *J. Am. Chem. Soc.* **104** 5804 (1982)
57. N B Feilchenfeld, W H Waddell *Chem. Phys. Lett.* **98** 190 (1983)
58. C H Lee Go, W H Waddell *J. Am. Chem. Soc.* **106** 715 (1984)
59. R F Jennkins, W H Waddell, H W Richter *J. Am. Chem. Soc.* **109** 1583 (1987)
60. H Morita, S Mori, S Sakaguchi, H Hayashi *Photochem. Photobiol. A: Chem.* **59** 29 (1991)
61. H Morita, S Sakaguchi, H Hayashi *Photochem. Photobiol. A: Chem.* **61** 227 (1991)
62. H Morita, N Uchino, Y Nakamura, T Yamaoka *J. Appl. Polym. Sci.* **38** 1997 (1989)
63. C Decker in *Materials for Microlithography* Am. Chem. Soc. Symp. Ser. V. 266 (Eds L F Thompson, C G Willson) (Washington, DC: ACS, 1984)
64. V K Grishchenko, A F Maslyuk, S S Gudzera *Zhidkie Fotopolimerizuyushchiesya Kompozitsii* (Liquid Photopolymerising Compositions) (Kiev: Naukova Dumka, 1985)
65. N G Vindenina, P A Bondarenko, A S Rot, E F Kirkach, in *Kompozitsionnye Polimernye Materialy* (Composite Polymeric Materials) (Ed. E V Lebedev) (Kiev: Naukova Dumka, 1989) No. 41, p. 16
66. E T Lazarenko *Fotokhimicheskoe Formirovanie Pechatnykh Form* (Photochemical Origination of Printing Blocks) (Lvov: Vishcha Shkola, 1984)
67. C Decker, K Moussa *J. Appl. Polym. Sci.*, **34** 1603 (1987)
68. R A Lieberman *J. Rad. Curing* **11** 22 (1984)
69. C Decker, K Moussa *Makromol. Chem. Macromol.: Chem. Phys.* **191** 963; 1241 (1990)
70. J S Arney *J. Imaging Sci.* **33** 1 (1989)
71. B M Treushnikov, A S Esin, L L Pomerantseva, et al. *Zh. Nauchn. Prikl. Fotogr. Kinematogr.* **35** 119 (1990)
72. J V Crivello, J H W Lam *Macromolecules* **10** 1307 (1977)
73. J V Crivello *Polym. Eng. Sci.* **23** 953 (1983)
74. G Manivannan, J P Fouassier *J. Polym. Sci. A: Polym. Chem.* **29** 1113 (1991)
75. W E Feely, J C Imhof, C A Stein *Polym. Eng. Sci.* **34** 2747 (1986)
76. K Ichimura, A Kameyama, K Hayashi *J. Appl. Polym. Sci.* **34** 2747 (1987)
77. H Ito, C G Willson *Polym. Eng. Sci.*, **23** 1012 (1983)
78. H Ito, E Flores *J. Electrochem. Soc.* **135** 2322 (1988)
79. H Ito, E Flores, A F Renaldo *J. Electrochem. Soc.* **135** 2328 (1988)
80. E Reichmanis, F M Houlihan, O Nalamasu, T X Neenan *Chem. Mater.* **3** 394 (1991)
81. L Schlegel, T Ueno, H Shiraishi, et al. *Chem. Mater.* **2** 299 (1990)
82. S A MacDonald, H Schlosser, H Ito, et al. *Chem. Mater.* **3** 435 (1991)
83. J M J Frechet, S Matuszczak, B Reck, et al. *Macromolecules* **24** 1746 (1991)
84. G N Taylor, L E Stillwagon, F M Houlihan, et al. *Chem. Mater.* **3** 1031 (1991)
85. K Naiton, T Yamaoka, A Umehara *Chem. Lett.* 1869 (1991)
86. J V Crivello *Adv. Polym. Sci.* **62** 3 (1984)
87. E Kustermann, H-J Timpe, K Gabert, H Schulert *Wiss. Z.* **29** 287 (1987)
88. J R Foussier, D Burr, J V Crivello *Photochem. Photobiol. A: Chem.* **49** 317 (1989)
89. H-J Timpe, K P Kronfeld, U Lammel, et al. *Photochem. Photobiol. A: Chem.* **52** 111 (1990)
90. J V Crivello, J L Lee, D A Condon *J. Polym. Sci. A, Polym. Chem.* **25** 3293 (1987)
91. T Yamaoka, M Nishiki, K Koseki, M Koshiba *Polym. Eng. Sci.* **29** 856 (1989)
92. T Omote, K Koseki, T Yamaoka *J. Polym. Sci., Polym. Lett.* **28** 59 (1990)
93. T Yamaoka, H Watanabe, K Koseki, T Asano *J. Imaging Sci.* **34** 50 (1990)
94. F M Houlihan, A Shugard, R Gooden, E Reichmanis *Macromolecules* **21** 2001 (1988)
95. T X Neenan, F M Houlihan, E Reichmanis, et al. *Macromolecules* **23** 145 (1990)
96. L Schlegel, T Ueno, N Hayashi, T Iwayanagi *Jpn. J. Appl. Phys. B* **30** 3108 (1991)
97. S A M Hesp, N Hayashi, T Ueno *J. Appl. Polym. Sci.* **42** 877 (1991)
98. A V Vannikov, A D Grishina, M G Tedoradze *Mendeleev Commun.* (1) 34 (1991)
99. A V Vannikov, A D Grishina, M G Tedoradze *New Polym. Mater.* **4** 147 (1992)
100. M G Tedoradze, A D Grishina, A M Tolmachev, M A Kudinova *Zh. Nauchn. Prikl. Fotogr. Kinematogr.* **35** 475 (1990)
101. M Melicharek, R Nelson *J. Electroanal. Chem.* **26** 201 (1970)
102. V N Kondrat'ev (Editor) *Energiya Razryva Khimicheskikh Svyazei. Potentsialy Ionizatsii i Srodstvo k Elektronu* (Chemical Bond Dissociation Energies, Ionisation Potentials, and Electron Affinities) (Moscow: Nauka, 1974).
103. J Fulara, T Latowski *Pol. J. Chem.* **64** 369 (1990)
104. A Yu Kryukov, A V Vannikov, A V Anikeev, L I Kostenko *Chem. Mater.* **4** 803 (1992)
105. A Yu Kryukov, A A Pakhratdinov, E B Khailova, et al. *Vysokomol. Soedin.* **32** 399 (1990)
106. A D Grishina, M G Tedoradze, A V Vannikov, et al. *Khim. Vys. Energ.* (in the press, 1993)
107. R A Fotland *J. Photogr. Sci.* **18** 33 (1970)
108. A C Hazy, V P Petro *Laser Focus* **8** 32 (1972)
109. G J Smets, J Thoen, A Aerts *J. Polym. Sci. C* **51** 119 (1975)
110. A D Grishina A D Vannikov *Usp. Khim.* **48** 1393 (1979) [*Russ. Chem. Rev.* **48** 746 (1979)]
111. A V Vannikov, A D Grishina *Usp. Khim.* **56** 1105 (1987) [*Russ. Chem. Rev.* **56** 633 (1987)]
112. A D Grishina, A V Vannikov, Z P Gol'dman, et al. *Khim. Vys. Energ.* **24** 136 (1990)
113. A V Vannikov, A D Grishina, M G Tedoradze *Mendeleev Commun.* (2) 62 (1992)
114. A V Vannikov, A D Grishina, M G Tedoradze *J. Mater. Chem.* **2** 755 (1992)

Russian Chemical Reviews **62** (1) 51–64 (1993)
© 1993 Russian Academy of Sciences and Turpion Ltd

UDC 547.787

Reactions of 4,5-dihydro-5-oxo-1,3-oxazoles with oxygen-containing nucleophiles

V O Topuzyan, N S Nesunts

Contents

I.	Introduction	51
II.	Reactions with alcohols and phenols	51
III.	Reductive alcoholysis of unsaturated 5(4*H*)-oxazolones	57
IV.	Oxidative alcoholysis of 5(4*H*)-oxazolones	58
V.	Reactions with hydroxylamine derivatives and aminoalcohols	59
VI.	Intramolecular reactions of 5(4*H*)-oxazolones containing a hydroxy-group	61

Abstract. The literature data on the interaction of 4,5-dihydro-5-oxo-1,3-oxazoles with alkyl and aryl alcohols as well as aminoalcohols are surveyed. The intramolecular reactions of the oxazoles containing a hydroxy-group are examined. The bibliography includes 141 references.

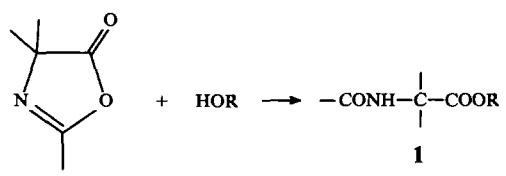
I. Introduction

Several reviews have been published since 1946 on the synthesis and chemical properties of 4,5-dihydro-5-oxo-1,3-oxazoles [(5(4*H*)-oxazolones)].[1–5] However, the reactions of 5(4*H*)-oxazolones with oxygen-containing nucleophiles are inadequately described in all these publications. Nevertheless, these reactions afford various compounds which are of both theoretical and practical interest.

At the present time, numerous studies devoted to the interaction of 5(4*H*)-oxazolones with oxygen-containing nucleophiles have accumulated in the literature. The aim of the present review is to survey the literature data on the interaction of both saturated and unsaturated 5(4*H*)-oxazolones with alcohols, phenols, aminoalcohols, and hydroxylamine derivatives. The intramolecular reactions of oxazolones containing a hydroxy-group are also discussed.

II. Reactions with alcohols and phenols

The reactions of 5(4*H*)-oxazolones with alkyl alcohols and aromatic alcohols proceed mainly with the cleavage of the 1,5-bond of the heterocycle, forming the corresponding esters of *N*-substituted aminoacids **1**:

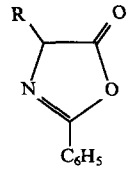


1

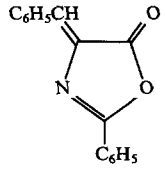
V O Topuzyan, N S Nesunts Laboratory of Synthesis of Biologically Active Derivatives of Aminoacids and Peptides, Institute of Fine Organic Chemistry, Academy of Sciences of the Republic of Armenia, 375014 Erevan, prosp. Azatutyan 26, Tel. (7-8852) 28 83 29

Received 22nd July 1992
Uspekhi Khimii **62** (1) 55–69 (1993); translated by A K Grzybowski

In this process, saturated and unsaturated 5(4*H*)-oxazolones exhibit different reactivities. As a rule, saturated 5(4*H*)-oxazolones are more reactive than their unsaturated analogues. 4-Benzyl-2-phenyl-5-oxazolone **2** (R = $C_6H_5CH_2$ reacts smoothly at room temperature with methanol, forming the methyl ester of *N*-benzoylphenylalanine, whereas 4-benzylidene-2-phenyl-5-oxazolone **3** remains unchanged under similar conditions.[2]



2



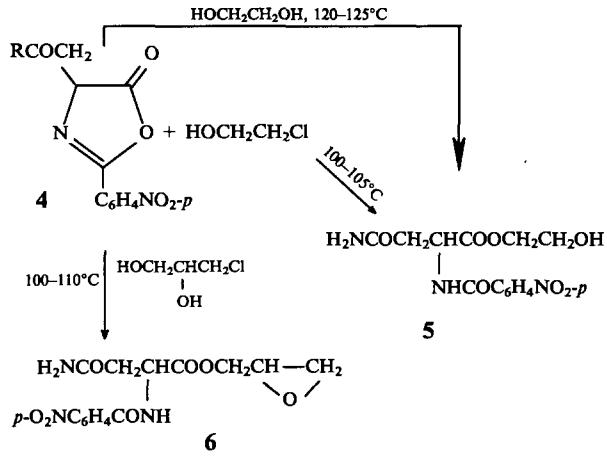
3

The inertness of unsaturated 5(4*H*)-oxazolones in relation to alcohols is indicated by their recrystallisation from ethanol, which has been described in most studies devoted to the synthesis of these compounds.

The rate of alcoholysis is also affected by the nature of the substituent in the 4-position in saturated 5(4*H*)-oxazolones. It has been noted[2] that the oxazolone **2** (R = $C_6H_5CH_2$) reacts with alcohols faster than 2-phenyl-5-oxazolones **2** (R = H), while 4-methyl-2-phenyl-5-oxazolone **2** (R = CH_3) reacts more slowly than the latter.

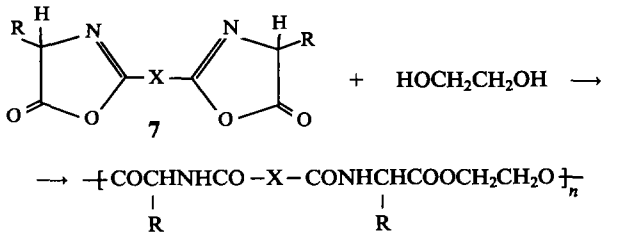
The alcoholysis also depends on the nature of the alcohol. Certain oxazolones react with methanol but are inert with respect to ethanol.[6] Secondary alcohols react with 5(4*H*)-oxazolones with difficulty, whilst tertiary alcohols frequently do not react at all.[4]

4-Carboxymethyl-2-(*p*-nitrophenyl-5-oxazolone **4** (R = OH) reacts with ethylenechlorohydrin at high temperatures (110–120 °C) to form the α-2-chloroethyl ester of *N*-*p*-nitrobenzoyl-DL-asparagine.[7,8] It is of interest to note that 4-aminomethyl-2-(*p*-nitrophenyl)-5-oxazolone **4** (R = NH_2) forms the 2-hydroxyethyl ester of the corresponding acid **5** under analogous conditions. The latter compound was also obtained by the reaction of the oxazolone **4** (R = NH_2) with 1,2-ethylene glycol.[7]

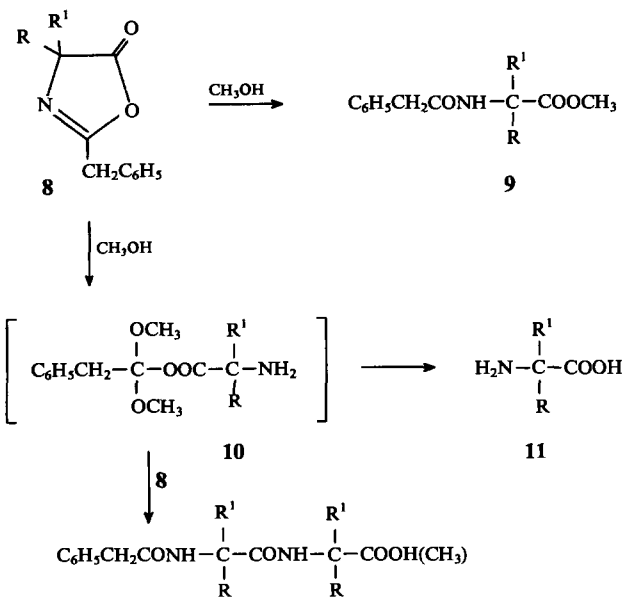


When the ratio of oxazolone **4** to ethylene glycol is 2 : 1 at 85–95 °C, the product of the reaction in dioxane is the bis-*O*-acylated glycol.[7] It was noted in the same communication that the oxazolone **4** (R = NH_2) reacts with glycerol-α-chlorohydrin [1-chloropropane-2,3-diol?] at high temperatures to form 2,3-epoxypropyl ether **6**.

The interaction of 2,2-bisoxazolones **7** with ethylene glycol at a temperature not exceeding 60 °C for 146 h leads to the formation of polymers:[9]

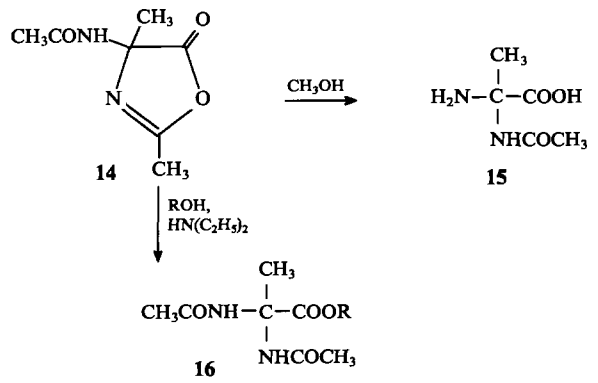


The reaction of unsaturated 5(4*H*)-oxazolones with ethylene glycol takes place at a higher temperature (150 °C).[10] Heating of glycerol containing 1–2% of an unsaturated 5(4*H*)-oxazolone to 200 °C leads to the formation of the monoglyceryl ester of a *N*-substituted aminoacid.[11,12]

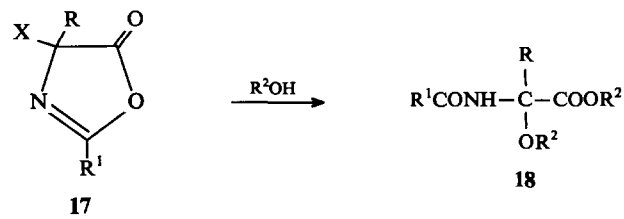


Certain saturated 5(4*H*)-oxazolones containing the benzyl substituent in the 2-position in the heterocycle behave in a non-standard manner on alcoholysis. Treatment of 2-benzyl-4-methyl-5-oxazolone **8** (R = H, R^1 = CH_3) or 2-benzyl-4,4-dimethyl-5-oxazolone **8** (R = R^1 = CH_3) with absolute alcohol does not, against expectation, lead to the formation of ester **9**. Under similar conditions, 2-benzyl-4-(*p*-methoxy-benzyl)-5-oxazolone **8** (R = H, R^1 = $CH_2C_6H_4OCH_3$-*p*) and 2-benzyl-4-isobutyl-5-oxazolone **8** [R = H, R = $CH_2CH\cdot(CH_3)_2$] not only undergo cleavage of the 1,5-bond with formation of the expected esters **9** but also react with the oxazolones as aminoalcohols with formation of the intermediate **10**. The latter can either decompose to the aminoacid **11** or its reaction with the oxazolone **8** can lead to the *N*-substituted dipeptide **12** or its ester **13**.[2]

The appearance of α-acetamidoalanine **15** in the methanolysis of 4-acetamido-2,4-dimethyl-5-oxazolone **14** is also explained by the formation of an intermediate analogous to compound **10**.[13] According to Nicolet,[14] the alcoholysis (methanolysis, ethanolysis) of the oxazolone **14** in the presence of diethylamine proceeds normally with formation of the ester **16**.

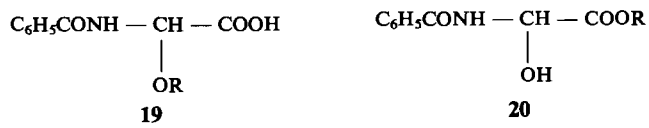


4-Halooxazolones **17** react smoothly with different alcohols.[15–20] The reaction with an excess of alcohol leads to the formation of *N*-substituted α-alkoxyaminoacids **18**. Under identical conditions the process proceeds with participation of both primary and secondary alkyl, arylalkyl, and alicyclic alcohols.[17]



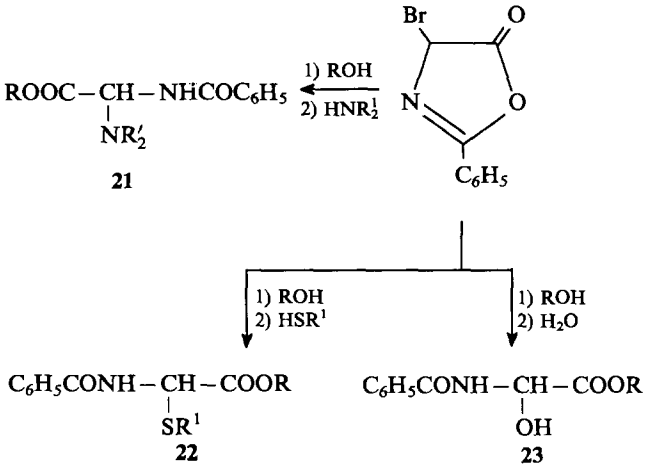
In the reaction of *tert*-butyl alcohol with 4-bromo-2-phenyl-5-oxazolone **17** (X = Br, R = H, R^1 = C_6H_5), *N*-benzoyl-α-*tert*-butoxyglycine **19** [R = $C(CH_{33}]$ and the *tert*-butyl ester of *N*-benzoyl-α-hydroxyglycine **20** [R = $C(CH_3)_3$] were obtained together with the *tert*-butyl ester of *N*-benzoyl-α-*tert*-butoxyglycine **18** [R = H, R^1 = C_6H_5, R^2 = $C(CH_3)_3$].

The analogous reaction with phenol leads to the formation of the phenyl ester of the aminoacid **20** (R = C_6H_5).[17] According to

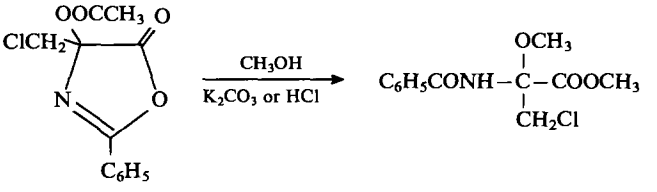


Chaman and co-workers,[15,17] the process under consideration, involving the alkoxides derived from alkyl alcohols, proceeds with greater difficulty than the reaction with the alcohols.

The study of the reaction of 4-halo-5(4*H*)-oxazolones with alcohols established[16,17] that opening of the oxazolone ring is proceeds faster than the substitution of the halogen atom by the alkoxy-group. This difference in reactivity has been used for the synthesis of esters of *N*-benzoylglycine with various substituents in the α-position compounds **21**–**23** (cf. Shemyakin and co-workers[17–20]).



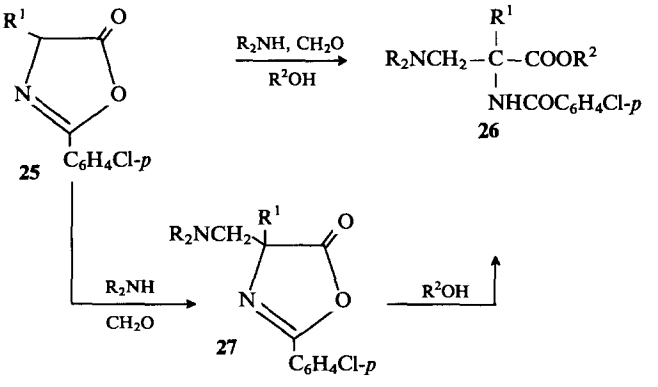
An α-alkoxyaminoacid ester is also formed in the reaction of 4-acetoxy-4-chloromethyl-2-phenyl-5-oxazolone **24** with methanol:[16]



24

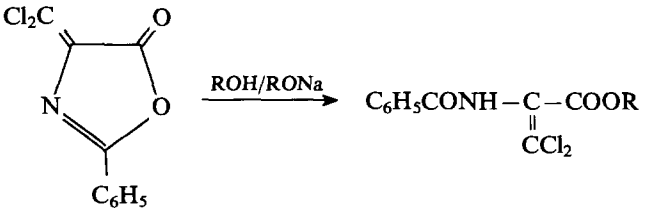
In the methanolysis of the oxazolone **24** in the presence of 10% potassium carbonate, the yield of the ester is 70%, whereas in the presence of hydrogen chloride the methanolysis proceeds with 50% yield. In the latter case, the corresponding α-methoxy-acid was also isolated from the reaction mixture in 15% yield.

The dialkylaminomethyl group in the 4-position of the saturated 5(4*H*)-oxazolone promotes alcoholysis. Under the conditions of the Mannich reaction,[21,22] carried out in methanol or ethanol, the oxazolone **25** gives rise to the formation of esters of 2-*N*-acylamino-3-dialkylaminopropionic acid **26**:



It was established that the product of the Mannich reaction — the oxazolone **27** — undergoes the ring opening reaction,[22] whereas according to other data[21] 2-*p*-chlorophenyl-5-oxazolones **25** are inert in relation to ethanol.

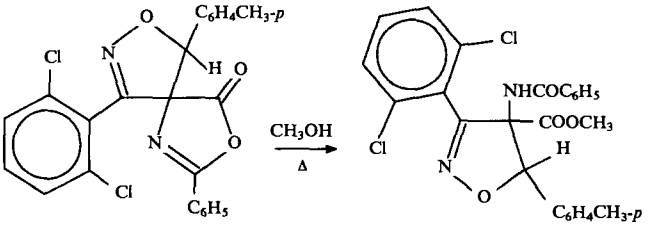
The alcoholysis of 4-dichloromethylene-2-phenyl-5-oxazolone **28** takes place on refluxing for up to 30 h with aliphatic alcohols (methanol, ethanol, isopropyl alcohol).[23] The process is accelerated in the presence of sodium alkoxides[24] but the substitution of halogen atoms is not then observed:



28

This phenomenon has been explained with the aid of Pearson's principle of hard and soft acids and bases (HSAB). Evidently the electrophilic centres in the oxazalone **28** — the carbon atoms of the dichloromethylene group and the carbon atom of the carbonyl group — clearly differ in their 'hardness'. The hard nucleophile — the alkoxide anion — therefore prefers to interact with the hard electrophilic centre located on the carbonyl group.[24]

4-Hydroxymethylene-2-phenyl-5-oxazolone readily undergoes alcoholysis by *p*-methoxybenzyl and 2,2,2-trichloroethyl alcohols when a benzene solution of the oxazolone and the corresponding alcohol are refluxed.[25] The spiro-oxazolones **29** also exhibit properties characteristic of 5(4*H*)-oxazolones; on refluxing, they react with methanol, affording the corresponding esters **30**:[26]



29 **30**

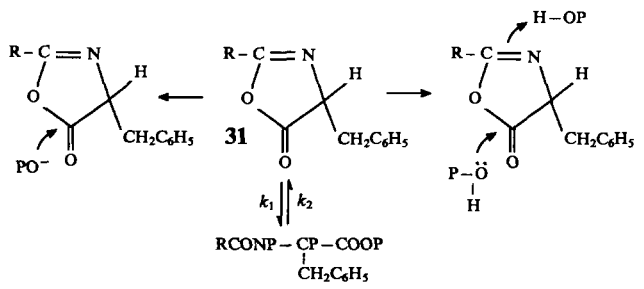
Among phenols, phenol itself and β-naphthol interact readily with 5(4*H*)-oxazolones.[27]

The reaction of saturated 5(4*H*)-oxazolones with phenols, especially *p*-nitrophenol, is also of theoretical importance in the study of the stereospecificity of peptide synthesis by the method of activated esters. One of the pathways leading to the racemisation of *N*-acylaminoacids in the formation of a peptide bond involves the intermediate formation of 5(4*H*)-oxazolones.[28] The question of both the formation of 5(4*H*)-oxazolones and of the opening of the oxazolone rings under the conditions of peptide synthesis has therefore become important. A number of studies have been devoted to such questions.[29–31]

The relative reactivities of 4-benzyl-2-benzyloxycarbonylaminomethyl-5-oxazolone **31** (R = $C_6H_5CH_2OCONHCH_2$) in relation to *p*-nitrophenol, dinitrophenol, and pentafluorophenol have been investigated.[29,30] According to Kovacs, et al.,[30] the above phenols can be arranged in the following sequence in terms of descending rate of opening of the oxazolone **31** ring: dinitrophenol, pentachlorophenol, *p*-nitrophenol. In all cases the rate of reaction depends on the phenol concentration. In the presence of triethylamine the series becomes *p*-nitrophenol, pentachlorophenol, dinitrophenol. Whereas in the absence of a tertiary amine the reactivity of phenols increases with enhancement of their acid properties, in the presence of triethylamine the opposite behaviour is observed. On this basis, one may conclude that the mechanisms of the opening of the oxazolone **31** ring by phenols and phenoxide anions differ.[29,30]

Thus the acidity of the phenols affects both the rate and the mode of the alcoholysis of 5(4*H*)-oxazolone. The comparatively less acid *p*-nitrophenol reacts slowly with the oxazolone **31**, as a result of which the resulting ester is racemic.[30]

Similar results were obtained in a study of the reaction of 4-benzyl-2-phenyl-5-oxazolone **31** (R = C_6H_5) with *p*-nitrophenol in the presence of tributylamine.[31] The determination of the rate constants for the forward (k_1) and reverse (k_2) reactions in the formation of the ester **32** (P = *p*-$NO_2C_6H_4$) for oxazolone : phenol : amine ratios of 1 : 10 : 10 shows that the equilibrium is displaced towards the formation of the ester.[31]



32

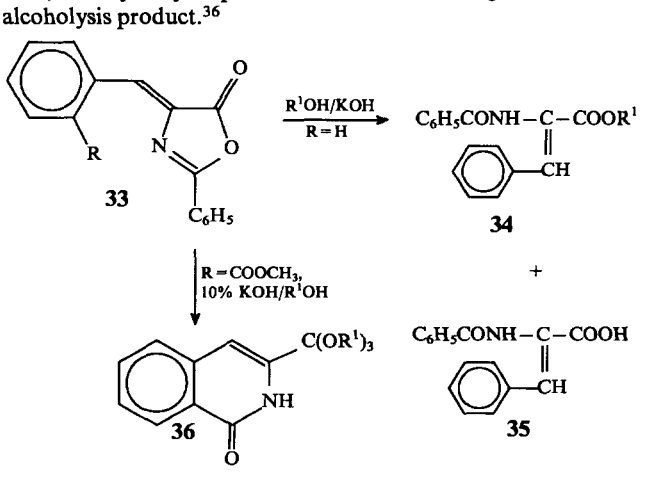
The kinetics of the reactions of 2-phenyl-5-oxazolone with substituted phenoxide anions have been investigated.[32]

p-Nitrophenyl *N*-benzamidoisobutyrate was obtained by the reaction of 4,4-dimethyl-2-phenyl-5-oxazolone with *p*-nitrophenol in the presence of triethylamine.[33] According to Suh et al.,[34] phenol reacts smoothly at pH 7 with unsaturated 5(4*H*)-oxazolones.

The reactions of oxazolones with alcohols and phenols are catalysed by both bases and acids.

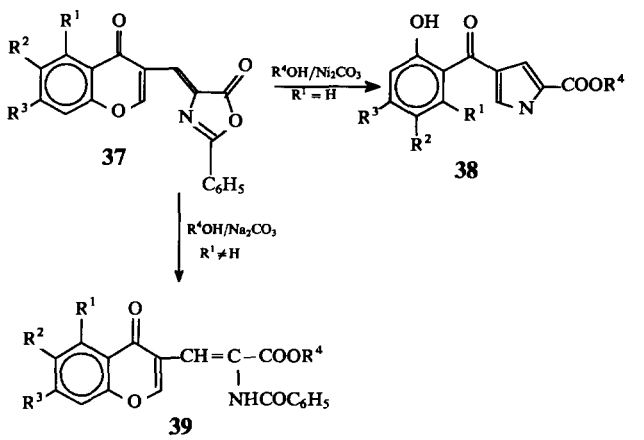
Potassium[10, 35–38] or sodium[10, 39–44] hydroxides have been used to catalyse the alcoholysis of unsaturated 5(4*H*)-oxazolones. There have also been studies where alkali metal salts were used for this purpose: potassium[45] and sodium[42, 46–48] carbonates and also sodium acetate[49, 50] and tetrahydroborate.[51] Evidently in all cases the reaction is accelerated by the alkoxide ion generated under these conditions, which leads to the cleavage of the 1,5-bond of the oxazolone ring. According to Tripathy and Mikerjee,[36] in the case of unsaturated 5(4*H*)-azlactones the addition of the alkoxide anion to the exocyclic double bond is not observed.

Analysis of the literature data shows that the amount of alkali used can affect the nature of the final products. The reaction of 4-benzylidene-2-phenyl-5-oxazolone **33** (R = H) with ethanol in the presence of catalytic amounts of potassium hydroxide leads to the formation of the ethyl ester of *N*-benzoyl-α,β-dehydrophenylalanine **34** (R^1 = C_2H_5 in a high yield. When an equivalent amount (in relation to the oxazolone) of alkali is used, the hydrolysis product **35** is detected together with the alcoholysis product.[36]



According to Stiller's data[35] the formation of only the acid **35** is observed in the reaction of the same oxazolone **33** (R = H) with a 10% alcoholic solution of potassium hydroxide. Evidently an increase in the amount of potassium hydroxide increases the concentration of hydroxide anions, increasing thereby the possibility of the competing reaction — the hydrolysis of the oxazolone. The formation of the ester **34** (R^1 = CH_3) and the acid **35** is also observed in the methanolysis of the oxazolone **33** (R = H) in a methanol – 1 M sodium hydroxide solution at room temperature.[43]

It is of interest to note that, in the presence of 10% potassium hydroxide in methanol or ethanol, 4-(*o*-methoxycarbonylbenzylidene)-2-phenyl-5-oxazolone **33** (R = $COOCH_3$) gives rise to the orthoformate **36** (R = CH_3 or C_2H_5).[35] The effect of the nature of the substituent in the 4-position on the product of the alcoholysis of 5(4*H*)-oxazolone is also observed in the reactions of unsaturated oxazolones **37** with alcohols (methanol, ethanol) in the presence of sodium carbonate.[46] Depending on R^1 in the benzene ring of the chromone residue of the oxazolone **37**, the reaction product can be the pyrrole **38** or the ester of the corresponding acid **39**:



It has been noted[46] that both the oxazolone **37** and the ester **39** are converted into the pyrrole **38** on refluxing in the presence of sodium methoxide regardless of R^1.

The results of a study carried out to determine the optimum conditions for the alcoholysis of a series of unsaturated 5(4*H*)-oxazolones in the presence of ethylene chlorohydrin and ethylene glycol have been published.[10] It was established that in the case of ethylene chlorohydrin it is necessary to avoid a high concentration of the hydroxide anion (a 5% KOH solution is optimal), while in the case of ethylene glycol base catalysis can be replaced by the corresponding increase in temperature.

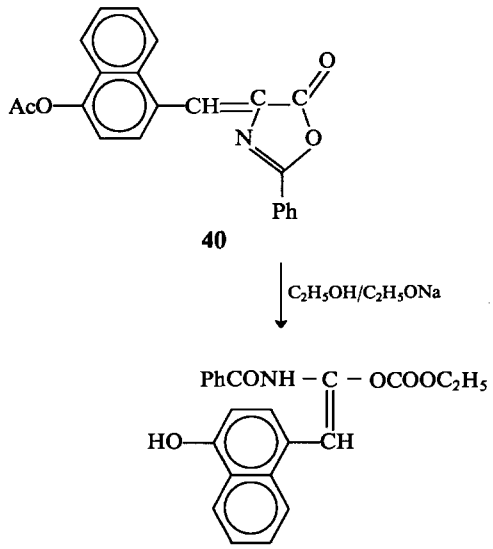
The influence of the electronic effects of the substituent in the 4-position in unsaturated 5(4*H*)-oxazolones on the rate of base-catalysed alcoholysis has been investigated.[39]

One of the common ways of catalysing the reactions of unsaturated 5(4*H*)-oxazolones with aliphatic alcohols is the method involving the use of the alkoxides derived from the same alcohols. The reaction proceeds mainly with the formation of the alkyl esters of *N*-substituted α,β-dehydroaminoacids with satisfactory results.[2, 24, 42, 46, 52–74]

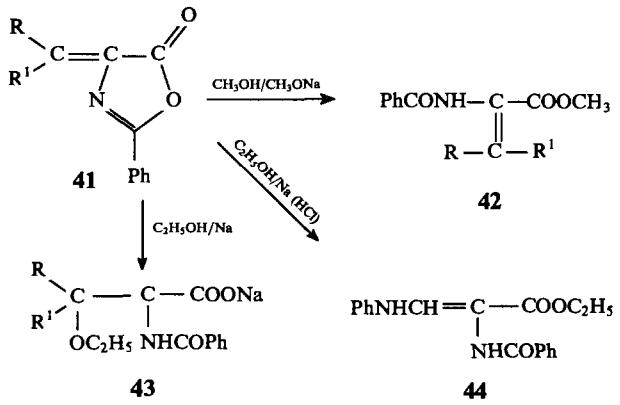
The ethanolysis of 4-[(4-acetoxy-1-naphthyl)methylene]-2-phenyl-5-oxazolone **40** in the presence of sodium ethoxide proceeds with simultaneous deacylation.[72]

It has been established[56] that the reaction of 4-isopropylidene-2-phenyl-5-oxazolone **41** (R = R^1 = CH_3) with methanol in the presence of sodium methoxide at pH 8.5 at room temperature is completed quantitatively after 4 h, whereas at 80 °C it leads to the formation of the methyl ester **42** (R = R^1 = CH_3) in 60% yield after 0.5 h. According to Zubareva et al.,[57] the methanolysis of the same oxazolone in the presence of comparatively small amounts

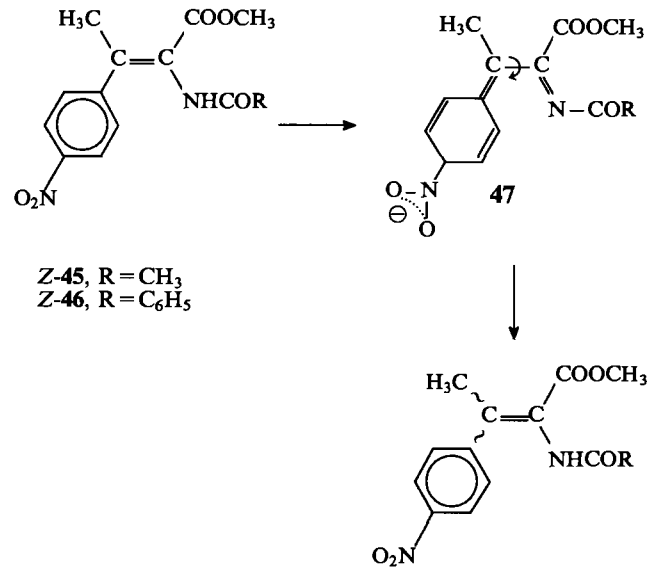
of sodium alkoxide leads to the expected ester **42** in 60% yield at room temperature after 20–25 h.



Cases are known where in the presence of sodium alkoxide the alcohol not only cleaves the 1,5-bond of the unsaturated 5(4*H*)-oxazolone but also adds to the exocyclic double bond of the heterocycle.[2, 4] 4-Ethylidene-2-phenyl-5-oxazolone **41** (R = H, R^1 = CH_3) is stable in boiling ethanol for 88 h. However, in the presence of sodium ethoxide the product was ethyl α-benzamido-β-ethoxybutyrate **43** (R = H, R^1 = CH_3).[2] The alkoxy-group in the 4-position increases the stability of the oxazolone ring in relation to alcohols.[4] However, according to the data quoted by Conforth,[2] the 2-phenyl-4-phenyl-4-phenylaminomethylene derivative **41** (R = H, R^1 = C_6H_5NH) reacts readily with ethanol in the presence of sodium ethoxide, giving rise to the ester of α-benzamido-β-phenylaminoacrylic acid **44**.[55]



One of the important questions concerning the alcoholysis of unsaturated 5(4*H*)-oxazolones is that of the configuration of the double bond in the reaction products. The study of this problem established[62] that reactions of *Z*- and *E*-4-arylethylidene-2-phenyl-5-oxazolones **41** (R = Ar, R^1 = CH_3) with sodium methoxide in methanol involve the stereospecific opening of the oxazolone ring with formation of the methyl esters of the corresponding *Z*- and *E*-acids. The same effect has been observed for 4-isobutylidene-2-phenyl-5-oxazolone **41** (R = C_2H_5, R^1 = CH_3) [56, 57] or 2-methyl(phenyl)-4-thienylmethylene-5-oxazolone **41** (R = thienyl, R^1 = H).[58, 68] However, in the case of *Z*-4-(α-*p*-nitrophenylethylidene)-2-phenyl-5-oxazolone **41** (R = 4-$NO_2C_6H_4$, R^1 = CH_3) the initial oxazolone isomer isomerises to form a mixture of the *Z*- and *E*-isomers of the expected ester with the *E*-isomer predominating.[62] The isomerisation of the *p*-nitrophenyl derivatives **45** and **46** can be explained by the fact that under alkaline reaction conditions the quinonoid compound **47**, in which rotation about the C–C bond becomes possible, may be formed:

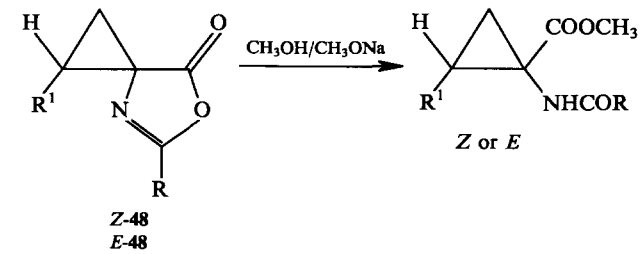


This conclusion is confirmed by the finding that the alcoholysis of the oxazolone *Z*-**46** in the presence of catalytic amounts of sulphuric acid proceeds without isomerisation.[62]

It is of interest to note that *Z*-4-benzylidene-2-phenyl-(methyl)-5-oxazolone **41** (R = H, R^1 = C_6H_5) undergoes alcoholysis in the presence of sodium alkoxide without change in the conformation of the double bond. However, the *E*-isomer leads to the formation of a mixture of the *Z*- and *E*-alkyl esters of *N*-substituted α,β-dehydrophenylalanine **42** (R = C_6H_5, R^1 = H) under the same conditions with the *Z*-isomer predominating.[53, 62]

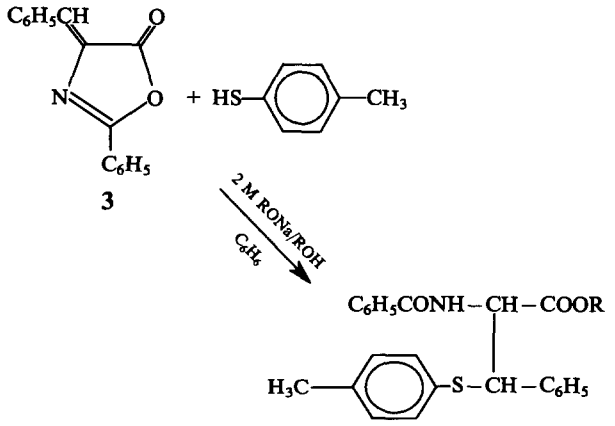
The alcoholysis of 4-(*p*-dimethylaminobenzylidene)-2-phenyl-5-oxazolone **41** [R = H, R^1 = 4-$(CH_3)_2NC_6H_4$] in the presence of alkali (NaOH) proceeds stereoselectively, while acid alcoholysis leads to the formation of a mixture of two geometrical isomers of the unsaturated ester **42** [R = H, R^1 = 4-$(CH_3)_2NC_6H_4$].[44]

The spiro-oxazolones **48** having both the *E*- and *Z*-conformations readily react with absolute methanol in the presence of catalytic amounts of sodium methoxides, being converted into the corresponding esters:[66, 67]



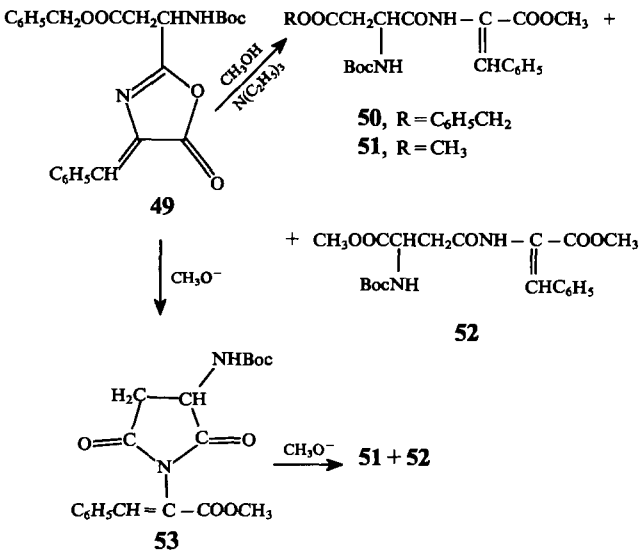
Z-48
E-48

It has been shown[2, 53] that the reaction of the oxazolone **3** with tolylmercaptan in the presence of sodium methoxide proceeds with formation of the corresponding ester of α-benzamido-β-phenyl-β-(*p*-tolylthio)propionic acids (see over):



The alcoholysis of 5(4*H*)-oxazolones also occurs in the presence of organic bases—amines. Both secondary[13] and tertiary[75–78] amines have been used for this purpose.

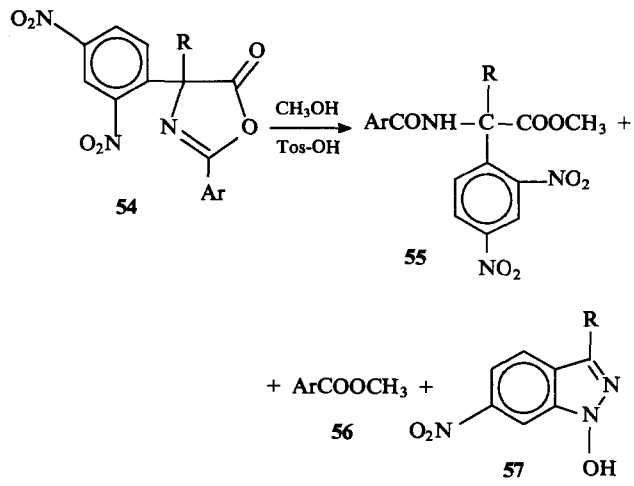
The methanolysis of the oxazolone **49** in the presence of triethylamine does not proceed unambiguously.[76] It affords a mixture of three compounds—the benzyl ester **50** and the methyl esters **51** and **52**. Evidently when the oxazolone ring is opened at the 1,5-bond on treatment with the nucleophile, the succinimide **53** is formed and leads to the formation of the unexpected methyl esters **51** and **52**.



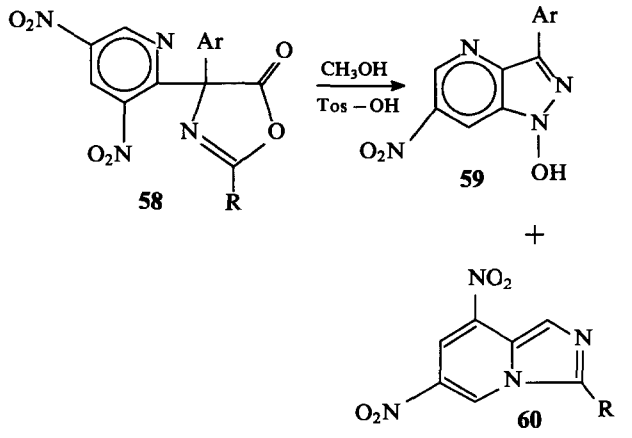
It has been noted[76] that the methanolysis of the oxazolone **49** in the presence of equimolar amounts of 4-dimethylaminopyridine leads unambiguously to the desired ester **50** without side products.

The opening of the oxazolone ring by alcohols is also catalysed by acids. Sulphuric acid,[79, 80] hydrochloric acid,[75, 81, 82] and toluene-*p*-sulphonic acid[83] have been used. In all cases the main reaction product is the alkyl ester of a *N*-substituted aminoacid.

According to D'Anello et al.,[83] on refluxing in methanol in the presence of catalytic amounts of toluene-*p*-sulphonic acid, 2-aryl-4-(*o*-nitrophenyl)-5-oxazolones **54** afford mixtures of methyl benzoate **56** and derivatives of 1-hydroxy-1*H*-indazole **57**. This reaction proceeds similarly also in ethanol and 1,2-ethylene glycol. However, in 2-propanol or *tert*-butyl alcohol, the main product is compound **57**. It is of interest to note that, both in the presence and absence of toluene-*p*-sulphonic acid in methanol, the oxazolone **54** (R = *iso*-C_3H_7) gives rise to the methyl ester of the corresponding acid **55** (R = *iso*-C_3H_7).

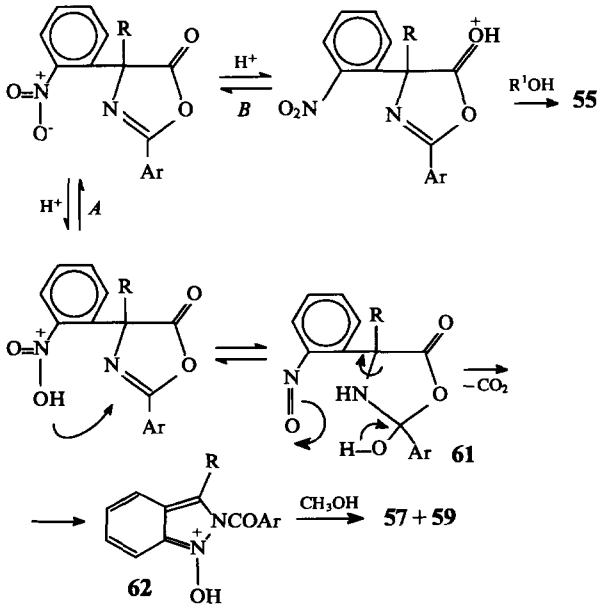


The reaction of 4-(β-nitropyridyl)oxazolones **58** with methanol in the presence of toluene-*p*-sulphonic acid has also been investigated.[83] It was established that the main reaction products are the indazole **59** and the imidazo[1,5-a]pyridine **60**:



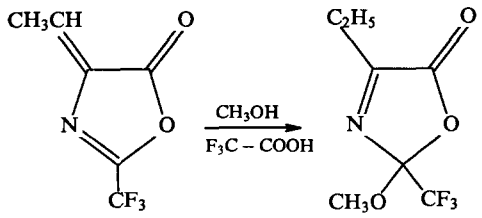
An ester analogous to compound **55** is formed in small amounts in this process.

The formation of compounds **57** and **59** can be explained by the nucleophilic attack by the oxazolone nitrogen atom on the protonated nitro-group (pathway *A*) with subsequent migration

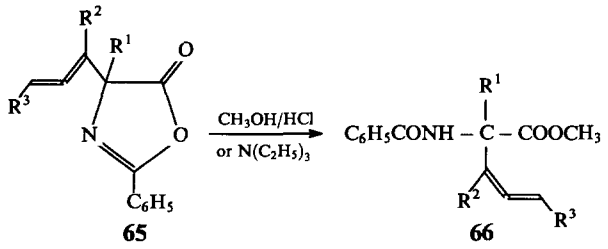


of the hydroxy-group to C(2) — an oxazolone carbon atom. After the evolution of carbon dioxide, the intermediate **61** formed in this process is converted into compound **62**, in which deacylation by the alcohol takes place with formation of compound **57** or **59**. The competing reaction — the catalytic opening of the oxazolone ring with formation of the aminoacid ester **55** (pathway *B*) — takes place simultaneously.

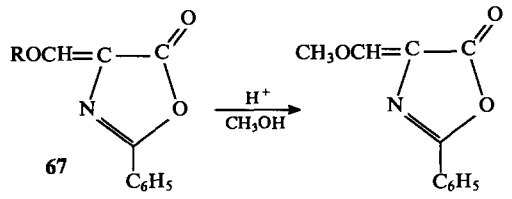
In the presence of trifluoroacetic acid, the reaction of a mixture of the *Z*- and *E*-isomers of 4-ethylidine-2-trifluoro-methyl-5-oxa-zolone **63** with methanol gives rise to the 1,4-adduct **64**:[84]



Methanolysis of the oxazolone **65** in the presence of hydrogen chloride leads to the formation of the corresponding ester **66** in a quantitative yield over a period of 15 min at room temperature. A similar result was obtained when the alcoholysis was carried out in the presence of triethylamine.[75]



In the presence of catalytic amounts of acid in methanol, the alkoxy-group of the alkoxymethyleneoxazolone **67** is substituted by the methoxy-group.[2]



The transalkylation of the alkoxy-group in compound **67** also proceeds in the presence of a platinum catalyst on heating with various alcohols.[85, 86]

The reactions of 5(4*H*)-oxazolones with epoxide resins proceed with ring opening.[87] The main products are the amidoesters containing the $-OOC-\overset{|}{C}-N-CO-$ fragment. The reaction in the absence of a catalyst is carried out at 190 °C. On the other hand the employment of catalysts usual for epoxide compositions makes it possible to reduce the reaction temperature to 140 – 150 °C. Both in the reactions with alcohols and in the case of the epoxide resins the chemical reactivity of 5(4*H*)-oxazolones depends on the polarity of the substituents in the 2- and 4-positions. Saturated 5(4*H*)-oxazolones react comparatively readily, while their unsaturated analogues require severe conditions.[87]

It has been shown[88, 89] that the reaction of saturated 5(4*H*)-oxazolones with hydroxylated polymers is catalysed by acids.

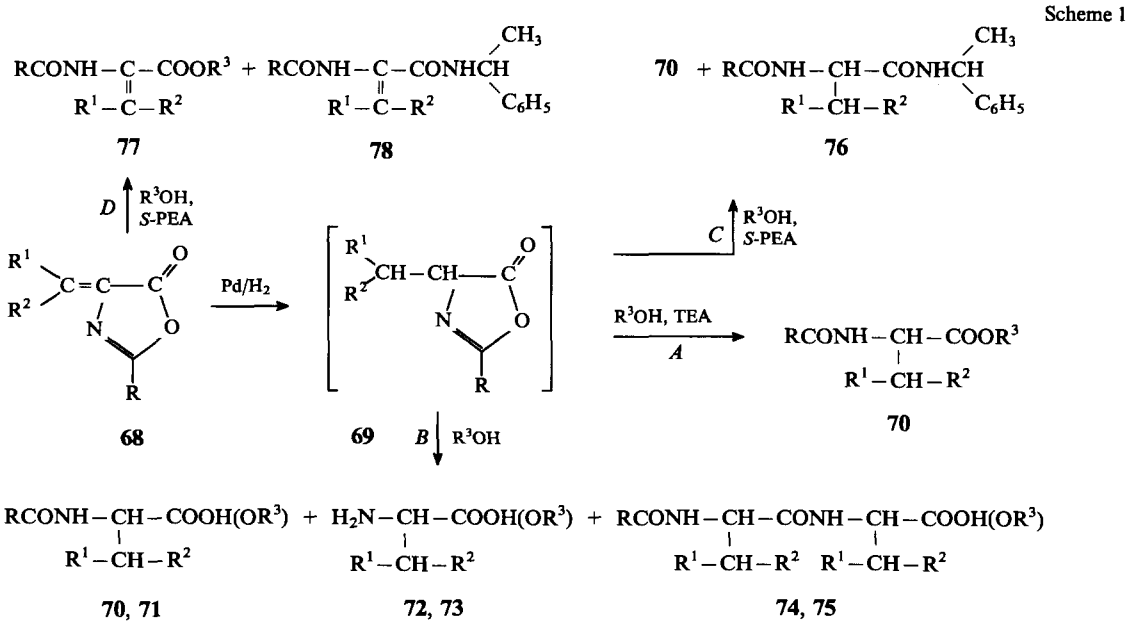
III. Reductive alcoholysis of unsaturated 5(4*H*)-oxazolones

A group of workers[90–97] achieved a very successful catalytic hydrogenation of unsaturated 5(4*H*)-oxazolones in alcohols. The catalyst is palladium obtained by reducing $PdCl_2$ in situ. The hydrogenation is carried out in the presence of triethylamine (TEA),[91] (*S*-(–)-α-phenylethylamine (*S*-PEA),[90–96] and (*S*)-(–)-*N*,*N*-dimethyl-α-phenylethylamine (*S*MPA).[94] According to Neupokoeva et al.,[91] the reductive alcoholysis of unsaturated 5(4*H*)-oxazolones can proceed in accordance with Scheme (1).

The unsaturated oxazolone **69** is obtained during hydrogenation, leading to a mixture of products **70** – **75** in the absence of a base (pathway *B*). The formation of the diacylated aminoacids **72** and **73** and their condensation products **74** and **75** can be explained by the interaction of the alcohol with the C(2) atom of the oxazolone **69** [the analogous process with 5(4*H*)-oxazolones was described above]. With decrease in the acidity of the alcohol (CH_3OH > C_2H_5OH > *iso*-C_3H_7OH), the cleavage of the 1,5-bond of the oxazolone **69** intensifies and leads to the formation of aminoacid esters **70**. In the presence of tertiary amines (TEA, *S*-MPA) the alcoholysis with formation of the ester **70** becomes the main reaction pathway (pathway *A*).

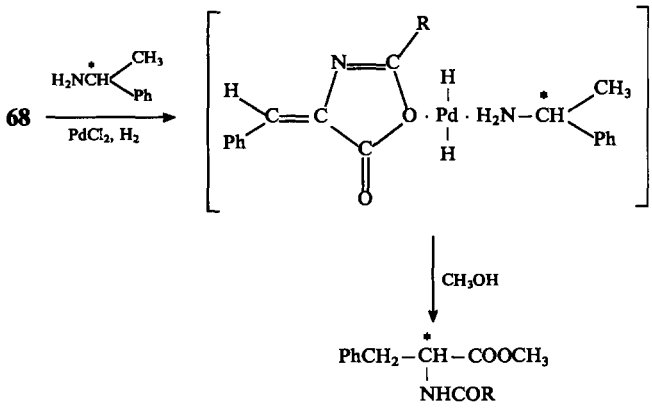
In the presence of *S*-PEA, the opening of the saturated [compound **69**] and unsaturated [compound **68**] oxazolones can

Scheme 1



take place under the influence of both the primary amine and the solvent (pathways *C* and *D*). Under these conditions, mainly the acylaminoacid ester[70] forms in methanol (pathway *C*).[91, 93-95, 97] On passing to alcohols with a higher molecular weight and a greater degree of branching of the molecule (C_2H_5OH, C_3H_7OH, *iso*-C_3H_7OH, C_4H_9OH, *sec*-C_4H_9OH, *tert*-C_4H_9OH), the content of the amide **76** increases.[93, 94] Furthermore, in connection with the decrease in the rates of hydrogenation of the unsaturated oxazolone **68** in the presence of *S*-PEA, unsaturated reaction products—the ester **77** and the amide **78**—are detected in the catalytic reaction mixture (pathway *D*).[91]

Reductive alcoholysis in the presence of the chiral amine *S*-PEA leads to the (*R*)-configuration of the ester **70** in the case of 2-alkyl(aryl)-4-benzylidene-5-oxazolone **68** (R^1 = H, R^2 = C_6H_5)[90] and to the (*S*-enantiometer in the case of 4-benzylidene-2-phenyl-5-oxazolone **68** (R = C_6H_5, R^1 = H, R^2 = C_6H_5).[97] The formation of the optically active methyl esters **70**) in the reductive methanolysis shows that in alcohols there is a possibility of the interaction of the oxazolone **68** with the hydrogen on the surface of the palladium catalysts modified by the chiral amine *S*-PEA without the migration of the reaction into the bulk phase.[90, 91] It has been suggested[93] that, in the enantioselective reductive methanolysis of unsaturated 5(4*H*)-oxazolones, the oxazolone **68** initially assumes a definite orientation in relation to the hydrogenating centre under the steric control of the chiral *S*-PEA coordinated to the catalytic palladium complex. This is followed by the formation of a coordinate bond between palladium and compound **68** and then by the saturation of the double bond and the opening of the oxazolone ring, which takes place within the complex without the elimination of the intermediate compounds.



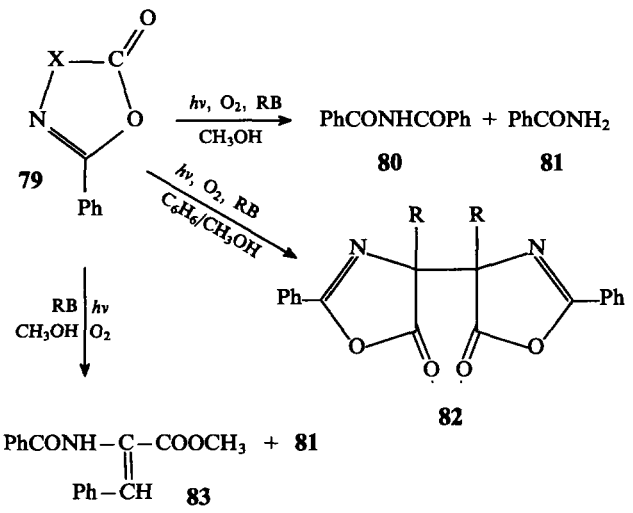
According to Khatskevich et al.,[94] the reductive methanolysis by the *Z*- and *E*-isomers of 4-*sec*-butylidene-5-oxazolones **68** (R^1 = CH_3, R^2 = C_2H_5) gives rise to the same diastereoisomeric composition of the aminoacid esters **70**. It follows from this that the *Z* – *E* isomerisation of the oxazolone **68** takes place in this process and that an identical mixture of isomers undergoes reduction. This is demonstrated by the finding that 4-*sec*-butylidene-5-oxazolone is not reduced in *tert*-butyl alcohol in the absence of a base and that the *Z*- and *E*-unsaturated oxazolones isomerise regardless of the initial compound **68**. In this case, the formation of *N*-substituted aminoacid esters takes place with a lower enantioselectivity than for 4-benzylidene-2-methyl-5-oxazolone **68** (R = CH_3, R^1 = H, R^2 = C_6H_5).[91] The reduction of both the *Z*- and *E*-isomers of 4-*sec*-butylidene-5-oxazolone in the presence of *S*-MPE leads to the optically active methyl ester **70** with a *threo* : *erythro* ratio of 63 : 67.[94]

When chiral phosphonic acid complexes of palladium are used as the catalyst, the double bond of the oxazolone **68** is hydrogenated initially and this is followed by the alcoholysis of the saturated oxazolone **69**.[97]

The reductive alcoholysis of unsaturated 5(4*H*)-oxazolones also proceeds in methanol in the presence of magnesium[98] or Raney nickel and sodium methoxide,[99] which leads to racemic methyl esters of *N*-substituted aminoacids.

IV. Oxidative alcoholysis of 5(4*H*)-oxazolones

Saturated and unsaturated 5(4*H*)-oxazolones react with alcohols in different ways in the presence of oxygen. The sensitised photochemical oxidation of 2,4-diphenyl-5-oxazolone **79** (X = CHC_6H_5) in methanol and in the presence of Rose Bengal (RB) for 0.5 h leads to the formation of 40% of the dibenzamide **80** (R = C_6H_5) and 49% of the benzamide **81**:

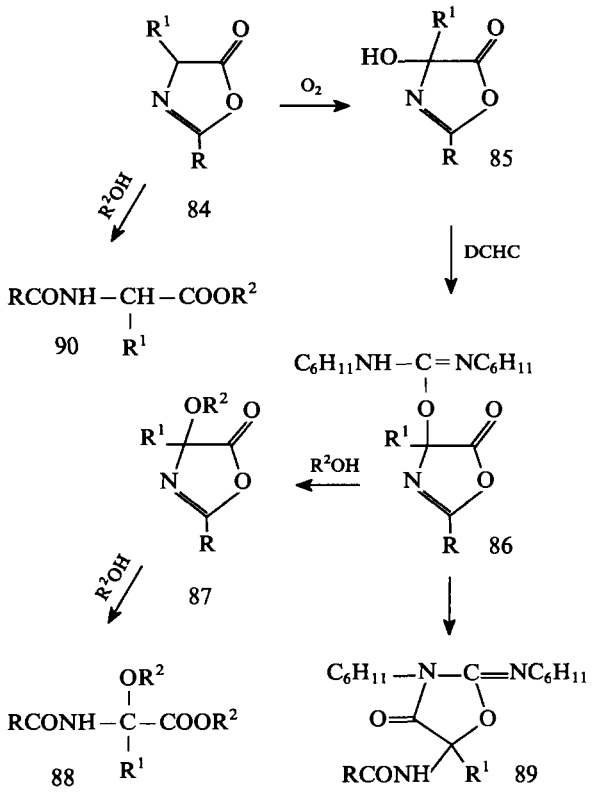


PhCONH–C(=CH–Ph)–COOCH3 + **81**

83

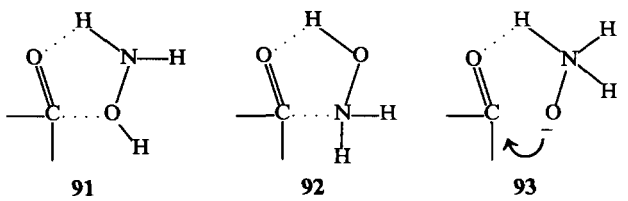
In a benzene–methanol mixture, the photochemical oxidation in the course of 0.25 h leads mainly to the formation of the dimer **82**.[100] Similar results were also obtained for 4-benzyl-2-phenyl-5-oxazolone **79** (X = $CHCH_2C_6H_5$), while, as in the case of its unsaturated analogue **79** (X = $C{=}CHC_6H_5$), the photochemical oxidation in the course of 0.25 h leads to the formation of a mixture consisting of 53% of the methyl ester **83** and 29% of the benzamide **81**.[100] When the photochemical oxidation of the unsaturated oxazolone **79** is prolonged to 0.75 h, the only product isolated from the reaction mixture is benzoic acid (yield 45%).

The interaction of the saturated oxazolones **84** with *N*,*N*-dicyclohexylcarbodiimide (DCHC) in methanol or ethanol and under an oxygen atmosphere also leads to the formation of a mixture of products.[101, 102] In the case of 2-benzyl-4-phenyl-5-oxazolone **84** (R = $CH_2C_6H_5$, R^1 = C_6H_5), the alkyl ester of α-alkoxy-*N*-phenylacetylphenylglycine **88** [R = $CH_2C_6H_5$, R^1 = C_6H_5, R^2 = CH_3 or C_2H_5 (37 and 27% respectively)], the alkyl ester of *N*-phenylacetylglycine **90** [R = $CH_2C_6H_5$, R^1 = C_6H_5, R^2 = CH_3 (7%)], and the oxazolone **89** [R = $CH_2C_6H_5$, R^1 = C_6H_5 (10% in methanol and 32% in ethanol)] were isolated from the reaction mixture.[102] It is suggested that the reaction proceeds via the oxidation of the oxazolone **84** to 4-hydroxy-oxazolone **85**, which interacts with DCHC to form the intermediate **86**. As a consequence of the attack by the alcohol, the latter gives rise to the ester **88** via compound **87** or undergoes an intramolecular rearrangement to compound **89**. When this reaction is carried out in 2,2,2-trichloroethanol, it leads to the formation of only the corresponding ester **90** (R = $CH_2C_6H_5$, R^1 = C_6H_5, R^2 = CH_2CCl_3). In the case of 2-benzyl-4-methyl-5-oxazolone **84** (R = $CH_2C_6H_5$, R^1 = CH_3), the oxidative alkoxylation product **88** is not detected, whereas in the case of 4-methyl-2-phenyl-5-oxazolone **84** (R = C_6H_5, R^1 = CH_3) compounds **88** and **90** (R = C_6H_5, R^1 = R^2 = CH_3) were isolated from the reaction mixture in 9% and 44% yields, respectively.[102]

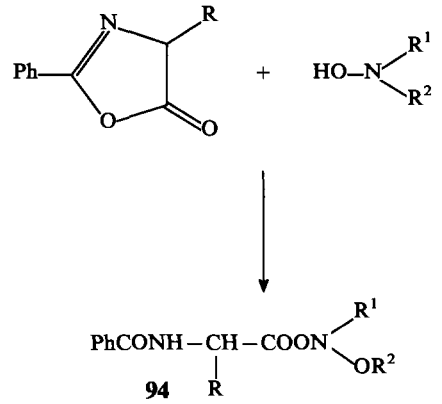


V. Reactions with hydroxylamine derivatives and aminoalcohols

Studies on the interaction of 5(4*H*)-oxazolones with hydroxylamine and its derivatives occupy a special place in the literature. The composition of reaction products is affected not only by the nature of the oxazolone but also by the reaction temperature and the solvent. Unsaturated 5(4*H*)-oxazolones react with hydroxylamine to form two products.[103] Evidently this entails the *N*- and *O*-acylation of hydroxylamine. In the presence of an excess of the latter, one product (the *O*-acyl derivative) vanishes. According to Goodman and Glaser,[103] hydroxylamine can attack 5(4*H*)-oxazolone along one of two pathways with the formation of products **91** and **92**. In addition, hydroxylamine can attack the 5(4*H*)-oxazolone in the form of the zwitter-ion **93**.



In the reaction of saturated 5(4*H*)-oxazolones with *N,N*-disubstituted hydroxylamine derivatives, the reaction product is an ester of the *N*-substituted aminoacid **94**.[103–105] According to the authors,[103] in the latter case a zwitter-ionic reaction mechanism takes place. Evidently, by virtue of the bifunctional attack by hydroxylamine and its derivatives, the opening of the oxazolone ring without racemisation becomes possible, particularly in the case of strong nucleophiles such as *N*-hydroxysuccinimide or 1-hydroxybenzotriazole, which have the properties of weak bases.[103–105]

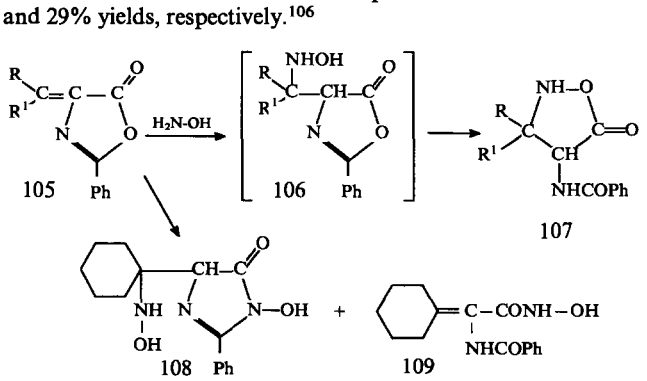


The reaction of hydroxylamine with unsaturated 5(4*H*)-oxazolones leads to different products. The reaction has been very effectively investigated by Ali and Khan.[106] Depending on the pH of the medium, the reactant ratio, the nature of the solvent, and temperature, different products are then obtained.

The hydroxamic acids **96** (26%) and **97** (51%) are obtained in the reaction of compound **95** (R = C_6H_5) with hydroxylamine at room temperature. When there is an excess of hydroxylamine, one obtains in the presence of sodium methoxide 20% of bis-(α-benzamidocinnamoyl)hydroxamic acid **101**, 4-(α-hydroxyaminobenzyl)-2-phenyl-5-oxazolone **99** (28%), 1-hydroxy-4-(α-hydroxyaminobenzyl)-2-phenyl-5-imidazolone **104** (35%), and 4-benzylidene-1-hydroxy-2-phenyl-5-imidazolone **98** (15%). The yield of the last product **98** increases sharply (to 58%) when pyridine is used instead of methanol. On heating hydroxylamine hydrochloride with the oxazolone **95** (R = C_6H_5) in acetic acid, compound **102** is obtained in 77% yield,[106] whereas in the presence of sodium hydroperoxide compound **100** is formed in 66% yield.[107] 4-Benzamido-4,5-dehydro-5-phenyl-5-isoxazolone **100** is formed in a high yield (76%) on exposure to light.[106] (see over)

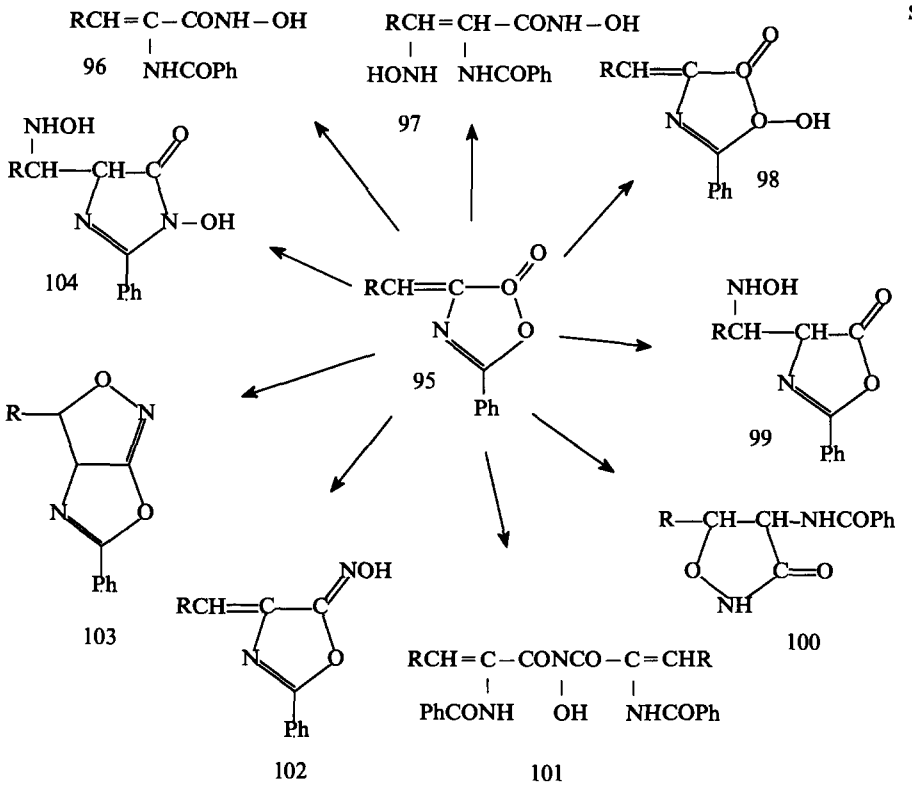
The reaction of hydroxylamine with 4-alkylidene-5-oxazolones **105** [107] proceeds, in contrast to 4-arylidene-5-oxazolones,[38] with formation of 3-alkyl-4-benzamido-5-oxo-1,2-oxazolidine **107**. The mechanism of this reaction involves[107] the addition, in weakly alkaline or neutral media, of a hydroxylamine molecule to the exocyclic double bond of the oxazolone, after which the resulting saturated oxazolone **106** undergoes intramolecular ring opening with formation of the isoxazolidine derivative.

The reaction involving 4-cyclohexylidene-2-phenyl-5-oxazolone **105** (R = R^1 = C_5H_{10}) in the presence of sodium methoxide in methanol affords a mixture of compounds **108** and **109** in 40% and 29% yields, respectively.[106]

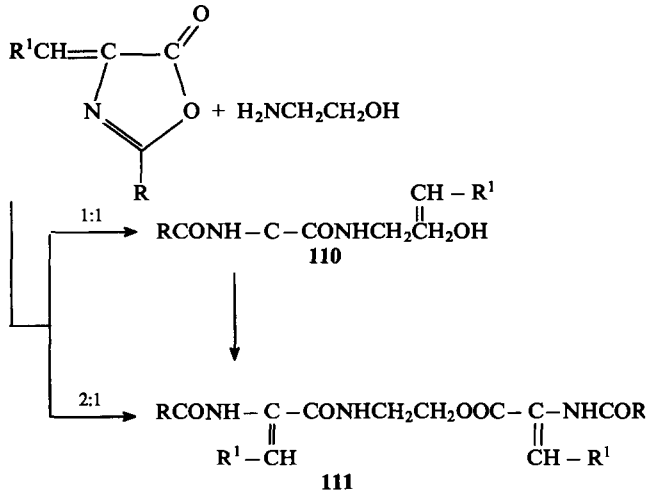


No studies on the reaction of unsaturated 5(4*H*)-oxazolones with *N,N*-di-substituted hydroxylamine derivatives have been described in the literature. However, there are communications devoted to the study of the reactions of these oxazolones with ethanolamine[108] and its derivatives.[109–121]

Scheme 2



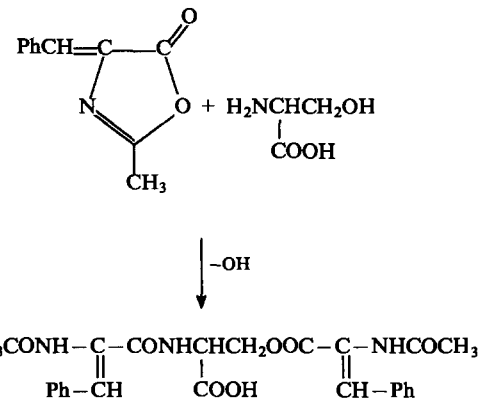
According to Lupsa,[108] owing to the comparatively high nucleophilicity of the amino-group, the interaction of equimolar amounts of monoethanolamine and an unsaturated 5(4*H*)-oxazolone leads to the formation of the 2-hydroxyethylamide **110**. On the other hand, when the oxazolone : aminoalcohol ratio is 2 : 1, the reaction product in the presence of 1–2% of a base (NaOH) is the *N,O*-diacylated aminoethanol **111**. Lupsa[108] also achieved the opening of the oxazolone ring by the 2-hydroxyethylamides **110** to give compound **111**.



The products of *N,O*-diacylation are also formed on reaction of 4-benzylidene-2-methyl-5-oxazolone with serine in the presence of alkali.[110, 111]

According to Botvinnik et al.,[110] saturated 5(4*H*)-oxazolones react with the hydroxy-group of *N*-benzoylserine or the ethyl ester of *N*-benzoylserine without ring opening.

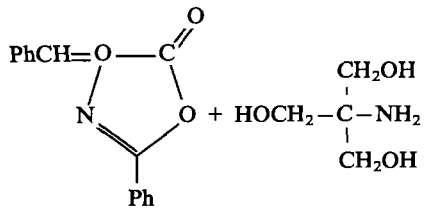
In the reactions of saturated 2,2-bis-5(4*H*)-oxazolones with ethanolamine, polymers with a regular structure have been obtained.[9]

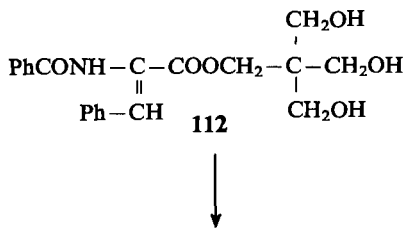


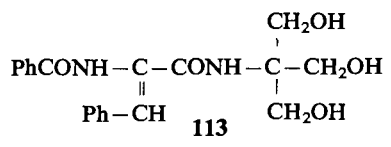
De Jersey and co-workers[112, 113] succeeded in isolating an ester of the α,β-dehydroaminoacid **112** in the reaction of the *Z*-isomer of 4-benzylidene-2-phenyl-5-oxazolone with tris-(hydroxymethyl)aminomethane in acetonitrile.It has been noted that the ester **112** is unstable, especially under alkaline conditions, and can be converted into the corresponding amide **113** as a consequence of an intramolecular rearrangement and an intermolecular interaction. The formation of an ester can be accounted for by the steric hindrance generated by the hydroxymethyl groups, on the one hand, and by the intramolecular hydrogen bond between the amino- and hydroxy-groups (which increases the nucleophilicity of the hydroxy-group), on the other.

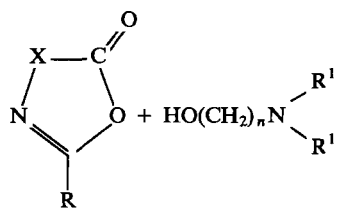
The interaction of dialkylaminoalkyl alcohols with both saturated,[114, 115] and unsaturated[115–118] 5(4*H*)-oxazolones leads to the formation of the corresponding esters of *N*-substituted aminoacids **115**.

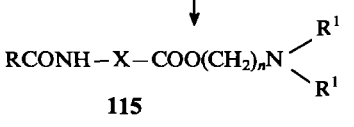
According to the data of Topuzyan et al.,[115] the reaction of the saturated oxazolone **114** (X = $CHCH_2C_6H_5$) with 2-dimethylaminoethanol takes place under milder conditions than the reaction with the unsaturated analogue **114** (X = $C=CHC_6H_5$). When *Z*-unsaturated 5(4*H*)-oxazolones are used, the heterocycle is opened stereoselectively by this aminoalcohol.[119]







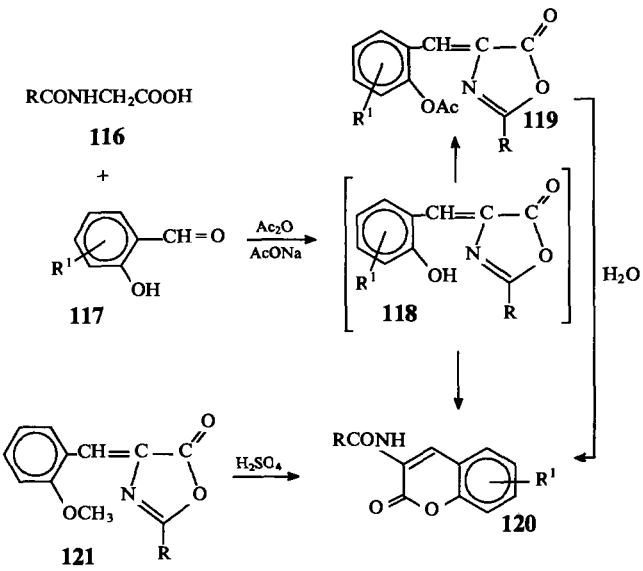




It has been established that the interaction of 2-dimethylaminoethanol with 4-benzylidene-2-phenyl-5-oxazolone involves general base catalysis.[120] The influence of the solvent[120] and certain additives (1-hydroxybenzotriazole, *N*-hydroxysuccinimide, imidazole, and *p*-nitrophenol)[121] on this reaction has been investigated. According to a patent,[118] the opening of the unsaturated oxazolone ring by dialkylaminoalkyl alcohols is accelerated in the presence of the alkoxides derived from the same aminoalcohols.

VI. Intramolecular reactions of 5(4*H*)-oxazolones containing a hydroxy-group

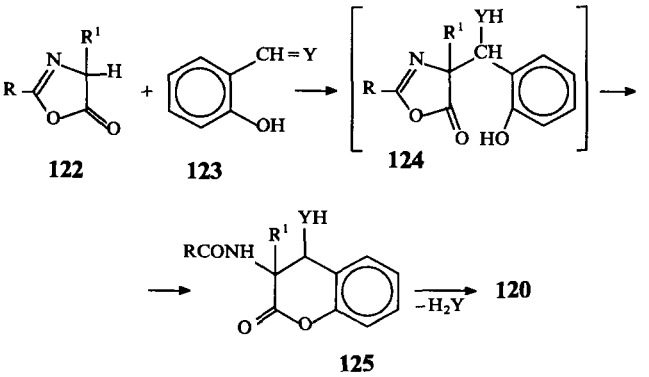
The synthesis of unsaturated 5(4*H*)-oxazolones from *N*-acylglycine **116** and derivatives of salicylaldehyde **117** involves the formation, under the conditions of the Erlenmeyer reaction, of a mixture of products consisting of the target oxazolone **119** and 3-*N*-acylcoumarin **120**.[122–124] Evidently this entails the intermediate formation of 2-aryl(alkyl)-4-(2-hydroxybenzylidene)-5-oxazolone **118**. The intramolecular hydrophilic attack by the hydroxy group of the latter on the carbon atom of the carbonyl group leads to the formation of the coumarin **120**. This hypothesis is confirmed by data indicating the formation of



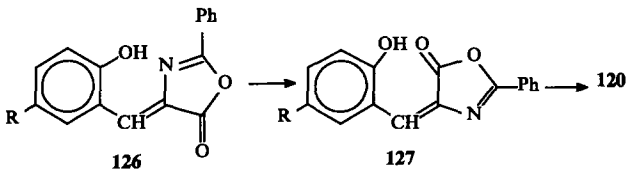
3-benzamidocoumarin **120** (R = C_6H_5, R^1 = H) from 4-(2-acetoxybenzylidene)-2-phenyl-5-oxazolone **119** (R = C_6H_5, R^1 = H)[125] and 4-(2-methoxy-benzylidene)-2-phenyl-5-oxazolone **121**[126] under the conditions involving the removal of the O-protecting groups in these compounds.

The formation of 3-acylaminocoumarins **120** is observed also in the reaction of the saturated oxazolones **122** with salicylaldehyde or its derivatives **123**.[127–129] The course of this reaction is appreciably influenced both by the substituent in the 2-position in the heterocycle **122** and by the substituent R in the second component **123**. According to Kumar and Mukerjee,[127] the use of salicylideneaniline **123** (Y = NC_6H_5) instead of salicylaldehyde leads to a decrease in the yield of acylaminocoumarins **120**. In the case of the oxazolone **122** (R = H), the corresponding coumarin **120** (R = R^1 = H) is obtained only when salicylaldehyde is used. The yield of the coumarin **120** increases in the following sequence of R: H < H < CH_3 < C_6H_5 < C_6H_5CH = CH.

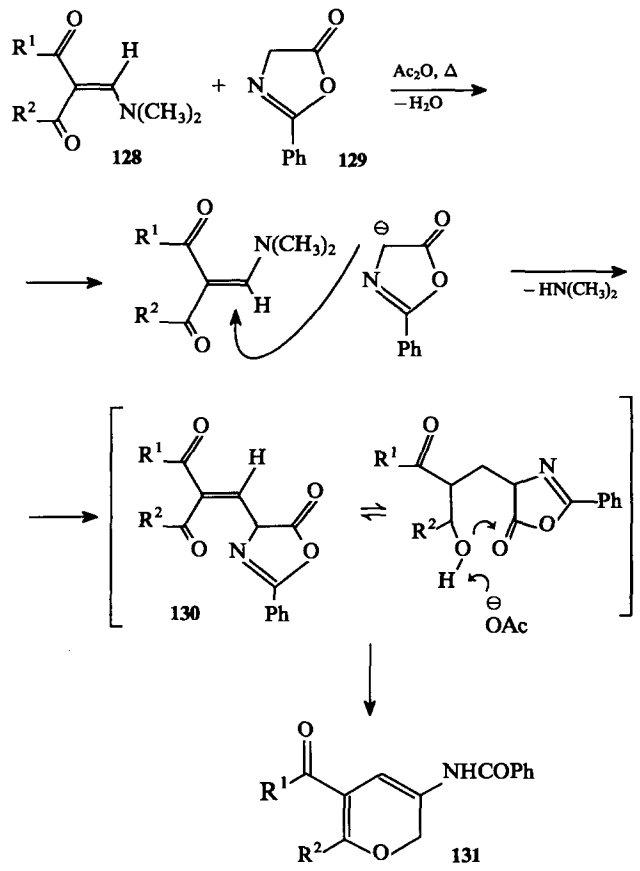
The study of the mechanism of the formation of acylaminocoumarins **120** showed[128] that the process proceeds via the formation of the dihydrocoumarin **125**. In the case of compound **122** (R = H), this intermediate **125** undergoes β-elimination, which leads to the coumarin **120**. In the reaction of 2,4-dimethyl-5-oxazolone **122** (R = R^1 = CH_3) with salicylaldehyde **123** (Y = O) or salicylideneaniline **123** (Y = NC_6H_5), the corresponding hydrocoumarin **125** (Y = O or NC_6H_5) was isolated, since under these conditions the β-elimination of the YH_2 group does not take place.



The acylcoumarins **120** have also been synthesised under the conditions of the photochemical[130] or electrochemical[131] conversion of the *Z*-oxazolone **126** into the *E*-isomer **127**:



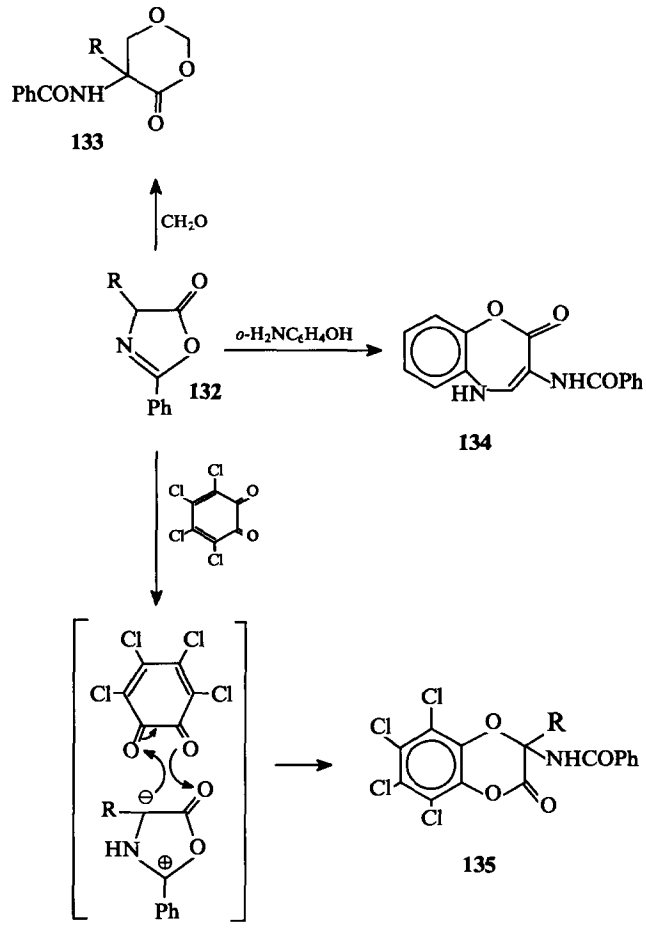
A method for the synthesis of 3-benzamido-2*H*-pyranones **131** via the reaction of esters of 2-acyl-3-dimethylaminoacrylic acids **128** ($R^1 = C_2H_5O$, $R^2 = CH_3$, C_6H_5) or 2-dimethylaminomethylene-1,3-diketones **128** ($R^1 = R^2 = CH_3$, C_6H_5) with 2-phenyl-5-oxazolone **129** has been described:[132]



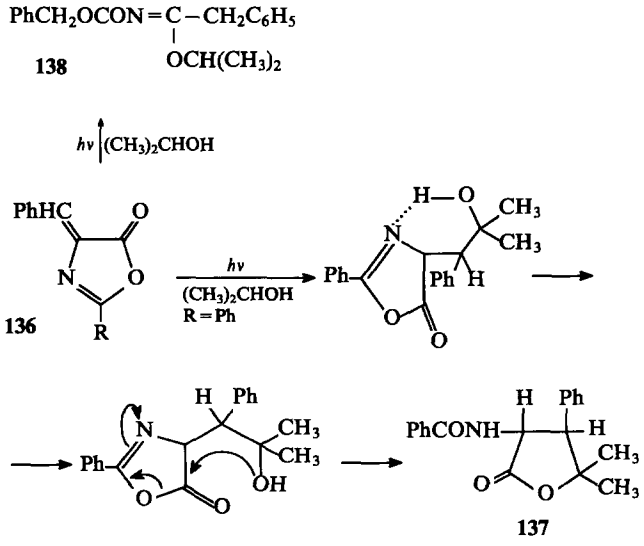
The reaction leads to nucleophilic substitution of the protonated dimethylamino-group in compound **128** and subsequent intramolecular attack by the carbonyl group of the oxazolone **130** on the alcoholic graph of the side substituent, which is completed by cyclisation to the pyran **131**.

The intramolecular opening of the ring in the saturated oxazolone **132** (R = H, alkyl) in the presence of alcohols is observed also in the hydroxymethylation of the heterocycle.[133–135] The reaction products are then 1,3-dioxan-4-ones **133**.

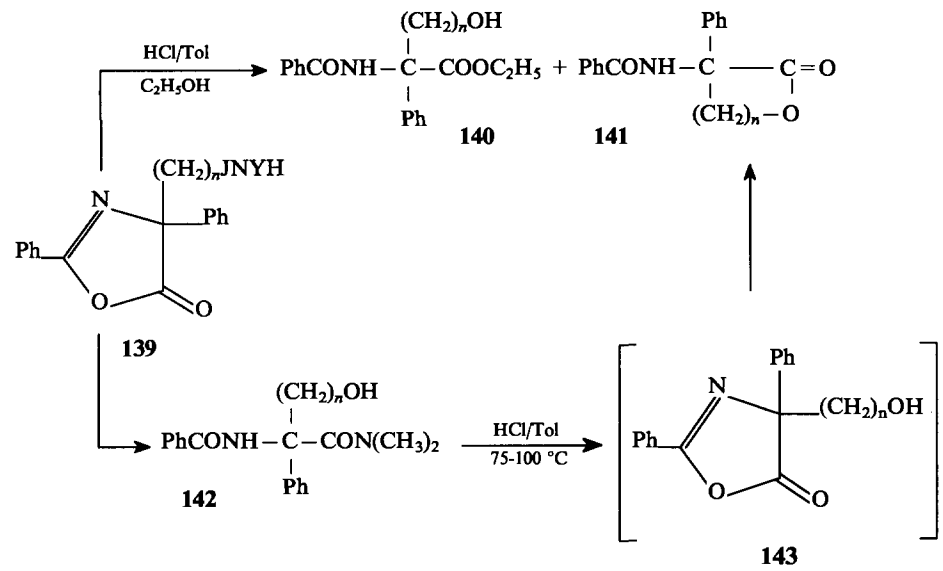
It has been found that the reaction of 4-ethoxycarbonyl-2-phenyl-5-oxazolone **132** (R = $COOC_2H_5$) with *o*-aminophenol leads to the formation of the benzoxazepin **134**,[136] while the reaction of the oxazolone **132** (R = H, alkyl, aryl) with chloranil affords benzodioxanes **135**.[137]



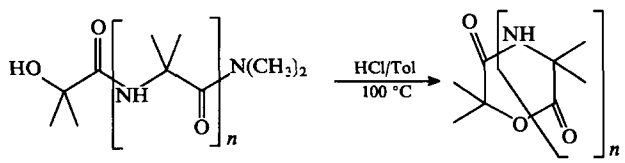
On irradiation with light in solution in 2-propanol, the unsaturated oxazolone **136** (R = C_6H_5) gives rise to the lactone **137** in 17% yield,[138, 139] while 4-benzylidene-2-benzyloxy-5-oxazolone **136** (R = $C_6H_5CH_2O$) affords compound **138** in 92% yield under analogous conditions.[140]



Under the conditions where the O-protecting group is removed from the saturated oxazolone **139** a mixture of the ethyl ester of the *N*-benzamidoacid **140** and the lactone **141** was obtained in the presence of ethanol.[141] It was noted in the same study that the lactonisation can occur when the dimethylamide of the *N*-substituted aminoacid **142** is heated in the presence of hydrogen chloride in toluene (tol.). This reaction proceeds via the intermediate formation of the oxazolone **143**.



Morpholinediones and more bulky cyclic compounds **144** (n = 1 – 4) are formed similarly:[142, 143]



Thus it is readily seen that the study of reactions of 5(4*H*)-oxazolones with oxygen-containing nucleophiles is important for the determination of the chemical properties of these heterocyclic systems and for the synthesis of organic compounds belonging to a wide variety of classes.

References

1. H E Carter *Organic Reactions* Vol. 3, p. 198 (1946)
2. J W Conforth *The Chemistry of Penicillin* (Princeton, NJ, 1949) p. 688
3. Y S Rao, R Filler *Synthesis* **2** 749 (1975)
4. S I Lur'e, E S Chaman *Reaktsii i Metody Issledovaniya Organicheskikh Soedinenii* (Reactions and Methods of Investigation of Organic Compounds) (Moscow: Khimicheskaya Literatura, 1959) p. 155
5. A K Mukerjee, P Kumar *Heterocycles* **16** (11) 1995 (1981)
6. F Bettzieche, R Menger *Z. Physiol. Chem.* **172** 56 (1927)
7. C H Budeanu, V Sunel *An. Stiint. Univ. "Al. I Cuzu Iasi." Sect. Ic* **18** 169 (1972)
8. C H Budeanu, V Sunel, I Iancu, et al. *Rev. Med.-Chir. (Romania)* **77** 817 (1973)
9. T M Frunze, V V Korshak, L V Kozlov *Izv. Akad. Nauk SSSR, Otd. Khim. Nauk* (3) 535 (1959)
10. I Lupsa *Rev. Chim. (Bucharest)* **25** 525 (1974)
11. Romanian P. 63 640; *Chem. Abs.* **92** 768 575 (1980)
12. Romanian P. 72 088; *Chem. Abs.* **97** 182 865 (1982)
13. M Bergmann, K Grafe *Z. Physiol. Chem.* **187** 183 (1930)
14. B H Nicolet *J. Biol. Chem.* **100** 287 (1933)
15. E S Chaman, M M Shemyakin *Zh. Obshch. Khim.*, **25** 1360 (1955)
16. O V Kil'disheva, M G Lin'kova, I L Knunyants *Izv. Akad. Nauk SSSR, Otd. Khim. Nauk* (2) 271 (1955)
17. M M Shemyakin, E S Chaman, L I Denisova *Dokl. Akad. Nauk SSSR* **106** 675 (1956)
18. M M Shemyakin, G A Ravdel', E S Chaman *Dokl. Akad. Nauk SSSR* **107** 706 (1956)
19. M M Shemyakin, L I Denisova, E S Chaman *Izv. Akad. Nauk SSSR, Otd. Khim. Nauk* (4) 690 (1959)
20. M M Chemiakin, E S Tchaman, I L Denisova, et al. *Bull. Soc. Chim. Fr.* (3) 530 (1959)
21. H J Petersen *Tetrahedron Lett.* **10** 1557 (1969)
22. H J Petersen *Acta Chem. Scan.* **25** 1502 (1971)
23. B S Drach, G N Mis'kevich, A P Martynyuk *Zh. Org. Khim.* **10** 2315 (1974)
24. B S Drach, G N Mis'kevich, A P Martynyuk *Zh. Org. Khim.* **14** 508 (1978)
25. G Just, B Y Chung, K Crozinger *Can. J. Chem.* **55** 274 (1977)
26. N G Agropoulos, E Coutouli-Argropoulos *J. Heterocycl. Chem.* **21** 1397 (1984)
27. H Lettre, M E Fernholz *Z. Physiol. Chem.* **266** 37 (1940)
28. E Gross, J A Meienhofer, in *The Peptides: Analysis, Synthesis, Biology* Vol. 1 *Major Methods of the Peptide Bond Formation* (Translated into Russian) (Moscow: Mir, 1983) p. 347
29. J Kovacs, L Kisfaludy, M Q Ceprini *Peptides. Proc. Eur. Peptide Symp.* (Amsterdam: North-Holland, 1967) p. 23; *Chem. Abs.* **68** 87 544 (1968)
30. J Kovacs, L Kisfaludy, M Q Ceprini, et al. *Tetrahedron* **25** 2555 (1969)
31. M Goodman, L Levine *J. Am. Chem. Soc.* **86** 2918 (1964)
32. T C Curran, C R Furrar, O Niazi, et al. *J. Am. Chem. Soc.* **102** 6828 (1980)
33. Y Jersey, P Willadsen, B Zerner *Biochemistry* **8** 1959 (1969)
34. J Suh, S S Yoon, E Or, et al. *Bioorg. Chem.* **16** 245 (1988)
35. E T Stiller *J. Chem. Soc.* 473 (1937)
36. P K Tripathy, A K Mikerjee *Synthesis* (5) 418 (1984)
37. P K Tripathy, A K Mikerjee *Indian. J. Chem., Sect. B* **25** 1059 (1986)
38. P K Tripathy, J Roy, A K Mikerjee *Indian J. Chem., Sect. B* **25** 1275 (1986)
39. V Farcasan, I Oprean, C Bodea *Rev. Roum. Chim.* **13** 647 (1968)
40. N K Kochetkov, E I Budovskii, Z I Khomutov, et al. *Zh. Obshch. Khim.* **29** 68 (1959)
41. J M Brown, P A Chaloner *J. Chem. Soc., Perkin Trans. 2* (6) 711 (1982)
42. USSR P. 529 154; *Byull. Izobret.* (35) (1976)
43. J M Brown, P A Chaloner *J. Am. Chem. Soc.* **102** 3040 (1980)
44. B L Moldaver, Z V Pushkareva *Zh. Obshch. Khim.* **31** 1560 (1961)
45. Japanese P. 7 558 063; *Chem. Abs.* **83** 193 075 (1975)
46. A O Fitton, J R Frost, H Suschitzky, et al. *Synthesis* (2) 133 (1977)
47. A K Saxena, P C Jain, N Anand *Indian J. Chem.* **13** 230 (1975)
48. N J O'Reilly, W S Derwin, H C Lin *Synthesis* (7) 550 (1990)
49. K B Niewiadomsky, H Suschitzky *J. Chem. Soc., Perkin Trans. 1* (7) 1679 (1975)
50. Y Omote, Y Fijinuma, N Suguiama, et al. *J. Chem. Soc., Chem. Commun.* (4) 1679 (1968)
51. J Roy *Indian J. Chem., Sect. B* **30** 433 (1991)
52. B H Nicolet *J. Biol. Chem.* **95** 389 (1932)
53. H E Carter, W C Risser *J. Biol. Chem.* **139**(1) 255 (1941)
54. B F Crowe, F F Nord *J. Org. Chem.* **15** 1177 (1950)

55. S I Lur'e, S M Mamofe, Kh M Ravikovich *Zh. Obshch. Khim.* **21** 1308 (1951)
56. S I Lur'e, R G Vdovina *Zh. Obshch. Khim.* **22** 1883 (1952)
57. N D Zubareva, I E Khatskevich, T N Kuznetsova, et al. *Izv. Akad. Nauk SSSR, Ser. Khim.* (4) 477 (1983)
58. C Cativiela, M D Diaz De Willagas, J A Majoral, et al. *Synthesis* (11) 899 (1983)
59. USSR P. 487 877; *Byull. Izobret.* (38) 57 (1975)
60. USSR P. 475 361; *Byull. Izobret.* (24) 55 (1975)
61. S V Krivun *Khim. Geterotsikl. Soedin.* (6) 757 (1976)
62. D Cativiela, M D Diaz De Willagas, E Melendes *Tetrahedron* **42** 583 (1986)
63. S Solyom, K Szilagui, L Toldy *Lieb. Ann. Chem.* (2) 153 (1987)
64. B Stanovnik, J Svete, M Tisler *J. Heterocycl. Chem.* **24** 1809 (1987)
65. B Stanovnik, J Svete, M Tisler, et al. *Heterocycles* **27** 903 (1988)
66. E M Kandel, A H Ald el Rahman, M N Khadeir *Pol. J. Chem.* **62** 787 (1988)
67. F Lopes-Arbeloa, K Goedeweeck, F Ruttens, et al. *J. Am. Chem. Soc.* **109** 3068 (1987)
68. C Cativiela, M D Diaz De Willagas, J A Majoral, et al. *J. Heterocycl. Chem.* **25** 851 (1988)
69. I Arenal, M Bernabe, E Fernandes-Avares, et al. *J. Heterocycl. Chem.* **20** 607 (1983)
70. I Arenal, M Bernabe, E Fernandes-Avares, et al. *Synthesis* (8) 773 (1985)
71. H E Carter, P Handler, D B Melwille *J. Biol. Chem.* **128** 359 (1939)
72. M A Vela, F R Frontzek, G W Horn, et al. *J. Org. Chem.* **55** 2913 (1990)
73. A M Islam, A M S El-Charief, I M Ismail, et al. *Egypt. J. Chem.* **26** 221 (1983)
74. E S Nicholas, D J Phelps *J. Chem. Eng. Data* **25** 89 (1980)
75. A S Castelhano, S Horne, G J Taylor, et al. *Tetrahedron* **44** 5451 (1988)
76. S W King, C H Stammer *J. Org. Chem.* **46** 4780 (1981)
77. S W King, J M Riordan, E M Holt, et al. *J. Org. Chem.* **47** 3270 (1982)
78. W Steglich, H Wegmann *Synthesis* (6) 481 (1980)
79. Yuan Yunchen, Yang Conggui *Dalian Gongxueyuan Xuebao* **23** 135 (1984); *Chem. Abs.* **102** 46234 (1985)
80. Ren Youda, Yuan Yuncheng, Yang Conggui, et al. *Coadeng Xuexiao Huahue Xuebao* **6** 518 (1985); *Chem. Abs.* **103** 215 753 (1985)
81. D Obrecht, H Heimgartner *Helv. Chim. Acta* **64** 482 (1981)
82. D Obrecht, H Heimgartner *Helv. Chim. Acta* **70** 102 (1987)
83. M D'Anello, E Erba, M L Gelmi, et al. *Chem. Ber.* **121** 67 (1988)
84. V Austel, V Steglich *Chem. Ber.* **108** 2361 (1975)
85. Japanese P. 180 063; *Chem. Abs.* **46** 4029 (1952)
86. S Tatsuoka, M Miyamoto, R Shi, et al. *J. Penicillin (Japan)* **1** 382 (1947); *Chem. Abs.* **43** 2618 (1949)
87. Z M Dobrokhotov, N R Makarov, R F Samoilovskikh *Plast. Massy* (9) 71 (1976)
88. US P. 2 522 192; *Chem. Abs.* **86** 18 524 (1977)
89. US P. 4 777 217; *Chem. Abs.* **110** 96 052 (1989)
90. E S Neupokoeva, E I Karpeiskaya, L F Godunova, et al. *Izv. Akad. Nauk SSSR, Ser. Khim.* (1) 139 (1979)
91. E S Neupokoeva, E I Karpeiskaya, L F Godunova, et al. *Izv. Akad. Nauk SSSR, Ser. Khim.* (1) 146 (1979)
92. L F Godunova, E S Levitina, E I Karpeiskaya, et al. *Izv. Akad. Nauk SSSR, Ser. Khim.* (4) 815 (1981)
93. G V Chel'tsova, E I Karpeiskaya, L N Kaigorodova, et al. *Izv. Akad. Nauk SSSR, Ser. Khim.* (1) 65 (1983)
94. I E Khatskevich, I K Kalnin', E I Karpeiskaya, et al. *Izv. Akad. Nauk SSSR, Ser. Khim.* (2) 359 (1983)
95. E I Karpeiskaya, M R Lutsenko, A I Lutsenko, et al. *Izv. Akad. Nauk SSSR, Ser. Khim.* (10) 2286 (1987)
96. E I Karpeiskaya, G V Chel'tsova, E I Klabunovskii, et al. *Izv. Akad. Nauk SSSR, Ser. Khim.* (5) 1082 (1980)
97. V A Pavlov, E N Rosotskina, E I Karpeiskaya, et al. *Izv. Akad. Nauk SSSR, Ser. Khim.* (5) 1087 (1980)
98. In Kwon Youn, Gyu Kwan Yon, Chwang Siek Pak *Tetrahedron Lett.* **27** 2409 (1986)
99. J M Roper, D P Bauer *Synthesis* (12) 1041 (1983)
100. V M Dixit, V Bhat, A M Trozzolo, et al. *J. Org. Chem.* **44** 4169 (1979)
101. Japanese P. 7 753 832; *Chem. Abs.* **87** 117674 (1977)
102. Tajima Kiyohiko *Chem. Lett.* (3) 279 (1977)
103. M Goodman, C B Glaser *J. Org. Chem.* **35** 1954 (1970)
104. P Kumar, A K Mukerjee *Synthesis* (9) 726 (1979)
105. L N Kaigorodova, E S Levitina, E I Karpeiskaya, et al. *Izv. Akad. Nauk SSSR, Ser. Khim.* (4) 813 (1984)
106. R M Ali, N H Khan *Synth. Commun.* **8** 497 (1978)
107. N K Kochetkov, R M Khomutov, E I Budovskii, et al. *Zh. Obshch. Khim.* **29** 4069 (1959)
108. I Lupsa *Rev. Chim. (Bucharest)* **26** 6 (1975)
109. M Bergmann, A Mickeley *Lieb. Ann. Chem.* **458** 44 (1927)
110. M M Botvinik, S M Avaeva, E A Mistryukov *Zh. Obshch. Khim.* **23** 971 (1953)
111. M Bergmann, A Mickeley *Lieb. Ann. Chem.* **458** 40 (1927)
112. J De Jersey, B Zerner *Biochemistry* **8** 1975 (1969)
113. J De Jersey, A K Fihelly, B Zerner *Bioorgan. Chem.* **9** 153 (1980)
114. V O Topuzyan, G P Alebyan, O L Mndzhoyan *Zh. Org. Khim.* **19** 827 (1983)
115. V O Topuzyan, Dzh A Gerasimyan, A S Edilyan, et al. *Khim.-Farm. Zh.* **20** 675 (1986)
116. R G Paronikyan, N S Nesunts, V O Topuzyan, et al. *Tezisy Dokladov VIII Molodezhnoi Konferentsii po Sinteticheskim i Prirodnym Fiziologicheski Aktivnym Soedineniyam* [Abstracts of Reports at the VIIIth Youth Conference on Synthetic and Natural Physiologically Active Compounds (Erevan, 1986)] p. 42
117. N S Nesunts, V O Topuzyan *Tezisy Dokladov X Molodezhnoi Konferentsii po Sinteticheskim i Prirodnym Fiziologicheski Aktivnym Soedineniyam* [Abstracts of Reports at the Xth Youth Conference on Synthetic and Natural Physiologically Active Compounds (Erevan, 1990)] p. 22
118. USSR P. 1 699 996; *Byull. Izobret.* (47) (1991)
119. M S Aleksanyan, A A Karapetyan, Yu T Struchkov, et al. *Arm. Khim. Zh.* **45** 249 (1992)
120. N S Nesunts, V O Topuzyan *Arm. Khim. Zh.* **44** 454 (1991)
121. N S Nesunts, V O Topuzyan *Arm. Khim. Zh.* **45** 156 (1991)
122. K N F Shaw, A McMillan, M D Armstrong *J. Org. Chem.* **21** 601 (1956)
123. W Ried, H G Gebhardtsbauer *Chem. Ber.* **89** 2933 (1956)
124. J P Lambooy *J. Am. Chem. Soc.* **76** 133 (1954)
125. J P Lambooy *J. Am. Chem. Soc.* **71** 3758 (1949)
126. D H Mariann, P B Russel, A R Todd *Biochem. J.* **45** 544 (1949)
127. P Kumar, A K Mukerjee *Indian J. Chem., Sect. B* **19** 704 (1980)
128. P Kumar, A K Mukerjee *Indian J. Chem., Sect. B* **20** 418 (1981)
129. P K Tripathy, A K Mukerjee *Indian J. Chem., Sect. B* **26** 61 (1987)
130. R Walter, T C Purcell, H Zimmer *J. Heterocycl. Chem.* **3** 235 (1966)
131. US P. 368 9391; *Chem. Abs.* **78** 3585 (1973)
132. J Svete, Z Cadez, B Stanovnik, et al. *Synthesis* (1) 70 (1990)
133. Polish P. 86 403; *Chem. Abs.* **91** 21107 (1979)
134. M Bukowska-Strzyzewska, W Wieczorek, Z J Kaminski, et al. *Proc. Eur. Pept. Symp., XVIII* (1984), p. 607; *Chem. Abs.* **103** 88 186 (1985)
135. M T Leplawy, A Olwa *Pol. J. Chem.* **53** 353 (1979)
136. BRD P. 117 678; *Chem. Abs.* **85** 177 510 (1976)
137. J M Riordan, C H Stammer *Tetrahedron Lett.* **17** 1247 (1976)
138. N Baumann, M-T Sung, E F Ullman *J. Am. Chem. Soc.* **90** 4157 (1968)
139. E F Ullman, N Baumann *J. Am. Chem. Soc.* **92** 5892 (1970)
140. J H Jones, M J Witty *J. Chem. Soc., Perkin Trans. 1* 858 (1980)
141. D Obrecht, H Heimgartner *Tetrahedron Lett.* **25** 1717 (1984)
142. D Obrecht, H Heimgartner *Tetrahedron Lett.* **24** 1921 (1983)
143. D Obrecht, H Heimgartner *Helv. Chim. Acta* **70** 329 (1987)

Russian Chemical Reviews **62** (1) 65–86 (1993) Russian Academy of Sciences and Turpion Ltd

UDC 543.87:577.113.4

Oxidative degradation of nucleic acids

D G Knorre, O S Fedorova, E I Frolova

Contents

I. Introduction 65
II. Activated oxygen species 65
III. Oxidation of the heterocycles in nucleic acids 68
IV. Oxidation of the carbohydrate fragments in nucleic acids 75
V. Conclusion 84

Abstract. The chemical mechanisms of the oxidative degradation of nucleic acids are surveyed and described systematically. The bibliography includes 141 references.

I. Introduction

The oxidative degradation of nucleic acids, induced by active forms of oxygen, is of interest from several points of view.

Firstly, in aerobic organisms biochemical processes and various physical and chemical influences (ionising radiation, UV light, etc.) result in the formation of free radicals and activated oxygen species: the superoxide radical-ion $O_2^{\cdot-}$), hydrogen peroxide (H_2O_2), and the free hydroxyl radical ($^{\cdot}OH$).[1–4] The damage to DNA induced by them plays an important role in mutagenic, carcinogenic, ageing, and other processes.

Secondly, many oxygen-dependent antitumour preparations (bleomycin) and low-molecular-weight complexes of variable-valence metal ions (Cu-1,10-phenanthroline, Fe-EDTA, Fe- and Mn-porphyrins, etc.) catalyse effectively the cleavage of nucleic acids with participation of active forms of oxygen.[5–9]

Thirdly, investigators have devoted increasing attention recently to designing synthetic molecules capable of binding specifically to DNA and cleaving the sugar phosphate skeleton like natural antibiotics of the type of bleomycin. Such compounds might find applications in the creation of the so called "chemical restrictases", i.e. reagents which, like restriction endonucleases, cleave nucleic acids in the vicinity of definite sequences, and of chemotherapeutic preparations which cause selective damage to nucleic acids.[10]

D G Knorre, O S Fedorova, E I Frolova Novosibirsk Institute of Bioorganic Chemistry, Siberian Division of the Russian Academy of Sciences, prosp. akad. Lavrent'eva 8, 630090 Novosibirsk, Fax (7-383-2) 35 16 65

Received 15 August 1992
Uspekhi Khimii **62** (1) 70–91 (1993); translated by A K Grzybowski

II. Activated oxygen species

Molecular oxygen is a four-electron oxidant and its stepwise reduction to water may be represented schematically as follows:[11–13]

$$E^0_{O_2/O_2^{\cdot-}} = -0.16\,V;\quad E^0_{HO_2^{\cdot}/HO_2^-} = 0.74\,V;$$

$$E^0_{HO^{\cdot}/HO^-} = 1.9\,V;$$

$$E^0_{O_2/HO_2^{\cdot}} = 0.13\,V;\quad E^0_{HO_2^{\cdot}/H_2O_2} = 1.43\,V;$$

$$O_2 \xrightarrow{e^-,H^+} HO_2^{\cdot}(H^+ + O_2^{\cdot-}) \xrightarrow{e^-,H^+} H_2O_2(H^+ + HO_2^-) \xrightarrow{e^-} HO^{\cdot} + OH^-$$

$$(E^0)'' = 0.3\ V \qquad e^-, H^+$$

$$(E^0)' = 0.815\ V \qquad 2H_2O$$

In reduction to both H_2O and to H_2O_2, molecular oxygen in aqueous solution is a powerful oxidant—the values of $(E^0)'$ are respectively 0.815 and 0.3 V. However, direct oxidation by oxygen, both two-electron and four-electron oxidation, hardly occurs. This is associated primarily with the fact that the O_2 molecule has a triplet ground state whereas the majority of organic substrates and their oxidation products have singlet ground states. The direct reaction of triplet O_2 with the substrate molecule is therefore spin-forbidden.

Several ways of overcoming this limitation are known: (1) successive one-electron reduction of the oxygen molecule to H_2O in conformity with a scheme such that each individual elementary reaction is spin-allowed; (2) activation of oxygen by enzymes or by the formation of complexes with transition metal ions; (3) transition of O_2 molecules to the excited singlet state.

The successive one-electron reduction of O_2 can be most simply achieved using variable-valence metal ions. Iron and copper ions are usually employed for this purpose. The process can be described by the following scheme:

$$M^{(n-1)+} + O_2 \rightarrow M^{n+} + O_2^{\cdot-}(HO_2^{\cdot}) \quad (1)$$

$$M^{(n-1)+} + O_2^{\cdot-}(HO_2^{\cdot}) \rightarrow M^{n+} + HO_2^-(H_2O_2) \quad (2)$$

$$M^{(n-1)+} + H_2O_2 \rightarrow M^{n+} + HO^{\cdot} + OH^- \quad (3)$$

$$M^{(n-1)+} + HO^{\cdot} \rightarrow M^{n+} + OH^- \quad (4)$$

The involvement of the metal ion is particularly significant in the first stage, because the reduction of O_2 to $O_2^{\cdot-}$ is characterised by a low oxidation–reduction potential $E^0 = -0.16$ V, i.e. is thermodynamically unfavourable.[11] Since the use of small amounts of metal ions is preferable, the occurrence of these reactions requires the presence of a coupled, readily oxidisable substrate H_2A (ascorbic acid, thiols, etc.) for the reduction of the metal ion to the lowest oxidation state:

$$M^{n+} + H_2A \text{ (or } HA^{\cdot}) \rightarrow M^{(n-1)+} + HA^{\cdot} \text{ (or } A + H^+) \quad (5)$$

Reaction (1) is reversible and $M^{(n-1)+}$ can be partly regenerated by the reaction

$$M^{n+} + O_2^{\cdot-} \rightarrow M^{(n-1)+} + O_2 \quad (6)$$

The rate constants for the competing reactions (2) and (6) are as a rule similar and are determined to a large extent[14] by the values of E^0 for the $M^{n+}/M^{(n-1)+}$ couple. Apart from reaction (2), the superoxide radical can be converted into hydrogen peroxide also via the disproportionation reaction (7) or via a reaction with an auxiliary reductant [reaction (8)]:

$$2O_2^{\cdot-} + 2H^+ \rightarrow O_2 + H_2O_2 \quad (7)$$

$$O_2^{\cdot-}(HO_2^{\cdot}) + H_2A \rightarrow HO_2^-(H_2O_2) + HA^{\cdot} \quad (8)$$

The hydrogen peroxide formed subsequently enters into reaction (5). The OH radical is the strongest oxidant among all the oxygen species examined and not only can it be reduced by metal ions [reaction (4)] but it can also accept an electron or can abstract a hydrogen atom from many organic substrates:

$$HO^{\cdot} + HX \rightarrow OH^- + H^+ + X^{\cdot} \quad (9)$$

Molecular oxygen reduction processes with participation of variable-valence metal ions have been described in greater detail in various other reviews, for example, those of Aust et al.[15] and Halliwell and Gutteridge.[16]

The one- and two-electron reduction of molecular oxygen in living organisms takes place in the course of various biochemical processes.[4] The formation of the superoxide radical is catalysed by the majority of NAD(P)H-dependent oxidases functioning within the composition of membrane complexes[17] and by flavin-dependent oxidases such as xanthine oxidase.[18] In the normal functioning of the mitochondrial respiratory chain, $O_2^{\cdot-}$ is formed in small amounts, but under the conditions of various disturbances in the operation of mitochondria the generation of $O_2^{\cdot-}$ as well as other active oxygen species increases sharply.[19]

Oxygen can be reduced to $O_2^{\cdot-}$ also by certain long-lived organic radicals (for example, semiquinone radicals) formed in the enzymic or photochemical reduction of anthraquinone antibiotics, riboflavin, and certain other compounds.[20]

Hydrogen peroxide can be formed via the disproportionation reaction (7), which can be both spontaneous or can be catalysed by special enzymes—superoxide dismutases. The direct enzymic reduction of O_2 to H_2O_2 without the intermediate formation of $O_2^{\cdot-}$ is characteristic of metabolic processes occurring in neutrophils and peroxisomes[21] and occurs, for example, in reactions catalysed by aminooxidases.[22]

The generation of hydroxyl radicals *in vivo* is apparently due primarily to the reduction of O_2 or H_2O_2 by transition metal ions.[6, 23, 24]

Active oxygen species are also formed under various external influences on living organisms, for example when the latter are acted upon by ionising radiation. The radiolysis of water[25–27] results in the formation of the following products:[27]

$H_2O \rightarrow$	$HO^{\cdot}$,	e_{aq}^-,	$H^{\cdot}$,	H_2O_2,	H_2	$H^+(H_3O^+)$
G	2.7	2.7	0.55	0.7	0.45	2.7

where G is the radiation-chemical yield (in dilute solutions) equal to the number of species formed per 100 eV of absorbed energy.

In aerated aqueous solutions, the solvated electron e_{aq}^- and $H^{\cdot}$ interact very rapidly with O_2, affording the superoxide radicals $O_2^{\cdot-}$ or $HO_2^{\cdot}$. Both H_2O_2 and $O_2^{\cdot-}$ can be reduced subsequently by the transition metal ions to OH radicals.

As a result of all these factors, the principal species in aerated solutions responsible for the oxidation of various substrates under the action of ionising radiation are OH radicals (>90%). In the study of reactions with participation of OH radicals, solutions are radiolysed in the presence of nitrous oxide N_2O, which promotes the conversion of e_{aq}^- into the OH radical.

Among the intermediates in the reduction of O_2 examined, OH radicals play the main role in the oxidative degradation of DNA. Under physiological conditions, the superoxide radical-ion is incapable of oxidising organic substrates. With the use of various systems for the generation of $O_2^{\cdot-}$, it has been shown that[28] it does not participate in the oxidative degradation of nucleic acids. Likewise H_2O_2 does not oxidise DNA under physiological conditions.[29–32] However, the introduction into the same systems of transition metal ions, which catalyse the reduction to the OH radicals of both the superoxide radical-ion and hydrogen peroxide via reactions (2), (3), and (7), leads to the degradation of nucleic acids.[28–30]

The OH radical is a powerful oxidant and is highly reactive. Under physiological conditions, it is able to abstract the hydrogen atom from the C–H bonds [reaction (10)] or it adds to unsaturated C=C double bonds [reaction (11)]:

$$R\text{-}H + \dot{O}H \longrightarrow \dot{R} + H_2O \quad (10)$$

$$\text{>C=C<} + \dot{O}H \longrightarrow \text{>}\dot{C}\text{–}C(OH)\text{<} \quad (11)$$

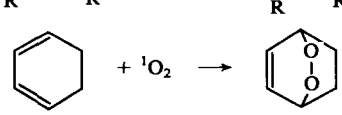
The rates of addition to the double bonds are usually higher than the rates of abstraction of the hydrogen atom from C–H bonds.[33]

The OH radicals interact with nucleic acids and model compounds such as nucleosides and nucleotides, the rate constant for the corresponding reactions being close to the diffusion-controlled values (Table 1).[25, 26, 33]

The dominant processes are addition to the double bonds of the heterocycles and the abstraction of hydrogen atoms from the C–H bonds of the pentose with formation of the corresponding free radicals. In aerated solutions, these radicals interact rapidly with oxygen O_2 to form peroxyl radicals. The subsequent reactions, leading ultimately to the modification of the heterocycles or to the cleavage of the pentose phosphate skeleton, will be examined in the later sections of this review.

Singlet oxygen can be formed as a result of photosensitisation and also as a side product in many biological oxidation processes.[34] Despite its considerable reactivity, singlet oxygen cannot react with alkanes and many aromatic systems. Interaction with alkenes to form allyl peroxides [reaction (12)] or endoperoxides [reaction (13)] is most characteristic of this species:[35]

$$R\text{–}C(R)=C(CHR_2)\text{–}R + {}^1O_2 \longrightarrow R\text{–}C(R)(OOH)\text{–}C(CR_2)\text{–}R \quad (12)$$



(13)

It has been shown that singlet oxygen does not oxidise the sugar phosphate skeleton in nucleic acids,[36, 37] but does react selectively with guanine residues, forming as a result modified fragments in which the sugar phosphate skeleton may be cleaved on treatment under alkaline conditions.[28]

The reduction of oxygen by variable-valence metal ions can occur with preliminary coordination of O_2 or species corresponding to its partial reduction. This results in the formation of oxo-complexes of metals, which are in high-valence states (Fe or Mn in the +4 or +5 oxidation states, Cu in the +3 state, etc.).[38] Such complexes can behave directly as oxidants or can generate OH radicals with transition of the metal to a lower oxidation state. The latter version has been postulated, for example, for the Fe·ATP complexes:[39]

$$Fe^{II} \cdot ATP + H_2O_2 \rightarrow \overset{O}{\underset{\|}{Fe^{IV}}} \cdot ATP + H_2O \quad (14)$$

$$\overset{O}{\underset{\|}{Fe^{IV}}} \cdot ATP + H^+ \rightarrow Fe^{III} \cdot ATP + {}^{\cdot}OH \quad (15)$$

Such oxo-complexes have been isolated and characterised by various chemical and physical methods for iron-porphyrins.[40-46] It has been shown that they can be obtained by the two-electron oxidation of iron(III)-porphyrins by peracids, hydroperoxides, or iodosobenzene (Por = porphyrin):

$$Fe^{III} \cdot Por + PhIO \rightarrow \overset{O}{\underset{\|}{Fe^{IV}}} \cdot Por^{\cdot +} + PhI$$

(RCO$_3$H, ROOH) (RCOOH, ROH)

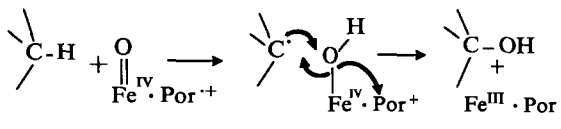
The structure of the oxo-complex containing iron in the +4 oxidation state and a porphyrin radical-cation stabilised by delocalisation in the π-system of the macrocycle has been generally accepted for iron-porphyrins.[42, 46]

The formation of high-valence metal oxo-species has been observed also for the porphyrin complexes of other transition metals. However, in the manganese and chromium complexes[47] the macrocyclic ligand does not participate in the oxidation and the metal is in the +5 oxidation state:

$$Mn^{III} \cdot Por + PhIO \rightarrow \overset{O}{\|}Mn^{V} \cdot Por + PhI$$

(RCO$_3$H, ROOH) (RCOOH, ROH)

Such oxo-complexes of high-valence metals are apparently weaker oxidants than OH radicals.[48] The following types of reactions are characteristic of them: the insertion of an oxygen atom in C–H bonds (hydroxylation) or addition to C=C bonds (epoxidation). It is believed that the first stage of the hydroxylation of alkanes involves the abstraction of the H atom from a C–H bond with subsequent transfer of the OH radical from the oxo-complex to the alkyl radical via the following mechanism:[49-51]

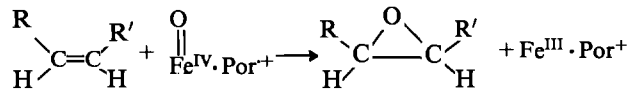


The selectivity of the reaction is achieved mainly as a result of the orientation of the oxygen atom in the complex relative to particular C–H bonds in the molecule being oxidised.[52] The hydroxylation of aldehydes with formation of carboxylic acids takes place in accordance with the same mechanisms.[53, 54]

Table 1. Rate constants for the reactions of OH radicals with nucleic acids and their components under neutral conditions.

Component	10^9 k/litre mol^{-1} s^{-1}
Heterocycles	
Thymine	5.6
Cytosine	4.7
Uracil	5.2
Adenine	4.4
Pentoses	
Ribose	1.6
Ribose-5′-phosphate	1.3
Nucleosides	
Thymidine	4.8
Cytidine	4.8
Uridine	4.3
Adenosine	4.0
Nucleotides	
TMP	5.3
CMP	4.5
dCMP	4.4
AMP	3.0
dAMP	3.5
dGMP	5.0
Polynucleotides	
poly (C)	1.2
poly (U)	1.25
poly (A)	0.9
poly (U+A)	0.5
DNA	0.3–0.8

The epoxidation of alkenes is achieved by the insertion of an oxygen atom in the C=C double bond:[47]



The oxidative degradation of DNA constitutes the basis of the action of the group of antibiotics of the class of bleomycin (Blm). It has been suggested[7, 55-56] that species of the type Blm·Fe^{V}=O participate in this process.

The hydrogen peroxide–Cu-1,10-phenanthroline complex system has found extensive applications in the oxidative degradation of DNA. There are two points of view on the mechanism of the oxidative cleavage of DNA in this system. According to one of them, a species bound to the metal and equivalent to the OH radical is responsible for the oxidation.[57, 58] According to the other, more widely adopted point of view, the Cu-1,10-phenanthroline complex is bound to DNA and interacts with H_2O_2 in the presence of reductants, generating OH radicals[8, 59, 60] via a mechanism analogous to that described by reactions (14) and (15) for the Fe·ATP complexes.[39] As a result, both free OH radicals and such radicals bound to the metal function in the system.

Thus, summarising all the factors described above, one may say that the free hydroxyl radicals, which are the products of the three-electron reduction of molecular oxygen, and, in certain systems, coordinated oxygen species in the form of oxo-complexes of metals in the highest oxidation states are primarily responsible for the degradation of nucleic acids under various oxidative conditions.

III. Oxidation of the heterocycles in nucleic acids

The oxidative modification of nucleic acid heterocycles by hydroxyl radicals has been studied in greatest detail under the conditions of γ-radiolysis, because this method of generation of OH radicals makes it possible to eliminate the involvement of other active species. These studies led to the isolation of a large number of products of the modification of the heterocycles and the mechanisms of the formation of some of them have been established. These investigations were carried out mainly on the free heterocycles and nucleosides. Further studies on nucleic acids showed that the data obtained on model compounds can be to a large extent transferred to the oxidation of polymeric molecules. The greatest progress has been achieved in the study of the oxidation of pyrimidine heterocycles.[25, 26, 61]

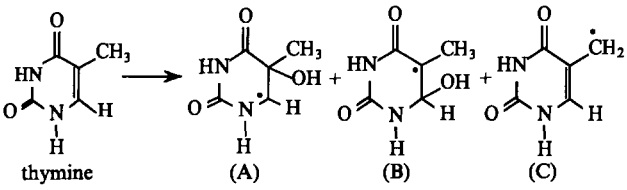
1. Anaerobic oxidation of pyrimidine heterocycles

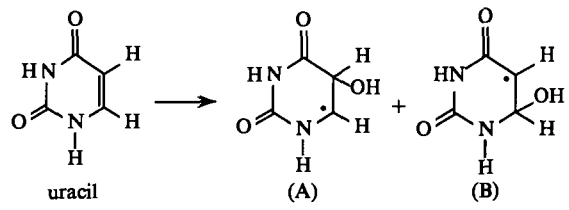
Hydroxyl radicals are electrophiles and attack preferentially sites with a high electron density, forming free radicals derived from the heterocycles. The structures of these radicals have been largely characterised on the basis of the structures of the products formed on γ-radiolysis in the presence of spin trapping agents—2-methyl-2-nitrosopropane or α-(1-hydroxy-4-pyridyl)-*N*-*tert*-butyl nitrone.[62-66] It was established that, as a result of the reaction with pyrimidines, the OH radicals add to the C(5) or C(6) carbon atoms, forming type (A) and type (B) radicals, while for thymine the abstraction of a H atom from the methyl group at the C(5) atom with formation of a type (C) radical is also observed.

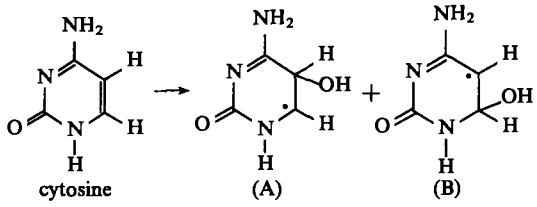
The three types of free radicals formed differ in their oxidation–reduction properties. The type (A) radicals, which are α-aminoalkyl derivatives, have the properties of reductants and can be determined quantitatively by reaction with oxidants such as benzoquinone, tetranitromethane, and tetracyanoferrate(III). The type (C) radical of thymine is also a reductant, although a weaker one, but it can be determined by reactions with strong oxidants. On the other hand, the type (B) radicals have oxidising properties by virtue of the presence of the mesomeric form—the oxyl radical—and can be determined with the aid of reductants such as *N,N,N′,N′*-tetramethylphenylenediamine and ascorbic acid. Such differences in the oxidation–reduction properties of the radicals formed made it possible to devise a method for their quantitative determination based on pulse radiolysis in the presence of the corresponding oxidants and reductants with the subsequent determination of their consumption.[67] It has been established with the aid of this method[68-70] that the preferential addition of the OH radicals to the C(5) position in the heterocycles is characteristic of all pyrimidines: to the extent of 87% for cytosine, 80% for uracil, and 56% for thymine. This is due to the greater electron density on the C(5) carbon atom. Only 10% of the OH radicals add to C(6) in the case of cytosine, 20% for uracil, and 35% for thymine. Less than 9% of the OH radicals participate in the abstraction of a hydrogen atom from the methyl group of thymine (Table 2).

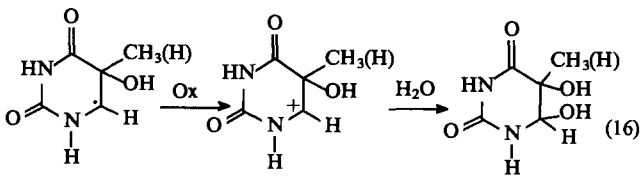
In the oxidation of type (A) radicals of thymine or uracil, the carbonium ion **1** is formed, the rapid solvolysis of which leads to the quantitative formation of glycols, namely the *cis*- or *trans*-form of 5,6-dihydroxy-5,6-dihydrothymine **2** or 5,6-dihydroxy-5,6-dihydroxyuracil **3**, by the following reaction:

The equality of the amount of type (A) radicals, estimated by the method of pulse radiolysis, and of the amount of the corresponding thymine or cytosine glycols, isolated chromatographically (Table 2), permitted the conclusion that the pyrimidine glycols are formed exclusively by the reaction involving the oxidation of type (A) radicals [reaction (16)].[68]







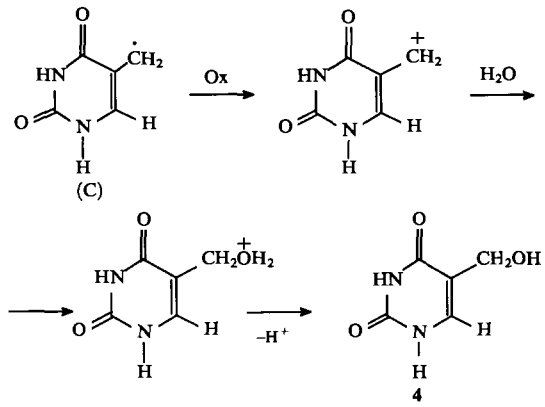


(16)

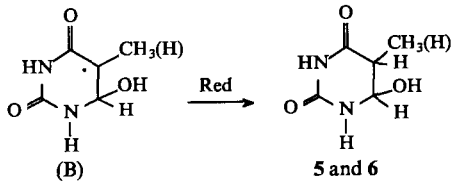
Table 2. The yields and oxidation-reduction properties of free radicals of the pyrimidines formed on reaction with hydroxyl radicals.[67-69]

Heterocycle	Radical	Oxidation–reduction properties	Yield/(%[OH])	
			pulse radiolysis	analysis of products
Thymine	(A)	reductant	56	57
	(B)	oxidant	35	–
	(C)	weak reductant	9	–
Uracil	(A)	reductant	80	77
	(B)	oxidant	20	–
Cytosine	(A)	reductant	87	–
	(B)	oxidant	10	–

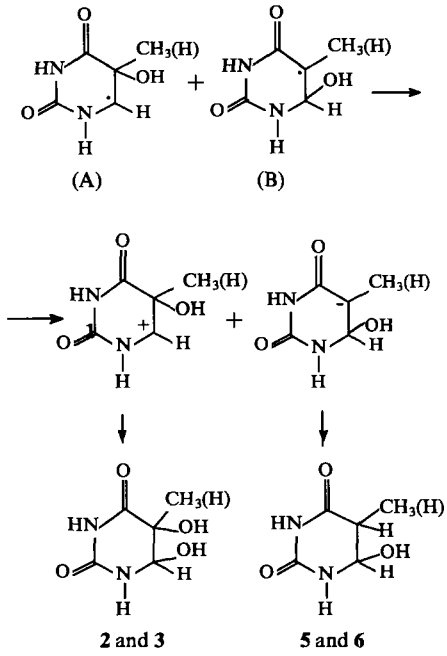
The oxidation of the type (C) thymine radical leads to the formation of 5-hydroxymethyluracil **4**.[71, 72]



The reduction of the type (B) thymine or uracil radicals leads to the formation of 6-hydroxy-5,6-dihydrothymine **5** or 6-hydroxy-5,6-dihydrouracil **6** respectively:

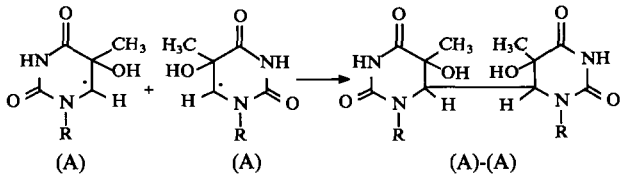


Since the oxidation–reduction properties of the radicals differ, it follows that, in the absence of exogenic oxidants or reductants, a type (A) radical may be oxidised by type (B) radicals to a carbonium ion with the subsequent formation of the glycols **2** or **3** and the 6-hydroxy-derivatives **5** or **6**.



Under these conditions, the yield of glycols is appreciably lower and amounts to one third of the yield of type (B) radicals, which are consumed also in the dimer formation reaction. The dimerisation reaction is likewise characteristic of other types of radicals [type (A) and type (C) radicals]:[73]

(B) + (B) → dimer (B),
(A) + (A) → dimer (A),
(C) + (C) → dimer (C),



The cytosine radicals behave similarly.[68] The *cis*- and *trans*-glycols of cytosine **7**, C–C cytosine dimers, 5-hydroxycytosine **8**, and, to a lesser extent, 6-hydroxycytosine **9** are formed in the course of further reactions of the cytosine radicals. Furthermore, the deamination of cytosine is observed, which results in the formation of uracil and the uracil glycols **3**.

Thus the main products of the oxidation of pyrimidines are glycols, hydroxyhydrates, and dimers, while in the oxidation of thymine 5-hydroxymethyluracil is also formed. The formation of these products in the γ-radiolysis of deaerated solutions of pyrimidines has been noted in studies by different investigators, although with some differences in their estimated amounts (Tables 3–5).[74–80]

Apart from these products, the radiolysis of pyrimidines in deaerated solutions (particularly for high doses) involves the formation of various urea derivatives: N^1-formyl-N^2-pyruvylurea **10**, *N*-formylurea **11**, and urea **12**. Their formation can be accounted for by the further oxidative degradation of the glycols.[78]

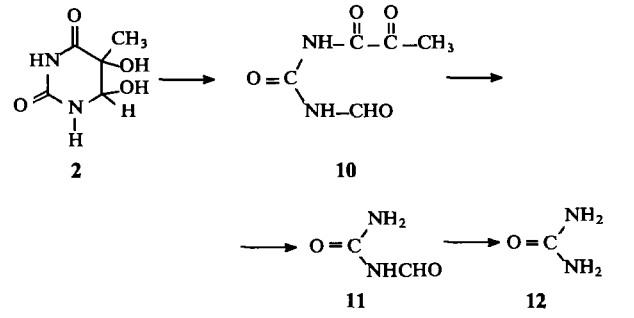


Table 3. The products of the γ-radiolysis of thymine in N_2O-saturated aqueous solutions.

Product	G[79]	G[25]
cis-5,6-Dihydroxy-5,6-dihydrothymine	1.45	–
trans-5,6-Dihydroxy-5,6-dihydrothymine	0.81	0.32
5-Hydroxy-5,6-dihydrothymine	–	0.08
6-Hydroxy-5,6-dihydrothymine	0.13	0.10
5-Hydroxymethyluracil	0.22	0.27
5-Hydroxy-5-methylbarbituric acid	0.11	–
N^1-Formyl-N^2-pyruvylurea	0.12	0.14
Urea	0.19	–
Dimers	0.26	–
Degradation of thymine	3.9	2.71

Table 4. The products of the γ-radiolysis of uracil in N_2O-saturated aqueous solutions.

Product	G^{75}		G^{76}		
	pH 5	pH 8.1	pH 4	pH 6	pH 8
cis-5,6-Dihydroxyl-5,6-dihydrouracil	0.2	0.4	0.32	0.30	0.18
trans-5,6-Dihydroxy-5,6-dehydrouracil	0.5	0.4			
6-Hydroxy-5,6-dihydrouracil	0.5	0.3	–	–	–
Isobarbituric acid	0.1	0.1	0.44	0.29	0.18
N^1-Formylurea	–	–	0.12	0.52	0.16
Dimers	3.1	0.7	3.30	4.38	1.60
Dehydration of uracil	4.4	1.9	4.25	5.51	2.11

2. Aerobic oxidation of pyrimidine heterocycles

Under aerobic conditions, the type (A), (B), and (C) radicals combine with oxygen, the reaction having a diffusion-controlled rate constant ($k \approx 2 \times 10^9$ litre mol^{-1} s^{-1}), forming the corresponding peroxyl radicals [reaction (17)], the decomposition of which leads to the formation of stable products.[25, 26]

Studies carried out in recent years on simple model compounds made it possible to formulate general principles governing the decomposition of organic peroxy-radicals.[25, 26] It usually takes place via a bimolecular mechanism with formation of a short-lived intermediate—a tetroxide, which can redissociate at low temperatures into two peroxy-radicals, while at room temperature it decomposes rapidly to stable products. The number of reactions involved in the decomposition of the tetroxide is small. Four main processes have been distinguished:

(1) the formation of an alcohol molecule, a carbonyl compound, and an oxygen molecule [reaction (18)]—Russell's concerted mechanism;

(2) the formation of two molecules of a carbonyl compound and a H_2O_2 molecule [reaction (19)];

(3) dissociation into two molecules of a carbonyl compound with a carbon atom having a lower degree of substitution, one oxygen molecule, and two alkyl radicals, which recombine with O_2 to form peroxy-radicals [reaction (20)];

(4) the products of all these reactions can be obtained also via a free-radical pathway through the formation of alkoxyl radicals [reaction (21)].

Tertiary peroxyl radicals do not undergo concerted decomposition via reactions of type (18)–(20), but do decompose via reaction (21), forming O_2 and tertiary alkoxyl radicals, which rapidly undergo β-elimination:

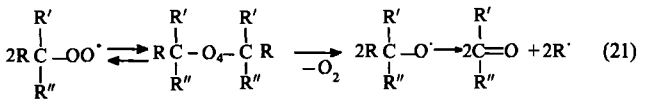
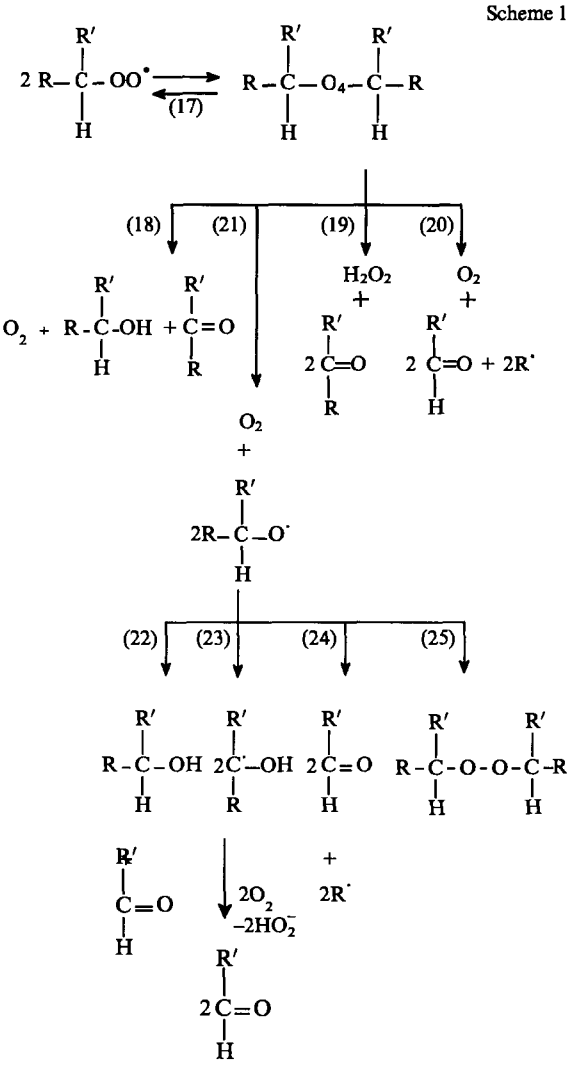


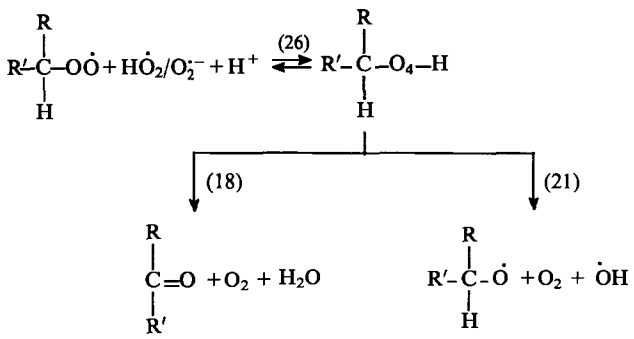
Table 5. The products of the γ-radiolysis of cytosine in N_2O-saturated aqueous solutions.

Product	G
cis-5,6-Dihydroxy-5,6-dihydrocytosine *trans*-5,6-Dihydroxy-5,6-dihydrocytosine	0.05
cis-5,6-Dihydroxy-5,6-dihydrouracil *trans*-5,6-Dihydroxy-5,6-dihydrouracil	0.15
6-Hydroxycytosine	0.07
5-Hydroxycytosine	1.4
5^6-Dihydroxycytosine	0.2
Dimers	3.2
Uracil	0.02

Scheme 1

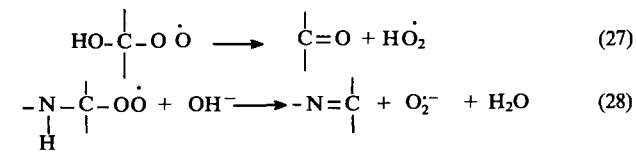


The rates of reaction of various peroxyl radicals, leading to the formation of tetroxides, differ greatly. Certain peroxyl radicals interact with rate constants close to the diffusion-controlled values, whilst others, particularly tertiary peroxyl radicals can have rate constants several orders of magnitude smaller.[33] However, usually more than one type of peroxyl radical is formed and tertiary peroxyl radicals, which interact with one another very slowly, are involved in reactions with primary or secondary peroxyl radicals. A similar situation occurs also with superoxide radical-ions. Owing to their comparatively low rate of disproportionation, they probably interact with other peroxyl radicals present [reaction (26)].



The resulting hydrotetroxide can decompose to an alkoxyl radical, molecular oxygen, and a OH radical via a reaction of type (21) or to a carbonyl compound, molecular oxygen, and water via a reaction of type (18).

If the peroxyl radical contains a OH or NH group in the α-position, then there is a possibility in this case of unimolecular decomposition with formation of the superoxide radical-ion. In the presence of the OH substituent, $O_2^{\cdot-}$ is formed spontaneously [reaction (27)], while in the presence of the substituent NH base catalysis is necessary [reaction (28)]:



On the basis of the mechanisms described, one may predict the pathways leading to the formation of the majority of the products identified in the γ-radiolysis of uracil in a N_2O/O_2-saturated aqueous solution (Table 6).

Since the OH radical adds preferentially to the C(5) position in uracil (80%), the main peroxyl radical is 5-hydroxy-6-peroxy-5,6-dihydrouracil **13**. The unimolecular reaction (28), involving the decomposition of the peroxyl radical **13** accompanied by the evolution of O_2 and requiring catalysis by OH^- ions, leads to the formation of 5-hydroxyisouracil **14** which can afford the *cis*- or *trans*-glycol **3** on interaction with H_2O and at pH 7 it can rearrange to isobarbituric acid **15**. In conformity with the foregoing, four mechanisms are possible for the bimolecular reaction (17) involving the decomposition of the peroxy-radical **13**. The first [mechanism (18)] leads to the formation of the *cis*- or *trans*-glycol **3** and dialuric acid **16** and is accompanied by the evolution of O_2. Two molecules of dialuric acid **16** and H_2O_2 are obtained via the second pathway [mechanism (19)]. In the third case [mechanism (20)], the C(5)–C(6) bond is ruptured

Scheme 2

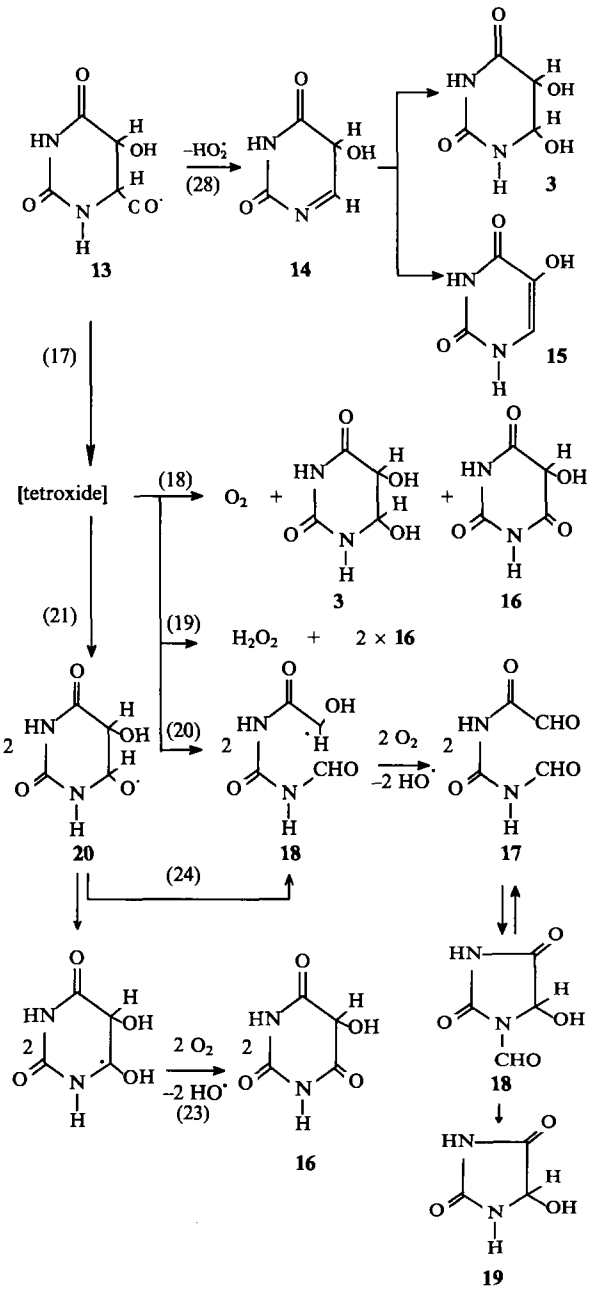


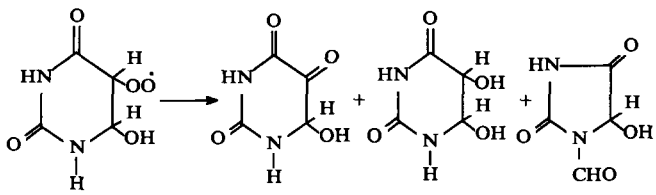
Table 6. The products of the γ-radiolysis of uracil in N_2O/O_2-saturated aqueous solutions.

Product	G^{82}		G^{81}	
	pH 6.0	pH 3.0	pH 6.5	pH 10
cis-5,6-Dihydroxy-5,6-dihydrouracil	0.42	0.6	0.9	1.4
trans-5,6-Dihydroxy-5,6-dihydrouracil	0.62	0.5	1.1	1.0
Isobarbituric acid	0.10	0	0.2	1.2
N^1-Formyl-N^2-glyoxylurea	0.72	–	–	–
N^1-Formyl-5-hydroxyhydantoin	–	1.6	1.4	0.2
5-Hydroxyhydantoin	0.18	0.4	0.4	0.3
Dialuric acid	–	0.9	0.4	0.2
Isodialuric acid	–	0.1	0.2	0.1
Alloxan	0.06	–	–	–
N^1-Formylurea	0.27	–	–	–
Urea	0.02	–	–	–
Oxalic acid and its ureides	0.13	–	–	–
Degradation of uracil	2.49	4.9	5.3	5.2

and the radical formed recombines with a O_2 molecule and, after the formation of HO_2^-, N^1-formyl-N^2-glyoxylurea **17** or its cyclic isomer N^1-formyl-5-hydroxyhydantoin **18** is produced. The latter readily loses the formaldehyde group and is converted into 5-hydroxyhydantoin **19**. The fourth pathway [mechanism (21)] leads to the formation of two alkoxyl radicals **20**, which are subsequently converted into dialuric acid **16** via pathway (23) or into N^1-formyl-5-hydroxyhydantoin **18** via pathway (24) [Scheme 2].

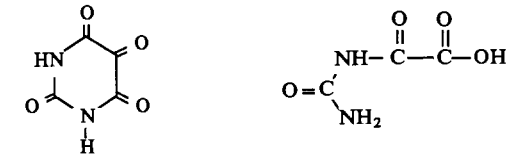
The unimolecular reaction (28) and the bimolecular reaction (17) compete. As shown in Table 6, the composition of the product varies with the pH of the medium and the power of the radiation.[81] At high pH, base catalysis renders the unimolecular reaction preferable, which results in isobarbituric acid (**15**) becoming the main product together with the glycols **3**, while the amount of N^1-formyl-5-hydroxyhydantoin **18** and dialuric acid **16** which are the main products of the bimolecular reaction, diminishes appreciably. At acid pH, there is a sharp change in the proportions of the product involving their inversion: N^1-formyl-5-hydroxyhydantoin and dialuric acid become the main products, while isobarbituric acid is not detected at all.

Evidently, only the bimolecular decomposition reaction is characteristic of the minor 6-hydroxy-5-peroxy-5,6-dihydrouracil **21** peroxyl radical. The main products are in this case the glycols **3** and N^1-formyl-5-hydroxyhydantoin **18**, as for the C(6)-peroxyl radical, and isodialuric acid **22** is formed instead of dialuric acid (Table 6).

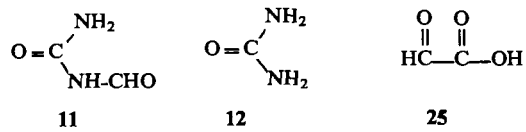


21 **22** **3** **18**

For high irradiation dose rates and doses,[82] alloxan **23**, *N*-formyl-urea **11**, urea **12**, oxalic acid and its ureide **24**, and glyoxalic acid **25** are detected to the products listed above. These compounds are the products of more far-reaching oxidation of uracil and become the main ones for high irradiation doses.



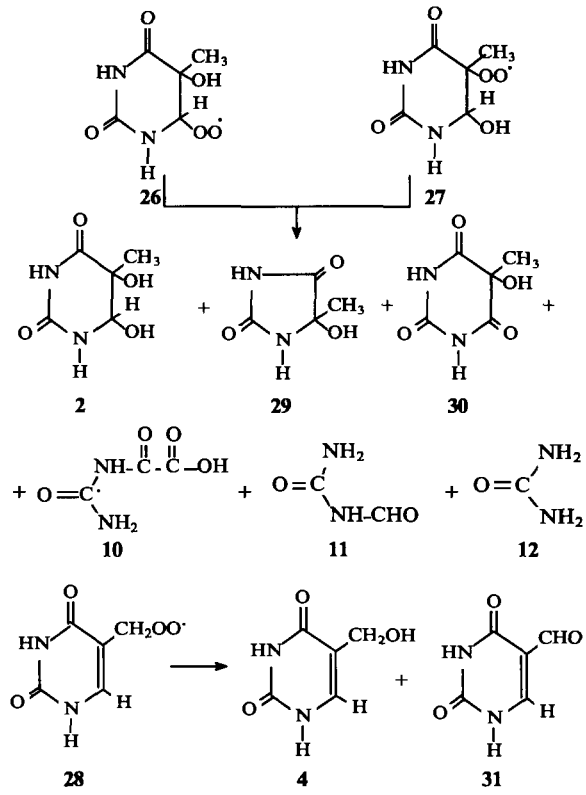
23 **24**



11 **12** **25**

In aerated aqueous thymine solutions, type (A), (B), and (C) radicals combine with O_2 and form respectively three types of peroxyl radicals: 5-hydroxy-6-peroxy-5,6-dihydrothymine **26** and 6-hydroxy-5-peroxy-5,6-dihydrothymine **27**, which are analogous to the uracil peroxyl radicals **13** and **21**, as well as 5-peroxymethyluracil **28**.

Overall, the mechanisms of the decomposition of the peroxyl radicals **26** and **27** do not differ from those described above for uracil peroxyl radicals. Table 7 presents the yields of different products of the anaerobic γ-radiolysis of thymine.[25, 79, 83–85] As in the γ-radiolysis of uracil, the oxidation of thymine entails the formation of the *cis*- and *trans*-glycols of thymine **2**, 5-hydroxy-5-methylhydantoin **29**, 5-hydroxy-5-methylbarbituric acid **30**,



26 **27** **2** **29** **30** **10** **11** **12** **28** **4** **31**

Table 7. The products of the γ-radiolysis of thymine in N_2O/O_2-saturated aqueous solutions.[86]

Product	*G*
cis-6-Hydroperoxy-5-hydroxy-5,6-dihydrothymine	0.3
trans-6-Hydroperoxy-5-hydroxy-5,6-dihydrothymine	0.7
cis-5-Hydroperoxy-6-hydroxy-5,6-dihydrothymine	0.08
trans-5-Hydroperoxy-6-hydroxy-5,6-dihydrothymine	0.17
cis-5,6-Dihydroxy-5,6-dihydrothymine	0.12
trans-5,6-Dihydroxy-5,6-dihydrothymine	0.12
cis-6-Hydroperoxy-5,6-dihydrothymine	0.03
trans-6-Hydroperoxy-5,6-dihydrothymine	0.03
5-Hydroperoxy-5,6-dihydrothymine	0.06
5-Hydroperoxymethyluracil	0.05
5-Hydroxy-5,6-dihydrothymine	0.02
6-Hydroxy-5,6-dihydrothymine	0.01
5-Hydroxymethyluracil	0.02
5-Hydroxy-5-methylhydantoin	0.15
5-Hydroxy-5-methylbarbituric acid	–
N^1-Formyl-N^2-pyruvylurea	0.5
N^2-Formylurea	0.07
Urea	0.08
Degradation of thymine	2.6

N^1-formyl-N^2-pyruvylurea **10**, *N*-formylurea **11**, and urea **12**. The decomposition of 5-peroxymethyluracil **28** leads to two main products: 5-hydroxymethyluracil **4** and 5-formyluracil **31**.

In addition, thymine hydroperoxides, obtained by the reduction of the peroxyl radicals, were isolated and characterised (Table 7).[86] The half-reaction time of the thymine hydroperoxides in aqueous solutions can reach 5 days at 37 °C.[25, 26] Four possible isomeric forms were isolated: the *trans*- and *cis*-forms of 6(5)-hydroxy-5(6)-peroxy-5,6-dihydrothymine and derivatives of type (A) and (B) radicals, the *trans*-isomers of the latter being formed preferentially. Hydroperoxymethyluracil—a derivative of the radical (C)—was also isolated.

Estimation of the products of the γ-radiolysis of cytosine in aerated aqueous solutions showed that 40% of the products isolated are the same as in the radiolysis of uracil (Table 8).[87, 88] This is apparently associated with the fact that the free-radical product formed from cytosine undergoes deamination in one of the first stages of the radiolysis. The free-radical products derived from uracil obtained as a result react via the mechanisms described for them above. The mechanism of the deamination has not yet been finally established.

In the decomposition of the peroxyl radicals derived from cytosine **32** and **33** which have not yet undergone deamination, the main products formed are *trans*-1-carbamoyl-2-oxoimidazolidine-4,5-diol **35** and 4-amino-N^1-formyl-5-hydroxy-2-oxo-Δ^3-imidazoline **36**. Compound **36** is apparently obtained via a mechanism similar to that of the formation of 5-hydroxyhydantoin and is subsequently converted on deamination into parabanic acid **37**. The formation of compound **35** can be explained by the dissociation of the C(4)–C(5) bond with formation of compound **34** which subsequently either cyclises to form compound **35** or undergoes further degradation to the biuret **38**. It is of interest to note that glycols are not formed in the radiolysis of cytosine in the presence of O_2 (Table 8). However, 5-hydroxycytosine, which may be a product of the dehydrogenation of the glycols, has been detected (Scheme 3):

Scheme 3

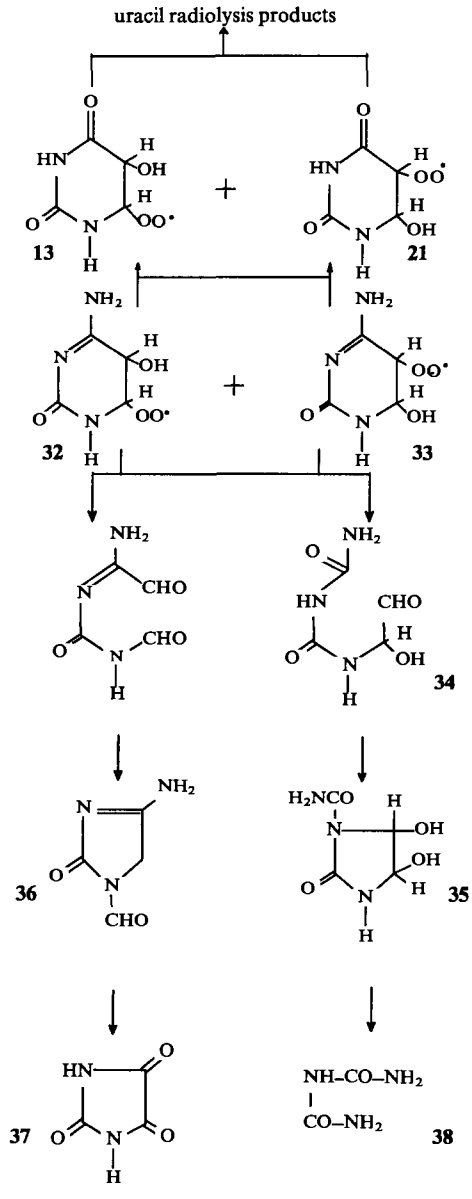


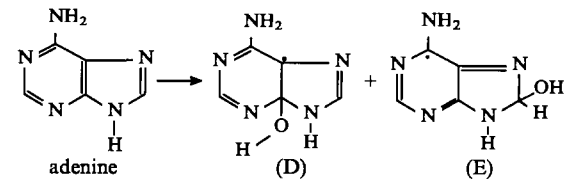
Table 8. The products of the γ-radiolysis of cytosine in N_2O/O_2-saturated aqueous solutions.[87, 88]

Product	*G*
cis-5,6-Dihydroxy-5,6-dihydrouracil	0.03
trans-5,6-Dihjydroxy-5,6-dihyrouracil	0.10
5-Hydroxyhydantoin	0.10
4-Amino-N^1-formyl-5-hydroxy-2-oxo-Δ^3-imidazoline	0.20
trans-1-Carbamoyl-2-oxoimidozilidine-4,5-diol	0.61
N^1-Formylurea	0.06
Parabanic acid	0.03
Biuret	0.06
Oxalic acid and its ureides	0.21
Degradation of cytosine	2.49

3. Oxidation of purine heterocycles

The advances in the study of the oxidation of purines by OH radicals on γ-radiolysis are not quite so considerable. This is because the methods for the investigation of the reactions of OH radicals, which have proved very useful in studies involving pyrimidines, encounter certain difficulties when applied to purine heterocycles. The use of EPR methods in combination with spin-trapping agents did not permit the unambiguous identification of the purine radicals formed on interaction with OH radicals.[89] Pulse radiolysis experiments combined with the study of the oxidation-reduction properties of the radicals obtained yield much information but their interpretation is also difficult. This is associated with the fact that the radicals formed in the reaction between free hydroxyls and purine heterocycles undergo rapid intramolecular rearrangements such as ring opening, dehydration, or dehydrogenation with formation of secondary radicals.

By means of pulse radiolytic methods it has been established[90–93] that, in its reaction with adenine, the OH radical adds preferentially to the C(4) carbon atom of the C(4)=C(5) double bond and to a lesser extent to the C(8) atom of the N(7)=C(8) double bond, forming respectively type (D) and (E)



radicals.

The type (D) radical is a weak oxidant, but as a result of dehydration it is converted into a type (F) radical, which is a powerful oxidant. The amount of radicals (F), determined by reaction with a reductant, was 81% for free adenine (Table 9). The reduction of the radical (F) leads to the formation of the initial adenine, which explains the observed low level of its degradation (30% relative to the amount of OH radicals).[93]

The type (E) radical is a reductant. Its yield, determined by reaction with an oxidant (Methyl Viologen), is 15% (Table 9). The oxidation of the radical (E) leads to the formation of 8-hydroxy-adenine **39**. When the γ-radiolysis was carried out in the presence of the oxidant $Fe(CN)_6^{3-}$, the yield of 8-hydroxyadenine was 18%, which agrees with the amount of the radical (E). However, the intramolecular reaction involving the opening of the imidazole ring with formation of the radical (G), which is an oxidant, is also characteristic of the radical (E). The reduction of the radical (G) leads to the formation of 4,6-diamino-5-formamidopyrimidine **40**.

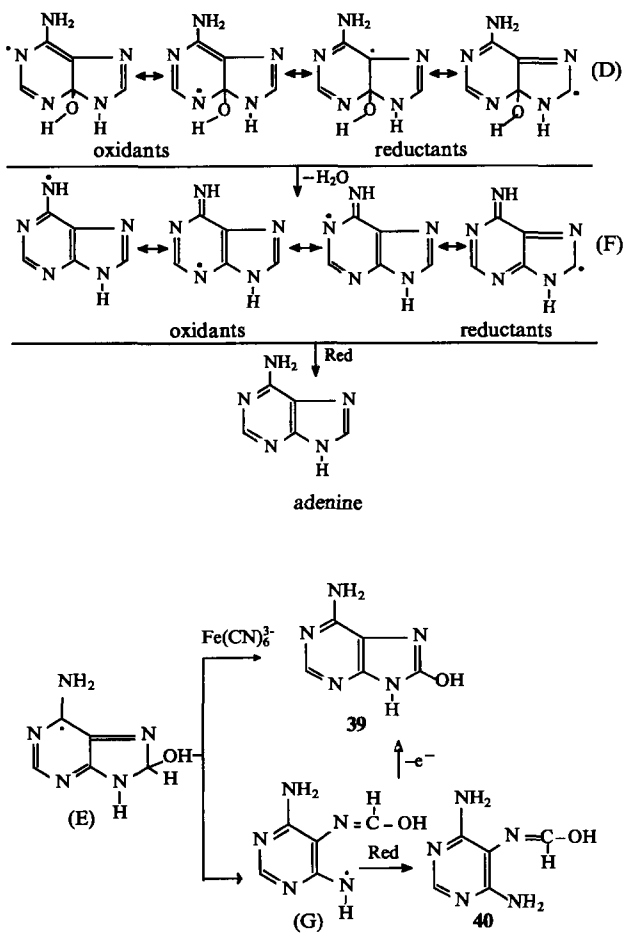
In the absence of exogenic oxidants, the yield of 8-hydroxyadenine **39** exceeds that of the derivative of **40** by a factor of 3. This confirms that the oxidation reaction is the main reaction pathway to the radical (E), which can be oxidised in this instance

Table 9. The yields and oxidation – reduction properties of the free radicals of purines formed by reaction with hydroxyl radicals.

Heterocycle	Radical	Oxidation–reduction properties	Yield, %[OH]$^{-1}$	Method of estimation
Adenine	(D)	oxidant	81	by reaction with TMPD
	(E)	reductant	15	by reaction with MV
	(E)	reductant	18	yield of 8-hydroxyadenine
Guanosine	(D)	oxidant	50	by reaction with TMPD
	(E)	reductant	25	yield of 8-hydroxyguanosine
	(H)	reductant	25	difference between the overall yield of the radicals formed by reaction with MV and the yield of the radical (E)

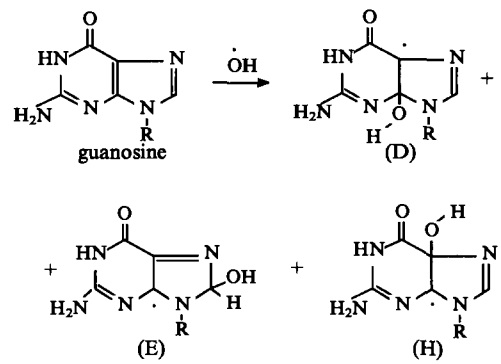
Notation: MV = Methyl Viologen;
TMPD = *N,N,N',N'*-tetramethylphenylenediamine.

by the radical (F) with formation of 8-hydroxyadenine and adenine. Compound **40** is apparently formed only as a result of the disproportionation of the radical (G).

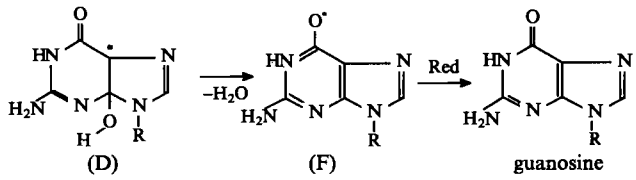


The addition of the OH radical to the C(5) carbon atom of adenine has been detected only in the case of *N*(6)-methyladenine and its contribution does not exceed 10–15%. Further reaction pathways for the radicals formed have not been characterised.

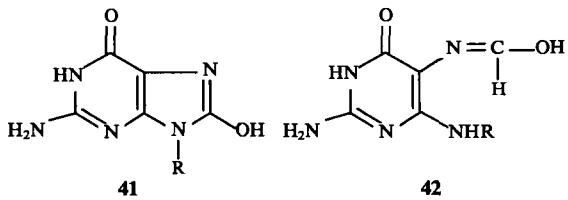
As a result of the interaction of OH radicals with guanosine or its 9-substituted analogues, the formation of approximately equal amounts of radicals of two types has been detected. One of these radicals has oxidising properties and the other has reducing properties (Table 9).[92] As in the case of adenine derivatives, OH radicals add to the C(4), C(8), and also, with appreciable yields, C(5) carbon atoms of guanosine, forming type (D), (E), and (H) radicals respectively:



Like the adenine radical (D), the type (D) guanosine radical is rapidly converted as a result of dehydration into a type (F) radical, which is a powerful oxidant. The yield of the radical (D) was determined by reaction with a powerful reductant and was found to be 50%. The reduction of the radical (F) leads to the formation of the initial guanosine,[93] lowering thereby the overall yield in the degradation of guanosine.



The radicals (E) and (H) have reducing properties. The same reaction pathways as for the adenine radical (E) are characteristic of the type (E) guanosine radical. Its oxidation and the reduction of its radical product (F), in which the imidazole ring has been opened, lead to the formation of 8-hydroxyguanosine **41** and 6-*N*-(2'-deoxy-D-*erythro*-pentofuranosyl)-2,6-diamino-5-formamido-4-hydroxypyrimidine **42** respectively. The amount of the radical (E), estimated from the yield of 8-hydroxyguanosine, was 25% (Table 9). The remaining 25% of radical products derived from guanosine were assumed to comprise a type (H) radical, the subsequent reaction pathways of which have not yet been established.



The interaction of purine radicals with molecular oxygen has been investigated very poorly. The rates of these reactions are lower than for the pyrimidine radicals. Furthermore, the type (D) radical is rapidly converted into a type (F) radical, which does not react with oxygen. The reactions of purine peroxyl radicals have not been characterised.

The 8-hydroxy-derivatives **39** and **41** and compounds **40** and **42**, in which the imidazole ring has been opened, have been detected as the main products of the oxidation of nucleic acid purines in different oxidation systems (Tables 10 and 11).[26, 94–98] Furthermore, in the oxidation of the dinucleotide d(CG) by the Cu-1,10-phenanthroline complex, the formation of *N*-(2′-deoxy-D-*erythro*-pentofuranosyl)formamide was detected. This compound is apparently the product of more far reaching oxidation of guanosine.[99]

Table 10. The products of the γ-radiolysis of adenine in N_2O-saturated aqueous solutions.[97]

Product	*G*
4,6-Diamino-5-formamidopyrimidine	0.2
8-Hydroxyadenine	0.35
6-Amino-8-hydroxy-7,8-dihydropurine	0.1
Degradation of adenine	1.0

Table 11. The products of the γ-radiolysis of guanosine in N_2O-saturated aqueous solutions.[96]

Product	*G*
6-*N*-(2′-Deoxy-α-D-*erythro*-pentofuranosyl)-2,6-diamino-5-formamido-4-oxopyrimidine	0.09
6-*N*-(2′-Deoxy-α-L-*erythro*-pentofuranosyl)-2^6-diamino-5-formamido-4-oxopyrimidine	0.25
5′,8-Cyclo-2′,5′-dideoxyguanosine	0.06
8-Hydroxyguanosine	0.24
Guanine	0.38
9-(2′-Deoxy-α-D-*erythro*-pentofuranosyl)guanine	0.03
9-(2′-Deoxy-β-D-*erythro*-pentofuranosyl)guanine	0.02
9-(2′-Deoxy-α-D-*erythro*-pentofuranosyl)guanine	0.02
9-(2′-Deoxy-α-L-*threo*-pentofuranosyl)guanine	0.03
9-(2′-Deoxy-β-D-*erythro*-pento-1,5-dialdo-1,4-furanosyl)guanine	0.08

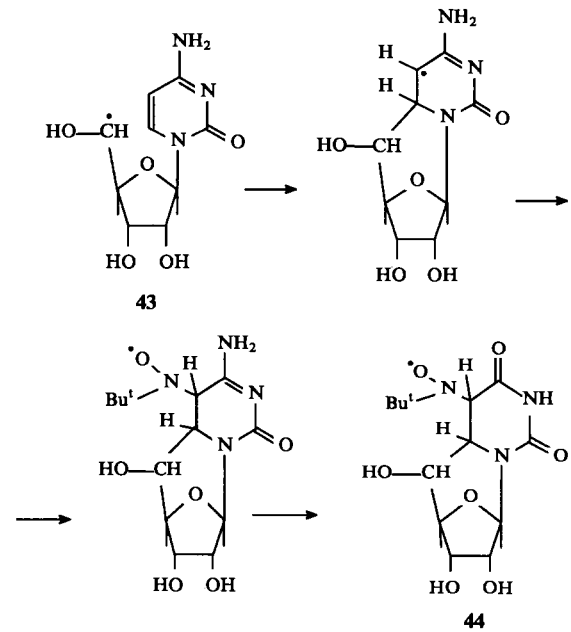
The majority of the products of the oxidation of heterocycles, characterised in terms of model compounds, have been detected also in the oxidation of DNA both *in vitro* and *in vivo* in different oxidation systems, namely on γ-radiolysis[100, 101] in the hydrogen peroxide–(Fe-EDTA)[31] or the superoxide radical ion–(Fe-EDTA)[29, 30] systems and also on oxidation by Cu-1,10-phenanthroline or Fe-bleomycin.[60, 102]

IV. Oxidation of the carbohydrate fragments in nucleic acids

1. General characteristics of the oxidation of the carbohydrate fragments of nucleic acids

The rate of reaction of hydroxyl radicals with ribose and 2′-deoxyribose is several times lower than for the heterocycles (Table 1). The reaction involves the abstraction of a H atom from all five carbon atoms in the pentose residue with not very different probabilities: approximately 25% each from the C(1′) and C(2′) carbon atoms, 20% each from the C(3′) and C(4′) atoms, and only 10% from C(5′).[103] This leads to the formation of a large number of modification products, which hinders the determination of the reaction pathways for particular primary radicals.

The use of spin-trapping agents made it possible to detect some of the ribose and deoxyribose free radicals formed in nucleic acids and their model compounds.[62, 63, 65] The stable products of the interaction of the C(4′), C(5′), and C(1′) radicals with 2-methyl-2-nitrosopropane have been isolated and characterised on γ-radiolysis of aqueous solutions of derivatives of uracil (uridine 3′-monophosphate and polyuridylic acid) and thymine (thymidine 5′-monophosphate). For cytosine derivatives (cytidine, deoxycytidine, cytidine 5′-monophosphate, cytidine 3′-monophosphate, and deoxycytidine 5′-monophosphate), it has been possible to detect by the reaction with 2-methyl-2-nitrosopropane only the C(4′) radical **43** and the radical product resulting from the further reaction of the C(5′) radical **44**:

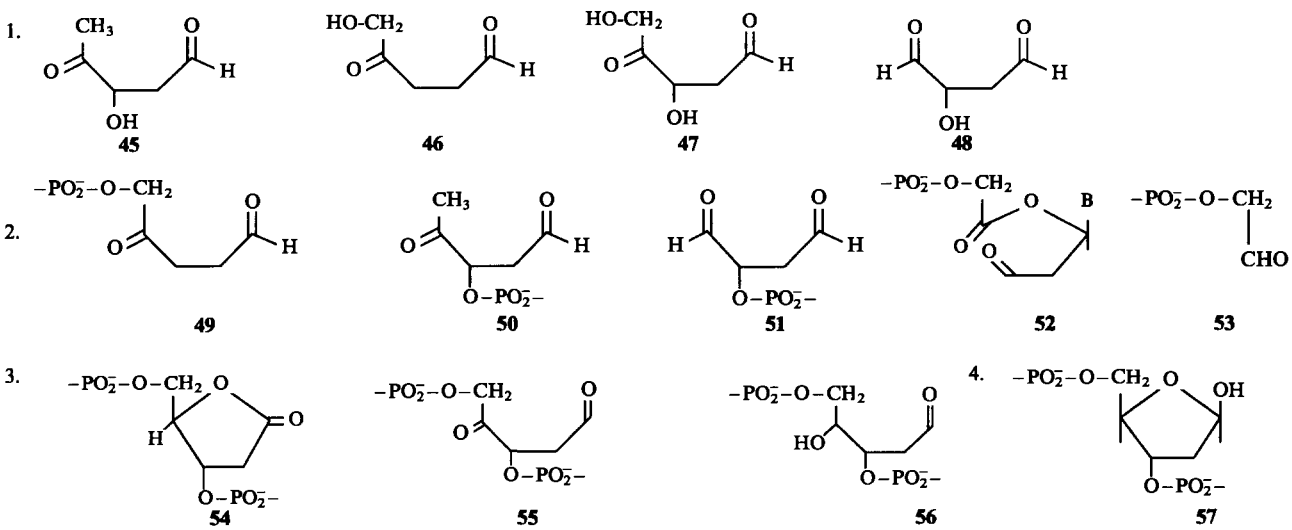


For purine nucleosides (deoxyadenosine, adenosine, guanosine, deoxyguanosine inosine) and their homopolymers poly(A) and poly(G), only the product derived from the C(4′) radical was identified.[58]

All the final products of the modification of the sugar residue which have been established (Table 12), formed on γ-radiolysis of aqueous DNA solutions, have been arbitrarily divided into 4 types:[25, 26, 61] (1) the pentose oxidation products **45–48** obtained on dissociation of both phosphoester bonds and on splitting off the unmodified heterocycles; (2) modification of the pentose residues linked to only one terminal phosphate group and containing or not containing the heterocycles **49–53**; (3) products in which both phosphate bonds are retained but the heterocyclic base has been split off and the pentose has been modified [compounds **54–56**]; (4) the product **57** with a non-purine/non-pyrimidine site formed as a result of the modification of the heterocycles leading to the cleavage of the glycosidic bond. The formation of type (1) and (2) products is accompanied by the rupture of the sugar phosphate skeleton of DNA and the isolation of intact heterocycles. Products of types (3) and (4) represent the so called alkali-labile sites, giving rise to breaks in the DNA chain after heating in an alkaline medium. Their formation is not always accompanied by the simultaneous splitting off of intact heterocycles, for example in the case of the product **52**.

Table 12. Products of the modification of the hydrocarbon residue on γ-radiolysis of aqueous solutions of DNA.

Product	Precursor radical	Without O_2	With O_2	Chain breaks	Alkali-labile sites
2'-Deoxyribolactone	C(1')	+	-	-	+
Erythrose bound to DNA	C(2')	-	+	-	+
2^5-Dideoxypentos-4-ulose	C(4')	+	-	+	-
2^5-Dideoxypentos-4-ulose bound to DNA	C(4')	+	-	+	-
2^3-Dideoxypentos-4-ulose	C(4')	+	-	+	-
2^3-Dideoxypentos-4-ulose bound to DNA	C(4')	+	-	+	-
2-Deoxypentos-4-ulose	C(4')	+	+	-	+
2-Deoxypentos-4-ulose bound to DNA	C(4')	+	+	-	+
Glycolic acid bound to DNA	C(4')	-	+	+	-
Compound abstracting malonodialdehyde	C(4')	-	+	+	-
2-Deoxytetrodialdose	C(5')	-	+	+	-
2-Deoxytetrodialdose bound to DNA	C(5')	-	+	+	-
Non-purine/non-pyrimidine sites	heterocycle	+	+	-	+



Studies on the mechanisms of the oxidation of the simplest DNA analogues made it possible to establish certain characteristic features in the reactions of the free radicals derived from sugar phosphate esters, on the basis of which the mechanisms of the OH-radical-induced oxidation of ribose and deoxyribose in nucleic acids to known final products were postulated. The principal features are listed briefly below. They were described in greater detail in other reviews.[25, 26, 61]

(1) α-Alcoholic and α-alkoxyalkyl radicals, containing a phosphate group in the β-position, are capable of splitting off the latter rapidly:

$$R\dot{C}OH-CH_2-O-PO_2^- \longrightarrow R-CO-\dot{C}H_2 + H^+ + PO_3^{2-} \quad (29)$$

$$RO\dot{C}H-CH_2-O-PO_2^- \longrightarrow \left[R-O-\overset{+}{\dot{C}}H-CH_2 \leftrightarrow R-O-CH-\overset{+}{\dot{C}}H_2\right] + PO_3^{2-} \quad (30)$$

$$\left[\quad\right] \xrightarrow{OH^-} RO-\dot{C}H-CH_2OH + RO-\underset{OH}{CH}-\dot{C}H_2$$

(2) Radicals of the type $RCHOH-\dot{C}O$ rapidly split off a CO molecule:

$$R-CH(OH)-C\dot{O} \rightarrow R-\dot{C}H-OH + CO \quad (31)$$

(3) The oxidation of the radicals by various oxidants leads to the formation of carbonium ions:

$$R\dot{H} + Ox \rightarrow R^+H + Ox^-, \quad (32)$$

(4) In the presence of oxygen, alkyl radicals rapidly combine with an oxygen molecule to form peroxyl radicals:

$$RR'R''C^{\cdot} + O_2 \rightarrow RR'R''C-OO^{\cdot} \quad (33)$$

(5) The peroxyl radicals decompose via the unimolecular or bimolecular mechanisms, described in the previous section.

A series of important data on the mechanism of the oxidation of the carbohydrate fragments have been obtained with the use of antitumour antibiotics (bleomycin, neocarzinostatin) and metal complexes (Cu-1,10-phenanthroline, Mn-porphyrin) which bind to DNA and oxidise pentose selectively in a specific position (subsections 2, 4, and 5 of the present section).

The oxidation of pentoses in the C(4') position has been studied in greatest detail. This is due to two causes. Firstly, the oxidation in the C(4') position is the main pathway leading to the degradation of nucleic acids by the antitumour antibiotics of the bleomycin group.[7] Secondly, the dominant formation of the ribose C(4') radical on γ-radiolysis in aqueous solutions as a result of the additional abstraction of a H atom from the C(4') position

in the sugar by the free radical of a heterocycle in a neighbouring monomer unit is characteristic of certain homopolynucleotides—poly(U) and poly(dT).[104] The known pathways leading to the oxidation of the sugars in nucleic acids in different positions in ribose or deoxyribose by both free OH radicals and certain antibiotics and metal complexes are described below.

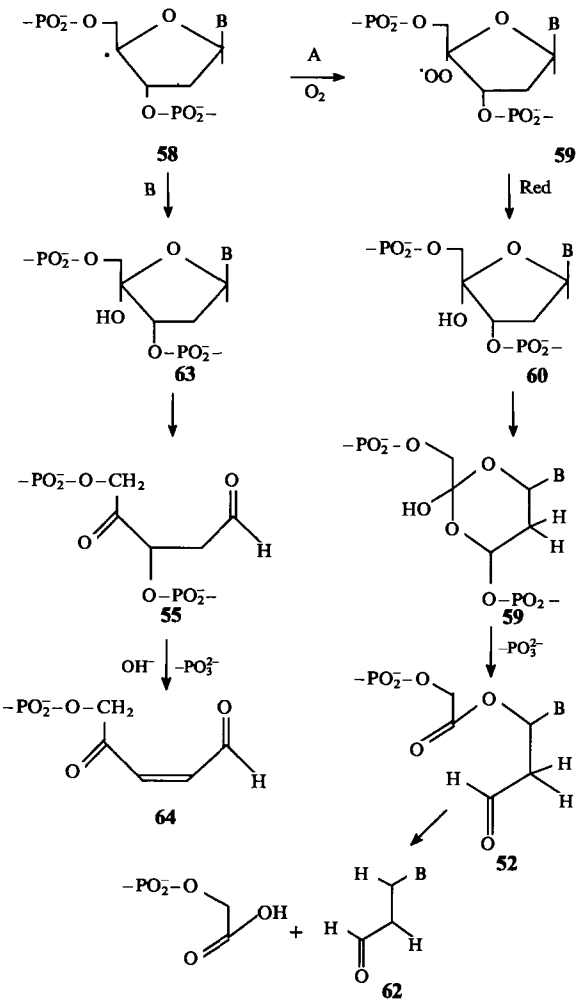
2. Oxidation of deoxyribose in the C(4′) position in the presence of bleomycin

Bleomycins are a group of glycopeptide antitumour antiobiotics inducing the degradation of DNA in the presence of Fe^{2+} ions and molecular oxygen.[7, 55, 105, 106]

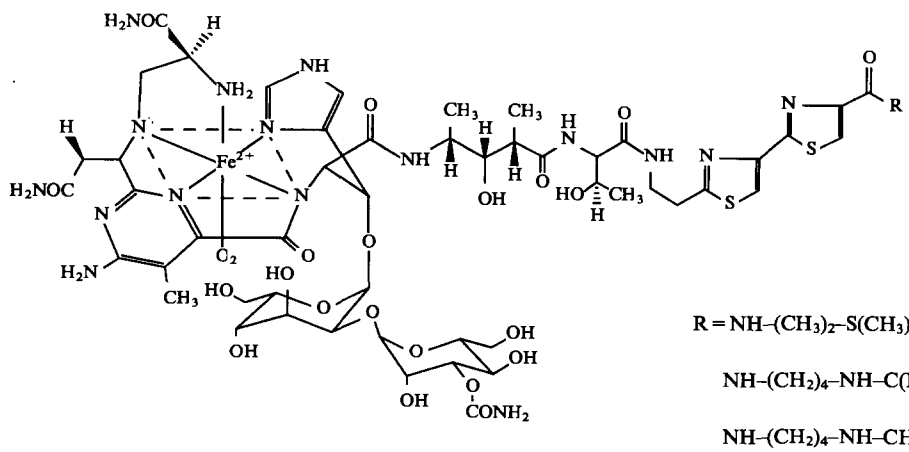
The oxidising unit is the so called 'activated bleomycin', which is a product of the two-electron reduction of the ternary complex Blm · Fe^{2+} · O_2, as already noted in Section II of this review, which is an oxo-complex of iron[50]. As a result of the degradation of DNA by the activated bleomycin, two types of monomeric products are detected: *trans*-propenals derived from the heterocycles (pathway A) and free heterocycles (pathway B). The formation of propenals requires the involvement of yet another oxygen molecule in addition to that used to activate bleomycin. This process is accompanied by the cleavage of DNA into two fragments, one of which contains a 5′-terminal phosphate and the other a 3′-terminal phosphoglycolate. The splitting off of the heterocycles does not require an additional oxygen molecule and leads to the formation of non-pyrimidine/non-purine sites in the oxidised deoxyribose residue, at which cleavage takes place only under alkaline conditions. At the normal oxygen pressure, the amount of the free heterocycles formed is virtually equal to the amount of heterocycle propenals. When the oxygen pressure is raised, reaction A takes place preferentially; under anaerobic conditions [Fe(III) and H_2O_2], pathway B is observed exclusively.[7, 55, 105, 106]

Experiments with different DNA containing tritium in the 4′-positions showed that the liberation of tritiated water is correlated with the formation of the sum of both monomeric products—propenals and free heterocycles.[55, 107] This shows that the first stage in both pathways is the abstraction of a hydrogen atom from the 4′-carbon atom of deoxyribose. The considerable isotope effect associated with the replacement of 4′-H by tritium or deuterium (by a factor of 7–11 and 4–5 respectively) permits the conclusion that the abstraction of a H atom from the C(4′) position in the pentose is the rate-limiting stage in both reactions.

Under aerobic conditions, the 4′-radical **58** rapidly interacts with oxygen, forming the 4′-peroxyl radical **59**. In order to demonstrate directly the occurrence of this process a series of experiments were carried out[108], in which the ^{16}O and ^{18}O oxygen isotopes were used. When $^{18}O_2$ was incorporated in the activated bleomycin and DNA was oxidised directly in the presence of $^{16}O_2$, no incorporation of the label in the product was detected. In the opposite situation, where the reaction medium contained $^{18}O_2$, the label was found to be incorporated in one of the oxidation products—3′-phosphoglycolate. Under these conditions, only one ^{18}O atom was incorporated in 3′-phosphoglycolate, while the other oxygen atom in this product originated from deoxyribose. The second oxygen atom of the peroxide group should apparently be included in the heterocycle propenal. However, so far it has not been possible to demonstrate this.



The subsequent stages, leading to the dissociation of the C(3′)–C(4′) bond, the cleavage of the sugar phosphate residue, and the formation of heterocycle propenals cannot yet be regarded as finally established. It appears that the 4′-peroxyl radical **59**

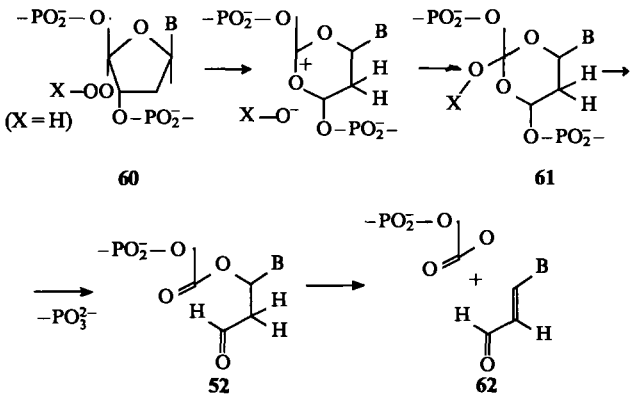


R = $NH-(CH_3)_2-S(CH_3)_2X^-$

$NH-(CH_2)_4-NH-C(NH_2)=NH$

$NH-(CH_2)_4-NH-CH(CH_3)-Ph$

subsequently accepts yet another electron from the reductant present and is converted into the fairly unstable 4′-peroxide **60**. It has been suggested that the peroxide **60** subsequently undergoes the Criegee rearrangement. During this rearrangement, the C(3′) atom migrates from the C(4′) atom to the O atom of the peroxide with the simultaneous heterolytic dissociation of the O–O bond. The C(2′) atom, activated by the appearance of the carbonyl group in the C(3′) positon in the intermediate **52**, can be deprotonated, initiating elimination via the C(2′)–C(1′) bond and the formation of the heterocycle propenal **62** and the phosphoglycolate product. In this mechanism, the appearance of the label in the phosphoglycolate product should be observed when DNA is oxidised in the presence of $^{18}O_2$, which has in fact been done:[108]

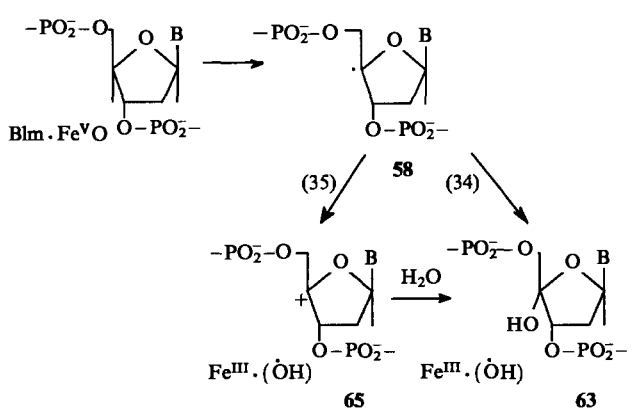


Confirmation has been obtained for this mechanism in a study[109] where it was shown, with 3′-^{18}O-labelled poly(dA-dT) as the substrate, that the 5′-phosphate products obtained on degradation by bleomycin contain the ^{18}O-label in the phosphate group. This indicates that the reaction proceeds via the pathway accompanied by the cleavage of the C(3′)–O(3′) bond.

Data in support of the existence of a precursor of the propenals **52** have been obtained.[110] The existence of a long-lived precursor of the heterocycle propenal, coprecipitated with DNA, was detected. This made it possible to demonstrate that the rate of formation of the propenals is an order of magnitude lower than the rate of appearance of single-strand breaks: $t_{1/2} \simeq 40$ min and $t_{1/2} \simeq 2.5-5$ min, respectively.

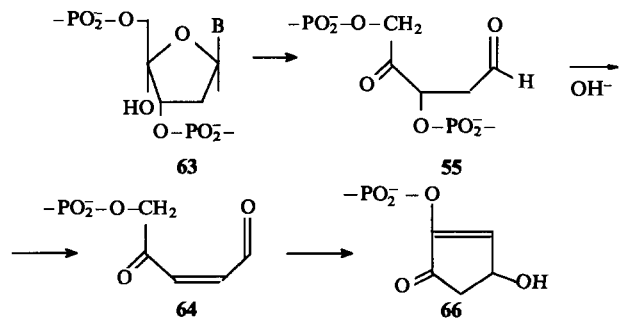
In a more detailed study of the rupture of the C(2′)–H bond, DNA selectively labelled with tritium was used:[111] poly(dA-[2′-proS-^{3}H]dU) and poly(dA-[2′-proR-^{3}H]dU). It was shown that the rigorously stereospecific elimination of 2′-proR-H takes place via anti-elimination with the exclusive formation of *trans*-propenals.

As noted previously, in the presence of a low O_2 content the oxidation of DNA proceeds via pathway B. After the abstraction of hydrogen from the C(4′) position, the splitting off of the heterocycles requires the addition of some kind of analogue of the OH radical. Two C(4′) hydroxylation mechanisms can be postulated.



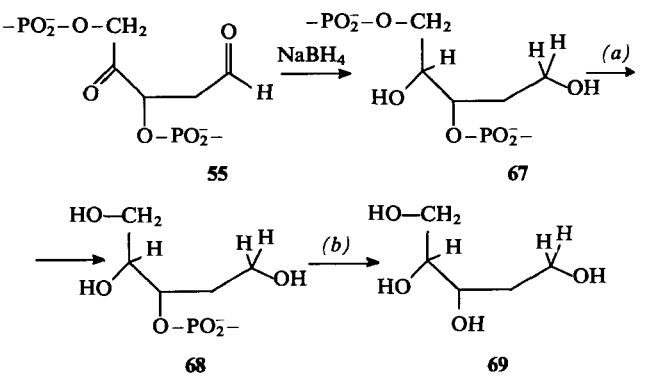
In the first case [reaction (34)], the C(4′) radical recombines with the hydroxyl radical bound to the antibiotic, resembling the mechanism proposed for cytochrome P-450 and metalloporphyrins.[111] In the second case [reaction (35)], the C(4′) radical can be oxidised by a second equivalent of the activated antibiotic, affording a carbonium ion, which rapidly interacts with water. The results of experiments using oxygen isotopes, which will be discussed below, support the second pathway.

The compound **63** formed is cleaved, giving rise to the free heterocycles. Under physiological conditions, the oxidised deoxyribose residue **55** remains bound to the DNA chain. Under alkaline conditions, the 3′-terminal fragment is split off in the form of a phosphomonoester. In the second fragment, the sugar oxidation product—3-hydroxyl-5-oxo-1-cyclopentenyl **66**— remains at the 3′-phosphate end:



Certain aspects of this mechanism have been confirmed experimentally. Sugiyama et al.,[112] using the model substrate d(CGCTTTAAAGCG) containing a single site in the third deoxycytidine, which is cleaved by bleomycin, isolated the product CpGpx and determined its structure by direct comparison with synthetic analogues. This compound corresponded to the product **66** postulated in the mechanism. However, a correlation was not traced in the above study between the amount of heterocycles isolated and the amount of alkali-labile products of the modification of deoxyribose.

An alternative approach to the identification of the product **55** has been proposed.[113, 114] After incubating the model substrate d(CGCGCG) under anaerobic conditions with Fe(III)·Blm and H_2O_2, the product of the oxidation of compound **55** was stabilised by reduction with $NaBH_4$. After the enzymic degradation of the polymer, the deoxyribose residue **69** was identified with the aid of chromatograph-linked mass spectrometry by comparison with synthetic analogues of 2-deoxy-D-*erythro*-pentitol and 2-deoxy-D-*threo*-pentitol:



(*a*) treatment with P1-nuclease and alkaline phosphatase;
(*b*) treatment with phosphodiesterase I and alkaline phosphatase.

The product **69** isolated corresponded to a mixture of diastereoisomers and its amount was correlated to the amount of heterocycles formed.

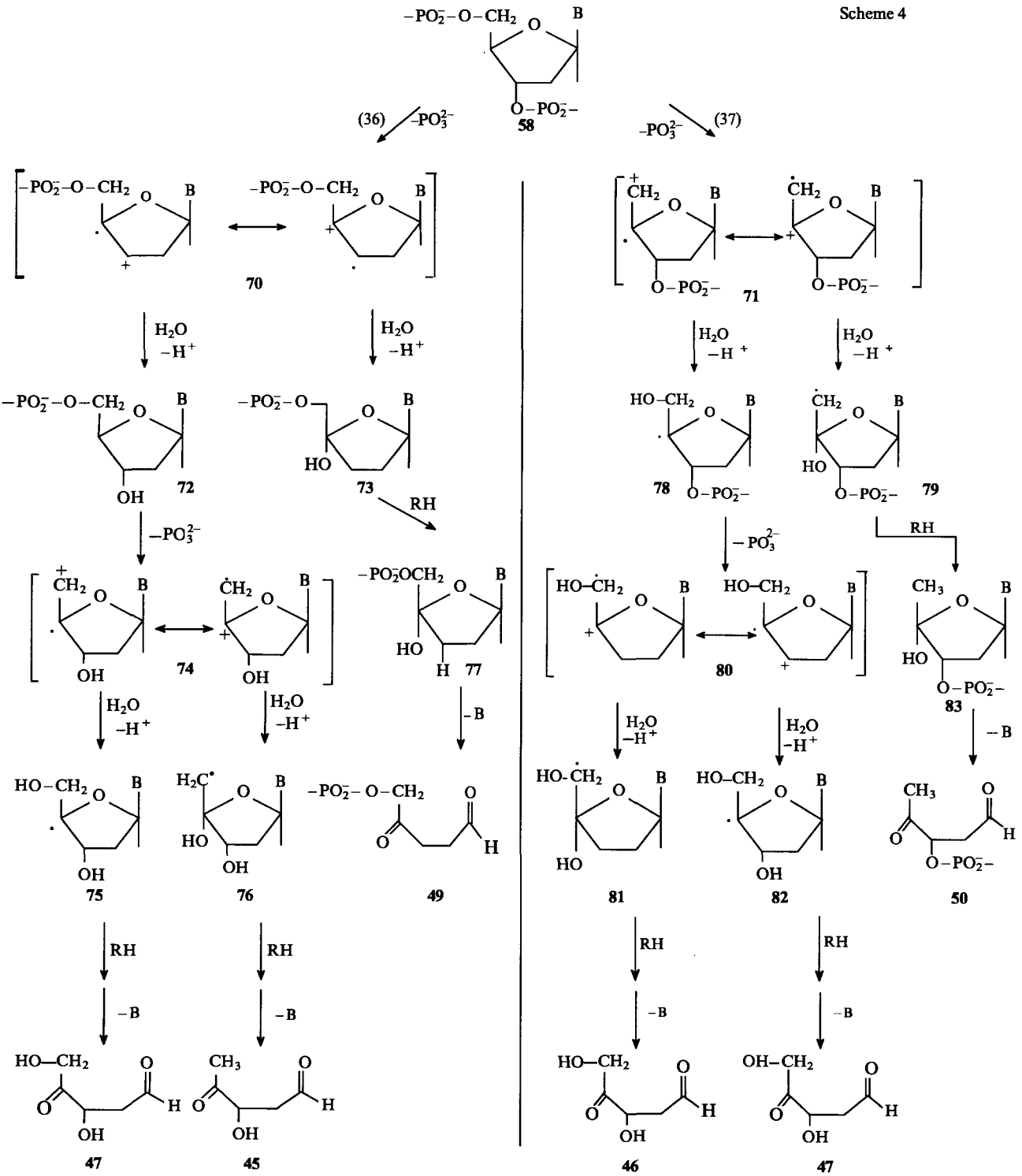
Using the approach described, the same workers[114] established the mechanism of the hydroxylation of the C(4') position. Using ^{18}O-labelled O_2 or H_2O, they showed that the source of oxygen in the 4'-keto-group of compound **64** is the solvent H_2O and the C(4') position is therefore hydroxylated via the second of the proposed pathways.

Thus wide scale investigations carried out in various laboratories made it possible to establish the mechanism of the oxidative fragmentation of DNA by bleomycin *in vivo*, although individual stages require further evidence.

3. Oxidation of pentose in the C(4') position by free OH radicals (according to γ-radiolytic data)

By analogy with bleomycin, the abstraction of a H atom by the OH radical from the C(4') carbon atom on γ-radiolysis leads to the splitting off of the free heterocycles and different modifications of the pentose. However, whereas the chain rupture under anaerobic conditions occurs only after treatment with alkali during oxidation with bleomycin, the splitting off of the heterocycle on γ-radiolysis is accompanied by rapid chain rupture.[25, 26]

Scheme 4



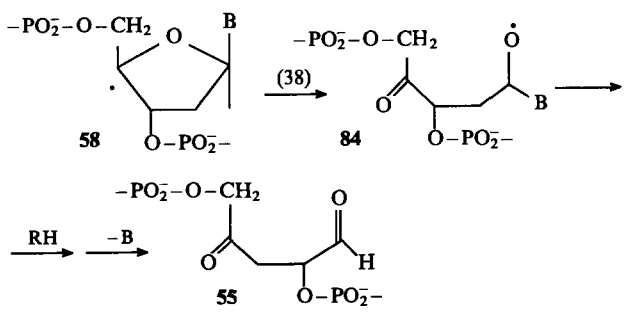
Consequently, the reactions of the C(4′) radicals leading to the final products are different in γ-radiolysis and in oxidation by bleomycin.

The C(4′) radical is a β-phospho-α-alkoxyalkyl radical, a characteristic feature of which has been shown, in simple models,[26] to involve the rapid elimination of the phosphate group. Since the ribose and deoxyribose C(4′) radicals contain two phosphate groups in the β-positions relative to the free valence, two competing reactions should be observed for them: the elimination of the phosphate group from the C(3′) atom [reaction (36)] and the C(5′) atom [reaction (37)]. It follows from the results of the study of model compounds that the elimination from the C(3′) atom should be faster, which is in fact reflected in the ratio of the final products (Table 12).

The postulated main reaction pathway for the deoxyribose C(4′) radical is presented in scheme 4. The radical-cation **70**, obtained when the phosphate group is split off from the C(3′) carbon atom [reaction (36)], can exist in two mesomeric forms with the positive charge located on the C(3′) or C(5′) atom. This radical-cation combines rapidly with a water molecule at one of the positively charged centres, forming respectively the C(4′)-β-phospho-α-alkoxyalkyl radical **72** again or the C(3′)-alkyl radical **73**. The radical **72** eliminates a second phosphate group and is converted into the radical-cation **74**. One nucleoside unit is fully eliminated from DNA at this stage. The intermediate **74** rapidly combines with a water molecule at the C(4′) or C(5′) position. The resulting alkyl radicals **75** and **76** are converted into the identified final products **45** and **47** respectively after reduction via a disproportionation reaction with any other radical and after the elimination of the intact heterocycle. The C(5′) radical is converted similarly via a disproportionation reaction into the unstable compound **77**, which is converted, after the heterocycle has been split off, into the detected product **49**. Although DNA is in fact cleaved at this stage, the oxidised nucleoside residue remains bound to the 3′-phosphate end of one of the DNA fragments.

The radical-cation **71** formed via the minor pathway (37) undergoes similar reactions, which result in the formation of the products **46**, **47**, and **50** (Table 12). They have also been detected as the final products of anaerobic γ-radiolysis of nucleic acids.[115]

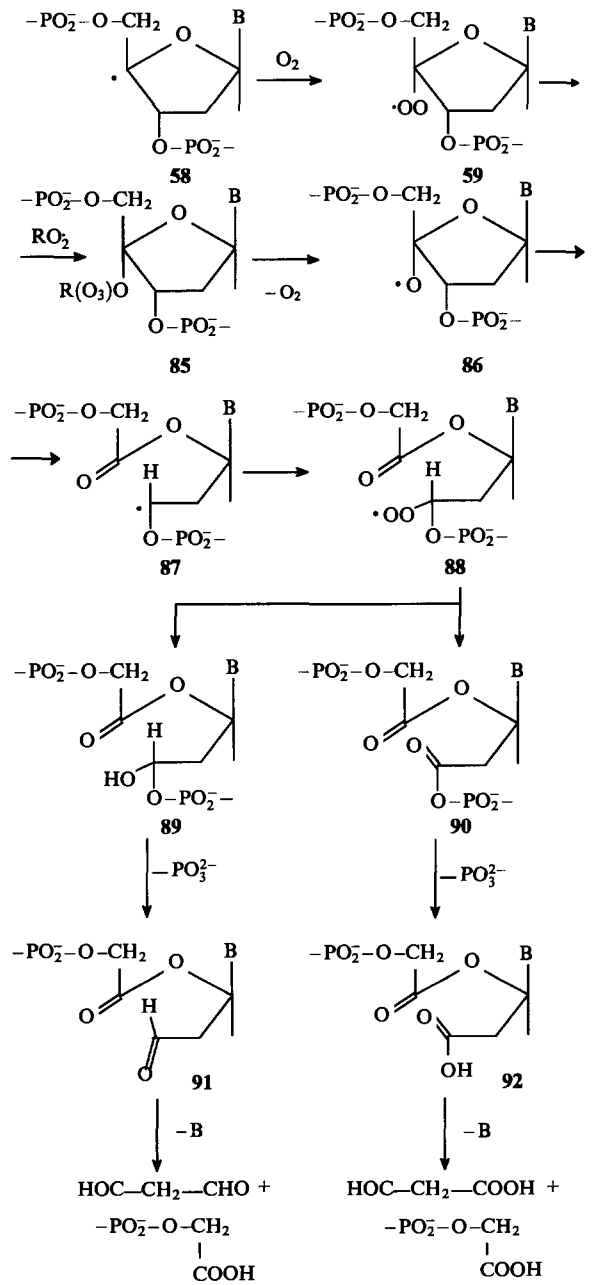
The isomerisation of the C(4′) radical to the C(1′) radical **84** [reaction (38)], accompanied by the opening of the furanose ring, may compete with the elimination reactions (36) and (37).[116] Reaction (38) prevents the cleavage of DNA. The alkyl radical **84** formed eliminates the heterocycle after reduction and is converted into the product **55**, analogous to the product of the anaerobic oxidation by bleomycin.



In the aerobic γ-radiolysis, the reactions of the C(4′) radical are much more complex than in the oxidation by bleomycin despite the fact that certain products are identical in both cases. Molecular oxygen, which adds to the C(4′) radical with a diffusion-controlled rate constant $k = 10^9$ litre mol^{-1} s^{-1}, fully suppresses the phosphate group elimination reactions (36) and (37). The peroxyl radicals formed were detected by EPR. They have an unusually long lifetime[117] (~0.2–3.3 s). The subsequent decomposition of the C(4′) peroxyl radicals leads to the cleavage of nucleic acids. The main products detected were fragments of nucleic acids containing the phosphate group at the 5′-end and fragments containing either the phosphate or the phosphoglycolate group at the 3′-end. In addition, heterocycle propenals and unidentified products, undergoing a reaction with thiobarbituric acid characteristic of malonaldehyde, were also detected.

The mechanism of the decomposition of the peroxyl radical **59** on γ-radiolysis most consistent with the experimental data has been proposed by Schulte-Frohlinde and Bothe.[104] According to this mechanism, the peroxyl radical decomposes via a bimolecular reaction with formation of the tetroxide **85**. The intermediate **59** is a tertiary peroxyl radical and, in conformity with the foregoing, decomposes solely via the radical mechanism (21) with formation of two oxyl radicals and an oxygen molecule. The rearrangement with selective cleavage of the C(3′)–C(4′) bond and the formation of the radical **87**, which again interacts with O_2, is characteristic of such oxyl radicals **86**. Being a secondary peroxyl radical, the radical **88** decomposes via the formation of a tetroxide intermediate in accordance with Russell's concerted bimolecular

Scheme 5



mechanism (18) described above. An hydroxy- or carbonyl group (compounds **89** and **90** respectively) appears with equal probability at the C(3') carbon atom as a result of this reaction. The phosphoester bond in the C(3') position undergoes rapid hydrolysis in the compounds **89** and **90** formed, which leads to the rupture of the sugar phosphate skeleton and the formation of the fragments **91** and **92**. The subsequent decomposition of these fragments is accelerated in an acid medium or on heating and leads to the formation of the intact heterocycle and the 5'-phosphoglycolate end group. According to some hypotheses, the hydrolysis of compound **91** can involve the formation of heterocycle propenals (see scheme 5).

As noted above, free OH radicals are formed also during the reduction of molecular oxygen by transition metal ion complexes, for example, Fe-EDTA. One might expect that nucleic acids are oxidised in such systems via the same mechanisms as in γ-radiolysis. The products of the degradation of DNA by the iron complex of methidiumpropyl-EDTA (MPE) in the presence of O_2 and a reductant or H_2O_2 have been most thoroughly characterised.[118] It was shown that the pentose phosphate skeleton is cleaved. For each break, one heterocycle is split off with formation of 5'-phosphate end groups and of 3'-phosphates and 3'-phosphoglycolates in approximately equal amounts. The mechanism of the degradation of DNA was not discussed in the above study.[118] Nevertheless, the formation of the products is consistent with the sequence of the reactions of the pentose C(4') radical proposed for γ-radiolysis, where the heterocycle is liberated in the presence of a deficiency of oxygen together with free 5'- and 3'-phosphate end groups, while in the presence of oxygen the 5'-phosphate and 3'-phosphoglycolate end groups and the heterocycle are formed. Indeed, if MPE · Fe(III) · H_2O_2 is used instead of MPE · Fe(II) · O_2, then 3'-phosphoglycolates are formed in significantly smaller amounts.

4. Oxidation in the C(5') position in the pentose

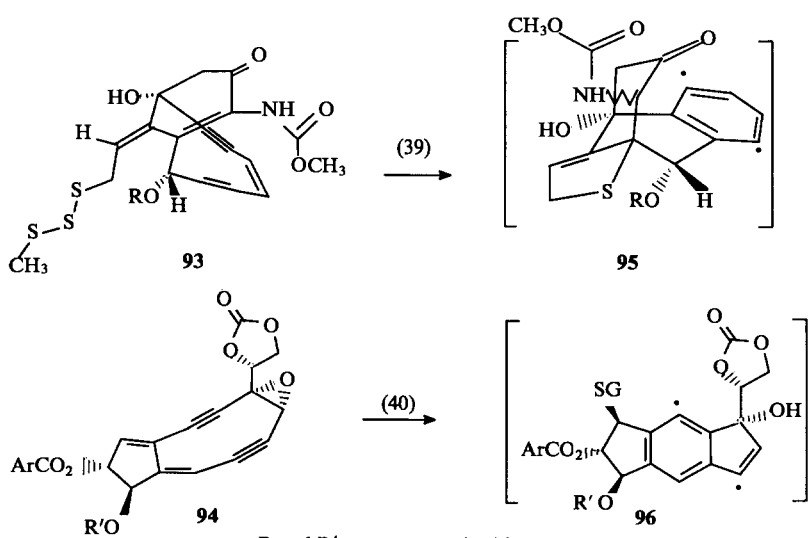
The preferential oxidation in the C(5') position in deoxyribose has been observed when DNA was cleaved by antibiotics of the diene-ene type such as neocarzinostatin **93** and calcomycin **94**.[119, 120] These antibiotics contain a bicyclodiene-ene structure, capable of being converted via reactions (39) and (40) into the biradicals **95** and **96**, which attack deoxyribose and abstract a H atom preferentially from the C(5') carbon atom.

The mechanism and the cleavage of DNA by neocarzinostatin has been investigated in greatest detail.[121–124] The neocarzinostatin biradical **95**, formed as a result of reduction by thiols, abstracts as a rule an H atom from the C(5') position in the pentose, which has been demonstrated in experiments with nucleic acids containing atoms of the ^2H or ^3H hydrogen isotope in different positions in deoxyribose. When the H atom at the C(5') atom was replaced, both covalent incorporation of a deuterium or tritium atom in the antibiotic molecule and an isotope effect in the DNA cleavage reaction were observed.[122, 125] The abstraction of a H atom from the C(4') or C(1') position is observed to a much lesser extent. The specificity of the reaction in relation to a particular position in deoxyribose is apparently due to the different accessibility of the H atoms of deoxyribose in different sections of DNA.

In the next stage, only covalent adducts between DNA and the antibiotics are formed under anaerobic conditions. On the other hand, under aerobic conditions, DNA is cleaved and the formation of two sets of cleavage products is observed. The main product (80%) involves single-strand breaks (T > A ≫ C > G) with formation at the cleavage site of a fragment with the 5'-phosphate end group and a fragment containing a nucleoside-5'-aldehyde at the 3'-end. Less than 20% of the breaks occur in one nucleoside with phosphates at both the 5'- and 3'-ends and accompanied by the spontaneous liberation of the heterocycles.

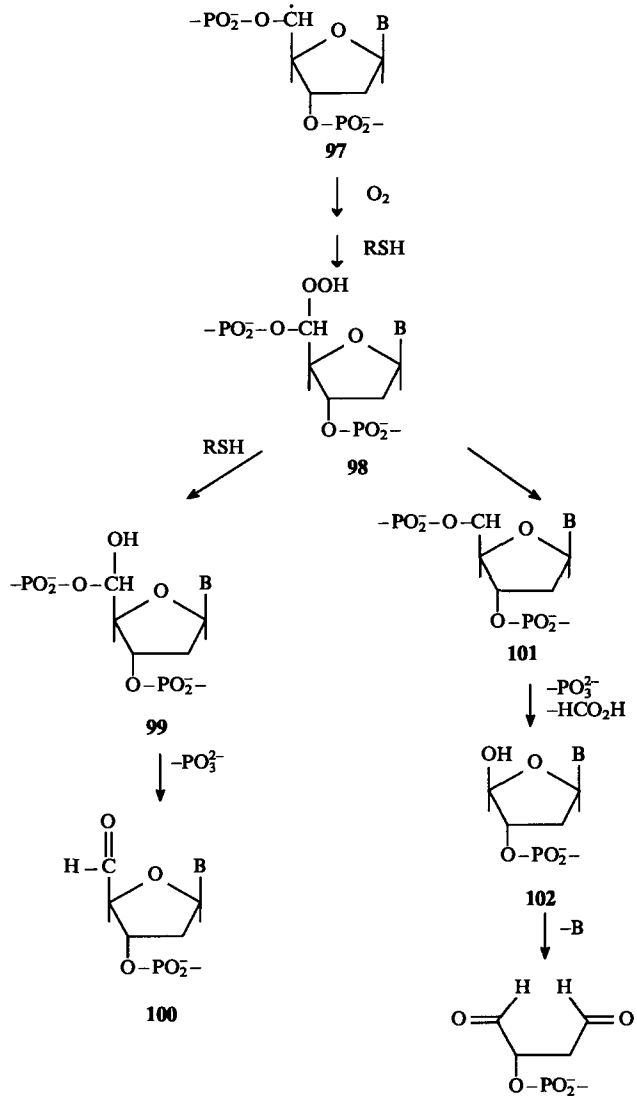
It has been shown [126] that under aerobic conditions the activation of the antibiotic is followed by the rapid absorption of an oxygen molecule via each antibiotic molecule and the subsequent utilisation of at least yet another reductant molecule. These results agree with the reaction in which the oxygen molecule adds to the radical **97**, generating a peroxyl radical, which is rapidly reduced by thiols to the hydroperoxide **98**. The use of $^{18}O_2$ made it possible to detect the incorporation of the oxygen isotope in one of the end products of the oxidation—nucleoside-5'-aldehyde.[127] The formation of the 5'-aldehyde end group has been demonstrated[124, 125] by reaction with $NaBH_4$, which leads to the reduction of the aldehyde group to the alcoholic group, and this was in its turn detected by phosphorylation catalysed by the T4 polynucleotidekinase. The use of a self-complementary short oligonucleotide,[124] having one site for oxidation by neocarzinostatin, made it possible to isolate all the final oxidation products and to establish their structures.

Two pathways leading to the decomposition of the hydroperoxide **98** have been postulated on the basis of the sum total of the results. Since the system contains a reductant (thiols), the peroxide group in the hydroperoxide **98** can be reduced to the hydroxy-group. The resulting compound **99** eliminates the phosphate group from the 5'-end, which ultimately leads to the rupture of the DNA chain and the formation of the 3'-phosphate and 5'-aldehyde (compound **100**) end groups. In addition, the hydroperoxide **98** can apparently undergo the Criegee rearrangement, which results in the formation of compound **101**. Compound **101** eliminates from the 5'-end a fragment containing the 3'-formyl

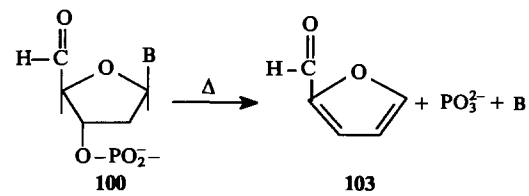


R and R' are monosaccharides

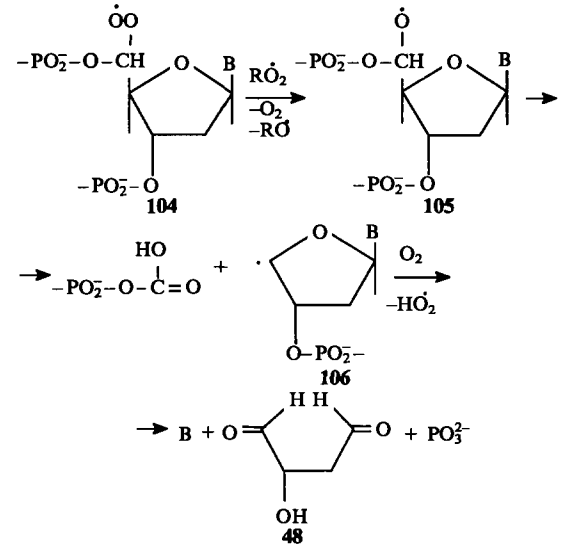
phosphate group, which hydrolyses spontaneously with the formation of the free 5′-phosphate end group. The second fragment contains the unstable compound **102**, which decomposes to compound **51**, liberating the heterocycle. It has been shown[127] that the amount of the nucleoside-5′-aldehyde increases with increase in the concentration of thiols, while the liberation of the free heterocycle diminishes. This confirms that the pathways leading to the formation of these products do indeed start from a single precursor—the hydroperoxide **98**—and that they compete with one another.



The selective oxidation of deoxyribose in the C(5′) position has been observed also for cationic metalloporphyrins.[128] However, as mentioned previously, in the case of metalloporphyrins the active oxidising species is apparently a high-valence metal oxocomplex, the most characteristic reaction of which is hydroxylation. Therefore, in the oxidation of DNA by metalloporphyrins, the first stage most probably involves the hydroxylation of the C(5′) carbon atom of the deoxyribose with the immediate formation of compound **99**. After the elimination of the phosphoester fragment from the C(5′) position, the nucleoside-5′-aldehyde fragment **100** is also formed. On further heating, it eliminates furfural **103**, splitting off the 5′-phosphate group.



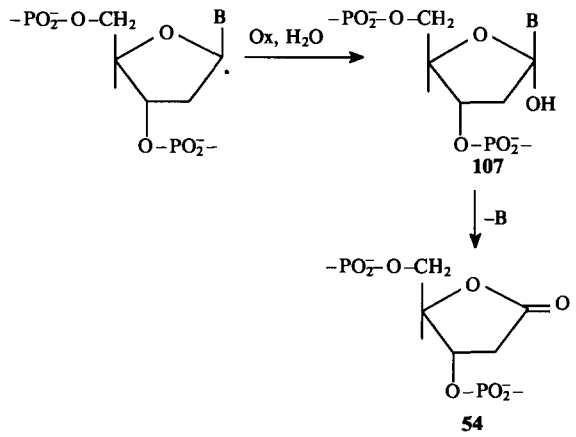
The formation of nucleoside-5′-aldehyde, accompanied by the splitting off of the phosphate, has been observed in the γ-radiolysis of aqueous solutions of D-ribose-5′-phosphate and guanosine 5′-phosphate under both anaerobic and aerobic conditions.[129] However, on γ-irradiation of aqueous DNA solutions, the formation of the nucleoside-5′-aldehyde was not observed. As regards the four-carbon fragment of deoxyribose of type **51**, linked to the 5′-phosphate end group of DNA, under aerobic conditions an analogous 2′-deoxytetradialdose is formed, but it is either linked to the 3′-phosphate end groups, as in **49**, or is present in the free state **96**.[30] The formation of such tetradialdose can be represented as a result of the conversion of the 5′-peroxyl radical **104**. The latter, being a secondary radical, can decompose via Russell's mechanism with formation of the oxyl radical **105**, which undergoes β-fragmentation, affording one DNA fragment with a 3′-formyl phosphate end group and another with the radical **106** linked to the 5′-phosphate group. At this stage, the DNA chain is cleaved betweren the C(4′) and C(5′) carbon atoms of deoxyribose. The radical **106**, which is a β-phospho-α-alkoxyl-akyl radical, rapidly eliminates the phosphate group from C(3′), recombines with an oxygen molecule, and the resulting peroxyl radical decomposes via a unimolecular mechanism with formation of the tetradialdose **48** and the liberation of the intact heterocycle.



5. Oxidation in the C(1′) position of the pentose

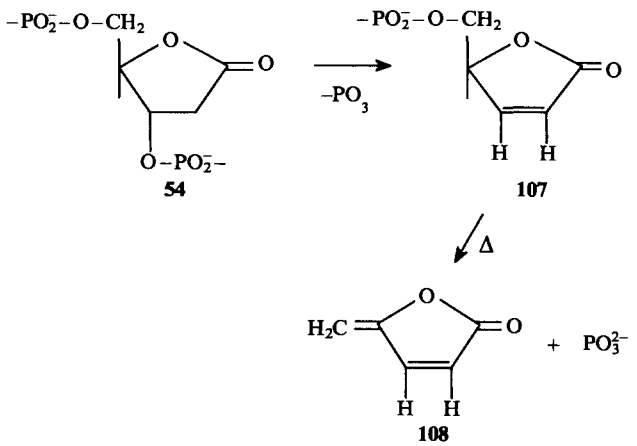
The oxidation in the C(1′) position leads to the formation of only one final product both on γ-radiolysis (under aerobic and anaerobic conditions) and on selective oxidation by certain 'chemical nucleases' (Cu-1,10-phenanthroline, Mn-porphyrins) although apparently via different mechanisms.

On γ-radiolysis under anaerobic conditions, the C(1′) radical can be oxidised with formation of a carbonium ion, the rapid solvolysis of which leads to the formation of compound **107**. The latter is unstable and rapidly splits off the heterocycle. The resulting lactone **54** remains bound to the sugar phosphate skeleton of DNA, as shown by Urata et al.[131] The presence of such a site can lead to the cleavage of DNA on heating or under acid conditions.



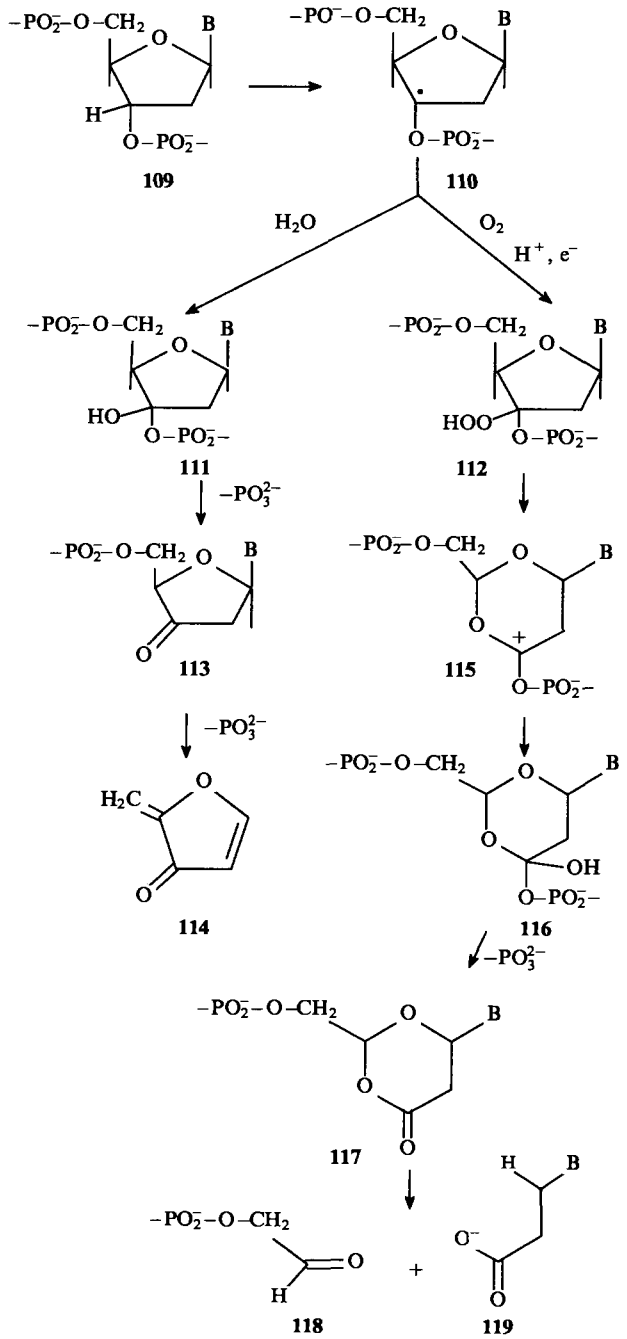
In the presence of molecular oxygen, the C(1′) radical should rapidly combine with oxygen to form a peroxyl radical, the subsequent reaction of which, apparently via Russell's mechanism, also leads to the formation of the lactone **54** bound to DNA.

The selective oxidation of DNA in the C(1′) position in deoxyribose is characteristic of certain metal complexes with affinity for DNA. This applies in the first place to Cu-1,10-phenanthroline[8, 132, 133] and Mn-tetra(4-methylpyridinium)porphyrin.[128, 134–136] The formation of coordinated active forms of oxygen is characteristic of such complexes and nucleic acids are oxidised via the hydroxylated C(1′) positions of deoxyribose, also with formation of compound **107**, which decomposes to the lactone **54**. However, it has been shown that compound **54** is unstable, so that its decomposition is also accompanied by the rupture of the DNA chain with liberation of the 3′-phosphate fragment and the 5′-intermediate. The latter gives rise to 5-methylene-2-5*H*-furanone **108** on heating with liberation of the 5′-phosphate end group. This difference between the stabilities of compound **54** in various oxidation systems has not so far been explained. It may be associated with the catalysis of the elimination of the phosphate group from the C(3′) position in the vicinity of the site where modification by metal complexes takes place. Such complexes may behave as Lewis acids.



6. Oxidation in the C(3′) position of the pentose

The oxidation in the C(3′) and C(2′) positions of the pentose has been investigated to a lesser extent because the majority of compounds catalysing the oxidative cleavage of DNA are bound to a small groove, whilst the C(3′) and C(2′) atoms are located in a large groove. Compounds have been discovered quite recently, which, on binding to DNA, are located in a large groove and catalyse the photochemical oxidative cleavage of DNA. These are mixed rhodium(III) complexes with two 9,10-phenanthrenequinone diimine molecules and one 2,2′-bipyridyl molecule or with two 1,10-phenanthroline molecules and one 9,10-phenanthrenequinone diimine molecule.[137] These complexes bind to DNA from the side of the large groove as a result of the intercalation of the 9,10-phenanthrenequinone diimine ligand. On irradiation, the latter is converted into a radical-cation,[138] which is capable of abstracting a hydrogen atom from deoxyribose. In conformity with crystallographic studies, on



intercalation from the side of the large groove the intercalator comes close to the C(3′)–H bond.[139]

The products of the oxidation of a short oligonucleotide duplex by such rhodium complexes have been isolated and characterised.[140] The mechanism of the oxidation of DNA in the C(3′)-position under both aerobic and anaerobic conditions has been proposed on the basis of the results. The radical **110** obtained is apparently oxidised by the rhodium(II) ion and then combines with water molecule. The compound **111** formed is unstable and as a result of several β-elimination processes splits off the 3′- and 5′-phosphate end groups and the free heterocycle. The oxidised deoxyribose residue is isolated in the form of 2-methylene-3-2*H*-furanone **114**.

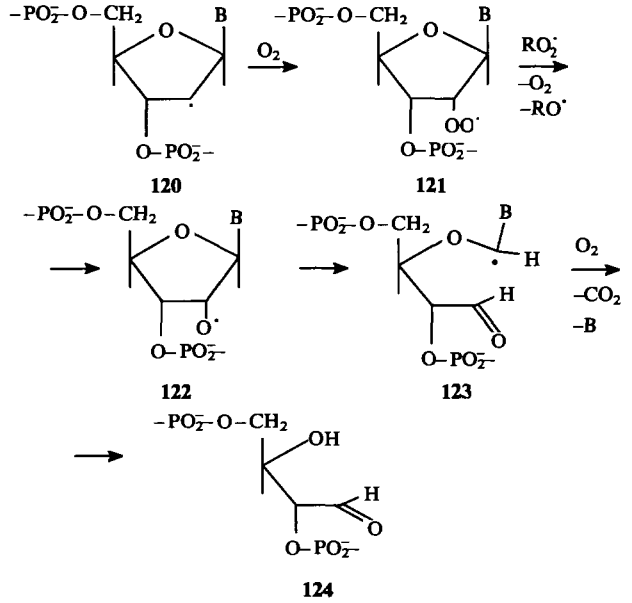
An alternative pathway is observed under aerobic conditions. In the first stage, an oxygen molecule adds rapidly to the C(3′) position and the resulting peroxyl radical is reduced. The hydroperoxide **112** undergoes the Criegee rearrangement, which leads to the rupture of the DNA chain with formation of 5′-phosphate and 3′-phosphoglycolaldehyde and groups (compound **118**). The heterocycles liberated contain a deoxyribose residue—propionic acid **119**.

Among the products of the γ-radiolysis of nucleic acids, products which might be formed as a result of the oxidation in the C(3′) position of the pentose were not identified. Only in the oxidation of deoxycytidine 5′-monophosphate was a product of the reaction of the C(3′) radical characterised,[117] but these results cannot be transferred to nucleic acids because the 3′-phosphate is absent in the given instance.

7. Oxidation in the C(2′) position of the pentose

Among the DNA oxidation products under aerobic conditions, only one compound was isolated for which a mechanism involving its formation from the C(2′) radicals may be postulated.[141]

Like other deoxyribose radicals, the radical **120** rapidly combines with an oxygen molecule and is converted into the peroxyl radical **121**, which decomposes via Russell's mechanism with formation of the oxyl radical **122**. The oxyl radical **122** undergoes fragmentation with rupture of the C(1′)–C(2′) bond and the resulting radical **123** can again combine with an oxygen molecule, which is followed by the elimination of the heterocycle and a CO_2 molecule. The ultimate formation of the four-carbon deoxyribose fragment (erythrose) **124** is not accompanied by the cleavage of the nucleic acid under physiological conditions.



V. Conclusion

Thus the main species responsible for the degradation of nucleic acids in various oxidising systems are usually free OH radicals. Hydroxyl radicals interact with nucleic acids and model compounds the rate constants of which are close to diffusion-controlled values and generate organic free radicals either by adding to the unsaturated bonds of the heterocycles or by abstracting a hydrogen atom from the pentose. The OH radicals interact preferentially with the heterocycles: in nucleotides and single-stranded nucleic acids, the ratio of the radicals formed from the heterocycles to the pentose radicals is 10–15. For double-stranded DNA, in which the heterocycles become less accessible, this ratio reaches 5–7. In a number of instances, the heterocycle radical may abstract a hydrogen atom from the C(4′)-position in the pentose of the preceding monomer unit, inducing the formation of this radical. In this case, the yield of the pentose radical reaches 40%.

In the oxidation of nucleic acids by a number of antibiotics or transition metal complexes, the oxidising species is a bound analogue of the OH radical—the oxo-complex of a high-valence metal. In this case, a selective interaction with the pentose takes place and its radicals become the main primary product of the oxidation reaction.

The pentose radicals obtained induce in the course of further reactions either direct cleavage of nucleic acids or modifications of pentose which lead to cleavage after treatment with alkali. In the presence of oxygen, only oxidation in the C(3′)-, C(4′)-, and C(5′)-positions in the pentose leads to the rupture of the nucleic acid target. In the absence of oxygen, only oxidation in the C(3′)- and C(5′)-positions is accompanied by the cleavage of the pentose phosphate skeleton. Oxidation in the C(1′)-position can induce the cleavage of nucleic acids only under the conditions of catalysis by transition metal complexes.

The appearance of radicals derived from heterocycles usually leads to irreversible modifications of the heterocycle in the course of further reactions. Some of these modifications may weaken the glycosidic linkage and may induce the formation of non-pyridine/non-purine sites, which is accompanied by the cleavage of the pentose phosphate skeleton under alkaline conditions. The stable modifications of the heterocycles, remaining bound to DNA, can have intrinsic coding properties different from those of the initial nucleoside, inducing mutations.

References

1. I Fridovich *Annu. Rev. Pharm. Tox.* **23** 239 (1989)
2. W Bors, M Saran, E Lengfelder et al. *Photochem. Photobiol.* **28** 629 (1978)
3. F Hutchinson *Progress in Nucleic Acids Research and Molecular Biology* **32** 115 (1985)
4. P A Cerutti *Science* **227** 375 (1985)
5. M E Vol'pin, D G Knorre, G N Novodarova, M Yu Tuvin, O S Fedorova, E N Frolova *Dokl. Akad. Nauk SSSR* **298** 363 (1988)
6. E J Gibbs, R F Pasternack *Seminars in Hematology* **26** 77 (1989)
7. J Stubbe, J W Kozarich, *Chem. Rev.* **87** 1107 (1987)
8. D S Sigman *Biochemistry* **29** 9097 (1990)
9. P B Dervan *Science* **232** 464 (1986)
10. D G Knorre, V F Zarytova, A G Badashkeeva, O S Fedorova *Biotekhnologiya* T.37 *Itogi Nauki i Tekhniki* [Biotechnology (Vol. 37 of the Series: Advances in Science and Engineering)] (Moscow: Izd. VINITI, 1991), Vol. 37, p 182
11. V M Berdnikov, O S Zhuravleva *Zh. Fiz. Khim.* 46 2658 (1972)
12. V M Berdnikov, N M Bazhin *Zh. Fiz. Khim.* 44 548 (1970)
13. H R Mahler, E H Cordes *Basic Biological Chemistry* (Translated into Russian) (Moscow: Mir, 1970)
14. E T Denisov *Kinetika Gomogennykh Khimicheskikh Reaktsii* (Kinetics of Homogeneous Chemical Reactions) (Moscow: Mir, 1978)

15. S D Aust, L A Morehouse, C E Thomas *J. Free Rad. Biol. Med.* **1** 3 (1985)
16. B Halliwell, J M C Gutteridge *Free Radicals in Biology and Medicine* (Oxford: Clarendon Press, 1986)
17. L A Morehouse, C E Thomas, S D Aust *Arch. Biochem. Biophys. (232) 366 (1984)*
18. J M McCord, I Fridovich *J. Biol. Chem.* (243) 5753 (1968)
19. D K Das, A George, X Liu, P S Rao *Biochem. Biophys. Res. Commun.* **165** 1004 (1989)
20. C A Chuaqui, A Petkau *Radiat. Phys. Chem.* **30** 365 (1987)
21. P Follin, C Dahlgren *Biochem. Biophys. Res. Commun.* **167** 970 (1990)
22. *Enzyme Nomenclature: Recommendations (1978) of the Nomenclature Committee of the International Union of Biochemistry* (New York: Academic Press, 1979) p. 82
23. G W Winston, D E Feierman, A I Cederbuum *Arch. Biochem. Biophys.* (232) 378 (1984)
24. G Czapski, S Goldstein *Bioelectrochem. Bioenergetics* **18** 21 (1987)
25. A S Bertinchamps, J Huttermann, W Kohnlein, R Teoule (Eds) *Effects of Ionising Radiation on DNA* (Berlin: Springer, 1978)
26. C von Sonntag (Ed.) *The Chemical Basis of Radiation Biology* (London: Taylor and Francis, 1987)
27. A J Swallow *Radiation Chemistry: An Introduction* (Translated into Russian) (Moscow: Atomizdat, 1976) p 278
28. J Cadet, R Teule *Photochem. Photobiol.* **28** 629 (1978)
29. O I Aruoma, B Halliwell, M Dizdaroglu *J. Biol. Chem.* **264** 13024 (1989)
30. O I Aruoma, B Halliwell, E Gajewski, M Dizdaroglu *J. Biol. Chem.* **264** 20509 (1989)
31. W F Blakely, A F Fuciarelli, B J Wegher, M Dizdaroglu *Radiat. Res.* **121** 338 (1990)
32. E M Link *Arch. Biochem. Biophys.* **265** 362 (1988)
33. Farhataziz, A B Ross, *Nat. Stand. Ref. Data System, Nat. Bur. Stand.* **59** (NSRDS-NBS-59) (1977)
34. A Singh *Photochem. Photobiol.* **28** 429 (1978)
35. D R Kearns *Chem. Rev.* **71** 395 (1971)
36. A W N Nieuwint, J M Aubry, F Arwert, et al. *Free Radical Res. Commun.* **1** 3 (1985)
37. E R Blazek, W R Midden, M J Peak *Photochem. Photobiol.* **45** (25) (1987)
38. P W White *Bioorgan. Chem.* **18** 440 (1990)
39. J D Rush, Z Maskos, W H Koppenol *FEBS Lett.* **261** 121 (1990)
40. T G Traylor, W-P Fann, D Bandyopadhyay *J. Am. Chem. Soc.* **111** 8009 (1989)
41. T G Traylor, F Xu *J. Am. Chem. Soc.* **112**(1) 178 (1990)
42. S Tsuchiya *J. Chem. Soc., Chem. Commun.* (10) 716 (1991)
43. W A Oertling, R T Kean, R Weaver, G T Babcock *Inorg. Chem.* **29** 2633 (1990)
44. S-M Chen, Y O Su *J. Chem. Soc., Chem. Commun.* (1) 491 (1990)
45. H Sugimoto, H-C Tung, D T Sawyer *J. Am. Chem. Soc.* **110** 2465 (1988)
46. E Bill, X-Q Ding, E L Bominaar, et al. *Eur. J. Biochem.* **188** 665 (1990)
47. T G Traylor, A R Miksztal *J. Am. Chem. Soc.* **111** 7443 (1989)
48. W H Koppenol, J F Liebman *J. Phys. Chem.* **88** 99 (1984)
49. N S Enikolopyan, L F Bogdanova, L V Karmilova, K A Askarov *Usp. Khim.* **54** 369 (1985) [*Russ. Chem. Rev.* **54** 215 (1985)]
50. T G Bowry, K V Ingold *J. Am. Chem. Soc.* **113** 5699 (1991)
51. R K Khanna, J S Sutherlin, D Lindsey *J. Org. Chem.* **55** 6233 (1990)
52. P A Grieco, T L Stuk *J. Am. Chem. Soc.* **112** 7799 (1990)
53. Y Watanabe, K Takehira, M Shimizu, et al. *J. Chem. Soc., Chem. Commun.* 927 (1990)
54. K R Rodgers, I M Arafa, H M Goff *J. Chem. Soc., Chem. Commun.* 1323 (1990)
55. G H McGall, J Stubbe, in *Nucleic Acids and Molecular Biology* Vol. 2, (Eds F Eckstein, D M J Lilley) (Berlin: Springer, 1988) p. 87
56. G Pratviel, J Bernadou, B Meunier *Biochem. Pharmacol.* **38** 133 (1989)
57. G R A Johnson, N B Nazhat *J. Am. Chem. Soc.* **109** 1990 (1987)
58. M Kuwabara, C Yoon, T Goyne, et al. *Biochemistry* **25** 7401 (1986)
59. T B Thederahu, M D Kuwabara, T A Larsen, B Sigman *J. Am. Chem. Soc.* **111** 3941 (1989)
60. M Dizdaroglu, O I Aruoma, B Halliwell *Biochemistry* **26** 8447 (1990)
61. M G Simic, L Grossman, A D Upton (Eds) *Mechanisms of DNA Damage and Repair* (New York: Plenum, 1986)
62. O Inanami, M Kuwabara, D Endoh, F Sato *Radiat. Res.* **108** 1 (1986)
63. O Inanami, M Kuwabara, F Sato *Radiat. Res.* **112** 36 (1987)
64. M Kuwabara, O Inanami, D Endoh, F Sato *Biochemistry* **26** 2458 (1987)
65. M Kuwabara, W Hiraoka, F Sato *Biochemistry* **28** 9625 (1989)
66. W Hiraoka, M Kuwabara, F Sato, et al. *Nucl. Acids Res.* **18** 1217 (1990)
67. S Fujita, S Steenken *J. Am. Chem. Soc.* **103** 2540 (1981)
68. S V Jovanovic, M G Simic *J. Am. Chem. Soc.* **108** 5968 (1986)
69. D K Hazra, S Steenken *J. Am. Chem. Soc.* **105** 4380 (1983)
70. C von Sonntag *Radiat. Phys. Chem.* **30**(5,6) 313 (1987)
71. G W Teebor, K Frenkel, M S Goldstein *Proc. Natl. Acad. Sci. USA* **81** 318 (1984)
72. K Frenkel, A Cummings, J Solomon, et al. *Biochemistry* **24** 4527 (1985)
73. M Dizdaroglu, M G Simic *Radiat. Phys. Chem.* (26) 309 (1985)
74. G A Infante, P Jirathana, J H Fendler, E J Fendler *J. Chem. Soc., Faraday Trans. 1* (69) 1586 (1973)
75. P C Shragge, A J Varghese, J W Hunt, C L Greenstock *Radiat. Res.* **60** 250 (1974)
76. K M Idriss Ali, G Scholes *J. Chem. Soc., Faraday Trans. 1* (76) 449 (1980)
77. S Nishimoto, H Ide, T Wada, T Kagiya *Int. J. Radiat. Biol.* **44** 585 (1983)
78. H Ide, Y W Kow, S S Wallace *Nucl. Acids Res.* **13** 8035 (1985)
79. R Teoule, J Cadet *J. Chem. Soc., Chem. Commun.* 1269 (1971)
80. M Dizdaroglu, M G Simic *Radiat. Res.* **100** 41 (1984)
81. M N Schuchmann, C von Sonntag *J. Chem. Soc., Perkin Trans. 2* 1525 (1983)
82. R Ducolomb, J Cadet, R Teoule *Bull. Soc. Chim. Fr.* 1167 (1973)
83. J Cadet, R Teoule *Bull. Soc. Chim. Fr.* (3,4) 885 (1975)
84. J Cadet, R Teoule *Bull. Soc. Chim. Fr.* (3,4) 891 (1975)
85. J Cadet, R Nardin, L Voituriez, et al. *Can. J. Chem.* **59** 3313 (1981)
86. J Cadet, R Teoule *Bull. Soc. Chim. Fr.* (3,4) 879 (1975)
87. M Polverelli, R Teoule *Z. Naturforsch. C* **29** 12 (1974)
88. M Polverelli, J Ulrich, R Teoule *Z.Naturforsch. C* **29** 64 (1974)
89. P O'Neill, S E Davies *Int. J. Radiat. Biol.* **49** 937 (1986)
90. A J S C Vieira, S J Steenken *J. Am. Chem. Soc.* **109** 7441 (1987)
91. A J S C Vieira, S J Steenken *J. Phys. Chem.* **91** 4138 (1987)
92. S Steenken *Chem. Rev.* **89**(3) 503 (1989)
93. A J S C Vieira, S J Steenken *J. Am. Chem. Soc.* **112** 6986 (1990)
94. S V Jovanovic, M G Simic *Biochem. Biophys. Acta* **1008** 39 (1989)
95. A Bonicel, N Mariaggi, E Hughes, R Teoule *Radiat. Res.* **83** 19 (1980)
96. M Berger, J Cadet *Z. Naturforsch. B* **40** 1519 (1985)
97. J J van Hemmen, J F Bleichrodt *Radiat. Res.* **46** 4476 (1971)
98. M Dizdaroglu *Biochemistry* **24** 4476 (1982)
99. S Uesugi, T Shida, M Ikehara, et al. *J. Am. Chem. Soc.* **104** 5494 (1982)
100. A F Fuciarelli, B J Wegher, E Gajewski, et al. *Radiat. Res.* **119** 219 (1989)
101. E Gajewski, G Rao, Z Nackerdien, M Dizdaroglu *Biochemistry* **29** 7876 (1990)
102. E Gajewski, O I Aruoma, M Dizdaroglu, B Halliwell *Biochemistry* **30** 2444 (1991)
103. D Schulte-Frohlinde, C von Sonntag *Isr. J. Chem.* **10** 1139 (1972)
104. D Schulte-Frohlinde, E Bothe *Z. Naturforsch. C* **39** 315 (1984)
105. S M Hecht (Ed.) *Bleomycin: Chemical, Biochemical and Biological Aspects* (New York: Springer, 1979)
106. S M Hecht *Acc. Chem. Res.* **19** 383 (1986)
107. J W Kozarich, L Worth, B L Franck, et al. *Science* **245** 1396 (1989)
108. G H McGall, L E Rabow, J Stubbe, et al. *J. Am. Chem. Soc.* **109** 2836 (1987)
109. S Ajmera, J C Wu, L Worth, et al. *Biochemistry* **25** 6586 (1986)
110. R M Burger, S J Projan, S B Horwitz, J Peisach *J. Biol. Chem.* **261** 15955 (1986)
111. J T Groves, R C Haushalter, M Nakamura, et al. *J. Am. Chem. Soc.* **103** 2884 (1981)
112. H Sugiyama, C Xu, N Murugesan, et al. *Biochemistry* **27** 58 (1988)
113. L E Rabow, J Stubbe, J W Kozarich *J. Am. Chem. Soc.* **112** 3196 (1990)

114. L E Rabow, G H McGall, J Stubbe, J W Kozarich *J. Am. Chem. Soc.* **112** 3203 (1990)
115. M Dizdaroglu, C von Sonntag, D Schulte-Frohlinde *J. Am. Chem. Soc.* **97** 2277 (1975)
116. H-P Schuchmann, R Wagner, C von Sonntag *Z. Naturforsch. B* **38** 1213 (1983)
117. D Schulte-Frohlinde, G Behrens, A Onal *Stud. Phys. Chem. Med.* **50** 103 (1986)
118. R P Hertzberg, P B Dervan *Biochemistry* **23** 3934 (1984)
119. I H Goldberg *Acc. Chem. Res.* **24** 191 (1991)
120. M D Lee, A G Ellestad, D R Borders *Acc. Chem. Res.* **24** 235 (1991)
121. S M Meschwitz, I H Goldberg *Proc. Natl. Acad. Sci. USA* **88** 3047 (1991)
122. B L Frank, L Worth, D F Christner, et al. *J. Amer. Chem. Soc.* **113** 2271 (1991)
123. L S Kappen, I H Goldberg, B L Frank, et al. *Biochemistry* **30** 2034 (1991)
124. H Kawabata, H Takeshita, T Fujiwara, et al. *Tetrahedron Lett.* **30** 4263 (1989)
125. L S Kappen, T E Ellenberger, I H Goldberg *Biochemistry* **26** 384 (1987)
126. L F Povirk, I H Goldberg *Biochemistry* **23** 6304 (1984)
127. D-H Chin, S A Carr, I H Goldberg *J. Biol. Chem.* **259** 9975 (1984)
128. G Pratviel, M Pitie, J Bernadou, B Meunier *Angew. Chem., Int. Ed. Engl.* **30** 702 (1991)
129. D Langfinger, C von Sonntag *Z. Naturforsch. C* **40** 446 (1985)
130. M Dizdaroglu, D Schulte-Frohlinde, C von Sonntag *Z. Naturforsch. C* **30** 826 (1975)
131. H Urata, K Yamamoto, M Akagi, et al. *Biochemistry* **28** 9566 (1989)
132. T E Goyne, D S Sigman *J. Am. Chem. Soc.* **109** 2846 (1987)
133. D S Sigman, A Spassky, in *Nucleic Acids and Molecular Biology* Vol. 3 (Eds F Eckstein, D M J Lilley) (Berlin: Springer, 1989) p. 13
134. J Bernadou, B Lauretta, G Pratviel, B Meunier *C.R. Acad. Sci.* Ser. 3 **309** 409 (1989)
135. G Gasmi, M Pasdeloup, G Pratviel, et al. *Nucl. Acid. Res.* **19** 2835 (1991)
136. G Pratviel, M Pitie, J Bernadou, B Meunier *Nucl. Acid. Res.* **19** 6283 (1991)
137. A M Pyle, E C Long, J K Barton *J. Am. Chem. Soc.* **111** 4520 (1989)
138. A M Pyle, M Chiang, J K Barton *Inorg. Chem.* **29** 4487 (1990)
139. A H G Wang, J Nathans, G van der Marel, et al. *Nature (London)* **276** 471 (1978)
140. A Sitlani, E C Long, A M Pyle, J K Barton *J. Am. Chem. Soc.* **114** 2303 (1992)
141. M Dizdaroglu, D Schulte-Frohlinde, C von Sonntag *Z. Naturforsch. C* **32** 1021 (1977)

Russian Chemical Reviews **62** (2) 87 – 104 (1993)
© 1993 Russian Academy of Sciences and Turpion Ltd

UDC 541.124/128.3:546.26-162

The chemical synthesis of diamond. Aspects of the general theory

A P Rudenko, I I Kulakova, V L Skvortsova

Contents

I.	Introduction	87
II.	The chemical synthesis of diamond from light carbon-containing molecules	88
III.	The stoichiometric and thermodynamic conditions of diamond and graphite polycondensation	89
IV.	The kinetic conditions of diamond and graphite polycondensation	92
V.	The polycondensation mechanism of the formation of diamond and non-diamond carbon	94
VI.	A model of the non-equilibrium growth of diamond crystals in a macroscopic open catalytic system	98
VII.	An analysis of the conditions of formation of diamond in experiments and in various natural deposits	100
VIII.	Summary	103

Abstract. The theory of the synthesis of diamond by the polycondensation of light carbon-containing molecules is examined, and the optimum stoichiometric, thermodynamic, and kinetic conditions for diamond and graphite polycondensation and the reverse conversion of diamond and graphite by water vapour and carbon dioxide are described. The formation of critical nuclei of diamond shows no specific restrictions, and can take place under static conditions. The growth of these nuclei and their transformation into macrocrystals require specific macrokinetic conditions, which can be produced only in non-equilibrium open catalytic systems. The conclusions from the theory are confirmed by analysis of the conditions of experiments on the growth of diamond crystals and the synthesis of diamond films on various supports, and of the formation and growth of diamond meta-crystals in nature. The bibliography contains 74 references.

I. Introduction

It is now becoming increasingly evident that diamond can be formed not only at high pressures and temperatures by the polymorphic transformation of graphite but also at medium and low pressures by the transformation of simple carbon-containing molecules. The extension of ideas about possible conditions of diamond formation applies not only to artificial synthesis but also to natural deposits. Until recently the formation of diamonds under natural conditions was assumed to be explained by the pallial (mantle) hypothesis [super-high pressure (SHP) conditions]. An important contribution to the establishment of the polygenetic hypothesis of diamond formation was made by work on the epitaxial growth of single crystals and the synthesis of diamond films from the gas phase at low pressures,[1-7] and also by facts revealed by the study of kimberlite[55-57] and non-kimberlite[66-70] diamond deposits. From the viewpoint of the polygenetic approach to diamond formation, which takes account of not only physical factors but also, and primarily, chemical factors, both the polycondensation of light carbon-containing species without SHP, and the polymorphic transformation of graphite into diamond by the action of SHP, but not without the involvement of certain chemical factors, are possible.

The possible high-pressure formation of diamond is confirmed by the present industrial production of diamonds by static synthesis at 1300 – 1400 K and 45 – 50 kbar, and also by the production of diamonds by explosion (detonation) at pressures up to 150 kbar, containing as the principal phase the hexagonal polytype of diamond — lonsdaleite. This is consistent with the discovery of lonsdaleite-containing polycrystalline diamonds in meteoric impact products with distinct traces of the action of SHP, and with the discovery of minerals formed at high pressures as inclusions in kimberlite diamonds. SHP was not critical, however, for the formation of kimberlite and more particularly non-kimberlite diamond deposits, similar to the Kokchetav deposit. The conservatism of various workers who consider that the high-pressure route is the only path to diamond formation is related to the neglect of chemical factors in diamond synthesis. Thus the solution to the problem of the genesis of natural diamonds lies not in the search for new evidence of their pallial (mantle) origin but in the accurate discrimination of the conditions for possible routes to the formation of diamond.

The present review provides a theoretical justification of the conditions of the chemical synthesis of diamond from small carbon-containing molecules without the use of high pressure. This synthesis is being successfully reproduced in laboratories, and is undoubtedly a source of diamonds in various types of natural deposit.

II. The chemical synthesis of diamond from light carbon-containing molecules

The general concept of the chemical synthesis of diamond from the gas phase at atmospheric pressure has been discussed.[8] The analysis of experimental data on the synthesis of diamond films by different authors has established the optimum conditions for the formation of diamond in relation to the atomic composition (H, C, O) of the original gas phase, its temperature, and the temperature of the support on which the diamond film is deposited.

A P Rudenko, I I Kulakova, V L Skvortsova Department of Petroleum Chemistry and Organic Catalysis, Faculty of Chemistry, Lomonosov Moscow State University, Leninskie Gory, 119899 GSP-3, Moscow V-234. Fax (7-095) 939 01 26

Received 29th October 1992
Uspekhi Khimii **62** (2) 99 – 117 (1993); translated by D A Paterson

The optimum range of diamond formation corresponds to a definite atomic ratio H : C : O. With increase in the temperature of the gas mixture there is a significant increase in the rate of diamond formation and a decrease in the influence of the nature of the original molecules. The deposition of diamond on the support, which may be practically any solid material, takes place at 700–1600 K; increasing the temperature of the support or going beyond the stoichiometric boundary of the diamond range (at H : C : O ratios characteristic of reducing conditions) gives 'non-diamond carbon'. All points of the H–C–O diagram corresponding to the syntheses carried out lie in a narrow diamond range close to the CO–H line, with rare exceptions, observed in experiments with mixtures enriched in oxygen or hydrogen and in experiments in which the influence of the nature of the original molecules and the support is appreciable.

In most of the studies analysed in the work cited,[8] increase in the temperature of the source of carbon (gas mixture or plasma) was the chief factor giving a high rate of formation of diamond films. Thus in addition to thermal heating, use was made of various methods of preparing the gas mixtures (high-frequency heating at low pressure, oxygen–acetylene flames, a high-voltage glow discharge, microwave or laser heating of plasma), which made possible a 10^2-10^3-fold increase in the rate of diamond formation, compared with thermal heating.

Naturally, increase in the temperature of the gas mixture from 400–800 K to 7000 K, leading to degradation of the molecules and levelling of the composition of the gas–plasma mixture, fully explains the fact that the position of the diamond range on the H–C–O diagram at high temperatures of preparation of the gas mixture is determined mainly by the H : C : O ratio in it, and not by the nature of the component molecules. This can be regarded as corresponding to a decrease in the role of chemical factors and an increase in the importance of physical factors in the formation of diamond films. This view is far from the truth, however, for the decisive role of chemical factors, even in experiments with a hot plasma, is related to the fact that the diamond range corresponds to a definite stoichiometric H : C : O ratio, and the formation of each new C–C bond in the diamond lattice is a chemical polycondensation process, taking place on the support at a comparatively low temperature and independent of the temperature of the plasma and the nature of the light carbon-containing species involved in the process.

Of course, with change in temperature the composition of the gas–plasma mixture changes, from that corresponding to the original mixture of components to some equilibrium composition, which is the same for all isostoichiometric mixtures. The specific mechanisms of formation of the new C–C bonds will differ in their elementary stages, but in all cases the process remains a chemical process. It is influenced strongly not only by stoichiometric but also by thermodynamic and kinetic conditions, and also by effects related to the non-equilibrium nature of open catalytic systems.

In the work cited,[8] most attention was paid to the stochiometric conditions of the synthesis of diamond from the gas phase, and no consideration was given to the other conditions of this chemical process, which are of no less importance for ensuring its stability. In the present review we have tried to fill this gap and to show the influence of various factors on the chemistry of the transformations of light carbon-containing molecules leading to the formation of diamond and non-diamond carbon and their conversion into gaseous products in the processes of chemical synthesis at low and medium pressures. Most attention is paid not to the formation of diamond films from the components of a high-temperature plasma[8] but to the heterogeneous-catalytic processes taking place under isothermal conditions with identical temperatures of the gas phase and the support or the nucleus of the diamond crystal. The last case reveals most fully and clearly the essential chemical nature of the diamond synthesis, which differs from the synthesis from a high-temperature plasma only in the details of the mechanism.

At low temperatures of the gas phase, the diamond material is formed by the polycondensation of the original molecules by a molecular mechanism. In a high-temperature plasma, the polycondensation involves both the undissociated original molecules and small molecules formed by the decomposition of the original molecules, and also ions and radical species. Thus the mechanism of the process may be to a large extent ionic and radical. In both cases, however, all the stages of the process take place at the temperature of the support, and diamond formation involves the polycondensation of light species with the necessary participation of the support and the diamond film growing on it. In other words, this is a heterogeneous-catalytic process. The catalysts may be the support, the diamond material formed on it, and various non-stoichiometric components of the gas phase.

The examination of the chemical aspect of the general theory of the synthesis of diamond from light carbon-containing molecules cannot be restricted to the question of diamond synthesis, without considering the polycondensation synthesis of graphite, graphite-like materials, and other condensation products (CP), often called 'non-diamond carbon'. The processes of diamond and graphite polycondensation are related chemical processes having the same stoichiometry and similar thermodynamics and differing only in the kinetic conditions and mechanisms. Thus the determination of the optimum kinetic conditions of diamond polycondensation compared with the conditions of graphite polycondensation is acquiring decisive importance in the development of the general theory of the chemical synthesis of diamond.

A basis for the discussion of the specific features of the kinetic conditions of diamond synthesis is provided by the results of systematic studies over many years in the following directions.

1. Work on the chemical synthesis of diamond at atmospheric pressure; the study of the chemistry of the surface of diamond crystals and the catalytic transformation of diamond in its reactions with gaseous and liquid media; the study of the mechanism of the oxidation of diamond material in its reaction with CO_2, H_2O, and other oxidants, and the conditions of the selective oxidation of graphite and other forms of non-diamond carbon in the presence of diamond; and the determination of the influence of various factors on the prevention of the oxidation of graphite under oxidising conditions.[9–14]

2. Work on the study of the nature and mechanism of formation of the polycondensation products of organic substances on heterogeneous catalysts, accompanying almost any organic catalytic reaction; the determination of the role of condensation products in stationary and non-stationary open catalytic systems; and the study of the influence of various factors on the polycondensation process, the degree of molecular condensation, the extent of aromatic condensation, the ratio of volatile and non-volatile condensation products, and the discrimination between the conditions for diamond and aromatic polycondensation.[15–18]

3. Work on the investigation of the conditions of diamond formation, the characteristics of the distribution of diamonds in deposits, and their mineral and geochemical associations with the surrounding medium; the establishment of correlations between the diamond-bearing character of various kimberlite pipes of Yakutia, the catalytic properties of the rock (in the oxidation of diamond by water vapour and carbon dioxide), and the oxidation potential and concentration of non-diamond carbon and bitumens[19–23] to develop a physicochemical criterion of diamond-bearing character; and the study of the properties of diamonds and the conditions of diamond formation in deposits of other types — metasomatic (Kokchetav), impact (Popigay), etc.

4. Work on the creation of models of the growth of diamond crystals and the abiogenic synthesis of hydrocarbons, bitumens, and graphite-like substances in the polycondensation of CO with H_2 and other light molecules in open catalytic systems,[19,24] and the development of the theory of non-equilibrium open catalytic systems[25,26] and evolution chemistry.[27]

III. The stoichiometric and thermodynamic conditions of diamond and graphite polycondensation

Published data[15-22,24,25] show that at the same temperatures at atmospheric or low pressures with the participation of heterogeneous catalysts (K), polycondensation of carbon-containing molecules A can take place with the formation of various solid products and the removal of various light molecules L:

$$nA \overset{K}{\rightleftharpoons} A_nK \rightarrow \{A_n - mL\}K + mL ,$$

$$A + \{A_n - mL\}K \rightleftharpoons \{A_{n+1} - mL\}K \rightarrow$$

$$\rightarrow \{A_{n+1} - (m+1)L\}K + L , \quad (i)$$

where $\{A_n - mL\}$, $\{A_{n+1} - (m+1)L\}$ represent the solid polyconden-sation products and other forms of non-diamond carbon or diamond.

Graphite (aromatic) and diamond polycondensation processes take place under their own specific kinetic conditions, but have the same or similar stoichiometric and thermodynamic parameters. Thus to distinguish the diamond range it is not sufficient to take as a basis the stoichiometric atomic ratio H : C : O, as was done in the work cited,[8] since in the same range the diamond and graphite polycondensation processes are equally probable.

In the work cited,[8] it was possible to distinguish the diamond range only because the diamond film syntheses examined were characterised by specific kinetic conditions which ensured that the experimental points lay in this range. Other factors were not examined. A definite role in the neglect of the kinetic conditions of the processes was also played by the observed[8] levelling of the influence of the nature of the molecules in equiatomic mixtures with increase in the temperature of the plasma. Although this is not inconsistent with the chemical nature of diamond synthesis, it reduces the stoichiometric conditions to the same equilibrium composition of the dissociation products of any isostoichiometric mixture, which is the case only for the highest-temperature plasma. If, however, the gas–plasma mixture contains undissociated molecules, or if an undissociated gas mixture heated to the temperature of the support is used, then it is obvious that the conditions of the polycondensation (1) for a definite atomic ratio H : C : O will differ not only in the kinetic factors but also in the stoichiometry and thermodynamics of the transformations of each of the equiatomic mixtures taken, according to each possible transformation direction.

This can be seen by examining the stoichiometry and thermodynamics of the reactions on which the polycondensation process (1) is based. We can take the series of simplest reactions giving graphite and diamond[15,19,24,25]

$$2CO \rightleftarrows C(\text{diamond}) + CO_2 , \quad (2)$$

$$2CO \rightleftarrows C(\text{graphite}) + CO_2 , \quad (2')$$

$$CO + H_2 \rightleftarrows C(\text{diamond}) + H_2O , \quad (3)$$

$$CO + H_2 \rightleftarrows C(\text{graphite}) + H_2O , \quad (3')$$

$$CH_4 + CO_2 \rightleftarrows 2C(\text{diamond}) + 2H_2O , \quad (4)$$

$$CH_4 + CO_2 \rightleftarrows 2C(\text{graphite}) + 2H_2O . \quad (4')$$

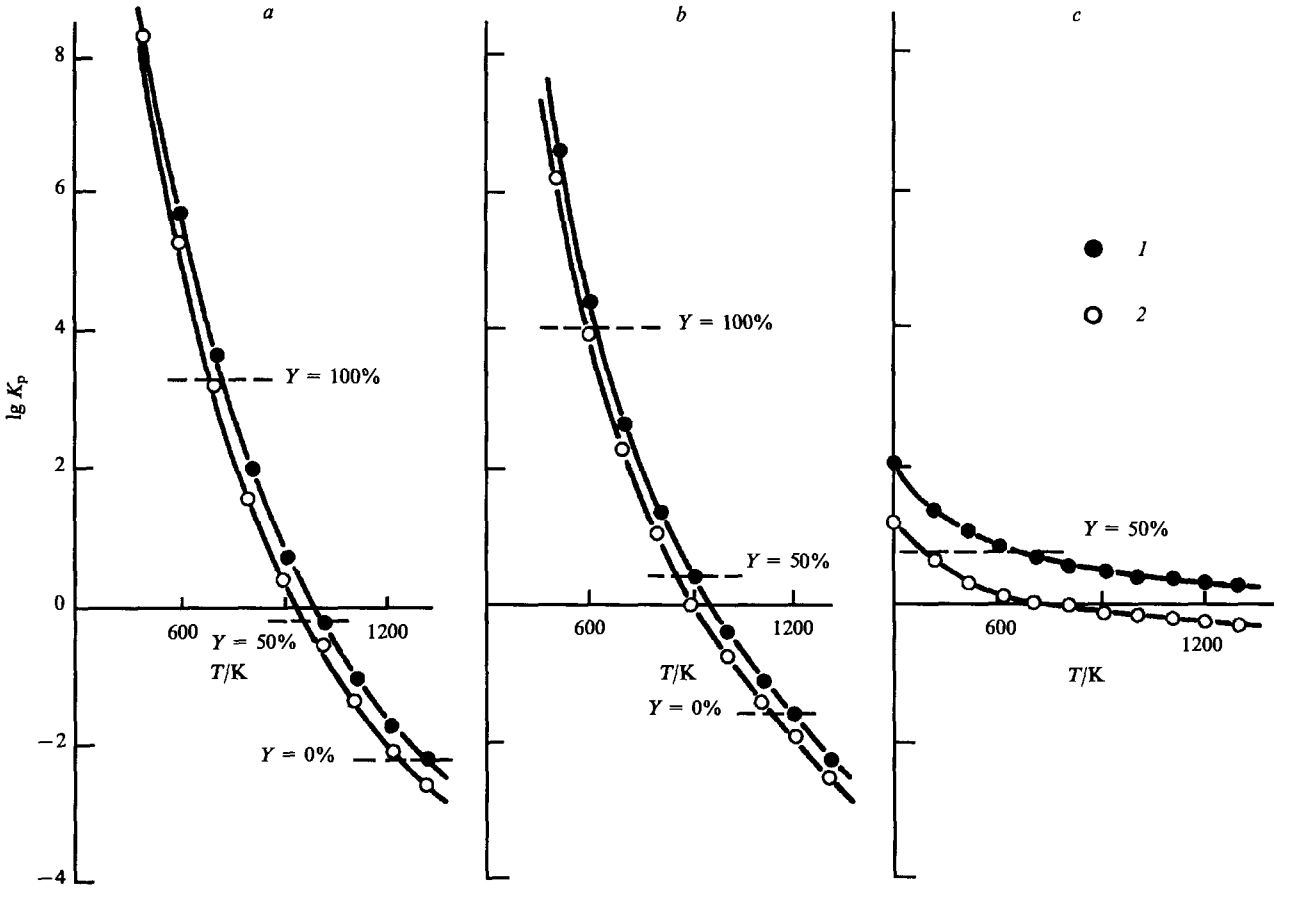


Figure 1. Thermodynamic conditions of the synthesis of graphite (*1*) and diamond (*2*) at P = 1 atm (Y is the degree of transformation); synthesis by the reactions: *a*, (2), (2′); *b*, (3), (3′); *c*, (4), (4′).

There are many analogous processes, for example

$$CH_3OH \rightleftarrows C(\text{diamond}) + H_2O + H_2 , \quad (5)$$

$$CH_3OH \rightleftarrows C(\text{graphite}) + H_2O + H_2 , \quad (5')$$

and also reactions involving solid components

$$CO + 2FeO \rightleftarrows C(\text{diamond}) + Fe_2O_3 , \quad (6)$$

$$CO_2 + 4FeO \rightleftarrows C(\text{diamond}) + 2Fe_2O_3 . \quad (7)$$

All these processes are thermodynamically possible, and the thermodynamic conditions for the diamond or graphite polycondensation processes to take place, although not the same, are nevertheless fairly similar (Fig. 1).

The thermodynamic conditions of different versions of the polycondensation (1) within a given type also differ from one another. For example, for the diamond polycondensation of methanol, in addition to version (5), it is possible to suggest at least another three:

$$2CH_3OH = C(\text{diamond}) + CO_2 + 4H_2 , \quad (8)$$

$$2CH_3OH = C(\text{diamond}) + CO + H_2O + 3H_2 , \quad (9)$$

$$2CH_3OH = C(\text{diamond}) + CH_2O + H_2O + 2H_2, \quad (10)$$

having different stoichiometries and thermodynamics (Fig. 2).

For diamond polycondensation from mixtures of different substances equiatomic with methanol we again have different thermodynamics for all four versions with different stoichiometries (Table 1).

There will be similar differences in the thermodynamic conditions for the processes of aromatic (graphite) polycondensation from the same original substances and mixtures. The calculations given were carried out for the formation of diamond and graphite, which are the products of the limiting stages of the polycondensation (1). The genealogical series of products of the diamond and graphite polycondensation processes (Tables 2 and 3 and Fig. 3), however, may also include the products of an intermediate stage of the polycondensation.

$$\left.\begin{array}{l} CH_3OH \\ C_2H_5OH + H_2O \\ C_2H_4 + 2H_2O \\ CH_2O + H_2 \end{array}\right\} \rightarrow \left\{\begin{array}{l} C(\text{diamond}) + H_2O + H_2 \\ C(\text{diamond}) + CO_2 + 4H_2 \\ C(\text{diamond}) + CO + H_2O + 3H_2 \\ C(\text{diamond}) + CH_2O + H_2O + 2H_2 \end{array}\right. \quad (11)$$

The extent of the polycondensation in these series is characterised by the ratio of the number of functional groups or hydrogen atoms on the peripheral parts of the polycyclic molecules of the condensation product to the total number of carbon atoms in the rings.[15,16] For example, for the hydrocarbon monomers A in the genealogical series of condensation products of the graphite series the atomic ratio H : C decreases from 1 to 0 on going from the simplest products (A = C_2H_2) to polycyclic aromatic hydrocarbons (PAH) and graphite, with a simultaneous increase in the specific (per monomer unit) decrease in the thermodynamic potential of process (1) (Fig. 4). In large crystals of diamond or graphite, or in carbon fibres, in which the polycyclic network of the PAH is coiled to form a tube, the H : C ratio approaches zero, but does not reach it. In the fullerenes[28] (C_{60} and others), however, the polycyclic carbon network is coiled into a closed sphere, leading to the limiting degree of aromatic polycondensation and a ratio H : C = 0.

The degree of aromatic polycondensation is related to the equilibrium degrees of transformation of A into different condensation products, which have their maximum values for the formation of the end member of this series, namely graphite. The degree of the transformation of A into diamond in all the parallel

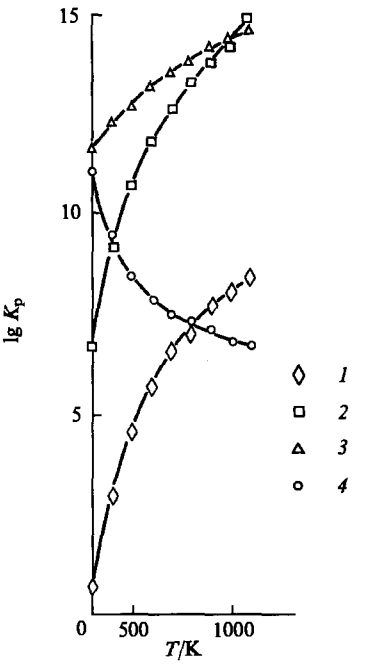


Figure 2. Thermodynamic conditions of the diamond polycondensation of methanol; synthesis by the reactions: *1*, (5); *2*, (8); *3* (9); *4*, (10).

reactions (2) and (2'), (3) and (3'), etc. is lower than the degree of transformation into graphite, and much higher than the equilibrium degree of transformation of CO + H_2 into PAH (see Fig. 4).

None of these differences, however, is significant for the polycondensation (1) taking place to give diamond or graphite, since the calculated thermodynamically equilibrium degrees of transformation characterise only the possibility that the reactions will take place spontaneously, and the question of whether they actually take place is determined by the kinetic conditions, which are different for each reaction.

The kinetic conditions include not only the actual characteristics of the interaction of the molecules and the mechanism of the reaction but also the effects of catalysts, other

Table 1. Values of lg K_p for the diamond polycondensation of CH_3OH, $C_2H_5OH + H_2O$, $C_2H_4 + 2H_2O$, and $CH_2O + H_2$ to give the products of reaction (11) for different degrees of transformation *Y*.

Reaction		*Y* (%)		
		100	50	0
CH_3OH		+1.69	−0.48	−4.00
$C_2H_5OH + H_2O$		+1.64	−0.60	−5.41
$C_2H_4 + 2H_2O$	$\rightleftarrows C(\text{diamond}) + H_2O + H_2$	+2.29	+0.13	−3.40
$CH_2O + H_2$		+2.00	0.00	−2.00
CH_3OH		+3.70	−0.73	−9.11
$C_2H_5OH + H_2O$		+4.30	−0.13	−8.51
$C_2H_4 + 2H_2O$	$\rightleftarrows C(\text{diamond}) + CO_2 + 4H_2$	+6.39	0.00	−9.14
$CH_2O + H_2$		+3.15	+0.35	−1.76
CH_3OH		+2.72	−1.71	−10.09
$C_2H_5OH + H_2O$		+1.62	−0.67	−7.60
$C_2H_4 + 2H_2O$	$\rightleftarrows C(\text{diamond}) + CO + H_2O + 3H_2$	+4.21	−0.13	−7.17
$CH_2O + H_2$		+3.15	+0.35	−1.76
CH_3OH		+2.80	−0.80	−8.60
$C_2H_5OH + H_2O$		+1.64	−0.60	−5.41
$C_2H_4 + 2H_2O$	$\rightleftarrows C(\text{diamond}) + CH_2O + H_2O + 2H_2$	+4.11	−0.10	−5.69
$CH_2O + H_2$		+2.00	0.00	−2.00

Table 2. Genealogical series of products of diamond polycondensation with allowance for the changes in the composition and size of the macromolecules.

Size of molecule (crystal)/mm	Diamond-hydrocarbons (C_nH_x)	Diamond-alcohols ($C_nO_xH_x$)	Diamond-ketones (C_nO_x)	Atomic ratio $C:C_{surf}$
		Molecular species		
3.5×10^{-7}	Adamantane	Tetrahydroxyadamantane-hexanone $C_{10}(OH)_4O_6$		1
$10^{-7}-10^{-6}$	Polycyclic	Polycyclic diamond-alcohols	Polycyclic diamond-ketones	1.3–13
$10^{-6}-10^{-4}$	Colloidal	Colloidal diamond-alcohols	Colloidal diamond-ketones	1.3–130
		Crystals		
$10^{-4}-10^{-1}$	Microcrystals of diamond with a hydrogen cover	Microcrystals of diamond with a hydroxyl cover	Microcrystals of diamond with a carbonyl cover	130–130×10^3
> 0.1	Macrocrystals of diamond with a hydrogen cover	Macrocrystals of diamond with a hydroxyl cover	Macrocrystals of diamond with a carbonyl cover	$> 130 \times 10^3$

non-stoichiometric components, and factors determining material exchange, the level of non-equilibrium character in the open system, etc. When favourable kinetic conditions are created, some of the thermodynamically possible reactions will take place, while others may be completely eliminated or largely suppressed, and in some cases this leads to diamond polycondensation under thermodynamic conditions favourable for graphite polycondensation.

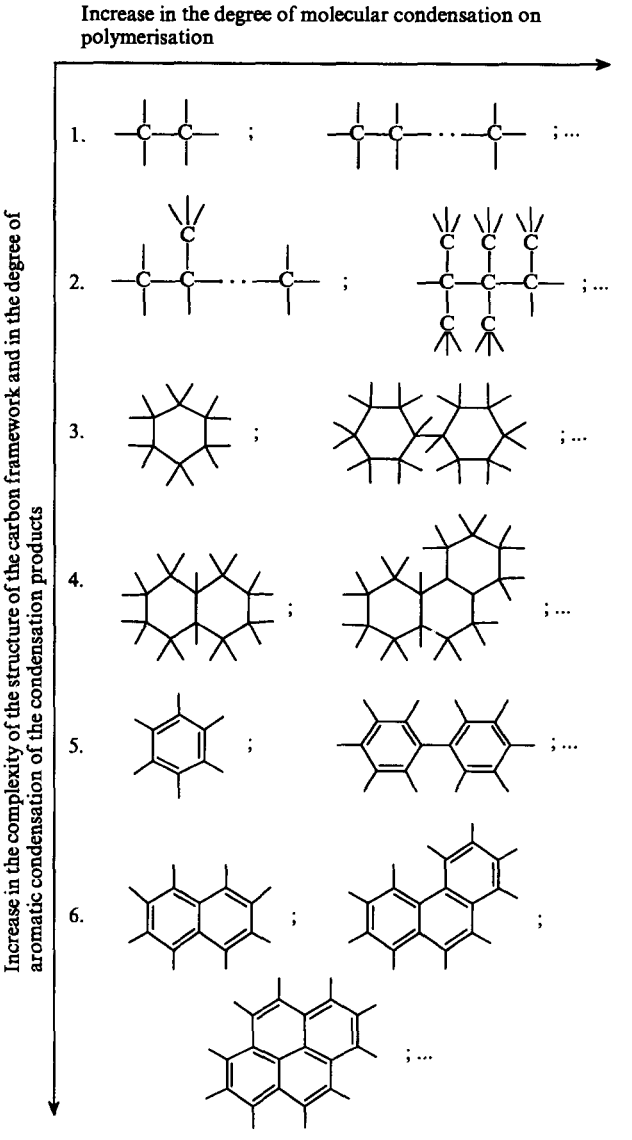
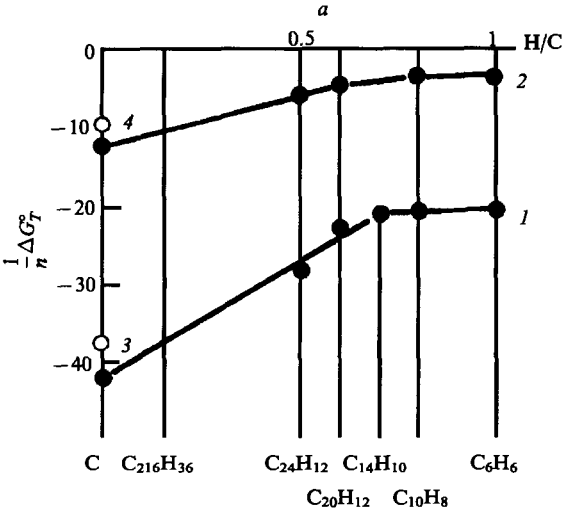


Figure 3. Natural genealogical classification of the condensation products of the graphite series.



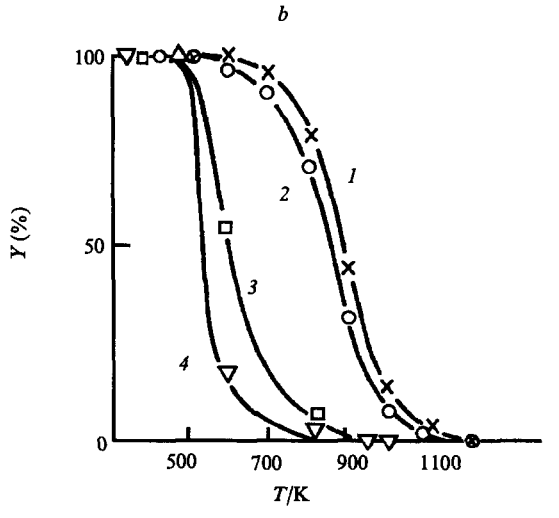


Figure 4. Relationship between the degree of polycondensation and the thermodynamic potential (*a*) and the equilibrium degree of transformation (*b*); *a*, dependence of the specific decrease in the Gibbs potential per monomeric unit on the atomic ratio H/C in the condensation products (CP) for their formation by the reactions $nC_2H_2 \rightleftharpoons \{(C_2H_2)_n\} \rightarrow \{(C_2H_2)_n\} - mH_2$ at 1000 K (*1*, *3*) and $CO + H_2 \rightarrow CP + H_2O$ at 700 K (*2*, *4*); *1*, *2*, CP of the graphite series; *3*, *4*, diamond; *b*, equilibrium degrees of transformation of a $CO + H_2$ mixture with the formation of graphite (*1*), diamond (*2*), coronene (*3*), and naphthalene (*4*).

Table 3. The crystal characteristics and functional groups in genealogical series of diamond polycondensation.

Series	Crystal habit	Face	a^*
Diamond-hydrocarbons >CH; >C(H)H	Octahedron, cubi-octahedron, rhombododecahedron	{111} {100}, {111} {100}	1.3
Diamond-alcohols >C—OH	Octahedron, rhombododecahedron	{111}, {100}	1.8
Diamond-ketones >C=O	Cube	{110}	2.6

* $C/C_{surf} = 10^a$ *a*.

IV. The kinetic conditions of diamond and graphite polycondensation

The most important factor creating favourable kinetic conditions for diamond polycondensation and the preservation and accumulation of diamond material with unfavourable conditions for the formation and preservation of graphite condensation products (non-diamond carbon) is the selection of catalysts and conditions for which the rate of formation of diamond (v_{di}) by reactions (2)–(5) is greater than the rate of formation of graphite (v_{gr}) by reactions (2′)–(5′) and, which is most important, the rate of oxidation of graphite $v_{o(gr)}$ is much greater than the rate of oxidation of diamond $v_{o(di)}$:

$$C(\text{diamond})[C(\text{graphite})] + H_2O(CO_2, O_2) \xrightarrow{v_o} CO + H_2. \quad (12)$$

The conditions

$$v_{di} > v_{gr}\,;\; v_{o(di)} \ll v_{o(gr)} \quad (13)$$

can obviously be produced in systems with a sufficiently high initial oxidation potential, in which reactions which are the reverse of reactions (2)–(5) or (2′)–(5′) and other polycondensation processes leading to the formation of diamond or graphite are possible. Thus the hatched diamond range established[8] on the H–C–O atomic diagram (Fig. 5) lies between a range with a high reduction potential (the range corresponding to hydrocarbons, whose polycondensation gives mainly graphite and other forms of non-diamond carbon) and a range with a high oxidation potential [the range corresponding to H_2O, CO_2, O_2, in which neither diamond nor graphite can be formed and preserved, since they undergo complete conversion according to Eqn. (12)].

This range should also be restricted in the direction corresponding to mixtures very rich in hydrogen, where hydrogenolysis of diamond and graphite with the rupture of C–C bonds is possible

$$C(\text{diamond})[C(\text{graphite})] + 2H_2 \rightarrow CH_4\,. \quad (14)$$

This process can take place, however, only when specific hydrogenolysis catalysts are present. The fact that diamond films have been synthesised in mixtures with a large excess of molecular hydrogen[8] is apparently due to the absence of these catalysts and the greater ease of hydrogenolysis of graphite compared with diamond.

The range very rich in carbon on the atomic diagram can be represented essentially by different types of solid polycondensation products. These products cannot be transferred to the vapour phase without degradation, and the possible synthesis of diamond from them reduces to the polymorphic transformation of graphite, for which the thermodynamic conditions are unfavourable without super-high pressure even with allowance for intermediate gasification

$$C(\text{graphite}) + CO_2 \rightarrow [2CO] \rightarrow C(\text{diamond}) + CO_2\,. \quad (15)$$

A number of experimental studies[9–12,15,16,19,20,24] have proved the existence of ranges with different oxidation potentials, in which it is possible to have polycondensation of hydrocarbons and other organic substances with the formation of condensation products of the graphite series and polycondensation of CO, H_2, CO_2, CH_4, H_2O mixtures with the predominant formation of diamond, and also complete conversion of diamond, graphite, and other condensation products by the action of water vapour, carbon dioxide, and certain other oxidants.

The hydrogenolysis of C–C bonds has been studied in the work[30,31] on the gasification of coals and on the hydrogenation of diamond in the presence of metallic catalysts.

It was established that: it is easy to find kinetic conditions favourable for graphite polycondensation, and much more difficult to find kinetic conditions favourable for diamond polycondensation;[15,16,19] there exist kinetic conditions under which graphite is oxidised, and diamond is not oxidised[11,12] or is oxidised much more slowly;[32] the nature of the catalysts has a strong influence on the rate of oxidation of diamond, and a mutual influence of different catalysts and substances in the vapour phase on the kinetics of the oxidation is observed, as far as its complete inhibition.[10,11] The formation of different functional groups on the diamond surface in its chemical reactions with the gas and liquid phases,[13,14] and the influence of the functional covering on the physical and chemical properties of diamond,[14] were established.

The data obtained brought us closer to an understanding of the mechanism of the oxidation of diamond by carbon dioxide and water vapour at 900–1300 K and of the reverse process, that is the synthesis of diamond by reactions (2)–(5). They made it possible to determine the necessary synthesis conditions and catalysts [since under conditions close to the equilibrium for

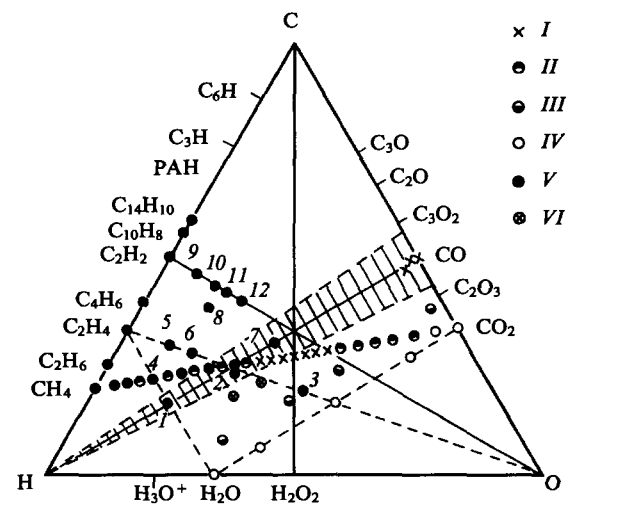


Figure 5. Diagram showing the stoichiometric conditions of the processes of diamond and graphite polycondensation and the conversion of diamond and graphite materials by oxidising agents, with points obtained in the experiments of the authors: *I*, the formation of diamond material on a diamond support by the growth of the diamond lattice; *II*, the graphitisation of a diamond support under the conditions of an experiment with $CH_4 + CO_2$ mixtures; *III*, the selective oxidation of graphite and the preservation of diamond in reaction (12); *IV*, the complete oxidation of graphite and diamond; *V*, the formation of condensation products of the graphite series from individual organic substances; *VI*, the formation of a diamond film outside the diamond range (from the data of Carrington and coworkers[35]); *1*, methanol; *2*, formaldehyde, acetic acid; *3*, formic acid; *4*, ethanol; *5*, acetone; *6*, acetaldehyde; *7*, pyruvic acid; *8*, acrolein; *9*, phenol; *10*, furan; *11*, dihydroxybenzenes; *12*, phloroglucinol.

reactions (2)–(5) the catalysts of the forward and reverse reactions are the same]. The catalysts chosen for these processes were the ions of the alkali, alkaline earth, lanthanide, and heavy elements present in kimberlites.[9–11] The most active were potassium among the alkali metals, strontium among the alkaline earth elements, lanthanum among the lanthanides, and chromium, nickel, cobalt, and iron among the heavy elements.

The above catalysts and conditions have been used repeatedly for the synthesis of diamond at 1073–1233 K and atmospheric pressure under isothermal conditions by growing diamond material on the faces of diamond crystals (seed crystals) and diamond powders by reactions (2)–(4). Since the conditions and results of these syntheses have not been described, they are given in the present review. Fig. 5 shows points corresponding to the stoichiometry of the original substances and mixtures in the diamond syntheses which we have carried out.

The results of some of the experiments on the synthesis of diamond can be considered.

Since the rate of growth of the diamond material under isothermal conditions at 1150 K was found to be very low (~ 1 μm d^{-1}) along the normal to the {111} face, the experiments were carried out not only on single crystals (in this case it is possible to monitor both the change in mass and the surface) but also on natural diamond powders with a particle size of 3–5 μm (in this case it is possible to monitor only the change in mass). The following gases and gas mixtures were used as the sources of carbon: CO, $CO + H_2$, $CO + H_2O$, $CO_2 + CH_4$. In the last case the influence of change in the composition of the mixture (from pure CO_2 to pure CH_4) on the course of the reaction was studied. The experiments with single crystals were carried out using KOH melts and solutions of manganese oxide in molten KOH, and also molten boron glasses containing the ions of chromium, copper, manganese, etc. The studies were carried out in platinum reactors at 700–1200 K. Typical results of the experiments are given in Fig. 6 for the single crystals, and in Fig. 7 for the diamond powders.

Fig. 6*a* shows that the growth of the diamond material on a diamond crystal takes place only in a narrow range of compositions of the $CH_4 + CO_2$ mixture, with a maximum rate at 30 vol.% CH_4 and 1180 K (with increase in temperature to 1230 K the height of the maximum decreases, and its position is displaced to 42 vol.% CH_4). In the ranges richer in CO_2 or CH_4, the diamond support shows a mass loss, taking place as a result of the graphitisation of diamond, accelerated by CO_2, and as a result of the direct oxidation of diamond by carbon dioxide. The mass characteristics of the diamond product, given in Fig. 6*a*, correspond to pure diamond, since after the experiments all the graphite obtained by the graphitisation, and the other non-diamond carbon deposited on the surface of the diamond crystals by the polycondensation of methane in the range of high CH_4 concentrations, were completely removed using Moissan mixture and perchloric acid.

The fact that the synthesis of diamond material takes place not only in the narrow zone where the weight increases but also in the graphitisation zones adjoining it is confirmed by the appearance on the {111} diamond faces of specific growth formations — reversed-parallel triangular and hexagonal indentations. In the oxidative solution of diamond by the action of CO_2, H_2O, and other oxidants, only directly-oriented triangular indentations are formed.[33] These facts indicate not only growth in the zone indicated but also recrystallisation of the diamond material.

The characteristics of the thermodynamics of the transformation of $CH_4 + CO_2$ mixtures with different compositions at different temperatures are hardly reflected in any way in the kinetics of the processes of growth, recrystallisation, and graphitisation of the diamond material (see Fig. 6*b*). This proves again that favourable thermodynamic conditions are not sufficient for diamond polycondensation to take place, and that the kinetic conditions are of the greatest importance.

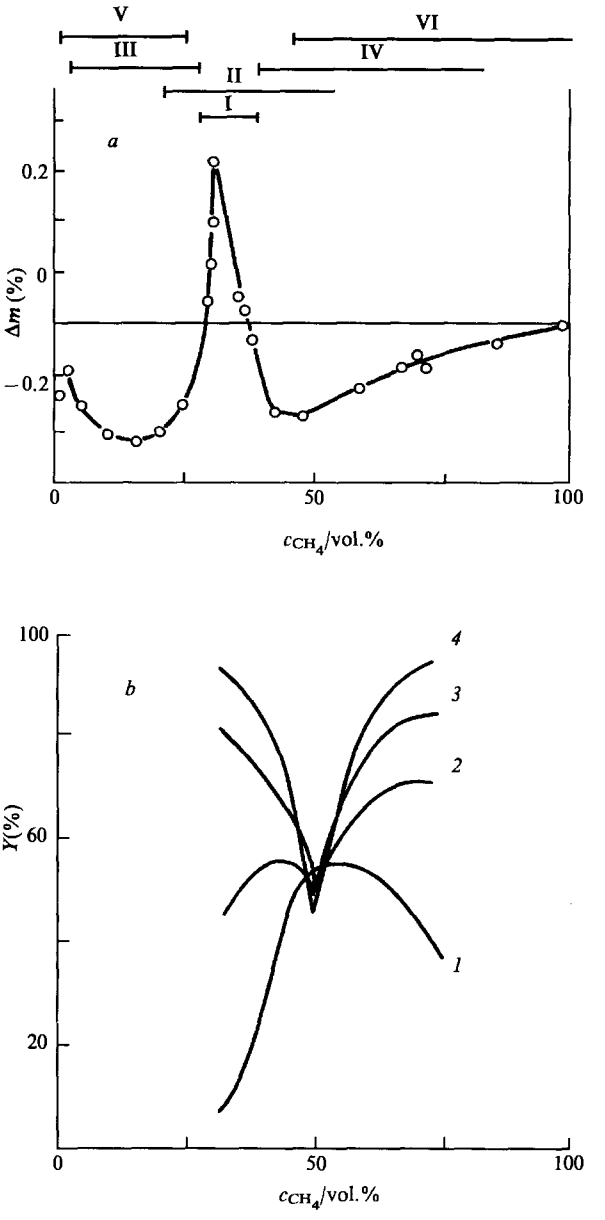


Figure 6. The results of experiments on the growth of diamond material on the {111} face of a diamond support by reaction (4) in a melt of the catalyst KOH (K_2CO_3); *a*, influence of the composition of the reaction mixture $CH_4 + CO_2$ on the change in the mass of the diamond support (T = 1180 K); ranges: *I*, growth of diamond; *II*, recrystallisation of diamond; *III*, *IV*, oxidation of diamond by CO_2; *V*, formation of condensation products of the graphite series from CH_4; *b*, equilibrium degree of transformation of $CH_4 + CO_2$ mixtures with different compositions into diamond at 673 (*1*), 873 (*2*), 1073 (*3*), and 1273 K (*4*).

The rate of growth of the diamond material on the powder in the polycondensation of CO depends markedly on the composition of the gas mixture, and is increased by small quantities of hydrogen (Fig. 7).

The data obtained indicate that at 1200 K the rate of growth of the diamond material corresponds to 0.8–1.5 carbon monolayers per hour; with decrease in temperature to 700 K it decreases to 0.06 monolayer per hour. This observation is consistent with published data,[34] according to which the rate of growth of diamond powders from CO at 1273 K has the values 0.0025 mass% per hour and 0.1 mass% per hour on powders with particle sizes of 53 μm and 1 μm respectively.

Fig. 5 shows that not all the points corresponding to diamond syntheses lie within the stoichiometric boundaries of the "diamond range" established by Bachmann and coworkers,[8] and that some are displaced considerably into the selective-oxidation zone. It is true that they do not lie in the complete-oxidation zone (the H_2O-CO_2-O triangle), but they lie below the lower boundary of Bachmann's diamond zone. The points corresponding to the formation of diamond films, established by Carrington and coworkers[35] and noted as exceptions by Bachmann,[8] also lie below this boundary. All these deviations are evidently not accidental, and are related to the fact that in the zone below the boundary indicated by Bachmann[8] as far as the upper boundary of the zone corresponding to the complete oxidation of diamond by water vapour and carbon dioxide (the line H_2O-CO_2), the formation of diamond is possible under certain kinetic conditions, while under other conditions it will be oxidised. These conditions are characteristic of non-equilibrium states of open catalytic systems, and they are extremely favourable for the recrystallisation and growth of crystals of the highest quality.

Thus in addition to Bachmann's diamond range, in which diamond and graphite may be formed under constant-growth conditions, it is also necessary to distinguish the recrystallisation diamond range $H-C_2O_3-CO_2-H_2O-H$ (Fig. 5), in which diamond may be formed mainly under growth–solution conditions. In this range and on its boundary with the Bachmann range, conditions are created for the formation of the purest diamond material without non-diamond carbon impurities. For example, to obtain a polycrystalline diamond film completely free from non-diamond carbon impurity (synthesis from microwave plasma) it is sufficient to add only 2.2 vol.% O_2 to the $CO+H_2$ mixture.[36]

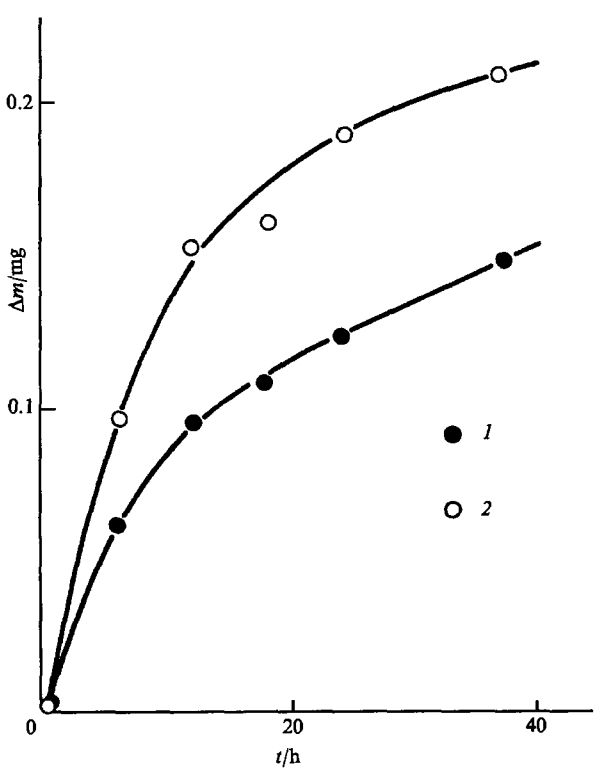


Figure 7. The growth of diamond material in the polycondensation of CO by reactions (2) and (3) on AP 3/5 natural diamond powder (T = 1123 K): *1*, input CO saturated with water vapour (32 mmHg); *2*, input CO saturated with water vapour (32 mmHg) after the establishment of the equilibrium $CO+H_2O \rightleftharpoons CO_2+H_2$; weight of powder in each series of experiments 6 mg; rate of supply of CO 0.5 litre h^{-1}; an increase in mass of 0.1 mg corresponds to the growth of 25 carbon monolayers.

The zones corresponding to the graphitisation of the diamond support by the action of CO_2 in experiments with CH_4+CO_2 mixtures extend both into the recrystallisation zone at high concentrations of CO_2 in the mixture and into the Bachmann diamond range and beyond it into the zone corresponding to the formation of non-diamond carbon with a high reduction potential, where graphitisation is accompanied by the additional formation of condensation products from the excess of methane (Figs. 5 and 6*a*). However, judging from studies of the nature and mechanism of formation of condensation products from individual organic substances,[15,16] the formation of condensation products of the graphite series by the polycondensation of various monomers A takes place readily throughout the entire $CH_4-C_2H_2-CO-C_2O_3-H_3O^+-CH_4$ zone (Fig. 5), including the Bachmann diamond range. This proves again that carrying out the polycondensation (1) under the stoichiometric conditions of the diamond range does not necessarily lead to the formation of diamond, which requires the creation of favourable kinetic conditions (13) for diamond polycondensation.

V. The polycondensation mechanism of the formation of diamond and non-diamond carbon

1. Polycondensation mechanism and genealogical series of condensation products

Without dwelling on the familiar facts that diamond and graphite are allotropic forms of carbon, crystallising in two different forms, we shall concentrate attention on the chemical and genetic aspects of the polymorphism and allotropy of carbon in diamond and graphite directly related to the chemical and genetic problems of their formation.

Formally, crystals of diamond and graphite are macromolecules; a single crystal of diamond is a three-dimensional macromolecule, and a single crystal of graphite is a stack of planar macromolecules. This approach leads to the recognition of the existence of a carbon ring and peripheral functional groups localising the free valences of the carbon atoms on the surfaces of the diamond crystal and the edges of the polycyclic graphite macromolecule emerging on to the faces of the graphite crystal prism.

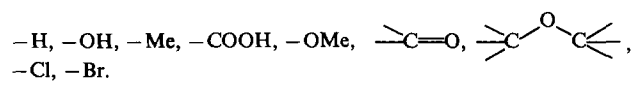
The introduction of each new carbon atom into the diamond or graphite lattice and the formation of the corresponding chemical bonds result from the processes of the polycondensation (1) of the original light carbon-containing molecules A with the reactive groups of the condensation product $\{A_n-mL\}$, which may be elements of the diamond or graphite lattice on the surface of the crystals. There are differences, however, in the details of the mechanism of the polycondensation giving the diamond or graphite material. There are also differences in the composition and structure of the condensation products which are the genealogical precursors of diamond and graphite, and the two directions of the polycondensation (1) have their own genealogical series (Tables 2 and 3 and Fig. 3). It is only in the lower stages of the polycondensation, involving the formation of linear and branched carbon–carbon chains and non-aromatic rings, that the compositions and structures of the condensation products are identical in the diamond and aromatic polycondensation series, with sp^3-configuration of the carbon atoms. The series differ completely, however, even at the stage corresponding to the formation of adamantane and its derivatives in the case of diamond polycondensation and to the formation of aromatic polycyclic compounds with sp^2-hybridisation of the carbon atoms in the case of graphite polycondensation.

The extent of the aromatic and diamond polycondensation in the genealogical series increases with decrease in the ratio of the number of surface functional groups to the number of carbon atoms in the ring of the macromolecule (Table 2).

Both the diamond and the graphite series may contain surface functional groups of different kinds, depending on the composition of the original monomers A, the conditions of the

polycondensation (1), and the subsequent chemical treatment of the condensation product. Thus for a monofunctional covering, the entire genealogical series of condensation products can be related to the corresponding class of organic substances, for example hydrocarbons, monohydric alcohols, etc. Thus the products of the diamond condensation of the original carbon-containing substances may contain series of diamond-hydrocarbons, diamond-alcohols, and diamond-ketones, differing chemically in their surface properties and even in their crystal habits (Tables 2 and 3).

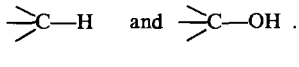
A particular functional covering can be produced on diamond not only by diamond polycondensation but also by special modifying chemical treatment of diamond crystals and powder. In particular, a hydrogen covering can be completely replaced by a hydroxyl covering, or vice versa, by treating diamond with water vapour or hydrogen respectively at 1073 K. This is reflected in the changes in the infrared spectra and the contact angles of wetting by water (in the range 0–90°). For different treatment conditions, the following groups have been detected on a diamond surface:[13,14,37,38]



Similar results have been obtained for graphites and coals. Thus the carbon material obtained by the polycondensation of benzene or ethylene contains the groups



and that obtained from acetone contains the alternating groups[15]



Many publications (for example by Rudenko and coworkers[15,16]) describe the mechanisms of the polycondensation (1) as series of simple repeatedly alternating reactions (addition of the monomer A, removal of different light molecules L, cyclisation, isomerisation, etc.) leading to the successive formation of all the more complex condensation products of the corresponding genealogical series. A particularly large number of studies have been devoted to the aromatic condensation of organic substances. The complexity of the mechanism of diamond polycondensation is indicated by the mechanism of the reverse processes of the oxidation of diamond by water vapour and carbon dioxide.[9,11]

2. Macrostructural forms of graphite and diamond polycondensation products

The formation of the diamond and graphite material is influenced considerably by the mechanism of formation of their macrostructural supermolecular forms. Additional macrokinetic conditions must be established, which when combined with the molecular mechanism of the polycondensation (1) lead to the production of a particular macrostructural form of the diamond or graphite material. For one combination this will be a polycrystalline diamond film, for another a three-dimensional polycrystalline aggregate, and for a third a single crystal of diamond, and the formation of a particular macrostructure will be determined not by the conditions of the polycondensation (1) but by the factors facilitating or preventing the formation of new crystallisation nuclei and determining the intensity and form of the reagent fluxes and the ratios of their rates to the rate of reaction (1), by factors related to the equilibrium in the open catalytic systems, etc.

It is well known that these macrokinetic factors influence the production of various macrostructural forms of graphite (carbonaceous) material,[15] which can be obtained as anisotropic films, polycrystalline or vitreous graphite, carbon spirals, dendrites, hollow carbon fibres, or spherical fullerene molecules.[28] For the production of particular macrostructures, specific additional conditions must be established. For example, the formation of graphite spirals and dendrites, which have an internal spiral structure, takes place during the polycondensation of n-hexanol only in the regions where screw dislocations emerge on the single crystals of nickel, and does not take place on defect-free regions of the face of cubic nickel.[39] Catalytic corrosion of the nickel crystal at the base of the carbon dendrite is observed, and nickel is transferred to the carbon material, in which the nickel is not present in the dispersed state but forms a spiral of crystalline hexagonal nickel, analogous to the graphite spiral (the concentration of nickel in the carbon dendrite reaches 6 mass%). These data indicate that the carbon spirals grow from the base.

Completely different conditions must be established in the formation of carbon fibres having the form of tubes with a constant diameter of ~500 Å and consisting of a polycyclic graphite macromolecule coiled coaxially with the axis of the fibre. The carbon fibres grow from the tip, and a necessary condition for their growth is the presence on the tip of the fibre of a catalyst crystal which is commensurate with the diameter of the fibre and which acts as the 'operator' for its growth.[40]

Fibres and spirals are also formed in the chemical synthesis of diamond. Filamentary acicular crystals of diamond with lengths up to 400 μm grow on diamond seed crystals in the presence of metallic catalysts (Fe, Ni, Mn, etc.) both at low pressures from the vapour phase[41,42] and under SHP conditions from solutions of carbon in the metals.[43,44] Diamond filaments and needles with a diameter : length ratio of 1 : 20 usually grow along the normal to the {110} face of the diamond seed crystal[42,43] at a rate of up to 200 μm h^{-1};[41] this is much greater than the rate of growth of diamond powders. These macrostructural forms are present at the tip of the metal catalyst crystal.[41,42]

Au does not bring about the formation of diamond filaments at low pressures,[42] but brings about the production of different skeletal forms of diamond and its dendrites under SHP conditions.[44] The production of diamond fibres in the form of spirals has been observed in the regions where screw dislocations emerge on a diamond seed crystal.[45] The growth of filamentary crystals of diamond has been observed[46] on the projections and edges of seed crystals on different supports (diamond, garnet, mica) by the action of the electron beam directly in an electron microscope in a high vacuum. The source of carbon was the residual vapour of the oil in a vacuum of 10^{-4}–10^{-6} mmHg. Thus the growth of diamond as single-crystal filaments is brought about by a number of specific factors, and pressure does not play a significant role.

Diamond spirals of filaments with a thickness of 0.6 μm with a step and diameter of 2.5 μm and a length of up to 75 μm were found by us in AP 5/3 diamond powder after experiments on its further growth by reaction (2) at 1220 K in the presence of a melt of MnO in B_2O_3. The diamond spirals were joined to the diamond seed crystal, and in one case the formation of two spirals joined by one seed particle and lying at an angle to one another was observed. In this case the growth of the diamond spirals apparently takes place on the diamond particles at regions corresponding to the emergence of screw dislocations, which have an increased ability to bring about diamond polycondensation. This is confirmed by the fact that the calculated rate of formation of diamond by the growth of the diamond spiral is greater by several powers of ten than the average rate of the layer growth of diamond material on the {111} face.

A unique theoretically possible macrostructural form of diamond material that can be distinguished corresponds to macrocrystals (molecular species) with dimensions of 100–1000 Å, having a high ratio of the number of surface carbon atoms, and hence number of functional groups, to the number of internal carbon atoms in the particle, and exhibiting colloidal

properties as a consequence of the polarity of the functional groups (Table 2). Colloidal diamonds should have unique physical and chemical properties, differing from those of diamond micro-powders and the organic substances formed by diamond polycondensation. In particular, colloidal diamonds should not have abrasive properties, and on the contrary may be good lubricants. Some parameters of detonation diamonds, produced by the explosion of chemical substances, are close to those corresponding to a colloidal form of diamond material.[47]

A unique position among the macrostructural forms of diamond material is occupied by epitaxial molecular films (several carbon atom layers) with a regular single-crystal structure. They may be formed by a chemical mechanism analogous to crystallisation, for example in any of the reactions (2)–(4), in the presence of non-equilibrium concentrations of the starting materials when the crystal faces of the support show a two-dimensional crystal-structural similarity (crystal-chemical correspondence) to the arrangement of the carbon atoms on one of the faces of diamond. The existence of this crystal-structural correspondence with a low value of the coefficient of surface tension with respect to diamond leads to the production of a strong field in the crystalline support, capable of initiating on it the growth of an isomorphous diamond lattice, which as it were extends the lattice of the support.

3. The formation of equilibrium epitaxial films of diamond and the non-equilibrium growth of macroscopic crystals of diamond

According to the model of the growth of diamond crystals in open catalytic systems,[19] two-dimensional diamond films may be the nuclei for the growth of diamond crystals. The growth of a microscopic diamond crystal requires a constant displacement of the equilibrium of reactions (2)–(4) to the right under the conditions of non-equilibrium of an open catalytic system, whereas the formation of macroscopic epitaxial film–nuclei can also take place in a closed system before its equilibrium is established.

When equilibrium is established in reactions (2)–(4) and the kinetic conditions of diamond polycondensation are established in the presence of a suitable matrix–crystal face, an equilibrium epitaxial diamond film of several carbon atom layers is necessarily formed, and will be stable under these conditions.

The possibility of the formation of two-dimensional equilibrium nuclei of a new phase on a support with the properties indicated is established by de Wolff's theory, and also by the principle of minimum Gibbs–Curie surface free energy and the crystal-growth theorems of Gibbs, Volmer, and others. Using these theories it is possible to calculate the work of formation of a two-dimensional critical (equilibrium) nucleus with allowance for its parameters, the specific inter-phase free energies at the nucleus–crystal–medium boundaries (ΔG), and also the critical size (l) and the rate of formation of a nucleus with super-critical perimeter (J)

$$\Delta G = -\frac{\varepsilon^2}{4\gamma h \Delta G_v}; \quad l = -\frac{\varepsilon}{2\gamma h \Delta G_v}; \quad J = la \exp\left(-\frac{\Delta G}{kT}\right),$$

where ε is the specific boundary free energy; γ a coefficient which makes it possible to calculate the area of the nucleus; γl^2 the area of the nucleus; h the height of the nucleus; ΔG_v the free energy of the medium,

$$\Delta G_v = \frac{kT}{\Omega} \ln \frac{p}{p_{equil}},$$

p the partial pressure of the gas; p_{equil} the equilibrium pressure of the gas; Ω the volume of one carbon atom in the crystal; and a a coefficient which depends on the frequency of the molecular collisions and on pressure.

Without knowing the values of a, γ, and ε it is impossible to calculate the specific parameters of the nuclei (for example the number of atomic layers in the epitaxial film). The above expressions have been used successfully[1] to determine the ratio of the rates and work of formation of epitaxial nuclei of diamond and graphite on the {111} face of a diamond support. It was shown that the equilibrium gas pressures for the formation of the diamond nuclei are twice those for the formation of graphite, and that the ratio of the rates of formation of the nuclei has a maximum value at a definite ratio of the partial and equilibrium pressures. Thus the most favourable range for the epitaxial growth of diamond will correspond to p/p_{equil}(graphite) = $2^{2.7}$.

From our viewpoint, however, this calculation, which is based on thermodynamic data, is of no significance for determining the most favourable range for the epitaxial synthesis of diamond, since this is determined entirely by the differences between the kinetic conditions for the synthesis of diamond and graphite.

At the same time it would be useful to know the specific parameters of the diamond critical nuclei obtained as equilibrium epitaxial films on the faces of minerals with the properties required for epitaxy.

It can readily be shown that there is a relationship between the thickness of the epitaxial diamond film, expressed as the number of carbon atomic layers (δ), and its two-dimensional size ($d = 2r$) and the equilibrium degree of transformation (Y) into diamond by reactions (2)–(4) at a definite temperature and pressure. A corresponding relationship should naturally exist for epitaxial films of graphite. The differences between the ratios of these parameters for diamond and graphite should not be of particular interest to us, since the formation of a particular epitaxial film is determined entirely by the kinetic conditions, and we are considering cases with kinetic conditions favourable for the synthesis of diamond.

For a microscopic volume with local equilibrium of the reactions, the quantities indicated are related to one another as follows:

$$\delta = \frac{c_{loc}}{c_1} Y\beta,$$

where c_{loc} is the number of carbon atoms in the volume of the local equilibrium, in a hemisphere with a volume of $(\frac{2}{3})\pi r^3$; c_1 the number of carbon atoms in one monolayer with an area of πr^2; and β the relative volume concentration of the substance A in the volume of the local equilibrium (if the volume is occupied by a gas, $\beta = 1$; if it is occupied by a solution of A in a melt or by a solid, $\beta \neq 1$). A model of the region of local equilibrium on the surface of the support is shown in Fig. 8.

Having determined the values of c_{loc} and c_1 with allowance for the fact that only half of the starting materials A in reactions (2) and (3) corresponds to the number of carbon atoms taken in the calculation,

$$c_{loc} = \frac{1}{3}\pi r^3 \frac{N_A}{V_0},$$

(V_0 is the volume of a mole of gas under normal conditions, and N_A is Avogadro's number) and

$$c_1 = \frac{\pi r^2}{\gamma},$$

(γ is the area occupied by one carbon atom on the {111} face of diamond, equal to 5.5 Å^2), we obtain

$$\delta = \frac{1}{3}\frac{\beta\gamma r Y N_A P_0}{273R}. \quad (16)$$

The results of the calculation of δ for different values of r and different temperatures of the equilibrium of reactions (2) and (3) for $\beta = 1$ and $P_0 = 1$ atm are given in Table 4. The value of δ is

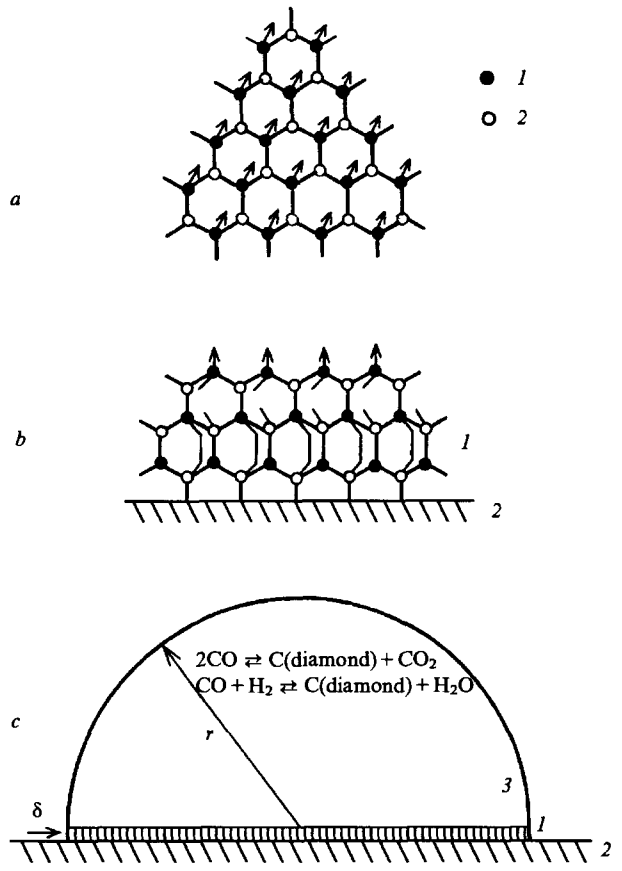


Figure 8. The formation of an equilibrium epitaxial film of diamond on supports showing a crystal-structural correspondence with the arrangement of the carbon atoms on the {111} face of diamond; *a*, view of a critical nucleus from above; the arrows indicate the free valences of carbon, lying at an angle of 90° to the {111} surface and localised by the functional groups; *1*, *2*, carbon atoms of the upper and lower sheets respectively; *b*, view of a critical nucleus from the side; *1*, three-layer epitaxial film of diamond; *2*, face of the mineral support; *c*, model of the region of local equilibrium on the surface of the support, bringing about the epitaxial growth of the diamond film; *1*, epitaxial film (nucleus) with thickness δ and diameter $d = 2r$; *2*, support; *3*, hemisphere bounding the range of local equilibrium of reactions (2) and (3).

proportional to the pressure (P) as it increases from the normal value (P_0) to the critical value (P_{cr}), and is independent of pressure for $P_0 > P_{cr}$.

Table 4 shows that the thickness of the epitaxial film in the critical nuclei of diamond may be greater, the greater the size of the nucleus and the volume of the local equilibrium in which the film is formed, and the lower the temperature of the synthesis. The increase in δ and δ/d with decrease in temperature reaches a limiting value at 400–600 K. The ratio of the thickness of the film to the diameter δ/d in the limit is independent of the diameter of the nucleus and is equal to 3300.

Thus the formation and preservation of the equilibrium epitaxial diamond films which are the critical nuclei for the crystallisation of diamond do not require exotic conditions, and can take place in a static closed system. The only factors making possible the formation of these films are the presence of the starting materials A for the diamond polycondensation in the local volume and the establishment of favourable kinetic conditions, including the presence of suitable matrix–minerals for the epitaxial growth of the diamond material.

In some cases the factor of epitaxial growth of critical diamond nuclei may be particularly favourable. This is indicated by the accelerating action of fullerenes on the synthesis of

Table 4. Number of atomic layers of carbon (δ) in the equilibrium epitaxial film of diamond for different nucleus diameters and reaction temperatures, calculated with the use of Eqn. (16).

T/K	Y (%)	d/μm		
		1	10	100
	$2CO \rightleftarrows C(diamond) + CO_2$			
400	100	1.4	13.6	135.5
500	100	1.4	13.6	135.5
600	99.90	1.4	13.5	135.4
700	98.85	1.3	13.4	134.0
800	92.75	1.3	12.6	125.7
900	71.06	1.0	9.6	96.3
1000	31.51	0.4	4.3	42.7
1100	8.21	0.1	1.1	11.1
	$CO + H_2 \rightleftarrows C(diamond) + H_2O$			
400	100	1.4	13.6	135.5
500	99.93	1.3	13.4	134.3
600	98.95	1.3	13.4	134.1
700	92.93	1.3	12.6	126.0
800	71.99	1.0	9.8	97.5
900	32.43	0.4	4.4	43.9
1000	8.60	0.1	1.2	11.7
1100	2.20	0.03	0.3	3.0

diamond films on a silicon support.[47] The deposition of C_{60} on silicon increases the rate of growth of the film by a factor of 10^4, and the deposition of C_{70} increases it by a factor of 10^{10}. Thus the presence on silicon of spherical fullerene molecules, whose surface consists of a 'parquet' of six-membered and five-membered carbon rings, increases the rate of diamond formation by a factor of at least 10^4, and the presence of the pyrene structural elements in the C_{70} molecule leads to a further increase in the rate of growth of the diamond film by a factor of 10^6. This case evidently shows not only the more favourable crystal-structural correspondence between the structural elements of the fullerenes and diamond, compared with the silicon lattice, but also the accelerating action of the spherical deformations of the pyrene and triphenylene structural elements of the fullerenes.

Pressure is not a decisive factor, since epitaxial films may be formed at low, high, and super-high pressures. Thus since minerals capable of bringing about the epitaxial growth of diamond are widely distributed, it may be concluded that the appearance of nuclei for the crystallisation of diamond has never been the limiting stage of the formation of diamond deposits in nature. In nature, an excess of diamond nuclei should evidently exist. At the same time, when all other favourable conditions for diamond polycondensation are established, the formation of natural deposits containing diamond macro-crystals might have been limited by a range of additional macroscopic conditions required to bring about the growth of crystals under the non-equilibrium conditions of an open catalytic system functioning for a prolonged period.

The macrokinetic conditions for the formation of diamond nuclei and for their growth to give macro-crystals differ considerably, despite the same optimum conditions of competition between the processes of formation and conversion of diamond and graphite materials (13). It is possible to have combinations of conditions leading to competition between the processes of the formation of nuclei (n) and the growth of crystals (c), between the processes of the formation and the oxidative solution of the diamond material of nuclei and crystals (o), and also between the processes of the formation of small and large crystals. The ratio of the degrees of transformation (Y_n, Y_c, Y_o) of the substance in these processes with the formation and oxidation of the diamond material, and the conditions for movement into

the recrystallisation zone shown in Fig. 5, are given by the diagram in Fig. 9. The vertices of the diagram correspond to 100% transformation in the formation of the diamond material as nuclei, the growth of crystals, and the oxidation of diamond material. The diagram contains zones corresponding to the complete oxidation of the diamond material (Y_oAOC), the preferential formation of the diamond material as nuclei (Y_nAOB), and the growth of diamond crystals (Y_cBOC).

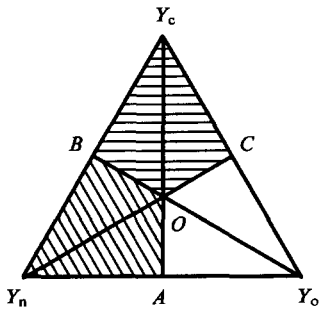


Figure 9. Diagram showing the degrees of transformation of the material in the competing processes of diamond formation and the oxidation of the diamond material (the vertices correspond to 100% degrees of transformation); Y_nAOB is the zone of nucleus formation; Y_cBOC the zone of crystal growth; Y_oAOC the zone of complete oxidative solution of the diamond material; the AOC the recrystallisation line.

Under the conditions of diamond polycondensation corresponding to the vertex Y_n, only the formation of nuclei takes place, and under the conditions corresponding to the apex Y_c, all the diamond material formed grows into crystals; on going from Y_n to Y_c, the number of nuclei (crystals) formed decreases sharply from infinitely large to 1. Under growth conditions without competition between the processes of nucleus formation and crystal growth and the processes of oxidation of the diamond material, however, the quality of the diamond crystals will be poor, because of various inclusions, dislocations, and polycrystalline aggregates.

Under conditions bringing about the dynamic process of growth and oxidation of diamond in the recrystallisation zone, corresponding to the line AOC in Fig. 9,

$$Y_{di} = Y_l = Y_o = 50\%;\ V_c = V_o;\ Y_{di} = Y_n + Y_c;\ Y_n \to 0,$$

the formation of large defect-free crystals of the highest quality is possible. The formation of new nuclei is almost completely suppressed

$$V_c \geqslant V_o;\quad V_n = 0.$$

These conditions were created in an experiment on the further growth of single crystals of diamond from $CH_4 + CO_2$ mixtures in alkaline melts. Fig. 6*a* shows that the recrystallisation zone includes the range of observed increase in the weight of the diamond material, and is appreciably broader than this range, that is recrystallisation changes in the diamond crystal are observed, corresponding both to an increase in its mass as a result of the formation of new diamond material and to a mass loss as a result of oxidation. Other examples of recrystallisation changes in single crystals of diamond and powders are known.[10, 23, 49]

For example, excellent photographs have been obtained[49] of successive recrystallisation changes on the surface of single crystals of diamond under the catalytic action of molten NaOH containing Ni^{2+} ions at 1100 K in a gaseous medium containing air.

Moving from the vertex Y_c to the point C in Fig. 9 corresponds to the change from reducing conditions of diamond polycondensation to oxidising conditions. According to the results of studies[10, 23] of the change in the habit of diamond crystals during partial oxidative solution and data[36, 50] on the relationship between the habit of diamond crystals and the oxidation potential of the growth medium, this is reflected in a change in the morphology of the diamond crystals formed. Thus under reducing conditions a $CO + H_2$ mixture gives cubic crystals; when traces of O_2 are added to the mixture, cubo-octahedral crystals are formed; and at an O_2 concentration of 2.2%, only octahedral diamond crystals are formed.[36] Increase in the oxidation potential of a kimberlite deposit, characterised by the change in the ratio Fe^{III}/Fe^{II}, leads to a change from octahedral diamond crystals with smooth faces to rhombododecahedral and rounded forms as a result of oxidative solution.[50] With further increase in the oxidation potential, however, when $v_o > v_c$, combustion of the finer diamond crystals with preservation of the large crystals will take place, and the size of distribution of the diamond crystals will change, as confirmed by the displacement of the maximum of this distribution towards large diamonds and the absence of fine diamonds in a number of kimberlite pipes of Yakutia.[51]

VI. A model of the non-equilibrium growth of diamond crystals in a macroscopic open catalytic system

When the polycondensation process (1) takes place in a macroscopic open catalytic system (a flow reactor) with the constant supply of the original light carbon-containing molecules A or their mixtures with the product A + L at a rate w_f and the removal of the light reaction products L, non-stationary conditions may be established

$$A \to \left\{ \frac{nA_n \to \{A - mL\} + mL}{\sum\{A_n - mL\}_i K} \right\} \to L, \qquad (17)$$

when the condensation product $\{A_n - mL\}$ formed by the reactions (2)–(4), (2′)–(4′), etc. remains in the constitution sphere of the system on the catalyst K and gradually accumulates as the diamond or graphite material $\sum\{A_n - mL\}_i$. The removal of the products L = CO_2, H_2O, etc. capable of oxidising the condensation product, and the displacement of the equilibrium in the system, lead to the establishment of a stationary (stable) non-equilibrium, and continuous growth of the diamond or graphite material takes place. When the products of reactions (2)–(4) and (2′)–(4′) enter the system (17) together with the starting materials, however, the rate of exchange of the materials and the effect of non-equilibrium growth of the condensation products decrease. We have used this model to describe the growth of diamond crystals in kimberlite deposits[19] and the abiogenic synthesis of hydrocarbons,[24] and also to describe non-stationary polymolecular processes involving the condensation products.[17]

As noted above, the direction of process (1) towards the formation of diamond material requires favourable kinetic conditions. If these conditions are observed, then a definite decrease in the intensity of material exchange and in the non-equilibrium character of the system (17) as a result of the retarding action of the products is favourable for the formation of large diamond crystals of good quality, since it moves the process into the dynamic conditions of growth and oxidation characteristic of the recrystallisation zone. This corresponds to the zone situated between the lower boundary of Bachmann's diamond range and the line $H_2O - CO_2$ in Fig. 5 or the lines AO and OC in Fig. 9.

At the same time, the continuous growth of diamond crystals on top of the initially formed equilibrium epitaxial films is possible only under non-equilibrium conditions. The apparent contradiction arises because the growth of the crystals, as well as the formation of epitaxial films, can take place at different degrees of non-equilibrium, but when equilibrium is reached, only the epitaxial film can be formed and exist.

The macroscopic open catalytic system (17), in which favourable kinetic conditions are created for diamond polycondensation by reactions (2)–(4), can exist for wide variations in the specific kinetic and macrokinetic conditions: from limiting non-equilibrium to close to equilibrium; from reactions taking place in the kinetic range to reactions taking place in the diffusion range; from conditions leading to the formation of only epitaxial films (nuclei) to conditions leading to the growth of single crystals; and from conditions leading to an increase in the number of nuclei to conditions preventing the formation of new nuclei and bringing about the growth of large crystals. A diagram of such a macroscopic open catalytic system with allowance for varied local conditions of diamond synthesis is given in Fig. 10. These conditions are characterised by different combinations of the rate of flow of the materials

$$w_f = w_{lf} + w_{diff},$$

(where w_{lf} is the rate of linear flow along the gas-transport channels, pores, and cracks, and w_{diff} the rate of diffusion through the pores) and the rate of formation and accumulation of the diamond material in the crystallisation centres

$$v_c = \frac{d[\{A_n - mL\}]}{dt},$$

which is a function of temperature, the rate of flow of the materials, and the composition of the mixture A + L, that is

$$v_c = \varphi[T, w_f, (A + L)].$$

In Fig. 10, *A* is the gas-transport channel through which the reacting mixture A + L moves under the influence of a pressure gradient at a rate w_{lf}; *B* the porous environment of the gas-transport channel, in which the reacting mixture diffuses under the influence of a pressure gradient at a rate w_{diff}; the total rate of flow through the non-equilibrium zone is $w_f = w_{ef} + w_{diff}$; *C* is the boundary of the non-equilibrium zone, at which $v_c = 0$ at $(A + L)_{equil}$; within the zone $v_c > 0$; $v_c < w_f$; *I* is the kinetic range in which diamond polycondensation takes place, including the extrakinetic range (*I'*) on the walls of the gas-transport channel ($v_c > v_{diff}$; $v_c < w_{lf}$; $w_{diff} < w_{lf}$) and the intrakinetic range (*I''*) in the porous wall ($v_c < w_{diff}$); and *II* the diffusion range in which diamond polycondensation takes place ($v_c > w_{diff}$).

With allowance for possible gradients in the pressure and in the concentrations of the starting materials A at the inlet and outlet of the system (Fig. 10), the model can be used to describe diamond polycondensation in the preparation of polycrystalline diamond films on supports by the reaction of the latter with a gas–plasma flux of original carbon-containing substances, for processes in ordinary catalytic flow reactors, and in the natural open catalytic systems produced in the fractures, cracks, and other gas-transport channels in the degassing paths in the earth's minerals.

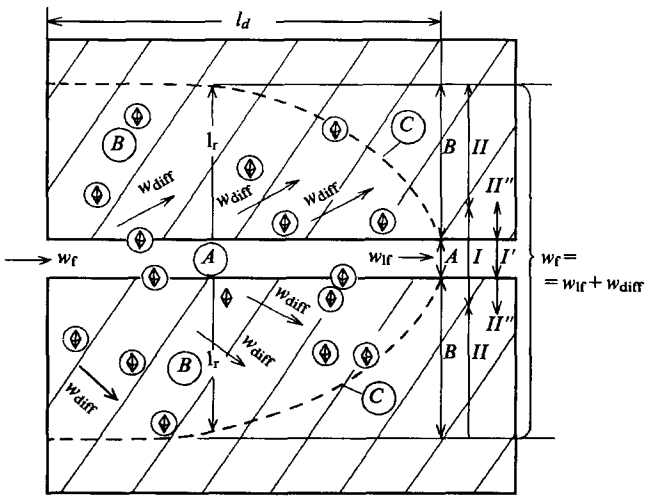


Figure 10. Model of the non-equilibrium zone in the macroscopic open system (17), bounded by the longitudinal and transverse ranges corresponding to the conditions for the growth of diamond crystals.

In the last cases the model makes it possible to describe not only the processes of diamond synthesis taking place at

$$v_c < w_f,$$

in the kinetic range but also syntheses in the diffusion paths, when

$$v_c > w_{diff}.$$

These conditions are ensured by the porosity of the catalysts in experimental flow reactors or by the porosity and diffusion gas-permeability of the rocks surrounding the fluid-transport channels in natural diamond deposits.

For constant values of *T*, w_f, and w_{diff}, the rate of growth of the diamond crystal will depend only on the composition of the mixture of carbon-containing starting materials and products passing into the system and into each local zone in which individual crystals grow

$$v_c = \varphi(A + L),$$

and for the equilibrium composition of the mixture, $v_c = 0$ ($v_c > 0$ only for a non-equilibrium composition).

Thus the growth of diamond crystals in the polycondensation reactions (2)–(4) etc. will be determined entirely by the macroscopic conditions maintaining non-equilibrium in the system (17).

According to the theory of open catalytic systems,[25,26] the extent to which a macroscopic open system deviates from equilibrium (ρ) is directly related to the potential degree of transformation $\tilde{Y}$ of the original mixture A + L in the system. The relationship between these parameters and the composition of the gas mixture entering the system (17) is shown in Fig. 11*a*. The figure shows that the maximum degree of non-equilibrium character $\rho = 1$ and the maximum value of the potential degree of transformation for the forward reactions (2)–(4), determined from the equation

$$\tilde{Y} = \frac{M_A(c) - M_A(equil.)}{M_A(c)}.$$

[$M_A(c)$ and $M_A(equil.)$ are the mole fractions of the substance A in mixtures with the current and equilibrium compositions respectively], are reached when the pure starting material A is supplied, and that these quantities are equal to zero when the equilibrium mixture is supplied. The same applies to the back reactions (2)–(4) when super-equilibrium quantities of oxidising products (CO_2, H_2O) are supplied to the system (17), if $\tilde{Y}$ is determined in terms of the mole fractions of L in the mixtures A + L.

By taking account of the fact that the composition A + L will change, approaching the equilibrium composition $(A + L)_{equil}$, along the direction of flow of the reaction mixture in the system as a result of reaction (1), it is possible to determine the longitudinal distance to which the polycondensation process will extend, l_d. This distance will be greater, the greater the difference between the composition of the entering mixture $(A + L)_{current}$ and the equilibrium composition (Fig. 11*b*). In the same way it is possible to estimate the transverse distance l_r to which non-equilibrium conditions of diamond polycondensation will extend in a macroscopic reactor (Fig. 10). In both cases the boundary of the non-equilibrium range in which the growth of diamond crystals is possible is determined by the approach of the composition of the mixture to the equilibrium composition, that is the actual range is finite.

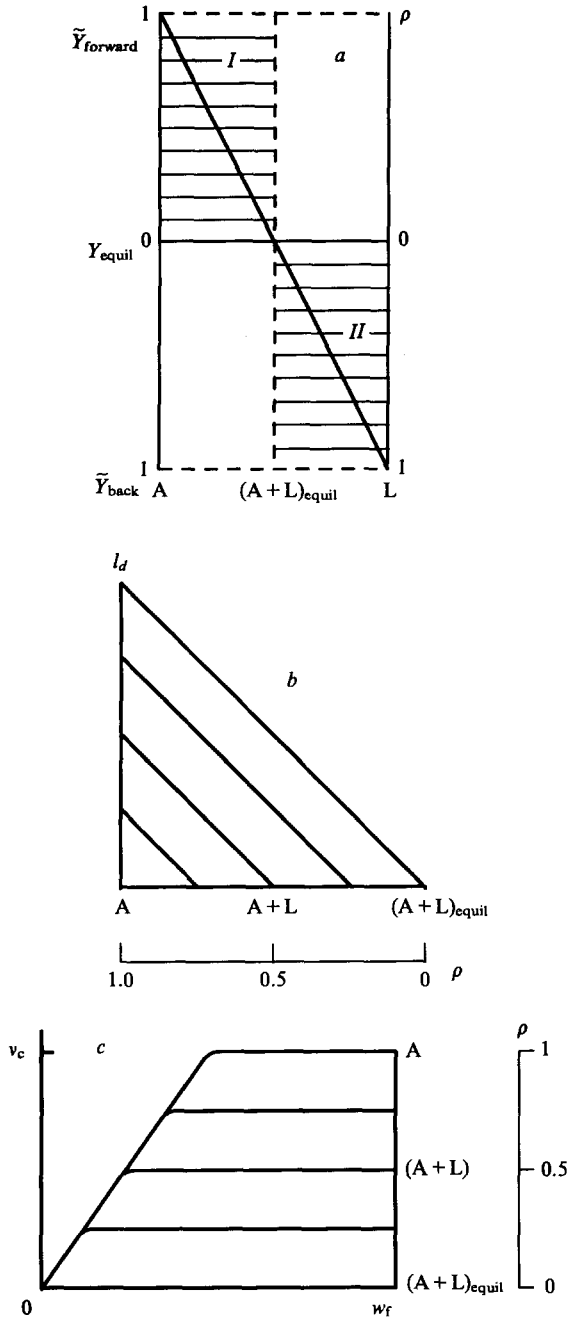


Figure 11. Relationship between the potential degree of transformation (*a*), the longitudinal distance to which the non-equilibrium conditions extend (*b*), and the rate of growth of diamond crystals (*c*) on the one hand and the rate of flow and the extent to which the composition of the reaction mixture entering the open catalytic system deviates from the equilibrium composition on the other; *a*: *I*, diamond polycondensation by reaction (1); *II*, conversion by reaction (12).

The non-equilibrium of system (17) as a whole and in each local zone in it, however, will be determined not only by the composition of the reaction mixture entering the system and the changes which it undergoes in reaction (1) but also by the ratio of the rate of polycondensation v_c and the rate of flow w_f and by the actual value of w_f (Fig. 11*c*). Non-equilibrium conditions in the open system are established with the condition that, essentially, reaction (1) is of zeroth order with respect to A, and there is a decrease in the value of v_c as the composition of the entering mixture approaches the equilibrium composition $(A+L)_{equil}$ and in the value of w_f at which the change to the non-equilibrium range takes place.

The last feature acquires great importance in the establishment of recrystallisation conditions (Fig. 9) at the boundary between the growth and the oxidative solution of diamond. These conditions are favourable for the prevention of the formation of new nuclei, for the oxidative solution of excess nuclei and fine crystals, and for the growth of the largest crystals of highest quality.

VII. An analysis of the conditions of formation of diamond in experiments and in various natural deposits

1 Experiments on the growth of polycrystalline diamond films from plasma on different supports and the epitaxial growth of single crystals

All known facts in the chemical synthesis of diamond at low pressures, both as polycrystalline films on different supports and in the growth of the diamond lattice in epitaxial films and single crystals, are consistent with the proposed model of the polycondensation growth of diamond material under the non-equilibrium conditions of open catalytic systems. In all observed cases of the formation and accumulation of diamond material in macroquantities, kinetic conditions have always been observed for the diamond condensation of the original light molecules [by reactions (2)–(4) etc.] in the non-equilibrium zones of the open catalytic systems, including primarily the macrokinetic conditions ensuring stationary non-equilibrium in the diamond crystal growth zones.

The slight differences between the kinetic and macrokinetic parameters in observed cases of diamond synthesis at low pressures do not go beyond the range of optimum conditions. Thus in the growth of polycrystalline diamond films on supports in a gas–plasma stream, the observed ratio of the rate of formation of the diamond material to the rate of flow is

$$v_c \ll w_f,$$

ensuring stable zeroth order of reaction (1) with respect to the original carbon-forming material and the maximum degree of non-equilibrium character. The process of diamond material formation takes place in the kinetic range (range *I* in Fig. 10), or more precisely in the extra-kinetic range (*I'*) on the wall of the gas-transport channel A.

In the case of the growth of a single-crystal lattice on a diamond seed crystal (in a solution of metal oxides in a molten alkali metal hydroxide), studied by us (Fig. 6), however, reaction (1) took place in the diffusion zone (zone *B* in Fig. 10), in which the transport of the reacting material to the growing diamond crystal took place from the gas-transport range A by diffusion through the melt, and

$$w_{diff} \ll w_f.$$

Reaction (1) in the diffusion zone was dependent on the thickness of the catalyst layer and took place either in the intra-kinetic range (range *II'* in Fig. 10), when

$$v_c < w_{diff},$$

or in the intra-diffusion range (range *II* in Fig. 10), when

$$v_c > w_{diff}.$$

The two sets of conditions are equally favourable for the growth of the diamond crystal, since they lie within the range of non-equilibrium of the open catalytic system. The boundaries of the non-equilibrium zone for constant values of w_f and w_{diff}, however, are determined only by the depletion of the reaction mixture in the direction of the fluxes of w_f and w_{diff} and by the approach of its composition to the equilibrium composition (range *C* in Fig. 10).

2. Facts indicating the growth of diamond metacrystals in the solid phase of kimberlite deposits

The optimum conditions for the growth of diamond crystals according to the model(17) can readily be established in kimberlite pipes, which are the funnels of characteristic volcanoes with an explosive action, filled with breccia, that is a porous rock with a large number of gas-transport channels, through which the degassing of the minerals of the earth took place (and in some cases is still taking place) from deep fractures, to which the pipes are confined. The gases liberated contain all the starting materials and products of reactions (2)–(4), and the kimberlites contain all known active catalysts of the formation of epitaxial nuclei and the synthesis of diamonds, from heavy metal ions to alkali metal ions.

In different parts of the pipe there may arise local regions with the properties of the non-equilibrium open catalytic system (17), having favourable micro- and macro-kinetic conditions for diamond polycondensation (1), corresponding to the model given in Fig. 10. The growth of diamond crystals will take place with ideal exchange of the materials in the system (17), when $v_c \ll w_f$ and the gas mixture A + L has a non-equilibrium composition. These conditions are established in the gas-transport channels.

The growth of diamond crystals will also take place in the diffusion zones (range *B* in Fig. 10), where $w_{diff} \ll w_f$: in the intra-kinetic range for $v_c < w_{diff}$ or in the intra-diffusion range for $v_c > w_{diff}$. In the diffusion zones of the porous solid filling the pipe, the rate of growth v_c will decrease in the radial direction relative to the transport channel as the composition of the mixture approaches the equilibrium composition $(A + L)_{equil}$; at the boundary of the non-equilibrium zone (range *C* in Fig. 10), reaction (1) necessarily moves into the intra-kinetic range as a result of the decrease in v_c to $v_c < w_{diff}$, and at the boundary of the non-equilibrium zone the reaction stops ($v_c = 0$). The growth of the diamond crystals also stops with decrease in the flow rate ($w_{diff} \to 0$).

In any case—when the composition A + L approaches the equilibrium composition or when the open system becomes static—the growth of the diamond crystals stops. The absence of direct removal of CO_2 and H_2O from the growing crystal under the specific conditions of a kimberlite deposit may be replaced by another mechanism of displacement of the equilibrium in reactions (2)–(4), leading to further growth.

This mechanism may be the accumulation of CO_2 and H_2O by the surrounding solid material, accompanied by allochemical changes in it

$$2CO \rightleftarrows C(\text{diamond}) + CO_2;\ CO_2 + M = MCO_3\ , \qquad (18)$$

$$CO + H_2 \rightleftarrows C(\text{diamond}) + H_2O\ ;$$

$$4H_2O + 3Mg_2SiO_4 = Mg_6[Si_4O_{10}](OH)_8\ . \qquad (19)$$

Carbonate and serpentine coatings, which do not oxidise diamond, should be formed round the diamond crystals. Special experiments have shown that at 1073–1273 K an oxidising action is shown only by free CO_2, and not by molten carbonates,[8,9] and that diamond does not dissolve in silicate melts.[9]

The carbonate and serpentine coatings detected round kimberlite diamonds and various characteristics of their composition and structure confirm that reactions (18) and (19) take place.[19,22,53] In kimberlite pipes of Yakutia, the primary contacts of diamonds with kimberlites and eclogites in fact indicate allochemical changes in the surrounding rock, revealed not only by the formation of layer mineral coatings but also by aureoles of chemical changes in the surrounding rock.[19,22] Cataclastic changes in the surrounding rock have also been revealed[19] by the formation of oriented micro-cracks and micro-displacements as a result of the increase in the volume of the diamond meta-crystal growing in the solid medium; this should be observed if reactions (18) and (19) take place with a constant supply of the starting materials of reactions (2) and (3) to the growing crystal.

The secondary contacts of diamond crystals with kimberlite breccia, taken by Rudenko and coworkers[53] as a typical case, are not accompanied by allochemical or cataclastic changes in the surrounding rock, and in this case the diamonds are xenocrysts. In the primary contacts, the growth of diamond as a meta-crystal in the solid medium is confirmed by the observed fractionation of carbon isotopes in reaction (18). For example, according to published data,[54] the carbonate carbon of the coating is lighter ($\delta^{13}C$ from −6.7‰ to −7.6‰) than the carbon of the carbonates in the surrounding kimberlite ($\delta^{13}C$ from −6.9‰ to −8.2‰) situated outside the zone of chemical changes.

These facts not only confirm the model of the growth of diamond crystals in the catalytic system (17) as a whole but also make it possible to deduce its details with allowance for the chemical and metasomatic processes (18) and (19), which maintain the disequilibrium in the system and ensure favourable conditions for diamond polycondensation.

The favourable kinetic conditions for diamond polycondensation, created in the formation of kimberlite deposits, are extended by the possible inclusion in the synthesis of reactions (6) and (7), which also take place under conditions corresponding to the constant displacement of the equilibrium as a result of the binding of the products with oxidising properties by surrounding solid minerals. Minerals containing divalent iron are converted into minerals containing trivalent iron, and the thermodynamic equilibrium of reactions (6) and (7) is displaced completely to the right ($\lg K_p$ at 1000 K has the values 35.6 and 71.1 respectively).

The duration of the preservation of the stationary non-equilibrium in reactions (6), (7), (18), and (19) ensuring the growth of the diamond crystal in the solid phase will naturally be determined by the concentration of the appropriate minerals in the local volume accessible for allochemical changes. For reactions (6) and (7) these are minerals containing Fe^{II}, for reaction (18) they are alkaline earth metal oxides and silicates, and for reaction (19) they are olivine and other silicates. Reactions (6), (7), (18), and (19), which extend the favourable conditions for diamond polycondensation, have undoubtedly been of considerable importance in the formation of kimberlite deposits.

The model of the growth of diamond crystals in non-equilibrium open catalytic systems is consistent with many other facts established during the exploration and exploitation of kimberlite deposits:[55,56] the existence of diamond-bearing and non-diamond-bearing kimberlite pipes with similar chemical compositions and locations,and a decrease in diamond-bearing character with depth;[55,57,61] the non-equilibrium nature of the distribution of diamonds along horizons and the correlation of the distribution with the characteristics of the morphology of the crystals;[54,56,57,60,62] and the correlation of the diamond-bearing character of individual sections of the pipes with the catalytic activity of the kimberlites in the reactions which are the reverse of reactions (2) and (3), and with the concentration of juvenile bitumens and the oxidation potential. This is also confirmed by the presence in the pipes of xenoliths of diamond-bearing and non-diamond-bearing eclogites with identical compositions,[63,64] the rare occurrence of diamond-bearing eclogites and the very high concentration of diamonds in them, the uniformity of the morphological characteristics and dimensions of eclogite diamonds, and the non-uniformity of the distribution of diamond crystals in the xenolith of eclogite, which are confined to the surface of the xenolith or to cracks intersecting the xenolith.[64–66] For example, in a xenolith of a diamond-bearing eclogite intersected by a serpentine vein, found in the Mir pipe in Yakutia, all the diamonds were confined to this vein.[66]

All these facts can be explained using the model of the chemical synthesis and growth of diamond crystals in open catalytic systems under non-equilibrium conditions. This model may be established under crustal conditions in the formation of kimberlite pipes or veins in degassing paths in the interior of the earth, and are not associated with super-high pressures.

The same facts cannot be explained, however, by assuming that diamonds are formed in the mantle at super-high pressures and removed from it.

The pallial (mantle) hypothesis is not consistent with the kinetic conditions of the formation and preservation of diamonds examined above. In the equilibrium magma of the mantle, only equilibrium epitaxial films of diamond on the faces of various minerals can be formed independently of the pressure by reactions (2)–(4) and exist for an unlimited time. Diamond crystals formed in the mantle at super-high pressure as a result of the polymorphic transformation of graphite under reducing conditions can exist for a long time only in the absence of CO_2 and H_2O, which is unlikely. Under non-equilibrium conditions in the mantle when open catalytic systems are produced, diamond crystals can be formed by reactions (2)–(4), etc., as in the crust, without super-high pressures. They will exist, however, so long as the non-equilibrium of system (17) is preserved and the exchange of materials continues, but will undergo combustion by the reverse reactions (2) and (3), or graphitisation, when these conditions break down {for example if there is a change in the composition of the mixture of light molecules A + L passing through the system (17) and super-equilibrium concentrations $[CO_2]$ and $[H_2O]$ appear in it as a result of the removal of the magma into the crust or on to the surface and as a result of a decrease in pressure}.

3. Facts relating to the growth of diamond crystals under the metasomatic conditions of the earth's crust without super-high pressure

Certain specific conditions of the formation of kimberlite pipes and paragenetic associations of diamond with high-pressure minerals have led a number of workers to assume that a leading role is played by the mantle production of kimberlite diamonds, that is by high pressures and temperatures. The recently established existence of non-kimberlite diamonds,[67–71] which eliminates completely high-pressure conditions for their formation, however, not only makes it necessary to doubt again the universal mantle hypothesis but also provides convincing confirmation of the model of the growth of diamond crystals in non-equilibrium open systems.

Metasomatic diamonds of the Kokchetav deposit. In the eighties, the Kokchetav (Kumdykul'skoe) deposit of fine diamonds with a cubic habit was discovered in Kazakhstan, occurring together with flaky graphite formations as a vein, localised in an old fracture, and formed as a result of metasomatic changes in the surrounding rocks by the reaction of the latter with products of the earth's degassing, passing along the fracture.[67–69] Diamonds with dimensions of 0.02–0.07 mm are present in very high concentrations in garnet–mica gneiss, garnet pyroxenites, marbles, and skarns. These minerals were formed as a result of metasomatic changes by the reaction of all types of rock intersected by the diamond-containing vein with gaseous fluids at 1000–1300 K and pressures not exceeding 6–9 kbar. At the same time, diamonds have not been found at a distance from the vein in corresponding surrounding rocks which have not undergone metasomatic changes. In the diamond-containing rocks the diamonds are found as inclusions in crystals of practically all the minerals (almandite, pyroxene, mica, quartz, etc.), and are often localised in micro-cracks and in the contacts between granules of other minerals.† In the axial zone of the deposit, richest in diamonds, there are very fine crystals (0.02–0.07 mm), and the less rich peripheral zones contain the largest crystals (up to 0.1–0.5 mm), and also contain pseudomorphs of graphite after diamond, not found in the other zones. In addition to diamonds, the diamond-containing rocks contain flaky graphite, formed at the same time as the diamond. The concentration of this graphite is 10^2 times the diamond concentration.

All this indicates the polycondensation of juvenile carbon-containing gases in the non-equilibrium open catalytic system (17), taking place in the diamond and graphite directions simultaneously and accompanied by the metasomatic transformation of the rocks surrounding the fluid-transport channels. The polycondensation has taken place under strongly reducing conditions with the predominant formation of graphite material, as shown not only by the higher yields of graphite material compared with diamond but also by the predominance of the cubic habit of the diamond crystals.[67] In this case the diamond material has been obtained under conditions leading to the preferential growth of nuclei (zone Y_nAOB in Fig. 9), as confirmed by the very high concentration of fine crystals in the rock and by the abundance of negative skeletal forms.

The model (17) is also consistent with the observed[69] distribution of diamonds relative to the axis of the diamond-containing ore vein. In the peripheral regions of the vein with a high oxidation potential and diffusion flow conditions, situated at the boundary of the non-equilibrium zone under conditions with $v_c < w_{diff}$, close to the conditions of the recrystallisation zone (COA in Fig. 9), the formation of nuclei has been retarded, and the diamond material has been deposited as larger crystals. This model is also consistent with the formation of paramorphs of graphite after diamond in the peripheral regions of the vein at the boundary of the non-equilibrium zone (range C in Fig. 10). The graphitisation of diamond

$$C(\text{diamond}) \rightarrow C(\text{graphite}),$$

accelerated by CO_2, will have favourable conditions as the composition of the diffusing gases (CO, H_2, CO_2) approaches the equilibrium composition and with the corresponding increase in the CO_2 concentration after the completion of the metasomatic changes, and also after the weakening or complete cessation of degassing, which gives non-equilibrium concentrations of the starting materials of reactions (2), (3), etc. The non-equilibrium character of the open catalytic system (17), which ensures favourable conditions for the synthesis of diamond and prevents graphitisation, disappears.

Pseudomorphs of graphite after diamond in the Beni Bouchera deposit (Morocco). Equally convincing confirmation of the model being considered is provided by the discovery of pseudomorphs of graphite after octahedral crystals of diamond[70, 71] in the laminated pluton of the ultrabasic rocks of the Beni Bouchera deposit, formed at temperatures of 770–1070 K and pressures not exceeding 5 kbar. In this deposit, between layers of flaky graphite, there is a lens of clinopyroxenites, in which all the graphite is present as pseudomorphs after graphite crystals with dimensions of 0.2–8 mm. The paramorphs constitute up to 15% of the volume of the rock. The concentration and size of the pseudomorphs are greatest at the centre of the lens.

In contrast to the metasomatic diamonds of the Kokchetav deposit, all the primary diamonds of the diamond-containing layer of the Beni Bouchera deposit have been completely converted into graphite pseudomorphs. The formation of the primary diamonds in this case has been associated with metamorphic changes in the cupola section of the pluton during its degassing and the movement of the carbon-containing fluids, and diffusion processes have predominated in the flux of fluids directed along the pressure gradient, that is

$$w_{diff} > w_f.$$

As a result of this last feature, the metamorphised part of the pluton has been formed as rhythmic layers. The production of this rhythmic diffusion stratification of the pluton indicates the prolonged action of the fluxes of the directed exchange of materials in this macroscopic open system and the development of self-organisation processes characteristic of these non-equilibrium systems.[72]

† The concentration of diamond granules is so high that it has been possible to study the distribution of their inclusions in the crystals of other minerals, in microcracks, and in the space between the granules from micrographs.[67–69]

The existence of the macroscopic open system (17) in the pluton degassing flux, which has given a mixture

$$\text{C(diamond)} + \overset{\downarrow}{\overline{\text{CO}_2 \rightarrow [2\text{CO}] \rightarrow \text{C(graphite)} + \text{CO}_2}} ,$$

of carbon-containing light molecules and other substances which bring about metasomatic changes in part of the pluton and the enclosing sedimentary rocks, has led to the development of all forms of the polycondensation process (1) and to the appearance of a zone most favourable for diamond polycondensation, together with zones in which ordinary flaky graphite has been formed. The conversion of diamond into graphite, irreversible at low pressures, has taken place, however, after the completion of the production of the pluton and the formation of the diamond and graphite deposits.

As in the case of the Kokchetav deposits, the start of graphitisation has been due mainly to a decrease in the non-equilibrium character of system (17) of diamond polycondensation as a result of a change in the composition of the entering gases, since only diamond polycondensation can oppose graphitisation under the same temperature conditions. The more favourable nature of the kinetic conditions for diamond polycondensation compared with graphite polycondensation reduces to the appropriate ratio of the rates (13). The graphitisation of diamond will become possible if a change in the composition of the gas-forming components or the cessation of the material exchange flux through the system (17) bring the conditions for reactions (2) and (2′) close to the equilibrium conditions and the reverse reactions (2) and (2′) take place to an insignificant extent in the presence of prepared crystals of diamond and graphite at a CO_2 concentration slightly greater than its equilibrium value.

The mechanism of this topochemical process may be the intermediate local conversion of diamond with the participation of CO_2 as catalyst, and the driving force may be the decrease in the thermodynamic potential in the polymorphic transformation of the diamond lattice into the graphite lattice. At super-high pressures, the reverse reaction (15) may take place with the same catalyst.

VIII. Summary

A large number of experimental facts and observations of natural phenomena confirm the model of the polycondensation synthesis of diamond from light-carbon-containing molecules by reactions of the type

$$2\text{CO} \rightleftarrows \text{C(diamond)} + \text{CO}_2 ,$$

$$\text{CO} + \text{H}_2 \rightleftarrows \text{C(diamond)} + \text{H}_2\text{O} ,$$

$$\text{CH}_4 + \text{CO}_2 \rightleftarrows 2\text{C(diamond)} + 2\text{H}_2\text{O} ,$$

at low pressures (not corresponding to the super-high pressures of the graphite $\rightleftharpoons$ diamond phase transformation). The chemical synthesis of diamond crystals has been observed in various open non-equilibrium catalytic systems differing in the scale of the observations.

The theory of this synthesis takes account of the stoichiometric, thermodynamic, and kinetic conditions of diamond polycondensation and the growth of diamond films and crystals. It defines the boundary and optimum conditions for the establishment of this complex process against a background of the aromatic polycondensation of the same original carbon-containing molecules leading to the production of graphite and other forms of non-diamond carbon. The general level of the oxidation potential and the difference between the kinetic conditions of diamond and graphite polycondensation is of considerable importance for determining the optimum conditions.

In addition to the conditions of the formation of new C–C bonds in the growth of the diamond lattice, the proposed theory examines the kinetic and macrokinetic conditions of formation of equilibrium epitaxial diamond films on crystal faces showing a crystal-structural correspondence with the arrangement of the carbon atoms on the faces of diamond, and also the conditions of the growth of macroscopic diamond crystals. It has been shown that equilibrium epitaxial films on appropriate supports (diamond critical nuclei) should be formed easily under static conditions. Their thickness, expressed as the number of carbon atomic layers, depends on the temperature and the size of the region of local equilibrium containing the original molecules of the polycondensation, but the ratio of the thickness of the film to the diameter is always constant and equal to 3×10^{-4}. At the same time the growth of the critical nuclei to give diamond macro-crystals requires special and rare (compared with those for the formation of the nuclei themselves) macrokinetic conditions. The growth of diamond macro-crystals by successive chemical synthesis is possible only in an open catalytic system operating in stationary fashion and ensuring a constant supply of the original carbon-containing molecules and the removal of product (CO_2 and H_2O) capable of displacing the equilibrium in the reverse direction.

The theory of the chemical synthesis of diamond essentially substantiates the possibility of the so-called metastable crystallisation of diamonds from the fluid or gas phase without super-high pressure, postulated by various authors in the formation of natural[73] and synthetic[2,74] diamonds. From the viewpoint of this theory, however, the actual term "metastable crystallisation of diamond" does not correspond to reality, since in it, metastability is defined with respect to the range of thermodynamic stability of diamond in the graphite $\rightleftharpoons$ diamond process, previously assumed to be the only possible route for the formation of diamond. We are dealing, however, with other processes of diamond synthesis with different thermodynamics, having its own ranges of stability of the diamond material under both equilibrium and non-equilibrium conditions.

References

1. B V Deryagin, D V Fedoseev *Rost Almaza i Grafita iz Gazovoi Fazy* (The Growth of Diamond and Graphite from the Gas Phase) (Moscow: Nauka, 1977)
2. D V Fedoseev, V P Varnin, B V Deryagin *Usp. Khim.* **53** 753 (1984) [*Russ. Chem. Rev.* **53** 435 (1984)]
3. Y H Lee, K J Bachmann, J T Glass, Y M Le Grice, R J Nemanich *Appl. Phys. Lett.* **57** 1916 (1990)
4. M A Cappelli, T G Owano, C H Kruger *J. Mater. Res.* **5** 2326 (1990)
5. N Ohtake, M Yoshikawa *New Diamond* 24 (1990)
6. K Hirabayashi *New Diamond* 29 (1990)
7. Y Muranaka, H Yamashita, H Miyadera *J. Vac. Sci. Technol.* **119** 76 (1991)
8. P K Bachmann, D Leers, H Lydtin *Diamond and Related Materials* **1** (1) 12 (1991)
9. A P Rudenko, I I Kulakova, A A Balandin *Vestn. Mosk. Univ., Ser. 2, Khim.* **8** (5) 105 (1967)
10. A P Rudenko, I I Kulakova, V L Shturman, in collected papers *Novye Dannye o Mineralakh SSSR* (New Data on the Minerals of the USSR) No. 28 (Moscow, 1979) p. 105
11. I I Kulakova, A P Rudenko, in collected papers *Kataliz: Fundamental'nye i Prikladnye Issledovaniya* (Catalysis: Fundamental and Applied Studies) (Moscow: Izd. MGU, 1987) p. 199
12. O Yu Zhdankina, I I Kulakova, A P Rudenko *Vestn. Mosk. Univ., Ser. 2, Khim.* **26** (5) 497 (1985)
13. F M Tapraeva, A N Pushkin, I I Kulakova, A P Rudenko, A L Elagin, S V Tikhomirov *Zh. Fiz. Khim.* **64** 2445 (1990)
14. A N Pushkin, F M Tapraeva, I I Kulakova, A P Rudenko *Sverkhtverdye Materialy* (3) 5 (1987)
15. A P Rudenko, in collected papers *Sovremennye Problemy Fizicheskoi Khimii* (Present-Day Problems in Physical Chemistry) Vol. 3 (Moscow: Izd. MGU, 1968) p. 263

16. A P Rudenko, I I Kulakova, S Ya Kurganova, in collected papers *Nauchnye Osnovy Kataliticheskoi Konversii Uglevodorodov* (Scientific Principles of the Catalytic Conversion of Hydrocarbons) (Kiev: Nauk. Dumka, 1977) p. 164
17. Ngo Thi Thuan, A P Rudenko *Vestn. Mosk. Univ., Ser. 2, Khimi.* **27** (5) 504 (1986)
18. V S Savel'ev, I I Kulakova, A P Rudenko *Geterogennyi Kataliz. Ch. 2 (Tr. V Mezhdunar. Simpoz.) Varna, 1983* (Proceedings of the Fifth International Symposium on Heterogeneous Catalysis, Varna, 1983, Part 2) p. 157
19. A P Rudenko, I I Kulakova *Geokhimiya* (7) 261 (1989)
20. I I Kulakova, A I Oglobina, A P Rudenko, V N Florovskaya, A I Botkunov, V L Skvortsova *Dokl. Akad. Nauk SSSR* **267** 1458 (1982)
21. F V Kaminskii, I I Kulakova, A I Ogloblina *Dokl. Akad. Nauk SSSR* **238** 985 (1985)
22. A I Botkunov, I I Kulakova, N N Krivitskaya, M E Ramenskaya, A P Rudenko, V L Shturman, in collected papers *Kompleksnye Issledovaniya Almazov, Vyp. 153 (Tr. TsNIGRI)* (Multipronged Studies of Diamonds. No. 153, Proceedings of the Central Geological Prospecting Scientific Institute) (Moscow, 1980) p. 69
23. I I Kulakova, O Yu Zhdankina, A P Rudenko, E D Nadezhdina *Mineral. Zh.* **11** (2) 52 (1989)
24. A P Rudenko, I I Kulakova *Zh. Vses. Khim. O-va im. D I Mendeleeva* **31** 518 (1986)
25. A P Rudenko *Teoriya Samorazvitiya Otkrytykh Kataliticheskikh Sistem* (The Theory of the Spontaneous Development of Open Catalytic Systems), (Moscow: Izd. MGU, 1969)
26. A P Rudenko *Zh. Fiz. Khim.* **61** 1457 (1987)
27. A P Rudenko *Zh. Vses. Khim. O-va im. D I Mendeleeva* **25** 390 (1980)
28. H W Kroto, A W Allaf, S P Balm *Chem. Rev.* **91** 1213 (1991)
29. Jpn. P. 59-35 092, *Ref. Zh. Khim.* 10M248P (1985)
30. A P Grigor'ev, S Kh Livshits, P P Shamaev *Kinet. Katal.* **18** 948 (1977)
31. S Kh Livshits, A P Grigor'ev, V V Koval'skii *Kinet. Katal.* **28** 313 (1987)
32. N Uchida, T Kurita, K Uematsu, K Saito *J. Mater. Sci. Lett.* **9** 249 (1990)
33. A V Varshavskii *VI Mezhdunarod. Konf. po Rostu Kristallov* (VI International Conference on Crystal Growth) Vol. 4 (Moscow, 1980) p. 134
34. US P. 3 030 187, 3 030 188, *Ref. Zh. Khim.* 17M116P, 17M117P (1963)
35. W A Carrington, L M Hanssen, K A Snail, D B Oakes, J E Butler *Metall. Trans. A* **20** 1282 (1989)
36. Y Muranaka, H Yamashita, H Miyadera, in *Diamond and Diamond-like Carbon Coatings* (New York: Elsevier, 1990) p. 1
37. J M Thomas, S Evans *Diamond Res.* 31 (1978)
38. V G Aleshin, A A Smekhnov, G P Bogatyreva, V B Kruk *Khimiya Poverkhnosti Almaza* (The Chemistry of the Surface of Diamond), (Kiev: Nauk. Dumka, 1990)
39. A A Balandin, A P Rudenko, G Stegner *Izv. Akad. Nauk SSSR, Otd. Khim. Nauk* (5) 762 (1961)
40. R A Buyanov, V V Chesnokov, A D Afanas'ev *Kinet. Katal.* **20** 207 (1979)
41. B V Deryagin, D V Fedoseev, V M Luk'yanovich, et al. *Dokl. Akad. Nauk SSSR* **181** 1094 (1968)
42. B V Deryagin, L L Builov, V M Zubkov, et al. *Kristallografiya* **14** 535 (1969)
43. Yu A Levitin, V P Butuzov, E M Nikiforova, et al. *Kristallografiya* **18** 435 (1973)
44. A Yoshida, Y Miyamoto, S Kume, M Koizumi, in *International Seminar "Superhard Materials"* Vol. 1 (Kiev, 1981) p. 36
45. A V Bochko, B V Deryagin *Dokl. Akad. Nauk SSSR* **196** 1056 (1971)
46. V D Zamozhskii, A N Luzin *Dokl. Akad. Nauk SSSR* **224** 369 (1975)
47. K V Volkov, V V Danilenko *Fiz. Goreniya i Vzryva* **26** (3) 123 (1990)
48. R J Meilunas *Appl. Phys. Lett.* **59** 3461 (1991)
49. K A Cherian, in *Diamond and Diamond-like Carbon Coatings* (New York: Elsevier, 1990) p. 127
50. Z V Bartoshinskii *Zap. Vses. Mineral. O-va, Ser. 2* **98** 560 (1960)
51. K P Argunov, V M Zuev, T M Nikiforova, V I Pritsepa, in *Tez. Dokl. IV Vsesoyuz. Soveshch. po Almazam (Simferopol', 1980)* (Summaries of Papers Presented at the Fourth All Union Conference on Diamonds, Simferopol', 1980) (Novosibirsk, 1980) p. 209
52. A I Ponomarenko, Z Specius *Zap. Vses. Mineral. O-va, Ser. 2* **110** 298 (1981)
53. A P Rudenko, I I Kulakova, V L Skvortsov, N N Krivitskaya, V L Bobrov, in *IX Vses. Simpoz. po Stabil'nym Izotopam v Geokhimii* (Ninth All Union Symposium on Stable Isotopes in Geochemistry) Vol. 1 (Moscow, 1982) p. 126
54. A I Botkunov, L A Fokina, in *Tez. Dokl. IV Vses. Soveshch. po Almazam (Simferopol' 1980)* (Summaries of Papers Presented at the Fourth All Union Conference on Diamonds, Simferopol', 1980) (Novosibirsk, 1980) p. 90
55. F F Brakhfogel', in *Tez. Dokl. IV Vses. Soveshch. po Almazam (Simferopol', 1980)* (Summaries of Papers Presented at the Fourth All Union Conference on Diamonds, Simferopol', 1980) (Novosibirsk, 1980) p. 54
56. A I Botkunov *Zap. Vses. Mineral. O-va, Ser. 2* **93** 427 (1964)
57. A I Botkunov *Zap. Vses. Mineral. O-va, Ser. 2* **99** 603 (1970)
58. V S Trofimov *Geologiya Mestorozhdenii Prirodnykh Almazov* (The Geology of Natural Diamond Deposits) (Moscow: Nedra, 1980)
59. V K Marshintsev, A V Lapin *Dokl. Akad. Nauk SSSR* **226** 681 (1976)
60. M A Gnevushev, Z V Bartoshinskii, A P Zinkov *Tr. Yakutsk. Fil. Sib. Otd. Akad. Nauk SSSR* (6) 105 (1961)
61. V V Zuenko, N S Makovskaya, A D Khar'kiv, N A Chernetskaya *Geol. Geofiz.* (4) 7 (1973)
62. Yu M Bilenko *Geol. Geofiz.* (10) 78 (1982)
63. A A Marakushev, A I Botkunov, S A Shcheka *Mineral. Zh.* **4** (4) 14 (1982)
64. N V Sobolev, N P Pokhilenko, E S Efimova *Geol. Geofiz.* (12) 63 (1984)
65. V S Sobolev, B S Nai, N V Sobolev, et al. *Dokl. Akad. Nauk SSSR* **188** 1141 (1969)
66. V I Mikheenko, B I Vladimirov, N I Nenashev, et al. *Dokl. Akad. Nauk SSSR* **190** 1440 (1970)
67. L D Lavrova *Priroda* (12) 62 (1991)
68. V A Pechnikov, Yu A Podkuiko, in *III Vses. Soveshch. po Geokhimii Ugleroda* (Third All-Union Conference on the Geochemistry of Carbon) (Moscow, 1991) p. 298
69. T B Ekimova, L D Lavrova, M A Petrova, E D Nadezhdina, S S Gorokhov, in *III Vses. Soveshch. po Geokhimii Ugleroda* (Third All-Union Conference on the Geochemistry of Carbon) (Moscow, 1991) p. 296
70. V V Slodkevich *Zap. Vses. Mineral. O-va, Ser. 2* **111** 13 (1982)
71. V V Slodkevich, in *Samorodnoe Mineraloobrazovanie v Magmaticheskom Protsesse. Tez. Dokl.* (Summaries of Papers Presented at the Conference on Natural Mineral Formation in the Magmatic Process) (Yakutsk, 1981) p. 149
72. K O Kratts, E N Eliseev (Eds) *Zakonomernosti Razvitiya Slozhnykh Sistem* (Regularities in the Development of Complex Systems) (Leningrad: Nauka, 1980)
73. N S Nikol'skii *Dokl. Akad. Nauk SSSR* **256** 954 (1981)
74. T R Anthony *Vacuum* **41** 1356 (1990)

Russian Chemical Reviews **62** (2) 105–120 (1993)
© 1993 Russian Academy of Sciences and Turpion Ltd

UDC 541.183

Use of IR spectroscopy in studies of catalysts based on molybdenum heteropoly compounds supported on oxides

A A Davydov, O I Goncharova

Contents

I. Introduction	105
II. Molybdenum heteropoly compounds	105
III. Supported molybdenum oxide catalysts. Formation, identification, and acidic properties of surface compounds	110
IV. Thermal stability of molybdenum compounds, decomposition mechanism, role of modifiers	116
V. Conclusions	118

Abstract. Experimental data on the use of IR spectra to identify compounds formed on the surface of various supports during the deposition of heteropoly compounds are reviewed. The spectral properties of the heteropoly compounds are analysed according to their type, to the character of the central ion, and to the form of the support. The first attempts to study the acidic properties of systems of this type are reported. The prospects of identifying the compounds formed on the surface of the carriers during the preparation of supported catalysts containing molybdenum or tungsten are examined. The bibliography includes 124 references.

I. Introduction

Heteropoly compounds (HPC) [heteropoly acids (HPA) and their salts] are now widely used in heterogeneous catalysis. They are effective catalysts of important chemical processes,[1–4] and they are also convenient as model catalytic systems, offering a useful combination of acid and oxidation–reduction properties which allows the composition and structure of the catalytically active centre to be strictly determined. Furthermore the HPC allow controlled variations of both the acidic and the oxidation–reduction function of the catalytic system, and in this sense they are superior to the zeolites.

The heteropoly compounds of molybdenum are good starting compounds for the preparation of multicomponent catalysts containing molybdenum, which includes most of the heterogeneous catalysts used in a variety of chemical processes such as partial oxidation.[4,5] Indeed, these compounds make possible the preparation of previously stipulated and exactly defined catalyst compositions with good mixing and complete interaction of the components, which allow the function of each of the components to be clearly displayed.

The role of HPC as precursors of active and selective catalysts has been pointed out more than once[5,6] in published work. the composition of many well known (including industrial) catalysts containing molybdenum probably included compounds of the HPC type. These can be formed in the course of the catalytic reaction (at least, on the surface of the heterogeneous system, where they cannot be observed by traditional methods such as X-ray diffraction analysis).

Supported catalysts offer several advantages,[7] of which the most important for HPC are probably a high mechanical strength and a developed specific surface. Furthermore a great saving in the expensive molybdenum compounds can be achieved by using supported catalysts. It has been shown[8] that in oxide catalysts the carrier can experience strong chemical interactions with the supported compound.

Published data on the character of the interaction of supported heteropoly compounds with the surface of the carrier are few.[8] It has been shown that when ammonium paramolybdate (APM) $(NH_4)_6Mo_7O_{24}$ is supported on carriers such as SiO_2, TiO_2, and Al_2O_3 the Si–Mo,[9] Ti–Mo,[10] and Al–Mo heteropoly compounds[11,12] can be synthesised on the surface of the catalysts under the influence of the cations of the support. These compounds are stable up to high temperatures. We may therefore assume that compounds of this type containing molybdenum as the active component will find extensive application as catalysts for the partial oxidation of hydrocarbons.[7] Therefore a more general formulation of the published information, a critical assessment of the reliability with which these compounds have been identified, and a determination of their properties are currently important problems.

II. Molybdenum heteropoly compounds

Traditional phase analysis methods, including X-ray phase analysis (XPA), have not been applied to HPC because of the dehydration of these materials and of the small content of the active component in supported catalysts. Vibrational spectroscopy offers some important advantages in these systems.[8–11,13] However, one of the difficulties in the study of supported systems is that the spectrum of the support usually overlaps the spectral region of the active component, making the latter difficult to resolve. Therefore the spectrum of the active component is often revealed by a procedure based on compensation for the spectrum of the support.[8–11,14]

1. IR spectra of massive heteropoly compounds

The IR spectra of HPC have been studied in detail. They adequately characterise HPC belonging to different structure types. In Fig. 1 we show the IR spectra of massive HPC containing 6 and 12 Mo atoms (Mo_6-HPC and Mo_{12}-HPC). In the spectra of Mo_6-HPC (spectra *4–6*) at 400–700 cm^{-1} we find strong absorption bands near 650 (ν_{as}) and 450 cm^{-1} (ν_s), assigned to the vibrations of the Mo–O–Mo bridging bonds.[15–17]

A A Davydov, O I Goncharova Institute of Catalysis, Siberian Division of the Russian Academy of Sciences, 5 prosp. akad. Lavrent'eva, 630 090 Novosibirsk, Fax (7-383-2) 35 57 66

Received 14th May 1992
Uspekhi Khimii **62** (2) 118–134 (1993); translated by J I Carasso

Furthermore the vibrations of the Mo=O multiple bonds[15-17] can be seen at 880–950 cm^{-1}. We should stress the difference between the spectra of the Mo_6-HPC in which the central atoms are triply charged (Fe^{3+} or Al^{3+}) ions (spectra *5* and *6*) or doubly charged ions (Cu^{2+}, Co^{2+}, spectrum *4*).† In the latter case the absorption bands assigned to $\nu_{Mo=O}$ and $\nu_{Mo-O-Mo}$ are shifted towards lower frequencies (925 and 635 cm^{-1} respectively) in comparison to the Al–Mo–HPC (945 and 665 cm^{-1}) and Fe–Mo–HPC spectra (945 and 645 cm^{-1}).

In the IR spectra of Mo_{12}- and $Mo_{11}Co$-HPC (Fig. 1, spectra *1–3*)‡ strong absorption bands are not found at 400–700 cm^{-1}, in contrast to the spectra of Mo_6-HPC. According to generally accepted suggestions[15-17] the IR absorption spectra of Mo_{12}-HPC in the 900–1000 cm^{-1} region correspond to the vibrations of the Mo=O end bonds (for example, the 965 cm^{-1} band in the spectra of P–Mo-HPC, spectrum *2*), whereas at 700–900 cm^{-1} we observe the stretching vibrations of the Mo–O–Mo bonds (absorption band at 780 cm^{-1} in the spectrum of Si–Mo-HPC, spectrum *1*). We note that the replacement of one molybdenum cation in the $SiMo_{12}O_{40}$ heteropoly anion by a different transition metal ion (mixed HPC, spectrum *3*) shifts the absorption band at 900–1000 cm^{-1} towards lower frequencies by 20–30 cm^{-1}. We also observe the appearance of an absorption at 720–730 cm^{-1}, which is not seen in the spectra of the Si–Mo-HPC.[18-20]

Thus the IR spectra of Mo_6-HPC in the region of 400–700 cm^{-1} differ markedly from those of Mo_{12}-HPC, whereas the IR spectra of mixed HPC at 700–1000 cm^{-1} differ from those of Si–Mo_{12}-HPC. These differences in the IR spectra of HPC belonging to different structure types allow the behaviour of the HPC supported on oxide carriers to be studied by IR spectroscopy.

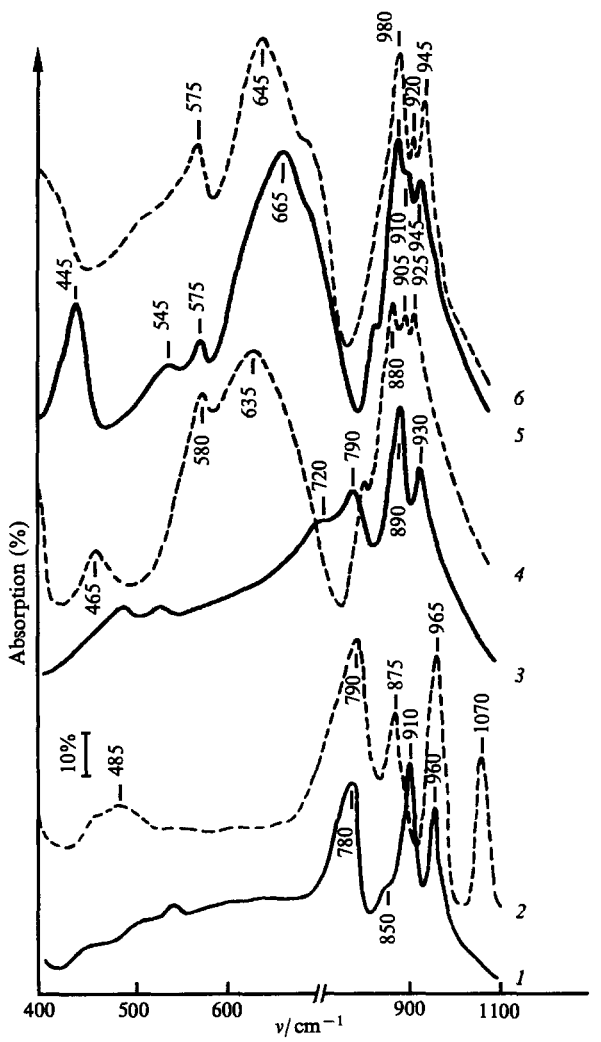


Figure 1. IR spectra of massive HPC dried at 373 K:
1) Cu_2SiMo_{12}, *2*) $Cu_{2/3}PMo_{12}$, *3*) $(NH_4)_6SiMo_{11}Co$, *4*) $(NH_4)_4CoMo_6$, *5*) $(NH_4)_3AlMo_6$, *6*) $(NH_4)_3FeMo_6$.

2. IR spectra of supported heteropoly compounds and effect of the support on their structure

The IR spectra of catalysts prepared by depositing the HPC $(NH_4)_{6-n}M^{n+}Mo_6$ (M = Cu^{2+}, Co^{2+}, Fe^{3+}) on SiO_2 are almost identical (spectra *3–5* of Fig. 2), but they differ markedly from the spectra of the unsupported (bulk) Mo_6-HPC of the transition metals (spectra *4–6* of Fig. 1): the strong absorption bands at 400–700 cm^{-1} are replaced by strong bands at 730–970 cm^{-1}, which are not found in the spectra of bulk Mo_6-HPC. As was stated above, these spectral features are also found in Mo_{12}-HPC and in mixed HPC. Comparing the spectra of Mo_6-HPC supported on SiO_2 (spectra *3–5* of Fig. 2) with the spectra of Mo_{12}- and $Mo_{11}Co$-HPC shows an analogy with the IR spectrum of the mixed $Mo_{11}Co$-HPC (spectrum *3* of Fig. 1). This suggests that when the Mo_6-HPC of copper, cobalt, and iron are supported on SiO_2 they become rearranged into mixed Si–Mo–M-HPC, i.e. molybdenum ions are replaced by transition metal cations.

The IR spectra of samples prepared by supporting $(NH_4)_4CuMo_6$ (spectrum *7* of Fig. 2) and $(NH_4)_4CoMo_6$ (spectrum *8* of Fig. 2) on Al_2O_3 are almost identical, and differ significantly from the spectrum of unsupported $(NH_4)_4CoMo_6$ (spectrum *4* of Fig. 1): for example, their $\nu_{Mo=O}$ and $\nu_{Mo-O-Mo}$ frequencies are shifted (by 20 and 30 cm^{-1} respectively) towards longer wavelengths as compared with the absorption bands at 925 and 635 cm^{-1} observed for the bulk compounds. These shifts in the position of the IR absorption bands can be used to distinguish the Mo_6-HPC of doubly charged cations from the HPC of triply charged cations. Comparing the spectra of these catalysts (Fig. 2, spectra *7* and *8*) with the spectrum of the NH_4 salt of the Al–Mo-HPA (where HPA is a heteropoly acid) supported on Al_2O_3 (Fig. 2, spectrum *6*) shows marked similarities, with coinciding maxima of the most characteristic absorption bands. This suggests that the deposition of the molybdenum heteropoly compounds of Cu and Co on Al_2O_3 causes the formation of Al compounds, involving the Al surface atoms of the support. Under these conditions the copper and cobalt cations usually continue to be the salt formers. The change in colour of the samples (from blue to green for the copper HPC and from light brown to lilac for the cobalt HPC) confirms the change in state of the Mo_6-HPC of copper and cobalt when supported on Al_2O_3.

An analysis of the IR results for samples prepared by supporting $(NH_4)_3FeMo_6$ on Al_2O_3 shows that in this case $FeMo_6O_{24}H_6^{3-}$ is converted into $AlMo_6O_{24}H_6^{3-}$. In the IR spectra of these catalysts in the $\nu_{Mo-O-Mo}$ region (spectrum *9* of Fig. 2) the characteristic absorption of the Fe–Mo-HPC at 645 cm^{-1} (spectrum *6* of Fig. 1) is replaced by an absorption band at 665 cm^{-1}, proper to the spectrum of the Al–Mo-HPC (spectrum *5* of Fig. 1), and furthermore an absorption at 445 cm^{-1} (belonging to the spectrum of Al–Mo-HPC, spectrum *5* of Fig. 1) is also seen. However, at 880–950 cm^{-1} these two compounds behave identically.

Thus the MMo_6-HPC (where M = Cu, Co, Fe) are unstable. When supported they react with the oxide carrier, and they decompose even at the drying stage. On an SiO_2 surface the silicon ions of the carrier form mixed Si–Mo–M-HPC in which transition metal cations replace molybdenum ions:

$$(NH_4)_{6-n}M^{n+}Mo_6O_{24}H_6 + SiO_2 \xrightarrow{373\ K} \longrightarrow (NH_4)_{8-n}SiMo_{11}M^{n+}O_{40}H_2/SiO_2 .$$

† The IR spectra of the Mo_6-HPC of copper and cobalt are identical.
‡ The IR spectra of the Cu and Co salts of Si–Mo- and P–Mo-HPC are similar to those of the corresponding heteropoly acids.

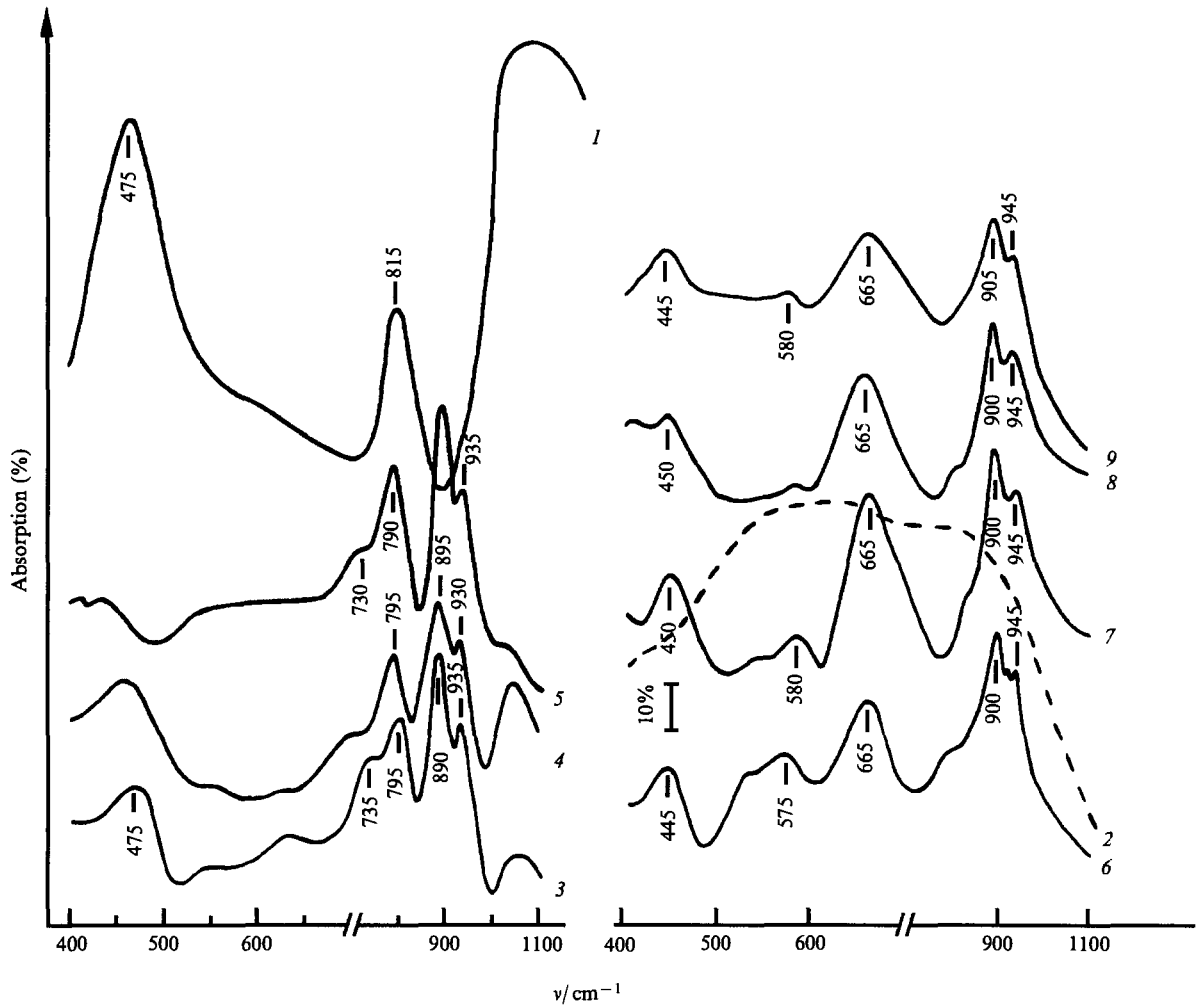


Figure 2. IR spectra of the carriers SiO_2 (*1*) and Al_2O_3 (*2*) and of the samples prepared by supporting Mo_6-HPC on these carriers: *3*) $(NH_4)_4CoMo_6/SiO_2$ (16.5% Mo), *4*) $(NH_4)_4CuMo_6/SiO_2$ (16% Mo), *5*) $(NH_4)_3FeMo_6/SiO_2$ (15% Mo), *6*) $(NH_4)_3AlMo_6/Al_2O_3$ (16.1% Mo), *7*) $(NH_4)_4CuMo_6/Al_2O_3$ (17.6% Mo), *8*) $(NH_4)_4CoMo_6/Al_2O_3$ (16% Mo), *9*) $(NH_4)_3FeMo_6/Al_2O_3$ (16.5% Mo).

When supported on Al_2O_3 the M–Mo_6-HPC (M = Cu, Co, Fe) are converted into Al–Mo_6-HPC with the participation of Al atoms from the carrier surface:

$$(NH_4)_{6-n}M^{n+}Mo_6O_{24}H_6 + Al_2O_3 \xrightarrow{373\ K} \longrightarrow (NH_4)_xM_{(3-x)/n}AlMo_6O_{24}H_6/Al_2O_3 .$$

These processes are of interest from the standpoint of the chemistry of HPC, but they have only very recently begun to be discussed in published work. Results so far available suggest that the tendency of surface atoms to form complexes with molybdenum depends on their nature, and in particular that this property is more clearly developed in Si and Al atoms than in Cu^{2+}, Co^{2+}, and Fe^{3+}. As a result the aluminium and silicon atoms on the carrier surface can displace copper, cobalt, and iron from the central ion position in the mixed HPC.

The IR spectra of Si–Mo_{12}- and P–Mo_{12}-HPC supported on SiO_2 or TiO_2 are identical to the spectra of their copper and cobalt salts on the same supports. The form of the spectra is independent of the content of HPC on the support (5–25 wt.% Mo). In the spectra of P–Mo_{12}-HPA on SiO_2 and TiO_2, we find absorption bands at 790, 875, and 965 cm^{-1} which are also seen in the spectra of massive P–Mo_{12}-HPA (spectrum *2* of Fig. 1). We note that the absorption band at 1065 cm^{-1} seen in the spectra of massive P–Mo-HPC cannot be reliably resolved in the IR spectra of these compounds supported on SiO_2 because of the strong absorption of the carrier in this region (spectrum *1* of Fig. 2). In the spectra of Si–Mo_{12}-HPC supported on SiO_2 and TiO_2 absorption bands can be seen at 780, 865, 910, and 960 cm^{-1}: these are characteristic of the heteropoly anion (HPAn) $SiMo_{12}O_{40}^{4-}$ (spectrum *1* of Fig. 1).

On the whole the good agreement between the IR spectra of bulk P–Mo_{12}- and Si–Mo_{12}-HPA (and their salts) and of the samples supported on SiO_2 and TiO_2 suggests that the structure of the anion of Mo_{12}-HPA is preserved when the material is supported on these carriers.[9,10]

A different state of affairs is found for Mo_{12}-HPC supported on Al_2O_3. The IR spectra of samples prepared by depositing the Cu and Co salts of Si–Mo_{12}-HPA on Al_2O_3 (~15% Mo) are similar. Fig. 3 (spectrum *2*) shows as an example the spectrum of Co_2SiMo_{12}/Al_2O_3, which differs markedly from the characteristic spectrum of the $SiMo_{12}O_{40}^{4-}$ HPA (spectrum *1* of Fig. 1), and is almost identical to the IR spectrum of the NH_4 salt of the Al–Mo-HPA supported on Al_2O_3 (spectrum *6* of Fig. 2). These results indicate the decomposition of $SiMo_{12}O_{40}^{4-}$ when the Cu and Co salts of Si–Mo_{12}-HPA are supported on Al_2O_3 in concentrations of ~15% Mo. Under these conditions Al–Mo_6-HPC are formed on the support. Unlike its salts, the Si–Mo_{12}-HPA itself is preserved when supported on Al_2O_3: the IR spectrum of the Si–Mo_{12}-HPA/Al_2O_3 sample (16.8% Mo) (spectrum *1* of Fig. 3) is similar to that of the massive heteropoly acid (spectrum *1* of Fig. 1).

The IR spectra of the catalysts prepared by supporting the P–Mo-HPA and its Cu and Co salts on Al_2O_3 (concentration of HPC ~15% Mo) are similar (spectra *3* and *4* of Fig. 3), and almost indistinguishable from the spectrum of $(NH_4)_3AlMo_6/Al_2O_3$

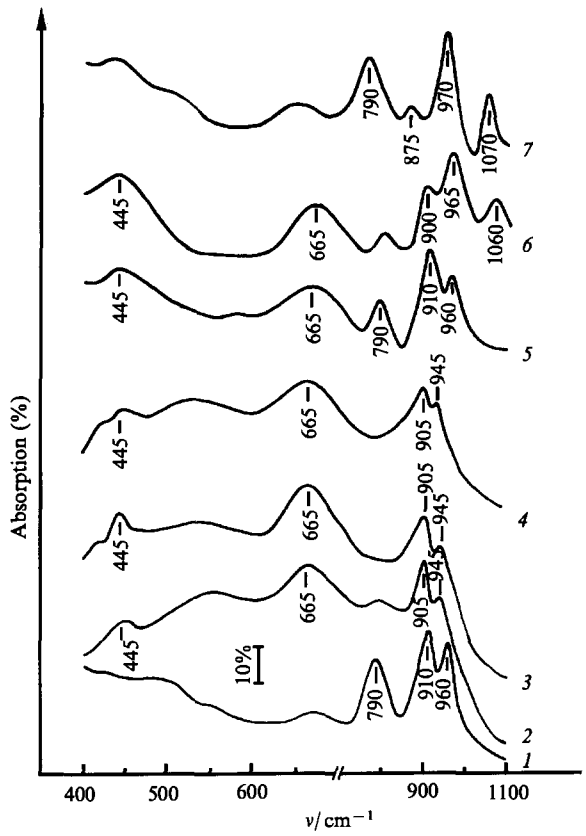


Figure 3. IR spectra of samples prepared by supporting Mo_{12}-HPC on Al_2O_3 and drying at 373 K:
1) H_4SiMo_{12} (16.8% Mo) *2*) Co_2SiMo_{12} (15.5% Mo)
3) $Cu_{3/2}PMo_{12}$ (14.6% Mo) *4*) H_3PMo_{12} (13.3% Mo)
5) Co_2SiMo_{12} (27.3% Mo) *6*) $Co_{3/2}PMo_{12}$ (21.5% Mo)
7) H_3PMo_{12} (23.4% Mo).

(spectrum *6* of Fig. 2). Absorption bands characteristic of the P–Mo_{12}-HPC are not observed in the spectra of these samples.

The totality of these results convincingly shows that at low concentrations (~15% Mo) on the surface of an Al_2O_3 support Mo_{12}-HPC (like Si–Mo_{12}-HPA) is decomposed with formation of Al–Mo_6-HPC by reacting with the aluminium atoms of the Al_2O_3 surface, whereas copper and cobalt cations tend to behave as salt formers:

$$M_xAMo_{12}O_{40} + Al_2O_3 \xrightarrow{373\ K} M_yAlMo_6O_{24}H_6/Al_2O_3 .$$

Fig. 3 also shows the IR spectra of catalysts with large concentrations of Mo_{12}-HPC on Al_2O_3 (23–27 wt.% Mo, spectra *5*–*7*). It can be seen that increasing the concentration of P–Mo_{12}-HPA and its salts (or of the salts of Si–Mo_{12}-HPA) on the support produces, in addition to a weak band at 665 cm^{-1}, characteristic of Al–Mo_6-HPC, absorption bands typical of $SiMo_{12}O_{40}^{4-}$ (780, 860, 910, and 960 cm^{-1}, spectrum *5* of Fig. 3) and of $PMo_{12}O_{40}^{3-}$ (790, 875, 965, and 1065 cm^{-1}, spectra *6* and *7* of Fig. 3). This suggests that at high concentrations the main part of the Mo_{12}-HPC is retained unchanged on the Al_2O_3 surface.

Thus the Mo_{12}-HPC are preserved (irrespectively of their concentration on the surface) when deposited on SiO_2 or TiO_2, whereas on the surface of Al_2O_3 the P–Mo_{12}-HPA and its salts, as well as the salts of Si–Mo_{12}-HPA, decompose at low concentrations with formation of Al–Mo_6-HPC.

These results have been explained[8] in terms of the acid–based properties of the substrates and of the pH stability range of the supported HPC.

As reported,[21,22] the substrates can be arranged in the following order of decreasing acidity: $SiO_2 > TiO_2 > Al_2O_3$. We know that P–Mo-HPA is stable over a very narrow range of pH (0.8–1.5), whereas for Si–Mo-HPA the range is much wider (from 1 to 4).[23,24] Solutions of the Cu and Co salts of Si–Mo- and P–Mo-HPA are also acidic: pH ~2 for $M_{3/2}PMo_{12}$ and pH ~4 for M_2SiMo_{12}.[23] The Mo_6-HPC are stable at higher pH values (2–5.5), and in particular the $AlMo_6O_{24}H_6^{3-}$ anion is preserved up to pH 5.5.[23]

The stability of the structure of Mo_6-HPC when supported on SiO_2 and TiO_2, even at low concentrations of Mo, is probably due to the relatively high acidity of these supports. With a more basic support (such as Al_2O_3) and at low concentrations of Mo_{12}-HPC on the support the heteropoly compound decomposes, lowering the acidity of the medium. As we have shown,[11] under these conditions we observe the formation of Al–Mo_6-HPC, whose anion is stable in less acidic media. At higher concentrations of the HPC on the Al_2O_3 (up to 20–25 wt.% of Mo) the structure of the supported material is retained, probably as a result of the increased acidity of the medium.

Si–Mo-HPA (unlike P–Mo, see above) does not decompose when supported on Al_2O_3, even at low concentrations on the carrier. This is probably due to the wider stability range of Si–Mo-HPA as compared with P–Mo-HPA. On the other hand the salts of the Si–Mo-HPA decompose under these conditions, probably because of the lower acidity of their solutions.

We could therefore have expected that the creation of a strongly acid medium on the surface of samples with a low concentration of HPC on the Al_2O_3 would regenerate the Mo_{12}-HPC after this compound had been decomposed with formation of Al–Mo_6-HPC. To test this hypothesis samples prepared by depositing P–Mo- and Si–Mo-HPC on Al_2O_3 (~15% Mo) were treated with a solution of hydrochloric acid (1 : 1). In the IR spectra of these samples (see Fig. 4, spectra *2*, *4*, and *6*) we found, in contrast to the spectra of the initial catalysts (spectra *1*, *3*, and *5*), absorption bands at 790, 875, 965, and 1065 cm^{-1}, characteristic of P–Mo_{12}-HPA (spectra *2* and *4*) and at 790, 910, and 960 cm^{-1}, characteristic of Si–Mo_{12}-HPA (spectrum *6*), i.e. the increased acidity of the medium induces the reverse conversion of Al–Mo_6-HPC into Si–Mo_{12}- and P–Mo_{12}-HPC.

Thus a study of the interactions of the Mo_6- and Mo_{12}-HPC with the oxide supports leads to the following conclusions. The M–Mo_6 molybdenum heteropoly compounds containing copper, cobalt, or iron as the central atom M are unstable. When supported they interact with the carrier, and as a result mixed Si–Mo–M heteropoly compounds are formed on the SiO_2 surface. On a γ-Al_2O_3 surface the Mo_6-HPC of the transition metals decompose with formation of salts of the Al–Mo_6-HPA. The phase composition of catalysts prepared by depositing Mo_{12}-HPC on supports depends on the acid–base properties of the support and on the pH stability range of the supported HPC. Whereas the structure of P–Mo_{12}- and Si–Mo_{12}-HPC is retained when the compounds are supported on SiO_2 and TiO_2, irrespective of their concentration on the carrier, deposition on Al_2O_3 causes decomposition of the compounds (when present at low concentrations) and the formation of Al–Mo_6-HPC. Thus the composition of the compounds on the surface of basic carriers can be controlled either by varying the concentration of the supported heteropoly compounds or by treating the carriers with solutions of mineral acids.

3. Acidic properties of molybdenum heteropoly compounds

The number of publications dealing with the acidic properties of supported HPC is small. We have described[25] a study of the acidic properties of P–Mo-HPA supported on various oxide carriers (SiO_2, TiO_2, Al_2O_3), and also of Si–Mo-HPA and the salts of P–Mo-HPA on SiO_2. The adsorption of molecules of a base (pyridine[25,26] or ammonia[9]) on these HPC was studied by IR spectroscopy.

It was found that the IR spectra of pyridine adsorbed on any of the HPC in the 1300–1650 cm^{-1} region were similar. The presence of an absorption band at 1540 cm^{-1}, assigned to vibrations in the pyridinium ion, was interpreted[25] as evidence of the presence in all the catalysts of Brønsted-acid centres (BAC)

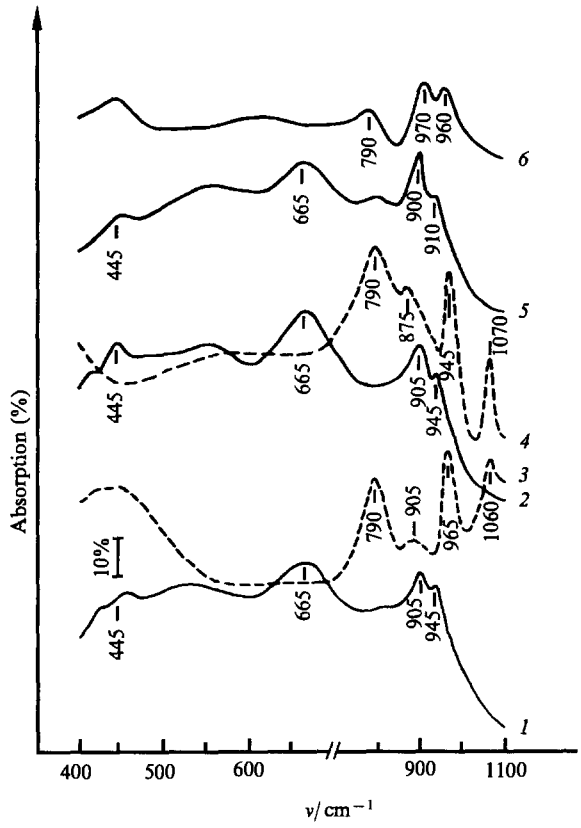


Figure 4. IR spectra of samples prepared by supporting Mo_{12}-HPC on Al_2O_3: *1*) and *2*) H_3PMo_{12} (13.3% Mo), *3*) and *4*) $Co_{3/2}PMo_{12}$ (14.1% Mo), *5*) and *6*) Cu_2SiMo_{12} (16.6% Mo). The spectra *2*, *4*, and *6* were recorded after treating the samples with a solution of HCl.

which protonate the pyridine molecule. The absorption band found at 1450 cm^{-1} denotes the formation of complexes of pyridine with aprotic centres of the catalyst.

Effect of the concentration of HPA. We studied the dependence of the concentration of proton centres (in μmol PyH^+ m^{-2}) on the content of P–Mo- and Si–Mo-HPA on SiO_2 and of P–Mo-HPA on Al_2O_3. All these dependences are of the same type, suggesting that in the region of low concentration of HPA on the carriers (7–15 wt.% of Mo) the amount of BAC increases in proportion to the concentration of HPA. At still higher concentrations of P–Mo- and Si–Mo-HPA on the carrier (up to 20–28 wt.% of Mo) the concentration of mobile protons (in μmol PyH^+ m^{-2}) stays unchanged, but the specific surface decreases.

The increase in the concentration of BAC with increasing content of HPA (in the region of 7–15 wt.% of Mo) was attributed to the increased coverage of the carrier surface by HPA molecules. A further increase in the content of HPA causes agglomeration of the molecules, which lowers the specific surface of the samples while the concentration of the proton centres per m^2 stays constant.

Since according to Okuhara et al.[27] the acidity measured for massive HPA is the bulk value, our results[25] indicate that in the case of supported HPA the main role is played by the surface properties.

The strength of the proton centres (in units of *PA*, or proton affinity[26]) was characterised by the frequency of the stretching vibrations band of the pyridinium ion, which depends on the basic properties of the acidic residue.[25]

The strength of the proton acid centres was unaffected by varying the content of P–Mo- and Si–Mo-HPA on SiO_2 or of P–Mo-HPA on Al_2O_3: the parameter ν^c_{NH} (defined as the position of the centre of gravity of the ν_{NH} band)§ is 2900 cm^{-1} for all the samples of P–Mo- and Si–Mo-HPA on SiO_2, and 2600 cm^{-1} for the HPA supported on Al_2O_3.

The acidic properties of the different HPC were compared at high concentrations of these compounds on the carrier.

Comparing the acidic properties of HPA with P and Si central atoms supported on SiO_2 showed that the concentration of BAC is greater by a factor of 1.4 in H_3PMo_{12}/SiO_2 than in H_4SiMo_{12}/SiO_2 over the whole range of concentrations of the HPA on the carrier. The strength of the proton centres (as previously defined[26]) was the same for P–Mo- and Si–Mo-HPA supported on SiO_2: ν^c_{NH} = 2900 cm^{-1}.

Effect of the type of carrier. It was reported[23] that the concentration of mobile protons in P–Mo-HPA supported on SiO_2 is much higher than in the same compound on Al_2O_3 over a wide range of concentrations of the HPA. The concentration of BAC in P–Mo-HPA supported on TiO_2 (13.7% of Mo) is 0.4 μmol m^{-2}, i.e. three or four times lower than the concentration of BAC in P–Mo-HPA on SiO_2 (13.6% of Mo), for which this quantity is 1.5 μmol m^{-2} (for samples conditioned at the same temperature of 423 K).

By comparing the ν^c_{NH} values obtained for P–Mo-HPA samples on different carriers it was shown that the centres of gravity ν^c_{NH} for HPA/TiO_2 and HPA/Al_2O_3 are strongly shifted towards lower frequencies. Their calculated ν^c_{NH} values were about 2600 cm^{-1}, as compared with 2900 cm^{-1} for HPA/SiO_2. Therefore supporting the P–Mo-HPA on TiO_2 and on Al_2O_3 lowers the strength of the proton centres.

Qualitative results on the change in the number of BAC caused by an increase in the conditioning temperature of Si–Mo-HPA and P–Mo-HPA (and its salts) deposited on SiO_2 were obtained by studying the adsorption of pyridine on these samples. The concentration of mobile protons on all the samples fell when the pretreatment temperature was increased, the effect being most marked following an increase in temperature from 523 to 723 K. The strength of the proton centres (the shift in ν^c_{NH}) was unaffected by increasing the conditioning temperature of the HPC/SiO_2.

Effect of replacing the protons in the HPA by metal cations. This effect was studied[25] for P–Mo-HPA and its sodium and copper salts supported on SiO_2.

Replacing some of the protons in P–Mo-HPA/SiO_2 by Na^+ produces a large change in the proton-donor capacity of the acid centres (as shown by the changes in the contour of ν^c_{NH}). Upon introducing sodium cations the centre of gravity of ν^c_{NH} is shifted towards lower frequencies (the calculated ν^c_{NH} is 2800 cm^{-1} for the salts and 2900 cm^{-1} for the acid). Similar effects were noted in a study[27] of the decrease in the desorption temperature of pyridine from the Na^+ salts of P–W-HPA as compared with its desorption from the acid itself. For the Cu^+ salts of P–Mo-HPA this decrease in the strength of the proton centres was not observed: ν^c_{NH} was the same for H_3PMo_{12}/SiO_2 and $Cu_{3/2}PMo_{12}/SiO_2$.

The change in the concentration of mobile protons caused by the replacement of H^+ by metal cations in P–Mo-HPA showed[25] that for conditioning temperatures between 423 and 723 K the number of BAC (in μmol PyH^+ m^{-2}) decreases monotonically as the concentration of sodium or of copper in the HPC is increased. However, even in the fully substituted salts Na_3PMo_{12}/SiO_2 and $Cu_{3/2}PMo_{12}/SiO_2$ a small number of mobile protons is still detectable.

Lewis-acid centres. As reported[28], the massive HPA and their salts can be classified as proton acids. The concentration of Lewis-acid centres (LAC) in these catalysts is negligibly small (the amplitude of the absorption band due to co-ordinated pyridine is small in comparison with the absorption band of PyH^+).

§ The position of the centre of gravity of the ν_{NH} band of the pyridinium ion was determined from the outline of the ν_{NH} line at 3400–1800 cm^{-1} (see Okuhara et al.[27]).

Studies of the acidic properties of HPC supported on a carrier have shown[9, 25] that the absorption bands which characterise the ions of co-ordinated pyridine and NH_3 are relatively strong. The concentration of LAC in P–Mo-HPA/SiO_2 has been measured, and the dependence of the concentration of LAC on the composition of the HPC and on their heat-treatment temperature was determined.[25]

Thus the results discussed above show that IR spectroscopy can be conveniently used to establish the presence of HPC on carriers (at least, on SiO_2, Al_2O_3, and TiO_2 as carriers). The method can also be used to monitor the formation of similar compounds during the preparation of traditional supported catalysts containing molybdenum. However, it should be noted that in this case the problem is much more complex than the problems considered above. This is due partly to the large number of phases present in the traditional catalysts (as has been repeatedly pointed out in published papers) and partly to the use of very high conditioning temperatures, which cannot fail to cause decomposition of the HPC, even in the case of compounds formed on the carrier surface during the preparation of the catalyst. Nevertheless the possibility of stabilising these compounds by an appropriate choice of support has now been established: in other words, the carrier should be treated as one of the components of the resulting HPC.[9–11]

As was shown by Mastikhin et al.,[29] important information on the changes in acidity of the HPA induced by the support can be obtained by using the PMR method.

III. Supported molybdenum oxide catalysts. Formation, identification, and surface properties of surface compounds

In this section we shall dwell on two aspects of the study of supported molybdenum oxide catalysts: (1) the development of methods of studying supported catalysts, and (2) the analysis of published data on the identification of the compounds formed on the surface of various carriers during their interaction with molybdenum oxide compounds. Of course, equal attention will be paid to the identification of other compounds formed on the surface of the carriers during this interaction. There are recent reports of the formation of HPC on the carrier surface during the deposition of molybdenum and tungsten oxide compounds (including the traditional methods) as a result of the far-reaching interaction of the supported compounds with the carrier.

X-Ray phase analysis is often not suited to the study of oxide systems formed on the surface of carriers, especially when the active component is present at low concentration. In this case IR spectroscopy is the most attractive method, widely used to establish the phase composition of oxide systems including catalysts amorphous to X-rays.[30, 31] To a first approximation the study of supported compounds by IR spectroscopy is similar to the study of adsorbed molecules:[32] in both cases the basic problem is to identify the type of compound formed by the interaction of the supported compound with the surface and to make apparent the changes taking place during this interaction, i.e. in this case IR spectroscopy is used mainly as a method of analytical control, showing the presence of various compounds of interest.¶ This application of IR spectroscopy suffers from the limitations imposed by the use of vibrational spectroscopy in surface chemistry: (1) the inability to provide a complete spectrum of the surface compound, due both to the overlap of the absorption bands of the active component with those of the support, and to the low concentration of the surface compound, and (2) the simultaneous formation on the carrier surface of several compounds and the overlap of the absorption bands belonging to different structures. For supported molybdenum oxide systems these limitations are even more serious because of the need to identify an inorganic surface compound on the surface of an inorganic carrier.

Because of these difficulties spectral compensation methods seem to be the most attractive: they have been reviewed in depth,[14] and are widely used by several workers to establish the nature of the active component,[8–11, 33] including supported molybdenum oxide compounds formed on the surface of carriers.[8–11]

1. Formation and identification of Al–Mo oxide compounds

Aluminium molybdenum oxide catalysts are being intensively studied everywhere because of the extreme importance of hydrodesulphurisation processes in petroleum refining, in which Al–Mo and Al–W systems promoted with cobalt and nickel are the most widely used industrial catalysts. Several reviews[33–36] of the structure and physicochemical properties of Al–Co–Mo hydro-refining catalysts have been published. The study of unpromoted Al–Mo catalysts is also of interest because these materials are active in many hydrocarbon conversion reactions: oxidation, hydrogenation, isomerisation, dehydrogenation, polymerisation, olefin metathesis, and paraffin condensation.

Several methods of preparing Al–Mo catalysts are available: the adsorption of $MoO_2(OH)_2$ on Al_2O_3 from the gas phase,[37] fixing metal-organic complexes on the Al_2O_3 surface,[38, 39] the adsorption of molybdate ions by the carrier from solutions,[40–44] and coprecipitation from solutions of ammonium paramolybdate (APM) and $Al(NO_3)_3$.[45, 46] The simplest and most widely used method relies on impregnation of the formed Al_2O_3 carrier with solutions of ammonium paramolybdate followed by drying and roasting of the catalyst at given temperatures.[37, 47–54]

Depending on the concentration and pH of the APM solution, surface compounds of different composition can be obtained on the carrier.[42, 43, 49–54] This is primarily due to the presence of different associations in the APM solution, depending on the pH and on the concentration.[55, 56] Increasing the pH and lowering the concentration shifts the equilibrium towards the formation of molybdates containing molybdenum ions in a tetrahedral coordination (MoO_4^{2-}). At low pH and high concentrations the dominant species are the isopoly molybdates, in which the molybdenum ions have an octahedral coordination.[50, 54] Furthermore the γ-Al_2O_3 carrier itself has acid–base properties,[22, 50, 54, 57, 58] and therefore an equilibrium determined by the initial pH and concentration of the solution and by the type of carrier is established at the interface with the molybdenum solutions.[42, 43, 50, 54] By using a more acidic carrier (SiO_2) the polymeric compounds can be stabilised at much lower molybdenum concentrations (down to 10%) than on the more basic Al_2O_3. On the strongly basic MgO the formation of octahedral molybdenum polyanions was not detected at any concentration of APM.[54, 59]

The surface OH groups of the carrier can interact with the molybdenum anions with formation of surface compounds. A large decrease (or complete suppression) of the fluorescence background accompanying the Raman spectrum and attributed to the OH groups on the Al_2O_3 surface has been noted[51] after the deposition of APM on the carrier, suggesting a reaction of the APM with the OH groups. A Raman study of Al–Mo catalysts prepared by impregnating Al_2O_3 carriers with APM solutions of pH between 6 and 11 led to the conclusion[50] that at low molybdenum concentrations (1–3 wt.% MoO_3) only MoO_4^{2-} ions are formed on Al_2O_3 even at pH 6, when the impregnating solution contains $Mo_7O_{24}^{6-}$ ions. The dissociation of the $Mo_7O_{24}^{6-}$ ions is attributed[50] to an increase in the pH of the

¶ This does not exclude the use of IR spectroscopy as a structural technique. If the limitations defined below can be overcome the results of IR spectroscopy can be used to establish the structural parameters of the supported compound.

solution due to the increased concentration of OH^- ions in solution produced by the ion-exchange adsorption

$$Al-OH + MoO_4^{2-} \leftrightarrows AlOMoO_3^- + OH^-.$$

The presence of tetrahedral molybdenum ions on the surface of Al–Mo catalysts prepared by adsorption of molybdate ions from dilute solutions APM at a high pH (8.6) has been established.[42, 43] Adsorption from concentrated solutions of APM or at low pH (4.0) results in the stabilisation of octahedral Mo polyanions[42, 43] on the Al_2O_3 surface; these are retained when the sample is dried.

According to Giordano et al.[53] the Al–Mo catalysts (before being heated) contain tetrahedral ions weakly interacting with the OH groups of the Al_2O_3. During the subsequent activation of the catalysts by oxidative high-temperature treatment further interaction of the molybdenum compounds with the carrier surface takes place.

Under these conditions stable monomeric molybdate complexes (MoO_4^{2-}) are formed at low molybdenum concentrations.[52] Experimental confirmation of the formation of a monolayer of tetrahedrally coordinated molybdenum ions has been obtained by different methods, including IR, Raman, and UV spectroscopy, XPS, and others.[37, 50, 52, 53, 60] According to most of the authors at low concentration (5–10 wt.% MoO_3) the whole of the molybdenum in the roasted catalysts is present in a highly dispersed state, and mainly as tetrahedral ions.[52, 53, 61–63] Increasing the concentration of MoO_3 (to 16 wt.%) increases the fraction of the molybdenum in octahedral coordination and forms polymolybdate structures. At even higher molybdenum concentrations the MoO_3 and $Al_2(MoO_4)_3$ phases are formed.[44–46, 50, 52–54, 59, 61, 64]

The degree of crystallinity of the compounds formed in the $MoO_3-Al_2O_3$ system depends on the concentration of molybdenum, and the extent of reaction depends on the heat treatment temperature.[45, 46] An X-ray study of amorphous molybdenum compounds by atomic radial distribution and ESR methods has shown[46] that polymolybdates containing molybdenum in an octahedral coordination are formed, in addition to the MoO_3 and $Al_2(MoO_4)_3$ phases, during the interaction of APM with Al_2O_3. An analysis of aqueous extracts from Al–Mo catalysts led to the same conclusion.[44] According to these results MoO_3 and $Al_2(MoO_4)_3$ are sparingly soluble in water, whereas a large fraction of the supported molybdenum is transferred to the solution when the Al–Mo catalysts are treated with water. The UV spectra of the aqueous extracts suggest the presence of molybdenum isopoly anions. It was therefore concluded[44] that in addition to the MoO_3 and $Al_2(MoO_4)_3$ phases observed by XPA (which are sparingly soluble and cannot pass into the solution) isopoly compounds are also formed on the surface of the Al–Mo catalysts, especially at high molybdenum concentrations. These are apparently responsible for the activity in the hydrogenolysis of thiophen. However, no attempt was made to identify these isopoly compounds directly on the surface of the catalysts.

Shmidt et al.[48] have established the presence in ignited Al–Mo catalysts of three different forms of molybdenum: water-soluble (W), soluble in ammonia (M), and insoluble in either water or ammonia (S). They claim that the water-soluble form is a compound containing molybdenum in an octahedral coordination (and assumed to be active towards the dehydrogenation of cyclohexane), but the nature of this compound was not examined in that study.[48]

In their discussion of the nature of the active centres created on the Al–Mo catalysts and responsible for the oxidation of propene to acetone Giordano et al.[47, 53] assumed that the compounds possessing acidic and oxidising properties and active in the conversion of propene into acetone could be reduced heteropoly acids or compounds of the $Mo_4O_{10}(OH)_2$ type (though the structure and properties of the heteropoly acids were not investigated in that work).

Several studies of the reduction of Al–Mo catalysts have been reported, and some of these have been reviewed in depth.[35, 36] Only a few features of that work call for comment here. The degree of reduction of Al–Mo catalysts increases with the reduction temperature. The reduction of the supported MoO_3 is much less complete than that of the massive compound.[65] It has been shown[53, 66] that the tetrahedral molybdenum ions are more difficult to reduce than the octahedral. On the whole the reduction of Al–Mo catalysts increases the degree of inhomogeneity of the molybdenum because of the different reducibilities of the molybdenum compounds of different composition.[53]

Studies aimed at identifying the molybdenum compounds formed by reduction and at determining their thermal stability and their stability in catalytic reaction[11, 67] have relied mainly on IR spectroscopy.

A special study[11] was made of the sequence of reactions of the molybdenum oxide compounds on the surface of Al_2O_3 during the thermal conditioning of the sample. In particular, in the IR spectrum of the 25% $MoO_3-Al_2O_3$ catalyst dried at 383 K (spectrum *4* of Fig. 5) we find, in addition to the absorption band at 920 cm^{-1}, a group of strong bands at 450, 665, 900, and 945 cm^{-1}, which is characteristic (according to published data) of polymolybdates.[35, 43] The presence of a strong band with a maximum at 945 cm^{-1} indicates the formation of a compound containing molybdenum in an octahedral coordination. By combining these results with those of previous studies by XPA and ESR,[46] and by Raman[50] and by UV and IR spectroscopy,[52] and also with recently formulated propositions,[53, 68] we may conclude that these compounds are polymeric formations consisting of MoO_6 octahedra or heteropoly compounds of molybdenum and aluminium.

In order to identify the resulting polymolybdate we compared[8] the IR spectra of a 25% $MoO_3-Al_2O_3$ catalyst and of ammonium paramolybdate (an isopoly compound), whose molecule consists of seven MoO_6 octahedra (spectrum *8* of Fig. 5), and of the heteropoly Al-Mo compound $(NH_4)_3AlMo_6O_{24}H_6$, whose anion is constructed from six MoO_6 octahedra connected by their edges into a ring (spectrum *9* of Fig. 5).[23, 69–71] In the latter compound the Al atom occupies the central octahedron. As can be seen from Fig. 5 and Table 1 the IR spectroscopic manifestations of the isopoly and the heteropoly compounds are quite different, which allows these compounds to be identified fairly reliably on catalyst surfaces.

By comparing the spectra *4*, *8*, and *9* of Fig. 5 with the spectral data in Table 1 we can see that the spectrum of the 25% $MoO_3-Al_2O_3$ catalyst dried at 383 K is essentially similar to that of the salt of the Al–Mo heteropoly acid: the maxima of the strongest absorption bands in the region of the Mo–O–Mo bridging bonds (445 and 665 cm^{-1}) are in identical positions, and include a triplet in the high-frequency region 880–950 cm^{-1} (Mo=O vibrations).[70] This suggests the formation on the Mo–Al catalyst surface of a compound similar in structure to the Al–Mo-HPA, and disproves the reported[46] formation of an isopoly compound.

It can also be seen from Fig. 5 that the spectrum of the supported HPA salt is more similar to that of the individual salt than is the spectrum of the compound formed on the surface of the 25% $MoO_3-Al_2O_3$ catalyst. This confirms our hypothesis of the effect of the surface aluminium atoms on the spectral characteristics of the heteropoly anion. When the salt of the HPA is deposited on the carrier the heteropoly anion is already formed, whereas during the interaction of ammonium paramolybdate and Al_2O_3 the anion is formed through the participation of aluminium atoms from the carrier surface.

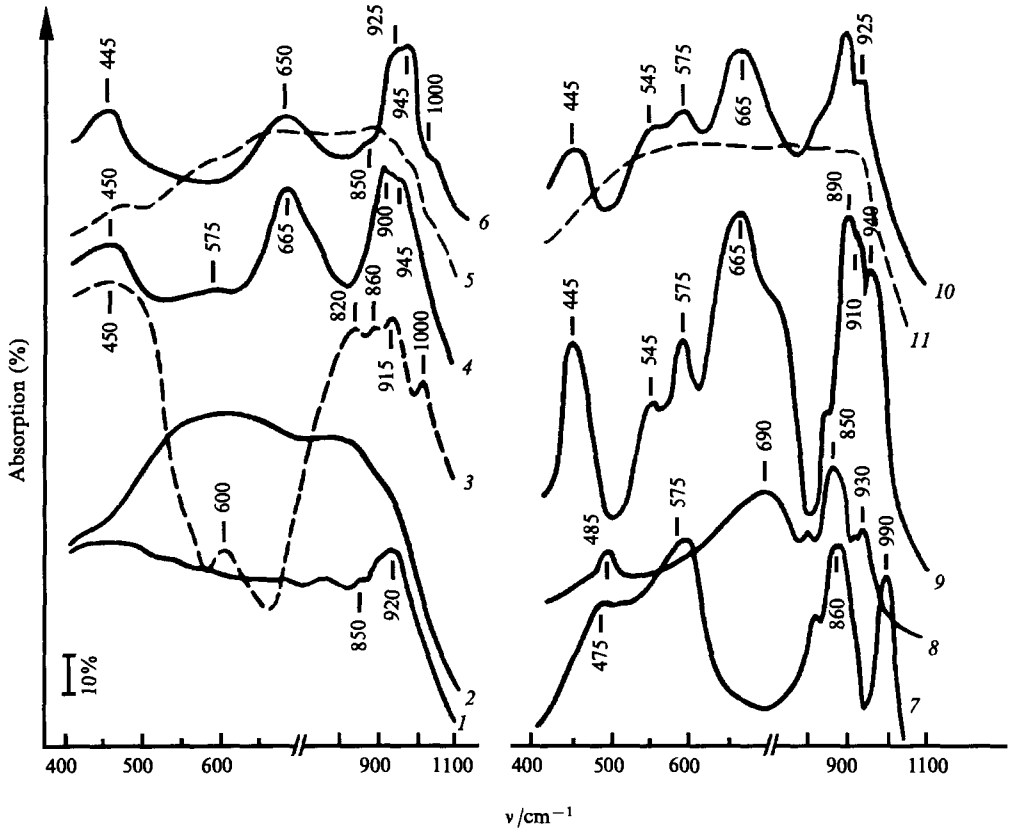


Figure 5. IR spectra of various molybdenum compounds and Mo–Al catalysts: *1*) 10% $MoO_3-Al_2O_3$; *2*) γ-Al_2O_3; *3*) $Al_2(MoO_4)_3$; *4*)–*6*) 25% $MoO_3-Al_2O_3$ at 383 (*4*) and 773 K (*5*), and after treatment with water (*6*); *7*) MoO_3; *8*) $(NH_4)_6Mo_7O_{24}$; *9*) individual $(NH_4)_3AlMo_6O_{24}H_6$; *10*) $(NH_4)_3AlMo_6O_{24}H_6$ supported on Al_2O_3 and dried at 383 K; *11*) ditto, heated at 573 K

In the latter case we can expect the effect of the carrier to be reflected by the IR spectra of the heteropoly anion. Obviously, the same is true of the differences in thermal stability of the heteropoly anions deposited on Al_2O_3 from solutions of their salts or formed by the reaction of ammonium paramolybdate with the carrier. The supported heteropoly compound dissociates even at 573 K (spectrum *11* of Fig. 5), whereas the polymolybdate formations on the surface of the Mo–Al catalysts are not decomposed at 773 K (spectrum *5* of Fig. 5).

Heating the 25% $MoO_3-Al_2O_3$ catalyst to 773 K apparently produces a large perturbation of the octahedral coordination of the molybdenum in the heteropoly compound, which manifests itself in the IR spectrum (spectrum *5* of Fig. 5) as a set of changes in the vibrations of the Mo = O bonds: the absorption band with a maximum at 890 cm^{-1} disappears, and the relative intensities of the bands at 925 and 945 cm^{-1} are increased. However, the character of the spectrum of the catalyst heat treated at 773 K suggests that the polyanion structure of the compound formed during the preparation of the catalyst from ammonium paramolybdate and Al_2O_3 is retained at these quite high temperatures.

Table 1. Position of the absorption bands (cm^{-1}) in the IR of various Mo compounds and Mo–Al catalysts.[14]

$[AlMo_6O_{24}H_6]^{3-}$	$(NH_4)_3[AlMo_6O_{24}H_6]$		Ammonium paramolybdate $(NH_4)_6Mo_7O_{24}$	Aluminium molybdate $Al_2(MoO_4)_3$	MoO_3	25% $MoO_3-Al_2O_3$	
	massive	deposited on Al_2O_3				383 K	773 K
1008 av	–	–	–	1000 av	990 s	–	1000 sh
945 s	945 s	945 s	930 s	–	–	945 s	945 s
922 v.s	910 av	925 av	910 w	915 w	–	920 s	925 s
895 s	890 s	890 s	–	–	–	900 s	–
–	–	–	850 v.w	860 w	860 v.w	–	850 w
–	–	–	–	820 w	820 av	–	–
660 v.s.	660 v.s	665 v.s	690 v.s	600 w	–	665 v.s	665 v.s
572 w	575 av	575 av	–	–	575 v.s	575 w	–
–	545 w	545 w	–	–	–	–	–
483 v.s	–	–	485 av	–	475 s	–	–
467 w	–	–	–	–	–	–	–
445 av	445 av	445 av	–	450 v.s	–	450 av	445 s

Note. Relative intensities of the absorption bands: v.s, very strong; s, strong; av, average; w, weak; v.w, very weak; sh, shoulder.

A comparison of the spectrum of the 25% $MoO_3-Al_2O_3$ catalysts heated at 773 K with the spectra of aluminium molybdate (spectrum *3* of Fig. 5) and of MoO_3 (spectrum *7*) shows that these phases are formed during the heat treatment of the catalyst. The presence of aluminium molybdate is indicated by the higher relative magnitude (as compared with the dried catalyst) of the absorption band at 445 cm^{-1}, and also by the appearance of a band at 920 cm^{-1} (spectrum *3*). The formation of MoO_3 is confirmed by the presence in the spectrum of the heated catalyst of an absorption band at 850 cm^{-1} and a shoulder at 1000 cm^{-1} (spectrum *7*). However, the absorption bands which characterise these phases are relatively weak, i.e. the predominant species on the surface of the heated catalyst are the paramolybdates.

As was pointed out above, one method of establishing the formation of HPC on the surface of carriers is by dissolution, since we know that all the heteropoly acids and many of their salts are readily soluble in water, unlike MoO_3 and aluminium molybdate. It was shown[68] that when these Mo–Al catalysts (with different aluminium contents) are treated with water the amount of molybdenum transferred to the solution is strongly dependent on its concentration in the initial sample. In other words the proportion of water-soluble molybdenum is negligibly small in a 5–10% $MoO_3-Al_2O_3$ sample, but it increases rapidly beyond this point and in a catalyst containing 25% of MoO_3 it amounts to about 50% of the molybdenum added to the sample.

The ^{27}Al NMR spectra of the aqueous extracts indicate the presence of the $AlMo_6O_{24}H_6^{3-}$ anion. It has been shown[11] that, as expected, treating a 25% $MoO_3-Al_2O_3$ catalyst (heated at 773 K) with water, i.e. removing the water-soluble molybdenum from it, produces a marked decrease in the absorption bands which characterise the polymolybdate (spectrum *6* of Fig. 5). This means that the water treatment of the catalyst removes the paramolybdate from the surface of the sample. These results, coupled with the detection of aluminium as well as molybdenum in the aqueous extracts, provide strong additional evidence of the formation of Al–Mo heteropoly compounds on the surface of Mo–Al catalysts with a high molybdenum content.

The presence of polymeric molybdenum compounds in the heat-treated 25% $MoO_3-Al_2O_3$ catalysts is additionally confirmed by the lines at 956, 891, and 345 cm^{-1} seen in the Raman spectra.[72]

Acidic properties. As was pointed out above proton acidity is a special feature of both supported and massive HPC. It should be noted that in order to account for the catalytic properties of Al–Mo catalysts in various reactions[40, 73–76] some workers have postulated the presence of strongly acid centres (including mobile protons) on the surface of these catalysts. Several studies of the acidity of these surfaces have been reported.[75–81] Information on the overall acidity of the catalysts can be obtained from titrations of the molybdenum oxides with *n*-butylamine[76, 77] and from their heats of immersion in pyridine.[75] However, results from different laboratories are usually inconsistent.

According to Parsons and Ternan[76] the acidity of Al–Mo catalysts increases monotonically with the molybdenum content form 2 to 30 wt.% of MoO_3, whereas Ragaini et al.[75] observed a non-monotonic change in the acidity with the content of MoO_3: samples containing 8 and 25 wt.% corresponded to maxima in the acidity. The maximum near 8 wt.% of MoO_3 was attributed[75] to the formation of the protonated $(HMoO_4)^{2-}$ and $(H_2Mo_2O_7)^{2-}$ [or $MoO(OH)^{2+}$] surface structures. At high concentrations (25 wt.% MoO_3) the acidity maximum was interpreted as the formation of $Mo_4O_{10}(OH)_2$ structures,[75] including the Mo^{5+} and Mo^{6+} ions. The decrease in the acidity at low concentrations (up to 4 wt.%) of MoO_3 is explained by the complete neutralisation of the most basic centres in the Al_2O_3 upon the addition of molybdenum. In the catalysts containing more than 27 wt.% of MoO_3 acid centres with H_0 between 6.8 and 3.3 were observed, and in catalysts containing less than 12.5 wt.% of MoO_3 the acid centres had $H_0 < 3.3$ (see Parsons and Ternan[76]).

Spectral studies of the acidity of Al–Mo catalysts by the pyridine adsorption method[78–81] have established the presence of both Lewis and Brønsted acid centres on the surface of these catalysts. The relative concentration of BAC increases with the concentration of molybdenum (from 9 to 25 wt.% of MoO_3),[78] and also when the catalyst is treated with water. Shmidt and coworkers showed[58] that Al–Mo catalysts have two types of BAC, characterised in the IR spectra of adsorbed ammonia by bands at 1450 and 1430 cm^{-1}, the band at the lower frequency being assigned to a compound containing octahedrally coordinated molybdenum ions. Unfortunately the nature of this compound was not established.

We have reported a study[11, 82] aimed at identifying the mutual relationship between the acidity (determined mainly by the BAC) and the formation of postulated molybdenum compounds on the carrier.

In an IR spectroscopic study of the adsorption of ammonia on 25% $MoO_3-Al_2O_3$ catalysts, for which the formation of a heteropoly molybdate had been established, we observed a large number of proton acid centres on the catalyst surface.[82] Kiviat and Petrakis[78] showed that these centres are due to the presence of heteropoly molybdate acidic compounds. Since treating the catalyst with water, which removes the polymolybdate from the surface, greatly lowers the concentration of BAC on the surface of the sample, the proton acidity of the 25% $MoO_3-Al_2O_3$ catalyst can be attributed to the formation of a water-soluble molybdenum compound on the Al_2O_3 surface. As was said above, this acidic compound could be a heteropoly compound of molybdenum and aluminium. The acidic centres (BAC) of these catalysts are relatively strong and can protonate propene, toluene, and ethylene molecules.[82]

Thus an analysis of the extensive published information shows that the formation of various compounds on the Al_2O_3 surface as a result of the deposition of a molybdenum oxide layer is determined by many factors of which the most important are the conditions and the methods used in the preparation of the catalytic system.

The formation on the Al–Mo catalysts of molybdenum ions in the tetrahedral and the octahedral coordination, in relative numbers depending on the composition and on the preparative conditions of the catalysts, is now fairly reliably established. The molybdenum ions in the tetrahedral coordination are present either as isolated MoO_3 units in the monolayer coverage of samples with a low molybdenum content or as aluminium molybdate at high molybdenum concentrations. In samples with a high molybdenum concentration (more than 10 wt.% of Mo) Al–Mo heteropoly compounds are formed on the surface in addition to the MoO_3 phase and to aluminium molybdate: these retain their polyanionic structure up to 773 K as a result of the interaction with the carrier, and are responsible for the strong proton acidity of these catalytic systems.

2. Formation and identification of Si–Mo oxide compounds

We shall assume that the chemical reactions in the Mo/SiO_2 system caused by the deposition of the active component are confined (at least, at low molybdenum concentrations) to the surface, and that bulk phases are not formed.† The state of the molybdenum ions in this system was studied by various methods, (mainly by optical, electronic, and ESR spectroscopy). Most of these studies were aimed at the local suroundings of the molybdenum ions (mainly because of the nature of the chosen methods).

The most important and complex problem seems to be to establish the relationship between the coordination state of the ion

† There are no reports of the formation of silicon molybdates or of solid solutions. The MoO_3 phase is usually observed only for high surface concentrations of molybdenum.

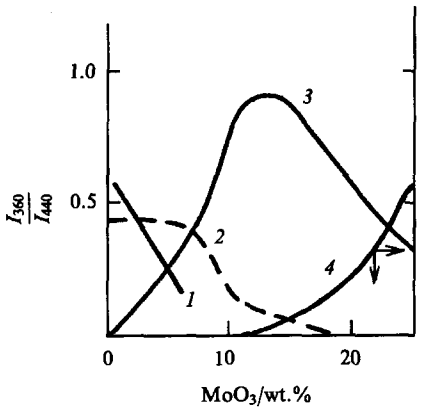


Figure 6. Distribution of the products in MoO_3/SiO_2 as a function of composition, established by titrations of: *1*) dimolybdates (DM), *2*) molybdosilicic acid (MSA), *3*) polymolybdates (PM). The proportion of MoO_3 (in relative units) was determined from the intensity ratio of the IR reflectance bands at 360 and 440 cm^{-1}.

and the type of chemical compound formed on the carrier. XPA is the method traditionally used to solve this problem. However, as in the case of the Mo/Al_2O_3 system, it is applicable only at high concentrations of molybdenum, and therefore vibrational spectroscopy plays an important role[9] in studies of the structure of the molybdenum compounds formed on the surface of SiO_2.

The coordination state of molybdenum at low concentrations was studied by ESR and UV spectroscopy.[83-85] The formation of tetrahedrally and of octahedrally coordinated molybdenum ions was observed. The coordination state of molybdenum was identified from the ESR spectra of Mo^{5+} (used as a paramagnetic probe) on the basis of the correspondence (well established in coordination chemistry) between the structure of the complex and the parameters of the ESR spectra.[86-88] The ESR results agree well with those of diffuse reflectance spectroscopy.[83, 84]

At low molybdenum concentrations tetrahedral molybdenum ions are found on the SiO_2 surface irrespectively of the method of preparing the catalyst. At higher concentrations octahedral molybdenum ions are usually formed as well as tetrahedral ions. However, there also reports of molybdenum ions in the two coordination states in a 1 : 1 ratio at low enough surface concentrations of molybdenum (0.1 Mo atom per 1 nm^2).[85] Whereas the tetrahedrally coordinated molybdenum ions are present as isolated ions in structures of the dimolybdate and MoO_3 type, the nature of the compounds in which the molybdenum is octahedrally coordinated is still problematic.

Castellan et al.[96] studied the Si–Mo system over a wide range of molybdenum concentrations by using a combination of physicochemical methods: XPA, optical spectroscopy, electron microscopy, acidometric titration, etc. From the results they constructed the phase diagram of molybdenum[96] as a function of the molybdenum content of the catalyst (Fig. 6). That work led to the suggestion that the molybdenum is present on the catalyst surface as isopoly and/or heteropoly acids, i.e. that it has a distorted octahedral coordination. In subsequent papers[97, 98] the same workers discussed the catalytic properties of the system towards propene disproportionation and oxidation reactions, and examined a scheme for the formation of products on different active centres.

Mo–Si oxide systems containing between 1 and 20 wt.% of Mo have been studied[9, 88, 89] by ESR and IR spectroscopy. The results were used to correlate the octahedral coordination of molybdenum with the formation of heteropoly compounds. By comparing the results of ESR studies of the state of the molybdenum as a function of the formation temperature of the sample it was concluded[88] that identical changes in the state of the molybdenum take place in the supported Si–Mo-HPA and in the molybdenum oxide catalyst synthesised on the SiO_2 surface (the anisotropic signal denotes stabilisation of the molybdenum in a distorted octahedral coordination of C_{4v} symmetry).

An identification by IR spectroscopy of the types of surface formation on silicon dioxide has been reported.[9] By comparing the IR spectra of SiO_2, MoO_3, and Si–Mo-HPA, and also Si–Mo-HPA supported on SiO_2, it was concluded that the most characteristic absorption bands of these compounds do not overlap (Fig. 7), thus allowing the molybdenum compounds to be identified spectroscopically even at low concentration on the SiO_2 surface. Since the strongest absorption for Mo_{12}-HPA (the Keggin structure) was observed at 700–1100 cm^{-1} and the low-frequency absorption bands are much weaker the absorptions above 700 cm^{-1} were mainly used in the identification of the HPC.

The IR spectrum of the Si–Mo oxide catalyst containing more than 5 wt.% of MoO_3 as the active component, prepared by impregnating SiO_2 with ammonium paramolybdate and drying it at 383 K (spectrum *5* of Fig. 7), was very similar to the spectrum of Si–Mo-HPA supported on SiO_2 (in which the observed absorptions cannot be assigned to ammonium paramolybdate, whose spectrum is also shown in Fig. 7 as spectrum *4*). This suggests the possible formation of Si–Mo-HPA on the SiO_2 surface.[9] Heating this system to 773 K has almost no effect on the form of the spectra (spectrum *6* of Fig. 7), showing that the heteropoly anions are retained on the SiO_2 surface up to quite high temperatures whereas the supported Si–Mo-HPA begins to decompose at 573 K. In the spectrum of the latter sample obtained by compensating for the spectrum of the carrier (spectrum *7* of Fig. 7) weak absorption bands characteristic of trace quantities of the MoO_3 phase are observed in addition to the absorption bands of the HPA. Heating the catalysts at 873 K lowers the intensity of the absorption bands characteristic of HPA and increases that of the MoO_3 bands. After heat treatment at 973 K only the MoO_3 bands can be seen.

Thus an analysis of the spectra of Si–Mo catalysts has shown that the interaction of ammonium paramolybdate with silica produces Si–Mo-HPA, whose thermal stability is higher than that of the heteropoly acid, both individual and supported on SiO_2.[9]

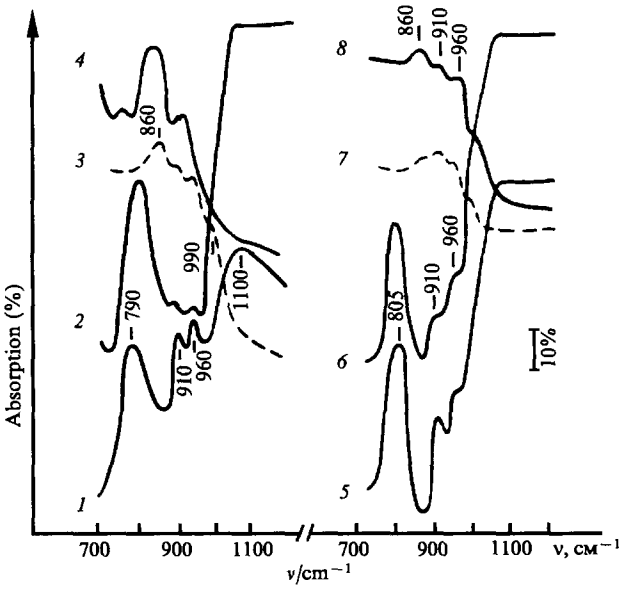


Figure 7. IR spectra of HPA/SiO_2 (spectra *1–3*), ordinary (*1*) and dehydrated at 573 K (*2*) and 673 K (*3*), of ammonium paramolybdate (spectrum *4*) and of a Si–Mo catalyst (spectra *5–8*) dried at 383 K (*5*) and dehydrated at 773 K (*6*, *7*) and 873 K (*8*). The spectra *3*, *7*, and *8* were obtained with compensation of the SiO_2.

Acidic properties. As was pointed out above, a distinguishing feature of the heteropoly acids is their proton acidity. Therefore in order to identify the type of compound formed on the surface of the carrier it is important to establish the nature of the mobile protons.

Studies[9, 91-94] of the acidic properties of Si–Mo oxide catalysts have confirmed the formation of a strong acid.

The IR spectra of ammonia adsorbed on both the HPA/SiO_2 and the Si–Mo catalyst dehydrated at 473 K show the formation of NH_4^+, i.e. the presence of mobile protons on the surface of these samples.[9] Raising the dehydration temperature of the sample from 473 to 573 and 873 K suppresses the intensity of the NH_4^+ absorption bands (as in the case of HPA/SiO_2) by lowering both the number and the strength of the BAC.[9]

The adsorption of ammonia on a Si–Mo catalyst hydrated after being heated to temperatures at which the heteropoly anions are not removed also denotes the presence of BAC. On the other hand after the complete breakdown of the heteropoly acid on the SiO_2 surface after heat treatment at 973 K the ammonium ion is not observed in the spectrum of ammonia adsorbed on the sample rehydrated after decomposition of the polyacid, i.e. in this case the hydration–dehydration processes are irreversible.[9]

Electron defect centres have also been observed on the surface of the Si–Mo system.[95] Thus, the adsorption of aromatic polycyclic hydrocarbon molecules on these catalysts is accompanied by electron transfer from the hydrocarbon to the molybdenum, which forms the corresponding cation radicals and reduces the Mo^{6+} to Mo^{5+}.

It should not be forgotten that an HPA which is thermally stable up to 773 K is formed on the Si–Mo catalysts in addition to MoO_3. This high stability can be attributed to the chemical interaction of the HPA with the carrier (~85–90% of the added molybdenum interacts with the surface according to the chemical analysis results). The thermal stability of this HPA is substantially higher than that of the bulk compound. The presence of mobile protons is associated with the presence of a Si–Mo-HPA on the carrier surface also in this system. The concentration of the protons depends on the degree of hydration of the heteropoly acid.

3. Formation and identification of Ti–Mo compounds

The physicochemical and catalytic properties of Mo/TiO_2 catalysts are largely determined by the method of preparation.[99-102] Catalysts having different phase compositions can be prepared. Thus, in the synthesis of Ti–Mo catalysts by the coprecipitation of molybdenum and titanium oxides, solid solutions based on titanium dioxide are formed. However, the situation is complicated by the formation of two modifications of TiO_2 under these conditions: anatase and rutile.[102, 103] A solid solution of molybdenum oxide in anatase is obtained when ammonium paramolybdate is added to titanium hydroxide paste.[101] The stability of molybdenum is fairly high: up to 25–30 wt.% of MoO_3. The formation of a solid solution is inferred from the abnormally high lattice parameters[104] of the TiO_2 phase, due to the difference in size of Ti^{4+} (r = 0.64 Å), Mo^{6+} (r = 0.66 Å), and Mo^{5+} (r = 0.65 Å). When the Mo–Ti catalyst was prepared by the impregnation of anatase with molybdic acid at low concentrations of Mo only the anatase phase was detected by X-ray diffraction (phases containing Mo could not be detected), and at high concentrations the MoO_3 phase was detected. In the synthesis of a Mo–Ti catalyst from molybdenum tartrate complexes an X-ray amorphous form was obtained.[101]

The effect of the pH used to precipitate the titanium hydroxide on the phase composition of the resulting Mo–Ti catalyst has been studied.[102] However, it was pointed out[89] that the measurements in the region of pH < 1.4 cannot be correct since titanium hydroxide is deposited at pH > 1.4 (see Goroshenko's monograph[103]). A detailed examination[87] of the influence of the method of preparation of the catalyst on the phase composition and on the state of the molybdenum ions showed that the presence of added ions favours the low-temperature formation of rutile and the stabilisation of the molybdenum on the lattice sites and in the interstitial positions of rutile. Molybdenum ions with an octahedral coordination stretched along the tetragonal axis are found in the lattice positions, whereas the interstitial ions are compressed along the same axis. In a catalyst prepared at a high pH without added ions the phase composition was found to depend on the total concentration of added molybdenum.[102]

For molybdenum concentrations up to 25–30 wt.% MoO_3 a solid solution based on TiO_2 is observed by X-ray diffraction. At high molybdenum concentrations MoO_3 is formed in addition to the solid solution. The XPA results were confirmed by IR spectroscopy.[104, 105] It was found that the IR spectrum of the solid solution is almost indistinguishable from the spectrum of titanium dioxide in the region of its characteristic vibrations.

It was also reported[105] that the surface composition of the Ti–Mo oxide catalyst (like that of the Sn–Mo oxide catalyst) differs markedly from the bulk composition by being more enriched in molybdenum. The IR spectrum of this surface layer also differs from the spectrum of the solid solution by the presence of bands characteristic of a compound containing molybdenum. It should be noted that a high proton acidity of the molybdenum compound formed on the surface of the TiO_2 support for concentrations of the active component greater than 5 wt.% of MoO_3 has been reported.[105, 106] This molybdenum compound is the active component (at least, in the oxidation of propene to acetone). However, the compound has not been identified.[105]

By using a combination of different methods (XPA, ESR, and IR spectroscopy) an attempt was made[10] to establish the phase composition of Ti–Mo oxide catalysts prepared by adding ammonium paramolybdate (APM) to a paste of titanium hydroxide and heating the product at 723 K (series A) or by impregnating TiO_2 (anatase) with a solution of APM and heating the product at 723 K (series C). In both cases an anatase phase with lattice parameters identical to those given in the literature was identified by XPA. In the series A catalysts the lattice constants of the anatase increased with the molybdenum content, pointing to the formation of a solid solution. No other phases were observed for Mo concentrations between 1 and 25 wt.% under these conditions. For molybdenum concentrations above 25 wt.% a MoO_3 phase was observed. In the series C catalysts there was no increase in the lattice parameters of anatase when the molybdenum content was increased. Adding 15 wt.% or more of Mo led to the formation of a MoO_3 phase. In this respect the most interesting samples are those of series C containing up to 15 wt.% of Mo, in which phases containing molybdenum are not detected by X-ray diffraction.

A detailed study of the IR and ESR spectral parameters of Ti–Mo oxide systems and of their changes in dehydration–rehydration processes at different temperatures, and a comparison of these spectra with those of Ti–Mo-HPA supported on TiO_2, showed[107, 108] that Ti–Mo-HPA (stable up to 723 K) is formed on the surface during the synthesis of Ti–Mo oxide catalysts. A similar state of affairs exists for the Si–Mo oxide system.

Thus in the Ti–Mo oxide catalysts prepared by adding APM to a paste of titanium hydroxide (series A) several phases are produced, depending on the molybdenum content: a solid solution of molybdenum in TiO_2, Ti–Mo-HPA, and MoO_3. For molybdenum concentrations below 10 wt.% almost the whole of the added molybdenum dissolves in the anatase to give a solid solution. Increasing the concentration of molybdenum in the catalyst results in the formation of new phases on the surface of the solid solution: Ti–Mo-HPA and MoO_3. As the concentration of molybdenum in the catalyst is increased still further the concentration of these phases increases.

In the Ti–Mo catalysts prepared by impregnating anatase with a solution of APM (series C) and heating the sample at 723 K Ti–Mo-HPA is formed for molybdenum concentrations lower

than 15 wt.%, but at higher concentrations MoO_3 is found as well as the HPA. The heteropolymolybdic acid thus obtained has a high thermal stability (up to 723 K).

Acidic properties. The HPA found on the surface of the Ti–Mo oxide catalysts is responsible for their Brønsted acidity.[10] The strong acidity of this type of catalyst and its role in the catalytic reactions have long been recognised,[101, 109–112] even before the formation of a HPA on the catalyst surface had been established.

IV. Thermal stability of molybdenum compounds, decomposition mechanism, role of modifiers

We shall now dwell on two problems directly related to the problems discussed above: the changes induced in the HPC by changes in temperature and the influence of the reaction medium on these changes.

1. Massive and supported heteropoly acids

We shall discuss these problems in terms of the most widely known HPA: molybdophosphoric and molybdosilicic.

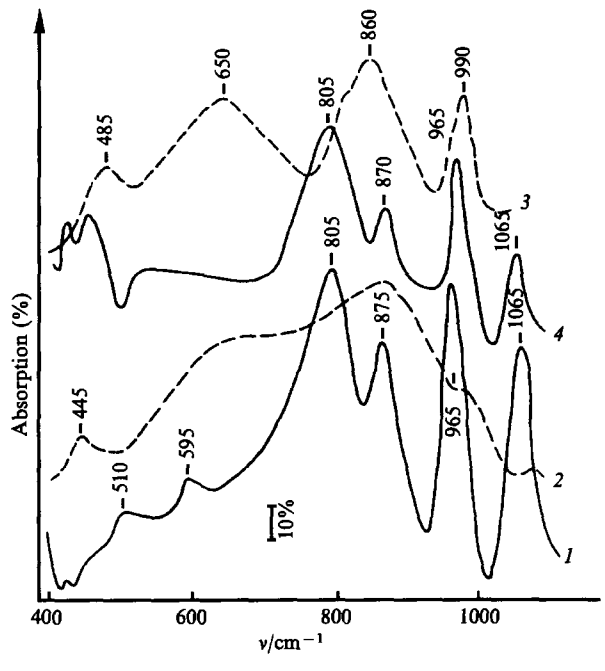


Figure 8. IR spectra of P–Mo-HPA heated at different temperatures: *1*) 673, *2*) 723, *3*) 773 (spectrum *4* relates to hydrated P–Mo-HPA heated at 723 K).

Table 2. Absorption bands in the IR spectra (700–1100 cm^{-1}) of Mo_{12}-HPC (the Keggin structure).

Si–Mo-HPA		P–Mo-HPA		NH_4-salt Ti–Mo-HPA
Ref. 113	Ref. 16	Ref. 113	Ref. 16	Ref. 113
999		1074	1070	1072
960	963	968	972	970
909	915	911		908
859	890	869	882	868
782	782	795	790	790

As was stated above, the IR spectra of Mo_{12}-HPA (the Keggin structure) are typical (Table 2), and those of P–Mo-HPA at 700–1100 cm^{-1} are characterised by strong absorption bands at 805, 875, 965, and 1065 cm^{-1} (Fig. 8). Heating the HPA for 2 h in a stream of air at 673 K does not change the contour of the spectrum, showing that the structure of the Keggin anion is retained. After thermal conditioning of the HPA at 723 K the intensity of the characteristic absorption bands of the HPA decreases rapidly and the shape of the spectrum changes: absorption bands appear at 445 cm^{-1} and in the 700–900 cm^{-1} range, with a maximum at 870 cm^{-1}. Subsequent treatment of the sample with water regenerates the HPA, as shown by the absorption bands at 805, 870, 965, and 1065 cm^{-1} in the spectrum of the hydrated sample (Fig. 8).

According to XPA results the sample heated at 723 K is a mixture of two phases: MoO_3 and a phase with a structure similar to that of Mo_4O_{11}. The MoO_3 phases persists after the treatment with water, but we see a change in the relative intensity of the main diffraction lines on the diffraction pattern of the hydrated sample. The phase with the Mo_4O_{11} structure disappears after the treatment with water.[67]

According to ESR results the state of the molybdenum ions is not markedly affected by heating the sample at 723 K: the molybdenum ions have distorted octahedral surroundings of oxygen atoms, similar to their surroundings in the HPA. In Mo_4O_{11} most of the molybdenum ions also have octahedral surroundings.

In the IR spectrum of the sample heated at 773 K we find absorption bands at 820, 865, and 1000 cm^{-1}, characteristic of MoO_3. After treating the sample with water we find a phase of P–Mo-HPA, and the MoO_3 phase cannot be detected by IR spectroscopy (it can be identified only by XPA).

By comparing the XPA and IR spectroscopy results we reach the following conclusions. After heat treatment of the P–Mo-HPA at temperatures below 623 K the structure of the Keggin anion is retained, whereas heating at 773 K and above causes breakdown of the anion structure and the formation of oxides. In the intermediate temperature region we observe a rearrangement of the Keggin anion with formation of a heteropoly molybdate (poly-oxide) with a structure similar to that of Mo_4O_{11}. We should stress the fact that the similarity between MoO_4 and the poly-oxide (which we shall call a P–Mo-anhydride) lies in their very close structure types, while their chemical natures are quite different. During the hydrolysis the heteropoly molybdate is rearranged into an anion with the Keggin structure, i.e. the process is reversed.

Allowing for these results the process induced by the heat treatment of P–Mo-HPA can be described by the scheme

$$\text{HPA} \leftrightarrows \text{P–Mo-anhydride} \rightarrow MoO_3 + P_2O_5 .$$

It follows from these results that in the region of 723 K the treatment with water produces a reversible rearrangement of the heteropoly anion into a phosphorus–molybdenum anhydride with a structure of the Mo_4O_{11} type. At 773 K this P–Mo-anhydride (poly-oxide) decomposes with formation of MoO_3. The dissociation of the heteropoly anion with an intermediate formation of a compound having the Mo_4O_{11} structure has been reported[18] for several HPA and their salts. It is interesting to note that the addition of water to the anhydride produces the HPA, whence it follows that the poly-oxide is a dehydration product of the HPA, and also that the coordination of the molybdenum ion is not significantly changed in the transition from the heteropoly anion to the poly-oxide: the distorted octahedral coordination is retained. As a result the reducibility of the molybdenum ions is the same in the HPA and in the poly-oxide.

The reduction temperatures of the Mo^{6+} ions to Mo^{5+} by hydrogen (with the corresponding temperatures for the reduction by atomic hydrogen shown in brackets) are listed below for some HPA, for phosphorus–molybdenum poly-oxide, and (for comparison) for MoO_3.

System	T/K
Si–Mo-HPA/SiO_2	373 (300)
Si–Mo-HPA	373 (300)
P–Mo-HPA	373–423
MoO_3	623

As can be seen, the poly-compounds are reduced at the same temperatures, which are much lower than the reduction temperature of MoO_3.

Similar results have been reported for supported systems.[67]

A study by IR spectroscopy and XPA of the change in phase composition as a function of the heating temperature of the P–Mo-HPA supported on SiO_2 showed that after being conditioned at 673 K the sample consists of a mixture of phases: HPA (the principal phase) and anhydride. Increasing the heating temperature to 723 K increases the content of heteropoly molybdate in the sample, and also produces a phase of molybdenum oxide. Therefore the rearrangement of the Keggin anion continues at 723 K. As in the case of massive HPA the heteropoly molybdate phase disappears during the subsequent hydrolysis, and the MoO_3 phase undergoes changes probably due to its texturing by the action of the water. After heat treatment at 773 K the structure of the anion is completely broken down (according to XPA results), and molybdenum oxide is formed: in other words we observe (on the whole) the same stages in the thermal dehydration of P–Mo-HPA supported on SiO_2 as in the dehydration of the massive HPA.

An analysis of the changes in the spectra of supported Si–Mo-HPA during heat treatment shows that above 673 K (or 573 K for the massive HPA) the compound dissociates with formation of MoO_3, as indicated by the appearance of new absorption bands at 860 cm^{-1} ($\nu_{Mo-O-Mo}$) and 990 cm^{-1} ($\nu_{Mo=O}$), which are the most characteristic lines in the MoO_3 spectrum, whereas the appearance of absorption bands in the region of 1100 cm^{-1} denotes the presence of SiO_2 (spectrum 2 of Fig. 7).[29] The complete decomposition of the supported Si–Mo-HPA with formation of MoO_3 and SiO_2 is observed at 773 K: in this case the IR spectrum is a superposition of the spectra of the individual MoO_3 and SiO_2. Thus, in spite of the fact that the deposition of the Si–Mo-HPA increases its thermal stability in comparison with the massive HPA, the nature of the transformations during the thermal conditioning is unchanged.

It should be noted that it has not yet been possible in this case to identify the intermediate compound (anhydride) from the IR spectra (the difficulty being even greater for the Si–Mo oxide catalysts) because of the low intensity of the characteristic absorption bands.[114] However, as in the case discussed above for P–Mo-HPA the spectral changes caused by hydration are reversible up to a dehydration temperature of 773 K for the Si–Mo oxide systems.

Modified catalysts. As has already been pointed out, modifiers are often added to complex catalysts containing molybdenum: for example, phosphorus (in the form of orthophosphoric acid).[115–117] The modifier alters the catalytic properties of the system. However, the role of the phosphorus is still unclear in most cases. There are reports of the formation of surface phases containing phosphorus and molybdenum during the modification by phosphorus,[115–118] i.e. the effect of phosphorus additions can be attributed to chemical changes leading to the formation of P–Mo-HPA and its salts, since the addition of orthophosphoric acid provides an element capable of acting as hetero-atom as well as lowering the pH of the medium.

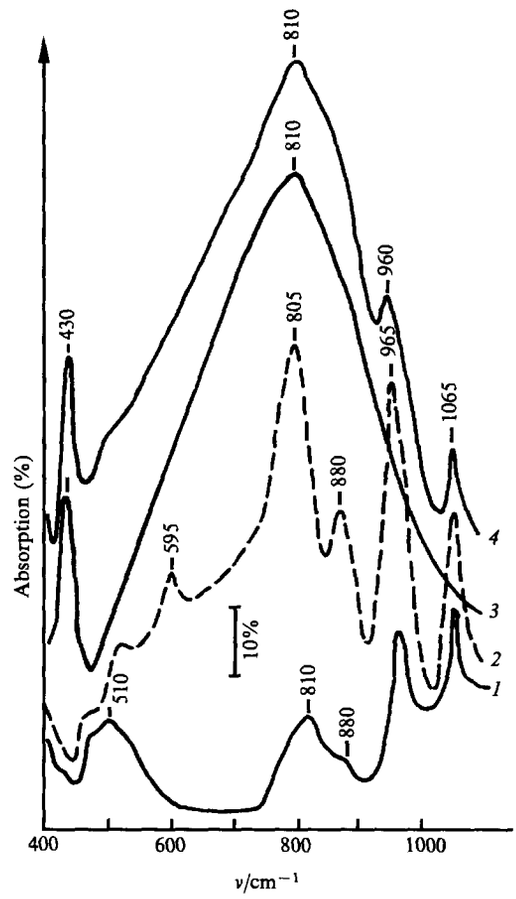


Figure 9. IR spectra of P–Mo-HPA (*1*), $CaMoO_4$ (*2*), and P–Mo-HPA supported on $CaMoO_4$ (*3* and *4*). For comparison we show the spectrum of P–Mo-HPA supported on $CaMoO_4$ taken with compensation for the molybdate absorption.

The possibility of forming P–Mo-HPA by modifying calcium molybdate with orthophosphoric acid has been investigated.[67] Bands at 800–900 cm^{-1}, characteristic of the HPA, were not seen in the IR spectrum of P–Mo-HPA supported on $CaMoO_4$, measured on a background of molybdate absorption (Fig. 9). Only the absorption bands at 960 and 1065 cm^{-1}, characteristic of the Mo = O vibrations and of the vibrations of the central PO_4 tetrahedron in the HPA anion respectively, are clearly seen (spectrum *4* of Fig. 9). The spectrum of supported HPA (with compensation for the absorption of the carrier) is indistinguishable from that of the massive HPA (spectrum *1* of Fig. 9), i.e. these results show that the P–Mo-HPA on the surface of $CaMoO_4$ can be identified reliably from the IR spectra.

The introduction of a superstoichiometric amount of molybdenum into $CaMoO_4$ by treating it with a solution of ammonium paramolybdate and heating the product at 773 K leads to the formation of a MoO_3 phase (Fig. 10). In this case, in addition to an absorption band at 430 cm^{-1} and a strong absorption in the 600–860 cm^{-1} region, characteristic of the molybdate, we find absorption bands at 475, 610, 820, 860, and 995 cm^{-1}, characteristic of molybdenum oxide (spectrum *2* of Fig. 10). By using the compensation procedure we can generate a spectrum for $CaMoO_4$ exactly similar to the initial spectrum, thus confirming that the symmetry of the molybdenum in $CaMoO_4$ is not affected by the addition of a superstoichiometric amount of MoO_3, i.e. indicating the formation of an individual phase of MoO_3. A similar effect has been observed in magnesium molybdate containing superstoichiometric MoO_3.[119]

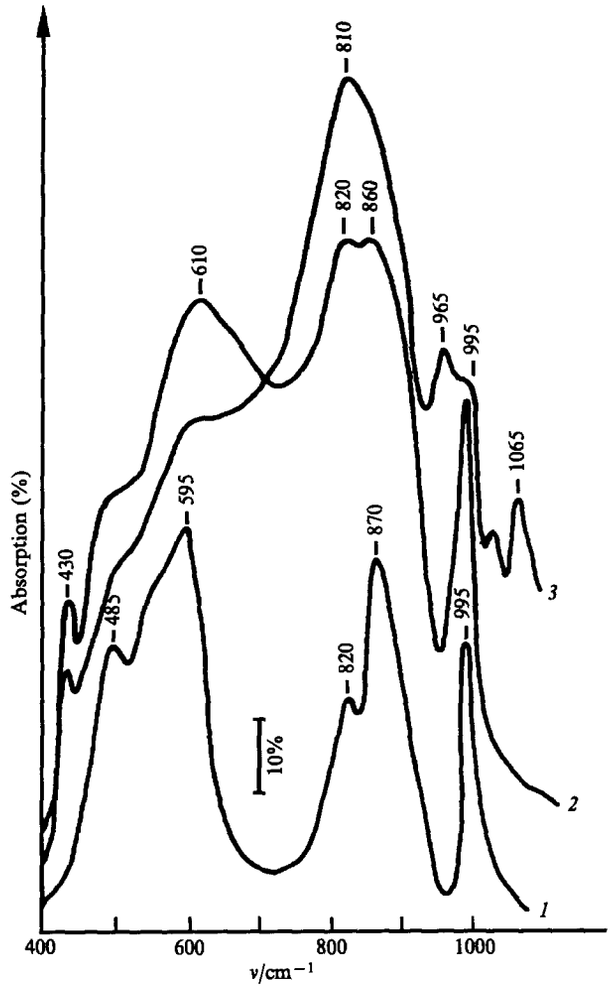


Figure 10. IR spectra of MoO_3 (*1*) and of $CaMoO_4$ modified by 10 wt.% of molybdenum (*2*); *3*) is the spectrum of the same sample after the addition of phosphorus.

Treating a $CaMoO_4-MoO_3$ catalyst with a solution of orthophosphoric acid produces substantial changes in the IR spectrum. The MoO_3 absorption band becomes weaker, and new absorption bands appear at 965 and 1065 cm^{-1} (spectrum *3* of Fig. 10). As was pointed out above, these bands are characteristic of P–Mo-HPA supported on molybdate.

Heating the catalyst at 623 K does not change the shape of the spectrum, confirming that the HPA is stable at this temperature. The absorption bands of the HPA are completely suppressed (i.e. the anion structure is broken down) only after heat treatment of the catalyst at 673 K.

Thus the modification of calcium molybdate with a superstoichiometric molybdenum content by treatment with phosphoric acid produces a P–Mo heteropoly acid stable up to 623 K.

V. Conclusions

The review of published data has shown that vibrational spectroscopy methods, now widely used in studies of the molecular structure of heteropoly compounds, can also be used successfully to identify these compounds when supported on carriers and when forming compounds on the carriers during the preparation of supported catalysts containing molybdenum and tungsten. We have not dwelt in detail on the interpretation of the spectra of HPC because this topic is already adequately reviewed.[13, 15–17, 24] However, it should be noted that in complex molecules a complete analysis of the normal vibrations is too laborious, and the absorption bands are usually assigned in the approximation of group vibrations.[16]

In the Keggin heteropoly anion we identify groups of atoms whose vibrations are not significantly influenced by the vibrations of the other atoms: 12 terminal Mo=O double bonds, 12 almost linear and 12 bridging Mo–O–Mo bonds, and 12 simple M–O bonds in which the oxygen atoms are shared by three molybdenum atoms and by the central hetero-atom.

It is generally accepted[16, 17] that the stretching vibrations of the bridging Mo–O–Mo bonds are observed in the 900–800 cm^{-1} region, and the vibrations of the Mo–O bonds below 600 cm^{-1}. Bands below 300 cm^{-1} are assigned to bending vibrations of the anion skeleton. The vibrations of the central tetrahedron appear at 1100–800 and at 600 cm^{-1}. The vibrations of the Mo=O bond appear at 900–1000 cm^{-1}.

The IR spectra of the Mo_{12}-HPA (the Keggin structure) are characteristic and can be used to identify the molecular structure of the heteropoly compounds.

We have shown that the Mo_6-HPC, in which the central atoms are transition metal ions (copper, cobalt, iron), are unstable. Strong chemical interactions with the carrier take place when these compounds are supported.

The observed influence of the acid–base properties of the carrier on the rearrangement of the heteropoly anion when supported is of great importance. On SiO_2 the Mo_6-HPA are converted into mixed Si–Mo_{12}–M-HPC, in whose coordination sphere the transition-metal cations replace the molybdenum ions. When supported on aluminium oxide the copper, cobalt, and iron heteropoly molybdates are converted into aluminium compounds (by reacting with the surface ions of the carrier).

The Mo_{12}-HPC are stable on SiO_2 and TiO_2 surfaces, but on Al_2O_3 they decompose (when at low concentrations) and they form Al–Mo_6-HPC at high concentrations.

This detailed review of the processes taking place on the surface of TiO_2, SiO_2, Al_2O_3 carriers during the formation of supported molybdenum catalysts has demonstrated the possibility of using vibrational spectroscopy in the identification of the compounds formed on the carrier surface and in establishing their origin.

Spectral criteria for the identification of HPC on carriers (even with inadequate spectral information) have been formulated, and they can be used to obtain reliable information on the resulting compounds. It was established that far-reaching interactions between the active component and the carrier usually take place, leading to the formation of new compounds. We have also examined the formation of different types of HPC on the carrier surface, depending on the acid–base properties of the carrier.

A detailed comparative analysis of published data on the occurrence of acidic properties (at least for the case of proton acidity) in these catalysts and supported HPC has shown that strong proton acidity is a necessary criterion for the formation of HPC on carrier surfaces during the preparation of catalysts.

Extensive evidence is now available of the important role of surface centres of this type (and of the role of the HPC formed on the surface of carriers) in catalytic processes.[3, 54, 67, 89, 106, 110, 120–124] It has been reported[67] that at least in some processes (for example, in the oxidation of propene and of methanol) the HPC are retained on the surface after its interaction with the reaction medium at the temperature and other conditions of the catalytic reaction.

The study of the decomposition of massive and of supported HPA has revealed the formation of acid anhydrides during their dehydration, and their reversible conversion into the initial HPC by hydration.

The possibility of forming HPC on the surface of molybdates with a superstoichiometric molybdenum content during their modification with acids (for example, phosphoric) has been demonstrated.

References

1. Y Konishi, Y Sakata, M Misono, Y Yoneda *J. Catal.* **77** 169 (1982)
2. K Kurzinger, G Emig, H Hoffmann, in *Proceedings of the Eighth International Congress on Catalysis, Berlin, 1984* Vol. 5, p. 499 (1982)
3. I V Kozhevinkov, K I Matveev *Usp. Khim.* **51** 1875 (1982) [*Russ. Chem. Rev.* **51** 1075 (1982)]
4. M Misono *Catal. Rev. Sci. Eng.* **29** 269 (1987)
5. N N Tumachenko, T P Gorshkova, D V Tarasova, in *Materialy Vsesoyuznogo Soveshchaniya "Nauchnye Osnovy Prigotovleniya Katalizatorov" Novosibirsk, 1983* (Proceedings of the All-Union Symposium on the Scientific Foundations of the Preparation of Catalysts, Novosibirsk, 1983) p. 24
6. Jpn. P. 57-12 830; *Ref. Zh. Khim.* 11N213R (1983)
7. L Ya Margolis *Okislenie Uglevodorodov na Geterogennykh Katalizatorakh* (Oxidation of Hydrocarbons on Heterogeneous Catalysts) (Moscow: Khimiya, 1977)
8. O I Goncharova, T M Yur'eva, A A Davydov *Kinet. Katal.* **27** 942 (1986)
9. O I Goncharova, A A Davydov, T M Yur'eva, T Kh Shokhireva *Kinet. Katal.* **24** 683 (1983)
10. O I Goncharova, A A Davydov, T M Yur'eva, T Kh Shokhireva *React. Kinet. Catal. Lett.* **20** 119 (1982)
11. O I Goncharova, A A Davydov, T M Yur'eva *Kinet. Katal.* **25** 152 (1984)
12. F Castellan, J C J Bart, A Vaghi, N Giordano *J. Catal.* **42** 162 (1976)
13. E N Yurchenko *Zh. Strukt. Khim.* **28** (3) 133 (1987)
14. A A Davydov, O I Goncharova *Zh. Prikl. Spektrosk.* **50** 76 (1989)
15. L P Kazanskii, A M Golubev, in *Khimiya Soedinenii Mo i W* (Chemistry of Molybdenum and Tungsten Compounds) (Novosibirsk: Nauka, 1979) p. 66
16. L P Kazanskii *Izv. Akad. Nauk SSSR, Ser. Khim.* 502 (1975)
17. E N Yurchenko, in *Metody Molekulyarnoi Spektroskopii v Khimii Koordinatsionnykh Soedinenii i Katalizatorov* (Molecular Spectroscopy in the Chemistry of Coordination Compounds and Catalysts) (Novosibirsk: Nauka, 1986) p. 254
18. C Rocchiccioli-Deltsheff, R Thouvenot *J. Chem. Res. (S)* 46 (1977)
19. E N Yurchenko, L G Detusheva, I P Olen'kova, O I Goncharova, G S Litvak *Izv. Akad. Nauk SSSR, Ser. Khim.* 56 (1984)
20. E N Yurchenko, I P Olen'kova, O I Goncharova, L G Detusheva, G S Litvak *Izv. Akad. Nauk SSSR, Ser. Khim.* 50 (1984)
21. N Giordano *Chim. Ind. (Milan)* **61** (4) 283 (1979)
22. G A Parks *Chem. Rev.* **65** 177 (1965)
23. G A Tsigdinas, in *Topics in Current Chemistry* Vol.76 (Berlin: Springer-Verlag, 1978) p. 1
24. L P Kazanskii, E A Torchenkova, V I Spitsyn *Usp. Khim.* **43** 1137 (1974) [*Russ. Chem. Rev.* **43** 525 (1974)]
25. E A Paukshtis, O I Goncharova, E N Yurchenko, T M Yur'eva *Kinet. Katal.* **27** 463 (1986)
26. E A Paukshtis, E N Yurchenko *Usp. Khim.* **52** 426 (1983) [*Russ. Chem. Rev.* **52** 242 (1983)]
27. T Okuhara, A Kasai, N Hayakawa, Y Yoneda, M Misono *J. Catal.* **83** 121 (1983)
28. M Misono, K Sakata, Y Yoneda, W Y Lece, in *Proceedings of the Seventh International Congress on Catalysis, Tokyo, 1980* B. 27
29. V M Mastikhin, S M Kulikov, A W Nosov, I V Kozhevnikov, I L Mudrakovsky *J. Mol. Catal.* **60** 65 (1990)
30. E N Yurchenko, G N Kustova, S S Batsanov, in *Kolebatel'nye Spektry Neorganicheskikh Soedinenii* (Vibrational Spectra of Inorganic Compounds) (Novosibirsk: Nauka, 1981) p. 82
31. S F West, L F Audrieth *J. Phys. Chem.* **59** 1069 (1955)
32. A A Davydov *IK-Spektroskopiya v Khimii Poverkhnosti Oksidov* (IR Spectroscopy in the Surface Chemistry of Oxides) (Novosibirsk: Nauka, 1984)
33. D A Arendarskii, E A Paukshtis, Z R Ismagilov, E N Yurchenko *React. Kinet. Catal. Lett.* **28** 195 (1985)
34. B C Gates, J R Katzer, G C A Schuit, in *Chemistry of Catalytic Processes* (translated into Russian) (Moscow: Mir, 1981) p. 399
35. M I Losev, A A Slinkin, in *Kinetika i Kataliz (Itogi Nauki i Tekhniki, Tom 7)* (Kinetics and Catalysis, Advances in Science and Technology, Vol. 7) (Moscow: VINITI, 1980) p. 3
36. F E Massoth *Adv. Catal.* **27** 265 (1978)
37. T Fransen, O Van der Meer, P Mars *J. Catal.* **42** 79 (1976)
38. A N Startsev, E A Demin, B N Kuznetsov, E M Chelganov, Yu I Ermakov *Izv. Vyssh. Uchebn. Zaved., Khim. Khim. Tekhnol.* **20** 1167 (1977)
39. B N Kuznetsov, O N Kimkhai, D Gutschik, A N Startsev, G K Boreskov *Z. Anorg. Allg. Chem.* **493** (10) 149 (1982)
40. N K Nag, T Fransen, P Mars *J. Catal.* **68** 77 (1981)
41. A A Lapez, F J Gill, J M Galleja, V Fernandes *J. Raman Spectrosc.* **11** 454 (1981)
42. L Wang, W K Hall *J. Catal.* **77** 232 (1982)
43. M A Aulmahn, G J Siri, M N Blanko, C V Caceres, H J Thomas *Appl. Catal.* **7** 139 (1983)
44. A A Spozhakina, N G Kostova, I A Tsolovski, D M Shopov *Kinet. Katal.* **23** 456 (1982)
45. L P Milova, L M Plyasova, N M Zaidman, S V Ketchik, G A Valiulina, K G Rikhter *Izv. Akad. Nauk SSSR, Neorg. Mater.* **17** 148 (1981)
46. S V Ketchik, L M Plyasova, K G Rikhter, L P Milova, N M Zaidman, V F Anufrienko, R G Ravilov *Izv. Akad. Nauk SSSR, Neorg. Mater.* **17** 153 (1981)
47. N Giordano, A Vaghi, J C J Bart, A Castellan *J. Catal.* **38** 11 (1975)
48. F K Shmidt, Kim En Xva, B V Timashkova, S M Krasnopolskaya, N E Baner, N N Orlova *React. Kinet. Catal. Lett.* **14** 283 (1980)
49. K N Irisova, N P Abramkina, V K Smirnov, B K Nefedov *Khim. Tekhnol. Topl. Masel* 16 (1983)
50. H Jeziorowski, H Knozinger *J. Phys. Chem.* **83** 1166 (1979)
51. H Knozinger, H Jeziorowski *J. Phys. Chem.* **82** 2002 (1978)
52. N Giordano, J C J Bart, A Vaghi, A Castellan, O Mattinatti *J. Catal.* **36** 81 (1975)
53. N Giordano, A Castellan, J C J Bart, A Vaghi, F Compadelli *J. Catal.* **37** 204 (1975)
54. N Giordano *Chim. Ind. (Milan)* **61** 283 (1979)
55. G W Keulks, J I Hall, C Daniel, K Jezuki *J. Catal.* **34** 79 (1974)
56. R Ripan, I Ceteanu *Inorganic Chemistry* (translated into Russian) (Moscow: Mir, 1972) Vol.2
57. K Tanabe *Solid Acids and Bases* (translated into Russian) (Moscow: Mir, 1973)
58. F K Shmidt, Kim En Khva, K P Zhdanova, B V Timashkova, N V Alekseeva, in *Gidrodinamika i Yavleniya Perenosa v Dvukhfaznykh Dispersnykh Sistemakh* (Hydrodynamics and Transport Phenomena in Two-phase Disperse Systems) (Irkutsk: Izd. Irkutsk. Univ., 1982) p. 113
59. G N Asmolov, O V Krylov *Kinet. Katal.* **11** 1028 (1970)
60. T Edmonds, P C H Mitchell *J. Catal.* **64** 491 (1980)
61. J Medema, C Van Stam, V H J De Beer, A J A Konings *J. Catal.* **53** 386 (1978)
62. M Che, F Figueras, M Forissier, J McAteer, M Peppin, J L Paptifaix, H Praliand, in *Proceedings of the Sixth International Congress on Catalysis* Vol.1 (London: The Chemical Society, 1976) p. 261
63. D S Zing, L L Makovsky, R E Tischer, F R Brown *J. Phys. Chem.* **84** 2898 (1980)
64. F R Brown, L L Makovski, K H Rhee *J. Catal.* **50** 162 (1977)
65. A Cimino, B A De Angelis *J. Catal.* **36** 11 (1975)
66. I Tikhy, T V Andrushkevich, L M Plyasova, in *Trudy Pervogo Mezhdunarodnogo Simpoziuma po Geterogennomu Katalizu* (Proceedings of the First International Symposium on Heterogeneous Catalysis) Part 2 (Varna, 1979) p. 99
67. T M Yur'eva, T Kh Shokhireva, O I Goncharova, G K Boreskov *Kinet. Katal.* **26** 1439 (1985)
68. O I Goncharova, G K Boreskov, T M Yurieva, E N Yurchenko, N N Boldyreva *React. Kinet. Catal. Lett.* **16** 349 (1981)
69. J M J G Lipsch, G C A Schuit *J. Catal.* **15** 174 (1969)
70. R K Mohana, R Gobetto, A Iannibello, A Zecchina *J. Catal.* **119** 512 (1989)
71. A F Wemmis, in *Structural Inorganic Chemistry* (Translated into Russian) (Moscow: Mir, 1987) Vol. 2, p. 694
72. O I Goncharova, Thesis, Novosibirsk, 1985
73. N Giordano, M Padovan, A Vaghi, J C J Bart, A Castellan *J. Catal.* **38** 1 (1975)
74. N Giordano, J C J Bart, A Vaghi *React. Kinet. Catal. Lett.* **2** 305 (1975)
75. V Ragaini, G Matarrese, N Giordano, J C J Bart *J. R. Netherl. Chem. Soc.* **97** (4) 97 (1978)

76. B J Parsons, M Ternan, in *Proceedings of the Sixth International Congress on Catalysis* (London: The Chemical Society, 1976) Vol. 2, p. 965
77. Sh Yamadaya, T Kabe, M Oba, V Miki *J. Nat. Chem. Lab. Ind.* **71** 483 (1976)
78. F E Kiviat, L Petrakis *J. Phys. Chem.* **77** 1232 (1973)
79. T Fransen, O Van der Meer, P Mars *J. Phys. Chem.* **80** 2103 (1976)
80. C P Cheng, G L Schader *Spectrosc. Lett.* **12** 857 (1979)
81. K Segawa, W K Hall *J. Catal.* **76** 133 (1982)
82. A A Davydov, O I Goncharova *Kinet. Katal.* **25** 905 (1984)
83. H Praliand, M Forissier *React. Kinet. Catal. Lett.* **8** 451 (1978)
84. *Proceedings of the Sixth International Congress on Catalysis* (London: The Chemical Society, 1976)
85. R Thomas, K Mittelmeijer, M C Hazeleger, F P Kerkhot, J Mouliyn, in *Chemistry and Uses of Molybdenum (Proceedings of the Third International Conference, Ann Arbor, Michigan, 1979)* p. 85
86. I N Marov, N A Kostromina *EPR i YaMR v Khimii Koordinatsionnykh Soedinenii* (ESR and NMR in the Chemistry of Coordination Compounds) (Moscow: Nauka, 1979)
87. F S Gadzhieva, G K Boreskov, V F Anufrienko *Dokl. Akad. Nauk SSSR* **265** b 638 (1983)
88. N G Maksimov, V F Anufrienko, T M Yurieva, T Kh Shokhireva, N N Chumachenko *React. Kinet. Catal. Lett.* **14** 93 (1980)
89. T Kh Shokhireva, Thesis, Novosibirsk, 1983
90. M Che, M Fournier, J P Launey *J. Chem. Phys.* **71** 1954 (1979)
91. M Akimoto, E Echigoja *J. Catal.* **29** 191 (1973)
92. M Akimoto, E Echigoja *Chem. Lett.* 305 (1972)
93. V Ragaini, G Mataresse, N Giordano, J C J Bart *Recl. Trav. Chim. Pays-Bas* **97** 97 (1978)
94. K Maruyama, H Hattori, K Tanabe *Bull. Chem. Soc. Jpn.* **50** 86 (1977)
95. C Naccache, J Bandiera, M Defaux *J. Catal.* **25** 334 (1972)
96. A Castellan, J C J Bart, A Vaghi, N Giordano *J. Catal.* **42** 162 (1976)
97. V Ragaini *J. Catal.* **42** 381 (1976)
98. N Giordano, M Meazza, A Castellan, J C J Bart, V Ragaini *J. Catal.* **50** 342 (1977)
99. T G Alkhazov, K Yu Adzhamov, A K Khanmamedova *Usp. Khim.* **51** 950 (1982) [*Russ. Chem. Rev.* **51** 542 (1982)]
100. F B Kasumov, N Kh Allakhverdova, K Yu Adzhamov *Azerb. Khim. Zh.* 19 (1978)
101. D Vanhove, S R Op, A Fernandes, M Blanchard *J. Catal.* **57** 253 (1979)
102. K M Kasumov, N Kh Allakhverdova, K Yu Adzhamov, K M Mekhtiev *Azerb. Khim. Zh.* 102 (1979)
103. Ya G Goroshenko *Khimiya Titana* (The Chemistry of Titanium) (Kiev: Naukova Dumka, 1970)
104. K Yu Adzhamov, A K Sengikhina, T G Alkhazov, K M Mekhtiev *Kinet. Katal.* **16** 686 (1975)
105. A A Davydov *React. Kinet. Catal. Lett.* **19** 377 (1982)
106. A A Davydov *Infrared Spectroscopy of Adsorbed Species on the Surface of Transition Metal Oxides* (Chichester: John Wiley, 1990)
107. Ru-Tao Kyi *Phys. Rev.* **128** 151 (1962)
108. G A Kravets, T Kh Shokhireva, V F Anufrienko, T M Yurieva *React. Kinet. Catal. Lett.* **19** 95 (1982)
109. M Ai *Bull. Chem. Soc. Jpn.* **49** 1328 (1976)
110. A A Davydov, A A Efremov, F B Kasumov, K Yu Adzhamov *React. Kinet. Catal. Lett.* **18** 29 (1981)
111. A Masamichi, E Echigoya *Bull. Chem. Soc. Jpn.* **46** 1909 (1973)
112. S Okasaki, N Ohsuka, T Iisuka, K Tanabe *J. Chem. Soc., Chem. Commun.* 654 (1976)
113. N E Sharpless, J S Manday *Anal. Chem.* **29** 1619 (1957)
114. A A Davydov, T G Kuznetsova, T V Andrushkevich *React. Kinet. Catal. Lett.* **30** 173 (1986)
115. F Rushala, P A Shiryaev, M Yu Kutyrev, M Ya Kushnarev, D P Shashkin *Kinet. Katal.* **22** 1307 (1981)
116. M Minra, Y Marikawa, T Shirasaki *J. Catal.* **39** 22 (1975)
117. US P 4 220 802; *Ref. Zh. Khim.*, 9N45P (1981)
118. US P 960 201
119. W Oganowska, J Hanuza, B Jezowska-Trzebiatowska, J Wrzyszla *J. Catal.* **39** 161 (1975)
120. Y Izumi, R Hasebe, K Urabe *J. Catal.* **84** 402 (1983)
121. Y Izumi, K Urabe *Chem. Lett.* 663 (1981)
122. C Rocchiccioli-Deltsheff, M Amirouche, G Herve, M Fournier, M Che, J-M Tatibouet *J. Catal.* **126** 591 (1990)
123. R Ohtsuka, J Kobayashi *Bull. Chem. Soc. Jpn.* **63** 2076 (1990)
124. R Ohtsuka, Y Morioka, J Kobayashi *Bull. Chem. Soc. Jpn.* **63** 2071 (1990)

Russian Chemical Reviews **62** (2) 121 – 141 (1993)
©1993 Russian Academy of Sciences and Turpion Ltd

UDC 547.1'13 : 547.559 : 546.76 : 541.13 : 541.67

Electrochemistry of diarenechromium complexes

L P Yur'eva, L N Nekrasov, S M Peregudova

Contents

I. Introduction 121
II. Electrochemical oxidation and reduction processes in the $Arene_2Cr^{+/0}$ and $Arene_2Cr^{2+/+}$ systems 122
III. Cathodic reduction of diarenechromium(0) complexes 131
IV. Characteristic features of the change in the reactivity of arenes under the influence of coordination to a chromium atom in one-electron transfer reactions 138

Abstract. The results of studies on the anodic oxidation and cathodic reduction of diarenechromium complexes are surveyed. The mechanisms of the multistage reactions involving the electrochemical reduction of the complexes are examined. Two aspects of their reactivity are analysed — the nature of the transmission of the electronic effect of substituents in the ligands to the reaction centre and the change in the properties of aromatic compounds as a result of the formation of a complex with a chromium atom. The bibliography includes 133 references.

I. Introduction

A characteristic property of transition metal π-complexes is their ability to enter into oxidation and reduction reactions. Such compounds can exist as neutral molecules and as ions. This is mainly associated with the possible occurrence of different oxidation states of the central metal atom, while the nature of the organic ligands remain unchanged. If the latter are also capable of undergoing oxidation – reduction reactions, the range of redox reactions involving π-complexes is significantly expanded.

The knowledge of the characteristic features of redox processes makes it possible to predict the reactivity of organometallic compounds in different chemical reactions. Electrochemical methods proved to be most effective in the study of redox processes. The high accuracy of the measurement of electrical quantities and the sensitivity of the electrochemical process characteristics to changes in the electronic structure of the molecules ensure a rigorous quantitative level of the investigation.

L P Yur'eva, S M Peregudova Laboratory of Organometallic Compounds, Nesmeyanov Institute of Organoelement Compounds, Russian Academy of Sciences, ul. Vavilova 28, 117813 GSP-1 Moscow,
Fax (7-095) 135 50 85
L N Nekrasov Department of Electrochemistry, Faculty of Chemistry, Lomonosov Moscow State University, Leninskie Gory, 19899 GSP-3 Moscow, Fax (7-095) 939 0126

Received 27th December 1992
Uspekhi Khimii **62** (2) 135 – 156; translated by A K Grzybowski

The problem of the reactivity of transition metal π-complexes of a particular type includes two important tasks: the study of the influence of the nature of organic ligands and of their substituents on the reactivity of the complexes and the determination of the nature of the change in the properties of the organic molecule as a result of its coordination to the metal atom. In relation to redox processes, the first task can be carried out by finding the standard potentials E_0 as a function of the nature and number of substituents in the ligands of the complex. In practice, instead of thermodynamic quantities E_0, use is usually made of the half-wave potentials $E_{1/2}$ of reversible electrochemical reduction or oxidation reactions of the corresponding complexes. The quantities $E_{1/2}$ are determined from polarisation measurements. Different types of polarography, voltammetry at rotating electrodes, cyclic voltammetry, and other methods are used for this purpose. The values of $E_{1/2}$ quoted in the literature do not as a rule include a correction for the interfacial potential jump at the liquid/liquid boundary, arising at the point of contact between solutions of different compositions. The lack of reliable information about the interfacial potential jumps hinders the comparison of the results obtained for the same system in different solvents. The occurrence of interfacial potential jumps as well as the possible differences in the capacities for solvation of the components of the oxidation – reduction system as a function of the nature of the solvent lead to different values of $E_{1/2}$ measured in different solvents relative to the same reference electrode. However, the above effects are not important if all the measurements for the test series of compounds are carried out in the same solvent under identical experimental conditions.

One of the most important problems in the chemistry of transition metal π-complexes is that of the influence of the coordination of the organic molecule to the transition metal atom on the properties of the former. In order to discover the general features of the effect of complex formation on the reactivity of the 'ligand', a comparative study of the electrochemical behaviour of a group of non-coordinated organic compounds and their π-complexes is carried out.

Among transition metal π-complexes, diarenechromium complexes occupy a special place. The discovery of dibenzenechromium and the determination of its sandwich structure[1,2] played an extremely important role in the establishment and development of modern organometallic chemistry. The characteristic features of the structure of complexes of the dibenzenechromium series, namely the presence of ligands of only one type, their aromatic nature, their ability to exist in a non-coordinated state, the formally zero valence of the

central metal atom in the uncharged complexes, as well as the reversibility of the electron transfer stages in the $Arene_2Cr^{+/0}$ and $Arene_2Cr^{0/-}$ systems render diarenechromium complexes exceptionally convenient for the solution of general problems of the reactivity of transition metal π-complexes.

A wide variety of redox processes, occurring both with retention of the sandwich structure and leading to its disruption, are characteristic of diarenechromium complexes:

$$2Arene + Cr^{3+} \overset{-\bar{e}}{\leftarrow} Arene_2Cr^{2+} \overset{-\bar{e}}{\leftrightarrows} Arene_2Cr^{+} \underset{+\bar{e}}{\overset{-\bar{e}}{\rightleftarrows}}$$

$$\leftrightarrows Arene_2Cr \underset{-\bar{e}}{\overset{+\bar{e}}{\rightleftarrows}} Arene_2Cr^{-} \xrightarrow{+m\bar{e}} \text{products.} \qquad (1)$$

Neutral complexes and singly charged paramagnetic cations are stable while the doubly charged cations and the radical-anions are unstable. Their formation in the course of the reaction has been demonstrated by electrochemical methods and EPR.

Chromium complexes are the only ones among the diarene π-complexes of Group VIA metal complexes whose electrochemistry has been investigated in fair detail. The electrochemical behaviour of molybdenum and tungsten analogues has been hardly studied.

The first electrochemical investigations of diarenechromium complexes[3-15] were performed soon after the synthesis of dibenzenechromium by Fischer.[1] In these investigations, a study was made, in relation to dibenzenechromium and its simplest derivatives containing alkyl and aryl groups in the benzene ligand, of redox processes in the $Arene_2Cr^{+/0}$ systems by polarography at the mercury dropping electrode (MDE). Electrochemical reduction reactions of neutral complexes were initially described for only two examples.[15,16] As the methods of synthesis developed, the range of available diarenechromium complexes expanded. This created preconditions for a systematic study of the reactivity of a large series of complexes of this type both in anodic oxidation and in cathodic reduction reactions. The range of electrochemical methods also expanded. Together with polarography at the MDE, cyclic voltammetry (CVA), the rotating disc electrode (RDE) method, and the rotating ring-disc electrode (RRDE) method came to be widely used.

The study of the polarisation characteristics of the oxidation–reduction processes with participation of chromium π-complexes led to the formulation of the characteristic features of the electrode reactions. The mechanism of the transmission of electronic effects of substituents in the complex molecule was established with the aid of correlation analysis. The nature of the changes in the properties of aromatic compounds in the complex formation process was discovered on the basis of comparative data on the reactivity of arenes and their chromium complexes in cathodic reduction reactions. The use of modern electrochemical experimental methods (CVA, RRDE) made it possible to determine the mechanisms of multistage electrochemical reduction reactions, to identify the unstable reaction intermediates, and to investigate their reactions.

A brief description of studies on the electrochemistry of diarenechromium complexes can be found in a number of publications.[17-26] The aim of the present review was to consider as fully as possible the results of studies over the last 10–15 years and also to discuss the characteristics of the electrochemical processes and the conclusions reached on their basis, which are important for the chemistry of transition metal π-complexes.

II. Electrochemical oxidation and reduction processes in the $Arene_2Cr^{+/0}$ and $Arene_2Cr^{2+/+}$ systems

The reversibility of the one-electron transfer stage

$$Arene_2Cr \underset{+\bar{e}}{\overset{-\bar{e}}{\rightleftarrows}} Arene_2Cr^{+} \qquad (2)$$

in protic[3-9,11-13] and aprotic[10,14,27-30] media is characteristic of all the diarenechromium complexes known at the present time. This confirms data obtained by the polarographic, CVA, RDE, and RRDE methods, according to which the half-wave potentials $E_{1/2}^{+/0}$ for the oxidation of the neutral form of the complex and the reduction of the corresponding cation are the same, while the slope of the polarisation curves is 0.06 V, which is close to the theoretical value for a reversible one-electron process. The same value is quoted in most studies for the difference between the potentials of the cathodic (pc) and anodic (pa) peaks on the cyclic voltammogram:

$$\Delta E_p = E_{pa} - E_{pc}$$

for a peak height ratio close to unity:[31] $i_{pc}/i_{pa} \simeq 1$. The polarisation characteristics of the processes, including the values of $E_{1/2}$, are unaffected by the nature of the material of the electrode and the composition and concentration of the supporting electrolyte. The limiting currents on the polarisation curves are diffusional in character.

The data encountered in certain studies which are formally inconsistent with the reversibility of the process, for example the difference between the potentials of the cathodic and anodic peaks on the cyclic voltammograms exceeding appreciably the value for a reversible reaction,[32,33] are in all probability a result of the inadequate accuracy of the experiment and the occurrence of ohmic potential drops in the solution, which has been confirmed convincingly[31] by the comparison of the values of ΔE_p measured with compensation for the ohmic potential drops (ΔE_p = 0.06 V) and without such compensation (ΔE_p = 0.12–0.14 V).

The reversibility of the electrode reactions observed with the aid of the experimental methods mentioned above is a consequence of the high standard exchange current density i_{00} in the test systems or, what amounts to the same thing, the high heterogeneous rate constants for the electron transfer stage at the equilibrium potentials k_s. In such cases, the kinetics of the overall process are wholly determined by the kinetics of the mass transfer stages, while the electrode potentials at each point on the polarisation curve are determined, in conformity with the thermodynamic Nernst formula for the electrode potential, by the logarithm of the ratio of the concentrations (activities) of the oxidised and reduced form of the electrochemically active substance at the electrode. The kinetic parameters of the electron transfer state (i_{00}, k_s, and the transfer coefficients α and β for the cathodic and anodic reactions respectively) can be determined directly using methods making it possible to remove the diffusional limitations and to investigate the kinetics. Thus, according to Gennett et al.,[34] the values of k_s for the bis(biphenyl)chromium$^{+/0}$ system, obtained in the course of impedance measurements by alternating current polarography in seven different solvents, are in the range from 0.3 (benzonitrile) to 4 cm s^{-1} (acetonitrile). Such values correspond to standard exchange current densities into the range 30–400 A cm^{-2} and characterise a very high reversibility of the reaction. The transfer coefficient α for this system proved to be 0.5±0.03.

The results of measurements of the rate constants for homogeneous electron exchange in solutions in hexane and benzene between the oxidised and reduced forms of methyl-substituted dibenzenechromium derivatives ($k_{ex} \sim 3 \times 10^8$ litre mol^{-1} s^{-1}), found by the ^1H NMR and EPR methods, as well as the low activation energies (E_a = 8.6 kJ mol^{-1}) characteristic of

diffusion-controlled reactions are consistent with the data presented above.[35] Similar data have been obtained for other derivatives of dibenzenechromium in dimethyl sulphoxide (DMSO).[28]

A high exchange current density is one of the conditions necessary to permit the use of a particular oxidation-reduction couple as a reference system for the measurement of electrode potentials. This feature as well as the fulfillment of a number of other conditions (closeness of the particles to the spherical shape and their large radius, low ionic charge, stability of both forms of the redox systems and their solubility in different solvents, and the constancy of the geometry of the ligands after electron transfer[36]) enabled the IUPAC Commission on Electrochemistry to recommend the bis(biphenyl)chromium $^{+/0}$ system together with the ferrocene/ferrocenium system for use as a reference electrode (as a portable electrode or as an internal standard) in electrochemical measurements in non-aqueous solvents.[37] Special studies[37,38] have shown that the potential difference between the two systems specified above in 22 organic solvents is virtually constant and the deviation from the average value of 1.124 V is ± 12 mV for an error of the measurements of ± 4 mV. This result indicates the virtually complete absence of effects due to the specific solvation of the cations and an insignificant change in the electrostatic component on passing from one solvent to another. The bis(biphenyl)chromium $^{+/0}$ couple proved to be the best reference system in non-aqueous media. It became possible to compare correctly the parameters of electrode reactions investigated in different organic solvents by potentiometric, voltammetric, and polarographic methods. A table representing a compilation of the half-wave potentials for the electrochemical reduction processes of a large number of metal cations, measured relative to the reference electrode under consideration, in 38 organic solvents has been published.[43] The use of bis(biphenyl)-chromium for similar purposes in aqueous solutions is not indicated in view of the instability of its cationic form, the insolubility of the neutral complex, and the pronounced adsorption phenomena.[39]

The data obtained from electrochemical measurements on the entropies of the electrochemical reduction reactions of bis-(biphenyl)chromium[40] and dibenzenechromium[34] cations in a number of solvents provide information about the temperature variation of the corresponding standard redox potentials. It has been established that the entropies of these reactions decrease linearly with increase in the acceptor number of the solvent.[40]

The change in the charge on the diarenechromium complexes in the course of the one-electron transfer process is accompanied by only a small reorganisation of the inner sphere of this species. Thus, on passing from the reduced to the oxidised form of dibenzene-chromium, the chromium–carbon bond length changes[41,42] by only 0.012 Å, whilst the free energy of the inner-sphere reorganisation ΔG_{is}^{+} is ~ 0.8 kJ mol^{-1}, which is at least 20 times lower than the free energy of the reorganisation of the outer sphere (the solvent). This enabled the authors[34] to use dibenzenechromium as one of the model objects for testing the theory of solvent reorganisation, constituting the basis of modern approaches to the treatment of the elementary electron transfer step in homogeneous oxidation–reduction and electrochemical reactions in condensed systems.[44,45]

Dibenzenechromium and its substituted derivatives are interesting objects for the study of the adsorption of organic cations at the interface. The low solubility of the salts of diarenechromium complexes in water is one of the main causes of the strong adsorption of the cations on the electrodes in aqueous media.[4] The appearance of adsorption waves (Brdicka waves) on the polarograms obtained in aqueous solutions of the iodides of certain alkyl-substituted dibenzenechromium derivatives is associated with this phenomenon.[7–9]

The adsorption of dibenzenechromium and bis(biphenyl)-chromium cations at the aqueous solutions/mercury and solution/air interfaces has been investigated[46,47] by the methods of electrocapillary curves and the maximum air pressure in the bubble. The adsorbability of these species is due to a number of factors: their positive charge, the squeezing effect at the interface owing to the breakdown of the structure of water, the interaction of the π-electrons of the aromatic system with the electrode surface, and the presence of the unpaired electron. The nature of the supporting electrolyte anion also exerts a strong influence on the adsorption. Comparison of the adsorption properties of dibenzenechromium, bis(biphenyl)chromium, and tetraethyl-ammonium cations established that the presence of the unpaired electron and of the π-electron system in the radical-cations of the π-complexes promotes their adsorption on mercury in the absence of the specific interaction of the supporting electrolyte anions with the electrode surface (for sulphate anions), but diminishes the adsorbability somewhat if such interaction does occur (for iodide anions). The appearance of adsorption peaks on the cyclic voltam-mograms of dibenzenechromium, bis(biphenyl)chromium, and dinaphthalenechromium, obtained at a platinum electrode in solutions in tetrahydrofuran (THF), has been noted.[48,49]

The existence of limiting diffusion currents on the electro-chemical reduction or electrochemical oxidation polarisation curves for chromium π-complexes, measured with the aid of the mercury dropping electrode or the rotating disc electrode, makes it possible to determine the diffusion coefficients of these com-pounds. The corresponding data for a series of derivatives of dibenzenechromium in several solvents have been published.[34,39,50]

Diarenechromium complexes are some of the most readily oxidisable transition metal π-complexes. Unsubstituted dibenz-enechromium is oxidised at high negative potentials. The measured value of $E_{1/2}$ (relative to the saturated calomel electrode) depends on the solvent: -0.71 V (DMF), -0.77 V (AN), -0.795 V (BN), -0.93 V (FA),[34] and -0.76 V (DMSO).[29] (The designations of the solvents are indicated in the footnote to Table 1.) Dibenzenemolybdenum is oxidised with somewhat greater difficulty than dibenzenechromium: $\Delta E_{1/2}$ is 0.1 V.[4] There are no literature data on the electrochemical oxidation of dibenzenetungsten.

Comparison[51] of the behaviour of dibenzenechromium, dibenzenevanadium, and cyclopentadienyl(cycloheptatrienyl)-chromium in the electrochemical oxidation reaction showed that the 18-electron dibenzenechromium is oxidised more readily than the 17-electron vanadium complex (the potentials $E_{1/2}$ in DME are -0.72 and -0.35 V respectively) and an asymmetric chromium complex with different ligands ($C_5H_5+C_7H_7$): for the latter, $E_{1/2}^{+/0} = -0.61$ V.

The half-wave potential is strongly influenced by the substituents in the arene ligand. Depending on the nature of the substituents and the number in the complex molecule, the values of $E_{1/2}^{+/0}$ vary from -1 to $+0.4$ V.

The half-wave potentials for the reversible redox transitions $+/0$ and $2+/+$ in the diarenechromium π-complexes are presented in Table 1.

The introduction of alkyl substituents into the dibenzene-chromium molecule shifts $E_{1/2}$ into the region of negative values.[4,6–9,12,27,53] On the other hand, the introduction of phenyl substituents hinders oxidation.[10] The principle of additivity then holds. For example, the shift of $E_{1/2}$ due to the introduction of one alkyl group is the same for the methyl and ethyl groups and amounts to 0.03 V. The validity of the principle of additivity has been indicated also in other studies.[29,31,62] The shift of $E_{1/2}$ after the introduction of one formyl group is 0.27 V, while the shift after the introduction of the cyano-group is 0.3 V (compounds **1**, **44**, **45**, **49**, **56**).† The maintenance of the principle of additivity as the phenyl groups accumulate in the dibenzene-chromium molecule is illustrated in Fig. 1. In a number of

†Here and henceforth the numbers of the compounds in Table 1 are quoted in the text.

Table 1. The potentials $E_{1/2}$ for the $Arene_2Cr^{0/+}$ and $Arene_2Cr^{2+/+}$ redox processes.

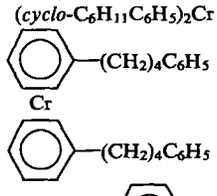
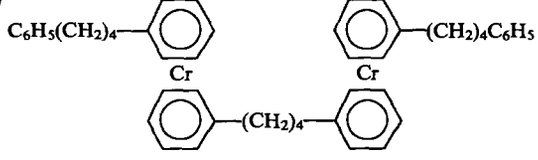
No.	Compound	$-E_{1/2}^{+/0}$/V ($-E_{1/2}^{2+/+}$)/V	Solvent	Supporting electrolyte	Method (electrode)	Ref.
1	$(C_6H_6)_2Cr$	0.97	H_2O	0.5 M LiCl	MDE	6
		0.835	C_2H_5OH	0.5 M LiCl	MDE	5
		0.807[a]	$CH_3OH:C_6H_6=4:1$	0.3 M NaOH	MDE	4
		0.81[a]	$CH_3OH:C_6H_6=4:1$	0.5 M LiCl	MDE	3
		1.04	FA	0.2 M $NaClO_4$	MDE	10
		0.81	DMF	0.2 M $NaClO_4$	MDE	10
		0.80	DMF	0.1 M NEt_4ClO_4	MDE	27
		0.81	DMF	0.1 M NEt_4ClO_4	(Pt)	52
		0.82	DMF	0.1 M NEt_4ClO_4	(Pt)	53
		1.3[b]	DME	0.1 M NBu_4ClO_4	MDE	14
		0.685	DME	0.1 M NBu_4ClO_4	CVA (CG)	54, 55
		0.72	DME	0.1 M NBu_4ClO_4	CVA (CG)	51
		(−1.14)	DME (−45 °C)	0.1 M NBu_4ClO_4	CVA (CG)	51
		(−0.94)[c]	THF (−80 °C)	0.05 M NBu_4PF_6	CVA (Pt)	48
		0.746	DMSO	0.1 M NBu_4ClO_4	CVA (Pt)	28
		0.76	DMSO	0.1 M NBu_4BF_4	RDE (Hg/Au)	29
		0.770	AN	0.1 M NBu_4PF_6	MDE, CVA (Hg)	34
		0.710	DMF	0.1 M NBu_4PF_6	MDE, CVA (Hg)	34
		0.930	FA	0.1 M NBu_4PF_6	MDE, CVA (Hg)	34
		0.795	BN	0.1 M NBu_4PF_6	MDE, CVA (Hg)	34
		0.80	CH_2Cl_2	0.1 M NBu_4PF_6	CVA (Pt)	56
2	$(CH_3C_6H_5)_2Cr$	0.885[a]	$CH_3OH:C_6H_6$ = 4:1	0.3 M NaOH	MDE	4
		0.775	$C_2H_5OH:C_6H_6$ = 7:3	0.5 M LiCl	MDE	12
		0.89	DMF	NEt_4ClO_4	(Pt)	53
		0.85	DMF	0.1 M NEt_4ClO_4	MDE	27
		1.04	H_2O	0.5 M LiCl	MDE	6
		0.82	DMSO	0.1 M NBu_4BF_4	RDE (Hg/Au)	29
3	$[1,2\text{-}(CH_3)_2C_6H_4]_2Cr$	1.06	H_2O	0.5 M LiCl	MDE	7
		0.93	DMF	0.1 M NEt_4ClO_4	MDE	27
		0.73	DME	NBu_4ClO_4	CVA (CG)	57
4	$[1,3\text{-}(CH_3)_2C_6H_4]_2Cr$	1.06	H_2O	0.5 M LiCl	MDE	7
		0.92	DMF	0.1 M NEt_4ClO_4	MDE	27
		0.88	DMSO	0.1 M NBu_4BF_4	RDE (Hg/Au)	29
		0.77	DME	0.1 M NBu_4ClO_4	CVA (CG)	58
5	$[1,4\text{-}(CH_3)_2C_6H_4]_2Cr$	1.06	H_2O	0.5 M LiCl	MDE	7
6	$[1,2,4\text{-}(CH_3)_3C_6H_3]_2Cr$	1.008[a]	$CH_3OH:C_6H_6$ = 4:1	0.3 M NaOH	MDE	4
		0.916	DMSO	0.1 M NBu_4ClO_4	CVA (Pt)	28
7	$[1,3,5\text{-}(CH_3)_3C_6H_3]_2Cr$	1.06	H_2O	0.5 M LiCl	MDE	6
		1.00[a]	$CH_3OH:C_6H_6$ = 4:1	0.3 M NaOH	MDE	4
		0.97	DMF	0.1 M NEt_4ClO_4	MDE	27, 53
		0.94	DMSO	0.1 M NBu_4BF_4	RDE (Hg/Au)	29
8	$[(CH_3)_6C_6]_2Cr$	1.12	H_2O	0.5 M LiCl	MDE	7
		1.63[d]	THF	NBu_4PF_6	CVA (Pt)	59
		(0.16)[d]	THF	NBu_4PF_6	CVA (Pt)	59
		0.94	DME	NBu_4ClO_4	CVA (CG)	51
		(−0.45)	DME (−45 °C)	NBu_4ClO_4	CVA (CG)	51
9	$(C_2H_5C_6H_5)Cr(C_6H_6)$	0.83	DMF	0.1 M NEt_4ClO_4	MDE	27
10	$(C_2H_5C_6H_5)_2Cr$	1.05	H_2O	0.5 M LiCl	MDE	8
		0.86	DMF	0.1 M NEt_4ClO_4	MDE	27
		0.81	DMSO	0.1 M NBu_4BF_4	RDE (Hg/Au)	29
11	$[(C_2H_5)_2C_6H_4]Cr(C_6H_5C_2H_5)$	0.89	DMF	0.1 M NEt_4ClO_4	MDE	27
12	$[(C_2H_5)_2C_6H_4]_2Cr$	0.92	DMF	0.1 M NEt_4ClO_4	MDE	27
13	$(iso\text{-}C_3H_7C_6H_5)_2Cr$	0.96	H_2O	0.5 M LiCl	MDE	6
		1.05	H_2O	0.5 M LiCl	MDE	9
14	$[1,3\text{-}(iso\text{-}C_3H_7)_2C_6H_4]_2Cr$	1.02	H_2O	0.5 M LiCl	MDE	9
15	$(cyclo\text{-}C_6H_{11}C_6H_5)_2Cr$	0.90	H_2O	0.5 M LiCl	MDE	6
16		0.82	DMSO	0.1 M NBu_4BF_4	RDE (Hg/Au)	29
17		0.82	DMSO	0.1 M NBu_4BF_4	RDE (Hg/Au)	29

Table 1 (contd).

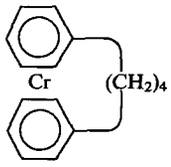
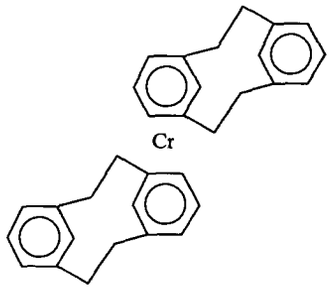
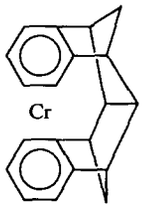
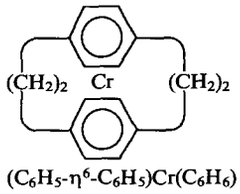
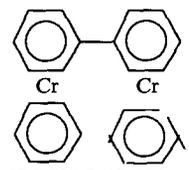
No.	Compound	$-E^{+/0}_{1/2}$/V ($-E^{2+/+}_{1/2}$)/V	Solvent	Supporting electrolyte	Method (electrode)	Ref.
18		0.79	DMSO	0.1 M NBu_4BF_4	RDE (Hg/Au)	29
19		0.82	DME	0.1 M NBu_4ClO_4	CVA (CG)	58
20		0.73	DME	0.1 M NBu_4ClO_4	CVA (CG)	57
21		0.74 (−1.24)	DME DME (−45 °C)	0.1 M NBu_4ClO_4	CVA (CG)	51
22	$(C_6H_5\text{-}\eta^6\text{-}C_6H_5)Cr(C_6H_6)$	0.87	H_2O	0.5 M LiCl	MDE	7
		0.78(5)	C_2H_5OH	0.5 M LiCl	MDE	5
		1.3[b]	DME	0.1 M NBu_4ClO_4	MDE	15
23	$(C_6H_5\text{-}\eta^6\text{-}C_6H_5)_2Cr$	0.669[e]	H_2O	1 M KCl	MDE	39
		0.66	H_2O	0.5 M LiCl	MDE	6
		0.72	C_2H_5OH	0.5 M LiCl	MDE	5
		0.697	$C_2H_5OH:C_6H_6 = 4:1$	0.1 M LiCl	MDE	11
		1.340[f]	THF	0.1 M NBu_4BF_4	CVA (Pt)	60
		1.10[b]	DMF	0.1 M NEt_4ClO_4	CVA (CG)	30
		0.74	DMF	0.1 M NEt_4ClO_4	(Pt)	53
		0.750	DMF	0.5 M $NaClO_4$	CVA (Pt)	10
		0.89	FA	0.5 M $NaClO_4$	CVA (Pt)	10
		0.645	DMSO	0.1 M NBu_4ClO_4	CVA (Pt)	28
		0.66	DMSO	0.1 M NBu_4BF_4	RDE (Hg/Au)	29
24	$(4\text{-}FC_6H_4\text{-}\eta^6\text{-}C_6H_5)Cr(\eta^6\text{-}C_6H_5C_6H_5)$	0.686	$C_2H_5OH:C_6H_6 = 4:1$	0.1 M LiCl	MDE	11
25	$(4\text{-}ClC_6H_4\text{-}\eta^6\text{-}C_6H_5)Cr(\eta^6\text{-}C_6H_5C_6H_5)$	0.679	$C_2H_5OH:C_6H_6 = 4:1$	0.1 M LiCl	MDE	11
26	$(4\text{-}BrC_6H_4\text{-}\eta^6\text{-}C_6H_5)Cr(\eta^6\text{-}C_6H_5C_6H_5)$	0.672	$C_2H_5OH:C_6H_6 = 4:1$	0.1 M LiCl	MDE	11
27	$[(C_6H_5)_3\text{-}\eta^6\text{-}C_6H_3]_2Cr$	0.53	DMSO	0.1 M NBu_4BF_4	RDE (Hg/Au)	24, 61, 62
28	$[(C_6H_5)_6\text{-}\eta^6\text{-}C_6]_2Cr$	0.28	DMSO	0.1 M NBu_4BF_4	RDE (Hg/Au)	24, 61, 62
29		0.82[e] 0.37	AN	0.1 M NEt_4BF_4	CVA	63
30	$(FC_6H_5)Cr(C_6H_6)$	0.57	DMSO	0.1 M NBu_4BF_4	RDE (Hg/Au)	62
31	$(FC_6H_5)_2Cr$	0.367	AN	0.1 M NBu_4ClO_4	CVA (Pt)	32
32	$(ClC_6H_5)_2Cr$	0.336	AN	0.1 M NBu_4ClO_4	CVA (Pt)	32
33	$[1,4\text{-}(CH_3)_2\text{-}2\text{-}ClC_6H_3]_2Cr$	0.516	AN	0.1 M NBu_4ClO_4	CVA (Pt)	32
34	$(IC_6H_5)_2Cr$	0.34	DMSO	0.1 M NBu_4BF_4	RDE (Hg/Au)	62

Table 1 (contd).

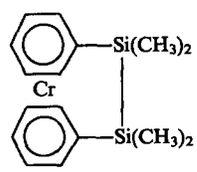
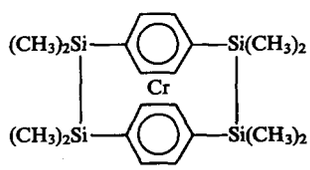
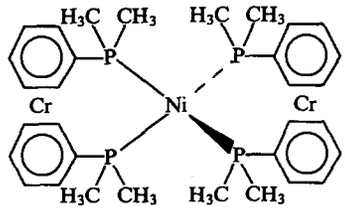
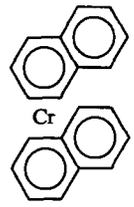
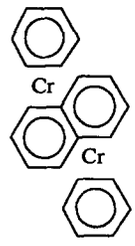
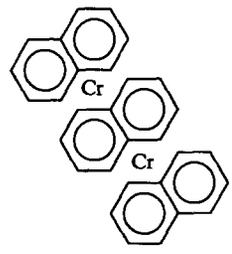
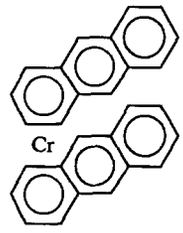
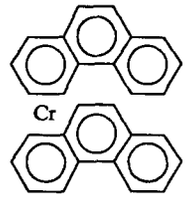
No.	Compound	$-E^{+/0}_{1/2}$/V ($-E^{2+/+}_{1/2}$)/V	Solvent	Supporting electrolyte	Method (electrode)	Ref.
35	$(CF_3C_6H_5)_2Cr$	0.24	DMSO	0.1 M NBu_4BF_4	RDE (Hg/Au)	62
		0.190	AN	0.1 M NBu_4ClO_4	CVA (Pt)	32
36	$[1,3\text{-}(CF_3)_2C_6H_4]_2Cr$	−0.385	AN	0.1 M NBu_4ClO_4	CVA (Pt)	32
37	$[1,4\text{-}(CF_3)_2C_6H_4]_2Cr$	−0.337	AN	0.1 M NBu_4ClO_4	CVA (Pt)	32
38	$(1,2\text{-}CF_3C_6H_4Cl)_2Cr$	−0.165	AN	0.1 M NBu_4ClO_4	CVA (Pt)	32
39	$(1,4\text{-}CF_3C_6H_4Cl)_2Cr$	−0.125	AN	0.1 M NBu_4ClO_4	CVA (Pt)	32
40	$(CH_3OC_6H_5)_2Cr$	0.767	AN	0.1 M NBu_4ClO_4	CVA (Pt)	32
41	$[(CH_3)_2NC_6H_5]Cr(C_6H_6)$	0.958	AN	0.1 M NBu_4ClO_4	CVA (CG)	31
42	$[(CH_3)_2NC_6H_5]_2Cr$	1.075	AN	0.1 M NBu_4ClO_4	CVA (CG)	31
43	$[(CH_3)_2NC_6H_5]Cr(C_6H_5COOCH_3)$	0.743	AN	0.1 M NBu_4ClO_4	CVA (CG)	31
44	$(HCOC_6H_5)Cr(C_6H_6)$	0.51	DMSO	0.1 M NBu_4BF_4	RDE (Hg/Au)	29
45	$(HCOC_6H_5)_2Cr$	0.27	DMSO	0.1 M NBu_4BF_4	RDE (Hg/Au)	29
46	$(CH_3COC_6H_5)Cr(C_6H_6)$	0.616	AN	0.1 M NBu_4ClO_4	CVA (CG)	31
47	$(CH_3COC_6H_5)_2Cr$	0.429	AN	0.1 M NBu_4ClO_4	CVA (CG)	31
		0.38	DMSO	NBu_4BF_4	RDE (Hg/Au)	29
48	$(C_6H_5CO\text{-}\eta^6\text{-}C_6H_5)Cr(C_6H_6)$	0.59	DMF	0.1 M NEt_4ClO_4	MDE	16, 53
49	$(NCC_6H_5)Cr(C_6H_6)$	0.46	DMSO	0.1 M NBu_4BF_4	RDE (Hg/Au)	62
50	$(NCC_6H_5)Cr(C_6H_5CH_3)$	0.49	DMSO	0.1 M NBu_4BF_4	RDE (Hg/Au)	62
51	$(NCC_6H_5)Cr(C_6H_5OCH_3)$	0.43	DMSO	0.1 M NBu_4BF_4	RDE (Hg/Au)	62
52	$(NCC_6H_5)Cr(C_6H_5COCH_3)$	0.28	DMSO	0.1 M NBu_4BF_4	RDE (Hg/Au)	62
53	$(NCC_6H_5)Cr(C_6H_5F)$	0.26	DMSO	0.1 M NBu_4BF_4	RDE (Hg/Au)	62
54	$(NCC_6H_5)Cr(C_6H_5Cl)$	0.27	DMSO	0.1 M NBu_4BF_4	RDE (Hg/Au)	62
55	$(NCC_6H_5)Cr(C_6H_5CF_3)$	0.18	DMSO	0.1 M NBu_4BF_4	RDE (Hg/Au)	62
56	$(NCC_6H_5)_2Cr$	0.14	DMSO	0.1 M NBu_4BF_4	RDE (Hg/Au)	62
57	$(CH_3OCOC_6H_5)Cr(C_6H_6)$	0.615	AN	0.1 M NBu_4ClO_4	CVA (Pt)	31
58	$(CH_3OCOC_6H_5)_2Cr$	0.407	AN	0.1 M NBu_4ClO_4	CVA (Pt)	31
59	$(C_2H_5OCOC_6H_5)Cr(C_6H_6)$	0.617	AN	0.1 M NBu_4ClO_4	CVA (Pt)	31
60	$(C_2H_5OCOC_6H_5)_2Cr$	0.421	AN	0.1 M NBu_4ClO_4	CVA (Pt)	31
		0.65	H_2O	0.1 M KCl	CVA (Pt)	64
61	$[1,2\text{-}(CH_3OCO)_2C_6H_4]Cr(C_6H_6)$	0.464	AN	0.1 M NBu_4ClO_4	CVA (Pt)	31
62	$[1,2\text{-}(CH_3OCO)_2C_6H_4]_2Cr$	0.157	AN	0.1 M NBu_4ClO_4	CVA (Pt)	31
63	$[1,2\text{-}(C_2H_5OCO)_2C_6H_4]_2Cr$	0.20	DMSO	0.1 M NBu_4BF_4	RDE (Hg/Au)	65
64	$[1,3\text{-}(CH_3OCO)_2C_6H_4]Cr(C_6H_6)$	0.409	AN	0.1 M NBu_4ClO_4	CVA (Pt)	31
65	$[1,3\text{-}(CH_3OCO)_2C_6H_4]_2Cr$	0.064	AN	0.1 M NBu_4ClO_4	CVA (Pt)	31
66	$[1,4\text{-}(CH_3OCO)_2C_6H_4]Cr(C_6H_6)$	0.407	AN	0.1 M NBu_4ClO_4	CVA (Pt)	31
67	$[1,4\text{-}(CH_3OCO)_2C_6H_4]_2Cr$	0.049	AN	0.1 M NBu_4ClO_4	CVA (Pt)	31
68	$(CH_3OCOCH_2C_6H_5)Cr(C_6H_6)$	0.782	AN	0.1 M NBu_4ClO_4	CVA (Pt)	31
69	$(CH_3OCOCH_2C_6H_5)_2Cr$	0.751	AN	0.1 M NBu_4ClO_4	CVA (Pt)	31
70	$(C_2H_5OCOCH_2C_6H_5)Cr(C_6H_6)$	0.797	AN	0.1 M NBu_4ClO_4	CVA (Pt)	31
71	$(C_2H_5OCOCH_2C_6H_5)_2Cr$	0.759	AN	0.1 M NBu_4ClO_4	CVA (Pt)	31
		0.70	DMSO	0.1 M NBu_4BF_4	RDE (Hg/Au)	29
72	$(CH_3OCOCH_2CH_2C_6H_5)Cr(C_6H_6)$	0.826	AN	0.1 M NBu_4ClO_4	CVA (Pt)	31
73	$(CH_3OCOCH_2CH_2C_6H_5)_2Cr$	0.837	AN	0.1 M NBu_4ClO_4	CVA (Pt)	31
74	$(C_2H_5OCOCH_2CH_2C_6H_5)Cr(C_6H_6)$	0.834	AN	0.1 M NBu_4ClO_4	CVA (Pt)	31
75	$(C_2H_5OCOCH_2CH_2C_6H_5)_2Cr$	0.840	AN	0.1 M NBu_4ClO_4	CVA (Pt)	31
		0.80	DMSO	0.1 M NBu_4BF_4	RDE (Hg/Au)	29
76	$(C_2H_5OCOCH=CHC_6H_5)_2Cr$	0.55	DMSO	0.1 M NBu_4BF_4	RDE (Hg/Au)	29
77	$(C_6H_5COCH=CH\text{-}\eta^6\text{-}C_6H_5)_2Cr$	0.50	DMSO	0.1 M NBu_4BF_4	RDE (Hg/Au)	29
78	$(C_6H_5C\equiv C\text{-}\eta^6\text{-}C_6H_5)_2Cr$	0.68	DMSO	0.1 M NBu_4BF_4	RDE (Hg/Au)	61, 62
79	$[(C_6H_5)_3Si\text{-}\eta^6\text{-}C_6H_5]_2Cr$	0.55	DME	0.1 M NEt_3ClO_4	CVA (CG)	66
80		0.69	DME	0.1 M NBu_4ClO_4	CVA (Pt)	67
81		0.66	DME	0.1 M NBu_4ClO_4	CVA (Pt)	67
82	$[(CH_3)_2PC_6H_5]Cr(C_6H_6)$	0.62	DME	0.1 M NBu_4ClO_4	CVA (CG)	68
83	$[(CH_3)_2PC_6H_5]_2Cr$	0.57	DME	0.1 M NBu_4ClO_4	CVA (CG)	68

Table 1 (contd).

No.	Compound		$-E_{1/2}^{+/0}$/V ($-E_{1/2}^{2+/+}$)/V	Solvent	Supporting electrolyte	Method (electrode)	Ref.
84			0.70	DME	0.1 M NBu_4ClO_4	CVA (CG)	68
85			1.190[d]	THF	NBu_4PF_6	CVA (Pt)	49
			(−0.196)[d]	THF	NBu_4PF_6	CVA (Pt)	49
			1.84[d]	EDA	NBu_4PF_6	CVA (Pt)	49
86			0.80[d]	THF	NBu_4PF_6	CVA (Pt)	49
			(−0.38)[d]	THF	NBu_4PF_6	CVA (Pt)	49
87			2.04[d]	EDA	NBu_4PF_6	CVA (Pt)	49
88			1.4[b]	DME	0.1 M NBu_4ClO_4	MDE	15
89			0.651	DMF	0.1 M NBu_4ClO_4	CVA (Pt)	69
			(−0.82)	DMF	0.1 M NBu_4ClO_4	CVA (Pt)	69
90	$(C_5H_5N)Cr(C_6H_6)$		0.560	DME	0.1 M NBu_4ClO_4	CVA (CG)	55
91	$(C_5H_5N)_2Cr$		0.445	DME	0.1 M NBu_4ClO_4	CVA (CG)	55
92	$(C_5H_5As)_2Cr$		0.51	DME	0.1 M NBu_4ClO_4	CVA (CG)	54
93	$(C_5H_5BR)_2Cr$	$R=CH_3$	−0.45	CH_2Cl_2	NBu_4PF_6	CVA (Pt)	70
94	$(C_5H_5BR)_2Cr$	$R=C_6H_5$	−0.53	CH_2Cl_2	NBu_4PF_6	CVA (Pt)	70

Note. The half-wave potentials $E_{1/2}$ were determined either directly from the polarisation curves (MDE, RDE) or were found as half the sum of the potentials of the cathodic (E_{pc}) and anodic (E_{pa}) peaks on the cyclic voltammograms. Unless stipulated otherwise, the electrode potentials listed in Table 1 and in the other tables and also quoted in the text were measured relative to the potential of the aqueous saturated calomel electrode. In the remaining cases, the reference electrode employed is indicated. The table also presents the experimental conditions (the method of measurement, the material of the electrode, the solvent, and the composition of the supporting electrolyte), the most important of which is the nature of the solvent when the process is reversible. The following abbreviations have been adopted in the table and in the text: CG = carbon glass, AN = acetonitrile, BN = benzonitrile, DMSO = dimethylsulphoxide, DMF = dimethylformamide, DME = dimethoxyethane, THF = tetrahydrofuran, FA = formamide, EDA = ethylenediamine.

Reference electrodes: [a] calomel electrode, 0.5 M LiCl, $CH_3-C_6H_6$; [b] $Ag/AgClO_4$; [c] Ag/AgCl/4 M aqueous LiCl; [d] $Ag/AgNO_3$; [e] Ag/AgCl; [f] $Ag/AgBF_4$.

Indeed, the kinetic stabilisation of the cation $Arene_2Cr^{2+}$ is achieved either with the aid of peripheral substitution in a dibenzenechromium molecule or as a result of a decrease in the experimental temperature. Thus, in the oxidation of bis(hexamethylbenzene)chromium in THF[59] and dimethoxyethane[51] at 20 °C and a reduced temperature, it was possible to observe two pairs of reversible peaks corresponding to two one-electron transitions. It was established by low-temperature cyclic voltammetry at a platinum electrode that dibenzenechromium and bis(biphenyl)chromium are also oxidised reversibly in dry THF to doubly charged cations, which are stable in terms of the time scale of the voltamperometric measurements below −80° and −60 °C respectively.[48,95] The anodic oxidation of the cation ({η^{12}-[2.2]paracyclophane}chromium)$^+$ **21** is reversible even at room temperature.[51]

The presence of cathodic peaks due to the electrochemical reduction of the cations $Arene_2Cr^{2+}$ on the cyclic voltammograms constitutes direct proof of the formation of these species during the anodic process. According to Elschenbroich et al.,[51] the lifetime of the doubly charged dibenzenechromium, bis(hexamethylbenzene)chromium, and {η^{12}-[2.2]paracyclophane}chromium cations in dimethoxyethane at −40 °C is several seconds, minutes, and hours respectively.

There are grounds for the assumption that the first stage of the anodic oxidation of the singly charged cations $Arene_2Cr^+$ [reaction (3)] consists as a rule of reversible electron transfer, preceding the chemical reaction with participation of doubly charged species, and determines to a large extent the half-wave potential for the overall irreversible process. We may note that the half-wave potential for the irreversible oxidation of $Arene_2Cr^+$ as well as for the reversible process (2) depends on the nature of the substituent in the arene ligand. Thus, in the presence of two electron-accepting substituents[31] COOR or COR in the dibenzenechromium molecule, the half-wave potential is 1.25 V, while in the presence of two electron-donating groups $N(CH_3)_2$ it amounts to 0.8 V.

During the electrochemical oxidation process, an electron is removed from the HOMO of the complex. In order to solve the problem of the nature of the frontier orbitals in transition metal π-complexes, Vlcek[5] proposed a method based on the comparison of the differences between the half-wave potentials for the reversible oxidation (or reduction) of two structurally similar complexes and the corresponding non-coordinated ligands. The relative contribution of the ligand MO and of the metal AO to the overall MO of the complex was estimated for the dibenzenechromium–bis(biphenyl)chromium system. The highest molecular orbital of the complex, in which electronic changes take place in the course of the electrochemical oxidation process, is a MO localised predominantly on the chromium atom[5,17] (the contribution of the ligand MO does not exceed 15%). Similar conclusions were reached in the study of diarene chromium complexes by quantum-chemical[82–85] and photo-electron spectroscopic (PES)[86,87] methods and also by the EPR of paramagnetic cationic complexes.[88]

The universality and reversibility of the one-electron oxidation of neutral diarenechromium complexes to the cationic form makes this reaction exceptionally convenient for the solution of problems associated with the transmission of the electronic effect of substituents in the dibenzenechromium molecule to the reaction centre (the chromium atom). The reversibility of the process rules out the influence on $E_{1/2}^{+/0}$ of heterogeneous factors associated with the specific features of the electrochemical process — the structure of the electrical double layer, adsorption, etc. For this reason, the value of $E_{1/2}$, which is close to the thermodynamic standard potential E_0, reflects objectively the influence of substituents on the reactivity of the complexes in redox reactions and can serve as its measure.

Table 3. Parameters of the correlation between $E_{1/2}^{+/0}$ and the substituent constants.[61,62]

Substituent constant	No. of points	ρ_π/V	$-b_1$/V	$-\rho$	r	S_{ρ_π}	S_{b_1}
σ_m^0	19	0.513	0.749	8.9	0.992	0.018	0.012
σ_m^+	20	0.520	0.760	9.0	0.990	0.017	0.011
σ_m	25	0.541	0.748	9.3	0.986	0.019	0.012
σ_p^0	17	0.396	0.635	6.8	0.964	0.028	0.019
σ_p	25	0.350	0.602	6.0	0.920	0.031	0.021
σ_I	23	0.456	0.717	7.9	0.814	0.071	0.047
σ_R	21	0.341	0.463	5.9	0.570	0.113	0.042

Note. b_1 and ρ_π are the parameters of the correlation equation; $\rho = \rho_\pi/0.058$; S_{ρ_π} and S_{b_1} are the standard deviations; r is the correlation coefficient; the constants σ were taken from Gordon and Ford[93] and Kochi and Hammond.[94]

In order to estimate quantitatively the electronic influence of substituents in the electrochemical oxidation of diarenechromium complexes, the correlations between $E_{1/2}^{+/0}$ and different σ constants of the substituents were analysed systematically in a number of studies[29,61,62] (Table 3). According to the Hammett–Zuman equation,[89] we have

$$E_{1/2} = b_1 + \rho_\pi \sum \sigma , \qquad (4)$$

where ρ_π is the polarographic reaction constant, b_1 the half-wave potential for the oxidation of dibenzenechromium, and $\Sigma\sigma$ the sum of the substituent constants. When the σ constants corresponding to only the resonance (σ_R) or the inductive (σ_I) mechanisms of the transmission of the influence of substituents are used, a linear relation is not obtained. The best correlation is observed between $E_{1/2}^{+/0}$ and the σ constants to which the main contribution comes from the inductive component: σ_m, σ_m^+, and σ_m^0.

The reversible oxidation of diarenechromium complexes is characterised by high absolute values of ρ, which indicates a high sensitivity of the dibenzenechromium system to the electronic influence of the substituents. High values of ρ are also observed in the series of oxidation–reduction reactions of ferrocene.[90] They are in general characteristic of reactions involving ions.[91] Compared with ferrocene, dibenzenechromium is a less conducting system. This can be inferred from the half-wave potential shift $\Delta E_{1/2}$ after the introduction of the same substituent (for example, CF_3) into the dibenzenechromium and ferrocene molecules. It amounts to 0.26 V in the first case[32,62] and 0.32 V in the second.[92]

The excellent correlation between $E_{1/2}^{+/0}$ and the σ constants of the *meta*-substituents led to the conclusion that the electronic influence of the substituents in the arene ligand on the reaction centre (the chromium atom) is transmitted predominantly via an inductive mechanism; the conjugation in the arene ligand exists only to the extent that this effect is reflected in the constants of the *meta*-substituent.[29,61,62]

The results of other studies carried out with a significantly smaller number of objects are on the whole similar. For example, a linear correlation between $E_{1/2}^{+/0}$ and the σ_m constants has been observed:[28]

$$E_{1/2}^{+/0} = -0.78 + 0.32 \sum \sigma_m . \qquad (5)$$

Two correlation equations have been obtained by Treichel et al.:[32]

$$E_{1/2}^{+/0} = -0.801 + 0.637\sigma_m , \quad r = 0.986 ; \qquad (6)$$

$$E_{1/2}^{+/0} = -0.530 + 0.413\sigma_p , \quad r = 0.976 . \qquad (7)$$

The similarity of the correlation coefficients precluded an ambiguous choice between these equations. It is noteworthy that the experimental data obtained in the above study[32] by cyclic

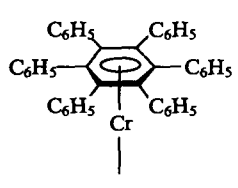
voltammetry are not quite correct. The potentials of the anodic and cathodic peaks are strongly distorted by the ohmic potential drops in solution, indicated by the difference between the potentials of the anodic and cathodic peaks, which exceeds the theoretical value (0.059 V) by a factor of 1.5–5. The deviation of the value of $E_{1/2}^{+/0}$ for dibenzenechromium from the correlation (7) is also striking: the experimental value is $E_{1/2}^{+/0} = -0.716$ V, while the value obtained from Eqn. (7) is $E_{1/2}^{+/0} = -0.530$ V.

The conclusion that the transmission of the electronic influence of substituents to the chromium atom is inductive was also reached in a study[53] where a correlation was observed between $E_{1/2}^{+/0}$ and the Taft substituent constants for six diarenechromium complexes.

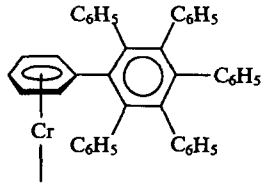
The results of the electrochemical study of the electronic effects in the diarenechromium π-complexes agree with data obtained by other physical methods. A correlation between the first ionisation potentials in the gas phase (IP_1) and the constants σ_m^0 has been established by photoelectron spectroscopy.[87] A correlation has been found between the chemical shift of fluorine and the constants σ_m^+ and σ_m^n (r = 0.958 and 0.952 respectively) with the aid of ^{19}F NMR for a series of heteroannularly disubstituted dibenzenechromium derivatives $(XC_6H_5)Cr(C_6H_5F)$.[96] Hence it follows that the electronic effects of the substituents at one of the arene ligands are exerted across the chromium atom on the indicator fluorine atom in the other ligand also predominantly via an inductive mechanism.

The correlation Eqn. (4) was used to confirm the structure of bis(iodobenzene)chromium.[97] The experimental value $E_{1/2}^{+/0} = -0.38$ V proved to be close to the value −0.40 V calculated by Eqn. (4).

An analogous approach was used to establish the structure of bis(hexaphenylbenzene)chromium obtained by the cyclotrimerisation of diphenylacetylene in the reaction with atomic chromium.[98] The observed[62] half-wave potential for the oxidation of the complex is −0.32 V, which confirms structure A assuming the additive influence of the phenyl ring on the oxidation potential (Fig. 1). If the alternative structure B is obtained, the half-wave potential for the oxidation of the complex would be close to $E_{1/2}^{+/0}$ for bis(biphenyl)chromium (−0.72 V).



A



B

The half-wave potentials $E_{1/2}^{+/0}$ for dibenzenechromium derivatives in DMSO have been compared[62] with the ionisation potentials IP_1 of the same complexes in the gas phase. A satisfactory correlation, described by the equation

$$E_{1/2}^{+/0} = -4.08(\pm 0.16) + 0.62(\pm 0.03)IP_1\,, \quad r = 0.990, \qquad (8)$$

was observed. The coefficient of IP_1 in the equation differs from unity and reflects the contribution of the solvation effects to the energetics of the oxidation reaction in solution in DMSO. The ionisation potentials of various diarenechromium complexes can be calculated using this equation with a fairly high degree of accuracy, which is important, because the experimental determination of the ionisation potentials is difficult compared with the determination of $E_{1/2}^{+/0}$. The existence of a correlation between $E_{1/2}^{+/0}$ and IP_1 shows that the photoelectron processes in the gas phase and the electrochemical oxidation in solution take place with participation of the same molecular orbitals localised predominantly on the chromium atom.

The parallel variation of the redox potentials of a number of sandwich chromium complexes (including three diarene complexes) and the potentials IP_1 of the same compounds in the gas phase was noted previously.[28]

A linear correlation has been observed[51] between the electrochemical potential $E_{1/2}(C_{12}H_{12}M^{+/0})$ for the dibenzene and cyclopentadienylcycloheptatrienyl complexes of chromium and vanadium and their IP_1 obtained from the photoelectron spectra:

$$IP_1 = 6.20 + 0.99E_{1/2}^{+/0}\,, \quad r = 0.995\,. \qquad (9)$$

The half-wave potentials $E_{1/2}$ vary in parallel with the appearance potentials of the molecular ions obtained from the mass spectra.[99]

It has been shown[100,101] that the standard redox potentials of a series of sandwich complexes of transition metals, including diarenechromium and diarenemolybdenum complexes, are linearly correlated with the gas-phase ionisation potentials of the corresponding metals.

III. Cathodic reduction of diarenechromium(0) complexes

Data on the electrochemical reduction of more than 30 diarenechromium complexes have now been published (Table 4).

The main difference between the cathodic reduction reactions and the processes examined in the previous section consists in the fact that they occur with participation of a molecular orbital the main contribution to which comes from the π orbital of the aromatic ligand. This conclusion is justified by the results of quantum-chemical calculations[85,102–106] carried out in different years for dibenzenechromium and dinaphthalenechromium molecules and has been confirmed by numerous experimental data. In particular, this is indicated by the similarity of the polarisation characteristics of the electrochemical reduction of free arenes and the corresponding diarenechromium complexes, including the similarity of the half-wave potentials $E_{1/2}$ for the electrochemical reduction of arenes ($E_{1/2}^{A}$) and the complexes ($E_{1/2}^{C}$)‡ (Table 5).

The application of Vlcek's methods[5,17–19] makes it possible to estimate the contribution of the lowest unoccupied molecular orbitals (LUMO) of the arene ligands in the complex, the results showing that it is the dominant contribution (~90%). This is also indicated by the parallel variation of $E_{1/2}^{A}$ and $E_{1/2}^{C}$ for symmetrical complexes (Table 5). Thus, depending on the nature and number of the substituents in the benzene ring, $E_{1/2}^{A}$ shifts towards positive values in the sequence $C_6H_5 < CF_3 < (C_6H_5)_3 < CN < COCH_3 < (COOC_2H_5)_2 < CHO < CH{=}CHCOOC_2H_5 < CH{=}CHCOC_6H_5$. The ease of the reduction of $Arene_2Cr$ increases in the same sequence. Only the CHO and $CH{=}CHCOOC_2H_5$ groups are an exception. They change places on passing from the arene to the complex.

The electron affinity is determined by the donor–acceptor properties of the substituents in the arene ring and also, and to an even greater degree, by the extent of the conjugated system. Among the compounds investigated,[50,65,107] benzylideneacetophenone and its complex are reduced more readily than the others, since this arene contains the most extensive conjugation system, although, judging from the value of $E_{1/2}^{+/0}$, the substituent $CH = CHCOC_6H_5$ is a moderately strong electron acceptor. A different picture is observed in the anodic oxidation of zerovalent chromium complexes where the electronic changes are localised not on the ligand π-orbitals but on the atomic orbitals of the metal.[62] In terms of their ability to hinder the oxidation of the complex, the above substituents can be arranged in the following sequence: $C_6H_5 < CH{=}CHCOOC_2H_5 < (C_6H_5)_3 < CH{=}CHCOC_6H_5 < COCH_3 < CHO < CF_3 < (COOC_2H_5)_2 < CN$, i.e. in this case the increase in the electron-accepting capacity of the substituent, characterised by the σ constant of the *meta*-substituents, is decisive.

‡Here and henceforth the superscripts A and C denote quantities referring to the free arenes and the chromium complexes respectively.

Table 4. The half-wave potentials $E_{1/2}$ for the cathodic reduction of diarenechromium(0) complexes.

No.	Compound	$-E^{C}_{1/2}$/V	Solvent	Supporting electrolyte	Method (electrode)	Ref.
1	$(C_6H_5\text{-}\eta^6\text{-}C_6H_5)Cr(C_6H_6)$	3.3[a]	DME	NBu_4ClO_4	MDE	15
2	$(C_6H_5\text{-}\eta^6\text{-}C_6H_5)_2Cr$	2.60	DMSO	NBu_4BF_4	RRDE (Hg/Au)	24, 61
3	$[(C_6H_5)_3\text{-}\eta^6\text{-}C_6H_3]_2Cr$	2.37	DMSO	NBu_4BF_4	RRDE (Hg/Au)	61
4	$(CF_3C_6H_5)_2Cr$	2.46	DMSO	NBu_4BF_4	RRDE (Hg/Au)	24, 61
5	$(HCOC_6H_5)Cr(C_6H_6)$	2.11	DMSO	NBu_4BF_4	RRDE (Hg/Au)	65
6	$(HCOC_6H_5)_2Cr$	1.80	DMSO	NBu_4BF_4	RRDE (Hg/Au)	65
7	$(C_2H_5OCOCH=CH\text{-}\eta^6\text{-}C_6H_5)_2Cr$	1.84	DMSO	NBu_4BF_4	RRDE (Hg/Au)	65
8	$(C_6H_5COCH=CH\text{-}\eta^6\text{-}C_6H_5)_2Cr$	1.42	DMSO	NBu_4BF_4	RRDE (Hg/Au)	50
9	$(CH_3COC_6H_5)_2Cr$	1.98	DMSO	NBu_4BF_4	RRDE (Hg/Au)	65
10	$(C_6H_5CO\text{-}\eta^6\text{-}C_6H_5)Cr(C_6H_6)$	1.91	DMF	NBu_4ClO_4	MDE	16
		1.92	DMF	NBu_4ClO_4	CVA (Pt)	108
11	$(C_6H_5CO\text{-}\eta^6\text{-}C_6H_5)_2Cr$	1.75	DMF	NBu_4ClO_4	CVA (Pt)	108
12	$(4\text{-}CH_3C_6H_4CO\text{-}\eta^6\text{-}C_6H_5)Cr(C_6H_6)$	1.97	DMF	NBu_4ClO_4	CVA (Pt)	108
13	$(4\text{-}CH_3C_6H_4CO\text{-}\eta^6\text{-}C_6H_5)_2Cr$	1.77	DMF	NBu_4ClO_4	CVA (Pt)	108
14	$(4\text{-}FC_6H_4CO\text{-}\eta^6\text{-}C_6H_5)Cr(C_6H_6)$	1.93	DMF	NBu_4ClO_4	CVA (Pt)	108
15	$(4\text{-}FC_6H_4CO\text{-}\eta^6\text{-}C_6H_5)_2Cr$	1.73	DMF	NBu_4ClO_4	CVA (Pt)	108
16	$(4\text{-}CF_3C_6H_4CO\text{-}\eta^6\text{-}C_6H_5)Cr(C_6H_6)$	1.65	DMF	NBu_4ClO_4	CVA (Pt)	108
17	$(4\text{-}CF_3C_6H_4CO\text{-}\eta^6\text{-}C_6H_5)_2Cr$	1.51	DMF	NBu_4ClO_4	CVA (Pt)	108
18	$(4\text{-}NC_5H_4CO\text{-}\eta^6\text{-}C_6H_5)Cr(C_6H_6)$	1.61	DMF	NBu_4ClO_4	CVA (Pt)	108
19	$(4\text{-}NC_5H_4CO\text{-}\eta^6\text{-}C_6H_5)_2Cr$	1.45	DMF	NBu_4ClO_4	CVA (Pt)	108
20	$[1,2\text{-}(C_2H_5OCO)_2C_6H_4]_2Cr$	1.87	DMSO	NBu_4BF_4	RRDE (Hg/Au)	65
21	$(NCC_6H_5)Cr(C_6H_6)$	2.52	DMSO	NBu_4BF_4	RRDE (Hg/Au)	109
22	$(NCC_6H_5)Cr(C_6H_5CH_3)$	2.54	DMSO	NBu_5BF_4	RRDE (Hg/Au)	109
23	$(NCC_6H_5)Cr(C_6H_5OCH_3)$	2.52	DMSO	NBu_4BF_4	RRDE (Hg/Au)	109
24	$(NCC_6H_5)Cr(C_6H_5F)$	2.39	DMSO	NBu_4BF_4	RRDE (Hg/Au)	109
25	$(NCC_6H_5)Cr(C_6H_5Cl)$	2.28	DMSO	NBu_4BF_4	RRDE (Hg/Au)	109
26	$(NCC_6H_5)Cr(C_6H_5CF_3)$	2.26	DMSO	NBu_4BF_4	RRDE (Hg/Au)	109
27	$(NCC_6H_5)Cr(C_6H_5COCH_3)$	1.97	DMSO	NBu_4BF_4	RRDE (Hg/Au)	109
28	$(NCC_6H_5)_2Cr$	2.18	DMSO	NBu_4BF_4	RRDE (Hg/Au)	65
29	$[(C_6H_5)_3Si\text{-}\eta^6\text{-}C_6H_5]_2Cr$	2.813	DME (−50 °C)	NEt_4ClO_4	CVA (CG)	66
30	$(\eta^6\text{-}C_{10}H_8)_2Cr$	3.126[b]	THF	NBu_4PF_6	CVA (Pt)	49
		1.84[b]	EDA	NBu_4PF_6	CVA (Pt)	49
31	$(C_6H_6)Cr(\mu\text{-}\eta^6,\eta^6\text{-}C_{10}H_8)Cr(C_6H_6)$	1.10[b]	THF	NBu_4PF_6	CVA (Pt)	49
32	$[(\mu\text{-}\eta^6,\eta^6\text{-}C_{10}H_8)Cr]_n$	2.04[b]	EDA	NBu_4PF_6	CVA (Pt)	49
33	$(C_{14}H_{10})_2Cr$	2.235	DMF	NBu_4ClO_4	CVA (CG)	69
34	$(C_5H_5As)_2Cr$	1.36	DME	NBu_4ClO_4	CVA (CG)	54
35	$(CH_3BC_5H_5)_2Cr$	1.26	CH_2Cl_2	NBu_4PF_6	CVA (Pt)	70
36	$(C_6H_5\text{-}\eta^6\text{-}BC_5H_5)_2Cr$	1.01	CH_2Cl_2	NBu_4PF_6	CVA (Pt)	70

Reference electrodes: [a] 1×10^{-3} M $Ag/AgClO_4$; [b] $Ag/AgNO_3$.

The agreement between the reaction constants ρ in the Hammett equation for the electrochemical reduction of the noncoordinated ketones $4\text{-}XC_6H_4COC_6H_5$ and their asymmetric complexes $(4\text{-}XC_6H_4COC_6H_5)Cr(C_6H_6)$ and the symmetrical complexes $(4\text{-}XC_6H_4COC_6H_5)_2Cr$ [108] as well as the small difference between the rate constants for the dimerisation of the radical-anions of benzylideneacetophenone and bis(benzylidene-acetophenone)-chromium can serve as additional arguments in support of the conclusion that the electronic changes in the course of the electrochemical reduction of the complexes are localised on the π-orbitals of the ligand.[50]

The structure of the radical-anions formed on electrochemical reduction or by chemical generation also confirms this conclusion. According to EPR data, the unpaired electron in the radical-anions of ketones,[108] trimethylsilyl-substituted derivatives of dibenzenechromium[110] and dibenzonitrilechromium,[111] as well as unsubstituted dibenzenechromium[112] and the isoelectronic cyclopentadienyl(cycloheptatrienyl)chromium[106] is localised on the molecular orbital the main contribution to which comes from the ligand π-orbital.

The involvement in the cathodic reduction of the zerovalent chromium π-complexes of the LUMO which has predominantly the character of the ligand π-orbital makes it possible to estimate the changes in the reactivity of the arenes due to the formation of complexes with the chromium atom by comparing the characteristic features of the electrochemical reduction of the chromium π-complexes and the corresponding arenes containing identical electrochemically active groups. This approach is characteristic of the majority of studies (in general not very numerous) of the cathodic reactions of diarenechromium(0) complexes.

Another feature of the electrochemical reduction reactions of diarenechromium complexes distinguishing them from the reversible reaction (2) is the greater complexity of the cathodic processes. The overall processes are as a rule irreversible, consist of many stages, and are characterised by the involvement of several electrons and protons, possible retardation of the electron transfer stages, and the presence of stages involving chemical reactions of the intermediates.

The choice of the potentials $E^{C}_{1/2}$ and $E^{A}_{1/2}$ as the reactivity criteria makes it necessary to justify the comparability of these quantities for complexes of different structure and also for pairs of complex–arene compounds with isotypical electroactive groups. This presupposes in its turn that the preliminary kinetic study of the mechanisms of the electrochemical reduction of the test compounds is carried out and the potential determining stage of the overall process is discovered under identical conditions. This problem, which is of independent interest also for electrochemical

Table 5. Comparative characteristics of the electrochemical reduction of arenes and diarenechromium complexes.[24, 61, 65, 107]

System	Compound	$-E^{A}_{1/2}$/V $-E^{C}_{1/2}$/V	$-\Delta E^{CA}_{1/2}$/V	$-\lg\frac{K^C}{K^A}$	$-E^{+/0}_{1/2}$/V
I	$C_6H_5C_6H_5$	2.50	0.10	1.7	0.66
	$(C_6H_5\text{-}\eta^6\text{-}C_6H_5)_2Cr$	2.60			
II	$C_2H_5OCOCH=CHC_6H_5$	1.76	0.08	1.4	0.55
	$(C_2H_5OCOCH=CHC_6H_5)_2Cr$	1.84			
III	$(C_6H_5)_3C_6H_3$	2.29	0.08	1.4	0.53
	$[(C_6H_5)_3\text{-}\eta^6\text{-}C_6H_3]_2Cr$	2.37			
IV	$C_6H_5COCH=CHC_6H_5$	1.37	0.05	0.9	0.50
	$(C_6H_5COCH=CH\text{-}\eta^6\text{-}C_6H_5)_2Cr$	1.42			
V	$CH_3COC_6H_5$	1.94	0.04	0.7	0.38
	$(CH_3COC_6H_5)_2Cr$	1.98			
VI	$HCOC_6H_5$	1.80	0.31	5.3	0.51
	$(HCOC_6H_5)Cr(C_6H_6)$	2.11	0	0	0.27
	$(HCOC_6H_5)_2Cr$	1.80			
VII	$CF_3C_6H_5$	2.46	0	0	0.24
	$(CF_3C_6H_5)_2Cr$	2.46			
VIII	$1,2\text{-}(C_2H_5OCO)_2C_6H_4$	1.88	−0.01	−0.2	0.20
	$[1,2\text{-}(C_2H_5OCO)_2C_6H_4]_2Cr$	1.87			
IX	NCC_6H_5	2.21	0.31	5.3	0.46
	$(NCC_6H_5)Cr(C_6H_6)$	2.52	−0.03	−0.5	0.14
	$(NCC_6H_5)_2Cr$	2.18			

kinetics, has been examined in greatest detail in several studies[50, 61, 65, 107, 109] of the mechanisms of the electrochemical reduction of 17 diarenechromium complexes with different substituents in DMSO.

The complexity of the kinetics of the multistage electrode processes necessitates the use of methods which yield, together with the usual polarisation characteristics, information about the appearance during the reaction of unstable intermediates (including free-radical or radical-ion intermediates), their nature, and properties.

In the study of the electrochemical reduction of chromium π-complexes, such methods were cyclic voltammetry at normal and reduced (cryoelectrochemical measurements) temperatures, EPR with electrochemical or chemical generation of paramagnetic species, and the method of a rotating ring-disc electrode.

The method of a rotation ring-disc electrode (RRDE), proposed by Frumkin and Nekrasov[113, 114] and representing a definite alternative to cyclic voltammetry, is based on the use of a single mechanical system consisting of two concentric electrodes—a disc and a ring—located in a single plane and separated by a thin insulating layer. The electrochemical reaction investigated is carried out at the disc electrode and the resulting unstable intermediate or stable final product of the reaction passes to the layer of solution near the electrode and is supplied by the convective stream of liquid to the ring, with the aid of which it can be detected in terms of its oxidation or reduction current. The comprehensive and in certain respects also unique possibilities of the method have led to its wide scale employment in electro-chemical kinetics, including studies on the electrochemistry of organic compounds.[115–118]

The existence of the reaction involving electrochemical oxidation to the cation, which is universal for the diarenechromium(0) complexes [reaction (2)], makes these compounds convenient objects for the study of their cathodic behaviour by the RRDE method. This reaction makes it possible to detect at the ring electrode all the intermediates of the cathodic process. The yield of the corresponding products can be inferred from the anodic limiting current at the ring and the dependence of the yield of the products on the rate of rotation of the electrode yields information about their stability in further reactions. The values of $E^{C}_{1/2}$ for the wave observed at the ring help to identify the species detected.

The first complex whose cathodic reduction was achieved proved to be benzene(biphenyl)chromium.[15] At the present time, the cathodic reduction reactions have been investigated for a wide range of diarenechromium complexes containing the COR, CN, C=C, C_6H_5, and other groups as substituents (Table 4).

Like benzene, unsubstituted dibenzenechromium has an extremely low electron affinity. The report of the direct electrochemical reduction of benzene to the radical-anion did not appear[119] until 1988 ($E_{1/2}$ = −3.38 V). Despite repeated attempts,[4, 56, 101] dibenzenechromium has not yet been reduced at the electrode, although it has been possible to obtain[112] its radical-anions chemically by treatment with potassium in dimethoxyethane in the presence of a crown-ether at −70 °C.

Compared with dibenzenechromium, its asymmetric analogue cyclopentadienyl(cycloheptatrienyl)chromium has a higher electron affinity:[51] it is reduced at carbon glass, the potential of the cathodic peak being E_{pc} = −2.90 V (DME, −35 °C). Ferrocene, which is isoelectronic with dibenzenechromium, is also reduced[120] at the cathode ($E_{1/2}$ = −2.93 V, DMF, −30 °C).

The introduction into the benzene or dibenzenechromium molecule of groups reducing the electron density in the benzene ring and increasing the extent of the conjugation chain ensures the electrochemical reduction of these compounds in the range of electrochemical potentials accessible to measurements.

The electrochemical reduction reactions of the majority of complexes investigated are usually characterised, like those of the non-coordinated arenes, by the presence of several waves on the polarisation curves corresponding to different macroscopic reaction stages. In the literature, attention is concentrated on the first cathodic waves, while the nature of the subsequent waves has been studied in less detail.

In the analysis of the characteristics of the cathodic process, the test compounds can be usefully divided into several groups. Each of these groups includes a series of π-complexes–corresponding arene systems. The formal criteria of the assignment of substances to a particular group are the number of added electrons n in the range of potentials of the first cathodic wave and the presence or absence of similarity in other process characteristics in this range of potentials in the electrochemical reduction of the π-complex and the arene in aprotic media.

Table 6. Parameters of the electrochemical reduction and oxidation of diarenechromium complexes and of the reduction of the corresponding arenes at an amalgamated gold rotating disc electrode in DMSO.[50,61,65]

Compound	Reduction									Oxidation		
	A wave			*B* wave			*C* wave			*Z* wave		
	$-E_{1/2}$/V	*n*	*b*/V	$-E_{1/2}$/V	*n*	*b*/V	$-E_{1/2}$/V	*n*	*b*/V	$-E^{+/0}_{1/2}$/V	*n*	*b*/V
$C_6H_5COCH=CHC_6H_5$	1.41	1	0.060				2.00	1	0.10			
$(C_6H_5COCH=CH\text{-}\eta^6\text{-}C_6H_5)_2Cr$	1.46	1	0.060	1.62	1	0.090	2.10	2	0.10	0.535	1	0.060
$C_2H_5OCOCH=CHC_6H_5$[a]	1.80	1	0.060				2.28	1	0.10			
$(C_2H_5OCOCH=CHC_6H_5)_2Cr$	1.88	1	0.070	2.09	1	0.100	2.82	1	0.10	0.59	1	0.060
$HCOC_6H_5$	1.84	1	0.060				2.30	1	0.08			
$(HCOC_6H_5)Cr(C_6H_6)$	2.15	1	0.060				2.56	1	0.08	0.55	1	0.058
$(HCOC_6H_5)_2Cr$	1.84	1	0.060	2.24	1	0.080	2.69	1	0.10	0.31	1	0.058

[a] Data of Nekrasov and Korotkov.[121]

The mechanisms of the reduction of the π-complexes combined in one group are identical or similar. Different mechanisms of the cathodic processes correspond to different groups of complexes, which constitutes in essence but not formally the basis of the adopted classification. The mechanism of the electrochemical reduction of arenes is in some cases fully identical with that for the π-complexes of the given group (carbonyl compounds, activated olefins), whilst in others, together with the general similarity, there is also an appreciable difference between them (nitriles).

The first group includes aldehydes, ketones, esters, and their vinylogues of the benzene and dibenzenechromium series. The similarity of the electrochemical behaviour under the conditions of the cathodic reaction is characteristic of compounds of this group.[16,50,65,108] In particular, it is manifested by the presence on the polarisation curves of one-electron reduction waves for both the free arenes and their chromium complexes and also by the similarity of the polarisation characteristics of each component of the Arene–$Arene_2Cr$ system (Table 6). In many instances, it has been possible with the aid of the RRDE method,[50,65] cyclic voltammetry, and EPR[108] to observe directly the formation of one-electron transfer products—radical-anions capable of dimerising.

Such similarity was first established[16] on the basis of classical polarographic data, potentiodynamic measurements, coulometry, and preparative electrolysis at a controlled potential and subsequent analysis of the reaction products when the electrochemical reduction reactions of aromatic carbonyl compounds and benzene(benzophenone)chromium were compared in DMF and aqueous alcoholic solutions of different acidity. The polarogram for the reduction of benzene(benzophenone)-chromium in DMF shows two one electron-waves with the potentials $E_{1/2}$ = −1.91 and −2.01 V. The first cathodic wave corresponds to the formation of the radical-anion, while the product of the two electron transfer is a dianion, which is unstable and is rapidly protonated to the alkoxide ion. The latter decomposes slowly in its turn in the bulk of the solution with rupture of the C–C bond and the formation of dibenzene-chromium. It follows from the comparison of the half-wave potentials for the reduction of benzene(benzophenone)chromium ($E_{1/2}$ = −1.91 V) and of the free benzophenone ($E_{1/2}$ = −1.72 V) that the coordination of the benzophenone molecule to the π-C_6H_6Cr fragment hinders the reduction reaction. Comparison of the values of $E_{1/2}$ for a series of ketones C_6H_5COX, where X = CH_3, $C_6H_6CrC_6H_5$, H, or C_6H_5, led the authors to the conclusion that dibenzenechromium resembles the methyl group as a substituent. The Taft substituent constant σ_T for the $C_6H_6CrC_6H_5$ group, found by interpolation, proved to be 0.19.

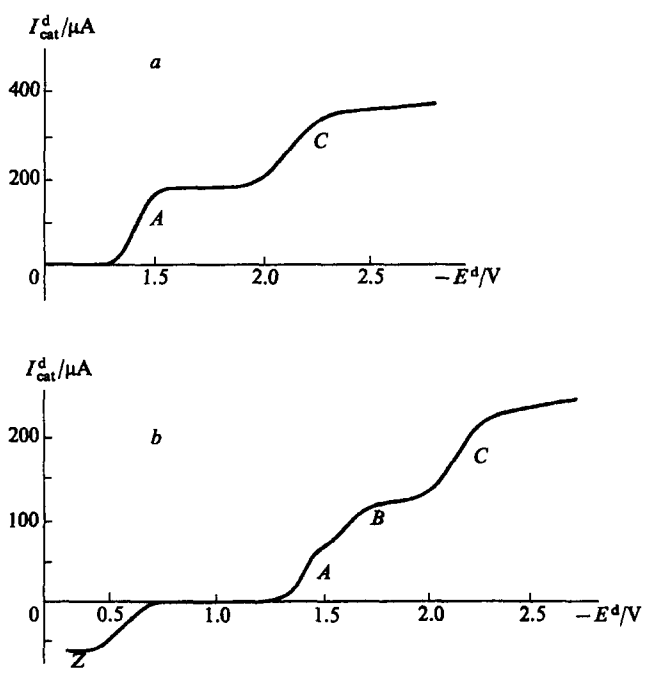


Figure 2. Polarisation curves at the rotating disc electrode in solutions of benzylideneacetophenone ($c = 2\times10^{-3}$ M) (*a*) and bis(benzylidene-acetophenone)chromium ($c = 9.4\times10^{-4}$ M) (*b*) in DMSO in the presence of 0.1 M $N(C_4H_9)_4BF_4$ (ω = 528 s^{-1}).

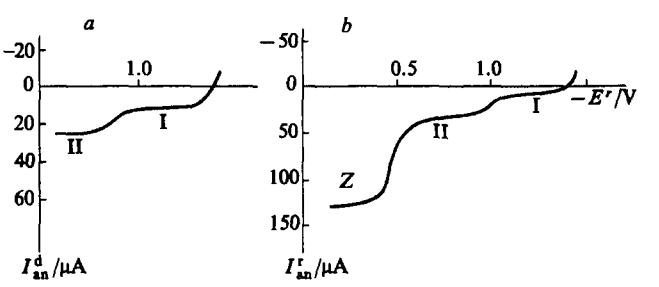


Figure 3. Polarisation curves for the anodic oxidation at the ring electrode of the products of the electrochemical reduction at the disc electrode of benzylideneacetophenone ($c = 4\times10^{-4}$ M) (*a*) and bis(benzylidene-acetophenone)chromium ($c = 2\times10^{-3}$ M) (*b*); E^d = −1.51 V, ω = 214 s^{-1}.

The polarisation characteristics ($E_{1/2}$, the slope b, the number of electrons n participating in the reaction) of all the electrochemical reduction waves (A, B, C) of a series of chromium π-complexes and the non-coordinated arenes, belonging to the first group of compounds, obtained with the aid of an amalgamated gold rotating disc electrode in solutions in DMSO with tributylammonium tetrafluoroborate ($TBABF_4$) as the supporting electrolyte, are presented in Table 6, which also contains analogous data on the Z waves for the electrochemical oxidation of the same complexes.

The kinetics and mechanisms of the electrochemical reduction of benzylideneacetophenone and bis(benzylideneacetophenone)-chromium have been investigated in greatest detail.[50] The polarisation curves for these compounds are presented in Fig. 2, while the corresponding quantitative characteristics are in Table 6. The A waves for the electrochemical reduction of both substances correspond to the reversible addition of one electron and the formation of radical-anions, detected by the RRDE method (I waves in Fig. 3):

$$C_6H_5CH=CHCOC_6H_5 \underset{-\bar{e}}{\overset{+\bar{e}}{\rightleftarrows}} C_6H_5CH=CHCOC_6H_5]^{\cdot-},$$

$$(C_6H_5CH=CHCOC_6H_5)_2Cr \underset{-\bar{e}}{\overset{+\bar{e}}{\rightleftarrows}}$$

$$\leftrightarrows (C_6H_5CH=CHCOC_6H_5)_2Cr]^{\cdot-}.$$

The cathodic B wave for the reduction of the complex can be related to the addition of an electron to the second ligand of the complex radial-anion. This wave is absent from the polarisation curve for the free arene. The C waves correspond to further reduction reactions of the radical species, and the Z waves (Figs. 2*b* and 3*b*) correspond to the electrochemical oxidation of the initial complex. The radical-anions derived from both compounds are unstable and enter into a dimerisation reaction, whose products are also detected at the ring electrode (II waves in Fig. 3).

Thus in the region of the potentials of the A waves, a two-stage reaction takes place: the reversible one-electron transfer stage is followed by the bimolecular chemical dimerisation reaction, which exerts a definite effect on the parameters of the electrode process (EC mechanism), as a consequence of which the A waves acquire a quasi-reversible character.[122]

The potentials $E^A_{1/2}$ and $E^C_{1/2}$, measured by the rotating electrode method under the conditions of the operation of the above electrochemical reduction mechanism, are[123,124] functions of the angular rate of rotation of the electrode ω, the depolariser concentration c, and the dimerisation constant of the radical species k_d:

$$E_{1/2} = E_0 + \frac{2.3RT}{3F}\lg 0.864\left(\frac{\nu}{D}\right)^{1/3} + \frac{2.3RT}{3F}\lg\frac{k_d c}{\omega}, \qquad (10)$$

where F is the Faraday constant, D the diffusion coefficient of the reactant, and ν the kinematic viscosity of the solution.

The experimental[50] dependences of $E^A_{1/2}$ and $E^C_{1/2}$ on $\lg\omega$ at different concentrations c are presented in Fig. 4. They consist of two linear sections—inclined and horizontal. The first reflects the influence of the dimerisation reaction on the half-wave potential. The rates obtained experimentally, $\Delta E^A_{1/2}/\Delta\lg\omega = -0.023$ V, $\Delta E^A_{1/2}/\Delta\lg c = -0.021$ V (for benzylideneacetophenone) and $\Delta E^C_{1/2}/\Delta\lg\omega = -0.021$ V [for bis(benzylideneacetophenone)-chromium] proved to be similar to the values predicted by theory for radical dimerisation ($2.3RT/3F = \pm 0.019$ V). For low concentrations c and high values of ω, the potentials $E^A_{1/2}$ and $E^C_{1/2}$ are independent of further increase in the rate of rotation of the electrode (the horizontal section of the curves in Fig. 4), since the rapid removal of the radical-anions from the layer near the electrode prevents the influence of their dimerisation on the electrode process, which becomes fully reversible under the given conditions. The radical-anions are then detected at the ring electrode with 100% yield, while the II oxidation waves for the dimers are absent. The rate constants for the dimerisation of the benzylideneacetophenone and bis(benzylideneaceto-phenone)-chromium radical-anions were calculated by Eqn. (10) from the experimental data obtained by the rotating disc electrode method:

$$k^A_d = (2.1 \pm 0.2) \times 10^4 \text{ litre mol}^{-1}\text{ s}^{-1},$$

$$k^C_d = (1.5 \pm 0.7) \times 10^4 \text{ litre mol}^{-1}\text{ s}^{-1}.$$

Similar values of k^A_d and k^C_d were also determined by an independent procedure using the RRDE method and a semiempirical calibration curve[125] relating the yield of the radical-anions at the ring electrode to the dimerisation rate constant:

$$k^A_d = (1.5 \pm 0.3) \times 10^4 \text{litre mol}^{-1}\text{ s}^{-1},$$

$$k^C_d = (1.2 \pm 0.5) \times 10^4 \text{ litre mol}^{-1}\text{ s}^{-1}.$$

The small difference between the rate constants for the dimerisation of the radical-anions of the π-complex and the free arene is striking.

A similar EC mechanism of the electrochemical reduction reactions is characteristic also of other classes of substances of the benzene and dibenzenechromium series forming part of the first group of compounds, including those listed in Table 6.

The mechanism is modified somewhat and simplified for benzophenone derivatives. Because of the high stability of the radical-anion of benzophenone itself and apparently also the radical-anions of the π-complexes containing benzophenone and its substituted derivatives as ligands,[108] the chemical stage of the reaction which follows electron transfer, does not occur in the layer near the electrode even when the solution is gently stirred.[126] The only potential-determining stage of the process is the reversible addition of an electron, a situation similar to that observed for the electrochemical reduction of benzylideneacetophenone and its chromium complex at comparatively high rates of rotation of the disc electrode.

The second group of compounds comprises mainly aromatic and complex nitriles (Table 7). An important feature of these substances is that nitriles of the dibenzenechromium series behave

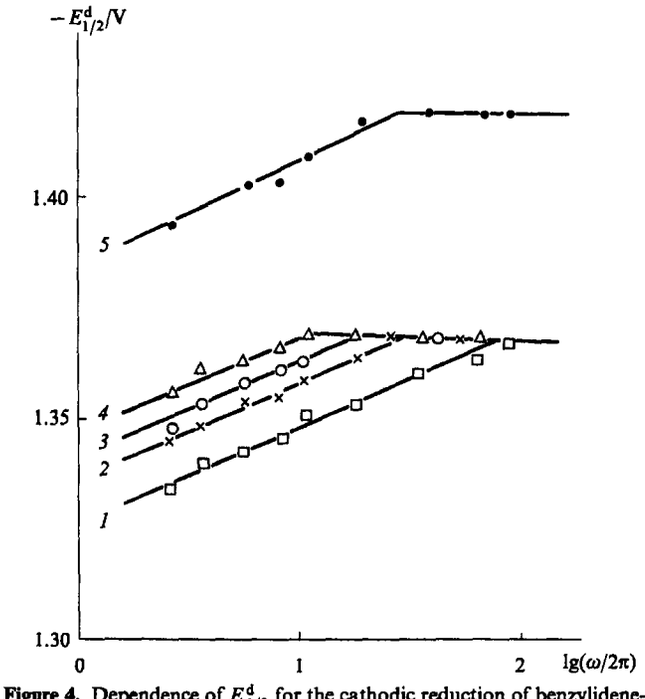


Figure 4. Dependence of $E^d_{1/2}$ for the cathodic reduction of benzylideneacetophenone (lines *1*–*4*) and bis(benzylideneacetophenone)chromium (line *5*) at a rotating disc electrode in solutions in DMSO on the logarithm of the angular rate of rotation of the disc electrode at different molar concentrations of the reactants: (*1*) 2×10^{-3}; (*2*) 8×10^{-4}; (*3*) 4×10^{-4}; (*4*) 2×10^{-4}; (*5*) 5.4×10^{-4}.

Table 7. Characteristics of the electrochemical reduction reactions of nitrile derivatives of benzene and dibenzenechromium.[109]

N	Compound	Cathodic wave *A*			Cathodic wave *B*		
		$-E_{1/2}$, V	*n*	Reaction products detected at ring electrode	$-E_{1/2}$, V	*n*	Reaction products detected at ring electrode
1	C_6H_5CN	2.25	1	$[C_6H_5CN]^{\cdot-}$			
2	$1,4\text{-}CH_3C_6H_4CN$	2.40	1	$[1,4\text{-}CH_3C_6H_4CN]^{\cdot-}$			
3	$1,3\text{-}C_6H_4(CN)_2$	1.74	1	$[1,3\text{-}C_6H_4(CN)_2]_2^{2-}$			
4	$1,2\text{-}C_6H_4(CN)_2$	1.62	1	$[1,2\text{-}C_6H_4(CN)_2]^{\cdot-}$	2.55	2	$[C_6H_5CN]^{\cdot-}$, CN^-
5	$1,4\text{-}C_6H_4(CN)_2$	1.62	1	$[1,4\text{-}C_6H_4(CN)_2]^{\cdot-}$	2.40	2	$[C_6H_5CN]^{\cdot-}$, CN^-
6	$1,2,4,5\text{-}C_6H_2(CN)_4$	0.66	1	$[1,2,4,5\text{-}C_6H_2(CN)_4]^{\cdot-}$	1.61	1	$[1,2,4,5\text{-}C_6H_2(CN)_4]^{2-}$
7	$(NCC_6H_5)Cr(C_6H_5CH_3)$	2.58	2	CN^-, $(C_6H_6)Cr(C_6H_5CH_3)$			
8	$(NCC_6H_5)Cr(C_6H_6)$	2.56	2	CN^-, $(C_6H_6)_2Cr$			
9	$(NCC_6H_5)Cr(C_6H_5OCH_3)$	2.56	2	CN^-, $(C_6H_6)Cr(C_6H_5OCH_3)$			
10	$(NCC_6H_5)_2Cr$	2.22	2	CN^-, $(C_6H_6)Cr(C_6H_5CN)$	2.56	2	CN^-, $(C_6H_6)_2Cr$
11	$(NCC_6H_5)Cr(C_6H_5F)$	2.43	2	$(NCC_6H_5)Cr(C_6H_6)$	2.56	2	CN^-, $(C_6H_6)_2Cr$
12	$(NCC_6H_5)Cr(C_6H_5Cl)$	2.32	2	$(NCC_6H_5)Cr(C_6H_6)$, Cl^-	2.56	2	CN^-, $(C_6H_6)_2Cr$
13	$(NCC_6H_5)Cr(C_6H_5CF_3)$	2.30	6	$(NCC_6H_5)Cr(C_6H_5CF_3)$, $(C_6H_6)Cr(C_6H_5CF_3)$, CN^-			
14	$(NCC_6H_5)Cr(C_6H_5COCH_3)$	2.01	1	$[(NCC_6H_5)Cr(C_6H_5COCH_3)]^{\cdot-}$	2.30	0.4	CN^-, unidentified complexes

differently from the nitriles of the aromatic series under the conditions of cathodic reduction in aprotic media (DMSO, THF).[109] The main difference consists in the absence of reversible one-electron waves from the polarisation curves for the electrochemical reduction of complexes **7–13**§ and their appearance in the reduction of the non-coordinated compounds **1–6**. Instead of the one-electron waves, the polarisation curves for the complex nitriles show one (mononitrile) or two (dinitrile) irreversible two-electron waves. A characteristic feature of the π-complexes, assigned to the second group of compounds, is the occurrence of a rapid chemical reaction with participation of the intermediate products of the one-electron transfer, leading to the elimination of the cyano-group or halogen atoms if the latter form part of the molecule.

In view of the uncertainty in the pathways leading to the reduction of nitriles of different structure, direct comparison of the characteristic features of the reduction of benzonitrile and its π-complexes, necessary for the quantitative comparison of the reactivities, proves insufficient to obtain objective information about the similarities and differences between the mechanisms of the electrochemical reduction of the two types of compounds. The approach based on a comparison of the electrochemical properties of complexes of the type $(NCC_6H_5)Cr(C_6H_5X)$ in a series of cyanobenzenes is more effective. For this reason, Table 7 includes, together with the characteristics of the electrochemical reduction of the π-complexes and free benzonitrile, also the analogous data for the isomers of dicyanobenzene and tetra-cyanobenzene.

In the range of potentials of the *A* wave for the electrochemical reduction of benzonitriles, stable radical-anions can be detected in quantitative yields by the RRDE method. An exception is *m*-dicyanobenzene, whose radical-anions are unstable. The reactivity of the radical-anions depends on the molecular structure. The radical-anions derived from mononitriles and 1,3-dicyanobenzene are not reduced at the electrode in the range of potentials accessible to measurements. A shift of the potential towards negative values by almost 1 V compared with $E^A_{1/2}$ for the formation of the radical-anions (*B* waves) is necessary for the electrochemical reduction of the radical-anions of the *ortho*- and *para*-isomers of dicyanobenzene and 1,2,4,5-tetracyanobenzene.

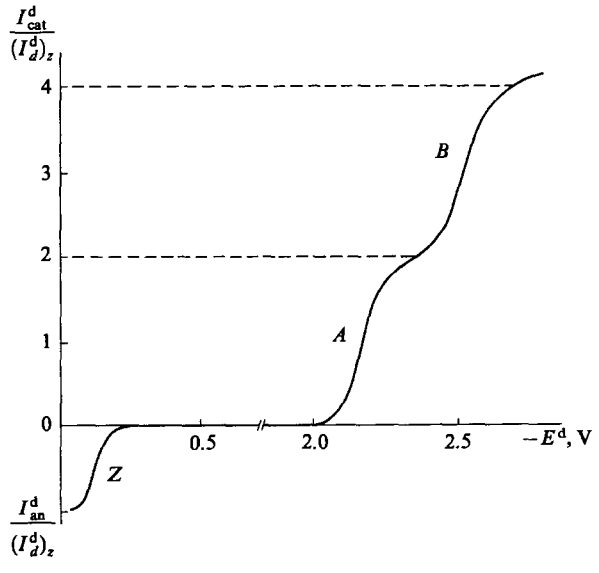


Figure 5. Normalised polarisation curve for the anodic oxidation and cathodic reduction of dibenzonitrilechromium at a rotating disc electrode in DMSO.

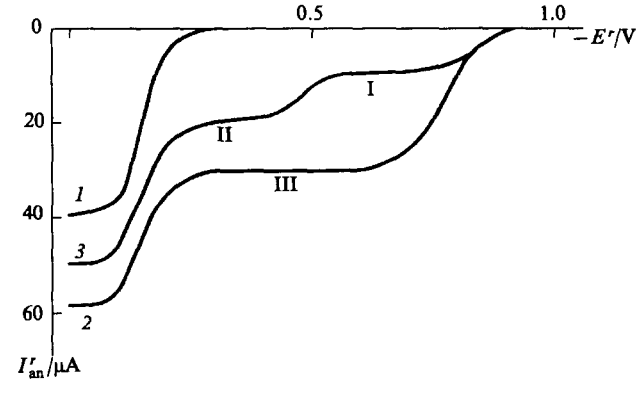


Figure 6. Polarisation curves for the electrochemical oxidation at the ring electrode of the product of the electrochemical reduction of dibenzonitrilechromium at the rotating disc electrode in DMSO at $E^d = -2.4$ V (line *1*) and -2.75 V (line *2*) and for the open circuit of the disc electrode ($I^d = 0$) (line *3*) ($\omega = 250$ s^{-1}). I–III numbers of the waves.

§ Here and henceforth the numbers of compounds in Table 7 are quoted in the text.

The electrochemical reduction of the radical-anions of 1,2- and 1,4-dicyanobenzenes leads to the elimination of one CN group and further reduction of the resulting benzonitrile and its radical-anion.

$$[C_6H_4(CN)_2]^{\cdot-} \xrightarrow[-CN^-,-B^-]{+\bar{e}+BH} C_6H_5CN \overset{+\bar{e}}{\rightleftarrows} [C_6H_5CN]^{\cdot-}$$

The irreversible two-electron *B* wave on the polarisation curves for the reduction of these compounds corresponds to this process. The increase in the number of cyano-groups in the molecule to four is responsible for the reversibility of the electrochemical reduction of the radical-anions of tetracyanobenzene to the dianions, which can be detected with 100% yield.[127]

A completely different picture is observed in the electrochemical reduction of the π-complex nitriles. With the exception of the complex $(NCC_6H_5)Cr(C_6H_5COCH_3)$, whose characteristics in the region of the potentials of the *A* and *B* waves permitted its assignment to the first group of substances, the radical-anions of the complex nitriles could not be detected in any instance by the RRDE method at room temperature, although the formation of the radical-anions of dibenzonitrilechromium as a result of chemical reduction with metallic potassium in dimethoxyethane at −70 °C has been demonstrated by the EPR method.[111] The two-electron *A* waves correspond to the elimination reaction of the CN group (compounds **7**–**10**), the stable products of which, namely the CN^- anion and the complexes $(C_6H_6)Cr(C_6H_5X)$ (X = H, CH_3, OCH_3, CN), can be detected at the amalgamated gold ring electrode.¶ In this respect, the nitriles of the dibenzenechromium series exhibit a greater similarity to the *ortho*- and *para*-isomers of dicyanobenzene than to benzonitrile.

Figure. 5 presents the polarisation curve for the electrochemical oxidation and reduction of the complex $(NCC_6H_5)_2Cr$ at the rotating disc electrode in solution in DMSO normalised with respect to the limiting current of the one-electron anodic oxidation of the complex to the cation (*Z* wave). Each of the cathodic waves (*A* and *B*) is of the two-electron type. Fig. 6 presents voltammograms of the anodic oxidation at the ring electrode of the products of the cathodic reduction of dibenzonitrilechromium at disc potentials E^d corresponding to the limiting currents of the *A* wave (curve *1*) and the *B* wave (curve *2*). In the region of the *A* wave, two products are formed, to which correspond two waves of equal height — the I wave ($E^{I}_{1/2} = -0.82$ V) and the II wave ($E^{II}_{1/2} = -0.46$ V). The current yields for each are 100%. The potentials $E^{I}_{1/2}$ and $E^{II}_{1/2}$ are characteristic of processes involving the formation of mercury cyanide and the oxidation of the complex $(C_6H_6)Cr(C_6H_5CN)$ to the cation respectively. Thus the following reaction takes place in the region of the potential of the *A* wave:

$$(NCC_6H_5)_2Cr \xrightarrow[-CN^-,-B^-]{+2\bar{e}+BH} (C_6H_6)Cr(C_6H_5CN)\ .$$

At the potentials of the *B* wave, a single III wave is observed at the ring electrode, its height exceeding by a factor of 3 that of the I wave on curve *1*. This finding is associated with the simultaneous occurrence of two anodic reactions with similar potentials $E_{1/2}$ — the oxidation of dibenzenechromium ($E^{+/0}_{1/2} = -0.76$ V) and the formation of $Hg_2(CN)_2$ as a result of the elimination of two cyano-groups from this initial complex. Consequently the following overall process takes place in the range of potentials of the *B* wave:

$$(NCC_6H_5)_2Cr \xrightarrow[-2CN^-,-2B^-]{+4\bar{e}+2BH} (C_6H_6)_2Cr\ ,$$

and the *B* wave itself characterises the elimination of the second cyano-group from the intermediate product — benzene(benzonitrile)chromium.

¶ The detection of the CN^- anions is based on the appearance in their presence in the layer near the ring electrode of the mercury oxidation wave with formation of mercury cyanide $Hg_2(CN)_2$ ($E_{1/2} = -0.82$ V).

Analysis of the reaction products by the RRDE method (Table 7) shows that, in the electrochemical reduction of the complex nitriles $(NCC_6H_5)Cr(C_6H_5X)$, where X = F, Cl, CF_3, the elimination of the CN group (*B* wave) is preceded by the elimination of the halogen (*A* wave).

An extremely important factor is the closeness of the slopes of the *A* wave for all the compounds included in Table 7 to 0.06 V regardless of the number of added electrons *n* and the reversible (aromatic nitriles) or irreversible (π-complexes) nature of the wave. This means that the electrochemical reduction of complex nitriles includes a chemical reaction between two electron transfer stages (ECE mechanism) and that the potential determining stage in the overall irreversible process is the reversible addition of the first electron to the initial molecule, which leads to the formation of unstable radical-anions.

The different behaviour at the cathode of free aromatic nitriles and their chromium complexes is due to the marked destabilisation of the radical-anions in the case of coordinated compounds, which diminishes the lifetime of these species compared with the radical-anions of the type $(XC_6H_4CN)^{\cdot-}$ by several orders of magnitude. The instability of the radical-anions of the complex nitriles is not related to their direct reduction at the electrode and is determined by their chemical decomposition via one of two possible pathways: the elimination of the cyano-group (halogen atom) from the radical-anion (a first-order reaction) with subsequent addition of a second electron to the free radical formed or disproportionation of the radical-anion (a second-order reaction) with partial regeneration of the initial complex, which again enters into the electrode reaction, and the formation of a dianion from which the cyano-group is eliminated in the form of the cyanide anion.

The mechanism of the process including the stage involving the reversible transfer of the first electron and the elimination of fluorine atoms operates[61] also in the reduction of trifluoromethylbenzene and its symmetrical chromium complex $(CF_3C_6H_5)_2Cr$. On the polarisation curve for the electrochemical reduction of this complex, it is possible to observe at low depolariser concentrations and for slow rotation of the electrode two waves corresponding to the addition of two (*A* wave) and four (*B* wave) electrons with subsequent formation of the complexes $(CF_3C_6H_5)Cr(C_6H_5CHF_2)$ and $(CF_3C_6H_5)Cr(C_6H_5CH_3)$.

The influence of proton-donating additives (benzoic acid, malonic ester, phenol, water) on the electrochemical reduction of complex nitriles has been investigated.[61] In the presence of additives, the elimination of the cyano-group is replaced by its partial or complete hydrogenation. In the presence of ammonium ions, which are reduced at the electrode more readily than the complex nitriles, the latter limiting current effect occurs[128, 129] — a decrease in the height of the two-electron cathodic waves for the electrochemical reduction of the nitriles to the one-electron level without change in $E_{1/2}$ and in the composition of the products of the cathodic reaction.[61] The cause of this phenomenon is either the interaction of the NH_4^+ ions as proton donor with the intermediate product of the electrochemical reduction of the nitriles (latent limiting current of the second kind) or the replacement of the electrochemical stage involving the addition of a second electron to the initial nitrile molecule by the stage in which the radical-anion is reduced chemically by the ammonium amalgam formed in the course of the reaction (latent limiting current of the first kind).

The third group of compounds includes aromatic hydrocarbons — phenylbenzenes and condensed systems as well as their chromium complexes. The electrochemical reduction reactions of the π-complexes containing naphthalene,[49] phenanthrene,[69] and biphenyl[48] as ligands were investigated by cyclic voltammetry, while the pairs of compounds[24, 61] $(C_6H_5)_2$–$[(C_6H_5)_2]_2Cr$ and $(C_6H_5)_3C_6H_3$–$[(C_6H_5)_3C_6H_3]_2Cr$ were studied by the RRDE method.

The first stage in the electrochemical reduction of aromatic hydrocarbons is known to be the reversible addition of an electron. The radical-anions formed are in many instances fairly stable and can be detected by various methods. Their destruction is attributed to the protonation reaction and subsequent transfer of a second electron either from the electrode or from a second radical-anion to the free radical.[130] The final products of the electrochemical reduction of aromatic hydrocarbons are partly hydrogenated compounds. There is every reason to assume that a similar mechanism, including a radical-anion protonation stage, operates also in the reduction of the corresponding π-complexes. The reversibility of the first electrochemical stage is indicated[61] by the slope of the cathodic wave $b \simeq 0.06$ V and the detection of the radical-anions of diphenanthrenechromium[69] and (naphthalene)-dibenzenedichromium.[49] The stability of the radical-anions of the non-coordinated phenylbenzenes appreciably exceeds that of the radical-anions of their π-complexes. Thus radical-anions have been detected in 50 and 100% yields by the RRDE method at the ring electrode at room temperature in the region of the first one-electron waves for the electrochemical reduction of biphenyl and a mixture of triphenylbenzene isomers respectively. In the electrochemical reduction of the corresponding complexes under the same conditions, the first cathodic waves in DMSO are characterised by $n = 4$ (biphenyl) and $n = 2$ (triphenylbenzene) and the radical-anions cannot be detected. The radical-anions of the π-complexes of condensed hydrocarbons are more stable, as a result of which the electrochemical reduction of diphenanthrene-chromium ($n = 1$) proves to be reversible.

There are incomplete literature data on the quasi-reversible one-electron cathodic reduction reactions of di(arsabenzene)-chromium[54] at 25 °C and bis(triphenylsilylbenzene)chromium[66] at −50 °C. The peaks due to the anodic oxidation of the radical-anions of both complexes were detected by cyclic voltammetry, which provides grounds for extending the conclusion that the first electron addition stage is reversible also to these compounds. As in the anodic oxidation reaction, di(arsabenzene)chromium behaves anomalously, being reduced at the cathode ($E^{C}_{1/2} = -1.36$ V) significantly more readily than free arsa-benzene ($E^{A}_{1/2} = -2.08$ V).

Thus, despite the irreversibility of many processes and the significant differences in the nature of the chemical stages of the reaction (dimerisation or protonation of the radical-anion, elimination of electroactive groups), the principal potential determining stage common to all the compounds of the benzene and dibenzenechromium series examined is the reversible addition of the first electron to the depolariser molecule.

IV. Characteristic features of the change in the reactivity of arenes under the influence of coordination to a chromium atom in one-electron transfer reactions

The establishment of the reversibility of the first electron addition stage in the electrochemical reduction reactions of free arenes and diarenechromium complexes is important from the standpoint of the possibility of using irreversible or quasi-reversible cathodic processes in the study of the reactivities of these compounds. On the one hand, there is a prospect of obtaining quantitative data concerning the influence of substituents in complexes, containing identical electrochemically active groups, on the ease of their reduction. In combination with correlation analysis, this makes it possible to assess the nature of the transmission of the electronic effects of substituents in one of the ligands to the reaction centre in the second ligand. Thus the potentials $E^{C}_{1/2}$ for the electro-chemical reduction of the heteroannularly substituted complex nitriles (compounds **7**–**13** in Table 7) are satisfactorily correlated[109] with the sets of substituent constants $\sigma^0_p, \sigma^0_m, \sigma_m$, and σ^+_m ($r = 0.961-0.972$). This indicates the predominantly inductive mechanism of the transmission of electronic effects in the molecule of the complex and agrees with conclusions reached as a result of the study of the reversible anodic oxidation reactions of the diarenechromium(0) complexes[29,61,62] and the ^{19}F NMR spectra.[96]

On the other hand, a basis appears for a quantitative comparison of the reactivities of the free and metal-coordinated arenes in similar electrochemical reduction reactions. A necessary precondition for the solution of this problem is the identity, noted above, of the reaction centres in the arenes and their π-complexes in cathodic reduction. We may note that the identical type of the main potential determining one-electron stage in the electrochemical reduction of the classes of compounds examined justifies the comparison of the potentials $E^{C}_{1/2}$ and $E^{A}_{1/2}$ of the first cathodic waves regardless of the total number of added electrons, which need not necessarily be identical in reactions involving an arene and its π-complex (electrochemical reduction of aromatic and complex nitriles).

For fully reversible processes, the half-wave potential difference $\Delta E^{CA}_{1/2}$ serves as a measure of the change in the reactivity of the arene as a result of its coordination to a chromium atom:

$$\Delta E^{CA}_{1/2} = E^{C}_{1/2} - E^{A}_{1/2} \simeq E^{C}_{0} - E^{A}_{0} = \frac{2.3RT}{F} \lg \frac{K^{C}}{K^{A}} , \qquad (11)$$

where K^{C} and K^{A} are the equilibrium constants of the corresponding redox processes. The quantity $\Delta E^{CA}_{1/2}$ characterises the overall effect of the change in the reactivities of the reactant in the electrochemical reduction reaction and of the radical-anion in the subsequent chemical reaction. Thus when the rotating disc electrode method is used in the case of the dimerisation of the radical-anions, the potentials $E^{C}_{1/2}$ and $E^{A}_{1/2}$ are defined by Eqn. (10) and their difference for $c = \text{const}$ and $\omega = \text{const}$ is defined by the equation

$$\Delta E^{CA}_{1/2} = \frac{2.3RT}{F} \lg \frac{K^{C}}{K^{A}} + \frac{2.3RT}{3F} \lg \frac{k^{C}_{d}}{k^{A}_{d}} + \frac{2.3RT}{9F} \lg \frac{D^{A}}{D^{C}} . \qquad (12)$$

Estimation of the contributions of the second and third terms on the right-hand side of the equation to $\Delta E^{CA}_{1/2}$ showed[50] that, at least for the first group of compounds, these terms can be neglected to a first approximation and the experimental quantity

$$\Delta E^{CA}_{1/2} \simeq \frac{2.3RT}{F} \lg \frac{K^{C}}{K^{A}} ,$$

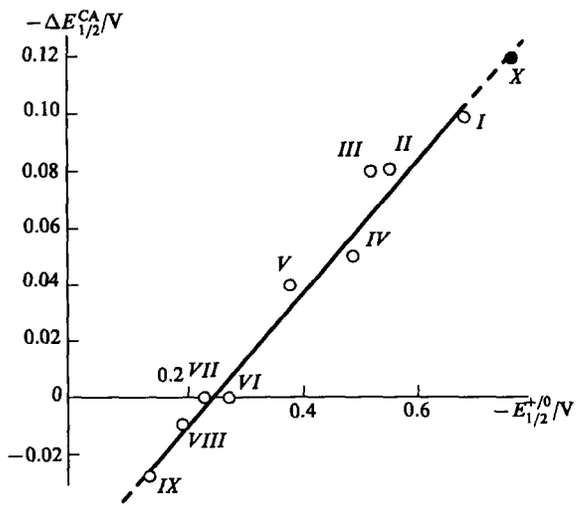


Figure 7. Correlation between $\Delta E^{CA}_{1/2}$ and $E^{+/0}_{1/2}$. The numbering of the points corresponds to the numbering of the Arene–Arene$_2$Cr systems in Table 5; X = calculated value of $\Delta E^{CA}_{1/2}$ for the C_6H_6–$(C_6H_6)_2Cr$ system.

characterises virtually only the change in the reactivity of the arene in the electrochemical reduction reaction as a result of its coordination to the metal atom.

The quantities $\Delta E_{1/2}^{CA}$ and $\lg(K^C/K^A)$ for a series of systems are presented in Table 5. Analysis of the data in the table permits the conclusion that the formation of π-complexes leads as a rule to a shift of the half-wave potential. The most marked difference is observed on passing from the free arene XC_6H_5 to the asymmetric complex $(XC_6H_5)Cr(C_6H_6)$, in which the arene (benzaldehyde, benzonitrile) is coordinated to the benzenechromium fragment. The value $\Delta E_{1/2}^{CA} = -0.31$ V corresponds to a decrease in the equilibrium constant of the electrochemical reduction reaction of the complex K^C by five orders of magnitude compared with K^A for the arene. Thus the fragment π-C_6H_6Cr plays the role of a very powerful donor relative to the arene, inducing an increase in electron density in the aromatic ring. On formation of symmetrical complexes $(XC_6H_5)_2Cr$, the difference $\Delta E_{1/2}^{CA}$ is significantly smaller and, depending on the nature of the substituent X and also on the number of substituents in the ligands, changes both in absolute magnitude and in sign. These results are fully consistent with data[108] for the Arene–(Arene)$Cr(C_6H_6)$–$(Arene)_2Cr$ system.

It has been established in a study of the characteristics of the cathodic processes for nine pairs of Arene–$Arene_2Cr$ compounds (Table 5)[65, 107] that there is a linear relation between the half-wave potential difference for the electrochemical reduction reactions involving each pair of substances $\Delta E_{1/2}^{CA}$ and the half-wave potential $E_{1/2}^{+/0}$ for the reversible anodic oxidation of the neutral form of the π-complex to the singly charged cation (Fig. 7):

$$\Delta E_{1/2}^{CA} = a' + \alpha' E_{1/2}^{+/0}, \quad (13)$$

where $a' = 0.072 \pm 0.007$ V, $\alpha' = 0.25 \pm 0.015$, and $r = 0.991$.

Since $\Delta E_{1/2}^{CA}$ is defined by Eqn. (11) and $E_{1/2}^{+/0}$ is a linear function[24, 61, 62] of the constants of the *meta*-substituents (σ_m, σ_m^0, σ_m^+), Eqn. (13) can be transformed into

$$\Delta E_{1/2}^{CA} = b' + \beta' \sum \sigma, \quad (14)$$

$$\lg \frac{K^C}{K^A} = g' + \gamma' \sum \sigma, \quad (15)$$

where $b' \simeq -0.125$ V, $\beta' = 0.13$, $g' \simeq -2.17$, $\gamma' = 2.2$, and $\sum\sigma$ is the sum of the Hammett constants of the *meta*-substituents.

Eqns. (13)–(15) correspond to the principle of linear free energy relationships and relate the change in the free energy as a result of the coordination of the arene to the metal atom involving the formation of a symmetrical π-complex to the free energy of the redox reaction (2) or other reactions involving the complexes, the logarithms of the equilibrium constants (rate constants) of which are correlated with the constants of the *meta*-substituents in the aromatic ring.

The unusual feature of Eqns. (13)–(15) and the significant difference between them and the Hammett correlation equations consist in the fact that the quantities $\Delta E_{1/2}^{CA}$ characterise pairs of compounds differing from one another in the nature of the reaction centre—in the electrochemically active group. The existence under these conditions of the linear relations (13)–(15) shows that the correlation equations obtained are based on a cause common to all the Arene–$Arene_2Cr$ systems investigated—the transition of the free arene to the state in which it is coordinated to chromium atom, i.e. on complex formation. In relation to this process, the electroactive groups play the role of substituents in the arene and do not participate directly in the process but do influence the distribution of electron density in the molecule. The electrochemical cathodic reduction reaction is in essence an indicator reaction, which makes it possible to determine the free energy change on transition of the arene to the state where it is coordinated to a chromium atom.

It follows from Eqns. (14) and (15) that the overall effect of the coordination of the arene to chromium consists of two components. The first component, characterised by the first term (b', g') is constant for all the symmetrical diarene-chromium complexes investigated and is responsible for the retardation of the cathodic reaction relative to the electrochemical reduction of the free arene. The second component (the $\beta'\sum\sigma$ and $\gamma'\sum\sigma$ terms) is variable and is determined by the nature and number of substituents in the arene ligands. Substituents with electron-accepting properties compensate to some extent for the inhibition of the reaction induced by the constant component of the coordination effect. In the presence of electron-accepting substituents, which give rise to $E_{1/2}^{+/0} > -0.3$ V, the overall effect of complex formation changes sign and the π-complex is reduced more readily than the corresponding free arene.

The relations obtained make it possible to calculate the potentials $E_{1/2}^C$ and hence also E_0^C for the electrochemical reduction reactions of symmetrical chromium π-complexes, provided that the corresponding values for the free arenes are known. This is of special interest in those cases where the cathodic process does not occur in the range of potentials accessible to measurements. Thus, according to Eqn. (14) the half-wave potential for the electrochemical reduction of dibenzene-chromium should be displaced approximately by 0.125 V towards negative values compared with $E_{1/2}^A$ for benzene. Since the potential for the $C_6H_6^{0/-}$ redox transition found experimentally[119] in solution in dimethoxyethane at −90 °C proved to be −3.38 V, the potential $E_{1/2}^C$ for dibenzene-chromium under these conditions should be about −3.5 V, i.e. should be in the range of potentials of the reduction of the solvent or the supporting electrolyte. This has been confirmed by Gavrilov et al.,[48] who were unable to observe the peak due to the electrochemical reduction of dibenzenechromium before the onset of the reduction of the supporting electrolyte under the conditions of the electrochemical reduction of benzene.

The available experimental data permit certain conclusions concerning the influence of coordination to chromium on the stability of the radical-anions—the intermediates in the electrochemical reduction of arenes and their complexes. In the case of compounds of the first group, the coordination of the arene to the metal has comparatively little effect on the stability of the radical-anions, especially in the presence of a double bond in the side chain [benzylideneacetophenone–bis(benzylideneaceto-phenone)-chromium, ethyl cinnamate–bis(ethyl cinnamate)-chromium]. The stability of the radical-anions falls somewhat as a result of the acceleration of the dimerisation reaction in the sequence $[C_6H_5CHO] > [(C_6H_5CHO)Cr(C_6H_6)] > [(C_6H_5CHO)_2Cr]$, which can be inferred from the decrease in the yield of the radical-anions at the ring electrode. The radical-anions of the complexes in the second group (nitriles) are appreciably less stable than the radical-anions of benzonitrile. They rapidly eliminate CN^- anions and are converted into neutral radicals, which are reduced at the electrode.

Table 8.

Compound	G/V
$(C_6H_6)_2Cr$	2.7
$(CF_3C_6H_5)_2Cr$	2.2
$(NCC_6H_5)_2Cr$	2.0
$(C_6H_5$-η^6-$C_6H_5)_2Cr$	1.9
$[(C_6H_5)_3$-η^6-$C_6H_3]_2Cr$	1.8
$[1,2$-$(C_2H_5OCO)_2C_6H_4]_2Cr$	1.7
$(CH_3COC_6H_5)_2Cr$	1.6
$(HCOC_6H_5)_2Cr$	1.5
$(C_2H_5OCOCH=CHC_6H_5)_2Cr$	1.3
$(C_6H_5COCH=CH$-η^6-$C_6H_5)_2Cr$	0.9

The difference in the behaviour of the radical-anions of the π-complexes belonging to the first and second groups of compounds is apparently due to the different nature of the distribution of the electron density.[131,132] In the radical-anions of free benzonitrile, the spin density is localised predominantly in the *para* and *ortho*-positions in the benzene ring and to a lesser extent on the cyano-group. On the other hand, in the presence of carbonyl groups (C=O, CH=CH−C=O), in the benzene ring, an appreciable proportion of the spin density in the radical-anion is on a carbon atom in the side chain. Naturally, the changes in electron density in the benzene ring induced by the coordination to chromium lead in the case of nitriles to a more significant changes in the stability of the radical-anions than in the case of carbonyl and vinyl derivatives.

Yet another aspect of the problem of the reactivity of the diarenechromium complexes is associated with the concept of the electrochemical gap G defined as the difference between the half-wave potentials for the anodic oxidation and cathodic reduction reactions of the complex.[133] The potentials $E_{1/2}$ characterise the relative energies of the frontier orbitals, while G characterises the difference between the energies of the HOMO and LUMO (energy gap).

Compounds of the benzene series are characterised by a wide electrochemical gap. Thus $G > 6$ V for benzene. The complex formation reaction between benzene and chromium leads to a marked narrowing of the gap (to 2.7 V) due to the fact that the HOMO of the complex is localised on the metal and lies appreciably above the HOMO of benzene, whereas the LUMO of the complex and the arene are of the same type and their energies are similar (see Table 8).

As mentioned above, in the diarenechromium complexes, the HOMO is influenced primarily by the electronegativity of the substituents in the ligands, whereas for the LUMO the conjugation effects are of greatest importance. The different character of the influence of substituents on the $E_{1/2}$ for the electrochemical oxidation and reduction processes, established in a number of studies,[24,29,61,62,65] alters the electrochemical gap. The gap is widest in dibenzenechromium and its derivatives containing substituents with a weak mesomeric effect (CN, CF_3) and is narrowest in complexes whose ligands have a long conjugation chain (ethyl cinnamate, benzylideneacetophenone).

The above analysis of studies on the chemistry of diarenechromium complexes demonstrates the interest in these compounds by chemists concerned with different disciplines. This is due to the characteristic features of the structure and chemical properties of dibenzenechromium and its derivatives and also the possibility of using them as convenient model compounds for the elucidation of general problems of the reactivity of transition metal π-complexes. Studies on these lines, to a large extent based on the investigation of the reversible electron transfer reaction in neutral complex/single charged cation systems, are most numerous and are of direct interest for organoelement chemistry and the chemistry of coordination compounds. The above reaction has also proved useful in the solution of certain problems of theoretical electrochemistry (a test of the theory of the reorganisation of the solvent, the creation of new reference electrodes suitable for the comparison of the results of electrochemical measurements in non-aqueous media of different nature). During the last 25 years, undoubted progress has been achieved also in the study of the kinetics and mechanisms of multistage cathodic processes with participation of diarenechromium(0) complexes.

However, one should note that at the present time the literature contains virtually no published study of preparative electrochemistry—not only on the synthesis of chromium complexes but also on the introduction of functional groups into the latter, although the results of the investigation of the kinetics of redox processes open the way in principle to the electrosynthesis of new compounds of the given class.

References

1. E O Fischer, W Hafner *Z. Naturforsch. B* **10** 665 (1955)
2. E Weiss, E O Fischer *Z. Anorg. Allg. Chem.* **286** 142 (1956)
3. C Furlani, E O Fischer *Z. Elektrochem.* **61** 481 (1957)
4. C Furlani, G Sartory *Ric. Sci.* **28** 973 (1958)
5. A A Vlček *Z. Anorg. Allg. Chem.* **304** 109 (1960)
6. I A Korshunov, L N Vertyulina, G A Razuvaev, Yu A Sorokin, G A Domrachev *Dokl. Akad. Nauk SSSR* **122** 1029 (1958)
7. I A Korshunov, L N Vertyulina, G A Domrachev *Zh. Obshch. Khim.* **32** 9 (1962)
8. L N Vertyulina, G A Domrachev, I A Korshunov, G A Razuvaev *Zh. Obshch. Khim.* **33** 285 (1963)
9. L N Vertyulina, I A Korshunov, Yu A Sorokin *Zh. Obshch. Khim.* **35** 1133 (1965)
10. H S Hsiung, G H Brown *J. Electrochem. Soc.* **110** 1085 (1963)
11. H P Schröer, A A Vlček *Z. Anorg. Allg. Chem.* **334** 205 (1964)
12. A Rusina, H P Schröer *Collect. Czech. Chem. Commun.* **31** 2600 (1966)
13. C Furlani *Ric. Sci.* **36** 989 (1966)
14. R E Dessy, F E Stary, R B King, M Waldrop *J. Am. Chem. Soc.* **88** 471 (1966)
15. R E Dessy, R B King, M Waldrop *J. Am. Chem. Soc.* **88** 5112 (1966)
16. S Valcher, G Casalbore *J. Electroanal. Chem.* **50** 359 (1974)
17. S P Gubin *Pure Appl. Chem.* **23** 463 (1970)
18. L I Denisovich, S P Gubin *Usp. Khim.* **46** 50 (1977) [*Russ. Chem. Rev.* **46** 27 (1977)]
19. S P Gubin, L I Denisovich *Elektrokhimiya (Itogi Nauki i Tekhniki)* [Eletrochemistry (Advances in Science and Engineering)] (Moscow: Izd. VINITI) Vol. 13, p. 94
20. N G Conelly, W E Geiger *Adv. Organomet. Chem.* **23** 1 (1984)
21. A P Tomilov, I N Chernykh, Yu M Kargin *Elektrokhimiya Elementoorganicheskikh Soedinenii. Elementy I, II, III Grupp Periodicheskoi Sistemy i Perekhodnye Metally* (Electrochemistry of Organoelement Compounds. Group, I, II, and III Elements and Transition Metals) (Moscow: Nauka, 1985)
22. V V Strelets *Usp. Khim.* **58** 496 (1989) [*Russ. Chem. Rev.* **58** 297 (1989)]
23. T V Magdesieva, K P Butin, O A Reutov *Usp. Khim.* **57** 1510 (1988) [*Russ. Chem. Rev.* **57** 864 (1988)]
24. L P Yur'eva, N N Zaitseva, I A Uralets, S M Peregudova, D N Kravtsov, A Yu Vasil'kov, V A Sergeev *Metalloorg. Khim.* **3** 783 (1990)
25. D De Montazon, R Poilbane, P Zemoine, M Gross *Electrochim. Acta* **23** 1247 (1978)
26. R C Kapoor, J Kishan *J. Sci. Ind. Res.* **38** 674 (1979)
27. I A Suskina, B G Gribov, R A Idrisova, L I Denisovich, S P Gubin *Izv. Akad. Nauk SSSR, Ser. Khim.* 425 (1971)
28. T T-T Li, C H Brubaker *J. Organomet. Chem.* **216** 223 (1981)
29. L P Yur'eva, S M Peregudova, L N Nekrasov, A P Korotkov, N N Zaitseva, N V Zakurin, A Yu Vasil'kov *J. Organomet. Chem.* **219** 43 (1981)
30. H S Hao, Y C Fann, R C Kapoor *Bul. Electrochem.* **5** 382 (1989)
31. H Brunner, H Koch *Chem. Ber.* **115** 65 (1982)
32. P Treichel, G Essenmacher, H Efner, K J Klabunde *Inorg. Chim. Acta* **48** 41 (1981)
33. N Ito, T Saji, K Suga, S Aoyagui *J. Organomet. Chem.* **229** 43 (1982)
34. T G Gennett, D F Milner, M J Weaver *J. Phys. Chem.* **89**, 2787 (1985)
35. C Elschenbroich, U Zenneck *J. Organomet. Chem.* **160** 125 (1978)
36. Z M Koepp, H Wendt, H Strehlow *Z. Elektrochem.* **64** 483 (1960)
37. G Gritzner, J Kuta *Pure Appl. Chem.* **56** 462 (1984)
38. G Gritzner *Inorg. Chim. Acta* **24** 5 (1977)
39. G Gritzner *Monatsh. Chem.* **106** 947 (1975)
40. J S Yaworsky *Polyhedron* **6** 2151 (1987)
41. E Keulen, K Jellinek *J. Organomet. Chem.* **5** 490 (1966)
42. B Morosin *Acta Crystallogr.* **B30** 838 (1974)
43. G Gritzner *Elektrokhimiya* **28** 1208 (1992)
44. L I Krishtalik *Elektrodnye Reaktsii. Mekhanizm Elementarnogo Akta* (Electrode Reactions. The Mechanism of the Elementary Step) (Moscow: Nauka, 1979)
45. R R Dogonadze, A M Kuznetsov, in *Dvoinoi Sloi i Elektrodnaya Kinetika* (The Double Layer and Electrode Kinetics) (Moscow: Nauka, 1981) p. 283
46. V M Gerovich, M I Podgornaya, B B Damaskin *Elektrokhimiya* **21** 1340 (1985)

47. B B Damaskin, V M Gerovich, M I Podgornaya *Elektrokhimiya* **22** 117 (1986)
48. A B Gavrilov, S V Kukharenko, V V Strelets *Metalloorg. Khim.* **3** 406 (1990)
49. B F Bush, J J Lagowski *J. Organomet. Chem.* **386** 37 (1990)
50. L N Nekrasov, L P Yur'eva, S M Peregudova *J. Organomet. Chem.* **238** 185 (1982)
51. Ch Elschenbroich, E Bilger, B Metz *Organometallics* **10** 2823 (1991)
52. S Valcher *Ric. Sci. Rend. Ser. A.* **8** 1007 (1965)
53. S Valcher, G Casalbore, M Mastragostino *J. Electroanal. Chem.* **51** 226 (1974)
54. C Elschenbroich, J Kroker, W Massa, M Wünsch, A J Asche III *Angew. Chem., Int. Ed. Engl.* **25** 571 (1986)
55. C Elschenbroich, J Koch, J Kroker, M Wünsch, W Massa, G Baum, G Strock *Chem. Ber.* **121** 1983 (1988)
56. U Koelle, W Holzinger, J Müller *Z. Naturforsch. B* **34** 759 (1979)
57. C Elschenbroich, J Schneider, H Prinzbach, W D Fessner *Organometallics* **5** 2091 (1986)
58. C Elschenbroich, J Schneider, H Mellinghoff *J. Organomet. Chem.* **333** 37 (1987)
59. R J Markle, J J Lagowski *Organometallics* **5** 595 (1986)
60. S I Bailey, W P Leung, I M Ritchi *Electrochim. Acta* **30** 861 (1985)
61. S M Peregudova, Candidate's Thesis in Chemical Sciences, Institute of Organoelement Compounds, Moscow, 1990
62. L P Yur'eva, S M Peregudova, D N Kravtsov, A Yu Vasil'kov, L N Nekrasov, N L Asfandiarov, M M Timoschenko, Yu V Chizhov *J. Organomet. Chem.* **336** 371 (1987)
63. C Elschenbroich, J Heck *Angew. Chem., Int. Ed. Engl.* **16** 479 (1977)
64. G A Razuvaev, G A Domrachev, V D Zinov'ev *Dokl. Akad. Nauk SSSR* **223** 617 (1975)
65. L P Yur'eva, L N Nekrasov, S M Peregudova, A P Korotkov, L N Vykhodtseva, N N Zaitseva, Yu A Shevelev *J. Organomet. Chem.* **238** 197 (1982)
66. C Elschenbroich, J Hurley, B Metz, W Massa, G Baum *Organometallics* **9** 889 (1990)
67. C Elschenbroich, J Hurley, W Massa, G Baum *Angew. Chem., Int. Ed. Engl.* **27** 684 (1988)
68. C Elschenbroich, G Heikenfeld, M Wünsch, W Massa, G Baum *Angew. Chem., Int. Ed. Engl.* **27** 414 (1988)
69. C Elschenbroich, E Bilger, R Moeckel *Z. Naturforsch. B* **38** 1357 (1983)
70. U Koelle *J. Organomet. Chem.* **157** 327 (1978)
71. Yu A Sorokin, G G Petukhov *Zh. Obshch. Khim.* **35** 2135 (1965)
72. C Elschenbroich *J. Organomet. Chem.* **14** 157 (1968)
73. A N Nesmeyanov, L P Yur'eva, S N Levchenko, N N Zaitseva *Izv. Akad. Nauk SSSR, Ser. Khim.* 2865 (1974)
74. A N Nesmeyanov, L P Yur'eva, N N Zaitseva *Izv. Akad. Nauk SSSR, Ser. Khim.* 922 (1976)
75. P L Timms *J. Chem. Soc., Chem. Commun.* 1033 (1969)
76. V Graves, J J Lagowski *Inorg. Chem.* **15** 577 (1976)
77. A N Nesmeyanov, V A Sergeev, N V Zakurin, A Yu Vasil'kov, A S Kogan, L P Yur'eva, N N Zaitseva, I A Uralets *J. Organomet. Chem.* **217** 195 (1981)
78. C Elschenbroich, J Heck *J. Am. Chem. Soc.* **101** 6773 (1979)
79. F Hein, W Kleinwächter *Monatsber. Dtsch. Akad. Wiss. Berlin* **2** 607 (1960)
80. E O Fischer, C Elschenbroich, C G Kreiter *J. Organomet. Chem.* **7** 481 (1967)
81. C Elschenbroich, R Möckel *Angew. Chem., Int. Ed. Engl.* **16** 870 (1977)
82. E M Shustorovich, M E Dyatkina *Dokl. Akad. Nauk SSSR* **128** 1234 (1959)
83. M F Guest, I H Hillier, B R Higginson, D R Lloyd *Mol. Phys.* **29** 113 (1975)
84. J Weber, M Geoffroy, A Goursot, E Penigault *J. Am. Chem. Soc.* **100** 3995 (1978)
85. J Weber, E P Kündig, A Goursot, E Penigault *Can. J. Chem.* **63** 1734 (1985)
86. S Evans, J C Green, S E Jackson *J. Chem. Soc., Faraday Trans. 2* **68** 249 (1972)
87. Yu V Chizhov, M M Timoshenko, L P Yur'eva, N N Zaitseva, I A Uralets, D N Kravtsov, N L Asfandiarov *J. Organomet. Chem.* **361** 79 (1989)
88. R Prins, F J Reinders *Chem. Phys. Lett.* **3** 45 (1969)
89. P Zuman *Substituent Effects in Organic Polarography* (New York: Plenum, 1967)
90. E G Perevalova, S P Gubin, S A Smirnova, A N Nesmeyanov *Dokl. Akad. Nauk SSSR* **155** 857 (1964)
91. Yu A Zhdanov, V I Minkin *Korrelyatsionnyi Analiz v Organicheskoi Khimii* (Correlation Analysis in Organic Chemistry) (Rostov-on-Don: Izd. Rostov. Univ., 1966)
92. P G Gassman, C R Winter *J. Am. Chem. Soc.* **108** 4228 (1986)
93. A J Gordon, R A Ford *A Chemist's Companion* (Translated into Russian) (Moscow: Mir, 1976)
94. J K Kochi, G S Hammond *J. Am. Chem. Soc.* **75** 3452 (1953)
95. V V Strelets *Elektrokhimiya* **28** 490 (1992)
96. V A Sergeev, L P Yur'eva, A S Peregudov, A Yu Vasil'kov, I A Uralets, N N Zaitseva, D N Kravtsov *Izv. Akad. Nauk SSSR, Ser. Khim.* 2576 (1987)
97. L P Yur'eva, N N Zaitseva, D N Kravtsov *Metalloorg. Khim.* **2** 411 (1989)
98. L P Yur'eva, N N Zaitseva, N V Zakurin, A Yu Vasil'kov, N I Vasyukova *J. Organomet. Chem.* **247** 287 (1983)
99. J Müller, P Göser *J. Organomet. Chem.* **12** 163 (1968)
100. V V Strelets, S V Kukharenko *Nouv. J. Chim.* **8** 785 (1984)
101. V V Strelets, S V Kukharenko *Metalloorg. Khim.* **1** 692 (1988)
102. D W Clack, K D Warren *J. Organomet. Chem.* **152** 60C (1978)
103. G A Domrachev, N N Vyshinskii *Dokl. Akad. Nauk SSSR* **194** 583 (1970)
104. J K Burdett, E Canadell *Organometallics* **4** 805 (1985)
105. J H Osborne, W C Trogler, P D Morand, C G Francis *Organometallics* **6** 94 (1987)
106. C Elschenbroich, F Gerson, F Stohler *J. Am. Chem. Soc.* **95** 6956 (1973)
107. L P Yur'eva, L N Nekrasov, S N Peregudova *Dokl. Akad. Nauk SSSR* **264** 876 (1982)
108. C Elschenbroich, J Heck, F Stohler, J Heinzer *Chem. Ber.* **117** 23 (1984)
109. L N Nekrasov, S M Peregudova, L P Yur'eva, D N Kravtsov, I A Uralets, N N Zaitseva *J. Organomet. Chem.* **365**, 269 (1989)
110. C Elschenbroich, J Heck *J. Organomet. Chem.* **229** 139 (1982)
111. S P Solodovnikov, L P Yur'eva, N N Zaitseva *Izv. Akad. Nauk SSSR, Ser. Khim.* 2392 (1982)
112. C Elschenbroich, E Bilger, J Koch, J Weber *J. Am. Chem. Soc.* **106** 4297 (1984)
113. A N Frumkin, L N Nekrasov *Dokl. Akad. Nauk SSSR* **126** 115 (1959)
114. A Frumkin, L Nekrasov, B Levich, Yu Ivanov *J. Electroanal. Chem.* **1** 84 (1959)
115. L N Nekrasov *Elektrokhimiya (Itogi Nauki i Tekhniki)* [Electrochemistry (Advances in Science and Engineering)] (Moscow: Izd. VINITI, 1981) Vol. 17, p. 148
116. W J Albery, M L Hitchman *Ring-Disc Electrodes* (Oxford: Clarendon Press, 1971)
117. M R Tarasevich, E I Khrushcheva, V Yu Filinovskii *Vrashchayushchiisya Diskovyi Elektrod s Kol'tsom* (The Rotating Ring-Disc Electrode) (Moscow: Nauka, 1987)
118. L N Nekrasov *Polyarografiya. Problemy i Perspektivy* (Polarography. Problems and Prospects) (Riga: Zinatne, 1977)
119. S V Kukharenko, V V Strelets *Elektrokhimiya* **24** 1379 (1988)
120. N El Murr, A Chaloyard, E Laviron *Nouv. J. Chim.* **2** 15 (1978)
121. L N Nekrasov, A P Korotkov *Elektrokhimiya* **16** 168 (1980)
122. S G Mairanovskii *Kataliticheskie i Kineticheskie Volny v Polyarografii* (Catalytic and Kinetic Waves in Polarography) (Moscow: Nauka, 1966)
123. Z Galus, R N Adams *J. Electroanal. Chem.* **4** 248 (1962)
124. L Nadjo, J M Saveant *J. Electroanal. Chem.* **44** 327 (1973)
125. A P Korotkov, L N Nekrasov *Elektrokhimiya* **18** 39 (1982)
126. L N Vykhodtseva, L N Nekrasov, E V Bulatkina, D V Ioffe *Elektrokhimiya* **21** 1138 (1985)
127. L N Vykhodtseva, L N Nekrasov, S M Peregudova *Vestn. Mosk. Univ., Ser. 2, Khim.* **28** 452 (1987)
128. W Kemula, Z Grabowski *Roczn. Chem.* **25** 350 (1951)
129. A V Sokirko, Yu I Kharkats *Elektrokhimiya* **25** 34 (1989)
130. R Dietz, in *Organic Electrochemistry, an Introduction and a Guide* Book 1 (Eds M M Baizer, H Lund) (Moscow: Khimiya, 1988) p. 243
131. P Rieger, G Fraenkel *J. Chem. Phys.* **37** 2811 (1962)
132. S P Solodovnikov, A I Prokof'ev *Usp. Khim.* **39** 1276 (1970) [*Russ. Chem. Rev.* **39** 591 (1970)]
133. K P Butin, V V Strelets, O A Reutov *Metalloorg. Khim.* **3** 814 (1990)

Russian Chemical Reviews **62** (2) 143 – 168 (1993)
© 1993 Russian Academy of Sciences and Turpion Ltd

UDC 542.943 : 547.235 : 547.556

Regioselective methods of synthesis of asymmetrically substituted diazene oxides

S G Zlotin, O A Luk'yanov

Contents

I.	Introduction	143
II.	Oxidation of asymmetrically substituted azo-compounds	143
III.	Reactions of *syn*-diazotates with alkylating agents	147
IV.	Reactions of nitro- and nitroso-compounds with amino-derivatives	148
V.	Interaction of anions containing the N_2O_2 fragment with electrophiles	160
VI.	Other methods of synthesis of asymmetrically substituted diazene *N*-oxides	163
VII.	Conclusion	165

Abstract. Regioselective methods of synthesis of asymmetrically substituted diazene oxides, in which the diazene oxide group is linked to carbon, oxygen, sulphur, nitrogen, and phosphorus atoms, are examined. Data on the reaction conditions, yields, and structures of azoxy-products are presented. The bibliography includes 232 references.

I. Introduction

The first azoxy-compounds were synthesised almost 150 years ago,[1] but almost up to the middle of the present century these were mainly compounds containing identical structural fragments at the nitrogen atoms of the diazene *N*-oxide group. The vigorous development of the chemistry of the diazene *N*-oxides was stimulated by the isolation from natural sources of compounds of this type exhibiting a high biological activity (carcinogenic,[2-9] antibacterial,[10-16] tuberculostatic,[7-8] fungicidal,[10,16-18] and nematocidal[19,20]) and also of the discovery in the series of asymmetrically substituted *N,N'*-diaryldiazene *N*-oxides of substances exhibiting the properties of liquid crystals.[21-30]

Although a series of reviews has been devoted to the chemistry of azoxy-compounds,[31-35] the regioselective methods of synthesis of asymmetrically substituted compounds of the given series are dealt with in a fragmentary fashion in these publications. Furthermore, since the appearance of the last of the published reviews[34] more than ten years have elapsed, which makes it timely to survey the large amount of synthetic data which have been published during this period.

This review is devoted to the consideration of modern methods of synthesis of asymmetrically substituted diazene *N*-oxides from compounds which do not contain the diazene *N*-oxide group.

The data are classified in terms of the N→O, C–N, and N=N bonds formed with participation of the nitrogen atoms of the diazene group. The reactions involving the alkylation of anions containing the N_2O_2 structural fragments (salts of *N*-nitrosohydroxylamines, *N*-nitroamines, and hyponitrous acid), accompanied by the formation of a C–O bond separated from the diazene *N*-oxide group and leading to the formation of O-substituted azoxy-compounds which have been actively investigated in recent years (*N'*-alkoxydiazene *N*-oxides, O,N-disubstituted nitroamines) are included in the review as a separate section.

In order to cover more fully the synthetic data and to facilitate the use of the review, a considerable proportion of the information has been arranged systematically in the form of tables containing detailed data on the initial compounds and reagents, the reaction conditions, and the yields and structures of the azoxy-products. Only studies where details of the methods used in carrying out the reactions are given and the structures of the asymmetrically substituted azoxy-compounds have been reliably demonstrated have been included, as a rule, in the sources quoted.

II. Oxidation of asymmetrically substituted azo-compounds

When an azo-compound is treated with oxygen-containing oxidants, a mixture of diazene *N*-oxides with different positions of the oxygen atom in the diazene *N*-oxide group is as a rule formed:[34]

$$R^1-N=N-R^2 \xrightarrow{Ox} \underset{\mathbf{A}}{R^1-\overset{\uparrow}{\underset{O}{N}}=N-R^2} + \underset{\mathbf{B}}{R^1-N=\overset{\uparrow}{\underset{O}{N}}-R^2} \quad (1)$$

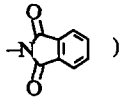
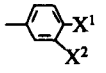
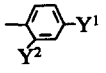
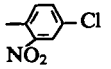
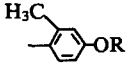
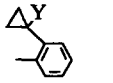
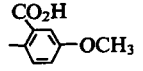
However, in a number of instances, the structural features of the starting substances ensure the preferential or exclusive formation of one of the regioisomeric oxidation products (Table 1).

The influence of the electronic and steric nature of the substituents at the nitrogen atoms of the azo-group on the regiospecificity of the oxidation process is clearly manifested in the series of *N,N'*-diaryldiazenes. The oxidation of *p*-nitro-[38] and *p*-alkoxy-diaryldiazenes[38-40] proceeds fairly selectively, in contrast to the oxidation of the majority of other asymmetric aromatic azo-compounds containing substituents in the *meta*- and *para*-positions in the aromatic ring, and makes it possible to synthesise azoxy-products in which the oxidised nitrogen atom is linked to the unsubstituted aromatic ring[38-40] (Table 1). The phenomenon of the identical directing effect of groups having completely different electronic characteristics has not yet received a satisfactory theoretical explanation,[34,38] but it can be used successfully in synthetic practice.

S G Zlotin, O A Luk'yanov Laboratory of Organic Synthesis, Zelinskii Institute of Organic Chemistry, Russian Academy of Sciences, Leninskii prosp. 47, 117913 Moscow, Fax (7-095)135 53 28

Received 12th November 1992
Uspekhi Khimii **62** (2) 157 – 183 (1993); translated by A K Grzybowski

Table 1. Conditions in the reactions of asymmetric azo-compounds with oxidants and the ratios and yields of the isomeric oxidation products.

R^1	R^2	Oxidant	Solvent	Reaction temperature/ °C	Reaction time/h	A/B ratio	Overall yield of oxidation products (%)	Ref.
$-C_6H_5$	$-C_6H_4-R$-*m, p* ($R = NO_2, SO_2CH_3, SO_2C_6H_5, NHC(O)CH_3, NHSO_2C_6H_4CH_3$-*p*, $OC(O)CH_3$, $OC(O)C_6H_5$, F, Cl, Br, )	36% H_2O_2	CH_3CO_2H	50	20–60	1.07–1.73	–	36, 37
$-C_6H_5$	$-C_6H_4-NO_2$-*p*	t-$C_4H_9OOH/MoO_2(dpm)_2$	C_6H_6	60	24	>100	73	38
		CH_3CO_3H	CH_3CO_2H	60	20	>100	84	38
		m-$ClC_6H_4CO_3H$	$CHCl_3$	60	24	>100	86	38
$-C_6H_5$	$-C_6H_4-OCH_3$-*p*	t-$C_4H_9OOH/MoO_2(dpm)_2$	C_6H_6	60	4	>100	81	38
		t-$C_4H_9OOH/Mo(CO)_6$	C_6H_6	60	24	0.89	88	38
		CH_3CO_3H	CH_3CO_2H	60	20	2.85	75	38
$-C_6H_4-X$-*p* ($X = H, n$-$C_4H_9, OC(O)CH_3$)	$-C_6H_4-Y$-*p* ($Y = CH_3, OCH_3, OC_2H_5, Cl$)	40% CH_3CO_3H	40% CH_3CO_3H	118	12	0.78–1.22	70–85	39
$-C_6H_4-Cl$-*p*	$-C_6H_4-OC_2H_5$-*p*	30% H_2O_2	CH_3CO_2H (glacial)	118	5	>100	50	40
			CH_3CO_2H (80%)	118	5	<0.01	51	40
 ($X^1 = H, CH_3, Cl, OCH_3$; $X^2 = H, Cl$)	 ($Y^1 = H, CH_3, Cl, OCH_3, CO_2CH_3$; $Y^2 = CH_3, Cl, OCH_3, CO_2CH_3, CO_2H$)	90% H_2O_2	CH_3CO_2H	25	12–24	5–24	82–92	41, 42
$-C_6H_4-Cl$-*p*		30% H_2O_2	CH_3CO_2H	70–75	1	>100	79	43
$-C_6H_4-C_4H_9$-*p*	 ($R = C_nH_{2n+1}$, $n = 1-6$)	30% H_2O_2	CH_3CO_2H (glacial) + $(CH_3CO)_2O$	20	24	>100	47–91	44
$-C_6H_5$	 (Y = H, CH_3)	30% H_2O_2	CH_3CO_2H	70–80	–	>100	38–75	45, 46
$-C_6H_4-OCD_3$-*p*		CH_3CO_3H	$CHCl_3$	20	18	2.67	55	47

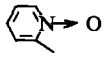
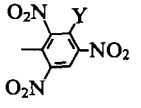
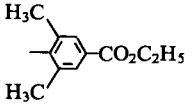
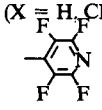
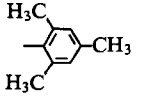
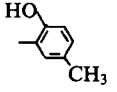
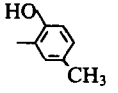
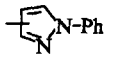
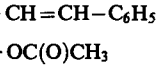
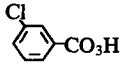
$-C_6H_5$		30% H_2O_2	CH_3CO_2H	–	–	> 100	–	48
$-C_6H_5$	 ($Y^1 = N\rightarrow O, Y^2 = CH$; $Y^1 = CH, Y^2 = N\rightarrow O$)	30% H_2O_2	CH_3CO_2H	–	–	2 – 3	–	48
$-C_6H_4-NO_2$-*p*	 (Y = H, Cl, $-N=N-C_6H_4-NO_2$-*p*)	CrO_3 + 98% HNO_3	98% HNO_3	70 – 80	2 – 3	> 100	40 – 92	49, 50
$-C_6H_5$		30% H_2O_2	CH_3CO_2H	–	–	> 10	80	51
$-C_6H_4-X$-*p* (X = H, CH_3, OCH_3, Br, Cl)	$-C_6Cl_5$	CF_3CO_3H	$CHCl_3$	61	2	> 100	> 95	52
		CF_3CO_3H	$CHCl_3$	61	2	< 0.01	75	53
$-C_6F_5$	$-C_6H_5$	CF_3CO_3H	CH_2Cl_2	40	5	> 100	87	54
$-C_6H_5$		90% H_2O_2	CH_3CO_2H	25	24	0.38	90	41
$-C_6H_4-X$-*o* (X = OCH_3, CH_3, Br, Cl)		30% H_2O_2	CH_3CO_2H	75 – 80	18	< 0.01	15 – 33	55
$-C_6H_5$	$-CH_3$	$C_6H_5CO_3H$	CH_2Cl_2	0	12	~ 10	–	56
$-C_6H_4-X$-*p* (X = H, Br)	$-CH_2-C_6H_4-Cl$-*p*	$C_6H_5CO_3H$	$(C_2H_5)_2O$	0	16	~ 10	~ 100	57
$-C_6H_4-X$ (X = H, Cl, Br, NO_2, OCH_3, CO_2CH_3)	$-C\equiv N$	85% H_2O_2	CF_3CO_2H	45	0.2 – 7.0	> 100	17 – 84	58-60
$-C_6H_4-X$-*p* (X = CH_3, Cl, NO_2, CO_2CH_3, CO_2H)	$-C(O)NH_2$	30% H_2O_2	HCO_2H or AcOH	40	~ 10	> 100	70 – 80	15, 61, 62

Table 1 (cont.).

R^1	R^2	Oxidant	Solvent	Reaction temperature/ °C	Reaction time/h	A/B ratio	Overall yield of oxidation products (%)	Ref.
	$-C\equiv N$	85% H_2O_2	CF_3CO_2H	45	–	> 100	65–70	63
$-C_6H_4-X$ [a] (X = H, Cl, Br, NO_2, OCH_3, CH_3)	$-CO_2Y$ (Y = CH_3, C_2H_5), $-C(O)C_6H_5$	85% H_2O_2 + maleic anhydride	CH_2Cl_2	40	0.5–1.5	> 100	70–90	58, 64
$-C_6H_4-X$ (X = H, CH_3, OCH_3, Cl, $CO_2C_2H_5$)	$-NH-C_6H_4-Y$ (Y = H, CH_3, OCH_3, Cl, $CO_2C_2H_5$, NO_2)	$C_6H_5CO_3H$	$(C_2H_5)_2O$ or $C_6H_5CH_3$	0	10–112	> 100 [b]	40–100	65
$-CH_3$ [c]		40% CH_3CO_3H	$(C_2H_5)_2O$	20	2	> 100	21	66
$-CX_2-OC(O)CH_3$ (X = CH_3, X_2 = $-(CH_2)_5-$)	$-CH_3$, $-C_6H_5$	40% CH_3CO_3H	CH_2Cl_2 or $(C_2H_5)_2O$	20	2–3	> 100	50–78	67
$-C(CH_3)=CH_2$	$-CH_3$	40% CH_3CO_3H	$(C_2H_5)_2O$	36	several hours	> 100	44	68
	$-CH_3$	40% CH_3CO_3H	$(C_2H_5)_2O$	20	1	> 100	66	68
$-CH=C(CH_3)_2$	$-CH_3$	40% CH_3CO_3H	$(C_2H_5)_2O$	20	1	< 0.01	34	68
$-C(CH_3)=C(CH_3)_2$	$-CH_3$		$(C_2H_5)_2O$	exothermic reaction	1	< 0.01	42	68
$-CH_3$	$-C(O)N(CH_3)_2$	90% H_2O_2 + 	CH_2Cl_2	40	3	> 100	50	69

[a] The initial arylazo-compounds may be generated *in situ* by oxidising the corresponding hydrazo-compounds and can be introduced into the process without isolation and purification.

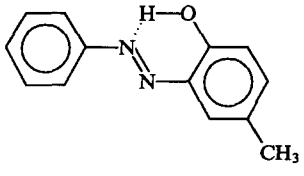
[b] For X ≠ Y, a mixture of the isomers $X-C_6H_4-\overset{\overset{O}{\uparrow}}{N}=N-NH-C_6H_4-Y$ and $X-C_6H_4-NH-N=\overset{\overset{O}{\uparrow}}{N}-C_6H_4-Y$ is formed. The component in which the oxidised nitrogen atom is linked to the aromatic ring containing a substituent with weaker electron-accepting properties predominates.

[c] The initial azo-compounds are generated *in situ* by oxidising the corresponding hydrazones.

In the case of *N,N'*-diaryl(heteroaryl)diazenes[53,54] containing substituents in the *ortho*-position relative to the azo-group, the sterically more accessible nitrogen atom, linked to the unsubstituted aromatic ring, is oxidised preferentially, the regioselectivity of the process reaching 75–100%.[41,47] Alkyl,[41,44] cycloalkyl,[45,46] alkoxy-,[41] ester,[41] carboxy,[42,47] and nitro-groups,[43] as well as halogen atoms[41] can be used as regio-controlling *ortho*-substituents. The *N*-oxide fragment of the heterocycle in the *ortho*-position relative to the azo-group exerts a similar directing effect[48] (Table 1).

The introduction of a second *ortho*-substituent into the aromatic ring as a rule fully inhibits the oxidation of the nitrogen atom of the azo-group linked to this ring.[49–52] The regiospecificity of the oxidation reactions of *N*-tetrafluoro-pyridyl-*N'*-(2,4,6-trimethylphenyl)diazene[53] and *N*-pentafluoro-phenyl-*N'*-phenyldiazene,[54] leading to the formation of azoxy-compounds in which the oxidised nitrogen atom is linked to the aromatic ring containing more bulky substituents in the *ortho*-position, therefore appears anomalous. A possible cause of the unexpected mode of oxidation of the above compounds may be, according to Miller and Furin, the increase in the nucleophilicity of the α-nitrogen atom induced by the decrease in the effectiveness of the interaction between the lone pair of the latter and the π-systems of the perfluoro- and 2,4,6-trimethyl-substituted aromatic rings.[54]

Processes involving the protonation of the reaction centre and the ability of the nitrogen atoms of the azo-group to participate in the formation of intramolecular hydrogen bonds can also exert a significant influence on the mode of oxidation of *N,N'*-diaryldiazenes. Thus, whereas the majority of *ortho*-substituents direct the oxidation of the N=N bond to the most remote nitrogen atom, in the case of *N*-(2-hydroxy-5-methylphenyl)-*N'*-aryldiazenes[41,55] (Table 1) a different mode of oxidation takes place preferentially, which is apparently due to the "blocking" of the lone pair of the β-nitrogen atom by the hydrogen atom of the hydroxy-group.[41]



The important role of the protonation of the reaction centre is confirmed by the different regiospecificities of the oxidation of *N*-(*p*-chlorophenyl)-*N'*-(*p*-alkoxyphenyl)-diazene[40] and *N*-phenyl-*N'*-(*p*-alkoxyphenyl)diazene[38] in media of different acidity (Table 1).

The oxidation reactions of asymmetrical azo-compounds in which one of the atoms is linked to an aromatic or heterocyclic system and the other to alkyl,[56,57] nitrile,[58,60,63] amino-carbonyl,[15,61,62] ester,[58,64] keto-,[58] or amino-group[65] are characterised as a rule by a high regioselectivity (Table 1). The reaction products are in this case usually asymmetrically substituted diazene *N*-oxides in which the oxygen atom is fixed in the α-position relative to the aromatic or heteroaromatic ring. The choice of the oxidant is determined by the stability under reaction conditions of the functional groups present in the molecule. Thus the synthesis of *N'*-cyanodiazene *N*-oxides from the corresponding cyanodiazenes[58–60,63] requires the use of 85% H_2O_2, because a more dilute hydrogen peroxide solution induces the hydrolysis of the nitrile group to the amide group.[15,58]

The oxidation of *N*-aryl-*N'*-(arylamino)diazenes (1,3-diaryltriazenes)[65] proceeds with participation of the nitrogen atom of the amino-group. The reaction results in the formation of a mixture of isomeric oxidation products (triazene oxides) in which the oxidised nitrogen atom is linked to one of the aromatic rings forming part of the molecule (preferentially to the ring containing electron-donating substituents).[65]

Data on the regioselective oxidation reactions of asymmetrically substituted aliphatic azo-compounds are limited to information about the oxidation of *N,N'*-dialkyldiazenes containing the acetoxy-group in the α-position relative to the azo-group[66,67] and about reactions with participation of *N*-alkenyl-[68] and *N*-dimethylaminocarbonyl-*N'*-alkyldiazenes[69] (Table 1).

The mode of reaction depends very greatly on the detailed characteristics of the structure of the initial compounds; slight changes in the structure of the substrates being oxidised (for example, in the number and disposition of the substituents at the double bond) entail a change in the site where the oxygen atom is attached in the azoxy-products formed. In our view, one should adopt a critical attitude to the conclusion[68] that the oxidation products have a regiostructure because it was based only on ^{1}H NMR spectroscopic data and is not supported by other reliable results (^{13}C and ^{14}N NMR and X-ray diffraction).

Thus oxidation of asymmetric azo-compounds to diazene *N*-oxides by oxygen-containing oxidants takes place regioselectively only in those cases where the substituents R^1 and R^2, linked to the nitrogen atoms of the azo-group, differ appreciably in their electronic and steric structures. The regiospecificity of the process is frequently unexpected and is not always susceptible to a simple interpretation from the standpoint of the structures of the initial compounds. The complexity of the detailed allowance for all the factors determining the direction of attack by the oxygen atom of the oxidant on a particular atom in the azo-group and the unpredictability of the mode of oxidation associated with this factor greatly reduce the synthetic value of the method and hinder its use for the specific synthesis of asymmetrically substituted diazene *N*-oxides.

III. Reactions of *syn*-diazotates with alkylating agents

In 1969 Moss and coworkers[70,71] proposed a direct method of synthesis of asymmetrically substituted *N,N'*-dialkyldiazene *N*-oxides and *N*-arylalkyl-*N'*-alkyldiazene *N*-oxides from *syn*-alkyldiazotates and alkylating agents (Table 2).

An intramolecular version of the reaction has been described:[79]

$$R^1-N=N-O^-K^+ + R^2X \rightarrow R^1-\overset{\overset{O}{\uparrow}}{N}=N-R^2 . \qquad (2)$$

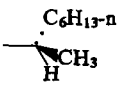
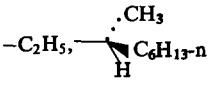
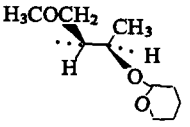
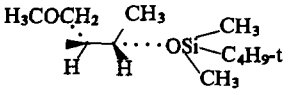
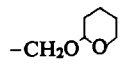
The reaction is regiospecific (the oxidised nitrogen atom in the azoxy-products formed is linked to the substituent R^2, which forms part of the alkylating agent). It involves nucleophilic attack by the N^2 atom of the diazotate anion on the electron-deficient carbon centre of the alkylating agent[80] and leads to complete or partial inversion of the configuration of the latter.[73]

The stereoselectivity of the reaction and the configurational stability of the alkyldiazotates make it possible in a number of instances to construct optically active azoxy-compounds with chiral centres at both nitrogen atoms of the diazene *N*-oxide group[73–75] (Table 2). In particular, the complete synthesis of elaiomycin[75]—a natural diazene *N*-oxide with powerful antibactericidal and carcinogenic properties—was achieved for the first time by the method considered.[7,81]

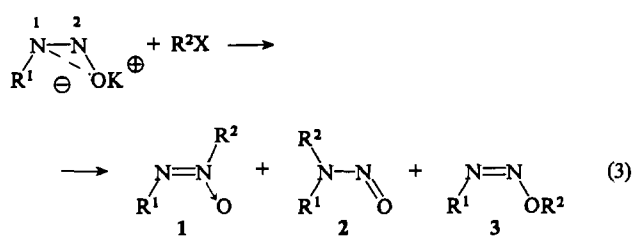
A serious disadvantage of Moss's method is the formation, together with the target azoxy-compounds **1**, of isomeric dialkylnitrosoamines **2** and diazoesters **3**—the products of alkylation at the N^1 and O atoms of the ambident diazotate anion.[80,82]

The diazoesters **3** are extremely unstable compounds and decompose under the reaction conditions, affording a mixture of nitrogen-free substances.

Table 2. Reaction conditions and the yields of products of the reactions of *syn*-alkyldiazotates with alkylating agents.

R^1	R^2	X	Solvent	Reaction temperature/°C	Time/h	Yield of product (%)[a]	Ref.
$-C_4H_9$-i, $-C_8H_{17}$-n, $-CH(CH_3)C_6H_5$, $-C_8H_{17}$-i	$-C_2H_5$	[b]	CH_2Cl_2	–	–	46 – 64	70, 71
$-C_8H_{17}$-n, $-CH(CH_3)C_6H_5$	$-C_2H_5$, $-C_4H_9$-n, $-C_3H_7$-i, $-C_4H_9$-i	I	HMPA	40	7	28 – 47	70, 71
$-C_8H_{17}$-i	$-CH_3$, $-C_3H_7$-n, $-CH_2CH=CH_2$	Br, I	HMPA	0–5	–	17 – 40	72
$-C_2H_5$, 	$-C_2H_5$, 	Cl, I	HMPA, CH_2Cl_2	–	–	20 – 50	73
	$-C_8H_{17}$-n	I	HMPA	20	15	65	74
$-CH(CH_3)C_6H_5$, $-CH(CH_3)C_6H_{11}$-cyclo	$-C_2H_5$	[b]	CH_2Cl_2	–30	2	53	11
	$-CH_3$	I	HMPA	25	12	29	75
$-CH(CH_3)C_6H_5$	$-C_2H_5$	I	THF	35	8	28	76
	$-CH_3$	I	Glyme	20	4	13	77
$-C_2H_5$	$-CH_3$	I	HMPA EPA	25 25	20 20	37 12	78 78

[a] The yields of products have been calculated relative to the *N*-nitrosourethanes used to obtain the *syn*-diazotates *in situ*.
[b] $(C_2H_5)_3OBF_4$ was used as the alkylating agent.
Note. HMPA = hexamethylphosphoramide; THF = tetrahydrofuran (Translator).



(3)

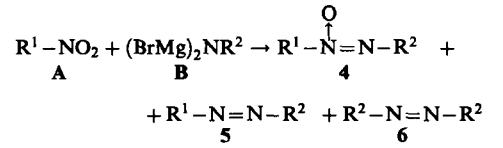
The influence of various factors on the mode of alkylation has been discussed in detail.[35] It is noteworthy that necessary conditions for the preferential formation of azoxy-compounds by Moss's reactions are the use of alkyldiazotates having the *syn*-configuration relative to the N=N bond[82] and the use of highly polar aprotic solvents, such as hexamethylphosphoramide[78] or glyme,[77] as the medium for carrying out the processes. However, even when the above conditions are maintained, it is not always possible to obtain the required azoxy-products.[77] The impossibility of using the more readily available *anti*-alkyldiazotates for the synthesis of diazene *N*-oxides[82] and also the impossibility of obtaining aromatic diazotates,[35] which are alkylated exclusively at the oxygen atom of the diazotate anion, significantly restricts the applications of Moss's reaction.

IV. Reactions of nitro- and nitroso-compounds with amino-derivatives

A more universal approach to the synthesis of asymmetrically substituted diazene *N*-oxides is based on the reactions of nitro- or nitroso-compounds with amino-derivatives. By varying the structures of the initial compounds, this procedure makes it possible to synthesise in one stage a wide range of products with the required combinations of substituents at the nitrogen atoms of the diazene *N*-oxide group.

1. Reactions of nitro-compounds with dimagnesyl derivatives of amines

In 1983 Japanese investigators[83] observed that aromatic nitro-compounds afford diazene *N*-oxides in their reactions with organodimagnesium derivatives of arylamines:

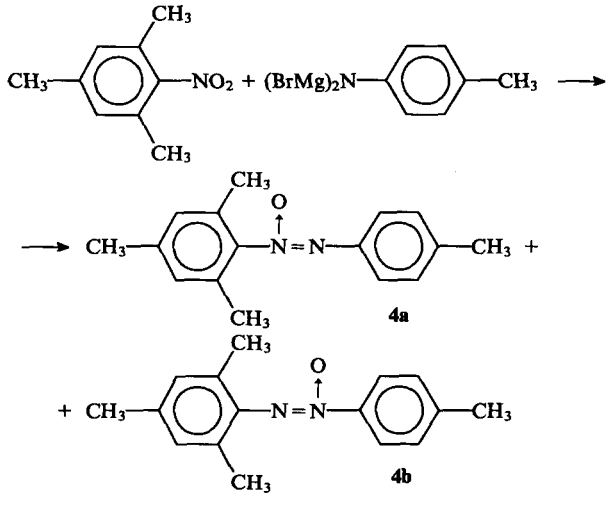


(4)

This reaction served as the basis of a new method of synthesis of asymmetrically substituted *N,N'*-diaryl(heteroaryl)diazene *N*-oxides. Its advantages are the ready availability of the initial compounds and the possibility of obtaining azoxyarenes with a fixed disposition of the oxidised nitrogen atom.

The reaction may be used to synthesise substituted *N,N'*-diaryldiazene *N*-oxides. Nitroarenes and dimagnesyl derivatives of arylamines containing alkyl, alkoxy-, and carbonyl substituents as well as halogen atoms in the aromatic ring enter into this reaction (Table 3). Azoxy-derivatives of naphthalene,[87,88] benzothiazole,[89] pyridine,[90] and ferrocene,[91] as well as polynuclear aromatic polyazoxy-compounds[92,93] have been obtained with its aid (Table 3). The synthesis of asymmetrically substituted azoxy-products from aliphatic nitro-compounds has been described.[94] The yields of diazene *N*-oxides **4** in this reaction reach 20–80% depending on the structure of the initial substances.

Unfortunately, together with the azoxy-compounds **4**, an appreciable amount of side products are formed during the reaction. These include in the first place, the diaryldiazenes **5** and **6**. The formation of the azo-compounds **5** and **6** can be explained[89–91] by the deoxygenation of the azoxyarenes **4** by the excess of the organomagnesium reagent $(BrMg)_2NR^2$ and by the oxidative dimerisation of the latter as a result of electron transfer from the reagent to the substrate. In this instance, the main factors influencing the relative yields of the products are the reactant ratio and the effectiveness of the one-electron transfer estimated from the oxidation-reduction potentials of the initial compounds.[86] Thus the introduction of electron-accepting substituents into the aryliminodimagnesyl reagent leads[83,84] to some increase in the yield of the azoxy-products **4**, while an increase in the ratio [B]/[A] is accompanied as a rule by an increase in the fraction of diaryldiazenes.[90] In a number of instances, the concept of the preliminary association under reaction conditions of the molecules of the initial compounds was used to account for the observed proportions of the products:[86,89]



The interaction of nitro-compounds with dimagnesyl derivatives of arylamines takes place as a rule regiospecifically and leads to the formation of azoxy-products in which the oxidised nitrogen atom is linked to the substituent R^1 forming part of the initial nitro-compound. This factor was used to obtain the isomeric *N,N'*-diaryldiazene *N*-oxides, which cannot be obtained by other methods and which differ in the position of the oxidised nitrogen atom in the diazene *N*-oxide group.[83,85,86,88,92] Substances having the properties of liquid crystals[29] and components of photosensitive compositions[88] have been synthesised in this way.

The only example of the isomerisation of the azoxy-group under the reaction conditions is the formation of isomeric azoxyarenes **4a** and **4b** from the sterically hindered 1-nitro-mesityl and *N,N*-bis(bromomagnesio)toluidine. The fraction of the rearrangement product **4b** increases with increase in the amount of the organometallic reagent, which indicates the involvement in the latter in the isomerisation process.[85]

Thus the interaction of nitro-compounds with dimagnesyl derivatives of arylamines constitutes a promising method of synthesis of asymmetrically substituted *N,N'*-diaryldiazene *N*-oxides of different structure. The wide scale employment of this reaction in synthetic practice has been held back, however, by the appreciable influence of the structure of the starting materials on the mode of this reaction and by the difficulty of isolating the target azoxy-compounds from the multicomponent mixtures of products formed in the course of the process. Furthermore, despite the data of Okubo et al.,[92] it is necessary to assess critically the possibility of synthesising with the aid of this method azoxyarenes carrying, apart from the azoxy-group, other functional group substituents sensitive to the action of bases.

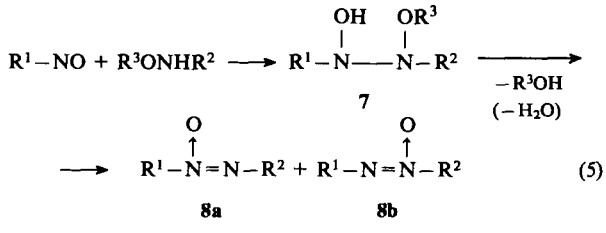
2. Synthesis of asymmetrically substituted diazene *N*-oxides by the reactions of nitroso-compounds with amino-derivatives

In our view, the synthesis of asymmetrically substituted diazene *N*-oxides from organic amino- and nitroso-compounds is the most promising. N-Substituted and O,N-disubstituted hydroxylamines as well as amino-derivatives containing an *N*–halogen bond are used as the amine component. It is noteworthy that reactions of this type were frequently considered in the chemical literature as special methods permitting the synthesis of definite fairly narrowly defined types of azoxy-compounds: triazene *N*-oxides,[95,96] *N'*-alkoxydiazene *N*-oxides,[97,98] *N'*-fluorodiazene *N*-oxides,[99,100,110] etc. In the present review, the processes involving the formation of the diazene *N*-oxide group from nitroso-compounds and amino-derivatives are presented for the first time as a general method of synthesis of carbo- and hetero-substituted azoxy-compounds.

a. Reactions of nitroso-compounds with N-substituted and O,N-disubstituted hydroxyl amines

The traditional method of synthesis of asymmetrically substituted azoxy- compounds involves reactions of aliphatic and aromatic nitroso-compounds with *N*-alkyl- and *N*-aryl-hydroxylamines (Table 4). The reactions are carried out as a rule in organic solvents (C_2H_5OH,[54,56,102] CH_3OH,[103,104] aqueous tetrahydrofuran,[104] and CH_2Cl_2[105]) over a wide temperature range. The use of UV irradiation, promoting the dissociation of dimeric nitrosoalkanes to the monomers, has a favourable effect.[104] Depending on the structure of the compounds involved in the reaction, the yields of the azoxy-products range from 5 to 85%.

A possible reaction mechanism involves the formation of the N=N bond between the nitrogen atoms of the hydroxyamino- and nitroso-groups and the elimination of one of the oxygen-containing substituents from the intermediate **7** with formation of the final reaction products.[104]



(5)

The observed regiospecificity of the process is determined by the structure of the OR^3 fragment and that of the substituents R^1 and R^2. Thus the use of N-substituted *O*-methyl-[104] and *O*-pivaloyl-hydroxylamines,[42] containing the readily removed methoxy- (R^3 = CH_3) and pivaloyl [R^3 = $C(O)C_4H_9$-t] groups, permits the regiospecific synthesis of diazene *N*-oxides in which

Table 3. The ratios of the reactants and the yields of the products of the reactions of nitro-compounds with dimagnesyl derivatives of arylamines (tetrahydrofuran, 55 °C, 1.5–5.0 h).

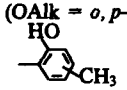
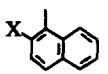
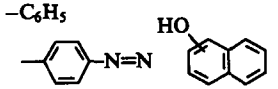
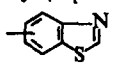
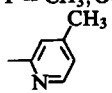
R^1	R^2	A/B molar ratio	Yields of products (%)			Ref.
			4	5	6	
$-C_6H_4-Hal$ (Hal = *o*, *m*, *p*-Cl, *o*, *p*-Br, *o*, *p*-I, *o*, *p*-F)	$-C_6H_4-Y$-*p* (Y = H, OCH_3, CH_3)	2.0–8.0	14–71	9–45	6–22	83–85
$-C_6H_4-X$-*p* (X = H, OCH_3, Cl)	$-C_6H_4-Hal$ (Hal = *m*, *p*-Cl)	2.0–5.0	65–81	10–15	6–12	83, 84
$-C_6H_4-Alk$ (Alk = *o*, *p*-CH_3, *m*-C_2H_5, *p*-C_3H_7)	$-C_6H_4-Y$ (Y = *o*, *m*, *p*-OCH_3, *m*-C_2H_5, *p*-CH_3, *p*-C_5H_{11}, *p*-$OC_6H_{13}-OC_{17}H_{35}$)	1.2–4.2	11–62	12–71	1–24	29, 83–86
$-C_6H_4-OAlk$ (OAlk = *o*, *p*-OCH_3, *p*-$OC_8H_{17}-OC_{22}H_{45}$)	$-C_6H_4-CH_3$-*p*	1.2–6.2	24–44	14–52	4–17	83, 85, 86
	$-C_6H_4-Y$-*p* (Y = CH_3, Cl)	2.0–8.0	14–43	7–33	6–12	87
 (X = H, OH)	$-C_6H_4-Y$-*p* (Y = H, Alk, OAlk)	2.0–3.0	13–40	~13	~4	87, 88
$-C_6H_5$	$-C_{10}H_7$-α	2.0	63	–	–	88
	$-C_6H_4-CH_3$-*p*	3.0	34–36	41–44	7	87
$-C_6H_4-[N=N-C_6H_4-N(CH_3)_2$-*p*$]$-*p*	$-C_6H_4-CH_3$-*p*	3.0	55	18	9	87
	$-C_6H_4-Y$-*p* (Y = CH_3, OCH_3, Cl)	2.0–7.0	17–74	0–34	4–31	89
$-C_6H_4-X$-*p* (X = CH_3, OCH_3, Cl)		1.1–10.0	1–24	7–74	4–14	90
$-C_5H_4FeC_5H_5$	$-C_6H_4-Y$-*p* (Y = H, CH_3, OCH_3, Cl)	5.0	52–73	9–34	4–12	91
$-C_6H_4-(X-C_6H_4-NO_2$-*p*$)$-*p* (X = CH_2, O, S)	$-C_6H_4-CH_3$-*p*	5.0	26–29 (bis-azoxy) 30–32 (azoxy-azo)	8–10	22–29	92, 93
$-C_6H_4-CH_3$-*p*	$-C_6H_4-[O-C_6H_4-N(MgBr)_2$-*p*$]$-*p*	0.63	12 (bis-azoxy) 13 (azoxy-azo)	–	–	92
$-C_6H_4-NO_2$-*m*, *p*	$-C_6H_4-CH_3$-*p*	5.0–6.0	26–43 (bis-azoxy) 11–15 (azoxy-azo)	0	18–25	92
$-C_6H_4-X$-*p* (X = CHO, $C(O)C_6H_4CH_3$-*p*)	$-C_6H_4-CH_3$-*p*	5.0	30–38	25–28	13–18	92
C_4H_9-t	$-C_6H_5$	2.5	35	–	–	94

Table 4. Reaction conditions and the yields of products in the reactions of nitroso-compounds with N-substituted and O,N-disubstituted hydroxylamines ($R^1 \neq R^2$).

R^1	R^2	R^3	Solvent	Reaction temperature/°C	Reaction time/h	Yield of **8a** (%)	Yield of **8b** (%)	Ref.
$-C(CH_3)_2CH_2CH_2CH(CH_3)_2$	$-CH_3$	H	–	110	2.0	57	–	56, 101
$-CF_3$	$-CH_3$, $-C_2H_5$, $-CH(CH_3)_2$, $-C_6H_5$	H	C_2H_5OH	–50	–	not quoted	–	102
$-C_6H_5$	$-CF_3$	H	C_2H_5OH	78	2.0	~5	–	102
$-C_6F_5$	$-C_6H_5$	H	C_2H_5OH	20	1.0	34	–	54
$-C_6H_5$	$-C_6F_5$	H	C_2H_5OH	20	24.0	–	70	54
$-C_6H_5$	$-CH(CH_3)C(NOH)C_6H_5$ (*syn*-isomer)	H	DMF	0	0.25	30	–	103
$-C_6H_5$	 (*syn*-isomer)	H	CH_3OH (CH_3ONa)	–10	0.33	30	–	103
$-C_6H_5$	$-CH_3$, $-CH_2C_6H_5$	H	C_2H_5OH, THF–H_2O	0–78	10.0	68–69	–	56, 104
$-C_4H_9$-t	$-CH_3$	H	THF–H_2O or without solvent	38–100	1.0–2.0	52–63	1	56, 104
$-CH_3$	$-C_4H_9$-t	H	CH_3OH (*hv*)	45	–	7	–	104
$-C_6H_{11}$-cyclo	$-CH_3$	H	CH_3OH	10–65 (*hv*)	–	70–76	7–14	104
		CH_3	THF–H_2O	50	–	55	–	104
$-CH_3$	$-C_6H_{11}$-cyclo	H	CH_3OH	45 (*hv*)	–	6	38	104
		CH_3	THF–H_2O	50		16	–	104
$-CH_2C_6H_5$, $-CH(CH_3)C_6H_5$	$-CH_3$	H	$CH_3OH - H_2O$	0–65 (*hv*)	–	39–64	16–18	104
$-C_6H_4-CH_3$-*o*	$-CH_3$	H	$THF - H_2O$	0	–	60	7	104
$-C_6H_5$, $-C(CH_3)_2NO_2$	$-CH_2CH(OH)CH_2OC_6H_5$	H	CH_2Cl_2	0–10	72	27–50	–	105
$-C_6H_3Cl_2$-*m*, *p*	$-C_6H_4-Cl$-*p*	$-C(O)C_4H_9$-t	–	–	–	not quoted	–	42
$-C_6H_4-Cl$-*p*	$-C_6H_3Cl_2$-*m*, *p*	$-C(O)C_4H_9$-t	–	–	–	not quoted	–	42

the nitrogen atom forming part of the initial nitroso-compound is oxidised. The stabilisation of the adducts **7**, formed from N-monosubstituted hydroxylamines and containing two hydroxy-groups (R^3 = H) is usually achieved as a result of the splitting off of the OH group from the nitrogen atom linked to the least sterically hindered hydrocarbon substituent[104] or the substituent having weaker electron-accepting properties.[54]

However, reactions with participation of N-substituted hydroxylamines most often lead to the formation of both possible regioisomers (Table 4).[104] In certain cases, the reaction proceeds via an alternative rather than the expected pathway.[102,104] Such unpredictability of the regiospecificity of the reaction significantly hinders the use of the method for the synthesis of asymmetrically substituted diazene *N*-oxides with the required structure.

$$Ar^1NO + HONHAr^2 \longrightarrow \underset{\mathbf{9a}}{[Ar^1NHO]^{\bullet}} + \underset{\mathbf{9b}}{[Ar^2NHO]^{\bullet}} \xrightarrow[(-H_2O)]{} \longrightarrow \begin{cases} Ar^1-\overset{\uparrow O}{N}=N-Ar^1 \\ Ar^1-\overset{\uparrow O}{N}=N-Ar^2 \\ Ar^2-\overset{\uparrow O}{N}=N-Ar^1 \\ Ar^2-\overset{\uparrow O}{N}=N-Ar^2 \end{cases} \quad (6)$$

Ar^1, Ar^2 = Ph, *p*-C_6H_4Cl, *p*-$C_6H_4CH_3$.

The reaction of nitroso-compounds with N-monosubstituted hydroxylamines (R^3 = H) is unsuitable for the selective synthesis of asymmetrically substituted aromatic diazene *N*-oxides. In this case, one observes the formation of a mixture of azoxy-arenes — the products of the disproportionation of the aminoxyl radicals **9a** and **9b** detected by the EPR method.[106-109]

The reaction of nitroso-compounds with O,N-disubstituted hydroxylamines (Table 4) has not come to be widely used in synthetic practice owing to the low availability of the initial compounds and the low yields of the azoxy-products.[42,104]

b. The reaction of nitroso-compounds with amino-derivatives containing N–halogen bonds

The method of synthesis of asymmetrically substituted azoxy-compounds based on the reaction of nitroso-compounds with amino-derivatives containing reactive N-halogen bonds has developed appreciably in recent years (Table 5).

$$R^1-NO + XYNR^2 \xrightarrow{Cat} R^1-\overset{\uparrow O}{N}=N-R^2 \quad (7)$$

Derivatives of ammonia,[99,112,118,119,124] aliphatic amines,[105,112-115] the amides of carboxylic[112] and sulphonic[114,116,120-122] acids, urethane,[64,111,112,114,149] urea,[112] tetrafluorohydro-azine,[99,100,121,123,125-128] and 4-(dichloroamino)tetrafluoropyridine[53] are used as the amino-derivatives and aliphatic,[99,100,105,112,113,115,123-132,134,149] aromatic,[53,64,99,105,112-116,118-123,133] and heterocyclic[117,122] *C*-nitroso-compounds are used as the nitroso-derivatives (Table 5). The initial nitrosoalkanes can be introduced into the reaction in a pure state or can be generated *in situ* from olefins,[100,125] *gem*-dinitroalkanes,[126] and oximes[123,132,133] under the reaction conditions.

The reactions occur as a rule at room temperature in organic solvents. Processes with participation of tetrafluorohydrazine,[125,127-131,134] which are frequently carried out by heating the components up to 60–80 °C in the absence of a solvent, are an exception.

A wide variety of asymmetrically substituted azoxy-compounds containing various functional group substituents were synthesised in this way: esters,[64,100,111,112,114-116,121,131,149] carboxy-derivatives,[116,122] sulphoxy-derivatives,[120-122] nitriles,[100,113,114] nitro-derivatives,[64,99,105,115,120,124,126,129] carbonyl derivatives,[111,112] hydroxy-derivatives,[105,123] difluroamino-derivatives,[100,123,125,132] halo-derivatives,[99,112,118,119,121,123-125] etc. The method is applicable to the synthesis of azoxy-compounds in which the diazene *N*-oxide group is linked to a carbon, chlorine, bromine, fluorine, or sulphur atom (Table 5). The involvement of bisnitroso-compounds in the reaction ensures a single-stage synthesis of azoxy-products containing two diazene *N*-oxide groups.[112,113,133]

The reaction is regiospecific. In all cases, its products are asymmetrically substituted diazene *N*-oxides, in which the nitrogen atom of the initial nitroso-compound is oxidised. The chemical nature of the substituent R^2 in the amino-derivative does not affect the mode of reaction.

Whereas the regiospecificity of this process is independent of the nature of the amino-derivative, the reactivity of *N*-haloamines in the given reaction is determined by the type of halogen atom forming part of their composition. *N*-Bromo-derivatives of amines and amides containing the exceptionally reactive N–Br bonds exhibit a high reactivity in reactions with nitroso-compounds.[114] The more stable *N*-chloroamines are distinguished by a greater inertness and interact with nitroso-compounds only in the presence of promoting agents (zerovalent silver,[112] pyridine,[116,118,120-122] alkali metal hydroxides,[113] and Ag^+, K^+, Cu^+, Cu^{2+}, Co^+, Co^{2+}, and Fe^{2+} halides or cyanides[53,64,105,111,112,114]). Among the *N*-fluoroamines, only difluoroammonia and tetrafluorohydrazine, containing N–H and N–N bonds weakened by fluorine atoms and tending as a result to dissociate, have been involved in the reactions with nitroso-compounds (Table 5).

The mechanism of the reaction of nitroso-compounds with *N*-haloamines has not been studied in detail owing to the low stability of the latter. However, it has been suggested that in most cases a radical process mechanism operates and includes the following stages: (1) homolytic dissociation of the N–Y bond in the R^2NXY molecule; (2) the addition of the *N*-haloaminyl radicals **10** formed to the nitroso-compound present in the system; (3) stabilisation of the spin-active adducts **11** as a result of the elimination of the halogen atom.

$$R^2-\overset{X}{\underset{Y}{N}} \xrightarrow[-\dot{Y}]{} R^2-\dot{N}-X \xrightarrow{R^1-NO} \underset{\mathbf{10}}{} \longrightarrow \underset{\mathbf{11}}{R^2-\overset{X}{N}-\overset{O^{\bullet}}{N}-R^1} \xrightarrow[-\dot{X}]{} R^2-\overset{\uparrow O}{N}=N-R^1 \quad (8)$$

X = Cl, Br, F; Y = Cl, Br, H, NF_2.

This mechanism has been confirmed by the EPR detection of the $\dot{N}F_2$ and $R^1-N(\dot{O})-NF_2$ radicals formed in the reaction of nitroso-compounds with tetrafluorohydrazine[128] and by the first order of the reaction of *N*,*N*-dibromoalkylamines with nitrosobenzene.[114] The increase in the reactivity of *N*-haloamines with decrease in the strength of the N–halogen bond and the role of promoting agents, involving the substitution of chlorine atoms in the amino-group by the more reactive bromine

Table 5. Reaction conditions and the yields of the products of the reactions of nitroso-compounds with *N*-haloamines, *N*-haloamides, and halohydrazines.

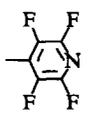
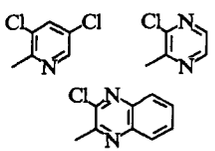
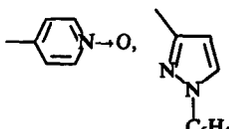
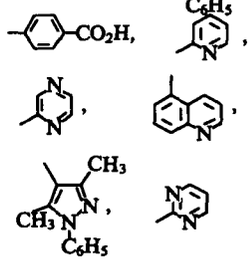
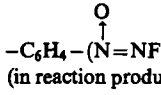
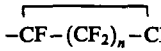
R^1	R^2	X	Y	Catalyst (Cat)	Solvent	Reaction temperature/°C	Reaction time/h	Product yield relative to to R'NO (%)	Ref.
$-C_6H_5$, $-\overline{CCl-(CH_2)_4}CH_2$	$-Alk$, $-CO_2C_2H_5$, $-C(O)C_6H_5$, $-C(O)N(CH_3)_2$	Cl	Cl	CuCl	CH_3CN	20	12	38–83	111, 112, 149
$-C_6H_5$	$-C_4H_9$-t, $-CO_2C_2H_5$	Cl	Cl	Ag^0, CuCN, CuBr, CuI, Cu_2S, $FeCl_2$, $CoBr_2$, KI, AgCN	CH_3CN	20	12	35–90	112
$-C_6H_5$, $-C_4H_9$-t, $-$Ad-1, $-C(CH_3)_2CN$, $-\overline{CZ-(CH_2)_4}CH_2$, (Z = Cl, CN)	$-C_4H_9$-t, $-C(CH_3)_2CN$, $-$Ad-1, $-\overline{C(CN)(CH_2)_4-CH_2}$	Cl	Cl	KOH, NaOH	CH_3OH-H_2O	20	1.0–2.0	36–80	113
$-C_6H_5$, $-\overline{CZ-CHZ-(CH_2)_3-CH_2}$	$-$Alk-t, $-CO_2C_2H_5$, $-SO_2-C_6H_4-CH_3$-*p* (Z = Cl, Br)	Br Cl	Br Cl	– $CuBr_2$, $CoBr_2$	CH_2Cl_2 or CH_3CN CH_3CN	0–20 0–20	~0.2 0.75	70–92 70–92	114 114
$-C_6H_5$, $-C(CH_3)_2NO_2$	$-CH_2CO_2$Alk	Br	Br	–	CH_2Cl_2	20	0.5–0.7	75–100	115
$-C_6H_4-Z$ (Z = H, Cl, Br, NO_2, OCH_3, CH_3, CO_2H)	$-CO_2$Alk	Cl	Cl	CuCl	CH_3CN	20	–	~50	64, 116
$-C_6H_5$, $-C_6H_4-CH_3$-*o*, 1,3,5-$(CH_3)_3C_6H_2-$, $-C_6F_5$		Cl	Cl	CuCl	CH_3CN	20	12	20–56	53
$-C_6H_5$, $-C(CH_3)_2NO_2$	$-CH_2CH(OH)CH_3$, $-CH_2CH_2OH$	Cl	Cl	$CuBr_2$	CH_3CN	0–2	0.5	64–98	105
	–Alk	Br	Br	–	–	–	–	–	117
$-C_6H_5$	Cl	Cl	H		CH_2Cl_2	20	0.3	43	118
$-C_6H_5$	Cl	Cl	Cl	KI	CH_2Cl_2	20	12	60	112
$-C_6H_5$, 1,3,5-$Cl_3C_6H_2-$	Br	Br	Br	–	CH_2Cl_2, CH_3CN	0	1.0	85–90	119

Table 5 (cont.).

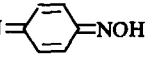
R^1	R^2	X	Y	Catalyst (Cat)	Solvent	Reaction temperature/°C	Reaction time/h	Product yield relative to to R'NO (%)	Ref.
$-C_6H_4-Z$ (Z = H, CH_3, NO_2, NR_2, CO_2H, $CO_2C_2H_5$)	$-SO_2-C_6H_4(Z)$ (Z = H, CH_3)	Cl	Na			80	2–4	50–92	116, 120, 121
	$-SO_2-C_6H_4-(Z)$-*p* (Z = H, CH_3)	Cl	Na			80	2–4		122
	$-SO_2-C_6H_4-(Z)$-*p* (Z = H, CH_3)	Cl	Na	$Cl^-N^+(CH_3)_3CH_2C_6H_5$	$CHCl_3/H_2O$	–	–		122
$-C_6H_4-Z$ (Z = H, *p*-Alk, *p*-Br, *p*-OH, *o*-$CO_2C_2H_5$)	F	F	NF_2	–	C_6H_5Cl, $CHCl_3$	0–70	2–3	30–90	99, 121, 123
$-C_6H_4-R$ (R = C_4H_9-t, $C(CH_3)_2Z$, CF_3)	F	F	H		CH_2Cl_2	20	–	23–50	99
$-\overline{CH(NO_2)-(CH_2)_4-CH_2}$	F	F	H	$BF_3-H_3PO_4$	HNF_2	–23	0.75	53	124
$CHR'(NF_2)-CR''R'''-$ (R', R'' = H, Alk; R''' = H, Alk, CO_2CH_3, CN)	F	F	NF_2	–	$CHCl_3$ –	20 80	19.0 8.0	34–48 [a] ~42 [a]	100 125
$-C(NO_2)_2-C_3H_7$-n	F	F	NF_2	–	CH_3OH	20	20.0	6 [b]	126
$-CF_3$	F	F	NF_2	–	–	120 20	1.0 6.0	45 23	127 128
$-CF_2CF_2NO_2$	F	F	NF_2	–	–	25	74.0	67	129
$-C(CF_3)_2CF_2OC_2H_5$	F	F	NF_2	–	–	80	3.0	35	130

$-CZ'Z''-CO_2C_2H_5$ ($Z', Z'' = F, Cl, CF_3$)	F	F	NF_2	–	–	70–80	4.0	24–45	131
$-CZ'Z''NF_2$ ($Z', Z'' =$ Alk)	F	F	NF_2	–	$CH_3CO_2C_2H_5$	60–80	8.0	~20[c]	132
					Freon-112	80	7.0–8.0	~35[c]	123
$-C_6H_4-NO$-*p* (in initial compound)	F	F	NF_2	–		20	–	61[d]	133
 (in reaction product)									
$-C(CH_3)_2Cl$	F	F	NF_2	–	–	0	4.0	61	128
 (n = 2, 3)	F	F	NF_2	Pyrex glass	–	55	16.0	–	134

[a] Yield calculated relative to XCH=CYZ.

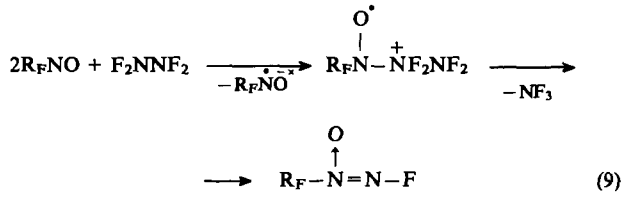
[b] Yield calculated relative to $C_3H_7C(NO_2)_2Na$.

[c] Yield calculated relative to XYC=NOH.

[d] Yield calculated relative to  .

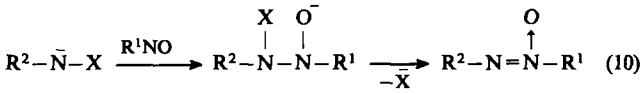
atoms[114] or the initiation of oxidation-reduction reactions of the amine component accompanied by the dissociation of the N–halogen bond therefore become understandable.[112,113]

In the reactions involving perfluoronitrosoalkanes, which exhibit an exceptionally high electron affinity,[110] a radical-anion mechanism is more probable. This has been confirmed by the EPR method, with the aid of which the presence of the $R_FNO^{-\cdot}$ radical-anions in the reaction mixture has been detected.[128]



(9)

The ionic mechanism apparently operates in the reaction of nitroso-compounds with the anions of the *N*-chloroamides of sulphonic acids[120–122] and dihaloamine derivatives in the presence of bases.[99,112,113,118]



(10)

X = F, Cl; R^2 = O_2SAr, Cl, F.

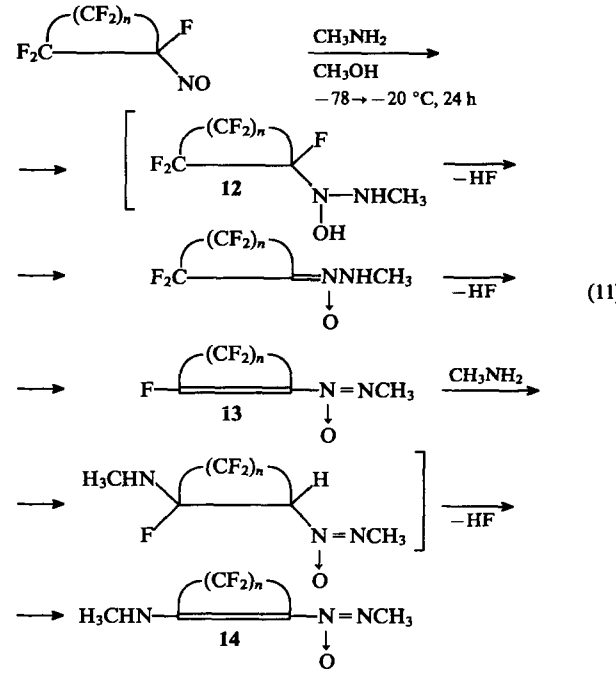
The "nitrene" mechanism of the reactions of nitroso-compounds with *N*-haloamines, *N*-haloamides, and *N*-halohydrazines, involving the formation of the nitrenes $R_2\ddot{N}$ and their addition to the N=O bond, is least probable in view of the absence of the characteristic products of the rearrangement and insertion of the nitrenes in the C–H bonds of the solvent.[113,114]

Thus the reaction of nitroso-compounds with amino-derivatives containing N–halogen bonds constitutes a convenient selective method of synthesis of asymmetrically substituted azoxy-compounds. The principal deficiency of the method is associated with the difficulty of isolation, the low stability, and the risk of explosion of the initial *N*-halo-compounds containing two and more N–halogen bonds. An additional restriction of the application of the reaction is the inability of *N*-haloamines to form the diazene *N*-oxide group in the reaction with *N*- and *O*-nitroso-compounds.[128]

c. Reactions of nitroso-compounds with compounds containing the NH_2 group

In view of the low stability of *N*-hydroxy- and *N*-halo-derivatives of amines, which limits their wide scale application, the direct synthesis of diazene *N*-oxides from nitroso-compounds and amino-derivatives containing an unsubstituted amino-group is extremely attractive. The reaction of nitroso-compounds with mono-substituted amines is known to entail usually the formation of asymmetrically substituted diazenes.[135–139] however, in a number of instances (when use is made of the characteristic features of the structures of certain types of starting compounds or when the reaction is carried out in the presence of oxidants), it is possible to drive the process towards the formation of diazene *N*-oxides.

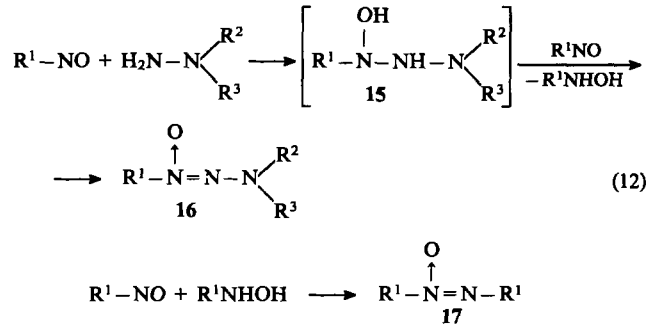
Thus the products of the reaction of perfluoronitrosocyclobutane and cyclopentane with methylamine are methylazoxyperfluorocycloalkenes **14**. The reaction probably proceeds via the nucleophilic addition of methylamine to the N=O bond. The resulting adduct **12** is stabilised under these conditions by eliminating a HF molecule and by the addition of methylamine to the activated double bond of the azoxyalkene **13**.[140] The dehydrofluorination process is preferred to the usual process involving the dehydration of type **12** intermediates apparently because of the thermodynamic stability of the conjugated π-system forming part of compound **13**.



(11)

n = 2, 3

The reaction of nitroso-compounds with 1,1-dialkyl-,[96,144] 1-alkyl-1-aryl-,[96,141–144] and 1,1-diaryl-hydrazines,[96,142,143] leading to triazene 1-oxides, also takes place with retention of the NO bond (Table 6). Various nitrosoarenes, including those containing substituents in the aromatic ring,[141–144] and tertiary nitrosoalkanes[96] enter into this reaction. The latter probably proceeds via a stage involving the formation of the 1-hydroxy-triazane **15**, which is oxidised to the product **16** by the excess nitroso-compound.[96,144]



(12)

The side products of this oxidation-reduction reaction are hydroxy-aminoderivatives R^1NHOH and the products of their condensation with R^1NO — symmetrically substituted diazene *N*-oxides **17**.[96] The necessity for the use of an appreciable excess of the nitroso-compound (completion of the reaction requires 3 moles of the nitroso-compound per mole of hydrazine) and the marked dependence of the yields of triazene 1-oxides on the structure of the starting materials (Table 6) are serious disadvantages of the method, which lowers its preparative value.

In order to intensify the reactions leading to the formation of the diazene *N*-oxide group, the reactions of nitroso-compounds with primary amino-derivatives are carried out in the presence of compounds capable of oxidising the nitrogen atoms of the amino-groups but inert with respect to the nitroso-compound present in the system (Table 7). Mercury oxide,[96,145] diethyl azodicarboxylate,[144] lead tetraacetate,[96–98,148,150,151] phenyl iodosoacetate,[98,116,146,152,153,155] as well as halogenating agents [sodium hypochlorite,[113] bromine,[156] dibromoisocyanurate (DBI),[157–161]] and the *tert*-butyl hypochlorite–iodine[154] and *tert*-butyl hypochlorite–sodium methoxide[158] systems have been used as

Table 6. Reaction conditions and the yields of the products of the reactions of nitroso-compounds with 1,1-disubstituted hydrazines in the absence of an oxidant.

R^1	R^2	R^3	Solvent	$\frac{(R^1NO)}{(H_2NNR^2R^3)}$	Reaction temperature/°C	Reaction time/h	Yield (%)[a]	Ref.
$-C_6H_5$	$-C_6H_5$	$-C_6H_5$	C_2H_5OH	3:1	−5 – +5	0.45	79	96, 143
$-C_6H_5$	$-CH_3$	$-CH_3$	C_2H_5OH	3:1	−5 – +20	0.45	74	96
$-C_6H_5$, $-C_6H_4-Br$-*p*	$-C_6H_5$	$-CH_3$	C_2H_5OH	3:1	−5 – +20	0.45	75	96, 143
$-C_4H_9$-t	$-C_6H_5$	$-C_6H_5$	C_2H_5OH	3:1	20	580	10	96
$-C_6H_3Cl_2$-2,6	$-CH_2C_6H_5$	$-CH_2C_6H_5$	THF	2:1	20	24	50	144
$-C_6H_3Cl_2$-2,6	$-CH_3$	$-CH_3$	THF	2:1	20	24	24	144
$-C_6H_4-Cl$-*p*	$-C_6H_5$	$-CH_3$	THF	1:1	−60 – +20	1.0	14	144
$-C_6H_4-N(CH_3)_2$-*p*	$-C_6H_5$	$-CH_3$	THF	1:1	−60	1.0	5	144

Note. The table does not include the results of studies in which the experiment was not described and no information was given about the yields of products (references to these investigations can be found in a monograph[95]).
[a] The yield calculated relative to the hydrazine component is quoted.

such substances. The promising nature of the reaction of nitroso-compounds with amino-derivatives in the presence of oxidants is indicated by the finding that it was possible to involve in this reaction aliphatic,[96–98, 146, 148, 150, 152, 157–159, 161] aromatic,[96, 113, 116, 145, 146, 152–154, 156, 158–161] and heterocyclic[98, 152, 153, 155, 158, 161] *C*-nitroso-compounds as well as *N*-nitroso-compounds.[147]

Among amino-derivatives, alkyl- and cycloalkyl-amines,[113, 146, 154, 157] cyanamide,[116, 146, 152, 153, 155, 158, 228–231] urethane,[152, 158] urea,[158] the amides of phosphoric[161] and sulphonic[146, 152] acids, 1,1-disubstituted derivatives of hydrazine,[96, 144–147, 156, 160] and alkoxyamines[97, 98, 148, 150, 151] were used. Such a wide range of substances involved in the given reaction ensures the synthesis with its aid of a wide range of carbo- and hetero-substituted azoxy-compounds whose diazene *N*-oxide group is linked to carbon,[113, 116, 146, 152–154, 157–159] oxygen,[97, 98, 148, 150, 151] nitrogen,[96, 144–147, 156, 160] and sulphur[146, 152] atoms.

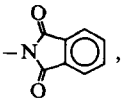
$$R^1-NO + H_2N-R^2 \xrightarrow{Ox} R^1-\overset{\overset{O}{\uparrow}}{N}=N-R^2 \qquad (13)$$

The majority of reactions of the given type take place readily under exceptionally mild conditions (at room or lower temperatures in inert organic solvents) and can be used to obtain azoxy-products containing various, including labile, functional groups.

The regiospecificity of the method is valuable. Regardless of the structure of the nitroso- and amino-compounds involved in the process and of the oxidant employed, the nitrogen atom forming part of the initial nitroso-compound is oxidised. The chemistry of the process is determined by the structure of the amine component and by the chemical nature of the oxidant. The mechanism of reaction (13) in the presence of oxidants such as mercury oxide or ethyl azodicarboxylate (a three-component reaction) is apparently similar to that of the corresponding two-component reaction (12) with the sole difference that in the given instance the intermediate **15** is dehydrogenated to the corresponding triazene 1-oxide by the oxidant present in the system.[96, 144] The synthetic result of the use of the oxidant is an increase in the effectiveness of the process, which can be carried out in the absence of an excess of the nitroso-compound.

When $Pb(OAc)_4$ and $C_6H_5I(OAc)_2$ are used as oxidants, the reaction of nitroso-compounds with amino-derivatives probably proceeds via a different pathway. Here the role of the oxidant consists in the formation of an electron-deficient centre of the nitrene type at the nitrogen atom of the amino-group, which subsequently interacts with the nitroso-compound to form the required diazene *N*-oxides.[96, 97, 147, 148, 151, 152]

$$R^2NH_2 \xrightarrow[\text{or } C_6H_5I(OAc)_2]{Pb(OAc)_4} [R^2N:] \xrightarrow{R^1NO} R^2-\overset{\overset{O}{\uparrow}}{N}=N-R^1 \qquad (14)$$

$R^2 =$  , $-OAlk$, $-CN$, $-CO_2C_2H_5$, $-SO_2C_6H_5$.

In the case of $C_6H_5I(OAc)_2$, a coordination process mechanism involving the formation and dissociation of the bond between the nitrogen atom of the amine component and the hypervalent iodine atom, has also been proposed.[146] When $Pb(OAc)_4$ and $C_6H_5I(OAc)_2$ are used, it is useful to involve in the reaction amino-derivatives capable of forming fairly stable nitrenes on treatment with oxidants: *N*-aminophthalimide, alkoxyamines, and cyanamide.[162, 163] Reactions with participation of the amides of arenesulphonic acids and urethane, whose nitrene derivatives are less stable, are characterised by a lower effectiveness.[152] The use of 1,1-dialkylhydrazines, incapable of forming stable nitrenoids in neutral media,[164] as amino-derivatives leads to the formation of 1,1,4,4-tetraalkyltetrazenes — the products of the oxidative dimerisation of the initial amino-compounds — instead of the expected triazene *N*-oxides.[96]

$$PhNO + H_2N-N(CH_3)_2 \xrightarrow{Pb(OAc)_4} \begin{cases} Ph-\overset{\overset{O}{\uparrow}}{N}=N-N(CH_3)_2 \\ (H_3C)_2NN=NN(CH_3)_2 \end{cases} \qquad (15)$$

Finally, in the presence of halogenating agents,[113, 154] the reactions of nitroso-compounds with amino-derivatives probably proceed via a stage involving the formation of *N*-halo-derivatives

Table 7. Reaction conditions and the yields of the products of the reactions of nitroso-compounds with primary amino-derivatives in the presence of oxidants.

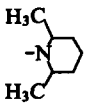
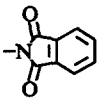
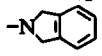
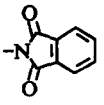
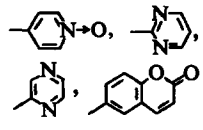
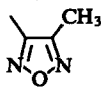
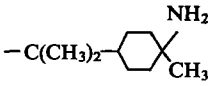
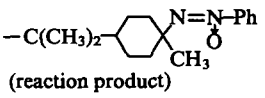
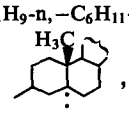
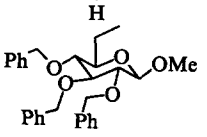
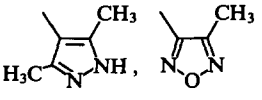
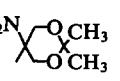
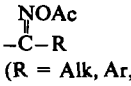
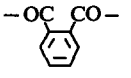
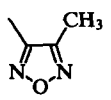
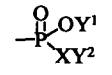
R^1	R^2	Oxidant (Ox)	Solvent	Reaction temperature/ °C	Reaction time/h	Yield of product (%)	Ref.
$-C_6H_4-N(CH_3)_2$-*p*	$-N(CH_3)_2$	HgO	C_2H_5OH	25	16.0	25	145
$-C_6H_5$		HgO	$CH_3CO_2C_2H_5$	25	16.0	71	145
$-C_6H_5$		HgO	$CH_3CO_2C_2H_5$	25	16.0	74	145
$-C_6H_4-F$-*o*	$-N(CH_3)_2$	HgO	$CH_3CO_2C_2H_5$	25	16.0	12	145
$-C_4H_9$-t	$-N(CH_3)_2$, $-N(C_6H_5)_2$	HgO	C_2H_5OH	20	1.0	29–46	96
$-C_6H_4-Cl$-*p*	$-N(CH_3)C_6H_5$	$(H_5C_2O_2CN{=})_2$	THF	−60	1.0	30	144
$-C_6H_4-N(CH_3)_2$-*p*	$-N(CH_3)C_6H_5$	$(H_5C_2O_2CN{=})_2$	THF	−60	1.0	75	144
$-C_4H_9$-t, $-C_6H_4-X$ (X = H, *o*, *p*-CH_3, *p*-$N(CH_3)_2$, *p*-CO_2CH_3)		$Pb(OAc)_4$	CH_2Cl_2 (K_2CO_3)	20	0.5–1.0	79–94	96
		$C_6H_5I(OAc)_2$	CH_2Cl_2	20	18.0	60–68	146
$-N(CH_3)_2$,  , 		$Pb(OAc)_4$	CH_2Cl_2 (K_2CO_3)	0→20	0.5–1.0	69–79	147
$-C_4H_9$-t, $-C(CH_3)_2CH_2CH_3$	$-OC_nH_{2n+1}$ ($n = 1-4$), $-OCH_2CH{=}CH_2$	$Pb(OAc)_4$	CH_2Cl_2 (K_2CO_3)	−45 +20	1.0 0.5	60–70 60–70	97, 148 97, 148
$-CH(C_6H_5)_2$ [a]	$-OCH(C_6H_5)_2$	$Pb(OAc)_4$	CH_2Cl_2	0	0.2	32	150
$-N(CH_3)_2$, $-N(C_2H_5)_2$	$-OC_nH_{2n+1}$ ($n = 1-3$)	$Pb(OAc)_4$	CH_2Cl_2 (K_2CO_3)	−45	–	13–47	151
$-C(CH_3)_2NO_2$, $-C(NO_2)-(CH_2)_4-CH_2$	$-OCH_3$	$Pb(OAc)_4$	CH_2Cl_2 (K_2CO_3)	−45 +20	1.0 0.5	8–16 8–16	98 98
$-C_4H_9$-t, $-C_6H_4-X$ (X = H, Cl, $N(CH_3)_2$, NHAc, C(O)NHAr, $-O_2S-N$ )	$-CN$	$C_6H_5I(OAc)_2$	CH_2Cl_2, $CHCl_3$, DMF	30	~1.0	85–95	152, 228–230
$-C_6H_4-COOH$-*o*, *p*	$-CN$	$C_6H_5I(OAc)_2$	Py	30	1.0	50–77	116
 (X = CH, N), 	$-CN$	$C_6H_5I(OAc)_2$	CH_2Cl_2	30	~1.0	35–90	146, 153, 155, 231
$-C_6H_4-X$-*o* (X = H, CH_3)	$-O_2S-Ar$, $-CO_2C_2H_5$	$C_6H_5I(OAc)_2$	CH_2Cl_2	30	4.0	~30–50	146, 152
$-C_6H_4-X$-*o* (X = H, CH_3), $-C_4H_9$-t	$-C_4H_9$-t, 	$C_6H_5I(OAc)_2$	CH_2Cl_2	20	18.0	55–67	146
$-C(NO_2)-(CH_2)_4-CH_2$, $-C(CH_3)_2OC(O)CH_3$ [b],	$-OCH_3$	$C_6H_5I(OAc)_2$	CH_2Cl_2	35	4.0	17–53	98
$-C_6H_5$, 							

Table 7 (cont.).

R^1	R^2	Oxidant (Ox)	Solvent	Reaction temperature/ °C	Reaction time/h	Yield of product (%)	Ref.
$-C_6H_5$	$-C_4H_9$-t	NaOCl	$CH_3OH - H_2O$	20	2.0	83	113
$-C_6H_5$	 (initial compound)	NaOCl	$CH_3OH - H_2O$	20	2.0	75	113
	 (reaction product)						
$-C_6H_5$	$-C_4H_9$-n, $-C_6H_{11}$-cyclo,  , 	t-$C_4H_9OCl - I_2$	C_6H_6	20	16.0	62–97	154
$-C_6H_5$	$-N(R)CH_3$ ($R = CH_3, CH_2CH_2CN$)	Br_2	$HBr - (C_2H_5)_2O$	−20 – +15	4–10	63–75	156
	$-CH_3, -CH_2CH_2NH_2$	DBI	CH_2Cl_2	0–20	24	86–92	157
($R = CH_3$, Br)							
$-C_6H_5, -C(CH_3)_2NO_2$	$-CN, -CO_2C_2H_5$	DBI	CH_2Cl_2	−20 – +20	3.0	32–95	158
$-C(CH_3)_2Br$, $-C(CH_3)BrNO_2$ [c], 	$-C(O)NH_2$	t-$C_4H_9OCl - CH_3O^-$	CH_3OH	−60 – +20	5.0	29–56	158
$-C_6H_5$, 	 ($R = Alk, Ar, CO_2C_2H_5$)	DBI	CH_2Cl_2, $CHCl_3$	20	5.0	14–65	159
$-C_6H_5$	$-NR'R''$ ($R', R'' = CH_3$, CH_2CH_2CN, $-CO(CH_2)_2-$, 	DBI	CH_2Cl_2, THF – $(C_2H_5)_2O$	−40 – +20	5.0	57–98	160
$-C_6H_5, -C(CH_3)_2NO_2$, $-C(CH_3)_2Br$, 	 ($Y^1, Y^2 = Alk, Ar$; $X = O, NR^3$)	DBI	CH_2Cl_2	20	12.0	47–92	161, 232

[a] The nitroso-compound was obtained *in situ* by oxidising $H_2NOCHPh_2$.

[b] The nitroso-compound is formed *in situ* from acetone oxime.

[c] The nitroso-compound was obtained *in situ* by brominating a salt of ethanenitrolic acid.

of amines[157,158,161] or hydrazines,[160] which interact with nitroso-compounds via one of the pathways examined in section I.3 [via a radical pathway[154] — reaction (8), with participation of diazenium cations[156] — reaction (9), or with participation of the anions of *N*-haloamines[158] — reaction (10)].

Reaction (16) is superior to reaction (7) since in this case there is no necessity to isolate and purify the intermediates with the N–halogen bond, generated *in situ*, which makes it possible to involve successfully in the reaction amino-compounds whose halo-derivatives are distinguished by an extremely low stability (cyanamide,[158] 1,1-disubstituted hydrazines,[156,160] ethers of amidoximes,[159] etc.).

$$AlkNH_2 \xrightarrow[X = Hal]{X^+} \begin{bmatrix} AlkNHX \\ AlkNX_2 \end{bmatrix} \xrightarrow{R^1NO} AlkN{=}\overset{\overset{O}{\uparrow}}{N}R^1 \qquad (16)$$

Overall, the oxidative condensation of nitroso-compounds with substances containing a primary amino-group constitutes one of the most promising approaches to the formation of C-, N-, P-, and O-substituted diazene *N*-oxides of different structure.

V. Interaction of anions containing the N_2O_2 structural fragment with electrophiles

A specific method of synthesis of asymmetrically substituted azoxy-compounds in which the nitrogen atoms of the diazene *N*-oxide group are linked to two oxygen atoms involves the reaction of anions containing the N_2O_2 structural fragment (salts of N-substituted *N*-nitrosohydroxylamines, primary *N*-nitroamines, *N*-nitroamides of hyponitrous acid) with electrophiles. This reaction is accompanied by the formation of the C–O bond the elements of which do not form part of the diazene *N*-oxide group and is therefore considered separately from the chemically related reaction involving the alkylation of *syn*-diazotates [see section III, reaction (2)]. The early studies of reaction (17) and the general principles governing the alkylation of ambient anions with N–N bonds were described in another review.[35] This review deals with the present state of the problem and considers primarily studies carried out in recent years which have greatly expanded the applications and preparative possibilities of the method.

$$R^1{-}N{-}\overset{\ominus}{N}{-}\dot{O}\,Cat^{\oplus} + XR^2 \longrightarrow \underset{\mathbf{18}}{R^1{-}\overset{\overset{O}{\uparrow}}{N}{=}N{-}OR^2} + \underset{\mathbf{19}}{R^1{-}\overset{N=O}{\overset{|}{N}}{-}OR^2} \qquad (17)$$

The alkylation (sulphonylation, stannylation) of salts of N-substituted *N*-nitrosohydroxylamines, which makes it possible to synthesise regiospecifically azoxy-products in which the alkoxy-substituent is linked to the distal nitrogen atom of the diazene *N*-oxide group, has come to be most widely used in synthetic practice among reactions of the type considered (Table 8). The range of *N*-nitrosohydroxylamine salts involved in this reaction is fairly wide: these are the salts of aliphatic and aromatic *N*-nitrosohydroxylamines, including those containing different functional group substituents in the molecule. The cations of alkali[166,167,172,173,176,178–182] and alkaline earth metals,[170] silver,[165,166,168,169,185] ammonia,[165–167,181,182,184] and organic bases[174] were used as counterions. The electrophiles were alkyl halides, dialkyl sulphates, oxirans, toluene-*p*-sulphonyl chloride, and anhydrides of trifluoromethanesulphonic acid, and compounds with the Sn–Cl bond (Table 8).

The reactions are carried out in hydroxylated solvents,[165–167,170–173,175–177,179,181,183] dimethyl sulphoxide,[166,175,176,178–180,186] chlorohydrocarbons,[182] ether,[166,168,169,185] acetonitrile,[174] and sulphur dioxide[184] at −10 to +80 °C.

A favourable effect is achieved by carrying out the reaction in the presence of a base, which neutralises the products of the side processes. An important advantage of the reaction is the possibility of synthesising with its aid *N'*-alkoxydiazene *N*-oxides containing different functional groups in the hydrocarbon fragments of the molecule. Thus alkylation of salts of *N*-nitrosohydroxylamines containing carbonyl[175–177] or ester[178,180] groups proceeds with retention of the above substituents and makes it possible to synthesise in one stage the corresponding *N*-alkyl-*N'*-alkoxydiazene *N*-oxides. Further-more, the formation of the diazene *N*-oxide fragment proceeds smoothly also in the presence in the anion being alkylated of a carboxy-group, which is transformed into an alkoxycarbonyl group under the reaction conditions.[179,180]

N'-Alkoxydiazene *N*-oxides containing functional groups in the alkoxy-component of the molecule are formed in the reaction of salts of *N*-nitrosohydroxylamines with alkylating agents containing functional groups.[166,168,172–174] The involvement of oxirans in the reaction is accompanied by the regioselective opening of the oxiran ring and the formation of hydroxylated *N'*-alkoxydiazene *N*-oxides, in which the diazene *N*-oxide fragment is linked to the most hydrogenated carbon atom of the given compound.[172,173]

The interaction of salts of *N*-nitrosohydroxylamines with sulphonic acid chlorides[181–184] and tin halides[185,186] makes it possible to synthesise azoxy-products (unavailable by other methods) containing a fragment comprising several directly linked heteroatoms: $-\overset{\overset{O}{\uparrow}}{N}{=}N{-}O{-}E{-}$ (E = S, Sn). The products of the alkylation of nitrosohydroxylamines by tin dihalides have a unique structure. In this case the reaction proceeds with participation of both halogen atoms and leads to the formation of bisdiazene *N*-oxides in which the heteroatomic chain consists of nine heteroatoms (Table 8).[185]

Azoxy-compounds containing two diazene *N*-oxide groups can be obtained also by the reaction of salts of *N*-nitrosohydroxylamines with epibromohydrin[172,173] (Table 8) and by alkylating the dianions of 1,1-bis(*N'*-nitrosohydroxyamine)alkanes (Table 9).[167,187,188] The 1,1-bis(*N'*-alkoxy-*N*-oxodiazeno)-alkanes **20** proved unexpectedly stable. Such compounds can be purified by heating with acids and alkalis.[167,169]

$$R^1{-}CH(N{-}\overset{\ominus}{N}{-}\dot{O})_2 \cdot 2Cat^{\oplus} + XR^2 \longrightarrow \underset{\mathbf{20}}{R^1{-}CH(\overset{\overset{O}{\uparrow}}{N}{=}N{-}OR^2)_2} \qquad (18)$$

Kinetic studies have shown that the alkylation reactions of salts of mono- and bis-(*N*-nitrosohydroxyamino)alkanes with dimethyl sulphate are first order with respect to each component and proceed via a bimolecular nucleophilic substitution mechanism.[171,190] The stringent requirements which must be met by the transition state of the process are confirmed by the high negative entropies of activation for the reaction (−63 to −127 J mol^{-1} K^{-1})[171,190] and by the decrease in the yield of the azoxy-products with increase in the three-dimensional branching of the alkylating agent.[165]

The alkylation reaction is complicated in many instances by the low stability of the salts of the initial *N*-nitrosohydroxylamines and the associated impossibility of isolating them in a pure state. The salts obtained by nitrosating the corresponding hydroxyamino-derivatives,[181] Grignard reagents,[170,181,183] or carbonyl compounds[175–178,180] in an alkaline medium are as a rule highly contaminated by side products, which lower appreciably the yields of the *N'*-alkoxydiazene *N*-oxides synthesised from them. The appreciable influence of the quality

Table 8. Reaction conditions and yields of the products of the reactions of salts of N-substituted *N*-nitrosohydroxylamines with electrophiles.

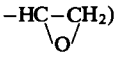
R^1	R^2	Catalyst	X	Solvent	Reaction temperature/°C	Reaction time/h	Yield of **18** (%)[a]	Ref.
$-C_6H_5$	$-CH_3$, $-C_2H_5$, $-C_3H_7$-i $-C_4H_9$-n, $-C_4H_9$-i, $-C_4H_9$-t, –Ad-1	NH_4, Ag	Br, SO_4CH_3	C_3H_7OH, H_2O	60	2–12	5–60	165–167
$-C_6H_5$, $-CH_3$	$-C_2H_5$, $-CH_2OR^3$ (R^3 = CH_3, C_2H_5, C_3H_7-i, $C(O)CH_3$)	Ag	Cl, Br, I	$(C_2H_5)_2O$	20–36	6–15	47–82	168, 169
$-C_2H_5$, $-C_3H_7$-i, $-C_4H_9$-n, $-CH_2C_4H_9$-t	$-CH_3$	MgBr, MgCl	SO_4CH_3	CH_3OH (H_2O)	65–90	2–3	18–43[b]	170
$-CH_3$, $-C_4H_9$-n, $-CH_2C_4H_9$-t	$-CH_3$	K, Na	SO_4CH_3	H_2O	60–90	1–2	71–80	170, 171, 189
$-C_6H_5$	$-CH_2Y$ (Y = $-CH=CH_2$, $-C_6H_5$, $-C\equiv CH$, 	Na, Ag	Cl, Br	$(C_2H_5)_2O$, DMSO, $(CH_3)_2CO$–H_2O, C_2H_5OH	20–78	1.5–36	20–47	166, 167, 172, 173
$-C_6H_5$	$-CH_2CH_2Y$ (Y = Br, OH, OAc)	Na	Cl, Br	DMSO, $(CH_3)_2CO$–H_2O, C_2H_5OH–H_2O	54–80	4–20	15–27	166
$-C_6H_5$	 (R^3 = H, CH_3; R^4 = H, CH_3, CH_2OH, CH_2OCH_3, $CH_2OC_6H_5$, $CH_2ON=N(O)C_6H_5$)	Na	[c]	$(CH_3)_2CO$–H_2O	50–60	8–18	19–48	172, 173
$-CH_3$	$-CH_2CH=CH_2$	NEt_4	Br	CH_3CN	20	2.0	34 (yield of **19**: 55%)	174
$-CHR^3R^4$ (R^3, R^4 = Alk, cyclo-Alk)	$-CH_3$, $-C_2H_5$, $-C_3H_7$-n, $-C_4H_9$-n	Na	Br	DMSO	55	1.5	25–30[d]	175, 176
$-CR^3R^4-C(O)C_6H_5$ (R^3, R^4 = Alk, cyclo-Alk)	$-CH_3$	Na	I	CH_3OH	55	3–5	54–62[e]	175, 176
$-CR^3R^4-C(O)CHR^3R^4$ (R^3, R^4 = Alk, cyclo-Alk)	$-CH_3$, $-C_2H_5$, $-C_4H_9$-n	Na	I	CH_3OH	60	3.0	50–85[e]	176, 177
$-CR^3R^4\overset{O}{\overset{\|}{C}}CR^3R^4\overset{O}{\overset{\|}{N}}=NOCH_3$ (R^3, R^4 = Alk, cyclo-Alk)	$-CH_3$	Na	I	CH_3OH	60	3.0	45–50[e]	177
$-CH(CO_2CH_3)_2$	$-CH_3$, $-C_2H_5$, $-C_3H_7$-i	Na	I	DMSO	50–60	2.0	10–15[e]	178
$-CH(R)COONa$ (in initial compound) $-CH(R)COOR^2$ (in product) (R = H, Alk, cyclo-Alk)	$-CH_3$, $-C_2H_5$, $-C_3H_7$-i, $-C_4H_9$-n	Na	I, SO_4CH_3	DMSO, H_2O	60–65	1–10	12–25	179–180
$-CH(R)COOCH_3$ (R = Alk, cyclo-Alk)	$-CH_3$	Na	I	DMSO	60	4.0	45–50[f]	180
$-CH_3$, $-CH_2C_3H_7$-i	$-O_2S-C_6H_4CH_3$-*p*	Na, K	Cl	H_2O, CH_2Cl_2	20	12	27–52[j]	181, 182
$-C_6H_{11}$-cyclo $-(CH_2)_n-C_6H_5$ (n = 1,2)	$-O_2S-C_6H_4CH_3$-*p*	Na, NH_4	Cl	$(CH_3)_2CO$–H_2O, CH_2Cl_2	20	0.5	4–20[b]	182, 183
$-C_6H_4-Cl$-*p*	$-CH_3$, $-O_2S-C_6H_4CH_3$-*p*	Na	Cl, SO_4CH_3	H_2O, $(CH_3)_2CO$–H_2O	20	0.6–0.8	24–32[h]	167, 181
$-C_6H_4-Y$-*p* (Y = H, CH_3)	$-O_2S-C_6H_4CH_3$-*p*	NH_4	Cl	H_2O	20	12	55–63	181

Table 8. (cont.).

R^1	R^2	Catalyst	X	Solvent	Reaction temperature/°C	Reaction time/h	Yield of **18** (%)[a]	Ref.
$-CH_3$	$-O_2SCF_3$	NH_4	OSO_2CF_3	SO_2	−10	0.25	not quoted	184
$-C_6H_5$, $-C_6H_{11}$-cyclo	$-SnR_3$ (R = Alk, C_6H_5)	Ag, K	Cl	$(C_2H_5)_2O$, DMSO	20	20	87–90	185,186
$-C_6H_5$	$-SnR_2-$ (R = Alk)	Ag	Cl	$(C_2H_5)_2O$	–	–	~90[i]	185

[a] The product **19** was not isolated.
[b] Yield calculated relative to R^1X (X = halogen).
[c] The compounds $H_2C(O)CR^3R^4$ where used as alkylating agents.
[d] Yield calculated relative to $R^1C(O)X$.
[e] Yield calculated relative to R^1H.
[f] Yield calculated relative to $CH(R)(CO_2CH_3)_2$.
[j] Yield calculated relative to R^1MgBr.
[h] Yield calculated relative to R^1NHOH.
[i] The reaction product is $(PhN(O)=NO)_2SnR_2$.

of the initial compounds on the effectiveness of the alkylation reaction is confirmed by the increase in the yields of the azoxy-products when purified salts of *N*-alkyl-*N*-nitrosohydroxylamines are involved in the reaction.[170,181]

Another factor which complicates the alkylation reaction is the ambident nature of the anions of *N*-nitrosohydroxylamines. Both oxygen atoms of the RN_2O_2 group can participate in the process, which leads to the formation, together with the required *N'*-alkoxydiazene *N*-oxides **18**, of isomeric O,N-disubstituted *N*-nitrosohydroxylamines **19** [reaction (17)]. There is virtually no quantitative information in the literature about the ratio of the isomeric products of the alkylation of salts of *N*-nitrosohydroxylamines. This is due to the low chemical and thermal stabilities of compounds **19**, which usually decompose under the reaction conditions. It is only known[174] that the main product of the alkylation of the tetraethylammonium salt of *N*-methyl-*N*-nitrosohydroxylamine with allyl bromide is *O*-allyl-*N*-methyl-*N*-nitrosohydroxylamine **19**, whereas the yield of the required *N*-methyl-*N'*-allyloxydiazene *N*-oxide **18** does not exceed 34% (Table 8). The lack of systematic data precludes the estimation of the influence of the structure of the interacting compounds and the reaction conditions on the mode of alkylation, which hinders deliberate regulation of the process.

On the basis of general considerations, the formation of *N'*-alkoxydiazene N-oxides might have been expected in the reaction of salts of hyponitrous acid, containing the ambident anion $N_2O_2^{2-}$, with alkylating agents. However, only one example of the reactions of hyponitrites accompanied by the formation of the diazene *N*-oxide group has been described in the literature. This involves the alkylation of silver hyponitrite with diphenylmethyl chloride. The reaction is carried out in a benzene–hexane mixture at 20 °C for 3.5 h; the yield of *N*-diphenylmethyl-*N'*-diphenylmethoxydiazene *N*-oxide **21** does not exceed 11%.[191]

$$2Ph_2CHCl + Ag_2N_2O_2 \longrightarrow \underset{\mathbf{21}}{Ph_2CHN(O)=N-OCPh_2} \qquad (19)$$

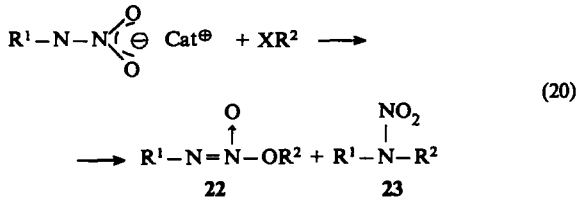
In the remaining cases the products of the alkylation of the ambident anions $N_2O_2^{2-}$ are unstable esters of *trans*-hyponitrous acids.[192]

Whereas the synthesis of *N'*-alkoxydiazene *N*-oxides is extremely widely represented in the chemical literature, less attention has been devoted to the synthesis of isomeric azoxy-

Table 9. Reaction conditions and yields of the products of the reactions of salts of 1,1-bis(*N'*-hydroxy-*N*-oxodiazeno) alkanes with alkylating agents.

R^1	R^2	Catalyst	X	Solvent	Reaction temperature/°C	Reaction time/h	Yield of **20** (%)	Ref.
H	$-CH_3$, $-C_2H_5$	NH_4	SO_4R^2	H_2O (8% NH_3)	20	31	9–33	167
H	$-CH_2CH_2Cl$	Ag	I	C_2H_5OH	20	120	37	167
CH_3	$-CH_3$	Na	SO_4CH_3	H_2O	20 60	31 1–2	20 20	187 187
H	$-CH_3$, $-C_2H_5$, $-C_3H_7$, $-C_4H_9$-n	Na	SO_4CH_3 Br	H_2O, DMSO	60	1–5	25–36	188
H	$-C_6H_{11}$-cyclo $-CH_2C\equiv CH$	Na	Cl, I	DMSO	60	5	2–4	188
H	$-C_4H_9$-t	Ag	Br	$(C_2H_5)_2O$	20	8	3	188

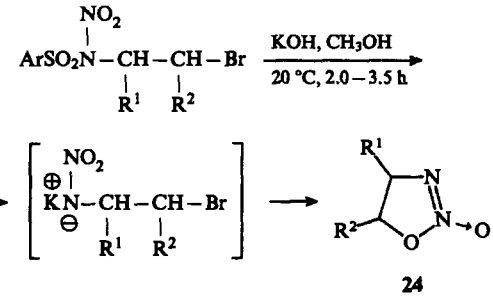
compounds **22** (Table 10), in which one of the nitrogen atoms of the diazene *N*-oxide groups is linked to two oxygen atoms. A general approach to the synthesis of structures of this type involves the interaction of salts of *N*-nitroamines and *N*-nitroamides with alkylating and acylating agents or the interaction of the corresponding CH acids with diazomethane (Table 10).



(20)

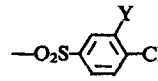
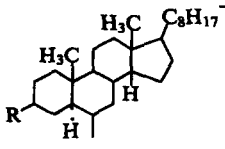
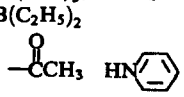
Like other reactions involving the alkylation of ambident anions containing the N_2O_2 fragment, the above processes are complicated by the formation, together with the azoxy-compounds **22**, of the isomeric products which in the given instance are secondary nitroamines **23**. The involvement in the reaction of the silver salts of nitroamines[169,193] and nitroamides[197–199] and increase in the size and degree of branching of the groups R^1 and R^2 in the interacting compounds[196,198,200] help to drive the process towards the preferential formation of the diazene *N*-oxide group. A decrease in the polarity of the solvent also promotes an increase in the yield of the *O*-alkylation products.[198]

When the initial compound contains a nitroamino-group and a halogen atom in vicinal positions, the reaction takes place intramolecularly[201] with the selective formation of cyclic azoxy-products **24**.



R^1 = H, CH_3; R^2 = H, CH_3.

Table 10. Reaction conditions and the yields and ratios of the products of the reactions of salts of *N*-nitroamines with alkylating agents.

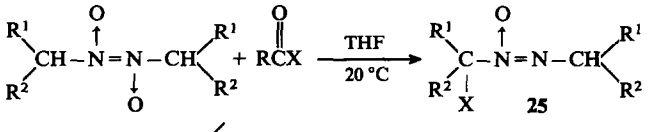
R^1	R^2	Catalyst	X	Solvent	Reaction temperature/°C	Reaction time/h	Yield of **22** (%)	Yield of **23** (%)	Ratio **22**/**23**	Ref.
$-CH_3$	$-C_2H_5$	Ag	I	–	–	–	Mixture of *cis*- and *trans*-isomers (1 : 4)	[a]	–	169
$-C_3H_7$-i	$-CH_3$	K	I	C_2H_5OH	20	48	9	60	0.15	193
		Ag	I	$(C_2H_5)_2O$	36	1.5	45	4	12.5	193
		K	SO_4CH_3	H_2O	20		21	18	1.20	193
		H	[b]	$(C_2H_5)_2O$	20		20	54	0.38	193
$-CH_3$, $-C_5H_{11}$-i	$-C_3H_7$-i	Ag	I	$(C_2H_5)_2O$	36	4–6	39–51	<4	>12.5	193
$-CH_3$, $-C_2H_5$, $-C_3H_7$, $-C_6H_{11}$-cyclo, $-C_4H_9$-t	$-CH_3$, $-C_2H_5$, $-C_3H_7$-i	Ag	Br, I	$(C_2H_5)_2O$	36	4.12	–	[a]	–	194
$-CH_3$, $-C_2H_5$	$-CH_2OCH_3$	Na	Cl	CH_3CN	70	0.3	28–38	23–36	0.77–1.39	195
					20	12.0	28–38	23–36	0.77–1.39	195
$-CH_3$	$-CH_3$	H	[b]	$(C_2H_5)_2O$	0	12.0	22	38	0.58	196
$-C_2H_5$, $-C_3H_7$-i, $-C_4H_9$-t	$-CH_3$	H	[b]	$(C_2H_5)_2O$	0	12.0	53–60	10–24	2.2–6.5	196
$-O_2S-C_6H_4-CH_3$-*p*	$-CH_2C_6H_5$	Ag	Cl	$(C_2H_5)_2O$	20	170	37	10	3.7	197
	$-CH_3$	Ag	Br	$(C_2H_5)_2O$	20	48–72	9–15	61–66	0.15–0.22	198
	$-C_2H_5$	Ag	Br	$(C_2H_5)_2O$	20	48–72	34–46	28–35	1.20–1.31	198
	$-C_3H_7$-n	Ag	Br	$(C_2H_5)_2O$	20	48–72	52	26	2.0	198
	$-C_3H_7$-i	Ag	Br	$(C_2H_5)_2O$	20	48–72	71	18	4.0	198
(Y = H, NO_2)	–Ad	Ag	Br	$(C_2H_5)_2O$	20	48	65	0	>100	198
$-O_2S-C_6H_4-CH_3$-*p*	$-Si(CH_3)_3$, $-B(C_2H_5)_2$	Ag	Cl	CH_2Cl_2	–30–20	1	~100	0	>100	199
				$(CH_3CO)_2O$–Py	20	0.5	73	0	>100	200
(R = H, Cl, OH)										

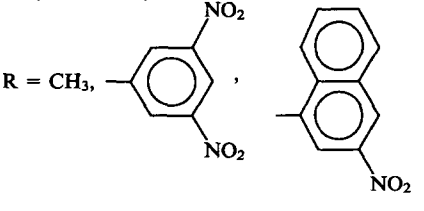
[a] The product was not isolated.
[b] CH_2N_2 was used as the alkylating agent.

Thus the alkylation of ambident anions containing the N_2O_2 structural fragment is a fairly common method of synthesis of asymmetrically substituted azoxy-compounds, in which the diazene *N*-oxide group is linked directly to an oxygen atom. Linear and cyclic azoxy-products, including those with different functional groups, can be obtained by means of this reaction. The principal disadvantage of the method is the uncertainty in the course of the reactions due to the dual reactivity of the alkylated anions and hence the low yields of the target azoxy-compounds.

VI. Other methods of synthesis of asymmetrically substituted diazene *N*-oxides

Apart from the alkylation of anions containing the N_2O_2 fragment, a number of other special methods of synthesis of asymmetrically substituted diazene *N*-oxides, used to obtain a narrow range of azoxy-products with specific structures, have been described in the literature. However, these methods have not found extensive applications in synthetic practice because of their limited applicability, low availability of the initial compounds, and also the inconvenient preparative aspect of the process. We shall consider some of these reactions. Thus the reaction of the dimers of primary and secondary nitrosoalkanes with acid halides leads to the formation of α-haloalkyldiazene *N*-oxides **25** containing a halogen atom in the α-position relative to the oxidised nitrogen atom of the diazene *N*-oxide fragment.[202]
When the reaction is carried out in the presence of Ag_2CO_3, its products are the corresponding α-acyloxyalkyldiazene *N*-oxides **26**.

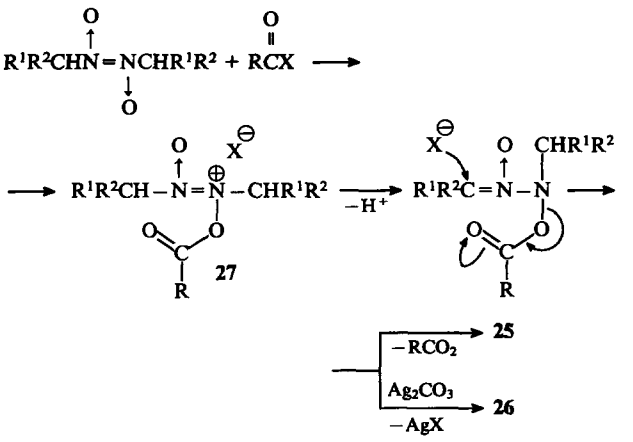


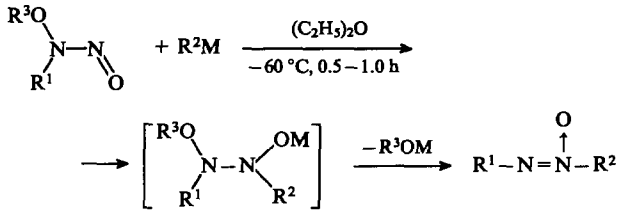


R^1	R^2	X	Yield of **25** (%)
$-C_3H_7$-i	H	Cl	65
$-C_3H_7$-i	H	Br	41
$-(CH_2)_5-$		Cl	25
$-CCl(CH_3)_2$	H	Cl	74

It has been suggested that the process proceeds via a stage involving the formation of *O*-acyl derivatives of diazene *N,N'*-dioxides **27**, which are stabilised by conversion into the final reaction products via the addition of a halide anion or (in the presence of Ag_2CO_3) via a rearrangement.[202]

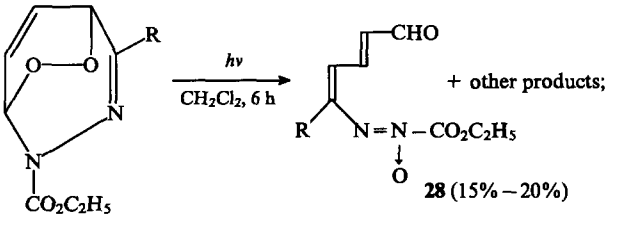
The regiospecific formation of the azoxy-group is observed in the reaction of *N*-nitroso-*O,N*-dialkylhydroxylamines with certain organometallic reagents, but the yields of the asymmetrically substituted azoxyalkanes do not as a rule exceed 20–30% in this case and the reaction has no preparative value.[203]





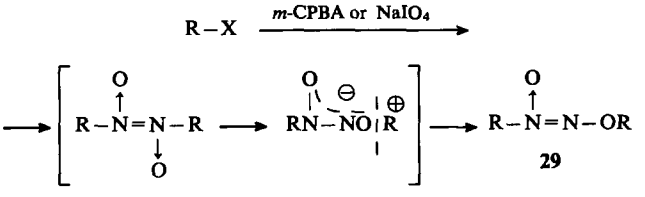
R = H, CH_3

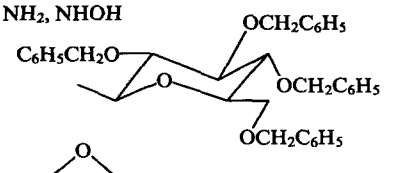
The photolysis of 1*H*-diazepine 1,2-epidioxides leads to the formation of a mixture of products,[204] one of which is the azoxyalkene **28** with functional group substituents.

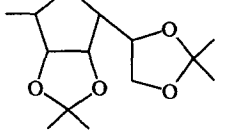


R^1, R^3 = Alk; R^2 = Alk, Ar; M = Li, MgBr.

The reaction of the amino- and hydroxyamino-derivatives of glucopyranose and mannose with oxidants results unexpectedly in the formation of the azoxy-derivatives **29** of the corresponding carbohydrates, containing the $-N{=}N(O)-$ structural fragment.[205]

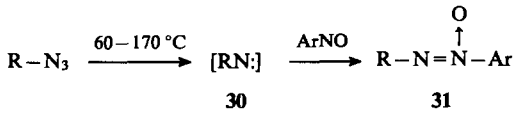


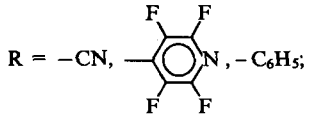
X = NH_2, NHOH
R = 
(yield 32%),

R = 
(yield 44%).

The authors explained this unusual mode of reaction by the heterolytic cleavage of the N–R bond in the dimeric nitroso-compounds (primary oxidation products) and the subsequent recombination of the ion pair, which leads to the product **29**. The driving force of the process is in this case the thermodynamic stability of the anions of the nitrosohydroxylamines and the cyclic oxonium cations.

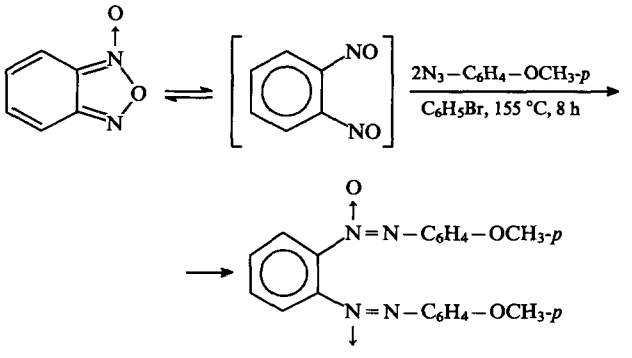
The formation of the diazene *N*-oxide group has been noted in the reaction of aromatic nitroso-compounds with cyanazides,[59,60] aryl azides,[206] and heteroaryl azides.[53] The most probable reaction pathway involves the addition of cyano-, aryl-, and heteroaryl-nitrenes **30**—the products of the thermal decomposition of the corresponding azide-derivatives—to nitrosoarenes with formation of the final reaction product **31**.





Ar = $-C_6H_4X$ (X = H, NO_2, $N(CH_3)_2$).

Together with nitroso-compounds, benzofuroxan can be made to react with aryl azides. It recyclises under the reaction conditions to *o*-dinitrosobenzene.[207]



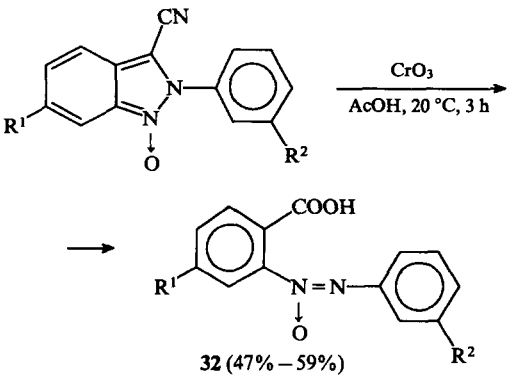
In view of the severe conditions in the thermolysis of the azides and the associated risk of explosion in the process as well as the low yields of the azoxy-products, this reaction cannot be regarded as a preparative method of synthesis of asymmetrically substituted diazene *N*-oxides.

A specific method of synthesis of *N,N'*-diaryldiazene *N*-oxides **32** with various substituents in the aromatic rings involves the oxidation of 2-aryl-3-cyanoindazole-1-oxides with chromium trioxide.[208,209]

Despite its regiospecificity, the reaction has not found wide scale application in synthetic practice, apparently owing to the low availability of the initial compounds.

VII. Conclusion

The data examined in this review show that studies designed to expand the applications of the known regioselective methods of synthesis of asymmetrically substituted diazene *N*-oxides and to develop new ones have been actively prosecuted in recent years in both our own and foreign scientific centres. A wide range of asymmetrically substituted azoxy-compounds, whose diazene *N*-oxide group is linked to carbon, oxygen, sulphur, nitrogen, and phosphorus atoms, has become available as a result. The range of the possible practical applications of these substances is extremely wide. Thus many of the newly synthesised asymmetrically substituted diazene *N*-oxides can be regarded as potential medicinal drugs (antibacterial,[7,10,12–16,59–61,63,122,153,214–217] antimicrobial,[218,219] antitumour,[12–16,63,122,153,220] anti-inflammatory,[145,221] immunodepressant,[222–224] anticonvulsive,[225,226] and analgesic[227]) as well as chemical plant protecting agents (nematocides,[19,20] fungicides,[16–18,186,228–231] and insecto-acaricides[161]), as components of liquid crystal compositions,[21–30] as gas-generating substances,[213] and as high-performance phases for gas–liquid chromatography.[30,210–212]



R^1, R^2 = H, NO_2

Bearing in mind the dynamics of the development of the synthetic and applied studies in this field, one may expect the preparation in the next few years of new diazene *N*-oxides which can find wide scale applications in various branches of science, industry, medicine, and agriculture.

References

1. N Zinin *J. Prakt. Chem.* **36** 93 (1845)
2. B Lythgoe, N V Riggs *J. Chem. Soc.* 2716 (1949)
3. B W Langley, B Lythgoe, N V Riggs *J. Chem. Soc.* 2309 (1951)
4. A Cooper *Proc. R. Soc. London* **74** 450 (1940)
5. K Nishida, A Kobayashi, T Nagahama *Bull. Agric. Chem. Soc. Jpn.* **19** 77 (1955); *Chem. Abstr.* **50** 13756 (1956)
6. N V Riggs *Chem. Ind.* 926 (1956)
7. L E Anderson, P R Burkholder, J Ehrlich, H S Sun *Antibiot. Chemother.* **6** 100 (1956)
8. S Yamashita *J. Antibiot.* **10** 224 (1957)
9. C L Stevens, B T Gillis, J C French, T H Haskell *J. Am. Chem. Soc.* **80** 6088 (1958)
10. W J McGahren, M P Kunstmann *J. Am. Chem. Soc.* **91** 2808 (1969)
11. W J McGahren, M P Kunstmann *J. Org. Chem.* **37** 902 (1972)
12. M Yamato, H Jinuma, H Nagahawa *J. Antibiot.* **39** 184 (1986)
13. M Yamato, T Takeuchi, H Umezawa, M Sakata, H Hayashi, M Hori *J. Antibiot.* **39** 1263 (1986)
14. H Umezawa, T Takeuchi, H Iinuma, M Ito, M Ishizuka, Y Kurakata, Y Umeda, Y Nakanishi, T Nakamura, A Obayashi, O Tanabe *J. Antibiot.* **28** 87 (1975)
15. A Gasco, A Serafino, V Mortarini, E Menziani *Tetrahedron Lett.* 3431 (1974)
16. T Okuda, N Nakayama, A Fujiwara *Nippon Kingakkai Kaiho* **23** 225 (1982); *Chem. Abstr.* **99** 191453b (1983)
17. M Nakayama, Y Takahashi, H Itoh, K Kamiya, M Shiratsuchi, G Otani *J. Antibiot.* **42** 1535 (1989)
18. Y Takahashi, M Nakayama, J Watanabe *J. Antibiot.* **42** 1541 (1989)
19. S Omura, K Otoguro, N Imamura, H Kuga, Y Takahashi, R Mosuma, Y Tanaka, H Tanaka, Su Xue-hui, You En-tai *J. Antibiot.* **40** 623 (1987)
20. N Imamura, H Kuga, K Otoguro, H Tanaka, S Omura *J. Antibiot.* **42** 156 (1989)
21. Polish P. 129463 (C1.C09K3/34) 1986; *Chem. Abstr.* **110** 125625d (1989)
22. Jpn. P. 58 69 280/83 69 280 (C1.C09K3/34) 1983; *Chem. Abstr.* **106** 93744r (1987)

23. R Dabrowski, K Kenig *Bull. Pol. Acad. Sci. Chem.* **34** 183 (1986); *Chem. Abstr.* **106** 41 951m (1987)
24. Jpn. P. 61 183 256/86 183 25 6 (C1.C07C 105/00) 1986; *Chem. Abstr.* **106** 224 617b (1987)
25. Jpn. P. 61 30 561/86 30 561 (C1.C07C 105/00) 1986; *Chem. Abstr.* **105** 143 707h (1986)
26. Jpn. P. 61 73 792/86 73 792 (C1.C09K 19/50) 1986; *Chem. Abstr.* **105** 162 383r (1986)
27. Jpn. P. 60 188 488/85 188 488 (C1.C09K 19/42) 1985; *Chem. Abstr.* **104** 139 869z (1986)
28. Jpn. P. 60 47 093/85 47 093 (C1.C09K 19/42) 1985; *Chem. Abstr.* **103** 14 659d (1985)
29. Jpn. P. 60 32 757/ [85 32 757] (C1.C07C 105/00) 1985; *Chem. Abstr.* **103** 71 042w (1985)
30. A V Bulanova, M S Vigdergauz, L S Lazareva, USSR P. 13 30 552 (G01N30/02) 1987; *Byull. Izobret.* **30** 199 (1987); *Chem. Abstr.* **107** 228 137p (1987)
31. H E Bigelow *Chem. Rev.* **9** 117 (1931)
32. S R Sandlers, W Karo, in *Organic Functional Group Preparations* (New York: Academic Press, 1968) Vol.1
33. J W Timberlake, J C Stowell In *The Chemistry of Hydrazo, Azo and Azoxy Groups* (Ed. S Patai) (New York: Interscience, 1975). p. 1
34. V N Yandovskii, B V Gidaspov, I V Tselinskii *Usp. Khim.* **50** 296 (1981) [*Russ. Chem. Rev.* **50** 164 (1981)]
35. V N Yandovskii, B V Gidaspov, I V Tselinskii *Usp. Khim.* **49** 449 (1980) [*Russ. Chem. Rev.* **49** 237 (1980)]
36. A Risaliti, A Monti *Gazz. Chim. Ital.* **91** 299 (1961)
37. A Risaliti *Gazz. Chim. Ital.* **93** 585 (1963)
38. N A Johnson, E S Gould *J. Org. Chem.* **39** 407 (1974)
39. R E Rondeau, M A Berwick, R N Steppel, M R Serve *J. Am. Chem. Soc.* **94** 1096 (1972)
40. U Hang, J Pelzung, H Usbeck *Pharmazie* **24** 442 (1969)
41. M A Berwick, R E Rondeau *J. Org. Chem.* **37** 2409 (1972)
42. N Novak, K A Martin, J L Heinrich, K M Peet, L K Mohler *J. Org. Chem.* **55** 3023 (1990)
43. B T Newbold *J. Org. Chem.* **27** 3919 (1962)
44. B M Bolotin, L K Tarygina, R V Poponova, D E Ostromyslenskii *Zh. Org. Khim.* **11** 782 (1975)
45. S S Mochalov, A N Fedotov, V Yu Plotkin, Yu S Shabarov *Zh. Org. Khim.* **16** 612 (1980)
46. A N Fedotov, I N Shishkina, S S Mochalov *Zh. Org. Khim.* **23** 112 (1987)
47. N Boden, R Bushby, L D Clark *J. Chem. Soc., Perkin Trans. 1* 543 (1983)
48. E Buncel, S R Keum, M Cygler, K J Varughese, G I Birnbaum *Can. J. Chem.* **62** 1628 (1984)
49. G P Sharnin, B I Buzykin *Zh. Org. Khim.* **4** 1622 (1968)
50. G P Sharnin, B I Buzykin *Zh. Org. Khim.* **6** 1476 (1970)
51. C J Byrne, D Christoforou, D A R Happer, M P Hartshorn *J. Chem. Soc., Perkin Trans. 2* 147 (1988)
52. E T McBee, G W Calundann, C J Morton *J. Org. Chem.* **37** 3140 (1972)
53. R E Banks, J M Farhat, R Fields, R G Pritchard, M M Salen *J. Fluorine Chem.* **28** 325 (1985)
54. A O Miller, G G Furin *J. Fluorine Chem.* **36** 247 (1987)
55. V M Dziomko, K A Dunaevskaya *Zh. Org. Khim.* **31** 3385 (1961)
56. J P Freeman *J. Org. Chem.* **28** 2508 (1963)
57. J N Brough, B Lythgoe, P Waterhouse *J. Chem. Soc.* 4069 (1954)
58. V Mortarini, A Serafino, E Menziani, A Gasco *Gazz. Chim. Ital.* **106** 1107 (1976)
59. V Mortarini, M A Bianco, A Gasco *Chim. Ind. (Milan)*, **59** 385 (1977); *Chem. Abstr.* **87** 200 967d (1977)
60. V Mortarini, G Rua, A Gasco, *Eur. J. Med. Chem.-Chim. Ther.* **12** 59 (1977)
61. Jpn. P. 76 26 844 (C1. C07C 125/08) 1976; *Chem. Abstr.* **85** 94 106 (1976)
62. H Umezawa, T Takeuchi, H Yimuma *J. Antibiot.* **28** 37 (1975)
63. R Fruttero, A Gasco, C Tironi, G Schioppacassi *Eur. J. Med. Chem.-Chim. Ther.* **17** 482 (1982)
64. V Mortarini, R Calvino, A Gasco, B Ferrarotti *Eur. J. Med. Chem.-Chim. Ther.* **15** 475 (1980)
65. T Mitsuhashi, O Simamura *J. Chem. Soc. B* 705 (1970)
66. B T Gillis, M P La Montagne *J. Org. Chem.* **33** 762 (1968)
67. B T Gillis, K F Schimmel *J. Org. Chem.* **32** 2865 (1967)
68. B T Gillis, J D Hagarty *J. Org. Chem.* **32** 95 (1967)
69. B Fugmann, W Steglich *Angew. Chem.* **96** 71 (1984)
70. R A Moss, M J Landon *Tetrahedron Lett.* 3897 (1969)
71. R A Moss, M J Landon, K M Luchter, A Mamontov *J. Am. Chem. Soc.* **94** 4392 (1972)
72. R A Moss, G M Love *Tetrahedron Lett.* 4701 (1973)
73. R A Moss, G M Love *J. Am. Chem. Soc.* **95** 3070 (1973)
74. R A Moss, T B K Lee *J. Chem. Soc., Perkin.Trans. 1* 2778 (1973)
75. R A Moss, M Matsuo *J. Am. Chem. Soc.* **99** 1643 (1977)
76. C S Cooper, A L Peyton, R J Weinkam *J. Org. Chem.* **48** 4116 (1983)
77. J A Kepler, G F Taylar *J. Org. Chem.* **52** 453 (1987)
78. J E Saavedra *J. Org. Chem.* **55** 6373 (1990)
79. D J Northington, W M Jones *J. Org. Chem.* **37** 693 (1972)
80. R A Moss *Acc. Chem. Res.* **7** 421 (1974)
81. J Ehrlich, L E Anderson, G L Coffey *Antibiot. Chemother.* **4** 338 (1954)
82. R A Moss, C E Powell *J. Am. Chem. Soc.* **98** 283 (1976)
83. M Okubo, T Takahashi, K Koga *Bull. Chem. Soc. Jpn.* **56** 199 (1983)
84. M Okubo, K Koga *Bull. Chem. Soc. Jpn.* **56** 203 (1983)
85. M Okubo, Y Inatomi, N Taniguchi, K Inamura *Bull. Chem. Soc. Jpn.* **61** 3581 (1988)
86. M Okubo, K Matsuo, A Yamauchi *Bull. Chem. Soc. Jpn.* **62** 915 (1989)
87. M Okubo, T Nakashima, H Shiku *Bull. Chem. Soc. Jpn.* **62** 1621 (1989)
88. Jpn. P. 60 184 245/85 184 245 (C1.G03C1/72) 1985; *Chem. Abstr.* **104** 120 172v (1986)
89. M Okubo, K Asao, H Hyakutake *Bull. Chem. Soc. Jpn.* **60** 3781 (1987)
90. M Okubo, C Sugimori, M Tokisada, T Tsutsumi *Bull. Chem. Soc. Jpn.* **59** 1644 (1986)
91. T Tsutsumi, M Okubo, N Yasuoka, Y Katsube *Bull. Chem. Soc. Jpn.* **61** 237 (1988)
92. M Okubo, H Aratani, T Gondo, K Koga *Bull. Chem. Soc. Jpn.* **56** 788 (1983)
93. Jpn. P. 58 201 757/83 201 757 (C1.C07C 113/04) 1983; *Chem. Abstr.* **100** 19 1 555a (1984)
94. E T Apasov, A V Kalinin, Yu A Strelenko, V A Tartakovskii *Izv. Akad. Nauk SSSR, Ser. Khim.* 2873 (1988)
95. V Ya Pochinok, in *Triazeny* (Triazenes) (Kiev: Izd. Kiev. Gos. Univ., 1968)
96. L Hoesch, B Koppel *Helv. Chim. Acta* **64** 864 (1981)
97. Yu P Artsybasheva, B V Ioffe *Zh. Org. Khim.* **18** 1802 (1982)
98. O A Luk'yanov, G A Smirnov, A M Vasil'ev *Izv. Akad. Nauk SSSR, Ser. Khim.* 2155 (1990)
99. T E Stevens, J P Freeman *J. Org. Chem.* **29** 2279 (1964)
100. S F Reed *J. Org. Chem.* **32** 3869 (1967)
101. I G Aston, D M Jankins *Nature* **167** 863 (1951)
102. V A Ginsburg, L L Martynova, N F Priveznetseva, Z A Buchek *Zh. Obshch. Khim.* **38** 2505 (1968)
103. S A Amitina, L B Volodarskii *Khim. Geterotsikl. Soedin.* 131 (1973)
104. K G Taylor, S R Isaac, M S Clark *J. Org. Chem.* **41** 1135 (1976)
105. O A Luk'yanov, Yu B Salamonov, S I Zherebyat'ev, Yu A Strelenko *Izv. Akad. Nauk SSSR, Ser. Khim.* 1110 (1989)
106. Y Ogata, M Tsuchida, Y Takagi *J. Am. Chem. Soc.* **79** 3397 (1957)
107. G A Russell, E J Geels *J. Am. Chem. Soc.* **87** 122 (1965)
108. G A Russell, E J Geels, F J Smentowski, K Y Chang, J Reynolds, G Kaupp *J. Am. Chem. Soc.* **89** 3821 (1967)
109. R Konaka, K Kuruma, S Terebe *J. Am. Chem. Soc.* **90** 1801 (1968)
110. I L Knunyants, Ya A Sizov, O V Ukharov *Usp. Khim.* **52** 976 (1983) [*Russ. Chem. Rev.* **52** 554 (1983)]
111. V Nelson, P Kovacic *J. Chem. Soc., Chem. Commun.* 312 (1975)
112. V Nelson, Serianz, P Kovacic *J. Org. Chem.* **41** 175 (1976)
113. F R Sullivan, E Luck, P Kovacic *J. Org. Chem.* **39** 2967 (1974)
114. R C Zawalski, P Kovacic *J. Org. Chem.* **44** 2130 (1979)
115. O A Luk'yanov, Yu B Salamonov, A G Bass, Yu A Strelenko, N F Karpenko *Izv. Akad. Nauk SSSR, Ser. Khim.* 352 (1990)
116. R Calvino, R Fruttero, A Gasco *J. Antibiot.* **39** 864 (1986)

117. K I Pashkevich, G L Rusinov, I E Filatov, Yu V Kulikov *Azotsoderzhashchie Geterotsikly. IV Vsesoyuznaya Konferentsiya po Khimii Azotsoderzhashchikh Geterotsiklicheskikh Soedinenii (Tezisy Dokladov). Novosibirsk 1987* [Nitrogen-Containing Heterocycles. The IVth All-Union Conference on the Chemistry of Nitrogen-Containing Heterocyclic Compounds (Abstracts of Reports). Novosibirsk, 1987] p. 120
118. W G Le Noble, W S Chang *Synthesis* 106 (1973)
119. A M Churakov, E L Goncharova, S L Ioffe, Yu A Strelenko, V A Tartakovskii *Izv. Akad. Nauk SSSR, Ser. Khim.* 953 (1990)
120. W L Farrar, J M Gulland *J. Chem. Soc.* 368 (1944)
121. T E Stevens *J. Org. Chem.* **33** 855 (1968)
122. R Fruttero, C Tironi, R Calvino *Pharmazie* **43** 551 (1988)
123. A V Fokin, V I Zimin, Yu N Studnev, M A Ponsov *Izv. Akad. Nauk SSSR, Ser. Khim.* 719 (1970)
124. K Baum *J. Org. Chem.* **34** 2049 (1969)
125. A V Fokin, V I Zimin, Yu N Studnev, V F Korotkov *Zh. Org. Khim.* **6** 880 (1970)
126. K Baum *J. Org. Chem.* **35** 2844 (1970)
127. J W Frazer, B E Holder, E F Worden *J. Inorg. Nucl. Chem.* **24** 45 (1962)
128. A N Medvedev, K N Smirnov, S S Dubov, V A Ginsburg *Zh. Obshch. Khim.* **38** 2462 (1968)
129. J W Frazer, V L Duval *J. Inorg. Nucl. Chem.* **25** 1066 (1963)
130. R A Bekker, B L Dyatkin, I L Knunyants *Izv. Akad. Nauk SSSR, Ser. Khim.* 1060 (1967)
131. I L Knunyants, B L Dyatkin, R A Bekker *Dokl. Akad. Nauk SSSR* **170** 337 (1966)
132. A V Fokin, V I Zimin, Yu N Studnev *Izv. Akad. Nauk SSSR, Ser. Khim.* 975 (1969)
133. A V Fokin, Yu N Studnev, M A Ponsov *Zh. Obshch. Khim.* **38** 1903 (1968)
134. H M Mardsen, J M Shreeve *J. Inorg. Chem.* **23** 3654 (1984)
135. G G Moskadenko, V F Sedova, V P Mamaev *Izv. Akad. Nauk SSSR, Ser. Khim.* 702 (1987)
136. L M Mironovich, V K Promonenkov, S E Bogushevich *Khim. Geterotsikl. Soedin.* 833 (1987)
137. Y M Wu, L Y Ho, C H Cheng *J. Org. Chem.* **50** 392 (1985)
138. D W Rangnekar, S V Dhamnaskar *J. Heterocycl. Chem.* **25** 1663 (1988)
139. C C Schmitt, C A Moritz, M G Pizzolatti, R A Yunes *Bull. Chem. Soc. Jpn.* **62** 3684 (1989)
140. H Hope, C B Shoemaker, D P Shoemaker *J. Org. Chem.* **50** 1136 (1985)
141. O Fisher, L Wacker *Chem. Ber.* **22** 622 (1889)
142. E Bamberger, A Stiegelmann *Chem. Ber.* **32** 3554 (1899)
143. E Bamberger *Helv. Chim. Acta* **14** 242 (1931)
144. K Kano, M Koga, J P Anselme *Bull. Soc. Chim. Belg.* **96** 137 (1987)
145. J L Miesel, US P. 3 989 680 CIF (C1.C07C 107/04) 1976; *Chem. Abstr.* **85** 20 819g (1976)
146. R M Moriarty, T E Hopkins, J Prakash, B K Vaid, R K Vaid *Synth. Commun.* **20** 2353 (1990)
147. L Hoesch *Helv. Chim. Acta* **64** 890 (1981)
148. Yu P Artsybasheva, I V Suvorova, B V Ioffe *Zh. Org. Khim.* **17** 435 (1981)
149. J Wrobel, V Nelson, J Sumiejski, P Kovacic *J. Org. Chem.* **44** 2345 (1979)
150. F A Carey, L J Hayes *J. Am. Chem. Soc.* **92** 7613 (1970)
151. Yu P Artsybasheva, B V Ioffe *Zh. Org. Khim.* **23** 1168 (1987)
152. R Fruttero, G Mulatero, R Calvino, A Gasco *J. Chem. Soc., Chem. Commun.* 323 (1984)
153. R Fruttero, R Calvino, A Distilo, A Gasco, I Galatulas, R Bossa *Pharmazie* **43** 499 (1988)
154. D H R Barton, G Lamotte, W B Motherwell, S C Narang *J. Chem. Soc., Perkin Trans. 1* 2030 (1979)
155. C Tironi, R Fruttero, A Distilo, P Aresea, R Bossa, J Galatulos, M Ninci *Anticancer Res.* **9** 609 (1989)
156. S G Zlotin, O V Prokshits, O A Luk'yanov *Izv. Akad. Nauk SSSR, Ser. Khim.* 2668 (1990)
157. S G Zlotin, E A Vinogradova, A I Podgurskii, Yu A Strelenko, O A Luk'yanov *Izv. Akad. Nauk SSSR, Ser. Khim.* 1656 (1990)
158. S G Zlotin, N V Airapetova, E A Vinogradova, A I Podgurskii, Yu A Strelenko, O A Luk'yanov *Izv. Akad. Nauk SSSR, Ser. Khim.* 2821 (1990)
159. O A Luk'yanov, Yu B Salamanov, A G Bass, Yu A Strelenko *Izv. Akad. Nauk SSSR, Ser. Khim.* 109 (1991)
160. S G Zlotin, O V Prokshits, N F Karpenko, O A Luk'yanov *Izv. Akad. Nauk SSSR, Ser. Khim.* 1679 (1990)
161. S Zlotin, M Sharashkina, Yu Strelenko, O Luk'yanov *Mendeleev Commun.* 49 (1991)
162. W Lwowski (Editor) *Nitrenes* (New York: Wiley Interscience, 1970)
163. M A Kuznetsov, B V Ioffe *Usp. Khim.* **58** 1271 (1989) [*Russ. Chem. Rev.* **58** 732 (1989)]
164. M A Kuznetsov *Usp. Khim.* **48** 1054 (1979) [*Russ. Chem. Rev.* **48** 563 (1979)]
165. V N Yandovskii, A D Misharev, I V Tselinskii, E Yu Dobrodumova, U Traore *Zh. Org. Khim.* **16** 292 (1980)
166. V N Yandovskii, A D Misharev, I V Tselinskii, U Traore *Zh. Org. Khim.* **14** 2505 (1978)
167. M V George, R W Kierstead, G F Wright *Can. J. Chem.* 37 679 (1959)
168. O A Luk'yanov, T I Zhiguleva *Izv. Akad. Nauk SSSR, Ser. Khim.* 1422 (1982)
169. A H Lamberton, H M Yusuf *J. Chem. Soc.* 397 (1969)
170. I N Zyuzin, D V Lempert *Izv. Akad. Nauk SSSR, Ser. Khim.* 831 (1985)
171. G A Marchenko, O G Yakovleva, V Z Latynova, L N Punegova, D A Semanov, V V Cherevin, Yu M Kargin, I V Tselinskii *Zh. Org. Khim.* **24** 1585 (1988)
172. V N Yandovskii, E Yu Dobrodumova, I V Tselinskii, U Traore *Zh. Org. Khim.* **14** 2461 (1978)
173. V N Yandovskii, E Yu Dobrodumova, I V Tselinskii, A D Misharev, U Traore *Zh. Org. Khim.* **16** 284 (1980)
174. I N Zyuzin *Izv. Akad. Nauk SSSR, Ser. Khim.* 2626 (1985)
175. V N Yandovskii, B V Gidaspov, I V Tselinskii *Dokl. Akad. Nauk SSSR* **289** 381 (1986)
176. V N Yandovskii, B V Gidaspov, I V Tselinskii, V S Kuznetsov *Zh. Org. Khim.* **23** 10 (1987)
177. V N Yandovskii, B V Gidaspov, I V Tselinskii *Dokl. Akad. Nauk SSSR* **289** 120 (1986)
178. V N Yandovskii, G M Frolova, I V Tselinskii *Zh. Org. Khim.* **18** 503 (1982)
179. V N Yandovskii, V S Kuznetsov, I V Tselinskii, G M Frolova *Zh. Org. Khim.* **18** 508 (1982)
180. V N Yandovskii, T I Doshechkina, I V Tselinskii, V S Kuznetsov *Zh. Org. Khim.* **19** 489 (1983)
181. T E Stevens *J. Org. Chem.* **29** 311 (1964)
182. E H White, C P Lewis, M A Ribi, T J Ryan *J. Org. Chem.* **46** 552 (1981)
183. J P Freeman, L D Littwitz *J. Org. Chem.* **35** 3107 (1970)
184. G A Olah, R Herges, K Laali, G A Segal *J. Am. Chem. Soc.* **108** 2054 (1986)
185. V N Yandovskii, U Traore, V S Zavgorodnii *Zh. Obshch. Khim.* **48** 708 (1978)
186. W Reuther, P Raff, E H Pommer, H P Heidenreich, BRD P. 2 633 452 (C1.C07F 7/22) 1978; *Chem. Abstr.* **88** 191 061v (1978)
187. L O Atovmyan, N I Golovina, I N Zyuzin *Izv. Akad. Nauk SSSR, Ser. Khim.* 1309 (1987)
188. V N Yandovskii, E Yu Dobrodumova, I V Tselinskii *Zh. Org. Khim.* **16** 933 (1980)
189. G A Marchenko, L F Chertanova, M Yu Antipin, Yu T Struchkov, L N Punegova *Dokl. Akad. Nauk SSSR* **294** 1169 (1987)
190. G A Marchenko, O G Yakovleva, V Z Latyshova, L N Punegova, V V Cherevin, Yu M Kargin, I V Tselinskii *Zh. Org. Khim.* **25** 2040 (1989)
191. E M Y Quinga, Y Bieker, M P Dziobak, G D Mendenhall *J. Org. Chem.* **54** 2769 (1989)
192. M N Hughes *Quart. Rev. Chem. Soc.* **22** 1 (1968)
193. P Bruck, A H Lamberton *J. Chem. Soc.* 3997 (1955)
194. P Bruck, A H Lamberton *J. Chem. Soc.* 4198 (1957)
195. B Unterhalt, D Thamer *Synthesis* 302 (1973)
196. B Unterhalt, D Thamer *Arch. Pharm.* **307** 731 (1974)
197. M J Gillibrand, A H Lamberton *J. Chem. Soc.* 1883 (1949)
198. O A Luk'yanov, N I Shlykova, V A Tartakovskii *Izv. Akad. Nauk SSSR, Ser. Khim.* 659 (1976)

199. S L Ioffe, L M Leont'eva, L M Makarenkova, A L Blyumenfel'd, V F Pyaterikov, V A Tartakovskii *Izv. Akad. Nauk SSSR, Ser. Khim.* 1146 (1975)
200. M S Ahmad, S K Paza *Indian J. Chem.* **26B** 261 (1987)
201. O A Luk'yanov, A A Onishchenko, V P Gorelik, V A Tartakovskii *Izv. Akad. Nauk SSSR, Ser. Khim.* 1294 (1973)
202. M A Ribi, E H White *Helv. Chim. Acta* **58** 120 (1975)
203. A C M Meesters, H Rueger, K Rajeswari, M H Benn *Can. J. Chem.* **59** 264 (1981)
204. T Takashi, A Heihachiro, H Hirishi, I Hiroshi *Chem. Pharm. Bull.* **26** 2205 (1978)
205. B M Aebischer, H W Hanssen, A T Vasella *J. Chem. Soc., Perkin Trans. 1* 2139 (1982)
206. A B Bulacinski, B Nay, E F V Schriven, H Suschitzky *Chem. Ind. (London)* 746 (1975)
207. A B Bulacinski, E F V Scriven, H Suschitzky *Tetrahedron Lett.* 3577 (1975)
208. L C Behr *J. Am. Chem. Soc.* **76** 3672 (1954)
209. L C Behr, E G Alley, O Levand *J. Org. Chem.* **27** 65 (1962)
210. M S Vigdergauz, G V Dmitrieva, L A Onuchak, G V Senitskaya *Izv. Akad. Nauk SSSR, Ser. Khim.* 197 (1988)
211. G S Fedchenko, M S Vigdergauz, T M Lesteva *Zavod. Lab.* **54** 22 (1988)
212. V I Pakhomova, M S Vigdergauz *Zavod. Lab.* **51** 17 (1985)
213. R E McLeay, US P. 4 228 069 (C1.C07C 107/02) 1980; *Chem. Abstr.* **94** 66 734q (1981)
214. W J McGahren, M P Kunstmann *J. Am. Chem. Soc.* **92** 1587 (1970)
215. W J McGahren, M P Kunstmann *J. Org. Chem.* **37** 902 (1972)
216. Jpn. P. 77 71 444 (C1.C07C 125/08) 1977; *Chem. Abstr.* **87** 167 770j (1977)
217. E Gadoni, A Miglietta, A Olivero, L Gabriel *Biochem. Pharmacol.* **38** 1121 (1989); *Chem. Abstr.* **110** 205 096x (1989)
218. A Miglietta, E Gadoni, A Olivero, L Gabriel, R Calvino *Med. Sci. Res.* **16** 267 (1988); *Chem. Abstr.* **109** 286s (1988)
219. A Miglietta, A Olivero, E Gadoni *Med. Sci. Res.* **16** 471 (1988); *Chem. Abstr.* **109** 85 819r (1988)
220. K Hiroyuki, H Toshiyuki, N Koushi *J. Med. Chem.* **32** 1098 (1989)
221. J L Miesel, US P. 3 962 434 CIF (C1.424 – 226) 1974; *Chem. Abstr.* **85** 56 997c (1967)
222. BRD P. 2 208 368 (C1.C07C, A61K) 1973; *Chem. Abstr.* **79** 146 271s (1973)
223. BRD P. 2 301 820 (C1.C07C, A61K) 1974; *Chem. Abstr.* **81** 104 976m (1974)
224. P B Stewart, G J Possanza, F G Hess *J. Immunol.* **110** 1180 (1973)
225. A Kumar, S K Mukerjee, S K Bhattacharya *Pharmazie* **38** 66 (1983)
226. A Kumar, S K Mukerjee, S K Bhattacharya *Pharm. Res.* **49** (1985); *Chem. Abstr.* **102** 125 427x (1985)
227. A Kumar, S K Mukerjee, S K Bhattacharya *Sci. Pharm.* **51** 278 (1983); *Chem. Abstr.* **100** 120 594b (1984)
228. W W Wood, T W Naisby, A C G Gray, Eur. Pat. Appl. EP 411 716 (C1.C07C291/08) 1991; *Chem. Abstr.* **115** 28 866d (1991)
229. W W Wood, T W Naisby, A C G Gray, Eur. Pat. Appl. EP 411 719 (C1.C07C291/08) 1991; *Chem. Abstr.* **115** 71 092k (1991)
230. A C G Gray, T W Naisby, S J Turner, T M Machin, Eur. Pat. Appl. EP 411 720 (C1.C07C 323/48) 1991; *Chem. Abstr.* **115** 71 093k (1991)
231. M Pearson, A C G Gray, T W Naisby, W W Wood, S J Turner, T M Machin, Eur. Pat. Appl. EP 371 560 (C1.A01N43/04) 1990; *Chem. Abstr.* **114** 23 803a (1991)
232. S G Zlotin, M V Sharashkina, Yu A Strelenko, O A Luk'yanov *Izv. Akad. Nauk SSSR, Ser. Khim.* 1148 (1992)

Russian Chemical Reviews **62** (2) 169 – 192 (1993)
© 1993 Russian Academy of Sciences and Turpion Ltd

UDC 547.725.3.07 : 547.414.28

The synthesis and properties of unsaturated nitro-compounds of the furan series

R A Karakhanov, V I Kelarev, Yu N Polivin

Contents

I. Introduction	169
II. Methods of synthesis of furylnitroalkenes	169
III. Structure and reactivity of furylnitroalkenes	174
IV. Chemical properties	179
V. Practical applications of furylnitroalkenes	188

Abstract. A systematic account is provided of data in the field of the chemistry of unsaturated nitro-compounds of the furan series. The methods of synthesis of nitroalkenes of the furan series and the characteristic features of the structure and reactivity of furylnitroalkenes are examined. The general characteristics and distinctive features of the chemical reactions of furylnitroalkenes are discussed and their applications are noted. The bibliography includes 212 references.

I. Introduction

The chemistry of unsaturated nitro-compounds is a promising and vigorously developing field in modern organic chemistry. This is associated with the progress achieved in the methods of synthesis of such compounds and their high reactivity.[1-6]

During the last decades, investigators have devoted much attention to unsaturated nitro-compounds of the furan series, since they are used as synthons in the synthesis of physiologically active substances, natural products, and various furan derivatives with a functional group in the side chain and also because of their high biological activity.

Considerable data have now accumulated in the literature on the synthesis, chemical reactions, and practical applications of furylnitroalkenes, which are, however, scattered in numerous article and patent sources. Some general information about furylnitroalkenes has been briefly described in monographs.[1,7,8]

In the present review we attempted to give a systematic account and to examine critically the most significant, from our point of view, aspects of the chemistry of furylnitroalkenes: data on modern methods of synthesis, structure, reactivity, and the synthetic possibilities of these furan derivatives as well as their practical applications.

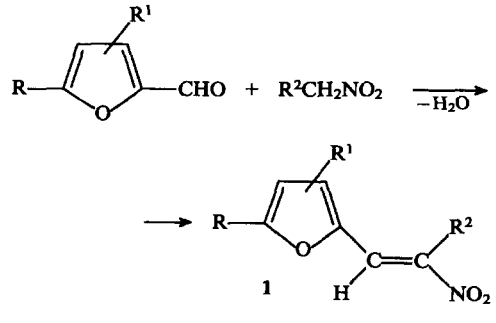
R A Karakhanov, V I Kelarev, Yu N Polivin Gubkin State Academy of Petroleum and Gas, Leninskii prosp. 65, 117917 GSP-1 Moscow, Fax (7-095) 135 8895

Received 28th November 1992
Uspekhi Khimii **62** (2) 184 – 207 (1993); translated by A K Grzybowski

II. Methods of synthesis of furylnitroalkenes

The most thoroughly investigated representatives of unsaturated nitro-compounds in the furan series are conjugated β-(5-R-2-furyl)nitroalkenes. Various methods of synthesis of conjugated heteroarylnitroalkenes have now been developed, among which the most important is the reaction involving the condensation of heteroaromatic aldehydes with primary nitro-compounds in the presence of basic catalysts — solutions of alkalies, alkali metal alkoxides, primary aliphatic amines, ammonium acetate, etc.[1-3]

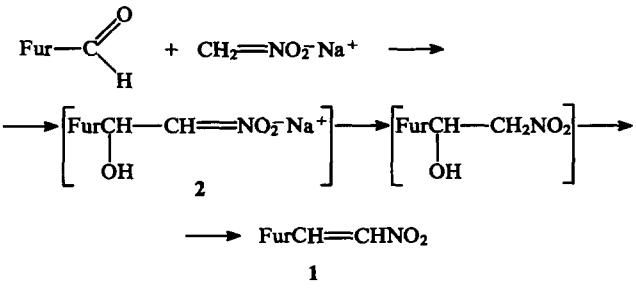
Numerous β-nitroalkenes, formed as a result of the condensation of furfural or ring-substituted furfurals with nitromethane,[9-35] nitroethane,[13,19,23,28,36-45] 1-nitropropane,[37,39,46] 1-nitrobutane,[37] 2-methyl-1-nitropropane,[46] 1-nitropentane,[39] 3-methyl-1-nitrobutane,[46] phenylnitromethane,[36,47-51] chloronitromethane,[12,52] bromonitromethane,[23,47] and nitroacetic acid derivatives — the methyl ester[53] and the nitrile,[54,55] have been described. It is noteworthy that these reactions (with the exception of the condensation involving methyl nitroacetate) take place stereoselectively and lead to the nitroalkenes **1**, having the (*E*)-configuration, which has been confirmed by spectroscopic methods.



R = H, Me, Cl, Br, I, NO_2, $HOCH_2$, MeOOC, CN, Me_2N, morpholino, PhN(Me), aryl, arylthio, $MeSO_2$, $PhSO_2$, 3-$NO_2C_6H_4O$, heteroarylthio; R^1 = H, 4-Cl, 4-Br, 3-I, 3-NO_2; R^2 = H, Me Et, Pr^n, Pr^i, Bu^n, Bu^i, Ph, 4-ClC_6H_4, Cl, Br, NC, MeOOC, $MeOOCCH_2$.

In the synthesis of β-nitroalkenes of the above type, alkali metal hydroxides or alkoxides as well as primary amines (methylamine, butylamine, 1-aminopentane, etc.) are usually employed as condensing agents. Two main preparative methods of synthesis of β-(5-R-2-furyl)nitroalkenes **1** have been developed accordingly.

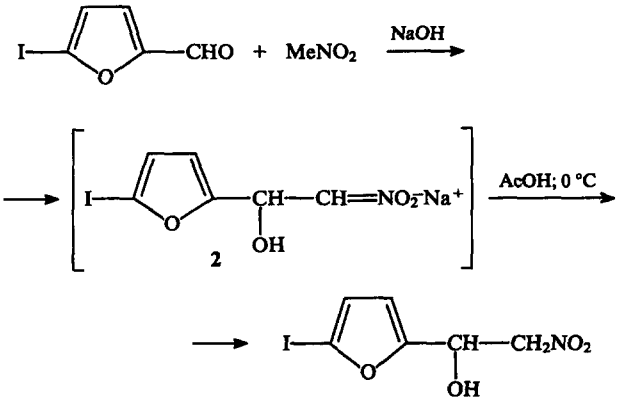
According to the first method, an equimolar mixture of an aldehyde of the furan series and nitromethane in methanol or ethanol is gradually treated, whilst cooling (−15 to −10 °C), with equivalent amounts of an aqueous or alcoholic solution of alkali or a sodium alkoxide solution in the corresponding alcohol. The reaction is accompanied by an appreciable heat change and is completed by the formation of an insoluble salt of the β-nitroalcohol **2**, which is then dissolved by adding water. On subsequent acidification with a dilute solution of an inorganic acid, the β-nitroalkene **1** is isolated in 50%–92% yield (method *A*).[9-23,26-28,30-35,56-58]



Here and henceforth Fur = 2-furyl.

This reaction should be regarded[1,3] as the result of the nucleophilic attack by the nitromethane anion on the electron-deficient carbon atom of the carbonyl group of 5-R-furfural, which leads initially to the aldol condensation product — a salt of the β-nitroalcohol **2**. There are no literature data concerning the mechanism of the dehydration of salts of β-nitroalcohols by inorganic acid solutions.

It has been reported[30] that, when the reaction mixture in the reaction of 5-iodofurfural with nitromethane and NaOH (1 : 1 : 1 molar ratios) is acidified cautiously with acetic acid, it is possible to isolate the unstable 1-(5-iodo-2-furyl)-2-nitroethanol. This finding constitutes confirmation of the formation in the given reaction of the salt **2** as an intermediate.

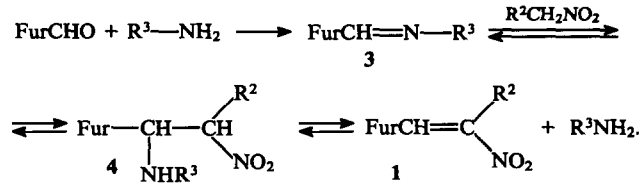


The study[59] of the kinetics of the condensation of furfural with nitromethane in aqueous alcohol in the presence of KOH also confirmed the intermediate formation of the salt **2**. The kinetic curves for the decrease in the furfural concentration are described by the equation for first-order reversible reactions under pseudo-unimolecular conditions with respect to furfural or by the equation for second-order reactions at comparable concentrations of furfural and nitromethane.

The condensation of furfural with nitromethane,[21] in which a solution of $Ca(OH)_2$ is used as condensing agent, is of interest for industrial application. It is noteworthy that alkalies and alkali metal alkoxides proved to be effective condensing agents in the reactions of furfural and its substituted derivatives not only with nitromethane but also with nitroethane,[19,23,28,36,40,41,43] chloronitromethane,[12,52] and bromonitromethane.[23,47] However, in the case of phenylnitromethane, 1-nitropropane, and 1-nitrobutane, the use of alkaline catalysts leads to appreciable charring of the reaction mixture.

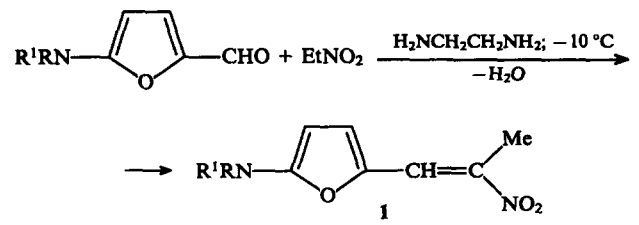
The second method (method *B*) of synthesis of β-(5-R-2-furyl)-nitroalkenes **1** represents a modified Knoevenagel reaction using methylamine, butylamine, 1-aminopentane, ethylenediamine, or piperidine as the catalysts.[13,29,36-38,41,42,44-48] In this method, an equimolar mixture of the furan aldehyde, and nitroalkane in dry ethanol is kept at 20 °C for 3–10 days[47,60] or is refluxed for several hours[13,37,61,62] with 5–10 mol% of a primary amine: under these conditions, the yield of the nitroalkenes **1** is 35–85%.

The mechanism of the catalytic action of primary amines apparently reduces to the formation of the azomethines **3** as intermediates, which react with nitroalkanes to form adducts — unstable β-nitroamines **4**. The latter decompose to the β-nitroalkene **1** and an amine under the influence of the excess nitroalkene:[1,3]



Although a clear cut correlation between the influence of substituents in the furfural ring on the reactivity of the carbonyl group in condensation reactions with nitroalkanes and the yields of β-nitroalkenes **1** are not quoted in the literature, nevertheless certain qualitative features of these reactions can be traced on the basis of the available data. For example, it has been noted[47] that the rate of condensation of 5-R-furfurals with bromonitromethane (method *A*) and phenylnitromethane (method *B*) diminishes in the sequence H > CH_3 > Cl > Br > NO_2 depending on the nature of the substituent R. Thus β-(5-nitro-2-furyl)-α-phenylnitroethylene was obtained in 26% yield only after keeping the reaction mixture at 20 °C for 14 days. On raising the temperature, appreciable charring was observed. The authors[12] were unable to synthesise α-bromo-β-(5-nitro-2-furyl)-nitroethylene by the direct condensation of 5-nitrofurfural with bromonitromethane under the conditions of method *A*; on the other hand, the condensation of 5-nitrofurfural with chloronitromethane and NaOH in aqueous methanol leads to α-chloro-β-(5-nitro-2-furyl)nitroethylene in 41% yield.

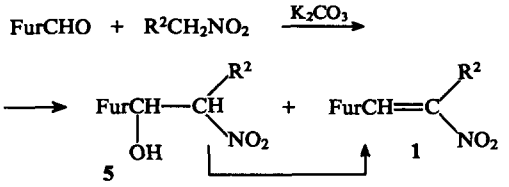
Attempts to obtain β-(5-dimethylamino-2-furyl)nitroethylene by the condensation of 5-dimethylaminofurfural with nitromethane in the presence of alkaline agents proved unsuccessful.[18] However, *N*,*N*-disubstituted 5-aminofurfurals[41,42] react with nitroethane in the presence of catalytic amounts of ethylenediamine at −10 to 0 °C, affording the corresponding β-nitroalkenes **1** in satisfactory yields (50%–80%).



R = R^1 = Me; R = Ph, R^1 = Me; RR^1N = morpholino.

According to patent data,[44] 5-(4-chlorophenyl)-2-(2-nitroprop-1-enyl)furan is formed in 50% yield on refluxing 5-(4-chlorophenyl)furfural in nitroethane in the presence of piperidine.

It has been reported[46] that the condensation of furfural with primary nitroalkanes in ethanol in the presence of K_2CO_3 or $KHCO_3$ results in the formation, together with β-(2-furyl)nitroalkenes **1**, also of the corresponding β-nitroalcohols **5**—the products of aldol condensation, their yield reaching 70%.

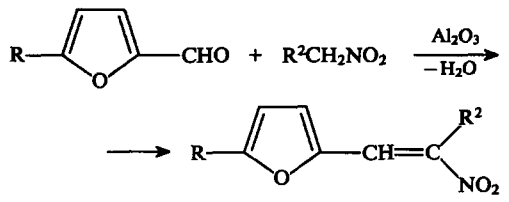


R^2 = H, Me, Et, Pr, Pr^i, Bu^i.

The dehydration of the β-nitroalcohols **5** leads to the β-nitroalkenes **1**; for example,[63] treatment of 1-(2-furyl)-2-nitroethanol **5** (R^2 = H) with dicyclohexylcarbodiimide in the presence of Cu_2Cl_2 in ether (35 °C, 24 h) affords β-(2-furyl)nitroethylene **1** in 66% yield.

Anion-exchange resins have also been used as catalysts in the condensation of furfural with nitromethane.[64,65] β-(2-Furyl)-nitroethylene was synthesised in 38%–46% yield in the presence of the AN-2F anion-exchange resin. The catalytic activities of various anion-exchange resins have been investigated[65] and it has been established that they decrease in the following sequence: EFE-10P > AN-2F > PE-9 > AN-9F. The strongly basic EFE-10P anion-exchange resin, containing quaternary ammonium groups, proved to be the most active catalyst in the above reaction. When this catalyst was used, the yield of β-(2-furyl)nitroethylene was 78%–86% (40 °C, 5 h).

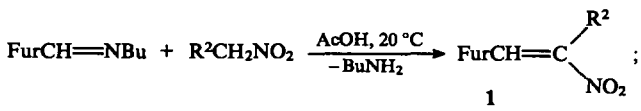
In 1985, Italian workers[39] proposed an effective method of synthesis of β-nitroalkenes of the furan series in 70%–93% yields by condensing equimolar amounts of 5-R-furfurals with nitroalkanes and carboxylic nitroacid esters on the surface of chromatographic Al_2O_3 without a solvent (20 °C, 30–48 h).



R = H, Me; R^2 = Me, Et, Bu^n, $MeOOCCH_2$, $MeOOC(CH_2)_5$, 2-methyl-1,3-dioxolan-2-ylmethyl.

The authors note that this reaction apparently involves the intermediate formation of the corresponding β-nitroalcohols **5**, which are subsequently dehydrated.

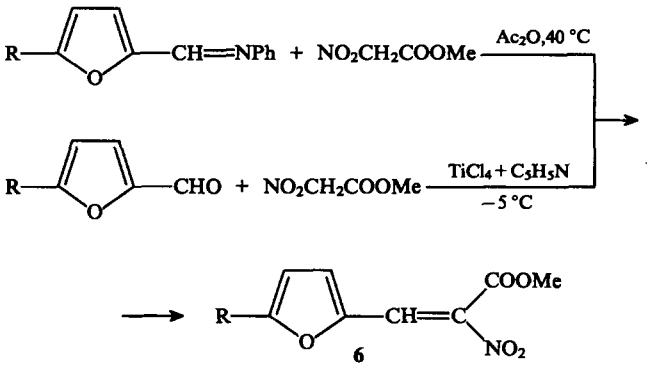
Robertson[49,50] used the condensation of phenyl- or 2-chlorophenyl-nitromethane with *N*-furfurylidenebutylamine in order to synthesise β-(2-furyl)-α-arylnitroethylenes (**1**, R = R^1 = H, R^2 = Ph, 2-ClC_6H_4):



R^2 = Ph, 2-ClC_6H_4.

The reaction was carried out by keeping equimolar amounts of the reactants in glacial acetic acid for several hours at 20 °C.

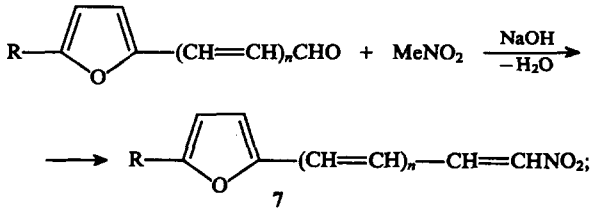
Czechoslovak scientists[53] synthesised the methyl esters of β-(5-R-2-furyl)-α-nitroacrylic acids **6** by condensing methyl nitroacetate with *N*-(5-R-furfurylidene)anilines in acetic anhydride (40–50 °C, 10 h: yield 30%–45%) or with 5-R-furfurals in the presence of $TiCl_4$ and pyridine in CCl_4 (–5 to 0 °C, 24 h; yield 77%–85%). However, the latter method has not come to be widely used for the synthesis of furylnitroalkenes.



R = H, Br, I, Me, MeOOC, NO_2.

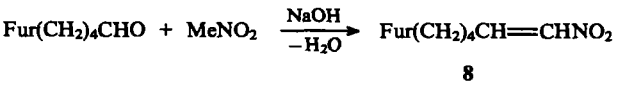
It is noteworthy that the reaction with 5-nitrofurfural takes place stereoselectively[53] to form the (*E*)-isomer of compound **6**. On the other hand, the condensation of other furan aldehydes with nitroacetic acid ester results in the formation of a mixture of (*E*)- and (*Z*)-stereoisomeric nitroalkenes **6** in which the (*Z*)-isomer predominates.

There are isolated literature data[29,66,67] concerning the synthesis of conjugated nitrodienes and nitrotrienes of the furan series **7**. Compounds of this type were synthesised in 70%–75% yield by condensing β-(2-furyl)acroleine or 5-(2-furyl)penta-2,4-dienal with nitromethane in the presence of NaOH (method *A*):

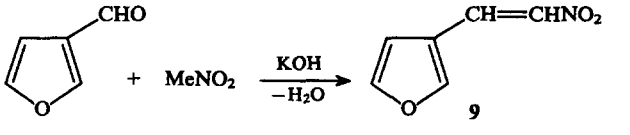


n = 1, 2; R = H, NC.

6-(2-Furyl)-1-nitrohex-1-ene **8** was synthesised in 47% yield by condensing 5-(2-furyl) pentanal with nitromethane and NaOH at 0 °C.[68]



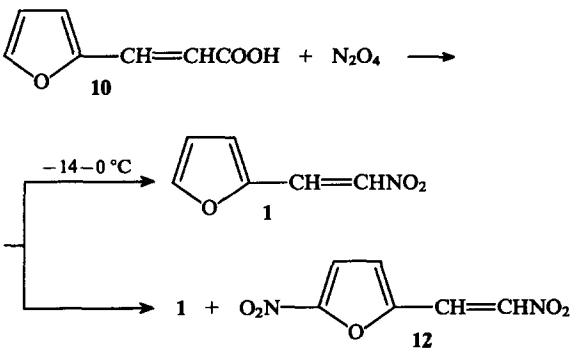
Data concerning the synthesis[69,70] of β-(3-furyl)nitroethylene **9** in 80%–86% yield by the condensation of 3-formylfuran, which is difficult to obtain, with nitromethane in the presence of KOH in methanol appeared in the literature in recent years.



β-Nitroalkenes of the furan series have been obtained using as the starting compounds β-(2-furyl)acrylic acids, which are formed in a high yield on condensation of furfural or substituted furfurals with malonic acid in the presence of piperidine.[7,71]

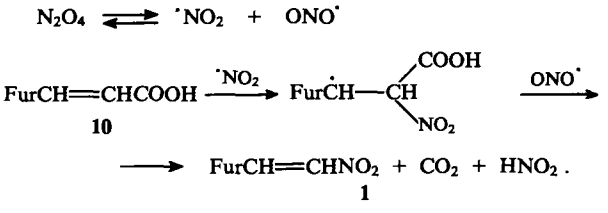
The nitration of (*E*)-β-(2-furyl)acrylic acid **10** with concentrated nitric acid in acetic anhydride has been described.[8,72–76] (*E*)-β-(5-Nitro-2-furyl)acrylic acid **11** was isolated as the main reaction product in all the investigations. It has been established[77] that (*E*)-β-(2-furyl)nitroethylene (**1**, R = R^1 = R^2 = H) and (*E*)-β-(5-nitro-2-furyl)nitroethylene **12** are formed under these

conditions as side products. The last two substances have also been obtained by passing nitrogen dioxide through a solution of the acid **10** in benzene, acetic acid, or acetic anhydride.[78]



When the acid **10** is nitrated with an equimolecular amount of nitrogen tetroxide in ether[79] at −12 to −14 °C or in benzene and acetic acid[78] at 0 °C, the nitro-group enters preferentially the side chain and the main reaction product is β-(2-furyl)nitroethylene **1** (yield 16%–18%).

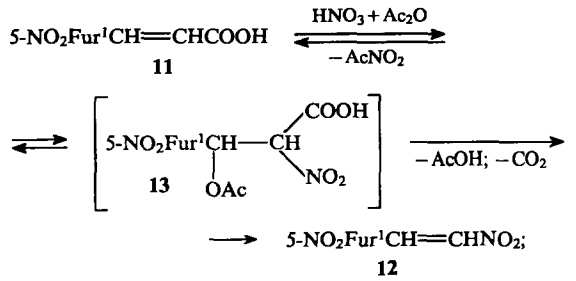
At a higher temperature, the ring is also nitrated;[78] the reaction products contain up to 15% of the β-nitroalkene **12**. According to Sitkin and Klimenko,[79] the synthesis of β-nitroethylene **1** from the acid **10** proceeds at reduced temperatures by a radical mechanism, which can be represented schematically as follows:



Together with the nitroalkene **1**, oxalic acid, formed as a result of the partial oxidation of the nitroalkene **1**, was isolated in the above reaction as a side product; the reaction was accompanied also by the formation of tarry products.

When the acid **10** is acted upon by a large excess of N_2O_4 at −10 °C, products of nitration in the furan ring are obtained[79] — β-(5-nitro-2-furyl)acrylic acid **11** (51.5%) and insignificant amounts of the β-nitroalkene **12**.

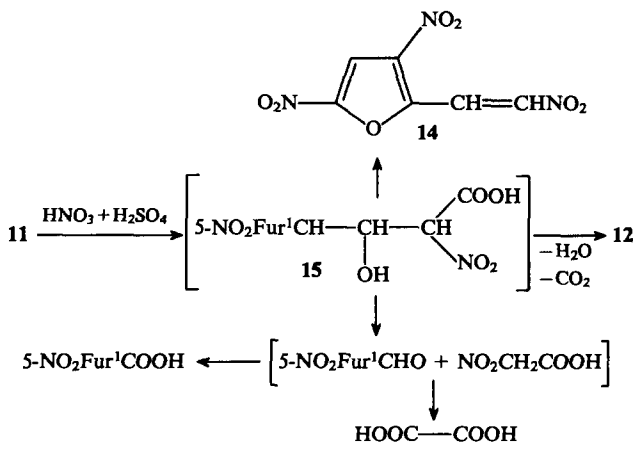
When the acid **11** is nitrated with fuming HNO_3 in acetic anhydride[80] (−20 °C; or 20 °C, 4 h), the nitroalkene **12** is formed in 15% yield:



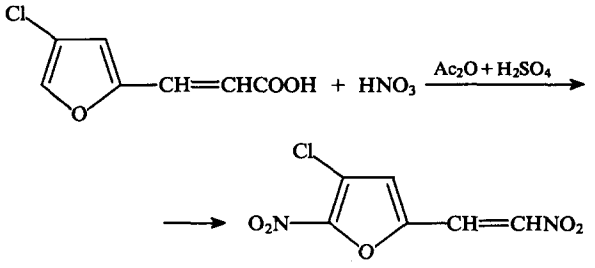
here and henceforth 5-NO_2Fur^1 = 5-nitro-2-furyl.

The unstable adduct **13** — the product of the addition of acetyl nitrate, formed in the mixture of acetic anhydride and fuming HNO_3, is an intermediate in this reaction.

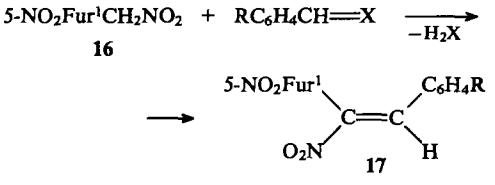
The authors established that the β-nitroalkene **12** is formed in 77% yield when the acid **11** is refluxed with 10% HNO_3; 5-nitrofurfural and 5-nitrofuran-2-carboxylic acid were isolated as side products under these conditions. Treatment of the acid **11** with the nitrating mixture comprising fuming nitric acid and concentrated sulphuric acid[80] at 5 °C affords 13% of β-(3,5-dinitro-2-furyl)nitroethylene **14** together with the β-nitroalkene **12**. The intermediate under these conditions is the unstable adduct **15** — the product of the addition of the elements of HNO_3 to the double bond; 5-nitrofuran-2-carboxylic acid and oxalic acid are formed as side products.



When β-(4-chloro-2-furyl)acrylic acid is nitrated with fuming HNO_3 in acetic anhydride (molar ratios 1 : 4 : 10) in the presence of catalytic amounts of H_2SO_4 at −10 to −5 °C, β-(4-chloro-5-nitro-2-furyl)nitroethylene is obtained in 70% yield.[23]



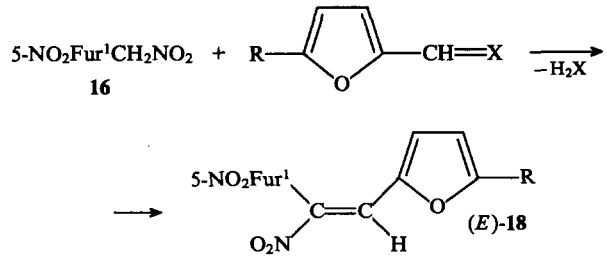
Condensation of 2-nitromethyl-5-nitrofuran **16** with aromatic aldehydes, ammonium acetate, and acetic acid in benzene (refluxing for 3–5 h) or with *N*-benzylidenebutylamines in acetic acid at 20 °C leads to α-nitro-α-(5-nitro-2-furyl)-β-arylethylene **17** having the (*E*)-configuration.[81–83]



X = O, NBu; R = H, 4-Me, 4-MeO, 2-MeO, 4-Me_2N, 2-F, 4-Cl, 4-NC, 2-NO_2, 4-NO_2, 4-AcNH.

The authors note that the first method makes it possible to obtain the β-nitroalkenes **17** in a satisfactory yield (25%–30%) only from benzaldehydes containing electron-donating substituents. The α-nitroalkenes **17** are synthesised by the second method from benzaldehydes with electron-accepting groups (yield 41%–84%).

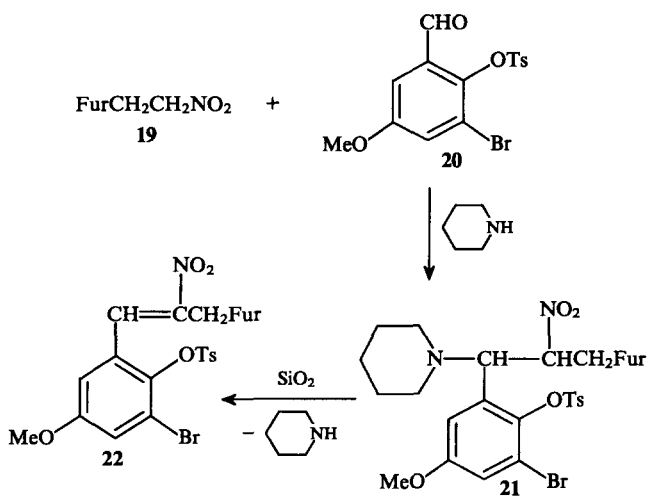
(*E*)-α-nitro-α-(5-nitro-2-furyl)-β-(5-R-2-furyl)ethylenes **18** were obtained in 28%–91% yield under analogous conditions from the nitromethyl derivative **16** and the 5-substituted furfurals or *N*-(5-R-furfurylidene)butylamines.[84]



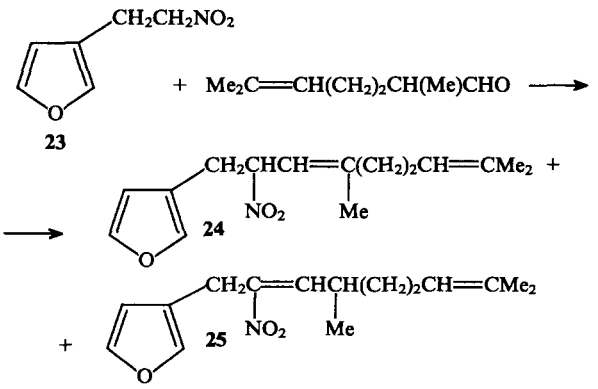
X = O, NBu; R = H, Me, Br, I, Ph, 4-ClC_6H_4, 2-ClC_6H_4, 4-BrC_6H_4, 4-MeC_6H_4, 4-$NO_2C_6H_4$.

However, the condensation of compound **16** with 5-nitrofurfural or with *N*-(5-nitrofurfurylidene)butylamine results in the formation of a 1:2 mixture of (*E*)- and (*Z*)-α,β-di(5-nitro-2-furyl)nitroethylene (**18**, R = NO_2) in 48% yield.

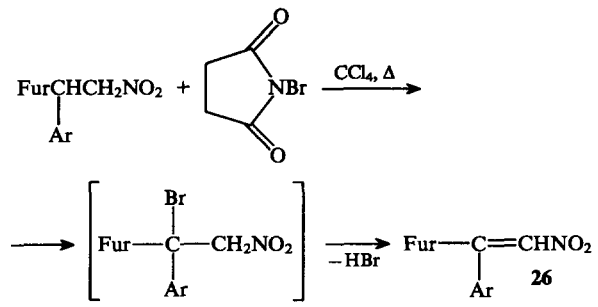
The condensation of 2-(2-furyl)-1-nitroethane **19** with a derivative of salicylaldehyde **20** in the presence of piperidine under the conditions of the Knoevenagel reaction[85] leads to the β-nitroamine **21** (yield 65%), the deamination of which on the surface of silica gel affords the nitroalkene **22** in 65% yield.



2-(3-Furyl)-1-nitroethane **23** reacts with 2,6-dimethylhept-5-enal in the presence of *N*,*N*-dimethylethylenediamine in toluene (refluxing for 2 h) to form a mixture of the allylic nitro-compound **24** (yield 46%) and the conjugated nitroalkene **25** (yield 25%).[70] On refluxing with triethylamine in benzene, the latter isomerises quantitatively to the nitroalkene **24**, which is a key compound in the synthesis of the pheromone dendrolasin.

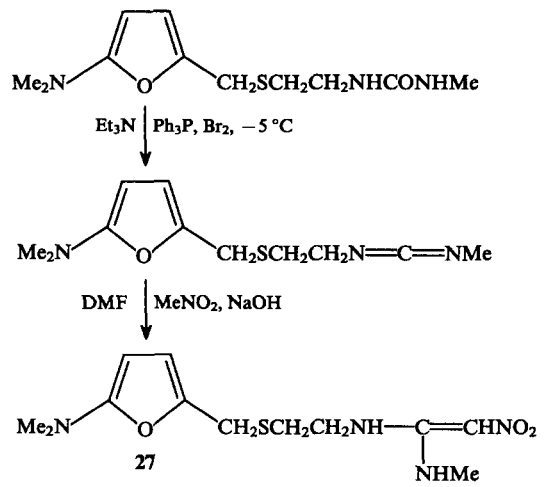


The bromination of 1-aryl-1-(2-furyl)nitroethanes by treatment with *N*-bromosuccinimide in CCl_4 (refluxing for 1 h) results in the formation of β-aryl-β-(2-furyl)nitroethylenes **26** in the form of a mixture of the (*E*)- and (*Z*)-isomers in 40%–43% yield.[86]



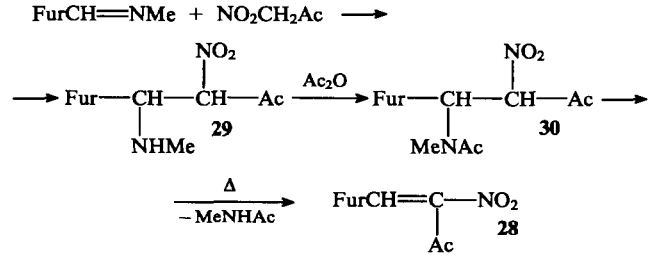
Ar = Ph, 3,4-$(OCH_2O)C_6H_3$.

An effective method of synthesis of the ulcerostatic preparation ranitidine **27**, which is nitrovinyl derivative of the furan series, in accordance with the scheme shown below has been reported.[87]



There exist also isolated data concerning the synthesis of unsaturated nitroketones of the furan series. By condensing furfurylidenemethylamine with nitroacetone in the presence of acetic anhydride, Dornow[88] synthesised 4-(2-furyl)-3-nitrobut-3-en-2-one **28** in 17% yield.

The unstable β-nitroamine **29** is formed initially and reacts with acetic anhydride, affording the *N*-acetyl derivative **30** (yield 67%). After brief heating, the latter splits off *N*-methylacetamide and is converted into the unsaturated ketone **28**. The author notes that, in the absence of acetic anhydride the nitroketone **28**, formed as a result of the deamination of the β-nitroamine **29**, combines with a second acetone molecule, giving rise to an unstable diadduct. This reaction is catalysed by the methylamine liberated; acetic anhydride binds the amine and reduces its basicity, weakening thereby its catalytic effect.



In 1969 German scientists[89] synthesised an unsaturated nitroketone of another type—1-(2-furyl)-4-nitrobut-2-en-1-one **31**, which is an interesting and promising synthon for the preparation of various furan derivatives with functional groups in the side chain. Compound **31** is formed in 80% yield on reaction of

equimolar amounts of 2-acetylfuran and 2-dimethylamino-1-nitroethylene in the presence of potassium ethoxide (60–70 °C) with subsequent hydrolysis (20 °C) of the intermediate potassium salt **32**.

$$\text{FurAc} + \text{Me}_2\text{NCH}{=}\text{CHNO}_2 \xrightarrow[-\text{Me}_2\text{NH}]{\text{EtOK}-\text{EtOH}} \text{FurCOCH}{=}\text{CH}-\text{CHNOO}^-\text{K}^+ \xrightarrow{\text{HOH}} \underset{\mathbf{31}}{\text{FurCOCH}{=}\text{CHCH}_2\text{NO}_2}$$

32

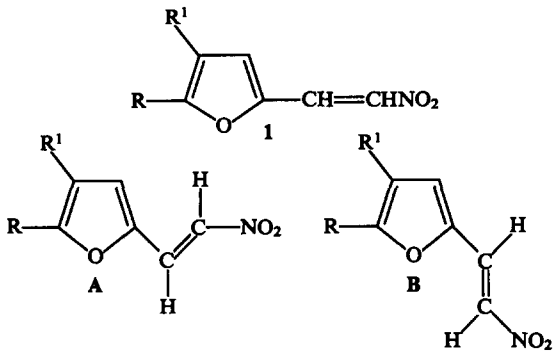
The authors note that this nitroketone is highly reactive and enters into many reactions characteristic of α,β-unsaturated ketones and primary nitrocompounds.

III. Structure and reactivity of furylnitroalkenes

1. The dipole moments of furylnitroalkenes

Important information about the steric structure and reactivity of β-(5-R-2-furyl)nitroalkenes has been obtained by studying their dipole moments.[1,62,90–94] The low aromaticity of furan[95,96] makes it possible to expect a strong π-interaction in the chain between the double bond of the vinyl fragment and the NO_2 group with participation of the furan ring and its substituents in the 5-position.

β-(5-R-4R¹-2-Furyl)nitroethylenes **1** are regarded[49,91] as planar *trans*-isomers which can exist in two forms — *trans*-(*S*)-*trans* (form *A*) and *cis*-(*S*)-*trans* (form *B*), depending on the positions of the double bonds of the furan and the vinyl group relative to the C(2)–Cβ bond.



R = H, Me, Cl, Br, I, NO_2; R¹ = H; R = Br, I; R¹ = Br.

The low aromaticity of the system makes the *trans*-(*S*)-*trans* structure, i.e. structure *A*, energetically more favourable.[41,91] The observed discrepancies between the experimental and calculated dipole moments ($\Delta\mu = \mu_{exp} - \mu_{calc}$) are then attributed to the interaction moment (μ_{int}) arising as a result of the π-conjugation in the molecule.

By analogy with 5-halofurfurals,[93] negative values of μ_{int} should be expected for β-(5-halo-2-furyl)nitroethylenes (**1**; R = Cl, Br, I; R¹ = H, Br) as a consequence of the $-J$ effect of these substituents. However, a higher value of μ_{exp} compared with μ_{calc} is observed for all the compounds of this series (Table 1). This is apparently caused by the stronger electron-accepting properties of the β-nitrovinyl group compared with the aldehyde group.[3,41,94] The electronic interaction of the halogen with the furan ring in the given compound should therefore be expressed by the $+M$ effect. Hence it is of interest to note that an increase in μ_{int} is observed for β-nitroalkenes **1** in the following sequence of substituents 5-R: I < Br < Cl (0.13, 0.30, and 0.76 D).

Table 1. The dipole moments of (*E*)-β-(5R-4R¹-2-furyl)-α-R²-nitroethylenes.[41,90–92,97]

R	R¹	R²	Dipole moments/D		
			μ_{exp}	μ_{calc}	μ_{int}
H	H	H	4.94	4.81	0.13
Me	H	H	4.76	5.31	0.45
Cl	H	H	4.97	4.21	0.76
Br	H	H	4.65	4.35	0.30
I	H	H	4.81	4.68	0.13
NO_2	H	H	4.15	3.56	0.59
Br	Br	H	3.70	3.03	0.67
I	Br	H	3.52	3.39	0.13
H	H	Me	4.87	5.07	−0.20
Me	H	Me	5.46	5.31	0.15
Cl	H	Me	4.35	4.31	0.04
Br	H	Me	4.24	4.35	−0.11
I	H	Me	4.38	4.68	−0.30
NO_2	H	Me	4.05	3.56	0.49
Morpholino	H	Me	5.66	–	–
MeNPh	H	Me	6.97	6.27	0.70
Me_2N	H	Me	6.62	6.28	0.34
Br	Br	Me	3.23	3.03	0.20
I	Br	Me	3.40	3.39	0.01
H	H	Ph	5.17	5.07	0.10
Me	H	Ph	5.66	5.31	0.35
Cl	H	Ph	4.59	4.21	0.35
Br	H	Ph	4.22	4.35	−0.13
I	H	Ph	4.45	4.68	−0.23
NO_2	H	Ph	3.88	3.56	0.32
Br	Br	Ph	3.41	3.03	0.38
I	Br	Ph	3.29	3.39	−0.10
H	H	Br	4.71	4.70	0.01
Me	H	Br	5.49	4.99	0.50
Cl	H	Br	4.40	4.22	0.18
Br	H	Br	4.44	4.31	0.13
I	H	Br	4.30	4.46	−0.16
NO_2	H	Br	3.77	4.54	−0.77
Br	Br	Br	3.41	3.50	−0.09
I	Br	Br	3.71	3.59	0.12
H	H	Cl	4.80	4.71	0.09
Br	H	Cl	4.32	4.30	0.02
NO_2	H	Cl	3.67	4.52	−0.85

The experimental dipole moments of β-(5-R-4-R¹-2-furyl)-α-methylnitroethylenes **33** are lower by 0.2–0.6 D than the corresponding values for β-(5-R-4-R¹-2-furyl)nitroethylenes **1** (Table 1).[41,92]

The dipole moment probably changes as a result of the breakdown of the planar configuration due to steric hindrance between the methyl group, the nitro-group, and the oxygen of the furan ring. Rotation about the Cα–N and C(2)–Cβ bonds weakens the π-interaction involving the electrons of the substituents in the 5-position in the vinyl group and of the NO_2 group, which decreases the dipole moment. The angle of rotation can then be estimated approximately from the formula

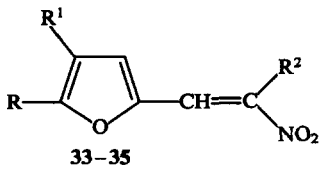
$$\mu = \mu_{int} \cos^2\theta ,$$

where $\Delta\mu = \mu_{exp} - \mu_{calc}$ for the β-nitroalkene **33**, and θ is the effective angle of rotation.

The angle θ is approximately 60° for β-(5-methyl-2-furyl)-α-methylnitroethylene (**33**, R = Me, R¹ = H, R² = Me), where appreciable changes in the dipole moment of the C(5)–Me bond due to the breakdown of conjugation do not occur because the methyl group has weak electron-donating properties.[41]

The introduction of the phenyl group in the α-position should induce an even greater breakdown of the planar configuration via the rotation of the Cα–N and C(2)–Cβ bonds. However, the values of μ_{exp} for β-(5-R-4-R¹-2-furyl)-α-phenylnitroethylenes **34**

occupy an intermediate position between those for the nitroethylenes **1** and the α-methylnitroethylenes **33**. This is apparently caused by the simultaneous rotation of the phenyl group, which creates conditions for the minimum deviation of the principal fragment of the molecule from the planar structure.[91]



33–35

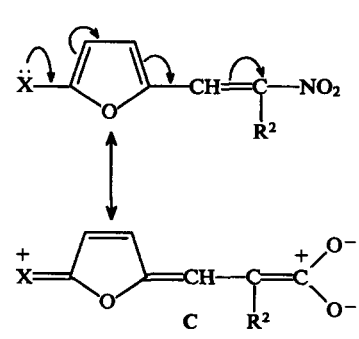
R = H, Me, Cl, Br, I, NO_2, Me_2N, morpholino, PhNMe; R^1 = H;
R = Br, I; R^1 = Br;
33: R^2 = Me; **34**: R^2 = Ph; **35**: R^2 = Cl, Br.

It has been suggested[41] that the $+M$ effect of the halogens predominates in the β-(5-halo-2-furyl)nitroethylenes **1** owing to the strong electron-accepting properties of the nitrovinyl fragment and the planar configuration of these molecules. On the other hand, the decrease in the degree of conjugation in the non-coplanar molecules of β-(5-halo-2-furyl)-α-R^2-nitroethylenes (**33**, **34**; R^2 = Me, Ph) promotes the appearance of the usual electron-accepting properties of the halogen in the 5-position. The latter follows from the appreciably smaller (R = Cl) and even negative (R = Br, I) values of μ_{int}. Evidently this is associated with the fact that the interaction of the electron-accepting nitrovinyl group with the substituent in the furan ring weakens when the planar conformation of the molecules breaks down.[91]

On the other hand, more favourable conditions for the planar molecular structure arise for β-(5-R-4-R^1-2-furyl)-α-halonitroethylenes (**35**; R^2 = Cl, Br).[91] High values of μ_{int}, characteristic of planar-(5,R-4-R^1-2-furyl)nitroethylenes **1**, are typical for these compounds. The high degree of conjugation in these compounds can be accounted for by the operation of two factors: the smaller bulk of the halogens compared with the methyl and phenyl groups and the greater electronegativity of the α-halo-α-nitrovinyl fragment.

2. Electronic absorption spectra of furylnitroalkenes

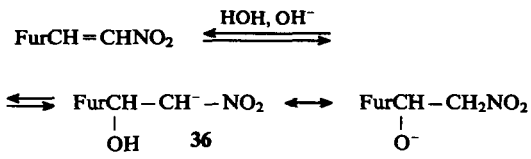
There are three absorption bands in the UV spectra of β-(5-R-4-R^1-2-furyl)-α-R^2-nitroalkenes **1** and **33–35** in the ranges 205–245, 234–282, and 322–428 nm. The first two bands can be assigned to the $\pi-\pi^*$ and $n-\pi^*$ electronic transitions in the furan, the aryl substituents, and the vinyl group.[18,98] The most intense band in the spectra of the given compounds (322–428 nm; the *K* band) refers to the $\pi-\pi^*$ transition throughout the conjugated polyene system and yields important information about the planarity of the system.[1,18,91,98,99] The observed bathochromic shift compared with 2-vinylfuran (261 nm) is associated with the appearance of the dipolar structure **C** as a consequence of direct polar conjugation:



C

We may note that the corresponding absorption band of β-nitrostyrene (309 nm)[1] lies below that of β-(2-furyl)nitroethylene **1** (346 nm) as a consequence of the stronger electron-donating properties of the furyl group.[95]

It has been reported[59,100] that, when the UV spectrum of the β-nitroethylene **1** is recorded in aqueous ethanol at pH 11.5–12.6, the absorption band at λ_{max} = 346 nm vanishes and a band appears at λ_{max} = 252–255 nm. This finding can be accounted for by the appearance of the stable mesomeric ion **36**.



The extinction coefficient ε for this nitroalkene (ε = 24 516) is approximately three times greater than for *cis*-β-(2-furyl)acrylic acid (ε = 9780), which is also evidence in support of the *trans*-conformation of furylnitroethylenes.[100]

In the UV spectra of β-(2-furyl)-α-R^2-nitroethylenes, and absorption *K* band undergoes a bathochromic shift as R^2 is varied in the sequence H (346) < Me (348) < Ph (353) < Cl (358) < Br (365) < CN (371 nm).[18,47,55,59,91,100] The appreciable bathochromic shift and the hyperchromic effect for β-(2-furyl)-α-nitroacrylonitrile (λ_{max} = 371 nm; ε = 21 500) compared with β-(2-furyl)nitroethylene indicates an increased contribution of the dipolar structure **C** to the ground state of the molecule.[55]

A bathochromic shift of the absorption *K* band is observed in the spectra of β-(5-R-2-furyl)nitroethylenes **1**. It increases in the following sequence of substituents R: H (346) < NO_2 (350) < Cl (358) < Br (355) < I (357) < Me (367) < PhS (370) < NMe_2 (428 nm).[18,55,59,80,91,100] The relatively small shift of the absorption maximum for R = NO_2 is associated with the non-coplanarity of this substituent relative to the nitrovinyl fragment.[91] The UV spectrum of β-(3,5-dinitro-2-furyl)nitroethylene **14** exhibits a hypsochromic shift of the *K* band (λ_{max} = 340 nm) as a consequence of the decrease in the mobility of the π-electron system induced by the introduction of the second nitro-group into the furan ring.[80]

The appreciable bathochromic shift of the *K* band in the spectra of β-(5-dimethylamino-2-furyl)-R^2-nitroethylenes (R^2 = H, λ_{max} = 428 nm; R^2 = Me, λ_{max} = 480 nm) can be explained by the possibility of direct polar conjugation in the molecules of these compounds and by the approach to a planar structure.[91]

The absorption maxima of the *K* band in the spectra of different β-(5-halo-2-furyl)-α-R^2-nitroethylenes can be arranged in the following sequence based on increasing wavelengths as a function of the substituents R^2;[18,47,91] Cl < Br < I. This is characteristic also of 4-halonitrobenzenes.[101] This sequence is the reverse of that observed for the changes in the dipole moment μ_{int} in terms of the same substituents, which can be explained by the greater $+M$ effect of the chlorine atom compared with bromine and iodine. The decrease in the C(5)–halogen bond polarity,§ which depends on this factor, is particularly appreciable for chloro-derivatives in view of the insignificant contribution of the π-interaction with the unoccupied *d* orbitals of the halogen atom. The latter feature is most favourable for halogens with a large radius.[102] It is essential to note that both the $+M$ and $-M$ effects of the halogens lead simultaneously to the stabilisation of the ground and excited states, which in fact accounts for the observed order of the bathochromic shifts for the group of furylnitroalkenes examined.

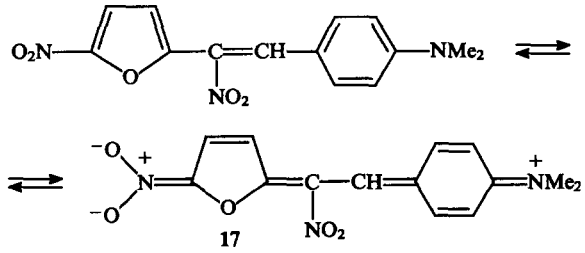
§The decrease in the C(5)–halogen polarity leads to an increase in the resulting molecular dipole moment.[41,91]

As the conjugation chain increases, the UV spectra of nitropolyenes of the furan series $Fur(CH=CH)_nNO_2$ **7** exhibit a bathochromic shift of the absorption *K* band ($n = 0$, $\lambda_{max} = 310$; $n = 1$, $\lambda_{max} = 346$; $n = 2$, $\lambda_{max} = 380$; $n = 3$, $\lambda_{max} = 410$ nm) and an increase in its intensity.[67,103]

R^2	λ_{max}/nm		
	Cl	Br	I
H	352	355	357
Me	353	355	362
Ph	360	363	369
Br	369	375	367

The electronic absorption spectra of α-nitro-α-(5-nitro-2-furyl)-β-(R-phenyl)ethylenes **17** contain two absorption bands in the range 216–275 and 298–318 nm,[81,82] which can be assigned to the electronic transitions in furan[104] and benzene.[99] Apart from the above absorption bands, compounds of this type, containing electron-donating groups in the aryl fragment, have yet another absorption band in the long-wavelength region (R = 4-MeO, λ_{max} = 363; R = 2-MeO, λ_{max} = 362; R = 4-NMe_2, λ_{max} = 370; R = 4-AcNH, λ_{max} = 460 nm).[81,82] This can be explained by the appearance of the corresponding quinnoid structure.

In the spectra of other α-nitroalkenes **17** (R = 2-F, 4-Cl, 4-NC, 4-NO_2, 2-NO_2), there is no absorption in this region, which is an indication of the incomplete coplanarity of the above compounds. Conjugation can also be prevented by the partial displacement of the 5-nitrofuryl and aryl fragments from the plane of the double bond induced by the bulky α-nitro-group.[81]



17

The UV spectra of (*E*)-α-nitro-α-(5-nitro-2-furyl)-β-(5-R-2-furyl)ethylenes **18** contain two absorption bands in the ranges 295–345 and 357–440 nm (*K* band).[84] It is noteworthy that, for example, the molecules of α-(5-nitro-2-furyl)-β-phenylethylene and α-(5-nitro-2-furyl)-β-(phenyl-2-furo)ethylene are planar systems and contain in the UV spectra an intense *K* band in the visible region. On the other hand, in the spectra of their α-nitro-analogues, this band has undergone a hypsochromic shift by 15–20 nm, which indicates the non-planarity of the molecules of these compounds.

The hypsochromic shift of the *K* band and the hyperchromic shift in the UV spectrum of (*E*)-α,β-di(5-nitro-2-furyl)ethylene (λ_{max} = 372 nm, $\lg\varepsilon$ = 4.15) relative to the (*Z*)-isomer (λ_{max} = 392 nm, $\lg\varepsilon$ = 4.18)[84] are noteworthy. This is apparently associated with the fact that the steric strain involving the substituents at the double bond in the (*E*)-isomer is greater than that in the (*Z*)-isomer and hence in the former case the system deviates more appreciably from planarity.

An appreciable hypsochromic shift of the *K* band is observed also in the spectra of the methyl esters of (*Z*)-β-(5-R-2-furyl)-α-nitroacrylic acids **6** (R = H, λ_{max} = 313; R = Br, λ_{max} = 321; R = I, λ_{max} = 333; R = Me, λ_{max} = 325; R = MeOOC, λ_{max} = 320 nm).[53]

3. IR spectra of furylnitroalkenes

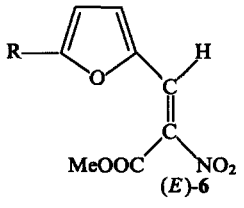
In the IR spectra of furylnitroalkenes there are intense absorption bands in the range 1610–1660 cm^{-1}, which are characteristic of conjugated double bonds in the *trans*-isomers of ethylene compounds.[105] The absorption band at 1660–1670 cm^{-1} is associated with the stretching vibrations of the C–C bonds of the furan ring,[100,104] which is typical for furan derivatives with unsaturated substituents in the 2-position. Absorption maxima in the range 1510–1550 and at 1340 cm^{-1} correspond[105,106] to the asymmetric and symmetric stretching vibrations of the NO_2 group.

The IR spectroscopic data confirm the features of the variation of the configurations of β-(5-R-4R^1-2-furyl)-α-R^2-nitroethylenes (**1**, **33**, **34**; R^2 = H, Me, Ph). The most planar molecules (**1**, R^2 = H) are characterised by a low-frequency $\nu_{C=C}$ absorption (1635–1642 cm^{-1}).[91,100] The deviation from the planar configuration on passing from R^2 = Ph (**34**) and specially to R^2 = Me (**33**) increases the $\nu_{C=C}$ absorption frequency (1640–1655 and 1653–1663 cm^{-1}) respectively.

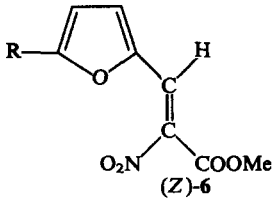
It was noted above that more favourable conditions for a planar molecular structure are created in β-(5-R-4-R′-2-furyl)-α-halonitroethylenes **35**. The high degree of conjugation in these compounds is reflected also in the $\nu_{C=C}$ frequency (1610–1628 cm^{-1}), which is reduced compared with compounds **1**, **33**, and **34**.[47,91]

The appreciable decrease in the $\nu_{C=C}$ absorption frequency in the spectra of N-substituted β-(5-amino-2-furyl)-α-methylnitroethylenes (**33**, R = Me_2N, PhNMe, morpholino) (1638–1645 cm^{-1}) compared with the remaining compounds of the same series (R = H, Me, Cl, Br, NO_2; 1653–1632 cm^{-1}) is noteworthy.[91] This can be explained by the direct polar conjugation in the β-(5-amino-2-furyl)-α-nitroethylene molecules and their approach to a planar structure.

The (*E*)- and (*Z*)-isomers of the methyl esters of β-(5-R-2-furyl)-α-nitroacrylic acids **6** differ in the absorption frequencies ν_{as} and ν_s of the α-nitro-group. The absorption bands due to these vibrations in the spectra of the (*E*)-isomers are at higher frequencies (1540–1542 and 1321–1330 cm^{-1}) than the analogous bands in the structure of the (*Z*)-isomers (1549–1552 and 1373–1375 cm^{-1}).[53]



(*E*)-**6**

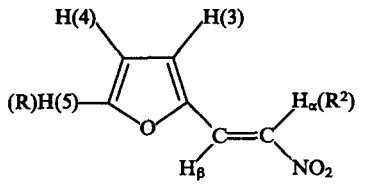


(*Z*)-**6**

The vibrations of the C=C valence bonds in the IR spectra of α-nitro-α-(5-nitro-2-furyl)-β-arylethylenes **17** are represented by moderately intense absorption bands in the range 1654–1670 cm^{-1}.[81,82] The introduction of electron-donating substituents (Me, MeO, NMe_2) into the benzene ring induces a bathochromic shift of the bands; electron-accepting substituents (NO_2, CN) induce the opposite shift. In the region of the symmetrical stretching vibrations of the NO_2 group in the spectra of these compounds, two absorption bands are observed at 1310–1340 and 1350–1360 cm^{-1}. The band at the higher frequency corresponds to the vibrations of the nitro-group in the furan ring.[81]

In the spectra of α-nitro-α-(5-nitro-2-furyl)-β-(5-R-2-furyl)-ethylenes **18**, absorption maxima in the range 1640–1655 cm^{-1} (R = H, Me, Br, I, NO_2) or in the range 1650–1662 cm^{-1} (R = aryl) refer to the C=C bond stretching vibrations.[84] The asymmetric stretching vibrations of the NO_2 group are represented by absorption bands at 1540–1560 cm^{-1}, while the

Table 2. ^{1}H NMR spectroscopic data for β-(5-R-2-furyl)-α-R^2-nitroethylenes



R	R^2	δ (ppm)					SSCC/Hz				Solvent	Ref.
		H(3)	H(4)	H(5)	H_α	H_β	J_{34}	J_{35}	J_{45}	$J_{\alpha\beta}$		
H	H	7.15	6.67	7.80	7.57	7.90	3.55	0.72	1.83	13.30	Acetone-d_6	8, 108, 109
H	H	6.81	6.53	7.25	7.66	7.37	3.48	0.72	1.82	13.26	CS_2	8, 109
H	H	7.00	6.65	7.70	7.53[a]	7.81[b]	3.60	–	1.80	13.00	CCl_4	110
H	H	6.03	6.05	7.01	7.04	7.55	3.40	–	1.80	13.50	C_6D_6	110
H	H	6.89	6.56	–	7.53	7.70	3.53	–	–	13.10	$CDCl_3$	18
H	E	6.90	6.67	7.56	–	7.80	–	–	–	–	$CDCl_3$	39
H	B	6.93	6.70	7.60	–	7.90	–	–	–	–	$CDCl_3$	39
NO_2	H	5.33	6.21	–	6.78	6.72	4.03	–	–	13.10	$CDCl_3$	18
NO_2[b]	H	–	8.25	–	8.20	8.46	–	–	–	14.00	Acetone-d_6	80
Br	H	6.51	6.83	–	7.66	7.50	3.51	–	–	13.10	$CDCl_3$	18
PhS	H	6.50	6.74	–	7.51	7.29	3.50	–	–	13.10	$CDCl_3$	18
$PhSO_2$	H	6.89	7.24	–	7.66	7.55	3.47	–	–	13.80	$CDCl_3$	18
3-$NO_2C_6H_4$	H	6.25	7.53	–	7.95	7.80	3.80	–	–	13.40	$CDCl_3$	18
Me_2N	H	7.16	7.38	–	8.15	8.07	3.79	–	–	13.50	$CDCl_3$	18

[a] Calculated from Pasqual's equation:[111] δ_{H_α} = 7.65 ppm; δ_{H_β} = 8.10 ppm.
[b] β=(3,5-Dinitro-2-furyl)nitroethylene.

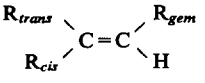
symmetric vibrations are represented by two bands at 1315–1340 cm^{-1} (the α-nitro-group) and 1355–1365 cm^{-1} (the nitro-group in the furan ring).

4. ^{1}H NMR spectra of furylnitroalkenes

The ^{1}H NMR spectra of β-(5-R-2-furyl)-α-R^2-nitroethylenes **1** and **33–35** contain the resonance bands of three or two protons of the furan ring in the form of doublets with chemical shifts and spin–spin coupling constants usual for these compounds.[104,107,108] Table 2 lists the chemical shifts of the most characteristic protons in the ^{1}H NMR spectra of certain furylnitroalkenes. Depending on the nature of the substituents R in the furan ring and of the solvent, the signals due to the protons of the furan ring are observed in the ranges 5.33–7.16 ppm for H(3), 6.05–7.53 ppm for H(4), and 7.01–7.80 ppm for H(5).

The protons attached to the double bond in β-(5-R-2-furyl)-nitroethylenes **1** give rise to doublet signals in the ranges 6.78–8.20 ppm (H_α) and 6.72–8.46 ppm (H_β) with spin–spin coupling constants of 13.0–14.0 Hz, which is characteristic of protons in the *trans*-position at the double bond.[105] Thus the spin–spin coupling constants ($^3J_{\alpha\beta}$) of the protons in the nitrovinyl group constitute yet another confirmation of the (*E*)-configuration of nitroethylenes of the given type.

It has been shown[110] that the chemical shifts of the vinyl protons in the spectra of β-(2-furyl)nitroethylene **1** are satisfactorily correlated with the values calculated from Pasqual's equation[111] taking into account the additive increments for different protons:

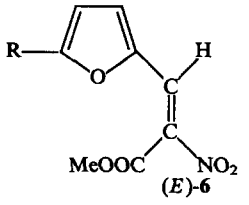


$$\delta_H = 5.25 + \Sigma z_i$$

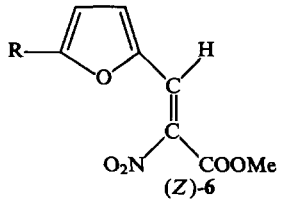
$z_i^{gem} = 2.00$; $z_i^{trans} = 0.46$; $z_i^{cis} = 1.67$.

Kovac and coworkers[53] noted that the (*E*)- and (*Z*)-isomers of the methyl esters of β-(5-R-2-furyl)-α-nitroacrylic acids **6** may be identified from the difference between the chemical shifts of the β-proton and the protons of the methoxy-group. The signal of the H_β vinyl proton in the spectra of the (*E*)-isomers is located downfield relative to the spectra of the (*Z*)-isomers (Table 3). Thus an appreciable shift of the signal due to this proton is induced by the greater magnetic anisotropy of the nitro-group compared with the carbonyl group. The H_β chemical shifts of the (*E*)- and (*Z*)-isomers of these nitroalkenes have also been calculated from Pasqual's equation using the additive increments:[112] δ_{H_β} is 8.75 ppm for the (*E*)-isomer and 8.10 ppm

Table 3. ^{1}H NMR spectroscopic data[53] for the (*E*)- and (*Z*)-isomeric methyl esters of β-(5-R-2-furyl)-α-nitroacrylic acids **6**.



(*E*)-**6**



(*Z*)-**6**

R	Isomer	δ_{H_β}[a] (ppm)	$\Delta\delta_{H_\beta}$ (ppm)	δ_{MeO} (ppm)	$\Delta\delta_{MeO}$ (ppm)
H	*Z*	7.25	0.50	3.81	0.06
	E	7.75		3.87	
Br	*Z*	7.20	0.55	3.81	0.09
	E	7.75		3.90	
I	*Z*	7.20	0.50	3.81	0.14
	E	7.70		3.95	
Me	*Z*	7.22	0.53	3.80	0.10
	E	7.75		3.90	
MeOOC	*Z*	7.37	0.40	3.86	0.14
	E	7.77		4.00	
NO_2	*Z*	7.28	0.49	3.86	0.15
	E	7.77		4.01	

[a] Calculated values: δ_{H_β} = 8.10 ppm for the (*Z*)-isomer; δ_{H_β} = 8.75 ppm for the (*E*)-isomer.

for the (*Z*)-isomer. The experimental and calculated H_β chemical shifts differ by approximately 1 ppm, which is an indication of the deviation of the system from planarity.

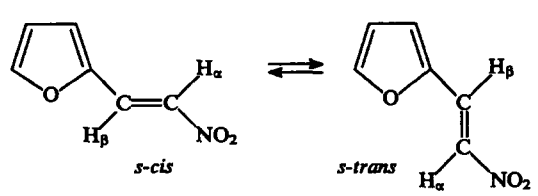
In the ^1H NMR spectra of the (*E*)-α-nitro-α-(5-nitro-2-furyl)-β-(R-phenyl) ethylenes **17**, the resonance signal of the vinyl proton is observed in the range 8.45–8.81 ppm,[81] which agrees well with the calculated value for the (*E*)-isomer (8.23 ppm). The signals due to the protons of the furan fragments are manifested as doublets at 6.77–7.17 ppm [H(3) and 7.36–7.80 ppm [H(4)] with $J_{3,4}$ = 3.7–3.9 Hz, which is characteristic of 2-substituted 5-nitrofurans.[8] The authors note that the substituent in the phenyl group hardly affects the signal of the vinyl proton. This may be due to the non-planarity of the given systems, where there is no mesomeric influence of the substituents.

The absence of an effect by the substituent R in the furan fragment on the chemical shift of the vinyl proton is also characteristic of (*E*)-α-nitro-α-(5-nitro-2-furyl)-β-(5-R-2-furyl)-ethylenes **18**. The chemical shift is observed in the range 8.44–8.53 ppm.[84] In the case of the (*E*)- and (*Z*)-isomers of α, β-di-(5-nitro-2-furyl)nitroethylene, the chemical shift of the above proton agrees well with the calculated data: 8.58 ppm for the (*E*)-isomer of compound **18** (calculated value 8.23 ppm) and 7.31 ppm for the (*Z*)-isomer (calculated value 7.45 ppm).

It is known[8,113] that the constants for the long-range (across five bonds) spin–spin coupling (^5J) between the β-proton in the side chain and the protons in the heterocyclic ring are highly stereospecific and are used to determine the most preferred configurations of the substituents in the side chain. Table 4 lists the experimental long-range spin–spin coupling constants for β-(2-furyl)nitroethylene as well as their values calculated using different methods of the molecular orbital theory.[114]

The results of the calculations of the populations of the conformational states and of the barriers to internal rotation by the molecular orbital method both at the level of the non-empirical (*ab initio*) and semiempirical (INDO2-MO-FRT, CNDO/2, etc.) approximations and the high stereospecificity show that the *s-trans*-conformer of β-(2-furyl)nitroethylene predominates in polar and non-polar salts. The value of $^6J_{\beta5}$ indicates the existence of an associative bond between H_α and H_β across the heteroatom.[109]

Table 4. The long-range spin–spin coupling constants for the ^1H NMR spectrum of β-(2-furyl)nitroethylene.[109,114]



SSCC	Experimental values for *s-trans*/Hz		Calculated values/Hz			
	CS_2	acetone-d_6	*s-trans* [a]	*s-cis* [a]	*s-trans* [b]	*s-cis* [b]
$^4J_{\alpha3}$	−0.42	−0.40	−1.01	−0.94	−1.23	−0.16
$^5J_{\alpha4}$	0.22	0.29	0.14	0.93	0.04	0.49
$^5J_{\alpha5}$	0.54	0.53	0.67	−0.22	0.56	0.09
$^5J_{\beta3}$	0.58	0.58	0.62	0.41	–	–
$^6J_{\beta4}$	0.06	0.03	−0.22	−0.10	–	–
$^6J_{\beta5}$	0.50	0.48	0.40	0.51	–	–

[a] The INDO-MO-FRT method.
[b] The CNDO-2 method.

The authors[114] concluded that the constant ^5J, incorporating $^5J_{\alpha5}$ and $^5J_{\alpha4}$, is highly stereospecific from the comparison of the experimental spin–spin coupling constants and the values predicted by calculation using the method of finite perturbations. The above constant reflects the transmission of the spin–spin coupling via the σ-electronic mechanism.

5. Quantum-chemical calculations for furylnitroalkene molecules and their reactivity

It was noted above that, among the possible planar structures of the series of β-(R-2-furyl)nitroalkenes **1**, two sterically unhindered forms can be realised: *trans-s-trans* (form **A**) and *cis-s-trans* (form **B**).[41,91]

The planar structures **A** and **B** should be energetically more favourable compared with the analogous structures of the furan aldehydes and ketones owing to the presence in them of a strong intramolecular π–π conjugation between the furan ring and the nitrovinyl fragment, demonstrated by the method of dipole moments and UV spectroscopic data.

Quantum-chemical calculation (EHM method) of the energies of the conformers **A** and **B** of β-(2-furyl)nitroethylene showed that the energy difference between the two planar conformers is comparatively small (ΔE = 0.143 kcal mol^{-1}) and the extent to which the non-planar form with a perpendicular disposition of the molecular fragments (O–C–C–H_β dihedral angle of 90°, *s*-90-conformer[114]) is unfavourable on energy grounds is much greater (E^* ≃ 10 kcal mol^{-1}).[97] The high degree of equalisation of the π-bonds C(2) ⋯ C_β ⋯ C_α ⋯ N in the planar structures of β-(2-furyl)nitroethylene is also consistent with this finding. Thus an appreciable energy barrier to rotation indicates a high stability of the above conformers and a low probability of their spontaneous interconversion.[97,114]

Certain β-(5-R-2-furyl)-α-R^2-nitroethylenes (**1** and **6**; R = H, NO_2; R^2 = H, MeOOC) have been characterised[115] by the Hückel molecular orbital method from the standpoint of their π-electronic structure. The quantum-chemical data obtained by the above investigators were compared with the physical properties (geometry and IR, UV, and ^1H and ^{13}C NMR spectra).

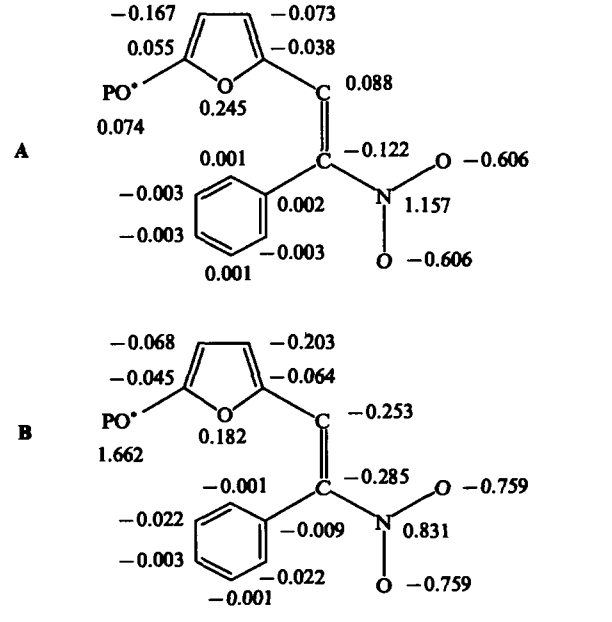


Figure 1. Distribution of the π-electron density of β-(5-chloro-2-furyl)-phenylnitroethylene **34** in the static (**A**) and transition (**B**) states: PO*—pseudo-orbital.

In order to consider the reactivity of furylnitroalkenes relative to nucleophiles, the π-electronic structures and the energies of the molecules in the static and transition (ST) states were calculated by the Hückel molecular orbital method for β-(5-chloro-2-furyl)-α-R^2-nitroethylenes (**1**, **33**, and **34**; R^2 = H, Me, Ph) (Fig. 1).[91,116] It was assumed that in the transition state the nucleophile and the chlorine atom being substituted can be represented in terms of a pseudo-orbital (PO) whose parameters have been published.[116-118]

The data on the distribution of π-electron density in the molecule of β-(5-chloro-2-furyl)-α-phenylnitroethylene **34** in the static and transition states show that nucleophilic substitution of the chlorine atom in the transition state is accompanied by a shift of π-electron density to the NO_2 group, while the phenyl group hardly participates in the electron shifts.[91] As a result of such displacement of π-electron density, the transition state energy is lowered i.e. the nitro group activates the nucleophilic substitution reactions.

Table 5 presents certain reactivity indices for β-(5-chloro-2-furyl)-α-R^2-nitroethylenes. The difference between the π-electron energies of the molecule in the static and transition states in units of the resonance integral $\beta(\Delta E^{\pi/\beta})$ is the π-electronic component of the activation energy and characterises the capacity for the nucleophilic substitution of the chlorine atom.[117] The π-electron density q^7 in the static approximation characterises the capacity for addition to multiple bonds.

The π-electron density at the C_β atom decreases in the sequence H > Ph > M, so that an increase in the capacity of the double bond to combine with nucleophiles in the same sequence should be expected.[91]

It is noteworthy that the above calculated quantities refer to hypothetical planar molecular models. If, on the other hand, account is taken of the breakdown of the planar configuration in compounds **33** (R^2 = Me) and **34** (R^2 = Ph) and of the associated decrease in the delocalisation of the π-electron cloud, then the differences in the capacity for nucleophilic addition in the sequence of R^2 substituents H > Ph > Me should be even more appreciable.

The quantity $\Delta E^{\pi/\beta}$ changes little as a function of the substituent R^2 and such variation is different for the variants of the parameters of the NO_2 group being compared.[117] It has therefore been suggested[91] that the interaction of the substituent R^2 with the NO_2 group alters the degree of its conjugation with the multiple bond and controls the rate of nucleophilic substitution of the chlorine atom. As a result of the electronic effects associated with the nature of the substituent R^2 and the change in configuration, the polarity of the C(5)–Cl bond (and hence also the rate of the nucleophilic substitution of the chlorine atom) diminishes after the introduction of the substituent R^2 in the following sequence: Me > Ph > H > Cl > Br.

Thus, comparison of the effects of the substituent R^2 on the behaviour in relation to nucleophiles permits the following conclusions.

1. β-(5-Halo-2-furyl)-α-methylnitroethylenes (**33**, R^2 = Me) exhibit the greatest tendency to undergo halogen substitution reactions.

Table 5. The reactivity indices for β-(5-chloro-2-furyl)-α-R^2-nitroethylenes.[91,117]

Variant	Index	R^2		
		H	Me	Ph
1	$\Delta E^{\pi/\beta}$	2.861	2.893 [a]	2.834
	q^7	0.092	0.080 [a]	0.088
2	$\Delta E^{\pi/\beta}$	1.952	1.946	1.958
	q^7	0.192	0.128	0.172

[a] Estimated by the perturbation theory method.[116]

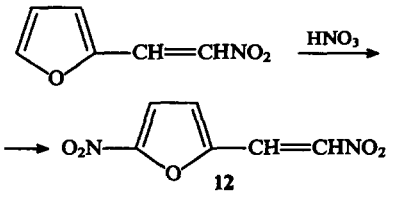
2. Addition reactions are more characteristic of β-(5-halo-2-furyl)nitroethylenes (**1**, R^2 = H) and β(5-halo-2-furyl)-α-halonitroethylenes (**35**; R^2 = Cl, Br).

According to patent data,[119] the interaction of β-(5-halo-2-furyl)-α-R^2-nitroethylenes **1** and **33**–**35** with morpholine leads to the polymerisation of the nitroalkenes when R^2 = H (**1**) and to the substitution of the halogen by morpholine R^2 = Me (**33**); for R^2 = Ph (**34**), products of the substitution and addition of the amine to the double bond were detected in the reaction mixture.

IV. Chemical properties

1. Substitution reactions in the furan ring

The most thoroughly investigated reaction of this type is the nitration of β-(2-furyl)nitroethylene **1** which leads to β-(5-nitro-2-furyl)nitroethylene **12**.



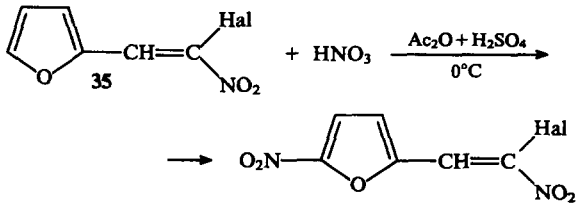
12

Nazarova[12] carried out the nitration with a tenfold excess of fuming HNO_3 in acetic anhydride at −5 to 0 °C and obtained compound **12** in 60.5% yield. Sasaki[72] used a fivefold excess of concentrated HNO_3 in acetic anhydride for nitration, whereupon the yield of the nitroalkene **12** did not exceed 35%.

The study of the nitration of β-(2-furyl)nitroethylene is of definite theoretical interest from the standpoint of the development of the theory of the nitration of furans. It is known[8] that the first elementary step in the nitration of acidophobic furans is the formation of oxonium compounds, which then either rearrange to 2,5-dihydrofuran derivatives or decompose with the opening of the furan ring to butane-1,4-diol derivatives, which char rapidly.

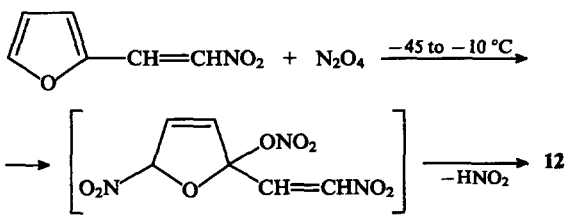
In the nitration of β-(2-furyl)nitroethylene **1**, this reaction pathway is excluded as a consequence of the influence of the electron-accepting NO_2 group, which lowers the tendency of the furan oxygen to be protonated and hence stabilises the entire furan system. Hillers and Nerklava[120] established that the nitration of compound **1** can be most usefully carried out with fuming HNO_3 in acetic anhydride (molar ratios $1:HNO_3:Ac_2O$ = 1:4:10) in the presence of catalytic amounts of H_2SO_4 at −10 to −5 °C; under these conditions, the yield of the nitroalkene **12** is 70%–80%. The authors showed that in this instance the true nitrating agent is the nitronium ion formed in HNO_3 solutions in acetic anhydride, particularly in the presence of H_2SO_4.

Nitration of β-(2-furyl)-α-halonitroethylenes (**35**; R^2 = Cl, Br) under similar conditions results in the formation of β-(5-nitro-2-furyl)-α-halonitroethylenes in 85%–88% yield.[47,52,91]

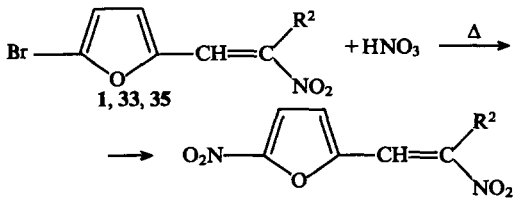


Hal = Cl, Br.

It has been shown[121] that the nitroalkene **12** is formed in 57% yield on treatment of β-(2-furyl)nitroethylene with a 50-fold excess of nitrogen tetroxide at low temperatures in ether.

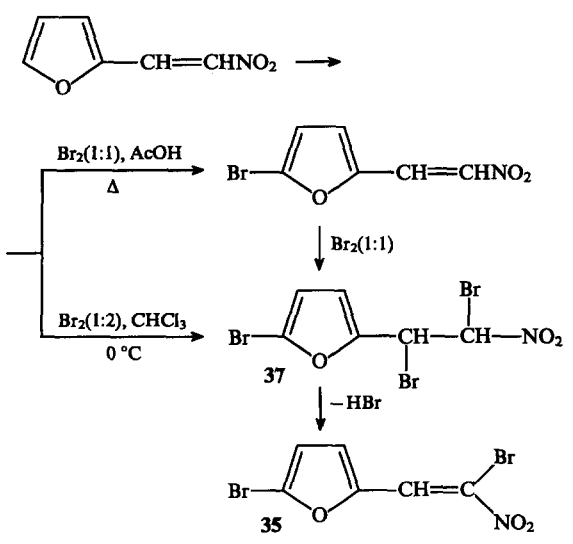


When β-(5-bromo-2-furyl)-α-R^2-nitroethylenes (**1**, **33**, and **35**) are heated with dilute HNO_3, the bromine atoms in the furan ring are substituted with formation of the corresponding 5-nitro-derivatives.[12,41,43,47,52,91] It is noteworthy that 5-bromofurfural does not afford 5-nitrofurfural under these conditions.



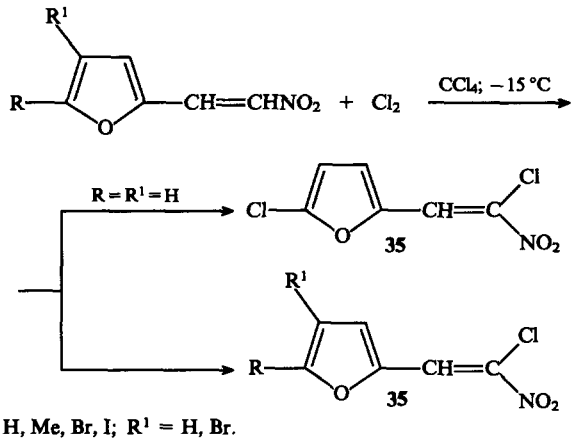
R^2 = H, Me, Cl. Br.

When β-(2-furyl)nitroethylene **1** is refluxed with an equimolar amount of bromine in acetic acid, β-(5-bromo-2-furyl)nitro-ethylene (**2**, R = Br) is formed.[12] Under similar conditions, β-(5-bromo-2-furyl)-α-chloronitroethylene (**35**; R = Br, R^2 = Cl) is obtained from β-(2-furyl)-α-chloronitroethylene. On the other hand, the bromination of compound **1** (molar ratio **1** : Br_2 = 1 : 2) in chloroform in the cold or bromination of β-(5-bromo-2-furyl)nitroethylene affords the unstable tribromo-derivative **37**, which decomposes on storage and distillation. Its dehydrobrom-ination with an aqueous solution of alkali at 20 °C leads to the synthesis of β-(5-bromo-2-furyl)-α-bromonitroethylene (**35**; R = R^2 = Br) in 64% yield.[52]



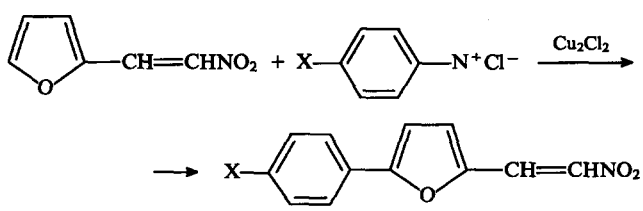
According to patent data,[122] chlorination of the nitroalkene **1** in chloroform or CCl_4 at −15 °C results in the simultaneous substitution of the hydrogen atoms in the 5-position in the furan ring and in the α-position in the vinyl fragment with formation of β-(5-chloro-2-furyl)-α-chloronitroethylene **35**. Chlorination of other β-(5-R-4-R^1-2-furyl)nitroethylenes under analogous conditions leads to the corresponding α-chloronitroalkenes **35** in 61% – 96% yield.

Oleinik and coworkers[98,123,124] reported for the first time the synthesis of (*E*)-β-(5-aryl-2-furyl)nitroethylenes (**1**; R = aryl) in 40% yield by arylating under the conditions of the Meerwein reaction (aqueous acetone, 40 °C) β-(2-furyl)nitroethylene with diazonium salts (molar ratio 1 : 1) containing electron-accepting substituents in the benzene ring.



R = H, Me, Br, I; R^1 = H, Br.

The authors' EPR spectroscopic study of the intermediates in the Meerwein arylation reaction permitted the conclusion that the given process has a radical mechanism.[124]



X = Cl, Br, NO_2.

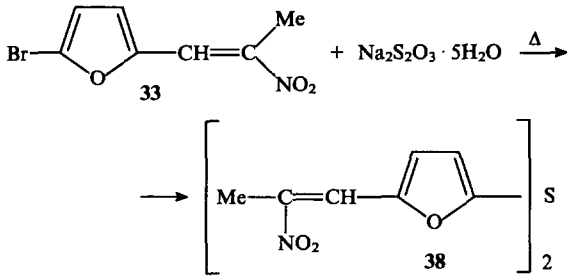
The influence of certain factors on the reactivity of β-(5-halo-2-furyl)-α-R^2-nitroethylenes relative to nucleophiles was examined in Section III.

It is known[93] that mainly the $-J$ effect of the halogens is manifested in 5-halofurfurals, as a result of which the C(5) atom of the furan ring acquires a positive charge, which increases in the sequence I < Br < Cl. The mobility of the halogens relative to the nucleophiles increases in the same sequence. On the other hand, in the case of β-(5-halo-2-furyl)nitroalkene the $n-\pi$ interaction with the furan nucleus is a $+M$ effect, which should diminish the positive charge on the C(5) atom and hinder substitution by nucleophiles compared with halofurfurals. The latter is manifested particularly strongly for β-(5-chloro-2-furyl)-α-R^2-nitroethylenes (**1**, **33**, and **35**; R^2 = H, Me, Ph, Cl, Br), which is indicated by the maximum value of μ_{int} in this instance (Table 1).

It has been shown[43,45] that when β-(5-halo-2-furyl)-α-methyl-nitroethylenes **33** are acted upon by nucleophiles (secondary amines, $Na_2S_2O_3$), the halogen in the 5-position in the furan ring is substituted, whereas in the case of β-(5-halo-2-furyl)nitro-ethylenes **1**, polymerisation or addition to the double bond takes place. These findings can be accounted for as follows. The direct polar conjugation in the planar structure of compound **1** (R^2 = H) leads to the appearance of a high positive charge on the β-atom of the vinyl fragment. The $+M$ interaction of the halogens in the 5-position with the furan ring in these compounds lowers simultaneously the effective positive charge on the C(5) atom of the furan. On the other hand, the introduction of the methyl group in the 5-position disturbs the planar configuration of the molecule and lowers the degree of conjugation, and hence promotes an increase in the positive charge on the C(5) atom of the furan ($-J$ effect of the halogen) and nucleophilic substitution.

The interaction of β-(5-bromo-2-furyl)-α-methylnitroethylene **33** with sodium thiosulphate in aqueous alcohol (refluxing for 2 h) leads to bis[5-(β-nitroprophenyl)-2-furyl] sulphide **38**.[43]

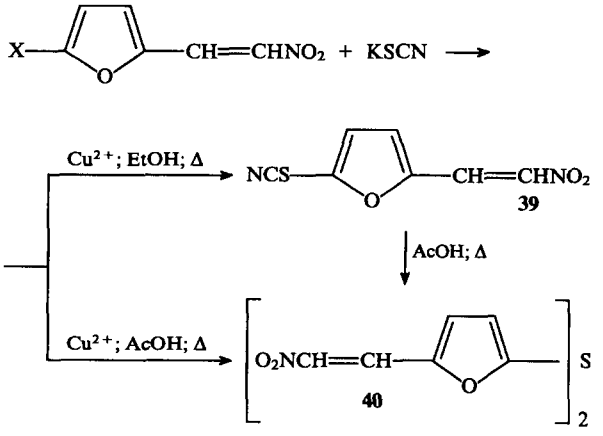
It is noteworthy that β-(2-furyl)-α-methylnitroethylene does not combine with sodium thiosulphate at the double bond, the methyl group apparently reducing the reactivity of the latter.[43]



On the other hand, Nazarova and coworkers[125,126] established that, on treatment with potassium thiocyanate or sodium sulphide, β-(5-halo-2-furyl)nitroethylenes form the products of the substitution of the halogen in the furan ring, i.e. in the reaction with the above reagents they behave similarly to the nitroalkenes **33**.

The reaction involving the exchange of bromine for the thiocyanato-group in the nitroalkenes **1** occurs only after prolonged refluxing of the reactants in anhydrous solvents (acetone, methanol, ethanol) in the presence of copper or cobalt salts. Under these conditions, β-(5-thiocyanato-2-furyl)nitroethylene **39** is formed in 78%–85% yield. This compound is more stable than 5-thiocyanatofurfural.[125]

The interaction of compound **1** with potassium or barium thiocyanate in acetic acid in the presence of copper or cobalt salts leads to the sulphide **40**, which is also formed on hydrolysis of the thiocyanate **39** in acetic acid.[126] The reaction of β-(5-halo-2-furyl)-α-R^2-nitroethylenes (compounds **1** and **33**; R^2 = H, Me) with sodium sulphide affords Na derivatives of β-(5-mercapto-2-furyl)-α-R^2-nitroethylenes **41**, whose treatment with formic acid gives rise to the corresponding mercaptans **42**. The sulphides **40** (R^2 = H, Me) are synthesised by the reaction of the Na derivatives **41** with β-(5-halo-2-furyl)nitroethylenes **1** and **33**.[126]

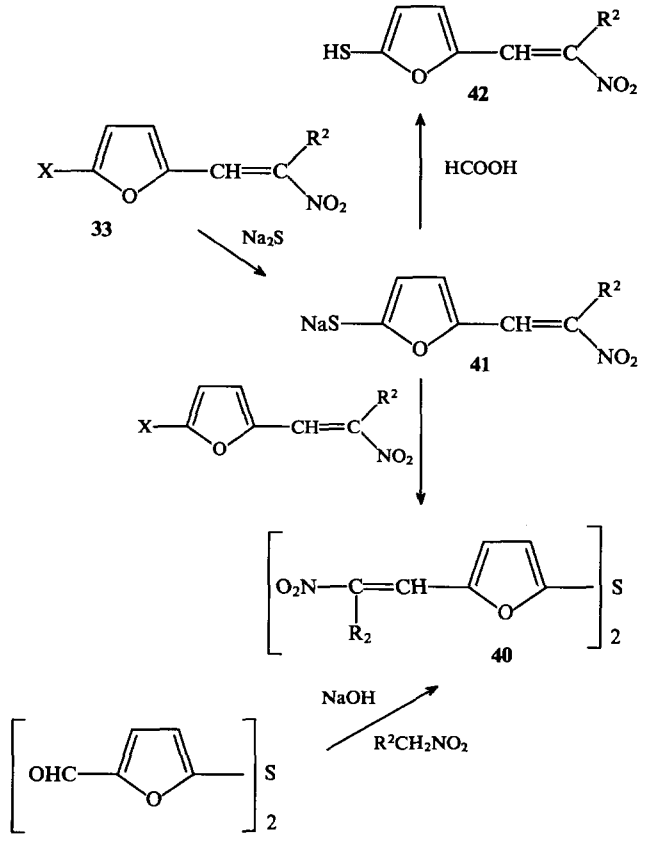


X = Cl, Br, I.

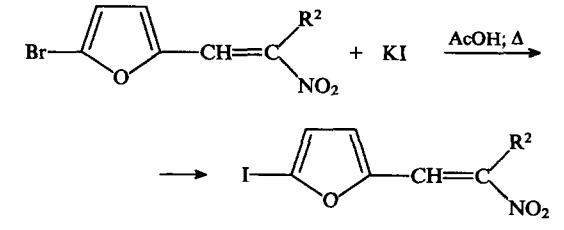
The structures of the sulphides **38** and **40** were confirmed also by unambiguous synthesis — the condensation of bis(5-formyl-2-furyl) sulphide with nitromethane or nitroethane in the presence of alkali.

A preparative method of synthesis of β-(5-iodo-2-furyl)-α-R^2-nitroethylenes (**1**, **33**, and **35**; R^2 = H, Me, Cl, Br) involves the nucleophilic substitution of bromine atoms in the corresponding 5-bromo derivatives.[12,30,43,47] The reaction involving the exchange of bromine for iodine occurs when the substrates are refluxed with potassium iodide in acetic acid for several hours; the target 5-iodo-derivatives are then formed in 50%–82% yield.

We may note that the chlorine or bromine atoms in the β-(5-nitro-2-furyl)-α-halonitroethylenes do not exchange for iodine under analogous conditions.[30]



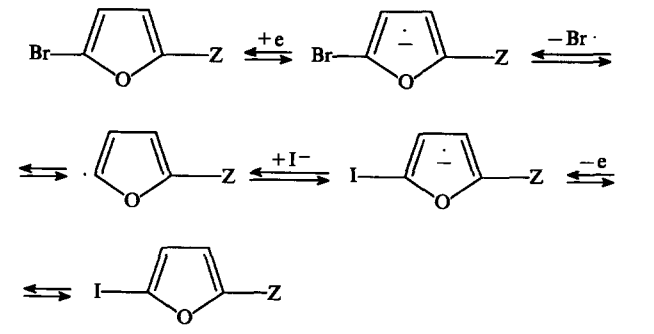
X = Br, I; R^2 = H, Me.



R^2 = H, Me, Cl, Br.

The kinetics of the exchange of bromine for iodine in β-(5-bromo-2-furyl)-nitroethylene have been investigated.[127] It was established that the reaction is reversible and is inhibited by oxidants (atmospheric oxygen, aromatic nitro-compounds, Schiff bases). The authors proposed a cryptoreductive reaction mechanism, which can operate in accordance with two schemes. According to Scheme 1, which includes the reversible electron transfer from the reducing supporting electrolyte generated by

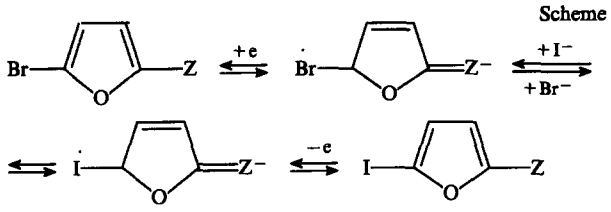
Scheme 1



Z = CH=CHNO$_2$.

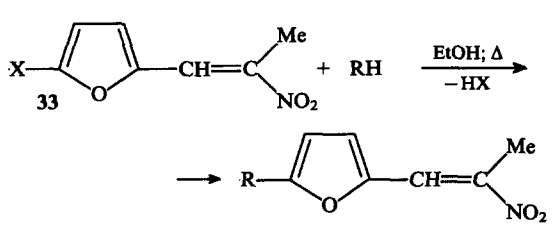
iodide anions to the halofuran molecule, the intermediate formation of a radical-anion with subsequent elimination from the latter of a bromide ion is postulated. The resulting furyl radical reacts with one of the halide ions of the reaction mixture with formation of either the initial or final products. On the other hand, one can assume that the furyl radical is not formed in this reaction as a kinetically independent species: without emerging from the reaction 'cage', it interacts with a second anion, which is also incorporated in the activated complex. In the limiting case, there is a possibility in this instance of a synchronous reaction involving the mutual exchange of the halogens in the radical-anions (illustrated in Scheme 2 in mesomeric form with separation of the radical and ionic fragments)—in terms of Bunnett's terminology,[128] this mechanism can be designated as $S_{RN}2$.

Scheme 2



It is noteworthy that, in terms of the decreasing rate of exchange of bromine for iodine, the substituents Z can be arranged in the following sequence: CH=CHCOPh > CHO > Ac > $CH=CHNO_2$, which is inconsistent with the activating strength of the above groups in reactions proceeding via the classical multistage mechanism of the 'addition–elimination' type.[127] The latter is characteristic, for example, of the reactions of 2-substituted 5-halofurans with secondary amines.[129]

Certain features of the interaction of furylnitroalkenes with secondary amines were noted in Section III. Nazarova and coworkers[45,119] established that the nucleophilic substitution of a halogen by secondary amine residues takes place most smoothly with β-(5-halo-2-furyl)-α-methylnitroethylenes **33**.

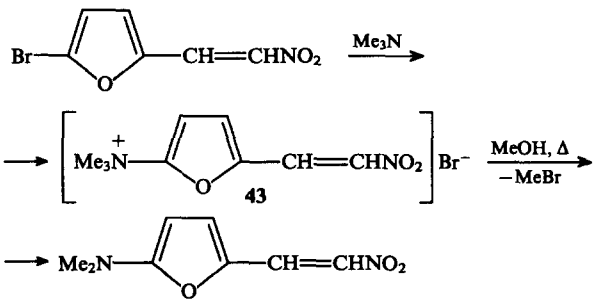


X = Br, I; R = morpholino, PhNMe.

The structure of the substitution products was confirmed by unambiguous synthesis from the corresponding N-substituted 5-aminofurfurals. The authors note that, when piperidine, diethylamine, or dimethylamine is introduced into the reaction, the double bond is also subjected to nucleophilic attack. The reaction of β-(5-bromo-2-furyl)nitroethylene with secondary amines proceeds very vigorously and leads to the products of the polymerisation of the initial alkene.

As a result of the study of the kinetics of the interaction of β-(5-halo-2-furyl)nitroethylenes **1** with secondary amines (dimethylamine, piperidine, and morpholine), Novikov and coworkers[130] showed that the halogen exchange reaction takes place against the background of the reversible interaction of the amine with the nitrovinyl group. The latter reaction is then 'asymmetric' as regards mechanism—the addition process takes place as a base-catalysed multistage reaction, while elimination is a synchronous unimolecular process.

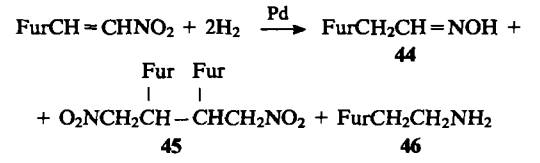
The interaction of the bromo-derivative **1** with trimethylamine in benzene affords the quaternary ammonium salt **43** in quantitative yield. On refluxing in methanol, the salt is converted into β-(5-dimethylamino-2-furyl)nitroethylene in 51% yield.[13]



2. Reduction of furylnitroalkenes

Depending on the chosen reduction method, the nature of the reductant, and the process conditions, the reduction of unsaturated nitro-compounds results in the formation of different classes of organic compounds.[1-3] From this standpoint, furylnitroethylenes are not an exception among other nitroalkenes.

Freidlin and coworkers[31] investigated the hydrogenation of β-(2-furyl)nitroethylene in the presence of palladium black in different solvents at atmospheric pressure and 25 °C. The reaction is zero order with respect to the nitroalkene and the rate of absorption of hydrogen remains constant up to the complete conversion of the initial compound. The main reaction products are furylacetaldehyde oxime **44** and a hydrodimer—2,3-di(2-furyl)-1,4-dinitrobutane **45**. 1-Amino-2-(2-furyl)ethane **46** is formed in very small amounts.



In the hydrogenation of compound **1** in a 1 : 1 ethanol–acetic acid mixture, the yield of the oxime **44** reaches 97%. When the hydrogenation is carried out in ethanol or dioxan, the yield of the oxime **44** reaches 25%–54% together with the hydrodimer **45**; the dimerisation reaction is suppressed in the presence of weak organic acids (HCOOH, CH_3COOH). We may note that under comparable conditions the nitroalkene **1** is hydrogenated at approximately the same rate as β-nitrostyrene; the rate of hydrogenation of the thiophene analogue—β(2-thienyl)nitroethylene—is appreciably lower.[131]

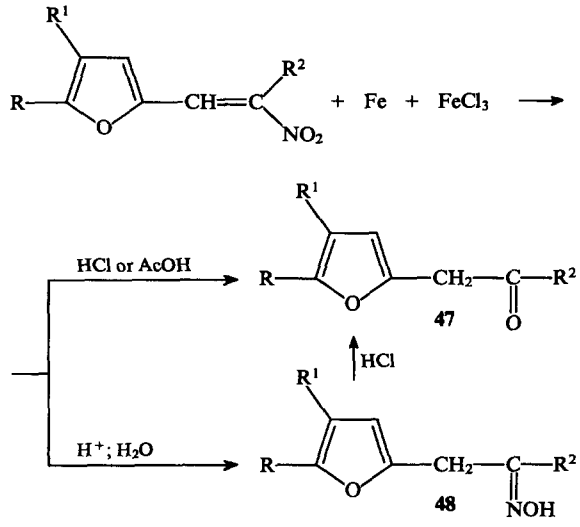
The reduction of β-(2-furyl)nitroethylene **1** with zinc dust in acetic acid results in the formation of the oxime **44** in 60%–70% yield.[16,57]

The reduction of β-(5-R-4R^1-2-furyl)-α-R^2-nitroethylenes with iron filings and $FeCl_3$ in hydrochloric acid (85–95 °C, 5–6 h)[37,48,132,133] or in acetic acid (80–100 °C, 1.5 h)[44] leads to ketones of the furan series with the carbonyl group in the 2-position in the side chain (compounds **47**) or to their oximes **48**, which are difficult to obtain by other methods.

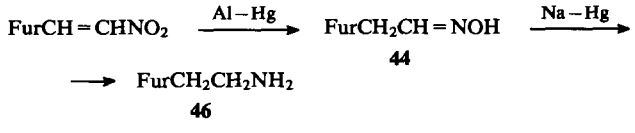
It has been established that an increase in the excess of acid promotes the formation of the ketones **47**, whose yield is usually 35%–70%, while a decrease in its amount raises the yield of the ketoximes **48**.

It has been recommended[132] that β-(4-methyl-2-furyl)-α-methylnitroethylene be reduced with an Fe + $FeCl_3$ mixture in 30% HCl, this being followed by treatment of the reaction product with a solution of $TiCl_3$ and ammonium acetate in water.

Japanese workers[14] synthesised 1-amino-2-(2-furyl)ethane **46** by the stepwise reduction of β-(2-furyl)nitroethylene with aluminium amalgam in ether and then with sodium amalgam in an ethanol–acetic acid mixture.

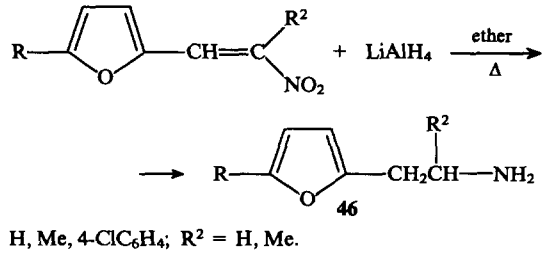


R = H, Me, 4-ClC$_6$H$_4$; R^1 = H, Me; R^2 = Me, Et, Pr, Ph.



The C=C bond, which is inert to the action of lithium tetrahydroaluminate, is readily reduced when it is conjugated with electron-accepting groups.[134] Lithium tetrahydroaluminate has therefore been used successfully for the reduction of a wide variety of nitroalkenes.[1] The structure of the reaction product depends to a large extent on the reduction conditions, primarily on temperature.

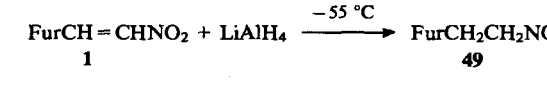
For example, in the reduction of furylnitroalkenes in boiling ether (molar ratio nitroalkene : $LiAlH_4$ = 1 : 2) the reaction is completed by the formation of the corresponding furylethylamines **46** in 52% – 65% yield.[13,25,38,98,135]



R = H, Me, 4-ClC$_6$H$_4$; R^2 = H, Me.

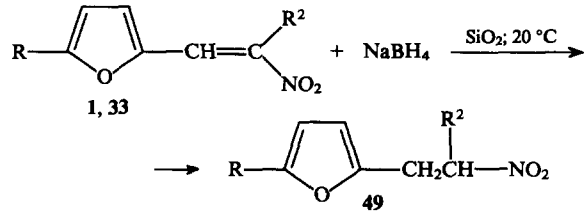
It is noteworthy that this method is the most effective procedure for the synthesis of 2-amino-1-(5-R-2-furyl)propanes (**46**; R = H, Me; R^2 = Me) — non-toxic analogues of the familiar preparation amphetamine.[38]

The reduction of β-(2-furyl)nitroethylene with 0.5 equiv. of $LiAlH_4$ at a low temperature (−55 to −60 °C) does not involve the nitro-group and only the double bond is reduced, the process being completed by the formation of 2-(2-furyl)-1-nitroethane **49**. However, the reaction is accompanied by appreciable charring and the yield[136] of the nitroalkene **49** does not exceed 16%.



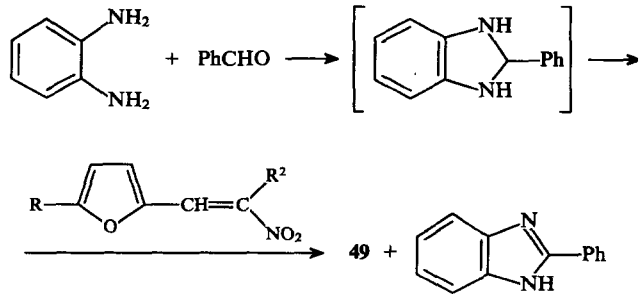
When the nitroalkene **1** is reduced with trimethoxyhydroborate and sodium tetrahydroborate in ether (−40 °C, molar ratios 1 : 1 : 3) or with lithium tetrahydroborate in ether (−73 °C, molar ratio 1 : 0.5),[136] the yield of the nitroalkane **49** can be raised to 28% – 31%.

According to Bogacheva,[137] on reduction of furylnitroalkenes **1** and **33** with sodium tetrahydroborate (molar ratio 1 : 4) in the presence of silica gel in a chloroform – 2-propanol mixture (20 °C, 2 – 4 h), the corresponding 1-nitro-1-R^2-2-(5-R-2-furyl)ethanes **49** can be obtained in 33% – 43% yield.

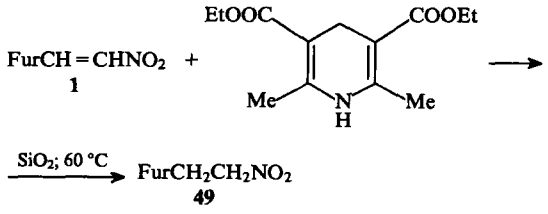


R = H, Me, NO$_2$; R^2 = H, Me.

2-Phenylbenzimidazoline, generated *in situ* from *o*-phenylenediamine and benzaldehyde, has been used as the selective reductant for the double bond in the furylnitroalkenes **1** and **33**.[137,138] This method affords the nitroalkanes **49** in 45% – 65% yield when nitroalkenes react with *o*-phenylenediamine and benzaldehyde (molar ratios 1.0 : 1.2 : 1.2) in 1-butanol at 20 °C.

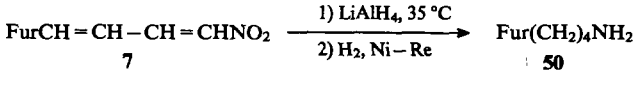


Japanese workers[139,140] proposed an effective method for the selective reduction of the double bond in conjugated nitroalkenes by reaction with the diethyl ester of 2,6-dimethyl-1,4-dihydropyridine-3,5-dicarboxylic acid (Hantzch's ester) in the presence of silica gel. When β-(2-furyl)nitroalkene is reduced with this reagent in benzene (60 °C, 20 h), the yield of the nitroalkane **49** reaches 93%. The authors note that the reduction does not occur in the absence of silica gel.



The reduction of β-(3-furyl)nitroethylene **9** by this method leads to a 94% yield of 2-(3-furyl)-1-nitroethane,[70] which is a key compound in the synthesis of various limonoid structures[69] and the pheromone dendrolasin.[70]

The reduction of 1-(2-furyl)-4-nitrobutadiene **7** with an excess of lithium tetrahydroaluminate in boiling ether affords, instead of the expected 4-amino-1-(2-furyl)butane **50**, a mixture of four unidentified incomplete reduction products.[141] Without additional purification, this mixture was subjected to catalytic hydrogenation over Raney nickel (methanol, 20 °C, initial hydrogen pressure 120 atm); under these conditions, the amine **50** is formed in 61% yield.



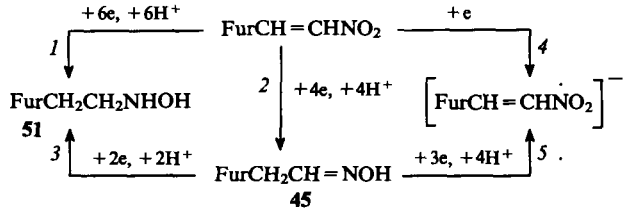
The authors note that the catalytic hydrogenation of the nitrodiene **7** with the aim of obtaining compound **50** in one stage leads to tarry products even under mild conditions.

The reduction of the potassium salt of the aci-form of 1-(2-furyl)-4-nitrobut-2-en-1-one **32** with sodium tetrahydroborate in water at 20 °C results in the formation[89] of the unstable sodium salt of 1-(2-furyl)-4-nitrobut-2-en-1-ol, which is converted into the nitrodiene **7** in 56% yield after acidification.

$$\text{FurCOCH=CHCH=NOO}^-\text{K}^+ \xrightarrow[H_2O]{NaBH_4} \text{FurCHCH=CHCH=NOO}^-\text{Na}^+ \xrightarrow{H^+} \underset{\text{OH}}{\text{FurCHCH=CHCH=NOO}^-\text{Na}^+} \longrightarrow \underset{7}{\text{FurCH=CHCH=CHNO}_2}$$

Takamoto[142] obtained 1-amino-2-(2-furyl)ethane **46** from β-(2-furyl)nitroethylene (yield 91%) by electrochemical reduction using amalgamated nickel as the cathode and a lead plate as the anode (the catholyte was an ethanol–acetic acid mixture and the anolyte was dilute H_2SO_4). The electrolysis was carried out at 30–35 °C at a current of 4–45 A.

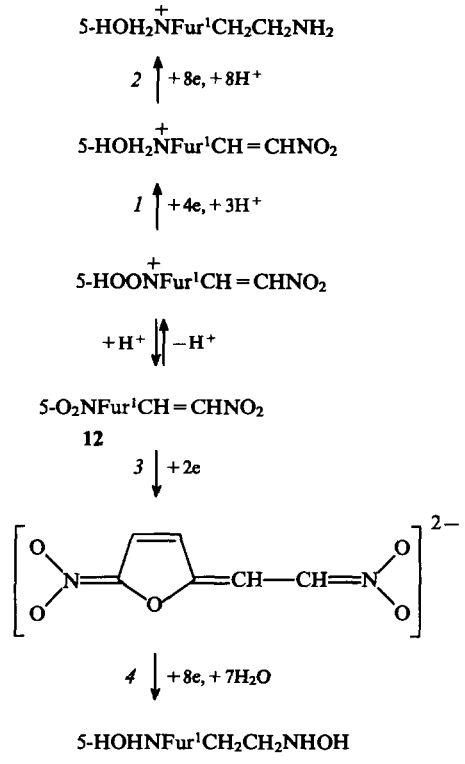
Reikhman et al.[143] investigated the mechanism of the polarographic reduction of β-(2-furyl)nitroethylene as a function of the mixture composition as well as the protolytic reactions of the compound. On the basis of the polarographic data recorded in aqueous alcoholic Britton–Robinson buffer solutions in the pH range from 2–12 in the presence of 0.1 M LiCl as the supporting electrolyte, the authors proposed the following mechanism of the polarographic reduction of this nitroalkene:



In acid solutions with a low ethanol content, 6-electron reduction to the substituted hydroxylamine **51** (reaction *1*) takes place. In neutral media, there is 4-electron reduction (reaction *2*) to the oxime **45** and the subsequent stage involving the addition of two further electrons (reaction *3*) is displaced towards negative potentials (−0.85 to −1.30 V) and is manifested by separate wave B, the half-wave potential $E_{1/2}$ of which corresponds to the electrochemical reduction potentials of oximes.[8,144,145]

In an alkaline medium, the 4-electron process *2* is split into 1-electron (reaction *4*) and 3-electron (reaction *5*) stages. The waves become clearly separated at pH > 10, where a dimunition of all the waves is observed. The latter is apparently due to the fact that the anionic form of compound **1** is polarographically inactive. in solutions with a high alcohol content at pH < 7, the reduction takes place in two stages (reactions *2* and *3*). In alkaline media and in DMF, distinct processes *4* and *5* take place.

In the electrochemical reduction of β-(5-nitro-2-furyl)-nitroethylene **12**, two reaction centres are reduced simultaneously.[8,145,146] In aqueous and 10% aqueous alcoholic Britton–Robinson buffer solutions in an acid medium (pH ⩽ 3) at potentials in the range 0 to −0.1 V, the 4-electron reduction of the nitro-group, characteristic of derivatives of 5-nitrofuran takes place (stage *1*). At more negative potentials (−0.3 to −0.7 V) the subsequent 8-electron wave, corresponding to the electrochemical reduction of the nitro-group conjugated with a double bond (stage *2*), takes place.



In more alkaline media (pH > 6), the primary step in the electrochemical reduction of this compound is the direct addition of two electrons (stage *3*) to the entire system of conjugated π-bonds of the molecule and is followed at potentials of −1.45 V by the 8-electron process *4* involving the electrochemical reduction of the dianion formed. This somewhat unusual mechanism of the electrochemical reduction is supported by the presence on the polarogram of a distinct 2-electron wave, by the independence of its $E_{1/2}$ of the pH, and also by the similarity to the mechanism of the chemical reduction of *p*-dinitrobenzene.[146]

At pH 9, the polarogram shows a sharp decrease in the height of all the waves. Spectrophotometric studies indicate the occurrence in these solutions of irreversible chemical reactions, whose products are polarographically inactive.[146]

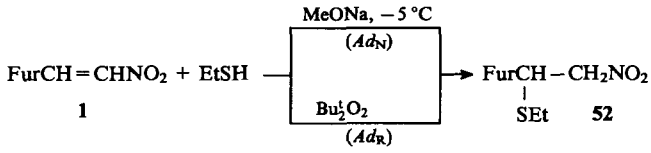
It has been shown[147] that β-aryl-α-(5-nitro-2-furyl)-α-nitroethylenes **34** are reduced at a mercury dropping electrode with two or three one-electron waves ($E^1_{1/2} = -0.6$ V, $E^2_{1/2} = 1.25$ V, and $E^3_{1/2} = -1.4$ V relative to 1 M LiCl at a calomel electrode). Unstable radicals with a lifetime of several seconds and with the unpaired electron centred on the nitro-group (according to EPR data) arise under these conditions.

3. Reactions involving addition to the double bond

It was noted in Section III that the tendency of furylnitroalkenes to undergo nucleophilic addition at the activated double bond depends primarily on the structure of the nitroalkenyl fragment.

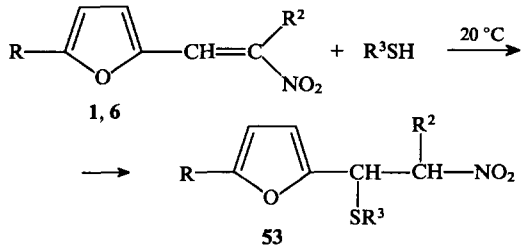
In considering reactions of this type, account must be taken not only of the appreciable polarity and ready polarisability of the activated double bond but also of the high probability of the delocalisation of the negative charge in the transition state. These factors determine the exceptionally high reactivity of furylnitroalkenes with respect to nucleophiles such as amines, alcohols, phenols, and mercaptans. As a result of the addition of these reagents, with formation of C–S, C–O, and C–N bonds, a wide variety of β-substituted nitroalkyl derivatives of the furan series may be synthesised. However, one should note that in the majority of cases the adducts formed are (in contrast to the analogous adducts in the series of aliphatic, acyclic, and aromatic nitroalkenes[1–3]) thermodynamically unstable, decomposing fairly rapidly and charring.

Ethanethiol adds to the double bond of β-(2-furyl)nitroalkene via both nucleophilic and radical mechanisms[148] with formation of the stable 2-ethylthio-2-(2-furyl)-1-nitroethane **52**.



The nucleophilic addition was carried out in the presence of an equimolar amount of sodium methoxide in methanol at −5 to 0 °C, while the radical addition was carried out by heating the reactants in the presence of *tert*-butoxide in sealed tubes, the yield of the adduct being appreciably higher in the latter case (~85%).

In a series of investigations by Czechoslovak workers[149-155] undertaken to investigate the mechanism of the biological activity of furylnitroalkenes **1** and **6** and to establish the structure–reactivity correlation for these compounds, a study was made of the interaction with various mercaptans in methanol at 20 °C, which leads to 1-R²-2-(R³-thio)-2-(5-R-2-furyl)-1-nitroethanes **53**.



R = H, Me, Br, I, MeOOC, NO_2; R^2 = H, MeOOC; R^3 = $PhCH_2$, $HOOCCH_2$, $HOCH_2CH_2$, $H_2NCH_2CH_2$.

The authors explain the cytotoxic and antimicrobial activities of the vinylfuran derivatives by the action of these biocides on the main processes of the energy metabolism of the cell, primarily on glycolysis. The basis of this interaction is the inhibition of certain enzymes — hexokinase, phosphofructokinase, and glycerol-3-phosphate dehydrogenase. These enzymes are deactivated as a result of the direct chemical modification of their catalytically active HS groups. The capacity of the furylnitroalkenes to undergo the nucleophilic addition of mercapto-derivatives constitutes an index of their antimicrobial and cytotoxic additivities.[156]

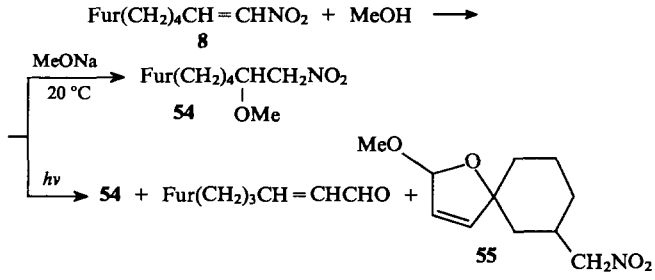
Kinetic study of the reactions of furylnitroethylenes with thiols showed that these reactions proceed via a nucleophilic addition mechanism and that the attack of the mercapto-anion is directed to the electron-deficient carbon atom of the double bond. It has been established that in an aqueous buffer system (pH 4.9) the reactions have second-order rate constants; the activity of furylnitroalkenes increases with enhancement of the electron accepting character of the substituent both in the 5-position in the furan ring and in the α-position in the nitrovinyl fragment. Using the Hammett constants, it has been established that this rule is quantitative. for example, in a study[151] of the reaction of the methyl esters of β-(5-R-2-furyl)-α-nitroacrylic acids **6** with mercaptoacetic acid (25 °C, aqueous Clark buffer, pH 4.9), it was found that $\lg K = 1.134\sigma_r + 7.125$ (correlation coefficient $r = 0.971$, $n = 6$).

Depending on the nature of the substituents R and R^2, furylnitroethylenes can be arranged in the following sequence in terms of the decrease in their reactivity in reactions with mercaptans:[151-153] NO_2, COOMe > COOMe, COOMe > I, COOMe > Br, COOMe > H, COOMe > Me, COOMe > NO_2, H > H, H.

The reactivity of mercaptans in the reactions with furylnitroethylenes increases with increase in their basicity. For example, the following sequence has been established for the reactions of mercaptans with β-(5-nitro-2-furyl)nitroethylene (25 °C, pH 4.4) in terms of the variation of the reactivity of the mercaptans:[153] $HSCH_2COOH$ (pK_a = 10.22) ≫ $HSCH_2CH_2OH$ (pK_a = 9.72) > $PhCH_2SH$ (pK_a = 9.43) > glutathione (pK_a = 8.56) > $HSCH_2CH_2NH_2$ (pK_a = 8.35) > $HSCH_2CH\cdot(NH_2)COOH$ (pK_a = 8.15).

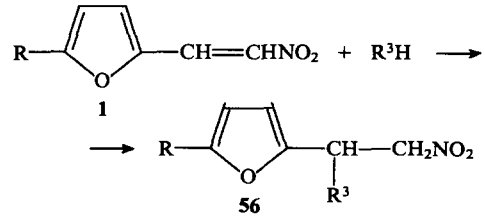
However, one should note that in the above investigations the authors carried out only kinetic measurements (mainly spectrophotometrically) and did not isolate or identify the adduct **53** formed.

The addition of methanol to the double bond of 6-(2-furyl)-1-nitrohex-1-ene **8** at 20 °C in the presence of calytic amounts of sodium methoxide has been reported.[68] Under these conditions, the yield of the methoxy-derivative **54** was 47%. The authors note that, when a solution of compound **8** in methanol is irradiated with UV light (450 W high-pressure Hg lamp argon-filled), 6-(2-furyl)hex-2-enal and 2-methoxy-6-nitromethyl-1-oxaspiro-[4.5]dec-3-ene **55** are formed together with the methoxy-derivative **54**.



As a result of the nucleophilic addition of amines to the double bond of β-(5-R-2-furyl)nitroethylenes **1**, the β-nitroamines **56** are formed.[18,155,157]

The interaction of β-(5-bromo-2-furyl)- and β-(5-nitro-2-furyl)-nitroethylenes with pyrrolidine and morpholine in ethanol, acetone, DMF, or DMSO leads even at 20 °C to appreciable charring and the formation of unstable adducts. Stable adducts could be obtained[18] only in the reaction of β-(2-furyl)- and β-(5-phenylthio-2-furyl)-nitroethylenes with 4-phenylpiperazine, whereupon the corresponding β-nitroamines **56** (R = H, PhS; R^3 = 4-phenylpiperazino) were isolated in 80%–90% yield.



R = H, Br, NO_2, PhS, $PhSO_2$, 4-$MeC_6H_4SO_2$; R^3 = pyrrolidino, piperidino, morpholino, 4-phenylpiperazine, BuNH, PhNH, $HOOCCH_2NH$

The study of the kinetics of the reaction of β-(2-furyl)nitroethylene with secondary amines showed that the reaction is second-order with respect to the substrate and first-order with respect to the nucleophile.[18,157] The rate of reaction at 25–45 °C increases with increase in the nucleophilicity of the reagents: pyrrolidine > piperidine > morpholine. A high rate constant for the reaction of the nitroalkene **1** with pyrrolidine is observed in non-polar solvents, diminishing with increasing solvent polarity in the sequence heptane > toluene > diethyl ether > DMSO > methanol.[18,157]

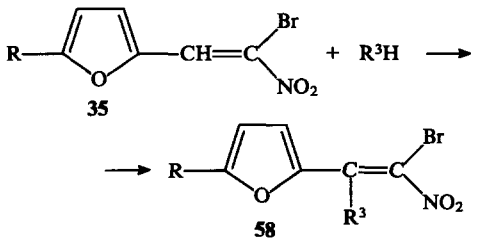
In terms of its influence on the rate of addition of secondary amines to the nitroalkenes **1** (MeOH, 25 °C), the substituents R can be arranged in the following sequence: $PhSO_2$ > 4-$MeC_6H_4SO_2$ > PhS ≃ Br > H, i.e. strongly electron-accepting groups induce an increase in the rate of reaction.[18,157]

The kinetics of the interaction of the methyl esters of β-(5-R-2-furyl)-α-nitroacrylic acid esters **6** and β-(5-nitro-2-furyl)nitroethylene with butylamine aniline, and certain aminoacids have been investigated[155,156] and it has been shown that in the case of amines the second-order rate constant is appreciably lower than in the case of mercaptans.

The interaction of the nitroalkene **1** with an equimolar amount of hydroxylamine in methanol leads[158] to the stable 2-hydroxyamino-2-(2-furyl)-1-nitroethane **57** in 80% yield.

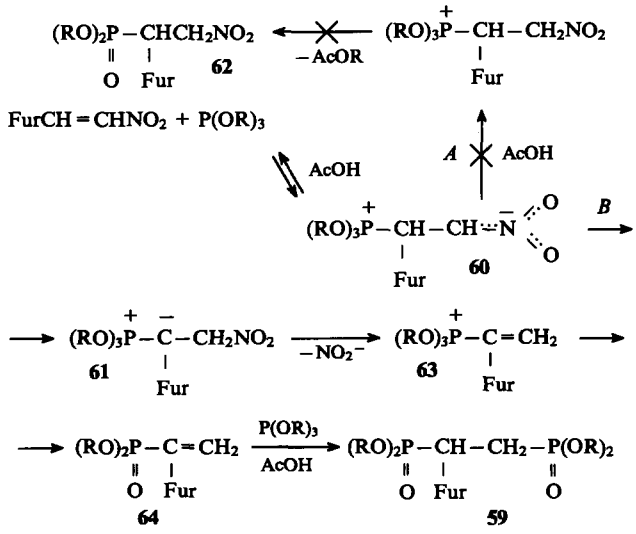
$$\underset{\mathbf{1}}{FurCH{=}CHNO_2} + NH_2OH \longrightarrow \underset{\mathbf{57}}{FurCH(NHOH){-}CH_2NO_2}$$

It has been reported[159] that α-bromo-β-(5-R-2-furyl)nitroethylenes **35** react with alcohols and secondary amines via an addition–elimination type of mechanism with formation of β,β-disubstituted nitroethylenes **58**.



Conjugated nitroalkenes can react with trivalent phosphorus acid esters in different ways depending on the nature of the nitroalkene, the groups surrounding the phosphorus atom, and the medium.[160,161]

It has been established that the interaction of β-(2-furyl)nitroethylene with trialkyl phosphites in acetic acid at 40 °C proceeds less vigorously than the reaction with β-nitrostyrene; under these conditions, 4 moles of the phosphite are consumed per mole of the alkene. As a result of the reaction, it was possible to isolate[162,163] 1,2-bis(dialkylphosphinyl)-1-(2-furyl)ethanes **59**. According to the proposed reaction mechanism,[163] the adduct formed initially as a result of addition to the double bond (the betaine **60**) can be either protonated in acetic acid (pathway *A*) or can be converted into the phosphinilide **61** as a result of the migration of the proton from the α- to the β-carbon atom (pathway *B*).



R = Me, Et

The dialkyl esters of 1-(2-furyl)-2-nitroethylphosphonic acid **62**, which should form as a result of the protonation of the intermediate betaine **60**, were not detected in the reaction mixture. This shows that the rate of migration of the protons from the C_α to the C_β atom in the adduct **60** appreciably exceeds the rate of its protonation even in a solvent such as acetic acid.

The phosphinilide **61** is stabilised as a result of the elimination of the nitrite anion with formation of the cation **63**, which is subsequently converted into 1-(dialkoxyphosphinyl)1-(2-furyl)-ethylene **64** in conformity with the second stage of the Arbuzov reaction. However, the latter could not be detected in the reaction mixture, owing to the high rate of addition of trialkyl phosphite to it, which leads to the final product **59**.

According to patent data,[164] the reaction of the nitroalkene **1** with diphenyl(trimethylsilyl)phosphine oxide leads to the corresponding β-nitroethylphosphine oxide **65**, in 80% yield.

$$\underset{\mathbf{1}}{FurCH{=}CHNO_2} + Ph_2P(O)SiMe_3 \longrightarrow \underset{\mathbf{65}}{Ph_2P(O){-}CH(Fur){-}CH_2NO_2}$$

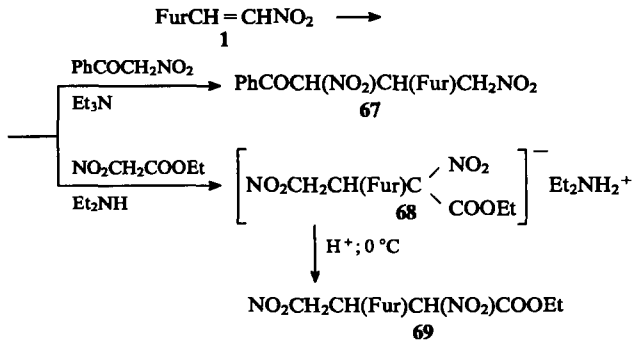
Reactions involving addition to nitroalkenes of the furan series with formation of new C–C bonds are of considerable theoretical and practical interest. Furylnitroalkenes enter fairly readily into the Michael reaction with a wide variety of CH acids, forming stable β-substituted β-furylnitroalkenes. For example, the interaction of β-(2-furyl)nitroethylene **1** with compounds containing activated methyl groups (2,4,6-trinitrotoluene, 9-methylacridine, and the quinaldine and 2-methylbenzothiazole methiodides) in benzene (20–80 °C, 1–2 h) in the presence of triethylamine, leads to the formation of the monoadducts-[3-R^3-2-(2-furyl)-1-nitropropanes] **66** in 63%–84% yield.[165]

$$\underset{\mathbf{1}}{FurCH{=}CHNO_2} + R^3Me \xrightarrow{Et_3N} \underset{\mathbf{66}}{R^3{-}CH_2{-}CH(Fur){-}CH_2NO}$$

R^3 = 2,4,6-$(NO_2)_3C_6H_2$, 9-acridinyl, 1-methyl-2-quinolinylinium iodide, 3-methyl-2-benzothiazolylinium iodode.

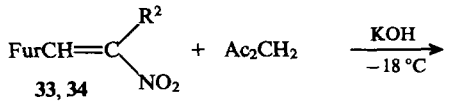
The reaction of the nitroalkene **1** with benzoylnitromethane in the presence of catalytic amounts of triethylamine in benzene (80 °C, 5–10 min) leads to the α,γ-dinitroketone **67** in 50%–54% yield.[166]

The interaction of β-(2-furyl)nitroethylene **1** with ethyl nitroacetate takes place only in the presence of equimolar amounts of diethylamine and leads to the formation of the diethylammonium salt **68**, whose acidification at 0 °C affords ethyl 3-(2-furyl)-2,4-dinitrobutanoate **69** in 25% yield.

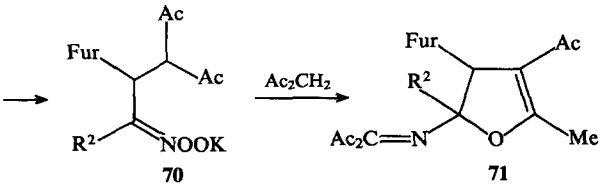


German workers[168,169] reported the reactions of β-(2-furyl)-α-R^2-nitroethylenes (**33** and **34**; R_2 = Me, Ph) with acetylacetone. The interaction of these reagents in aqueous methanol at −18 °C in the presence of equimolar amounts of alkali leads to the salts of 5-acinitro-5-R^2-3-acetyl-4-(2-furyl)pentan-2-ones **70** in 80%–88% yield.[168]

When the reaction is carried out in an excess of the β-diketone,[169] 3-acetyl-5-(diacetylmethylene)amino-4-(2-furyl)-2-methyl-5-R^2-4,5-dihydrofurans **71** are formed in low yields.



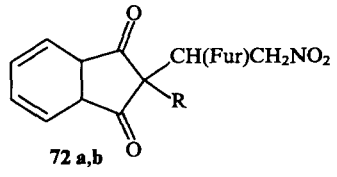
33, 34



70 71

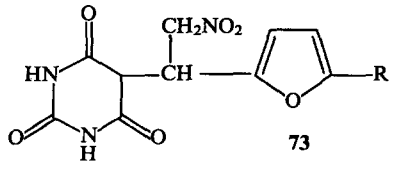
R^2 = Me, Ph.

The interaction of β-(2-furyl)nitroethylene with indan-1,3-dione and 2-phenylindan-1,3-dione (phenylin) in benzene (20 °C) in the presence of triethylamine led to the synthesis of the corresponding diadducts **72a** or the monoadducts **72b** in 50%–56% yield.[170]



72 a,b

a: R = $NO_2CH_2CH(Fur)$, b: R = Ph.



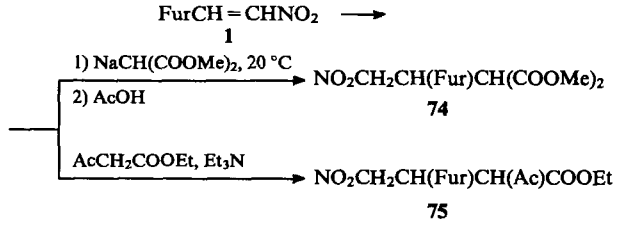
73

R = H, Me, NO_2.

When equimolar amounts of β-(5-R-2-furyl)nitroethylenes and barbituric acid are refluxed in aqueous ethanol, the monoadducts **73** are obtained in 73%–90% yield.[171] The authors note that the reaction of furylnitroethylenes with barbituric acid proceeds under more severe conditions than the reaction with β-nitrostyrene,[1] which is due to the more pronounced electron-donating influence of the furyl fragment compared with the phenyl group. The reactions could not be carried out at room temperature both in the presence and absence of a basic catalyst. On heating in the presence of alkaline catalysts (i.e. catalysts typical for the Michael reaction), partial or even complete charring takes place.

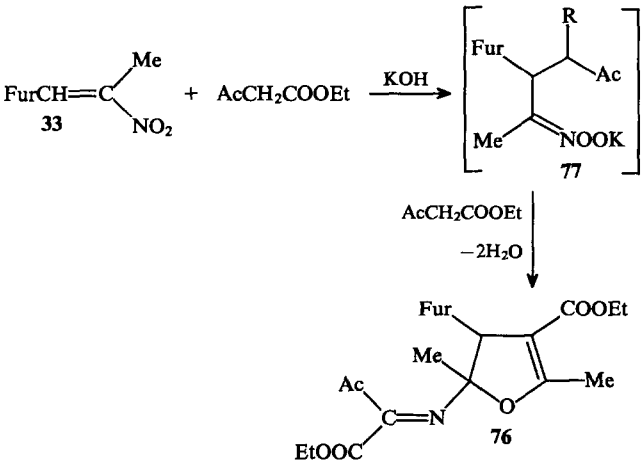
The reaction of sodiomalonic ester with β-(2-furyl)nitroethylene **1** and subsequent treatment with acetic acid lead to an 87% yield of the ester of 3-(2-furyl)-2-methoxycarbonyl-4-nitrobutanoic acid **74**—a valuable intermediate for the synthesis of furyl-containing γ-aminoacids and pyrrolidinones.[172,173]

The mode of interaction of acetoacetic ester with furylnitroalkenes depends primarily on the structure of the latter. For example, the ester of 2-acetyl-3-(2-furyl)-4-nitrobutanoic acid **75** was obtained in 60%–82% yield by the reaction of acetoacetic ester with β-(2-furyl)nitroethylene in the presence of triethylamine (benzene, 20 °C, 48–144 h).[174,175]



On the other hand, the interaction of acetoacetic ester with β-(2-furyl)-α-methylnitroethylene **33** and KOH (in molar proportions of 3 : 1 : 1) in ether led to the isolation of the ester of 5-[acetyl(ethoxycarbonyl)methyleneamino]-4-(2-furyl)-2,5-dimethyl-4,5-dihydrofuran-3-carboxylic acid **76** in 26% yield.[176] The authors believe that the potassium salt **77** of the aci-form of the 1 : 1 adduct is an intermediate in this reaction. It reacts subsequently with a second molecule of acetoacetic ester to form the dihydrofuran **76**.

It is noteworthy that there are still no literature data concerning the involvement of furylnitroalkenes in the Michael reaction with reactive CH acids such as nitro- and *gem*-dinitroalkanes, trinitromethane, benzyl cyanide, cyanoacetic ester, dimedone, cyclopentane-1,3-dione, etc.

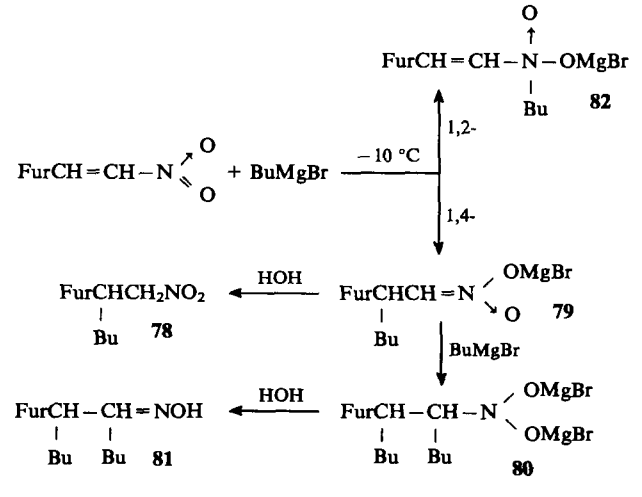


33 **77** **76**

Unsaturated nitro-compounds are capable of reacting with organometallic compounds, forming nitroalkanes derived from isonitroso-compounds, oximes, and hydroxylamine.[1-3] However, there is only one communication in the literature[177] about the reaction of β-(2-furyl)nitroethylene with butylmagnesium bromide, which leads to 2-(2-furyl)-1-nitrohexane **78** in 33% yield.

The 1,4-addition of the Grignard reagent to the conjugated system of the nitroalkene **1** affords predominantly complex **79**, whose hydrolysis leads to the nitroalkene **78**. However, by virtue of the presence of the $-C=N \rightarrow O$ system in complex **79**, it becomes possible to add a second molecule of the Grignard complex and to form complex **80**, which is converted into the oxime **81** on hydrolysis. The Grignard reagent adds partly to the 1,2-positions with formation of complex **82**, whose hydrolysis leads to a *N,N*-disubstituted hydroxylamine.

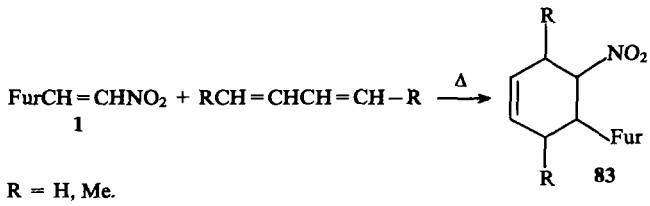
The authors note that, in order to suppress the nitroalkene polymerisation side reaction, it is useful to carry out the process at 10 °C with an excess of the Grignard reagent.



82 **78** **79** **81** **80**

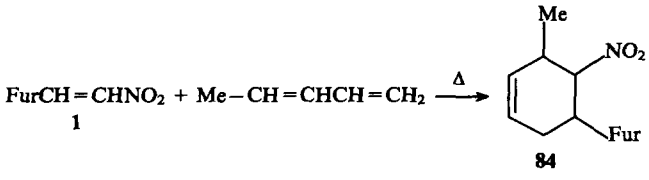
4. The cycloaddition reaction

According to the data of Kataev and Matveeva,[178] heating (150 °C, 10–16 h) of β-(2-furyl)nitroethylene **1** with butadiene and hexa-2,4-diene (molar ratio 1 : 3) in the presence of hydroquinone in a sealed tube affords a 45% yield of 5-(2-furyl)-4-nitrocyclohexenes **83**. The authors note that the reaction is accompanied by appreciable charring.

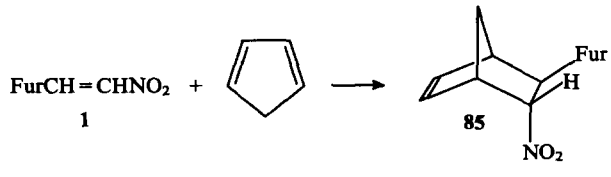


R = H, Me.

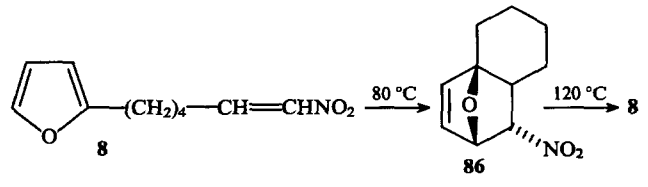
The study of the cycloaddition of the nitroalkene **1** to penta-2,4-diene showed that the reaction proceeds regioselectively with formation of only one regioisomer[178] — 5-(2-furyl)-3-methyl-4-nitrocyclohexene **84** in 55% yield.



endo-3-(2-Furyl)-2-nitrobicyclo[2.2.1]hept-5-ene **85** can be obtained in 78% yield by the reaction of the nitroalkene **1** with an equimolar amount of cyclopentadiene.[179] The stereochemistry of the process and the relative reactivity of the nitroalkene **1** with respect to cyclopentadiene are correlated with quantum-chemical CNDO/2 calculations.

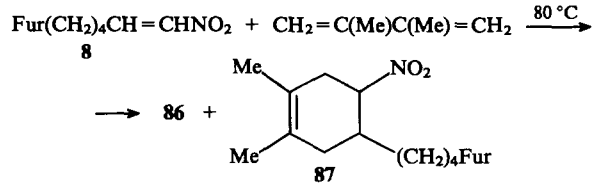


When 6-(2-furyl)-1-nitrohex-1-ene **8** is refluxed in benzene with catalytic amounts of pyridine, an intramolecular Diels–Alder reaction takes place with formation of the tricyclic adduct **86** in 52% yield.[68] On heating to 120 °C, the latter is reconverted into the initial compound **8**:



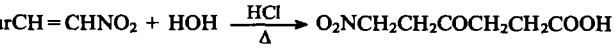
Prolonged (182 h) heating of the nitroalkene **8** with 2,3-dimethylbutadiene (molar ratio 1 : 10) in benzene produces a mixture containing 13.4% of the cyclic adduct **86**, 42.8% of 5-[4-(2-furyl)butyl]-1,2-dimethyl-*p*-nitrocyclohexene **87**, and 22% of compound **8**. Compound **8** is apparently formed as a result of the retroreaction of the adduct **86**.

Heating on compound **86** with 2,3-dimethylbutadiene (molar ratio 1 : 20) in benzene (80 °C, 251 h) affords a mixture containing 36.7% of compound **8**, 25.9% of compound **86**, and 30.8% of cyclohexene **87**.[68]



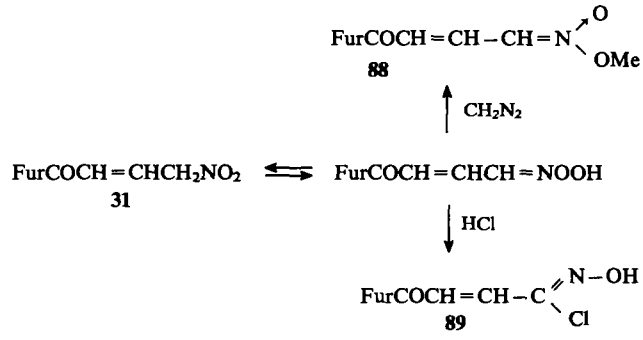
5. Other reactions of furylnitroalkenes

When β-(2-furyl)nitroethylene **1** is heated with concentrated hydrochloric acid, the furan ring is cleaved with formation of 6-nitro-4-oxocaproic acid.[180]

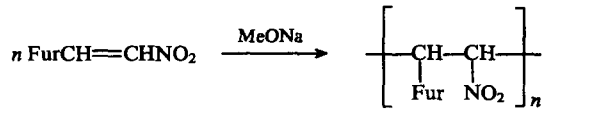


Methylation of 1-(2-furyl)-4-nitrobut-2-en-1-one **31** with diazomethane affords a 50% yield of the *o*-methyl ester of the acinitro-form **90**.[89]

Treatment of a solution of the nitroketone **31** in dioxane with concentrated hydrochloric acid gives rise to the chloride of the corresponding hydroxamic acid **89** in 45% yield.[89]



Studies on the polymerisation of β-(2-furyl)nitroethylene in the presence of anionic initiators (sodium methoxide, sodium ethoxide, etc.) have been reported.[180–182] The reactions were carried out in the temperature range −15 to 20 °C in different solvents — toluene, THF, and DMF. In the presence of cationic and radical initiators, the polymerisation of β-(2-furyl)nitroethylene was not observed.

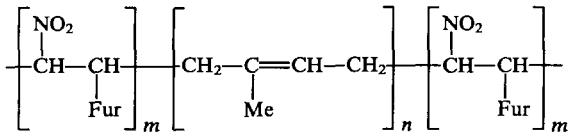


It has been shown that, with increase in the solvating capacity and polarity of the solvent, the yield of the polymer increases.[181] For example, when the polymerisation is carried out in toluene (0 °C, 150 min) the yield of the polymer is 15%, while in THF and in DMF the yields are 68% and 55% respectively. The polymer formed under these conditions is of the rigid-chain type and has no glass point in the range 20–250 °C.

The rate of polymerisation of β-(2-furyl)nitroethylene increases with increase in temperature and initiator and monomer concentrations; the molecular weight of the polymer rises as the temperature and initiator concentration are reduced and the monomer concentration is increased.[181] The study of the kinetics of the polymerisation reaction showed that the activation energy for the process in THF at temperatures in the range −15 to 20 °C is 2.8 kcal mol^{-1}.

It has been established[181-183] that the rate of anionic polymerisation of nitroalkenes increases in the sequence $FurCH=CHNO_2 < PhCH=CHNO_2 < MeCH=CHNO_2$. As the electron-accepting properties of the substituent in the nitroalkene molecule of the type $R-CH=CHNO_2$ are enhanced (Me < Ph < 2-furyl), the electron density at the double bond increases, which induces a decrease in the reactivity of the nitroalkenes in anionic polymerisation reactions.

Copolymerisation of β-(2-furyl)nitroethylene with isoprene resulted in the synthesis of block-copolymers of the B–A–B type.[183-185]



$m = 5-65$, $n = 400-3200$.

Under static conditions, the copolymers can be synthesised only in the presence of cationic initiators, for example dilithiopolyisoprene or dipotassiopolyisoprene. The reaction was carried out in benzene at temperatures in the range 10–70 °C and the block-copolymers were then obtained in 35%–65% yield. The composition of the copolymers included up to 30 mol% of the nitroalkene.

It has been established[185] that the statistical copolymerisation of isoprene with furylnitroethylene can be achieved also in the presence of $SnCl_4$ in solution in chloroform at temperatures in the range −50 to 50 °C.

It has been noted[181] that 1-(2-furyl)-4-nitrobuta-1,3-diene (**7**, $n = 1$) does not exhibit a tendency to undergo anionic polymerisation owing to the influence of steric effects. In the presence of sodium methoxide, 1-(2-furyl)-6-nitrohexa-1,3,5-triene (**7**, $n = 2$) gives rise to a dimer in yields up to 12%.

V. Practical applications of furylnitroalkenes

Unsaturated nitro-compounds of the furan series are used widely in organic synthesis as starting materials and intermediates of the preparation of various functional derivatives of the furan series, which are difficult to obtain by other methods, and also for the synthesis of biologically active substances and natural products.

Furylnitroalkenes are also of significant interest because of their high physiological activity. For example, β-(5-nitro-2-furyl)-nitroethylenes **12**, used in medical practice under the name nitrofurylene, effectively suppresses the growth of pathogenic fungi.[186,187] In this respect, its activity corresponds to the activity of the most active of the known antifungal antibiotics — nystatin, griseofulvin, etc. Clinical experience gained using this preparation indicates the virtual absence of resistance of the microflora to it and its satisfactory transferability.[188]

β-(5-Chloro-2-furyl)-α-R^2-nitroethylenes (**1** and **33**; R^2 = H, Me) exhibit a powerful lachrymatory activity.[28] This ability diminishes for substituents[23] R in the 5-position in the furan ring in the following sequence: Cl > Br > I > Me > H. The introduction of the nitro- or thiocyanate group in the 5-position weakens the irritant activity and enhances the bacteriostatic properties. For example,[47,125] β-(5-thiocyanato-2-furyl)nitroethylene **39** is capable of arresting the growth of the Siberian ulcer bacillus and of the staphylococcus at dilutions of 1 : 10000.

The introduction of the methyl group in the side chain is not reflected significantly in the nature of the physiological activity,[65] while the presence of a chlorine atom at the double bond of the side chain greatly enhances the bactericidal properties and leads to the appearance of new valuable qualities. For example, α-chloro-β-(5-nitro-2-furyl)nitroethylene **35** exhibits the capacity to inhibit the growth of the blue rot bacillus, but it is fairly toxic.[47]

β-[5-(4-R-phenyl)-2-furyl]-α-R^2-nitroethylenes (R = Cl, NO_2; R^2 = H, Me) have been patented as substances with bactericidal activity.[35]

The antibacterial activity of the methyl esters of β-(5-R-2-furyl)-α-nitroacrylic acids **6** has been reported.[53] The authors note that the 5-nitrofuryl derivative exhibits the highest activity among compounds of this type.

Czechoslovak workers[189-199] carried out a systematic study of the pharmacological activity of substituted vinylfurans, including furylnitroethylenes. It was established that furylnitroalkenes possess antimicrobial,[189-191] cytotoxic,[193] chemotherapeutic,[194,195] carcinogenic,[196-198] and in certain cases mutagenic activities. It was shown that the antimicrobial and cytotoxic activities are associated with the reactivity of the furylnitroalkenes in relation to nucleophiles — mainly low-molecular-weight thiols.[196] The mutagenic activity is associated with the presence of the nitro-group in the 5-position in the furan ring.[191,192,196] Together with the reactivity of furylnitroalkenes, their lipophilic-hydrophilic properties are very important physicochemical parameters which determine the intensity of the biological activity.[189] Attempts to establish quantitative structure–activity correlations in the series of furylnitroalkenes have been reported.[190,191,193,197]

It is noteworthy that β-(5-methanesulphonyl-2-furyl)-nitroethylene exhibits a high antimicrobial activity,[33] while β-(5-cyano-2-furyl)nitroethylene and 4-(5-cyano-2-furyl)-1-nitrobuta-1,3-diene possess only a slight activity.[29]

It has been established that furylnitroalkenes inhibit the activity of alcohol dehydrogenase[195,200-202] and xenobiotic receptors[198] and the fermentation of HS-enzymes[196,200] and are also effective antagonists of histamine.[203]

Furylnitroalkenes exhibit an appreciable fungicidal activity.[31,35,47,204,205] Hillers et al.[206] established that the nitrofurylene **12** is an effective fungicidal preparation. After the introduction of nitrofurylene as an additive to cotton, acetate, or polyester fibres, materials with fungicidal properties are obtained.[207] β-(5-Iodo-2-furyl)nitroethylene[208] and β-(5-aryl-2-furyl)nitroethylenes[209] also exhibit an appreciable fungicidal activity.

β-(2-Furyl)-α-methylnitroethylene **33** has been patented as an effective insecticide.[17] Furylnitroalkenes of different structure have been tested also as repellents.[210,211] It was established that they are excellent agents against rodents. According to patent data,[212] β-(2-furyl)-α-R^2-nitroethylenes (R^2 = alkyl, Ph) can be used as effective nematocides.

Copolymers of isoprene with β-(2-furyl)nitroethylene can be used as multifunctional additives to motor oils, thermoplastic elastomers, emulsifiers in hydrophobic emulsions for drilling in petroleum and gas deposits, and also as components of inhibited thin-film coatings.[181,183-185]

References

1. V V Perekalin, A S Sopova, E S Lipina *Nepredel'nye Nitrosoedineniya* (Unsaturated Nitro-compounds) (Moscow: Khimiya, 1982)
2. H Feuer *The Chemistry of the Nitro and Nitroso Groups* (Translated into Russian) (Moscow: Mir, 1972, Vol. I; 1973, Vol. II)
3. S S Novikov, G A Shvekhgeimer, V V Sevast'yanov, V A Shlyapochnikov *Khimiya Alifaticheskikh i Atsiklicheskikh Nitrosoedinenii* (The Chemistry of Aliphatic and Acyclic Nitro-compounds) (Moscow: Khimiya, 1974)
4. A Baranski, V I Kelarev *Khim. Geterotsikl. Soedin.* 435 (1990)
5. V V Perekalin *Zh. Org. Khim.* **21** 1171 (1985)
6. R S Varma, G W Kabalka *Heterocycles* **24** 2645 (1986)
7. A P Dunlop, F N Peters *The Furans* (New York: Reinhold, 1953)
8. E Lukevics (Editor) *Uspekhi Khimii Furana* (Advances in the Chemistry of Furan) (Riga: Zinatne, 1978)
9. B Priebs *Ber.* **18** 1362 (1895)
10. J Thille, H Landers *Ann.* **369** 300 (1909)
11. O Moldenhauer, W Irion, D Mastaglio, R Pfluger, H Doser *Ann.* **583** 50 (1953)
12. Z N Nazarova *Zh. Obshch. Khim.* **24** 575 (1954)

13. W McCarthy, R Kuhl *J. Org. Chem.* **21** 1118 (1956)
14. J Yabuta, K Kambe *Proc. Imp. Acad. Tokyo* **4** 120 (1928)
15. S Fujise, O Takenchi, T Kamioka, K Tiba *Ber.* **68** 1272 (1935)
16. M M Runde, E W Scott, J B Johnson *J. Am. Chem. Soc.* **52** 1284 (1930)
17. DDR P. 7178; *Ref. Zh. Khim.* 40677 (1955)
18. R Kada, V Knoppova, J Kovac, J Malenakova *Collect. Czech. Chem. Commun.* **49** 2496 (1984)
19. K Mitsunobu, O Hachiro, S Toshio, N Toshiro *Takamine Kenkynsto Nempo* **13** (2) 216 (1961); *Chem. Abs.* **57** 16451 (1962)
20. C Grundmann, W Rucke *Chem. Ber.* **85** 939 (1953)
21. K Schumann, R Kalchen *Chem. Technol.* **7** 175 (1955)
22. H Jutaka, O Ryasaku, T Jun *Daigaku Yakugaku Kenkyu Nempo* **18** 1 (1969); *Chem. Abs.* **74** 12968 (1971)
23. Z N Nazarova, S S Goryaev *Zh. Org. Khim.* **11** 1955 (1975)
24. E W Scott, J R Johnson *J. Am. Chem. Soc.* **54** 2549 (1932)
25. Yu K Yur'ev, N S Zefirov, R A Ivanova *Zh. Obshch. Khim.* **33** 3512 (1963)
26. G C McCowan, P W Brian, H G Hemming *Applied. Biol.* **35** (1) 25 (1948)
27. O Moldenhauer, W Irion, D Mastaglio, R Pfluger, H Marwitz *Ann.* **583** 646 (1953)
28. Z N Nazarova, F T Pozharskii *Zh. Obshch. Khim.* **28** 1503 (1958)
29. H Nakao, M Fukushima, S Sugawara *J. Pharm. Soc. Jpn.* **93** 1526 (1973)
30. Z N Nazarova *Zh. Obshch. Khim.* **25** 539 (1955)
31. R O Owens, H M Novotny *Contribution Boyce Thompson Ins.* **20** (2) 151 (1959)
32. R Kada, J Kovac *Collect. Czech. Chem. Commun.* **43** (12) 2037 (1978)
33. A Toshio, H Hayasho, K Shogo, N Takeshi *J. Pharm. Soc. Jpn.* **86** 735 (1966)
34. Jpn. P. 69-09902P; *Ref. Zh. Khim.* 30421P (1981)
35. Jpn. P. 63-4079; *Chem Abs.* **59** 11427 (1963)
36. J Kasiwagi *Bull. Chem. Soc. Jpn.* **2** 110 (1927)
37. H B Hass, A G Susie, R L Heider *J. Org. Chem.* **15** 8 (1950)
38. W O Foye, S Tovivieh *J. Pharm. Sci.* **65** (5) 591 (1979)
39. G Rosini, R Ballini, M Petrini, P Sorreti *Synthesis* 151 (1985)
40. S S Goreev in *Molodye Uchenye – Nauchno-Tekhnicheskomu Progressu* (The Contribution of Young Scientists to Scientific and Technical Progress) (Rostov-on-Don: Izd. Rostov. Gos. Univ., 1973) p. 78
41. M G Grunfest, Yu V Kolodyazhnyi, G F Potemkin, Z N Nazarova, O A Osipov *Zh. Org. Khim.* **7** 1057 (1971)
42. Z N Nazarova, V S Pustovarov *Khim. Geterotsikl. Soedin.* 586 (1969)
43. Z N Nazarova, G F Potemkin *Zh. Obshch. Khim.* **34** 157 (1964)
44. US P. 4209448 CIF; *Ref. Zh. Khim.* 30421G (1981)
45. Z N Nazarova, G F Potemkin, O A Pustovarova *Khim. Geterotsikl. Soedin.* 1128 (1967)
46. S Kanao *J. Pharm. Soc. Jpn.* **50** 1019 (1927); *Chem. Abs.* **22** 1588 (1928)
47. Z N Nazarova, G F Potemkin *Khim.-Farm. Zh.* **6** (10) 5 (1972)
48. B Reichert, W Kuhn *Ber.* **74B** 328 (1941)
49. D N Robertson *J. Org. Chem.* **25** (1) 47 (1960)
50. US P. 2899429 CIF; *Chem. Abs.* **54** 4341 (1960)
51. C T Bahner, H E Dickson, L Moore *J. Am. Chem. Soc.* **70** 1982 (1948)
52. I P Tsukervanik, G F Potemkin *Dokl. Akad. Nauk Uzbek. SSR* (8) 26 (1951)
53. D Vegh, J Kovac, M Dandarova *Collect. Czech. Chem. Commun.* **41** 2422 (1976)
54. W Ried, E Kohler *Ann.* **598** (2) 145 (1956)
55. A S Polyanskaya, V V Perekalin, N I Absokalova, Z N Demireva, A N Sokolova, Z A Abdulkina *Zh. Org. Khim.* **15** 2057 (1979)
56. L Bouveult, A Wahl *C.R. Acad. Sci.* **134** 41 (1902)
57. L Bouveult, A Wahl *Bull. Soc. Chim. Fr.* **29** (3) 521 (1903)
58. H Kaufmann *Chem. Ber.* **52** 1422 (1919)
59. G L Kamalov, L G Bogatskaya, T Kyun, I G Luk'yanenko, A V Bogatskii *Dokl. Akad. Nauk SSSR* **232** 1077 (1977)
60. E Knoevenagel, L Walter *Chem. Ber.* **37** 4502 (1904)
61. O Schales, H A Graefe *J. Am. Chem. Soc.* **74** 4486 (1952)
62. D E Worrall, L Cohen *J. Am. Chem. Soc.* **66** 842 (1944)
63. P Knochel, D Seebach *Synthesis* 1017 (1982)
64. A V Topchiev, V P Alanin, V A Sporano *Dokl. Akad. Nauk SSSR* **139** 396 (1961)
65. Kh R Rustamov, R Usmanov *Uzb. Khim. Zh.* **4** 44 (1963)
66. O Moldenhauer, T D Mastaglion, M Rohmer, P Senger, H Marwitz *Ann.* **583** 80 (1953)
67. V P Alanin, N A Sokolov *Zh. Org. Khim.* **1** 2245 (1965)
68. A Radva, Q Chen, Huaxne Xuebgi **44** 675 (1986); *Ref. Zh. Khim.* IZh194 (1987)
69. E J Corey, J G Reid, A G Myers, R W Hahl *J. Am. Chem. Soc.* **109** 918 (1987)
70. M Fujii *Bull. Chem. Soc. Jpn.* **61** 4029 (1988)
71. A A Ponomarev *Sintezy i Reaktsii Furanovykh Soedinenii* (The Syntheses and Reactions of Furan Compounds) (Saratov: Izd. Saratov. Gos. Univ., 1960)
72. T Sasaki *Bull. Chem. Soc. Jpn.* **27** 398 (1954)
73. K K Venters, S Hillers, V Cirule *Izv. Akad. Nauk Latv. SSR* **2** 131 (1962)
74. Jpn. P. 62-10688; *Chem. Abs.* **59** 3895 (1963)
75. H Saikachi, A Tonoka *J.Pharm. Soc. Jpn.* **83** 240 (1963)
76. J Kovac, R Frimm, A Jurasek, in *Sb. pr. Chemickotechnol. Fak. SVST* (Bratislava, 1971) p. 65
77. J Kovac, E Komalova, F Povazanec *Chem. Zvesti* **25** 63 (1971)
78. J Kovac, in *Sb. pr. Chemickotechnol. Fak. SVST* (Bratislava, 1972) p. 45
79. A I Sitkin, V I Klimenko in *Khimiya i Tekhnologiya Furanovykh Soedinenii* (The Chemistry and Technology of Furan Compounds) (Krasnodar: Izd. Krasnodar. Politekh. Inst., 1979) p. 78
80. J Kovac, R Brenzy *Collect. Czech. Chem. Communs.* **42** 1880 (1977)
81. I Strokova, A Jurasek, M Dandarova, J Kovac *Collect. Czech. Chem. Commun.* **43** 463 (1978)
82. Czech. P. 187135; *Chem. Abs.* **96** 35063 (1982)
83. A Jurasek in *III Vsesoyuznaya Nauchnaya Konferentsiya po Khimii i Tekhnologii Furanovykh Soedinenii (Tezisy Dokladov)* [The IIIrd All-Union Scientific Conference on the Chemistry and Technology of Furan Compounds (Abstracts of Reports)] (Riga: Zinatne, 1978) p. 173
84. I Strokova, A Jurasek, M Dandarova, J Kovac *Collect. Czech. Chem. Commun.* **43** 3252 (1978)
85. W H Darlington, J Szmuszkowicz *Tetrahedron Lett.* **29** 1883 (1988)
86. M M Campbell, N Cosford, J Li, M Sainsbury *Tetrahedron* **43** 1117 (1987)
87. F Moimas, C Angeli, G Commiso, P Zanon, D Enio *Synthesis* 509 (1985)
88. A Dornow *Ann.* **594** 191 (1955)
89. T Severin, P Adhikary, I Schnabel *Ber.* **102** 1325 (1969)
90. V R Vasil'eva, V V Perekalin, V G Vasil'eva *Zh. Obshch. Khim.* **61** 2171 (1961)
91. M G Grunfest, G F Potemkin, Yu V Kolodyazhnyi, V V Zverev, Z N Nazarova, O A Osipov *Zh. Org. Khim.* **8** 404 (1972)
92. V N Vasil'eva, V V Perekalin, V G Vasil'ev *Zh. Obshch. Khim.* **31** 2175 (1961)
93. M G Kogan, V S Pustovarov, Z N Nazarova, O A Osipov *Zh. Org. Khim.* **4** 2216 (1968)
94. Yu A Zhdanov, V I Minkin in *Korrelyatsionnyi Analiz v Organicheskoi Khimii* (Correlation Analysis in Organic Chemistry) (Rostov-on-Don: Izd. Rostov. Gos. Univ., 1966) p. 57
95. S V Tsukerman, V D Orlov, V M Nikitchenko, Yu S Rozun, V D Lavrushin, Yu K Ur'ev *Teor. Eksp. Khim.* **2** 399 (1966)
96. L M Sitkina, A F Pozharskii, A M Simonov *Zh. Obshch. Khim.* **37** 10 (1967)
97. A S Kuzharov, V N Sheinker, R M Minyaev, Z N Nazarova, V I Minkin, O A Osipov *Zh. Fiz. Khim.* **50** 2380 (1976)
98. A F Oleinik, G A Modnikova, T I Voznyakova, E I Burgova, K Yu Novitskii *Khim. Geterotsikl. Soedin.* 452 (1975)
99. C N R Rao, in *Electronic Spectra in Chemistry* (Translated into Russian) (Moscow: Mir, 1964) p. 54
100. L G Bogatskaya, G L Kamalov, L G Luk'yanenko *Zh. Org. Khim.* **13** 1072 (1977)
101. W E Forbes *Can. J. Chem.* **38** 1104 (1960)
102. J N Murrell, S F A Kettle, J M Tedder *Valence Theory* (Translated into Russian) (Moscow: Mir, 1968) p. 415
103. N A Sokolov, V P Alaniya *Zh. Prikl. Spektrosk.* **8** 348 (1968)
104. A R Katritzky (Editor) *Physical Methods in Heterocyclic Chemistry* (Translated into Russian) (Moscow: Khimiya, 1966) p. 430
105. R M Silverstein, G C Bassler, T C Morrill *Spectroscopic Identification of Organic Compounds* (Translated into Russian) (Moscow: Mir, 1977) p. 203

106. T Ya Paperno, V V Perekalin, in *Infrakrasnye Spektry Nitrosoedinenii* (Infrared Spectra of Nitro-compounds) (Leningrad: Izd. LGPI, 1974) p. 49
107. S Watarai, K Yamamura, N Kinugasa *Bull. Chem. Soc. Jpn.* **40** 1448 (1967)
108. N Bhacca, L F Johnson, J N Shoolery *High Resolution NMR Spectra Catalog.* (New York: Varian Associates, 1962)
109. T N Huckerby *Tetrahedron Lett.* **12** 353 (1971)
110. G Descotes, J Bahurel, M Buorillot, G Pingeon, R Rostaina *Bull. Soc. Chim. Fr.* 282 (1970)
111. C Pasqual, J Meier, W Simon *Helv. Chim. Acta.* **49** 164 (1966)
112. U E Matter, C Pasqual, E Pretsch, A Pross, W Simon, S Sternhell *Tetrahedron* **25** 691 (1969)
113. B Roques, M C Fournie-Zaluski *Org. Magn. Reson.* **3** 305 (1971)
114. E J Parr, R E Wasylishen, T Schaefer *Can. J. Chem.* **54** 3216 (1976)
115. D Ilavsky, V Kery, J Kovac, J Hubac, in *Sb. pr. Chemickotechnol. Fak. SVST* (Bratislava, 1977–1978) p. 69
116. M V Bazilevskii in *Metod Molekulyarnykh Orbit i Reaktsionnaya Sposobnost' v Organicheskoi Khimii* (The Molecular Orbital Method and Reactivity in Organic Chemistry) (Moscow: Khimiya, 1969) p. 63
117. S Cavva, M Raimondi, M Simonetta *Tetrahedron* **22** 2673 (1966)
118. V V Zverev *Teor. Eksp. Khim.* **5** 834 (1969)
119. USSR P. 184 874; *Byul. Izobret.* **16** (1966)
120. S Hillers, M Berklava *Izv. Akad. Nauk Latv. SSSR* (5) 115 (1959)
121. A I Sitkin, V N Klimenko. A I Fridman *Zh. Org. Khim.* **10** 2625 (1974)
122. USSR P. 491 613; *Ref. Zh. Khim.* 200338 (1976)
123. T I Vozyukova, T F Oleinik, K Yu Novitskii, in *III Vsesoyuznaya Nauchnaya Konferentsiya po Khimii i Tekhnologii Furanovykh Soedinenii (Tezisy Dokladov)* [The IIIrd All-Union Scientific Conference on the Chemistry and Technology of Furan Compounds (Abstracts of Reports)], Zinatne, Riga, 1978, p. 100
124. A F Oleinik, K Yu Novitskii, in *III Vsesoyuznaya Nauchnaya Konferentsiya po Khimii i Tekhnologii Furanovykh Soedinenii (Tezisy Dokladov)* [The IIIrd All-Union Scientific Conference on the Chemistry and Technology of Furan Compounds (Abstracts of Reports)] (Riga: Zinatne, 1978) p. 37
125. Z N Nazarova, L E Nivorozhkin *Zh. Obshch. Khim.* **30** 3297 (1960)
126. Z N Nazarova, G F Potemkin *Zh. Org. Khim.* **1** 1709 (1965)
127. V N Novikov *Khim. Geterotsikl. Soedin.* 1601 (1976)
128. J F Bunnett, J K Kim *J. Am. Chem. Soc.* **92** 7463 (1970)
129. V N Novikov. L D Babeshkina *Khim. Geterotsikl. Soedin.* 1465 (1976)
130. V N Novikov, S V Borodaev, L D Babeshkina, in *III Vsesoyuznaya Nauchnaya Konferentsiya po Khimii i Tekhnologii Furanovykh Soedinenii (Tezisy Dokladov)* [The IIIrd All-Union Scientific Conference on the Chemistry and Technology of Furan Compounds (Abstracts of Reports)] (Riga: Zinatne, 1978) p. 35
131. L Kh Freidlin, E F Litvin, V M Chursina *Khim. Geterotsikl. Soedin.* 22 (1969)
132. N Fukamiya, S Yasuda *Chem. Ind.* London, 126 (1979)
133. G N Dorofeenko, L V Dulenko *Khim. Geterotsikl. Soedin.* 417 (1969)
134. M Ferles *Chem. Listy* **64** (2) 188 (1970)
135. I F Bel'skii, Z K Minashkina, O G Kesarev *Izv. Akad. Nauk SSSR, Ser. Khim.* 2093 (1970)
136. H Shechter, D E Ley, E B Robertson *J. Am. Chem. Soc.* **78** 4984 (1956)
137. E S Bogacheva, Candidate's Thesis in Chemical Sciences, Gubkin Moscow Institute of Petroleum and Gas, Moscow, 1989
138. H Chikashita, Y Morita, K Jtoh *Synthetic Commun.* **15** 527 (1985)
139. K Nakamura, M Fujii, S Oka, A Ohno *Chem. Lett.* 523 (1985)
140. Jpn. P. 61-76444; *Chem. Abs.* **105** 97 002 (1986)
141. I M Skvortsov, N A Bustyakova, A A Stolyarchuk, N N Ivanova *Khim. Farm. Zh.* **11** (5) 66 (1977)
142. P Takamoto *J. Pharm. Soc. Jpn.* **48** 22 (1927)
143. G Reihmanis, J Stradins, R Gavars, S Hillers *Zh. Obshch. Khim.* **41** 906 (1971)
144. J Stradins, V Kadis, S Hillers *Khim. Geterotsikl. Soedin.* 1587 (1973)
145. J Stradins, V Kadis, S Hillers *Khim. Geterotsikl. Soedin.* 147 (1974)
146. J Stradins, G Reihmanis *Izv. Akad. Nauk Latv. SSSR Ser. Khim.* 470 (1973)
147. J Cernak, A Stasko, F Tomanovic, L Nemethy, I Strokova *Chem. Zvesti* **37** (3) 385 (1983)
148. A I Vil'davskaya, I G Sulimov, K B Rall' *Zh. Org. Khim.* **5** 1326 (1969)
149. L Drobnika *Collect. Lect. IIIth Intern. Symposium of Furan Chemistry* (Riga, 1979) p. 50
150. E Sturdik, L Drobnika, S Balaz, V Marko *Biochem. Pharmacol.* **28** 2525 (1979)
151. E Sturdik, S Balaz, V Marko, L Drobnika *Sb. pr. Chemickotechnol. Fak. SVST* (Bratislava, 1977–1978) p .245
152. E Sturdik, T Liptai, S Balaz, L Drobnika *Collect. Czech. Chem. Commun.* **47** 1523 (1982)
153. S Balaz, E Sturdik, L Drobnika *Collect. Czech. Chem. Commun.* **47** 1659 (1982)
154. E Sturdik, L Drobnika, S Balaz *Collect. Czech. Chem. Commun.* **48** 336 (1983)
155. M Roseberg, S Balaz, E Sturdik, A Kuchar *Collect. Czech. Chem. Commun.* **52** 425 (1987)
156. M Rosenberg, E Sturdik, T Liptai, J Bella *Collect. Czech. Chem. Commun.* **50** 470 (1985)
157. R Kada, V Knoppova, J Kovac *Topics in Furan Chemistry. Proceedings of IVth Symposium on Furan Chemistry* (Bratislava, 1983) p. 135
158. C D Hurd, J Patterson *J. Am. Chem. Soc.* **75** 285 (1953)
159. D Calleias, K Jahnisch, A Weigt *Abstract of Vth Intern. Symposium on Furan Chemistry* (Riga, 1988) p. 71
160. E E Borisova, R D Gareev, G A Guseva, L M Kozlov, I M Shermergon *Dokl. Akad. Nauk SSSR* **226** 1330 (1976)
161. N M Vafina, T A Zyablikova, A V Il'yasov, I M Shermergon *Zh. Obshch. Khim.* **52** 35 (1982)
162. N M Vafina, I M Shermergon *Zh. Obshch. Khim.* **50** 2137 (1980)
163. N M Vafina, Yu Ya Efremov, T A Zyablikova, A V Il'yasov, I M Shermergon *Zh. Obshch. Khim.* **52** 2432 (1982)
164. DDR P. 156816; *Chem. Abs.* **98** 198441 (1983)
165. V V Perekalin, A S Polyanskaya *Dokl. Akad. Nauk SSSR* **112** 441 (1957)
166. V V Perekalin, K Bayer *Zh. Obshch. Khim.* **30** 943 (1960)
167. A Dornow, A Frese *Ann.* **581** 211 (1953)
168. F Bogerg, M Ruhr, K H Garburg, A Garming *J. Heterocycl. Chem.* **23** 759 (1987)
169. F Bogerg, K H Garburg, K J Gorlich, E Pipereit, E Redelfs, M Ruhr *J. Heterocycl. Chem.* **23** 1853 (1986)
170. V V Perekalin, K S Parfenova *Dokl. Akad. Nauk SSSR* **124** 592 (1959)
171. V G Kul'nevich, G P Fedoseeva in *Nauchnye Trudy Kubanskogo Gosudarstvennogo Universiteta* (Scientific Reports from the Kuban State University) (Krasnodar, 1977) p. 57
172. M M Zobacheva, V V Perekalin *Dokl. Vys. Shkoly* **40** 740 (1958)
173. V V Perekalin, M M Zobacheva *Zh. Obshch. Khim.* **29** 2905 (1959)
174. A F Shalygin, L V Kuprik in *Voprosy Prikladnoi Khimii* (Problems of Applied Chemistry) (Chelyabinsk: Izd. Chelyabinsk. Gos. Ped. Inst., 1967) p. 52
175. V S Grineva, M M Zobacheva, V V Perekalin *Zh. Org. Khim.* **8** 411 (1972)
176. F Bogerg, K H Garburg, K J Gorlich, E Pipereit, M Ruhr *Ann.* **6** 911 (1984)
177. G Buckley, E Ellery *J. Chem. Soc.* 1497 (1947)
178. E G Kataev, V S Matveeva *Zh. Obshch. Khim.* **23** 405 (1953)
179. J Bouguignon, G Le Nard, G Queguiner *Can. J. Chem.* **63** 2354 (1985)
180. M Okawara *J. Chem. Soc. Jpn., Ind. Chem. Sect.* **56** 90 (1953)
181. V P Alaniya, Doctoral Thesis in Chemical Sciences, Moscow Institute of the Petrochemical and Gas Industry, Moscow, 1975
182. J Jagur-Grodzinki *Encycl. Polymer Sci. Technol.* **9** 315 (1968)
183. N G Kuznetsov, Candidate's Thesis in Chemical Sciences, Moscow Institute of the Petrochemical and Gas Industry, Moscow, 1977
184. USSR P. 539927; *Byul. Izobret.* **15** (1977)
185. V P Alaniya, E G Gorlov, N G Kuznetsov *Vysokomol. Soedin, Ser. B* **21** 452 (1979)
186. M U Lidaks *Khim. Geterotsikl. Soedin.* 5 (1985)
187. L N Yakovlev, R T Glushkov in *Sinteticheskie Lekarstvennye Sredstva* (Synthetic Medicinal Drugs) (Moscow: Meditsina, 1983) p. 272

188. S Hillers, B Press, A Sile, M Berklava in *Materialy III Nauchno Prakticheskoi Konferentsii Gigienistov, Epidemiologov, Mikrobiologov i Infektsionistov Latv. SSR, Riga* (Proceedings of the IIIrd Scientific and Applied Conference of Hygienists, Epidemiologists and Specialists in Microbiology and Infections, the Latvian SSR, Riga) (Riga, 1960) p. 46
189. E Sturdik, L Drobnika, S Balaz, M Antalik *Sb. pr. Chemickotechnol. Fak. SVST* (Bratislava, 1979–1981, published 1986) p. 109
190. S Balaz, A Cuchar, E Sturdik, M Rosenberg, L Stibranyi, D Slavsky *Collect. Czech. Chem. Commun.* **50** 1642 (1985)
191. L Drobnika, E Sturdik *Folia Microbiol.* **25** 467 (1980)
192. E Sturdik, M Rosenberg, L Stibrany, S Balaz, O Chereno, L Eblinger, D Slavsky, D Vegh *Chem. Biol. Interact.* **53** 145 (1985)
193. E.Sturdik, M Behova, S Miertus, S Balaz, M Rosenberg, M Studnikova, L Ebringer, L Stibranyi, D Slavsky *Chem. Biol. Interact.* **58** 69 (1985)
194. S Balaz, M Rosenberg, M Tieny, E Sturdik, I Augustin *Pharmacochem. Libr.* **10** 325 (1987)
195. S Balaz, E Sturdik, V Sitkey, M Rosenberg, I Augustin *Farm. Obzor (SVST)* **56** (5) 225 (1987)
196. S Balaz, E Sturdik, I Augustin, D Ieasky *Biologia (Bratislava)* **42** (12) 1161 (1987)
197. S Balaz, E Sturdik, I Augustin, B Skarka *Biologia (Bratislava)* **42** (12) 1171 (1987)
198. S Balaz, M Rosenberg, E Sturdik, I Augustin *Cesk. Farm. (SVST)* **36** (4) 145 (1987)
199. S Balaz, E Sturdik, M Rosenberg, I Augustin, B Skarka *J. Theor. Biol.* **131** 115 (1988)
200. L Drobnika, E Sturdik, J Kovac, D Vegh *Neoplasma* **28** (3) 281 (1981)
201. S Balaz, E Sturdik, V Sitkey, M Rosenberg, I Augustin *Stud. Biophys.* **114** 23 (1986)
202. S Balaz, E Sturdik, I Augustin, D Vegh, L Stibranyi, J Kovac *Chem. Biol. Interact.* **63** 195 (1987)
203. R C Young, R C Mitchell, T H Brown, C R Ganellin, R Griffiths, M Jones, K K Rana *J. Med. Chem.* **31** 656 (1988)
204. J C McGowan, P W Drian, H G Hemming *Ann. Applied. Biol.* **35** 25 (1948)
205. DDR P. 234 782; *Chem. Abs.* **105** 185 867 (1986)
206. S Hillers, A Zile, M Berklava, L Kruzmetra, S Germane, B Press, *Eksp. Klin. Khimioterapiya* 111 (1970)
207. K L Glazomitskii, L D Mazo, I M Akim, E S Roskin in *III Mezhdunarodnyi Simpozium po Khimicheskim Voloknam. Leningrad, 1977* (The IIIrd International Symposium on Chemical Fibres. Leningrad 1977) p. 228
208. L K Gorshkov, V I Mishin *Tr. Sel'skokhoz. Inst. Zaochnogo Obrazovaniya* No. 106 (Balashikha,1975) p. 9
209. S Somasekhara, D M Desai, A C Padhya *Indian J. Microbiol.* **14** (2) 89 (1974)
210. US P. 2 889 246; *Chem. Abs.* **55** 1018 (1960)
211. E W Schaefer, W A Bowles *Arch. Environ. Contam. Toxicol.* **14** 111 (1985)
212. USSR P. 191 956; *Ref. Zh. Khim.* 6N704 (1968)

Russian Chemical Reviews 1993 **62** (2) 193–202
© 1993 Russian Academy of Sciences and Turpion Ltd

UDC 547.1'28

Spirocyclic compounds of the siloxane series

M A Sipyagina (deceased), E A Stepanova, N M Buzyreva, T V Vasetchenkova, E A Chernyshev

Contents

I. Introduction	193
II. Synthesis of organospirocyclosiloxanes	193
III. Conversion reactions of organospirocyclosiloxanes	199
IV. Certain physicochemical properties of organospirocyclosiloxanes	200

Abstract. Monomeric and oligomeric spirocyclic compounds of the siloxane series, the methods of their synthesis, some of their physicochemical properties, and the reactions leading to their conversion into polymers of different structure are examined. The bibliography includes 69 references.

I. Introduction

The term spirocyclic is given to compounds whose molecules consist of two or several cyclic fragments linked to one another via a common atom, which enters simultaneously into the compositions of two neighbouring rings.[1]

In spirocyclic compounds of the siloxane series, either a silicon atom or the atom of any other element whose valence is four may be found in the spiro-position. The silicon atoms at the spiro-nodes of organospirocyclosiloxanes are involved in a fairly rigid tetrahedral coordination.[2] According to X-ray diffraction data, the Si–O bonds in the spiran group are somewhat shortened compared with the Si–O bonds in the cyclic fragment of the molecule, which is usually attributed to the more complete involvement of the central silicon atom in $p_\pi - d_\pi$ conjugation with the four oxygen atoms surrounding it.[2] The cyclic fragments in the molecules of organospirocyclosiloxanes can differ also in their strain. The most strained cyclic fragments play the role of chemically active centres responsible for the conversion of the spirocyclic compounds into oligomers and polymers.

By creating spirocyclic molecules of different composition and by altering the size of the cyclic fragments and their strain, it is possible to obtain three-dimensionally cross-linked polymers with a controllable network density and with different properties.

The fundamental principles of the synthesis of such compounds have already been described.[3] Individual communications concerning the distinctive features of polymeric materials based on spirocyclic oligomers and polymers can also be encountered.[4]

The aim of the present review is the examination of the methods of synthesis of spirocyclic monomers and oligomers and the procedures for their conversion into polymers of different structure.

M A Sipyagina, E E Stepanova, N M Buzyreva, T V Vasetchenkova, E A Chernyshev Department of the Synthesis of Organoelement and Inorganic Polymers, Lomonosov Moscow Institute of Fine Chemical Engineering, prosp. Vernadskogo 86, 117 Moscow V-571
Fax (7-095)430 79 83

Received 14 April 1992
Uspekhi Khimii **62** (3) 208–217 (1993); translated by A K Grzybowski

II. Synthesis of organospirocyclosiloxanes

The complexity of the synthesis of organospirocyclosiloxanes consists in the fact that many of them may polymerise during synthesis and isolation owing to the opening of the strained cyclic fragments, forming polymers with three-dimensional structures.

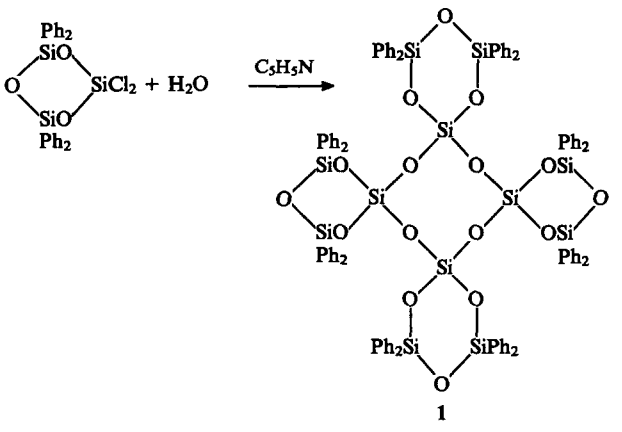
The majority of the traditional methods of synthesis of organosilicon compounds have been tried in order to obtain spirosiloxanes but not all of them proved to be suitable.

1. Hydrolytic polycondensation

The simplest spirocyclic compounds of the siloxane series (together with other polysiloxanes) were first obtained in very low yields by hydrolytic polycondensation (HPC). Thus octamethylspiro[5.5]pentasiloxane was isolated in 1% yield from a complex mixture produced by the thermal rearrangement of the products of the cohydrolysis of dichlorodimethylsilane and silicon tetrachloride.[5] Subsequently a series of cyclic compounds were isolated in 3%–7% yield from the products of the cohydrolysis of the same monomers and a spirocyclic structure was assigned to them on the basis of elemental analysis and their molecular weights.[6] The authors do not present more rigorous proof of the structures of the compounds synthesised. After the appearance of these studies, the literature contained for a long time no publications devoted to the synthesis of organospiropolysiloxanes by the hydrolytic polycondensation method. This can evidently be explained by the fact that the hydrolytic polycondensation of monomers with different functional groups is very difficult to control. Furthermore, the appreciable difference between the rates of hydrolysis and subsequent condensation of the initial monomers leads in the given instance to a sharp decrease in the yield of the target products and hinders their isolation.[5]

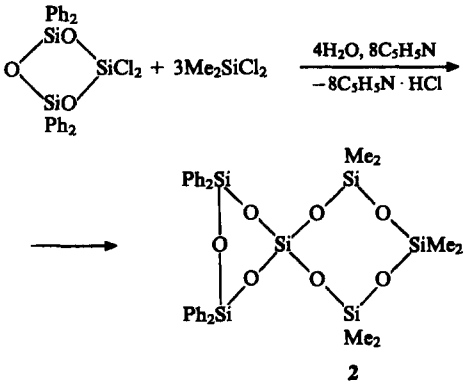
Studies dealing in fair detail with the hydrolytic polycondensation of chlorine-containing organocylcosiloxanes and their copolycondensation with organochlorosilanes have appeared in recent years.[7, 8] It has been established that the products of the hydrolytic polycondensation of these monomers are a mixture of cyclic compounds which cannot always be fully separated.

However, by selecting reaction conditions for each specific case, the authors were able to isolate a series of individual spirocyclic compounds (albeit in low yields) from the complex range of products, whose structure was confirmed by X-ray diffraction and IR and ^{1}H NMR spectroscopy. Thus the spiropentacyclic compound **1** was isolated in a yield reaching 30% from the products of the hydrolytic polycondensation of 2,2-dichlorotetraphenyl-cyclotrisiloxane in ether in the presence of a hydrogen chloride acceptor and a less than stoichiometric amount of water.[8]



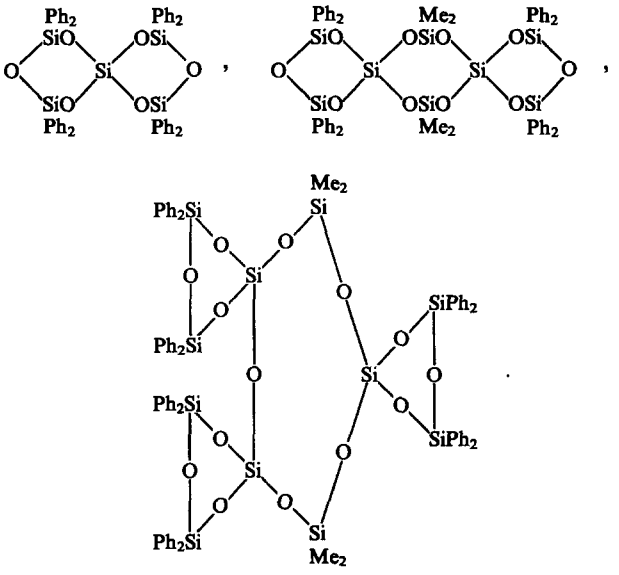
1

In the hydrolytic cocondensation of 2,2-dichlorotetraphenyl-cyclotrisiloxane with dichlorodimethylsilane, the formation of a mixture of bicyclic, tricyclic, and tetracyclic organospirosiloxanes, containing simultaneously tetraphenylcyclotrisiloxane and dimethyl-siloxane units, is formed only when the cohydrolysis is carried out with an equimolar amount of water in the presence of a hydrogen chloride acceptor.[8] The composition of the mixture formed then depends only slightly on the ratio of the initial reactants. For example, the hydrolytic polycondensation of 2,2-dichlorotetra-phenylcyclotrisiloxane and dichlorodimethylsilane in proportions of 1 : 3 with an equimolar amount of water in the presence of pyridine leads to a mixture of spirocyclic compounds which can be vacuum distilled. The main reaction product[8] is 8,8,10,10,12,12-hexamethyl-2,2,4,4-tetraphenylspiro[5.7]hexasiloxane **2**, which was isolated in 21.4% yield.

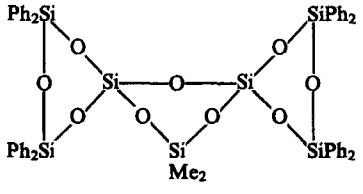


2

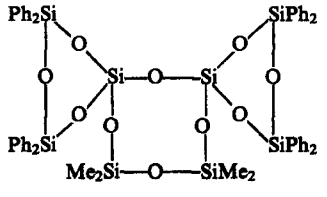
The following compounds are also isolated from the products of this reaction in much lower yield, not exceeding 3%:



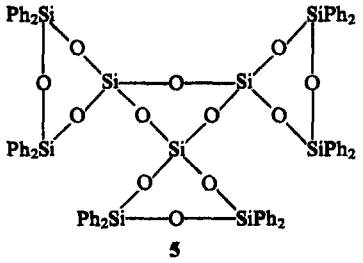
The spirotricyclic and spirotetracyclic compounds **3**–**5** were isolated in 3.5%–9% yield from the mixture of products formed and identified after the cocondensation of 2,2-dichlorotetra-phenylcyclotrisiloxane with dichlorodimethylsiloxane (2 : 1 reactant ratio) and with 1,3-dichlorotetramethyldisiloxane.[8]



3

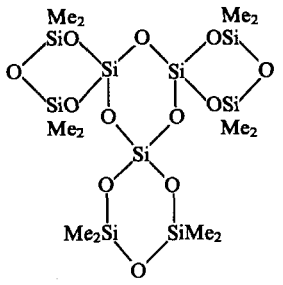


4



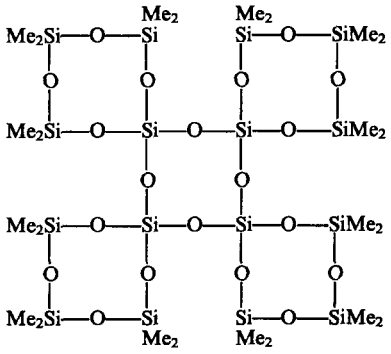
5

The hydrolytic polycondensation of chlorine-containing cyclosiloxanes with methyl groups attached to the silicon atom is no less complex. Thus the hydrolytic polycondensation of 2,2-dichlorotetramethylcyclotrisiloxane with the stoichiometric amount of water in the presence of a hydrogen chloride acceptor leads to a mixture of spirocyclic compounds,[7] from which only one compound, namely the spirotetracyclic compound **6**, was isolated in 22% yield.



6

The spiropentacyclic compound **7**, whose structure was determined by X-ray diffraction, was isolated from the products of the hydrolytic polycondensation of 2,2-dichlorohexamethylcyclotetrasiloxane under conditions similar to those described above.[7, 9]



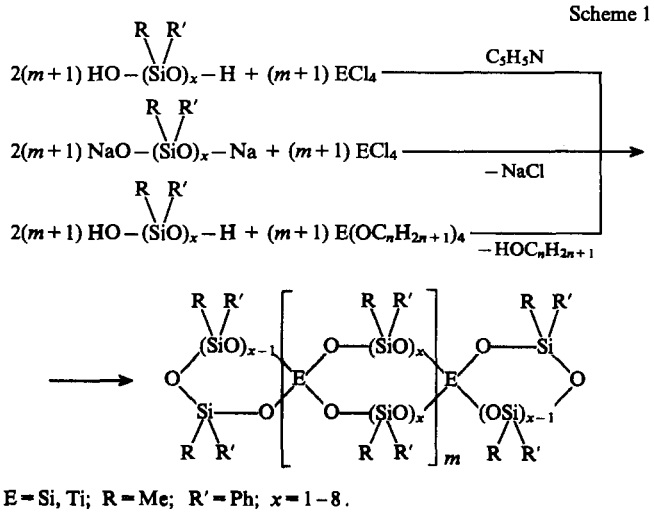
7

Thus the hydrolytic polycondensation of organochlorosiloxanes and organochlorocyclosiloxanes proceeds in a complex manner and leads under the conditions indicated to a mixture of spirocyclic compounds which are difficult to separate and whose yield in each specific case is determined both by the composition and structure of the initial polymers and by the reaction conditions. By virtue of the causes discussed above, it is difficult to obtain by this method organospirocyclosiloxane with a specified disposition and ratio of siloxane units.

2. Heterofunctional condensation

The method most widely used for the synthesis of organospirocyclosiloxanes is based on the heterofunctional condensation (HFC) reaction of di- and tetra-functional organosilicon compounds. In contrast to hydrolytic polycondensation, this method has been used for the specific synthesis of both the simplest spirobicyclic compounds[10–15] and for the synthesis of polyspirocyclic systems.[7, 16–21] The yield of organospirocyclosiloxanes in these reactions depends on the ratio of the initial reactants, their composition and structure, and the reaction conditions. The heterofunctional condensation of bifunctional organosilanes and linear organosiloxanes with tetrafunctional monomers of the type EX_4 (where E = Si or Ti and X = Cl or OC_nH_{2n+1}) is frequently used for the synthesis of organospirosilosiloxanes.[3, 16–19, 22–24] In this case, the initial reactants are taken in proportions of 2 : 1. α, ω-Dihydroxy- or α, ω-disodio-oxyorganosiloxanes are used as the bifunctional component. In the general case, the reaction can be represented by Scheme 1.

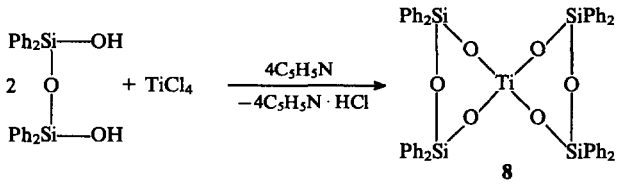
Scheme 1



E = Si, Ti; R = Me; R′ = Ph; $x = 1-8$.

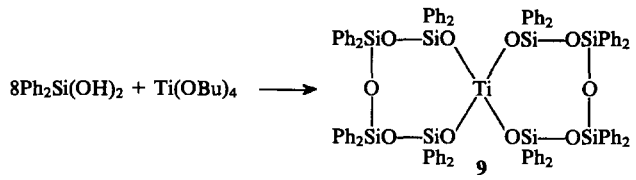
Methylphenylspirocyclosiloxanes, the properties of which have been described,[15, 25, 26] were obtained by means of these reactions. All the compounds synthesised were isolated in 42% to 62% yields and were identified by IR spectroscopy and X-ray diffraction. It is also essential to note that, in the case of the reaction of α, ω-dihydroxyorganosiloxanes with tetrafunctional monomers of the type ECl_4, the reaction proceeds in the direction indicated only in the presence of an acceptor which binds the hydrogen chloride evolved. In the absence of the latter, chlorine-containing cyclosiloxanes, in the molecules of which two chlorine atoms are linked to the silicon atom, are formed preferentially.[14]

Spirobicyclic and polyspirocyclic siloxanes containing titanium as the spiran atom have been obtained by the heterofunctional condensation of linear α, ω-dihydroxyorganosiloxanes with titanium tetrachloride or tetrabutoxytitanium and were identified.[12, 27, 28]



8

The reactions of α,ω-dihydroxyorganosiloxanes with titanium tetrachloride as well as silicon tetrachloride are carried out in the presence of a hydrogen chloride acceptor in anhydrous organic solvents. Under the conditions indicated,[12] the reaction of 1,3-dihydroxytetraphenyldisiloxane with titanium tetrachloride leads to the formation of octaphenyltetrasiloxyspiro[5.5]titanate **8**, which was isolated from the reaction products in a yield of about 14%. The analogous compound **9** with bulky cyclic fragments have been obtained by the reaction of dihydroxydiphenylsilane with tetrabutoxytitanium.[27]

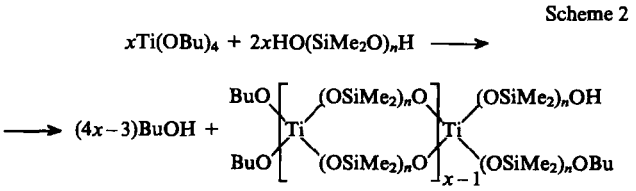


9

Both compounds were characterised by IR spectroscopy and elemental analysis.

Condensation of tetrabutoxytitanium with α,ω-dihydroxypolydimethylsiloxanes[28] having the general formula $HO(SiMe_2O)_nH$, where n is 2, 3, or 4, takes place in conformity with Scheme 2.

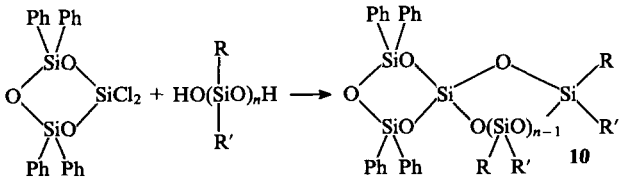
Scheme 2



It has been shown by ^{1}H NMR spectroscopy that the main reaction pathway involves the interaction of the butoxy-groups of tetrabutoxytitanium with the hydroxy-groups of the siloxane. In vacuum at an elevated temperature, the reaction takes place readily with formation of butyl alcohol, the degree of its completion reaching 90%.

One of the versions of the heterofunctional condensation reaction, leading to the formation of organospirocyclosiloxanes, involves the interaction of the bifunctional organosilanes already mentioned and linear organosiloxanes with cyclic di- and tetrafunctional monomers.[7, 10, 11, 29, 30] A series of organodichlorotricyclosiloxanes, organotetrachlorotricyclosiloxanes, and organotetrachlorotetracyclosiloxanes, containing methyl, phenyl, and vinyl substituents at the silicon atom, have now been obtained.[12, 14, 29–31] The study of nucleophilic substitution reactions in organochlorocyclosiloxanes showed that they take place without the cleavage of the siloxane bonds in the rings.[31, 32] This makes it possible to use them as cyclic synthons for the preparation of mixed organospirocyclosiloxanes containing simultaneously different organic substituents in neighbouring rings.[10, 11]

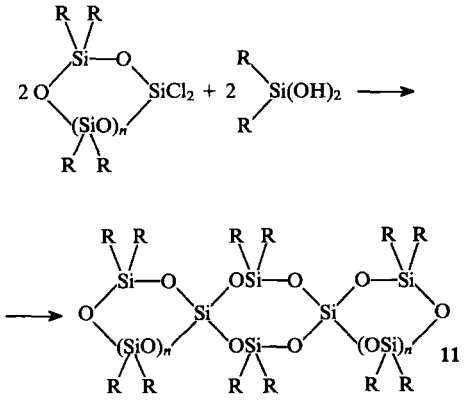
The reactions of organochlorocyclosiloxanes with diorganodihydroxysilanes and α,ω-dihydroxyorganosiloxanes proceed in a complex manner. The yield of organospirocyclosiloxanes depends in this instance to a large extent on the reaction conditions and the organic substituents at the silicon atom. For the equimolar ratio of the initial reactants in the presence of a hydrogen chloride acceptor,[10, 11, 29] the main reaction products are the spirobicyclosiloxanes **10** and spirotricyclosiloxanes **11** having both identical and different sizes of the cyclic fragments in the molecule.[7]



10

for n = 1:	R = R′ = Me	R = Me	R = Me,
for n = 2:	R = R′ = Me	R′ = Ph	R′ = Bu^i

The yield of organospirocyclosiloxanes in these reactions varies from 20% to 48%, the yield of spirobicyclosiloxanes increasing on replacement of the methyl surrounding groups in the diorganodihydroxysiloxane molecule by more bulky substituents, which probably diminish the tendency of diorganodihydroxysiloxanes to enter into homocondensation reactions. The structure of the spirosiloxane thus obtained was confirmed by IR and ^{1}H NMR spectroscopy.

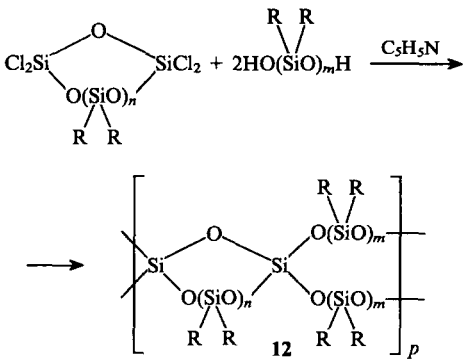


11

R = Me; n = 1, 2.

In contrast to α,ω-dihydroxymethylphenylsiloxanes, the condensation of α,ω-dihydroxyphenylvinylsiloxanes does not lead to the formation of spirocyclic compounds.[12] This is apparently associated with the considerable tendency of compounds in which the silicon atom is surrounded by aliphatic groups to undergo homocondensation.

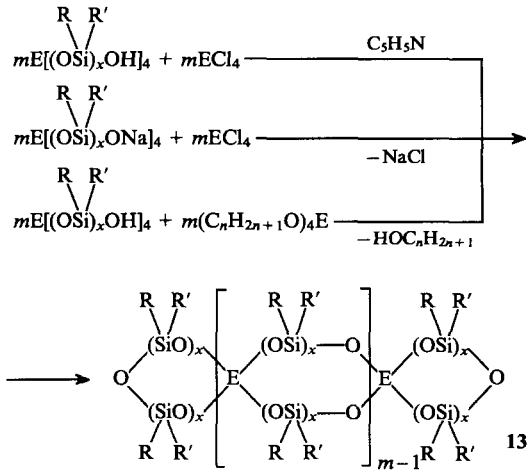
Under conditions analogous to those described above,[30] the oligoorganospirocyclosiloxanes **12** were obtained by the condensation of tetrachlorotetraphenylcyclotetrasiloxane and tetrachlorooctaphenylcyclohexasiloxane with dihydroxydiphenylsilane and 1,3-dihydroxytetraphenyldisiloxane.



12

R = Ph; n = 2, 4; m = 1, 2.

Organospirocyclosiloxanes can also be obtained as a result of the heterofunctional condensation of two tetrafunctional compounds. In this case, a tetrafunctional monomer of the type EX_4 (where E = Si or Ti and X = Cl or OC_nH_{2n+1}) is taken as one of the reactants, while the other is a tetrafunctional compound with a branched or cyclic structure.[3, 16–19, 33–35] Thus the condensation of tetrafunctional compounds having a branched cross-shaped structure with the tetrafunctional monomers indicated above, in proportions of 1 : 1,[3, 16–19] leads to the organospirocylcosiloxanes **13**.

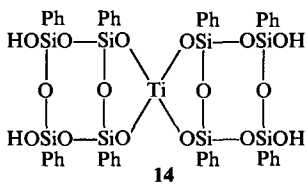


13

E = Si, Ti; R = Me; R′ = Ph; x = 3, 4.

It is noteworthy that the condensation of tetrafunctional monomers with cross-shaped compounds containing a branching titanium atom proceeds readily. The yield of the polycondensation products reaches 63–65% in this case. On passing to compounds with a branching silicon atom, the reaction is retarded and the yield of the reaction product falls to 10%. This mode of reaction is probably due to differences in the steric structure of the above compounds and the influence of the central atom. Nor can one rule out the catalytic action of the titanium atom, which exists in such compounds in a coordinatively unsaturated state.

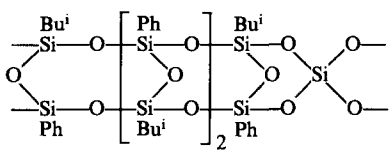
The condensation of tetrafunctional monomers with tetrafunctional cyclic compounds results in the formation of compounds with a spiroladder structure, in contrast to the reaction with tetrafunctional branched organosiloxanes.[33-35] For example, compound **14** was obtained and isolated by the reaction of tetrahydroxytetraphenylcyclotetrasiloxane with tetrabutoxytitanium in proportions of 2 : 1.[34, 35]



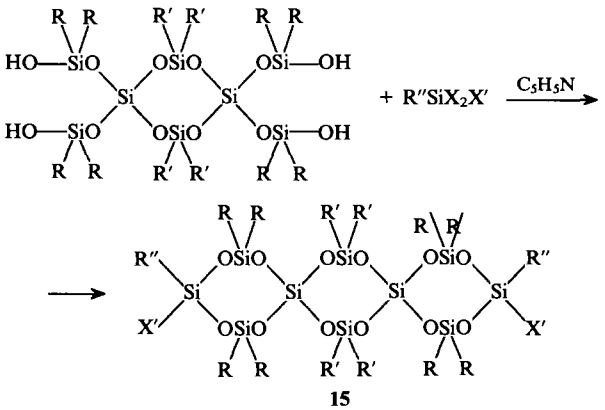
14

Further condensation of this compound leads to a titanophenylsiloxane oligomer containing spirocyclic fragments.[34]

Polyphenylisobutylsiloxane with a spiroladder molecular structure was obtained by the heterofunctional condensation of tetrafunctional polycyclic compounds with carbon tetrachloride. Its elementary unit has the following structure:[33]



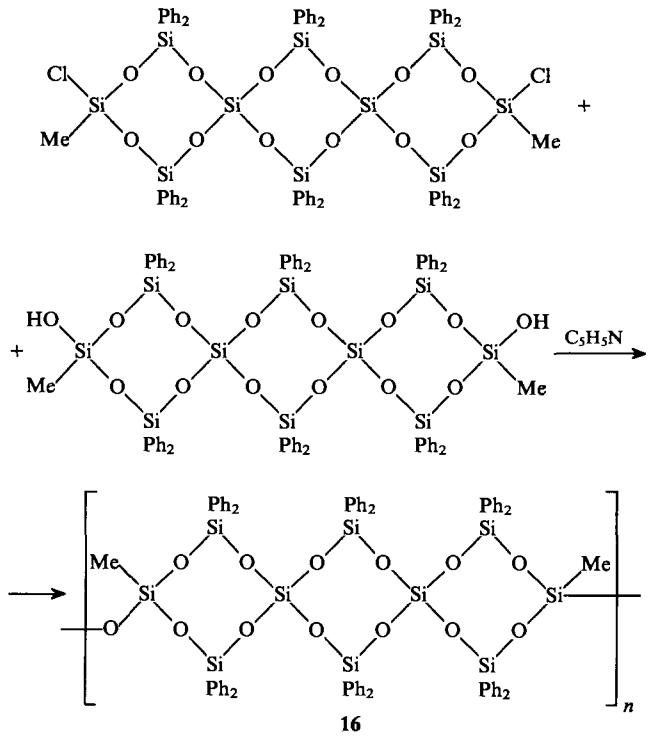
In those cases where the groups surrounding the siloxane chain comprise only phenyl substituents, polymers similar structure are not formed, which is probably due to steric hindrance.[33] Communications describing the synthesis of organospirotricyclic compounds **15** and polymers based on them by the heterofunctional condensation of tetrafunctional branched organocyclosiloxanes and bifunctional organospirocyclosiloxanes with di- and tri-functional organosilicon compounds have been published in recent years.[20, 21, 36-38]



15

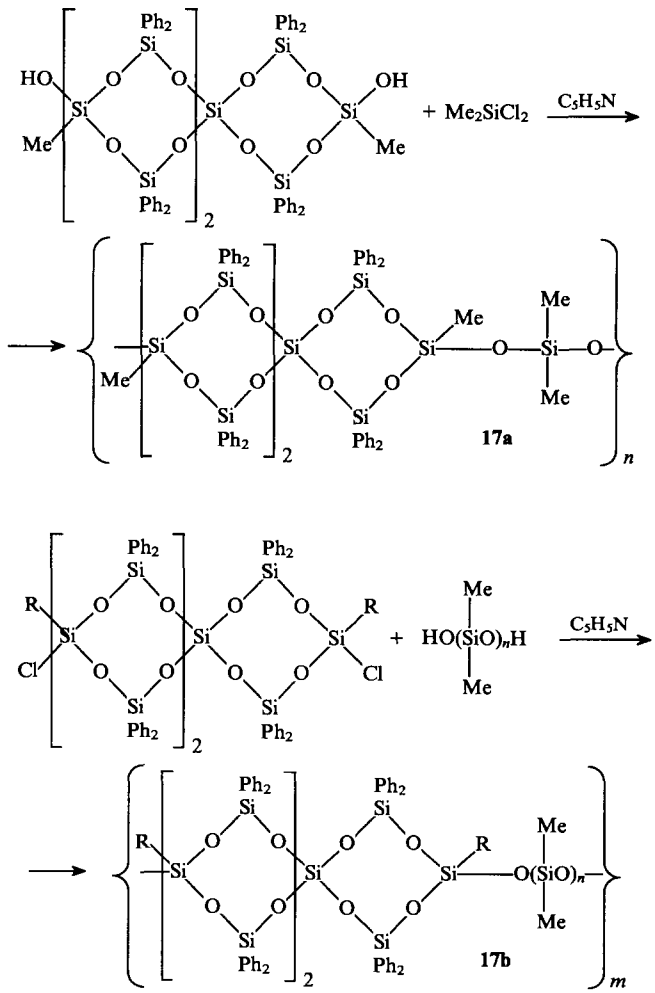
R = R′ = Ph; R″ = Me, Ph; X = Cl; X′ = Cl, OEt, CH=CH$_2$;
R = Et; R′ = R″ = Ph; X = Cl; X′ = Ph;
R = Et; R′ = R″ = Ph; X = X′ = Cl;
R = R″ = Me; R′ = Ph; X = X′ = Cl;
R = Me; R′ = R″ = Ph; X = X′ = Cl.

The products of this reaction, carried out in dilute solutions in the presence of pyridine, are bifunctional spirotricyclosiloxanes (yield from 50% to 75%), whose structure has been confirmed by X-ray diffraction and IR and NMR spectroscopy. The bifunctional organospirocyclosiloxanes obtained by this reaction are capable of interacting with various bifunctional organosilicon compounds and with one another, which leads to the formation of spirocyclolinear polyorganosiloxanes **16** and **17**, whose macromolecules contain rigid fragments with a spiran structure joined together either by an oxygen atom[20, 37] or by dimethylsiloxane units.[20, 37]



16

As in the previous case, the polycondensation reaction is carried out in organic solvents in the presence of pyridine at 50–150 °C.



R = Me, n = 8;
R = Ph, n = 70, 242;
m = 20–60.

For the equimolar ratio of the initial reactants, the yield of the polymers under the conditions indicated reaches 86–92%.

In conclusion, one should note the extensive synthetic possibilities of the heterofunctional condensation method. Spirocyclic compounds with various organic groups surrounding the silicon atom and with different bulk of the cyclic fragments can be obtained by this method in fairly high yields. Both monomeric and oligomeric and polymeric forms of organospirocyclosiloxanes have been obtained by this method and identified.

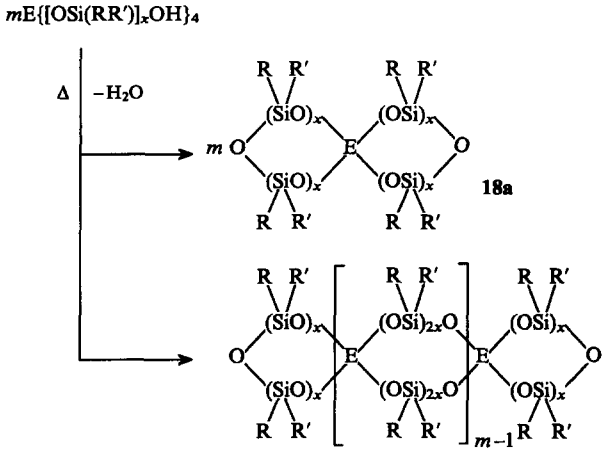
3. Polycondensation of tetrafunctional compounds

The polycondensation of tetrafunctional compounds has been investigated at the present time only for oligomers. The synthesis of organospirocyclosiloxanes by the polycondensation of tetrafunctional cross-shaped oligomers having the general formula

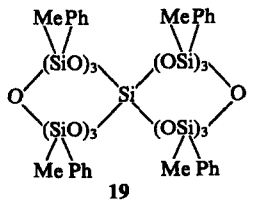
$$E\{[OSi(RR')]_xOH\}_4,$$

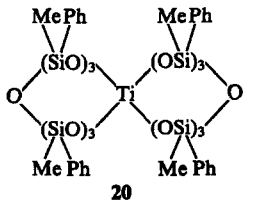
where E = Si, Ti; R = CH_3; R' = C_6H_5, $x = 2-4$, has been described.[3, 15, 16–19]

The block polycondensation of such compounds[15, 39, 40] at 150 °C takes place both intermolecularly and intramolecularly and leads in both cases to the spirocyclic compounds **18**.



The overall yield of the polycondensation products then reaches 70–75%.[15, 40] The spirocyclic structure of the products obtained by this method was demonstrated by isolating the individual compounds and by identifying them by IR spectroscopy and X-ray diffraction. For example, the spirocyclic compounds **19** and **20** were isolated (and identified[15]) in 15 and 10% yields respectively from the products of the polycondensation of tetrakis(3,5,7-trimethyl-3,5,7-triphenylsiloxano-7-hydroxy)silane and tetrakis(3,5,7-trimethyl-3,5,7-triphenylsiloxano-7-hydroxy)-titanium.



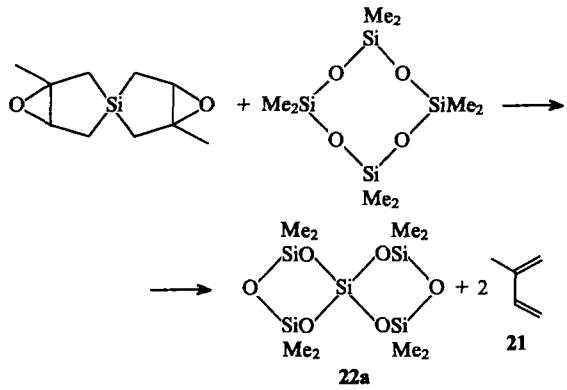


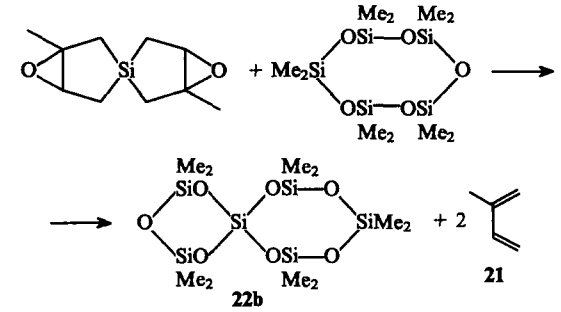
It is also noteworthy that the formation of spirocyclic compounds is observed only in the condensation of oligomers with low values of x.

The above method of synthesis of organospirocyclosiloxanes was not developed further because of its laborious nature.

4. Instantaneous vacuum pyrolysis

Communications describing the synthesis of organospirocyclosiloxanes by the "instantaneous" vacuum pyrolysis of dialkyldiepoxysilaspiroalkanes with organocyclosiloxanes have appeared in the literature in recent years.[41–43] The reaction proceeds in a complex manner via a series of intermediate stages accompanied by the formation of the monomeric silicon dioxide O=Si=O and the so called silanones—reactive intermediates containing silicon–oxygen bonds (silanone intermediates). The final reaction products are[41] isoprene **21** and the corresponding spirosiloxane **22**.





The copyrolysis of 2,3 : 7,8-diepoxy-2,7-dimethyl-5-silaspiro-[4.4]nonane with hexamethylcyclotrisiloxane has been studied in greatest detail. According to the authors,[42] it proceeds stepwise in accordance with Scheme 3.

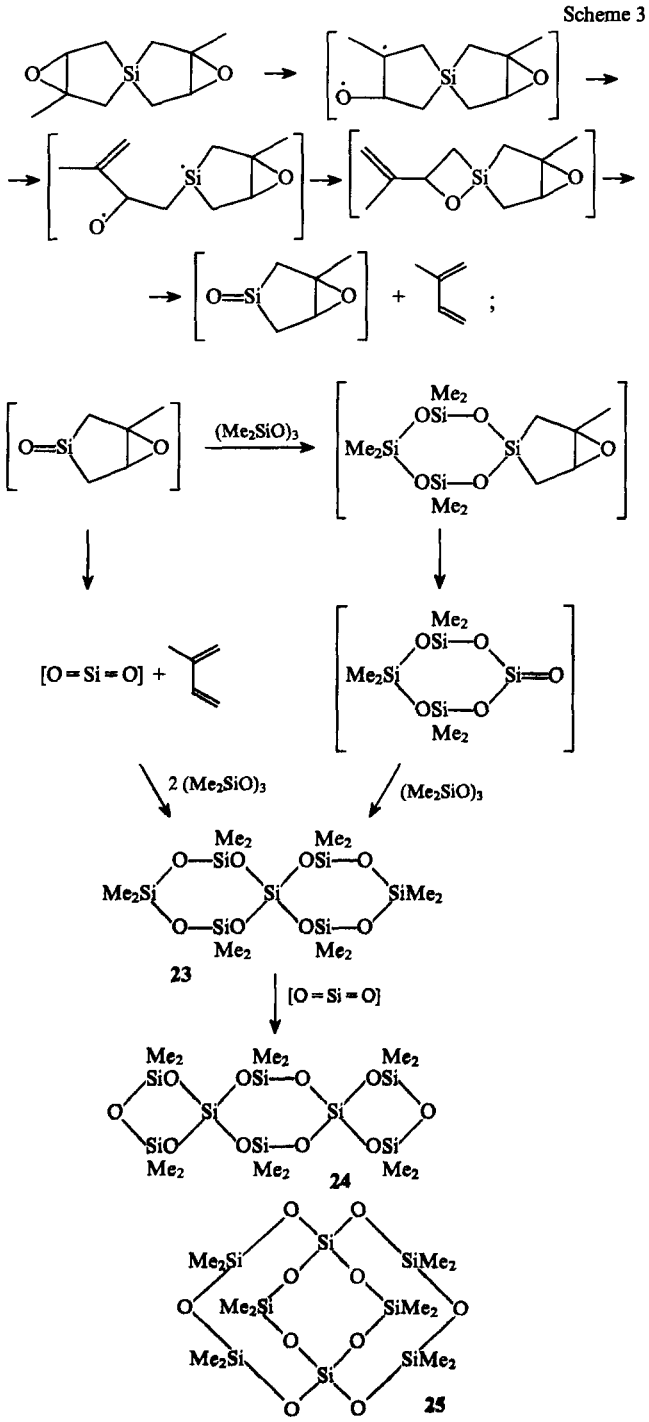
It has been suggested that the reaction begins with the dissociation of the C–O single bond of the bicycle epoxide and with formation of a biradical. The subsequent reactions with its participation lead to silanone intermediates, which are inserted in the Si–O single bonds of the cylcosiloxane and this entails a rearrangement of the siloxane skeleton and ultimately leads to the formation of the corresponding spirosiloxane and isoprene. However, the authors claim[42] that the reaction does not stop at this point and that, together with isoprene and the corresponding spirobicyclosiloxane **23**, a compound with a higher molecular weight is formed. According to X-ray diffraction data, this compound is the spirotricyclosiloxane **24**, which is a product of the interaction of the spirobicyclosiloxane with a second molecule of [O=Si=O]. The interaction of the spirobicyclosiloxane **23** with [O=Si=O] can also lead to the spirotricyclosiloxane **25** according to the results of another study.[43]

The pyrolysis of the above compounds is carried out *in vacuo* at 520 °C. Despite the short residence time of the reactants in the reaction zone, the spirosiloxanes formed under these conditions can probably undergo further reactions. This can be inferred from the low yield of the target products. Thus in most cases of the copyrolysis of 2,3 : 7,8-diepoxy-2,7-dimethyl-5-silaspiro[4.4]-nonane with substituted cyclotrisiloxanes and cyclotetrasiloxanes

(hexaethylcyclotrisiloxane, trimethyltrivinylcyclotrisiloxane, heptamethylcyclotetrasiloxane, heptamethylvinylcyclotetrasiloxane, heptamethylphenylcyclotetrasiloxane, and chloromethylheptamethylcyclotetrasiloxane) the yield of the organospirocyclosiloxanes does not exceed 9%–12%.[41, 42] The structures of all the compounds obtained by this method were confirmed by X-ray diffraction and by ^{29}Si NMR spectroscopy.

Thus, despite the fact that the mechanism of the copyrolysis of dialkyldiepoxysilaspiroalkanes with organocyclosiloxanes has not been elucidated completely and the yield of the target products is low, the method considered is in our view preparative in relation to the synthesis of organospirocyclosiloxanes, is fairly novel, and requires further development.

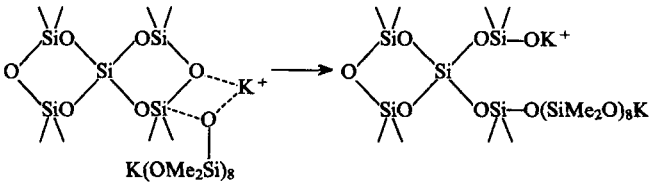
Scheme 3



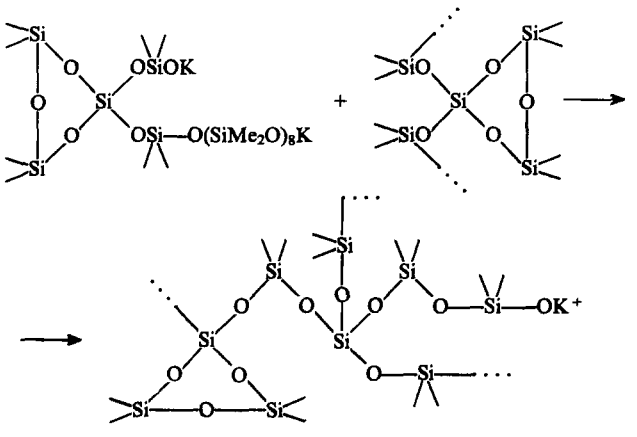
III. Conversion reactions of organospirocyclosiloxanes

The principal reactions involving the conversion of organospirocyclosiloxanes into polymers of different structure are their polymerisation and copolymerisation with organocyclosiloxanes. According to modern ideas, organospirocyclosiloxanes exhibit a functionality of two and four in polymerisation reactions and can form both linear polycyclic polymers and polymers with a three-dimensional structure.[11, 44–49] The catalytic polymerisation of organospirocyclosiloxanes has been little investigated and, in contrast to the polymerisation of organocyclosiloxanes, has a more complex mechanism. In the polymerisation of a spirocyclic compound, the growing polymer chain can enter into two competing reactions. There is then a possibility of either the addition to it of another monomer unit, leading to branching, or the formation of a ring.[11, 45]

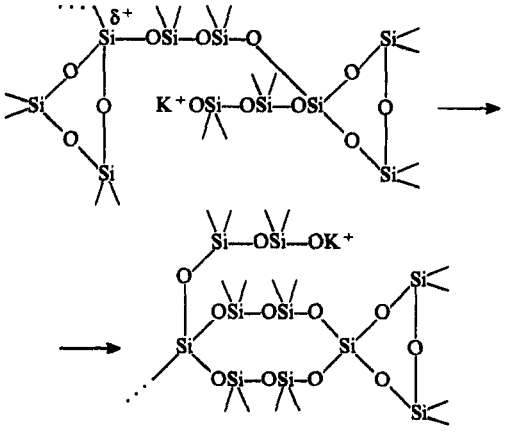
Initiation:



Interchain interaction:

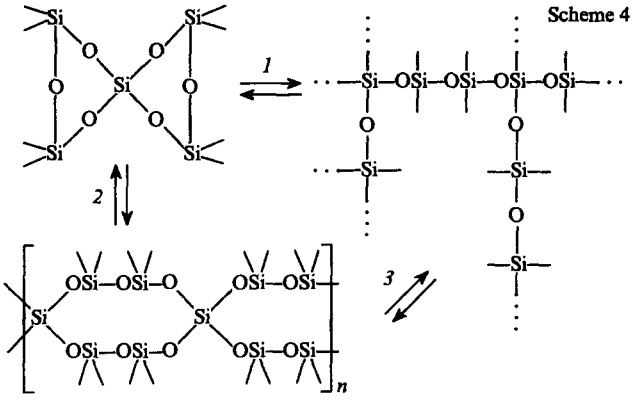


Intrachain cyclisation:



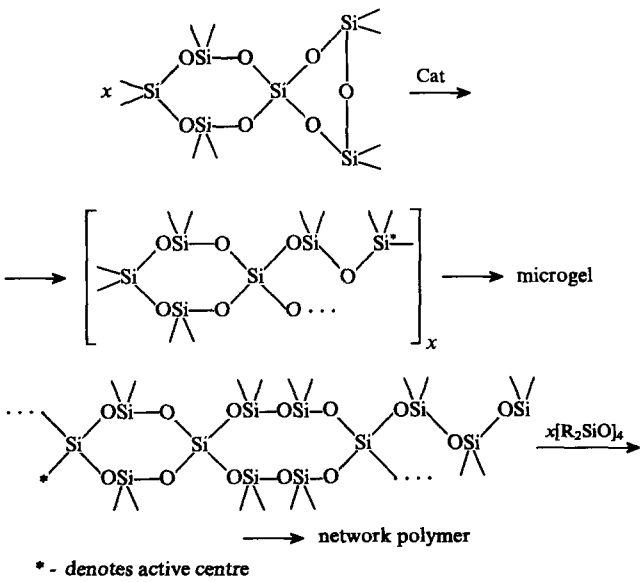
In a general form, the polymerisation of organospirocyclosiloxanes can be represented by Scheme 4, from which it is seen that the polymerisation of organospirocyclosiloxanes develops in the given instance in two directions (reactions *1* and *2* in

Scheme 4). The existence of equilibrium between the soluble and three-dimensionally cross-linked polymers (reaction *3*) has also been established.

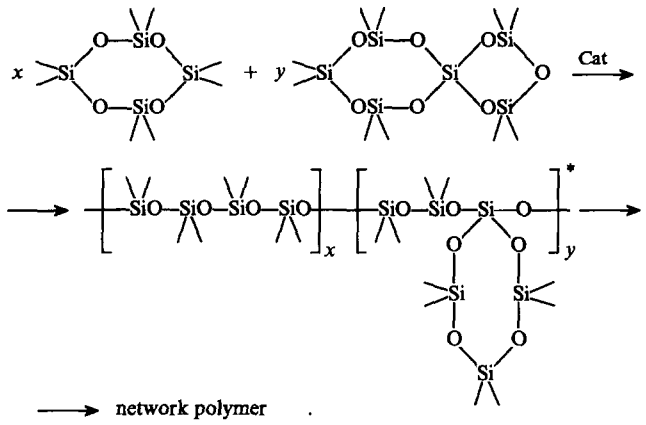


The preferential occurrence of the process via a particular pathway depends mainly on the composition and structure of the initial monomers and also on the reaction conditions. For example, in the case of the anionic polymerisation of spirobicyclic compounds containing only methyl groups at the silicon atom, polymers with a three-dimensional structure are formed.[11, 13] The replacement of some of the methyl groups by phenyl groups leads to a decrease in the equilibrium yield of the gel fraction and, after the complete replacement of methyl groups by phenyl groups or tolyl groups, fully soluble polymers are formed.[14, 44, 46] Consequently pathway *1* predominates for spirosiloxanes with methyl substituents, while pathway *2* is the main one for spirocyclosiloxanes surrounded by phenyl groups. Both pathways operate for spirosiloxanes containing simultaneously both methyl and phenyl groups. It has also been established that there is a definite gel-formation temperature for the process under consideration, above which the formation of a three-dimensional polymer is thermodynamically impossible.[11, 45]

The joint catalytic polymerisation of organospirocyclosiloxanes with organocyclosiloxanes takes place in an even more complex manner and also leads to polymers with a three-dimensional structure.[13, 50–53] In this case, the linear sections of the polymer macromolecules are formed as a result of the polymerisation of the organocyclosiloxane, while the organospirosiloxane, plays the role of a branching agent.[50] A network polymer is formed in this case either as a result of the



homopolymerisation of the spirosiloxane and the formation of microgel particles with subsequent polymerisation of the organocyclosiloxane on the resulting active centres[50] or as a result of the formation in the first stage of the process of a linear polymer containing cyclic fragments, which subsequently passes to an insoluble state as a result of the opening of these fragments by catalytically active centres.[50, 52] The predominance of a particular process is determined by the reactant ratio:

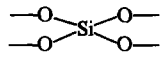


An example of a process leading to three-dimensional polymers may also be provided by the copolymerisation reactions of organospirocyclosiloxanes with linear dihydroxypolydimethylsiloxanes.[54] As in the previous cases, the spirosiloxane plays the role of a branching agent and the polymer chains are cross-linked as a result of the opening of the siloxane rings by the silanolate anions located at the ends of the polymer chains or arising as a result of the exchange between the proton of a hydroxy-group of the dihydroxypolydimethylsiloxane and the cation of the silanolate group of the initiator (Scheme 5).[55]

The subsequent attack by the cyclic fragments of the polymer chain leads to cross-linking. It has been shown that the introduction of α,ω-dihydroxypolydimethylsiloxanes (n = 24–270) into the polymerisation-exchange process makes it possible to obtain three-dimensionally cross-linked polymers with a regular distribution of branching nodes in the network.[56]

IV. Certain physicochemical properties of organospirocyclosiloxanes

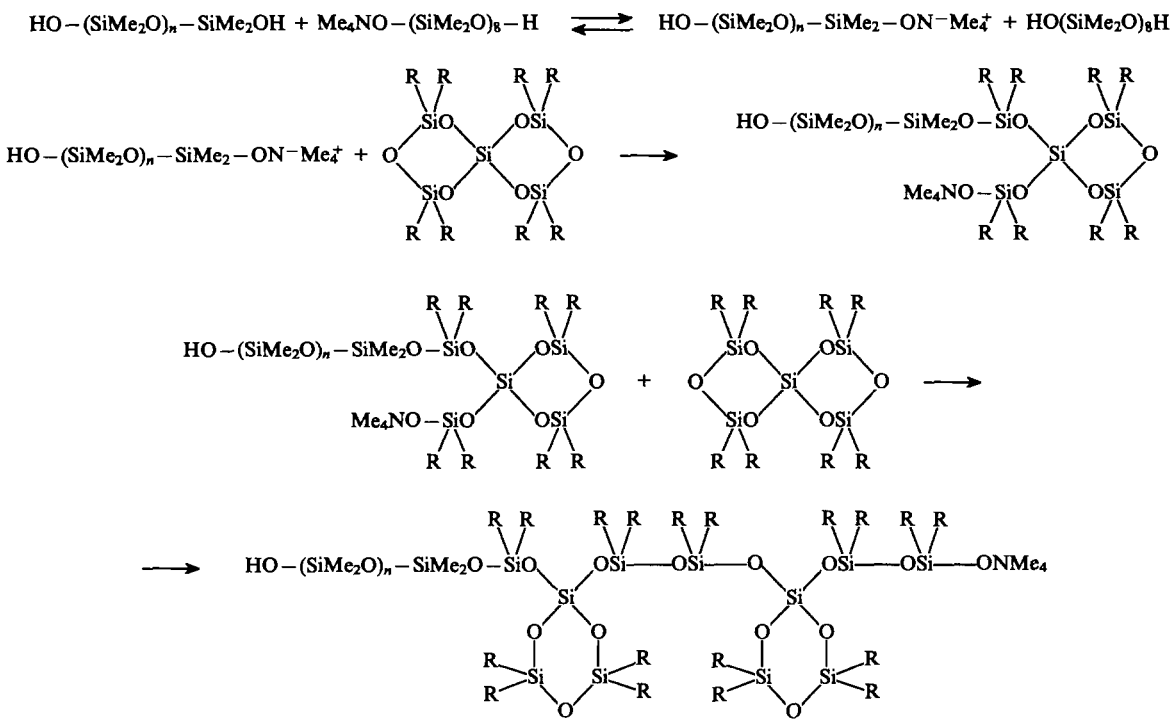
A specific feature of organospirocyclosiloxanes, which distinguishes them from simple organocyclosiloxanes, is the presence of the group



which can be detected with the greatest reliability by means of NMR spectroscopic data. The study of the ^{29}Si NMR spectra of a series of organospirocyclosiloxanes with different surrounding organic groups and different ring sizes showed that signals in the range 6–30 ppm, referring to the silicon atoms of the siloxane rings, and signals in the range 95–105 ppm, corresponding to the silicon atom in the spiro-position, are characteristic of these compounds.[21, 41, 42]

The ring conformations and the geometrical features of the spiro-nodes of organospirocyclosiloxanes[2, 9, 42, 57–62] and organospirocyclosilazoxanes[63, 64] have been determined by X-ray diffraction. It has been shown that the silicon atoms at the spiro-nodes have a fairly rigid tetrahedral coordination; this structural feature is retained also on substitution of the oxygen atoms in the spiro-environment by nitrogen atoms.[64] As already mentioned above, the Si–O bonds at the spiro-nodes of siloxanes are usually somewhat shortened compared with the Si–O bonds of the cyclic

Scheme 5



fragments. On substitution of some of the oxygen atoms in the spiro-environment by nitrogen atoms in the molecules of organospirocyclosilaxanes, the shortening of the Si–O bond lengths becomes extremely insignificant or is altogether absent, which has been attributed to the lower electronegativity of nitrogen compared with oxygen.[62–64]

The trisiloxane rings forming part of spirocyclosiloxanes have an almost planar structure close to that of the molecules of organocyclotrisiloxanes.[58] Analysis of the conformations of the tetrasiloxane rings in the molecules of spirotricyclosiloxanes and spiropentacyclosiloxanes showed that the central rings in these compounds are appreciably flattened compared with the spiro-linked rings surrounding them, which in the authors view[9, 61] is due to steric factors.

The manifestation of the skeletal vibrations of the Si–O bonds of organospirocyclosiloxanes in the IR spectra is also of interest. As a result of the differences between the Si–O bonds of the spiro-node and the siloxane side fragments noted above, one may expect that the characteristic features of the structure of organospirocyclosiloxanes will be manifested in the IR spectra of these compounds.

The most intense absorption in the IR spectra of organo-spirocyclosiloxanes is observed in the range 1020–1100 cm^{-1}. It is characteristic of antisymmetrical stretching vibrations of the Si–O–Si bridge bonds. It has been shown in a number of studies that the Si–O bond vibrations in spirosiloxanes are manifested by a characteristic split ν_{as}(SiOSi) band with two maxima.[3, 8, 10, 15, 29, 31] The positions of these maxima depend on the number of silicon atoms in the ring. On passing from spirocyclic compounds with a smaller number of silicon atoms in the cyclic fragment to compounds with a larger number of such atoms, the ν_{as}(SiOSi) band undergoes a hypsochromic shift. At the same time, the symmetrical stretching vibration frequency ν_s(SiOSi) in the spectra of organospirocyclosiloxanes increases compared with the corresponding vibration in simple organocyclosiloxanes.[3, 15] The observed features of the IR spectra of the spirocyclic compounds of the siloxane series have been attributed[3, 15] to the presence of a branching centre and have been assigned to the vibrations of the Si–O–Si groups adjoining the central spiro-atom and constituting together with the latter a single structural nucleus. However, hitherto there is no unanimous view in the interpretation of the characteristics of the IR spectra of the above compounds. A number of investigators believe that a similar splitting of the ν_{as}(SiOSi) band is characteristic also of the spectra of linear and cyclic compounds containing more than four siloxane units.[2, 65–67]

In the case of spirocyclic compounds containing titanium as the spiro-atom,[3, 12, 15, 27, 28, 68, 69] the IR spectra show, apart from the splitting of the ν_{as}(SiOSi) band into two maxima mentioned above, an intense absorption in the range 910–930 cm^{-1} due to the vibrations of the TiOSi fragment.

In comparing the methods of synthesis of organospiro-cyclosiloxanes examined in this review, one should note that the heterofunctional condensation method is at present the most thoroughly developed and preparatively and technologically most convenient, ensuring a fairly high yield of the target products. Spirocyclic oligomers, on the basis of which a series of composite materials with unique properties have been developed, have now been obtained by this method. These materials are used successfully in various branches of modern engineering.

References

1. R S Cahn, O C Dermer *An Introduction to Chemical Nomenclature* (Translated into Russian) (Moscow: Khimiya, 1983)
2. V E Shklover, Yu T Struchkov *Usp. Khim.* **59** 518 (1980) [*Russ. Chem. Rev.* **59** (1980)]
3. K A Andrianov *Dokl. Akad. Nauk SSSR* **191** 347 (1970)
4. V A Mostyaev, S I Pekarskaya, M A Sipyagina, A S Rodichev, V D Lavrentsov, Z D Kasatochkina in *Elektronnaya Tekhnika* (*Radiodetali i Radiokomponenty*) [Electronic Engineering (Radio Units and Radio Components)] (Moscow, 1985) p. 60
5. D W Scott *J. Am. Chem. Soc.* **68** 356 (1946)
6. US P. 2 418 051; *Chem. Abs.* **51** 514 508 (1957)
7. A B Zachernyuk, A A Zhdanov, V E Shklover *Zh. Obshch. Khim.* **57** 562 (1987)
8. K A Andrianov, A B Zachernyuk, G V Solomatin *Dokl. Akad. Nauk SSSR* **236** 601 (1977)
9. V E Shklover, Ju T Struchkov, A B Zachernyuk, A A Zhdanov *Cryst. Struct. Commun.* 1771 (1982)
10. K A Andrianov, A B Zachernyuk, B D Lavrukhin, N G Vasilenko *Dokl. Akad. Nauk SSSR* **204** 1112 (1972)

11. K A Andrianov, A B Zachernyuk *Vysokomol. Soedin.* **16A** 1435 (1974)
12. K A Andrianov, N A Kurasheva, L I Kuteinikova *Zh. Obshch. Khim.* **46** 1533 (1976)
13. R Mayo Frank *J. Polym. Sci.* **55** 65 (1961)
14. T C Wu, C A Hirt *J. Organomet. Chem.* **11** 17 (1968)
15. K A Andrianov, M A Sipyagina, N P Gashnikova *Izv. Akad. Nauk SSSR, Otd. Khim. Nauk* 2493 (1970)
16. US P. 3 817 917 (1974)
17. B P. 1 329 180 ; *Chem. Abs.* **80** 37 626m (1974)
18. BRD P. 2 138 824; *Chem. Abs.* **79** 6100k (1973)
19. French P. 2 151 510 (1973)
20. A A Zhdanov, N A Kurasheva, E S Khynku *Izv. Akad. Nauk Kaz. SSR* 38 (1981)
21. A A Zhdanov, E S Khynku, O B Gorbatsevich, B D Lavrukhin *Zh. Obshch. Khim.* **56** 1076 (1986)
22. K A Andrianov, N A Sipyagina, N A Dyudina, E I Voronina, in *V Vsesoyuznaya Konferentsiya po Khimii i Primeneniyu Kremniiorganicheskikh Soedinenii (Tezisy Dokladov)* [The Vth All-Union Conference on the Chemistry and Applications of Organosilicon Compounds (Abstracts of Reports)] (Tbilisi: IIKht, 1980) p. 237
23. K A Andrianov, M A Sipyagina, N A Dyudina in, *Khimiya i Tekhnologiya Organicheskikh Proizvodstv, T.7, Mezhvuzovskii Tematicheskii Sbornik* (The Chemistry and Technology of Organic Manufacturing Processes, Vol. 7., Intercollegiate Topical Collection) (Moscow: MIKhM, 1977) p. 67
24. K A Andrianov, M A Sipyagina, A G Kolchina, N A Dyudina, L M Kostryukova, in *Khimiya i Tekhnologiya Organicheskikh Proizvodstv, T.7, Mezhvuzovskii Tematicheskii Sbornik* (The Chemistry and Technology of Organic Manufacturing Processes, Vol. 7., Intercollegiate Topical Collection) (Moscow: MIKhM, 1977) p. 77
25. K A Andrianov, V I Elinek, M A Sipyagina, E P Agapova *Izv. Akad. Nauk SSSR, Otd. Khim. Nauk* 2145 (1971)
26. K A Andrianov, M A Sipyagina, V Ya Kovalenko, A G Kolchina, T S Bebchuk *Izv. Akad. Nauk SSSR, Otd. Khim. Nauk* 1318 (1972)
27. V A Zeitler, C A Brown *J. Am. Chem. Soc.* **79** 4618 (1957)
28. K A Andrianov, N A Kurasheva, B D Lavrukhin, L I Kuteinikova *Vysokomol. Soedin.* **14A** 2450 (1972)
29. K A Andrianov, A B Zachernyuk, B D Lavrukhin *Dokl. Akad. Nauk SSSR* **204** 593 (1972)
30. S M Meladze, O V Mukbaniani, L M Khananashvili, G G Andronikashvili *Vysokomol. Soedin.* **23B** 590 (1981)
31. A B Zachernyuk, E A Burlova, A A Zhdanov *Zh. Obshch. Khim.* **55** 1368 (1985)
32. K A Andrianov, A B Zachernyuk *Khim. Geterotsikl. Soedin.* 1183 (1972)
33. K A Andrianov, V N Tsvetkov, M G Vitovskaya, N N Makarova, P N Lavrenko, T I Garmonova, E P Astapenko, S V Bushin *Vysokomol. Soedin.* **13A** 2746 (1971)
34. K A Andrianov, V S Tikhonov, I Yu Klement'ev in *Uchenye Zapiski MITKhT* (Scientific Reports from the Moscow Institute of Fine Chemical Engineering) (Moscow: Izd. MITKhT, 1974) Vol. 1, p. 70
35. K A Andrianov, V S Tikhonov, I Yu Klement'ev, N A Babkina *Tr. MITKhT* **3** 67 (1974)
36. A A Zhdanov, E F Khynku, N A Kurasheva, V E Shklover *Dokl. Akad. Nauk SSSR* **250** 1392 (1980)
37. A A Zhdanov, N A Kurasheva, E S Khynku *Vysokomol. Soedin.* **22B** 624 (1980)
38. E S Khynku, O V Gorbatsevich, in *VI Vsesoyuznaya Konferentsiya po Khimii i Primeneniyu Kremniiorganicheskikh Soedinenii, Riga, 1986 (Tezisy Dokladov)* [The VIth All-Union Conference on the Chemistry and Applications of Organosilicon Compounds. Riga, 1986 (Abstracts of Reports)] (Riga: Inst. Org. Sinteza Akad. Nauk Latv. SSR, 1986) p. 239
39. N P Gashnikova, M A Sipyagina, K A Andrianov, in *VI Vsesoyuznaya Konferentsiya po Khimii i Primeneniyu Kremniiorganicheskikh Soedinenii, Moskva, 1968 (Tezisy Dokladov)* [The VIth All-Union Conference on the Chemistry and Applications of Organosilicon Compounds. Moscow, 1968 (Abstracts of Reports)] (Moscow: Izd. NIITEKhIM, 1968) p. 35
40. K A Andrianov, M A Sipyagina, in *Kremniiorganicheskie Soedineniya. Vyp. III. Moskva, 1966 (Tr. Soveshch.)* [Organosilicon Compounds. No. III, Moscow, 1966 (Conference Proceedings)] (Moscow: Izd. NIITEKhIM, 1967) p. 47
41. D J Clifford, W P Weber *J. Organomet. Chem.* **308** 187 (1986)
42. G K Genry, D R Dowd, G Mannuel, W P Weber *Organometallics* 1818 (1986)
43. W P Weber, S A Kazoura, G Mannuel, G Bertrand, in *VIIth International Symposium on Organosilicon Chemistry, (Abstracts of Papers) Kyoto 1984* p. 99
44. K A Andrianov, A B Zachernyuk *Vysokomol. Soedin.* **16B** 307 (1974)
45. K A Andrianov *Vysokomol. Soedin.* **20A** 243 (1978)
46. K A Andrianov, A B Zachernyuk *Pure Appl. Chem.* **48** 251 (1976)
47. K A Andrianov, M A Sipyagina, N A Dyudina, Yu V Zherdev, N P Gashnikova *Dokl. Akad. Nauk SSSR* **241** 1089 (1978)
48. K A Andrianov, A B Zachernyuk *Polym. Prepr.* **16** 442 (1975)
49. V V Korshak *Uspekhi v Oblasti Sinteza Elementoorganicheskikh Polimerov* (Advances in the Synthesis of Organoelement Polymers) (Moscow: Nauka, 1988)
50. K A Andrianov, E A Burlova, A B Zachernyuk *Vysokomol. Soedin.* **19B** 211 (1977)
51. K A Andrianov, G V Vinogradov, Yu G Yanovskii, A B Zachernyuk, E A Burlova, S I Sergeenkov *Dokl. Akad. Nauk SSSR* **232** 810 (1977)
52. A B Zachernyuk, E A Burlova, A A Zhdanov *Vysokomol. Soedin.* **29A** 1548 (1987)
53. E A Burlova, A B Zachernyuk, A A Zhdanov, in *VI Vsesoyuznaya Konferentsiya po Khimii i Primeneniyu Kremniiorganicheskikh Soedinenii, Riga, 1986 (Tezisy Dokladov)* [The VIth All-Union Conference on the Chemistry and Applications of Organosilicon Compounds. Riga, 1986 (Abstracts of Reports)] (Riga: Inst. Org. Sinteza Akad. Nauk Latv. SSR, 1986) p. 26
54. K A Andrianov, A B Zachernyuk, E A Burlova *Dokl. Akad. Nauk SSSR* **236** 873 (1977)
55. K A Andrianov, A I Chernyshev, V A Temnikovskii, V V Yastrebov, V M Kopylov *Teor. Eksp. Khim.* **11** 678 (1975)
56. USSR P. 529 181; *Byul. Izobret.* **35** (1976)
57. N G Bokii, Yu T Struchkov *Zh. Strukt. Khim.* **9** 722 (1968)
58. V E Shklover, M G Bokii, Yu T Struchkov, K A Andrianov, A B Zachernyuk *Zh. Strukt. Khim.* **15** 857 (1974)
59. V E Shklover, Yu T Struchkov, K A Andrianov, A B Zachernyuk *Zh. Strukt. Khim.* **19** 116 (1978)
60. V E Shklover, Yu T Struchkov, G V Solomatin, A B Zachernyuk, K A Andrianov *Zh. Strukt. Khim.* **20** 309 (1979)
61. I L Dubchak, V E Shklover, Yu T Struchkov *Zh. Strukt. Khim.* **5** (24) 121 (1983)
62. I L Dubchak, V E Shklover, Yu T Struchkov, E S Khynku, A A Zhdanov *Zh. Strukt. Khim.* **25** (4) 74 (1984)
63. V E Shklover, T Ad'yaasuren, G V Kotrelev, E A Zhdanova, V S Svistunov, Yu T Struchkov *Zh. Strukt. Khim.* **21** (2) 94 (1980)
64. Yu E Ovchinnikov, V E Shklover, Yu T Struchkov, A B Zachernyuk, A A Zhdanov, V B Isaev *Metalloorg. Khim.* **1** 1121 (1988)
65. A N Lazarev *Kolebatel'nye Spektry i Stroenie Silikatov* (The Vibrational Spectra and Structure of Silicates) (Leningrad: Nauka, 1968)
66. A N Lazarev, I S Ignat'ev, T S Tenisheva *Kolebaniya Prostykh Molekul so Svyazami Si–O* (The Vibrations of Simple Molecules with Si–O Bonds) (Leningrad: Nauka, 1980)
67. J Haslam, H A Willis *Identification and Analysis of Plastics* (Translated into Russian) (Moscow: Khimiya, 1971) p. 431
68. V A Zeitler, C A Brown *J. Phys. Chem.* **61**(7) 1174 (1957)
69. V A Leither, C A Brown *J. Am. Chem. Soc.* **79** 4616 (1957)

Russian Chemical Reviews **62** (3) 203 – 226 (1993)
© 1993 Russian Academy of Sciences and Turpion Ltd

UDC 621.37 + 541

Macroscopic kinetics of thermochemical processes on laser heating: current state and prospects

N V Karlov, N A Kirichenko, B S Luk'yanchuk

Contents

I.	Introduction	203
II.	History of the problem	204
III.	Thermochemical processes stimulated by laser radiation in homogeneous media	205
IV.	Thermochemical processes in the laser heating of metals	211
V.	Physicochemical processes in the laser heating of liquids	215
VI.	Some technological applications	218

Abstract. The characteristic features of the kinetics and dynamics of processes occurring on laser heating of chemically reactive media are analysed. Attention is concentrated on effects due to the macroscopic disequilibrium and the feedbacks between various degrees of freedom of thermochemical systems. Processes stimulated by laser radiation in homogeneous media, the phenomena occurring on laser heating of metals, and the physicochemical processes occurring on laser heating of liquids are considered. Examples of certain technological applications of laser thermochemistry are presented: laser-induced precipitation of a substance from the gas phase, etching and modification of surfaces, synthesis of compounds, etc. The bibliography includes 123 references.

I. Introduction

Among the effects associated with the chemical reactions of substances in the field of a powerful light wave, the photochemical and thermochemical effects differ significantly. Until the end of the 1970s, mainly photochemical processes were investigated. However, during the last decade, there has been a sharp growth of interest in thermochemical processes. This is associated with their wide occurrence and the prospects for their employment to create new progressive technologies in many branches of industry, and effective research methods in the field of nonlinear dynamics.

The characteristic features of the kinetics of thermochemical processes occurring on laser heating of chemically reactive media are associated principally with two factors: with the disequilibrium due to the nonstationary and/or inhomogeneous occurrence of reactions and with the mutual influence (feedback) between the chemical state of the medium and energy and mass transfer processes in the field of the laser radiation. Therefore the main problems in modern laser thermochemistry are as follows: analysis of the mechanisms of the generation of feedbacks between the chemical, thermal, and other degrees of freedom† of the system in various problems; the discovery of the most typical nonlinear features and analysis of the influence of various feedback channels on the kinetics and dynamics of thermochemical processes; the study of self-organisation phenomena induced by the laser radiation during the heating of the test substances; the search for the possible ways of achieving an effective control of thermochemical processes with the aid of lasers.

The complexity of such studies is due to the great variety of specific conditions under which nonlinear thermochemical processes take place, the wide range of variation in the rates of chemical reactions, the different phase states of the reactants (solids, liquids, and gases), and the multiplicity of procedures for the laser heating of chemically reactive media.

In the present review, we have tried to describe the ideas and theoretical and experimental results constituting the basis of modern research into the nonlinear dynamics of laser-induced thermochemical processes. If one compares them with studies carried out within the framework of the macroscopic kinetics and physics of combustion, where the role of disequilibrium and of the feedbacks between different degrees of freedom of the system is also significant, then two factors should be noted. First, the thermochemical processes occurring under the influence of laser radiation are frequently characterised by a high level of disequilibrium. For example, in the laser-induced chemical precipitation of a substance from the gas phase, the temperature may vary at rates up to 10^{10} K s^{-1} and there is a possibility of temperature gradients up to 10^{7} K cm^{-1}. The latter factor leads, in particular, to an intense interaction of the thermal, concentration, charge, and other fluxes and can ultimately alter radically the kinetics of the respective processes. Second, laser radiation is itself capable of generating new feedback channels in

N V Karlov Moscow Institute of Physics and Technology, Institutskii per. 9, Dolgoprudnyi, 141700 Moscow Region, Russian Federation, Fax (7-095) 485 44 72
N A Kirichenko, B S Luk'yanchuk Laboratory of the Macrokinetics of Nonequilibrium Processes, Institute of General Physics, Russian Academy of Sciences, ul. Vavilova 38, 117942 Moscow V-333, Russian Federation, Fax (7-095) 135 02 70

Received 22nd December 1992
Uspekhi Khimii **62** (3) 223 – 248 (1993); translated by A K Grzybowski

† The degree of freedom is a concept which arose from classical mechanics. In nonlinear dynamics, this concept is used to designate some kind of dynamic characteristic describing the state of the system, for example temperature, concentration of the reactants, etc. The term 'degree of freedom' is frequently used in relation to each differential first-order equation describing the variation of physically different characteristics (thermal degree of freedom, chemical degree of freedom, etc.). The reader may become acquainted with the principal concepts of nonlinear dynamics in the book by M I Rabinovich and D I Trubetskov, *Vvedenie v Teoriyu Kolebanii i Voln* (Introduction to the Theory of Vibrations and Waves) (Moscow: Nauka, 1984).

the system and of altering the dynamic properties of the medium. These factors do in fact indicate the specific features of the laser heating of chemically reactive media compared with heating by nonlaser sources.

II. History of the problem

Quantitative methods for the description of the dynamics of chemical systems arose long after the formulation of the fundamental theoretical ideas in mechanics, optics, theory of electricity, hydrodynamics, and classical electrodynamics. The first fundamental equations of the law of mass action were proposed by Guldberg and Waage, while the mathematical laws of chemical reactions were first formulated and elucidated by van't Hoff.‡ Arrhenius explained the mechanism of the temperature variation of the reaction rate constants and formulated the second fundamental law of chemical kinetics (the Arrhenius equation).

The fundamentally nonlinear nature of these laws makes it possible to understand the theoretical difficulties and problems in the analysis of the dynamics of chemical systems which arose in the initial stage of the development of chemical kinetics. These difficulties were overcome only as a result of the development and application to chemical systems of the ideas and methods of the theory of nonlinear oscillations. (The role which chemical systems have played in the formulation of nonlinear concepts and images such as autowave, reverberator, dissipative structure, etc. is in its turn also well known.)

During the period from 1928 to 1940, Semenov, Zel'dovich, Frank-Kamenetskii, Kharitonov, Todes, and others carried out fundamental studies in the field of the chemical kinetics and physics of combustion, where the dynamics of chemical systems with feedbacks between chemical, thermal, and other degrees of freedom came to the fore. These investigations served as the basis of a new scientific discipline — macroscopic kinetics, within the framework of which the most important basic models, specifying the mechanisms and dynamic manifestations of the action of feedbacks in thermochemical systems, were created and developed.[1,2] Studies on oscillatory chemical reactions have played an important role in the development of macrokinetics.[3-6]

Studies on chemical thermodynamics, devoted to the investigation of the states of equilibrium in chemical systems, served as an ideologically important addition to the research into chemical kinetics. This branch of research, associated with the names of Gibbs, Helmholtz, van't Hoff, van der Waals, Nernst, and others, underwent a qualitatively new development when the ideas of chemical thermodynamics began to be applied to the analysis of nonequilibrium systems. As a result of studies by Onsager, the linear nonequilibrium thermodynamics was created, while studies by Prigogine led to the formulation of nonlinear nonequilibrium thermodynamics and completed the process of merging chemical kinetics and chemical thermodynamics into a single integral science.

Laser thermochemistry constitutes in essence a development and a generalisation of the ideas of macroscopic kinetics and nonequilibrium thermodynamics in relation to a substance placed in the field of laser radiation.

Immediately after the creation of lasers, it was by no means a simple matter to decide whether this introduced anything new into chemistry. Lasers were used initially in photochemistry as sources with a high spectral brightness. The most important discoveries were made when quantum electronics 'assimilated' the IR range. These discoveries are well known (see, for example, Refs 7-12). They include the multiphoton IR photodissociation of molecules, selective as regards substances, which permits laser separation of isotopes, the elimination of small amounts of impurities from gases, etc., as well as effects associated with the generation of a disequilibrium at the level corresponding to the separation between the vibrational and translational temperatures, which permit the laser control of radical synthesis (in particular permit the synthesis of thermally less stable compounds on IR photolysis of more stable compounds — for example the synthesis of CF_3I by the photolysis of CF_3Br in an iodine atmosphere[13]).

Studies in the field of reactions initiated by laser heating developed more slowly. According to Tal'roze's estimates,[14] 170 studies devoted to the thermochemical effect of laser radiation were published in 1977. Among them, it is possible to distinguish three groups of investigations the results of which were of value for subsequent research into the nonlinear dynamics of thermochemical processes.

1. Experimental and theoretical studies devoted to the development of thermochemical instability in reactions involving the heterogeneous oxidation of metals in air under the influence of laser radiation.[15-17]

2. Studies on the thermal bistability and dissipative structures on heating gaseous media by optical radiation.[11,18,19] In a number of investigations,[15-19] attention was first drawn to the fact that a new feedback channel between the chemical and thermal degrees of freedom of the system is created in the field of laser radiation. This feedback is achieved via a change in the absorption characteristics of the system during chemical reaction. In particular, when radiation is absorbed preferentially by the chemical reaction product, a positive feedback is generated in the system, leading to thermochemical instability, bistability, etc.

3. Studies undertaken to determine the conditions governing the separation between the vibrational and translational temperature on laser stimulation of homogeneous reactions (see, for example, Refs 7, 9-14, 20-22). These investigations showed that, at pressures of the gas mixture above 1 torr under typical experimental conditions with continuous-wave CO_2 lasers, the thermal mechanism of chemical reactions predominates in the majority of substances. For this reason, all the remarkable properties of IR-photochemical processes, attention to the possible manifestation of which was drawn already in the studies by Askar'yan (1964) and other workers (for the history of this problem, see Dunskaya[23]), therefore occur as a rule only at fairly low gas pressures. On the other hand, in experiments (see, for example, Oraevskii[9] and Molin et al.[11]) at high pressures of the gas mixture, a marked difference is observed between the products of laser and nonlaser pyrolysis. A marked dependence of the yield of the reaction on the wavelength of the laser radiation, threshold phenomena, etc. were observed. The experimental results clearly indicated a specific disequilibrium of the chemical process during the IR-laser heating of the gases, but the fundamental details of the generation of such disequilibrium remained obscure. The observed discrepancy between the seemingly photochemical behaviour of a number of reactions and the explicit thermal regime governing the injection of the energy of the laser radiation aroused a lively controversy between supporters of particular mechanisms for these reactions. It was of interest to note that at approximately this time a controversy of a similar nature arose concerning the thermal and nonthermal nature of the laser-induced annealing of semiconductors.[24,25]

Thus towards the end of the 1970s, the situation was objectively prepared for the vigorous development of research into the dynamics of the laser heating of chemically reactive media, analysis of the dynamics of heating in the IR spectral range being particularly timely.

‡ Van't Hoff's book *An Outline of Chemical Dynamics* was published in 1884. It laid the foundations for the development of chemical kinetics and, in Semenov's words, outlined the path for its development during the next half century.

III. Thermochemical processes stimulated by laser radiation in homogeneous media

1. The macroscopic disequilibrium and feedbacks

The interaction of light with matter is a complex nonlinear process, which can be arbitrarily divided into several stages: the absorption of light by matter; energy and matter transfer (processes involving heat and mass exchange with the surrounding medium, redistribution of energy among the internal degrees of freedom); the chemical reaction proper. Definite degrees of freedom, the evolution of which actually determines the behaviour of the system, correspond to these stages. The nature of such evolution can change significantly as a result of the interaction (feedbacks) between various degrees of freedom.

Certain types of feedbacks generated in the presence or absence of radiation may be indicated.

1. Purely thermal feedbacks, arising as a consequence of changes in temperature caused by the evolution or absorption of heat in the course of various physicochemical processes. This alters the rates of chemical reactions and transfer processes. Such feedbacks play a key role in problems of the physics of combustion,[1,2] the stability of ideal mixing flow reactors,[5] etc.

2. Selective feedbacks due to local changes in the absorptance of the medium during the process (owing to changes in its chemical composition, density, etc.). As a result of these feedbacks, the local amounts of radiant energy introduced into the test substance are altered.

3. The feedbacks due to various nonlinear optical effects leading to a change in the spatial distribution of the radiation density.

4. Kinetic feedbacks. For example, in the case of multi-pathway chemical reactions, the rate of reaction via one pathway depends on the rates of reaction via the other pathways as a consequence of the change in the chemical composition of the medium. Such feedbacks are responsible for the development of auto-oscillations in Belousov–Zhabotinskii reactions.

In connection with the foregoing, the question arises of the construction and study of the basic mathematical models taking into account the most significant mechanisms affecting the process dynamics. Such study constitutes the basis for the subsequent construction of a theory permitting a quantitative comparison with the experiment. The mathematical procedures necessary for this are provided by the theory of nonlinear oscillations and the theory of stability, bifurcations, and catastrophes.

In the analysis of the chemical action of laser radiation towards the end of the 1970s, use was frequently made of the idea that, if an amount of energy E is introduced into the medium with the aid of laser radiation in the absence of heat and mass transfer, then the chemical result of such thermal action of the radiation should not depend on the particular substance (starting material, reaction product, or buffer component) which absorbs this energy. On the other hand, the dependence of the chemical result not only on the amount of absorbed energy but also on the wavelength of the laser radiation was regarded as indirect proof of a nonequilibrium distribution of the molecules among the vibrational–rotational energy levels. However, it was shown later that, generally speaking, this hypothesis is incorrect. This can be understood from the following considerations.

Evidently the radiant energy absorbed by the reactant determines the change in the temperature of the medium. On the other hand, the chemical result depends on the ratio of the rate of change of temperature $(dT/dt)/T$ and the rate of relaxation of the chemical composition $(dN/dt)/N$. If $(dN/dt)/N \gg (dT/dt)/T$, then the chemical composition is close to equilibrium for the given temperature. In this case, the concentration of the reacted substance (N) depends on the temperature and is determined by the constant for the chemical equilibrium in the reactor, i.e. for a slow change in temperature, the corresponding process is close to equilibrium. For the reverse ratio of the chemical and thermal rates, the process is of a nonequilibrium type. A well-known example, illustrating this fact, is provided by the quenching of the chemical composition on rapid cooling of the reactor. In the general case, the chemical result is a functional of temperature and depends on the way in which this temperature has been reached.

We shall now take into account the change in the absorptance capacity of the medium. Since the different components absorb radiation in different ways at different wavelengths, a feedback is established in the system between the chemical and thermal degrees of freedom. For example, this feedback is positive if radiation is absorbed by the reaction product.[18,19] Thus the dynamics of the change in temperature and hence the chemical result of the laser radiation depend in general not only on the amount of energy absorbed but also on the wavelength of the laser radiation.

We shall now consider the very simple reaction

$$A \rightarrow B + \text{heat}. \tag{1}$$

The dependence of the dynamics of this reaction on the wavelength can be conveniently characterised by the selectivity parameter

$$\mu = \frac{\sigma_A - \sigma_B}{\sigma_A + \sigma_B},$$

where σ_A and σ_B are the cross-sections for the absorption of radiation by substances A and B. When μ changes, there is a possibility of a change in the nature of the feedback, in the reactor dynamics, and, naturally, in the chemical result of the exposure to laser radiation. Depending on the chosen values of the parameters, the system can reach a stable stationary state or an auto-oscillatory regime[18,26] and the effect of the limit at the red end of the spectrum as well as threshold and other phenomena normally characteristic of photochemical reactions may be observed.

2. Bifurcations in the chemical state of the medium

In order to demonstrate the characteristic features of reactions in the field of laser radiation, we shall examine the simplest situation where only the reversible reaction

$$A \rightleftarrows B + \text{heat} \tag{2}$$

takes place in a chemical reactor with ideal mixing. The equation for the kinetics of this reaction is

$$\frac{dc}{dt} = k_1(1 - c) - k_2 c, \tag{3}$$

where c is the concentration of the product B and k_1 and k_2 are the rate constants for the forward and reverse reactions, which depend on temperature in accordance with the Arrhenius law:

$$k_1(T) = k_1^{(0)} e^{-T_1/T}, \quad k_2(T) = k_2^{(0)} e^{-T_2/T}. \tag{4}$$

The change in the temperature of the medium T is determined from the heat balance equation

$$C\frac{dT}{dt} = AP + W\frac{dc}{dt} - P_1(T), \tag{5}$$

where A is the absorptance of the medium, P the power of the radiation, W the heat of reaction, P_1 the power associated with heat losses, and C the total heat capacity of the medium.

The characteristics of the laser-induced heating are determined by the explicit dependence of the absorptance of the medium A on its chemical composition and temperature and also on the wavelength of the radiation. To make the treatment concrete, we shall assume that the reactor is optically thin in the direction of propagation of the radiation. Then

$$A = [(1 - c)\sigma_A + c\sigma_B]Nh, \tag{6}$$

where N is the total number of species of substances A and B per unit volume and h is the optical thickness of the reactor.

We shall consider separately the visible and infrared wavelength ranges. In the visible range, the energy of a quantum of the laser radiation $\hbar\omega$ is high, i.e. $\hbar\omega \gg kT$, the temperature dependence of the absorption cross-sections σ_A and σ_B is as a rule extremely weak, and one can assume that σ_A, σ_B = const. Analysis of Eqns (3)–(6) shows that the chemical system considered passes from any kind of initial conditions to a stable stationary state. Allowance for photochemical pathways with participation of electronically excited molecules does not alter this conclusion. There may be several final stationary states (this entails hysteresis phenomena when parameters such as the power and wavelength of the radiation are changed).

The number of stationary states changes when the parameters pass through certain critical (bifurcation) values, in the vicinity of which even slight changes in the latter lead to a sharp alteration of the chemical result. The point is that, starting from the same initial state, the system is able to enter the region of attraction by other final states after passing through the bifurcation point. In this connection, one should note that laser control in the vicinity of bifurcation values does not require much energy expenditure. In other words, even small influences can yield a major effect.

In contrast to the visible region, in the IR region $\hbar\omega \approx kT$ and the absorption cross-sections depends strongly on temperature. As a result, new dynamic regimes arise in the system — the number of stationary states increases and stable auto-oscillations in temperature and concentration and more complex types of hysteresis phenomena become possible.[27]

The foregoing explains the complexity of the behaviour of even simple chemical systems under the influence of laser radiation.

3. Transient regimes and metastable ordering

Sometimes not only the final states but also transient processes are of practical interest. This is associated with the fact that in chemistry transient processes may be extremely long. Furthermore, particular products of interest may be formed in the intermediate stages, vanishing as the final state is approached.

As an example, we shall consider the imidisation reaction in the field of the continuous radiation from a CO_2 laser.[28] The essential feature of the reaction is as follows. The starting material — the polyamidoacid (PAA) — is heated and water molecules are split off and removed. This results in the formation of a thermostable polymeric aromatic polyimide (PI) (polypyromellitimide), which has useful mechanical and electrical insulating properties. Studies have shown that the quality of the polyimide is higher the more complete the removal of water. In the usual technology for the manufacture of the polyimide (under isothermal conditions), the complete removal of water requires that the process be carried out at higher temperature ($T \gtrsim 670-770$ K, where the rate of evaporation increases); however, under these conditions polyimide thermal degradation processes begin and, in addition, the water formed may cause the hydrolysis of the polyimide. As a result, the degree of imidisation is usually 75%–80%.

If the polyamidoacid is heated with the aid of the radiation from a CO_2 laser, water is in fact fully removed and a degree of imidisation >95% is attained. This can be explained by the fact that water absorbs strongly the CO_2 laser radiation and the laser-induced heating of the polyamidoacid therefore develops as follows. The absorptance of the medium is initially low and at moderate temperatures water is evolved. Then, when a fairly large amount of water has formed, the degree of absorption of the radiation increases and this results in the heating of the substance, leading to the rapid evaporation of water. Subsequently the absorptance again falls and the temperature of the medium diminishes to a level at which there is virtually no degradation of the polyimide. The time during which the system is heated and water is fully removed is short and is insufficient for the development of hydrolysis and thermal degradation of polyimide. Thus a self-organising disequilibrium regime arises where the medium 'knows itself' at which instant it has to heat up more intensely, i.e. the optimum course of the reaction is ensured by the internal dynamic resources of the system and not by the time variation of external controlling parameters.

Compared with monotonic heating in a thermostat, the positive effect during laser-induced heating is attained as a result of the 'timely' rise and decrease in temperature. Such character of the thermal process is confirmed by the results of experiments and numerical modelling.

From a formal mathematical point of view, the polyimidisation reactions during heating in a thermostat and during laser-induced heating differ in the number of occasions when the rate of reaction reaches an extremum (bifurcations in the transient regimes).[30] Such nonmonotonic changes in the rate during laser-induced heating are characteristic of many reactions. For example similar transient oscillations in temperature and rate of reaction occur over a certain range of parameters even during the laser-induced heating of a binary gas mixture involving a reversible reaction.[18]

In the example of the laser-induced polyimide formation reaction examined above, a feedback is established as a result of the change in the absorptance of the system when the chemical composition of the medium is altered. Another mechanism of the appearance of a feedback is determined by the concentration- and temperature-induced changes in the parameters of the heat exchange leading to effects of the type of thermal explosion.[1] It is not difficult to understand that this mechanism can also lead to a different kind of bifurcations in transient regimes.

Thus, even in spatially uniform systems (for example in an ideal mixing reactor), nontrivial changes in both the stationary states and in the transient processes may occur. Table 1 presents the principal mechanisms of the feedbacks and the corresponding nonlinear thermochemical phenomena observed in the laser-induced heating of chemically reactive media. The table also indicates the feedbacks investigated in the usual (nonlaser) macrokinetics.

We have spoken hitherto about point systems. On passing to distributed systems, where heat and mass transfer processes play a significant role, the range of possible regimes expands sharply. The occurrence of diffusion and thermal conductivity can lead to phenomena involving the spontaneous loss of symmetry and spatiotemporal self-organisation and also to the formation of various nonequilibrium structures.[4,6,34] The theoretical dynamics of the corresponding processes is described by coupled diffusion equations:

$$\frac{\partial u}{\partial t} = \nabla(D\nabla u) + Q(u)\,, \tag{7}$$

where u is the vector of state, D the matrix of the diffusion coefficients (in the general case it is nondiagonal and depends on u), and Q the vector of nonlinear sources. A multiplicity of different problems, including the problems of the chemical dynamics of the reactor, reduce to an equation of type (7). In essence the spatiotemporal self-organisation is determined by the presence in Eqn (7) of new feedback channels between spatial gradients (fluxes) of the corresponding quantities. If the feedback generated is positive, then in distributed system instabilities may develop, leading to the formation of either dissipative structures or autowaves.

As an example we shall consider the appearance of thermal diffusion instability during the laser-induced heating of binary gas mixtures.[19,35] In the field of the laser radiation, the temperature gradients may be high and the thermal diffusion mechanism of the transport of matter may be significant. The thermal diffusion flux of the light component (B_l) is usually directed towards the hotter region of the medium, while that of the heavy component (B_h) is directed towards the colder region. This factor leads to separation in space of the components of the nonuniformly heated $B_l + B_h$ gas mixtures.

We shall consider the heating of an optically and thermally thin gas-containing cell (oriented along the x axis) by radiation incident on the cell at right angles to the x axis and having an intensity distribution $I(x) = I$ = const. ($0 < x < L$), where L is the length of the cell. It is assumed that the radiation is absorbed selectively by the light component of the gas. The appearance of instability in the homogeneous state of the gas is due to the fact

Table 1. Typical feedbacks and nonlinear phenomena in macroscopic kinetics.

Feedback mechanisms	Type of nonlinearity	Nonlinear phenomena	Ref.
Heat of zero-order reaction	$P_{exo} = Wk_0 e^{-T_0/T}$	Thermal explosion, thermochemical bistability	29, 1, 3
Heat of reaction of order α	$P_{exo}(N,T) = Wk_0 N^{\alpha} e^{-T_0/T}$	Thermokinetic oscillations	1, 5
Concentration-induced changes in absorption	$\sigma_A = \sigma_A(T)$, $\sigma_B = \sigma_B(T)$	Thermochemical bistability, auto-oscillations, bifurcation of transient regimes, self-stabilisation, Belousov–Zhabotinskii reactions	3, 18, 28
Temperature- and concentration-induced changes in absorption	$\sigma_A = \text{const}$, $\sigma_B = 0$, nonequilibrium chemical kinetic equation	Thermochemical bistability, auto-oscillations	26
Concentration-induced change in heat capacity	$C = C_1 c + C_2(1-c)$	Bifurcations in transient regimes	30
Change in the parameters of heat and mass exchange	$\eta = \eta(v, T)$, $\sigma_0 = \sigma_0(N, T)$	Crisis in heat exchange, thermal explosion, auto-oscillations	2, 31
	$v \neq 0$ (exposure to gas stream)	Auto-oscillations, dissipative structures	32, 33

Note. To make the illustration concrete, the results are presented for the reaction A $\rightleftharpoons$ B. Notation employed: P_{exo} is the power evolved in the reaction, k_0 and T_0 are the parameters of the rate of an Arrhenius-type reaction, N is the amount of the initial reaction component, c is its concentration, σ_A and σ_B are the cross-sections for the absorption of radiation by substances A and B, η is the Newtonian heat exchange coefficient, σ_0 is the blackbody coefficient for the radiative heat exchange, v is the velocity of the gas stream, and C is the heat capacity.

that, in the presence of local temperature fluctuations, a thermal diffusion flux directed to the hot region arises. A local increase in the concentration of the absorbing component and a further growth of temperature gradients then occur. However, by virtue of the thermal conductivity and the usual diffusion, the instability can develop only when the intensity of the radiation I exceeds a critical value. Such a mechanism has been proposed by Nitzan et al.[19] Stabilisation is achieved by virtue of some kind of nonlinear factors. Thus if there is a feedback $B_l \rightleftharpoons B_h$ between the components of the medium, the principal stabilisation mechanism consists in the fact that, in conformity with the reaction kinetics, an effective 'sink' of the light component B_l arises at the points with an excess of the latter, while a 'source' of this component arises at the points where its amount is deficient.

As a result of the development of the instability, the system passes to a stable stationary inhomogeneous state with distributions of temperature and concentrations of the gas components which are periodic with respect to the length of the cell.[19, 35] As a consequence of this transition, the average (with respect to space) absorptance of the medium changes. It is found that, over a wide range of values of the parameters, the absorptance diminishes, i.e. the fraction of absorbed energy of the radiation decreases.[36] In other words, the behaviour of the system corresponds qualitatively to the Le Chatelier principle familiar in classical thermodynamics. Nevertheless, this claim is invalid in the general case, i.e. one may indicate a range of parameters in which the average absorptance increases when the medium passes to the inhomogeneous state.

The breakdown of the Le Chatelier principle reflects the fact that the system is far from thermodynamic equilibrium. We may recall that the latter is manifested by the existence of bistability, which is impossible in the case of weak energy and mass exchange between the system and the surrounding medium.

Structure formation phenomena, similar to those examined above, have been widely discussed in various branches of physics and similar equations have been used for their description. Thus the dynamics of a homogeneous two-component system near the instability threshold depends only slightly on the specific form of nonlinearity and can be frequently described by one of the following equations:¶[36]

¶ See, for example, also the book *Nelineinye Volny. Dinamika i Evolyutsiya* (Nonlinear Waves. Dynamics and Evolution) (Moscow: Nauka, 1989) p. 113.

$$\frac{\partial u}{\partial \tau} = -\frac{\partial^2}{\partial x^2}\left(\frac{\partial^2 u}{\partial x^2} + \beta u + \varepsilon u^2 - u^3\right), \quad 0 < x < L, \tag{8}$$

or

$$\frac{\partial u}{\partial \tau} = \left[\beta - \left(\frac{\partial^2 u}{\partial x^2} + k_0^2\right)^2\right] u + \varepsilon u^2 - u^3, \quad 0 < x < L, \tag{9}$$

where τ, x, and L are respectively the dimensionless time, the coordinate, and the linear dimension of the system, u the deviation of any characteristic of the system (for example, temperature) from its value in the equilibrium homogeneous state, $\beta \simeq I - I_c$ characterises the extent by which the radiation intensity I exceeds the threshold intensity I_c, and the parameter ε is determined by the properties of the medium and describes the quadratic nonlinearity of the system. Eqns (8) and (9) can be obtained as special cases of Eqn (7). They have been proposed for the description of convective and thermoconvective instabilities in liquids, phase transitions in nuclear matter, and the separation of alloys and suspensions into layers.

Eqns (8) and (9) can be investigated by the known methods of the qualitative theory of nonlinear boundary problems. In the first place, it is evident that they have the homogeneous stationary solution $u = 0$. By linearising Eqns (8) and (9) in the vicinity of this solution and assuming that

$$\delta u = (\delta u)_0 \exp(\gamma \tau + iqx), \tag{10}$$

it is easy to find the dependence of the increment γ on the wave number q, which assumes the form

$$\gamma = q^2(\beta - q^2) \tag{11}$$

in the case of Eqn (8), and

$$\gamma = \beta - (q^2 - k_0^2)^2 \tag{12}$$

in the case of Eqn (9). If $\beta > 0$, there is always a range of wave numbers q in which $\gamma > 0$, i.e. the perturbations increase exponentially with time.

We shall now consider Eqn (8) in greater detail. It follows from Eqn (11) that perturbations with the wave numbers $q_m = (\frac{1}{2}\beta)^{1/2}$ grow at the fastest rate (γ is a maximum). The formation in the system of a spatially periodic structure with a period $\lambda_m \simeq 2\pi/q_m$ is therefore to be expected. Numerical integration of Eqn (8) confirms this conclusion. However, it can be demonstrated rigorously that only those solutions of Eqn (8) the period of which is $\lambda_a = 2L$ are asymptotically (at $\tau \to \infty$) stable.

Hence it follows that, for sufficiently large values of L, solutions with a period $\lambda \simeq \lambda_m$ are unstable and arise only as intermediate (transition) states.[37] Since states with $\lambda \simeq \lambda_m$ arise almost inevitably in the course of the evolution of the test system, they can be naturally referred to as metastable structures and the appearance of such states can be called metastable self-organisation. The term 'metastable structure' will also be applied because the lifetime of such structures is long: they decompose only under the influence of longer-wavelength perturbations, the time of the increase of which is long (since this process requires the synchronisation of the motion of more extensive sections of the medium). We may note that metastable ordering phenomena are characteristic of many nonlinear dynamic systems. They can arise, for example, in the thermal diffusion separation of gas mixtures, and in the laser-induced annealing and quenching of nonequilibrium vacancies in the surface layers of metals.[38]

4. Thermal diffusion oscillations during nonuniform heating of gas mixtures

We shall consider the heating of a chemically inert gas mixture by a beam of continuous laser radiation. We shall assume that the radiation is absorbed by the heavy component of the mixture via a resonance mechanism. The gas layer is assumed to be optically thin along the axis of the beam. The mathematical model of the process[39] includes diffusion (taking into account concentration and thermal diffusion) and thermal conductivity equations. In the latter, account must be taken of the fact that in the IR region of the spectrum the absorptances of many molecular gases depend strongly on temperature and are often described by the formula

$$A(N,T) = \beta N \exp\left(-\frac{T_a}{T}\right),$$

where N is the molecular density of the absorbing component of the medium.

If the radiation has a uniform intensity distribution with respect to the cross-section of the cell, then only stationary states are stable. In the same case, when the radiation beam has a finite radius stable nonstationary regimes become possible. The mechanism of the generation of oscillations in temperature and the concentrations of the components is as follows. Under the influence of radiation, the mixture is heated and temperature gradients directed towards the axis of the laser beam arise. As a result of thermal diffusion, the heavy component of the mixture is expelled from the beam, so that the absorptance of the medium diminishes, the gas cools, the temperature gradients diminish, and concentration diffusion returns the absorbing component to the region within the limits of the laser beam. The process is then repeated.

We shall now present the results of the numerical analysis of this process.[39] It was found that oscillatory regimes are possible in a restricted range of powers (P) and radii (r_0) of the radiation beam. This region is illustrated in Fig. 1*a*. It is divided into two subregions with different dynamic regimes. For the parameters in the subregion I, the system executes simple auto-oscillations, which are represented on the phase plane by a closed curve without self-intersections (the so called limiting cycle S^1).

On passing to the subregion II, the oscillations are become more complex as a result of the cascade of bifurcations involving the doubling of the period. Typical phase portraits of the complex limiting cycles are presented in Figs 1*b*–1*e*.

In the subregion II in Fig. 1*a*, the system is extremely sensitive to the choice of the radiation parameters. Therefore, under the conditions of a real experiment, when the radiation parameters have been determined with insufficient accuracy or fluctuate, it is difficult to obtain the required complex dynamic regime in a pure form. As regards the characteristic values of the periods of the oscillations, we may point out that, in the vicinity of the stability threshold of the stationary state, they are $\sim(5-10)r_0^2/D$. For typical experimental conditions with diffusion coefficient $D = 0.1$ cm^2 s^{-1} and the laser beam radius $r_0 = 1$ cm, this estimate yields a characteristic time of the order of 1 min.

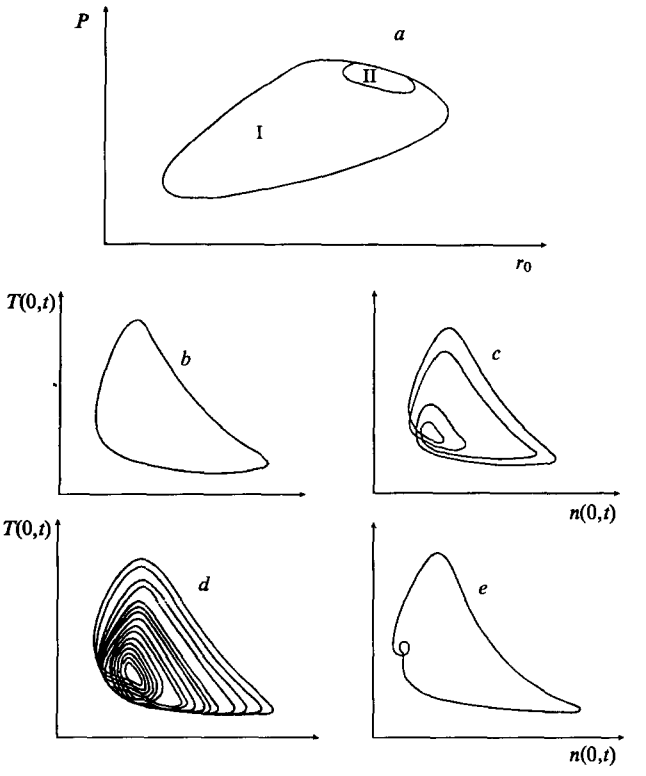


Figure 1. The region of existence of thermodiffusional oscillations (*a*) and typical phase portraits (*b*–*e*).

The diffusional oscillations examined above have been observed in experiments on the laser-induced heating of gas mixtures.[40] Fig. 2 presents the time variations of the power of the laser radiation which has passed through a cell containing a mixture of air and SF_6 as well as a mixture of NH_3 and SF_6. The radiation was absorbed selectively by the heavy component (SF_6). The oscillograms show that the heavy component is periodically ejected outside the limits of the laser beam. The characteristic process times show that there are no gas-dynamic motions of the medium (turbulence, convection) and that mass transfer is diffusional.

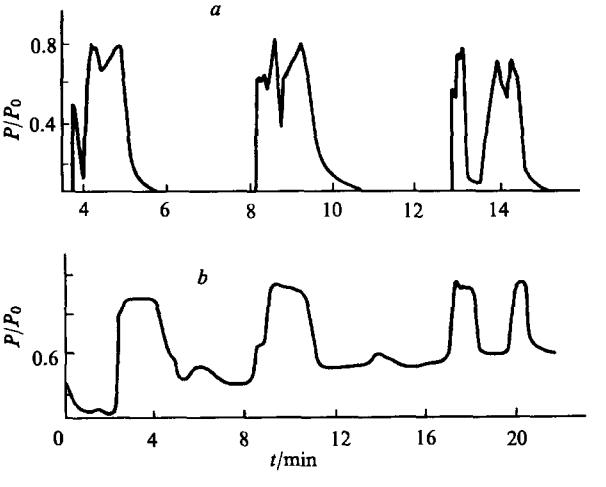


Figure 2. Time variation of the power of the laser radiation which has passed through a cell with SF_6+air (*a*) and SF_6+NH_3 (*b*) mixtures.[39] Power of the radiation incident on the cell $P_0 = 5$ W; length of the cell 20 cm; pressure (torr): (*a*) $P_{SF_6} = 2$, $P_{air} = 20$; (*b*) $P_{SF_6} = 2.5$, $P_{NH_3} = 19$.

5. Travelling fronts and 'chemical solitons'

Hitherto we have spoken of the heating of a gas mixture placed in an optically thin cell. On the other hand, if the optical thinness condition is infringed, there is a possibility of the appearance of qualitatively new dynamic regimes. In particular, combined waves may appear in which the concentration of the reactants and temperature differ markedly from the background values (travelling pulse or 'chemical soliton'). We shall consider this phenomenon in relation to the laser-induced heating of a gaseous medium involving a reversible chemical reaction.

Suppose that the gas mixture has been placed in a long thin cell illuminated from the end-face by radiation with a power P. As mentioned above, in a gaseous medium with a reversible chemical reaction there is a possibility of the phenomenon of thermochemical bistability on heating by laser radiation at a suitable wavelength. This means that, in a certain range of radiant powers ($P_1 < P < P_2$), there exist two stable stationary states differing in temperature and the concentrations of the components. The attenuation of radiation in accordance with the Bouguer (Beer–Lambert) law and transfer processes are not taken into account in this treatment, but they can in fact lead to new interesting effects.

Suppose that in the initial instant the system is in its lowest state as regards concentrations and temperature. If the medium in a certain part of the cell is transferred to a state with an increased concentration of the absorbing component, then the absorption of radiation in this region increases and heating of the gas begins. As a result of heat conduction and the absorption of the energy of the laser radiation, the neighbouring regions also begin to heat up. The size of the absorbing zone then increases until the radiant power behind it becomes less than W_1 — the minimum value necessary for the existence of bistability. The zone formed begins to move towards the laser beam, because, as a result of heat conduction, the region ahead of the zone heats up and the absorption in the latter increases, while the region behind the zone cools as a result of heat losses and the decrease in the heating power. This leads to the formation of a travelling pulse — a localised region in which the medium is in a high-temperature and strongly absorbing state. We may note that a similar phenomenon is observed not only in laser-induced thermochemical processes but also in many others, for example, in the generation of plasma in optical breakdown.[41]

The phenomenon considered above is formally described in terms of the following boundary-value problem.[42] The change in the concentration n of substance B is defined by the equation for reaction kinetics taking into account diffusion:

$$\frac{\partial c}{\partial t} = D\frac{\partial^2 c}{\partial z^2} + k_A(1-c)\exp\left(-\frac{T_A}{T}\right) - k_B n \exp\left(-\frac{T_B}{T}\right). \qquad (13)$$

We shall assume that $T_A > T_B$, i.e. the equilibrium concentration of substance B,

$$c = \left[1 + \frac{k_B}{k_A}\exp\left(\frac{T_A - T_B}{T}\right)\right]^{-1} \equiv c(T), \qquad (14)$$

increases with temperature.

We shall assume that radiation is absorbed only by substance B

$$\frac{\partial I}{\partial z} = -\beta c I, \quad \beta = \text{const}, \quad I|_{z=0} = I_0, \qquad (15)$$

while the change in the gas temperature is described by the thermal conductivity equation

$$\frac{1}{a}\frac{\partial T}{\partial t} = \frac{\partial^2 T}{\partial z^2} - \frac{1}{k}\frac{\partial I}{\partial z} - \frac{\eta}{k}(T - T_i), \qquad (16)$$

where η is the heat loss per unit length of the cell and T_i the initial temperature of the medium.

We shall assume that the length of the cell exceeds significantly the spatial size of the travelling pulse. Fig. 3 illustrates the dynamics of the formation of a chemical soliton.

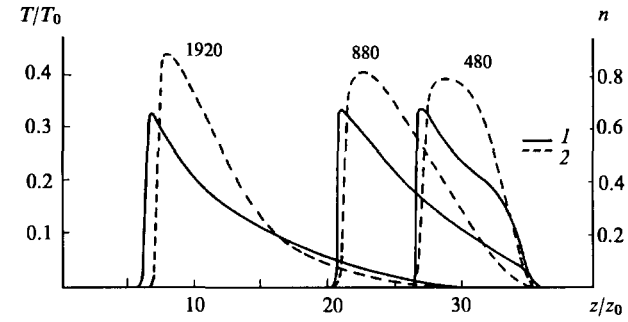


Figure 3. Dynamics of the formation of a chemical soliton. The dimensionless temperature (T/T_0), distance (z/z_0), and concentration c are plotted along the coordinate axes; the numerals opposite the curves denote the dimensionless time (t/t_0): (*1*) temperature profile; (*2*) concentration profile.

The switching caused by longitudinal bistability leads to additional characteristic modulation (kinks) of the intensity of the radiation at the outlet from the medium. For example, if the time variation of the radiation intensity at the inlet to the medium has the form of a triangle (Fig. 4*a*) with an amplitude higher than a certain critical value, the transmitted pulse has the form of a trident (Fig. 4*b*). Phenomena of this kind have been observed in the interaction of laser radiation with semiconductors.[43] The time constant corresponding to the mechanism of the chemical nonlinearity makes it possible to observe kinks in the range of intensities and for durations of laser action differing by several orders of magnitude from those where kinks are observed in semiconductors.

In a medium with a nonuniform energy exchange [the quantity T_i in Eqn (16) is, for example, a monotonically increasing linear function of the coordinate], a cyclic process may occur, consisting of stages involving the 'self-initiation' of the travelling pulse at the remote end of the cell, its subsequent propagation towards the beam, and its 'self-quenching' at the inlet to the reactor (Fig. 5). In terms of external features, such a system may be called a chemical analogue of the Gunn diode. The amplitude, width, velocity, and other parameters of a chemical soliton during its propagation in the medium may vary periodically (or even stochastically). Together with bifurcations, leading to identical changes in the system dynamics throughout the length of the reactor, there is a possibility of bifurcations leading to the appearance of dynamic regimes qualitatively different in different parts of the reactor. This can be manifested, for example, by the fact that part of the reactor is traversed by the 'chemical soliton' as a 'two-hump' species whilst another part is traversed by the soliton as a 'one-hump' species. From the formal point of view, such transformations correspond to bifurcations involving the doubling of the period along the spatial coordinate.

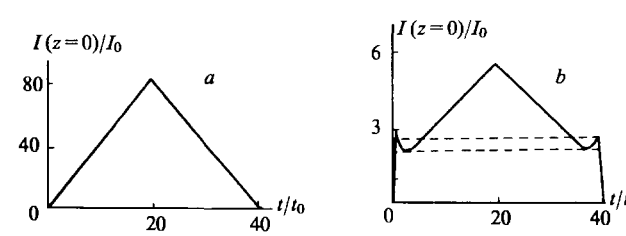


Figure 4. Time modulation of the triangular pulse arising during passage through a bistable medium.[44] Time profile of the incident (*a*) and transmitted (*b*) radiation.

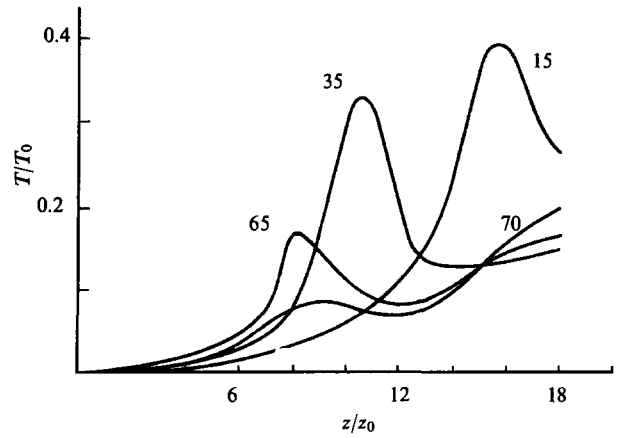


Figure 5. Chemical analogue of the Gunn diode: temperature profile of the field for different times in a medium with a nonuniform energy exchange. The legend is the same as in Fig. 3.

6. Nonlinear optical phenomena in a chemical reactor

The phenomena examined above belong to the class of nonlinear amplitude effects. Even these alone lead to complex dynamics of chemical processes in an optically thick reactor. In reality, together with amplitude effects there are also phase distortions of the wave front associated with the change in the refractive index of the medium during the reaction.

We shall consider this in greater detail. We shall suppose that a chemical reaction A → B takes place in the medium and that the initial substance A and the reaction product B have different optical properties. If the refractive index of substance B (n_B) is greater than that of substance A (n_A), a positive feedback is established, leading to instability. The mechanism of the instability is as follows. In the presence of perturbations, the medium is more strongly heated in the regions with increased intensity compared with the neighbouring regions and the reaction is activated sooner. As a result, the refractive index in these regions increases more rapidly, since $n_B > n_A$, which leads to the deviation of the light rays in this region and to a further increase in the local radiation intensity. The propagation of the radiation in a medium with a chemical inertial nonlinearity is described by the system of thermal conductivity and reaction kinetic equations (taking into account diffusion) together with the Maxwell equations specifying the distributed feedback.

Two cases are distinguished: those of narrow[44] and wide[45] radiation beams. A narrow beam is understood as one for which the radiation intensity distribution across a transverse section is nonuniform. A wide beam corresponds to the situation where the incident radiation is spatially uniform (planar wave).

We shall consider the characteristics of the formation of thermal structures in a nonuniform field of laser radiation. In the course of the development of instability, the optical nonuniformity of the medium increases and the self-focusing of the radiation take place. The self-focusing begins if

$$EN > (EN)_c , \tag{17}$$

where $E = \pi r_0^2 I_0 t$ is the energy of the radiation, N the concentration of the reaction products formed during time t, and $(EN)_c$ is determined by the parameters of the medium, the radiation wavelength, and the constants characterising the rate of reaction.[44] The effective width of the beam $r(z, t)$ may vary nonmonotonically along the beam z axis by virtue of the competition between the diffraction divergence and the focusing action of the 'chemical' lens: constrictions appear in the beam, their number varying in the course of the reaction. As can be seen from Fig. 6, when the self-focusing condition (17) is fulfilled, a beam constriction is generated, which moves from the point in which the radiation enters into the bulk of the medium ($z = 0$) and then, as the initial substance is 'burnt off' and the optical uniformity is restored, it moves in the opposite direction. The law governing the motion of the constriction can be explained qualitatively by considering the medium as an effective lens the focal distance R of which varies with time. The beam profile is now described by the expression

$$f(z) = \sqrt{\left(1 - \frac{z}{R}\right)^2 + \mu\left(\frac{z}{r_0}\right)^2} , \tag{18}$$

where the diffraction parameter $\mu = (kr_0)^{-2}$ and k is the radiation wavenumber.

The position of the constriction z_m corresponds to the minimum in the function $f(z)$:

$$f_{min} = f(z_m) = \sqrt{\frac{\mu(R/r_0)^2}{1 + \mu(R/r_0)^2}} , \quad z_m = \frac{R}{1 + \mu(R/r_0)^2} . \tag{19}$$

Hence it follows that, when $R = \infty$, i.e. when the medium is optically uniform, we have $z_m = 0$. Then, as R diminishes (the optical power of the lens increases), z_m reaches a maximum for a certain value of R and then begins to decrease as R diminishes further ($z_m \simeq R$ when $R \to 0$).

If the variation of the refractive index as a function of the radius is sufficiently great, then, when the beam passes from an optically denser medium to a less dense one, conditions for internal reflection may be fulfilled, as a consequence of which new constrictions appear on the beam — the beam acquires a corrugated profile. The appearance of constrictions implies the appearance of hot spots in which the reaction proceeds more vigorously. Evidently, this phenomenon may lead to the inclusion of high-temperature reaction pathways and hence to a qualitative change in the chemical composition of the reaction products. Under such conditions, it is difficult to predict the chemical result of the action of the laser radiation on the medium.

If the incident radiation has a spatially uniform intensity distribution, different aberrations of the radiation may be observed in the cross-section depending on the initial form of small perturbations — subdivision into 'filaments', the appearance of a nonstationary ring structure, etc. The instability can be convective (displacement) in nature: an intensity maximum arises at the inlet to the medium ($z = 0$) in an elementary tube, and then migrates into the bulk of the medium. The appearance of the maximum and its migration are caused, on the one hand, by the intensification of the optical strength of the chemical lens

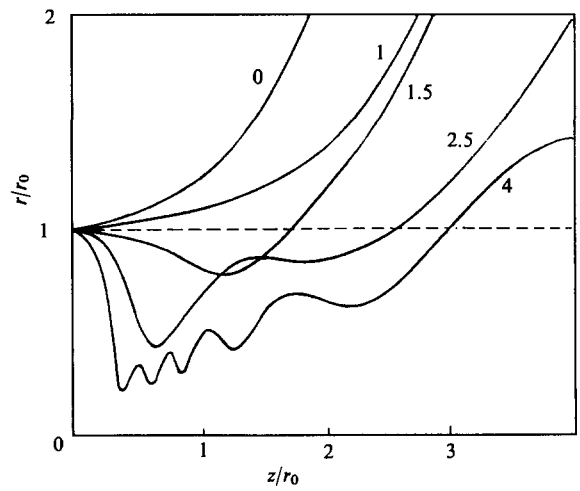


Figure 6. The profile of a radiation beam at different times during the reaction; r = beam radius, z = coordinate along the reactor axis, r_0 = radius of incident beam; the numbers opposite the curves denote dimensionless times.

during the reaction and, on the other, by two stabilising factors: the Bouguer attenuation of the radiation in the medium and the wave relaxation, which moves behind the instability front and is caused by the joint action of heat conduction and diffusion. The relaxation wave leads to the equalisation of the optical density of the medium, as a result of which the beams deviate only slightly from the initial direction before the attainment of the perturbation front.[45]

IV. Thermochemical processes in the laser heating of metals

1. Kinetics and dynamics of heterogeneous reactions and the morphology of the surface

Three major problems are associated with the laser stimulation of heterogeneous reactions.

The first refers to the reaction kinetics. During the last 10–15 years, many investigators observed that the kinetics of heterogeneous reactions in the field of the laser radiation are frequently characterised by different kinetic constants and even by different forms of the kinetic laws from those of the kinetics of isothermal processes (numerous reference data are available for the latter). This means that, for the development of the laser technology, it is essential to carry out an extensive set of studies in order to discover the form of the kinetic laws and the values of the corresponding kinetic constants, their dependence on the intensity and wavelength of the laser radiation, etc. As for homogeneous reactions, it is possible to differentiate photochemical and thermochemical effects. The photochemical effects are characteristic of laser-induced processes involving the oxidation of semiconductors and metals, the oxides of which have semiconducting properties. The 'red limit' of such photoactivity is usually in the visible or UV regions of the spectrum. On the other hand, the effects associated with the thermochemical influence of laser radiation on the reaction kinetics are associated with either high heating rates or high spatial temperature gradients in the oxidised layer.

The second problem concerns the kinetics of oxidation reactions. The observation of thermochemical instability and the first theoretical models of the development of instability on formation of strongly absorbing oxides have played an important role in this connection.[16] Such instability characterises the nonlinear dynamics of a system with a positive feedback in the initial stage. In later stages, where different stabilisation mechanisms begin to operate, the process dynamics become more complex. The experimental observation of the nonmonotonic dependence of the change in the absorption by metallic targets during their laser-induced heating in air has played an important role in the development of these studies.[17] It was found that the sign of the feedback, arising as a consequence of the change in absorption, can change during the process. More complex manifestations of the nonlinear dynamics of thermochemical processes were observed subsequently.

Finally, the third problem is that of the morphology of the surface in the laser initiation of heterogeneous reactions. As early as the beginning of the 1970s, studies on the heat-induced strengthening of metals and alloys led to the observation (see, for example, Rykalin et al.[46]) that in laser-induced heating the morphology of the surface is different from that found on heating in a furnace. The causes of this phenomenon were inadequately investigated at the time. Nowadays, numerous new results have been obtained. It is noteworthy that investigations of the structural changes in the surface under the influence of laser radiation are important for many technological applications, for example, in microelectronics, in integrated optics, in the laser-induced stabilisation of surfaces, etc.

2. The effect of laser radiation on the kinetics of heterogeneous reactions

The heterogeneous reactions at the solid–gas interface (oxidation, reduction, nitride formation, etc.) are known[47] to consist of many stages, the transfer of reactants in the gas or solid phase frequently playing the role of the rate-limiting stage. Accordingly, the kinetics of such reactions have a number of features in common with the kinetics of homogeneous reactions whose rate is limited by the diffusional transport of the components. Under these conditions, heterogeneous reactions should be more sensitive to changes in the parameters of the laser radiation than homogeneous reactions, because the diffusion coefficients of atoms in a solid vary more markedly with temperature than in gases (the variation is exponential and not of the power type).

However, as early as 10–15 years ago it was claimed that, for example, in metal oxidation reactions laser radiation exerts no specific influence on the reaction kinetics: the kinetics are exactly the same as during the heating of the target in a furnace. On the other hand, early experiments[48] already showed that the oxidation of copper in air under the influence of laser radiation is faster than in the furnace at the same temperature of the metal.

We shall consider the phenomena associated with the high rates of laser heating. For continuous emission, such rates are attained at the stage involving the development of thermodynamic instability, while for pulsed or repetitively pulsed emission they are attained in each individual pulse. Here it is significant that during rapid heating the distributions of the reactants deviate markedly from those which are established during slow heating. Evidently this is associated with the finite rate of diffusional transport of the components (oxidant and the metal) and with the migration of the metal–reaction product interface, the effective constants of which are functionals of the concentrations. Strictly speaking, the kinetic constants are not of this kind. For example, in relation to the oxidation of metals, the corresponding constants must be found by solving a system of equations for the diffusion of metal and oxidant ions in the layer of reaction products. The changes in the kinetics caused by the high rates of laser heating in heterogeneous reactions have been discussed.[48–52] Under stationary conditions, the kinetics of the heterogeneous oxidation are influenced by the nonuniformity caused by the spatial localisation of the reaction owing to the finite nature of the diameter of the laser beam and the temperature gradients in the oxidised layer. We shall consider the influence of these nonuniformities. The limited size of the laser beam leads, in particular, to the phenomenon of the diffusional limitation of the reaction as regards the supply of the oxidant from the gas phase (see, for example, Bunkin et al.[26] and Prokhorov et al.[49]).

The temperature gradients along the surface of the oxide layer are as a rule significantly lower than across it. The influence of these gradients on the reaction kinetics is various. The temperature gradients along the surface influence the transport of atoms via surface diffusion and thermal diffusion. This entails a change in the spatial distribution of the rate of reaction along the radial coordinate, which alters qualitatively the dependence of the increment in the instability of the planar oxidation front on the parameters of the laser radiation and the perturbation wave number.[53]

The temperature gradients across the oxide layer are more significant. They influence the transport of reactants in the solid phases. There are several mechanisms of the influence of such gradients on the reaction kinetics. The mechanisms determined by the temperature dependence of the diffusion coefficients and the thermal diffusion flux of atoms are fairly evident. Their effect in different models of the laser-induced oxidation has been investigated, for example, by Buzykin and coworkers.[54, 55] The phenomena caused by the influence of the temperature gradient on the electrical transport are of special interest. Owing to the high field of the thermo-e.m.f. in an oxide with semiconducting properties, the temperature gradients can lead to both

acceleration and retardation of the reaction. This has been demonstrated experimentally for the oxidation of copper (acceleration) and cobalt (retardation).[56]

Another important factor is accelerated diffusion via the grain boundaries and microcracks formed in the oxide film under the influence of thermal stresses. To a first approximation, the corrections to Wagner's parabolic law, caused by the increased permeability of the oxide, lead to a paralinear oxidation law. It has been observed experimentally[57] that, in the laser-induced heating of cobalt to 1300 K, a linear oxidation law holds up to an oxide thickness $h \simeq 10^5$ A, after which it is replaced by a parabolic law. On the other hand, under isothermal conditions (during oxidation in a furnace) the parabolic law is observed already for thicknesses $h > 10^2$ Å. Such 'extension' of the linear law into the region of high thicknesses may be associated with increased permeability of the oxide layer together with other causes (for example thermal diffusion).

The mechanisms of the influence of the generation of non-equilibrium point defects on the changes in the oxidation kinetics have been investigated vigorously in recent years.[38] The simplest mechanism of such influence may involve a change in the diffusion coefficients of atoms in the oxide, which, according to the Dienes–Damask theory[58] is described by an equation of the following form:

$$D(T) = D_0(T)\frac{N}{N_0(T)},$$

where $D_0(T)$ is the 'equilibrium' value of the diffusion coefficient at the given temperature and N is the concentration of non-equilibrium vacancies which exceeds significantly the equilibrium concentration $N_0(T)$ for the pulsed-periodic application of laser radiation. Such mechanisms make it possible to explain the accelerated growth of the oxide film in the 'low temperature' region which has been observed experimentally.[59]

Thus the studies of the last 10 years have yielded a result of practical and theoretical importance, namely that the kinetics of the laser-induced and isothermal oxidation are different. These differences depend greatly on the nature of the metal and the gas composition of the atmosphere and on the parameters of the target and the laser radiation. The specific mechanisms responsible for such differences proved to be varied. A number of them were discussed above.

3. Laser-induced oxidation

We shall now turn to the dynamics of oxidation reactions under the influence of laser radiation. In the simplest case, the rate of reaction can be characterised by the change in the thickness of the oxide layer dx/dt. This quantity depends on the temperature of the substance and can be expressed in the form

$$\frac{dx}{dt} = f(x, T). \tag{20}$$

In order to determine the reaction dynamics, it is essential to solve Eqn (20) simultaneously with the thermal conductivity equation. We shall consider such dynamics in relation to the problem of the growth of thick ($x > 10^3$ Å) compact oxide layers. In such layers, the reactants are transported by diffusion, which leads to the so called parabolic law

$$\frac{dx}{dt} = \frac{d(T)}{x}, \tag{21}$$

where the quantity $d(T)$ has come to be referred to as the parabolic law constant. At a constant temperature, the thickness of the oxide varies, according to Eqn (21), in conformity with the characteristic diffusion law $x^2 = 2dt$. The temperature variation $d(T)$ is frequently determined by the Arrhenius factor:

$$d(T) = d_0 \exp\left(-\frac{T_d}{T}\right), \tag{22}$$

which is valid within fairly wide temperature ranges.

The dynamics of such a system may be complex. The reason for this is that feedbacks arise in the system between the rates of heating and the rates of chemical reactions. The optical channel for the feedback, arising as a consequence of the dependence of the absorptance A of the irradiated specimen on the thickness of the oxide layer, plays a significant role in the laser-induced oxidation. The optical feedback may be both positive (along the section where the absorptance increases, $dA/dx > 0$) and negative ($dA/dx < 0$).

The positive feedback leads to thermochemical instability. We shall consider this phenomenon in greater detail.

The laser-induced heating of a thermally thin metallic film in an oxidising gas medium is described by the kinetic equations (21) and (22) and the heat balance equation (the heat of reaction is neglected):

$$mc_1\frac{dT}{dt} = PA(x) - P_1(T), \tag{23}$$

where m is the mass of the plate, c_1 is its specific heat, and P_1 is the power associated with the heat loss. Taking into account only the convective heat exchange, we assume that $P_1(T) = \eta S(T - T_1)$, where S is the total area of the heated specimen and η is the heat exchange coefficient.

An explosive increase in temperature (thermochemical instability) is observed after the thickness of the oxide film has increased so much that the change in absorption begins to alter significantly the heat balance, i.e. thermochemical instability develops after the elapse of a certain characteristic time, referred to as the activation time t_a, and not immediately after the start of irradiation. Under typical conditions, this time is proportional to $\exp(T_d/T_0)$, where T_0 is the quasi-stationary temperature to which the specimen is heated when its initial absorptance is equal to the absorptance of the unoxidised metal.

For nonuniform laser irradiation, the temperature maximum is located on the beam axis. Since the activation time increases exponentially with decrease in temperature and the temperature diminishes on moving away from the centre of the beam, an effective self-compression of the temperature field takes place in the course of development of thermochemical instability.

We may note that, by virtue of the temperature dependence defined by Eqn (22), the reaction takes place effectively in the vicinity of the centre of the laser beam. The size of the region may be small, compared not only with the characteristic width of the thermal field but also with the radius of the reaction-initiating beam itself. The above factor is important for laser technology, since it makes it possible to localise the chemical reaction. The effect involving the sharpening and localisation of the temperature field has been observed in experiments on the laser-induced heating of metals in air.[60] This is illustrated in Fig. 7, which shows the time variation of the spatial distribution of the temperature field for the heating of a titanium target by the radiation from a CO_2 laser. Evidently the self-acceleration of the temperature rise is accompanied by the self-compression of the temperature field.

We emphasise that the non-uniformity of the distribution of the radiation intensity is essential for the appearance of localisation effects only at the beginning. It serves as a 'seed' of the instability, which can then develop also in a uniform field. Therefore even small fluctuations in the distribution of the radiation intensity or in the optical characteristics of the test substances play an important role in laser-induced thermochemical processes.

For many metal oxides, the absorptance varies nonmonotonically with increase in thickness. This can be associated with interference due to the penetration of the light beam through a dielectric film the optical thickness of which is a multiple of an integral number of half-waves. Owing to interference oscillations in absorption, the sign of the feedback changes periodically, which results in the pulsation of the heating rate. Such pulsations are of a transient character and are not observed for asymptotic states (at $t \to \infty$).

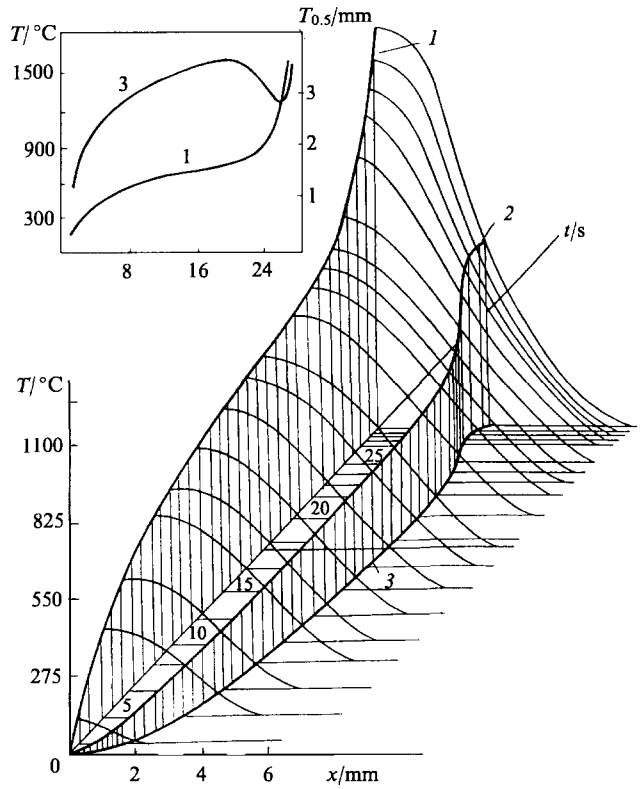


Figure 7. Time evolution of the spatial temperature profile of a titanium plate during its heating by the continuous radiation from a CO_2 laser:[60] power of the laser 40 W: (*1*) temperature $T(0, t)$; (*2*) temperature $0.5T(0, t)$; (*3*) effective radius of the localisation of the temperature field $r_{0.5}$, i.e. the value of the coordinate r for which $T(r_{0.5}, t) = 0.5T(0, t)$.

Another positive feedback channel is provided by the heat of a chemical reaction, which is responsible for the self-inflammation phenomenon[1] and for the appearance of auto-oscillations in a flow reactor with an exothermic reaction.[5] The heat of reaction plays a significant role in laser-induced inflammation processes. The following model, describing the qualitative features of the inflammation of tungsten, has been proposed:[61]

$$\frac{dx}{dt} = \frac{d}{x}\left(\exp\left(-\frac{T_d}{T}\right) - \upsilon_0 \exp\left(-\frac{T_s}{T}\right)\right),$$

$$mc_1 \frac{\partial T}{\partial t} = PA(x) - P_1(T) + \rho SW \frac{d}{x} \exp\left(-\frac{T_d}{T}\right) - \tag{24}$$

$$-\rho SL\upsilon_0 \exp\left(-\frac{T_s}{T}\right),$$

where W is the specific heat of the chemical reaction, L the specific heat loss on sublimation, ρ the density of the test substance, υ_0 the pre-exponential factor, and the subscripts s and d refer respectively to sublimation and diffusion processes.

In the kinetic equation, account was taken of the change in the thickness of the oxide layer x due to oxidation in accordance with the parabolic law (the first term) and the sublimation of the oxide WO_3 (the second term). The first term on the right-hand side of the heat balance equation describes the absorption of the laser radiation, the second term describes the heat losses caused by heat exchange with the surrounding medium, the third describes the evolution of energy in the reaction, and the fourth describes the loss of energy in sublimation. Analysis shows that there may be a limiting cycle on the phase plane of such a system, corresponding to the auto-oscillatory laser-induced combustion regime. The transitions between different regimes, for example, the trigger and auto-oscillatory regimes, can be achieved by altering the target parameters (mass, thickness) and the power of the incident laser radiation. All the regimes predicted by the theory—passive, latent, trigger, and auto-oscillatory—have been observed experimentally.

A model analogous to that defined by Eqn (24) can be used for the description of the laser-induced oxidation of molybdenum. In this case, the oxide MoO_3 at $T > 800$ °C is in the liquid phase and intense evaporation takes place from the surface of the liquid. The kinetic equation has the same form as Eqn (24), but for molybdenum $T_d < T_s$. The heat balance equation also retains its form, but the quantity W in it has the significance of the difference between the heat of the oxidation reaction and the heat of fusion. For MoO_3, this difference is negative ($W < 0$). Accordingly, the auto-oscillations are significantly associated with the presence of the MoO_3 melt. Experiments[57] confirmed the presence of the auto-oscillatory regime in the oxidation of molybdenum. The oscillations proved to be extremely stable and were observed for a long time— sometimes more than an hour. Part of the experimental oscillogram is presented in Fig. 8.

The oscillatory reactions examined are fairly simple from the standpoint of kinetics, being described by a single differential equation. As the kinetics become more complex, whereupon parallel or consecutive reactions arise, the oscillatory oxidation regimes can change similarly. An example is provided by the catalytic heterogeneous oxidation of ammonia in air on the surface of copper oxide and under the influence of the radiation of a CO_2 laser. The increase in the complexity of the oscillations, occurring apparently via a cascade of bifurcations associated with the doubling of the period, has been observed experimentally.[62]

An increase in the complexity of oscillations also takes place when the problem is transformed into one of the distributed type, i.e. under conditions where radial heat conduction phenomena play a significant role. Thus the transition from the stationary regime in the combustion of titanium to a stochastic regime on changing the conditions in the focusing of the laser radiation onto the surface of the specimen has been demonstrated.[63]

The nature of the complex oscillatory combustion regimes is determined to a large extent by the nature of the metal. We shall consider the case of tungsten. Suppose that the surface of a thin tungsten plate with a radius R is heated by a beam of laser radiation in which the intensity is distributed over the cross-section in accordance with the expression

$$I(r) = I_0 \exp\left(-\frac{r^2}{r_0^2}\right).$$

In contrast to Eqn (24), it is now necessary to take into account also the effects of radial heat conduction in the heated specimen. In the limit where $r_0 \gg R$ and the characteristic spatial scale of the changes in the variables is large compared with R, the effects of heat conduction are evidently insignificant. In conformity with the theory of nonlinear oscillations, there is then a possibility either of the attainment of stationary states or of simple auto-oscillations, depending on the radiation intensity. Such phenomena were discussed above.

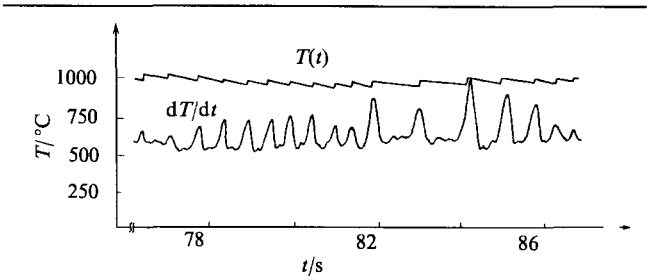


Figure 8. Experimental oscillogram of the $T(t)$ and dT/dt signals in the auto-oscillatory oxidation of molybdenum.[57]

Heat conduction and the nonuniformity of the radiation field lead not only to a quantitative but also to a qualitative change in the process dynamics. We shall fix the power of the radiation $P = \pi r_0^2 I_0$ and shall vary the focusing (i.e. the beam radius r_0) on the surface of the specimen. Numerical analysis leads to the following findings.[64]

In the first place, the presence of the simplest types of attractors—stable stationary states—was established. By virtue of the nonuniformity of the radiation field, the temperature $T(r)$ and the thickness of the oxide $x(r)$ are also found to be nonuniform and $x(r)$ may prove to be a nonmonotonic function of the coordinate r. With increase in the radiation beam radius r_0, the simplest nonstationary ordering arises. This is the limiting cycle S^1, corresponding to the situation where during the period of the oscillations the temperature $T(r, t)$ and the thickness of the oxide $x(r, t)$ reach a maximum once. The process is localised in a region of the order of magnitude of the size of the beam. On further increase in r_0, the dynamics become more complex—cycles S^n are generated corresponding to the situation where in the course of one period the number of local maxima reaches n, with $n > 1$. The increase in complexity takes place as a consequence of consecutive bifurcations associated with the doubling of the period as r_0 increases. This is followed by a range of values of r_0 to which stochastic regimes of different complexity correspond. Fig. 9 presents a diagram illustrating the change in the dynamic regimes as the parameters of the radiation are altered.

We may note that, apart from the complex oscillatory regimes examined above, the model under discussion describes the appearance of rotating spiral waves (reverberates) similar to those observed in the Belousov–Zhabotinskii reactions. Fig. 10 presents examples of the profiles of the temperature field in the form of single- and two-arm spirals rotating around the radiation beam axis. In the laser-induced heating of metals, such rotating structures are observed fairly frequently.

Another mechanism for the increase in the complexity of the dynamics operates when metals of the type of titanium are heated.

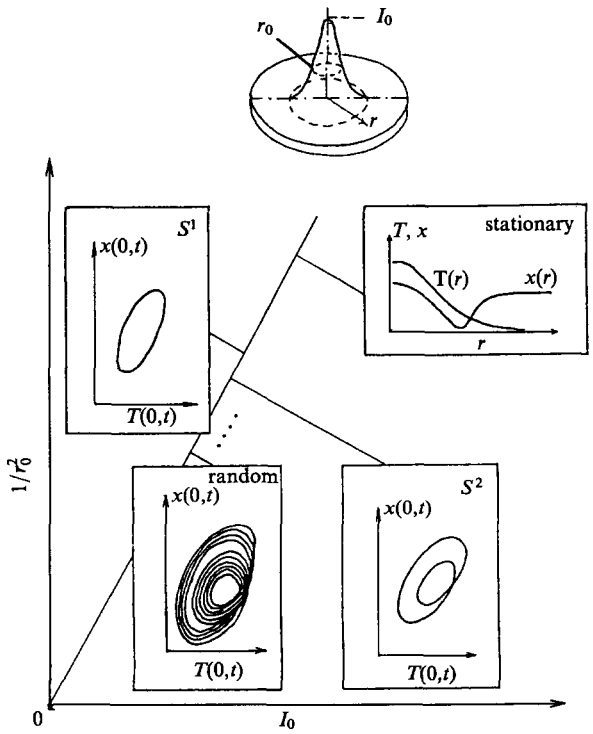


Figure 9. Dependence of the metallic target (tungsten) combustion regime on the beam radius r_0 for a fixed total power of the radiation $P = \pi r_0^2 I_0$.

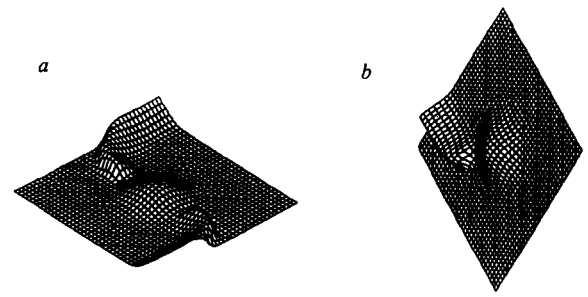


Figure 10. Rotating two-arm (*a*) and single-arm (*b*) spiral temperature field waves for nonuniform laser-induced heating of tungsten.[65]

It is determined by the transport of reactants or reaction products in the gaseous medium surrounding the heated specimen.[66] During the oxidation of the metal, oxygen is removed selectively from the surrounding medium, so that in the vicinity of the target surface the rate of reaction diminishes owing to the deficiency of the oxidant. There is a corresponding decrease also in the rate of consumption of oxygen. As a result of diffusion, its concentration increases again, the reaction is accelerated, and the process is repeated. The foregoing illustrates the possibility of the appearance of auto-oscillatory combustion regimes owing to the diffusion transport of the reactant (oxidant) in the gaseous medium.

Finally, yet another mechanism of the increase in complexity, qualitatively similar to the previous one, is induced by the diffusional transport of reactants through the layer of the oxide.[67] Other heterogeneous reactions with auto-oscillations have also been observed and other mechanisms of auto-oscillations, associated, for example, with the formation of oxide nitrides, the dissolution of scale, etc., have also been observed.

4. Laser-induced reduction

We have examined the dynamics of heterogeneous thermochemical processes due to the presence of a positive feedback between the chemical and thermal degrees of freedom of the system. Such a feedback was generated by the increase in the absorptance of the test substance or in the evolution of energy in the reaction. The opposite situation is one where a negative feedback is established on decrease in the absorptance of the substance or for a negative heat change (endothermic reaction). We shall consider the dynamics of systems with a negative feedback in relation to the reduction of metal oxides to the metals under the influence of laser radiation. In such a system, the negative feedback is established by virtue of the decrease in the absorptance of the test substance from A_{ox} (absorptance of the oxide) to A_m (absorptance of the metal). We have $A_{ox} > A_m$, which leads to a decrease in the energy introduced into the test substance and to a lowering of the heating rate.

We shall illustrate the characteristic features of the dynamics of the reduction reaction in relation to the laser-induced heating of a thermally thin specimen of oxidised metal. This problem is described by the heat balance equation

$$mc_1 \frac{dT}{dt} = PA(x) - P_l(T), \tag{25}$$

and the kinetic equation

$$\frac{dx}{dt} = d\exp\left(-\frac{T_d}{T}\right), \tag{26}$$

where x is the thickness of the layer of metal produced by the reduction process. For an absorptance $A(x)$, one can assume that

$$A(x) \simeq A_{ox}(1 - \beta x), \qquad \beta x \ll 1. \tag{27}$$

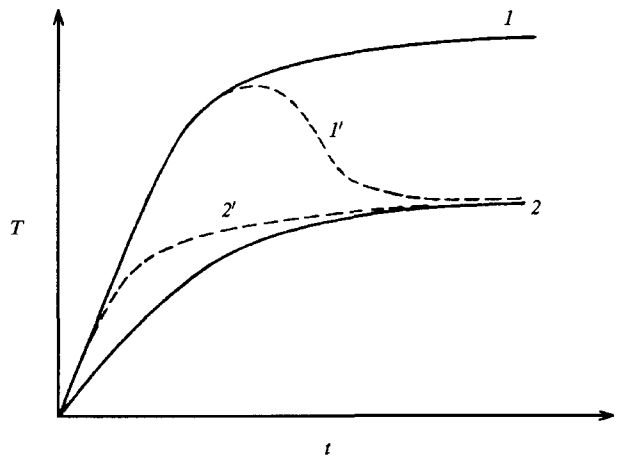


Figure 11. Time variation of the temperature of the specimen for $A(x) = A_{ox}$ (curve *1*) and $A(x) = A_m$ (curve *2*). (*1'*) activated reduction regime; (*2'*) nonactivated reduction regime.

For larger values of x, we have $\beta x \simeq 1$ and we can use the relation

$$A(x) \simeq \frac{x_0}{x}, \tag{28}$$

where x_0 is a characteristic scaling factor. In the reduction of Cu_2O to metallic copper, $x_0 \simeq 15$ Å and Eqn (28) fits satisfactorily the exact relation in the range of copper film thicknesses 50 Å $< x <$ 1000 Å. Fig. 11 presents curves illustrating the variation of the temperature of the specimen for two constant absorptances — corresponding to the pure oxide and the pure metal. In the reduction of the specimen, its heating begins in the state of the pure oxide, i.e. the specimen temperature follows initially curve *1* corresponding to the greater absorptance of the oxide. In the concluding state of the process, laser radiation acts on metallic film (complete reduction) and the temperature $T(t)$ should therefore tend asymptotically to curve *2* (heating of the pure metal). If the heating rate is high (large power of the radiation), the reaction begins in the early stages of the process. The transition from curve *1* to curve *2* takes place for a monotonic increase in temperature (curve *2'*). For slow heating, the reaction is unable to develop appreciably during the characteristic time of the establishment of the quasi-stationary temperature, so that heating takes place for a long time along curve *1*, the departure from it (curve *1'*) occurring at fairly late stages of the process. This in fact explains the nonmonotonic temperature variation for low powers.

The results of the direct numerical integration of Eqns (25) and (26) for the reduction of the lower oxide of copper to the metal under a hydrogen atmosphere are presented in Fig. 12.

We may note that in the laser-induced reduction the effects of heat conduction and of the nonuniformity of the heating process lead, as in the combustion processes discussed above, to changes in the dynamics.

There are numerous experimental situations where feedback channels of different signs exist simultaneously. For example, we have the negative feedback due to the change in absorptance and the positive feedback due to the exothermicity of the reaction. Such a situation is typical for the surface synthesis of titanium nitride on heating a titanium target in a nitrogen atmosphere with exposure to continuous IR radiation. In this case the chemical reaction may be a self-stabilising process for one set of parameters or a process with inflammation or thermochemical instability for another set. Such a combination of processes makes it possible to explain different complex transient pulsations in the heating rate which are not linked directly to the change in the power of the laser radiation, or, for example, to the interference oscillations in the absorption.

V. Physicochemical processes in the laser heating of liquids

We have considered hitherto processes in gaseous media or at solid–gas interfaces. Thermochemical processes initiated by laser radiation in a liquid are also of considerable interest.

1. Thermoelectrochemical instability in the laser-induced heating of absorbing electrolytes

Technologies based on the laser stimulation of electrochemical processes at conducting support–electrolyte solution interfaces have developed vigorously in recent years.[69,70] In the absence of laser radiation, such processes are the concern of classical electrochemistry.[71] The fundamental characteristic of electrochemical processes under equilibrium conditions is the electrochemical potential φ defined by the Nernst formula

$$\varphi = \varphi_0 + \frac{RT}{z_i F} \ln\left(\frac{a_i}{a_m}\right), \tag{29}$$

where z_i is the charge of the potential-generating ion and a_i and a_m are respectively the activities of the ion and the metal.

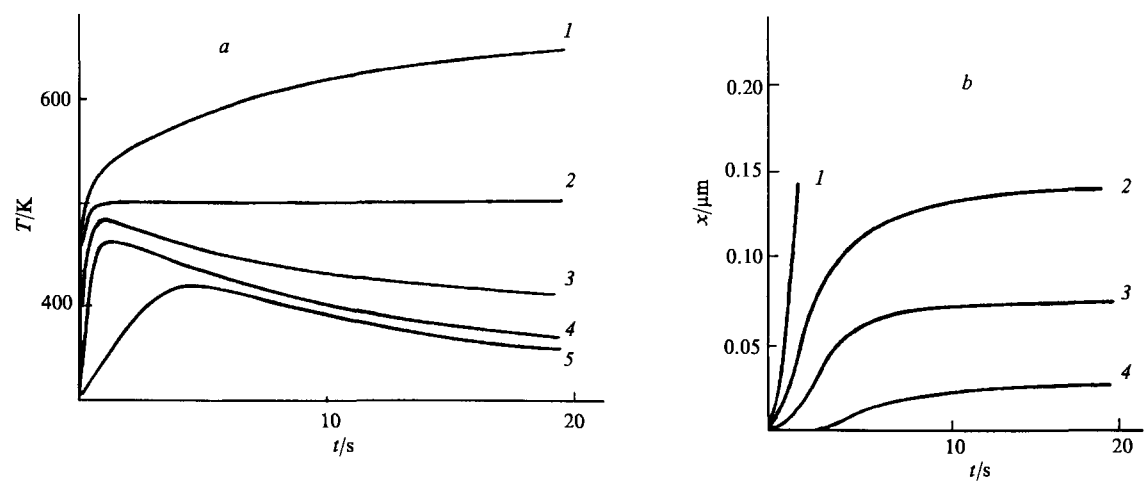


Figure 12. Variation of the temperature (*a*) and thickness of the copper layer (*b*) during its formation by the reduction of Cu_2O under a hydrogen atmosphere:[68] target mass 50 mg; target area 0.4 cm^2; continuous-wave CO_2 laser; power of the radiation (W): (*1*) 42; (*2*) 21; (*3*) 10; (*4*) 5; (*5*) 1.

The hierarchy of the electrode processes depends on the positions of the substances in the series of standard electrode potentials φ_0. For example, in order to precipitate from solutions metals which lie to the left of the material of the support in the above series, it is necessary to apply an external potential U exceeding the corresponding difference between the electrode potentials. However, the laser-induced precipitation of metals can take place in the absence of an external potential (see, for example, von Gutfeld[70] and Bunkin et al.[72]). Von Gutfeld[70] put forward the idea that the precipitation takes place under the influence of the e.m.f. of a microvoltaic cell associated with the temperature variation of the electrode potential $\varphi = \varphi_0(T)$. It was found[73] that the e.m.f. of the voltaic concentration cell associated with the local changes in the activity a_i of the potential-generating ions in solution also makes a comparable contribution. The change in activity is in its turn correlated with the change in the concentration of ions in solution as a result of thermal diffusion during nonuniform laser-induced heating.

We shall now discuss the characteristic features of the laser-induced heating of absorbing electrolytes. The absorption bands of the ionic complexes in solutions are fairly broad, but they are nevertheless well separated in many cases. At the radiation wavelengths in the vicinity of the absorption maximum of the corresponding complexes, the heating rate of the solution is determined mainly by their concentration. For example, in aqueous $CoCl_2$ solutions, the Co^{2+} absorption maximum corresponds to a wavelength of 510 nm,[74] whilst in aqueous $CuSO_4$ solutions the Cu^{2+} absorption maximum is at 800 nm. The sign of the thermal diffusion constant in solutions is such that positively charged metal ions migrate as a rule from the less heated to the more heated region. In nonpolar solvents with such a value of the thermal diffusion constant for the absorbing component of the solution, a positive feedback arises between the thermal and concentration degrees of freedom, which leads to thermal diffusion instability[75] analogous to the thermal diffusion instability in gases.[19] In electrolyte solutions, the development of thermal diffusion instability is complicated by the electrical interaction between the ionic complexes. Furthermore, the change in the distributions of the thermal and concentration fields entails a change in the distribution of the electrochemical potential. Therefore a thermal electrochemical instability may develop in electrolyte solutions.[76] It consists in an avalanche-like increase in the electrochemical potential.

Experimental studies have shown[74,76] that there is a range of parameters in which nonstationary changes in the electrochemical potential are observed: from simple and quasi-harmonic to complex stochastic oscillations. The oscillations are complicated by the cascade of bifurcations associated with the doubling of the period and by the increase in the complexity of the form of the limiting cycle (Fig. 13). A similar qualitative result was obtained in a theoretical study of the purely thermal diffusion instability in a mixture of gases.[39]

The spatially nonuniform distribution of the electrochemical potential on the surface of a metallic support coated by a layer of electrolyte solution leads to the formation of a microvoltaic cell, which permits electrochemical etching and precipitation.[70,74] Thus a microvoltaic cell with an e.m.f. of ~ 0.6 V can be induced with the aid of a CW YAG-laser having a power up to 50 W. The size of the cell amounts to tens of micrometers and the precipitation current density reaches ~ 1 A cm^{-2}, which is higher by several orders of magnitude than the values used in traditional electrochemistry. The laser-induced microvoltaic cell therefore permits the establishment of high-speed and at the same time low-temperature ($T < 373$ K) regimes in the laser treatment of conducting surfaces. This is of significant technological interest.

High-speed laser processes in the liquid-phase treatment of semiconductor surfaces can be achieved similarly. For this type of laser treatment, the use of the pulsed-periodic radiation of a copper vapour-based laser proved the most effective. Under these conditions, high rates of the photogeneration of electron–hole pairs in the semiconductor and fairly high temperature gradients in the electrolyte solutions are also ensured simultaneously. The formation of a microvoltaic cell is due in this case to the semiconducting nature of the support. Calculations have shown[77] that, in the deposition of metals on the surface of gallium arsenide, a microvoltaic cell with an e.m.f. of ~ 0.5 V is formed mainly due to the Dember effect (i.e. due to the appearance of an e.m.f. as a consequence of the separation in space of the charges of electrons and holes) and the thermo-e.m.f. in the semiconductor, the Dember effect making the main contribution ($\sim 75\%$).

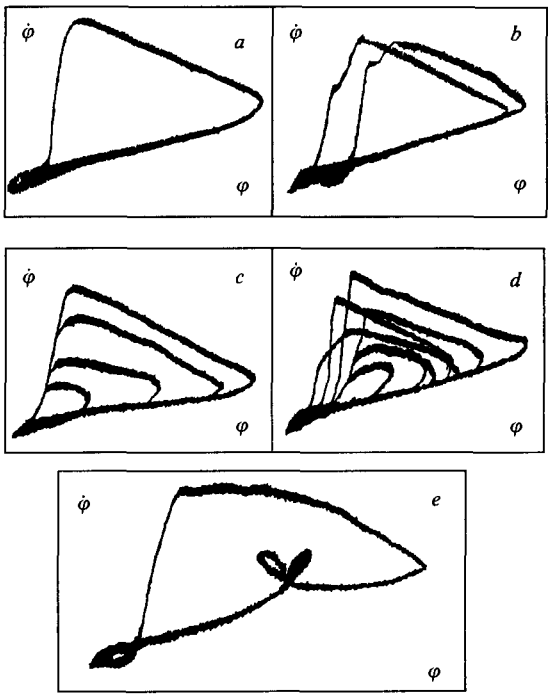


Figure 13. Phase portraits in terms of the variables φ, $\dot{\varphi}$ on the screen of an oscilloscope with a memory, obtained during the heating of an aqueous $CuSO_4$ solution by the radiation from a continuous-wave YAG-laser: (*a*)–(*d*) changes in the phase portrait as a result of the bifurcations involving the doubling of the period as the power of the laser radiation is varied; (*e*) increase in the complexity of the form of the simple limiting cycle (appearance of an additional 'small loop') as the beam width and the solution concentration are varied.

2. Dissipative structures in the laser-induced heating of thin layers of liquid

When the intensity of the laser radiation is insufficient for the bulk-phase ebullition or surface evaporation of the liquid it does nevertheless excite in the latter surface and bulk-phase hydrodynamic flows. These flows are caused by the convective instability of the nonuniformly heated stationary liquid.

Such convective flows play an important role in laser-induced thermochemical processes associated with the initiation of thermochemical and thermoelectrochemical reactions in solutions and also in processes associated with the formation of a melt on the surface of the test substance in the synthesis of surface compounds.

There exist several mechanisms for the influence of 'laser convection' on reaction kinetics. The rates of many processes in solutions are limited by the rate of supply of the reactant to the reaction zone. Initiation of convective flows promotes the removal of diffusional limitations and the acceleration of both pyrolytic and electrochemical reactions. In absorbing solutions, the situation is more complex because hydrodynamic flows are involved directly in the establishment of different feedbacks between the thermal and other degrees of freedom of the system. In particular, the eddies in the convective flows under the

conditions of nonuniform laser heating of the liquid can greatly intensify the effects of the thermal diffusion separation of the solution similarly to the situation arising in gas thermal diffusion columns with a heated filament in the centre. The hydrodynamic intensification of the separating effect can be characterised by the 'rate of rotation' of the convective eddy in the region of the separation of the test substance during the activation of the thermal diffusion instability. For example, according to Bunkin et al.,[78] the velocity of the convective streams initiated during the laser-induced heating of an aqueous $CuSO_4$ solution by the radiation of a continuous-wave YAG-laser with a power of 5–30 W is 1–30 cm s^{-1} and the rate of rotation of the eddy reaches $\sim 10^3$.

The 'hydrodynamic' feedback between the distributions of the temperature and concentration in the presence of laser-induced convection is established as follows. The increase in temperature gradient in the liquid increases the Rayleigh number. As the latter increases, the effectiveness of the thermal diffusion separation rises, as a result of which the region acted upon by the laser radiation is enriched in the absorbing ions. This increases the temperature gradient in the liquid, and so on. Experiments[73] showed that the effective thermal diffusion coefficient in the system acted upon by the laser radiation can reach values of $\sim 10^{-2}$ cm^2 s^{-1}. This exceeds by three orders of magnitude the molecular thermal diffusion coefficient of the ions in an electrolyte solution.

However, for large Rayleigh numbers (Ra > 5000), turbulence develops, leading to a sharp increase (by five orders of magnitude) in the effective normal diffusion coefficient, as a consequence of which the enriched region rapidly 'dissipates' and the homogeneity of the solution is restored. According to this scenario, auto-oscillations of the electrochemical potential, accompanied by the formation of bubbles and by the ebullition of the solution, may arise.

The development of hydrodynamic and thermal diffusion instabilities is accompanied in many instances by the formation of structures on the surface of the liquid differing from the familiar structures of the type of Benard or Marangoni cells. Among them, structures with a disturbed axial symmetry are of special interest. The appearance of such structures in a layer of a V_2O_5 melt during the laser-induced oxidation of vanadium in air has been noted.[79] It has been shown[80] that, on exposure to the continuous radiation of a YAG-laser with a power up to 150 W, there are three qualitatively different types of structures with a disturbed axial symmetry and three different scenarios for the increase in their complexity as the parameters of the laser radiation are altered (Fig. 14).

In wide beams (Fig. 14*a*), the formation of rotating spiral waves, the number of arms of which varied in the course of the oxidation process (with increase in the thickness of the fused layer of the oxide V_2O_5), has been observed. In the later stages of the oxidation process, the arms of the spiral closed, forming a stationary cellular structure. The rate of rotation of the spiral wave was 0.25–0.3 rev. s^{-1}. In beams having diameters of moderate size (Fig. 14*b*), stationary radial arms appeared, their number increasing as oxidation proceeded. Finally, following sharper focusing (Fig. 14*c*), a reverberator arose—a circular diffuse spot from which hot protuberances broke away periodically, rotating in one direction or another.

The effects observed in experiments[79,80] can be qualitatively explained as follows. During nonuniform laser-induced heating, surface flows arise in the liquid owing to the Marangoni effect together with bulk-phase flows associated with the instability of the radially and nonuniformly heated liquid. As a result, a flow with toroidal symmetry is initiated in the liquid layer, the flow rate becoming zero on the surface of the solid metal. This flow is analogous to the Couette flow between two rotating cylinders closed to form a torus. At certain rates of rotation of the cylinders, Taylor instabilities may develop in the Couette flow, as a result of which toroidal Taylor eddies arise along the entire length of the cylinder at regular intervals. The wave vector k of the resulting structure is then directed at a nonzero angle relative to the vector

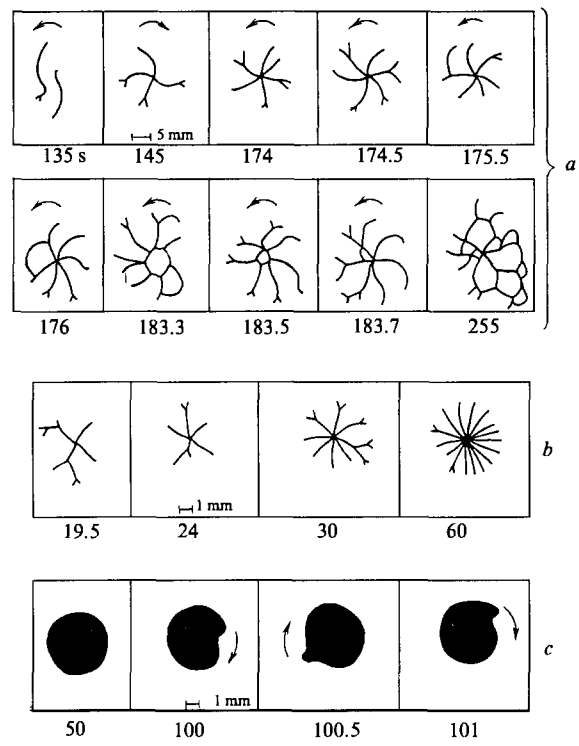


Figure 14. Dynamics of the variation of the thermal field during the heating of vanadium in air by the continuous radiation of an YAG-laser:[80] power of the laser 150 W; lines are streams of V_2O_5 melt at an elevated temperature; (*a*) wide beam 24 mm in diameter; (*b*) medium beam 18 mm in diameter; (*c*) focused beam 12 mm in diameter. The arrows in figures *a* and *c* indicate the direction of rotation of the structures and the numerals represent the times elapsed since the instant when the laser was switched on (seconds).

of the linear rate of rotation of the cylinders. For the geometry of the experiments considered, such instabilities lead to the loss of axial symmetry and to the appearance of isolated radial arms of the flow. In order that the structure obtained should rotate, the imaginary part of the increment at the instant of the loss of stability by the primary flow should be nonzero.

It has not so far been possible to create computer models of three-dimensional nonstationary structures in hydrodynamic streams, based on a direct numerical solution of hydrodynamic equations. For this reason, phenomenological or simplified models, obtained from hydrodynamic equations subject to certain assumptions, are frequently considered. Such are, for example, the Swift–Hohenberg, Kuramoto–Sivashinskii, etc. equations. The spiral waves of the type considered above are described satisfactorily by the phenomenological Arnol'd–Kirichenko equation:[81]

$$\frac{\partial w}{\partial t} = \left[\beta - A\left(k_r^2 + \frac{\partial^2}{\partial r^2}\right)^2 - 2C\left(k_r^2 + \frac{\partial^2}{\partial r^2}\right)\left(k_\varphi^2 + \frac{\partial^2}{\partial \varphi^2}\right) - \right.$$

$$\left. - B\left(k_\varphi^2 + \frac{\partial^2}{\partial \varphi^2}\right)^2\right] w + aw^2 - w^3 , \qquad (30)$$

where w is the order parameter having the significance of the deviation of the temperature from its value in the equilibrium homogeneous state, β the parameter of the supercritical state, r and φ are polar coordinates, and A, B, C, k_r, and k_φ are constants.

Numerical analysis of Eqn (30) makes it possible to describe various spatially nonuniform structures arising on development of thermocapillary instability in a thin layer of liquid. Some examples of such structures are presented in Fig. 15. The results of the calculations (Figs 15*a* and 15*b*) describe qualitatively

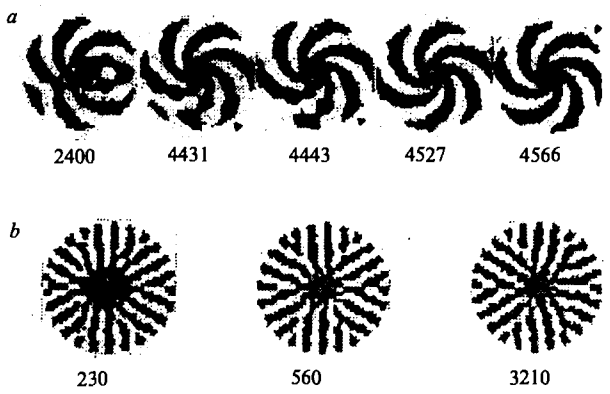


Figure 15. Two-dimensional structures found in the numerical solution of Eqn. (30) for different values of the parameters and different initial conditions (the numerals represent dimensionless times).[81]

correctly the experimentally observed structures (Figs 14*a* and 14*b*). We emphasise that the nonuniformity of the heat source is important for the appearance of these structures. This distinguishes them, for example, from the spiral waves in the Belousov–Zhabotinskii reactions arising in an initially homogeneous system.

VI. Some technological applications

1. Processes with participation of the gas phase: laser-induced precipitation and etching of a substance, separation of gases, and the synthesis of powders

The self-organisation phenomena considered above frequently lead to undesirable technological consequences. Processes with feedbacks due to the heat of a chemical reaction and the change in absorption are most dangerous in this respect. The few examples of a useful effect of the self-organisation phenomena (of the type of self-organising disequilibrium in the polyimide formation and the sharpening and localisation effects discussed above) merely emphasise the validity of the foregoing.

In addition, the dynamics of processes in the field of IR radiation are significantly more complex than in the field of radiation in the visible and UV regions. Therefore the application of the IR lasers such as the CO_2 or CO lasers is in many cases ineffective despite their great technological sophistication and excellent energy parameters. As a result of this, lasers working in the visible and UV ranges, primarily argon and excimer lasers, are mainly used in modern technologies.

Thus in order to achieve stable thermochemical processes, it is necessary to eliminate effects due to the concentration-induced change in absorption, laser radiation in the visible and UV ranges and thermally neutral or even endothermic reactions should be used, and the chemical reaction should be carried out in a region the size of which should not exceed the characteristic scale of unstable perturbations, i.e. a focused laser beam with a diameter not exceeding tens and sometimes even a few micrometers should be employed.

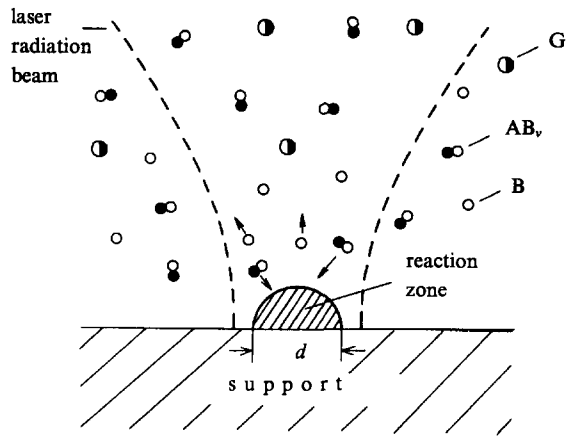


Figure 16. Typical geometry of the irradiation zone in experiments on the laser-induced deposition of a substance from the gas phase ($d = 2r_0$).

Virtually all these requirements are met in the modern technology for the laser-induced precipitation of a substance from the gas phase.[82,83] In the literature this process is frequently designated by LCVD (from the English language term Laser-induced Chemical Vapour Deposition). This technology is already used by a number of companies for the solution of certain problems in microelectronics, integrated optics, etc. and the processes achieved are indeed distinguished by their stability and by the high quality of their technological characteristics.

However, feedbacks cannot be fully excluded from laser-stimulated chemical processes. In the case of LCVD, the main cause of the disequilibrium is high temperature gradients (up to 10^6-10^7 K cm^{-1}), which lead to the interaction of different flows.

In many experiments on LCVD, the gas mixture is transparent to the laser radiation, while the deposit is thermally thin. A simplified scheme of the irradiation zone is illustrated in Fig. 16. The gas pressure usually selected is, on the one hand, not too great to avoid the appearance of an intense eddy convection in the gravitational field, and, on the other, is not too small to make sure that the thermal jump at the solid–gas interface is negligible. Typical ranges of pressures, temperatures, and activation energies for certain LCVD reactions are presented in Table 2.

In many instances, the LCVD process can be represented by the unimolecular decomposition reaction

$$AB_\nu + G \rightarrow A\downarrow + \nu B\uparrow + G, \qquad (31)$$

where AB_ν is a molecule of the gas being decomposed, G a molecule of the diluent gas, A a molecule (atom) of the substance forming the solid deposit, B a molecule of the gaseous fraction of the reaction product, and ν a stoichiometric coefficient. The processes involving the formation of solid carbon in the pyrolysis of methane and other hydrocarbons and the deposition of silicon on pyrolysis of monosilane may serve as examples of

Table 2. Activation energies for certain reactions involving the deposition of material from the gas phase at high temperatures.[83]

Reaction	T/K	Pressure range in mixture/mbar	ΔE/kJ mol^{-1}
$C_2H_2 + H_2 \rightarrow 2C\downarrow + H_2\uparrow + H_2$	1900–2450	50–1000	197.7±0.6
$C_2H_4 + H_2 \rightarrow 2C\downarrow + 2H_2\uparrow + H_2$	2000–2250	300–1000	242.7±1.3
$C_2H_2 + H_2 \rightarrow 2C\downarrow + 3H_2\uparrow + H_2$	2200–2250	300–1000	495.4±2
$CH_4 + H_2 \rightarrow C\downarrow + 2H_2\uparrow + H_2$	2850–3100	500–1000	180.8±1.4
$SiH_4 + H_2 \rightarrow Si\downarrow + 2H_2\uparrow + H_2$	1000–1800	10–1000	183.9±4

type (31) reactions. The elementary rate J of such reactions is described by the unimolecular decomposition law

$$J = k_0 N c_s \exp\left(-\frac{\Delta E}{k_B T_s}\right), \quad (32)$$

where N is the total density of the molecules in the gas, c_s the concentration of the substance AB_ν on the surface of the deposit, ΔE the activation energy for the chemical reaction, k_0 the pre-exponential factor, k_B the Boltzmann constant, and T_s the temperature of the surface. At low temperatures, the concentration of the substance AB_ν is virtually identical throughout the volume (kinetic region). At high temperatures, the rate of formation of the deposit is determined by the rate of supply of the reactant to the reaction zone (diffusional region) rather than by the rate of the elementary step involving the chemical decomposition of the molecules.

The diffusional rate limitation effect can be clearly observed in LCVD processes.[83] However, its manifestations are qualitatively different for equimolecular ($\nu = 1$) and nonequimolecular ($\nu \neq 1$) reactions. Among the reactions listed in Table 2, only that involving the deposition of carbon in the decomposition of acetylene is equimolecular.

The characteristic features of the kinetics of equimolecular reactions are determined mainly by factors such as the temperature dependence of the density and the diffusion coefficient, the existence of a thermal diffusion flux of the substance, and the presence of a diluent gas. On the other hand, the nonlinearity caused by the diffusional thermal effect as well as the concentration- and temperature-induced changes in the thermal conductivity are insignificant. In particular, thermal diffusion can lead to large (of 1–2 orders of magnitude) quantitative differences in the rate of reaction, depending on the choice of the diluent gas G.[84]

In nonequimolecular reactions, for example

$$Mo(CO)_6 \rightarrow Mo\downarrow + 6\,CO\uparrow ,$$

a directed gas flow (chemical convection) arises owing to the inconstancy of the number of molecules in the gas phase.[85,86] This effect exerts a strong influence on the reaction kinetics. In a theoretical analysis of the LCVD process, the viscosity and the nonisobaric effects are usually neglected and it is also assumed that the specific heats of the medium c_p and c_v as well as the thermal diffusion constant α are invariant. The kinetics of the LCVD process can then be described by a system of three equations: two continuity equations (for AB_ν molecules and for the gas as a whole) and the heat transfer equation (the equation for the thermal conductivity in a moving gas). This model presupposes a series of nontrivial phenomena due to the interaction of the diffusion and convective streams of the test substance. For example, for $\nu > 1$ the convective gas flow is directed away from the surface of the deposit into the bulk of the medium and therefore should seemingly inhibit the reaction. Indeed, at relatively low temperatures of the deposit this is what happens. However, at high temperature, over a certain range of values of the parameter $b = \nu - 1$, the convective flow directed from the reaction zone ($b > 0$) promotes not the retardation but actually the acceleration of the deposition of the substance. For simplicity, we shall assume that there is no thermal diffusion flow. The cause of this result is then the interaction of the flows, which takes place in accordance with the following scheme. Convection itself at $\nu > 1$ prevents diffusion (the displacement flow is directed in opposition to the diffusion flow) and at the same time it promotes the transfer of the more heated gas into the bulk of the medium and hence additional heating of the medium around the deposit. Such heating increases the diffusion coefficient, which entails an increase in the diffusion flux. The overall result is determined by the competition between two effects — the increase in the convective displacement and the increase in the opposed diffusion flux. If this leads to an increase in the concentration of the gas being decomposed in the vicinity of the surface of the support, then, by virtue of the concentration dependence of the rate of diffusion, a positive feedback arises between the concentration and diffusion fluxes.

Analysis shows that, when account is taken of the thermal diffusion flux, a complex system of feedbacks is generated between the convective, diffusion, thermal diffusion, and thermal fluxes. As a result, the overall effect cannot be determined merely on the basis of the principle of the superposition of independent material fluxes.

One of the consequences of the interaction of the fluxes is the possibility of the formation of a diffusion barrier in the vicinity of the zone where the nonstoichiometric reaction takes place.[86] This barrier is overcome by means of thermal diffusion, while ordinary diffusion and convection behind the diffusion barrier transfer the substance in the direction away from the deposit.

Thus the transfer of the test substance, which determines the reaction kinetics under the nonequilibrium conditions typical for LCVD, is complex even in the absence of a change in the absorptance of the substance or additional energy evolution by the chemical reaction itself. High temperature gradients entail effects, which cannot be eliminated, associated with the parametric interaction of different fluxes arising by virtue of the temperature and concentration dependences of the kinetic coefficients.

We have considered hitherto the LCVD process without paying attention to the form of the deposit obtained, actually assuming that it is spherically symmetrical. On the other hand, in many practical applications the spatial distribution of the deposit plays an important role. It is determined by the type of reaction and its conditions. Consider, for example, the laser-induced tungsten deposition reaction

$$WF_6 + 3H_2 + G \underset{k_{se}}{\overset{k_{sd},\,k_v}{\rightleftharpoons}} W\downarrow + 6HF + G . \quad (33)$$

In contrast to the reaction (31), the above reaction is not unimolecular. The forward pathway involves the decomposition of tungsten hexafluoride, which may occur both on the surface (rate constant k_{sd}) and in the bulk phase (k_v). The reverse reaction (etching) takes place on the surface and is characterised by the rate constants k_{se}. Different activation energies correspond to all three pathways, so that different reactions can predominate in different temperature ranges. Furthermore, the reaction rates depend greatly on the partial pressures of the components of the gas mixture. The combination of all these factors actually determines

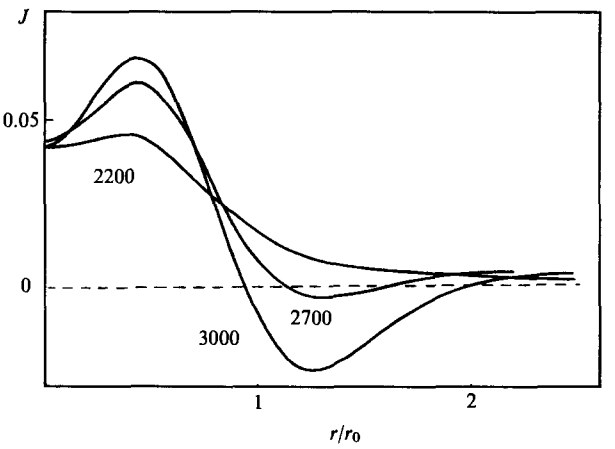


Figure 17. Typical spatial profiles of the deposit formed under the influence of laser radiation under the conditions of the diffusional limitation of the reaction for open surface and bulk-phase deposition reaction pathways and in the presence of the reverse reaction (etching).[83] The numerals opposite the curves denote the surface temperatures along the beam axis (in kelvins).

the form of the deposit produced. If the forward reaction (k_{sd}) predominates, the deposit is well localised within the limits of the radiation zone. On the other hand, if the bulk-phase reaction (k_v) predominates, then tungsten atoms are transported over large distances by diffusion in the gas and the characteristic dimensions of the deposit can appreciably exceed the size of the irradiation spot. As a result of etching, the thickness of the deposit diminishes and this can lead to the formation of a deposited substance profile which is nonmonotonic with respect to the radius. We may also note that the complex form of the deposit may be caused by the diffusional rotation of the transport of reactants in the gas phase as well.[87] Figs 17 presents the results of calculations[88] illustrating the foregoing. The minima on the curve are associated with the etching and/or diffusional limitation. The parts of the curve below the 'zero' level correspond to the etching of the support. The experimental results indicate the validity of the foregoing.[89] Fig. 18 presents photomicrographs of tungsten deposits obtained on decomposition of WF_6 and WCl_6.

Laser deposition from the gas phase is used in microelectronics not only in order to obtain localised deposits but also for the deposition of stripes with the aid of a moving laser source. The so called direct drawing regime is used for this purpose. As an example, Fig. 19 presents photographs of stripes of tungsten deposited by this method on silicon plates. The significant technological characteristics of the deposit are its height and width, conductivity, adhesion to the support, etc. It is fairly difficult to select a laser deposition regime in which the stripes possess the required technological characteristics.

The attempts to use lasers for the deposition of local structures by LCVD methods (for example from the vapours of organometallic compounds) were undertaken as early as the end of the 1960s.[91] However, the results of these studies were in most cases negative — it was not possible to ensure the required technological parameters. During this period, many specialists shared the view that the poor quality of the stripes is mainly caused by the inadequate characteristics of the lasers themselves. Almost fifteen years were needed in order to understand that the 'technological' difficulties have deep physical roots. They are associated with the capacity of nonequilibrium systems to undergo self-organisation.

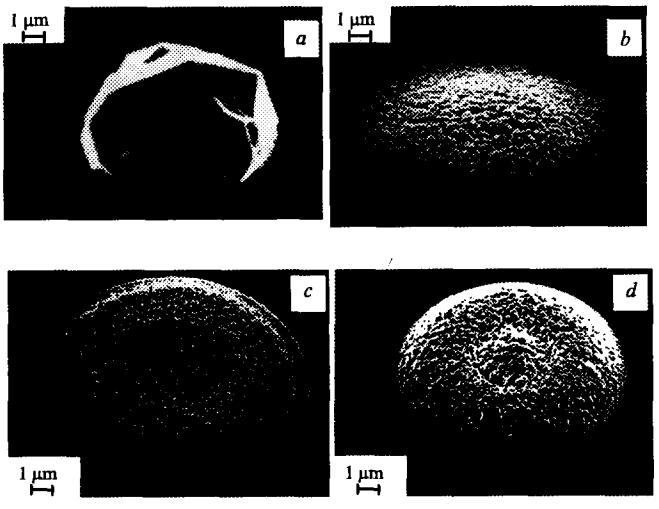


Figure 18. Photomicrographs of tungsten deposits in the decomposition of WF_6 (*a* and *b*) by the radiation of an argon laser (λ = 514.5 nm) and in the decomposition of WCl_6 by the radiation of a dye laser (λ = 680 nm) (*c* and *d*) at different partial pressures and for different irradiation conditions.

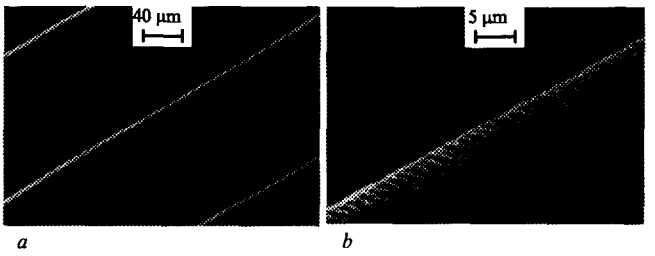


Figure 19. Photomicrographs of tungsten stripes deposited from a $WF_6 + H_2$ mixture on silicon plates under the influence of the radiation from a Kr^+ laser (λ = 647.1 nm).[90]

For a theoretical determination of the form of the deposited stripe it is necessary to solve chemical kinetic equations simultaneously with the equations for the thermal field generated by the moving laser source. In contrast to the problems discussed above, in problems of this kind the negative feedback between the deposition kinetics and temperature, determined by the influence of the form of the stripe itself on the distribution of the thermal field, proved to be significant. Since the thermal conductivity of the metallic stripe is many times greater than the thermal conductivity of the support (particularly a dielectric support), an additional heat flux arises from the irradiation zone towards the side away from the direction of movement of the source. Such outflow of heat is higher the greater the cross-section of the stripe. The presence of such 'geometrical' feedback together with other factors (for example, the change in absorption) leads to numerous instabilities and self-organisation phenomena: the deposits are formed in many cases with an internal structure, with various pulsations in the thickness and width of the stripe, etc.[83] In order to discover the optimum treatment conditions, it is in many cases necessary to employ the methods of the self-organisation theory.

The related problem of the high-temperature laser synthesis of powders from the gas phase is closely associated with LCVD processes. Many refractory compounds (boron nitride and carbide, silicon nitride, the oxides of certain metals, etc.) can be synthesised in the form of finely dispersed powders with particle sizes ranging from tens to hundreds of ångströms if the laser radiation is focused directly in the gas mixture.[92] Such powders have practical applications as abrasive materials and they can also be pressed and sintered in the form of shaped specimens. Examples are provided[92] by the synthesis of silicon carbide powders, i.e.

$$SiH_4 + CH_4 \rightarrow SiC\downarrow + 4H_2\,, \tag{34}$$

or

$$2SiH_4 + C_2H_4 \rightarrow 2SiC\downarrow + 6H_2\,, \tag{35}$$

and also the synthesis of silicon nitride, i.e.

$$4NH_3 + 3SiH_4 \rightarrow Si_3N_4\downarrow + 12H_2\,. \tag{36}$$

The reactions frequently have high activation energies and a high temperature is therefore required to carry them out. There is no special difficulty in attaining a local temperature of several thousand degrees with the aid of lasers. The particles formed in the course of the elementary reactions subsequently coalesce and form clusters. Similar processes have been observed at high temperatures also in the reactions occurring in the laser-induced deposition of a substance.[83] In this case the growth of the deposit is no longer a result of the elementary process (31) considered above, but is due to the transport of clusters in the gaseous medium and their subsequent deposition on the support.

Different mechanisms of the laser-induced nucleation are possible. For example, if the gaseous medium absorbs weakly the laser radiation, the reaction can be initiated first in the vicinity of impurity absorbing centres (impurity species, dust particles, etc.) and can then attain a self-supporting regime due to absorption in the cluster itself. A similar mechanism can operate in the nucleation in LCVD processes.[83]

The kinetics proper of the growth of the cluster constitute a separate problem. The cluster can grow both as a result of 'sticking' to other clusters and as a result of the increase in its intrinsic volume. In particular, if the synthesis on the surface of the nucleus takes place more effectively than in the bulk of the gas, then the cluster may grow via the same mechanism as the deposit in LCVD.

Effects associated with the change in activation energy due to strong surface tension forces play a significant role for microclusters. The physicochemical properties of microclusters differ markedly from those of the corresponding macroformations.[93]

In discussing LCVD processes above, we spoke of molecular mass transfer due to conventional diffusion, thermal diffusion, and chemical convection. By virtue of nucleation, other mass transfer mechanisms are also possible. For example, in the usual (nonlaser) problems of the chemical deposition of a substance, clusters migrate via thermophoresis,[94] as a result of which the particles are expelled from the more heated to the less heated region. It would therefore seem that microclusters should not settle at all on the heated surface. However, experiments have demonstrated an effective flux of clusters onto the heated surface. Direct experimental measurements of the distribution of temperature in the boundary layer over the heated deposition surface[95] showed that, owing to the considerable evolution of energy on coalescence of the microclusters, caused by the decrease in their surface energy, an additional intense heating of the gas takes place in the cluster growth zone. For example, on formation of carbon clusters from hydrocarbons, cluster formation leads to additional heating of the gas regardless of whether the decomposition reaction itself is exothermic or endothermic. This results in the establishment of a nonmonotonic distribution of temperature with a maximum which is separated from the heated wall by 200–500 μm. The temperature at the maximum exceeds by 300–500 K that of the wall itself.[95] As a consequence, a thermophoretic force directed towards the wall is generated. On the other hand, in the case of the laser-induced synthesis of powders, apart from thermophoresis, other forces acting on the particles arise, for example forces associated with the radiometric effect (at low gas pressures), etc.

In nonequimolecular reactions, the force due to the difference between the flux recoil momenta (associated with the chemical convection in the gas) on the 'hot' and 'cold' sides of the particle, also acts on the microparticle. In contrast to thermophoresis and the radiometric force, which expel the particle with the 'cold' side in front, the directional forces associated with the chemical convection depend on the stoichiometry of the reaction. This phenomenon can be properly referred to as 'chemophoresis'. The chemophoretic effect can be readily understood with the aid of the following considerations.

Suppose that a spherically symmetrical particle with a radius R is in a temperature field $T(z)$ with a constant gradient $\gamma = \mathrm{d}T/\mathrm{d}z$. Then the boundary condition for the rate of migration of a gas v on the surface of the particle is

$$v = bc_{AB}k_0 \exp\left(-\frac{T_a}{T}\right), \tag{37}$$

where c_{AB} is the concentration of the substance AB_ν on the surface of the particle, $b = \nu - 1$, and $T_a = \Delta E/k_B$. We shall assume that the reaction proceeds in the kinetic region (c_{AB} = const.). The temperature of the surface of the particle is

$$T = T(\theta) = T_0 + \gamma R\cos\theta, \tag{38}$$

so that the temperature drop across the particle is $2\gamma R$. The component of the gas momentum, summed over the surface, is

$$P_z \simeq Mbc_{AB}k_0 \int_0^\pi \left[2\pi R^2 \sin\theta\cos^2\theta \times \right.$$
$$\left. \times \exp\left(-\frac{T_a}{T_0 + \gamma R\cos\theta}\right)\right]\mathrm{d}\theta =$$
$$= Mbc_{AB}k_0 \exp\left(-\frac{T_a}{T_0}\right)2\pi R^2\varphi, \tag{39}$$

where in the limit $\gamma R \ll T_0$ we have

$$\varphi \simeq \int_{-1}^{1} y^2 \exp(-\xi y)\,\mathrm{d}y = \left(\frac{2}{\xi} + \frac{4}{\xi^3}\right)\sinh\xi - \frac{4}{\xi^2}\cosh\xi,$$

$$\xi = \frac{T_a}{T_0^2}\gamma R.$$

By virtue of the symmetry of the problem, all the remaining components of the momentum (P_x and P_y) become zero. Hence, as a result of the recoil, the particle acquires a nonzero momentum equal to $-P_z$. It is seen from Eqn (39) that the chemophoretic force depends not only on the gradient γ but also on the temperature T_0. Its pressure dependence is therefore different from that of the force due to the radiometric effect and is determined by the reaction kinetics. It is also noteworthy that the chemophoretic force may be considerable.

The laser-induced etching process is closely related to deposition. The etching effects arise when the chemical interaction of the surface atoms of the support (for example, a silicon plate) with the reactive molecules or radicals of the gas phase results in the formation of a more volatile substance (for example, a $SiCl_4$ molecule), which leads to the removal of the solid phase. Chemically reactive molecules can arise in the gas phase on laser-induced thermal dissociation of, for example, halogen-containing gases (for the specific features of such processes, see Karlov et al.[96]). Whilst referring the readers to the original communications as regards the details of this technology (see, for example, Bäuerle,[83] Takai et al.[97] as well as the references quoted therein), we may note that channels with a width and depth ranging from several to several tens of micrometers can be formed in semiconductors, ferrites, and other materials by means of laser-induced chemical etching. The rate of the laser-induced etching can greatly exceed[97] the rate of the plasma-chemical etching[98] usually employed in microelectronics. Apart from the evident applications of the laser-induced etching technology in microelectronics, to which many of the investigations have been directed, this technology can also be employed in micromechanics[99] (preparation of miniature mechanical components, for example, in accelerometers, with dimensions corresponding to several tens of micrometres, etc.).

Among the problems of the kinetics of the laser-induced etching, we may note the diffusional limitation of the reaction (as regards the supply of the etching agent and the removal of the volatile reaction products) similar to that examined above for the LCVD process. In the range of high temperatures, diffusional limitation should restrict the rate of reaction. On the other hand, experiments[97] have shown that the rates of etching are high compared with those which could occur under the conditions of diffusional limitation. One of the explanations of this technologically favourable effect is that, at the high pressures of the gas mixtures used for etching, an intense gravitational convection develops which removes the diffusional limitation.

There exist also purely chemical problems of etching associated with the multistage nature of many reactions and the participation in the latter of intermediate surface products.[100] As in the case of LCVD, further development of the technology of the laser-induced chemical etching requires special research which would make it possible to understand more fully the nature of the process and the possibility of its optimisation.

Laser-induced separation of gases is based on the thermal diffusion effect. In the usual thermal diffusion columns, a heated filament is used as the source generating a nonuniform thermal field.[101] Such a column operates also in the case where the function of the heated filament is assumed by a beam of laser radiation absorbed in the gas mixture. However, as we have seen above, laser radiation can intensify the effect associated with the thermal diffusion separation of the mixture as a result of the positive feedback established between the concentration and thermal degrees of freedom of the system. In the usual thermal diffusion column, convection in the gravitational field plays an

important role in intensifying the separation effect.[101] Laser radiation can enhance also this convective effect as a result of the positive feedback between convection, thermal diffusion, and the heat evolved. The existence of different kinds of positive feedbacks renders the separation of the gas mixture in a laser thermal diffusion column more effective than in the usual column. This has been confirmed by direct experiments.[102]

2. Processes at the interface between two solid phases: direct drawing, etching, and synthesis

The action of laser radiation on the surface of a solid on which films of other solids have been deposited leads to the modification of the properties of the film and/or the surface of the solid (support). With the aid of such solid-phase sandwich structures, it is possible to achieve virtually all types of microchemical treatment of the surface: deposition of metals, etching of the surface, syntheses of various compounds on the surface of the support. One is dealing with a solid-phase microtreatment technology which is an alternative to the traditional technologies (plasma, gas-phase, and liquid-phase technologies).

Certain metal salts, for example those of formic and oxalic acids, readily decompose on heating to the pure metal and volatile components. The decomposition of copper formate may serve as an example:

$$Cu(HCOO)_2 \rightarrow Cu\downarrow + H_2O\uparrow + CO\uparrow + CO_2\uparrow. \qquad (40)$$

The process temperature under the usual conditions is 598 K. Copper formate is deposited on the surface in the form of a powder or a suspension. The thin surface layer is then acted upon by a laser, which results in the formation of copper stripes on various supports.[91] It is possible to obtain solid films of organic substances by using various solvents, which then volatilise during drying. Metallic stripes, formed from the resinates of various metals,[83] triphenylphosphine complexes of univalent gold,[103] etc. are deposited by this procedure.

The laser-induced decomposition of certain substances, for example poly(vinyl chloride) films, results in the formation of free radicals, chlorine molecules, etc., which can etch the support. Multilayer structures of the support–decomposable film–glass type are used in the experiment. Laser radiation acts from the side of the transparent glass. Under these conditions, one can obtain etched channels in the glass several ångströms deep and several tens of micrometres wide.

The most detailed studies have been carried out on the laser-induced synthesis of substances from thin films.[104,105] Extremely pure compounds of various elements, including compounds of the type $A^{III}B^{V}$ (AlSb, AlAs), $A^{II}V_x^{VI}$ (CdTe, CdSe, ZnSe), $A^{IV}B^{VI}$ ($GeSe_2$, GeSe), ternary compounds ($CuInSe_2$), etc. have been synthesised. This technology can be used to record information on high-capacity optical discs and also in microelectronics and integrated optics.

Many scientific problems are associated with the preparation of compounds from thin-film structures. We shall elucidate some of them in relation to the synthesis of the binary compounds A+B → AB (in particular of AlSb from aluminium and antimony films). Experiments have shown[104] that, when such a structure is heated in an ordinary furnace up to the melting point of aluminium (933 K), about 100 s is required for the formation of the AlSb film. The reason for this is fairly simple: the initial AlSb layer is formed at the site of contact between aluminium and antimony. The melting point of AlSb (1353 K) exceeds the melting points of its constituent elements. The solid film formed therefore separates the components in space. In this case, the rate of reaction is limited by the diffusion of atoms through the layer of AB, as happens in reactions involving the heterogeneous oxidation of metals. On the other hand, under the conditions of pulsed laser action, which heats the film to the same temperature, the synthesis takes place effectively during the laser pulse of 10 ns. If the validity of the estimated temperature is accepted and it is postulated that the formation of the film is limited by diffusion, then this means that the coefficients of the diffusion of atoms through the AlSb layer acted upon by laser radiation should be anomalously high (of the order of 10^{-2} cm^2 s^{-1}). We recall that the phenomenon of the anomalously rapid diffusion first attracted attention in the analysis of the laser-induced annealing of semiconductors.[24,25] Experiments have shown[104] that in the laser-induced synthesis of films there is a threshold energy equal to the energy necessary to fuse aluminium. On the other hand, if the multilayer structure prepared is subjected to preliminary annealing at 623 K for 30 min and longer, then the threshold energy required for the synthesis increases by 60% and corresponds to the melting point of AlSb. The possible explanations of the results of these experiments are as follows: in contrast to experiments in a furnace, exposure to laser radiation does not result in the formation of a planar AlSb layer but instead the liquids are rapidly mixed with subsequent chemical reaction; owing to the heat of the chemical reaction in the film, under certain irradiation conditions, 'inflammation' takes place over a brief period, as a result of which the film of the compound synthesised melts.

The presence of a melt is indicated, for example, by structures of the type of Benard bridges (Fig. 20), which were observed in the synthesis of CdSe and a number of other films. However, there is also evidence that the laser-induced synthesis is accelerated also in the solid phase of the film. It may be that such increased 'permeability' of the solid films is associated with the presence in the latter of non-equilibrium vacancies. This mechanism of the acceleration has been discussed.[38] The experimental results can also be interpreted as the effect of the decrease in the melting point[104] of the solid film presaturated by nonequilibrium vacancies.[104]

Finally, yet another interesting problem, observed in the course of a study of the laser-induced synthesis of thin-film compounds, is that of the presence of large (up to 1 μm, i.e. many times greater than the thickness of the film) single crystals of many compounds (AlSb, $GeSe_2$, $CuInSe_2$, etc.) on irradiation of the initial structure with 10^{-6} s laser pulses. In order to account for these effects, the idea of the 'polymerisation' of liquids, in particular $GeSe_2$, has been put forward.[104] We may note that the rapid crystallisation of films from the melt in the synthesis of compounds differs significantly from the analogous process in the laser-induced annealing of semiconductors, where there is epitaxial growth of the film, for example of silicon, from the melt on an orienting support. In the synthesis of thin-film compounds, there is no orienting support and the crystal nuclei formed are oriented at random. Therefore, in the rapid laser-induced synthesis, polycrystalline or amorphous films should be



Figure 20. Photomicrograph of the convective ridges formed in the synthesis of the CdSe sandwich structure on glass in air;[104] power of the laser 1 W; typical cell size ~10 μm; ratio of the ridge width to thickness ~50.

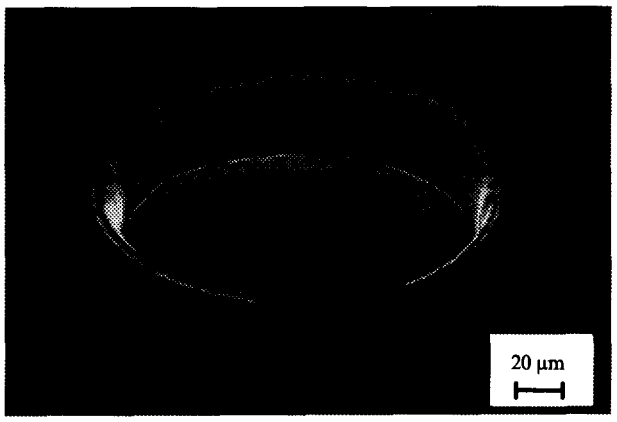


Figure 21. Crater formed in a $LiNbO_3$ single crystal on exposure to a XeCl excimer laser (500 pulses with an overall energy density of 2.7 J cm^{-2}). The half-height diameter of the beam was 175 μm.

observed depending on the rate of cooling, which does in fact frequently occur. On the other hand, the formation of large single crystals during rapid crystallisation on a nonorienting support is possible because of the orienting forces of the external mechanical stresses.[106] One should therefore analyse carefully the experimental conditions in order to eliminate fully the possibility of the generation of such stresses.

Other features of the laser-induced synthesis have also been noted—such as the retention of the high stoichiometry of the compounds obtained, the dependence of the orientation of the synthesised film on the wavelength of the laser radiation observed in certain cases, etc.[104, 105]

3. Laser-induced ablation of polymers

An important aspect of laser chemistry is associated with the phenomenon of laser-induced ablation, i.e. the effect of the removal of material under the influence of radiation, in which the resulting crater contains no traces of the melt or any kinds of mechanical failures (Fig. 21). The properties of the laser-induced ablation make it an attractive procedure for various applications in microelectronics, medicine, and other fields.[107-109]

The laser-induced ablation of polymers is usually carried out with the aid of excimer lasers. The characteristic features of this process are as follows: the existence of an irradiation energy density threshold, the change in the optical properties of the substance in the course of exposure to radiation, a nonequilibrium distribution with respect to the velocities of the products removed.

The existence of the threshold may be due to different causes. One of them is thermal sublimation with a pronounced Arrhenius temperature dependence of propagation of the velocity of the sublimation front.[109] Another cause is the development in the substance of elastic stresses,[107] which must reach critical values necessary for removing a significant amount of mass. Yet another cause may be multiphoton (or stepwise) absorption,[107, 108] which requires fairly high light intensities.

The change in the optical properties of the test substance may be associated both with irreversible processes, for example, with thermochemical or photochemical reactions,[107] as well as reversible processes, for example with the passage of light due to the saturation of the populations of the levels between which the transition responsible for the absorption of light takes place.[110]

The distribution with respect to composition and velocities of the products removed is of great interest.[107] Indeed, the products of the ablation of polymers include both low-molecular-mass fragments (pure carbon, simple organic molecules, and small clusters) as well as fragments with a moderate molecular mass close to that of the monomers (or part of the monomers) of the initial substance. In addition, the removal of large clusters (lumps of the initial polymer) and large carbon particles is observed. The latter is of particular interest in connection with the synthesis[111] of macromolecular carbon C_{60}. In the velocity distribution of products, the equilibrium (Maxwellian) fraction and the fraction comprising nonequilibrium fast particles are clearly differentiated.[107] So far this complex pattern cannot be convincingly explained within the framework of the concept of secondary photolysis or multiphoton absorption.

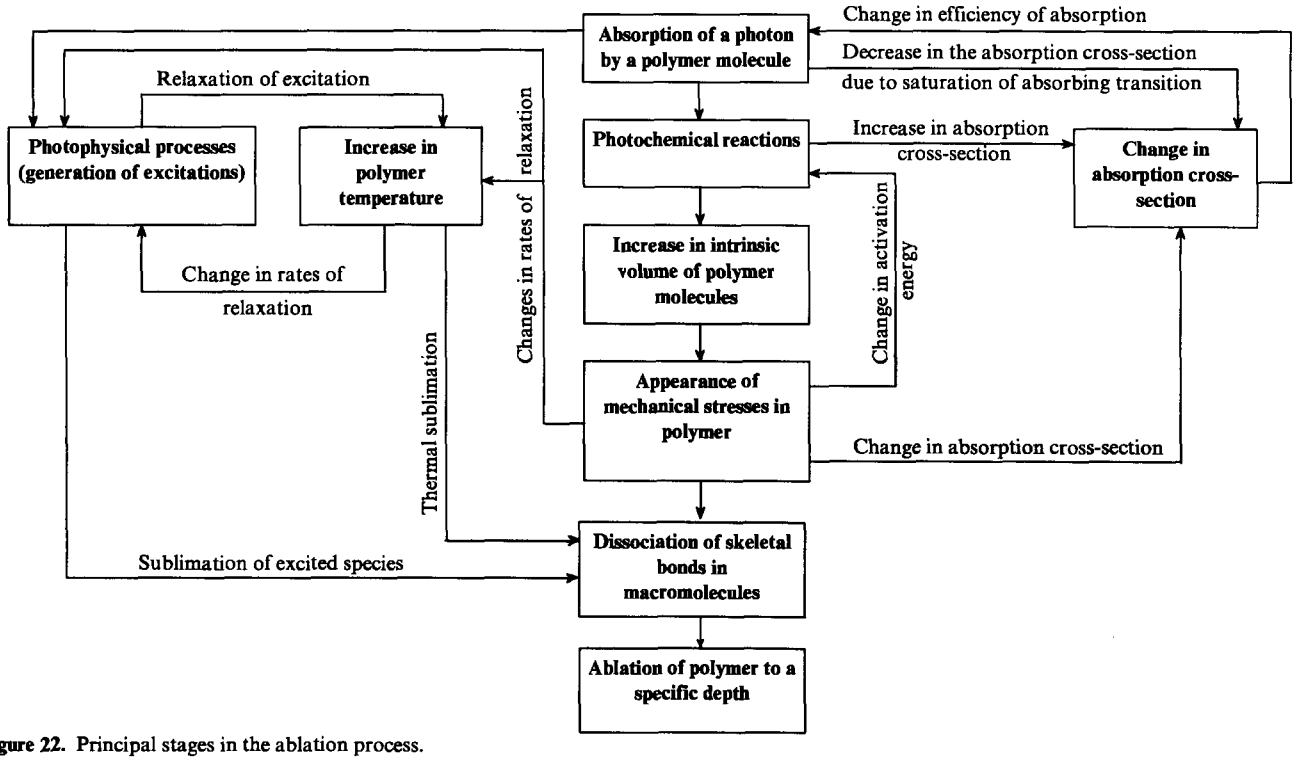


Figure 22. Principal stages in the ablation process.

The data on the dynamics of the development of mechanical stresses in the system and the dynamics of the removal of material during ablation[107] agree better with the thermal sublimation model than with the model involving the photothermomechanical removal, according to which the main bulk of the substance is carried away in the relaxation wave after the operation of the laser radiation pulse has ceased.

The behaviour of species in an electronically excited state plays an important role in the ablation process. The presence of such species in strongly absorbing polymers is not open to doubt.[110] Together with the change in the optical properties,[110] there exist many other pathways by means of which the excited species can affect the kinetics and dynamics of the laser-induced ablation. The sublimation of these species takes place with a reduced activation energy, which permits the assumption of the existence of a cold sublimation regime at a surface temperature below the melting point. Furthermore, such sublimation alters the velocity distributions of the species eliminated.

The characteristic features of the ablation can also be associated with the relaxation process during fusion. In view of the relative slowness of these processes even at temperatures appreciably greater than the melting point,[112] sublimation may be faster than fusion. This probably explains the absence of traces of fusion even at high surface temperatures.

Finally, mention may be made of an important factor associated with the influence of mechanical stresses in the substance on the activation energies of various processes.[113] Such stresses may arise both owing to the usual thermoelasticity and owing to the different volume of the products of the chemical reactions compared with the starting material.[114] Many other factors can also play an important role in the ablation processes. A scheme of the principal stages in the ablation process, similar to that quoted by Kitai et al.,[112] is presented in Fig. 22. Evidently the process is fairly complex and its complete description is almost impossible. Therefore simplified models have to be often used. The most pronounced simplification consists in the fact that the process is assumed to be purely photophysical and of the threshold type, i.e. the entire substance in which the density of the absorbed energy φ exceeds a certain threshold density φ_0 is removed. In this case the thickness of the layer of the substance removed is

$$h = \frac{1}{\alpha}\ln\left(\frac{\varphi}{\varphi_0}\right), \qquad (41)$$

where α is the absorption coefficient for the radiation. This empirical formula reproduces qualitatively the behaviour $h = h(\varphi)$ in the vicinity of the ablation threshold and is therefore frequently used in the analysis of the experimental data (as a rule without justification).

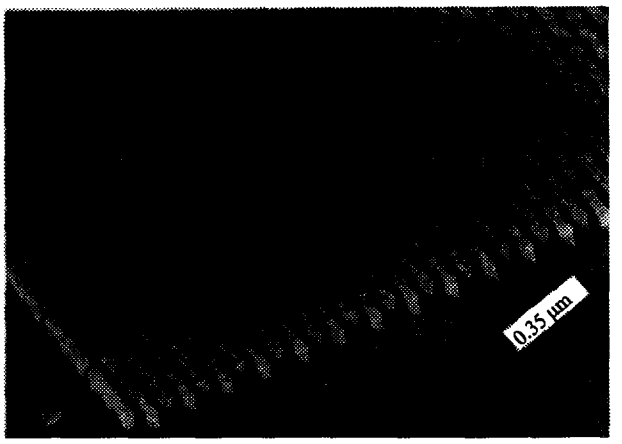


Figure 23. Specimen prepared from a multilayer photoresist with the aid of a KrF laser.[120]

Owing to the large number of positive feedbacks, the laser-induced ablation is characterised by many instabilities and spontaneously generated structures (some of them have been observed experimentally in a number of investigations[115–119]). However, it is possible to select empirically conditions under which polymers can be treated effectively and phototemplates for submicron lithography may be obtained. An example of one such structure is presented in Fig. 23.

* * *

Within the framework of a short review, it is difficult to provide an exhaustive list of the technological applications of laser thermochemistry. The foregoing text merely illustrates certain aspects of the applied research. The list may be significantly expanded, for example by including studies in the field of laser thermolithography,[121] microtreatment of a surface in a liquid,[70,74] selective laser-induced extraction from liquids,[122] etc. However, we believe that even the present review is sufficient to demonstrate that laser thermochemistry[123] is a rapidly developing field, which is of great scientific interest and has numerous practical applications.

References

1. D A Frank-Kamenetskii *Diffuziya i Teploperedacha v Khimicheskoi Kinetike* (Diffusion and Heat Transfer in Chemical Kinetics) (Moscow: Nauka, 1987)
2. A G Merzhanov, E N Rumanov *Usp. Fiz. Nauk* **151** 553 (1987)
3. A M Zhabotinskii *Kontsentratsionnye Avtokolebaniya* (Concentration-induced Auto-oscillations) (Moscow: Nauka, 1974)
4. G Nicolis, I Prigogine *Self-organisation in Nonequilibrium Systems* (New York: Wiley, 1977)
5. B V Vol'ter, I E Sal'nikov *Ustoichivost' Rezhimov Raboty Khimicheskikh Reaktorov* (Stability in the Regimes Governing the Operation of Chemical Reactors) (Moscow: Khimiya, 1981)
6. V A Vasil'ev, Yu M Romanovskii, V G Yakhno *Avtovolnovye Protsessy* (Autowave Processes) (Ed. D S Chernyavskii) (Moscow: Nauka, 1987)
7. V L Tal'roze, P P Barashev *Zh. Vses. Khim. O-va im. D I Mendeleeva* **18** 15 (1973)
8. A Ben-Shaul, Y Haas, K L Kompa, R D Levine *Lasers and Chemical Change* (Berlin: Springer, 1981)
9. A N Oraevskii *Vestn. Akad. Nauk SSSR* **6** 132 (1982)
10. V S Letokhov *Nelineinye Selektivnye Fotoprotsessy v Atomakh i Molekulakh* (Nonlinear Selective Photoprocesses in Atoms and Molecules) (Moscow: Nauka, 1983)
11. Yu N Molin, V N Panfilov, A K Petrov *Infrakrasnaya Fotokhimiya* (Infrared Photochemistry) (Novosibirsk: Nauka, 1985)
12. V M Akulin, N V Karlov *Intensivnye Rezonansnye Vzaimodeistviya v Kvantovoi Elektronike* (Intense Resonance Interactions in Quantum Electronics) (Moscow: Nauka, 1987)
13. V N Bagratashvili, Doctoral Thesis in Physical-Mathematical Sciences, Karpov Physicochemical Institute, Moscow, 1986
14. V L Tal'roze, in *Gazodinamicheskie Lazery i Lazernaya Fotokhimiya* (Gas-Dynamic Lasers and Laser Photochemistry) (Moscow: Izd. Mosk. Gos. Univ., 1987) p. 105
15. J F Asmus, F S Baker, in *Records of 10th Symposium on Electron, Ion and Laser Beam Technology, San Francisco, 1969*, p. 241
16. V P Veiko, G A Kotov, M N Libenson *Dokl. Akad. Nauk SSSR* **208** 587 (1973)
17. M I Arzuov, V I Konov, S M Metev *Fiz. Khim. Obrab. Mater.* **5** 19 (1978)
18. A Nitzan, J Ross *J. Chem. Phys.* **59** 241 (1973)
19. A Nitzan, P Ortoleva, J Ross *J. Chem. Phys.* **60** 3134 (1974)
20. A N Oraevskii, V A Savva *Kratk. Soobshch. Fiz.* **7** 50 (1970)
21. N D Artamonova, V T Platonenko, R V Khokhlov *Zh. Eksp. Teor. Fiz.* **58** 2195 (1970)
22. P P Barashev, V L Tal'roze *Khim. Vys. Energ.* **3** 30 (1971)
23. I M Dunskaya *Lazery i Khimiya* (Lasers and Chemistry) (Moscow: Nauka, 1979)
24. J A Van Veehten *Solid State Commun.* **39** 1285 (1981)

25. V V Kopaev, Yu V Kopaev, S N Molotkov *Mikroelektronika* **12** 499 (1983)
26. F V Bunkin, N A Kirichenko, B S Luk'yanchuk *Izv. Akad. Nauk SSSR, Ser. Fiz.* **45** 1018 (1981)
27. F V Bunkin, N A Kirichenko, B S Luk'yanchuk *Kvantovaya Elektron. Mosk.* **11** 1183 (1984)
28. N V Karlov, E K Karlova, N A Kirichenko, V S Luk'yanchuk, O V Neklyudova, I Ya Ravich, A N Sapetskii, T N Toroptseva *Kvantovaya Elektron. Mosk.* **9** 2049 (1982)
29. N N Semenov *Tsepnye Reaktsii* (Chain Reactions) (Moscow: Nauka, 1986)
30. F V Bunkin, N A Kirichenko, B S Luk'yanchuk *Izv. Akad. Nauk SSSR, Ser. Fiz.* **49** 1054 (1985)
31. A G Merzhanov, E N Rumanov *Gorenie bez Topliva* (Combustion without Fuel) (Moscow: Znanie, 1978)
32. N A Kirichenko, A G Korepanov, B S Luk'yanchuk *Kvantovaya Elektron. Mosk.* **7** 2049 (1980)
33. S V Selishchev, in *Vozdeistvie Kontsentrirovannykh Potokov Energii na Metally* (The Effect of Concentrated Energy Fluxes on Metals) (Moscow: Nauka, 1985) p. 170
34. H Haken *Synergetics* (Translated into Russian) (Moscow: Mir, 1980) *Synergetics: Hierarchies of the Instabilities in Self-organising Systems and Devices* (Translated into Russian) (Moscow: Mir, 1985)
35. F V Bunkin, N A Kirichenko, B S Luk'yanchuk, Yu Yu Morozov *Kvantovaya Elektron. Mosk.* **10** 2136 (1983)
36. F V Bunkin, N A Kirichenko *Dokl. Akad. Nauk SSSR* **277** 1357 (1984)
37. F V Bunkin, N A Kirichenko, Yu Yu Morozov *Pis'ma Zh. Eksp. Teor. Fiz.* **41** 378 (1985)
38. V I Boiko, B S Luk'yanchuk, E R Tsarev, in *Lazernaya Generatsiya Neravnovesnykh Defektov v Tverdom Tele. Trudy IOFAN* (Laser-Induced Generation of Nonequilibrium Defects in a Solid. Transactions of the Institute of General Physics, Academy of Sciences) (Moscow: Nauka, 1991) Vol. 30, p. 6
39. F V Bunkin, N A Kirichenko, Yu Yu Morozov *Izv. Akad. Nauk SSSR, Ser. Fiz.* **51** 1162 (1987)
40. F V Bunkin, N A Kirichenko, B S Luk'yanchuk, G A Shafeev *Kvantovaya Elektron. Mosk.* **9** 1864 (1982)
41. Yu P Raizer *Lazernaya Iskra i Rasprostranenie Razryadov* (The Laser Spark and the Propagation of Discharges) (Moscow: Nauka, 1973)
42. N D Arnol'd, N A Kirichenko, B S Luk'yanchuk, A V Sheludyakov *Longitudinal Bistability and Travelling Pulses in the Propagation of Laser Radiation in Media with Nonlinear Absorption* Preprint from the Institute of General Physics, Academy of Sciences, Moscow, 1989, No. 35
43. M R Taghizadch, I Janossy, S D Smith *Appl. Phys. Lett.* **46** 331 (1985)
44. F V Bunkin, N A Kirichenko, B S Luk'yanchuk *Kvantovaya Elektron. Mosk.* **9** 704 (1982)
45. N A Kirichenko *Instability of a Laser Radiation Beam in a Chemically Reactive Medium* Preprint from the Physicochemical Institute of the Academy of Sciences, Moscow, 1982, No. 196
46. N N Rykalin, A A Uglov, I V Zuev, A N Kokora *Lazernaya i Elektronno-Luchevaya Obrabotka Materialov* (Laser and Electron Beam Treatment of Materials) (Moscow: Mashinostroenie, 1985)
47. P Barre *Kinetics of Heterogeneous Processes* (Translated into Russian) (Moscow: Mir, 1976)
48. M I Arzuov, F V Bunkin, N A Kirichenko, V I Konov, B S Luk'yanchuk *Pis'ma Zh. Eksp. Teor. Fiz.* **27** 230 (1978)
49. A M Prokhorov, V I Konov, I I Ursu, I N Mihailescu *Vzaimodeistvie Lazernogo Izlucheniya s Metallami* (Interaction of Laser Radiation with Metals) (Moscow: Nauka, 1988)
50. F V Bunkin, N A Kirichenko, V I Konov, B S Luk'yanchuk *Kvantovaya Elektron. Mosk.* **7** 1548 (1980)
51. V A Bobyrev, F V Bunkin, N A Kirichenko, B S Luk'yanchuk, A V Simakin *Kvantovaya Elektron. Mosk.* **9** 695 (1982)
52. M Wautelet *Appl. Phys. A* **50** 131 (1990)
53. D T Alimov, F V Bunkin, I V Edvabnyi, N A Kirichenko, B S Luk'yanchuk, P K Khabibulaev *Poverkhnost'* **9** 82 (1982)
54. O G Buzykin, A V Burmistrov, M N Kogan *Poverkhnost'* **9** 91 (1982)
55. O G Buzykin, A V Burmistrov *Poverkhnost'* **10** 91 (1983)
56. D T Alimov, V A Bobyrev, N A Kirichenko, B S Luk'yanchuk, Yu N Mitin, A I Omel'chenko, A V Simakin, P K Khabibulaev *Dokl. Akad. Nauk SSSR* **268** 850 (1983)
57. V A Bobyrev, F V Bunkin, N A Kirichenko, B S Luk'yanchuk, A V Simakin, G A Shafeev *Poverkhnost'* **4** 134 (1984)
58. A C Damask, G J Dienes *Point Defects in Metals* (New York: Gordon and Breach, 1963)
59. M I Arzuov, F V Bunkin, N A Kirichenko, V I Konov, B S Luk'yanchuk *Pis'ma Zh. Eksp. Teor. Fiz.* **5** 193 (1979)
60. V A Bobyrev, F V Bunkin, N A Kirichenko, B S Luk'yanchuk, S A Ubaidullaev *Fiz. Khim. Obrab. Mater.* **3** 19 (1988)
61. V A Bobyrev, F V Bunkin, N A Kirichenko, B S Luk'yanchuk, A V Simakin *Kvantovaya Elektron. Mosk.* **10** 793 (1983)
62. G A Shafeev *Experimental Study of the Ammonia Oxidation Reactions Stimulated by Laser Radiation* Preprint from the Institute of General Physics, Academy of Sciences, Moscow, 1984, No. 194
63. V A Bobyrev, F V Bunkin, N A Kirichenko, V S Luk'yanchuk, A V Simakin *Pis'ma Zh. Eksp. Teor. Fiz.* **32** 608 (1980)
64. T S Akhromeeva, F V Bunkin, N A Kirichenko, S P Kurdyumov, G G Malinetskii, A A Samarskii *Izv. Akad. Nauk SSSR, Ser. Fiz.* **51** 1154 (1987)
65. N A Kirichenko, Yu Yu Morozov *Modelling of Spiral Waves in Laser-Induced Heating of Metals* Preprint from the Institute of General Physics, Academy of Sciences, Moscow, 1990, No. 92
66. N A Kirichenko *Izv. Akad. Nauk SSSR, Ser. Fiz.* **53** 1215 (1989)
67. N R Anisimov *Pis'ma Zh. Eksp. Teor. Fiz.* **8** 1320 (1982)
68. F V Bunkin, N A Kirichenko, B S Luk'yanchuk, A N Sapetskii *Poverkhnost'* **6** 98 (1982)
69. Yu A Gurevich, Yu V Pleskov *Fotoelektrokhimiya Poluprovodnikov* (Photoelectrochemistry of Semiconductors) (Moscow: Nauka, 1983)
70. R J von Gutfeld, in *Laser Processing and Diagnostics. Springer Series in Chemistry and Physics* (Ed. D Bäuerle) (Berlin: Springer, 1984)
71. E B Damaskin, O A Petrii *Osnovy Teoreticheskoi Elektrokhimii* (Fundamentals of Theoretical Electrochemistry) (Moscow: Vysshaya Shkola, 1978)
72. F V Bunkin, B S Luk'yanchuk, G A Shafeev *Pis'ma Zh. Eksp. Teor. Fiz.* **39** 464 (1984)
73. N F Bunkin, A K Dmitriev, B S Luk'yanchuk, G A Shafeev, T Szorenyi *Appl. Phys. A* **40** 159 (1986)
74. B S Luk'yanchuk, G A Shafeev, in *Lasers — Physics and Applications. Proceedings of the 5th International School in Quantum Electronics* (Ed. A I Spasov) (Singapore: World Scientific, 1989) p. 359
75. F V Bunkin, B S Luk'yanchuk, G A Shafeev *Kvantovaya Elektron. Mosk.* **12** 2391 (1985)
76. F V Bunkin, B S Luk'yanchuk, G A Shafeev *Izv. Akad. Nauk SSSR, Ser. Fiz.* **50** 1176 (1986)
77. Z C Wu, D A Jelski, T F George, L Nanai, I Hevesi, F V Bunkin, M R Brook, B S Luk'yanchuk, G A Shafeev *Chem. Mater.* **1** 353 (1989)
78. N F Bunkin, B S Luk'yanchuk, G A Shafeev *J. Inform. Rec. Mat.* **15** 323 (1987)
79. N F Bunkin, N A Kirichenko, B S Luk'yanchuk, A V Simakin, G A Shafeev, L Nanai, I Hevesi *Acta Phys. Hung.* **54** 111 (1983)
80. D T Alimov, V A Bobyrev, F V Bunkin, B S Luk'yanchuk, S A Ubaidullaev, P K Khabibullaev *Izv. Akad. Nauk SSSR, Ser. Fiz.* **51** 1144 (1987)
81. N D Arnol'd, N A Kirichenko *Zh. Eksp. Teor. Fiz.* **101** 1395 (1992)
82. D Bäuerle (Ed.) *Laser Processing and Diagnostics. Springer Series in Chemistry and Physics* (Berlin: Springer, 1984) Vol. 39
83. D Bäuerle *Chemical Processing with Lasers. Springer Series in Materials Science* (Berlin: Springer, 1986) Vol. 1
84. D Bäuerle, B S Luk'yanchuk, K Piglmayer *Appl. Phys. A* **50** 385 (1990)
85. N Kirichenko, K Piglmayer, D Bäuerle *Appl. Phys. A* **49** 51 (1990)
86. B S Luk'yanchuk, K Piglmayer, N Kirichenko, D Bäuerle *Physica A* **180** 285 (1992)
87. N A Kirichenko *Izv. Akad. Nauk SSSR, Ser. Fiz.* **55** 1333 (1991)
88. N Kirichenko, D Bäuerle *Thin Solid Films* **218** 1 (1992)
89. Z Toth, P Kargl, C Grivas, K Piglmayer, T Szorenyi, D Bäuerle *Appl. Phys. B* **54** 189 (1992)
90. D Bäuerle *Appl. Phys. B* **46** 261 (1988)
91. V P Veiko, M N Libenson *Lazernaya Obrabotka* (Laser Treatment) (Leningrad: Lenizdat, 1973)
92. J I Steinfeld (Ed.) *Laser-Induced Chemical Reactions* (Translated into Russian) (Moscow: Mir, 1984)
93. S Sugane, Y Nishina, S Ohnishi (Eds) *Microclusters . Springer Series in Materials Science* (Berlin: Springer, 1984) Vol. 4
94. S P Bakanov, B V Deryagin, V I Roldugin *Usp. Fiz. Nauk* **129** 255 (1979)

95. S Yu Volkov, V V Smirnov, V P Yazan *Pis'ma Zh. Eksp. Teor. Fiz.* **16** 54 (1990)
96. N V Karlov, B S Luk'yanchuk, E V Sisakyan, G A Shafeev *Kvantovaya Elektron. Mosk.* **12** 803 (1985)
97. M Takai, J Tsichimoto, I Tokuda, H Nakai, K Gamo, S Namba *Appl. Phys. A* **45** 305 (1988)
98. N G Einsbruch, D M Brown (Eds) *Plasma Processing for VLSI* (Translated into Russian) (Moscow: Mir, 1987)
99. J C Peterson *V Mire Nauki* (In the World of Science)1986
100. N V Karlov, A M Prokhorov *Usp. Fiz. Nauk* **123** 57 (1977)
101. A K Kikoin, I K Kikoin *Molekulyarnaya Fizika* (Molecular Physics) (Moscow: Nauka, 1976)
102. F Bachman *IR-Laser Induzierte Reactionen: Beiträge zum Temperaturprofil und zum Nachweis von Primärproduktion* Preprint, Max-Plank-Institut für Quantenoptik, MPO-57, 1981
103. F V Bunkin, K I Grandberg, B S Luk'yanchuk, E G Perevalova, G A Shafeev *Kvantovaya Elektron. Mosk.* **13** 1227 (1986)
104. L D Laude, M Wautelet, R Andreev *Appl. Phys. A* **40** 133 (1986)
105. L D Laude, in *Interfaces under Laser Irradiation* (Eds L D Laude, D Bäuerle, M Wautelet) (Dordrecht: Martinus Nijhoff, 1987) p. 301
106. Yu A Bityurin, S V Gaponov, A I Gudkov, V L Mironov *Kvantovaya Elektron. Mosk.* **11** 181 (1984)
107. R Srinivasan, B Braren *Chem. Rev.* **89** 1303 (1989)
108. S Lazare, V Granier *Laser Chem.* **10** 25 (1989)
109. D Bäuerle, B Luk'yanchuk, P Schab, X Z Wang, E Arenholz, in *Laser Ablation of Electronic Materials. Basic Mechanisms and Applications* (Eds E Fogarassy, S Lazare) (Amsterdam: Elsevier, 1992) p. 39
110. R Sauerbrev, G H Pettit *Appl. Phys. Lett.* **55** 421 (1989)
111. E E B Campbell, G Ulmer, B Hasselberger, H G Busmann, I V Hertel *J. Chem. Phys.* (1990)
112. M Kitai,V L Popkov, V A Semchishen *Macromol. Chem. Macromol. Symp.* **37** 257 (1990)
113. V R Regel', A I Slutsker, E E Tomashevskii *Kineticheskaya Priroda Tverdykh Tel* (Kinetic Nature of Solids) (Moscow: Nauka, 1984)
114. B J Garrison, R Srinivasan *J. Appl. Phys.* **57** 2909 (1985)
115. Y Novis, J J Pireaux, A Brezini, E Petit, R Caudano, P Lutgen, G Fyder, S Lazare *J. Appl. Phys.* **64** 365 (1988)
116. H Niino, A Yabe, S Nagano, T Miki *Appl. Phys. Lett.* **54** 2159 (1989)
117. H Niino, M Nakano, S Nagano, A Yabe, T Miki *Appl. Phys. Lett.* **55** 510 (1989)
118. H Niino, N Shimoyama, A Yabe *Appl. Phys. Lett.* **57** 2368 (1990)
119. E Arenholz, V Svorak, T Kefer, J Heitz, D Bäuerle *Appl. Phys. A* **53** 330 (1991)
120. Y Horiike, N Hayasaka, M Sekine, T Aricado, M Nakase, H Okano *Appl. Phys. A* **44** 313 (1987)
121. I M Karpman, M N Libenson, E B Yakovlev *Lazernaya Termolitografiya v Proizvodstve Integral'nykh Skhem* (Laser Thermolithography in the Manufacture of Integrated Circuits) (Leningrad: Izd. LDNTP, 1981)
122. N V Karlov, E K Karlova, B N Laskorin, A M Prokhorov, N P Stupin, L B Shurmel' *Kvantovaya Elektron. Mosk.* **6** 2190 (1979)
123. N V Karlov, N A Kirichenko, B S Luk'yanchuk *Lazernaya Termokhimiya* (Laser Thermochemistry) (Moscow: Nauka, 1992)

Russian Chemical Reviews **62** (3) 227 – 236 1993
© 1993 Russian Academy of Sciences and Turpion Ltd

UDC 548.52 + 66.065

Crystal sensorics

I V Melikhov

Contents

I.	Introduction	227
II.	Fundamentals of crystal sensor action	227
III.	Theory	228
IV.	Basic relationships	228
V.	Methods of increasing the sensitivity	232
VI.	Diagnostic systems	233
VII.	Conclusions	234

Abstract. The phenomena responsible for the dependence of the rate of nucleation, growth, and aggregation of crystals on the concentration and state of trace impurities in the supersaturated medium are discussed. Methods of increasing the sensitivity of the crystallisation to the presence of trace impurities are described. Data on diagnostic systems capable of detecting ultrasmall quantities of impurities from their effect on crystallisation are presented. The bibliography includes 210 references.

I. Introduction

In recent years the well known effects of impurities on crystallisation has stimulated the development of a new field of science: the crystal diagnostics of impurities. The term crystal diagnostics describes the detection, identification, and determination of the amount and state of molecular or colloidal impurities in liquid or in gaseous media from their effect on the crystallisation of a specially chosen substance: the crystallisant. At present crystal diagnostics are used in many laboratories throughout the world. The method now has its own theory and research methodology, and it can claim remarkable success in the determination of extremely small amounts of impurities, down to a few thousand and even hundreds of molecules. Thus we can assert that the foundations of a special field of knowledge (the sensitivity of crystallisation to the presence of small traces of impurities, i.e. crystal sensorics) have already been laid.

The recent developments in crystal sensorics can be attributed to two reasons. One is the unexpectedly large effect of some trace components on crystallisation,[1-3] which stimulated theoretical studies and led to a deeper understanding of the role of microcomponents. The second is the ever-increasing concern with the behaviour of trace components in ecological problems.[4, 5] The need to determine tens of thousands of different ions, complexes, isomers, conformers, and aerosol species present at concentrations down to 10^{-9} g cm^{-3} has been met only in the chemistry of the hydrosphere and of the atmosphere,[6, 7] and the best solution of these problems is not always clear.[8] In some cases a suitable solution has been provided by crystal sensorics. Thus, Kogan[9] determined small quantities (20 – 50 atoms cm^{-3}) of lead by using pyridine-2,6-dicarboxylic acid. Under certain conditions he found that in the condensation of this compound from a vapour containing lead the number of condensate particles was equal to the number of lead atoms.

In 1980 Ansorge and Maeyer[10] found that the reduction of silver nitrate by formaldehyde in a solution containing traces of protein can be controlled so that one silver microcrystal appears on each protein molecule. In this way they could estimate the amount of protein in the sample (approximately 10^6 molecules) from the number of Ag microcrystals. Lastly, in 1983 Kucher[11] used solid hydrazine to detect traces of aldehyde in the atmosphere. The conditions of the reaction were chosen to make the number of resulting hydrazone crystals proportional to the concentration of aldehydes. By counting the hydrazone crystals aldehydes in air could be detected at concentrations down to 10^{-9} g cm^{-3}. These studies[10, 11] led to the development of crystal-sensor diagnostic systems whose most important properties are listed below.

II. Fundamentals of crystal sensor action

It has been established experimentally that when a liquid (or gas) containing a microscopic component is supersaturated with respect to a crystallisant, crystallisation centres appear in its volume and grow, relieving the supersaturation.[2] On the other hand if the crystals are formed in large numbers they coalesce and grow together into aggregates. In the presence of trace components these processes follow paths different from those of the same processes in the pure liquid. As a result the kinetic parameters of the crystallisation (induction period, rate, number of crystals produced) and the morphological properties of the crystals (size, shape, and defect density) depend on the nature of the microcomponent.[12] The dependence is specific. If several trace components are present simultaneously in the system it is usually possible to choose the crystallisant and the crystallisation conditions which make the contribution of one of the trace components to the process predominant. Under these conditions by varying the crystallisation conditions we can ensure that the action of the trace component is selective and restricted either to the formation of the nucleation centres or to their growth and aggregation.

Experiments have also shown that if the trace component is sparingly soluble and is present in the medium (liquid, or gaseous) in amounts which make it supersaturated with respect to the trace

I V Melikhov Department of Chemistry, Lomonosov Moscow State University, Leninskie gory, 119899 GSP-3 Moscow V-234, Fax (7-095) 939 01 26

Received 9th December 1992
Uspekhi Khimii **62** (3) 249 – 259 (1993); translated by J I Carasso

component itself the concentration and state of the latter can be assessed from the kinetics of its spontaneous crystallisation.[13] It may therefore be useful to define the following limiting types of crystal sensor behaviour.

1. Impurity nucleation sensor action, i.e. the ability of the crystallisant to vary its rate of nucleation in response to the presence of the trace component.

2. Growth-related impurity sensor action, i.e. the ability of the crystallisant to vary its growth rate and surface features in response to the presence of the trace compound.

3. Impurity aggregation sensor action, i.e. the change in the rate of aggregation, size, and shape of the crystalline aggregates of the crystallisant under the influence of the trace component.

4. Spontaneous crystal sensor action, i.e. the ability of the trace component to vary the kinetic parameters of its spontaneous crystallisation and the properties of its crystals in response to changes in its concentration and state in the medium.

The sensor behaviour of any of these types can be characterised quantitatively by the functions $B_j(C, \Gamma)$, where B_j is the crystallisation parameter (or property of the crystal) which is sensitive to the trace component of concentration C and parameters of state Γ in the liquid. The simplest characteristics of the sensor behaviour could be the partial sensitivity factor A_j, the limit of detection Π, and the total sensitivity factor A:

$$A_j = B_{0j}^{-1}\left[C\frac{\partial B_j}{\partial C} + \Gamma\frac{\partial B_j}{\partial \Gamma}\right], \quad \Pi = \lim_{B_j \to B_{0j}} C, \qquad (1)$$

$$A = \sum_{j=1}^{n} A_j .$$

Here B_{0j} is the value of the parameter B_j in the absence of the trace component, and n is the number of crystallisation parameters and of properties of the crystals included in the diagnostic. Phenomena close to crystal sensor behaviour include catalysis with formation of a solid product, and photographic sensitivity. In the former case the crystallisant is formed in the medium by a chemical reaction, accelerated by the catalyst (trace component). In the latter the trace component is formed by a photochemical reaction.[14] In this respect both cases differ from the crystal sensor behaviour, in which the trace component and the crystallisant are both present in the medium initially.

III. Theory

The foundations of the theoretical studies of crystal sensorics include the models of condensation, crystal growth, and aggregation of colloids in a medium free from impurities (background models) and in the presence of trace component (working models). Most of the models are macrokinetic, with the nucleation and growth of the crystals expressed in terms of kinetic coefficients which require experimental determination.[15-18] Models in which the kinetic coefficients are expressed through the parameters of the molecular motion in the medium and on the surface of the crystals have also been developed.[19, 20]

The base model is the model of condensation in a dilute but slightly supersaturated vapour (or solution) in the presence of an impurity and of a carrier gas (to remove the heat of condensation), allowing for the formation of clusters of crystallisant and of impurity molecules and for their growth by the incorporation of free molecules or of other clusters.[21-26] The base models usually assume the existence of a critical size, below which the clusters can be treated as quasi-equilibrium formations. The probability of cluster formation is determined by the free energy of the formation, calculated quantum-chemically[27, 28] or estimated by processing data from molecular dynamics and from Monte Carlo calculations.[29-31]

Models of crystal growth include self-association and molecular adsorption processes, surface diffusion, surface clustering,[32-35] and interaction with growth steps.[36-38] The modelling of the aggregation allows for the successive addition of single microcrystals,[39-41] the equilibrium breakdown of the aggregated phase into fragments,[42-45] and the amalgamation of aggregates.[46-50] Recent developments have been reported in the numerical modelling of aggregation and fragmentation by the cluster dynamics and the Monte Carlo method,[51-55] and also analytical solutions of the kinetic balance equations describing the populations of aggregates.[56-60] The background models are the most generally used, the working models being confined to a small group of substances. Therefore the possibility of predicting the effect of the properties of the impurity and of the crystallisant on the rate of crystallisation is very limited at present.

IV. Basic relationships

1. Mechanism of the nucleation sensor action

In order to induce crystal sensor action we must generate a supersaturation with respect to the crystallisant in the diagnostic medium. In the supersaturated medium the molecules (or ions) of the crystallisant and the trace component combine to form clusters which grow by adding on single molecules or by the mutual aggregation of the clusters themselves.[61-72] The frequencies of the addition and removal of molecules vary irregularly with the size of the clusters (with a general trend for a decrease in the frequency of removal with increasing cluster size).[64] As a rule a cluster size can always be found for which the frequency of addition is smaller and that of removal is much greater than for both the smaller and the larger clusters. For example, in aqueous alkaline solutions of Fe(III) salts the critical cluster is the tetramer $[Fe(OH)_3]_4$,[65] whereas in solutions of 1,1′-diethyl-2,2′-cyanine chloride it is the pentamer.[72] When the number of molecules in the cluster is increased to $n = 500-1000$ regrouping can take place, and the structure of the cluster tends towards the structure typical of the macrocrystal.[61] After the rearrangement the properties of the cluster are indistinguishable from those of the massive body.[62, 63]

In a medium containing trace components heteroclusters containing molecules of both the crystallisant and the trace component can be formed. They grow, and become rearranged, in different ways from the homoclusters (consisting only of crystallisant molecules), as was established experimentally and by calculations.[73-79] In particular, heteroclusters are characterised by exchange reactions such as[80]

$$[Fe_6C(CO)_{16}]^{2-} + RhCl_3 \xrightarrow[80\%]{40\ ^\circ C,\ 2\ s} [Fe_5RhC(CO)_{16}]^{2-} + FeCl_3 .$$

No quantitative data on the kinetics of the growth of heteroclusters are yet available. Indirect information can be obtained from the frequency of the appearance of microcrystals: this involves the assumption that critical clusters are instantaneously converted into microcrystals. From the rate of appearance of the microcrystals we may conclude that in some cases the heteroclusters are formed many orders of magnitude faster than the homoclusters. Many solutions in which microcrystals are not formed even after several days in the absence of impurities produce crystal immediately when an impurity is added.[2] For example, in aqueous solutions an impurity of $PbCl_2$ accelerates the formation of K_4MnCl_6 microcrystals by more than 10^6.

Precise measurements have shown that the number of microdrops of water formed in a moderately supersaturated vapour containing ionised air molecules is proportional to the number of these molecules, the frequency of drop formation being at least three orders of magnitude greater than in the absence of ions.[76, 77] Atomic and molecular impurities have similar effects. Thus, if atomic lead ($10-100$ atoms cm^{-3}) is introduced into a stream of very pure saturated pyridine-2,6-dicarboxylic acid (dipicolinic acid) vapour, by cooling the vapour and measuring (after some time) the concentration of drops of the acid it can be shown[9] that if the supercooling is substantial each lead atom generates one drop of the acid (Figure 1). In a mixture of dilute $Fe_2(CO)_9$ vapour

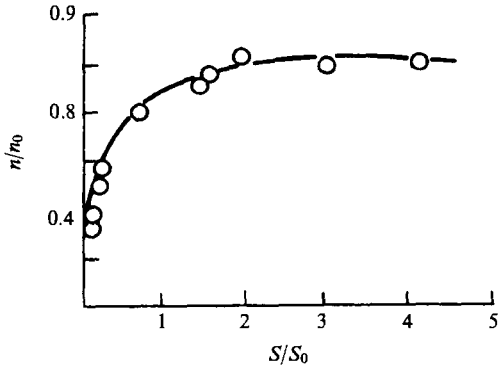


Figure 1. Dependence of the number of drops of dipicolinic acid in the vapour upon the supersaturation:[9] n and n_0 are the numbers of drops and of lead atoms in unit volume of the vapour, $S = [(C/C_\infty) - 1]$ is the supersaturation of the vapour, C_∞ is the concentration of the acid in the saturated vapour, and S_0 is the reference supersaturation.

($10^3 - 10^{18}$ molecules cm^{-3}) and slightly supersaturated dioxyethyl sebacate (DES) vapour drops of DES are nucleated exclusively on the $Fe_2(CO)_9$.[78] This means that in this case the rate of formation of critical heteroclusters is 10^5 times higher than in homoclusters.

In all the cases mentioned so far the heteroclusters develop so rapidly that each molecule of the trace component becomes overgrown with crystallisant and is converted into a microscopic drop or crystal, and thus produces a large number of homoclusters of the crystallisant of critical size. In these cases the crystals decorate the molecules of the trace component. Decoration of the molecules takes place also during the crystallisation of silver in solutions of large aminoacid or protein molecules.[10] Thus, if $AgNO_3$ is added to a solution of DNA or of protein, and a reducer (formaldehyde) is then added, silver microcrystals are nucleated and grow only on the protein molecules.[81-83] These microcrystals are strongly bound to the protein and follow it during the electrophoretic separation.[10] Evidently the $AgNO_3$ and the formaldehyde are taken up by the protein like the Cu(II) and Ni(II) salts[84, 85] and small organic molecules.[86] In the bound state the $AgNO_3$ and the formaldehyde can interact and deposit silver on the parts of the protein molecule between the domains.[87]

However, cases of full predominance of the heteroclusters over the homoclusters are only seldom met. Often the two types develop with comparable speeds, and as a result the effect of the trace components on the nucleation is less marked, and confined to relatively high concentrations.

It has been established experimentally[88-94] that the effect of the trace components on the nucleation is selective. They can both accelerate and retard the process, and often similar compounds have different effects.[88] In particular, organic substances can affect the crystallisation of metals (Cu, Ni, Co, Fe, Ag, Au, Ru, Rh, Pt, Pd, Re, Sn, Te, In, Cd, Bi, Pb) from aqueous solutions by the reduction of their salts (for example, by borohydride).[89, 90] Compounds containing nitrogen and sulphur (thiocyanates, polysulphides, dithionates, thiocarbamide, dithiocarbamates, thioaminoacids, dithiols, thiazines) lower the rate of nucleation at concentrations of $10^{-4} - 10^{-3}$ mol dm^{-3}, whereas other substances are effective only at concentrations of $10^{-2} - 10^{-1}$ mol dm^{-3}. Under these conditions the mutual enhancement of the inhibitors' effects is non-additive.[91]

As was concluded by processing the results of Tsebul'skaya et al.,[94] in the crystallisation of nickel the rate of nucleation B_N depends on the concentration C of the impurity as described by the formula

$$B_N = B_{N,0}[1 - a(C/C_r)^{1/2}]^{-1}, \qquad (2)$$

where $B_{N,0}$ is the rate of nucleation in the absence of the impurity, a is an empirical parameter, and C_r is the critical concentration.

For an alkyldimethylamine impurity $a = -1$ and $C_r = (3.5 \pm 0.2) \times 10^{-4}$ mol dm^{-3}; for methionine, cysteine, thiocarbamide, 5-nitrobenzimidazole, and the tetraalkylammonium bromides $a = -1$ and $C_r = 10^{-5} - 10^{-4}$ mol dm^{-3}, and C_r is independent of the length of the alkyl chain in the tetraalkylammonium molecules; for cetylpyridinium chloride $a = 1$ and $C_r = 5 \times 10^{-2}$ mol dm^{-3}.

It follows from formulae (1) and (2) that the limit of detection of these impurities from their influence on nucleation (assuming a minimum significance level of 5% in the difference between B_N and B_{N0}) is $\Pi = 2.5 \times 10^{-3}\ C_r = 10^{-8} - 10^{-4}$ mol dm^{-3}. The sensitivity factor of the nucleation towards these impurities is $A_N = -0.5a(C/C_r)^{1/2}(B/B_{N0})^2$ if the influence of the impurities is determined exclusively by their concentration, i.e. if $\Gamma = 0$.

The rate of nucleation is also dependent on the presence of colloidal impurities. In some solutions impurity particles about 1 nm in diameter are known to behave as giant clusters which absorb the crystallisant and are rapidly converted into crystals. It has been reported[95-97] that if a polystyrene strip is immersed in a solution of $PdCl_2$ and $SnCl_2$ (0.1 – 1.0 g dm^{-3}) in hydrochloric acid, washed with water, and then transferred to a solution of $NiCl_2$ containing a reducing agent, nickel hemispheres (which can easily be developed and counted) are formed on the surface. The following processes are probably involved. In the initial solution in hydrochloric acid the reaction $SnCl_2 + PdCl_2 = Pd + SnCl_4$ produces colloidal palladium, deposited on the polystyrene surface as particles 0.3 – 1 nm in diameter. These are not removed from the surface by washing, and when the strip is immersed in a solution of $NiCl_2$ they grow by nickel deposition. After some time each colloidal particle of palladium is converted into a nickel hemisphere large enough to be easily counted. New nickel particles are not nucleated on the surface during this time, and the rate of nucleation is controlled exclusively by the palladium particles. A similar state of affairs is found in the crystallisation of copper and of many other metals.[89]

2. Growth sensor action

The effect of trace components on the growth of crystals depends on the relative energies of the interactions between crystallisant, trace component, and solvent molecules. If the trace component interacts with the solvent more strongly than with the crystallisant the effect is principally an acceleration of the growth by the salting-out of the crystallisant. With comparable interaction energies the predominant effect is contributed by the formation of solvated impurity–crystallisant complexes, which can both accelerate and suppress the growth. On the other hand, if the impurity interacts with the crystallisant more strongly than with the solvent, adsorption blocking of the surface by the impurity takes place, and usually suppresses the growth. Many workers have discussed these effects,[37, 98-120] but a generally valid dependence of the growth rate on the concentration and state of the impurity has not yet been formulated. It has been shown experimentally[105-107] that the growth of many salt crystals in weakly supersaturated solutions containing trace impurities is described by the isotherm

$$B_G = B_{G0}\left[Q + \frac{1-Q}{1 + C/C_v}\right], \qquad (3)$$

where B_G and B_{G0} are the normal growth rate of the crystals with and without the impurity, Q is the maximum possible decrease in the growth rate under the influence of the impurity, and C_v is an empirical parameter, dependent on the supersaturation. From (1) and (2) we obtain

$$\Pi = \frac{C_v b}{1 - Q - b}, \qquad A_N = \frac{Q-1}{(1+C/C_v)^2}\,\frac{C}{C_v}, \qquad (4)$$

where b is the smallest statistically significant relative deviation of B_G from B_{G0}. According to formula (4) the growth rate is

sensitive to the impurity at a concentration of the order of C_v. At lower concentrations the amount of impurity is too small (and at higher concentrations it is too great) to produce a significant change in B_G.

There is evidence[37, 105–110] that for many (and possibly for all) of the crystallisants special impurities can be found for which $Q \to 0$ (superinhibitors). For example, hydroxyethylene-1,1'-diphosphonic acid (for $C_v = 10^{-8}$ mol dm^{-3}) is a superinhibitor for calcite,[105] triethylenediaminetetramethylenephosphonic acid ($C_v = 10^{-6}$ mol dm^{-3}) for gypsum, and $CrCl_3$ ($C_v = 5 \times 10^{-7}$ mol dm^{-3}) for KH_2PO_4 and $NH_4H_2PO_4$.[109, 110]

An important example of inhibition is the cyanide retardation of the growth of AgHal crystals by iron and cobalt cyanides during the preparation of photographic emulsions.[111] The acceleration of the growth of crystals by an impurity has also been reported.[112–114]

If the crystal grows by the layer mechanism not only the normal growth rate (i.e. the rate of growth of a face at right angles to the surface) but also the parameters of the surface morphology of the crystal are sensitive to the impurity.[98–114] In layer growth the crystallisant is deposited on the surface of the crystal in successive layers.[37] It was experimentally found that molecules of the trace component deposited on the sides of the steps formed by the growth layers can suppress the attachment of molecules of the crystallisant to those steps (poisoning of the steps). Furthermore the adsorbed impurity can form a molecular fence on the faces, which inhibits the extension of the layers over the face (cut-off retardation of the growth).[98–101] This effect makes the surface morphology sensitive to the impurity. It was shown[109, 110] that the steepness of the growth hillocks on the faces of growing crystals of KH_2PO_4 is no less sensitive to the presence of $CrCl_3$ than is the normal growth rate (Fig. 2). At low supersaturations the faces have a complex morphology and the crystals grow very slowly. The growth rate becomes appreciable only at supersaturations in excess of some threshold value S_r. By processing published data[109, 110] it was shown that the threshold supersaturation S_r for KH_2PO_4 crystals is

$$S_r = S_0[1 + 1.1C/C_K], \quad (5)$$

where S_0 is the threshold supersaturation in the pure solution, and C and C_K are the concentrations of $CrCl_3$ and of the crystallisant in the solution. It follows from (1) and (5) that if the threshold supersaturation is used as the diagnostic criterion, a detection limit of $\Pi = 9.1 \times 10^{-7}\, bC_K$ can be achieved for chromium. For a claimed[109] significance level of the deviation of $b = 0.05$, $\Pi = 4.5 \times 10^{-8}\, C_K$. Even lower limits of detection can be reached by choosing a crystallisant for which crystal growth takes place through the formation of intermediate surface compounds incorporating the impurity. It was established that metal crystals grow faster under the influence of impurity–crystallisant complexes which transfer an electron.[115] For example, the crystals of a series of metals dissolved as their chlorides MCl_2 in the presence of an alkali M'OH and of a reducing agent RH grow as a result of the reaction[83, 116]

$$RH + 2M'OH + MCl_2 = ROH + H_2O + M + 2M'Cl. \quad (6)$$

The reducing agent and the chloride interact when adsorbed on the crystal faces. The M adatoms produced in this way combine to form surface clusters, and subsequently ultramicrocrystals, which arrange themselves in a layer as in the layer growth mechanism.[117–119] In the absence of the impurity the reaction (6) is slow. However, if a crystal of copper or nickel is treated (before growth) for 40 s with a 10^{-3} mol dm^{-3} solution of cetylpyridinium chloride (CPC), its growth is accelerated by a substantial factor as a result of a charge-transfer reaction within the complex:

$$RH + CPC + MCl_2 \to [RH(CPC)MCl_2] \xrightarrow{2M'OH}$$

$$\to ROH + H_2O + M + 2M'Cl + CPC. \quad (7)$$

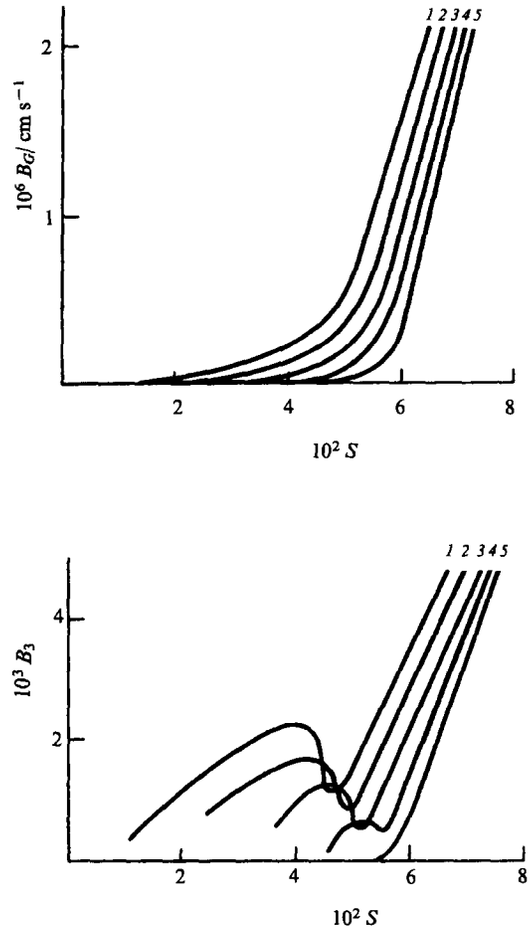


Figure 2. Dependence of the growth parameters of a KH_2PO_4 crystal on the supersaturation S for different contents of $CrCl_3$ in the solution.[109, 110] B_G is the normal growth rate, B_3 is the steepness of the growth hillocks; concentration of trace component: *1*) 0, *2*) 1.5, *3*) 3.3, *4*) 4.5, *5*) 6 ppm.

In reaction (7) the CPC acts as a catalyst, and the sensitivity of the crystal growth to this process can be maximised by choosing the most favourable conditions.

The action of trace components on faces with different surface morphologies is usually selective. As a result, the trace components can affect the habit of the crystals. Only $CdCl_2$, $MnCl_2$, $PbCl_2$, $ZnCl_2$, $HgCl_2$ influence the habit of NaCl crystals growing in an aqueous solution at low supersaturations: no other soluble chloride has any effect.[120] $CdCl_2$ and $ZnCl_2$ favour the formation of (111) faces instead of the more usual (100) for $\Pi = 5 \times 10^{-3}$ and 5×10^{-2} mol dm^{-3} respectively, but their analogue $HgCl_2$ produces (110) faces.[120]

3. Aggregation sensitivity

Crystalline aggregations are often formed as a result of collisions between the crystals. Thus, collisions can cause the crystals to merge, and finally to intergrow.[121–133] The most important manifestations of the effect of impurities on these process are the following.

1. Electrolyte impurities usually affect the coagulation threshold in accordance with the Deryagin–Landau–Verwey–Overbeek (DLVO) theory.[129] Low-molecular-mass electrolytes affect the properties of the electrical double layer, and therefore also the configuration of the aggregations and the radial distribution function of the crystals in the bulk of the aggregations.[134, 135] This effect is usually observed at electrolyte concentrations $C > 10^{-3}$ mol dm^{-3}.[129, 136]

2. Most trace impurities affect the aggregation as a result of specific adsorption.[134] For example, during the precipitation of

nickel by borohydride from an aqueous solution of $NiCl_2$ the primary Ni microcrystals (2–25 nm in size) are incorporated into spherical aggregations 100–200 nm in size if the solution contains alkylmethylamine oxide ($C = 5 \times 10^{-3}$ mol dm^{-3}) and 20–50 nm in size in the presence of 2-mercaptobenzimidazole or 6-methyl-2-thiouracil (5×10^{-4} mol dm^{-3}). On the other hand in a pure solution or in the presence of 6-methyluracil (5×10^{-4} mol dm^{-3}) aggregation of the microcrystals is not observed.[137]

In the crystallisation of $BaSO_4$ from an aqueous solution (37 °C, pH ~7)[128] in the presence of 1-hydroxy-1,1′-disulphonic acid the size of the aggregations decreases three-fold even for an impurity concentration $C = 2 \times 10^{-4}$ mol dm^{-3}, and in the crystallisation of AgI in the presence of $C_8H_{17}OC_6H_4 \cdot (OCH_2CH_2)_xOH$ ($x = 10-70$)[138] the same effect is reached for $C = 10^{-7}-10^{-8}$ mol dm^{-3}. If the impurity molecule is large enough it can be adsorbed on several crystals simultaneously.[139, 140] This effect was noted[141] in the flocculation of SKS-30ARK latexes and of polystyrene in the presence of polyethyleneimine (M = 4500) at a concentration $C = 4 \times 10^{-9}$ mol dm^{-3}. This type of adsorption has been observed only in aqueous gold and silver sols with microcrystals of about 50 nm.[142] In these sols aggregations containing $10-10^5$ microcrystals are formed within a few minutes of the addition of homo- and copolymers of aza-crown ethers (M = 55 000), in concentrations $C = 5 \times 10^{-6}-3 \times 10^{-5}$ mol dm^{-3}, irrespectively of the acidity of the sols. Measurements showed that the sol microcrystals had a negative charge, whereas the macromolecules were positively charged in an acid medium and uncharged in an alkaline medium. The similarity between the effects of the polymer in acid and in alkaline media suggests that charge neutralisation of the microcrystals does not play a major role in their mutual coupling, caused by the specificity of the adsorption. Conversely, in SiO_2, S, FeOOH, As_2S_3, and $CuFe(CN)_6$ sols the crown ethers induce aggregation only in an acid medium because of the charge neutralisation of the microcrystals. As a result the crown ethers affect only the gold and silver microcrystals in an alkaline medium. This observation suggests new diagnostic possibilities for crown ethers.

3. If the impurity macromolecule is much larger than the microcrystals it can act as an aggregation centre. In this case the microcrystals adhere to the impurity molecule and intergrow into a large aggregation long before homoclusters of the microcrystals are formed. The frequency of incorporation of the microcrystals is usually much greater on the large than on the small aggregations.[143] Therefore the overgrown impurity molecules rapidly grow into large particles from whose numbers the number of impurity molecules can be inferred. The reality of this interpretation has been demonstrated in a study[144] of the addition of a multitude of hydroxyapatite microcrystals to a molecule of DNA. Bacterial cells can be used as the aggregation centres in these studies:[145, 146] in the presence of biologically active impurities the bacteria add on microcrystals either selectively or in other ways.[146–148] For example, cells of *Bacillus sp. 1AC7* in an aqueous alkaline colloidal solution of gold can remove almost all the gold microcrystals in 1 h. By adding to the solution 2,4-dinitrophenol ($C = 10^{-6}$ mol dm^{-3}), gramicidin D (10^{-6} mol dm^{-3}), or pentachlorophenol (5×10^{-9} mol dm^{-3} most of the microcrystals can be removed from the surface of the cells. Increasing the concentration of these impurities by an order of magnitude removes the microcrystals completely.[146] Obviously, a colloidal solution of gold containing bacteria can be used as an aggregation sensor of the presence of pentachlorophenol offering a very low detection limit.

4. Spontaneous crystal sensor action

If the trace component undergoes a topochemical reaction with the crystals of the crystallisant it can be detected by the change in surface topology of the crystals. For example, if a crystal of fluoroapatite is introduced into a stream of water containing small quantities of H_3PO_4 its surface develops etch pits in which

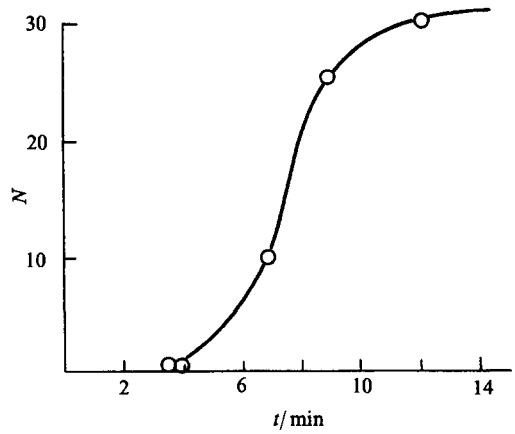


Figure 3. Rate of nucleation of microcrystals of sodium cyclophospate during the dehydration of $Na_3P_3O_9.6H_2O$.[152] Humidity of the air 26%; temperature 40 °C; N is the number of microcrystals on the (100) faces of the initial monocrystal ($F = 3$ mm^2).

$Ca(H_2PO_4)_2$ microcrystals are subsequently formed.[149–151] At the contact between a monocrystal of cyclophosphate ($Na_3P_3O_9 \cdot 6H_2O$) and moist air microcrystals of anhydrous cyclophosphate are produced on the crystal faces at a rate shown in Fig. 3.[152] The rate of nucleation of cyclophosphate crystals is sensitive to the water content of the air.

Monocrystals of fluoroapatite and of cyclophosphate hexahydrate also can be used as sensors for the presence of impurities. They should offer an enhanced sensitivity for the microcomponent if their surface morphology is determined by a microscopic method after a lengthy exposure to a stream of the medium under study. In this approach the long exposure and the small size of the morphological elements compensate for the low concentration of the trace component. Changes in morphology are revealed unambiguously if the size d of the new surface elements exceeds the resolution of the microscope and their number n is large enough. This requirement can be expressed as $d^2n > q$, where q is the minimum coverage of the surface by the new elements which can be identified unambiguously.[150] For an exposure time t and a growth rate of the topographic elements $B_G = B_{G0}C/C_K$ we have, for $d = B_G t$,

$$\Pi = (q/n)^{1/2} C_K / B_{G0} t, \tag{8}$$

where C_K is the solubility of the crystallisant. The new morphological elements are usually nucleated on active centres of the surface, so that the number n depends on the structural perfection of the monocrystal.[153–156] In monocrystals with a developed dislocation structure $n = 10^8-10^{10}$ cm^{-2}, and therefore a limit of detection $\Pi = (10^{-8}-10^{-7})C_K$ can be expected for the typical values $q = 10^{-6}$ and $B_{G0} t = 1$ cm.

Another method of revealing the trace component consists in localising its crystallisation on the surface of a specially provided collector and depositing on this surface the trace component from the largest possible volume of the medium.[157–161] The mass of the trace component removed from a volume V on a collector having a surface F is $\rho d^3 nF = CV$. Therefore if the condition $d^2n > q$ is obeyed we have

$$\Pi = \rho q^{3/2} \frac{F}{n^{1/2} V}, \tag{9}$$

where ρ is the content of the trace component in a unit volume of the reaction product.

If the reaction has a high activation energy, the process can be localised by heating the collector. Thus, in the pyrolytic reduction of silicon tetrachloride (activation energy 330 kJ mol^{-1}) or zirconium tetrachloride by hydrogen the product is collected quantitatively on the heated walls of the reactor.[157, 158] In the

pyrolysis of methylchlorosilane in a stream of hydrogen by a heated tungsten wire SiC was detected[159, 160] in 60–80% yield. TiC, NbC, HfC, BN, TiN, and TiB_2 have been obtained in a similar way.[158] An unusual method of localisation was reported by Givargizov.[161] If a single crystal of silicon heated to 1200 K is introduced into a stream of $SiCl_4$ vapour in H_2 carrier gas and a drop of molten gold is placed on the surface of the crystal the $SiCl_4$ is reduced on the drop surface and the resulting silicon dissolves in the gold. The drop becomes supersaturated in silicon, which crystallises at the contact surface with monocrystal. This produces a filamentary growth tipped with a drop of gold which collects $SiCl_4$ from the vapour. On the remainder of the monocrystal surface the reduction is negligibly slow. This technique was used to crystallise many trace components on collectors of various types.[161]

5. Selectivity of the effect of the trace component

The formation of excited and ionised forms of the trace component results in changes in the rate of crystallisation. This effect is observed as an acceleration of the crystallisation under the influence of an external ionising radiation.[162–165] The photolytic crystallisation of cadmium from the vapour of CdR_2 onto a silicon substrate was achieved by a preliminary exposure of the substrate to CdR_2 vapour followed by a brief irradiation with a laser beam (λ = 193 nm).[166, 167] If the substrate is not pretreated with the vapour, but is simply irradiated, crystallisation of cadmium is not observed. If the substrate, after being treated with vapour, is irradiated with a beam of irregular cross-section, the cadmium crystallises only on the illuminated part and its microcrystals are localised on an islet whose shape matches exactly the shape of the beam. Obviously, in this case the cadmium crystallisation centres are the radicals or ions adsorbed on the substrate.

Selective action has been observed[168] in metallic clusters of 2–10 atoms. Microcrystals of AgBr were irradiated as a layer with an Ag_n^+ ion beam, and after treatment with a reducing agent the microcrystals which had been reduced to silver were counted. The ion beam was produced in a mass spectrometer: it consisted of identical clusters accelerated to an energy of 8 eV per atom. The density of the beam and the exposure were chosen to produce at least 10 clusters for each microcrystal. It was found that after irradiation with a beam of Ag^+, Ag_2^+, or Ag_3^+ ions the microcrystals were not reduced. On the other hand irradiation with a beam of Ag_4^+ or with beams of larger clusters reduced 80% or more of the microcrystals.

In the crystallisation of metals by reaction (6) only the ultramicrocrystals of other metals, of given sizes, acted as crystallisation centres over a wide range of supersaturation.[89, 90] For example, in the crystallisation of nickel on polystyrene the crystallisation centres were particles of palladium (0.3–1 nm) or of silver (3–80 nm).

Alkyldimethylamine oxides do not affect the crystallisation of nickel, when present in solution in a molecular form, up to the micelle formation threshold, but they strongly retard the process when in the micellar form.[94] As reported,[94] near the micelle formation threshold the oxide lowers the rate of growth of nickel crystals from 1.7 ± 0.2 to 1.7×10^{-3} nm s^{-1}. Clearly, the microcrystals remain most of the time within the micelles, and the former rate characterises the growth outside the micelle whereas the latter refers to growth within the micelle.

V. Methods of increasing the sensitivity

Crystal diagnostics are most conveniently carried out under conditions of minimum B_{0j} but maximum number and size of the crystals formed under the influence of the impurity [Eqn (1)]. This objective can be achieved by the following procedures.

1. Lowering the supersaturation of the medium

At low supersaturations crystallisation in the absence of impurities is characterised by a long induction period.[169–174] Therefore in the diagnosis of impurities the supersaturation is lowered to a level for which the diagnosis time is substantially shorter than the induction period. The induction period t_0 has been measured by several workers.[2, 169–174] All their measurements are consistent with the formula

$$t_0 = KN_0S^{-n}\frac{RT^2}{H}M\frac{\mathrm{d}\ln C_K}{\mathrm{d}T}\exp\left(\frac{E}{RT}\right), \qquad (10)$$

where K and n are empirical parameters, N_0 is the minimum number of crystals which can be reliably determined, S is the supersaturation, M is the mass of one mole of crystallisant, and E is the activation energy for the nucleation of the crystals.

As has been reported,[2, 169, 173] the parameter K increases upon changing from anhydrous substances to crystal hydrates and from salts of univalent metals to salts of multivalent metals, i.e. as the composition of the crystallisant becomes more complex. In $Cu(NO_3)_2 \cdot 3H_2O$, $Na_2S_2O_3 \cdot 5H_2O$, $MnCl_2 \cdot 4H_2O$, and $Cd(NO_3)_2 \cdot 4H_2O$ and in many other complex crystallisants the K value is so high that in the absence of impurities their crystallisation is suppressed up to very high supersaturations. These crystallisants can be used at fairly high as well as at low supersaturations.

2. Overgrowing the primary crystals

The size of the crystals is increased by lowering the supersaturation S of the medium until new crystals cease to be nucleated, and holding it at this level for a long time.[175] In this case the crystals which had been nucleated before the decrease in supersaturation grow to an easily detected size without a change in their number. In a study[176, 177] of the overgrowing of ultramicrocrystals of metals in supersaturated zinc vapour it was shown that the rate of overgrowing can be controlled by electrically charging the ultramicrocrystals, and that the growth is completely suppressed at high enough negative charges. This suggests new prospects of controlling the overgrowing (in either direction) without altering the supersaturation.

3. Multiplication of the crystals

It has been established that a single primary crystal can produce a multitude of secondary crystals by three mechanisms.

Relay crystallisation. If drops of the supercooled melt of crystallisant (amorphous particles) are added to a medium containing a primary crystal the latter crystallises the drops with which it comes in contact. This effect was observed in a layer of amorphous $Ca_3(PO_4)_2$ powder as the formation of a group of secondary crystals round each primary crystal upon heating the medium,[178, 179] and also in a study[180] of an aqueous emulsion of molten hexachloro-*m*-xylene. Fig. 4 shows the result of the contactless crystallisation of a melt of *p*-bromoaniline dispersed in water and supercooled by 30 °C.[181] The drops of the melt and the primary crystal were deposited on an inert substrate and were not in mutual contact, but as a result of the dendritic overgrowth of the primary crystal the dendrite branches reached the nearest drops and crystallised them.

It has been established that ultramicrocrystals of silver are formed as a latent image in layers of AgBr crystal exposed to light. Treating the layer with a reducing solution produces growth of the ultramicrocrystal.[182–185] At a low and negative redox potential of the solution each ultramicrocrystal grows until it occupies the whole of the AgBr crystal in which it had been nucleated, but it does not extend to the neighbouring crystals.[182] On the other hand at a high negative potential each primary ultramicrocrystal emerges from its mother crystal and reaches the surface of the neighbouring crystals, inducing their reduction. As a result each microcrystal is surrounded by a cluster of secondary crystals.[183]

Multiplication by a topochemical process. It has been noted that when primary AgBr crystals are added to a solution of KI saturated with AgBr, microcrystals of AgI are nucleated at the corners of these crystals.[185] Their growth is accompanied by the dissolution of the adjacent parts of the AgBr crystal. However, the

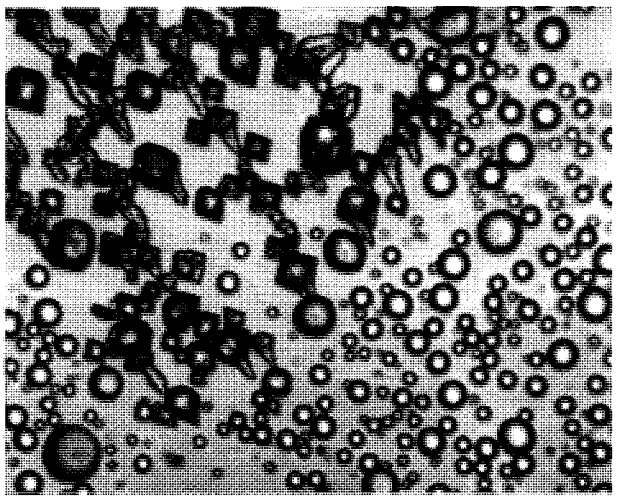


Figure 4. Relay crystallisation of a melt of *p*-bromoaniline dispersed in water (×20).[181]

microcrystals become separated from the mother crystals before reaching even one tenth of their size, and are replaced by new AgI microcrystals. In this way each primary crystal of AgBr generates hundreds of secondary AgI crystals. The same process is found in the interaction of fluoroapatite crystal with a mixture of sulphuric and phosphoric acid.[186]

Crystal showers. If a suspension of primary crystals is strongly stirred or irradiated with ultrasound the crystals can be broken down into a multitude of small fragments which grow to the size of the primary crystals as a result of overgrowth. This process has been observed in aqueous suspensions of $(NH_4)_2SO_4$, KCl, K_2SO_4, $CuSO_4 \cdot 5H_2O$, and $KAl(SO_4)_2 \cdot 12H_2O$.[187-190] A shower of secondary crystals is formed also by sliding a monocrystal of $MgSO_4 \cdot 7H_2O$ on a polished glass plate in a supersaturated solution of magnesium sulphate.[191]

VI. Diagnostic systems

Various systems based on nucleation and on growth sensor action have already been developed. Conditions suitable for the exploitation of aggregation sensor action have been formulated.[192, 193]

1. System for monitoring the concentration of carbonyl compounds

Fig. 5 shows a system developed for monitoring the concentrations of carbonyl compounds with $C = 10^{-7}-10^{-4}$ mol dm^{-3}. The system is prepared by depositing on an inert film an aerosol of a solution of the developer (a suitable hydrazide). After being dried the film is covered with a large number of microcrystals of the reagent.

The dried film acts as a crystal sensor. It is stored out of contact with the substance to be determined, and at the beginning of the experiment it is introduced into a stream of the gas to be analysed. After contact with the film the gas becomes supersaturated with the product, and ultramicrocrystals of the product are formed on the surface of the microcrystals of the reagent. The number of nucleated crystals is greater, the higher the concentration of the compound being monitored in the gas stream. The reagent is chosen so that the rate of nucleation is much smaller than the growth rate of the ultramicrocrystals. Therefore each nucleus grows over the whole volume of the mother microcrystal immediately after being nucleated, and the increase in the number of microcrystals of the product on the film is equal to the rate of nucleation. After being exposed to the flow the film is treated with a supersaturated solution of the product in order to overgrow the ultramicrocrystals to a conveniently detected size, ensuring that the supersaturation is kept below the level at which new crystals could be produced ($t \ll t_0$). When the crystals have been enlarged they are determined by counting them or by measuring any property which is dependent on their number. The sensitivity of the system increases when the drop size of the aerosol is decreased, the working area of the film is increased, and the supersaturation level used in the overgrowing is lowered. This system has been used to detect ketones, keto-esters, keto-acids, and other carbonyl compounds in gases and in solutions. 40 reagents offering a limit of detection of the carbonyl compound $II = 10^{-7}$ mol dm^{-3} have been found.[11]

2. Peptide visualisation system

The peptide visualisation system[81, 82] can be used to display and to determine amounts of protein down to 10^{-10} g. A layer of polyacrylamide gel[194] is deposited on a glass plate, and the solution of protein is admitted from the inlet side. The plate is then treated with a 0.1% solution of $AgNO_3$, and (after being washed) with a solution of formaldehyde (0.01–0.1%). Silver microcrystals are nucleated and grow on the protein molecules, which become decorated with silver.[82] The layer is examined by electrophoresis, and the localisation region of the protein is examined with a

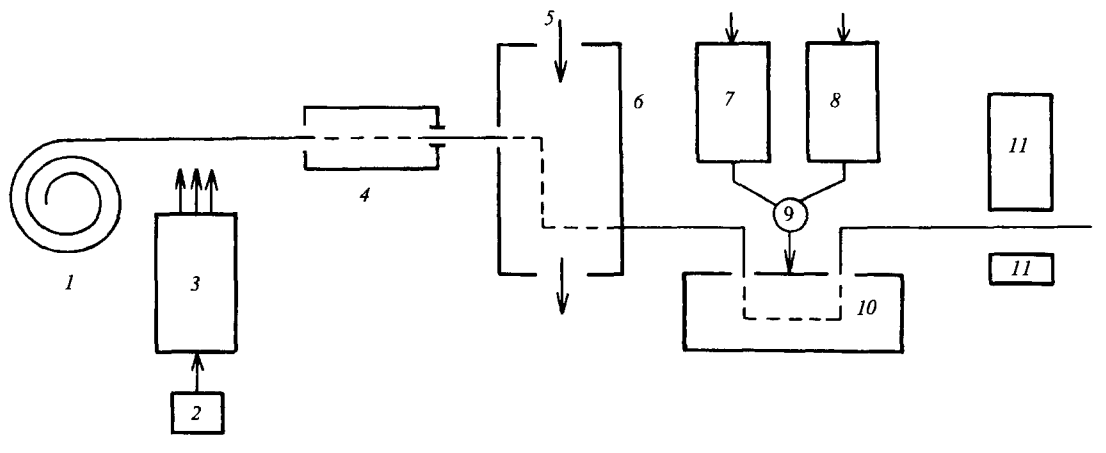


Fig. 5. System for monitoring the concentration of formaldehyde in a medium:[11] *1*) polymer film, *2*) methanolic solution of the hydrazide of *p*-hydroxybenzoic acid, *3*) aerosol generator, *4*) drying chamber, *5*) flow of gas (or liquid) containing formaldehyde, *6*) exposure chamber, *7*) aqueous solution of formaldehyde, *8*) aqueous solution of *p*-hydroxybenzoic acid hydrazide, *9*) mixer, *10*) chamber of contact of the film with the supersaturated solution of the hydrazone of *p*-hydroxybenzoic acid, *11*) photographic recording apparatus.

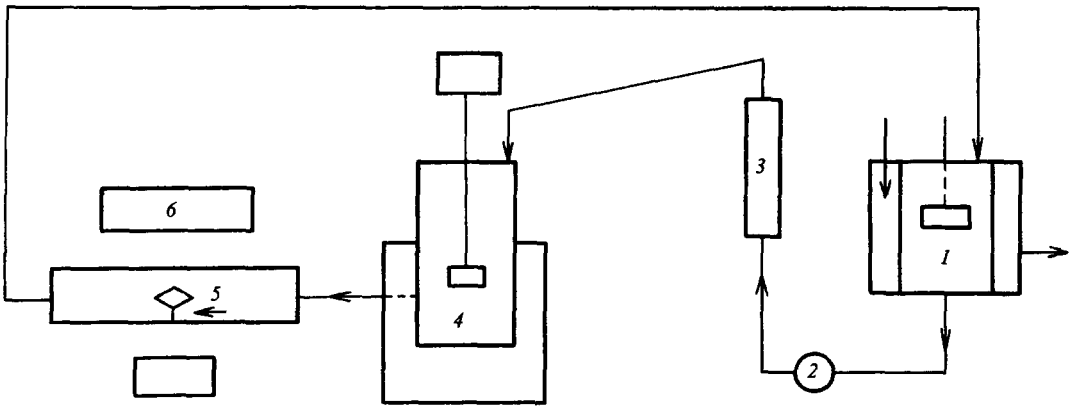


Figure 6. System for impurity diagnosis from the growth of crystals:[26] *1*) block for preparing a saturated solution of the crystallisant; *2*) pump; *3*) flow meter; *4*) cooling unit; *5*) growing crystal; *6*) block for monitoring the properties of the crystal *in situ*.

microphotometer. Occasionally the layer is treated, before the silver nitrate treatment, with a 0.01% solution of $KMnO_4$, which also stains the protein molecules with microcrystals of manganese dioxide.[81] A wide range of protein and DNA mixtures can be diagnosed from the position of the localisation region and from the intensity and nature of their coloration. The sensitivity is increased by treating the gel, after the formation of the silver microcrystals, with a mixture of iron cyanide and potassium bromide in order to convert the silver into AgBr. The AgBr is then converted into the sulphide by treating it with thiourea containing the ^{35}S radio-nuclide, which has a high specific radio-activity.[195, 196] In this case the localisation regions are delineated by autoradiography, which lowers the limit of detection of the protein by an order of magnitude.[83] Future improvements of the systems are expected to lower this limit still further.[82]

3. Growth systems

The basic system for monitoring the growth of crystals (Fig. 6) is designed for continuously recording the growth rate and the morphology of the growing faces.[29, 197] For β-methylnapthalene the growth rate is determined from the change in the interference colour of the crystals: this allows layers 2 nm thick to be determined.[198] By using the growing face of the crystal as one of the mirrors of a Michelson interferometer Rashkovich and Shekunov[199] were able to study the dynamics of the motion of layers more than 10 nm thick, and by including a Mach–Zehnder interferometer they lowered the thickness of the layer to 4 nm. Phase-contrast and reflection microscopy in conjunction with sensitive telephoto cameras and high-contrast video amplifiers allowed the *in situ* observation of the deposition of mono-molecular layers on the faces of calcium iodide, potassium hydrogen phthalate, and barium nitrate.[200–202] Other workers,[203] by including ellipsometry and low-angle scattering of synchrotron X-radiation, were able to demonstrate the effect of impurities on the composition and the crystal structure of the layers.

4. Autoradiographic system of detecting high-molecular-mass substances

The system relies on introducing into the molecule to be detected the ^3H, ^{35}S, ^{32}P, and ^{33}P radio-nuclides by isotope exchange or other methods.[204–206] The labelled substance is placed in contact with a layer of nuclear photographic emulsion which is then developed and examined in an electron microscope.[207–208] The system was used[209–210] for example, to detect DNA in aqueous solutions with a limit of detection $\Pi = 10^{-12}$ mol dm^{-3}. Under these conditions each molecule of DNA appeared in the field of the electron microscope as a circular conglomeration of silver microcrystals 0.4 μm in diameter.

VII. Conclusions

It has been established experimentally that crystal sensorics can offer a high sensitivity and selectivity in the detection of impurities. By using growth and aggregation sensor action a limit of detection of 10^{-9} mol dm^{-3} can be achieved. Intrinsic and nucleation sensor action give limits of 10^{-15} and 10^{-18} mol dm^{-3} respectively. These successes can be claimed even though crystal sensorics are a relatively new development: the theoretical foundations have been laid, but experimental data are still disconnected and incapable of answering the main question, i.e. of establishing the relationship between crystal sensorics and the nature of the impurity, the crystallisant, and the solvent. Working crystal sensorics systems offer an illustration of the problem rather than a scientifically well founded model. Very little use has been made so far of the fundamental methods of increasing the sensitivity (for example, crystal multiplication), and of the experimentally established special features of the crystallisation (for example, the transfer of the growing microcrystals into the volume of the micelles, or the formation of crystal islets on the illuminated substrate surface). Nevertheless recent progress in the use of crystal sensor systems strongly suggests that wide-ranging applications will be found in the near future.

References

1. R Buckley *Growth of Crystals* (Translated into Russian) (Moscow: Inostr. Lit., 1954)
2. L N Matusevich *Kristallizatsiya iz Rastvorov v Khimicheskoi Promyshlennosti* (Crystallisation from Solutions in the Chemical Industry) (Moscow: Khimiya, 1968)
3. I V Melikhov *Khim. Promst. (Moscow)* 461 (1992)
4. K Ya Kondrat'ev *Global'nyi Klimat i Ego Izmenenie* (The Global Climate and Its Changes) (Leningrad: Nauka, 1987)
5. P Werneck *Chemistry of the Natural Atmosphere* (New York: Academic Press, 1988)
6. T Pollock *Dioxins and Furans: Questions and Answers* (Philadelphia: Academy of Natural Sciences, 1989)
7. J H Seinfeld *Atmospheric Chemistry and Physics of Air Pollution* (New York: Wiley, 1986)
8. W T Sturges, R M Harrison *Atmos. Environ.* **23** 1083 (1989)
9. Ya I Kogan *Dokl. Akad. Nauk SSSR* **197** 121 (1971)
10. W Ansorge, A Maeyer *J. Chromatogr.* **202** 45 (1980)
11. US P. 4 380 587
12. I V Melikhov *Teor. Osn. Khim. Tekhnol.* **22** 168 (1988)
13. A Nielsen *Kinetics of Precipitation* (London: Pergamon Press, 1964)
14. K V Chibisov *Priroda Fotograficheskoi Chuvstvitel'nosti* (Nature of Photographic Sensitivity) (Moscow: Nauka, 1980)

15. A D Randolph, M A Larson *Theory of Particulate Processes* (New York: Academic Press, 1971)
16. I V Melikhov *Zh. Fiz. Khim.* **63** 476 (1989)
17. M J Haurslow *AIChE J.* **36** 1748 (1990)
18. P Marchal, R David, J P Klein, J Vilermaux *Chem. Eng. Sci.* **43** 59 (1988)
19. S Andrien, F A d'Avitaya, J S Pfister *J. Appl. Phys.* **65** 2681 (1989)
20. A I Rusanov, F M Kuni *J. Colloid Interface Sci.* **100** 264 (1984)
21. I V Melikhov *Kristallizatsiya. N. 2 (Trudy Vses. Nauch.-Issled. Inst. Khim. Reaktivov i Osobochistykh Khim. Veshchestv)* [Crystallisation No. 2 (Proceedings of the All-Union Research Institute for Chemical Reagents and Specially Pure Substances)] (Moscow: IREA, 1977) p. 5
22. A P Grinin, F M Kuni, V B Kurasov *Kolloidn. Zh.* **52** 430 (1990)
23. I V Alekseeva, A S Kabanov *Kolloidn. Zh.* **52** 227 (1990)
24. R Hagenloch, S K Friedlander *J. Colloid Interface Sci.* **133** 185 (1989)
25. Yu M Petrov *Klastery i Malye Chastitsy* (Clusters and Small Particles) (Moscow: Nauka, 1986)
26. S P Delineshev, G Blisnakov *Cryst. Res. Technol.* **17** 1323 (1982)
27. B Z Gorbunov *Kolloidn. Zh.* **52** 653 (1990)
28. T Hoffend, H Price, Y T Tan, P R Baukema, A J Hopfinger *J. Colloid Interface Sci.* **130** 568 (1989)
29. C Yang, Z Chen, M A El-Sayed *J. Phys. Chem.* **91** 3002 (1987)
30. J P Elrden, P Bennema, T A Cherepanova *Prog. Cryst. Growth Charact.* **1** 219 (1978)
31. E N Brodskaya, A I Rusanov *Kolloidn. Zh.* **48** 3 (1986)
32. Z Adamczyk, M Zembaba, B Siwek, P Warszynski *J. Colloid Interface Sci.* **140** 123 (1990)
33. M Ohara, R C Reid, in *Modelling Crystal Growth Rates from Solution* (Englewood Cliffs, NJ: Prentice-Hall, 1973) p. 85
34. J Garside *AIChE Symp. Ser.* **80** 23 (1984)
35. A V Osipov *Metallofiz.* **12** 44 (1990)
36. G H Nancollas *Adv. Colloid Interface Sci.* **10** 215 (1979)
37. A A Chernov, in *Sovremennaya Kristallizatsiya, Tom 3* (Modern Crystallisation, Vol. 3) (Moscow: Nauka, 1980) p. 7
38. T Sugimoto, K Miyake *J. Colloid Interface Sci.* **140** 348 (1990)
39. W R Schowalter *Adv. Colloid Interface Sci.* **17** 129 (1982)
40. J Bacon, E Dickinson, R Parker *Faraday Discuss. Chem. Soc.* **76** 165 (1983)
41. Yu A Buevich, K S Kuvalkin *Kolloidn. Zh.* **47** 857 (1985)
42. J Lyklema *Adv. Colloid Interface Sci.* **17** 307 (1982)
43. J Edwards, D H Everett, T O'Sullivan, I Pangalou, B Vincent *J. Chem. Soc., Faraday Trans.* **80** 2599 (1984)
44. W Y Shin, I A Aksay, R Kikucy *J. Chem. Phys.* **86** 5127 (1987)
45. Yu A Buevich, A O Ivanov *Kolloidn. Zh.* **53** 436 (1991)
46. P Meakin *J. Colloid Interface Sci.* **112** 187 (1986)
47. H M Lindsay, M Y Lin, D A Weitz *Faraday Discuss. Chem. Soc.* 153 (1987)
48. M Uwaha, Y Saito *J. Cryst. Growth* **99** 175 (1990)
49. R Jullien *New J. Chem.* **14** 239 (1990)
50. T G Dewey *Chem. Phys.* **150** 445 (1991)
51. P Meakin *J. Colloid Interface Sci.* **134** 235 (1990)
52. M Doi, D Chen *J. Chem. Phys.* **90** 5271 (1989)
53. A C Balazs, J Y Hu, A P Lentvorski, S Lewandovski, L Christopher *Phys. Rev. A* **41** 2109 (1990)
54. P M Adler *Faraday Discuss. Chem. Soc.* 145 (1987)
55. E Dickinson, C Elvingson, S R Euston *J. Chem. Soc., Faraday Trans.* **85** 891 (1989)
56. R D Vigil, R M Ziff *J. Colloid Interface Sci.* **133** 257 (1989)
57. V G Dubrovskii *Kolloidn. Zh.* **52** 243 (1990)
58. F M Kuni, A P Grinin *Kolloidn. Zh.* **52** 277 (1990)
59. M M R Williams *Ann. Nucl. Energy* **17** 161 (1990)
60. R D Cohen *J. Chem. Soc., Faraday Trans.* **86** 2133 (1990)
61. V P Zagorodnikov, M N Vargaftik, D I Kochubei, et al. *Izv. Akad. Nauk SSSR, Ser. Khim.* 849 (1989)
62. I V Melikhov, V F Komarov, Yu A Kozel *Kolloidn. Zh.* **53** 515 (1991)
63. M A Larson, J Garside *J. Cryst. Growth* **76** 88 (1986)
64. A Hodreau, B Cabaud, P Melinon *Surf. Sci.* **106** 125 (1981)
65. I V Melikhov, E D Kozlovskaya, L B Berliner, M A Prokofiev *J. Colloid Interface Sci.* **117** 1 (1987)
66. I L Frost, D W James *J. Chem. Soc., Faraday Trans.* **78** 3223 (1982)
67. I T Rusli, G L Schrader, M A Larson *J. Cryst. Growth* **97** 345 (1989)
68. M K Cerreta, K A Berglund *J. Cryst. Growth* **84** 577 (1987)
69. Y C Chang, A S Meyerson *AIChE J* **32** 1567 (1986)
70. E L Cussler *AIChE J* **26** 43 (1980)
71. D Hayes, K H Schmidt, D Meisel *J. Phys. Chem.* **93** 6100 (1989)
72. T Tanako, H Sajo, M Iwasaki *J. Soc. Photogr. Sci. Technol. Jpn.* **50** 22 (1987)
73. S Davis, K J Klabunde *Chem. Rev.* **82** 153 (1982)
74. V Akhmedov, K J Klabunde *J. Mol. Catal.* **45** 193 (1988)
75. I I Moiseev, M N Vargaftik *Usp. Khim.* **59** 1931 (1990) [*Russ. Chem. Rev.* **59** 1133 (1990)]
76. A W Castleman, I N Tang *J. Chem. Phys.* **57** 3672 (1972)
77. H Rabeony, P Mirabel *J. Chim. Phys.* **83** 219 (1986)
78. A I Kogan *Dokl. Akad. Nauk SSSR* **161** 388 (1965)
79. V E Lopatin, N M Mikova, S P Gubin *Koord. Khim.* **10** 715 (1984)
80. S P Gubin *J. Pure Appl. Chem.* **58** 567 (1986)
81. W Ansorge *Biochem. Biophys. Methods* **11** 13 (1985)
82. A Wallase H P Saluz *Nature* **357** 608 (1992)
83. A Wallase, H P Saluz *Anal. Biochem.* **203** 34 (1992)
84. A Dixon, J W B Sarkar *J. Biol. Chem.* **249** 5872 (1974)
85. S M Pedersen *Biochem. Pharm.* **35** 2661 (1987)
86. T J Peters *Adv. Protein Chem.* **37** 161 (1985)
87. X M He, D C Carter *Nature* **358** 209 (1992)
88. J Nyvlt, in *Crystalline Materials: Growth and Characterization* (Eds R Rodriguez-Clemente, C Parici) (Zurich: Trans. Tech. Publ., 1992) p. 1
89. M Shalkauskas, A Vashkyalis, in *Khimicheskaya Metallizatsiya Plastmass* (Chemical Metallisation of Plastics) (Leningrad: Khimiya, 1985) p. 53
90. V V Sviridov, T N Vorob'eva, T V Gaeskaya, L I Stepanov *Khimicheskoe Osazhdenie Metallov iz Vodnykh Rastvorov* (Chemical Deposition of Metals from Aqueous Solutions) (Minsk: Izd. Universitetskoe, 1987)
91. V P Bobrovskaya *Zh. Nauchn. Prikl. Fotogr. Kinematogr.* **28** 354 (1983)
92. A Henglein, T Praske *Ber. Bunsenges. Phys. Chem.* **82** 471 (1978)
93. V V Sviridov, T V Gaeskaya, V P Bobrovskaya *Izv. Akad. Nauk Beloruss. SSR, Ser. Khim. Nauk* 31 (1983)
94. L S Tsebul'skaya, T V Gaevskaya, V V Sviridov, E A Semenenko *Zh. Nauchn. Prikl. Fotogr. Kinematogr.* **34** 31 (1989)
95. J P Morton, M Schlesinger *J. Electrochem. Soc.* **115** 16 (1968)
96. R L Cohen, R L Meck, K W West *Plat. Surf. Finish.* **63** 52 (1976)
97. E Matijevic, A M Poskanzer, P Zuman *Plat. Surf. Finish.* **67** 38 (1980)
98. G M Bliznakov *Kristallografiya* **4** 150 (1960)
99. N Cabrera, D A Vermilyea, in *Growth and Perfection of Crystals* (New York: Wiley, 1958) p. 393
100. L N Rashkovich, A A Mkrtchan, A A Chernov *Kristallografiya* **30** 380 (1985)
101. M H J Hottenhuis, C B Lucosius *J. Cryst. Growth* **94** 708 (1989)
102. M H J Hottenhuis, C B Lucosius *J. Cryst. Growth* **91** 623 (1988)
103. I Owezarek, K Sangwal *J. Cryst. Growth* **102** 574 (1990)
104. M P C Weijnen, W G J Marchel, G M Rosmalen *Desalination* **47** 81 (1983)
105. G H Nancollas, S J Zawacki, in *Industrial Crystallization 84* (Eds S J Jancic, E J de Jong) (Amsterdam: Elsevier, 1984) p. 51
106. P G Kotsoukos, Z Amjad, G H Nancollas *J. Colloid Interface Sci.* **83** 599 (1981)
107. J Christoffersen, M R Christoffersen, S B Christensen, G H Nancollas *J. Cryst. Growth* **62** 254 (1983)
108. P G Kotsoukos, G H Nancollas *J. Phys. Chem.* **85** 2403 (1981)
109. A A Chernov, L N Rashkovich, A A Mkrtchan *Kristallografiya* **32** 737 (1987)
110. L N Raskovich, B Yu Shekunov, in *Rost Kristallov, Tom 18* (Crystal Growth, Vol. 18) (Moscow : Nauka, 1990) p. 124
111. USSR P. 554 522; *Byul. Izobr.* **14** 130 (1977)
112. M Todorova, T Ivanova, A Stankova *Godishnik Sofiiskogo Universiteta, Khimicheskii Fakul'tet* **41** 147 (1980)
113. S Khambaty, M A Larson *Ind. Eng. Chem. Fundam.* **17** 160 (1978)
114. P H Karpinski, J Budz, M A Larson, in *Industrial Crystallization 84* (Eds S J Jancic, E J de Jong) (Amsterdam: Elsevier, 1984) p. 85
115. Yu S Polyakov, G A Branitskii, I V Korchevskaya *Zh. Nauchn. Prikl. Fotogr. Kinematogr.* **34** 200 (1989)
116. J E A M Meerakker *J. Appl. Electrochem.* **11** 395 (1981)
117. A Masson, J J Metois, R Kern *Surf. Sci.* **27** 463 (1971)

118. V D Frechette, J C Pulver, P R Rossington *J. Am. Ceram. Soc.* **64** 463 (1982)
119. V M Ievlev, L I Trusov, V A Kholmyanskii *Strukturnye Prevrashcheniya v Tonkikh Plenkakh* (Structural Transformations in Thin Films) (Moscow: Metallurgiya, 1982)
120. R Kern, in *Rost Kristallov, Tom 8* (Crystal Growth, Vol. 8) (Moscow: Nauka, 1968) p. 5
121. F Family, D P Landau (Eds) *Kinetics of Aggregation and Gelation* (Amsterdam: Elsevier, 1984)
122. N B Ur'ev *Vysokokontsentrirovannye Dispersnye Sistemy* (Very Concentrated Dispersed Systems) (Moscow: Khimiya, 1980)
123. B I Deryagin, N V Churaev, V M Muller *Poverkhnostnye Sily* (Surface Forces) (Moscow: Nauka, 1987)
124. I V Melikhov, V G Pechnikov *Zh. Fiz. Khim.* **44** 2239 (1970)
125. P Thilssen, K Meyer, G Heinicke *Grundlagen der Tribochemie* (Berlin: Academie-Verlag, 1967)
126. G Barnocky, in *Disord. and Mixing: Conv. Diffus. and React. Random Mater. and Process* (Proc. NATO Adv. Study Inst. Disord. and Mixing. Cargese, June 15–27, 1987) p. 265
127. R Conti, A W Nienow *Chem. Eng. Sci.* **35** 543 (1980)
128. M C Leeden, G M Rosmalen, in *Industrial Crystallization 84* (Eds S J Jancic, E J de Jong) (Amsterdam: Elsevier, 1984) p. 325
129. B V Deryagin *Teoriya Ustoichivosti Kolloidov i Tonkikh Plenok* (Theory of the Stability of Colloids and Thin Films) (Moscow: Nauka, 1986)
130. D L Feke, N D Prabhu *Langmuir* **1** 691 (1985)
131. T Kimura, M Nakamura *J. Soc. Power Technol. Jpn.* **27** 597 (1990)
132. E Pfefferkorn, S Stoll *J. Colloid Interface Sci.* **138** 261 (1990)
133. M Carpineti, F Ferry, M Giglio *Phys. Rev. A* **42** 7347 (1990)
134. A A Baran *Polimersoderzhashchie Dispersnye Sistemy* (Disperse Systems Containing Polymers) (Kiev: Naukova Dumka, 1986)
135. E Dickinson *Colloids Surf.* **39** 143 (1989)
136. A A Cahill, P G Cummins, E J Staples, L Thompson *Colloids Surf.* **18** 189 (1986)
137. T V Gaevskaya, N V Amelina, V V Sviridov, P G Ten *Kolloidn. Zh.* **52** 1167 (1990)
138. D Tezak, N Batina, B Cosovic *Croat. Chem. Acta* **58** 814 (1986)
139. B Vincent *Adv. Colloid Interface Sci.* **4** 193 (1974)
140. A A Baran, I M Solomentseva *Khim. Tekhnol. Vody* **5** 120 (1983)
141. V N Berezhnikov, P E Kashlinskaya, T N Poyarkova *Kolloidn. Zh.* **53** 822 (1991)
142. L A Tsar'kova, V L Lishchinskii, A A Rakhnyanskaya, N V Pertsev, V S Pshezhetskii *Kolloidn. Zh.* **53** 709 (1991)
143. S Kim, C F Zukoski *J. Colloid Interface Sci.* **139** 198 (1990)
144. V Kibal'chits, Thesis, Moscow, 1980
145. F D Ovcharenko, N V Pertsov, Z R Ul'berg, L G Marochko, B S Kogan *Dokl. Akad. Nauk Ukr. SSR, Ser. B* 42 (1984)
146. Z R Ul'berg, V I Karamushka, T G Gruzina, A S Dukhin, S V Garbara, N I Grishchenko *Kolloidn. Zh.* **52** 172 (1990)
147. D W Urry *Membranes Transp.* **2** 285 (1982)
148. O N Oktyabrskii, G V Smirnova *Biofizika* **31** 459 (1986)
149. I V Melikhov, S V Dorozhkin, A L Nikolaev, E D Kozlovskaya, V N Rudin *Zh. Fiz. Khim.* **64** 3242 (1990)
150. C V Dorozhkin, A L Nikolaev, I V Melikhov, G V Saparin, V G Bliadze *Scanning* **14** 112 (1992)
151. I V Melikhov, V E Bozhevol'nov, E D Kozlovskaya, A L Nikolaev *Zh. Fiz. Khim.* **64** 3249 (1990)
152. E A Prodan, S I Pytlev *Zh. Fiz. Khim.* **57** 1998 (1983)
153. R L Dentscher, S Fletcher *J. Electroanal. Chem.* **239** 17 (1988)
154. V V Boldyrev, M I Tatarintseva, T I Samsonova, B B Bokhonov *Dokl. Akad. Nauk SSSR* **260** 122 (1981)
155. E A Prodan *Neorganicheskaya Topokhimiya* (Inorganic Topochemistry) (Minsk: Nauka i Tekhnika, 1986)
156. T Sugimoto, K Miyake *J. Colloid Interface Sci.* **140** 335 (1990)
157. J Nishizava, H Nihira, in *4th Intern. Conf. Vapor. Growth and Epitaxy* (Proc. Nogoy, 1978) p. 128
158. A V Emyashev *Gazovaya Metallurgiya Tugoplavkikh Soedinenii* (Gas Metallurgy of Refractory Compounds) (Moscow: Metallurgiya, 1987)
159. P Popper, I Riley *Proc. Br. Ceram. Soc.* 99 (1967)
160. E V Pridutskii, in *Karbidy i Splavy na Ikh Osnove* (Carbides and Carbide Melts) (Kiev: Naukova Dumka, 1976) p. 74
161. E I Givargizov *Rost Nitevidnykh i Plastinchatykh Kristallov iz Para* (Growth of Filiform and Platelet Crystals from the Vapour), (Moscow: Nauka, 1977)
162. USSR P. 21 125 (1930)
163. Jpn P. 23 929
164. Jpn P. 60-96 759; *Chem. Abs.* **103** 164 863 (1985)
165. GDR P. 226 907; *Chem Abs.* **104** 91 562 (1985)
166. D J Ehrlich, R M Osgood, T F Deutsch *Appl. Phys. Lett.* **38** 946 (1981)
167. C J Chen, R M Osgood *Phys. Rev. Lett.* **50** 1705 (1983)
168. P Fayet, F Granzer, G Hagenbart, E Moisar, B Pischel, L Woste *Z. Phys. D : At. Mol. Clusters* **3** 299 (1986)
169. A V Shlykov, S V Gorbachev *Zh. Fiz. Khim.* **29** 607 (1955)
170. M Kind, A Mersmann *Chem. -Ing.-Tech.* **55** 720 (1983)
171. Y Harano, H Yamamoto, T Miura *J. Chem. Eng. Jpn.* **13** 439 (1986)
172. J Nyvlt, V Sohnel, M Matuchova, M Broul, in *The Kinetics of Industrial Crystallization* (Amsterdam: Elsevier, 1985) p. 20
173. E V Khamskii *Peresyshchennye Rastvory* (Supersaturated Solutions) (Leningrad: Nauka, 1975)
174. M V Tovbin, S I Krasnova *Zh. Fiz. Khim.* **25** 161 (1951)
175. S K Rakhmanov, G A Ragoisha, G A Branitskii, V V Sviridov *Zh. Fiz. Khim.* **4**, 2565 (1980)
176. J F Hamilton *J. Phys.* **38** 181 (1977)
177. G A Ragoisha, V V Sviridov *Zh. Fiz. Khim.* **61** 1433 (1987)
178. T Kanazawa, T Umegaki, N Uchiyama *J. Chem. Technol.* **32** 399 (1982)
179. I V Melikhov, E D Kozlovskaya, L B Berliner *Zh. Fiz. Khim.* **62** 765 (1988)
180. I V Melikhov, V G Kel'ner, A M Pekler *Teor. Osn. Khim. Tekhnol.* 17 31 (1983)
181. I V Melikhov, A Pamiatnikh *J. Crystal Growth* **102** 885 (1990)
182. I S Ratner *Zh. Nauchn. Prikl. Fotogr. Kinematogr.* **11** 324 (1966)
183. E P Senchenkov, K V Chibisov *Zh. Nauchn. Prikl. Fotogr. Kinematogr.* **13** 446 (1968)
184. A P Kartuzhanskii, L K Kudryashova, V A Reznikov *Zh. Nauchn. Prikl. Fotogr. Kinematogr.* **34** 378 (1989)
185. A P Kartuzhanskii, L K Kudryashova, V A Reznikov *Zh. Nauchn. Prikl. Fotogr. Kinematogr.* **33** 295 (1988)
186. I V Melikhov, S V Dorozhkin, A L Nikolaev, V N Rudin *Izv. Akad. Nauk SSSR, Neorg. Mater.* **28** 872 (1992)
187. E Yamamoto, Y Harano *J. Chem. Eng. Jpn.* **13** 393 (1980)
188. P J Daudey, E J Jong, in *Industrial Crystallization 84* (Eds S J Jancic, E J de Jong) (Amsterdam: Elsevier, 1984) p. 15
189. A Mersmann *Chem. Eng. Process.* **23** 213 (1988)
190. S Heffels, E J Jong *Chem. Eng. Technol.* **13** 63 (1990)
191. M Elwenspoek, P Bennema, in *Industrial Crystallization 84* (Eds S J Jancic, E J de Jong) (Amsterdam: Elsevier, 1984) p. 267
192. W L Goffe *Photogr. Sci. Eng.* **15** 304 (1971)
193. M Tam, P S Vincett *IEEE J.* N 1A-19, 766 (1983)
194. U K Laembi *Nature* **227** 680 (1970)
195. J R Fyson, G I P Levenson *J. Photogr. Sci.* **28** 194 (1980)
196. A Owunwanne, L E Wheaton, B H Carrol, R E O'Mara *J. Appl. Photogr. Eng.* **8** 104 (1982)
197. G Bliznakov, E Kirkova *J. Phys. Chem.* **206** 271 (1957)
198. M I Kozlovskii, G G Lemmlein *Kristallografiya* **3** 271 (1958)
199. L N Rashkovich, B Yu Shekunov *Kristallografiya* **35** 160 (1990)
200. K Tsukamoto *J. Cryst. Growth* **61** 199 (1983)
201. M H J Hottenhuis, C B Lacasius *J. Cryst. Growth* **78** 379 (1986)
202. K Tsukamoto, I Sunagawa *J. Cryst. Growth* **71** 183 (1985)
203. D Cunningham, R J Davey, K J Roberts, J N Sherwood, T Shripatt *J. Cryst. Growth* **99** 211 (1989)
204. M R Evan, C A Read *Nature* **358** 520 (1992)
205. A P Feinberg, B Vogelstein *Analyt. Biochem.* **132** 6 (1983)
206. D A Melton *Nucleic Acids Res.* **12** 7035 (1984)
207. H A Ficher, H Korr, H Theile, G Werner *Naturwissenschaften* **58** 101 (1971)
208. L A Buchel, E Delain, L Bouteille *J. Microsc.* **112** 223 (1978)
209. Yu P Sivolap, V D Rusov, L P Khoroshevskaya, V M Mosyuk *Biofizika* **25** 921 (1979)
210. V D Rusov, T N Zelentsova, M Yu Semenov, V I Zakharov, S N Kravchenko *Zh. Nauchn. Prikl. Fotogr. Kinematogr.* **32** 401 (1987)

Russian Chemical Reviews **62** (3) 237–242 (1993)
© 1993 Russian Academy of Sciences and Turpion Ltd

UDC 548.0:612.315.592

Synthesis of thin-layer structures by the ionic layer deposition method

V P Tolstoi

Contents

I. Introduction	237
II. Conditions for the synthesis of thin-layer structures by ionic layer deposition	238
III. Preparation of thin layers of various compounds	238
IV. Conclusions	241

Abstract. A review is presented of ionic layer deposition, one of the methods of synthesising thin-layer structures of a predetermined composition with very precise thickness control on the surface of a support. Conditions for the synthesis of ultra-thin films of metal oxides, hydroxides, phosphates, chromates, sulphides, and tellurides on the surface of metals, semiconductors, and dielectrics are discussed. The advantages of the method are pointed out, including the possibility of synthesising layers in an automatic regime under mild conditions at room temperature on substrates of complex shape by using simple apparatus. The problems which prevent the wider use of the method are formulated, and ways of solving them are suggested. The bibliography includes 69 references.

I. Introduction

Recent developments in various fields of technology such as submicroelectronics, the production of catalysts and sorbents, and protective coatings have stimulated more demanding requirements for methods of synthesising thin-layer structures. Thus, specific technological problems in the synthesis of thin-layer structures currently being studied include controlling the disposition of different atoms to within one monolayer of the structural units.

This review covers existing methods of high-precision synthesis of thin-layer structures. One of these methods (ionic layer deposition) is examined in greater detail, because it appears to deserve wider recognition from specialists in solid-state surface chemistry.

The methods used to deposit thin layers of solid substances on the surface of various supports can be arbitrarily classified as physical or chemical. The former include methods in which the material to be deposited is evaporated in a vacuum or an inert medium by thermal, electron-beam, cathodic, or magnetron evaporation.[1–5] In the chemical methods the layer is formed by deposition from the gas or the liquid phase as a result of a chemical reaction initiated by thermal energy, by a plasma, by a change in pH, etc.[6,7] A feature common to all these methods is that the layer is formed as a result of a shift in the chemical equilibrium between the reactants in the gas or the liquid phase and the growing layer, in the direction of layer formation. This allows the thickness of the layer to be controlled though the concentration and temperature of the reactants as well as through the temperature of the substrate, the deposition time, and other parameters. However, changes in these parameters do not offer thickness control at the level of a monolayer of structural units.

Essentially new conditions of high-precision layer synthesis have been formulated for the preparation of thin-layer structures: conditions offering an unusual type of chemical assembly.[8–12] The most important of these is a special preparation of the substrate surface. A layer of functional groups is then formed on the prepared surface, and used to induce the chemisorption of bifunctional molecules containing atoms of the layer to be synthesised and of molecules of another reactant, not less than bifunctional, giving new functional groups which contribute to further chemisorption reactions. This removes the excess of reactants. As a result, the direct synthesis is replaced, in the complex conditions created by the thermodynamics of the process, by a stepwise synthesis with acts of irreversible chemisorption alternating in a predetermined sequence.

These ideas have been used in a series of studies[13–17] of the synthesis of various metal oxides (TiO_2, Cr_2O_3, etc.) on the surface of dispersed solids (mainly silica), and also of multizone layers based on these materials. Readily hydrolysed chlorides and water are most commonly used as reactants. The method of synthesis of layers of a single composition has been called molecular layer deposition. Organometallic compounds have also been used for this purpose,[18–21] for example $Ti(OC_2H_5)_4$, $Si(OC_2H_5)_4$, $Al(OC_3H_7)_3$, $Zn(CH_3)_2$, $Cd(CH_3)_2$, H_2S, etc. The advantages of this method include, in addition to a precise control of the layer thickness, the ability to deposit layers on the surface of porous supports having a complex shape.

This approach has been used in conjunction with molecular beam epitaxy[22] to expose the support in an ultra-high vacuum to alternating beams of atoms of different elements which react on the support but not in the gas phase. The method is also used to prepare various thin-layer materials used in microelectronics (for example, $Ga_{1-x}Al_xAs$).

A definite analogy has been reported also with the atomic beam epitaxy method,[23–25] in which a layer of ZnS is deposited on the substrate surface by heating the substrate above the evaporation temperature of both the reactants (in this case, zinc and sulfur), and the chemisorption of zinc and sulfur atoms is

V P Tolstoi Institute of Chemistry, St Petersburg State University, Universitetskii prosp. 2, Staryi Petergof, 198904 St Petersburg, Fax (7-812) 428 66 49

Received 8th September 1992
Uspekhi Khimii **62** (3) 260–265 (1993); translated by J I Carasso

obtained by successively exposing the surface to these atoms. The method has been used in the synthesis of high-purity layers of ZnS, CdS, ZnSe, CdSe, etc.

These methods require the use of vacuum or high-vacuum apparatus, or flow apparatus filled with a purified inert gas. The molecular layer deposition method has also been used[26] for synthesis experiments in inert solvents.

This interest in the preparation of layers by using liquid reactants is not new, mainly because the apparatus requirements are much simpler for synthesis in the liquid phase. Thus, the impregnation method is now widely used in the development of catalysts and sorbents.[27] An inert matrix is immersed in a solvent containing the substance to be deposited, and (without washing away the excess of reactants) the system is then heated or treated with another reagent which converts the deposited substance into a sparingly soluble compound. This technique infringes one of the fundamental requirements of precision synthesis by failing to remove the excess of reactants.

Evidently, the most stringent control over the synthesis conditions of the layers from the liquid phase can be exercised by using ion exchange reactions, now widely applied for the modification of solids.[28-30] However, the application of ion exchange reactions in the synthesis of thin-layer structures involves serious difficulties, mainly associated with the fact that these reactions are reversible, and therefore the layer produced in the first few layer deposition cycles can be lost in experiments involving repeated depositions.

II. Conditions for the synthesis of thin-layer structures by ionic layer deposition

The layer synthesis from solutions on a substrate surface was first proposed by Iler,[31] who prepared layers of silicon oxide by using charged particles of colloidal silica as the initial structural units for layer deposition. Treating the surface of a substrate carrying a charge opposite to that of the colloidal silica particles resulted in the deposition of a layer of the particles. A subsequent treatment of the substrate and the deposited layer with a salt solution produced charge reversal in the supported particles, with deposition of a second layer.

The application of these ideas to the synthesis of layers with very precise thickness control, with cations and anions used as the main structural building blocks, is complicated first and foremost by the reversibility of the ion exchange reactions taking place on the surface.

Nevertheless it has been shown[32,33] that the silica gel containing PO_4^{3-} as a substituent is an effective sorbent for the Hf^{4+}, Zr^{4+}, and Sn^{4+} ions. It has also been shown[34] that Ca^{2+}-substituted silica gel can be used as an anion exchanger for PO_4^{3-}. An increased adsorption of PO_4^{3-} ions on Zn^{2+}-substituted silica gel (as compared with the H^+-substituted silica gel) has also been reported.[35] It was suggested that one layer of metal phosphate is formed on the surface by the interaction with the solution.

These results can be explained by the well-known Fajans rule:[36] ions are adsorbed most effectively on a surface if they form a sparingly soluble or a weakly dissociated compound with an oppositely charged ion in the substrate.

Thus it may be possible to prepare thin-layer structures by using the principles of the chemical assembly of solid substances, realised by the molecular layer deposition method (which relies on the irreversible adsorption of easily hydrolysed metal chloride molecules). In other words, ions can be used for the synthesis instead of molecules, thus producing an ionic type of layer deposition.

The irreversible adsorption reactions of anions and cations, giving sparingly soluble compounds as a result of the interaction, provide the foundations of the ionic layer deposition method. In this approach the thickness of the layer is determined by the number of cycles of ionic layer deposition performed, including the removal of the excess of reagents between cycles. In this case the support behaves alternately as a cation exchanger and as an anion exchanger, which allows the now well-understood ion exchange concepts to be used. The conditions for the most complete ion exchange and the exchange capacity are well established for almost all the types of ion exchanger: furthermore, the appropriate thermodynamic and kinetic relationships have been obtained, sequences of exchanging ions have been formulated, and reaction mechanisms have been proposed.[37-47]

However, there is as yet no systematic treatment of the basic process involved in the synthesis by the ionic layer formation method (namely, the problem of the conditions for which the ion exchange reactions are irreversible). To some extent this state of affairs is exactly the opposite of the problems encountered in developing effective ion exchangers, since a long operating life in that case requires a knowledge of the reversibility conditions of the adsorption of ions on the surface. Very little is known about the ability of the layers synthesised in the first stages of layer deposition to take part in later ion exchange reactions during repeated exposures of the support to the reactants, and also about the properties of the layers synthesised in this way.

III. Preparation of thin layers of various compounds

Synthesis of manganese oxide and chromium hydroxide layers. At first sight layers of metal hydroxides and oxides can be synthesised by successively depositing layers of metal and of hydroxyl ions on the surface by the scheme

$$[M]OH + M_1^{n+} \rightarrow [M]OM_1^{(n-1)+},$$
$$[M]OM_1^{(n-1)+} + OH^- \rightarrow [M]OM_1(OH)_{(n-1)}.$$

However, this expectation is not fulfilled, since the layer of hydroxide formed after the first cycle redissolves in subsequent exposures to a solution of the metal salt, even at the highest pH values, by the reaction

$$[M]OM_1(OH)_{(n-1)} + H^+ \rightarrow [M]OH + M_1(OH)^+_{(n-1)}.$$

Therefore the writer proposed a method of synthesising hydroxide layers by converting the ions of the adsorbed metal layer into a higher valency state, for which the interaction with the solution of the metal salt is not reversible.[48] Layers of MnO_2 were synthesised in this way from $Mn(NO_3)_2$ or $MnSO_4$ and $KMnO_4$. As a result of these reactions every manganese ion was converted into the Mn^{4+} state of oxidation by the scheme

$$[M]OH + MnOH^+ \rightarrow [M]OMnOH + H^+,$$
$$[M]OMnOH + MnO_4^- \rightarrow [M]O(MnO_2)_2OH.$$

A more substantial adsorption of Mn^{2+} ions on the substrate surface was obtained by adding NaOH to a solution of $MnSO_4$ to give a pH value differing by a few tenths of a pH unit from the $Mn(OH)_2$ precipitation value. After each treatment the excess of reagent was removed by washing the sample with an aqueous solution saturated with Mn^{4+} ions. This suppressed the dissolution of the MnO_2 layer even at the stage of washing the support and its layer free from the excess of each of the reagents.

The synthesised layers were studied spectrophotometrically in the visible and UV regions and by IR spectroscopy. Their composition was found to correspond to hydrated MnO_2, and a regular increase in the layer thickness with the number of layering cycles was demonstrated.

The coating of the surface of carbon steel with a layer of chromium hydroxide has also been reported.[49,50] In this case the support was treated successively, several times, with aqueous solutions of H_2CrO_4, CrO_3, and $Na_2S_2O_3$ or $NaNO_2$, and washed free from the excess of reagent with water after each exposure. Irreversibility of the adsorption of the $HCrO_4^-$ ions on the surface of the growing layer of hydroxide was achieved by an intermediate heating of the substrate bearing a thin layer of CrO_3 solution to

150–200 °C. This heating stage evaporated the water and resulted in binding the $HCrO_4^-$ (for example) to the FeOH groups of the surface by forming Fe–O–Cr groups:

$$[Fe]OH + H_2CrO_4 \xrightarrow{T} [Fe](OCrO_2OH)_{ads}(CrO_3)_x ,$$

$$[Fe](OCrO_2OH)_{ads}(CrO_3)_x \xrightarrow{H_2O} [Fe](OCrO_2OH)_{ads} ,$$

$$[Fe](OCrO_2OH)_{ads} + Red \rightarrow [Fe]OCr(OH)_2 .$$

After this treatment in a reducing solution the adsorbed Cr^{6+} ions were converted into the Cr^{3+} ions of a layer of chromium hydroxide, which is insoluble at the given pH value.

A practically important result of these syntheses is a marked increase in the corrosion resistance of the steel surface, depending on the number of layer deposition cycles. Thus, whereas a repeated treatment with solutions of oxidiser and reducer produces a negligibly small change in the corrosion resistance, an alternating treatment by the ionic layer deposition mechanism gives an almost 15-fold improvement after 10 layer deposition cycles, as shown by measurements in a 2% solution of $CuSO_4$. It is also important to note that the observed corrosion resistance values greatly exceed the level of protection offered by existing methods of depositing chromate conversion coatings.

Synthesis of layers of barium phosphate and zinc chromate. Reference was made above to some studies[32–35] of the increased adsorption of PO_4^{3-} ions on the surface of cation-exchanged forms of silica gel and of metal ions which form sparingly soluble compounds with PO_4^{3-} on the surface of phosphate-substituted silica gel. However, no detailed mechanism of these interactions has yet been suggested.

A recent Patent[51] discloses a method of synthesising a layer of barium phosphate on a carbon steel surface by using $Ba(NO_3)_2$ and Na_2HPO_4 as reagents with an intermediate washing of the sample with water to remove the excess reactants and products:

$$[Fe]OH + Ba^{2+} \rightarrow [Fe]OBa^+ ,$$

$$[Fe]OBa^+ + HPO_4^{2-} \rightarrow [Fe]OBaHPO_4^- .$$

A result of practical value from this work was the achievement of an almost 10-fold increase in the corrosion resistance of the metal as compared with the existing method of producing phosphate conversion layers. This difference can probably be ascribed to a lower porosity of the coatings obtained by the new method.

Great interest has been shown in the synthesis of binary oxide layers not only on pure metal surfaces but also on a metal coated with a layer of oxide prepared (for example) by a passivation treatment. In this case we have shown[52] that a synthesis by the ionic layer deposition of $ZnCrO_4$ on a layer of the same compound on zinc (obtained in a passivating chromate solution) produces a greatly increased corrosion resistance of the surface after 10 layer deposition cycles, and solves the practically important problem of increasing to 200 °C the thermal stability of the passivating conversion layer, which had a limit of 60 °C before the layer deposition treatment. The reagents used in this study were $Zn(CH_3COO)_2$ and Na_2CrO_4. Irreversibility of the adsorption of CrO_4^{2-} on the $ZnCrO_4$ surface was achieved by an intermediate heating of the sample with a layer of Na_2CrO_4 solution at 150–200 °C for 1–2 min:

$$[Zn](ZnCrO_4)_mZnOH + Na_2CrO_4 \xrightarrow{T} \rightarrow [Zn](ZnCrO_4)_m(ZnCrO_4^-)(Na_2CrO_4)_x ,$$

$$[Zn](ZnCrO_4)_m(ZnCrO_4^-)(Na_2CrO_4)_x \rightarrow \rightarrow [Zn](ZnCrO_4)_m(ZnCrO_4^-)_{ads} ,$$

$$[Zn](ZnCrO_4)_m(ZnCrO_4^-)_{ads} + Zn(CH_3COO)_2 \rightarrow \rightarrow [Zn](ZnCrO_4)_m(ZnCrO_4)Zn^+_{ads} .$$

Synthesis of layers of copper and zinc sulphides. The first studies of the synthesis of ultra-thin layers of CuS were carried out by the method proposed by Rotrekl et al.[53] in the early 1970s. The method has been developed for the deposition of an electrically conducting layer on the surface of a dielectric. These layers are strongly bound (chemically) to the surface, and their electrical resistance is relatively low. Therefore they produce effective current-carrying layers for the electrochemical metallisation of dielectrics (and especially of plastics). Published work in this area has already been reviewed.[54]

In most cases the layers of CuS were synthesised by using solutions of $CuSO_4$ and Na_2S as reagents. When a layer is deposited on supports made of various materials (wood, fibrous silicates, unglazed porcelain) the first stage can be the adsorption of either Cu^{2+} or S^{2-} ions. To increase the thickness of the deposited layer the substrate should be washed free from the excess of Cu^{2+} with hot water, which hydrolyses the surface compounds of Cu^{2+} and inhibits their removal. In treatments by 3–5 exposures the sample is not usually washed free from the excess of S^{2-} ions: this also favours the deposition of thicker layers. In this way the resistance of a layer of CuS was lowered to 10^3–10^4 Ω cm^{-1} after three treatments. Even lower resistances have been obtained[56] by adding Zn^{2+} ions to the solution of $CuSO_4$.

All these studies had one feature in common: they aimed to solve a specific technological problem (in this case, the production of an electrically conducting layer). Little attention was paid to the special aspects of the synthesis or to the mechanism of the reactions.

These problems were adequately studied (in the case of ZnS and CdS layers) by Nikolau et al.,[56–60] who proposed the term SILAR (Successive Ionic-Layer Adsorption and Reaction) for the above method of synthesising metal sulphide layers. Other names have been used for the same procedure in the Russian literature: ionic layer epitaxy[61] and layer chemisorption.[62] We believe that all these names only partially reflect the true nature of the processes taking place on the surface, since the ionic layer deposition may not involve epitaxy, and the dominant process in the synthesis could be the interaction of layers of physisorbed ions. In this review we shall retain the term which has been adopted in the Russian literature, and call the process (by analogy with molecular layer deposition) ionic layer deposition. This term is only slightly different from the term proposed by Nikolau.

It has been established[56] that in the synthesis of a layer of ZnS on the surface of ITO the maximum growth rate (3.0–3.1 Å per cycle of layer deposition) is obtained by using a 5 M solution of $ZnCl_2$ and a 2.8 M solution of Na_2S. For CdS the maximum rate of 1.3–1.4 Å per cycle was obtained for a 5 M solution of $CdCl_2$ and a 2.8 M solution of Na_2S. The maximum surface coverages during the adsorption were calculated from the growth rates: $\Phi_{Zn} = 0.72$ and $\Phi_S = 0.72$ (for ZnS) and $\Phi_{Cd} = 0.23$ and $\Phi_S = 0.2$ (for CdS).

In order to identify the mechanism of the adsorption of Zn^{2+}, Cd^{2+}, and S^{2-} the ξ potentials were measured[58] in solutions of different concentrations and different pH. Three critical points were found on the experimental curves: CR1, CR2, and CR3. At pH values lower than CR1 (2.3 for ZnS and 1.8 for CdS) the sulphide surface is positively charged owing to the adsorption of H^+ on the sulfur adsorption centres. For pH values between CR1 and CR2 (up to 7.5 for ZnS and up to 10 for CdS) the charge can be both negative (because of the ionisation of Brönsted-acid centres) and positive (because of the adsorption of the Zn^{2+} and Cd^{2+} ions on these centres or of the chemisorption of $ZnOH^+$ on the S^{2-} ions). At pH > 9 for ZnS and pH > 11 for CdS the surface is charged negatively because of the adsorption of OH^- ions on $Zn(OH)_2$ and $Cd(OH)_2$.

If one allows for these results and for data on the growth rate of layers in solutions of reagents of different concentrations, the following model can be proposed for the growth of the layer.

As we know, the dissolution of $ZnSO_4$ and Na_2S in water is accompanied by dissociation and hydrolysis:

$$ZnSO_{4\,aq} \leftrightarrows Zn^{2+}_{aq} + SO^{2-}_{4\,aq} ,$$

$$Zn^{2+}_{aq} + H_2O \leftrightarrows ZnOH^{+}_{aq} + H^{+}_{aq} ,$$

$$Na_2S \leftrightarrows 2Na^{+}_{aq} + S^{2-}_{aq} ,$$

$$S^{2-}_{aq} + H_2O \overset{(HS^-)}{\rightleftharpoons} HS^{-}_{aq} + OH_{aq} .$$

As soon as the ZnS support is immersed in a solution of $ZnSO_4$ the Zn^{2+} and $ZnOH^+$ ions react with the HS^-_{ads} to form more ZnS:

$$Zn^{2+}_{aq} + HS^{-}_{ads} \rightarrow ZnS + H^{+}_{aq} ,$$

$$ZnOH^{+}_{aq} + HS^{-}_{ads} \rightarrow ZnS_{ads} + H_2O .$$

Under these conditions only the number of zinc ions determined by the number of adsorption centres on the surface is taken up by the substrate, and the synthesis takes place under the condition

$$[HS^{-}_{ads}] \geqslant \frac{SP_{ZnS} K_1 [H^+]}{[Zn^{2+}_{aq}]} ,$$

where SP ($\cong 2 \times 10^{-22}$) is the solubility product of ZnS and K_1 ($\cong 1 \times 10^{-15}$) is the protonation constant of S^{2-}. The following condition must also be fulfilled in order to avoid layer formation by the precipitation of colloidal ZnS:

$$[HS^{-}_{aq}] < \frac{SP_{ZnS} K_1 [H^{+}_{aq}]}{[Zn^{2+}_{aq}]} .$$

Beyond this point we find a superequivalent adsorption of Zn^{2+} and $ZnOH^+$ on the ZnS, and the charge on the surface becomes positive.

When the substrate is washed in distilled water some of the zinc ions are removed from the surface, but the pH at the surface is changed to 7 by the water, causing hydrolysis of the zinc ions which opposes the desorption.

If the substrate is then immersed in a solution of Na_2S, the S^{2-} and HS^- ions react on the surface, giving a layer of ZnS:

$$Zn^{2+}_{ads} + S^{2-}_{aq} \rightarrow ZnS ,$$

$$ZnOH_{ads} + HS^- \rightarrow ZnS + H_2O .$$

Because of their higher mobility the OH^- ions can reach the surface more rapidly when $[S^{2-}] = [OH^-]$, and react with formation of $Zn(OH)_2$. However, since the solubility product of $Zn(OH)_2$ (1.2×10^{-17}) is much greater than that of ZnS, the first formations are rapidly converted into ZnS and the positive surface charge disappears. The layer of ZnS is formed when the following condition is satisfied:

$$[Zn^{2+}_{ads}] \geqslant \frac{SP_{ZnS} K_1 [H^{+}_{aq}]}{[HS^{-}_{aq}]} .$$

To avoid the precipitation of colloidal particles of ZnS we also require that

$$[Zn^{2+}_{aq}] < \frac{SP_{ZnS} K_1 [H^{+}_{aq}]}{[HS^{-}_{aq}]} .$$

Thus the complete synthesis includes several different stages of diffusion and adsorption of ions.

As can be seen from the above description of the ionic layer deposition mechanism it should be possible to dope the layer with various ions and to create a distribution of the doping impurity over the thickness of the layer by exposing the substrate to solutions of various salts. This approach has been used in a study[59] of the synthesis of electroluminescent layers of ZnS and CdS doped with indium and manganese incorporated into the structure of the layer from solutions of $InCl_3$ and $KMnO_4$.

Layers of ZnS and CdS have also been produced[61-63] by using silicon and germanium in the (111) orientation as substrates and $Zn(NO_3)_2$, $Cd(NO_3)_2$, and Na_2S as reagents. Solid solutions of $Zn_{1-x}Cd_xS$ were synthesised from mixed aqueous solutions of $Zn(NO_3)_2$ and $Cd(NO_3)_2$.

The resulting layers, up to 200 nm thick, had a smooth mirror-like surface; the layer thickness produced by one layer deposition cycle was 3.2 Å for ZnS and 2.9 Å for CdS, corresponding to ~90% coverage of the surface by adsorbed ions.

Electron-diffraction studies of these materials showed that for ZnS the growth of the layer on the substrate surface begins with the formation of crystallites having a lattice of the wurtzite type, but when the layer thickness is increased (after 30–40 cycles) polycrystallites begin to grow with a lattice of the sphalerite type. The growth of CdS on Si(111) begins with the formation of a polycrystalline cubic structure, in which some of the crystallites are oriented in the (111) plane as the layer thickness is increased. On the other hand $Zn_{1-x}Cd_xS$ solid solutions are obtained only when the mole fraction of Cd in the solution is 0.0001–0.003, the most perfect layers being formed for $x = 0.0002$. When $x = 0.003$ the structure of the layer corresponds to the CdS cubic lattice.

Kutepov et al.[63] have studied the effect of the concentration and temperature of the solutions on the refractive index of the ZnS layers. It was established that the lowest density is found in layers grown from concentrated solutions and from solutions with identical concentrations of the reactants but prepared at low temperatures, and also in layers synthesised from the most dilute solutions. The highest refractive index was observed for solutions with a 5-fold excess of the concentration of $Zn(NO_3)_2$ over the concentration of Na_2S and at high temperatures.

In addition to ZnS, CdS, and $Zn_{1-x}Cd_xS$, layers of PbS have been synthesised by using aqueous solutions of $Pb(CH_3COO)_2$ and Na_2S as reagents on a Si(111) surface. These layers had a mirror-smooth surface and were strongly held on the substrate. After 100–200 deposition cycles their thickness was 30–50 nm, corresponding to a growth rate close to a monolayer per cycle. The structure of the PbS layers was assigned to the block monocrystal type, with a small disorientation of the blocks and a block size of 0.1 μm.

Klechkovskaya et al.[62] explained published results[56-63] on the growth mechanism of sulfide layers by postulating that the lattice parameters and the structural parameters of the substrate play a dominant role in the formation of the structure of the growing film (especially during the first stages of layer deposition). However, it was noted that under the conditions of the experiments the ordinary growth mechanism is predominant, including the adsorption of ions of both components, the formation of three-dimensional growth centres (which are not oriented with respect to the substrate in the initial stages when the mismatch of the lattice parameters is large), and their coalescence with a preferred orientation and the subsequent growth of a new layer on the substrate surface.

The growth mechanism suggested[61,63] for metal sulfide layers differs from the mechanism proposed by Nikolau,[58] probably because of the nature of the substrate materials. Thus, the former workers[61-63] used silicon and germanium as substrates, whereas Nikolau[58] used mainly ITO and molyb-denum, which adsorb S^{2-} ions as well as incorporating them in the structure of the layer growing on their surface. On the other hand when silicon or germanium are used as substrates allowance must be made for the reversibility of the adsorption of the Zn^{2+} and Cd^{2+} ions on SiOH and GeOH. Thus it has been shown[64] that in the adsorption of salts of these metals from aqueous solutions monolayer coverage of the surface by OH groups does not take place, and that when the sample is subsequently washed free from the excess of reagents the metal in the Si–O–M bond is replaced by a proton. Clearly, the first treatments do not form continuous layers of the sulfides on the surface. We must also allow for the possible adsorption, from solutions of metal salts at concentrations greater than

0.01 – 0.001 M, of clusters of metal hydroxides, formed (as reported[65–67]) during the ageing of the solutions. The subsequent treatment of these layers in a solution of sodium sulfide, which has a strongly alkaline reaction, should produce a partial dissolution of the hydroxides with precipitation of the sulfides by the destructive epitaxial interaction mechanism. Under these conditions a continuous layer cannot be produced during the initial stages of the treatment. A possible explanation of the mechanism of the three-dimensional growth of the layer may be found in the suggested[68] superequivalent adsorption of the ions on the surface at solution concentrations greater than 0.001 M.

A substantial contribution to the uncontrolled growth of the layer comes also from the incomplete removal of the excess of reagents from the substrate. In this case the thickness of the prepared layer is determined by the kinetic parameters of the washing operation. In spite of its importance this topic is not adequately dealt with in published papers.[56–63]

Synthesis of layers of cadmium telluride on a gold electrode surface. It has been pointed out[57] that the ionic layer deposition method can be used to synthesise layers on electrode surfaces by controlling the adsorption processes through the electric field. Clearly, the ions which interact on the surface have a charge, and their motion can therefore be controlled by an electric field.

Thus, Shtikin et al.[69] deposited, in a thin-walled electrochemical cell, two monolayers of CdTe on the surface of a gold single crystal which had been previously cleaned in an ultra-high vacuum. The reagents were a 1.0 μM solution of $CdSO_4$ in an acetate buffer and a 0.4 μM solution of TeO_2 in H_2SO_4 (pH 2.2). The potential of the electrode was varied between −0.6 and 0.8 V at a rate of 2 mV s^{-1} while measuring the current in the cell filled with each reagent successively. Two peaks, corresponding to the adsorption of the Cd^{2+} and the Te^{2-} ions, were detected in the current – voltage curves.

The composition of these layers was studied by low-energy electron diffraction and Auger spectroscopy, and a structure-chemical model of the arrangement of the atoms in the layer was constructed. This suggested a high degree of perfection of the layers and good control over the conditions of synthesis.

IV. Conclusions

The experimental information reviewed above makes clear several advantages of the ionic layer deposition method, such as the possibility of depositing layers of various substances (including pure substances and multicomponent binary compounds of the main classes of solids), the high precision of control over the layer thickness, and the ability to prepare layers in automated regimes at low temperatures on objects of complex shape. In spite of the simplicity of the method, the synthesis of a layer on the surface relies on several processes in parallel: the adsorption and desorption of the ions, their multistage hydrolysis, and diffusion from the bulk to the surface layer.

In all the substrate – growing layer systems considered here these processes allow the synthesis to be carried out by a chemical assembly mechanism and the growth of the layer to be controlled very precisely. Allowance is needed for the effect of the concentration and temperature of the reactants, the pH of the solutions and of the wash liquid, the time of treatment and of washing out the reagents, and the method of surface preparation before the synthesis. This is specially true of the synthesis of two or more regions in the layer, including the addition of a doping impurity with a prescribed distribution over the thickness of the layer. All these aspects constitute a fairly complex physico-chemical problem. Therefore at present it is as important to identify the general features of the synthesis in each class of materials (for example, metal sulfides and phosphates) as to produce still more experimental information on the synthesis of the layers, or to systematise it: this approach should allow the prediction and selection of the synthesis conditions for new types of layers. Special attention should be paid to the synthesis by the ionic layer deposition method of layers which cannot be prepared by other methods (for example, owing to the involatility of the starting compounds in the case of synthesis from the gas phase or because of thermal instability).

References

1. L S Palatnik, I I Papirov *Epitaksial'nye Plenki* (Epitaxial Films) (Moscow: Nauka, 1971)
2. *Tekhnologiya Tonkikh Plenok* (Thin Film Technology) (Moscow: Sovetskoe Radio, 1977)
3. B A Movchan, I S Malashenko *Zharostoikie Pokrytiya Osazhdaemye v Vakuume* (Heat-resistant Coatings Deposited in a Vacuum) (Kiev: Naukova Dumka, 1983)
4. L I Kostryzhskii, O V Lebedinskii *Mnogokomponentnye Vakuumnye Pokrytiya* (Multicomponent Vacuum Coatings) (Moscow: Mashinostroenie, 1987)
5. *Thin Films, Interdiffusion and Reactions* (Translated into Russian) (Moscow: Mir, 1982)
6. N V Suikovskaya *Khimicheskie Metody Polucheniya Tonkikh Plenok* (Chemical Method of Preparing Thin Films) (Leningrad: Khimiya, 1971)
7. G N Krylova *Interferentsionnye Pokrytiya* (Interference Coatings) (Leningrad: Mashinostroenie, 1973)
8. V B Aleskovskii, in *Tezisy Dokladov Nauchno-tekhnicheskoi Konferentsii LTI Imeni Lensoveta, Leningrad 1965* (Abstracts of Papers Presented to the Scientific and Technical Conference at the Lensovet Technical Institute, Leningrad, 1965), p. 66
9. V B Aleskovskii *Zh. Prikl. Khim.* **47** 2145 (1974)
10. V B Aleskovskii *Vestn. Akad. Nauk SSSR* **6** 48 (1975)
11. V B Aleskovskii *Stekhiometriya i Sintez Tverdykh Soedinenii* (Stoichiometry and Synthesis of Solid Compounds) (Leningrad: Nauka, 1980)
12. S I Kol'tsov, V B Aleskovskii *Zh. Prikl. Khim.* **39** 299 (1966)
13. S I Kol'tsov *Zh. Prikl. Khim.* **42** 1023 (1969)
14. A A Malygin, S I Kol'tsov, V B Aleskovskii *Zh. Obshch. Khim.* **49** 1936 (1979)
15. S I Kol'tsov, V E Drozd, V B Aleskovskii *Dokl. Akad. Nauk SSSR* **229** 1145 (1976)
16. V M Smirnov, S I Kol'tsov, V B Aleskovskii *Izv. Vyssh. Ucheb. Zaved., Khim. Khim. Tekhnol.* **17** 1759 (1974)
17. A A Malygin, S I Kol'tsov, in *Napravlennyi Sintez Tverdykh Veshchestv. Vypusk 1* (Controlled Synthesis of Solid Substances, No. 1) (Leningrad: Izd. Leningr. Univ., 1983) p. 17
18. L P Bogdanov, V P Tolstoi in *Tezisy Dokladov Pyatogo Vsesoyuznogo Soveshchaniya po Sintezu, Issledovaniyu, Svoistvam, i Tekhnologii Primeneniya Lyuminoforov, Stavropol, 1988* (Abstracts of Papers Presented to the Fifth All-Union Conference on the Synthesis, Investigation, Properties, and Application Technology of Phosphors, Stavropol, 1988) p. 94
19. V B Aleskovskii, V E Drozd, V I Gubaidullin, A I Romanychev *Dokl. Akad. Nauk SSSR* **291** 136 (1986)
20. V E Drozd, V B Aleskovskii, A I Romanychev *Zh. Prikl. Khim.* **52** 12 (1989)
21. V B Aleskovsky, V E Drozd *Acta Polytech. Scand.* **195** 155 (1990)
22. *Molecular Beam Epitaxy and Heterostructures* (Translated into Russian) (Moscow: Mir, 1989)
23. US P. 4058430
24. M Ahonen, M Pessa *Thin Solid Films* **65** 301 (1980)
25. M Pessa, O Jylhä, M A Herman *J. Cryst. Growth* **67** 255 (1984)
26. Yu V Plyuto, E S Smol, I V Babich *Kinet. Katal.* **32** 775 (1991)
27. V A Dzis'ko *Osnovnye Metody Prigotovleniya Katalizatorov* (Basic Methods of Preparation of Catalysts) (Novosibirsk: Nauka, 1983)
28. G V Lisichkin, G V Kudryavtsev, A A Serdan, et al. *Modifitsirovannye Kremnezemy* (Modified Silicas) (Moscow: Khimiya, 1986)
29. F Hartley *Immobilised Complexes in Catalysis* (Translated into Russian) (Moscow: Mir, 1989)
30. Yu I Ermakov, V A Zakharov, B N Kuznetsov *Zakreplennye Kompleksy na Okisnykh Nositelyakh v Katalize* (Immobilised Complexes on Oxide Supports in Catalysis) (Novosibirsk: Nauka, 1980)

31. R K Iler *Colloid Chemistry of Silica and the Silicates* (Translated into Russian) (Moscow: Mir, 1982)
32. H Kautsky, H Wesslay *Z. Naturforsch. B* **9** 569 (1954)
33. US P 3 634 286
34. M F Smirnova, A P Dushina, V B Aleskovskii, in *Ionnyi Obmen i Ionity* (Ion Exchange and Ion Exchangers) (Leningrad: Nauka, 1970) p. 130
35. A M D Bollond, A M Posner, J Qvirk *Aust. J. Soil. Res.* **15** 279 (1977)
36. K Fajans *Radio Elements and Isotopes* **4** 34 (1939)
37. C B Amphlett *Inorganic Ion Exchangers* (Translated into Russian) (Moscow: Mir, 1966)
38. *Ionnyi Obmen i Sorbtsiya iz Rastvorov* (Ion Exchange and Sorption from Solutions) (Minsk: Izd. Akad. Nauk. Beloruss.SSR, 1963)
39. R Griessbach *Theorie und Praxis des Ionenaustausches* (Translated into Russian) (Moscow: Inostr. Lit., 1963)
40. Yu V Egorov *Statistika Sorbtsii Mikroelementov Oksigidratami* (Statistics of the Sorption of Trace Elements by Oxide Hydroxides) (Moscow: Nauka, 1975)
41. K M Saldadze, V D Kopylova-Valova *Kompleksnye Ionity* (Complex Ion Exchangers) (Leningrad: Khimiya, 1980)
42. Yu A Kokotov, P P Zolotarev, G E El'kin *Teoreticheskie Osnovy Ionnogo Obmena* (Theoretical Foundations of Ion Exchange) (Leningrad: Khimiya, 1986)
43. V S Soldatov, V A Bychkova *Ionoobmennye Ravnovesiya v Mnogokomponentnykh Sistemakh* (Ion-exchange Equilibria in Multicomponent Systems) (Moscow: Nauka i Tekhnika, 1988)
44. F A Belinskaya, E D Makarov, in *Ionometriya i Ionnyi Obmen* (Ionometry and Ion Exchange) No. 1 (Leningrad: Izd. Leningr. Univ., 1976) p. 21
45. F A Belinskaya, in *Ionometriya i Ionnyi Obmen* (Ionometry and Ion Exchange) No. 6 (Leningrad: Izd. Leningr. Univ., 1988) p. 76
46. E S Boichinova, in *Ionometriya i Ionnyi Obmen* (Ionometry and Ion Exchange) No. 4 (Leningrad: Izd. Leningr. Univ., 1984) p. 20
47. *Sorbenty na Osnove Silikagelya v Radiokhimii* (Sorbents Based on Silica Gel in Radiochemistry) (Moscow: Atomizdat, 1977)
48. USSR P 1 386 600; *Byul. Izobr.* **13** 114 (1988)
49. USSR P 1 560 627; *Byul. Izobr.* **16** 105 (1990)
50. L P Bogdanov, V P Tolstoi, V B Aleskovskii *Zashchita Metallov* **3** 470 (1990)
51. USSR P. 1 475 980; *Byul. Izobr.* **4** 708 (1990)
52. L P Bogdanov, V P Tolstoi *Zashchita Metallov* **3** 485 (1991)
53. B Rotrekl, I Gudnichek, A Komarek *Poverkhnostnaya Obrabotka Plastmass* (Surface Treatment of Plastics) (Leningrad: Khimiya, 1972)
54. N S Golovchanskaya, S S Kruglikov, in *Itogi Nauki i Tekhniki. Seriya Elektrokhimiya* (Advances in Science and Technology. Electrochemistry Series) Vol. 25 (Moscow: VINITI, 1987) p. 28
55. I I Stavnitser, A P Eichis, N I Kletsko *Metallizatsiya Plastmass* (Metallisation of Plastics) (Moscow, 1984)
56. V F Nikolau *Appl. Surf. Sci.* **22/23** 1061 (1985)
57. US P 4 675 207A
58. V F Nikolau, J C Menard *J. Cryst. Growth* **42B** 128 (1988)
59. V F Nikolau, M Dupuy, M Brunel *J. Electrochem. Soc.* **137** 2915 (1990)
60. V F Nikolau, J C Menard *J. Colloid Interface Sci.* **148** 551 (1992)
61. V N Maslov, M B Muradov, V V Klechkovskaya, in *Protsessy Rosta Poluprovodnikovykh Kristallov i Plenok* (Growth Processes of Semiconductor Crystals and Films) (Novosibirsk: Nauka, 1988) p. 89
62. V V Klechkovskaya, V N Muradov, M B Maslov *Kristallografiya* (1) 182 (1989)
63. A M Kutepov, V N Maslov, V S Petrov *Dokl. Akad. Nauk SSSR* **304** 900 (1989)
64. V N Vorob'ev, F N Khasanov, in *Adsorbtsiya i Adsorbenty* (Adsorbtion and Adsorbents) No. 10 (Kiev: Naukova Dumka, 1982) p. 44
65. K A Burkov, V M Sidyakov, L A Myund, in *Problemy Sovremennoi Khimii Koordinatsionnykh Soedinenii* (Problems in Modern Coordination Chemistry) (Leningrad: Izd. Leningr. Univ., 1978) p. 20
66. K A Burkov, V M Sidyakov, L A Myund *Zh. Prikl. Khim.* **52** 53 (1979)
67. V A Nazarenko, V P Antonovich, S S Nevskaya *Gidroliz Ionov v Rastvorakh* (Hydrolysis of Ions in Solutions) (Moscow: Nauka, 1979)
68. O A Demin, K P Tikhomolova, N G Sharova *Vestn. Leningr. Univ.* **25** 57 (1990)
69. B W Gregory, D W Suggs, J L Stickney *J. Electrochem. Soc.* **138** 1279 (1991)

Russian Chemical Reviews **62** (3) 243–259 1993
© 1993 Russian Academy of Sciences and Turpion Ltd

U.D.C. 542.91 + 547.241 + 547.539.151

Phosphorus-containing nucleophiles in reactions with polyfluorinated organic compounds

G G Furin

Contents

I. Introduction 243
II. Reactions of phosphorus-containing nucleophiles with unsaturated perfluorinated compounds 222
III. P-Nucleophiles as synthons in the synthesis of perfluorinated organic compounds without phosphorus atoms 253
IV. Conclusion 257

Abstract. The review presents a compilation of new experimental data on the reactions of phosphorus-containing nucleophiles [triphenylphosphine, trialkylphosphines, trialkyl phosphites, phosphorus tris(diethylamide), etc.] with perfluorinated olefins and aromatic and heterocyclic compounds, leading to substances both with and without a phosphorus atom. It is shown that the interaction of phosphorus tris(diethylamide) and trialkylphosphines with organic polyfluoro-compounds and perfluoroolefins leads to the formation of phosphoranes, the decomposition of which is accompanied by the generation of aryl and alkenyl anions. The reactions of these anions with C-electrophiles and compounds containing mobile halogen atoms are examined. In addition, the pathways in the Arbuzov reaction involving a series of unsaturated perfluorinated compounds are analysed. Possible applications of these reactions in organic synthesis are demonstrated. The bibliography includes 120 references.

I. Introduction

The interest shown by investigators in the chemistry of organophosphorus compounds can be explained by their high reactivity and a unique set of properties, which make these substances valuable objects for theoretical research and impart to them practical importance.[1] However, organophosphorus compounds containing polyfluorinated alkyl and aryl substituents began to be investigated only recently. Bearing in mind the mutual influence of the fluorine and phosphorus atoms on the properties of the entire molecule, one can postulate that such compounds have many interesting properties.

The methods of synthesis of organophosphorus compounds are based on reactions involving the nucleophilic substitution of fluorine atoms in unsaturated organofluorine compounds on treatment with P-nucleophiles (compounds of trivalent phosphorus). Three types of reactions are then possible:

(1) substitution reactions without change in the valence of the phosphorus atom (one of the substituents at the phosphorus atom undergoes the usual exchange for a perfluorinated substituent);

(2) substitution reactions accompanied by the oxidation of the phosphorus atom (they lead to the formation of phosphonium salts, phosphoranes, and phosphinic and phosphonic acid esters in which the phosphorus atom is in pentacoordinate and tetracoordinate states);

(3) reactions in which compounds of tricoordinate phosphorus play the role of a synthon, the final product of such reactions being compounds with a new C–C bond and without a phosphorus atom.

Whereas the reactions of the first two types have long been known and have been thoroughly investigated for a wide range of P-nucleophiles, those of the third type are in fact characteristic of the polyfluorinated compounds. They have come to constitute one of the methods of synthetic organic chemistry used to introduce various perfluorocarbon groups into the molecule. One can now note that these procedures have a great future.

The introduction of a fluorine atom into organophosphorus compounds leads to extensive possibilities both in the synthesis of biologically active compounds and in the determination of the relation between the chemical structure and properties of compounds of this class. At the present time, the stage involving the accumulation of experimental data on the synthesis of compounds of this class may be regarded as completed and attention should now be concentrated on the study of their structures, reactivities, and reaction mechanisms. A series of experimental data on the reactions of triethyl phosphite with perfluoroisobutene and aromatic polyfluoro-compounds have been compiled in a number of reviews.[2–4] On the other hand, inadequate attention has been devoted in the literature to questions of the reactivity of other P-nucleophiles in reactions with organic polyfluoro-compounds. At the same time, the biological activity and unique properties of materials based on fluorine-containing organophosphorus compounds have created a basis for their practical use, so that systematic treatment and analysis of the accumulated extensive data are urgently required and the publication of a review on this topic should stimulate further research on these lines.

The arrangement of the data is based on the nature of the P-nucleophile because the latter actually introduces significant differences into the behaviour of perfluorinated compounds and determines the nature of the products formed.

G G Furin. Novosibirsk Institute of Organic Chemistry, Siberian Division of the Russian Academy of Sciences. prosp. ak. Lavrent'eva 9, 630090 Novosibirsk, Fax (7-383-2) 35 47 52.

Received 1 July 1992
Uspekhi Khimii **62** (3) 267–283 (1993); translated by A K Grzybowski

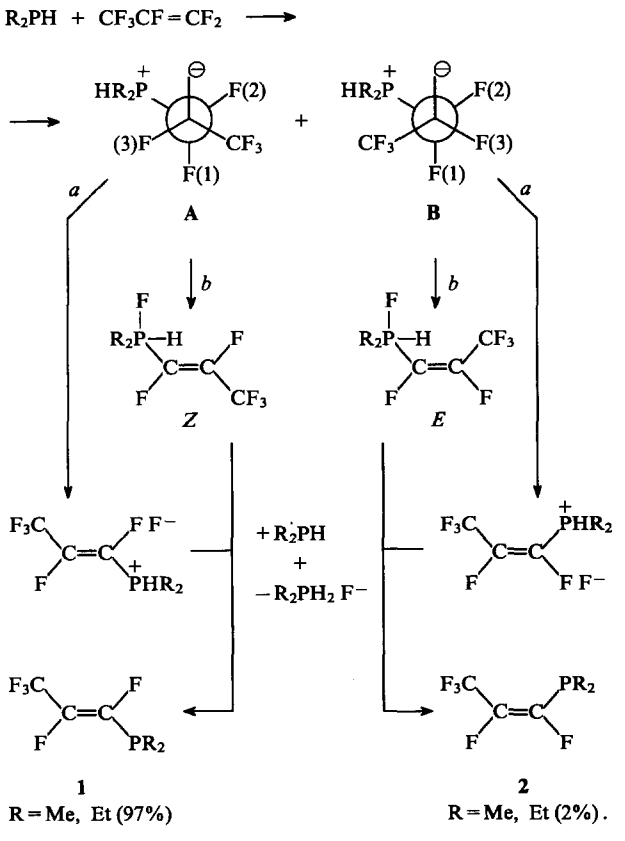
II. Reactions of phosphorus-containing nucleophiles with unsaturated perfluorinated compounds

Nucleophilic reactions of derivatives of trivalent phosphorus are some of the most important and varied in the chemistry of organophosphorus compounds. One of the most widely used is the reaction of trialkyl phosphites and dialkyl phosphonites with alkyl halides and other alkylating agents, accompanied by the formation of phosphonic and phosphinic acid esters.[5] By virtue of the high electronegativity of the fluorine atom, its introduction into an organic molecule influences significantly the charge characteristics of the carbon atom, increasing its positive charge.[3] Nucleophilic substitution reactions become characteristic of compounds of this type and the nature of the products formed depends significantly on the structure of the initial compound.

1. Reactions with trialkyl-, dialkyl-, and triphenylphosphines

Trivalent phosphorus compounds, which are highly nucleophilic, are known to react readily with substances incorporating electronegative halogen, sulphur, and oxygen atoms. In conformity with their nucleophilicity, phosphines can be arranged in the following sequence in terms of their reactivities: $PPh_3 > Ph_2POEt > PhP(OEt)_2 > P(OEt)_3$. When halogen-containing compounds are acted upon by phosphines and phosphites, compounds of two types may be formed, in which the phosphorus atom either retains its valence (new phosphines and phosphites) or its valence increases (for example, with formation of phosphoranes). We shall consider reactions occurring with retention of the valence of the phosphorus atom.

It has been shown[6,7] that hexafluoropropene reacts with dialkylphosphines R_2PH, affording perfluoropropenyl derivatives and phosphonium fluoride $R_2P^+H_2F^-$. The reaction proceeds via the intermediate formation of two 1,3-betaines as a result of the nucleophilic attack by the phosphorus atom on the C(1) atom. The intermediate **A** is more favourable on energy grounds than **B**, because the steric hindrance generated by the bulky CF_3 and PR_2H groups is smaller in the latter.



The intermediates **A** and **B** can be stabilised in two ways: either as a result of the migration of the F(1) ion (pathway *a*) in the *trans*-position with respect to the electron pair of the C(2) atom (the quasi-phosphonium ions formed are deprotonated, affording the corresponding phosphines) or as a result of the 1,2-migration of the fluorine atom to the phosphorus atom (pathway *b*) [the (*Z*)- and (*E*)-fluorophosphoranes formed in this process are subsequently dehydrofluorinated].

In the reaction of tri(*tert*-butyl)phosphine with hexafluoropropene, the fluorine atom at the C(1) atom is substituted and the phosphine **3**, isobutene, and tri(*tert*-butyl)phosphonium fluoride are formed. The last two compounds are obtained from the initial phosphine and fluorotrimethylmethane — one of the products of the reaction of the perfluoroolefin with phosphine.

In contrast to this, in the reaction of phenylphosphine with

$$CF_3CF=CF_2 + P(Bu^t)_3 \longrightarrow [CF_3CF=CF-P(Bu^t)_3]^+F^- \xrightarrow{P(Bu^t)_3} CF_3CF=CFP(Bu^t)_2 + Me_2C=CH_2 + (Bu^t)_3\overset{+}{P}HF^-.$$

3

tetrafluoroethylene, nucleophilic addition to the double bond takes place with formation of phenyltetrafluoroethylphosphine **4**.[8]

In the presence of an excess of tetrafluoroethylene, the disubstituted phosphine $PhP(CF_2CHF_2)_2$ is formed as well as compound **4**. In the presence of an inhibitor of the polymerisation of tetrafluoroethylene and for the 1 : 1 reactant ratio, the yield of compound **4** is 84%. The adduct resulting from the addition of phenylphosphine to 1,1-difluoroethylene is formed in approximately the same yield.

$$CF_2=CF_2 + PhPH_2 \xrightarrow{150^\circ C} PhPHCF_2CHF_2.$$

4

Diethylphosphine reacts with perfluorobut-2-yne at −78 °C with formation of the *trans*-isomer **5**.[9]

$$CF_3C\equiv CCF_3 + Et_2PH \longrightarrow Et_2P(CF_3)C=CHCF_3$$

5 (45%).

According to Fild et al.,[10] the reaction of CF_2Br_2 with organylbis(trimethylsilyl)phosphine $RP(SiMe_3)_2$ and diorganyl(trimethylsilyl)phosphine R_2PSiMe_3 (R = Ph, Bu^t, Me) leads to the formation of the diphosphetan **6** and R_2PCF_2Br respectively.

$$RP(SiMe_3)_2 + CF_2Br_2 \longrightarrow \text{(6)};$$

6

$$R_2PSiMe_3 + CF_2Br_2 \longrightarrow R_2PCF_2Br.$$

The structure of compound **6** was confirmed by X-ray diffraction analysis and ^{19}F and ^{31}P NMR spectroscopy. It is suggested that the diphosphetan **6** is formed via an intermediate phosphaalkene as a result of its subsequent thermal decomposition.

The reaction of diphenyltrimethylsilylphosphine with CF_3I at 20 °C leads to the formation of diphenyltrifluoromethylphosphine in 78% yield.[11] The same compound is obtained in a satisfactory yield by the reaction of CF_3I with triphenylphosphine at 185–200 °C.[12]

Table 1. Fluorophosphoranes obtained by the reaction of tributylphosphine with perfluoroolefins.[15]

Olefin	Reaction product	Yield (%)	*E*/*Z*
$CF_3(CF_2)_2CF=CF_2$	$CF_3(CF_2)_2CF=CFPF(Bu^n)_3$	81	100 (*Z*)
$CF_3(CF_2)_4CF=CF_2$	$CF_3(CF_2)_4CF=CFPF(Bu^n)_3$	83	100 (*Z*)
$CF_3CPh=CF_2$	$CF_3CPh=CFPF(Bu^n)_3$	84	91/9
$CF_3CF_2CPh=CF_2$	$CF_3CF_2CPh=CFPF(Bu^n)_3$	87	92/8

Trimethylphosphine reacts with trifluoroiodomethane to form dimethyltrifluoromethylphosphine and tetramethylphosphonium iodide.[13, 14]

$$Me_3P + ICF_3 \longrightarrow [Me_3PCF_3]^+I^- \xrightarrow{Me_3P} Me_2PCF_3 + [Me_4P]^+I^-.$$

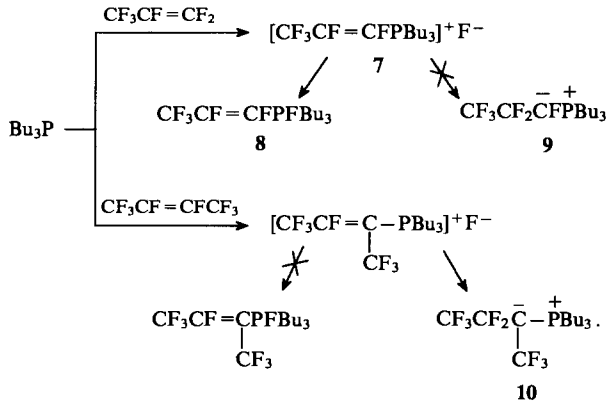
Reactions of another type, specific to perfluorinated organic compounds, involve the formation of fluorophosphoranes. Thus it has been shown[15] that tributyl- and trimethyl-perfluoropropenylfluorophosphoranes are formed in the reaction of hexafluoropropene with tributyl- and trimethylphosphines respectively.

$$CF_3CF=CF_2 + R_3P \longrightarrow CF_3CF=CFPFR_3$$

R = Me, Bu^n.

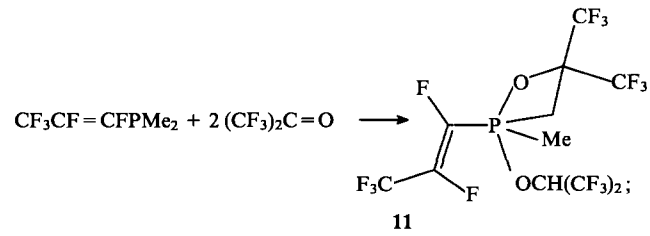
Other perfluoroalk-1-enes react similarly (Table 1), the *trans*-isomers being mainly formed (Scheme 1).

Scheme 1

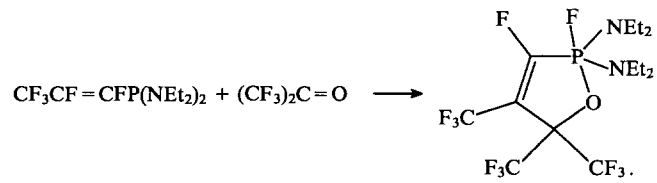


The primary step in these reactions involves the attack by the nucleophilic phosphorus atom on a carbon atom, leading to the quasi-phosphonium salt **7**, from which compound **8** is formed as a result of the 1,2-migration of the fluoride anion to the phosphorus atom. The phosphorus ylide **9** is not obtained in this reaction. On the other hand, in the case of perfluorobut-2-ene the main reaction product is believed[15] to be in fact the ylide **10** of this kind, while the corresponding phosphorane is not formed. The structure of compound **10** was confirmed by ^{31}P and ^{19}F NMR spectroscopy.

A series of phosphines react with carbonyl compounds. Thus it has been shown[6, 7] that dimethylperfluoropropenylphosphine and bis(diethylamino)perfluoropropenylphosphine react with hexafluoroacetone, affording cyclic phosphorus compounds: 1,2-oxaphosphetan **11** and 1,2-oxaphospholen **12** respectively.

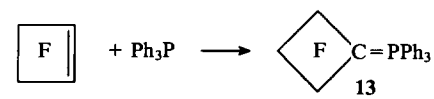


11



12

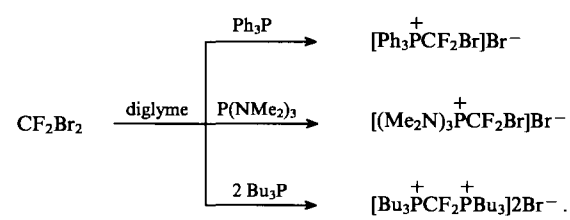
By allowing triphenylphosphine to react with perfluorocyclobutene, Stochel et al.[16] obtained, instead of a phosphorus ylide, 2,2,3,3,4,4-hexafluoro(triphenylphosphoranylidene)cyclobutane **13**, the structure of which was later confirmed by X-ray diffraction.[17]



13

Perfluorobutadiene also reacts with triphenylphosphine to form 1 : 1 adducts, which consist of relatively unstable cyclic phosphoranes.

When the polyfluoroolefin molecule contains other halogen atoms as well as those of fluorine, stable phosphonium salts are formed. For example, the reaction of dibromodifluoromethane with triphenylphosphine[18] or tris(dimethylamino)phosphine[19] affords phosphonium salts in quantitative yields. A diphosphonium salt is formed in the presence of an excess of the phosphine. The reaction is of the S_N2 type.



2. The Arbuzov reactions of perfluorinated compounds

Trialkyl phosphites induce the dehalogenation of certain vicinal dihalo-derivatives.[21]

$$(EtO)_3P + BrCF_2CFBrCl \longrightarrow CF_2=CFCl + (EtO)_2P(O)Br + EtBr.$$

Table 2. Reactions of haloperfluoroalkanes with triethyl phosphite.[20]

Initial compound	Reaction product	Yield (%)
$I(CF_2)_6CFClCF_2Cl$	$I(CF_2)_6CF=CF_2$,	23,
	$I(CF_2)_6CF=CFP(O)(OEt)_2$	50
$I(CF_2)_4CFClCF_2Cl$	$I(CF_2)_4CF=CF_2$,	38,
	$I(CF_2)_4CF=CFP(O)(OEt)_2$	46
$I(CF_2)_2CFClCF_2Cl$	$I(CF_2)_2CF=CFP(O)(OEt)_2$	43.5
$ClCF_2CFCl(CF_2)_4CFClCF_2Cl$	$(EtO)_2(O)PCF=CF(CF_2)_4CF=CFP(O)(OEt)_2$	17

When trialkyl phosphites are heated with $Cl(CF_2CFCl)_nCl$, olefins are formed.[22] Having observed this property of trialkyl phosphites, the authors suggest that the reaction proceeds via the formation of the product **14** of the usual Arbuzov rearrangement, which subsequently decomposes, affording diethyl phosphorochloridate and a polyfluoroolefin.

$$CFCl_2CF_2CFClCF_2Cl + P(OEt)_3 \longrightarrow$$
$$\longrightarrow \underset{\mathbf{14}}{CFCl_2CF_2CFClCF_2P(O)(OEt)_2} \longrightarrow$$
$$\longrightarrow CFCl_2CF_2CF=CF_2 + ClP(O)(OEt)_2.$$

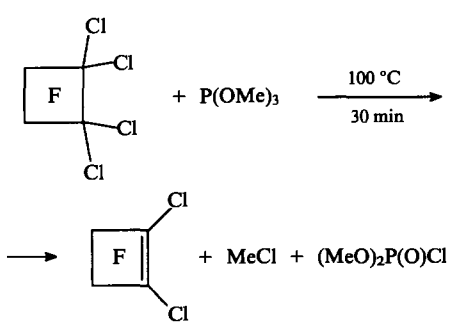
It has been shown[20, 23, 24] that the reactions of triethyl phosphite with α,β-dichloro-ω-iodoperfluoroalkanes does indeed involve dehalogenation, but the products are a mixture of ω-iodoperfluoroalk-1-enes and diethyl esters of ω-iodoper-fluoroalk-1-enylphosphonic acids (Table 2).

$$RCF(X)-CY_2(Cl) \xrightarrow[[-XCl]]{P(OEt)_3} [RCF=CY_2] \xrightarrow[-EtY]{P(OEt)_3}$$
$$\longrightarrow RCF=CYP(O)(OEt)_2$$

X = F, Y = Cl, R = $CFCl_2$;
X = Cl, Y = F, R = $I(CF_2)_2$, $I(CF_2)_4$, $I(CF_2)_6$.

Knunyants and Pervova[23] suggest a different mechanism of the dehalogenation process, consisting in the initial splitting off of two halogen atoms in vicinal positions with formation of diethyl phosphorochloridate and ω-iodoperfluoroalk-1-ene, which interacts with triethyl phosphite, affording the product of the Arbuzov rearrangement. Only in the reaction of triethyl phosphite with dichloroiodotrifluoroethane is the halogen split off without the formation of the corresponding phosphonates. Chlorotrifluoroethylene is then obtained in a quantitative yield.

The results of a study[25] in which it was shown that the dehalogenation of polyhalogenated cyclobutanes by trimethyl phosphite leads to polyfluorocyclobutenes are consistent with these ideas.



The defluorination of perfluoro-*N*-fluoropiperidine by triphenylphosphine, leading to perfluoro-1-azacyclohexene, was described previously.[26]

In the reaction of chlorofluoroalkanes with triethyl phosphite, attack by the chlorine atom on the phosphite molecule results in the intermediate formation of the phosphonium salt **16**.[27]

$$(EtO)_3P + CCl_3(CF_2)_nCl \longrightarrow$$
$$\longrightarrow \underset{\mathbf{16}}{[(EtO)_3PCl]^+[CCl_2(CF_2)_nCl]^-} \longrightarrow$$
$$\longrightarrow \underset{\mathbf{17}}{CCl_2=CF(CF_2)_{n-1}Cl} + \underset{\mathbf{18}}{EtCCl_2(CF_2)_nCl} +$$
$$+ \underset{\mathbf{19}}{(EtO)_2P(O)CCl=CF(CF_2)_{n-1}Cl} + (EtO)_2P(O)Cl.$$

The further reaction of the salt **16** leads to the dehalogenation and alkylation products **17** and **18** respectively. Furthermore, the Arbuzov reaction with participation of the olefin **17** affords compound **19**.

Certain perfluorohaloalkanes also enter into the Arbuzov reaction. In the presence of bromine as well as fluorine atoms in the alkyl group, the Arbuzov reaction then proceeds with participation of the bromine atoms (Table 3).[28]

$$CFXY_2 + P(OR)_3 \xrightarrow[25-50\ °C,\ 24\ h]{\text{triglyme}} (RO)_2(O)PCFXY + RY.$$

On the other hand, the compounds CF_3Cl, CF_3I, and $CFCl_3$ are inert under the conditions of the Arbuzov reaction.[29, 30]

The Arbuzov reaction with participation of polyfluorinated alkyl halides can be carried out under UV irradiation. Thus the reaction of perfluoroalkyl iodides with triethyl phosphite under UV irradiation,[31] leading to diethyl perfluoroalkylphosphonate **20**, has been achieved. The reaction probably proceeds in accordance with the following mechanism:

$$CF_3I \xrightarrow{h\nu} \dot{C}F_3 + \dot{I},$$
$$\dot{C}F_3 + (EtO)_3P \longrightarrow CF_3\dot{P}(OEt)_3 \xrightarrow{CF_3I}$$
$$\longrightarrow \underset{\mathbf{21}}{[CF_3P(OEt)_3]^+I^-} + \dot{C}F_3;$$
$$[CF_3P(OEt)_3]^+I^- \longrightarrow \underset{\mathbf{20}}{CF_3P(O)(OEt)_2} + EtI.$$

Table 3. Reactions of dibromodifluoromethane and tribromofluoromethane with trialkyl phosphites $P(OR)_3$ (data of Burton and Flynn[28]).

$CFXY^2$	R	Solvent	Yield (%)
CF_2Br_2	Me	triglyme	55
	Et	diethyl ether	95
	Et	triglyme	55
	Bu^n	diethyl ether	65
	Pr^i	triglyme	42
$CFBr^3$	Et	diethyl ether	78
	Et	triglyme	60
	Pr^i	diethyl ether	22

The trifluoromethyl radical, formed on dissociation of trifluoromethyl iodide, attacks a molecule of triethyl phosphite, giving rise to a phosphoranyl radical. The latter is oxidised by trifluoromethyl iodide to the quasi-phosphonium salt **21**, which decomposes with liberation of ethyl iodide and diethyl trifluoromethylphosphonate **20**. The reaction is carried out in an excess of trifluoromethyl iodide over a period of 10 h, the yield of the phosphonate being 51%.

Pentafluoroiodobenzene reacts with triethyl phosphite at the C–I bond also only on exposure to UV radiation (350 nm), whereupon diethyl pentafluorophenylphosphonate **22** is formed.

$$C_6F_5I + (EtO)_3P \longrightarrow \underset{\mathbf{22}\ (32\%)}{C_6F_5P(O)(OEt)_2} + EtI.$$

The reaction of dichlorotrifluoroethyl hexafluoroiodopropyl ether **23** with triethyl phosphite in the presence of *tert*-butyl peroxide takes place similarly.[32] The trivalent phosphorus derivative **24** is formed initially and is then oxidised to the phosphonate **25**.

$$\underset{\mathbf{23}}{CF_2ClCFClO(CF_2)_3I} + P(OEt)_3 \xrightarrow{(Bu^tO)_2} \underset{\mathbf{24}}{CF_2ClCFClO(CF_2)_3P(OEt)_2} \xrightarrow{Bu^tOOH} \underset{\mathbf{25}}{CF_2ClCFClO(CF_2)_3P(O)(OEt)_2}.$$

It is seen from these examples that an advantage of photochemical initiation of the Arbuzov reaction is the possibility of synthesising fluorine-containing phosphonates from available reagents in one stage.

The CH_2Br group and not CF_2Br participates in the reaction of the bromo-derivative **26** with triethyl phosphite, although the positive charge on the carbon atom of the CF_2Br group is higher than that on the carbon atom of CH_2Br.[33] Under these conditions, the (*Z*)-isomer of diethyl 4-bromo-3,4,4-trifluorobut-2-enylphosphonate **27** is formed. Steric factors probably play a role in this instance.

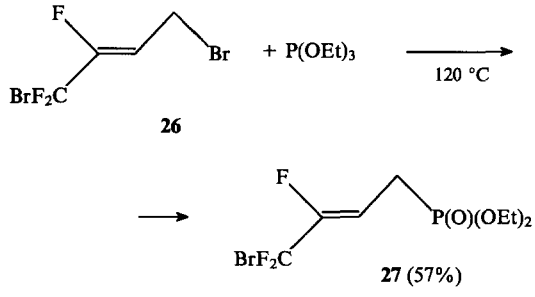


Table 4. Reactions of polyfluoroolefins with trialkyl phosphites.[36]

Fluorooelfin	Trialkyl phosphite	Reaction product	Yield (%)
$CF_2=CFCl$	$(EtO)_3P$	$CFCl=CFP(O)(OEt)_2$	10
$CF_2=CF_2$	$(Pr^iO)_3P$	$CF_2=CFP(O)(OPr^i)_2$	26
$CF_3CF=CF_2$	$(Pr^iO)_3P$	$CF_3CF=CFP(O)(OPr^i)_2$	48
$(CF_3)_2C=CF_2$	$(BuO)_3P$	$(CF_3)_2C=CFP(O)(OBu)_2$	35
$CF_3CF=CF_2$	$MeP(OPr^i)_2$	$CF_3CF=CFP(O)(OPr^i)$ | Me	51
$(CF_3)_2C=CF_2$	$(Pr^iO)_3P$	$(CF_3)_2C=CFP(O)(OPr^i)_2$	50

In contrast to perfluoroalkyl halides, perfluoroolefins react readily with trialkyl phosphites to form the esters of perfluoroalkenylphosphonic acids (Table 4).[34–36] Thus perfluoroisobutene reacts vigorously with triethyl phosphite even at −35 to 30 °C, affording the fluorophosphorane **28**, which is stable under the usual conditions. The phosphorane decomposes at 120 °C with formation of diethyl perfluoroalkenylphosphonate **29**.[37]

$$(CF_3)_2C=CF_2 + P(OEt)_3 \xrightarrow{-35\ ^\circ C} \underset{\mathbf{28}}{(CF_3)_2C=CFPF(OEt)_3} \xrightarrow{120\ ^\circ C} \underset{\mathbf{29}}{(CF_3)_2C=CFP(O)(OEt)_2}.$$

Perfluoroolefins behave similarly.[34–39]

The interaction of perfluoroolefins with triethyl phosphite takes place in two stages: the first stage of the reaction involves the formation of triethoxyperfluoroalkenylfluorophosphorane **28**, which then decomposes under more severe conditions with formation of the final products of the Arbuzov rearrangement—compound **29**. In the reaction of hexafluoropropene with triethyl phosphite, the intermediate fluorophosphorane cannot be detected, but the final product is diethyl pentafluoropropenylphosphonate.[37] The decomposition of the intermediate fluorophosphorane takes place via two pathways and leads, on the one hand, to ethyl fluoride and the full ester of perfluoroalkenylphosphonic acid and, on the other, to the fluoride of the acid ester of perfluoroalkenylphosphonic acid and diethyl ether.[37] This constitutes the specificity of the Arbuzov reaction for unsaturated perfluorinated compounds.

$$\underset{\mathbf{28}}{(CF_3)_2C=CFPF(OEt)_3} \longrightarrow \begin{cases} (CF_3)_2C=CFP(O)(OEt)_2 + EtF \\ (CF_3)_2C=CFPF(O)(OEt) + Et_2O. \end{cases}$$

The reactivity of perfluoroolefins in the reaction with triethyl phosphite diminishes in the following sequence:

$$\boxed{F} > (CF_3)_2C=CF_2 > CF_3CF=CF_2 \approx CF_2=CF_2.$$

When one fluorine atom is replaced in perfluoroethylene by another halogen atom, a fluorine and not a chlorine[36] or iodine[40] atom participates in the reaction with phosphites.

Thus the reaction of trifluoroiodoethylene with tris(isopropyl) phosphite[40] affords the *trans*-di(isopropyl) ester of phosphonic acid **30**.

$$CF_2=CFI + (Pr^iO)_3P \longrightarrow \begin{cases} \xrightarrow[60\ h]{80^\circ C} \underset{\mathbf{30}\ (67\%)}{CFI=CFP(O)(OPr^i)_2} \\ \xrightarrow[80\ h]{100^\circ C} \underset{\mathbf{31}}{(Pr^iO)_2(O)P\diagdown\ \diagup F\ C=C\ F\diagup\ \diagdown P(O)(OPr^i)_2}. \end{cases}$$

However, when an excess of tri(isopropyl) phosphite is used, the iodine atom is also substituted with formation of the corresponding ester of the diphosphonic acid **31**. The reaction of trifluoroiodoethylene with other trialkyl phosphites (R = Pr^i, Et, Me) takes place similarly. We may note that in the case of bromotrifluoro- and chlorotrifluoro-ethylenes, the esters of phosphonic acids are obtained in very low yields. Thus the presence of an iodine atom at the double bond activates the fluorine atom involved in the reaction with trialkyl phosphites.

The interaction of pentafluoroazapropene $CF_3N=CF_2$ with triethyl phosphite leads to the formation of the stable trialkoxytetrafluoroazapropenylfluorophosphorane $CF_3N=CFPF(OR)_3$.[41]

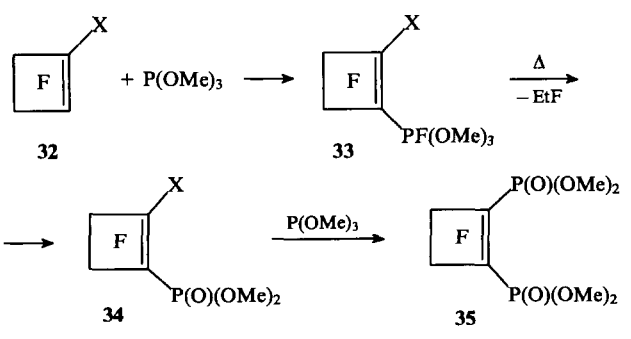
The bisphosphonate $(RO)_2P(O)CF=CFP(O)(OR)_2$ **32**, where R = Et or Pr^i, is formed when tetrafluoroethylene is treated with $(RO)_2POSiMe_3$.[42]

The reaction of triethyl phosphite with allenes results in the formation of the corresponding perfluorinated 1,3-dienylphosphonic acid esters.[43] Thus the corresponding 1,3-dien-2-ylphosphonate was obtained from tetrakis(trifluoromethyl)allene and triethyl phosphite probably as a result of the occurrence of a reaction of the S_N2 type.

$$(CF_3)_2C=C=C(CF_3)_2 \xrightarrow{P(OEt)_3} (CF_3)_2C=\underset{\displaystyle (EtO)_3PF}{\overset{\displaystyle CF_3}{\underset{|}{C}}}-\overset{\displaystyle CF_3}{\overset{|}{C}}=CF_2 \xrightarrow[-EtF]{\Delta} (CF_3)_2C=\underset{\displaystyle O=P(OEt)_2}{\overset{\displaystyle CF_3}{\underset{|}{C}}}-\overset{\displaystyle CF_3}{\overset{|}{C}}=CF_2 .$$

The synthesis of diethyl 2-trifluoromethylperfluoropenta-1,3-dien-3-yl-phosphonate from perfluoro-2-methylpent-2-ene and triethyl phosphite has been described[44] from the standpoint of the initial formation of tris(trifluoromethyl)allene as a result of the defluorination of the initial perfluoroolefin by triethyl phosphite and its subsequent reaction with the latter.

$$(CF_3)_2C=CFC_2F_5 + P(OEt)_3 \longrightarrow [(CF_3)_2C=C=CFCF_3] + F_2P(OEt)_3 \xrightarrow{P(OEt)_3} CF_2=\underset{\displaystyle O=P(OEt)_2}{\overset{\displaystyle CF_3}{\underset{|}{C}}}-\overset{\displaystyle CF_3}{\overset{|}{C}}=CFCF_3 .$$



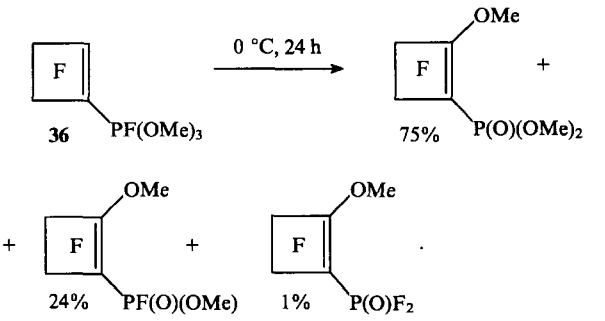
X = F, Cl, Br, I.

X	Yield of **33** (%)	Yield of **34** (%)
F	43	–
Cl	100	60
Br	100	49
I	100	45

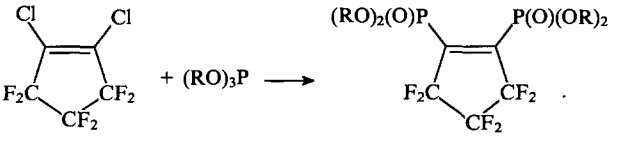
Perfluorocycloalkenes can also be introduced into the Arbuzov reaction. Thus it has been shown[45, 46] that 3,3,4,4-tetrafluoro-1-halocyclobut-1-enyl-2-(trimethoxy)fluorophosphorane is formed as a result of the exothermic reaction of 1-halopentafluorocyclobut-1-ene **32** with trimethyl phosphite.

The phosphorane **33** is stable at 0 °C for several days. Its controlled decomposition leads to dimethyl cyclobutenylphosphonate **34**. On treatment of the ester **34** with an excess of trimethyl phosphite, the tetramethyl ester of 3,3,4,4-tetrafluorocyclobutenylenediphosphonic acid **35** is formed.

On the other hand, the decomposition of 1,3,3,4,4-pentafluorocyclobutenyl-(trimethoxy)fluorophosphorane **36** leads to a mixture of tetrafluorocyclobutenes, in which the fluorine atom at the multiple bond is replaced by the methoxy-group.

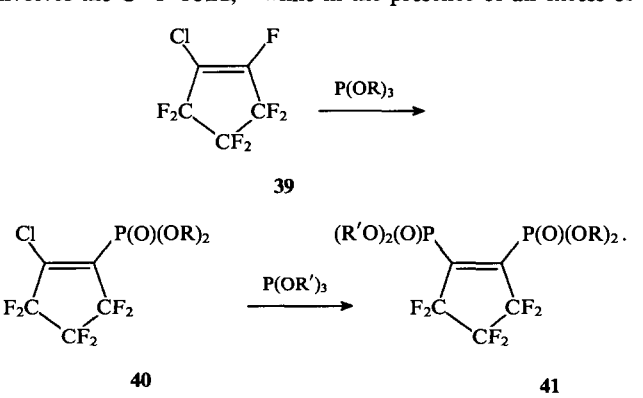


The reaction between 1,2-dichloro-3,3,4,4,5,5-hexafluorocyclopentene **37** and trialkyl phosphite affords tetraalkyl hexafluorocyclopentenylenediphosphonates **38**.[47]



R	Me	Et	Bu	$CH_2CH=CH_2$	Ph
Yield of **38** (%)	40	74	93	92	75

In the presence of two different halogen atoms at the double bond, for example of a chlorine and a fluorine atom, the reaction involves the C–F bond,[48] while in the presence of an excess of



R	Yield of **40** (%)	R	R'	Yield of **41** (%)
Et	33	Et	Et	50
Bu	88	Bu	Et	72.5
Me	38	CH_2CF_3	CH_2CF_3	51

trialkyl phosphite both atoms are substituted.[49] Thus the dialkyl ester of 2-chloro-3,3,4,4,5,5-hexafluorocyclopent-1-enylphosphonic acid **40** is obtained in the reaction of 1-chloro-2,3,3,4,4,5,5-heptafluorocyclopent-1-ene **39** with trialkyl phosphites, while in the presence of an excess of the phosphite the product is tetraalkyl 3,3,4,4,5,5-hexafluorocyclopent-1-en-1,2-ylenediphosphonate **41**.

It has been shown[50] that 2-chloro-1-ethylthiofluorocyclopent-1-ene is converted into diethyl 2-ethylthio-3,3,4,4,5,5-hexafluorocyclopent-1-enylphosphonate (yield 63.7%).

Arbuzov type reactions can be achieved also by treating hexafluoropropene with ethyl and isopropyl methylphosphonites.[51] The yield of the corresponding phosphinate esters **42** was 45% to 55%. The replacement of phosphites by phosphonites makes it possible to carry out the reactions under milder conditions.

$$CF_2{=}CFCF_3 + MeP(OR)_2 \xrightarrow[8-10\ h]{100-120\ ^\circ C} \underset{\mathbf{42}}{\overset{CF=CFCF_3}{\overset{|}{MeP(O)OR}}} + R-F$$

R = Et, Pr^i.

Knunyants et al.[52] introduced the chlorides of dialkylphosphinous, dialkylphosphorous, and *N,N,N',N'*-tetraalkylphosphorodiamidous acids into reactions with perfluoroolefins and, depending on the substituents and the reaction conditions, obtained different products of the reactions of the intermediate perfluoroisobutylfluorophosphoranes **43**, in particular the ester of perfluoroisobutenylphosphinic acid **44**.

$$(CF_3)_2C{=}CF_2 + X-PCl-Y \longrightarrow \underset{\mathbf{43}}{[(CF_3)_2C{=}CFPFClXY]} \xrightarrow[X=Y=OEt]{\Delta} (CF_3)_2C{=}CFPF(O)(OEt)$$

44

X = Y = Et, EtO, Me_2N, Et_2N.

The reactivities of the chlorides of the above acids in relation to perfluoroisobutene proved to be lower than the reactivity of their full esters. Thus, whereas perfluoroisobutene reacts with triethyl phosphite at −30 °C, the acid chlorides react with the above olefin only at an elevated temperature, except for *N,N,N',N'*-tetraethylphosphorodiamidite, which reacts at room temperature. Knunyants et al.[52] derived the following reactivity series for the above reagents:

$$(Et_2N)_2PCl > (Me_2N)_2PCl > (EtO)_2PCl > Et_2PCl.$$

They explain the above decrease in reactivity by the decrease in the capacity of the substituents X for $p-d$ conjugation with the phosphorus atom. In the last compound, there is no $p-d$ conjugation.

It has been shown[6] that the reactions of the phosphites $(R^2O)_2POSiMe_3$ (R^2 = Et, $SiMe_3$) with the perfluoroolefins $R^1CF=CF_2$ ($R^1 = CF_3$, SF_5) give rise to fluorotrimethylsilane and the fluoroalkenylphosphonates **45** and **46** in conformity with the Arbuzov rule (Scheme 2). It is suggested that the reaction follows the pathway described above for perfluoroisobutene. In the case of $F_5SCF=CF_2$, the (*E*)-isomer **45** formed exclusively, whereas in the case of $F_3CCF=CF_2$ the product with the *cis*-configuration **46** is obtained in very small amounts, which indicates the occurrence of slight interaction between the substituents Et and $SiMe_3$, on the one hand, and the fluorine atoms of the CF_3 group, on the other.

It has been shown[53-55] that the derivatives of perfluoromethacrylic acid **47**, which is no less reactive than perfluoroisobutene, react with trialkyl phosphites to form the fluorophosphoranes **48**.

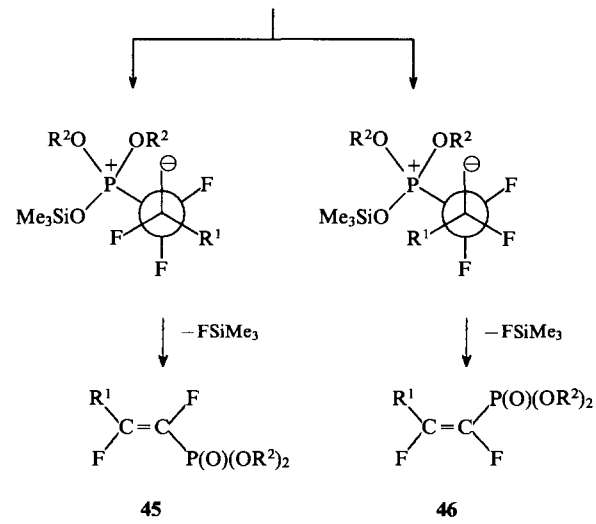
$$(RO)_3P + CF_2{=}\underset{CF_3}{\overset{|}{C}}-C(O)X \longrightarrow \underset{\mathbf{48}}{(RO)_3PFCF{=}\overset{|}{\underset{CF_3}{C}}-C(O)X}$$

47

R = Me, Et; X = OMe, OEt, NMe_2.

Scheme 2

$$(R^2O)_2POSiMe_3 + R^1CF{=}CF_2$$



45 **46**

R^1	R^2	Yield of **45** (%)	Yield of **46** (%)
CF_3	Et	97	3
	$SiMe_3$	99	1
SF_5	Et	100	–
	$SiMe_3$	100	–

The phosphoranes **48** proved to be stable compounds, which decompose only on heating to 115–120 °C. They could be actually vacuum distilled without decomposition. It was then found unexpectedly that the main products of the decomposition of the phosphoranes **48** are alkyl phosphorodifluoridites **49** and the acetals of the substituted ketones **50**.

$$\underset{\mathbf{48}}{(RO)_3PFCF{=}\overset{|}{\underset{CF_3}{C}}COOR^1} \longrightarrow$$

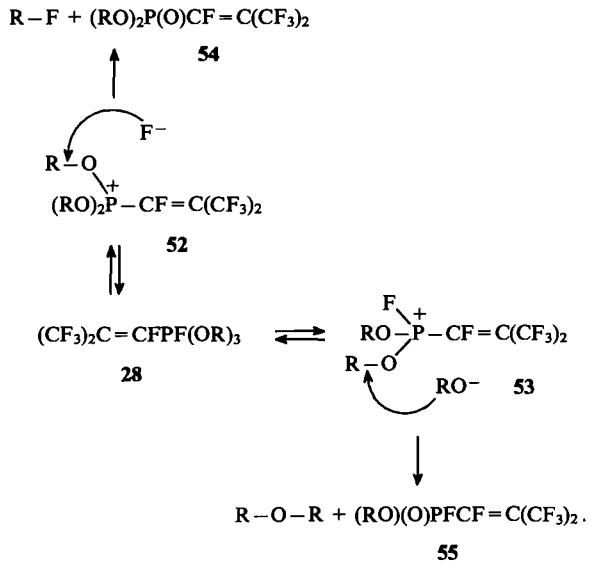
$$\longrightarrow \underset{\mathbf{51}}{(RO)_2(O)P-CF{=}\overset{|}{\underset{CF_3}{C}}COOR^1} + R-F$$

$$\longrightarrow \underset{\mathbf{49}}{RO-PF_2} + \underset{\mathbf{50}\ (70\%-90\%)}{(RO)_2C{=}\overset{|}{\underset{CF_3}{C}}COOR^1}$$

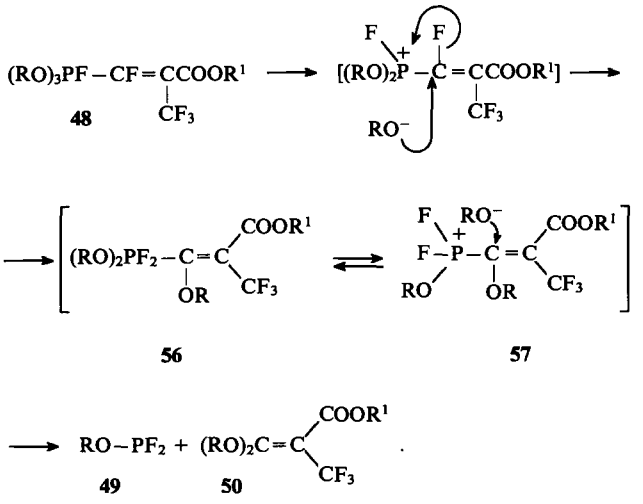
R = Me, Et; R^1 = Me, Et.

The Arbuzov reaction products **51** are not formed at all from the phosphoranes **48** or are obtained only in small amounts. On the other hand, the first stage of the decomposition of the phosphorane **28** is reversible dissociation leading to quasiphosphonium cations of type **52** or **53** and the anions F^- or RO^-. The authors explained this difference in the behaviour of the phosphoranes **28** and **48** by the much greater electrophilicity of the carbon atom of the CF group in the phosphoranes **48** compared with the phosphoranes **28**. In the decomposition of the phosphoranes **28**, the carbon atom of the alkyl group R functions as the electrophilic centre.

Attack by an alkoxide or fluoride ion on the carbon atom leads to the ester **54** or to the acid fluoride **55**.



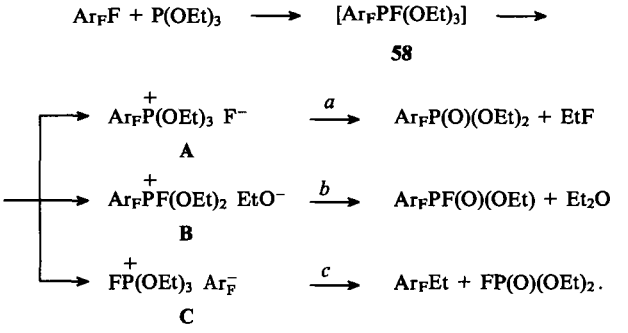
On the other hand, in the phosphoranes **48** the nucleophilic alkoxide anion attacks the β-carbon atom of the acrylic system with formation of the new phosphorane **56**. The dissociation of the latter leads to the quasi-phosphonium salt **57**, which is split into the acetal **50** and the alkyl phosphorodifluoridite **49** as a result of the attack by the alkoxide anion on the same carbon atom.



The possibility of carrying out the Arbuzov reaction with participation of aromatic polyfluoro-compounds of the type C_6F_5X (X = Cl, Br, F, H, OMe) and triethyl phosphite has been discussed.[56] Later this reaction was investigated in greater detail in relation to the interaction of pentafluorobenzonitrile, decafluorobiphenyl, and pentafluoropyridine with triethyl phosphite. The reaction takes place at 140–150 °C with formation of the diethyl esters of polyfluoroarylphosphonic acids in 25–30% yield and is accompanied by a series of side processes: triethyl phosphite, diethyl ethylphosphonate, diethyl phosphonofluoridate, and diethyl ether were detected in the reaction mixtures. An increase in temperature diminishes the yield of phosphonic acid esters. Markovskii et al.[58] determined the factors influencing the occurrence of the side reactions characteristic of compounds of the aromatic polyfluoro-series. In view of the fact that the rate of nucleophilic substitution diminishes significantly in the sequence $C_6F_5NO_2 > C_6F_5CF_3 > C_6F_5H$, a similar sequence might have been expected for the rate of the Arbuzov reaction. However, analysis of the compositions of the reaction mixtures showed that the overall yield of the phosphorylated polyfluorobenzenes increases, contrary to expectation, on passing from pentafluoronitrobenzene to pentafluorobenzene. Furthermore, compounds formed as a result of the reduction and alkylation processes were detected among the reaction products and their amount was actually found to decrease in the above series (Table 5).

This finding, which cannot be explained in terms of the S_N2 nucleophilic substitution mechanism, may indicate the influence on the Arbuzov reaction of factors specific to compounds of the aromatic polyfluoro-series. Apparently, the specific features lie in the fact that a mechanism similar to that proposed by Knunyants et al.[54] for the reaction between perfluoroisobutene and triethyl phosphite operates in the case of aromatic polyfluoro-compounds. A dominant role is assigned in this mechanism to the intermediate polyfluoroaryltriethoxyfluorophosphorane **58**, the reactions of which actually lead to the observed set of products (Scheme 3). The type of the reactions of the phosphorane **58** should be determined both by the stability of the phosphonium cations **A**, **B**, and **C** formed and by the stability of the polyfluoroaryl anion.

Scheme 3



Indeed, with increase in the stability of Ar_F^-, the yield of the alkylation (ethyltetrafluorobenzene Ar_FEt) and reduction (tetrafluorobenzenes Ar_FH) products as well as diethyl phosphorofluoridates should increase (pathway *c*), while the yield of diethyl esters of polyfluoroarylphosphonic acids should diminish (pathway *a*) (Table 5). The reduction process comes down in this instance to the reaction of the polyfluoroaryl anion with a proton from the medium. Indeed, when the reaction of triethyl phosphite with octafluorotoluene or pentafluoropyridine is carried out in the presence of methanol as a source of protons, the yields of heptafluorotoluene and 2,3,5,6-tetrafluoropyridine increase.

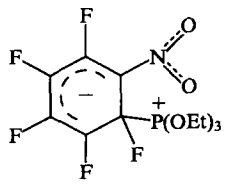
We may note that, together with 4-ethyl-2,3,5,6-tetrafluoronitrobenzene, 2-ethyl-3,4,5,6-tetrafluoronitrobenzene is formed in the reaction of triphenyl phosphite with pentafluoronitrobenzene. This is due to the *ortho*/*para* directing effect of the nitro-group in the nucleophilic substitution reaction.[59]

Table 5. The products of the Arbuzov reaction in $Ar_FF + P(OEt)_3$ reaction mixtures (data of Markovskii et al.[58]).

Ar_F	$Ar_FP(O)(OEt)_2$	$Ar_FPF(O)(OEt)$	Ar_FEt	Ar_FH
$4\text{-}NO_2C_6F_4$	2.2 [a]	0	4.2; 30.0 [a]	3.8; 44.1 [a]
$4\text{-}CF_3C_6F_4$	8.5	5.0	12.8	14.5
$4\text{-}HC_6F_4$	44.0	0	traces	2.0

[a] The product of *ortho*-sustitution relative to the NO_2 group is quoted.

The dominant yield of the product of *ortho*-substitution (Table 5) may be due to the formation of the more favourable transition complex **59** as a result of the interaction of the oxygen of the nitro-group with the phosphorus atom.



59

In addition, triethyl phosphate and the ethyl esters of (1′-ethylethoxy) (4-trifluoromethyl-2,3,5,6-tetrafluorophenyl)-phosphinic and bis(4-trifluoromethyl-2,3,5,6-tetrafluorophenyl)-phosphinic acids were detected among the products of the reaction of octafluorotoluene with triethyl phosphite. The authors[59] explain the formation of the phosphonous acid ester **60** as well as the appearance of the H^+ cation in the system by the following reactions of the phosphonium cation:

$$[Ar_FP(OEt)_3]^+ \longrightarrow \underset{\mathbf{60}}{Ar_FP(OEt)_2} + [OEt]^+ \longrightarrow H^+ + MeCHO.$$

Compound **60** can react in its turn both with acetaldehyde and with octafluorotoluene. The fact that, despite the presence of a 20% excess of triethyl phosphite relative to octafluorotoluene, the entire triethyl phosphite is consumed can be explained by the oxidation of triethyl phosphite with acetaldehyde to triethyl phosphate[60] and also by the rearrangement of triethyl phosphite to diethyl ethylphosphonate.

The results obtained in the reaction of octafluorotoluene and pentafluoropyridine with triethyl phosphite in the presence of Lewis acids ($FeCl_3$, $ZnCl_2$, $SnCl_4$) can serve as yet another confirmation of the formation of the polyfluoroaryl anion. A Lewis acid is known to promote the occurrence of the Arbuzov reaction by activating the carbonium centre.[61] However, octafluorotoluene and pentafluoropyridine do not enter into the Arbuzov reaction and their interaction with triethyl phosphite is unaffected by the presence of Lewis acids. Perfluorobitolyl and octafluoro-4,4′-bipyridyl are then formed as the main products together with the phosphorylation, reduction, and alkylation products. It is natural to suppose that the formation of octafluorobiphenyl derivatives is induced by the generation of polyfluoroaryl anions during the reaction and their subsequent interaction with pentafluorobenzene derivatives.

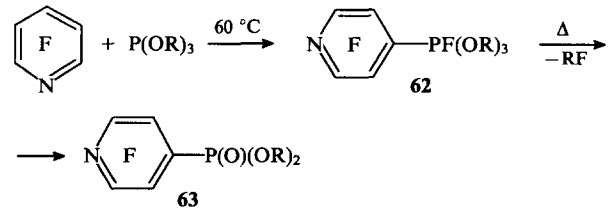
It may be that the diethyl esters of 4-trifluoromethyl-2,3,5,6-tetrafluorophenylphosphonic and 2,3,5,6-tetrafluoropyridyl-phosphonic acids can afford the activated complex **61** in their reactions with $FeCl_3$ as a consequence of the coordination of the Lewis acid to the phosphoryl oxygen atom, from which the corresponding anion Ar_F^- is generated on thermolysis.

$$\underset{\mathbf{61}}{Cl_3Fe...O=P(OEt)_2-Ar_F} \longrightarrow FeCl_3 + [O=P(OEt)_2]^+ + Ar_F^-.$$

However, in the reaction of octafluorotoluene and pentafluoropyridine with the corresponding alkylphosphonic acid esters in the presence of $FeCl_3$ under the conditions of the Arbuzov reaction, the initial compounds are returned unchanged and 1% of a polymeric product is formed. Evidently the Lewis acids play an active role in the stage involving the postulated formation of triethoxypolyfluoroarylfluorophosphorane **58**, which is in equilibrium with quasi-phosphonium compounds containing fluoride and heptafluorotoluene or tetrafluoropyridine anions. The formation of the stable anions $FeCl_3 \cdot Ar_F^-$ and $FeCl_3F^-$ actually determines the further course of the reaction. The $FeCl_3 \cdot Ar_F^-$ anions are apparently more active nucleophiles than the $FeCl_3F^-$ anions. They enter vigorously into competing reactions with the phosphonium cation and the initial compound, forming the corresponding alkylation products.

On the other hand, the reaction of tris(trimethylsilyl) phosphite with pentafluoropyridine, pentachloropyridine, and 3-cyanotetrachloropyridine in the presence of catalytic amounts of nickel chloride leads to the formation of the corresponding phosphonates in virtually quantitative yields. The reaction takes place at 150 °C over a period of 30 min.[62] The authors[62] note that under non-catalytic conditions tris(trimethylsilyl) phosphite reacts with pentafluoropyridine more effectively than do trialkyl phosphites. The yield of the final products is 60–69%.

Boenigk and Hagele[63] were able to isolate the stable trialkoxy-(2,3,5,6-tetrafluoro-4-pyridyl)fluorophosphorane **62** (stable for several days) in the reaction of pentafluoropyridine with trialkyl phosphites (R = Et, Pr^i) at 60 °C. When the temperature is raised, the phosphorane **62** decomposes with formation of dialkyl esters of 2,3,5,6-tetrafluoro-4-pyridylphosphonic acid **63** and alkylation (4-alkyl-2,3,5,6-tetrafluoropyridine) and reduction (2,3,5,6-tetrafluoropyridine) products. On passing from triethyl phosphite to triisopropyl phosphite, an increase in the yield (up to 90%) of diisopropyl 2,3,5,6-tetrafluoro-4-pyridylphosphonate is observed.

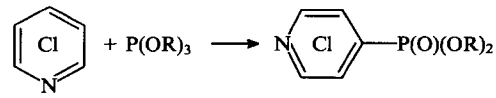


62 **63**

R = Et (50%, 80 °C, 24 h);
Pr^i (90%, 90 °C, 10 h).

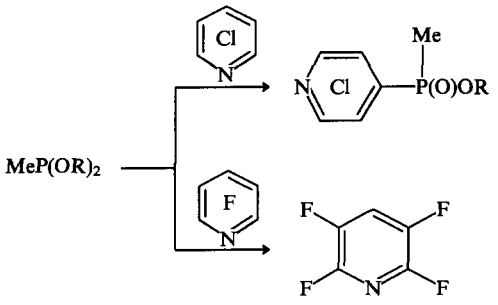
On the other hand, when trimethyl phosphite is introduced into the reaction with pentafluoropyridine, dimethyl 2,3,5,6-tetrafluoro-4-pyridylphosphonate is not formed, the reduction product 2,3,5,6,-tetrafluoropyridine and trimethyl phosphate being obtained instead.

When pentafluoropyridine is replaced by pentachloropyridine, the formation of a stable phosphorane is not observed, the dialkyl esters of 2,3,5,6-tetrachloro-4-pyridylphosphonic acid being isolated as the main products.



R = Me (45%, 120 °C, 15 h); Et (48%, 150 °C, 15 h);
Pr^i (60%, 130 °C, 16 h).

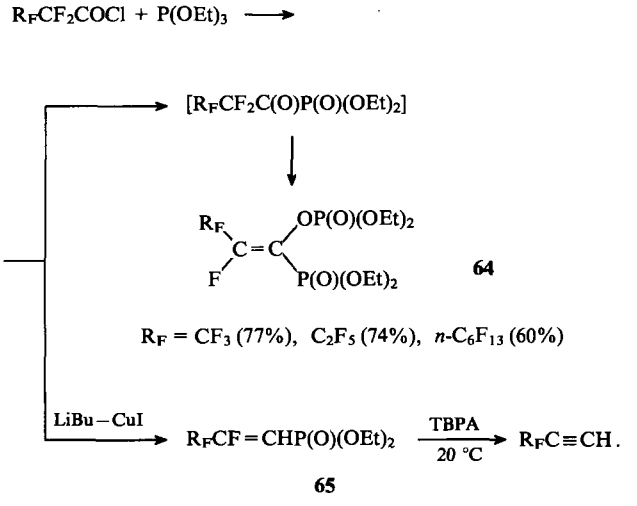
It has been shown[64] that pentachloropyridine enters into the Arbuzov reaction with dialkyl esters of methylphosphonous acid, affording the corresponding phosphinic acid ester, whereas pentafluoropyridine reacts with these esters to form the reduction product — 2,3,5,6-tetrafluropyridine.



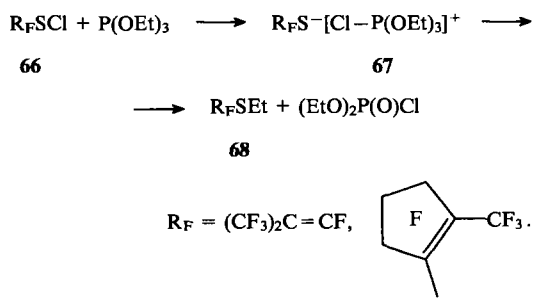
R = Et (20%), Pr^i (14%).

Trialkyl phosphites react with the chlorides of carboxylic perfluoroacids[65] giving rise to the phosphonic acid esters **64**. However, when this reaction was carried out in the presence of LiBu–CuI at temperatures ranging from 0 °C to room temperature, diethyl perfluoroalkenylphosphonate **65** was obtained (Scheme 4).[66] A convenient method of synthesis of perfluoroalkylacetylenes, involving treatment of the ester **65** with tetrabutylphosphoramidite (TBPA), was developed on the basis of this reaction.

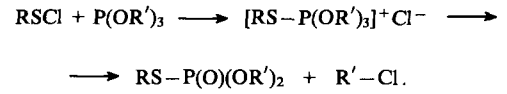
Scheme 4



The unsaturated sulphenyl chlorides **66**, containing fluorine atoms in the carbon chain, react with triethyl phosphite via the chlorine atom with formation of the unstable intermediate **67**, the decomposition of which leads to ethyl perfluoroalkenyl sulphides **68** and diethyl phosphorochloridate.[67]

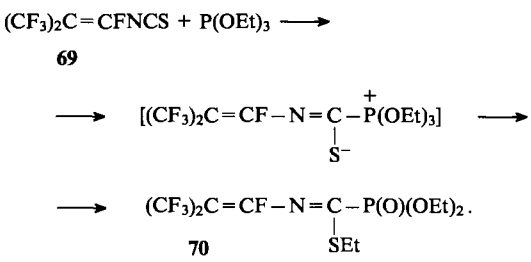


Trialkyl phosphites react with non-fluorinated sulphenyl chlorides via the sulphur atom, affording alkyl halides and phosphates.[68]

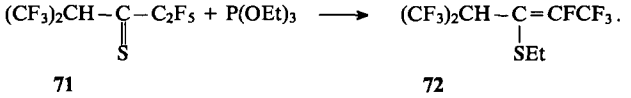


Trifluoromethanesulphenyl chloride reacts with trimethyl phosphite via two pathways simultaneously, which results in the formation of the sulphide CF_3SMe and the phosphorothioate $CF_3SP(O)(OMe)_2$.

The reaction of perfluoroisobutenyl isothiocyanate **69** with triethyl phosphite leads to the formation of the diethyl ester of the phosphonic acid **70** as a result of the nucleophilic atack by the trivalent phosphorus atom on the carbon atom of the C = S bond. Under these conditions, the fluorine atoms attached to the double bond are not substituted.[69]

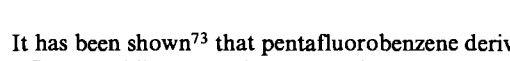


On the other hand, treatment of the thione **71** with triethyl phosphite affords the product **72**, which contains no phosphorus atom.[70]

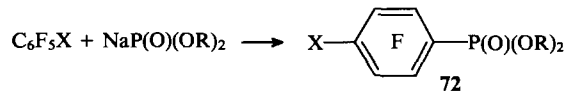


3. The Michaelis–Bekker reaction in the series of aromatic polyfluoro-compounds

The reactions of perfluoroolefins with dialkyl phosphites have been achieved only under radical conditions,[71] which resulted in the formation of a mixture of telomeric fluorinated alkylphosphonic acid esters of the type $H(CF_2CF_2)_nP(O)(OR)_2$ (n = 1–7). Alkyl esters of difluoromethylphosphonic acid were synthesised from chlorodifluoromethane and sodium dialkyl phosphite.[72]



It has been shown[73] that pentafluorobenzene derivatives and pentafluoropyridine enter into the Michaelis–Bekker reaction with the sodium salts of dimethyl and diethyl phosphites in tetrahydrofuran and afford the corresponding esters of polyfluoroarylphosphonic acids **72** in 10–60% yields.



X = NO_2, CN, CF_3, H, F, OMe;
R = Me, Et.

The low yield of the polyfluoroalkylphosphonic acid esters may be due to the interaction of the nucleophile with the phosphorus atom.[74] The Michaelis–Bekker reaction takes place similarly with pentachlorobenzene,[75] hexachlorobenzene,[76] and certain chlorine-containing heterocyclic compounds.[77] Iodobenzene interacts with the sodium salt of diethyl phosphite to form diethyl phenylphosphonate only when the reaction is carried out under irradiation.[77]

III. P-Nucleophiles as synthons in the synthesis of perfluorinated organic compounds without phosphorus atoms

As shown above, the reactions of phosphines with perfluoroolefins and aromatic polyfluoro-compounds lead initially to the formation of fluorophosphoranes, which proved to be extremely stable in some cases. The stability of fluorophosphoranes is determined by the electronegativity of the atoms of the substituents attached to the phosphorus atom: its increase entails an increase in the stability of the phosphorane.

The cleavage of the P–X bonds in phosphoranes generates a stable phosphonium cation. Such cleavage is controlled by thermodynamic factors. Because of this, the cleavage of the P–C bond, and not P–F and P–O, is energetically more favourable.[78] The thermolysis of phosphorane accompanied by the formation of the P=O bond is even more effective.

These factors suggested that the generation of carbanions, the transfer of the organic fragment in the form of an anion, and the formation of a new C–C bond may be expected for phosphoranes having a specific structure. In synthesis, the phosphorane need not necessarily be isolated beforehand. The most important factor is that a phosphorane of this kind should be formed during the reaction, whereupon the entire process can be carried out in one stage. We shall consider certain examples of reactions in which trialkylphosphines or triphenylphosphines are reactants in the synthesis of fluorophosphoranes, the subsequent interactions of which with unsaturated polyfluorinated compounds can lead to the formation of new C–C bonds. In this case, there is a possibility that the entire process can be achieved in one stage. We shall therefore consider primarily the reactions of trialkylphosphines or triphenylphosphine with organic perfluoro-compounds containing mobile fluorine atoms.

1. Reactions of organic perfluoro-compounds with trialkyl- and triphenyl-phosphines in the presence of C-electrophiles

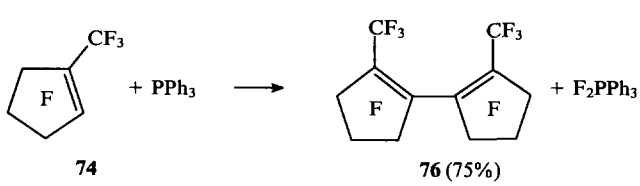
It has been found[79] that the reactions of fluoroolefins having three perfluoroalkyl substituents with phosphines lead to the reductive dimerisation of the olefins, as a result of which conjugated dienes are formed. Thus, when perfluoro-2-methylpent-2-ene **73** is acted upon by phosphorus tris(diethylamide) or perfluoro-1-methylcyclopent-1-ene **74** is acted upon by triphenylphosphine, perfluoro-3-ethyl-2,5-dimethylocta-2,4-diene **75**

$$(CF_3)_2C{=}CFC_2F_5 + P(NEt_2)_3 \xrightarrow[-F_2P(NEt_2)_3]{}$$

73

$$\longrightarrow (CF_3)_2C{=}\overset{C_2F_5}{\overset{|}{C}}{-}CF{=}C(CF_3)C_3F_7$$

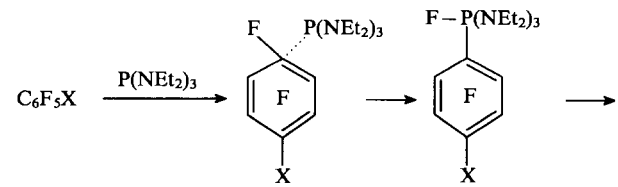
75 (61%)



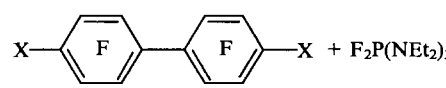
74 **76** (75%)

and perfluoro-1-methyl-2-(2′-methylcyclopent-1′-enyl)-cyclopent-1-ene **76** are formed respectively.

According to the data of Markovskii et al.,[80] the reaction of compounds of the type C_6F_5X with phosphorous tris-(diethylamide) results in the formation of symmetrically substituted octafluorobiphenyls, while in the reaction with pentafluoropyridine the product is octafluoro-4,4′-bipyridyl (yield 50–60%).



$$\longrightarrow [4\text{-}XC_6F_4]^- + [FP(NEt_2)_3]^+ \longrightarrow$$



X = CF_3, COOMe.

Presumably, in the reactions of perfluoroalkenes or substituted perfluorobenzenes, the trivalent phosphorus atom attacks in the first stage the electrophilic carbon atom involved in the multiple bond or in the benzene ring with subsequent migration of the fluoride anion to the phosphorus atom. The resulting phosphorane is thermally unstable and decomposes, affording a phosphonium cation and a perfluoroalkenyl or pentafluorophenyl anion, which subsequently react with the initial substrates, affording the reaction products. The pentafluorophenyl anion generated in this way reacts further both with the initial aromatic polyfluoro-substrate and with other compounds having more mobile halogen atoms. For example, the addition of chlorotrimethylsilane to a mixture of octafluorotoluene and phosphorus tris(diethylamide) leads to 4-trifluoromethyltetrafluorophenyltrimethylsilane.[81] Pentafluoropyridine and 3-chlorotrifluoropyrimidine have also been introduced into this reaction.

$$C_6F_5R + Me_3SiCl + P(NEt_2)_3 \longrightarrow$$

$$\longrightarrow 4\text{-}RC_6F_4SiMe_3 + P(NEt_2)_3FCl$$

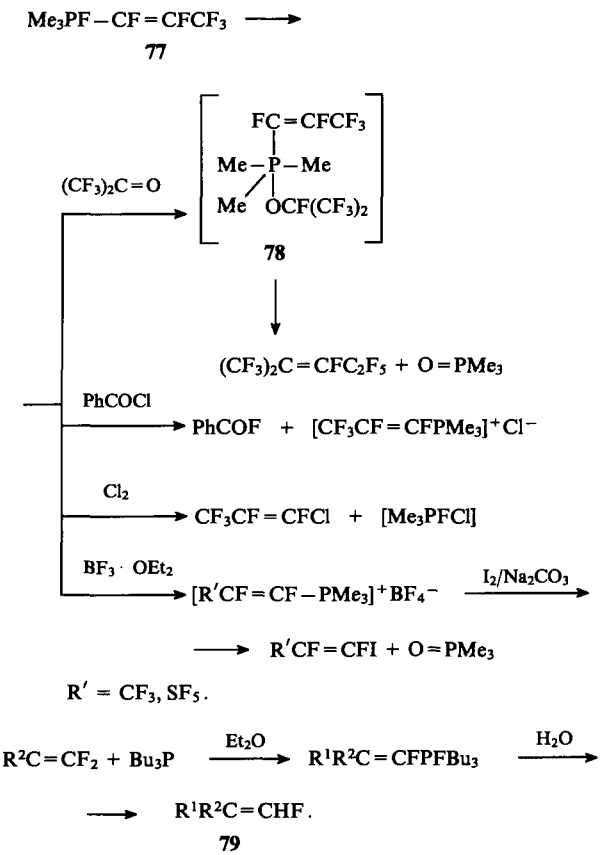
R = CF_3, CN, COOEt.

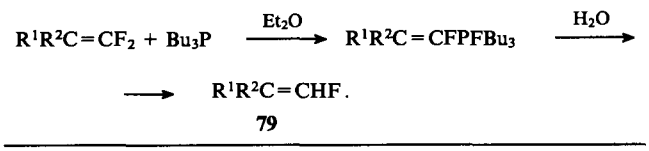
This opens a pathway to the synthesis of various polyfluoro-derivatives of Group IV–VI elements, which were previously difficult to obtain. It is particularly significant that compounds containing strong electron-accepting substituents in the benzene ring can be obtained by this method.

It has been shown[82] that the phosphorane **77**, formed in the reaction of triphenylphosphine with hexafluoropropene, reacts further with hexafluoroacetone in the presence of the fluoride ion, affording triphenylphosphine oxide and perfluoro-2-methylpent-2-ene. The authors assume that these products are obtained as a result of the decomposition of the phosphorane **78**. Scheme 5 presents other reactions of the phosphorane **77**.

Using this approach, a method has been developed for the reduction of perfluoroolefins. The first stage of this reaction involved the formation from the perfluoroolefin and tributylphosphine of a fluorophosphorane, the subsequent hydrolysis of which leads to the olefin **79**. This reaction can be regarded

Scheme 5

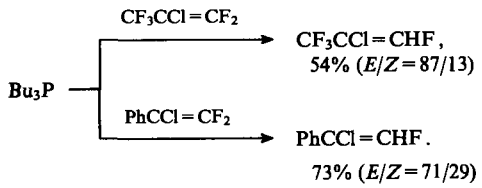




R^1	R^2	*E*/*Z*	Yield of **79** (%)
CF_3	F	100(*E*)	97
$CF_3(CF_2)_2$	F	100(*E*)	72
$CF_3(CF_2)_4$	F	100(*E*)	85
Ph	CF_3	12/88	100
Ph	C_2F_5	100(*Z*)	47
4-$MeOC_6H_4$	CF_3	9/91	100

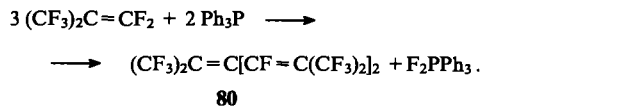
formally as substitution of a fluorine atom at the multiple bond by a hydrogen atom.[83, 84]

Since treatment of chloroperfluoroolefins with tributylphosphine involves a fluorine atom and not the chlorine atom, a fluorine atom is formally split off from the final product.



Hydrolysis of the *cis*-isomer of vinylphosphorane in moist dimethylformamide (DMF) proceeds stereoselectively. When the reaction of β,β-difluorostyrene with tributylphosphine is carried out in the presence of $BF_3.OEt_2$, the *trans*-isomer of the vinylphosphonium salt is obtained and subsequently hydrolysed. The selectivity of the formation of the (*Z*)- and (*E*)-isomer is 100%, but it diminishes after the introduction into the alkene, together with the perfluoroalkyl group, of substituents such as phenyl and *p*-methoxyphenyl.

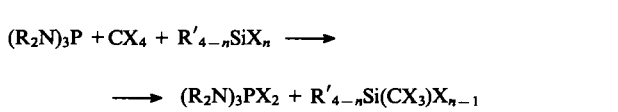
In contrast to the examples mentioned above, where triphenylphosphine behaves as a nucleophile and the final product contains a phosphorus atom, in the reaction with perfluoroisobutene it behaves as a defluorinating agent and the final product—1,1-divinylalkene **80**—does not contain a phosphorus atom.[85]



The authors suggest that the triene **80** is formed from an intermediate fluorophosphorane.

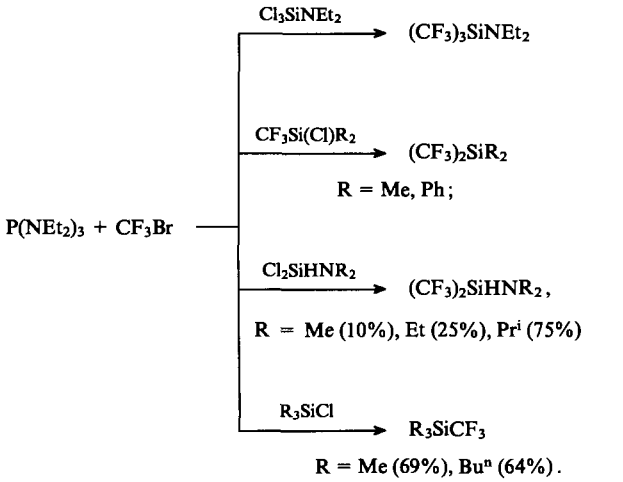
2. The use of perfluoroalkyl bromides (or bromopolyfluorobenzenes)-phosphorus tris(dialkylamide) systems as nucleophiles

If the aromatic compounds contain a halogen atom with a low mobility, for example, iodine or bromine, there is a possibility of a situation where the rate of nucleophilic substitution of such a halogen by trivalent phosphorus derivatives is very low and there is only polarisation of the C–halogen bond under the influence of the phosphorus atom. However, in this case too it is possible to make use of the nucleophilic properties of such a complex. It has been found that the phosphorous tris(diethylamide)–alkyl bromide system is a unique nucleophile. This system has found extensive applications in organic synthesis in recent years owing to the formation in the intermediate stage of the trihalomethanide ion, which is highly reactive towards proton-donating agents and electrophiles.[86, 87]



Ruppert and coworkers[88, 89] showed that bromotrifluoromethane enters into this reaction. It was later found that the $CF_3Br–P(NEt_2)_3$ system is fairly universal and can be used as the reagent for the introduction of the trifluoromethyl group. Thus it has been shown[90, 91] that this system is effective in the synthesis of various organosilicon compounds (Scheme 6).

Scheme 6



Instead of halotrimethylsilanes, it is possible to use trimethylsilyl azide, trimethyl isothiocyanate, and trimethyl isocyanate.[92, 93] A number of workers[94–99] have used the $CF_3Br–P(NEt_2)_3$ system for the trihalomethylation of organophosphorus compounds containing P–halogen bonds, while Burger et al.[100] used it for the methylation of boron compounds.

$$R_nE-X + CF_3Br + P(NEt_2)_3 \longrightarrow$$
$$\longrightarrow R_nE-CF_3 + [XP(NEt_2)_3]Br$$

E = P, Si, B.

Wakselman and Tordeux[101] used the $CF_3Br-P(NEt_2)_3$ system for the direct introduction of the trifluoromethyl group into anilines.

Bardin et al.[102] used the $C_6F_5Br-P(NEt_2)_3$ system instead of $CF_3Br-P(NEt_2)_3$. A method of synthesis of polyfluoroaryl-substituted silanes, germanes, and stannanes was developed on its basis.

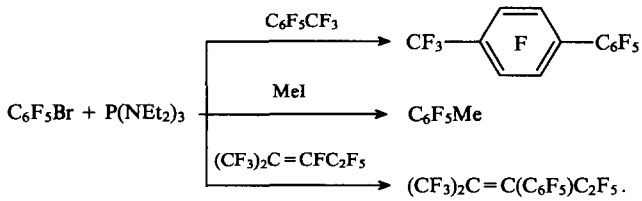
$$4\text{-}R'C_6F_4Br + P(NEt_2)_3 + R_3MX \longrightarrow$$
$$\longrightarrow 4\text{-}R'C_6F_4MR_3 + (NEt_2)_3PXBr$$

R = Me, Et; R′ = F, PrO, CF_3;
M = Si (66%), Ge (57%), Sn (50%); X = Cl, Br.

Pentachlorobenzene, bromobenzene, 3-bromo-1-trifluoromethylbenzene, and benzyl bromide do not react under these conditions. Pentafluoroiodobenzene reacts with the above system, giving rise to methyl(pentafluorophenyl)silane.

The nucleophilic phosphorus atom in the $C_6F_5Br-P(NEt_2)_3$ system attacks the bromine atom, affording a phosphonium cation and a carbanion. The subsequent reactions of these species depend on the presence of C-electrophiles. It has been shown,[102, 103] that this system is convenient for the introduction of the polyfluoroaryl fragment into aromatic polyfluoro-compounds and perfluoroolefins. Certain reactions are illustrated in Scheme 7 below.

Scheme 7

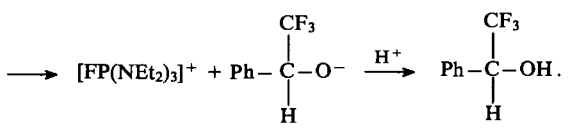


The interaction of CF_3Br with $P(NR_2)_3$ (R = Me, Et) leads to the phosphonium salt **81** in a virtually quantitative yield.[104] The structure of the latter was confirmed by NMR spectroscopic data and X-ray diffraction.

$$(R_2N)_3P + BrCF_3 \longrightarrow [CF_3P(NR_2)_3]^+Br^-.$$
81 (95%–100%)

On the other hand, in the reaction of CF_3I and $P(NEt_2)_3$ other products are formed, namely $CF_3P(NEt_2)_2$ and the salt $[P(NEt_2)_4]^+I^-$.[105] The salt **81** is stable up to the melting point. The high positive charge on the phosphorus atom in this compound promotes the reaction with the fluoride anion (arising from CsF, TASF, etc.). The fluorophosphorane **82** is formed as an intermediate in this reaction. It reacts, for example, with benzaldehyde to form the alcohol **83**.

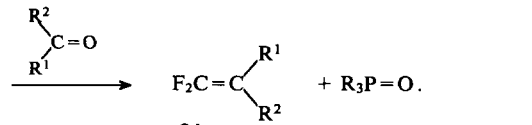
$$[CF_3P(NEt_2)_3]^+Br^- + F^- \longrightarrow [(Et_2N)_3PFCF_3] \xrightarrow{PhCHO}$$
81 **82**



83 (73%)

Phosphonium salts may react with salts of type **81** also via a different pathway. Thus, in the presence of an excess of this P-nucleophile, the corresponding ylide, having pronounced nucleophilic properties, is formed. It reacts with aldehyde and ketones, forming terminal olefins.[106]

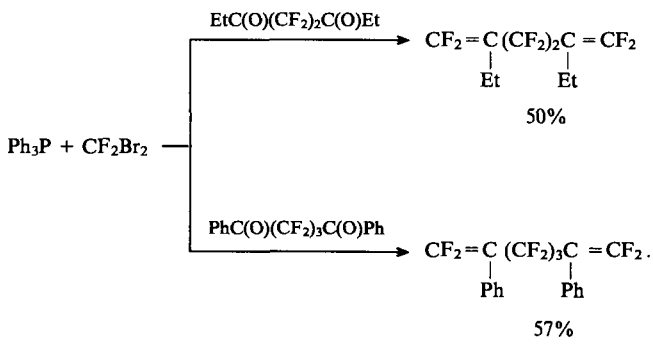
$$[R_3PCF_2Br]Br^- + R_3P \longrightarrow [R_3P-CF_2] + [R_3PBr]Br^- \longrightarrow$$



84

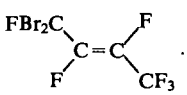
R	R^1	R^2	Yield of **84** (%)
Ph	Ph	H	65
	C_6F_5	H	20
	Ph	CF_3	85
	C_6H_{11}	CF_3	90
	Ph	C_2F_5	82
	3-BrC_6H_4	CF_3	83
NMe_2	Ph	Me	81
	Ph	Et	82
	Et	Et	75
	Me	Me	60
	Ph	CF_3	25

Polyfluorinated ketones react similarly.



The PPh_3-CFBr_3 system is capable of reacting with perfluoroolefins, substituting a fluorine atom at the double bond by the $CFBr_2$ group.[107]

$$Ph_3P + CFBr_3 + CF_3CF=CF_2 \longrightarrow$$



$P(NEt_2)_3$ may be used instead of triphenylphosphine.[108]

$$P(NEt_2)_3 + BrCF_2X + Me_3SiCl \longrightarrow$$
$$\longrightarrow Me_3SiCF_2Cl + [(Et_2N)_3PX]^+Br^-$$

X = Cl, Br, I.

The reaction of the $CF_3Br-P(NEt_2)_3$ system with benzaldehyde[109] leads to the formation of the phosphonium salt **85**, which decomposes at 140 °C, affording α-bromophenylethane and not the alcohol **83**. Owing to the ease of formation of a phosphorus compound with P=O bond, in this case the intermediate carbonium ion reacts with the bromide anion,

giving rise to the final reaction product. The reaction is general in character. Perfluoroalkyl bromides with different carbon chain lengths (from 2 to 6) have been used as reactants in it.

$$PhCHO + CF_3Br + P(NEt_2)_3 \longrightarrow$$

$$\longrightarrow [PhCH(CF_3)OP(NEt_2)_3]^+Br^- \xrightarrow{140\ ^\circ C}$$

85 (77%)

$$\longrightarrow PhCHBrCF_3 + O{=}P(NEt_2)_3.$$

99% 95%

According to the data of Kolomeitsev et al.,[110] chloro- and bromo-alkanes **86** react in the presence of $P(NEt_2)_3$ with $PhCH_2SCN$, affording the product **87** resulting from the substitution of the CN group.

$$PhCH_2SCN + F(CX_2)_mY \xrightarrow[CH_2Cl_2,\ -70\ ^\circ C]{P(NEt_2)_3} PhCH_2S(CX_2)_mF$$

86 **87**

X = Cl, F; Y = Cl, Br; m = 1–3.

The interaction of the $C_2F_5I-P(NEt_2)_3$ system with benzoyl chloride[111] in a non-polar solvent results in the formation of the product of the substitution of the chlorine atom — the corresponding ketone (yield 58%).

The reaction of the partly fluorinated aliphatic-aromatic ketones **88** with $CF_3Br-P(NEt_2)_3$ leads to the formation of the tertiary alcohol **89**.

$$PhCOC_2F_5 + CF_3Br + P(NEt_2)_3 \xrightarrow[-70\ ^\circ C,\ 5\ h]{H^+} Ph-\underset{\displaystyle C_2F_5}{\overset{\displaystyle CF_3}{\overset{|}{\underset{|}{C}}}}-OH.$$

88 **89** (56%)

On the other hand, in the case of benzoyl fluoride, the reaction is very slow and leads to the ultimate formation not of a tertiary alcohol but of the products of the esterification of benzoic acid by the latter. The yield of the ester is 81%.

In the presence of $P(NEt_2)_3$, polyfluoroalkyl iodides react with various aroyl chlorides to form aryl polyfluoroalkyl ketones (Table 6).[112]

$$R_FI + ArCOCl + P(NEt_2)_3 \longrightarrow ArCOR_F + ClP(NEt_2)_3.$$

The primary step in this reaction is nucleophilic attack by the phosphorus atom on the iodine atom. The subsequent nucleophilic attack by the anionoid polyfluoroalkyl group on the electrophile present in the reaction mixture affords the corresponding ketone and phosphorane.[113] The reaction between the phosphonium ylide and acetyl halide usually leads to the ylide acylation product. The Wittig reaction also occurs here. This has been used to obtain olefins from acyl halides.[114]

Table 6. Reactions of polyfluoroalkyl iodides with aroyl chlorides in the presence of phosphorus tris(diethylamide).[112]

ArCOCl	R_FI	Time/h	Yield (%)
4-ClC_6H_4COCl	$CF_3(CF_2)_5I$	6	41
2,4-$Cl_2C_6H_3COCl$	$CF_3(CF_2)_7I$	6	36
4-ClC_6H_4COCl	$Cl(CF_2)_4I$	3.5	42
PhCOCl	$Cl(CF_2)_4I$	6	43
2,4-$Cl_2C_6H_3COCl$	$Cl(CF_2)_4I$	4	43
4-ClC_6H_4COCl	$Cl(CF_2)_6I$	5	41
PhCOCl	$Cl(CF_2)_6I$	6	41
2,4-$Cl_2C_6H_3COCl$	$Cl(CF_2)_6I$	6.5	40

$$R_3P + CFX_3 \longrightarrow [R_3\overset{+}{P}-\overset{-}{C}F-\overset{+}{P}R_3]X^- + R_3PX_2,$$

R = Bu, Ph; X = Cl, Br **90** (90–95%)

$$\mathbf{90} + R_FCOF \longrightarrow R_3\overset{+}{P}-CF-\overset{+}{P}R_3\cdot X^- \longrightarrow$$

$$\longrightarrow R_3P{=}O + \underset{\displaystyle F}{\overset{\displaystyle X^-}{\overset{|}{\underset{|}{R_3\overset{+}{P}}}}}-C{=}C\begin{matrix}F\\R_F\end{matrix} \xrightarrow{H_2O}$$

91

$$\longrightarrow \begin{matrix}H\\F\end{matrix}\!\!>\!C{=}C\!<\!\begin{matrix}F\\R_F\end{matrix} + R_3P{=}O.$$

92

R_F	Yield of **91** (%)	Yield of **92** (%)
C_2F_5	80	62
Pr^n	82	52
CF_2Cl	73	50
$MeOOCCF_2$	70	20
$CF_3(CF_2)_2OCF(CF_3)$	75	49

Various alkyl halides may be used to obtain phosphorus ylides. The $PPh_3-CF_2Br_2$[106] and PPh_3-CClF_2COONa[115] systems were used to synthesise 2-phenylpentafluoropropene from 4-$RC_6H_4COCF_3$.

$$4\text{-}RC_6H_4COCF_3 + Ph_3P + CClF_2COONa \longrightarrow \begin{matrix}4\text{-}RC_6H_4\\CF_3\end{matrix}\!\!>\!C{=}CF_2$$

R = H (75.9%), Me (81.9%), OMe (90.7%), F (66.6%).

A convenient method of synthesis of 1,1-bis(trifluoromethyl)-alkenes **93** from aldehydes and 2,2-dichlorohexafluoropropane in the presence of triphenylphosphine has been developed.[116]

$$Cl_2C(CF_3)_2 + Ph_3P + RCHO \longrightarrow$$

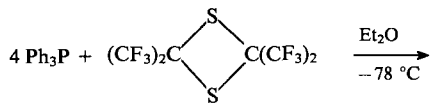
$$\longrightarrow \begin{matrix}H\\R\end{matrix}\!\!>\!C{=}C\!<\!\begin{matrix}CF_3\\CF_3\end{matrix} + Ph_3P{=}O + Cl_2PPh_3$$

93

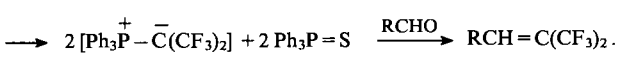
R = Et (31%), Pr (22%), 4-ClC_6H_4 (88%), 4-$MeOC_6H_4$ (27%), C_6H_{11} (4%), $Cl_2C{=}CH$ (83%), Ph (54%), $Me_2CHCHCl$ (62%).

The mechanism of this reaction is so far obscure. Two pathways have been suggested: either the carbanion reacts directly with the aldehyde or the phosphorus ylide is formed as an intermediate and then reacts with the aldehyde.

The phosphorus ylide **94** can be obtained also by the reaction of triphenylphosphine with tetrakis(trifluoromethyl)-1,3-dithietan.[117] Its subsequent interaction with aldehydes leads to the corresponding perfluoroolefins.



$$4\,Ph_3P + (CF_3)_2C\langle S\rangle C(CF_3)_2 \xrightarrow[-78\ ^\circ C]{Et_2O}$$



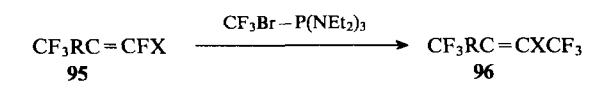
$$\longrightarrow 2\,[Ph_3\overset{+}{P}-\overset{-}{C}(CF_3)_2] + 2\,Ph_3P{=}S \xrightarrow{RCHO} RCH{=}C(CF_3)_2.$$

94

R	Ph	C_6F_5	$Me(CH_2)_5$
Yield of olefin (%)	99	100	100
R	MeCHPh	PhCH=CH	4-$MeOC_6H_4$
Yield of olefin (%)	61	60	52

The effectiveness of the PPh_3–F_3CCCl_3 system in reactions with aldehydes, which lead to the formation of trifluoromethylolefins, has been demonstrated.[118] The reaction with aromatic and α,β-unsaturated aliphatic aldehydes proceeds with a high stereoselectivity [the (*Z*)-isomers are formed exclusively], whereas the reaction with other aliphatic aldehydes affords a mixture of the (*Z*)- and (*E*)-isomers in proportions ranging from 2 : 1 to 3 : 1.

The highly reactive perfluoroolefins **95** react under mild conditions with the CF_3Br–$P(NEt_2)_3$ system, giving rise to monosubstitution products **96**.[119]



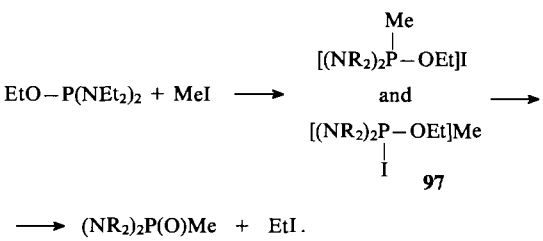
$$\underset{\mathbf{95}}{CF_3RC{=}CFX} \xrightarrow{CF_3Br-P(NEt_2)_3} \underset{\mathbf{96}}{CF_3RC{=}CXCF_3}$$

R = CF_3, X = F; R = F, X = C_2F_5; R = $CONEt_2$, X = F.

In the reaction of perfluoro-2-methylpent-2-ene and perfluoromethacrylamide with the above system, the products of the substitution of two fluorine atoms are formed together with the monosubstituted products (the yields are 45 and 34% respectively). The reaction with perfluoroisobutene gives rise to a mixture of isomeric perfluorodienes, whilst the reaction with octafluorotoluene affords a mixture of isomeric perfluoroxylenes in a yield of only 7%.

3. Reactions with phosphines containing P–O and P–N bonds simultaneously

In an early study, Michaelis[120] reported two stable quasi-phosphonium salts **97**, formed when methyl iodide is acted upon by alkyl *N,N,N',N'*-tetraalkylphosphorodiamidites. The salts decompose in accordance with the scheme.



$$EtO-P(NEt_2)_2 + MeI \longrightarrow \underset{\text{and}}{\overset{Me}{\underset{|}{[(NR_2)_2P-OEt]I}}} \longrightarrow$$

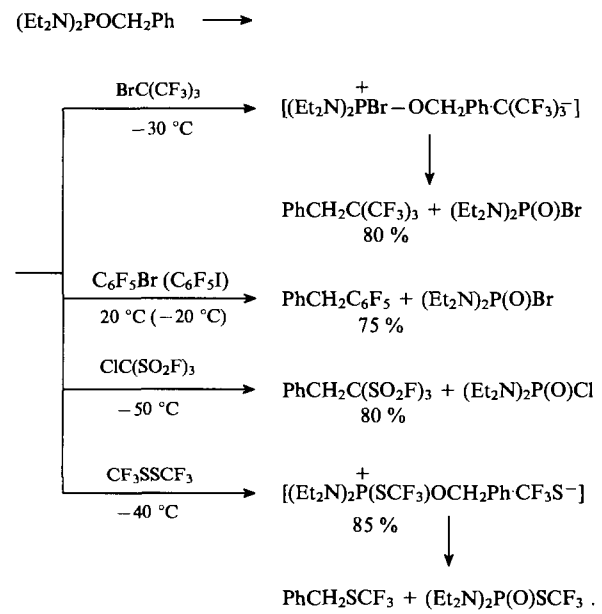
$$[(NR_2)_2P-\underset{|}{\overset{Me}{OEt}}]I$$

97

$$\longrightarrow (NR_2)_2P(O)Me + EtI.$$

Wakselman and Tordeux[101] developed the research based on this observation and showed that such phosphorodiamidites react exothermally with fluorine-containing electrophiles incorporating mobile groups such as Br, SCF_3, etc., forming *N,N,N',N'*-tetraethylphosphorodiamidic halides and fluorinated compounds with new C–C bonds. Thus it became possible to synthesise a series of phosphorus-containing compounds which are otherwise difficult to obtain. Some examples of these reactions are presented in Scheme 8.

Scheme 8



$$(Et_2N)_2POCH_2Ph \longrightarrow$$

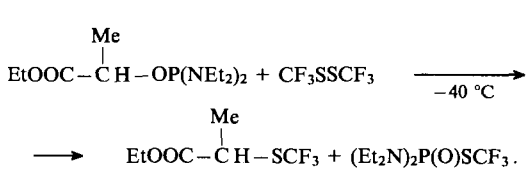
$$\xrightarrow[-30\ ^\circ C]{BrC(CF_3)_3} [(Et_2N)_2\overset{+}{P}Br-OCH_2Ph\cdot C(CF_3)_3^-] \longrightarrow PhCH_2C(CF_3)_3 + (Et_2N)_2P(O)Br \quad 80\,\%$$

$$\xrightarrow[20\ ^\circ C\,(-20\ ^\circ C)]{C_6F_5Br\ (C_6F_5I)} PhCH_2C_6F_5 + (Et_2N)_2P(O)Br \quad 75\,\%$$

$$\xrightarrow[-50\ ^\circ C]{ClC(SO_2F)_3} PhCH_2C(SO_2F)_3 + (Et_2N)_2P(O)Cl \quad 80\,\%$$

$$\xrightarrow[-40\ ^\circ C]{CF_3SSCF_3} [(Et_2N)_2\overset{+}{P}(SCF_3)OCH_2Ph\cdot CF_3S^-] \quad 85\,\% \longrightarrow PhCH_2SCF_3 + (Et_2N)_2P(O)SCF_3.$$

Instead of the benzyl residue, other groups can also be used, for example:



$$EtOOC-\underset{|}{\overset{Me}{CH}}-OP(NEt_2)_2 + CF_3SSCF_3 \xrightarrow[-40\ ^\circ C]{}$$

$$\longrightarrow EtOOC-\underset{|}{\overset{Me}{CH}}-SCF_3 + (Et_2N)_2P(O)SCF_3.$$

IV. Conclusion

The examples presented in this review show that phosphorus-containing nucleophiles play an important role not only in the synthesis of organophosphorus compounds containing perfluorinated substituents but also in reactions where they behave as synthons. This has made it possible to develop novel methods of synthesis of compounds with new C–C bonds. There is no doubt that all these features have enriched synthetic organic chemistry by a series of new approaches to the specific synthesis of interesting organic compounds. Further development of this field of chemistry and the discovery of new possibilities in the reactions of phosphorus-containing nucleophiles with unsaturated halogen-containing substances may be expected. The author does not claim to have given an exhaustive bibliographic survey in the present review, but the latter reflects fully the principal aspects of studies both in the field of methods of synthesis of organofluorine compounds and as regards the principal trends in the development of methods for the introduction of organophosphorus fragments into various molecules and also in the application of organo-phosphorus synthons in the synthesis of compounds with new carbon–carbon bonds. The author hopes that the review will be useful not only to investigators working in the field of the organic chemistry of fluorine but also to a wider range of chemists concerned with synthesis.

References

1. E E Nifant'ev *Khimiya Fosfororganicheskikh Soedinenii* (The Chemistry of Organophosphorus Compounds) (Moscow : Izd. Mosk. Gos. Univ., 1971)
2. V V Tyuleneva, E M Rokhlin, I L Knunyants *Usp. Khim.* **51** 3 (1982) [*Russ. Chem. Rev.* **51** 1 (1982)]
3. G G Furin, in *Reaktsionnaya Sposobnost' Poliftoraromaticheskikh Soedinenii* (The Reactivity of Aromatic Polyfluoro-Compounds) Ed. G G Yakobson (Novosibirsk: Nauka, 1981) p. 97
4. A A Kadyrov, E M Rokhlin *Usp. Khim.* **57** 1488 (1988) [*Russ. Chem. Rev.* **57** 852 (1988)]
5. R G Harvey, E R De Sombre, in *Topics in Phosphorus Chemistry* (New York: Interscience, 1964) Vol. 1, p. 57
6. U Allwörden, G-V Röschenthaler *Chem. -Ztg.* **112** 69 (1988)
7. G-V Röschenthaler, in *The Third Regular German–Soviet Symposium on Fluorine Chemistry, Schmitten/Taunus, 3 October 3 1990. Abstracts* p. 105
8. G W Parshall, D C England, R V Lindsey *J. Am. Chem. Soc.* **81** 4801 (1959)
9. R E Banks, A C Harrison, R N Haszeldine *J. Chem. Soc., Chem. Commun.* 338 (1966)
10. M Fild, P G Jones, K Ruhnau *J. Fluorine Chem.* **54** 388 (1992)
11. J Brierly, J I Dickstein, S Tripett *Phosphorus Sulfur* **7** 167 (1979)
12. M A A Beg, H C Clarc *Can. J. Chem.* **40** 283 (1962)
13. R N Haszeldine *J. Chem. Soc.* 4259 (1952)
14. R N Haszeldine, B O West *J. Chem. Soc.* 3631 (1956)
15. D J Burton, S Shinya, R D Howells *J. Am. Chem. Soc.* **101** 3689 (1979)
16. R F Stochel, F Megson, M T Beachem *J. Org. Chem.* **33** 4395 (1968)
17. M A Howells, R D Howells, N C Baenziger, D J Burton *J. Am. Chem. Soc.* **95** 5366 (1973)
18. D G Naae, D J Burton *J. Fluorine Chem.* **1** 123 (1971)
19. D G Naae, D J Burton *Synth. Commun.* **3** 197 (1973)
20. D J Burton *J. Fluorine Chem.* **23** 339 (1983)
21. G Kamai *Izv. Akad. Nauk SSSR, Otd. Khim. Nauk* 923 (1952)
22. H D Davis, R Harace, US P. 2 742 510 (1956)
23. I L Knunyants, E Ya Pervova *Izv. Akad. Nauk SSSR, Ser. Khim.* 1409 (1962)
24. B Boutevin, Y Hervand, Y Pietrasanta *Phosphorus Sulfur* **11** 373 (1982)
25. G Bauer, G Hagele, P Sartori *Z. Naturforsch. B* **34** 1249 (1979)
26. R E Banks, V Murtagh, E Tsiliopoulos *J. Fluorine Chem.* **52** 389 (1991)
27. A E Platt, B Tittle *J. Chem. Soc. C* 1150 (1967)
28. D J Burton, R M Flynn *J. Fluorine Chem.* **10** 329 (1977)
29. G Kamai *Dokl. Akad. Nauk SSSR* **79** 795 (1951)
30. A F Isbell, US P. 266 675 (1961); *Chem. Abstr.* **58** 11394 (1963)
31. D J Burton, R M Flynn *Synthesis* 615 (1979)
32. K Masao, A Katsuyki, A Yonezoh, Y Masaaki *Rep. Res. Lab. Asahi Glass Co.* **32** 117 (1982)
33. N Matsuo, A S Kende *Bull. Chem. Soc. Jpn.* **64** 3193 (1991)
34. I L Knunyants, E Ya Pervova, V V Tyuleneva *Dokl. Akad. Nauk SSSR* **129** 576 (1959)
35. I L Knunyants, E Ya Pervova, V V Tyuleneva *Izv. Akad. Nauk SSSR, Ser. Khim.* 1576 (1963)
36. I L Knunyants, R N Sterlin, V V Tyuleneva, L N Pinkina *Izv. Akad. Nauk SSSR, Ser. Khim.* 1123 (1963)
37. I L Knunyants, V V Tyuleneva, E Ya Pervova, R N Sterlin *Izv. Akad. Nauk SSSR, Ser. Khim.* 1797 (1964)
38. U Allwörden, G-V Röschenthaler *Chem. -Ztg.* **109** 81 (1985)
39. I L Knunyants, R N Sterlin, V V Tyuleneva *Izv. Akad. Nauk SSSR, Ser. Khim.* 1123 (1963)
40. R Dittrich, G Hagele *Phosphorus Sulfur* **10** 127 (1981)
41. A F Gontar', N A Til'lunova, E G Bykhovskaya, I L Knunyants *Izv. Akad. Nauk SSSR, Ser. Khim.* 2379 (1977)
42. A A Kadyrov, E M Rokhlin, M V Galakhov *Izv. Akad. Nauk SSSR, Ser. Khim.* 1885 (1988)
43. N P Gambaryan, D P Del'tsova, V A Livshits, E G Ter-Gabrielyan *Izv. Akad. Nauk SSSR, Ser. Khim.* 2344 (1986)
44. G G Furin, A V Rogoza *1-i Ukrainsko–Nemetskii Simpozium po Khimii Ftora, Odessa, 20–25 Sentyabrya 1992. Tezisy Dokladov* [The 1st Ukrainian–German Symposium on Fluorine Chemistry, Odessa, 20–25 September 1992, Abstracts] p. 18
45. G Bauer, G Hagele *Z. Naturforsch. B* **34** 1252 (1979)
46. G Bauer, G Hagele *Angew. Chem.* **89** 493 (1977)
47. A W Frank *J. Org. Chem.* **30** 3663 (1965)
48. A W Frank *J. Org. Chem.* **31** 1917 (1966)
49. A W Frank *J. Org. Chem.* **31** 1521 (1966)
50. J D Park, C K Furuta *Tetrahedron Lett.* **10** 393 (1969)
51. S Z Ivin, V K Promorenko, E A Fokin *Zh. Org. Khim.* **39** 1058 (1969)
52. I L Knunyants, E G Bykhovskaya, V N Volkovitskii, V F Plotnikov, M V Galakhov, L I Ragulin *Zh. Vses. Khim. O-va im. D. I. Mendeleeva* **17** 598 (1972)
53. U Utebaev, E M Rokhlin, E P Lur'e, I L Knunyants *Izv. Akad. Nauk SSSR, Ser Khim.* 142 (1976)
54. I L Knunyants, U Utebaev, E M Rokhlin, E P Lur'e, E I Mysov *Izv. Akad. Nauk SSSR, Ser. Khim.* 875 (1976)
55. U Utebaev, E M Rokhlin, E P Lur'e, I L Knunyants *Izv. Akad. Nauk SSSR, Ser. Khim.* 1463 (1975)
56. E T McBee, J Stark, R Hurnaus, T Hodgins *V Mezhdunarodnyi Simposium po Khimii Ftora (Tezisy Dokladov)* [The Vth International Symposium on the Chemistry of Fluorine (Abstracts of Reports)] (Moscow: Nauka, 1969)
57. L N Markovskii, G G Furin, Yu G Shermolovich, G G Yakobson *Izv. Akad. Nauk SSSR, Ser. Khim.* 2839 (1977)
58. L N Markovskii, G G Furin, Yu G Shermolovich, G G Yakobson *Zh. Obshch. Khim.* **49** 531 (1979)
59. L S Kobrina, G G Furin, G G Yakobson *Zh. Org. Khim.* **6** 512 (1970)
60. A J Kirby, S G Warren *The Organic Chemistry of Phosphorus* (Translated into Russian) (Moscow: Mir, 1971) p. 97
61. T F Kozlova, A F Granov, N M Mel'nikov *Zh. Obshch. Khim.* **45** 1392 (1975)
62. N N Demik, M I Kabachnik, Z S Novikova, I P Beletskaya *Izv. Akad. Nauk SSSR, Ser. Khim.* 2432 (1992)
63. W Boenigk, G Hagele *Chem. Ber.* **116** 2418 (1983)
64. W Boenigk, U Fischer, G Hagele *Phosphorus Sulfur* **16** 263 (1983)
65. T Ishihara, T Maekawa, T Ando *Tetrahedron Lett.* **24** 4299 (1983)
66. T Ishihara, T Maekawa, T Ando *Tetrahedron Lett.* **25** 1377 (1984)
67. R A Bekker, V Ya Popkova *Izv. Akad. Nauk SSSR, Ser. Khim.* 1123 (1982)
68. E Kühle *Chemistry of the Sulfenic Acids* (Stuttgart, 1973)
69. S R Sterlin, B L Dyatkin, L G Zhuravkova, I L Knunyants *Izv. Akad. Nauk SSSR, Ser. Khim.* 1176 (1969)
70. R A Bekker, V Ya Popkova *Izv. Akad. Nauk SSSR, Ser. Khim.* 1123 (1982)
71. J Bittls, R Joyce, US P. 2 559 754; *Chem. Abstr.* **46** 1026 (1952)
72. L Z Soborovskii, N F Baina *Zh. Org. Khim.* **29** 1144 (1959)
73. L N Markovskii, G G Furin, Yu G Shermolovich, G G Yakobson *Izv. Akad. Nauk SSSR, Ser. Khim.* 867 (1981)
74. J Burdon, I N Roznikov, G M Perry *J. Chem., Soc. C* 2615 (1969)
75. M C Demareq *Bull. Soc. Chim. Fr.* 1716 (1969)
76. W Boenigk, G Hagele *Chem. Ber.* **117** 2287 (1984)
77. *Reaktsii i Metody Issledovaniya Organicheskikh Soedinenii* (Reactions and Methods for the Investigation of Organic Compounds) (Moscow: Khimiya, 1966) p. 41
78. R F Hudson *Structure and Mechanism in Organo-phosphorus Chemistry* (London: Academic Press, 1966)
79. A A Stepanov, I N Rozhkov, I L Knunyants *Izv. Akad. Nauk SSSR, Ser. Khim.* 701 (1981)
80. L N Markovskii, G G Furin, Yu G Shermolovich, O N Tychkina, G G Yakobson *Zh. Obshch. Khim.* **49** 710 (1979)
81. V V Bardin, L S Pressman, L N Rogoza, G G Furin *J. Fluorine Chem.* **54** 298 (1991)
82. R Bohlen, G-V Röshchenthaler *Z. Anorg. Allg. Chem.* **578** 47 (1989)
83. D J Burton, S Shin-ya, R D Howells *J. Fluorine Chem.* **15** 543 (1980)
84. D J Burton, T D Spawn, P L Heize, A R Bailey, S Shin-ya *J. Fluorine Chem.* **44** 167 (1989)
85. I L Knunyants, E G Ter-Gabrielyan, Yu V Zeifman, Z V Safronova, N P Gambaryan, E I Mysov, A I Lutsenko, P V Petrovskii *Dokl. Akad. Nauk SSSR* **228** 1344 (1976)
86. A P Marchenko, V V Miroshnichenko, G N Koidan, A M Pinchuk *Zh. Obshch. Khim.* **50** 1897 (1980)
87. G N Koidan, A P Marchenko, A M Pinchuk *Zh. Obshch. Khim.* **60** 709 (1990)
88. I Ruppert, K Schlich, W Volbach *Tetrahedron Lett.* **25** 2195 (1984)

89. V Volbach, I Ruppert *Tetrahedron Lett.* **24** 5509 (1983)
90. G P Stahly, D R Bell *J. Org. Chem.* **54** 2873 (1989)
91. H Beckers, H Burger, R Eujen *Z. Anorg. Allgm. Chem.* **563** 38 (1988)
92. I Ruppert *J. Fluorine Chem.* **29** 98 (1985)
93. A P Marchenko, S I Shaposhnikov, G N Koidan, A V Kharchenko, A M Pinchuk *Zh. Obshch. Khim.* **58** 2230 (1988)
94. R Appel, E Hiester *Chem. Ber.* **114** 2649 (1981)
95. W Volbach, I Ruppert *Tetrahedron Lett.* **24** 5509 (1983)
96. A P Marchenko, G N Koidan, G O Baram, A A Kudryavtsev, A M Pinchuk *Zh. Obshch. Khim.* **60** 961 (1990)
97. G N Koidan, G O Baram, E A Romanenko, A P Marchenko, A M Pinchuk *Zh. Obshch. Khim.* **60** 1423 (1990)
98. V A Olenik, G N Koidan, A P Marchenko, A M Pinchuk *Zh. Obshch. Khim.* **58** 482 (1988)
99. W P Dailey, P Ralli, D Wasserman, D M Lemal *J. Org. Chem.* **54** 5516 (1989)
100. H Burger, M Grunwald, G Pawelke *J. Fluorine Chem.* **31** 89 (1986)
101. C Wakselman, M Tordeux *J. Chem. Soc., Chem. Commun.* 1701 (1987)
102. V V Bardin, L N Aparina, L S Pressman, G G Furin *Izv. Akad. Nauk SSSR, Ser. Khim.* 2153 (1989)
103. V V Bardin, L S Pressman, L N Rogoza, G G Furin *J. Fluorine Chem.* **53** 213 (1991)
104. A A Kolomeitsev, V N Movchun, Yu L Yagupolskii *First Soviet–British Symposium on Fluorine Chemistry (Abstracts)* (Novosibirsk, 1991) p. 160
105. H G Ang *J. Inorg. Nucl. Chem.* **30** 1715 (1968)
106. D G Naae, H S Kesling, D J Burton *Tetrahedron Lett.* **16** 3789 (1975)
107. D J Burton, S W Hanzen, G S Shaw *6th Winter Conference Daytona Beach, FL, 1983*
108. V Broicher, D Geffken *J. Organomet. Chem.* **381** 315 (1990)
109. A Kruse, G Siegemund, A Schumann, I Ruppert, Ger. Offen DE 3 801 248 (1989); *Chem. Abstr.* **112** 77537 (1990)
110. A A Kolomeitsev, N V Ignat'ev, R F Skripnik *J. Fluorine Chem.* **54** 318 (1991)
111. A Kruse, G Siegemund, I Ruppert, Eur. Pat. Appl. EP 302 331 (1989); *Chem. Abstr.* **111** 77 646 (1989)
112. W-Y Huang, C-M Hu, Y-O He, H-F Zhou *J. Fluorine Chem.* **48** 145 (1990)
113. Y O Elmig umi, H J Emeleus *J. Inorg. Nucl. Chem.* **32** 3211 (1970)
114. D J Burton, D G Cox *J. Am. Chem. Soc.* **105** 650 (1983)
115. D J Burton, F E Herkes *Tetrahedron Lett.* **6** 1883 (1965)
116. M Hanack, C Korhummel *Synthesis* 944 (1987)
117. D J Burton, Y Inouye *Tetrahedron Lett.* **17** 3397 (1976)
118. Xingya Li, Weimin Fu, Shengming Ma, Xikui Jiang *Xuanxue Xuebao* **47** 360 (1989); *Chem. Abstr.* **111** 173 568 (1989)
119. L S German, E I Mysov, E G Ter-Gabrielyan *Izv. Akad. Nauk SSSR, Ser. Khim.* 491 (1990)
120. A Michaelis *Annalen* **326** 129 (1903)

Russian Chemical Reviews **62** (3) 261 – 278 (1993)

© 1993 Russian Academy of Sciences and Turpion Ltd

UDC 547.484.2 + 547.214;547.233

Asymmetric synthesis of fluorine- and phosphorus-containing analogues of aminoacids

V P Kukhar', N Yu Svistunova, V A Solodenko, V A Soloshonok

Contents

I. Introduction	261
II. Enantioselective formation of the C–C bond	261
III. Enantioselective formation of the C–P bond	269
IV. Enantioselective formation of the C–H bond	271
V. Enantioselective formation of the C–N bond	274
VI. Asymmetric synthesis with the use of enzymes	275

Abstract. The available literature data on the methods for the asymmetric synthesis of fluorine- and phosphorus-containing aminoacids are surveyed. The chemical and enzymic methods of the asymmetric synthesis of the above compounds are considered. The bibliography includes 139 references.

I. Introduction

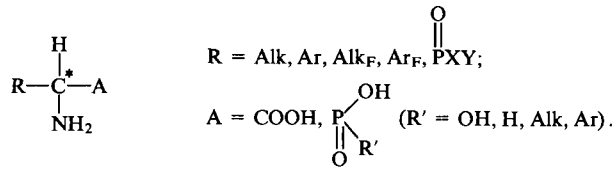
The synthesis of organoelement analogues of natural products and in the first place of element-containing aminoacids is one of the most vigorously developing fields in modern organic chemistry.[1] There exist natural element-containing aminoacids; bromine-,[2] chlorine-,[3] fluorine-,[4] and phosphorus-containing aminoacids[5, 6] have been isolated from various sources. The unique biological activity of natural element-containing aminoacids has served as a powerful stimulus which initiated vigorous research in this field.

Numerous element-containing aminoacids have been synthesised hitherto, among which special emphasis must be laid on fluorine- and phosphorus-containing aminoacids. The majority of these aminoacids are metabolites of the 'normal' aminoacids. They exhibit the properties of highly selective (as regards the specificity of their activity) inhibitors of enzyme reactions and they possess high carcinostatic, bactericidal, cytotoxic, and other forms of biological activity. Thus more than 20 studies devoted to various aspects of the synthesis and biological activity of fluorine-,[7–24] phosphorus-,[25–35] boron-,[36] and selenium-containing aminoacids[37] have now been published.

Analysis of the literature data shows that the most urgent problem in the chemistry of organoelement aminoacids is that of the development of methods of synthesis of these compounds in an enantiomerically pure form, which is dictated by modern requirements in biology and medicine. Unfortunately, in most cases racemic synthesis is considered in the reviews quoted above and the main aspects of the asymmetric synthesis of element-containing aminoacids (the nature of the enantioselectivity, the optical purity, and the absolute configuration) are hardly discussed.

The present review deals with the methods of asymmetric synthesis of fluorine- and phosphorus-containing aminoacids published up to the middle of 1992 inclusive. We were guided by the fundamental classical definition of asymmetric synthesis, given in the monograph of Morrison and Mosher,[38] as a process in which a prochiral molecule or its fragment is converted into a chiral molecule with unequal amounts of the stereoisomeric products. The process takes place under the influence of chiral reagents, part of the initial molecule, or the catalyst. The methods of synthesis of enantiomerically pure or optically active organoelement aminoacids (C–F, C–P) involving the direct introduction of the element into complete aminoacid enantiomers or involving enzymic or chemical separation of racemic compounds will therefore not be considered in the present review.

The entire data are described in five main sections depending on the type of bond formed at the chiral centre of the α-aminoacid, while syntheses using enzymes have been collected in a separate section.



II. Enantioselective formation of the C–C bond

The asymmetric synthesis of element-containing aminoacids is most widely represented by examples of the enantioselective formation of the C–C bond on alkylation of chiral Schiff bases. These can be readily obtained from the esters of the simplest aminoacids and chiral carbonyl compounds, which can be regenerated and used in new syntheses. The formation of Schiff bases increases the CH acidity of the aminoacid fragment and permits the generation of a carbanion under the influence of bases of different strengths and its subsequent reactions with various electrophiles.[39]

Camphor and its derivatives are frequently used as the chiral carbonyl compound in the above synthesis, which is due to their ready availability in both enantiomerically pure forms.

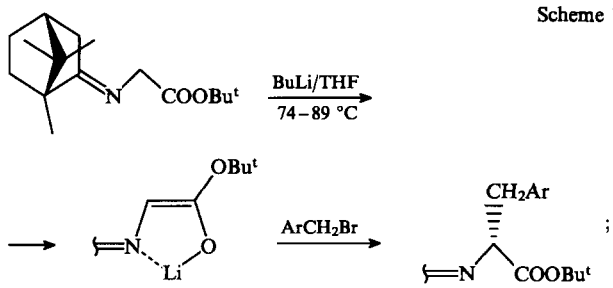
V P Kukhar', N Yu Svistunova, V A Solodenko, V A Soloshonok Institute of Bioorganic Chemistry and Petrochemistry, Academy of Sciences of the Ukraine, Murmanskaya ul. 1, 252660 Kiev-94, Fax (7-044) 543 5152

Received 14th December 1992
Uspekhi Khimii **62** (3) 284 – 302 (1993); translated by A K Grzybowski

In most cases the chiral Schiff base is deprotonated with butyllithium or lithium diisopropylamide and the carbanion formed is made to react with alkyl halides, carbonyl compounds, or Michael acceptors.

Thus the (*R*)-enantiomers of *p*-fluoro- and *p*-trifluoromethylphenylalanines have been synthesised[40] by alkylating the Schiff base formed from the *tert*-butyl ester of glycine and (*R*)-camphor with the corresponding benzyl bromides (Scheme 1).

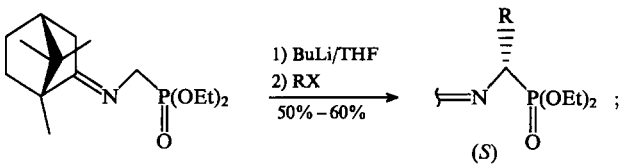
Scheme 1



Ar = 4-FC_6H_4, 4-$CF_3C_6H_4$.

The attack by the lithium derivative comes predominantly from the *re*-side [the side opposite to the C(8) atom of camphor], affording products with a diastereo-isomeric excess (d.e.) > 98% (F) and 79% (CF_3), which is controlled kinetically. It is of interest to note that high values of d.e. are observed in this synthesis only when benzyl and allyl halides are used as alkylating agents (in the case of EtBr, d.e. = 33%). This has been attributed[40] to the additional $\pi-\pi$ interaction in the transition state between the π-system of benzyl or allyl halides, which has a positive character after the partial dissociation of the C–Br bond, and the π-system of the enolate. This hypothesis has been confirmed by the dependence of the d.e. on the nature of the substituent in the benzene ring and benzyl bromide. A series of (*S*)-α-aminoalkylphosphonic acids have been synthesised by a similar procedure using the Schiff base obtained from (*R*)-camphor and diethyl aminomethylphosphonate (the phosphonoglycine synthon),[41] the maximum enantioselectivity of the alkylation being achieved, as in the study of McIntosh et al.,[40] in the case of allyl and benzyl halides (Scheme 2).

Scheme 2



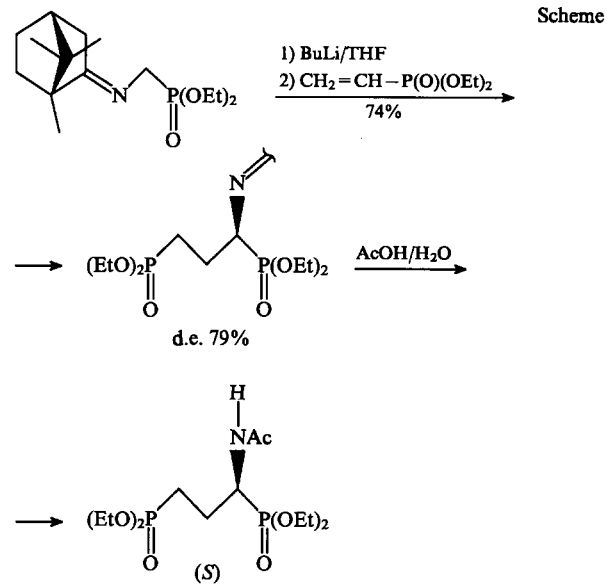
R	$CH_2CH=CH_2$	$PhCH_2$	$CH_2-C\equiv CH$
d.e. (%)	>95	>95	71

R	Me	Et	Pr	$MeOCH_2$
d.e. (%)	11	69	77	56

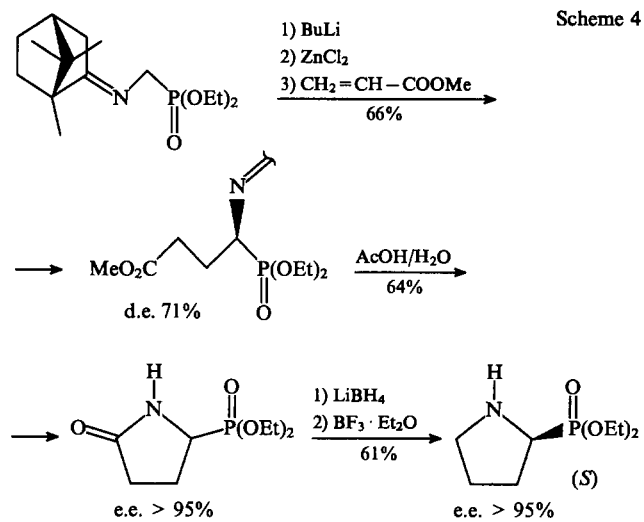
The possibilities of the phosphonoglycine synthon may be expanded by using it for the Michael addition to activated carbon–carbon double bonds.[42]

The kinetically controlled addition of vinylphosphonate or methyl acrylate to the lithium derivative of the Schiff base takes place with high values of the d.e., affording esters of the phosphono-analogues† of (*S*)-$Glu^{\alpha,\omega\text{-}P}$ and (*S*)-$Glu^{\alpha\text{-}P}$. The ester of (*S*)-phosphonoproline was obtained from the latter in two stages (Scheme 3 and 4).

Scheme 3



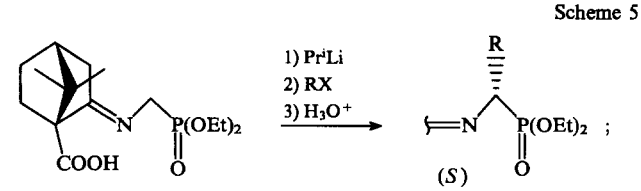
Scheme 4



e.e. = enantiomeric excess.

The use of (*R*)-ketopinoic acid (a camphor derivative), instead of camphor itself, for the synthesis of the chiral phosphonoglycine synthon hardly affects the enantioselectivity of the alkylation and leads to the (*S*)-phosphonic acid with high values of d.e. only in the case of the allyl and benzyl derivatives (Scheme 5).[43]

Scheme 5

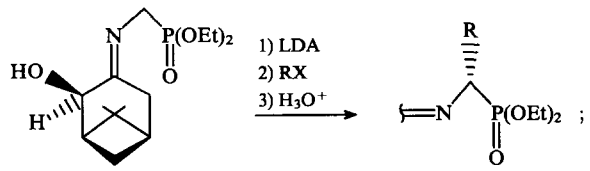


R	Me	Et	CH_2Ph	$CH_2CH=CH_2$
Yield (%)	67	68	93	65
d.e. (%)	15.1	62	79	92

† Three-letter designations of aminoacids with the superscript 'P' are used to designate the phosphorus analogues of natural aminoacids. In the case of the phosphorus analogues of aspartic and glutamic acids, the additional superscripts α, β, and γ, indicating the position of the phosphorus-containing group, are introduced.

The phosphonoglycine synthon, obtained from (1*R*, 2*R*, 5*R*)- or (1*S*, 2*S*, 5*S*)-2-hydroxypinan-3-one, gives a more stable stereochemical result which depends little on the nature of the alkylating agent (Scheme 6).[41, 44–46]

Scheme 6



(1*R*, 2*R*, 5*R*) (*R*)
(1*S*, 2*S*, 5*S*) (*S*)

R	Me	Et	$PhCH_2$	$CH_2=CHCH_2$
Yield (%)	90	85	71	70
d.e. (%)	74–85	95	83	74

R	$CH_2-C\equiv CH$	$(CH_2)_5I$	$(CH_2)_2OTHP$
Yield (%)	85	72	85
d.e. (%)	83	69	~100

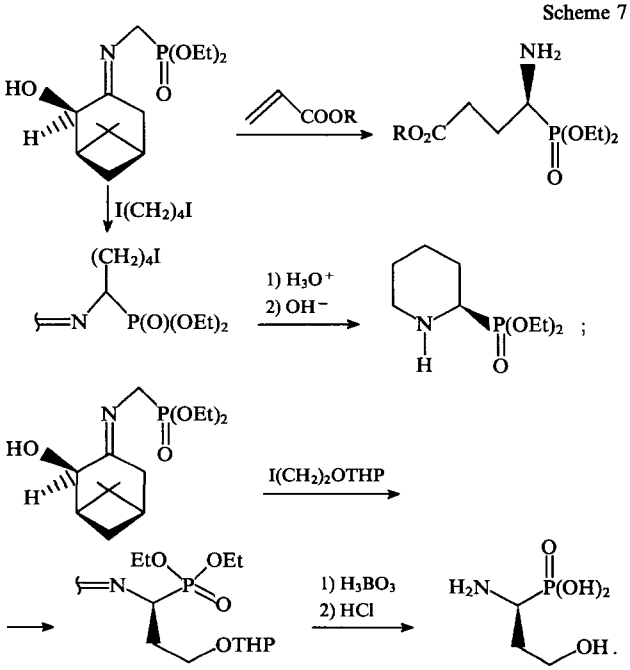
LDA = *N*-lithium diisopropylamide, OTHP = *O*-tetrahydropyranyl.

In this case, phosphonic aminoacids can be obtained with a high optical purity even when their alkyl groups are small.

The nature of the asymmetric induction in the alkylation of the Schiff base obtained from phosphonoglycine and hydroxypinanone has not been discussed,[44, 45] but one can postulate the important role of the hydroxy-group in the α-position relative to the C=N bond in the coordination of the metal during the reaction. Thus the replacement of LDA by *tert*-BuOK in this synthesis leads to the alkylation of the hydroxyl (MeI) and a decrease in the diastereoselectivity of the alkylation of the Schiff base from 85% to 45% (R = Me).

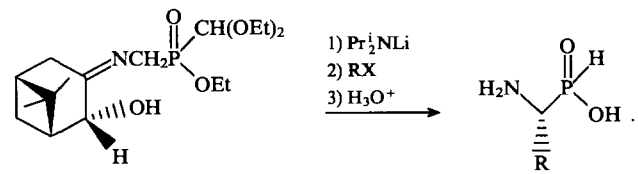
The use of α,ω-dihaloalkanes makes it possible to obtain cyclic phosphonic aminoacids (proline homologues), which is illustrated in relation to the synthesis of (*S*)- or (*R*)-homoproline, while the Michael addition of methyl acrylate affords the α-phosphonic analogue of glutamic acid with 87% enantiomeric purity, from which the esters of (*S*)- and (*R*)-Pro^{P} were obtained in several stages (Scheme 7).[44]

Scheme 7



The only example of the asymmetric synthesis of α-aminoalkylphosphonous acids also involves the stereoselective alkylation of a chiral Schiff base obtained from (1*R*, 2*R*, 5*R*)-2-hydroxy-3-pinanone and ethyl aminomethyl(diethoxymethyl)-phosphinic acid with benzyl bromide (d.e. > 99%) and methyl iodide (d.e. 56%).[47] After the hydrolysis of the alkylation products under mild conditions, optically active phosphonous analogues of phenylalanine (*R*)-Phe^{P-H} (d.e. > 99%) and alanine (*R*)-Ala^{P-H} (d.e. 46%) were isolated (Scheme 8).

Scheme 8



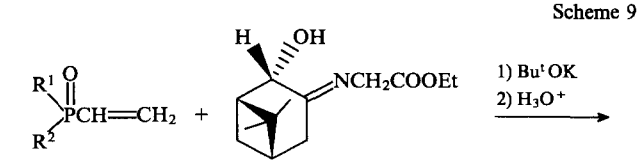
(1*R*, 2*R*, 5*R*) (*R*)

The use of the Schiff base derived from (1*S*, 2*S*, 5*S*)-2-hydroxy-3-pinanone leads to the formation of another enantiomer of the phosphonous analogue of phenylalanine–(*S*)-Phe^{P-H} (e.e. > 99%).

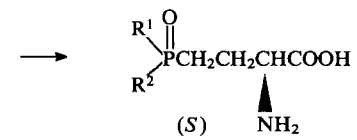
The authors note the dependence of the stereoselectvity of the alkylation of the Schiff base on the nature of its acid function: the diastereoselectivity of the benzylation ($PhCH_2Br$) increases appreciably in the sequence COOEt < $P(O)(OEt)_2$ < P(O)··$(OEt)CH(OEt)_2$ and amounts to 75%, 83%, and 99% respectively.

The addition of chiral Schiff bases derived from hydroxypinanones to vinylphosphonates and vinylphosphinates has been used for the asymmetric synthesis of α-amino-γ-phosphonobutyric acid [(*S*)-(+)-Glu$^{\gamma\text{-P}}$] and (*S*)-(+)-phosphinotricin [(*S*)-(+)-Glu$^{\gamma\text{-P-Me}}$] as well as their (*R*)-(−)-enantiomers (Scheme 9).[48]

Scheme 9



R^1 = Me, R^2 = OMe (1*S*, 2*S*, 5*S*)
$R^1 = R^2$ = OEt



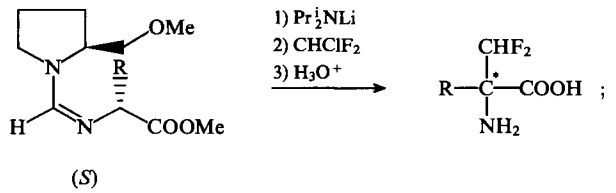
R^1 = Me, R^2 = OH,
$R^1 = R^2$ = OH.

The stereoselectivity of the process is appreciably higher in addition to vinylphosphinate (d.e. 73% and 79%) than in addition to vinylphosphonate (45% and 50%) and decrease by 25% – 30% in the presence of additives which effectively solvate the cation (hexamethylphosphoramide, crown-ether). On this basis, the authors conclude that the coordination of the electron pairs of the nitrogen atom and of the oxygen atom of the phosphoryl group to the metal ion (K^+) exerts a decisive influence on the stereoselectivity of the addition reaction.

The use of chiral inducing reagents of another type — proline derivatives — in the asymmetric synthesis of element-containing aminoacids has been demonstrated in relation to the synthesis of α-difluoromethylalanine and α-difluoromethylphenylalanine by alkylating with chlorodifluoromethane the lithio-derivative of

the Schiff base obtained from (*S*)-1-dimethoxymethyl-2-methoxymethylpyrrolidine and the esters of the corresponding aminoacids (Scheme 10).[49]

Scheme 10



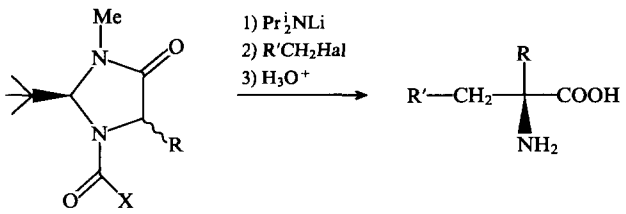
(*S*)

R = Me, CH_2Ph.

The enantioselectivity of the reaction and the absolute configuration of the aminoacids formed are not discussed in the above communication.[49] However, the [1,5]-asymmetric induction occurring in this instance is as a rule weak.[50]

The alkylation of rigid cyclic synthons usually takes place with a higher diastereoselectivity than in the case of linear systems. The advantages of using cyclic synthons have been demonstrated particularly convincingly in the studies by Seebach et al.,[51] Schöllkopf,[51] and Belokon' et al.[53] Thus the lithio-derivative obtained from (*S*)-1-*tert*-butoxycarbonyl-2-(*tert*-butyl)-3-methyl-4-imidazolidinone (R = H) is alkylated diastereospecifically with *p*-fluoro- or pentafluoro-benzyl bromides, affording, after the hydrolysis of the alkylation products, (*S*)-*p*-fluoro- and (*S*)-pentafluoro-phenylalanines with an optical purity >98% (Scheme 11).[54, 55]

Scheme 11



R = H, Me; R′ = 4-FC_6H_4, C_6F_5, 2-FC_6H_4, 3-FC_6H_4; X = CH_2Ph, $OCMe_3$.

The alkylation of the alanine synthon (R = Me) with fluorobenzyl halides led to the formation of the isomeric (*S*)-α-methyl derivatives of *o*-, *m*-, and *p*-fluorophenylalanines with an equally high optical purity.[56]

The lithio-derivative of imidazolidinone (R = H) as well as another chiral glycine synthon used by Seebach, namely benzyl-(*R*)-2-(*tert*-butyl)-5-oxo-3-oxalidine carboxylate, have been used in the synthesis of (2*S*, 3*S*)-trifluorothreonine‡ and (2*S*, 3*R*)-*p*-trifluoromethyl- and (2*S*, 3*R*)-*o*-fluorophenylserines (Scheme 12).[57, 58]

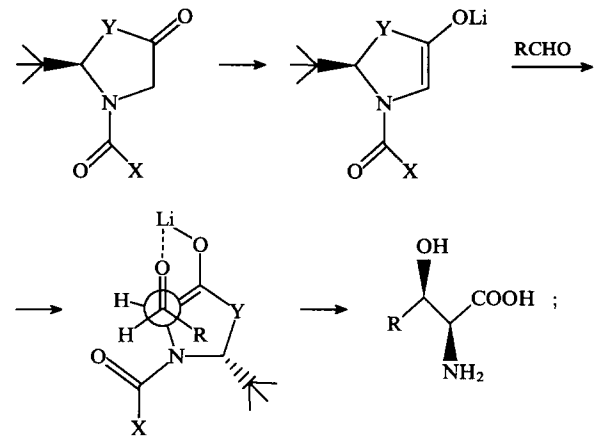
The high stereoselectivity of the reaction can be explained by the preference for one of the possible transition states in which minimum steric interactions and maximum overlap of the donor and acceptor π-systems of the reacting molecules are insured.

The alkylation of the lithio-derivative of the chiral bislactim ether with ω-phosphonoalkyl bromides (Schöllkopf's method) takes place with a high stereoselectivity, which has been used for the asymmetric synthesis of optically active carboxylic α-amino-ω-phosphono-acids and their esters (Scheme 13).[59]

The phosphorus-containing bislactim ether formed in the first stage can be realkylated, which ultimately leads to α-substituted γ-phosphonic analogues of (*S*)-glutamic acid.

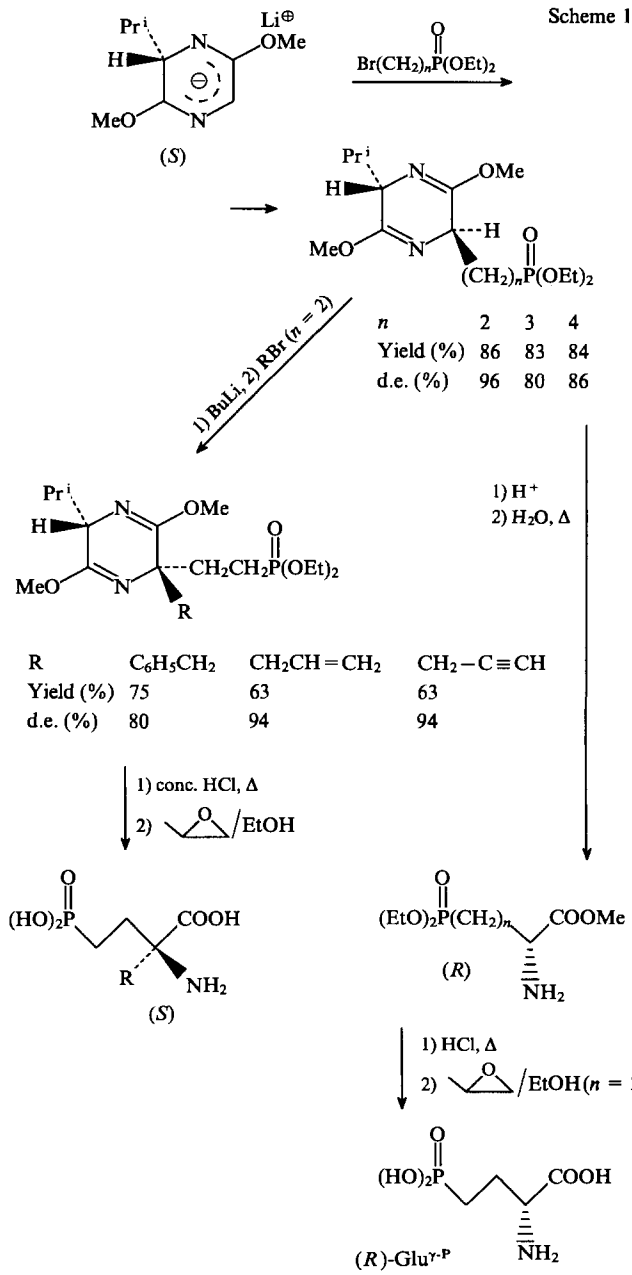
‡ Seebach et al.[58] erroneously attributed the (2*S*, 3*R*)-configuration to the aminoacid obtained.

Scheme 12



R = CF_3, 4-$CF_3C_6H_4$, 4-FC_6H_4; X = Ph, $PhCH_2O$; Y = O, NMe.

Scheme 13

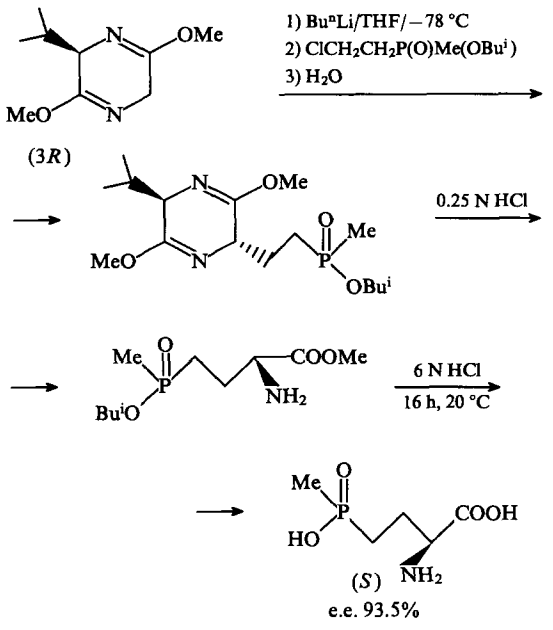


n	2	3	4
Yield (%)	86	83	84
d.e. (%)	96	80	86

R	$C_6H_5CH_2$	$CH_2CH=CH_2$	$CH_2-C\equiv CH$
Yield (%)	75	63	63
d.e. (%)	80	94	94

Both enantiomers of phosphinotricin were obtained by Schöllkopf's method involving the alkylation of the lithio-derivative of the bislactim ether containing a valine residue as the stereodifferentiating group (Scheme 14).

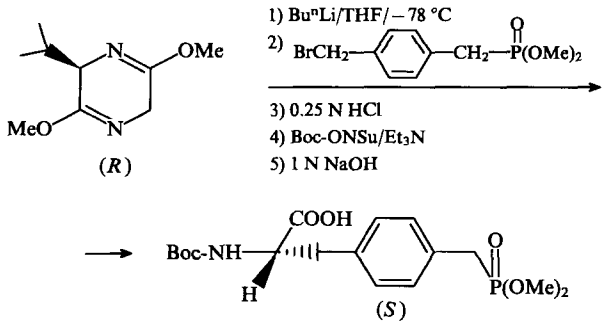
Scheme 14



As in all the syntheses by Schöllkopf's method, in this case the chiral anion is alkylated with a high degree of stereoselectivity (93.5%), affording phosphorus-containing (*S*)- or (*R*)-amino-acids when the (*R*)- or (*S*)-bislactim ethers are used respectively.[60]

The same method has been employed to synthesise an analogue of phosphonotyrosine—*p*-phosphonomethyl-(*S*)-phenyl-alanine, which was subsequently incorporated in the peptide chain of angiotensin in the search for biologically active peptides (Scheme 15).

Scheme 15

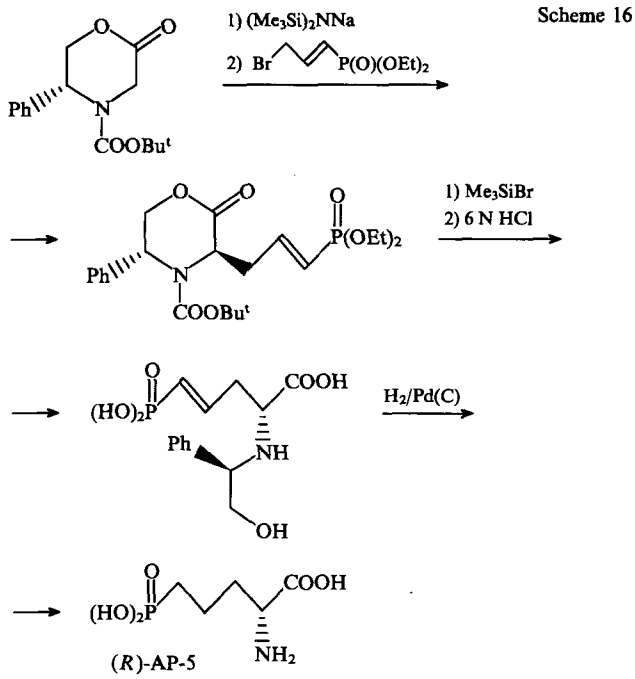


In order to estimate the optical purity of the product, the P- and N- substituted aminoacid was condensed with the methyl ester of (*S*)-leucine and the content of the diastereoisomeric dipeptides obtained was determined by high performance liquid chromatography (HPLC): the ratio of the (*S*,*S*)- and (*R*,*S*)-dipeptides was 95.3 : 4.7.[61]

Alkylation of the chiral oxazinone, obtained from D-phenyl-glycinol, has been used in the first enantioselective synthesis of (*R*)-(−)-2-amino-5-phosphonopentanoic acid (AP-5).[62] This compound is a selective antagonist of *N*-methyl-D-aspartate and is widely used in biochemical research.[63] The glycine synthon employed requires an active alkylating agent. In this instance, 3-phosphonoallyl bromide was used for this purpose (Scheme 16).

After the removal of the protecting groups and the hydrogenation of the carbon–carbon double bond, the target phosphorus-containing aminoacid was obtained in a high yield, its optical purity being estimated as 'high' from high performance liquid chromatographic data and the analysis of the NMR data for the diastereoisomeric precursors.

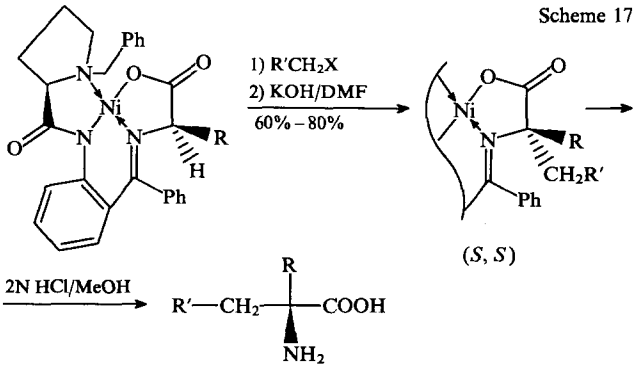
Scheme 16



In Belokon's chiral glycine synthon, the carboxy-group of the Gly (or Ala) fragment is not esterified and is not bound in a ring by a covalent bond, as in the previous methods. Nevertheless, the nickel(II) complexes of the glycine Schiff base are rigid cyclic systems in which [1,7]-asymmetric induction occurs as a result of the distortion of the chelate rings, which leads, when (*S*)-proline is used, to the shielding of the *re*-side of the methylene group of glycine by the benzene ring of the *o*-aminobenzophenone fragment. In order to generate the corresponding carbanion in these complexes, it is sufficient to use ordinary KOH in a dry organic solvent (DMF, MeCN), or NEt$_3$, or diazabicyclooctane in methanol or CHCl$_3$.

Alkylation with the appropriate fluorine-substituted benzyl chlorides or bromides of the nickel(II) complex of the Schiff base obtained from glycine and (*S*)-2-[*N*-(benzylprolyl)amino]-benzophenone afforded a series of (*S*)-phenylalanines containing from one to five fluorine atoms (as well as other halogens—Cl and Br) in the benzene ring as well as the trifluoromethyl group in the *para*- or *meta*-position.[64, 65] The attempts to obtain by this method (*S*)-*o*-trifluoromethylphenylalanine were unsuccessful, apparently owing to the steric effect of the trifluoromethyl group. The use of the nickel(II) complex of the Schiff base derived from alanine makes it possible to obtain fluorine-substituted α-methylphenylalanine derivatives (Scheme 17).

Scheme 17

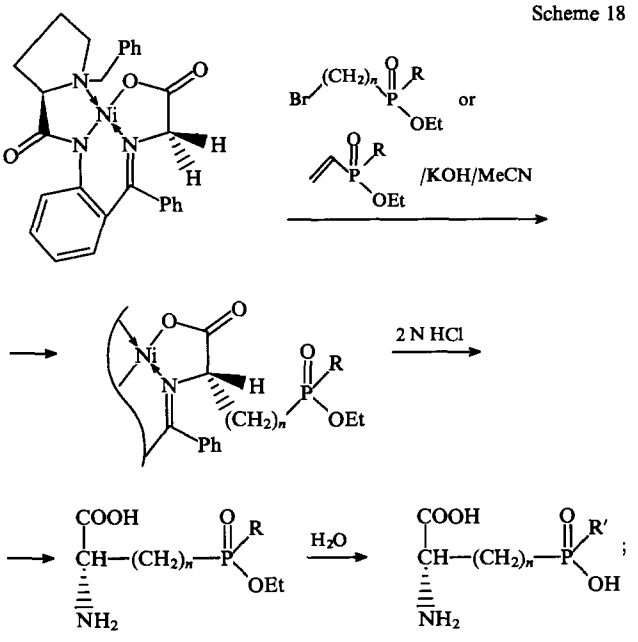


R = H, Me; R' = 2-FC$_6$H$_4$, 3-FC$_6$H$_4$, 4-FC$_6$H$_4$, 2-Cl,6-FC$_6$H$_3$, 4-CF$_3$C$_6$H$_4$, 2-F,6-BrC$_6$H$_3$, 2,6-Cl$_2$C$_6$H$_3$; X = Br, Cl.

The high chemical (50% – 80%) and optical (~90% d.e.) yields in the stage involving the alkylation of the nickel complexes render this method preparative.

The (*S*)-enantiomers of ω-phosphonic and ω-phosphinic analogues of carboxylic α-aminoacids have been obtained by alkylating the nickel complex of glycine with the corresponding phosphonoalkyl bromides or, in a synthesis of homoglutamic acid and phosphinotricin, with vinyl phosphonate and vinyl phosphinate (Scheme 18).[66, 67]

Scheme 18



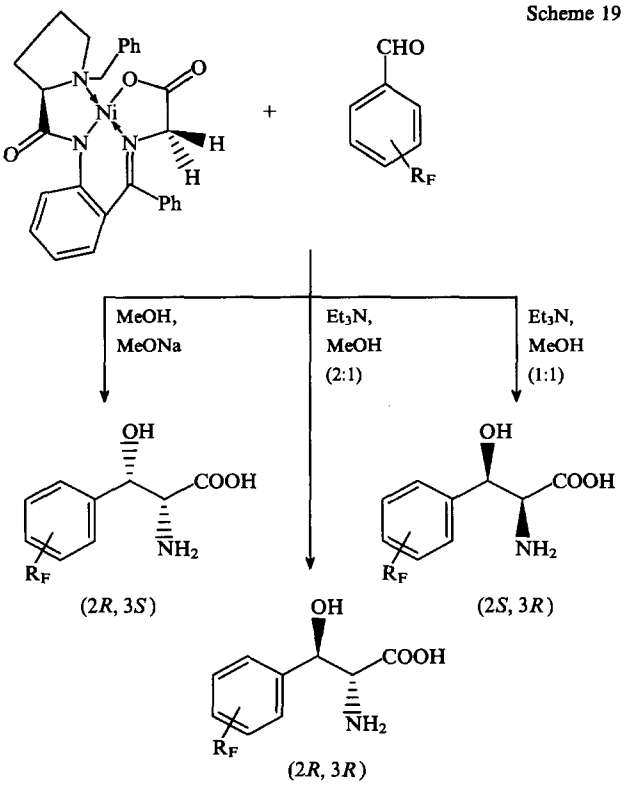
n = 2, 3; R = Me, OEt; R′ = Me, OH.

The enantioselectivity of the alkylation of the nickel complex with the diesters of ω-haloalkylphosphonic acids is >90%, while the kinetically controlled Michael addition takes place with only 60% diastereoselectivity. However, thermodynamic control (in the presence of MeONa) leads[67] to a 95 : 5 ratio of the diastereoisomeric complexes.

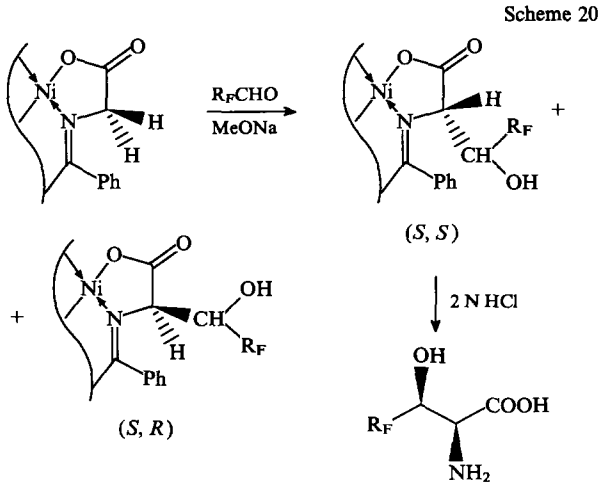
From the standpoint of the stereochemical result (diastereoselectivity of the alkylation), the method considered has no advantage over the Seebach or Schöllkopf methods in the synthesis of α-aminoacids, while its application to the synthesis of α-amino-β-hydroxyacid produces a unique result associated with the fact that at high pH the ionised β-hydroxy-group of the aminoacid fragment can substitute the carboxy-group at the nickel atom in the coordination plane, which results in the inversion of the absolute configuration at the α-carbon.[68] Thus, depending on the conditions in the condensation of the nickel(II) complexes of the Schiff bases obtained from glycine and fluorobenzaldehydes, the corresponding β-(fluorophenyl)serines with the absolute (2*R*, 3*S*)-, (2*R*, 3*R*)-, and (2*S*, 3*R*)-configurations respectively of the chiral atoms were obtained in an optically pure form (Scheme 19).[69–71]

An interesting example of the critical influence of the fluorine-containing substituent on the stereochemical outcome of the reaction has been demonstrated in the condensation of a chiral glycine complex with aliphatic perfluorinated aldehydes.[71] The interaction of fluoral or its hydrate (hemiacetal) with the glycine complex in methanol under the influence of MeONa leads to the formation of (2*R*, 3*S*)-4,4,4-trifluorothreonine, whereas acetaldehyde afford (2*R*, 3*S*)-threonine under analogous conditions (Scheme 20).[68]

Scheme 19



Scheme 20

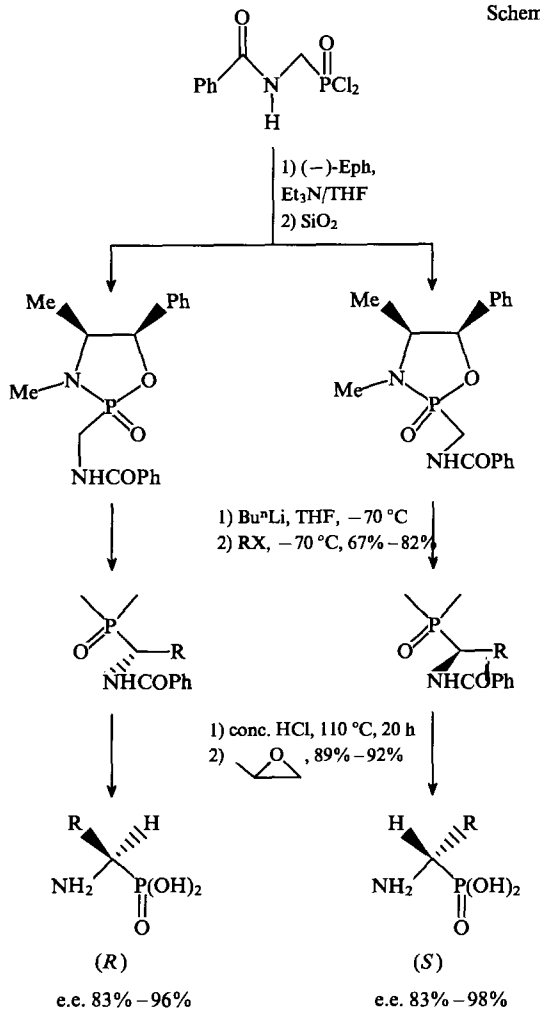


The same method has been used to synthesise (2*R*, 3*S*)- and (2*S*, 3*R*)-ω-phosphonic analogues of glutamic and homoglutamic acids with a β-hydroxy-group.[72, 73] The phosphonate group in the ω-position in the corresponding aldehyde does not exert in this instance any influence on the stereochemistry of the reaction.

In the examples examined above, the chiral auxiliary reagent is bound to the amino-group of the glycine or phosphonoglycine synthon. In an alternative approach, the chiral auxiliary reagent is bound to the acid functional group of the aminoacid. In the case of carboxylic α-aminoacids, it led to disappointingly low optical yields[50] but in the synthesis of phosphonic α-aminoacids it afforded a remarkable result. This was based on the possibility of obtaining cyclic esters, amides, or amidoesters in which the stereodifferentiating fragment is bound directly to the phosphorous atom ('chiral phosphorus').

Thus epimeric (with respect to the phosphorus atom) 2-benzamidomethyl-3,4-dimethyl-2-oxo-5-phenyl-2λ^5-1,3,2-oxazaphospholidines have been obtained from the dichloride of *N*-benzamidomethylphosphonic acid and (−)-ephedrine (Eph). After resolution on SiO_2, they were used[74] in the synthesis of the (*R*)- and (*S*)-enantiomers of Ala^P, Phe^P, and 1-aminobut-3-enylphosphonic acid (Scheme 21).

Scheme 21



RX = MeI, $PhCH_2Br$, $CH_2=CHCH_2I$.

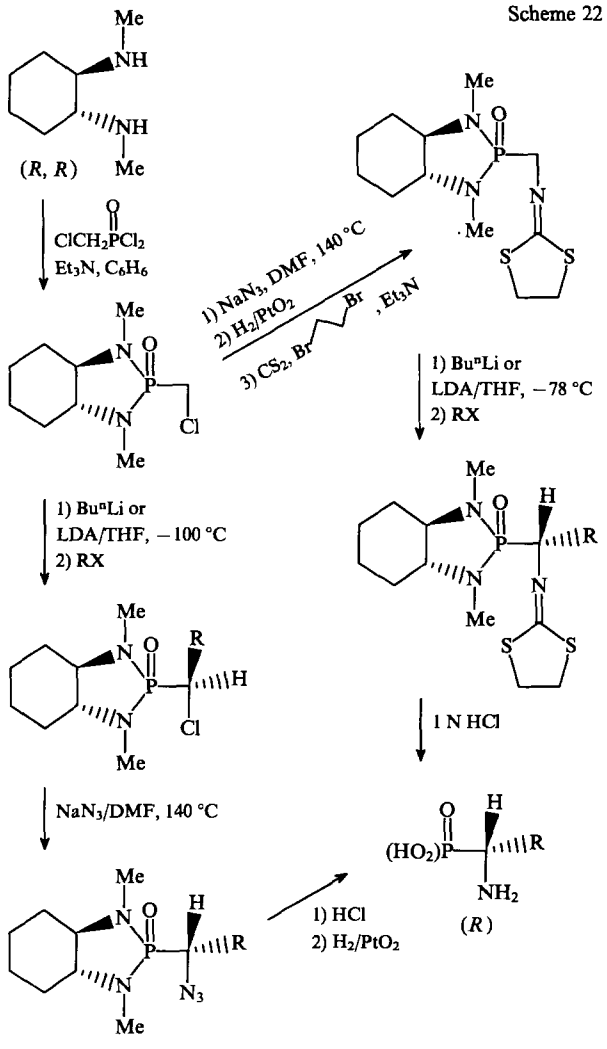
The diastereoselectivity of the alkylation reaction depends on the bulk of the substituent in the alkylating agent and is in the range form 58%−73% (MeI) to 84%−92% ($PhCH_2Br$). The chemical yield of the alkylation product is 67%−82%.

It is of interest to note that the diastereoselectivity of the alkylation of oxazaphospholidines diastereoisomeric with respect to the phosphorus atom is not the same. Thus in the case of the diastereoisomer with the (S^P)-configuration, this parameter is appreciably higher (up to 15%).

A method has been described in which a ligand with C_2 symmetry, namely (1*S*, 2*S*)- or (1*R*, 2*R*)-1,2-bis(methylamino)-cyclohexane, was used as the chiral inducing fragment bound to the phosphorus atom.[75, 76] The chiral methyliminodithiolan obtained from it can be alkylated with a high degree of diastereoselectivity (up to 98% d.e.), affording, after the removal of the protecting groups, phosphonic α-aminoacids in a satisfactory chemical yield and with a satisfactory chemical purity (Scheme 22).[75]

Another version of the method involves the alkylation of the chiral chloromethylphosphonate with subsequent replacement of chlorine by the amino-group and leads to optically active phosphonic α-aminoacids with the same stereoconfiguration,

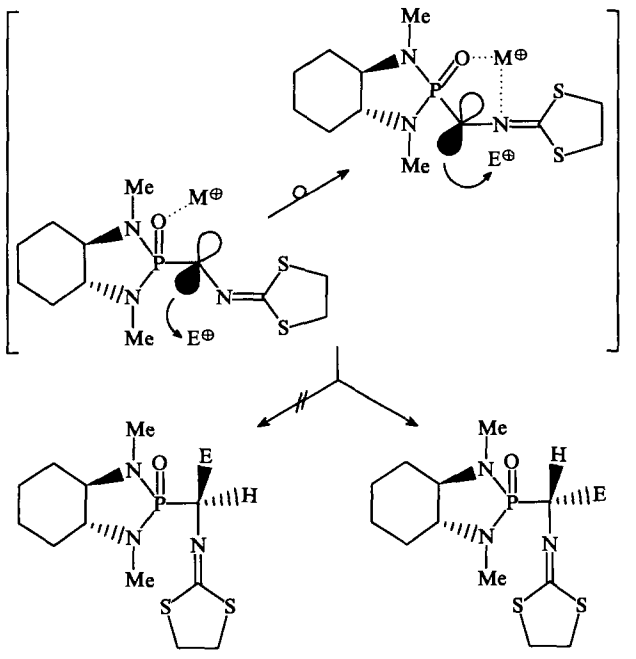
Scheme 22



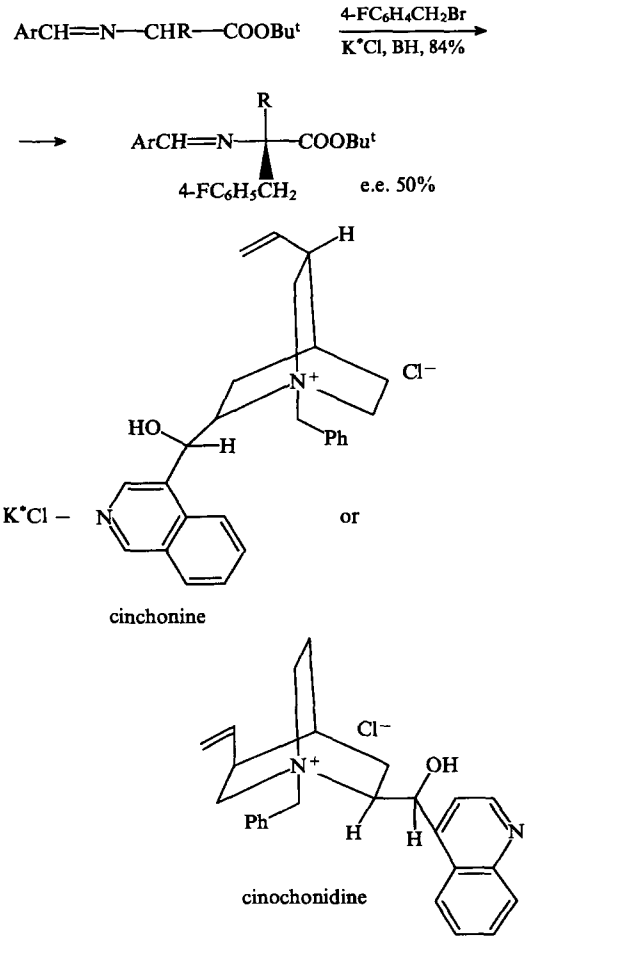
despite the fact that the sequence of reactions employed involves the replacement of chlorine by the azido-group as a result of a reaction of the S_N2 type with inversion of the configuration at the C_α-atom. This is associated with the fact that in the given instance, while a high degree of stereoselectivity in the alkylation reaction is retained, the absolute configuration of the alkylation product is different from that in the alkylation of the corresponding methyliminodithiolan. The authors assume[75] that in the case of the methyliminodithiolan the metallation of the latter is followed initially by the formation of a chelate with participation of the nitrogen atom in the iminothiolan fragment, leading to the complete inversion of the configuration of the carbanion, and then by alkylation predominantly the 'opposite side' of the anion (Scheme 23).

There is no doubt that the most effective method of using optically pure compounds in asymmetric synthesis involves their application as catalysts. Major advances in asymmetric catalysis have been achieved in the hydrogenation of unsaturated bonds, while instances of the enantioselective formation of a C−C bond in the presence of a chiral catalyst are still fairly rare.[50] Two widely known methods for the catalytic asymmetric synthesis of α-aminoacids, developed by O'Donnell and Hayashi, have been used successfully for the preparation of element-containing aminoacids. Thus alkylation with alkyl halides of the Schiff bases of the *tert*-butyl esters of glycine or alanine under phase transfer conditions in the presence of quaternary salts of cinchonine or cinochonidine makes it possible to obtain the corresponding α-aminoacids, including *p*-fluorophenylalanine, with a moderate enantiomeric excess (Scheme 24).[77, 78]

Scheme 23



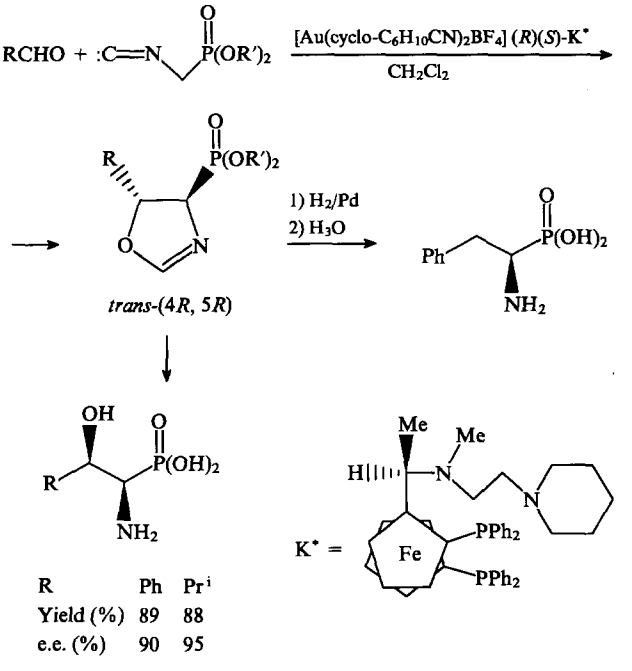
Scheme 24



The use of the quaternary cinchonine salt as the catalyst yields an excess of the (*R*)-aminoacid, while 'pseudoenantiomeric catalysis' by the cinochonidine salt leads to the formation of (*S*)-4-fluorophenylalanine.

Optically pure α-phosphonic analogues of phenylalanine and β-alkyl(aryl)serines can be obtained by the asymmetric aldol reaction [condensation ?] between isocyanomethylphosphonates and various aldehydes in the presence of catalytic amounts of chiral ferrocenylphosphine complexes of gold(I) (Scheme 25).[79–81]

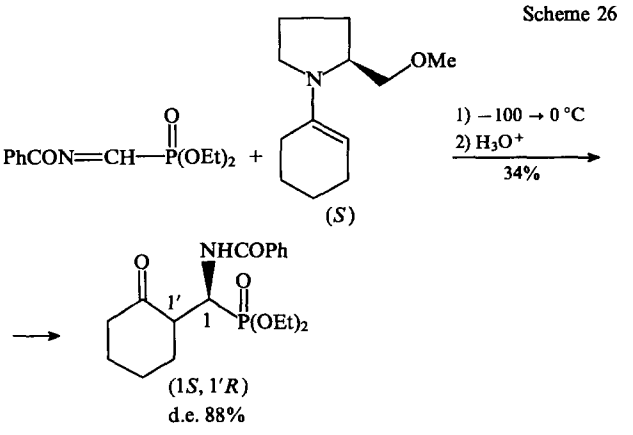
Scheme 25



The highest enantioselectivities of the reaction (94%) were obtained when diphenyl isocyanomethylphosphonate was used. It is noteworthy that only one hundredth of a mole of the catalyst is sufficient for effective asymmetric catalysis in this reaction.

The only example of the asymmetric synthesis of phosphonic aminoacids (with formation of a C–C bond) using the substituent group itself as the chiral auxiliary group is the nucleophilic addition of a chiral enamine to an acyliminoalkylphosphonate,[82] which affords the target aminoacid with a 88% diastereoisomeric excess (Scheme 26).

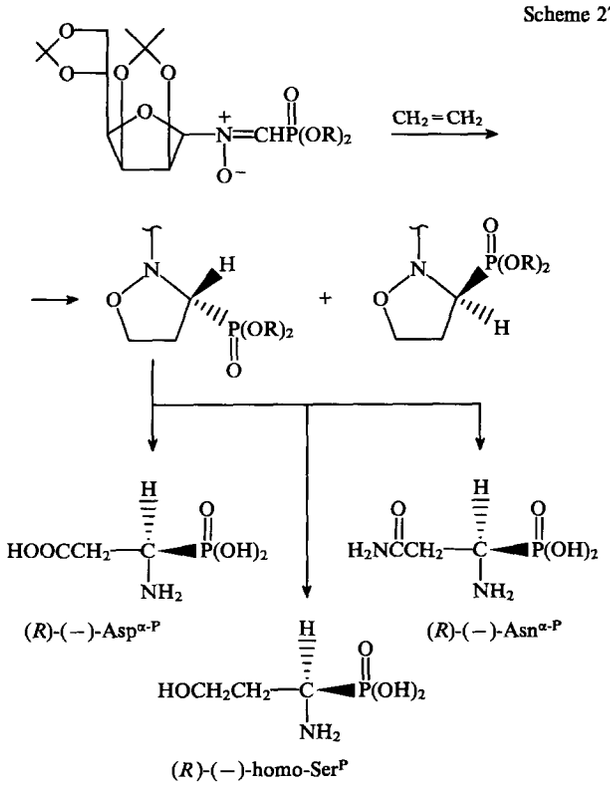
Scheme 26



N-Glycosyl-*C*-dialkoxyphosphonylnitrones based on α-D-mannofuranose combine with ethylene, forming diastereoselective cyclic adducts (yield 80%–85%) in proportions of 3 : 1, diastereoisomers with the configuration of the aminoalkylphosphonate fragment corresponding to that of natural L-aminoacids being formed preferentially. After the chromatographic separation, the dominant diastereoisomers were converted in high yields[83] into (*R*)-(–)-phosphonic analogues of homoserine, aspartic acid, and asparagine (Scheme 27).

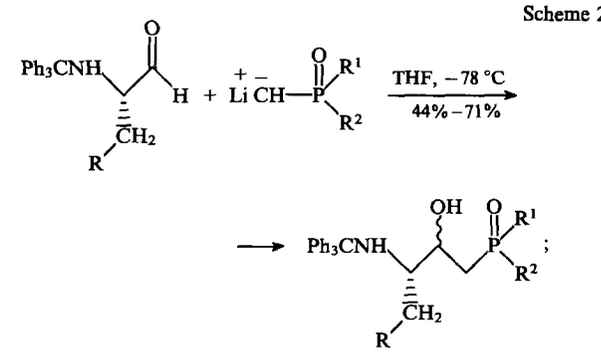
Phosphonic acid analogues of statine—an unusual natural carboxylic γ-amino-β-hydroxy-acid with two chiral centres [4-(*S*)-amino-3-(*S*)-hydroxy-6-methylheptanoic acid], forming part of the natural peptide pepstatin,[84] have been synthesised by

Scheme 27



adding a stabilised anion, generated from the dialkyl ester of methylphosphonic acid by treatment with butyllithium or sodium bis(trimethylsilyl)amide, to enantiomeric α-(*N*-trimethylamino)-aldehydes obtained from the corresponding *L*-aminoacids.[85] It was found that the diastereoselectivity of the addition depends only slightly on the nature of this group in the initial amino-aldehyde and on the ester groups in the phosphonate anion: the ratio of the (2*R*, 3*S*)- and (2*S*, 3*S*)-diastereoisomers formed varies within narrow limits—from 2.3 : 1 to 3.0 : 1 (Scheme 28).

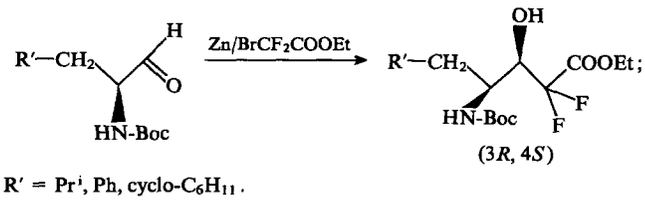
Scheme 28



R = Pr^i, cyclo-C_6H_{11}, Ph; R^1 = R^2 = MeO, BuO; R^1R^2 = $O(CH_2)_3O$.

The possibility of introducing the esters of bromodifluoroacetic acid into the Reformatskii reaction[86] has been used in the asymmetric synthesis of 2,2-difluoro-substituted analogues of statine (Scheme 29).

Scheme 29



R' = Pr^i, Ph, cyclo-C_6H_{11}.

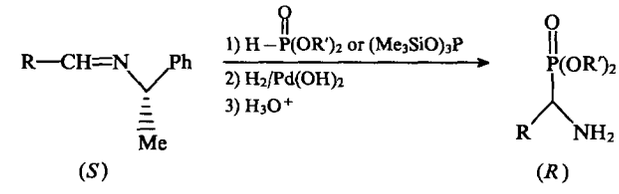
Two methods have been proposed for the condensation of *N-tert*-butoxycarbonyl-(*S*)-leucinal with bromodifluoroacetic ester in the presence of activated zinc.[87–91] Refluxing of the reagents in tetrahydrofuran (THF) affords a mixture of the (3*R*, 4*S*)- and (3*S*, 4*R*)-diastereoisomers in proportions of ~9 : 1, which is associated with the partial racemisation of the initial (*S*)-leucinal on heating. Milder condensation conditions at low temperatures under the influence of ultrasound lead to a 7 : 3 mixture of the (3*R*, 4*S*)- and (3*S*, 4*R*)-diastereoisomers. Almost the same stereochemical result was obtained on using the (*S*)-enantiomers of α-aminoaldehydes containing the phenyl or cyclohexyl group instead of the isopropyl group.

III. Enantioselective formation of the C–P bond

The nucleophilic addition of hydrophosphoryl compounds with a carbon–nitrogen double bond has been used extremely widely for the asymmetric synthesis of phosphonic α-aminoacids. This approach was used for the first time more than twenty years ago, and, although the optical yield of the aminoacids in these syntheses is as a rule not very high, the method still continues to attract the attention of investigators in view of its simplicity and accessibility.

In the first syntheses of this type,[92–95] the Schiff bases derived from α-phenylethylamine enantiomers were used as the chiral inducing agent. The addition of acid phosphites to the corresponding aldimines under the conditions of acid catalysis (organic and inorganic acids, Lewis acids) takes place with a fairly high diastereoselectivity only in the case of bulky substituents in the aldehyde fragment in the initial aldimine (R = Ph, Pr^i; up to 80% d.e.) and decreases on passing to small aliphatic substituents (R = Me, Et) (Scheme 30). The attempts to increase the stereoselectivity of the addition by increasing the bulk of the substituent in the second reactant (the phosphite), by employing tris-(trimethylsilyl) phosphate, did not produce the desired result.[95]

Scheme 30



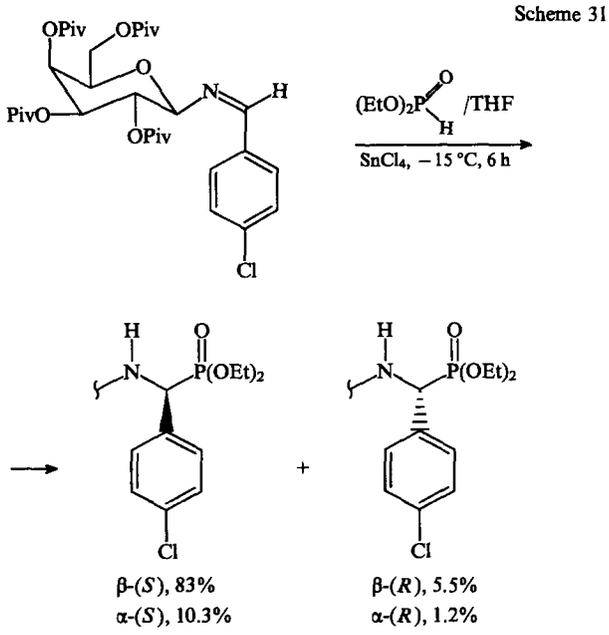
R = Me, Et, Pr^i, Ph.

A satisfactory result, within the framework of this method, has been obtained using Schiff bases obtained from aldehydes and pivaloylated glycosylamines (Scheme 31).

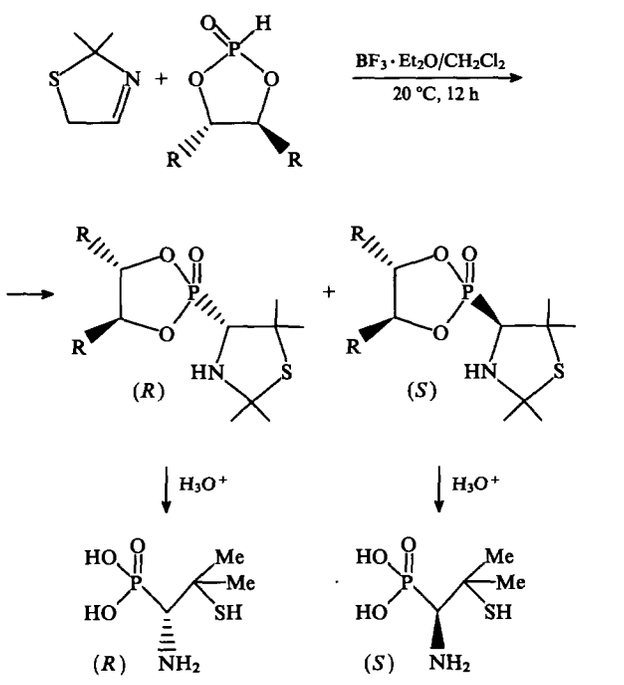
The nucleophilic addition of the acid phosphite in the reaction catalysed by $SnCl_4$ proceeds with high chemical and optical yields, affording as the main product (*S*)-amino-substituted phosphonates when β-D-galactosylimine (shown in Scheme 31) is used and (*R*)-amino-substituted phosphonates when α-D-arabino-pyranosylimine is used.[96] The resolution of the optical isomers is complicated in this case by the α,β-anomerisation of the products, but it can be achieved effectively by a combination of crystallisation and chromatographic methods.

In the syntheses of this type, the chiral inducing group can also be located at the phosphorus atom (nucleophilic diastereoselective addition of the chiral phosphite to the achiral azomethine), which has been demonstrated in relation to the synthesis of the enantiomers of the phosphonic analogue of penicillamine,[97] where the diastereoisomers are formed in the first stage in the proportions (*R*) : (*S*) = 2 : 1 (Scheme 32).

Scheme 31



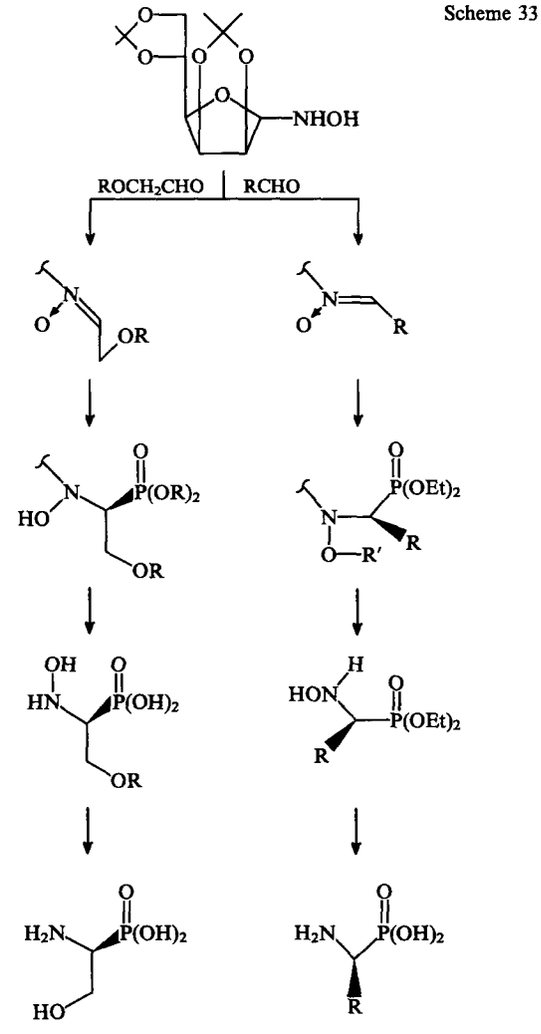
Scheme 32



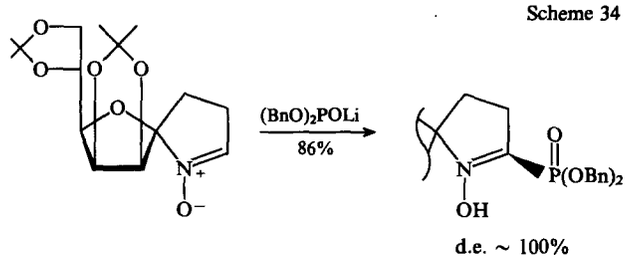
Hydrophosphoryl compounds can be added to, apart from Schiff bases, a series of other compounds with a C=N bond, which has been used for the asymmetric synthesis of α-amino-substituted phosphonic acids. Considerable advances have been achieved by Vasella and coworkers,[98-100] who investigated the reactions involving the addition of phosphites to *N*-α-D-mannofuranosylnitrones (Scheme 33).

This method[98] makes it possible to obtain aminoacids with small alkyl substituents (Ala^P, Val^P) in high optical yields, although the chemical yield does not exceed 50%. The diastereoselectivity of the addition of lithium dialkyl phosphites to *N*-glycosyl-*C*-alkylnitrones is 78%–93%, decreasing appreciably when potassium dialkyl phosphites are used.[98] We may note that 100% diastereoselectivity is observed in addition of lithium dibenzyl phosphite to *N*-glycosylspironitrone (Scheme 34).[100]

Scheme 33



Scheme 34



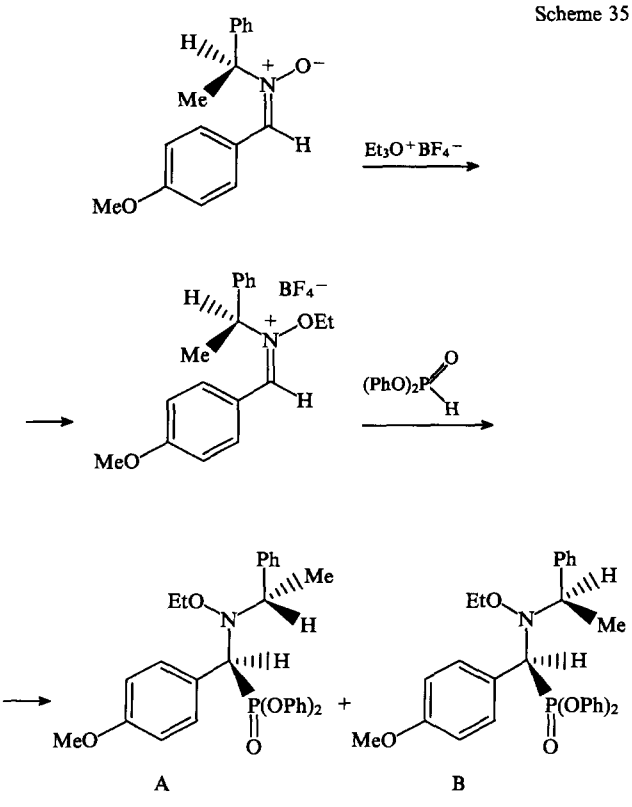
d.e. ~ 100%

The synthetic possibilities of the method are not limited to the synthesis of α-aminoalkylphosphonic acids. One of the advantages of the method is the possibility of isolating optically active *N*-hydroxy-α-aminoalkylphosphonic acids which cannot be obtained by other methods. In addition, the use of the corresponding aldehydes with protected functional groups makes it possible to obtain β-hydroxy-α-aminoalkylphosphonic acids (Ser^P) and γ-alkylthio-α-aminoalkylphosphonic acids (Met^P).[99]

It has been found that *N*-glycosyl-*C*-arylnitrones do not interact with the anions of dialkyl phosphites but do readily combine with tris(trimethylsilyl)phosphite in the presence of Lewis acids ($ZnCl_2$, $HClO_4$) with a diastereoselectivity of 79%–93%, which has been used to obtain optically active phosphonic analogues of phenylglycine.[99] The interesting inversion of the absolute configuration of the α-aminoalkylphosphonate on changing the relative amount of the catalyst present ($ZnCl_2$) is noteworthy. This made it possible to obtain both enantiomers of the phosphonic analogue of phenylglycine using the same reagents.

After *O*-ethylation, the nitrone with the chiral α-phenylethyl substituent at the nitrogen atom gives rise to an oxoiminium salt,[101] which combines diastereoselectively with diphenyl phosphite to form two diastereoisomers in proportions of 3 : 2. The absolute configurations of the diastereoisomers, which can be resolved by chromatography on an alumina column, were determined, but the authors suggest that the diastereoisomer A should be formed preferentially as a result of the attack on the C = N bond from the *si*-side (Scheme 35).

Scheme 35



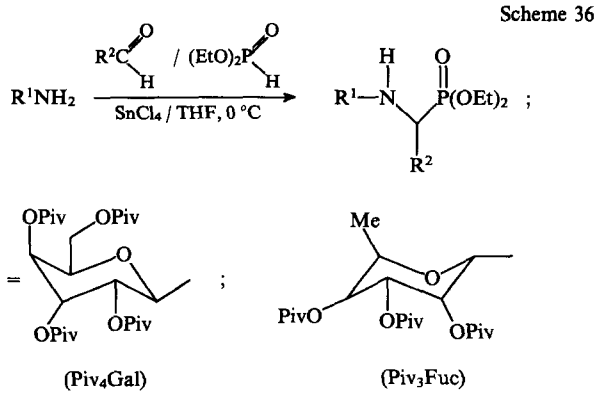
The *N*-acyliminoester obtained from (−)-ω-camphanic acid combines with dialkyl phosphites to form diastereoisomeric adducts from which optically active phosphonic analogues of phenylalanine [(+)- and (−)-Phe^P] were obtained[102] by the reductive elimination of the alkylthio-group and subsequent hydrolysis.

Other methods for the formation of the carbon–phosphorus bond, widely used in the synthesis of racemic α-aminoalkylphosphonic acids,[31] are represented by only isolated examples in the asymmetric synthesis of aminoalkylphosphonates. Thus β-D-galactosylamine and β-L-fucopyranosylamine have been used as the amino components in the Kabachnik – Fields reaction. Asymmetric induction, leading preferentially to (*S*)- and (*R*)-α-aminoalkylphosphonates respectively (from 42 to 96% d.e.), was then observed.[96] The level of this induction was virtually the same as in the addition of acid phosphites to the Schiff bases derived from the corresponding glycosylamines (Scheme 36).

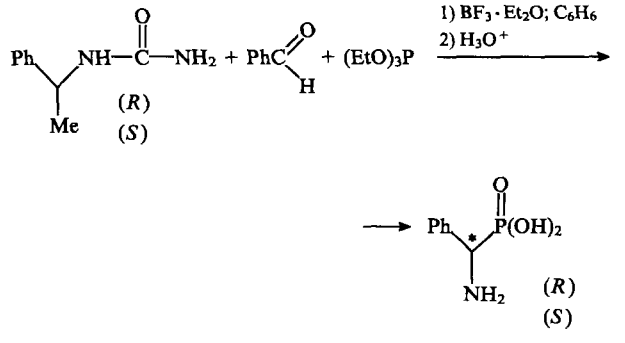
The intereaction of neutral phosphites with aldehydes and ureas or carbamates (a non-classical version of the Arbuzov reaction) has also been used for the asymmetric synthesis of a series of α-aminoalkylphosphonic acids. *N*-Monosubstituted ureas, obtained from (*R*)- and (*S*)-α-phenylethylamine,[103] or carbamates based on (−)-menthol or 1,7,7-trimethylspiro{bicyclo-[2.2.1]heptane-3,2′-indan}-2-ol, obtained from (*R*)-(+)-camphor, were introduced into the reaction (Scheme 37).[104]

The optical purity of the aminoalkylphosphonic acids obtained by this method — the phosphonic analogues of alanine, valine, and phenylglycine, as well as 1-amino-propylphosphonic acid — is low (e.e. = 8.3% – 42.2%), but one should note the inversion of the stereochemical outcome of this reaction relative to the reaction,

Scheme 36



Scheme 37



examined above, involving the addition reaction of acid phosphites with the C = N double bond. Thus, when the urea based on (*R*)-α-phenylethylamine is used, (*R*)-aminoalkylphosphonic acids are formed preferentially, while the addition of acid phosphites to aldimines based on (*S*)-α-phenylethylamine leads to (*S*)-aminoalkylphosphonates.[92, 103]

In the presence of titanium tetrachloride, triethyl phosphite effects the stereoselective opening of the homochiral acetals based on (+)-(2*S*, 4*S*)-pentanediol. The principal diastereoisomers, which are readily separated by column chromatography, were converted by the Swern oxidation into α-hydroxyalkylphosphonates with the (*R*)-configuration (e.e. > 95%), which were converted in their turn into α-azidoalkylphosphonates via reactions which occur with inversion of the configuration of the chiral centre (the Mitsunoba reaction or the reaction of sodium azide with the corresponding methanesulphonate) (Scheme 38).[105]

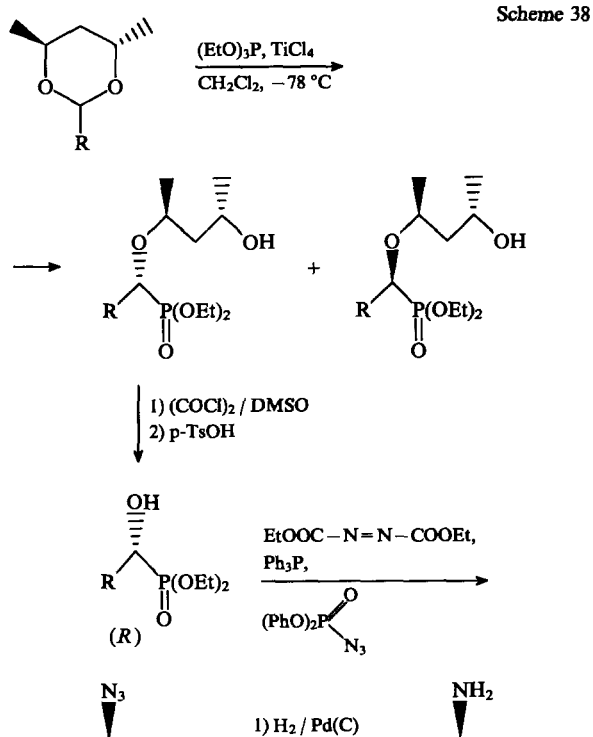
The catalytic hydrogenation of the azides leads to α-aminoalkylphosphonates, the hydrolysis of which afforded (*S*)-α-aminoalkylphosphonic acids (Val^P and Leu^P).

The base-catalysed diastereoselective addition of dimethyl phosphite to the chiral aldehyde obtained from L-phenylalanine leads to the formation of diastereoisomeric β-amino-α-hydroxyalkylphosphonates. Depending on the solvent and base used, the ratio of the *anti*- and *syn*-isomers varies from 1.2 : 1 (DBU/DMF) to 12 : 1 (KF/DMF) (Scheme 39).[106] The *anti*-diastereoisomer was used to synthesise an effective renin inhibitor.

IV. Enantioselective formation of the C–H bond

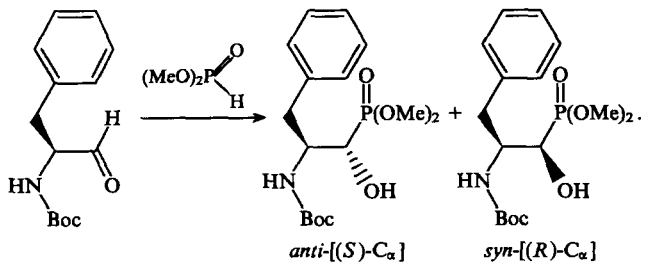
The reduction of the prochiral derivatives of α,β-dehydroaminoacids to the corresponding optically active aminoacids is one of the most vigorously developing fields of asymmetric synthesis. The rigidity of the intermediate complexes between the α,β-dehydroaminoacids and the catalyst is an important factor influencing the enantioselectivity of the reduction. It has been suggested that this factor is the cause of the lower optical yields in the reduction of (*E*)-dehydroaminoacids compared with the (*Z*)-isomers.[107]

Scheme 38



R	Pr^i	Bu^i	$PhCH_2$
d.e. (%)	86	88	82

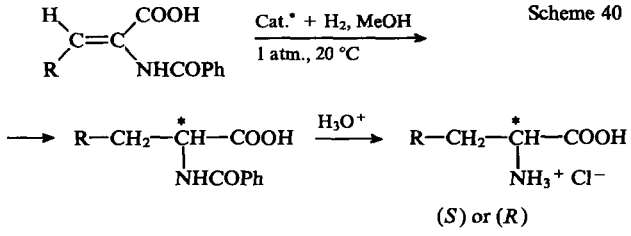
Scheme 39



The wide scale employment of rhodium catalysts is restricted by the necessity to select both the catalyst and the reaction conditions for each new substrate.[50]

In a recently published study,[108] a whole series of rhodium catalysts for the reduction of the corresponding (*Z*)-α-*N*-benzamido-β-(fluorophenyl)acrylic acids or their esters were investigated in order to achieve the asymmetric synthesis of fluorine-substituted phenylalanines. The best result (e.e. ≃ 90%) was obtained using rhodium complexes with PROPRAPHOS and *O*,*N*-bis(diphenylphosphino)-2-*exo*-hydroxy-3-*endo*-methylaminonorbornene as the chiral ligand (Scheme 40).

Scheme 40



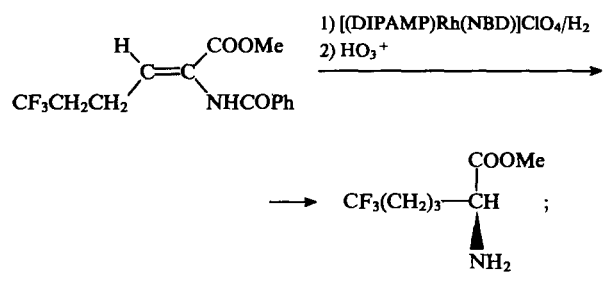
(*S*) or (*R*)

R = 2-FC_6H_4, 3-FC_6H_4, 4-FC_6H_4, 4-$CF_3C_6H_4$, C_6F_5.

It is noteworthy that in the reduction of (*Z*)-α-*N*-benzamido-β-pentafluorophenylacrylic acid a higher optical yield is observed than in the reduction of the monofluoro-substituted analogue under identical conditions.

Methyl (*Z*)-α-*N*-benzamido-β-3,3,3-trifluoropropylacrylate was reduced to the methyl ester of (*S*)-*N*-benzoyl-6,6,6-trifluoronorleucine in the presence of the rhodium complex of (1*R*, 2*R*)-1,2-ethanediylbis[(*o*-anisylphenyl)phosphine] (DIPAMP) with the same optical yield (e.e. = 90%) (Scheme 41).[109, 110]

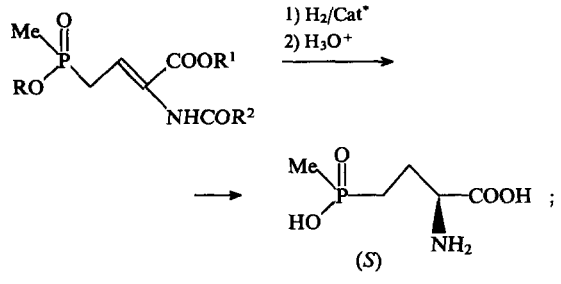
Scheme 41



NBD = *norbornadiene*

The asymmetric synthesis of phosphorus-containing amino-acids using rhodium catalysts was demonstrated in relation to the synthesis of (*S*)-phosphinotricin (Scheme 42).[111]

Scheme 42



Cat* = (*R*, *R*)-NORPHOS, (*S*, *S*)-CHIRAPHOS

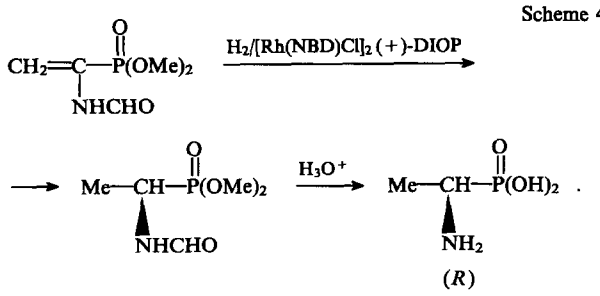
The best optical yield in the reduction stage was obtained using the rhodium complex of (*S*, *S*)-CHIRAPHOS (e.e. 91%).

In the cases examined above, the presence of fluorine or phosphorus atoms in the substituent in the γ-position in the corresponding acrylic acid does not apparently exert a significant influence on the catalytic process. The study of the possibility of using rhodium catalysts in the synthesis of α-aminoalkylphosphonic acids in which the phosphono-group adjoins the C=C double bond and can participate in the formation of the transition complex with the rhodium catalysts has therefore aroused much interest.

Schöllkopf et al.[112] showed that α-(*N*-formamido)vinylphosphonate, obtained by the Horner–Wittig reaction from *N*-formamidomethylenediphosphonate and paraformaldehyde, can be reduced in the presence of the rhodium complex of (+)-2,3-*O*-isopropylidene-2,3-dihydroxy-1,4-bis-(diphenylphosphino)butane [(+)-DIOP], which results in the formation of (*R*)-(−)-α-(*N*-formamido)ethylphosphonate with an enantiomeric excess of 76% (Scheme 43).

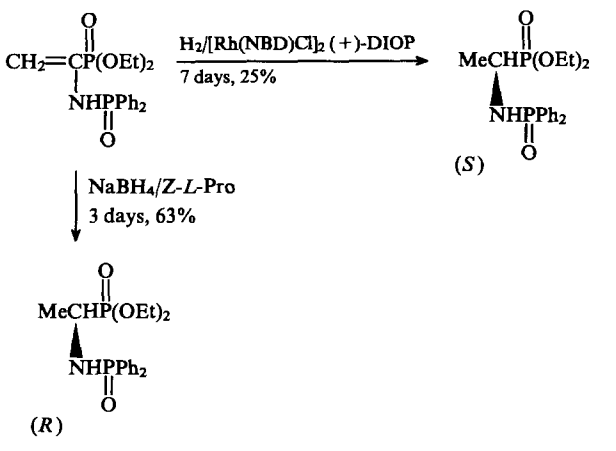
The attempts to use (+)-DIPAMP or (+)-NORPHOS instead of (+)-DIOP as the chiral ligands were unsuccessful—hydrogenation did not take place at the normal pressure. The asymmetric hydrogenation process in the presence of rhodium catalysts depends not only on the chiral ligand employed but also on the structure of the substrate. Thus the reduction of α-(*N*-diphenylphosphinylamino)vinylphosphonate in the presence of the chiral rhodium catalyst based on (+)-DIOP takes place extremely slowly and with a low asymmetric induction [e.e. ~ 3%;

Scheme 43



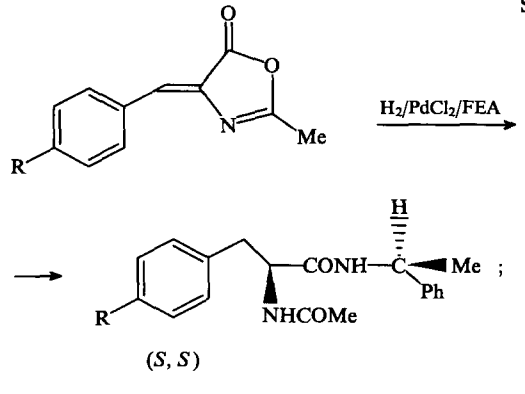
(*S*)-aminoalkylphosphonate predominates]. It is of interest that the reduction of this substrate with sodium tetrahydroborate in the presence of *N*-benzyloxycarbonyl-*L*-proline results in the preferential formation[113] of the (*R*)-aminoalkylphosphonate (e.e. 12%) (Scheme 44).

Scheme 44



The hydrogenation of azlactones in the presence of $PdCl_2$ and added (*S*)-α-phenylethylamine (PEA) (up to 55% d.e.) has been used to synthesise fluoro-derivatives of (*S*)-phenylalanine (Scheme 45).[114, 115]

Scheme 45

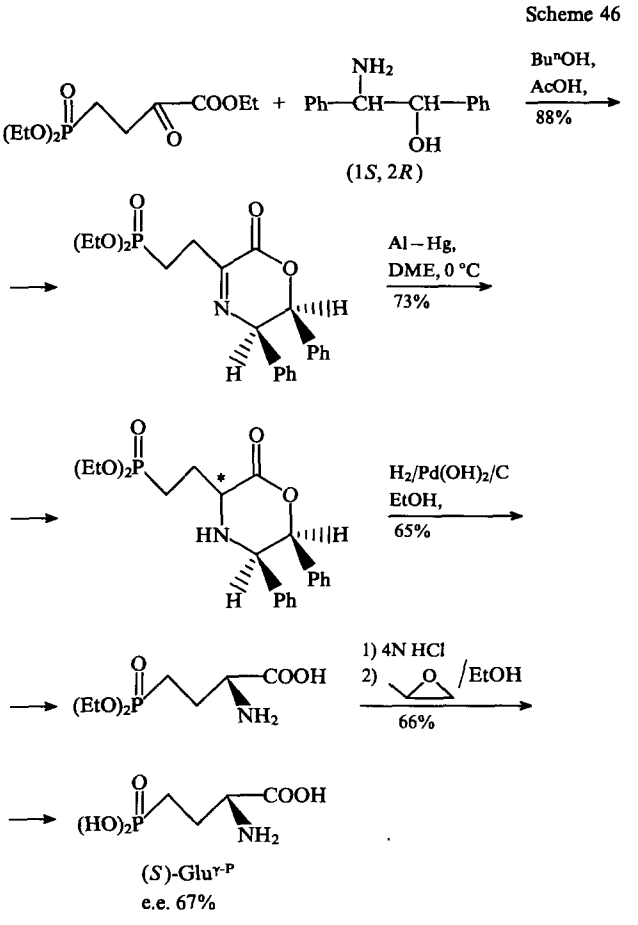


R = F, $OCHF_2$.

The dihydrooxazinone obtained from the ester of a γ-phosphono-α-ketoacid and the optically active (+)-*erythro*-2-hydroxy-1,2-diphenylethylamine, acted upon by aluminium amalgam, undergoes stereoselective reduction with formation of the corresponding tetrahydrooxazinone, which is subsequently converted by a standard procedure into the γ-phosphonic analogue of (*S*)-glutamic acid (e.e. 67%) (Scheme 46).[116]

The hydrogenation of the C=N double bond takes place more effectively in the presence of catalysts such as Raney nickel and platinum or palladium on carbon but under these conditions there is also simultaneous decomposition of the oxazinone ring,

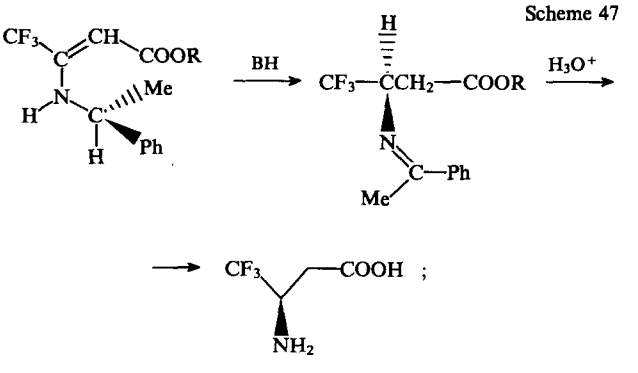
Scheme 46



playing the role of the stereodifferentiating fragment, which results in the formation of the racemic product.

The asymmetric version of the general method of synthesis of α-difluoromethylamines and -aminoacids via the irreversible isomerisation of α-trifluoromethyl-*N*-benzylimines[117] has been proposed for the enantioselective synthesis of (*S*)- and (*R*)-β-trifluoromethyl-β-alanine (Scheme 47).

Scheme 47



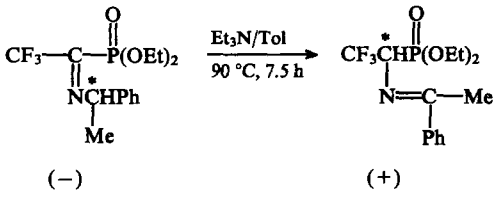
R = Me, Et.

The isomerisation in the above process, the [1,3]-proton shift, takes place on heating in the presence of bases (DBU, DBO) with a moderate enantioselectivity (up to 75% e.e.), which is determined by the preferential proton transfer from the *re*- or *si*-sides of the intermediate [1,3]-azaallyl anion. The catalytic version of this isomerisation [chiral enamine, chiral base (cinchonidine)] has also been examined but the asymmetric outcome of the reaction did not exceed 10% e.e.

N-(α-phenylethyl)trifluoroacetimidoylphosphonate, obtained from (−)-α-phenylethylamine, also undergoes a [1,3]-H shift on heating in the presence of triethylamine, which proceeds with a

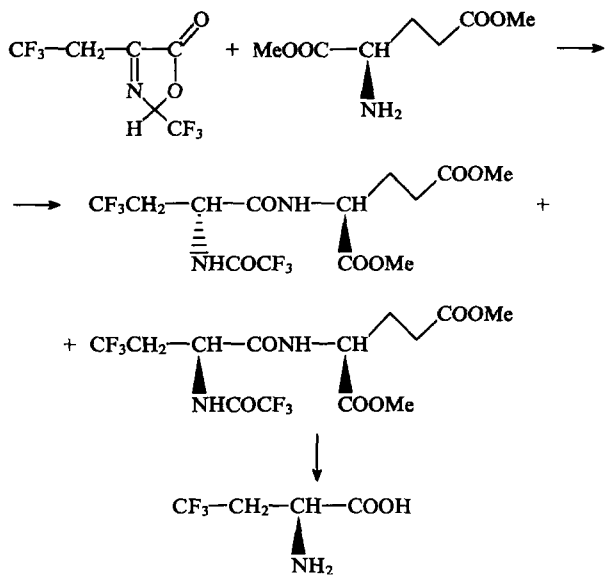
low asymmetric induction (e.e. 22%) and results in the formation of an optically active phosphonic analogue of trifluoroalanine (Scheme 48).[119]

Scheme 48



An asymmetric process has been proposed for the synthesis of the *L*-enantiomer of 4,4,4-trifluoro-2-aminobutyric acid. It consists of the stereoselective opening of the ring in 4-(2,2,2-trifluoroethyl)-2-trifluoromethyl-Δ^3-5-oxazolinone by the dimethyl ester of *L*-glutamic acid, which affords a mixture of diastereoisomeric dipeptides in the proportions (*L*, *L*) : (*D*, *L*) = 83 : 17. Optically pure *L*-4,4,4-trifluoro2-aminobutyric acid has also been obtained after repeated crystallisation of a diastereoisomeric mixture with subsequent elimination of the *L*-glutamic acid residue (Scheme 49).[120]

Scheme 49



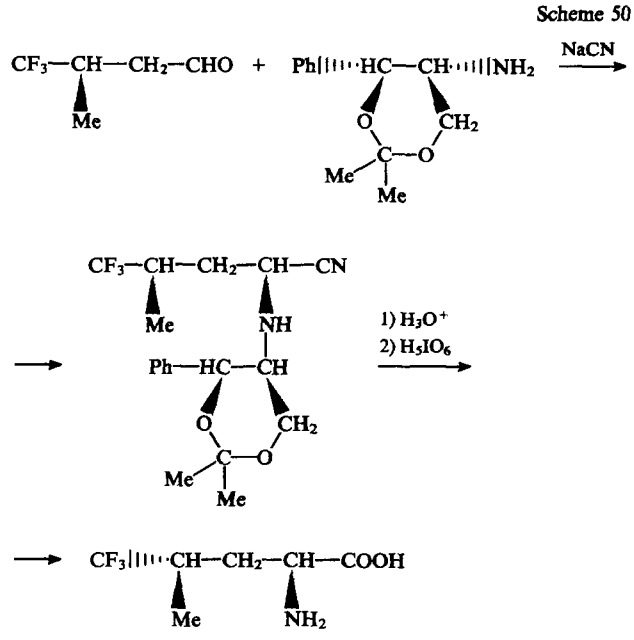
V. Enantioselective formation of the C–N bond

The asymmetric synthesis of (2*S*, 4*R*)-5,5,5-trifluoroleucine from the optically pure (3*R*)-3-trifluoromethylbutanal and (4*S*, 5*S*)-5-amino-2,2-dimethyl-4-phenyl-1,3-dioxane was carried out by the strecker reaction.[121] The reaction takes place with a moderate diastereoselectivity (d.e. 60%), affording the target aminoacid with the α-(*S*)-configuration of the chiral carbon atom (Scheme 50).

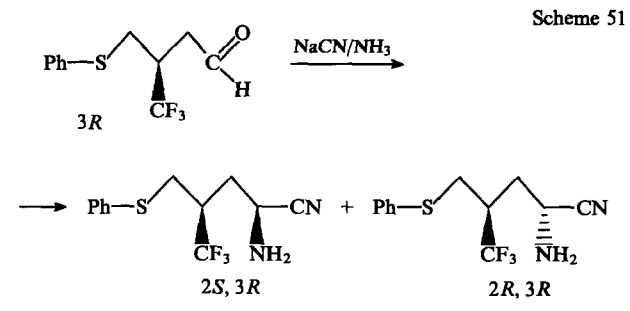
The asymmetric induction is apparently determined in this instance by the stereochemical structure of the substituent at the nitrogen atom, while the chiral centre in the aldehyde fragment has virtually no stereodifferentiating effect. Thus the Strecker synthesis using the 4-phenylthio-derivative of (3*R*)-3-trifluoromethylbutanal affords a mixture of the corresponding diastereoisomeric aminonitriles in proportions of ~1 : 1, from which the optically pure (2*R*, 3*R*)- and (2*R*, 3*S*)-5,5,5-trifluoroleucines were obtained after resolution, the hydrolysis of the nitrile group, and desulphurisation (Scheme 51).[122]

The use of ω-formylalkylphosphonates and (*S*)-α-phenylethylamine in the Strecker synthesis makes it possible to achieve the asymmetric synthesis of the (*S*)-enantiomers of the ω-phosphonic

Scheme 50

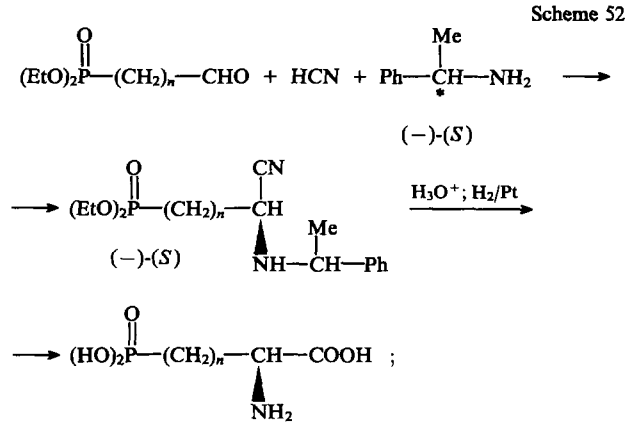


Scheme 51



analogues of aspartic and glutamic acid with e.e. up to 50% (Scheme 52).[123]

Scheme 52

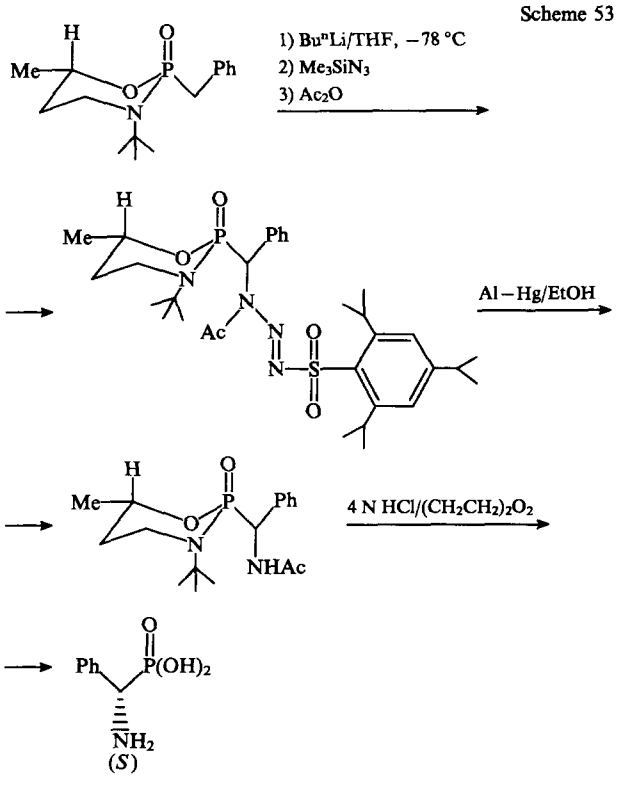


n = 1, 2.

The asymmetric electrophilic amination of stabilised phosphorus-containing carbanions, developed recently by Denmark, is a promising aspect of the asymmetric synthesis of α-aminoalkylphosphonic acids. The electrophilic amination of a series of chiral oxazaphosphorinanes and oxaphospholidines, obtained from the dichlorides of alkylphosphonic acids and the corresponding chiral 1,3- or 1,2-aminoalcohols has been investigated.[124] Trimethylsilyl azide was used as the aminating agent. It was established that the stereochemical outcome of the reaction depends on the structure of the stereodifferentiating aminoalcohol fragment, the nature of the *P*-alkyl substituent,

and the choice of the amination method and it has been shown that under optimum conditions it is possible to achieve an extremely high level of asymmetric induction. This was demonstrated in relation to the synthesis of the (*S*)-enantiomer of the phosphonic analogue of phenylglycine with an optical purity of 92% in accordance with Scheme 53.

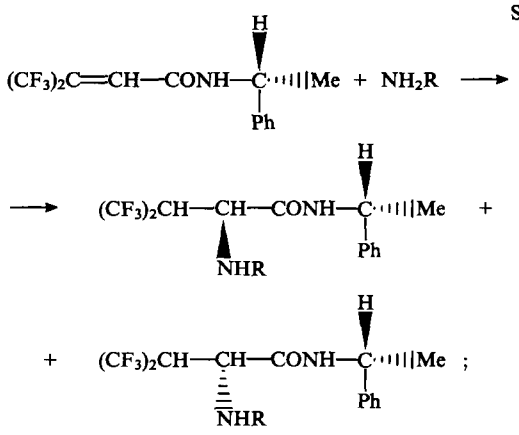
Scheme 53



When the *P*-benzyl substituent in the oxazaphoshorinane was replaced by the ethyl substituent or the 2-phenylethyl group, an appreciable decrease in the stereoselectivity of the amination was observed.

A simpler but much less effective method of asymmetric amination has been investigated by Solodin and coworkers[125, 126] in order to synthesise optically active hexafluorovaline (Scheme 54).

Scheme 54

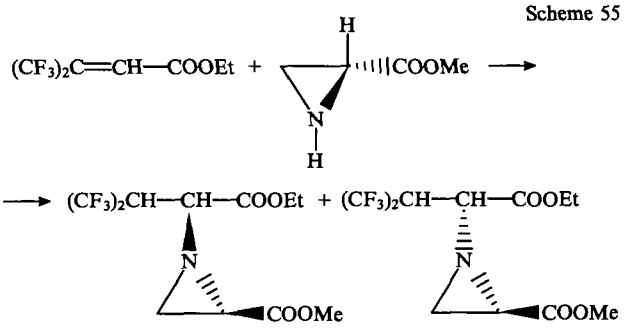


R = H, CH_2Ph.

It has been stated[125] that the addition of ammonia or benzylamine to the chiral *N*-phenylethylamide of 3,3-bis-(trifluoromethyl)acrylic acid leads to the formation of the corresponding hexafluorovaline derivatives with 20% – 41% d.e. However, neither the nature of the asymmetric induction nor the fact that the diastereoisomer is formed in excess were discussed.

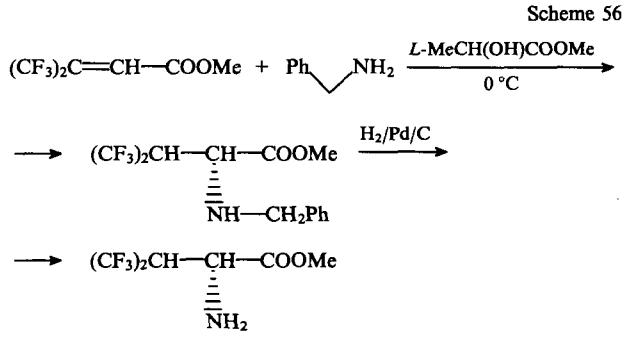
The asymmetric synthesis of hexafluorovaline derivatives can be achieved also by the addition of the chiral esters of (*S*)- or (*R*)-aziridine-2-carboxylic acids to ethyl 3,3-bis(trifluoromethyl)-acrylate. The stereochemical aspects of the addition were not discussed (Scheme 55).[126]

Scheme 55



The addition of benzylamine to methyl 3,3-bis(trifluoro-methyl)acrylate in a chiral medium (solution in *L*-methyl lactate) made it possible to obtain the methyl ester of (*R*)-hexafluoro-valine with a low optical purity (9.2%) (Scheme 56).[125]

Scheme 56



VI. Asymmetric synthesis with the use of enzymes

One of the promising methods of the industrial production of the *L*-enantiomers of proteinogenic aminoacids is their enzymic synthesis.[127] The enantiomeric purity of the aminoacids obtained approaches 100%. Salt suspensions in the culture liquid, disrupted cells, or the purified enzymes in a free state can be used as the source of enzymes effecting the asymmetric synthesis. The economy and simplicity of the method ensure a lower, compared with the chemical asymmetric synthesis, cost of the aminoacids obtained. This field is developing particularly vigorously at the present time in Japan.

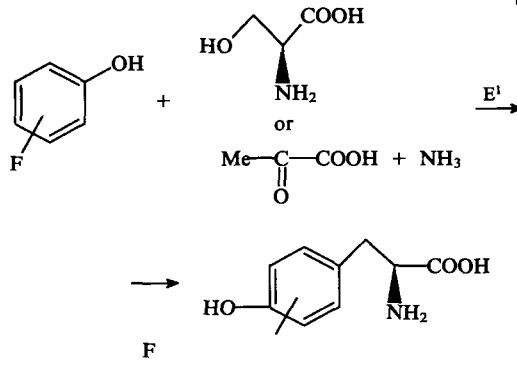
The possibility of obtaining element-containing aminoacids by enzymic synthesis arises from the fact that the majority of the enzymes used in this method have a fairly broad substrate specificity.

Thus β-tyrosinase (E^1), used successfully for the synthesis of various halogen-containing (Cl, Br) tyrosine analogues, was also employed to obtain (*S*)-2-fluoro- and (*S*)-3-fluoro-tyrosines in 75 and 50% yields respectively (Scheme 57).[128–133]

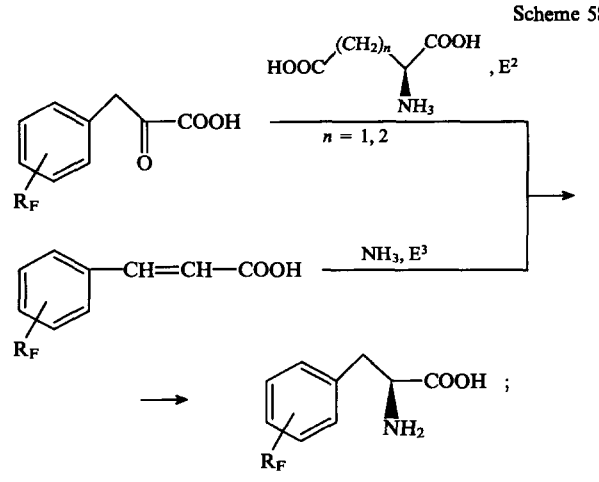
Fluorophenols and (*S*)-serine or a mixture of pyruvic acid and ammonia are used as starting compounds in the synthesis.

β-Phenylpyruvic acid with fluorine atoms or the trifluoro-methyl group in the benzene ring can be converted into the corresponding fluorine-substituted (*S*)-phenylalanines with a chemical yield up to 90% using the transaminase (E^2) from *Alcaligenes falcalis* and aspartic or glutamic acid as the donor of the amino-group (Scheme 58).[14, 132, 134]

Scheme 57



Scheme 58



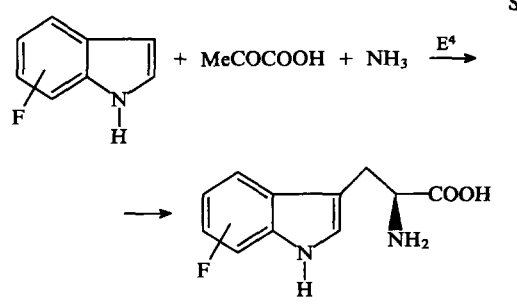
R_F = F, F_5, CF_3.

The rate of the enzymic transamination of phenylpyruvic acid depends on the nature of the substituents in the benzene ring and decreases appreciably on passing from the monofluoro- to the pentafluoro-, and trifluoro-methyl derivatives.

Phenylalanine ammonium lyase (E^3), can also be used for the synthesis of fluorophenylalanines, but this enzyme is more substrate-specific than the transaminase and cannot be employed for the synthesis of trifluoromethylphenylalanines.[14]

All the isomeric (*S*)-4-, (*S*)-5-, (*S*)-6-, and (*S*)-7-fluoroindoles as well as the (*S*)-5,7-di- and (*S*)-trifluoroindoles can also be obtained with an optical yield up to 90% from the corresponding fluoroindoles, pyruvic acid, and ammonia in the presence of tryptophanase (E^4) (Scheme 59).[14, 135]

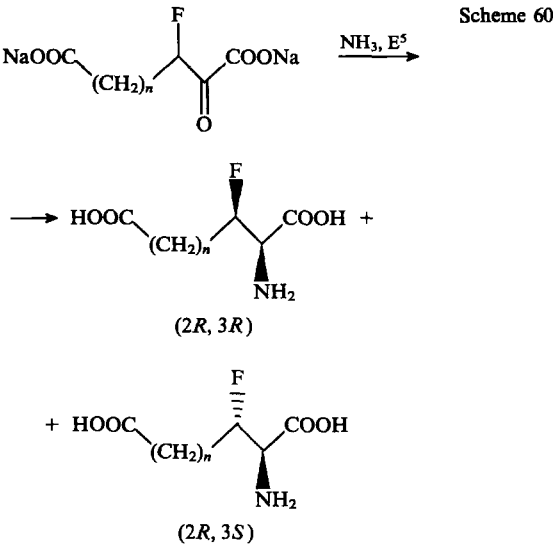
Scheme 59



The methods examined have also been used to synthesise ^{13}N- and ^{11}C-labelled aromatic fluoro-derivatives of amino-acids.[133, 135]

Optically pure (2*R*, 3*R*)- and (2*R*, 3*S*)-3-fluoroglutamic acids have been synthesised effectively from (*R*, *S*)-3-fluoro-2-oxo-glutaric acid under the influence of glutamate dehydrogenase (E^5) (Scheme 60).[136, 137]

Scheme 60



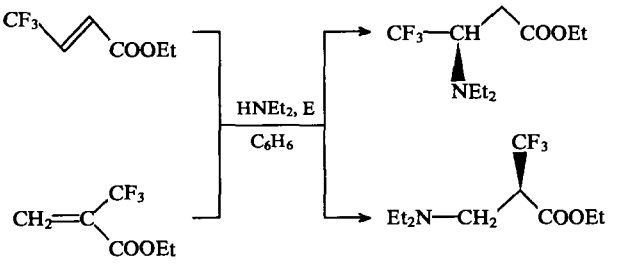
n = 0, 1.

The (2*R*, 3*R*)- and (2*R*, 3*S*)-diastereoisomers are formed in almost identical chemical and stereochemical yields (e.e. 97 and 98% respectively), which indicates the absence of any kind of stereodifferentiating effect on the fluorine atom in the initial racemate of 3-fluoro-2-oxoglutaric acid.

The racemate of 3-fluoro-2-oxosuccinic acid was converted by similar procedure in the presence of aspartate dehydrogenase into a mixture of the diastereoisomeric (2*R*, 3*R*)- and (2*R*, 3*S*)-3-fluoroaspartic acids, isolated in an optically pure form by ion exchange chromatography.[138]

Yet another example of the use of enzymes in the asymmetric synthesis of fluorine-containing aminoacids is the Michael addition of diethylamine in benzene to esters of trifluoromethylacrylic acids catalysed by lipases, amidases, or esterases.[139] The enantiomeric purity of the (−)-β-diethylamino-derivatives of aminoacids obtained in the reaction catalysed by the lipase MY from *Candida cylindracea* approaches 40%, but the absolute configuration of the aminoacid was not discussed (Scheme 61).[13]

Scheme 61



	Yield (%)	e.e. (%)
Lipase MY	47	37
α-Chymotrypsin	36	19
Esterase (from pig liver)	41	8

* *
*

As can be seen from the foregoing, the asymmetric synthesis of element-containing analogues of carboxylic aminoacids has passed through the foundation stage and is now in the dynamic development stage. Both traditional methods of synthesis of aminoacids (for example the alkylation of glycine synthons or the hydrogenation of α,β-dehydroaminoacids) as well as specific approaches associated with the characteristic features of the

chemistry of the corresponding elements are used for the asymmetric synthesis of element-containing aminoacid analogues. The latter appraoches are particularly valid in relation to phosphonic analogues of aminoacids, for the synthesis of which special methods of the chemistry of organophosphorus compounds have been used — the addition of hydrophosphoryl compounds to azomethines and aldehydes and the Arbuzov and Kabachnik–Fields reactions. The development of the methods of asymmetric synthesis has led to the availability of a wide range of optically active fluorine- and phosphorus-containing aminoacid analogues. On the other hand, by no means all the problems associated with the synthesis of specific enantiomerically pure element-containing aminoacid analogues with a high optical purity have found optimum solutions within the framework of the existing methods, which means that further development of the methods of asymmetric synthesis is required.

It may be expected that further research in the field of the asymmetric synthesis of element-containing aminoacid analogues will be directed primarily to the search for new highly effective chiral reagents and to the development of catalytic methods for the asymmetric synthesis of the of these compounds. There is no doubt that the use of enzymes also constitutes a promising approach to the synthesis of enantiomerically pure element-containing aminoacid analogues.

References

1. D Seebach *Angew. Chem.* **29** 1320 (1990)
2. K E Kassuhlke, D J Faulkner *Tetrahedron* **47** 1809 (1991)
3. S Hunt, in *Chemistry and Biochemistry of Amino Acids* (Ed. G C Barret) (London: Chapman and Hall, 1985) p. 55
4. M Sanada, T Mijano, S Iwadare *J. Antibiot.* **39** 259 (1986)
5. M Horiguchi, M Kandatsu *Nature* **184** 901 (1959)
6. E Bayer, K H Gugel, H Hagele, H Hagenmaier, S Jessipow, W A Konig, H Zahnor *Helv. Chim. Acta* **55** 224 (1972)
7. M Sieler, M J Jung, J Koch-Waser, in *Enzyme-activated Irreversible Inhibitors* (Amsterdam: Elsevier, 1978) p. 396
8. C Walsh *Tetrahedron* **38** 871 (1982)
9. J Kollonitsch *Isr. J. Chem.* **17** 53 (1978)
10. J Kollonitsch, in *Biomedicinal Aspects of Fluorine Chemistry* (Eds R Filler et al.) (Amsterdam: Kodansha/Elsevier Biomedical, 1982) p. 93
11. Y Kobayashi, I Kumadaki, T Taguchi, in *Progress in the Technology of Fluorine Compounds* (Ed. N Ishikawa) (Translated into Russian), (Moscow: Mir, 1984) p. 526
12. J T Welch *Tetrahedron* **43** 3123 (1987)
13. M J Jung *Bioorg. Chem.* **14** 429 (1986)
14. N Ishikawa, in *Fluorine Compounds. Synthesis and Applications* (Translated into Russian) (Moscow: Mir, 1990) p. 307
15. J T Gorig, in *Biomedicinal Aspects of Fluorine Chemistry* (Ed. R Filler et al.) (Amsterdam: Kodansha/Elsevier Biomedical, 1982) p. 163
16. E S Garnett, G Firnau, C Nahmias *Nature* **305** 137 (1983)
17. D F Loncrini, R Filler *Adv. Fluorine Chem.* **6** 43 (1970)
18. F Weygand, W Oettmeier *Usp. Khim.* **39** 622 (1970) [*Russ. Chem. Rev.* **39** 290 (1970)]
19. V P Kukhar', V A Soloshonok *Usp. Khim.* **60** 1680 (1991) [*Russ. Chem. Rev.* **60** 850 (1991)]
20. V P Kukhar', Yu L Yagupol'skii, V A Soloshonok *Usp. Khim.* **59** 149 (1990) [*Russ. Chem. Rev.* **59** 89 (1990)]
21. J T Welch, S Eswarakrishnan *Flourine in Bioorganic Chemistry* (New York: Wiley, 1991)
22. M R Kilbourn *Fluorine-18 Labelling of Radiopharmaceuticals* (Washington DC: National Academy Press, 1990) p. 95
23. V P Kukhar', Yu L Yagupol'skii, I I Gerus, M G Kolycheva *Usp. Khim.* **60** 2047 (1991) [*Russ. Chem. Rev.* **60** 1050 (1991)]
24. P Bravo, G Resnati *Tetrahedron: Asymmetry* **1** 661 (1990)
25. K Yamauchi *Nippon Nogei Kagaku Kaishi* **65** 1508 (1991); *Chem. Abstr.* **116** 17 236t (1991)
26. A N Pudovik, I V Gur'yanova, E A Ishmaeva, in *Reaktsii i Metody Issledovaniya Organicheskikh Soedinenii* (Reactions and Methods for the Investigation of Organic Compounds) (Moscow: Khimiya, 1968) Vol. 19.
27. K A Petrov, V A Chauzov, T E Erokhina, in *Reaktsii i Metody Issledovaniya Organicheskikh Soedinenii* (Reactions and Methods for the Investigation of Organic Compounds) (Moscow: Khimiya, 1974) Vol. 43, p. 2045
28. D Redmore, in *Topics in Phosphorus Chemistry* Vol. 8 (Eds M Grayson and E J Griffith) (New York: Wiley, 1976) p. 515
29. K Prajer, J Rachson *Z. Chem.* **15** 209 (1975)
30. L Maier *Phosphorus Sulfur* **14** 295 (1983)
31. V P Kukhar', V A Solodenko *Usp. Khim.* **56** 1504 (1987) [*Russ. Chem. Rev.* **54** 859 (1987)]
32. R L Hildebrand, J Gurley-Joseph, H J Lubansky, in *Topics in Phosphorus Chemistry* Vol. 11 (Eds M Grayson, E J Griffith) (New York: Wiley, 1983) p. 297
33. V L Ryzhkov, M I Kabachnik, L M Tarasevich, T Ya Medved', N A Zeitlenok, M K Marchenko, V A Vagzhanova, E F Ulanova, N V Cheburkina *Dokl. Akad. Nauk SSSR* **98** 849 (1954)
34. E K Baylis, C D Campbell, J G Dingwall *J. Chem. Soc., Perkin Trans. 1* 2845 (1984)
35. V P Kukhar', N M Solodenko, V A Solodenko *Ukr. Biokhim. Zh.* **60** 95 (1988)
36. B Spielvogel, A Mephail, Report 1987, ARO-20852.10-CH, Order No. AD-A184838; *Chem. Abstr.* **110** 212 884t (1989); from *Gov. Rep. Announce. Index (U.S.)* **88** (2) 803 800 (1988)
37. N Esaki, H Tanaka, K Soda *Chem. Abstr.* **110** 2 132 862 (1989); *Kagaku Zokan (Kyoto)* **115** 205 (1988)
38. J D Morrison, H S Mosher *Asymmetric Organic Reactions* (Translated into Russian) (Moscow: Mir, 1973)
39. N K Kochetkov (Ed.) *Obshchaya Organicheskaya Khimiya* (General Organic Chemistry) (Moscow: Khimiya, 1982) Vol. 3 p. 476
40. J M McIntosh, R K Leavitt, P Mishra, K C Cassidy, J E Drake, R Chadha *J. Org. Chem.* **53** 1947 (1988)
41. U Schöllkopf, R Schutze *J. Liebigs Ann. Chem.* 45 (1987)
42. U Groth, L Richter, U Sch *Tetrahedron* **48** 117 (1992)
43. M Ferrary, G Jommi, G Miglierini, R Pagliarin, M Sisti *Synth. Commun.* **22** 107 (1992)
44. R Jacquier, F Ouazzani, M-L Roumestant, Ph Viallefont *Phosphorus Sulfur* **36** 73 (1988)
45. S K Cho, Y J Kim *Taehan Hwahakh Chi* **33** 257 (1989); *Chem. Inform.* **35** 145 (1989)
46. F Ouazzani, M-L Roumestant, Ph Viallefont, A E Mallaoui *Tetrahedron: Asymmetry* **2** 913 (1991)
47. B McCleery *J. Chem. Soc., Perkin Trans. 1* 1319 (1989)
48. N Minowa, M Hirayama, S Fukatsu *Tetrahedron Lett.* **25** 1147 (1984)
49. M Kolb, J Barth *Tetrahedron Lett.* **20** 2999 (1979)
50. K A Kochetkov, V M Belikov *Usp. Khim.* **56** 1832 (1987) [*Russ. Chem. Rev.* **56** 1045 (1987)]
51. D Seebach, M Boes, R Naef, B Schweizer *J. Am. Chem. Soc.* **105** 5390 (1983)
52. U Schöllkopf *Pure Appl. Chem.* **55** 1799 (1983)
53. Yu N Belokon', V I Bakhmutov, N I Chernoglazova, K A Kochetkov, S V Vitt, N S Garbalinskaya, V M Belikov *J. Chem. Soc., Perkin Trans. 1* 305 (1988)
54. R Futzi, D Seebach *Tetrahedron* **44** 5277 (1988)
55. D Seebach *Liebigs Ann. Chem.* 1215 (1989)
56. BDR P 334 855 p. 9029 (1986)
57. D Blaser, D Seebach *Liebigs Ann. Chem.* 1067 (1991)
58. D Seebach, E Juaristi, D D Miller, Ch Schickli, Th Weber *Helv. Chim. Acta* **70** 237 (1987)
59. U Schöllkopf, U Busse, R Lonsky, R Hinrichs *Liebigs Ann. Chem.* 2150 (1986)
60. H-J Zeiss *Tetrahedron Lett.* **28** 1255 (1987)
61. M Cushman, E-S Lee *Tetrahedron Lett.* **33** 1193 (1992)
62. P L Ornstein *J. Org. Chem.* **54** 2251 (1989)
63. R H Evans, A A Fransis, A W Jones, D A S Smith, J C Watkins *Br. J. Pharmacol.* **75** 65 (1982)
64. V A Soloshonok, Yu N Belokon', V P Kukhar', N I Chernoglazova, M B Saporovskaya, V I Bakhmutov, M T Kolicheva, V M Belikov *Izv. Akad. Nauk SSSR, Ser. Khim.* 1630 (1990)

65. V P Kukhar', Yu N Belokon', V A Soloshonok, N Yu Svistunova, A B Rozhenko, N A Kuz'mina *Synthesis* 117 (1993)
66. V A Soloshonok, N Yu Svistunova, V P Kukhar', V A Solodenko, N A Kuz'mina, A B Rozhenko, S V Galushko, I P Shishkina, A O Gudima, Yu N Belokon' *Izv. Akad. Nauk SSSR, Ser. Khim.* 397 (1992)
67. V A Soloshonok, Yu N Belokon', N A Kuz'mina, V I Maleev, N Yu Svistunova, V A Solodenko, V P Kukhar' *J. Chem. Soc., Perkin Trans. 1* 1525 (1992)
68. Yu N Belokon', A G Bulychev, S V Vitt, Yu T Struchkov, A S Batsanov, T V Timofeeva, V A Tsyryapkin, M G Rizhov, L A Lysova, V I Bakhmutov, V M Belikov *J. Am. Chem. Soc.* **107** 4252 (1985)
69. V A Soloshonok, V P Kukhar', S V Galushko, M T Kolycheva, A B Rozhenko, Yu N Belokon' *Izv. Akad. Nauk SSSR, Ser. Khim.* 1166 (1991)
70. V A Soloshonok, V P Kukhar', A S Batsanov, M A Galakhov, Yu N Belokon', Yu T Struchkov *Izv. Akad. Nauk SSSR, Ser. Khim.* 1548 (1991)
71. V A Soloshonok, V P Kukhar', S V Galushko, A B Rozhenko, N A Kuz'mina, Yu N Belokon' *Izv. Akad. Nauk SSSR, Ser. Khim.* 1906 (1991)
72. V A Soloshonok, N Yu Svistunova, V P Kukhar', N A Kuz'mina, Yu N Belokon' *Izv. Akad. Nauk SSSR, Ser. Khim.* 687 (1992)
73. V A Soloshonok, N Yu Svistunova, V P Kukhar', A O Gudima, N A Kuz'mina, Yu N Belokon' *Izv. Akad. Nauk SSSR, Ser. Khim.* 1172 (1992)
74. M Sting, W Steglich *Synthesis* **2** 132 (1990)
75. S Hanessian, J L Bennani *Tetrahedron Lett.* **31** 6465 (1990)
76. S Hanessian, J L Bennani, D Delorme *Tetrahedron Lett.* **31** 6461 (1990)
77. M J O'Donnell, W D Bennett, S Wu *J. Am. Chem.* Soc. **111** 2353 (1989)
78. M J O'Donnell, S Wu *Tetrahedron: Asymmetry* **3** 591 (1992)
79. Y Ito, M Sawamura, T Hayashi *J. Am. Chem. Soc.* **108** 6405 (1986)
80. M Sawamura, Y Ito, T Hayashi *Tetrahedron Lett.* **30** 2247 (1989)
81. A Togni, S D Rastor *Tetrahedron Lett.* **30** 1071 (1989)
82. T Schrader, R Kober, W Steglich *Synthesis* 372 (1986)
83. A Vasella, R Volffray *Helv. Chim. Acta* **65** 1953 (1982)
84. H Umezawa, T Aoyagi, H Morishima, M Matsuzaki, M Hamada, T Takeuchi *J. Antibiot.* **23** 259 (1970); *Chem. Abstr.* **73** 54 423 (1970)
85. J F Dellaria, R G Maki, H H Stein, J Cochon, D Whittorn, K Marsh, D J Hoffman, J J Plattner, Th J Perun *J. Med. Chem.* **33** 534 (1990)
86. E A Halliman, J Fried *Tetrahedron Lett.* **25** 2301 (1984)
87. S Thaisrivong, D T Pals, W M Kati, S R Turner, L M Thomasco *J. Med. Chem.* **28** 1553 (1985)
88. S Thaisrivong, D T Pals, W M Kati, S R Turner, L M Thomasco, W Watt *J. Med. Chem.* **29** 2080 (1986)
89. N P Peet, J P Burkhart, M R Angelastro, E L Giroux, Sh Mendi, Ph Bey, M Kolb, B Neises, D Sohirlin *J. Med. Chem.* **33** 394 (1990)
90. H L Sham, Ch A Rempel, H Stein *J. Chem. Soc., Chem. Commun.* 904 (1990)
91. M H Gelb, J P Svaren, R H Abeles *Biochemistry* **24** 1813 (1985)
92. W F Gilmore, H A McBride *J. Am. Chem. Soc.* **94** 4361 (1972)
93. T Slowiak, W Sawka-Dobrowolska, J Kowalik, P Mastalerz, M Soroka, E Zon, in *Khimiya i Primenenie Fosfororganicheskikh Soedinenii (Tr. VI Konferentsii)* [The Chemistry and Applications of Organophosphorus Compounds (Proceedings of the VIth Conference)] (Kiev: Naukova Dumka, 1981) p. 306
94. T Slowiak, W Sawka-Dobrowolska, J Kowalik, P Mastalerz, M Soroka, E Zon *Tetrahedron Lett.* **18** 3965 (1977)
95. J Zon *Pol. J. Chem.* **55** 643 (1981)
96. S Laschat, H Kunz *Synthesis* 90 (1992)
97. I Hoppe, V Schöllkopf, M Nieger, E Egeret *Agnew. Chem.* **97** 1066 (1985)
98. R Huber, A Knierzinger, J-P Obrecht, A Vasella *Helv. Chim. Acta* **68** 1730 (1985)
99. R Huber, A Vasella *Helv. Chim. Acta.* **70** 1461 (1987)
100. B Bernet, E Krawczyk, A Vasella *Helv. Chim. Acta* **68** 2299 (1985)
101. S Schatzmiller, B-Z Dolitzky, R Meirovich, R Neidlin, Ch Weik *Liebigs Ann. Chem.* 161 (1991)
102. A K Kotynski, W T Stec *J. Chem. Res. (S)* 41 (1978)
103. J W Huber, W F Gilmore *Tetrahedron Lett.* **20** 3049 (1979)
104. T Oshikawa, M Jamashita *Bull. Chem. Soc. Jpn.* **62** 3177 (1989)
105. T Jokomatsu, S Shibuya *Tetrahedron: Asymmetry* **3** 377 (1992)
106. D V Patel, K Rielly-Ganvin, D E Ryono *Tetrahedron Lett.* **31** 5587 (1990)
107. I Ojima, T Kogure, N Yoda *J. Org. Chem.* **45** 4728 (1980)
108. H-W Krause, H-J Kreuzfeld, Ch Dobler, S Taudien *Tetrahedron: Asymmetry* **3** 555 (1992)
109. I Ojima *Actual. Chim.* 171 (1987)
110. I Ojima, K Kato, K Nakahaschi *J. Org. Chem.* **54** 4511 (1989)
111. H-J Zeiss *J. Org. Chem.* **56** 1783 (1991)
112. U Schöllkopf, I Hoppe, A Thiele *Liebigs Ann. Chem.* 555 (1985)
113. B Krzyzanowska, S Pilichowska *Pol. J. Chem.* **62** 165 (1988)
114. L F Godunova, E I Karpeiskaya, E S Levitina, E I Klabunovskii, Yu L Yagupol'skii, M T Kolycheva *Izv. Akad. Nauk SSSR, Ser. Khim.* 1359 (1987)
115. L F Godunova, E S Levitina, E I Karpeiskaya, E I Klabunovskii, Yu L Yagupol'skii, M T Kolycheva *Izv. Akad. Nauk SSSR, Ser. Khim.* 404 (1989)
116. X-Y Jiao, W-J Chen, B-F Hu *Synth. Commun.* **22** 1179 (1991)
117. V A Soloshonok, V P Kukhar', Yu L Yagupol'skii, I I Gerus *Zh. Org. Khim.* **24** 993 (1988)
118. V P Kukhar', V A Soloshonok, S V Galushko, A B Rozhenko *Dokl. Akad. Nauk SSSR* **310** 886 (1990)
119. P P Onys'ko, T V Kim, E I Kiseleva, A D Sinitsa, M Yu Kornilov *Zh. Obshch. Khim.* **60** 1304 (1990)
120. W Steglich, H U Heininger, H D Worschank, F Weygang *Angew. Chem.* 822 (1967)
121. K Weinges, E Kromm *Liebigs Ann. Chem.* 90 (1985)
122. T Taguchi, Y Kobayashi *Tetrahedron Lett.* **27** 5117 (1986)
123. J M Villanueva, N Collignon, A Guy, Ph Savignac *Tetrahedron* **39** 1299 (1983)
124. S E Denmark, N Chatani, S V Pansare *Tetrahedron* **48** 2191 (1992)
125. A V Eremeev, I V Solodin, F D Polyak *Izv. Akad. Nauk Latv. SSR, Ser. Khim.* 345 (1985)
126. I V Solodin, F D Polyak, A V Eremeev, I A Vosekalna, E Liepins, I I Chervin, R G Kostyanovskii *Khim. Geterotsikl. Soedin.* 1355 (1985)
127. I V Tysyachnaya, V I Yakovleva, A K Aren *Prikl. Biokhim. Mikrobiol.* **17** 645 (1981)
128. T Nagasawa, T Utagawa, J Goto *Eur. J. Biochem.* **117** 33 (1981)
129. T E Walker, C Matheny, C B Storm, H Hayden *J. Org. Chem.* **51** 1175 (1986)
130. USSR P. 1 351 974, 1986; *Byul. Izobret.* **42** 89 (1987)
131. V I Lozinsky, N G Faleev, A L Zubov *Biotechnology Lett.* **11** 43 (1989)
132. H Tanaka, K Uchida, M Yamabe *J. Fluorine Chem.* **35** 253 (1987)
133. Jpn. P. 03.151.889; *Chem. Abstr.* **116** 37 534s (1991)
134. Jpn. P. 63.148.991; *Chem. Abstr.* **110** 210 974m (1989)
135. Jpn. P. 03.151.888; *Chem. Abstr.* **116** 37 535t (1991)
136. A Vidal-Cros, M Gaudry, A Marquet *J. Org. Chem.* **50** 3163 (1985)
137. A Vidal-Cros, M Gaudry, A Marquet *J. Org. Chem.* **54** 498 (1989)
138. Y Kobayashi, I K Kumadaki *Kagaku (Chemistry)* **32** 538 (1977)
139. T Kitszume, K Murata *J. Fluorine Chem.* **36** 339 (1987)

Russian Chemical Reviews **62** (3) 279–290 (1993)
© 1993 Russian Academy of Sciences and Turpion Ltd

UDC 541.128 + 541.49 + 547.97

The catalase, peroxidase, and oxidase properties of the coordination compounds of manganese

A Ya Sychev, V G Isac

Contents

I.	Introduction	279
II.	Catalase properties. The mechanisms of the catalytic decompositon of H_2O_2	279
III.	Peroxidase properties. Oxidation of organic substrates	282
IV.	Oxidase properties	284
V.	Manganese compounds as catalysts of processes in the environment	286
VI.	Conclusion	287

Abstract. The experimental data on the oxidation–reduction catalysis by coordination compounds of manganese(II) of reactions involving the decomposition of H_2O_2 and the oxidation of organic substances by hydrogen peroxide and molecular oxygen are surveyed and modern ideas on these topics are described. The bibliography includes 170 references.

I. Introduction

Coordination compounds of transition metals are known to promote the occurrence of many industrially important technological processes under milder conditions than traditional heterogeneous catalysts, sometimes with a much greater activity and selectivity. The role of the active centre also in enzyme-like (analogue) systems designed to effect particular catalytic processes in homogeneous media has been attributed to the coordination compounds of transition metals. The study of the oxidation–reduction catalysis by transition metal compounds has made a definite contribution to the development of the theory of homogeneous catalysis. Homogeneous catalysis by coordination compounds in the liquid phase is a rapidly developing field of physical chemistry.

The interest in the study of the catalase, peroxidase, and oxidase properties of coordination compounds of manganese has been aroused by the presence of the latter in the active centres of manganese-containing catalases[1,2] and also by the discovery of the role of manganese in the oxidation of H_2O_2 to O_2 (in the photosystem II in photosynthesis),[1–5] in the dismutation of the superoxide radical in the living cell,[6,7] and in the catalytic oxidation–reduction reactions of organic substances in the tricarboxylic acid cycle (the Krebs cycle),[8] as well as the unique ability of the manganese ion to undergo relatively readily the change in the oxidation state from +2 to +7.

The coordination compounds of manganese with ligands containing nitrogen, oxygen, and both nitrogen and oxygen are effective catalysts of the decomposition of hydrogen peroxide, the liquid-phase oxidation of various organic compounds by molecular oxygen (synthetic molecular oxygen transferring agents have been obtained on the basis of manganese complexes), and also the oxidation of substrates by periodate and other oxidants, in contrast to the aquo-ions. There are numerous data on the reactivity of manganese complexes in such reactions and on the mechanisms of their catalytic action.[9,10]

All the studies devoted to the catalytic decomposition of hydrogen peroxide and the oxidation of substrates in the presence of manganese compounds can be divided into two large groups: studies of a phenomenological character[11–26] and studies in which the detailed kinetic characteristics of processes under the influence of catalysts were obtained and the mechanism of the corresponding process was established.[9,10,27–60]

From the practical point of view, studies in which the high peroxidase and oxidase activities of manganese complexes were established are of special interest.[10] Such complexes can be used to develop new highly sensitive and selective kinetic methods for the determination of microamounts of Mn^{2+} and also for the synthesis of new compounds. Since manganese complexes are effective catalysts of the oxidation by hydrogen peroxide (and its decomposition) and by oxygen of organic compounds, the investigation of the possibility of using such systems for the purification of waste water (especially from dye industries) is of special interest.

II. Catalase properties. The mechanisms of the catalytic decomposition of H_2O_2

Many transition metal compounds, including a series of coordination compounds of manganese, exhibit catalase activity.[11–60] In some studies, only the presence of catalase activity in particular manganese complexes was stated,[11–26] in others a comparative analysis of their activities was carried out, whilst in a third group attempts were made to elucidate the mechanism of the decomposition of hydrogen peroxide by manganese(II) complexes. At the same time, during the last 20 years a series of novel investigations have been carried out[10,31–60] † in which the

A Ya Sychev, V G Isac Department of Physical Chemistry, Moldavian State University, ul. Mateevicha 60, 277009 Kishinev, Moldova, Fax (7-042-2) 24 06 65

Received 11th November 1992
Uspekhi Khimii **62** (3) 303–315 (1993); translated by A K Grzybowski

† The results of the study of the catalytic properties of manganese aquo-ions permit an unambiguous conclusion: Mn^{2+} aquo-ions have no catalase, peroxidase, and oxidase activity.[10] On the other hand, they exhibit a definite catalytic activity in reactions involving the oxidation of certain substrates by periodate.[50] The Mn^{3+} aquo-ions catalyse the H_2O_2 decomposition reactions[61,62] and reactions involving the oxidation of organic substrates by molecular oxygen,[63–67] but the mechanisms proposed for these processes[61–67] cannot be regarded as being even qualitatively well-founded.

kinetics of the process and the composition and stability of the catalytically active complex were established and the mechanisms of the catalytic decomposition of hydrogen peroxide were justified on the basis of systematic investigations. It has now been established that the coordination compounds of manganese(II) with triethylenetetramine (Trien),[11,26,38] diethylenetriamine (Dien),[39,42] tetraethylenepentamine,[13] α,α′-bipyridyl (Bipy),[11] *o*-phenanthroline (Phen),[1,48,51] 2,2′,2″-terpyridyl,[11] 2- and 3-aminopyridines,[11] 2,9-dimethyl- and 4,7-diphenyl-1,10-phenanthrolines,[11] diethanolamine,[11,36,40] *N,N′,N″*-trimethyldiethylenetriamines,[11] acetylacetone (Acac),[31,32] the hydrogen carbonate ion,[29,33] histidine (His),[28,52] glycine (Gly),[43-45] sorbitol,[10] sucrose,[10] 8-hydroxyquinoline,[23,55] a series of α-aminoacids (Am),[46,47] and certain other substances[58-60] possess catalase activity.

The above compounds can be regarded as functional models of catalase (because, like the enzyme catalase itself, they catalyse the decomposition of H_2O_2 to O_2 and H_2O). It has come to be assumed that they possess catalase activity.

The catalase activity in the Mn(II)–Phen–H_2O_2 system is known to be determined[48,49] by the complex $Mn(Phen)_2^{2+}$, while in the Mn(II)–HCO_3^-–H_2O_2 system it is determined by the complex[10] $Mn(HCO_3)_2$. The decomposition of H_2O_2 is catalysed by the complex $MnEn_2^{2+}$ (En = ethylenediamine) in the Mn(II)–En–H_2O_2 system,[36,40] by the complex $Mn(Bipy)_2^{2+}$ in the Mn(II)–Bipy–H_2O_2 system, and by the complexes $MnTrien^{2+}$ and $MnTEA_2^{2+}$ (TEA = triethanolamine) in the Mn(II)–Trien–H_2O_2[27,38] and Mn(II)–TEA–H_2O_2[54] systems respectively. The complexes $Mn(Am)_2$ and $Mn(Am)_3$, incorporating bidentate and tridentate aminoacids and H_2O_2 in the corresponding systems,[46,47] $MnDien_2^{2+}$,[35,42] and the dinuclear complexes Mn_2His_3 [52] and $MnAcac_2$ [31,32] have the same properties.

Complexes having this composition manifest as a rule a high peroxidase activity. This has been confirmed by the results of studies on the oxidation reactions of various organic compounds in the Mn(II)–ligand–H_2O_2–S (S is the substrate) systems. The hydrogen carbonate ion,[68-70] triethylenetetramine,[71-74] ethylenediamine,[72] diethylenetriamine,[75,76] acetylacetone,[77,78] *o*-phenanthroline,[79-81] α,α′-bipyridyl,[50,78-81] and glycine[82] have been used as the ligands. The substrates are indigomonosulfonate, indigocarmine, indigotetrasulfonate, murexide, and carmine, which do not form complexes (or form only weak complexes) with Mn^{2+}, and also chelating ligands lumomagneson, lumogallion, alizarin C, tiron, and catechol.

A number of manganese complexes exhibit also oxidase activity. The catalytic oxidation of organic substances by molecular oxygen is carried out as a rule in non-aqueous media. The catalysts of such processes are manganese stearate and a series of manganese complexes:[83-86] porphyrin,[87-90] phthalocyanine,[91,92] caprylate,[93] carboxylate,[93] naphthenate,[94] tripropyl phosphate,[94] and other complexes.[95-97] The oxidation in the presence of manganese stearate $MnSt_2$ has been studied in greatest detail.

On the basis of literature data, manganese(II) complexes can be arranged in the following sequence in terms of their catalase activity:

$$Mn(HCO_3)_2 > MnTrien_2 > MnHis_2^{2+} > MnDien_2^{2+} >$$
$$> MnAcac_2^{2+} > MnEn_2^{2+} > MnBipy_2^{2+} > MnPhen_2^{2+} >$$
$$> MnAla_3 > MnVal_3 > MnGly_3 \simeq MnTre_2 >$$
$$> Mn(\beta\text{-Phen-}\alpha\text{-Ala})_3 > MnSer_2 > MnAsp_2 \simeq Mn(Aspa)_2$$

(Ala = alanine, Val = valine, Tre = threonine, Ser = serine, Asp = asparagine, and Aspa = aspartic acid).

The manganese(II) hydrogen carbonate complexes exhibit the highest catalase activity. In terms of their activity in the hydrogen peroxide decomposition reactions, they are inferior only by an order of magnitude to the iron(III) complex of triethylenetetramine — the most effective catalyst of the decomposition of hydrogen peroxide among low-molecular-mass compounds.‡

‡ The complex Fe^{3+}Trien has been called 'inorganic catalase' in the literature.[98]

Manganese complexes with ligands containing nitrogen and oxygen and both nitrogen and oxygen are catalytically active in the reactions involving the decomposition of hydrogen peroxide and the oxidation of substrates. Coordinatively unsaturated complexes catalyse the above processes as a rule, but coordinatively saturated complexes as well as a series of dinuclear compounds exhibit a catalytic activity in certain cases. The following oxidation–reduction reactions can occur in the course of the process:

$$L_nMn(II) \underset{+2e}{\overset{-2e}{\rightleftharpoons}} L_nMn(IV)\,,$$

$$L_nMn(III) \underset{+e}{\overset{-e}{\rightleftharpoons}} L_nMn(IV)\,,$$

$$L_nMn(III) \xrightarrow{e} L_nMn(II)\,.$$

Depending on which oxidation–reduction reactions occur in the decomposition of hydrogen peroxide by specific coordination compounds of manganese(II), the process proceeds via a radical-ion (radical-chain or cyclic) or ion-molecule mechanisms.

The radical-ion (radical-chain) mechanism of the decomposition of hydrogen peroxide operates in the following systems: Mn(II)–HCO_3^-–H_2O_2, Mn(II)–Triene–H_2O_2, Mn(II)–His–H_2O_2–H_3BO_3, Mn(II)–Phen–H_2O_2, and Mn(II)–Bipy–H_2O_2.[28,31,33,37,38,50,51] The kinetics and mechanisms of the decomposition of hydrogen peroxide by manganese(II) complexes of HCO_3^- and triethylenetetramine have been examined.[33,37,38,52] The catalase activity of these systems is due respectively to the complexes $Mn(HCO_3)_2$ and $MnTrien_2$.

The radical mechanism of the process has been confirmed by data on the inhibiting effect of the specific $\dot{O}H$ and $\dot{O}_2$ radical acceptors on the catalase process[27,30,37,38] and the fact that the rate of chain propagation (the rate of gas evolution) W_{O_2} exceeds appreciably the rate of initiation W_i [the ratio of these rates is $\sim 10^3$ for the Mn(II)–HCO_3^-–H_2O_2 system[30]]. This has been established[37,38] by introducing into the reaction medium before the start of the process a $\dot{O}H$ indicator (*N,N*-dimethyl-*p*-nitrosoaniline) and a $O_2^{\cdot-}$ acceptor (tetranitromethane). In both systems, $O_2^{\cdot-}$ radical-ions are generated on initiation of the process, and the radicals ·OH are formed in the subsequent stages. Data obtained by the spectrophotometric detection of the manganese(III) complexes indicate the generation in the system also of manganese(IV) complexes.[10,37,38,99] These results served as a basis for the formulation of the radical-chain mechanism of the decomposition of hydrogen peroxide by the complexes $Mn(HCO_3)_2$ and $MnTrien^{2+}$ in the following form:[10]

initiation:

$$Mn(II)L + H_2O_2 \longrightarrow Mn(IV)L + 2\,OH^-\,,$$
$$Mn(IV)L + HO_2^- \longrightarrow Mn(III)L + O_2^{\cdot-} + H^+\,;$$

chain propagation:

$$Mn(IV)L + O_2^{\cdot-} \longrightarrow Mn(III)L + O_2\,,$$
$$Mn(III)L + H_2O_2 \longrightarrow Mn(IV)L + \dot{O}H + OH^-\,,$$
$$\dot{O}H + H_2O_2 \longrightarrow O_2^{\cdot-} + H^+ + H_2O\,;$$

chain termination:

$$Mn(III)L + O_2^{\cdot-} \longrightarrow Mn(II)L + O_2$$

(L = 2 HCO_3^- or Trien).

Comparison of the rate constants and the corresponding concentrations in solution showed that[33,37] the following stage also occurs in the Mn(II)–HCO_3^-–H_2O_2 system:

$$\dot{O}H + HCO_3^- \longrightarrow CO_3^{\dot{-}} + H_2O ,$$

$$CO_3^{\dot{-}} + H_2O_2 \longrightarrow HCO_3^- + O_2^{\dot{-}} + H^+ .$$

The above reactions ensure the additional generation of the $O_2^{\dot{-}}$ radical-ions in the chain propagation process. This promotes the effective decomposition of hydrogen peroxide in the presence of the $Mn(HCO_3)_2$ complex. The decomposition of hydrogen peroxide in the Mn(II)–HCO_3^-–H_2O_2 system via this mechanism has also been confirmed by the results of other investigations.[100,101]

A similar mechanism operates in the decomposition of hydrogen peroxide in the Mn(II)–His–H_2O_2 system in borate buffer solutions.[31,102]

A somewhat different mechanism is observed in the Mn(II)–Phen(Bipy)–H_2O_2 systems. As noted above, the catalysts are the complexes $MnPhen_2^{2+}$ and $MnBipy_2^{2+}$.[48–51] The catalase process in the above systems is influenced by inhibitors such as specific $\dot{O}H$ radical acceptors (in particular, *N,N*-dimethyl-*p*-nitroso-aniline).[50] On the other hand, the gas evolution process is effectively inhibited by ascorbic acid, hydroquinone, *p*-benzoquinone, and tetranitromethane.[50,51] The radical-chain nature of the mechanism is indicated by the finding that in this case $W_{O_2}/W_i \simeq 10^3$.[50] Since $\dot{O}H$ radicals are not generated in these systems, one can justify the occurrence of a two-electron transfer stage:[50,51]

$$Mn(II)L_2 + H_2O_2 \longrightarrow Mn(IV)L_2 + 2\,OH^-$$

(L = Phen, Bipy).

The interaction of manganese(IV) compounds with hydrogen peroxide includes consecutive one-electron transfer steps with the generation of $O_2^{\dot{-}}$ in the reaction medium (this has been demonstrated by the method of inhibitors[50]). The complete process mechanism in the Mn(II)–Phen(Bipy)–H_2O_2 system under stationary conditions is as follows:[50]

initiation:

$$L_2Mn(III) + HO_2^- \longrightarrow L_2Mn(II) + HO_2^{\dot{}} ;$$

chain propagation:

$$L_2Mn(II) + H_2O_2 \longrightarrow L_2Mn(IV) + H_2O,$$

$$L_2Mn(IV) + H_2O_2 \longrightarrow L_2Mn(III) + HO_2^{\dot{}} + H^+ ,$$

$$HO_2^{\dot{}} \longrightarrow O_2^{\dot{-}} + H^+ ,$$

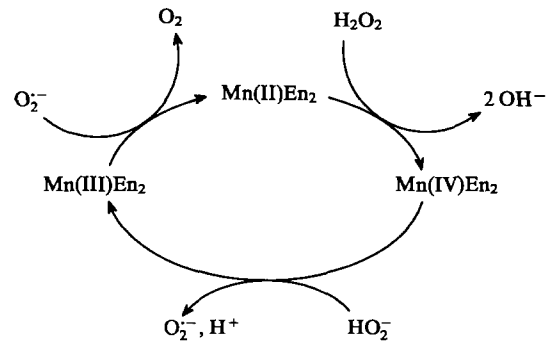
$$L_2Mn(III) + O_2^{\dot{-}} \longrightarrow L_2Mn(II) + O_2 ;$$

chain termination:

$$L_2Mn(II) + HO_2^{\dot{}} \longrightarrow L_2Mn(III) + HO_2^- .$$

Thus the characteristic features of the radical-chain mechanism of the decomposition of hydrogen peroxide by manganese complexes are as follows: the generation of the $O_2^{\dot{-}}$ and $\dot{O}H$ radical species (or of $O_2^{\dot{-}}$ alone) in the reaction volume; the formation of manganese(IV) and manganese(III) compounds owing to the catalase process; a significantly greater rate of chain propagation compared with the rate of initiation.

The formation of the $O_2^{\dot{-}}$ radical-ions has been observed also in the Mn(II)–En–H_2O_2 and Mn(II)–His–H_2O_2 systems, but in this case a distinctive feature of the process is the equality of the rates of gas evolution and initiation. This provided a basis for the classification of the given mechanism as of the radical-ion cyclic type. In relation to catalysis by the $MnEn_2^{2+}$ complex, this mechanism assumes the form shown below.[36,52,53,72] The radical-ion cyclic mechanism also operates in the Mn(II)–ethylenediaminetetramethyl phosphate–H_2O_2 system.[58] In the Mn(II)–His–H_2O_2 system, the reaction proceeds via a radical-ion mechanism with participation of dinuclear complexes of the type His–Mn(II)–His–Mn(II)–His (the formation of the latter has been demonstrated by EPR.[10,52,60]



The ion-molecule mechanism differs from that examined above primarily by the fact that free radicals are not formed in the reaction system. The absence of the inhibition of the catalase process by specific acceptors of the $\dot{O}H$ and $O_2^{\dot{-}}$ radical species (at concentrations such that they compete with the other reactants for free radicals) suggests that an ion-molecule mechanism of the decomposition of hydrogen peroxide operates in the system. In such cases, the reaction can proceed with formation of mono- or di-peroxo-compounds and may be accompanied by oxidation–reduction processes within the complex catalyst.[9] If such compounds are not formed, the mechanism includes stages involving the transfer of two electrons from the complex catalyst to hydrogen peroxide and conversely. This is clearly illustrated by the following general scheme:

$$Mn(II)L_n + H_2O_2 \longrightarrow Mn(IV)L_n + 2\,OH^- ,$$

$$Mn(IV)L_n + HO_2^- \longrightarrow Mn(II)L_n + H^+ + O_2 .$$

The decomposition of hydrogen peroxide proceeds via this mechanism in the Mn(II)–Dien–H_2O_2,[39,42] Mn(II)–sorbitol–H_2O_2,[10] Mn(II)–sucrose–H_2O_2,[10] Mn(II)–Gly–H_2O_2,[43–45] Mn(II)–Ala–H_2O_2,[46] and Mn(II)–Val (ser, Tre, Asp)–H_2O_2[46,47] systems. If the second stage is rate-limiting in the above mechanism, then one can write the following expression for the Mn(II)–Dien–H_2O_2 system:

$$W = \frac{k_2 K_{H_2O_2}[MnDien_2][H_2O_2]}{[H^+]} .$$

This expression agrees with the experimental equation, which confirms the reality of the proposed mechanism. The ion-molecule mechanism of the catalysis by manganese(II) complexes of sorbitol, sucrose, and a number of aminoacids has been demonstrated similarly.[10,43–47] In fact, the same mechanism operates also in the Mn(II)–Acac–H_2O_2 system.[31,32] The decomposition of hydrogen peroxide by trivalent manganese compounds in the Mn(III)–5,10,15,20-tetrakis-(2,6-dimethyl-3-sulfonatophenyl) porphyrinate–H_2O_2 system also proceeds via an ion-molecule mechanism.[59]

Thus one may conclude that hydrogen peroxide is capable of oxidising manganese(II) compounds to monomeric manganese(IV) compounds in neutral (and in a number of cases also weakly alkaline) media. One cannot rule out the possibility that such a process consists of two consecutive one-electron transfers without the emergence of the $\dot{O}H$ radicals from the inner sphere into the reaction volume,[50] but there is no rigorous evidence in support of the mechanism (with participation of manganese complexes).

At the same time, the unique ability of hydrogen peroxide to oxidise manganese(II) compounds to the permanganate ion is manifested in alkaline media. This has been demonstrated in relation to the catalytic decomposition of H_2O_2 by the manganese(II) complexes of triethanolamine.[10] The hypothetical

mechanism of this process, in which free radicals are not formed in the reaction volume (this has been demonstrated by the method of inhibitors), is as follows:[10]

$$Mn(II) + H_2O_2 \longrightarrow Mn(IV) + 2\,OH^-,$$

$$Mn(IV) + H_2O_2 \longrightarrow Mn(VI) + 2\,OH^-,$$

$$2\,Mn(VI) \longrightarrow Mn(V) + Mn(VII),$$

$$Mn(V) + Mn(II) \longrightarrow Mn(III) + Mn(IV),$$

$$Mn(III) + H_2O_2 \longrightarrow Mn(V) + 2\,OH^-,$$

$$Mn(V) + H_2O_2 \longrightarrow Mn(VII) + 2\,OH^-$$

[Mn(II)–Mn(V) are understood as the corresponding complexes, while Mn(VI) and Mn(VII) form the MnO_4^{2-} and MnO_4^- ions in alkaline media].

Thus in the systems of the type Mn(II)–ligand–H_2O_2 considered, manganese(III) manganese(IV) species (compounds) as well as $\dot{O}H$ and $O_2^{\cdot-}$ are generated and it is to be expected that they should ensure the effective oxidation of organic compounds.

III. Peroxidase properties. Oxidation of organic substrates

The high reactivity of many coordination compounds of manganese in catalytic hydrogen peroxide decomposition reactions has stimulated studies of the use of the Mn(II)–ligand–H_2O_2 systems for the oxidation of substrates and also of the application of manganese complexes as catalysts of the oxidation of organic compounds by molecular oxygen and periodate. The aim of such studies has been the search for new catalysts of the peroxidase oxidation of substrates, the establishment of the mechanism of the catalytic effect of the coordination compounds of manganese and of the role of the ligand environment of the central metal ion in this process, of the nature of the substrate being oxidised, of the experimental conditions (aerobic, anaerobic), and of the relation between the catalase and peroxidase properties of the manganese complexes, and the development on this basis of a new procedure for the synthesis of organic substances of practical importance and of new catalymetric analytical methods, and also the discovery of the general features of the catalytic oxidation of organic substrates.

The kinetics and mechanisms of the peroxidase activity of the coordination compounds of manganese with various ligands, including oxygen-containing (the monodentate hydrogen carbonate ion,[68-70] the bidentate acetylacetone,[77,78] and the tridentate triethanolamine[10]), nitrogen-containing (the bidentate ethylenediamine,[72] phenanthroline,[50] and bipyridyl,[50] the tridentate diethylenetriamine,[75,76] and the tetradentate triethylenetetramine[71,72,74]), as well as both nitrogen- and oxygen-containing (the tridentate histidine), have been investigated in detail hitherto in the oxidation reactions of organic substrates — both substrates with a weak capacity for the formation of complexes with Mn^{2+} (indigomonosulfonate, indigocarmine, indigotetrasulfonate, murexide, carmine, Procion Blue, Direct Bordeaux 150, Disperse Violet K) as well as ligands forming fairly stable complexes with Mn^{2+} (lumomagneson, lumogallion, alizarin, alizarin C, tiron, catechol). Alcohols are oxidised similarly under aerobic conditions (monohydric — methanol, ethanol, and isopropyl alcohol; dihydric — ethylene glycol; polyhydric — glycerol). In systems of the type Mn(II)–ligand–H_2O_2–substrate, the coordination compounds of manganese catalyse the oxidation of substrates and one can therefore regard them as functional models of peroxidase.¶

Among the reactions where molecular oxygen is used as the oxidant, the oxidation reactions of 8-pentadecanone and hexadecanone catalysed by manganese stearate have been investigated in greatest detail.[83-86] Systems incorporating porphyrin complexes, sodium tetrahydroborate, olefins, or other organic compounds[87-92] as well as the oxidation reactions of α-aminoacids, α-ketoacids, and other compounds, catalysed by the coordination complexes of manganese(II) with Schiff bases[94-97] have also been studied in detail.

The above analysis of the mechanisms operating in the Mn(II)–ligand–H_2O_2 systems shows that, in the course of the decomposition of hydrogen peroxide by manganese complexes, intermediate species (compounds $\dot{O}H$, $O_2^{\cdot-}$, $L_nMn(IV)$, and $L_nMn(III)$, with a high oxidising capacity, are generated in the reaction medium. The oxidation–reduction potentials of the corresponding pairs are as follows:

Pair	φ/V	Ref.
Mn^{4+}/Mn^{3+}	1.63	103
Mn^{3+}/Mn^{2+}	1.51	9
Mn^{4+}/Mn^{2+}	1.57	103
$\dot{O}H/H_2O$	2.83	104
$O_2^{\cdot-}/O_2$	−0.16	104

Subsequently, when the substrate S is introduced additionally into such systems, it can be oxidised by precisely these species. The mechanism of the oxidation reaction can include the following stages:

$$\dot{O}H + S \longrightarrow P_1,$$

$$O_2^{\cdot-} + S \longrightarrow P_2,$$

$$L_nMn(III)[L_nMn(IV)] + S \longrightarrow P_3 + L_nMn(II)[L_nMn(III)],$$

$$L_nMn(III)S[L_nMn(IV)S] \longrightarrow P_4 + L_nMn(II)[L_nMn(III)],$$

$$L_nMn(IV)S[L_nM(IV)\,S] \longrightarrow P_5 + L_nMn(II).$$

The substrate may be oxidised by active species (compounds) in the reaction volume (outside the first sphere of the complex catalyst). In this case, the mechanism is classified as of the outer-sphere type.[10,37,68,70,105] If the substrate S is oxidised by manganese ions in high oxidation states within the coordination sphere of the complex catalyst, an inner-sphere mechanism operates.[10,37,68,70,106]

The outer-sphere mechanism. In the systems where the radical-chain decomposition of hydrogen peroxide with generation of $\dot{O}H$ radicals takes place, various organic dyes are oxidised effectively.[37,68,71,72,74,82,105] The results of the study of the kinetics of the oxidation of the substrates having a weak complex-forming capacity (organic dyes, alcohols) shows that the same coordination compounds of manganese which determine the catalase activity of the given systems catalyse the above process. One can postulate that in the Mn(II)–HCO_3^-–H_2O_2,[33] Mn(II)–Trien–H_2O_2,[38,72] and Mn(II)–His–H_2O_2–H_3BO_3[31] systems the substrates are oxidised by the $\dot{O}H$ and $O_2^{\cdot-}$ radical species as well as the Mn^{4+} and Mn^{3+} ions forming part of the composition of the corresponding complexes. The above species (compounds) compete with one another for the substrate molecule. In terms of their 'oxidising strength', they can be arranged in the following sequence:[10]

$$\dot{O}H > L_nMn(IV) > L_nMn(III) > O_2^{\cdot-}.$$

The experimental results[10,37,53,105,107] indicate the dominant role of the $\dot{O}H$ radicals in the oxidation of the above substrates, in particular, potassium indigotetrasulfonate, murexide, and carmine.

The same type of kinetics of the catalase and peroxidase processes in the Mn(II)–ligand–H_2O_2 and Mn(II)–ligand–H_2O_2–S systems (where HCO_3^-, Trien, and His are used as the ligands, while the substrates are organic compounds with a weak complex-forming capacity), the equality of the rates of conversion

¶ The enzyme peroxidase is an effective catalyst of the decomposition of H_2O_2 and the oxidation of substrates by the intermediate compounds formed on decomposition of the peroxide. It has therefore come to be assumed that the above manganese compounds possess peroxidase activity.

of the substrate under aerobic and anaerobic conditions, and also the fact that the interaction of the selected substrates S with ȮH results in the formation of inactive substrate radicals permitted the conclusion that the reaction

$$\dot{O}H + S \longrightarrow S \text{ oxidation products}$$

can be included in the mechanism of the catalase decomposition of hydrogen peroxide as the chain termination stage.[10, 37, 53, 68, 105]

Thus substrates with weak complex-forming capacity in relation to Mn^{2+} do not affect the fundamental process mechanism. The radical-chain mechanism of the decomposition of hydrogen peroxide, established for the catalase process, is retained under these conditions.

In the systems considered, the mechanism of the oxidation of substrates by ȮH radicals is of the outer-sphere type. The above data permit the conclusion that the outer-sphere mechanism of the oxidation of substrates with a weak complex-forming capacity in relation to Mn^{2+} {$pK_s < 3$ for $K_s[S]/K_s[L] < 1$, where K_s is the stability constant} can operate in all catalytic systems of the metal–ligand–H_2O_2 type in which hydrogen peroxide undergoes a radical-chain decomposition with generation of ȮH radicals and a relatively inactive substrate radical is formed. In such systems, the mechanisms of the catalase and peroxidase activities of the complex catalyst should be to a certain extent similar. The mechanism becomes complicated when, as a result of the interaction with ȮH radicals, the oxidation of substrates involves the formation of reactive substrate radicals, which, possessing reducing properties, can react with manganese(III) and manganese(IV) compounds and, under aerobic conditions, also with molecular oxygen. The oxidation of alcohols (methanol, ethanol, isopropyl alcohol, ethylene glycol, and glycerol) in the Mn(II)–HCO_3^-–H_2O_2 systems under aerobic conditions can serve as an example.[108, 109]

Analysis of the results of a number of studies[108–110] shows that at certain concentrations of the test substances in the Mn(II)–HCO_3^-–H_2O_2–ROH systems the role of hydrogen peroxide reduces to the preparation of the alcohol (by converting it into the alkoxy-radical R_α) for interaction with oxygen. Consequently molecular oxygen participates in the oxidation of alcohols as a consequence of the formation of the reactive substrate radical R_α, which leads to an increase in the complexity of the process mechanism, namely to the appearance of a series of new stages:[10, 37, 53, 110]

$$R_\alpha + O_2 \longrightarrow RO_2^\cdot ,$$

$$RO_2^\cdot \longrightarrow ROHO + HO_2^\cdot ,$$

$$RO_2^\cdot + ROH \longrightarrow R_\alpha + RCHO + H_2O_2 .$$

These do not occur in the absence of substrates or in their presence if the substrate radical formed is inactive. Since alcohols are oxidised in the reaction volume (outside the coordination sphere of the catalyst), such a mechanism may be also referred to as of the outer-sphere type. The results of studies on the Mn(II)–HCO_3^-–H_2O_2–ROH systems under aerobic conditions permit the conclusion that alcohols and other organic compounds are oxidised effectively by hydrogen peroxide under aerobic conditions provided that the catalyst is a complex with a distinct catalase activity and that H_2O_2 decomposes via a radical-chain mechanism with generation of ȮH radicals. The following conditions must be maintained if this is to be achieved:

$$\frac{k_{S+\dot{O}H}[S]}{k_{\dot{O}H+H_2O_2}[H_2O_2]} \gg 1 \quad \text{and} \quad \frac{k_{S+\dot{O}H}[S]}{k_{P+\dot{O}H}[P]} \gg 1,$$

where $k_{S+\dot{O}H}$, $k_{\dot{O}H+H_2O_2}$, and $k_{P+\dot{O}H}$ are the corresponding rate constants for the interaction of ȮH with the alcohol (or the organic substrate S), hydrogen peroxide, and other system components (P). The above relations may serve as criteria for the selection of catalysts for the liquid-phase oxidation of alcohols (and other organic compounds) under mild conditions.

It is noteworthy that the active principle in the oxidation of organic substrates with a weak complex-forming capacity in relation to Mn^{2+} in the Mn(II)–HCO_3^-–H_2O_2, Mn(II)–Trien–H_2O_2, and Mn(II)–His–H_2O_2–H_3BO_3 system is the ȮH radical. However, such radicals are not generated in the disproportionation of hydrogen peroxide by manganese(II) complexes of *o*-phenanthroline, α,α′-bipyridyl, histidine (in the absence of borate buffer), ethylenediamine, diethylenetriamine, acetylacetone, and other compounds. At the same time, indigocarmine, potassium indigomonosulfonate and indigotetrasulfonate, murexide, and carmine are effectively oxidised in the above systems.[37, 68, 70, 72, 111] The results of the study of the kinetics and mechanisms of the decomposition of hydrogen peroxide and of the oxidation of substrates have shown that manganese(IV) compounds are the oxidant in the given instance. The general process mechanism can be represented as follows:

$$L_nMn(II) + H_2O_2 \longrightarrow L_nMn(IV) + 2\,OH^- ,$$

$$L_nMn(IV) + S \longrightarrow L_nMn(II) + P \text{ (S oxidation products)}.$$

The oxidation of substrates by manganese(IV) compounds has been demonstrated in cases where the catalysts are manganese(II) complexes of phenanthroline and bipyridyl,[50] as well as the acetylacetonate and histidine complexes.[10, 53, 78, 111]

Thus one may conclude that, in the oxidation–reduction decomposition of hydrogen peroxide by manganese(II) coordination compounds without the formation of hydroxyl radicals in the reaction medium, substrates having a weak complex-forming capacity in relation to Mn^{2+} are oxidised by manganese(IV) via an outer-sphere mechanism. The process takes place as a result of two-electron transfer. One cannot rule out the possibility that, when substrates incapable of being oxidised via a two-electron mechanism are used, consecutive one-electron transfer steps take place involving also manganese(III) compounds in the oxidation process.

The inner-sphere mechanism. The nature of the substrate oxidised affects the mechanism of the catalytic decomposition of hydrogen peroxide, particularly if the substrate has a chelating capacity and is able to form fairly stable complexes with Mn^{2+} ($pK_s > 3$). Such substrates are lumomagneson, lumogallion, alizarin, and alizarin C, the kinetics and mechanisms of the oxidation of which in the Mn(II)–ligand–H_2O_2 systems have been thoroughly investigated.[10, 37, 53, 69, 106] The above substrates, which play simultaneously the role of a ligand (S_L), are effectively oxidised [especially in a system such as Mn(II)–HCO_3^-–H_2O_2]. A distinctive feature of these processes is the fact that free hydroxyl and superoxide radicals are not generated in the reaction volume, but the substrates are oxidised within the coordination sphere of the metal complex catalyst (the inner-sphere mechanism).

A similar fundamental mechanism operates in the oxidation of lumomagneson in the Mn(II)–Triene–H_2O_2 and Mn(II)–En–H_2O_2 systems[106, 112] and in the oxidation of tiron and catechol in the Mn(II)–Phen(Bipy)–H_2O_2 systems.[50] The characteristic difference between the process in the above systems and that occurring in the latter without a substrate (the radical-chain mechanism) consists in the absence of the inhibiting effect and a diminishing role of radical acceptors in the course of the reaction. These data indicate unambiguously that hydrogen peroxide is decomposed and the substrate oxidised via a fundamentally new mechanism, differing from the mechanism of the catalase process. The substrate is oxidised in these systems via an inner-sphere mechanism[50, 106, 112] [as in the Mn(II)–HCO_3^-–H_2O_2–S_L systems]. The general process mechanism[106, 112] can be represented by the following set of stages:

$$Mn(II) + S_L \rightleftarrows Mn(II)S_L ,$$

$$Mn(II)S_L + H_2O_2 \longrightarrow Mn(IV)S_L + 2\,OH^- ,$$

$$Mn(IV)S_L \longrightarrow Mn(II) + P \text{ (S_L oxidation products)};$$

[Mn(II)–Mn(IV) are understood as the corresponding complexes $MnEn_2$ and MnTrien]. One cannot rule out the possibility that a peroxo-complex of the type $Mn(II)S_LH_2O_2$ is formed in the reaction of the complex catalyst with hydrogen peroxide, as has been suggested[69] for the catalysis by the manganese hydrogen carbonate complex, but this has not been confirmed experimentally. A somewhat different sequence of stages (within the framework of the same fundamental mechanism) occurs in the oxidation of tiron and catechol in the Mn(II)–Phen(Bipy)–H_2O_2 system:[50]

$$L_2Mn(II) + H_2O_2 \longrightarrow L_2Mn(II)HO_2^+ + H^+,$$

$$L_2Mn(II)HO_2^+ \longrightarrow L_2Mn(IV) + H_2O,$$

$$L_2Mn(IV) + S_L \rightleftarrows L_2Mn(IV)S_L,$$

$$L_2Mn(IV)S_L \longrightarrow L_2Mn(II) + P$$

(L = Phen, Bipy).

The mechanism of the oxidation of substrates of the type S_L in the Mn(II)–Acac–H_2O_2 system is much more complex,[77,78] since in this case a dinuclear complex participates in the reactions with hydrogen peroxide.

The coordination compounds of manganese [systems of the type Mn(II)–ligand–H_2O_2] and in the first place the hydrogen carbonate complexes exhibit a high peroxidase activity, so that they could be used in the development of new catalymetric methods for the determination of microamounts of Mn^{2+}, for preparative purposes, as polymerisation initiators, and for the removal of organic impurities from waste waters.

Catalymetric analytical methods. The effective catalytic activity of manganese compounds in reactions involving oxidation by hydrogen peroxide of various indicator substances made it possible to use them for the development[113–116] of catalytic methods for the determination of microamounts of manganese. Such indicator substances are alizarin C in the presence of HCO_3^- (the lower limit of the detection of Mn^{2+} ions is 0.4 ng ml^{-1}),[117] Catechol Violet in the presence of ethylenediamine (0.5 ng ml^{-1}),[118] lumomagneson (0.1 ng ml^{-1}),[119] sodium carminate in the presence of ethylenediamine and lead (0.1 ng ml^{-1}),[120] H-acids in the presence of ethylenediamine (0.1 ng ml^{-1}),[121] and Pyrogallol Red in the presence of bipyridyl (0.01 ng ml^{-1}).[122]

Catalymetric methods for the determination of Mn^{2+}, based on the oxidation with hydrogen peroxide of indigosulfonic acids,[117,123] *o*-dianisidine, Variamine Blue, gallion, and other indicator substances,[113–116] have been proposed. A series of kinetic methods have been developed in which use is made of the catalytic oxidation of dyes by molecular oxygen, for example, in the Mn(II)–morin–O_2 system,[124] or by periodate.[10,114–116,125]

The method based on catalytic oxidation with hydrogen peroxide in the presence of the manganese hydrogen carbonate complex of alizarin, alizarin C, and other organic dyes, is especially selective.[117,125] This method is highly sensitive: the lower limit of the detection of Mn^{2+} ions in the oxidation reaction is 0.4 ng ml^{-1}.

Catalymetric methods for the determination of microamounts of manganese in specially pure substances have found the widest application.[114]

A general deficiency of the kinetic methods developed for the determination of microamounts of Mn^{2+} is the large error of the determination caused by the occurrence of a rapid background reaction. Therefore one of the important tasks is the search for such new systems in which the rate of the background reaction is low or the development of methods of inhibiting the background reaction in known systems.

IV. Oxidase properties

Many coordination compounds of the 3*d* transition metals in low oxidation states are capable of binding reversibly molecular oxygen, as a consequence of which they are classified as synthetic O_2 transferring agents.[126–128] The coordinated oxygen is in an activated state in many compounds, which permits its use to effect various oxidation–reduction processes, in particular for the oxidation of organic substrates, in which transition metal complexes behave as catalysts. The coordination of molecular oxygen to transition metal complexes is one of the most effective methods of activating this commonest and cheapest oxidant.

A number of coordination compounds of manganese also have notable properties, although very little information is available about such compounds (O_2 transferring agents) and also about the reactivity of coordinated O_2 in manganese complexes. The reversible binding of molecular oxygen by manganese complexes takes place as a rule in non-aqueous media. The formation of oxygenated manganese complexes with porphyrin,[129] *para*-substituted *meso*-tetraphenylporphyrins,[130] dibutylcatechol, semiquinone,[131] picoline,[132] pyridine,[133] *N*,*N*-bis(salicylidene)ethylenediamine,[134] tetraphenylporphyrin,[135] threonyl- and phenyl-dialkylphosphines,[136] tripropylphosphine,[138] and others[137–140] has now been demonstrated. Certain coordination compounds of manganese(II) are oxygenated irreversibly. As a consequence of the activation of O_2, the central ion in the coordination sphere of the complex is oxidised with formation of manganese(III) and manganese(IV) complexes. It has been established that such oxygenation occurs in a series of porphyrin complexes,[141] in manganese complexes of phthalocyanine,[132] Schiff bases,[142,143] and triethanolamine,[144] and also in the gluconate[145] and sorbitol[146] complexes.

Studies on the activation by manganese complexes of molecular oxygen in the oxidation of organic substrates by the latter are of special interest. Such complexes may be regarded (subject to certain assumptions) as functional models of oxidases. As mentioned above, manganese stearate and a series of porphyrin, phthalocyanate [phthalocyanine?], and other complexes are used as catalysts of the oxidation of substrates by molecular oxygen. Thus, in catalysis by manganese(III) aquo-ions, the latter oxidise the substrates, forming at the same time radicals and manganese(II).[62–65] In the subsequent stages, manganese(II) is oxidised by the reaction products to manganese(III), i.e. the catalytic process includes the redox reactions:

$$Mn(III) \underset{-e}{\overset{+e}{\rightleftarrows}} Mn(II)$$

and a radical-chain or a radical-ion (non-chain) mechanism of the oxidation of substrates by molecular oxygen. The role of manganese(III) ions consists in preparing the substrate (by converting it into a radical) for the subsequent interaction with oxygen.

Catalysis by manganese(II) aquo-ions occurs apparently only when the substrate has a chelating capacity and a metal–substrate complex effectively reacting with oxygen is formed during the process. The oxidation of the substrate proceeds most probably within the coordination sphere of the metal–substrate complex under the influence of the manganese ions in the highest oxidation states.[65,147–149]

Coordination compounds of manganese are more effective catalysts of the oxidation of substrates by molecular oxygen. In such processes the initial stage involves the formation of an intermediate compound incorporating the complex catalyst and O_2, in which the latter is in fact activated. The mechanism of the activation of O_2 has not been ultimately elucidated. It has been suggested that there is no spin density and no appreciable negative charge on the oxygen in such an intermediate complex, so that O_2 is bound in a quasi-singlet state ($^1\Delta_g$).[88] One may therefore expect

the manifestation by the oxygen in such complexes of the chemical reactivity characteristic of O_2 in its singlet state.§

The composition of the intermediate active oxygen complex formed has been given in a number of studies[83,91] as $L_n(Mn(II)^{\delta+}\ldots O_2^{\delta-}$. For example, the mechanism of chain initiation in the oxidation by molecular oxygen of a series of organic substrates (8-pentadecanone, hexadecanone) in the presence of manganese stearate has been expressed as follows:

$$MnSt_2 + O_2 \longrightarrow MnSt_2^{\delta+}\ldots O_2^{\delta-},$$

$$MnSt_2^{\delta+}\ldots O_2^{\delta-} + RH \longrightarrow \begin{cases} MnSt_2OH + RO, \\ MnSt_2OOH + R. \end{cases}$$

In most studies, it is assumed that the process proceeds via a stage involving the formation of a ternary catalyst–O_2–substrate complex, the decomposition of which leads to the formation of the reaction products.[88]

If the substrates are oxidised with trivalent manganese compounds used as the catalysts, an additional reductant (usually tetrahydroborate) is introduced into the system. The process mechanism under such conditions becomes appreciably more complex, which hinders its rigorous justification. It has been established reliably that in such cases the manganese(III) compounds are initially reduced to manganese(II) compounds, after which the substrate–O_2–catalyst ternary complex is formed. A process of this kind occurs in the oxidation of cholesterol, androst-5-en-5β-ol, and a number of aliphatic olefins in the presence of porphyrin complexes of manganese(III).

The general mechanism can be represented in the following form:[90,151]

$$TPPMn(III) + NaBH_4 \rightleftarrows TPPMn(II) + P_1,$$

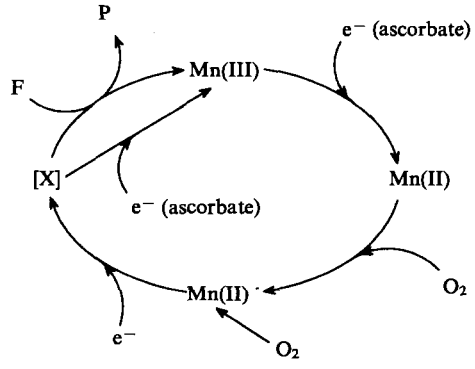
$$TPPMn(II) + S + O_2 \rightleftarrows S{-}O{-}O{-}Mn(II)TPP,$$

$$S{-}O{-}O{-}Mn(II)TPP \longrightarrow TPPMn(III) + P_2,$$

$$S{-}O{-}O{-}Mn(II)TPP \longrightarrow P_3,$$

$$TPPMn(II) \longrightarrow P_4,$$

where P_1 are the $NaBH_4$ reaction products, P_2 the olefin oxidation products, P_3 and P_4 the catalyst reaction and dehydration products respectively, [and TPP is tripyhenylphosphine]. A similar mechanism has been proposed also for the oxidation of olefins in the Mn(III)(TPP)–O_2–ascorbic acid–olefin system;[87] and the formation of a complex between O_2 and the catalyst, and the fact that $O_2^{\cdot-}$ and H_2O_2 are not involved in the process have been demonstrated. The mechanism can be represented by a sequence of stages.



[Mn(II) and Mn(III) are understood as the corresponding complexes with TPP, F is the olefin, and P is its oxidation product]. Competition between the ascorbate ion and the substrates for the active species [X] is postulated.

The mechanisms of substrate oxidation presented above are of the inner-sphere type. Complete schemes for the oxidation of substrates with formation of the experimentally established final products have been put forward in a number of studies[88,89,93] taking into account the operation of the inner-sphere mechanism. Such mechanisms must be regarded as tentative, because they have been set up purely speculatively in order to express clearly the possible pathways leading to the formation of the oxidation products.

Substrates may be oxidised by oxygen also via an outer-sphere mechanism, for example in the oxidation of hydrazine [the Mn(III)–Hm–O_2–N_2H_4 system, where Hm = haemoglobin]:

$$Mn(III){-}Hm + O_2 \rightleftarrows Mn(III)_2Hm\ldots O_2,$$

$$Mn(III)_2Hm\ldots O_2 + N_2H_4 \longrightarrow Mn(III)Hm + N_2 + 2\,H_2O.$$

An outer-sphere mechanism operates also in the Mn(II)–L–O_2–leuco-base (LO) systems:[10]

$$MnL_2 + O_2 \rightleftarrows MnL_2O_2,$$

$$MnL_2O_2 + LO \longrightarrow MnL_2 + LO \text{ oxidation products}$$

(L = Phen, Bipy).

A distinctive feature of this process is that it occurs in neutral aqueous media and that the rate of oxidation of the leuco-base increases appreciably when the system is irradiated with UV light (λ = 314–334 nm).

An outer-sphere mechanism (without the activation of O_2 in the coordination sphere of the complex catalyst) also operates in the liquid-phase oxidation of organic substances in the presence of initiators or when manganese(III) complexes, which react effectively with the substrate, are used as the catalysts.[84,97]

It is noteworthy that occasional studies on the oxidation reactions of organic substances by molecular oxygen in the presence of manganese ions and coordination compounds do not permit the development of a unique point of view on their mechanisms. At the same time, one may conclude that such systems may be used for the synthesis of certain organic compounds of practical interest.

Many studies devoted to the liquid-phase oxidation of organic compounds by molecular oxygen in the presence of manganese ions had preparative aims. For example, optimum conditions have been found {[$MnSt_2$] = 16.5 mmol litre^{-1}, 393 K} for the oxidation of 8-pentadecanone by oxygen, in which the yield of caprylic and oenanthic acids (51.9%) is a maximum.[88]

The main products of the liquid-phase oxidation of *n*-pentane in solution in acetic acid in the presence of 10^{-3} mole of manganese acetate per mole of *n*-pentene are lower aliphatic carboxylic acids.[152]

Preparative methods of synthesis of new organic substances with manganese complexes used as catalysts have also been described in a number of other studies.[10,84,89,92–94,96,147] The manganese(II)–ligand–H_2O_2 systems, in which ȮH radicals are generated, can be used to obtain aldehydes (ketones) from the corresponding alcohols.[103,104,116] By virtue of their high effectiveness in the hydrogen peroxide decomposition reactions, manganese(II) complexes are suitable for the elimination of H_2O_2 at high concentrations from waste waters.[153]

§ Questions concerning the activation of O_2 by coordination compounds have been considered in detail in a number of communications.[126,131,150]

V. Manganese compounds as catalysts of processes in the environment

One of the consequences of the increasing amount of anthropogenic waste discharged into the atmosphere is the precipitation of acid rain, the main components of which are sulfuric and nitric acids. The oxidation processes in the atmosphere, leading, for example, to sulfur(IV) (in the form of SO_2) and sulfur(VI) (in the form of H_2SO_4) are usually accelerated catalytically by transition metal ions and compounds, particularly those of manganese and iron. The concentrations of the latter in rain water are usually $\sim 2.6 \times 10^{-7}$ and $\sim 3.8 \times 10^{-6}$ M respectively.[154] This is sufficient to exert a strong catalytic effect on many processes.[10, 149, 155] The oxidants are usually O_2, H_2O_2, or their reactive activation products — the $\dot{O}H$ and $H\dot{O}_2$ radicals.

Metal (manganese, iron) complexes participate in the oxidation of sulfur(IV) by ozone in the aqueous phase of the atmosphere.[156, 157] Furthermore, compounds of these metals may concentrate in the moist aerosol particles and there is therefore a possibility of an appreciable increase in the rate of oxidation of SO_2.

The mechanisms of this process under laboratory conditions and in the real atmospheric moisture can differ appreciably (for example, the SO_2 oxidation reactions in the water of a mist, in rain water, or in aerosol water). The rate of oxidation of SO_2 in aerosols diminishes in the following sequence of metal salts:

$$Mn(NO_3)_2 > MnCl_2 > Cu(NO_3)_2 > MnSO_4 > CuSO_4 > CuCl_2.$$

This indicates the strong influence of the nature of the ligand. For example, the formation of complexes with participation of manganese ions and various volatile organic ligands leads to the appearance of fairly effective catalysts activating the molecules of the oxidant (O_2, H_2O_2) and the substrate (SO_2). The rate of the catalytic oxidation of SO_2 depends on a multiplicity of causes: on the ratio of the manganese ions and ligand molecules, on the pH of the medium, and other factors. The observed rates of this oxidation process at different sites and at different times can therefore also be different. However, an appreciable fraction of sulfur dioxide in a water drop within the mist is usually rapidly converted into sulfuric acid. For example, during summer approximately half of the atmospheric SO_2 and NO_2 waste is converted into H_2SO_4 and HNO_3 after 180 and 14 h respectively.[158] The detailed mechanisms of these processes have so far been poorly determined.

The overall reaction involving the catalytic oxidation of sulfur(IV) to sulfur(VI) by oxygen can be as follows:

$$SO_2(aq) + H_2O + \tfrac{1}{2}O_2 \xrightarrow{Mn^{2+}L_n} \longrightarrow H_2SO_4 \rightleftarrows HSO_4^- + H^+.$$

The study of the model $Mn(II) - SO_2(aq) - HSO_3^- - O_2$ system showed that the order of the reaction with respect to manganese is two (there is a possibility of the participation of species of the type of Mn_2^{4+}). A radical-chain mechanism has been postulated:[159]

$$Mn^{2+} + HSO_3^- \rightleftarrows MnHSO_3^+ ,$$

$$2\,Mn^{2+} \rightleftarrows Mn_2^{4+} ;$$

intiation:

$$Mn_2^{4+} + HSO_3^- \xrightarrow{slow} Mn_2HSO_3^{3+} ,$$

$$Mn_2HSO_3^{3+} + O_2 \xrightarrow{fast} 2\,Mn^{2+} + \dot{O}H + SO_4^{\cdot -} ,$$

$$\dot{O}H + HSO_3^- \longrightarrow H_2O + SO_3^{\cdot -} ;$$

branching:

$$SO_4^{\cdot -} + HSO_3^- \longrightarrow HSO_4^- + SO_3^{\cdot -} ,$$

$$SO_3^{\cdot -} + O_2 \longrightarrow SO_5^{\cdot -} ,$$

$$SO_5^{\cdot -} + HSO_3^- \longrightarrow SO_4^{\cdot -} + HSO_4^- ,$$

$$MnHSO_3^+ + HSO_3^- \longrightarrow Mn(HSO_3)_2 ,$$

$$Mn(HSO_3)_2 + O_2 \longrightarrow Mn^{2+} + 2\,HSO_4^- ;$$

termination:

$$SO_5^{\cdot -} + \text{organic compound} \longrightarrow \text{inert products.}$$

This mechanism of the oxidation of sulfur(IV) to sulfur(VI) corresponds to the following rate equation:[159]

$$\frac{d}{dt}[S(VI)] = \left[10 \exp\left(\frac{6.4 - 4\sqrt{I}}{1 + \sqrt{I}}\right)\right][Mn^{2+}]^2 + \left[10 \exp\left(\frac{3.5 - \sqrt{I}}{1 + \sqrt{I}}\right)\right][Mn^{2+}][HCO_3^-] ,$$

where I is the ionic strength.

In contrast to the catalytic oxidation of sulfur(IV) to sulfur(VI) in the presence of iron compounds, in the case of compounds of manganese the catalyst is its dinuclear form Mn_2^{4+} [apparently in the form of some kind of complex, for example, $(MnSO_2)_2^{4+} \cdot O_2$].[160] A powerful oxidant (the $\dot{O}H$ radical), participating in the process, is formed under these conditions.

One of the problems in passing from the model mechanism to the mechanism of the oxidation of SO_2 in the atmosphere is the presence in the latter of both manganese(II) and iron(III) compounds. They exert jointly a much greater catalytic effect than they do separately, as under laboratory conditions. In addition there is a possibility of a difference between the mechanisms due to the difference between the concentrations of the interacting substances under laboratory conditions and in the atmosphere. Thus, at low SO_2 (HSO_3^-) concentrations, the following mechanism of the oxidation of sulfur(IV) by oxygen has been proposed:

$$Mn^{3+} + HSO_3^- \xrightarrow{k_1} HSO_3^{\cdot} + Mn^{2+} , \quad (1)$$

$$HSO_3^{\cdot} + O_2 \xrightarrow{k_2} HSO_5^{\cdot} , \quad (2)$$

$$HSO_5^{\cdot} + HSO_3^- \xrightarrow{k_3} HSO_5^- + HSO_3^{\cdot} , \quad (3)$$

$$HSO_3^- + HSO_5^- \xrightarrow{k_4} 2\,HSO_4^- , \quad (4)$$

$$HSO_5^{\cdot} + HSO_5^{\cdot} \xrightarrow{k_5} S_2O_6^{2-} + 2\,O_2 . \quad (5)$$

Then

$$\frac{d}{dt}[SO_4^{2-}] = k_3 \frac{k_1^{1/2}}{k_5}[HSO_3^-]^{3/2}[Mn]^{1/2} ,$$

if it is assumed that the rate is determined by stage (3).

On raising the concentration of SO_2 (HSO_3^-), the mechanism may change and the reaction

$$HSO_3^{\cdot} + HSO_3^- \xrightarrow{k_6} H_2S_2O_6 + e^- , \quad (6)$$

will appear instead of stage (5). The chain termination stage is now represented by reaction (6) instead of reaction (5) and the rate is determined by stage (2). In this case

$$\frac{d}{dt}[SO_4^{2-}] = k_2 \frac{k_1}{k_6}[Mn^{2+}][O_2] .$$

The catalytic oxidation of SO_2 by oxygen in the presence of the chloride of the tetraolylporphyrin (II) complex of manganese [Mn(III)II] and a reductant can be represented schematically in the following way:[162]

$$SO_2 \cdot H_2O \rightleftharpoons HSO_3^- + H^+ \rightleftharpoons SO_3^{2-} + 2H^+,$$

$$Mn^{3+}\Pi...O_2 \xrightarrow{+e^-} Mn^{3+}\Pi...O_2^- \xleftarrow{Mn^{3+}\Pi} O_2^- \xleftarrow{+e^-} O_2$$

$$+O_2 \uparrow\downarrow -O_2$$

$$Mn^{3+}\Pi \xrightarrow{+e^-} Mn^{2+}\Pi \xrightarrow{+O_2} Mn^{4+}\Pi...O_2^-$$

$$\downarrow +HSO_3^-$$

$$Mn^{3+}\Pi + SO_4^{2-} + HSO_3^{\cdot} + OH^-,$$

$$HSO_3^{\cdot} + O_2 \longrightarrow HSO_5^{\cdot},$$

$$HSO_5^{\cdot} + HSO_3^- \longrightarrow HSO_5^- + HSO_3^{\cdot},$$

$$HSO_5^- + HSO_3^- \longrightarrow 2\,HSO_4^-,$$

$$HSO_4^- + H^+ \rightleftharpoons H_2SO_4.$$

The initiation stage involves the reduction of MnΠ, O_2, or MnΠ ... O_2. The catalyst promotes the coordination and specific reduction of O_2 to the peroxide ions O_2^{2-} and also the generation of the active form of the substrate ($H \cdot SO_3^{\cdot}$ radicals), which is the initiator of the autoxidation of sulfur(IV). The oxide ($Mn^{3+}\Pi$ ... O_2), superoxide ($Mn^{3+}\Pi$ ... O_2^-), and peroxide ($Mn^{4+}\Pi$ ... O_2^{2-}) complexes formed were detected spectrophotometrically.

Hydrogen peroxide plays an even more important role than O_2 as the oxidant in the catalytic conversion of SO_2 into H_2SO_4 in the atmosphere. The H_2O_2 concentration in an atmospheric moisture drop is $\sim 10^{-6}$–10^{-4} M.[163] Typical catalytic oxidation–reduction systems are then produced:

$$M^{z+} - H_2O_2 - SO_2,\ M^{z+} - L - H_2O_2 - SO_2$$

(M = Mn, Fe, Cu, etc),

in which sulfur dioxide is oxidised to sulfuric acid:

$$SO_2 + H_2O_2 \xrightarrow{Mn^{z+}\ (Mn^{z+}L)} H_2SO_4.$$

Thus in the majority of the aqueous atmospheric systems (pH < 5) the main oxidant for SO_2 is H_2O_2.[164] At pH > 5, other oxidants [OH, O_3, Fe(III)–O_2] begin to play an important role and the contribution of H_2O_2 to the oxidation reaction diminishes. Similar catalytic oxidation–reduction systems arise in atmospheric water with participation of O_3 and O_2.

The conditions in certain model experiments on the catalytic oxidation of SO_2 were close to the atmospheric conditions [the concentrations of the reacting components — Mn(II), SO_2, and H_2O_2, acidity, and temperature].[165] Thus the concentration of manganese(II) was 10^{-6} to 4×10^{-6} M, which corresponds to its content in the atmosphere. Under these conditions, the rate of oxidation of sulfur(IV) is given by

$$-\frac{d}{dt}[S(VI)] = k[S(IV)][Mn(II)].$$

In different studies, the order of the reaction with respect to manganese(II) varied from 1 to 2. The rate constant for this reaction at pH 3–6 remained invariant also for $[Mn(II)]_0 = 10^{-6}$ M and amounted to 5.1×10^3 litre mol^{-1} s^{-1}, which was approximately 6 times greater than the value of k at the same iron(III) concentration. The reaction involving the catalytic oxidation of sulfur(IV) to sulfur(VI) proceeds via the formation of the complex $Mn(II)(HSO_3^-)_x^{2-x}$, the composition of which has not been ultimately determined. It is of interest that similar manganese hydrogen carbonate complexes $[Mn(HCO_3)_2]$ are[10] active catalysts of the decomposition of H_2O_2 with subsequent formation of $HO_2^{\cdot -}$ and $\dot{O}H$ free radicals species. The sequence of metals forming the catalyst is as follows when account is taken of the rate constants for the oxidation of sulfur(IV) to sulfur(VI):

Mn(II) > Fe(III), Cu(II) ≫ non-catalytic reaction.

Thus the non-catalytic and catalytic oxidation of SO_2 to H_2SO_4 by various oxidants (especially H_2O_2) is the most important process leading to the acidification of rain water. Apparently the key catalysts of this process (together with iron compounds) are manganese compounds and the rates of formation of SO_4^{2-} (mol litre^{-1} s^{-1}) in model experiments are described by the expressions

$$\frac{d}{dt}[SO_4^{2-}] = 0.142[Mn(II)] \text{ at } [SO_2] > 4 \times 10^{-5}\ M,$$

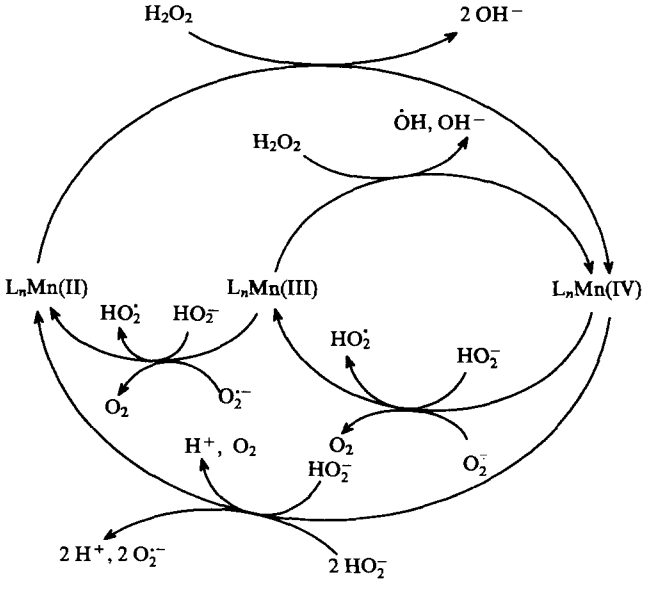
$$\frac{d}{dt}[SO_4^{2-}] = 0.142[Mn][SO_2]^{3/2} \text{ at } [SO_2] < 4 \times 10^{-5}\ M.$$

The mechanism of the oxidation of SO_2 in the atmosphere apparently involves free radical species.

In the atmosphere, 20%–40% of the acidity is caused by the oxidation of NO_x to nitric acid.[166] This reaction can also occur under the influence of catalysts.[167–170] However, the number of reliable data concerning the mechanism of this process is much smaller than for the mechanism of the oxidation of sulfur and they will not therefore be considered here.

VI. Conclusion

Many coordination compounds of manganese(II) with ligands containing nitrogen, oxygen, and both nitrogen and oxygen can be regarded as functional models of catalase (they catalyse the decomposition of H_2O_2 to O_2), peroxidase (they catalyse reactions involving the oxidation of organic and inorganic compounds by hydrogen peroxide oxidation products), superoxide dismutase (they catalyse the destruction of superoxide radical-ions O_2^-), and oxidase (they activate O_2 in the oxidation reactions of various compounds). The set of oxidation–reduction reactions which can occur in Mn(II)–ligand–H_2O_2 systems with participation of the complex catalyst is reflected by the following general scheme:



In each specific case, the mechanism of the decomposition of H_2O_2 by manganese complexes includes a definite set of oxidation–reduction reactions (presented above). The operation of a radical-ion (chain or cyclic) or ion-molecule mechanism is determined by the ligand environment of Mn^{2+} and the process

conditions. A clear relationship between the composition of the complex, the ligand environment in which the manganese ion exists, its reactivity, and the mechanism of the catalytic action has not so far been established.

The catalase-active coordination compounds of manganese(II) possess also a definite peroxidase activity because the catalytic decomposition of hydrogen peroxide generates ȮH radicals and manganese(IV) and manganese(III) compounds which have a high oxidising capacity. If a radical-chain mechanism of the decomposition of hydrogen peroxide operates in the systems with generation of ȮH radicals, the latter make the main contribution to the oxidation of the substrates. When an ion-molecule or a radical-ion cyclic mechanism of the decomposition of hydrogen peroxide operates, the oxidant consists mainly of manganese(IV) compounds. Substrates with relatively weak complex-forming capacity in relation to Mn^{2+} {$pK_s < 3$ for $K_s[L]/K_s[S] \gg 1$} are oxidised via an outer-sphere mechanism in the Mn(II)–ligand–H_2O_2 systems. Substrates forming fairly stable compounds with Mn^{2+} {$3 < pK_s < 8$ for $K_s[L]/K_s[S] \geqslant 1$} are oxidised within the coordination sphere of the complex catalyst (inner-sphere oxidation mechanism). If reactive substrate radicals are formed in the reaction volume, molecular oxygen participates in the oxidation process under aerobic conditions and the role of H_2O_2 reduces to the preparation of the substrate, by converting it into an active radical, for subsequent oxidation by molecular oxygen.

The liquid-phase catalytic oxidation by molecular oxygen in the presence of coordination compounds of manganese proceeds as a rule in non-aqueous media. Oxygen is activated mainly as a consequence of the formation of an intermediate active catalyst–O_2 compound and the mechanism of the oxidation of the substrate is then of the outer-sphere type. A ternary complex of the type MnL_n-O_2-S is sometimes formed in the course of the process. In such cases an inner-sphere mechanism of the oxidation of the substrate operates. The factors determining the operation of a particular oxidation mechanism, which permit a purposeful search for catalytically active manganese compounds and also characterise the role of the substrate and the medium in the liquid-phase oxidation by molecular oxygen, have by no means been fully established.

The high reactivity of individual manganese complexes can be used to develop catalymetric analytical methods (tens of such methods are already known) for preparative purposes (for the synthesis of particular organic compounds via liquid-phase oxidation) and for the solution of other applied problems (-elimination of organic contaminants from waste waters, etc.). The role of manganese compounds as catalysts of the processes occurring in the environment has been demonstrated on model systems for the conversion of sulfur(IV) (as SO_2) into sulfur(VI) (as H_2SO_4), which play an important role in the formation of acid rain.

References

1. S V Khangulov, V V Barynin, V R Melik-Adomyan, A I Grebenko, N V Voevodskaya, L A Blyumenfel'd, S N Dobryakov, V B Il'yasova *Bioorg. Khim.* **12** 741 (1986)
2. S V Khangulov, N V Voevodskaya, V V Barynin, A I Grebenko, V R Melik-Adomyan, *Biofizika* **32** 960 (1987)
3. G M Chenial *Ann. Rev. Plant. Physiol.* **21** 467 (1970)
4. G M Chenial, I F Martin *Biochim. Biophys. Acta* **197** 219 (1970)
5. M Galvin *Science* **184** 375 (1974)
6. M Pick, I Raboni, F Yost, J Fridovich *J. Am. Chem. Soc.* **96** 7329 (1974)
7. B B Keele, J M McCord, J Fridovich *J. Biol. Chem.* **245** 6176 (1970)
8. I A Chernavin, in *Fiziologiya i Biokhimiya Mikroelementov v Katalize* (The Physiology and Biochemistry of Microelements in Catalysis) (Moscow: Vys. Shkola, 1970) p. 70
9. A Ya Sychev *Okislitel'no-Vosstanovitel'nyi Kataliz Kompleksami Metallov* (Oxidation-Reduction Catalysis by Metal Complexes) (Kishinev: Shtiintsa, 1976)
10. A Ya Sychev, V G Isac *Koordinatsionnye Soedineniya Margantsa* (Coordination Compounds of Manganese) (Kishinev: Shtiintsa, 1990)
11. R P Pantaler, L D Alfimova, A M Bulgakova *Zh. Anal. Khim.* **30** 1834 (1975)
12. S L Davydova, N N Plate, T P Brin *Zh. Fiz. Khim.* **42** 258 (1968)
13. N M Reibel' *Zh. Fiz. Khim.* **40** 1112 (1966)
14. G F Reshetnikova, A G Muftakhov, N V Kapitsa, in *Tezisy Dokladov III Vsesoyuznogo Soveshchaniya po Khimii Koordinatsionnykh Soedinenii Kobal'ta, Margantsa, Nikelya. Tbilisi, 1974* (Abstracts of Reports at the IIIrd All-Union Conference on the Chemistry of the Coordination Compounds of Cobalt, Manganese, and Nickel. Tbilisi, 1974) p. 168
15. J H Wang *J. Am. Chem. Soc.* **77** 4715 (1955)
16. R P Pantaler, L E Alfimova, M E Globus, A M Bulgakov *Zh. Neorg. Khim.* **22** 1559 (1977)
17. W Langenbeck, K Dehler *Chem. Ber.* **89** 2458 (1956)
18. W Langenbeck, M Augustin, F H Richter *J. Prakt. Chem.* **27** 64 (1965)
19. W Langenbeck, M Augustin, F H Richter *Chem. Ber.* **94** 831 (1961)
20. H W Krause *Chem. Ber.* **95** 777 (1962)
21. D T Richens, D T Sawyer *J. Am. Chem. Soc.* **101** 3681 (1979)
22. E R Nightingale *Anal. Chem.* **31** 146 (1959)
23. M A Suwyn, R E Hamm *Inorg. Chem.* **6** 142 (1967)
24. T E Jones, R E Hamm *Inorg. Chem.* **13** 1940 (1974)
25. M Oishi, Y Mishida, S Kida *Chem. Lett.* 409 (1982)
26. J Dolezal, O Gurtler *Talanta* **15** 299 (1968)
27. A Ya Sychev, V G Isac *Zh. Fiz. Khim.* **47** 593 (1973)
28. A Ya Sychev, V G Isac *Zh. Fiz. Khim.* **47** 244 (1973)
29. A Ya Sychev, V G Isac, Dao Van Lap *Zh. Fiz. Khim.* **51** 363 (1977)
30. A Ya Sychev, V G Isac, Dao Van Lap *Zh. Fiz. Khim.* **52** 107 (1978)
31. A Ya Sychev, V G Isac, Chan Thi Thanh Phuong *Izv. Akad. Nauk Mold. SSR, Ser. Biol. Khim. Nauk* **6** 66 (1984)
32. A Ya Sychev, V G Isac, Chan Thi Thanh Phuong *Zh. Fiz. Khim.* **58** 332 (1984)
33. A Ya Sychev, V G Isac, U Pfanmueller *Zh. Fiz. Khim.* **57** 760 (1983)
34. A Ya Sychev, S S Budnikov, V G Isac *Izv. Akad. Nauk Mold. SSR, Ser. Biol. Khim. Nauk* **2** 54 (1986)
35. A Ya Sychev, V G Isac, Chan Thi Thanh Phuong *Zh. Fiz. Khim.* **58** 2331 (1984)
36. D G Batyr, V G Isac, A A Kirienko *Koord. Khim.* **10** 1372 (1984)
37. V G Isac, A Ya Sychev *Okislitel'no–Vosstanovitel'nyi Kataliz Kompleksami Perekhodnykh Metallov* (Oxidation–Reduction Catalysis by Transition Metal Complexes) (Kishinev: Izd. Mold. Gos. Univ., 1984)
38. D G Batyr, V G Isac, A A Kirienko, S V Kil'mininov *Disproportionation of Hydrogen Peroxide in the Mn(II)–triethylenetetramine–H_2O_2 System* (Moscow, 1984) Article deposited at the All-Union Institute of Scientific and Technical Information (VINITI), N 5779-84
39. D G Batyr, V G Isac, A A Kirienko, N B Unkulitsa *Koord. Khim.* **9** 1085 (1983)
40. V G Isac, A A Kirienko *Izv. Akad. Nauk Mold. SSR, Ser. Biol. Khim. Nauk* **4** 82 (1981)
41. D G Batyr, V G Isac, A A Kirienko *Koord. Khim.* **10** 1372 (1984)
42. D G Batyr, V G Isac, S O Travin, A A Kirienko *Koord. Khim.* **12** 1065 (1986)
43. D G Batyr, V G Isac, S V Kil'mininov *Kinetics and Fundamental Mechanism of the Disproportionation of H_2O_2 by Coordination Compounds of Manganese(II) and Glycine* (Moscow, 1985) Article deposited at the All-Union Institute of Scientific and Technical Information (VINITI), N8353-V (1985)
44. D G Batyr, V G Isac, S V Kil'mininov, Yu A Kharitonov *Koord. Khim.* **13** 3 (1987)
45. D G Batyr, V G Isac, S V Kil'mininov *Koord. Khim.* **13** 367 (1987)
46. D G Batyr, V G Isac, S V Kil'mininov *Koord. Khim.* **13** 1371 (1987)
47. D G Batyr, V G Isac, S V Kil'mininov, Chan Thi Thanh Phuong *Izv. Akad. Nauk Mold. SSR, Ser. Biol. Khim. Nauk* **6** 46 (1986)
48. Ya D Tiginyanu, A Ya Sychev, V M Berdnikov *Zh. Fiz. Khim.* **45** 1723 (1971)
49. Ya D Tiginyanu, A Ya Sychev, V M Berdnikov *Zh. Fiz. Khim.* **45** 2533 (1971)
50. Ya D Tiginyanu, Doctoral Thesis in Chemical Sciences, Moscow State University, Moscow, 1984
51. Ya D Tiginyanu, V M Berdnikov *Zh. Fiz. Khim.* **59** 349 (1985)

52. V G Isac, A Ya Sychev *Oxidation–Reduction Catalysis of the Disproportionation of Hydrogen Peroxide by Coordination Compounds of Manganese. The Catalase Activity* (Kishinev: Mold. Gos. Univ., 1985) Article deposited at MoldNIINTI, N 568-M (1985)
53. V G Isac, Abstract of Doctoral Thesis in Chemical Sciences, Rostov-on-Don, 1990
54. V G Isac, A Ya Sychev, L B Voziyan *Catalytic Properties of Mn(II) Complexes of Triethanolamine* (Kishinev: Mold. Gos. Univ., 1986) Article deposited at MoldNIINTI, N 655-M (1986)
55. V G Isac *Manganese Complexes of 8-Hydroxyquinoline in the Catalytic Decomposition of H_2O_2* (Kishinev: Mold. Gos. Univ., 1990) Article deposited at the MoldNIINTI, N 1159-M (1990)
56. D G Batyr, V G Isac, S V Kil'mininov *Coordination Compounds of Manganese(II) and Glycine* (Kishinev: Mold. Gos. Univ., 1989) Article deposited at MoldNIINTI, N 1145-M (1989)
57. Ya D Tiginyanu, A P Moravskii, V F Shuvalov, V M Berdnikov *Kinet. Katal.* **24** 1038 (1983)
58. E N Rizkolle, J J Anis, L H Knafil *Polyhedron* **109** 7865 (1987)
59. P N Bolasubramanion, E S Schmidt, T C Bruice *J. Am. Chem. Soc.* **109** 7865 (1987)
60. Chan Thi Thanh Phuong, Abstract of Candidate's Thesis in Chemical Sciences, Kishinev, 1984
61. G Davies, L J Kirschenbaum, K Kustin *Inorg. Chem.* 7 146 (1968)
62. C F Walls, D Mays *J. Chem. Soc. A* 665 (1968)
63. M Constantini, A Droward, M Jouref, B Brossard, I Varagnat *J. Mol. Catal.* 7 98 (1980)
64. J Reinado *Analyst* **112** 771 (1987)
65. E G Denisov, N I Mitskevich, V E Agabekov *Mekhanizmy Zhidkofaznogo Okisleniya Kislorodsoderzhashchikh Soedinenii* (The Mechanisms of the Liquid-Phase Oxidation of Oxygen-Containing Compounds) (Minsk: Nauka i Tekhnika, 1975)
66. O S Fedorova *React. Kinet. Catal. Lett.* **8** 371 (1978)
67. N N Lebedev, N G Digurov, T V Bukharina, in *Tezisy Vsesoyuznoi Konferentsii po Zhidkofaznomu Okisleniyu Organicheskikh Soedinenii. Okislenie-86* (Abstracts of Reports at the All-Union Conference on the Liquid-Phase Oxidation of Organic Compounds. Oxidation-86) (Lvov, 1986) Vol. 1, p. 114
68. V G Isac, U Pfanmueller, A Ya Sychev *Zh. Fiz. Khim.* **57** 1969 (1983)
69. A Ya Sychev, U Pfanmueller, V G Isac *Zh. Fiz. Khim.* **57** 1974 (1983)
70. A Ya Sychev, U Pfanmueller, V G Isac *Zh. Fiz. Khim.* **57** 2217 (1983)
71. D G Batyr, V G Isac, S V Kil'mininov *Koord. Khim.* **12** 949 (1986)
72. D G Batyr, V G Isac, A A Kirienko, Yu Ya Kharitonov *Koord. Khim.* **12** 435, (1986)
73. V G Isac, A Ya Sychev *Peroxidase Properties of Manganese(II) Compounds. General Features* (Kishinev: Mold. Gos. Univ., 1988) Article Deposited at MoldNIINTI, N 916-M (1988)
74. D G Batyr, V G Isac, A A Kirienko, S V Kil'mininov *Izv. Akad. Nauk Mold. SSR, Ser. Biol. Khim. Nauk* **5** 46 (1985)
75. D G Batyr, V G Isac, A A Kirienko, I G Povar *Koord. Khim.* **11** 266 (1985)
76. D G Batyr, V G Isac, A A Kirienko, I G Povar *Koord. Khim.* **11** 628 (1985)
77. A Ya Sychev, V G Isac, Chang Thi Thanh Phuong *Zh. Fiz. Khim.* **59** 771 (1985)
78. A Ya Sychev, V G Isac, Chang Thi Thanh Phuong *Zh. Fiz. Khim.* **59** 773 (1985)
79. Ya D Tiginyanu, V P Lozovan *Izv. Vyssh. Uchebn. Zaved., Khim. Khim. Tekhnol.* **21** 1314 (1978)
80. Ya D Tiginyanu, V P Lozovan *Izv. Vyssh. Uchebn. Zaved., Khim. Khim. Tekhnol.* **18** 1229 (1978)
81. Ya D Tiginyanu *Koord. Khim.* **2** 933 (1976)
82. D G Batyr, V G Isac, S V Kil'mininov, S M Fedorova *Peroxidase Properties of Coordination Compounds of Manganese(II) and Glycine. The Outer-Sphere Mechanism of the Oxidation of Substrates* (Kishinev: Mold. Gos. Univ., 1990) Article deposited at MoldNIINTI, N 1167-M (1990)
83. O P Dmitrieva, V E Agabekov, N I Mitskevich *Dokl. Akad. Nauk Beloruss. SSR* **25** 329 (1981)
84. R V Kucher, L I Opeida, T V Novikova *Dokl. Akad. Nauk Ukr. SSR* **5** 37 (1987)
85. I I Korsak, V E Agabekov, V I Bondurko, et al. *Vestsi Akad. Navuk Beloruss. SSR, Ser. Khim. Navuk* **2** 21 (1980)
86. I I Korsak, V E Agabekov, N I Mitskevich *Vestsi Akad. Navuk Beloruss. SSR, Ser. Khim. Navuk* 1 37 (1979)
87. I Tobushi, N Koga *J. Am. Chem. Soc.* **101** 6456 (1974)
88. E A Lukashova, A B Solov'eva, A L Chugreev, N S Enikolopyan *Dokl. Akad. Nauk SSSR* **294** 1167 (1987)
89. A B Solov'eva, V I Mel'nikov, K K Livnitskii *Izv. Akad. Nauk SSSR Ser. Khim.* **10** 2327 (1983)
90. E A Lukashova, A B Solov'eva, G Ya Malinovskii *Kinet. Katal.* **26** 56 (1985)
91. N S Enikolopyan, K A Bogdanova, K A Askarov *Usp. Khim.* **52** 20 (1983) [*Russ. Chem. Rev.* **52** 13 (1993)]
92. A B Solov'eva, T I Karakazova, K A Bogdanova *Dokl. Akad. Nauk SSSR* **269** 160 (1983)
93. N G Ariko, T P Kenigsberg, N I Mitskevich *Neftekhimiya* **22** 653 (1982)
94. St Lunâk, S Veprek-Siska *React. Kinet. Katal. Lett.* **16** 305 (1981)
95. N P Butina, V S Pshezhetskii, D I Stom *Vysokomol. Soedin.* **626** 813 (1984)
96. A R Eichhorn (Ed.) *Inorganic Chemistry* [G L Eichhorn, Inorganic Biochemistry?] (Translated into Russian) (Moscow: Mir 1978) p. 82
97. V D Komisarov, E T Denisov *Kinet. Katal.* **10** 513 (1969)
98. T P Vorob'eva, E G Isac, A P Purmal', A Ya Sychev *Zh. Fiz. Khim.* **48** 1731 (1974)
99. A Ya Sychev, U Pfanmueller, V G Isac *Zh. Fiz. Khim.* **57** 1690 (1983)
100. E R Stadtman, B S Berlett, P B Chock *Proc. Natl. Acad. Sci. USA* **87** 384 (1990)
101. M B Yim, B S Berlett, P B Chock, E R Stadtman *Proc. Natl. Acad. Sci. USA* **87** 394 (1990)
102. V G Isac, A Ya Sychev, Chan Thi Thanh Phuong, in *Sintez, Modifikatsiya i Issledovaniya Polimernykh i Koordinatsionnykh Soedinenii* (The Synthesis, Modification, and Study of Polymeric and Coordination Compounds) (Kishinev: Sitiintsa, 1989) p. 36
103. I E Kalinichenko, E N Matveeva, A G Pilipenko *Kinet. Katal.* **23** 626 (1982)
104. Yu I Skurlatov, Doctoral Thesis in Chemical Sciences, Moscow State University, Moscow, 1980
105. V G Isac, A Ya Sychev *Peroxidase Properties of Manganese(II) Compounds. II. Oxidation of Organic Dyes by OH Radicals* (Kishinev: Mold. Gos. Univ., 1988) Article Deposited at MoldNIINTI, N 911-M (1988)
106. V G Isac, A Ya Sychev *Peroxidase Properties of Manganese(II) Compounds. VI. Inner-Sphere Oxidation of Organic Dyes* Kishinev (Kishinev: Mold. Gos. Univ., 1988) Article deposited at MoldNIINTI, N 915-M (1988)
107. A Ya Sychev, V G Isac, U Pfanmueller *Zh. Fiz. Khim.* **53** 2790 (1979)
108. A Ya Sychev, Mai Hui Him, V G Isac *Zh. Fiz. Khim.* **58** 906 (1984)
109. V G Isac, A Ya Sychev *Izv. Akad. Nauk Mold. SSR, Ser. Biol. Khim. Nauk* **3** 74 (1987)
110. A Ya Sychev, V G Isac *Peroxidase Properties of Manganese(II) Compounds. III. The Influence of Molecular Oxygen* (Kishinev: Mold. Gos. Univ., 1988) Article deposited at MoldNIINTI, N 912-M (1988)
111. A Ya Sychev, V G Isac *Peroxidase Properties of Manganese(II) Compounds. IV. Oxidation by Manganese(IV) Compounds* (Kishinev: Mold. Gos. Univ., 1988) Article deposited at MoldNIINTI, N 923-M (1988)
112. D G Batyr, V G Isac, A A Kirienko, S V Kil'mininov *Koord. Khim.* **12** 949 (1986)
113. K B Yatsimirskii *Kineticheskie Metody Analiza* (Kinetic Analytical Methods) (Moscow: Khimiya, 1967)
114. S U Kreingol'd *Katalimetriya v Analize Reaktivov i Veshchestv Osoboi Chistoty* (Catalymetry in the Analysis of Reagents and Specially Pure Substances) (Moscow: Khimiya, 1983)
115. H Muller, M Otto, G Werner *Catalytic Methods in Trace Analysis* (Translated into Russian) (Moscow: Mir, 1983)
116. A K Lavrukhina, L V Yukina *Analiticheskaya Khimiya Margantsa* (Analytical Chemistry of Manganese) (Moscow: Nauka, 1974)
117. A Ya Sychev, V G Isac, U Pfanmueller *Zh. Anal. Khim.* **33** 1351 (1978)
118. P Bartkus, S Kalesnikaite, L Siaurukaite, E Jasinskiene *Nauch. Tr. Vyssh. Uchebn. Zaved. Lit. SSR, Khim. Khim. Tekhnol.* **8** 37 (1967)
119. S U Kreingol'd, E A Bozhevol'nov, N S Petrovskaya *Metody Analiza Khimicheskikh Reaktivov i Preparatov* (Methods for the Analysis of Chemical Reagents and Preparations) (Moscow: Izd. IREA, 1966) No. 13
120. P Bartkus, E Jasinskiene *Nauch. Tr. Vyssh. Uchebn. Zaved. Lit. SSR, Khim. Khim. Tekhnol.* **11** 25 (1969)

121. V I Martsokha, S U Kreingol'd, L I Sosenkova, in *Sbornik Nauchnykh Trudov VNII Lyuminoforov i Osobo Chistykh Veshchestv* (Collected Reports from the All-Union Institute of Phosphors and Specially Pure Substances) (Moscow, 1977) No. 16, p. 49
122. Chen Gnochu, Fansi Huasjua *Anal. Chem.* **15** 910 (1987)
123. A Ya Sychev, V G Isac, U Pfanmueller *Izv. Akad. Nauk Mold. SSR, Ser. Biol. Khim. Nauk* **4** 88 (1979)
124. P Bartkus, E Jasinskiene *Zh. Anal. Khim.* **23** 1622 (1968)
125. V G Isac, A Ya Sychev *Peroxidase Properties of Manganese(II) Compounds. VIII. Application of the Results in Catalymetry* (Moscow: Mold. Gos. Univ., 1988) Article deposited at MoldNIINTI, N 917-M (1988)
126. Yu I Bratushko *Koordinatsionnye Soedineniya 3d-Perekhodnykh Metallov s Molekulyarnym Kislorodom* (Coordination Compounds of 3*d* Transition Metals with Molecular Oxygen) (Kiev: Naukova Dumka, 1987)
127. E Bayer, P Schretzmann *Structure and Bonding* (Translated into Russian) (Moscow: Mir, 1969)
128. Yu I Bratushko, Abstract of Doctoral Thesis in Chemical Sciences, Kiev, 1991
129. B M Hoffman, C J Wechler, F Basolo *J. Am. Chem. Soc.* **98** 5473 (1976)
130. R D Jones, D A Summervile, F Basolo *J. Am. Chem. Soc.* **100** 4416 (1978)
131. K D Magers, C G Smith, D G Sawyer *J. Am. Chem. Soc.* **100** 989 (1978)
132. A B P Lever, J P Wilshire, S K Quan *Inorg. Chem.* **21** 761 (1981)
133. S D Miller, F D Oliver *J. Inorg. Nucl. Chem.* **34** 1873 (1972)
134. C J Borehan, B Chiswell *Inorg. Chem. Acta* **24** 77 (1977)
135. A Dedien, M M Rohmer *J. Am. Chem. Soc.* **99** 8050 (1977)
136. H D Burcett, V F Newberry, W E Hill, S D Worda *J. Am. Chem. Soc.* **105** 4097 (1983)
137. Li Guang-Nian, Li Guang-Qing *Acta Chem. Sci.* **43** 1053 (1985)
138. K B Yatsimirskii, Yu I Bratushko *Teor. Eksp. Khim.* **18** 367 (1982)
139. N Herron, D H Busch *Inorg. Chem.* **22** 3470 (1983)
140. I Ocura, N K Thuan, T Kaii *J. Mol. Catal.* **5** 125 (1979)
141. I A Duncan, A Harriman, G Parter *J. Chem. Soc., Faraday Trans. 2* **76** 227 (1980)
142. D J Cookson, T D Smith, J F Boas, R Pilbrow *J. Chem. Soc., Dalton Trans.* 1791 (1976)
143. T Yarino, T Matsushito, I Masuda, K Shinra *J. Chem. Soc., Chem. Commun.* 1317 (1970)
144. K Togokichi *Nippon Kagaku Zasshi* **80** 575 (1960)
145. M E Bodini, D T Sawyer *J. Am. Chem. Soc.* **98** 8366 (1976)
146. D T Richens, C G Smith, D T Sawyer *Inorg. Chem.* **18** 707 (1979)
147. A Y Sychev, I M Reibel', L P Podgornaya *Zh. Fiz. Khim.* **43** 676 (1969)
148. I L Benet, F H Hernande, J M Eseriche, R M Zaez *Analyst* **111** 1325 (1986)
149. H S Hertog, E Kooyman *J. Mol. Catal.* **6** 357 (1966)
150. A Ya Sychev, S O Travin G G Duka, Yu I Skurlatov *Kataliticheskie Reaktsii i Okhrana Okruzhayushchei Sredy* (Catalytic Reactions and Protection of the Environment) (Kishinev: Shtiintsa, 1983)
151. A B Solov'eva, A I Samokhvalova, E I Karakozova *Kinet. Katal.* **25** 1080 (1984)
152. S P Prokipchuk, B V Ivakh, in *Tezisy Dokladov 6 Vsesoyuznoi Nauchnoi Konferentsii po Okisleniyu Organicheskikh Soedinenii v Zhidkoi Faze. Okislenie-86* (Abstracts of Reports at the 6th All-Union Conference on the Oxidation of Organic Compounds in the Liquid Phase. Oxidation-86) (Lvov, 1986) Vol. 2, p. 43
153. V G Isac, A Ya Sychev, L B Voziyan, in *Mezhvuzovskii Sbornik* (Intercollegiate Collection) (Kishinev, 1991) p. 89
154. G Gravenhorst, S Beilke, M Betz, H-M Gheovgii, in *Effects of Acid Precipitation on Terrestrial Ecosystems* (Eds T C Hutchinson, M Havis) (New York: Plenum, 1980) p. 41
155. F E Brickman, G J Olson, W P Iverson, in *Atmospheric Chemistry* (Ed. E D Goldberg) (Berlin: Springer, 1982) p. 231
156. H Harirson, T V Larson, C S Monkman *Atmos. Environ.* **16** 1039 (1982)
157. M R Hoffman, D J Jasov, in *SO_2, NO_2 and NO Oxidation Mechanisms: Atmospheric Considerations* (Ed. G Calbert) (Boston: Ann Arbor Science, 1984) p. 101
158. G E Zaikov, S A Maslov, V L Rubailo *Kislotnye Dozhdi i Okruzhayushchaya Sreda* (Acid Rain and the Environment) (Moscow: Khimiya, 1991)
159. A Huss, P K Lim, C A Eckert *J. Phys. Chem.* **86** 4224 (1982)
160. M J Matteson, W Stober, H Luther *Ind. Eng. Chem., Fundam.* **6** 677 (1969)
161. S A Penkett, in *Chemistry of Multiphase Atmospheric Systems* (Ed. W Jaeschke) (Berlin: Springer, 1986) p. 507
162. V V Volod'ko, A A Revin *Kinet. Katal.* **32** 1362 (1991)
163. R G Zika *J. Geophys. Res.* **87** 5015 (1982)
164. D W Gunz, M R Hoffman *Atmos. Environ.* **24** 1601 (1990)
165. T Ibusuki, H M Barnes *Atmos. Environ.* **18** 145 (1984)
166. F W Lurmann, J R Yong, G M Hidy, in *Chemistry of Multiphase Atmospheric Systems* (Ed. W Jaeschke) (Berlin: Springer, 1986) p. 773
167. L W Richards *Atmos. Environ.* **17** 397 (1983)
168. C L Jones, J H Seinfeld *Atmos. Environ.* **21** 2370 (1987)
169. B G Heikes, A M Tompson *J. Geophys. Res.* **88** 10883 (1983)
170. W R Stockwell, J L Calvert *J. Geophys. Res.* **88** 6673 (1983)

Russian Chemical Reviews **62** (4) 291 – 321 (1993)
© 1993 Russian Academy of Sciences and Turpion Ltd

UDC 538.737

Metal-containing liquid-crystal phases

A P Polishchuk, T V Timofeeva

Contents

I. Introduction	291
II. Metal-containing ionic liquid crystals	291
III. Liquid-crystal coordination compounds	294
IV. Conclusion	310

Abstract. Data on the synthesis, structures, and properties of ionic, coordination, organometallic, and organoelement compounds with liquid-crystal properties are surveyed. The substances examined are new in the chemistry of liquid-crystal compounds. Their potential applications are described. The bibliography includes 211 references.

I. Introduction

Liquid crystals have been known for more than 100 years but the number of structural types and of classes of chemical compounds capable of exhibiting mesomorphic properties has increased significantly only during the last 15 – 20 years. For example, discotic, columnar, and nematic phases,[1-3] cup-shaped liquid crystals,[4] and columnar associated species in which the molecules are linked by a system of hydrogen bonds have been added recently to the structural types of low-molecular-mass liquid crystals alone.[5,6] New classes of mesogenic chemical compounds include also coordination compounds, usually complexes of mesogenic ligands with various metals,[7,8] as well as certain organometallic and organoelement compounds. Furthermore, new data have appeared recently on salts of organic acids possessing mesomorphic properties, which have been known for a long time.[9]

Evidently the physical properties of the compounds listed above should differ from those of classical organic mesogenic substances. Thus metal containing mesogenic substances are usually paramagnetic and this leads to new possibilities for their practical use.

In the present review, we have attempted to survey data on the methods of synthesis (in those cases where they are not trivial), structures, and properties of new metal-containing mesogenic substances. Furthermore, we endeavoured to trace, wherever possible, the relation between molecular structure, type of packing in the crystal, and the nature of the existing intermolecular interactions, on the one hand, and the tendency manifested (or not manifested) by the given compound to form definite types of mesophases, on the other. Such analysis permits a deeper understanding of the characteristics of the structures of liquid crystal phases, the discovery in many cases of new types of mesophases, and also the prediction of the presence of mesogenic activity in specific compounds.

It is noteworthy that analysis of the authors' own studies occupies an appreciable place in the present review, since the studies by foreign investigators have been described in fair detail in the review of Giroud-Godquin and Maitlis.[7] Unfortunately, the latter review includes hardly any work published in Soviet journals and we believe that the present article should fill this gap.

In analysing the relevant data, one can employ different approaches to the classification of the test objects. We believe that it is most useful to arrange mesogenic metal-containing compounds in groups in the following way: ionic compounds, coordination compounds (the most numerous group which can be subdivided in terms of the types of ligands), organoelement compounds, and organometallic compounds. However, one should bear in mind the arbitrary nature of this classification and the possibility of assigning the same compound to different groups simultaneously.

We shall not dwell on the structural classification of the types of liquid crystals, since it has been described in fair detail in a monograph[10] and also in other reviews.[3,11] We shall restrict consideration to principal low-molecular-mass thermotropic liquid crystals, since high-molecular-mass as well as lyotropic liquid crystals constitute separate independent groups.

II. Metal-containing ionic liquid crystals

Ionic liquid crystals have long been known. A characteristic feature of these compounds — the possibility of the separate existence of the cationic and anionic components of the molecules in the mesophase (in contrast to molecular liquid crystals in which the metal is firmly coordinated to the ligand atoms) — gives rise to a series of new properties of such phases. Typical representatives of ionic liquid crystals are carboxylic acid salts.

1. Carboxylic acid salts

As early as 1910, Vorländer[12] first observed the liquid-crystal state on fusion of salts of long-chain carboxylic acids referred to as soaps.

Structural studies at high temperatures on the anhydrous thermotropic mesophases of a series of homologues of salts of long-chain aliphatic acids $C_nH_{2n+1}COOH$ (n = 9 – 19, odd values of n) have been described in a number of communications.[13-16] The following structures were established in these investigations on the basis of X-ray diffraction data: layered (smectic) structures with an ordered or disordered

A P Polishchuk Laboratory for Spectroscopic Methods, Institute of Physics, Academy of Sciences of the Ukraine, prosp. Nauki 46, 252028 GSP-650 Kiev, Ukraine
T V Timofeeva Laboratory for X-Ray Diffraction Studies, A N Nesmeyanov Institute of Organoelement Compounds, Russian Academy of Sciences, ul. Vavilova 28, 117813 GSP-1 Moscow. Fax (7-095)135 50 85.

Received 22nd October 1992
Uspekhi Khimii **62** (4) 319 – 350 (1993); translated by A K Grzybowski

disposition of aliphatic chains, discotic structures with an orthogonal lattice (for example, in the sodium salts of aliphatic acids), and columnar (ribbon) structures with a hexagonal packing of the columns. In layers of homologues of the same metal, it is possible to observe the entire set of structural types described. For example, calcium carboxylates are characterised below 100 °C by a layered structure with the disposition of the alkyl chains at right angles to the plane of the layer, while in the range from 120 to 180 °C they are characterised by hexagonal packing of cylindrical associated species.[16] Unfortunately, X-ray diffraction studies on the mesophase do not permit the determination of the detailed pattern in the packing of the molecules in discs and cylinders[13-16] and the most likely hypotheses concerning their structures can be formulated only on the basis of X-ray diffraction studies of the corresponding single crystals.

At the beginning of the 1970s, it was observed that the homologues of the salts of lower carboxylic acids also exhibit thermotropic mesomorphism.[17] Their structures and thermodynamic, transport, and optical properties have been reviewed.[9]

The observation of mesophases in such compounds, which have been called ionic liquid crystals (ILC), was fairly unexpected since the presence of extended molecules, usually one of the main conditions for the manifestation of mesomorphism, is not characteristic of these substances. It is believed[9] that the species constituting these mesophases are quasi-globular associated formations containing metal cations (Na^+, K^+, Ba^{2+}, Tl^+, Cd^{2+}, Cs^+) and carboxylate anions (n-$C_nH_{2n+1}COO^-$, $2 \leqslant n < 7$). The latter do not exhibit an explicit anisometry (the length to width ratio does not exceed 2). Furthermore, in contrast to the classical molecular liquid crystals, ionic liquid crystals are characterised by a high ratio of the electrostatic charges on the constituent components to the total number of atoms, which leads to the predominance of Coulombic forces over van der Waals forces in the formation of their structure. Ionic liquid crystals have an intrinsic conductivity which exceeds by 6–8 orders of magnitude the impurity conductivity in classical organic liquid crystals. Data obtained by Meisel et al.[18] indicate that the charge transfer in the carboxylate melts is effected mainly by metal cations.

The structure of the mesophases of ionic liquid crystals has been investigated by X-ray diffraction, ^1H NMR, and ^{23}Na NMR for sodium butyrate and isovalerate[19-21] and by X-ray diffraction for potassium caproate (hypotheses concerning the structure were put forward on the basis of X-ray diffraction studies on single crystals[22]) and thallium and sodium n-alkanoates.[23-25] It has recently been possible to investigate a series of crystal structures of such salts and this yielded more refined and detailed information about the structure of the mesophases.

There have been few structural studies on the single crystals and thermotropic mesophases of metal alkanoates and complete X-ray diffraction analysis has been achieved mainly for certain hydrated formates and acetates.[26] The reason for this is the difficulty of obtaining single crystals of salts of this group. However, reports have recently appeared concerning structural studies on such salts, in particular barium butyrate ($BaBut_2$), which forms a smectic phase A:

$$\text{Crystal (C)} \xrightarrow{240\ ^\circ\text{C}} \text{smectic phase (SmA)} \xrightarrow{304\ ^\circ\text{C}} \text{isotropic liquid (IL).}$$

This compound was synthesised by the method described by Hazlewood et al.[27]

The crystal structure of $BaBut_2$ contains two symmetrically independent barium atoms, each of which is coordinated to eight oxygen atoms.[28] The coordination of the barium atoms can be described in terms of a polyhedron, the lower and upper bases of

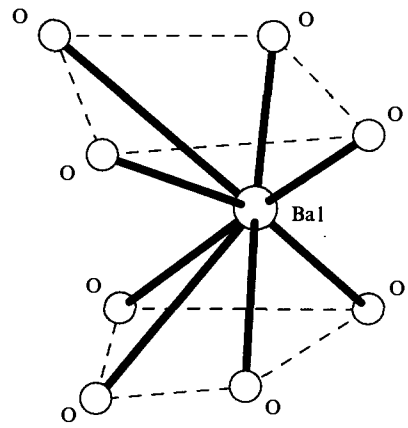


Figure 1. Coordination of the Ba(1) atom in the $BaBut_2$ structure.[28] The angle between the planes formed by the oxygen atoms is 9°.

which comprise irregular rectangles rotated relative to one another (Fig. 1). In this coordination, the barium atom is, as it were, compressed by two 'oxygen lids', on either side of which the alkyl chains of the butyrate anions are disposed. The metal–oxygen bonds are significantly ionic (the sum of the ionic radii is less than or equal to the Ba–O distances found in the crystal: 2.687–2.936 Å). It should be especially noted that Mirnaya et al.[28] established for the first time the disposition of the metal cations and the carboxylate groups of the anions for ionic liquid crystals. Since the type of packing of the molecules in the mesogenic crystal can be to some extent inherited by the mesophase, the observed coordination of the metal should be retained, at least in broad outline, also in the mesophase, as has been observed, for example, for metal complexes of Schiff bases and a number of other compounds.[5,6,8] The packing of the molecules in the $BaBut_2$ crystal has an explicit bilayer character and within each double layer hundreds of barium and oxygen atoms form electrically charged cation–anion strata separated from one another by layers of alkyl substituents (Fig. 2). One may postulate that during fusion the 'acceleration' of the alkyl substituents occurs before the breakdown of the barium–oxygen strata. As a result, the sliding of the alkyl layers relative to one another becomes possible, which favours the formation of the smectic mesophase.

Low angle scattering studies on the vitrified $BaBut_2$ mesophase showed[28] that the thickness of the bilayer (14.02 Å) is somewhat smaller than that of the corresponding bilayer in the crystal (14.63 Å). This may be associated with the partial compression of the layers in the mesophase due to the strong electrostatic interactions between neighbouring bilayers. The same effect has been observed also for homologues of thallium n-alkanoates,[29] where there are considerable possibilities for conformational changes in the alkyl chains. The addition of different amounts of sodium butyrate (20, 40, and 50 mol%) to the $BaBut_2$ melt hardly alters the interlayer distance in the mesophase. This can be explained by the similar polarising capacities of both cations and also by the fact that the changes in composition indicated do not entail appreciable changes in the nature of the electrostatic interactions in the cation–anion stratum and hence in the bulk of the stratum.

The smectic mesophase A has been observed[30] also for the hydrated form of cadmium isovalerate, the structure of which is in broad outline similar to that of $BaBut_2$.

$$\text{C} \xrightarrow{180\ ^\circ\text{C}} \text{SmA} \xrightarrow{237\ ^\circ\text{C}} \text{IL}$$

The metal atom in the crystal occupies a specific position on the twofold axis and is coordinated to six oxygen atoms, two of which belong to water molecules. The coordination environment of the

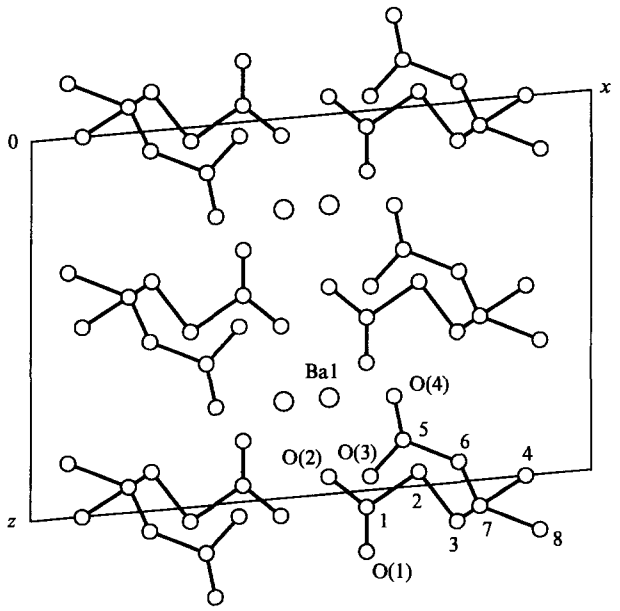


Figure 2. The packing of the first independent barium butyrate molecule in projection onto the *xz* plane.

cadmium atom is represented by a polyhedron, the lower and upper bases of which comprise triangles made up of oxygen atoms and linked by a twofold crystallographic axis. The angle between them is 14.8°. The disposition of the molecules in the cadmium complex is of the double layer type, as in the $BaBut_2$ crystal: the cadmium and oxygen atoms form strata between which the alkyl chains are accommodated. The presence in the structure of two water molecules leads to the formation of two chains of hydrogen bonds which join together the anions within one bilayer.

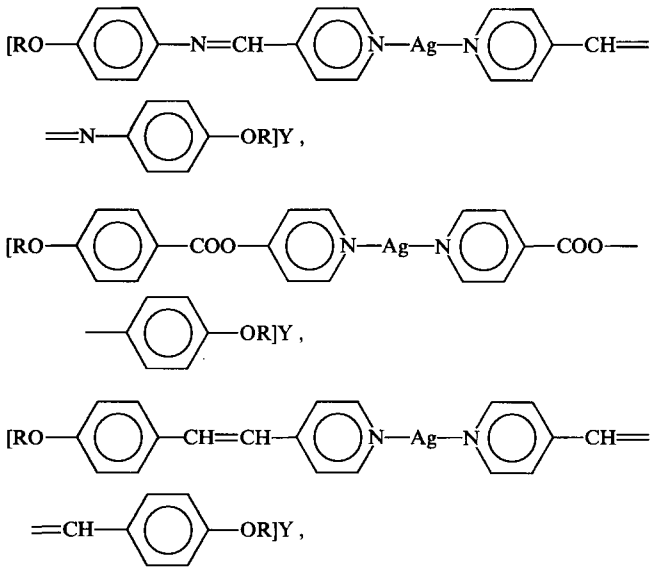
The thickness of the bilayers in the mesophase (14.1 Å) exceeds appreciably the thickness of the layers in the crystal (12.29 Å). This can be explained by the inclined disposition of the molecules in the crystal relative to the plane of the layer, which changes to an orthogonal disposition on passing to the smectic phase A. IR spectroscopic studies have shown that, when crystals of cadmium isovalerate are heated and pass to the mesophase, there is only partial loss of water, the presence of which is responsible for the mesomorphism (the anhydrous substance does not form the mesophase).[30]

The absence of mesomorphism in magnesium butyrate hydrate ($MgBut_2.4H_2O$), the crystal structure of which is also characterised by a bilayer disposition of the molecules,[30] can be attributed to the high polarising capacity of the cation, as a result of which the condition for the existence of ionic liquid crystals, namely $Z_k/r_k^2 < 1.05$ (Z_k and r_k are respectively the charge and radius of the cation) is not fulfilled because of the small radius of the metal.[31] However, we believe that the presence in the crystal of a branched three-dimensional network of hydrogen bonds is also unfavourable for the manifestation of mesomorphism. Furthermore, water molecules shield the Mg^{2+} cation in such a way that the second butyrate anion is not linked directly to the metal cation. The presence of such a bond is apparently essential for the formation of ionic liquid crystals.

It is noteworthy that ionic liquid crystals and their binary mixtures are promising materials for the preparation of supercooled mesomorphic substances—liquid-crystal glasses. Furthermore, ionic liquid crystals exhibit a high optical sensitivity, which can be varied by the application of even weak electric fields.

2. Salts of complex cations

Silver salts with complex cations and various anions constitute a fairly numerous group of ionic liquid crystals:[32, 34]



where $Y = BF_4^-$, NO_3^-, $CF_3SO_3^-$, or $C_{12}H_{25}SO_4^-$ and $R = C_nH_{2n+1}$. Wider ranges of conditions for the existence of mesophases and a greater variety of polymorphic modifications than for salts with imino-ligands are characteristic of salts with ester ligands in this group. The greatest number of mesomorphic phases has been observed for salts with stilbazole ligands and the dodecyl sulphate anion (DOS), this being particularly notable for the alkoxy-homologues with $n > 5$.

Fig. 3 presents the phase diagram for the homologues of the last of the salts listed above [derivatives of *trans*-4-alkoxy-4′-stilbazole (TAS)]. The columns on the diagram correspond to phase transitions investigated by differential scanning calorimetry and X-ray diffraction, including the procedure using synchrotron radiation. For example, on the X-ray diffraction pattern for the $[Ag(TAS)_2][DOS]$ ($R = C_3H_7$) nematic phase, a peak was found corresponding to a distance of 33.1 Å, in good agreement with the length of the complex anion, which is 35.1 Å. For the homologue with $R = C_{12}H_{25}$, the phase at 138 °C was identified as cubic with a unit cell parameter of 73.4 Å. This isotropic cubic phase (M_I on the phase transitions scheme—see Fig. 3) proved to be similar to the phase D found earlier for biphenylcarboxylic acids.[35] The properties of salts with other anions (NO_3^-, $CF_3SO_3^-$) are close to

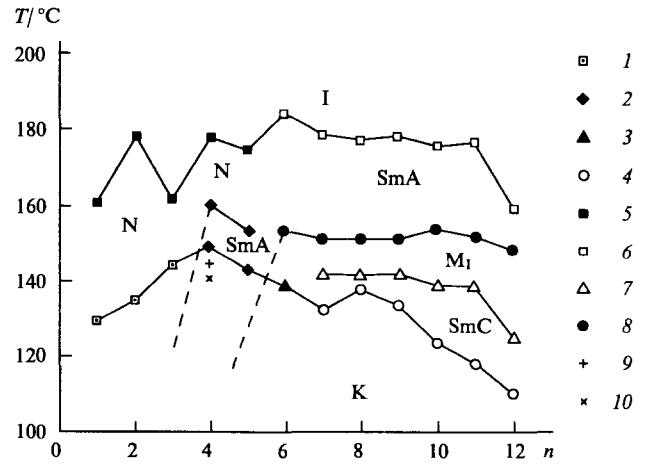


Figure 3. Phase diagram for the $[Ag(TAS)_2][DOS]$ homologues.[34] The region of existence of the SmA phase is indicated by dashed lines. Phase transitions: (*1*) C → N; (*2*) C → SmA and SmA → N; (*3*) C → M_I; (*4*) C → SmC; (*5*) N → I; (*6*) SmA → I; (*7*) SmC → M_I; (*8*) M_I → SmA; (*9*) SmA → N_R; (*10*) N_R → SmC; N = nematic phase, N_R = reverse nematic phase; C = crystal; I = isotropic liquid.

those found for the DOS salts, but they do not form so many polymorphic phases. The pronounced poly-morphism of the silver salts examined may find applications in electrochemistry.

III. Liquid-crystal coordination compounds

At the present time coordination compounds constitute the most numerous group of metal-containing liquid-crystal substances which has also been investigated in greatest detail. Their behaviour is similar to that of classical organic liquid crystals, since, in contrast to ionic liquid crystals, they represent molecular phases. However, the presence of a metal naturally gives rise to a series of new properties.

In this section we shall consider complexes with carboxylate, β-diketonate, salicylaldiminate, and other ligands, the majority of which are also mesogenic compounds in the noncoordinated state. Comparison of the structures of the mesophases of the coordination compounds and the free ligands is of interest in many instances since it makes it possible to predict the trend in the variation of the properties of these compounds.

1. Complex mesogenic substances with carboxylate ligands

Copper stearate was the first to be investigated among the mesogenic carboxylates.[36] The method of synthesis, the structures of the solid and liquid crystal phases, and the mobilities of the molecules of the above compound and other carboxylates of the type $M_2(\mu\text{-}O_2CC_nH_{2n+1})_4$, where $n > 4$ and M = Cu, Ru, Rh, or Mo, have been investigated by many workers.

Divalent metal carboxylates are usually obtained by the exchange reactions between alkali metal salts of aliphatic acids and the salts of the corresponding divalent metals. Furthermore, it is possible to obtain them by fusing aliphatic acids together with metal hydroxides.[37] The molecular structure of the carboxylates is fairly well known[38-40] on the basis of X-ray diffraction data for single crystals of copper alkanoates with n = 4, 8, and 10. Their molecules are dinuclear complexes in which each copper atom is involved in a square-bipyramidal coordination and is surrounded by four oxygen atoms in the equatorial plane. One of the vertices of the pyramid is occupied by the copper atom and another is occupied by an oxygen atom of a neighbouring complex (Fig. 4). The average Cu–O distance for all five oxygen atoms is 2.01 Å and the Cu–Cu distance is 2.59 Å. The molecules in the crystals of the alkanoates investigated are packed in stacks in such a way that the axis of the stack passes through the centres of gravity of the molecules.

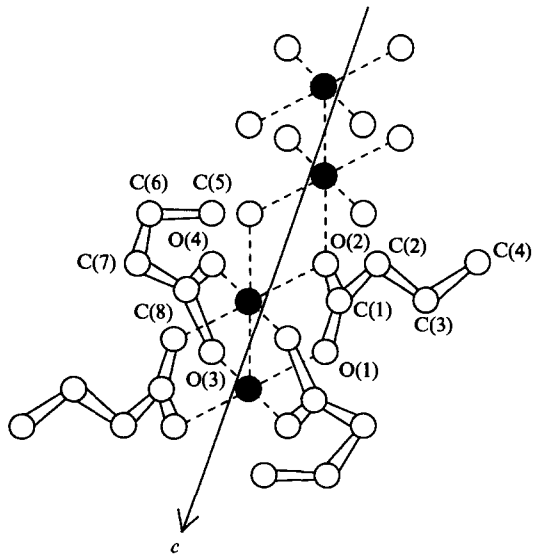


Figure 4. The structure of the copper carboxylate complex (n = 4) in the crystal.[38] The arrow indicates the direction of the column.

Systematic studies have been made[41-45] on copper carboxylates with n = 4–24 by differential scanning calorimetry, optical microscopy, X-ray diffraction of the mesophase, and EXAFS spectroscopy. X-Ray diffraction study of the mesophase showed[45] that, at temperatures above 120 °C, copper carboxylates form a columnar discotic phase with a planar hexagonal lattice. In the mesophases investigated, the nuclei of the dinuclear complexes are arranged along the axis of the column and, regardless of the length of the alkyl chains, the distance between the neighbouring complexes in the column is 4.7 Å. The distances between the columns themselves vary as a function of the length of the alkyl chains and amount to 15–25 Å. We may note that the disposition of the molecules in the mesophases considered (Fig. 5) and in the single crystals of these compounds is similar. It is believed[42] that the mesophases of the copper carboxylates are the first example of a thermotropic columnar liquid crystal phase in which the molecules with four equivalent substituents (the intrinsic symmetry of the molecule approaches the quaternary symmetry) form a hexagonal phase. EXAFS spectroscopic data confirmed that the metal–metal distance in the dinuclear complex remains unchanged when the crystal passes to the mesomorphic state.[43]

The carboxylate complexes of tetrakis[2,2-(dioctyl)acetate-*O*,*O*′]dicopper(II) have been investigated.[46] A distinctive feature of these complexes with branched substituents is the fact that the temperature of the range corresponding to the existence of the mesophase is reduced below room temperature and reaches −20 °C. It may be that, apart from the chain branching, this is influenced also by the presence of impurity ions in the mesophase. X-Ray diffraction study made it possible to assign this mesophase to the discotic columnar hexagonal type with distances of 4.6 Å between the discs and 21.5 Å between the columns. Molecular complexes between the above copper carboxylate and pyrazine and 4,4′-bipyridyl also form mesophases, the structure of which has not yet been established unambiguously.

A similarity in the behaviour and structure has been noted for divalent rhodium carboxylates and the analogous copper complexes.[47] According to EXAFS spectroscopic data, the Rh–Rh distance in the dimeric complex $Rh_2(\mu\text{-}O_2CC_7H_{15})_4$ is 2.38 Å, while the intermolecular distance Rh...Rh, which completes the coordination of the metal atom, is 3.16 Å. The presence of the additional coordination in the mesophase has been confirmed also by Raman spectroscopic data.[48] This suggested that the authors dealt in this instance for the first time with a columnar type complex in which there is a chain of metal–metal bonds within the discotic column. Mesophases with a similar structure have been observed also for dinuclear chromium and molybdenum complexes,[49,50] in the latter case the metal atoms being linked by a quadruple bond. Similar phases have been found for dinuclear ruthenium(II) complexes. The synthesis and properties of the mixed valence ruthenium complexes $Ru(RCO_2)_4X$, where R = C_8H_{17} or $C_{11}H_{23}$ and X = Cl or RCOO, have been described.[51] It was found that the complexes with X = Cl are nonmesogenic, while those with X = RCOO form hexagonal (R = $C_{11}H_{23}$) or orthogonal (R = C_8H_{17}) columnar mesophases.

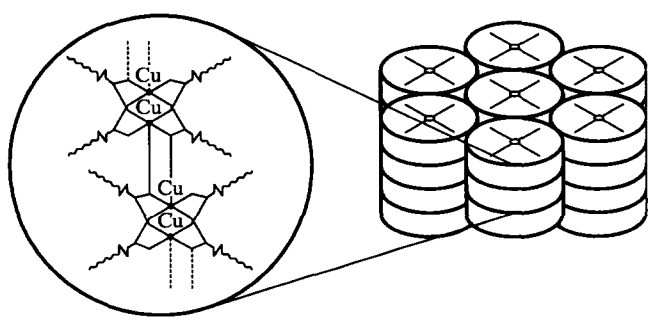
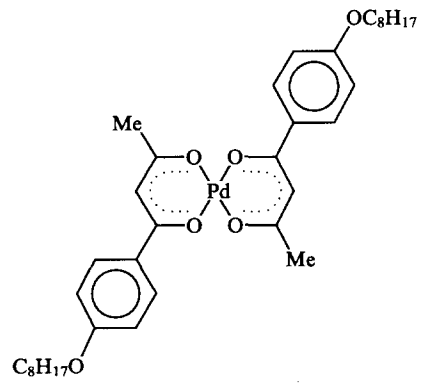


Figure 5. The columnar mesophase of copper carboxylates.[7]

These compounds are apparently the first example of liquid crystals with a mixed valence.

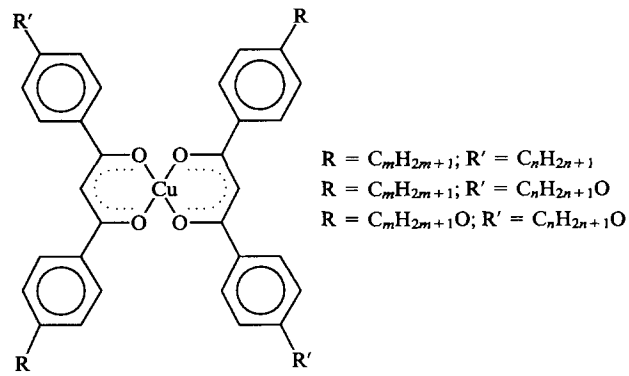
2. Mesogenic complexes of β-diketonates

The diligand complexes of β-diketones, especially those with palladium and copper having suitable substituents, exhibit mesomorphic properties in many cases. These complexes can be obtained by the reaction of β-diketones with the salts of the corresponding metals. Mesomorphism was first observed and described[52] for the palladium complex, the molecule of which is rod-shaped.



It has been stated[52] that, although the above complexes exhibit mesomorphism (according to differential scanning calorimetric data), it has not been possible to investigate it by optical methods owing to the darkening of the specimens on heating. The analogous copper complexes with alkyl substituents of different lengths do not exhibit mesomorphism.[53]

The copper complexes, first described by Giroud-Godquin and Billard,[54,55] in which the β-diketonate ligands each have two phenyl groups with the same or different terminal substituents in the *para*-position, are assumed to be much more promising mesogenic substances.



Complexes of this type tend to form highly ordered discotic, especially layered, phases. The complexes of β-diketonates with identical alkyl substituents at the phenyl groups have higher melting points and clarification temperatures than the same complexes with different substituents. For example, the range of existence of the mesophase is 71–122 °C for $n = 7$ and $m = 13$, 89.5–128.5 °C for $n = m = 10$, and 95.1–113.4 °C for $n = m = 12$. It has been established[7] that the region corresponding to the existence of the mesophase is wider for complexes with terminal alkyl substituents than for complexes with alkoxy-substituents. On the other hand, the analogous nickel diketonate complexes do not form mesophases at all.[55]

The structures of the single crystals of two complexes of this series with R = R' = $C_8H_{17}O$ and R = R' = C_8H_{17} have been established.[56–58] We may note that hitherto this has been achieved only for very few compounds forming discotic phases. According to X-ray diffraction data, the copper atom has a square planar configuration and the angle of rotation of the benzene rings relative to the plane of the central nucleus does not exceed 20°. As in other mesogenic molecules,[5,8] the alkyl chains are characterised by high thermal factors, indicating their appreciable mobility, which decreases even further in the mesophase.

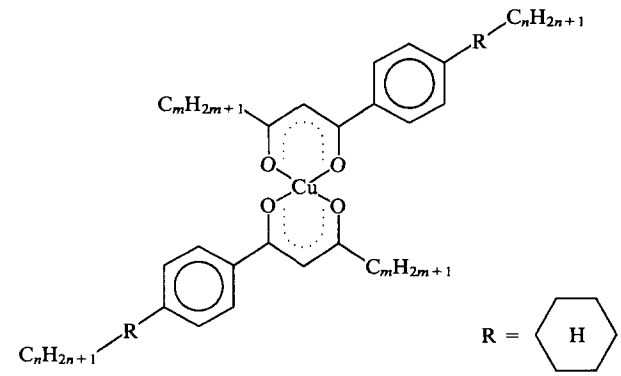
The packing of the molecules in the crystal with R = OC_8H_{17} is of the layered-columnar type.[57] In contrast to the usual discotic phases, the molecules in the column are grouped into centrosymmetric dimers and each column is surrounded by six neighbouring columns, but their relative disposition is far from being of the hexagonal type. The central part of the column is surrounded on all sides by alkyl substituents belonging to the given column and neighbouring columns (Fig. 6).

The columnar arrangement is not, however, characteristic of all compounds of this series. Thus X-ray diffraction data for the mesophase of molecules with R = R' = $C_{12}H_{25}$[59] made it possible to attribute to it a layered structure with a uniform distribution of molecules in the layer and without a columnar ordered arrangement.

It has been shown[60,61] that an increase in the number of substituents in the benzene rings of 1,3-diphenyl-β-diketones also makes it possible in a number of instances to obtain discotic compounds. Discotic phases have been observed for phenyl-substituted copper complexes with hydroxyalkyl substituents in the 3- and 4-positions, but have not been found for 3,5-diphenyl-substituted complexes. The analogous nickel complexes do not form mesophases. Mesophases have also not been observed for a number of other complexes with alkyl substituents.[62]

In the presence of substituents in the benzene rings, imparting to the β-diketone compounds a significant anisometry (for example in the case of copper complexes[63,64] with R = Ar-$C_{10}H_{21}$ and R' = Me, Et, OMe, OEt, or OPr), the type of the mesophase formed changes. It becomes nematic, retaining at the same time features characteristic of discotic nematic phases. It is believed[65] that this group of compounds is the first example of biaxial nematic metallomesogenic substances.

Similar complexes with one phenyl and one alkyl substituent in the β-diketone ligand also form nematic phases.[66]



It has been possible to investigate the crystal structures of two of them with $n = 3$ and $m = 1$, and with $n = 3$ and $m = 8$.[66] The structure of the first molecule is nearly planar (with the exception of a slight rotation of the benzene rings, by not more than 12°, relative to the plane of the metal chelate ring). On the other hand, the second molecule is significantly nonplanar: not only the benzene rings have been displaced from the central plane (by not more than 21°) but also the alkyl substituent (by ~40°). Evidently, the compound constructed from rod-shaped molecules with $n = 3$ and $m = 1$ exhibits nematic properties. The molecules with $n = 3$ and $m = 8$ are packed in the crystal in layers, which indicates the possibility of the existence of the smectic phase. However, the compound forms only a monotropic nematic phase. In our view, this can be explained precisely by the presence in the crystal of layers, which must be disrupted to achieve the transition to the nematic phase directly from the solid phase. Apparently such disrupting effect on the layered structure

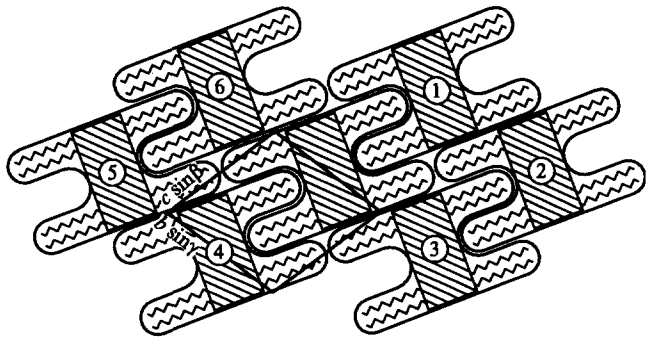
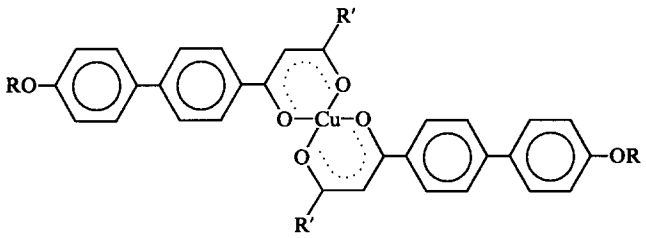


Figure 6. Columns in the crystal[57] of a copper β-diketonate complex (R = OC_8H_{17}). The dimers are surrounded by a continuous line and their central parts are shaded. The numerals denote the nearest neighbours of the dimer.

is exerted by the added 4-cyano-4′-(4″-*n*-pentylcyclohexyl)-biphenyl. The reason for the absence of the smectic phase can be found by analysing the energy of the intermolecular interaction, for example by the method used by Polishchuk et al.[8]

At first sight it is entirely natural to postulate, on the basis of the shape of the molecule, the presence of a nematic mesogenic phase for compounds having the general formula



the synthesis, properties, and structure of which have been described in the case of homologues with R′ = Me, R = C_nH_{2n+1}, and n = 8–12, 16, or 18.[67]

All the homologues indicated, except that with n = 8, form the so called orthogonal columnar ordered discotic mesophase D_{ho}, which had not been mentioned initially in the classification of discotic mesophases proposed by Destrade et al.,[68] but which has been recently added to this classification.[69] The mesophase of the homologue with n = 16 has been studied in greatest detail by X-ray diffraction. The results made it possible to construct a model of the mesophase (Fig. 7). The molecules of this homologue are rod-shaped and not disc-shaped and the authors therefore assume that the elementary units from which the columns are made up are molecular dimers. Similar dimers had been detected also previously in the crystal structures of discotic substances, in particular in the complexes, mentioned above, described by Usha et al.[56] and Muhlberger and Haase.[66] The dimers (Fig. 7*a*) are arranged in an ordered fashion along the column axis (Fig. 7*b*). The disposition of the columns is characterised by a planar orthogonal lattice $C2/m$ symmetry having the parameters indicated in Fig. 7*c*. This example confirms yet again that not only the shape of the molecule but also the nature of their aggregation within the mesophase is important for the formation of a columnar discotic phase. In our view, however, this phase should not be referred to as discotic, since it contains no disc-shaped molecules and should probably be assigned to the class of phases made up of columnar associated nondiscotic molecules, for example, of the kind described by Polishchuk and coworkers.[5,6]

As a result of the introduction into the above complexes of more bulky substituents R′, for example, C_4H_9, C_8H_{17}, and $C_{12}H_{25}$, the molecules become less anisometric and cease to form discotic phases of type D_{ho}, forming instead enantiotropic or

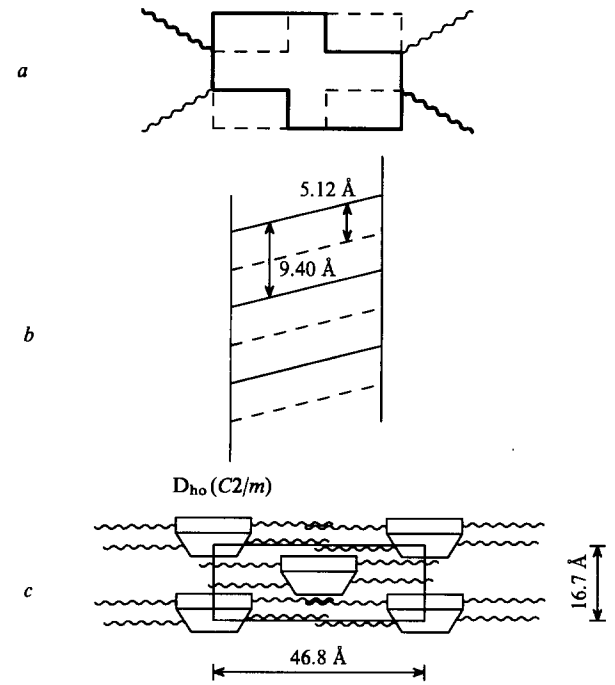


Figure 7. 'Discotic' phase made up of rod-shaped molecules:[67] (*a*) schematic illustration of the structure of the molecular dimer; (*b*) disposition of the dimers in stacks (interdimer distance 9.40 Å, intradimer distance 5.12 Å); (*c*) schematic illustration of the packing of the columns in the orthogonal mesophase — the parallelopipeds represent the central parts of the molecular dimers.

monotropic nematic phases.[70] The phase transitions in these compounds are illustrated schematically in Table 1. The nature of the nematic mesophase is determined by the ratio of the lengths of the substituents R and R′, i.e. by the shape of the molecule. The replacement of the small methyl groups (Fig. 8*a*) by the more bulky n-butyl groups (Fig. 8*b*) prevents the formation of the discotic phase D_{ho} and, on still further increase in their length and hence in the mobility and disorder of the terminal alkyl substituents, the nematic phase can be obtained only from the isotropic liquid on rapid cooling. After prolonged maintenance of the melt at a temperature several degrees below the clarification temperature, the formation of helicoidal mesophases was

Table 1. Phase transition temperatures (°C) in nematic copper β-diketonate complexes.

R	R′	Phase transition
C_4H_9	C_4H_9	C $\xleftrightarrow{201.0}$ N $\xleftrightarrow{205.3}$ IL
C_8H_{17}	C_4H_9	C $\xleftrightarrow{170.0}$ N $\xleftrightarrow{176.3}$ IL
$C_{12}H_{25}$	C_4H_9	C $\xleftrightarrow{111.5}$ C_2 $\xleftrightarrow[\text{slow}]{153.3}$ IL; C_2 $\xrightarrow{\text{fast}}$ N $\xrightarrow{}$ IL
C_8H_{17}	C_8H_{17}	C $\xleftrightarrow[\text{slow}]{166.9}$ IL; C $\xrightarrow{155,\ \text{fast}}$ N $\xrightarrow{}$ IL
$C_{12}H_{25}$	$C_{12}H_{25}$	C_1 $\xrightarrow{108.5}$ C_2 $\xrightarrow{128.5}$ C_3 $\xrightarrow{139.5}$ IL; C_3 $\xrightarrow{}$ C_4 $\xleftrightarrow[\text{slow}]{147.5}$ IL; C_4 $\xrightarrow[\text{fast}]{137.0}$ N $\xrightarrow{}$ IL

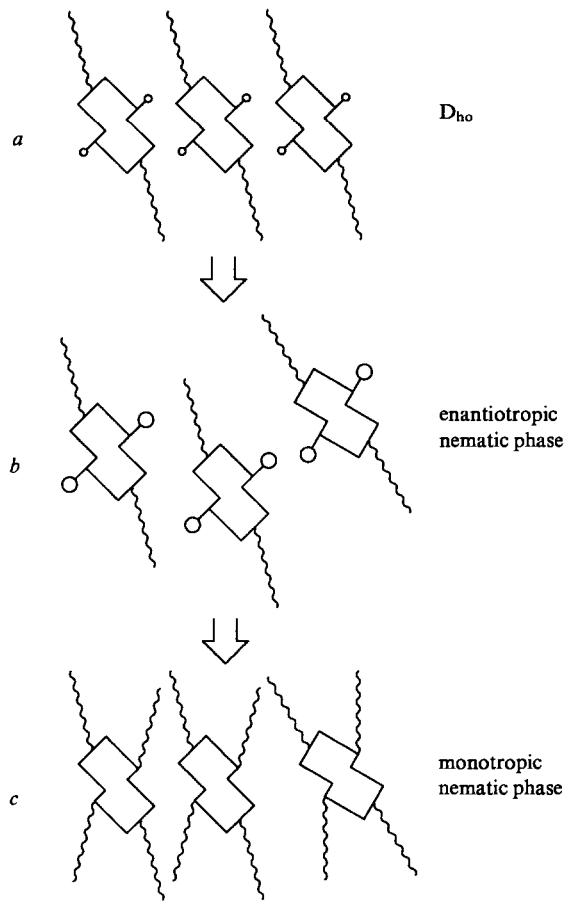
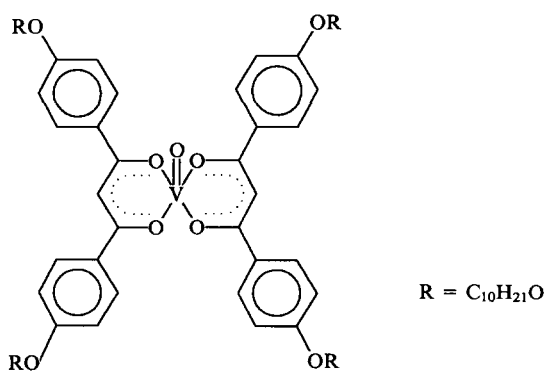


Figure 8. Three types of molecules forming the 'discotic' (*a*), enantiotropic (*b*), and monotropic (*c*) nematic phases.[70]

observed for compounds exhibiting monotropic nematic mesomorphism (Fig. 8*c*). It is of interest that the corresponding noncoordinated ligands form smectic phases.[70]

Nematic mesophases of the enantiotropic or monotropic types[71] (except for one case where a smectic mesophase was found) have also been observed for a large number of similar complexes in which one of the phenyl rings has been replaced by a cyclohexyl or fluorophenyl ring.[71] In contrast to the previous group of complexes, here the mesomorphism of the ligands themselves is more varied. Nematic phases and smectic mesophases of different types have been observed for such ligands.

So far few mesogenic complexes of other metals with β-diketonate ligands have been found. One may mention the octahedral complex of trivalent iron[7] $Fe(RCOCHCOR)_3$, which

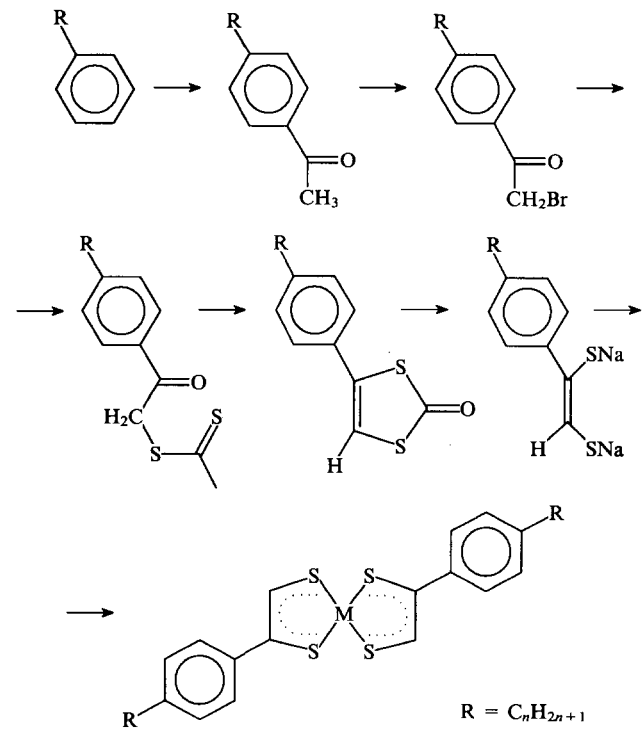


R = $C_{10}H_{21}O$

is apparently the first example of an octahedral metallomesogenic substance, and mesogenic oxovanadium(IV) complexes[72] for which discotic hexagonal columnar phases D_h have been found.

3. Mesogenic dithiol metal complexes

Dithiol complexes have structures similar to those of carboxylate complexes and, depending on the nature of the terminal substituents, it is possible to observe nematic, smectic, or discotic phases for such compounds. We shall describe the first series of dithiols, one of the most thoroughly investigated, which have been synthesised in accordance with the following scheme.[73-76]

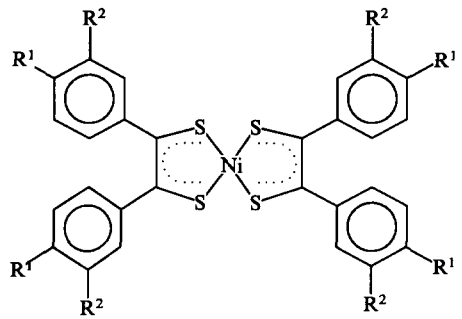


The above complexes (M = Ni, Pt)[75] exhibit nematic mesomorphism for n = 4 and 5 and form the SmA phase when $n \geqslant 6$.

A structural study on a single crystal of the nickel complex (n = 8) showed[76] that the coordination of the metal atom is planar and the substituents are distributed in the *trans*-orientation, which is the reason why the molecule has the shape extended to the maximum degree. The molecules in the crystal are packed in layers, which is apparently a precondition for the manifestation by these compounds of smectic mesomorphism.

It has been suggested that the molecules of dithiol complexes, having appreciable electron-accepting properties, can form charge-transfer complexes (CTC) with electron-donating molecules, for example, with liquid-crystal derivatives of tetrathiofulvalene.[77] However, it has been found that the compounds synthesised do not form charge-transfer complexes.[77] On the other hand, they can be used in a mixture with cyanobiphenyls as laser dyes.[78] Finally, it has been noted[75] that palladium complexes do not exhibit the properties of liquid crystals for the entire series of homologues, in contrast to the analogous nickel and platinum complexes. The authors believe that the reason for this difference is the dimerisation of the palladium complexes as a result of the metal–metal interaction, which predominates over the dispersion forces.

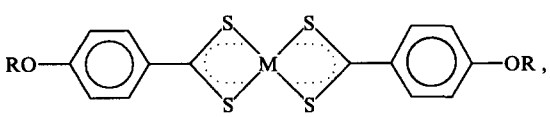
Complexes with two phenyl substituents in each dithiol ligand, whose structure is similar to that of the diphenyl-substituted β-diketonates, also exhibit discotic mesomorphism, the type of mesophases being different for complexes with monosubstituted and disubstituted phenyl groups.



For the monosubstituted phenyl derivatives with four substituents $R^1 = p\text{-}C_nH_{2n+1}$ (n = 8–12), R^2 = H and $R^1 = p\text{-}C_nH_{2n+1}O$ (n = 7–12), R^2 = H, the formation of only layered discotic phases has been established.[79,80] The search for columnar phases in compounds of the above type has continued, since these compounds could have interesting electrochemical properties. It has been observed[81] that the introduction of two alkyl substituents $R^1 = R^2 = p\text{-}C_nH_{2n+1}$ (n = 6, 8) does not lead to the formation of a mesophase at all, while the compound with the alkoxy-substituents $R^1 = R^2 = p\text{-}C_{10}H_{21}O$ forms a hexagonal phase D_{hd} with disordered columns (the hexagonal lattice parameter is 32.7 Å and the distance between the mobile alkyl chains is 4.4 Å). Subsequently the entire series of complexes with $R^1 = R^2 = p\text{-}C_nH_{2n+1}O$ (n = 1–12) was investigated systematically.[82] It was found that all the complexes with $n \geqslant 5$ form enantiotropic discotic phases D_{hd}, while the first members of the series (n = 2–4) form monotropic discotic phases. The half-wave potential for the reduction of these complexes is independent of the length of the substituents and its values are close to −0.05 to 0.06 V. This is somewhat smaller than the value for the unsubstituted complex, which indicates the independence of the electrochemical properties of the mesogenic nature of the specimens.

4. Metal dithiocarboxylate complexes

By analogy with metal carboxylates, it was natural to expect the manifestation of mesogenic activity by thiocarboxylates. Their synthesis and study by differential scanning calorimetry and X-ray diffraction[83] did indeed confirm the validity of such hypotheses. The mesogenic properties of the complexes $M(C_nH_{2n+1}OC_6H_4CS_2)_2$,



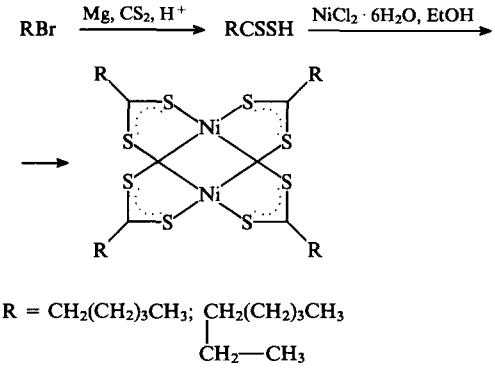
where M = Zn, Ni, or Pd and n = 4–10, were investigated.

An analogous mercury complex, described by Adams et al.,[83] has also been mentioned.[7] The replacement of the metal in the complex leads to the appearance of different types of mesophases. For example, for n = 8 the zinc complex forms only nematic phases, whereas the palladium and nickel complexes give rise to several smectic phases in addition to the nematic phases. This may be associated with the different types of coordination of the metal in these complexes. Thus a tetrahedral coordination is usually characteristic of zinc, although in the case of the complex with n = 4 dimers were found in the crystal in which the eight-membered ring Zn–S–C–S–Zn–S–C–S is present. In the crystal of the planar palladium complex, the metal atoms are involved in an additional coordination as a result of the interaction with the sulfur atoms of neighbouring molecules (the intramolecular Pd–S distances are 2.29–2.35 Å and the intermolecular Pd ... S distances are 3.38 Å). A similar molecular packing was found also in the mercury complex: the Hg–S distances within the complex are significantly nonequivalent, amounting to 2.41 and 2.96 Å, while the lengths of the Hg ... S intermolecular contacts are 3.36 Å.

It has been stated[84] that the palladium and nickel complexes exhibit a significant dichroism: after the passage of light along the molecular axes, the extinction coefficient is appreciably higher than in the case where light is transmitted at right angles. This property may be used to devise displays of the 'guest–host' type. For example, the nickel complex can serve as the guest in the cell, while the host is an organic liquid-crystal compound. If the molecules are oriented at right angles to the direction of light in the absence of an electric field and parallel to this direction in the presence of the field, then in the former case the cell is coloured purple while in the latter it is transparent.

Gold(III) alkoxydithiobenzoate complexes $ROC_6H_4CS_2AuCl_2$, forming SmA phases on heating, have been investigated.[84]

Apart from the nickel(II) bisthiocarboxylate complexes, the synthesis and properties of nickel(II) tetrakisdithiocarboxylate complexes have been described.[84,85]



Two series of tetrakis-complexes with linear and branched alkyl substituents were obtained.

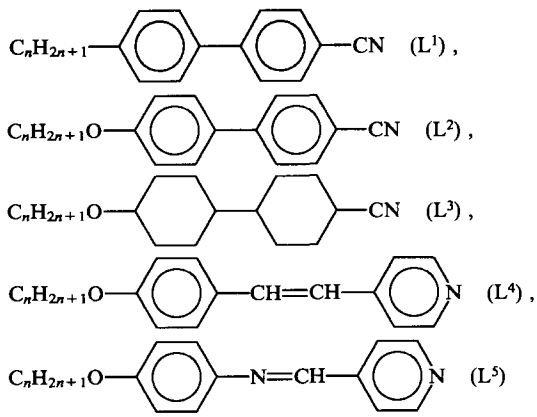
The results of differential scanning calorimetric and X-ray diffraction studies have shown that complexes with linear chains form monotropic lamellar (layered) discotic phases of the type D_l, whereas the presence of an enantiotropic discotic phase with a hexagonal columnar ordered arrangement of the type D_{hd} is characteristic of complexes with a branched alkyl chain. On heating of the given substance or on its dissolution in chloroform, the tetrakis-complexes are converted into the bis-complexes.

5. Mesogenic metal complexes with monodentate nitrogen-containing ligands

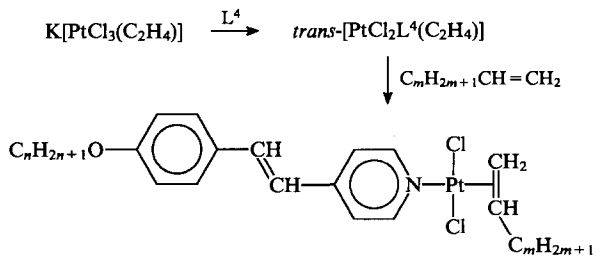
The widely known organic mesogenic substances, containing a nitrogen atom capable of forming a coordinate bond, can serve as monodentate ligands. Such mesogenic substances form metal complexes in reactions with platinum group metal halides or carbonyls. The complexes may contain one or two mesogenic ligands. Their properties have been thoroughly investigated. For example, the mesogenic properties of the free ligands and complexes with different metals have been compared.[7,86]

The majority of complexes of the type ML^2Cl_2 (M = Pt, Pd; n < 9) exhibit only nematic mesomorphism. With increase in chain length, smectic SmA and/or SmC phases are also observed.

The introduction into the complex of two different ligands, for example π-olefin and monostilbazole ligands, leads to an appreciable decrease in the temperature of the appearance of the mesophase. Such complexes were synthesised in accordance with the following scheme:[7]

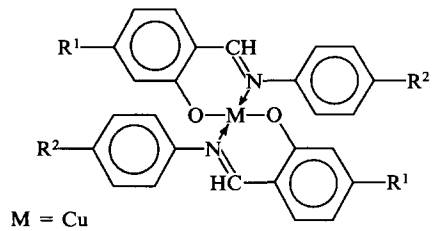


The presence of L^4 and L^5 ligands makes it possible to classify these complexes both as coordination and as organometallic compounds. The mesogenic properties of the complexes depend on the overall length of the alkyl chains of the two ligands. For $m+n < 8$, such complexes are nonmesogenic, forming a SmA phase with increase in chain length. They are monotropic for $m+n = 8-11$ and enantiotropic for $m+n > 11-13$.



6. Salicylideneamine metal complexes

The liquid-crystal properties of copper complexes of Schiff bases have been vigorously investigated in recent years. The synthesis of such compounds was first described by Ovchinnikov et al.[87] They obtained Schiff bases as a result of the interaction of 4-*n*-heptyl-oxy-2-hydroxybenzaldehyde with substituted anilines, after which the corresponding complexes were isolated by treating the bases obtained with copper acetate in ethanol.



M = Cu
$R^1 = OC_7H_{15}$
R^2 = H, F, CH_3, OC_nH_{2n+1} ($n = 1-8$)

In order to elucidate the influence of the nature of the metal atom on the mesomorphic properties, the analogous compounds with M = Zn, Co, Ni, Pd, and also VO were synthesised[88] ($R^1 = p$-OC_7H_{15}; $R^2 = p$-OC_8H_{17}). These compounds were obtained by refluxing in ethanol the corresponding metal acetate (potassium tetrachloropalladate was used for the palladium complex) with 4-heptyloxysalicylaldehyde and subsequent addition of 4-octyloxyaniline to the reaction mixture.

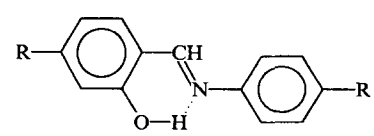
Studies by polarisation polythermal microscopy and differential scanning calorimetry showed that the substances obtained (Table 2) can be divided into two groups in terms of the nature of the phase transitions. The first includes copper, palladium, and vanadyl complexes, which have the properties of liquid crystals manifesting smectic or nematic mesomorphism. The second group includes cobalt, zinc, and nickel complexes, which in most cases do not form mesophases.

In order to establish the relation between the structure and liquid-crystal properties, single crystals of the metal complexes of the above series were investigated by X-ray diffraction, EPR spectroscopy, and electronic spectroscopy and also by the method involving low-angle X-ray scattering in the mesophase. Conformational calculations and calculations of the intermolecular interaction energy (IMIE) in the crystal were carried out on the basis of structural data.

In considering the complexes **1**–**13** in Table 2, we concentrated attention on the geometry of the metal chelate unit, because the ability of the metal complexes to exhibit mesomorphism is to a large extent determined by the coordination of the metal atom. Depending on the type of coordination of the metal, the molecules can assume a form with different degrees of anisometry, which plays a decisive role in the formation of the mesophase. Furthermore, as will be shown below, the liquid-crystal properties depend significantly on the possibility of the additional intermolecular coordination of the metal atom.

From the standpoint of understanding the causes responsible for the mesophase, compounds **1** and **2** proved to be the most important.[8,89] The crystal structures of these complexes are made up of two systems of symmetrically independent molecules with different coordinations of the copper atoms. In compound **1**, both molecules exist[8] in specific positions at the centre of symmetry and on the twofold axis (Fig. 9). The centrosymmetric molecules contain a copper atom involved in *trans*-square planar coordination, while the copper atom in the molecules on the two-fold axis is involved in a tetrahedral coordination characterised by a dihedral angle of 60° (angle of twist) between the coordination planes of copper, nitrogen, and oxygen of the two ligands. In the structure of complex **2**,[89] one of the independent molecules is also located at the centre of symmetry, which predetermines the *trans*-square planar coordination of the metal, while the other occupies a general position with an approximate C_2 crystallographic symmetry and an angle of twist of 31°. A similar disposition of two independent molecules has been found[90] for the crystal of compound **3**, which is isostructural with compound **2**. The different coordinations of the copper atoms in the crystals of compounds **1**–**3** lead to different Cu–O and Cu–N bond lengths. For the tetrahedral coordination, these bonds are shorter, which is characteristic of complexes of the type considered.[100]

Comparison[8] of the conformations of the ligands in compound **1** with that of the similar noncoordinated nematogenic molecules of *p*-ethoxy-[101] and *p*-(n-propoxy)-salicylidene-*p*-(n-butyl)aniline[102] (ESBA and PSBA respectively) showed that the formation of the complexes does not entail significant changes in the conformation of the ligands. In particular, both in the complexes and in the noncoordinated molecules the benzene rings of the nitrogen atom have been significantly rotated relative to the chelate unit, while the benzene rings condensed with the unit are virtually coplanar with the latter (in ESBA and PSBA, the six-membered chelate ring, closed by a hydrogen bond, is entirely planar, while in the metal complexes the planar fragment of the chelate unit is made up of five nonmetal atoms). In both cases, the significant rotations of the benzene rings can be accounted for by intramolecular steric interactions.



R = OC_2H_5 (ESBA),
R = OC_3H_7 (PSBA),

Analysis of the configurations of the planar molecular complexes showed[95] that such molecules are incapable of forming the discotic mesophases postulated initially.[87] A discotic mesophase is not formed owing to the lack of an overall planar anisometry characteristic of it.[2] This is associated with the

Table 2. Phase transition temperatures (°C) and the type of coordination of the metal atoms in complexes of Schiff bases.

No.	M	R^1	R^2	N	SmC	SmA	Isotropic liquid	Coordination of metal	Ref.
1	Cu	OC_7H_{15}	OCH_3			132.9	140.0	Planar[d], tetrahedral	8
2	Cu	OC_7H_{15}	OC_5H_{11}		148.0	151.0	168.0	"	89
3	Cu	OC_7H_{15}	OC_6H_{13}		149.0	152.0	168.0	"	90
4	Co	OC_7H_{15}	OCH_3				137.0	Tetrahedral	91
5	Co	OC_3H_7	OC_7H_{15}				122.0	Octahedral	91
6[a]	Pd	OC_7H_{15}	OCH_3			203.0	226.0	Planar	92
7	Pd	OC_7H_{15}	OC_6H_{13}		158.3	171.0	180.0	"	93
8[b]	Ni	OC_7H_{15}	OCH_3				138.0 155.0	"	94
9	Cu	OC_7H_{15}	F			130.1	150.5	Square-pyramidal	95
10	Cu	OC_7H_{15}	CH_3				150.1	"	96
11	Cu	OC_7H_{15}	CN	(190)[c]			202.0	Square-bipyramidal	97
12	Cu	OC_7H_{15}	NO_2				220.0	"	98
13	Cu	H	$COOPhC_9H_{19}$	196.0			201.0	Planar	99

[a] A phase transition is observed in the crystal at 129 °C.
[b] Two melting points (see text).
[c] Temperature of the appearance of the monotropic nematic phase.
[d] Two independent molecules.

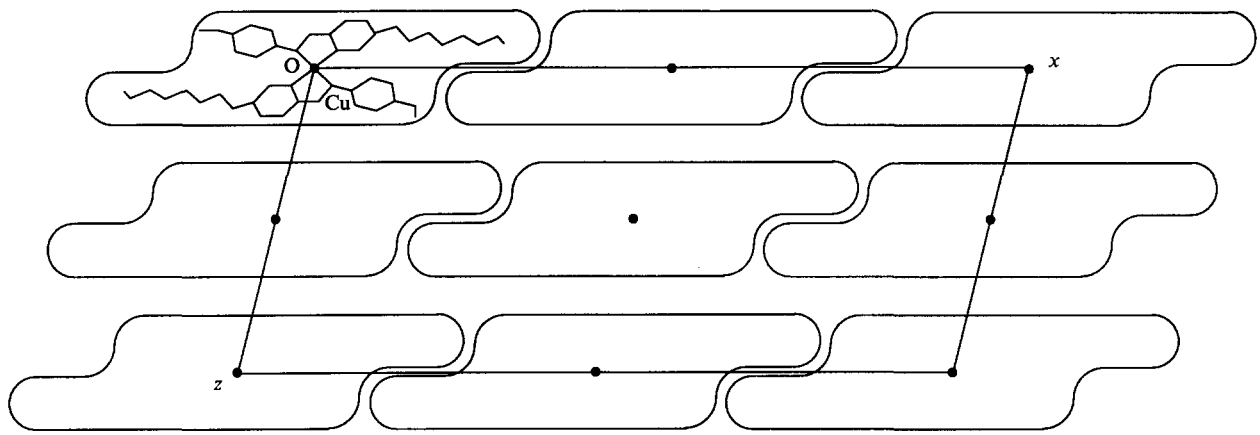


Figure 9. Arrangement of the molecules in the structure of a crystal of compound **1** located at the centres of symmetry. Individual molecules are involved in a projection – hollow type of arrangement. A similar type of packing is observed also for molecules located on twofold axes.[8]

rotation of the benzene rings[90] and with the stepped form of the coordination unit in molecules with the *trans*-square planar coordination of the metal atom.[95]

It was stressed for the first time[95] that, for the manifestation of mesomorphism, the square planar coordination is preferable to the tetrahedral coordination. Molecules with a *trans*-square planar coordination of the metal are characterised by a shape extended to the maximum extent by virtue of the parallel arrangement of the axes of the ligands (the angle of twist is 0°). On the other hand, the tetrahedral coordination leads to the rotation of the ligands relative to one another, which results in a decrease in the anisometry of the molecules. Thus the angle between the long axes of the ligands in the tetrahedral† molecules of compound **1** is[8] approximately 20°, but the most striking decrease in anisometry was manifested in a tetrahedral cobalt complex[91] (Table 2, compound **4**), in which the analogous angle of rotation is about 100° (Fig. 10). The absence of anisometry in the molecules has also been observed for an octahedral cobalt complex[91] (Table 2, compound **5**; Fig. 11).

†Here and subsequently in the text, the terms tetrahedral and planar molecules imply molecules with the corresponding coordination of the metal atom.

Thus the tetrahedral and octahedral coordinations of the cobalt atoms in complexes **4** and **5** actually preclude the formation of the mesophase in these compounds. The same causes

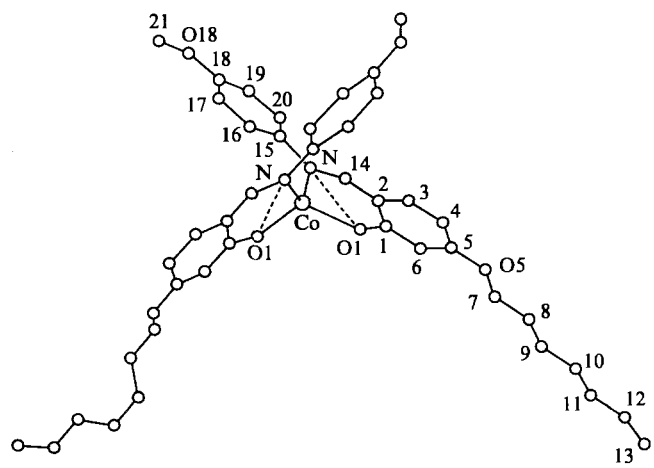


Figure 10. Molecular structure of a tetrahedral cobalt complex.[91]

apparently explain the absence of mesomorphism in zinc complexes with similar ligands as in complex **4**, because these compounds have the same structures.[91] An additional confirmation of the similarities of the structures of the zinc complexes and compound **4** is provided by the description[103] of the structure of a zinc complex of a Schiff base (R^1 = H; R^2 = CH_3), in which the metal atom has a tetrahedral coordination.

The presence in complexes **1**–**3** of two types of coordination of copper atoms indicates the conformational nonrigidity of the coordination metal unit. Therefore both planar and tetrahedral molecules may be present in the smectic phase.[8] This hypothesis was confirmed by the results of EPR studies. Bichkantaev et al.[104] investigated a single crystal of compound **1**, the EPR spectrum of which consists of a single Lorentzian line for all orientations of the crystal despite the presence of different types of complexes. The g-factors and their directions {g_1 = 2.2080, $\mathbf{n}_1$ = (0, 1, 0); g_2 = 2.0985, $\mathbf{n}_2$ = (0.866, 0, 0.5); g_3 = 2.0590, $\mathbf{n}_3$ = [$\mathbf{n}_1$, $\mathbf{n}_2$]} are inconsistent with the magnetic parameters of the individual complexes and are a result of the partial averaging of molecular g-factors due to spin exchange. The knowledge of the crystal structure of complex **1** made it possible to find the molecular magnetic parameters of each of the two types of complexes: $g_\perp^p \simeq 2.049$ and $g_\parallel^p \simeq 2.190$ ($g_o^p \simeq 2.096$) for the planar molecules and $g_\perp^t \simeq 2.068$ and $g_\parallel^t \simeq 2.298$ ($g_o^t \simeq 2.144$) for the tetrahedral molecules (g_i^t is greater than g_i^p, which is characteristic of distorted copper complexes). These g-factors made it possible to interpret subsequently the EPR spectra of the tested complexes in different phase states. In particular, it has been established for compounds **1**–**3** as well as other homologues of this series[105] that the isotropic melt actually consists of planar complexes giving rise to only one line in the EPR spectrum. Two independent lines with g-factors close to the values found for the planar and tetrahedral molecules in a single crystal of compound **1** are present in the spectrum of the mesophase (Fig. 12). It is postulated that the viscous mesophase proper is in fact formed by planar complexes, while the tetrahedral complexes are present in it as isotropic 'impurity' drops of low viscosity,[105] i.e. these molecules are separated in space.

The conformational changes in the chelate unit (*trans*-square planar → tetrahedral coordination), arising in some of the molecules during the liquid → smectic mesophase phase transition, suggest that the planar molecules are favoured by energy factors compared with the tetrahedral molecules. The corresponding calculations[89] based on the real molecular structures of compound **1** show that the conformational energy of the planar molecules is indeed smaller by ~5 kcal mol^{-1} than that of the tetrahedral molecules.

We believe that there is no doubt about the fact that two types of coordination of the metal atoms occur for copper complexes in the smectic mesophase, i.e. both planar and tetrahedral molecules are present in the mesophase. However, the specific structure of such a mesophase requires further refinement, because the claim[105] that the planar and tetrahedral complexes are separated in space is not unquestioned. Such separation actually implies the separation of the mesophase into layers, as a result of conformational transformations due to the different coordinations of the copper atoms. However, one should bear in mind that the tetrahedral complexes are nevertheless fairly anisometric, although to a lesser extent than the planar complexes, because the rotations of the ligands (~20° in compound **1** and ~10° in compounds **2** and **3**) are not so pronounced as in the classical tetrahedral complex **4** (~100°). It therefore appears doubtful that the planar molecules displace the tetrahedral molecules from their matrix, which would result in the latter being grouped together to form nonmesogenic 'impurity' drops.

The available information about the crystal packing in mesogenic substances is very useful, since certain features of the disposition of the molecules, i.e. different types of molecular associated species which are retained to some extent in the liquid-crystal state, are inherent in the mesogenic crystal. This was first pointed out by Bernal and Crowfoot[106] as early as 1933. It is essential to note that molecular packing is analysed not only with geometrical criteria (the presence or absence of layer motifs, parallel arrangement of molecules) but also energetic criteria[107] involving the analysis of the energy of molecular pair interactions. Here use is made of the concept of the structural subclass describing the relative orientation and symmetry of the molecular associated species most strongly bound by nonvalence interactions. The search for such associated species is based on the calculation of the intermolecular interaction energy by the method of atom–atom potentials. This procedure was first applied to liquid crystals by Polishchuk et al.[108] The advantage of this method, like that of conformational calculations, also based on the atom–atom approximation, consists in the fact that it operates with the structures of specific molecules and not with the approximation to the latter in the form of structureless formations (rods, discs, etc.).

A layered disposition of molecules is characteristic of the crystalline complexes **1**–**3** (Fig. 9). For compound **1**, this has been confirmed by the IMIE calculation, according to which the intralayer energy exceeds the interlayer energy by a factor of ~3.5.[8] We may note that the crystals of compounds **1**–**3** are unique objects as regards both structure (they consist of different conformers) and magnetic properties, because the magnetic interaction between the molecules within the limits of the layer is much stronger than between the layers, i.e. these objects constitute dimeric magnetic systems (see, for example, Bichkantaev et al.[104]). This is associated with the fact that the closest distance between the copper atoms in the layer is 6.5 and 5.5 Å whilst that between the layers is 21.8 and 24.7 Å for compounds **1** and **2** respectively (in the crystal of compound **3**, these distances are close to those in that of compound **2**). The data indicated above have led to the conclusion[8,89,90] that the explicit layered character of the molecular packing in compounds **1**–**3** actually predetermines the smectic mesomorphism of the above compounds.

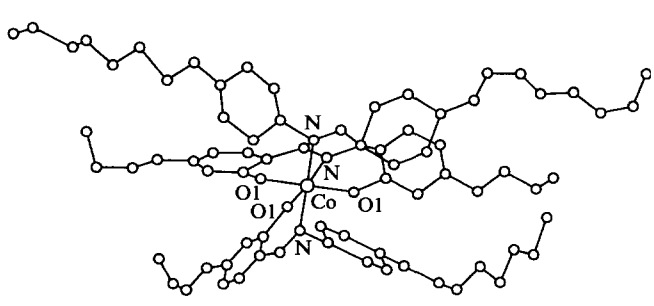


Figure 11. Molecular structure of an octahedral cobalt complex.[91]

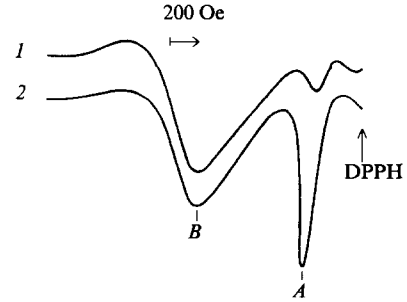


Figure 12. EPR spectrum of the mesophase of a copper complex[88] (R^1 = OC_7H_{15}; R^2 = OC_8H_{17}). External magnetic field: (*1*) parallel to the director; (*2*) perpendicular to the director; (*A*) perpendicular component of the spectrum of planar molecules (g = 2.047); (*B*) isotropic spectrum of tetrahedrally distorted complexes (g = 2.113). DPPH = diphenylpicrylhydrazyl.

Low-angle X-ray studies have shown that the thicknesses of the SmA layers in compounds **1** and **2** (d_1 = 23.6 Å, d_2 = 26.0 Å) agree with the lengths of the ligands in the corresponding complexes. Comparison of these quantities with the overall length of the molecules (30 Å in compound **1** and 26 Å in compound **2**) made it possible to put forward[109] the following models of the structures of these phases. In the case of compound **2** and also of its isostructural homologue **3** (d_3 = 26.1 Å),[90] in which the length of the molecular complexes is approximately equal to the length of their ligands, the structure of the SmA phase is usual in the sense that the thickness of the layers is specified by the overall length of the metal complexes. This is associated with the fact that in the complexes, having a transoid form, the geometrical parameters of the substituents R^1 and R^2 (Table 2) are approximately the same. On the other hand, owing to the different nature of R^1 and R^2, the overall length of the transoid complex **1** exceeds the dimensions of its ligands by a factor of approximately 1.3. Therefore the most reliable model of the layered structure of the mesophase of compound **1** is believed[109] to be that based on the crystal packing of the projection–hollow type. Fig. 9 illustrates schematically the molecular packing in the mesophase, showing the mutual migration of molecules from one layer to the other. We may note that the closest interlayer distances in the crystals of compounds **1** ($a/2$ = 21.8 Å) and **2** (c = 24.7 Å) are similar to the thickness of the layers in the mesophases (23.6 and 26.0 Å). A similar picture is observed in the smectic mesophases of the homologues with $R^1 = OC_7H_{15}$ or $OC_{12}H_{25}$ and $R^2 = C_4H_9$. Low-angle X-ray studies[110] indicate the mutual interlayer penetration of the fused alkyl 'tails' and the possible formation of pairs of copper atoms within the layers.

In order to confirm the importance of the *trans*-square planar coordination of the metal atom for the establishment of liquid-crystal properties in complexes of Schiff bases, structural and spectroscopic studies have been carried out[92] on the palladium complex **6**. It is of interest to compare the coordinations of the metal atoms and the mesomorphic properties of the palladium and copper complexes.

The replacement of copper in compound **1** by palladium does not entail a significant change in the structure of the planar molecules.[92] However, in contrast to the crystals of compounds **1**–**3**, in which both planar and tetrahedral molecules are present, the crystal structure of compound **6** is made up of only planar molecular complexes located at the centres of symmetry. The *trans*-square planar coordination of the palladium atom then remains unchanged in all phase states. This is indicated by the presence of the absorption band with λ_{max} = 402 nm in the electronic spectra of both crystalline modifications of the solution and the vitrified mesophase.[92] A similar absorption band has been attributed[111] to the square planar coordination of the palladium atom in complexes of Schiff bases.

The layered disposition of the molecules in complex **6** (Fig. 13) has been confirmed by IMIE calculations.[92] It has been noted that the presence of only planar molecules in compound **6** alters the intermolecular interaction compared with compound **1**. It is believed that the planar molecules, arranged one on top of another, interact more strongly than only tetrahedral or planar and tetrahedral molecules. This is due to the greater number of van der Waals contacts between the planar molecules, which increases their intermolecular interaction energy. The energies of the maximum pair interactions of the molecules in the layers of compounds **6** (−13.5 kcal mol^{-1}) and **1** (−11.0 kcal mol^{-1}) may be quoted to confirm this. Under these conditions, the layers in compound **6** are energetically more distinct ($U_{layer}/U_{interlayer} \simeq 5$ for compound **6** and 3.5 for compound **1**), which naturally predetermines the formation of a layered mesophase. According to Polishchuk et al.,[92] the above factors influence appreciably the range of existence of the smectic mesophase and its thermal stability, which are appreciably greater for compound **6** than for compound **1** (Table 2).

Despite the inclination of the long axes of the molecules of compound **6** relative to the layer boundary, the layered packing is similar in crystals of compounds **1** and **6**; in both cases, the arrangement of the molecules is of the projection–hollow type. Evidently, in the formation of the SmA phase the inclination of the molecules of compound **6** changes, but the characteristic features of close packing remain. This is indicated by the equal thicknesses of the smectic layers: d_6 = 23.7 Å and d_1 = 23.6 Å. Thus, in both cases the periodicity of the smectic layers is determined not by the overall length of the complexes but by the sizes of their ligands, which corresponds to distance of 22.64 Å in the crystal of compound **6** (Fig. 13).

The *trans*-square planar coordination of the metal atom has been observed also in the palladium complex **7**, having the same substituents as compound **3** (Table 2). However, in contrast to the crystal of compound **3**, in compound **7** there are only planar molecules, forming layers and evidently, as for complexes **1** and **6**, such coordination leads to higher phase transition temperatures in compound **7** than in compound **3**.

The absence of mesomorphism in the nickel complex **8** proved unexpected.[94] This complex has the same structural characteristics as the palladium complex **6** because these compounds are isostructural. It has been established that the crystals of compound **8** fuse at two temperatures (138° and 155 °C) but they do not form a mesophase, which is indicated by the absence of textures characteristic of liquid crystals in observations under a polarisation microscope. It has been noted[94] that, after the first fusion (138 °C), a dark green isotropic amorphous phase is formed, the outward form of which changes little in the second phase transition (155 °C). It is remarkable that, on repeated heating (after 24 h) of the cooled melt of compound **8**, the phase transition occurs at 348 °C and is accompanied by the decomposition of the specimen.

The authors[94] see the reason for such behaviour in the change of the coordination of the nickel atom during the fusion of the

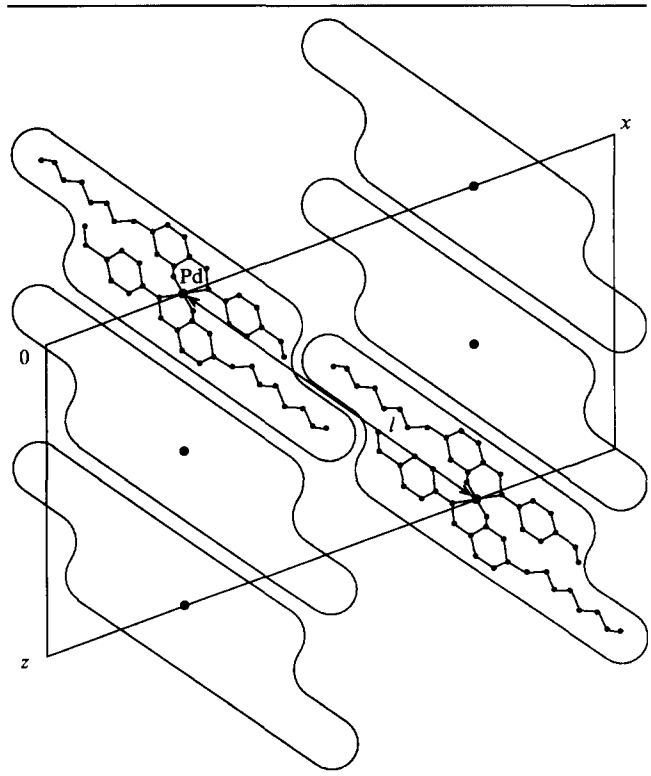


Figure 13. Molecular packing in a palladium complex. The overall form of the molecules arranged in accordance with the projection–hollow principle is indicated; l = distance between the molecules in neighbouring layers in the direction of long axes.

substance. Nickel complexes with a planar geometry of the coordination unit are diamagnetic, while those with a nonplanar coordination are paramagnetic.[112-114] The crystals of compound **8**, with a square planar coordination of the nickel, are indeed diamagnetic, which is indicated by the absence of an EPR signal in the powder of this compound at −196 °C. However, after heating to 140 °C and subsequent cooling of the melt to −196 °C, two broad lines appear in the EPR spectrum with effective *g*-factors of ~7 and ~3, indicating the transition of the test substance to the paramagnetic state. A similar situation arises[94] on fusion of the initial specimen of complex **8** to 160 °C.

Unfortunately, owing to the short spin relaxation times of the nickel compounds, their EPR signal can be recorded only at temperatures close to that of liquid nitrogen. The configurational transitions of the molecules involving a change in the coordination of nickel cannot therefore be observed by the EPR method during the heating of the specimen and directly in the melt. Studies have therefore been made[94] on the electronic spectra of the diamagnetic complex **8**, which showed that in solution in chloroform the spectrum exhibits absorption bands with maxima at 354 and 610 nm. On the other hand, an additional maximum appears in the region of 1005 nm in the spectrum of the melt after the first phase transition. These bands are retained also after the second phase transition with a slight change in their shape. According to Yamada and Takeuchi,[112] these data show that the diamagnetic complex **8** retains in solution its initial planar configuration of the unit, but on fusion and in the melt it most probably assumes a tetrahedral configuration. On the basis of the above facts, it is concluded[94] that the planar molecules of the initial specimen of compound **8** assume the tetrahedral configuration during fusion (there is a possibility of another nonplanar configuration — the octahedral configuration), which is an unfavourable factor for the establishment of the liquid-crystal state.

It is stated in a review[115] that an equilibrium mixture of isomers with planar and nonplanar structures exists as a rule in solutions of nickel complexes of Schiff bases and that the free energy of their interconversion is low (ΔG = 0.15–0.20 kcal mol^{-1} depending on the nature of the substituents in the ligands). One may postulate that the equilibrium in the melt of complex **8** is displaced towards the isomer with a nonplanar metal chelate unit. Finally, it has been noted[94] that yet another possible cause of the absence of mesomorphism in compound **8** may be a significant change in molecular structure, for example, polymerisation of the compound on fusion; the polymeric specimen then melts with decomposition at a high temperature (348 °C).

The square planar coordination of the copper atoms is very often built up to the tetragonal-pyramidal or octahedral configuration as a result of an additional intermolecular interaction. The influence of such coordination on the liquid-crystal properties of metal complexes of Schiff bases has been analysed.[95-98] Thus the copper atoms in the isostructural crystals of compounds **9** and **10** (Table 2) are in general positions and have the *trans*-square planar coordination. However, in contrast to compounds **1**–**3**, this coordination is built up to the square pyramidal as a result of the Cu ... O intermolecular interaction [the oxygen atom belongs to the metal chelate ring of a neighbouring molecule (the corresponding Cu ... O distances are 2.60 Å for compound **9**[95] and 2.62 Å for compound **10**[96])]. Such additional interaction leads to the formation of centrosymmetric coordination dimers (Fig. 14) in which the distance between the copper atoms is 3.44 Å in compound **9** and 3.46 Å in compound **10**, which is appreciably less than in compounds **1**–**3**.

The dimers in the crystals of compounds **9** and **10** form a layered packing and under these conditions the intermolecular interaction energy in the layer exceeds the interlayer energy by a factor of 3.5 for compound **9** and 4.4 for compound **10**. We may note that, in the calculation of the intermolecular interaction energy, an attempt was made[8,95] to take into account not only the dispersion component (the '6-exp' potential) of the nonvalence interactions but also the electrostatic component. However, this could not be done correctly because

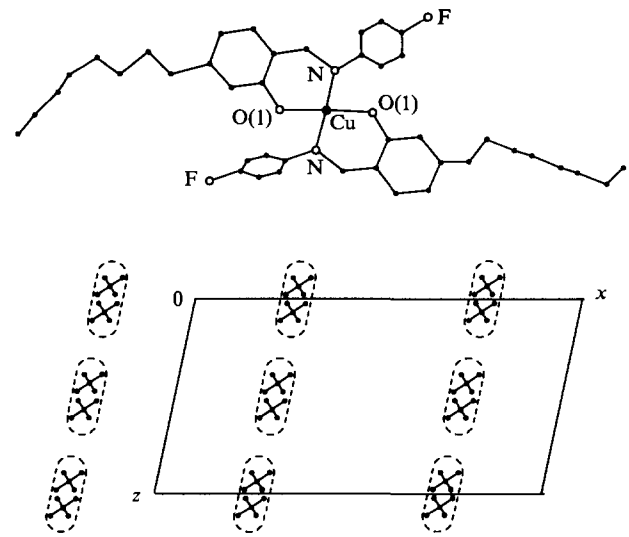


Figure 14. Molecular structure of the copper complex **9** and the packing of the central parts of the complex species in the crystal.[95] The centrosymmetric dimers are indicated by dashed lines.

it proved impossible to take into account accurately the charge distribution of the copper, nitrogen, and oxygen atoms by the semi-empirical methods employed. On the other hand, it was established that the additional intermolecular coordination enhances the interaction of the molecules in the dimers via the electrostatic component.

The observed ratio of the intermolecular interaction energies within the layers and between them for complexes **9** and **10** suggests the manifestation of smectic mesomorphism by the latter. However, an enantiotropic smectic mesophase is observed only for compound **9** (Table 2). It was assumed earlier that compound **10** does not exhibit liquid crystal properties at all (whilst the corresponding ligand does form a nematic phase[87]), but its more thorough investigation led to the observation of the monotropic SmA phase.[96] On cooling of the isotropic liquid, this phase appears just before the onset of crystallisation and exists in a very short time interval and over a very narrow temperature range. According to Polishchuk et al.,[96] the different mesomorphic behaviour of the isostructural compounds **9** and **10** can be accounted for by the different dissociation energies of the coordination dimers. This has been confirmed[95,96] by calculations of the intermolecular interaction energy: U_{dim} (**9**) = −13.9 kcal mol^{-1}; U_{dim} (**10**) = −15.2 kcal mol^{-1}. It has been noted[96] that the existence of dimers by itself need not necessarily be accompanied by the disappearance of liquid-crystal properties. Furthermore, if the dimers are characterised by an adequate anisometry, then mesomorphism is extremely likely. This is clearly seen in relation to *p*-n-alkoxybenzoic acids.[116] The O ... H–O bonds in these substances lead to the formation of dimers the anisometry of which exceeds significantly that of individual molecules. On the other hand, the dimers detected in compounds **9** and **10** have a smaller anisometry than the initial complexes of the monomeric compound. The length of such coordination dimers in fact remains the same as that of the monomer, while its transverse dimensions (or at least one of them) increase approximately by a factor of two. In this case, the dissociation energy of the dimers should play a decisive role in the formation of the mesophase. Its value should not be very great, so that the dimers do not decompose during the heating of the crystals even before the formation of the isometric liquid.

The hypothesis that the liquid-crystal properties depend on the presence or absence of coordination dimers has been confirmed by EPR studies. It has been noted[96] that he EPR spectra of compounds **9** and **10** are identical and that they are characterised by the presence of a fine structure and a forbidden

transition ($\Delta M_s = \pm 2$) (Fig. 15). When powdered compound **9** is heated, the EPR spectrum is modified at the instant of the formation of the SmA phase (130.1 °C, Table 2): the fine structure vanishes and a spectrum characteristic of monomeric copper complexes appears (Fig. 12).[105] The spectra indicate the absence of dimers over the entire range of existence of the SmA phase and also in the isotropic phase on further heating. We may note that the mesophase of compound **9** is characterised by a layer thickness of 22.4 Å, which is close to the length of an individual ligand. This finding indicates, as for the smectic phases of compounds **1** and **6**, an arrangement of the molecules of the projection–hollow type, which is characteristic also of the crystal structure itself, where the distance between the molecules in neighbouring layers is equal to half the maximum period $a/2$ = 19.91 Å.

Heating of compound **10** entails the same changes in the EPR spectrum as in the spectrum of compound **9**. However, in this case the fine structure due to the dimeric organisation of the molecules vanishes at the instant of fusion of the substance to the isotropic liquid (150.1 °C), in which only monomeric complexes are present.

Thus EPR data show that the dimers in compound **10** decompose at a higher temperature than in compound **9**, which is the reason for the monotropic smectic mesomorphism of compound **10**. In other words, the temperature range of the possible existence of the mesophase in compound **10** is, as it were, 'jumped over' on heating by virtue of the higher dissociation energy of the dimers compared with compound **9**. At the same time, the temperatures of the transition to the isotropic liquid are virtually identical for both compounds.

The negative influence of the additional intermolecular coordination on the formation of the mesophase was manifested even more evidently in the isostructural copper complexes **11** and **12** containing polar ligands. These compounds were obtained by procedures similar to those used for the compounds described by Ovchinnikov et al.[87]—by refluxing in absolute ethanol equivalent amounts of the 4-heptyloxy-*N*-(4′-cyanophenyl)- and 4-heptyloxy-*N*-(4′-nitrophenyl)-2-benzylidenehydroxyamine with copper acetate for compounds **11** and **12** respectively. In the crystal structures of compounds **11**[97] and **12**[98], the copper atoms occupy general positions and are characterised by a *trans*-square planar coordination. As in complexes **1**–**10**, the benzene rings in these compounds, condensed with chelate rings, are parallel to the planar fragments of the chelate rings, while the phenyl substituents at the nitrogen atoms have undergone significant rotation. At the same time, the presence of the polar CN and NO_2 groups in the ligands builds up the coordination of the copper atoms to the square-bipyramidal as a result of the Cu...N intermolecular interaction for compound **11** and the Cu...O interaction for compound **12**. Such additional coordination promotes the formation in these crystals of the so called infinite coordination strata, the thickness of which is determined by the transverse dimensions of the molecules (Fig. 16). The thickness of the layered associated species is determined by the length of the molecule and this constitutes the main difference between strata and layers. The presence of strata has been confirmed by calculations of the intermolecular interaction energy (without taking into account the electrostatic component), according to which the energy of the interaction of the molecules in the strata is approximately six times greater than that between them.[97] One has to assume that the additional intermolecular coordination intensifies to an even greater extent the interactions of the molecules in the strata via the electrostatic component, which is evidently responsible for the high temperatures of the conversion of compounds **11** and **12** into the isotropic state (Table 2).

According to Polishchuk and coworkers,[97,98] the formation of the mesophase by compounds **11** and **12** is accompanied by the disruption of the infinite coordination strata and the disappearance of the additional intermolecular coordination, which is similar to the decomposition of the dimers in compounds **9** and **10**. Indeed, when the crystals are heated, an isotropic liquid consisting of individual molecules with the anisometry of the molecular complexes characteristic of the square planar coordination of copper is formed. During the heating of the isotropic melt of compound **11**, the planar molecules form a nematic mesophase in a narrow temperature range near 10 °C, which vanishes following the onset of the restoration of the additional coordination, i.e. on crystallisation. In the case of compound **12**, the intermolecular coordination is evidently restored faster on cooling of the isotropic melt, as a result of which the crystallisation of the specimen sets in immediately. The absence of the liquid-crystal state for compound **12** (in contrast to the monotropic mesomorphism of complex **11**) is associated, according to the authors,[98] with the stronger additional interaction in the latter case. This is indicated indirectly by the intermolecular coordination distances. When account is taken of the van der Waals radii of the oxygen atoms (1.29 Å)[117] and nitrogen atoms (1.50 Å),[118] they are smaller for the complexes with the NO_2 group (Cu...O = 2.88, 2.91 Å[98]; Cu...N = 3.10, 3.47 Å[97]).

Thus analysis of the above studies[96–98] indicates the negative influence of the additional intermolecular coordination in

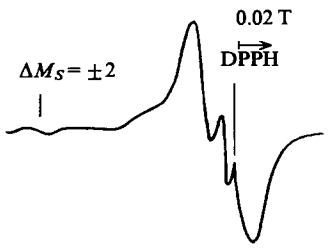


Figure 15. EPR spectrum of the powdered crystalline copper complex **10** at room temperature.[96] The presence of the fine structure and of the forbidden transition $\Delta M_S = \pm 2$ is due to the presence of coordination dimers.

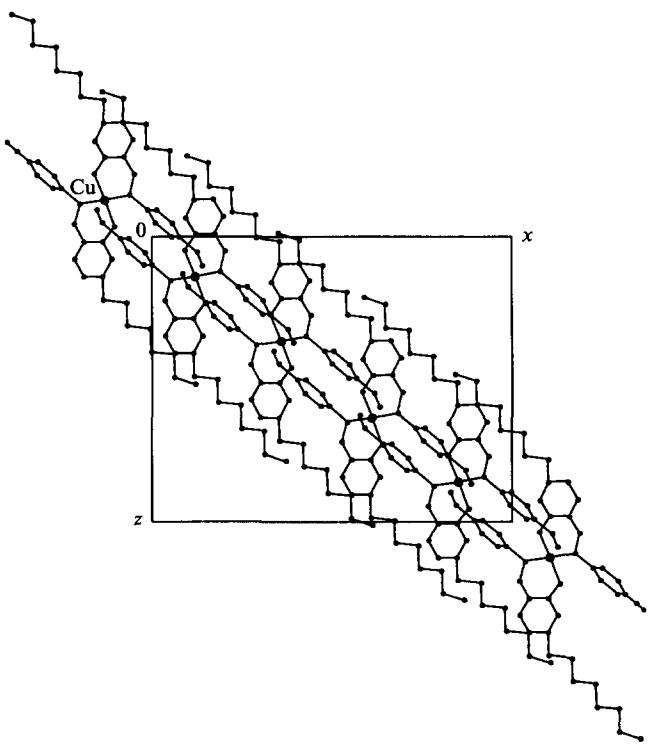


Figure 16. Molecular packing in strata in the crystalline copper complex **11**. Only the central stratum is shown. The thickness of the strata is determined by the transverse dimensions of the molecules.

compounds **10**–**12** and the establishment of the liquid-crystal state, which is expressed either by the presence of only monotropic mesomorphism or by the absence of any kind of liquid-crystal properties. This claim is supported by the finding that individual ligands of the above complexes do exhibit mesomorphism.[87,119]

Among all the complexes of Schiff bases considered here, compound **13** exhibits the maximum molecular anisometry. In the crystal, its molecules are located[99] at the centres of symmetry and are characterised by a *trans*-square planar coordination of the copper atoms. The increase in the length of the mesogenic molecules intensifies the lateral interaction between them, which ensures the appearance of the smectic mesophase. We may note that the copper complexes tend in the main to exhibit smectic mesomorphism (Table 2), while their ligands form a nematic phase. This has been explained in a study,[96] where it was stated that transoid metal complexes are longer by a factor of 1.3–1.4 than their ligands. Furthermore, the lateral interaction of the metal complexes intensifies as a result of the greater number of benzene rings in the central part of the molecules. Taking these facts into account, one would expect the formation of the smectic phase of compound **13**, particularly since its ligands exhibit these properties (smectic phase A at 43–148 °C and a nematic phase at 148–164 °C). However, this compound forms only a nematic mesophase (Table 2), which is caused, according to Polishchuk et al.,[99] by the characteristics of the molecular packing, especially by the presence of chain associated species. Calculations of the intermolecular interaction energy showed that energetically segregated chains of molecules are formed in the crystal in the direction along the x axis and that the energy of the strongest interaction in them is -16.4 kcal mol^{-1}. The assembly of such chains forms strata parallel to the crystallographic xy plane. It is emphasised[99] that the energetic preference for the formation of strata (the interaction of the molecules within the strata is more than 8 times more intense than the interaction between the strata) is in the main associated with an intrachain interaction, which contributes about 55% to the total energy of the interaction of molecules in the strata. It has also been suggested[99] that this interaction intensifies still more via the electrostatic component, because the coordination of the copper atoms in the chains is close to the square-bipyramidal owing to the additional Cu ... O (3.94 Å) intermolecular interaction.

According to the authors,[99] the intense interaction between the molecules in the chain inhibits smectic isomorphism just as the dimers or coordination strata prevent the formation of the mesophase in complexes **10**–**12** examined above. However, such interactions were apparently insufficient to inhibit also the nematic phase. When complex **13** is heated, the formation of the nematic phase entails the rupture of the chain associated species without affecting at the same time the parallel arrangement of the long molecular axes characteristic of this mesophase. On cooling the melt of compound **13**, such associated species are not restored immediately owing to thermal motion and the temperature range of the existence of the nematic phase is appreciably extended (ΔT = 75 °C) compared with the analogous region arising on heating (ΔT = 5 °C, Table 2). In other words, the chain associated species in compound **13** prevent the appearance of the smectic mesophase both on heating and on cooling and, furthermore, cause significant narrowing of the temperature range corresponding to the existence of the nematic mesophase during the heating of the specimen.

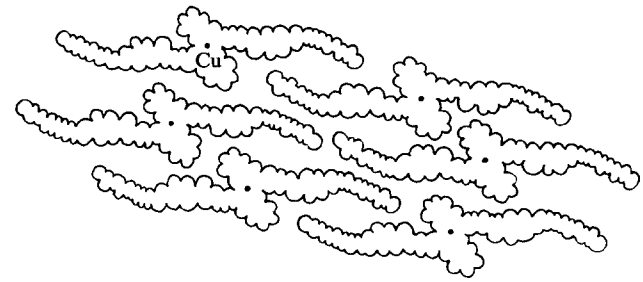
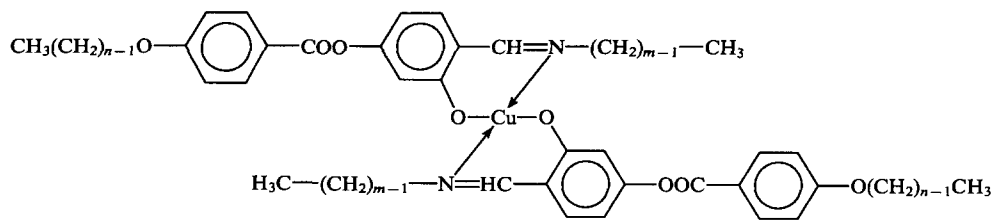


Figure 17. Model of the molecular packing in the nematic phase of the copper complex **13**.

Together with the description of the dependence of the liquid-crystal properties on the additional coordination of the metal atom, much attention has been devoted by Polishchuk et al.[97–99] to the analysis of the geometrical characteristics of the molecular associated species. In particular, it is emphasised that[97] the formation of molecular strata is unfavourable for the manifestation of smectic mesomorphism. As mentioned above, the thickness of the strata in compounds **11** and **13** is determined by the transverse dimensions of the molecules, whereas in the classical smectogenic crystals the thickness of the layer is comparable to the longitudinal dimensions, i.e. the length of the molecules. Furthermore, in smectogenic crystals the interlayer interaction energy is largely determined by the 'end-face' interactions between the alkyl chains of the molecules in neighbouring layers (see, for example, Fig. 9). On heating such crystals, the 'fusion' of the chains, characterised in the crystalline state by high thermal parameters,[8] begins at lower temperatures compared with the central rigid fragments. As a result of such partial fusion, there is a possibility of almost free sliding of the smectic layers relative to one another. Such nature of the fusion with the initial increase in the mobility of the terminal alkyl substituents has been demonstrated by NMR[120] and EPR methods with the aid of spin labels in the aromatic and aliphatic parts of the molecules.[121] On the other hand, in crystals with a stratified structure the sliding of the strata relative to one another is difficult, because not only the atoms of the alkoxy-chain but also those of the central rigid fragments, characterised by significantly weaker thermal vibrations, participate in the contacts between the strata.

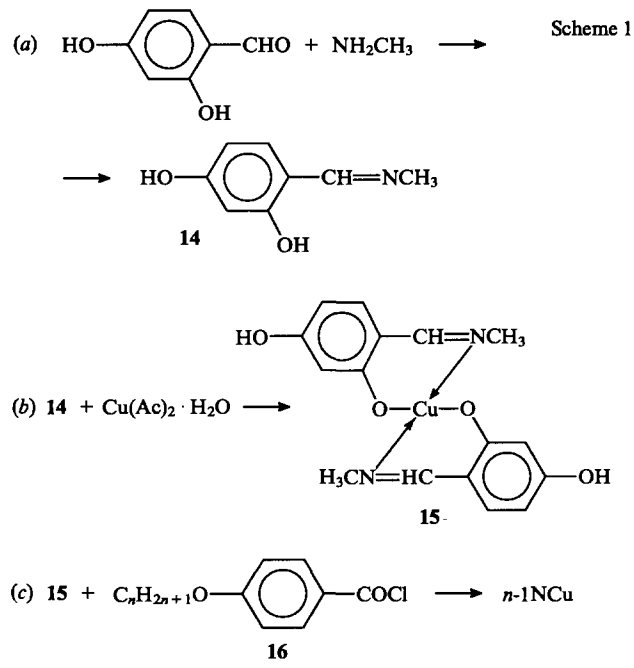
As in the smectic mesophases of compounds **1**, **6**, and **9**, the periodicity of the nematic phase in compound **13** (l_{13} = 34.0 Å) is determined by the length of the ligands (~37 Å). This leads to molecular packing of the projection–hollow type. However, in contrast to the smectic mesophases, in the nematic mesophase of compound **13** the intermolecular end-face contacts are varied. In particular, contacts between the carbon atoms of the condensed benzene rings, contacts between the same rings and the alkoxy-chains, and finally contacts between the chains themselves occur in this case (Fig. 17).

A series of studies devoted to new copper complexes with similar ligands have been published recently. Thus the synthesis and characteristics of the phase transitions in the metal complexes *n*-*m*NCu with the structural formula have been described by Caruso and coworkers.[122,123] The compounds with m = 1 and n = 6–14 (*n*-1NCu) were synthesised as follows.[122]

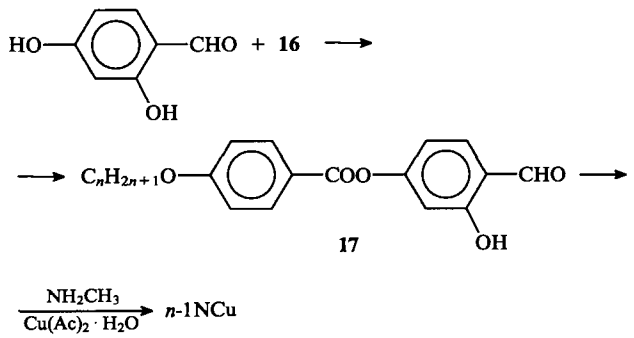


Complex *n*-*m*NCu

Scheme 1



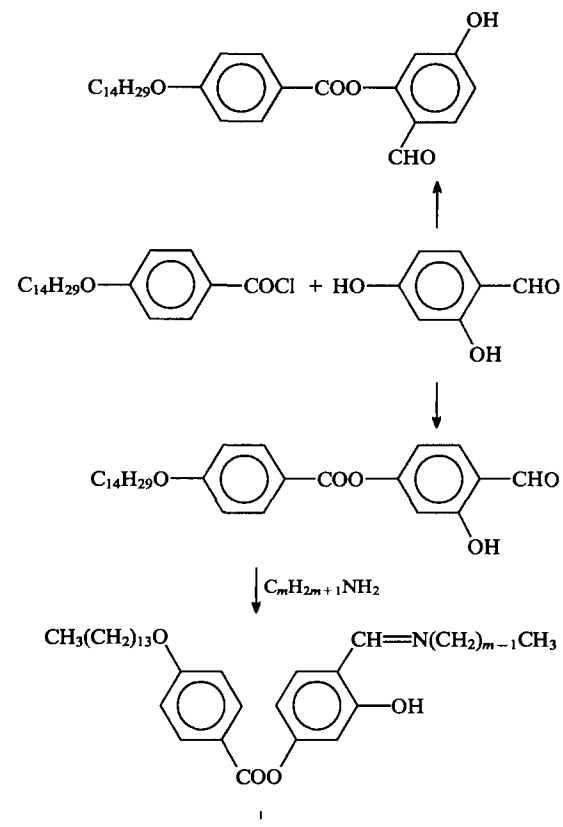
Scheme 2



The compounds with n = 7, 10, and 14 were obtained in accordance with Scheme 1, whilst all the others were obtained in accordance with Scheme 2. All the compounds with n = 6–14 can be obtained in accordance with one of the two schemes, but the authors[122] quote two schemes in order to illustrate different versions of the synthesis. All the compounds are enantiotropic mesogenic substances. For n = 6–9, only the nematic phase is observed, but, with increase in n from 10 to 13, both nematic and smectic phases appear. Finally, for n = 14 only the SmC phase exists. It is noted that in the above homologues there is no even-odd effect in the temperatures of the transition to the isotropic state and the enthalpies per unit mass are appreciably smaller compared with the usual organic mesogenic substances containing symmetrical alkoxy-chains of the corresponding length. It is of interest that in all the smectogenic homologues with n = 10–14 solid-crystal transitions were observed. Thus, in the compounds 13-1NCu and 14-1NCu, these transitions have been confirmed by X-ray powder diffraction studies. It is emphasised here that the layered character of the packing in the crystalline modifications, which are precursors of the mesophase, is correlated with the smectic mesomorphism.

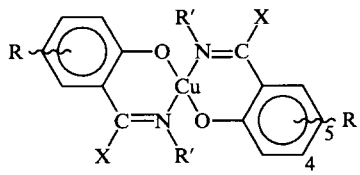
Data have been published[123] on the liquid-crystal properties in the homologous series of copper complexes containing alkylamino-groups with m = 2–15. The need to elucidate the dependence of the mesogenic properties on the length of the alkylamino-groups in the complex 14-1NCu, which itself forms only the SmC phase, led to the synthesis of these compounds.

The compounds with m = 2–15 (14-mNCu) were synthesised in accordance with the following scheme.

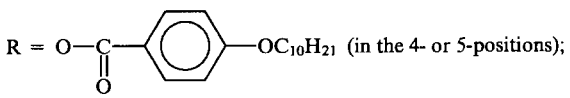


In the series of metal complexes 14-mNCu obtained, only the homologue with m = 2 has no liquid-crystal properties. This has been explained[123] by the impairment of the conditions for the effective packing of molecules along their short axis, which is induced by changes in molecular structure compared with the smectogenic homologue with m = 1. Evidently the conformation of the ethyl groups at the nitrogen atoms weakens the lateral interaction between the molecules. The presence of only the nematic phase N is characteristic of the homologues with m = 3–9, while the presence of the mesophases N and SmC is characteristic of the homologues with m = 10–15. Low-angle X-ray studies on the compounds 14-14NCu and 14-15NCu showed[123] that the periodicities of their smectic layers, amounting to 35.3 and 36.3 Å respectively, are significantly smaller than the analogous periodicity for the compound 14-1NCu (43.3 Å).[122] These results show that, despite the identical type of the mesophases (SmC), the molecular packing within smectic layers changes appreciably. These changes are most probably associated with the inclination of the long molecular axes with respect to the boundary of the layer, which is smaller for 14-1NCu. The majority of the compounds of the 14-mNCu series undergo solid-crystal phase transitions, which are not always reproducible and which depend on the rate of heating and cooling of the specimens. It has also been noted[123] that the crystals of certain homologues, obtained from solution and the melt, have different structures and melt at different temperatures. We emphasise that the solid-crystal polymorphism, characteristic of liquid-crystal compounds, is as a rule associated with conformational changes in the mobile groups, in particular in aliphatic chains. Cholesteryl benzoate, for which six modifications have been found[124] and the single crystals of three of them have been investigated by X-ray diffraction,[125] may serve as a typical example.

A more detailed analysis of the dependence of the liquid-crystal properties on the structural characteristics of the molecule has been carried out[126] for complexes of the type

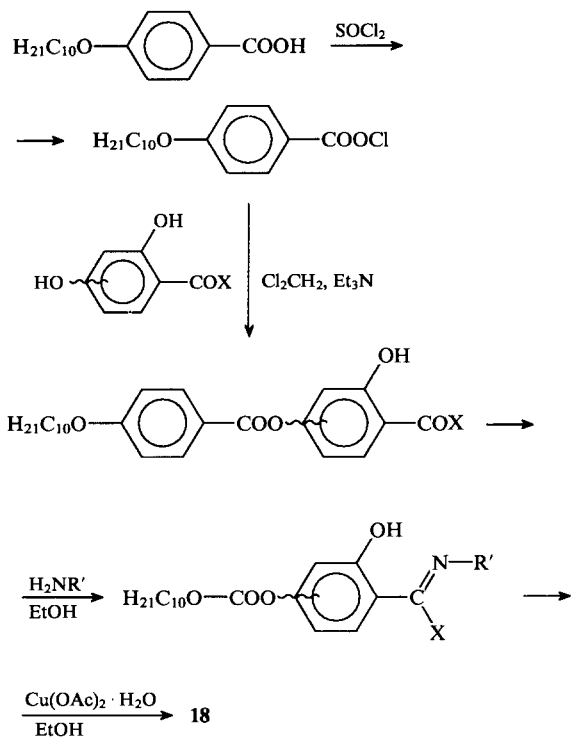


18



R' = CH_3, *p*-$C_{10}H_{21}$, $C_6H_4OC_{10}H_{21}$; X = H, CH_3.

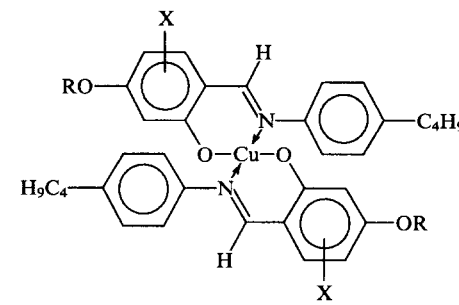
They were synthesised as follows:

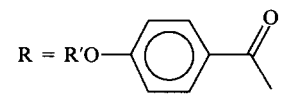


Mesomorphism is characteristic of complexes of this kind (Table 3). Its manifestation is legitimately attributed to the molecular shape, which depends significantly on the disposition of the substituents (Figs 18 and 19). Table 3 shows that the complexes with X = H and R in the 4-position possess liquid-crystal properties and for R' = $C_6H_4-OC_{10}H_{21}$ two smectic phases, SmC and SmI, have been found. The latter has been identified as SmG.[10,127] The authors[126] mention particularly the different types of mesophases for *N*-alkylimines. For complexes with R' = CH_3, there exist both SmC and N mesophases, while for R' = *p*-$C_{10}H_{21}$ there is only an N mesophase. The reason for this is that the long and conformationally mobile decyl groups, parallel to the main molecular axis (Fig. 18), interfere with the establishment of the packing equivalent to the smectic mesophase. They can serve as a shield preventing interaction between the rigid aromatic rings of the molecules. On the other hand, the comparatively small size of the methyl groups makes it possible to increase the effectiveness of this interaction, which results in the appearance of the more ordered mesophase SmC and the thermal stability increases by 90 °C (Table 3). We may note that the interaction between the central parts of the mesogenic molecules should be optimum for the formation of the smectic mesophase. When the layers are insufficiently distinct in energetic terms, they do not persist during fusion. As a consequence of the unduly intense interaction (the presence of coordination dimers, chains, networks, etc.), the melting point increases and the temperature range corresponding to the smectic mesophase can be 'jumped over' under these conditions and in many cases there may be no mesomorphism at all. We believe that the second factor is the reason why only the nematic mesophase arises[128] at 223 °C in one of the representatives of the 2,4-hydroxy-derivatives of the complexes considered (X = H, R' = $C_6H_4-C_5H_{11}$, n = 4). It has been established that the copper atom is involved in a distorted square-pyramidal coordination with an angle of twist of 22° between the two coordination planes formed by copper, oxygen, and nitrogen atoms and is also involved in an additional interaction (Cu ... O = 3.04 Å) with the ester carbonyl group of a neighbouring molecule.

The overall structure of 2,5-dihydroxy-derivatives of the complexes differs appreciably from that of the 2,4-disubstituted derivatives. Such complexes can be represented schematically by a long rod with side substituents R', which prevent a parallel ordered arrangement of the molecules in the mesophase (Fig. 19). This is why only the *N*-methylamine complex (R' = CH_3, X = H) forms a mesophase (Table 3). For longer substituents R', such molecules undergo a decrease in their anisometry, as happens on replacement of a copper atom in complex **18** (see above) by a cobalt atom. The absence of liquid-crystal properties in the complexes with X = CH_3 is due to the steric effects of the methyl groups, which distort the square planar coordination of copper in the direction of tetrahedral coordination.[126]

The mesomorphism of copper complexes with halide substituents in the 3- and 5-positions has been examined.[129] It was noted that the overall anisometry of the molecular complexes and the transition temperatures vary little as a





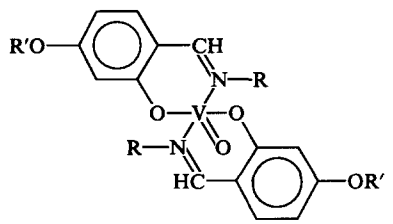
R' = C_nH_{2n+1}, n = 4, 8, 12, 16;
X = Cl, Br (in the 3- or 5-positions).

function of the positions of the halogen atoms.

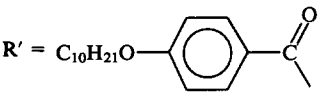
Complexes of other metals [VO[130,131] and iron(III)[132]] with Schiff bases have been investigated in lesser detail hitherto. In particular, the VO complexes (R = Me, C_5H_{11}, $C_{10}H_{21}$, etc.) described[131] have a square-pyramidal coordination and form both nematic and smectic (SmC) paramagnetic mesophases.

The synthesis of these compounds has been undertaken in order to obtain a biaxial nematic mesophase, but this attempt proved unsuccessful. Nevertheless, it has been observed that these compounds have a series of interesting properties.

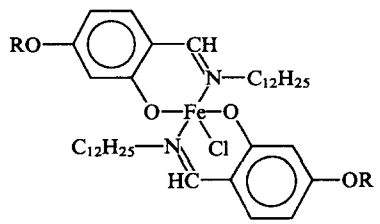
Thus the low viscosity of the nematic mesophase permits a ready orientation of the molecule by a magnetic field, such orientation remaining unchanged also in the solid-crystal state (in the presence of a magnetic field), which indicates the similarity of the molecular packing in these states.



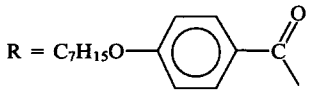
R = Me, *p*-C_5H_{11}, *p*-$C_{10}H_{21}$, C_6H_4–OMe, C_6H_4–OEt, $C_6H_4-OC_5H_{11}$, $C_6H_4-OC_{10}H_{21}$;



The paramagnetic mesogenic iron(III) complex **19** (g_1 = 2.096, g_2 = 4.30) forms a smectic phase (85–151 °C) and is probably characterised by a square-pyramidal coordination of the metal atom.[132]

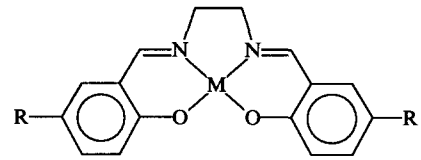


19



Another type of coordination of the metal atom to salicylideneanime ligands occurs in di(5-substituted) salicylideneethylenediamine complexes of nickel(II) and copper(II) described by Paschke et al.[133]

The formation of type SmA smectic phase is characteristic of these complexes. It has been possible to carry out an X-ray diffraction study on a single crystal of the nickel(II) hydrate complex with R = OC_6H_{13}. Layered associated molecular formations, characteristic of crystalline precursors of smectic mesophases, were not detected in the crystal. The molecules in the crystal form centrosymmetric dimers, which are arranged in stacks with a superimposed 'herringbone' pattern. However, on the basis of these results, one cannot conclude that there is no similarity between the structures of the solid- and liquid-crystal phases, since the hydrate of the complex was investigated by X-ray diffraction and the presence of water molecules might have exerted a significant influence on its packing in the crystal.

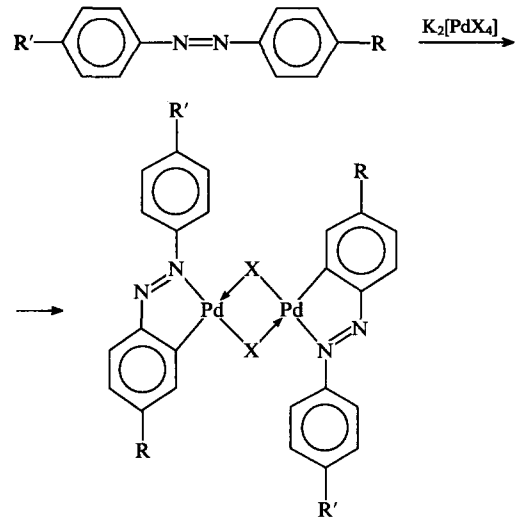


R = OC_nH_{2n+1}, C_nH_{2n+1}, n = 5–10.

7. Mesogenic palladium complexes

Mesogenic palladium complexes are usually segregated in a separate group, since mesogenic compounds in which the metal atom forms part of a cyclic fragment have been found only among them. A distinctive feature is that the palladium atom in the complexes forms a Pd–C(sp^2) σ-bond with a carbon atom of the benzene ring, i.e. such compounds can be regarded as organometallic.

The synthesis of liquid crystals of cyclopalladate complexes has been described for the first time by Chedini et al.[134]



X = Cl; R = OEt or Et; R′ = $COOC_4H_9$, $COOC_5H_{11}$, $COOC_6H_{13}$, or $COO(CH_2)_8CH=CH_2$.

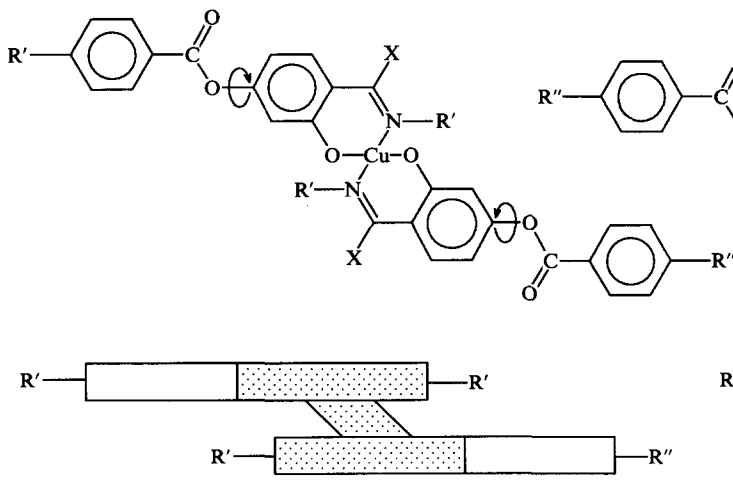


Figure 18. Structural formula and representation of the overall form of the molecule of a 2,4-disubstituted copper complex[126] (R″ = $OC_{10}H_{21}$). The rigid central fragment of the molecule is shown dotted.

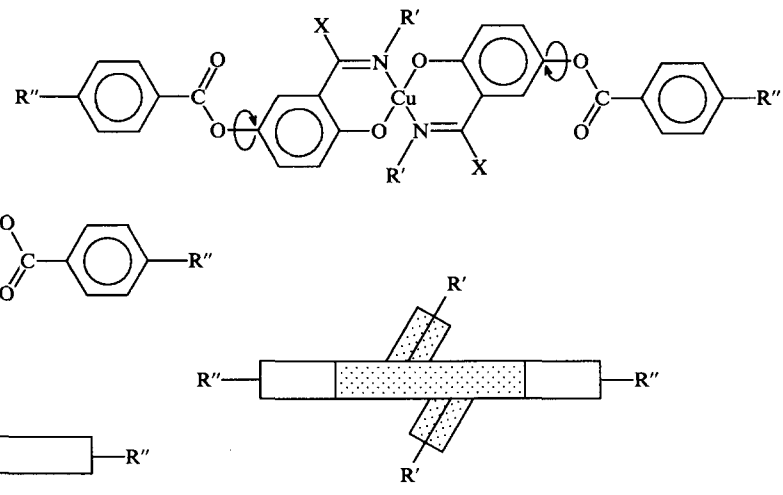


Figure 19. Structural formula and representation of the overall form of the molecule of a 2,5-disubstituted copper complex[126] (R″ = $OC_{10}H_{21}$).

Table 3. Characteristics of the phase transitions in complexes **6**.

X	Position of R	R′	Phase transition temperatures/ °C
H	4	$C_6H_4-OC_{10}H_{21}$	C $\xrightarrow{120.6}$ SmI $\xrightarrow{163.6}$ SmC $\xrightarrow{247.9}$ N $\xrightarrow{248.5}$ I
H	5	$C_6H_4-OC_{10}H_{21}$	$C_1 \xrightarrow{59.2} C_2 \xrightarrow{119.0} C_3 \xrightarrow{119.2}$ I
H	4	p-$C_{10}H_{21}$	C $\xrightarrow{115.7}$ N $\xrightarrow{134.0}$ I
H	5	p-$C_{10}H_{21}$	C $\xrightarrow{103.9}$ I
H	4	CH_3	C $\xrightarrow{173.9}$ SmC $\xrightarrow{178.2}$ N $\xrightarrow{224.0}$ I
H	5	CH_3	C $\xrightarrow{187.4}$ SmC $\xrightarrow{237.5}$ N $\xrightarrow{265.7}$ I
CH_3	4	$C_6H_4-OC_{10}H_{21}$	$C_1 \xrightarrow{106.5} C_2 \xrightarrow{184.3} C_3 \xrightarrow{201.0} C_4 \xrightarrow{228.0}$ I
CH_3	5	$C_6H_4-OC_{10}H_{21}$	C $\xrightarrow{190.0}$ I
CH_3	4	p-$C_{10}H_{21}$	C $\xrightarrow{142.3}$ I
CH_3	5	p-$C_{10}H_{21}$	C $\xrightarrow{115.6}$ I

These compounds form a nematic phase at a fairly high temperature (~200 °C), which rises in the sequence I > Br > Cl (R = OEt, R′ = C_6H_{13}).[135,136]

The results of optical, calorimetric, and IR spectroscopic studies on certain mesogenic azobenzene compounds and their metallocyclic palladium complexes with R = CH_3 or C_2H_5, R′ = C_nH_{2n+1}, and n = 1, 2, 7, and 12 have been compared.[137] The mesophase consists of a 1 : 1 mixture of complexes in which R and R′ change places. These investigations enabled the authors to observe an optically biaxial nematic mesophase in the palladium complexes. The presence of the biaxial nematic phase in these complexes was detected by observing the conoscopic pattern, which was found to contain split monoaxial crosses.[137] This effect (the splitting of the crosses) intensifies still more on imposition of a magnetic field. It has also been noted that the changes in the enthalpies and entropies of the N → I phase transitions are appreciably smaller for the complexes than for the ligands. According to Galerne,[138] this is associated with the molecular biaxial arrangement. It is emphasised[137] that the order parameter P_2 for the complexes is systematically lower than the analogous value for the corresponding ligands (Fig. 20).

The authors discussed this change in P_2 within the framework of the theory of Luckhurst et al.[139] for biaxial molecules and concluded that the incomplete agreement with this theory can be accounted for either by the inaccurate expression for the pseudopotential or by the fact that the biaxial ordering occurs only at a local level, where P_2 is merely one of the components of the order parameter tensor. We emphasise that in the complexes described the biaxial nature of the nematic phase is due to the molecular structure, because the length of the molecules in the complexes is identical with the length of the molecules of the monoaxial ligands, while the width is approximately twice as great.

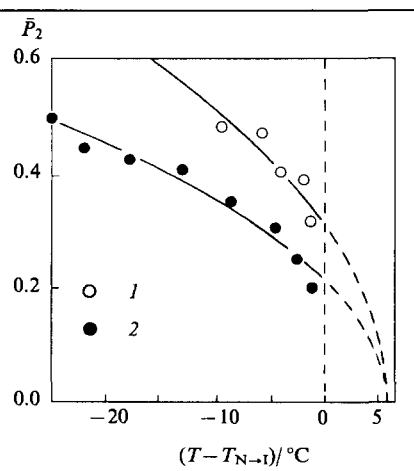
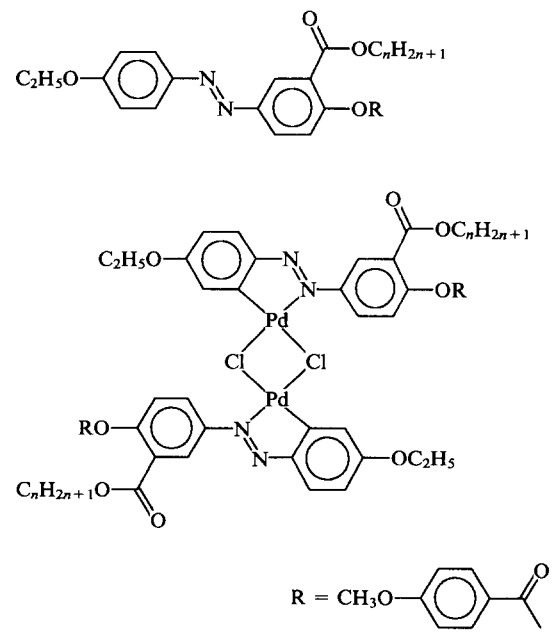


Figure 20. Temperature variation of the order parameter P_2. $T_{N\to I}$ is the temperature of the phase transition N → I; (*1*) complex; (*2*) ligand.

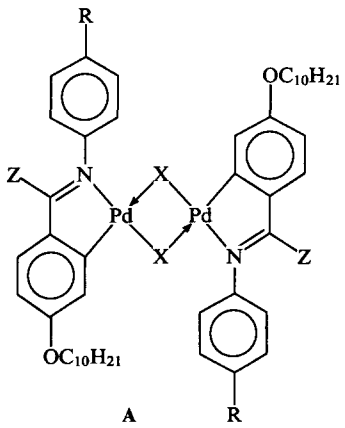
Similar complexes have been obtained from ligands containing three benzene rings and which have been described by Hoshino et al.[140] The ligand and the complex have the following form:



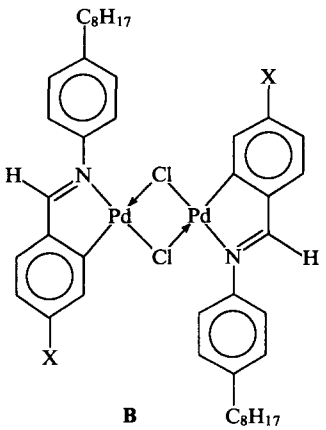
The homologous series with n = 1–10, 12, 14, 16, and 18 has been investigated. Both the ligands and the complexes proved to be nematogenic compounds, the temperature ranges corresponding to the existence the mesophases of these homologues varying in parallel. The average melting point of the complexes is higher by 87 °C and the clarification temperature is higher by 126 °C than the corresponding temperatures for the ligands. ^{1}H NMR data suggested that the most favourable conformation, at least for long-chain homologues, is that in which each substituent

$COOC_nH_{2n+1}$ occupies a position between the main phenyl-containing chains of the ligands. According to Hoshino et al.,[140] this conformation is most favourable for the formation of a nematic phase by the above compounds.

The synthesis of complexes of two types from the corresponding Schiff bases and $Pd_3(OAc)_6$ has been described.[141–144] Complexes A form mainly mesophases of the SmA type with the following bridging groups: X = Cl, Br, or SCN; the acetate-bridged complexes are in most cases nonmesogenic, which may be associated with the distortion of the planarity of the central part of the molecules. Mesomorphic behaviour is also characteristic of chloride complexes of type B.



A



B

In contrast to the complexes mentioned above, a complex with a different type of acetate bridge (X = $MeCO_2$), obtained from the symmetrical 4,4′-bis(alkoxybenzylidene)hydrazine $C_nH_{2n+1}OC_6H_4CH = N-N = CHC_6H_4OC_nH_{2n+1}$ (n = 7, 10, 12, 14), forms an SmC mesophase. Evidently the μ-acetate ligands distort the planarity of the central part of the molecular complexes, which made it necessary to segregate them[145] as a new type of structure referred to as 'open book' structures (Fig. 21).

Special mention should be made that, according to NMR data, an optically active complex of this series (n = 10) (Fig. 21) contains a mixture of the *trans*-λ-R,R-, *trans*-δ-R,R-, and *cis*-R,R-isomers.[146] This compound forms an enantiotropic SmC* phase and is the first organometallic ferroelectric substance. However, its electrooptical response is significantly weaker than for organic calamitic phases SmC* owing to its high viscosity, which is probably due to its large molecular volume.

8. Liquid-crystal complexes of phthalocyanines

Mesogenic phthalocyanines (Pc) constitute a new class of potential liquid-crystal one-dimensional conductors,[147–150] in which the direction with maximum conduction coincides with the direction of the columns. The columns themselves are made up of flat polar

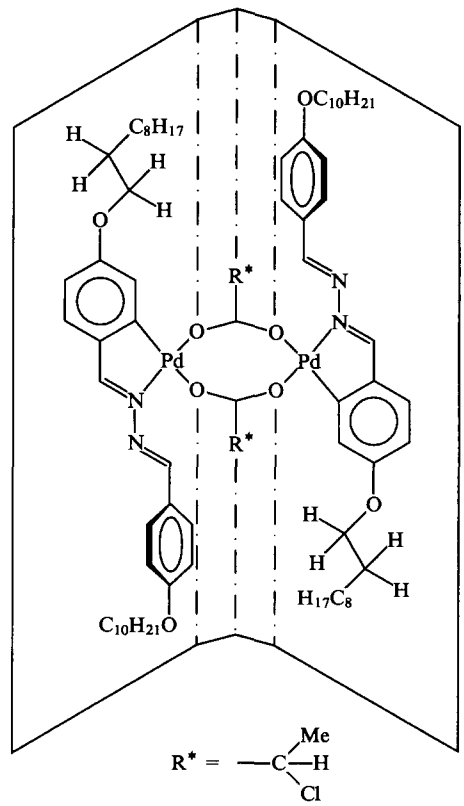
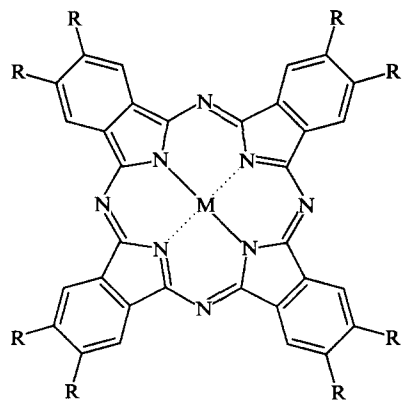


Figure 21. An optically active complex having the open book conformation.[146]

aromatic nuclei separated by neutral fused paraffin chains. It is possible to obtain phthalocyanine complexes of different metals: Fe, Co, Ni, Cu, Zn, and Pt. This allows one to vary their electronic properties. The presence of stacks with a fairly strong interaction of the molecules within them and appreciably weaker interactions of the molecules between the stacks is characteristic of such compounds in the crystalline and liquid-crystal states. Thus such interaction gives rise to anisotropy of the electronic transport properties.

The mesomorphic, structural, optical, and electrical properties of a large number of phthalocyanine compounds having the general formula



M = 2H, Cu,
R = OC_nH_{2n+1}, n = 6–12.

have been examined in detail in a review article.[151]

The copper complexes (CuPc) were synthesised by deprotonating the free ligands with sodium pentyloxide and subsequent interaction with anhydrous copper(II) chloride. Low-angle X-ray studies[151] showed that all the Pc homologues

and the corresponding copper complex CuPc form a discotic ordered hexagonal mesophase D_{ho}. According to electron-diffraction data, the molecular stacks in the crystals are then disposed along the long axes of the acicular crystals, for which ~20–25 diffraction lines are observed. The indexing of these lines showed that the crystals belong to the orthorhombic system with $Z = 4$. The calculated densities (1.1 g cm^{-3} for $n = 12$ and 1.4 g cm^{-3} for $n = 6$) of the complexes CuPc agree with the values established previously (1.6 g cm^{-3} for CuPc[152] and 1.1 g cm^{-3} for the phthalocyanine complex with R = $CH_2OC_{12}H_{25}$[148]). In all cases the (001) reflections correspond to a distance of ~4.3 Å between neighbouring molecules within each stack. This fairly large distance indicates an inclined disposition of the molecules relative to the axes of the stacks. This is also indicated indirectly by the change in the unit cell parameters a and b as a function of n (Fig. 22). On average, both parameters increase with increase in n, but van der Pol et al.[151] suggest that the more marked change in the parameter b indicates a change in the inclination of the molecules precisely relative to this direction.

The electron diffraction pattern of the mesophase in the region of low angles contains five reflections ($l/d = 1 : \sqrt{3} : \sqrt{4} : \sqrt{7} : \sqrt{9}$) corresponding to a hexagonal lattice, the broad diffuse reflection (4.6 Å) corresponding to the disordered structure of the aliphatic chains. At the same time, the X-ray diffraction patterns of all the homologues of Pc and CuPc contain an intense and sharpened reflection (3.4 Å) due to the ordered arrangement of the molecular discs within one column. Finally, the weak and broad reflection (7.0 Å) is attributed to some kind of ordering within the columns, but one cannot rule out the possibility that this is a second-order manifestation of the 3.4 Å periodicity.

The dependence of the distances D between the columns in Pc and CuPc (parameter of the planar hexagonal unit cell) on the length of the alkyl chain is almost linear (Fig. 23).

Comparison of the values of D found with the calculated diameter of the nuclei (taking into account the oxygen atoms) D_c = 16.8 Å and with the length of the extended n-alkyl chain indicates an appreciable interpenetration of the alkyl chains of neighbouring columns up to their contact with the phthalocyanine nuclei of neighbouring columns. The fact that the value D_c = 16.8 Å does not differ greatly from that established (13.9 Å) for unsubstituted phthalocyanine[153] and is close to the model estimates (17.0 Å) led the authors[151] to the conclusion that the planes of the nuclei of the phthalocyanine molecules in the mesophase are on average disposed at right angles to the axis of the column (if they were inclined, the value of D_c would be even

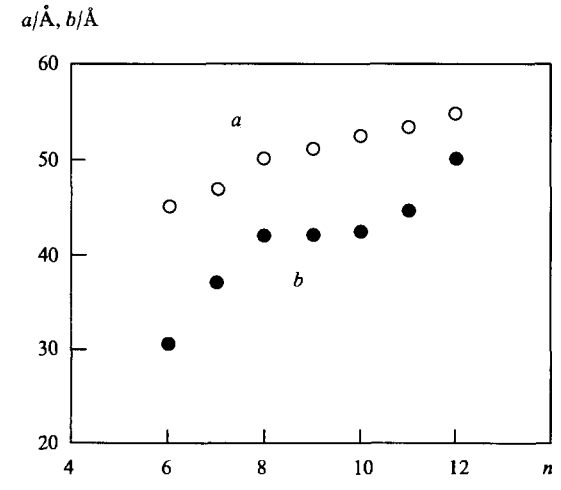


Figure 22. Dependence of the parameters a and b of the orthorhombic lattice on n in the homologous series of complexes CuPc.

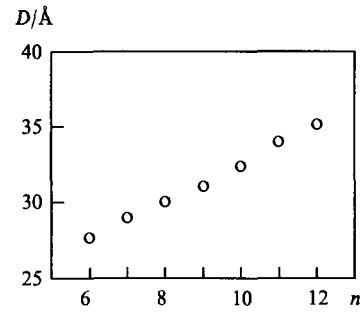


Figure 23. Variation of the distance between the columns in Pc and CuPc as a function of the length of the alkyl chain.[151]

smaller). Such stacked arrangement of the nuclei of the molecules is in fact favourable for the exciton and electron migration through the column. We may note that the inclined disposition of the molecules is frequently encountered in discotic mesophases. Thus the study of freely suspended films of triphenylene hexa-n-dodecanoate using synchroton radiation established[154] that in both phases, D_{hd} and D_{rd}, the nuclei of the molecules are inclined relative to the column axes at an angle of ~28°. An even more marked inclination has been observed in the columnar orthogonal mesophase D_{rd} of triphenylene hexahexyloxybenzoate, in the structure of which the molecular planes form an angle of about 40° with the column axes.[155]

The electrical conductivities of the CuPc metal complexes in the form of compressed discs (n = 8, 12) have been measured. Such measurements have become possible by virtue of the high viscosity of the mesophase, the conductivity of which increases with increase in temperature. On passing from the crystalline to the liquid-crystal state, a slight increase in the conductivity is observed: $\sigma_{n=8} = 5 \times 10^{-8}\ \Omega^{-1}\ m^{-1}$ and $\sigma_{n=12} = 7 \times 10^{-8}\ \Omega^{-1}\ m^{-1}$ at 175 °C. The activation energies for the mesophases of the above homologues E_a = 0.5–0.6 eV are appreciably smaller than for the unsubstituted crystal (R = H, $\sigma = 6 \times 10^{-8}\ \Omega^{-1}\ m^{-1}$, E_a = 1.4 eV). The measured difference can be explained by the fact[151] that a more effective overlap of the orbitals of the central parts of the molecules in the stacks occurs in the mesophase. We may recall that the central parts of the molecules in the mesophase are arranged at right angles to the stack axes, as a result of which there is an appreciable decrease in the forbidden gap between the valence and conductivity bands. This conclusion agrees with the measurements of the microwave conductivity with time resolution.[151]

It was noted above that the conductivities of the compounds CuPc with n = 8 and 12 are of the same order of magnitude. This demonstrates the independence of this property of the length of the alkyl chains. At the same time, the conductivity increases sharply after the introduction of electron-donating or electron-accepting compounds into these materials, because this leads to the appearance of free electrons or holes. Thus the addition of I_2 to CuPc (n = 8) in proportions of 1 : 1 by weight leads to an increase in conductivity by four orders of magnitude.[151] A gigantic increase in conductivity (by 9–10 orders of magnitude) compared with the initial MPc has been observed[156] in crystals of the nonstoichiometric compounds $MPcI_x$ ($x < 3$; M = Cu, Ni, Pt, Co, 2H). It is believed that the high conductivity is caused in this case by the incomplete oxidation of the MPc molecules within the stacks by the I_3^- anions, which results in the formation of 'holes'. Bearing in mind the fact that the conductivity of PcH_2I_x is of the same order of magnitude as that of the metal complexes $MPcI_x$, Peterson et al[156] concluded that the conductivity of these materials depends not so much on the metal–metal overlap as on the π–π or π–d overlap. This is attributed to the fact that the holes formed on partial oxidation can be concentrated either on the metal or on the ligand.

In the studies discussed, the conductivity was measured for powdered specimens and nonoriented mesophases, which naturally reduced its value. The small size of the CuPc (n = 8 and 12) single crystals and their acicular form, for which the molecular stacks are arranged along the long axis, made it impossible for the investigators to carry out measurements on single crystals. For comparison, we may point out that the conductivity of the single crystal specimen of (Qn) $(TCNQ)_2$, measured[157] at room temperature in the direction along the stacks ($\sigma = 10^4\ \Omega^{-1}\ m^{-1}$; $E_a \simeq 0$ eV), exceeds significantly the conductivity of the powder of this compound ($\sigma = 4 \times 10^2\ \Omega^{-1}\ m^{-1}$; $E_a \simeq 0.03$ eV).[158] We may note that an even greater conductivity in the direction of the chain axis has been observed for a single crystal of the Krogmann salt $K_2Pt(CN)_4Br_{0.30}\cdot 3H_2O$ ($\sigma = 3 \times 10^4\ \Omega^{-1}\ m^{-1}$).[159]

The phthalocyanine with R = $CH_2OC_{12}H_{25}$ forms a disordered hexagonal discotic mesophase D_{hd} with distances between the molecules in the columns of ~4.5 Å and a hexagonal lattice parameter of 31.2 Å.[148] The X-ray diffraction patterns of the mesophase show an additional intense reflection due to the periodic distortion of the columns with a wavelength of 20.5 Å. On the other hand, the copper complex of this compound forms an ordered mesophase D_{ho} in which the distance between the plane of the metallocycles is 3.8 Å and that between the columns is 34.0 Å.[147]

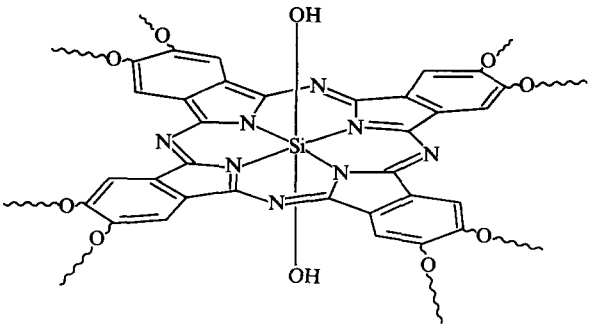
The introduction of other substituents into the phthalocyanine nucleus does not as a rule alter the columnar character of the mesophase formed, although the latter may be characterised by different structural types. For example, a series of polymorphic mesophases have been found for the copper complexes of phthalocyanine with chiral substituents R = $C_{12}H_{25}OC^*H(Me)CH_2OCH_2CH_2$, whereas the analogous complexes with nonchiral substituents form only one mesophase.[160] The influence of the length of the substituent on the type of mesophase has been investigated[161] for the copper complexes of phthalocyanine with R = $C_nH_{2n+1}OC_6H_4$ (n = 8, 10, 12, 18) and the analogous free nonmetallated phthalocyanines. For n = 12 and 18, the nonmetallated phthalocyanines form hexagonal phases with disordered columns D_{hd}, while the copper complexes form orthogonal phases D_{rd} (with $C2/m$ symmetry).

The copper complexes of phthalocyanines in which the substituents are crown-ethers, in particular 15-crown-5, are unusual. It has been suggested[162] that such molecules can form channels through which ions may be transported.

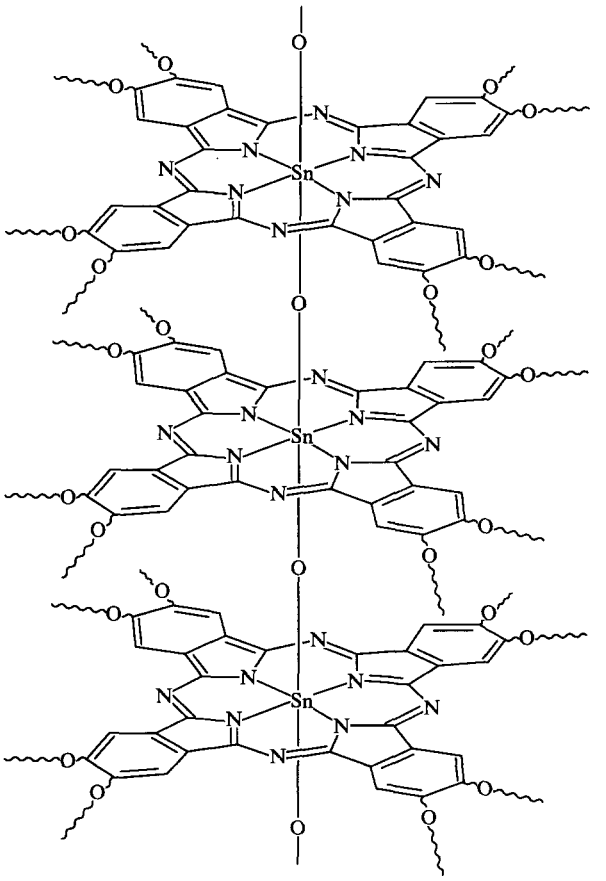
The complexes of phthalocyanines with other metals (Co, Ni, Pb, Zn, Mg) also form mesophases,[163-165] which, by virtue of their bright colour, have found extensive and varied applications.

Unusual discotic mesophases have been found[166-169] for two forms of bis(phthalocyanine)lutetium $Lu\{(ROCH_2)_8C_{32}H_8N_8\}_2$ ($LuPc_2$) with R = $C_{12}H_{25}$. It is emphasised that the red oxidised form, constituting a salt of the anion $SbCl_6^-$, is more stable than the green neutral form. X-Ray diffraction study of the $LuPc_2$ (R = $C_{18}H_{37}$) mesophase showed[7] that the distance between the columns is 37.0 Å, while the periodicity within the column (7.3 Å) is equal to twice the thickness of the phthalocyanine rings (Fig. 24). It is of interest that the form of the X-ray diffraction pattern at room temperature remains unchanged up to the transition of the isotropic phase, which indicates the similarity of the crystal and liquid-crystal structures. The conductivities of these phases are also approximately the same ($1.8 \times 10^{-7}\ \Omega^{-1}\ m^{-1}$ for the neutral form) and the probability of electron jumps within the columns is greater by a factor of 10^7 than the probability of the jumps between them for the same activation energy.

The phthalocyanine complexes in which the metal (Si or Sn) atoms are linked by oxygen bridges can be classified as liquid-crystal polymers. They are formed on heating from dihydroxy-complexes of the type:[170-172]

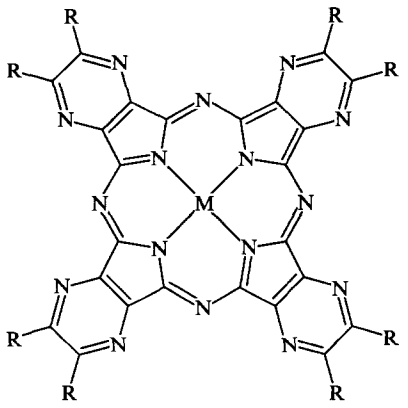


Bridged tin complexes form a columnar mesophase in the temperature range 59–114 °C, which is characterised[170] by a rectangular planar unit cell (25.2 Å × 30.7 Å) in which the distance between the metal atoms is 3.85 Å. The liquid isotropic phase of this compound is slowly transformed into a highly viscous anisotropic material, which contains polymer type bonds $(-O-Sn-)_n$ and a new temperature of transition to the isotropic phase (290 °C).



The analogous silicon phthalocyanine complex (n > 4) forms a hexagonal columnar mesophase of type D_{hd} in the temperature range from 20 to 300 °C. During heating in air at 180 °C, water evaporates, which is accompanied by the oligomerisation of the specimen to dimers, trimers, and higher oligomers.[171,172] We may note that a dimeric organisation of molecules, due to antiferroelectric pairing, has been observed in the phthalocyanine complexes of lead,[173] which form discotic mesophases with intercolumn distances of 26.9, 31.0, and 36.0 Å for R = $C_8H_{12}OCH_2$, $C_{12}H_{25}OCH_2$, and $C_{18}H_{37}OCH_2$ respectively.[174]

The synthesis and properties of substituted tetrapyrazinoporphyrazines and their complexes, similar to the phthalocyanine complexes, have been described.[175-177]



Discotic phases D_{rd} (with $C2/m$ symmetry) with an orthogonal centred cell and a disordered disposition of molecules in the column have been found for the complexes with M = Cu, Ni, or Co and R = $C_{12}H_{25}$. The similar phthalocyanine complexes have an analogous structure. The nonmetallated tetrapyrazinoporphyrazines form hexagonal columnar mesophases also with a disordered disposition of the molecules in the columns (D_{hd}). The compounds investigated are π-acceptor mesogenic substances. They are reduced more readily than the analogous phthalocyanine derivatives and this feature can be used to create discotic liquid crystals with mixed columns.

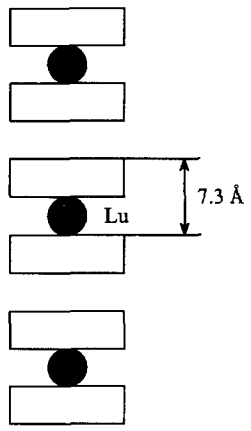
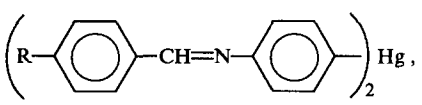


Figure 24. The structure of the columns in $LuPc_2$.

9. Organometallic and organoelement liquid-crystal compounds

Some of the first liquid-crystal compounds synthesised were organometallic mesogenic compounds. In particular, Vorländer obtained in 1923 the diarylmercury derivatives[7]

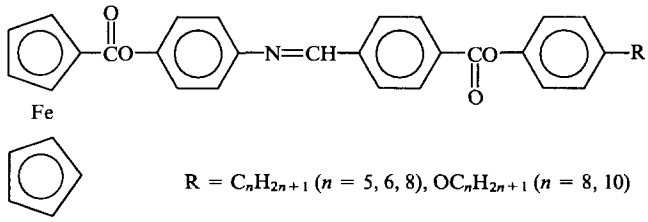


which exhibit smectic mesomorphism. The first example of a liquid-crystal π-complex (a ferrocene derivative) was described[178] in the middle 1970s. At the present time the number of studies devoted to such complexes is continually increasing. The first mentions of mesogenic materials belonging to the class of organoelement silicon derivatives were made at the beginning of the 1950s,[170,180] but such studies underwent a vigorous development only recently.

a. Ferrocene derivatives

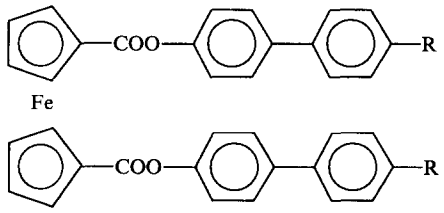
Ferrocene derivatives with Schiff bases as substituents are some of the first liquid-crystal smectic transition metal complexes obtained. They were synthesised by the reaction of the corresponding benzal-dehyde derivative with 4-aminophenyl-ferrocenyl carboxylate.[178]

Mesogenic ferrocene diesters, forming monotropic smectic mesophases,[181] were synthesised subsequently.[181]



R = C_nH_{2n+1} (n = 5, 6, 8), OC_nH_{2n+1} (n = 8, 10)

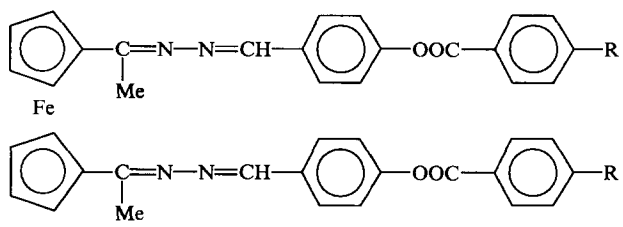
An X-ray diffraction study of one of these compounds (R = OC_5H_{11}) was carried out.[182] It showed that the molecule in the crystal occupies a specific position (at the centre of symmetry) and has a transoid form. The plane of the carbonyl group is coplanar with the plane of the cyclopentadienyl ring, but is almost perpendicular to the nearest benzene ring. The dihedral angle between the benzene rings (23°) is appreciably smaller than in the crystals[183,184] and mesophases[185] of various cyanobiphenyls.



R = OC_5H_{11}, C_6H_{13}.

Low-angle X-ray studies on the mesophase yielded little information compared with the study of the single crystals, which was attributed[182] to the thermal instability of the mesophase. However, for the homologue with R = C_6H_{13} it has nevertheless been possible to establish a layer periodicity (~47 Å) at the instant when the specimen consisted of a mixture of crystals and the mesophase. This quantity corresponds to an extended transoid molecular shape. Taking this factor into account and also the fact that in the crystal with R = OC_5H_{11} the molecule has the transoid form, the authors[182] concluded that the smectic phase contains precisely such molecules. It is emphasised that the bulky substituents in the mesogenic diesters prevent the torsional vibrations of the cyclopentadienyl rings around the C_5 axis.[186]

A nematic type of mesophase has been observed in the mesogenic series of compounds



R = OC_nH_{2n+1} (n = 1–8).

As in the case of the ferrocene diesters, the most probable form of these molecules is either U-shaped or S-shaped. In order to establish reliably the structure of the nematic mesophase of such compounds, a structural study was carried out[187] on a single crystal of 1,1′-bis[4′-(n-propoxy)benzoyl-4″-methyldiphenoxy-

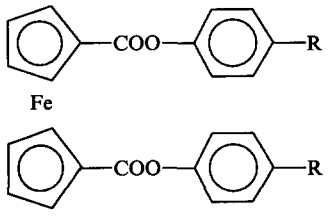
azinomethyl]ferrocene‡ (PBIFF, R = OC_3H_7), forming a mesophase in the temperature range 210–220 °C. Evidently, depending on the U- or S-shaped molecular structure, the nematic phase can be constructed in two ways (Fig. 25) within approximately the same characteristic periodicity of the mesophase ($d_1 \simeq d_2$) in both cases.

A molecule in the PBIFF crystal occupies a general position and has a U-shape in which the long axes of the ligands are almost parallel (Fig. 26). The conformations of two crystallographically independent ligands are similar; in each of them the carbonyl group is coplanar with one benzene ring [C(16)–C(21)] and has rotated by approximately 50° relative to the plane of the other ring [C(9)–C(14)], the planar fragments of one ligand being parallel to the analogous fragment of the other.

In the crystal (Fig. 27), the molecules are packed in an antiparallel arrangement, forming layers, and an interpenetration of the ferrocene component of the molecules from one layer into the other is observed. Despite the layered character of the packing, [the layers are energetically appreciably less distinct ($U_{layer}/U_{interlayer} \simeq 2.8$) than in the metal complexes of Schiff bases], the contacts between the rigid ferrocene components of the molecules rule out the possibility of the formation of a smectic mesophase, because such layers cannot slide freely relative to one another. On the other hand, the antiparallel arrangement of the molecules does not conflict with the structure of the nematic phase. The investigation described[187] permits the conclusion that the nematic phase of PBIFF consists of cisoid molecules. The presence in the crystal of energetically indistinct layers agrees with X-ray diffraction studies on mesophases of this series,[188] from which it follows that the molecules in the nematic phase can form small lamellar associated species.

We may note that the S-shape of the mesogenic ferrocene molecules is more favourable than the U-shape for the formation of the smectic mesophase, since mobile alkyl substituents would be involved in the interlayer contacts on either side for this shape. Conformational calculation carried out for disubstituted ferrocenes showed[187] that the U-shape is more favourable for an isolated molecule, whereas in the crystal and in the mesophase the energies of the U- and S-shaped forms may be similar when account is taken of the nonvalence intermolecular interactions.

Yet another series of ferrocene derivatives



with R = OC_7H_{15}, $OC_{10}H_{21}$, OH, and OCH_2Ph has been described.[189] For R = OC_7H_{15} and $OC_{10}H_{21}$, the compounds form a nematic phase, the phase of the compound with R = OH being characterised by the largest temperature range (hydrogen bonds can probably be formed under these conditions). For the homologue with R = OCH_2Ph, a mesophase is not formed.

b. Organoelement liquid crystals

The majority of the thermotropic mesophases known at the present time are made up of molecules having an anisometric shape — rods or discs. At the same time, data are being published with an increasing frequency concerning the formation of mesophases by compounds the molecules of which do not possess the classical anisometry. The unusual mesophase formed by one of the representatives of the series of silanediols $R_2Si(OH)_2$

‡ 1,1′-Bis[*p*-(*p*′-n-propoxybenzoyloxy)benzylidenehydrazono(α-ethyl)]-ferrocene? [Translator].

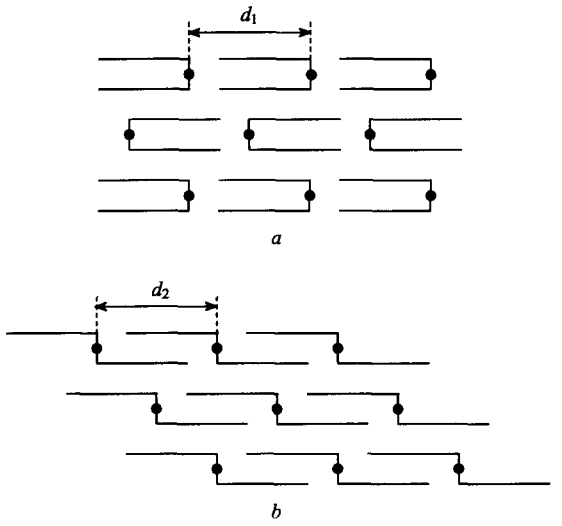


Figure 25. The structure of the cisoid (*a*) and transoid (*b*) molecules in the nematic mesophase of disubstituted ferrocene.[187]

(R = Bu^i)—diisobutylsilanediol (DISD)—may be included among them.[179,180]

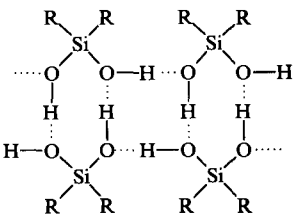
As early as 1952, the unusual behaviour of DISD on fusion was noted.[179] It is due to the existence of a mesophase in the temperature range 89.5–101.5 °C. For other derivatives of this series with R = Me, Et, Ph, Pr^i, or Bu^t, the manifestation of mesomorphism was not observed.[179,180] The DISD mesophase was initially identified as smectic, consisting of extended chains of hydrogen-bonded molecules. The accumulated data on the structures of liquid crystals and especially the discovery of discotic mesophases[1] made it necessary to return to the investigation of the structure of this unusual mesophase after almost 30 years.[190]

Calorimetric study of DISD demonstrated the similarity of the enthalpies of the phase transitions

$$C \xrightarrow[7.6\ kJ\ mol^{-1}]{89.5\ °C} LC \xrightarrow[7.2\ kJ\ mol^{-1}]{101.5\ °C} IL.$$

According to Bunning et al,[190] this shows that only some of the hydrogen bonds present in the crystal are disrupted in the first phase transition, while some remain and are disrupted only on transition to the isotropic liquid. We may note that discotic mesophases, where there are no hydrogen bonds, are also characterised by similar enthalpies of the phase transitions C → LC and LC → IL.[54] It has been emphasised[190] that the textures of the DISD mesophase resemble those of discotic materials and their continuous miscibility with a classical discotic compound, namely hexa(n-heptyloxy)benzene, has been observed.

The X-ray diffraction patterns of the DISD mesophase contain[190] two diffuse rings corresponding to interplanar distances of 4.7 and 11.0 Å. The crystal structure of this compound has not been established, but the parameters of a nearly hexagonal triclinic cell with $a \simeq 12$ Å have been found. It has been possible to carry out a structural study on single crystals for a



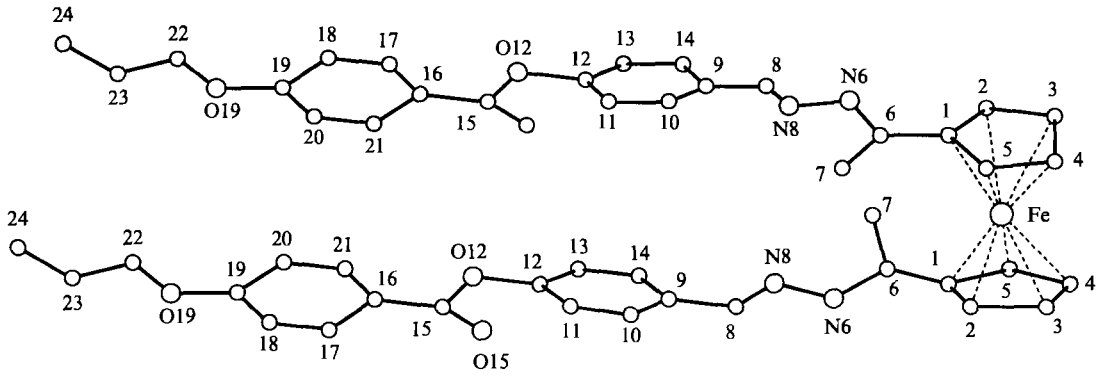


Figure 26. The structure of the PBIFF molecule.

series of DISD homologues.[191-193] Thus hydrogen-bonded strips made up of dimers have been observed for crystals with R = Pr^i and Bu^t.

On the basis of the above data, it was concluded[190] that the DISD mesophase is discotic. The role of discoid molecules is assumed in this case by the hydrogen-bonded dimers. In the DISD crystal, these dimers are joined together by hydrogen bonds into inclined stacks (Fig. 28) with an approximately hexagonal arrangement. It is believed that during heating, in the transition of the crystal to the mesophase, the interdimer hydrogen bonds are broken, while the intradimer hydrogen bonds are retained. However, it is noteworthy that the latter requires significant evidence, since it is not entirely clear why selective and not random dissociation of hydrogen bonds takes place (in crystals with R = Pr^i and Bu^t, all these bonds have virtually the same lengths and hence similar energies).

In the related series of lower-melting disiloxanediols,[194] thermotropic mesomorphism proved to be a more general property. It has been observed for compounds with alkyl substituents having the normal structure (R = n-C_nH_{2n+1}, n = 2–4), but not for compounds with R = Me, Ph, or isoalkyl.

The results of X-ray diffraction studies on single crystals and mesophases as well as IR spectroscopic, calorimetric, and optical studies on compounds of the class of DISD and its analogues have been surveyed,[5,6,195-197] which has made it possible to characterise fairly fully the mesophases examined and to assign them to a new structural type.

The crystal structures of three nonmesogenic and two mesogenic compounds of the DISD series are now known. Studies have shown that 1,3-dihydroxy-1,1,3,3-tetraalkyldisiloxanes (DTADS), namely DTPDS (R = Pr^n),[195] DTMDS (R = Me),[6] DTEDS (R = Et),[197] and DTPDS (R = Ph),[198] have the same molecular packing in the crystals and the same system of intermolecular cooperative hydrogen bonds, without dimeric organisation, regardless of the fact that their crystals belong to different structural classes.

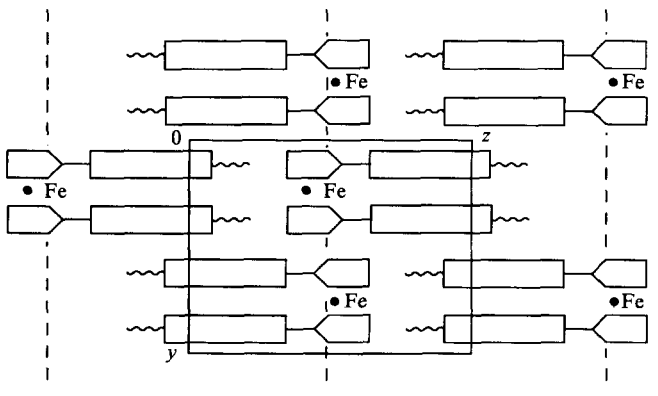
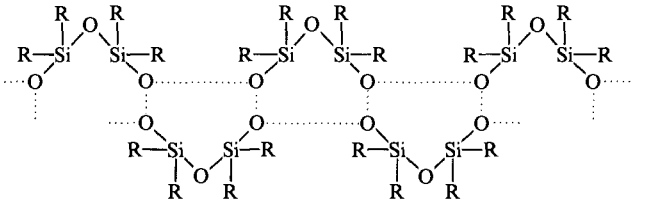


Figure 27. The layered packing of the molecules in the PBIFF crystal. The layer boundaries are shown dashed.[187]



The system of hydrogen bonds in the DTMDS crystal can be described as two chains of hydrogen-bonded molecules linked by transverse hydrogen bonds into infinite strips with 2_1 symmetry and extended along the b axis (Fig. 29). In contrast to DTMDS, the crystal of which contains one system of independent molecules, in the DTPDS crystal the analogous strips are formed by six independent molecules A–E (Fig. 30), while in DTEDS

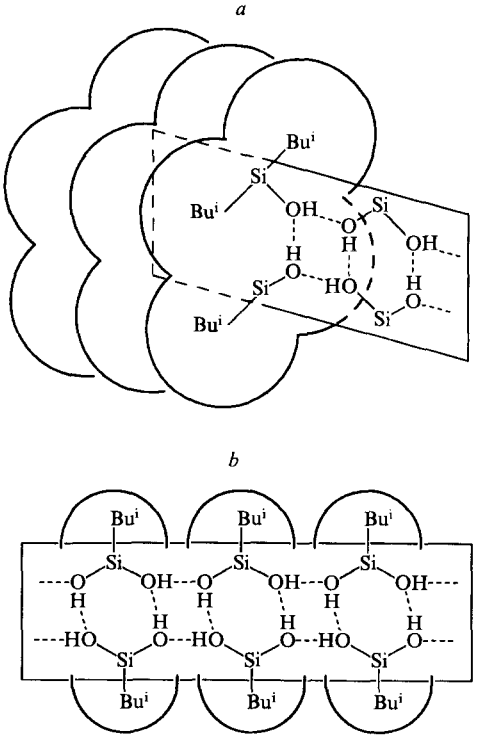
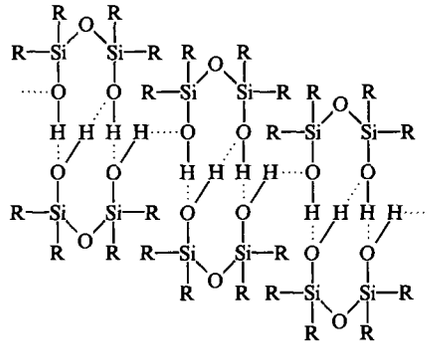


Figure 28. The structure of the dimeric discotic DISD phase: (*a*) perspective view along the column; (*b*) view at right angles to the column.

centrosymmetric hydrogen-bonded strips are formed by two independent molecules. Similar strips are observed also in the DTPDS crystal, but here they are made up of three symmetrically independent molecules. In the majority of the crystals which we examined there are conformational differences between symmetrically independent molecules, which is indicated by the differences between the SiOSi bond angles and the pseudotorsional (H)SiO ... OSi(H) angles characterising the overall molecular conformation.

In the crystal of the isopropyl homologue of DTPDS, i.e. $Pr^i_2(OH)SiOSi(OH)Pr^i_2$, the hydrogen bond system is somewhat different, although here too strips of hydrogen-bonded molecules are observed.[199]



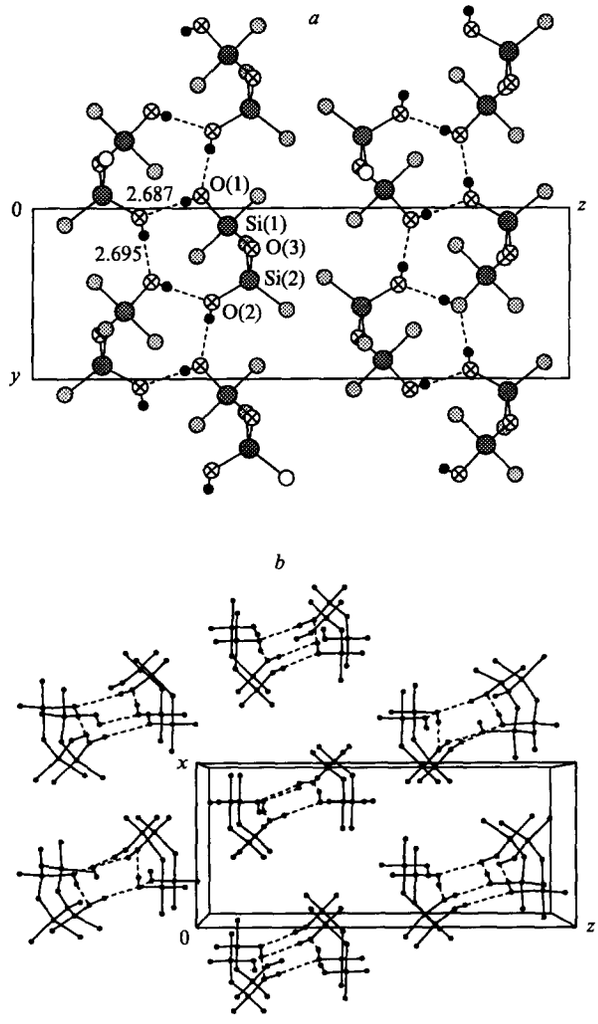


Figure 29. Projection of the crystal structure of DTMDS onto the *yz* (*a*) and *xz* (*b*) planes:[6] (*a*) view at right angles to the column; (*b*) view along the column.

In this structure, made up of two crystallographically independent molecules, three out of the four hydrogen bonds combine the molecules into dimers whilst the fourth hydrogen bond combines the dimers into strips.

The shape of the molecular strips in the structures of disiloxanediols, considered along the long axis, i.e. the crystallographic *b* axis (Fig. 30), is of great interest. These strips are approximately cylindrical, the surface layer of the quasi-cylinders, especially in the Pr^n and Et homologues, being framed by conformationally flexible alkyl substituents. The alkyl environment of the quasi-cylindrical strips (columns) is very similar to that in columnar discotic mesophases.[2] The similarity of the alkyl frame around the quasi-cylindrical strips in the crystal to the structure of the columns in the mesophase is manifested by the presence in the crystal of several independent molecules with different conformations of the alkyl substituents and by the lack of order in the arrangement of these substituents.

The quasi-cylinders formed by hydrogen bonds in the crystals of three alkyl homologues are arranged pseudohexagonally in the *ac* plane. The parameter of the planar pseudohexagonal unit cell in the crystal is $a = 12.66$ Å for DTPDS and $a = 10.69$ Å for DTEDS. According to X-ray diffraction studies on the mesophases of the corresponding compounds,[194] the parameters of the planar hexagonal unit cells are 12.58 and 11.10 Å, i.e. are close to those observed in the crystal. The hexagonal type of the cells and the similarity of the parameters permit the conclusion that the crystalline and liquid crystal phases in DTPDS and DTEDS are structurally continuous. The diffractometer trace for the Bu^n derivative (DTBDS), the structure of the single crystal of which could not be investigated, indicates that its mesophase also belongs to the hexagonal type.

The characteristic features of the textures of the mesophases of the compounds DTEDS, DTPDS, and DTBDS have been investigated.[5] It was shown that they resemble the textures of the hexagonal columnar discotic phases.[200,201] A model of the structures of DTEDS, DTPDS, and DTBDS, similar to the structure of the DISD mesophase in which the hydrogen-bonded dimers play the role of discoid units and their assembly forms the column, was proposed initially.[194] However, the crystal structures of the homologues investigated suggested another model, namely

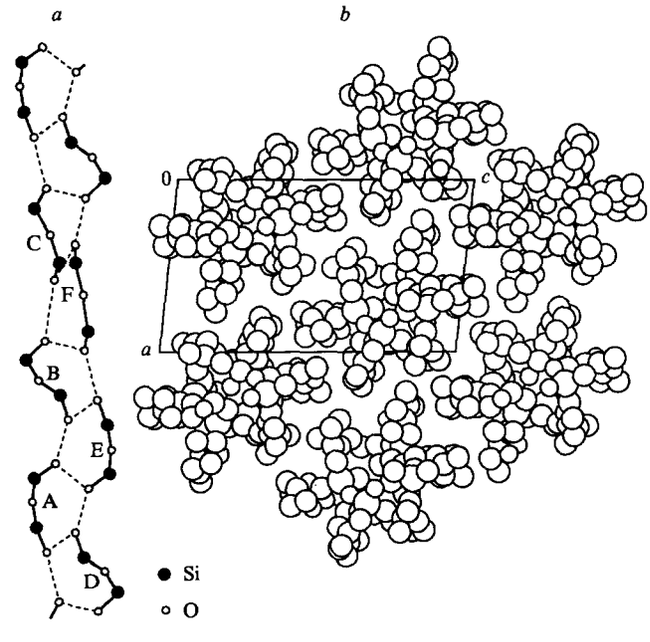
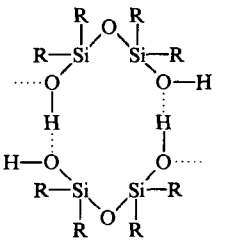


Figure 30. Projection of the crystal structure of DTPDS onto the *bc* (*a*) and *ac* (*b*) planes: (*a*) view at right angles to the column; (*b*) view along the column. The arrangement of the quasi-cylindrical molecular columns is pseudohexagonal.[196]

the presence in the mesophases of columns of hydrogen-bonded molecules (observed in crystals) and not of dimers.



Spectroscopic studies[5,196] have demonstrated the retention of a considerable number of 'crystalline' hydrogen bonds in the mesophase, i.e. in the crystal → liquid-crystal phase transition columns of hydrogen-bonded molecules, present in the crystals, may be retained. Furthermore apart from the similarity of the parameters of the hexagonal cells, the similarity between the crystal and liquid-crystal structures of disiloxanes was demonstrated by optical measurements of the refractive index along and at right angles to the columns. It was found that $n_{\parallel} < n_{\perp}$ both in the DTPDS crystal and in the mesophase.[5] Naturally, in contrast to the crystals, in the liquid-crystal state these columns have finite and different lengths and there is no translational order along their long axes, but there is a certain long-range orientational order. In the perpendicular direction, the long-range translational order is manifested by the occurrence of a planar hexagonal cell.

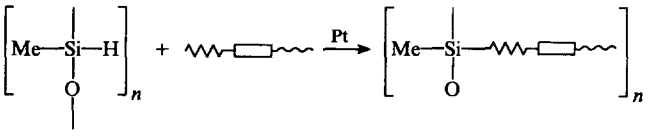
The absence of mesomorphic properties from the Ph and Me homologues is due to the fact that in DTPDS the outer layer of the column is made up of the rigid Ph substituents, while in DTMDS the surrounding layer of alkyl groups is minimal. The absence of the mesophase from diisopropyldisiloxanediol can be explained by the fact that in this case there is no infinite system of hydrogen-bonded molecules but dimers connected by hydrogen bonds do exist.

In our view, the DTEDS, DTPDS, and DTBDS mesophases, made up of molecular columns constructed as a result of the formation of cooperative hydrogen bonds and surrounded by alkyl substituents, should be assigned to a new structural type of liquid crystals. This type has been called[5,6] 'mesophases with columnar hydrogen-bonded associated species', since such liquid-crystal phases differ significantly in the mode of their formation both from phases made up of rod-shaped molecules and phases constructed from discoid molecules. The DISD mesophase can also be assigned to this class, because it is more likely that, in the transition to the liquid-crystal state, the hydrogen bonds are ruptured at random and the mesophase is formed not so much by free dimers or other associated species (for example trimers)¶ as by columns formed by hydrogen bonds.

c. Cyclic siloxanes

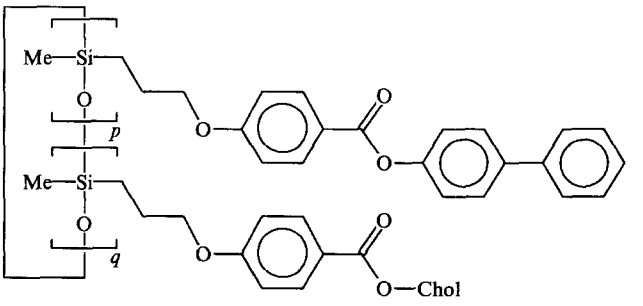
There exist many data on the mesomorphism of polylinear siloxanes. The mesomorphic properties of these polymers are manifested both in the presence[202,203] and absence[204,205] of mesogenic side substituents.

Low-molecular-mass cyclic siloxanes with mesogenic substituents, exhibiting liquid crystal properties, were obtained at the beginning of the 1980s.[206] One of the methods of synthesis of such compounds is hydrosilylation of cyclic siloxanes in accordance with the scheme[207]



¶ J E Lydon, personal communication.

Derivatives of biphenylenes, esters, and cholesteryl (Chol) benzoate can be used as substituents. In a number of instances derivatives with substituents of two types are also possible.



Even small siloxane rings are appreciably flexible.[208] This makes it possible to postulate that, although the mobility of the long mesogenic substituents in the molecules of cyclic siloxanes is limited by their incorporation in a ring, it does have sufficient degrees of freedom. Computer modelling showed that such molecules can have different configurations and can form both discotic and nematic phases.[209]

The study of the phase state of the cyclic siloxanes with the ring sizes $p+q = 4-7$[207] and 4–24[210] demonstrated the presence of mesophases of the nematic and smectic types for these compounds. The properties of such mesophases depend both on the number of chain units and on the dimensions of the side substituents. For example, virtually no change in the thickness of the layers with increase in the size of the ring is observed for type SmA mesophases with the same side substituents.[207]

X-Ray diffraction studies on the mesophases made up of siloxane rings with two types of substituents showed that they possess a high degree of order. In the analysis of the structure of a type SmA mesophase, three types of molecules were considered:[211] discotic, cylindrical, and conical (Fig. 31), and it was concluded that the cylindrical type is most likely. It has been noted that the thickness of the layer is usually determined by the

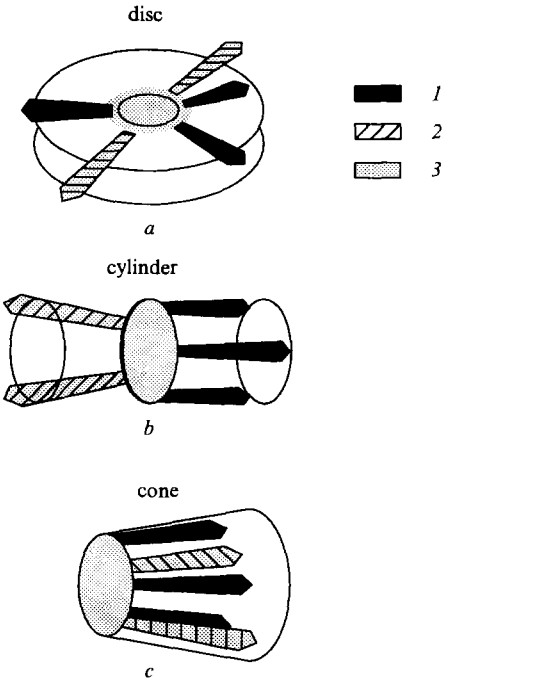


Figure 31. Molecules made up of cylindrical siloxanes with two types of substituents.[213] Molecules: (*a*) discotic; (*b*) cylindrical; (*c*) conical; (*1*) biphenyl nuclei; (*2*) cholesteryl nuclei; (*3*) cyclic siloxane.

length of the large substituent and can change when the ratio of the substituents $p:q$ in the ring is altered.[211] According to the results of optical studies, the layers in smectic specimens have a helicoidal twist (Fig. 32). The latter factor and also the tendency of the above compounds to vitrify create good prospects for their application in optical systems.

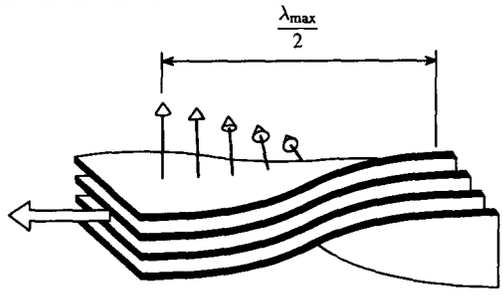


Figure 32. Helicoidal twisting of the smectic layers in cyclic siloxanes.[213]

IV. Conclusion

The above analysis of the literature and the authors' own data permits certain conclusions concerning the structural aspects of metallomesogenic substances. Despite the fact that metal complexes have not been investigated as extensively as classical organic liquid crystals, nevertheless one may say that, as in the case of organic liquid crystals, for the manifestation of mesomorphism the molecules of metal complexes must possess either intrinsic anisometry or they must form anisometric associated species the shape of which may differ significantly from that of the initial molecules. The discotic mesophases of β-diketones, made up of extended molecules, may serve as an example. Special mention should be made of the fact that in metal complexes the anisometry of the molecule depends significantly on the coordination of the metal atom, which has been manifested most clearly in the complexes with Schiff bases.

The presence of additional intermolecular coordination can have a dual effect on the mesomorphic properties. If this coordination leads to the formation of anisometric associated species, for example, columns in columnar phases, mesomorphism is possible. However, in the majority of cases such coordination plays a negative role, because the coordination dimers, strata, etc. are as a rule characterised by a lower anisometry. The EPR spectra of copper complexes of Schiff bases indicate unambiguously the absence of additional coordination in the mesophase.

In ionic liquid crystals, the smectic mesomorphism is due to the bilayer nature of the ordering of the molecules in which the metal and oxygen atoms within the bilayer form cation–anion strata separated by layers of alkyl substituents. It is of interest that in the strata the metal atom is located between oxygen planes and that water molecules are involved in the formation of such planes in the structure of, for example, $Cd(Isoval)_2 \cdot 2H_2O$. Apparently this is the first compound in which the presence of water molecules determines the appearance of the liquid-crystal state.

The mesophases based on silanediols are a striking example of the dependence of the mesomorphism on the type of aggregation of the molecules. The unusual feature of these substance consists in the fact that their molecules, which have no anisometry, form columnar associated species via hydrogen bonding, which give rise to hexagonal mesophases. The completely new structure of these mesophases (mesophases with columnar hydrogen-bonded associated species) is in many respects determined by the conformational flexibility of the molecules.

Finally, we may note that X-ray diffraction data for single crystals are very useful for the understanding of the relationship between the structure of the molecules and their ability to form liquid crystals. Such studies make it possible to determine reliably the molecular and crystal structures and then to extrapolate them to the mesophase in which the principal features of the crystal structure (layers, columns, coordination of the metal atoms, etc.) are retained. As regards the practical use of the compounds examined in this review, the prospects for their application have already been outlined.[7] We only wish to note the ability of ionic liquid crystals to form stable anisotropic glasses, which can be used for various spectroscopic purposes.

References

1. S Chandrasekhar, B K Sadashiva, K A Suresh *Paramana* **9** 41 (1977)
2. A M Levelut *J. Chem. Phys.* **80** 149 (1983)
3. D V Timofeeva, P M Zorkii, A P Polishchuk, in *Problemy Kristallokhimii* (Problems of Crystal Chemistry) (Moscow: Nauka, 1990) p. 149
4. L Lin *Mol. Cryst. Liquid Cryst.* **146** 41 (1987)
5. A P Polishchuk, T V Timofeeva, M Yu Antipin, N N Makarova, Yu T Struchkov, O D Lavrentovich *Metalloorg. Khim.* **4** 147 (1991)
6. A P Polishchuk, T V Timofeeva, N N Makarova, M Yu Antipin, Yu T Struchkov *Liquid Cryst.* **9** 433 (1991)
7. A-M Giroud-Godquin, P M Maitlis *Angew. Chem. Int. Ed. Engl.* **30** 375 (1991)
8. A P Polishchuk, T V Timofeeva, M Yu Antipin, Yu T Struchkov, Yu G Galyametdinov, I V Ovchinnikov *Kristallografiya* **31** 466 (1986)
9. T A Mirnaya, V D Prisyazhnyi, V A Shcherbakov *Usp. Khim.* **58** 1429 (1989) [*Russ. Chem. Rev.* **58** 821 (1989)]
10. J W G Goodby, G W Gray *Smectic Liquid Crystals* (Glasgow, 1984)
11. P M Zorkii, A P Polishchuk, T V Timofeeva *Usp. Khim.* **58** 1971 (1989) [*Russ. Chem. Rev.* **58** 1119 (1989)]
12. G W Gray *Molecular Structure and the Properties of Liquid Crystals* (London: Academic Press, 1962)
13. A Skoulios, V Luzzati *Acta Crystallogr.* **14** 278 (1961)
14. B Gallot *Acta Crystallogr.* **15** 826 (1962)
15. B Gallot, A Skoulios *Acta Crystallogr.* **14** 419 (1961)
16. P Spegt, A Skoulios *Acta Crystallogr.* **17** 198 (1964)
17. A R Ubbelohde, H J Michels, J J Duruz *Nature (Londom)* **228** 50 (1970)
18. T Meisel, K Seybold, J Roth *J. Therm. Anal.* **12** 361 (1977)
19. J J Duruz, A R Ubbelohde *Proc. Roy. Soc. London* **330** 1 (1972)
20. J E Bonekamp, T Eguchi, S Plesko, J Johnas *J. Chem. Phys.* **79** 1203 (1983)
21. J E Bonekamp, B Hegemann, J Johnas *Mol. Cryst. Liquid Cryst.* **87** 13 (1982)
22. T R Lomer *Acta Crystallogr.* **5** 14 (1952)
23. G Pelzl, H Sackmann *Mol. Cryst. Liquid Cryst.* **15** 75 (1971)
24. J E Bonekamp, I Artaki, M L Phillips, S Plesko, J Jonas *J. Phys. Chem.* **87** 4991 (1983)
25. M L Phillips, T M Barbara, S Plesko, J Jonas *J. Chem. Phys.* **84** 5143 (1986)
26. C L Grombridge, R K Harris, K J Packer, M B Hursthouse, N P C Walker *J. Solid State Chem.* **59** 306 (1985)
27. F J Hazelwood, E Rohdes, A R Ubbelohde *Proc. Roy. Soc. London A* **322** 281 (1971)
28. T A Mirnaya, A P Polishchuk, V I Molochaeva, A S Tolochko *Kristallografiya* **36** 377 (1991)
29. J Lindau, S Diele, H Kruger, H D Dorfler *Z. Phys. Chem. (Leipzig)* **262** 775 (1981)
30. A P Polishchuk, T A Mirnaya, A S Tolochko *Kristallografiya* (in the press) (1992)
31. T A Mirnaya, Candidate's Thesis in Chemical Sciences, Institute of General and Inorganic Chemistry, Academy of Sciences of the Ukrainian SSR, Kiev, 1984.
32. D W Bruce, D A Dunmur, E Lalinde, P M Maitlis, P Styring *Nature (London)* **323** 791 (1986)
33. D W Bruce, D A Dunmur, P M Maitlis, P Styring, M A Esteruelas, L A Oro, M B Ros, J L Serrano, E Sola *Chem. Mater.* **1** 479 (1989)
34. D W Bruce, D A Dunmur, S A Hudson, E Lalinde, P M Maitlis, M P McDonald, R Orr, P Styring, A S Cherodian, R M Richardson, J L Feijoo, G Ungar *Mol. Cryst. Liquid Cryst.* **206** 79 (1991)
35. G Etherington, A J Leadbetter, X J Wang, G W Grau, T Tajbkhsh *Liquid Cryst.* **1** 209 (1986)

36. A S C Lowrence *Trans. Faraday Soc.* **34** 660 (1938)
37. O B Akopova, V I Bobrov , N S Shabyshev, A A Onishchenko, in *Tezisy Dokladov VIII Vsesoyuznogo Simpoziuma po Mezhmolekulyarnomu Vzaimodeistviyu i Konformatsiyam Molekul* (Abstracts of Reports at the VIIIth All-Union Symposium on Intermolecular Interaction and Molecular Conformations), Novosibirsk, 1990, p. 67
38. M J Bird, T R Lomer *Acta Crystallogr. Sect. B* **28** 242 (1972)
39. T R Lomer, K Perera *Acta Crystallogr. Sect. B* **30** 2912 (1974)
40. T R Lomer, K Perera *Acta Crystallogr. Sect. B* **30** 2913 (1974)
41. H Abied, D Guillon, A Skoulios, P Weber, A-M Giroud-Godquin, J C Marchon *Liquid Cryst.* **2** 269 (1987)
42. A-M Giroud-Godquin, J C Marchon, D Guillon, A Skoulios *J. Phys. Lett. (Fr.)* **45** L681 (1984)
43. P Maldivi, D Guillon, A-M Giroud-Godquin, J C Marchon, H Abied, H Dexpert, A Skoulios *J. Chim. Phys. (Fr.)* **86** 1651 (1989)
44. A-M Giroud-Godquin, J M Latour, J C Marchon *Inorg. Chem.* **24** 4452 (1985)
45. H Abied, D Guillon, A Skoulios *Coloid Polym. Sci.* **266** 579 (1988)
46. G S Attard, P R Cullum *Liquid Cryst.* **8** 299 (1990)
47. A-M Giroud-Godquin, J C Marchon, D Guillon, A Skoulios *J. Phys. Chem.* **90** 5502 (1986)
48. O Poizat, D P Strommen, P Maldivi, A-M Giroud-Godquin, J C Marchon *Inorg. Chem.* **29** 4851 (1990)
49. P Maldivi, A-M Giroud-Godquin, J C Marchon, D Guillon, A Skoulios *Chem. Phys. Lett.* **157** 552 (1989)
50. R Y Cayton, M H Chisholm, F D Darrington *Angew. Chem.* **29** 1481 (1990)
51. F Cukienik, P Maldivi, A-M Giroud-Godquin, J C Marchon *Liquid Cryst.* **9** 903 (1991)
52. B J Bulkin, R K Rose, A Santoro *Mol. Cryst. Liquid Cryst.* **43** 53 (1977)
53. K Ohta, M Yokoyama, S Kusabayashi, H Mikava *J. Chem. Soc., Chem. Commun.* 392 (1980)
54. A-M Giroud-Godquin, J Billard *Mol. Cryst. Liquid Cryst.* **66** 147 (1981)
55. A-M Giroud-Godquin, J Billard *Mol. Cryst. Liquid Cryst.* **97** 287 (1983)
56. K Usha, K Vijayan, B K Sadashiva *Mol. Cryst. Liquid Cryst.* **5** 67 (1987)
57. K Usha, K Vijayan *Mol. Cryst. Liquid Cryst.* **174** 39 (1989)
58. K Usha, K Vijayan, B K Sadashiva *Mol. Cryst. Liquid Cryst.* **201** 13 (1991)
59. H Sakashita, A Nishitani, Y Sumiya, H Terauchi, K Ohta, I Yamamoto *Mol. Cryst. Liquid Cryst.* **163** 211 (1988)
60. P Terech, C Chachaty, J Guillard, A-M Giroud-Godquin *J. Phys. (Fr.)* **48** 663 (1987)
61. A-M Giroud-Godquin, M M Gauthier, J Sigaud, F Hardouin, M F Achard *Mol. Cryst. Liquid Cryst.* **132** 35 (1986)
62. K Ohta, H Ema, H Muroki, I Yamamoto, K Matsuzaki *Mol. Cryst. Liquid Cryst.* **147** 61 (1987)
63. S Chandrasekhar, B K Sadashiva, B S Srikanta *Mol. Cryst. Liquid Cryst.* **151** 93 (1987)
64. S Chandrasekhar, B K Sadashiva, B S Srikanta *Mol. Cryst. Liquid Cryst.* **166** 231 (1989)
65. S Chandrasekhar, B R Ratna, B K Sadashiva, V N Raja *Mol. Cryst. Liquid Cryst.* **165** 123 (1988)
66. B Muhlberger, W Haase *Liquid Cryst.* **5** 251 (1989)
67. K Ohta, O Takenaka, H Hasebe, Y Morizumi, T Fujimoto, I Yamamoto *Mol. Cryst. Liquid Cryst.* **195** 135 (1991)
68. C Destrade, P Foucher, H Gasparoux, H T Nguen *Mol. Cryst. Liquid Cryst.* **106** 121 (1984)
69. N L Morris, R G Zimmermann, G B Jameson, A W Dalziel, R W Reuss, R G Weiss *J. Am. Chem. Soc.* **100** 2177 (1988)
70. K Ohta, O Takenaka, H Hasebe, Y Morizumi, T Fujimoto, I Yamamoto *Mol. Cryst. Liquid Cryst.* **195** 123 (1991)
71. N J Thompson, G W Gray, J W Goodby, K J Toyne *Mol. Cryst. Liquid Cryst.* **200** 109 (1991)
72. P Styring, S Tantrawong, D R Beattie, J W Goodby *Liquid Cryst.* **10** 581 (1991)
73. A-M Giroud, U T Muller-Westerhoff *Mol. Cryst. Liquid Cryst.* **41** 11 (1977)
74. A-M Giroud, A Nazzal, U T Muller-Westerhoff *Mol. Cryst. Liquid Cryst.* **56** 225 (1980)
75. U T Muller-Westerhoff, A Nazzal, R J Cox, A-M Giroud *Mol. Cryst. Liquid Cryst.* **56** 249 (1980)
76. M Cotrait, J Gaultier, C Polycarpe, A-M Giroud, U T Muller-Westerhoff *Acta Crystallogr. Sect. C* **39** 833 (1983)
77. U T Muller-Westerhoff, A Nazzal, R J Cox, A-M Giroud *J. Chem. Soc. Chem. Commun.* 497 (1980)
78. K L Marshal, S D Jacobs *Mol. Cryst. Liquid Cryst.* **159** 181 (1988)
79. K Ohta, A Takagi, H Muroki, I Yamamoto, K Matsuzaki, T Inabe, Y Maruyama *J. Chem. Soc., Chem. Commun.* 883 (1986)
80. K Ohta, A Takagi, H Muroki, I Yamamoto, K Matsuzaki *Mol. Cryst. Liquid Cryst.* **147** 15 (1987)
81. K Ohta, H Hasebe, H Ema, M Moriya, T Fujimoto, I Yamamoto *Mol. Cryst. Liquid Cryst.* **208** 21 (1991)
82. K Ohta, H Hasebe, M Moriya, T Fujimoto, I Yamamoto *Mol. Cryst. Liquid Cryst.* **208** 33 (1991)
83. H Adams, N A Bailey, D W Bruce, R Dhillon, D A Dunmur, S E Hunt, E Lalinde, A A Maggs, R Orr, P Styring, M S Wragg, P M Maitlis *Polyhedron* **7** 1861 (1988)
84. K Ohta, H Ema, I Yamamoto, K Matsuzaki *Liquid Cryst.* **3** 1671 (1988)
85. K Ohta, Y Morizumi, H Ema, T Fujimoto, I Yamamoto *Mol. Cryst. Liquid Cryst.* **208** 55 (1991)
86. H Adams, N A Bailey, D W Bruce, D A Dunmur, E Lalinde, M Marcos, C Ridgway, A J Smith, P Styring, P M Maitlis *Liquid Cryst.* **2** 381 (1987)
87. I V Ovchinnikov, Yu G Galyametdinov, G I Ivanova, L M Yagofarova *Dokl. Akad. Nauk SSSR* **276** 126 (1984)
88. Yu G Galyametdimov. I G Bikchantaev, I V Ovchinnikov *Zh. Obshch. Khim.* **58** 1326 (1988)
89. A P Polishchuk, M Yu Antipin, T V Timofeeva, Yu T Struchkov, Yu G Galyametdinov, I V Ovchinnikov *Kristallografiya* **36** 642 (1991)
90. A Roviello, A Sirigu, P Iannelli, A Immirzi *Liquid Cryst.* **3** 115 (1988)
91. A P Polishchuk, M Yu Antipin, A I Yanovskii, T V Timofeeva, Yu T Struchkov, Yu G Galyametdinov, I V Ovchinnikov *Kristallografiya* **36** 98 (1991)
92. A P Polishchuk, M Yu Antipin, T V Timofeeva, Yu T Struchkov, Yu G Galyametdinov, I V Ovchinnikov *Kristallografiya* **35** 699 (1990)
93. P Iannelli, A Immirzi, U Caruso, A Roviello, A Sirigu *Acta Crystallogr., Sect. C* **45** 879 (1989)
94. A P Polishchuk, M Yu Antipin, T V Timofeeva, Yu T Struchkov, Yu G Galyametdinov, I G Bichkantaev, I V Ovchinnikov *Kristallografiya* **36** 389 (1991)
95. A P Polishchuk, M Yu Antipin, T V Timofeeva, Yu T Struchkov, Yu G Galyametdinov, I V Ovchinnikov *Kristallografiya* **33** 111 (1983)
96. A P Polishchuk, M Yu Antipin, T V Timofeeva, Yu T Struchkov, Yu G Galyametdinov, I V Ovchinnikov *Koord. Khim.* **16** 490 (1990)
97. A P Polishchuk, M Yu Antipin, R G Gerr, T V Timofeeva, Yu T Struchkov, I V Ovchinnikov *Kristallografiya* **34** 122 (1989)
98. A P Polishchuk, M Yu Antipin, T V Timofeeva, Yu T Struchkov, Yu G Galyametdinov, I V Ovchinnikov *Kristallografiya* **35** 693 (1990)
99. A P Polishchuk, M Yu Antipin, T V Timofeeva, Yu T Struchkov, Yu G Galyametdinov, I V Ovchinnikov *Kristallografiya* **34** 353 (1989)
100. B J Hathway, P G Hodgson *J.Inorg. Nucl. Chem.* **35** 4071 (1973)
101. O S Filipenko, L O Atovmyan, B L Tarnopol'skii, E Sh Safina *Zh. Strukt. Khim.* **29** 80 (1989)
102. V I Ponomarev, O S Filipenko, K O Atovmyan *Dokl. Akad. Nauk SSSR* **246** 321 (1979)
103. T Sogo, V Romero, A Sousa *Z. Naturforsch. B* **43** 611 (1988)
104. I G Bichkantaev, A P Polishchuk, I V Ovchinnikov *Zh. Strukt. Khim.* **28** 157 (1987)
105. I G Bichkantaev , Yu G Galyametdinov, I V Ovchinnikov *Zh. Strukt. Khim.* **28** 61 (1987)
106. J D Bernal, D Crowfoot *Trans. Faraday Soc.* **29** 1032 (1933)
107. P M Zorkii, V K Bel'skii, in *Sovremennye Problemy Fizicheskoi Khimii* (Modern Problems in Physical Chemistry) (Moscow: Izd. Moskov. Gos. Univ., 1970), No. 4, p. 397
108. A P Polishchuk, T V Timofeeva, M Yu Antipin, Yu T Struchkov *Kristallografiya* **29** 931 (1984)

109. A P Polishchuk, T V Timofeeva, M Yu Antipin, Yu T Struchkov, in *Tezisy Dokladov VIII Vsesoyuznogo Simpoziuma po Mezhmolekulyarnomu Vzaimodeistviyu i Konformatsiyam Molekul* (Abstracts of Reports at the VIIIth All-Union Symposium on Intermolecular Interaction and Molecular Conformations), Novosibirsk, 1990, Part 2, p. 59
110. M Ghedini, S Armentano, R Bartolino, G Torquati, F Rustichelli *Solid State Commun.* **64** 1191 (1987)
111. S Yamada, K Yamanouchi *Bull. Chem. Soc. Jpn.* **42** 2543 (1969)
112. S Yamada, A Takeuchi *Coord. Chem. Rev.* **43** 187 (1982)
113. Yu N Kukushkin, N S Palina, V N Yakovlev *Koord. Khim.* **11** 579 (1985)
114. E Ernst, M O'Connor, R Holm *J. Am. Chem. Soc.* **89** 6104 (1961)
115. G V Panova, N K Vikulova, V M Potapov *Usp. Khim.* **49** 1234 (1980) [*Russ. Chem. Rev.* **49** 655 (1980)]
116. R F Bryan, P Hartley *Mol. Cryst. Liquid Cryst.* **62** 259 (1990)
117. Yu V Zefirov, P M Zorkii *Zh. Strukt. Khim.* **15** 118 (1974)
118. L Pauling in *The Nature of the Chemical Bond* (New York: Cornell University Press, 1960) p. 260
119. Yu G Galyametdinov, G I Ivanova *Izv. Akad. Nauk SSSR, Ser. Khim.* 1997 (1989)
120. M Dvolaitzky, F Poldy, C C Taupin *Phys. Lett. A.* **45** 445 (1980)
121. J A Murphy, J W Doane, L J Hgu, D L Fishel *Mol. Cryst. Liquid Cryst.* **22** 133 (1973)
122. U Caruso, A Roviello, A Sirigu *Liquid Cryst.* 7 421 (1990)
123. U Caruso, A Roviello, A Sirigu *Liquid Cryst.* 7 431 (1990)
124. M Kuhnert-Brandstatter, D Seidel *Mikrochim. Acta* **1** 243 (1982)
125. A P Polishchuk, V I Kulishov, T V Timofeeva, M Yu Antipin, Yu T Struchkov *Mol. Cryst. Liquid Cryst.* **128** 367 (1985)
126. M Marcos, P Romero, J L Serrano, J Barbera, A M Levelut *Liquid Cryst.* 7 251 (1990)
127. D Demus, L Richter *Textures of Liquid Crystals* (Halle: Verlag Chemie, 1978)
128. N Hoshino, H Murakami, Y Matsunaga, T Inabe, Y Maruyama *Inorg. Chem.* **29** 1177 (1990)
129. E Bui, J P Bayle, F Perez, L Liebert, J Courtieu *Liquid Cryst.* **8** 513 (1990)
130. Yu G Galyametdinov, I G Ivanova, I V Ovchinnikov *Zh. Obshch. Khim.* **54** 2796 (1984)
131. J I Serrano, P Pomero, M Marcos, P J Alonso *J. Chem. Soc. Chem. Commun.* 859 (1990)
132. Yu G Galyametdinov, I G Ivanova, I V Ovchinnikov *Izv. Akad. Nauk SSSR, Ser. Khim.* 1931 (1989)
133. R Paschke, D Balkow, U Baumeister, H Hartung, J R Chipperfield, A B Blake, P G Nelson, G W Gray *Mol. Cryst. Liquid Cryst.* **188** 105 (1990)
134. M Chedini, M Longeri, R Bartolino *Mol. Cryst. Liquid Cryst.* **84** 207 (1982)
135. M Chedini, S Licoccia, S Armentano, R Bartolino *Mol. Cryst. Liquid Cryst.* **108** 269 (1984)
136. M Chedini, S Armentano, R Bartolino, F Rustichelli, G Torquati, N Kirov, M Petrov *Mol. Cryst. Liquid Cryst.* **151** 75 (1987)
137. C C Versace, R Bartolino, M Chedini, F Neve, S Armentano, M Petrov, N Kirov *Liquid Cryst.* **8** 481 (1990)
138. Y Galerne *Mol. Cryst. Liquid Cryst.* **165** 180 (1988)
139. G R Luckhurst, C Zannoni, P L Notdio, U Segre *Mol. Phys.* **30** 1345 (1975)
140. N Hoshino, H Hasegawa, Y Matsunaga *Liquid Cryst.* **9** 267 (1991)
141. J Barbera, P Espinet, E Lalinde, M Marcos, J L Serrano *Liquid Cryst.* **2** 833 (1987)
142. M A Ciriano, P Espinet, E Lalinde, M B Ros, J L Serrano *J. Mol. Struct.* **196** 327 (1989)
143. M Marcos, M B Ros, J L Serrano *Liquid Cryst.* **8** 1129 (1988)
144. M B Ros, N Ruiz, J L Serrano, P Espinet *Liquid Cryst.* **9** 77 (1991)
145. P Espinet, E Lalinde, M Marcos, J Perez, J L Serrano *Organometallics* **9** 555 (1990)
146. P Espinet, J L Extebarria, M Marcos, J Perez, A Remon, J L Serrano *Angew. Chem. Int. Ed. Engl.* **28** 1065 (1989)
147. C Piechocki, J Simon, A Skoulios, D Guillon, P Weber *J. Am. Chem. Soc.* **104** 5245 (1982)
148. D Guillon, A Skoulios, C Piechocki, J Simon, P Weber *Mol. Cryst. Liquid Cryst.* **100** 275 (1983)
149. J J Andre, M Bernard, C Piechocki, J Simon *J. Phys. Chem.* **90** 1327 (1986)
150. D Leliere, M A Petit, J Simon *Liquid Cryst.* **4** 707 (1989)
151. J F Van der Pol, E Neeleman, J W Zwikker, R J M Nolte, W Drenth, J Aerts, R Visser, S J Picken *Liquid Cryst.* **6** 577 (1989)
152. C J Brown *J. Chem. Soc. A* 2488 (1968)
153. B Honigmann, H V Lenne, R Schrodel *Z. Kristallogr.* **122** 185 (1965)
154. C R Safinya, K S Liang, W A Varady *Phys. Rev. Lett.* **53** 1172 (1984)
155. A M Levelut, F Hardouin, H Gasparoux *J. Phys. (Fr.)* **42** 147 (1981)
156. J L Peterson, C S Schramm, D R Stojakovic, B M Hoffman, T J Marks *J. Am. Chem. Soc.* **99** 286 (1977)
157. V Walatka, J H Perlstein *Mol. Cryst. Liquid Cryst.* **15** 269 (1971)
158. W J Siemons, P E Bierstedt, G Kepler *J. Chem. Phys.* **39** 3523 (1963)
159. H R Zeller, A Beck *J. Phys. Chem. Solids* **35** 77 (1974)
160. H I Cho, Y Lim *Chem. Lett.* 2107 (1987)
161. K Ohta, T Watanabe, S Tanaka,T Fujimoto, I Yamamoto, P Bassoul, N Kucharczyk, J Simon *Liquid Cryst.* **10** 357 (1991)
162. D Guillon, P Weber, A Skoulios, C Piechoki, J Simon *Mol. Cryst. Liquid Cryst.* **130** 223 (1985)
163. M J Cook, M F Daniel, K J Harrison, N B McKeown, A J Thomson *J. Chem. Soc., Chem. Commun.* 1086 (1987)
164. M J Cook, A J Dunn, S D Howe, A J Thomson, K J Harrison *J. Chem. Soc., Perkin Trans. 1* 2453 (1988)
165. C Sirlin, L Bosio, J Simon,V Ahsen, E Yilmazer, O Bekaroglu *Chem. Phys. Lett.* **139** 362 (1987)
166. C Piechocki, J Simon, J J Andre, D Guillon, P Petit, A Skoulios, P Weber *Chem. Phys. Lett.* **122** 124 (1985)
167. F Castaneda, C Piechocki, V Plichon, J Simon, J Vaxiviere *Electrochim. Acta* **31** 131 (1986)
168. Z Belarbi, M Maitrot, K Ohta, J Simon, J J Andre, P Petit *Chem. Phys. Lett.* **143** 400 (1988)
169. Z Belarbi, C Sirlin, J Simon, J J Andre *J. Phys. Chem.* **93** 8105 (1989)
170. C Sirlin, L Bosio, J Simon *J. Chem. Soc., Chem. Commun.* 379 (1987)
171. C Sirlin, L Bosio, J Simon *J. Chem. Soc., Chem. Commun.* 236 (1988)
172. C Sirlin, L Bosio, J Simon *Mol. Cryst. Liquid Cryst.* **155** 231 (1988)
173. C Piechocki, J C Boulou, J Simon *Mol. Cryst. Liquid Cryst.* **149** 115 (1987)
174. P Weber, D Guillon, A Skoulios *J. Phys. Chem.* **91** 2242 (1987)
175. K Ohta, T Watanabe, T Fujimoto, Y Yamamoto *J. Chem. Soc., Chem. Commun.* 1611 (1989)
176. K Ohta, H Hasebe, H Ema *J. Chem. Soc., Chem. Commun.* 1610 (1989)
177. K Ohta, T Watanabe, H Hasebe, Y Morizumi, T Fujimoto, I Yamamoto *Mol. Cryst. Liquid Cryst.* **196** 13 (1991)
178. J Malthete, J Billard *Mol. Cryst. Liquid Cryst.* **34** 117 (1976)
179. C Eaborn *J. Chem. Soc.* 149 (1952)
180. C Eaborn, N H Hartshorne *J. Chem. Soc.* 549 (1955)
181. J Bhatt, B M Fung, K M Nicholas, C D Poon *J. Chem. Soc., Chem. Commun.* 1439 (1988)
182. M A Khan, J C Bhatt, B M Fung, K M Nicholas, E Wachtel *Liquid Cryst.* **5** 285 (1989)
183. G V Vani *Mol. Cryst. Liquid Cryst.* **99** 21 (1983)
184. W Haase, H Paulus, R Pendzialek *Mol. Cryst. Liquid Cryst.* **100** 21 (1983)
185. S Sinton, A Pines *Chem. Phys. Lett.* 76 263 (1980)
186. E A Seibold, L E Sutton *J. Chem. Phys.* **23** 1967 (1955)
187. A P Polishchuk, T V Timofeeva, M Yu Antipin, Yu T Struchkov, Yu G Galyametdinov, I V Ovchinnikov *Kristallografiya* **37** 705 (1992)
188. L I Mineev, I I Sushkin, T E Kalinnikova, in *Zhidkie Kristally. Mezhvuzovskii Sbornik Nauchnykh Trudov* (Liquid Crystals. Intercollegiate Collection of Scientific Reports) (Ivanovo: Izd. Ivanovsk. Gos. Univ., 1987), p. 38
189. P Singh, M D Raush, R W Lenz *Liquid Cryst.* **9** 19 (1991)
190. J D Bunning, J E Lydon, C Eaborn, P H Jaksen, J W Goodby, G W Gray *J. Chem. Soc., Faraday Trans. 1* 713 (1982)
191. L Parkanyi, G Bocelli *Cryst. Struct. Commun.* 7 335 (1978)
192. N H Buttrus, C Eaborn, P B Hitchcock, A K Saxena *J. Organomet. Chem.* **248** 291 (1985)
193. N H Buttrus, C Eaborn, P B Hitchcock, P D Lickis *J. Organomet. Chem.* **302** 159 (1986)
194. N N Makarova, N N Kuz'min, Yu K Godovskii, E A Matukhina *Dokl. Akad. Nauk SSSR* **300** 372 (1988)
195. A P Polishchuk, N N Makarova, M Yu Antipin, O D Lavrentovich, N A Golovina, G A Puchkovskaya, Yu K Godovskii *Kristallografiya* **35** 446 (1990)

196. A P Polishchuk, N N Makarova, T V Timofeeva, N A Golovina, Yu T Struchkov *Kristallografiya* **35** 452 (1990)
197. A P Polishchuk, M Yu Antipin, T V Timofeeva, V A Odinets, A A Zhdanov *Kristallografiya* **36** 92 (1991)
198. V E Shklover, Yu T Struchkov, I V Karpova *Zh. Strukt. Khim.* **26** 125 (1985)
199. W Clegg *Acta Crystallogr. Sect. C* **39** 901 (1983)
200. J Bouligand *J. Physique* **41** 1307 (1980)
201. F Livolautf, J Bouligand *J. Physique* **47** 1813 (1986)
202. H Finkelmann, G Rehage *Makromol. Chem. Rapid Commun.* **3** 859 (1982)
203. S Diele, B Hisgen, B Reck, H Ringsdorf *Makromol. Chem. Rapid Commun.* **7** 267 (1986)
204. Yu K Godovsky, N N Makarova, V S Papkov, N N Kuzmin *Makromol. Chem. Rapid Commun.* **6** 797 (1985)
205. I L Dubchak, A I Pertsin, A A Zhdanov *Vysokomol. Soedin., Ser. A* **29** 567 (1987)
206. F-H Kreuzer *Proceedings 11 Freiburger Arbeitstagung Flussigkristalle* (1981) p. 5
207. F-H Kreuzer, D Andrejewski, W Haas, N Haberle, G Riepl, P Spes *Mol. Cryst. Liquid Cryst.* **199** 345 (1991)
208. T V Timofeeva, I L Dubchak, V G Dashevsky, Yu T Struchkov *Polyhedron* **3** 1109 (1984)
209. D R R Everitt, C M Care, R M Wood *Mol. Cryst. Liquid Cryst.* **153** 55 (1987)
210. R D C Richards, W D Hawthorn, J S Hill, R L Grane, R J Linville *J. Chem. Soc., Chem. Commun.* 95 (1990)
211. T J Bunning, H E Klei, E T Samulski *Liquid Cryst.* **10** 445 (1991)

Russian Chemical Reviews **62** (4) 323 – 336 1993
© 1993 Russian Academy of Sciences and Turpion Ltd

UDC 543.422:547.458.8

Low-frequency IR spectroscopy in the study of the structures of cellulose and cellulose nitrates

R M Mukhamadeeva, R G Zhbankov, V F Sopin, G N Marchenko

Contents

I.	Introduction	323
II.	Monosaccharides and disaccharides. Methyl β-D-glucoside nitrates	324
III.	Celluloses with different degrees of structural order	327
IV.	Celluloses of different origin and with different structural modifications	328
V.	Formation of the structure of cellulose nitrate	330
VI.	Kinetics of the nitration of celluloses of different biological origin and with different structural modifications	331

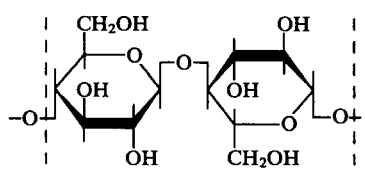
Abstract. The application of low-frequency IR spectroscopy in the structural analysis of polymers is examined. The vibrations of crystal lattices and polymer chains as well as deformation and torsional vibrations manifested in the low-frequency part of the IR spectrum are discussed. Studies in this field are reviewed critically and the experimental and theoretical data concerning the interpretation of the low-frequency spectra of monosaccharides, polysaccharides, and their nitro-derivatives are surveyed. Attention is concentrated on the establishment of 'spectrum–structure' correlations for cellulose in the course of its physical modification and chemical reactions (nitration). The bibliography includes 79 references.

I. Introduction

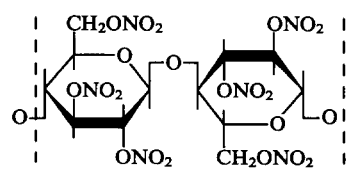
The high practical value of cellulose and its derivatives, especially its ethers and esters, has necessitated the study of the structural features of macromolecules in the course of their physical and chemical modifications. The structure of the polymer at the molecular and supermolecular levels of its organisation is associated with the packing of the macromolecules, intramolecular and intermolecular interactions, and the spatial orientation of the individual structural fragments.[1–15] The study of slight structural changes in the polymer requires the use of spectroscopic characteristics which are especially sensitive to such changes. The region of the 'atypical' low-frequency vibrations (30–700 cm^{-1}) is most sensitive to the changes in the structure of the polymers.[9–12] The interpretation of the spectrum in this region is impossible without theoretical calculations. Extensive experimental and theoretical data on model compounds of cellulose and cellulose nitrates (monosaccharides and disaccharides) have now accumulated. Their comparative analysis has made it possible to discover a series of spectroscopic features characterising the structural features of these low-molecular-mass polymer analogues.

A rigorous theoretical analysis of the vibrational spectra of such polymers is as yet impossible. On the other hand, in a number of recent studies it has been possible to find fairly rigorous correlations of the 'spectrum–structure–property' type in the analysis of the experimental spectra of cellulose in the course of its physical and chemical (nitration) modification and by comparing them with the spectra of model systems. The present review is devoted to the analysis of these investigations.

The cellulose macromolecule consists of a linear chain made up of β-D-glucose residues connected by 1,4-β-D-glycoside linkages.[1–3] The elementary unit of cellulose comprises two glucopyranose rings **1**. Different conformers can arise as a result of the change in the spatial orientation of the pyranose rings relative to one another and the hindered internal rotation of the OH and CH_2OH groups. In cellulose nitrates **2**, the hydroxy-groups have been substituted by nitrate groups and the polymer can contain units substituted to different extents (tri-, di-, and monosubstituted as well as unsubstituted units). Monosaccharides, disaccharides, and their nitro-derivatives are analogues of the structural fragments in the monomeric unit of cellulose and cellulose nitrates.



1



2

R M Mukhamadeeva A E Arbuzov Institute of Organic and Physical Chemistry, Russian Academy of Sciences, ul. ak. Arbuzova 8, 420083 Kazan-83, Russian Federation. Fax (7-432-2) 75 22 53

R G Zhbankov Laboratory of Molecular Spectroscopic Analysis, Institute of Physics, Academy of Sciences of Belarus, prosp. Skoryny 70, 220200 Minsk, Belarus

V F Sopin, G N Marchenko Institute of Chemical Products, 420033 Kazan-33, Russian Federation

Received 18th February 1993
Uspekhi Khimii **62** (3) 351 – 364 (1993); translated by A K Grzybowski

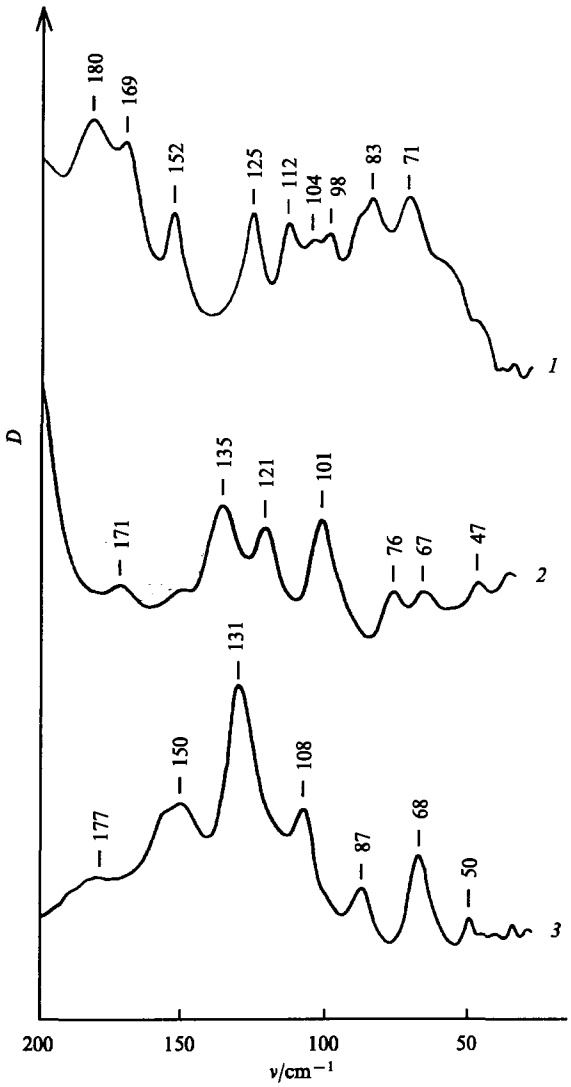


Figure 1. IR spectra of monosaccharides: (*1*) β-D-glucose; (*2*) β-D-mannose; (*3*) methyl β-D-glucoside.

II. Monosaccharides and disaccharides. Methyl β-D-glucoside nitrates

The experimental and theoretical methods of vibrational spectroscopy have been used fairly successfully for the analysis of monosaccharides, disaccharides, and their derivatives. It has been established that the vibrations at frequencies of 750–950 cm^{-1} depend on the type of the anomer: D-glucose, D-mannose, and D-galactose.[16–18] It has been shown[19, 20] that this dependence persists on formation of disaccharides and polysaccharides. Analysis of the low-frequency vibrations in the spectra of the monosaccharides was initiated in a number of studies,[21–23] which are mainly descriptive in character and do not contain correlations with the structural features of the molecules. Individual attempts have been made[24] to find the relationship between the structures of monosaccharides and disaccharides and their spectra. In particular, according to the authors, vibrations at frequencies in the range 500–700 cm^{-1} characterise the crystal structure of the compounds, while the vibrations at frequencies in the range 800–1 000 cm^{-1} characterise the type of configuration (α-, β-) of the glycoside bond in the disaccharides. The authors did not analyse the 40–500 cm^{-1} spectral range. A detailed study of the low-frequency vibrations resorting to data derived from theoretical calculations of the spectra of monosaccharides, disaccharides, and their nitro-derivatives[25–34] made it possible to solve a number of problems associated with the determination of the structure-

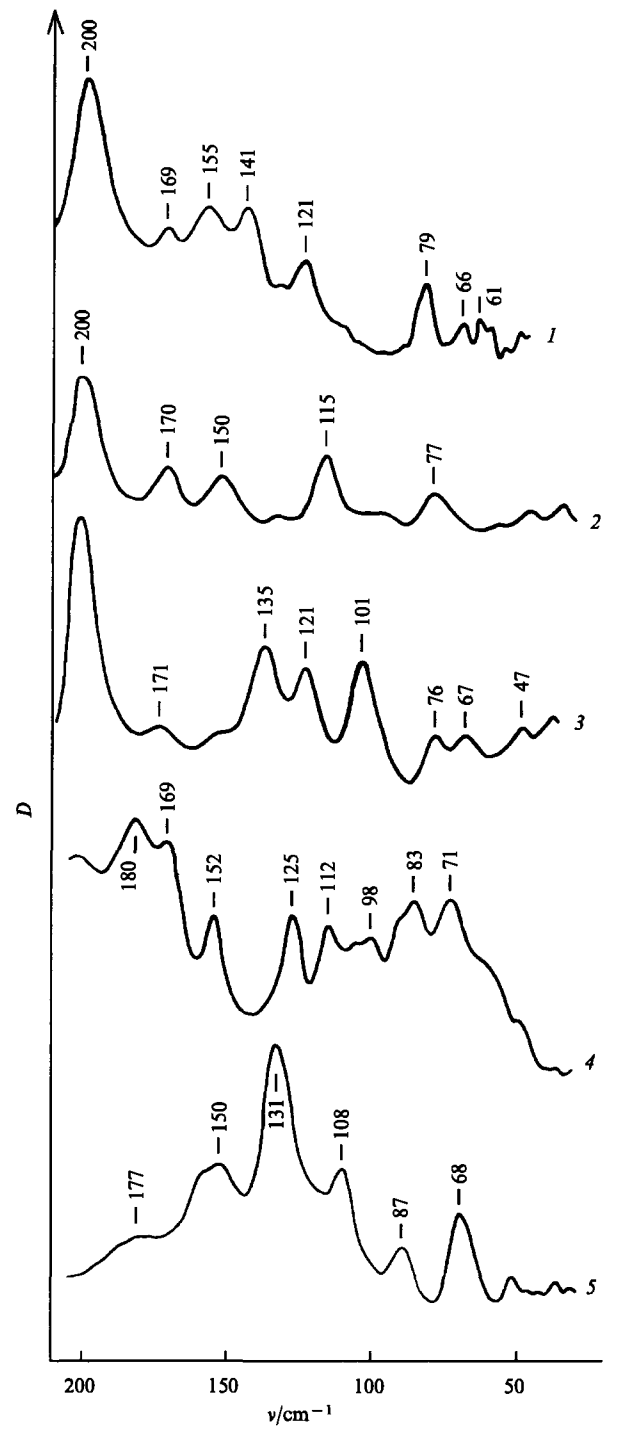


Figure 2. IR spectra of monosaccharides: (*1*) α-D-glucose; (*2*) α-D-galactose; (*3*) β-D-mannose; (*4*) β-D-glucose; (*5*) methyl β-D-glucoside.

sensitive absorption bands. Monosaccharides with different chemical structures of the fragments at the C(1) and C(5) atoms of the pyranose ring (OH, OCH_3, CH_2OH, H) (Table 1) and different configurations of the hydroxy-group at the C(1) atom [axial (*A*) and equatorial (*E*)], exhibiting rotational isomerism due to the rotation about the C–O bond, have been analysed.[26, 28, 29] In disaccharides, it is essential to note the difference between the types of glycoside bond connecting the glucose residues (the α- and β-configurations). The frequency ranges of the intermolecular vibrations of the crystal lattices (30–200 cm^{-1}) and of the intramolecular vibrations (150–700 cm^{-1}) were established in the above studies. The spectra of crystals of monosaccharides with a hydroxy-group at the C(1)

Table 1. Monosaccharides.

Compound	C(1)	C(5)	
α-D-Glucose	H	H	CH_2OH
β-D-Mannose	OH	H	CH_2OH
β-D-Glucose	OH	H	CH_2OH
Methyl β-D-glucoside	OCH_3	H	CH_2OH
α-D-Galactose	H	H	CH_2OH
α-L-Sorbose	OH	H	H
β-D-Xylose	OH	H	H
Arabinose	H(OH)	H	H
Ribose	H(OH)	H	H
Rhamnose	H(OH)	CH_3	H

atom (β-D-glucose, β-D-mannose are characterised by moderately intense absorption bands near 80, 120, and 170 cm^{-1} (Fig. 1). When the OH group is substituted by OCH_3, the 'crystallinity' bands undergo a slight hypsochromic shift owing to the change in the hydrogen bonds determining the crystal packing. This is also indicated by the results of Husain et al.,[34] who showed that, when the influence of the configurations of the CO(CH) bonds in the side fragments of the saccharide on the low-frequency vibrations is considered, it is essential to take into account the nearest structural elements. For the configurations *AEEEE* (α-D-glucose), *EAEEE* (β-D-mannose), and *AEEAE* (α-D-galactose) of the CO bonds at the atoms of the pyranose ring, the spectra show clearly an absorption band near 200 cm^{-1} (Fig. 2), while for the *EEEEE* configuration (β-D-glucose, methyl β-D-glucoside) this absorption is absent. In the region of the bands due to the 'crystallinity' of the disaccharide and the monosaccharides which it comprises, for example α-D-glucose and maltose or β-D-glucose and cellobiose, the spectra of all the substances were found to contain absorption bands at 200–220 cm^{-1} and 150–170 cm^{-1} (Fig. 3). This is explained by the similarity of the parameters of the crystal structures of the monosaccharide and disaccharides.

The uncharacteristic nature of the intramolecular vibrations in the range 200–700 cm^{-1}, deduced from theoretical calculations,[30–35] and their high sensitivity to slight structural changes in the crystal packing complicate the interpretation of the spectrum. Nevertheless, by analysing the spectra of crystalline and fused specimens and by resorting to calculated data for the steric structures of the saccharides, it has been possible to discover[26, 28, 29] the spectroscopic manifestations of different types of spatial orientation of individual fragments. It was shown that the position of the absorption band in the range 200–400 cm^{-1}, determined by the τ(CO) and τ(CC) torsional vibrations, depends on the orientation of the hydroxy-group at C(1) (Fig. 4). In the case of the axial disposition of the bond (α-D-glucose and α-D-sorbose), an intense absorption is observed near 300 cm^{-1}, while for the equatorial disposition (β-D-glucose, methyl β-D-glucoside, and β-D-xylose) it is observed near 312–325 cm^{-1}. The higher τ(CO) frequency for the equatorial orientation of the CO bond may be associated with its 'strained' state owing to the interaction with the lone pair of the oxygen of the pyranose ring. Calculations of the steric structures and the vibrational spectra of monosaccharides differing in the stereochemical disposition of the CO bonds at the C(1)–C(4) atoms confirmed the dependence of the torsional vibrations on the configuration of this group.[32] However, the calculations demonstrated a different trend in the variation of the frequencies on passing from axial to equatorial anomers. This can be explained by the fact that, in the calculations

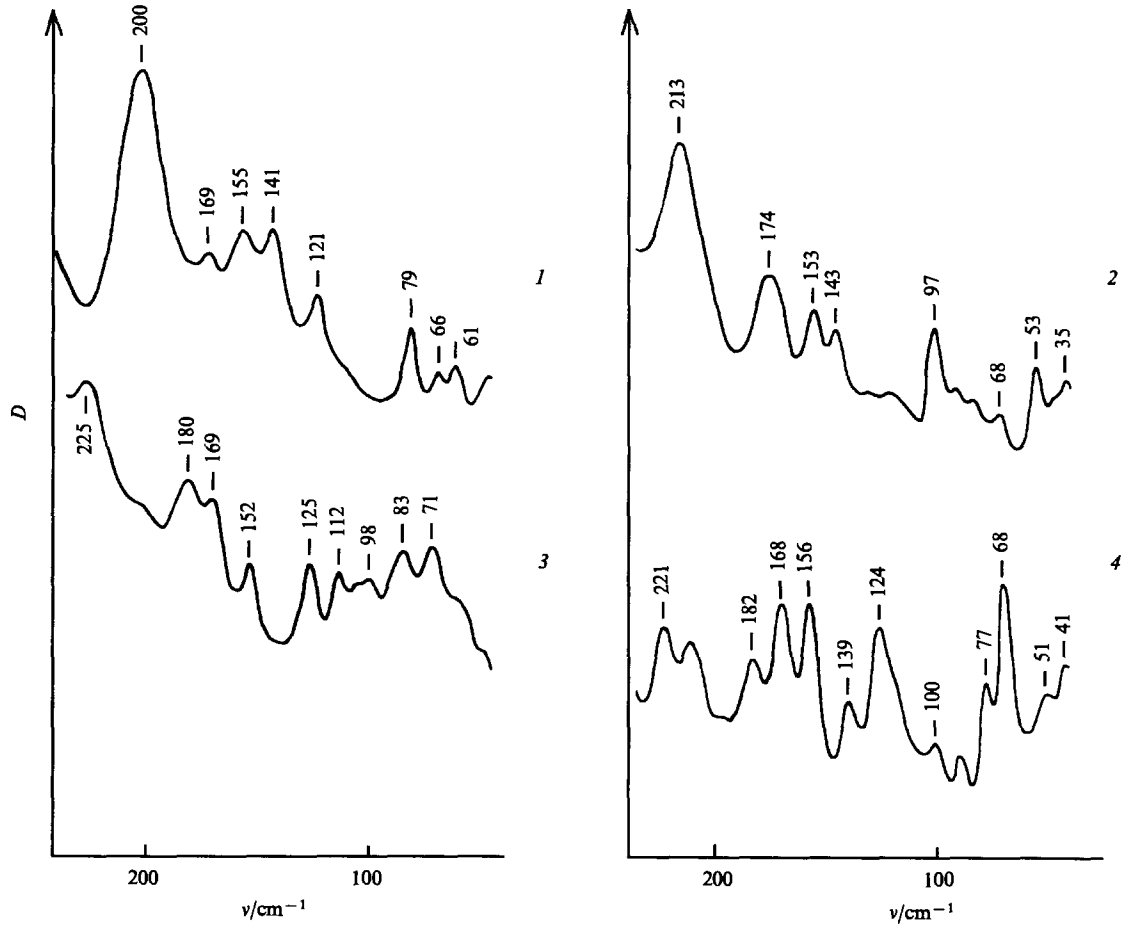


Figure 3. IR spectra of monosaccharides and disaccharides: (*1*) α D-glucose; (*2*) maltose; (*3*) β-D-glucose; (*4*) cellobiose.

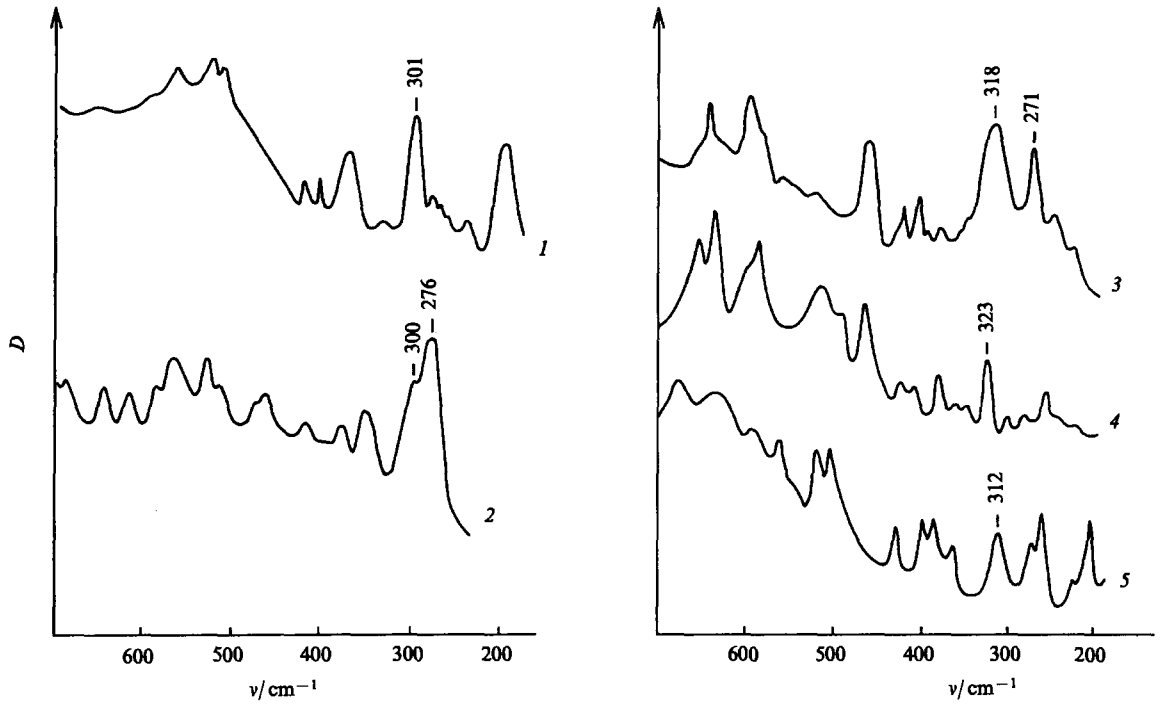


Figure 4. IR spectra of monosaccharides: (*1*) α-D-glucose; (*2*) α-L-sorbose; (*3*) β-D-glucose; (*4*) methyl β-D-glucoside; (*5*) β-D-xylose.

performed for isolated systems, no account was taken of the effects of the intermolecular interactions and of the crystal packing. Indeed, theoretical analysis of the spectrum of α-D-glucose taking into account the crystal field[33] demonstrated the dependence of the torsional vibration frequencies on the intermolecular interactions—the hydrogen bonds, determining the crystal packing of the molecules. Together with this, according to the calculations,[25, 29, 31, 32] the torsional vibrations and frequencies in the range 280–330 cm^{-1} are determined by the orientation of the CO bond of the hydroxy-methyl group at the C(6) atom. The conformational sensitivity of the torsional vibrations has been examined in fair detail in two investigations.[25, 29] The influence of the orientation of the hydroxymethyl group on the τ(CO) torsional vibrations in the range 160–400 cm^{-1} proved to be the most significant: variation of the frequencies by 30–60 cm^{-1} depending on the orientation of the CO and OH bonds of the CH_2OH fragment was observed. An increase in the complexity of the τ(CO) absorption band contour owing to the appearance of new constituent components was noted on fusion of the monosaccharides. One of the possible causes of this is the conformational transformations accompanying the fusion of the specimens. The influence of the spatial disposition of the structural fragments of monosaccharides and disaccharides on the vibration frequencies in the range 400–700 cm^{-1} has been treated systematically.[29, 35] According to calculations, this range contains the frequencies of the deformation vibrations of the CCO and COH groups at the C(1) and C(6) atoms, as well as those of the torsional vibrations of the C–OH bond. It has been shown that the transition from the *gauche*- to the *trans*-orientation of the C(6)–O(6) bond [relative to the C(5)–H(5) bond] is accompanied by an increase in the δ(CCO) and δ(COH) frequencies (620 and 470 cm^{-1}) by 30–40 cm^{-1}. The calculations made it possible to explain the experimentally observed differences between the spectra of the crystals and melts of β-D-glucose and methyl β-D-glucoside in the range 400–660 cm^{-1} by the difference between the conformations of the fragments at the C(1) and C(6) atoms. The dependence of the frequencies in the range 400–660 cm^{-1} on the configuration has also been noted.[29] A distinctive feature of the spectrum of the monosaccharide with the axial orientation (α-D-glucose) is the appearance of absorption bands at 514, 529, and 566 cm^{-1}. This frequency range is sensitive to the type of bonding of the glucose residues in the disaccharides. In the case of the α-configuration of the C–O–C group (maltose), the spectrum shows distinct absorption bands at 518 and 541 cm^{-1}. An intense absorption at 465 and 486 cm^{-1} is characteristic of the β-con-figuration (cellobiose).

The nitro-derivatives of monosaccharides and disaccharides are models of the monomeric unit of cellulose nitrate. The low-frequency spectra of selectively substituted methyl β-D-glucoside nitrates, namely 2,3-dinitro-, 2,3,6-trinitro-, and 2,3,4,6-tetranitro-methyl β-D-glucosides (Fig. 5), were first analysed by Mukhamadeeva and coworkers.[26, 29] According to the calculations, the frequencies and modes of the normal vibrations[36–39] corresponding to the absorption bands in the range 400–660 cm^{-1} are determined mainly by deformation vibrations involving the CCO, CON, and ONO group of atoms; in the frequency range 200–400 cm^{-1}, they are determined by the τ(CO) and τ(NO) torsional vibrations and δ(CCO) and δ(ONO) deformation vibrations. The characteristic features of the intermolecular interactions and the conformations of the hydroxy- and nitro-groups in the crystals and melts determine the contours and positions of the absorption bands. The sensitivity of the deformation vibrations at 400–660 cm^{-1} to the spatial orientation of the nitrate groups was predicted by calculations.[29, 37, 38] A characteristic feature of the spectra of methyl β-D-glucoside nitrates is absorption in the range 540–548 cm^{-1} (Fig. 5). According to calculations, these frequencies are characteristic of deformation vibrations involving nitrate groups: ON(2)O in the dinitrate, ON(6)O and CON(6) in the trinitrate, and ON(2)O and ON(4)O in the tetranitrate of methyl β-D-glucoside. It has been proposed that the absorption in this frequency range be used for the analysis of the nitrate groups. The frequencies in the range 30–200 cm^{-1} are sensitive to the presence of a crystal structure and the nature of the packing of the molecules in the crystal (Fig. 5).

Analysis of the spectra of model compounds made it possible to interpret the low-frequency spectra of cellulose and its nitrates.

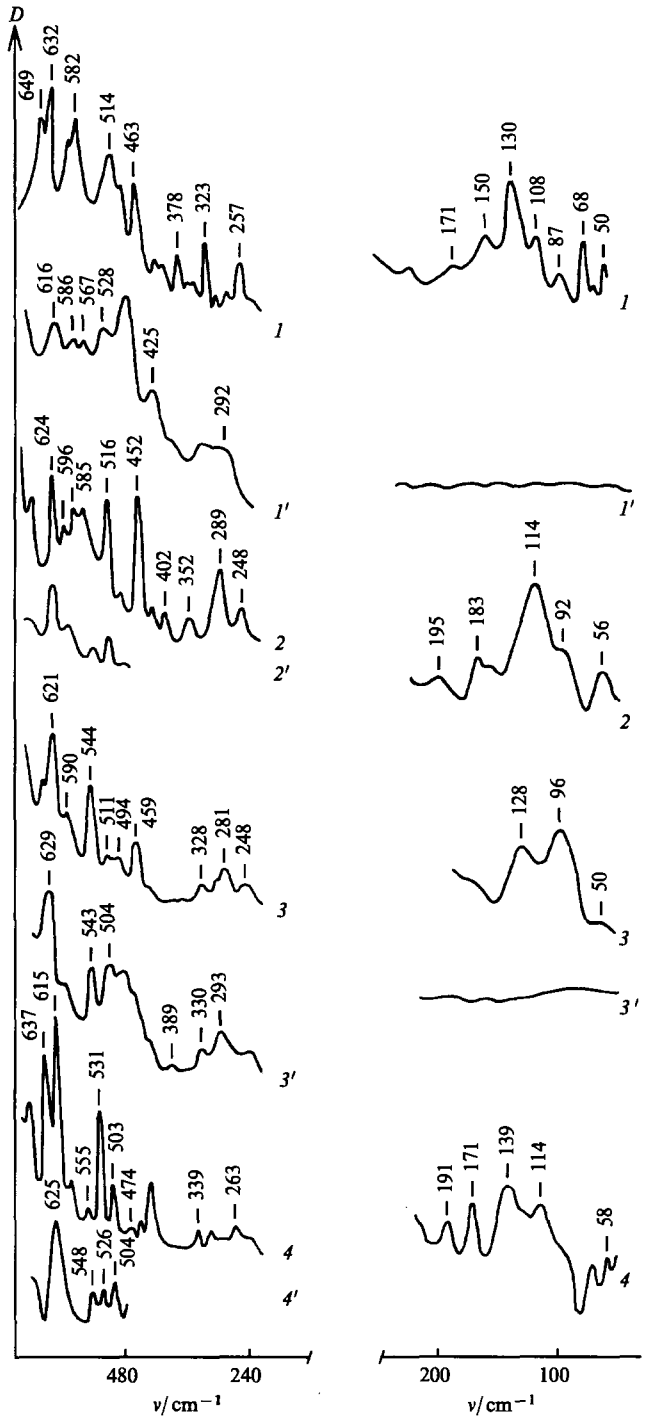


Figure 5. IR spectra of methyl β-D-glucoside nitrates: (*1*) methyl β-D-glucoside; (*2*) methyl 2,3-dinitro-β-D-glucoside; (*3*) methyl 2,3,6-trinitro-β-D-glucoside; (*4*) methyl 2,3,4,6-tetranitro-β-D-glucoside; (*1'*)–(*4'*) spectra of the corresponding melts.

III. Celluloses with different degrees of structural order

The properties of a polymer are determined by the structure of both its elementary unit and of the macromolecule as a whole.[9, 40] The intermolecular interaction forces between the polymer chains are significantly weaker than the intramolecular forces and, to a first approximation, their influence on the vibrational spectrum can be regarded as a perturbing factor. As mentioned above, in the interpretation of the spectrum of cellulose use is made of the comparative analysis of the spectra of the polymer and of the corresponding low-molecular-mass analogues. The identity of the structural elements of cellulose, β-D-glucose, and cellobiose is responsible for a series of similar absorption bands in the range of the δ(CCO), δ(CCH), and δ(COH) deformation frequencies and the τ(CO) and τ(CC) torsional frequencies at 200–700 cm^{-1} (Fig. 6). The complex diffuse contour of the absorption bands in the spectrum of cellulose compared with those of the low-molecular-mass analogues can be explained by a characteristic feature of the structure of its macromolecules: the multiplicity of intermolecular and intramolecular interactions and the conformational properties of the fragments of the polymer chain. In the range of the vibration frequencies of the crystal lattices (30–200 cm^{-1}), the differences between the spectra of cellulose and the model compounds are more significant (Fig. 7). The spectrum of cellulose shows moderately intense bands at 70, 100, and 170 cm^{-1}. A series of bands characteristic of mono-saccharides and disaccharides vanish. The reason for this is the complex structural organisation of the highly ordered cellulose formations.[28, 29]

The intermolecular order (two- and three-dimensional), determined by the conformation of the macromolecular chain and the system of intermolecular interactions, and the intramolecular order, characterised by the conformations of the pyranose rings and the hydroxy-groups and by the mutual spatial disposition of the elementary units, are distinguished in the structure of cellulose. The existing experimental methods[41–44] make it possible to estimate the degree of order in the polymer.

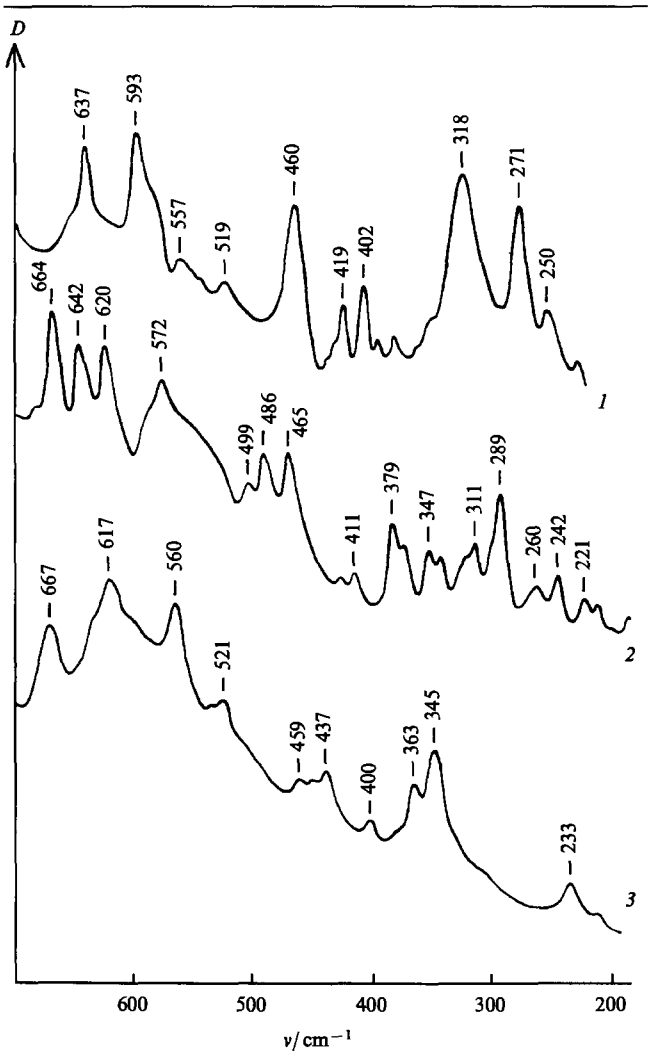


Figure 6. IR spectra (200–700 cm^{-1}): (*1*) β-D-glucose; (*2*) cellobiose; (*3*) cellulose.

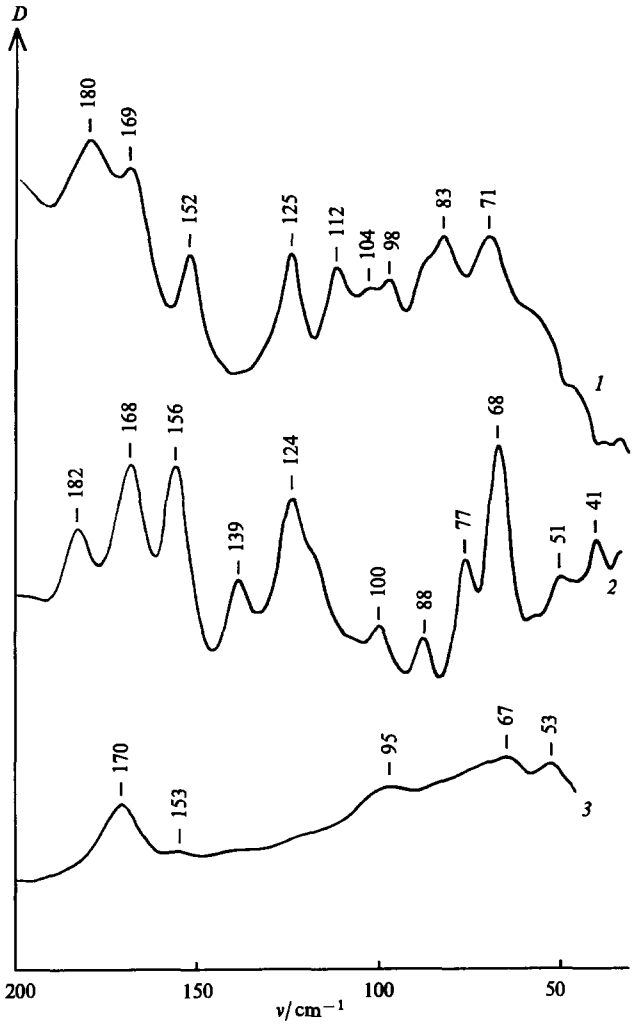


Figure 7. IR spectra (30–200 cm^{-1}): (1) β-D-glucose; (*2*) cellobiose; (*3*) cellulose.

X-Ray diffraction methods permit the estimation of the intermolecular three-dimensional order. The degree of intramolecular order associated with the rotation of the CH_2OH groups in the ordered sections of cellulose can be determined by analysing the IR absorption in the ranges 1 200–1 400 and 800–900 cm^{-1}.[3, 4] The study of the spectra in the range 30–200 cm^{-1} on these lines is particularly valuable, because low frequencies are characteristic of vibrations of the more complex structural elements—crystal lattices and polymer chains.[11, 12] A detailed quantitative analysis of the low-frequency absorption bands in the spectra of cotton and wood celluloses with different degrees of order has been carried out.[28, 29] Below 200 cm^{-1}, no distinct absorption bands were observed in the spectrum of disordered cellulose. Bands at 70, 100, and 170 cm^{-1}, which are a manifestation of the crystalline structure and can be used for the quantitative determination of the degree of order in cellulose, are characteristic of highly ordered cellulose.[29] According to the existing methods for the spectroscopic estimation of the degree of order in polymers,[9] the Beer–Lambert law for the optical density of the 'crystallinity' band (170 cm^{-1}) is defined by a relation of the type

$$D_{rel} = \varepsilon_{rel} K ,$$

where D_{rel} is the ratio of the optical density of the absorption band at 170 cm^{-1} to the optical density of the 'standard' absorption band at 520 cm^{-1} (the intensity of this absorption band is independent of the treatment of celluloses), ε_{rel} is the relative extinction coefficient at the above frequencies, and K is the degree of order (the volume concentration of the ordered fraction). The coefficient ε_{rel} can be determined by measuring D_{rel} in the spectrum of microcrystalline cellulose with a known degree of order—$K = 0.64$ (Magdalev et al.[43]); in this case $K = 0.54D_{rel}$. The spectroscopic estimates of the degree of order in natural celluloses based on low-frequency spectra and X-ray diffraction studies are presented in Table 2. Thus quantitative estimation not only of the intramolecular degree of order but also of the intermolecular degree of order (two- and three-dimensional) is possible with the aid of IR spectroscopy.

Table 2. Estimates of the degree of order in celluloses from spectroscopic and X-ray diffraction data.

Cellulose	IR spectroscopy[29]	X-Ray diffraction analysis[42, 43]
Microcrystalline	–	0.64
Cotton	0.45	0.50
Wood	0.36	0.41
Mercerised	0.14	0.42
Treated with liquid ammonia	0.22	–

IV. Celluloses of different origin and with different structural modifications

Cellulose can exist in different structural modifications.[1] The main ones are cellulose I (CI)—natural cellulose—and cellulose II (CIII), obtained from natural cellulose by reaction with concentrated solutions of alkali (NaOH). Treatment of CI and CII with liquid ammonia and subsequent removal of NH_3 vapour yields cellulose III (CIII).

Significant differences between CI and CII are observed in the study of these structural modifications by IR spectroscopy.[3–7, 45–47] Compared with the spectra of CI, the spectra of CII exhibit a broadening of the ν(OH) absorption band (3 000–3 600 cm^{-1}) and a change in the intensities of the absorption bands at 1 300–1 500 and 900 cm^{-1}. The spectral differences between CI and CII reflect the differences between the systems of hydrogen bonds and the orientations of the hydroxymethyl and hydroxy-groups noted in theoretical calculations.[48–51] The spectral changes in the structural transition from CI and CII (in the mercerisation process) have been established in a number of studies.[45–47] The process was monitored by measuring the optical densities of the 1 375 and 1 325 cm^{-1} absorption bands. A linear dependence of the absorption band intensities at 900 and 1 430 cm^{-1} on the sodium hydroxide concentration was established.[46] The spectroscopic characteristics of CI and CII have been explained by the conformations of the hydroxymethyl groups—the hydroxymethyl groups in the disordered regions make the main contribution to the absorption band at 900 cm^{-1} in the spectrum of natural cellulose, while in the spectrum of cellulose hydrate the main contribution comes from the hydroxymethyl groups in the ordered regions. Analysis of the characteristics of the ν(OH) absorption band (3 000–3 600 cm^{-1}) showed[45] that the cellulose mercerisation process is associated with the increase in the number of energetically weaker hydrogen bonds. A number of studies have been made on the low-frequency spectra of celluloses modified in different ways.[52–54] The most marked differences occur in the IR spectra in the frequency range 300–500 cm^{-1}. Differences in the range 200–600 cm^{-1} have also been observed in the Raman spectra of CI and CII. According to the results of Atalla and Dimick,[53] these spectroscopic features are due to the specific characteristics of the mutual orientation of the D-glucose residues in the polymer chain. A detailed study has been made[26, 29] of the spectra of different structural modifications of cellulose in the frequency range 30–700 cm^{-1} using data for model compounds. Characteristic features were observed in the spectra of celluloses I, II, and III in the frequency range corresponding to the vibrations of the ordered structural elements—crystal lattices and

polymer chains (30–200 cm^{-1}). The lattice vibrations in CI and CIII have frequencies of 100 and 170 cm^{-1}, while those in CII have frequencies of 125 and 170 cm^{-1}. A complex multicomponent absorption with maxima at 364 and 344 (CI), 380 and 351 (CII), and 349 cm^{-1} (CIII) was noted in the frequency range 200–400 cm^{-1}. These vibrations are sensitive to conformations[29] and are determined by the spatial orientation of the hydroxymethyl groups. Calculations showed that[29] the vibrations with frequencies of 340 cm^{-1} are characteristic of the *gauche*-orientation of the CO bond in the CH_2OH group regardless of the disposition of OH. These vibrations are more distinctive in CI, which indicates the predominance of the *gauche*-conformation in this structural modification. The data obtained agree also with the results of conformational calculations on the isolated cellulose I helix.[48–51] According to Mukhamadeeva,[29] the more distinct manifestation of the component at 380 cm^{-1} is due to the presence of the *gauche*-conformation of the CO bond for the *gauche*, *trans*-orientation of the hydroxy-group. The ratio of the intensities of the components of the 300–400 cm^{-1} absorption band is used for the comparative estimation of the conformational composition of the hydroxymethyl groups in various celluloses. Table 3 shows that the conformations of the hydroxymethyl groups are similar in celluloses of different origin and prepared in different ways but are different in CI and CII. Analysis of the spectra of model disaccharides[28, 29] demonstrated the possibility of estimating the comparative orientations of glucose residues along the glycoside linkage from the absorption bands in the frequency range 500–600 cm^{-1}. In the spectra of celluloses, the 520 and 560 cm^{-1} bands are most distinct in this range. The quantitative estimate based on the intensities of these absorption bands (Table 3) indicates significant differences between the celluloses as a function of their modification. The origin and the method of preparation of the cellulose have less influence on the degree of order in the macromolecules and on the conformational properties of individual fragments.

Low-frequency IR spectra have also been used to discover the mechanism of the structural (physical) modification of cellulose when it is treated with a solution of sodium hydroxide. The heterogeneity of the physical structure of cellulose is known to be responsible for the presence of two stages in the mercerisation process. In the initial stage, the interfibre space is filled (impregnation of pores) and this is followed by the diffusion of the reagent into the cellulose fibres. It was important to detect the second stage of the reaction. The principal structural changes in the cellulose at the molecular and supermolecular levels occurred at this instant. Three stages in the structural changes in cotton and wood celluloses have been differentiated[29] on the basis of spectroscopic data. In the first stage (Fig. 8), the structure of the celluloses is almost unaltered for a sodium hydroxide content up to 8%. In this case, the interfibre pores are filled with the alkaline solution. In the second stage of mercerisation, involving the penetration of the reagent into the fibre (8%–14%), there is a sharp change in the intensity ratios of the spectra of the absorption bands D_{560}/D_{520} (D_1), reflecting the characteristics of the orientation of the elementary units of the macromolecules, and D_{363}/D_{344} (D_2) and $D_{1\,430}/D_{900}$ (D_3), associated with the spatial orientation of the side fragments, particularly the CH_2OH groups. The hypsochromic shift of the ν(OH) absorption band maximum is induced by the increase in the number of energetically weaker hydrogen bonds[15, 55]—changes in the system of intramolecular hydrogen bonds of the type O(2)–H ... O′(6)H and O′(6)H ... O(2). These features are closely related to the conformational composition of the hydroxymethyl groups. Analysis of the 'crystallinity' band (170 cm^{-1}) showed that the second mercerisation stage (8%–12%) is accompanied by a sharp increase in the disorder in the cellulose chains (the degree of crystallinity K decreases from 0.44 to 0.16). At a solution concentration of 14%–18% (third mercerisation stage), the spectral changes associated with the structural transformations outlined above are gradually completed.

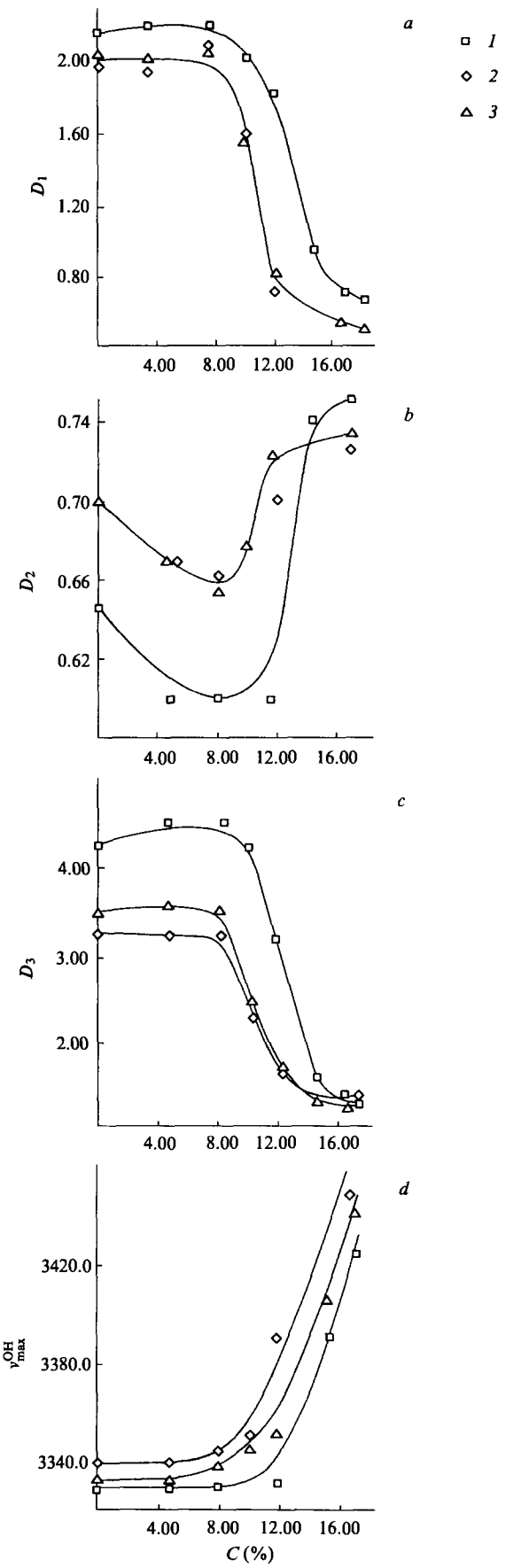


Figure 8. Dependence of the intensities D_1 (*a*), D_2 (*b*), and D_3 (*c*) and of the ν(OH) maxima (*d*) of the absorption bands on the concentration of sodium hydroxide (*C*, %): (*1*) cotton cellulose; (*2*) wood cellulose fibres; (*3*) wood cellulose paper.

Table 3. Intensity ratios of the low-frequency bands of different celluloses.[28, 29]

D_{rel}	Origin			Method of preparation			Structural modification		
	CC	WCF	WCP	SFI	SFA	NA	I	II	III
363/344	0.65	0.73	0.70	0.72	0.70	0.71	0.65	0.85	0.78
560/520	2.18	2.22	2.06	2.02	2.41	2.32	2.18	0.61	1.35

Note. CC = cotton cellulose, WCF = wood cellulose in the form of fibres, WCP = wood cellulose in the form of paper, SFI = cellulose obtained by the sulfite method, SFA = cellulose obtained by the sulfate method, NA = cellulose obtained by the nitric acid method.

A method has been proposed for monitoring the amount of CI which has been converted into CII in terms of the optical densities of the low-frequency absorption bands.[28, 29]

V. Formation of the structure of cellulose nitrate

The nitration of cellulose takes place, like the mercerisation process, in a heterogeneous medium, the rate of nitration being determined by the ratio of the rate of diffusion of the reagent into the fibre to the rate of the chemical reaction. The chemical reaction and the diffusion of the reagent are related in their turn to the accessibility of the reaction centres (hydroxy-groups) and the structure of the initial cellulose.[1] IR spectroscopy combined with other physicochemical methods, particularly with X-ray diffraction analysis and high-resolution ^{13}C NMR spectroscopy in the solid phase, is a fairly effective method for the investigation of the formation of the cellulose nitrate structure.[3, 7] The spectra of cellulose nitrate in the frequency range 600–4000 cm^{-1} contain absorption bands characteristic of the nitrate groups: an intense absorption in the frequency ranges 1500–1700 cm^{-1} and 1200–1300 cm^{-1}, due respectively to the antisymmetrical and symmetrical $\nu(NO_2)$ vibrations, and moderately intense absorption bands at 650, 750, and 840 cm^{-1} referring to ν(NO) and $\delta(ONO_2)$.[56, 57] In addition, the IR spectra of incompletely esterified specimens contain in the frequency range 3100–3600 cm^{-1} a diffuse absorption due to the residual OH groups. The position of the maximum of this band indicates the presence in cellulose nitrate (CN) of weak hydrogen bonds of the type OH ... ONO_2.[56] The molecular structure of cellulose nitrate has been analysed[58–60] as a function of the origin of the cellulose and the composition of the nitrating mixture. The degree of asymmetry of the ν(OH) absorption band contour has been used to estimate spectroscopically the uniformity of the substitution of the hydroxy-groups.[61] It was shown that, during the nitration of cellulose with nitric acid in a medium with methylene chloride, the hydroxy-groups are substituted fairly uniformly. This is associated with the ability of methylene chloride to loosen the packing of the polymer chains, which facilitates the penetration of the nitrating agent to the reaction centres.[58]

It has been proposed in a number of studies[57, 62–66] that the $\nu_{as}(ONO_2)$ absorption band (1500–1700 cm^{-1}) be used for analytical purposes in order to determine the nitrogen content and the locations of the nitric groups. However, the study of model compounds[62, 63] and cellulose nitrates in different stages of aggregation[4, 64] demonstrated that the determination of these structural parameters yields uncertain results. The complex contour of the $\nu_{as}(NO_2)$ absorption band is due to the superposition of the effect due to the crystal packing of the molecules, intermolecular interactions, the environment of the nitrate groups, and their conformational state. The spectroscopic manifestation of each of the above effects is determined by the state of aggregation of the cellulose nitrate test specimen and the degree of its esterification.

A theoretical study of the conformational properties of the monomeric and dimeric fragments of the cellulose trinitrate (CTN) macromolecules within the framework of the method of atom–atom potentials has been described.[65, 66] The stable conformations, determined by the rotation about the CO and CC bonds, were established. It was shown that, in the case of the nitrate groups at the C(2) and C(3) atoms, four rotational isomers can be formed preferentially. The CH_2ONO_2 group has a large number of stable conformations. The conformations of the dimeric fragment (elementary unit) of the cellulose trinitrate molecule have been calculated.[66] In the analysis of the potential surface as a function of the torsional angles at the glycosidic bond, which determine the conformation of the chain skeleton, two regions with low energies were discovered in the ranges from 0° to 20° and from 20° to 40°. It was established that the allowed region of possible cellulose nitrate conformations is smaller than a similar region in cellulose, which indicates a lower conformational liability of the monomeric units of cellulose trinitrate compared with cellulose. The steric forms of the macromolecules produced are determined mainly by the orientation of the side fragments.[3] As in the case of cellulose trinitrate, the conformational analysis of partly substituted cellobiose nitrates demonstrated the presence of two deep minima on the potential surface.[67] The authors noted only a slight difference in the steepness of the potential energy surfaces for partly and fully substituted cellobiose nitrates. Furthermore, in the partly substituted cellobiose nitrates the formation of intramolecular hydrogen bonds of the type O(3)H ... O(5) and O(3)H ... O(2)H or O(3)H ... O(2)NO_2 has been postulated. They are important for the stabilisation of cellobiose nitrate. The possibility of the formation of hydrogen bonds in partly substituted cellulose nitrates had been confirmed earlier in an analysis of experimental spectra.

A number of studies have been made on the low-frequency spectra of cellulose nitrates.[29, 68–71] The high sensitivity of the low-frequency vibrations to the characteristics of the crystal and molecular structures enabled the authors to solve a series of practical problems associated with the assessment of the kinetics of the nitration of cellulose. In the nitration of celluloses, the chemical reactions involve the formation of new structures.[3] The establishment of the relationship between the stages in the chemical synthesis, determined by the kinetic and diffusional processes, and the stages in the structural transformation, characterised by the disordering of the cellulose chains, the mutual orientation of the monomeric units, and the conformational state of the fragments of the macromolecules, is important. The spectra of cellulose nitrates with different degrees of substitution (γ) have been investigated.

Fig. 9 presents the low-frequency spectra of cellulose and cellulose nitrate. The frequencies and the assignments of the vibrations are given in Table 4. Analysis of the model compounds showed that the range of intramolecular vibrations of the macromolecules (200–700 cm^{-1}) and the frequency range of the intermolecular vibrations of the ordered polymer chains (30–200 cm^{-1}) can be differentiated arbitrarily in the spectra. During nitration, virtually the entire low-frequency spectrum changes. In the range of frequencies of the intramolecular vibrations, there are significant changes in the range 480–600 cm^{-1}. The multicomponent absorption observed in this frequency range is due to mixed vibrations with participation of the CCO, CON, and ONO groups of atoms.[29, 36–39] The positions of the bands and their intensities depend on the degree of substitution. Thus, for low values of γ, the spectra contain distinct bands with maxima at 560 and 520 cm^{-1}. The intensity of the 560 cm^{-1} band diminishes

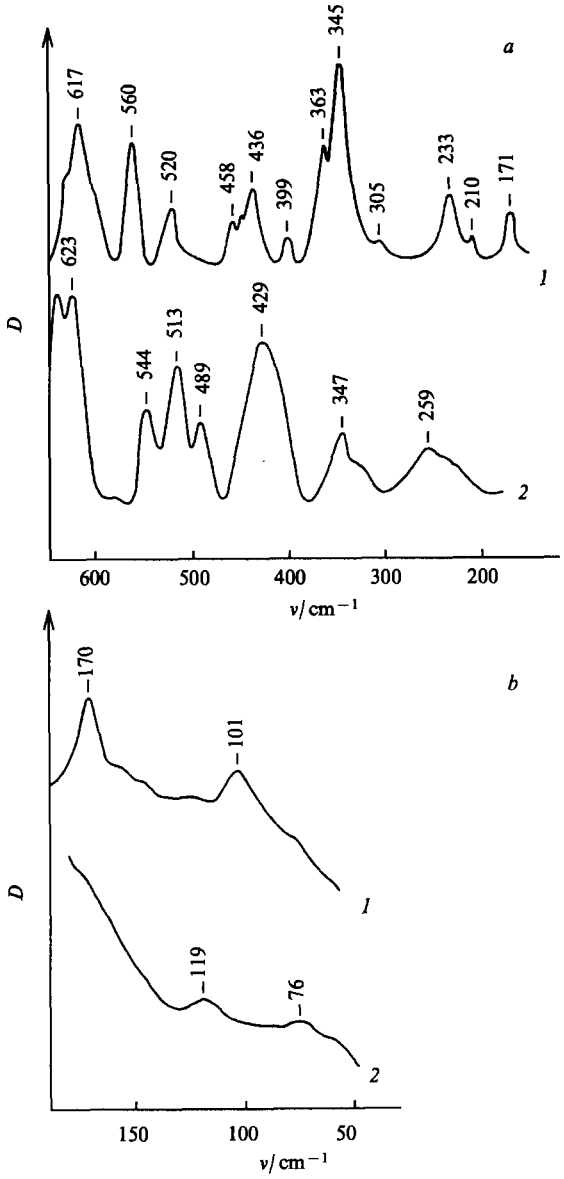


Figure 9. IR spectra of cellulose (curves *1*) and cellulose nitrate (curves *2*) (200–700 cm^{-1}).

with the increase in the degree of substitution. This has been explained by the characteristic features of the environment of the carbon atom involved in the glycosidic C–O–C linkage and by the orientation of the monomeric units. These structural changes are most significant in the first stage of the chemical synthesis (up to a degree of substitution of 1.6). The conclusions reached for vibrations at frequencies of 480–600 cm^{-1} are important. The increase in the absorption intensity at 544 cm^{-1} is explained by the substitution of the hydroxy-groups located at the C(6) atom. The triplet structure of this absorption band with maxima at 490, 513, and 544 cm^{-1}, manifested in the spectra for degrees of substitution in excess of 1.6 (the second stage of the chemical synthesis), has been attributed to the formation of the trinitrate units in the cellulose nitrate.

In the frequency range 300–500 cm^{-1}, where the δ(CCO), δ(CON), δ(ONO), τ(CO), and τ(NO) vibrations are manifested according to calculations,[29, 38] the increase in the intensity of the 436 cm^{-1} absorption band entails a decrease in the intensity of the absorption at 344 cm^{-1}. These spectral changes during the nitration processes have been attributed to the increase in the content of nitrate groups and the decrease in the number of residual hydroxy-groups. The spectra in this range are sensitive to conformations.[27–29, 38] For degrees of substitution of 1.6–1.8,

Table 4. Experimental and theoretically calculated frequencies of the normal vibrations of cellulose nitrate.[29, 38]

Frequency/cm^{-1}		Assignment
experiment	calculation	
644s	643[a]	δ[CON(2)] δ[ON(6)O] δ[CC(4)O]
623s	626[a]	δ[CON(2)] δ[CON(3)] δ[CC(2)O]
593sh	601[a]	δ[ON(3)O] δ[CC(1)O] δ[CC(3)O]
580w	–	–
576w	560[a]	δ[C(2)C(1)O(5)] δ[C(4)C(5)O(5)]
544m	540	δ[ON(6)O] δ[C(4)C(5)O(5)]
513m		
490m	484[a]	δ[ON(6)O] δ[ON(2)O] δ[CON(3)]
450sh	441	δ[ON(2)O] δ[CON(6)]
428s	425	δ[ON(3)O] δ[ON(2)O]
370sh	–	–
348m	360[a]	τ[N(6)O]
332sh	322[a]	δ[OC(1)O] δ[C(4)C(5)O(6)]
307sh	303[a]	τ[N(6)O]
280sh	–	–
253m	247[a]	τ[N(6)O]
242sh	–	–
120w	–	–
80w	–	–

Note. Absorption bands: s = strong (intense), m = moderately intense, and sh = shoulder.

[a] Vibration frequencies sensitive to conformations.

the conformational structure of the nitrate and the residual hydroxy-groups is virtually stabilised. In the frequency range 200–300 cm^{-1}, the frequencies of the τ(CO) and τ(NO) torsional vibrations shift from 233 to 251 cm^{-1} with increase in the degree of substitution of cellulose. The reason for this is the increase in the barrier to the internal rotation of the nitrate groups compared with the hydroxy-groups.

The absorption at 170 cm^{-1} has been used to analyse the changes in the crystal structure of cellulose. A significant disordering in the cellulose chains for a degree of substitution of 1.6 has been observed. At the same time, the appearance of new absorption bands at 80 and 120 cm^{-1} has been noted in the spectra of cellulose nitrates with increase in γ. They were assigned to the low-frequency vibrations of the cellulose nitrate macromolecules in the ordered regions. The disruption of the crystal structure of cellulose and the presence of elements of an ordered structure in cellulose nitrates for a degree of substitution of 1.6 have been confirmed also by the results of X-ray diffraction analysis.[67]

VI. Kinetics of the nitration of celluloses of different biological origin and with different structural modifications

The chemical reactions of cellulose and the formation of the structure of cellulose nitrates are in many respects determined by the biological origin and the structural modification of cellulose and by the conditions in its nitration. A number of studies[58, 59, 72] have been devoted to the X-ray diffraction analysis of the characteristic features of the formation of the crystal structures of different cellulose nitrates. By means of high-resolution ^{13}C and ^{15}N NMR spectroscopy,[73, 77] the establishment of the monomeric composition of cellulose nitrate was analysed. A number of studies[28, 29, 69–71] were devoted to investigations on the low-frequency IR spectra of the nitrates of cotton celluloses (CCN), wood celluloses in the form of fibres (WCNF) and paper (WCNP), as well as the nitrates of different types of cellulose (CCNII, CCNIII). The influence of the composition of the nitrating mixture on the formation of the structure of cellulose nitrate has

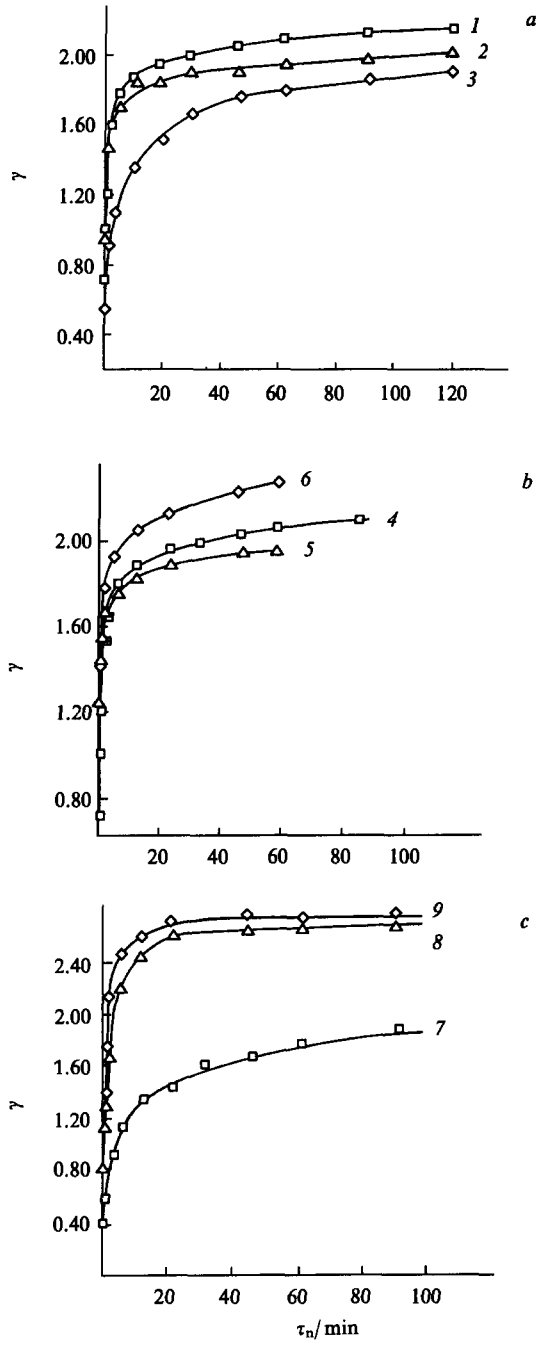


Figure 10. Kinetics of the nitration process: (*a*) cotton cellulose (curve *1*), wood cellulose fibres (curve *2*), and wood cellulose paper (curve *3*); (*b* cotton cellulose I (curve *4*), cotton cellulose II (curve *5*), cotton cellulose III (curve *6*); (*c*) cotton cellulose in reaction mixtures with different water contents (%): (*7*) 15; (*8*) 5; (*9*) 0.

also been investigated. The kinetic relations obtained are presented in Fig. 10. They are described fairly satisfactorily by an equation similar to that put forward in Refs. 78 and 79:

$$\gamma = \gamma_0[1-\exp(-k\tau^{\alpha})] ,$$

where $K = k^{1/\alpha}\alpha$ is the reaction rate constant. The parameters of this equation are listed in Table 5. The physical modification of cellulose and the composition of the nitrating mixture exert the strongest influence on the reaction rate constant K. The transition from the first (kinetic) to the second (diffusional) stage of the chemical synthesis takes place for degrees of substitution from 1.6 to 2.2.

Fig. 11 presents the spectra of cellulose nitrates with low degrees of substitution (γ = 0.5–1.8). Judging from the spectra, ordered cellulose chains are retained in nitrated cotton and wood celluloses for the above values of γ regardless of the composition of the nitrating mixture. In the cellulose nitrates subjected to a preliminary treatment (CCNII, CCNIII), the 'amorphisation' of the cellulose chains takes place virtually in the first seconds of the nitration process. The changes in the structure of the fragments of the macromolecules can be monitored on the basis of the frequencies of the intramolecular vibrations in the range 480–600 cm^{-1} [δ(CCO), δ(CON), δ(ONO)]. The ratio of the intensities of the 520 and 560 cm^{-1} absorption bands characterises the features of the environment of the C–O–C glycosidic linkage (Fig. 12). The relation can be represented approximately by a mathematical expression of the following type:

$$D_1 = D_{1,0}\exp(-B\gamma) ,$$

where D_1 and $D_{1,0}$ are the relative optical densities for a degree of substitution γ and for γ close to zero respectively and B are experimental constants. Their values for the spectra of the nitrates of different celluloses are presented in Table 6. The dependence of the relative optical density of the 544 cm^{-1} absorption band on the degree of substitution (Fig. 12), characterising the accumulation of nitrate groups at the C(6) atom, has been represented approximately by a mathematical expression of the type

$$D_2 = D_{2,0}[1-\exp(-A\gamma^{n})] .$$

The experimental constants A and n are listed in Table 7. The constants $D_{2,0}$, A, and B are maximum for CCNII and CCNIII. Bearing in mind the feature, noted above, involving the existence of order in the residual cellulose chains in cellulose nitrates with low degrees of substitution, the authors suggest that the characteristics of the spatial orientation of the monomeric units and the substitution of the primary hydroxy-groups on nitration of CCII and CCIII are associated mainly with the "amorphous" regions, while those in the nitration of cotton and wood celluloses are associated with sections of the polymer which are non-uniform as regards the degree of order. For $\gamma > (1.6-2.0)$ (the second stage of the chemical synthesis), the contour of the absorption band at 480–600 cm^{-1} in the spectra of cellulose nitrates (Fig. 13) assumes the form of a triplet with maxima at about 490, 514, and 544 cm^{-1} regardless of the biological origin of the celluloses

Table 5. The constants of the kinetic equation for the nitration of cellulose, $\gamma = \gamma_0[1-\exp(-k\tau^{\alpha})]$.

Constant	CCN	WCFN	WCPN (15%)	CCIIN	CCIIIN	WCPN (5%)	WCPN (0%)
γ_0	2.13	2.01	1.86	1.99	2.30	2.70	2.75
k	0.83	0.93	0.39	1.46	1.24	0.70	1.00
K	0.14	0.33	0.08	1.09	0.60	0.26	0.47
α	0.38	0.40	0.51	0.27	0.27	0.52	0.47
δ[a]	0.09	0.08	0.11	0.04	0.10	0.06	0.04

Note. CCN, WCFN, and WCPN are the nitrates of cotton cellulose and wood cellulose in the form of fibres and paper respectively; the water content in the $HNO_3 : H_2SO_4 : H_2O$ = 50 : 50 : 0, 58 : 37 : 5, and 58 : 27 : 15 nitrating mixtures are given in brackets.

* Here and henceforth δ denotes the error of the fit (%).

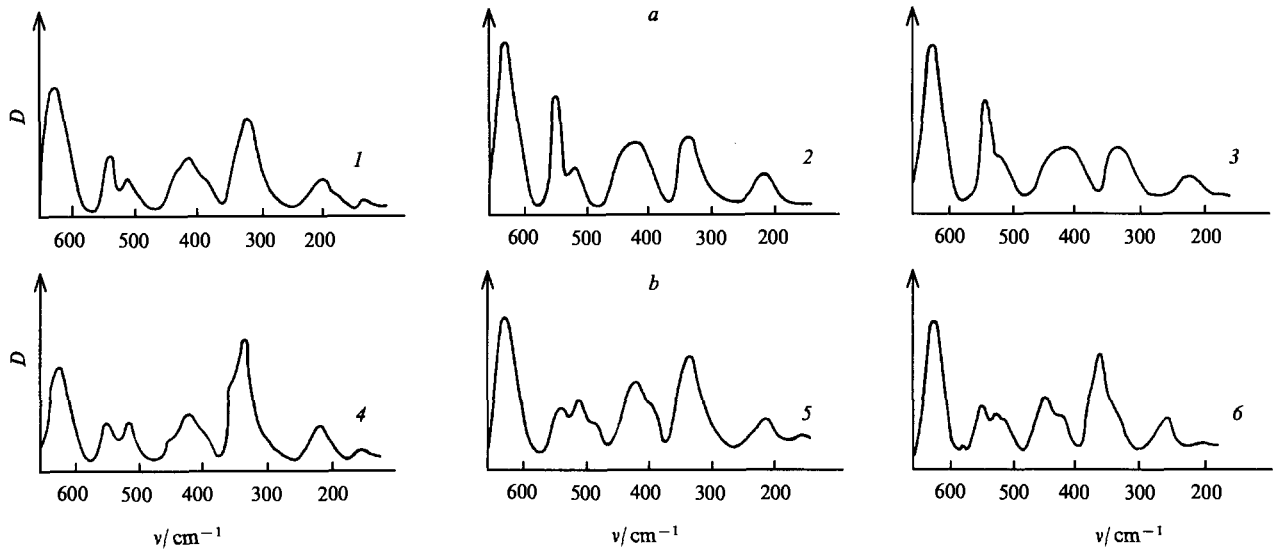


Figure 11. IR spectra of cellulose nitrates with degrees of substitution of 0.5–1.8 (the first of the chemical synthesis): (*a*) cellulose nitrate from cotton cellulose I (curve *1*), cotton cellulose II (curve *2*), and cotton cellulose III (curve *3*); (*b*) cellulose nitrates obtained in reaction mixtures with different water contents (%): (*4*) 0; (*5*) 5; (*6*) 15.

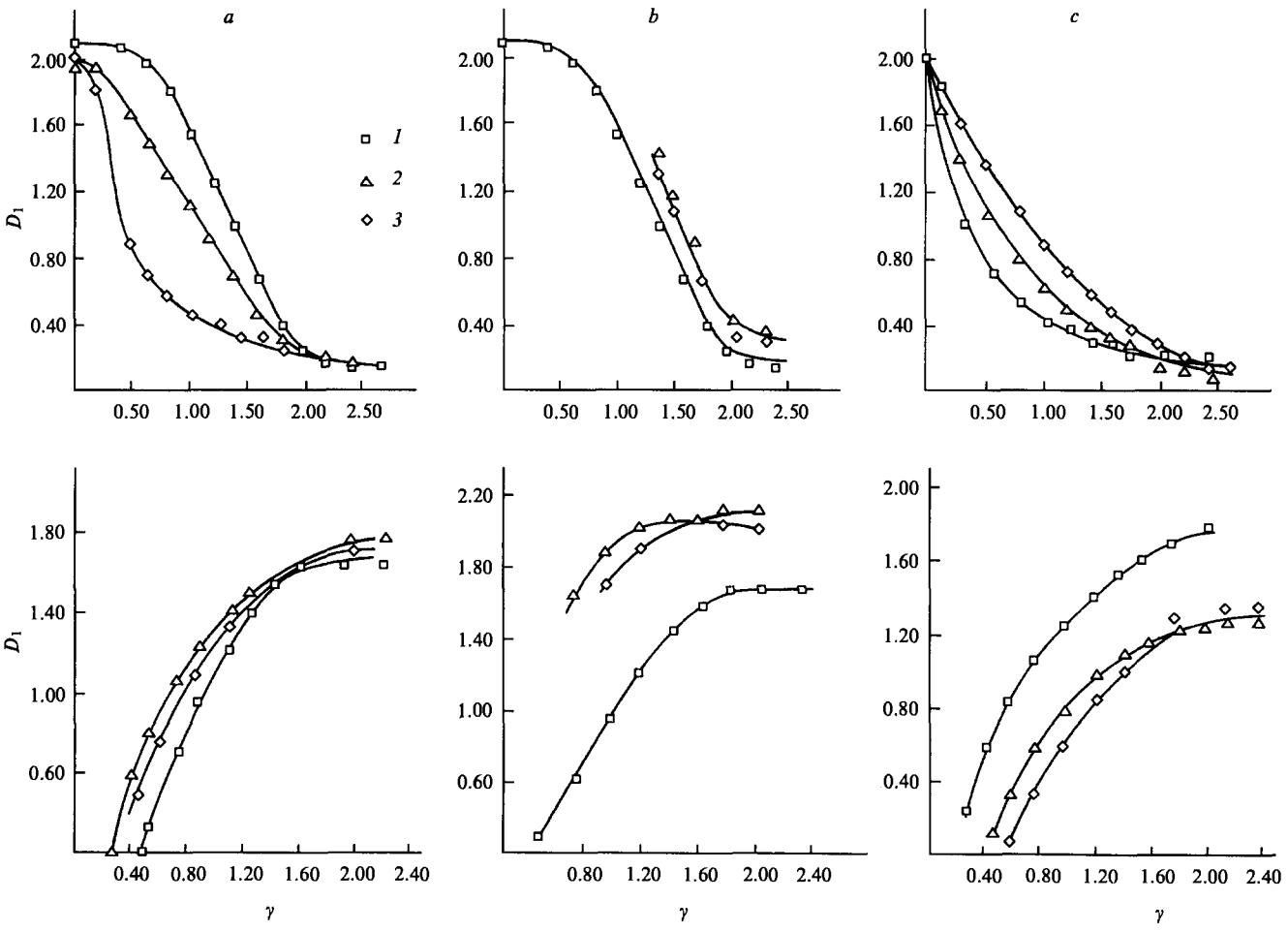


Figure 12. Dependence of the absorption band intensity ratios D_1 and D_2 on the degree of substitution γ: (*a*) nitrated cotton cellulose (curve *1*), nitrated wood cellulose fibres (curve *2*), and nitrated wood cellulose paper (curve *3*); (*b*) nitrated cotton cellulose I (curve *1*), nitrated cotton cellulose II (curve *2*), and nitrated cotton cellulose III (curve *3*); (*c*) cellulose nitrates obtained in reaction mixtures with different water contents (%): (*1*) 0; (*2*) 5; (*3*) 15.

Table 6. Parameters of the equation $D_1(560/520\ cm^{-1}) = D_{1,0}(560/520\ cm^{-1})\exp(-B\gamma)$.

Constant	CCN	WCPN	WCPN (25%)	CCIIN	CCIIIN	WCPN (5%)	WCPN (0%)
$D_{1,0}$	6.09	2.90	1.14	10.08	10.52	2.31	2.80
B	1.45	1.16	0.77	1.53	1.62	1.31	1.21
δ	0.15	0.13	0.14	0.14	0.12	0.04	0.15

Table 7. Parameters of the equation $D_2(544/520\ cm^{-1}) = D_{2,0}(544/520\ cm^{-1})[1-\exp(-A\gamma^n)]$.

Constant	CCN	WCFN	WCPN	CCIIN	CCIIIN	WCPN (5%)	WCPN (0%)
$D_{2,0}$	1.70	1.80	1.85	2.15	2.00	1.33	1.34
A	0.75	0.90	1.13	2.11	2.11	0.77	0.47
n	2.62	1.34	1.91	2.83	2.05	2.77	1.26
δ	0.05	0.12	0.04	0.10	0.13	0.08	0.05

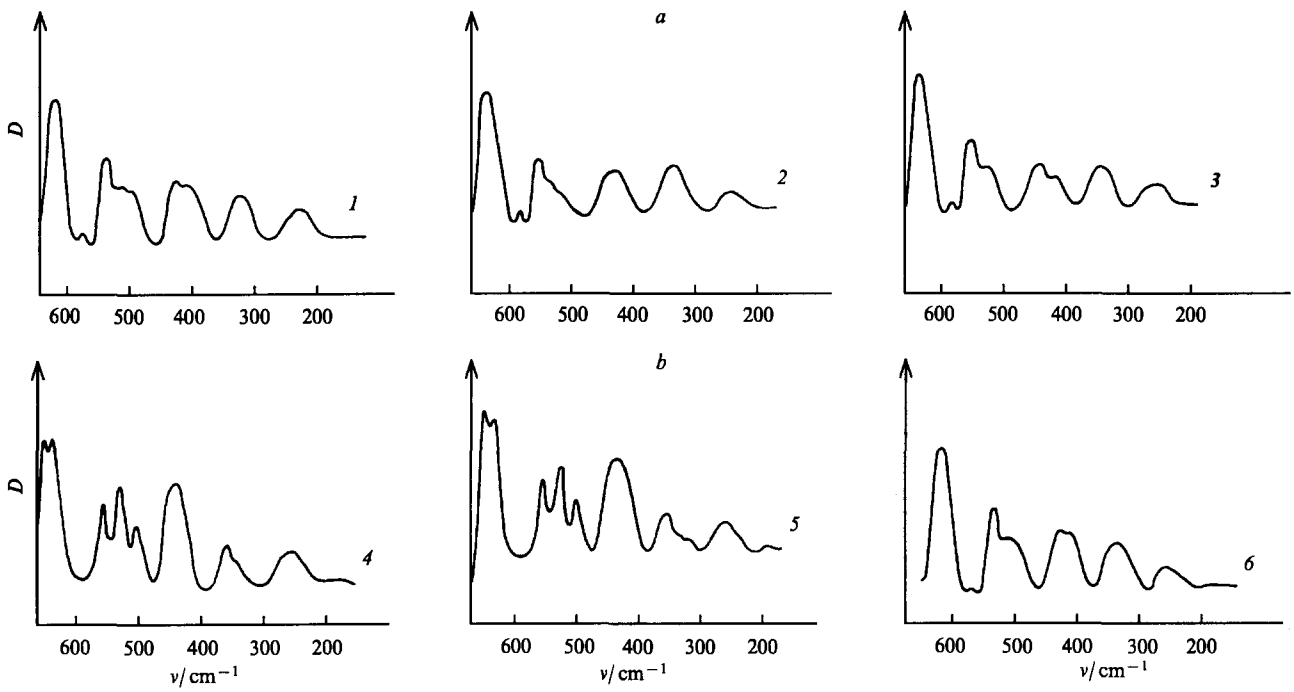


Figure 13. IR spectra of cellulose nitrates with degrees of substitution of 1.6–2.8 (second stage of the chemical synthesis): (*a*) cellulose nitrates from cotton cellulose I (curve *1*), cotton cellulose II (curve *2*), and cotton cellulose III (curve *3*); (*b*) cellulose nitrates obtained in reaction mixtures with different water contents (%): (*4*) 0; (*5*) 5; (*6*) 15.

and their structural modification. Comparison with experimental and calculated spectra of model compounds led to the conclusion that trinitrate units are formed when the nitrate groups are located at the C(2), C(3), and C(6) atoms. The triplet structure is distinctly manifested on nitration of cellulose under anhydrous conditions. The structural data for the cellulose nitrate molecules obtained from the spectra agree well with the results of the study of the monomeric composition of cellulose nitrates by ^{13}C NMR spectroscopy:[74–76] the cellulose nitrate specimens obtained in anhydrous nitrating mixtures and such mixtures diluted with water are characterised respectively by 75% and 46% contents of trinitrate units in the polymer chain.

*
* *

The data presented indicate the important role of low-frequency IR spectroscopy in the study of the structural features of monosaccharides and polysaccharides, including cellulose and its nitrates. Comparison of the experimental spectra with the results of calculations of the frequencies and modes of the normal vibrations and also of the steric structure of monosaccharides, disaccharides, and their nitro-derivatives permitted a detailed interpretation of the low-frequency vibrations. The frequency ranges of the vibrations of the crystal lattices (30–200 cm^{-1}) and intramolecular (deformation and torsional) vibrations (200–700 cm^{-1}) were established. It is shown that the frequencies of the 'lattice' vibrations are determined by the structure of monosaccharides and disaccharides: by the chemical structure of the side fragments (OH, OCH_3, CH_2OH, CH_2ONO_2), the spatial orientation of the OH groups (axial or equatorial), and the characteristic features of the bonding of the glucose residues (the α- and β-configurations). The observation of the conformational sensitivity of the δ(CCO), δ(CON), τ(CO), and τ(NO) vibrations in the range

$200-700\ cm^{-1}$ and the identification of the spectral manifestations of the location of the nitrate groups at the C(2), C(3), and C(6) atoms of the pyranose ring are important.

The use of the analysis of model compounds for the interpretation of the low-frequency spectra of cellulose and cellulose nitrates in order to solve a number of structural problems is of special interest and practical value: the determination of the three-dimensional degree of order in cellulose and cellulose nitrates and physically and chemically modified cellulose. Spectroscopic study of the mechanism of the physical modification of cellulose on treatment of the latter with aqueous solutions of alkali made it possible to identify three stages in the structural changes in the polymer determined by the degree of order in the macromolecules, the conformational state of the hydroxymethyl groups, and the system of hydrogen bonds. Analysis of the formation of the molecular crystal structures of cellulose nitrate demonstrated that the principal structural changes in cellulose nitrate, associated with the disorder in the cellulose chains and the spatial orientation of the fragments of the macromolecules, nitrate groups, and the residual hydroxy-groups, occurs in the first stage of the chemical synthesis for a degree of substitution in cellulose nitrate less than 1.6.

References

1. Z A Rogovin *Khimiya Tsellulozy* (The Chemistry of Cellulose) (Moscow: Khimiya, 1972)
2. I A Tarchevskii, G N Marchenko *Biosintez i Struktura Tsellyulozy* (The Biosynthesis and Structure of Cellulose) (Moscow: Nauka, 1985)
3. R G Zhbankov *Infrakrasnye Spektry i Structura Uglevodov* (The Infrared Spectra and Structure of Carbohydrates) (Minsk: Nauka i Tekhnika, 1972)
4. R G Zhbankov, P V Kozlov *Fizika Tsellyulozy i Ee Proizvodnykh* (The Physics of Cellulose and Its Derivatives) (Minsk: Nauka i Tekhnika, 1983)
5. R G Zhbankov *Infrakrasnye Spektry Tsellyulozy i Ee Proizvodnykh* (The Infrared Spectra of Cellulose and Its Derivatives) (Minsk: Nauka i Tekhnika, 1964)
6. R G Zhbankov *Infrared Spectra of Cellulose and Its Derivatives* (New York: Consultants Bureau, 1966)
7. R G Zhbankov, R N Marupov, N V Ivanova, A N Shishko *Spektroskopiya Khlopka* (The Spectroscopy of Cotton) (Moscow: Nauka, 1976)
8. L M Sverdlov, N A Kovner, V P Krainov *Kolebatel'nye Spektry Mnogoatomnykh Molekul* (Vibrational Spectra of Polyatomic Molecules) (Moscow: Nauka, 1970)
9. J Dechant, R Danz, W Kimmer, R Schmolke *Infrared Spectroscopic Studies of Polymers* (Translated into Russian) (Moscow: Khimiya, 1976)
10. A Finch, P N Gates, K Radcliffe, F Dixon, F F Bentley *Chemical Applications of Far Infrared Spectroscopy* (Translated into Russian) (Moscow: Mir, 1973)
11. P C Painter, M M Coleman, J L Koenig *The Theory of Vibrational Spectroscopy and Its Application to Polymeric Materials* (Translated into Russian) (Moscow: Mir, 1986)
12. S P Firsov, R G Zhbankov *Zh. Prikl. Spektrosk.* **39** 249 (1983)
13. V P Panov, R G Zhbankov *Konformatsiya Sakharov. Fizicheskie Metody Issledovaniya* (The Conformation of Sugars. Physical Research Methods) (Minsk: Nauka i Tekhnika, 1975)
14. V G Dashevskii *Konformatsionnyi Analiz Organicheskikh Molekul* (Conformational Analysis of Organic Molecules) (Moscow: Khimiya, 1982)
15. V P Panov, R G Zhbankov *Vnutri- i Mezhmolekulyarnye Vzaimodeistviya v Uglevodakh* (Intramolecular and Intermolecular Interactions in Carbohydrates) (Minsk: Nauka i Tekhnika, 1988)
16. S A Barker, E J Bourne, M Stacey *J. Chem. Soc.* 171 (1954)
17. V V Sivchik, R G Zhbankov *Zh. Prikl. Spektrosk.* **28** 1038 (1978)
18. R G Zhbankov, V V Sivchik, T E Kolosova *Zh. Prikl. Spektrosk.* **32** 827 (1980)
19. V V Sivchik, R G Zhbankov *Zh. Prikl. Spektrosk.* **27** 853 (1977)
20. V M Andiranov, R G Zhbankov *Zh. Strukt. Khim.* **21** 85 (1980)
21. M Hineno, H Yoshinaga *Spectrochim. Acta A* **28** 2263 (1972)
22. M Hineno, H Yoshinaga *Spectrochim. Acta A* **29** 301 (1973)
23. M Hineno, H Yoshinaga *Spectrochim. Acta A* **30** 411 (1974)
24. V M Tul'shinsky, S E Zurabyan, K A Azankozhoev *Carbohyd. Res.* **51** 1 (1976)
25. R M Mukhamadeeva, V I Kovalenko, A Kh Plyamovatyi, in *XX Vsesoyuznyi S'ezd po Spektroskopii (Tezisy Dokladov)* [The XXth All-Union Congress on Spectroscopy (Abstracts of Reports)] (Kiev, 1988) p. 344
26. R M Mukhamadeeva, R G Zhbankov, V I Kovalenko, V F Sopin, G N Marchenko *Zh. Prikl. Spektrosk.* **53** 188 (1990)
27. R M Mukhamadeeva, R G Zhbankov, V F Sopin, G N Marchenko *Zh. Prikl. Spektrosk.* **53** 1007 (1990)
28. R M Mukhamadeeva, R G Zhbankov, V F Sopin, G N Marchenko, Preprint No. 599, Institute of Physics, Academy of Sciences of Beloruss. SSR, Minsk (1990)
29. R M Mukhamadeeva, Candidate's Thesis in Physico-mathematical Sciences, Institute of Physics, Academy of Sciences of the Beloruss. SSR, Minsk (1991)
30. M Hineno *Carbohyd. Res.* **56** 219 (1977)
31. V M Andrianov, R G Zhbankov, V G Dashevskii *Zh. Strukt. Khim.* **21** 35 (1980)
32. V M Andrianov, R G Zhbankov, V G Dashevskii *Zh. Strukt. Khim.* **21** 42 (1980)
33. V M Andrianov, R G Zhbankov, V G Dashevskii *Zh. Prikl. Spektrosk.* **38** 240 (1983)
34. S K Husain, J B Hasted, D Rosen *Infrared Phys.* **24** 209 (1984)
35. V V Sivchik, R G Zhbankov *Zh. Prikl. Spektrosk.* **32** 910 (1980)
36. N V Ivanova, T E Kolosova, E A Korolenko, L G Bazhnik, R G Zhbankov, L K Prikhodchenko *Zh. Prikl. Spektrosk.* **46** 852 (1987)
37. V M Andrianov, R G Zhbankov *Zh. Prikl. Spektrosk.* **45** 245 (1986)
38. V M Andrianov, R G Zhbankov *Zh. Strukt. Khim.* **28** 35 (1987)
39. M V Korolevich, R G Zhbankov, V V Sivchik, G N Marchenko, L V Zabelin *Dokl. Akad. Nauk SSSR* **294** 629 (1987)
40. R G Zhbankov, D K Buslov *Zh. Prikl. Spektrosk.* **27** 647 (1977)
41. L Mary, R O'Connor *J. Appl. Polym. Sci.* **8** 1311 (1964)
42. V W Tripp, in *Cellulose and Cellulose Derivatives* (E Is N M Bikales, L Segal) (Translated into Russian) (Moscow: Mir, 1974) p. 214
43. E T Magdalev, V F Sopin, L I Vershinin, in *Vsesoyuznaya Konferentsiya "Metody Issledovaniya Tsellyulozy" (Tezisy Dokladov)* [All-Union Conference on "Methods for the Investigation of Cellulose" (Abstracts of Reports)] (Riga, 1988) p. 19
44. P K Chidambareswaran, S Srecnivasan, N V Patil *J. Appl. Polym. Sci.* **27** 709 (1982)
45. I Levdik, in *Metody Issledovaniya Tsellyulozy* (Methods for the Investigation of Cellulose) (Ed. V Karliv) (Riga: Zinatne, 1981) p. 258
46. A M Shishko, R G Zhbankov *Khim. Drevesiny* 3 (1982)
47. D K Buslov, R G Zhbankov, L V Zabelin *Dokl. Akad. Nauk SSSR* **264** 348 (1982)
48. O K Nugmanov, A I Pertsin, in *Konformatsii i Funktsii Biologicheskikh Molekul* (The Conformations and Functions of Biological Molecules) (Ed. G Cipens) (Riga: Zinatne, 1984) p. 143
49. A J Pertsin, O K Nugmanov, G N Marchenko *Polymer* **27** 597 (1986)
50. A I Pertsin, O K Nugmanov, V F Sopin, G N Marchenko, A I Kitaigorodskii *Vysokomol. Soedin. A* **23** 2147 (1981)
51. O K Nugmanov, A I Pertsin, L V Zabelin, G N Marchenko *Usp. Khim.* 56 1339 (1987) [*Russ. Chem. Rev.* **54** 764 (1987)]
52. J Michell *Cellulose Chem. Technol.* **8** 439 (1974)
53. R H Atalla, B E Dimick *Carbohyd. Res.* **49** 1 (1975)
54. V P Firsov, R G Zhbankov, N N Avsenev, in *Materialy I Vsesoyuznoi Konferentsii po Spektroskopii Kombinatsionnogo Rasseyaniya Sveta* (Proceedings of the 1st All-Union Conference on Raman Spectroscopy) (Kiev: Naukova Dumka, 1975) p. 106
55. R G Zhbankov, D K Buslov *Zh. Prikl. Spektrosk.* **38** 33 (1983)
56. R I Sarybaeva, L M Shchelokhova *Khimiya Azotnokislykh Efirov Tsellyulozy* (The Chemistry of Cellulose Nitrate Esters) (Frunze: Ilim, 1985)
57. V P Panov, R G Zhbankov *Infrakrasnye Spektry i Struktura Nitratov Tsellyulozy* (The Infrared Spectra and Structure of Cellulose Nitrates) (Minsk: Izd. Inst. Fiz. Akad. Nauk Beloruss. SSR, 1970)

58. E M Belova, N G Gustova, E T Magdalev, V N Mirsheva, V I Kovalenko, V F Sopin, in *Vsesoyuznaya Konferentsiya "Khimiya, Teknologiya i Primenenie Tsellyulozy i Ee Proizvodnykh" (Tezisy Dokladov)* [All-Union Conference on "The Chemistry, Technology, and Applications of Cellulose and Its Derivatives" (Abstracts of Reports)] (Cherkassy, 1985) p. 128
59. V I Kovalenko, N G Gustova, E N Belova, V N Mirsheva, V F Sopin, in *Vsesoyuznaya Konferentsiya "Khimiya, Teknologiya i Primenenie Tsellyulozy i Ee Proizvodnykh" (Tezisy Dokladov)* [All-Union Conference on "The Chemistry, Technology, and Applications of Cellulose and Its Derivatives" (Abstracts of Reports)] (Cherkassy, 1985) p. 129
60. R G Zhbankov, N V Ivnova, T E Kolosova, in *Vsesoyuznaya Konferentsiya "Khimiya, Teknologiya i Primenenie Tsellyulozy i Ee Proizvodnykh" (Tezisy Dokladov)* [All-Union Conference on "The Chemistry, Technology, and Applications of Cellulose and Its Derivatives" (Abstracts of Reports)] (Cherkassy, 1985) p. 130
61. N Petropavlovsky *J. Polym. Sci.* **16** 3187 (1968)
62. T Urbanski, M Witanowski *Trans. Faraday Soc.* **59** 1039 (1963)
63. Y Oyuimi, T V Brill *Spectrochim. Acta* **42** 1001 (1986)
64. A N Krasovskii, A V Filippov, G Ya Gumenyuk *Khim. Drevesiny* **3** 87 (1987)
65. V P Panov, R G Zhbankov, R A Malakhov *Vysokomol. Soedin. A* **12** 2435 (1970)
66. V M Panov, R G Zhbankov, R A Malakhov *Vysokomol. Soedin. A* **15** 1648 (1973)
67. D A Winkler *Polymer* **27** 765 (1986)
68. R M Mukhamadeeva, R G Zhbankov, V F Sopin, G N Marchenko *Zh. Prikl. Spektrosk.* **53** 851 (1990)
69. R M Mukhamadeeva, V I Kovalenko, in *Tezisy Dokladov Konferentsii "Fiziko-khimicheskie Metody Issledovaniya v Oblasti Khimii, Biologii"* (Abstracts of Reports Presented at the Conference *"Physico-chemical Methods of Investigation in the Field of Chemistry, Biology"*) (Kazan, 1987) p. 11
70. R M Mukhamadeeva, R G Zhbankov, V I Kovalenko, in *Tezisy Dokladov XX Vsesoyuznogo S'ezda po Spektroskopii* (Abstracts of Reports presented at the XXth All-Union Meeting on Spectroscopy) (Kiev, 1988) p. 345
71. R M Mukhamadeeva, R G Zhbankov, V F Sopin, in *Vsesoyuznaya Konferentsiya "Khimiya, Tekhnologiya i Primenenie Tsellyulozy i Ee Prozvodnykh" (Tezisy Dokladov)* [All-Union Conference "Chemistry and Technology of the Application of Cellulose and Its Derivatives" (Abstracts of Reports)] (Cherkassy, 1990) p. 188
72. E M Belova, V I Kovalenko, V N Marsheva, in *Vsesoyuznaya Konferentsiya "Khimiya, Tekhnologiya i Primenenie Tsellyulozy i Ee Proizvodnykh" (Tezisy Dokladov)* [All-Union Conference "Chemistry and Technology of the Application of Cellulose and Its Derivatives" (Abstracts of Reports)] (Cherkassy, 1985) p. 127
73. N M Azancheev, V F Sopin, V I Kovalenko, E N Sergeev, E M Belova *Vysokomol. Soedin. B* **30** 295 (1988)
74. E T Lipmaa, R ETeeyaer, R G Zhbankov *Dokl. Akad. Nauk SSSR* **271** 1150 (1983)
75. N M Azancheev, E N Sergeev, V F Sopin, V I Kovalenko, E M Belova, G N Marchenko *Vysokomol. Soedin. A* **29** 1001 (1987)
76. N M Azancheev, E N Sergeev, V F Sopin, G N Marchenko *Vysokomol. Soedin. B* **30** 295 (1988)
77. E N Sergeev, N M Azancheev, V F Sopin, V I Kovalenko, E M Belova, G N Marchenko *Vysokomol. Soedin. B* **30** 299 (1988)
78. B Ya Vytenskii, E P Kuznetsova, N I Klenkova *Zh. Prikl. Khim.* **34** 185 (1966)
79. B V Erogeev *Dokl. Akad. Nauk SSSR* **52** 515 (1946)

Russian Chemical Reviews **62** (4) 337–358 (1993)
© 1993 Russian Academy of Sciences and Turpion Ltd

UDC 547.512

The chemistry of acetylcyclopropane

B A Czeskis, N M Ivanova, A M Moiseenkov (deceased), O M Nefedov

Contents

I. Introduction	337
II. Methods of synthesis of acetylcyclopropane	337
III. Chemical properties of acetylcyclopropane	338
IV. The use of acetylcyclopropane in the synthesis of natural and practically useful compounds	352

Abstract. Data on the synthesis chemical reactions of acetylcyclopropane are presented. A systematic account is given in terms of the reactions of the functional groups of the above compound (methyl, carbonyl, and cyclopropyl). The extensive possibilities of acetylcyclopropane as a convenient five-carbon building block in organic synthesis are demonstrated. The bibliography includes 268 references.

I. Introduction

During the more than one hundred years that have elapsed since W A Perkin, Jr[1] first described the synthesis of acetylcyclopropane (ACP) and especially during the last decades, extensive structural data have accumulated on the use of this five-carbon synthon in organic synthesis. The presence of the keto-group in acetylcyclopropane in combination with a three-membered carbocycle is responsible for the specific bifunctional properties of this compound and, apart from the multiplicity of classical reactions characteristic of methyl ketones, it is possible to carry out with this compound also reactions involving the opening and retention of the cyclopropane fragment. Organic compounds of various classes have been synthesised from acetylcyclopropane. Acetylcyclopropane and its derivatives are widely used in the preparation of substances which have found applications in engineering, agriculture, and medicine.

Despite the existence of fairly extensive data on the chemical reactions of acetylcyclopropane, they have not so far been treated systematically and the present review was undertaken to fill this gap.

II. Methods of synthesis of acetylcyclopropane

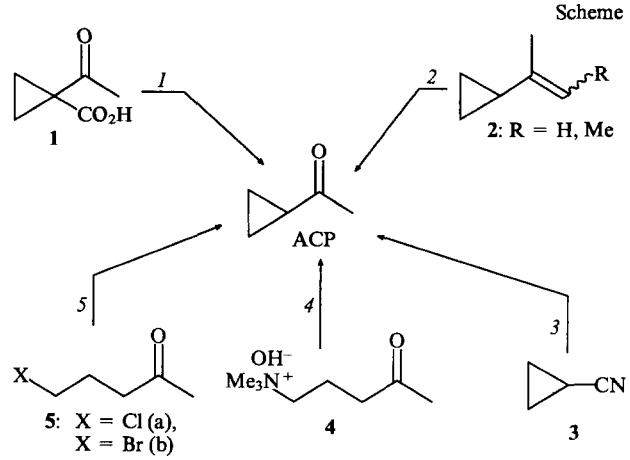
Acetylcyclopropane was first synthesised in a moderate yield in 1887 by the thermolysis of acetylcyclopropanecarboxylic acid **1** (Scheme 1).[1] At the present time, acetylcyclopropane is a commercially available product. A compilation of the methods of its synthesis known at the end of the 1950s has been published.[2]

B A Czeskis, A M Moiseenkov, O M Nefedov ¶ Laboratory of Polyunsaturated Compounds (¶ Laboratory of the Chemistry of Carbenes and Small-Ring Compounds), N D Zelinskii Institute of Organic Chemistry, Russian Academy of Sciences, Leninskii prosp. 47, 117913 Moscow, Russian Federation. Fax (7-095)135 53 28
N M Ivanova 'Kaprolaktam' Joint Stock Company, 606000 Dzerzhinsk, Nizhnii Novgorod Region, Russian Federation

Received 3rd February 1993
Uspekhi Khimii **62** (4) 365–386 (1993); translated by A K Grzybowski

Apart from the thermolysis mentioned above, these include the oxidation of alkenes **2**.[3,4] Grignard synthesis from the cyano-derivatives **3**,[5] thermal decomposition of the ammonium salt **4** in the presence of KOH,[6] as well as cyclisation of γ-acetylpropyl halides **5**.[2] These and related methods are in fact most widely used.

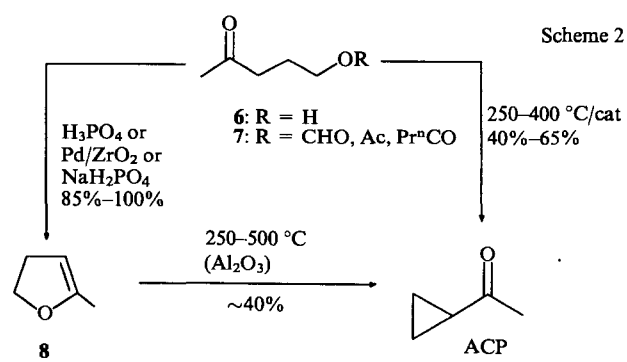
Scheme 1



(*1*) Δ(30%);
(*2*) $KMnO_4$ or O_3 (~50%);
(*3*) MeMgBr (40%);
(*4*) Δ/KOH (45%);
(*5*) EtONa or KOH (40%–95%).

The methods of synthesis of acetylcyclopropane developed during the last three decades, among which special mention should be made of the synthesis of acetylcyclopropane from acetylpropyl alcohol **6** and some of its derivatives, are summarised below (Scheme 2).[7–13]

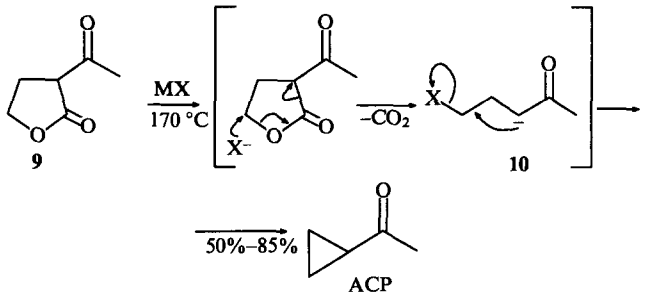
Scheme 2



The cyclodehydration of compound **6** proceeds readily and affords the dihydrofuran **8**,[7,14,15] the (thermo)catalytic isomerisation of which in a flow system leads to acetylcyclopropane.[7-11,13,16] The efficiency of this stage depends on a series of parameters (the temperatures used, contact time with the catalyst, etc.) and can reach 40% for a low overall conversion of the ketoalcohol **6**. The use of the esters **7** makes it possible to increase the yield of acetylcyclopropane to 65%.[11,12] The catalysts used in this process are zeolites[12] or metal oxides, mainly transition metal oxides.[11,12]

Acetylcyclopropane can be obtained by the thermolysis of α-acetylbutyrolactone **9** in the presence of catalytic amounts of alkali ,metal halides (Scheme 3).[17-20]

Scheme 3

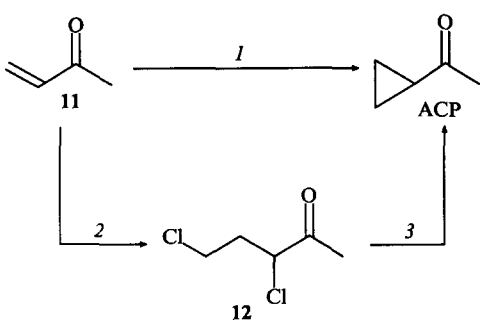


MX = NaI, NaBr, LiCl.

The reaction evidently proceeds via stages involving the opening of the five-membered ring and the generation of the carbanion **10**, which subsequently undergoes intramolecular cyclisation.[17,18] The maximum yield of acetylcyclopropane was achieved under these conditions using NaI in hexamethylphosphoramide (HMPA).[17]

One of the evident approaches to the synthesis of acetylcyclopropane involves the transformation of methyl vinyl ketone **11** (Scheme 4).

Scheme 4

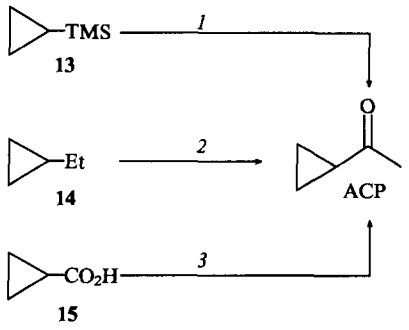


(*1*) CH_2I_2–Zn/Cu (50%), CH_2I_2–Zn/Ag (60%), CH_2Br_2–Ni(0)/Zn/NaI (> 95%);
(*2*) CH_2Cl_2/MeCN, CuCl, Bu^n_4NBr, *hν*;
(*3*) e^- (45% from **11**).

The classical version of the Simmons–Smith reaction leads in this instance to acetylcyclopropane in approximately 50% yield.[21] The use of a modified version of this method, in which the Zn/Cu couple has been replaced by the Zn/Ag couple, proved to be somewhat more effective.[21] A virtually quantitative yield of acetylcyclopropane was achieved when CH_2Br_2 and the complex Ni(0)/Zn/NaI were involved in the reaction.[22] Finally, the possibility of converting compound **11** into a cyclopropane derivative using CH_2Cl_2 as the methylenating agent has been demonstrated by the two-stage version of this process, including the cathodic dechlorination of the intermediate photoadduct **12**.[23]

A small group of methods is based on the use of cyclopropane precursors (Scheme 5). Thus the acylation, catalysed by a Lewis acid, of the cyclopropylsilane **13**, which was obtained in its turn by the Simmons–Smith conversion of trimethylvinylsilane into a cyclopropane derivative, leads smoothly to acetylcyclopropane virtually without the competing reaction involving the opening of the three-membered ring.[24] The oxidation of ethylcyclopropane **14** by ozone in the presence of SiO_2 is also characterised by a satisfactory yield of acetylcyclopropane.[25] The single-stage conversion of the acid **15** into acetylcyclopropane on treatment with LiMe,[26] in principle related to the conversion into acetylcyclopropane of the nitrile **3** of the above acid on treatment with MeMgBr, is almost just as effective.

Scheme 5



(*1*) AcCl/$AlCl_3$–CH_2Cl_2 (60%);
(*2*) O_3/SiO_2 (~60%);
(*3*) MeLi (~65%).

It follows from the data presented that, among the various methods of synthesis of acetylcyclopropane available at present, the procedures based on γ-acetylpropyl chloride **5a** and the corresponding alcohol **6** are the most attractive and technologically most sophisticated.

III. Chemical properties of acetylcyclopropane

Numerous reactions of acetylcyclopropane, occurring both with participation of its carbonyl or methyl group and with the opening of the three-membered carbocycle, have now been described. This will be the subject of the further consideration of the literature data available at present, which do not so far contain information about the direct introduction of functional groups into the cyclopropane fragment of this molecule.

1. Reactions involving the carbonyl group

Reactions of this type constitute the commonest series of reactions of acetylcyclopropane. They are similar to the known reactions of aliphatic ketones.

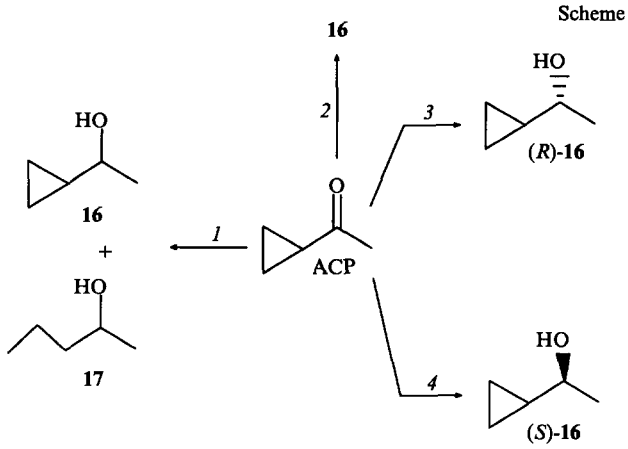
a. Reduction

Acetylcyclopropane is an extremely popular substrate for the study of the properties of new reductants. In particular, it has become one of the first objects to which the Bouveault–Blanc reaction has been applied.[27] The reduction of acetylcyclopropane by the Bouveault–Blanc method leads to a mixture of secondary alcohols with cyclic (compound **16**) and linear (compound **17**) structures (Scheme 6).[27,29] Hydrogenation of acetylcyclopropane over a nickel catalyst is also accompanied to a significant extent by the opening of the three-membered ring,[28] which can be appreciably suppressed by using platinum[30] and can be almost entirely excluded in the presence of a chromium-containing catalyst.[28] The complete retention of the cyclopropane ring is attained when a zinc-based catalyst is employed,[31,32] although the degree of conversion of acetylcyclopropane is then fairly low.

Acetylcyclopropane is reduced chemoselectively by Bu^n_3SnH under mild conditions but with a moderate yield.[33] The Meerwein–Pondorf reduction of acetylcyclopropane makes it possible to obtain the alcohol **16** in ~90% yield[29] under

conditions involving the rapid decomposition of the intermediate organoaluminium complexes, inducing the formation of high-molecular-mass side products.[34] The same complications may arise in the treatment of the reaction mixtures formed as a result of the hydride reduction of the acetylcyclopropane with the aid of lithium tetrahydroaluminate ($LiAlH_4$)[28,31,35-39] or KBH_4.[40]

Scheme 6



(*1*) Na/EtOH (~50%), H_2/Ni-Ra (~70%, **16**:**17** ≃1:1), H_2/Pt (~50%), H_2/Cr_2O_3, 100°C (90%);
(*2*) H_2/Zn, 160°C (45%), H_2/Zn–Cu, 125°C (65%), Bu^n_3SnH/Bu^n_4NCl (~25%), Bu^n_3SnH/Bu^n_4NF (~45%), $(Pr^iO)_3Al/Pr^iOH$ (~90%), $LiAlH_4/Et_2O$ (~75%), KBH_4/MeOH (~75%);
(*3*) enzymes from the fungus *Pseudomonas* (> 60%);
(*4*) (*R*)-β-isopinocamphenyl-9-borabicyclo[3.3.1]nonane.

Data on the enantioselective reduction of acetylcyclopropane have been published recently. Thus the chemoenzymic method, using the enzyme system from fungi of the genus *Pseudomonas*, makes it possible to obtain the optically pure (> 98%) isomer (*R*)-**16** in a satisfactory yield.[41-43] Its enantiomer (*S*)-**16** has been synthesised with an optical purity of 69% with the aid of the bulk-phase chiral tetrahydroborate reagent.[44]

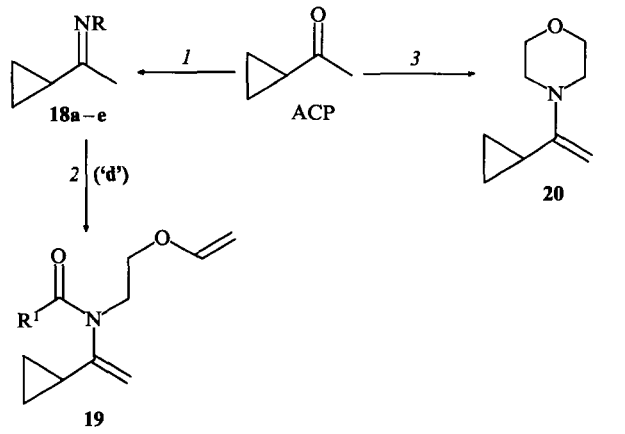
b. Synthesis of nitrogen-containing derivatives

The interaction of acetylcyclopropane with various nitrogen-containing bases afforded a large number of its different derivatives involving the carbonyl group—from the simple oxime[45,46] and hydrazones[47-54] to structurally more complex systems, some of which serve as the starting materials in the synthesis of medicinal preparations and herbicides.[46,49,55-58]

The interaction of acetylcyclopropane with primary amines leads smoothly to the Schiff bases **18a–e** (Scheme 7),[58-63] which have recently found synthetic applications on an increasingly wide scale. In particular, the acylation of the imine **18d** leads to the smooth formation of the vinylamides **19**, which are of interest as monomers; in this reaction, only the nitrogen atom is subjected to electrophilic attack in the initial molecule.[61-63] The direct conversion of acetylcyclopropane into the enamine **20** has been achieved, admittedly only in a low yield, by the Lewis-base catalysed reaction of acetylcyclopropane with morpholine.[64,65]

The primary amine **21** was obtained by the reductive amination of acetylcyclopropane[66,67] (Scheme 8).† In contrast to the hydrogenation over Raney nickel, in this case the reaction is not accompanied by the opening of the cyclopropane ring, which can be explained by the partial deactivation of the catalyst in the presence of NH_3.[66] Nucleophilic substitution of the hydroxy-group by the amino-group in the intermediate cyanohydrins, arising in the interaction of acetylcyclopropane with HCN, leads to the aminonitriles **22a**[55,56,68] and **22b**.[69]

Scheme 7



18: R = Bu^n(**a**), cyclo-C_6H_{11}(**b**), CH_2CH_2OEt (**c**), $CH_2CH_2OCH=CH_2$ (**d**), $CH_2CH_2CO_2TMS$ (**e**),
19: R^1 = Me, Et, Pr^n, Bu^n, Ph

(*1*) RNH_2/H^+, boiling PhH (50%–90%);
(*2*) R^1COCl/NEt_3, PhH (70%–80%);
(*3*) morpholine/$TiCl_4$, pentane (> 30%).

The reaction of acetylcyclopropane with *o*-phenylenediamine affords the aminal **23**.[70] Another representative of substances of this class is the amidonitrile **24**, which exhibits mutagenic properties. It was synthesised by the condensation of 2-cyano-aziridine with acetylcyclopropane and subsequent hydrolysis of one of the two nitrile groups in the molecule of the intermediate adduct.[57]

Individual α-cyclopropyl-containing secondary amines have been obtained from the Schiff bases **18a–d**. Thus the aminoester **25** has been synthesised in an almost quantitative yield by the hydride reduction of the imine **18d**.[61] The alkoxide-catalysed addition of dialkyl phosphites to the azomethine bond in the imines **18a–d** involves the Arbuzov rearrangement, affording high yields of the aminoalkylphosphonates **26a–d**, among which compounds with insecticidal properties were found.[58]

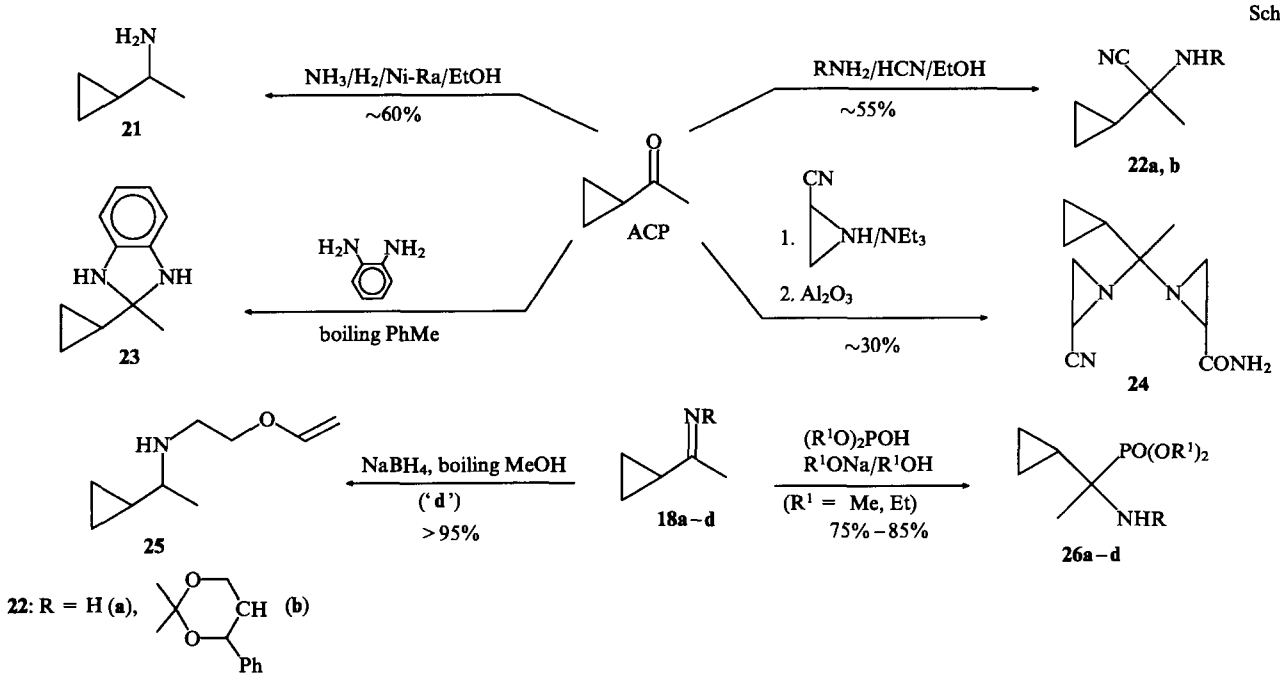
c. Enolic derivatives of acetylcyclopropane

On treatment with strong bases of the type of lithium tetramethylpiperidide (LTMP),[71] lithium diisopropylamide (LDA),[72] $NaNH_2$,[73] KH,[74] LiH,[75] and even NEt_3,[20,76-79] acetylcyclopropane is deprotonated under mild conditions, which leads to a simple and regioselective synthesis of its enolic derivatives (Scheme 9). Thus treatment of lithium acetylcyclopropane enolate with isobutyl chlorocarbonate leads to the smooth formation of the enol carbonate **27**.[71] The TMS-ester‡ **28**, which has found extensive synthetic applications, is obtained similarly to the interaction of Me_3SiCl with the acetylcyclopropane enolate generated *in situ* by various methods,[20,72-74,76-79] for example by treatment with NEt_3 in dimethyl formamide (DMF).[76-79] The yield of compound **28** is in this case ~65%, diminishing somewhat when catalytic amounts of $ZnCl_2$ are used,[20] although overall this version of the silylation reaction is comparatively more convenient, because it simplifies the isolation of the ether. The deprotonation of acetylcyclopropane with the aid of LDA, $NaNH_2$, or KH promotes an increase in the yield of compound **28**. The LiH obtained *in situ* by the hydrogenation of the complex Bu^nLi-TMEDA (TMEDA = tetramethylethylenediamine) partly reduces acetylcyclopropane, affording, after treating the reaction

† The absence from the schemes of information about the yield and/or the proportions of the products (for example, in ACI[e] → **23**) always implies the absence of such data from the original sources.

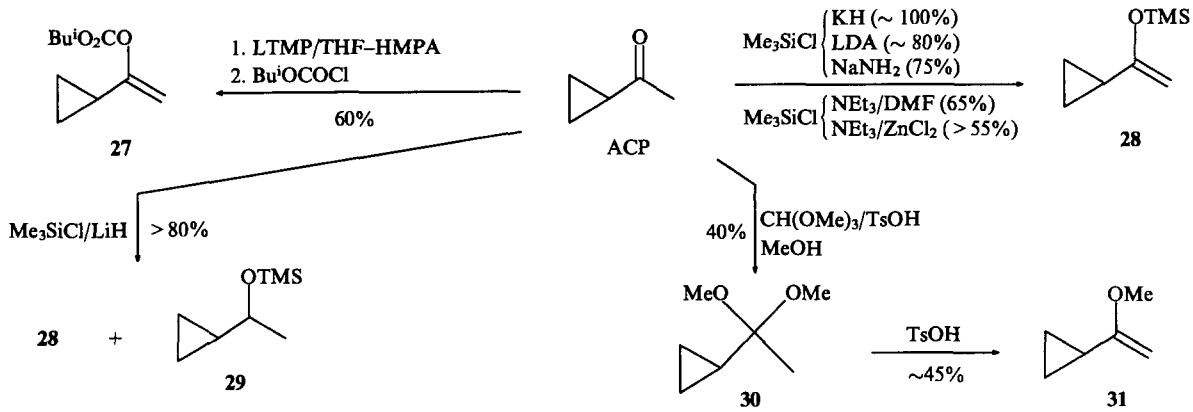
‡ TMS = trimethylsilyl (translator).

Scheme 8



26: R = Bu^n (**a**), cyclo-C_6H_{11} (**b**), CH_2CH_2OEt (**c**), $CH_2CH_2OCH=CH_2$ (**d**).

Scheme 9



mass with Me_3SiCl, a mixture of the ethers **28** and **29** in proportions of ~2:3.[75]

The methyl ether **31** was synthesised in a moderate yield by eliminating the elements of MeOH from the dimethyl ketal **30** obtained by a standard method.[80]

d. Conversion into olefins and related reactions of acetylcyclopropane

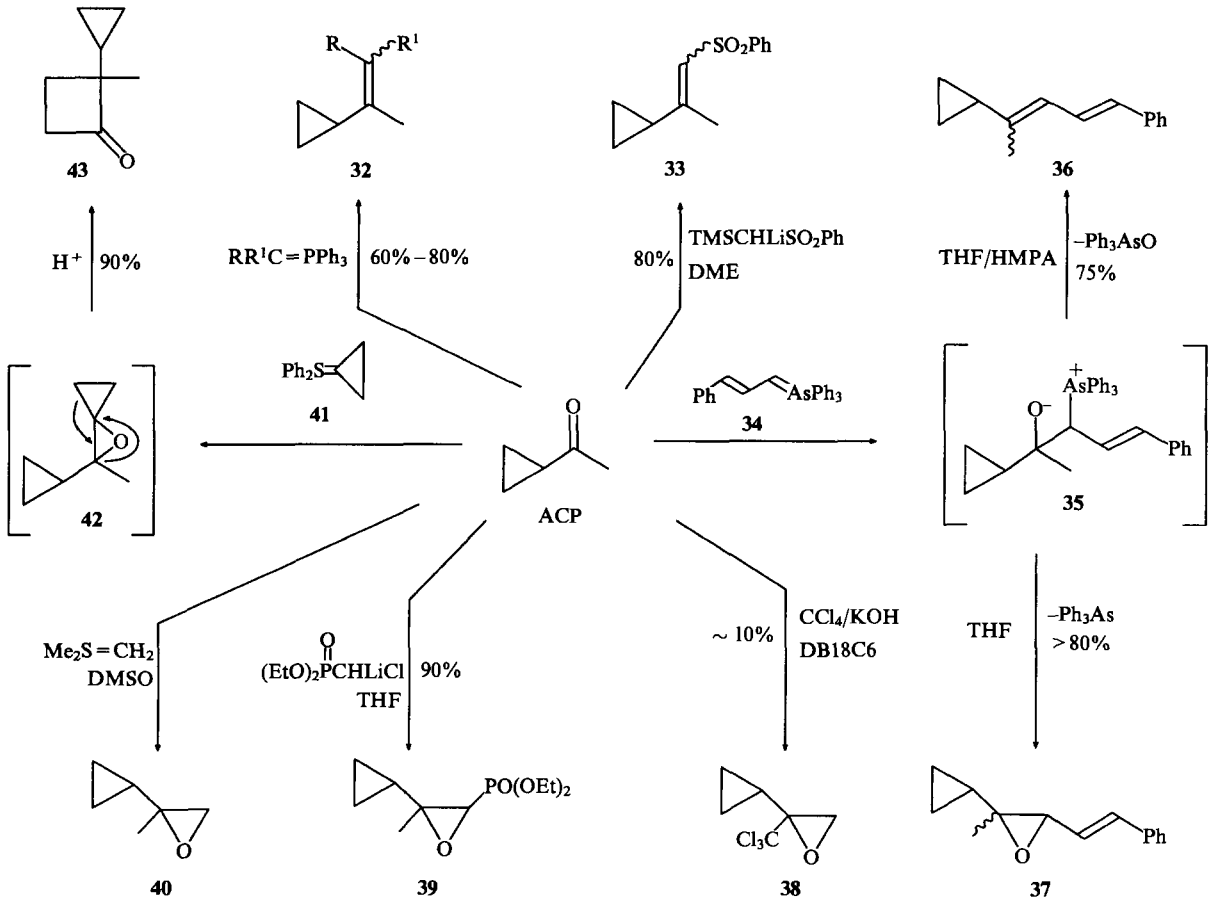
Reactions of acetylcyclopropane with phosphorus, arsenic, and sulfur ylides, leading to the corresponding olefins and epoxides, are widely represented in the literature. For example, the Wittig conversion of acetylcyclopropane into olefins proceeds without complications, affording vinylcyclopropanes **32** in preparative yields and with the expected ratio of the stereoisomers[81–87] (Scheme 10). The Peterson reaction of acetylcyclopropane with the lithio-derivative of trimethylsilylbenzenesulfonylmethane leads similarly to the smooth formation of a mixture of the vinyl sulfones **33** ($Z:E \simeq 3:1$).[88]

The arsorane **34** interacts with acetylcyclopropane via one of two possible pathways depending on the reaction conditions. Thus, when a 1:1 THF–HMPA (HMPA = hexamethylphosphoramide) mixture was used as the solvent, the product **36** of the olefin formation reaction was obtained exclusively ($E:Z \simeq 1:1$),[89,90] whereas in tetrahydrofuran (THF) only the epoxide **37** is formed.[89] The authors correctly explain this effect by the ability of HMPA to stabilise the positive charge in the betaine intermediate **35**, which should diminish the polarity of the C–As bond and thereby promote the generation of the alkene.[89]

The substituted oxiran **38** has been synthesised by the reaction of acetylcyclopropane with CCl_4 in the presence of alkali and the crown-ether, although the yield was low.[91] The mechanism of this reaction has not been explained.

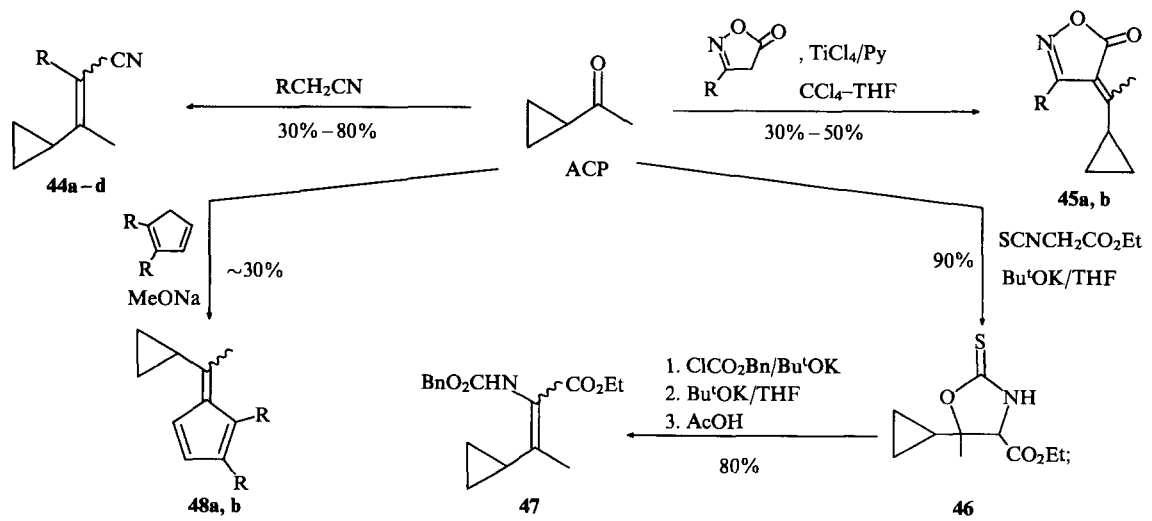
The epoxide **39** has been obtained almost quantitatively by condensing acetylcyclopropane with the lithio-derivative of diethyl chloromethylphosphonate, evidently via an intermediate chlorohydrin stage.[92] This reaction is in principle related to the Corey–Chaykovsky reaction with the sole difference that the leaving group is in this instance the chlorine atom and not the sulfonium group. The involvement in this reaction of acetylcyclopropane and dimethylsulfonium methylide leads to the epoxide **40**.[93] The analogous interaction with the ylide **41** affords a high yield of the cyclobutanone **43**, which evidently arises as a result of the ready rearrangement of the intermediate spiroepoxide **42**.[94,95]

Scheme 10



32: R = H, R^1 = Me, OMe; R = R^1 = Me; RR^1 = $(CH_2)_2$, $(CH_2)_3$;
DB18C6 = dibenzo-18-crown-6.

Scheme 11



44: R = CN (**a**), Bz (**b**), CO_2Et (**c**), $CONH_2$ (**d**);
45: R = Me (**a**), Ph (**b**);
48: R = H (**a**), RR = $(CH{=}CH)_2$ (**b**);
Bn = benzyl, Bz = benzoyl.

The Knoevenagel reaction with participation of acetylcyclopropane has been used to obtain the unsaturated nitriles **44a–d**[96,97] (Scheme 11), which have served, in their turn, as key intermediates in the synthesis of 2-aminothiophenes and some of their derivatives with antitumour activity. It is noteworthy that the effectiveness of the condensation depends on the nature of both the initial malononitrile and the chosen catalyst. For example, on catalysis with an ion-exchange resin[97] or an AcOH/$AcONH_4$ mixture,[98] the yield of the dinitrile **44a** (or the ester **44c**) is 50%, falling to 30% in the case of the amide **44d**.[97] The use of the AcOH–β-alanine system as the catalyst makes it possible to obtain the nitriles **44a**[99] and **44b**[96] in 81% and 58% yields respectively. The stereochemistry of the olefins **44b–d** remains unelucidated.

The Lewis acid-catalysed condensation of acetylcyclopropane with 3-methylisoxazolone leads stereoselectively to the adduct **45a**, which is a mixture of isomers ($E:Z$ = 85:15).[100] In the case of the 3-phenyl derivative, both stereoisomers of compound **45b** are formed in approximately equal amounts.[100]

The reaction of ethyl isothiocyanatoacetate with acetylcyclopropane in the presence of *tert*-BuOK affords the oxazolidinethione **46** as a result of the intermolecular cyclisation of the intermediate tertiary alcohol.[101,102] The product of the acylation of compound **46** isomerises under the influence of the excess of *tert*-BuOK, which is accompanied by the elimination of COS. This leads ultimately to the vinylcyclopropanes **47** in an overall yield >70%.[102] Finally, condensation of acetylcyclopropane with CH acids, catalysed by a strong base, led to the formation of the corresponding fulvenes **48a**[103] and **48b**[104] in moderate yields.

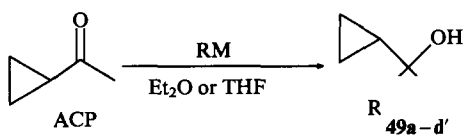
Thus conversion into olefins and nucleophilic reactions of acetylcyclopropane of a similar nature provide an easy access to functionalised vinylcyclopropanes and related epoxides, which have a high synthetic potential.

e. Reactions of acetylcyclopropane with organometallic compounds

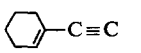
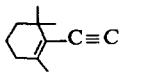
The data described above cover only a small number of examples of the use of acetylcyclopropane as a convenient and readily available compound for the study of the properties of various nucleophiles, leading at the same time to products with a wide variety of synthetic applications. The main bulk of the data published until recently refer to the synthesis and subsequent chemical reactions of cyclopropyl alcohols **49** formed in the reactions of acetylcyclopropane with various organometallic compounds—primarily with Grignard reagents (Scheme 12).

It is seen from the data presented that the Grignard reaction involving acetylcyclopropane proceeds as a whole with fairly high yields, which decrease, as was to be expected, when sterically bulky allyl halides are used. In the case of MeMgI, a significant amount (~15%) of 1-iodo-4-methylpent-3-ene—the acyclic product of the cyclopropylcarbinyl rearrangement (CPCR)—is

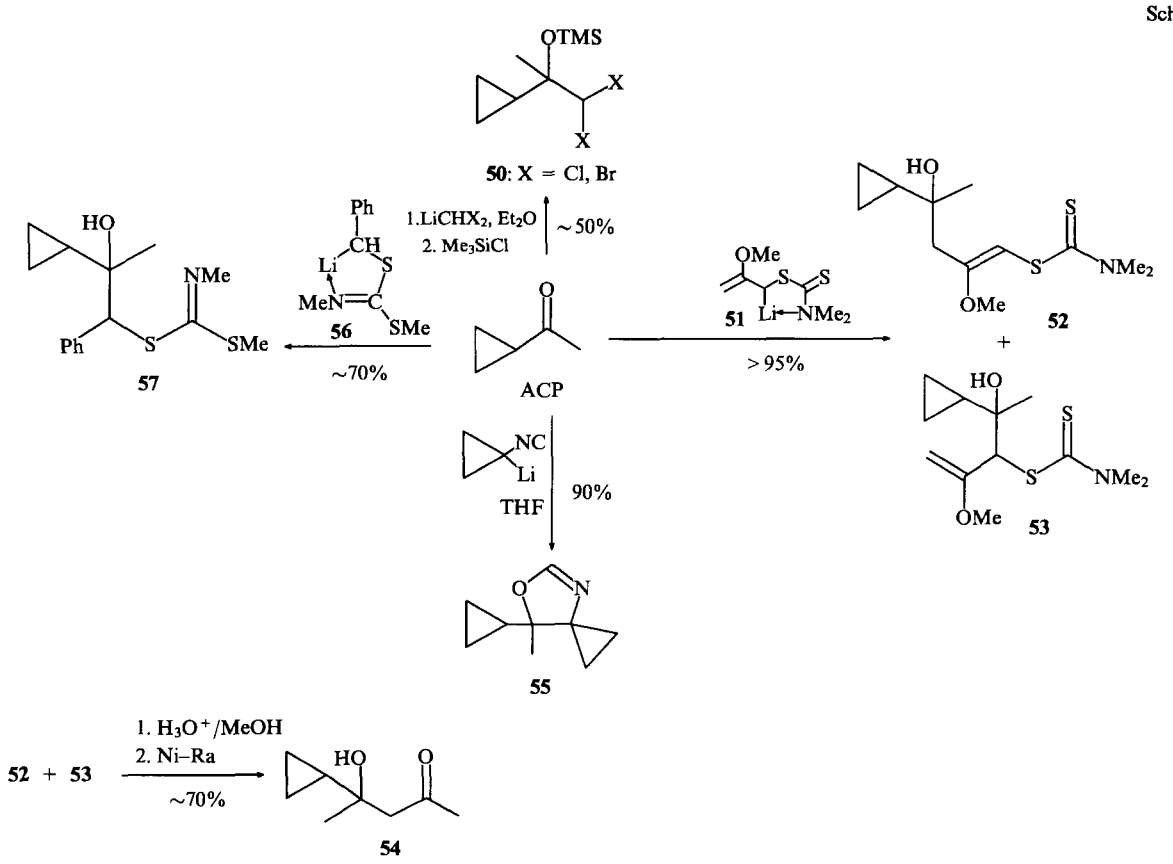
Scheme 12



M = Li, Na, K, MgCl, MgBr, MgI

No.	R	M	Yield of **49** (%)	Ref.
a	Me	Li	61	105
		MgX (X = Cl, Br, I)	55–90	34, 106–115
b	Et	MgBr	54–81	107, 109, 112, 113, 116–119
c	Pr^n	MgX (X = Cl, Br)	51–57	107, 120–122
d	Pr^i	MgBr	27–51	123
e	Bu^n	MgBr	52–84	107, 124, 125
f	Bu^t	MgCl	19	126
g	$HO(CH_2)_4$	MgCl	81	127
h	$CH_2=CH$	MgX (X = Cl, Br)	50–83	128–130
i	(*Z*)-MeCH=CH	MgBr	82	131
k	$CH_2=CHCH_2$	MgBr	48–96	131–134
l	(*E*)-$MeCH=CH(CH_2)_2$	MgBr	>70	135, 136
m	$EtMeC=CH(CH_2)_2$	MgBr	72	136
n	$CH_2=CHCMe=CH(CH_2)_2$	MgBr	94	129
o	$Pent^iMeC=CH(CH_2)_2$	MgBr	57	136
p	$H(CH_2CMe=CHCH_2)_nCH_2$			
	$n=1$	MgBr	70–91	110, 111, 136, 137
	$n=2$	MgBr	46–69	110, 111, 132, 136
	$n=3$	MgBr	57	111
r	Ph	Li	>91	138
		MgBr	57–65	139, 140
s	Bn	MgX (X = Cl, Br)	57–85	141, 142
t	$o\text{-}CNC_6H_4CH_2$	Li	~100	143
u	$HC\equiv C$	Na	77–88	129, 144, 145
		K	50–90	146–148
v	$MeC\equiv C$	MgBr	90	131
w	cyclo-$PrC\equiv C$	Li	82	149
		MgBr	73	149
x		MgBr	80	150
y		MgBr	80	150
z	$PhC\equiv C$	K	84	151
		MgBr	95	151
a'	$HOCH_2C\equiv C$	K	70	132
b'	$HC\equiv C\text{–}CH_2$	MgBr	88	131
c'	$C(SMe)_3$	Li	83	152, 153
d'	$TMS\text{–}C\equiv C\text{–}C$ 	Li	78	154

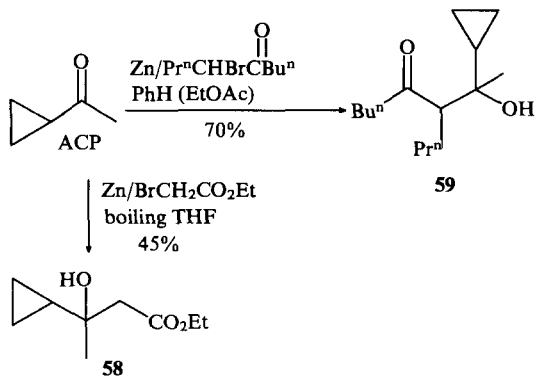
Scheme 13



formed together with the corresponding cyclopropyldimethylcarbinol **49a**.[112,114] Sodium[129,144,145] and potassium acetylides[132,146–148,151] interact with acetylcyclopropane without complications, affording the corresponding ethynylmethylcarbinols. Substituted acetylides have been used successfully under these conditions as Iotsich reagents or as alkali metal derivatives.

Examples of the interaction of certain functionalised organolithium reagents are presented in Scheme 13. Thus silylation of the products of the condensation of dihalomethyllithium with acetylcyclopropane leads to the trimethylsilyl ether **50**, which can readily undergo β-elimination on treatment with bases to form *gem*-dihaloalkenes.[155] The introduction of the acetonyl fragment into the acetylcyclopropane molecule has been achieved with the aid of the lithio-derivative of the dithiocarbamate **51**, which interacts with acetylcyclopropane, affording a mixture of the regioisomers **52** and **53** in proportions of 4 : 1.[156] Their hydrolysis and subsequent reductive desulfurisation of the intermediate dithio-carbamates led to the formation of the β-hydroxyketone **54** in a high overall yield.

Scheme 14

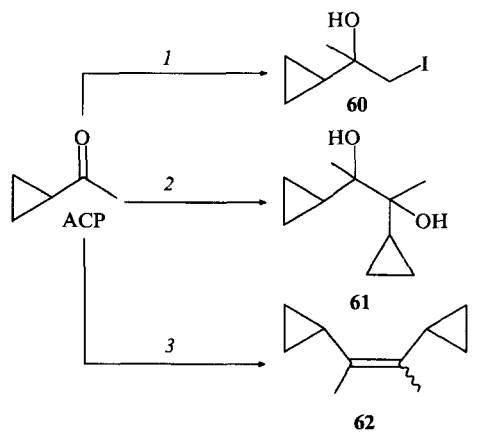


The reaction of the lithio-derivative of isocyanocyclopropane with acetylcyclopropane leads to an intermediate isocyano-derivative, which undergoes spontaneous intramolecular cyclisation to the oxazoline **55**.[157] Yet another example of the use of acetylcyclopropane for the synthesis of various heterocycles is provided by its reaction with the metallated dithioimide **56**, which leads to the carbinol **57** — a precursor of oxathiolans.[158]

Another interesting but hitherto inadequately developed approach to the synthesis of functionalised cyclopropylmethylcarbinols involves the use of organozinc reagents. For example, the synthesis of the tertiary alcohols **58**[159] and **59**[160] from acetylcyclopropane by the Reformatskii reaction has been described (Scheme 14).

The radical–ion reactions with participation of acetylcyclopropane have also been investigated extremely inadequately.

Scheme 15



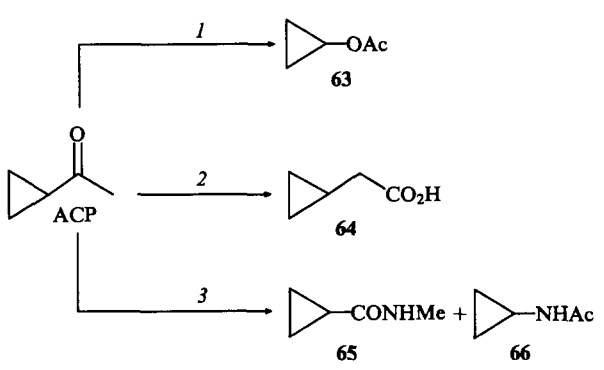
(*1*) CH_2I_2/Sm(0)–THF (60%);
(*2*) Al/Hg (30%), $TiCl_4$/Mg–Bu^{t}OH (60%);
(*3*) $TiCl_3$/$LiAlH_4$–THF (30%).

Reactions of this kind include, for example, the Sm(0)-initiated iodomethylation of acetylcyclopropane with CH_2I_2, which leads effectively to the iodohydrin **60** related to the carbinols **49**[161] (Scheme 15). The conversion of acetylcyclopropane into the vicinal glycol **61**, which takes place smoothly under the influence of aluminium amalgam, also belongs to this class.[162] The yield of compound **61** increases by a factor of 2 when low-valence titanium ions, suppressing the opening of the three-membered ring, are used.[163] When the McMurry reagent[164] is employed, the final products are tetra-substituted olefins **62**, which evidently arise via the pinacol **61** stage.[165]

f. Other reactions of acetylcyclopropane involving the carbonyl group

In conclusion of this Section, we shall consider the individual reactions of acetylcyclopropane in which this compound was used simply as a standard carbonyl substrate, the products of the reaction of which have not so far found a fitting synthetic application. Thus the Baeyer–Villiger oxidation of acetylcyclopropane with the aid of CF_3CO_3H affords smoothly the acetate **63** (Scheme 16).[166] On the other hand, acetylcyclopropane is resistant to the action of weaker peracids of the type of perbenzoic acid.[167] The conversion of acetylcyclopropane into cyclopropyl acetic acid **64** by the Willgerodt–Kindler reaction takes place only with an insignificant yield.[168] Under the conditions of the Schmidt reaction, acetylcyclopropane affords a mixture of both expected regioisomeric amides **65** and **66**,[169–171] the ratio of which in a strongly acid medium depends on the pH of the reaction mixture and can be logically explained by the different rates, under such conditions, of the competing migration to the nitrogen atom of the methyl and cyclopropyl residues in the key intermediate.[170,171]

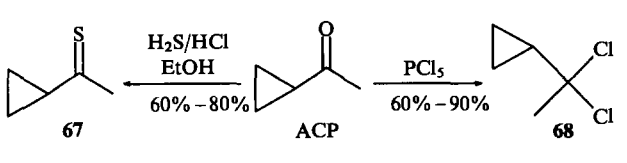
Scheme 16



(*1*) CF_3CO_3H/Na_2HPO_4 (~55%);
(*2*) S/Pi/Δ (~10%) (Pi = piperidine);
(*3*) NH_3 (90%).

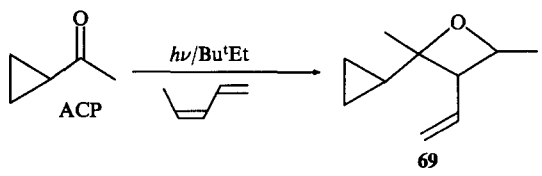
The thione **67** and the *gem*-dichloro-derivative **68**, obtained in high yields by treating acetylcyclopropane with H_2S in an alcoholic solution of HCl[172,173] and with PCl_5 in chlorinated solvents[73,174–176] respectively (Scheme 17), may be of definite synthetic interest. The yield of the dichloro-derivative **68** increases appreciably when the reaction is carried out in the presence of a base (pyridine,[177,178] Na_2CO_3[179]), although partial dehydrochlorination of the product is then observed.

Scheme 17



The photochemical [2 + 2]cycloaddition with participation of the central C=C bond of (*Z*)-piperylene and the carbonyl group of acetylcyclopropane leads regiospecifically to the oxetan **69**, the geometry of which has not been established;[180] the reaction is complicated by the formation of significant amounts of the photodimer of (*Z*)-piperylene (Scheme 18). Other examples of the involvement of acetylcyclopropane in photochemical reactions with retention of the three-membered ring are lacking in the literature.

Scheme 18



Thus the reactions with participation of the carbonyl group of acetylcyclopropane considered above illustrate the extensive possibilities of the use of this ketone for the introduction of the ethylcyclopropane carbon skeleton into various organic compounds, making available thereby a large number of oxygen- and nitrogen-containing derivatives of acetylcyclopropane — important intermediates in organic synthesis.

2. Reactions with participation of the methyl group of acetylcyclopropane

Numerous reactions based on the use of acetylcyclopropane as a typical CH acid, reacting, in contrast to other aliphatic cyclic methyl ketones, with participation of only the methyl group, have been described nowadays. Such unique regiospecificity is the main reason why ways of using acetylcyclopropane as an effective C_5 building block in the synthesis of certain biologically active substances are being sought. The activation of the carbonyl functional group of acetylcyclopropane by its conversion into the imino- or enol form proves to be superfluous in many instances, although it does promote an increase in the yield of the target product and sometimes an enhancement of the chemoselectivity of reactions with certain electrophiles.

a. Synthesis of α-functionalised derivatives of acetylcyclopropane

Treatment of acetylcyclopropane with Br_2 in methanol affords smoothly and selectively the monobromo-derivative **70**[181–185] (Scheme 19). The reaction of acetylcyclopropane with 2,4-dinitrobenzenesulfenyl chloride, leading to a virtually quantitative yield of the ketosulfide **71**, is just as selective.[186] The methanesulfonate **72a**,[187] the toluene-*p*-sulfonate **72b**,[188] and the phosphate **72c**[189] have been obtained by the reaction of acetylcyclopropane with the corresponding derivatives of trivalent iodine. In all the cases indicated, the process evidently includes a stage in which the enolic form of acetylcyclopropane is generated.[187,188]

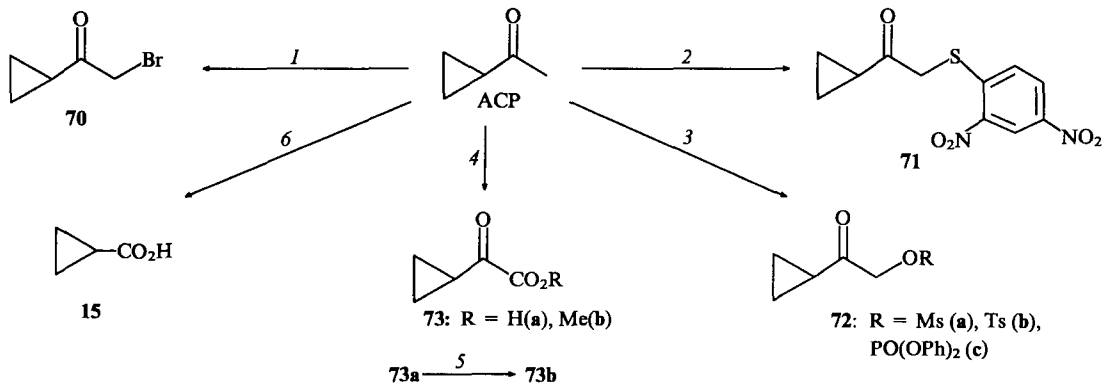
The oxidation of acetylcyclopropane with $KMnO_4$ leads to cyclopropylglyoxalic acid **73a**, which is characterised as the keto-ester **73b**.[190,191] The use of NaOBr as the oxidant opens an effective pathway to cyclopropanecarboxylic acid **15**.[70]

b. Reactions leading to the formation of a new carbon–carbon bond

The Neff methylation of acetylcyclopropane by treatment with $NaNH_2$ (Scheme 20) is characterised by low selectivity. A mixture of all three possible products **74–76** is then formed with the dimethyl derivative **74** predominating.[125]

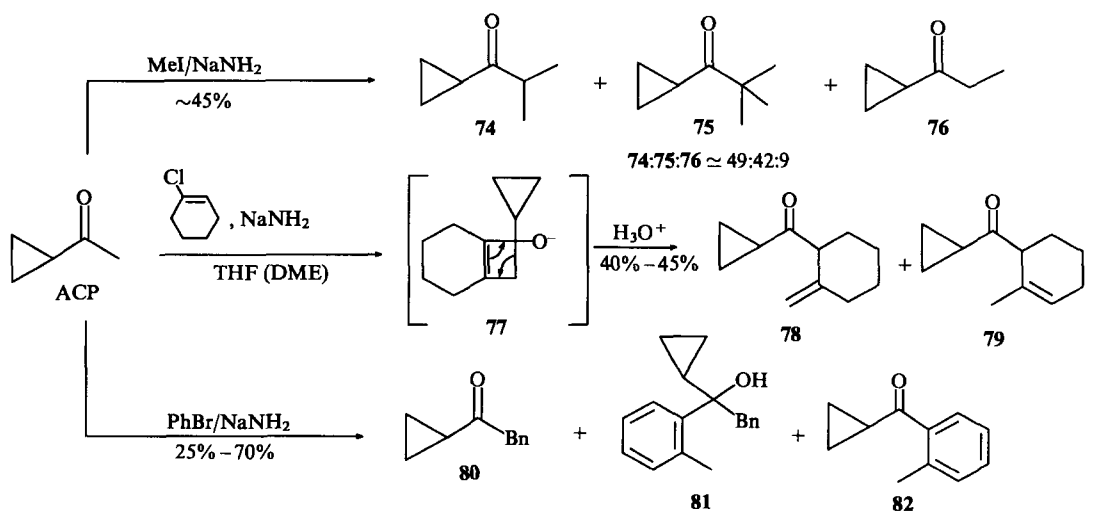
The condensation of acetylcyclopropane with 1-chlorocyclohexene in an aprotic medium, catalysed by a strong base, leads to the unsaturated ketones **78** and **79** in proportions of ~4 : 1.[192] Cyclohexyne is apparently formed initially and then interacts with the acetylcyclopropane enolate anion, affording the product **77**.

Scheme 19



(*1*) Br_2/MeOH (75% – 90%);
(*2*) 2,4-$(NO_2)_2C_6H_3SCl$, boiling CCl_4 (~95%);
(*3*) PhI(OH)OR, boiling MeCN (60% – 90%);
(*4*) $KMnO_4/Na_2CO_3$, H_2O–MeOH;
(*5*) CH_2N_2/Et_2O (> 60% from ACP), $Me_2SO_4/BnMe_3N^+Br^-$, H_2O–CH_2Cl_2 (> 65% from ACP);
(*6*) NaOBr, H_2O (~80%).

Scheme 20

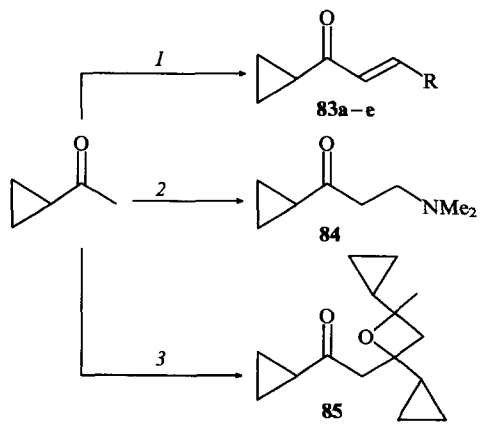


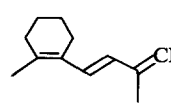
Isomerisation of the cyclobutene fragment in the adduct **77** leads to the main product **78**. Its allyl isomer **79** is probably obtained as a result of the shift of the exocyclic C = C bond on treatment with the base. The reaction of acetylcyclopropane with the dehydrobenzene generated from bromobenzene proceeds similarly, affording the product of phenylation at the methyl group **80**, the alcohol **81** and the ketone **82**, related to cyclohexene, the ratio of the latter depending on the reaction conditions.[193]

The condensation of acetylcyclopropane with trioxane in the presence of an equimolar amount of the salt CF_3CO_2H.PhNHMe affords a high yield of cyclopropyl vinyl ketone **83a**, which is evidently formed from the intermediate thermally unstable Mannich base[194] (Scheme 21). When this reaction is carried out in the classical version, the β-dimethylaminoketone **84** is formed smoothly. Its thermal decomposition led to the isolation of only the polymerisation product of the expected vinyl ketone **83a** instead of the vinyl ketone itself.[195]

Fairly numerous examples of the involvement of acetylcyclopropane in the base-catalysed condensation of the aldol-crotonic type with aliphatic[126,195–197] and aromatic[182,198–206] aldehydes have been described. The reaction undoubtedly proceeds via the corresponding aldol, which has been detected, for example, for isobutyraldehyde;[195,196] further dehydration leads to the formation of the thermodynamically preferred (*E*)-isomers **83b–e**, the yield of which depends on the nature of the aldehyde.

Scheme 21



83: R = H (a), Pr^i (b), cyclo-C_6H_{11} (c),  CH (d), Ar (e)

(*1*) $(CH_2O)_3/CF_3CO_2H$·PhNHMe (~75%) (for **83a**), RCHO/NaOH or Bu^tOK (30% – %90%) (for **83b–e**);
(*2*) CH_2O/Pr^iOH, Me_2NH·HCl (60%);
(*3*) KOH/Δ (25%).

The main cause of the decrease in the effectiveness of the reaction in the case of aliphatic aldehydes is their competitive reactions (self-condensation, polycondensation, and others).[195,196] The cyclopropyl tetraenyl ketone **83d**, prepared by this method (yield ~90%), was used in the synthesis of a retinal analogue.[197]

Direct condensation of the aldol–crotonic type of ketones with acetylcyclopropane is an uncharacteristic reaction in view of the tendency of the latter to form condensation products. In particular, when acetylcyclopropane was boiled (refluxed?) in the presence of powdered KOH, a compound was isolated, to which the structure of the oxetan trimer **85** with an unknown configuration was attributed.[126]

The involvement of acetylcyclopropane in a Claisen type reaction makes it possible to obtain a large series of β-dicarbonyl compounds **86** (Scheme 22). It may be catalysed by Lewis acids, for example BF_3,[207] although bases are used more often and more effectively ($NaNH_2$,[207] MeONa, EtONa,[208,209] NaH[210,211]). The result of the reaction, leading to the β-dicarbonyl derivatives **86a–g** depends significantly on the nature of the substrate. Thus condensation of acetylcyclopropane with acid anhydrides is as a rule less effective than the condensation with esters. For example, in the $NaNH_2$-initiated interaction of acetylcyclopropane with ethyl acetate, the yield of acetoacetylcyclopropane **86a** is 75%. The replacement of AcOEt by Ac_2O lowers the yield of compound **86a** almost by 20%.[207] The condensation of acetylcyclopropane with $(EtCO)_2O$, leading to the diketone **86b**, is characterised by an even lower yield (< 20%).[207]

The reaction of acetylcyclopropane with carbonates is in many respects determined by the choice of the catalyst. The best result is achieved usually when NaH is employed. Thus the replacement of $NaNH_2$ by NaH makes it possible to raise the yield of the β-ketoester **86e** from 55% to 85%.[211] Similarly diethyl oxalate reacts smoothly with acetylcyclopropane in the presence of only EtONa with formation of the highly reactive diketoester **86g**.[207] The ketoamide **87**, related to compound **86** and used as an intermediate in the synthesis of certain medicinal preparations, has been obtained by treating lithium acetylcyclopropane enolate with fluorinated aryl isocyanide and subsequent hydrolytic decomposition of the intermediate adduct.[212] Finally, one should note that the reaction of acetylcyclopropane with propiolates proceeds initially as the Claisen condensation and is terminated by the cyclisation of the intermediate acetylenic diketones to γ-pyrones **88**, which are formed in moderate overall yields.[213]

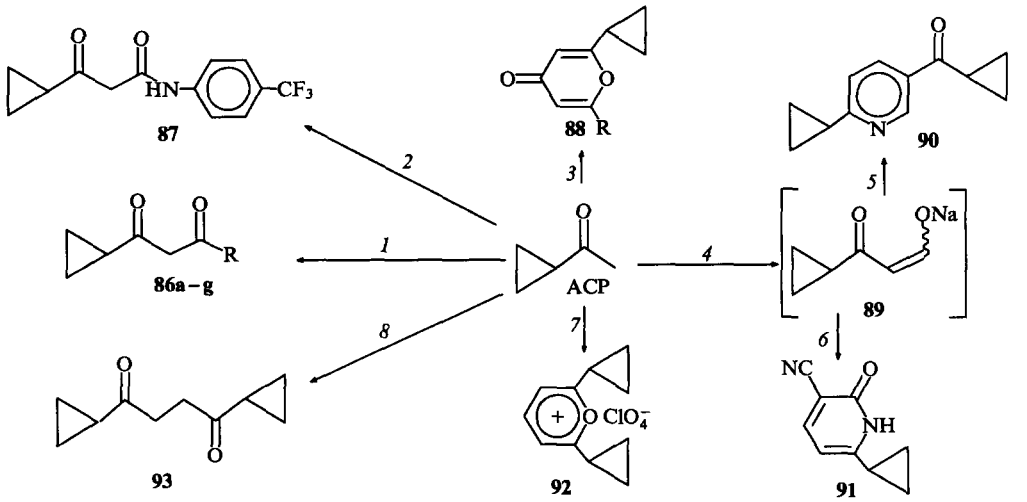
The Claisen condensation examined above, leading to the β-dicarbonyl compounds **86**, implies in the case of the formate the formation of the corresponding labile β-ketoformyl derivative. One of the interesting synthetic applications of the fairly stable sodium enolate **89**[214,215] involves its simple conversion into certain six-membered heterocycles. Thus, on treatment with ammonium acetate in acetic acid, the enolate **89** dimerises readily to the pyridine **90**[215] and reacts smoothly with cyanoacetamide in the presence of Pi.AcOH (Pi = piperidine), affording the pyridone **91**.[214] The thermal reaction of acetylcyclopropane with orthoformic ester, initiated by $HClO_4$, takes place similarly and proceeds evidently via the stage of a 1,5-dicarbonyl intermediate to the pyrylium salt **92**.[216]

In conclusion, one should note that the synthetic possibilities of enolates of type **89** as highly reactive intermediates are far from being exhausted. In particular, the lack of data on their involvement in a reaction of the Michael type and in radical-ion reactions is noteworthy. The latter apparently include the copper(II)-catalysed dimerisation of the lithium acetylcyclopropane enolate to the 1,4-diketone **93**.[217]

c. Certain reactions of activated acetylcyclopropane

Examples of the use of three readily available activated derivatives of acetylcyclopropane — the imine **18b**, the silyl ether **28**, and the hydrazone **94** — are considered below. With their aid, it is possible to achieve more effective regioselective and chemoselective reactions involving the methyl group than with the methyl ketone itself. Thus the direct chlorination of acetylcyclopropane proceeds non-selectively, affording a complex mixture of chloro-derivatives which are difficult to separate.[59] On the other hand, the ketimine **18b** reacts smoothly with *N*-chlorosuccinimide (NCS) and is converted, after the hydrolysis of the intermediate Schiff base, into the dichloroketone **95**[59] (Scheme 23).

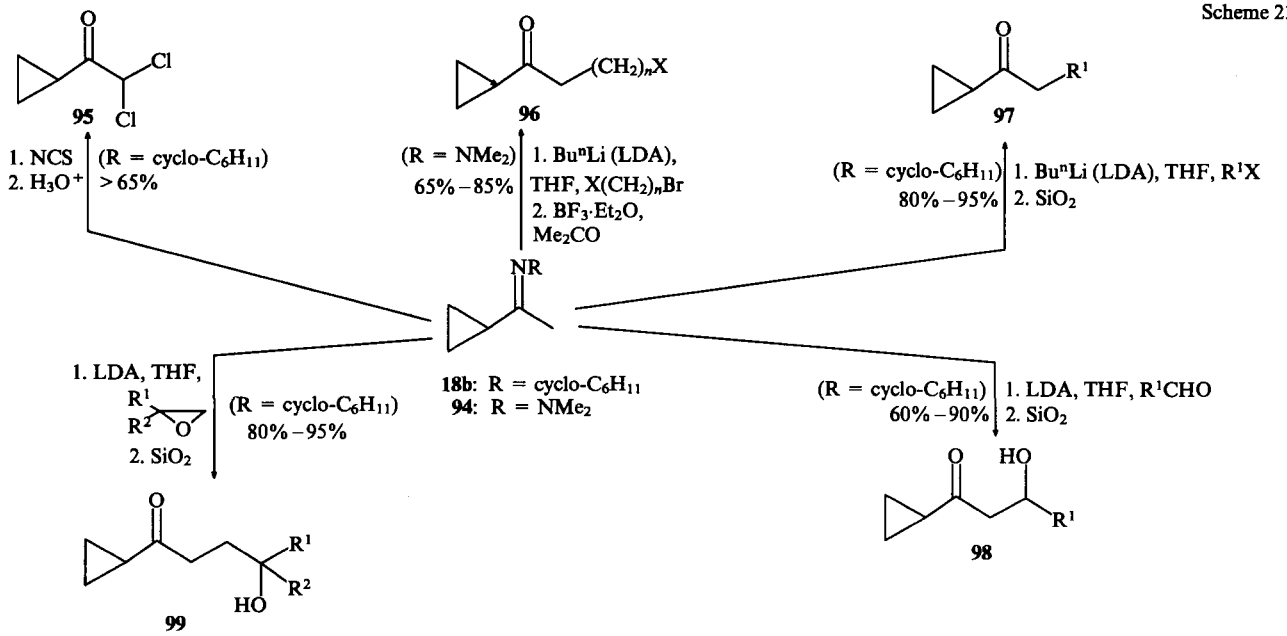
Scheme 22



88: R = H, *o*-ClC_6H_4, *p*-ClC_6H_4, *p*-$MeOC_6H_4$
86: R = Me (**a**), Et (**b**), Ph(**c**), OMe (**d**), OEt (**e**), OPh (**f**), CO_2Et (**g**)

(*1*) RCO_2R^1/BF_3 or NaH, or $NaNH_2$, or R^2ONa (20% – 85%);
(*2*) LTMP/THF, then *p*-$F_3CC_6H_4NC$, and then HCl;
(*3*) $RC{\equiv}CCO_2Et$, EtONa (25% – 60%);
(*4*) HCO_2Et, MeONa;
(*5*) AcOH, NH_4OAc (~80%);
(*6*) $NCCH_2CONH_2$, Pi·AcOH, boiling H_2O (~55%);
(*7*) $HC(OEt)_3/HClO_4$, Δ (~10%);
(*8*) LDA/CuCl, THF–DME (> 45%).

Scheme 23

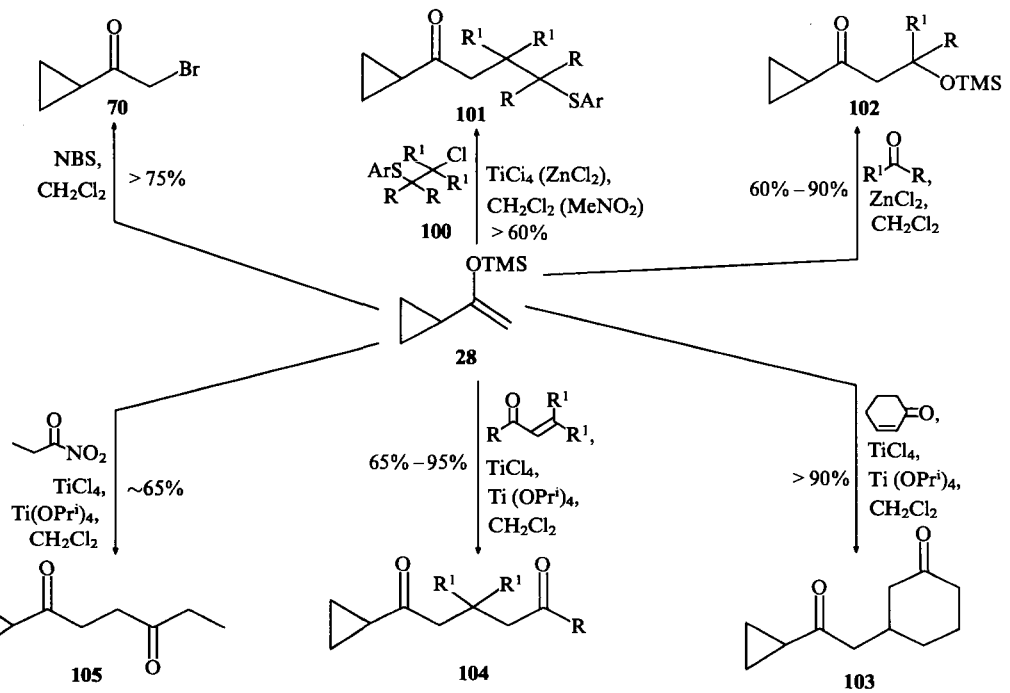


96: X = Cl, $n = 3, 4$; X = Br, $n = 5$;
97: R^1 = Me, Pr^n, n-C_7H_{15}, n-C_9H_{19}, $Me_2C{=}CHCH_2$, (*E*)-$Bu^nCH{=}CH(CH_2)_3$, (*Z*)-$Bu^nCH{=}CH(CH_2)_7$;
98: R^1 = Et, Bu^n, n-C_6H_{11}, n-C_8H_{17}, (*E*)-$MeCH{=}CH$, (*Z*)-$Bu^nCH{=}CH(CH_2)_3$;
99: $R^1 = R^2 = H$; $R^1 = H$, $R^2 = Me$; $R^1 = Me$, $R^2 = CH_2{=}CH$.

Alkylation of the products of the deprotonation of the dimethylhydrazone **94** with ω-haloalkyl bromides affords, after the hydrolytic cleavage of the corresponding adducts, the ketones **96** in high overall yields.[218] Similarly the lithio-derivative of the imine **18b** interacts readily and selectively with primary alkyl halides, aldehydes, and epoxides, affording the ketones **97**, the β-hydroxyketones **98**, and the γ-hydroxyketones **99** respectively after the hydrolysis on silica gel of the imines formed.[219–223]

Treatment of the silyl ether **28** with *N*-bromosuccinimide leads to the monobromo-derivative **70**[224] (Scheme 24) without any appreciable advantage compared with the same reaction using acetylcyclopropane itself. On the other hand, the employment of compound **28** leads to the possibility of obtaining the products of the alkylation of acetylcyclopropane by sterically very greatly hindered electrophiles of the type of vicinal arylthiochloro-derivatives **100** on treatment with Lewis acids. The γ-arylthio-substituted ketones **101** have been effectively synthesised by this method.[225,226] The interaction of aliphatic aldehydes and ketones with the silyl ether of the enol **28** is effectively catalysed by $ZnCl_2$. This reaction results in the smooth formation of β-siloxyketones

Scheme 24



101: R = H, R^1 = Me; R = CMe_2, R^1 = H;
102: R = H, R^1 = Et, Pr^i, Bu^n, n-C_6H_{11}, n-C_8H_{17}, $MeCH{=}CH$, (*E*)-$Bu^nCH{=}CH(CH_2)_2$; R = Me, R^1 = Me, cyclo-Pr;
104: R = R^1 = Me; R = Et, R^1 = H.

102, which makes it possible to solve the problem of the synthesis from acetylcyclopropane of the product of its aldol-crotonic condensation with carbonyl compounds.[227-231]

An extremely interesting synthetic application of the silyl ether **28** is based on the little investigated possibility of involving acetylcyclopropane in a reaction of the Michael type. Thus the reaction of compound **28** with conjugated ketones in the presence of mixed titanium(IV) salts leads to high yields of the 1,5-diketones **103** and **104**.[72] When nitrobutene was used as the acceptor, the 1,4-diketone **105** was obtained.[72]

Thus the large set of selective transformations of acetylcyclopropane involving its methyl group, presented in this Section, opens an extremely effective pathway to various functionalised cyclopropyl ketones, many of which are important synthons.

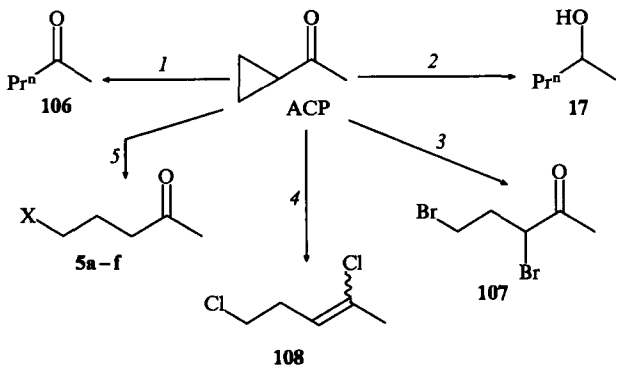
3. Reactions with participation of the cyclopropane fragment

The data examined above demonstrate the properties of acetylcyclopropane as a typical representative of aliphatic methyl ketones. The presence of the cyclopropane residue in its molecule is responsible for additional synthetic possibilities associated with the transformation of the strained three-membered carbocycle. The data described below refer to this feature of the acetylcyclopropane molecule and its derivatives and, mainly, to the ability of the corresponding secondary and tertiary amines to undergo the cyclopropylcarbinyl rearrangement (CPCR).

a. Hydrogenolysis and heterolysis of acetylcyclopropane

Catalytic hydrogenation of acetylcyclopropane leads in many instances to the initial opening of the three-membered ring and the formation of the ketone **106**, which is capable of being further reduced to the alcohol **17**[31,232-234] (Scheme 25). The maximum yield of the ketone **106** was attained when 10% Pd/C was used as the catalyst;[31,232,233] when it is replaced by the mixed Pd–Ni catalyst, the complete conversion of acetylcyclopropane into the alcohol **17** is observed.[234] The pentanone **106** has also been obtained in a high yield by the homolytic reduction of acetylcyclopropane via its photolysis or thermolysis in the presence of the $Bu^n_3SnH/AIBN$ couple (AIBN = azobisisobutyronitrile).[235-237] The Birch radical-ion reduction of acetylcyclopropane leads non-selectively to a mixture of both expected products — **17** and **106**.[34]

Scheme 25



5: X = Cl (**a**), Br (**b**), I (**c**), SPh (**d**), $P^+Ph_3Br^-$ (**e**), SePh (**f**)

(*1*) H_2/Cu, 80 °C (~20%), H_2/Pd–C (90%), $Bu^n_3SnH/AIBN/h\nu(\Delta)$(85%), Na/NH_3 (in a mixture with compound **17**);
(*2*) H_2/Cu, 125 °C (55%), H_2/Pd–Ni (> 90%);
(*3*) Br_2/CH_2Cl_2 ($CHCl_3$, AcOH) (~30%);
(*4*) PCl_5/boiling CH_2Cl_2;
(*5*) Py·HCl (> 80%), P_2I_4 (~90%), Me_3SiX (X = Cl, Br, I) (85% – 95%), $AlCl_3$/PhSH (Me_3SiSPh) (35% – 45%); Ph_3P·HBr (> 90%), PhSeLi (90%).

The results of the hitherto little investigated interaction of various cationoid reagents with acetylcyclopropane may be of great synthetic interest. The electron-accepting nature of the acetyl residue of acetylcyclopropane induces via an inductive mechanism the polarisation of the C–C 'banana' bond,[238] as a result of which this molecule resembles to some extent electrophilic olefins. The competition (evidently in favour of the C=O group) between the intermolecular and intramolecular coordination of the electrophile to the acetylcyclopropane molecule should promote additional polarisation of the above bond and hence an increase in the reactivity of the cyclopropane fragment.

In conformity with the foregoing considerations, the bromination of acetylcyclopropane in chlorinated hydrocarbons leads to a moderate yield of the acyclic dibromo-derivative **107**.[239,240] When the reaction is carried out in acetic acid, its effectiveness is not significantly affected but it becomes complicated by a competing process leading to the formation of appreciable amounts of γ-bromoketone **5b**.[240] Taking into account the data examined above in the synthesis of the α-bromoketone **70**, the data discussed here may serve as a good illustration of the influence of the polarity of the medium on the result of the electrophilic reaction in relation to a chemically fairly simple substrate. The conversion of acetylcyclopropane into a mixture of (*E*)- and (*Z*)-dichloro-derivatives **108** under the influence of PCl_5 in boiling CH_2Cl_2 may be referred to the same type of reactions.[241]

Data obtained recently on the interaction of acetylcyclopropane with soft acids may have significantly more important synthetic consequences. Thus the γ-chloroketone **5a** is formed smoothly when acetylcyclopropane is treated with pyridinium chloride.[242,243] There is no information about a similar reaction with pyridinium bromide, although it is known that in the case of the related pyridinium iodide, which has reducing properties, a complex mixture of substances of unknown structure is produced.[243] However, the γ-iodoketone **5c** can be obtained in a high yield by treating acetylcyclopropane with P_2I_4 under mild conditions.[244]

The use of available or generated *in situ* trimethylsilyl halides is a universal and effective procedure for transforming acetylcyclopropane into the γ-haloketones **5a–c**,[245,246] with *O*-silyl ethers as reaction intermediates. The $AlCl_3$-catalysed effective transformation of acetylcyclopropane into the γ-phenylthioalkyl ketone **5d** on treatment with thiophenol or its trimethylsilyl derivative[246] and the synthesis of the phosphonium salt **5e** on treatment of acetylcyclopropane with PPh_3·HBr have been achieved in conformity with the same principle.[247]

In conclusion of this Section, the absence of data on the anionoid opening of the acetylcyclopropane ring and hence on its involvement in a series of synthetically useful transformations should be noted. So far the effective conversion of acetylcyclopropane into the ketoselenide **5f** on treatment with PhSeLi may serve as the only example of this kind.[248]

b. The cyclopropylcarbinyl rearrangement

The data discussed below refer to the chemistry of secondary and tertiary cyclopropylcarbinols, readily obtainable from acetylcyclopropane, which have recently found extensive applications by virtue of their unique ability to undergo the cyclopropylcarbinyl rearrangement on treatment with protic and Lewis acids.[249-251] It is now well known that such rearrangement of secondary alcohols takes place highly stereoselectively, affording as a rule, high yields of the corresponding (*E*)-olefins. Thus cyclopropylmethylcarbinol **16** readily isomerises under the conditions of the Julia reaction (48% HBr) to the homoallyl bromide **110a**[35,36,38-40] (Scheme 26). A similar transformation can be readily achieved with the aid of $MgBr_2$ and this approach has proved extremely effective also for the preparation of the iodide **110b** from compound **16** on treatment with MgI_2.[112] Another version of the transformation of cyclopropylcarbinols into homoallyl iodides involves the use of 40% HI in DME (dimethoxyethane?). This method was applied to the synthesis

of the anisyl derivative **111** from the alcohol **109a** prepared by the two-stage reduction of the enone **83e** (R = *m*-$MeOC_6H_4$).[182] The conversion of the alcohol **109b**, obtained from the ketoester **86e**, into the bromoester **112** has been achieved successfully on treatment with a solution of $ZnBr_2$ in 48% HBr.[211,252] It was shown recently that the cyclopropylcarbinyl rearrangement of the saturated (compounds **109c–i**) and allylic (compounds **114a–f**) cyclopropylcarbinols obtained from acetylcyclopropane takes place readily under mild conditions under the influence of trimethyl silyl halides and catalytic amounts of zinc halides, affording the corresponding (*E*)-homoallyl halides **113a–i** and **115a–i** in high yields.[219–223,227–231] The method makes it possible to obtain equally effectively both the bromides **113c–i** and **115e–i** and the chlorides **113a, b** and **115a–d**. In contrast to the saturated alcohols, the allyl alcohols **114** are capable of rearranging with the aid of HCO_2H and AcOH to the transoid homoallyl formates and acetates of the type **116a, b** and **116c, d** respectively.[253]

Numerous tertiary cyclopropylmethylcarbinols **49**, readily obtained in one stage from acetylcyclopropane, have been involved in the classical Julia reaction with the use of 48% HBr (Scheme 27). In contrast to the secondary carbinols, tertiary cyclopropylcarbinols afford under these conditions as a rule mixtures of (*E*)- and (*Z*)-stereoisomeric bromides **117** in different proportions, mainly with one of them predominating. The ethynylcarbinols **49u, v** are an exception. Their Julia conversion under the conditions indicated leads almost wholly to the (*Z*)-isomers **117u, v**,[129,131] which has been used successfully in one of the simple schemes for the total synthesis of the juvenile hormone I.[256] There is as yet no rational explanation of this unique steric effect, although in purely qualitative terms it may reduce to the fact that the conformation of the transition state in the rearrangement is determined by the minimum overlap of the cyclopropyl substituent with the methyl substituent, which is significantly more bulky than the ethynyl substituent.[129]

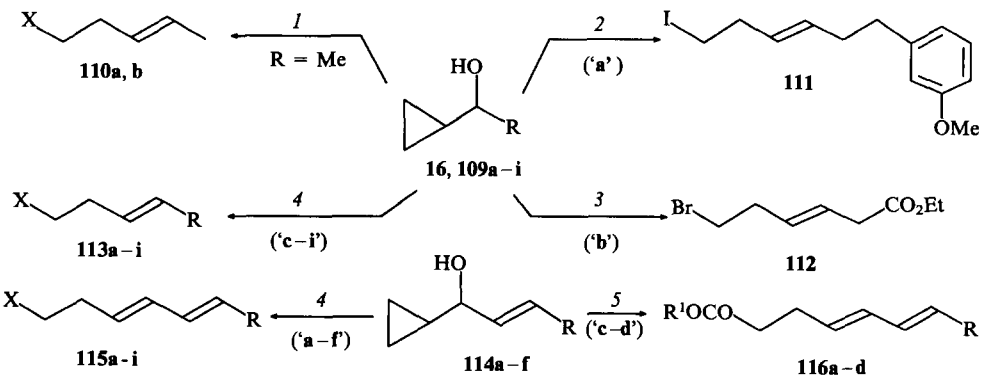
The homoallyl bromides **117**, which are stereochemically inhomogeneous as regards the trisubstituted C=C bond, have nevertheless found practical applications in the synthesis of various natural products, predominantly of the isoprenoid series.

The cyclopropylcarbinyl rearrangement of alcohols **49** proceeds almost always with high yields and without complications and for this reason only certain features of this reaction are noted below. Thus the formation of up to 14% of the olefin hydrobromination product **117a** has been noted in the isomerisation of compound **49a**.[111] The conversion of the homoallyl alcohol **49k** is partly (~15%) accompanied by a shift of the terminal double bond of the product **117k** with formation of a conjugated diene.[131]

Scheme 28 presents other versions of the procedure for carrying out the cyclopropylcarbinyl rearrangement of tertiary carbinols **49** different from that in the standard Julia method. Thus the unusual LiBr/TsOH/AcOH/Ac_2O system has been used to obtain the 3,5-dienyl bromide **117h** without explanation of its advantage over 48% HBr.[130] As in the case of secondary cyclopropylcarbinols, the tertiary carbinols rearrange smoothly and almost quantitatively under the influence of $MgBr_2$ and MgI_2 to the corresponding homoallyl halides **117** with the (*E*)-isomer predominating in the case of compound **117b**.[112]

The use of aqueous HCl to convert cyclopropylcarbinol into homoallyl chlorides is characterised by the absence of regioselectivity. Thus in the four instances of this reaction, only one, leading to the homoprenyl chloride **118a**, can be regarded as unambiguous.[106] Apart from the expected olefins **118e, r, u**, in the remaining three cases the corresponding dienes and their hydrochlorination products as well as the corresponding cyclobutyl chlorides were detected.[124,139,258]

Scheme 26



16: R = Me;

109: R = *m*-$MeOC_6H_4(CH_2)_2$ (**a**), CH_2CO_2Et (**b**), Et (**c**), Bu^n (**d**), n-C_8H_{17} (**e**), n-$C_{10}H_{21}$ (**f**), (*E*)-$Bu^nCH=CH(CH_2)_4$ (**g**), (*Z*)-$Bu^nCH=CH(CH_2)_8$ (**h**), $HO(CH_2)_3$ (**i**);

110: X = Br (**a**), I (**b**);
X = Cl: R = Bu^n (**a**), n-C_8H_{17} (**b**);
X = Br: R = Et (**c**), Bu^n (**d**), n-C_8H_{17} (**e**), n-$C_{10}H_{21}$ (**f**), (*E*)-$Bu^nCH=CH(CH_2)_4$ (**g**), (*Z*)-$Bu^nCH=CH(CH_2)_8$ (**h**), $HO(CH_2)_3$ (**i**);

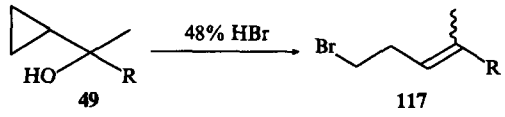
114: R = Et (**a**), Pr^i (**b**), Bu^n (**c**), n-C_8H_{17} (**d**), (*E*)-MeCH=CH (**e**), (*Z*)-$Bu^nCH=CH(CH_2)_3$ (**f**);

115: X = Cl: R = Pr^i (**a**), Bu^n (**b**), n-C_8H_{17} (**c**), (*E*)-MeCH=CH (**d**);
X = Br: R = Et (**e**), Pr^i (**f**), Bu^n (**g**), n-C_8H_{17} (**h**), (*Z*)-$Bu^nCH=CH(CH_2)_3$ (**i**);

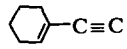
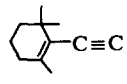
116: R^1 = H: R = Bu^n (**a**), n-C_8H_{17} (**b**);
R^1 = Me: R = Bu^n (**c**), n-C_8H_{17} (**d**);

(*1*) 48% HBr (> 80%), Et_2O·MgX (70% – 90%);
(*2*) 40% HI–DME (75%);
(*3*) 48% HBr/$ZnBr_2$;
(*4*) Me_3SiX/ZnX_2, CH_2Cl_2 (65% – 100%);
(*5*) R^1CO_2H (60% – 90%).

Scheme 27



49 117

No.	R	E / Z	Yield of 117 (%)	Ref.
a	Me	–	75	110, 111, 115
b	Et	3:1	98	117, 118
c	Pr^n	5:2	79	120–122
g	$HO(CH_2)_4$	[a]	87	127
h	$CH_2=CH$	3:1	85	128, 129, 254, 255
i	(*Z*)-MeCH=CH	3:2	90	131
k	$CH_2=CHCH_2$	4:1	78	131–133
l	(*E*)-MeCH=$CH(CH_2)_2$	7:1	67	135
m	$EtMeC=CH(CH_2)_2$	[a]	70	136
o	$Pent^iMeC=CH(CH_2)_2$	[a]	75	136
p	$H(CH_2CMe=CHCH_2)_nCH_2$			
	$n=1$	[a]	83	110, 111, 129, 132, 136
	$n=2$	[a]	84	110, 111, 132, 136
	$n=3$	[a]	61	111
s	Bn	5:1	85	142
u	$HC\equiv C$	1:19	88	128, 129, 144, 145, 256
v	$MeC\equiv C$	1:16	90	131, 257
x		[a]	98	150
y		[a]	96	150
b'	$HC\equiv CCH_2$	4:1	87	131
e'	EtO_2CCH_2	[a]	78	160

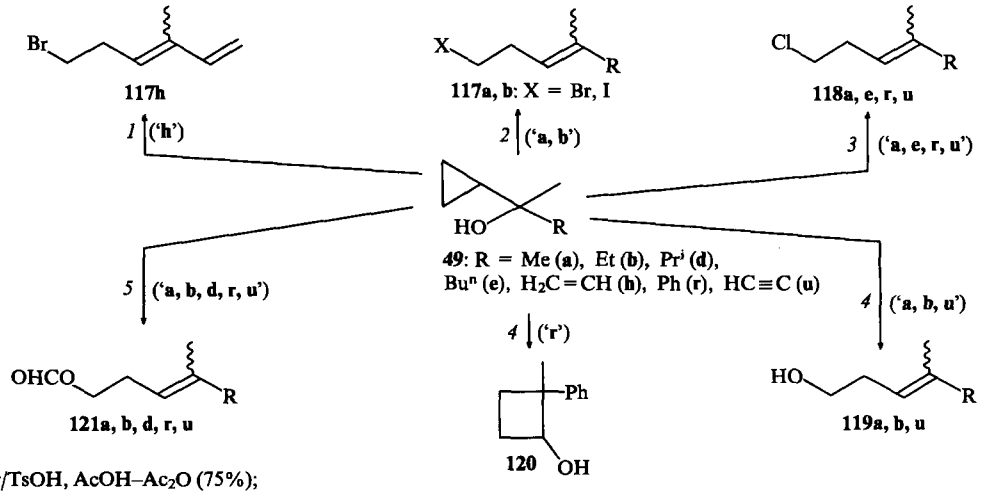
[a] Data on the isomeric composition are not available.

Extremely varied products were obtained when aqueous H_2SO_4 was used for the cyclopropylcarbinyl rearrangement of tertiary alcohols. For example, in the case of compounds **49a, b, u**, mixtures of the homoallyl alcohols **119a, b, u**, together with the products of their dehydration, intramolecular cyclisation, and dimerisation were isolated in low yields.[109, 139, 147] Under the same conditions, the benzyl alcohol **49r** is converted predominantly into cyclobutanol **120**.[139]

The selectivity of the isomerisation of tertiary cyclopropylcarbinols under the influence of HCO_2H depends to a significant extent on the conditions in this reaction. Thus heating of compounds **49a, b, r, u** with 20%–50% aqueous solutions of HCO_2H affords a complex mixture of substances with a low content of the formates **121a, b, r, u**.[108, 116, 140, 258] On the other hand, the use of 98% HCO_2H in THF leads smoothly to the formates **121a, b, d**.[259, 260]

A successful modification of the two-stage synthesis, examined above, of homoallyl halides from cyclopropyl ketones via a stage involving tertiary carbinols consists in the treatment with 50% H_2SO_4 of the alkoxide formed in the reaction between a Grignard reagent and acetylcyclopropane (Scheme 29).

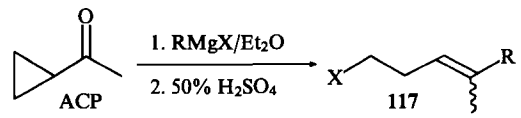
Scheme 28



I

(*1*) LiBr/TsOH, AcOH–Ac_2O (75%);
(*2*) $Et_2O{\cdot}MgX_2$ (~100%);
(*3*) 20%–36% HCl (45%–75%);
(*4*) 10%–50% H_2SO_4 (25%–45%);
(*5*) 20%–98% HCO_2H (40%–60%).

Scheme 29

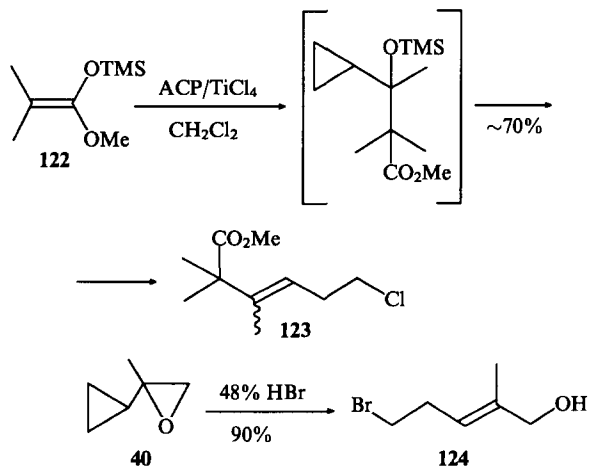


No.	R	X	E/Z	Yield of 117 (%)	Ref.
a	Me	Br	–	88	261
e	Bu^n	Br	4:1	60	262
m	$EtMeC=CH(CH_2)_2$	Br	[a]	62	136
n	$Bu^nMeC=CH(CH_2)_2$	Br	[a]	67	262
o	$Pent^iMeC=CH(CH_2)_2$	Br	7:2	46	136
p	$H(CH_2CMe=CHCH_2)_nCH_2$				
	$n=1$	Br	[a]	77	136
	$n=2$	Br	3:1	60	136
r	$EtMeC=CH(CH_2)_2$	I	[a]	62	136
t	$Pent^iMeC=CH(CH_2)_2$	I	3:1	49	136
w	$H(CH_2CMe=CHCH_2)_nCH_2$				
	$n=1$	I	7:2	72	136, 263
	$n=2$	I	7:2	41	136
z	$MeOCHMe(CH_2)_3$	Cl	3:1	61	264

[a] Data on the isomeric composition are not available.

A large number of halides **117**, used in the synthesis of pheromones, juvenile hormones, and other biologically active substances, have been synthesised by this single-stage method. Yet another example of the cyclopropylcarbinyl rearrangement without the isolation of the intermediate tertiary alcohol consists in the $TiCl_4$-initiated condensation of acetylcyclopropane with the ketene acetal **122**, which leads smoothly to a mixture of the stereoisomeric homoallyl chlorides **123** (Scheme 30).[265]

Scheme 30

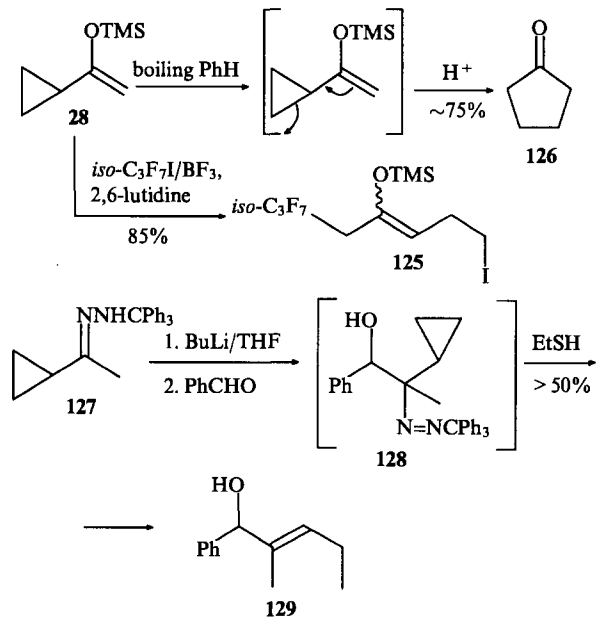


In conclusion, mention should be made of the isomerisation of the epoxide **40**, which takes place in accordance with the mechanism of the cyclopropylcarbinyl rearrangement under the influence of 48% HBr and is distinguished by a high stereoselectivity [> 96% of the (*E*)-isomer] and affords an almost quantitative yield of the bromohydrin **124**.[93]

c. Other reactions with participation of the three-membered ring

Individual examples of the involvement of certain derivatives of acetylcyclopropane in reactions via the carbonyl group, which proceed formally with participation of the acetyl and cyclopropane fragments of this molecule, have been described. Thus, treatment of the trimethylsilyl ether **28** with perfluoroisopropyl iodide in the presence of a base and BF_3 leads selectively to a mixture of the isomeric siloxyiodo-derivatives **125** ($Z:E$ = 4:1)[266] (Scheme 31). The reaction apparently proceeds via a radical ion mechanism involving the cyclopropyl-carbinyl rearrangement at an intermediate stage.

Scheme 31



The thermolysis of the enolate **28** induces its rearrangement with ring expansion and the formation of the cyclopentanone **126** in a high yield after the hydrolysis of the intermediate trimethylsilyl ether.[76]

The deprotonation and subsequent treatment with benzaldehyde of the hydrazone **127**, readily obtainable from acetylcyclopropane, afford the intermediate azo-compound **128**, which undergoes under mild conditions the radical homoallyl rearrangement to the (*E*)-olefin **129** with a stereochemical purity of 93%.[52]

Thus the reactions of acetylcyclopropane and its derivatives with participation of the three-membered ring permit convenient and in many instances the most rational synthesis of various acyclic functionalised compounds, including ketones and saturated and unsaturated halides and alcohols.

IV. The use of acetylcyclopropane in the synthesis of natural and practically useful compounds

Some of the reactions of acetylcyclopropane examined above served as a basis for a series of schemes for the specific synthesis of pheromones, terpenoids, steroids, vitamins, prostanoids, alkaloids, as well as medicinal preparations and herbicides.

1. Synthesis of acetogenin pheromones

The use of acetylcyclopropane as the five-carbon (*E*)-fragment served as the basis for the stereoselective synthesis of a whole series of acetogenin transoid pheromones of the insects of the order Lepidoptera. The pheromones, having the structure of (*E*)-homoallyl acetates **130–132**, were obtained in one stage and in high yields from the corresponding bromides **113e, h** and **115h** (Scheme 32).[222,228,229,267]

The synthesis of a large number of other acetogenin pheromones, including alkene (**133**[219–221,223,231,267]), diene (**134**[220,267] and **135**[39,221,223]), as well as triene (**136**[221,222]) representatives has been achieved with the aid of various methods for increasing the length of the carbon–carbon linear chain in the homoallyl halides **110a, 113c, d, i**, and **115h, e, i** (Scheme 33).

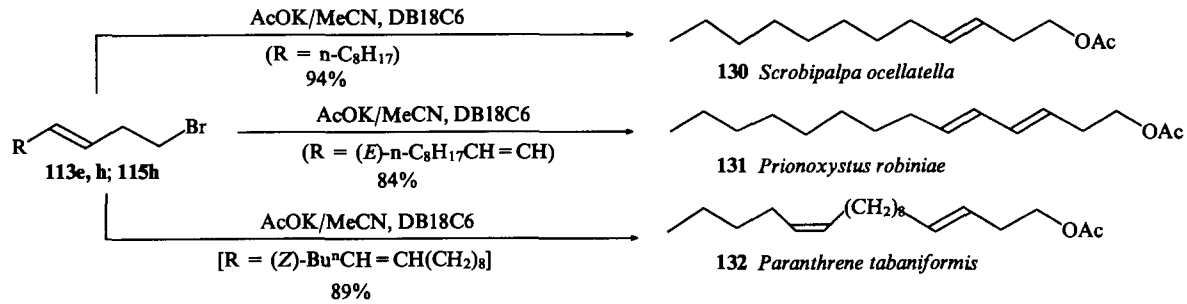
2. Synthesis of terpenoids

The method developed by Julia for the synthesis of homoallyl bromides has served as a key procedure in the synthesis of acyclic terpenoids based on acetylcyclopropane.[35,115,117,120–122,135,145,150,160,256,257,261–264,268]

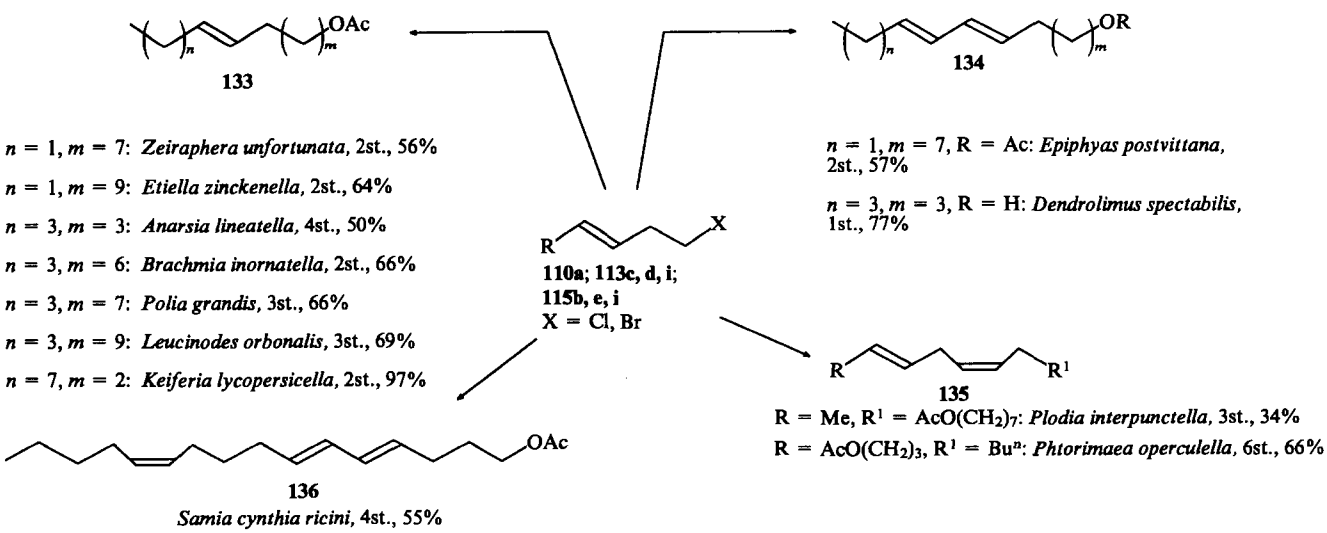
One of the simplest syntheses of linalool **137** includes the metallation of the bromide **117a** and subsequent condensation of the resulting lithio-derivative with methyl vinyl ketone[11] (Scheme 34). In many cases, acetylcyclopropane is introduced into a Grignard reaction with the homoallyl bromide prepared from it; repetition of this operation ensures the successive growth of the linear isoprenoid chain.[110,111,129,132,133,137,262] This simple procedure has been used, in particular, for the synthesis of the (*E*)- and (*Z*)-isomers of homogeraniol **138** (*n* = 1) and homofarnesol **138** (*n* = 2) by the reaction of the Grignard reagents obtained from the bromides **117a** and **117p** (*n* = 1) with acetylcyclopropane and the subsequent cyclopropylcarbinyl rearrangement of the cyclopropylcarbinols formed. The conversion of the bromide **117p** into the corresponding alcohols **138** was carried out by their standard acetolysis and the hydrolysis of the acetates in the final stage.[111]

It is noteworthy that the advantages of this universal method are partly abolished by the absence, already mentioned above, of the stereoselectivity in the rearrangement of the tertiary cyclopropylcarbinols. The syntheses of the racemates of saturated isoprenoids based on acetylcyclopropane are free from this disadvantage.[118,121,122,211,252,262] Thus (±)-5,9-dimethylheptadecane **139**, which is the sex pheromone of the apple leafminer moth *Leucoptera malifoliella*, has been obtained by the cross-coupling of the homoallyl bromide **117n** with pentylmagnesium bromide in the presence of the Cauchy reagent [sic. lithium copper chloride in original paper. (Translator)] and the subsequent hydrogenation of the resulting diene.[262] The bromide **117n** was synthesised for this purpose from acetylcyclopropane and Bu^nMgBr via its C_5-norhomologue **117e** involving two applications of the cyclopropylcarbinyl rearrangement.

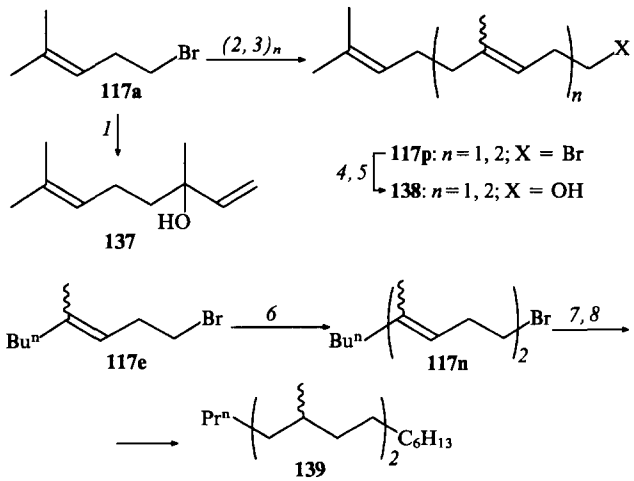
Scheme 32



Scheme 33



Scheme 34



(*1*) Li/Et_2O, then $MeC(O)CH{=}CH_2$ (~20%);
(*2*) Mg, then ACP (55% – 80%);
(*3*) 48% HBr (~80%);
(*4*) AcOK/AcOH;
(*5*) K_2CO_3/MeOH (~75% from **117p**);
(*6*) Mg, then ACP, then 50% H_2SO_4 (~70%);
(*7*) Pe^nMgBr, Li_2CuCl_4/THF;
(*8*) H_2/Pd–C (85% from **117n**).

3. Conversion into steroids, vitamins, and a prostanoid synthon

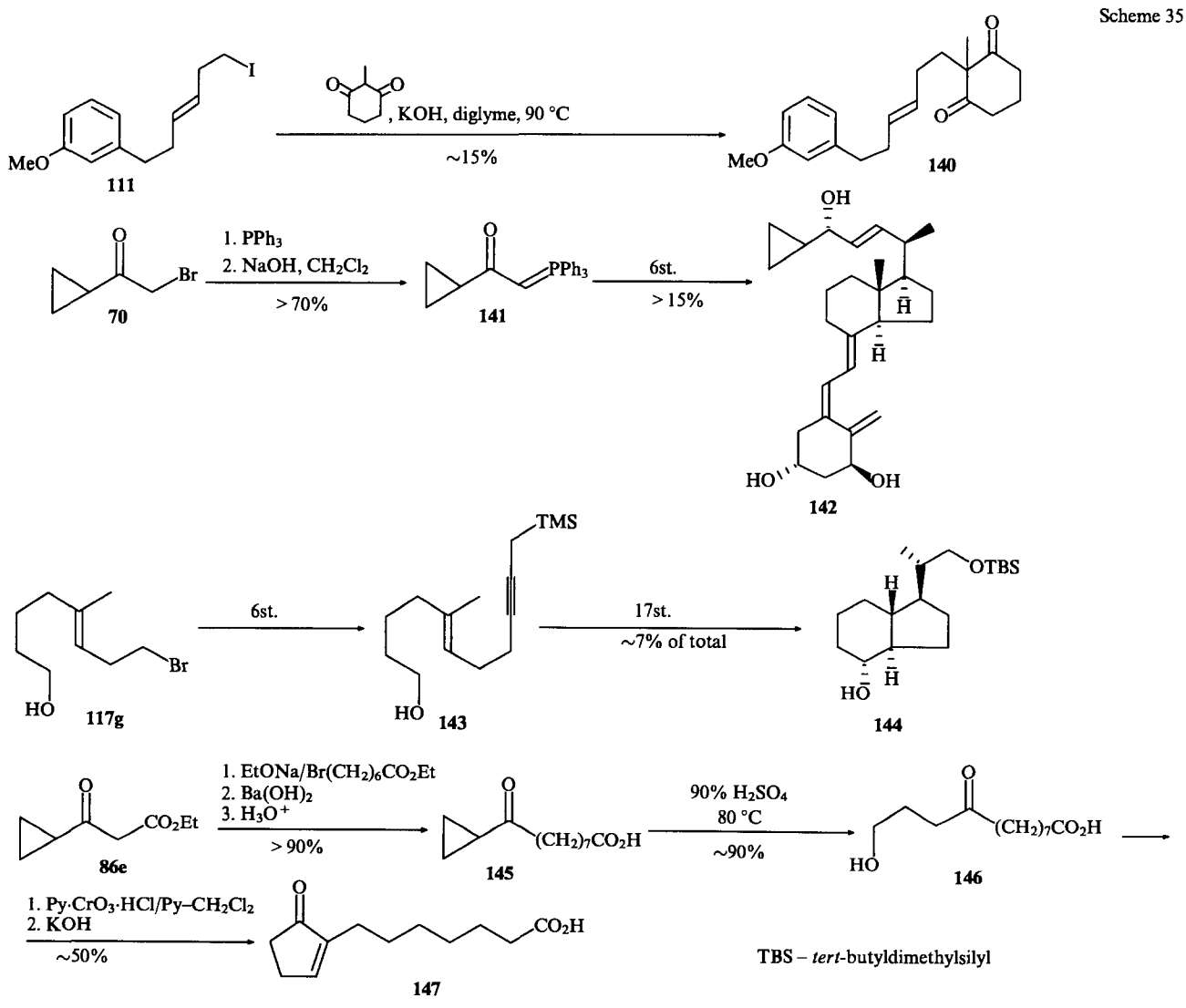
The homoallyl iodide **111**, prepared in three stages from acetylcyclopropane, has been used in the synthesis of D-homodehydrooestranes by Torgov's method. The key stage in this process is the alkylation by the iodide **111** of 2-methylcyclohexane-1,3-dione with formation of the diketone **140** (Scheme 35).[182]

The cyclopropyl analogue of vitamin B **142**, which exhibits a high physiological activity,has been synthesised using in one of the stages the phosphorane **141** prepared from the bromoketone **70**.[184]

The key intermediate **144** in the synthesis of vitamin D_3 was obtained in 25 stages from acetylcyclopropane.[127] The main strategy reduces in this case to the formation in the early stages of the functionalised *trans*-perhydroindan skeleton, which is achieved on the basis of the unsaturated silane **143**, prepared in its turn from the available homallyl bromide **117g**.

The increase in the length of the ketoester **86e** by a six-carbon fragment and the subsequent hydrolytic opening of the cyclopropane residue in the ketone **145** by heating it with concentrated H_2SO_4 lead to the ketol **146**, which is converted by the oxidation and intramolecular condensation of the intermediate ketoaldehyde into the cyclopentenone **147** — a widely used prostanoid synthon.[210]

Scheme 35

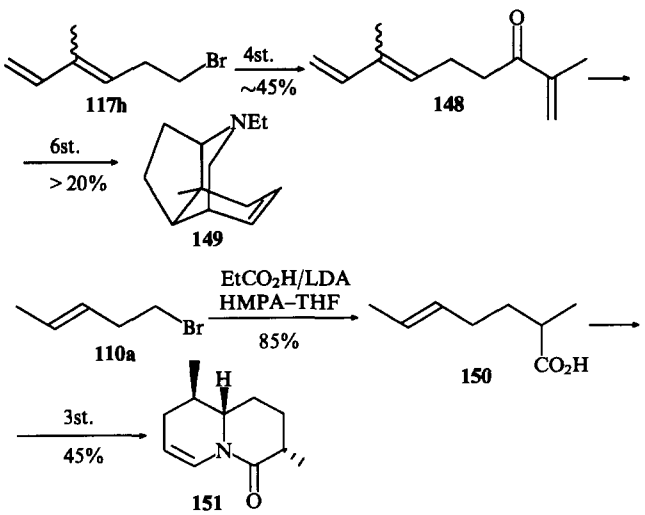


TBS – *tert*-butyldimethylsilyl

4. Synthesis of alkaloid fragments

Acetylcyclopropane has served as the starting compound in the model syntheses of the hexacyclic diterpene alkaloids of the aconitine series and also of tricyclic sesquiterpene alkaloids of the nupharidine type. In the first case, the increase in the length of the carbon chains of the homoallyl bromides **117h** afforded the key trienones **148**, transformed subsequently into the tricyclic aminoalkene **149** (Scheme 36).[254,255] In the second case, alkylation of the dilithio-derivative of propionic acid with the bromide **110a**, readily obtained from acetylcyclopropane, led to the unsaturated acid **150**, which is a key intermediate for conversion into the quinolizidinone **151**.[38]

Scheme 36



5. Synthesis of medicinal preparations and herbicides

A whole series of substances of practical importance have been synthesised from acetylcyclopropane (Schemes 37 and 38).

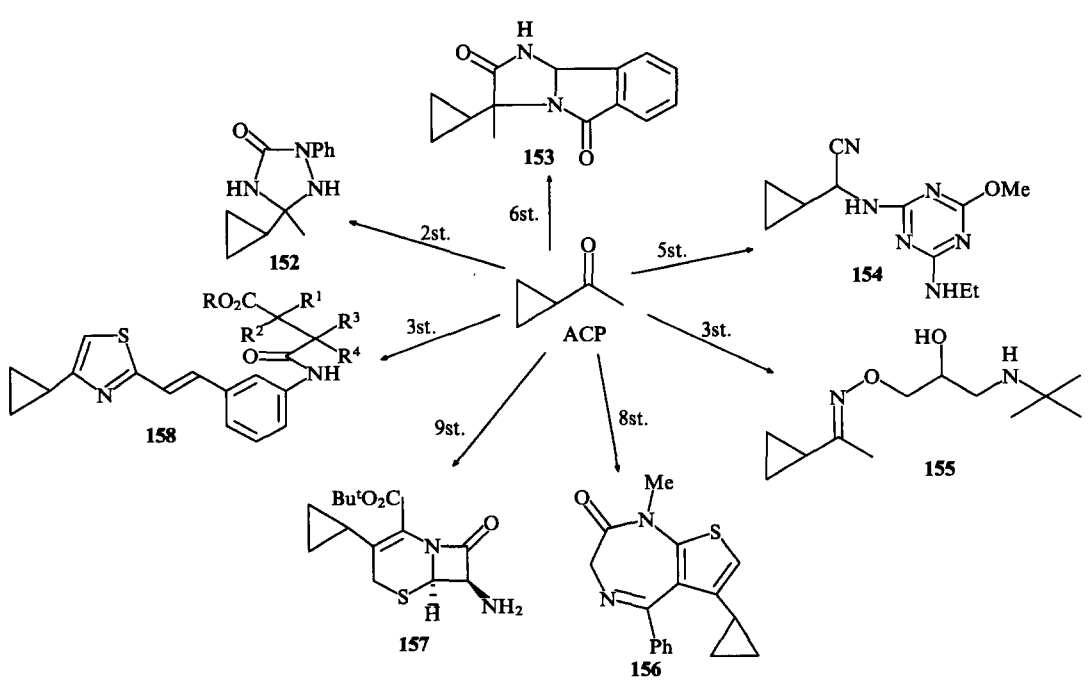
In the first stages of the syntheses of each of compounds **152–164**, the transformations of acetylcyclopropane discussed above were employed. The intermediates used in the syntheses were as follows: acetylcyclopropane hydrazone for the synthesis of compound **152**;[49] the aminonitrile **22** for the syntheses of compounds **153**[56] and **154**;[55] acetylcyclopropane oxime for the synthesis of compound **155**;[46] the vinylnitrile **44b** for the synthesis of compound **156**;[96] the bromoketone **70** for the syntheses of compounds **157**[224] and **158**;[185] the alkoxydiketones **86d, e** for the syntheses of compounds **159a, b**[208] and **160a, b**;[209] the ketoamide **87** for the synthesis of compound **161**;[212] the ketone **83e** for the syntheses of compounds **162**,[205,206] **163**,[203] and **164**.[199]

A high herbicidal activity was found in the polynitrogen heterocyclic representatives **152–154** while the ketoxime **155** was found to possess antiglaucoma activity. The diazepinone **156** exhibits pronounced antitumour properties,. while the azetidinone **157** has bactericidal properties. The thiazole derivatives **158** were found to have antiallergic activity, while the enaminoketones **159a, b** and the isoxazoles **160a, b** showed an analgesic activity. The fluorine-containing isoxazole **161** is recommended as a powerful antiarthritic drug, while the oxazole **162** is recommended as an antiviral agent. Finally, anti-inflammatory properties were found in a derivative of the aminoalcohol **163**, while the substituted pyrrolidines **164** were found to lead to the loss of appetite in dogs.

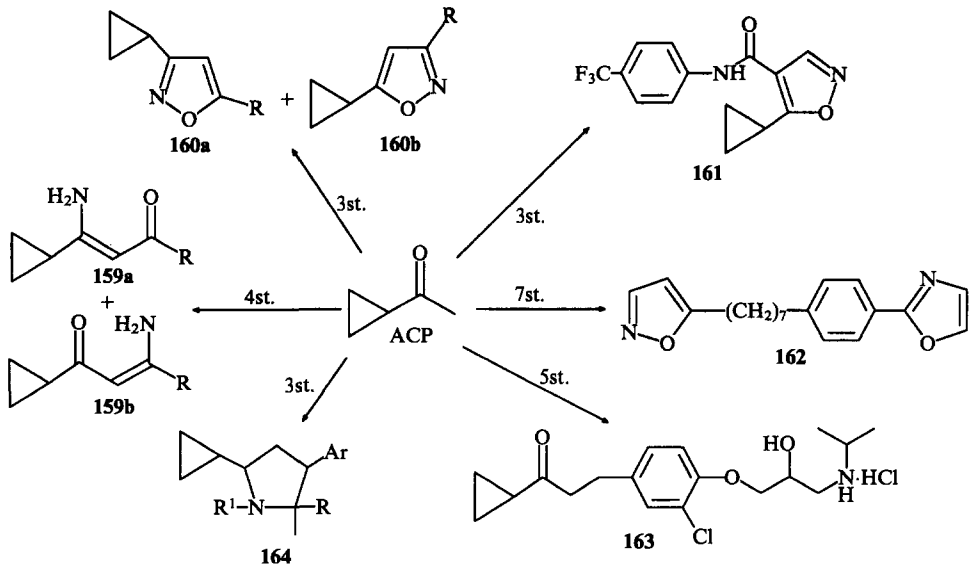
It is noteworthy that all the compounds examined above, with the exception of compound **162**, contain in their structure a three-membered ring, which is transferred from the initial acetylcyclopropane molecule.

The data described in this review illustrate the abundance of the chemical reactions of acetylcyclopropane, characteristic not only of methyl ketones but also of cyclopropylcarbinol derivatives. The possibilities in the selective transformations of acetylcyclopropane with participation of the methyl, carbonyl, or cyclopropyl groups serve as a basis for the extensive synthetic use of this commercially readily available C_5 building block. There is no doubt that this application will develop vigorously.

Scheme 37



Scheme 38



References

1. P C Freer, W H Perkin, Jr *J. Chem. Soc.* **51** 820 (1887)
2. A P Meshcheryakov, V G Glukhovtsev *Izv. Akad. Nauk SSSR, Otd. Khim. Nauk* 1490 (1959)
3. N Kizhner, V Klavikordov *Zh. Russ. Fiz.-Khim. O-va* **43** 595 (1911)
4. V A Slabey, P H Wise *Natl. Advis. Comm. Aeronaut. Tech. Note* 2398 22 (1951); *Chem. Abstr.* **46** 5535 (1952)
5. P Bruylants *Bull. Soc. Chim. Belg.* **36** 519 (1927)
6. Ya M Slobodin, N A Selezneva *Zh. Obshch. Khim.* **23** 886 (1953)
7. A G Rakhimkulov, I M Kolesnikov, V A Poteryakhin *Zh. Prikl. Khim.* **55** 1902 (1982)
8. N I Shuikin, I F Bel'skii, R A Karakhanov *Dokl. Akad. Nauk SSSR* **125** 1051 (1959)
9. D M A Armitage, C L Wilson *J. Am. Chem. Soc.* **81** 2437 (1959)
10. Ch Sh Kadyrov *Uzb. Khim. Zh.* **3** 83 (1962)
11. O M Nefedov, V M Shostakovskii, I E Dolgii, I K Anikeev, V N Pavlychev, Yu M Luchko *Izv. Akad. Nauk SSSR, Ser. Khim.* 234 (1978)
12. O M Nefedov, V M Shostakovskii, I E Dolgii, V S Fedorov, O A Ktatorov, M F Sisin, M A Volkova, V N Pavlychev, V S Asmolov, USSR P. 591 451 (5.2.78); *Byull. Izobret.* **5** 72 (1978); O M Nefedov, I E Dolgii, V M Shostakovskii, M F Sisin, USSR P. 663 694; *Byull. Izobret.* **19** 80 (1979)
13. V A Poteryakhin, V F Sabitova, V N Pavlychev, A I Yudaev, A G Rakhimkulov, USSR P. 642 289 (15.1.79); *Byull. Izobret.* **2** 95 (1979)
14. T E Londergan, N L Hause, W R Schmitz *J. Am. Chem. Soc.* **75** 4456 (1953)
15. V S Asmolov, G Kh Yamilova, V M Shostakovskii, R A Karakhanov, O M Nefedov, USSR P. 584 006 (15.12.77); *Byull. Izobret.* **46** 55 (1977)
16. J D Butler, R D Laundon *J. Chem. Soc. C* 173 (1969)
17. M Asaoka, K Miyake, H Takey *Chem. Lett.* 1149 (1975)
18. S Takei, Y Kawano *Tetrahedron Lett.* **16** 4389 (1975)
19. T Saburo, K Yasuhito, Jpn. P. 76 105 037 (17.9.76); *Chem. Abstr.* **86** 550 55c (1977)
20. W Weber, A de Meijere *Synth. Commun.* **16** 837 (1986)
21. J M Denis, C Girard, J M Conia *Synthesis* **10** 549 (1972)
22. H Kanai, N Hiraki, S Iida *Bull. Chem. Soc. Jpn.* **56** 1025 (1983)
23. M Mitani, Y Yamamoto, K Koyama *J. Chem. Soc., Chem. Commun.* 1446 (1983)
24. M Grignon-Dubois, J Dunogues *Synthesis* **11** 737 (1976)
25. E Proksch, A de Meijere *Angew. Chem.* **88** 802 (1976)
26. H Kanghals, C Ruchardt *Chem. Ber.* **114** 3831 (1981)
27. N Ya Dem'yanov, S A Pinegin *Zh. Russ. Fiz.-Khim. O-va* **43** 510 (1911)
28. V A Slabey, P H Wise *J. Am. Chem. Soc.* **71** 3252 (1949)
29. Ya M Slobodin, I N Shorokh *Zh. Obshch. Khim.* **21** 2001 (1951)
30. B A Kazanskii, M Yu Lukina, L G Sal'nikova *Izv. Akad. Nauk SSSR, Otd. Khim. Nauk* 1401 (1957)
31. L Kh Freidlin, A P Meshcheryakov, V I Gorshkov, V G Glukhovtsev *Izv. Akad. Nauk SSSR, Otd. Khim. Nauk* 2237 (1959)
32. L Kh Freidlin, V I Gorshkov *Dokl. Akad. Nauk SSSR* **131** 1109 (1960)
33. J Schibata, T Yoshida, A Baba, H Matsuda *Chem. Lett.* 307 (1991)
34. R Van Volkenburgh, K W Greenlee, J M Derfer, C E Boord *J. Am. Chem. Soc.* **71** 3595 (1949)
35. W Biernacki, W Sobotka *Rocz. Chem.* **51** 469 (1977)
36. R M Coates, P D Senter, W R Baker *J. Org. Chem.* **47** 3597 (1982)
37. R T Hrubiec, M B Smith *J. Org. Chem.* **49** 431 (1984)
38. Y C Hwang, F W Fowler *J. Org. Chem.* **50** 2719 (1985)
39. E D Matveeva, A L Kurts, A V Blokhin *Bioorg. Khim.* **14** 839 (1988)
40. M Julia, S Julia, S-Y Tchen *Bull. Soc. Chim. Fr.* 1849 (1961)
41. E Keinan, E K Hafeli, K K Seth, R Lamed *J. Am. Chem. Soc.* **108** 162 (1986)
42. C Hansch, J-P Bjorkroth *J. Org. Chem.* **51** 5461 (1986)
43. G-J Shen, Y-F Wang, C Bradshaw, C-H Wong *J. Chem. Soc., Chem. Commun.* 677 (1990)
44. M M Midland, J I McLoughlin *J. Org. Chem.* **49** 1316 (1984)
45. Ya M Slobodin, I N Shorokh *Zh. Obshch. Khim.* **2** 208 (1952)
46. G Leclers, M Bouzoubaa, G Andermann, G de Burlet, C Cannet, J Himber, P. 87 378 (31.8.83); *Chem. Abstr.* **100** 5849b (1984)
47. C H Herr, F C Whitmore, R W Schiessler *J. Am. Chem. Soc.* **67** 2061 (1945)
48. R van Volkenburgh, K W Greenlee, J M Derfer, C E Boord *J. Am. Chem. Soc.* **71** 172 (1949)
49. P Wirth, V Schmied-Kowarzik, P Weinhold, D Gudel, German P. 2921307 (29.11.79); *Chem. Abstr.* **92** 128 933y (1980)
50. D G Mislankar, B Mugrage, S D Darling *Tetrahedron Lett.* **22** 4619 (1981)
51. W A Harrmann, C Weber, M L Ziegler, C Pahl *Chem. Ber.* **117** 875 (1984)
52. J E Baldwin, R M Adlington, J C Bottaro, J N Kohle, J M Newington, M W D Perry *Tetrahedron* **42** 4235 (1986)
53. M W Maichrzak, M Bekhazi, I Tse-Sheepy, J Warkentin *J. Org. Chem.* **54** 1842 (1989)
54. P S Engel, A M Culotta *J. Am. Chem. Soc.* **113** 2686 (1991)
55. M Kuchne, C Vogel, US P. 3 766 182 (16.10.73); *Chem. Abstr.* **80** 70 847g (1974)
56. M Los, US P. 4 041 045 (9.8.77); *Chem. Abstr.* **87** 168034j (1977)
57. W Kampe, M Thiel, E Fauland, U Bucker, G Hebold, German P. 2 656 240 (15.6.78); *Chem. Abstr.* **89** 109 037f (1978)
58. B U Minbaev, S O Mataeva, B D Abiyurov *Zh. Obshch. Khim.* **60** 1070 (1990)
59. W Coppens, N Schamp *Bull. Soc. Chim. Belg.* **8** 643 (1972)
60. G Schulz, W Steglich *Angew. Chem.* **89** 255 (1977)

61. V V Zamkova, B U Minbaev, A E Lyuts, S O Mataeva, Z M Muldakhmetov *Izv. Akad. Nauk Kaz. SSR, Ser. Khim.* **3** 30 (1990)
62. B U Minbaev, S O Mataeva, V M Shostakovskii, Z M Muldakhmetov *Dokl. Akad. Nauk SSSR* **311** 878 (1990)
63. B U Minbaev, S O Mataeva, V M Shostakovskii *Zh. Org. Khim.* **26** 545 (1990)
64. D Pocar, R Stradi, P Trimarco *Tetrahedron* **31** 2427 (1975)
65. R Carlson, L Nilsson, C Rappe, A Babadjamian, J Metzger *Acta Chem. Scand., Ser. B* **32** 85 (1978)
66. P M Adrov, V N Yandovskii, V N Borodin, M I Komendantov, N I Shenberg *Zh. Org. Khim.* **12** 1827 (1976)
67. V N Yandovskii, P M Adrov, M I Komendantov, N I Shenberg, USSR P. 546 606 (15.2.77); *Byull. Izobret.* **6** 72 (1977)
68. N D Zelinsky, E F Dengin *Ber. D. Chem. Ges.* **55** 3354 (1922)
69. K Weinges, H Blackholm *Chem. Ber.* **113** 3098 (1980)
70. R C Elderfield, J R McCarthy *J. Am. Chem. Soc.* **73** 975 (1951)
71. R A Olafson, J Cuomo, B A Bauman *J. Org. Chem.* **43** 2073 (1978)
72. P A Grieco, Y J Ohfune *J. Org. Chem.* **43** 2720 (1978)
73. L Fitjer, J-M Conia *Angew. Chem.* **85** 347 (1973)
74. C A Brown *J. Org. Chem.* **39** 3913 (1974)
75. R Pi, T Friedl, P R von Schleyer, P Klusener, L Brandsma *J. Org. Chem.* **52** 4299 (1987)
76. S A Monti, F G Cowherd, T W McAninch *J. Org. Chem.* **40** 858 (1975)
77. P Amice, L Blanco, J-M Conia *Synthesis* **3** 196 (1976)
78. L Blanco, P Amice, J-M Conia *Synthesis* **4** 291 (1981)
79. A Hofland, H Steinberg, T J de Boer *Recl. Trav. Chim. Pays-Bas* **104** (12) 350 (1985)
80. E Taskinen *Acta Chem. Scand., Ser. B* **28** 357 (1974)
81. N A Donskaya, T V Akachinskaya, Yu S Shabarov *Zh. Org. Khim.* **12** 1596 (1976)
82. G Rousseau, P Le Perchec, J-M.Conia *Tetrahedron* **32** 2533 (1976)
83. G Rousseau, P Le Perchec, J-M Conia *Tetrahedron Lett.* **18** 45 (1977)
84. G Rousseau, P Le Perchec, J-M.Conia *Tetrahedron Lett.* **18** 2517 (1977)
85. T V Akhachinskaya, M Bakhbukh, Yu K Grishin, N A Donskaya, Yu A Ustynyuk *Zh. Org. Khim.* **14** 2317 (1978)
86. G Rousseau, P Le Perchec, J-M Conia *Tetrahedron* **34** 3475 (1978)
87. G Rousseau, P Le Perchec, J-M Conia *Tetrahedron* **34** 3483 (1978)
88. D Craig, S V Ley, N S Simpkins, G H Whitham, M J Prior *J. Chem. Soc., Perkin Trans. 1* 1949 (1985)
89. J B Ousset, C Mioskowski, G Solladie *Synth. Commun.* **13** 1193 (1983)
90. J B Ousset, C Mioskowski, G Solladie *Tetrahedron Lett.* **24** 4419 (1983)
91. I E Dolgii, I B Shvedova, USSR P. 1 212 007 (7.12.87); *Byull. Izobret.* **45** 253 (1987)
92. P Coutrot, P Savignac *Synthesis* 34 (1978)
93. H Nakamura, H Yamamoto, H Nozaki *Tetrahedron Lett.* **14** 111 (1973)
94. B M Trost, M J Bogdanowicz *J. Am. Chem. Soc.* **95** 5321 (1973)
95. M J Curry, D R Stevens *J. Chem. Soc., Perkin Trans. 2* 1391 (1980)
96. R Beetzsen, K Lamprecht, R Beetzjun, U Heidrich, W Timpe, J Siegfried, German P. 2 813 996 (5.10.78); *Chem. Abstr.* **90** 6430v (1979)
97. T P Surikova, V D Zakharova, S S Molchanov, Yu S Shabarov *Khim. Geterotsikl. Soedin.* 1045 (1988)
98. A J Bellamy, J B Kerr *Acta Chem. Scand., Ser. B* **33** (5) 370 (1979)
99. O A Svishchuk, M V Sukharenko *Ukr. Khim. Zh.* **41** 462 (1975)
100. H-J Wollweber, C Wentrup *J. Org. Chem.* **50** 2041 (1985)
101. D Hoppe, R Follmann *Chem. Ber.* **109** 3047 (1976)
102. D Hoppe, R Follmann *Chem. Ber.* **109** 3062 (1976)
103. G A Olah, G K S Prakash, G Liang *J. Org. Chem.* **42** 661 (1977)
104. F Z Galin, V K Ignatyuk, S N Lakeev, R G Rakhimov, V S Sultanova, G A Tolstikov *Zh. Org. Khim.* **25** 103 (1989)
105. H O House, W C Liang, P D Weeks *J. Org. Chem.* **39** 3102 (1974)
106. T A Favorskaya, Sh A Fridman *Zh. Obshch. Khim.* **15** 421 (1945)
107. V A Slabey, P H Wise *J. Am. Chem. Soc.* **74** 1473 (1952)
108. T A Favorskaya, N V Shcherbinskaya *Zh. Obshch. Khim.* **23** 1485 (1953)
109. T A Favorskaya, N V Shcherbinskaya, E S Golovacheva *Zh. Obshch. Khim.* **23** 1878 (1953)
110. M Julia, S Julia, R Guegan *C.R. Acad. Sci.* **248** 820 (1959)
111. M Julia, S Julia, R Guegan *Bull. Soc. Chim. Fr.* **6** 1072 (1960)
112. J P McCormick, D L Barton *J. Chem. Soc., Chem. Commun.* 303 (1975)
113. P C Traas, H Boelens, H J Takken *Recl. Trav. Chim.* **95** (3) 57 (1976)
114. N I Yakushkina, L F Germanova, V D Klebanova, L I Leonova, I G Bolesov *Zh. Org. Khim.* **12** 2141 (1976)
115. G Buchbauer *Monatsh. Chem.* **109** 289 (1978)
116. T A Favorskaya, N V Shcherbinskaya *Zh. Obshch. Khim.* **23** 1667 (1953)
117. J P Kutney, M J McGrath, R N Young, B R Worth *Can. J. Chem.* **57** 3145 (1979)
118. P L Guss, J H Timlinson, P E Sonnet, A T Proveaux, US P. 408 569 (1.4.83); *Chem. Abstr.* **99** 87 906r (1983)
119. A G Bessmertnykh, Yu N Bubnov, T I Voevodskaya, N A Donskaya, A Yu Zykov *Zh. Org. Khim.* **26** 2348 (1990)
120. V G Kovalev, A Kh Khusid, V P Konyukhov, S F Nedopekina, Ya L Neimark *Zh. Org. Khim.* **11** 1183 (1975)
121. P L Guss, J H Timlinson, P E Sonnet, J R McLaughlin, US P. 461 299 (17.4.84); *Chem. Abstr.* **101** 23 207r (1984)
122. T Chuman, P L Guss, R E Doolittle, J R McLaughlin, J H Timlinson, US P. 207 591 (1.1.89); *Chem. Abstr.* **111** 169 400b (1989)
123. V A Slabey *J. Am. Chem. Soc.* **74** 4963 (1952)
124. T A Favorskaya, T N Gulyaev, E S Golovacheva *Zh. Obshch. Khim.* **23** 2014 (1953)
125. S C Bunce *J. Am. Chem. Soc.* **77** 6616 (1955)
126. A P Meshcheryakov, V G Glukhovtsev *Izv. Akad. Nauk SSSR, Otd. Khim. Nauk* 780 (1958); 176 (1962); O M Nefedov, V G Glukhovtsev, S V Zakharova, A Ya Shteinshneider, R N Shafran *Izv. Akad. Nauk SSSR, Ser. Khim.* 896 (1972)
127. S Hatakeyama, H Numata, K Osanai *J. Chem. Soc., Chem. Commun.* 1893 (1989)
128. M Julia, S Julia, D Stalla-Bourdillon *C.R. Acad. Sci.* **253** 951 (1961)
129. M Julia, S Julia, D Stalla-Bourdillon, C Descoins *Bull. Soc. Chim. Fr.* **10** 2533 (1964)
130. J H Babler, H J Coghlan, D J Giacherio *J. Org. Chem.* **42** 2172 (1977)
131. M Julia, C Descoins, C Risse *Tetrahedron Suppl. Pt II* **8** 443 (1966)
132. O A Svishchuk, M N Vysotskii, S L Grinberg *Ukr. Khim. Zh.* **41** 846 (1975)
133. W Biernacki, W Sobotka *Rocz. Chem.* **51** 1105 (1977)
134. M J Curry, D R Stevens *J. Chem. Soc., Perkin Trans. 1* 1756 (1980)
135. W Biernacki, W Sobotka *Rocz. Chem.* **51** 2369 (1977)
136. W Biernacki, A Gdula *Synthesis* 37 (1979)
137. W Biernacki, W Sobotka *Rocz. Chem.* **51** 979 (1977)
138. S S Hall, F J McEnroe *J. Org. Chem.* **40** 271 (1975)
139. T A Favorskaya, Sh A Fridman *Zh. Obshch. Khim.* **20** 581 (1950)
140. T A Favorskaya, N V Shcherbinskaya, S E Chernobel'skaya *Zh. Obshch. Khim.* **20** 855 (1950)
141. A P Molchanov, R R Kostikov *Zh. Org. Khim.* **20** 2118 (1984)
142. M E Krafft *Tetrahedron Lett.* **30** 539 (1989)
143. Y Ito, K Kobajashi, T Saegusa *Chem. Lett.* 1563 (1980)
144. M Julia, C Descoins *Bull. Soc. Chim. Fr.* 1933 (1962)
145. E D Morgan, L D Thompson *J. Chem. Soc., Perkin Trans. 1* 399 (1985)
146. A P Golovchanskaya *Zh. Obshch. Khim.* **11** 608 (1941)
147. T A Favorskaya, L S Bresler *Zh. Obshch. Khim.* **27** 1179 (1957)
148. A A Gevorkyan, A S Melikyan, P I Kazaryan, S V Avakyan *Arm. Khim. Zh.* **30** 791 (1977)
149. O M Nefedov, I E Dolgii, I B Shvedova, E A Baidzhigitova *Izv. Akad. Nauk SSSR, Ser. Khim.* 1339 (1978); K N Shavrin, I V Krylova, G P Okonnishnikova, I E Dolgy, O M Nefedov *J. Chem. Soc., Perkin Trans. 2* 1875 (1991)
150. M Julia, C Descoins *Bull. Soc. Chim. Fr.* 1939 (1962)
151. T A Favorskaya, K A Kononova, M I Titov *Zh. Obshch. Khim.* **29** 2894 (1959)
152. J N Denis, S Desauvage, L Hevesi, A Krief *Tetrahedron Lett.* **22** 4009 (1981)
153. R J Israel, R K Murray *J. Org. Chem.* **50** 1573 (1985)
154. N H Andersen, A D Denniston, D A McCrae *J. Org. Chem.* **47** 1145 (1982)
155. P Entmayer, G Kobrich *Chem. Ber.* **109** 2175 (1976)
156. T Nakai, H Shiono, M Okawara *Tetrahedron Lett.* **16** 4027 (1975)

157. R Harms, U Schollkopf, M Muramatsu *Liebigs Ann. Chem.* 1194 (1978)
158. D Hoppe, R Follmann, L Beckmann *Liebigs Ann. Chem.* 1765 (1980)
159. F G Saitkulova, G G Abashev, I I Lapkin *Izv. Vyssh. Uchebn. Zaved., Khim. Khim. Tekhnol.* **16** 1458 (1973)
160. O A Svishchuk, K D Basalkevich, M M Vysotskii *Ukr. Khim. Zh.* **41** 216 (1975)
161. T Imamoto, T Takeyama, H Koto *Tetrahedron Lett.* **27** 3243 (1986)
162. U M Dzhemilev, R I Khusnutdinov, V A Dokichev, S I Lomakina, L M Khalilov, G A Tolstikov, O M Nefedov *Izv. Akad. Nauk SSSR, Ser. Khim.* 2071 (1981)
163. J-M Pons, M Santelli *J. Org. Chem.* **54** 877 (1989)
164. J E McMurry *Acc. Chem. Res.* **7** 281 (1974)
165. E V Dehmlow, A Eulenberger *Liebigs Ann. Chem.* 1112 (1979)
166. W D Emmons, G B Lucas *J. Am. Chem. Soc.* **78** 2287 (1955)
167. S L Friess *J. Am. Chem. Soc.* **71** 14 (1949)
168. J E Phodes, L Vargas *J. Org. Chem.* **38** 4077 (1973)
169. S C Bunce, J B Cloke *J. Am. Chem. Soc.* **76** 2244 (1954)
170. L E Fikes, H Shechter *Tetrahedron Lett.* **17** 2525 (1976)
171. L E Fikes, H Shechter *J. Org. Chem.* **44** 74 (1979)
172. D Paquer, J Vialle *C.R. Acad. Sci.* **274** 1846 (1972)
173. C Fournier, D Paquer, M Vazeux *Bull. Soc. Chim. Fr. Pt 2* 2753 (1975)
174. M Hanack, T Bassler *J. Am. Chem. Soc.* **91** 2117 (1969)
175. C E Hudson, N L Bauld *J. Am. Chem. Soc.* **94** 1158 (1972)
176. W Schoberth, M Hanack *Synthesis* **12** 703 (1972)
177. I E Dolgii, I B Shvedova, K N Shavrin, USSR P. 555 079 (25.4.77); *Byull. Izobret.* **15** 65 (1977)
178. I E Dolgii, K N Shavrin, O M Nefedov *Izv. Akad. Nauk SSSR, Ser. Khim.* 135 (1987)
179. I E Dolgii, I B Shvedova, K N Shavrin, O M Nefedov, USSR P. 572 445 (15.9.77); *Byull. Izobret.* **34** 51 (1977); O M Nefedov, I E Dolgii, I B Shvedova, USSR P. 578 293; *Byull. Izobret.* **40** 69 (1977)
180. C W Funke, H Cerfontain *J. Chem. Soc., Perkin Trans. 2* 1902 (1976)
181. N S Hussain, T Ravindranathan, B D Tilak *Indian J. Chem., Sect. B* **16** 721 (1978)
182. V K Jinaraj, Z Muljiani, T Ravindranathan, B D Tilak *Ind. J. Chem., Sect. B* **22** 841 (1983)
183. M C Pirrung, G M McGeehan *Angew. Chem.* **97** 1074 (1985)
184. M J Calverley *Tetrahedron* **43** 4609 (1987)
185. G F Field, J R Vermeuler, W J Zally, Eur. P. 355 353 (28.2.90); *Chem. Abstr.* **113** 172 006z (1990)
186. C Rappe, R Gustafsson *Acta Chem. Scand.* **22** 2967 (1968)
187. J S Ladaya, G F Koser *J. Org. Chem.* **53** 210 (1988)
188. G F Koser, A G Relenyi, A N Kolas, S Rebrovic, R H Wettach *J. Org. Chem.* **47** 2487 (1982)
189. G F Koser, J S Lodaya, D G Ray *J. Am. Chem. Soc.* **110** 2987 (1988)
190. I Basnak, J Farkas *Collect. Czech. Chem. Commun.* **40** 1038 (1975)
191. D Laurie, E Lucas, D C Nonhebel, C J Suckling, J C Walton *Tetrahedron* **42** 1035 (1986)
192. P Caubere, J J Brunet *Tetrahedron* **73** 4835 (1972)
193. P Caubere, G Guillaumet *Bull. Soc. Chim. Fr.* 4643 (1972)
194. J L Gras *Tetrahedron Lett.* **19** 2965 (1978)
195. L I Smith, E R Rogier *J. Am. Chem. Soc.* **73** 3840 (1951)
196. A T Nielsen, D W Moore, K Highberg *J. Org. Chem.* **26** 3691 (1961)
197. A D Kaulen, L V Khitrina *Bioorg. Khim.* **15** 1484 (1989)
198. S C Bunce, H J Dorsman, F D Popp *J. Chem. Soc.* 303 (1963)
199. E Sommerfeld, D von Bezold, P Schutz, W Heusler, German P. 2 446 317 (10.4.78); *Chem. Abstr.* **83** 43183t (1975)
200. G D Diana, W B Hinshaw, US P. 3 878 200 (15.4.75); *Chem. Abstr.* **83** 27 869r (1975)
201. G D Diana, W B Hinshaw, US P. 3 891 671 (24.6.75); *Chem. Abstr.* **83** 96 770p (1975)
202. J C Collins, US P. 3 917 718 (4.11.75); *Chem. Abstr.* **84** 30 648u (1976)
203. M Miehe, German P. 2 736 106 (23.2.78); *Chem. Abstr.* **89** 6096v (1978)
204. J C Collins, US P. 4 275 201 (23.6.81); *Chem. Abstr.* **95** 186 875d (1981)
205. G D Diana, Eur. P. 137 242 (17.4.85); *Chem. Abstr.* **103** 141 941q (1985)
206. G D Diana, US P. 4 843 087 (27.6.89); *Chem. Abstr.* **112** 118 810y (1990)
207. G W Cannon, H L Whidden *J. Org. Chem.* **17** 685 (1952)
208. W J Fanshawe, G E Wiegand, L S Crawley, S R Safir, US P. 3 957 805 (18.5.76); *Chem. Abstr.* **85** 143 084w (1976)
209. W J Fanshawe, L S Crawley, S R Safir, G E Wiegand, E C Cooley, US P. 3 997 530 (14.12.76); *Chem. Abstr.* **87** 38 992j (1977)
210. E Wada, T Nakai, M Okawara *Chem. Lett.* 1121 (1977)
211. W Muller-Bore, P Deufel, A Schon, W Hertee, German P. 2 848 095 (14.5.80); *Chem. Abstr.* **93** 132 355z (1980)
212. W T Han, Eur. P. 326 108 (2.8.89); *Chem. Abstr.* **112** 55 842n (1990)
213. N H Al-Jobour, M Y Shandala *J. Heterocycl. Chem.* **17** 941 (1980)
214. R P Mariella, L F A Peterson, R C Ferris *J. Am. Chem. Soc.* **70** 1494 (1948)
215. K Miyano, T Sakasai, H Hamano *Chem. Pharm. Bull.* **26** 2328 (1978)
216. M Regitz, S G Khbeis *Chem. Ber.* **117** 2233 (1984)
217. Y Ito, T Konoike, T Harada, T Saegusa *J. Am. Chem. Soc.* **99** 1487 (1977)
218. M Vaultier, P H Lambert, R Carrie *Bull. Soc. Chim. Fr.* 83 (1986)
219. A M Moiseenkov, B A Czeskis, N M Ivanova, O M Nefedov *Mendeleev Commun.* 13 (1991)
220. B A Czeskis, N M Ivanova, A M Moiseenkov, O M Nefedov *Izv. Akad. Nauk SSSR, Ser. Khim.* 1555 (1991)
221. A M Moiseenkov, B A Czeskis, N M Ivanova, O M Nefedov *J. Chem. Soc., Perkin Trans. 1* 2639 (1991)
222. N M Ivanova, B A Czeskis, A M Moiseenkov, O M Nefedov *Izv. Akad. Nauk SSSR, Ser. Khim.* 2521 (1991)
223. N M Ivanova, B A Czeskis, A M Moiseenkov, O M Nefedov *Izv. Akad. Nauk SSSR, Ser. Khim.* 2362 (1992)
224. M J B Pearson, G B P Burton, S C M Fell, Eur. P. 354 757 (14.2.90); *Chem. Abstr.* **113** 191954l (1990)
225. M A Ibragimov, V A Smit, M I Lazareva *Izv. Akad. Nauk SSSR, Ser. Khim.* 2177 (1982)
226. M A Ibragimov, V A Smit, M I Lazareva *Izv. Akad. Nauk SSSR, Ser. Khim.* 392 (1985)
227. N M Ivanova, B A Czeskis, A M Moiseenkov, O M Nefedov *Izv. Akad. Nauk SSSR, Ser. Khim.* 225 (1990)
228. B A Czeskis, N M Ivanova, A M Moiseenkov, O M Nefedov *Izv. Akad. Nauk SSSR, Ser. Khim.* 2025 (1990)
229. A M Moiseenkov, B A Czeskis, N M Ivanova, O M Nefedov *Org. Prep. Proced. Int.* **22** 215 (1990)
230. N M Ivanova, B A Czeskis, E V Rubanova, V G Yatsynin, A M Moiseenkov, O M Nefedov *Izv. Akad. Nauk SSSR, Ser. Khim.* 640 (1991)
231. B A Cheskis, N M Ivanova, A L Il'ichev, A M Moiseenkov, O M Nefedov, USSR P. 1 719 390 (15.3.92); *Byull. Izobret.* **10** 92 (1992)
232. R Fraisse-Jullien, C Frejaville, V Toure *Bull. Soc. Chim. Fr.* 4444 (1968)
233. A L Schultz *J. Org. Chem.* **36** 383 (1971)
234. M V Smirnova, A A Grigor'ev, E V Pinkhasik, V N Pavlychev, V I Zavorodov, T V Kolomnina, USSR P. 1 397 423 (23.5.88); *Byull. Izobret.* **19** 95 (1988)
235. M Pereyre, J-Y Godet *Tetrahedron Lett.* **11** 3653 (1970)
236. J -Y Godet, M Pereyre *Bull. Soc. Chim. Fr., Pt II* 1105 (1976)
237. M Degueil-Castaing, A Rahm, N Dahan *J. Org. Chem.* **51** 1672 (1986)
238. W A Bernett *J. Chem. Educ.* **44** 17 (1967)
239. N A Donskaya, T V Akhachinskaya, T V Leonova, E V Shulishov, Yu S Shabarov *Zh. Org. Khim.* **16** 563 (1980)
240. G T Katvalyan, Doctoral Thesis in Chemical Sciences, Gubkin State Academy of Petroleum and Gas, Moscow, 1991
241. C O Parker, T E Stevens *J. Org. Chem.* **37** 922 (1972)
242. N Di Bello, L Pellacani, P A Tardella *Synthesis* 3 227 (1978)
243. E Giacomini, M A Loreto, L Pellacani, P A Tardella *J. Org. Chem.* **45** 519 (1980)
244. J. N Denis, A Krief *J. Chem. Soc., Chem. Commun.* 229 (1983)
245. R D Miller, D R McKean *J. Org. Chem.* **46** 2412 (1981)
246. R K Dieter, S Pounds *J. Org. Chem.* **47** 3174 (1982)
247. H-J Cristau, Y Beziat, C E Niangoran, H Christol *Synthesis* 648 (1987)
248. A B Smith, R M Scarborough *Tetrahedron Lett.* **19** 1649 (1978)

249. D Wendish, in *Methoden der Organischen Chemie (Houben-Weyl) B. IV/3* (Ed. E Muller) (Stuttgart: Georg Thieme, 1971) p. 415
250. A S Arora, I K Ugi, in *Methoden der Organischen Chemie (Houben-Weyl) B. V/1b* (Ed. E Muller) (Stuttgart: Georg Thieme, 1972) p. 912
251. D Tunemoto, K Kondo *J. Synth. Org. Chem. Jpn.* **35** 1071 (1977)
252. H Wolf, U Matzel, E-J Brunke, E Klein *Tetrahedron Lett.* **20** 2339 (1979)
253. B A Czeskis, N M Ivanova, A M Moiseenkov *Izv. Akad. Nauk SSSR, Ser. Khim.* 853 (1991)
254. K Shishido, K Hiroya, K Fukumoto, T Kametani *Tetrahedron Lett.* **27** 1167 (1986)
255. K Shishido, K Hiroya, K Fukumoto, T Kametani *J. Chem. Res. Synop.* **4** 100 (1989)
256. K Mori, A Sato, M Matsui *Agric. Biol. Chem.* **36** 1931 (1972)
257. K Mori, A Sato, M Matsui *Tetrahedron* **28** 3739 (1972)
258. T A Favorskaya *Zh. Obshch. Khim.* **11** 1246 (1941)
259. A M Moiseenkov, B A Czeskis, O M Nefedov *Synthesis* **10** 932 (1985)
260. B A Czeskis, A M Moiseenkov, O M Nefedov *Dokl. Akad. Nauk SSSR* **289** 637 (1986)
261. G Cahiez, J Rivas-Enterrios, J P Cleri *Tetrahedron Lett.* **29** 3659 (1988)
262. F Rama, L Capuzzi *Synth. Commun.* **19** 1051 (1989)
263. W Biernacki *Pol. J. Chem.* **54** 777 (1980)
264. W Biernacki, A Gdula *Pol. J. Chem.* **55** 1063 (1981)
265. G Wenke, E N Jacobsen, G E Totten, A C Karydas, Y E Rhodes *Synth. Commun.* **13** 449 (1983)
266. K Miura, M Taniguchi, K Nozaki, K Oshima, K Utimoto *Tetrahedron Lett.* **31** 6391 (1990)
267. B A Czeskis, N M Ivanova, A M Moiseenkov, O M Nefedov *Izv. Akad. Nauk SSSR, Ser. Khim.* 2539 (1990)
268. W Biernacki, W Sobotka *Rocz. Chem.* **51** 469 (1977)

Russian Chemical Reviews **62** (4) 359–385 (1993)
© 1993 Russian Academy of Sciences and Turpion Ltd

UDC 547.259+541.138

Redox potentials and electronic structures of organic complexes of ruthenium and rhodium

T V Magdesieva, K P Butin

Contents

I. Introduction 359
II. Theoretical ideas on the structures of transition metal complexes 359
III. Electrochemical properties of ruthenium and rhodium complexes 365

Abstract. The redox properties of mononuclear and polynuclear rhodium and ruthenium complexes are examined. Attention is concentrated on the possible locations of the electronic changes in the redox transitions. The relation between the electrochemical parameters of the complexes and electronic spectroscopic data is traced. Extensive reference data are presented on the oxidation and reduction potentials of mononuclear and polynuclear rhodium and ruthenium complexes. The bibliography includes 133 references.

I. Introduction

Transition metal dinuclear and polynuclear complexes in which the central ions are linked to one another by different bridging ligands (inorganic ligands of the type of CN, SCN, OCN, etc. and organic ligands of the type of polyazabiphenyls and polyazaterphenyls) have been investigated very vigorously during the last decade. This applies particularly to ruthenium(II) compounds, which have proved extremely useful in many applied investigations. Such complexes are employed widely as photoluminescent substances, mediators of photochemical processes,[1, 2] and materials for non-linear optics.[3, 4]

In essence, the polynuclear complexes can be regarded as mononuclear complexes which contain organometallic ligands. For example, in the compound $L_nM^1CN \rightarrow M^2L_n$ one of the ligands is L_nM^1CN. Such ligands are of undoubted interest, since they contain transition metal atoms and tend to undergo redox transitions. In our view, the polynuclear complexes can serve as convenient models for the study of intramolecular electron transfer (charge transfer) processes from the metal (in the above example this is M^2) to the ligand (L_nM^1CN) (MLCT) or from the ligand to the metal (LMCT) both under the conditions of photochemical excitation and in electrochemical or chemical oxidation-reduction reactions.[5, 6]

Complexes of rhodium and ruthenium, the organometallic compounds of which have been investigated most widely, are considered in the present review. The theoretical ideas concerning the structure of transition metal complexes are discussed briefly in the first part within the framework of the molecular orbital method. The redox and spectroscopic properties of mononuclear complexes of ruthenium and rhodium are considered next, since such data are essential for the subsequent analysis of the electronic structures of the polynuclear bridged metal complexes to which the next section is devoted. In conclusion, tables giving compilations of the experimental oxidation and reduction potentials of mononuclear and polynuclear ruthenium and rhodium complexes are presented with an indication of specific experimental conditions (electrode material, solvent, supporting electrolyte, reference electrode) and also of the most probable locations of the electronic changes in the involved molecules of the complexes occurring in redox transitions (in those cases where such assignment to particular locations is possible). We suggest that such data will be useful to a wide range of chemists as regards comparison of the reactivities of these compounds in homogeneous reactions of different nature and not only in electronic processes.

T V Magdesieva, K P Butin Department of Organic Chemistry, Faculty of Chemistry, Lomonosov Moscow State University, Leninskie Gory, 119899 Moscow. Fax (7-095) 939-01 26

Received 4th January 1993
Uspekhi Khimii **62** (4) 387–413 (1993); translated by A K Grzybowski

II. Theoretical ideas on the structures of transition metal complexes

1. The redox levels of the octahedral complexes

The highly symmetrical transition metal complexes with six identical monodentate ligands L, for example $[Co(NH_3)_6]^{3+}$ or $Cr(CO)_6$, have the structure of a regular octahedron. If the metal–ligand bond is formed exclusively by the lone pair of the ligand and the π orbitals are not involved in the bonding, then the perturbation of the nine atomic orbitals (*d*, *s*, *p*) of the metal by the six group orbitals of the L_6 ensemble, having the O_h symmetry, results in the formation of the following energy levels of the complex ML_6 in the octahedral field: six bonding levels (σ), six antibonding levels (σ^*), and three degenerate non-bonding levels (t_{2g}) corresponding to the d_{xy}, d_{yz}, and d_{xz} orbitals of the metal, which are relatively little perturbed as regards energy and form (Fig. 1).[7] In the 18-electron complexes, all the bonding σ orbitals and t_{2g} orbitals are fully occupied. Consequently, in the simplest case, where the ligand is exclusively the donor of the lone pair of electrons and the molecular orbitals of the ligand (for example, π-type orbitals) not involved in bonding have low energies, the redox levels responsible for the oxidation potential (E^{Ox}, Fig. 1*c*) are the t_{2g} levels, which are the highest occupied molecular orbitals (HOMO) of the complex. Since the t_{2g} orbitals are largely located on the metal, it is usual to say that in the oxidation of ML_6 the electronic changes are 'localised on the metal atom'.

The position of the t_{2g} levels depends not only on the nature of the metal and its oxidation state but also on the donor strength of the ligands: if the ligands are strong donors (Fig. 1*a*) then the t_{2g} levels are raised, whilst in the case where they are weak donors (Fig. 1*b*) they are lowered, which is reflected in the oxidation potentials of the complexes.

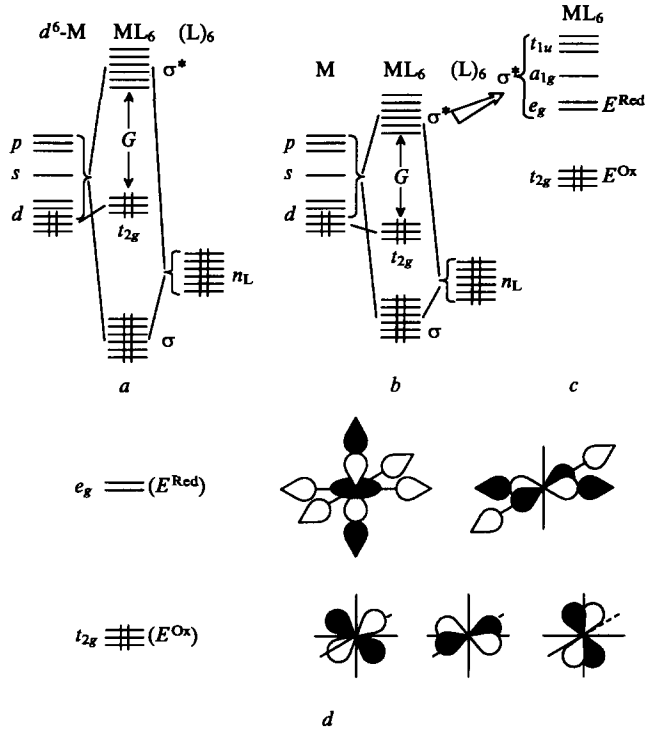


Figure 1. Energy levels of the octahedral complexes: (*a*) strong *n*-donor ligands; (*b*) weak *n*-donor ligands; (*c*) redox levels (t_{2g} and e_g) of the octahedral complex;[7] (*d*) the form of the frontier orbitals of the complex ML_6.

The six antibonding levels of the σ* type are divided into three blocks (Fig. 1*c*): the three degenerate t_{1u} orbitals have the highest energy, the a_{1g} orbital has a lower energy, and the two degenerate e_g levels have the lowest energy. The last levels are the redox levels responsible for the reduction of the complex (E^{Red}, Fig. 1*c*).

The form of the e_g orbitals is such that it is impossible to state *a priori* where the electronic changes during reduction are located: 'on the metal' or 'on the ligand', since, in contrast to the t_{2g} orbitals, the contributions of the ligand orbitals to the e_g levels can be significant. Therefore a special discussion of this problem is necessary in each specific case. The position of the e_g levels depends on the electron-donating capacity of the ligands. If the ligands are strong donors (Fig. 1*a*), then the splitting of the levels into the σ and σ* blocks is much more pronounced than in the case of weak donor ligands (Fig. 1*b*). As a result, the energy gap *G* between the highest occupied (t_{2g}) and lowest unoccupied (e_g) levels in the case of weak donor ligands is smaller than for the ligands with a greater electron-donating capacity. The chemical consequences of the change in the donor strength of the ligands are well known. Thus the octahedral complexes ML_6 with weak donor ligands are thermodynamically less stable and they pass more readily to paramagnetic moderate-spin or high-spin states, absorb light at longer wavelengths, etc. From the standpoint of redox chemistry, the transition from strong to weak ligands is expressed by a decrease in the electrochemical gap *G*,[8-10] defined as the difference between the redox potentials E^{Ox} and E^{Red} of the given compound.

$$ML_6^{\cdot+} \underset{E^{Ox}}{\overset{-\bar{e}}{\rightleftarrows}} ML_6 \underset{E^{Red}}{\overset{+\bar{e}}{\rightleftarrows}} ML_6^{\cdot-},$$

$$G = E^{Ox} - E^{Red}.$$

The quantity *G* is related to the constant for the equilibrium between the 17-electron radical-cation and the 19-electron radical-anion derived from the ML_6 molecule.

$$ML_6^{\cdot+} + ML_6^{\cdot-} \overset{K}{\rightleftarrows} 2ML_6;$$

$$\ln K = -(F/RT)G.$$

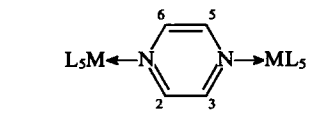
With decrease in *G*, *K* also diminishes, i.e. the equilibrium shifts to the left. This means that the 17-electron radical-cation (RC) and the 19-electron radical-anion (RA) are no longer quite so strongly destabilised relative to the 18-electron neutral complex ML_6 as in the case of compounds with large values of *G*. A complex with a narrow electrochemical gap, particularly in the case where it is uncharged and contains no strongly polar groups, i.e. has a moderate 'absolute electronegativity',[11] should be characterised by a tendency to enter into radical reactions. Similar considerations have been used in the classification of organomercury compounds in terms of their electrochemical potentials.[8]

Since the e_g levels of strong [donor?] ligands lie above those for the weak ligands, their complexes are reduced with a greater difficulty (i.e. the potentials E^{Red} have high negative values) and the 19-electron radical-anions formed, with an unpaired electron and a σ* orbital of the e_g type, are less stable.

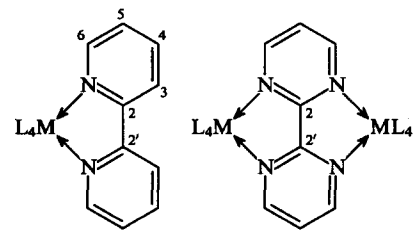
There exists a whole range of experimental evidence concerning the instability of 19-electron radical-anions in the case of strong donor ligands. For example, since CO is a strong *n*-donor, on bombardment with electrons in an argon matrix at −196 °C $Cr(CO)_6$ affords the 17-electron radical-anion $Cr(CO)_5^{\cdot-}$ as the main product,[12] while $Co(NH_3)_6^{3+}$ (NH_3 is a weaker donor than CO) combines with an electron to form the high-spin 19-electron $Co(NH_3)_6^{2+}$ cation, which does not decompose.[13]

2. Bidentate chelating and bridge-forming nitrogen-containing heterocycles

Pyrazine (pz) **1** is a bridge-forming ligand, 2,2′-bipyridyl (bpy) **2** is a chelating ligand, and 2,2′-bipyrimidyl (bpm) **3** is both a bridge-forming and a chelating ligand.



1



2 **3**

These and similar ligands form stable complexes with many transition metals: their structures can be readily modified by introducing various substituents altering the σ-donor and π-acceptor properties of the molecules. An appreciable proportion of the present review is devoted to the description of complexes with precisely these or similar ligands.

In the pyrazine molecule, the two lone pairs of the nitrogen atoms, directed to the opposite sides, interact with one another in such a way that they become non-equivalent. This is manifested by the fact that the ionisation potential of one lone pair is higher by 1.72 eV than that of the other.[14] Ideas concerning the interaction of electron pairs 'through space' and 'through the bond' are usually employed to account for this effect.[15-18] Direct interaction through space leads to the formation of symmetrised n_+ and n_- levels, the energies of which differ little owing to the

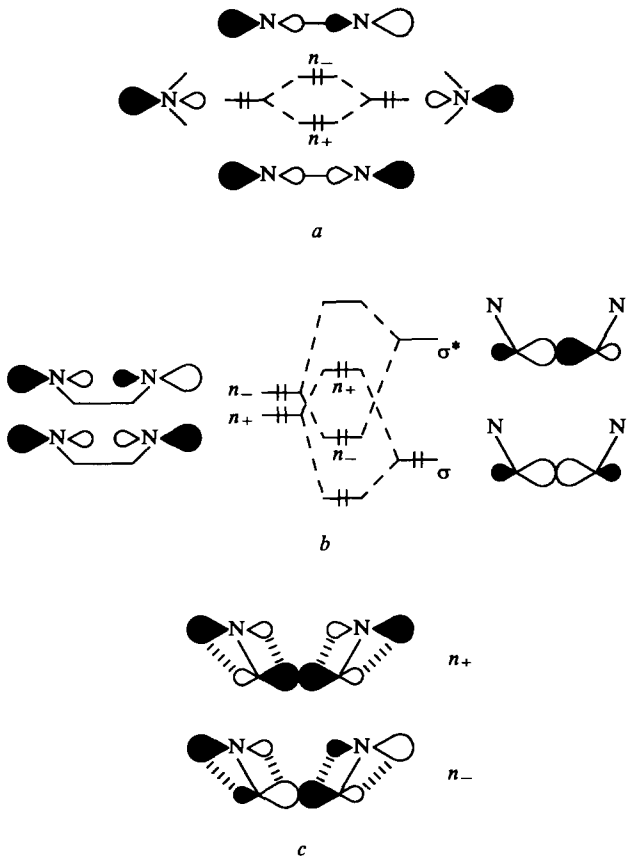


Figure 2. Interaction of the orbitals of the lone pairs of the nitrogen atoms in the pyrazine molecule: (*a*) through space; (*b*) through the C(2)–C(3) bond; (*c*) the form of the n_- and n_+ orbitals.

weak overlap as a consequence of the relatively large distance between the nitrogen atoms (Fig. 2*a*). We suggest that, as usual, combination in phase (n_+) has a lower energy than combination in antiphase (n_-). However, calculations and experiment have shown that the splitting between the levels n_+ and n_- is much greater than expected and moreover the n_+ level lies not below but above the n_- level by 1.72 eV.[7] Such an 'unnatural' order in the disposition of the levels can be explained by the fact that the lone pairs of the nitrogen atoms interact not only through space but also through C–C σ-bonds. Fig. 2*b* illustrates the interaction of the n_+ and n_- orbitals with the σ and σ* orbitals of the C(2)–C(3) bond in the pyrazine molecule. Compared with the weak 1,4-interaction between the nitrogen centres, the above 1,2-interactions of ($n_+ \pm \sigma$) and ($n_- \pm \sigma$) are strong. This leads to a greater splitting of the n_+ and n_- levels and to a change in their sequence. A similar interaction takes place with participation of the C(5)–C(6) bonds.

The molecular orbitals of complex **1** are constructed by a linear combination of the n_- and n_+ orbitals of pyrazine with the frontier orbitals of the two ML_5 fragments obtained by removing one ligand from the octahedral complex ML_6. The frontier orbital of the ML_5 fragment has the form shown in Fig. 3*a*.[7] On combining the bonding (M_+) and antibonding (M_-) combinations of the two frontier orbitals with the M_+ and M_- orbitals of the pyrazine lone pairs respectively, we obtain the pattern in the splitting of the levels shown in Fig. 3*b*. Since the M_+ and n_+ orbitals have more similar energies than the M_- and n_- orbitals, the M_+/n_+ splitting is greater than the M_-/n_- splitting. This renders the two M–N bonds in complex **1** equivalent, although in the pyrazine molecule the energies of the two electron pairs differ by 1.72 eV (see above).

Fig. 4 presents orbital diagrams for the chelate complex **2**: $L_4M(bpy)$. The ML_4 fragment has two almost degenerate frontier orbitals,[7] which are designated by the symbols M_+ and M_-

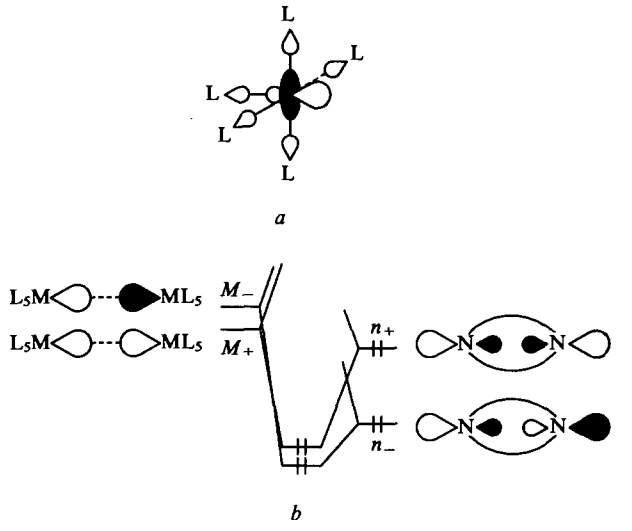


Figure 3. The form of the frontier orbital of the ML_5 fragment (*a*) and the orbital diagram for the interaction of the combination of two frontier orbitals in phase (M_+) and out of phase (M_-) with the n_+ and n_- orbitals of the lone pairs of pyrazine (*b*).

(Fig. 4*a*). In the 2,2′-bipyridyl molecule, the nitrogen *n* orbitals interact with one another through space and through the C(2)–C(2′) bonds similarly to the interaction of the orbitals in pyrazine. This interaction differs quantitatively from that in pyrazine, since the nitrogen lone pairs in the bipyridyl molecule are directed at an angle of 60° to one another and to the C(2)–C(2′)–L bond line. However, the qualitative pattern in the splitting of the levels of the lone pairs in he 2,2′-bipyridyl and pyrazine molecules is the same. The interaction of the M_+ and M_- orbitals with the n_+ and n_- orbitals (Fig. 4*b*) leads to strong chelate bonding (Fig. 4*c*).

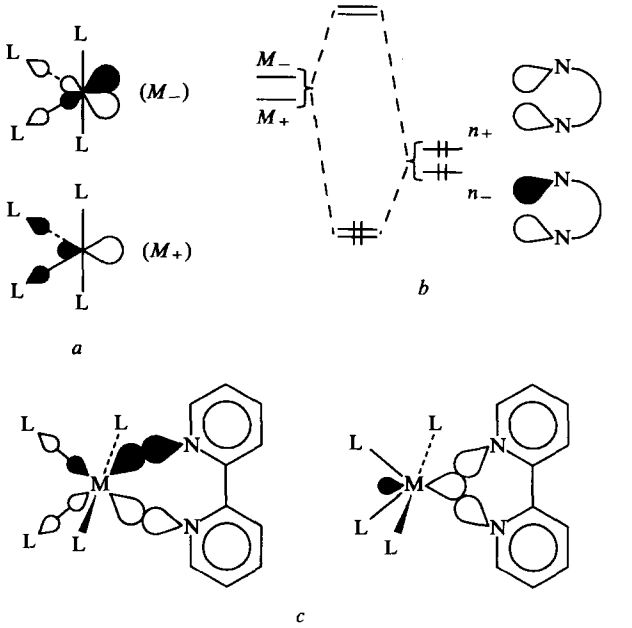
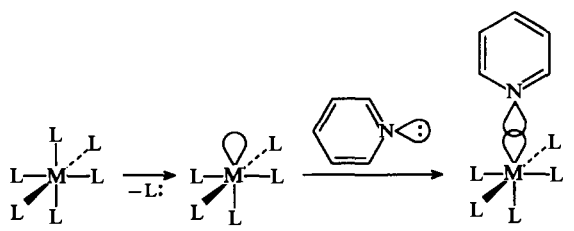


Figure 4. The form of the frontier orbitals of the ML_4 fragment (*a*), the diagram for the interaction of the frontier orbitals with the n_+ and n_- orbitals of the lone pairs in the 2,2′-bipyridyl molecule (*b*), and the form of the bonding molecular orbitals in the $L_4M(bpy)$ molecule (*c*).

3. The π-bonds in the octahedron

On passing from simple Lewis ligands of the type of NH_3, aliphatic amines, and phosphines to ligands containing p or π orbitals (these comprise CO, CN^-, SCN^-, Cl^-, and many organic ligands, including nitrogen-containing heterocycles) the positions of the redox levels can change greatly. We shall consider, for example the situation where one, two, or three of the simple ligands L in the octahedral complex ML_6 are replaced by pyridine molecules.



The pyridine nitrogen atom has a lone pair located in the plane of the ring. This pair participates in the formation of the usual coordinate bond in the complex L_5MPy (Py = pyridine). Pyridine (photochemical ionisation potential IP = 9.7 eV[18]) is a stronger lone pair donor than NH_3 (IP = 10.9 eV) but weaker than $N(CH_3)_3$ (IP = 8.5 eV), i.e. in the series of nitrogen-containing bases it is a moderately strong donor. However, in contrast to NH_3 and NR_3, there is a π-system in the pyridine molecule which can interact with the t_{2g} levels of the complex.

Fig. 5 illustrates the form of the two highest occupied and the two lowest unoccupied π orbitals of pyridine. Evidently in the coordinated pyridine molecule there is a possibility of interaction of the occupied d_{yz} level of the metal with the π LUMO and the π-bonding pyridine orbital, lying a little below the HOMO, because all three orbitals have the same symmetry b_1. This results in the stabilisation of both the π-bonding and d_{yz} levels, which increases the stability of the complex compared with the complex in which there is no π bonding.

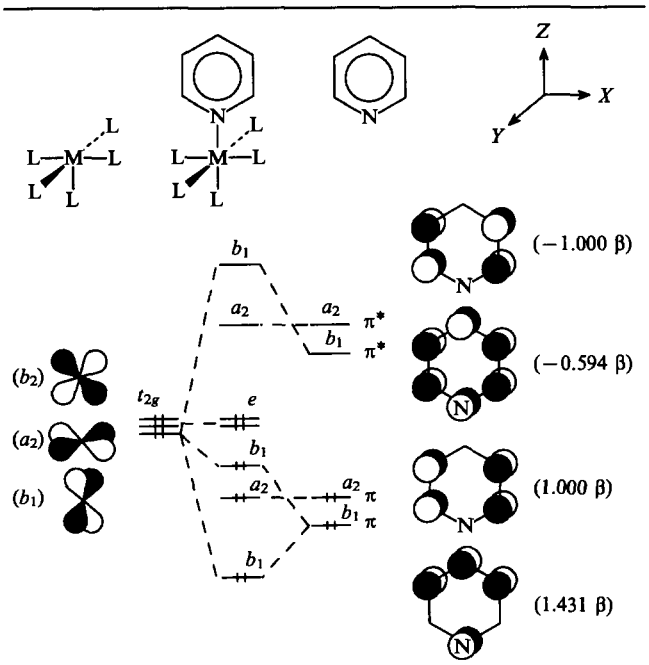
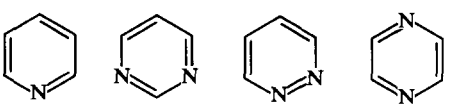


Figure 5. The π levels of the octahedral complex $L_5M(Py)$. The energies of the two highest occupied and the two lowest unoccupied π levels of the pyridine molecule, calculated by the Hückel method, are indicated in brackets.

The diagram in Fig. 5 corresponds to the case where the perturbation exerted by the π* molecular orbital of the ligand (reducing the energy of the t_{2g} level) is greater than the perturbation by the π molecular orbital (which increases the energy of the level). This type of splitting is more pronounced the lower the energy of the $\pi(b_1)$ orbital and the smaller the difference between the energies of the $\pi^*(b_1)$ and t_{2g} orbitals. In the series of free ligands pyridine, pyrimidine, pyridazine, and pyrazine, the ionisation potentials for the n and $\pi(b_1)$ levels, determined experimentally by photoelectron spectroscopy in the gas phase,[19] as well as the half-wave potentials $E_{1/2}$ for reduction in dimethylformamide (DMF), characterising the position of the $\pi^*(b_1)$ level,[20] vary as follows:

		Pyridine	Pyrimidine	Pyridazine	Pyrazine
					
IP/eV	n:	9.7	9.7	9.3	9.3
	$\pi(b_1)$:	10.5	10.5	11.3	13.3
$-E^{Red}_{1/2}$/ V (n.c.e.):		2.20	1.82	1.66	1.51

Evidently, on passing from pyridine to pyrimidine, the stabilising π-acceptor effect of the ligand should change little, but for pyridazine and pyrazine the effect intensifies, since the energy of the destabilising $\pi(b_1)$ orbital and of the stabilising $\pi^*(b_1)$ orbital diminishes. Compared with pyridine and pyrimidine, pyridazine and pyrazine also have higher n levels, which is indicated by the corresponding ionisation potentials, i.e. they are stronger Lewis bases. Consequently the stability of the pyridazine and pyrazine complexes increases as a result of the intensification of not only the π-acceptor but also of the σ-donor properties.

The π-bonding of two or three azine molecules, located at the vertices of the same face of the octahedron entails a decrease in two or three t_{2g} levels of the metal (Fig. 6). This means that, if the

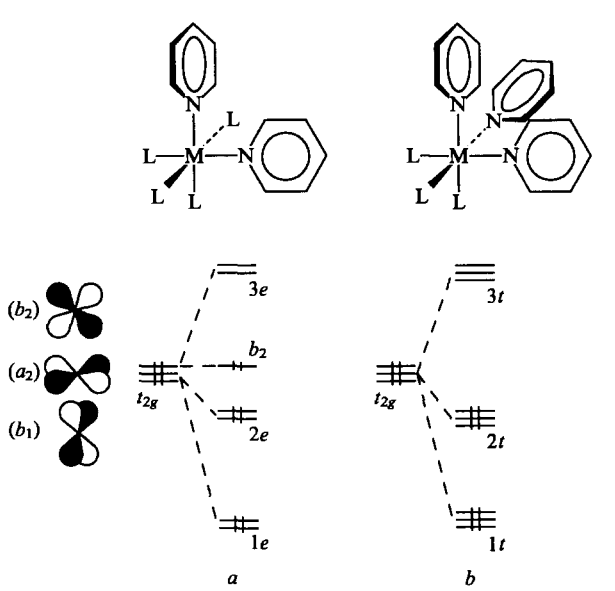
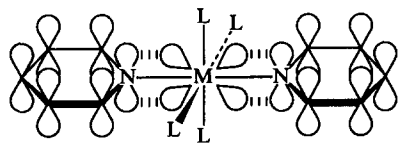


Figure 6. The π-bonding in the coordination of two (*a*) and three (*b*) pyridine molecules in orthogonal planes.

redox levels in the oxidation of the complexes are t_{2g} orbitals, then the oxidation potential of the complex $ML_3(azine)_3$ should increase relative to the oxidation potential of ML_6 (the oxidation should be hindered). A further increase in the number of ligands to six in the complex $M(azine)_6$ does not introduce significant changes into the perturbation pattern, since the π-systems of the two *trans*-ligands interact with only one of the t_{2g} orbitals, for example:

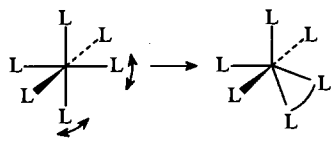


The positions of the $2t$ levels apparently change little (Fig. 6*b*).

If the ligand has fairly low acceptor π* orbitals but exhibits a π- or *p*-donor function, then the energy of the corresponding (in terms of symmetry) t_{2g} level increases, which destabilises the complex and diminishes its oxidation potential. Such ligands include, for example, Cl^- and other halide ions, ethers, or organic ligands of the Lewis *n*-type, which have electron-donating π-subsystems, in particular 4-mercaptopyridine.[21]

4. Geometrical distortions in the octahedron

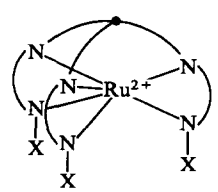
On coordination to bidentate ligands L–L, the structure of the regular octahedron is geometrically distorted when the length of the bridge is inadequate or the bridge is insufficiently flexible. These distortions are illustrated below schematically by arrows:



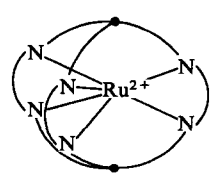
Analysis of the influence of the change in the bond angles between the L–M–L *cis*- and *trans*-bonds (see, for example Albright et al.[7] and the literature quoted therein) shows that the degenerate t_{2g} and e_g levels are lowered in the distorted octahedron. It was stated above that π-acceptor or π-donor ligands also create energy differences between the levels of the t_{2g} set. Since π overlap is a function of angular changes, the distortions in the octahedron also alter the degree of π bonding in the octahedron.

Geometrical distortions play an important role in 16-electron octahedral complexes ML_6. In order that such molecules should be in a low spin state, it is necessary that one of the t_{2g} levels should lie appreciably above the other two. This is achieved as a result of the combination of π bonding (if it is possible) with the geometrical distortions in the octahedron.

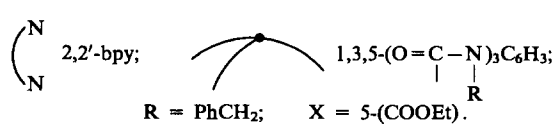
Particularly pronounced geometrical changes in the octahedron are observed in the case of the so called 'capped' ligands as well as ligands of the 'bicapped' type. The origin of these terms is clear from the three-dimensional formulae of compounds **4** and **5**, investigated by Barigelletti et al.,[22] presented below.



4
'capped'



5
'bicapped'



In this case, the six nitrogen atoms are arranged around the central metal ion, forming a trigonal prism. The six *n* orbitals of nitrogen, directed towards the centre of symmetry (D_{3h}), form six symmetrised group orbitals, the conventional representations of which are given in Fig. 7.

Fig. 7 shows that there is no fundamental difference between the octahedral and prismatic complexes: in both cases, the occupied t_{2g} levels (a_{1g} + e_{2g}) play the role of the HOMO, while the unoccupied e_g levels play the role of the LUMO.

Distortions can also arise owing to the rigidity of the bridging bidentate ligand. Thus the pyridine rings in 2,2'-bipyridyl cannot be located in the same plane owing to the repulsion of the hydrogen atoms in the 3- and 3'-positions, i.e. the molecule is twisted relative to the C(2)–C(2') axis; this alters the symmetry of the complex and the strength of bonding with the central metal ion.

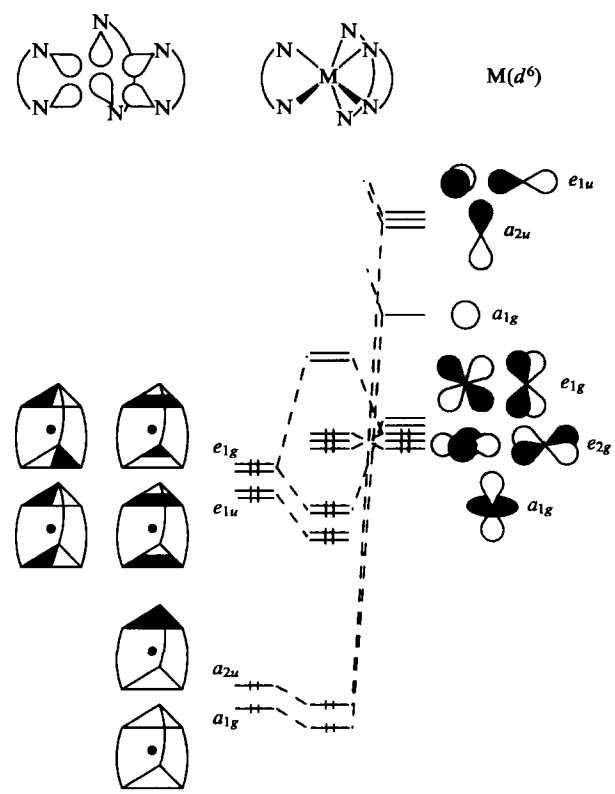


Figure 7. Molecular σ orbitals of the 'capped' and 'bicapped' complexes **4** and **5**.

5. Electrochemistry and photochemistry

In the general case, the electronic transitions in the spectra of transition metal complexes ML_6 can be divided into three types:[23]

(1) transitions between levels located predominantly on the metal, for example, the familiar d–d transition;

(2) transitions between levels predominantly located on ligands (for example, the π–π* transitions in aromatic ligands);

(3) transitions in which an electron is transferred from the metal to the ligand (MLCT) or, conversely, from the ligand to the metal (LMCT).

The possible electronic transitions for the symmetrical octahedral complex ML_6, in which the ligands L have π-systems, are illustrated schematically in Fig. 8. We may note that in the 17-electron complexes there is a possibility, apart from the transitions shown in Fig. 8, also of the $\pi L \rightarrow M(t_{2g})$ and $\sigma L \rightarrow M(t_{2g})$ transitions, while in the 19-electron complexes $M(e_g) \rightarrow \pi^* L$ transitions are possible. Among the transitions shown in Fig. 8, three (*c*, *d*, and *f*) correspond to the charge-transfer (CT) bands. In the spectra of 18-electron d^6 complexes with azine ligands, the

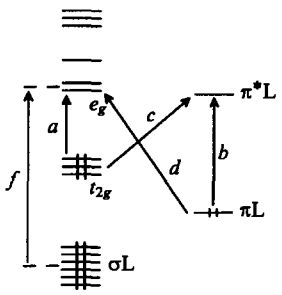


Figure 8. Schematic illustration of the main electronic transitions in the spectra of the complex of ML_6 with π-ligands. Transitions: (*a*) *d*–*d*; (*b*) πL→π*L; (*c*) $M(t_{2g})$→π*L(MLCT); (*d*) πL→$M(e_g)$ (LMCT); (*f*) σL→$M(e_g)$.

longest-wavelength band corresponds as a rule to the MLCT transition[1] $M(t_{2g})$→π*L, since the π and π* orbitals of these ligands are fairly low. This band usually has a low intensity, rarely exceeding 10^4 litre mol^{-1} s^{-1}, and in terms of this feature it can be distinguished from the more intense π→π* band. Thus the frontier orbitals of the azine complexes are $M(t_{2g})$ (HOMO) and π*L (LUMO).

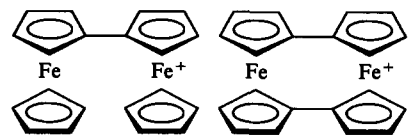
For this reason, one can assume that in the general case the electronic changes occurring on electrochemical oxidation of such complexes should be localised 'on the metal', while in the electrochemical reduction they should be localised 'on the azine ligand'. Naturally, one is dealing with the so called 'primary electronic changes'. Electron transfer may be followed by intramolecular electron transfer (IET), as a result of which the electron in the radical-cation or radical-anion formed may be located in a region completely different from that to which it was initially transferred.

Dinuclear compounds of the type M^1–μ-L–M^2, where μ-L is a bridging ligand, for example, pyrazine, 4,4′-bipyridyl, cyanide, etc. while M^1 and M^2 are two different or identical organometallic residues, are of great interest. As a rule, complexes in which M^1 and M^2 are in oxidation states differing by unity are the most important. If the two metallic centres can interact with one another via a bridge, then there is a possibility of an IET process, which in the given instance is referred to as an intervalence [mixed valence ? Ed.] transition:

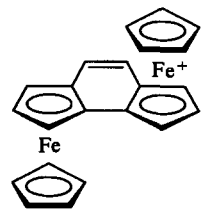
$$(M^1)^+ - \mu\text{-L} - M^2 \longrightarrow M^1 - \mu\text{-L} - (M^2)^+ .$$

Robin and Day[24] proposed that mixed-valence complexes be divided into three classes in terms of the degree of delocalisation of the valence electrons. Compounds in which there is no interaction of any kind between centres with different oxidation states, i.e. the valences are fixed, are referred to as class I and the properties of these complexes are simply the sum of the properties of the two different centres. The fully delocalised systems, in which the two centres with different oxidation states are indistinguishable by methods with characteristic times greater than the time required for electron transfer, are referred to as class III. Compounds of class II occupy an intermediate position between classes I and III. In this case, there is a weak interaction between M^1 and M^2.

The intervalence transitions are usually investigated by spectroscopic methods. The biferrocenyl cations **6** and **8** and a number of others were particularly thoroughly investigated (see Richardson[6] and the references quoted therein). The electronic spectrum of the cation **6** in acetonitrile contains absorption bands at 545, 840, and, which is particularly important, at 1800 nm (ε = 750) in the near infrared. The 1800 nm band is not observed in the spectra of either Fc–Fc or Fc^+–Fc^+. On this basis, it was attributed to an intervalence or IET transition occurring as a consequence of optical excitation. The Mössbauer spectrum shows clearly that the cation **6** contains iron(II) and iron(III) and that a thermal electron exchange takes place at a rate of about 10^7 s^{-1}. Thus the ion **6** belongs to class II in terms of the classification of Robin and Day.



6 **7**

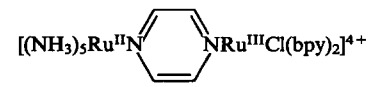


8

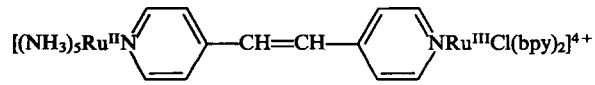
Electrochemical measurements have also shown that the cation **6** contains divalent and trivalent iron. Oxidation (E^{Ox} = 0.64 V in CH_3CN) and reduction (E^{Red} = 0.31 V) involve iron(II) and iron(III) respectively.[25]

Thus in the mixed-valence complexes the redox centres in the anodic and cathodic processes are different metal ions. However, in dinuclear bridged complexes of the type L_nM–μ-L–ML_n with two identical metals in the same oxidation state and with the same ligand environment, the electronic changes on reduction may be localised on the bridging or terminal ligand.

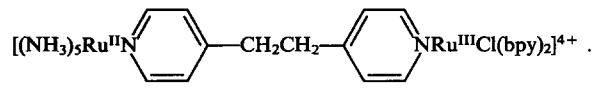
The band in the near infrared corresponds to charge transfer between two metallic centres (MMCT). It has been observed for many bridged bimetallic ruthenium complexes, for example, for the pyrazine and dipyridylethylene complexes presented below (the extinction coefficients are given in brackets):[26]



960 nm (530)



680 nm (< 300)



MMCT (band absent)

However, on passing to the dipyridylethane bridge, the MMCT band vanishes as a consequence of the absence of conjugation between the pyridine rings.

It is natural to expect that there should be a linear correlation between the energy of the long-wavelength charge-transfer band and the electrode potentials of the complexes, because the same frontier orbitals are involved both in photo-excitation and in electrode processes. The correlation equation is

$$G = ah\nu_{CT} + b, \qquad (1)$$

where G is the 'electrochemical gap' (in volts), defined as the difference between the oxidation (E^{Ox}) and reduction (E^{Red}) potentials of the given complex ($G = E^{Ox} - E^{Red}$), $h\nu_{CT}$ is the energy of the charge-transfer band or the 'spectral gap' (in eV), and a and b are constants. From general considerations, it is to be expected that a should be close to unity.

There have been a number of studies in which measurements were made of three parameters simultaneously ($h\nu_{CT}$, E^{Ox}, and E^{Red}) in fairly wide series of ruthenium complexes.[27–37]

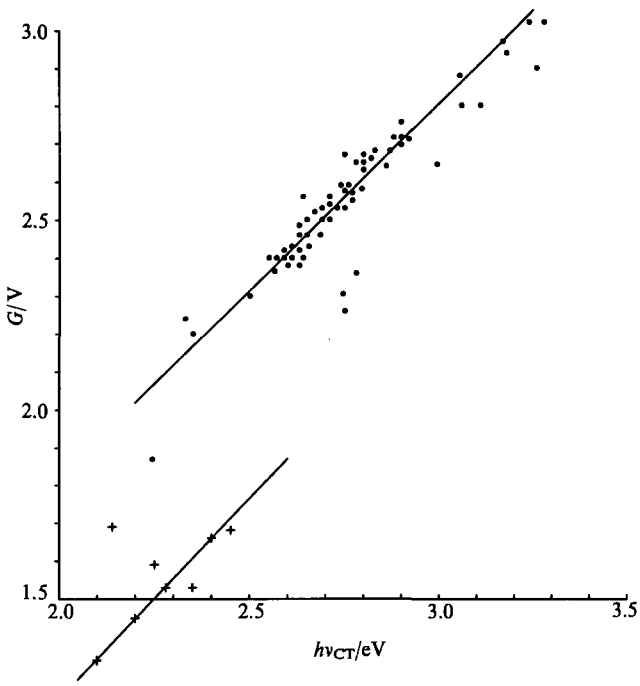
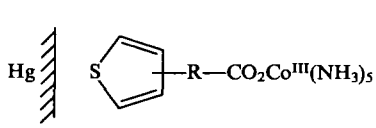


Figure 9. Relation between G and $h\nu_{CT}$ for ruthenium(II) complexes based on data in Refs 27–33.

Fig. 9 presents the relation between the spectral and electrochemical gaps for ruthenium(II) complexes constructed on the basis of the results of these studies. Evidently there is a linear relation between G and $h\nu_{CT}$ with a slope close to unity. A number of points deviate from the overall straight line, the deviation of the points in the lower left-hand corner of the diagram, designated by crosses, being most pronounced. They form their own straight line with a slope which is also close to unity. The reason for this is apparently that the majority of the 70 points plotted on the graph correspond to compounds with bidentate ligands of the type of α,α′-bipyridyl, 2,2′-bipyrimidyl, and similar compounds. On the other hand, the crosses correspond to compounds with six monodentate ligands, for example, $Ru(NH_3)_5L$, $(Py)Ru(NH_3)_4L$, $(3\text{-ClPy})Ru(NH_3)_4L$ (where L = 4-cyano-*N*-methylpyridinium), etc.[28] The shift of the points is caused by the change in the constant b in Eqn. (1). This constant probably depends largely on solvation. Indeed, it has been shown that MLCT depends exceptionally strongly on the solvent [nitromethane, acetonitrile, propylene carbonate, acetone, DMF, and dimethyl sulfoxide (DMSO) have been investigated] and this solvatochromism cannot be accounted for simply in terms of the dielectric properties of the solvents. There is evidence that the charge transfer depends on the specific interaction of the solvent with a coordinated NH_3 molecule.

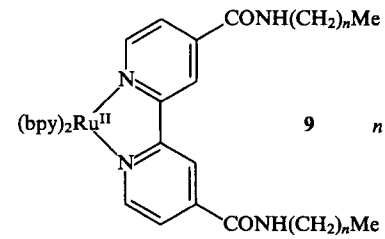
When the redox properties of the complexes are considered, it is essential to take into account primarily also the possibility of the specific interaction with the electrode material. For example, the pentamminecobalt(III) complex containing a carboxylate ion with a thienyl substituent as the sixth ligand is reduced at a mercury cathode not at the metal atom but initially at the thienyl group with subsequent electron transfer to the metal via the IET process described above.[38] This is associated with the strong specific interaction of the sulfur atom with mercury, which is responsible for the following orientation on the electrode:



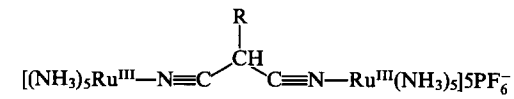
III. Electrochemical properties of ruthenium and rhodium complexes

1. Mononuclear ruthenium complexes

There has been a particular growth of interest in the chemistry of ruthenium complexes in recent years because ruthenium compounds have been finding increasing application in various fields. For example, since complexes containing ruthenium in different oxidation states are more stable than the analogous iron complexes, they can serve as a convenient model for the study of various redox reactions in biological systems where a ruthenium atom replaces an iron atom. In this connection, studies have been made[39] on the redox properties of tetra(*o*-aminophenyl)porphyrins containing ruthenium(II) combined with various axial ligands. Certain ruthenium compounds are of interest as nonlinear optical materials. Thus ruthenocene and its derivatives exhibit a second-order nonlinear optical effect.[3] Similar properties have been observed in recent years also in other ruthenium complexes, in particular those containing bipyridyl (compound **9**) and bridging (compound **10**) ligands.[4, 40]



9 $n = 1, 5, 11, 15, 17$



10

R = H, Bu^t

Considerable attention has been devoted to the study of polypyridylruthenium(II) complexes (Tables 1 and 2). More than 200 bidentate (LL) polypyridyl ligands used in the chemistry of ruthenium(II) have been examined in a review,[2] which also presents the oxidation-reduction potentials of a large number of the homoleptic complexes $Ru(LL)_3^{2+}$ synthesised. It is important to note that the different one-electron transitions observed on cyclic voltammograms for the ruthenium(II) complexes can be readily related in many instances to specific donor or acceptor orbitals.

Polypyridylruthenium(II) complexes are oxidised with participation of the t_{2g} orbitals d_{xy}, d_{xz}, and d_{yz}, which are located on the metal atom. This results in the formation of low-spin ruthenium(III) complexes with the $4d^5$ configuration, which are resistant to ligand substitution. This has been confirmed with the aid of orbital diagrams.[41]

$$[Ru^{II}(LL)_3]^{2+} \rightleftharpoons [Ru^{III}(LL)_3]^{3+} + \bar{e}\,.$$

It has been established that the Ru(II)/Ru(III) redox transitions in complexes with polypyridyl ligands lie within a narrow range of potentials [about 1.53 V relative to the saturated calomel electrode (s.c.e.)]. The replacement of one or several polypyridyl ligands can significantly alter these potentials. Thus the substitution of one bpy in $Ru(bpy)_3^{2+}$ by two chloride ions affords $Ru(bpy)_2Cl_2$ and lowers the oxidation potential to 0.63 V, while the introduction of two CO molecules instead of bpy increases the oxidation potential of $[Ru(bpy)_2(CO)_2]^{2+}$ to 2.18 V.

Table 1. Data on the electrochemical oxidation of mononuclear ruthenium complexes.

Complex[a]	E/V	ECLS[b]	Conditions[c]	Ref.
4 ('capped')	1.54	$Ru^{II/III}$	Pt, MeCN, Bu_4NClO_4, s.c.e.	22
5 ('bicapped')	1.55	$Ru^{II/III}$	Pt, MeCN, Bu_4NClO_4, Ag	22
$Ru(bpy)_3^{2+}$	1.26	$Ru^{II/III}$	Pt, MeCN, Bu_4NClO_4, Ag	2, 44
$[Ru(5,5'\text{-}(EtO_2C)_2bpy)_3]^{2+}$	1.55	$Ru^{II/III}$	Pt, MeCN, Bu_4NClO_4, Ag	22
$[Ru(bpy)_2bpt]^+$	0.85	$Ru^{II/III}$	CG, MeCN, Bu_4NClO_4, n.h.e.	1
$Ru(2,3\text{-}dpp)(CO)_2Cl_2$	1.90	$Ru^{II/III}$	Pt, MeCN, Et_4NClO_4, s.c.e.	106
$Ru(2,5\text{-}dpp)(CO)_2Cl_2$	1.86	$Ru^{II/III}$	Pt, MeCN, Et_4NClO_4, s.c.e.	106
$[Ru(bpy)(biq)(Me_2bpy)]^{2+}$	1.30	$Ru^{II/III}$	Pt, MeCN, Bu_4NClO_4, s.c.e.	42
$[Ru(bpy)(biq)(phen)]^{2+}$	1.35	$Ru^{II/III}$	Pt, MeCN, Bu_4NClO_4, s.c.e.	42
$[Ru(bpy)(biq)(pq)]^{2+}$	1.39	$Ru^{II/III}$	Pt, MeCN, Bu_4NClO_4, s.c.e.	42
$[Ru(bpy)(biq)(i\text{-}biq)]^{2+}$	1.29	$Ru^{II/III}$	Pt, MeCN, Bu_4NClO_4, s.c.e.	42
$[Ru(bpy)(biq)(pzpm)]^{2+}$	1.42	$Ru^{II/III}$	Pt, MeCN, Bu_4NClO_4, s.c.e.	42
$[Ru(bpy)(biq)(biImH_2)]^{2+}$	1.09	$Ru^{II/III}$	Pt, MeCN, Bu_4NClO_4, s.c.e.	42
$[Ru(bpy)(biq)(bpm)]^{2+}$	1.46	$Ru^{II/III}$	Pt, MeCN, Bu_4NClO_4, s.c.e.	42
$[Ru(bpy)(biq)(taphen)]^{2+}$	1.46	$Ru^{II/III}$	Pt, MeCN, Bu_4NClO_4, s.c.e.	42
$[Ru(bpy)(biq)(dinapy)]^{2+}$	1.27	$Ru^{II/III}$	Pt, MeCN, Bu_4NClO_4, s.c.e.	42
$[Ru(dinapy)_3]^{2+}$	1.01	$Ru^{II/III}$	Pt, MeCN, Bu_4NClO_4, s.c.e.	44
$[Ru(bpy)_2(biBzImH)_2]^{2+}$	1.12	$Ru^{II/III}$	Pt, MeCN, Bu_4NClO_4, s.c.e.	101
$Ru(chd)_3(BPh)$	1.22	$Ru^{II/III}$	Pt, CH_2Cl_2, Bu_4NBF_4, s.c.e.	70
$Ru(chd)_3(BBu^n)$	1.17	$Ru^{II/III}$	Pt, CH_2Cl_2, Bu_4NBF_4, s.c.e.	70
$Ru(chd)_3(BOMe)$	1.14	$Ru^{II/III}$	Pt, CH_2Cl_2, Bu_4NBF_4, s.c.e.	70
$Ru(chd)_3(BF)$	1.33	$Ru^{II/III}$	Pt, CH_2Cl_2, Bu_4NBF_4, s.c.e.	70
$Ru(chd)_3(BOMe)$	1.21	$Ru^{II/III}$	Pt, CH_2Cl_2, Bu_4NBF_4, s.c.e.	70
$Ru(chd)_3(BOEt)$	1.20	$Ru^{II/III}$	Pt, CH_2Cl_2, Bu_4NBF_4, s.c.e.	70
$Ru(chd)_3(BOPr^n)$	1.20	$Ru^{II/III}$	Pt, CH_2Cl_2, Bu_4NBF_4, s.c.e.	70
$Ru(chd)_3(BOPr^i)$	1.20	$Ru^{II/III}$	Pt, CH_2Cl_2, Bu_4NBF_4, s.c.e.	70
$Ru(chd)_3(BOBu^n)$	1.21	$Ru^{II/III}$	Pt, CH_2Cl_2, Bu_4NBF_4, s.c.e.	70
$Ru(chd)_3(BOn\text{-}C_5H_{11})$	1.21	$Ru^{II/III}$	Pt, CH_2Cl_2, Bu_4NBF_4, s.c.e.	70
$Ru(chd)_3(BOn\text{-}C_{10}H_{21})$	1.22	$Ru^{II/III}$	Pt, CH_2Cl_2, Bu_4NBF_4, s.c.e.	70
$Ru(dpg)(BBu^n)$	1.34	$Ru^{II/III}$	Pt, CH_2Cl_2, Bu_4NBF_4, s.c.e.	70
$Ru(dpg)(BOMe)$	1.43	$Ru^{II/III}$	Pt, CH_2Cl_2, Bu_4NBF_4, s.c.e.	70
$Ru(dmg)(BBu^n)$	1.15	$Ru^{II/III}$	Pt, CH_2Cl_2, Bu_4NBF_4, s.c.e.	70
$Ru(dmg)(BOMe)$	1.23	$Ru^{II/III}$	Pt, CH_2Cl_2, Bu_4NBF_4, s.c.e.	70
$[RuBr(CO)_2(\eta^5\text{-}C_5Ph_5)]$	1.76	$Ru^{II/III}$	Pt, CH_2Cl_2, Bu_4NPF_6, s.c.e.	68
$[RuMe(CO)_2(\eta^5\text{-}C_5Ph_5)]$	1.49	$Ru^{II/III}$	Pt, CH_2Cl_2, Bu_4NPF_6, s.c.e.	68
$[RuBr(CO)(PPh_3)L]$	1.07	$Ru^{II/III}$	Pt, CH_2Cl_2, Bu_4NPF_6, s.c.e.	68
$L = \eta^5\text{-}C_5Ph_5$				
$[RuBr(CO)(PEt_3)L]$	1.01	$Ru^{II/III}$	Pt, CH_2Cl_2, Bu_4NPF_6, s.c.e.	68
$L = \eta^5\text{-}C_5Ph_5$				
$[RuBr(CO)\{P(OMe)_3\}L]$	1.12	$Ru^{II/III}$	Pt, CH_2Cl_2, Bu_4NPF_6, s.c.e.	68
$L = \eta^5\text{-}C_5Ph_5$				
$[RuMe(CO)(PEt_3)L]$	0.73	$Ru^{II/III}$	Pt, CH_2Cl_2, Bu_4NPF_6, s.c.e.	68
$L = \eta^5\text{-}C_5Ph_5$				
$[RuEt(CO)(PEt_3)L]$	0.71	$Ru^{II/III}$	Pt, CH_2Cl_2, Bu_4NPF_6, s.c.e.	68
$L = \eta^5\text{-}C_5Ph_5$				
$[Ru(COMe)(CO)(PEt_3)L]$	0.67	$Ru^{II/III}$	Pt, CH_2Cl_2, Bu_4NPF_6, s.c.e.	68
$L = \eta^5\text{-}C_5Ph_5$				
$[Ru(CMe{=}CMe_2)(CO)(PEt_3)L]$	0.59	$Ru^{II/III}$	Pt, CH_2Cl_2, Bu_4NPF_6, s.c.e.	68
$L = \eta^5\text{-}C_5Ph_5$				
$[Ru(salen)(Ph_3P)]Cl$	0.49	$Ru^{III/IV}$	CG, MeCN, Bu_4NClO_4, $Ag/AgNO_3$	129
$[Ru(salen)(Py)]ClO_4$	0.76	$Ru^{III/IV}$	CG, MeCN, Bu_4NClO_4, $Ag/AgNO_3$	129
$[Ru(salen)(N_3)]$	0.48	$Ru^{III/IV}$	CG, MeCN, Bu_4NClO_4, $Ag/AgNO_3$	129
$[Ru(salen)(Ph_3P)(oTs]$	0.76	$Ru^{III/IV}$	CG, MeCN, Bu_4NClO_4, $Ag/AgNO_3$	129
$[Ru(salen)(CN)_2]^-$	0.37	$Ru^{III/IV}$	CG, MeCN, Bu_4NClO_4, $Ag/AgNO_3$	129
$[(bpy)(tpy)Ru(H_2O)]^{2+}$	0.80	$Ru^{II/IV}$	Pt, H_2O, Bu_4NOH, s.c.e.	130
$RuCl_2(Bu^tCN)_4$	0.99	$Ru^{II/III}$	Pt, MeCN, Bu_4NClO_4, s.c.e.	131
$RuCl_2(2,4,6\text{-}Me_3C_6H_2CN)_4$	1.26	$Ru^{II/III}$	Pt, MeCN, Bu_4NClO_4, s.c.e.	131
$RuCl_2(4\text{-}Br\text{-}2,6\text{-}Me_2C_6H_2)_4$	1.20	$Ru^{II/III}$	Pt, MeCN, Bu_4NClO_4, s.c.e.	131
$RuCl_2(Bu^tCN)_2(Ph_3P)_2$	0.79	$Ru^{II/III}$	Pt, MeCN, Bu_4NClO_4, s.c.e.	131
$RuCl_2L_2(Ph_3P)_2$	0.85	$Ru^{II/III}$	Pt, MeCN, Bu_4NClO_4, s.c.e.	131
$L = 2,4,6\text{-}Me_3C_6H_2$				
$Ru(phen)_3^{2+}$	1.31	$Ru^{II/III}$	Pt, MeCN, Bu_4NClO_4, s.c.e.	117
$Ru(dpp)_3^{2+}$	1.68	$Ru^{II/III}$	Pt, MeCN, Bu_4NClO_4, s.c.e.	117
$Ru(dpq)_3^{2+}$	1.65	$Ru^{II/III}$	Pt, MeCN, Bu_4NClO_4, s.c.e.	117
$Ru(phen)_2(dpq)^{2+}$	1.42	$Ru^{II/III}$	Pt, MeCN, Bu_4NClO_4, s.c.e.	117
$Ru(phen)_2(dpp)^{2+}$	1.39	$Ru^{II/III}$	Pt, MeCN, Bu_4NClO_4, s.c.e.	117
$Ru(bpy)_2(dpp)^{2+}$	1.33	$Ru^{II/III}$	Pt, MeCN, Bu_4NClO_4, s.c.e.	117
$Ru(dpk)_2Cl_2$	0.61	$Ru^{II/III}$	CG, DMF, Bu_4NClO_4, s.c.e.	132
$Ru(dpk)(CO)Cl_2$	0.88	$Ru^{II/III}$	CG, DMF, Bu_4NClO_4, s.c.e.	132

Table 1. (continued)

Complex [a]	E/V	ECLS [b]	Conditions [c]	Ref.
$[Ru(dpk)(MeCN)_2]^{2+}$	1.31	$Ru^{II/III}$	CG, DMF, Bu_4NClO_4, s.c.e.	132
$[Ru(bpy)_2(dpk)]^{2+}$	1.34	$Ru^{II/III}$	CG, DMF, Bu_4NClO_4, s.c.e.	132
$Ru(o\text{-}NH_2)TPP(CO)$	0.88	$Ru^{II/III}$	Pt, MeCN, Et_4NClO_4, Ag/AgCl	39
	1.20			
$Ru(o\text{-}NH_2)TPP(Py)_2$	0.15		Pt, MeCN, Et_4NClO_4, Ag/AgCl	39
	0.38			
$Ru(o\text{-}NH_2)TPP(MeCN)_2$	0.12		Pt, MeCN, Et_4NClO_4, Ag/AgCl	39
	0.28			
$Ru(dmqH)_2(Ph_3P)_2$	0.44	$Ru^{II/III}$	Pt, CH_2Cl_2, Bu_4NClO_4, Ag/AgCl	76
	1.00	$Ru^{III/IV}$		
	0.40	$Ru^{II/III}$	Au, CH_2Cl_2, Bu_4NClO_4, Ag/AgCl	
	1.00	$Ru^{III/IV}$		
	0.40	$Ru^{II/III}$	CG, CH_2Cl_2, Bu_4NClO_4, Ag/AgCl	
	1.00	$Ru^{III/IV}$		
$Ru(dpqH)_2(Ph_3P)_2$	0.57	$Ru^{II/III}$	Pt, CH_2Cl_2, Bu_4NClO_4, Ag/AgCl	76
	1.13	$Ru^{III/IV}$		
	0.58	$Ru^{II/III}$	Au, CH_2Cl_2, Bu_4NClO_4, Ag/AgCl	
	1.12	$Ru^{III/IV}$		
	0.58	$Ru^{II/III}$	CG, CH_2Cl_2, Bu_4NClO_4, Ag/AgCl	
	1.14	$Ru^{III/IV}$		
$Ru(chdH)_2(Ph_3P)_2$	0.37	$Ru^{II/III}$	Pt, CH_2Cl_2, Bu_4NClO_4, Ag/AgCl	76
	0.96	$Ru^{III/IV}$		
	0.38	$Ru^{II/III}$	Au, CH_2Cl_2, Bu_4NClO_4, Ag/AgCl	
	0.98	$Ru^{III/IV}$		
	0.38	$Ru^{II/III}$	CG, CH_2Cl_2, Bu_4NClO_4, Ag/AgCl	
	0.99	$Ru^{III/IV}$		
$Ru(dmgH)_2(Ph_3P)(Py)$	0.42	$Ru^{II/III}$	Pt, CH_2Cl_2, Bu_4NClO_4, Ag/AgCl	76
	0.89	$Ru^{III/IV}$		
$Ru(quin)_2(Ph_3P)_2$	0.14	$Ru^{II/III}$	Pt, CH_2Cl_2, Bu_4NClO_4, Ag/AgCl	76
	1.15	$Ru^{III/IV}$		
$Ru(bgdH)_2(Ph_3P)_2$	0.23	$Ru^{II/III}$	Pt, CH_2Cl_2, Bu_4NClO_4, Ag/AgCl	76
	0.78	$Ru^{III/IV}$		
	1.04			
$Ru(bgdH)_2(Ph_3P)(MeIm)$	0.23	$Ru^{II/III}$	Pt, CH_2Cl_2, Bu_4NClO_4, Ag/AgCl	76
	0.73	$Ru^{III/IV}$		
	0.95			
$[Ru(NH_3)_5(Py)]^{2+}$	0.29	$Ru^{II/III}$	GG, H_2O, CF_3COOH/CF_3COONa, n.h.e.	59–61
	0.30	$Ru^{II/III}$	GG, H_2O, $MeC_6H_4OSO_3H/MeC_6H_4OSO_3K$, n.h.e.	59
$[Ru(NH_3)_5(isn)]^{2+}$	0.38	$Ru^{II/III}$	GG, H_2O, $MeC_6H_4OSO_3H/MeC_6H_4OSO_3K$, n.h.e.	59
$[Ru(NH_3)_5(4\text{-}acpy)]^{2+}$	0.39	$Ru^{II/III}$	GG, H_2O, $MeC_6H_4OSO_3H/MeC_6H_4OSO_3K$, n.h.e.	59
(E)-$[Ru(NH_3)_4(4\text{-}pic)_2]^{2+}$	0.42	$Ru^{II/III}$	GG, H_2O, CF_3COOH/CF_3COONa, n.h.e.	61
(E)-$[Ru(NH_3)_4(4\text{-}pic)(Py)]^{2+}$	0.45	$Ru^{II/III}$	GG, H_2O, CF_3COOH/CF_3COONa, n.h.e.	61
(E)-$[Ru(NH_3)_4(4\text{-}pic)(isn)]^{2+}$	0.50	$Ru^{II/III}$	GG, H_2O, CF_3COOH/CF_3COONa, n.h.e.	61
(Z)-$[Ru(NH_3)_4(4\text{-}pic)(isn)]^{2+}$	0.54	$Ru^{II/III}$	GG, H_2O, CF_3COOH/CF_3COONa, n.h.e.	61
(E)-$[Ru(NH_3)_4(4\text{-}pic)(pz)]^{2+}$	0.61	$Ru^{II/III}$	GG, H_2O, CF_3COOH/CF_3COONa, n.h.e.	61
(E)-$[Ru(NH_3)_4(4\text{-}pic)L]^{2+}$ L = 4-acpy	0.52	$Ru^{II/III}$	GG, H_2O, CF_3COOH/CF_3COONa, n.h.e.	61
(E)-$[Ru(NH_3)_4(Py)_2]^{2+}$	0.49	$Ru^{II/III}$	GG, H_2O, $MeC_6H_4OSO_3H/MeC_6H_4OSO_3K$, n.h.e.	59
(Z)-$[Ru(NH_3)_4(Py)_2]^{2+}$	0.51	$Ru^{II/III}$	GG, H_2O, $MeC_6H_4OSO_3H/MeC_6H_4OSO_3K$, n.h.e.	59
(E)-$[Ru(NH_3)_4(Py)(isn)]^{2+}$	0.55	$Ru^{II/III}$	GG, H_2O, CF_3COOH/CF_3COONa, n.h.e.	61
(Z)-$[Ru(NH_3)_4(Py)(isn)]^{2+}$	0.58	$Ru^{II/III}$	GG, H_2O, CF_3COOH/CF_3COONa, n.h.e.	61
(E)-$[Ru(NH_3)_4(Py)(pz)]^{2+}$	0.65	$Ru^{II/III}$	GG, H_2O, CF_3COOH/CF_3COONa, n.h.e.	61
(E)-$[Ru(NH_3)_4(4\text{-}acpy)(Py)]^{2+}$	0.55	$Ru^{II/III}$	GG, H_2O, CF_3COOH/CF_3COONa, n.h.e.	61
(E)-$[Ru(NH_3)_4(pz)(isn)]^{2+}$	0.70	$Ru^{II/III}$	GG, H_2O, CF_3COOH/CF_3COONa, n.h.e.	61
(Z)-$[Ru(NH_3)_4(Py)(isn)]^{2+}$	0.75	$Ru^{II/III}$	GG, H_2O, CF_3COOH/CF_3COONa, n.h.e.	61
(E)-$[Ru(NH_3)_4(isn)L]^{2+}$ L = 4-acpy	0.61	$Ru^{II/III}$	GG, H_2O, CF_3COOH/CF_3COONa, n.h.e.	61
(Z)-$[Ru(NH_3)_4(isn)L]^{2+}$ L = 4-acpy	0.66	$Ru^{II/III}$	GG, H_2O, CF_3COOH/CF_3COONa, n.h.e.	61
(E)-$[Ru(NH_3)_4(pz)L]^{2+}$ L = 4-acpy	0.74	$Ru^{II/III}$	GG, H_2O, CF_3COOH/CF_3COONa, n.h.e.	61
(E)-$[Ru(NH_3)_4(4\text{-}acpy)_2]^{2+}$	0.60	$Ru^{II/III}$	GG, H_2O, CF_3COOH/CF_3COONa, n.h.e.	61
(E)-$[Ru(NH_3)_4(pz)_2]^{2+}$	0.78	$Ru^{II/III}$	GG, H_2O, NaCl, n.h.e.	61
(Z)-$[Ru(NH_3)_4(pz)_2]^{2+}$	0.86	$Ru^{II/III}$	GG, H_2O, NaCl, n.h.e.	61
$[Ru(NH_3)_5(pz)]^{2+}$	0.49	$Ru^{II/III}$	GG, H_2O, NaCl, n.h.e.	61
$[Ru(bpy)_2(biImH_2)]^{2+}$	1.04	$Ru^{II/III}$	Pt, MeCN, Bu_4NBF_4, s.c.e.	50
$[Ru(bpy)_2(biBzImH_2)]^{2+}$	1.12		Pt, MeCN, Bu_4NBF_4, s.c.e.	50
$[Ru(bpy)_2(PBzImH)]^{2+}$	1.17		Pt, MeCN, Bu_4NBF_4, s.c.e.	50
$[Ru(bpy)_2(OBzImH)]^{2+}$	0.39		Pt, MeCN, Bu_4NBF_4, s.c.e.	50

Table 1. (continued)

Complex[a]	E/V	ECLS[b]	Conditions[c]	Ref.
$[Ru(bpy)_2(PBzIm)]^+$	0.72		Pt, MeCN, Bu_4NBF_4, s.c.e.	50
$[Ru(bpy)_2(biBzImH)]^+$	0.72		Pt, MeCN, Bu_4NBF_4, s.c.e.	50
$[Ru(bpy)_2(biBzIm)]$	0.43		Pt, MeCN, Bu_4NBF_4, s.c.e.	50
$[Ru(bpy)_2(OBzIm)]^+$	0.09		Pt, MeCN, Bu_4NBF_4, s.c.e.	50
$[Ru(2,3\text{-dpp})(bpy)_2]^{2+}$	1.31	$Ru^{II/III}$	Pt, MeCN, Et_4NClO_4, s.c.e.	103

Note. [a] The abbreviations of the ligand names are given in the text of the corresponding sections. Those not mentioned in the text are as follows: dpk = 2,2'-bipyridyl ketone; R_2dsc = dialkyl-substituted diselenocarbamate; (o-NH_2)TPP = tetra-o-aminophenylporphyrin; tpy = 2,2',6',2''-terpyridine; PBzImH = 2-(2-pyridyl)benzimidazole; OBzImH = 2-(o-hydroxyphenyl)benzimidazole; PImH = 2-(2-pyridyl)imidazole; $Fc^{+/0}$ = ferrocene-ferrocenium cation redox couple.

[b] ECLS denotes the most probable sites where the electronic changes are localised in the redox transitions. An empty column means that the assignment is difficult. The symbol L indicates that the reduction involves one of the ligands.

[c] In all tables, the conditions in the electrochemical measurements are listed in the following order: material of the working electrode, solvent, supporting electrolyte, reference electrode.

Table 2. Data on the electrochemical reduction of mononuclear ruthenium complexes.

Complex	$-E$/V	ECLS	Conditions	Ref.
4 ('capped')	0.86	L	Pt, MeCN, Bu_4NClO_4, s.c.e.	22
	0.99			
	1.17			
5 ('bicapped')	1.01	L	Pt, MeCN, Bu_4NClO_4, Ag	22
	1.20			
	1.38			
$[Ru(bpy)_3]^{2+}$	1.35	L	Pt, MeCN, Bu_4NClO_4, Ag	2, 44
	1.54			
	1.79			
$[Ru(5,5'\text{-}(EtO_2C)_2bpy)_3]^{2+}$	0.74	L	Pt, MeCN, Bu_4NClO_4, Ag	22
	0.86			
	1.03			
$[Ru(bpy)_2bpt]^+$	1.46	bpy	CG, MeCN, Bu_4NClO_4, n.h.e.	1
	1.72			
	2.28			
	2.45			
	2.52			
$Ru(2,3\text{-dpp})(CO)_2Cl_2$	1.04	dpp	Pt, MeCN, Et_4NClO_4, s.c.e.	106
$Ru(2,5\text{-dpp})(CO)_2Cl_2$	0.93	dpp	Pt, MeCN, Et_4NClO_4, s.c.e.	106
$[Ru(bpy)(biq)(Me_2bpy)]^{2+}$	0.92	biq	Pt, MeCN, Bu_4NClO_4, s.c.e.	42
	1.39	bpy		
	1.72	Me_2bpy		
$[Ru(bpy)(biq)(phen)]^{2+}$	0.90	biq	Pt, MeCN, Bu_4NClO_4, s.c.e.	42
	1.38	bpy		
	1.68	phen		
$[Ru(bpy)(biq)(pq)]^{2+}$	0.88	biq	Pt, MeCN, Bu_4NClO_4, s.c.e.	42
	1.19	pq		
	1.62	bpy		
$[Ru(bpy)(biq)(i\text{-biq})]^{2+}$	0.92	biq	Pt, MeCN, Bu_4NClO_4, s.c.e.	42
	1.39	bpy		
	1.66	i-biq		
$[Ru(bpy)(biq)(pzpm)]^{2+}$	0.89	biq	Pt, MeCN, Bu_4NClO_4, s.c.e.	42
	1.38			
	1.65			
$[Ru(bpy)_2(dinapy)]^{2+}$	1.66	dinapy	Pt, MeCN, Bu_4NClO_4, s.c.e.	42
	1.26			
	1.83			
$[Ru(bpy)(biq)(bpm)]^{2+}$	0.82	biq	Pt, MeCN, Bu_4NClO_4, s.c.e.	42
	1.10	bpm		
	1.56	bpy		
$[Ru(bpy)(biq)(taphen)]^{2+}$	0.65	taphen	Pt, MeCN, Bu_4NClO_4, s.c.e.	42
	1.00	biq		
	1.51	bpy		
$[Ru(bpy)(biq)(dinapy)]^{2+}$	0.66	dinapy	Pt, MeCN, Bu_4NClO_4, s.c.e.	42, 44, 53
	0.99	biq		
	1.71	bpy		
$[Ru(dinapy)_3]^{2+}$	0.82	dinapy	Pt, MeCN, Bu_4NClO_4, s.c.e.	44
	1.07			
	1.40			

Table 2. (continued)

Complex	$-E$/V	ECLS	Conditions	Ref.
$[Ru(salen)(Ph_3P)Cl]$	0.52	$Ru^{III/II}$	CG, MeCN, Bu_4NClO_4, $Ag/AgNO_3$	129
$[Ru(salen)(Ph_3P)(Py)]^+$	0.47	$Ru^{III/II}$	CG, MeCN, Bu_4NClO_4, $Ag/AgNO_3$	129
$[Ru(salen)(Ph_3P)(N_3)]$	0.64	$Ru^{III/II}$	CG, MeCN, Bu_4NClO_4, $Ag/AgNO_3$	129
$[Ru(salen)(Ph_3P)(PBu_3)]^+$	0.47	$Ru^{III/II}$	CG, MeCN, Bu_4NClO_4, $Ag/AgNO_3$	129
$[Ru(salen)(Ph_3P)(OTs)]$	0.65	$Ru^{III/II}$	CG, MeCN, Bu_4NClO_4, $Ag/AgNO_3$	129
$[Ru(salen)(CN)_2]^-$	1.06	$Ru^{III/II}$	CG, MeCN, Bu_4NClO_4, $Ag/AgNO_3$	129
$[Ru(bpy)_2(CO)_2]^{2+}$	1.03	$Ru^{II/I}$	Pt, MeCN, Bu_4NClO_4, s.c.e.	128
$[Ru(phen)_2(CO)_2]^{2+}$	1.07	$Ru^{II/I}$	Pt, MeCN, Bu_4NClO_4, s.c.e.	128
$[Ru(dmbpy)_2(CO)_2]^{2+}$	1.13	$Ru^{II/I}$	Pt, MeCN, Bu_4NClO_4, s.c.e.	128
$[Ru(phen)_3]^{2+}$	1.34	phen	Pt, MeCN, Bu_4NClO_4, s.c.e.	117
	1.47			
$[Ru(dpp)_3]^{2+}$	0.95	dpp	Pt, MeCN, Bu_4NClO_4, s.c.e.	117
	1.12			
	1.39			
$[Ru(dpq)_3]^{2+}$	0.62	dpq	Pt, MeCN, Bu_4NClO_4, s.c.e.	117
	1.80			
	1.06			
$[Ru(phen)_2(dpp)]^{2+}$	1.07	dpp	Pt, MeCN, Bu_4NClO_4, s.c.e.	117
	1.35	phen		
$[Ru(bpy)_2(dpp)]^{2+}$	1.06	dpp	Pt, MeCN, Bu_4NClO_4, s.c.e.	117
	1.48	bpy		
$[Ru(phen)_2(dpq)]^{2+}$	0.79	dpq	Pt, MeCN, Bu_4NClO_4, s.c.e.	117
	1.50	phen		
$Ru(dpk)_2Cl_2$	1.06	dpk	CG, DMF, Bu_4NClO_4, s.c.e.	132
$Ru(dpk)(CO)Cl_2$	0.79	dpk	CG, DMF, Bu_4NClO_4, s.c.e.	132
$[Ru(dpk)_2(MeCN)_2]^{2+}$	0.81	dpk	CG, DMF, Bu_4NClO_4, s.c.e.	132
$[Ru(bpy)_2(dpk)]^{2+}$	1.06	dpk	CG, DMF, Bu_4NClO_4, s.c.e.	132
$Ru(bqdH)_2(Ph_3P)_2$	1.18		Pt, CH_2Cl_2, Bu_4NClO_4, Ag/AgCl	76
	1.14		Au, CH_2Cl_2, Bu_4NClO_4, Ag/AgCl	
	1.16		CG, CH_2Cl_2, Bu_4NClO_4, Ag/AgCl	
$Ru(bqdH)_2(Ph_3P)(MeIm)$	1.13		Pt, CH_2Cl_2, Bu_4NClO_4, Ag/AgCl	76
	1.13		Au, CH_2Cl_2, Bu_4NClO_4, Ag/AgCl	
	1.12		CG, CH_2Cl_2, Bu_4NClO_4, Ag/AgCl	
$[Ru(bpy)_2(biImH_2)]^{2+}$	1.66	bpy	Pt, MeCN, Bu_4NClO_4, s.c.e.	50
	1.96			
$[Ru(bpy)_2(biBzImH_2)]^{2+}$	1.60	bpy	Pt, MeCN, Bu_4NClO_4, s.c.e.	50
	1.90			
$[Ru(bpy)_2(PBzImH)]^{2+}$	1.49	bpy	Pt, MeCN, Bu_4NClO_4, s.c.e.	50
	1.76			
$[Ru(bpy)_2(OBzImH)]^{2+}$	1.67	bpy	Pt, MeCN, Bu_4NClO_4, s.c.e.	50
	2.00			
$[Ru(bpy)_2(PBzIm)]^+$	1.46	bpy	Pt, MeCN, Bu_4NClO_4, s.c.e.	50
	1.70			
$[Ru(bpy)_2(biBzImH)]^+$	1.53	bpy	Pt, MeCN, Bu_4NClO_4, s.c.e.	50
	1.86			
$[Ru(bpy)_2(biBzIm)]$	1.58	bpy	Pt, MeCN, Bu_4NClO_4, s.c.e.	50
	1.87			
$[Ru(bpy)_2(OBzIm)]^+$	1.63	bpy	Pt, MeCN, Bu_4NClO_4, s.c.e.	50
	1.94			
$Ru(2,3\text{-dpp})(bpy)_2^{2+}$	1.06	dpp	Pt, MeCN, Et_4NClO_4, s.c.e.	103
	1.50			

Polypyridylruthenium(II) complexes can be reduced with participation of orbitals located both on the metal atom and on the ligand. If the ligand field is strong and (or) the ligands are readily reducible, then the reduction proceeds with participation of the π^* orbital of the ligand. A similar picture is usually observed for polypyridylruthenium(II) complexes.[1, 2, 35, 41, 42, 44] The reduced form retains the low-spin $4d^6$ configuration and the reduction process is reversible:

$$[Ru^{II}(LL)_3]^{2+} + \bar{e} \rightleftharpoons [Ru^{II}(LL)_2(LL^-)]^+ .$$

Thus the additional electron is localised on a specific ligand. It is of interest that the complex $[Ru(bpy)_3]^{2+}$ may be reduced with consumption of $6\bar{e}$, affording $[Ru^{II}(bpy)_3]^{4-}$. If the complex is heteroleptic, then the ligands are reduced consecutively in a sequence determined by the energies of their π^* orbitals.

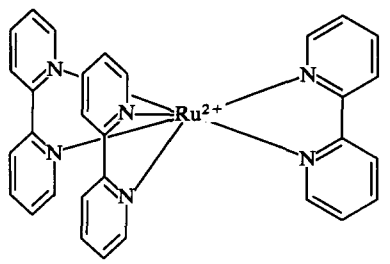
If the ligand field is weak, and (or) the ligands are difficult to reduce, then the e_g orbital, with an octahedral symmetry and largely located on the metal ion, may assume the role of the LUMO. In this case, the reduction product is an unstable low-spin d^7 system, in which one ligand is rapidly split off, which makes the reduction process irreversible:

$$[Ru^{II}(LL)_3]^{2+} + \bar{e} \rightleftharpoons [Ru^{I}(LL)_3]^+ \longrightarrow [Ru^{I}(LL)_2]^+ + LL.$$

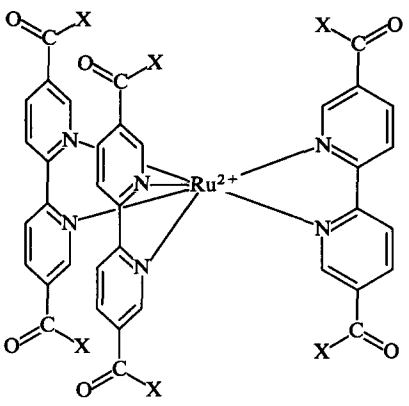
However, such processes are uncharacteristic of polypyridylruthenium complexes.

The electrochemical behaviour of the 'capped' (compound **4**) and 'bicapped' (compound **5**) see above) polypyridylruthenium(II) complexes and the comparison with their initial $Ru(bpy)_3^{2+}$ **11** and $Ru[5,5'\text{-}(EtO_2C)_2bpy]_3^{2+}$ **12**, a characteristic feature of which

is the distortion of the octahedral coordination sphere of the metal, are of interest.[22]



11

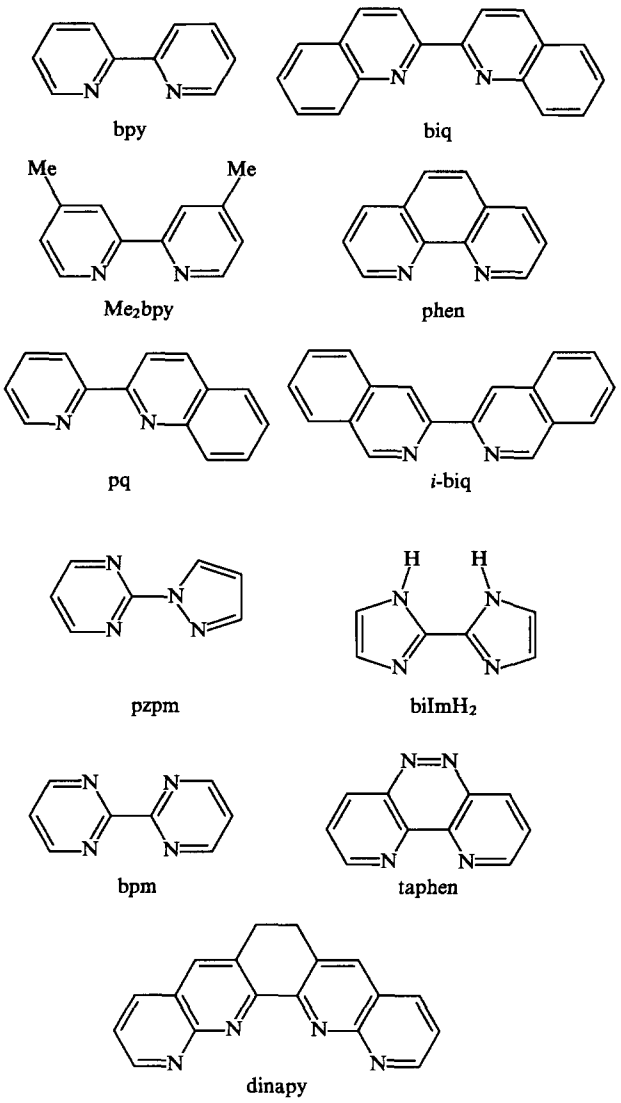


12

X = OC_2H_5

Complexes **4** and **5** are oxidised with one one-electron wave corresponding to oxidation 'at the metal atom' and are reduced with three one-electron waves corresponding to the reduction of the three bidentate ligands. The observed redox processes are reversible with the exception of the oxidation of compound **5**, as a result of which the process is kinetically controlled (i.e. the electron transfer is slow) even though stable species are formed. The low rate of electron transfer in the oxidation of compound **5** has been explained by steric hindrance, which precludes the approach of the metal atom to the electrode surface. Complexes **4**, **5**, and **12** are oxidised at identical potentials, which are more positive than for complex **11**. The equality of the oxidation potentials of compound **5** and **12** is surprising. In this case, one should apparently take into account the difference between the solvation energies of the oxidised and reduced forms and also the strain in the metal–ligand bonds due to the presence of the cage structure.

Electrochemical and spectroscopic data for the trisheteroleptic complexes $[Ru(LL)(LL)'(LL)'']^{2+}$ are very rarely encountered in the literature. The electrochemical behaviour of a series of nine recently synthesised complexes of the type $[Ru(bpy)(biq)(LL)]^{2+}$ (LL = Me_2bpy, phen, pq, *i*-biq, pzpm, $biImH_2$, bpm, taphen, and dinapy) has been investigated.[42] These complexes are especially interesting because the redox processes in them proceed with participation of orbitals located on four different centres: M, LL, LL', and LL''. The electrochemical behaviour of $[Ru(bpy)(biq)(LL)]^{2+}$ is qualitatively similar to that of other polypyridylruthenium(II) complexes:[2, 41, 43] a single metal oxidation wave and a series of three waves corresponding to the reduction of the ligands are observed on the cyclic voltammogram. In order to assign the reduction waves to a particular ligand, a comparison was made with the known reduction potentials of homoleptic[2, 29, 33, 41, 44–49] and bisheteroleptic[2, 29, 33, 44–47, 49–51] complexes. For LL = Me_2bpy and phen, the first reduction wave was attributed to biq, the second to bpy, and the third to the LL ligands. For LL = pq, the order in which the ligands are reduced is as follows: biq is reduced initially, is followed by pq, and finally bpy is reduced. In the case of LL = *i*-biq, the interpretation of the first two waves (biq and bpy)

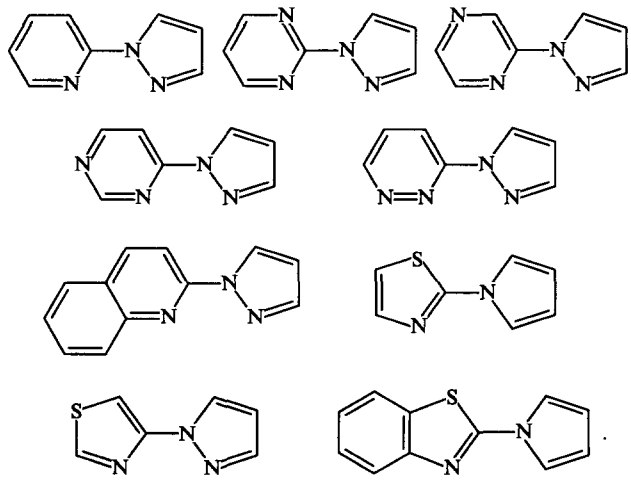


is not open to doubt, while the third wave may correspond both to the second stage of the reduction of biq and to the reduction of *i*-biq. For LL = pzpm, data on homoleptic complexes were not obtained. However, examination of the correlations between the spectroscopic and electrochemical quantities leaves no doubt that the biq ligand is the first to be reduced. Clear-cut data have not been obtained for LL = $biImH_2$, but it is clear from the first reduction potential (−1.66 V relative to the s.c.e.) of $[Ru(bpy)_2(biImH_2)]^{2+}$ that $biImH_2$ is reduced with more difficulty than bpy.[50] The first reduction potential of $[Ru(bpy)(biq)(biImH_2)]^{2+}$ was therefore attributed to the biq ligand. For LL = bpm, the sequence of the reduction waves is probably as follows: biq, bpm, bpy. The taphen ligand is very unusual, its π^* orbital being located mainly on the peripheral nitrogen atoms and having a low energy.[52] The most probable sequence in the reduction of the ligands of $[Ru(bpy)(biq)(taphen)]^{2+}$ is as follows: taphen is reduced initially and is followed by biq and bpy. Judging from the homoleptic complexes,[44, 53] dinapy is reduced more readily than biq, so that the order of the reduction of the ligands in $[Ru(dinapy)(biq)(bpy)]^{2+}$ should be as follows: dinapy, biq, bpy.

It has been shown[42, 54, 55] that in the polypyridylruthenium(II) complexes reduction involves in the first place the π^* orbital, with which the appearance in the spectra of the band due to charge transfer from the metal to the ligand (MLCT) is also associated. One can therefore expect a linear correlation[2, 29, 30, 33, 42, 45, 56, 57] between the energy of the absorption (or emission) maximum and the electrochemical gap $G = [E_{1/2}Ru(LL)_3^{III/II} - E_{1/2}Ru(LL)_3^{II/I}]$, which is a measure of the difference between the energies of

the HOMO and the LUMO of the ruthenium(II) complexes. Such correlation has indeed been observed for a series of polypyridyl complexes investigated (Fig. 9), with the exception of $[Ru(taphen)_3]^{2+}$.[42, 45] For this complex, both the long-wavelength absorption band and the emission band correspond to excited states with a higher energy than might have been expected on the basis of the reduction potential. This can be accounted for by the participation of the ligand biq in the spectral transitions, whereas the π^* orbital of the ligand taphen, localised mainly on the peripheral nitrogen atoms, participates in the redox transition. It is not clear why emission takes place from a high (with participation of biq) charge-transfer state and not from a low state (with participation of taphen).[42, 52] It may be that ligand–ligand interactions occur in the complexes investigated, which may be due both to electronic perturbations, transmitted mainly by the metal, and steric interactions of ligands such as biq.

The majority of studies devoted to the polypyridyl-ruthenium(II) complexes constitute in essence attempts to select the necessary properties of the ground and excited states of the complexes by replacing one or several bpy ligands by other nitrogen-containing chelating ligands, mainly by six-membered aromatic nitrogen-containing heterocycles (azines). Electrochemical studies on complexes containing five-membered aromatic heterocycles (azoles) have been recently initiated.[32] It has been shown[32] that such ligands modify to a greater extent the properties of ruthenium complexes, since the π-excess azoles differ radically from the π-deficient azines. The study of various heteroleptic complexes $[Ru(bpy)_2(LL')]^{2+}$ and homoleptic complexes $[Ru(LL')_3]^{2+}$ showed that the reduction involves the ligand and is almost always reversible.[32] In this case, the symbol LL′ designates bidentate ligands containing five- and six-membered heterocycles having the following structures:



For the series of complexes $[Ru(bpy)_{3-x}(LL')_x]^{2+}$, the dependence of E^{Ox} on x is linear for a wide range of LL′. The slope of the straight line can be used to estimate the relative contributions of the π-donor and π-acceptor properties of the ligands LL′.[32, 58]

In the study of the redox transitions of $[Ru(NH_3)_5L]^{III/II}$ (L = py-X; X = Me, Cl, $CONH_2$, CF_3, COMe, CHO, COOH, H),[59] it was noted that complexes with unsaturated π-ligands have appreciably more positive reduction potentials than the hexammine or aquo-complexes. The electron-accepting substituents X in $[Ru(NH_3)_5(py\text{-}X)]^{2+}$ increase the formal potentials E_f, i.e. the π-acceptor properties of the ligands facilitate the reduction of the oxidised complex. If yet another ammonia molecule in the complex is replaced by the ligand L′, with strong π-acceptor and weak σ-donor properties, the ruthenium(II) complex is stabilised relative to the ruthenium(III) complex, which means that the redox transition in $[Ru(NH_3)_4LL']^{III/II}$ is facilitated.[60] This is confirmed by the results of a study[61] in which measurements were made of the reduction potentials of a series of *trans*-$[Ru(NH_3)_4LL']^{3+}$ [L,L′ = pyridine, 4-picoline (4-pic), isonicotanimide (isn), 4-acetylpyridine (4-acpy), pyrazine (pz), or pyrazinium (pzH^+)] with a fixed ligand L. In terms of their ability to facilitate the reduction of the ruthenium complex, the ligands investigated can be arranged in the sequence pz > 4-acpy > isn > py > 4-pic. Comparison of the redox potentials of *cis*- and *trans*-$[Ru(NH_3)_4(isn)L]^{2+}$ showed that the *cis*-isomers are reduced more readily than their *trans*-analogues. Taking into account the fact that only one of the *d* orbitals of the metal participates in the bonding to both heterocyclic ligands, one may conclude that the heterocyclic ligands in *trans*-$[Ru(NH_3)_4(isn)L]^{2+}$ are coplanar.

The ruthenium and rhodium complexes are interesting because they can serve as convenient models for the study of the influence of the metal atom coordination on the properties of the ligands. For example, by comparing the rate of the alkaline hydrolysis of the CN group in the pentammine complexes $[M(NH_3)_5(RCN)]^{n+}$ (M = Ru, Rh; R = Me, Ph; n = 2, 3), it is possible to estimate the electronic influence of the central atom on the organic ligand.[62] The ruthenium(II) and rhodium(III) complexes are isoelectronic ($4d^6$) and differ only in the charge, while the ruthenium(III) and rhodium(III) complexes have the same charge but differ in the number of *d* electrons of the metal [Ru(III)—$4d^5$]. It was found that complexes containing ruthenium(III) are hydrolysed much more readily than their $4d^6$ rhodium(III) and ruthenium(II) analogues. This is due to the ability of ruthenium(III) to function as a π-acceptor (by virtue of the t_{2g} vacancy in the *d* orbitals) and to stabilise the negative charge arising when the nitrile carbon atom is attacked by the OH group. The ruthenium(II) complex hardly undergoes alkaline hydrolysis, since it is an electron donor in relation to the π-acceptor unsaturated organic ligands.

The capacity of ruthenium(III) for reverse π-bonding has been confirmed also by electrochemical studies on pentammine-ruthenium(II) complexes containing quinone diimine ligands.[63] Thus the abstraction of one electron alters radically the influence of the metal atom on the ligands. The determination of the potentials and of the nature of the redox transitions can therefore be extremely useful for the elucidation of the change in the electronic properties of the central metal atom and the ligands bound to it.

The olefin complexes of ruthenium(II) have been investigated.[64–66] $[Ru(CO)_2L(\eta^4\text{-cot})]^{2+}$ (where L = CO or PPh_3 and cot = cyclooctatetraene) is oxidised at a platinum electrode in a single irreversible one-electron stage.[64] Complexes of the type $[Ru(NH_3)_5(olefin)]^{2+}$, where styrene, *p*-vinylbenzoic acid, cyclohexa-1,3-diene, and a number of others were used as the olefins, have been investigated by cyclic voltammetry.[65] The introduction of substituents into the aromatic rings of the ligands does not affect the electrochemical oxidation potential, while the pentammine environment is more likely to compensate for the charge on the ruthenium centre than a polycarboxylate environment.

The electrochemistry of the mixed-ligand ruthenium(II) and ruthenium(III) complexes containing various β-diketonate ligands has been studied.[67] The *d*-π molecular orbitals, formed from the t_{2g} orbitals d_{xy}, d_{xz}, and d_{yz} of ruthenium, assume the role of the HOMO and the LUMO of the tris(β-diketonato)ruthenium complexes. Linear correlations have been found[67] between the ligand composition and the $E_{1/2}$ for the oxidation and reduction of the complexes. For example, the reduction potentials of the mixed-ligand complexes can be estimated from these linear relations when the $E_{1/2}$ for the reversible redox transitions in the corresponding homoleptic complexes are known:

$$E^{III/II}(L''_nL'_{3-n}) = (n/3)E^{III/II}(L''_3) + (1-n/3)E^{III/II}(L'_3)\ .$$

The ligand η^5-C_5Ph_5 is known to stabilise paramagnetic complexes, which makes it possible to investigate[68] by cyclic voltammetry the ruthenium(II) complexes containing this ligand, in particular $[RuBr(CO)_2(\eta^5\text{-}C_5Ph_5)]$, $[RuBr(CO)L(\eta^5\text{-}C_5Ph_5)]$ [where L = PPh_3, PEt_3, $P(OMe)_3$], $[Ru(CO)LL'(\eta^5\text{-}C_5Ph_5)]^+$

[where L = PEt_3 or $P(OMe)_3$; L′ = CO, C_2H_4, PEt_3, MeHC=CHMe, $P(OMe)_3$], [$RuMe(CO)_2(\eta^5\text{-}C_5Ph_5)$], and [$RuR(CO)(PEt_3)(\eta^5\text{-}C_5Ph_5)$] (where R = Me, Et, COMe, CH=CHMe). It is seen from the analysis of the oxidation potentials that:

(1) the C_5Ph_5 ligands stabilise the cations $[Ru^{III}Br(CO)L(\eta^5\text{-}C_5Ph_5)]^+$ [L = PPh_3, PEt_3, $P(OMe)_3$] and $[Ru^{III}R(CO)(PEt_3).(\eta^5\text{-}C_5Ph_5)]^+$ (R = Me, Et, COMe);

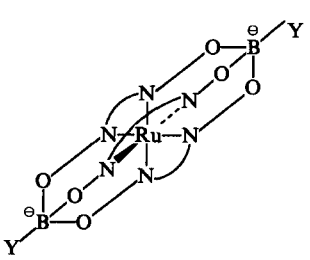
(2) the substitution of CO by L lowers the equilibrium potentials E^0;

(3) bromides are oxidised with greater difficulty than complexes containing σ-bound organic groups;

(4) the π-donor properties of the ligand have little influence on E^0.

The oxidation of sandwich complexes having the composition $(\eta^5\text{-}C_9H_7)Ru(\eta^5\text{-}L)$ (L = C_5H_5, C_5Me_5, C_9H_7) has been investigated.[69] The reversible transfer of one electron leads to the formation of 17-electron radical-cations, the stability of which depends on the properties of the η-ligand and the nucleophilicity of the medium.

The influence of the steric and electronic effects on the stability of boron-containing ruthenium(II) and ruthenium(III) complexes has been investigated.[70] The cathodic (I_{pc}) and anodic (I_{pa}) currents have been determined by cyclic voltammetry for the quasi-equilibrium couple Ru(II/III); their ratio I_{pc}/I_{pa} served as a criterion of the stability of the ruthenium(III) complex. The increase in I_{pc}/I_{pa} for a series of substituents Y, i.e. $n\text{-}C_{10}H_{21}O > n\text{-}C_5H_{11}O > Bu^nO > Pr^nO > EtO > MeO \simeq Pr^iO$, permits the conclusion that the stability of the ruthenium(III) complex increases with increase in the length of the chain of the alkoxy-groups. However, it is believed that this effect is not related to the electronic or steric effects of the alkoxy-substituents, whereas the decrease in I_{pc}/I_{pa} on passing from $Ru(chd)_3(BOPr^n)_2$ to $Ru(chd)_3(BOPr^i)_2$ indicates a decrease in the stability of the high-valence complex with increase in the bulk of the alkoxy-groups.



Here O—N N—O is

(1) a 1,2-cyclohexanone dioxime residue (chd) with Y = Ph, Bu^n, Me, F or OR (R = Me, Et, Pr^n, Bu^n, $n-C_5H_{11}$, $n-C_{10}H_{21}$),

(2) a diphenyl-glyoxime residue (dpg) with Y = Bu^n or OMe, or

(3) a dimethyl-glyoxime residue (dmg) with Y = Bu^n or OMe.

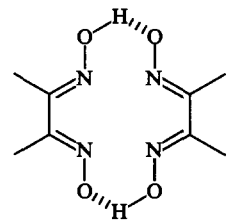
The study of the high-valence ruthenium(IV) complexes is of special interest, since they may prove to be promising catalysts (see, for example, Refs 71–73). The ruthenium(IV) complexes are relatively rare, and only a few of them have been reliably characterised (see Refs 74–76 and the literature quoted therein).

Ruthenium(II) complexes containing macrocyclic ligands which are difficult to oxidise can be readily oxidised at platinum, gold, or carbon glass electrodes with formation of hexacoordinate complexes formally corresponding to ruthenium(III) and ruthenium(IV), for example:[76]

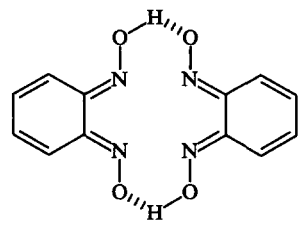
$$Ru(dmgH)_2(PPh_3)_2 \rightleftharpoons [Ru(dmgH)_2(PPh_3)_2]^+ + \bar{e},$$

$$[Ru(dmgH)_2(PPh_3)_2]^+ \rightleftharpoons [Ru(dmgH)_2(PPh_3)_2]^{2+} + \bar{e}.$$

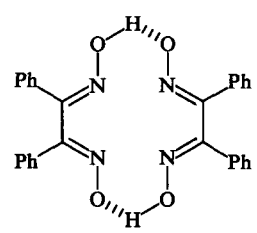
The ruthenium(III) complexes are relatively stable at room temperature, while the formation of the formally tetravalent ruthenium(IV) complexes frequently requires cooling to −78 °C.



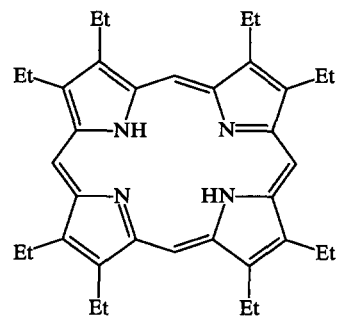
$(dmgH)_2$



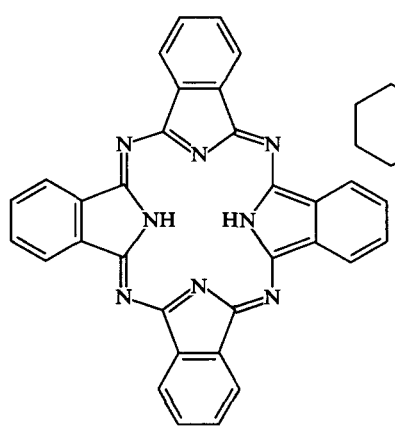
$(bgdH)_2$



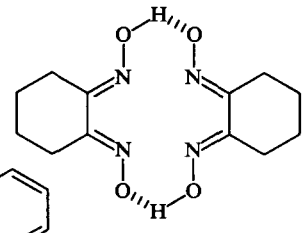
$(dpgH)_2$



P_0



P_c



$(chdH)_2$

It has been shown[76] that the stability of the ruthenium(IV) complexes increases significantly on replacement of nitrogen- or oxygen-containing donors (*N*-methylimidazole, DMSO, pyridine, etc.) by phosphine ligands. However, the formation of a high-valence ruthenium(IV) complex on oxidation of the complex $[Ru(bpy)_2(biBzIm)]^{2+}$ (where $biBzImH_2$ = 2,2′-bibenzimidazole) can be observed by cyclic voltammetry at a carbon glass (CG) electrode at a potential scanning rate $> 5\ V\ s^{-1}$.[77] In contrast to the complex $[Ru(bpy)_3]^{2+}$, for which the second anodic wave corresponds to the oxidation of the ligand,[78] it was shown in this case[77] that the oxidation takes place at the ruthenium atom and that a low-spin d^5 [ruthenium(III)] complex is indeed formed.

The replacement of the nitrogen-containing macrocyclic system by other ligands, for example, 8-hydroxyquinoline, lowers the stability of the ruthenium(IV) complexes. The ability of nitrogen-containing macrocycles to stabilise metals in high oxidation states is known. For example, the complex $[Hg^{III}(N_4)]^{3+}$ (where N_4 = 1, 4, 8, 11-tetraazacyclotetradecane) with a lifetime of about 5 s at −78 °C has been obtained by electrochemical oxidation.[79, 80] Ruthenium(IV) complexes not containing macrocyclic ligands could not be isolated, although electrochemical evidence for their formation has been obtained.[81, 82] It is noteworthy that a true ruthenium(IV) complex is obtained only

if the ligand is not oxidised. In certain cases, the ligand may be oxidised after the electron transfer from the metal atom, i.e. there is a possibility of an intramolecular reaction involving electron transfer from the ligand to the metal, which means that the ruthenium(IV) complex cannot be claimed to be the final product of the electron transfer. The involvement of ligands such as dimethylglyoxime and its derivatives in such processes is unlikely, so that complexes containing them are extremely convenient for the synthesis of ruthenium(IV) compounds. There exists another point of view, according to which ruthenium(IV) complexes may be regarded as ruthenium(III) radicals.[77] The oxidation of the complex $Ru(dtc)_3$ (where dtc = dithiocarbamate) leads to the formation of heptacoordinate ruthenium(IV) complexes of the type $[Ru(dtc)_3Solv]^{2+}$ (Solv = solvent molecule)[83] or dimeric ruthenium(III) complexes. Similarly the oxidation of ruthenocene affords $[Ru^{IV}Cp_2Solv]^{2+}$.[84] The heptacoordinate ruthenium(IV) complexes are more stable than the hexacoordinate complexes.[76]

In conclusion one should note that, in order to be able to compare the electronic properties of different compounds on the basis of electrochemical parameters (current, potential), one has to be sure that the diffusion coefficient is constant for the given series of compounds. Measurements have been made[85] of the diffusion coefficients of a large series of ruthenium(II) complexes in solution in acetonitrile using a rotating disc electrode and it was shown that the diffusion coefficient remains almost constant, while the rate of electron transfer increases with decrease in the redox potential.

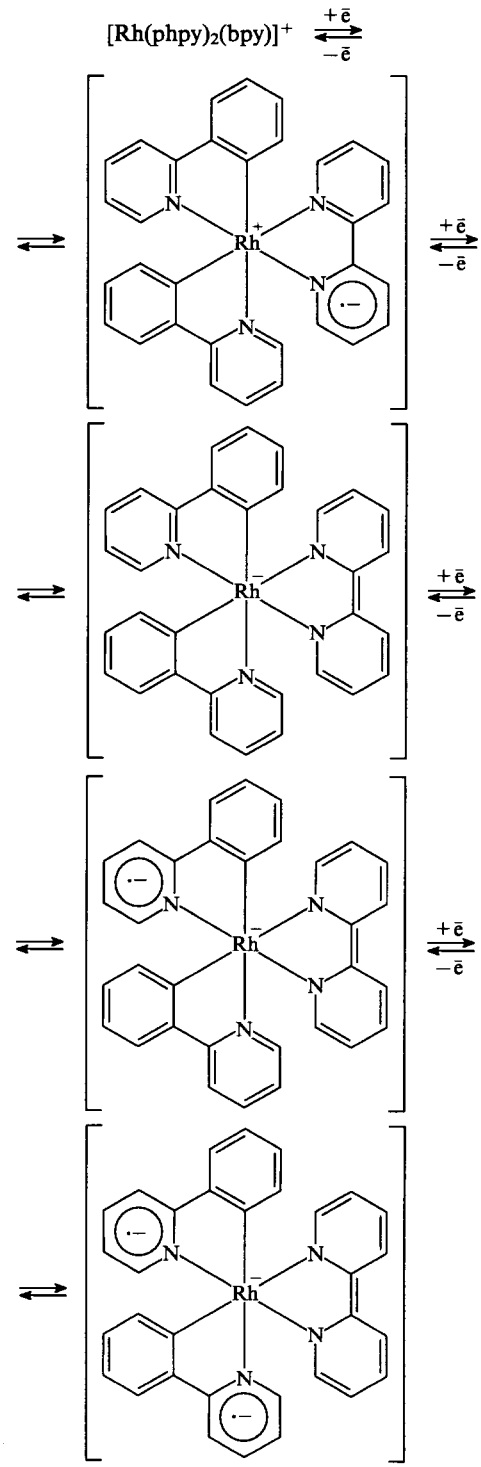
2. Electrochemical properties of mononuclear rhodium complexes

Comparison of the electrochemical properties of complexes containing metal atoms in the d^6 and d^8 configurations, for example, ruthenium(II) (d^6) and rhodium(I) (d^8) compounds, is of definite interest from the theoretical point of view. The energy difference between HOMO and LUMO is much smaller if the central metal atom has the d^8 configuration and not the d^6 one. This is apparently due to the fact that in the former case the unoccupied orbital is a ligand orbital, whilst the HOMO is localised on the metal atom.[86] For metal complexes with the d^6 configuration, both the HOMO and the LUMO are localised on the metal. This is confirmed, for example, by data on the electrochemical oxidation and reduction of dienerhodium(I) complexes containing cycloocta-1,5-diene (cod) or norbornadiene (nbd) ligands with 2,2′-bipyrimidine (bpym) (Tables 3 and 4).[86]

Extensive studies have been made on rhodium(III) complexes containing bipyrimidine and a number of other ligands capable of forming ortho-metallated derivatives, for example $[Rh(phpy)_2(phen)]^+$, $[Ru(thpy)_2(phen)]^+$, $[Rh(phpy)_2(biq)]^+$, $[Rh(phpy)_2(bpy)]^+$, and $[Rh(thpy)_2(bpy)]^+$, where phen = 1,10-phenanthroline, biq = 2,2′-biquinoline, and $phpy^-$ and $thpy^-$ denote the *ortho*-C-deprotonated forms of 2-phenylpyridine and 2-(2-thienyl)pyridine.[87–90] The *ortho*-metallated complexes constitute a new potential class of mediators for photochemical and chemiluminescence reactions. Four reversible waves are observed in the reduction of $[Rh(phpy)_2(bpy)]^+$ at a platinum disc electrode and a mercury dropping electrode in DMF at a low temperature (−54 °C).[87, 89] On the basis of the behaviour of the homoleptic complexes $Ru(bpy)_3^{2+}$,[33, 43] $Ir(bpy)_3^{3+}$, and $Ir(phpy)_3$,[89] as well as the dimer $[Ru(phpy)_2Cl]_2$,[91] one may conclude that the appearance of such a large number of reduction waves should be associated not only with ligand orbital association processes but also with the acceptor orbitals localised on the pyridine rings of the individual ligands. The first wave has been attributed to the reduction of the ligand bpy, while the group of three closely spaced waves is associated with the reduction of the two $phpy^-$ ligands and the second stage of the reduction of bpy (Scheme 1).

Three reversible waves are observed in the electrochemical reduction of $[Rh(phpy)_2phen]^+$ and $[Rh(phpy)_2(biq)]^+$. Thus each heteroleptic complex has virtually the same set of reduction waves regardless of whether the ligands are linked to a

Scheme 1



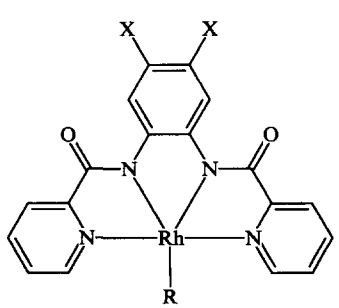
rhodium(III) atom or to, for example, an iridium(III) atom and the process proceeds consecutively with respect to each of the pyridine rings present in the molecule;[87] the difference between the wave [half-wave?] potentials is 0.2–0.3 V. The oxidation of rhodium(III) complexes listed above, with *ortho*-metallated nitrogen-containing ligands, takes place at the metal atom.

The correlations between the electrochemical parameters and electronic spectroscopic data for rhodium complexes have been examined.[87, 92–94] Cyclic voltammetric data[87] have shown that N,N-coordinated ligands are reduced more readily than the N,C-coordinated ones (for example, $phpy^-$). This shows that the π^* LUMO is to a large extent associated with the N,N-coordinated ligands. However, it follows from the absorption spectra[87] that the MLCT band with minimum energy corresponds to the electron transfer from the metal to the N,C-coordinated ligands and not to

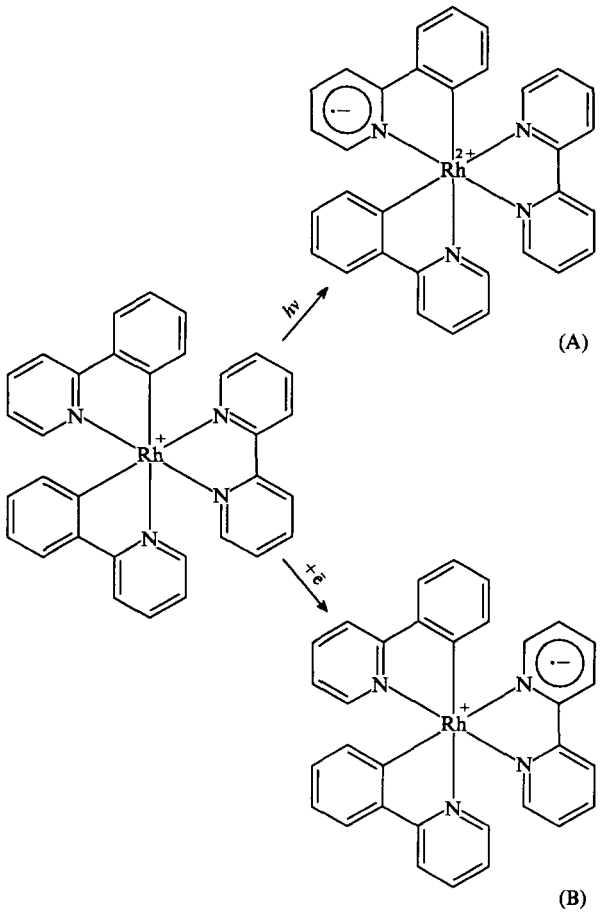
Table 3. Data on the electrochemical oxidation of mononuclear rhodium complexes.

Complex	E/V	ECLS	Conditions	Ref.
$[N(CH_2CH_2PPh_2)_3Rh(CN)]$	−0.19	$Rh^{I/II}$	Pt, CH_2Cl_2, Bu_4NClO_4, s.c.e.	93
	0.23	$Rh^{II/III}$		
	−0.19	$Rh^{I/II}$	Pt, THF, Bu_4NClO_4, s.c.e.	
	0.19	$Rh^{II/III}$		
$[P(CH_2CH_2PPh_2)_3Rh(CN)]$	−0.13	$Rh^{I/II}$	Pt, CH_2Cl_2, Bu_4NClO_4, s.c.e.	93
	0.38	$Rh^{II/III}$		
	−0.12	$Rh^{I/II}$	Pt, THF, Bu_4NClO_4, s.c.e.	
	0.34	$Rh^{II/III}$		
$[N(CH_2CH_2PPh_2)_3Rh(C\equiv CPh)]$	−0.45	$Rh^{I/II}$	Pt, CH_2Cl_2, Bu_4NClO_4, s.c.e.	93
	0.02	$Rh^{II/III}$		
	−0.39	$Rh^{I/II}$	Pt, THF, Bu_4NClO_4, s.c.e.	
	0.02	$Rh^{II/III}$		
$[P(CH_2CH_2PPh_2)_3Rh(C\equiv CPh)]$	−0.29	$Rh^{I/II}$	Pt, CH_2Cl_2, Bu_4NClO_4, s.c.e.	93
	0.38	$Rh^{II/III}$		
	−0.27	$Rh^{I/II}$	Pt, THF, Bu_4NClO_4, s.c.e.	
	0.31	$Rh^{II/III}$		
$[P(CH_2CH_2PPh_2)_3Rh(C\equiv C-CO_2Et)]$	−0.21	$Rh^{I/II}$	Pt, CH_2Cl_2, Bu_4NClO_4, s.c.e.	93
	0.33	$Rh^{II/III}$		
	−0.18	$Rh^{I/II}$	Pt, THF, Bu_4NClO_4, s.c.e.	
	0.28	$Rh^{II/III}$		
$[Rh(bpb)Me]\cdot H_2O$	0.31	$bpb^{0/+}$	CG, MeCN, Bu_4NBF_4, $Fc^{+/0}$	95
	0.81			
$[Rh(bpb)Et]\cdot H_2O$	0.31		CG, MeCN, Bu_4NBF_4, $Fc^{+/0}$	95
	0.82			
$[Rh(bpb)Cl_2]^-$	0.35		CG, MeCN, Bu_4NBF_4, $Fc^{+/0}$	95
	0.91			
$[Rh(bpb)(Py)]^+$	0.77		CG, MeCN, Bu_4NBF_4, $Fc^{+/0}$	95
	1.21			
$[Rh(bpb)(PPh_3)]^+$	0.70		CG, MeCN, Bu_4NBF_4, $Fc^{+/0}$	95
	1.25			
$[Rh(bpc)Me]\ H_2O$	0.48	$bpc^{0/+}$	CG, MeCN, Bu_4NBF_4, $Fc^{+/0}$	95
	0.94			
$[Rh(bpc)Cl_2]^-$	0.50		CG, MeCN, Bu_4NBF_4, $Fc^{+/0}$	95
	0.99			
$[Rh(bpb)(CN)_2]^-Na^+$	0.61		CG, MeCN, Bu_4NBF_4, $Fc^{+/0}$	95
	1.07			
$[Rh(ppz)_2bpy]^+$	1.27	$Rh^{III/IV}$	Pt, DMF, Et_4NClO_4, s.c.e.	88
$[Rh(3\text{-}Clppz)_2(bpy)]^+$	1.25		Pt, DMF, Et_4NClO_4, s.c.e.	88
$[Rh(4\text{-}NO_2ppz)_2(bpy)]^+$	1.24		Pt, DMF, Et_4NClO_4, s.c.e.	88
$[Rh(ppz)_2(biq)]^+$	1.20		Pt, DMF, Et_4NClO_4, s.c.e.	88
$[Rh(4\text{-}NO_2ppz)_2(biq)]^+$	1.09		Pt, DMF, Et_4NClO_4, s.c.e.	88
$[(NP_3)Rh(C\equiv CPh)]$	−0.45	$Rh^{I/II}$	Pt, CH_2Cl_2, Bu_4NClO_4, s.c.e.	94
$[(NP_3)Rh(C\equiv CCOOEt)]$	−0.26		Pt, CH_2Cl_2, Bu_4NClO_4, s.c.e.	94
$[(PP_3)Rh(C\equiv CPh)]$	−0.29		Pt, CH_2Cl_2, Bu_4NClO_4, s.c.e.	94
$[(PP_3)Rh(C\equiv CCOOEt)]$	−0.21		Pt, CH_2Cl_2, Bu_4NClO_4, s.c.e.	94
$[(NP_3)RhCN]$	−0.19		Pt, CH_2Cl_2, Bu_4NClO_4, s.c.e.	94
$[(PP_3)RhCN]$	−0.30		Pt, CH_2Cl_2, Bu_4NClO_4, s.c.e.	94
$[Rh(cod)(bpym)]^+$	0.96	$Rh^{I/II}$	Pt, MeCN, Et_4NClO_4, s.c.e.	86
$[Rh(nbd)(bpym)]^+$	1.10		Pt, MeCN, Et_4NClO_4, s.c.e.	86
$[Rh(R_2dtc)_3]$				
R = Me	1.13		Pt, CH_2Cl_2, Bu_4NClO_4, Ag/AgCl	133
Et	1.12			
Pr	1.02			
$[Rh(Et_2dsc)_3]$	0.78		Pt, CH_2Cl_2, Bu_4NClO_4, Ag/AgCl	133

the more readily reducible N,N-coordinated ligands. The reasons why the energies of the Rh→N,C and Rh→N,N transitions do not reflect the energies of the corresponding π^* orbitals are probably as follows. First, the octahedral t_{2g} d orbitals of the metal are split in different ways owing to the different electron-donating capacities of the N,N- and N,C-ligands and the d orbitals of the metal participating in the Rh→N,C transitions have a higher energy than the d orbitals involved in the Rh→N,N transitions. Secondly, owing to the different nature of the Rh–N,C and Rh–N,N bonds, the interaction between the outer electron shells in the excited state (A) and in the radical (B) may differ greatly, so that on photoexcitation the radical cation (A) is more stable while on electrochemical reduction radical (B) is more stable (see over).

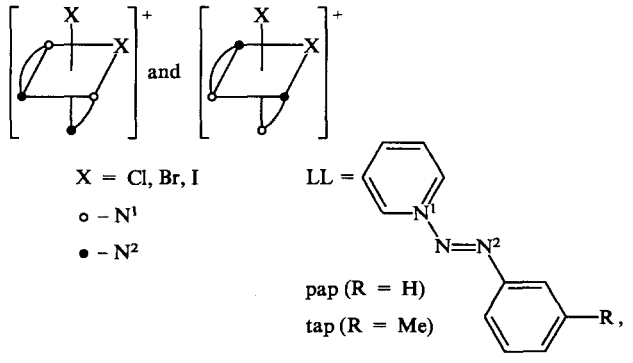


X = H, Cl;
R = Me, Et, Pr.



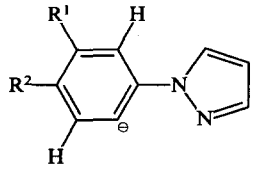
The dianionic amide chelating ligands containing a pyridine fragment are capable of stabilising transition metals in high oxidation states, which makes it possible to obtain fairly stable rhodium(IV) complexes. The electrochemical oxidation of such complexes has been investigated,[95] but the attempts to find a correlation between λ_{max} in the electronic absorption spectra of these compounds and their oxidation potentials were also unsuccessful. Thus the simplified picture of the 'localisation of the electronic changes' associated with the spectroscopic and electrochemical transitions ('on the metal' or 'on the ligand'), widely used for transition metal compounds, does not always yield a satisfactory description, particularly in the case of systems containing *ortho*-metallated ligands, where the metal–ligand bonds are significantly covalent.

The redox properties of 2-arylazopyridinerhodium(III) complexes $[RhX_2(LL)_2]ClO_4$, having the structure



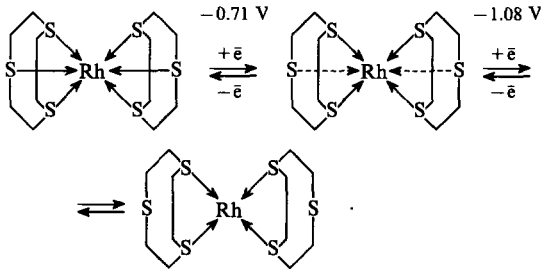
have been investigated by cyclic voltammetry at a platinum electrode.[96] The studies were carried out over a wide range of potentials: from 2.0 to −1.5 V. Three cathodic waves were observed, but the reduction products were unstable and were not isolated in a pure form. The EPR spectra of the electrolysis products at a reduced temperature (−13 °C) showed that the unpaired electron in the reduction products $[RhCl_2(LL)_2]$ and $[RhCl_2(LL)_2]^-$ is located on orbitals with a predominant ligand character, i.e. reduction takes place 'at the azo-group'.

The electrochemical behaviour of mixed-ligand rhodium(II) complexes containing neutral pyridine (bpy) and quinoline (biq) as well as anionic 1-phenylpyrazole ligands substituted in the benzene ring has been studied.[97] The results are in many respects similar to those observed for other cyclo-metallated rhodium(III) complexes:[88, 92] the reduction proceeds in the first place at the bpy ligand, while the oxidation is irreversible and belongs to processes 'localised on the metal'.



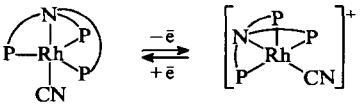
ppz⁻ ($R^1 = R^2 = H$)
(3-Clppz)⁻ ($R^1 = Cl$, $R^2 = H$)
(4-NO_2ppz)⁻ ($R^1 = H$, $R^2 = NO_2$)

Cyclic voltammetry at a platinum electrode of the homoleptic hexathia-coordinate complex $[Rh(LLL)_2](PF_6)_3$ (LLL = 1,4,7-trithiacyclononane) indicates the occurrence of two chemically reversible reduction processes, corresponding to the redox transitions Rh(III/II) and Rh(II/I). The cathodic reactions can be represented schematically as follows:[98]



The 19-electron complexes $[Rh(LLL)_2]^{2+}$ are less stable than the corresponding complexes $[Pd(LLL)_2]^{3+}$, which also have a central atom with the d^7 configuration. This is associated with the smaller formal charge on the rhodium atom. In the rhodium(I) complex, the metal has so many electrons that it is coordinated to only four and not six sulfur atoms. The cation $(Rh(LL)_2]^+$ is a very powerful reductant.

The redox properties of 18-electron pentacoordinate trigonal-bipyramidal rhodium(I) complexes containing σ-cyanide and σ-acetylide ligands, [(LLLL)Rh(CN)] and [(LLLL)Rh(C ≡ CPh)] [where LLLL = $N(CH_2CH_2PPh_2)_3$ or $P(CH_2CH_2PPh_2)_3$], were subjected to a comparative analysis.[93] It was found that there is little difference in the electrochemical behaviour of these complexes. π- and σ-bonding with the transition metal atom is characteristic of the cyanide and acetylide ligands. As a result of the one-electron oxidation of the above complexes, a stable paramagnetic rhodium(II) complex having the structure of a square pyramid is formed, for example:



Further oxidation of the rhodium(II) complex leads to the unstable rhodium(III) species, which rapidly decompose with formation of dicyanide complexes:

$$2[(LLLL)Rh(CN)]^{2+} \longrightarrow [(LLLL)Rh(CN)_2]^+ + [(LLLL)Rh]^{3+}.$$

Table 4. Data on the electrochemical reduction of mononuclear rhodium complexes.

Complex	$-E$/V	ECLS	Conditions	Ref.
$[Rh(phpy)_2(bpy)]^+$	1.84	bpy	Pt, DMF, Et_4NOH, $Ag/AgNO_3$	87, 89
	2.49			
	2.76			
$[Rh(phpy)_2(phen)]^+$	1.43	phen	Pt, DMF, Et_4NOH, $Ag/AgNO_3$	87
	2.12			
	2.42			
$[Rh(phpy)_2(bic)]^+$	1.00	bic	Pt, DMF, Et_4NOH, $Ag/AgNO_3$	87
	1.60			
	2.40			
$[RhCl_2(pap)_2]ClO_4 \cdot H_2O$	0.02	pap	Pt, MeCN, Et_4NOH, s.c.e.	96
	0.34			
	1.05			
$[RhCl_2(tap)_2]ClO_4 \cdot H_2O$	0.03	tap	Pt, MeCN, Et_4NOH, s.c.e.	96
	0.24			
	1.36			
[Rh(bpb)Me] H_2O	2.16	$Rh^{III/II}$	CG, MeCN, Bu_4NBF_4, $Fc^{+/0}$	95
[Rh(bpb)Et] H_2O	2.20		CG, MeCN, Bu_4NBF_4, $Fc^{+/0}$	95
$[Rh(bpb)Cl_2]^-$	1.98		CG, MeCN, Bu_4NBF_4, $Fc^{+/0}$	95
$[Rh(bpb)(Py)]^+$	1.70		CG, MeCN, Bu_4NBF_4, $Fc^{+/0}$	95
$[Rh(bpb)(Ph_3P)]^+$	1.30		CG, MeCN, Bu_4NBF_4, $Fc^{+/0}$	95
[Rh(bpc)Me] H_2O	2.15		CG, MeCN, Bu_4NBF_4, $Fc^{+/0}$	95
$[Rh(bpc)Cl_2]^-$	1.51		CG, MeCN, Bu_4NBF_4, $Fc^{+/0}$	95
$[Rh(bpc)(CN)_2]^-$	2.33		CG, MeCN, Bu_4NBF_4, $Fc^{+/0}$	95
$[Rh(ppz)_2(bpy)]^+$	1.46	bpy	Pt, DMF, Et_4NClO_4, s.c.e.	88
	2.09			
$[Rh(3\text{-}Clppz)_2(bpy)]^+$	1.42		Pt, DMF, Et_4NClO_4, s.c.e.	88
	2.02			
$[Rh(4\text{-}NO_2ppz)_2(bpy)]^+$	1.16		Pt, DMF, Et_4NClO_4, s.c.e.	88
	1.50			
$[Rh(ppz)_2(biq)]^+$	1.02	biq	Pt, DMF, Et_4NClO_4, s.c.e.	88
	1.64			
$[Rh(4\text{-}NO_2ppz)_2(biq)]^+$	0.92	biq	Pt, DMF, Et_4NClO_4, s.c.e.	88
	1.18	ppz		
	1.33			
	1.72			
$[Rh(cod)(bpym)]^+$	0.83	bpym	Pt, MeCN, Et_4NClO_4, s.c.e.	86
	0.90			
$[Rh(nbd)(bpym)]^+$	0.83		Pt, MeCN, Et_4NClO_4, s.c.e.	86
	0.91			
$Rh(Me_2dtc)_3$	2.02		Pt, CH_2Cl_2, Bu_4NClO_4, Ag/AgCl	133
	1.90		Hg, CH_2Cl_2, Bu_4NClO_4, Ag/AgCl	133
$Rh(Et_2dtc)_3$	2.11		Pt, CH_2Cl_2, Bu_4NClO_4, Ag/AgCl	133
	1.97		Hg, CH_2Cl_2, Bu_4NClO_4, Ag/AgCl	133
$Rh(Pr_2dtc)_3$	2.23		Pt, CH_2Cl_2, Bu_4NClO_4, Ag/AgCl	133
	2.10		Hg, CH_2Cl_2, Bu_4NClO_4, Ag/AgCl	133
$Rh(Et_2dsc)_3$	2.13		Pt, CH_2Cl_2, Bu_4NClO_4, Ag/AgCl	133
	1.99		Hg, CH_2Cl_2, Bu_4NClO_4, Ag/AgCl	133

Without knowing the structures of the intermediates, it is difficult to explain the pathway leading to the formation of the final dicyanide complex. The initial dimerisation with formation of a bridged tetracation $[(LLLL)Rh(\mu\text{-}CN)_2Rh(LLLL)]^{4+}$ and its subsequent decomposition appear most likely. Dicationic rhodium(III) acetylide complexes are more stable than the cyanide complexes. As expected, the acetylide ligands proved to be better donors, although not very much better, than the cyanide ions.

Terminal rhodium(II) and rhodium(III) complexes of acetylene have been obtained[94] by electrolysis at a controlled oxidation potential of the neutral rhodium(I) complexes [(LLLL)Rh(C≡CR)], where R = Ph, COOEt, or CHO. Comparison of the stretching vibration frequencies of the C≡C bond in a series of complexes $[(LLLL)Rh(C{\equiv}CR)]^{n+}$ (n = 0–2) or of the redox potentials in a series of complexes [(LLLL)RhX] (X = Cl, H, C ≡ CR, CN or CO) indicates a fairly considerable interaction between the d–π-orbital of the metal and the π* orbital of the acetylide. Such interaction is reflected in the properties of the carbon–metal bond in the rhodium(I) and rhodium(II) complexes. On passing from ligands without π-acceptor properties (H, Cl) to strong π-acceptors, the potential E_0 of the Rh(I)/Rh(II) redox couple increases in the sequence Cl > H > C≡CR > CN > CO. The σ-acetylide compounds lie halfway between the hydride and cyanide complexes, E^0 depending on the electronic properties of the substituent at the C≡C bond.

The study of the electrochemical properties of the porphyrins[99] made it possible to deduce a series of empirical rules whereby it is possible to determine the direction of the redox process. According to one of them, the electronic changes involve the ligand environment if in the electrochemical reduction process the difference between $E_{1/2}$ for the metalloporphyrin and $E_{1/2}$ for the free porphyrin is negative. This conclusion is based on the hypothesis that the metal exerts a positive inductive effect and therefore shifts the σ-electron density closer to the ligand. A similar approach has been used in an electrochemical study of tetra(3,5-di-*tert*-butyl-4-hydroxyphenyl)dodecachlorophthalocyanine complexes

of various metals, including rhodium and ruthenium.[100] The oxidation and reduction processes can be described by means of the following scheme:

$$PcMX_n \begin{cases} \xrightleftharpoons{+\bar{e}} (PcMX_n)^- \xrightleftharpoons{+\bar{e}} (PcMX_n)^{2-} \\ \xrightleftharpoons{-\bar{e}} (PcMX_n)^+ \xrightleftharpoons{-\bar{e}} (PcMX_n)^{2+} \end{cases}$$

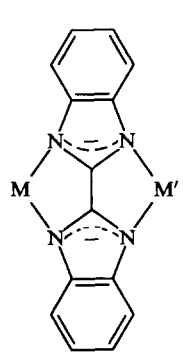
Pc = phthalocyanine, X = axial ligand.

It was shown that the magnesium, zinc, copper, and nickel complexes are oxidised and reduced with participation of the ligand, while the rhodium, ruthenium, osmium, cobalt, palladium, and platinum complexes are oxidised 'at the ligand' and their reduction takes place with participation of the metal ion.

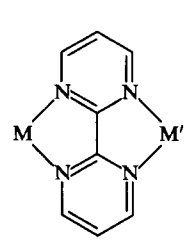
3. Polynuclear ruthenium and rhodium complexes

The redox chemistry of polymetallic complexes containing different bridging ligands is of special interest. Many natural products contain such fragments. By varying the structure of the bridging ligand, it is possible to alter the degree of metal–metal interaction and also the rate of the inner-sphere electron transfer. Complexes of metals in the same valence state as well as mixed-valence bimetallic complexes are known. Despite the fact that the study of the electrochemical properties of homonuclear and heteronuclear polymetallic complexes with organic ligands was begun comparatively recently, numerous interesting data, significantly expanding our ideas concerning their structure and properties, have already been obtained. The key component in such systems is the bridging ligand, since many properties of the complexes depend on the size, form, and electronic nature of the bridge; in certain cases, the bridge participates directly in electrochemical and photochemical processes.

Investigations of a series of 2,2′-bibenzimidazolyl (biBzIm) bridged homobinuclear and heterobinuclear complexes $[(bpy)_2M(biBzIm)M'(bpy)_2]^{n+}$ (n = 2–4; M = Ru, Os; M′ = Ru) and their fragments (mononuclear complexes) $[M(bpy)_2(biBzImH_2)]^{2+}$, $[M(bpy)_2(biBzIm)]$, and $[M'(bpy)_3]^{2+}$ have been performed.[101] The 2,2′-bibenzimidazolyl bridging ligand is structurally similar to the 2,2′-bipyrimidyl (bpm) ligand.



M(biBzIm)M′



M(bpm)M′

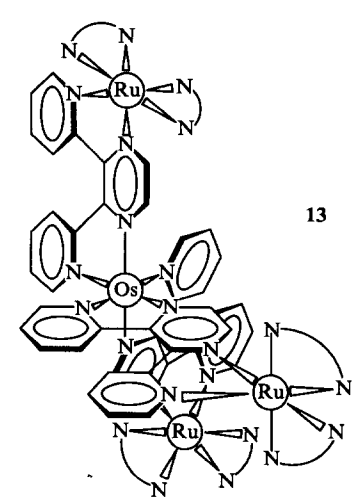
The distance between the metallic centres in these two complexes is in fact the same but the charges on the ligands are different; biBzIm has a charge of 2–, while bpm is neutral. All the dinuclear bisimidazolyl complexes investigated (with the exception of the ruthenium-nickel complex) give rise to two one-electron reversible waves on oxidation, whilst the complex containing ruthenium and nickel gives rise to one wave corresponding to the Ru(II)/Ru(III) transition. The potentials of the two oxidation waves of the heterobinuclear [Ru, Os] and [Ru, Co] complexes were compared with the potentials of the corresponding mononuclear complexes $[M(bpy)_3]^{2+}$, which made it possible to attribute the first electrode process (at the lower potential) to the Os(II)/Os(III) and Co(II)/Co(III) transitions and the second to the Ru(II)/Ru(III) transition. Comparison of the oxidation potentials of the dinuclear and mononuclear complexes $[M(bpy)_2(biBzImH_2)]^{2+}$ shows that the first oxidation potentials of the dinuclear complexes $[(bpy)_2M(biBzIm)M'(bpy)_2]^{n+}$ are lower by 0.3 V than the potentials of the corresponding mononuclear complexes. Hence it was concluded[101] that biBzIm exhibits electron-donating properties in the dinuclear complexes. On the other hand, the first oxidation potential of the dinuclear complex $[(bpy)_2Ru(bpm)Ru(bpy)_2]^{4+}$ is higher by 0.4 V than that of the corresponding mononuclear complex, which indicates the electron-accepting character of the bmp bridge. The potential of the Ru(II)/Ru(III) redox transition in the dinuclear complexes depends only on the charge of the second metal ion. This made it possible to conclude that the electron delocalisation via the biBzIm bridge is relatively slight and that electrostatic interactions have become an important potential-determining factor. Knowing the difference between the potentials of the different redox couples, it is possible to calculate the comproportionation constant (K_{com}).

$$[M^{II}-biBzIm-M^{II}]^{2+} + [M^{III}-biBzIm-M^{III}]^{4+} \rightleftharpoons 2[M^{II}-biBzIm-M^{III}]^{3+}$$

For example, $K_{com} = 8.2 \times 10^4$ for M = $Ru(bpy)_2$.[101]

2,3-Di(2-pyridyl)pyrazine (dpp) is an interesting nitrogen-containing bridging ligand. The complex $[Ru(dpp)_3]^{2+}$ is of great practical importance,[102] since it is capable of forming polymetallic chains, which makes it possible to obtain a new class of polynuclear complexes capable of accumulating solar energy. The strength of the electronic interaction between the metal atoms in the ground state of the bimetallic and polymetallic complexes depends on the distance between the metal atoms and on the degree of conjugation in the π-system of the bridging ligand. The transmission of the influence along the bridge can be estimated by comparing the potentials E^{Ox} of complexes of the type $[(LL)_2Ru^{II}(\mu\text{-}L)]^{2+}$ (LL = bpy or phen and μ-L = dpp, dpq, or bpm is the bridging ligand) with the first oxidation potentials of the corresponding complexes $[(LL_2Ru^{II})_2(\mu\text{-}L)]^{4+}$. The small difference between the oxidation potentials of the monometallic and bimetallic complexes (eg. ΔE = 10 mV) indicates an insignificant change in the energy of the t_{2g} orbitals and hence a weak interaction between the two metallic centres in the bimetallic complex. If the interaction had been stronger, the bimetallic complex would have been oxidised at more positive potentials and ΔE could have reached several hundreds of millivolts.

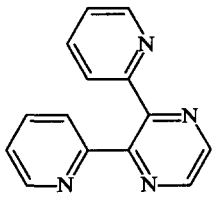
The redox properties of the heterometallic complex $Os[(\mu\text{-}2,3\text{-}dpp)Ru(bpy)_2]_3^{8+}$ **13**,[103] its homometallic analogue $Ru[(\mu\text{-}2,3\text{-}dpp)Ru(bpy)_2]_3^{8+}$ **14**,[102] and also the mononuclear



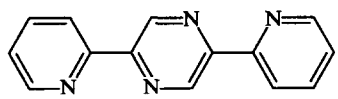
13

complexes $[Ru(2,3\text{-dpp})(bpy)_2]^{2+}$ **15**[104, 105] and $[Os(2,3\text{-dpp})_3]^{2+}$ **16**[105] have been investigated by cyclic voltammetry. A single one-electron reversible wave, attributed to the oxidation of the metal, was observed in the electrochemical oxidation of the mononuclear complexes. When the homotetrametallic complex **14** is oxidised, it gives rise to a three-electron wave corresponding to the oxidation of the peripheral ruthenium atoms. Oxidation at the central ruthenium atom is not observed, since the atom is bound to three strong π-acceptor dpp bridging ligands. In the oxidation of compound **13**, a one-electron reversible wave followed by a three-electron quasi-reversible wave is observed. The first anodic process was attributed to the oxidation of the osmium atom and the second to the oxidation of the three ruthenium atoms. In the reduction of compounds **13**, **14**, and **16**, three one-electron waves, associated with the reduction of the three dpp ligands (since they are reduced much more readily than bpy), were observed. It has been noted[102, 103] that the bridging ligands are as a rule reduced more readily to an extent of approximately 0.4 V than the structurally similar terminal ligands. The several indistinct waves observed at potentials more negative than −1.35 V probably correspond to further reduction of dpp and the one-electron reduction of the bpy ligands. The sequence in the reduction of the ligands in complex **15** is similar: dpp followed by bpy. On the basis of the reversibility of all three reduction waves for the tetrametallic complexes, one may postulate that these systems can serve as multielectron oxidising agents in the ground state.

A study[106] of the mononuclear and dinuclear ruthenium(II) complexes $[Ru(L)(CO)_2Cl_2]$ and $(\mu\text{-}L)[Ru(CO)_2Cl_2]_2$, containing the 2,3- and 2,5-isomers of di(2-pyridyl)pyrazine (dpp) as the bridging ligands, showed that the interaction between the metallic centres depends not only on the structure of the bridge but also on the nature of the ligands bound to the metal.



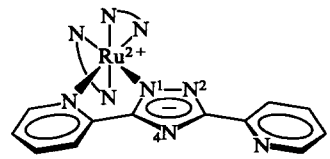
2,3-dpp



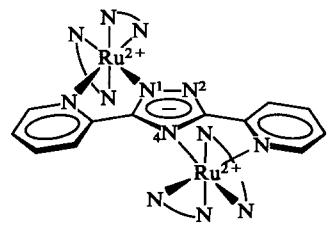
2,5-dpp

Monometallic and bimetallic complexes were oxidised with a single irreversible wave at a potential of about 2.0 V. Since the oxidation waves were observed only for the complexes and not for the free ligands, they apparently correspond to the oxidation of the metal ion. The high positive oxidation potentials agree well with the electron-accepting character of the CO ligands. The oxidation potentials of the monometallic and bimetallic complexes are similar, whence one may conclude that the bond between the two metallic centres is very weak. This can be accounted for by the strong mesomeric effect of the CO ligands. The first reduction wave for all the compounds of the given series is reversible and corresponds to the reduction of the aromatic ligand (dpp). Its potential diminishes in the sequence free ligand, mononuclear complex, dinuclear complex. This is associated with the fact that the electron density on the ligands diminishes on coordination to the electron-deficient ruthenium atom. A satisfactory linear correlation has been observed between the reduction potentials and the energies of the MLCT bands in the electronic spectra (see Section II.5).

The electrochemical behaviour at the carbon glass electrode of the polypyridine bisheteroleptic complexes has been investigated:[1, 107, 108] the mononuclear complex $[Ru(bpy)_2(bpt)]^+$ **17** and the dinuclear $[Ru(bpy)_2]_2(bpt)^+$ **18** [bpt = anion of 3,5-bis(2-pyridyl)-1,2,4-triazole].



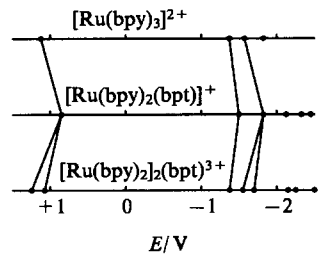
17



18

The anion bpt^- is particularly interesting, because, in contrast to the majority of other polypyridine bridging ligands, it carries a negative charge and exhibits a high σ-donor and low π-acceptor capacity. The redox potentials were measured using differential pulse polarography. The mononuclear complex **17** gives rise to one oxidation wave[107] and five reduction waves.[1, 108] The dinuclear complex **18** is oxidised in two stages,[107] while on reduction it gives rise to six waves, the first of which is a two-electron wave.[108] The protonated bpt^- anion (Hbpt) is not reduced at potentials up to −2.8 V. Scheme 2 illustrates the changes in E^{Red} and E^{Ox} on passing from $[Ru(bpy)_3]^{2+}$ to $[Ru(bpy)_2(bpt)]^+$ and then to the dinuclear complex.

Scheme 2



In particular, it follows from the analysis of Scheme 2 that, by virtue of the non-equivalence of the disposition of the two $[Ru(bpy)_2]^{2+}$ fragments relative to the bridge, two well-separated oxidation waves are obtained for the dinuclear complex, the difference between the potentials of which is 0.32 V. This permits the calculation of the comproportionation constant by using the equation $RT\ln K_{com} = F(\Delta E)$.

$$[M^{III}, M^{III}] + [M^{II}, M^{II}] \overset{K_{com}}{\rightleftharpoons} 2[M^{II}, M^{III}] .$$

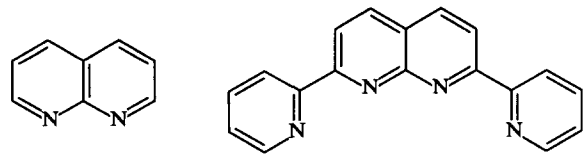
The value $K_{com} = 2.4 \times 10^5$ obtained indicates a fairly strong interaction between the metallic centres.

The first and second reduction potentials of $[Ru(bpy)_2bpt]^+$ are satisfactorily correlated with the corresponding reduction potentials of $[Ru(bpy)_3]^{2+}$ and hence can be attributed to the reduction of the coordinated bpy ligands.

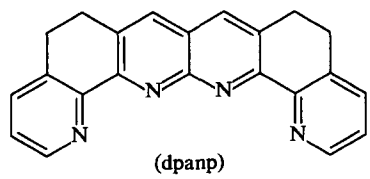
The splitting of the waves on passing from the mononuclear to the dinuclear compound in the reduction process is much smaller than the splitting observed in the oxidation process, so that the two centres involved in the reduction (ligands) are further apart than the two centres involved in the oxidation.

Detailed analysis of the electrochemical data obtained led to the conclusion[107] that the bridging bpt^- ligand hardly participates in the formation of the π LUMO of the complex.

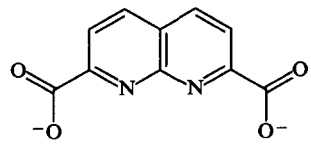
There exists a series of dinuclear copper, nickel, rhodium, and ruthenium complexes in which 1,8-naphthyridine (np) and its derivatives participate as the bridging ligands.[109, 110]



(np) (dpnp)



(dpanp)



$(dcnp)^{2-}$

These complexes are remarkable, because the small distance between the two metal nuclei leads to synergistic effects,[111, 112] especially in the homogenous catalysis.[113, 114] The oxidation of the rhodium complexes proceeds with participation of the orbitals localised on the metallic centres, while the reduction involves the ligand. It is of interest to note that the 2Ru(III)/Ru(III), Ru(II) transition in the complex $[Ru_2(OAc)_3(dcnp)]$ takes place very readily (0.33 V), while the Ru(III), Ru(II)/2Ru(II) transition is fairly difficult to achieve (−1.11 V), which indicates a greater stability of the system of the $[Ru^{III}, Ru^{II}]$ type. The stability of the $[Ru^{III}, Ru^{II}]$ complex can be estimated with the aid of the comproportionation constant

$$[Ru^{II}, Ru^{II}] + [Ru^{III}, Ru^{III}] \overset{K_{com}}{\rightleftharpoons} 2[Ru^{II}, Ru^{III}],$$

$$\ln K_{com} = \frac{F}{RT}(E_2^0 - E_1^0),$$

where E_2^0 and E_1^0 are the potentials of the 2Ru(III)/Ru(III), Ru(II) and Ru(III), Ru(II)/2Ru(II) redox transitions.

$K_{com} = 2.5 \times 10^{24}$ for the $[Ru_2(OAc)_3(dcnp)]$ complex,[110] which is one of the most stable mixed-valence complexes. For the analogous complex containing chloride instead of acetate ligands, $K_{com} = 3.5 \times 10^{23}$.[115] For comparison, we may point out that, for example, in the case of bimetallic ruthenium complexes, containing the bidentate bridging ligands 2,3-dpp and 2,3-di(2-pyridyl)quinoxaline (2,3-dpq), the comproportionation constant is of the order of 10^3. This value is the most typical for systems of this kind.[116]

It also follows from the electrochemical data[110] that the interaction between the metal atoms in the isovalent $[Ru^{II}, Ru^{II}]$ complex containing the dpp and dpq ligands is weak. The data presented indicate the important role of the aromatic bridging ligands in the redistribution of electrons between the two metallic centres.

The irreversible reduction wave of the complex $[Ru_2(OAc)_3(dcnp)]^-$ [formally corresponding to the 2Ru(II)/Ru(II)Ru(I) transition] is observed at very high cathodic potentials and has been attributed[110] to electron transfer to an orbital localised on the $(dcnp)^{2-}$ ligand.

The dependence of the distribution of electron density between the metal and the ligands on the introduction of a second substituent into the molecule has been investigated in relation to dienerhodium complexes containing bipyrimidine ligands.[86] Comparison of the spectroscopic and electrochemical properties of the mononuclear and dinuclear complexes $[Rh(nbd)(bpym)]^+$, $[Rh(cod)(bpym)]^+$, $[Rh(nbd)]_2(bpym)^{2+}$, and $[Rh(cod)]_2(bpym)^{2+}$ (where nbd = norbornadiene and cod = cycloocta-1,5-diene) showed[86] that in all cases the lowest excited state corresponds to the MLCT transition (Rh→bpym), while reduction involves in the first place the bpym ligand. The energy levels participating in the MLCT transition and also those associated with one-electron oxidation and reduction are very similar for the mononuclear and dinuclear complexes.

However, luminescence is observed for the mononuclear complexes but not for the dinuclear one. The reason for this is apparently the interaction of the two metallic centres. We may note that the potentials of the first and second reduction waves for $[Rh(cod)]_2(bpym)^{2+}$ are approximately equal to the reduction potential of the mononuclear complex (Tables 4 and 6), which shows that the introduction of the second Rh atom does not induce an appreciable change in the π^* level (b_1) of the bridging bipyrimidyl ligand. The dinuclear complexes are oxidised ($E_{1/2}$ = 1.0 V) with somewhat more difficulty than the mononuclear ones, which agrees fully with the electrostatic requirements. The potential of the second oxidation wave of the dinuclear rhodium complex is more positive by 0.42 V than that of the first wave. For the polynuclear ruthenium(II) complexes, the quantity $\Delta E_{1/2} = E^2_{1/2} - E^1_{1/2}$ can be regarded as a quantitative measure of the interaction between the two metallic centres.[117] Using a similar test, one may conclude that the interaction of the two rhodium(I) atoms in the $[Rh(cod)]_2(bpym)^{2+}$ ion is very significant.

In order to investigate the nature of the bonding in the cyanide-bridged rhodium and ruthenium complexes having the general formula $M^1-CN\rightarrow(M_2)^+$ [where M^1 and(or) M^2 = $(\eta^5\text{-}C_5H_5)Rh(\eta^3\text{-}C_3H_5)$ or $(\eta^6\text{-}Ph)Ru(\eta^3\text{-}C_3H_5)$], a study was made of their oxidation and reduction reactions and also of the corresponding characteristics of their mononuclear fragments.[118] All the complexes are reduced in the first place at the 'cationic' fragment (M^{2+}). This results in the formation of the cyanide M^1CN, which is reduced in the second stage:

$$M^1-CN\rightarrow(M^2)^+ \xrightarrow{+\bar{e}} M^1CN \xrightarrow{+2\bar{e}} \text{products} + CN^-.$$

The fact that the first electron transfer is followed by the chemical stage involving the cleavage of the bridge has been confirmed by the irreversible nature of the reduction process and also by the very great similarity between the potential of the second stage in the reduction of the bridged complex and the potential E^{Red} of the mononuclear cyanide complex forming part of its composition. The mechanism of the oxidation of complexes of this type is much more complex. The number of electrons involved in the oxidation depends greatly on the structure of the complex. The irreversibility of all the oxidation waves shows that the radical-cation formed initially undergoes rapid consecutive reactions. Detailed analysis of the electrochemical parameters showed that the centres at which the electronic changes are localised in the oxidation of the complexes can be different, but the bridge is not cleaved in the oxidation of any of the complexes investigated.[118] This demonstrates a fairly high strength of the $N\rightarrow M^+$ bond and the delocalisation of the charge on the cationic fragment over the entire $M^1-C\equiv N\rightarrow(M^2)^+$ chain. The oxidation at the 'cationic' metal atom observed for the complexes $RhCNRu^+$ and RhCNRh, which at first sight appears unlikely, can be accounted for by the charge redistribution. Comparison of the spectroscopic and electrochemical data has shown[118] that linear correlations between the electrochemical potentials and the frequency of the CN group stretching vibrations occur for a series of compounds in which the electronic changes are localised at the same centre.

The electrochemical behaviour of the mixed-valence cyanide-bridged complexes $[(NH_3)_5RuCNRu(bpy)_2CN]^{3+}$ and $[(NH_3)_5RuCNRu(bpy)_2CNRu(NH_3)_5]^{6+}$, which can be designated by [3.2] and [3.2.3] in conformity with the oxidation state of the ruthenium atoms, has been investigated[34] by polarographic and cyclic voltammetric methods and by electrolysis at a controlled potential. The oxidation potentials of the complexes [3.2] and

Table 5. Data on the electrochemical oxidation of dinuclear ruthenium and rhodium complexes.

Complex	E/V	ECLS	Conditions	Ref.
$Os[(\mu\text{-}2,3\text{-}dpp)Ru(bpy)_2]_3^{8+}$	1.25	$Os^{II/III}$	Pt, MeCN, Et_4NClO_4, s.c.e.	103
	1.55	$Ru^{II/III}$		
$Ru[(\mu\text{-}2,3\text{-}dpp)Ru(bpy)_2]_3^{8+}$	1.50	$Ru^{II/III}$	CG, MeCN, Bu_4NClO_4, s.c.e.	102
$[Ru(bpy)_2]_2(bpt)]^+$	1.04	$Ru^{II/III}$	CG, MeCN, Bu_4NClO_4, s.c.e.	107, 108
	1.34			
$(\mu\text{-}2,3\text{-}dpp)[Ru(CO)_2Cl_2]_2$	2.00	$Ru^{II/III}$	Pt, MeCN, Et_4NClO_4, s.c.e.	106
$(\mu\text{-}2,5\text{-}dpp)[Ru(CO)_2Cl_2]_2$	1.92	$Ru^{II/III}$	Pt, MeCN, Et_4NClO_4, s.c.e.	106
$(fulv)Ru_2(CO)_4$	1.05	$Ru_2^{I/II}$	Pt, THF, Bu_4NBF_4, n.h.e.	125
$(fulv)RuMo(CO)_5$	1.03	$Ru^{I/II}$	Pt, THF, Bu_4NBF_4, n.h.e.	125
$[(bpy)_2Ru(BiBzIm)Ru(bpy)_2]^{2+}$	0.77	$Ru^{II/III}$	Pt, MeCN, Bu_4NClO_4, s.c.e.	101
	1.06	$Ru^{II/III}$		
$[(bpy)_2Ru(BiBzIm)Os(bpy)_2]^{2+}$	1.01	$Ru^{II/III}$	Pt, MeCN, Bu_4NClO_4, s.c.e.	101
	0.39	$Os^{II/III}$		
$[(bpy)_2Ru(BiBzIm)Co(bpy)_2]^{2+}$	1.01	$Ru^{II/III}$	Pt, MeCN, Bu_4NClO_4, s.c.e.	101
	0.37	$Co^{II/III}$		
$[(bpy)_2Ru(BiBzIm)Ni(bpy)_2]^{2+}$	0.78	$Ru^{II/III}$	Pt, MeCN, Bu_4NClO_4, s.c.e.	101
$[(Rh\,cod)_2bpym]^{2+}$	1.00	Rh^{I}, $Rh^{I/II}$	Pt, MeCN, Et_4NClO_4, s.c.e.	86
	1.42	Rh^{II}, $Rh^{I/II}$		
$[Ru(phen)_2]_2(dpp)^{4+}$	1.41	Ru^{II}, $Ru^{II/III}$	Pt, MeCN, Bu_4NClO_4, s.c.e.	117
$[Ru(bpy)_2]_2(dpp)^{4+}$	1.44	Ru^{II}, $Ru^{II/III}$	Pt, MeCN, Bu_4NClO_4, s.c.e.	117
	1.65	Ru^{III}, $Ru^{II/III}$		
$[(phen)_2Ru(dpp)Ru(bpy)_2]^{4+}$	1.41	Ru^{II}, $Ru^{II/III}$	Pt, MeCN, Bu_4NClO_4, s.c.e.	117
	1.61	Ru^{III}, $Ru^{II/III}$		
$[Ru(bpy)_2]_2(dpq)^{4+}$	1.48	Ru^{II}, $Ru^{II/III}$	Pt, MeCN, Bu_4NClO_4, s.c.e.	117
	1.64	Ru^{III}, $Ru^{II/III}$		
$[Ru(phen)_2]_2(dpq)^{4+}$	1.47	Ru^{II}, $Ru^{II/III}$	Pt, MeCN, Bu_4NClO_4, s.c.e.	117
	1.62	Ru^{III}, $Ru^{II/III}$		
$[(phen)_2Ru(dpq)Ru(bpy)_2]^{4+}$	1.51	Ru^{II}, $Ru^{II/III}$	Pt, MeCN, Bu_4NClO_4, s.c.e.	117
	1.69	Ru^{III}, $Ru^{II/III}$		
$Ru_2(CO)_6L$	1.24		Pt, MeCN, Et_4NClO_4, s.c.e.	126
L = [C(Me) = C(Ph)COC(Me) = C(Ph)]	1.38		Pt, CH_2Cl_2, Et_4NClO_4, s.c.e.	126
$Ru_2(CO)_6L$	1.27		Pt, MeCN, Et_4NClO_4, s.c.e.	126
L = [C(Ph) = C(Ph)COC(Ph) = C(Ph)]				
$Ru_2(CO)_5(Ph_3P)L$	1.03		Pt, MeCN, Et_4NClO_4, s.c.e.	126
L = [C(Ph) = C(Me)COC(Ph) = C(Me)]	1.16		Pt, CH_2Cl_2, Et_4NClO_4, s.c.e.	126
$Ru_2(CO)_5(Ph_3As)L$	1.05		Pt, MeCN, Et_4NClO_4, s.c.e.	126
L = [C(Ph) = C(Me)COC(Ph) = C(Me)]	1.29		Pt, CH_2Cl_2, Et_4NClO_4, s.c.e.	126
$Ru_2(CO)_5(Ph_3Sb)L$	1.07		Pt, MeCN, Et_4NClO_4, s.c.e.	126
L = [C(Ph) = C(Me)COC(Ph) = C(Me)]	1.24		Pt, CH_2Cl_2, Et_4NClO_4, s.c.e.	126
$\{[(tpy)ClRu]_2(dpp)\}^{2+}$	0.94	$Ru^{II/III}$	Pt, MeCN, Bu_4NPF_6, s.c.e.	102
$\{Ru[(dpp)Ru(dpy)_2]_3\}^{8+}$	1.50	$Ru^{II/III}$	Pt, MeCN, Bu_4NPF_6, s.c.e.	102
$\{Ru[(dpp)Ru(phen)_2]_3\}^{8+}$	1.43	$Ru^{II/III}$	Pt, MeCN, Bu_4NPF_6, s.c.e.	102
$\{Ru[(dpp)Ru(tpy)Cl]_3\}^{5+}$	1.06	$Ru^{II/III}$	Pt, MeCN, Bu_4NPF_6, s.c.e.	102
$Rh_2(hp)_4$	0.82		Pt, MeCN, Bu_4NBF_4, Ag, $AgCl/Cl^-$	122
$Rh_2(chp)_4$	1.43		Pt, MeCN, Bu_4NBF_4, Ag, $AgCl/Cl^-$	122
$Rh_2(mhp)_4$	1.16		Pt, MeCN, Bu_4NBF_4, Ag, $AgCl/Cl^-$	122

Table 6. Data on the electrochemical reduction of dinuclear ruthenium and rhodium complexes.

Complex	$-E$/V	ECLS	Conditions	Ref.
$Os[(\mu\text{-}2,3\text{-}dpp)Ru(bpy)_2]_3^{8+}$	0.55	dpp	Pt, MeCN, Et_4NClO_4, s.c.e.	103
	0.65			
	0.77			
$Ru[(\mu\text{-}2,3\text{-}dpp)Ru(bpy)_2]_3^{8+}$	0.56	dpp	Pt, MeCN, Et_4NClO_4, s.c.e.	103
	0.74			
	0.89			
$[Ru(bpy)_2]_2(bpt)]^+$	1.40	bpy	CG, MeCN, Bu_4NClO_4, s.c.e.	108
	1.63			
	1.67			
	2.23			
	2.33			
	2.74			
$(\mu\text{-}2,3\text{-}dpp)[Ru(CO)_2Cl_2]_2$	0.62	dpp	Pt, MeCN, Et_4NClO_4, s.c.e.	106
$(\mu\text{-}2,5\text{-}dpp)[Ru(CO)_2Cl_2]_2$	0.38	dpp	Pt, MeCN, Et_4NClO_4, s.c.e.	106
$(fulv)Ru_2(CO)_4$	1.65	$Ru^{I/II}$	Pt, THF, Bu_4NBF_4, n.h.e.	125

Table 6 (continued).

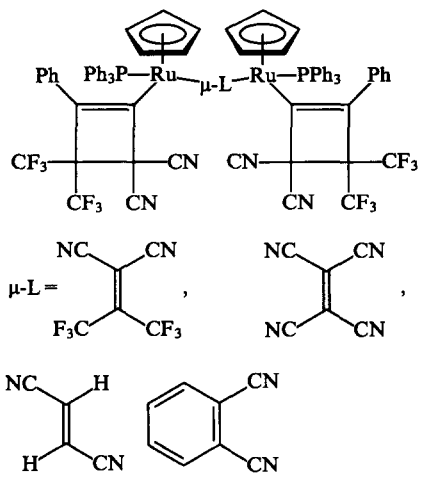
Complex	$-E$/ V	ECLS	Conditions	Ref.
$[(triphos)RhH(\mu\text{-}Cl)_2HRh(triphos)]^{2+}$	0.84	$Rh^{III/II}$	Pt, DMF, Et_4NClO_4, s.c.e.	123
$[(triphos)Rh(\mu\text{-}S)_2Rh(triphos)]^{2+}$	0.45	$Rh^{II/I}$, Rh^{II}	Pt, CH_2Cl_2, Et_4NClO_4, s.c.e.	123
	1.00	Rh^{I}, $Rh^{II/I}$		
$[(triphos)Rh(\mu\text{-}S)_2Co(triphos)]^{2+}$	0.06	$Rh^{II/I}$, Co^{II}	Pt, CH_2Cl_2, Et_4NClO_4, s.c.e.	123
	0.98	Rh^{I}, $Co^{II/I}$		
$[Ru_2(OAc)_3(dcnp)]^{+}$	1.28	$Ru^{III/II}$, Ru^{II}	Pt, MeCN, Et_4NClO_4, s.c.e.	110
	0.57	$Ru^{II/I}$, Ru^{II}		
	1.21	Ru^{I}, $Ru^{II/I}$		
$[Rh_2(OAc)_4(MeCN)_2]$	1.00	$Rh^{III/II}$, Rh^{II}	Pt, MeCN, Et_4NClO_4, s.c.e.	110
	1.08	Rh^{II}, $Rh^{II/I}$		
$[Rh_2(OAc)_3(dpanp)]^{+}$	1.33	$Rh^{III/II}$, Rh^{II}	Pt, MeCN, Et_4NClO_4, s.c.e.	110
	0.68	Rh^{II}, $Rh^{II/I}$		
	1.36	Rh^{I}, $Rh^{II/I}$		
$[Rh_2(OAc)_3(dcnp)]^{-}$	0.98	$Rh^{III/II}$, Rh^{II}	Pt, MeCN, Et_4NClO_4, s.c.e.	110
	0.95	Rh^{II}, $Rh^{II/I}$		
	1.80	Rh^{I}, $Rh^{II/I}$		
$[Ru_2(dpnp)(bpy)_2Cl_2]^{2+}$	1.34	Ru^{III}, $Ru^{III/II}$	Pt, MeCN, Et_4NClO_4, s.c.e.	110
	0.64	$Ru^{III/II}$, Ru^{II}		
	0.76	Ru^{II}, $Ru^{II/I}$		
	1.35	Ru^{I}, $Ru^{II/I}$		
$[Ru_2(dpnp)(OAc)_3]^{+}$	0.72	$Ru^{III/II}$, Ru^{II}	Pt, MeCN, Et_4NClO_4, s.c.e.	110
	0.62	Ru^{II}, $Ru^{II/I}$		
	1.37	Ru^{I}, $Ru^{II/I}$		
$[Ru_2(dcnp)(OAc)_3]^{-}$	0.33	Ru^{III}, $Ru^{III/II}$	Pt, MeCN, Et_4NClO_4, s.c.e.	110
	1.11	$Ru^{III/II}$, Ru^{II}		
	1.86	Ru^{II}, $Ru^{II/I}$		
$\{[Rh(cod)]_2(bpym)\}^{2+}$	0.82	bpym	Pt, MeCN, Et_4NClO_4, s.c.e.	86
$\{[Ru(phen)_2]_2(dpp)\}^{4+}$	0.78		Pt, MeCN, Et_4NClO_4, s.c.e.	117
	1.41			
$\{[Ru(bpy)_2]_2(dpp)\}^{4+}$	0.64		Pt, MeCN, Et_4NClO_4, s.c.e.	117
	1.13			
	1.40			
$[(phen)_2Ru(dpp)Ru(bpy)_2]^{4+}$	0.60		Pt, MeCN, Et_4NClO_4, s.c.e.	117
	1.15			
	1.40			
$\{[Ru(bpy)_2]_2(bpq)\}^{4+}$	0.40		Pt, MeCN, Et_4NClO_4, s.c.e.	117
	1.09			
	1.40			
$\{[Ru(phen)_2]_2(dpq)\}^{4+}$	0.37		Pt, MeCN, Et_4NClO_4, s.c.e.	117
	1.10			
$[(phen)_2Ru(dpq)Ru(bpy)_2]^{4+}$	0.36		Pt, MeCN, Et_4NClO_4, s.c.e.	117
	1.08			
	1.41			
$Ru_2(CO)_6L$	1.25		Pt, MeCN, Et_4NClO_4, s.c.e.	126
L = [C(Me) = C(Ph)COC(Me) = C(Ph)]	1.39		Pt, CH_2Cl_2, Et_4NClO_4, s.c.e.	126
$Ru_2(CO)_6L$	1.12		Pt, MeCN, Et_4NClO_4, s.c.e.	126
L = [C(Ph) = C(Ph)COC(Ph) = C(Ph)]				
$Ru_2(CO)_5(Ph_3P)L$	1.45		Pt, MeCN, Et_4NClO_4, s.c.e.	126
L = [C(Ph) = C(Me)COC(Ph) = C(Me)]	1.57		Pt, CH_2Cl_2, Et_4NClO_4, s.c.e.	126
$Ru_2(CO)_5(Ph_3As)L$	1.36		Pt, MeCN, Et_4NClO_4, s.c.e.	126
L = [C(Ph) = C(Me)COC(Ph) = C(Me)]	1.51		Pt, CH_2Cl_2, Et_4NClO_4, s.c.e.	126
$Ru_2(CO)_5(Ph_3Sb)L$	1.35		Pt, MeCN, Et_4NClO_4, s.c.e.	126
L = [C(Ph) = C(Me)COC(Ph) = C(Me)]	1.47		Pt, CH_2Cl_2, Et_4NClO_4, s.c.e.	126
$[(tpy)ClRu]_2(dpp)^{2+}$	0.85	dpp	Pt, MeCN, Bu_4NPF_6, s.c.e.	102
	1.32			
	1.60	tpy		
$Ru[(dpp)Ru(bpy)_2]_3^{8+}$	0.56	dpp	Pt, MeCN, Bu_4NPF_6, s.c.e.	102
	1.12			
	1.24	bpy		
$Ru[(dpp)Ru(tpy)Cl]_3^{5+}$	0.60	dpp	Pt, MeCN, Bu_4NPF_6, s.c.e.	102
	0.72			
	0.84			
$[(triphos)Rh(\mu\text{-}S)_2Rh(triphos)]^{2+}$	0.45	Rh^{II}, $Rh^{II/I}$	Pt, CH_2Cl_2, Et_4NClO_4, s.c.e.	124
	1.10	Rh^{I}, $Rh^{II/I}$		
$[(triphos)Rh(\mu\text{-}S)_2Rh(triphos)]^{2+}$	0.06	Rh^{II}, $Co^{II/I}$	Pt, CH_2Cl_2, Et_4NClO_4, s.c.e.	124
	0.98	Co^{I}, $Rh^{II/I}$		

[3.2.3] are similar to the corresponding potentials for $[Ru(bpy)_2(CN)]^{2+}$, while the reduction potentials are virtually identical with the cathodic potentials of the pentammineruthenium(III) complexes. The compound [3.2] undergoes one-electron reversible reduction, while in the reduction of the compound [3.2.3] two consecutive one-electron reversible transitions are observed. These have similar standard potentials and lead to the formation of the complexes [3.2.2] and [2.2.2]. The comproportionation constant, determined electrochemically for the equilibrium

$$[3.2.3]+[2.2.2] \overset{K_{com}}{\rightleftharpoons} 2[3.2.2],$$

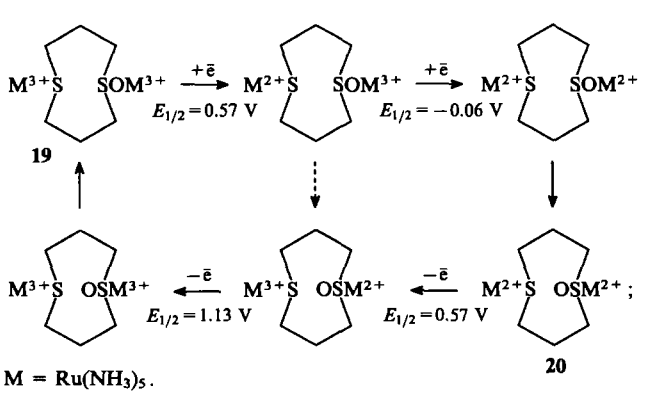
is 24, whence it follows that the amount of the complex [3.2.2] in the half-electrolysed [3.2.3] solution is about 70%.

Dinuclear complexes containing complex nitrile bridges as well as their constituent mononuclear fragments have also been investigated by cyclic voltammetry.[119]



Two reversible one-electron oxidation waves, corresponding to the Ru(II)/ Ru(III) transitions, were observed for the dinuclear complex in which the bridging group is $(CN)_2C=C(CF_3)_2$. When the two rhodium atoms are linked by phthalodinitrile, a single two-electron oxidation wave is observed. The waves observed on reduction of dinuclear complexes of this type are quasi-reversible and correspond to the transfer of one electron to the nitrile ligand. The electron transfer in the dinuclear complex may be accompanied by isomerisation. The redox properties of (1,5-dithiacyclooctane 1-oxide)bis(pentammine)ruthenium(II) **19** may serve as one of the striking examples of such a process.[120] The electrochemical behaviour of the dinuclear system is presented in Scheme 3.

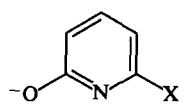
Scheme 3



M = $Ru(NH_3)_5$.

Evidently there are two types of mixed-valence complexes, one of which may be obtained only by the reduction of the stable form **19**, while the other can be obtained only by the oxidation of the stable form **20**.

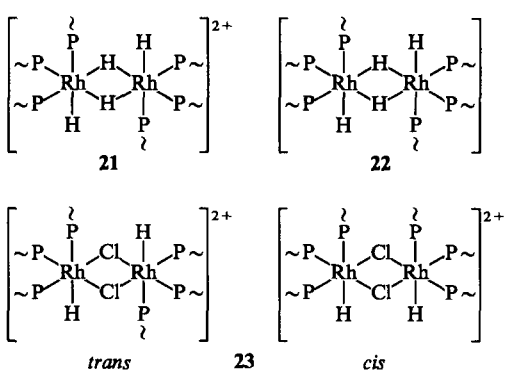
The electrochemical oxidation and reduction of the dinuclear rhodium, manganese, and cobalt complexes containing the methylene bridge has been studied.[121] The oxidation of the dirhodium complexes $Rh_2(hp)_4$, $Rh_2(chp)_4$, and $Rh_2(mhp)_4$ containing substituted *o*-hydroxypyridyl anions as the ligands has been investigated[122] by cyclic and a.c. voltammetry.



hp (X = H)
chp (X = Cl)
mhp (X = Me)

The oxidation potentials of the dirhodium fragment in such complexes depend not only on the nature of the substituent in the pyridine rings of the ligands but also on the solvent. They shift to the more cathodic with increase in the electron-donating strength of the solvent. A correlation has been found[124] between the oxidation potentials of these three complexes and the Taft resonance parameters of the substituents in the pyridine ring. The products of the one-electron oxidation of complexes containing the $[Rh_2]^{4+}$ fragments have been characterised spectroelectrochemically.

It is of interest to compare the electrochemical properties of complexes containing different inorganic bridging ligands. The electrochemical reduction of the dinuclear rhodium complexes $[(triphos)RhH(\mu\text{-}X)_2RhH(triphos)]^{n+}$ [X = H, Cl; *n* = 2, 0; triphos = $MeC(CH_2PPh_2)_3$], containing two hydride or chloride bridges, has been investigated.[123]

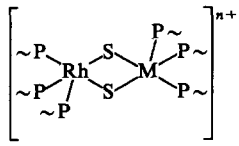


Complex **21** is reduced at the platinum electrode in two reversible one-electron stages:

$$[(triphos)RhH(\mu\text{-}H)_2RhH(triphos)]^{2+} \overset{+\bar{e}}{\underset{-\bar{e}}{\rightleftharpoons}}$$
$$\rightleftharpoons [(triphos)RhH(\mu\text{-}H)_2RhH(triphos)]^{+} \overset{+\bar{e}}{\underset{-\bar{e}}{\rightleftharpoons}}$$
$$\rightleftharpoons [(triphos)RhH(\mu\text{-}H)_2RhH(triphos)] .$$

The complete electrochemical reversibility of these redox transitions shows that a significant structural reorganisation does not take place within the limits of the skeleton of the complex. As was to be expected, the oxidation potentials of complex **22** are identical with the potentials of the reduction wave of complex **21**. The presence of chloride bridges in the molecule alters sharply its redox properties and reversible electron transfer becomes impossible. The cyclic voltammogram for complex **23** shows a two-electron reduction peak, while the presence of several small anodic peaks, revealed by reverse scanning, indicates the occurrence of rapid fragmentation reactions accompanying the electron transfer.

Homobinuclear and heterobinuclear complexes having the general formula $[(triphos)Rh(\mu\text{-}S)_2M(triphos)]^{n+}$ (M = Rh, Co, n = 2; M = Pt or Fe, n = 1), and containing sulphide bridges have been investigated.[124]



Two consecutive cathodic processes were observed in all cases, the species formed in each stage being relatively stable:

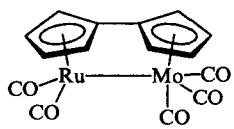
$$[Rh^{III}, M^{III}] \underset{-\bar{e}}{\overset{+\bar{e}}{\rightleftharpoons}} [Rh^{III}, M^{II}] \underset{-\bar{e}}{\overset{+\bar{e}}{\rightleftharpoons}} [Rh^{II}, M^{II}] .$$

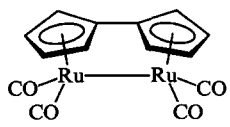
The difference between the potentials of the redox transitions in the two stages makes it possible to calculate[124] the compro-portionation constant:

$$[Rh^{III}, M^{III}] + [Rh^{II}, M^{II}] \overset{K_{com}}{\rightleftharpoons} 2[Rh^{III}, M^{II}] .$$

It is equal to 2×10^9 for the dirhodium complex, while in the case where M = Co we have $K_{com} = 3 \times 10^{15}$. The coordination polyhedron of each metal atom does not change and there is only some increase in the distance between the metal atoms in the consecutive reduction stages.[124]

Yet another type of dinuclear complex exists which contains simultaneously both a bridging ligand and a direct metal–metal bond. The bimetallic fulvalene complexes of ruthenium and molybdenum belong to this class.[125]

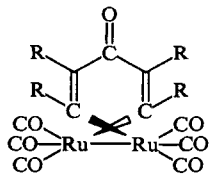




These complexes are oxidised in one two-electron irreversible stage. The irreversibility of the wave can be explained by the reaction of the dication formed with the solvent. The oxidation potentials of these and similar complexes with other metals are between 1.0 and 1.1 V (relative to the normal hydrogen electrode) regardless of the nature of the metals in the complexes. This led to the conclusion that an electron is removed from the orbital localised on the ligand. The reduction of the complexes depends greatly on the nature of the metal. Cyclic voltammetric and coulometric data support the *ece*-mechanism of the reduction process, (i.e. the alternation of stages: electrochemical, chemical, electrochemical — see diagram at the top of the next column).

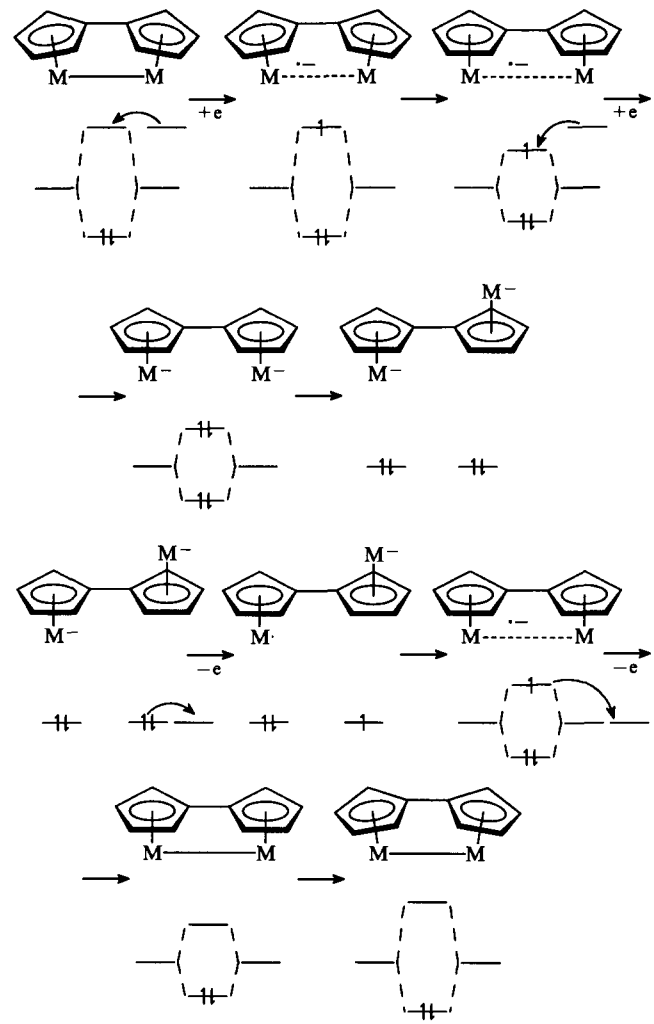
Presumably the first electron, transferred to the antibonding orbital of the M–M bond, lowers its order; this entails the initial formation of a radical-anion, the steric structure of the species changes, and the latter is reduced more readily than the initial complex.

The electrochemical behaviour of 'flyover-bridged' ruthenium complexes having the structure



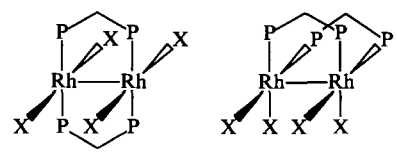
R = Alk, Ph.

has been investigated.[126] Both the anodic and cathodic processes take place with participation of one electron. The presence of



ligands having a higher ratio of the σ-donor and π-acceptor properties than CO renders the reduction process thermo-dynamically harder and favours oxidation.

Dirhodium complexes containing the $[Rh_2]^{4+}$ fragments are used widely as catalysts.[111, 112] The electrochemical properties of the complexes $Rh_2Cl_2(OOCMe)_2(dppm)_2$ and $Rh_2Cl_4(dppm)_2$ (dppm = diphenylphosphinomethane) have been investigated. The existence of structures of two types is possible for such complexes:



X = Cl, MeCOO.

Both complexes are oxidised and reduced irreversibly and their potentials E^{Red} and E^{Ox} differ very significantly. The difficulty of obtaining the $[Rh_2^{5+}]$ species, indicated by the oxidation potentials of these compounds (1.47 and 1.44 V respectively), is apparently due to the fact that the diphenylphosphinomethane and chloride ligands stabilise fairly effectively the $[Rh_2^{4+}]$ fragment. The complex $Rh_2Cl_2(dppm)_2(Ph_2PC_6H_4)_2$ is oxidised much more readily (0.86 V relative to Ag/AgCl) than the first two.

The relative ease of the $Rh_2^{4+} \rightarrow Rh_2^{5+}$ oxidative transition for the third complex suggests that $[Rh_2Cl_2(dppm)_2(Ph_2PC_6H_4)_2]^+$ can be readily obtained chemically, which was in fact subsequently achieved using NO^+ as the oxidising agent.[127]

References

1. F Barigelletti, L Decola, V Balzani, J Reedijk, R Hage, J G Haasnoot, J G Vos *Inorg. Chem.* **28** 4344 (1989)
2. A Juris, V Balzani, F Barigelletti, S Campagna, P Belzer, A Von Zelewsky *Coord. Chem. Rev.* **84** 85 (1988)
3. H S Nawla *Appl. Organomet. Chem.* **5** 349 (1991)
4. P A Cahill *Mater. Res. Soc. Proc.* **109** 319 (1988)
5. V Balzani, F Bolletta, M Ciano, M Maestry *J. Chem. Educ.* **60** 447 (1983)
6. D E Richardson *Comments Inorg. Chem.* **3** 367 (1985)
7. T A Albright, J K Burdett, M N Whanglo, in *Orbital Interactions in Chemistry* (New York: Wiley, 1985)
8. K P Butin, T V Magdesieva, R D Rakhimov, O A Reutov *Zh. Org. Khim.* **23** 2481 (1987)
9. K P Butin, O A Reutov *Metalloorg. Khim.* **1** 94 (1988)
10. K P Butin, V V Strelets, O A Reutov *Metalloorg. Khim.* **3** 814 (1990)
11. R G Pearson *J. Chem. Educ.* **64** 561 (1987)
12. P A Breeze, J K Burdett, J J Turner *Inorg. Chem.* **20** 3369 (1981)
13. N E Kime, J A Ibers *Acta Crystallogr. B* **25** 168 (1969)
14. K A Muszkat, J Schaublin *Chem. Phys. Lett.* **13** 301 (1972)
15. R Hoffman *Acc. Chem. Res.* **4** 1 (1971)
16. R Gleiter *Angew. Chem. Int. Ed. Engl.* **13** 696 (1974)
17. A Paddon-Row *Acc. Chem. Res.* **15** 245 (1982)
18. V F Traven', in *Elektronnaya Struktura i Svoistva Organicheskikh Molekul* (The Electronic Structure and Properties of Organic Molecules (Moscow: Khimiya, 1989) p. 289
19. C Batich, E Heilbronner *J. Am. Chem. Soc.* **95** 928 (1973)
20. I Nenner, G F Schulz *J. Chem. Phys.* **62** 1747 (1975)
21. B P Kennedy, A B Lever *Can. J. Chem.* **50** 3488 (1972)
22. F Barigelletti, S Grammenudi, A Von Zelewsky, F Ebmeyer, L Decola, F Vogtle *J. Am. Chem. Soc.* **111** 4662 (1989)
23. A B Lever *J. Chem. Educ.* **51** 612 (1974)
24. M B Robin, P Day *Adv. Inorg. Chem. Radiochem.* **10** 247 (1967)
25. W H Morrison, D N Hendrickson *J. Chem. Phys.* **59** 380 (1973)
26. J S Sutton, P M Sutton, H Taube *Inorg. Chem.* **18** 1017 (1979)
27. R J Crutchley, A B Lever *Inorg. Chem.* **21** 2276 (1982)
28. J C Curtis, B P Sullivan, T J Meyer *Inorg. Chem.* **22** 224 (1983)
29. D P Rillema, G Allen, T J Meyer, D Conrad *Inorg. Chem.* **22** 1617 (1983)
30. F Barigelletti, A Juris, V Balzani, P Belser, A Von Zelewsky *Inorg. Chem.* **26** 4115 (1987)
31. S Campagna, G Denti, G De Rosa, L Sabatino, M Ciano, V Balzani *Inorg. Chem.* **28** 2565 (1989)
32. P J Steel, E C Constable *J. Chem. Soc., Dalton Trans.* 1389 (1990)
33. Y Ohsawa, K W Hanck, M K De Armond *J. Electroanalyt. Chem.* **175** 229 (1984)
34. S Rottia, C Paradisi, C A Bignozzi *J. Electroanalyt. Chem.* **200** 105 (1986)
35. T Saji, S Aoyagui *J. Electroanalyt. Chem.* **58** 401 (1975)
36. T Saji, S Aoyagui *J. Electroanalyt. Chem.* **60** 1 (1975)
37. E S Dodsworth, A B Lever *Chem. Phys. Lett.* **119** 61 (1985)
38. T T-T Li, H Y Liu, M J Weaver *J. Am. Chem. Soc.* **106** 1233 (1984)
39. A Bettelheim, D Ozer, R Harth, R W Murray *J. Electroanalyt. Chem.* **246** 139 (1988)
40. H Sakaguchi, H Nagamura, T Nagamura *Chem. Lett.* 1715 (1989)
41. A J Bard, R E Hemingway, N E Tokel-Tak-Voryan *J. Am. Chem. Soc.* **95** 6582 (1973)
42. A Juris, S Campagna, V Balzani, G Gremaud, A Von Zelewsky *Inorg. Chem.* **27** 3652 (1988)
43. M K De Armond, C M Carlin *Coord. Chem. Rev.* **36** 325 (1981)
44. R P Thummel, F Lefoulon, S Chirayil *Inorg. Chem.* **26** 3072 (1987)
45. A Juris, P Belser, F Barigelletti, A Von Zelewsky, V Balzani *Inorg. Chem.* **25** 256 (1986)
46. P Belser, A Von Zelewsky *Helv. Chim. Acta* **63** 1675 (1980)
47. A Juris, F Barigelletti, V Balzani, P Belser, A Von Zelewsky *Inorg. Chem.* **24** 202 (1985)
48. P Benhard, H Lehmann, A Ludi *J. Chem. Soc., Chem. Commun.* 1216 (1981)
49. P Belser, A Von Zelewsky, A Juris, F Barigelletti, V Balzani *Chem. Phys. Lett.* **89** 101 (1982)
50. M A Haga *Inorg. Chim. Acta* **75** 29 (1983)
51. J V Caspar, T J Meyer *Inorg. Chem.* **22** 2444 (1983)
52. F Barigelletti, A Juris, V Balzani, P Belser, A Von Zelewsky *Phys. Chem.* **90** 5790 (1986)
53. A Juris, F Barigelletti, V Balzani, P Belser, A Von Zelewsky *Isr. J. Chem.* **22** 87 (1982)
54. A A Vlček *Coord. Chem. Rev.* **43** 39 (1982)
55. D E Morris, Y Ohsawa, D P Segers, M K De Armond, K W Hanck *Inorg. Chem.* **23** 3010 (1984)
56. P Ghosh, A Chakravorty *Inorg. Chim. Acta* **83** 2242 (1984)
57. E S Dodsworth, A B Lever *Chem. Phys. Lett.* **124** 152 (1986)
58. M Haga, G P Sato, T Matsumura, K Shimizu *J. Chem. Soc., Dalton Trans.* 371 (1989)
59. T Matsubara, P C Ford *Inorg. Chem.* **15** 1107 (1976)
60. H S Lim, D J Barclay, F C Anson *Inorg. Chem.* **11** 1460 (1972)
61. M L Bento, E Tfouni *Inorg. Chem.* **27** 3410 (1988)
62. A Zanella, P C Ford *Inorg. Chem.* **14** 42 (1975)
63. K Rieder, H Hauser, H Siegenhaler *Inorg. Chem.* **14** 1902 (1975)
64. N G Connelly, P G Graham, J B Sheridan *J. Chem. Soc., Dalton Trans.* 1619 (1986)
65. M G Elliott, S Zhang, R Shepherd *Inorg. Chem.* **28** 3036 (1989)
66. J M Calvert, D L Peebles, R J Nowak *Inorg. Chem.* **24** 3111 (1985)
67. Y Hoshino, Y Yukawa, T Maruyama, A Endo, K Shimizu, G P Sato *Inorg. Chim. Acta* **174** 41 (1990)
68. N G Connelly, I Manners *J. Chem. Soc., Dalton Trans.* 283 (1989)
69. L I Denisovich, M G Peterleitner, A Z Kreindin, in *Abstracts of the 9 FECHEM Conference on Organometallic Chemistry, Heidelberg, 1991* p. 92
70. J G Muller, K J Takeuchi, J J Grzybowsky *Polyhedron* **8** 1391 (1989)
71. S Goswami, A P Chakravarty, A Chakravorty *J. Chem. Soc., Chem. Commun.* 106 (1982)
72. C M Che, W O Lee *J. Chem. Soc. Chem. Commun.* 891 (1988)
73. F P Guengerich, T L Macdonald *Acc. Chem. Res.* **17** 9 (1984)
74. F A Cotton, G Wilkinson, in *Advances in Inorganic Chemistry* (4-th Edn) (New York: Wiley-Interscience, 1980) p. 912
75. S Bhattacharya, A Chakravorty, F A Cotton, R Mukherjee, W Schwotzer *Inorg. Chem.* **23** 1709 (1984)
76. A M Bond, M Khalifa *Austral. J. Chem.* **41** 1389 (1988)
77. A M Bond, M Haga *Inorg. Chem.* **25** 4507 (1986)
78. J G Gaudiello, P G Bradley, V A Norton, W H Woodruff, A J Bard *Inorg. Chem.* **23** 3 (1984)
79. R L Deming, A L Allred, A R Dahl, A W Herlinger, M D Kestner *J. Am. Chem. Soc.* **98** 4132 (1976)
80. F A Cotton, G Wilkinson, in *Advances in Inorganic Chemistry* (4-th Edn) (New York: Wiley-Interscience, 1980) p. 608
81. A Giraudeau, P Lemoine, M Gross, J Rose, P Braunstein *Inorg. Chim. Acta* **62** 117 (1982)
82. Y Takeuchi, A Endo, K Shimizu, G P Sato *J. Electroanalyt. Chem.* **185** 185 (1985)
83. A M Bond, R L Martin *Coord. Chem. Rev.* **54** 23 (1984)
84. T P Smith, D J Iverson, A W Droege, K S Kwan, H Taube *Inorg. Chem.* **26** 2882 (1987)
85. M Morita, T Matsumura, K Tanaka, Y Matsuda, Y Tanaka *Bull. Chem. Soc. Jpn.* **61** 2711 (1988)
86. L De Cola, M Ciano, F Barigelletti, M P Carcia, L A Oro *Inorg. Chim. Acta* **172** 181 (1990)
87. D Sandrini, M Maestri, V Balzani, U Maeder, A Von Zelewsky *Inorg. Chem.* **27** 2640 (1988)
88. M Maestri, D Sandrini, V.Balzani, U Maeder, A Von Zelewsky *Inorg. Chem.* **26** 1323 (1987)
89. Y Ohsawa, M K De Armond, K A King, K W Hanck, S Sprouse, R J Watts *J. Phys. Chem.* **91** 1047 (1987)
90. J E Anderson, T P Gregory *Abstr. Papers Am. Chem. Soc.* **199** 180 (1990)
91. S Sprouse, K A King, P J Spellane, R J Watts *J. Am. Chem. Soc.* **106** 6647 (1984)
92. E S Dodsworth, A B P Lever, H J Morgans *Abstr. Papers Am. Chem. Soc.* **195** 610 (1988)
93. C Bianchini, M Peruzzini, M F Ottaviani, F Laschi, F Zanobini *Organometallics* **8** 893 (1989)
94. C Bianchini, A Meli, M Peruzzini, A Vacca, F Laschi, P Zanello *Organometallics* **9** 360 (1990)
95. S T Mak, V W W Yam, C M Che, T C W Mak *J. Chem. Soc., Dalton Trans.* 2555 (1990)
96. A K Deb, S Goswami *J. Chem. Soc., Dalton Trans.* 1635 (1989)

97. D Sandrini, M Maestri, M Ciano, U Maeder, A Von Zelewsky *Helv. Chim. Acta* **73** 1306 (1990)
98. A J Blake, M Schroder, R O Gould, T I Hyde, A J Holder *J. Chem. Soc., Dalton Trans.* 1861 (1988)
99. V G Mairanovskii, in *Porfiriny: Spektroskopiya, Elektrokhimiya, Primenenie* (Porphyrins: Spectroscopy, Electrochemistry, and Applications) (Ed. N S Enikolopyan) (Moscow: Nauka, 1987) p. 127
100. K P Butin, E P Milaeva, R D Rakhimov, I N Chechulina, Yu G Bundel' *Metalloorg. Khim.* **2** 1283 (1989)
101. M Haga, S Yamabe, T Matsumura *Inorg. Chem.* **26** 4148 (1987)
102. R W Murphy, J K Brewer, G Gettliffe, J D Petersen *Inorg. Chem.* **28** 81 (1989)
103. S Campagna, G Denti, L Sabatino, S Serroni, V Balzani, M Ciano *J. Chem. Soc., Chem. Commun.* 1500 (1989)
104. Y Fuchs, T Dieter, S Lofters, A D Baker, H D Gafnoy, R Morgan, W Shi, T C Strokas *J. Am. Chem. Soc.* **109** 2691 (1987)
105. J K Brewer, R W Murphy, R S Spurlin, J D Petersen *Inorg. Chem.* **25** 882 (1986)
106. S Campagna, L Sabatino, G Denti, G Derosa, M Ciano *Inorg. Chem.* **28** 2565 (1989)
107. R Hage, A H Dijkhuis, J G Haasnoot, R Prins, E B Buchanan, G J Vos *Inorg. Chem.* **27** 2185 (1988)
108. R Hage, J G Haasnoot, D J Stufkens, T L Snoeck, G J Vos, K J Reedij *Inorg. Chem.* **28** 1413 (1989)
109. A L Balch, R D Cooper *J. Organomet. Chem.* **169** 97 (1979)
110. J P Collin, A Jouaiti, J P Sauvage, W C Kaska, M A McLoughlin, N L Keder, W T Harrison, G D Stucky *Inorg. Chem.* **29** 2238 (1990)
111. K R Mann, R A Bell, H B Gray *Inorg. Chem.* **18** 2671 (1979)
112. C P Kubiak, C Woodcock, R Eisenberg *Inorg. Chem.* **21** 2119 (1982)
113. T R Felthouse *Prog. Inorg. Chem.* **29** 73 (1982)
114. N Petiniot, A F Noels, A J Anciaux, in *Fundamental Research in Homogeneous Catalysis* Vol. 3 (Ed. M.Tsutsui) (New York: Plenum, 1978) p. 421
115. E Binarira-Soriaga, Thesis, University of California, Santa Barbara, 1985
116. A W Wallace, W R Murphy, J D Petersen *Inorg. Chim. Acta* **166** 47 (1989)
117. J D Petersen, in *Supramolecular Photochemistry* (Ed. V Balzani) (Dordrecht: Reidel, 1987) p. 135
118. K P Butin, T V Magdesieva, G A Pirogova, A Z Rubezhov, A A Bezrukova, V S Khandkarova *Metalloorg. Khim.* **6** 335 (1993)
119. M I Bruce, T W Hambley, M J Liddell, A G Swincer, E R T Tiekink *Organometallics* **9** 2886 (1990)
120. M Sano, H Taube *J. Am. Chem. Soc.* **113** 2327 (1991)
121. W E Geiger, T Gennett, W A Herrmann, W K Mcvicar *Organometallics* **6** 1634 (1987)
122. D A Tocher, J H Tocher *Inorg. Chim. Acta* **131** 69 (1987)
123. C Bianchini, J A Ramirez, A Meli, P Zanello, A Vacca, F Laschi *Inorg. Chem.* **27** 4429 (1988)
124. C Bianchini, A Meli, F Laschi, A Vacca, P Zanello *J. Am. Chem. Soc.* **110** 3913 (1988)
125. R Moulton, T W Weidman, K P Vollhardt, A J Bard *Inorg. Chem.* **25** 1846 (1986)
126. D Osella, P Zanello, R Gobetto, F Laschi, M Botta *Organometallics* **7** 283 (1988)
127. A F Cotton, K R Danbar, M G Verbrugger *J. Am. Chem. Soc.* **109** 5498 (1987)
128. H Ishida, K Fujiki, T Ohba, K Ohkubo, K Tanaka, T Terada *J. Chem. Soc., Dalton Trans.* 2155 (1990)
129. W Hungleung, Che Chi-Ming *Inorg. Chem.* **28** 4619 (1989)
130. J L Campos, W F De Giovani, J R Romero *Synthesis* 597 (1990)
131. Y Yamamoto, T Tanase, T Date, Y Kade, K Kobayashi *J. Organomet. Chem.* **386** 365 (1990)
132. A Basu, N Y Sapre, T G Kasar *Inorg. Chem.* **27** 4539 (1988)
133. A M Bond, D R Mann, R Colton *Inorg. Chem.* **28** 54 (1989)

Russian Chemical Reviews **62** (4) 387–407 (1993)
© (1993) Russian Academy of Sciences and Turpion Ltd

UDC 577.113.7;547.963.92

Imperfectly matched nucleic acid complexes and their biochemical manifestation

M A Zenkova, G G Karpova

Contents

I.	Introduction	387
II.	Theoretical estimates of the specificity of the interaction of nucleic acids	388
III.	Thermodynamic parameters of the formation of perfectly and imperfectly matched duplexes and the characteristic features of their steric structure	388
IV.	Accuracy of the interaction of RNA and DNA molecules with oligonucleotides and their derivatives	395
V.	Conclusion	403

Abstract. The review is devoted to the analysis of experimental data on the selectivity of the interaction of nucleic acids with antisense oligonucleotides and their derivatives, which lead to the prospect of achieving a highly selective influence on many biochemical and molecular-genetic processes in living organisms. Theoretical estimates of the level of specificity of the interaction of nucleic acids and the thermodynamic parameters of the formation of perfectly and imperfectly matched complementary complexes are examined in the review. Attention is concentrated on the complementation accuracy of the interaction of DNA and RNA with oligonucleotides and their derivatives in various model systems both *in vitro* and *in vivo*. Data on the specificity of the inhibition of translation with the aid of antisense oligonucleotides in model systems *in vitro* are analysed. The question of the influence of the steric structure of the nucleic acid molecule on the accuracy and efficiency of the interaction with antisense oligonucleotides and their derivatives is discussed. The bibliography includes 247 references.

I. Introduction

The selective interaction between nucleic acids is of cardinal importance in ensuring the occurrence of key life processes. It is sufficient to recall that the specific interaction of complementary nucleic acid sequences constitutes the basis of the double helix DNA structure established by Watson and Crick. The principle of complementarity in fact determines the selective interaction of nucleic acids with antisense RNA, oligonucleotides, and their derivatives. (Such compounds are referred to as antisense on the basis of their ability to form a complementary complex with the selected nucleic acid sequence — the NA target, which is a sense sequence.) All this leads to the prospect of being able to exert a site-specific ('addressed') influence on many key biochemical and molecular-genetic processes occurring with participation of nucleic acids both *in vitro* and in the living cell *in vivo*.[1,2] By virtue of the numerous interesting possibilities of this approach, including specific influence on intracellular processes, as well as the advances in the field of oligonucleotide synthesis, the method of site-specific action, based on the use of antisense oligonucleotides, has attracted increasing attention in recent years.[3–5]

One of the versions of this approach, first formulated at the end of the 1960s, has been called complementarily addressed (site-specific in modern parlance) modification.[6–8] It is based on two processes: in the first, a reactive derivative of the oligonucleotide, complementary to a specific section of the NA target, forms with this section a specific complementary complex and thus directs (addresses) the action of the reactive part of the molecule; in the second, there is a direct chemical reaction (alkylation, photomodification, cleavage) with a nucleic acid base near this section. This approach is regarded nowadays as the most universal method whereby nucleic acids can be highly selectively influenced in order to suppress the development of viral infections and the tumour process induced by mutations in protooncogenes, which are responsible for the malignant degeneracy of the cell.[5,9]

For the wide scale employment of this approach both in research and for therapeutic purposes, it is important that the interaction of the oligonucleotide or its reactive derivative with the NA target should occur with a high selectivity. According to statistics,[1] the sequence of a random 17-unit oligonucleotide is repeated in the human genome only once and one may therefore expect an extremely effective interaction of the NA target with oligonucleotides of this length. However, a fairly extensive set of experimental data, showing that the specificity of the interaction of nucleic acids (the formation of a perfectly matched complementary complex) is low has now accumulated. There is a high probability of the formation of imperfectly matched (containing noncanonical base pairs or loops) or partial (only part of the antisense oligonucleotide is in the complex) complexes with different sections of the NA target. Furthermore, the efficiency of complex formation with an antisense oligonucleotide is influenced enormously by the steric structure and by the accessibility of the selected section for the binding of the NA target. The same problem arises also when oligonucleotides or their derivatives are used for site-specific mutagenesis or as hybridisation probes.

The experimental data on the selectivity of the interaction of nucleic acids which have accumulated hitherto are analysed in the present review. They are examined in order of increase in the complexity of the model system investigated: from perfectly and

M A Zenkova, G G Karpova Laboratory for the Structure and Functions of Ribosomes, Novosibirsk Institute of Bioorganic Chemistry, Siberian Division of the Russian Academy of Sciences, prosp. akad. Lavrent'eva 8, 630090 Novosibirsk. Tel. (7-383-2) 35 16 68; Fax (7-383-2) 35 16 65.

Received 7th December 1992
Uspekhi Khimii **62** (4) 414–435 (1993); translated by A K Grzybowski

imperfectly matched complementary complexes formed by oligonucleotides to the interaction of antisense oligonucleotides with high-molecular-mass nucleic acids in systems *in vitro*. To facilitate the assimilation of such data, the first Section of the review quotes theoretical estimates of the level of selectivity of the interaction of nucleic acids and the second quotes the thermodynamic parameters of the formation of perfectly and imperfectly matched complementary complexes. The section devoted to the interaction of reactive derivatives of oligonucleotides with NA targets is based largely on the results of studies carried out at the Novosibirsk Institute of Bioorganic Chemistry of the Siberian Division of the Russian Academy of Sciences. It should be noted that the present review analyses only those studies concerning the interaction of high-molecular-mass NA targets with oligonucleotides in which the level of accuracy of the interaction of the nucleic acids was estimated or if sufficient experimental data were available to make such an estimate.

II. Theoretical estimates of the specificity of the interaction of nucleic acids

One of the sources of errors in the application of site-specific influences to nucleic acids is the possibility of the formation of imperfectly matched complexes. Theoretical estimates of the level of modification of nucleic acids in imperfectly matched complexes have been carried out.[10-12]

The influence of temperature and the concentration of the reagent (reactive oligonucleotide) on the specificity of the interaction of the oligonucleotide probe and the NA target has been analysed.[10] In order to estimate the contribution of the imperfectly matched complexes, it was suggested that the discrimination parameter (∇), characterising the ratio of the degrees of binding of the reagent in the regular and imperfectly matched complexes, be used to estimate the contribution of imperfectly matched complexes. The final expression for ∇ is as follows:

$$\nabla = \{\alpha - \lg[X]\}\frac{n-n'}{n'},$$

where [X] is the concentration of the reagent and n and n' are the lengths of the perfectly and imperfectly matched duplexes. Hence it follows that the value of ∇, i.e. the discrimination between perfectly and imperfectly matched duplexes, is determined by the length of these duplexes and depends logarithmically on the probe concentration, diminishing significantly with its increase. According to estimates made for oligonucleotide concentrations of 10^{-8} and 10^{-2} M, the parameter ∇ attains the maximum value at a reaction temperature equal to the melting point (T_m) of the perfectly matched duplex.

The ratio r' of the sum of the equilibrium nonspecific binding constants $\sum K_n^i = K_n$ for different types of imperfectly matched complexes [noncanonical pairs ('mismatch'), dangling ends, and 'extra' or projecting bases ('bulge') in the target and the oligonucleotide] to the formation constant of the perfectly matched duplex K_s ($r' = K_n/K_s$) has been estimated[11] with the aid of a statistical approach. The results enabled the authors to reach the following conclusions. The main contribution to K_n comes from complexes with dangling ends. In order to diminish the fraction of such complexes, it is necessary to employ reagents containing G · C pairs at the ends, because the difference between the stabilities of the perfectly and imperfectly matched duplexes, associated with the absence of the terminal G · C pair from the imperfectly matched complex, is 5–6 times greater than that due to the absence of the terminal A · T pair. The fraction of binding into imperfectly matched complexes can be significantly reduced if long oligonucleotides are employed or the condition $K_s x_0 \ll 1$, where x_0 is the oligonucleotide concentration, is maintained. It is noteworthy that all the calculations in the above study[11] were performed subject to certain assumptions. Thus the authors assumed that the terminal noncanonical pairs are fully fused and do not contribute to the stability of the duplex. The numerical changes in the free energy of the duplex associated with the formation of noncanonical pairs, calculated from the data of Aboul-ela et al.,[13] were averages and did not take into account the immediate environment. The degree of destabilisation of the duplex induced by the extra base was determined from experimental data of the same study for the extra cytosine and was assumed to be the same for all the bases. However, the assumptions made by the authors should not alter fundamentally the conclusions reached.

The kinetic aspects of the specificity of the interaction of the addressed reagent and the matrix have been examined[12] and it was shown that the nonspecificity of the interaction of the oligonucleotide reagent and the matrix may be of two types. Firstly, there is the nonspecificity associated with the reaction outside the complex, previously considered in a number of studies.[14-16] Secondly, the nonspecificity is induced by the formation of imperfectly matched complexes. The results of the analysis of the possible level of the nonspecific modification of both types for the 302-membered DNA fragment by reagents of different lengths (6–14 units) showed that the contribution of the nonspecific modification of the second type increases with decrease in the length of the nucleotide part of the reagent. It is noteworthy that the nonspecificity of the modifications of both types depends on the reagent concentration: the specificity of the modification of the NA target falls with increase in the reagent concentration.

III. Thermodynamic parameters of the formation of perfectly and imperfectly matched duplexes and the characteristic features of their steric structure

1. Perfectly matched duplexes

According to modern ideas, the characteristic features of the behaviour of double-helix nucleotide structures in solution are determined by the interactions between the heterocyclic bases, the influence of the solvent, the ionic strength, and the electrostatic interactions of the phosphate groups. In the complementary complex, the change in the state of each nucleotide unit cannot take place independently of the neighbouring units, which is responsible for the cooperative nature of the formation and dissociation of the double helix structures. Thermodynamic data for the DNA duplexes have been examined in detail in a number of reviews.[17-19] Natural RNA produce the right-handed *A* form of the double helix, which differs from the *B* form of DNA by the pitch of the helix in eleven bases (one more than in the *B* form of DNA). The most important differences between DNA and RNA involve the conformation of the nucleotide: in RNA the sugar residue has the C(3′)-*endo*-conformation, whilst in DNA it has the C(2′)-*endo*-conformation. The differences between the sugar conformations lead to the appearance of differences in the distances between the phosphates of the polynucleotide chain: 5.9 Å in the RNA duplexes and 7 Å in the DNA duplexes.[20] The relative stability of the *B* form of the DNA duplexes depends on the sequence of chains forming the duplex or, in other words, the stability of the base pair is determined by its immediate neighbours.[13,21-24] The overall stability and the conditions governing the fusion of any DNA duplex can be predicted on the basis of its primary structure, provided that the parameters ΔG_0, ΔH_0, and ΔS_0 are known for each pair of nearest neighbours[24] (Table 1). The free energy of formation of the perfectly matched duplex (ΔG_0) is determined by the sum of the free energies of formation of the pairs of nearest neighbours (ΔG_x) and can be readily estimated from the data in Table 1 by the formula

$$\Delta G_0 = -(\Delta G_{in} + \Delta G_{sym}) + \sum_x \Delta G_x,$$

Table 1. Thermodynamic parameters of the formation of pairs of nearest neighbours in DNA duplexes[24] (1 M NaCl, 25 °C, pH 7.0).

Pair	$-\Delta H_0$ / kcal mol^{-1}	$-\Delta S_0$ / cal mol^{-1} K^{-1}	$-\Delta G_0$ / kcal mol^{-1}
AA/TT	9.1	24.0	1.9
AT/TA	8.6	23.9	1.5
TA/AT	6.0	16.9	0.9
CA/GT	5.8	12.9	1.9
GT/CA	6.5	17.3	1.3
CT/GA	7.8	20.8	1.6
GA/CT	5.6	13.5	1.6
CG/GC	11.9	27.8	3.6
GC/CG	11.1	26.7	3.1

where ΔG_{in} is the change in the ΔG_0 of formation of the duplex as a result of initiation and ΔG_{sym} is a quantity which explains the difference between the entropies of the duplex formed by a self-complementary sequence and the duplex formed by two complementary sequences; ΔG_{in} = 5 kcal mol^{-1} for the complex originating from the G · C pair and 6 kcal mol^{-1} for the complex originating from the A · U pair; ΔG_{sym} = 0.4 kcal mol^{-1} for the duplex formed by a self-complementary sequence and is zero for the complex formed by two complementary sequences. ΔH_0 and ΔS_0 for the formation of the perfectly matched duplex are determined similarly. The thermodynamic parameters of the formation of a long DNA duplex can be readily determined from the three-dimensional diagram presented in a review.[19]

Table 2 lists the thermodynamic parameters of the formation of the G · C or A · U pairs in RNA duplexes obtained by the method of nearest neighbours.[25-28] The thermodynamic parameters of the formation of each duplex are determined in the same way as for the DNA duplexes.[24]

The most characteristic feature of the secondary structure of RNA is the formation of hairpins. The groups at the ends of the hairpin usually comprise 4–6 bases and stabilise the entire hairpin. The quantity $\Delta\Delta G_0$ depends to a large extent on the sequence of bases in the loop and on the base pair closing the loop, varying from −3 to 1.5 kcal mol^{-1}.[29-33] Under these conditions, all the bases even in the short groups (3–5 nucleotides) are stacked together with the ribose ring and each ribose residue has the N conformation, which enables the nucleotide to stretch to the maximum length.[20,30] In the general case, the loops formed by deoxyribooligonucleotides stabilise the entire hairpin to a somewhat lesser extent, but the dependence of the stabilising effects on the base sequence in the loop is retained.[32,33]

The only form in which the double helix RNA exists is the *A* conformation. Depending on the conditions in their formation and the sequence, DNA duplexes can exist in the form of the *A* and *B* conformations or the left-handed *Z* conformation. According to a number of data,[18,19,34-37] the *A* form of the helix is more characteristic of the RNA–DNA duplex, although under certain conditions and depending on the sequence, other conformations can also occur. A comparative analysis of the thermodynamics and kinetics of the formation of hybrid duplexes has been carried out.[18,35,37-41] On the basis of the analysis of the fusion curves and NMR spectroscopic data, the following stability series has been established for RNA–DNA duplexes: $dA_5 \cdot dT_5 > rA_5 \cdot dT_5 > rA_5 \cdot rU_5 > dA_5 \cdot rU_5$ (T_m = 27.5, 22.9, 19.1, and 0 °C respectively).[35] It is noteworthy that very few data are available on the stabilities of the RNA–DNA duplexes and they are contradictory. For the majority of the duplexes investigated, it has been found that the hybrid duplexes are less stable than the corresponding RNA or DNA duplexes.[42] Evidently the stability of the hybrid duplexes, like that of deoxyribo- and ribo-analogues, is determined by their primary structure.

Table 2. Thermodynamic parameters of the formation of pairs of nearest neighbours in RNA duplexes[28] (1 M NaCl, 25 °C, pH 7.0).

Pair	$-\Delta H_0$ / kcal mol^{-1}	$-\Delta S_0$ / cal mol^{-1} K^{-1}	$-\Delta G_0$ / kcal mol^{-1}
AA/UU	6.6	18.4	0.9
AU/UA	5.7	15.5	0.9
UA/AU	8.1	22.6	1.1
CA/GU	10.5	27.8	1.8
CU/GA	7.6	19.2	1.7
GA/CU	13.3	35.5	2.3
GU/CA	10.2	26.2	2.1
CG/GC	8.0	19.4	2.0
GC/CG	14.2	34.9	3.4
GG/CC	12.2	29.7	2.4
Initiation	0	10.8	−3.4
Symmetry of duplex	0	1.4	−0.4

2. Imperfectly matched nucleic acid duplexes

Interest in imperfectly matched nucleic acid duplexes arose initially apparently in the course of the study of the mechanisms of the transmission of kinetic information. In replication, transcription, or reverse transcription, the accuracy of the transmission of genetic information is ensured by the complementary interactions of nucleic acids, but this entails also the inclusion of error bases.[43,44] On the other hand, complexes of this type are formed in codon–anticodon interactions on formation of the steric structure of RNA (G · A and G · U pairs). The formation of imperfectly matched duplexes is widely used in the technique of site-specific mutagenesis.

a. Duplexes with dangling bases at the ends

Terminal unpaired bases, adjoining a long double helix (core), are a characteristic element of the secondary structure of RNA and are involved in many biological processes. The addition of an unpaired base at the 3′- and 5′-end of the RNA duplex stabilises the core duplex as a result of the stacking interaction of the dangling base with the last complementary pair of the duplex. The paired base at the 3′-end of the RNA duplex stabilises the duplex to a greater extent under these conditions than the 'dangling' 5′-end; the difference between the melting points of such duplexes is 8 °C at an oligonucleotide concentration of 10^{-4} M. The addition of a 3′-terminal unpaired base is comparable to the addition of the A · U pair. The stabilising effect of the noncomplementary bases at the ends of the RNA duplex diminishes in the sequence[45,46] 3′-A > 3′-U > 5′-A ≃ 5′-U. Similar results were obtained in the study of the influence of unpaired bases at the ends on the stability of the core duplexes[28,47] GGCC/GGCC, CCGG/CCGG, and CGCG/CGCG. The stabilising effect of unpaired terminal bases increased in the sequence 3′-C < 3′-U < 3′-G ≃ 3′-A and the increase in the free energy of the duplex as a result of the stabilising effect of the unpaired bases at the ends was then 10%–20%, 30%–70%, and 60%–95% of the increase in ΔG_0 due to the formation of the corresponding complementary pair. On average, the 5′- and 3′-noncomplementary bases contribute −0.2 and −(0.4–1.8) kcal mol^{-1} to the ΔG_0 of formation of an RNA duplex.[48,49]

The influence of the unpaired terminal base on the stability of the core DNA duplex is the opposite of the influence of the dangling base on the RNA duplex: the DNA duplexes are stabilised to a greater extent by the unpaired base at the 5′-end.[50,52] A study of the structure and thermodynamic features of the behaviour of the core duplexes containing unpaired thymidine residues at the 5′- and 3′-ends showed that the addition of a dangling 5′- or 3′-thymidine to the core duplex increases the T_m of the duplex. The 5′-terminal thymidine exerts a greater stabilising effect: T_m = 8.3–9.3 °C and 5.0–3.0 °C for the unpaired 5′- and 3′-thymidine residues respectively. Analysis of the circular dichroism (CD) spectra of the core duplexes and their derivatives with unpaired thymidine residues at the 3′- or 5′-ends

showed that the entire duplex, including the dangling end, is in the *B* conformation whilst the unpaired base is in a stack with the core duplex.[52]

b. Duplexes with extra (bulging) bases

The inner loop, consisting of a single base, or the extra (bulging) base are frequently encountered elements of the secondary structure of DNA and RNA. The special interest in projecting bases is associated with the fact that in DNA such a base is a 'hot' spot for mutations, whilst in RNA an extra adenosine frequently appears at the protein binding sites. The main question concerning this element of the secondary structure is whether the extra base belongs to the double helix or whether it forms an inner loop and is displaced from the stack.

The extra adenine in the duplex **1** is involved in a stacking interaction with neighbouring cytidine and guanine residues and does not form an inner loop. The conformation of the complementary pairs on either side of the projecting base is not altered, but the phosphodiester linkage opposite the extra adenine is somewhat lengthened, which leads to the loosening of the structure of the duplex and to a slight change in the torsional angles of the phosphodiester linkage. The melting point of the duplex with bulging adenine is lower by 19 °C than T_m for the perfectly matched duplex, but the fusion of such a duplex takes place cooperatively, including the bulging adenine.[53,54]

$^{5'}$CGC^{A}GAATTCGCG$^{3'}$ / $_{3'}$GCG–CTTAAGCGC$_{5'}$ **1**

$^{5'}$CAAA^{C}AAAG$^{3'}$ / $_{3'}$GTTT–TTTC$_{5'}$ **2**

The activation energy for the formation of the duplex **1** ($E_{act\text{-}A}$) is appreciably higher than the activation energy for the formation of the perfectly matched complex.[55] Whereas the rate-limiting stage in the formation of the perfectly matched duplexes is the formation of the nucleation core,[35] in the duplex with projecting adenine complex formation is inhibited at a defective section of the structure,[55] which leads to an appreciable increase in the activation energy and a broadening of the temperature range in which duplex **1** fuses.

The NMR spectra of nonexchanging protons and the nuclear Overhauser effect (NOE) spectra of the imino-protons of the bases, located on either side of the extra cytidine in duplex **2**, led to the conclusion that such cytidine is outside the helix and that the conformation of the A · T pair adjoining it is greatly modified. Duplex **2** is highly destabilised compared with the perfectly matched complex (T_m for duplex **2** is lower by 15 °C than T_m for the perfectly matched complex and $\Delta\Delta G$ = 2.9 kcal mol^{-1}). The decrease in the stability of the duplex has an enthalpy origin and is a consequence of the breakdown of the stacking interactions in this duplex.[56] At a low temperature (about 0 °C), the projecting cytidine is outside the duplex and, on raising the temperature (>40 °C), the fraction of conformations in which the extra cytidine forms part of the helix increases.[57]

The extra adenine and guanine adjoining the G · C pair (duplexes **A** and **G**) participate in the stacking interactions with the adjoining bases and are clearly part of the double helix (Scheme 1).

Scheme 1

$^{5'}$GATGGGCAG$^{3'}$ / $_{3'}$CTACCCGTC$_{5'}$ **N**

$^{5'}$GAT–GGGCAG$^{3'}$ / $_{3'}$CTA$_{C}$CCCGTC$_{5'}$ **C**

^{5}GAT–GGGCAG$^{3'}$ / $_{3'}$CTA$_{A}$CCCGTC$_{5'}$ **A**

$^{5'}$GAT–GGGCAG$^{3'}$ / $_{3'}$CTA$_{G}$CCCGTC$_{5'}$ **G**

The destabilising effect of these bases is strictly localised and does not extend over the entire duplex. The bulging cytidine is in the $C_{(4)}$ backbone of duplex **C** and is, as it were, delocalised over the $C_{(4)}$ sequence. This decreases the destabilising effect of the extra cytidine on the double helix; T_m for duplex **C** is higher by 5.7 °C than for duplex **A** or **G**.[58,59] Comparison of the structures of ribo- and deoxyribo-duplexes containing bulging uridine or thymidine (duplexes **3** and **4**) showed that the bulging thymidine in **4** is built into the double helix without causing any appreciable distortions in the *B* form of DNA, while the extra uridine in duplex **3**, having the same composition, is outside the helix. The regular structure of the *A* form of RNA is also unaffected under these conditions.[60,61]

$^{5'}$r(CUGG^{U}GCGC)$^{3'}$ / $_{3'}$(GACC–CGCG)r$_{5'}$ **3**

$^{5'}$d(CTGG^{T}GCGC)$^{3'}$ / $_{3'}$(GACC–CGCG)d$_{5'}$ **4**

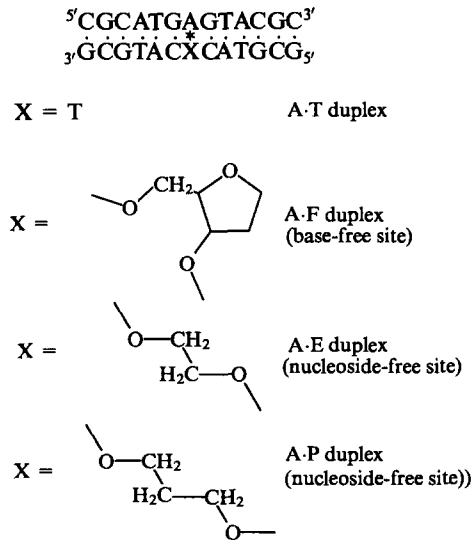
There are comparatively few experimental data concerning the influence of the projecting base on the structure and stability of RNA duplexes. The study of the thermodynamic behaviour of 14 synthetic ribooligonucleotides, assuming in solution the hairpin shape with four bases in the loop and one projecting base in the stem, showed that the introduction of the extra base into the double helix region destabilises the duplex. The magnitude of the effect is determined by the type of base: the greatest destabilising effect is shown by the extra adenine and guanine ($\Delta\Delta G_A^{37\,°C}$ = 3.3 kcal mol^{-1} and $\Delta\Delta G_G^{37\,°C}$ = 3.5 kcal mol^{-1}) and the smallest is exerted by the extra uridine ($\Delta\Delta G_U^{37\,°C}$ = 2.7 kcal mol^{-1}).[31]

c. Duplexes with point breaks

Point breaks as well as nonpurine and nonpyrimidine sites are frequently encountered in the DNA structure. However, comparatively few data have accumulated at the present time concerning the influence of such damage to DNA on the structure and stability of the DNA duplexes. Similar data on RNA duplexes are altogether lacking. Four 12-unit duplexes of identical composition with a point break have been investigated by NMR and NOE spectroscopy. It was found that they all have a helix in the *B* form and differ slightly in stability from the perfectly matched duplex. Fusion of the duplex with a point break takes place cooperatively. Apparently the point break does not alter appreciably either the stability or the structure of these DNA duplexes.[62] Somewhat different results for the influence of point breaks on the stability of a DNA duplex have been obtained in another study.[63] The introduction of a point break into the ring structure diminishes T_m for such a duplex by 27 °C (1 M NaCl).

The introduction of a base-free site into the structure of the duplex lowers the melting point of the duplex by 10–12 °C compared with the perfectly matched duplex. The destabilisation of the duplex by a 'hole' is comparable to the effect of the introduction into the duplex of a T · T pair (T_m = 66, 53–56, and 56 °C for the perfectly matched 13-unit duplex, the duplex with a nonpyrimidine site in the 7-position, and the duplex with a T · T pair in the 7-position respectively.[64] The influence of the base-free site and the nucleoside-free site on the structure of the DNA duplex has been investigated in greatest detail[65] in relation to the duplex having the composition shown in the next column.

The changes in all the thermodynamic parameters induced by the damage to the duplex resulting from the formation of a 'hole' are very great (ΔT_m = 13.9, 12.9, and 14.4 °C for the duplexes A · F, A · E, and A · P respectively) and greatly exceed the values predicted for such duplexes by the nearest neighbours method. The results show that these changes in the stability of the duplex are associated with the absence of a base and not the absence of a sugar residue. The cooperative nature of the helix–coil transition hardly changes on passing from the duplex A · T to the duplexes A · F and A · E. This suggests[57,65] that the sugar phosphate skeleton of the DNA molecule is in fact responsible for the cooperative nature of the helix–coil transition on fusion.

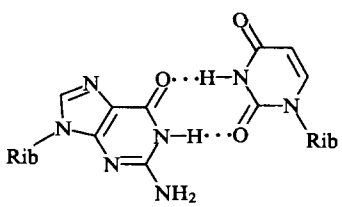


The data presented permit the conclusion that, although the introduction of a point break lowers the stability of the DNA duplex, it does not affect its structure, whereas nonpurine and nonpyrimidine sites lead to appreciable changes in the structure of the duplex as a result of the disturbance of the stacking interactions in the double helix.

d. Duplexes containing noncanonical base pairs

Noncanonical or irregular base pairs are very often encountered in the molecules of both RNA and DNA. All noncanonical pairs can either form an inner loop made up of two bases, or can participate in the stacking interactions of the double helix, or can form a noncanonical ('wobble') pair. In analysing any noncanonical pair, it is essential to answer the following questions: (1) what structural changes are introduced by the given irregular pair into the conformation of the duplex; (2) what thermodynamic and kinetic parameters of the formation of the duplex are altered under the influence of the given noncanonical pair; (3) in what way are hydrogen bonds formed in the given noncanonical pair. All these questions have been examined in detail in a review.[18] This section presents data concerning only the influence of noncanonical pairs on the stability of RNA and DNA duplexes.

The G · U or G · T pair. The G · U pair is one of the most thoroughly investigated, most frequently encountered, and most stable of the irregular pairs. The formation of hydrogen bonds in the G · U pair, put forward by Watson and Crick, is illustrated in the scheme below:



G · U

X-Ray diffraction analysis of an 8-unit duplex with two central G · T pairs as well as NMR spectroscopy of poly(dGT) [the appearance in the spectra of two signals in the region of 11 p.p.m. (resonance of the >N–H...O = C< hydrogen bond) and two signals in the region of 8 ± 0.5 p.p.m. (-resonance of the free NH_2 group)] yielded rigorous experimental evidence showing that the bases in the G · T and G · U pairs in long DNA or RNA duplexes are paired and built into the double helix.[22, 23, 54, 66–69]

The G · T pairs exert extremely little influence on the overall structure of the duplex and hardly disturb the stacking interactions in it. On formation of such a pair, small changes occur only in the torsional angle of the *N*-glycoside component of uridine, which is the main reason for the destabilisation of duplexes with G · U pairs compared with perfectly matched duplexes.[66, 70] Comparison of three 8-unit duplexes,[71] containing two G · T, two G · C, or two A · T pairs in the 3- and 4-positions, showed that both G · T pairs participate in the formation of the double helix, but the rotation of the helix at the G · T pair is by 44.3° (instead of 31.5° for the classical pair), while at the G · C pair, which follows G · T, the rotation is by only 22°.

The melting point of the 8-unit duplex with two G · T pairs in the centre is lower by 20 °C than T_m for the perfectly matched duplex (52 and 72 °C respectively), while $\Delta\Delta G_0 = 2-3$ kcal mol^{-1}.[66, 71] Similar results have been obtained in the X-ray diffraction analysis of an 8-unit duplex containing two I · T pairs in the centre.[72] It was found that a thermodynamically more favourable situation arises if the two G · T pairs follow one another and are not separated by classical pairs. The degree of destabilisation of the duplex ($\Delta\Delta G_0$) is in this case 1 kcal mol^{-1} per G · T pair.[71]

The rate of exchange of the protons of the G · T pairs[22, 23] in the 3- and 10-positions in a 12-unit duplex at 35 °C exceeds (approximately by an order of magnitude) the rate of exchange of the protons of the G · C pairs in the same positions in the duplex, which indicates a looser structure of the G · T pair, more accessible to the solvent, compared with the G · C pair. Data confirming the formation of the looser structure in duplexes with G · T pairs have also been obtained in other studies.[67, 68]

Comparison of the thermodynamic parameters of the formation of 16 duplexes containing an inner G · U or A · U pair revealed that the G · U pair stabilises the duplex (compared with the loop at this site) and that its contribution to ΔG_0 of formation of the duplex depends on the immediate environment.[73] If the G · U pair adjoins an A · U pair, then the increase in the free energy of the duplex is $-(0.5-0.7)$ kcal mol^{-1}, but, when it adjoins a G · C pair, then $\Delta G_0(G \cdot U) \simeq \Delta G_0(A \cdot U) = -(1.3-1.9)$ kcal mol^{-1}. On average, the inner G · U pair is less stable to the extent of 0.7 kcal mol^{-1} than the A · U pair.[48, 70, 73] The greater stability of the G · U pair with a G · C pair on its side, compared with the G · U pair adjoining an A · U pair, can be explained by more effective stacking interactions of the G · U and G · C pairs compared with the G · U and A · U pairs. Comparison of the ribo-duplexes containing a central G · U, G · C, or A · U pair showed that the T_m of the duplex with a G · U pair is approximately equal to the T_m of the duplex shortened by one unit. The G · U pair itself is a site of instability in the double helix.[74]

The G · A pair. This 'wobble' pair is of special interest, because it is the usual element forming the steric structure of RNA.[75] At neutral pH, one can postulate four different versions of the formation of hydrogen bonds in the G · A pair (Fig. 1).[75, 76] It is noteworthy that the conformation *a* has been predicted and detected in the RNA double helix,[75] while the conformation *b* has been confirmed experimentally in a study of model DNA duplexes.[77, 78] Until recently, there was no experimental confirmation of the existence of the conformations *c* and *d* for the G · A pair. In the conformations *a* and *b*, there is a characteristic propeller-like disposition of the bases relative to one another (the angle of rotation is 24.8°), which facilitates the formation of hydrogen bonds between guanine and adenine.[77, 79] The G · A pair fits satisfactorily into the double helix of the *B* form, causing virtually no disturbance to the stacking interactions in the duplex, while the changes in the torsional angles of the bases are within the limits characteristic of canonical base pairs.[77, 80, 81] The destabilising effect of the G · A pair is manifested by a decrease in the T_m of the duplex by 10 °C per G · A pair compared with the perfectly matched duplex. The perturbations introduced by the G · A pairs are local in character and are not propagated along the helix.[13, 77]

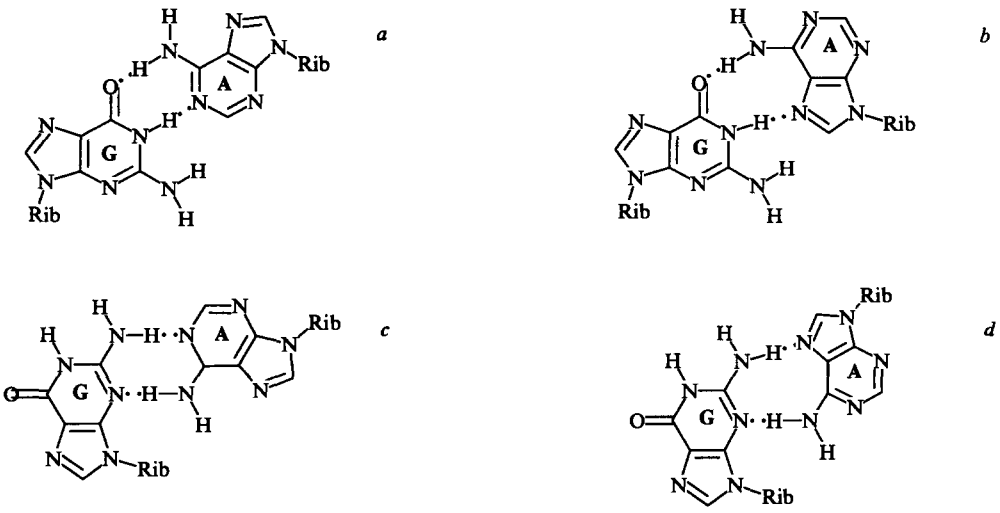


Figure 1. Four versions of the formation of hydrogen bonds in the G · A pair.

Comparative study of 13 dodecamers, differing in the number of G · A pairs, their positions, and their environments, revealed the influence of the nearest neighbours on the stability of the imperfectly matched duplex with such noncanonical pairs. It was found that the most stable sequences, containing two adjoining G · A pairs, have thermodynamic parameters of formation approximately equal to the parameters of formation of the perfectly matched duplex. However, the same sequences with a single G · A pair are appreciably destabilised compared with the perfectly matched duplex.[82,83]

In a comparatively recent study of a 10-unit duplex formed by the oligonucleotide d(ATGAGCGAATA), containing four G · A pairs and a noncomplementary adenine unit at the 3'-end, direct evidence was obtained for the existence of the conformation *d* of the G · A pair. This duplex produced the *B* form of the double helix and was distinguished by an anomalously high stability, approximately equal to the stability of the perfectly matched complex, which was explained by the very effective stacking interactions between the bases of the opposite chains (G_3 with G_7 and A_4 with A_8).[84] The study of the contribution of the hydrogen bonds formed within the G · A pairs to the stability of the RNA duplexes (not less than -1.4 kcal mol^{-1} per pair) makes it possible to explain this anomalously high stability of the imperfectly matched duplex with G · A pairs.[83]

The A · A pair. The A · A pair does not form stable hydrogen bonds. The incorporation of the d(A · A) pair in the double helix takes place as a result of the stacking of adenine units with neighbouring bases and is accompanied by the distortion of the planar structure of the heterocyclic base, in order to decrease the overlap of the exocyclic amino-groups of the adenine units, and by appreciable rearrangements of the sugar phosphate skeleton of the duplex.[85]

The G · G pair. Indirect evidence for the existence of this pair has been obtained in a number of studies,[86-88] but the existence of this wobble pair in a duplex was first demonstrated by Cognet et al.[89] According to two-dimensional NMR data, the bases of this pair participate effectively in the stacking interactions of the double helix and the double helix itself has the classical *B* form. The imino-protons of the bases participate in the formation of the hydrogen bond of the G · G pair; one of the guanine units assumes the normal *anti*-conformation, whilst the other assumes the *syn*-conformation or one close to it. Such a pair has a symmetrical structure and does not introduce perturbations into the regular structure of the *B* form of DNA. There are no data on the thermodynamic stability of duplexes with G · G pairs.

Purine–purine pairs cause a marked destabilisation of the double helix. Comparison of the thermal stabilities of oligomer-polymer duplexes having the structures $dG_ndG_{12}A_mC_x$ and $dG_ndG_{10}G_mC_x$ (n = 100, m = 0–6, x = 5–41) with different numbers of d(A · G) and d(G · G) pairs showed that the destabilisation of the duplex is proportional to the number of noncanonical pairs.[87] The presence of a cluster of noncanonical G · A or G · G pairs does not, however, affect the cooperative nature of the fusion of the duplex, which constitutes additional confirmation that the irregular purine–purine pairs are built into the regular double helix. Long DNA duplexes, containing one noncanonical pair, are resistant to the action of S1 nuclease. The increase in the length of the section with noncanonical pairs from 2 to 6 bases increases the sensitivity of the duplex to S1 nuclease: the duplex is cleaved by S1 nuclease under identical conditions to the extent of 4% and 30% for duplexes with one and six G · G pairs respectively.[87]

The influence of nearest neighbours on the destabilising effect of the purine–purine noncanonical pair has been investigated.[70,74,82] According to NMR spectroscopic data, 5-unit duplexes are not formed if the G · A or G · G pairs are flanked by A · U pairs, whereas duplexes in which the G · A or G · G pairs are flanked by G · C pairs are fairly stable (T_m = 26 °C). Data confirming the marked dependence of the stability of the duplex with purine–purine pairs on its base sequence have also been published.[82,84,87,90]

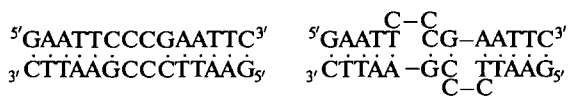
The A · C pair. According to literature data,[77,91] the A · C pair is stabilised by one hydrogen bond between the N(6) protons of the amino-group of adenine and the N(3) or O(2) protons of cytidine, but the possibility of the formation of an A · C pair, stabilised by two hydrogen bonds in the case of adenine in the tautomeric form, is not ruled out. The rate of exchange of the imino-protons in the G · C and A · T pairs adjoining a noncanonical A · C pair in a duplex with two A · C pairs increases compared with the perfectly matched duplex by factors of 3 and 2 respectively. Consequently the destabilising influence of the A · C pair is not localised and is propagated along the double helix.[91] The incorporation of an A · C pair in a DNA duplex is accompanied by small changes in the sugar phosphate skeleton of the duplex, ensuring the occurrence of stacking interactions between the A · C pair and the adjoining bases.[92] The introduction of an A · C pair into the centre of a 17-unit duplex lowers its melting point compared with the perfectly matched duplex by 10 °C. The stability of the duplexes containing noncanonical pairs diminishes in the sequence[93] G · C > A · T > G · U > A · C. Comparative analysis of data on the hybridisation of 11-, 14-, and 17-unit oligonucleotides with the DNA of the phage φX 174 and with the

DNA of a mutant phage in which a point exchange of G · A has taken place at the oligonucleotide binding site demonstrated that all three probes are bound much more weakly with the mutant DNA. The introduction of one A · C pair into the duplex lowers the dissociation temperature of these probes by 12 °C, which corresponds to the 'loss' of approximately three G · C pairs.[94]

The U · U pair. The existence of the U · U pair has not been demonstrated experimentally. The five-membered self-complementary oligonucleotide AGUCU exists preferentially in the single-stranded form. The U · U pair in the centre of the duplex leads to its complete destabilisation, while the duplex with the G · C pair at the same site has[74] a melting point of 25 °C.

The T · T pair. According to NMR data, the T · T pair is not stabilised by a hydrogen bond,[13] but it can be built into the double helix under these conditions with minimum disturbances to the structure of the duplex and leads to a decrease in its T_m compared with the perfectly matched 12-unit duplex by 11 °C. This pair forms a locally unstable section in which the dissociation of the duplex is initiated on raising the temperature simultaneously with a process occurring from the end of the duplex.[51,95] The T · T pair destabilises the duplex to the greatest extent[13,85] if it is incorporated in the ATA/TTT sequence, exerting the least effect in the CTG/GTC sequence.

The C · C pair. There is at present no experimental evidence in the literature for the formation of hydrogen bonds between the bases of the C · C pair. The absence of hydrogen bonds stabilising the C · C pair as well as the poor overlap (stacking) of the unpaired cytosine with the adjoining bases of the duplex lead to the bulging of the C · C pair with formation of an inner loop.[70,74] It has been shown[96] that duplex **5** exists not in the form of a hairpin with an inner loop comprising four cytidine units but has the structure **6** with bulging cytidine units. Such rearrangement of the duplex is accompanied by a change in the sugar phosphate skeleton only in the looped out nucleotide, whereas the entire remainder of the duplex has the *B* form of DNA.



5 **6**

The appearance of the C · C pair in the duplex causes an appreciable increase in the enthalpy of formation of the duplex: $\Delta H_0 = -77$ kcal mol^{-1} for $[(Ap)_3A(pU)_4]_2$ and $\Delta H_0 = -43$ kcal mol^{-1} for $[(Ap)_4C(pU)_4]_2$, and reduces its melting point by 10–17 °C, which corresponds to the loss of two A · U pairs.[97]

In the study of the crystal structure of the dodecameric RNA duplex containing three noncanonical pairs in the centre, it was observed that four noncomplementary bases do not form an inner loop, giving rise to a fairly regular helix incorporating the G · U and U · C pairs.[98] These results are the first experimental evidence for the existence of the U · C pair in the crystal. This pair forms one hydrogen bond and is stabilised by hydrogen bonds with water molecules, forming bridges between the nitrogen atom of the heterocyclic base and the oxygen atom attached to phosphorus. The authors mention particularly the influence of the hydrogen bonds between the OH groups of ribose, the oxygen atoms at the phosphorus, and the water molecules on the stabilisation of the duplex structure.[98]

3. Comparative analysis of the influence of noncanonical base pairs on the stability of DNA and RNA duplexes

It is quite evident that the less the stability of an imperfectly matched complex, formed fortuitously by an oligonucleotide and the NA target, differs from the stability of the perfectly matched duplex, the higher the level of their nonspecific interaction. Comparison of the destabilising influence of various structural anomalies (noncanonical pairs, projecting bases, dangling ends) in order to discover those which destabilise the duplex to the least extent is therefore extremely urgently required. An extensive set of experimental data, including also the thermodynamic parameters of the formation of imperfectly matched complexes with structural anomalies, has now accumulated, but these data are somewhat heterogeneous and do not permit unambiguous conclusions about the degree of the destabilising influence of each separate noncanonical base pair or some other structural anomaly in the duplex.[13,18] It is noteworthy that the destabilising influence of each structural anomaly depends also on the environment in which it is located i.e. on the nearest neighbours.[13,84,89] Thus the core component of the duplex usually remained unchanged in studies where the relative stabilities of different noncanonical pairs were estimated. This was the reason for the considerable discrepancies between the estimates of the stability of noncanonical base pairs obtained by different workers:[13,23,99]

T · G > G · G = G · A > G · T > A · G = C · T >
T · C = A · A = T · T > C · A > C · C > A · C;[13]
G · T = T · G > A · G > T · T = C · T > G · A = G · G >
T · C > A · A > A · C > C · A > C · C;[99]
G · T > G · A > A · A = T · T = C · A > C · T.[23]

Noncanonical base pairs are arranged in order of decreasing stability.

Considerable discrepancies are observed not only in the estimates of the relative stabilities of various noncanonical base pairs but also in the absolute differences between the thermodynamic parameters for perfectly and imperfectly matched complexes incorporating the same noncanonical pair. Thus, the destabilising influence of the A · C pair with a constant environment can be determined from the results of different studies:[13,100] $\Delta\Delta G_0$(A · C) = 2.7 kcal mol^{-1} (Ref. 100) and 3.5 kcal mol^{-1} (Ref. 13). However, such a difference between the destabilising effect of the given noncanonical base pair cannot be accounted for by the differences either between the experimental conditions or between the lengths of the duplexes investigated.

The destabilising effect of different noncanonical bases on the stability of core duplexes has been studied in greatest detail in several investigations.[13,56,99,100] Corresponding parameters for the destabilisation of the duplex owing to the formation of noncanonical pairs as a function of nearest neighbours have been determined experimentally.[13] These data are presented in Table 3.

The influence of all possible noncanonical pairs on the thermodynamics of the formation of a 17-unit DNA duplex (with mismatches located within the centre of the duplex) has been investigated.[99] On the basis of the analysis of the ΔH_0 and ΔS_0 for a noncanonical base pair, i.e. the parameters which describe the stacking interactions of the given pair with the adjoining bases, the authors classified different mismatches in terms of their involvement in the formation of the duplex: (1) Wobble pairs or irregular pairs stabilised by hydrogen bonds. These are characterised by a strong stacking interaction with the adjoining bases. Such pairs do not disturb either the overall stacking of the duplex or the conformations of the sugar phosphate residue; the entropy of formation of the wobble pair is approximately equal to the entropy of the Watson–Crick pair, while the enthalpy of formation is somewhat lower. The T · G, G · G, C · A, A · A, and A · G pairs belong to the class of wobble pairs. (2) Open pairs, i.e. pairs which do not form hydrogen bonds but are involved in the stacking interaction with

Table 3. Destabilisation of the double helix by the formation of noncanonical base pairs.[13]

Base pairs	ΔG_0 kcal mol^{-1}	ΔH_0 kcal mol^{-1}	ΔS_0 cal mol^{-1} K^{-1}
A–T–A / T–G–T	0	−8.1	−27
A–G–A / T–G–T	0.2	−6.0	−20
A–G–A / T–A–T	0.3	−5.1	−18
A–G–A / T–T–T	0.7	0.8	1
A–A–A / T–G–T	1.2	7.6	22
A–C–A / T–T–T	1.2	−5.7	−23
A–T–A / T–C–T	1.5	−2.5	−13
A–A–A / T–A–T	1.5	10.6	31
A–T–A / T–T–T	1.5	−7.1	29
A–C–A / T–A–T	1.9	7.2	38
A–C–A / T–C–T	2.0	−7.8	−33

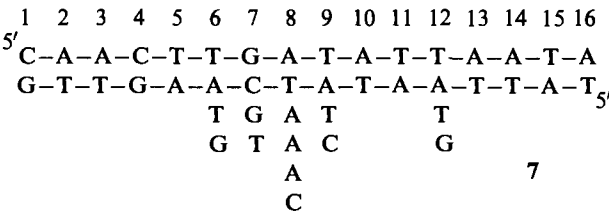
the bases of the chain. Such pairs introduce the greatest perturbation and destabilise the duplex. (3) Weak pairs linked by only one hydrogen bond; the stacking interaction is unlikely in this instance. The enthalpy of formation of a weak pair is approximately equal to half the enthalpy of formation of a wobble pair.

It is noteworthy that the melting points of the duplexes differing only in the orientation of the irregular pair are not the same although the environment of these pairs and hence the interplanar contacts do not change. Data obtained recently indicate the extremely anomalous influence of adjacent inverted G · A pairs on the stability of DNA duplexes.[82,84] The replacement of two canonical pairs in the decameric duplex by two isolated G · A pairs lowers the association constant by a factor of $10^3-4\times10^5$. Four inverted G · A pairs arranged in pairs destabilise the duplex by a factor of 4.5, but, in the presence of the same number of G · C pairs in this duplex as in the perfectly matched complex, an anomalously stable duplex is produced (the association constant increases by a factor of 5–40). Similar data have been obtained[90] also for ribo-duplexes containing a G · A pair.

The influence of the location of the noncanonical pairs on the stability of duplex **7**, which is a fragment of the DNA of the bacteriophage φX 174 and is the binding site of the gene A protein, has been investigated.[100] Duplexes containing noncanonical pairs fuse at a lower temperature than the perfectly matched duplex **7**. The destabilisation of the duplex is greater when the irregular pair substitutes a G · C not a A · T pair and also if the noncanonical pair is located closer to the centre of the duplex (cf. the duplexes 8-AA and 12TG in Scheme 2).

Three probable structures were analysed for all the duplexes in Scheme 2: (1) the formation of inner loops. This process should be accompanied by the loss of the stacking interaction of two base pairs, an appreciable increase in ΔH_0, and a change in the free energy of the duplex ($\Delta\Delta G_0$) in the range 5.5–7.0 kcal mol^{-1}. (2) The formation of a structure with bulging bases. This should be accompanied by the elimination from the stacking interaction of one base pair and should involve $\Delta\Delta G_0$ = 7.0 kcal mol^{-1}. (3) The formation of a noncanonical base pair. This process is characterised by the retention or slight alteration of the values of ΔH_0 and low values of $\Delta\Delta G_0$. According to the thermodynamic parameters presented above, these duplexes, illustrated in the scheme, form noncanonical pairs and not any other structures.

Scheme 2



Duplex	T_m °C	$-\Delta G_0$ kcal mol^{-1}	$\Delta\Delta G_0$ kcal mol^{-1}
7	52.0	15.8	–
6-TG	45.1	13.2	2.6
7-GT	42.9	12.7	3.1
8-AA	42.1	12.6	3.2
8-AC	40.6	12.1	3.7
9-TC	43.0	13.1	2.7
12-TG	46.9	14.0	1.8

The influence of the terminal noncanonical pair on the stability of the duplex has been studied only for oligoribo-nucleotide duplexes.[49,101] The free energy increment following the addition of the terminal noncanonical pair to the core duplex was on average −0.5 to −2.3 kcal mol^{-1} depending on the form of the noncanonical pair and the last base of the core duplex: $\Delta\Delta G_0$(G · U) ≃ $\Delta\Delta G_0$(A · U) ≃ −1.3 kcal mol^{-1}; the addition of a pyrimidine–pyrimidine or purine–pyrimidine pair (but not G · U) increased the stability of the duplex by −0.5 kcal mol^{-1}, while the addition of a purine–purine pair had an effect comparable to that of the addition of a dangling end (the contribution to ΔG_0 by this pair is −0.2 kcal mol^{-1}). It has been shown[102] that the stabilising influence of the terminal mismatch increases in the sequence A · C ≃ A · A < A · G ≃ A · U (data obtained for the CCGG/GGCC core duplex).

Comparative analysis of the data presented in a number of studies[13,49,56,99,101] permits the claim that the addition of the weakest noncanonical pair U · C at the end of the duplex does not alter its stability, while the appearance of an isolated G · U pair in the central part of the duplex causes its appreciable destabilisation.

The study of Gillam et al.[42] is the only one in which the stabilities of imperfectly matched heteroduplexes were compared. The melting points of the mismatched duplexes were determined from the temperature dependence of the degree of binding of the oligonucleotides to d(pT)$_9$ immobilised on a resin. The following noncanonical pairs were analysed: T · dC; T · rC; T · dG; T · rG; T · T; T · U. Ribooligonucleotides form less stable duplexes with immobilised d(pT)$_9$ than do deoxyribooligonucleotides. Only duplexes containing the T · rG pair are an exception. The destabilising effect of this pair is much smaller than that of the dT · dG pair. The stability of the duplex with the T · rG pair corresponds to that of the duplex shortened by one A · U pair. Furthermore, the influence of the position of the irregular pair in the duplex on its stability was demonstrated in the same study. The terminal irregular pair induces a minimal destabilisation of the double helix (ΔT_m = 4 °C for dT$_9$ · dA$_8$ and dT$_9$ · dA$_8$G) compared with the irregular pair at the centre of the duplex (ΔT_m = 15 °C for dT$_9$ · dA$_8$ and dT$_9$ · dA$_5$GA$_3$).

In considering the problem of the reparation of the noncanonical pairs,[88,90] the authors conclude that the stable pairs (G · T and T · G), introducing minimal perturbations into the DNA structure, are repaired most effectively. The degree of reparation is 93% for the G · T pair and 55% for the T · G pair, whereas other mismatches are recognised by the cell repair system to a much lesser extent. The degree of reparation is less than 5% for the A · G and C · T pairs and 42% for the G · A pair.

The experimental data considered in this Section indicate unambiguously that the greatest contribution to the decrease in the complementary accuracy of the interaction of nucleic acids should come from imperfectly matched complexes with structural

anomalies at the ends of the duplex, which agrees with theoretical estimates of Perelroyzen and Vologodskii.[11] However, one should not forget at the same time the possibility of the formation of imperfectly matched complexes with an increased stability, e.g. such as the duplexes with inverted noncanonical G · A pairs.

IV. Accuracy of the interaction of RNA and DNA molecules with oligonucleotides and their derivatives

A number of approaches have been developed in recent years for the investigation of the structure and functions of nucleic acids based on the use of antisense oligonucleotides and their derivatives.[1] The antisense oligonucleotides, which are complementary to different sequences in the composition of single-stranded and double-stranded nucleic acids, have the ability to form specific complexes with these nucleic acids (duplexes and triplexes), which prevents the interaction of the nucleic acids with ribosomes and DNA or RNA polymerases both *in vitro* and *in vivo*.[2,9]

There exist several main requirements on which these approaches are based. Firstly, oligonucleotide derivatives must permeate the cell and must be sufficiently stable under *in vivo* conditions. Secondly, oligonucleotides or their derivatives must form a complex with the selected nucleic acid sequence. Thirdly, the formation of the complex must inhibit the functions of the given nucleic acid. Fourthly, the antisense oligonucleotides must not interact with other sequences in the cell apart from the one chosen.[9] It is quite evident that the last two principles are closely interrelated—a specific interaction with the selected sequence is impossible without the formation of a highly stable complementary complex.

The thermodynamic parameters of the formation of perfectly matched DNA and RNA duplexes as well as the defects in the double helix having a destabilising effect on the duplex were examined in the previous Sections. All these data were obtained in the study of model oligomeric duplexes. The next section will deal with studies on the interaction of oligonucleotides or their derivatives with the NA target, in which the accuracy of the interaction of the oligonucleotide with the selected nucleic acid was estimated.

1. Model systems

a. Oligonucleotides with the usual phosphodiester linkage

The specificity and effectiveness of complex formation by a series of synthetic oligonucleotides with a length corresponding to 8–14 units (ON) with the M13mp3 phage DNA have been investigated.[103] Two oligonucleotides out of the eleven investigated [one a 12-unit oligonucleotide (ON-12) and the other a 14-unit oligonucleotide (ON-14)], complementary to the 3366-3377 and 2216-2230 sections of the phage DNA respectively, were bound at 4 °C to the DNA target at more than one site (the ON-12 and ON-14 concentrations were 2 μM). The binding of these oligonucleotides to the DNA target with formation of imperfectly matched complexes was confirmed by the elongation of ON-12 and ON-14 as primers under the influence of DNA polymerase at 20 °C. It is noteworthy that under the same conditions two 10-unit oligonucleotides, forming with the M13mp3 DNA duplexes with a length equivalent to 10 base pairs and containing a central G · T pair, were not built up by DNA polymerase, while a 13-unit oligonucleotide containing an analogous noncanonical pair was built up by the enzyme until the phage DNA was replicated.

The influence of noncomplementary pairs in the matrix · primer duplex on the effectiveness of the chain elongation reaction with the aid of the Taq DNA polymerase and the AMV reverse transcriptase has been investigated in a series of studies.[104–108] The presence of a single mismatch within the matrix · primer duplex did not produce an appreciable effect on the yield of the product of the amplification of the HIV-1 gag-region, whereas the presence of a noncanonical base pair at the 3′-end affected the yield of the PCR-product. The 3′-terminal T · C, T · G, T · T, G · G, and A · C pairs were amplified with the same effectiveness as the perfectly matched duplex, whereas the A · G, G · A, and C · C pairs at the 3′-end of the duplex decreased the overall yield of the PCR product by a factor of 100 and the A · A pair decreased it by a factor of 20. The influence of the G · A and A · G mismatches on the yield of the product was the same. The minimum effect on the yield of the PCR-product was exerted by mismatches generated by T with G and by C with T. The presence of two irregular pairs in the vicinity of the 3′-end of the primer · matrix duplex (the last four bases of the duplex), one of the mismatches being 3′-terminal (apart from the irregularly paired thymidine), leads to the virtually complete cessation of the elongation reaction.[104] It is noteworthy that the data on the thermodynamic stability of such imperfectly matched duplexes do not explain the results obtained by the authors. Similar data have been obtained[105] for the elongation of an imperfectly matched primer · matrix duplex with the aid of the AMV reverse transcriptase. The decrease in the overall concentration of dNTP from 800 to 50 μM[104] or from 200 to 2 μM[106] led to the elongation mainly of only the perfectly matched duplex (the G · G and C · T mismatches respectively). With increase in the temperature of the annealing of the primer · matrix duplex from 44 to 55 °C, only the perfectly matched duplex was elongated, while no elongation was observed in the duplexes with the 3′-terminal A · A and T · T mismatches.[107] The elongation of only the perfectly matched duplex could be achieved also using shorter primers: 10 out of the 12 possible noncanonical pairs at the 3′-end of the duplex completely stopped the elongation if short (10-unit) primers were employed.[108]

Analysis of a series of oligonucleotides, complementary to the Shine–Dalgarno sequence in the *E. coli* 16S rRNA, forming with the latter perfectly (AGAGGAGGU, ON/r) and imperfectly matched complexes (GGAAGGAGC, ON/i-1; GGAGAAGC, ON/i-2; AUUUCUUCUAUG, ON/i-3) showed that the effectiveness of the inhibition of the binding of Qβ RNA to the 70S ribosomes of *E. coli* depends on the stability of the 16S rRNA · oligonucleotide duplex: ON/r: ΔG = 16.9 kcal mol^{-1}, binding inhibited by 87.2%: ON/i-1: ΔG = −11.1 kcal mol^{-1}, binding inhibited by 56.6%; ON/i-2: ΔG = −7.9 kcal mol^{-1}, binding inhibited by 42.6%; ON/i-3: ΔG = −1.1 kcal mol^{-1}, no inhibition observed.[109] The oligonucleotide 'probing' of the 16S rRNA molecule forming part of the composition of the 30S ribosomal subparticles in *E. coli* by 8–15 unit oligonucleotides demonstrated that, at an oligonucleotide concentration of 1 μM, there is a possibility of the formation of an imperfectly matched complex with exposed RNA sections, containing five classical Watson–Crick pairs at the 3′-end of the duplex.[110]

The site-specific cleavage of mRNA of prothymosin-α, isolated from the cytoplasm of lymphocytes stimulated by the staphylococcal enterotoxin, in the presence of a 12-unit oligonucleotide (GCAGGGCGTCTC) and RNase H takes place within both perfectly and imperfectly matched duplexes. The imperfectly matched ON-12 binding site was identified from the size of the hydrolysis product and was found to contain three irregular pairs (structure **8**).[111]

$^{5'}$GAGAGGCCCGCCCGCCC$^{3'}$ fragment of mRNA
$_{3'}$CTCTGCGGGACG$_{5'}$
8

The mRNA of γ-interferon was cleaved in the same investigation in the presence of a 24-unit oligonucleotide ON-24 (at a concentration of 1 μM). Although, apart from forming a complex with the 603–625 sequence of the mRNA of γ-interferon, ON-24 can form an imperfectly matched duplex with a length equivalent to seven base pairs with the TGCCTGC sequence of mRNA, the products of the cleavage of RNA at this site were not detected. Evidently the difference between the

stabilities of the perfect and imperfect ON-24 · mRNA of γ-interferon duplexes proved insufficient for discrimination between these sites by RNase H.

The accuracy of the formation of the duplex is particularly important in site-specific mutagenesis. 8–12-Unit oligonucleotides containing the base to be replaced in the centre proved to be most convenient for the introduction of point mutations into the DNA molecule.[112] The stability of the imperfectly matched duplex containing one noncanonical pair proved to be the decisive parameter on which depended the yields of the mutant DNA. The yield of the mutant DNA increased from 0.05 to 20% on reducing the hybridisation temperature from 33 to 0 °C for the 8-unit oligonucleotide with the G · T pair in the centre. The use of a 10-unit oligonucleotide with a similar irregular pair[113] increased the yield of the mutant DNA to 38% at 10 °C. When the base to be replaced was shifted from the 3'-end to the centre of the oligonucleotide, the yield of the mutant DNA rose from 8 to 20% respectively. Although duplexes with an irregular pair at the end are in fact more stable, the oligonucleotides forming such duplexes are probably poor primers for DNA polymerase.[113]

When oligonucleotides complementary to the mutation site were used, it was shown that the effectiveness of the correction of the DNA sequence with the aid of DNA polymerase is linked directly to the stability of the oligonucleotide (primer) · DNA duplex. With increase in the length of the primer from 11 to 17 bases, the yield of the 'corrected' phage φX 174 DNA (the mutant strain am3 was corrected) increased from 0.02 to 13.9%. Furthermore, the two oligonucleotides placed one immediately behind the other (in a tandem fashion) (simulation of point dissociation) were more effective in the synthesis of the 'corrected' DNA than short oligonucleotides [yield of φX 174 phage DNA (%): 1.2 for ON-11 + ON-6 and 0.02 and 0 for ON-11 and ON-6 respectively; 14.0 for ON-14 + ON-6 and 1.9 for ON-14; 32.5 for ON-17 + ON-6 and 13.9 for ON-17].[114]

The pentadecadeoxyribonucleotide, fully complementary to the RNA segment (synthesised on the *E. coli* tryptophan operon) responsible for the regulation of attenuation, was used[115] to investigate the role of the secondary structure of RNA in the termination of transcription. The essential feature of the approach employed in the above study[115] is that the oligomer is bound in a complex with a selected section of the synthesised transcript, preventing thereby the formation of the corresponding 'terminator' secondary structure in this segment of RNA and behaving therefore as an antiterminator. It was shown that, in the presence of a 500-fold excess of the oligomer (2 μM, 37 °C) relative to the matrix, the yield of the transcript exceeded by a factor of approximately four the yield of the product in the control experiment (without the oligonucleotide). On the other hand, the yield of the transcript synthesised in the presence of the same oligomer (and under the same conditions) on the *Ser. marcescens* tryptophan operon exceeded the yield of the product in the control experiment by a factor of only 1.2. In the latter case, the oligomer might have formed a duplex containing two noncanonical pairs with the corresponding section of the transcript, in contrast to the perfectly matched complex formed by the oligomer with the selected section of RNA synthesised on the *E. coli* tryptophan operon.

A general approach to the formation of oligonucleotide probes for mRNA with an unknown primary structure has been proposed[116] (if it is assumed that the aminoacid sequence of the corresponding protein is at least partly known). This approach is based on the use as the primer or the probe of an oligonucleotide complementary to the section of mRNA coding for tetrapeptides consisting of the aminoacids Phe, Tyr, His, Asn, Asp, Cys, Gln, Lys, Glu, Trp, and Met. Taking into account the degeneracy of the code, such an oligonucleotide will form with mRNA a duplex containing either G · C or G · U pairs. Furthermore, T · G or T · A pairs may be encountered. The probe, constructed in accordance with this principle for gastrin mRNA (containing two G · U pairs) was hybridised with the mRNA, but its efficiency as a primer was lower by a factor of 2 than the efficiency of the oligonucleotide fully complementary to the given section. Furthermore, in the case of oligonucleotides with two G · U pairs, the primer underwent both hybridisation and elongation only on denaturation of the mRNA.

The exact selection of hybridisation conditions makes it possible to distinguish the RNA or DNA sequences containing at least one replacement at the probe binding site.[117,118] Thus the presence of one G · T pair (instead of G · C) at the centre of the binding site for a 14-unit oligonucleotide (ON-14-B) decreased the degree of its hybridisation with the rabbit β-globin mRNA to 8% compared with the degree of hybridisation of the oligonucleotide fully complementary to the same section (ON-14-A) {1 M NaCl, 37 °C, [ON-14-A] = [ON-14-B] = 0.15×10^{-9} M}. The dissociation temperatures of the complexes[117] mRNA · ON-14-A and mRNA · ON-14-B differed by 5 °C.

The hybridisation of 23-unit oligonucleotides with the initial and mutant DNA depended on the type of irregular pair at the oligonucleotide binding site. The oligonucleotide ON-23, complementary to the adenovirus Ad-2 DNA, was hybridised also with the DNA of the Cyt-15 mutant strain. The duplex ON-23 · Cyt-15 DNA contained the T · T pair. On the other hand, the oligonucleotide ON-23M, complementary to the Cyt-15 DNA, gave rise to a very weak signal due to hybridisation with the Ad-2 DNA. In the latter case the duplex contained the A · A pair, which can be explained by the greater destabilising effect of this pair on the double helix than the effect of the T · T pair.[118]

The differences between the stabilities of the perfectly matched duplex and the duplex containing one irregular pair were used to diagnose sickle cell anaemia. The 19-unit oligonucleotides ON-19-A, complementary to the normal globin mRNA (mRNA-A), and ON-19-S, complementary to a mutant mRNA (mRNA-S), gave rise to cross-hybridisation at 45 °C (level of hybridisation 10%–15%); the complex mRNA-A · ON-19-S contained one A · A pair, while the complex mRNA-S · ON-19-A contained one T · T pair. An increase in the hybridisation temperature to 55 °C led[119] to a rigorously specific interaction of the above oligonucleotides with the corresponding mRNA. The accuracy of the interaction of short probes with lengths equivalent to 7, 9, or 12 oligonucleotide units proved low and led to intense cross-hybridisation. Thus the 9-unit and 12-unit probes, complementary to the gene for the phage T4 lysozyme, were hybridised to the extent of 15%–18% with the DNA of the lysozyme-free G223 phage and 10% with the total RNA of *E. coli*.[120] At a hybridisation temperature lower by 15–20 °C than the melting point of the perfectly matched complex, the 12–15-unit oligonucleotides were effectively hybridised with the DNA of the *lac* operon (of not only the wild strain but also of a series of mutant strains) with formation of duplexes containing noncanonical pairs of the type C · A, G · A, T · T, etc. The degree of cross-hybridisation depended under these conditions on the type of the irregular pair: the degree of hybridisation for oligonucleotides forming a complex with the G · A pair was lower than for those forming a complex with the C · A pair. An increase in the hybridisation temperature from 30 to 37 °C made it possible to avoid the cross-hybridisation of these probes.[121]

b. Nonionic analogues of oligonucleotides

Nonionic analogues of oligonucleotides (phosphotriesters, methylphosphonates) have been proposed as antisense oligonucleotides for the inhibition of the expression of genes *in vivo*. Unchanged oligonucleotides readily permeate into the cell via passive diffusion. The use of nonionic analogues of oligonucleotides as inhibitors of the translation of mRNA or the expression of genes has been examined in detail in a number of reviews.[1–3,122]

In the study of the binding of ethyl phosphotriesters of oligonucleotides complementary to the anticodon loop (dTpTpCpA, ON-I) and the CCA-end (dGpGpT, ON-II) of yeast and *E. coli* $tRNA^{Phe}$, it was observed that the constants for

the binding of these derivatives to $tRNA^{Phe}$ are higher than for the unmodified oligonucleotide. At 0 °C (1 M NaCl, 10 mM, Mg^{2+}), the binding constant (K_x) was 3600 litre mol^{-1} for ON-I and 2400 litre mol^{-1} for the diester analogue.[123] As expected, at 0 °C ON-II at a concentration of 270 μM inhibited the aminoacylation of all five tRNA investigated (specific to Phe, Lys, Tyr, Pro, and Leu) to approximately the same extent (60% – 80%). At a concentration of 364 μM, ON-I inhibited the aminoacylation of $tRNA^{Phe}$ as a result of the formation of a perfectly matched duplex with the tetranucleotide sequence in the anticodon loop of $tRNA^{Phe}$. Together with this finding, the inhibition of the aminoacylation reactions of other tRNA was also observed[124] in the presence of ON-I: by 35% for $tRNA^{Leu}$, by 12% for $tRNA^{Lys}$, and by 0.7% for $tRNA^{Pro}$. When the methyl phosphate derivatives (the modified phosphate is designated by an asterisk) of the oligonucleotides dAp*Ap*Ap*A (M-ON-1) and dGp*Gp*U (M-ON-2), complementary to the sequence in the anticodon loop of $tRNA^{Lys}$ and the CCA-end of tRNA respectively, were used as the aminoacylation reaction inhibitors, the nonspecific inhibition of the aminoacylation of $tRNA^{Phe}$ by 9% and of $tRNA^{Leu}$ by 12% was observed in the presence of M-ON-1 (0 °C). In the presence of a similar oligonucleotide derivative dAp*Ap*Gp*A (M-ON-3), forming with the anticodon loop of $tRNA^{Lys}$ a duplex with one G · U pair, the level of inhibition of the aminoacylation reaction of $tRNA^{Lys}$ was 35% (whereas for M-ON-1 it was 88%), while the degrees of aminoacylation of $tRNA^{Phe}$ and $tRNA^{Lu}$ did not change.[125]

The experimental data on the thermodynamics of the duplexes formed by phosphodiester and methylphosphonate oligonucleotides are represented in the most complete form in the communications of Quartin and Wetmur[126] and Miller et al.[127] The change in the free energy of the duplex as a consequence of the introduction of one methylphosphonate linkage instead of the diester linkage is $\Delta\Delta G_0 = -0.75$ kcal mol^{-1} (1 M NaCl, 25 °C) regardless of the type of base in the oligonucleotide. These duplexes are additionally stabilised as a result of the decrease in the overall charge per pair of nearest neighbours containing the methylphosphonate linkage.[126]

The increase in the stability of the duplexes formed by methyl phosphate derivatives of oligonucleotides influences the complementation accuracy of the interaction of such derivatives with nucleic acids and their fragments. The photomodification of a 35-membered oligonucleotide by dodecameric methylphosphonates carrying 4'-aminoalkyl-4,5',8-trimethylpsoralen at the 5'-end has been investigated.[128] It was shown that the degree of photomodification of the ON target depends greatly on the accuracy of the formation of the duplex with the reagent (Table 4). Noncanonical pairs adjoining the reactive component of the derivative reduced sharply the degree of photomodification of the target. These results agree well with data obtained in a study[129] where it was shown that the biological and biochemical activity of oligonucleoside methylphosphonates falls sharply when defects appear in the duplex.

Table 4. The influence of the accuracy of the formation of the duplex on the degree of photomodification of a 35-unit oligonucleotide by the psoralen derivative of a methylphosphonate dodecamer.[128]

Duplex	Degree of photomodification (%)
Perfectly matched	85
Central T·pair	53
3'-Terminal T · C pair	58
5 G · T pairs at one pair intervals	33
3 T · C pairs at one pair intervals	19
4 T · C pairs at one pair intervals	0

c. Phosphorothioate analogues of oligonucleotides

The phosphorothioate analogues of oligonucleotides, containing a sulfur instead of an oxygen atom at the phosphorus atom, also belong to oligonucleotide derivatives with a modified phosphodiester linkage. The replacement of an oxygen atom by a sulfur atom increases the resistance of such derivatives to the action of intracellular nucleases.[130] The thermodynamic parameters of the formation of duplexes between the usual DNA or RNA and the phosphorothioate derivatives of oligonucleotides have been published.[1,131–134] Unfortunately, there are no data concerning the accuracy of the interaction of the phosphorothioate derivatives of oligonucleotides with model NA targets.

d. Derivatives of oligonucleotides containing α-anomeric units

During the last few years, methods have been developed for the synthesis of oligonucleotides resistant to the action of nucleases and consisting of the α-anomers of nucleotides (see the relevant reviews[135–137]). α-Oligonucleotides form a double helix with a complementary chain consisting of natural β-anomers of α-anomers of nucleotides. Both chains of the α · β duplex have a parallel orientation and the duplex itself belongs, according to NMR data, to the *B* conformation of DNA and has a right-handed twist to the extent of 70 ± 10%.[138] The melting point of duplexes[140] of the type α · β{α[(Tp)$_7$T] · β[d(pA)$_8$]} (30 °C) is higher than the T_m of the corresponding β · β duplex (24 °C),[139] which indicates the greater stability of the α · β duplexes compared with the β · β duplexes. On the other hand, the melting point of the heterooligomeric duplexes of the type α[d(TCTAAAC)] · · β[d(AGATTTG)] hardly differs from that of the corresponding β · β duplex (33 and 36 °C respectively).[141] Detailed thermodynamic studies of the duplexes β[d(CCTTCC)] · β[d(GGAAGG)], α[d(CCTTCC)] · β[d(GGAAGG)], and β[d(CCTTCC) · ·α[d(GGAAGG)] permitted the conclusion that the stability of the α · β duplexes depends on the nature of the bases in the α-chain (purine or pyrimidine) at least for homopurine or homopyrimidine sequences.[142] Comparison of the β · β duplexes mentioned above (T_m = 19 °C) with the α · β duplexes (T_m = 28 °C) showed that the α · β duplexes are more stable in 1 M NaCl than the β · β duplexes, provided that the α-chain consists of pyrimidine bases.[136] The duplexes of the α-oligonucleotides [α(T$_p$)$_7$T] with natural RNA [poly(rA)] are more stable than the analogous duplexes with poly(dA) (T_m = 29 and 17 °C respectively), while the β-dT$_8$ · poly(rA) duplex is less stable than dT$_8$ · poly(dA) (T_m = 14 and 17 °C respectively).[143] Data on the accuracy of the interaction of α-oligonucleotides with natural DNA or RNA targets are lacking in the literature.

e. Derivatives of oligonucleotides bound covalently to duplex-stabilising groups

The oligonucleotides bound covalently via an oligomethylene bridge to a dye molecule form duplexes with an increased stability (ΔT_m = 20 – 30 °C) as a result of the intercalation of the dye in the mRNA · antisense oligonucleotide double helix.[131,144,145] The synthesis and the mechanism of the action of such oligonucleotide derivatives have been considered in detail in a number of reviews.[5,146,147] The stability of the duplex poly(rA) · dT$_{6-8}$ increases appreciably (ΔT_m = 20 – 30 °C) if the oligothymidylate is bound covalently via one of the ends to 9-aminoacridine.[139,144,148] Another dye — *N*-(2-hydroxyethyl)-phenazinium — has been used[149,150] to increase the stability of the DNA duplexes. The oligonucleotide carrying a phenazinium residue at the 5'-end activated the replication of the M13mp7 bacteriophage DNA to the extent of 65%, while the free oligonucleotide showed no inactivation activity.[150] Unfortunately, the accuracy of the interaction with the NA target was not specially estimated in the studies devoted to such oligonucleotide derivatives. All the investigations were performed either on homopolymer matrices or on short DNA fragments.

2. Inhibition of the translation of mRNA

In recent years, antisense oligonucleotides and their derivatives have been used rigorously as specific inhibitors of the expression of genes.[1,5,151,152] The approach is based on the hypothesis[158-161] that, after the formation of a duplex with an antisense oligonucleotide, mRNA either loses the ability to be translated by the ribosome[153-157] or is cleaved by RNase H.

Standard cell-free protein-synthesising systems [the lysate of rabbit reticulocytes, the extract from wheat germ (WGE), and the oocytes of *Xenopus laevis*] are used to study the inhibiting activity of oligonucleotides or their derivatives on the translation of mRNA. The activity of RNase H is particularly high in the wheat germ extract.[159,162,163] Tests showed that the low activity of RNase H in a freshly prepared lysate of rabbit reticuloycytes is sufficient to hydrolyse exogenic mRNA with an antisense nucleotide.[160] In *Xenopus laevis* oocytes, RNase H activity is observed in the nucleus and in the cytoplasm.[159,164]

The most readily available mRNA of rabbit[157,159,165-169] or mouse[160] globins were used as the matrix. In addition, viral RNA sometimes served as a matrix: from the Rous sarcoma (RSV),[170,171] the Sendai virus,[172] the encephalomyocarditis virus,[173] and the tobacco mosaic virus.[174] Since the level of specificity of the inhibition of the translation was estimated in some investigations, the results of the latter will be considered in greater detail.

It has been shown[170] that the translation of 35S RNA from the Rous sarcoma virus (RSV) was effectively translated in WGE in the presence of the 13-unit oligonucleotide d(AATGGTAAATGG), complementary to the 3'- and 5'-terminal sequences of this RNA. Simultaneously with the suppression of the translation of the RSV RNA (approximately to the extent of 88%), the inhibition of the translation of AMV (avian myeloblastosis), the rabbit globin mRNA, and the BMV (broom mosaic virus) RNA to the extent of 57, 25, and 30% respectively has been observed (the data are quoted for a RNA : ON-13 ratio of 1 : 20 at 25 °C). The degree of inhibition of the translation of all the types of RNA increased with increase in the ON-13 concentration, but at low ON-13 concentrations (RNA : ON-13 = 1 : 2) mainly the translation of the oncovirus RNA (RSV and AMV RNA) was inhibited — to the extent of 27% and 10% respectively. Analysis of the sequence showed that ON-13 could form an imperfectly matched complex with AMV RNA with a length equivalent to 13 base pairs and containing three noncanonical pairs — two in the centre and one at the 3'-end. The degree of homology of the above oligomer with BMV RNA and globin RNA was not determined.

The inhibition of the translation of the mRNA in WGE as a result of the formation of an imperfectly matched complex with an antisense oligonucleotide has been observed.[164] All three oligonucleotides investigated, specific to β-globin mRNA, had incomplete complementation sites on the α-globin mRNA. Thus ON-17 could form with α-globin mRNA an imperfectly matched duplex comprising ten base pairs, three of which were noncanonical, ON-12 could form an imperfectly matched duplex consisting of seven base pairs with a central A · C pair, and finally ON-8 could form a duplex containing seven base pairs with a terminal irregular pair. The inhibition of the translation of the α-globin mRNA was observed only in the presence of ON-8 (the degrees of inhibition of β- and α-globin mRNA were 65% and 15% respectively). Apparently, in the case of ON-17 and ON-12 the difference between the stabilities of the perfectly and imperfectly matched duplexes, formed by these oligonucleotides with the β- and α-globin mRNA, was sufficiently high to prevent altogether the formation of an imperfectly matched complex at 25 °C and a concentration of the oligonucleotides of 10 μM or the complex was not recognised by RNase H.

The formation of an imperfectly matched complex between the α-globin mRNA and a 30-unit oligonucleotide complementary to the 270-300 fragment of the β-globin mRNA was detected from the cleavage of α-globin mRNA in the presence of saturation concentrations of the 30-unit oligomer in the *Xenopus laevis* oocytes.[159] The degree of homology between the α-globin mRNA and ON-30 was 60%. The non-specific inhibition of the translation of globin mRNA by oligonucleotides complementary to the 5'-nontranslatable sequence has been observed.[160] This finding was accounted for by the high level of homology between the nontranslatable sequences in the α- and β-globin mRNA. As a result of the high degree of homology (about 50%) between the 5'-terminal sequences of all the mRNA of the Sendai virus, the 20-unit oligonucleotide, complementary to the 1-20 fragment of the nucleocapsidyprotein (NP) mRNA reduced the yields of the products of the translation of all the mRNA of this virus due to the formation of a partial complex with a length equivalent to ten base pairs and a 10-unit sequence, which is virtually common to all the mRNA of the Sendai virus.[172]

The nonspecific inhibition of the translation of the BMV RNA in the lysate of rabbit reticulocytes (RRL) by a 15-unit oligonucleotide complementary to the vesicular stomatitis virus (VSV) was explained by the inhibition of the translating capacity of ribosomes as a result of the binding of the above ON-15 to 18S rRNA. The level of the nonspecific inhibition of the translation of the BMV RNA depended on the ON-15 concentration and showed a distinct tendency towards saturation. The maximum attained degree of inhibition of the translation was 88% and 43% in the presence of 40 μM ON-15 and 41% and 2% in the presence of 10 μM ON-15 for VSV and BMV RNA respectively.[175] Although, according to the authors claim there is no homology between the BMV RNA, 18S rRNA, and the above ON-15, the inhibition of the translation of the BMV RNA as a result of the formation of an imperfectly matched complex with the oligonucleotide appears more likely than nonspecific inhibition of the translating activity of ribosomes.

It has been shown[173] that the translation of the encephalomyocarditis viral RNA in the RRL is inhibited approximately to the extent of 60% with the aid of 25 μM 13-unit oligonucleotide, which forms a perfectly matched complex with the 751-763 section. The replacement of the central G · C pair of this duplex by the G · A pair (one base of ON-13 is altered) leads to a fourfold decrease in the degree of inhibition of the translation (down to 14%) at the same ON-13 concentration.

Interesting data on the complementation accuracy of the interaction of antisense oligonucleotides or their methylphosphonate analogues with a NA target have been obtained in a series of studies by Miller and coworkers[165-167,176,177] of the inhibition of the translation of rabbit globin mRNA *in vitro*. Phosphodiester oligonucleotides with a length equivalent to 8-10 units inhibited the translation of the globin mRNA in the RRL and WGE (0-200 μM solution of the (oligonucleotide, 0.3 μg of mRNA). The above oligomers were fully complementary to the sequences located in the 5'-nontranslatable region and the region of the AUG codon in either α- or β-globin mRNA. All the oligonucleotides synthesised formed a duplex with the selected mRNA sequences, which was demonstrated by building up these oligonucleotides (as primers) using a reverse transcriptase. However, despite the fact that these oligonucleotides were effective translation inhibitors, the complementation accuracy of their interaction with mRNA was low. For example, the ON-12 oligonucleotide inhibited the translation of the α-globin mRNA (it was complementary to its 28-39 section) by 97% in the RRL and by 100% in the WGE at a concentration of 100 μM. However, the ON-12 inhibited simultaneously the translation of the β-globin mRNA by 96 and 100% in the RRL and WGE respectively. At a ON-12 concentration of 5 μM, the degree of inhibition of the translation of α- and β-globin mRNA was 15 and 14% in the RRL and 75 and 14% in the WGE respectively. Similar results were obtained for all seven nucleotides investigated.[165]

Short 4-12 unit oligonucleoside methylphosphonates (M-ON), exactly complementary to the same sections of the globin mRNA as the phosphodiester oligonucleotides used by

Blake et al.,[165] have been investigated.[166,176] The prehybridisation of M-ON with mRNA increased the degree of inhibition of the translation of the mRNA in the RRL by 20%–30%. It is surprising that at 37 °C the M-ON-4 (Cp*Cp*Ap*T) (complementary to the 37–40 and 54–57 sections in α- and β-globin mRNA respectively) at a concentration of 100 μM did not inhibit the translation of mRNA, while at a concentration of 200 μM the degree of inhibition of the translation of α- and β-globin mRNA was 28% and 42% respectively. As in the study of Murakami et al.,[167] the M-ON complementary to the α-globin mRNA inhibit the translation of both mRNA to approximately the same extent, particularly at high M-ON concentrations (200 μM) and when the stage involving the transhybridisation of the mRNA with the M-ON is carried out.

Direct comparison of the inhibiting activities of the ON and M-ON permits the conclusion that the M-ON are not more effective and specific translation inhibitors than the phosphodiester oligonucleotides. The low specificity of the ON and M-ON with lengths equivalent to 4–12 units as well as their low effectiveness in inhibiting translation can be explained by several causes. Firstly, the 5'-nontranslatable region in the rabbit α- and β-globin mRNA exhibits a high degree of homology. Therefore, apart from the binding site selected on one mRNA, each nucleotide can form also imperfectly matched complexes with the other mRNA. However, the authors, in discussing the possibility of the formation of such complexes, seek only those sections of the mRNA which can form with the M-ON or ON a continuous duplex with a length equivalent to not less than four base pairs (the so called partial duplex[47]) and fully reject the possibility of the formation of longer duplexes containing noncanonical pairs or, in other words, imperfectly matched complexes.[165,166] Secondly, the influence of the secondary structure of mRNA on complex formation is not considered.[175]

A low specificity of the action of short M-ON (9-unit oligonucleotides) has also been observed in the inhibition of the translation of the mRNA of the N, NS, and GVSV proteins in the RRL at 30 °C. On concentrating M-ON-9 (complementary to the N protein mRNA, section 14–22), the inhibition of the synthesis of the N protein by 77% was accompanied by the inhibition of the syntheses of the NS and M proteins by 38% and 43% respectively.[178] The low specificity of the inhibition of the translation observed at high concentrations (100–150 μM) of M-ON-9, was explained by the formation of partial complexes between M-ON-9 and other VSV mRNA. Furthermore, despite the absence of experimental evidence, the authors suggest[178] that the secondary structure of the mRNA exerts a strong influence on the specificity and effectiveness of the inhibition of the translation.

The site-specific inhibition of the translation takes place also when the M-ON forms with the mRNA a duplex containing noncanonical pairs. Three octamers (M-ON-8_{1-3}), complementary to the AUG region of the codon for the ras p21 BALB protein mRNA, inhibited translation of the mRNA in conformity with the stability of the duplexes formed. Thus M-ON-8_1[177] inhibited the synthesis of the protein by 97%; M-ON-8_2, forming with the mRNA a duplex containing one irregular pair in the centre, caused 31% inhibition; whereas M-ON-8_3, forming with the mRNA a duplex with two noncanonical pairs in the centre, inhibited the translation to the extent of 9%.

At a certain temperature and certain concentrations of the antisense oligonucleotides, the degree of inhibition of the translation of mRNA depends on the length of the oligonucleotide employed, i.e. on the stability of the duplex. The 12-unit oligonucleotide complementary to the initiator region of trypanosomal mRNA is less effective in inhibiting translation[179] (degree of inhibition 20%–25%) than ON-22 and ON-34 (translation inhibited to the extent of 65%–70% and 95%–100% respectively) at 25 °C and a concentration of 15 μM. The decisive importance of the stability of the mRNA · ON duplex in inhibiting the translation of the given mRNA in the RRL and WGE can be additionally illustrated by data from other studies.[180,181] Thus the 12-unit oligonucleotide complementary to the 2-13 sequence of the *T. brucei* mRNA inhibits the translation of the mRNA but not that of *T. vivax* (another species of African trypanosomes) at 22 °C. It was found that ON-12 forms with the *T. vivax* mRNA a duplex (its dissociation temperature is 22 °C) containing two irregular pairs — G · A and T · T.

It has been demonstrated[145,182] that the 18-unit oligonucleotide carrying at the 3'-end a 9-aminoacridine residue inhibits the expression of pKH113 by 55% (at an ON-18 concentration of 30 μM). A slight inhibition of the expression of pBR322 (by 10%) is observed simultaneously, evidently owing to the formation of an imperfectly matched complex with a length equivalent to 11 units and containing two noncanonical base pairs at the 5'-end of the duplex (G · T and C · T) in the 3234 region of the pBR322 nucleotide residue.

In all the studies examined in this section, short (4-13)-unit oligonucleotides at high concentrations (40–200 μM) were used to inhibit the translation of mRNA *in vitro*. The low specificity of the inhibition of the translation was apparently associated with the fact that the difference between the stabilities of the imperfectly and perfectly matched complexes at high concentrations of the oligonucleotides virtually disappeared and both types of duplexes functioned as inhibitors of the initiation of translation (binding to ribosomes) or served as substrates of the RNase H.

The specificity of the inhibition of the translation of mRNA *in vitro* increases sharply when long antisense oligonucleotides are employed. Thus the translation of the mRNA of trypanosomes was inhibited specifically (degree of inhibition 95%–100%) by 22- and 34-unit oligonucleotides at a concentration of 25 μM in the WGE. The BMV RNA, the degree of translation of which in the presence of the same oligonucleotides remained unchanged, was employed as a control.[179] The translation of the tobacco mosaic virus (TMV) RNA was inhibited specifically (to the extent of 90%–95%) by two 26-unit oligonucleotides (at a concentration of 10 μM) in the RRL at 30 °C. Under the same conditions, the level of translation of the BMV RNA remained unaltered.[174] Specific inhibition of the translation of the rabbit β-globin mRNA in the presence of the α-globin RNA was achieved using 20–25- and 48-unit oligonucleotides at a concentration of 5.3 μM (2.6 μM for ON-48) at 37 °C in the RRL. The level of inhibition was[169] 55%–88% for ON-20(25) and 80%–98% for ON-48.

The use of antisense oligonucleotides with lengths equivalent to 21–49 units, complementary either to the translation initiation region or the part of the mRNA molecule coding for the enzyme dehydrofolate reductase–thymidylate synthetase of *Plasmodium falciparum*, led to the inhibition of the translation of mRNA in the RRL system by not more than 60% at a concentration of the 49-unit oligonucleotide of 190 μM. The main reason for the low inhibiting capacity of such long oligonucleotides relative to their length and concentration employed is apparently the inaccessibility of sections of the mRNA for the formation of such a long duplex.[156] Unfortunately, there are at present insufficient data to discuss the specificity of the inhibition of translation of the mRNA of the rabbit globins with the aid of 17-unit phosphorothioate oligonucleotide derivatives (S-ON) or α-oligomers having the same length in the RRL, WGE, and *Xenopus laevis* oocytes.[157,168]

3. Accuracy of the interaction of the oligonucleotides and their derivatives with the NA target *in vivo*

Antisense oligonucleotides and their derivatives can be regarded as possible future therapeutic antitumour, antiviral, and antibacterial agents. This explains the enormous interest in the study of the action of antisense oligonucleotides *in vivo*. The mechanism of the permeation of oligonucleotide derivatives into the cell and their utilisation have been examined in detail in a number of studies.[159,183–187]

a. *Xenopus laevis* oocytes

The *Xenopus laevis* oocytes are some of the simplest *in vivo* systems.[188] Exogenic mRNA and DNA, introduced into the *Xenopus* oocytes by microinjections, are expressed in the given system; under these conditions, the nuclear cytoplasmic transcripts are equally accessible for the interaction with (19–20)-unit oligonucleotides and antisense RNA.[189,190] As in the *in vitro* translation system, one of the mechanisms of the action of the oligonucleotides *in vivo* involves[189] oligonucleotide-specific cleavage of the exogenic mRNA by the endogenic RNase H. Unfortunately, there are no literature data concerning the influence of the accuracy of the interaction of antisense oligonucleotides on the degree of inhibition of the translation or transcription of exogenic mRNA or DNA in the *Xenopus laevis* oocytes. Oligonucleotides with a length corresponding to 18–23 nucleotide residues[191] inhibit by 85%–98% the translation of the mRNA of interleukins IL-2 and IL-3 in the *Xenopus laevis* oocytes at a concentration less than 1 μM; on the other hand, the inhibition of the synthesis of β-tubulin in the same system requires a concentration of the 27-unit oligonucleotide of 20 μM.[192]

b. The accuracy of the antiviral activity of oligonucleotides

The majority of studies of the functioning of antisense oligonucleotides *in vivo* have been carried out on cultivated cell strains infected with viruses. This is evidently associated with the fact that sequences of viral RNA or DNA and the characteristic features of the development of the viral infection of the cell are known for many viruses and also with the relative simplicity of the determination of the effect of an antisense oligonucleotide on the viral gene. Studies on the antiviral effect of antisense oligonucleotides have been carried out on the viruses of the Rous sarcoma (RSV),[193] vesicular stomatitis (VSV),[178,194] herpes (HSV),[129] human immunodeficiency (HIV),[195–200] and influenza.[201–203] However, the mechanism of the antiviral action of antisense oligonucleotides has not been demonstrated in any of the above studies. Furthermore, direct evidence has not been obtained for the formation of a duplex between the oligonucleotide and the viral RNA or DNA *in vivo*. Nevertheless, numerous experimental data have accumulated which it would be of interest to examine from the standpoint of the specificity of the interaction of oligonucleotides or their derivatives with the NA target.

Thus the virtually quantitative inhibition of the multiplication of the Rous sarcoma virus in a culture of fibroblasts from chick embryos took place[193] on treatment with a 13-unit protected oligonucleotide complementary to the 3′- and 5′-terminal sequences of the RVS RNA at an ON-13 concentration in the medium of 2 μM. Some data on the dependence of the degree of inhibition of the viral infection on the accuracy of the interaction of the oligonucleotide with the NA target have been obtained[129] in a study of the inhibition of the replication of the HVS DNA by the octanucleoside methylphosphonate d(TpCp*Cp*Tp*Cp*Cp*Tp*G) (M-ON-8). This octanucleoside methylphosphonate is complementary to the acceptor site for the splicing of the HSV-1 mRNA 4 and 5. A virtually quantitative inhibition of the multiplication of the virus (the extent of 90%–95%) occurred on treatment with 75 μM M-ON-8, added to the medium simultaneously with the virus or before the latter. When M-ON-8 was added to the medium (at a concentration of 150 μM) 1 h after infection, the degree of inhibition of the development of the virus did not exceed 40%. Simultaneously with the inhibition of the HSV, the synthesis of a number of low-molecular-mass proteins of the host cell by M-ON-8 to the extent of 10%–30% occurred. Furthermore,[139] M-ON-8 was able to form a complex with a length equivalent to 6 base pairs in the acceptor site for the splicing of the IE mRNA 4 and 5 of the HSV-2 genome and hence to inhibit the multiplication of the HSV-2 virus (by 70% at an M-ON-8 concentration of 5 μM) just as effectively as that of the HSV-1 virus. Moreover, M-ON-8 could form a partial duplex with a length equivalent to 7 base pairs with the mRNA of the L protein of the VSV and with the 72–80 sequence of the rabbit β-globin mRNA. In conformity with the above findings, M-ON-8 (150 μM) inhibited the synthesis of the VSV L protein by 85% during multiplication in the mouse L cells and the translation of the β-globin mRNA by 75%–78% in the RRL *in vitro*.[166]

The increase in the length of the antisense oligonucleotide with increase in concentration made it possible to achieve rigorously selective inhibition of the multiplication of the virus. It has been shown[194,204] that a 15-unit oligonucleotide (at a concentration in the medium of 200–400 mM), bound covalently by the 3′-end to poly-L-lysine, inhibits specifically (by 85%–98%) the multiplication of the VSV, without inhibiting at the same time either the synthesis of the host protein or the encephalomyocarditis virus. The function of poly-L-lysine (molecular mass 14000) is to stimulate the permeation of the antisense oligonucleotide into the cell.

In contrast to model systems, antisense oligonucleotides can inhibit *in vivo* the development of the virus at any ripening stage. For example, for the human immunodeficiency virus (HIV), the target acted upon by antisense oligonucleotides may be the 5′-end of the viral RNA and the regions of all the initiator codons, the sections of the viral RNA involved in the splicing process (the donor and acceptor splicing sites), and the polyA backbone. Furthermore, with the aid of oligonucleotides it is possible to affect the activity of the viral reverse transcriptase, the region of the viral genome responsible for transactivation (the TAR region), and many other stages in the ripening of the virus. It has been shown[196,205] that the greatest inhibition of the multiplication of the HIV virus in the Molt-3 cells is observed in the interaction of ON-20 with the splice acceptor site (5349-5368) of the tat III gene. The repeating sequences, the nontranslatable 5′-regions of the mRNA of viral proteins, and the polyA backbone at the 3′-end of viral RNA are next as regards sensitivity to antisense nucleotides. It has been shown that the effectiveness of the inhibition of the virus depends on the length of the antisense oligonucleotide. Thus ON-12, ON-15, and ON-20, complementary to the 5349-5368 sequence, inhibit the development of synsytium by 64%, 64%, and 73% at concentrations in the medium of 26.0, 19.7, and 15.4 μM respectively.

Oligonucleotides forming complexes with viral RNA containing noncomplementary bases at the 3′-end of the oligonucleotide are effective inhibitors of viral revertase [reverse transcriptase]. Thus ON-26 and ON-14, which form with viral RNA duplexes having three and two noncomplementary bases at the 3′-end of the oligonucleotide, inhibit the enzyme activity of the HIV revertase by 80% and 75% respectively. The inhibition[205] of the synthesis of the viral proteins p15 and p24 in the presence of the same nucleotide takes place to the extent of 4%–8% only.

Tests of the antiviral activity of 15- and 20-unit oligonucleotides containing a modified linkage (phosphorothioates, butylphosphoramidates, phosphoromorpholidates, phosphoropiperazidates) led to the observation that not only antisense oligonucleotides but also ON-20 with a random sequence and homooligomers with the same length exhibit an anti-HIV activity.[196,199,200,206,207] According to the authors, there is a possibility here of several mechanisms of action of such oligonucleotides. Firstly, since the homooligomers are better substrates for the HIV revertase than the heterooligomers, they can function as competing inhibitors of the viral revertase. Secondly, the homooligonucleotides can form imperfectly matched long duplexes, which are sufficiently stable to be cleaved by RNase H. Thirdly, one cannot fully rule out a completely different inhibition mechanism. It is noteworthy that, whereas the homooligomers and oligonucleotides with a random sequence inhibit effectively the development of HIV when added to the medium simultaneously with the virus or even before the latter, the antisense oligonucleotides inhibit HIV satisfactorily also in chronically infected cells.[197,199,200] This difference can apparently be explained by the fact that any oligonucleotide and virus added to the medium simultaneously or with a small time interval (early

infection) have more possibilities for interaction (the oligonucleotide may prevent the permeation of the virus into the cell, may intensify the action of RNase H). It has been shown[197] that, in the early stages of the infection with the HIV virus, the concentrations of phosphorothioate derivatives of oligonucleotides [an antisense oligonucleotide (S-ON-I), an oligonucleotide forming an imperfectly matched duplex with eight mismatches (S-ON-II), and S-dA_{20}] necessary to inhibit the development of syncytia are approximately the same. In a chronic infection, the attainment of the same level of inhibition requires an increase in the S-ON-I, S-ON-II, and S-dA_{20} concentrations by factors of 3, 8, and 11 respectively. Similar results were obtained in other investigations.[196,206] In order to achieve 50% inhibition of the HIV virus in chronically infected cells, it was necessary to use concentrations of the antisense ON-20, the ON-20 with a random sequence, and $(dA)_{20}$ of 12, 46, and 60 μg ml^{-1}. Two random ON-20 oligonucleotides (manifesting an anti-HIV activity and serving as a control for antisense ON-20), complementary to the 5349-5368 and 280-299 HIV RNA sequences, were subjected to computer analysis.[206] It was found that the ON-20 with a random sequence, complementary to the 5349-5368 fragment, can form a perfectly matched duplex, having a length equivalent to six base pairs, with the 917–928 section or a duplex, having a length equivalent to 12 base pairs and containing two noncanonical pairs, with the same sequence. The ON-20 oligonucleotide, which is random as regards the 280–299 sequence, can form in the 8421-8437 region either a six-unit duplex or a duplex having a length equivalent to 17 base pairs with four irregular pairs. Furthermore, sequences such as T_4, T_5, A_4, and A_5 are encountered in the HIV genome 49, 13, 149, and 50 times respectively. Thus the antiviral activity of the "random" oligonucleotides and homooligomers may be associated with their ability to form imperfectly matched complexes with HIV RNA having a length equivalent to four base pairs and more and a stability which is sufficient for the manifestation of the activity of RNase H.

Oligonucleotides with a modified phosphodiester linkage exhibit a stronger antiviral activity than those with the usual phosphodiester linkage despite the virtually identical stabilities of the duplexes; O-ON-20 (T_m of the duplex 55 °C, determined at an oligonucleotide concentration of 5 μM) inhibits syncytia by 68% at a concentration in the medium of 100 μg ml^{-1}. The inhibition effected by MO-ON-20 (T_m of the duplex 51.5 °C, 5 μM), S-ON-20 (T_m of the duplex 49 °C, 5 μM), and *N*-butylphosphoramidate-ON-20 (T_m of the duplex 45 °C, 5 μM) is to the extent of 90%, 90%, and 100% respectively at concentrations in the medium of 25 μg ml^{-1} in each case.[197,199,206,207]

The study of the anti-HIV activity of antisense oligonucleotides with a modified phosphodiester linkage (phosphorothioates and nucleoside methylphosphonates) yielded a considerable amount of experimental data indicating a different inhibition mechanism, which rules out the formation of a complementary complex or, in other words, a sequence-independent inhibition of the development of the virus. Thus the methylphosphonate derivative of the 8-unit oligonucleotide d(CpCAATTCT) (the underlined nucleotides have been modified), complementary to the splice acceptor site of the HIV-1 tat-3 gene, inhibited specifically the development of synsytium and the activity of the viral revertase at a concentration of 100 μM. The synthesis of the viral RNA was inhibited both by the 8-unit nucleotide and by the oligonucleotide complementary to it (sense sequence).[198]

In the study of the antiviral activity of phosphorothioate derivatives of hetero- and homo-oligomers, it was observed that the 14-unit phosphorothioate analogues (25 μM) have the same inhibiting activity (93%–95%) as the analogous derivatives of oligonucleotides having the same sequence as the HIV RNA (78%–100%). In addition it has been observed that the decisive factor is the length of the phosphorothioate derivative:[195,199,208,209] the inhibiting effect of oligocytidine phosphorothioates increases in the sequence $d(p_SC) < d(p_SC)_{14} < d(p_SC)_{28}$. It has been suggested that such derivatives are inhibitors of the DNA polymerase activity of the reverse HIV transcriptase. It is also possible that the production of interferon is stimulated under the influence of phosphorothioate analogues of oligonucleotides.[195] The complete inhibition of the reproduction of HIV-1 in H9 cells has been achieved[209] with the aid of the phosphorothioate derivative of a 27-unit oligonucleotide (25 μM) complementary to the regular HIV-1 gene rev. The mechanism of such effective action of the above derivatives has not been ultimately elucidated. Phosphorothioate analogues of 2′-*O*-methylribooligonucleotides with a length equivalent to 10–30 units also exhibited an antiviral activity, while the 2′-*O*-methylated oligoribonucleotides and their deoxy-analogues did not inhibit HIV in MT-4 cells.[210]

c. Inhibition of the expression of genes *in vivo*

The expression of the c-myc gene constitutes a good model for the study of the inhibition of gene expression under the influence of antisense oligonucleotides,[211–214] since the lifetime of the c-myc mRNA and proteins is 20–30 min. In the study of the expression of the c-myc gene, T-lymphocytes of human peripheral blood, stimulated by phytohaemagglutinin (PTH), are usually employed. Antisense oligonucleotides are added to the medium up to a concentration of 30 μM 4 h before the stimulation of the T-lymphocytes by PTH. It has been shown[211] that a 15-unit oligonucleotide complementary to the first five codons for c-myc mRNA inhibits the mitogen-stimulated proliferation of cells to the extent of 80%, while an oligonucleotide with a random or coding sequence does not have an inhibiting effect on the cell proliferation. A similar pentadecamer induced in another study[212] a decrease in the level of synthesis of c-myc protein by 50%–80%. The inhibition of the expression of the c-myc gene is associated with the decrease in cell growth and the induction of myeloid differentiation. Treatment of HL cells with antisense 15-unit oligonucleotides (4 μM, 37 °C), which form complexes containing from 2 to 12 irregular base pairs (T_m = 56 °C and 41 °C for the perfectly matched duplex and the duplex with two G · T pairs respectively) did not alter the time required for the doubling of the number of cells. In the presence of the fully complementary nucleotide, the cell doubling time increased by a factor greater than 2.

The rigorously specific inhibition of the expression of the c-myc gene by the antisense 15-unit oligonucleotide complementary to the first five codons of the c-myc RNA apparently occurs[213] because, according to the calculated secondary structure of the c-myc mRNA, the ON-15 binding site is in the region of the loop, i.e. is open to interaction with ON-15. The specific inhibition of the expression of the c-myc gene, associated with the decrease in the level of both the c-myc protein and the c-myc mRNA, was achieved with the aid of a 17-unit antisense nucleotide bound covalently to poly-L-lysine.[214] At the concentrations employed (less than 1 μM), neither the random oligonucleotide nor one forming an imperfectly matched complex with six mismatches exerted an appreciably inhibiting effect on the expression of the c-myc gene.

Apart from the studies listed above, there is an enormous number of others devoted to the action of antisense oligonucleotides on different mRNA and genes in which the level of specificity of the interaction could not be determined simply. The inhibiting effect of the oligonucleotide was followed either from the enzyme activity of, for example, chloramphenicol : acetyl transferase[215] or from the inclusion of ^3H TTP in Balb/c3T3 cells after incubation with an oligonucleotide complementary to PCNA mRNA.[216]

4. Interaction of reactive derivatives of oligonucleotides with NA targets

The mechanism of the inhibiting activity of antisense oligonucleotides on different biochemical and molecular-genetic processes *in vitro* and *in vivo* includes as one of the main stages the formation of a complementary complex between the oligonucleotide and the NA-target. As shown in previous Sections, the stability of the ON-NA target duplex is one of the decisive parameters for the effective inhibition of both the translation of mRNA and the expression of genes.

In order to create more effective inhibitors, derivatives of oligonucleotides capable of forming duplexes with an enhanced stability have been devised. Thus the introduction into the oligonucleotide of intercalators such as acridine, *N*-(2-hydroxyethyl)-phenazinium, and ethidium bromide leads to an appreciable stabilisation of the duplex, but the complex formation itself remains an equilibrium process. Furthermore, it is well known that the translating ribosome possesses unwinding activity, i.e. the ability to melt fairly stable duplexes.[153,154] On the other hand, it has been shown in a number of studies that, in order to inhibit the translation of mRNA, RNase H is necessary apart from the complex formation with the antisense oligonucleotide. However, not all the heteroduplexes are cleaved by the RNase. For example, the derivatives of oligodeoxyribooligonucleotides with a modified phosphodiester linkage (phosphorothioates) are very stable in the cell and form stable complexes with RNA, which are not substrates of RNase H.

Derivatives of antisense oligonucleotides which would not only form a stable duplex with the NA target but would also damage the nucleic acid molecule as a result of a site-specific interaction, or, in other words, contain the reactive unit, are therefore very promising. There is then a possibility of several types of reactive groups bound covalently to the antisense oligonucleotide:

(1) alkylating groups which lead to the formation of a covalent bond between the oligonucleotide and the NA target;

(2) groups capable of being photoactivated, the activity of which is induced by UV radiation, resulting also in the formation of a covalent bond between the 'addressed' reagent and the nucleic acid;

(3) cleaving groups, that is groups such as Fe · EDTA, Cu · 1, 10-phenanthroline, and Fe(Co, Mn) · porphyrins, as a result of the activity of which the sugar phosphate skeleton of the nucleic acid is cleaved.

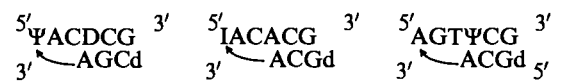
The methods of synthesis of oligonucleotides, the properties important for their use, and the results of the specific action of these derivatives on NA targets have been examined in a number of reviews.[5,9,217–222]

The majority of studies on the site-specific modification or site-specific damage of the NA target have been carried out on model matrices: synthetic oligonucleotides, homopolymers, short DNA fragments (up to 400 bases), tRNA, and 16S rRNA, oligonucleotides of different lengths being used. The advantages of the reactive groups used were demonstrated, the effectiveness of the reaction was estimated, and modification conditions were selected in these studies. In some investigations, the positional specificity of the modification was determined.[216–220] The specificity of the modification (complementation accuracy) was studied only in a few investigations, which will be examined in the present section.

Certain data on the accuracy of the interaction of the reagent and the NA target may be found in a series of communications (see the relevant reviews[2,5,9,219,221,229]) on the site-specific modification of nucleic acids by oligonucleotide derivatives containing the *N*-2-chloroethyl-*N*-methylaminophenyl group bound either to the 3′-end of the oligonucleotide via a benzylidene linkage or to the 5′-end via phosphoramide linkage.

The first experiments on the site-specific modification of natural nucleic acids (23S + 16S rRNA of *E. coli*) by derivatives of tetra-, penta-, and hexaadenylates carrying the 2′,3′-*O*-[4-*N*-(2-chloroethyl)-*N*-methylamino]benzylidene group (=CHRCl) at the 3′-end of $(Ap)_{n-1}A=CHRCl$ ($n = 4-6$)[229–231] demonstrated the highly effective modification of 16S + 23S rRNA. At a concentration of the reagents less than or equal to the concentration of the NA target, between 70 and 98% of the reagent present in the reaction medium was consumed on the alkylation of the RNA. This process was not distinguished by chemical selectivity—all the bases, except uridine, were modified.[230] The degree of modification of 16S + 23S rRNA was[230] 5 mol of $(Ap)_4A=CHRCl$ per mole of RNA at 20 °C and about 30 mol at 5 °C. According to the analysis of the sequence, in 16S and 23S rRNA there are no U_5 and longer fragments capable of ensuring the formation of a sufficiently long duplex with the reagent and only three U_4 and 24 U_3 sequences. Reagents of the type $(Ap)_{n-1}A=CHRCl$ ($n = 4-6$) apparently formed either partial duplexes with the U_3 and U_4 sequences or imperfectly matched complexes incorporating the U_3 and U_4 backbones. The values of $R_{x(app)}$ for the binding of the reagents $(Ap)_{n-1}A=CHRCl$ ($n = 4-6$) to RNA, found by Karpova,[229] proved to be similar and corresponded to $(3-7)\times10^5$, 7×10^5, and $(3-7)\times10^5$ litre mol^{-1} for reagents with $n = 6$, 5, and 4 respectively. Comparison of the values of $K_{x(app)}$ with those of K_x estimated by the method of Uhlenbeck et al.[97] showed that $K_{x(app)}$ is approximately equal to K_x for the duplex $A_4 \cdot U_4$.

The selectivity of the site-specific modification of nucleic acids was first estimated in the determination of the points where yeast $tRNA_I^{Val}$ was modified by the reagent d(pCpG)rA=CHRCl.[232,233] It was shown that three bases in $tRNA_I^{Val}$ with the same disposition relative to its CpG sequence, are alkylated. The modification occurred in the following duplexes:



where the arrow indicates the tRNA sequence. The adenine residue in these duplexes either forms an irregular pair or does not participate in complex formation.[234]

Subsequently, a similar analysis of the accuracy of the interaction of the addressed reagent and the NA target was carried out for the $ClRCH_2NH$ reagents. It was shown[235] that the reagent $ClRCH_2NH$-p(dAACCA) alkylates selectively the G_{24} $tRNA^{Phe}$ base of *E. coli*. Judging from the position of the modification point, G_{24} is alkylated in the imperfectly matched complex



where the arrow indicates the *p*-NA-CH_2-RCl group, whereas the section of the $tRNA^{Phe}$ molecule to which the reagent was addressed is involved in the formation of the secondary structure.

The reagent $ClRCH_2NH$-p(dATTTTCA), fully complementary to the sequence in the anticodon loop of $tRNA^{Phe}$, modifies three guanine residues:[236] G_{10}, G_{24}, and $G_{28/29}$. Whereas the alkylation of $G_{28/29}$ most probably takes place when it is part of the composition of a perfectly matched duplex with the selected sequence, G_{10} and G_{24}, which have similar secondary and tertiary structures, are apparently modified when they are part of the composition of an imperfectly matched complex with the corresponding sequence in the D-loop.



The ratios of the rates of the addressed and unaddressed (outside the complex) modifications (f) for $G_{24}+G_{10}$ and $G_{28/29}$ are 58 and 460 respectively, i.e. the level of the nonspecific modification is 2% for G_{10} and G_{24} and less than 0.3% for $G_{28/29}$. The results of the analysis of the modification points of tRNA indicate an enormous influence of the steric structure on the selectivity of the site-specific modification.

Interesting results have been obtained in studies[150,237] on the site-specific modification of the 302 unit DNA fragment by $-NHCH_2RCl-$ and $>CHRCl$ derivatives of 6-14-unit oligonucleotides. It was shown that, by virtue of the formation of an inner hairpin, the 144–149 section is entirely inaccessible for the binding of the reagent $ClRCH_2NH$-pd(TTCCC)rA, whereas the open 261–266 section is modified by this reagent. The modification of this fragment when the latter forms part of an imperfectly matched duplex with an oligo-G-sequence near its 5'-end has also been observed. In addition, the alkylation of G_{179}, which is apparently close to the reagent binding section (261–274), has been noted.[16,149,237-237]

The problem of the selectivity of the site-specific modification has been investigated in greatest detail in a series of studies[240-244] in relation to the modification of the 16S rRNA of *E. coli*, the length of which is equivalent to 1542 nucleotides, by oligonucleotide derivatives carrying the $>CHRCl$ group at the 3'-end. In such a long target, having a fairly complex steric structure, one may encounter, together with sequences fully complementary to the oligonucleotide address, also incompletely complementary fragments. Such fragments may be detected with the aid of a special program for the analysis of nucleic acid sequences — context analysis.[245] For example, according to the data of such analysis, the reagent complementary to the 771–781 region may form imperfectly matched complexes, containing at least five canonical base pairs, also with 12 sections of 16S rRNA. Estimation of the interaction energy showed[240] that at least three out of the twelve imperfectly matched duplexes of the reagent with the target have a stability which does not differ greatly from that of the fully complementary duplex, namely the duplexes with the sequences 442–452, 663–683, and 883–893. It has been demonstrated experimentally that this reagent does indeed modify 16S rRNA along eight sections and that four of these are modified to approximately the same extent (771–781, 442–452, 663–673, and 883–893). This apparently means that the reagent does not interact via all the bases with the fully complementary section, since the complementation section is involved in the formation of the secondary structure. A similar influence of the steric structure on the effectiveness of the site-specific modification has been demonstrated also in the alkylation of 16S rRNA by other reagents[240-242] and in the site-specific modification[235,236] of $tRNA^{Phe}$.

The influence of temperature and the reagent concentration on the selectivity of the modification has been investigated.[243] At 20 °C, the increase in the reagent concentration from 1.3×10^{-1} to 2.5×10^{-6} M entailed the increase in the overall limiting degree of modification of 16S rRNA from 0.05 to 0.62, whereas the modified fraction in the perfectly matched complex fell from 0.38 to 0.22. On raising the modification temperature from 20° to 40 °C at a reagent concentration of 4×10^{-5} M, the overall degree of modification fell from 2.57 to 0.64, but the modified fraction in the perfectly matched complex increased under these conditions from 0.24 to 0.35. Thus, despite the complexity of the model investigated, its modification is likewise determined by the stability of the duplexes formed by the reagent with the NA target. The additional stabilisation of the 16S rRNA · reagent duplex with the aid of an auxiliary effector oligonucleotide [complementary to the section of 16S rRNA immediately adjoining the reagent binding section, carrying at its 5'-end the *N*-(2-hydroxyethyl)-phenazinium residue and stabilising the duplex as a result of the cooperative interaction with the reagent[246]] led to an increase by a factor greater than 2 in the modified fraction of the RNA in the perfectly matched complex but did not affect under these conditions the modification of the imperfectly matched duplexes.[244]

Unfortunately there are virtually no data on the selectivity of the inhibition with the aid of reactive oligonucleotide derivatives of any biochemical processes occurring with participation of nucleic acids. In this connection, one may mention only two studies where the inhibition of the translation of mRNA with the aid of reactive oligonucleotide derivatives was investigated. It has been shown[247] that preliminary incubation of the total mRNA of the cells of the MOPC 21 mouse plasmocytoma with the $ClRCH_2NH$ derivative of an 11-unit oligonucleotide complementary to the sequence of the light chain of immunoglobulin G (coding for the variable section of the protein) leads to the quantitative inhibition of the synthesis of not only the light but also the heavy chain of Ig-G in the RRL.

Similar results have been obtained in a study[221] in which psoralen derivatives of 12-unit oligonucleotides were used to inhibit the synthesis of mouse α- or β-globins in the RRL. The reagent, fully complementary to the α- or β-globin mRNA, inhibited the synthesis of both globins to approximately the same extent. However, the authors of the above studies do not discuss the results from the standpoint of the specificity of the interaction of derivatives of antisense oligonucleotides with mRNA.

V. Conclusion

The data presented in the review show that the problem of increasing the complementary accuracy of the interaction of RNA and DNA with antisense oligonucleotides and their derivatives is a principal one in the study of effect of site-specific interaction on nucleic acids both *in vitro* and *in vivo*. The experimental data available at present on the thermodynamics of perfectly matched duplexes and duplexes with structural anomalies, obtained in the study of the interaction of model oligonucleotides, permit the hope that, by virtue of the destabilising effect of one or several mismatches, extra bases, or loops, a fairly selective interaction may be achieved between the NA target on the oligonucleotide complementary to the selected section.

In the case of site-specific modification, the problem of increasing the complementation accuracy reduces in essence to the exclusion from the reaction sphere of imperfectly matched complexes between the NA target and the 'addressed' reagent. As can be seen from the data discussed, in certain cases highly selective interaction may be achieved in systems *in vitro* either by carrying out the modification at a temperature close to the melting point of the perfectly matched complex or by using fairly low concentrations of the 'addressed' reagent ($10^{-8}-10^{-9}$ M). However, it is then necessary to take into account the fact that, simultaneously with the increase in the selectivity of the modification, the degree of alkylation of the nucleic acid along the selected section will diminish. Furthermore, in systems *in vitro* an increase in the selectivity of the site-specific modification can be achieved by employing effector oligonucleotides stabilising the duplex, which are complementary to the sequence of the NA target adjoining the binding site of the 'addressed' reagent and carrying the *N*-(2-hydroxyethyl)phenazinium residues at one or both ends. Although impressive advances have in fact now been achieved in the application of this approach to increase the selectivity and effectiveness of the site-specific modification of synthetic oligonucleotides and fragments of single-stranded DNA with a weak secondary structure, there are so far insufficient data to postulate that this approach will prove just as productive when applied to high-molecular-mass nucleic acids having a complex steric structure.

Evidently, in inhibition with the aid of antisense oligonucleotides and their derivatives of processes such as translation, transcription, and others, occurring in systems *in vitro* let alone *in vivo*, the accuracy of the effect is determined not only by the differences between the stabilities of the perfectly

and imperfectly matched complexes but also by the steric structure of the NA target, the interaction of the antisense oligonucleotides with other biopolymers involved in the process investigated, and also the mechanism of the inhibition of the given process with the aid of the antisense oligonucleotide. For example, translation is inhibited because mRNA is either cleaved by RNase H or loses the capacity to be translated by the ribosome after the formation of a duplex with the antisense oligonucleotide. Therefore one can hardly assume that the approaches developed for model systems where synthetic oligonucleotides or fragments of single-stranded DNA are used as matrices can be sufficiently effective in increasing the specificity of the inhibition of the above processes.

In our view, the methodology of the approaches used to increase the specificity of the influence on the genetic apparatus requires profound physicochemical and biochemical studies in model systems involving different stages of the processes which ensure the storage, replication, and utilisation of hereditary information (replication, transcription, reparation, translation, etc.) in cells and viruses. The possibility of establishing the primary structure of virtually any nucleic acid allows the creation of specific oligonucleotide and polynucleotide addresses to a great variety of sections of the generic apparatus in living organisms, and the development on this basis of new approaches designed to increase the selectivity of the specific influence, which take into account fully both the characteristics of the steric structure of the given nucleic acid and the imperfect direct repetitions of selected complementation sections, as well as data on the thermodynamics of perfectly and imperfectly matched duplexes.

Thus the problem of the complementation accuracy of the interaction of antisense oligonucleotides and their derivatives with nucleic acids is at present one of the most acute problems in the study of site-specific influences on nucleic acids.

References

1. C A Stain, J S Cohen *Cancer Res.* **48** 2659 (1988)
2. N I Grineva *Vestn. Akad. Med. Nauk SSSR* **2** 83 (1981)
3. S Agrawal, P S Sarin *Advanced Drug Delivery Rev.* **6** 251 (1991)
4. Y Euguchi, T Itoh, J-I Tomizawa *Annu. Rev. Biochem.* **60** 631 (1991)
5. D G Knorre, V V Vlassov, V F Zarutova, A V Lebedev *Sov. Sci. Rev. B* **12** 269 (1990)
6. A M Belikova, V F Zarytova, N I Grineva *Tetrahedron Lett.* **37** 3557 (1967)
7. N I Grineva, V F Zarytova, D G Knorre *Izv. Sib. Otd. Akad. Nauk SSSR, Ser. Khim. Nauk* **12** 118 (1968)
8. N I Grineva, G G Karpova *FEBS Lett.* **32** 351 (1973)
9. J S Cohen *Topics in Molecular and Structural Biology.* Vol. 12. *Oligonucleotides. Antisense Inhibitors of Gene Expression* (Eds J S Cohen) (London: Macmillan Press, 1989)
10. J E Hearst *Photobiochem. Photobiophys, Suppl.* 23 (1987)
11. M P Perelroyzen, A V Vologodskii *Nucleic Acids Res.* **16** 4693 (1988)
12. D G Knorre, O S Fedorova *Khim. Fiz.* **10** 869 (1991)
13. F Aboul-ela, D Koh, I Tinoco Jr, F Martin *Nucleic Acids Res.* **13** 4811 (1985)
14. N I Grineva, D G Knorre, V A Kurbatov *Dokl. Akad. Nauk SSSR* **201** 609 (1971)
15. D G Knorre, I V Kutyavin, A S Levina, N P Pichko, L M Podust, O S Fedorova *Bioorg. Khim.* **12** 230 (1986)
16. V V Vlasov, D G Knorre, I V Kutyavin, S V Mamaev, L M Podust, O S Fedorova *Bioorg. Khim.* **13** 1221 (1987)
17. N I Sokolova, V G Kagramonova, N G Dolinnaya *Usp. Khim.* **44** 104 (1975) [*Russ. Chem. Rev.* **44** 56 (1975)]
18. N G Dolinnaya, O I Gryaznova *Usp. Khim.* **58** 1318 (1989) [*Russ. Chem. Rev.* **58** 758 (1989)]
19. H H Klump, in *Biochemical Thermodynamics* (Ed. M N Jones) (Amsterdam: Elsevier, 1988) p. 100
20. J R Wyatt, J D Puglisi, I Tinoco Jr *Bio Essays* **11** 100 (1989)
21. L A Marky, K J Breslauer *Biopolymers* **21** 2185 (1982)
22. D J Patel, S A Kozlowski, L A Marky, J A Rice, C Broka, K Itakura, K J Breslauer *Biochemistry* **21** 428 (1982)
23. D J Patel, S A Kozlowski, L A Marky, J A Rice, C Broka, J Dallas, K Itakura, K J Breslauer *Biochemistry* **21** 437 (1982)
24. K J Breslauer, R Frank, H Blocker, L A Marky *Proc. Natl. Acad. Sci. USA* **83** 3746 (1986)
25. R L Ornstein, J R Fresco *Biopolymers* **22** 2001 (1983)
26. R Kierzek, M H Caruthers, C E Longfellow, D Swinton, D H Turner, S M Freier *Biochemistry* **25** 7840 (1986)
27. S M Freier, R Kierzek, M H Caruthers, T Neilson, D H Turner *Biochemistry* **25** 3209 (1986)
28. S M Freier, R Kierzek, D H Jaeger, N Sugimoto, M H Caruthers, T Neilson, D H Turner *Proc. Natl. Acad. Sci. USA* **83** 9373 (1986)
29. C A G Haasnoot, J H J den Hartog, J F de Rooij, J H van Boom, C Altona *Nucleic Acids Res.* **8** 169 (1980)
30. D R Groebe, O C Uhlenbeck *Nucleic Acids Res.* **16** 11725 (1988)
31. D R Groebe, O C Uhlenbeck *Biochemistry* **28** 742 (1989)
32. V P Antao, S Y Lai, I Tinoco Jr *Nucleic Acids Res.* **19** 5901 (1991)
33. V P Antao, I Tinoco Jr *Nucleic Acids Res.* **20** 819 (1992)
34. B Hartmann, R Lavery *J. Biomol. Struct. Dyn.* **7** 363 (1989)
35. F H Martin, I Tinoco *Nucleic Acids Res.* **8** 2295 (1980)
36. H T Steely, Jr, D M Gray, R L Ratliff *Nucleic Acids Res.* **14** 10071 (1986)
37. S-H Chou, P Flynn, B Reid *Biochemistry* **28** 2435 (1989)
38. A Pardi, I Tinoco Jr *Biochemistry* **21** 4686 (1982)
39. J W Nelson, I Tinoco Jr *Biochemistry* **21** 5289 (1982)
40. C H Lee, J G Wetmur *Biopolymers* **11** 1485 (1972)
41. J G Hoggett, G Maass *Ber. Bunenges. Phys. Chem.* **75** 45 (1971)
42. S Gillam, K Waterman, M Smith *Nucleic Acids Res.* **2** 625 (1975)
43. L L Gerchman, D B Ludlum *Biochem. Biophys. Acta* **308** 310 (1973)
44. R S Lasken, M F Goodman *J. Biol. Chem.* **259** 11491 (1984)
45. M Petersheim, D H Turner *Biochemistry* **22** 256 (1983)
46. M Petersheim, D H Turner *Biochemistry* **22** 269 (1983)
47. S M Freier, B J Burger, D Alkema, T Neilson, D H Turner *Biochemistry* **22** 6198 (1983)
48. M Sugimoto, R Kierzek, S M Freier, D H Turner *Biochemistry* **25** 5755 (1986)
49. M Sugimoto, R Kierzek, D H Turner *Biochemistry* **26** 4554 (1987)
50. D J Patel, S A Kozlowski, L A Marky, J A Rice, C Broka, K Itakura, K J Breslauer *Biochemistry* **21** 451 (1982)
51. J-R Mellema, R van der Woerd, G A van der Marel, J H van Boom, C Altona *Nucleic Acids Res.* **12** 5061 (1984)
52. M Senior, R A Jones, K J Breslauer *Biochemistry* **27** 3879 (1988)
53. D J Patel, S A Kozlowski, L A Marky, J A Rice, C Broka, K Itakura, K J Breslauer *Biochemistry* **21** 445 (1982)
54. D J Patel, A Pardi, K Itakura *Science* **216** 581 (1982)
55. J G Chu, I Tinoco Jr *Biopolymers* **22** 1235 (1983)
56. K M Morden, J G Chu, F H Martin, I Tinoco Jr *Biochemistry* **22** 5557 (1983)
57. M W Kalnik, C-N Chang, A P Crollmann, D J Patel *Biochemistry* **27** 924 (1988)
58. S A Woodson, D M Crothers *Biochemistry* **26** 904 (1987)
59. S A Woodson, D M Crothers *Biochemistry* **27** 3130 (1988)
60. J Th van der Hoogen, C Erkelens, E de Vroom, G A van der Marel, J H van Boom, C Altona *Eur. J. Biochem.* **173** 295 (1988)
61. J Th van den Hoogen, A A van Beuzekom, H van den Elst, G A van der Marel, J H van Boom *Nucleic Acids Res.* **16** 2971 (1988)
62. J M L Pieters, R M W Mans, H van den Elst, G A van der Marel, J H van Boom, C Altona *Nucleic Acids Res.* **17** 4551 (1989)
63. D A Eril, R A Joues, W K Olson, N K Sinha, K J Breslauer *Biochemistry* **28** 268 (1989)
64. S Adam, J P Ridous, P Bourtayre, E Taillandier, S Pochet, T Hieynh-Dinh, J Igolen *J. Biomol. Struct. Dyn.* **6** 167 (1988)
65. G Vesnaver, C-N Chang, M Eisenberg, A P Grollman, K J Breslauer *Proc. Natl. Acad. Sci. USA* **86** 3614 (1989)
66. G Kneale, T Brown, O Kennard *J. Mol. Biol.* **186** 805 (1985)
67. T A Early, J Olmsted III, D R Kearns, A G Lexius *Nucleic Acids Res.* **5** 1955 (1978)
68. S Ikuta, R Eritja, B E Kaplan, K Itakura *Biochemistry* **26** 5646 (1987)
69. E Quignard, G Fazakerly, G van der Marel, J H van Boom, W Guschlbauer *Nucleic Acids Res.* **15** 3397 (1987)
70. P J Romaniuk, D W Hughes, R J Grigoire, R A Bell, Th Neilson *Biochemistry* **18** 5109 (1979)
71. D Rabinovich, T Haran, M Eisenstein, Z Shakked *J. Mol. Biol.* **200** 151 (1988)

72. W B T Cruse, J Aymani, O Kennard, T Brown, A G C Jack, C A Leonard *Nucleic Acids Res.* **17** 55 (1989)
73. L He, R Kierzek, J SantaLucia, A E Walter, D H Turner *Biochemistry* **30** 11124 (1991)
74. D Alkema, P A Hader, R A Bell, T Neilson *Biochemistry* **21** 2109 (1982)
75. W Traub, J L Sussmann *Nucleic Acids Res.* **10** 2701 (1982)
76. V I Poltev, N V Shulypina *J. Biomol. Struct. Dyn.* **3** 739 (1986)
77. D J Patel, S A Kozlowski, K Ikuta *Biochemisty* **23** 3207 (1984)
78. X E Gao, D J Patel *J. Am. Chem. Soc.* **110** 5178 (1989)
79. E P Nikonowicz, R P Meadows, P Fagan, D G Gorenstein *Biochemistry* **30** 1323 (1991)
80. G G Prive, U Heimann, S Chandrasegaran, L Kan, M L Kopka, R E Dickerson *Science* **238** 498 (1987)
81. W N Hunter, T Brown, O Kennard *J. Biomol. Struct. Dyn.* **4** 173 (1986)
82. Y Li, G Zon, W D Wilson *Biochemistry* **30** 7566 (1991)
83. J SantaLucia, R Kierzek, D H Turner *J. Am. Chem. Soc.* **113** 4313 (1991)
84. Y Li, G Zon, W D Wilson *Proc. Natl. Acad. Sci. USA* **88** 26 (1991)
85. F H Arnold, S Wolk, Ph Creez, I Tinoco Jr *Biochemistry* **26** 4068 (1987)
86. J B Dodgson, R D Wells *Biochemistry* **16** 2367 (1977)
87. J B Dodgson, R D Wells *Biochemistry* **16** 2374 (1977)
88. G V Fazakerly, E Quignard, A Woisad, W Guschlbauer, G A van der Marel, J H van Boom, M Joues, M Radman *EMBO J.* **5** 3697 (1985)
89. J A H Cognet, J Gabarro-Arpa, M Le Bret, G A van der Marel, J H van Boom, G V Fazakerly *Nucleic Acids Res.* **19** 6771 (1991)
90. J SantaLucia, R Kierzek, D H Turner *Biochemistry* **29** 8813 (1990)
91. X Gao, D J Patel *J. Biol. Chem.* **262** 16973 (1987)
92. M H Sarma, G Gupta, R H Sarma *Biochemistry* **26** 7707 (1987)
93. N N Anand, D M Brown, S A Salisbury *Nucleic Acids Res.* **15** 8167 (1987)
94. R B Wallace, J Shaffer, R F Murphy, J Bonner, T Hirose, K Itakura *Nucleic Acids Res.* **6** 3543 (1979)
95. A G Cornelis, J H J Haasnoot, J F den Hargot, M de Rooij, J H van Boom, C Altona *Nature (London)* **281** 235 (1979)
96. R V Hosur, A Sheth, K V R Chary, M Ravikumar, G Govil, T Zu-Kan, T Miles *Biochem. Biophys. Res. Commun.* **139** 1224 (1986)
97. O C Uhlenbeck, F H Martin, P Doty *J. Mol. Biol.* **57** 217 (1971)
98. S R Holbrook, C Cheong, I Tinoco, Jr, S-H Kim *Nature (London)* **353** 579 (1991)
99. H Werntges, G Stiger, D Riesner, H-J Fritz *Nucleic Acids Res.* **14** 3773 (1986)
100. N Tibanyenda, S H De Bruin, C A G Haasnoot, G A van der Marel, J H van Boom, C W Hilberts *Eur. J. Biochem.* **139** 19 (1984)
101. N Sugimoto, R Kierzek, D H Turner *Biochemistry* **26** 4559 (1987)
102. D R Hickey, D H Turner *Biochemistry* **24** 3987 (1985)
103. G R Titeeva, R V Vinogradov, Yu A Berlin *Bioorg. Khim.* **12** 1484 (1986)
104. S Kwok, D E Kellog, N McKinney, D Spasik, L Goda, C Levenson, J J Sninsky *Nucleic Acids Res.* **18** 999 (1990)
105. C R Newton, A Graham, L E Heptinstall, S J Powell, C Summers, N Kalsheker, J C Smith, A F Markham *Nucleic Acids Res.* **17** 2503 (1989)
106. T Ehlen, L Debeau *Biochem. Biophys. Res. Commun.* **160** 441 (1989)
107. D J Wu, L Ugazzoli, B K Pol, R B Wallace *Proc. Natl. Acad. Sci. USA* **86** 2759 (1989)
108. H Okayama, D T Curei, M L Brantly, M D Halmes, R G Crystal *J. Lab. Clin. Med.* **114** 105 (1989)
109. T Tanigushi, C Weissmann *Nature (London)* **275** 770 (1978)
110. L S Lasater, H M Olson, P A Cann, D G Glitz *Biochemistry* **27** 4687 (1988)
111. S L Berger *Analytical Biochem.* **161** 272 (1987)
112. M J Zoller, M Smith *Methods Enzymol. B* **100** 468 (1983)
113. M Smith *Nucleic Acids Res., Symp. Ser.* **7** 387 (1980)
114. A Razin, T Hirose, K Itakura, A D Riggs *Proc. Natl. Acad. Sci. USA* **57** 4268 (1978)
115. M E Winkler, K Mullis, J Barnett, I Stroynowski, Ch Yanofsky *Proc. Natl. Acad. Sci. USA* **79** 2181 (1982)
116. K L Agrawal, J Brunstedt, B E Noyes *J. Biol. Chem.* **259** 1023 (1981)
117. R B Wallace, M J Johnson, T Hirose, T Miyake, E H Kawashima, K Itakura *Nucleic Acids Res.* **9** 879 (1981)
118. A Murasugi, N Takemori, S Hashimoto *J. Biochem.* **102** 627 (1987)
119. B J Conner, A A Reyes, C Morin, K Itakura, R L Teplitz, R B Walla *Proc. Natl. Acad. Sci. USA* **80** 278 (1983)
120. M T Doel, M Smith *FEBS Lett.* **34** 99 (1973)
121. J W Szostak, J I Stiles, B-K Tyl, P Chui, F Sherman, R Wu *Methods Enzymol.* **68** 419 (1979)
122. P S Miller, in *Topics in Molecular and Structural Biology* Vol. 12 *Oligonucleotides. Antisense Inhibitors of Gene Expression* (Ed. J S Cohen) (London: Macmillan, 1989) p. 79
123. P S Miller, J C Barrett, P O P Ts'o *Biochemistry* **13** 4887 (1974)
124. J C Barrett, P S Miller, P O P Ts'o *Biochemistry* **13** 4897 (1974)
125. P S Miller, K B McParland, K Jayaraman, P O P Ts'o *Biochemistry* **20** 1874 (1981)
126. R S Quartin, J G Wetmur *Biochemistry* **28** 1040 (1989)
127. P S Miller, N Dreon, S M Pulfold, K B McParland *J. Biol. Chem.* **255** 9659 (1980)
128. B K Lee, A Murakami, K R Blake, S-B.Lin, P S Miller *Biochemistry* **27** 3197 (1988)
129. C C Smith, L Aurelian, M P Reddy, P S Miller, P O P Ts'o *Proc. Natl. Acad. Sci. USA* **83** 2787 (1986)
130. F Eckstein *Annu. Rev. Biochem.* **54** 367 (1985)
131. C A Stein, C Subasinghe, K Shinozuka, J S Cohen *Nucleic Acids Res.* **16** 3209 (1988)
132. C A Stein, K Mori, S L Loke, C Subasinghe, K Shinozuka, J S Cohen, J M Neckers *Gene* **72** 333 (1988)
133. A Andrus, T Geiser, G Zon *Nucleosides Nucleotides* **8** 967 (1989)
134. L Kibler-Herzog, G Zon, B Uznaushi, G Whittier *Nucleic Acids Res.* **19** 2979 (1991)
135. C Helene, N T Thuong *Antisense RNA and DNA: Conf. Cold Spring Harbor* Cold Spring Harbor, NY, 1988, p. 47
136. J-L Imbach, B Rayner, F Morvan *Nucleosids Nucleotides* **8** 627 (1989)
137. B Rayner, C Malvy, J Paoletti, B Lebleu, C Paoletti, J-LImbach, in *Topics in Molecular and Structural Biology*. Vol. 12 *Oligonucleotides. Antisense Inhibitors of Gene Expression* (Ed. J S Cohen) (London: Macmillan, 1989), p. 119
138. F Morvan, B Rayner, J-L Imbach, S Thenet, J R Bertrand, J Paoletti, C Malvy, C Paoletti *Nucleic Acids Res.* **15** 3421 (1987)
139. M Durand, J C Maurizot, U Asseline, C Barbier, N T Thuong, C Helene *Nucleic Acids Res.* **17** 1823 (1989)
140. C Gagnor, J R Bertrand, S Thenet, M Lemaitre, F Morvan, B Rayner, C Malvy, B Lebleu, J-L Imbach, C Paoletti *Nucleic Acids Res.* **15** 10419 (1987)
141. G Lancelot, U Asseline, N T Thuong, C Helene *Biochemistry* **24** 2521 (1985)
142. J Paolettie, D Bazile, F Morvan, J-L Imbach, C Paolettie *Nucleic Acids Res.* **17** 2693 (1989)
143. M Durand, N T Thuong, J C Marizot *Biochem. Biophys. Res. Commun.* **162** 505 (1989)
144. U Asseline, N T Thuong, F Toulme, M Delarue, T Montenay-Garestier, C Helene *EMBO J.* **3** 795 (1984)
145. J J Toulme, H M Krisch, N Loreau, N T Thuong, C Helene *Proc. Natl. Acad. Sci. USA* **83** 1227 (1986)
146. N T Thuong, U Asseline, T Montenay-Garestier, in *Topics in Molecular and Structural Biology*. Vol. 12 *Oligonucleotides. Antisense Inhibitors of Gene Expression* (Ed. J S Cohen) (London: Macmillan, 1989), p. 25
147. C J Marcus-Sekura *Analytical Biochem.* **172** 289 (1988)
148. J Sun, U Asseline, D Rouzand, T Montenay-Garestier, N T Thuonge, C Helene *Nucleic Acids Res.* **15** 6149 (1987)
149. V F Zarytova, I V Kutyavin, M A Podyminogin, V N Sil'nikov, G V Shishkin *Bioorg. Khim.* **13** 1212 (1987)
150. V V Vlassov, V F Zarytova, I V Kutiavin, S V Mamaev *FEBS Lett.* **231** 352 (1988)
151. D A Melton (Ed.) *Antisense DNA and RNA: Conf. Cold Spring Harbor* (Cold Spring Harbor, NY, 1988)
152. J J Toulme, C Helene *Gene* **72** 51 (1988)
153. S A Liebhaber, F E Cash, S H Shakin *J. Biol. Chem.* **259** 15597 (1984)
154. S H Shakin, S A Liebhaber *J. Biol. Chem.* **261** 16018 (1986)

155. T G Lawson, B K Ray, J T Dodds, J A Grifo, R D Abramson, W C Marrick, D F Betsch, H L Weith, R E Thach *J. Biol. Chem.* **260** 13979 (1986)
156. C Sartorius, R M Franklin *Nucleic Acids Res.* **19** 1613 (1991)
157. C Boiziau, R Kurfurst, C Cazenave, V Roig, N T Thuong, J-J Toulme *Nucleic Acids Res.* **19** 1113 (1991)
158. M-T Haeuptle, R Frank, B Dobberstein *Nucleic Acids Res.* **14** 1427 (1986)
159. P Dash, I Lotan, M Knapp, E R Kandel, P Goelet *Proc. Natl. Acad. Sci. USA* **84** 7896 (1987)
160. R Y Walder, J A Walder *Proc. Natl. Acad. Sci. USA* **85** 5011 (1988)
161. C Cazenave, N Loreau, N T Thuong, J-J Toulme, C Helene *Nucleic Acids Res.* **15** 4717 (1987)
162. J Minshull, T Hunt *Nucleic Acids Res.* **14** 6433 (1986)
163. J-R Bertrand, J-L Imbach, C Paoletti, C Malvy *Biochem. Biophys. Res. Commun.* **164** 311 (1989)
164. C Cazenave, N Loreau, J-J Toulme, C Helene *Biochimie* **68** 1063 (1986)
165. K R Blake, A Murakami, P S Miller *Biochemistry* **24** 6132 (1985)
166. K R Blake, A Murakami, S A Spitz, S A Glave, M Paramiswara, M P Reddy, P O P Ts'o *Biochemistry* **24** 6139 (1985)
167. A Murakami, K R Blake, P S Miller *Biochemistry* **24** 4041 (1985)
168. C Cazenave, C A Stein, N Loreau, N T Thuong, L M Neckers, C Subasinghe, C Helene, J S Cohen, J-J Toulme *Nucleic Acids Res.* **17** 4255 (1989)
169. J Goodchild, E Carroll III, J R Greenberg *Arch. Biochem. Biophys.* **263** 401 (1988)
170. M L Stephenson, P C Zamecnik *Proc. Natl. Acad. Sci. USA* **75** 285 (1978)
171. E Wickstrom *J. Biochem. Biophys. Methods* **13** 97 (1986)
172. K C Gupta *J. Biol. Chem.* **262** 7492 (1987)
173. S Sankar, K-C Cheah, A G Porter *Eur. J. Biochem.* **184** 39 (1989)
174. C Crum, J D Johnson, A Nelson, D Roth *Nucleic Acids Res.* **16** 4569 (1988)
175. E Wickstrom, W S Simonet, K Medlock, I Ruis-Robles *Biophys. J.* **49** 15 (1986)
176. P S Miller, C H Agris, L Aurelian, K R Blake, A Murakami, M P Reddy, S A Spitz, P O P Ts'o *Biochemie* **67** 769 (1985)
177. P S Miller, L Aurelian, K R Blake, E Chang, J M Kean, B L Lee, S-B Lin, A Murakami, P O P Ts'o *Antisense RNA and DNA: Conf. Cold Spring Harbor* (Cold Spring Harbor, NY, 1988) p. 41
178. C H Agris, K R Blake, P S Miller, M P Reddy, P O P Ts'o *Biochemistry* **25** 6268 (1986)
179. A W C A Cornelissen, M P Verspieren, J-J Toulme, B W Swinkels, P Borst *Nucleic Acids Res.* **14** 5605 (1986)
180. P Verspieren, A W C A Cornelissen, N T Thuong, C Helene, J-J Toulme *Gene* **61** 307 (1987)
181. P Verspieren, N T Thuong, C Helene, J-J Toulme *Antisense RNA and DNA. Conf. Cold Spring Harbor* (Cold Spring Harbor, NY, 1988) p. 53
182. C Helene, T Montenay-Garestier, T Saison, M Takasugi, J-J Toulme, U Asseline, G Lancelot, J C Meanrizot, F Toulme, N T Thuong *Biochimie* **67** 777 (1985)
183. M Ceruzzi, K Draper *Nucleosides Nucleotides* **8** 815 (1989)
184. J W Jaroszewski, J S Cohen *Adv. Drug Delivery Rev.* **6** 235 (1991)
185. J-P Leonetti, N Mechti, G Degols, C Gagnor, B Leableu *Proc. Natl. Acad. Sci. USA* **88** 2702 (1991)
186. Y Shoji, S Akhtar, A Periasamy, B Herman, R L Juliano *Nucleic Acids Res.* **19** 5543 (1991)
187. L A Yakubov, E A Deeva, V F Zarytova, A S Ryte, L V Yurchenko, V V Vlassov *Proc. Natl. Acad. Sci. USA* **86** 6454 (1989)
188. B D Hames, S J Higgins (Eds), *Transcription and Translation* (Translated into Russian) (Moscow: Mir, 1987) p. 102
189. J Shuttleworth, A Colman *EMBO J.* **7** 427 (1988)
190. W M Wormingston *Proc. Natl. Acad. Sci. USA* **83** 8639 (1986)
191. E S Kawasaki *Nucleic Acids Res.* **13** 4991 (1985)
192. C Jessus, C Cazenave, R Ozon, C Helene *Nucleic Acids Res.* **16** 2225 (1988)
193. P C Zamecnik, M L Stephenson *Proc. Natl. Acad. Sci. USA* **75** 280 (1978)
194. M Lemaitre, B Bayard, B Lebleu *Proc. Natl. Acad. Sci. USA* **84** 648 (1987)
195. M Matsukura, K Shinozuka, G Zon, H Mitsuya, M Reitz, J S Cohen, S Broder *Proc. Natl. Acad. Sci. USA* **84** 7706 (1987)
196. S Agrawal, J Goodchild, M P Civeira, A H Thornton, P A Sarinet, P C Zamecnik *Proc. Natl. Acad. Sci. USA* **85** 7079 (1988)
197. S Agrawal, P S Sarin *Adv. Drug Delivery Rev.* **6** 251 (1991)
198. J A Zaia, J J Rossi, G J Murakawa, P A Spallone, D A Stephens, B E Kaplan, R Eritza, P B Wallace, E M Cantin *J. Virol.* **62** 3914 (1988)
199. C A Stein, R Pal, A L DeVico, G Hoke, S Mumbauer, O Kinstler, M G Sarngadharam, R L Letsinger *Biochemistry* **30** 2439 (1991)
200. T Vickers, B F Baker, P D Cook, M Zounes, R W Buckheit Jr, J Germany, D E Ecker *Nucleic Acids Res.* **19** 3559 (1991)
201. A Zerial, N T Thuong, C Helene *Nucleic Acids Res.* **15** 9909 (1987)
202. V V Vlassov, V V Gorn, N J Nomokonova, T N Fokina, L V Yurchenkot *Nucleosides Nucleotides* **10** 649 (1991)
203. V V Vlassov, E I Frolova, T S Godovikova, E M Ivanova *Nucleosides Nucleotides* **10** 645 (1991)
204. J-P Leonetti, G Degols, P Milhaud, C Gagnor, M Lemaitre, B Lebleu *Nucleosides Nucleotides* **8** 821 (1989)
205. P C Zamecnik, J Goodchild, J Taguchi, P S Sarin *Proc. Natl. Acad. Sci. USA* **83** 4143 (1986)
206. S Agrawal, T Ikeuchi, D Sun, P S Sarin, A Konopka, J Maizel, P C Zamecnik *Proc. Natl. Acad. Sci. USA* **86** 7790 (1989)
207. S Agrawal, J Goodchild, M Civeira, P S Sarin, P C Zamecnik *Nucleosides Nucleotides* **8** 819 (1989)
208. M Matsukura, G Zon, K Shinozuka, G A Stein, H Mitsuya, J S Cohen, S Broder *Gene* **72** 343 (1988)
209. M Matsukura, G Zon, K Shinozuka, M Robert-Guroff, T Shimada, G A Stein, H Mitsura, F Wong-Staal, J S Cohen, S Broder *Proc. Natl. Acad. Sci. USA* **86** 4244 (1989)
210. S Shibahara, S Mukai, H Morisawa, H Nakashima, S Kobayashi, I Yamamoto *Nucleic Acids Res.* **17** 239 (1989)
211. R Heikkila, G Schwab, E Wickstrom, S L Loke, D H Pluznik, R Watt, L M Neckers *Nature (London)* **328** 445 (1987)
212. G Degols, J-P Leonetti, N Mechti, B Lebleu *Nucleic Acids Res.* **19** 945 (1991)
213. J T Holt, R L Redner, A W Nienhuis *Mol. Cell. Biol.* **8** 963 (1988)
214. E L Wickstrom, T A Bacon, A Gonzalez, D L Freeman, G H Lyman, E Wickstrom *Proc. Natl. Acad. Sci. USA* **85** 1028 (1988)
215. C J Marcus-Sekura, A M Wolrner, K Shinozuka, G Zon, G V Quinnan Jr *Nucleic Acids Res.* **15** 5749 (1987)
216. D Jaskulski, J Kim de Riel, W E Mercer, B Calabretta, R Baserga *Science* **240** 1544 (1988)
217. C Helene, J-J Toulme, in *Topics in Molecular and Structural Biology* Vol. 12 *Oligonucleotides. Antisense Inhibitors of Gene Expression* (Ed. J S Cohen) (London: Macmillan, 1989) p. 137
218. P B Dervan, in *Topics in Molecular and Structural Biology* Vol. 12 *Oligonucleotides. Antisense Inhibitors of Gene Expression* (Ed. J S Cohen) (London: Macmillan, 1989) p. 197
219. D G Knorre, V V Vlassov *Progr. Nucleic Acids Res. Mol. Biol.* **32** 291 (1985)
220. D G Knorre, V V Vlassov, V F Zarytova, G G Karpova, in *Advances in Enzyme Regulation.* Vol .24. (Oxford: Pergamon Press, 1986) p. 277
221. J M Kean, A Murakami, K R Blake, C D Cishman, P S Miller *Biochemistry* **27** 9113 (1988)
222. U Pieles, U Englisch *Nucleic Acids Res.* **17** 285 (1989)
223. R B Meyer Jr, J C Tabone, G D Hurst, T M Smith, H Gamper *J. Am. Chem. Soc.* **111** 8517 (1989)
224. G B Dreyer, P B Dervan *Proc. Natl. Acad. Sci. USA* **82** 968 (1985)
225. J C Francois, T Saison-Behmoaras, M Chassignol, N T Thuong, J C Sun, C Helene *Biochemistry* **27** 2272 (1988)
226. T Le Doan, L Perronault, D Praseuth, N Habhout, J-P Decout, N T Thuong, J Lhomme, C Helene *Nucleic Acids Res.* **15** 7749 (1987)
227. C H B Chen, D S Sigman *Proc. Natl. Acad. Sci. USA* **83** 7147 (1986)
228. N I Grineva, G G Karpova, G G Shamovskii *Mol. Biol.* **8** 358 (1974)
229. G G Karpova *Izv. Sib. Otd. Akad. Nauk SSSR, Ser. Khim. Nauk* **4** 82 (1987)
230. N I Grineva, G G Karpova *Mol. Biol.* **8** 832 (1974)
231. N I Grineva, G G Karpova *Bioorg. Khim.* **1** 588 (1975)
232. N I Grineva, G G Karpova, L M Kuznetsova, T A Chimitova, T V Vekstern, L P Shershneva, A A Baev *Mol. Biol.* **10** 1260 (1976)
233. N I Grineva, G G Karpova, L M Kuznetsova, T V Vekstern, A A Baev *Nucleic Acids Res.* **4** 1609 (1977)

234. A M Belikova, N I Grineva, G N Kabasheva *Tetrahedron* **29** 2277 (1973)
235. O I Gimautinova, I I Gorshkova, G G Karpova, I V Kutyavin, D M Graifer *Mol. Biol.* **18** 1419 (1984)
236. O I Gumautdinova, V V Gorn, I I Gorshkova, D M Graifer, G G Karpova, D A Mundus, N M Teplova *Bioorg. Khim.* **12** 490 (1986)
237. V V Vlassov, S A Gaidamakov, V F Zarytova, D G Knorre, A S Levina, A A Nikonova, L M Podust, O S Fedorova *Gene* **72** 313 (1988)
238. E B Brosalina, V V Vlasov, I V Kutyavin, S V Mamaev, A G Pletnev, M A Podyminogin *Dokl. Akad. Nauk SSSR* **285** 1475 (1985)
239. E B Brosalina, V V Vlasov, I V Kutyavin, S V Mamaev, A G Pletnev, M A Podyminogin *Bioorg. Khim.* **12** 240 (1986)
240. I I Gorshkova, M A Zenkova, G G Karpova, A S Levina, V V Solov'ev *Mol. Biol.* **20** 1084 (1986)
241. M A Zenkova, G G Karpova, A S Levina *Mol. Biol.* **23** 1056 (1989)
242. M A Zenkova, G G Karpova, A S Levina, S V Mamaev, V V Solov'ev *Bioorg. Khim.* **16** 788 (1990)
243. M A Zenkova, O S Fedorova, A S Levina, S V Mamaev, G G Karpova *FEBS Lett.* **269** 26 (1990)
244. M A Zenkova, G G Karpova, A F Levina, S V Mamaev, Yu N Nazarova, O S Fedorova *Bioorg. Khim.* **17** 470 (1991)
245. N A Kolchanov, V V Solov'ev, A A Zharkikh *Dokl. Akad. Nauk SSSR* **273** 741 (1983)
246. I V Kutiavin, M A Podyminogin, J N Bashina, O S Fedorova, D G Knorre, A S Levina, S V Mamaev *FEBS Lett.* **238** 35 (1988)
247. V V Vlasov, A A Godovikov, V F Zarytova, E M Ivanova, N Yu Nomokonova *Mol. Biol.* **24** 173 (1990)

Russian Chemical Reviews **62** (5) 409–418 (1993)
© 1993 Russian Academy of Sciences and Turpion Ltd

UDC 539.211 + 542.973 + 541.128

Studies of heterogeneous catalytic systems and of their models by scanning tunnelling microscopy

Sh K Shaikhutdinov, D I Kochubei

Contents

I. Introduction	409
II. Principles of the scanning tunnelling microscopy method	410
III. Studies of surfaces by scanning tunnelling microscopy	410

Abstract. Studies of carbon materials, oxides, metals, clusters, and model catalysts, of potential interest in the field of heterogeneous catalysis, are reviewed. The principles of the method and its possible applications are discussed. 127 references.

I. Introduction

Progress in heterogeneous catalysis is largely dependent on improvements in our understanding, at the molecular level, of surface structures and of surface processes. Various methods of studying surfaces are used for this purpose. Workers in this field have tried for many years to see atoms by observations in an optical microscope. This visualisation of the surface structure at the atomic level was made possible by the development, in 1981, of scanning tunnelling microscopy (STM).[1]

The principle of the STM effect is based on recording the tunnelling current between the sample and a needle scanning the sample surface (Figure 1). We know that in the case of a one-dimensional potential barrier[2] the tunnelling current is exponentially dependent on the width and height of the barrier (the distance between the tip of the needle and the surface, i.e. the tunnelling length, and the work function of the sample and needle materials respectively). This exponential dependence accounts for the high resolving power of the STM method (~ 1 Å in the plane of the surface and 0.1 Å at right angles to it). Furthermore, studies by STM offer the additional advantage that the measurements are non-destructive, are aimed at the surface layer itself, and can be made in liquids and in gases as well as in a vacuum. The main weaknesses of the method, which limit the range of applications of STM, include the stringent elimination of all mechanical vibrations, the small size (up to 10 μm^2) of the scanning region, and (perhaps most importantly) the fact that the measurements are confined to electrically conducting samples. The latter limitation provided a stimulus for the development of a whole family of new microscopes based on the STM concept: these include the atomic force microscope, which can be used with non-conducting as well as with conducting materials, the magnetic force microscope, the thermal microscope, and others.[3]

Recent studies of scanning tunnelling microscopy and of similar methods of surface analysis have shown that the analytical possibilities of these techniques are increasingly wide-ranging.[4, 5]

In spite of many suggestions of potential applications of STM in studies of catalytic systems, the first reports of studies of actual catalysts have only recently appeared. Evidently, difficulties have been encountered firstly because heterogeneous catalysts usually consist of a multiphased system on a highly dispersed (and often non-conducting) carrier, and secondly because at present surface structures are studied by STM without an element analysis. Therefore research must be confined to model systems consisting of metal single crystals, small particles on a conducting substrate, metal oxides, and carbonaceous materials. The present review is aimed at materials of these types.

STM began to be used here later than in some other countries, and this partly accounts for our lag in this field. We hope that this review will stimulate the interest of Russian physical chemists and encourage them to study by STM the atomic structure of reactions on surfaces more widely.

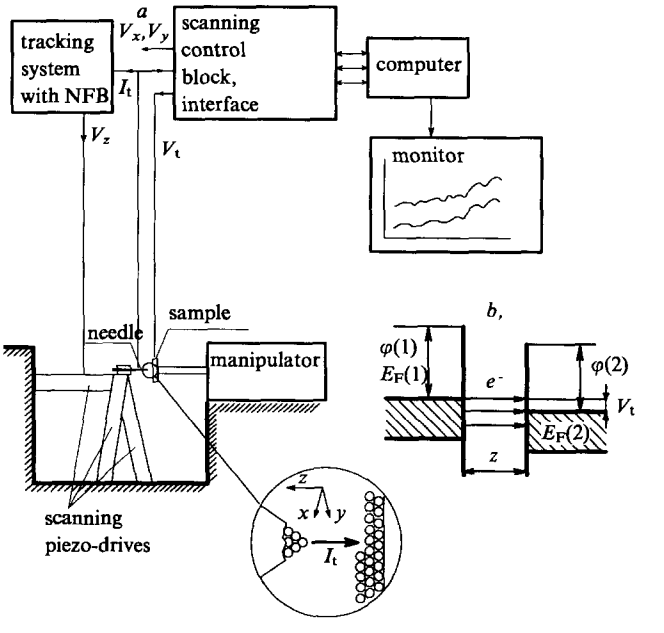


Figure 1. Block diagram of the STM (*a*) and schematic representation of the tunnelling process between the metallic needle and the sample (*b*). E_F is the Fermi energy, φ is the work function of the sample, V_t is the tunnelling voltage, I_t is the tunnelling current, z is the tunnelling distance, $V_{x,y}$ is the voltage applied to the scanning piezo-drives, V_z is the voltage applied to the z piezo-drives of the feedback system.

Sh K Shaikhutdinov, D I Kochubei G K Boreskov Institute of Catalysis, Siberian Section of the Russian Academy of Sciences, prosp. ak. Lavrent'eva 5, 630090, Novosibirsk. Fax (7-383-2) 35 57 56

Received 16th March 1993
Uspekhi Khimii **62** (5) 443–454 (1993); translated by J I Carasso

II. Principles of the scanning tunnelling microscopy method

Various types of STM have already been developed, including designs in which tunnelling microscopy is combined with other analytical methods of surface analysis.[6-8] A block diagram of an STM and of its component parts is shown † in Figure 1. Elements common to all types of STM include a vibration isolation system, which limits the amplitude of external perturbations of the tunnelling length to 0.05 Å; a system which allows the needle to be brought gradually closer to the surface until a tunnel current is obtained; an electronic system with negative feedback (NFB), which maintains the required tunnel current; a scanning needle with a tip having the smallest possible radius of curvature (ideally, terminating in a single atom), which mainly determines the spatial resolution of the apparatus; a frame scanning apparatus, based on piezoelectric ceramics (piezo-drives); a computer system for controlling the scan and for collecting and processing the required data.

In the topographic regime the negative feedback loop keeps the tunnel current constant throughout the scan. Under these conditions the vertical displacement Δz of the piezo-drive relative to the scanning plane reflects the geometry of the surface, and the STM picture is a $\Delta z(x, y)$ representation. In the fast scanning (constant height) regime the negative feedback loop does not follow the outline of the surface, and under these conditions the changes in the tunnel current ΔI are recorded, and the structure of the surface is obtained as a $\Delta I(x, y)$ representation. The latter regime can be used with relatively smooth surfaces, as in layer structures or single crystals, on which collisions between the needle and the surface are less likely.

An absolute calibration of the three-dimensional STM representation is usually obtained with samples of highly oriented pyrolytic graphite or samples containing monoatomic steps.

Obviously, the one-dimensional tunnelling model is a simplified first approximation which offers a qualitative interpretation of the STM picture. Attempts to develop a theory of three-dimensional tunnelling have met serious computational difficulties.

The tunnel current under conditions of weak binding between the electronic states on the surface of the needle and the sample is given by the expression[9]

$$I \approx \int_{-\infty}^{\infty} \rho_s(E+eV)\rho_t(E)|M(E)|^2[f(E)-f(E+eV)]\mathrm{d}E, \quad (1)$$

where E is the energy of a given electronic state, M is a matrix element of the electronic transition, $f(E)$ is the Fermi function, $\rho(E)$ is the state density function in the sample (s) and in the needle (t), and V is the tunnelling voltage.

At low voltages, and on the assumption that the point of the needle can be described by a hemisphere with its centre at the point $\mathbf{r}$ and that the wave function which describes the electronic structure of the surface has the form of an s-type atomic function, formula (1) can be simplified to[10,11]

$$I \sim V\rho_s(\mathbf{r}, E_F)\rho_t(E_F), \quad (2)$$

where $\rho_s(\mathbf{r}, E_F)$ and $\rho_t(E_F)$ are the densities of states at the Fermi level in the sample and in the needle respectively.

It is clear from Eqn (2) that in the topographic regime (I = const) the z-displacement of the STM needle, for which $\rho_t(x, y)$ is constant during the scan, takes place over a contour of constant local density of electronic states on the sample surface.

The results obtained by STM reflect not so much the geometric topography of the surface as its electronic structure, which is itself determined by the arrangement of the atoms. For example, the true position of the carbon atoms on the STM picture of the graphite surface is unquestionable. However, the image of a single atom adsorbed on an ideally smooth surface scanned by an atomically sharp needle can have different heights, depending on the tunnelling voltage, and it can even appear as a hollow.[12,13] This is due to the dependence of the electronic state density on the applied tunnelling voltage [see Eqn (1)]. This phenomenon complicates the interpretation of the observed STM picture, but it also allows the surface states to be probed. For small needle potentials, expressions of the following general form have been obtained for the differential conductivity:[14,15,18]

$$\frac{\mathrm{d}I}{\mathrm{d}V} \sim \rho_s(\mathbf{r}, V)T(V),$$

where $T(V)$ is the transparency of the barrier for a tunnelling voltage V.

By establishing the dependence of the tunnel current on the voltage we can measure the density of electronic states above and below the Fermi level, and in particular we can obtain direct information on the position of the energy gap in semiconductors. Experimentally this is done by suppressing the negative feedback during the time needed to measure the current–voltage characteristic. If this procedure is applied at all the scanning points on the surface the method is called scanning tunnelling spectroscopy (STS). It has yielded spectroscopic representations $[I(x, y, V)]$ of Si(111)–(7×7)[16,17] and GaAs(110)–(1×2) structures,[18] from which the atoms on the surface could be identified.

Thus more detailed information on the structure of the surface can be obtained by recording the STM image for different values of the tunnel voltage.

The parameters which mainly determine the tunnelling by electrons are the height and shape of the tunnel barrier. From the simplified formula for the tunnelling current

$$I \propto V\exp(-az\sqrt{\varphi}),$$

where a is a constant, it follows that the average barrier height φ can be determined by measuring the changes in barrier current (ΔI) produced by changes in the tunnelling distance z,

$$\varphi \approx \left(\frac{\Delta \ln I}{\Delta z}\right)^2.$$

The work function of the material of the sample is obtained in this way.[2] These measurements are usually made by the phase detection method: this gives the STM representation as a $\varphi(x, y)$ dependence, which often offers a contrast better than that of a $\Delta z(x, y)$ topogram of the surface. It should be noted that the measured absolute values of the work function are often much lower than the known values, even when the experiment is carried out in a high vacuum. Usually this is attributed to adsorbates on the surface of the sample or of the needle.[19] Another possible explanation is that at short distances between the needle and the sample the height of the barrier decreases until a point contact is produced.[20-22]

Thus in order to analyse the processes taking place in STM and the experimental results obtained by this method we require additional information, including new theoretical models of the electronic structure of the surface.

III. Studies of surfaces by scanning tunnelling microscopy

1. Carbon materials

Highly oriented pyrolytic graphite (HOPG) is one of the materials most extensively studied by scanning tunnelling microscopy. It offers a number of advantages for the development of the STM technique, including a flat hexagonal layer structure extending over thousands of angstroms, and it is chemically inert. Nevertheless the STM pictures show some unusual features even for this relatively simple material.

Thus, samples of HOPG have shown an anomalously high atomic corrugation (the Δz_{max} value for an atomically flat surface

†The present writers have constructed an STM on the basis of an SO-03 Auger spectrometer.

with periodic packing), making neighbouring atoms non-equivalent in the STM picture and producing a trigonal rather than hexagonal symmetry in the resulting map.[23, 24]

One possible explanation of the anomalous corrugation, reaching ~1 Å, is that the tunnelling current is proportional to the local density of electronic states. According to theoretical calculations[11, 14, 25] the contours of constant density of states at the Fermi level show corrugations with an amplitude of ~0.8 Å, whereas in the total charge density contours the corrugations are only 0.2 Å high.

However, giant corrugations up to 8 Å in amplitude are often observed: these cannot be explained in terms of changes in the local charge density. One explanation proposed for this phenomenon assumes that at small tunnelling distances the interaction between the point and the sample produces elastic shifts of the surface atoms of graphite, and thus enhances the observed amplitude of the corrugations.[26] An alternative explanation relies on the shift of impurities and adsorbates (rather than of the graphite atoms themselves) on the surface of the sample or of the needle. Thus, it has been shown by electron microscopy[27] that when graphite is scanned in air microscopic carbon whiskers are formed on the tip of the needle: their deformation under the action of interatomic forces centred on the sample is assumed to result in giant corrugations.

The apparently trigonal symmetry of the basal plane of HOPG is usually attributed to the asymmetry of the local charge density distribution between neighbouring atoms. The local electron density on the surface is lower on the carbon atoms located above the atoms of the second layer, and therefore their image is suppressed in the STM picture.[28]

Another special feature of HOPG is the presence of surface superstructures, detected as a regular variation of the amplitude of the atomic corrugation of the graphite.[29–32] The lattice periodicity of the superstructures can reach hundreds of angstroms. Evidently, these superstructures can be classified into two groups.[33] The first includes superstructures whose period and amplitude depend on the angular mismatch between neighbouring graphite layers. In this case the STM picture reflects a real property of the surface: the difference in azimuthal orientation between the first two layers of graphite atoms. In the second group we find superstructures with constant period and amplitude, which show a sharp transition to the normal graphite structure. In this case the STM picture does not reflect the real structure of the surface: it is due to the presence on the tip of the needle of a crystalline graphite layer plane-parallel to the surface. The second class of superstructures is the more common, suggesting ready contamination of the point.

Effects arising from the formation of structures differing from the normal graphite structure can complicate the study of molecules adsorbed on HOPG, especially when the adsorbate is accommodated with a periodic packing.

The symmetry type of the STM picture of HOPG is determined by the electronic structure of the neighbouring carbon atoms, which is strongly influenced (as was pointed out above) by their interaction with the atoms of the underlying layer. This effect has been allowed for[34–39] in studies of graphite intercalation compounds (GIC) whose Fermi surface was controlled[40] by introducing electron donors or acceptors.

Thus, the STM pictures[34] of a GIC of the donor type (MC_8, M = K, Rb, Cs) show a 2×2 structure over a wide range of tunnel voltage and current (Figures 2*a* and 2*b*), determined by the distribution in space of a layer of donors under a layer of graphite.[37, 38] In the $CuCl_2$–HOPG system, which contains a GIC of the acceptor type,[35] the STM picture depended on the sign of the tunnelling voltage. When the electrons are tunnelling from the needle into the sample (at the electron localisation sites shown in Figure 2*d*) the STM picture has a clearly developed hexagonal symmetry. This indicates equivalence of the carbon atoms in the elementary cell of the basal plane, corresponding to a large decrease in the interaction between planes. When the polarity is inverted the STM picture is determined by the layer of acceptors and by their distribution under the upper graphite layer. However, a similar dependence of the STM image on the sign of the applied voltage is not found in compounds of graphite with electron donors. This means that in GIC of the donor type both occupied and unoccupied states are present near the Fermi level, and can contribute to the tunnelling. In the case of intercalation by a donor the charge transfer is relatively large, and if the packing of the donor layer matches that of the graphite the modulation of the electron density in the surface layer by the intercalated metal is more marked than in compounds of the acceptor type, in which the charge transfer is small and the packing is unmatched.[35]

A study of the $KHgC_4$ and $KHgC_8$ systems detected[39] a matched 2×2 superstructure in addition to the hexagonal graphite structure. This work led to the conclusion[34, 39] that the 2×2 structure is the result of a periodic arrangement of the potassium ions beneath a graphite layer. Furthermore a new orthorhombic superlattice was detected for the $KHgC_8$ complex, with parameters $a = b = 8.9$ Å and $\angle\gamma = 89°$, whose orientation is independent of the orientation of the graphite lattice. This structure is believed to be related to the waves of charge density observed in layer systems based on metal chalcogenides.

It can be seen that tunnelling microscopy offers valuable new information in studies of intercalation compounds.

Important new topics in the study of carbon materials include defect structures on the surface, the processes induced by bombarding the surface with various particles, and the amorphisation of graphite.[41–44] In particular, treating pyrolytic graphite with a methane plasma in a high-frequency discharge produces a strong modification of the surface:[44] the bombardment by the plasma ions yields amorphous formations ~50 Å in diameter which increase in number (but not in size) as the exposure time is increased. Obviously, regions of amorphous carbon are formed on defects induced by the plasma ions. In samples which had not been bombarded reproducible patterns could not be obtained because the operation of the STM was destabilised by the formation of an electrically insulating layer on the surface.

Recently reported[45–49] studies of other carbon materials have greater practical interest than the studies of HOPG. Thus, graphite structures obtained by the pyrolysis of various hydrocarbons have been examined,[45, 46] as well as carbon fibres.[47, 49] As could have been expected, pyrolytic graphites have a planar structure, but unlike the HOPG they contain large structurally

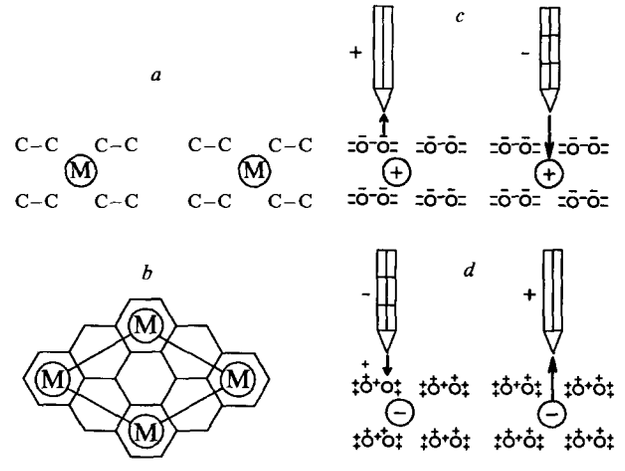


Figure 2. (2×2) structure of an intercalation graphite compound of the MC_8 type.[34, 35]
(*a*) transverse section; (*b*) top view of the basal plane; localisation sites of the tunnelling electrons in compounds of graphite with electron donors (*c*) and acceptors (*d*) for different polarities of the tunnelling voltage.

inhomogeneous regions determined by the method of preparing the graphite. The structure of the carbon fibre also depends on the method of synthesis, and on the temperature of heat treatment. For example, high-temperature graphitisation of the fibre results in ordering of the structure at the atomic level, as is clearly shown by the STM pictures.[47]

Scanning tunnelling microscopy has been used successfully in studies of the processes involved in the etching of the basal plane of graphite during the gasification of HOPG in air.[50, 51] This work has made clear the unique possibilities of the method in studies of reaction kinetics at the molecular level.

Heating a clean, freshly cleaved HOPG surface at 773 – 873 K in air produces a uniform distribution of circular etch pits one monolayer deep over the surface. The concentration of these pits varies between 0.1 and 13 μm^{-2} in different samples. Their diameter (but not their number) increases linearly with the time of heat treatment. The rate constant for the removal of carbon on one active centre calculated[50] from kinetic data is 0.5 s^{-1}. A typical activational temperature dependence of the growth rate of the diameter for the monolayer etch pits has been observed[51] between 773 and 973 K. The activation energy determined from these data is 127 kJ mol^{-1}, which is close to the value[51] obtained gravimetrically (147 kJ mol^{-1}). Successive heating and cooling cycles increase the size of the old pits as well as producing new pits. Therefore the etching is controlled by the presence of vacancies or impurities on the surface. Increasing the heat treatment temperature above 973 K produces a large number of concentric pits one monolayer deep, and at 1173 K the STM picture consists of conical craters.

Many different types of tracks, channels, and craters are seen on samples which have been stored in air for long periods or exposed to chemically active (or even inert) materials before being heat treated. Since in these cases the STM pictures are independent of the nature of the impurity on the HOPG surface it has been suggested[50] that the carbon gasification centres may be formed by the mechanical interaction of the impurity particles and the graphite particles.

2. Metals

Attempts to achieve a resolution sufficient to observe atoms on a clean metal surface have long been unsuccessful, though some workers have observed monatomic steps and reconstructions of the surface of single crystals induced by gases.[52–54] The lack of resolution on an atomic scale on metallic surfaces has been interpreted as a manifestation of the high level of delocalisation of the electron density in metals. The first report of atomic resolution on a close-packed surface of monocrystalline gold was published[55] in 1987. The anomalously high amplitude (up to 0.5 Å) of the atomic corrugations was stressed. By analogy with graphite this phenomenon was ascribed to the presence of local surface states near the Fermi level. In the following year another group of workers[56] proposed a different explanation of the atomic resolution which they had observed on an Al(111) monocrystal. A reasonably reproducible method of modifying the point of the STM to give an enhanced resolution was proposed: it was based on the experimental observation that the point is elongated by ~25 Å when a pulse of increased tunnelling voltage is applied to it over a gold or aluminium sample. It was suggested that this pulse induces the transfer of a small cluster of material from the substrate to the tip of the needle, thus increasing the contrast of the image. The same workers attribute the anomalously high corrugations to elastic deformations of the resulting cluster by the interatomic forces which it experiences from both sides (the needle and the sample).

Different theoretical interpretations of the anomalous amplitude of the atomic corrugations on metal surfaces have already been proposed. According to one of these the resolution of a tungsten needle[57] can be ascribed to the elimination of all impurities from the needle, giving ideally clean tungsten, whose d_{z^2} atomic function has a smaller radius of curvature than the generally adopted s wave function model of the electronic structure of the point. An alternative theory[58] postulates that for small tunnelling gaps (in which the atomic corrugations of metals surfaces are observed) large changes in the electronic structure of the surface can take place, and the tunnelling current can no longer be assumed to flow between unperturbed electronic states In this case localised electronic states induced by the point above the Fermi level appear on the surface. It was shown that their energy distribution and the effective height and width of the tunnelling barrier are very different in the regions above the atoms and above the vacancies. As a result the contrast of the STM representation of the metal surface increases until atomic resolution is achieved. The amplitude of the atomic corrugation calculated by this model (~0.3 Å) is close to the experimentally observed value (0.1 – 0.5 Å).

The achievement of resolution on an atomic scale on metals stimulated new studies of metal surfaces, including processes leading to their reconstruction. The positions of the atoms on a reconstructed metal were first established for the (111) gold surface.[59, 60] We know that gold is the only metal with a face-centred cubic (f.c.c.) packing in which reconstruction of the (111) face into a hexagonal close-packed (h.c.p.) structure is observed. Woll et al.[59] and Barth et al.[60] were able to visualise $(23 \times \sqrt{3})$ elementary cells forming a structure of parallel lines (Figure 3*a*). A more detailed study[60] also revealed superstructures identified as 120° breaks in the lines approximately 250 Å apart, producing a zigzag pattern in the STM (Figure 3*b*). Surface steps and bulk defects do not impede the passage of the lines, though they affect the details of the picture. It is interesting to note that these lines are always closed. These results suggest a model of the reconstruction consisting in a transition from f.c.c. to h.c.p. packing in the upper atomic layer.

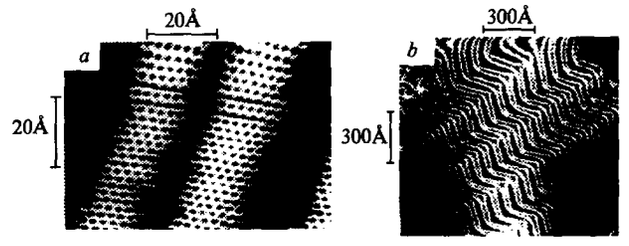


Figure 3. STM image[60] with atomic resolution of the reconstructed Au(111) surface.
(*a*) structure of parallel lines, the frame defines the elementary $23 \times \sqrt{3}$ cell, difference in height between the black and the white areas 0.2 Å; (*b*) structure of the zig-zag lines.

Scanning tunnelling microscopy results have also shown[61] that carefully prepared, clean (110) faces of platinum and gold undergo a thermodynamically stable (1×2) reconstruction by the 'absent rows' model rather than through impurity effects (Figure 4). The (1×2) reconstruction remains stable even near a screw dislocation. Increasing the concentration of impurity (mainly calcium) decreases the relative proportion of regions with a (1×2) structure and increases the proportion of (1×7) and (1×5) structures. Ultimately, at high impurity concentrations, we obtain a (1×3) structure consisting of (111) micro-facets.

An analysis of sequential STM representations of an Au(110)-(1×2) structure, obtained in a period of several hours in an ultra-high vacuum,[62] revealed a substantial motion of the surface atoms. The structural changes were found to be related to defects on the steps (i.e. to kinks) on the (100) microfacets, confirming the earlier hypothesis of an important contribution to mass transfer from these defects.

A study of the fine structure of the steps on an Ag(111) face showed that at room temperature this structure includes an irregularity of subatomic dimensions, indicating a motion of the atoms along the steps between successive frames of the scan.

Lowering the temperature to 27 K in order to lower the mobility of the atoms removes the kinks from the steps.

In situ studies by STM of the Ag(111) surface gave visual evidence[64] that an increase in temperature converts an initially regular (though stepped) surface into a disordered system as a result of the surface diffusion of atoms, with an effective transition temperature of ~350 K. The list of metals which have been studied by STM is continually growing. In particular, studies of chromium monocrystals have been reported.[65, 66]

Studies of the interaction of gases with the structure of the surface are of special interest. These are conveniently classified into two groups. The first includes the visualisation of adsorbed molecules and the identification of their adsorption sites, the second deals with surface reconstruction processes induced by gases.

The adsorption sites of the molecules can be determined only when the STM offers atomic resolution. One of the earliest studies of the adsorption of oxygen[67] was carried out on an Al(111) monocrystal surface. Even at low coverages (up to 5% of a monolayer) islets of adsorbed oxygen uniformly distributed over the surface can be distinguished, but they appear as depressions 10–20 Å in diameter rather than as prominences. This confirms that the STM image describes the local distribution of electron density. After being annealed at 800 K the sample shows some characteristic surface formations: a mound surrounded by a ring of six depressions, with three aluminium atoms round each depression. These structural features were interpreted as oxide nuclei.

The STM image of molecules adsorbed on a substrate is the result of changes in the local electron density not only at the site of the adsorbate but also on the neighbouring atoms of the substrate, as was demonstrated[68] for carbon atoms adsorbed on Al(111). As can be seen from Figure 5, the carbon atom adsorbed on a hexagonal metal lattice has a trigonal symmetry. The images of the six aluminium atoms nearest to this carbon atom differ markedly from those of the more remote atoms. Three of them are bound to the carbon and appear as pits, whereas the other three seem to project above the surface. The authors conclude from these results that the apparent changes in the vertical position of the aluminium atoms are more probably due to a redistribution of the electron density than to genuine structural changes.

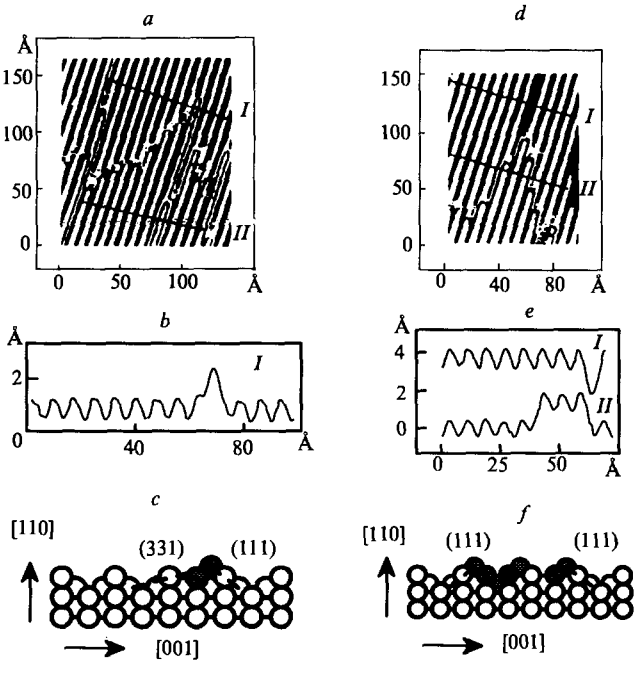


Figure 4. STM images[61] of the reconstructed Au(110) surface.
(*a*) top view of the region with a (1 × 2) structure; (*b*) transverse section along the line *I* shown in Figure 4*a*; (*c*) model of the structure of the surface along the line *I*, showing the structure of the microfacets; (*d*) top view of the region of the surface with (1 × 2) and (1 × 3) structures; (*e*) transverse sections along the lines *I* and *II* shown in Figure 4*d*; (*f*) model of the structure of the surface along the lines *I* (open circles) and *II* (filled circles).

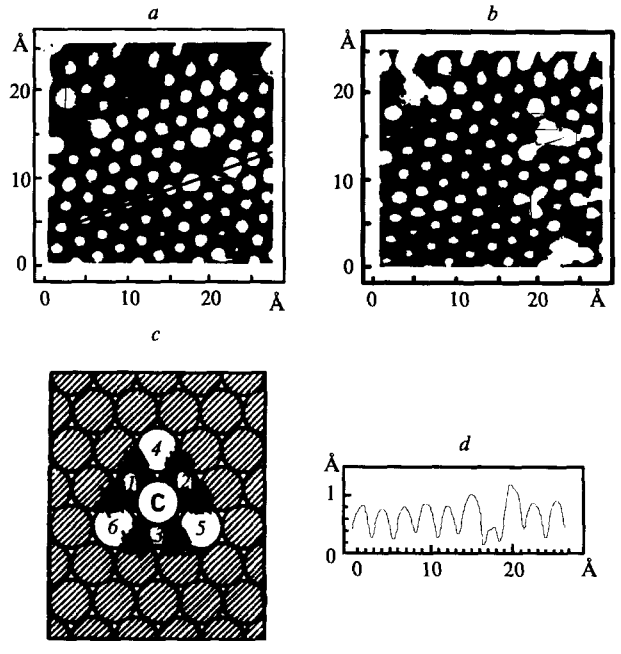


Figure 5. Successive STM representations[68] of the Al(111) surface with adsorbed carbon atoms.
(*a*) $V = -20$ mV, $I = 41$ nA; (*b*) $V = -70$ mV, $I = 41$ nA; (*c*) model of the atomic surroundings of an adsorbed carbon atom; aluminium atoms of the first (*1*–*3*) and of the second coordination sphere are shown (*4*–*6*); (*d*) transverse section along the [110] direction shown in Figure 5*a*.

The scanning tunnelling microscopy method has also been used[69] in studies of the adsorption of oxygen on a Ni(100) single crystal. At 400 K and 15% coverage square pits with a side of ~4 Å were found in the STM pictures, and ascribed to oxygen atoms. These pits are located over cavities of the square nickel lattice. Unlike the oxygen atoms adsorbed on Al(111) the oxygen atom on Ni(100) do not tend to form islets and appear to be uniformly distributed over the surface. However, a more detailed study revealed some ordering of the adatoms on the surface. Statistical evidence of interaction between the adatoms up to the third nearest neighbour was obtained. Gradually increasing the coverage of the surface produces first a $p(2 \times 2)$ and then a $c(2 \times 2)$ packing of the adsorbed layer.

Studying the distribution of the adsorbed molecules over the surface gives information on their interaction. Thus, the formation of sulfur clusters on the Re(0001) face has been observed[70, 71] in this way. At low surface coverages (up to 25% of a monolayer) the sulfur atoms are located over the c.p.h. cavities of the Re lattice, forming $p(2 \times 2)$ or (less often) $c(\sqrt{3} \times 5)$ structures. At higher surface loadings the more close-packed $(\sqrt{3} \times \sqrt{3})R30°$ structure is replaced by clusters of three, four, or six atoms, but not by dimers, indicating the presence of three-centre interaction. The authors suggest[70, 71] that this interaction takes place through the substrate, because the distance between the sulfur atoms in the clusters is much greater than the interatomic distance in the S_2 and S_8 molecules. This assumption is also confirmed by the absence of a similar effect when the S/Mo(001) system is studied in the air.[72]

Scanning tunnelling microscopy has been successfully applied in a study of the structure of surfaces during the adsorption of

aromatic compounds. Ordered (3×3) circular formations, occasionally with a resolved fine structure ascribed to benzene rings, have been observed[73] in the coadsorption of benzene and CO (up to saturation) on a Rh(111) surface. In a study of the adsorption of naphthalene on Pt(111) it was found[74] that the adsorbed molecules can be accommodated in three positions differing by a 120° rotation of the molecule in the plane. At low coverages the naphthalene molecules are distributed uniformly, and they can rotate round their axis and move over the surface, as was demonstrated by comparing successively recorded STM pictures. The mobility of the adsorbate is greatly suppressed at higher coverages.

With large molecules the site of attachment to the substrate is difficult to determine, because several such sites may be involved, but under these conditions the visualisation of the molecule by STM can be improved until the structure of the molecule is resolved. Thus, the electron density distribution in copper phthalocyanine adsorbed on a Cu(100) substrate has been established in this way.[75] It was pointed out that this was made possible only by a correct choice of the metal support, since the phthalocyanine molecule can move along the surface (like silver phthalocyanine on a polycrystalline silver foil[76]).

The adsorption of molecules is often accompanied by reconstruction of the surface, but different types of reconstruction can be encountered, depending on the nature of the adsorbate and of the metal, on the type of face, on the temperature and on the coverage.[77]

The O/Cu system has been studied most intensively by scanning tunnelling microscopy.[78–83] On the STM pictures of the clean Cu(110) surface the monatomic steps were found to have the shape of a fringe.[78] This was interpreted as evidence of a substantial amount of diffusion of the copper atoms over the surface. Quantitative estimates of the diffusion coefficient obtained from successive STM pictures showed that a monolayer of copper adatoms (removed from the steps) can be formed in less than 20 s at room temperature. When adsorbed oxygen is present on the surface the wandering copper adatoms are captured by the oxygen atoms and the surface is reconstructed, giving a (2×1) structure formed from O–Cu–O chains extending above the base plane and oriented in the [001] direction. At higher coverages the chains combine into islets elongated in the same direction, denoting a greater probability of capture of the wandering adatom at the end of the chain than on its side. The larger islets are less mobile, but individual chains can be captured by them to produce even larger islets. By visualising the dynamics of this process[79] at about 1 frame s^{-1} it can be shown that copper atoms are transferred from the steps to the terraces on the surface. This leads to the so-called additional rows model, which differs from the missing rows model by stipulating mass transfer in the opposite sense. At even greater exposures the (2×1) structure is converted into a $c(6 \times 2)$ structure. In this case the formation of islets of the new structure beings on the steps.

Unlike the Cu(110) face, the Cu(100) gives a $(2\sqrt{2} \times \sqrt{2})R45°$ structure under the influence of oxygen. Under these conditions successive STM pictures show[80] that the nucleation and growth of islets takes place on the terraces, and that the steps are almost unaffected. The islets grow preferentially in the [010] and [001] directions. This is taken[80] as direct evidence that the reconstruction of the (100) face takes place by the missing rows model with formation of O–Cu–O chains in the [001] direction, which then coalesce in the [010] direction to give islets.

Two previously unknown structures containing 29 and 44 (1×1) cells respectively have been discovered[84] in the O/Cu(111) system. They were ascribed to the mixing of the hexagonal lattice of the $Cu_2O(111)$ face with the (1×1) copper lattice.

Surface reconstruction under the influence of alkali metals is well known, but only one study of this effect has so far been reported:[85] the mechanism of the reconstruction of the Cu(110) face induced by potassium. It was shown that at low coverages the potassium atoms are uniformly distributed as single atoms or as chains of 2 or 3 atoms in the [110] direction, and that these species (unlike oxygen) are not captured by surface steps. It is suggested that copper atoms under the potassium atom are squeezed out and migrate along the surface, ultimately landing on steps. Increasing the coverage to 15% of a monolayer results in growth of the chains, with formation of (1×4) and (1×3) structures. At still higher coverages the reconstruction ceases and the well known (1×2) structure is observed.

STM studies of the morphology of Pt(111) samples after the ion bombardment and annealing[86, 87] have made an important contribution to our understanding of the role of defects in surface processes. Irrespectively of the nature of the ion (He^+, or Ar^+) trigonal craters are formed on the metal surface at low doses and for annealing temperatures below 700 K. Increasing the annealing temperature results in the formation of monolayer pits and islets, whether the anneal is carried out during the bombardment or after it. This shows that an increase in temperature produces a substantial mass transfer between the layers. The islets formed under these conditions have a trigonal symmetry, indicating thermodynamic equilibrium. It is assumed[86, 87] that these processes are common to all metals with an f.c.c. lattice [at least, on the (111) face].

Real polycrystalline systems have not been studied in depth so far. They were used as samples during the initial stages of the development of tunnelling microscopy. Thus, Gimzewski et al.[88] compared the topographies of silver films evaporated on substrates at different temperatures with the aim of establishing the effect of surface roughness on the enhancement in hyper Raman scattering. Some studies of the epitaxy of metallic layers on metals should also be noted.[89]

The above STM studies of metals were carried out on monocrystalline samples under vacuum conditions, in conjunction with data obtained by electron-spectroscopy and structural methods of analysis such as low-energy electron diffraction, Auger spectroscopy, X-ray spectroscopy, UV electron spectroscopy, etc. Of course, under these conditions the information content of the scanning tunnelling microscopy method is substantially enhanced. Comparing different methods allows us to use scanning tunnelling microscopy in cases where alternative methods are unsatisfactory, for example owing to the small size of the metallic particles, to their very low concentration, or to their amorphous structure.

3. Clusters and small particles

The development of tunnel microscopy has stimulated considerable interest from workers engaged in the study of clusters. Applying STM to cluster studies usually involves the following steps: depositing the substance of interest on a flat, electrically conducting substrate in concentrations low enough to allow the atomic structure of the substrate to be observed; a quantitative element analysis of the composition of the surface; visualising the particles in the STM. In spite of the apparent simplicity of this approach only a few studies of clusters by scanning tunnelling microscopy have been reported. Difficulties are met even at the stage of choosing a substrate. A clean surface and ultra-high vacuum conditions are needed when monocrystals of metals or of semiconductors (of the silicon type) are chosen. In this respect pyrolytic graphite is more convenient, but (as was said above) there may be problems in interpreting the STM representation because of the possible formation of anomalous superstructures on the graphite substrate. Difficulties are also met in ensuring uniform deposition of the clusters because of the possibility of very rapid diffusion on the inert pyrographite surface, and also of uneven evaporation of the solvent when the clusters are deposited from a solution. Lastly, treating HOPG with acetone produces a regular structure with a period of ~4 Å (which eventually disappears), and treatment with a solution of $[Et_4N]_3[Re_7C(CO)_{21}]$ in acetone produces a hexagonal structure with a period of 10 Å in addition to amorphous aggregated formations.[90]

A more uniform distribution of the particles is obtained by molecular beam deposition in a stream of inert gas or by thermal evaporation in a vacuum, with condensation of the atoms on a substrate. Ligand-free particles of different size can be obtained by varying the deposition conditions. Clusters with a ligand coat and molecular complexes are usually deposited from solutions on a graphite or gold substrate. Often the deposition of the particles and the element analysis of the surface are carried out in a vacuum, and the STM study in the air (sometimes including a repeated check for changes in composition of the surface during the vacuum treatment). However, some ambiguity in the interpretation of the results cannot be avoided in these experiments.

The potential advantages of STM in studies of small particles were first demonstrated by the observation of isolated particles of silver, gold, and aluminium on a graphite substrate.[91, 92] In spite of the high mobility of the adatoms relatively stable single atoms of the metal could be detected near the larger particles. Dimers and linear trimers were also seen in the STM pictures. It should be noted that atoms were never observed over the cavities in the graphite lattice: from this result, and from an analysis of the interatomic distances, the authors suggested the presence of a strong interaction between the metal and the carbon substrate, which is suppressed by increasing the size of the particle.

This conclusion was tested by statistical studies[93] of the position of the metal atoms, and by determining the length of the metal–metal bonds in the platinum dimers and trimers. It was found that the position of the metal atoms was stable in time. An analysis of the position of the single metal atoms with respect to the graphite lattice showed that no preferential binding site could be identified, though the metal atom had the highest probability of lying above a carbon atom not directly bound to the lower layer. The average Pt–Pt distance in the dimers was 2.45 ± 0.26 Å, i.e. close to the lattice parameter of the graphite. However, the relatively wide distribution of the Pt–Pt bond lengths made it impossible to establish unambiguously whether this agreement was fortuitous or whether it was the result of platinum–carbon interactions. The trimers were mostly linear, or arranged as equilateral triangles. The average bond length of the trimers was 2.66 ± 0.32 Å, suggesting a predominant effect from the metal–metal bonds.

Humbert et al.[94] studied clusters of gold and palladium deposited by the atomic beam method in a Knudsen cell on a single crystal of natural graphite at 623 K. Under these deposition conditions the particles grow as a result of the diffusion of adatoms over the surface. According to transmission electron microscopy results the particles were condensed mainly along the graphite steps. The STM images revealed both large (~100 Å) and small particles (~15 Å), with a ratio of height to diameter of ~0.1, indicating a strong compression of the particles.

The preferential formation of flat structures is confirmed by a statistical analysis of more than 200 particles of platinum on graphite at different coverages. When the coverage is increased from 10% to 50% of a monolayer the particle diameter increases from 47 to 80 Å, whereas the average height (3.8 Å) stays practically constant. Unfortunately, these results were obtained by working in the air, which gave an oxygen content of the surface 3–4 times higher than in the initial sample immediately after evaporation of the metal. Therefore it is not clear whether the results apply to particles of platinum or of its oxide.[95]

In order to establish the effect of exposure to air on the observed form of the clusters Humbert et al.[96] compared the STM pictures obtained by depositing palladium particles in a vacuum and in air. The clusters were deposited by the atomic beam method on to a graphite substrate heated to 573 K, previously irradiated in a low-energy (50 eV) ion beam with a dose of less than 10^{12} ions cm^{-2} in order to increase the concentration of adsorbed particles on the surface. According to those workers the shape of the larger particles (> 100 Å) was unaffected by deposition in air. On the other hand an unexplained corrugation of atomic dimensions was seen on the surface of the smaller particles (15 Å) in air.

Clusters of gold deposited by a molecular beam on an atomically flat gold substrate were used to examine possible explanations of the compression of the particles observed in the STM, including artefacts associated with the production of the STM image.[97] The authors concluded that the compression occurs only in particles of size smaller than a critical size determined by the nature of the substance. The compression is due to plastic deformation, which lowers the surface energy at the contact with the substrate.

More recent papers have described STM studies of large Au_{55} clusters stabilised by ligands[98, 99] and of Pd_{561} clusters,[99] deposited from solutions on HOPG or gold substrates. The difficulty of working with these materials is stressed: the surface mobility is high, especially on graphite, and the cluster can be entrained by the point until it is transferred to the needle of the microscope. Therefore the results so far are only tentative. Similar investigations of the visualisation of heteropoly acids (hydrogen tungstophosphate)[90, 100] and BiI_3 clusters[101] have been reported.

A new class of carbon compounds (the fullerenes) has recently come to the fore in the study of clusters. Their properties have been studied by various physical methods, including scanning tunnelling microscopy.[102, 103] After mild evaporation of C_{60} and C_{70} clusters on to a gold substrate regular close-packed spherical structures spaced at a distance of ~11 Å between centres were observed on the surface. Furthermore after deposition on the Au(110) face [but not on the (111) face] C_{60} showed intramolecular structure both in air and in an electrochemical cell containing a solution of $HClO_4$.[104] A model of the electron tunnelling which allows for superexchange interactions was developed from the STM images obtained in this work.

The present writers believe that studies of clusters and of small particles by scanning tunnelling microscopy will develop mainly in the following directions: the achievement of intramolecular resolution (for example, at low temperatures); studies of the dynamics of the cluster behaviour in adsorption processes and during changes in temperature; studies of electronic structure. All these directions need new theoretical models to be developed in order to interpret the STM representations of the clusters.

4. Model catalysts

Alumina or silica are often used in industrial catalysts as carriers with a highly developed surface. Unfortunately these carriers are electrically insulating, and therefore the catalysts cannot be studied by scanning tunnelling microscopy. Substrates of carbon materials or of 3*d* metal oxides have been used for STM studies of model catalysts. Studies of transition-metal oxides are also of independent interest because these materials are themselves catalysts for many processes. Titanium oxide has been studied most intensively by scanning tunnelling microscopy.

The TiO_2 surface partially reduced in hydrogen has been studied in air as a function of the conditions of surface treatment (polishing and etching),[105] and the effect of the potential applied to the sample in an electrochemical cell on the STM picture has also been examined.[106] It was found that stable images of *n*-TiO_2 are obtained only when negative potentials are applied to the sample, suggesting a system of energy bands typical of semiconductors. The band structure of the oxide was established by tunnelling microscopy (TS) on *n*-TiO_2(001) samples[107, 108] and reduced TiO_2(110) samples.[109] The measurements were made in air. The edges of the energy gap were determined from the tunnelling spectra.[107] A hysteresis observed[108] in the tunnelling spectra was ascribed to surface states induced within the energy gap by the electric field.

From the tunnelling spectroscopy results the width of the energy gap was found[109] to be only 1.7 eV [(+0.25)–(–1.35) eV relative to the Fermi level], i.e. much smaller than the bulk value (~3.0 eV). (The possibility of this effect being due to the presence

of a large number of states near the band edges cannot be excluded, since the measurements were made in air.) Of course, a stable STM picture cannot be obtained when the applied tunnelling voltage brings the Fermi level of the metal of the needle within the forbidden band of the oxide. However, the adsorption of phenol, for example, on the titanium oxide surface produces a surface state within the energy gap ~0.45 eV below the Fermi level. Scanning for this potential difference produced STM images of the phenol, which appeared to be adsorbed parallel to the plane of the oxide. These workers adopted the approach used in scanning tunnelling spectroscopy: they scanned the sample at a predetermined tunnelling voltage.

Rohrer et al.[110] obtained atomic resolution on a sample of reduced $TiO_2(110)$ by careful surface preparation and by operating the STM in an ultra-high vacuum. The STM image showed some clearly developed lines alternating (with a period of 8.5 Å in the [111] direction) with a less well developed corrugation having a period of 3.4 Å along the lines. This picture was interpreted as an ordered packing of two-dimensional defects (crystal lattice shifts).

As in the case of titanium oxide, atomic resolution could not be obtained in an STM study[111] of ZnO(0001) monocrystals. Attention was paid mainly to the effect of surface geometry on the electronic structure of the surface. The STM pictures of the ZnO crystal contained a large number of steps in the [1010] and [1120] directions. The tunnelling spectroscopy results suggest that these steps lead to the formation of surface states in the forbidden energy gap which are probably responsible for the chemical reactivity of the surface.

The scanning tunnelling microscopy method can be used to study strong metal–substrate interactions. According to one of the models the effect is caused by the decoration of the metallic particle by the carrier, with formation of new active centres on the metal–oxide interface. One approach to the study of these interactions is to use oxide samples deposited on a metallic substrate (i.e. a reversed-phase model of the catalyst), because the electrical conductivity of the oxides is low and the effects of surface charge are substantial.

Thus, STM has been used[112] to study islets of MnO_x deposited on a Ni(111) substrate during the adsorption of CO. Measurements of the perimeter of the particles as a function of the mean coverage revealed a correlation with data for the thermal desorption of CO. These results confirm the earlier conclusion that the increased rate of hydrogenation of CO is associated with the CO adsorption centres at the metal–oxide interface.

Islets 20 Å in diameter, in the form of rings, were observed[113] on Rh(111) at submonolayer coverages of TiO_x. The ring shape was obtained only when negative tunnelling voltages were applied to the sample, and therefore its origin must be electronic. These observations were explained in terms of partial reduction of the TiO_2 at the perimeter of the particle.

Unlike TiO_2 zirconium oxide (ZrO_2) is not easily reducible as a substrate. ZrO_2/Pd(100) systems have been studied by scanning tunnelling microscopy. The results[114] suggest the presence of different types of region in this system. The first is assigned to metallic palladium, the second to semiconducting zirconium oxide. The third region is seen only on samples prepared by thermal oxidation in air at 673 K of $Zr(OC_2H_5)_4$ sublimed on a Pd(100) substrate. According to EXAFS spectroscopy results this region may be associated with palladium oxide. It has been suggested that in an oxidising atmosphere the zirconium oxide is uniformly distributed over the whole surface of the substrate. After treatment in hydrogen at 773 K for one hour the oxide islets develop a bulk structure with a sharp metal–oxide boundary. It is suggested that this boundary prevents the decoration of the metal particles by the reduced oxide when zirconium oxide is used as the carrier.

One method of visually resolving the phases in the STM picture relies on the large difference in work function between the metal and the substrate. This conclusion was reached in one of the first studies of model catalysts: ultra-dispersed particles of gold and platinum on carbon substrates, and of titanium oxide.[115] The same approach was used in the Pt/Ga_2O_3 system.[116] The metal particles were identified with a greater contrast by superposing the $\varphi(x, y)$ distribution map on the topogram of the same area of the surface. By comparing the maps thus obtained before and after an anneal of the sample at 1100 K large differences in the structure of the sample were detected. Before the anneal the platinum islets were circular and of similar size, but after being annealed the surface developed a patchwork appearance with the islets concentrated mainly along the grain boundaries of the Ga_2O_3: this may account for the decrease in the free platinum surface (according to Auger spectroscopy results) and in the catalytic activity towards the oxidation of CO (according to mass spectrometry results).

It is well known that catalytic activity is largely determined by the method of preparation of the catalyst: its previous history, and its treatment and conditioning. Therefore studies of all these stages are of interest. In this respect the studies of the effect of various pretreatments on the morphology of platinum particles on a graphite surface are particularly meaningful.[117,118] The particles were obtained by various methods, including the reduction in hydrogen of tetrachloroplatinic(II) acid H_2PtCl_4 or of tetra-ammineplatinum nitrate for 2 h at 723 K. A graphite surface (clean, or treated with nitric acid for 50 h at room temperature) was used as substrate. Detailed studies by STM were carried out at each stage. Thus, the modification of graphite by HNO_3 produced a more uniform distribution of the precursor, and the platinum salt gave smaller associations than the H_2PtCl_4. The size and the distribution of the reduced particles were less dependent on the nature of the precursor, but their microstructure and morphology were strongly influenced by the previous history of the sample. Thus, in the reduction from tetra-ammineplatinum on a substrate treated with HNO_3 the reconstruction of the platinum surface into a structure close to $(111)(\sqrt{3} \times \sqrt{3})$ induced by atmospheric oxygen was visualised for the first time for small particles.

The dynamics of the changes in the morphology of the particles on a graphite surface during the reduction of platinum from H_2PtCl_4 were studied under conditions analogous to those used in the preparation of the platinum catalyst.[118] It was shown that for short reduction times (0.5 h, 723 K) rod-shaped particles are formed, both large (1000–2000 Å long and 100–500 Å high) and small (280 Å long and 30 Å high). This large scatter suggests a partial reduction of the precursor. After being reduced for 2 h the particles break down into crystallites, ellipsoid in shape, and ultimately (after 60 h) they produce particles with a nominal diameter of ~170 Å and ~20 Å high, showing a well faceted surface. On the other hand the platinum particles evaporated in a vacuum and treated with hydrogen at 623 K for 0.5 h are spherical, with a diameter of 25–100 Å and an atomically disordered surface structure.

The study of the shape of the particles reduced from H_2PtCl_4 for different times showed that the crystallite shape is determined mainly by the reduction conditions and is less dependent on the precursor, on the type of graphite substrate, and on the method of deposition. It was found that a small proportion of the crystallites is spherical (with a ratio of length to width not greater than 1.2), and that the proportion of these increases with the reduction time though not above 40%. This is surprising, since crystallites of platinum in thermodynamic equilibrium (a metal with an f.c.c. structure) should be spherical. Studies of the degree of sphericity of the particles could be of interest in relation to the thermodynamics of small supported particles.

Molybdenum disulfide occupies a special place among model catalysts, because it has a layer structure similar to that of graphite, built of S–Mo–S packets. The atomically flat surface of MoS_2 makes this a convenient substrate for visualising deposited molecules; furthermore molecules can, in principle, be intercalated between the layers, and this should help to explain

the nature of superconductivity in structures of reduced dimensionality (see Heckl et al.[119]). The strong localisation of the electron density makes atomic resolution possible, confirming the hexagonal packing of the upper layer.[120] However, the element which appears in the STM image has not yet been identified.[121–123]

Monolayer particles of MoS_2 deposited on a pyrolitic graphite substrate have been studied in this way.[123] It was found that if the layer of sulfide is surrounded by water molecules its surface undergoes a (2×1) reconstruction. When the sample is dried an STM picture identical to that of the surface of the bulk crystal is observed. By combining the results obtained from STM and EXAFS measurements the authors constructed a model in which the molybdenum had distorted octahedral surroundings in solvated samples. The aim of those studies was to determine the mechanism of the action of hydrodesulfurisation catalysts.

Only a few studies of industrial catalysts by scanning tunnelling microscopy have been reported so far.[124–127] The first dealt with the surface topography of an iron–zirconium alloy (the precursor of an ammonia synthesis catalyst).[124]

Besenbacher et al.[125] observed a very dispersed structure in a passivated ammonia synthesis catalyst containing iron. In addition to pores and cracks they found parallel ridged structures corresponding to the crystallographic orientation of magnetite grains. They suggested that these lines appear in the STM as a result of the FeO/Fe epitaxy accompanying the passivation of the catalyst, and that they correspond to the [110] direction of the iron lattice.

Studies of the platinum–rhodium gauze catalyst used in HCN synthesis showed that the surface roughness of this catalyst varies with the conditions of the reaction.[126] However, the increase in the surface area of the catalyst during the activation calculated from STM data (as compared with the initial surface) was not more than two-fold, which is an order of magnitude less than the values obtained by other methods. Therefore the authors concluded that the main contribution to the increase in area is provided by the formation of crystallites more than 1 μm in diameter, and not by changes in morphology on a submicrometre scale.

Ex situ studies of the morphological changes in a supported Ag/SiC catalyst (for the conversion of ethylene glycol into glyoxal) were made possible by the formation of a conducting layer of silver over the whole surface of the carrier.[127] According to the scanning tunnelling microscopy results the silver particles are sintered into larger flat formations under the conditions of the reaction. Additions of small quantities of diethyl phosphite to improve the selectivity of the reaction produce a marked change in the topography of the catalyst, giving a surface of the fractal type, probably as a result of chemical erosion.

Thus tunnelling microscopy is often the only suitable method of studying catalytic systems. The amount of information which it yields on model catalysts depends on the specific properties of the system of interest.

* * *

The results discussed above show that scanning tunnelling microscopy is a powerful instrumental method of studying the surface of electrically conducting systems. Further improvements in the method for *in situ* temperature and adsorption studies and the application of the scanning tunnelling spectroscopy method in conjunction with fast scanning regimes should offer new prospects of studying the kinetics of surface processes at the atomic-molecular level.

References

1. G Binnig, H Rohrer *Rev. Mod. Phys.* **59** 615 (1987)
2. J G Simmons *J. Appl. Phys.* **34** 1793 (1987)
3. R Pool *Science* **247** 634 (1990)
4. R J Behm (Ed.) *Scanning Tunneling Microscopy and Related Methods* (Dordrecht: Kluver, 1989)
5. N S Maslova, V I Panov *Usp. Fiz. Nauk* **157** 185 (1989)
6. Y Kuk, P J Silverman *Rev. Sci. Instrum.* **60** 165 (1989)
7. V S Edel'man *Prib. Tekh. Eksp.* 5 25 (1989)
8. D W Pohl *IBM J. Res. Devel.* **30** 417 (1986)
9. J Bardeen *Phys. Rev. Lett.* **6** 57 (1961)
10. J Tersoff, D R Hamann *Phys. Rev. B* **31** 805 (1985)
11. J Tersoff *Phys. Rev. Lett.* **57** 440(1986)
12. N D Lang *Phys. Rev. Lett.* **55** 230 (1985)
13. N D Lang *Phys. Rev. Lett.* **56** 1164 (1986)
14. A Selloni, P Carnevali, E Tossati, C D Chen *Phys. Rev. B* **31** 2602 (1985)
15. C J Chen *J. Vac. Sci. Technol. A* **6** 312 (1988)
16. R J Hamers, R M Tromp, J E Demuth *Phys. Rev. Lett.* **56** 1972 (1986)
17. R M Tromp, R J Hamers, J E Demuth *Phys. Rev. B* **34** 1388 (1986)
18. R M Feenstra, J A Stroscio, A P Fein *Surf. Sci.* **181** 295 (1987)
19. J M Gomez-Rodriguez, J Gomez-Herrero, A M Baro *Surf. Sci.* **220** 152 (1989)
20. N Garsia *IBM J. Res. Devel.* **30** 533 (1986)
21. N D Lang *Phys. Rev. B* 37 10 395 (1988)
22. J K Gimzewski, R.Moller. *Phys. Rev. B* **36** 1284 (1987)
23. G Binnig, H Fuchs, Ch Gerber, H Rohrer, E Stoll *Europhys. Lett.* **1** 31 (1986)
24. S Park, C R Quate *Appl. Phys. Lett.* **48** 112 (1986)
25. I P Batra, N Garsia, H Rohrer, H Salemink, E Stoll, S Ciraci *Surf. Sci.* **181** 126 (1987)
26. J M Soler, A M Baro, N Garsia, H Rohrer *Phys. Rev. Lett.* **57** 444 (1986)
27. T Tiedje, J Varon, H Deckman, J Stokes *J. Vac. Sci. Technol. A* **6** 372 (1987)
28. D Tomanek, S G Louie, H J Mamin, D W Abraham, R E Thomson, E Ganz, J Clarke *Phys. Rev. B* **35** 7790 (1987)
29. T R Albrecht, H A Mizes, J Nogami, S Park, C F Quate *Appl. Phys. Lett.* **52** 362 (1988)
30. J E Bucley, J L Wragg, H W White, A Bruckdorfer, D L Worcester *J. Vac. Sci. Technol. B* **9** 1079 (1990)
31. M Kuvabara, D R Clarke, D A Smith *Appl. Phys. Lett.* **56** 2396 (1990)
32. P I Oden, T Thundat, L A Nagahara, S M Lindsay, G B Adams, O F Sankey *Surf. Sci.* **254** L454 (1991)
33. M Sawamura, J F Womelsdorf, W C Ermler *J. Phys. Chem.* **95** 8823 (1991)
34. S Kelty, Ch Lieber *Phys. Rev. B* **40** 5856 (1989)
35. C H Olk, J Heremans, M S Dresselhaus, J S Speck, J T Nicholls *J. Vac. Sci. Technol. B* **9** 1055 (1991)
36. S Gautier, S Rousset, J Klein *J. Vac. Sci. Technol. A* **6** 360 (1988)
37. A Selloni, C D Chen, E Tosatti *Phys. Scr.* **38** 297 (1988)
38. X.-R.Qin, G.Kirczenow *Phys. Rev. B* **41** 4976 (1990)
39. S Kelty, Ch Lieber *J. Vac. Sci. Technol. B* **9** 1068 (1991)
40. M S Dresselhaus *Intercalation in Layered Materials* (New York: Plenum, 1986)
41. R Coratger, A Claverie, F Ajustron, J Beauvillain *Surf. Sci.* **227** 7 (1990)
42. L Porte, C H de Villeneuve, M Phaner *J. Vac. Sci. Technol. B* **9** 1064 (1991)
43. G M Shedd, P E Russel *J. Vac. Sci. Technol. A* **9** 1261 (1991)
44. G J Vandentop, P A P Nascente, M Kawasaki, D F Olgetree, G A Samorjai, M Salmeron *J. Vac. Sci. Technol. A* **9** 2273 (1991)
45. V Elings, F Wudl *J. Vac. Sci. Technol. A* **6** 412 (1991)
46. L M Siperko *J. Vac. Sci. Technol. B* **9** 1061 (1991)
47. S N Magonov, H-J Cantow, J-B Donnet *Polym. Bull.* **23** 555 (1990)
48. W P Hoffman, V B Elings, J A Gurley *Carbon* **26** 754
49. N M D Brown, H-X You *Surf. Sci.* **237** 273 (1990)
50. H Chang, A J Bard *J. Am. Chem. Soc.* **113** 5588 (1991)
51. X Chu, L D Shmidt *Carbon* **29** 1251 (1991)
52. Y Kuk, P J Silverman *Appl. Phys. Lett.* **48** 1597 (1986)

53. G Binnig, H Rohrer, Ch Gerber, E Weibel *Surf. Sci.* **131** L379 (1983)
54. W Hosler, R J Behm, E Ritter *IBM J. Res. Devel.* **30** 403 (1986)
55. V M Hallmark, S Chiang, J F Rabolt, J D Swalen, R J Wilson *Phys. Rev. Lett.* **59** 2879 (1987)
56. J Wintterlin, J Wiechers, H Brune, T Gritsch, H Hofer, R J Behm *Phys. Rev. Lett.* **62** 59 (1989)
57. C J Chen *Phys. Rev. Lett.* **65** 448 (1990)
58. E Tekman, S Ciraci *Phys. Rev. B.* **42** 1860 (1990)
59. ChWoll, S Chiang, R J Wilson, P H Lippel *Phys. Rev. B* **39** 7988 (1989)
60. J V Barth, H Brune, G Ertl, R J Behm *Phys. Rev. B* **42** 9307 (1990)
61. T Gritsch, D Coulman, R J Behm, G Ertl *Surf. Sci.* **257** 297 (1991)
62. J K Gimzewski, R Berndt, R R Schlittler *J. Vac. Sci. Technol. B* **9** 897 (1991)
63. J F Wolf, B Vicenzi, H Ibach *Surf. Sci.* **249** 233 (1991)
64. J W M Frenken, R J Hamers, J E Demuth *J. Vac. Sci. Technol. A* **8** 293 (1990)
65. R Wiesendanger, H J Gunhterodt *Surf. Sci.* **235** 1 (1990)
66. N M D Brown, H-X You *Surf. Sci.* **233** 317 (1990)
67. J Wintterlin, H Brune, H Hofer, R J Behm *Appl. Phys. A* **47** 99 (1988)
68. H Brune, J Wintterlin, G Ertl, R J Behm *Europhys. Lett.* **13** 123 (1990)
69. E Kopatzki, R J Behm *Surf. Sci.* **245** 255 (1991)
70. D F Olgetree, R Q Hwang, D M Zeglinski, A Lopez Vazquez de Parga, G A Samorjai, M Salmeron *J. Vac. Sci. Technol. B* **9** 886 (1991)
71. R Q Hwang, D M Zeglinski, A Lopez Vazquez-de-Parga *Phys. Rev. B* **44** 1914 (1991)
72. B Marchon, P Bernhardt, M E Bussel *Phys. Rev. Lett.* **60** 1166 (1988)
73. S Chiang, R J Wilson, C M Mate, H Ohtani *J. Microsc.* **152** 567 (1988)
74. V M Hallmark, S Chiang, Ch Woll *J. Vac. Sci. Technol. B* **9** 1111 (1991)
75. P H Lippel, R J Wilson, M D Miller *Phys. Rev. Lett.* **62** 171 (1989)
76. J K Gimzewski, E Stoll, R R Schlitter *Surf. Sci.* **181** 267 (1987)
77. G A Somorjai *Catal. Lett.* **12** 17 (1992)
78. J Wintterlin, R Shuster, D J Coulman, G Ertl *J. Vac. Sci. Technol. B* **9** 902 (1991)
79. F Besenbacher, F Jensen, E Lagsgaad, K Mortensen, I Stensgaard *J. Vac. Sci. Technol. B* **9** 874 (1991)
80. F Jensen, F Besenbacher, E Lagsgaad, I Stensgaard *Phys. Rev. B* **42** 9206 (1990)
81. F M Chua, Y Kuk, P J Silverman *Phys. Rev. Lett.* **63** 386 (1989)
82. Y Kuk, F M Chua, P J Silverman *Phys. Rev. B* **41** 12393 (1990)
83. R Feidenhansl, F Grey, M Nielsen, F Besenbacher, F Jensen, E Langsgaad, I Stensgaard, K W Jacobsen, J K Norskov, R L Johnson *Phys. Rev. Lett.* **65** 2027 (1990)
84. F Jensen, F Besenbacher, E Lagsgaad, I Stensgaard *Surf. Sci.* **259** L774 (1991)
85. R Shuster, J V Barth, G Ertl. *Surf. Sci.* **247** L229 (1991)
86. T Michely, G Comsa *Surf. Sci.* **256** 217 (1991)
87. T Michely, G Comsa *J. Vac. Sci. Technol. B* **9** 862 (1991)
88. J K Gimzewski, A Humbert, J G Bednorz, B Reihl *Phys. Rev. Lett.* **55** 951 (1985)
89. D D Chambliss, R J Wilson *J. Vac. Sci. Technol. B* **9** 928 (1991)
90. J V Lyding, J S Hubachek, G Gammie, S Scala, R Brockenbrough, J R Shapley, M P Keyes *J. Vac. Sci. Technol. A* **6** 363 (1988)
91. D W Abraham, K Sattler, E Ganz, H J Mamin, R E Thompson, J Clarke *Appl. Phys. Lett.* **49** 853 (1986)
92. E Ganz, K Sattler, J Clarke *Surf. Sci.* **219** 33 (1989)
93. U Muller, K Sattler, J Xhie, N Venkatesvaran, G Raina *J. Vac. Sci. Technol. B* **9** 829 (1991)
94. A Humbert, M Dayez, S Sanday, C L Chapon, C R Henry *J. Vac. Sci. Technol. A* **8** 311 (1990)
95. S Eppell, G S Chottiner, D A Scherson, G Pruett *Langmuir* **6** 1316 (1990)
96. A Humbert, M Dayez, S Granjeaud, P Ricci, C L Chapon, C R Henry *J. Vac. Sci. Technol. B* **9** 804 (1991)
97. Y Z Li, R Reifenberger, E Choi, R P Andres *Surf. Sci.* **250** 1 (1991)
98. C Becker, Th Fries, K Wandelt, U Kreibig, G Schmid *J. Vac. Sci. Technol. B* **9** 810 (1991)
99. L E C Van de Leemput, J W Gerritsen, P H H Rongen, R T M Smokers, H A Wierenga, H van Kempen, G Schmid *J. Vac. Sci. Technol. B* **9** 814 (1991)
100. B Keita, L Nadjo *Surf. Sci.* **254** L443 (1991)
101. D Sarid, T Henson, L S Bell, C J Sandrof *J. Vac. Sci. Technol. A* **6** 424 (1988)
102. R J Wilson, G Mejer, D S Bethune, R D Johnson, D Chambliss, M S de Vries, H E Hunziker *Nature (London)* **348** 621 (1990)
103. J L Wragg, J E Chamberlain, H W White, W Kratchmer, D R Huffman *Nature (London)* **348** 623 (1990)
104. Y Zhang, X Gao, M J Weaver *J. Phys. Chem.* **96** 510 (1992)
105. S E Gilbert, J H Kennedy *J. Electrochem. Soc.* **135** 2385 (1988)
106. K Itaya, E Tomita *Chem. Lett.* **2** 285 (1989)
107. F-R Fan, A J Bard *J. Phys. Chem.* **94** 3761 (1990)
108. S E Gilbert, J H Kennedy *Surf. Sci.* **225** L1 (1990)
109. K Sakamaki, S Matsunaga, K Itoh, A Fujishima, Y Gohshi *Surf. Sci.* **219** L531 (1989)
110. G S Rohrer, V E Henrich, D A Bonnell *Science* **250** 1239 (1990)
111. G S Rohrer, D A Bonnell *Surf. Sci.* **247** L195 (1990)
112. Y B Zhao, Tz-S Lin, Y-W Chung *J. Catal.* **125** 207 (1990)
113. H Ch Wang, D F Olgetree, M Salmeron *J. Vac. Sci. Technol. B* **9** 853 (1991)
114. K Asakura, Y Iwasawa, S K Purnell, B A Watson, M A Barteau, B C Gates *Catal. Lett.* **15** 317 (1992)
115. M Komyama, S Morita, N Micoshiba *J. Microsc.* **152** 197 (1988)
116. W Hanreider, A Scholz, H Meixner *Surf. Sci.* **243** 166 (1991)
117. K L Yeung, E E Wolf *J. Vac. Sci. Technol. B* **9** 798 (1991)
118. K L Yeung, E E Wolf *Catal. Lett.* **12** 213 (1992)
119. W M Heckl, F Ohnesorge, G Binnig, M L Specht, M Hashmi *J. Vac. Sci. Technol. B* **9** 1072 (1991)
120. G W Stupian, M S Leung *Appl. Phys. Lett.* **51** 1560 (1987)
121. M Weimer, J Kramar, C Bai, J D Baldescwiller, W J Kaiser *J. Vac. Sci. Technol. A* **6** 336 (1988)
122. T R Coley, W A Goddard III, C Baldescwiller *J. Vac. Sci. Technol. B* **9** 470 (1991)
123. X R Qin, D Yang, R F Frindt, J C Irwin *Phys. Rev. B* **44** 3490 (1991)
124. R Schlogl, R Wiesendanger, A J Baiker *J. Catal.* **108** 452 (1987)
125. F Besenbacher, E Lagsgaard, I Stensgaard, P Stoltze, H Topsoe *Catal. Lett.* **8** 273 (1991)
126. B A Cowans, K A Jurman, W N Delgass, Y Z Li, R Reifenberger, T A Koch *J. Catal.* **125** 501 (1990).
127. P Gallezot, S Tretjak, Y Christidis, G Mattioda, A Schouteeten, Y-W Chung, T S Sriran *Catal. Lett.* 13 305 (1992)

Russian Chemical Reviews **62** (5) 419–435 (1993)
© 1993 Russian Academy of Sciences and Turpion Ltd

UDC 541.67:541.142

The fullerenes — new allotropic forms of carbon: molecular and electronic structure, and chemical properties

V I Sokolov, I V Stankevich

Contents

I.	Introduction	419
II.	Topological and metric characteristics of polyhedral carbon clusters	420
III.	Quantum chemistry of the fullerenes	421
IV.	Mechanism of formation of the fullerenes and of endohedral complexes	428
V.	Classification of the forms of carbon with a regular structure	429
VI.	Chemical properties of carbon clusters	430
VII.	Conclusions	433

Abstract. In the early 1970s Osawa (and also Bochvar and Gal'pern) theoretically discussed the possibility of the existence of polyhedral carbon clusters, and predicted some of their properties. In 1985 it was established by spectral methods that carbon clusters containing an even number of atoms (mainly C_{60} and C_{70}) are formed under certain conditions when graphite is evaporated under the influence of laser radiation. These discoveries stimulated extensive studies of the synthesis of polyhedral carbon clusters of various molecular masses, and descriptions of their molecular and electronic structure and of their chemical properties. The most important results achieved in these areas of research are reviewed. The bibliography contains 194 references.

I. Introduction

A remarkable discovery in the chemistry of one of the best known of all the elements (carbon) was reported during the late 1980s. A group of workers, including Kroto (UK, Sussex University) and Heath, O'Brien, Curl, and Smalley (USA, Rice University),[1] studied the mass spectra or graphite vapour obtained by laser irradiation of a solid sample and observed peaks corresponding to masses 720 and 840. They suggested that these peaks correspond to the individual molecules C_{60} and C_{70}, and that the C_{60} molecule is a truncated icosahedron with an I_h symmetry while C_{70} is a more extended structure with an ellipsoidal (D_{5h}) symmetry type (Figures 1 and 2). This paper was followed by a report[2] of the observation of a peak with $m/e = 859 = (720 + 139)$ in the mass spectrum of the vapour of graphite doped with La atoms, from which it was concluded that the internal cavity of the spheroidal C_{60} molecule can incorporate a lanthanum atom with formation of the endohedral La @ C_{60} complex. Both these hypotheses were subsequently confirmed quite unambiguously.

V I Sokolov, I V Stankevich A N Nesmeyanov Institute of Organoelement Compounds, Russian Academy of Sciences, ul Vavilova 28, 117813 Moscow. Fax (7-095) 125 50 85

Received 14th January 1993
Uspekhi Khimii **62** (5) 455–472; translated by J I Carasso

Polyhedral carbon clusters were called fullerenes [and their prototype, C_{60}, buckminsterfullerene (BF)] from the name of the distinguished American architect Richard Buckminster Fuller (1895–1983).† The publication of these results stimulated wide-ranging studies of the spectroscopic and other physical properties of the structure of fullerene[3] clusters.

The next step forward was taken in 1990 by Krätschmer, Lamb, Fostiropoulos, and Huffman,[4] who developed a method of preparing gramme quantities of carbon clusters by burning graphite electrodes in an electric arc in a helium atmosphere at an optimised (subatmospheric) pressure. In a study of the preparative conditions of carbon clusters in specific assemblies it was shown that the deposited soot contains a mixture of these clusters, which can be separated by extraction. As reported,[5–7] the content of carbon clusters can vary between 3% and 44%. The most selective method of separating the carbon clusters is by successive extraction with different solvents.[5] The clusters isolated in this way included molecules containing up to 200 carbon atoms. The ratio of the main components (C_{60}/C_{70}) is usually $(80 \pm 5)/(20 \pm 5)$. Approximately 1% of the graphite black consists of the heavier clusters. Other workers[6,7] detected even heavier carbon clusters in graphite black, as well as the oxide $C_{60}O$.

The most laborious part of the process is the separation of the components, since as a result of the very small structural differences between the components the properties of the various polyhedral carbon clusters such as solubility and adsorbability are also very similar. Separation can be achieved only by column or liquid chromatography methods, which are time-consuming as well as requiring large amounts of solvents.[8,9] These methods can separate some of the higher fullerenes as well as C_{60} and C_{70}.[10] However, some important technical improvements have now been introduced into the processes: these offer a faster separation, a better yield of pure products, and a more modest consumption of solvents.[11–14].

The detection of polyhedral carbon clusters in the soot deposits formed by burning benzene and other hydrocarbons[15] was unexpected. The ratio of the main components varies according to the combustion conditions, and the proportion of C_{70} can be as high as 85%. However, it has not yet been established whether this method is of preparative value.

† The C_{60} cluster, of icosahedral I_h symmetry, has the shape of a truncated icosahedron, similar to a football. Therefore this cluster has also been called carbo-*s*-icosahedron, footballene, or soccer ball.

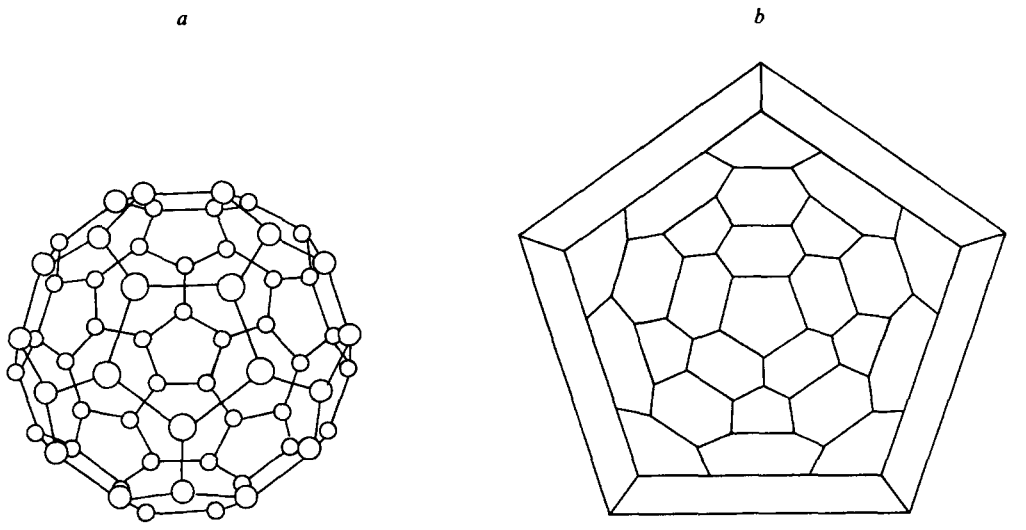


Figure 1. I_h-C_{60} carbon cluster (*a*) and its molecular diagram (*b*).

These methods of preparative synthesis of carbon clusters made a substantial number of fullerenes available to researchers and made possible the detailed study of their physical and chemical properties. Various derivatives of the fullerenes were also produced. Papers describing the synthesis of crystalline samples of C_{60} and of doped systems of the A_nC_{60} type attracted special attention. The salts of BF with alkali metals (n = 3) have superconducting properties at T_c = 18 K (A = K) and at T_c = 28 K (A = Rb).[16,17] Some reports of the preparation of superconducting doped fullerenes with higher values of T_c have not been confirmed. The highest adequately reproducible critical temperature T_c so far reported for the fullerene series is 33 K (for the caesium–rubidium salt Cs_2RbC_{60}).[18]

The main aim of the present review is to assess the current state of research on the molecular and electronic structure and on the chemical properties of the fullerenes (with the use of information available up to the second half of 1992). Because of the wide scope and of the rapidly increasing number of publications on this topic the review cannot claim to be exhaustive. Several reviews of the fullerenes have already appeared,[19,20] but it is difficult to disagree with the statement[21] that any such review should be treated as out of date even on the day of its publication unless transmitted by electronic mail. However, the conceptual and the analytical parts of recent publications should be of more lasting value.

II. Topological and metric characteristics of polyhedral carbon clusters

Various convex polyhedra are used to model the structure of carbon clusters. The topological characteristics of the clusters, defined by systems of two-centre carbon–carbon bonds, are described in terms of these polyhedra. However, it follows from the theory of valency that not all polyhedra are equally suitable for describing the carbon skeleton. The most successful for this purpose[22] are the polyhedra with faces consisting of five-, six-, seven-, or possibly eight-membered rings.‡

We shall call F the number of faces of the polyhedron, V the number of vertices, and E the number of edges. A simple relationship, known as Euler's theorem, exists between these quantities: $V+F-E = 2$. According to the theory of valency each carbon atom in the polyhedral cluster should have either three or two neighbours. It follows that in the topological method of modelling these structures the choice of polyhedra can be confined to figures in which all the vertices have an order of three. These polyhedra can be represented as planar uniform molecular diagrams of order three. By placing new vertices on some of their edges we obtain molecular diagrams which describe the topology of carbon clusters containing atoms with a coordination number of two.[23] Polyhedra with a greater number of vertices are difficult to represent clearly as three-dimensional figures. Therefore planar images (Schlegel diagrams) are used to describe the higher fullerenes. Two diagrams of this type are shown in Figures 1 and 2 for the clusters C_{60} (truncated icosahedron) and C_{70}. We shall denote as n_i the number of faces having i angles. In this case the following equality applies to polyhedra of this class:

$$3n_3 + 2n_4 + n_5 = 12 + n_7 + 2n_8 + 4n_{10} + \ldots$$

It follows directly from this formula that if the faces of a convex polyhedron in which all the vertices are of order three consist exclusively of five- and six-membered rings we must have n_5 = 12. In other words any polyhedron of this type [(5,6)-polyhedron] has not less than 20 vertices, and contains 12 five-membered rings.§ Furthermore the following formulae, which apply to the system, can be useful for discussing the topology of the clusters:

$$2E = 3V, \quad 2E = \sum jn_j, \quad n_6 = \tfrac{1}{2}V - 10 - 2n_7$$

(for polyhedra with faces consisting of five-, six-, and seven-membered rings respectively).

(5,6)-Polyhedra in which none of the pentagonal faces are contiguous are of special interest from the chemical point of view. The truncated icosahedron has the smallest number of vertices among the polyhedra of this class (V = 60).

The other criteria used in the selection of polyhedra and useful for describing the carbon skeletons are based on an analysis of their metric characteristics, consistent with the topology of the polyhedron. These characteristics include the length of the edge and the angles between the edges and between the faces. The values of these parameters, calculated for polyhedra with an ideal geometry, are used to determine the size of the corresponding carbo-polyhedra and to infer the degree of strain of their σ-frame, defined in terms of the distortions of the bond angles from their ideal values.[25–31] Table 1 shows the geometric characteristics of three polyhedra: the dodecahedron, the *s*-octahedron, and the *s*-icosahedron.

‡ We know that in some polyhedra all of the faces are regular polygons. If all these polygons are equal the resulting polyhedron is called Platonic or regular. If some of the faces are different, though formed by regular polygons, the polyhedron is called Archimedean or semiregular.[24]

§ The dodecahedron is the simplest member of the family of (5,6)-polyhedra, with n_6 = 0 six-membered rings.

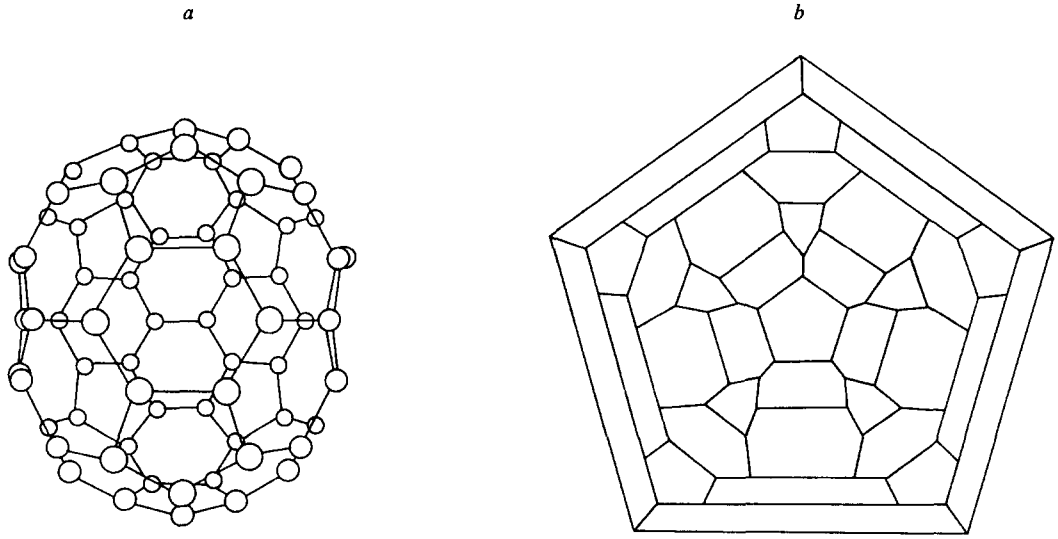


Figure 2. D_{5h}-C_{70} carbon cluster (*a*) and its molecular diagram (*b*).

We shall now examine in more detail some of the methods of constructing polyhedra to be used in the molecular modelling of the structure of carbon clusters.

The triangulation method.
Methods of designing carbon clusters of icosahedral symmetry have been discussed in several papers.[27,29,32,33] These clusters are conveniently generated by the triangulation of a sphere circumscribed about the icosahedron. The first stage is the triangulation of each face of the regular icosahedron, which divides it into small equilateral triangles. This procedure is described in terms of two integers b and c, with $b \geqslant c \geqslant 0$, and leads to a triangulation of the sphere containing V vertices: $V = 20(b^2+bc+c^2)$. Among these vertices 12 have a degree of five, and the remainder have a degree of six. If $b = c$, or $bc = 0$, the deltahedron¶ corresponding to this sphere has the I_h symmetry group. In other cases the polyhedra have the I symmetry group. Furthermore by joining the centres of adjacent faces we convert the deltahedron into a dual polyhedron: a (5,6)-polyhedron of icosahedral symmetry. In this way we can model the structures of giant fullerenes of icosahedral form. The method can also be used to model the structure of clusters of tetrahedral and even lower symmetry groups.[33] Figure 3 shows the self-repeating fragments of some of the icosahedral clusters with a large number of vertices.

The method based on the triangulation of a sphere is widely used in geodesy and in architecture. The general principles governing the application of this approach to the construction of geodesic domes were formulated by R Buckminster Fuller. The structure of the C_{60} cluster can be interpreted as the combination of two hemispheres covered with a network of five- and six-membered rings.

The leapfrog method.
The method of constructing carbo-polyhedra now known as the leapfrog method was proposed by Fowler.[34] Its application involves starting, for example, from a (5,6)-polyhedron with a relatively small number of vertices. A new vertex is then inserted at the centre of each face of the polyhedron, and connected (by new edges) to the nearest existing vertices. The next stage produces a dual polyhedron. This procedure yields a polyhedron with a number of vertices three times greater than in the original polyhedron. The essential features of the leapfrog method are illustrated in Figure 4.

¶ The term deltahedron denotes a polyhedron in which all the faces are triangular.

The petal method.
This method of constructing polyhedra was proposed for the modelling of structures having an axis of symmetry of fairly high order (5, 6, or 7). It relies on the construction of a self-repeating fragment consisting of several condensed rings. The fragments (or petals) are then interconnected to form new faces (Figure 5). The petal method has also been used in the design of chiral and of polar carbo-polyhedra.[28,29,35]

The spiral method.
This method relies on representing the structure of a polyhedron as a planar diagram in which the vertices lie on concentric circles. In this case the structure of the polyhedron can be coded as a sequence of numbers denoting the size of the rings met along a spiral path which begins at the central ring and then passes in turn through the faces of the neighbouring rings.[36] A path of this type for the C_{60} cluster is illustrated in Figure 6. To progress from the topological description of the carbon clusters to a more detailed analysis of their structure and to a prediction of their physicochemical properties we must apply physicochemical methods such as those of quantum chemistry and of molecular mechanics.

III. Quantum chemistry of the fullerenes

The quantum-chemical models of carbon clusters of the polyhedral type described in papers published up to 1985 were based on classical convex polyhedra (the dodecahedron and the truncated icosahedron).[25,37,42] The π-electron model, known to be a convenient method of describing planar conjugated hydrocarbons and their hetero analogues,[43] has been applied to the C_{20} (carbo-dodecahedron) and C_{60} (carbo-*s*-icosahedron) carbon clusters. Strictly speaking a π electron system cannot exist in a polyhedral molecule, which is non-planar and has an approximately spherical surface. However, the bonds in a carbo-polyhedron can be described by the following procedure, which is used in classical (planar) conjugated systems: each carbon atom contributes three hybrid orbitals and three electrons to the formation of three two-electron (localised) σ-bonds with neighbouring atoms. The fourth electron is placed in a hybrid ρ-orbital orthogonal to the three σ-orbitals oriented along the bonds to the neighbouring atoms.[25,29,31] Bochvar et al.[25,38,39] discussed the structure of the ρ-electron system by using the Hückel approximation in conjunction with the concepts adopted in that theory to describe the classical π-electron systems.

Table 1. Some geometric characteristics of polyhedra.[30]

Characteristic	Dodecahedron	*s*-Octahedron	*s*-Icosahedron
Number of vertices	20	24	60
Number of faces	12 pentagons	6 quadrangles + 8 hexagons	12 pentagons + 20 hexagons
Diameter of inscribed sphere (for a CC bond length of 1.40)	3.118	3.429	6.348
Angle between edges and radius vector/°	110.90	108.26	101.65

Some relevant aspects of the Hückel theory should be stressed in order to make clear the significance of the results obtained in the many calculations of carbo-polyhedra in the ρ approximation published in the last 5–7 years. We should note first of all that the Hückel method is essentially topological. In its simplest variant it merely takes account of the nature of nearest neighbours (i.e. of the presence of chemical bonds) and ignores the metric characteristics of the molecule. Two empirical parameters are used in the Hückel method: the Coulombic (α) and the resonance integral (β). These quantities are used to describe the Hamiltonian for the π-electron system and to calculate the one-electron energy levels ε_i as the linear functions

$$\varepsilon_i = \alpha + x_i\beta,$$

where x_i are the characteristic numbers of the molecular diagram which describes the σ skeleton of the carbo-polyhedron. Energy levels with $x_i > 0$ are called bonding, and those with $x_i < 0$ are called antibonding. The energy level $\varepsilon_i = \alpha$ is called nonbonding. A similar terminology is used for the molecular orbitals (MO).

The fundamental concept of the Hückel theory is the formation of closed electron shells. This property is found in systems in which all the bonding MO are doubly occupied in the ground state, and the nonbonding and antibonding energy levels are vacant. If the molecule in the ground state possesses unoccupied as well as doubly occupied bonding orbitals the system is said to have a pseudo-closed shell. The presence of a closed electron shell denotes a kinetically stable system. The stability usually increases with the width of the energy gap $\Delta\varepsilon$ which separates the antibonding from the bonding energy levels. The systems which contain unoccupied bonding energy levels can have an increased tendency towards the formation of anions. The presence of occupied antibonding energy levels stabilises the oxidised forms. The case of an occupied nonbonding level usually requires a more detailed analysis.

Various form of resonance energy are used, in addition to the delocalisation energy, to calculate the stabilisation of the ρ-electron systems of carbo-polyhedra: these include the topological resonance energy,[29,44,45] the resonance energy of Hess and Schaad,[46] calculated by the fused rings method,[47] and some other similar characteristics. All these quantities are commonly used to determine the degree of aromaticity of classical conjugated hydrocarbons. However, these calculations have also been used[27–29,48,49] to establish the relative stability of unsaturated polyhedral carbon clusters.

Since 1985, when the original paper by Kroto et al.[1] was published, the fullerene problem has stimulated increasing theoretical interest. Many studies by quantum-chemical methods in various approximations of the electronic structure of footballene (I_h-C_{60}) were published, as well as studies of its isomers, anions, cations, and of polyhedral carbon clusters with different numbers of atoms, including the higher fullerenes. Calculations were made in the restricted and the expanded Hückel,[26–34,36–39,42,48–64] MNDO,[64–71] and AMI methods,[72–74] in the nonempirical MO LCAO SCF method in different basis sets,[71,73,75–77] in the CNDO[30,39,78] and INDO methods,[79] and in the Pariser–Parr–Pople method allowing for configuration interaction,[80–82] the X_α method,[83,84] and the methods of molecular mechanics with estimates of the vibration frequencies.[83–89] We shall examine in some detail some of these papers, highlighting those which appear to have played a dominant role in our understanding of the special features of the chemical structure of polyhedral carbon clusters.[29,36,66,69]

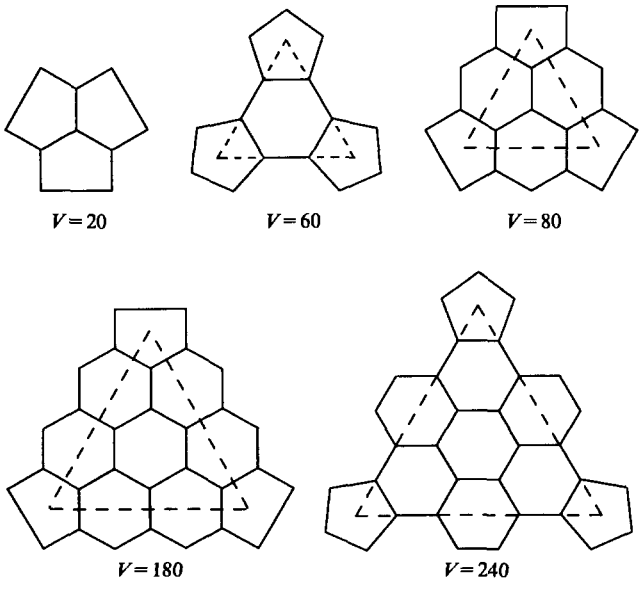


Figure 3. Self-repeating fragments of some icosahedral clusters.

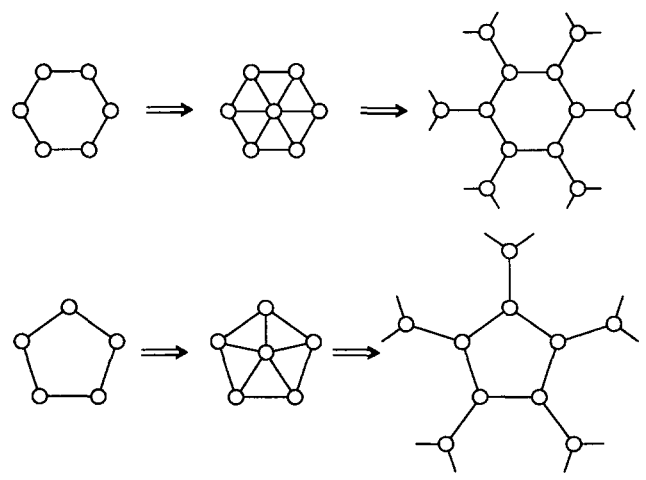


Figure 4. Scheme illustrating the construction of the higher fullerenes by the addition of one corner at the centre of each face of the initial (5,6) polyhedron.

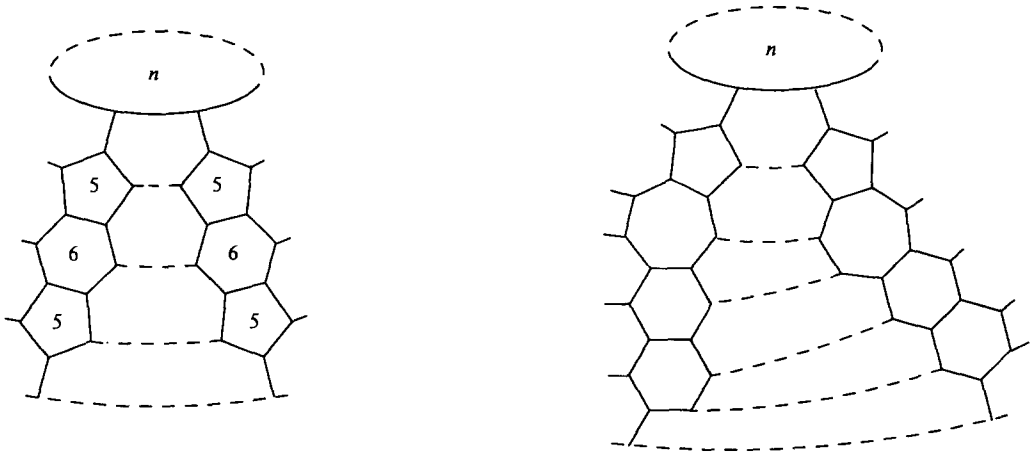


Figure 5. Examples of the basic fragments used in the design of carbon clusters with 5th- and 6th-order symmetry axes.

Schmalz and coworkers[29] developed a simple method of designing polyhedral structures with the D_{nd} and D_{nh} symmetry groups and used it to model the electronic structure of more than 30 carbon clusters of that type in the topological approximation. An analysis of their results[29] led to the formulation of several rules governing the stabilisation of polyhedral structures. The following are the most important:

1. Stable carbon clusters are polyhedra in which each carbon atom has a coordination number of 3.
2. The carbo-polymers containing only five- and six-membered rings are the most stable.
3. The most symmetric carbon clusters are the most stable.
4. Five-membered rings in the polyhedra should be isolated.
5. The shape of the carbo-polymers should be approximately spherical.

Some corollaries of these rules should be noted. For example, it follows from the first rule that the number of vertices in the cluster should be even (odd clusters of larger size have not been reported), and from the second rule we conclude that any polyhedron in this class should contain exactly 12 pentagons. No limit is placed on the number of hexagons. Footballene (I_h-C_{60}) is the smallest cluster which satisfies the fourth rule.

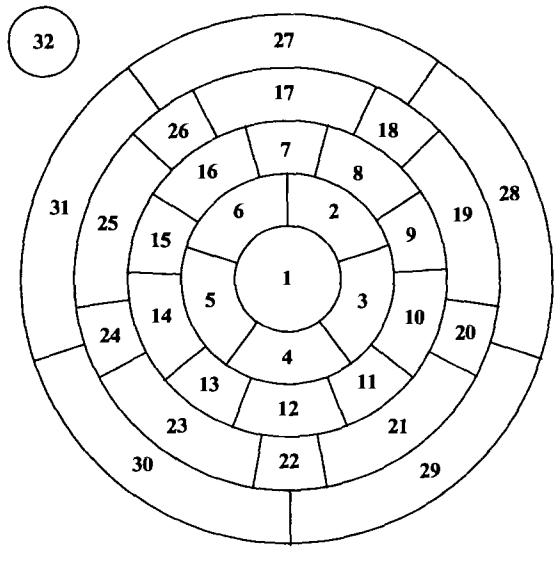


Figure 6. Structures of the I_h-C_{60} cluster coded with a system of concentric rings. Faces numbered clockwise in a spiral path. The code for the I_h-C_{60} cluster is 566 666 565 656 565 665 656 565 656 666 65. The first number of this code is the number of sides of the ith face. The last number corresponds to the infinite face of the molecular diagram [D E Manolopoulos, J C May, S E Down *Chem. Phys. Lett.* **181** 105 (1991)].

The number of isomers of the polyhedral C_n structures should increase rapidly with the number of atoms, even if only the (5,6)-polyhedra are considered. The C_{20} carbododecahedron has no isomers in this class of polymers, but (for example) in the polymer with $n = 78$ we find 21 822 isomers. Therefore the listing of all possible polyhedral structures with a given number of atoms is not an easy problem. The problem becomes even more complex when *a priori* estimates of the energetic and of the spectral characteristics of these structures are required. Hückel's topological approximation is often used as a rapid method of analysis, and the most probable structures are identified as a result of these calculations and studied in more detail. Papers in which Hückel's method is used account for a substantial proportion of the theoretical publications on the electronic structure of carbon clusters. Therefore it is natural to ask to what extent the Hückel approximation is suitable for solving problems in the structural chemistry of the fullerenes.

Let us consider, in this context, the results of some studies which are not only of intrinsic interest but also confirm the usefulness of the Hückel method for analysing the properties of carbon clusters. We note first of all that in the case of the most widely studied cluster (C_{60}) all the higher-level methods of calculation give a scheme of one-electron energies similar to that given by the Hückel method.[20]

Newton and Stanton[66] reported calculations on footballene and on some other carbon clusters by the MNDO method. In the case of C_{60} the authors[66] analysed the structure of the frontier orbitals and established that the HOMO are functions consisting (to within 97%) of the radial p-orbitals of the carbon atoms.

Bakowies and Thiel[69] studied approximately 30 carbon clusters of very different structure: clusters of icosahedral and of tetrahedral symmetry, and spherical or barrel-shaped clusters with groups of D_{nd} and D_{nh} symmetry. The choice of the systems was largely dictated by the results of MNDO calculations with full optimisation of the geometry. The structures examined included a giant C_{540} cluster of icosahedral symmetry. Schmalz et al.[29] determined the geometric characteristics and the heats of formation of the clusters. They found that the heats of formation of some of these carbon superclusters are directly proportional to the energy of delocalisation calculated by the Hückel approximation, which includes corrections for the resonance integrals (associated with the deviation of the cluster structure from a spherical form).

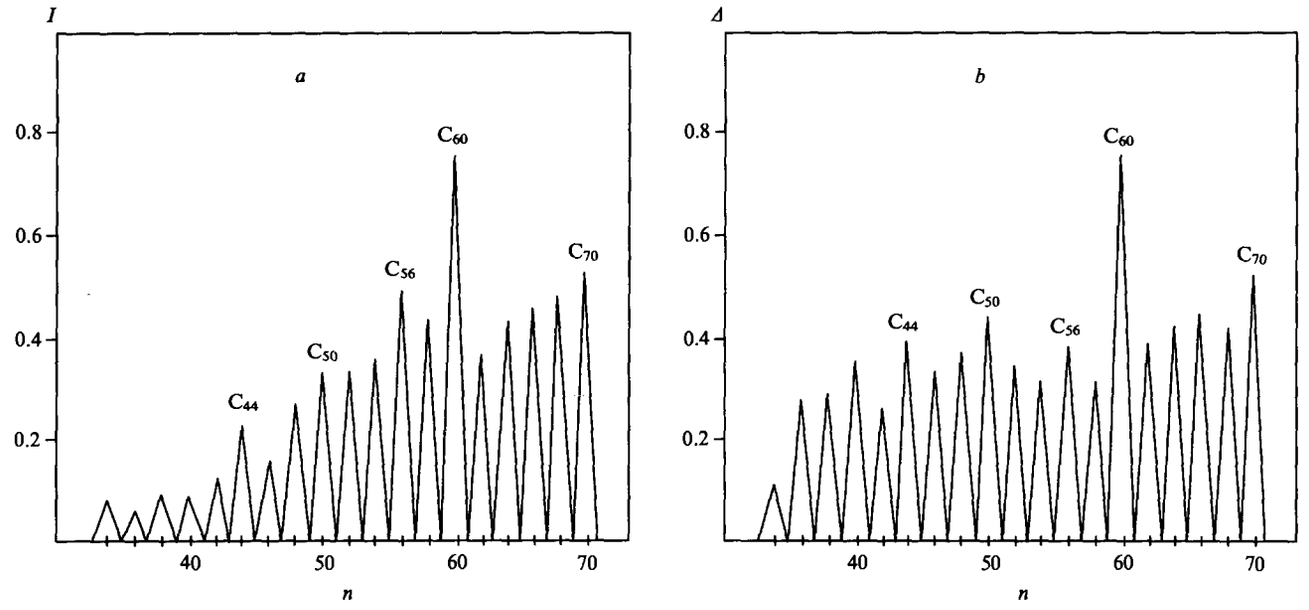


Figure 7. Relative intensities in the mass spectra of the C_n carbon clusters for $34 \leqslant n \leqslant 70$ (*a*). Energy gaps separating the filled from the empty energy levels (in the ground state) of the C_n clusters (*b*). The width Δ of these energy gaps was calculated in the topological approximation by the Hückel method and expressed in units of the resonance integral β.

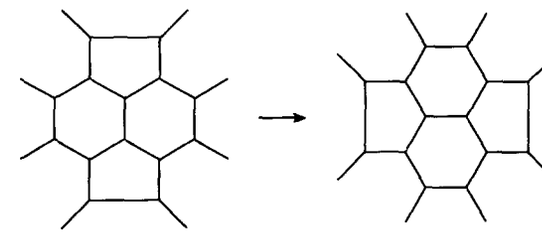
An interesting paper by Manolopoulos et al.[36] reports a correlation between the intensities of the mass spectra of the ions obtained from C_n^+ carbon clusters, where $34 \leqslant n \leqslant 70$, produced by laser evaporation of graphite, and the values of the energy gap $\Delta\varepsilon$ in the ρ-electron spectra calculated by the simple Hückel method for the corresponding fullerenes (Figure 7). Among all the possible isomers of the C_n clusters they chose those with the largest energy gap $\Delta\varepsilon$.

It is clear from this brief analysis that in systems of the polyhedral type with an almost spherical form it is convenient to use the Hückel approximation, since this method gives valuable information on the electronic properties of the systems. Let us examine in greater detail some of the characteristics of the geometry and of the electronic structure of the C_{60} and C_{70} clusters and of carbo-polyhedra with a greater number of atoms, and also of endohedral complexes.

1. C_{60} clusters

Many isomers can be constructed from 60 carbon atoms: one of these is the I_h-C_{60} cluster. Its geometric characteristics were established by electron diffraction[92] and X-ray structural analysis† (the structure of the osmium derivatives has been reported[93]), and calculated by various quantum-chemical methods.[49,54,66,68,72,73,75,76] Bonds of two types are found in the I_h-C_{60} cluster: r_1, specific to the five-membered rings, and r_2, common to the pentagonal and the hexagonal faces. All the methods of calculation indicate an alternation of the two bond lengths (r_1 and r_2), in keeping with the experimental results ($r_1 = 1.401$, $r_2 = 1.456$ Å).[92,93] The C_{60} isomers can be constructed in different ways. For example, from the dodecahedral C_{20} structure a new structure (C_{60}) consisting of three-membered and ten-membered rings can be obtained by truncating the vertices. A series of C_{60} isomers was generated by the petal method.[29] Isomers of the fullerene type can be obtained from I_h-C_{60} as a result of Stone–Wales regrouping in the pyracyclene fragments.[63] However, this operation leads to the appearance in the new isomer structures of adjacent five-membered rings (pentalene fragments), which destabilise the carbon cluster.

† H B Burgi, E Blanc, D Schwarzenbach, S Liu, Y Lu, M M Kappes, J A Ibers *Angew. Chem.* **104** 667 (1992).



It follows from the results of extensive theoretical studies that the icosahedral BF structure is the most stable of the polyhedral C_{60} isomers. The stability of the I_h-C_{60} footballene is usually attributed to the presence of 12 equivalent (partially overlapping) corannulene structural fragments, each containing a five-membered ring surrounded by five hexagons, which ensure that the pentagons are mutually isolated. Qualitative considerations indicating instability of structures containing adjacent five-membered rings are confirmed by calculations[71] by the semiempirical MNDO method and by the nonempirical MO LCAO SCF method in the two-exponential 3-21G basis, applied to C_{60} isomers containing two, three, and four pairs of adjacent five-membered rings. It was established that the most stable isomer of this type has a C_{2v} symmetry and an energy 2 eV higher than the energy of the I_h-C_{60} isomer. Each pair of adjacent five-membered rings makes approximately the same contribution (1.0 ± 0.2 eV) to the destabilisation energy of the I_h-C_{60} structure.

The effect of the pentalene fragments on the stability of the C_{60} isomers was discussed by Stanton[70] in relation to the photodissociation reactions of the C_{60} cluster, and also of some other carbon clusters studied by O'Brien et al.[94] MNDO calculations of the equilibrium geometry, of the heats of formation, and of the ionisation potentials of several carbon clusters (C_{62}, C_{60}, C_{58}, C_{56}, C_{54}, C_{52}, and C_{50}) have also been reported.[70] Estimates of the heats of isomerisation of these polyhedral clusters by the Stone–Wales mechanism have been obtained, as well as estimates of the heats of elimination of the C_2, C_4, and C_6 fragments from footballene (C_{60}) and from the C_{62} cluster. These calculations also confirm the conclusion that the presence of pentalene fragments destabilises the carbon clusters. It was found that the elimination of C_2 from the C_{62} cluster is strongly endothermic ($\Delta H = 99$ kcal mol^{-1}), but the heat of this

reaction is much smaller than that of the reaction $C_{60} \rightarrow C_{58} + C_2$ (ΔH = 273 kcal mol^{-1}). We also note that the same workers[70] described the structure of one of the most stable polyhedral isomers of C_{30}.

These results indicate that the structure of footballene is more stable than that of its polyhedral isomers. However, under certain conditions other isomers can also exist as metastable high-energy species. It has been shown[95] that a series of C_{60} isomers is present in the flame produced by the combustion of benzene.

2. Aromaticity of the C_{60} fullerene

The Japanese workers Yoshida and Osawa[37] have proposed a definition of a new class of conjugated molecules, which they called superaromatics. They assigned to this class of compounds molecules of polyhedral form which contain electrons in molecular orbital delocalised on the surface of a three-dimensional structure having an almost spherical symmetry.‡ They suggested as an illustration the hypothetical C_{60} molecule with the structure of a truncated icosahedron. This C_{60} molecule possesses a system of mobile electrons which contributes additional stabilisation to the polyhedron, as in the benzene molecule. Independently of the work of Yoshida and Osawa[37] polyhedral analogues of the classical aromatic systems (containing only carbon) were discussed by Bochvar and Gal'pern.[25,38] They produced[25] the first quantitative estimates of the resonance energy (or delocalisation energy) for this unusual type of conjugated molecule. It was concluded[25] that the C_{60} cluster has a greater resonance energy than the benzene molecule, and that in keeping with the quantum-mechanical criterion of aromaticity the C_{60} molecule should be assigned to a new class of aromatic systems.

We should stress the fact that the term 'aromaticity' has long been used in organic chemistry. It is associated with the presence of a large group of physicochemical properties (listed, for example, by Vol'pin[90]). However, the use of the term aromaticity has always been ambiguous to some extent, depending on whether the main stress of the argument lay on the chemical properties or on the molecular and the electronic structure (compare, for example, the definitions of this term given in Refs 90 and 91).

An analysis of the chemical properties of footballene shows that this molecule cannot be classified as an aromatic compound. Indeed, most of the known derivatives of footballene were prepared by addition reactions at multiple bonds (see Section VI).

However, according to the physical criteria the C_{60} molecule can be assigned to the group of aromatic systems [for example, the C–C bond lengths in C_{60}, though different for the (6, 6) and the (6, 5) bonds, are close to the bond lengths in graphite; furthermore the C_{60} system absorbs light at relatively long wavelengths, has a closed electron shell, and its resonance energy is relatively high].

The resonance energy is often used as a measure of the stability of the system relative to some standard structures. Comparative estimates of the resonance energy of C_{60} have been calculated[29] by different methods: Hückel's method, the methods of Hess and Schaad and of Randic, the conjugated rings method, and some others. The results are consistent with the aromaticity of BF in the sense of the quantum-chemical criteria, though according to most of these criteria the aromaticity of BF is lower than that of benzene.

Thus the aromaticity concept developed for the classical conjugated molecules cannot be applied to molecules of the fullerene type. The term 'pseudoaromaticity' gives a more accurate description of the formation of a single delocalised π-electron system, with a definite energy gain. The most important physical properties of BF are listed below.[18]

Structural data

Cubic crystal structure:
- $Fm\bar{3}m$ (T > 260 K)
- $Pa\bar{3}$ (T < 260 K)

Diameter of carbon cage: 7.1 Å

Bond lengths:
- C=C 1.391 Å,
- C–C 1.455 Å

Nonvalence distance between C_{60} molecules in the crystal: 3.1 Å

Bulk modulus: 18 GPa

Density: 1.65 g cm^{-3}

Spectral characteristics

Electron affinity: 2.6–2.8 eV

Ionisation potential: 7.6 eV

Energy gap: 1.9 eV

^{13}C NMR chemical shift: 142.68 p.p.m.

Vibration frequencies:
- IR: 528, 577, 1183, 1429 cm^{-1}
- Raman: 1250, 1422, 1467, 1573 cm^{-1}

Refractive index: 2.2 (630 nm)

3. The C_{70} cluster

The structure of the C_{70} cluster was determined by electron diffraction[96] and X-ray structural analysis of the iridium derivatives,[97] and calculated by various quantum chemical methods (see, for example, Ref. 77). It was established[96] that the C_{70} cluster has a fullerene structure with an ellipsoidal shape, described by the D_{5h} symmetry group. The C–C bond length varies between 1.37 and 1.47 Å. The shortest bonds are those connecting the vertices of two different pentagons; the longest are found within the five-membered rings. The 'height' of the molecule is 7.8 Å. As reported,[96] the equatorial part of C_{70} has a diameter of 6.94 Å and is narrowed by 0.05 Å. The lengths of the C–C bonds found by the XSA method for the iridium derivative of C_{70}[97] agree on the whole with the values obtained[96] by electron diffraction.

Formally the D_{5h}-C_{70} cluster can be obtained from two halves of the C_{60} cluster by inserting five pairs of carbon atoms in the equatorial plane.

The D_{5h}-C_{70} cluster, like the I_h-C_{60}, contains only isolated five-membered rings. In the spheroidal I_h-C_{60} molecule the carbon atoms are equivalent: they can be readily divided into pairs contributing to the formation of bonds between adjacent five-membered rings, which are equivalent in pairs. The I_h-C_{60} structure can also be described in terms of pyracyclene fragments or fragments of the corannulene type, which are structurally equivalent in pairs. However, the ellipsoidal D_{5h}-C_{70} structure cannot be described in terms of the fragments of a single type defined above. In the D_{5h}-C_{70} molecule corannulene and pyrene structural units can be distinguished in addition to the pyracyclene fragments.

The nonequivalence of the carbon atoms in the C_{70} molecule results in different values of the chemical shifts in the ^{13}C NMR spectra. Five types of atoms are present in the C_{70} molecule, with a corresponding number of signals. The following interpretation of the chemical shifts in the D_{5h}-C_{70} cluster has been proposed:[98] the signal at 130.8 p.p.m. is assigned to the carbon atoms of the ten pyrene fragments, the signals which appear in the range of 147.8–150.8 p.p.m. are assigned to the three different carbon atoms of the pyracyclene fragments, and the signal at 144.4 p.p.m. is assigned to the corannulene carbon atoms.

This interpretation of the chemical shifts in the D_{5h}-C_{70} cluster was used in subsequent work to model the structure of higher fullerenes in terms of their NMR spectra.[10]

‡ An English translation of part of the relevant paper,[37] kindly supplied by Professor Osawa, was used in the preparation of this review.

4. C_n clusters with $n > 70$

As was pointed out above, the number of isomers of the C_n clusters increases rapidly as n increases, even if the analysis is confined to fullerenes containing five- and six-membered rings. However, the number of isomers is greatly decreased if only the clusters which obey the isolated pentagons rule are considered. For C_{78} the number of isomers containing only isolated pentagons is five; for C_{84} it is 24, and for C_{90} it is 46.[55] However, the number of these isomers also increases fairly rapidly as n is increased. Therefore qualitative methods of predicting the structure and the properties of polyhedral clusters containing more than 70 atoms are of interest. One of these methods is based on the Hückel approximation. It was used by Fowler et al.[57,60] to formulate a group of rules analogous to the classical $(4n+2)$ Hückel rule, which must be satisfied by a closed electron shell. The most generally applicable of these rules can be formulated as follows.[60]

Rule 1. The isomers of the C_n clusters with $n = 60+6k$, $(k \geqslant 1)$ include at least one molecule with a closed electron shell for each integral value of k.

Rule 2. The isomers of the C_n clusters having a fifth-order axis of symmetry with $n = 70+30k$ or $n = 84+36k$ include at least one molecule with a closed electron shell for each integral value of $k \geqslant 0$.

Rule 3. The cluster C_{3m} obtained from the cluster C_m by a 'leapfrog' operation has a closed electron shell.

In the presence of a closed electron shell the difference between the HOMO and the LUMO energy ($\Delta\varepsilon$) is often used as a measure of the relative stability of carbon clusters. As was said above, this quantity is sufficiently well correlated with the intensities of the mass spectra of the $C_{34}-C_{70}$ carbon clusters obtained by the laser evaporation of graphite. However, the estimates of the stability of the higher fullerenes based on the width of the energy gap $\Delta\varepsilon$ are not always reliable. Thus, three structures (of D_{6h}, T_d, and D_2 symmetry) have been proposed[60] for the C_{84} cluster. A fourth isomer, of D_{7d} symmetry, was later added to this list.[99] The main parameters of the electronic structure of these four isomers, calculated by Hückel's method, are shown in Table 2.

It can be seen that the energy characteristics of the D_{7d}-C_{84} structure are close to the corresponding values for footballene (C_{60}). Furthermore the energy gap $\Delta\varepsilon$ for D_{7d}-C_{84} differs from the value for footballene by only $0.011\,|\beta|$, and therefore the structure of D_{7d}-C_{84} should be the preferred structure. However, calculations[71] by the MNDO and the nonempirical variant of the MO LCAO SCF method in the 3-21G basis showed that this is not the case. It was established[71] that the three structures of the C_{84} cluster with D_{6h}, T_d, and D_{7d} symmetry actually correspond to local minima on the potential energy surface, and that the D_{6h}-C_{84} structure is more stable than T_d-C_{84} [by 23.4 kcal mol^{-1} (MNDO) or by 18.2 kcal mol^{-1} (*ab initio*)]. Furthermore the energy of the D_{7d}-C_{84} structure is higher by several tens of kcal mol^{-1} than the energy of the T_d-C_{84} structure.

Table 2. Energy characteristics of the C_{84} isomers calculated by the Hückel method.[99]

Cluster	Symmetry	HOMO (β)	LUMO (β)	$\Delta\varepsilon$ ($\lvert\beta\rvert$)[a]	E_d (β)[b]
C_{84}	T_d	0.572	−0.124	0.696	0.559
	D_{6h}	0.529	0	0.529	0.558
	D_2	0.497	−0.117	0.614	0.558
	D_{7d}	0.607	−0.139	0.746	0.556
C_{60}	I_h	0.618	−0.139	0.757	0.553

[a] $\Delta\varepsilon$ is the width of the forbidden band
[b] E_d is the delocalisation energy per electron

This example shows that topological methods can give erroneous results in the comparison of the energy characteristics of the higher fullerenes. However, were it not for the topological approximation there would have been no progress in the search for possible structures, in the detection of isomers, in the interpretation of the NMR spectra, and in some other aspects of the structural chemistry of the fullerenes. A paper by Fowler et al.[100] in which the topological isomers of C_{84} of the fullerene type are characterised is noteworthy in this respect.

The structures of the higher fullerenes with a number of carbon atoms $\leqslant 84$ have also been discussed.[57-59,67] Table 3 shows reported data on the structure of the C_n carbon clusters with $60 \leqslant n \leqslant 78$, which satisfy the isolated pentagon rule and have a closed electron shell. The table also gives the characteristics of the ^{13}C NMR spectra and the heats of formation of the isomers, calculated by the molecular mechanics method.

Table 3. C_n fullerenes with closed and with pseudo-closed electron shells for $60 \leqslant n \leqslant 78$, ^{13}C NMR spectra, and calculated heats of formation.

Structure	Line intensity	ΔH_f°/kcal mol^{-1}
I_h-C_{60}	1(60c)	573.0
D_{5h}-C_{70}	3(10c), 2(20c)	–
D_{6h}-C_{72}	2(24c), 2(12c)	–
D_{3h}-C_{74}	1(2c), 4(4c), 4(12c)	–
D_2-C_{76}	19(4c)	–
C_{2v}-C_{78}	18(4c), 3(2c)	695.7
D_{3h}-C_{78}	13(6c)	697.8
C_{2v}-C_{78}	17(4c), 5(2c)	694.3
D_{3h}-C_{78}	5(12c), 3(6c)	702.3
D_{3h}-C_{78}	5(12c), 3(6c)	697.8

Note. Data for two symmetries (C_{2v} and D_{3h}) are given for the C_{78} fullerene

Fullerenes with a large number of atoms (giant fullerenes), including the extended carbon structures of the fullerene type, have been studied extensively.[59,101-106] Methods of modelling their structure have stimulated most interest. Thus, Kroto[101] proposed using spherical models for the giant fullerenes. The suggested structures are very attractive at first sight. Furthermore quantum-chemical calculations[69] for large clusters suggest that even a giant fullerene of icosahedral symmetry as large as C_{540} may be stable. Nevertheless the formation of hollow giant fullerenes of the spheroidal type seems unlikely, because these molecules must include a large proportion of empty space. It is difficult to believe that in the synthesis of the giant clusters C_n by the evaporation of graphite or by the combustion of benzene the inner cavity of the cluster is not filled by other smaller species formed from carbon atoms, or by other (impurity) atoms. Therefore the possibility that giant fullerenes have a more complex structure cannot be excluded. For example, these clusters may have a structure of the onion bulb type. Some of the giant fullerenes could be cylindrical, or they could have more complex cellular structures. Carbon clusters of these types (capsulenes, barrelenes, tubulenes, kegs, torenes, etc.) have been widely discussed.[31,64,102-108]

Cylindrical structures can be described as homologous series. Thus, Gal'pern et al.[64] have examined the molecular and the electronic structure of barrelenes of general formula C_m ($m = 36+12n$). In the limit, cylindrical carbon clusters can be treated as infinite macromolecules, and their corresponding endohedral complexes (containing linear chains of atoms within the carbon cylinder §) can be treated as molecular conductors.[106]

§ The possible formation of isolated homoatomic chain macromolecules consisting of atoms of the first or of the second period has long been a topic of discussions among specialists.[109] The formation of lead conductors within carbon microtubes up to 2 nm in diameter has recently been reported [P M Ajayan, S Iijima *Nature (London)* **361** 333 (1993)].

The properties of the carbon cylinders depend on the radius and on the character of the end groups. Carbon clusters with a closed electron shell should have the form of cylinders closed at the ends (capsulenes, barrelenes). Open carbon cylinders can have no independent existence, because they include many radical centres at their ends. However, by saturating the free valencies of these radicals we can create cylindrical macromolecules having favourable properties as electronic conductors. Mathematical models of these systems, including their toroidal analogues, were first discussed by Heilbronner[110] in 1954 from the standpoint of a study of the electronic structure of homologous series of polynuclear aromatic hydrocarbons. More recently renewed interest has been shown in the search for new classes of quasi-one-dimensional conductors.[111,112]

The production of filiform carbon crystals, probably composed of microtubulenes, has been reported.[103]

In principle the possible formation of carbon structures with carbon atoms distributed over surfaces of various types should also not be excluded. For example, Lenosky et al.[104] have considered the case of surfaces with a negative curvature.

5. Endohedral fullerene complexes

Let us now turn to inclusion compounds of the $M_n @ C_m$ type. The first results of quantum-chemical calculations on these systems were reported by Bochvar et al.,[38,39] who applied the CNDO/2 method with partial optimisation of the geometry to the system $M^+ @ C_{24}$, with M = Li, Na. In these calculations the C_{24} cluster was assumed to be a truncated octahedron. According to the results the introduction of a Li cation at the centre of the carbo-*s*-octahedron stabilises the C_{24} system, whereas Na^+ has a destabilising effect. This is because in the case of Li the whole of the positive charge is transferred to the carbon skeleton whereas with Na 30% of the charge remains on the metal atom. A high energy barrier has to be overcome in order to extract the M^+ cation through the centre of the hexagonal face. This effect ensures the kinetic stability of $M^+ @ C_{24}$.

Relatively few calculations on endohedral clusters have been published. Special interest was stimulated by detailed calculations on Li^+C_{60} by Bakowies and Thiel,[69] who considered the case of Li^+ present both within and outside the C_{60} cluster. It was found that the formation of the endohedral $Li^+ @ C_{60}$ cluster requires a large consumption of energy (ΔH = 30 kcal mol^{-1}), whereas the formation of an exohedral cluster, with the Li^+ located outside the carbon cage over a pentagonal or hexagonal ring, results in a substantial gain in energy.

The charge on the Li atom is positive varying between 0.5 and 0.8 a.u. The position of the Li cation at the centre of the cage does not correspond to the absolute minimum: the cation can move almost freely within the polyhedron to a point 1.4 Å from the centre. However, as in the case of $M^+ @ C_{24}$, the emergence of the M^+ cation from the carbon cage requires overcoming a high potential barrier (> 75 kcal mol^{-1}), which ensures the kinetic stability of this type of endohedral complex.

Nonempirical calculations of the clusters $X @ C_{60}$ (X = O, F, K, Ca, Mg, Cr, Ba, La, Eu, U) have been reported. Chand et al.[113] used the Hartree–Fock method in conjunction with a relativistic potential for the core electrons. It was assumed that the impurity atom is located at the centre of the carbon cage. Calculations in the approximation of an energy functional dependent on the local electron density[114] were carried out with the exchange-correlation potential proposed by Barth and Hedin.[115] By analysing the Mulliken populations it was established that a charge of $\sim 2.85e$ is retained on the carbon skeleton. The highest occupied energy level corresponds to the MO localised on the carbon atoms.

From the calculations[113] on the $M @ C_n$ inclusion compounds it can be seen that the role of the atom (or ion) within the carbon cage is principally to donate electrons to the ρ-electron shell of the carbon core. The extent of electron transfer and the stability of the system depend on the relative values of the redox properties of the additive atom and of the carbon cluster. Thus the La atom donates two 6*s* electrons to the delocalised system of the carbon cage, occupying two vacant orbitals of the C_{60} clusters, and the third valence electron remains localised on the 5*d*-AO. We may conclude from the results of the calculation[113] that the $La @ C_{60}$ complex should have chemical properties similar to those of fullerene in a triplet excited state. The electronic structure of the endohedral $M @ C_n$ complexes has been discussed also by other workers.[116–119]

The acceptor capacity of the C_n clusters can be evaluated qualitatively at the level of the Hückel approximation. Thus it was shown[56] that the C_n^{2-} dianions with n = 74, 82, and 88 are the most stable of these species. It is stressed that these dianions are convenient structures for the formation of endohedral complexes with metals which donate two electrons to the ρ system of the surrounding cage. In particular, the stability of the C_{3v}-C_{82}^{2-} cluster is specially noted. This conclusion agrees with experimental data indicating the existence of a long-lived $La @ C_{82}$ cluster and defining the charge distribution pattern in the system.[56]

6. Unstable fullerenes

Most of the theoretical papers in which polyhedral carbon clusters are discussed are mainly concerned with structures which satisfy variously defined stability criteria and in particular with clusters having a closed electron shell. The presence of an open electron shell in a polyhedral C_n cluster denotes a fairly high reactivity. Such a cluster is kinetically unstable, and difficult to isolate. However, knowing the geometry of the ground state and the electronic structure of the C_n cluster with an open electron shell it is often possible to make a qualitative estimate of the stable derivatives of such a cluster. Therefore the unstable structures also are of interest, and it is reasonable to treat them as intermediates whose stabilisation under prescribed conditions can lead to the creation of new types of materials.

Let us examine some examples. The simplest member of the fullerene family is the carbododecahedron C_{20}. The earliest calculations on the cluster C_{20}, made first in the Hückel ρ approximation[25] and then by the expanded Hückel method,[38] showed that this fullerene has an open electron shell and that its ground state should be triplet. Recent nonempirical calculations by Parasuk and Almlöf[120] confirmed this conclusion from which it follows that the C_{20} cluster should be a chemically active species. One of the methods of preparing stable, less reactive systems relies on passing from the C_{20} cluster to its carborane derivative $C_{18}B_2$.[25,121]

The D_{6h}-C_{36+12n} family of clusters of the barrelene type has been discussed.[64,122] It was established that these clusters have an open electron shell. However, it appeared that the highest partially occupied doubly degenerate level is a bonding level and that two electrons are not sufficient to fill it. Therefore it was concluded that the D_{6h}-C_{36+12n} clusters can readily form dianions.[64] They can be stabilised in the solid phase by the addition of alkali metal atoms.

Another interesting method of stabilising polyhedral clusters was proposed by Guo et al.[117] It was shown that the most stable C_{28} isomer has a tetrahedral (T_d) type of symmetry (Figure 8). At each corner of the tetrahedron we find a group of three condensed pentagonal rings: the carbon atoms shared by the three rings lie exactly at the corners of the tetrahedron. The electronic ground state of the C_{28} cluster has the $^5A_2$ configuration. One of the four unpaired electrons is located on a molecular orbital of a_1 symmetry, whereas the other three are on orbitals of t_2 symmetry. The tetrahedral C_{28} cluster can be formally treated as a super-atom with a valency of four, able to form compounds analogous to those of the quadrivalent carbon atom in the sp^3 hybridisation state.

Furthermore, calculations[117] by the nonempirical SCF method showed that the $C_{28}H_4$ molecule (of T_d symmetry) should be extremely stable. This molecule could be appropriately called supermethane. However, there is an alternative method of

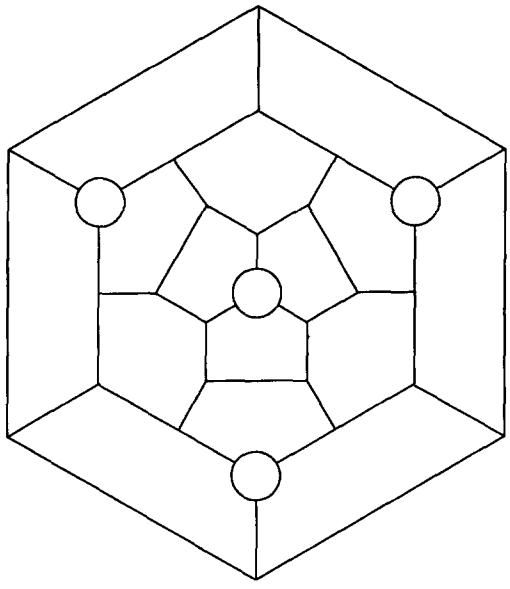


Figure 8. Molecular diagram for the C_{28} cluster of tetrahedral symmetry. The corners denoted by open circles correspond to carbon atoms lying on third-order axes of symmetry.

stabilising C_{28}: by introducing into the inner cavity of the polyhedron a quadrivalent atom such as Ti or U to form endohedral M @ C_{28} compounds. Mass spectral data for samples obtained by laser evaporation of a recently prepared composite (graphite – UO_2) were also reported.[117] These suggest the existence of U @ C_{28} clusters.

We should also point out that by analogy with the carbon atom in the sp^3 hybridisation crystal lattices of the diamond type can be constructed from the C_{28} super-atom, as well as some other lattices. The C_{28} super-atom can find applications in the design of superaliphatic hydrocarbons $[(C_{28}H_2)_m(C_{28}H_3)_n]$.

7. Polyhedral clusters of atoms of other elements

The synthesis of polyhedral clusters of carbon atoms strongly stimulated the search for analogous structures composed of atoms of elements of group IV of the Periodic Table, or of mixed clusters of atoms of elements from groups III and V, For example, Nagase and Kobayachi[123] have discussed the stability of the O_h-Si_{24} cluster, of the icosahedral Si_{60} cluster, and of the endohedral M @ Si_{60} complexes, where M = Ne, F^-, or Na^+. The calculations were carried out by the Hartree–Fock–Roothaan method. A two-exponential basis was used for Si_{60}, and an effective nonempirical potential for the cores of the Si atoms. The structure of the Si_{60} cluster was optimised by postulating the retention of the I_h symmetry group. It was established that bonds of two types are present in the Si_{60} cluster: bonds shared by two hexagons have a length of 2.189 Å, and those shared by a pentagon and a hexagon have a length of 2.266 Å. The highest occupied energy level (−6.5 eV) has a five-fold degeneracy, and the lowest unoccupied level (−2.5 eV) is triply degenerate. The structure of the Si_{60} cluster was found to be stable with respect to certain distortions which lower the symmetry. It was shown that the Na^+ @ Si_{60} complex is much more stable than F^- @ Si_{60}, unlike the X @ C_{60} complexes (X = Na^+, F^-), to which the inverse order of stability applies. The structure of the Si_{24} cluster was calculated on the assumption that the O_h symmetry group is retained. It was pointed out that the total potential energy surface does not contain a local minimum corresponding to this structure.

It should be noted that problems relating to the structure of clusters of silicon atoms have been widely discussed in the literature.[124, 125] The results of mass-spectral analyses suggest that silicon (unlike carbon) tends to form clusters with an odd number of atoms.[124] The greater length of the Si – Si (as compared with the C–C) bond may assist the formation of three-dimensional structures on whose surface partially conjugated Si_m chains are accommodated. This model was constructed for the Si_{45} cluster[125] by the molecular mechanics method. Evidently the structure of the Si_{45} cluster[124] is a reflection of the greater tendency of Si atoms to form single bonds.

We know that the elements of the third period do not form aromatic compounds.[126] Therefore the problem of synthesising the silicon analogue of footballene is of great interest to theoreticians as well as to experimentalists.

The ability of boron atoms to form polyhedral structures of composition C_nB_m is beyond doubt.[121] Similarly, the replacement of some carbon atom in a polyhedral cluster by nitrogen is not incompatible with the general principles of valency theory. However, it is reasonable to ask whether the homonuclear N_n or B_n clusters can exist.

In the former case the clusters could play the role of Lewis superbases, in the latter they could be superacids. The possibility of combining boron and nitrogen atoms within the same molecule has already been established in nature for a small molecule: borazole, a very stable compound of aromatic character.

The study of the possible existence of N_n clusters has a long history, and is directly related to the stability of hexa-azabenzene (the cyclic molecule N_6), which has been discussed extensively (see for example, the work of Gal'pern et al.,[127] and Stankevich et al.[128] and the references quoted in those papers).

It was concluded[127, 128] that the repulsion between the neighbouring unshared electron pairs could be responsible for instability of the cyclic N_6 molecule. In principle this destabilising factor should also be found in polyhedral systems. Chen Cheng et al.[129] reported the results of calculations by the MINDO/3, MNDO, and AMI methods for a dodecahedral N_{20} cluster. The equilibrium geometry was identified, and the heat of formation of the cluster was calculated as well as the heats of the reactions $10N_2 \rightleftharpoons N_{20} \rightleftharpoons 20N$. All three methods lead to the conclusion that a local energy minimum exists for the N_{20} cluster. The following values (in Å) were obtained for the N–N bond lengths: 1.484 (AMI), 1.426 (MNDO) and 1.347 (MINDO/3). The N_{20} cluster was found to be more stable than a system of 20 nitrogen atoms but less stable than a system of 10 nitrogen molecules (AMI, MNDO).

The stability and the electronic structure of polyhedral clusters of the mixed type $(C_nB_mN_k)$ were discussed by Xia et al.,[130] who calculated by the MNDO method the electronic structure of the 60-atom systems C_{60}, B_2C_{58}, N_2C_{58}, BNC_{58}, $C_{12}B_{24}N_{24}$, and $B_{30}N_{30}$, and obtained their heats of formation. It was established that all the mixed systems have a stability close to that of C_{60}. According to these workers[130] it should be easier to synthesise the $B_{30}N_{30}$ than the C_{60} cluster, but no attempt appears to have been made so far to prepare that cluster.¶

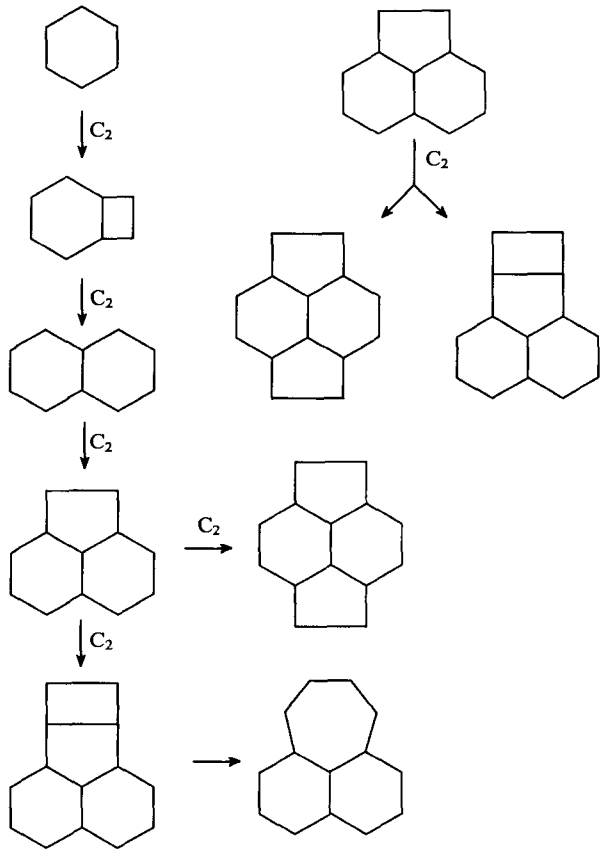
IV. Mechanism of formation of the fullerenes and of endohedral complexes

The mechanism of formation of the fullerenes is not known in detail. There are only some general considerations on the growth of the carbon cluster by the successive addition of C_2 particles, which are thought to be predominant in graphite vapour.[131] Experimental morphological observations (the spiral growth of cylindrical tubes in tubulenes[97]) cannot be extended to the closed molecules of the higher fullerenes.

The main structural difference between the fullerenes and graphite is the presence of pentagons in the former. The first pentagon (surrounded by hexagons) leads to the formation of

¶ Reports of the synthesis of M_8C_{12} systems, where M = Ti, Zr, V, have recently appeared [B C Guo, K P Kerns, A W Gastleman *Science* **256** 515 (1992)]. Dodecahedral structures, with each M atom associated with three C atoms, were assigned to these molecules.

corannulene (a nonplanar structure), and the formation of a heptagon can lead to the same result.[132] The formation of even a single nonhexagonal ring is a prerequisite for the eventual conversion of the structure into a closed figure. The formal scheme described in the next section explains the formation of nonhexagons during the initial stages of the process.



The presence of pentagons is the critical stage in the *de novo* formation of endohedral metal complexes. It should be noted first of all that endohedral complexes have been described only for group III metals (lanthanum, yttrium, and scandium). These metals are characterised by the formation of π-cyclopentadienyl (cp) complexes with η^5 coordination, and π-arene complexes with η^6 coordination are practically unknown in this case. According to the hypothesis formulated by one of us[132] this difference is critical in the formation of endohedral metal fullerenes with the participation of intermediates of the $(\eta^5\text{-}C_5H_5)_nM$ type (n = 1, 2) with a closed fullerene shell. Thus η^5 coordination with several cp ligands is also characteristic of other metals (for example, uranium), and in these transition metals, as in nickel and iron, η^5 coordination is preferred over η^6.

If the $(\eta^5\text{-}C_5H_5)_nM$ intermediates are important in the synthesis of endohedral complexes it may be preferable to introduce into the graphite electrode the already prepared cp_2M-X complex instead of the metal salt (or, indeed, the oxide) in view of the high affinity of the group III metals for oxygen, which may produce an undesirable competition for the metal. The prepared cp–M fragment is stable in an inert gas atmosphere, and it can arrange itself in hexagons during high-temperature dehydrogenation, which favours the formation of endohedral complexes of the fullerenes with other metals possibly in high yields. The *de novo* synthesis of endohedral fullerene complexes thus described, i.e. the synthesis at the instant of the formation of the fullerene spheroid itself, was complemented by another approach different in principle. It was shown mass-spectrometrically[133–137] that when an inert gas is bombarded with a beam of accelerated C_n^+ cation radicals endohedral $X@C_n$ complexes are formed with the inert gases (helium or neon) in an ionised form. A special technique was developed to reduce the $He@C_{60}$ reversibly in the gas phase and to detect it.[137] These studies were recently reviewed by Schwarz.[138]

V. Classification of the forms of carbon with a regular structure

Known forms of carbon with a regular structure are most rationally classified as molecular or covalent crystals. Molecular crystals are composed of individual molecules (carbon clusters) of finite size: the fullerenes. Covalent crystals are characterised by polymeric structures.

The structures of covalent crystals are conveniently described in terms of infinite graphs. In this method of description diamond corresponds to a uniform graph of order 4. By constructing such a graph in three dimensions we can easily represent the diamond structure, which corresponds to the closest packing of carbon atoms.

Graphite is described by a disconnected graph consisting of an infinite number of two-dimensional lattices. Each of these lattices can be realised as a hexagonal grid on a plane. The third allotropic form of carbon (carbyne[139]) is described in terms of an infinite number of simple, rectilinear paths.

The real structures of diamond, graphite, and carbyne suggest a three-dimensional, a quasi-two-dimensional, and a quasi-one-dimensional character for these allotropic modifications of carbon, accurately reflected by the theory of hybridisation.

In addition to the above, there are many other methods of regularly filling a three-dimensional space with carbon atoms. Some of these are described in the monograph by Wells,[24] who used infinite graphs with coordinates. The construction of nets of trigonal carbon atoms has also been described:[140,141] it was shown that in addition to diamond, graphite, and carbyne, which display (in the ideal case) the sp^3, sp^2, and sp hybridisation of the atomic orbitals, crystalline modifications of carbon with an intermediate hybridisation are possible, and also mixed forms of carbon containing tetragonal, corner, and trigonal atoms.

A mechanism allowing the regrouping of several nets of this type into planar graphite layers has been proposed.[142] In the crystals the graphite layers are at a distance of 3.35 Å from each other. This defines the 'thickness' of the graphite layer, i.e. its extent in a direction perpendicular to the plane. Since this is infinitely small in comparison with the size of the graphite plane the three-dimensional structure of the graphite layer can be characterised by the effective dimensionality $2+\varepsilon$ where $0 < \varepsilon \ll 1$. Similarly the van der Waals interaction defines the thickness of the carbyne filament. The three-dimensional structure of the carbyne molecule can be described as $1+\delta$, where $0 < \delta \ll 1$. Obviously, on this scale the effective dimensionality of diamond is described by the number 3, corresponding to that of three-dimensional space.

Let us now consider a fragment of a hexagonal net on a plane, in the shape of an infinite band. This fragment can be rolled into a hexagonal net (tubulene), drawn over the lateral surface of a cylinder, and in this way chiral tubulenes of different size can be produced.

The tubulene form of carbon is intermediate between diamond and the fullerenes. The growth of carbon tubes of different diameter has been observed experimentally by Iijima.[103]

If the network on a plane consists of 5- and 6-membered rings it can be treated as the result of defect formation in an ideal hexagonal system. Toroidal structures (the torenes) can be formed from fragments of this net in the form of an infinite band. A combination of tubulenes can give tubular systems with bifurcations, and also structures whose atoms are located on a surface having a negative curvature.[104]

We should also note that the structures of all the forms listed above can be interpreted as the result of 'grafts' between chain carbon molecules.

Some workers suggest[20] that the mechanism of formation of the fullerenes from carbon vapour includes a process of the grafting type as one of its initial stages.

The classification of the regular carbon structures proposed by one of us[35] is shown in Figure 9.

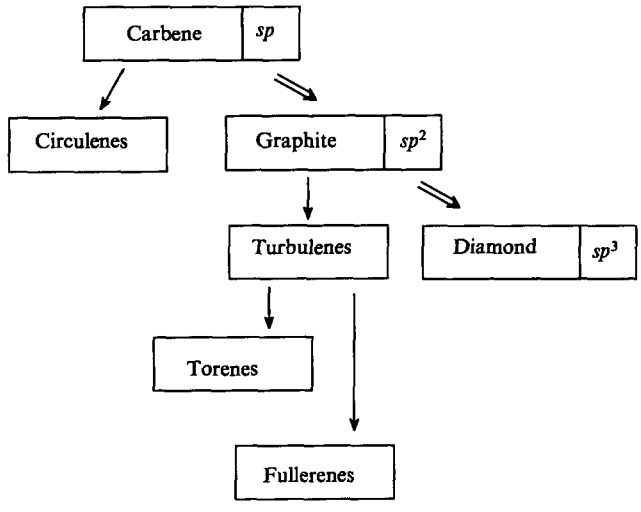


Figure 9. Classification of the regular carbon structures.[35]

VI. Chemical properties of carbon clusters

The unique structural features of the fullerenes, causing unsaturation of all the bonds in the absence of substituents, make only two types of primary reaction possible in this system: the withdrawal of electrons and the addition of electrons or of groups. The replacement of already present groups and their removal are secondary reactions of the derivatives. It follows from the above that the fullerenes are electrophilic and good electron acceptors. They readily undergo addition of nucleophiles, and also of free-radical and of carbenoid species. Nearly all the reactions studied in fullerenes took place on C_{60} or its mixtures with C_{70}. Nothing is known about the chemical properties of the higher fullerenes.

1. Reactivity of C_{60}

a. Addition of hydrogen and halogens

The addition of several hydrogen molecules takes place under the conditions of the Birch reaction in the presence of an alkali metal in ammonia or in an amine, giving $C_{60}H_{36}$ as the main product, from which (as reported[143]) the $C_{60}H_{60}$ fullerene can be obtained. Dihydrofullerene $C_{60}H_2$ was obtained by selective hydrozirconylation of C_{60} followed by hydrolysis.[144]

$$C_{60} + cp_2Zr(H)Cl \longrightarrow C_{60}H(Zr\,cp_2Cl) \xrightarrow{H_2O} C_{60}H_2$$

8% ($\delta_H = 5.07$ p.p.m.)

A theoretical evaluation of all the possible isomers of $C_{60}H_2$ has been reported:[145] many of the isomers are found to be stable.

Buckminsterfullerene adds on some fluorine atoms in the presence of XeF_2, and complete fluorination is observed when solid C_{60} is treated with gaseous fluorine.[146,147] The fullerene $C_{60}F_{60}$ is a colourless crystalline substance soluble in THF and in acetone. Its ^{19}F NMR spectrum contains only one singlet line. The chlorination and bromination reactions are reversible, and iodine undergoes almost no addition. Chlorination and bromination yield a mixture of products containing (on average) 22 chlorine atoms and 28 bromine atoms respectively. Some bromofullerenes have been isolated in a pure form. The halogen atoms in the halogenofullerenes are easily replaced by nucleophilic OH or NH_2 groups.[148-150]

b. Electrochemical reduction

The electrochemistry of the fullerenes has been studied by a few groups of workers. By examining a continuously increasing range of electrolytes and solvents it was shown that 6 electrons can be added sequentially and reversibly to C_{60}.[151] It is interesting to note that no difference was observed between the first ionisation potentials of C_{60} and C_{70}.[152] The C_{60}^{n-} anions are anion radicals for odd values of n, but for even n the spin pairing problem prevents the observation of the ESR spectrum under certain conditions. Some work on the electrochemistry of BF derivatives has been published recently.[153]

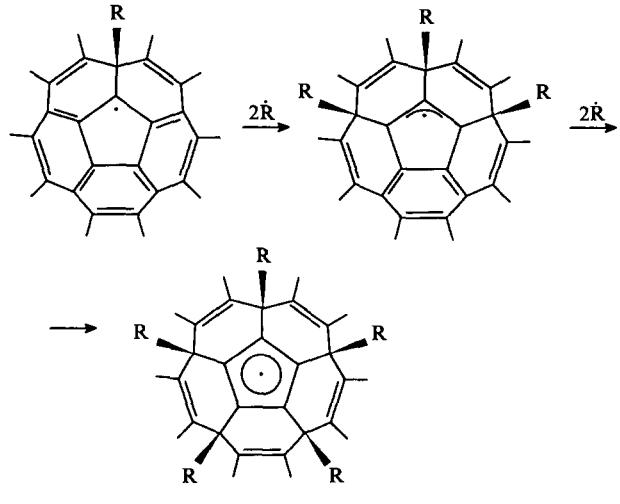
c. Reduction by metals

The transfer of electrons from alkali metals to fullerenes has been studied in reasonable detail both in solutions and in films. The stimulus for this work was the discovery of superconductivity in the M_3C_{60} phase.[17] The highest critical temperature observed for the caesium–rubidium salt Cs_2RbC_{60} was 33 K. We note that the superconducting salts are ion radicals and have a face-centred cubic lattice.[154] Changing from Cs_2RbC_{60} to Cs_3C_{60} produces a different type of lattice, and the superconductivity disappears.

Other metals and their salts can also transfer electrons to the fullerenes. However, these compounds have not been adequately studied. It was recently shown that the C_{60} anion radical is formed during the homogeneous reduction of C_{60} by samarium(II) iodide in THF.[155]

d. Addition of free radicals

Krusic et al.[156] observed the very easy addition to C_{60} of free radicals with their centre over the carbon, oxygen, or sulphur atoms. By using ESR they established the structure of some of the most stable radical products of repeated additions. An analysis of the hyperfine splitting lines showed that the most stable radicals are those of the allyl and cyclopentadienyl type, with three or five benzyl radicals added at the (6, 6) bonds.[157] The benzyl radical used in this work was labelled with the ^{13}C isotope at the methylene group.



We have studied the addition to C_{60} and C_{70} of free radicals in which the spin density was concentrated on an atom which had a magnetic moment (phosphorus, boron, tin, etc.).[158-160] This approach is useful because it allows the hyperfine splitting in the ESR spectra to be observed without introducing an isotopic label. The addition of the phosphoryl radical, conveniently generated by the photolysis and thermolysis of the mercury salt $Hg[P(O)(OR)_2]_2$, was studied in most detail. The spin density in

the phosphoranylfullerenyl radical was almost fully localised on three carbon atoms of the short-range surroundings. We studied the kinetics of the reversible dimerisation of this radical.

$$2C_{60}^{\cdot}-P(O)(OR)_2 \rightleftharpoons [C_{60}-P(O)(OR)_2]_2$$

e. Ion-radical salts

In addition to the salts with alkali metals mentioned above other ion-radical salts have also been described.† The electrolysis of C_{60} in a mixture of THF and CH_2Cl_2 in the presence of tetraphenylphosphinium chloride gave the paramagnetic salt $Ph_4P^+ \ldots C_{60}^- \ldots (Ph_2PCl)_2$.[161] The interaction of C_{60} with the electron-donor complex of low-valency chromium **1** in toluene solution gave the salt **2** as a result of electron transfer from **1** to the fullerene.

$$C_{60} + \underset{\mathbf{1}}{(TPP)Cr(II)} \underset{THF}{\overset{PhMe}{\rightleftharpoons}} \underset{\mathbf{2}}{C_{60}^-(TPP)Cr(III)^{\cdot+}}$$

The addition of THF causes dissociation of salt **2**. The reaction of BF in toluene solution with a 20-fold excess of tetrakis-(dimethylamino)ethylene produces the salt $C_{60}(TDAE)_{0.86}$. This ion-radical salt undergoes a ferromagnetic transition at 16.1 K, which is the highest reported temperature for an organic ferromagnetic.[163]

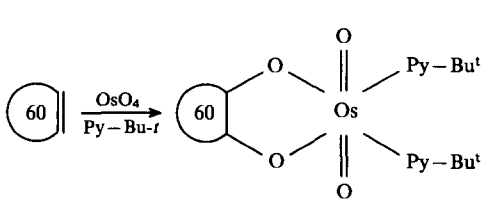
f. Oxidation and reactions with Lewis acids

Buckminsterfullerene C_{60} forms a cation radical under the influence of Lewis acids (for example, SbF_5).[164] However, in order to obtain stable derivatives from these cation radicals it is convenient to use $AlCl_3$, which yields the polyarylated fullerenes $C_{60}H_nAr_n$ ($n \simeq 12$).[165]

$$C_{60} \xrightarrow[AlCl_3]{ArH\ (exc.)} C_{60}H_nAr_n$$

Oxidation with oxygen. Buckminsterfullerene reacts with oxygen only when irradiated:[166] the triplet state of C_{60} is formed first, and energy transfer from this state produces singlet oxygen which reacts directly with the fullerene. Under these conditions some of the carbon–carbon bonds are broken and carbonyl groups are formed, with evolution of CO and CO_2. One direction of the reaction produces the oxides $C_{60}O$ and $C_{70}O$, which are usually found in mixtures of fullerenes.[167]

Oxidation with OsO_4. The oxidation of olefins by osmium tetroxide with opening of the double bond and formation of 1,2-diol ethers is well known. This reaction has been observed with C_{60}.



The conditions needed to produce the pure mono-derivative have been identified, and an X-ray diffraction analysis of the compound has been reported.[87, 168–170] The first experimental data on the geometry of the BF were obtained for this compound.

†A complex with the (+)-DIOP ligand (the first optically active organometallic derivative in the fullerene series) was obtained in a similar way [V V Bashilov et al. *Izv. Ross. Akad. Nauk, Ser. Khim.* 428 (1993)].

g. Fullerenes as ligands

The presence of a continuous 'electron cloud' in a fullerene polyhedron allows us, in principle, to select different numbers of electrons as participants in the bonding to give metal complexes. The formation of the following types of complex can be postulated:

η^1 — a simple complex with a σ bonding at one vertex (an even number of groups can be found in a non-free-radical product),
η^2 — a π-olefin complex at an edge or the geometrically equivalent double σ bonding at neighbouring vertices,
η^3 — a π-allyl complex,
η^4 — a π complex of the trimethylenemethane or 1,3-diene type,
η^5 — a π-cyclopentadienyl complex,
η^6 — a π-arene complex.

The stable complexes so far identified all belong to the first two types. Other types do not appear to have been prepared as yet. The last two types are of special interest because double π complexes of metals with nonadjacent hexagonal faces of C_{60} should be chiral and therefore could occur in an optically active form.[171]

Reactions with low-valency complexes of the transition metals. The analogy between fullerenes and the electron-acceptor olefins is clearly seen in the formation of π complexes with some transition metals. The reaction of C_{60} with ethylene-bis-(triphenylphosphine)platinum results in the addition of between 1 and 6 L_2Pt fragments: the first and the second of these complexes have been characterised by X-ray structural analysis.[172–174] In the $(\eta^1\text{-}C_{60}).(PtL_2)_6$ complex the six L_2Pt groups are disposed octahedrally, forming a molecule with the T_h symmetry. The reaction of C_{60} with tetrakis-(triphenylphosphene)palladium gives the complex $(\eta^2\text{-}C_{60})Pd(PPh_3)_2$,

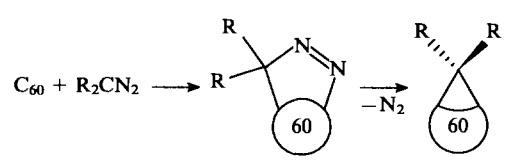
$$C_{60} + (Ph_3P)_4Pd \longrightarrow (\eta^2\text{-}C_{60})Pd(PPh_3)_2 ,$$

whose structure[175] is very similar to that of its platinum analogue: the only difference is that the coordinated C–C bond is less stretched and has approximately the same length as the corresponding bond in the initial fullerene.‡ The reaction of C_{60} with the zero-valent $Pd_2(dba)_3$ complex yields insoluble oligomeric products of composition $C_{60}Pd_x$.[176]

$$C_{60} + Pd_2(dba)_3 \longrightarrow C_{60}Pd_x + dba .$$

In the olefin complexes with Ir(I) the olefin can be removed by buckminsterfullerene, whereas the CO, PPh_3 and $P(OMe)_3$ molecules remove the fullerene from the complex.[177–179]

Reactions with diazo compounds. Fulleroids. A new type of product was obtained by Wudl[180–182] from the reaction between buckminsterfullerene and diaryldiazo compounds. The first stage was probably [3 + 2]-cyclo-addition with formation of pyrazolene. However, after one hour a mixture of products of composition $C_{60}[CR_2]_n$ (where n = 1–6, R = Ar) was precipitated from a toluene solution.



3

‡The electrochemical synthesis of the salt $[(Ph_3P)_2N]^+C_{60}^-$ has recently been reported [H Moriyama, H Kobayashi, A Kobayashi, T Watanabe *J. Am. Chem. Soc.* **115** 1185 (1993)]. Single crystals of this salt have been studied by the X-ray structural method.

A remarkable feature of the fullerene structure is the breaking of one C–C bond in the reaction with carbenes, forming a bridge consisting of a tetrahedral carbon atom with two aryl substituents. The structures **3** formed in this way were called fulleroids. This is still the only way so far reported of preparing fullerenes with an odd number of carbon atoms: all the other fullerenes known at present have an even number of carbon atoms.

All the 6 homologous fullerenes with $n = 1-6$ (R = Ph) have been isolated and characterised spectroscopically (and also by X-ray structural analysis in the case of the first homologue). The methanoannulene structure for the compound **3** is suggested by the large distance between the carbon atoms of the pair (1.84 Å) and also by comparing the NMR spectra of this compound with those of the Vogel model compounds.[183]

The addition of the Ar_2C species to the final product takes place at a (6, 6) bond, but it was established that two additional isomers can be formed and then be converted into the main isomer. Surprisingly, in a recent study[184] of the reaction of C_{60} with unsubstituted diazomethane the addition of CH_2 was found to take place on a (6, 5) junction. Thus the regioselectivity of the formation of the fulleroid depends on the nature of the substituents on the carbene carbon (Figure 10).

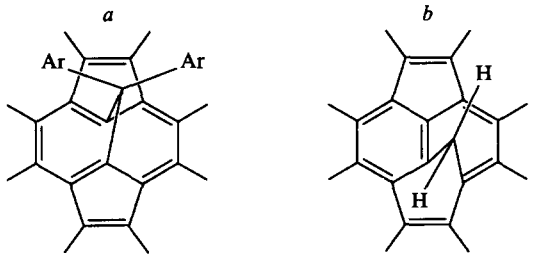


Figure 10. Fragments of the surface of $C_{60}CR_2$ fulleroids. *a* with the carbene added across the (6,6) bond, *b* with the carbene added across the (6,5) bond.

A recent publication[185] suggests that the thermolysis of azides in the presence of C_{60} produces azafulleroids; in one of these, the azide $Me_3SiCH_2CH_2OCH_2N_3$ with the ^{15}N isotopic label, it was shown that the nitrene group breaks a (5, 6) carbon bond.

We should stress the difference in structure between the adducts of C_{60} with a true (carbon) carbene or nitrene and with a platinum (or palladium) carbenoid (see above). Obviously, for carbon and nitrogen the most favourable process is the breaking of the strained cyclopropane fragment, giving two σ bonds, whereas with a transition metal the η^2 coordination is preferred.

2. Reactivity of C_{70}

Studies with C_{60}/C_{70} mixtures failed to detect a significant difference in reactivity between the two. Therefore, since pure C_{70} is more difficult to prepare than pure C_{60} its chemical properties have been less widely studied.

Balch et al.[179] have described the synthesis and the structure of the complex of iridium(I) with C_{70}.

$$Ir(CO)(PPh_3)_2Cl + C_{70} \longrightarrow (\eta^2\text{-}C_{70})Ir(CO)(PPh_3)Cl$$

Precise information on the geometry of fullerene-70 itself was inferred from the structure of this complex. Iridium is added across a (6, 6) edge at the 'sharp' end of the egg-shaped molecule. As reported,[179] the freedom of this end of the molecule from departures from a spheroidal shape favours bond formation. The iridium complex of C_{70} could not be obtained from the η^5-indenyl derivative of iridium.[178]

The reaction of C_{70} with the $^{\bullet}P(O)(OR)_2$ phosphoranyl radicals has been studied by ESR.[160] The primary products were found to be three different phosphoranylfullerenyl radicals corresponding to addition at nonequivalent corners of a nongraphite type (i.e. not at the junction of three hexagons).

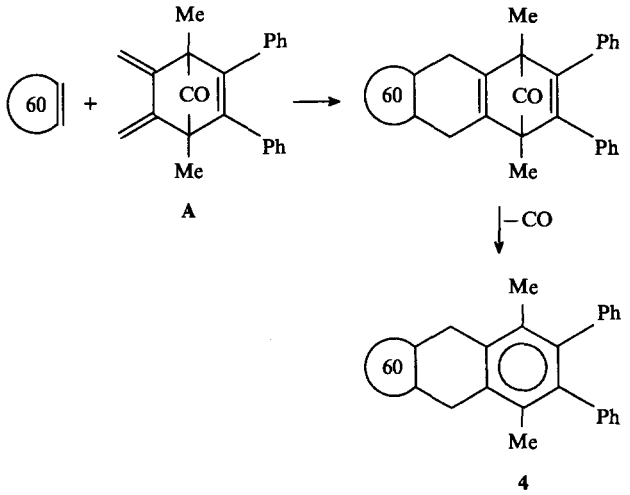
3. Other chemical properties

Inclusion compounds in which hydrophobic fullerenes act as guests for the inclusion of appropriate hosts within molecules or lattices are of special interest. It should be possible to separate the different fullerenes by this method. However, so far only one detailed publication has appeared,[185] describing the structure of the inclusion compound of C_{60} and hydroquinone with a stoichiometry of 1 : 3. The formation of a complex of γ-cyclodextrine with C_{60} has also been reported.[187] However, the formation of the inclusion compound was inferred only from the evidence of the absorption spectrum of a dilute aqueous solution.

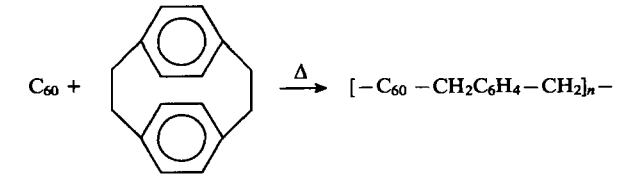
For many reactions of the fullerenes no corroborated data are available, but tentative advance reports can be found in papers on related topics. Thus, we know that fullerenes react with anthracene, cyclopentadiene, phosphines, and amines but only the adduct of C_{60} with morpholine has been described in sufficient detail.[188] A light yellow substance whose analysis indicated the addition of 6 equivalents of the amine was precipitated from a solution of C_{60} in morpholine. The ^1H NMR spectra of this compound suggest the presence of a dynamic process, interpreted as the motion of H atoms over the surface of the spheroid.

Reliable descriptions of two cases of cycloaddition at a double bond of fullerenes in purely carbon systems are available.

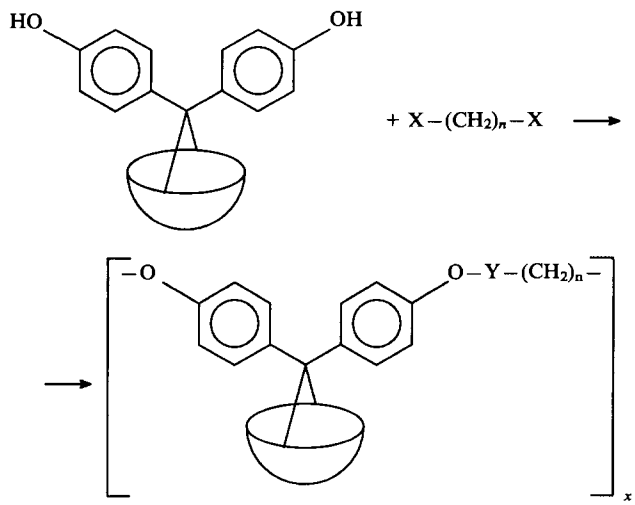
The reaction with dehydrobenzene takes place as a [2+2] cycloaddition, leading to adducts of the biphenylene type.[189] To identify the product of the Diels–Alder [4+2] reaction a special diene was used (structure A), whose adduct with fullerene undergoes partial aromatisation thus preventing the retro-decomposition.[190] The stable end product **4** was characterised by X-ray structural analysis.



The prospects of including fullerenes in polymeric systems have been examined. Thus polydiazo compounds can be converted into polyfullerenes of the 'pendant chain' type.[182] By exploiting the tendency of benzyl radicals to combine with fullerenes a polymer in which the C_{60} spheroids are connected in a chain by xylylene radicals was synthesised: pyrolysis of this material gives [2,2]-paracyclophane.[191]



Clearly, multiple grafting of the chains with formation of net polymers is possible. Polymers of the polyester and polyurethane types have been obtained[192] from a fulleroid containing two *p*-hydroxyphenyl groups and derivatives of dibasic carboxylic acids.



X = –COCl, *n* = 8, Y = –CO–
X = –NCO, *n* = 6, Y = –CO–NH–

Very useful information is given by a quantitative study[193] of the solubility of C_{60}. The best solvent is carbon disulfide, in which the solubility of C_{60} greatly exceeds the solubility in any other solvent. The solvents can be arranged in the following series of decreasing ability to dissolve the fullerenes: carbon disulfide ≫ toluene > benzene > mesitylene ≫ carbon tetrachloride > methylene chloride ≫ tetradecane > dodecane > decane > cyclohexane > dioxan ≈ hexane > isooctane ≈ octane ≫ pentane.

We also have a report[194] of the preparation of mixed polyhedral carbon–lanthanide clusters (C_nLn_m) in a solution of the iron–carbon eutectic.

No information on the biological activity of the compounds of the fullerene series has been published so far. Nevertheless their ability to generate singlet oxygen under UV irradiation justifies the expectation of oxidation catalysis *in vivo*, which implies biological activity.

VII. Conclusions

This review has dealt only with the most interesting and promising directions in the chemistry of the fullerenes. Evidently, during the next few years these areas will be actively developed, and will stimulate increasing interest in both experimentalists and theoreticians.§ These directions include, in particular:

— the development of new cheaper and more convenient methods and schemes for the preparation and separation of the pure C_{60} and C_{70} fullerenes;

— the synthesis of fullerenes containing a greater number of carbon atoms;

— the development of methods of synthesis of heterofullerenes consisting of polyhedra of noncarbon atoms (boron, nitrogen, transition metals, etc.), and the synthesis of new endohedral complexes;

— the development of reliable theoretical methods of predicting the physicochemical properties of carbon clusters and of their hetero-analogues and endohedral complexes;

— the computer modelling of the mechanism of formation of fullerenes, tubulenes, torenes, and other carbon clusters;

— the creation of methods of selective functionalisation (i.e. the preparation or individual fullerene derivatives);

— the preparation of optically active fullerene derivatives and their study by chiro-optical methods;

— the creation of a fund of information on the biological activity of the fullerenes and of their derivatives, and the assessment of the ecological safety of the fullerene derivatives.

§This expectation is supported by the appearance of a new international and interdisciplinary journal: *Fullerene Science and Technology*. The first issue of this journal was produced in February 1993 by Marcel Dekker.

References

1. H W Kroto, J R Heath, S C O'Brien, R F Curl, R E Smalley *Nature (London)* **318** 162 (1985)
2. J R Heath, S C O'Brien, Q Zhang, Y Lui, R F Curl, H W Kroto, R E Smalley *J. Am. Chem. Soc.* **107** 7779 (1985)
3. R M Baum *Chem. Eng. News* **63** (51) 20 (1985)
4. W Krätschmer, L D Lamb, K Fostiropoulos, D R Huffman *Nature (London)* **347** 354 (1990)
5. D H Parker, P Wurz, K Chatterjee, K R Lykke, J E Hunt, M J Pellin, J C Hemminger, D M Guen, L M Stock *J. Am. Chem. Soc.* **113** 7499 (1991)
6. F Diederich, R Ettl, V Rubin, R E Whetten, R Beck, M Alvarez, S Anz, D Sensharma, F Wudl, K C Khemani, A Koch *Science* **252** 548 (1991)
7. S Shinohara, H Sato, Y Saito, M Takayama, A Izuoka, T Sugawara *J. Phys. Chem.* **95** 8449 (1991)
8. D M Cox, S Behal, M Disko, S M Corun, M Greaney, C S Hsu, E B Kollin, J Millar, J Robins, R D Sherwood, P Tindall *J. Am. Chem. Soc.* **113** 2490 (1991)
9. R Taylor, J P Hare, A Abdul-Sade, H W Kroto *J. Chem. Soc., Chem. Commun.* 1423 (1990)
10. F Diederich, R L Whetten *Acc. Chem. Res.* **25** (3) 119 (1992)
11. W A Scrivens, P V Bedworth, J M Tour *J. Am. Chem. Soc.* **114** 7917 (1992)
12. A Gügel, M Becker, D Hammel, L Mindach, J Räder, T Simon, M Wagner, K Müllen *Angew. Chem.* **104** 666 (1992)
13. M S Meier, V P Selegue *J. Org. Chem.* **57** 1924 (1992)
14. J J Stry, M T Coolbaugh, E Turos, J F Garvey *J. Am. Chem. Soc.* **114** 7914 (1992)
15. J B Howard, J T McKinnon, Y Makarovsky, A Lafleur, M E Johnson *Nature (London)* **352** 139 (1991)
16. A F Hebard, M J Rosseinsky, R C Haddon, D W Murphy, S H Glarum, T T M Palstra, A P Ramirez, A R Kortan *Nature (London)* **350** 600 (1991)
17. R C Haddon *Acc. Chem. Res.* **25** 127 (1992)
18. K Prassides, H W Kroto *Phys. World* **4** 44 (1992)
19. W Weltner, R J Van Zee *Chem. Rev.* **89** 1713 (1989)
20. H W Kroto, A W Allaf, S P Balm *Chem. Rev.* **91** 1213 (1991)
21. Z Gasyna, P N Schatz, J P Hare, T J Dennis, H W Kroto, R Taylor, D R M Walton *Chem. Phys. Lett.* **183** 283 (1991)
22. H P Schultz *J. Org. Chem.* **30** 1361 (1965)
23. I V Stankevich, in *Primenenie Teorii Grafov v Khimii* (Application of the Theory of Graphs in Chemistry) (Eds N S Zefirov, S I Kuchanov) (Novosibirsk: Nauka, 1988) p. 7
24. A F Wells *Three-Dimensional Nets and Polyhedra* (New York: Wiley, 1977)
25. D A Bochvar, E G Gal'pern *Dokl. Akad. Nauk SSSR* **209** 610 (1973)
26. A D J Haymet *Chem. Phys. Lett.* **122** 421 (1985)
27. D J Klein, W A Seitz, T G Schmalz *Nature (London)* **323** 703 (1986)
28. T G Schmalz, W A Seitz, D J Klein, G E Hite *Chem. Phys. Lett.* **130** 203 (1986)
29. T G Schmalz, W A Seitz, D J Klein, G E Hite *J. Am. Chem. Soc.* **110** 1113 (1988)
30. D A Bochvar, E G Gal'pern, I V Stankevich *Zh. Strukt. Khim.* **30** 38 (1989)
31. R C Haddon, L E Brus, K Raghavachari *Chem. Phys. Lett.* **131** 165 (1986)
32. P W Fowler *Chem. Phys. Lett.* **131** 444 (1986)

33. P W Fowler, J E Cremona, J I Steer *Theor. Chim. Acta* **73** 1 (1988)
34. P W Fowler, J I Steer *J.Chem. Soc., Chem. Commun.* 1403 (1987)
35. V I Sokolov *Dokl. Ross. Akad. Nauk* **325** 540 (1992)
36. D E Manolopoulos, J C May, S E Down *Chem. Phys. Lett.* **181** 105 (1991)
37. Z Yoshida, E Osawa *Aromaticity (Japan)* (Kyoto: Kagakudojin, 1971) p.174
38. D A Bochvar, E G Gal'pern, in *Fizicheskie i Matematicheskie Metody v Koordinatsionnoi Khimii (Sed'moe Vsesoyuznoe Soveshchanie: Tezisy Dokladov)* (Abstracts of Papers Presented to the Seventh All-Union Conference on Physical and Mathematical Methods in Coordination Chemistry) (Kishinev, 1980) p. 144
39. D A Bochvar, E G Gal'pern, M V Nikerov, I V Stankevich, in *Dvenadtsatyi Mendeleevskii S'ezd po Obshchei i Prikladnoi Khimii* (Twelfth Mendeleev Session on General and Applied Chemistry) (Baku, 1981) p. 162
40. I V Stankevich, M V Nikerov, D A Bochvar *Usp. Khim.* **53** 1101 (1984) [*Russ. Chem. Rev.* **53** 640 (1984)]
41. D A Bochvar, M V Nikerov, I V Stankevich *Sov. Sci. Rev. B. Chem.* **9** 483 (1987)
42. R A Davidson *Theor. Chim. Acta* **58** 193 (1981)
43. A Streitwieser *The Molecular Orbitals Method for Organic Chemists* (Translated into Russian) (Moscow: Mir, 1965)
44. J Aihara *J. Am. Chem. Soc.* **98** 2750 (1976)
45. I Gutman, M Milun, N Trinajstic *J. Am. Chem. Soc.* **99** 1692 (1977)
46. B A Hess, L J Schaad *J. Am. Chem. Soc.* **93** 2413 (1971)
47. M Randic *Chem. Phys. Lett.* **38** 68 (1976)
48. D J Klein, T G Schmalz, G E Hit *J. Am. Chem. Soc.* **108** 1301 (1986)
49. M Randic, S Nikolic, N Trinajstic *Croat. Chem. Acta* **60** 595 (1987)
50. P N D'yachkov, T B Babenko, N V Kharchevnikova *Dokl. Akad. Nauk SSSR* **328** 477 (1993)
51. J Aihara, H Hosoya *Bull. Chem. Soc. Jpn.* **61** 2657 (1988)
52. A D J Haymet *J. Am. Chem. Soc.* **108** 319 (1986)
53. R Balasabramainan, X Lin *Int. J. Quant. Chem., Quant. Chem. Symp.* **22** 319 (1988)
54. M Ozaki, A Takahashi *Chem. Phys. Lett.* **127** 242 (1986)
55. D E Manolopoulos, P W Fowler *Chem. Phys. Lett.* **181** 1 (1991)
56. P W Fowler, D E Manolopoulos *Nature (London)* **355** 428 (1992)
57. P W Fowler, R C Batten, D E Manolopoulos *J. Chem. Soc., Faraday Trans.* **87** 3103 (1991)
58. D E Manolopoulos *J. Chem. Soc., Faraday Trans.* **87** 2861 (1991)
59. P W Fowler *J. Chem. Soc., Faraday Trans.* **86** 2073 (1990)
60. P W Fowler *J. Chem. Soc., Faraday Trans.* **87** 1945 (1991)
61. P W Fowler, J Woolrich *Chem. Phys. Lett.* **127** 78 (1986)
62. R C Haddon, L E Brus, K Raghavachari *Chem. Phys. Lett.* **125** 456 (1986)
63. A J Stone, D J Wales *Chem. Phys. Lett.* **128** 501 (1986)
64. E G Gal'pern, I V Stankevich, L A Chernozatonskii, A L Chistyakov *Pis'ma Zh. Eksp. Teor. Fiz.* **55** 469 (1992)
65. M L McKee, W C Herndon *J. Mol. Struct.* **153** 75 (1987)
66. M D Newton, R E Stanton *J. Am. Chem. Soc.* **108** 2469 (1986)
67. D Bakowies, W Thiel *Chem. Phys.* **151** 309 (1991)
68. R E Stanton, M D Newton *J. Phys. Chem.* **92** 5314 (1988)
69. D Bakowies, W Thiel *J. Am. Chem. Soc.* **113** (10), 3705 (1991)
70. R E Stanton *J. Phys. Chem.* **96** 111 (1992)
71. K Raghavachari, C M Rohlfing *J. Phys. Chem.* **96** 2463 (1992)
72. J M Rudzinski, Z Slanina, M Togasi, E Osawa, T Tizuka *Thermochim. Acta* **141** 155 (1987)
73. J M Schulman, R L Disch, M A Miller, R C Peck *Chem. Phys. Lett.* **141** 45 (1987)
74. Z Slanina, J M Rudzinski, E Osawa *Collect. Czech. Chem. Commun.* **52** 2831 (1987)
75. R L Disch, J M Schulman *Chem. Phys. Lett.* **125** 465 (1986)
76. H P Lüthi, J Almlöf *Chem. Phys. Lett.* **135** 357 (1991)
77. J Baker, P W Fowler, P Lazzeretti, M Melagoli, R Zanasi *Chem. Phys. Lett.* **184** 182 (1991)
78. S Larsson, A Volossov, A Rosen *Chem. Phys. Lett.* **137** 501 (1987)
79. T I Shibuya, M Yoshitani *Chem. Phys. Lett.* **137** 13 (1987)
80. M Kataoka, T Nakajima *Tetrahedron* **42** 6437 (1986)
81. I Laszlo, L Udvardi *Chem. Phys. Lett.* **136** 418 (1987)
82. F Negri, G Orlando, F Zerbetto *J. Am. Chem. Soc.* **114** 2909 (1992)
83. P D Hall *J. Am. Chem. Soc.* **108** 6087 (1986)
84. A Rosen, B Wästberg *J. Chem. Phys.* **90** 2525 (1989)
85. S Z Cyvin, E Brensdal, B N Cyvin *Chem. Phys. Lett.* **143** 377 (1988)
86. Z C Wu, D A Jelski, T F Georwe *Chem. Phys. Lett.* **137** 291 (1987)
87. D E Weeks, W G Harter *Chem. Phys. Lett.* **144** 366 (1988)
88. D E Weeks, W G Harter *J. Chem. Phys.* **90** 4744 (1989)
89. R C Jowrey, M M Ross, J H Callahan *J. Phys. Chem.* **96** 4755 (1992)
90. M E Vol'pin *Usp. Khim.* **29** 298 (1960) [*Russ. Chem. Rev.* **29** 129 (1960)]
91. D Lewis, D Peters *Facts and Theories of Aromaticity* (London: MacMillan, 1975)
92. K Hedberg, L Hedberg, D S Bethune, C A Brown, H C Dorn, R D Johnson, M de Vries *Science* **254** 826 (1991)
93. J M Hawkins, A Meyer, T A Lewis, S D Loren, F J Holander *Science* **252** 312 (1991)
94. S C O'Brien, J R Heath, R F Curl, R E Smalley *J. Chem. Phys.* **88** 220 (1988)
95. R M Baum *Chem. Eng. News* 25 (1992)
96. D R McKenzie, C A Davis, D J H Cockayne, D A Miller, A M Vassallo *Nature (London)* **355** 622 (1992)
97. A L Balch, V J Catalano, J W Lee *J. Am. Chem. Soc.* **131** 8953 (1991)
98. R D Johnson, G Meijer, J R Salem, D S Bethune *J. Am. Chem. Soc.* **113** 3919 (1991)
99. E G Gal'pern, V I Sokolov, I V Stankevich, A L Chistyakov *Izv. Akad. Nauk, Ser. Khim.* 2193 (1992)
100. P W Fowler, D E Manolopoulos, R P Ryan *J. Chem. Soc., Chem. Commun.* 408 (1992)
101. H Kroto *Pure Appl. Chem.* **62** 407 (1990)
102. L A Chernozatonskii *Phys. Lett.* **166** 55 (1992)
103. S Iijima *Nature (London)* **354** 56 (1991)
104. T Lenosky, X Gonze, M Teter, V Elser *Nature (London)* **355** 333 (1992)
105. P M Ajayan, S Iijima *Nature (London)* **358** 23 (1992)
106. C Jin, T Guo, Y Chai, A Lee, R E Smalley, in *Proceedings of 1st Italian Workshop on Fullerenes: Status and Perspectives. 6-7 February, 1992, Carlton Hotel, Bologna, Italy*
107. D Ugarte *Nature (London)* **359** 707 (1992)
108. V I Sokolov *Dokl. Akad. Nauk* **325** 991 (1992)
109. I V Stankevich, O B Tomilin *Zh. Strukt. Khim.* **18** 799 (1977)
110. E Heilbronner *Helv. Chim. Acta* **37** 921 (1954)
111. S Kivelson, O L Chapman *Phys. Rev.* **28** 7236 (1983)
112. M A Haase, R W Zoellner *J. Org. Chem.* **57** 1031 (1992)
113. A H H Chand, W C Ermler, R M Pitzer *J. Chem. Phys.* **94** 5004 (1991)
114. A Rosen, B Wäestberg *J. Am. Chem. Soc.* **110** 8701 (1988)
115. U Barth, L Hedin *J.Phys.* **5** 1629 (1972)
116. Y Chai, T Guo, C Jin, R E Haufler, L P F Chibante, J Fure, L Wang, J M Alford, R E Smalley *J. Phys. Chem.* **95** 7564 (1991)
117. T Guo, M D Diener, Y Chai, M J Alford, R E Haufler, S M McClure, T Ohno, J H Weaver, G E Scuseria, R E Smalley *Science* **257** 1661 (1992)
118. J Cioslowski *J. Am. Chem. Soc.* **113** 4139 (1991)
119. R E Smalley, in *Fullerenes* (Eds G S Hammond, V J Kuck) ACS Symp. Ser. 481 (1992) p. 141
120. V Parasuk, J Almlöf *Chem. Phys. Lett.* **184** 187 (1991)
121. D A Bochvar, E G Gal'pern *Izv. Akad. Nauk SSSR, Ser. Khim.* 2367 (1974)
122. L A Chernozatonskii *Phys. Lett.* **160** 392 (1991)
123. S Nagase, K Kobayachi *Chem. Phys. Lett.* **187** 291 (1991)
124. E Kaxiras *Phys. Rev. Lett.* **64** 551 (1990)
125. E Kaxiras *Chem. Phys. Lett.* **163** 323 (1989)
126. N P Gambaryan I V Stankevich *Usp. Khim.* **58** 1945 (1989) [*Russ. Chem. Rev.* **58** 1103 (1989)]
127. E G Gal'pern, I V Stankevich, A L Chistyakov, V B Shur, M E Vol'pin *Dokl. Akad. Nauk SSSR* **302** 1384 (1988)
128. I V Stankevich, A L Chistyakov, V B Shur, M E Vol'pin *Dokl. Akad. Nauk SSSR* **313** 118 (1990)
129. Chen Cheng, Lu Li-Hwa, Yang-Yung Wei *J. Mol. Struct.* **253** 1 (1992)
130. X Xia, D A Jelski, J Bowser, T G George *J. Am. Chem. Soc.* **114** 6493 (1992)
131. R E Smalley *Acc. Chem. Res.* **25** 98 (1992)
132. V I Sokolov *Izv. Akad. Nauk, Ser. Khim.* 10 (1993)
133. T Weiske, D K Böhme, J Hrusak, W Krätschmer *Angew. Chem.* **103** 898 (1991)
134. T Weiske, J Hrusak, D K Böhme, H Schwarz *Helv. Chim. Acta* **75** 79 (1992)
135. T Weiske, H Schwarz *Angew. Chem.* **104** 639 (1992)

136. K A Caldwell, D E Gibbin, C S Hsn, D Cox, M L Gross *J. Am. Chem. Soc.* **113** 8519 (1991)
137. T W Weiske, T Wong, W Krätschmer, J K Terlouw, H Schwarz *Angew. Chem. Int. Ed. Engl.* **31** 183 (1992)
138. H Schwarz *Angew. Chem. Int. Ed. Engl.* **31** 293 (1992)
139. V V Korshak, Yu P Kudryavtsev, A M Sladkov *Vestn. Akad. Nauk SSSR* **1** 70 (1978)
140. M V Nikerov, D A Bochvar, I V Stankevich *Zh. Strukt. Khim.* **23** 16 (1982)
141. K M Merz, R Hoffmann, A T Balaban *J. Am. Chem. Soc.* **106** 6742 (1987)
142. V I Sokolov *Zh. Strukt. Khim.* **25** 175 (1984)
143. R E Haufler, J Conceicao, L P F Chilante *J. Phys. Chem.* **94** 8634 (1990)
144. S Ballenweg Doctorate Thesis, Heidelberg University, Heidelberg (1992)
145. N Matsuzawa, D A Dixon, T Fukunaga *J. Phys. Chem.* **96** 7594 (1991)
146. J H Holloway, E G Hope, R Taylor, G J Langley, A G Avent, T J Denis, J P Hare, H W Kroto, D R M Walton *J. Chem. Soc., Chem. Commun.* 966 (1991)
147. H Selig, C Lifshitz, T Peres, J E Fischer, A R McGhie, W J Romanow, J P McCauley, A B Smith *J. Am. Chem. Soc.* **113** 5475 (1991)
148. G A Olah, I Bucsi, C Lambert, R Anisfeld, N J Trivedi, D K Sensharma, G K S Prakash *J. Am. Chem. Soc.* **113** 9385 (1991)
149. P E Birkett, P B Hitchcock, H W Kroto, R Taylor, D R M Walton *Nature (London)* **357** 479 (1992)
150. F N Tebbe, J Y Becker, D B Chase *Science* **256** 822 (1992)
151. D Dubois, K M Kadish, S Flanagan, Z J Wilson *J. Am. Chem. Soc.* **113** 4364; 7773 (1991)
152. P M Allemand, A Koch, F Wudl, Y Rubin, F Diederich, M M Alvarez, S J Auz, R L Whetten *J. Am. Chem. Soc.* **113** 1050 (1991)
153. S A Lerke, B A Parkinson, D H Evans, P J Fagan *J. Am. Chem. Soc.* **114** 7807 (1992)
154. R C Haddon, A F Hebard, M Rosseinsky, D J Murphy, in *Fullerenes* (Eds G S Hammond, V J Kuck) ACS Symp. Ser. 481 (1992) p. 71
155. S P Solodovnikov, V V Bashilov, V I Sokolov *Izv. Akad. Nauk, Ser. Khim.* 2809 (1992)
156. P J Krusic, E Wasserman, B A Parkinson, B Malone, E R Holler *J. Am. Chem. Soc.* **113** 6274 (1991)
157. P J Krusic, E Wasserman, P N Keizer, J R Morton, K F Preston *Science* **254** 1183 (1991)
158. B L Tumanskii, V V Bashilov, S P Solodovnikov, V I Sokolov *Izv. Akad. Nauk, Ser. Khim.* 1457 (1992)
159. B L Tumanskii, V V Bashilov, N N Bubnov, S P Solodovnikov, V I Sokolov *Izv. Akad. Nauk, Ser. Khim.* 1936 (1992)
160. B L Tumanskii, V V Bashilov, N N Bubnov, S P Solodovnikov, V I Sokolov *Izv. Akad. Nauk, Ser. Khim.* 1938 (1992)
161. P M Allemand, A Koch, K C Khemani, G Srdanov, F Wude, Y Rubin, F Diederich, M M Alvarez, S J Auz, R L Whetten *J. Am. Chem. Soc.* **113** 2780 (1991)
162. A Penicaud, J Hsu, C A Reed, A Koch, K C Khemani, P M Allemand, F Wude *J. Am. Chem. Soc.* **133** 6698 (1991)
163. P M Allemand, K C Khemani, A Koch *Science* **253** 301 (1991)
164. J W Bausch, G K S Prakasch, G A Olah, D S Tse, D C Zorents, Y K Bae, R Malhotra *J. Am. Chem. Soc.* **113** 3205 (1991)
165. G A Olah, I Bucsi, C Lambert, R Amiszfeld, N J Trivedi, D K Sensharma, G K S Prakasch *J. Am. Chem. Soc.* **113** 9387 (1991)
166. G H Kroll, P J Benning, Y Chen, T R Ohno, J H Weaver, L P F Chibante, R E Smalley *Chem. Phys. Lett.* **181** 112 (1991)
167. K M Greegan, J L Robbins, W K Robbins, J M Miller, R D Sherwood, R J Tindall, D M Cox, J P McCauley, D R Jones, R T Gallagher, A B Smith III *J. Am . Chem. Soc.* **114** 1103 (1992)
168. J M Hawkins, T A Lewis, S D Loren, A Meyer, J R Heath, Y Shibato, R J Saykally *J. Org. Chem.* **55** 6250 (1990)
169. J M Hawkins, A Meyer, S D Loren, R Nunlist *J. Am. Chem. Soc.* **113** 9394 (1991)
170. J M Hawkins *Acc. Chem. Res.* **25** 150 (1992)
171. V I Sokolov *Dokl. Akad. Nauk* **326** 647 (1992)
172. P J Fagan, J C Calabrese, B Malone *Science* **252** 1160 (1991)
173. P J Fagan, J C Calabrese, B Malone *J. Am. Chem. Soc.* **113** 9408 (1991)
174. P J Fagan, J C Calabrese, B Malone *Acc. Chem. Res.* **25** 134 (1992)
175. V V Bashilov, P V Petrovski, V I Sokolov, I A Gurey, S V Lindeman, Yu T Struchkov *Organometallics* (in press, 1993)
176. H Nagashima, A Nakaoka, Y Saito, M Kato, T Kawanishi, K Itoh *J. Chem. Soc., Chem. Commun.* 377 (1992)
177. A L Balch, V J Catalano, J W Lee *Inorg. Chem.* **30** 3981 (1991)
178. R S Koefod, M F Hugdens, J P Shapley *J. Am. Chem. Soc.* **113** 8957 (1991)
179. A L Balch, V J Catalano, J W Lee, M M Olmstead *J. Am. Chem. Soc.* **114** 5455 (1992)
180. T Suzuki, Q Li, K C Khemani, F Wudl, Ö Almarsson *Science* **254** 1186 (1991)
181. F Wudl *Acc. Chem. Res.* **25** 157 (1992)
182. T Suzuki, Q Li, K C Khemani, F Wudl, Ö Almarsson *J. Am. Chem. Soc.* **114** 7300 (1992)
183. E Vogel *Pure Appl. Chem.* **54** 1015 (1982)
184. T Suzuki, Q Li, K C Khemani, F Wudl *J. Am. Chem. Soc.* **114** 7301 (1992)
185. M Prato, Q C Li, F Wudl, V Lucchini *J. Am. Chem. Soc.* **115** 1148 (1993)
186. O Ermer *Helv. Chim. Acta* **74** 1339 (1991)
187. T Andersson, K Nielsson, M Sundahl, G Westmann, O Wennerström *J. Chem. Soc., Chem. Commun.* 604 (1992)
188. A Hirsch, Q Li, F Wudl *Angew. Chem. Int. Ed. Engl.* **30** 1309 (1991)
189. S H Hoke II, J Molstad, D Dilettato, M J Jay, D Karlson, B Kahr, R G Cooks *J. Org. Chem.* **57** 5069 (1992)
190. Y Rubin, S Khan, D I Freedberg, C Yeretzian *J. Am. Chem. Soc.* **115** 344 (1993)
191. A D Loy, R A Assink *J. Am. Chem. Soc.* **114** 3978 (1992)
192. S Shi, K C Khemani, Q C Li, F Wudl *J. Am. Chem. Soc.* **114** 1065 (1992)
193. N Sivaraman, R Dhamodaran, I Kaliappan, T G Srinivasan, P R V Rao, C K Mathews *J. Org. Chem.* **57** 6077 (1992)
194. V V Levitskii, S V Dozmorov, USSR P 158 700; *Byull. Izobr.* **31** (1991)

Russian Chemical Reviews **62** (5) 437–446 (1993)
© 1993 Russian Academy of Sciences and Turpion Ltd

UDC 546.763

Inhibitors of the crystallisation of amorphous materials

L A Reznitskii, S E Filippova

Contents

I.	Introduction	437
II.	Crystallisation of oxides that are amorphous to X-rays	438
III.	Crystallisation of solid solutions of oxides	439
IV.	Crystallisation of chemical compounds from coprecipitated hydroxides that are amorphous to X-rays	441
V.	Crystallisation of amorphous metal alloys	442
VI.	Conclusion	445

Abstract. The problems arising in the choice of additives that will improve the temporal and thermal stability of the non-crystalline state of materials are discussed. Transition metal oxides and amorphous metal alloys form suitable subjects for studying the effect of crystal-chemical and energy factors on the stabilisation of amorphous substances. Data on the stabilisation of the amorphous matrix by introducing alloying additives which form solid solutions with isovalent and heterovalent substitution in the cationic sublattice, chemical compounds, and alloys, are reviewed. Criteria for selecting inhibitors that will stabilise the amorphous state of a material are formulated. The bibliography comprises 63 references.

I. Introduction

In the technology of the production of many inorganic materials, e.g. oxides and metal alloys, use is often made of metastable and amorphous modifications of substances. The use of amorphous oxides in the preparation of complex coordination compounds makes it easier for solid state reactions to occur. Such oxides are used in energy-saving technologies that allow homogeneous materials to be produced under optimum conditions. Amorphous metal alloys possess special magnetic properties and resistance to corrosion; this makes them interesting topics for research. One of the problems in studying the amorphous state of a material is to find the factors affecting its time-dependent and thermal stability. This review is only concerned with an analysis of certain general structural and energy characteristics of the non-crystalline state of a solid which can be used to formulate criteria for searching for inhibitors that will hinder the transition of the amorphous to the crystalline state. As the non-crystalline state of matter is as widespread as the crystalline state, we may expect that general physicochemical principles will also be satisfied for amorphous materials.[1]

When analysing publications on the physicochemical properties of amorphous compounds we encounter the problem of comparing the properties of materials with the same or similar compositions but which have sometimes been produced under extremal conditions. For example, in the production of amorphous metal strips the rate of quenching reaches 10^8–10^{10} deg s^{-1}. This makes comparison (and recommendations) difficult because the thermodynamic functions of a substance are dependent on the method of preparation if the material is not in an equilibrium state. In a practical respect the temperatures of relaxation (T_{rel}) and crystallisation (T_{cr}) of amorphous materials, at which irreversible changes in the structure takes place, are very important, as is also, in a number of cases, the loss of valuable technological qualities. These temperatures sometimes vary by some tens of degrees for similar specimens produced in different laboratories. One must therefore concentrate on criteria for the correctness of the measurements of thermodynamic properties. Such measurements are valid if the internal state of the system remains unchanged during the measurement of the property. In this respect the certification of amorphous compounds produced by chemical methods is simpler and more reliable because such methods are milder and more easily reproduced and monitored.

Chemical methods for obtaining complex coordination compounds frequently involve the use of coprecipitation of metal hydroxides followed by dehydration which produces an intermediate state that is amorphous to X-rays. The crystallisation of such amorphous oxides sometimes has an 'explosive' character and is accompanied by a chemical reaction between the oxides giving a 100% yield of the substance being prepared. Oxides play an important role in chemical thermodynamics and can be used as models for the study of physicochemical aspects of the metastable state of matter.

Measurements of the heat capacity (C_p) and crystallisation temperature of amorphous compounds are fully valid if the time over which the property is measured is shorter than the relaxation time of the system. In most instances the thermodynamic properties of amorphous materials are measured with the use of differential thermal analysis (DTA) and/or differential scanning calorimetry (DSC) with a rate of heating less than 10 deg min^{-1}, which is much higher than the rate of relaxation of the system at temperatures a long way from the relaxation and crystallisation temperatures. This guarantees reproducibility of the properties of the specimens because the conditions under which heat is absorbed and evolved are reversible. The thermodynamic properties of metastable and amorphous modifications of solids can serve as characteristics of their stability and reactivity.

L A Reznitskii, S E Filippova Department of General Chemistry, Lomonosov Moscow State University, 119899 Moscow.
Fax (7-095) 939 01 71

Received 22nd December 1992
Uspekhi Khimii **62** (5) 474–484 (1993); translated by G J Bullen

Most transition metal oxides and metal alloys belong to the category of coordination compounds. Structural studies on amorphous materials of different provenance indicate that the metal atoms have coordination polyhedra (CP), the various modes of linking of which provide short-range order in these materials in the absence of translational symmetry. A knowledge of the distinctive features and types of CPs is essential for an understanding of the reaction mechanisms in crystalline and non-crystalline states of solids and the use of the CP as a structural fragment which is common to both states enables them to be discussed from a common standpoint.

Examples indicating the polyhedral structure of amorphous oxides are given below. In films of amorphous oxides (e.g. Fe_2O_3, Al_2O_3, Nb_2O_5, and WO_3) obtained by pyrolysis of organometallic compounds in an O_2 atmosphere the first coordination number (CN) of the metal is smaller than in known crystal structures. The parameters of the structure of amorphous phases are determined by analysing the radial distribution function (RDF).[2] For example, an analysis of the RDF of an amorphous Fe_2O_3 film showed that the Fe–O distance (1.95 Å) is smaller than the corresponding distance in crystalline α-Fe_2O_3 (2.01 Å). The iron atoms in amorphous Fe_2O_3 are located in both octahedral and tetrahedral holes in a disordered packing of oxygen atoms. The presence of such holes is characteristic of the metastable modification γ-Fe_2O_3. The short-range order in the amorphous α-Fe_2O_3 is similar to that in γ-Fe_2O_3. The first coordination peak in the RDF at an Fe–O distance of 1.95 Å and the fact that $5 < CN < 6$ indicates that amorphous Fe_2O_3 can be described with the use of the most likely structural elements (MLSE).[3] A similar approach was developed elsewhere.[4]

The quantitative relationships between the types of polyhedra may vary depending on the method by which the amorphous materials have been obtained. For example, the model for the structure of an amorphous film of Al_2O_3 is a linear group of three polyhedra, two of which are AlO_6 octahedra with a shared edge and the third is an AlO_4 tetrahedron which shares a corner with one of the octahedra. For a film obtained by pyrolysis of aluminium isopropoxide at 670 K with 50 vol.% O_2 in the gas phase on an NaCl base, the mean CN(Al) is 5.3. If the O_2 concentration is raised to 75 vol.% the MLSE is a group of three AlO_4 tetrahedra, two of which have a shared face and the third is linked to them by a corner.[5]

The model of MLSE for an amorphous film of Nb_2O_5 is a linear group of three polyhedra: two tetragonal pyramids and one tetrahedron linked by corners, with a mean CN(Nb) of 4.5. The model of MLSE for amorphous WO_3 is a group of tetragonal pyramids and octahedra with a mean CN(W) of 5.5. In crystalline WO_3 the octahedron is the main coordination polyhedron. Thus the models of the atomic groupings can be regarded as subcells of the structure of amorphous oxides which are joined together to form a chain without any long-range order and are space-filling. This enables models for amorphous oxides to be obtained.[6]

A similar situation is observed in studies of amorphous alloys. The amorphous state of metal alloys is characterised by atomic short-range order and it is thermodynamically metastable.[7] Fragments of the crystal structure of metal alloys are retained in the amorphous state and the chief 'amorphising' elements are boron, carbon, and phosphorus. The stability of amorphous alloys against diffusion decomposition is associated with the presence in the alloy of fragments with rigid metal–non-metal covalent bonds. These fragments may have a composition corresponding to a stable or metastable crystalline state and a similar nearest coordination sphere.[8] To describe the Fe–B system (alloys with the approximate composition $Fe_{0.8}B_{0.2}$ form the subject of experimental studies particularly frequently) a trigonal prism model with an Fe_3C type CP has been used.[9] The tendency to amorphisation is related to the variation in the type of linking of these prisms. Clearly, the more stable such fragments the more difficult it is for disintegration of the amorphous alloy to occur on its crystallisation.

The view that transition metal oxides can be regarded as inorganic polymers with M–O covalent bonds and that the structure of the polymers can be modelled by a three-dimensional chain composed of deformed oxygen polyhedra[10] is valid. Most transition metal oxides are semiconductors or insulators. According to Ioffe "all the main properties of a semiconductor, including its band structure, are determined by the short-range order — the chemical bonds within one unit cell of the crystal".[11]

These preliminary remarks are, of necessity, fragmentary in nature but they indicate that the structures of the first coordination spheres of amorphous and crystalline structures have similar features and it is only in the more distant coordination spheres that differences are observed. It may therefore be expected that when explaining the reasons responsible for the features of the crystallisation of amorphous compounds, irrespective of their nature, the energy and crystal-chemical properties of the coordination polyhedra will be of predominant importance.

For most amorphous oxides and metal alloys, which are investigated by thermal methods, simultaneous structural studies are not carried out. The crystallisation of amorphous compounds may be accompanied by a change in the CN in the nearest neighbours. The enthalpies of the change in CN of some cations with oxygen nearest neighbours are known[12] and they are less than 5% of the enthalpies of atomisation of the oxides. Hence, to a first approximation, the effect of a change in the coordination of the metal cation when amorphous oxides and their solid solutions crystallise can be neglected (such data are not yet available for some cations). Furthermore, the ratio of the different polyhedra in the MLSE may vary depending on the method used to obtain the amorphous compound. Therefore it will henceforth be assumed that the coordination numbers of the cations are the same in the primary matrix and in the alloying constituent.

II. Crystallisation of oxides that are amorphous to X-rays

The general criteria for searching for inhibitors that will stabilise the amorphous state of a solid can be recognised by experimental studies of the crystallisation of simple amorphous (to X-rays) oxides, solid solutions, and chemical compounds with different polyhedral structures. The principal method for obtaining amorphous oxides is the careful decomposition of the hydroxide at low temperatures. Suitable model subjects are the oxides Fe_2O_3, Cr_2O_3, Al_2O_3, and ZrO_2, solid solutions based on them, and chemical compounds formed by them; these are widely used in electronic engineering. The phase transformations occurring on dehydration of the hydroxides and subsequent crystallisation of the amorphous oxides are normally studied by DTA, DSC, X-ray phase analysis, and Raman spectroscopy. By using these methods the sequence of chemical and physical changes can be reconstructed.

The preparation and crystallisation of amorphous Fe_2O_3, forming α-Fe_2O_3, had already been described by Mendeleev[13]

Table 1. *Temperatures of commencement of crystallisation and enthalpies of crystallisation of oxides from the amorphous state.*

Oxide	T_{cr} / K	$-\Delta H_{cr}$ / kJ mol^{-1}	$-\Delta H_{fus}$ / kJ mol^{-1}	$-\Delta H_{cr}/\Delta H_{fus}$	Ref.
Fe_2O_3	533	37.9±2.3	–	–	14
	533	134	–	–	17
Cr_2O_3	653	22.3±1.5	125	0.18	15
	663	50		0.40	17
Al_2O_3	443	58	111	0.52	17
ZrO_2	666	21.0±0.5	90	0.23	16
TiO_2	523	63	68	0.93	17

Table 2. Temperatures and enthalpies of crystallisation of amorphous oxides.

Oxide	$\frac{T_{cr}}{K}$	$\frac{-\Delta H_{cr}}{kJ\ mol^{-1}}$	$\frac{a_0}{Å} \pm 0.005$	$\frac{c_0}{Å} \pm 0.005$
$Sc_{0.04}Fe_{1.96}O_3$	535	32.7±1.0	5.046	13.754
$Sc_{0.1}Fe_{1.9}O_3$	579	24.8±0.4	5.054	13.764
$In_{0.1}Fe_{1.9}O_3$	524	34.2±2.1	5.057	13.782
$Ga_{0.2}Fe_{1.8}O_3$	519	41.2±4.5	5.036	13.748
$Al_{0.1}Fe_{1.9}O_3$	593	33.9±2.3	5.018	13.704
Fe_2O_3	533	37.9±2.3	5.036	13.748
$(Yb_{0.1}Fe_{1.9}O_3)$[a]	603	–	–	–
$(Tm_{0.1}Fe_{1.9}O_3)$[a]	646	–	–	–
$(La_{0.1}Fe_{1.9}O_3)$	709	–	–	–

[a] According to initial mixture; the crystallisation products are α-Fe_2O_3 + $MFeO_3$.

who remarked on the spontaneous heating of dehydrated $Fe_2O_3 \cdot 1.5H_2O$.

Hydroxides of iron, chromium, and zirconium have been obtained by precipitation from solutions of the nitrates with ammonia solution[14-16] The DSC thermograms of hydroxides previously dried (100–120 °C) show endothermic effects due to the removal of water. After this the materials were oxides amorphous to X-rays. At higher temperatures exothermic effects due to crystallisation were observed, and these effects are sometimes 'explosive' in character.

The changes occurring in the hydroxides on heating have been assessed from X-ray phase analysis and Raman spectroscopic data. In the Raman spectra the bands due to M–O–H and H–O–H stretches disappear as the temperature is increased. The temperatures and enthalpies of crystallisation of the amorphous oxides are given in Table 1. T_{cr} and ΔH_{cr} from different publications show marked differences, i.e. undoubtedly the method of preparing the amorphous compounds affects their properties. As short-range order exists in the amorphous phase the value of ΔH_{cr} for the amorphous material cannot be larger in absolute magnitude than ΔH_{fus} for the crystalline material.

Publications on the determination of ΔH_{cr} for Fe_2O_3 have been analysed critically.[14] It was shown, in particular, that the value of ΔH_{cr} for Fe_2O_3 found by quantitative differential thermal analysis (−134 kJ mol^{-1} [17]) is obviously too high. This method is inaccurate and therefore the values of ΔH_{cr} for Fe_2O_3 and the other oxides (TiO_2, Al_2O_3, Cr_2O_3) must be regarded as estimates.

The enthalpies of fusion of crystalline M_2O_3 (M = Al, Cr, Ti, Sc) are 100–125 kJ mol^{-1} but the entropies of fusion are ~46 J mol^{-1} K^{-1}.[18] Since hematite α-Fe_2O_3 dissociates to magnetite and O_2 at 1 700 K (which is much lower than the melting points of the other M_2O_3, *viz.* 2 100–2 700 K), it is unlikely that the enthalpy of crystallisation of Fe_2O_3 would be of the same order of magnitude (100–125 kJ mol^{-1}) or even exceed the enthalpies of fusion of the thermodynamically stable oxides. The ratios $\alpha = \Delta H_{cr}/\Delta H_{fus}$, indicating the high energy capacity of the amorphous oxides, are also given in Table 1.

III. Crystallisation of solid solutions of oxides

The effect of adding 5–10 mol% of oxides on T_{cr} and ΔH_{cr} of amorphous Fe_2O_3 and ZrO_2 has been investigated.[15, 19-23] The main aim of this research was to find oxides which might stabilise the amorphous state of the primary matrix in the model specimens. Small amounts of additives can be introduced into a matrix of the main component and may form a solid solution, if this is permitted by the size factor, or form a chemical compound with the main component.

1. Formation of solid solutions with isovalent substitution

Studies of the effect of M_2O_3 additives (M = Al, Ga, Cr, Sc, In, La, Tm, Yb) on the variation in T_{cr} of amorphous Fe_2O_3 led to the following conclusions. In the same type of processes of solid-solution formation there is a correlation between increasing crystallisation temperature and an increase in the bond energy ε(M–O) as compared to ε(Fe–O). The higher ε(M–O) the higher the temperature of commencement of reorganisation of fragments of the structure of amorphous oxides that are formed by dehydration of coprecipitated hydroxides with subsequent crystallisation of the solid solutions based on hematite. Such solutions are formed by introducing the oxides of aluminium, chromium, gallium, indium, and scandium but the introduction of lanthanum, thulium, and ytterbium oxides, whose cations are larger, leads to crystallisation of a two-phase mixture of the orthoferrite-perovskites $MFeO_3$ with Fe_2O_3. T_{cr} and $-\Delta H_{cr}$, obtained by the DSC method, for the amorphous oxides $M_xFe_{2-x}O_3$ are given, together with their rhombohedral lattice parameters, in Table 2; crystal-chemical and energy characteristics of M^{3+} cations, and the bond energies ε(M–O) in the oxides, calculated by a method proposed previously,[24] are given in Table 3.

The increase in T_{cr} on the introduction of lanthanum, terbium [thulium? (Ed. of translation)], and ytterbium oxides is determined mainly by the high M–O bond energies. On crystallisation in an iron oxide matrix a chemical reaction takes place to form islets of a new phase: the orthoferrite $MFeO_3$. The new phase, which is distributed uniformly throughout the whole volume of the oxides crystallising, inhibits the formation of hematite and consequently the upper temperature boundary of the exothermic effect is not recorded and the large lanthanide ions do not enter into the hematite structure.

The change in the CN of the metal on insertion into the hematite structure (CN = 6, octahedron) also has an effect on the temperature range for crystallisation. The insertion of Ga^{3+} and Cr^{3+} ions, with radii similar to that of Fe^{3+}, leads to differing thermograms. The crystallisation range of the Ga–Fe solid solution is more extended than the Cr–Fe crystallisation range, reflecting the diffusion difficulties associated with the change in

Table 3. Crystal-chemical and energy characteristics of M^{3+} ions and bond energies ε(M–O) in the oxides M_2O_3.

Property	In^{3+}	Ga^{3+}	Fe^{3+}	Cr^{3+}	Sc^{3+}	Al^{3+}	Yb^{3+}	Tm^{3+}	La^{3+}
ε(M–O)[a]/ kJ g^{-1} electron^{-1}	179	195	199	222	–	255	–	–	–
ε(M–O)[b]/ kJ g^{-1} electron^{-1}	178.5	197	199	222	283	255	238	257	282
$r(M^{3+})$[a]/ Å	0.80	0.62	0.65	0.62	0.75	0.53	0.87	0.88	1.03
ΔT_{cr}/ K	−9	−7	–	40	46	60	70	112	176
$\Delta\varepsilon$/ J g^{-1} electron^{-1}	−20	−2	–	23	84	56	39	58	83
Crystallisation products	Solid solution based on hematite α-Fe_2O_3 + $MFeO_3$								

Note. ΔT_{cr} is the change in the crystallisation temperature of Fe_2O_3 per 5 mol% of additive and $\Delta\varepsilon = \varepsilon(M-O) - \varepsilon(Fe-O)$; the scale of $\Delta\varepsilon$ shows the enthalpy of formation of the paired-electron bonds per 1 g-mol of electrons.

[a] CN = 6.

[b] In the individual oxide.

the CN of one of the gallium ions in the thermodynamically stable modification β-Ga_2O_3. This modification may be produced in the crystallisation of the coprecipitated hydroxides. In β-Ga_2O_3 one of the cations is tetrahedrally, and the other octahedrally, coordinated by O^{2-} ions. The structure of Cr_2O_3 is however similar to that of Fe_2O_3 and there is therefore no change in the CN of chromium on formation of a $Cr_2O_3-Fe_2O_3$ solid solution.

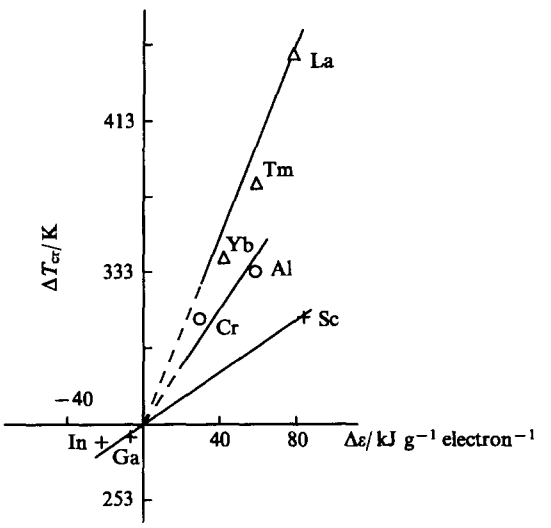


Figure 1. The change in the temperature of commencement of crystallisation of amorphous oxides $\Delta T_{cr} = T_{cr}[(M_xFe_{1-x})_2O_3] - T_{cr}(Fe_2O_3)$ plotted as a function of the bond energy difference Δε.

The function $\Delta T_{cr}(\Delta\varepsilon)$ is shown in Fig. 1 for three groups of additive cations: Al and Cr; In, Ga, and Sc; and La, Tm, and Yb. For the cations in the first group a CN of 6, which is characteristic of them in the pure oxides and in a thermodynamically stable state, is retained in the solid solution. The CN of the cations in the second group changes on formation of the solid solution. On insertion of the additive cations in the third group crystallisation of the two-phase mixture α-Fe_2O_3 + $MFeO_3$ takes place. For all three groups of additive cations the dominant factor affecting the stabilisation of the amorphous state of iron oxide is the metal–oxygen bond energy.

2. Formation of solid solutions with heterovalent substitution

The effect of heterovalent additives on the stability of the amorphous oxide has been investigated in the case of ZrO_2. Crystallisation of amorphous ZrO_2 on heating in a calorimeter leads to the formation of the metastable cubic modification, in contrast to the crystallisation of amorphous Fe_2O_3 in which the stable phase α-Fe_2O_3 is formed. The high-temperature cubic modification of ZrO_2, which is formed by crystallisation from the melt, is stabilised at low temperatures by the introduction of lanthanide oxide additives. The introduction of 5 mol% $MO_{1.5}$ leads to stabilisation of the cubic modification of ZrO_2 which persists down to 1 070 K and on subsequent cooling to 300 K. T_{cr} and ΔH_{cr} for the cubic solid solutions are shown in Table 4 and Fig. 2. ε(M–O) and the radius of the lanthanide ion (CN = 8) clearly have the main influence on T_{cr}. In Fig. 2 two coordinate fields, situated above and below the abscissa axis, can be distinguished. The ions occuring in the first field are those of yttrium, scandium, terbium, praseodymium, and neodymium, the insertion of which increases the temperature stability of the amorphous ZrO_2 matrix. The M–O bond energies in these oxides are greater than or almost the same as ε(Zr–O), which is equal to 268 kJ g^{-1} electron^{-1} in the cubic modification. In the second field the europium and ytterbium ions, which have ε(M–O) < ε(Zr–O), occur. The introduction of oxides with a lower chemical potential for oxygen favours an increase in the crystallisation temperature of the solid solution, i.e. these oxides are inhibitors of crystallisation of the amorphous state.

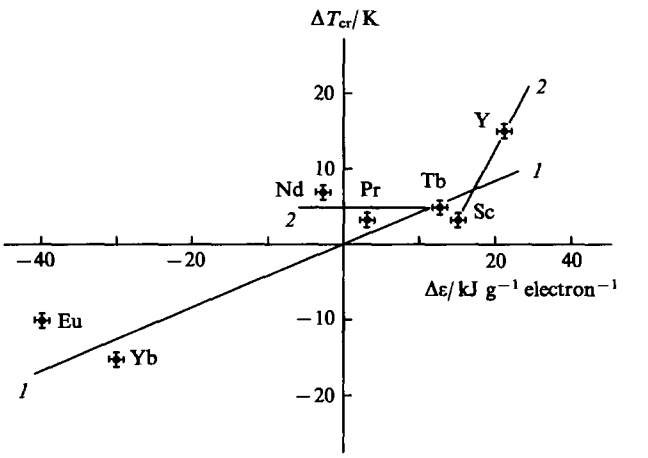


Figure 2. The change in the crystallisation temperature of solid solutions $\Delta T_{cr} = T_{cr}(Zr_{0.95}M_{0.05}O_{1.975}) - T_{cr}(ZrO_2)$ plotted as a function of the bond energy difference $\Delta\varepsilon = \varepsilon(M-O) - \varepsilon(Zr-O)$.

Table 4. Crystal-chemical and energy characteristics of the oxides $Zr_{1-x}M_xO_{2-x/2}$.

Oxide	ε(M – O) / kJ g^{-1} electron^{-1}	$r_{M^{3+}}$ / Å	$\Delta r_{M^{3+}}$ / %	T_{cr} / K	$-\Delta H_{cr}$ / kJ mol^{-1}
ZrO_2	268	0.84	–	666–715	21.0±0.46
$Zr_{0.95}Y_{0.05}O_{1.975}$	290	1.02	21	680–715	18.0±0.86
$Zr_{0.95}Sc_{0.05}O_{1.975}$	283	0.87	3.6	669–771	17.5±0.53
$Zr_{0.95}Pr_{0.05}O_{1.975}$	271	1.13	34	669–775	15.0±0.78
$Zr_{0.95}Nb_{0.05}O_{1.975}$	266	1.11	27	672–775	14.5±1.6
$Zr_{0.95}Eu_{0.05}O_{1.975}$	229	1.07	23	655–754	17.5±1.0
$Zr_{0.95}Tb_{0.05}O_{1.975}$	281	1.04	24	671–781	18.0±0.6
$Zr_{0.95}Yb_{0.05}O_{1.975}$	238	0.99	18	651–741	17.5±0.6

The large praseodymium and neodymium ions produce a slight increase in T_{cr} of amorphous ZrO_2 although their ε(M–O) values are close to ε(Zr–O). Y_2O_3, which has a high ε(Y–O) bond energy and also a large Y^{3+} cation, is an effective stabiliser of the amorphous state. In this instance the crystal-chemical and energy factors act in the same sense. The introduction of the large europium and ytterbium ions, which form oxides with lower M–O bond energies, does not have a stabilising influence. The straight line *1* in Fig. 2, which is drawn through all the points including the coordinate origin, confirms the dominant influence of the energy factor on T_{cr} but allowance for the crystal-chemical size factor adds a correction to the prediction. The broken line *2* also objectively reflects the influence of the additive on T_{cr} of the solid solution. It has been found[20] that introducing an M_2O_3 additive into the solid solution displaces ΔH_{cr} in a positive direction from −21 to −18 to −15 kJ mol^{-1}. The less negative values of ΔH_{cr} are due to the positive enthalpy of mixing (ΔH_{mix}) when heterovalent solid solutions are formed. An analysis of ΔH_{cr} with the aim of eliminating ΔH_{mix} showed that small ΔH_{mix} values are not at variance with the formation of solid solutions in the $Y_2O_3-ZrO_2$ system.

Table 5. Temperatures and enthalpies of crystallisation of the solid solutions $Zr_{1-x}Fe_xO_{2-x/2}$ and $Zr_{1-x}Mg_xO_{2-x}$.

Solid solution	T_{cr}/K	$-\Delta H_{cr}$/kJ mol^{-1}
$Zr_{0.75}Fe_{0.25}O_{1.875}$	851–943	12.0±1.5
$Zr_{0.5}Fe_{0.5}O_{1.75}$	921–1007	7.7±1.5
$Zr_{0.95}Mg_{0.05}O_{1.95}$	717–777	16.5±1.1
$Zr_{0.5}Mg_{0.5}O_{1.5}$	835–886	9.1±0.3

An unexpected result was obtained[21] regarding the effect of introducing Fe_2O_3 into ZrO_2 on T_{cr} for the solid solution $Zr_{1-x}Fe_xO_{2-x/2}$ (x = 0.25 and 0.50) (Table 5). The formation of the solid solution leads to an increase in T_{cr} compared to T_{cr} for the two amorphous oxides although $\varepsilon(Fe-O) < \varepsilon(Zr-O)$. This result is attributed to the polyhedral structure of the solid solution. Results obtained by the method of hyperfine structure of the X-ray absorption spectrum show[25] that in the cubic solid solution with x = 0.3 the ZrO_8 polyhedra are linked by their edges, the FeO_4 tetrahedra are linked by their edges to the ZrO_8 polyhedra and by two corners to other FeO_4 tetrahedra. The increase in T_{cr} is due to the formation of FeO_4 tetrahedra which are energetically less stable than FeO_6 octahedra which might appear on formation of the hematite structure. In order to form FeO_4 polyhedra a potential barrier must be overcome because the $FeO_6 \rightarrow FeO_4$ transition is accompanied by the absorption of heat (22.2 kJ mol^{-1}).[12] The small positive values of ΔH_{mix} which have been calculated[21] are not at variance with the formation of solid solutions in the $Fe_2O_3-ZrO_2$ system.

The introduction of the additive MgO has a similar effect on the increase in T_{cr} for ZrO_2.[23] In this instance the crystallisation is 'explosive' in character and T_{cr} increases compared to the value for zirconium dioxide by 200 K for every 5 mol% of MgO. MgO_8 polyhedra are formed in the cubic solid solution, the enthalpy change in the process MgO_6(octahedron)$\rightarrow MgO_8$(cube) being 71 kJ mol^{-1}.[24] To overcome the potential barrier on formation of the cubic environment of O^{2-} ions around the magnesium ion the amorphous oxides must be heated to $T > T_{cr}$ for ZrO_2, i.e. the reason for the stabilisation of the amorphous ZrO_2 is the same as when Fe_2O_3 is introduced although $\varepsilon(Mg-O) < \varepsilon(Zr-O)$.

Thus when the enthalpy of the change in the CN of the additive cations on their insertion into the solid solution has high positive values, a considerable increase in T_{cr} of the primary matrix is possible.

In research on the preparation of the adsorbents $xAl_2O_3 \cdot yZrO_2$, $xAl_2O_3 \cdot yY_2O_3$, etc.[26–28] the crystallisation temperature of coprecipitated hydroxides was shown to increase on formation of solid solutions. This phenomenon was called a protective effect from crystallisation of the components. The introduction of Al_2O_3 into a ZrO_2 matrix by heating the coprecipitated hydroxides $Al(OH)_3/Zr(OH)_4$ increases T_{cr} for tetragonal ZrO_2 by 400 K compared with the value for amorphous ZrO_2 (445 °C).[29] The energetics nature of this effect was not considered in these papers[26–29] although its interpretation may, in our opinion, be similar to that discussed above for the introduction of Fe_2O_3 and MgO into ZrO_2. The formation of Al_2O_3/ZrO_2 substitutional solid solutions will be accompanied by a change in the CN of aluminium on its insertion into zirconium positions with high CNs (7 or 8). This type of coordination is not typical of aluminium and in order to form AlO_7 or AlO_8 fragments a high potential barrier must be overcome. Magnus's crystal-chemical rules, which determine the possible CNs of cations from the ratio of the cation and anion radii, lead to the same conclusion. The enthalpy of the change in the coordination in the transition $AlO_6 \rightarrow AlO_n$ (n = 7 or 8) is not known but it probably has a high positive value. This inhibits the crystallisation of the oxides. The final products of the coprecipitation of the hydroxides $Al(OH)_3/Zr(OH)_4$ may be mixtures of polymorphs of ZrO_2 depending on the ratio of the aluminium and zirconium concentrations, the conditions used to precipitate the hydroxides, and whether the solid solutions are heated or maintained isothermally at high temperatures.[28, 30]

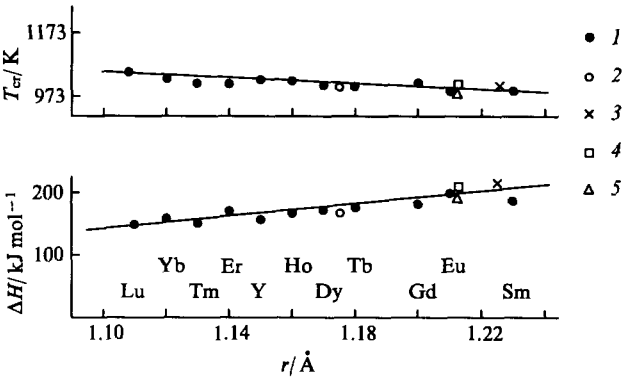


Figure 3. Variation of T_{cr} and ΔH_{cr} with the ionic radius of the lanthanide: *1*) lanthanide ions; *2*) $LuEu_2Fe_5O_{12}$, *3*) $Nd_{0.94}Gd_{2.06}Fe_5O_{12}$, *4*) $Lu_{0.48}Sm_{2.52}Fe_5O_{12}$, *5*) $La_{0.24}Gd_{2.76}Fe_5O_{12}$.

The effect of stabilisation of amorphous films based on ZrO_2 with Y_2O_3 introduced, which were obtained by electron-beam vaporisation, has been noted.[31] Crystalline films of ZrO_2 are obtained at as low a temperature as 420–470 K but the introduction of 10–20 mol% Y_2O_3 enables the amorphous state to be preserved up to 520–550 K. The crystallisation temperatures of the amorphous films are much lower than those of the amorphous compounds obtained from coprecipitated hydroxides but the introduction of Y_2O_3 into the film leads to stabilisation of the amorphous state.

IV. Crystallisation of chemical compounds from coprecipitated hydroxides that are amorphous to X-rays

The formation of chemical compounds with a more complex crystal structure than those of simple oxides or their solid solutions also increases the time-dependent and thermal stability of the amorphous state. Systematic studies have been carried out on the process of crystallisation of the ferrogarnets $E_3Fe_5O_{12}$, orthoferrites with the perovskite structure type $EFeO_3$ (E = a lanthanide ion), and compounds with the magnetoplumbite structure $MFe_{12}O_{19}$ (M = Pb, Sr, Ba).[32–37]

1. Formation of $E_3Fe_5O_{12}$

The distinctive features of the process of crystallisation of ferrogarnets from the amorphous (to X-rays) state of the oxides by DSC are associated with a change in the mechanism of the solid-state reaction. In the garnet structure there are three non-equivalent positions for the cations in an oxygen environment: $3E^{3+}$ are in EO_8 dodecahedra, $3Fe^{3+}$ in FeO_4 tetrahedra, and $2Fe^{3+}$ in FeO_6 octahedra. For the formation of the complex garnet crystal structure temperatures higher than T_{cr} for amorphous Fe_2O_3 are required (Fig. 3).

Lanthanide ferrites with the garnet structure are formed only for E = Sm ... Lu; larger lanthanide ions will not enter the garnet structure owing to steric hindrance. However, lanthanum, praseodymium, and neodymium ions can be inserted into the garnet structure if lanthanide ions with a smaller radius are introduced at the same time. The dependence of T_{cr} and ΔH_{cr} on the radius of the lanthanide is shown in Fig. 3. In general, ΔH_{cr} decreases and T_{cr} increases along the series Sm ... Lu. The formation of garnets with the large ions Sm ... Dy, and also the solid solutions $Lu_{0.48}Sm_{2.52}Fe_5O_{12}$, $La_{0.24}Gd_{2.76}Fe_5O_{12}$, $LuEu_2Fe_5O_{12}$, and $Nd_{0.94}Gd_{2.06}Fe_5O_{12}$ in which the mean radii of the lanthanide ions do not exceed the ionic radius of Sm^{3+}, is

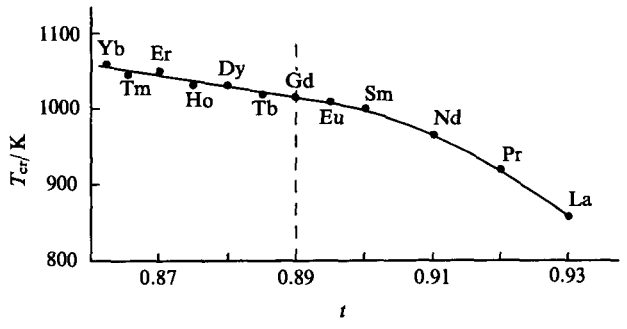


Figure 4. Dependence of T_{cr} for lanthanide orthoferrites on the stability factor t:

$$t = \frac{r_{Ln^{3+}} + r_{O^{2-}}}{\sqrt{2}(r_{Fe^{3+}} + r_{O^{2-}})}$$

accompanied by a single sharp exothermic effect within a narrow temperature range. The ferrogarnets of Ho ... Lu are formed by a more complex mechanism with an increasingly distinct separation into two crystallisation stages and a higher temperature range for the reaction. The decrease in ΔH_{cr} with increasing atomic number of the lanthanide is due to an increase in the degree of distortion of the EO_8 dodecahedra along the series Eu ... Lu. When the components are in a stoichiometric ratio crystallisation gives single-phase green garnets which have Raman spectra consistent with the published spectra. $Lu_3Fe_5O_{12}$ could not be prepared; all attempts gave a mixture of the garnet and the perovskite $LuFeO_3$ or the oxides.

The crystal-chemical factor is clearly dominant in the crystallisation of these coordination compounds which form three sublattices. On going from the state in the oxides ($6O^{2-} + 2\square$, where $\square$ represents a vacancy) there is a monotonic decrease in the enthalpy of the change in the CN of the lanthanide ions as the atomic number of the lanthanide increases, *viz.* $E(Gd^{3+}) = 33$, $E(Y^{3+}) = 71$, $E(La^{3+}) = -31$ kJ ($4O^{2-} + 3O^{2-} \rightarrow LaO_8$).[38] These individual values fit the straight line $E(E^{3+}) = f[r(E^{3+})]$, where r is the ionic radius of the lanthanide. The presence of the hydrates $E(OH)_3$ and $Y(OH)_3$ in the coprecipitated hydroxides increases T_{cr} for amorphous Fe_2O_3 from 260 to 720–770 °C, i.e. it promotes stabilisation of the amorphous state of the dehydrated oxides.

2. Formation of the orthoferrite-perovskites $EFeO_3$

Crystallisation of the coprecipitated hydroxides $E(OH)_3$/ $Fe(OH)_3$ to form lanthanide orthoferrites is observed in the range 850–1170 K. On formation of the orthoferrites of La ... Sm the DSC thermograms show a single exothermic peak due to crystallisation extending over a 70 K range. In the formation of $EuFeO_3$ the peak begins to split, the crystallisation of $GdFeO_3$ spans a range of 100 K, and at the end of the lanthanide series the crystallisation of thulium and ytterbium orthoferrites takes place in two stages extending over a range of 150 K. As for the ferrogarnets, the decrease in the ionic radius of the lanthanide at the end of the series is accompanied by a decrease in ΔH_{cr} of the orthoferrite and an increase in the thermal stability of the amorphous state. The dependence of T_{cr} on the stability factor is shown in Fig. 4. For perovskites with tervalent cations the lower limit of the t factor is 0.89. In the vicinity of $t = 0.89$ there is a change in the slope of the curve showing the dependence of T_{cr} (and ΔH_{cr}) on t and the peaks due to crystallisation start to split. The inhibiting effect of the E_2O_3 is shown by a 300–600 K increase in T_{cr}, or 6–13 K for each 1 mol% of the E_2O_3 additive if it is assumed that ΔT_{cr} is proportional to the amount of E_2O_3. These values of ΔT_{cr} are comparable with those observed when 5 mol% of ytterbium, thulium, or lutetium are introduced into Fe_2O_3 (15–30 K per mol% of the additive).

3. Formation of the hexaferrites $MFe_{12}O_{19}$

To prepare the hexaferrites $MFe_{12}O_{19}$ (M = Pb, Sr, Ba) with the magnetoplumbite structure the methods of obtaining coprecipitated hydroxides described previously[39–41] were used. The crystallisation of strontium and barium hexaferrites takes place in a single stage at 730 and 650 °C respectively. The complex coordination structure of the hexaferrites contains four types of CP in each formula unit: an MO_{12} cubo-octahedron, an FeO_5 trigonal bipyramid, two FeO_4 tetrahedra, and nine FeO_6 octahedra. This is a more complex structure than that of the perovskites or garnets. The formation of FeO_5 and FeO_4 polyhedra is energetically less favourable than the formation of FeO_6 octahedra and consequently the formation of the structure may be particularly inhibited when the crystal-chemical factor is added to the energy factor [$\varepsilon(Sr-O) > \varepsilon(Fe-O)$ and $\varepsilon(Ba-O) > \varepsilon(Fe-O)$].

A characteristic feature of the exothermic effect due to crystallisation of coprecipitated lead and iron hydroxides is that it is spread out over the range 390–670 °C on formation of $PbFe_{12}O_{19}$. Furthermore the products of the crystallisation reaction also contain α-Fe_2O_3; this is not inconsistent with the known metastability of $PbFe_{12}O_{19}$, whose enthalpy of formation from the oxides is estimated to be 37 kJ mol^{-1}.[42] In an attempt to synthesise $SrFe_{12}O_{19}$ a qualitatively similar thermogram was obtained by heating coprecipitated strontium and iron hydroxides; crystallisation of $SrFe_{12}O_{19}$ takes place at 567–777 °C. The higher temperature is due to the higher value of $\varepsilon(Sr-O)$. The formation of a mixture of the hexaferrite and hematite is also observed in this case.

The thermogram of coprecipitated barium and iron hydroxides shows a pronounced effect due to the 'explosive' formation of single-phase $BaFe_{12}O_{19}$ within the narrower temperature range 723–818 °C. The bond energies $\varepsilon(Sr-O) = 249$ and $\varepsilon(Ba-O) = 244$ kJ g^{-1} electron^{-1} agree with experimental error (± 10 kJ mol^{-1}) and overall the inhibiting effect of the large cations on the temperature of formation of the hexaferrites increases in the order Pb–Sr–Ba as $\varepsilon(M-O)$ increases. The increase in T_{cr} over the value for iron oxide is 130–460 K when 7.7 mol% of additive is introduced into the cationic sublattice, i.e. 16–60 K per mol% of the additive. This is the same order of magnitude as the increase in T_{cr} for the solid solutions based on hematite and containing 5–10 mol% of additive cations (see above). The increases in the crystallisation temperature (in K) occurring on formation of solid solutions of the oxides and chemical compounds with alloying additives introduced (calculated per 1 mol% of additive in the cationic sublattice) are given below:

Solid solution	$E_3Fe_5O_{12}$	$EFeO_3$	$MFe_{12}O_{19}$
14–30	17–20	6–13	14–60

We may conclude that the crystal-chemical (size) factor is predominant in inhibiting the crystallisation of the amorphous phase. However a definite answer to this problem is not possible in all instances. The bond energies must also be taken into account, especially if the effects of the bond energy and the size factor compensate each other to some extent.

V. Crystallisation of amorphous metal alloys

The chief 'amorphising' elements in transition metal (TM) alloys are boron, carbon, and phosphorus. One of the major problems in studying alloys (AAs) is to find the factors governing their thermal stability. We shall consider two factors which affect the stability of AAs: the nature of the metal and of the amorphising element. Both factors are, as a rule, connected with aspects of the metal–non-metal interaction and with thermodynamic stimuli of crystallisation of the AA.

Table 6. Bond energies $\varepsilon(M-X)$ and ΔH_f for compounds used to estimate the increase in thermal stability of AAs.

Compound	ε/ kJ g^{-1} electron^{-1}	$-\Delta H_f$/ kJ mol^{-1}
	Borides	
ScB_2	239.7	307.8
TiB_2	194.1	323.4
ZrB_2	210.5	328.0
HfB_2	213.4	329.3
VB_2	173.6	215.0
$TaB_{2.03}$	205.9	190.0
$NbB_{1.82}$	197.1	185.8
CrB_2	189.5	119.4
LaB_6	265.3	400.4
W_2B	194.0	68.2
WB	182.0	66.5
W_2B_5	181.6	199.6
Mn_2B	163.2	95.1
MnB	164.8	71.6
MnB_2	165.7	63.3
$AlB_{2.215}$	161.3	77.4
Fe_2B	186.1	67.9
FeB	174.3	64.6
Co_2B	188.3	58.1
CoB	176.6	69.5
Ni_2B	190.0	67.7
NiB	171.5	40.2
	Phosphides	
Fe_3P	162.1	164.1
Fe_2P	161.7	121.6
FeP	169.1	137.2
FeP_2	158.5	217.6
Co_2P	170.4	196.6
CoP	174.2	146.4
CoP_3	170.9	280.3
Ni_3P	174.0	219.7
Ni_2P	168.4	184.0
NiP_2	152.1	167.0
NiP_3	157.7	200.8
	Carbides	
Fe_3C	168.2	−25.2
Fe_2C	168.8	−20.6
Co_3C	168.7	−44.4
Co_2C	172.1	−16.8
Ni_3C	164.9	−75.3

An irreversible transition of an AA to the crystalline state is often of a diffusion character. As in the case of oxides, stability against diffusion decomposition can be attributed to the presence in the alloy of fragments with rigid metal–non-metal covalent bonds.[43] These fragments may have a composition corresponding to a stable or metastable composition of the crystalline compound or alloy and a similar nearest coordination sphere to that in the crystal. The tendency to amorphisation is dependent on the variation in the type of linking of the coordination polyhedra in the alloy. Clearly, the higher the chemical bond energy in such fragments the more difficult it is for diffusion decomposition of the AA to occur on its crystallisation.

The question of a correlation of the structure of AAs and the bond energies $\varepsilon(M-X)$ (X = B, C, P) with the thermodynamic stability of the alloys has been raised in a general form repeatedly. However, there has rarely been any estimation of $\varepsilon(M-X)$ in a quantitative form suitable for solving practical problems, particularly those associated with estimating the enthalpies of formation (ΔH_f) of the alloys. This is because, until recently, there were no reliable thermochemical data on ΔH_f for many borides, carbides, and phosphides. The regeneration of interest in fundamental investigations of the structural and thermodynamic properties of these compounds has promoted a substantial development of a simple model for calculating the bond energies $\varepsilon(M-X)$ and hence ΔH_f.

The calculation of $\varepsilon(M-X)$ was carried out using a simplified model which takes into account the structural, thermochemical, and electrophysical properties of the compounds. The basis of the calculation has been published[44–48] for the compounds MB_n, MC_n, MN_n, MC_nO_m, and MN_nO_m, where M is a transition metal.

In these calculations the enthalpy of atomisation (ΔH_a) of the compounds to the monoatomic gas state is represented by the sum of the bond dissociation energies. In the general case for metal-like compounds of the MX type we can write

$$\Delta H_a = E_{free} + E(M-X) + E(M-M) + E(X-X)$$

$$= \Delta H_aM + \Delta H_aX - \Delta H_fMX.$$

The terms in this equation allow for the partial contributions of the free electrons of the conduction band (E_{free}), the band of covalent metal–non-metal bonds [$E(M-X)$] and metal–metal bonds [$E(M-M)$], and also non-metal–non-metal bonds [$E(X-X)$] if they are formed, e.g. as in the higher borides. For some compounds the individual contributions cannot be taken into account (for example in lower borides of the MB type where the boron atoms can be regarded as isolated). Calculations of the bond energies $\varepsilon(M-X)$ and the enthalpies of formation of transition metal borides, carbides, and phosphides (Table 6) have been carried out.[48, 49] The method of calculation is fairly simple and does not involve quantum-chemical calculations.

The data in Table 6 show that in general within the Groups of the Periodic Table the bond energies $\varepsilon(M-B)$ increase as the atomic number of the metal increases. The same trend applies to other binary compounds (oxides, halides, nitrides, etc.). Within the Periods $\varepsilon(M-X)$ decreases as the atomic number of the element increases and is approximately constant for the elements in the iron triad. $\varepsilon(M-X)$ is approximately constant for the compounds within one system; this makes it possible to estimate ΔH_f for compounds recorded on the M–X equilibrium diagrams that are unstable or have not been studied, or to estimate the compositions of alloys from the mean values of $\varepsilon(M-X)$. The approximate constancy of $\varepsilon(M-X)$ is consistent with the known principle of transferability of the characteristics of a chemical bond in compounds.

The absolute deviations of the mean values of $\varepsilon(M-X)$ from the bond energies in the individual compounds do not exceed ± 10 kJ g^{-1} electron^{-1}, which is within the error of the thermodynamic quantities.

Alloying of the binary alloys with a third component (a transition metal or X) has an appreciable effect on the time-dependent and thermal stability of an AA. It is questionable whether the bond energies calculated using thermodynamic data for the crystalline state are adequate for the bond energies in an AA. A statistical analysis of ΔH_{cr} for 40 amorphous alloys with different chemical compositions showed that the mean value of ΔH_{fus} for substances forming AAs is 16.3 kJ g-atom^{-1} but ΔH_{cr} for the amorphous alloys is −7.5 kJ g-atom^{-1}. Thus for the transition liquid→amorphous material there is a margin of internal excess enthalpy per 1 g-atom of the AA of −8.8 kJ g-atom^{-1}.[50] The value 7.5 kJ g-atom^{-1} is close to the values of the enthalpies of phase transitions and represents the difference in the enthalpies of the amorphous and crystalline materials. This value is close to a theoretical estimate based on the assumption of a non-equilibrium electronic state for the interacting atoms.[51] Such estimates agree with the conclusion[1] that the main condition for obtaining a non-crystalline state of a solid is an excess binding enthalpy equal to $0.5\Delta H_{fus}$.

The short-range order in the AA corresponds to the arrangement of the atoms in the crystal structures of some actual

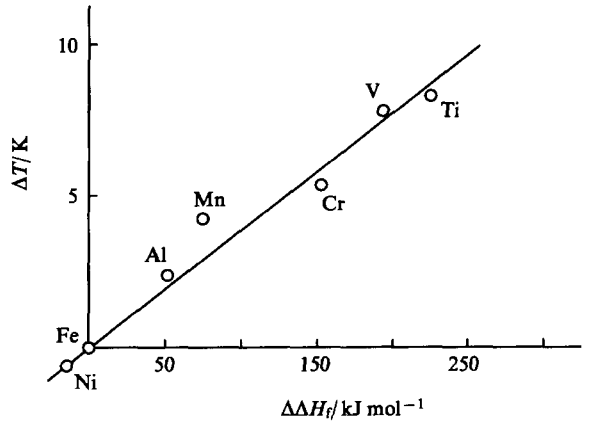


Figure 5. The change in the crystallisation temperature of the amorphous alloys $Fe_{80}M_5B_{15}$ for alloying with 1 atom % M plotted against the difference $\Delta\Delta H_f = \Delta H_f(M_3B) - \Delta H_f(Fe_3B)$ (3 atom % alloying in the case of Al).[52]

compounds that are present in the equilibrium diagrams (e.g. Co_3B or Ni_3B, where each boron atom is coordinated by nine metal atoms). The preservation in the AA of the coordination polyhedra that occur in the crystalline state makes it unnecessary to use the concept of variable valency to account for the energetics of the crystallisation of the AA.[51] The transition from the amorphous to the crystalline state can be treated as a form of polymorphic transformation. The amount 7.5 kJ g-atom^{-1} is only 1%–2% of the values of the enthalpies of atomisation of crystalline borides, carbides, and other compounds and the use of M–X bond energies calculated for compounds in the crystalline state for the amorphous alloys as well is therefore justified. It has been shown[50] that the ratio (α) of the experimental values of ΔH_{cr} for an AA and $\Sigma x_i \Delta H_i$ for the components of the alloy, where x_i is the mole fraction and ΔH_i the enthalpy of fusion of the ith component, is 0.3–0.5. This range of values corresponds to the excess enthalpy remaining in AAs obtained by various methods (spinning, condensation from the gas phase, cathode sputtering, etc.). It is easily seen that α for AAs is similar to α for oxides (see Table 1);† this indicates that the excess enthalpy in non-crystalline materials is approximately constant, irrespective of their chemical nature and method of preparation.

Let us consider two extreme cases in the variation of α. When $\alpha \rightarrow 1$ crystallisation of the amorphous material is accompanied by evolution of heat. The heat effect is similar in absolute magnitude to ΔH_{fus} of the crystal. The amorphous material retains the structure of the melt near to the equilibrium melting point. When $\alpha \rightarrow 0$ the quenched melt or other non-crystalline materials are similar in structure to the equilibrium crystal and there is no appreciable thermal effect on the thermogram. Such a material will have a similar diffraction pattern to the equilibrium crystal. In certain instances crystallisation of the AA gives strips containing a microcrystalline phase together with the amorphous phase.

For the methods used to obtain non-crystalline materials the degree of crystallinity could be described by the quantity $\beta = 1-\alpha$, so that $0.5 < \beta < 0.7$.

The introduction of 3d transition metals into an AA of the Fe_3B type increases the T_{cr} of the alloy if the 3d metal is in a Period to the left of iron. For $Fe_{80}M_5B_{15}$ (M = Ti ... Ni) T_{cr} increases, per 1 mol% M alloying content, in the order Mn–Cr–V–Ti but the introduction of nickel reduces T_{cr}.[52] Elsewhere[53] similar behaviour was observed for the series Ni–Co–Fe–Cr–V although different T_{cr} values are obtained by different authors owing to the use of different conditions for obtaining the AA and different rates of heating in the calorimeter. There is a linear relationship between the change in the crystallisation temperature of amorphous $Fe_{80}M_5B_{15}$ alloys when they are alloyed with metals and the difference in the enthalpies of formation of the alloys $\Delta\Delta H_f = \Delta H_f(M_3B) - \Delta H_f(Fe_3B)$ (Fig. 5).[48] $\Delta H_f(M_3B)$ was calculated on the basis of the bond energies ε(M–B) (see Table 6). There is obviously a connection between the decrease in the activity of boron on formation of borides with high ΔH_f values and the increase in the thermal stability of the AA. The thermal stability is associated with the formation of boron positions in the AA that have a lower energy and so inhibit crystallisation.[52] It can therefore be predicted that the T_{cr} of alloys of this type can be increased considerably by alloying with lanthanide, Sc, and Y borides.

It is clear from Table 6 that $\varepsilon(M-P) \simeq \varepsilon(M-C)$ and $\varepsilon(M-B)$ is ~10% higher. The similarity of the M–X bond energies in these compounds and the compatibility of the fragments facilitates alloying of amorphous alloys based on the Fe–B system with boron, carbon, and phosphorus. The formation of the more exothermic iron phosphides, for example, as compared to the borides, leads to a reduction in the thermodynamic activity of iron in the alloy. Analysis of experimental data on T_{cr} for AAs in M–X (M = Fe, Co, Ni) systems showed that T_{cr} is 610–680 K for the phosphides, 600–700 K for borides, and only 450 K for Fe_3C.[54] These values accurately reflect the main trends: Fe_3C, which is endothermic, has the lowest value of T_{cr} while the exothermic phosphides and borides have high thermal stability. Therefore the reason for the variation in T_{cr} of an amorphous material irrespective of its nature is the formation of more stable fragments of compounds that strengthen the matrix of the amorphous compound.

The validity of the conceptual approach based on a quantitative consideration of the energy non-equivalence of coexisting bonds is confirmed by recently published data on the effect of alloying the primary matrix with transition metal additives on the relaxation temperature. An analysis has been carried out[55] of publications[56–58] in which the effect of replacing iron in alloys with compositions close to Fe_4B or Fe_5B was determined. To a first approximation the compositions of the alloyed materials can be described as 95 mol% Fe_4B + 5 mol% M_4B (M = Co, V). The enthalpies of formation of the alloys were calculated[55] from the equation

$$\Delta H_f = 0{\cdot}95\Delta H_f(Fe_4B) + 0.05\Delta H_f(M_4B),$$

on the assumption that the enthalpy of mixing is zero. The reduction in the relaxation temperature when cobalt is introduced into the alloy $Fe_{0.81}B_{0.19}$ and the increase when vanadium is introduced are due to the fact that $\Delta H_f(Co_4B) < \Delta H_f(Fe_4B)$ but $\Delta H_f(V_4B) > \Delta H_f(Fe_4B)$. The enthalpies of formation of Co_4B, Fe_4B, and V_4B are −21, −25, and −213 kJ (mol M_4B)$^{-1}$ respectively. The introduction of vanadium, which forms a boride whose ΔH_f is more negative than $\Delta H_f(Fe_4B)$, favours a reduction in the activity of boron in the Fe–B system, hinders the diffusion mobility of fragments of the amorphous structure, and

Table 7. Transition temperatures of amorphous alloys and the calculated enthalpies of formation of the alloys.

Alloy	T_{rel}/K, T_{cr}/K	ΔT_{rel}/K, ΔT_{cr}/K	$-\Delta H_f(M_xB)$ / kJ mol^{-1}
$Fe_{0.81}B_{0.19}(Fe_{4.26}B)$	603	–	25
$Fe_{0.76}Co_{0.04}B_{0.20}(M_4B)$	595	−8	24.8
$Fe_{0.75}V_{0.04}B_{0.21}(M_{3.76}B)$	663	60	34.4
$Fe_{0.74}Co_{0.10}B_{0.16}$	688	–	24.7
$Fe_{0.74}Co_{0.05}Cr_{0.05}B_{0.16}$	733	45	34.2
$Fe_{0.74}Cr_{0.10}B_{0.16}$	763	75	43.5

Note. The values given for the first three alloys are T_{rel} from the data of Barricco et al.[56] (x = 4); those for the other alloys are T_{cr} from other data[57, 58] (x = 5). The possible error in ΔT_{rel} for the second alloy is ±50% owing the small scale of the figure in the paper.[56]

† We recall that the values of α from the data of Natarajan et al.[17] are estimated

Table 8. Changes in T_{cr} for the alloys $Fe_{79-x}B_{16}Si_5M_x$ (x = 4).

Element	T_{cr}/K	ΔT/K	ΔT/K per 1 mol%
V	806	30	7.5
Cr	790	14	3.5
Nb	816	40	10
Mo	814	38	9.5
Ni	773	−3	−0.8
Fe	776	–	–

increases the potential barrier to relaxation. The introduction of cobalt, on the other hand, reduces the relaxation temperature of the alloy (Table 7).

In the case of alloys with compositions close to M_5B studies have been made of the effect of T_{cr} of replacing the cobalt in $Fe_{0.74}Co_{0.10}B_{0.16}$ by chromium.[57, 58] Replacing 50%–100% of the cobalt by chromium leads to an increase in T_{cr} by 45–75 K. The introduction of chromium, vanadium, molybdenum, niobium, and nickel into the AA with the more complex composition $Fe_{79-x}B_{16}Si_5M_x$, which contains two amorphising elements (boron and silicon), gives similar results (Table 8).[59]

Barrue et al.[59] arranged the alloying elements in order of decreasing atomic radius: Nb > Mo > V > Cr, noting that there is a correlation between the size of the substituent atom and T_{cr} of the alloy. However, the size of the atom is larger for 4*d* elements than for their 3*d* analogues. Comparison of the pairs V–Cr and Nb–Mo indicates a semi-quantitative correlation: the increase in T_{cr} on introducing vanadium and niobium is more marked than on introducing chromium and molybdenum; this is consistent with the greater thermodynamic stability of borides of Group V elements compared with those of Group VI elements.

The change in T_{rel} and T_{cr} for AAs with the still more complex compositions $Fe_{39}Ni_{36}Cr_5P_{14}B_6$, $Fe_{76}Co_4B_{20}$, and $Fe_{75}V_4B_{21}$, as compared with the typical matrix $Fe_{81}B_{19}$ (Fe_4B), has been studied by DSC.[56] The introduction of chromium, phosphorus, and vanadium into $Fe_{81}B_{19}$ leads to the formation of chromium and vanadium borides and phosphides that are thermodynamically more stable than Fe_4B. An important feature of the method used[56] was an X-ray diffraction examination of both sides of the amorphous strip from the quenched melt; this confirmed the absence of crystallisation throughout the whole thickness. A study has been made of the effect of high-melting metals on the thermal stability of amorphous bands of Ni–M–B alloys (M = Zr, Nb, Mo; 13–14 mol% B, 5–14 mol% M).[60] The alloys containing zirconium retain an amorphous state at higher temperatures than those containing niobium and molybdenum and the crystallisation temperatures of the AAs increase linearly with increasing zirconium and molybdenum concentrations. This effect is consistent with the greater stability of zirconium borides as compared with molybdenum and niobium borides.

A comprehensive study of the dependence of T_{cr} on features of the electronic structure of the AAs $Fe_{75}B_{20}M_5$, where M = Ni, Co, Cr, V, Mo, W, and Nb, has been carried out.[53] Calorimetric studies showed that T_{cr} increases for this set of metals: 415, 467, 502, 566, 597, 611, and 613 °C, and this is consistent with the increase in the thermodynamic stability of M_4B fragments in sets of 3*d* and 4*d* metals. The similarity of T_{cr} for the niobium and vanadium [tungsten? Ed.] alloys is also consistent with the known diagonal similarity between elements in the Periodic Table.[61] The increase in T_{cr} for the alloys formed by metals in the same Group, e.g. the Group VI metals Cr–Mo–W, is consistent with the general tendency for the borides to have increasing ΔH_f values and hence for there to be increasing stability of the structural fragments. K_α emission spectra have been studied for the series under discussion (with the use of an electron microbeam as the excitation source). The shift of the K_α band of the compound, as compared with the K_α band of boron, from 1 to 1.35 eV as we pass along the series Ni ... Nb is due to an increase in the degree of overlap of the *d* electrons of the transition metal atoms with the 2*p* electrons of boron. This implies an increase in the M–B bond strength along this series, as is confirmed by thermodynamic calculations.

The introduction of 5 mol% of such elements as chromium, vanadium, molybdenum, niobium, tungsten, and tantalum into the alloy $Fe_{80}B_{20}$ increases T_{cr};[62] however the interpretation of the observed linear relationship $T_{cr} = f(Z/U)$, where Z is the atomic number of the element and U is the $M \rightarrow M^+$ ionisation potential, raises doubts as to the appropriateness of using such an argument for the function because there is no evidence that the M atoms are singly ionised in the borides.

There are wide discrepancies in the published values of the crystallisation temperatures for the replacement of the iron in FeB_n alloys by other transition metals. This is due to differences in the conditions of preparation of the AAs; the preparation is carried out under extremal conditions and is evidently not sufficiently reliably monitored (rate of quenching, thickness of the AA strip, possible deviations from the prescribed composition of the mixture due to evaporation of the components with different vapour pressures, methods of measuring T_{cr}, etc.). The use of high-sensitivity DSC enables observations to be made up to the crystallisation temperature of the alloy on changes in the solid state due to relaxation of the quenched alloy, the Curie temperature of the α-Fe phase which separates out, the crystallisation temperature of α-Fe, and, only after this, on T_{cr} for the alloy.[63] Consequently in working on this review we did not undertake the task of covering all the published literature in this field but have selected for investigation only the most representative topics which had been dealt with properly and contain reliable primary information. The increasing number of publications on the experimental thermodynamics of AAs means that it is necessary to look for criteria for choosing model AAs which might serve as key compounds in the chemical thermodynamics of non-crystalline materials. The use of such 'benchmarks' in research will contribute to a more reasoned comparison of the properties of the alloys.

VI. Conclusion

This review deals with the results of experimental studies of the conditions of crystallisation of amorphous materials in the presence of alloying additives that reduce the diffusion mobility or increase the thermodynamic stability of fragments of the amorphous matrix. Additives that are effective stabilisers of the amorphous state of coordination compounds (oxides) are oxides in which the metal–oxygen bonds are stronger than those in the primary matrix and the cations are larger than those in the primary matrix. A change in the CN of the additive cation on insertion into the amorphous matrix has an inhibiting effect when the enthalpy of the change in coordination during crystallisation of the amorphous phase has a high positive value. An increase in the crystallisation temperature of the solid solution is due to a potential barrier being overcome on formation of the less stable coordination polyhedron of the additive cation which is 'finely adjusted' to the polyhedron of the cation in the matrix. As a simplification it is assumed that the enthalpies of the change in the coordination of the cations in the primary matrix and in the additive are identical in the amorphous and crystalline states.

The crystal-chemical factor is dominant for the introduction of additives capable of forming compounds with a complex polyhedral structure and with the same crystal structure. The variation in the bond energies $\varepsilon(M-O)$ in a series of lanthanide oxides is not monotonic owing to the 'bivalence' of europium and ytterbium in the metallic state and the necessity, in contrast to the other lanthanides, to promote a third electron when the oxide E_2O_3 is formed. However, the crystallisation temperatures of the amorphous phases do increase monotonically with increasing atomic number of the lanthanide. The insertion of a new phase of compounds with a complex structure inhibits crystallisation and amorphous compounds must be heated to a higher

temperature even in those instances where the concentration of the additive is small but its insertion into the matrix of the primary material is impossible for crystal-chemical reasons.

The effects of introducing a third component into amorphous binary metal alloys on the thermal stabilisation are interpreted from the same conceptual standpoints. The main thermodynamic reason for an increase in the crystallisation temperature of the amorphous material irrespective of its chemical nature is the formation of fragments of more stable compounds which strengthen the amorphous matrix and inhibit diffusion processes.

The energy content of amorphous materials is 20% – 50% of the enthalpy of fusion of crystalline phases. The increase in the crystallisation temperature on the introduction of alloying components into amorphous oxides and metal alloys is 5 – 60 K per mol% of the component.

References

1. V V Bondar', in *Itogi Nauki i Tekhniki. Khimiya Tverdogo Tela* (Progress in Science and Technology. Solid-state Chemistry) (Moscow: Izd. VINITI, 1982) Vol. 2, p. 4
2. A L Tolstikhina, S A Semiletov *Izv. Akad. Nauk SSSR, Ser. Fiz.* **52** 1320 (1988)
3. S S Olevskii, M S Sergeev, A L Tolstikhina, V P Repko, P E Kandyba *Dokl. Akad. Nauk SSSR* **266** 113 (1992)
4. A Mosset, P Lecante, J Galy *Phil. Mag. B* **46** 137 (1982)
5. S S Olevskii, M S Sergeev, A L Tolstikhina, A V Koshienko, B I Kozyrkin, A S Avilov, B G Gribov *Poverkhn. Fiz. Khim. Mekh.* **4** 78 (1985)
6. S S Olevskii, M S Sergeev, A L Tolstikhina, A V Koshchienko, B I Kozyrkin *Poverkhn. Fiz. Khim. Mekh.* **8** 97 (1985)
7. Yu A Skakov, Zh Akhmetzhanov *Rasplavy* **3** 3 (1992)
8. A V Serebryakov *Izv. Vyssh. Ucheb. Zaved., Chern. Metall.* **7** 103 (1982)
9. Yu A Skakov *Izv. Vyssh. Ucheb. Zaved., Chern. Metall.* **7** 87 (1982)
10. L L Odynets *Poverkhn. Fiz. Khim. Mekh.* **12** 128 (1984)
11. A F Ioffe *Zh. Tekh. Fiz.* **27** 1153 (1957)
12. L A Reznitskii *Khimicheskaya Svyaz' i Prevrashcheniya Oksidov* (Chemical Bonding and Transformations in Oxides) (Moscow: Izd. Mosk. Gos. Univ., 1991)
13. D I Mendeleev, in *Osnovy Khimii* (Fundamentals of Chemistry) (Moscow, Leningrad: Goskhimizdat, 1947) Vol. 2, p. 263
14. L A Reznitskii, S E Filippova, A V Leonov, S N Grishenina *Izv. Akad. Nauk SSSR, Neorg. Mater.* **21** 439 (1985)
15. L A Reznitskii, S E Filippova, V K Portnoi *Izv. Akad. Nauk SSSR, Neorg. Mater.* **24** 1543 (1988)
16. L A Reznitskii *Izv. Akad. Nauk SSSR, Neorg. Mater.* **26** 1987 (1990)
17. M Natarajan, G V Chandrashekhar, C N R Rao *J. Chem. Eng. Data* **13** 235 (1968)
18. V P Glushko (Ed.) *Termodinamicheskie Svoistva Individual'nykh Veshchestv. Spravochnik* (Reference Book "Thermodynamic Properties of Individual Substances") (Moscow: Nauka, 1982) Vol. 4
19. L A Reznitskii, S E Filippova *Izv. Akad. Nauk SSSR, Neorg. Mater.* **26** 1481 (1990)
20. L A Reznitskii, S E Filippova *Izv. Akad. Nauk SSSR, Neorg. Mater.* **27** 1841 (1991)
21. L A Reznitskii, S E Filippova *Izv. Akad. Nauk SSSR, Neorg. Mater.* **27** 2211 (1991)
22. V I Strakhov, L I Mikhailova, T V Ivanova *Vliyanie Fe_2O_3 na Stabilizatsiyu Vysokotemperaturnoi Formy ZrO_2* (The Effect of Fe_2O_3 on the Stabilisation of the High-temperature Form of ZrO_2), manuscript deposited at ONIITEKhIM Cherkassy, No. 1171-Kh11 88 (6.12.88)
23. L A Reznitskii, S E Filippova *Izv. Akad. Nauk SSSR, Neorg. Mater.* **28** 1128 (1992)
24. G K Demenskii, L A Reznitskii *Vestn. Mosk. Gos. Univ., Khim.* **17** 57 (1976)
25. P Berhet, J Berthon, A Revcolevsky *Physica B* **158** 506 (1989)
26. L M Sharygin, S Ya Tret'yakov, V M Galkin *Izv. Akad. Nauk SSSR, Neorg. Mater.* **28** 1543 (1992)
27. L M Sharygin, V M Galkin, S M Vovk, Yu A Dorofeev *Izv. Akad. Nauk SSSR, Neorg. Mater.* **27** 295 (1991)
28. M S Khodzhamberdiev, M D Vol'kovskii, G Z Pinsker, E N Beresnev, I A Rozanov, V P Orlovskii, M G Komova *Izv. Akad. Nauk SSSR, Neorg. Mater.* **25** 76 (1989)
29. N V Kadoshnikova, G V Rodicheva, V P Orlovskii *Zh. Neorg. Khim.* **34** 316 (1989)
30. L M Sharygin, V M Galkin, S Ya Tret'yakov, A V Korenkova *Izv. Akad. Nauk SSSR, Neorg. Mater.* **24** 1673 (1988)
31. N V Krivosheev, O G Alekseev, E G Semin, E M Menchuk, M Ya Khodos, G A Teterin, A N Belov, V B Borisova *Izv. Akad. Nauk SSSR, Neorg. Mater.* **26** 308 (1990)
32. L A Reznitskii, S E Filippova, A V Leonov *Izv. Akad. Nauk SSSR, Neorg. Mater.* **21** 859 (1985)
33. L A Reznitskii, S E Filippova, L M Viting *Izv. Akad. Nauk SSSR, Neorg. Mater.* **21** 1060 (1985)
34. S E Filippova, L A Reznitskii, A V Leonov, L M Viting *Izv. Akad. Nauk SSSR, Neorg. Mater.* **21** 1805 (1985)
35. L A Reznitskii, S E Filippova, A V Leonov *Izv. Akad. Nauk SSSR, Neorg. Mater.* **22** 2037 (1986)
36. S E Filippova, L A Reznitskii *Izv. Akad. Nauk SSSR, Neorg. Mater.* **27** 2219 (1991)
37. L A Reznitskii, S E Filippova *Izv. Akad. Nauk SSSR, Neorg. Mater.* **29** (1993) (in the press)
38. L A Reznitskii *Sverkhprovod. Fiz. Khim. Tekh.* **6** 183 (1993)
39. K Haneda, C Mijakawa, H Kojiama *J. Am. Ceram. Soc.* **57** 354 (1974)
40. W Roos *J. Am. Ceram. Soc.* **63** 601 (1980)
41. S D Kulkarni, C E Deshpande, J J Shrotri *Thermochim. Acta* **153** 47 (1989)
42. L A Reznitskii *Zh. Fiz. Khim.* **66** 1931 (1992)
43. S D Kaloshkin, I A Tomilin *Izv. Vyssh. Ucheb. Zaved., Chern. Metall.* **3** 4 (1988)
44. L A Reznitskii *Izv. Akad. Nauk SSSR, Neorg. Mater.* **2** 953 (1966)
45. L A Reznitskii *Izv. Akad. Nauk SSSR, Neorg. Mater.* **4** 706 (1968)
46. L A Reznitskii, S E Filippova *Vestn. Mosk. Gos. Univ., Khim.* **22** 181 (1981)
47. L A Reznitskii, S E Filippova *Vestn. Mosk. Gos. Univ., Khim.* **23** 299 (1982)
48. L A Reznitskii *Zh. Fiz. Khim.* **61** 1800 (1987)
49. L A Reznitskii *Zh. Fiz. Khim.* **62** 2893 (1988)
50. L A Reznitskii *Zh. Fiz. Khim.* **61** 1085 (1987)
51. A S Mal'kovskii *Zh. Neorg. Khim.* **30** 180 (1985)
52. S D Kaloshkin, Thesis for the Degree of Candidate of Physico-mathematical Sciences, Moscow Institute of Steel and Alloys, Moscow, 1985
53. V O Abramov, A I Belokonov, R A Oganyan, Ya N Oganyan, E P Ozerova, G A Sharpataya, A N Shul'gin, in *Fizikokhimiya Amorfnykh Metallicheskikh Splavov. Tezisy Dokladov III Vsesoyuznogo Soveshchaniya* (The Physical Chemistry of Amorphous Metal Alloys. Abstracts of Papers for the Third All-Union Conference) (Moscow: Baikov Institute of Metallurgy, 1989) p. 78
54. V V Bondar', B R Gorobets, U Rashke, in *Itogi Nauki i Tekhniki. Khimiya Tverdogo Tela* (Progress in Science and Technology. Solid-state Chemistry) (Moscow: Izd. VINITI, 1982) Vol. 2, p. 15
55. L A Reznitskii *Zh. Fiz. Khim.* **53** 3074 (1989)
56. M Barricco, L Battezzati, G Riontino *J. Therm. Anal.* **30** 1259 (1985)
57. D Akhtar, V N Murthy, P Subrahmanian, R Jagannathan *J. Mater. Sci. Lett.* **5** 1148 (1986)
58. R P Mathur, V N Murthy, D Akhtar *J. Mater. Sci. Lett.* **6** 1019 (1987)
59. R Barrue, J Bigot, J C Fangieras, J C Perron, J F Rialland, J Robert, F Schwartz *Phys. Scr.* **37** 356 (1988)
60. V I Fadeeva, L M Kubalova, S E Filippova, in *Tezisy Dokladov III Vsesoyuznogo Soveshchaniya "Fizikokhimiya Amorfnykh Metallicheskikh Splavov"* (Abstracts of Papers for the Third All-Union Conference "The Physical Chemistry of Amorphous Metal Alloys") (Moscow, 1989), p. 65
61. L A Reznitskii, in *Khimicheskaya Svyaz' i Stroenie Veshchestva* (Chemical Bonding and the Structure of Materials) (Moscow: Izd. Mosk. Gos. Univ., 1988) p. 44
62. E G Darovskikh, Z A Samoilenko, A F Prokoshin *Izv. Akad. Nauk SSSR, Neorg. Mater.* **27** 1624 (1991)
63. E Illekova, L Kubicar *J. Therm. Anal.* **33** 673 (1988)

Russian Chemical Reviews **62** (5) 447 – 472 (1993)
© 1993 Russian Academy of Sciences and Turpion Ltd

UDC 547.467.2

Carbene reactions of diazoesters with σ-bonds as an effective method for the alkoxycarbonylmethylenation of organic compounds

E A Shapiro, A B Dyatkin, O M Nefedov

Contents

I. Introduction	447
II. Carbon – hydrogen bonds	448
III. Heteroatom – hydrogen bonds	453
IV. Carbon – carbon bonds	457
V. Carbon – heteroatom bonds	457
VI. Heteroatom – heteroatom bonds	466

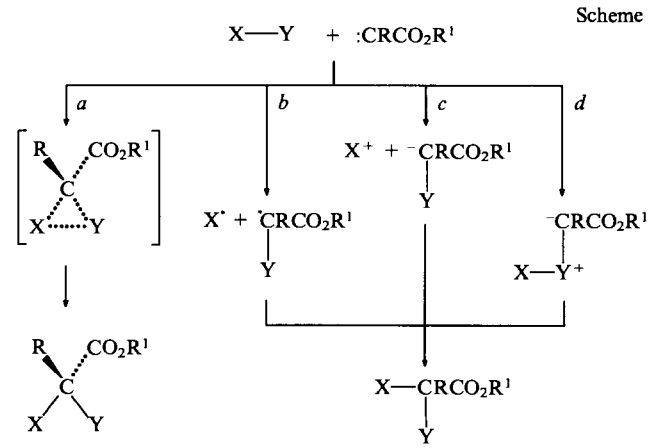
Abstract. Data on the carbene reactions of diazoesters with carbon – hydrogen, heteroatom – hydrogen, carbon – carbon, carbon – heteroatom, and heteroatom – heteroatom σ-bonds in organic molecules, demonstrating the synthetic possibilities of such reactions as an effective and universal method of the alkoxycarbonylmethylenation of organic compounds, are considered systematically. The bibliography includes 179 references.

I. Introduction

The reactions involving the carbene decomposition of the esters of diazoacetic and other carboxylic diazoacids (diazoesters) are widely used in organic synthesis for the preparation of the esters of cyclopropanecarboxylic and cyclopropenecarboxylic acids from unsaturated compounds.[1-8] The reactions of diazoesters with saturated compounds, leading in the general case to the insertion of the $CRCO_2R^1$ fragment in the X – Y σ-bonds as a result of the dissociation of these bonds and formation of new C – X and C – Y bonds, are much less well known. This reaction can be achieved either as a concerted process via a three-centre transition state with retention of the configuration of the asymmetric atom (pathway *a*) or as the opposite stepwise process involving racemisation, of the type of abstraction – recombination with participation of radical species (pathway *b*), dipolar intermediates (pathway *c*), or ylide structures (pathway *d*) (Scheme 1).

Clearly the operation of a particular pathway is mainly determined by the structure of the substrate and also by the mode of generation of the carbene. The synthetic importance of reactions of this type is due to the possibility of the introduction of functional groups at carbon atoms of saturated compounds. However, until recently, their use in organic synthesis was restricted because of the lack of convenient methods for the generation of alkoxycarbonylcarbenes (ACC) capable of entering into selective reactions with σ-bonds. The photolytic and thermal dediazotisation of diazoesters leads to the formation of extremely active carbenes, which react nonselectively with an acceptor to form a large number of products. Catalytic dediazotisation on treatment with traditional catalysts based on copper compounds leads to more selective carbenes but ensures the necessary preparative selectivity of the reactions of diazoesters with saturated compounds only in individual instances.

Scheme 1



Only the latest advances in the catalysis of the carbene decomposition of diazoesters and in first place the use of rhodium(II) compounds as catalysts of this process[9] led to the possibility of the wide scale employment of the insertion reactions for the alkoxycarbonylmethylenation of a wide variety of saturated compounds. Since the discovery of rhodium catalysis, extensive experimental data have accumulated, which, however, have not been treated systematically, although individual examples of reactions of this type have been included in virtually all the reviews devoted to the chemistry of diazoesters.[2-8,10]

In the present review, an attempt is made for the first time to consider systematically the literature data on the reactions of diazoesters with saturated compounds. The review is not exhaustive and its aim is to provide only a general idea about the synthetic possibilities of reactions of this type. For convenience, the entire data have been grouped in terms of the types of bonds involved in the reaction: carbon – hydrogen, heteroatom – hydrogen, carbon – carbon, carbon – heteroatom, and heteroatom – heteroatom. Within the groups, the classification is based on the type of compounds incorporating these bonds and the kind of heteroatom.

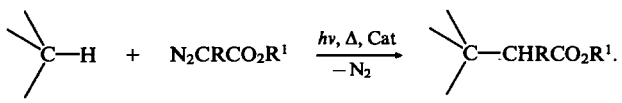
E A Shapiro, A B Dyatkin, O M Nefedov N D Zelinskii Institute of Organic Chemistry, Russian Academy of Sciences, Leninskii prosp. 47, 117913 Moscow. Fax (7-095) 135 52 28

Received 14th January 1993
Uspekhi Khimii **62** (5) 485 – 509 (1993); translated by A K Grzybowski

II. Carbon–hydrogen bonds

1. Aliphatic C–H bonds

Reactions involving the insertion of ACC in the C–H bonds of alkanes, alkenes, and alkynes are known. They can be represented by the following equation in a general form:

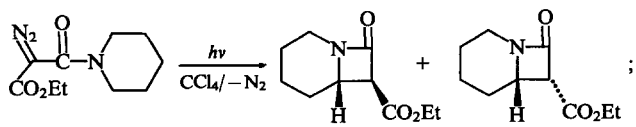


The reaction with alkanes is of limited synthetic applicability because the low selectivity of the highly reactive ACC in relation to primary, secondary, and tertiary C–H bonds and the ease of the dimerisation of carbenes usually lead to mixtures of products, although their overall yields reach 90% when rhodium(II) carboxylates are used as catalysts.[11] The rules governing the catalytic action of the above catalysts as a function of the structure of the substrate, diazoester, and the counterion and the catalyst concentration have been examined.[12,13] The formation of the products of insertion in the C–H bonds of alkanes in high yields (~90%) has been noted in the dediazotisation of diazoesters with an unsaturated alcoholic component, for example, prenyl diazoacetate in hexane in the presence of $CuCl_2$.

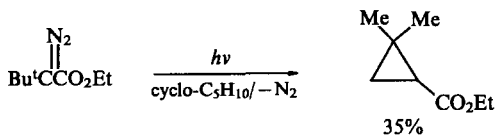
The intermolecular C–H insertion reaction has found a practical application in the modification of ethylenepropylene rubber, which is achieved by treating the latter with ethyl diazoacetate (EDA) at 210 °C (degree of functionalisation 5%–10%).[14]

The intramolecular C–H insertion reactions are of much greater synthetic importance. These reactions proceed with preparative yields even under the conditions of the photolysis or pyrolysis of diazoesters (Scheme 2).[15–17]

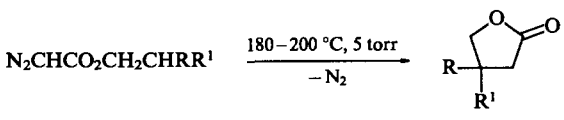
Scheme 2



overall yield 80%; 1 : 2 ratio



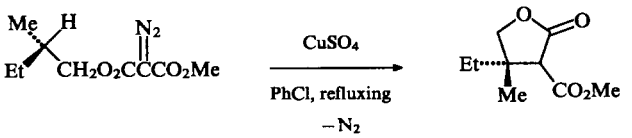
35%



20%

Preparative yields can be achieved also using copper compounds as catalysts of the dediazotisation of the diazoesters (Scheme 3).[18]

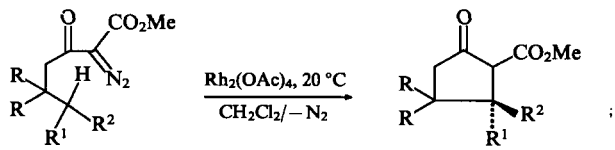
Scheme 3



48%

The use of rhodium(II) carboxylates makes it possible to carry out the reactions under milder conditions, which promotes an increase in the yields of products and the process selectivity (Scheme 4).[19,20]

Scheme 4



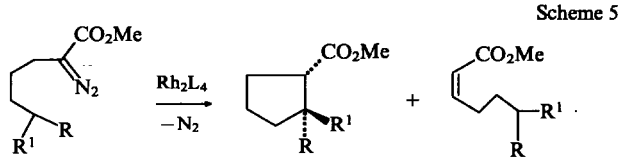
55%–77%

R = Me, Pr^i, C_8H_{17}, $H_2C{=}CH$, $Me_2C{=}CHCH_2$,
$R^1 = R^2$ = H, Me.

The reactivity of the C–H bonds in this reaction diminishes in the sequence C_{tert}–H > C_{sec}–H > C_n–H and all the bonds are more reactive than the C–H bonds of the benzyl and allyl types.[21,22]

When the molecule contains long unbranched hydrocarbon chains, the bond subjected to attack by the carbene centre is exclusively a C–H bond at the ε-carbon atom with formation of cyclopentane derivatives.[23] The insertion reaction is then complicated by the competing processes involving the elimination of a β-hydrogen atom with formation of acrylic acid derivatives, the relative contributions of these pathways depending on the ligand at the rhodium atom (Scheme 5).

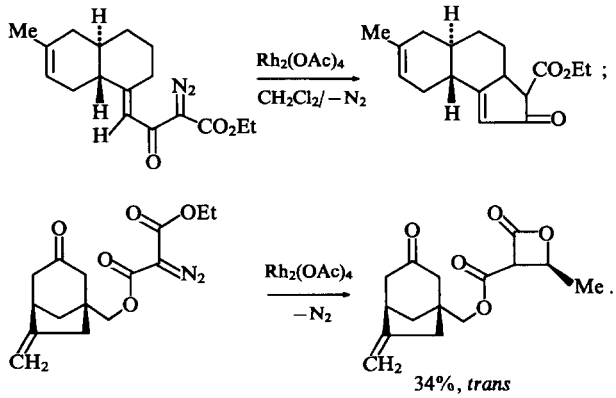
Scheme 5



	1		2	
L	R = H, $R^1 = C_7H_{15}$		R = Me, $R^1 = C_6H_4Me$–4	
	overall yield (%)	1 : 2 ratio	overall yield (%)	1 : 2 ratio
$OCOBu^t$	97	85:15	89	55:45
$OCOCF_3$	93	52:48	99	26:74

The steric factor can exert an even greater influence on the course of the process than the electronic factor, as a result of which the carbene may cyclise with participation of not the tertiary but the secondary carbon atom (Scheme 6).[24,25]

Scheme 6

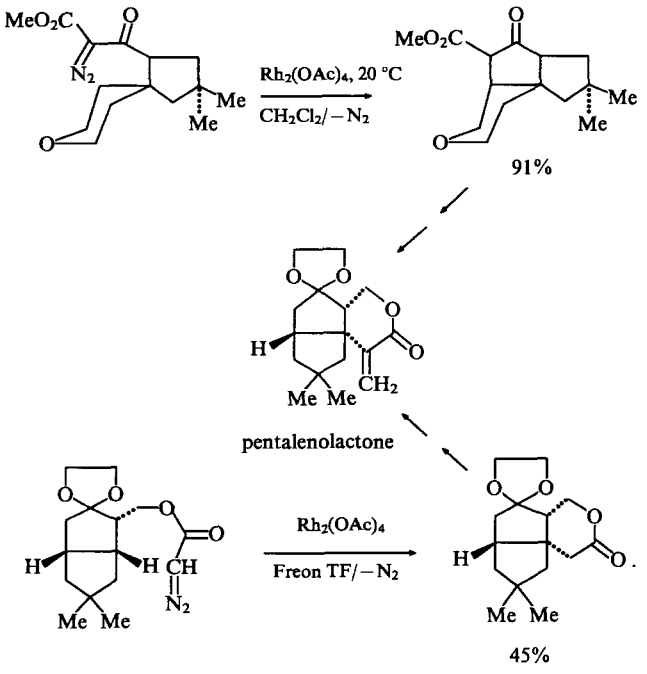


34%, *trans*

These examples demonstrate in addition the ability of rhodium compounds, in contrast to the copper catalysts, to effect the C–H insertion reactions even in the presence of a double bond.

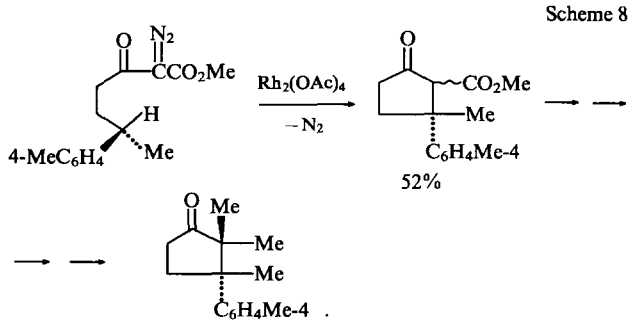
The marked sensitivity of the intramolecular insertion reactions to steric factors must be taken into account in choosing a strategy for the synthesis of the target products. Thus the two schemes proposed by Taber and Schuchardt[26] and Cane and Thomas[27] for the synthesis of pentalenolactone are based on the preferential attack by the carbene on the sterically most accessible bonds, although in the second case this leads to the formation of a six-membered and not a five-membered ring (Scheme 7).

Scheme 7



The intramolecular insertion reaction with participation of rhodium complexes of carbenes, generated by the dediazotisation of β-oxodiazoacetates, is distinguished by a high degree of stereoselectivity and proceeds with retention of the configuration of the attacked carbon atom, which enabled, for example, Taber et al.,[22] to use this reaction for the synthesis of α-cuparenone (Scheme 8).

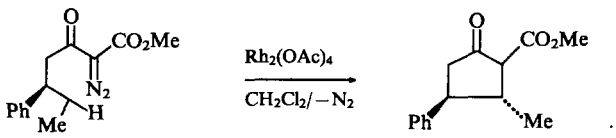
Scheme 8



α-cuparenone

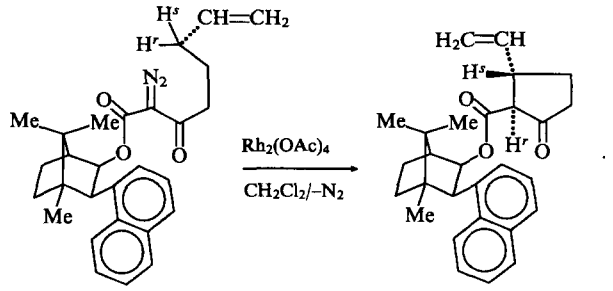
The same group of workers established that the substituents in α-acetyldiazoacetates increase the *trans*-selectivity of the intramolecular C–H insertion (Scheme 9)[28] and the enantioselectivity of the cyclisation to form the rhodium complex of a carbene from the chiral oxodiazoester precursor **3** (Scheme 10).[29] The bulky α-naphthyl substituent in the above diazoester effectively shields one of the sides of the acyl substituent and favours the insertion of the carbene centre in the C–H^r bond. The hydrolysis and decarboxylation of the esters thus obtained permit the enantioselective synthesis of cyclopentanones with an enantioselective excess (e.e.) up to 98%.

Scheme 9



66%, *trans*

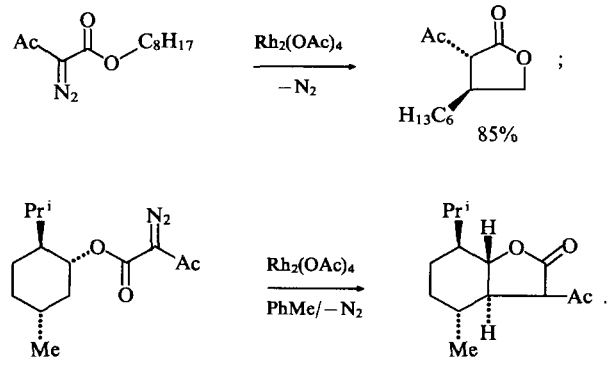
Scheme 10



3 e.e. 98%

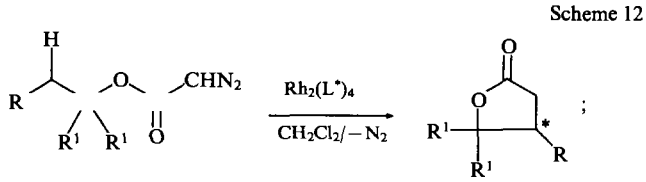
The C–H insertion reactions involving the alcoholic part of α-diazoacetates on treatment with rhodium(II) acetate and acetamide proceeds with a selectivity which is just as high. Thus it is possible to obtain γ-lactones with high regio- and diastereoselectivities and a virtually complete conversion of the diazoester (Scheme 11).[30]

Scheme 11



Data have been published recently on the asymmetric synthesis of lactones with a high enantioselectivity (enantiomeric excess up to 85%) via intramolecular C–H insertion reactions of carbenes generated from certain alkoxyethyl diazoacetates on treatment with chiral rhodium(II) carboxamides, in particular tetrakis(5-methoxycarbonylpyrrolidin-2-one)dirhodium(II) [Rh_2(MEPY)$_4$].[31] The configuration of the resulting lactone is then determined by that of the catalyst ligand and the substituent R (Scheme 12).

Scheme 12



R = MeO, EtO, $PhCH_2O$, Ph; 42%–56%

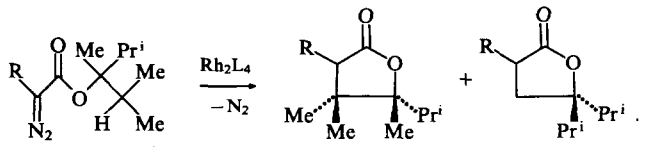
R^1 = H, Me; L* = (*R*)- or (*S*)-MEPY. e.e. 77%–85%

By 'grafting' this catalyst to the polyethylene, it is possible to achieve the enantioselective synthesis of lactones in a heterogeneous version, which simplifies significantly processes involving the recovery of the expensive rhodium catalysts.[32]

Unfortunately, the effectiveness of this catalyst is inferior to that of the homogeneous catalyst and is reduced sharply after its repeated use.

It is noteworthy that the intramolecular C–H insertion reactions with participation of the alcoholic components of diazoesters are extremely sensitive to the structure of the diazoester and the catalyst counterion. Thus, under the influence of rhodium(II) perfluorobutyrate, alkyl diazoacetates (ADA) and alkyl α-acyldiazoacetates cyclise with the preferential formation of the products of insertion in the C–H bonds formed by the primary carbon atom, the process selectivity being somewhat higher in the case of ADA (Table 1). On the other hand, under the influence of rhodium(II) acetate, the insertion takes place mainly, and in the presence of rhodium(II) acetamide, exclusively in tertiary C–H bonds.[30]

Table 1. The regioselectivity of the intramolecular C–H insertion reactions with participation of the alcoholic component of diazoacetates.



4 5

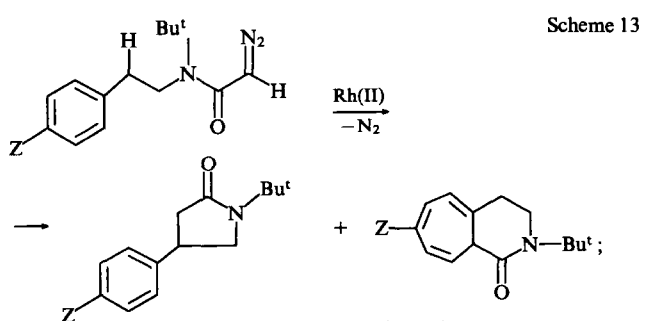
L	R = H		R = Ac	
	overall yield (%)	**4**:**5** ratio	overall yield (%)	**4**:**5** ratio
pfb	56	32:68	45	45:55
OAc	81	53:47	97	90:10
acam	96	>99:1	89	>99:1

Note. pfb = perfluorobutyrate and acam = acetamide.

The influence of the ligand on the selectivity of the rhodium(II)-catalysed C–H insertion processes has been demonstrated in relation to the intramolecular reactions of diazoamides. Thus in the case of substituted *N*-(*tert*-butyl)-*N*-ethyldiazoamides, the attack by the carbene centre can be directed to all the C–H bonds of the ethyl and *tert*-butyl fragments. However, depending on the counterion, it is possible to achieve the required specific cyclisation of the carbene with an appreciable enantioselectivity (Table 2).[33]

The dediazotisation of diazoamides containing an aromatic fragment proceeds either via insertion in the C–H bond at the δ-carbon atom or with participation of the multiple bonds of the aromatic substituent, depending on the ligand (Scheme 13).[34]

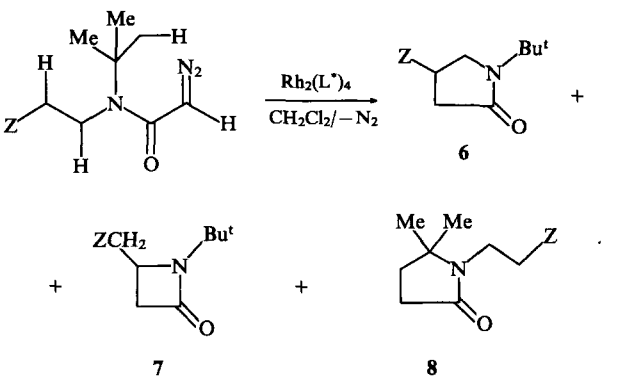
Scheme 13



Z = H, MeO, O_2N

$Rh_2(pfb)_4$, 80% (95:5);
Rh_2(caprylamide)$_4$, 65% (3:97);
$Rh_2(acam)_4$ 90% (0:100).

Table 2. The selectivity of the intramolecular C–H insertion reactions of diazoamides.



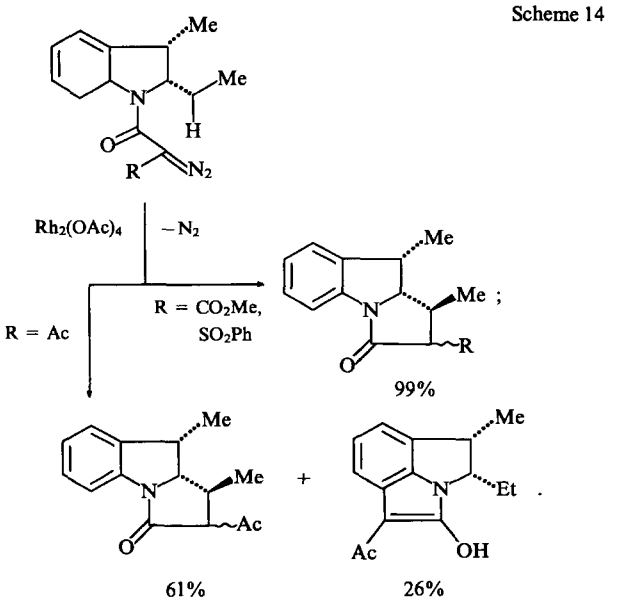
6 7 8

Z	L	Overall yield (%)	**6**:**7**:**8** molar ratios	Enantiomeric excess (%) **6**	**7**
Et	4-(*S*)-MEOX	82	91:9:0	71	80
OEt	4-(*S*)-MEOX	97	100:0:0	78	–
CO_2Et	5-(*R*)-MEPY	64	0:9:91	–	44
CO_2Et	4-(*S*)-BNOX	60	0:100:0	–	20

Note. 4-(*S*)-MEOX = 2-oxazolidine-4-(*S*)-carboxylate and 4-(*S*)-BNOX = 4-(*S*)-benzyloxazolidinone.

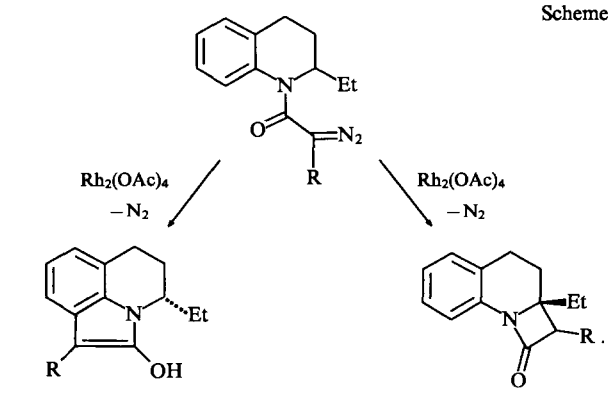
The substituents at the carbon atom of the diazo-group also affect significantly the regioselectivity of the dediazotisation of aromatic aryl-substituted diazoamides. Diazoamides with electron-accepting substituents, for example, Ac, CO_2R, or SO_2Ph, are dediazotised on treatment with $Rh_2(OAc)_4$ usually with the preferential formation of the products of insertion in aliphatic C–H bonds (Scheme 14), although the cyclisation of certain α-acyldiazoamides is accompanied by the formation of products of insertion in aromatic C–H bonds (Scheme 15).[35]

Scheme 14



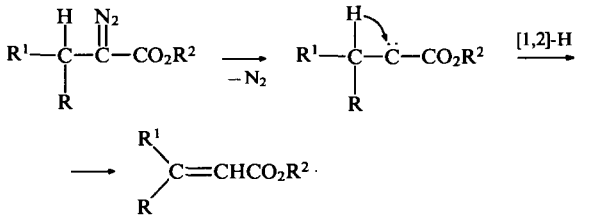
61% 26%

Scheme 15



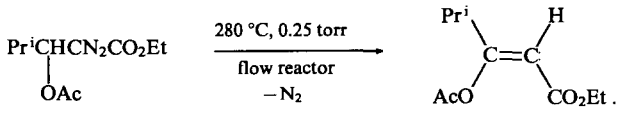
R = CO_2Me 88% R = Ac 61%

An interesting instance of intramolecular reactions of diazoesters with participation of C–H bonds is the [1,2]-hydride shift of the hydrogen atom to a neighbouring carbene centre with formation of acrylic acid derivatives.



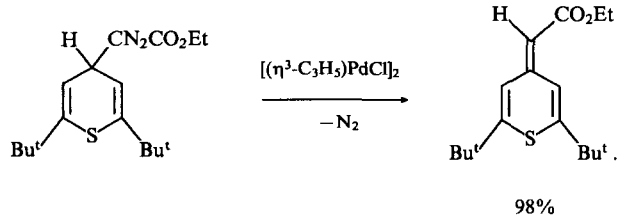
In the absence of active carbene acceptors, this rearrangement is the main pathway in the dediazotisation of diazoacetic acid esters on heating (Scheme 16)[36] and on treatment with catalysts based on transition metals (Schemes 17 and 18)[37,38] and Lewis acids (Scheme 19).[39]

Scheme 16



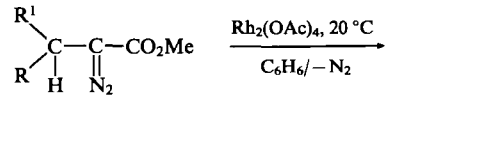
27%

Scheme 17



98%

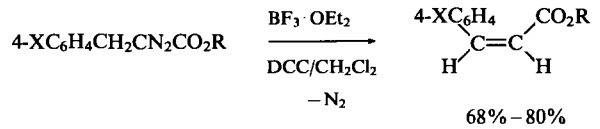
Scheme 18



R	R^1	Fraction of (Z)-isomer (%)	Overall yield (%)
Pr^i	H	~100	99
Ph	H	~100	~100
$PhCH_2O$	H	~100	90
Me	Et	57	95
$H_2C=CH$	H	~100	39[a]

[a] Another product is methylbicyclo[1.1.0]butanecarboxylate (yield 51%).

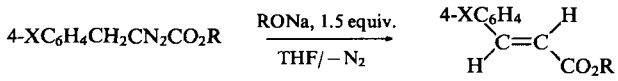
Scheme 19



DCC = dicyclohexylcarbodiimide;
X = H, NO_2, MeO; R = Me, Et.

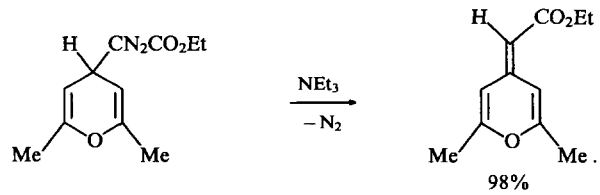
The yields of the acrylic acid derivatives thus obtained reach 98%, the (Z)-isomer predominating. Furthermore, in the case of the H-shift of the hydrogen atom in the methylene fragment, the reaction leads to the (Z)-isomer only. Similar reactions of diazoesters can be initiated also by bases.[39,40] However, in this case the reaction leads to the (E)-isomer (Scheme 20).

Scheme 20



X = H, NO_2, MeO; R = Me, Et

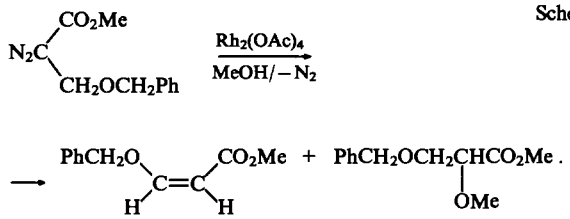
E, 59%–72%



98%

The migration of a hydrogen atom in the rhodium(II)-catalysed dediazotisation of certain diazoesters with an active methylene group proceeds to an appreciable extent even in the presence of methanol (Scheme 21),[37] which is an active carbene acceptor under these conditions (Section III).

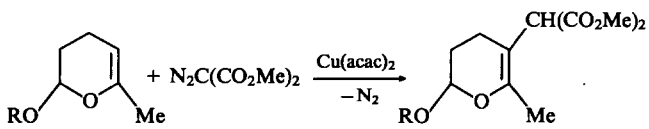
Scheme 21



80% (1:1)

A few examples of reactions involving the insertion of carbenes in the vinyl C–H bonds of alkenes are known. Thus, although the ACC generated by the photolysis or pyrolysis of alkyl diazoacetates afford predominantly cyclopropane adducts on reaction with olefins, the products of insertion in the vinyl C–H bonds are also formed in a small amount (3%–5%).[41] On the other hand, the catalytic dediazotisation of alkyl diazoacetates makes it possible to obtain the corresponding C–H insertion products with a high selectivity. In particular, the formation of vinyl insertion products has been observed in the reaction of dimethyl diazomalonate (MDM) with vinyl ethers in the presence of copper catalysts (Scheme 22).[42]

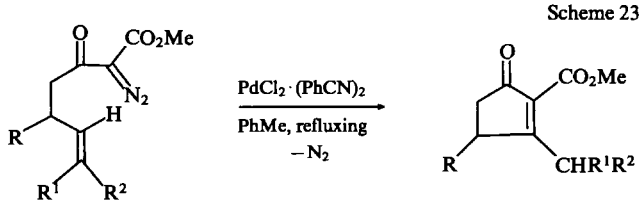
Scheme 22



76%–80%

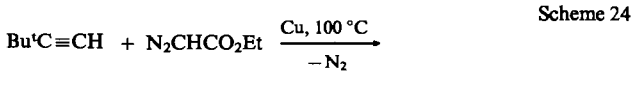
The intramolecular reaction of 2-diazo-3-oxohept-6-enoates on treatment with palladium(II), leading to methyl 3-alkylcyclopent-2-enecarboxylates in 34%–73% yields (Scheme 23), belongs formally to this type of reactions.[43]

Scheme 23



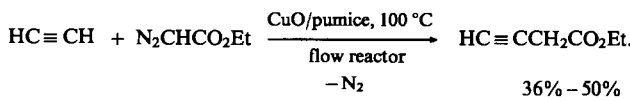
The reaction with ethyl diazoacetate under these conditions leads to the cyclopropane adduct only.[44] Instances of the insertion of ACC in a C–H bond at an *sp*-hybridised carbon atom in alkynes are also known. As in the case of alkenes, here the direct insertion of carbenes in these bonds with formation of the esters of alk-3-ynoic acids is scarcely possible, because the photolysis of alkyl diazoacetates in the presence of terminal alkynes leads only to products of C–H insertion in alkyl substituents together with cyclopropenes. The formal products of insertion in an acetylenic C–H bond in terminal acetylenes, observed[45] in the catalytic dediazotisation of alkyl diazoacetates, are most probably formed from the 1-pyrazoles produced initially (Scheme 24).[46]

Scheme 24



The only example of a preparative reaction of this type is the copyrolysis of acetylene with ethyl diazoacetate over a copper catalyst in a flow reactor, which leads to a butynoic acid ester in a yield up to 50% (Scheme 25).[47]

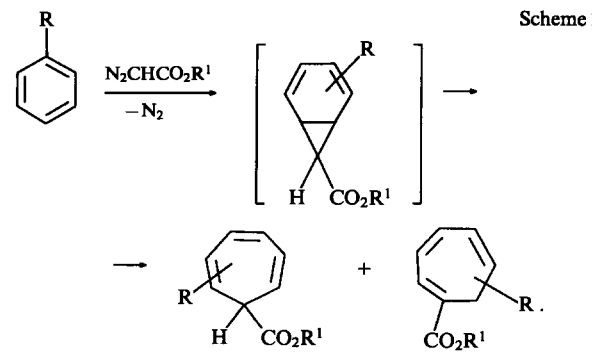
Scheme 25



2. C–H bonds in aromatic compounds of the benzenoid series

The carbenes generated by the dediazotisation of diazoesters add to the multiple bonds of aromatic compounds in the absence of more active acceptors (Scheme 26). However, bicyclo[4.1.0]-heptadienes are usually not identified in the reaction products because they readily isomerise to 1-*H*-cyclohepta-2,4,6-triene-carboxylates and the thermodynamically more stable 7-*H*-cyclo-hepta-1,3,5-trienecarboxylates.

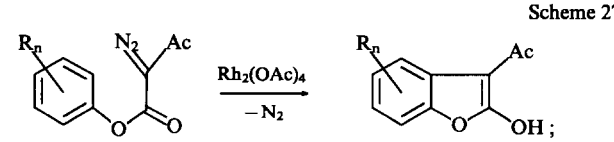
Scheme 26



Much attention has been devoted in recent years to the study of the intramolecular cyclisation reactions of ACC containing aromatic substituents. However, these reactions result in the formation not of cycloheptatriene derivatives but of the products of the formal insertion of the carbene in aromatic C–H bonds. Although it has still not been ultimately established whether this entails the concerted insertion of the carbene in a C–H bond or the isomerisation of the cyclopropane adduct formed initially, this reaction constitutes a convenient method of synthesis of polycyclic systems.

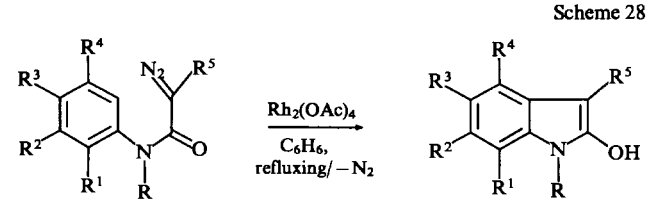
For example, the dediazotisation of phenyl α-acetyldiazo-acetates (Scheme 27)[48] or *N*-phenyldiazoamides (Schemes 28 and 29),[35,49,50] initiated by rhodium(II), is accompanied by the intramolecular cyclisation of the corresponding metal carbene complexes with formation of substituted enols of benzo[*b*]-furanone or oxindoles respectively in satisfactory yields.

Scheme 27



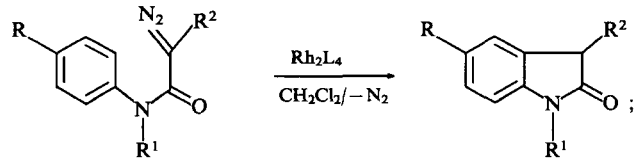
R = H, 2-Me, 2-Br, 3,4-OCH_2O; 92%–98%.

Scheme 28



R = Alk, CH_2Ph, R^5 = H, Ac;
R^1–R^4 = Alk or R^2+R^3 = CH=CHCH=CH. 77%–97%

Scheme 29

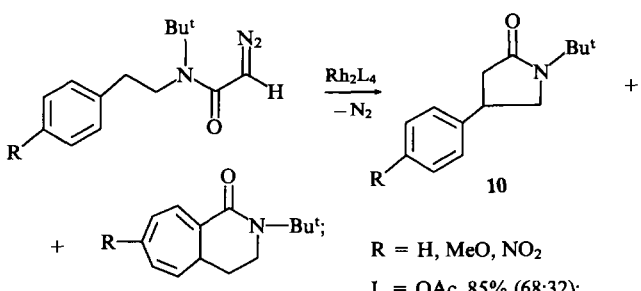


L = OAc, $OCOCF_3$, pfb, acam;

R = R^2 = H, R^1 = Me (86%),
R = MeO, R^1 = Bu, R^2 = SO_2Ph (98%).

At the same time, the cyclisation of *N*-(2-arylethyl)diazoamides on treatment with rhodium(II) compounds proceeds via two other competing pathways: with participation of the multiple bonds of the aromatic ring to form δ-lactams **9** containing a cycloheptatriene fragment and also with participation of α-C–H bonds of the alkyl chain to form γ-lactams **10** (Scheme 30).[51] The selectivity of this reaction depends decisively on the catalyst counterion. Thus the use of $Rh_2(OAc)_4$ leads to a mixture of the products indicated. The δ-lactams are formed exclusively in the presence of rhodium(II) perfluorobutyrate, while the γ-lactams are formed in the presence of rhodium(II) caprylamide.

Scheme 30

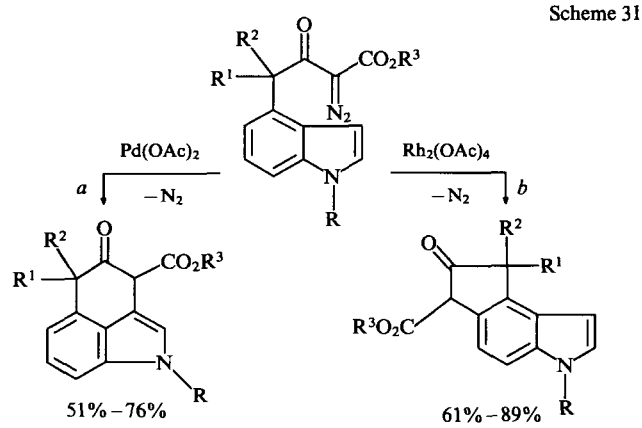


R = H, MeO, NO_2

L = OAc, 85% (68:32);
pfb, 80% (95:5);
caprylamide, 65% (3:97).

Another example of the influence of the nature of the dediazotisation catalyst on the chemoselectivity of the intramolecular cyclisation reactions of aromatic diazoesters is the cyclisation of α-(indolylacetyl)diazoacetates. In the presence of $Pd(OAc)_2$, the reaction proceeds with participation of the heterocyclic fragment (Scheme 31, pathway *a*), while on treatment with $Rh_2(OAc)_4$ it involves the benzene ring (pathway *b*).[52]

Scheme 31

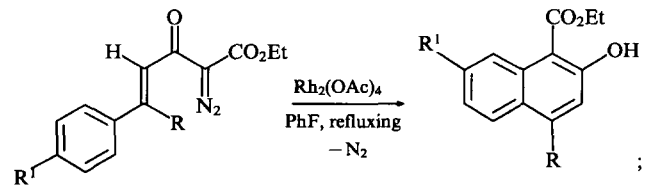


R = H, Ts, CH_2Ph;
R^1, R^2 = H, Alk; R^3 = Me, Et.

This course of the process is apparently determined by the different mechanisms of the catalytic action of palladium and rhodium compounds in the carbene reactions with participation of diazoesters, although in the case of palladium compounds the authors postulate the involvement not of carbene but of carbonium ion intermediates.

The intramolecular C–H insertion in the aromatic ring is preferable in certain cases even in the presence of a multiple bond in the molecule, as has been observed in the case of ethyl α-(arylvinylcarbonyl)diazoacetates, in which the double bond is deactivated by conjugation with the carbonyl group.[53] The reaction affords derivatives of β-naphthols in high yields (Scheme 32).

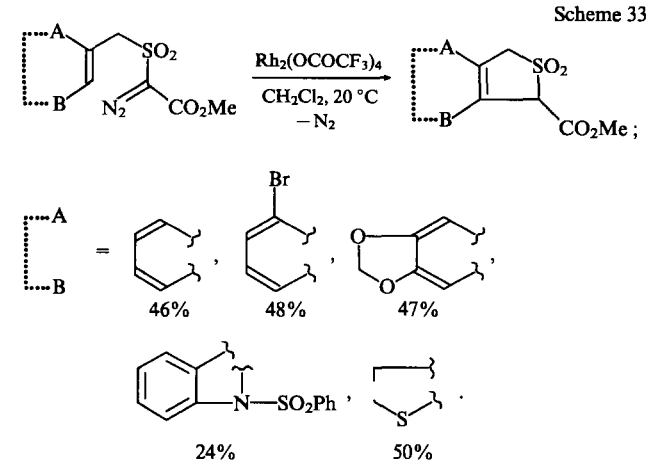
Scheme 32



R = Ph, R^1 = H (90%);
R = C_6H_4Me-4, R^1 = Me (76%);
R = C_6H_4Cl-4, R^1 = Cl (97%).

On treatment with rhodium(II) compounds, intramolecular cyclisation takes place also in the case of α-[aryl (or heteroaryl)-methanesulfonyl] diazoacetates, which leads to the corresponding benzo[*c*]thiophene 1,1-dioxides in moderate yields (24%–48%) (Scheme 33).[54]

Scheme 33

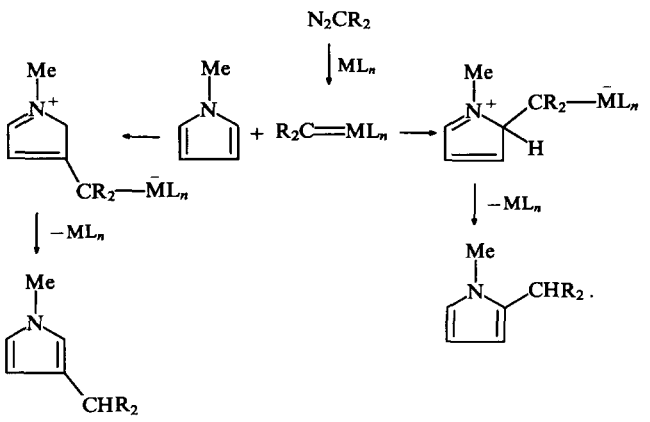


3. C–H bonds in heteroaromatic compounds

The nature of the multiple bonds in heteroaromatic compounds, which occupy an intermediate position between aromatic bonds of the benzenoid type and conjugated bonds of diene systems, as well as the presence of a nucleophilic heteroatom are responsible for the wide variety of reactions of compounds of this class with carbenes or their transition metal complexes. However, selective reactions of diazoesters with heteroaromatic compounds, accompanied by the formation of products of insertion in C–H bonds, are known.

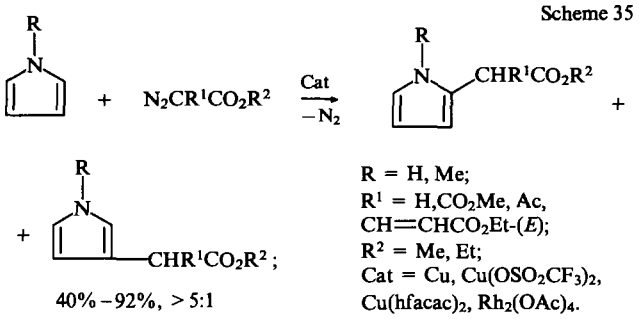
The commonest C–H insertion reactions occur in the pyrrole series, which can be explained by the greater aromatic character of the pyrrole ring.[55] As a result, the insertion products are formed as electrophilic substitution by the metal-carbene in the heteroaromatic ring via a metastable σ-complex (Scheme 34).

Scheme 34



The reactions of diazoesters with pyrrole itself and *N*-alkylpyrroles lead only to the products of formal insertion in the C–H bonds of the pyrrole ring, among which products of insertion in the α-C–H bonds predominate; the formation of N–H insertion products was not observed at all under these conditions (Scheme 35).[56–58]

Scheme 35

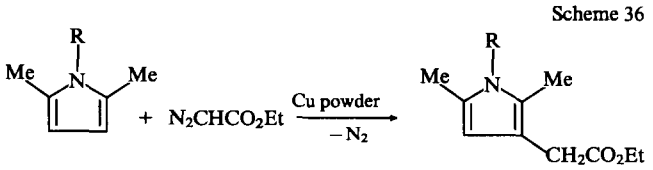


The regioselectivity of this reaction depends on the catalyst, the diazo-compound and the substituent at the nitrogen atom. The highest yields (up to 92%) and the highest reaction selectivity (>90%) in relation to the product of insertion in α-C–H bonds have been achieved in reactions involving dimethyl diazomalonate and homogeneous catalysts based on copper(II) compounds or $Rh_2(OAc)_4$. The reactions of ethyl diazoacetate and other diazoesters with pyrroles proceed in general with lower yields of the insertion products and a lower selectivity; rhodium compounds rapidly lose their activity in the dediazotisation of ethyl diazoacetate under these conditions and afford complex mixtures of products with traces of C–H insertion products.

The influence of *N*-alkyl substituents reduces to an increase in the fraction of the β-isomer with increase in the steric effect of this substituent in the series H < Me < Pr^i < Bu^t with the exclusive formation of the β-isomer in the case of the *tert*-butyl group.

Substituents in other positions in the pyrrole ring do not influence the regioselectivity of the reaction regardless of their nature, with the exception of the case where they occupy the 2- and 5-positions in the ring. The reaction of ethyl diazoacetates with such pyrroles leads to the product of insertion in the β-C–H bonds (Scheme 36).[59]

Scheme 36

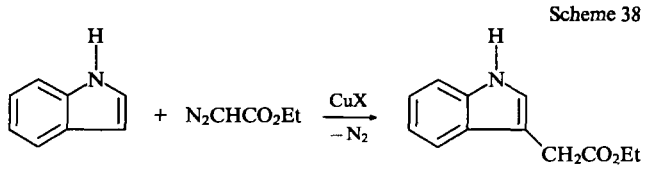


59%

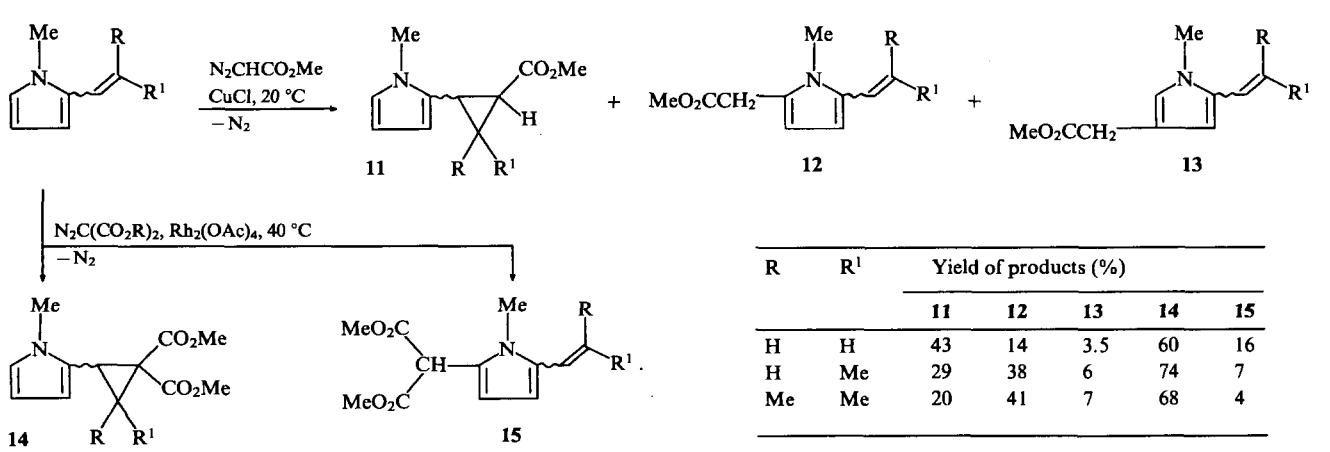
The possibility of competition between the reactions involving the attack by the carbene on the pyrrole ring and the alkenyl group arises in reactions with participation of 2-alkenyl-1-methylpyrroles, as a result of which cyclopropane adducts involving the exocyclic double bond are formed together with the C–H insertion products (Scheme 37).[60] The relative contributions of these reaction pathways are determined by the structure of the diazoesters and to a lesser extent of the substituent at the double bond. In reactions with participation of dimethyl diazomalonate, the alkylation of the pyrrole ring in the α-position predominates in all cases, while in the reaction involving methyl diazoacetate this process becomes the main one only in the presence of substituents at the double bond.

Certain other heteroaromatic nitrogen-containing compounds also behave similarly to pyrroles in reactions with diazoesters. Thus the esters of the corresponding heteroarylacetic acids are the main products of the reactions of ethyl diazoacetate with indoles[61] (Scheme 38) and furazans[62] (Scheme 39). The β-isomer predominates in the products of the reaction with indole under these conditions.

Scheme 38

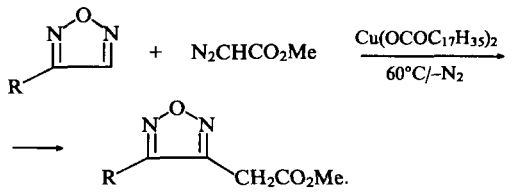


Scheme 37



R	R^1	Yield of products (%)				
		11	**12**	**13**	**14**	**15**
H	H	43	14	3.5	60	16
H	Me	29	38	6	74	7
Me	Me	20	41	7	68	4

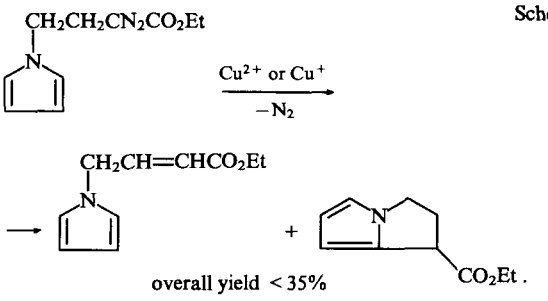
Scheme 39



9%–12% R = H, Ph, 2-thienyl.

Several examples of the intramolecular C–H insertion with participation of the pyrrole ring are known. Thus the carbenes generated by the dediazotisation of α-(2-pyrrolylethyl)diazoacetate (Scheme 40)[63] or α-(3-indolesulphonyl)diazoacetate[64] are converted into the corresponding polyheterocycles albeit with low yields (see Scheme 33).

Scheme 40



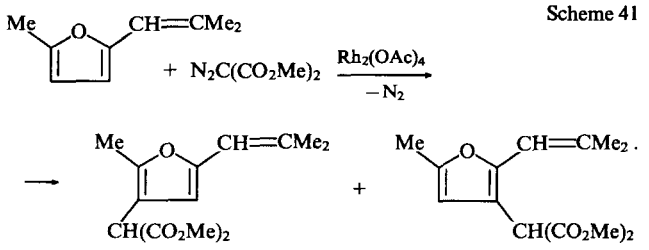
overall yield < 35%

On the other hand, the complexes of carbenes formed from 2-diazo-4-(4-indolyl)-3-oxobutanoates cyclise with participation of the indole ring in yields up to 76% (Scheme 31, pathway *a*).

In the series of thiophene and furan derivatives, only isolated instances of C–H insertion reactions are known. The reason for this is the low aromaticity of thiophene and furan compared with pyrrole and the presence of lone pairs at the O and S atoms, as a result of which the main primary reaction products are the corresponding S and O ylides. The subsequent reactions of these ylides lead in certain cases to C–H insertion products.

Thus the C–H insertion products, namely 3-furylmalonates, are formed in the reaction of 5-methyl-2-(2-methylprop-1-enyl)-furan with dimethyl diazomalonate (Scheme 41).[65]

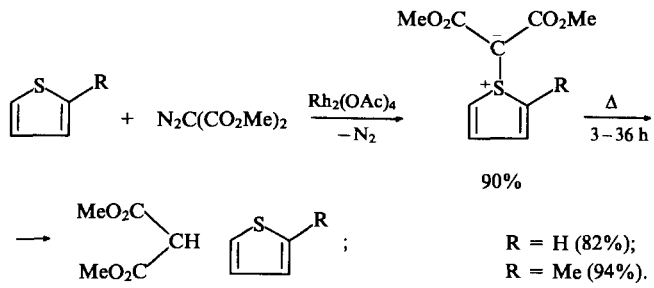
Scheme 41



80% (1:1)

Several examples of the formation of C–H insertion products in the reactions of dimethyl diazomalonate with thiophene are known. Thus the reaction of diazomalonates with thiophenes, catalysed by $Rh_2(OAc)_4$ at 20 °C, leads to the corresponding stable ylides in yields up to 90%. The thermal rearrangement of the ylides affords acceptable yields of 2-thienylmalonates, which are convenient synthons for the preparation of semisynthetic antibiotics of the β-lactam type, for example, cephalothin (Scheme 42).[66,67]

Scheme 42



90%

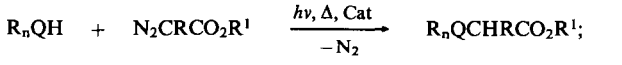
R = H (82%); R = Me (94%).

Other examples of the C–H insertion in reactions with thiophenes are examined in Section V devoted to reactions involving C–S bonds.

III. Heteroatom–hydrogen bonds

On irradiation, heating, or under the influence of catalysts, diazoesters react with compounds containing a heteroatom–hydrogen bond with formation of products of the insertion of the corresponding carbenes — esters of acetic acid derivatives.

Reactions involving insertion in the N–H, O–H, S–H, Si–H, Ge–H, and P–H bonds, which as a rule proceed selectively and with high yields of the insertion products, are now known.

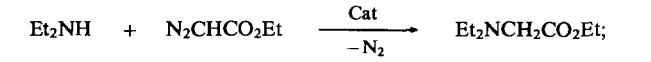


Q = N, O, S, Si, Ge.

1. N–H bonds

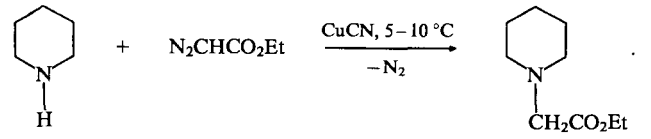
Regardless of the method of dediazotisation, both aliphatic (Schemes 43 and 44)[68] and aromatic primary and secondary amines (Schemes 45 and 46)[69,70] react with alkyl diazoacetates, affording high yields of *N*-alkylated glycine esters.

Scheme 43



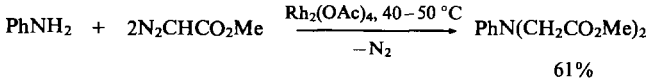
Cat = CuCN (72%), CuCl (33%).

Scheme 44



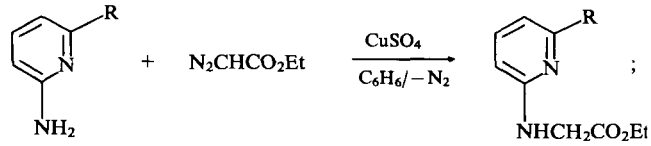
72%

Scheme 45



61%

Scheme 46

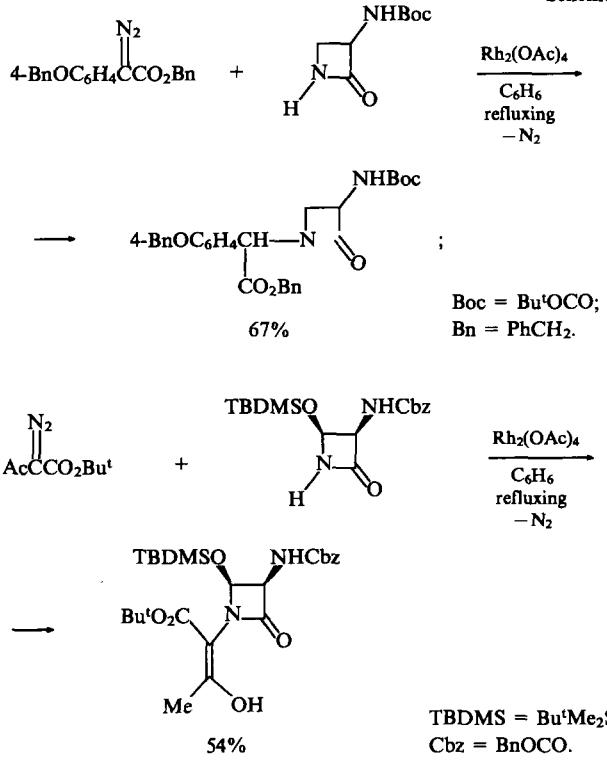


R = H, Me.

The intermolecular N–H insertion proceeds so readily that the catalytic dediazotisation of 2-alkylaminoethyl diazoacetates, even in the presence of olefins, leads not to cyclopropane adducts but exclusively to oligomers, which are formed as a result of the insertion of the carbene centre in the N–H bond of another molecule.[71]

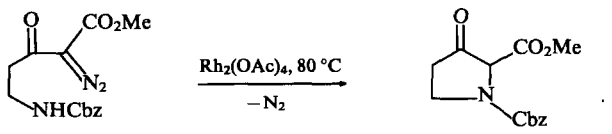
The use of rhodium(II) acetate as the catalyst makes it possible to achieve the intermolecular N–H insertion reactions with labile products such as azetidinones. In the case of 3-aminoazetidinones, this reaction is exclusively selective, involving only the ring nitrogen atom, and leads to *N*-alkylated azetidinones — synthons for the preparation of β-lactam antibiotics (Scheme 47).[72,73]

Scheme 47



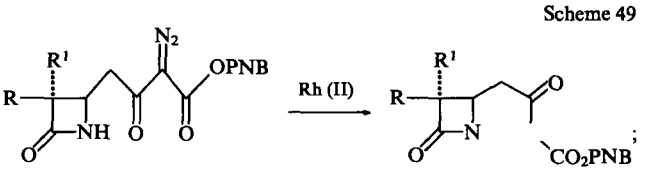
Examples of the intramolecular N–H insertion of carbenes, generated from diazoesters under the conditions of their dediazotisation by rhodium(II) compounds, are also known. However, these reactions take place effectively only in the case of compounds containing a N–H bond at a carbon atom in the δ-position. Thus the cyclisation of methyl 5-amino-2-diazo-3-oxopentanoate leads to methyl 3-oxopyrrolidine-2-carboxylate in 90% yield (Scheme 48).[74]

Scheme 48



The $Rh_2(OAc)_4$-catalysed intramolecular N–H insertion reaction with participation of the corresponding metal-carbene complexes derived from α-acyldiazoacetates containing an azetidinone fragment is used widely for the synthesis of β-lactam antibiotics (Scheme 49)[75] (for the references to studies up to 1985, see Maas[7]).

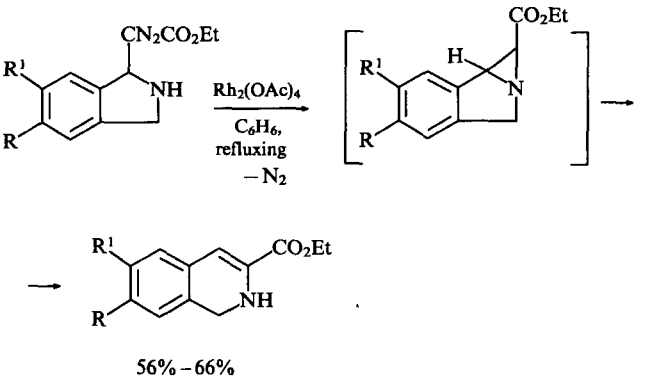
Scheme 49



PNB = $C_6H_4NO_2$-4. 50% – 100%

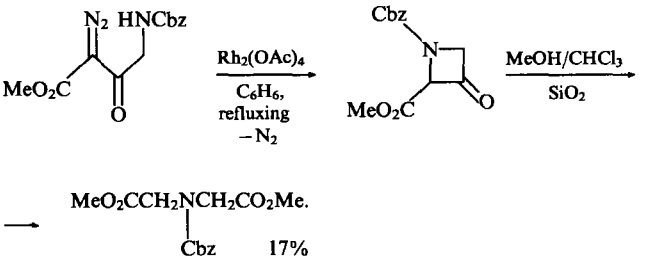
The number of examples of intramolecular cyclisation involving a more or less remote amino-group is extremely small. In particular, the cyclisation of β-aminodiazoesters has been described recently. The unstable aziridines formed initially in this case readily isomerise under the reaction conditions with the opening of the three-membered ring to give dihydroisoquinoline-carboxylates (Scheme 50).[76]

Scheme 50



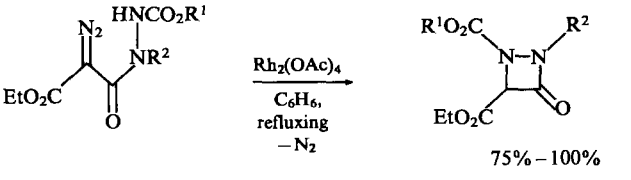
Intramolecular N–H insertion reactions with participation of a γ-amino-group are also known. For example, the $Rh_2(OAc)_4$-catalysed dediazotisation of the *N*-protected methyl 4-amino-2-diazo-3-oxobutanoate leads, admittedly with a low yield, to 3-oxoazetidine-2-carboxylate, which readily isomerises during isolation to a glycine derivative (Scheme 51).[74]

Scheme 51



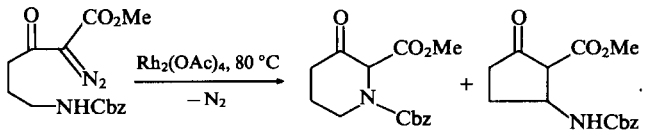
The monocarbazides of diazomalonates cyclise significantly more readily under these conditions, forming 1,2-diazetidinones in high yields (Scheme 52).[77]

Scheme 52



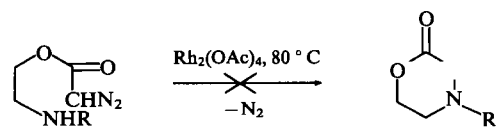
The intramolecular N–H insertion reaction involving diazoesters with an ε-amino-group is frequently complicated by the formation of side products of insertion in a C–H bond in the γ-position (Scheme 53)[74] or it does not occur at all, as happens in the reactions of 2-aminoethyl esters of diazoacetic acid (Scheme 54).[71]

Scheme 53



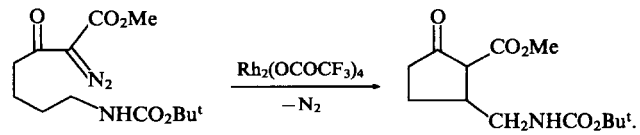
70% 10%

Scheme 54



The available information about the possibility of the N–H insertion with participation of more remote amino-groups is contradictory. Thus the cyclisation of methyl 7-*tert*-butoxycarbonylamino-2-diazo-3-oxoheptanoate leads exclusively to the products of insertion in a C–H bond at the ε-carbon atom (Scheme 55).[78]

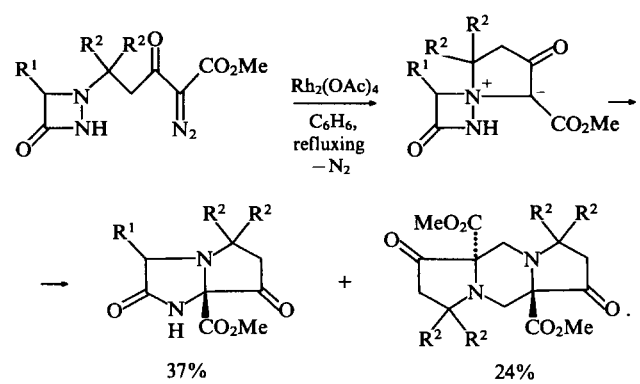
Scheme 55



73%

On the other hand, in the absence of C–H bonds at the ε-atom, as happens, for example, in methyl 2-diazo-5-(3-oxo-2*H*-1,2-diazetidinyl)-3-oxopentanoate, the products of insertion in a ring C–N bond of the diazetidine are formed, apparently via the intermediate formation of ylides (Scheme 56).[79]

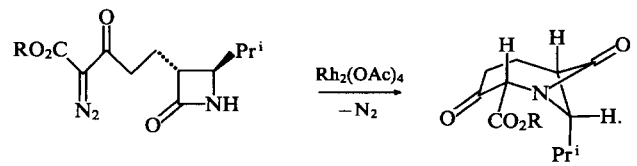
Scheme 56



37% 24%

However, the intramolecular insertion of the carbene centre in a N–H bond separated by a chain of five carbon atoms has been recently observed (Scheme 57).[80]

Scheme 57



50%

2. O–H bonds

The reactions of alkyl diazoacetates with hydroxyl-containing compounds, leading to the formation of the products of the insertion of the corresponding carbenes in the O–H bonds, are fairly varied. Thus certain organic acids, for example, trifluoromethanesulfonic acid, are capable of reacting with ethyl diazoacetate in liquid SO_2 even at −78 °C with formation of the corresponding sulfonate of glycolic acid in 73% yield (Scheme 58).[81]

Scheme 58

$$CF_3SO_2OH + N_2CHCO_2Et \xrightarrow[-78\,°C/-N_2]{\text{liquefied } SO_2} CF_3SO_2OCH_2CO_2Et.$$

However, other hydroxylated compounds (water, alcohols, carboxylic acids) afford the O–H insertion products only in the photolytic, pyrolytic, or catalytic dediazotisation of alkyl diazoacetates[68,82] or their α-metallated derivatives (Scheme 59).[83]

Scheme 59

$$ROH + N_2CR^1CO_2R^2 \xrightarrow[-N_2]{h\nu,\ \Delta,\ Cat} ROCHR^1CO_2R^2;$$

R = H, Alk, Ac; R^1 = H, HgMe; R^2 = Alk.

This reaction acquired preparative importance only after the discovery of catalysts based on rhodium compounds, which ensure preparative yields (in excess of 80%) of the products in the case of various diazoesters and a wide range of hydroxylated compounds.[7]

The high efficiency of these catalysts makes it possible to carry out reactions also with diazoacetic acid esters having a complex structure (Scheme 60).[84]

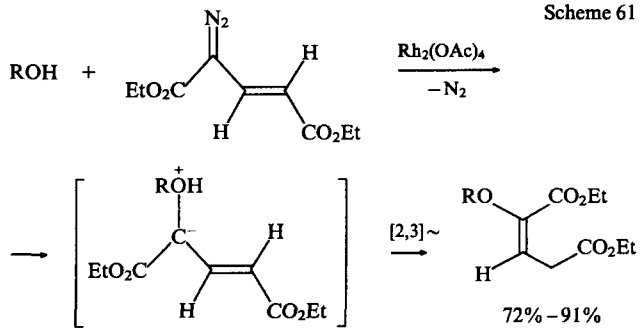
Scheme 60

$$H_2O + N_2CHCO_2CH_2C{\equiv}CH \xrightarrow[CH_2Cl_2/-N_2]{Rh_2(OAc)_4,\ 20\,°C}$$

$$\longrightarrow \underset{15\%}{HOCH_2CO_2CH_2C{\equiv}CH} + \underset{20\%}{O(CH_2CO_2CH_2C{\equiv}CH)_2}.$$

In the case of carbenes containing an allyl fragment, for example, the metal-carbene complex formed on dediazotisation of ethyl α-(2-ethoxycarbonylvinyl)diazoacetate on treatment with $Rh_2(OAc)_4$, the insertion reaction is accompanied by a [2,3]-sigmatropic rearrangement (Scheme 61).[85]

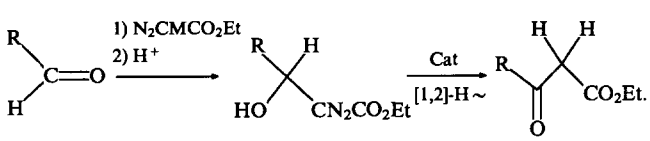
Scheme 61



R = Me, Et, Pr^i, Bu^t.

Instances of intramolecular reactions of diazoesters with participation of O–H bonds are known. However, these have a number of characteristic features compared with the analogous N–H insertion reactions. Thus the dediazotisation of α-diazo-β-hydroxyacetates, catalysed by rhodium(II) carboxylates, leads not to three-membered heterocycles (oxirans in the given instance), of the kind observed in the reactions involving β-amino-α-diazoacetates (Scheme 50), but to acyl acetates as a result of a [1,2]-H shift (Scheme 62).[36,86–89]

Scheme 62

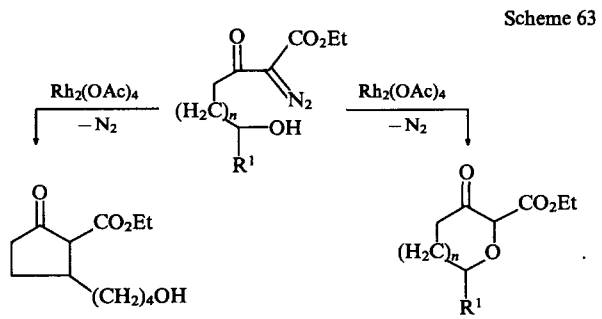


M – metal; Cat = Rh_2L_4; SnX_2;
R = H, Alk, Ph, $H_2C=CH$, *trans*-PhCH=CH.

71%–100%

Furthermore, similar cyclisations involving hydroxylated diazoesters lead readily to six-, seven-, and eight-membered cyclic esters in satisfactory yields,[90,91] whereas heterocycles containing more than six atoms cannot be obtained as a rule with the aid of similar N–H insertion reactions. However, the attempts to obtain oxygen-containing heterocycles with more than eight atoms by this procedure have led to the formation of cyclopentanones — the products of the competing C–H insertion (Scheme 63).[90]

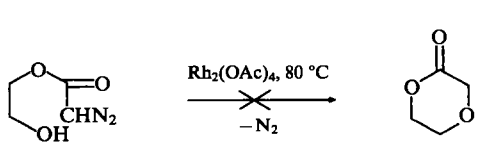
Scheme 63



n = 5, R^1 = H. n = 1–3, 24%–78%.

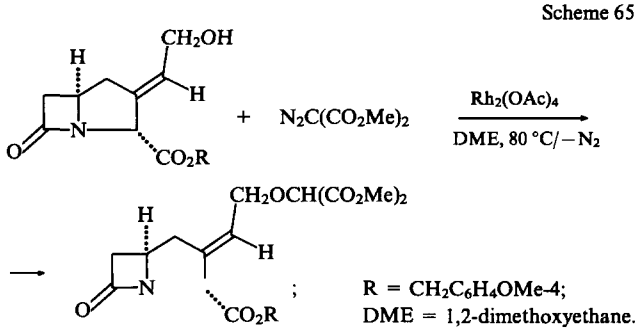
The attempt to obtain 1,4-dioxanone by the cyclisation of 2-hydroxyethyl diazoacetate was also unsuccessful. The dediazotisation of this diazoacetate led to the formation of oligomers, apparently as a result of intermolecular O–H insertion (Scheme 64).[92]

Scheme 64



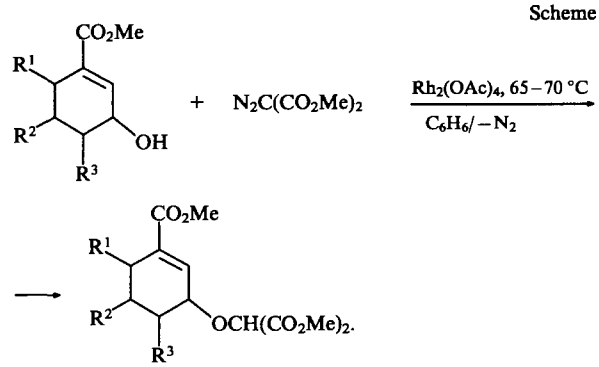
Special mention should be made of the reactions of carbenes, generated from diazoesters, with allyl and propargyl alcohols, because in this case the ACC are capable both of being inserted in the O–H bonds and of adding to the multiple bond with formation of cyclopropane or cyclopropene adducts.[93,94] However, instances are known where the interaction with allyl alcohol in accordance with the O–H insertion mechanism proceeds with a high selectivity and high yields of the corresponding esters (Schemes 65 and 66).[95–98]

Scheme 65



R = $CH_2C_6H_4OMe$-4;
DME = 1,2-dimethoxyethane.

Scheme 66

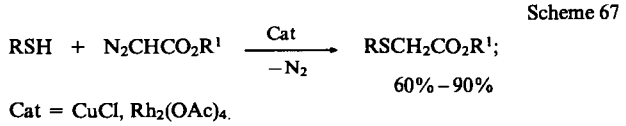


R^1	R^2	R^3	Yield (%)	Ref.
H	H	OCH_2CH_2OMe	75	96
H	H	$NHCO_2Bu^t$	94	97
H	–O–		82	98

3. S–H, Si–H, Ge–H, and P–H bonds

Isolated examples of the reactions of diazoesters with the S–H bond, leading to the formation of esters of thioglycolic acid, have been described in the literature. In the reactions with thiols, both CuCl[67] and $Rh_2(OAc)_4$ are used as the catalysts of the dediazotisation of alkyl diazoacetates (Scheme 67).[99]

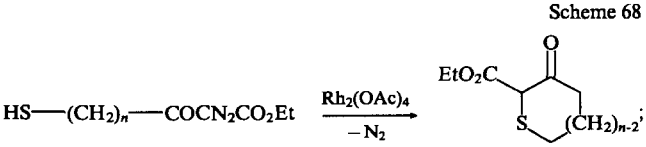
Scheme 67



Cat = CuCl, $Rh_2(OAc)_4$.

However, rhodium(II) compounds are usually employed for theintramolecular reactions of mercaptodiazoesters (Scheme 68).[73,77]

Scheme 68



n = 3 (73%), n = 4 (35%).

The reactions of diazoesters with mono-, di-, and trisubstituted hydrosilanes, leading to esters of acetic acids, are of preparative importance. The reactions proceed with high yields both under the conditions of the thermal decomposition of alkyl diazoacetates (Scheme 69) and on treatment with catalysts — copper compounds and $Rh_2(OAc)_4$ (Scheme 70).[100-102]

Scheme 69

$$PhMe_nSiH_{3-n} + N_2CHCO_2Et \xrightarrow[-N_2]{130-140\ ^\circ C} PhMe_nSiH_{2-n}CH_2CO_2Et;$$

n = 0 (59%), 1 (92%), 2 (94%).

Scheme 70

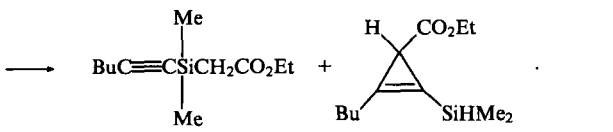
$$RR^1R^2SiH + N_2CHCO_2R^3 \xrightarrow[-N_2]{Cat} RR^1R^2SiCH_2CO_2R^3;$$

Cat = Cu, 94 °C (< 90%);
$Rh_2(OAc)_4/CH_2Cl_2$ (90%-94%).

Under these conditions, the addition to the triple bond in hydroxyacetylenes competes to only a slight extent with the Si–H insertion reactions (Scheme 71).[103]

Scheme 71

$$BuC{\equiv}CSiMe_2H + N_2CHCO_2Et \xrightarrow[-N_2]{150\ ^\circ C\ (or\ CuCl,\ 80\ ^\circ C)}$$



50%–60% 5%–15%

There are data indicating the possibility of the insertion of carbenes, generated by the dediazotisation of α-triethylgermyldiazoacetates, in the Ge–H bond of triethylgermane and in the Sn–H bond of trineopentylstannane (Scheme 72).[104] In the case of stannanes, this reaction proceeds in the absence of catalysts (Scheme 73).

Scheme 72

$$Et_3GeCN_2CO_2Et + Et_3GeH \xrightarrow[C_6H_6/-N_2]{Cu,\ 100\ ^\circ C} (Et_3Ge)_2CHCO_2Et.$$

66%

Scheme 73

$$(neo\text{-}C_5H_{11})_3SnCN_2CO_2Et + (neo\text{-}C_5H_{11})_3SnH \xrightarrow[C_6H_6/-N_2]{100\ ^\circ C}$$

$$\longrightarrow [(neo\text{-}C_5H_{11})_3Sn]_2CHCO_2Et.$$

It has been established recently that products of P–H insertion may be formed in 16%–39% yields under the conditions of the benzophenone-sensitised photolysis of certain diazoesters in the presence of dimethyl phosphorothioite (Scheme 74).[105,106]

This reaction proceeds more selectively under the conditions of catalytic dediazotisation of diazoesters by $Cu(acac)_2$; the yields of the corresponding P–H insertion products reach 83%.[107]

Scheme 74

$$N_2CRCO_2R^1 + (R^2O)_2\overset{\overset{S}{\|}}{P}H \xrightarrow[-N_2]{h\nu\ (Cat)} (R^2O)_2\overset{\overset{S}{\|}}{P}CHRCO_2R^1;$$

R = H, Ph, Ac, CO_2Me; R^1 and R^2 = Me, Et.

IV. Carbon–carbon bonds

The dediazotisation of certain α-diazocarboxylates may be accompanied not only by a [1,2]-H-shift (Section II, 1) but also by the [1,2]-shift of the carbon atom to the carbene centre generated with formation of the products of the formal insertion of the carbene in the C–C bond. Rearrangements of this type usually occur in the catalytic and photolytic decomposition of diazoacetates containing a cyclic substituent in the α-position. The dediazotisation of such diazoesters leads to ring expansion by one carbon atom and may serve as a convenient method for the formation of higher homologues of alicyclic compounds. The data concerning the [1,2]-carbon shift in a series of α-cyclyldiazoacetates are in Table 3.

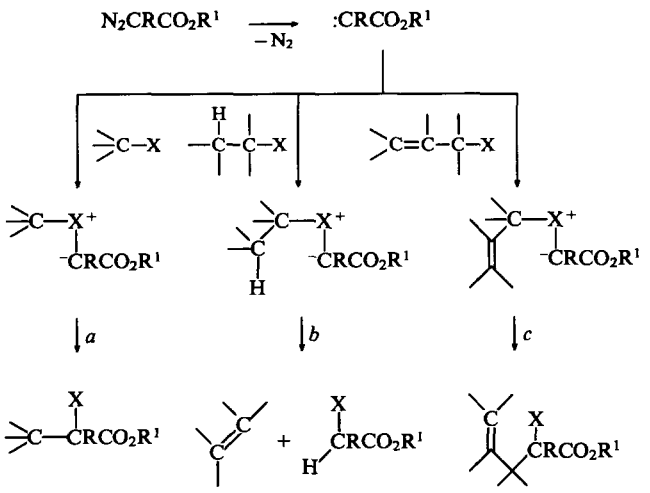
The [1,2]-carbon shift reactions are frequently accompanied by other reactions, for example, the [1,2]-hydride shift (Table 4, example 1). Combination of the [1,2]-H and [1,2]-C shifts in the transition metal-catalysed dediazotisation of certain α-diazo-β-hydroxycarboxylates without a hydrogen atom in the α-position leads to a mixture of α-acyl-α-alkylacetates (Table 4). In the case of cyclic α-diazo-β-hydroxycarboxylates (Table 4, examples 1–5), the analogous reactions are accompanied by the unexpected migration of the less substituted carbon atom and lead to the formation of 2-oxocyclocarboxylates.

High and in certain cases quantitative yields of target products as well as the availability of the initial α-diazo-β-hydroxycarboxylates, obtained by the reaction of carbonyl compounds with alkyl diazoacetates, make this reaction a convenient preparative method for the formation of higher homologues of carbonyl compounds.

V. Carbon–heteroatom bonds

Under the conditions of their dediazotisation, diazoesters react with various compounds containing carbon–heteroatom bonds. A common feature of this large group of reactions is the mechanism of the primary step, which consists in the attack by the carbene on the lone pair of the heteroatom with formation of an ylide. The subsequent reactions of these ylides, determined by the structure of the substrate, are fairly varied. The [1,2]-shift of the carbene fragment from the heteroatom to a neighbouring carbon atom occurs most frequently (the Stevens rearrangement) with formation of the product of the formal insertion of the carbene in the C–X (Scheme 75, pathway *a*), which is sometimes complicated by the elimination of a hydrogen atom attached to the β-carbon atom with transfer of the HX fragment from the substrate to the carbene (pathway *b*). In the case of allyl derivatives, the [2,3]-sigmatropic rearrangement of the ylide takes place effectively and leads to the insertion product (pathway *c*).

Scheme 75



All these processes, which lead to significant changes in the carbon skeleton of the initial molecule, take place selectively in many instances and constitute an effective pathway to the introduction of functional groups into acyclic heteroatomic compounds and the synthesis of carbofunctional heterocycles. Numerous studies devoted to the mechanistic aspects of the insertion reactions of this type have been described in detail in a number of reviews.[3,7,118–120] We shall deal with the synthetic possibilities of these reactions.

It has now been established that diazoesters are able to interact with C–Hal, C–N, C–O, and C–S bonds; individual examples of reactions involving C–Se are known; in conformity with the logic adopted for the presentation of data, they are considered in the Section devoted to the C–S insertion (Section V.4).

1. Carbon–halogen bonds

The interaction with monohaloalkanes leads to esters of monochloroacetic and ω-haloalkanoic acids as a result of β-elimination and C–H insertion respectively and usually proceeds nonselectively, as a result of which the reaction has no preparative value. The reaction of ethyl diazoacetate with bromotrinitromethane, which leads to the product of C–Br insertion in 67% yield, is an exception (Scheme 76).[121]

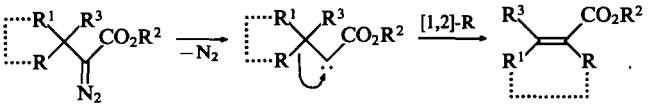
Scheme 76

$$(O_2N)_3CBr + N_2CHCO_2Et \xrightarrow[-N_2]{\text{ether, 20 °C}} (O_2N)_3CCHBrCO_2Et.$$

The reactions of diazoesters with allyl halides, which contain two reaction centres in the molecule (the double bond and the C–Hal bond), have been investigated quite vigorously. It was established that carbenes in the singlet state are equally involved in the addition to the double bond with formation of cyclopropane adducts and in the reaction with the C–Hal bond with formation of ylides, undergoing the [2,3]-rearrangement to the C–Hal insertion products; on the other hand, triplet carbenes add preferentially to the multiple bond.[3] This finding enabled Ando[119] to propose allyl halides as test reagents for the spin state of carbenes generated by the dediazotisation of alkyl diazoacetates.

The reaction of alkyl diazoacetates with allyl halides has acquired preparative importance after the appearance of catalysts based on rhodium(II) carboxylates, which make it possible to increase significantly the selectivity of the processes involving the insertion of carbenes in the C–Hal bond. The use of $Rh_2(OAc)_4$ for the dediazotisation of ethyl diazoacetate in the reaction with allyl iodide makes is possible to obtain the ester of 2-iodobut-3-enoic acid in a virtually quantitative yield (Scheme 77).[122]

Table 3. The formation of higher homologues of cyclic compounds via the [1,2]-carbon shift in alkoxycarbonylcarbenes.



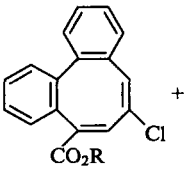
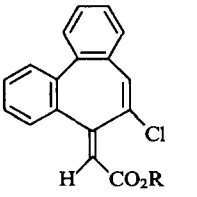
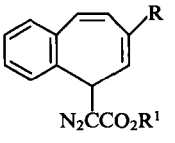
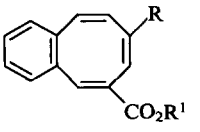
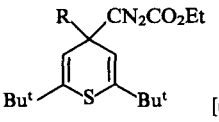
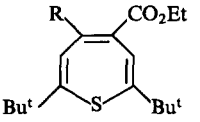
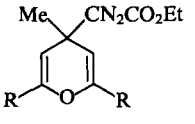
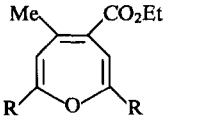
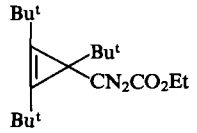
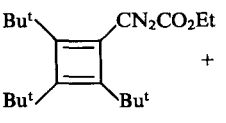
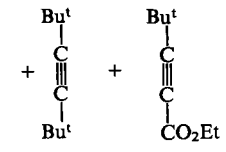
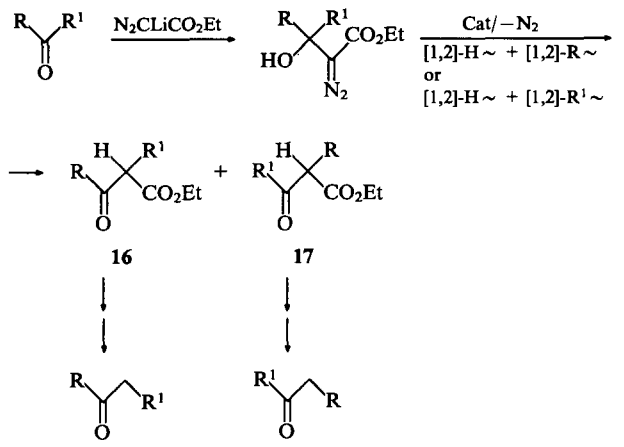
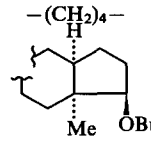
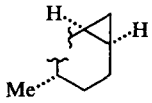
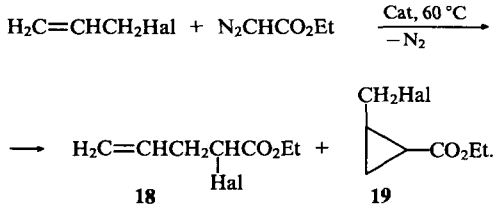
Diazoester	Dediazotisation conditions	Products (yield (%))	Ref.
 (R = Me, Et)	$Cu(acac)_2$, PhMe, refluxing	 (25) +  (10)	120
	$Cu(acac)_2$, PhMe, refluxing	 R = Br, R^1 = Me, Bu^t (70–86); R = Cl, R^1 = Me (64)	109, 110
	$[(\eta^3\text{-}C_3H_5)PdCl]_2$ $CHCl_3$, 0 °C	 R = CO_2Et; R = Me (99)	129, 112
	$[(\eta^3\text{-}C_3H_5)PdCl]_2$ C_6H_6, 0 °C	 R = Bu^t (92); R = Me, Ph (97–98)	128, 130
	*hv* C_5H_{12}, 20 °C	 +  54:23:23	98

Table 4. The formation of higher homologues of ketones by the successive [1,2]-H and [1,2]-C shifts in alkoxycarbonylcarbenes.



R	R^1	Catalyst[a]	Yield (%) (16:17 ratio)	Ref.
Et	Me	A	87 (6:5)	87
Bu	Me	B	86 (7:5)	87
Bu^t	Me	B	59 (1:0)	87
$PhCH_2$	Me	C	73 (5:8)	87
Ph	Ph	C	70 (cm[b])	87
$-(CH_2)_4CHMe-$		B	82 (1:0)	87
$-(CH_2)_4-$		A	~100 (cm[b])	116
		C	~100 (1:0)	87
		A	55 (cm[b])	117

Scheme 77

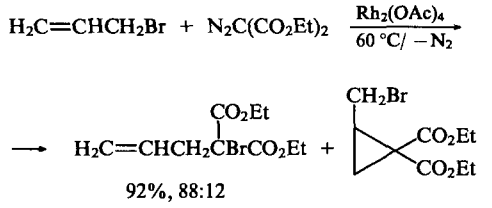


Cat	Hal	Yield (%)	
		18	19
$Rh_2(OAc)_4$	I	98%	–
$Rh_2(OAc)_4$	Cl	<2%	95%
$Rh_2(OAc)_4$	Br	30%	46%
Cu bronze	Br	50%	6%

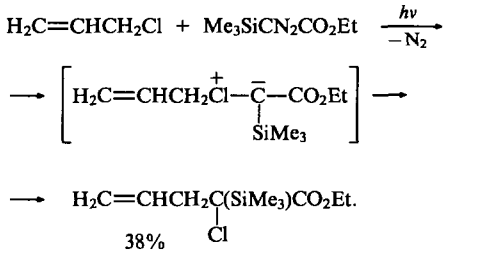
However, in the case of allyl bromide and chloride, the cyclopropane formation reaction is the main one; the decrease in the fraction of the C–Hal insertion products under these conditions in favour of cyclopropane adducts takes place in parallel with the decrease in nucleophilicity in the sequence I > Br > Cl, which confirms the ylide mechanism of the reaction. Thus allyl chloride affords the ester of 2-chloromethylcyclopropanecarboxylic acid in a yield exceeding 95% in the reaction with ethyl diazoacetate in the presence of $Rh_2(OAc)_4$. Nevertheless, when the same catalyst is used in the reaction with allyl bromide, the process proceeds nonselectively and leads to the formation of almost equal amounts of cyclopropane adducts and α-bromobutenoates, the use of copper bronze permitting some increase in the process selectivity as regards the insertion product.

Metal–carbene complexes generated from dimethyl diazomalonate on treatment with rhodium catalysts[122] and carbenes formed on photolysis of ethyl α-trimethylsilyldiazoacetate[123] show an even greater tendency to form ylides with allyl halides. In the first case (Scheme 78), the product of insertion in the C–Br bond of allyl bromide predominates even when $Rh_2(OAc)_4$ is used, whilst in the second (Scheme 79) the corresponding cyclopropane adduct is not formed at all.

Scheme 78

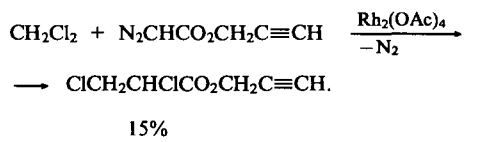


Scheme 79



The photolytic decomposition reactions of diazoesters in the presence of polyhaloalkanes, which were investigated vigorously in the 1950s,[3] have not found preparative applications because of their low selectivity. The synthetic possibilities of catalytic processes have been scarcely studied, although examples of such processes, described recently, yielded promising results. Thus, the ability of propargyl diazoacetate to afford the product of insertion in the C–Cl bond of methylene chloride in the presence of $Rh_2(OAc)_4$ has been established recently (Scheme 80).[84]

Scheme 80

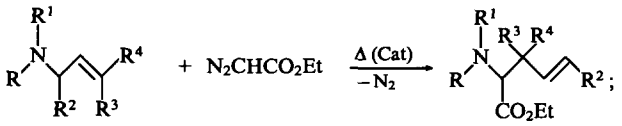


The analogous reaction does not take place with methyl diazoacetate.

2. C–N bonds

The number of examples of preparative syntheses based on the reactions of alkyl diazoacetates with amines, leading to products of the insertion of alkoxycarbonylcarbenes in the C–N bond, is limited. The interaction of ethyl diazoacetate with tertiary allyl amines on heating to 144–175 °C or on treatment with catalysts based on rhodium(II), copper(II), cobalt(II), and nickel(II), or zirconium(IV) compounds at 60 °C leads, as a result of the [2,3]-rearrangement, to esters of unsaturated *N,N*-dialkylamino-acids in high yields (Scheme 81).[124]

Scheme 81



30%–99%

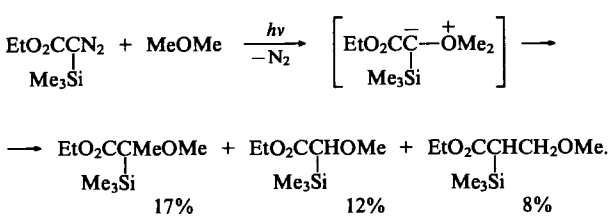
R, R^1 = alkyl or R + R^1 = $(CH_2)_n$ (n = 5–6) or $CH_2OCH_2CH_2$; R^2 = alkyl; R^3, R^4 = alkyl or $R^3 + R^4$ = α,ω-alkenyl.

The reaction is extremely sensitive to the catalyst concentration. The highest yields have been achieved for a catalyst : amine molar ratio of 1 : 800; with increase in catalyst concentration, there is an appreciable increase in the contribution of the competing addition of the carbene to the double bond.[125]

3. C–O bonds

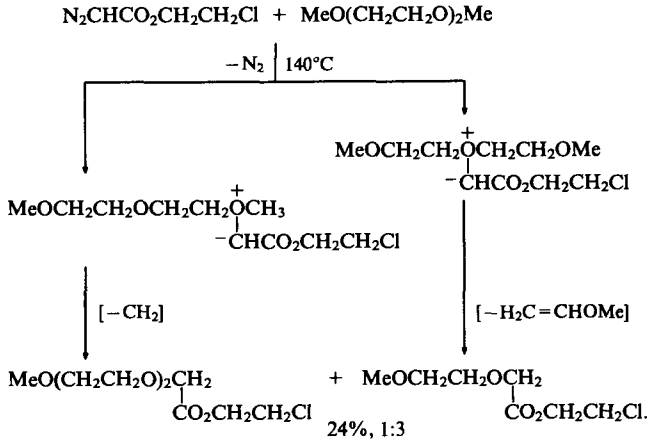
The reactions of diazoesters with acyclic ethers, initiated by irradiation (Scheme 82),[123] heating (Scheme 83),[126] or treatment with $Rh_2(OAc)_4$ (Scheme 84),[124] usually proceed nonselectively, leading to esters of alkoxyacetic acids as a result of the β-elimination reaction of the O ylides formed initially. The formation of C–O insertion products is observed in exceptional instances.

Scheme 82



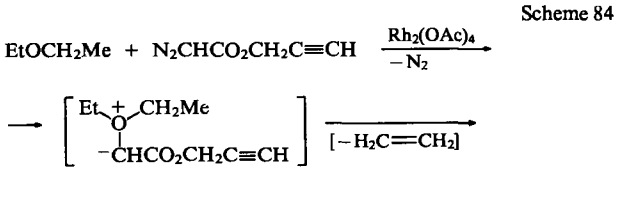
17% 12% 8%

Scheme 83



24%, 1:3

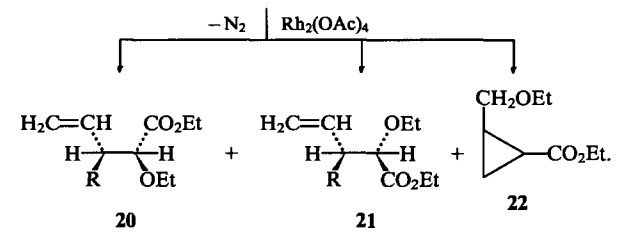
Scheme 84



30%

Although the reaction of ethyl diazoacetate with allyl ethyl ether in the presence of $Rh_2(OAc)_4$ does lead to C–O insertion products as a result of the [2,3]-rearrangement of the ylide, it too is complicated by the competing formation of cyclopropane adducts, the fraction of which may reach 30% (Scheme 85).[127]

Scheme 85

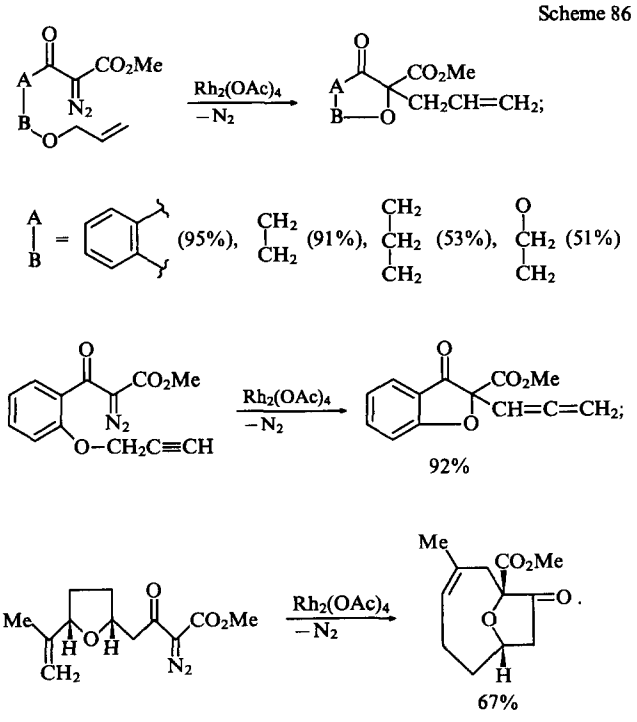


R	Configuration of double bond	Overall yield (%)	Product ratio		
			20	21	22/(20+21)
Ph	E	95	83	17	27
Ph	Z	95	6	94	26
Me	E	86	79	21	8
Me_3Si	E	68	97	3	6

The [2,3]-rearrangement itself then proceeds with a high degree of diastereoselectivity.

The $Rh_2(OAc)_4$-initiated intramolecular cyclisation of α-acyldiazoesters containing an allyloxy- or propargyloxy-fragment takes place with a high selectivity (Scheme 86).[128]

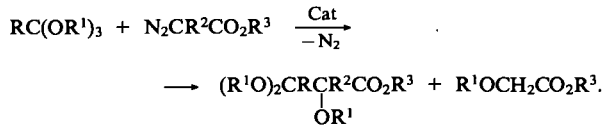
Scheme 86



These reactions lead to five- and six-membered oxacyclanones as a result of C–O insertion and the [2,3]-rearrangement.

The formation of products of the formal C–O insertion has been noted also in the reactions of ethyl diazoacetate with acetals and orthoesters. On treatment with BF_3 etherate, the reactions of diazoesters with orthoesters lead under these conditions exclusively to C–O insertion products. The metal-catalysed processes are less selective and are accompanied by β-elimination (Scheme 87).[129]

Scheme 87

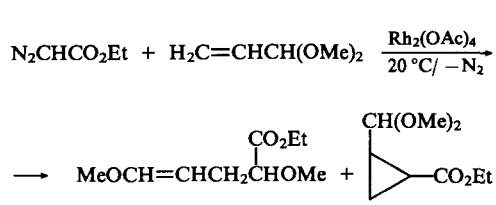


$BF_3 \cdot OEt_2$(Cat), 25 °C	45%–85%	< 5%
$Rh_2(OAc)_4$, 60 °C	3%–20%	11%–27%
$Cu(OTf)_2$, 20 °C	38%–46%	6%–20%

R = H, Me, Et; R^1 = Me, Et;
R^2 = H, CO_2Me; R^3 = Me, Et.

In the presence of $Rh_2(OAc)_4$, ethyl diazoacetate reacts with acrolein dimethyl acetal to form the product of the [2,3]-rearrangement of the O ylide together with the cyclopropane adducts (Scheme 88).[130]

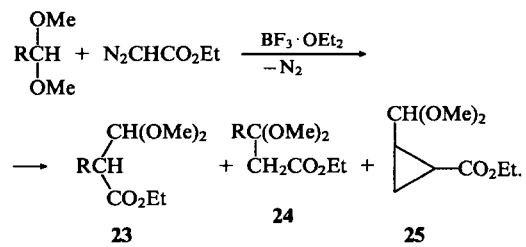
Scheme 88



76 : 24, overall yield 47%.

However, when this reaction is initiated by BF_3 etherate, the main and sometimes the only products are those of the formal C–C insertion — the diacetals of derivatives of formylacetic acid (together with small amounts of cyclopropane adducts) (Scheme 89).[131]

Scheme 89

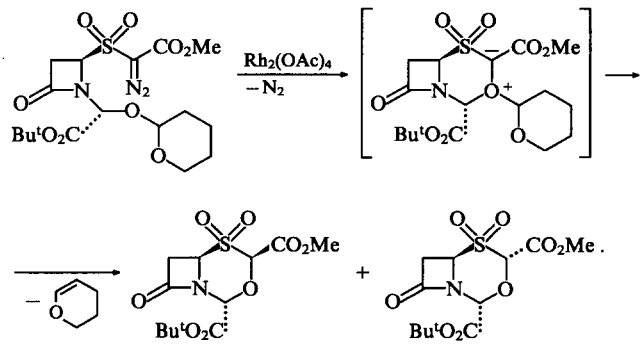


23 **24** **25**

R	T/°C	Overall yield (%)	Product ratio		
			23	**24**	**25**
$H_2C=CH$	−15	70	75	10	15
(*E*)-PhCH=CH	0	70	~100	< 1	< 1
Ph	25	85	~97	3	–
PhC≡C	25	22	~100	< 1	–

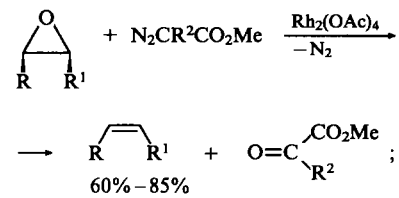
The β-elimination reaction of an endocyclic O ylide has been used recently for the preparative synthesis of antibiotics of the 3-oxacepham series (Scheme 90).[132]

Scheme 90



The reaction of diazoesters with cyclic oxa-compounds has a number of characteristic features, the decisive factor being the ring size. Dimethyl diazomalonate and methyl α-trimethylsilyldiazoacetate induce the deoxygenation of oxirans in the presence of $Rh_2(OAc)_4$, which proceeds with retention of the configuration of the initial oxirans in the olefins formed and with high yields of the latter (Scheme 91).[133]

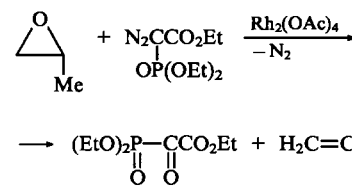
Scheme 91



R^2 = CO_2Me, $SiMe_3$.

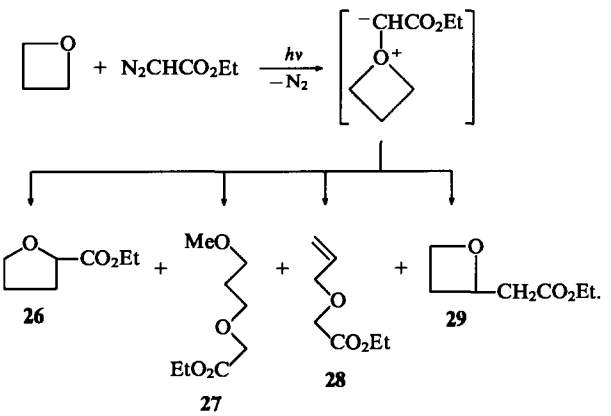
The analogous reaction of α-phosphoryldiazoacetate with methyloxiran has been used to synthesise oxophosphonates (Scheme 92).[134]

Scheme 92



On photolysis of ethyl diazoacetate in oxetan, the ylide formed is converted into the ester of tetrahydrofuran-2-carboxylic acid as the main product as a result of the Stevens rearrangement (Scheme 93).[135] However, in methanol the main process becomes the solvolysis of the ylide, which leads to ring opening and the formation of the ester of alkoxyacetic acid.

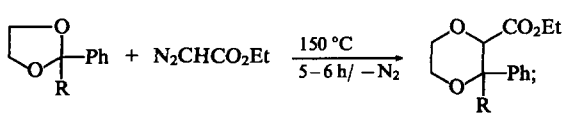
Scheme 93



Solvent	Overall yield (%)	Product ratio			
		26	27	28	29
Oxetan	54	70.3	–	12.2	17.5
MeOH	54	23.6	51.9	6.3	18.2

The interaction of ethyl diazoacetate with 1,3-dioxolans leads to 1,4-dioxanecarboxylates—the products of the formal C–O insertion of ethoxycarbonylcarbene—apparently as a result of the Stevens rearrangement of the corresponding O ylides (Scheme 94).[134]

Scheme 94



R = H (48.5%); Me (6.5%).

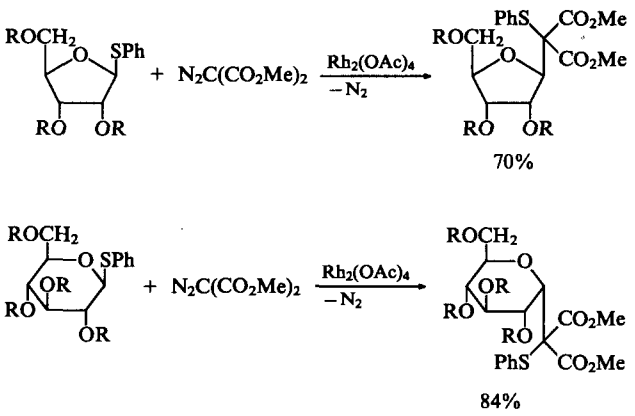
The low yields of the products formed (less than 50%) are due to the fairly severe reaction conditions (150 °C), but there are no literature data concerning the possibility of using milder conditions, for example, dediazotisation in the presence of $Rh_2(OAc)_4$.

4. C–S and C–Se bonds

The greater nucleophilicity of the sulphur atom compared with nitrogen or oxygen atoms is responsible for the high reactivity of sulphur-containing compounds and hence for the greater variety of the synthetic possibilities of their reactions with carbenes. This explains the special interest in the study of the reactions of diazoesters with compounds containing C–S bonds, which has been reflected in the large number of studies described in the literature. Furthermore, in the reactions of diazoesters with sulphur-containing compounds, it has been possible to isolate stable S ylides and to investigate the reactions of the latter, obtaining thereby direct evidence for their involvement in the formation of the final products.

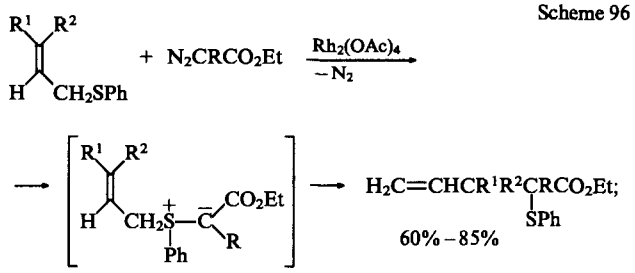
Diazoesters react with virtually any acyclic sulfides to form the C–S insertion products as a result of the [1,2]-shift of the carbene fragment in the S ylide formed initially (Scheme 95).[137]

Scheme 95

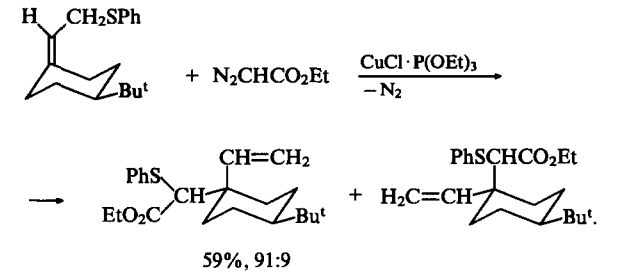


Allyl sulfides react under these conditions with a [2,3]-rearrangement (Scheme 96).[138,139]

Scheme 96



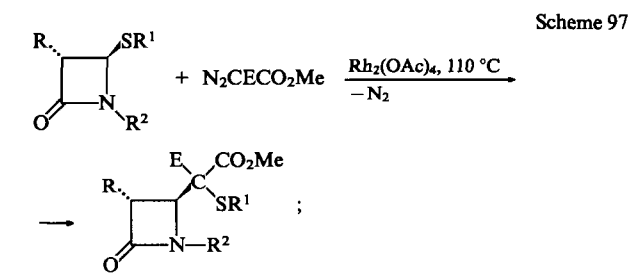
R = CO_2Et, $P(O)(OEt)_2$.



59%, 91:9

The attack on the sulfur atom in the carbenes generated from diazoesters takes place preferentially even in the presence in the substrate molecule of other heteroatoms, for example, oxygen or nitrogen (Scheme 97).[140]

Scheme 97

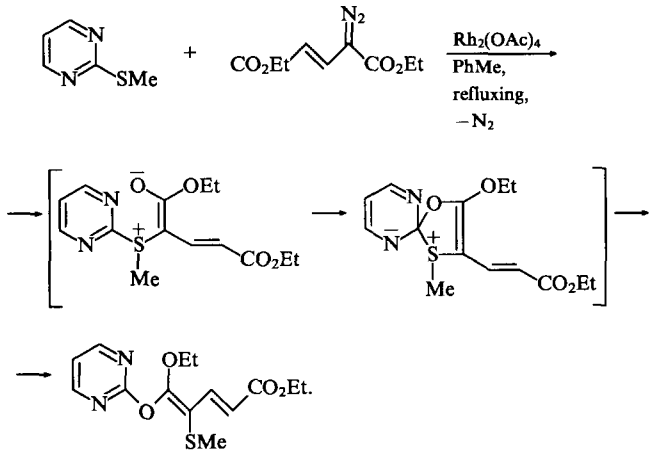


R, R^1 – Alk, Ph, CH_2Ph;
R^2 = H, $CH_2CO_2R^3$, $SiMe_2Bu^t$;
E = CO_2R^4, $P(O)(OEt)_2$.

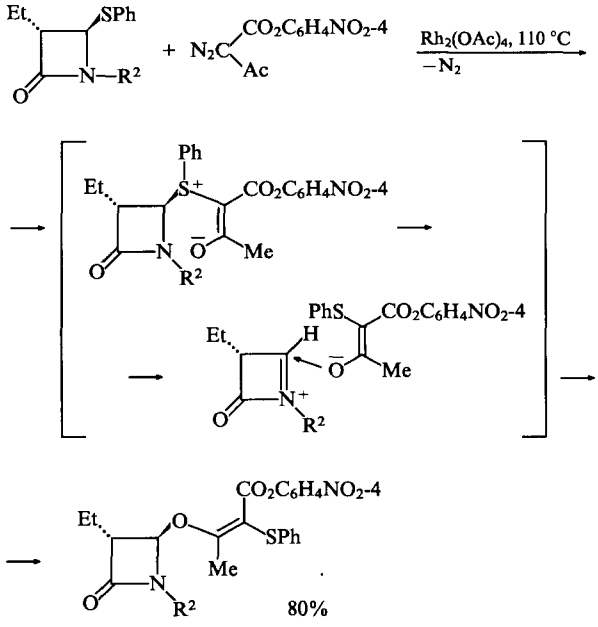
Furthermore, the interaction of such polyheteroatomic molecules with certain diazoesters, for example with ethyl α-(2-ethoxycarbonylvinyl)diazoacetate (Scheme 98)[141] or with 4-nitrophenyl α-acetyldiazoacetate (Scheme 99),[142] gives rise to

the possibility of the additional stabilisation of the cationic and ionic centres in the resulting S ylide which promotes its [1,4]-rearrangement with formation of an *O*-alkylated product.

Scheme 98

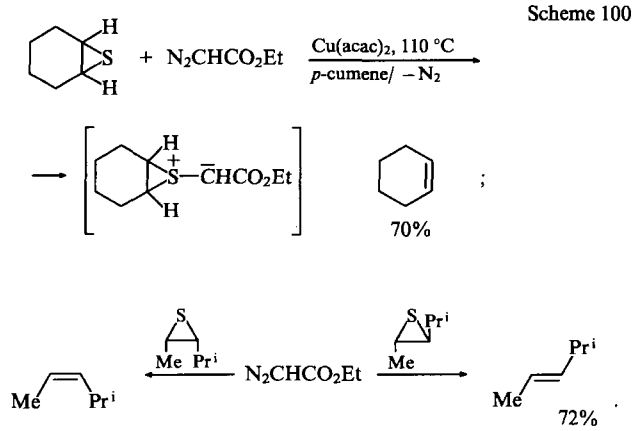


Scheme 99



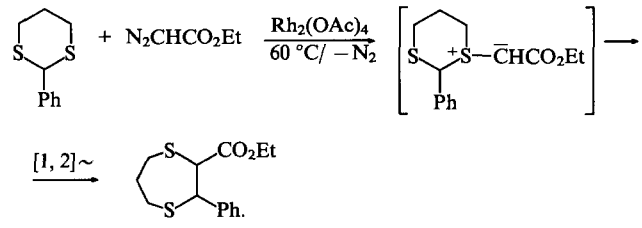
The carbene decomposition of alkyl diazoacetate in the presence of cyclic thioethers also leads to the formation of S ylides, the subsequent reactions of which are usually accompanied by a change in ring size. For example, as in the reactions with oxirans, the interaction of ethyl diazoacetate with thiirans is accompanied by selective desthiylation with formation of olefins retaining the initial configuration of the three-membered heterocycle (Scheme 100).[143]

Scheme 100



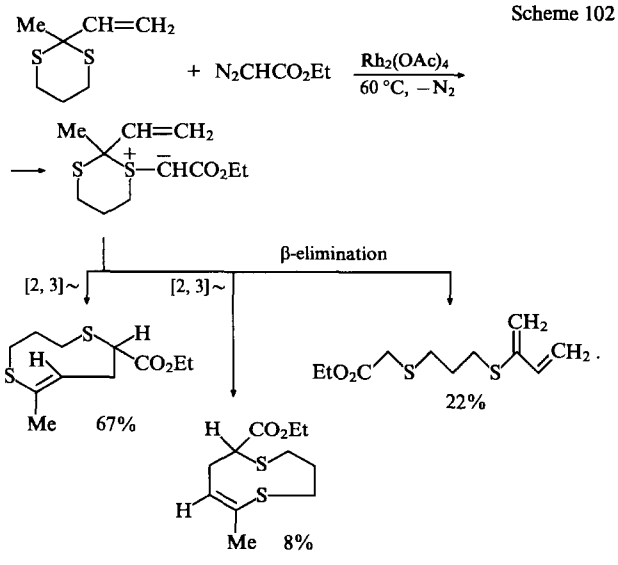
On the other hand, the $Rh_2(OAc)_4$-catalysed interaction of ethyl diazoacetate with 2-phenyl-1,3-dithiane is accompanied by the insertion of the ethoxycarbonylmethylene fragment into the six-membered ring as a result of the Stevens rearrangement of the S ylide formed initially and leads to the corresponding 1,4-dithiepan (Scheme 101).[129]

Scheme 101

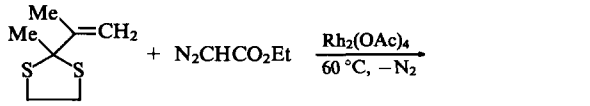


The interaction of alkyl diazoacetates with thiacyclanes containing an unsaturated fragment involves either the substrate ring expansion or ring contraction depending on whether the double bond is in the side chain or in the ring. Thus the $Rh_2(OAc)_4$-catalysed interaction of diazoesters with 2-vinyl-1,3-dithiane (Scheme 102),[129] 2-isopropenyl-2-methyl-1,3-dithiolan (Scheme 103),[129] and 2-vinyltetrahydrothiophene (Scheme 104)[144] leads, as a result of the [2,3]-sigmatropic rearrangement of the S ylides, to nine- and eight-membered thiacyclanes together with the acyclic β-elimination products.

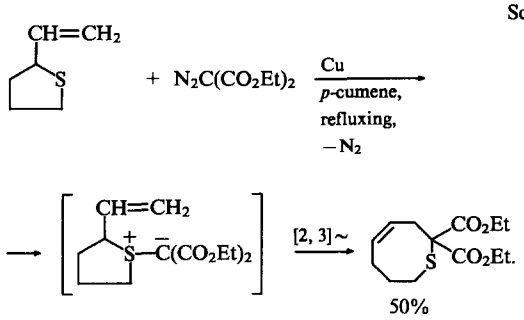
Scheme 102



Scheme 103

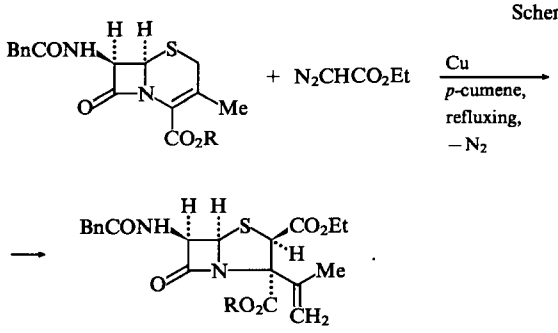


Scheme 104



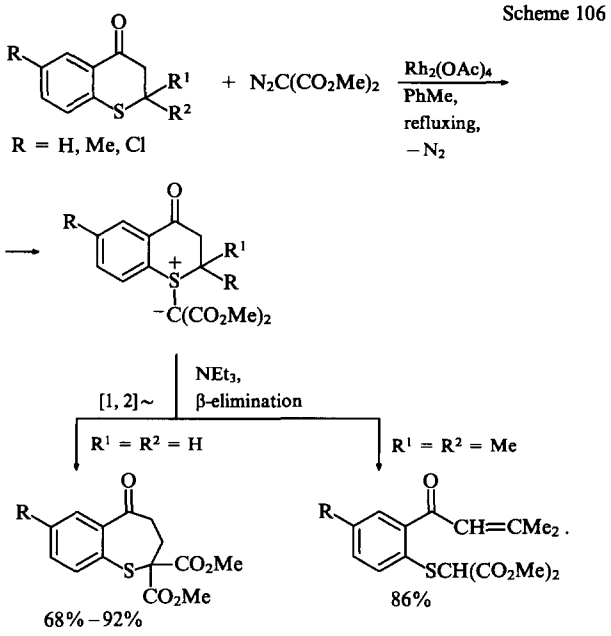
On the other hand, the reaction of ethyl diazoacetate with the esters of cephalosporanic acid, containing a double bond in the heterocycle, is accompanied by ring contraction with formation of the esters of 3-isopropenylpenicillanic acid (Scheme 105).[145]

Scheme 105



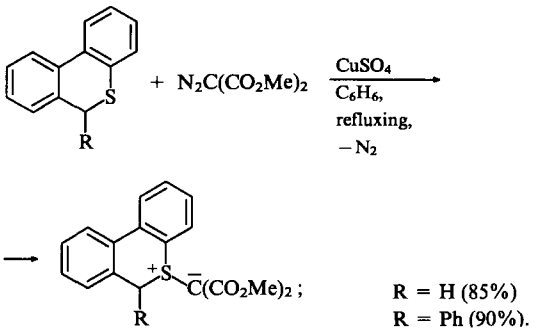
In contrast to alkyl diazoacetates, diazomalonates and diazomalononitriles react with thiacyclanes to form fairly stable S ylides, which can be isolated in a pure form as the main or even the only reaction products, which makes it possible to investigate their subsequent reactions. For example, the $Rh_2(OAc)_4$-catalysed decomposition of dimethyl diazomalonate in the presence of thiachromones leads to stable S ylides, the decomposition of which takes place only on treatment with triethylamine and leads to homothiachromones or thiobenzophenone as a result of the [1,2]-shift and β-elimination respectively (Scheme 106).[146]

Scheme 106

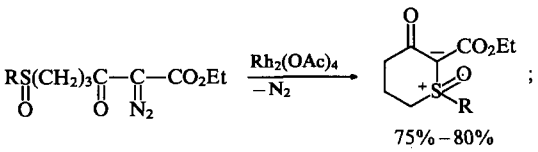


The S ylides formed are sometimes so stable that they do not rearrange even on fusion at temperatures above 100 °C (Schemes 107–109).[147–149]

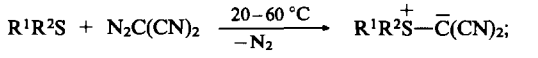
Scheme 107



Scheme 108

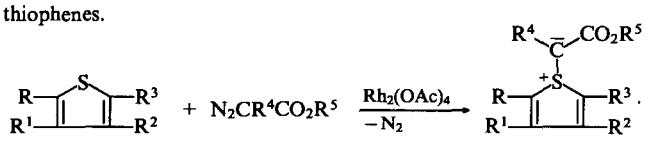


Scheme 109



As already mentioned above, stable ylides are also formed in yields up to 98% in $Rh_2(OAc)_4$-catalysed reactions of diazomalonates with thiophenes at 20 °C (Table 5).

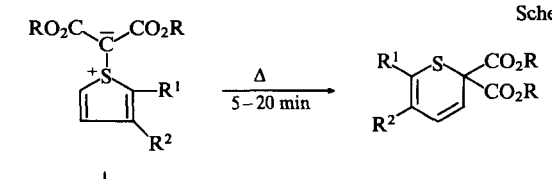
Table 5. The formation of ylides in the reactions of diazoesters with thiophenes.



R	R^1	R^2	R^3	R^4	R^5	Yield of ylide (%)	Ref.
H	H	H	H	CO_2Me	Me	95	150
Cl	H	H	Cl	CO_2Me	Me	~100	151
$HOCH_2$	H	H	H	CO_2Me	Me	92	151
Br	Me	H	H	CO_2Me	Me	86	151
Me	H	H	H	CO_2Me	Me	90	151
Br	H	H	H	CO_2Me	Me	95	151
Cl	Cl	Cl	Cl	SO_2CH_2Ph	Et	53	151
Cl	Cl	Cl	Cl	CONHTs	Et	88	72
CH=CHCH=CH	H	H		CO_2Me	Me	97	72
CH=CHCH=CH	Br	Br		Ac	Et	71	152
CH=CHCH=CH	H	H		Ac	Et	58	152
CH=CHCH=CH	H	H		Ac	Bu^t	88	152
CH=CHCH=CH	Cl	Cl		Ac	Et	84	152
CH=CHCH=CH	Br	Br		Ac	Bu^t	41	152
CH=CHCH=CH	Br	Br		CO_2Me	Me	65	152
$CH=CMe_2$	H	H	H	CO_2Me	Me	40	153

The thermal rearrangement of such ylides leads to acceptable yields of C–S insertion products (2*H*-thiopyrans), which are subsequently converted into the thermodynamically more stable (2-thienyl)malonates (Section II. 2).[154,155] The final composition of the products of the thermal isomerisation of S ylides is determined by the nature of the substituents, temperature, and duration of heating (Scheme 110). Thus brief heating (for less than 20 min) of thiophenium bis(*tert*-butoxycarbonyl)methylides leads to the corresponding 2*H*-thiopyrans in yields up to 98%. After more prolonged heating of the ylides, 2-substituted thiophenes are formed.

Scheme 110



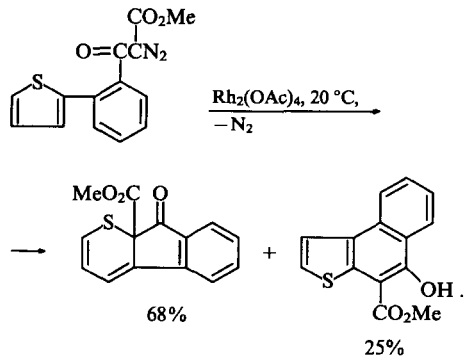
R	R^1	R^2	Yield (%)
Me	H	H	82
Me	Me	H	94

R	R^1	R^2	Yield (%)
Me	H	H	30
Me	Br	H	89
Bu^t	H	H	84
Bu^t	Me	H	98
Bu^t	I	H	60
Bu^t	$PhOCH_2$	H	97
Bu^t	Br	H	75
Bu^t	H	Br	22

The ease with which ylides rearrange to 2*H*-thiopyrans depends on the nature of the substituents. Thus the 2-phenoxymethyl-substituted ylide is converted into the corresponding 2*H*-thiopyran during crystallisation from methylcyclohexane, while the 3-bromo-substituted ylide is converted *in situ*.

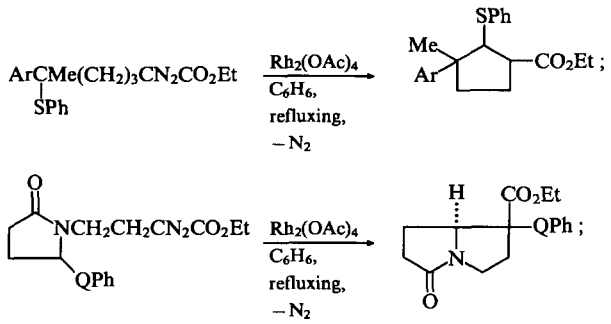
The formation of 2*H*-thiopyrans together with 2-substitution products has been observed also in the isomerisation of cyclic S ylides formed during the rhodium(II)-catalysed dediazotisation of the thienyl-substituted α-acyldiazoester (Scheme 111).[156]

Scheme 111



Similar intramolecular reactions of sulphur- and selenium-containing diazoesters constitute an effective synthetic method for the preparation of cyclic and condensed systems. For example, the metal-carbene complexes generated by the dediazotisation of 6-phenylthiodiazoalkanoates in the presence of $Rh_2(OAc)_4$ readily cyclise to five-membered rings (Scheme 112).[157,158]

Scheme 112

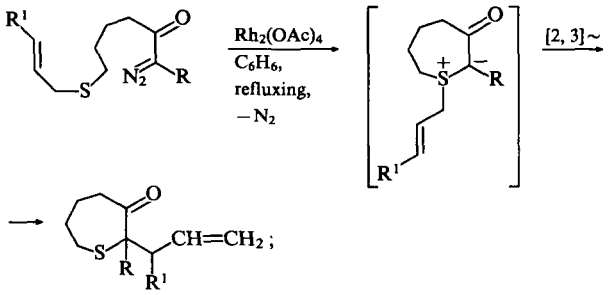


Q = S (55%), Se (36%).

Unfortunately, cyclic compounds containing six and more atoms in the ring cannot be obtained in this way because of the active competition by the C–H insertion reaction.[150]

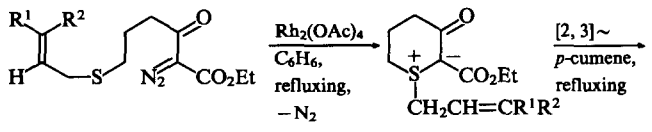
The formation of heterocycles containing more than five atoms in the ring is observed in the intramolecular reactions of the carbenes generated from diazoesters containing an allyl fragment. Thus the $Rh_2(OAc)_4$-catalysed dediazotisation of 7-allylthio-2-diazo-3-oxoheptanoates and 6-allylthio-2-diazo-3-oxohexanoates results in the formation of 3-thiepanones and 3-thianones in high yields (Schemes 113 and 114);[149] the C–H insertion products were not detected under these conditions.

Scheme 113



R = CO_2Et, R^1 = Ph (29%).

Scheme 114

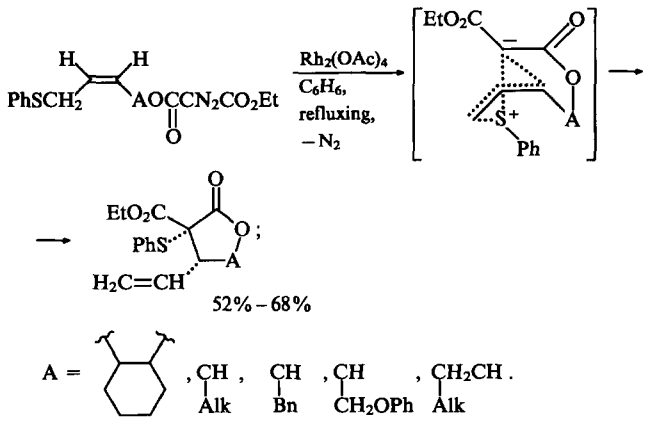


55–85%

R^1	R^2	Yield (%)
Me	Me	66
H	H	59
Ph	H	78
Me	H	71

The presence of the allyl fragment in the alcoholic component of the monoethyl diazomalonate molecule also makes it possible to synthesise vinyl-substituted five- and six-membered cyclic lactones as a result of the stereoselective [2,3]-rearrangement of the S ylide arising on cyclisation of the carbenes stabilised on rhodium(II) (Scheme 115).[149,160]

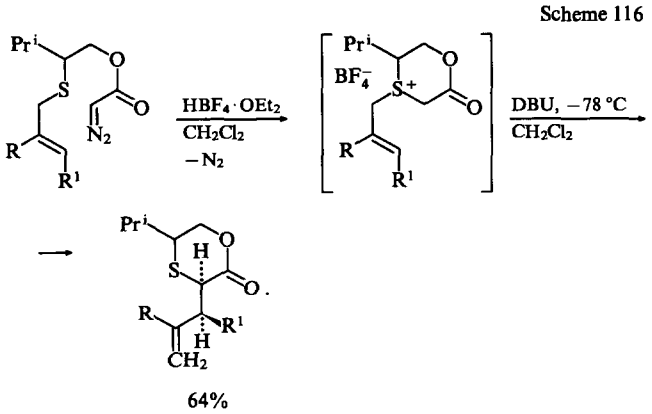
Scheme 115



52%–68%

The diastereoselectivity of this reaction can be increased significantly by using $HBF_4 \cdot Et_2O$ as the agent promoting the heterocyclisation of diazaesters and subsequently treating the resulting thiooxonium salt with 1,8-diazobicyclo[5.4.0]-undec-7-ene (DBU). Thiooxanones were obtained in this way from allylthioalkyl diazoacetates in satisfactory yields and with a high diastereoselectivity (in excess of 93%) (Scheme 116).[161]

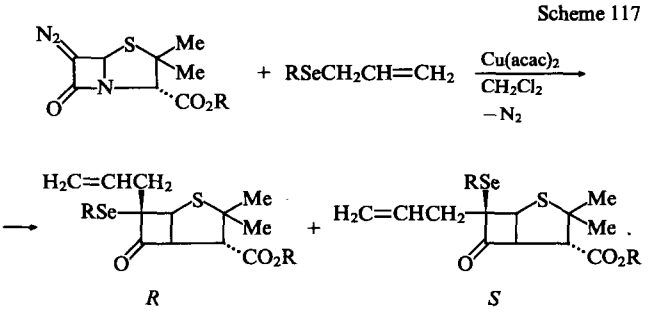
Scheme 116



64%

There are only isolated examples of reactions involving insertion in the C–Se bond. Thus the reaction of a cyclic diazoamide with allyl phenyl selenide in the presence of $Cu(acac)_2$ leads to a mixture of equal amounts of the corresponding isomeric C–Se insertion products with an overall yield of 64% (Scheme 117).[162]

Scheme 117



The analogous reaction of this diazoamide with allyl sulfides proceeds more selectively with the (*R*)-isomer predominating. Its fraction can reach 87%.

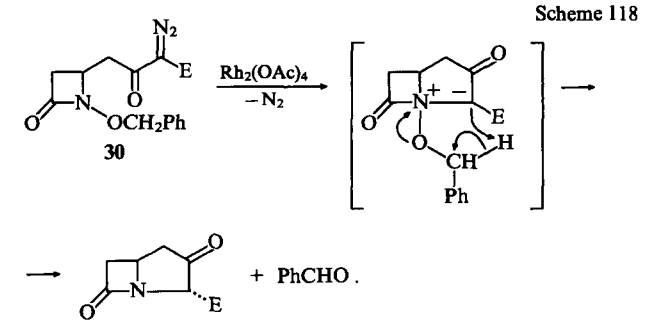
VI. Heteroatom–heteroatom bonds

The reactions of diazoesters involving the insertion of the carbene fragment in a heteroatom–heteroatom bond are presented in Table 6.

These reactions also take place with the intermediate formation of ylides. In the carbene reactions of diazoesters with organosilicon compounds (examples 5–7, Table 6), β-elimination and C–H insertion processes take place in the ylides formed apart from the [1,2]-shift, which lowers the preparative value of these reactions.

The reactions of ylides do not always lead to the products of the insertion of the carbene in the bond being attacked. Thus the intramolecular attack by the carbene centre on the N–O bond in the diazolactam **30** (E = CO_2Me) leads to an N ylide, the rearrangement of which is accompanied by the dissociation of the N–O bond and the formation of a N–C bond (Scheme 118).[178]

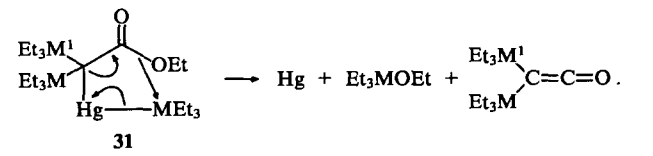
Scheme 118



30

It is suggested that the formation of organoelement ketenes as a result of the interaction of α-metallated diazoesters with bis(triethylsilyl)- or bis(triethylgermyl)-mercury (examples **20**–**22**) takes place owing to the decomposition of the unstable product **31** of the insertion of the carbene in the Hg–Si or Hg–Ge bond formed initially (Scheme 119).

Scheme 119



31

It is noteworthy that the formation of the formal insertion products is not always associated with the reactions of diazoesters via the carbene pathway. For example, although the interaction of ethyl diazoacetate with *tert*-butyl hypochlorite does lead to the product of the insertion of the carbene fragment $CHCO_2Et$ in the O–Cl bond (examples **1** and **2**, Table 6), the attempts to achieve

Table 6. Reactions of diazoesters with element–element bonds.

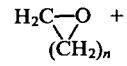
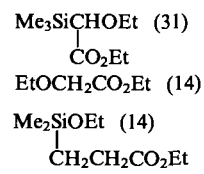
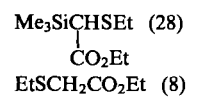
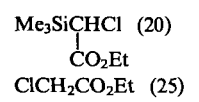
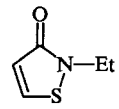
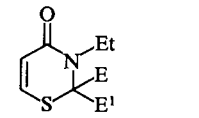
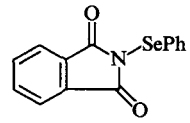
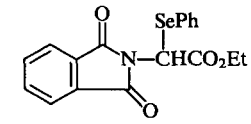
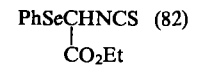
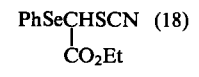
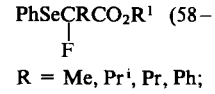
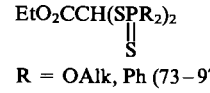
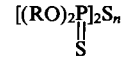
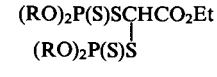
No.	Bond	Substrate	Diazoester	Reaction conditions	Products (yield (%))	Ref.
1	O–Cl	Bu^tOCl	EDA	−10 °C, CH_2Cl_2	$Bu^tOCHClCO_2Et$ (36)	163
2	O–Cl	Bu^tOCl	EDA	−10 °C, CH_2Cl_2/ROH	$(RO)_2CHCO_2Et$[a] R = Bu^t (36), Et (57)	163
3	O–Cl	$ROR^1 + SO_2Cl_2$	EDA	0 °C, darkness, CH_2Cl_2	$ROCHClCO_2Et$ R = R^1 = Et (75), R = Me, R^1 = $CH(OMe)_2$ (64) R = Me, R^1 = CH_2CH_2OMe (76)	164
4	O–Cl		EDA	0 °C, darkness, CH_2Cl_2	$Cl(CH_2)_nOCHClCO_2Et$ n = 1–4 (67.5–73)	164
5	Si–O	Me_3SiOEt	EDA	*hv*, MeCN	 $EtOCH_2CO_2Et$ (14) 	165
6	Si–S	Me_3SiSEt	EDA	*hv*, MeCN	 $EtSCH_2CO_2Et$ (8)	165
7	Si–Cl	Me_3SiCl	EDA	Cu/NEt_3, 80 °C	 $ClCH_2CO_2Et$ (25)	166
8	N–S		N_2CEE^1	$Rh_2(OAc)_4$, C_6H_6, refluxing	 E = E^1 = CO_2Et (70); E = Ac, E^1 = CO_2Et (74); E+E^1 = $COCMe_2OC(O)$ (74)	167
9	N–Se		EDA	20 °C, CH_2Cl_2	 (58)	168
10	S–Se	PhSeSCN	EDA	20 °C, CH_2Cl_2	 	169
11	Se–Se	PhSeSePh	EDA	Cu bronze, *p*-cumene, 100 °C	$(PhSe)_2CHCO_2Et$ (46)	169
12	Se–Se	PhSeSePh	MDM	100 °C	$(PhSe)_2C(CO_2Me)_2$ (32) $PhSeCH(CO_2Me)_2$ (12)	169
13	Se–F	PhSeF		CH_2Cl_2, 20 °C	 R = Me, Pr^i, Pr, Ph; R^1 = Me, Et	170
14	S–S	$[R_2P(S)S]_2$	EDA	Cu, 80 °C	 R = OAlk, Ph (73–97)	171
15	S–S		EDA	Cu, 80 °C		172

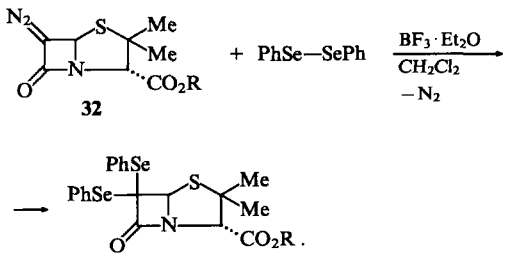
Table 6. (continued)

No.	Bond	Substrate	Diazoester	Reaction conditions	Products (yield (%))	Ref.
16	S–S	$[(RO)_2\overset{\overset{O}{\|}}{P}S]_2$	EDA	Cu, 80 °C	$(RO)_2P(O)SCHCO_2Et$ (67) $(RO)_2P(O)S$ $[(RO)_2P(O)CHS]_2$ (< 7) CO_2Et	173
17	S–P	$[(RO)_2\overset{\overset{O}{\|}}{P}S]_2$	EDA	80 °C, C_6H_6	$[(RO)_2P(O)CHS]_2$ CO_2Et R = Alk (11)	174
18	S–P	$[(RO)_2\overset{\overset{O}{\|}}{P}S]_2$	EDA	120 °C	$(RO)_2P\overset{\overset{S}{\|}}{O}CHSP(O)(OR)_2$ [b] CO_2Et	174
19	S–P	$[(RO)_2\overset{\overset{O}{\|}}{P}]_2S_n$	EDA	70–100 °C	$(RO)_2P(O)SCHCO_2Et$ (> 80) $(RO)_2P(O)S_n$	172
20	Hg–Si Hg–Ge	$Hg(MEt_3)_2$	N_2CCO_2Et $SiEt_3$	Cu, 100 °C, C_6H_{14}	Et_3Si $C{=}C{=}O$ Et_3M M = Si (58), Ge (92)	175
21	Hg–Ge	$Hg(GeEt_3)_2$	N_2CCO_2Et $SnEt_3$	Cu, 100 °C, C_6H_{14}	Et_3Sn $C{=}C{=}O$ (73) Et_3Ge	175
22	Hg–Ge	$Hg(GeEt_3)_2$	N_2CCO_2Et $GeEt_3$	Cu, 100 °C, C_6H_{14}	Et_3Ge $C{=}C{=}O$ (72) Et_3Ge	176

[a] Formed as a result of the solvolysis of the O–Cl insertion product.
[b] The yield is not indicated.

the capture of the carbene by the olefin under these conditions were unsuccessful. The formation of the O–Cl insertion products was observed also in the reaction of ethyl diazoacetate with ethers in the presence of SO_2Cl_2 (examples **3** and **4**, Table 6). Yet another example of reactions of this type is the $BF_3 \cdot Et_2O$-catalysed interaction of the cyclic diazoamide **32** with diphenyldiselenium, which leads to 6,6-di(phenylselenyl)penicillanate in a satisfactory yield (Scheme 120).[178]

Scheme 120



32

* * *

The data presented in this review clearly demonstrate, in relation to insertion reactions, the considerable potential possibilities of the use of the chemistry of diazoesters in organic synthesis. Quite recently, the principal application of diazoesters was still the reaction involving the conversion of olefins into cyclopropane derivatives. At the present time, progress in the field of homogeneous catalysis has made it possible to include in practical preparative organic synthesis also reactions which seemed to be exotic in earlier studies, such as the insertion of alkoxycarbonylcarbenes in a carbon–carbon or carbon–heteroatom bond. Study of the literature shows that the development of this branch of the chemistry of diazoesters has proceeded in two directions, which are of key importance for the expansion of the applications of these reagents in organic synthesis.

The first of these is associated with the increase in the selectivity of the reactions with participation of diazoesters. It involves mainly studies on the enantioselective and stereoselective synthesis of cyclic compounds by the catalytic dediazotisation of diazoesters. The aim of the second aspect was to expand the applications of insertion reactions with participation of diazoesters in organic synthesis. It has developed, in its turn, both in connection with the search for new reactions of diazoesters and their involvement in reactions with compounds of new classes such as the synthesis of new diazoesters for the construction of specified structures, in particular natural products.

The successful development of these two types of studies will depend, in our view, on the progress in the development of synthetic methods for the introduction of the functional diazo-group into the molecules of organic acid esters and also on the search for new effective and selective catalysts of the dediazotisation of diazoesters and the advances in the elucidation of the mechanisms of catalytic reactions undertaken to allow the regulation of such reactions.

References

1. E A Shapiro, A B Dyatkin, O M Nefedov *Diazoefiry* (Diazoesters) (Moscow: Nauka, 1992)
2. V Dave, E Warnhoff, in *Organic Reactions* Vol. 18 (Ed. W G Dauben) (New York: Wiley, 1970) p. 217
3. A P Marchand, N McBrockway *Chem. Rev.* **74** 431 (1974)
4. S D Burke, P A Grieco, in *Organic Reactions* Vol. 26 (Ed. W G Dauben) (New York: Wiley, 1979) p. 361
5. D S Wulfmann, G Linstrumelle, C F Cooper *The Chemistry of Diazonium and Diazo Groups* Vol. 2 (Ed. S Patai) (New York: Wiley, 1978)
6. M P Doyle *Chem. Rev.* **86** 919 (1986)
7. G Maas, in *Topics in Current Chemistry* Vol. 137 (Berlin: Springer, 1987) p. 77
8. J Adams, D M Spero *Tetrahedron* **47** 1765 (1991)
9. A J Hubert, A F Noel, A J Anciaux, P Teyssiè *Synthesis* **9** 600 (1976)
10. O G Kulinkovich *Usp. Khim.* **58** 1233 (1989) [*Russ. Chem. Rev.* **58** 711 (1989)]
11. A Demonceau, A F Noels, A J Hubert, P Teyssiè *Tetrahedron* **14** 688 (1981)
12. A Demonceau, A F Noels, A J Hubert, P Teyssiè *Bull. Soc. Chim. Belg.* **93** 945 (1984); A Demonceau, A F Noels, P Teyssiè, A J Hubert *J. Mol. Catal.* **49** L13 (1988); A Demonceau, A F Noels, A J Hubert *J. Mol. Catal.* **57** 149 (1989); A Demonceau, A F Noels, J-L Costa, A J Hubert *J. Mol. Catal.* **58** 21 (1990)
13. M E Alonso, M del C Garcia *Tetrahedron* **45** 69 (1989)
14. M Aglietto, R Alterio, R Bertani, F Galleschi, G Ruggeri *Polymer* **30** 1133 (1989)
15. G Lowe, J Parker *J. Chem. Soc., Chem. Commun.* 577 (1971)
16. E Buchner, M Fritsch, A Papendieck, H Witter *Liebigs Ann. Chem.* **278** 214 (1893)
17. I E Dolgii, E A Shapiro, G V Lun'kova, O M Nefedov *Izv. Akad. Nauk SSSR, Ser. Khim.* **7** 1652 (1979)
18. H Ledon, G Linstrumelle, S Julia *Tetrahedron Lett.* **14** 25 (1973)
19. D F Taber, R E Ruckle *J. Am. Chem. Soc.* **108** 7686 (1986)
20. D F Taber, E H Petty *J. Org. Chem.* **47** 4808 (1982)
21. D F Taber, K J Raman *J. Am. Chem. Soc.* **105** 5935 (1983)
22. D F Taber, E H Petty, K J Raman *J. Am. Chem. Soc.* **107** 196 (1985)
23. D F Taber, M J Hennessy, J P Louey *J. Org. Chem.* **57** 436 (1992)
24. P Ceccherelli, M Curini, M C Marcotullio, O Rosati, E Wenkert *J. Org. Chem.* **55** 311 (1990)
25. V G S Box, N Marinovic, G P Yiannikouros *Heterocycles* **32** 245 (1991)
26. D F Taber, J L Schuchardt *Tetrahedron* **43** 5677 (1987)
27. D E Cane, P J Thomas *J. Am. Chem. Soc.* **106** 5295 (1984)
28. D F Taber, R E Ruckle *Tetrahedron Lett.* **26** 3059 (1985)
29. D F Taber, K J Raman, M D Gaul *J. Org. Chem.* **52** 28 (1987)
30. M P Doyle, V Bagheri, M M Pearson, J D Edwards *Tetrahedron Lett.* **30** 7001 (1989)
31. M P Doyle, A van Oeveren, L J Westrum, M N Protopopova, T W Clayton Jr *J. Am. Chem. Soc.* **113** 8982 (1991)
32. M P Doyle, M Y Eismont, D E Bergbreiter, B Chen *J. Am. Chem. Soc.* in press (1993)
33. M P Doyle, M N Protopopova, W R Winchester, K L Daniel *J. Am. Chem. Soc.* in press (1993)
34. A Padwa, D J Austin, S F Hornbuckle, M A Semones, M P Doyle, M N Protopopova *J. Am. Chem. Soc.* **114** 1874 (1992)
35. A G Wee, B Liu, L Zhang *J. Org. Chem.* **57** 4404 (1992)
36. E Wenkert, P Ceccherelli, R A Fugiel *J. Org. Chem.* **43** 3982 (1978)
37. N Ikota, N Takamura, S D Young, B Canem *Tetrahedron Lett.* **22** 4163 (1981)
38. W Ando, S Kondo, K Nakayama, K Ichibori, H Kohoda, H Yamato, I Imai, S Nakaido, T Migita *J. Am. Chem. Soc.* **94** 3870 (1972)
39. N Takamura, T Mizoguchi, S Yamada *Tetrahedron Lett.* **14** 4267 (1973)
40. M Regitz, S G Khbeis *Chem. Ber.* **117** 2233 (1984)
41. M Jones Jr, W Ando, A Kulczycki Jr *Tetrahedron Lett.* **8** 1391 (1967); W von Doering, T Mole *Tetrahedron* **10** 65 (1960)
42. D F Taber, J C Amedio Jr, R G Sherrill *J. Org. Chem.* **51** 3382 (1986)
43. M E Alonso, R Fernandez *Tetrahedron* **45** 3313 (1989)
44. M E Alonso, M del C Garcia *J. Org. Chem.* **50** 988 (1985)
45. M Vidal, F Massot, P Arnaud *C. R. Acad. Sci.* **268C** 423 (1969)
46. M Vidal, M Vincens, P Arnaud *Bull. Soc. Chim. Fr.* **2** 657 (1972)
47. E A Shapiro, I E Dolgii, C M Nefedov *Izv. Akad. Nauk SSSR, Ser. Khim.* **9** 2096 (1980)
48. M Hrytsak, T Durst *J. Chem. Soc., Chem. Commun.* 1150 (1987)
49. N Etkin, S D Babu, C J Fooks, T Durst *J. Org. Chem.* **55** 1093 (1990)
50. M P Doyle, M S Shanklin, H Q Pho, S N Mahapatro *J. Org. Chem.* **53** 1017 (1988)
51. A Padwa, D J Austin, S F Hornbuckle, M A Semones, M P Doyle, M N Protopopova *J. Am. Chem. Soc.* **114** 1874 (1992)
52. M Matsumoto, N Watanabe, H Kobayashi *Heterocycles* **26** 1479 (1987)
53. E C Taylor, H M L Davies *Tetrahedron Lett.* **24** 5453 (1983)
54. S D Babu, M D Hrytsak, T Durst *Can. J. Chem.* **67** 1071 (1989)
55. D S Wulfmann, B Poling, in *Reactive Intermediates* Vol. 1. (Ed. R A Abramovitch) (New York: Plenum, 1980) p. 321
56. B E Marianoff *J. Org. Chem.* **44** 4410 (1979)
57. B E Marianoff *J. Org. Chem.* **47** 3000 (1982)
58. H M L Davies, W B Young, H D Smith *Tetrahedron Lett.* **30** 4653 (1989)
59. W Herz, R L Settine *J. Org. Chem.* **24** 201 (1959)
60. V M Shostakovskii, A U Musaev, A E Vasil'vitskii, A M Gumilev, O M Nefedov *Izv. Akad. Nauk SSSR, Ser. Khim.* 715 (1989); V M Shostakovsky, A E Vasilvitsky, A U Musaev, O M Nefedov *VI International Conference on Organic Synthesis, Moscow: Abstracts* (Moscow: Izd. Akad. Nauk SSSR, 1986) p. 176
61. US P. 2 079 416; *Chem. Abstr.* **91** 4343 (1937); J R Piper, F J Stevens *J. Heterocycl. Chem.* **3** 95 (1966); C A Payne, F J Stevens *J. Chem. Ind. Data* **10** 71 (1975)
62. A E Vasil'vitskii, A B Sheremet'ev, T S Novikova, L I Khmel'nitskii, O M Nefedov *Izv. Akad. Nauk SSSR, Ser. Khim.* 2876 (1989)
63. E Galeazzi, A Gurzmann, A Pinedo, A Saldana, D Torre, J M Muchowski *Can. J. Chem.* **61** 454 (1983)
64. R A Franich, G Lowe, J Parker *J. Chem. Soc., Perkin Trans. 1* **16** 2034 (1972)
65. A E Vasilvitsky, O M Nefedov, in *Chemistry of Carbenes and Small-sized Cyclic Compounds* (Ed. O M Nefedov) (Moscow: Mir, 1989) p. 142
66. R J Gillespie, A E A Porter, W E Willmott *J. Chem. Soc., Chem. Commun.* **1** 85 (1978)
67. T Bowles, R J Gillespie, A E A Porter, J A Rechka, H S Rzepa *J. Chem. Soc., Perkin Trans. 1* **4** 803 (1988)
68. T Saegusa, Y Ito, S Kobayashi, K Hirota, T Shimizu *Tetrahedron Lett.* 7 6131 (1966); *J. Org. Chem.* **33** 544 (1968)
69. R J Chorvat, K J Rorig *J. Org. Chem.* **53** 5779 (1988)
70. B Doma, B Vercek, B Stanovnik, M Tisler *Chimia* **28** 235 (1974)
71. E A Shapiro, T N Romanova, T A Bunkina, I E Dolgii, O M Nefedov *Izv. Akad. Nauk SSSR, Ser. Khim.* 1344 (1987)
72. R J Gillespie, A E A Porter *J. Chem. Soc., Perkin Trans. 1* **11** 2624 (1979)
73. M Hrytsak, T Durst *Heterocycles* **26** 2393 (1987)
74. M P Moyer, P L Feldman, H Rapoport *J. Org. Chem.* **50** 5223 (1985)
75. T J Sowin, A I Meyers *J. Org. Chem.* **53** 4155 (1988); D Häbich, H Hartwig *Tetrahedron Lett.* **28** 781 (1987); J Fetter, K Lempert, T Gizur, J Nyitrai, M Kajtar-Peredy, G Simig, G Hornyak, G Doleschall *J. Chem. Soc., Perkin Trans. 1* **2** 221 (1986); J D Buynak, M N Pao, H Pajouhesh, R Y Chandrasekaran, K Finn *J. Org. Chem.* **50** 4245 (1985); M Aratani, H Hirai, K Sawada, A Yamada, M Hashimoto *Tetrahedron Lett.* **26** 223 (1985)
76. J-M Liu, J-J Yong, Y-J Li, Ch-K Sha *J. Org. Chem.* **51** 1120 (1986)
77. C J Moody, C J Pearson, G Lawton *Tetrahedron Lett.* **26** 3171 (1985); *J. Chem. Soc., Perkin Trans. 1* **4** 899 (1987)
78. C J Moody, R J Taylor *Tetrahedron Lett.* **28** 5351 (1987)
79. E C Taylor, H M L Davies *J. Org. Chem.* **49** 113 (1984)
80. R M Williams, B H Lee, M M Miller, O P Anderson *J. Am. Chem. Soc.* **111** 1073 (1989)
81. E Vedejs, D A Engler, M J Mullins *J. Org. Chem.* **42** 3109 (1977)
82. H Chaimovich, R J Vaugham, F H Westheimer *J. Am. Chem. Soc.* **90** 4088 (1968); O P Strausz, T DoMinh, H E Gunning *J. Am. Chem. Soc.* **90** 1660 (1968); E A Shapiro, I E Dolgii, O M Nefedov *Izv. Akad. Nauk SSSR, Ser. Khim.* 2096 (1980)
83. S J Valenty, P S Skell *J. Org. Chem.* **38** 3937 (1973)
84. E A Shapiro, A B Dyatkin, O M Nefedov *Izv. Akad. Nauk SSSR, Ser. Khim.* 1051 (1991)
85. H M L Davies, H D Smith, O Korkov *Tetrahedron Lett.* **28** 1853 (1987)
86. R Pelliciari, R Fringuelli, E Sisani, M Curini *J. Chem. Soc., Chem. Commun.* 959 (1979)
87. K Nagao, M Chiba, S-W Kim *Synthesis* **3** 197 (1983); C R Holmquist, E J Roskamp *J. Org. Chem.* **54** 3258 (1989)

88. A Padwa, J S Kulkarni, Z Zhang *J. Org. Chem.* **55** 4144 (1990)
89. R Pellicciari, B Natalini, S Cecchetti, R Fringuelli *J. Chem. Soc., Chem. Commun.* 493 (1985)
90. C J Moody, R J Taylor *J. Chem. Soc., Perkin Trans. 1* **4** 721 (1989)
91. J C Heslin, C J Moody *J. Chem. Soc., Perkin. Trans. 1* **6** 1417 (1988)
92. J P Greenstein, M Winitz, in *Chemistry of the Amino Acids* Vol .2 (New York: Wiley, 1961) p. 925
93. A F Noels, A Demonceau, N Petiniot, A J Hubert, P Teyssiè *Tetrahedron* **38** 2733 (1982)
94. W Ando, I Imai, T Migita *J. Org. Chem.* **37** 3596 (1972)
95. B.P. 1 572 259 *Chem. Abstr.* **94** 103 343j (1981)
96. B Ganem, N Ikota, V B Muralidharan, W S Wade, S D Young, Y Yukimoto *J. Am. Chem. Soc.* **104** 6787 (1982)
97. C-Y Teng, B Ganem, S Z Doktor, B P Nichols, R K Bhatnagar, L C Vining *J. Am. Chem. Soc.* **107** 5008 (1985)
98. J H Hoare, P P Policastro, G A Berchthold *J. Am. Chem. Soc.* **105** 6264 (1983)
99. R Paulissen, H Reimlinger, E Hayez, A J Hubert, P Teyssiè *Tetrahedron Lett.* **14** 2233 (1973)
100. V Bagheri, M P Doyle, J Taunton, E E Claxton *J. Org. Chem.* **53** 6158 (1988)
101. H Watanabe, T Nakano, Y Araki, H Matsumoto, Y Nagai *J. Organomet. Chem.* **69** 389 (1974)
102. L P Danilkina, O V Dorokhova, Ya M Slobodin *Zh. Obshch. Khim.* **45** 2677 (1975)
103. V E Baikov, L P Danilkina, K A Ogloblin *Zh. Obshch. Khim.* **51** 2156 (1981)
104. O A Kruglaya, I B Fedot'eva, B F Fedot'ev, I D Kalikhman, E I Brodskaya, N S Vyazankin *Izv. Akad. Nauk SSSR, Ser. Khim.* 1887 (1976)
105. A M Polozov, N A Polezhaeva, B A Arbuzov *Zh. Obshch. Khim.* **57** 2200 (1987)
106. A M Polozov, A Ya Levin, E I Goldfarb, N A Polezhaeva, A Kh Mustafin *Zh. Obshch. Khim.* **59** 1262 (1989)
107. A M Polozov, N A Polezhaeva, A H Mustafin, A V Khotinen, B A Arbuzov *Synthesis* **6** 515 (1990)
108. S Arenz, M Böhshar, M Regitz *Chem. Ber.* **119** 1755 (1986)
109. M Böhshar, H Heydt, M Regitz *Chem. Ber.* **117** 3093 (1984)
110. M Böhshar, G Maas, H Heydt, M Regitz *Tetrahedron* **40** 5171 (1984)
111. K Yamamoto, A Matsukawa, I Murata *Chem. Lett.* **8** 1119 (1985)
112. K Nishino, S Yano, Y Kohashi, K Yamamoto, I Murata *J. Am. Chem. Soc.* **101** 5059 (1979)
113. K-L Hoffmann, G Maas, M Regitz *Chem. Ber.* **118** 3700 (1985)
114. K-L Hoffmann, G Maas, M Regitz *J. Org. Chem.* **52** 3851 (1987)
115. P Eisenbarth, M Regitz *Chem. Ber.* **115** 3796 (1982)
116. S Padwa, G S Kulkarni, Z Zhang *J. Org. Chem.* **55** 4144 (1990)
117. R Baudouy, J Gore, L Ruest *Tetrahedron* **43** 1099 (1987)
118. W Ando *Acc. Chem. Res.* **10** 179 (1977)
119. W Ando, in *The Chemistry of Diazonium and Diazo Group* (Ed. S Patai) (New York: Wiley, 1978) p. 341
120. A Padwa, S F Hornbuckle *Chem. Rev.* **91** 263 (1991)
121. A L Fridman, F A Gabitov, A D Nikolaeva *Zh. Org. Khim.* **7** 1126 (1971)
122. M P Doyle, W H Tamblyn, V Bagheri *J. Org. Chem.* **46** 5094 (1981)
123. A Sekiguchi, W Ando *J. Synth. Org. Chem. Jpn.* **35** 897 (1977)
124. U N Dzhemelev, R N Fakhretdinov, R M Marvanov, O M Nefedov *Izv. Akad. Nauk SSSR, Ser. Khim.* 588 (1984); R M Marvanov, R N Fakhretdinov, U M Dzhemelev *Izv. Akad. Nauk SSSR, Ser. Khim.* 1680 (1985); T V Mandel'shtam, A V Balycheva *Zh. Org. Khim.* **19** 232 (1983)
125. R M Marvanov, Candidate's Thesis in Chemical Sciences, Institute of Chemistry, Ufa, 1988
126. E A Shapiro, G V Lun'kova, I E Dolgii, O M Nefedov *Izv. Akad. Nauk SSSR, Ser. Khim.* 2529 (1984)
127. M P Doyle, V Bagheri, N K Harn *Tetrahedron Lett.* 5119 (1988)
128. M C Pirrung, J A Werner *J. Am. Chem. Soc.* **108** 6060 (1986)
129. M P Doyle. M L Trudell *J. Org. Chem.* **49** 1196 (1984); A Schönberg, K Praefcke *Tetrahedron Lett.* **5** 2043 (1964)
130. M P Doyle, J H Griffin, M S Chinn, D van Leusen *J. Org. Chem.* **49** 1917 (1984)
131. M P Doyle, M L Trudell, J W Terpstra *J. Org. Chem.* **48** 5146 (1983)
132. P H Crackett, P Sayer, R J Stoodley, C W Greengrass *J. Chem. Soc., Perkin Trans. 1* **5** 1235 (1991)
133. M G Martin, B Ganem *Tetrahedron Lett.* **25** 251 (1984)
134. C E McKenna, J N Levi *J. Chem. Soc., Chem. Commun.* 246 (1989)
135. K Friedrich, U Jansen, W Kirmse *Tetrahedron Lett.* **26** 193 (1985)
136. C D Gutsche, M Hillman *J. Am. Chem. Soc.* **76** 2236 (1954)
137. T Kametani, K Kawamura, T Honda *J. Am. Chem. Soc.* **109** 3010 (1987)
138. S Takano, S Tomita, M Takahashi, K Ogasawara *Chem. Lett.* **8** 1569 (1987)
139. G Andrews, D A Evans *Tetrahedron Lett.* **13** 5121 (1972)
140. K Prasad, P Kneussel, G Shulz, P Stütz *Tetrahedron Lett.* **23** 1247 (1982)
141. T Kametani, K Kawamura, T Akaji, C Fujita, T Honda *Heterocycles* **27** 2531 (1988)
142. T Kametani, N Kanaya, T Mochizuki, T Honda *Heterocycles* **19** 1023 (1982); *Tetrahedron Lett.* 221 (1983)
143. Y Hata, M Watanabe, S Inoue, S Oae *J. Am. Chem. Soc.* **97** 2553 (1975)
144. E Vedejs, J P Hagen *J. Am. Chem. Soc.* **97** 6878 (1975)
145. M Yoshimoto, S Ishihara, E Nakayama, N Soma *Tetrahedron Lett.* **13** 2923 (1972)
146. Y Tamura, Y Takebe, C Mukai, M Ikeda *Heterocycles* **15** 875 (1981)
147. L Benati, P C Montevecchi, P Spagnolo *J. Chem. Soc., Perkin Trans. 1* **4** 917 (1982)
148. C J Moody, R J Taylor *Tetrahedron* **46** 6524 (1990)
149. K Friedrich, J Rieser *Liebigs. Ann. Chem.* **4** 641 (1976)
150. R J Gillespie, J Murray-Rust, P Murray-Rust, A Porter *J. Chem. Soc., Chem. Commun.* 83 (1978)
151. O Meth-Cohn, E Vuorinen, T A Modro *J. Org. Chem.* **54** 4822 (1989)
152. E Vuorinen, A A Chalmers, J L M Dillen, T A Modro *Tetrahedron* **47** 8611 (1991)
153. V M Shostakovskii, A E Vasil'vitskii, V L Zlatkina, O M Nefedov *Izv. Akad. Nauk SSSR, Ser. Khim.* 2180 (1980)
154. R J Gillespie, A E A Porter, W E Willmott *J. Chem. Soc., Chem. Commun.* 85 (1978)
155. T Bowles, R J Gillespie, A E A Porter, J A Rechka, H S Rzepa *J. Chem. Soc., Perkin Trans. 1* **4** 803 (1988)
156. H Storflor, J Skramstrad, S Nordenson *J. Chem. Soc., Chem. Commun.* 208 (1984)
157. T Kametani, K Kawamura, M Tsubuki, T Honda *J. Chem. Soc., Chem. Commun.* 1324 (1985)
158. T Kametani, H Yukawa, T Honda *J. Chem. Soc., Perkin Trans. 1* **4** 833 (1988)
159. H M L Davies, van T Crisco *Tetrahedron Lett.* **28** 371 (1987)
160. F Kido, S C Sinha, T Abiko, M Watanabe, A Yoshikoshi *Tetrahedron* **46** 4887 (1990)
161. M J Kurth, S H Tahir, M M Olmstead *J. Org. Chem.* **55** 2286 (1990)
162. P J Giddings, D I John, E J Thomas *Tetrahedron Lett.* **21** 395 (1980)
163. B Zwanenburg, W Middelbos, G J K Hemke, J Strating *Recl. Trav. Chim. Pays-Bas* **90** 429 (1971)
164. W Middelbos, B Zwanenburg, J Strating *Recl. Trav. Chim. Pays-Bas* **90** 435 (1971)
165. W Ando, K Konishi, T Hagiwara, T Migita *J. Am. Chem. Soc.* **96** 1601 (1974)
166. E A Shapiro, I E Dolgii, O M Nefedov *Izv. Akad. Nauk SSSR, Ser. Khim.* 1915 (1979)
167. W D Grow, I Gosney, R A Ormiston *J. Chem. Soc., Chem. Commun.* 643 (1983)
168. T G Back, R G Kerr *J. Organomet. Chem.* **286** 171 (1985)
169. N Furukawa, F Takahashi, T Yoshimura, S Oae *Tetrahedron Lett.* **28** 3633 (1977)
170. R Pellicciari, M Curini, P Ceccherelli, R Fringnelli *J. Chem. Soc., Chem. Commun.* 440 (1979)
171. Y Usuki, M Iwaoke, Sh Tomoda *J. Chem. Soc., Chem. Commun.* 1148 (1992)
172. B A Khaskin, O D Sheluchenko, N A Torgasheva *Zh. Obshch. Khim.* **50** 1990 (1980)
173. B A Khaskin, N A Tolmacheva, T I Koroleva *Zh. Obshch. Khim.* **53** 1219 (1983)
174. B A Khaskin, O D Sheluchenko, N A Torgasheva *Zh. Obshch. Khim.* **53** 780 (1983)
175. B A Khaskin, O D Sheluchenko, N A Torgasheva *Zh. Obshch. Khim.* **52** 597 (1982)
176. O A Kruglaya, I B Fedot'eva, B V Fedot'ev, I D Kalikhman, V V Keiko, N S Vyazankin *Zh. Obshch. Khim.* **46** 930 (1976)
177. O A Kruglaya, I B Fedot'eva, B V Fedot'ev, I D Kalikhmann, E I Brodskaya, N S Vyazankin *J. Organomet. Chem.* **142** 155 (1977)
178. M A Williams, M J Miller *Tetrahedron Lett.* **31** 1807 (1990)
179. P J Giddings, D I John, E J Thomas *Tetrahedron Lett.* **21** 399 (1980)

Russian Chemical Reviews **62** (5) 473–491 1993
© 1993 Russian Academy of Sciences and Turpion Ltd

UDC 541.128

Fine organic synthesis with the aid of heteropolycompounds

I V Kozhevnikov

Contents

I. Introduction	473
II. Acid catalysis	473
III. Liquid-phase oxidation reactions	482
IV. Conclusion	487

Abstract. The use of heteropolycompounds (heteropolyacids and their salts) as acid and oxidation catalysts of fine organic synthesis reactions is examined. The use of heteropolycompounds in the synthesis of antioxidants, medicinal preparations, vitamins and other products produced on a small scale is discussed. Examples of the practical application of catalysis by heteropolycompounds are presented. The bibliography includes 177 references.

I. Introduction

Catalysis by heteropolycompounds (HPC) is one of the important aspects of the modern science of catalysis.[1–9] Studies in this field have been already prosecuted vigorously for 20 years. They permitted significant progress in the understanding of the mechanism of the catalytic effect of HPC at the molecular level and have led to the creation of a series of new industrial processes.

HPC have unique physicochemical properties. Catalysts based on them have a definite and well established structure. HPC catalyse effectively both acid-dependent and oxidation reactions and are frequently superior in their activity and/or selectively to known analogues.[2–4, 6] Their likely usefulness is indicated, in particular by the development and application in Japan of a series of new large-scale organic synthetic processes in which HPC are employed as catalysts (Table 1).[7] These processes include the oxidation of methacrolein to methacrylic acid, the hydration of olefins to alcohols, and polymerisation of tetrahydrofuran with ring opening (a stage in the synthesis of polyurethanes).

The use of HPC as catalysts of fine organic synthetic processes is very promising. By virtue of the high price of the products, the gain in selectivity as a result of the introduction of a more effective catalyst frequently covers severalfold the cost of the catalysts. Numerous studies have been carried out recently on the application of HPC as antioxidants, medicinal preparations, vitamins, biologically active substances, etc. There exist numerous patents for the application of HPC in fine organic synthesis. Some developments have already been applied in practice. The discussion of these new data is in fact the principal aim of the present review. The review is addressed primarily to synthetic chemists in order to draw their attention to the considerable possibilities which have arisen as a result of the application of HPC in synthetic practice. Attention is concentrated on acid-dependent and oxidation reactions of organic molecules in the liquid phase in homogeneous and heterogeneous systems. Certain new data concerning the preparation and properties of HPC-based catalysts are also considered. More complete information about the synthesis and the physicochemical and catalytic properties of HPC may be found in monographs and reviews.[1–14] The catalytic properties of HPC have been examined in greatest detail in a recently published review.[2]

I V Kozhevnikov G K Boreskov Institute of Catalysis, Siberian Division of the Russian Academy of Sciences, prosp. ak. Lavrent'eva 5, 630090 Novosibirsk 90. Fax (7-383-2) 35 57 56

Received 25 January 1993
Uspekhi Khimii **62** (5) 510–528 (1993); translated by A K Grzybowski

II. Acid catalysis

HPC are representatives of the large class of polynuclear complexes which combines a multiplicity of compounds differing in chemical composition and structure.[13] Despite their wide variety, until recently only the most stable and well investigated HPC have been used almost exclusively in catalysis. They contain the heteropolyanions $XM_{12}O_{40}^{x-8}$, where X is the central atom (Si^{4+}, P^{5+}, etc.), x is its oxidation state, and M is the metal ion (Mo^{6+}, W^{6+}, V^{5+}, etc.). The cations may be protons, metal ions, etc. These HPC have the well known Keggin structure (Fig. 1),[15] which includes the XO_4 tetrahedron surrounded by 12 MO_6 octahedra with common vertices and edges. Subsequently, for specially stipulated cases, HPC will be understood as compounds having this structure.

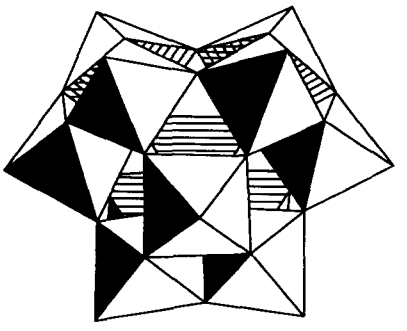


Figure 1. The structure of the heteropolyanion $XM_{12}O_{40}^{x-8}$ (α-isomer).[15]

Mainly the heteropolyacids $H_{8-x}[XM_{12}O_{40}]$ (HPA) are used in acid catalysis. Their high effectiveness as acid catalysts is due to a number of causes. In the first place, they are strong Brønsted acids, stronger than many of the usual acids employed as catalysts.[4] Heteropolyacids are readily soluble in water and

Table 1. Industrial heteropolyacid-catalysed processes.[7]

Reaction	Catalyst	Scale of industrial production/tonnes	Year of introduction
$CH_2=C(CH_3)CHO \xrightarrow{O_2} CH_2=C(CH_3)COOH$	Mo–V–P–HPA	95000	1982
$CH_2=C(CH_3)_2 \xrightarrow{H_2O} (CH_3)_3COH$	$H_3PMo_{12}O_{40}$	56000	1984
$CH_3CH=CHCH_3 \xrightarrow{H_2O} CH_3CH(OH)CH_2CH_3$	$H_3PMo_{12}O_{40}$	40000	1985
 $\xrightarrow{H_2O}$ $HO\text{-}[(CH_2)_4\text{-}O]_n\text{-}H$	$H_3PW_{12}O_{40}$	–	1987

oxygen-containing solvents and their thermal stability is high in the solid state. Because of this, they are used as both homogeneous and heterogeneous catalysts. Being 'soft' bases, heteropoly-anions (HPAN) are capable of effecting the specific coordination of the molecules of organic reagents, which may activate the latter in particular chemical reactions.[6, 7] The inertness of heteropoly-anions in relation to many side reactions, characteristic of organic reagents, which readily occur in the presence of the usual inorganic acids (sulfonation, chlorination, etc.), is important for homogeneous catalysis.[4] Because of the lability of their crystal structures and the high mobility of protons, solid heteropolyacids are capable of effecting not only the usual catalysis involving the active centres on their surface but they can also participate in bulk-phase catalytic action, like concentrated solutions of acids ('pseudoliquid phase').[6]

Data concerning the acid properties of heteropolyacids and their applications in acid catalysis have been examined in a number of reviews.[2, 4, 6]

1. Preparation of the catalysts

Heteropolyacids such as $H_3PW_{12}O_{40}$, $H_4SiW_{12}O_{40}$, and $H_3PMo_{12}O_{40}$ are used industrially in Russia and abroad in the form of hydrates. They are readily available. They are usually obtained by acidifying an aqueous solution containing the sodium salt of the heteroelement and sodium tungstate or molybdate and are isolated by extraction with ether.[10, 13, 14] Certain heteropoly-acids, in particular $H_3PMo_{12}O_{40}$ and mixtures of heteropolyacids having the composition $H_3PO_4 \cdot nMoO_3$ ($n = 6-9$), can be obtained by the direct reaction of the corresponding acids and oxides in solution without extraction with ether.[14, 16–18]

New possibilities in the synthesis of heteropolyacids have been provided by electrodialysis. This method makes it possible to obtain many heteropolyacids in quantitative yields from sodium salts.[19–25] An effective electromembrane method of synthesis of $H_3PW_{12}O_{40}$ by the reaction of Na_2WO_4 with H_3PO_4 in aqueous solution followed by the removal of Na^+ with the acid of a selective cation-exchange membrane has been developed and applied in industry.[22–24] The method is illustrated schematically in Fig. 2.

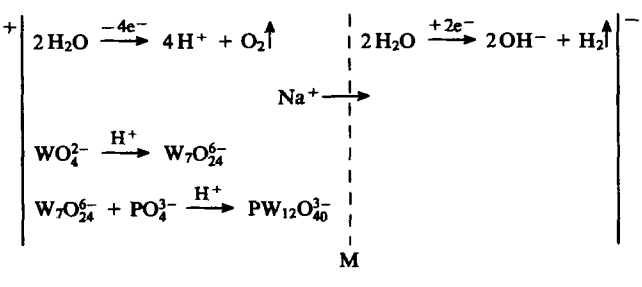


Figure 2. Schematic illustration of the synthesis of $H_3PW_{12}O_{40}$ with the aid of electrodialysis. M = cation-exchange membrane.

The $PW_{12}O_{40}^{3-}$ anion is formed in the anodic compartment of the electrodialyser from WO_4^{2-} and PO_4^{3-} taken in virtually stoichiometric proportions. The necessary acidification of the solution is achieved by electrolysing water. Heteropolyacids are synthesised in two stages.[21–24] In the first stage, in the absence of phosphate ions, WO_4^{2-} is converted into the isopolytungstate $W_7O_{24}^{6-}$. H_3PO_4 is then introduced and the electrochemical process is continued until completion. Under the influence of electric potential, Na^+ ions migrate from the anodic to the cathodic compartment through the cation-exchange membrane. This results in the concentration of aqueous $H_3PW_{12}O_{40}$ and NaOH solutions in the anodic and cathodic compartments respectively. The solution of the heteropolyacid is concentrated and the solid acid is crystallised out. Alkali is used to obtain Na_2WO_3 from WO_3 or H_2WO_4. Thus the process is waste-free. The yield of the heteropolyacid is close to 100% relative to tungsten. The Na^+ content in the final product does not exceed 0.01 wt.%. Other heteropolyacids, for example, $H_4SiW_{12}O_{40}$, $H_5PW_{11}TiO_{40}$, $H_5PW_{11}ZrO_{40}$, $H_6PW_{11}BiO_{40}$, $H_5PW_{11}CeO_{40}$, $H_6P_2W_{21}O_{17}$, and others, can be obtained similarly.[19, 21, 25]

As a rule, the tungsten acids are the best acid catalysts in the series of heteropolyacids. This is due to their greater acidity, resistance to hydrolysis, and thermal stability and also their lower oxidation potential compared with molybdic and vanadic acids.[4] However, cases are known also where Mo-HPA are used, for example, in industrial olefin-hydration processes.[7]

Massive heteropolyacids have a low specific surface ($1-5\ m^2\ g^{-1}$)[4, 26, 27] and are readily soluble in water and oxygen-containing organic solvents but are insoluble in hydrocarbons. The specific surface of insoluble salts, for example $Cs_{3-x}H_xPW_{12}O_{40}$,[28, 29] is $100-200\ m^2\ g^{-1}$. The porous structure of HPC has been examined.[30] Tungsten heteropoly-acids are stable up to ~400 °C.[31] The thermal stability of salts of heteropolyacids is higher than that of the acids themselves.

The strength and number of the acid centres of the hetero-polyacid can be regulated by selecting the outer-sphere cation, by replacing the central atom and the metal atom in the structure of the polyanion, and also by using carriers of different nature and by changing the concentration of the heteropolyacid on the latter.[4]

The disposition of heteropolyacids on inert carriers makes it possible to increase their surface area, but the strength of the acid centres is then somewhat reduced.[32] The deposited heteropoly-acids are usually obtained by impregnating or adsorbing the heteropolyacids from solutions on carriers. The adsorption of heteropolyacids from solutions in various solvents on silica gel, alumina, and activated charcoal has been investigated.[32, 33]

Silica gel is most often used as the carrier for the heteropolyacid in acid catalysis, whilst activated charcoal is more rarely employed; more basic carriers such as Al_2O_3 and MgO reduce the acidity of the heteropolyacid.[4, 34–36] When the heteropolyacid is deposited on SiO_2, its structure is retained.[34] According to X-ray diffraction data,[32, 34] a crystalline phase of the heteropolyacid appears on SiO_2 when the heteropolyacid content is >20%. Three forms of $H_4SiW_{12}O_{40}$ have been observed on the

Table 2. Dissociation constants of heteropolyacids in acetone at 25 °C.[4]

Acid	pK_1	pK_2	pK_3
$H_3PW_{12}O_{40}$	1.6	3.0	4.0
$H_4PW_{11}VO_{40}$	1.8	3.2	4.4
$H_4SiW_{12}O_{40}$	2.0	3.6	5.3
$H_3PMo_{12}O_{40}$	2.0	3.6	5.3
$H_4SiMo_{12}O_{40}$	2.1	3.9	5.9
H_2SO_4	6.6	+	+
HCl	4.3	+	+
HNO_3	9.4	+	+

SiO_2 surface by electron microscopy: isolated heteropolyacid molecules, 50 Å clusters, and 500 Å crystallites.[32] The ratios of these forms depend on the amount of deposited heteropolyacid.

Catalysts obtained by depositing the heteropolyacid on its insoluble isostructural salt, for example, $H_{3+n}PMo_{12-n}V_nO_{40}/K_3PMo_{12}O_{40}$ ($n = 0-3$) have attracted interest recently.[37, 38] Such systems have an increased thermal stability. They are apparently analogous to the insoluble acid salts of the type $Cs_{3-x}H_xPW_{12}O_{40}$.[28, 29]

Heteropolyacid-based catalysts are activated before use by thermal dehydration. For the complete removal of water from the heteropolyacid, it is sufficient to heat it *in vacuo* at 200–250 °C for 1–2 h.

2. Acid properties of heteropolyacids

Heteropolyacids are strong Brønsted acids,[1-9] whilst heteropolyanions are 'soft' weakly solvated bases.[39] In solutions, heteropolyacids are stronger than many usual inorganic acids such as H_2SO_4, HCl, HBr, HNO_3, etc. (Table 2). The strength of heteropolyacids with the Keggin structure depends only slightly on their composition. However, tungsten heteropolyacids are appreciably stronger than molybdenum heteropolyacids. The strongest and the most stable among the acids of the M_{12}-series is $H_3PW_{12}O_{40}$.[4] The dissociation constants of heteropolyacids in water,[40, 41] acetone, ethanol, and acetic acid[42, 43] and their Hammett acidity functions in water and water–acetic acid, water–dioxane, water–ethanol, and water–acetone mixtures[44, 45] have been measured. The activities of water in $H_3PW_{12}O_{40}$ solutions have been determined.[44]

Solid heteropolyacids exhibit purely Brønsted acidity[46, 47] and are stronger than traditional acid catalysts such as aluminosilicates, H_3PO_4/SiO_2, and HX and HY zeolites.[46] The acidity of massive and deposited heteropolyacids has been investigated by various methods. These include the indicator method,[48, 49] measurement of diffusion coefficients[50] and ionic conductivities,[49, 51] ion exchange,[52] thermal desorption of bases,[46] IR spectroscopy,[34, 46, 47, 53] broad band ^1H NMR[11, 31, 54, 55] and ^1H NMR (MAS),[56, 57] ESCA,[58] etc.

According to adsorption calorimetric data,[59] the protic centres of $H_3PW_{12}O_{40}$ are fairly homogeneous (Fig. 3) and their strength is close to that of H-mordenite.† After deposition on silica gel (20% HPA/SiO_2), the protic centres are weakened, their strength approaching that of the protic centres of the HX and HY zeolites, and the centres become less homogeneous.[59] The strength of the acid centres of the deposited $H_3PW_{12}O_{40}$ diminishes in the sequence of carriers $SiO_2 > Al_2O_3 >$ activated charcoal (Sibunit).[59] The cause of the reduced acidity of the heteropolyacids on charcoal is so far obscure.

The structure of the protic centres of heteropolyacid-based catalysts has been studied.[4]

Neutral salts of heteropolyacids are also used in acid catalysis because they are capable of forming protic centres on interaction with the reaction medium.[2, 4, 6] Two mechanism of the generation

† Centres on which the heat adsorption of ammonia exceeded 90 kJ mol^{-1} were classified as protic.[59]

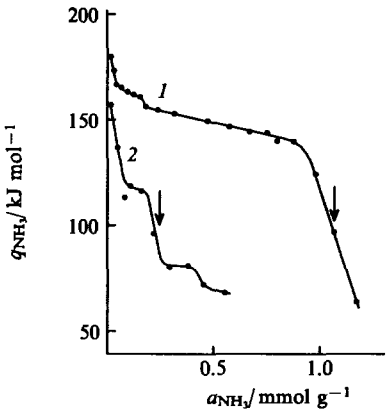


Figure 3. Differential heats of adsorption of NH_3 on $H_3PW_{12}O_{40}$ (*1*) and 20% $H_3PW_{12}O_{40}/SiO_2$ (*2*) at 150 °C. The position on the abscissa axis corresponding to the numbers of protic centres in the specimens are designated by arrows.[59]

of protic centres in heteropolyacid salts are distinguished[2, 6] — hydrolytic (for salts with the Al_3^+, Zn_2^+, etc. cations) and oxidation-reduction (for Cu^{2+}, Pd^{2+}):

$$Al^{3+} + H_2O \longrightarrow Al(OH)^{2+} + H^+ ,$$

$$Ag^+ + \frac{1}{2}H_2 \longrightarrow Ag^0 + H^+ .$$

The HPC containing simultaneously outer-sphere protons and transition metal cations are capable of acting as bifunctional catalysts. The hydroisomerisation of alkanes[2] on (Pt, Pd)/$H_3PW_{12}O_{40}$ may serve as an example.

The nature, strength, and number of acid centres can be regulated specifically by varying the chemical composition of the HPC, the type of carrier, the concentration of the HPC on the carrier, the conditions in the preliminary treatment of the catalyst, etc. The Keggin structure is retained over a wide range of acid properties of the HPC, which has been established reliably by spectroscopic methods (IR, ^{31}P, ^{17}O, ^{95}Mo, ^{183}W, ^{51}V, etc. MNR).[4, 11, 13] Because of these valuable properties, HPC are of great interest both for applied acid catalysis and as model systems for the study of fundamental problems of catalysis at the molecular level.

3. Mechanisms of acid catalysis by heteropolyacids

a. Homogeneous catalysis

The mechanism of the homogeneous acid catalysis by heteropolyacids is in principle similar to the mechanism of the catalysis by solutions of inorganic acids. In the simplest case, it can be represented schematically as follows:

$$S + HA \rightleftharpoons SH^+ + A^- ,$$

$$SH^+ \xrightarrow[(A^-)]{} P + HA ,$$

where S is the substrate, HA the catalyst, and P the product. Being stronger, heteropolyacids are capable of protonating the substrate and activating it for subsequent chemical reactions more effectively than the usual inorganic acids. As a result of this, heteropolyacids are as a rule much more active than inorganic acids.

Organic reactions in the presence of heteropolyacids and inorganic acids usually obey the same rules. Many examples of the parallel variation of the catalytic activity of heteropolyacids and their dissociation constants (the Brønsted equation) are known.[2, 4] In concentrated solutions of heteropolyacids, the rate

constant is found to depend on the Hammett acidity function H_0.[45, 60] Thus the rate constants for the hydration of isobutene in aqueous solution in the presence of $H_3PW_{12}O_{40}$ and $H_4SiW_{12}O_{40}$ at 25 °C obey the equation[60]

$$\lg k = -1.04H_0 - 3.46.$$

The same relation holds for H_2SO_4, HCl, HNO_3, and $HClO_4$. On this basis, it has been suggested[60] that the hydration of isobutene in the presence of heteropolyacids and inorganic acids proceeds via the generally accepted mechanism in which the rate-limiting stage is the conversion of the π-complex between the olefin and H^+ into a carbonium ion.

$$(CH_3)_2C{=}CH_2 \overset{H^+}{\rightleftharpoons} (CH_3)_2C^{\overset{H^+}{\cdot\cdot}}{=}CH_2 \longrightarrow (CH_3)_3C^+ \xrightarrow{H_2O} (CH_3)_3COH + H^+ .$$

At the same time, the mechanisms of the catalytic action of heteropolyacids and inorganic acids in solutions differ somewhat, which is associated with the greater degree of dissociation of heteropolyacids and the high charge on the heteropolyanions. This is manifested primarily by a strong salt effect, which is observed in ionising media, for example, in water.[45, 60] This is indicated by the variable order of the reaction with respect to the catalyst, exceeding unity. Thus the formal order of the isobutene hydration reaction with respect to the heteropolyacid in dilute solutions (0.02–0.1 M heteropolyacid) is 1.2–1.5, while in concentrated solutions (up to 0.5 M) it is 2.0–2.2.[60] In the presence of inorganic acids, the reaction is virtually first-order. The contribution of the salt effect to the rate constants for the reactions of a non-electrolyte with an ionic reagent can be estimated with the aid of the Sechenov equation. In the case of bimolecular reaction, we have

$$\lg k = \lg k_0 + (B - B^{\neq})[H^+],$$

where k is the second-order rate constant at the given concentration $[H^+]$, $k_0 = k$ at $[H^+] = 0$, and B and $B^{\neq}$ are the salting-out coefficients in the ground and transition states.[60] This equation holds satisfactorily in the hydration of isobutene in the presence of both heteropolyacids and inorganic acids. Hence it was concluded that the true order of the reaction with respect to the heteropolyacid unity, as in the case of inorganic acids, and that its increase with increase in the concentration of the heteropolyacid is due to the salt effect.[60] The values of k_0, B, $B^{\neq}$, and $B-B^{\neq}$ for the hydration of isobutene in the presence of

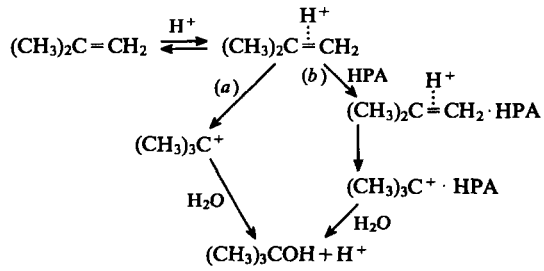
	$10^4 k^0$ / litre mol^{-1}	B / litre mol^{-1}	$B^{\neq}$ / litre mol^{-1}	$B-B^{\neq}$ / litre mol^{-1}
$H_3PW_{12}O_{40}$	20.0±3	−0.87	−3.0	2.1
$H_4SiW_{12}O_{40}$	17.0±4	−0.87	−3.0	2.1
HNO_3	3.8±0.4	−0.02	−0.2	0.2
H_2SO_4	5.0±1	+0.08	−0.2	0.3

different acids (at 25 °C) are given below:[60]

Evidently the constants k_0, extrapolated to $[H^+] = 0$, correspond approximately to the basicities of the acids, i.e. the rates of reaction per proton are similar regardless of the type of acid catalyst. Judging from the negative values of B and $B^{\neq}$, 'salting-in' i.e. a decrease in the level of the free energy of the ground and transition states due to the salt effect, almost always occurs. As was to be expected, the more polar transition state is 'salted-in' to a greater extent under these conditions. The fact that the salt effect $B-B^{\neq}$ is an order of magnitude higher for HPA than for inorganic acids is striking. This can be explained satisfactorily by the expected influence of ionic strength on the rate of the interaction of the polar molecule with an ion, because on complete dissociation of a 1–4 electrolyte ($H_4SiW_{12}O_{40}$) the ionic strength is ten times greater than on dissociation of a 1–1 electrolyte (HNO_3).

The kinetics of polar reactions involving ionic reagents are usually investigated in solutions with a fairly high constant ionic strength established by the addition of a neutral electrolyte in order to compensate for the salt effect. We may note that in the case of heteropolyacids the strong salt effect frequently renders this procedure relatively ineffective and this complicates the determination of the true order of the reaction with respect to HPA.

A number of workers have postulated the ability of 'soft' heteropolyanions to effect the specific coordination of organic molecules.[6, 7] Thus, a detailed study[2] of the hydration of isobutene in the presence of heteropolyacids made it possible to interpret the high order of the reaction with respect to the heteropolyacid on the hypothesis of a two-pathway mechanism:



Here (*a*) is the usual pathway which was already considered above and (*b*) is the pathway involving the formation of a complex between the heteropolyanion and the olefin, in which the latter is activated as a result of the coordination to the heteropolyanion. It has been suggested that the increase in the order of reaction with respect to the heteropolyacid may in fact be explained by the presence of pathway (*b*).

In reality both mechanisms of this industrially important reaction are probably in essence the same and the difference consists merely in the interpretation of the influence of the medium. In one case, this is done within the framework of the traditional approach involving allowance for the salt effect, where the medium is regarded as a continuum, whilst in the other this is done at the molecular level during the formation of weak complexes between the heteropolyanion and the substrate. In our view, further investigations in order to find evidence for the possibility of the formation of such complexes are of great interest.

b. Heterogeneous catalysis

In heterogeneous systems, heteropolyacids also exhibit a very high activity. As a rule, heteropolyacids are more active than traditional catalysts such as Al_2O_3, $Al_2O_3-SiO_2$, the HX and HY zeolites, etc., which is fully consistent with the relative strengths of the solid acids.[2, 4, 6] As already mentioned, heteropolyacids exhibit a purely Brønsted acidity, in contrast to oxide systems which have both Brønsted and Lewis acid centres.

Massive heteropolyacids possess very strong and fairly uniform protic centres, but their specific surface is low (1–5 $m^2\ g^{-1}$). Following deposition on an inert carrier, the accessible surface of the heteropolyacid increases, but the acid centres become weaker and less uniform.[59] For reactions occurring on moderately strong acid centres in the vapour or liquid phase, 20% HPA/SiO_2, where HPA = $H_3PW_{12}O_{40}$ or $H_4SiW_{12}O_{40}$, while SiO_2 is coarsely porous silica gel with a specific surface of 200–300 $m^2\ g^{-1}$, may serve as the optimum catalyst. Such a catalyst may be obtained by impregnating SiO_2 with an aqueous solution of the heteropolyacid with subsequent drying in air and activation by vacuum heat treatment at 200–250 °C. The heteropolyacid exists on the surface of this catalyst in the form of isolated molecules and 50 Å clusters; the Keggin structure of the heteropolyacid is retained under these conditions.[32]

Massive heteropolyacids behave in many respects like solutions, which provides a basis for the expectation of a similarity in

the mechanisms of the action of homogeneous and heterogeneous heteropolyacid-based catalysts. This is associated primarily with the fact that both in solution and in the solid state heteropolyacids have the same molecular (Keggin) structure. The high proton conductivity of the heteropolyacids and their ability to form solvates with polar organic molecules also play an important role.[2, 4, 6] These properties are manifested more strikingly in low-temperature reactions (< 300 °C), where the Keggin structure is retained.

The strength of solid heteropolyacid hydrates diminishes in the sequence[4]

$$H_3PW_{12}O_{40} > H_4SiW_{12}O_{40} \cong H_3PMo_{12}O_{40} > H_4SiMo_{12}O_{40},$$

which is identical with the series based on the strength of the heteropolyacids in solutions (Table 2). The catalytic activity of the heteropolyacids usually diminishes in the same sequence in both homogeneous and heterogeneous systems.[2, 4]

The hydrates of heteropolyacids exhibit a high proton conductivity.[2-4, 6] The migration of H^+ via the system of hydrogen bonds constituting the crystal structure of the heteropolyacid takes place with a low activation energy and virtually just as readily as in aqueous solutions, the electrical conductivity increasing with increase in the degree of hydration of the heteropolyacids. The anomalously high mobility of H^+ may be one of the reasons for the high catalytic activity of massive heteropolyacids, since it increases the effective concentration of H^+ in the surface region.

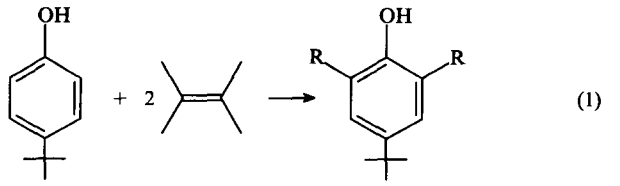
Solid heteropolyacids and their soluble salts have a high affinity for the molecules of polar substances such as alcohols, ketones, ethers, amines, etc. These substances are absorbed in large amounts in the bulk of the crystalline heteropolyacids with formation of solvates.[2-4, 6] The sorption of non-polar hydrocarbons (alkanes, olefins, arenes) is insignificant. They are adsorbed only on the surface of the heteropolyacids.

Because of the ease of sorption of polar molecules, their catalytic reactions can occur not only on the surface but also in the bulk of massive heteropolyacids. Solid heteropolyacids behave in relation to polar substances very similarly to concentrated solution, i.e. all the acid protons, and not only the surface protons, participate in the catalytic reaction. This phenomenon, unusual for heterogeneous acid catalysis, is designated by the term 'pseudoliquid phase'.[2, 6] In contrast to polar molecules, non-polar reagents are incapable of being absorbed in the bulk phase of heteropolyacids; they interact only with the surface of the catalyst. The 'pseudoliquid phase' apparently plays a significant role in reactions of polar substances at low temperatures, i.e. under conditions where the degree of sorption of the substrate in the bulk phase of the catalyst is high. In high-temperature processes, the contribution of the bulk phase reaction is probably not so significant. For a more detailed treatment, see other communications.[2, 4, 6]

4. Alkylation, dealkylation, and transalkylation of phenols

These reactions are of practical importance and are used widely in industry to obtain antioxidants, thermo- and photo-stabilisers, biologically active substances, etc. A wide variety of acid–base catalysts are used to carry them out: inorganic acids, sulfonic acids, cation-exchange resins, aluminosilicates, and metal salts and oxides.[61-64]

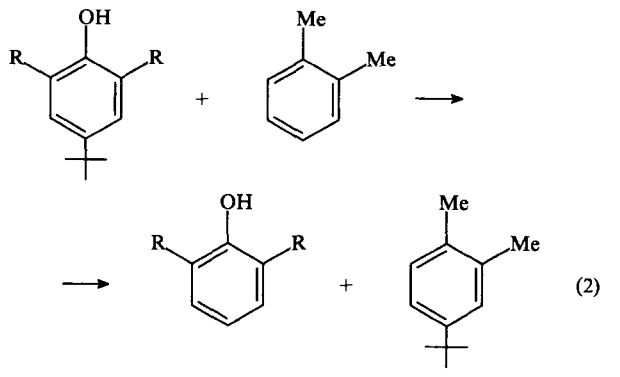
Heteropolyacids exhibit a high catalytic activity in reactions involving the alkylation of benzene and alkylbenzenes by olefins.[34, 65-67] Phenol is also readily alkylated on heteropolyacids, but the reaction in non-selective.[68-71] *p*-(*tert*-Butyl)phenol (TBP) is alkylated more selectively. Its reaction with cyclohexene, hex-1-ene, styrene, and benzyl chloride in the presence of the massive acids $H_3PW_{12}O_{40}$ and $H_4SiW_{12}O_{40}$ and the acids deposited on SiO_2 (1% relative to TBP) at 100–150 °C affords 2,6-dialkyl-4-*tert*-butylphenols in 63%–90% yield.[68, 69]



(1)

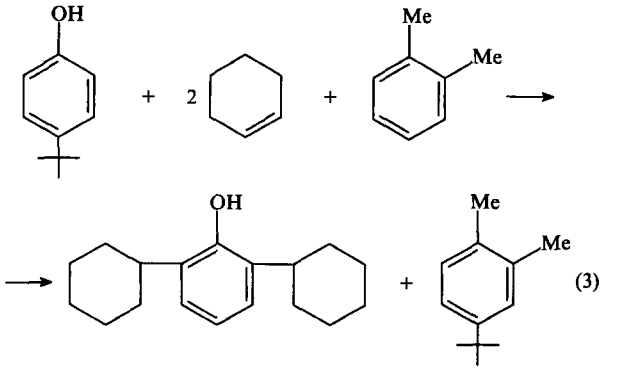
The most selective reaction is that with styrene: the yield reaches 90% for 100% conversion of TBP (100–110 °C, 1 h). In the case of α-methylstyrene, monoalkylation takes place preferentially and the yield of 4-*tert*-butyl-2-cumenylphenol is 70%.

The alkylation of TBP by olefins in the presence of heteropolyacids in *o*-xylene, which is an acceptor of the *tert*-butyl group, makes it possible to obtain 2,6-dialkylphenols without the intermediate isolation of 2,6-dialkyl-4-*tert*-butylphenol. The *tert*-butyl group is eliminated quantitatively via the reaction



(2)

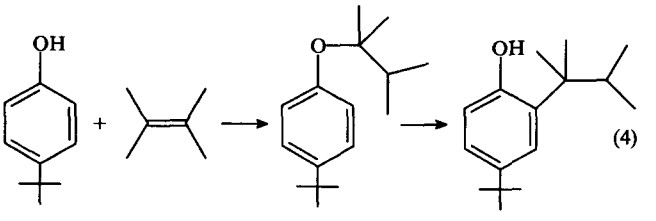
2,6-Dicyclohexylphenol was obtained in this way in 77% yield.[68, 69] The *tert*-butylxylene formed in this reaction can be used in the synthesis of pigments.



(3)

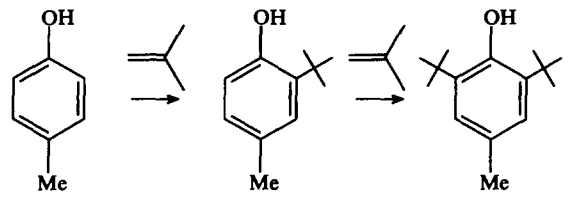
Heteropolyacids are insoluble in the reaction mass, are readily separated from the latter, and can be reused.

The alkylation of TBP apparently proceeds via a mechanism involving the formation of ethers as the primary products with their subsequent rearrangement to the *C*-alkylation products. This has been confirmed by the detection of ethers in the initial stage of the reaction.[68, 69]



(4)

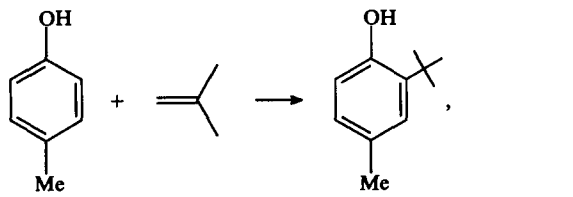
The acid alkylation of *p*-cresol by isobutene is an important industrial reaction used in the synthesis of phenolic antioxidants.[62]



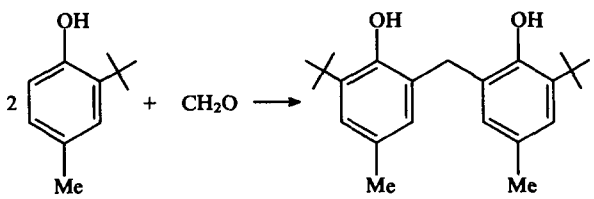
(5)

This reaction proceeds smoothly when the heteropolyacid is used as a heterogeneous catalyst. The activity of heteropolyacids in the *p*-cresol and TBP alkylation reactions (calculated per available proton) is greater by four orders of magnitude than the activity of sulfuric acid, which can be explained by the stronger acidity of the heteropolyacid.[68]

An industrial version of the alkylation of *p*-cresol by isobutene in the presence of $H_3PW_{12}O_{40}$ has been developed at the Institute of Catalysis of the Siberian Division of the Russian Academy of Sciences. This reaction is the first stage of the synthesis of the antioxidant Agidol-2 [2,2'-methylenebis(6-*tert*-butyl-4-methylphenol)], widely used to stabilise polymeric materials.[62]



(6)

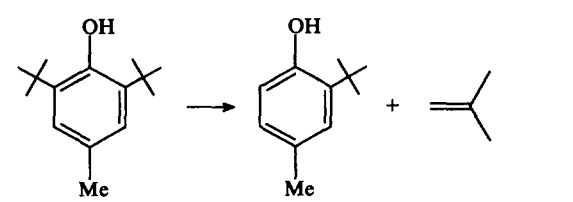


(7)

Agidol-2

The second stage [reaction (7)] is carried out by familiar method with HCl as the catalyst.[62] The use of a heteropolyacid instead of sulfuric acid made it possible to eliminate completely the formation of toxic cresol-sulfate waste water in the first stage of the process. The consumption of *p*-cresol was reduced, because its sulfonation and losses during neutralisation and washing were eliminated. The duration of the alkylation stage was shortened and charring was sharply reduced.

The dealkylation of derivatives of 2,6-di-*tert*-butylphenol to 2-*tert*-butylphenols is also widely used in the synthesis of phenolic antioxidants.

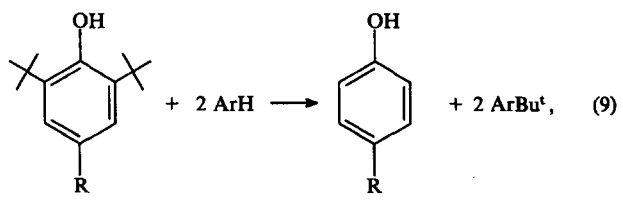


(8)

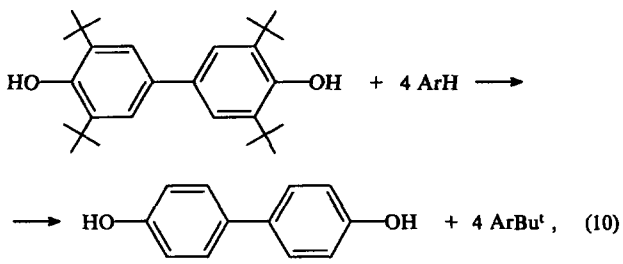
The acids $H_3PW_{12}O_{40}$ and $H_4SiW_{12}O_{40}$ are effective homogeneous and heterogeneous catalysts of this reaction, in which the substituents can be not only the methyl group but also H, Et, and CH_2CH_2COOMe.[72–74] The heterogeneous process takes place at 130–150 °C in the presence of a catalyst (<1%) in the substrate melt.[72, 73] Molybdenum heteropolyacids are rapidly deactivated as a result of their reduction by the reaction medium. Heteropolyacids are tens of times more active than heterogeneous catalysts such as cation-exchange resins, aluminosilicates, aluminium sulfate, etc. The homogeneous process is even more effective. In solution in acetic acid, dealkylation takes place even at 80 °C. The catalytic activity of heteropolyacids is correlated with their strength and exceeds by a factor greater than 100 the activity of sulfuric acid.[74]

The transalkylation of 2,6-di-*tert*-butylphenols in the presence of heteropolyacids has been studied in detail.[70, 75–77] This important reaction is used widely in organic synthesis for the regioselective introduction of functional groups in phenols.[78, 79] Aromatic compounds (ArH) such as benzene, toluene, *o*-xylene, naphthalene, etc. are used as acceptors of the *tert*-butyl group, while the catalysts are H_2SO_4, $4\text{-}MeC_6H_4SO_3H$, $MeSO_3H$, CF_3SO_3H, zeolites, aluminosilicates, and the perfluorosulfonic acid cation exchanger Nafion-H.[78–81]

Massive and deposited tungsten heteropolyacids (0.5–7%) are universal catalysts of the complete *trans*-de-*tert*-butylation of phenols



(9)



(10)

where R = H, Me, Et, $(CH_2)_2COMe$, $(CH_2)_2COOMe$, $(CH_2)_3OCOMe$, $(CH_2)_3Cl$, and $(CH_2)_3OCOC_{17}H_{35}$. These reactions take place at 100–140 °C with the molar ratio ArH : (2,6-di-*tert*-butylphenol) = 2 : 1 in 0.2–4 h with a yield of 92%–98%. The best *tert*-butyl group acceptors are toluene and *o*-xylene. The catalyst can be readily separated from the reaction mass and can be reused. Heteropolyacids are more active in the transalkylation reaction of phenols compared with other acid catalysts. Even Nafion-H, the strength of which is similar to that of superacids,[82] is appreciably inferior to heteropolyacids as regards activity in these reactions.[76, 81]

The de-*tert*-butylation reaction of 2,6-di-*tert*-butylphenols is first-order with respect to phenol and heteropolyacid. Its rate depends on the nature of ArH. This dependence is analogous to that observed in electrophilic substitution in aromatic compounds. The rate constant ratios k_{ArH}/k_{PhH} at 20 °C (2% $H_3PW_{12}O_{40}$) are given below:[77]

ArH	PhH	PhMe	PhBu^t	*o*-$Me_2C_6H_4$	*m*-$Me_2C_6H_4$
k_{ArH}/k_{PhH}	1.0	6.9	1.5	12	0.95

When catalysts on a carrier are used, the rate of reaction depends significantly on the amount of deposited heteropolyacids. Fig. 4 illustrates the dependence of the rate constants k_t and k_s for the de-*tert*-butylation of 2,6-di-*tert*-butyl-4-methylphenol on the amount of the acid $H_3PW_{12}O_{40}$ deposited on silica gel (k_t and k_s are the rate constants referred respectively to the total number of protons of the heteropolyacid in the catalyst and to the number of surface protic centres of the heteropolyacid). With increase in the amount of the deposited heteropolyacid, the strength of the protic

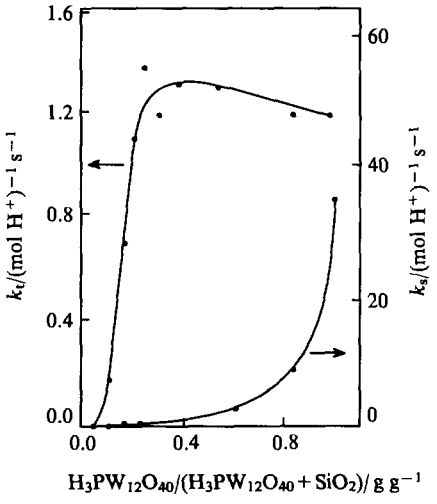
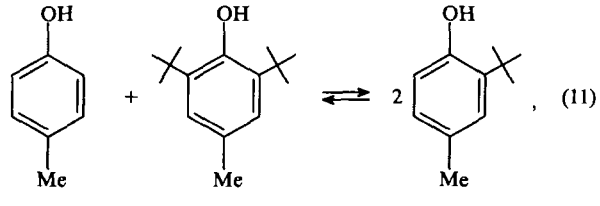


Figure 4. Dependence of the constants k_t and k_s on the ratio $H_3PW_{12}O_{40}/(H_3PW_{12}O_{40} + SiO_2)$.[77]

centres also increases and there is a simultaneous decrease in the surface area of the catalyst and hence a decrease in the number of accessible protic centres. Evidently k_t increases rapidly with increase in the concentration of the heteropolyacid on the carrier, reaches a maximum, and then slowly decreases. This type of dependence has been explained by the competitive influence of the increase in the strength of the acid centres, on the one hand, and the decrease in their number on the catalyst surface, on the other.[77] A similar dependence has been observed in the vapour phase dehydration of *tert*-butyl alcohol on $H_3PW_{12}O_{40}$ and $H_3PMo_{12}O_{40}$.[83] In contrast to k_t, the constant k_s increases monotonically with increase in the heteropolyacid concentration on the carrier, which indicates the existence of a correlation between the catalytic activity and the strength of the acid centres.[77]

Heteropolyacids are effective catalysts of the reaction



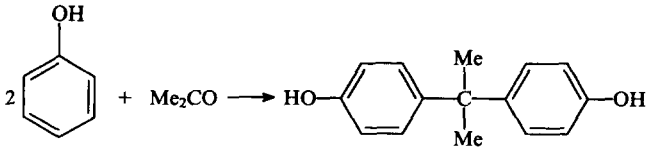
(11)

which, together with reaction (5) and (8), is used in industry for the synthesis of phenolic oxidants. In this case too, heteropolyacids are more active than sulfuric acid by four orders of magnitude per accessible proton.[76]

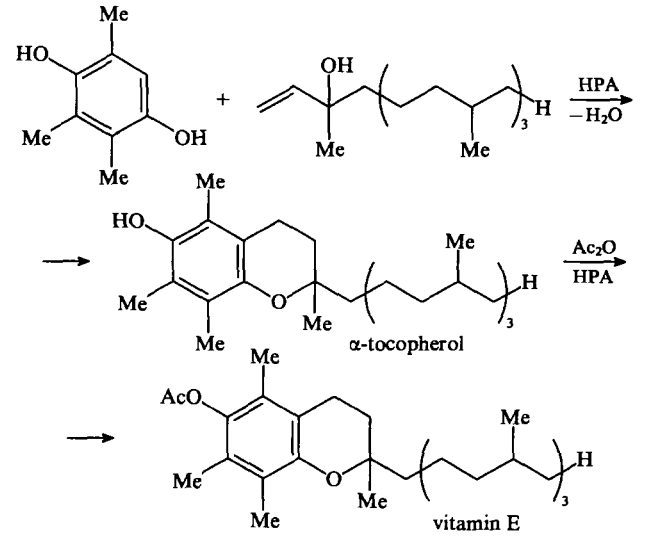
An industrial method of synthesis of 2-*tert*-butyl-4-methylphenol via reaction (11) using heteropolyacids instead of sulfuric acid has been developed at the Institute of Catalysis of the Siberian Division of the Russian Academy of Sciences. It has the same advantages as the alkylation of *p*-cresol via reaction (6) examined above.

5. Condensation reactions

Heteropolyacids have long been used as catalysts of condensation reactions.[4] They catalyse the condensation of acetone with formation of mesityl oxide and alkylbenzenes under both homogeneous[84, 85] and heterogeneous[86] conditions. Bisphenols are obtained by condensing phenols and ketones in the presence of a heteropolyacid:[87]

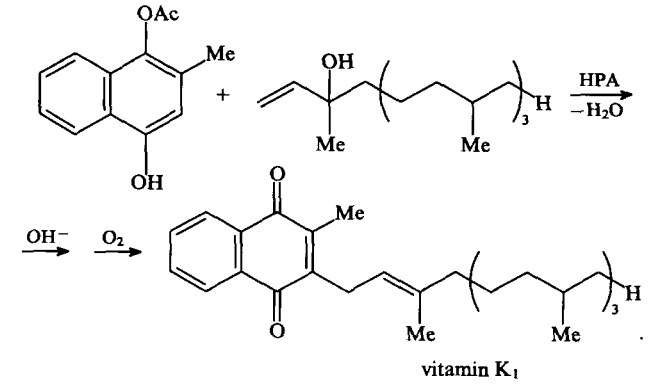


It has been established recently that heteropolyacids catalyse effectively the condensation stage in the synthesis of vitamins E, K_1, and C.[88-90] The acids $H_3PW_{12}O_{40}$ and $H_4SiW_{12}O_{40}$ catalyse the condensation of isophytol with 2,3,5-trimethylhydroquinone (TMHQ) with formation of α-tocopherol and the conversion of the latter into the acetate (vitamin E):[88, 89]

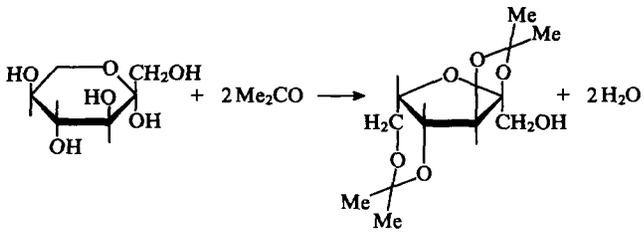


The condensation reaction proceeds both in homogeneous (in acetic acid and butanol) and heterogeneous (in toluene and *o*-xylene) systems. Heteropolyacids are introduced in an amount of about 1% relative to TMHQ. The yield of the product reaches 91%–92% and the content of vitamin E in the latter is 95%. In industry, $ZnCl_2$ or sulfuric acid is used as the catalyst for the synthesis of α-tocopherol.[91] When $ZnCl_2$ is employed, a high-quality product (yield ~80%) is obtained with a vitamin E content in excess of 95%.[92] A significant disadvantage of this method is the high consumption of the catalyst (about 1 mol of $ZnCl_2$ per mole of TMHQ) and the formation of a large amount of waste. When sulfuric acid is used, the product contains 10–20% of impurities which are difficult to separate from vitamin E.[93] The use of heteropolyacids instead of $ZnCl_2$ increases the yield of vitamin E by 10% without reducing the quality of the product. Heteropolyacids can be readily separated from the reaction mass without neutralisation and can be reused.

Heteropolyacids are also effective in the related condensation reaction between isophytol and 1-acetoxy-4-hydroxy-2-methylnaphthalene, which is a key stage in the synthesis of vitamin K_1.[88, 89] In this reaction, heteropolyacids are approximately 50 times more active than $ZnCl_2$ and aluminosilicates.[94]

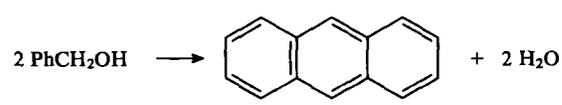


The reaction of L-sorbose with acetone — one of the stages in the synthesis of L-ascorbic acid (vitamin C) — takes place in acetone and the yield of diacetone-L-sorbase (DAS) in the presence of 0.1%–0.35% of $H_3PW_{12}O_{40}$ or $H_4SiW_{12}O_{40}$ as the catalyst is then 85%.[88, 90]



The water formed in the reaction is distilled away or eliminated by absorbing it with the NaA zeolite. The reaction of L-sorbose with acetone is carried out in industry in the presence of oleum (the yield of DAS is ~80%[91]). Oleum is added in a large amount (~5% relative to acetone), because it serves both as the catalyst and as the dehydrating agent. A disadvantage of this process is the large amount of sodium sulfate waste obtained when oleum is neutralised. Thus the use of heteropolyacids makes it possible to increase appreciably the yield of DAS and to diminish significantly the amount of waste on neutralisation of the catalyst.

Heteropolyacids catalyse the condensation of benzyl alcohol with formation of anthracene, but the yield of anthracene is lower than in the case where weaker solid acids, such as the HY zeolite and fluorinated alumina, are used.



In terms of the yield of product at 300 °C, the catalysts can be arranged in the following sequence (the yield expressed as a percentage is indicated in brackets): Al_2O_3 (14) < $H_4SiW_{12}O_{40}$ (25) < $H_3PW_{12}O_{40}$ (33) < F^-/Al_2O_3 (46) < HY (50). The reason for the lower activity of the heteropolyacids may be their small specific surface compared with HY and F^-/Al_2O_3 and also the absence of Lewis acid centres from the heteropolyacid if such centres are required for the given reaction.[95]

The polycondensation of benzyl alcohol is catalysed by $H_3PW_{12}O_{40}$ and $H_4SiW_{12}O_{40}$.[96] The chiral acid $H_6P_2Mo_{18}O_{62}$, having the Dawson structure, induces the asymmetric polycondensation of benzyl alcohol.[97] In the presence of the homogeneous *l*-brucine–$H_6P_2Mo_{18}O_{62}$ system, benzyl alcohol is converted into an optically active polybenzyl:

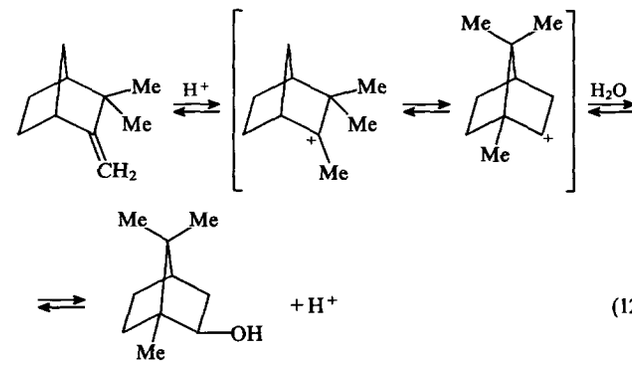
$$n\mathrm{PhCH_2OH} \longrightarrow \{\mathrm{C_6H_4CH_2}\}_n + (n-1)\mathrm{H_2O}\ .$$

When the non-chiral acid $H_6P_2Mo_{18}O_{62}$ is used, an optically inactive polybenzyl is produced.

6. Hydration reactions

The hydration of olefins in the presence of heteropolyacids has been thoroughly investigated in both liquid and vapour phases.[4] As already mentioned, the liquid-phase hydration of propene and butenes in the presence of heteropolyacids is used in industry to synthesise the corresponding alcohols.[7]

The acids $H_3PW_{12}O_{40}$ and $H_4SiW_{12}O_{40}$ proved to be excellent catalysts of the homogeneous hydration of camphene to isoborneol — an intermediate in the synthesis of camphor (50 °C, [HPA] = 0.05 in a Me_2CO–H_2O mixture):[98]



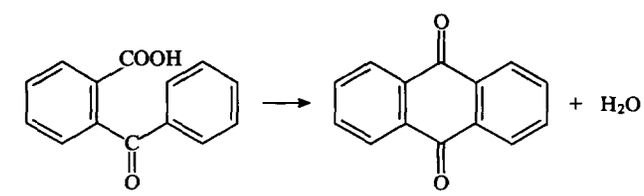
(12)

Isoborneol is virtually the only product of this reaction. The degree of conversion of camphene is 35%. The stronger acid $H_3PW_{12}O_{40}$ is somewhat more active than $H_4SiW_{12}O_{40}$. In the presence of sulfuric acid, reaction (12) proceeds much more slowly: under comparable conditions, the degree of conversion of camphene does not exceed 3%. This reaction may be of practical interest as a direct single-stage method of synthesis of isoborneol. The existing method of its synthesis consists of two stages and bornyl acetate is formed as an intermediate.

When cycloalkenes are hydrated in the presence of a catalyst consisting of a concentrated aqueous solution of an aromatic sulfonic acid and a tungsten heteropolyacid with the Keggin structure, cycloalkanols are formed with a selectivity >99%. The use of heteropolyacids makes it possible to increase the yield of the alcohols and to lower the corrosion activity of the reaction mixture.[99]

The hydration of phenylacetylene in the presence of a heteropolyacid at 60 °C has been investigated. Heteropolyacids are more active in this reaction than sulfuric or perchloric acid.[100]

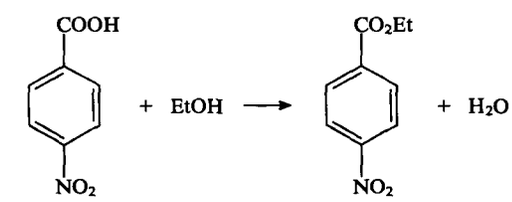
The heteropolyacid $H_3PW_{12}O_{40}$ can be used instead of sulfuric acid as the catalyst of the dehydration of *o*-benzoylbenzoic acid to anthraquinone.[101]



7. Esterification (etherification) reactions

Heteropolyacids are effective catalysts of the synthesis of ethers and esters.[4] Their use in esterification reactions in the synthesis of medicinal preparations is promising.

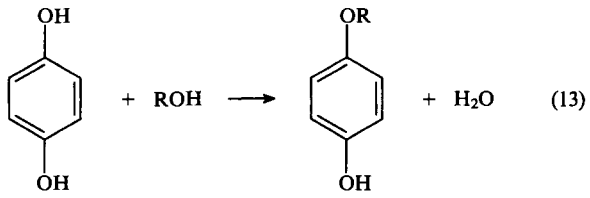
The ethyl ester of *p*-nitrobenzoic acid (PNBA) — an intermediate in the synthesis of the analgesic preparations anesthesin and novocain — was obtained in a yield >99% by esterifying PNBA with ethanol in the presence of $H_3PW_{12}O_{40}$ (3%–7%) at 75 °C.[102]



The water formed in the reaction is distilled away as the azeotrope with toluene. At the end of the reaction, the reaction mass divides into two separate phases. The upper layer contains ethyl *p*-nitrobenzoate mixed with toluene and the alcohol and the lower consists of a solution of the heteropolyacid in ethanol. As a result of this, the catalyst can be readily separated from the reaction product without neutralisation and can be reused. Activity is not lost under these conditions.

Sulfuric acid is used industrially as the catalyst for the synthesis of the ethyl ester of PNBA. This method is characterised by a low yield of the product (75%) and a large amount of waste formed as a result of the neutralisation of sulfuric acid.[103] Thus the application of heteropolyacids in this reaction makes it possible to increase significantly the yield of the product and to diminish the amount of waste. The catalytic activity of the heteropolyacids in the esterification of PNBA is close to that of the KU-2-8 cation-exchange resin[104]

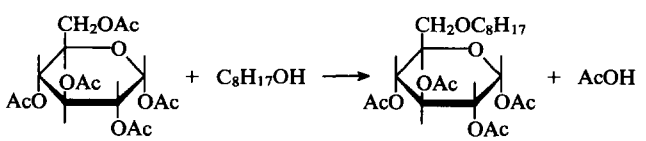
Massive heteropolyacids and heteropolyacids deposited on SiO_2, Al_2O_3, or TiO_2 are used as catalysts of the synthesis of hydroquinone monoethers, which are employed in the manufacture of medicinal preparations and perfumes, stabilisers, polymerisation inhibitors, etc. For example, the use of 1-hexanol in reaction (13) makes it possible to obtain the corresponding monoether with a selectivity of 99% in the presence of $H_3PMo_{12}O_{40}$ (3%) for a hydroquinone conversion of 83% (105 °C, 5 h).[105]



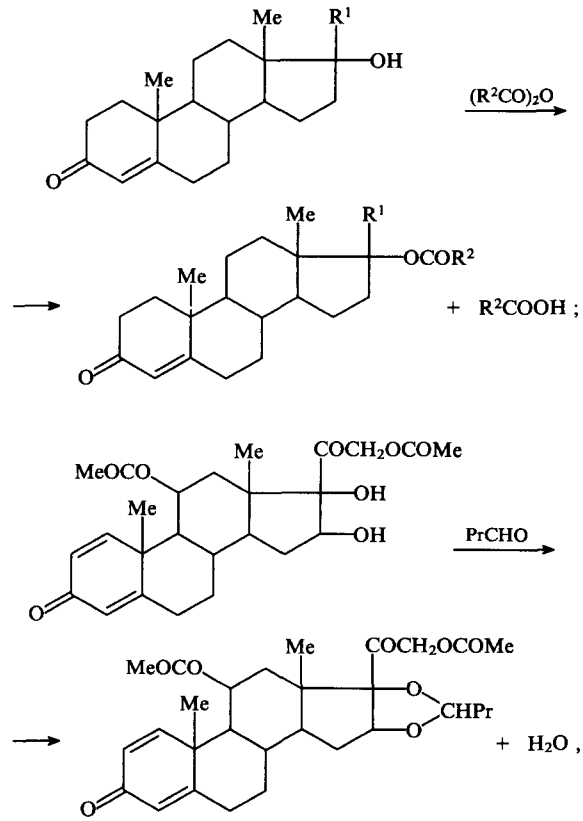
(13)

Dialkyl phthalates, which are used as plasticisers, have been obtained by esterifying phthalic anhydride with C_8-C_{10} alcohols at 100–120 °C in the presence of the homogeneous or heterogeneous $H_3PW_{12}O_{40}$ catalyst (1%–2%). In the latter case, the heteropolyacid deposited on activated charcoal was employed. The catalytic activity of the heteropolyacid is greatly superior to that of H_2SO_4 and toluene-*p*-sulfonic acid. The HPA/C catalyst is less active than the homogeneous catalyst, but has the advantage of being readily removed from the reaction mixture.[106]

The synthesis of glycosides using heteropolyacids as catalysts is of industrial importance.[7] There exist numerous patents concerning the use of this reaction. On interaction with alcohols in the presence of a heteropolyacid (85 °C, 4 h), monosaccharides are readily converted into glycosides in 47%–83% yield. Thus the reaction of pentaacetylglucose with 1-octanol in the presence of $H_3PMo_{12}O_{40}$ (3%) afforded octyl tetraacetylglucoside in 70% yield.[107] Glycosides have found applications as medicinal preparations.



The esterification of steroids and their conversion into acetals take place with quantitative yields in the presence of the catalysts $H_3PW_{12}O_{40}$ and 25% $H_3PW_{12}O_{40}/SiO_2$ (1.5%–9%) in MeCN, CH_2Cl_2, or C_6H_6 (40–82 °C, 0.5–4 h):



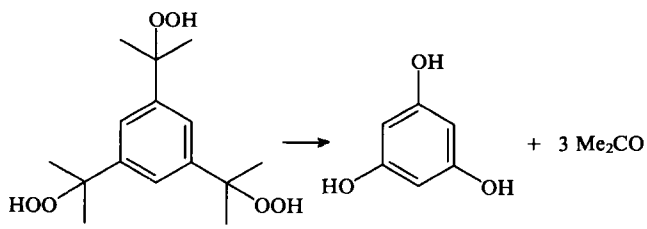
where R^1 = H or COMe and R_2 = Et or Pe.[108] These reactions represent stages in the synthesis of modified hormones.[109] In benzene, where the heteropolyacid is insoluble, such reactions proceed heterogeneously; the catalyst can be separated from the reaction mixture without neutralisation and can be reused. The activity of the heteropolyacid is close to that of $HClO_4$ and is much greater than that of 5-sulfosalicylic acid.

8. Other reactions

The acids $H_3PMo_{12}O_{40}$ and $H_4SiMo_{12}O_{40}$ catalyse the acylation of aromatic compounds (the Friedel–Crafts reaction).[110–112]

Heteropolyacids are highly active and selective homogeneous[36, 113] and heterogeneous[114, 115] catalysts for the decomposition of cumenyl hydroperoxide to phenyl and acetone. Phloroglucinol was obtained by means of a similar procedure involving the decomposition of 1,3,5-tris(hydroperoxy-isopropyl)benzene in the presence of a heteropolyacid at 50–100 °C with a selectivity of 97% and a hydroperoxide conversion of 89%.[116]

The hydrolysis of sucrose in the presence of $H_4SiW_{12}O_{40}$ has been investigated.[117]



III. Liquid-phase oxidation reactions

The liquid-phase oxidation of organic substances catalysed by heteropolyanions takes place in homogeneous or heterogeneous (two-phase) systems. In the latter case, phase transfer catalysts are frequently used. O_2, H_2O_2, alkyl hydroperoxides and, more rarely, other substances are used as oxidants. The oxidation-reduction properties of heteropolyacids, their synthesis, state in the solution, and applications as catalysts of liquid-phase oxidation have been examined in a number of reviews.[2, 3, 8, 13, 118-120]

1. Oxidation with oxygen

Mixed molybdovanadophosphoric heteropolyanions $PMo_{12-n}^{6+}V_n^{5+}O_{40}^{(3+n)-}$ (HPAN-n, n = 2–6) are used preferentially as catalysts in these reactions.[3, 8, 118-120] They have a fairly high oxidation potential [0.7 V relative to the normal hydrogen electrode (n.h.e.)] and are themselves capable of oxidising a large number of organic and inorganic substances. At the same time, the HPAN-n are reversibly acting oxidants, i.e. their reduced forms can be readily reoxidised to the initial HPAN-n with the aid of O_2.

$$\text{Red} + \text{HPA-}n + i\,H^+ \longrightarrow \text{Ox} + H_iHPA\text{-}n\,, \quad (14)$$

$$H_iHPA\text{-}n + i/4\,O_2 \longrightarrow \text{HPA-}n + i/2\,H_2O\,. \quad (15)$$

Here Red and Ox are respectively the i-electron reductant (substrate or the reduced form of the cocatalyst) and its oxidised form, $H_iHPA\text{-}n = H_i[H_{3+n}PMo_{12-n}^{6+}V_{n-i}^{5+}V_i^{4+}O_{40}]$ is a heteropolyblue, i.e. the reduced form of HPAN-n ($i \leqslant n$).[3, 8, 118-120] The reversibility of the oxidation-reduction reactions of HPAN-n in fact constitutes the basis of their use as catalysts of a large number of liquid-phase oxidation reactions. Certain other mixed heteropolyanions, having similar properties, for example, $H_3PMo_6W_6O_{40}$, are also used for this purpose.[121, 122]

The HPAN-n-catalysed oxidation reactions proceed via a multistage mechanism in conformity with Eqns. (14) and (15).[3] Reactions (14) and (15) can be carried out simultaneously in one reactor or separately. In the second case, direct contact between the organic substrate and O_2 is excluded. The catalysts may be the HPAN-n themselves (one-component systems) or their combinations with other compounds (two-component systems). Among the latter, the HPAN-n + Pd(II)/Pd(0) redox system is the most important. It is analogous to the catalytic system $CuCl_2$ + Pd(II)/Pd(0) used to oxidise ethylene to acetaldehyde (the Wacker process), but, in contrast to the latter, it can work in the absence of Cl^- ions, which increases the selectivity of the process and lowers the corrosion activity of the catalyst solution.[3] The use of the HPAN-n + Pd(II) system in liquid-phase oxidation reactions has been examined in a number of studies.[3, 8, 118-120] Other redox systems based on HPAN-n are also known. Their second component is Tl(III)/Tl(I),[123, 124] Pt(IV)/Pt(II),[125] Ru(IV)/Ru(III), Ir(IV)/Ir(III),[126] Br_2/Br^-,[127] and I_2/I^-.[128] In two-component systems, the substrate is usually oxidised by the cocatalyst and the HPAN-n ensures the regeneration of the cocatalyst via reactions (14) and (15).

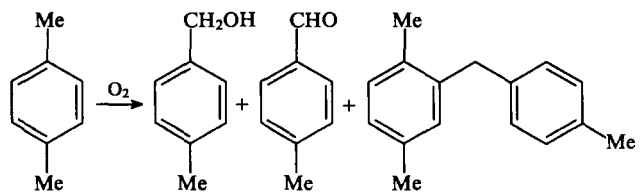
The HPAN + Pd(II) and HPAN + Rh(I) systems are also used in carbonylation hydroformylation, and hydrogenation reactions.[129-133]

Homogeneous catalysts based on HPAN-n consist as a rule of complex equilibrium mixtures of polyanions of different composition with products of the degradative dissociation of the heteropolyanion. All these species can function as the active form of the catalyst. Thus, in oxidation of hydrogen sulfide by the Mo_{12}-molybdophosphate at pH 3, the active role is played by isopolyanions for example, $Mo_7O_{24}^{6-}$ or $Mo_8O_{26}^{4-}$ in equilibrium with the heteropolyanion.[134] In the oxidation of alkylbenzenes and phenols by oxygen in the presence of HPAN-n, the true oxidant is most likely to be the VO_2^+ ions formed as the result of the dissociation of HPAN-n.[135-137]

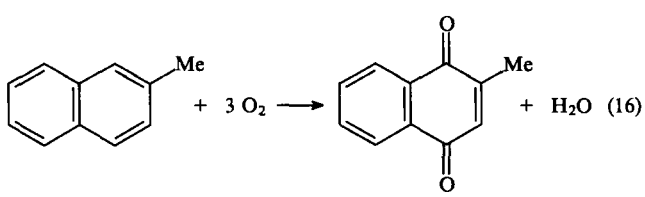
Free vanadium(IV) in the form of the VO^{2+} ion is hardly oxidised in acid aqueous solutions but is fairly readily oxidised when it is part of the compositions of HPAN-n [Eqn. (15)].[3] This reaction proceeds via a many-electron mechanism involving the consecutive transfer of three or four electrons in the complex of $H_iHPAN\text{-}n$ with O_2.[3] In contrast to the HPAN-n blues, the more readily oxidised blues derived from the tungsten heteropolyanions $PW_{12}O_{40}^{3-}$ and $SiW_{12}O_{40}^{4-}$ (E = 0–0.1 V) are oxidised by O_2 via a one-electron mechanism.[138]

a. Oxidation of arenes

Heteropolyanions in acetic acis solutions oxidise methylbenzenes with formation of a mixture of aromatic alcohols, aldehydes, and di- and poly-aryl methanes. In the presence of O_2, the reaction can proceed catalytically.[135] The true arene oxidants are probably the VO_2^+ ions which have emerged from the coordination sphere of HPAN-n. The rate of oxidation of arenes decreases in the sequence durene > mesitylene > p-xylene > toluene. The reaction apparently proceeds via the formation of aromatic radical-cations as intermediates.[135]



2-Methylnaphthalene (MN) is oxidised to 2-methyl-1,4-naphthoquinone by oxygen (3–8 atm) in the presence of 0.02–0.2 M HPAN-n as the catalyst. The reaction is carried out in a $AcOH-H_2O-H_2SO_4$ solution at 120–140 °C and its selectivity is 82% for a 2-methylnaphthalene conversion of 78%.[139] 2-Methyl-1,4-naphthoquinone is an intermediate in the synthesis of group K vitamins. It is obtained industrially by the stoichiometric oxidation of 2-methylnaphthalene by chromium trioxide in 40–50% yield.[91, 140] This reaction can be carried out catalytically with a higher yield with the aid of HPAN-n an O_2 as the oxidant:



Heteropolyanions catalyse the oxidative ring bromination of arenes with HBr as the brominating agent and O_2 as the oxidant.[127]

$$ArH + HBr + \frac{1}{2}O_2 \longrightarrow ArBr + H_2O\,.$$

The arenes brominated include benzene, its derivatives, naphthalene, thiophene, etc. The reaction proceeds in an $AcOH-H_2O-H_2SO_4$ solution at 50–100 °C. The bromination of the ring in arenes is effected by Br_2, which is formed as a result of the bromination of bromide ions by HPAN-n. In the case of alkylbenzenes, the alkyl groups are also oxidised. An advantage of this method is the possibility of using Br^- in the reaction instead of Br_2.

The HPAN-n + HBr system brominates phenol selectively in the *para*-position.[141]

Many stoichiometric reactions involving the oxidation of organic substances by palladium(II) compounds can be carried out catalytically with O_2 as the oxidant and the HPAN-n + Pd(II) two-component system as the catalyst.[3, 8, 118-120] Thus the

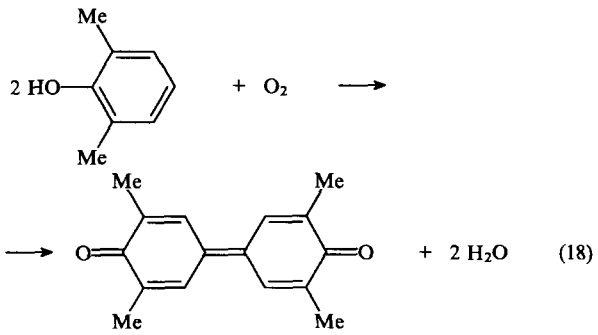
oxidative coupling of arenes in the presence of the HPAN-*n* + Pd(II) system makes it possible to obtain in a single stage biaryls — valuable intermediates in inorganic synthesis:

$$2\,ArH + \frac{1}{2}O_2 \longrightarrow Ar-Ar + H_2O, \quad (17)$$

where ArH = C_6H_6, PhAlk, PhCl, PhCOOH, $PhCF_3$, thiophene, etc.[142-144] The reaction proceeds under very mild conditions at 50–90 °C and an O_2 pressure of 1.5 atm. The selectivity in relation to biaryls is 70%–93%. It is noteworthy that in the absence of HPAN-*n*, reaction (17) requires a temperature of 150 °C and a pressure of 25 atm.[120] The mechanism of the oxidative coupling of arenes under the influence of palladium(II) has been examined in other reviews.[120, 145]

b. Oxidation of phenols

The compounds of many metals are capable of catalysing the oxidative coupling of phenols to diphenoquinones in solutions.[146] The coupling of 2,6-dialkylphenols (mainly 2,6-xylenol) under the influence of oxygen in the presence of copper complexes of amines is of practical importance:

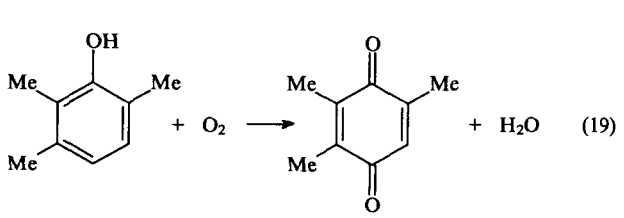


(18)

Diphenoquinones are used to synthesise bisphenols, which are used widely as stabilisers of polymers, oils, etc.[62]

The activity of heteropolyanions in reaction (18) is greater than that of copper compounds. The oxidative coupling takes place in H_2O, AcOH–H_2O, or MeOH–H_2O at 25–50 °C and an O_2 pressure of 1–5 atm. The diphenoquinones are insoluble under these conditions and can be readily isolated from the reaction mixture by crystallisation. The catalyst can be used repeatedly without loss of its activity. 2,2',6,6'-Tetramethyl- and 2,2',6,6'-tetra-*tert*-butyl-diphenoquinones have been obtained by this method in 100% yield relative to the initial phenol.[147]

The oxidation of 2,3,6-trimethylphenol (TMP) is of interest for the synthesis of 2,3,5-trimethyl-1,4-benzoquinone (TMBQ), which is an intermediate in the synthesis of vitamin E.[148] The oxidation of TMP by oxygen in the presence of HPAN-*n* as the catalyst in solution in aqueous acetic acid makes it possible to obtain TMBQ with a selectivity of 86% for 100% conversion of TMP.[136, 137]



(19)

2,2',3,3',6,6'-Hexamethyl-4,4'-bisphenol (HMBP), the product of the oxidative coupling of TMP, is also formed under these conditions. The process selectivity depends on the water concentration in the reaction mixture: with increase in [H_2O], the yield of HMBP increases owing to the decrease in the yield of TMBQ. The bisphenol HMBP itself undergoes oxidative conversion into TMBQ via the intermediate formation of hexamethyldiphenoquinone (HMDQ).

Evidence has been obtained that the activity of the oxidant arises through the VO_2^+ ions formed as a result of the dissociation of HPAN-*n*. A mechanism has been proposed for reaction (19) involving the one-electron oxidation of TMP (ArOH) by VO_2^+ ions with formation of TMBQ and vanadium(IV) followed by the oxidation of vanadium(IV) to vanadium(V) by oxygen in the coordination sphere of HPAN-*n*.[137]

$$\text{HPAN-}n \rightleftharpoons V(V) + \text{HPAN-}(n-1), \quad (20)$$

$$V(V) + ArOH \longrightarrow ArO^{\cdot} + V(IV) + H^+, \quad (21)$$

$$2\,ArO^{\cdot} \longrightarrow HMBD \xrightarrow{Ox} HMDQ \xrightarrow{Ox} TMBQ, \quad (22)$$

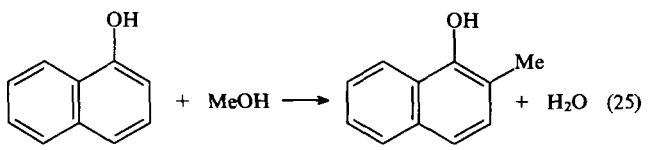
$$V(IV) + \text{HPAN-}n + H^+ \rightleftharpoons V(V) + H(\text{HPAN-}n), \quad (23)$$

$$4\,H(\text{HPAN-}n) + O_2 \longrightarrow 4\,\text{HPAN-}n + 2\,H_2O. \quad (24)$$

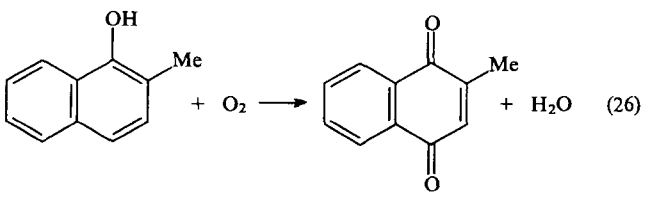
The stage involving the formation of the phenoxyl radical [reaction (21)] is probably rate-limiting.

The oxidation of sterically hindered phenols to benzoquinones by oxygen in the presence of manganese(II) complexes of heteropolytungstates has been investigated.[149]

A new two-stage method of synthesis of vitamin K_3 from 1-naphthol has been developed.[150] It involves the alkylation of 1-naphthol by methanol to 2-methyl-1-naphthol and the oxidation of the latter to 2-methyl-1,4-naphthoquinone.



(25)



(26)

The alkylation reaction (25) is carried out in the vapour phase in the presence of an iron–vanadium catalyst. The oxidation stage (26) is carried out in the liquid phase using HPAN-*n* as the catalyst. Reaction (25) proceeds with a selectivity in excess of 90% and reaction (26) with a selectivity of 83%. As a result of this, the ultimate selectivity greatly exceeds the selectivity in the industrial single-stage synthesis of vitamin K_3 by the stoichiometric oxidation of 2-methylnaphthalene by CrO_3.[91, 140]

2. Oxidation by hydrogen peroxide

The tungsten(VI) and molybdenum(VI) heteropolyanions catalyse various reactions involving the oxidation of organic substances by hydrogen peroxide in homogeneous or two-phase systems under the conditions of phase transfer catalysis. Such reactions include the epoxidation of olefins, the oxidation of alcohols, glycols, phenols, etc.[2] The active intermediates in these reactions are peroxoheteropolycomplexes. In many cases, it was possible to detect them spectroscopically[151, 152] and sometimes to isolate them.[153]

In the homogeneous oxidation of allyl alcohol by H_2O_2 in aqueous solution in the presence of $H_3PW_{12}O_{40}$ at pH 0.7–1.8, glycerol is formed in 64%–100% yield relative to the peroxide which has reacted (70–90 °C, 1–2 h). The primary product is probably an epoxide, which rapidly hydrolyses to glycerol in an acid medium. The peroxo-complexes of heteropolyacids containing up to four peroxo-groups linked to the $PW_{12}O_{40}^{3-}$

anion, have been detected in the reaction system by ^{31}P NMR. The heteropolyacid does not decompose during the reaction.[151]

The catalytic activity of heteropolyanions of different types in the homogeneous reaction involving the oxidation of cyclohexene by hydrogen peroxide in acetonitrile at 35 °C has been investigated. The heteropolyanions employed include $PW_{12}O_{40}^{3-}$ and the lacunary anion $PW_{11}O_{39}^{7-}$ and complexes with transition metal ions $PW_{11}O_{39}M^{x-}$, where M = Ni(II), Co(II), Cu(II), Fe(II), Cr(III), Ru(IV), Ti(IV), and V(V). The anion $PW_{11}O_{39}^{7-}$ shows the highest catalytic activity and selectivity in relation to epoxycyclohexane. The anion $PW_{12}O_{40}^{3-}$ is much less active. The cobalt (II), copper(II), and ruthenium(IV) complexes are inactive in the oxidation of cyclohexene but rapidly decompose H_2O_2. The nickel(II), titanium(IV), and vanadium(V) complexes are inert both in the oxidation of the substrate and in the decomposition of H_2O_2. The iron(II) and chromium(III) complexes are moderately active catalysts of the oxidation of cyclohexene, but the reaction proceeds nonselectively.[152]

Cyclopentene is oxidised by hydrogen peroxide to glutaraldehyde in the presence of the mixed heteropolyacids $H_3PMo_{12-n}W_nO_{40}$ (n = 1–9) in solution in tributyl phosphate (TBP) in 60% yield relative to the H_2O_2 employed (35 °C, 3 h). Water is removed from the H_2O_2–TBP system by vacuum distillation. Other heteropolyacids have been investigated in this reaction. The yield of glutaraldehyde (mol%) decreases in the sequence[154] $H_3PMo_{10}W_2O_{40}$ (16) > $H_3PMo_{12}O_{40}$ (47) > $H_4GeMo_{12}O_{40}$ (21) > $H_3PMo_{10}V_2O_{40}$ (6) > $H_3PW_{12}O_{40}$ (5) > $H_4SiMo_{12}O_{40}$ (1).

The two-phase system including immiscible aqueous and organic phases and a phase transfer catalyst is used widely in reactions involving oxidation by H_2O_2.[154–160] Convenient organic solvents are $1,2\text{-}Cl_2C_2H_4$, $CHCl_3$, CCl_4, C_6H_6, etc. The phase transfer catalysts employed are tetraalkylammonium (C_6–C_{18}) cetylpyridinium, etc. cations (Q^+). The catalytic system is usually prepared as follows. Active peroxo-complexes are formed initially in the aqueous phase from the tungsten(VI) or molybdenum(VI) starting compounds (for example, the heteropolyanions or $WO_4^{2+} + PO_4^{3-}$, etc.) and hydrogen peroxide. The initial heteropolyanions can then partly decompose on reaction with the excess H_2O_2.[161] Next the organic phase with the phase transfer catalyst dissolved in it is added. This results in the formation of Q^+ salts with peroxoheteropolyanions, which are soluble in the organic phase and are almost fully transferred to the latter. This is followed by the addition of the organic substrate, for example, an olefin, and the reaction begins. The oxidation takes place preferentially in the organic phase via the transfer of an oxygen atom from the peroxo-complex to the substrate. The peroxo-complexes are regenerated at the interface via the interaction of the heteropolyanion with the hydrogen peroxide in the aqueous phase. The mechanism of the catalytic epoxidation of the olefins by hydrogen peroxide in the two-phase system in the presence of $PW_{12}O_{40}^{3-}$ is illustrated schematically in Fig. 5.

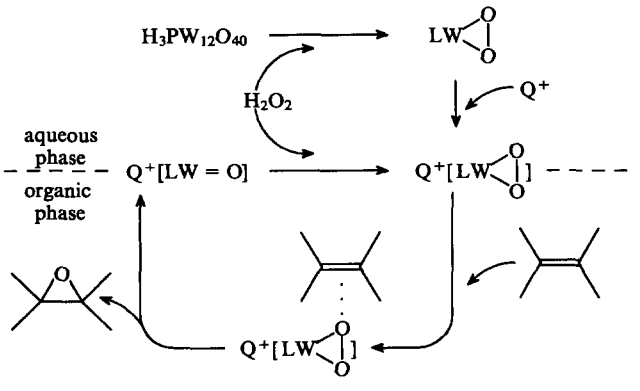


Figure 5. Epoxidation of olefins by hydrogen peroxide in a two-phase system.

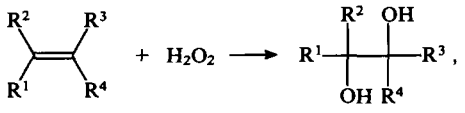
Tetrahexylammonium heteropoly-11-tungstates are active catalysts of the oxidation of cyclohexene by 30% aqueous H_2O_2 in the 1,2-dichloroethane–water two-phase system. The reaction proceeds in the organic phase and the main product is cyclohexanediol. The products of the oxidative cleavage of the ring—adipaldehyde and adipic acid—are also formed in 30%–45% yield. In contrast to the lacunary M_{11}-HPA, the saturated M_{12}-HPA proved to be virtually inactive.[156]

The tetrakis(diperoxotungsto)phosphate $Q_3^+[PW_4O_{24}]^{3-}$ [$Q^+ = N(C_6H_{13})_4^+$, $N(C_8H_{17})_3(CH_3)^+$, etc.] is an effective stoichiometric reagent for the epoxidation of olefins in aprotic solvents and is also an effective catalyst of this reaction with H_2O_2 in a two-phase system.[153, 158] This compound has been isolated and its structure has been characterised by X-ray diffraction[153] (Fig. 6).

The anion $PW_4O_{24}^{3-}$ has the C_2 symmetry and consists of a central PO_4 tetrahedron and four distorted $W(O_2)_2O_3$ pentagonal bipyramids linked to it via the oxygen atoms. The bipyramids are grouped into two pairs with common edges. Each tungsten atom is linked to two peroxide groups located in the equatorial plane of the pentagonal bipyramid. It is of interest to note that tungsten(VI) and molybdenum(VI) have the same coordination environment in their monomeric diperoxo-complexes, which are capable of the effective epoxidation of olefins.[159]

The epoxidation of oct-1-ene with 15% H_2O_2 in the presence of $PW_4O_{24}^{3-}$ in the 1,2-dichloroethane–water system affords epoxyoctane in 89% yield relative to the initial hydrogen peroxide for a H_2O_2 conversion of about 100% (70 °C, 1.5 h). The reaction is stereoselective: *cis*-hex-2-ene is converted solely into the *cis*-epoxide, while *trans*-hex-2-ene is converted into the *trans*-epoxide.[153]

The heteropolyanion in $Q_3^+[PW_4O_{24}]^{3-}$ catalyses the conversion in the two-phase system of water-insoluble olefins of different structure into water-soluble vicinal *trans*-glycols in 71%–88% yield (60–70 °C, 1–4 h, 2%–4% H_2O_2, pH 1.2–1.5)[158]



where R^1–R^4 = H, Me, Et, Bu, Ph, etc. The glycols formed are present almost entirely in the aqueous phase and can be readily isolated from the reaction mixture. The vicinal glycols are used for the preparation of cosmetics and perfumes, photographic materials, etc.

The epoxidation of oct-1-ene by hydrogen peroxide in the $CHCl_3$–H_2O system has been investigated under the conditions of phase transfer catalysis in the presence of the heteropolyanion $XM_{12}O_{40}^{n-}$ and $X_2M_{18}O_{62}^{n-}$ and the isopolyanions $M_xO_y^{z-}$ (M = Mo or W; X = P, Si, or B) as precursors of catalytically active peroxo-complexes. The state of the complexes in the system has been characterised by a number of spectroscopic methods.

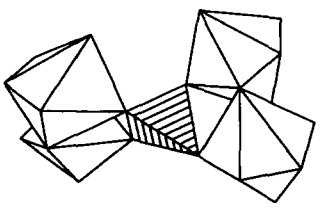


Figure 6. The structure of the peroxoheteropolyanion $PW_4O_{24}^{3-}$ (according to the data of Venturello et al.[153]).

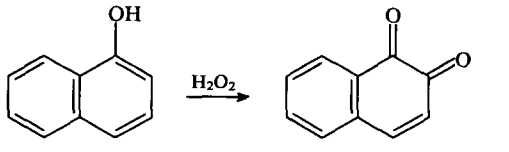
It was established that the anions $BW_{12}O_{40}^{5-}$, $SiW_{12}O_{40}^{4-}$, and $P_2W_{18}O_{62}^{6-}$ are altogether inactive and do not change during the reaction, while $PMo_{12}O_{40}^{3-}$ exhibits a low activity. On the other hand, $PW_{12}O_{40}^{3-}$ exhibits a high activity (the yield of the epoxide is 79% relative to oct-1-ene for a 95% selectivity) when the catalytic system is formed beforehand by the reaction of the heteropolyanion with H_2O_2 in aqueous solution in the absence of Q^+ and oct-1-ene. When all the reagents are mixed simultaneously, the activity of $PW_{12}O_{40}^{3-}$ is zero. A higher activity is shown by tunstic acid (yield 76%) and $H_2W_{12}O_{42}^{10-}$ (yield 67%), their activity being independent of the method used to carry out the reaction. Heteropolyanions having the Keggin structure decompose in the presence of an excess of H_2O_2 {$[H_2O_2]/[M]$ = 30–355 mol mol^{-1}} with formation of the peroxo-complexes $PM_4O_{24}^{3-}$ and $M_2O_{11}(H_2O)_2^{2-}$. It has been suggested that $PM_4O_{24}^{3-}$ is in fact the active species responsible for epoxidation when $PM_{12}O_{40}^{3-}$ is used under the conditions of phase transfer catalysis.[161]

The epoxidation of styrene–butadiene and isobutene–isoprene copolymers by hydrogen peroxide in the presence of $PW_4O_{24}^{3-}$ has been investigated.[162]

The cetylpyridinium salt of $PW_{12}O_{40}^{3-}$, which can be readily obtained by the reaction of $H_3PW_{12}O_{40}$ with three equivalents of cetylpyridinium chloride, catalyses a large number of reactions involving oxidation by hydrogen peroxide. They include the epoxidation of olefins, allyl alcohols, and α,β-unsaturated carboxylic acids, the oxidation of secondary alcohols to ketones, the oxidation of α,ω-diols to lactones, the oxidative cleavage of vicinal diols and olefins to give carboxylic acids, etc. These reactions proceed under mild conditions and with satisfactory yields.[157, 163, 164] Alkynes are also oxidised smoothly in this system to carboxylic acids.[165]

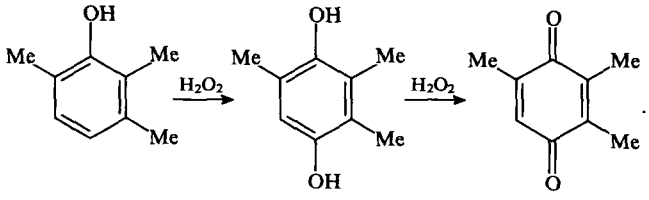
The oxidation of primary and secondary aliphatic and aromatic amines with 35% H_2O_2, catalysed by peroxo-heteropolytungstates, leads to the formation of oximes and nitro-compounds in a high yield in homogeneous or two-phase systems.[166]

α- and β-Naphthols ($\sim 10^{-3}$ M) are oxidised by H_2O_2 (2%–15%) to 1,2-naphthoquinone in 80%–98% yield at 20 °C in the 1,2-dichloroethane–water system in the presence of peroxoheterotungstates and trioctylbenzylammonium chloride (TOBAC).



When the naphthol concentration is increased, C–C coupling products are formed. The catalytic system is prepared by mixing PO_4^{3-}, WO_4^{2-}, and TOBAC in molar proportions of 8 : 4 : 3. It is suggested that the active form of the catalyst is the peroxo-complex $PW_4O_{24}^{3-}$. The reaction proceeds via the intermediate formation of semiquinone radicals, which have been detected by the EPR method.[167]

Heteropolyacids with the Keggin structure catalyse the oxidation of 2,3,5- and 2,3,6-trimethylphenol (TMP) to 2,3,5-trimethyl-1,4-benzoquinone (TMBQ) by hydrogen peroxide in solution in acetic acid with a selectivity of 65%–78% for a TMP conversion of 94%–100%.



The hydroxylation of the benzene ring catalysed by the heteropolyacid probably results in the initial formation of 2,3,5-trimethylhydroquinone, which is subsequently rapidly oxidised to TMBQ.[168] Apparently in this case the heteropolyacid behaves as a Brønsted acid catalyst. TMP is oxidised similarly by hydrogen peroxide in the presence of sulfuric acid.[169] In acetic acid in the presence of a strong inorganic acid, H_2O_2 is rapidly converted into peracetic acid, which is probably the true hydroxylating agent.[170]

The molybdovanadium isopolyacids $H_2V_{12-x}Mo_xO_{31}$ (x = 0–4) catalyse the oxidation of 1,2,4-trimethylbenzene to TMBQ by peracetic acid in solution in acetic acid (20 °C, 4 h) with a selectivity of 12%–31% for a trimethylbenzene conversion of 15%–22%.[171]

The oxidation of ethylbenzene by hydrogen peroxide in acetonitrile in the presence of $H_3PW_{12}O_{40}$, $H_3PMo_{12}O_{40}$, and their tetrabutylammonium salts has been investigated. The main reaction product is acetophenone (selectivity 100%, PhEt conversion 5%–17%).[172]

3. Oxidation by hydroperoxides

The epoxidation of hex-1-ene by isopropylphenyl hydroperoxide (IPPHP) in isopropyl alcohol in the presence of heteropolyacid salts at 110 °C proceeds with a selectivity of approximately 100% with respect to epoxyhexane for an IPPHP conversion >80%. The rate of reaction is described by the kinetic equation $w = k[\text{HPAN}]^p[\text{IPPHP}][C_6H_{12}]$, where p = 0.5–0.9 for [HPAN] = $(0.2–9)\times 10^{-5}$ M. The catalytic activity of heteropolyacid salts decreases in the sequence $Na_3PMo_{12}O_{40} \simeq AlPMo_{12}O_{40} > Na_4PMo_{11}VO_{40} > Na_4SiMo_{12}O_{40} \gg Na_3PW_{12}O_{40}$. The heteropolyacids themselves are ineffective in epoxidation because they catalyse the decomposition of IPPHP to phenol and acetone. It has been suggested that the reaction mechanism involves the decomposition of the heteropolyanion with formation of monomeric molybdenum(VI) complexes, which are the true epoxidation catalysts.[173]

Transition metal complexes of the lacunary heteropoly-11-tungstate (p-$Bu_4N)_4HPW_{11}O_{39}M$, where M = Mn(II), Co(II), Cu(II), Fe(II), etc., catalyse the oxidation of cyclohexanol and adamantane by butyl hydroperoxide (TBHP) in benzene. The selectivity in the formation of the oxidation products (cyclohexanone or 1-adamantanol, 2-adamantanol, and 2-adamantanone) reaches 90% relative to the TBHP which has reacted. Such complexes catalyse also the oxidation of olefins (cyclohexene, hex-1-ene, norbornene, and cyclooctene) by iodosobenzene and pentafluoroiodosobenzene in acetonitrile. The manganese(II) and cobalt(II) complexes exhibit the highest activity.[174, 175]

The compound $[(C_6H_{13})_4N]_5SiW_{11}O_{39}Ru(H_2O)$ catalyses the liquid-phase oxidation of alkanes and alkenes by oxidants such as TBHP, potassium persulfate, sodium periodate, and iodosobenzene.[176]

4. Other reactions

The stoichiometric oxidation sclareol (a labdanediol) by the $PW_{11}O_{39}Tl^{4-}$ anion containing thallium(III) has been investigated. The main reaction products are epoxy-derivatives of labdane.[177]

Table 3. Acid catalysis by heteropolyacids in liquid-phase fine organic synthetic reactions (catalysts: $H_3PW_{12}O_{40}$, $H_4SiW_{12}O_{40}$, $H_3PMo_{12}O_{40}$, HPA/SiO_2).

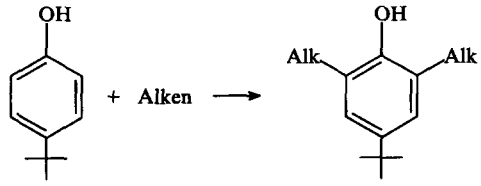
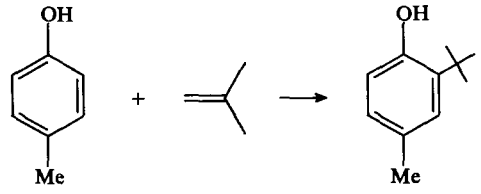
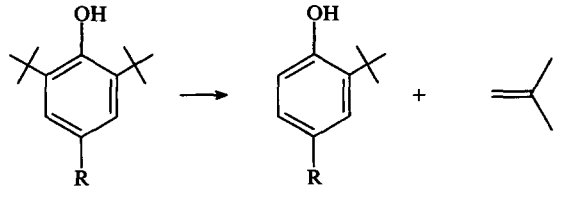
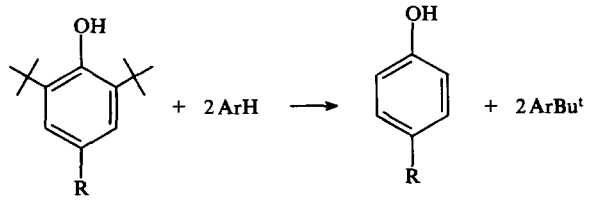
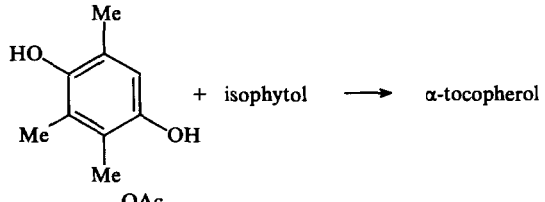
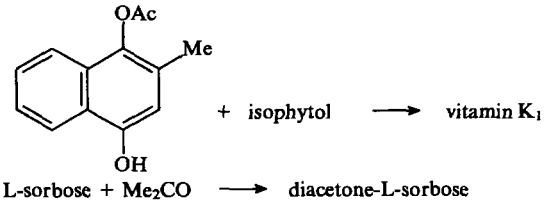
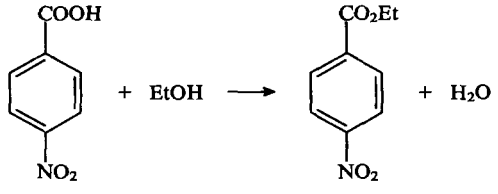
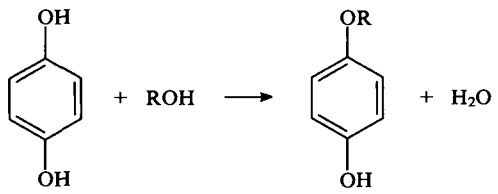
Reaction	T/ °C	Selectivity (%), (yield (%))	Ref.
(De)alkylation			
	100–150	(63–90)	68, 69
	90	80	68
	80–150	100	72–74
	100–140	(92–98)	76
Condensation			
	90–150	(92)	89
	110	(73)	89
L-sorbose + Me_2CO ⟶ diacetone-L-sorbose	56	(85)	90
Hydration			
camphene + H_2O ⟶ isoborneol	50	100	98
Esterification			
	100	99	102

Table 3 (continued).

Reaction	T/ °C	Selectivity (%), (yield (%))	Ref.
	105	99	105
monosaccaride + ROH ⟶ glycoside	85	(47–83)	107
testosterone + $(EtCO)_2O$ ⟶ testosterone propionate	40	99	108

IV. Conclusion

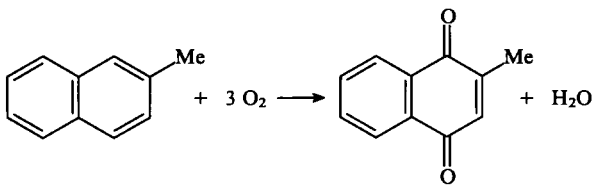
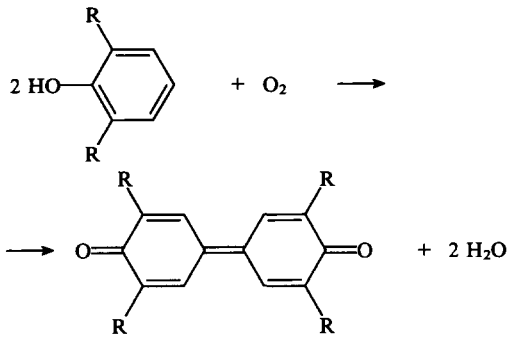
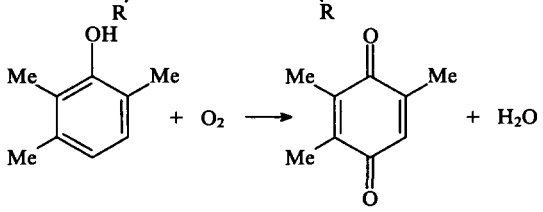
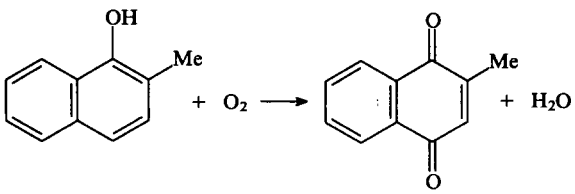
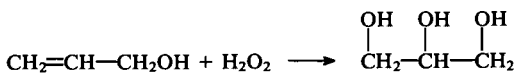
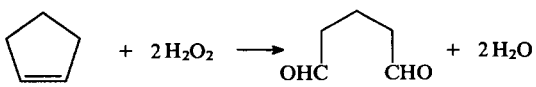
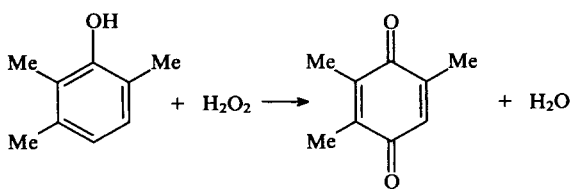
Considerable progress has been achieved during the last 20 years in the study of the catalysis by heteropolyacids. Their industrial use in organic synthetic processes has been initiated (Table 1). The employment of heteropolyacids in fine organic synthesis has given rise to considerable possibilities. The data obtained hitherto definitely indicate the likely usefulness of heteropolyacids as catalysts of fine organic synthetic reactions. Tables 3 and 4 give a compilation of the most important acid-dependent and oxidation reactions discussed in the present review. In many of them, heteropolyacids have significant advantages as regards their activity and/or selectivity compared with traditional catalysts. Some of these reactions are already being used in industry. Thus the heteropolyacid-catalysed alkylation and transalkylation of phenol derivatives is used in Russia for the synthesis of antioxidants. There are data[7] concerning the industrial application of hydropolyacids in the synthesis of glycosides in Japan. In the future the number of such processes will undoubtedly increase.

We may note the principal causes of the high effectiveness of heteropolyacid-based catalysts in organic synthesis compared with other catalytic systems. The advantages of heteropolyacids are manifested most strikingly in acid catalysis. The high effectiveness of heteropolyacids as acid catalysts is primarily due to their high Brønsted acidity, which exceeds the acidity of inorganic acids and traditional solid acid catalysts. This makes it possible to carry out the catalytic process at a lower catalyst concentration and/or a lower temperature, which tends to increase the process selectivity and permits an appreciable diminution of the amount of waste on neutralisation of the catalyst. Furthermore, by virtue of the inertness of their anions, heteropolyacids do not enter into side reactions with organic reagents, a feature typical for the usual inorganic acids (sulfonation, chlorination, nitrogenation, etc.). Heteropolyacids may be used as homogeneous or heterogeneous (massive and deposited) catalysts. In contrast to inorganic acids, heterogeneous heteropolyacid-based catalysts can be readily separated from the reaction products without neutralisation and can be reused. The heterogeneous systems are in many respects similar to concentrated solutions of heteropolyacids ('pseudoliquid phase') and exhibit a high catalytic activity in low-temperature reactions. In homogeneous systems the heteropolyacids are usually neutralised at the end of the reaction, as in the case of the inorganic acids. However, when heteropolyacids are used the amount of alkali consumed and hence the amount of waste is tens of times smaller. We may note that certain homogeneous systems divide into layers in the presence of heteropolyacids with formation of two immiscible phases, one of which contains the heteropolyacid and the other the reaction product. In such cases, the catalyst is also readily separated from the product and can be reused. Similar heterophase systems are used in the industrial polymerisation of tetrahydrofuran (Table 1)[2, 7] and in the esterification of *p*-nitrobenzoic acid with ethanol in the presence of $H_3PW_{12}O_{40}$, already noted above.[102]

The use of catalysts based on heteropolycompounds in liquid-phase oxidation reactions is also promising (Table 4). Heteropolycompounds can be employed as stoichiometric oxidants or catalysts together with oxidants such as O_2, H_2O_2, organic hydroperoxides, etc. The application of two-component catalysts incorporating transition metal complexes and a heteropolycompounds as cocatalysts appreciably expands the range of possible oxidation reactions.[3] The acid-base and oxidation-reduction properties of heteropolycompounds and the possibility of their specific regulation permit the employment of such compounds as bifunctional catalysts in processes involving coupled electron and proton transfer, which are fairly common in liquid-phase oxidation. An example of the bifunctional activity of HPC is provided by the vapour-phase oxidation of acrolein over $H_3PMo_{12}O_{40}$.[1, 2]

Much still remains to be done both in the field of fundamental research into the catalysis by HPC and in their practical employment. The unique physicochemical properties of HPC give rise to considerable potential possibilities for the investigation of the elementary steps in homogeneous and heterogeneous acid and oxidative catalysis. There is no doubt that the research into the mechanism of the catalytic activity of HPC will be continued and intensified at the molecular level with employment of HPC of different structural types. These systems are of special interest for the investigation of bifunctional catalysis and of the relation between homogeneous and heterogeneous catalysis. As regards practical application, the expansion of the research into the catalysis by HPC in fine organic synthesis, the development of new more effective methods of synthesis of HPC and catalysts based on them, methods for their isolation, regeneration, and utilisation, and the study of the corrosion activity of HPC solutions, their toxicity, etc. is of current interest.

Table 4. Liquid-phase oxidation reactions in the presence of heteropolycompounds.

Reaction	Catalyst	T/ °C	Selectivity (%), (yield (%))	Ref.
Oxidation by oxygen				
	HPAN-*n*	120–140	82	139
$ArH + HBr + \frac{1}{2}O_2 \longrightarrow ArBr + H_2O$	HPAN-*n*	50–100	100	127
$2\,ArH + \frac{1}{2}O_2 \longrightarrow Ar{-}Ar + H_2O$,	Pd(II)+HPAN-*n*	50–90	70–93	142–144
	HPAN-*n*	25–50	100	147
	HPAN-*n*	50–100	86	137
	HPAN-*n*	50–100	83	150
Oxidation by hydrogen peroxide				
	$H_3PW_{12}O_{40}$	70–90	64–100	151
	$H_3PMo_{10}W_2O_{40}$	35	(61)	154
olefin + H_2O_2 ⟶ epoxide + H_2O	$Q_3[PW_4O_{24}]$	70	(89)	153
olefin + H_2O_2 ⟶ glycol	$Q_3[PW_4O_{24}]$	60–70	(71–88)	158
α- or β-napthol + H_2O_2 ⟶ 1,2-naphthoquinone + H_2O	$Q_3[PW_4O_{24}]$	20	80–98	167
	$H_3PW_{12}O_{40}$	40	65–78	168
Oxidation by hydroperoxides				
hex-1-ene + ROOH ⟶ epoxide + ROH	$Na_3PMo_{12}O_{40}$	110	100	173

References

1. M Misono, K Sakata, Y Yoneda, W Y Lee, in *VII International Congress on Catalysis, Tokyo, 1980 (Preprints)* p. 27
2. Y Ono, in *Perspectives in Catalysis* (Eds J M Thomas, K I Zamaraev) (Oxford: Blackwell Sci. Publ., 1992) p. 431
3. I V Kozhevnikov, K I Matveev *Usp. Khim.* **52** 1433 (1983) [*Russ. Chem. Rev.* **52** 817 (1983)]
4. I V Kozhevnikov *Usp. Khim.* **56** 1417 (1987) [*Russ. Chem. Rev.* **56** 811 (1987)]
5. J B Moffat *Rev. Chem. Intermediates* **8** 1 (1987)
6. M Misono *Catal. Rev. Sci. Eng.* **29** 269 (1987)
7. M Misono, N Nojiri *Appl. Catal.* **64** 1 (1990)
8. I V Kozhevnikov, K I Matveev *Appl. Catal.* **5** 135 (1983)
9. I V Kozhevnikov *Kataliz Kislotami i Osnovaniyami* (Catalysis by Acids and Bases) (Novosibirsk: Izd. Novosibirsk. Univ., 1991)
10. G A Tsigdinos, in *Topics Current Chemistry* (Berlin: Springer, 1978) Vol. 76, p. 1
11. V I Spitsyn, E A Torchenkova, L P Kazanskii, in *Itogi Nauki i Tekhniki. Neorganicheskaya Khimiya* (Advances in Science and Engineering. Inorganic Chemistry) (Moscow: Izd. VINITI, 1984) Vol. 10, p. 65
12. M T Pope, A Muller *Angew. Chem. Intern. Ed. Engl.* **30** 34 (1991)
13. M T Pope *Heteropoly and Isopoly Oxometallates* (Berlin: Springer, 1983)
14. E A Nikitina *Geteropolisoedineniya* (Heteropolycompounds) (Moscow: Goskhimizdat, 1962)
15. J F Keggin *Proc. Roy. Soc. London A* **144** 75 (1934)
16. I V Kozhevnikov, USSR P. 676 317; *Byull. Izobret.* **28** (1979)
17. I V Kozhevnikov, K I Matveev, V E Tarabanko, USSR P. 706 109; *Byull. Izobret.* **48** (1979)
18. I V Kozhevnikov, Doctoral Thesis in Chemical Sciences, Institute of Catalysis, Siberian Division of the Academy of Sciences of the USSR, Novosibirsk, 1983
19. US P. 3 947 332
20. T Peng, E Wang, R Zheng *Kexue Tongbao* **31** 526 (1986)
21. O M Kulikova, R I Maksimovskaya, S M Kulikov, I V Kozhevnikov *Izv. Akad. Nauk, Ser. Khim.* 494 (1992)
22. S M Kulikov, O M Kulikova, R I Maksimovskaya, I V Kozhevnikov *Izv. Akad. Nauk SSSR, Ser. Khim.* 1944 (1990)
23. O M Kulikova, R M Maksimovskaya, S M Kulikov, I V Kozhevnikov *Akad. Nauk SSSR, Ser. Khim.* 1726 (1991)
24. O M Kulikova, Candidate's Thesis in Chemical Sciences, IKhPOS, Siberian Division of the Russian Academy of Sciences, Krasnoyarsk, 1992
25. G M Maksimov, R I Maksimovskaya, I V Kozhevnikov *Zh. Neorg. Khim.* **37** 2279 (1992)
26. T Okuhara, A Kasai, N Hayakawa, Y Yoneda, M Misono *J. Catal.* **83** 121 (1983)
27. T Komaya, M Misono *Chem. Lett.* 1177 (1983)
28. S Tatematsu, T Hibi, T Okuhara, M Misono *Chem. Lett.* 865 (1984)
29. T Okuhara, T Hibi, K Takahashi, S Tatematsu, M Misono *J. Chem. Soc., Chem. Commun.* 697 (1984)
30. J B Moffat *J. Mol. Catal.* **52** 169 (1989)
31. V F Chuvaev, K I Popov, V I Spitsyn *Dokl. Akad. Nauk SSSR* **255** 892 (1980)
32. S M Kulikov, M N Timofeeva, I V Kozhevnikov, V I Zaikovskii, L M Playsova, I A Ovsyannikova *Izv. Akad. Nauk SSSR, Ser. Khim.* 763 (1989)
33. M A Schwegler, P Vinke, M van der Eijk, H van Bekkum *Appl. Catal.* **80** 41 (1992)
34. Y Izumi, R Hasebe, K Urabe *J. Catal.* **84** 402 (1983)
35. K Nowinska, R Fiedorow, J Adamiec *J. Chem. Soc., Faraday Trans.* **87** 749 (1991)
36. I V Kozhevnikov, S M Kulikov *Kinet. Katal.* **22** 956 (1981)
37. K Bruckman, J Haber, E Lalik, E M Serwicka *Catal. Lett.* **1** 35 (1988)
38. E M Serwicka, K Bruckman, J Haber, E A Paukshtis, E N Yurchenko *Appl. Catal.* **73** 153 (1991)
39. Y Izumi, K Matsuo, K Urabe *J. Mol. Catal.* **18** 299 (1983)
40. L D Kurbatova, A A Ivakin, E M Voronova *Koord. Khim.* **1** 1481 (1975)
41. A A Ivakin, L D Kurbatova, L A Kapustina *Zh. Neorg. Khim.* **23** 2545 (1978)
42. I V Kozhevnikov, S M Kulikov, K I Matveev *Izv. Akad. Nauk SSSR, Ser. Khim.* 2213 (1980)
43. S M Kulikov, I M Kozhevnikov *Izv. Akad. Nauk SSSR, Ser. Khim.* 498 (1981)
44. S Ts Khankhasaeva, Candidate's Thesis in Chemical Sciences, Institute of Catalysis, Siberian Division of the Academy of Sciences of the USSR, Novosibirsk, 1989
45. I V Kozhevnikov, S Ts Khankasaeva, S M Kulikov *Kinet. Katal.* **29** 76 (1988)
46. M Misono, N Mizuno, K Katamura, A Kasai, Y Konishi, K Sakata, T Okuhara, Y Yoneda *Bull. Chem. Soc. Jpn.* **55** 400 (1982)
47. M Furuta, K Sakata, M Misono, Y Yoneda *Chem. Lett.* 31 (1979)
48. A K Ghosh, J B Moffat *J. Catal.* **101** 238 (1986)
49. R Ohtsuka, Y Morioka, J Kobayashi *Bull. Chem. Soc. Jpn.* **63** 2071 (1990)
50. T Utada, N Sugiura, R Nakamura, H Niiayama *J. Chem. Eng. Jpn.* **24** 417 (1991)
51. V F Chuvaev, A B Yaroslavtsev, E M Yaroslavtseva, E S Oniani *Zh. Neorg. Khim.* **36** 2101 (1991)
52. G B McGarvey, J B Moffat *J. Catal.* **128** 69 (1991)
53. E A Paukshtis, O I Goncharova, T M Yur'eva, E N Yurchenko *Kinet. Katal.* **27** 463 (1986)
54. V I Spitsyn, I V Potapord, L P Kazanskii *Dokl. Akad. Nauk SSSR* **243** 426 (1978)
55. V F Chuvaev, K I Popov, V I Spitsyn *Dokl. Akad. Nauk SSSR* **243** 973 (1978)
56. Y Kanda, K Y Lee, S Nakata, S Asaoka, M Misono *Chem. Lett.* 139 (1988)
57. V M Mastikhin, S M Kulikov, A V Nosov, I V Kozhevnikov, I L Mudrakovsky, M N Timofeeva *J. Mol. Catal.* **60** 65 (1990)
58. B Wiswanathan, M J Omana, T K Varadarajan *Chem. Lett.* **3** 217 (1989)
59. G I Kapustin, T R Brueva, A L Klyachko, M N Timofeeva, S M Kulikov, I V Kozhevnikov *Kinet. Katal.* **31** 1017 (1990)
60. I V Kozhevnikov, S Ts Khankhasaeva, S M Kulikov *Kinet. Katal.* **30** 50 (1989)
61. G Olah (Ed.) *Friedel–Crafts and Related Reactions* (New York: Wiley–Interscience, 1964)
62. B N Gorbunov, Ya A Guvich, I P Maslova *Khimiya i Tekhnologiya Polimernykh Materialov* (The Chemistry and Technology of Polymeric Materials) (Moscow: Khimiya, 1981)
63. A B Vol'-Epshtein, S G Gagarin *Kataliticheskie Prevrashcheniya Alkilfenolov* (Catalytic Reactions of Alkylphenols) (Moscow: Khimiya, 1973)
64. V V Ershov, G A Nikiforova, A A Volod'kin *Prostranstvenno-Zatrudnennye Fenoly* (Sterically Hindered Phenols) (Moscow: Khimiya, 1972)
65. A A Bakhshi-Zade, N A Smirnova, R I Shenderova, in *Neftekhimicheskie Sintezy* (Petrochemical Syntheses) (Baku, 1976) No. 3, p. 88
66. T Okuhara, T Nishimura, H Watanabe, M Misono *J. Mol. Catal.* **74** 247 (1992)
67. Y Izumi, N Natsume, H Takamine, I Tamaoki, K Urabe *Bull. Chem. Soc. Jpn.* **62** 2159 (1989)
68. I V Kozhevnikov, A I Tsyganok, M N Timofeeva, S M Kulikov, V N Sidelnikov *React. Kinet. Catal. Lett.* **46** 17 (1992)
69. I V Kozhevnikov, A I Tsyganok, M N Timofeeva, S M Kulikov, V N Sidel'nikov *Kinet. Katal.* **33** 535 (1992)
70. M N Timofeeva, Candidate's Thesis in Chemical Sciences, Institute of Catalysis, Siberian Division of the Academy of Sciences of the USSR, Novosibirsk, 1992
71. T Nishimura, H Watanabe, T Okuhara, M Misono *Shokubai (Catalyst)* **33** 420 (1991)
72. S M Kulikov, A P Krysin, I V Kozhevnikov, USSR P. 1 162 780; *Byull. Izobret.* **23** (1985)
73. S M Kulikov, I V Kozhevnikov, M N Fomina, A P Krysin *Kinet. Katal.* **27** 750 (1986)
74. S M Kulikov, I V Kozhevnikov, M N Fomina, A P Krysin *Izv. Akad. Nauk SSSR, Ser. Khim.* 752 (1987)
75. I V Kozhevnikov, S M Kulikov, M N Timofeeva, N G Chukaeva, O A Kholdeeva, A I Tsyganok, in *VII International Symposium on Homogeneous Catalysis, Lyon, 1990* p. 14
76. I V Kozhevnikov, S M Kulikov, M N Timofeeva, A P Krysin, T F Titova *React. Kinet. Catal. Lett.* **45** 257 (1991)

77. I V Kozhevnikov, M N Timofeeva *J. Mol. Catal.* **75** 179 (1992)
78. M Tashiro, A Fukata *Org. Prep. Pros. Int.* **8** 51 (1976)
79. M Tashiro, T Yamato *Org. Prep. Pros. Int.* **10** 143 (1978)
80. F R J Willemse, E C Kooyman, H B van Lamoen, D de Vos, J Wolters *Recl. Trav. Chim. Pays-Bas* **102** 206 (1983)
81. G Olah, G K S Prakash, P S Iyer, M Tashiro, T Yamato *J. Org. Chem.* **52** 1881 (1987)
82. G Olah, G K S Prakash, J Sommer *Superacids* (New York: Wiley–Interscience, 1985)
83. R Ohtsuka, Y Morioka, J Kobayashi *Bull. Chem. Soc. Jpn.* **62** 3195 (1989)
84. V F Chuvaev, A I Gasanov, V I Spitsyn, USSR P. 550 373; *Byull. Izobret.* **10** (1977)
85. S Ts Khankhasaeva, S M Kulikov, I V Kozhevnikov *Kinet. Katal.* **31** 216 (1990)
86. V N Ipatieff, C B Linn, US P. 2 425 096 (1947)
87. S Yamamatsu, Y Ishibashi, Y Susuki, Jpn. P. 2-454 397; *Chem. Abstr.* **113** 24665 (1990)
88. S M Kulikov, I V Kozhevnikov, N G Chukaeva, in *Tezisy Dokladov II Vsesoyuznoi Konferentsii "Kataliz i Kataliticheskie Protsessy Khim. Farm. Proizvodstv"* (Abstracts of Reports at the IInd All-Union Conference on "Catalysis and Catalytic Processes in the Manufacture of Chemopharmaceuticals") (Moscow, 1989) Part 1, p. 142
89. I V Kozhevnikov, S M Kulikov, N G Chukaeva, A T Kirsanov, A B Letunova, V I Blinova *React. Kinet. Catal. Lett.* **47** 59 (1992)
90. I V Kozhevnikov, I B Vasilieva, V V Zarutsky *React. Kinet. Catal. Lett.* **47** 83 (1992)
91. L O Shnaidman *Proizvodstvo Vitaminov* (Production of Vitamins) (Moscow: Pishchevaya Prom., 1973)
92. Jpn. P. 7 2 167 (1973)
93. R P Evstigneeva, I K Sarycheva, M S Bainova, G I Basilevskaya, USSR P. 4 607 23; *Byull. Izobret.* **1** (1977)
94. O V Aref'eva, E E Zhukova, V N Byzova, R P Evstigneeva *Izv. Vyssh. Uchebn. Zaved., Khim. Khim. Tekhnol.* **33** 70 (1990)
95. K Ganesan, C N Pillai *J. Catal.* **119** 8 (1989)
96. K Nomiya, T Ueno, M Miwa *Bull. Chem. Soc. Jpn.* **53** 827 (1980)
97. K Nomiya, M Miwa, Y Sugaya *Polyhedron* **3** 381 (1984)
98. M A Schwegler, H van Bekkum *Bull. Soc. Chim. Belg.* **99** 113 (1990)
99. O Mitsuo, Y Fukuoka, US P. 4 528 409
100. K Matsuo, K Urabe, Y Izumi *Chem. Lett.* 1315 (1981)
101. W C Hsin, C C Lai, M H Chou, Y T Chen, C T Su *Shih Yu (Taipei)* **24** 193 (1988); *Chem. Abstr.* **113** 134 556 (1990)
102. S M Kulikov, S Ts Khankhasaeva, I V Kozhevnikov, in *Tezisy Dokladov II Vsesoyuznoi Konferentsii "Kataliz i Kataliticheskie Protsessy Khim. Farm. Proizvodstv"* (Abstracts of Reports at the IInd All Union Conference on "Catalysis and Catalytic Processes in the Manufacture of Chemopharmaceuticals") (Moscow, 1989) Part 1, p. 119
103. S A Elgazin, V K Ivanov, A P Tyuvanova, USSR P. 455 943; *Byull. Izobret.* **1** (1975)
104. I L Parbuzina, V A Trofimov *Khim.-Farm. Zh.* 7 36 (1975)
105. K Taniguti, Jpn. P. 60-215 643; *Ref. Zh. Khim.* 22N101 (1986)
106. M A Schwegler, H van Bekkum, N A de Munk *Appl. Catal.* **74** 191 (1991)
107. R Kiromura, S Kitazawa, Y Takata, T Sakakibara, US P. 4 874 852
108. M N Timofeeva, V S Grosheva, B I Demchenko, I V Kozhevnikov *React. Kinet. Catal. Lett.* **45** 215 (1991)
109. J Fried, J A Edwards *Organic Reactions in Steroid Chemistry* Vol. 2 (New York: Van Nostrand–Reinhold, 1972)
110. K Nomiya, Y Sugaya, S Sasao, M Miwa *Bull. Chem. Soc. Jpn.* **53** 2089 (1980)
111. K Nomiya, H Saijoh, M Miwa *Bull. Chem. Soc. Jpn.* **53** 3719 (1980)
112. K Nomiya, S Sasao, M Miwa *Chem. Lett.* 1075 (1980)
113. I V Kozhevnikov, V M Mastikhin, K I Matveev, G N Kirichenko, Yu V Churkin, V I Glazunova *React. Kinet. Catal. Lett.* **3** 291 (1977)
114. J F Knifton, J R Sanderson, US P. 4 898 995 (1990)
115. J F Knifton, US P. 4 898 987 (1990)
116. M Tanaka, K Mizuno, Jpn. P. 6 0-61 546; *Ref. Zh. Khim.* 6N120 (1986)
117. K Arai, Y Ogiwara *Macromol. Chem., Rapid Commun.* **4** 181 (1983); *Chem. Abstr.* **99** 38736 (1983)
118. K I Matveev *Kinet. Katal.* **18** 862 (1977)
119. K I Matveev, I V Kozhevnikov *Kinet. Katal.* **21** 1189 (1980)
120. I V Kozhevnikov, K I Matveev *Usp. Khim.* **47** 1231 (1978) [*Russ. Chem. Rev.* **47** 649 (1978)]
121. K Urabe, F Kimura, Y Izumi, in *Proceedings of VII International Congress on Catalysis, Tokyo, 1980* p. 1478
122. H Ogawa, H Fujiwara, K Taya, S Teratani *Bull. Chem. Soc. Jpn.* **57** 1908 (1984)
123. T A Gorodetskaya, I V Kozhevnikov, K I Matveev *React. Kinet. Catal. Lett.* **16** 17 (1981)
124. T A Gorodetskaya, I V Kozhevnikov, K I Matveev, USSR P. 983 058; *Byull. Izobret.* **47** (1982)
125. Yu V Geletii, A E Shilov *Kinet. Katal.* **24** 486 (1983)
126. L N Arzamaskova, A V Romanenko, Yu I Ermakov *Kinet. Katal.* **21** 1068 (1980)
127. T A Gorodetskaya, I V Kozhevnikov, K I Matveev *Kinet. Katal.* **23** 992 (1982)
128. E V Gusevskaya, Candidate's Thesis, Institute of Catalysis, Siberian Division of the Academy of Sciences of the USSR, Novosibirsk, 1980
129. Y Izumi, Y Tanaka, K Urabe *Chem. Lett.* 679 (1982)
130. K Urabe, Y Tanaka, Y Izumi *Chem. Lett.* 1595 (1985)
131. Z Ainbinder, G W Parshall, US P. 4 386 217; *Chem. Abstr.* **99** 12 1 789 (1983)
132. A R Siedle, C G Markell, P A Lyon, K O Hodson, A L Roe *Inorg. Chem.* **26** 219 (1987)
133. Y Izumi, Y Satoh, H Kondoh, K Urabe *J. Mol. Catal.* **72** 37 (1992)
134. I V Kozhevnikov, O A Kholdeeva *Izv. Akad. Nauk SSSR, Ser. Khim.* 2663 (1983)
135. T A Gorodetskaya, I V Kozhevnikov, K I Matveev, V N Sidel'nikov, R I Maksimovskaya *Izv. Akad. Nauk SSSR, Ser. Khim.* 1010 (1984)
136. O A Kholdeeva, A V Golovin, I V Kozhevnikov *React. Kinet. Catal. Lett.* **46** 107 (1992)
137. O A Kholdeeva, A V Golovin, R I Maksimovskaya, I V Kozhevnikov *J. Mol. Catal.* **75** 235 (1992)
138. I V Kozhevnikov, O A Kholdeeva *Izv. Akad. Nauk SSSR, Ser. Khim.* 528 (1987)
139. T A Gorodetskaya, I V Kozhevnikov, K I Matveev, USSR P. 1 121 255; *Byull. Izobret.* **40** (1984)
140. V M Berezovskii *Khimiya Vitaminov* (The Chemistry of the Vitamins) (Moscow: Pishchevaya Prom., 1973)
141. R Neumann, I Assael *J. Chem. Soc., Chem. Commun.* 1285 (1988)
142. G U Mennenga, A I Rudenkov, K I Matveev, I V Kozhevnikov *React. Kinet. Catal. Lett.* **5** 401 (1976)
143. A I Rudenkov, G U Mennenga, L N Rachkovskaya, K I Matveev, I V Kozhevnikov *Kinet. Katal.* **18** 915 (1977)
144. V E Tarabanko, I V Kozhevnikov, K I Matveev *React. Kinet. Catal. Lett.* **8** 77 (1978)
145. I V Kozhevnikov *Usp. Khim.* **52** 244 (1983) [*Russ. Chem. Rev.* **52** 138 (1983)]
146. G W Parshall *Homogeneous Catalysis* (New York: Wiley–Interscience, 1980)
147. T A Gorodetskaya, I V Kozhevnikov, K I Matveev, USSR P. 1 155 580; *Byull. Izobret.* **18** (1985)
148. G S Chernikova, N G Baranova, U M Azizov, I B Afanas'ev *Khim.-Farm. Zh.* 1244 (1988)
149. D E Katsoulis, M T Pope *J. Chem. Soc., Dalton Trans.* 1483 (1989)
150. A P Krysin, T F Titova, K I Matveev, V F Odyakov, E G Zhizhina, B M Khlebnikov, G A Valeulina, A I Kishkan', in *Tezisy Dokladov Vsesoyuznoi Konferentsii po Khimii Khinonov i Khinoidnykh Soedinenii. Krasnoyarsk* (Abstracts of Reports at the All-Union Conference on the Chemistry of Quinones and Quinonoid Compounds. Krasnoyarsk) (Novosibirsk, 1991) p. 140
151. L I Kuznetsova, R I Maksimovskaya, M A Fedotov *Izv. Akad. Nauk SSSR, Ser. Khim.* 537 (1985)
152. N I Kuznetsova, L G Detusheva, L I Kuznetsova, M A Fedotov, V A Likholobov *Kinet. Katal.* **33** 516 (1992)
153. C Venturello, R D'Aloisio, J C J Bart, M Ricci *J. Mol. Catal.* **32** 107 (1985)
154. H Furukawa, T Nakamura, H Inagaki, E Nishikawa, C Imai, M Misono *Chem. Lett.* 877 (1988)
155. C Venturello, E Alneri, M Ricci *J. Org. Chem.* **48** 3831 (1983)
156. M Schwegler, M Floor, H van Bekkum *Tetrahedron Lett.* **29** 823 (1988)

157. Y Ishii, K Yamawaki, T Yoshida, M Ogawa *J. Org. Chem.* **53** 5589 (1988)
158. C Venturello, M Gambaro *Synthesis* 295 (1989)
159. G Amato, A Arcoria, F P Ballisteri, G A Tomaselli, O Bortolini, V Conte, F Di Furia, G Modena, G Valle *J. Mol. Catal.* **37** 165 (1986)
160. L J Csanyi, K Jaky *J. Catal.* **127** 42 (1991)
161. C Aubry, G Chottard, N Platzer, J-M Bregeault, R Thouvenot, F Chauveau, C Huet, H Ledon *Inorg. Chem.* **30** 4409 (1991)
162. X Jian, A S Hay *J. Polym. Sci.* **28** 285 (1990)
163. Y Ishii, Y Yamawaki, T Ura, H Yamada, T Yoshida, M Ogawa *J. Org. Chem.* **53** 3587 (1988)
164. T Oguchi, Y Sakata, N Takeuchi, K Kaneda, Y Ishii, M Ogawa *Chem. Lett.* 2053 (1989)
165. F P Ballistreri, S Failla, E Spina, G A Tomaselli *J. Org. Chem.* **54** 947 (1989)
166. S Sakaue, Y Sakata, Y Nishiyama, Y Ishii *J. Org. Chem.* **54** 289 (1992)
167. V V Berentsveig, T V Dovganyuk, E A Karakhanov *Kinet. Katal.* **32** 623 (1991)
168. M Shimizu, H Orita, T Hayakawa, T Takehira *Tetrahedron Lett.* **30** 471 (1989)
169. S Ito, K Aihara, M Matsumoto *Tetrahedron Lett.* **24** 5249 (1983)
170. O A Kholdeeva, I V Kozhevnikov *Izv. Akad. Nauk SSSR, Ser. Khim.* 2716 (1990)
171. L A Petrov, N P Lobanova, L Volkov, G S Zakharova, I P Kolenko, L Yu Buldakova *Izv. Akad. Nauk SSSR, Ser. Khim.* 1967 (1989)
172. D Attanasio, D Orru, L Suber *J. Mol. Catal.* **57** 21 (1989)
173. S M Kulikov, I V Kozhevnikov *Kinet. Katal.* **24** 42 (1983)
174. C L Hill, R B Brown *J. Am. Chem. Soc.* **108** 536 (1986)
175. M Faraj, C L Hill *J. Chem. Soc., Chem. Commun.* 1487 (1987)
176. R Neumann, C Abu-Gnim *J. Am. Chem. Soc.* **112** 6025 (1990)
177. G F Chernenko, M A Golikova, T V Romanchenko, E N Shmidt, K I Matveev, V A Pentegova *Izv. Sibir. Otd. Akad. Nauk SSSR, Khim. Nauki* **5** 29 (1989)

Russian Chemical Reviews **62** (5) 493 – 508 (1993)
© 1993 Russian Academy of Sciences and Turpion Ltd

UDC 541.15

Radiation-induced inactivation of proteolytic enzymes

M A Orlova

Contents

I. Introduction	493
II. Irradiation of proteases in the solid and immobilised states	494
III. The effect of ionising radiation on aqueous solutions of proteolytic enzymes	495
IV. Application of the method of radiation-induced inactivation of proteolytic enzymes	506

Abstract. Data on the mechanism of the inactivation of proteases under various conditions and the possible applications of these processes are surveyed. Serine, sulfhydryl, acid, and metal-containing proteases are considered. Attention is concentrated on the conformational changes in radiolytic processes: their dependence on the pH of the medium and the correlations with the change in the aminoacid composition of the enzymes. The bibliography includes 90 references.

I. Introduction

Ionising radiation occupies a special place in the series of influences on biological objects. This is associated, firstly, with the fact that there exists a natural radioactive background stimulating changes in the processes occurring on Earth. Secondly, the technological use of ionising radiation and nuclear processes has led to the possibility of the directed liberation of an enormous amount of energy and contamination of the ecosystem with the subsequent increase in the natural radioactive background and irradiation of the population with small doses; expressed quantitatively, this corresponds to an appreciable increase in the natural total annual irradiation dose received by the population, which up to 1986 was about 3×10^6 Gy person^{-1}.[1] It is evidently important to study such influences on the human organism as a whole and on its individual systems in order to discover the adaptive and protective mechanisms. The difference between ionising radiation and other physicochemical influences consists in the reduced wavelength (< 100 nm) and higher energy. The ionisation region begins with an energy in excess of 5 eV. The interaction of ionising radiation with matter, including biochemical objects, has been described in numerous monographs.[2-4] Without going into the details of the theoretical aspects of this process, we shall mention here only that the study of the indirect influence of ionising radiation through the radicals formed as a result of the radiolysis of the medium (in particular water) is more important and informative for biochemistry. The principal water radiolysis products are as follows:[5] H, OH, e_{aq}^-, O^{2-}, HO_2, H_2O_2. The radiation-chemical yield G (the amount of product formed per 100 eV of absorbed energy) depends on the presence of impurities (radical donors and acceptors), the pH of the solution, and other factors.[6]

The interaction of a biomolecule with these products leads to a change and degradation of structures, in particular those ensuring the functioning of the organism. The mechanisms of such processes have been described in another review for the simplest biomolecules (peptides, aminoacids, and proteins).[7]

The imbalance in the processes involving the activation and inactivation of enzyme systems, which in the case of low and chronic irradiation doses may not be manifested for a time but accelerates nevertheless the ageing of the systems of the organism, may be regarded as one of the ways in which the vital activity of an organism is disturbed. In view of this, there has been a growth of interest at the present time in the study of phenomena determining the relationship between the functioning of separate systems and combined influences, which presuppose the occurrence of synergism.[8] The necessity for such studies is associated with the sharp impairment of radioecology against the background of a disastrous ecological situation. The problem of discovering the consequences of the influence of small radiation doses as well as chemical reagents (radiomodifiers) on the results of radiolytic processes requires the creation of predictive models. Quite a large number have now been proposed — both purely biological and biochemical, including protease models.[9]

The development of radiotherapy is also closely related to problems of radiobiology and damage to individual portions of cells and microstructures of the organism.[10] This is partly a consequence of the use of new emitters (for example, neutron emitters[11,12] or emitters of beams of heavy ions[13,14]), which requires additional studies in the field of the relative biological effects of this influence on the principal components of the organism and different cells.

It has become evident in recent years that proteases play a decisive role in the processing of protein.[15] Many facts indicate that proteolytic enzymes perform the function of biological control in the organism, influencing objects important for life. A whole series of key metabolic enzymes are controlled directly by proteases. The mechanisms of the regulation of their activity can operate via the activation of zymogens, the inhibitor–protease balance, and the location of the protease with the substrate. It is therefore not surprising that, in the early stages of radiation and thermal lesions, changes were observed in proteolytic activity,[16] this finding being attributed to the pathology of the kallikrein–kinin system.

M A Orlova Department of Radiochemistry, Faculty of Chemistry, Lomonosov Moscow State University, Leninskie Gory, 119899 Moscow. Fax (7-095) 939 01 26; Tel. (7-095) 939 31 86

Received 4th February 1993
Uspekhi Khimii **62** (5) 529 – 544; translated by A K Grzybowski

The aim of the present review is a comprehensive examination of the mechanism of the radiolysis of proteases and the possible use of this process in medicine and bioengineering.

II. Irradiation of proteases in the solid and immobilised states

Irradiation of enzymes in the solid state constitutes the first stage in the study of the mechanism of their radiolysis, since it makes it possible to investigate the consequences of the direct action of radiation and not of the secondary products of the radiolysis of the medium. This also permits in many instances the determination of the relative molecular masses of both the individual enzymes and of complex biological formations. Studies on these lines, initiated in the 1950s,[17] have continued to this day as a result of a new assessment of the possibilities of the radiation method for the determination of relative molecular masses[18,19] and new computational methods.[20,21]

It is believed that, on irradiation of biochemical objects in the dry state, the site acted upon by the radiation is localised at the point of incidence, in contrast to solutions where the effective volume increases as a result of the diffusion of the water radiolysis products. Localisation is partly observed also on irradiation of frozen solutions,[22] although on subsequent heating to room temperature secondary reactions do occur. In all cases, the target theory is applicable[23] and the main quantitative characteristic of the process is the effect–dose relation, which is exponential for proteases. On the other hand, the deviations from the exponential function which are encountered permit inferences about the process mechanism, which may be complicated as a result of energy transfer in the biosystem.

On irradiation of an enzyme system, the energy transfer to the most radiosensitive component of the molecule can greatly increase the effective volume,[24] increasing it to the size of the entire biomolecule and this affects also the relative molecular masses determined. Since the inactivation of the system changes as a rule on raising the temperature, one should introduce a correction to the calculations of the molecular mass. This has been demonstrated.[25,26] The introduction of additives, i.e. irradiation of mixtures containing several components, also changes the degree of inactivation of the enzyme itself. For example, on irradiation of a mixture with glutathione[27] or another radioprotector, a decrease in the degree of inactivation of the enzyme is observed.

Theoretical problems concerning the determination of the sizes of complex equilibrium enzyme systems comprising several identical components[19] or identical functional units[20] have been examined.[19,20] In both cases, simple exponential effect–dose relations and more complex convex-concave curves may be observed, which depends on the oligomer–monomer equilibrium:

$$R + E \underset{}{\overset{K_d}{\rightleftharpoons}} RE ,$$

where R is the regulator unit, E the catalytic unit, and K_d the equilibrium dissociation constant.[9]

Depending on the size and concentrations of the components, the equilibrium constant, the relative activities of the free enzyme and the enzyme complex, and also the distribution of the components between the free and bound forms, the apparent size of the target and hence the relative molecular masses obtained also change during irradiation.

Analysis with the aid of the target theory likewise makes it possible to obtain an idea about the structural organisation of complex systems, which has been demonstrated in relation to a calmodulin-dependent phosphodiesterase[28] and the components of the adenylate cyclase system in erythrocytes.[29] The presence and the influence of the activator or inhibitor can also be determined from the form of the above relation.[20] In many instances it has been suggested that the role of the transfer of the energy of the oligomeric subunits be likewise estimated in this way when the dissociation of the oligomeric complex can be modelled.[20,28,30,31]

Examination of the form of the effect–dose relations and the application of the target theory on irradiation of a pure enzyme and enzyme complexes with different degrees of interaction of their components permit not only the development of a theoretical analysis but also the determination of the influence of the parameters on the cell populations[32] and also an understanding of the mechanism of the inactivation of a particular enzyme, which is itself a complex structural reacting unit.[33] The increase in the popularity of the method of radiation-induced inactivation for the determination of the dimensions of the systems is due to its simplicity, applicability to complex objects, and the possibility of using only partly purified preparations.

There are literature data on the inactivation of dry preparations of proteases: trypsin,[23,34–36] pepsin,[23] chymotrypsin, papain, subtilisin, and carboxypeptidase.[34,35] Two interrelated processes arise on irradiation: radical formation and inactivation. The radiation-chemical yield of radicals is $\sim 1-7$. γ-Irradiation yields information under these conditions about the distribution of carbon-based radicals (for example, in chymotrypsin at 195 K), preceding the secondary radicals observed at 295 K. The carbon-based radicals can be divided into two groups: those formed at a temperature below 195 K and independent of the aminoacid sequence and those formed above 195 K and depending on the conformation of a specific native enzyme.[37] The dose dependences are exponential and the inactivation reaction is first order for γ- and X-irradiation.

In order to investigate the damage caused in molecules by ionising radiation, it is convenient to employ subsequent tritiation, which has been used[38] to determine the changes which had occurred in α-chymotrypsin after γ-irradiation. On the basis of the aminoacid analysis of the tritiated specimens, the authors reached a conclusion about the conformational transformations, which entailed a change in the area of the accessible surface of the molecule and a greater importance of the hydrophobic residues.

In a number of studies, dry enzymes were irradiated in order to elucidate their radiation stabilities as such and to compare them with stabilities in relation to other methods of treatment. Figure 1 presents results characterising the loss of activity by certain dry proteases on irradiation.

It is noteworthy that the observed degree of inactivation of proteases may depend on the method of its determination, which hinders comparison of the results of different studies. In particular, this has been observed for chymotrypsin irradiated in a dry state.[35,36]

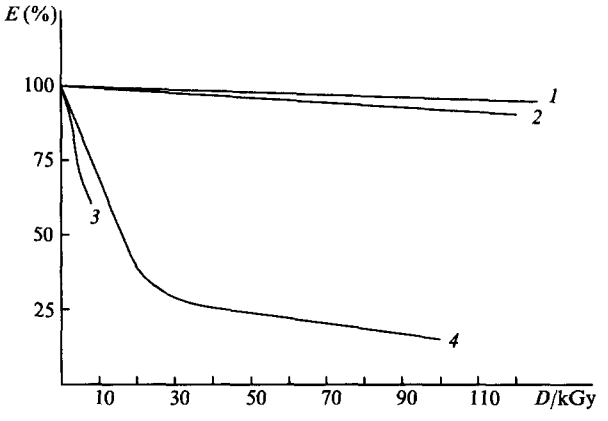


Figure 1. Radiation-induced inactivation of enzymes in the crystalline state: (*1*) α-chymotrypsin (X-rays);[39] (*2*) trypsin (γ-rays);[36] (*3*) glucosidase + catalase (X-rays);[39] (*4*) subtilisin-72 (X-rays).[39]

The stability of enzymes increases following their immobilisation and for this reason immobilised enzymes are actively employed in the national economy, especially in medicine. There exist three aspects of the study of the action of ionising radiation on immobilised enzymes. The first involves the use of ionising radiation for immobilisation itself. There exists an extensive literature on this question, which is not considered in the present review.

The second aspect involves the development of materials for the production of an image (for use in roentgenoscopy, autoradiography, and dosimetry). Thus α-chymotrypsin and subtilisin-72 have been bound[39] to various diazides and the vinylpyrrolidinone–acrolein copolymer on chromatographic paper in order to obtain a latent image and hence to detect X-radiation. The authors tested several versions of the method: solutions of the enzyme (2×10^{-3} M α-chymotrypsin, 1.1×10^{-3} M subtilisin) were deposited on a support and irradiated with X-rays at a dose rate of 200 rad s^{-1}; the enzyme and the diazide were deposited on a support and irradiated with X-rays transformed by a special screen into UV radiation at a wavelength of 365 nm; chromatographic paper was subjected to a preliminary treatment with *p*-azidobenzaldehyde diethyl acetal, the vinylpyrrolidinone–acrolein copolymer (VPA), or VPA modified by azide groups with subsequent exposure together with the enzyme. The subsequent development of the latent image by a suitable dye reveals a difference between the irradiated and nonirradiated sections. Exposure to X-rays of a carrier impregnated with an enzyme solution leads to the immobilisation of 0.05% of α-chymotrypsin and 0.01% of subtilisin.

The use of proteases for the preparation of dosimetric materials has been described.[40] Gelatin films containing small amounts of enzymes (chymotrypsin, papain, trypsin, and subtilisin) were exposed to the low-energy tritium β-radiation and development was carried out after irradiation in solutions of these enzymes. In both cases, irradiation hardly affected the activity of the enzyme but damaged the structure of gelatin, altering the degree of and conditions for its digestion by the enzyme. When the films are dyed, a half-tone image is formed and this method as well as the previous one can therefore be used to detect ionising radiation.

The third aspect of the studies involves an attempt to model the mechanism of the action of ionising radiation on immobilised systems via the investigation of the radicals generated. Such studies have been carried out for trypsin immobilised on dialdehyde-cellulose (DAC) by comparison with pure trypsin.[41,42] The range of γ-irradiation doses was 0.05–10 Mrad (0.5–100 kGy). Comparison of the EPR spectra of the immobilised and native trypsin as well as the support suggested that the increase in the stability of the immobilised trypsin is associated with the recombination of the trypsin radicals with the DAC radicals and with their migration to weakened bonds in the DAC. The activity of the immobilised trypsin does not then change, while native trypsin loses 25% of its activity for a dose of 10 Mrad (100 kGy).[42] Such increase in stability makes it possible to employ immobilised proteases in enzyme therapy using γ-sterilisation,[43] since the activity of γ-irradiated immobilised trypsin does not change during prolonged storage with a simultaneous decrease in the number of radicals. Trypsin immobilised on DAC can be stored under severe conditions for a long time. Comparison of the behaviour of the enzymes on γ-irradiation of their aqueous solutions and the enzymes immobilised on nylon fibres showed[44] that not all enzymes exhibit an appreciable increase in their resistance to radiation in the immobilised state; however, this does not apply to proteases.

III. The effect of ionising radiation on aqueous solutions of proteolytic enzymes

1. Serine proteases

The radiolysis of serine proteases in solution has been studied most fully. Questions associated with the mechanism of the radiation-induced damage to trypsin and chymotrypsin (the enzymes of the pancrease) and certain subtilisins (the enzymes from microorganisms produced by various strains of *B. subtilis*) have been examined in detail in the literature. The blood enzymes (thrombin and plasmin) have been much less investigated and as regards certain enzymes no information is encountered in the literature.

The main feature of the radiolytic damage to serine proteases is a fairly high stability of the active centres, containing a serine residue, in relation to the action of ionising radiation, whilst the conformational stability of the biomolecule is most vulnerable. It has been shown in a number of studies[45,46] that the main contribution to the inactivation of serine proteases comes from OH radicals obtained on radiolysis of water. This has been readily confirmed by irradiating chymotrypsin in N_2O, where the number of OH radicals increases as a result of the reaction

$$e_{aq}^- + N_2O + H_2O \rightarrow OH + OH^- + N_2 . \quad (1)$$

In this case, the corresponding increase in the radiation-chemical yield of the inactivation is observed.

The coefficients of susceptibility to damage (effectiveness of inactivation, i.e. the probability that the attack by a given active influence inactivates the enzyme) of chymotrypsin by various radicals, the number of which was regulated by controlling the irradiation conditions (Tables 1 and 2), have been published.[2,3] The rate constants for reactions with certain water radiolysis products are also known (Table 3). It has been shown that the changes induced by the OH and H radical species involve mainly tryptophan residues in chymotrypsin, while approximately 15%

Table 1. Radiation-chemical yields in radical formation (G_R) and inactivation (G_{in}) reactions in aqueous solutions of chymotrypsin and papain on γ-irradiation under different conditions.

Medium	Radicals	G_{in}	Effectiveness of inactivation, f	G_R	f/G_R
		Chymotrypsin[45]			
Air	OH	0.265	0.266	2.8	0.095
N_2O	2 OH, H	0.83	0.30	0.7	0.43
N_2O + *tert*-BuOH	H	0.091	0.091	0.7	0.13
Ar	OH, H	0.61	0.044	2.8 2.6	0.17
Ar + *tert*-BuOH	H	0.234	0.143	2.6	0.055
		Papain[47,48]			
N_2O	OH, H	–	–	5.9	0.43

Table 2. Effectiveness of the inactivation of enzymes by the water radiolysis products.

Reagent	Trypsin[75]	Chymotrypsin[45]
H	0.1	0.13
OH	0.05	0.137
e_{aq}^-	0.09	0.055
H_2O_2	0.04	–
HO_2	0.04	–
O_2	0.03	–

Table 3. The rate constants for the reactions of proteases with the water radiolysis products (γ-irradiation).

Substance	10^{-10} k/litre mol^{-1} s^{-1}			Ref.
	e^-_{aq}	OH	O_2^-	
Proteins	5	1–	$6<10^{-7}$	23
Chymotrypsin	–	3.7±0.4	–	49
Papain	4.1	4.7	–	48

of e^-_{aq} react at the S–S bonds. The next stage of the study was therefore the determination of the relationship between the damage to the tryptophan residues and the conformational stability.

A detailed analysis has been carried out of the mechanism of the inactivation of chymotrypsin.[49-51] A change in the accessible surface of the globule was detected by the $^1H-^3H$ exchange method.[46,50] The rate of exchange increased by 16% compared with the nonirradiated enzyme with increase in the irradiation dose from 30 to 50 Gy. The use of fluorescence, viscometric, and microcalorimetric methods made it possible to determine the radiation-chemical yield of the uncoiled molecules (G_{unc}) and to find the correlation between G_{unc} and the radiation-chemical yield of the damaged tryptophan residues $-G(-Trp)$[49] (Table 4). Data on the binding of proflavin[53] demonstrated the presence of local steric changes around the binding centres. Conformational changes were initially detected only after an irradiation dose of about 2 kGy,[46,49] but later they were discovered also at lower doses (< 1 kGy).[50,51] The change in the fluorescence quantum yield in irradiated chymotrypsin solutions, characterising the number of tryptophan residues, showed[52] that at pH 3 their decrease is correlated with the decrease in catalytic activity. At pH 7.8 (the pH optimum of the esterase activity), an increase in the number of accessible tryptophan residues was observed initially, decreasing following an increase in their dose. These data make it possible to infer the changes in the degree of uncoiling of the chymotrypsin globule as a function of pH. In particular, it appears that at low pH the area of the accessible surface of the globule is greater. The maximum change in this quantity was observed at pH 2.0, whereupon the radiation-chemical yield of the inactivation reaction increases.[53] For doses in excess of 0.6 kGy, the conformational changes became insignificant but the aminoacid composition of the enzyme changed sharply.[51]

Damage to the disulfide bridges occurred at higher irradiation doses and no longer played a significant role in the breakdown of catalytic activity. Thus, for a dose of 0.5 kGy, 5.5 S–S bonds were detected in chymotrypsin,[50] while for a dose of 0.8 kGy the number of such bonds was 4. It was found that the presence of S–S bonds is important for reducing the conformational changes on irradiation. This was demonstrated by comparing the γ-inactivation of chymotrypsin and subtilisin,[52] where the same degree of inactivation in subtilisin entails the decomposition of a smaller number of important aminoacid residues. This conclusion follows from the comparison of the ratios $G(-Trp)/G_{in}$. This quantity is 4.3 times smaller for subtilisin than for chymotrypsin, while G_{in} (subtilisin) is smaller than G_{in} (chymotrypsin) by a factor of 1.4 (Table 4). A similar difference has been observed also between the overall quantities $G(Tyr+Trp)/G_{in}$. The authors see an explanation of this effect in the presence of five S–S bonds in chymotrypsin (subtilisin is a single-stranded enzyme and has no disulfide bridges), which, as it were, 'maintain' the structure of the enzyme under the conditions where the tryptophan residues are damaged.

The change in the aminoacid composition of chymotrypsin for different irradiation doses has been investigated in a number of studies.[50-52] $5\times10^{-6}-10^{-5}$ M solutions at pH 3 (HCl)[50] and 7.8 (tris-HCl buffer)[52] were used. After irradiation with a dose of 0.5 kGy, a decrease in the number of tyrosine residues and, after a dose of 1.2 kGy also, in phenylalanine residues was observed together with the damage to the tryptophan residues.[50] For a dose of about 1.6 kGy, almost all the aminoacid residues are involved. The aminoacid compositions[52] of the irradiated solutions at pH 3 and 7.8 were compared. A common feature of these compositions is a decrease in the number of tyrosine, cysteine, phenylalanine, and lysine residues, but the doses required for this are smaller at pH 3. Thus the decomposition of one tyrosine residue requires about 0.025 kGy at pH 3 and approximately 0.6 kGy at pH 7.8. A greater radiation yield G_{decomp} for chymotrypsin at pH 3 compared with pH 6.9 has been observed.[49] Comparison of data from different studies shows that, by virtue of their more uncoiled conformation, the damage to the aminoacid residues on irradiation with high doses at pH 3 is stochastic and evidently the change in conformation is more important for catalytic activity than the change in the aminoacid composition (except for the aromatic aminoacid residues).

A correlation between the decrease in catalytic activity and the decomposition of tyrosine residues has been observed for irradiated subtilisin-BPN′ and subtilisin-72,[52,54] especially at pH 8.5 (the pH optimum of the activity of the enzyme).[52] At lower pH (for example, 5.5), this correlation is less marked, since there is a dependence on the decomposition of tryptophan residues. The degradation of the histidine residues forming part of the active centre of subtilisin-72 is observed at doses in excess of 5 kGy, whereupon the catalytic activity is almost completely lost. Histidine is more important for the radiation stability of subtilisin-BPN′. After γ-irradiation with a dose of 1.1 kGy, subtilisin-BPN′ loses two tyrosine residues and one tryptophan, one methionine, and one histidine residues[53,54] (Figure 2). The reaction with diisopropyl phosphorofluoridate shows that under these conditions 85% of the active centres are retained. For an irradiation dose of 2.4 kGy, changes appear in the leucine, proline, phenylalanine, serine, and alanine residues. The

Table 4. Comparison of the radiation-chemical yields in the uncoiling of enzyme molecules (G_{unc}) and inactivation (G_{in}) with the radiation-chemical yield in the decomposition of aminoacid residues.

Enzyme	Irradiation conditions	G_{unc}	G_{in}	$G(-Trp)$	$G(-Tyr)$	$G(-Trp)/G_{unc}$	$G(-Tyr)/G_{unc}$	Ref.
Trypsin	HCl, pH 3.0	0.37	–	0.9	–	2.4	–	49
Chymotrypsin	HCl, pH 3.0	0.43	–	1.2	–	2.8	–	49
Trypsin	H_2O, pH 6.6	0.32	–	0.7	–	2.2	–	49
Chymotrypsin	H_2O, pH 6.6	0.31	–	1.1	–	3.5	–	49
Trypsin	Glycine buffer, pH 6.9	0.26	–	0.6	–	2.3	–	49
Chymotrypsin	Glycine buffer, pH 6.9	0.18	–	0.6	–	2.5	–	49
Trypsin	Phosphate buffer	0.36	–	0.9	–	2.5	–	49
Chymotrypsin	Phosphate buffer	0.30	–	0.9	–	3.0	–	49
Subtilisin-72	0.1 M NaCl, pH 5.6	–	0.23	0.19	0.35	0.82	1.5	52
	0.1 M NaCl + NaOH, pH 8.5	–	0.29	0.20	0.55	0.69	1.9	52
	Acetate buffer, pH 5.0	–	0.19	0.22	0.73	1.2	3.9	52

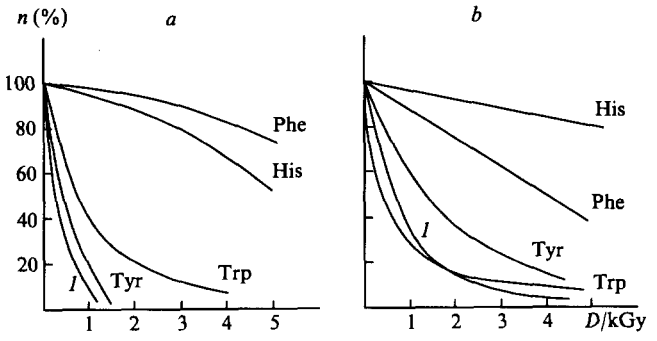


Figure 2. Variation of the number of aminoacid residues (n) in subtilisin-72 with the irradiation dose: (a) pH 8.5, 0.1 M NaCl + NaOH; (b) pH 5.0, 5×10^{-3} M acetate buffer; (1) variation of catalytic activity.

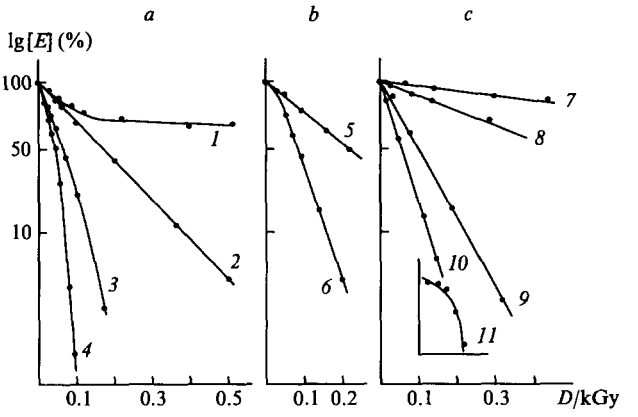


Figure 3. Dependence of the change in the catalytic activity of enzymes on the absorbed γ-radiation dose:[33] (a) α-chymotrypsin; (b) trypsin; (c) subtilisin-72; concentration (M): (1) 10^{-4}; (2) 7.5×10^{-6}; (3) 10^{-6}; (4) 10^{-7}; (5) 10^{-5}; (6) 10^{-6}; (7) 5×10^{-5}; (8) 5×10^{-6}; (9) 9×10^{-7}; (10) 3×10^{-7}; (11) 8×10^{-8}.

oxidation of methionine does not then lead to the inactivation of subtilisin-BPN',[54] but is significant for subtilisin-Carlsberg,[55] which differs, according to the data of Alden et al.,[56] from subtilisin-BPN' by the presence of a series of repeating segments in the polypeptide chain. For a dose of 0.55 kGy, the number of degraded tyrosine residues increases in subtilisin-72 compared with subtilisin-BPN', but the histidine residue is not degraded.[52] For a dose of 1.1 kGy, the difference between the numbers of degraded tyrosine residues increases still further. These data led to the conclusion that the tyrosine residues are more accessible in subtilisin-72.

Application of the electrophoretic method to irradiated subtilisin-BPN' demonstrated[53] the presence of a larger electric charge compared with the native enzyme, accompanied by the absence of changes in catalytic activity. This agrees with the earlier hypothesis that small irradiation doses lead to the formation of noninactivated molecules, which, however, differ conformationally from the native ones.

The appearance of active but partly damaged molecules has been confirmed by a change, even for low irradiation doses, in the kinetic parameters — the Michaelis constant (K_M) and the maximum rate of the catalytic reaction (V_{max}). Irradiation of dilute solutions increases K_M and diminishes V_{max} both in the case of chymotrypsin[57,58] and subtilisin-BPN' (Table 5).[54] Since the main damage to serine proteases caused by low doses is conformational damage associated with the disappearance of tryptophan residues (at least in chymotrypsin) and since in ribonuclease, which contains no tryptophan residues, there are no changes in K_M and V_{max},[59] the modification of the molecules is attributed to changes in the tryptophan residues. Other workers arrived at similar conclusions on the basis of the results of the irradiation of chymotrypsin and chymotrypsinogen.[60] The presence of modified molecules is reflected in the nature of the effect–dose relation, in particular deviations of the exponential function appear and the form of the curve depends on the initial enzyme concentration (Figure 3). A change in the radiation-chemical yield of the inactivation as a function of the initial enzyme concentration [E_0] has been observed[61-64] for trypsin and chymotrypsin (Table 6). This relation was described by the equation $G_{in} \simeq [E]^N$, where N is an integer. However, there is no concentration dependence if the active radicals (in this case OH radicals) react with the dissolved enzyme molecules faster than with one another, so that the decisive factor is the ratio of the number of the dissolved molecules to the number of active radicals. For trypsin, chymotrypsin, and subtilisin-72, the concentration ranges in which the dose dependences follow the exponential law have been determined:[33] $3 \times 10^{-6} - 5 \times 10^{-5}$ M for chymotrypsin, $2 \times 10^{-6} - 10^{-4}$ M for subtilisin-72, and above 10^{-6} M for trypsin. At lower concentrations, a deviation towards increasing inactivation is observed, whilst at higher concentrations ($> 10^{-4}$ M for chymotrypsin) an increase in dose

Table 5. The change in the kinetic parameters of irradiated proteolytic enzymes.

Enzyme	Irradiation conditions	Radiation	Dose/kGy	Substrate	Number of active centres	K_M/M	V_{max}/mol min^{-1} mg^{-1} [c]	Ref.
Subtilisin-72	0.1 M KCl, 30 °C, pH 7.5	γ	–	ATEE [a]	1.00	4.9×10^{-2}	7.6×10^{2}	54
	0.1 M KCl, 30 °C, pH 7.5	γ	0.95	ATEE	0.86	5.6×10^{-2}	7.6×10^{2}	54
	0.1 M KCl, 30 °C, pH 7.5	γ	1.66	ATEE	0.77	6.1×10^{-2}	6.6×10^{2}	54
Subtilisin-BPN'	0.1 M KCl, 30 °C, pH 7.5	γ	–	BTEE [b]	1.00	1.03×10^{-2}	3.46×10^{2}	54
	0.1 M KCl, 30 °C, pH 7.5	γ	1.2	BTEE	0.83	1.01×10^{-2}	2.66×10^{2}	54
	0.1 M KCl, 30 °C, pH 7.5	γ	1.66	BTEE	0.77	1.01×10^{-2}	2.08×10^{2}	54
α-Chymotrypsin	H_2O, 0 °C, pH 5.0, 60 mg ml^{-1}	X	–	ATEE	–	3.5×10^{-3}	100%	57
	H_2O, 0 °C, pH 5.0, 60 mg ml^{-1}	X	0.05	ATEE	–	5.2×10^{-3}	83%	57
	H_2O, 0 °C, pH 5.0, 60 mg ml^{-1}	X	–	ATEE	–	2.8×10^{-3}	100%	57
	H_2O, 0 °C, pH 5.0, 60 mg ml^{-1}	X	0.5	ATEE	–	5.4×10^{-3}	77%	57
	H_2O, 0 °C, pH 5.0, 60 mg ml^{-1}	X	0.75	ATEE	–	6.9×10^{-3}	66%	57

[a] ATEE = ethyl ester of *N*-acetyl-L-tryosine.
[b] BTEE = ethyl ester of *N*-benzoyl-L-tyrosine.
[c] V_{max} for α-chymotrypsin is expressed as a percentage of V_{max} for the nonirradiated enzyme.

Table 6. Dependence of the catalytic activity of serine proteases in aqueous solutions on the irradiation conditions.

Enzyme	Irradiation conditions	t/°C	Radiation	Dose rate/ Gy s^{-1}	[E]/M	Substrate	Dose/ Gy	D_{37}	G_{in}	G_{conf}	Residual enzyme activity (%)	Ref.
Trypsin	3×10^{-3} M H_2SO_4	2	X	0.075	4×10^{-3}	Haemoglobin	25.2	–	–	–	0	64
	3×10^{-3} M H_2SO_4	25	X	0.075	4×10^{-3}	Haemoglobin	25.2	–	–	–	49	64
	3×10^{-3} M H_2SO_4	37	X	0.075	4×10^{-3}	Haemoglobin	25.2	–	–	–	29	64
	5×10^{-3} M HCl, pH 3.0, air	20	X	0.075	2×10^{-4}	Haemoglobin	–	–	1.22 M/1000 r	–	–	63
	5×10^{-3} M HCl, pH 3.0, air	20	X	0.075	10^{-7}	Haemoglobin	–	–	0.057 M/1000 r	–	–	63
	H_2O air	20	X	0.075	10^{-3}	Haemoglobin	100	–	–	–	86	62
	10^{-3} M phosphate buffer, pH 6.1	20	X	0.075	10^{-3}	Haemoglobin	100	–	–	–	83	62
	10^{-2} M phosphate buffer, pH 6.1	20	X	0.075	10^{-3}	Haemoglobin	100	–	–	–	80	62
	10^{-1} M phosphate buffer, pH 6.1	20	X	0.075	10^{-3}	Haemoglobin	100	–	–	–	69	62
	2.5×10^{-3} M acetate buffer, pH 4.1	20	X	0.075	10^{-3}	Haemoglobin	100	–	–	–	50	62
	5×10^{-2} M acetate buffer, pH 4.1	20	X	0.075	10^{-3}	Haemoglobin	100	–	–	–	15	62
	10^{-3} M universal buffer, pH 5.3	20	X	0.075	10^{-3}	Haemoglobin	100	–	–	–	5	62
	5×10^{-3} M universal buffer, pH 5.3	20	X	0.075	10^{-3}	Haemoglobin	100	–	–	–	4	62
	HCl, pH 3.0, air	20	X	0.095	5×10^{-6}	*p*-Nitrophenyl ester of *N*-benzyloxy-carbonyl-L-tyrosine	–	17.5	–	–	–	65
	HCl, pH 3.0, N_2	20	X	0.095	5×10^{-6}	*p*-Nitrophenyl ester of *N*-benzyloxy-carbonyl-L-tyrosine	–	8.8	–	–	–	65
	HCl, pH 3.0, air	20	X	0.095	5×10^{-6}	*p*-Nitrophenyl ester of *N*-benzyloxy-carbonyl-L-leucine	–	8.3	–	–	–	65
	HCl, pH 3.0, air	20	X	0.095	5×10^{-6}	BTEE	–	21.8	–	–	–	65
	HCl, pH 3.0, N_2	20	X	0.095	5×10^{-6}	BTEE	–	8.2	–	–	–	65
	HCl, pH 3.0, air	20	X	0.095	5×10^{-6}	Methyl ester of *p*-toluene-sulfonyl-L-arginine	–	22.2	–	–	–	65
	HCl, pH 3.0, N_2	20	X	0.095	5×10^{-6}	Methyl ester of *p*-toluene-sulfonyl-L-arginine	–	8.3	–	–	–	65
	HCl, pH 3.0, air	20	X	0.095	5×10^{-6}	*p*-Nitroanilide of benzoyl-DL-arginine hydrochloride	–	18.2	–	–	–	65

Trypsin	HCl, pH 3.0, air	20	X	0.095	5×10^{-6}	*p*-Nitroanilide of benzoyl-DL-arginine hydrochloride	–	8.0	–	–	–	65
	HCl, pH 3.0, air	20	X	0.095	5×10^{-6}	β-Naphthylamide of benzoyl-DL-arginine hydrochloride	–	10.3	–	–	–	65
	HCl, pH 3.0, N_2	20	X	0.095	5×10^{-6}	β-Naphthylamide of benzoyl-DL-arginine hydrochloride	–	5.8	–	–	–	65
	HCl, pH 3.0, air	20	X	0.095	5×10^{-6}	Bovine serum albumin	–	13.1	–	–	–	65
	HCl, pH 3.0, N_2	20	γ	0.095	5×10^{-6}	Bovine serum albumin	–	6.0	–	–	–	65
	HCl, pH 3.0, air	20	γ	0.43	2×10^{-5} – $- 4 \times 10^{-4}$	Fluorescence of tryptophan residues	–	–	–	0.37	–	49
	H_2O, pH 6.6, air	20	γ	0.43	2×10^{-5} – $- 4 \times 10^{-4}$	Fluorescence of tryptophan residues	–	–	–	0.32	–	49
	Glycine buffer, pH 6.9, air	20	γ	0.43	2×10^{-5} – $- 4 \times 10^{-4}$	Fluorescence of tryptophan residues	–	–	–	0.26	–	49
	Phosphate buffer, pH 6.9	20	γ	0.43	2×10^{-5} – $- 4 \times 10^{-4}$	Fluorescence of tryptophan residues	–	–	–	0.36	–	49
Chymotrypsin	3×10^{-3} M H_2SO_4, air	20	X	0.075	2.8×10^{-4}	Haemoglobin	25.2	–	0.87 M/1000 r	–	–	61
	3×10^{-3} M H_2SO_4, air	20	X	0.075	6.4×10^{-6}	Haemoglobin	25.2	–	0.5 M/1000 r	–	–	61
	HCl, pH 3.0, air	37	X	17	2×10^{-4}	Casein	–	1.8×10^{4} –		–	–	60
	HCl, pH 3.0, N_2	37	X	17	2×10^{-4}	Casein	–	9.5×10^{3} –		–	–	60
	HCl, pH 3.0, air	20	X, γ	0.1 (P_X) 0.095 (P_γ)	5×10^{-6}	ATEE	–	150	–	–	–	50
	HCl, pH 3.0, air	20	X, γ	0.1 (P_X) 0.095 (P_γ)	5×10^{-6}	BTEE	–	170	–	–	–	50
	HCl, pH 3.0, N_2	20	X, γ	0.1 (P_X) 0.095 (P_γ)	5×10^{-6}	BTEE	–	117	–	–	–	50
	HCl, pH 3.0, air	20	X, γ	0.1 (P_X) 0.095 (P_γ)	5×10^{-6}	Methyl ester of *N*-acetyl-L-tyrosine	–	155	–	–	–	50
	HCl, pH 3.0, air	20	X, γ	0.1 (P_X) 0.095 (P_γ)	5×10^{-6}	Ethyl ester of L-tyrosine	–	136	–	–	–	50

Table 6 (continued)

Enzyme	Irradiation conditions	t/°C	Radiation	Dose rate/ Gy s^{-1}	[E]/M	Substrate	Dose/ Gy	D_{37}	G_{in}	G_{conf}	Residual enzyme activity (%)	Ref.
Chymotrypsin	HCl, pH 3.0, N_2	20	X, γ	0.1 (P_X) 0.095 (P_γ)	5×10^{-6}	Ethyl ester of L-tyrosine	–	99	–	–	–	50
	HCl, pH 3.0, air	20	X, γ	0.1 (P_X) 0.095 (P_γ)	5×10^{-6}	*p*-Nitrophenyl ester of *N*-benzyloxy-carbonyl-L-tyrosine	–	140	–	–	–	50
	HCl, pH 3.0, N_2	20	X, γ	0.1 (P_X) 0.095 (P_γ)	5×10^{-6}	*p*-Nitrophenyl ester of *N*-benzyloxy-carbonyl-L-tyrosine	–	68	–	–	–	50
	HCl, pH 3.0, air	20	X, γ	0.1 (P_X) 0.095 (P_γ)	5×10^{-6}	*p*-Nitrophenyl ester of *N*-benzyloxy-carbonyl-L-leucine	–	171	–	–	–	50
	HCl, pH 3.0, N_2	20	X, γ	0.1 (P_X) 0.095 (P_γ)	5×10^{-6}	*p*-Nitrophenyl ester of *N*-benzyloxy-carbonyl-L-leucine	–	84	–	–	–	50
	HCl, pH 3.0, air	20	X, γ	0.1 (P_X) 0.095 (P_γ)	5×10^{-6}	*p*-Nitrophenyl ester of *N*-benzyloxy-carbonyl-L-tryptophan	–	140	–	–	–	50
	HCl, pH 3.0, N_2	20	X, γ	0.1 (P_X) 0.095 (P_γ)	5×10^{-6}	*p*-Nitrophenyl ester of *N*-benzyloxy-carbonyl-L-tryptophan	–	76	–	–	–	50
	HCl, pH 3.0, air	20	X, γ	0.1 (P_X) 0.095 (P_γ)	5×10^{-6}	Glutaryl-L-phenylalanine β-naphthylamide	–	105	–	–	–	50
	HCl, pH 3.0, N_2	20	X, γ	0.1 (P_X) 0.095 (P_γ)	5×10^{-6}	Glutaryl-L-phenylalanine β-naphthylamide	–	54	–	–	–	50
	HCl, pH 3.0, air	20	X, γ	0.1 (P_X) 0.095 (P_γ)	5×10^{-6}	Glutaryl-L-phenylalanine *p*-nitroanilide	–	147	–	–	–	50
	HCl, pH 3.0, N_2	20	X, γ	0.1 (P_X) 0.095 (P_γ)	5×10^{-6}	Glutaryl-L-phenylalanine *p*-nitroanilide	–	76	–	–	–	50
	10^{-3} M phosphate buffer, pH 7, air	20	γ	0.12	1.6×10^{-6}	ATEE	–	45.9	0.265	–	–	45
	10^{-3} M phosphate buffer, pH 7, argon	20	γ	0.12	1.6×10^{-6}	ATEE	–	20	0.61	–	–	45
	10^{-3} M phosphate buffer, pH 7, N_2O	20	γ	0.12	1.6×10^{-6}	ATEE	–	14.5	0.83	–	–	45
	HCl, pH 3.0, air	20	γ	0.43	2×10^{-5} – 4×10^{-4}	Fluorescence of tryptophan residues	–	–	–	0.43	–	66
	H_2O, pH 6.2, air	20	γ	0.43	2×10^{-5} – 4×10^{-4}	Fluorescence of tryptophan residues	–	–	–	0.31	–	66

Chymotrypsin	Glycine buffer, pH 6.9	20	γ	0.43	2×10^{-5} – -4×10^{-4}	Fluorescence of tryptophan residues	–	–	–	0.18	–	66
	Phosphate buffer, pH 6.9	20	γ	0.43	2×10^{-5} – -4×10^{-4}	Fluorescence of tryptophan residues	–	–	–	0.30	–	66
	Phosphate buffer, pH 6.9	20	X	–	1.6×10^{-5}	Casein	–	40	–	–	–	65
	Phosphate buffer, pH 6.9	20	X	–	8×10^{-5}	Casein	–	50	–	–	–	65
	Phosphate buffer, pH 6.9	20	X	–	1.6×10^{-5}	ATEE	–	20	–	–	–	65
	Phosphate buffer, pH 6.9	20	X	–	8×10^{-5}	ATEE	–	40	–	–	–	65
	tris-HCl buffer, pH 7.8, air	20	γ	0.058	10^{-5}	ATEE	–	–	0.44	–	–	67
	tris-HCl buffer, pH 7.8, air	20	γ, *n*	0.55×10^{-4}	10^{-5}	ATEE	–	–	0.40	–	–	67
Subtilisin-BPN′	H_2O, pH 6, air	2	γ	0.125	0.42×10^{-4}	ATEE	550	–	–	–	76	53
	H_2O, pH 6, air	2	γ	0.125	0.42×10^{-4}	ATEE	550	–	–	–	84	53
	H_2O, pH 6, air	2	γ	0.125	0.42×10^{-4}	ATEE	550	–	–	–	98	53
Subtilisin-72	0.1 M NaCl, pH 5.5, air	20	γ	0.083	10^{-4}	ATEE	–	–	0.17	–	–	68
	5×10^{-3} M acetate buffer, pH 5, air	20	γ	0.083	10^{-4}	ATEE	–	–	0.15	–	–	68
	5×10^{-3} M acetate buffer, pH 5, air	20	γ	0.083	10^{-5}	ATEE	–	–	0.06	–	–	68
	5×10^{-3} M acetate buffer, pH 5, air	20	γ	0.083	5×10^{-6}	ATEE	–	–	0.05	–	–	68
	5×10^{-3} M acetate buffer, pH 5, air	20	γ	0.083	1×10^{-6}	ATEE	–	–	0.01	–	–	68
	0.1 M NaCl, pH 5.5, air	20	γ	0.083	1×10^{-5}	ATEE	–	–	0.12	–	–	68
	0.1 M NaCl, pH 5.5, air	20	γ	0.083	5×10^{-6}	ATEE	–	–	0.10	–	–	68
	0.1 M NaCl, pH 5.5, air	20	γ	0.083	1×10^{-6}	ATEE	–	–	0.09	–	–	68
Carboxy-peptidase A	N_2	20	γ	–	–	Haemoglobin	–	–	0.27	–	–	69
	N_2O	20	γ	–	–	Haemoglobin	–	–	0.44	–	–	69
	O_2	20	γ	–	–	Haemoglobin	–	–	0.26	–	–	69
	N_2O + *tert*-BuOH	20	γ	–	–	Haemoglobin	–	–	0.11	–	–	69

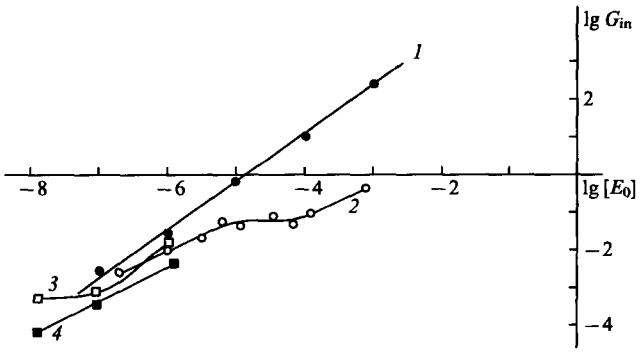


Figure 4. Dependence of the radiation-chemical inactivation yield (G_{in}) on the initial concentrations of chymotrypsin (curves *1* and *2*) and the angiotensin converting enzyme (curves *3* and *4*). For curve *1*, G_{in} was calculated along the initial section of the dose dependence plot and for curve *2* at a dose of 200 Gy; pH: (*1*) and (*2*) 7.8; (*3*) 7.5; (*4*) 9.0.

actually entails a decrease in inactivation compared with the expected value. The simplest calculation of the ratio of the active radicals derived from water and the enzyme molecules for a dose of 20 Gy demonstrated a relation between the observed deviations and the excess of either OH radicals ($< 10^{-6}$ M) or enzyme molecules ($> 10^{-5}$ M). Although the purity of the enzyme and also its possible immobilisation on glass can in fact alter the absolute value of G_{in} under these conditions, they do not affect the nature of the dose dependence. The curve relating G_{in} to the initial enzyme concentration is presented in Figure 4 in terms of logarithmic coordinates. For low doses, it is linear but for a dose of 0.2 kGy there is already a plateau in the chymotrypsin concentration range 5×10^{-6}–6×10^{-4} M. The authors therefore suggest that two inactivation regions, linked to the relation examined above, be distinguished: (1) the number of inactivated molecules is proportional to the initial enzyme concentration (a dose < 20 kGy in the case of chymotrypsin), i.e. a definite fraction of the molecules are inactivated; (2) the number of inactivated molecules ceases to depend on the initial concentration. Very low enzyme concentrations ($< 10^{-7}$ M), at which the excess of radicals is too high, and concentrations above 10^{-3} M, where the direct action of the radiation on the energy transfer process may become important as a result of aggregation, are possible exceptions.

The method used to determine the enzyme activity has a major influence on the value of G_{in} and the form of the effect–dose relation. Lynn[65] pointed out the absence of an exponential dose dependence in the case of trypsin when the catalytic activity was determined with the aid of casein and put forward an explanation based on the methodological characteristics of the determination, namely on the differences between the rates of the tryptic and chymotryptic digestion of the peptides formed.[71] The mixture of peptides varied depending on the degree of irradiation, and its solubility in trichloroacetic acid, used in this method, also varied. As already pointed out above, there are deviations from the exponential relation also when ester substrates are used, in particular, the ethyl ester of *N*-acetyl-L-tyrosine (ATEE).[33,65,71] The reason for and the extent of these differences have been investigated in numerous studies devoted to chymotrypsin,[33,60,65,71,72] trypsin,[65] and subtilisin-BPN′,[53] mainly in relation to casein and ATEE (Table 6). Substrates can be arranged in the following sequence in terms of increasing sensitivity: casein ≪ BTEE < ATEE. This fact confirms the conformational changes on irradiation. By virtue of the difference in the size of the biomolecules, the smallest conformational change affects the ability of the enzyme molecules to bind different substrates. Furthermore, casein apparently has several centres for binding to the enzyme by virtue of its structure, whereas in esters there is only one such centre. The difference between the specificities of ester substrates can be explained by different binding mechanisms.[53] Thus nine ester substrates have been used[72] and it has been shown that for some of them there is a relation between the loss of catalytic activity and the decomposition of the tryptophan derivatives, but this is not true of all substrates. Under these conditions, both catalytic stages—acylation of the active centre as well as deacylation—are acted upon by ionising radiation.

It is noteworthy that in all cases the purities of the enzyme and the substrate are very important for the sensitivity to radiation; this has been demonstrated specially in relation to casein.[65]

The reaction conditions, i.e. the composition of the medium, alter the radiation-chemical yield of active radicals and influence greatly G_{in}. The influence of different buffers on the latter is indicated in Table 6 and for subtilisin-72 has been described in a study[68] where the dependences of G_{in} on the initial enzyme concentration in the acetate buffer and in 0.1 M NaCl solution were compared. At a high enzyme concentration (10^{-4} M), the difference is insignificant, but in 10^{-6} M solution it already increases almost by an order of magnitude. The greatest effect of the acetate buffer on trypsin has been observed by McDonald.[62] On the other hand, the tris-HCl buffer hardly affected G_{in} for chymotrypsin.[51]

The presence of Ca^{2+} ions is important under irradiation. There are data indicating their binding to enzyme molecules (particularly those of the subtilisins), which leads to the observation of a protective effect, G_{in} diminishing for serine proteases as a result of the decrease in G_{unc}. It has been shown[51] that the presence of Ca^{2+} retards the decomposition of the tryptophan residues. The stabilising effect of Ca^{2+} is known also in thermal inactivation.[73] According to Nikol'skaya and coworkers,[51,68] the stabilising effect increases with increase in enzyme concentration; D_{50} (the dose at which 50% of the active enzyme remains) increases by a factor of 2. The stability increases also with increase in pH to 7.8 (D_{50} increases by a factor of 1.5 for a concentration of 10^{-6} M and by a factor of 3 for 10^{-4} M). The joint influence of calcium ions and the acetate buffer has been investigated for subtilisin-72.[68] In this case, competing processes are observed and the protective effect of Ca^{2+} ions is manifested when the effect due to the binding of Ca^{2+} to subtilisin molecules begins to exceed the destabilising effect of the increase in the ionic strength of the solution. There is a region in which the effects cancel out (in the given instance at an enzyme concentration of about 3×10^{-6} M).

The change in the inactivation of chymotrypsin and subtilisin as a function of the type of irradiation has been described[59,67] and is illustrated in Table 7. However, one should bear in mind that such variation depends as a rule on the dose rate of the source, which also influences the radiation stability of enzymes.

Table 7. Dependence of the inactivation constant ($k_{in,eff}$) on the type of radiation.[67]

Enzyme	Medium	pH	Radiation	$10^4\ k_{in,eff}$/min^{-1}
Chymotrypsin, 10^{-5} M	Tris-HCl buffer	7.8	γ	1.0
	Tris-HCl buffer	7.8	γ-n[a]	0.5
Subtilisin-72, 10^{-6} M	0.1 M NaCl	5.5	γ	0.9
	0.1 M NaCl	5.5	γ-n[a]	0.5

[a] Gamma-neutron field.

Many questions are associated with the influence of oxygen on the radiation-induced inactivation process. The results of the irradiation of serine proteases in air and in an inert gas atmosphere have been compared,[50,60] but the conclusions are not unambiguous. It is assumed[65] that, on irradiation in air, the principal role is assumed by OH radicals, whilst under anaerobic conditions it is assumed by both OH and H. According to the

results of Masuda et al.,[74] the yields $G(-SH)$ and $G(-Trp)$ are smaller under anaerobic conditions, whilst in the case of chymotrypsin a greater sensitivity was observed in the absence of oxygen.[57] One of the explanations of differences of this kind may be provided by the dependence on the medium in which the irradiation is carried out (the same competing processes involving the interaction of the enzyme with the active radicals and of the radicals with one another). Thus O_2^- ions are formed faster at pH 5.0 than H atoms and the effectiveness of the inactivation by them is much smaller.[57] The protective role of oxygen on irradiation in air has been observed.[72] In many instances the formation of H_2O_2 is decisive. This has been demonstrated in relation to subtilisin-Carlsberg.[55]

All the data considered above refer to the study of the enzymes *in vitro*. Another version of the study of the changes in the function of the enzyme under influence of ionising radiation constitutes studies *in vivo*. Investigations of this kind[75,76] have been performed to determine the changes in the fibrinolytic metabolism associated with the activity of plasmin. It has been shown that the fibrinolytic activity diminishes with increase in the γ-irradiation dose *in vivo* and this is associated in its turn with the decrease in the reactivity of the plasminogen activator. Unfortunately it was not possible to find any literature data on the mechanism of the radiolysis of the enzymes thrombin and plasmin themselves, but one can postulate that it is common to the serine proteases and involves a change in the conformation of the active centre.

2. Sulfhydryl proteases

Proteases containing cysteine in the active centres are of special interest in the study of their radiosensitivity in connection with the hypothesis of a unique mechanism of radiation sickness associated with the number of free sulfhydryl groups in the organism.[77] The radiolysis of one of the most thoroughly investigated sulfhydryl proteases (papain) has been examined in detail.[78,79] As already pointed out above, the majority of studies on the radiolysis of enzymes have been carried out in the region where the exponential effect–dose relation holds, the latter being as a rule a result of the combination of several nonexponential processes. The kinetics of the inactivation of papain have been described[78] and the following relation between the dose and the degree of inactivation has been obtained:

$$D\alpha = \frac{k' - k_1}{k_0} y + \frac{k_1 E_0 + k'_1 F + k_2 P}{k_0} \ln \frac{E_0}{E_0 - y}, \qquad (2)$$

where D is the dose in Roentgens, α the proportionality coefficient which converts the dose into the number of radicals ($It = \alpha D$), I the number of radicals (mol litre^{-1}) formed per unit time, k' the rate constant for the inactivation of the radicals by the active enzyme, k_1 the rate constant for the inactivation of the radicals by the inactivated enzyme, k_0 the rate constant for the inactivation of the enzyme by the radicals, E_0 the initial enzyme concentration, k'_1 the rate constant for the inactivation of the radicals by contaminants, F the concentration of contaminants in the enzyme, k_2 the rate constant for the inactivation of the radicals by radioprotectors, y the concentration of the inactivated enzyme, and P the concentration of the radioprotectors.

Eqn (2) is in principle applicable to any enzyme. It has linear and logarithmic components. Only when $k' = k_1$, i.e. if the active and inactivated enzymes react with the radicals in the same way, does the exponential relation hold for the dose–effect curves, since we then have

$$E = E_0 \exp(-k_0 D\alpha/[k_1 E_0 + k'_1 F + k_2 P]) = \\ = E_0 \exp(-KD). \qquad (3)$$

However, the authors observed that, for an exponential dose dependence of the X-inactivation of papain, the active enzyme molecules react with the water radiolysis products faster than the inactivated molecules. This made it necessary to examine in greater detail the inactivation kinetics. A family of curves was obtained with an increase in the inactivation yield as a function of the dose, which is associated with the decrease in the importance of the logarithmic part of Eqn (2) as k_0 increases. The theoretical ideas agreed well with the experimental data for the X-inactivation of 1.2×10^{-5} M solutions of papain in phosphate buffer at pH 7.4 and 0 °C. When $k' \neq k_1$, the radiosensitivity parameters change, which usually diminishes the degree of inactivation. Gaucher et al.[80] assumed that, when the enzyme is papain, then, in contrast to serine proteases, it reacts preferentially with the aquated electron e_{aq}^- being an SH-containing enzyme. The fundamental inactivation mechanism involves damage of the active centre by one of the water radiolysis products. Under these conditions, only one active group is important. The interaction of the radical with this group leads to the inactivation of the molecule, i.e. $(k' - k_1)/k_0 = 1$.

The hypothesis that the mechanism of the inactivation of papain (Pa) reduces to damage of the active centre has been confirmed by experiments with modified papain and also by the change in G_{in} in the presence of inhibitors.[81] When cysteamine monosulfoxide, which gives rise to the mixed disulfide Pa–S–S–R, and tetrathionate, forming the Pa–S–$S_2O_3^-$ ion, were used as the modifying agents, an increase in the radiation stability of such papain derivatives was observed (Table 8).[82]

Thus, in contrast to serine proteases, the inactivation of the sulfhydryl enzyme reduces partly to the damage of the active centre, mainly via a single impact mechanism, and this is responsible for the difference between k' and k_1 and leads to the deviation of the dose dependence from the exponential function. One should also note that e_{aq}^- can pass through the protein molecule very effectively, which should hinder the application of the target theory in calculations for SH enzymes. However, by virtue of the appreciable electron affinity of the disulfide bridges, such estimates are nevertheless possible.[48] As already mentioned, the dose curves for the serine proteases, which depend on the direct damage of the serine in the active centre, also do not always correspond to an exponential relation. It is difficult to account for these findings, because the authors[78,79] did not take into account the changes in the conformation of the papain molecule, assuming this process to be of secondary importance. However, it must inevitably occur as a result of the formation under the influence of ionising radiation of S–S bonds and mixed disulfides of the type Pa–S–S–R, which alters (usually strengthens) the molecular structure and inhibits complete degradation by influencing the conformation.

The observed conformational disturbances in papain have been shown[48,87] to occur due to the decomposition of the tyrosine and tryptophan residues with preferential damage to tyrosine residues, two of which (Tyr-61 and Tyr-67) are close to the active centre. In addition, the imidazole–thiol pair (Cys-25 and His-159) plays a major role in the inactivation of papain, which affects the interaction of the enzyme with the substrate.[86] Evidently, as for trypsin-like enzymes, in the case of papain the attack by the OH radicals and the accessibility of aromatic aminoacid residues to the latter are important apart from the effect of e_{aq}^-. Table 9 presents data on the reactivities of various aminoacid residues in papain relative to OH radicals. The tyrosine and tryptophan residues head this list. The overall rate constants for the reactions of papain with OH radicals and e_{aq}^- are listed in Table 3.

Thus the additivity of two processes, namely

$$Cys + e_{aq}^- \rightarrow E_{in},$$

$$Tyr(Trp) + OH \rightarrow E_{in} + E_{ac}^{\bullet},$$

Table 8. Change in the catalytic activity of sulfhydryl proteases on exposure to X-rays (t = 0 °C, substrate—haemoglobin).

Enzyme	Irradiation conditions	Dose rate/ Gy s^{-1}	Dose/ Gy	10^5 [E] / M	D_{37}/Gy[a]	Ionic yield	No. of SH groups per molecule	G_{in}[a]	Residual activity (%)[a]	Ref.
Papain	0.067 M phosphate buffer, pH 7.4, air	0.14	65	1.35	30 (70)	–	0.5	0 (40)	–	79
	0.067 M phosphate buffer, pH 7.4, air	0.16	–	0.9	–	0.79	0.5	–	–	79
	0.067 M phosphate buffer, pH 7.4, air, in the presence of catalase	0.14	63	1.2	85	0.41	0.5	–	50	79
	0.067 M phosphate buffer, pH 7.4, N_2	0.16	–	0.9	–	0.44	–	–	–	79
	0.067 M phosphate buffer, pH 7.4, N_2, in the presence of catalase	0.16	–	0.9	–	0.37	–	–	–	79
	0.067 M phosphate buffer, pH 7.4	0.145	300	1.5	–	–	–	–	– (27)	48
	Acetate buffer, pH 6.8, N_2O	1.5×10^{-4}	–	2.0	–	–	–	1.00 (0.54)	–	79
	Acetate buffer, pH 6.9, N_2, Bu^{i}OH	1.5×10^{-4}	–	2.0	–	–	–	1.00 (0.53)	–	85
	pH 6.9	1.5×10^{-4}	–	2.0	–	–	–	0.43 (0.11)	–	85
	pH 6.9, $(CNS)_2^-$	1.5×10^{-4}	–	2.0	–	–	–	1.00 (0.31)	–	85
Papain-S–S–R	0.067 M phosphate buffer, pH 7.4	0.145	300	1.5	–	–	0.4	–	– (82)	48

[a] The value obtained in the presence of cysteine is indicated in brackets.

(E^*_{ac} are the molecules of active but damaged molecules) generates the papain inactivation pattern. The decrease in the esterase activity of papain under these conditions is associated,[48] as for serine proteases, with the degradation of Trp-177. Furthermore, the abstraction of a H atom from the SH group contributes to the inactivation:

$$OH + Pa{-}SH \rightarrow Pa{-}S^{\cdot} + H_2O\,.$$

If aromatic aminoacid residues are in the vicinity of the S–S bridge, then the probability of inactivation increases to the extent determined by the sum of the processes. As shown by the γ-radiolysis of cysteamine disulfide[48] and cystine,[83,84] the effect of ionising radiation on disulfides and thiols generates numerous products, which then enter into secondary reactions. Similar processes affect also the inactivation of SH enzymes.

It is of interest that papain exhibits a greater radiosensitivity than other SH-containing enzymes, such as alcohol dehydrogenase and glyceraldehyde-3-phosphate dehydrogenase.[81] Its capacity for reactivation by cysteine is also higher. On the other hand, in view of the greater vulnerability of the active centre to the two reactions discussed above, papain is more radiosensitive also compared with serine proteases. However, one should take into

Table 9. The reactivity and accessibility of certain aminoacid residues in papain in relation to OH radicals.[48]

Aminoacid residue	n_{tot}	n_{exp}	$10^{-9}\,k_{(OH+AA)}$/ litre $mol^{-1}\,s^{-1}$	$n_{exp}\,k_{(OH+AA)}$	$\frac{n_{exp}\,k_{(OH+AA)}}{\Sigma\, n_{exp}\,k_{(OH+AA)}}$
Cysteine	1	1	12.3	12.3	0.04
Tryptophan	5	2.2	13.3	29.3	0.10
Tyrosine	19	13	10.1	131.3	0.47
Histidine	2	2	4.7	9.4	0.03
Phenylalanine	4	2	5.5	11.0	0.04

account the specific features and the sensitivity of the methods for the determination of catalytic activity, which, as shown in relation to chymotrypsin, are extremely important. Furthermore, in the determination of the activity of papain and in the calculation of G_{in} account must be taken of the fact that about 50% of the papain in the preparation may be in the oxidised (inactive) form, which hinders the comparison of data from different investigations if preliminary reactivation or purification has not been carried out.[85]

Experiments showed[48,80] that the radiation-induced inactivation of papain diminishes greatly following the addition of cysteine after irradiation, partly owing to the reaction

$$Pa^{\cdot} + Cys-SH \rightarrow Pa-H + Cys-S^{\cdot} .$$

The ratio G_{in} (in the presence of cysteine)/G_{in} (in the absence of cysteine) (relative yield) is presented in Figure 5. The protection by cysteine then depends on the real ratio [Pa]/[Cys]. Thus in nitrogen-purified solutions, it should be 1/(2–10). This is caused, apart from the reaction indicated above, by competing reactions with OH radicals and the faster reactions involving e_{aq}^-:

$$e_{aq}^- + R-SH \rightarrow R^{\cdot} + SH^- ,$$

$$Cys^{\cdot} + Cys-SH \rightarrow Cys-H + Cys-S^{\cdot} .$$

The species e_{aq}^- therefore cause a reversible inactivation, whereas OH radicals give rise to an irreversible inactivation.[85]

It is noteworthy that an increase in the pH of the solution increases as a rule G_{in}, although the relation between these quantities is not unambiguous.[81]

The influence of irradiation conditions on the radiation-induced inactivation of papain has been investigated. The authors[85] elucidated the effect on this process of the acetate, isobutyl alcohol, and CNS radicals. It was found that they all increase G_{in} (Table 8), evidently owing to the reaction

$$Pa-SH + R \rightarrow Pa-S^{\cdot} + RH .$$

The influence of hydrogen peroxide on the inactivation of papain has also been observed.[79,85,86] The peroxide gives rise to 60% of the reversible and 40% of the irreversible damage in papain.[85] The elimination of its influence by the addition of catalase diminishes the ionic yield, which hardly changes in air and under a nitrogen atmosphere. The dependence of the degree of inactivation on the presence of H_2O_2 can also be estimated from the increase in the radiation-induced inactivation of papain on reducing the dose rate in the absence of catalase.

Thus the principal difference between the mechanisms of the radiation-induced inactivation of the serine and sulfhydryl proteases consists in the fact that not only a disturbance of the conformation on degradation of the aromatic aminoacid residues but also the competing dominant process involving the single impact inactivation as a result of the damage to the active centre is observed in the latter case.

3. Other classes of proteases

Whereas the radiolysis of the serine and sulfhydryl proteases has been studied fairly completely, the remaining representatives of proteases are mentioned in the literature only incidentally.

The radiolysis of pepsin — an acid protease containing an asparagine residue in the active centre — has been examined.[70] It was shown that the overall characteristics of the inactivation of this enzyme are the same as for trypsin, chymotrypsin, and the subtilisins: in solution, the main reactive species is the OH radical; atomic hydrogen is extremely effective, but it makes a smaller contribution to the inactivation owing to its low yield. The similarity consists also in damage being sustained by the same radiation-sensitive aminoacid residue: Trp and Tyr, which was demonstrated by altering the degree of inactivation in the presence of Br_2^- and $(SCN)_2^-$ ions and also of *tert*-butyl alcohol. The parameters and conditions of the inactivation are presented in Table 6.

Figures 6 and 7 illustrate the inactivation of pepsin in the form of dose dependences and the changes in the pH dependence under various irradiation conditions. The pH dependence varies in the range pH 2–3. Taking into account also the changes for subtilisin[52] and the angiotensin converting enzyme (ACE) (Figure 7), one may say that the radiation-induced inactivation makes it possible to determine the conditions under which conformational changes in the molecule take place.

In the case of carboxypeptidase A, the effectiveness of the action of water radiolysis products on its enzyme activity does not differ from that for serine proteases,[69] despite the fact that the

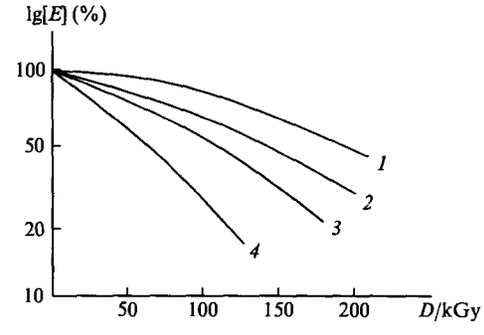


Figure 6. Dependence of the radiosensitivity of pepsin on the irradiation conditions:[69] (*1*) Ar + *tert*-BuOH; (*2*) O_2; (*3*) Ar; (*4*) N_2O.

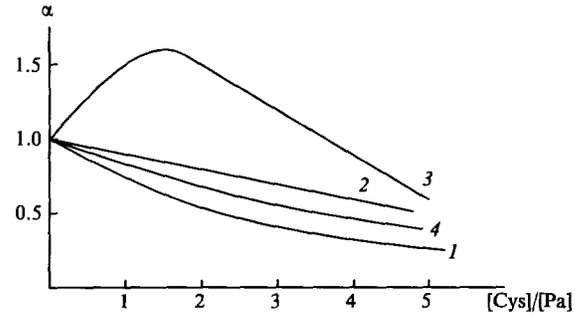


Figure 5. The relative inactivation yield (α) as a function of [Cys]/[Pa]: (*1*) calculated fraction of OH radicals reacting with papain in N_2-saturated solutions; (*2*) irreversible inactivation; (*3*) overall inactivation; (*4*) fraction corresponding to the interaction with papain of both radicals ($OH + e_{aq}^-$) in N_2-saturated solutions.

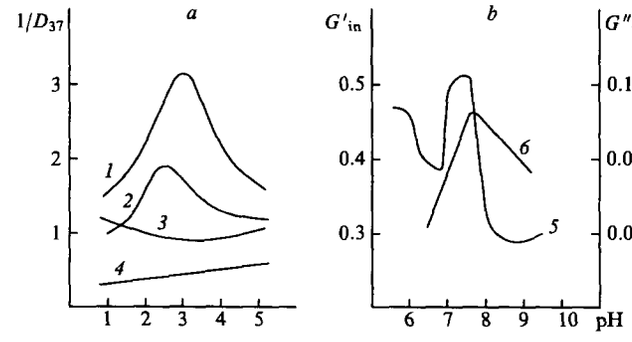


Figure 7. Variation of the radiosensitivity of pepsin[69] (*a*), subtilisin-72 [G'_{in}; curve *5* (*b*)],[52] and the angiotensin converting enzyme (ACE) [G''_{in}; curve *6* (*b*)] under different conditions: (*1*) N_2O + KBr; (*2*) N_2O; (*3*) O_2; (*4*) N_2O + KSCN.

active centre contains in this case a metal (Zn) ion. A similar radiation-chemical yield of the inactivation process is also observed (G_{in}, Table 6). All this confirmed that the inactivation of enzymes of this class takes place primarily via the alteration of the conformation and not via a single impact mechanism involving damage to the active centre. An appreciable dependence of the inactivation on the conformational state of the molecule has been observed also for a Zn-containing hydrolase—ACE, for the stability of which the number of decomposed aromatic aminoacid residues is important. Their decomposition to the extent of ~50% made the active centre accessible to radicals and caused a decrease in enzyme activity (Figure 8).

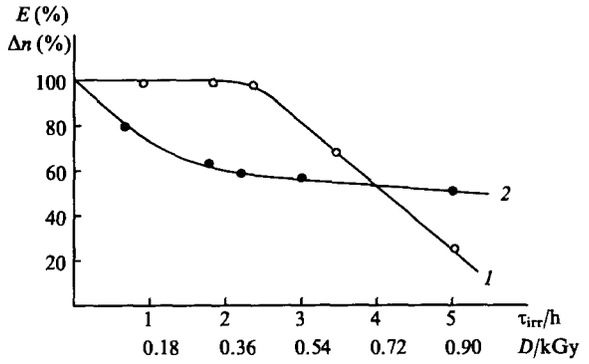


Figure 8. Variation of the catalytic activity E (curve *1*) and of the number of tryptophan and tyrosine residues (curve *2*) in the angiotensin-converting enzyme (γ-irradiation).

Overall, the radiation-induced inactivation of proteases like, incidentally, that of any other enzyme, can be represented by a scheme (Figure 9), the use of which gives rise to a greater complexity of the expressions obtained by Phihl and Sanner[79] and Gaucher et al.[80] Process *4* (Figure 9), which constitutes the mechanism of the inactivation proper, i.e. the modification of the biomolecule, depends on the coefficients of the effectiveness of the action of the water radiolysis products on the given enzyme, involving the active centre itself or its immediate environment. The highest yield and the highest effectiveness are those of the OH radicals and e^-_{aq}. The yield of H atoms, whose effectiveness is a maximum, is insufficient to influence greatly the inactivation, so that OH and e^-_{aq} actually make the main contribution to the given process. On irradiation of the pure enzyme, fundamental differences are observed between SH-containing enzymes and the remaining proteases regardless of whether their active centre contains serine, aspartic acid, or a metal atom. Apart from undergoing conformational damage due to the interaction of OH radicals with tryptophan and tyrosine residues, in the biomolecules containing a SH group the cysteine in the active centre is acted upon directly by e^-_{aq}, which increases their G_{in}. When the mechanism of the inactivation is identical, the area of the accessible surface of the molecule, characterising the extent to which it has been uncoiled, assumes fundamental importance.

Table 10. Accessible surface areas for different classes of proteases.

Enzyme	Accessible surface area/Å²	Ref.
Chymotrypsin	12996	88
Carboxypeptidase A	11260	89
Subtilisin	9790	88
Papain	9210	88

Table 10 presents certain accessible surface areas for metal-containing, SH-containing, and serine proteases. Comparison of the values of G_{in} (Table 6) shows that they are similar for chymotrypsin and carboxypeptidase. For subtilisin, which has a smaller accessible surface area, the radiation-chemical inactivation yield also diminishes. However, for papain, which has a different inactivation mechanism, a higher value of G_{in} is observed despite its smaller accessible surface area. Furthermore, the radiation stability of any protease depends on the accessibility of the aromatic aminoacid residues, especially Trp and Tyr, regardless of the stability in the active centre.

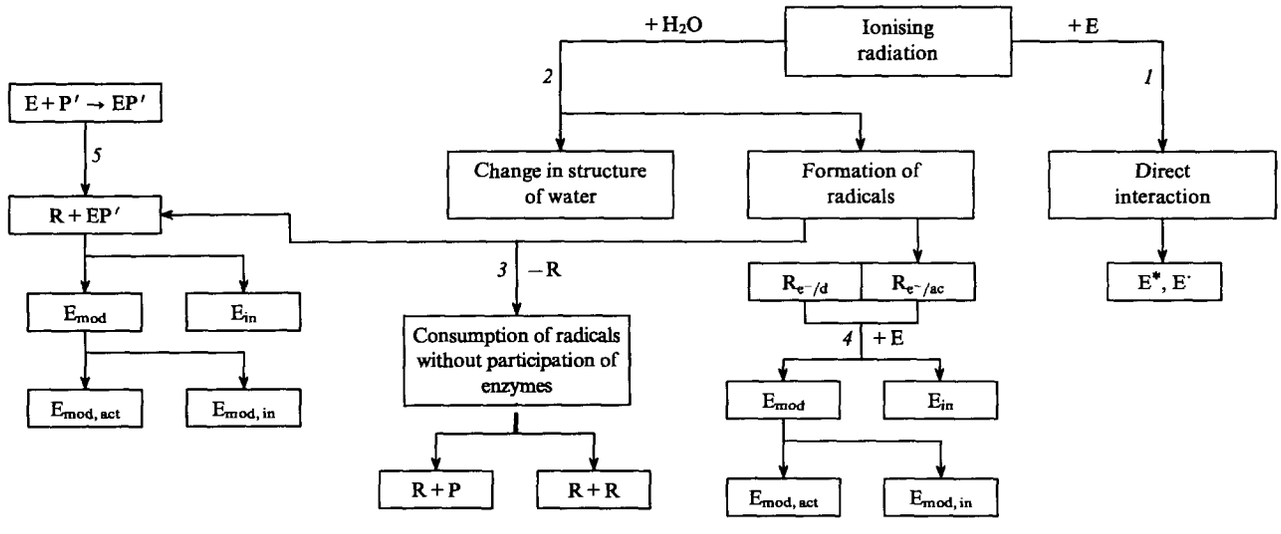


Figure 9. Schematic illustration of the interaction of enzymes with ionising radiation; E = native enzyme, E· = radical fragments of the enzyme molecule, E* = excited enzyme molecules, E_{in} = inactivated enzyme, E_{mod} = enzyme modified in any way, $E_{mod,act}$ = enzyme modified without change in activity, $E_{mod,in}$ = enzyme modified with a change in activity, R = radicals derived from water, $R_{e^-/d}$ = electron-donor radicals, $R_{e^-/ac}$ = electron-acceptor radicals, P and P′ = chemical impurity molecules present in solution.

IV. Application of the method of radiation-induced inactivation of proteolytic enzymes

There are fairly good prospects for the application of the radiation-induced inactivation method. This was partly discussed above.

The oldest and best known application of the radiation-induced inactivation method involves its use in the determination of the molecular masses of biomolecules. The possibility of characterising complex supermolecular formations is of special interest.[18] The application of the method for this purpose has been well developed and has been described in detail.[5,17,18,23,35] It is convenient, reliable, and is fairly widely used.

Medical applications of the results of the study of proteases with the aid of radiation are extremely promising. Immobilised enzymes, which, as stated above, are much more stable than the enzymes in solution, are used in this instance. An important factor is that the action of such materials on the organism is prolonged and requires very low enzyme concentrations.[41-43] Mainly the use of serine proteases, in particular trypsin, has been described. The aim of the preliminary radiation treatment is simultaneous immobilisation and sterilisation virtually without affecting the enzyme activity.

The methods for the generation of half-tone images by exposing protease-containing materials to different types of radiation give rise to extensive possibilities for the creation of dosimetric systems based on them.[40] The sensitivity of such materials can be increased (i.e. the lower limit of the doses determined can be reduced) by altering the material of the support, by introducing additives into the latter, and also by increasing the concentration of the enzymes (the latter is less desirable owing to the increase in the cost of the material and the possibility of partial radiolysis). Apart from purely dosimetric purposes, some of the systems examined[39] can serve as a material which provides an alternative to the X-ray films used in autoradiography and medicine.

In connection with the sharp impairment of the radioecological situation, various biochemical models designed to estimate the degree of risk from ionising radiation simultaneously with the risk from the usual domestic and medical factors (domestic chemistry, fertilisers, pesticides, medicines) have been widely developed in recent years.[8] In addition, another aim of these studies involves the possibility of screening the radioprotectors. In contrast to tests on animals, biochemical models are simpler and yield additional ideas concerning the mechanism of the action of the reagent under certain conditions. Among the models developed, there are also enzyme models, in particular hydrolase models.[9] An attempt was made to use enzyme models in the 1950s, but they proved to be ineffective because of the linear treatment of the results. It was found that the correlation between the effect of radiation on the organism and enzymes is more complex and is associated with the influence of effectors (activators and inhibitors), which leads to a greater or smaller imbalance in the systems of the organism under the influence of ionising radiation or other types of radiation. Figure 10 illustrates the correlation between the constant for the inhibition (K_{in}) of chymotrypsin by certain familiar radioprotectors and the dose characteristic (D_{80}) for which 80% of the enzyme remains active. The type of inhibition (competitive, noncompetitive) does not exert an appreciable influence on the above relation.[90] It must be borne in mind that any compounds used in man's daily life, including food components, medicines, perfumes, etc., may function as effectors. Thus many substances serve as radiomodifying agents, which alter the possible action of any type of radiation. The use of enzyme models may characterise the influence of the radiomodifying agent on a fully defined mechanism of the action of radiation — in particular the protease model yields information about the conformational mechanism.

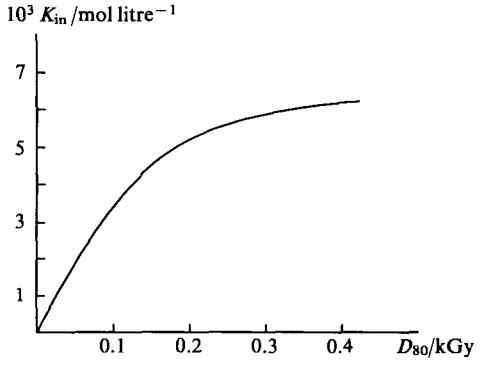


Figure 10. Dependence of the constant for the inhibition of chymotrypsin[90] by radiomodifying agents on D_{80}.

References

1. I Ya Vasilenko, Yu I Moskalev, V N Strel'tsov *Voprosy Onkologii* **31** 3 (1985)
2. N F Timofeev-Resovskii (Editor) *Pervichnye Radiobiologicheskie Protsessy* (Primary Radiobiological Processes) (Moscow: Atomizdat, 1973)
3. A V Savich (Ed.) *Radiatsionnoe Porazhenie i Vosstanovlenie Struktur i Funktsii Makromolekul* (Radiation Damage and Restoration of the Structures and Functions of Macromolecules) (Moscow: Meditsina, 1977)
4. N F Timofeev-Resovskii, A V Savich, M I Shal'nov *Vvedenie v Molekulyarnuyu Radiobiologiyu* (Introduction to Molecular Radiobiology) (Moscow: Meditsina, 1981)
5. A Swallow *Radiation Chemistry of Organic Compounds* (Translated into Russian) (Moscow: Inostr. Lit., 1963)
6. M V Vladimirova *Radiatsionnaya Khimiya Aktinoidov* (Radiation Chemistry of the Actinides) (Moscow: Energoizdat, 1983)
7. W M Garrison *Chem. Rev.* **87** 381 (1987)
8. M M Vilenchik *Radiobiologicheskie Effekty i Okruzhayushchaya Sreda* (Radiobiological Effects and the Environment) (Moscow: Energoizdat, 1983)
9. M A Orlova, S E Tkachenko, T P Trofimova, N N Troshina, V M Fedoseev, I V Golubtsov, V V Kuusk *Biochem. Biotechnol. Elect. Express Data* **1** 15 (1991)
10. J F Fowler *Phys. Med. Biol.* **29** 97 (1984)
11. L Rosenberg, M Awschalam, R K Ten Haben, B R Bennett *Health Phys.* **46** 407 (1984)
12. H Wakabayashi, Sh Suzuki, A Ite *J. Radiat. Res.* **24** 305 (1983)
13. P Andreo, A Brahme *Acta Radiol. Oncol. Rad. Ther. Phys. Biol.* **22** (1983) (Suppl. N 364. p.25)
14. L Frankenberg *Radiat. Res.* **97** 329 (1984)
15. V N Orekhovich, L A Lokshina, Yu E Eliseeva, L V Pavlikhin *Vestn. Akad. Med. Nauk SSSR* **8** 3 (1984)
16. N I Larionova, Doctoral Thesis in Chemical Sciences, Moscow State University, Moscow, 1992
17. E Pollard, A Buzzell, C Jeffrays, F Forro *Arch. Biochem. Biophys.* **33** 9 (1951)
18. J C Ellory *TJBS* 99 (1979)
19. M Houslay, J C Ellory, G Smith, T Hesketh, J Stein, G Warren, J C Metcalfe *Biochim. Biophys. Acta* **467** 208 (1977)
20. P Simon, S Swillens, J Dumont *Biochem. J.* **205** 477 (1982)
21. A S Verkman, K Skorecki, D A Ausiello *Proc. Natl. Acad. Sci. USA* **81** 150 (1984)
22. S R Levinson, J C Ellory *Biochem. J.* **137** 123 (1974)
23. K G Tsimmer *Problemy Kolichestvennoi Radiobiologii* (Problems of Quantitative Radiobiology) (Moscow: Gosatomizdat, 1962)
24. D P Alexander, D A Charlesby *Nature (London)* **173** 578 (1954)
25. R B Setlow *Proc. Natl. Acad. Sci. USA* **38** 166 (1952)
26. R B Setlow, B Doyle *Arch. Biochem. Biophys.* **46** 46 (1953)
27. A Norman, W Ginoza *Radiat. Res.* 7 440 (1957)
28. R L Kincald, E Kempner, V C Manganielle, G C Osborne, M Vaughan *J. Biol. Chem.* **256** 11351 (1981)
29. T B Nielsen, P M Lad, M S Preston, E Kempner, W Schlegel, M Rodbell *Proc. Natl. Acad. Sci. USA* **78** 722 (1981)

30. E Kempner, W Schlegel, J H Miller, J Z Hearon *J. Biol. Chem.* **255** 6826 (1980)
31. E Kempner, W Schlegel *Anal. Biochem.* **92** 2 (1979)
32. A K Valeev, O V Malinovskii *Radiobiologiya* **23** 624 (1983)
33. M A Orlova, I I Nikol'skaya, I V Golubtsov *Radiobiologiya* **27** 308 (1987)
34. R A Deering *Radiat. Res.* **5** 238 (1956)
35. E S Pollard, W R Guld, F Hutchinson, R B Setlow *Prog. Biophys.* **5** 238 (1955)
36. T K Hopkins, J D Spikes *Radiat. Res.* **37** 253 (1969)
37. P Riesz, F H White *Radiat. Res.* **44** 24 (1970)
38. F H White, P Riesz, H Kon *Radiat. Res.* **32** 744 (1962)
39. E V Lukasheva, N F Kazanskaya, I V Berezin *Vestn. Mosk. Univ., Ser. 2: Khim.* **27** 86 (1986)
40. M A Orlova, I I Nikolskaya, I V Golubtsov, N F Kazanskaya *Radiat. Eff. Lett.* **85** 143 (1984)
41. R V Virnik, V V Ryl'tsev, L G Vlasov, E V Dovbii, A T Kalashnik *Prikl. Biokhim. Mikrobiol.* **19** 533 (1983)
42. V V Ryl'tsev, L G Vlasov, T I Samoilova, L I Volkovinskaya, L N Bondareva, V D Zazhirei, S V Netrebenko, V I Khachiyants *Prikl. Biokhim. Mikrobiol.* **20** 694 (1984)
43. R V Virnik, V V Ryl'tsev, L G Vlasov, G I Samoilova, E V Dovbii, A T Kalashnik *Prikl. Biokhim. Mikrobiol.* **21** 106 (1985)
44. L Schachinger, Ch Schippel, E Altmann, B Diepold, Ch Yang, M Jaenke *Radiat. Environ. Biophys.* **24** 259 (1985)
45. G E Adams, K F Baverstock, R B Cundall, J L Redpath *Radiat. Res.* **54** 375 (1973)
46. K R Lynn, G Orpen *Int. J. Radiat. Biol.* **14** 363 (1968)
47. J R Clement, D A Armstrong, N A Gillis *Can. J. Chem.* **50** 2833 (1972)
48. J R Clement, D A Armstrong, H N V Klassen *Can. J. Chem.* **51** 2443 (1973)
49. A G Bezrukova, J Yu Ostashevsky *Int. J. Radiat. Biol.* **31** 131 (1977)
50. K R Lynn, G Orpen *Radiat. Res.* **39** 15 (1969)
51. I I Nikol'skaya, M A Orlova, I V Golubtsov *Radiobiologiya* **26** 302 (1986)
52. I I Nikol'skaya, M A Orlova, E V Bogaevskaya *Radiobiologiya* **26** 477 (1986)
53. K Outsuki, M Fukuhara, K Sumizu, H Hatano *J. Radiat. Res.* **11** 113 (1970)
54. K Outsuki *J. Radiat. Res.* **11** 120 (1970)
55. C E Stauffer, D Etson *J. Biol. Chem.* **244** 5333 (1969)
56. R A Alden, C S Wright, F C Westall, J Kraut *Subtilisin BPN': Tertiary Structure and Inhibitor Binding* (1970)
57. L K Mee *Radiat. Res.* **21** 501 (1964)
58. L K Mee *Radiat. Res.* **9** 151 (1958)
59. T W Smith, S J Adelstein *Radiat. Res.* **19** 213 (1963)
60. L A Mounter *Radiat. Res.* **12** 487 (1960)
61. E C Moore, M McDonald *Radiat. Res.* **3** 38 (1955)
62. M McDonald *J. Gen. Physiol.* **38** 581 (1955)
63. M McDonald *J. Gen. Physiol.* **38** 93 (1955)
64. M McDonald *Br. J. Radiol.* **27** 62 (1954)
65. K R Lynn *Radiat. Res.* **46** 268 (1971)
66. A G Bezrukova, I Yu Ostashevsky *Int. J. Radiat. Biol.* **31** 349 (1977)
67. M A Orlova, I V Golubtsov, I I Nikol'skaya *Vestn. Mosk. Univ., Ser. 2: Khim.* **28** 601 (1987)
68. M A Orlova, I I Nikol'skaya, E V Bogaevskaya, I V Golubtsov *Radiobiologiya* **26** 844 (1986)
69. PB Roberts *Int. J. Radiat. Biol.* **24** 143 (1973)
70. G E Adams, M I Pesener, R H Bisby, R B Cundall, J R Key *Int. J. Radiat. Biol.* **35** 497 (1979)
71. D Aronson, L Mee, C L Smith, in *Progress in Radiobiology, Proceedings of IV Internatinal Conference on Radiobiology, Cambridge, 1955* p. 61
72. K R Lynn *Radiat. Res.* **43** 525 (1970)
73. V V Mosolov *Proteoliticheskie Fermenty* (Proteolytic Enzymes) (Moscow: Nauka, 1971)
74. T Masuda, J Ovadia, L L Grossweiner *Int. J. Radiat. Biol.* **20** 447 (1971)
75. Ch Ts'ao, W F Ward *Radiat. Res.* **101** 394 (1985)
76. Ch Ts'ao, W F Ward, C D Port *Radiat. Res.* **96** 301 (1983)
77. E Ya Graevskii *Sul'fgidril'nye Gruppy i Radiochuvstvitel'nost'* (The Sulfhydryl Groups and Radiosensitivity) (Moscow: Atomizdat, 1969)
78. T Sanner, A Phihl *Radiat. Res.* **19** 12 (1963)
79. A Phihl, T Sanner *Radiat. Res.* **19** 27 (1963)
80. G M Gaucher, B L Mainman, G P Thompson, D A Armstrong *Radiat. Res.* **46** 457 (1971)
81. S Fuimoto, T Nakagawa, S Ishimitsu, A Ohara *Chem. Pharm. Bull.* **31** 992 (1983)
82. J W Purdie *Can. J. Chem.* **49** 725 (1971)
83. J W Purdie *J. Am. Chem. Soc.* **89** 226 (1967)
84. D W Grant, S N Mason, M A Link *Nature (London)* **192** 352 (1961)
85. G M Gaucher, D A Armstrong *Can. J. Chem.* **51** 2443 (1973)
86. W S Lin, G Maurice, M Lal, D A Armstrong *Can. J. Chem.* **54** 242 (1976)
87. G Beguta, A M Dancewicz *Int. J. Radiat. Biol.* **43** 249 (1983)
88. C Chetskia *Nature (London)* **254** 304 (1975)
89. C Chetskia *J. Mol. Biol.* **105** 1 (1976)
90. M A Orlova, S E Tkachenko, T P Trofimova, N N Troshina, V M Fedoseev *Vestn. Mosk. Univ., Ser. 2: Khim.* **34** (1993) (in the press)

Russian Chemical Reviews **62** (6) 509 – 526 (1993)
© 1993 Russian Academy of Sciences and Turpion Ltd

UDC 541.515:541.124

Relation between molecular and chemical dynamics for elementary radical reactions in viscous media

R R Rakhimov, A I Prokof'ev, Ya S Lebedev

Contents

I.	Introduction	509
II.	The influence of molecular mobility on the kinetics of bimolecular reactions of free radicals	509
III.	The influence of the mobility of the medium on the kinetics of intramolecular radical substitution reactions	511
IV.	Conformational transitions in free radicals. Relation between intramolecular mobility and the mobility of the medium	520
V.	Relation between the rotational mobility and the dynamics of spin exchange in nitroxyl biradicals	522
VI.	Conclusion	525

Abstract. Experimental data on the effect of viscosity on the kinetics of elementary chemical reactions of free radicals in solid matrices and viscous solutions are analysed. The dynamic effects in EPR spectroscopy are used for the simultaneous investigation of molecular and chemical dynamics. The intramolecular transformations in free radicals and the spin exchange in biradicals are considered. It is shown that the rates of such intramolecular reactions are controlled by the molecular dynamics of the chemical cage. The bibliography includes 58 references.

I. Introduction

The influence of the viscosity of the medium on the rates of chemical reactions is one of the 'classical' effects in physicochemical kinetics. However, new results, significantly supplementing and modifying the existing ideas, have been obtained in recent years. These ideas refer to diffusion-controlled reactions. If the direct chemical step is rapid, then the rate of a bimolecular reaction is determined by the frequency of the diffusional encounters of the reactants in the 'cage', while the rate of unimolecular decomposition is determined by the frequency of the release of the products from the cage. It has been shown comparatively recently that slow bimolecular reactions, for which the duration of the chemical step is many orders of magnitude greater than the duration of the diffusional approach, can also be controlled by the viscosity of the medium. This can be explained most simply by considering the rotational diffusion of molecules, already involved in an encounter within the cage, as the rate-limiting stage of the process: in this case, the rate of the reaction is proportional to the rotational diffusion coefficient (as in the usual diffusion-controlled processes, the rate is proportional to the translational diffusion coefficient) and is determined unambiguously by the viscosity of the medium.

R R Rakhimov, V I Nikitin Institute of Chemistry, Academy of Sciences of the Tajikistan Republic, ul. Aini 299, 734063 Dushanbe, Tajikistan
A I Prokof'ev, A N Nemeyanov Institute of Organoelement Compounds, Russian Academy of Sciences, ul. Vavilova 28, 117813 Moscow.
Fax (7-095)135 5085.
Ya S Lebedev N N Semenov Institute of Chemical Physics, Russian Academy of Sciences, ul. Kosygina 4, 117977 Moscow.
Fax (7-095)938 2156

Received 18th January 1993
Uspekhi Khimii **62** (6) 547 – 564 (1993); translated by A K Grzybowski

The influence of the viscosity of the medium on a series of intramolecular processes, which cannot be controlled by rotational mobility, has been observed experimentally in recent years. This necessitates the consideration of the microscopic (at the level of intramolecular dynamics) relation between the viscosity of the medium and the rates of chemical reactions. It was found that the viscosity influences intramolecular processes, which at first sight do not require any intramolecular rearrangements (for example, spin exchange or electron transfer in non-polar media).

The present review is not concerned with 'classical' diffusion-controlled reactions and its subject is only slow bimolecular reactions of free radicals and their intramolecular transformations. As will be shown below, it is precisely in the case of free radicals that the EPR method makes it possible to investigate simultaneously the reaction rates and the molecular mobilities of the reactants, i.e. to compare the frequencies of the molecular motions, whose relation with the viscosity of the medium is evident, with the frequencies of the chemical steps. Attention is concentrated on the analysis of the experimental results obtained in recent years.

II. The influence of molecular mobility on the kinetics of bimolecular reactions of free radicals

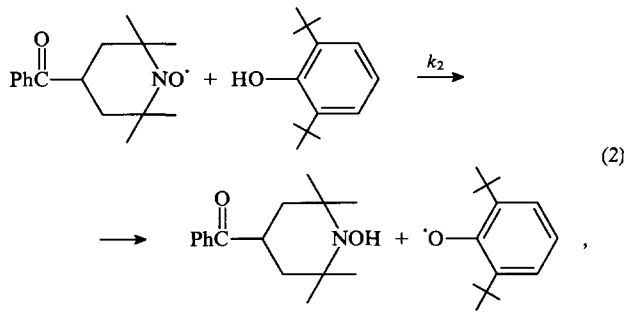
Together with the usual cage effect, consisting in the fact that the relatively immobile species comprising the medium prevent the release of radicals into space, in the case of radical reactions in solid matrices there exists the so called indirect cage effect leading to the retardation of the bimolecular chemical reaction proper.[1] It cannot be explained by diffusional limitations, since the observed bimolecular reaction rate constants are several orders of magnitude lower than the rate constants for the encounters of the reactants. The first effects associated with the influence of the mobility of the medium on the kinetics of slow bimolecular reactions in polymers were observed by Roginskii and coworkers[2–4] and Denisov and coworkers[5–9] The molecular mobility in polymers changed as a result of the change in the external pressure and the plasticisation of the polymer by chemically inert solvents. The interaction of the phenoxyl radical PhO$^{\cdot}$ with a polymeric peroxide, i.e.

$$\mathrm{PhO^{\cdot}} + \mathrm{ROOH} \xrightarrow{k_1} \mathrm{PhOH} + \mathrm{ROO^{\cdot}}, \qquad (1)$$

has been investigated and it has been shown that in polypropylene the reaction is accelerated on plasticisation.[2] The increase in the rate constants k_1 in the polymer is accompanied by a decrease in

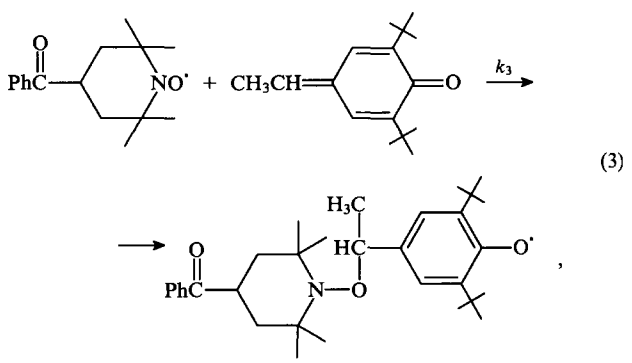
the activation energy and in the pre-exponential factor in the Arrhenius equation.

It has been shown[5,8] that the rate constants for bimolecular reactions involving the abstraction of a hydrogen atom by a nitroxyl radical from 2,6-di-*tert*-butylphenol, i.e.



(2)

and the addition of the same radical to the double bond of α-methyl-2,6-di-*tert*-butylmethylenequinone, i.e.



(3)

in plasticised polymers are determined unambiguously by the molecular mobility—the frequency of the rotation of the nitroxyl-radical involved in the reaction.

Another characteristic feature of the radical reactions in polymers is the levelling of the reactivity, i.e. rapid reactions are retarded much more markedly on passing to the solid phase. The levelling is manifested quantitatively by the fact that, for the same chemical reactions (occurring in the kinetic region), the rate constants in the solid phase (k_s) differ much less than those in the liquid phase (k_f) and that the relation $k_s \propto k_f^{1/2}$ holds approximately.[10] If the frequency of the rotation of the spin probe is measured in the same matrices, then the relation $k_s \propto v_c$ is seen to hold in the range of frequencies corresponding to the rotational mobility ($v_c = 10^8 - 10^9\ s^{-1}$). At higher frequencies, this type of relation is not observed.

If one uses indirect data, then the correlation between the rate constant and the mobility of the medium can be found in a much greater number of experiments. For example, a linear relation has been observed[11-13] between $\ln k_s$ and the fraction of the fluctuation volume f. The study of the rotational mobility of spin probes has shown that the same relation holds between $\ln v_c$ and f,[14] so that one may claim that in such cases a correlation is observed between the chemical reaction rate constant and the frequency of molecular reorientations. Data indicating the pressure dependence of k_s and v_c can be compared similarly.[14-16] These relations are of the same type:

$$\ln k_s, \ln v_c \propto -p/c,$$

where p is the pressure and c a coefficient characterising the change in the modulus of bulk compression with increase in pressure. Hence it also follows that $k_s \propto v_c^m$.

Thus the early experiments designed to investigate the influence of molecular mobility on the kinetics of elementary chemical reactions demonstrated the effectiveness of the spin probe method for understanding the kinetics of reactions in polymers.

Bimolecular substitition reactions in solid matrices (inhibition, oxidation chain propagation, etc.) are of special interest to investigators of the structure and stabilisation of polymers.[17] It is then necessary to develop reliable methods for the prediction of reactivities in solid phase reactions, the elementary rate constants of which in the liquid phase are known. It has been shown in relation to the substitution reaction (2)[18] that measurement of the molecular mobility of the spin probe in a solid polymer and the knowledge of the reaction rate constant in the liquid phase k_f make it possible to predict the reaction rate constant in the solid state k_s. The corresponding experimental data can be conveniently represented in the form of the relation between the reciprocal of the rate constant and the correlation time of the rotational mobility $\tau_c = 1/v_c$. For the elementary reactions considered in this review, the above relation can be represented phenomenologically in the following form:

$$\frac{1}{k} = \frac{1}{k_f} + \alpha\tau_c, \qquad (4)$$

where α is an empirical coefficient and k_f the rate constant under the conditions of unlimited molecular mobility ($\tau_c \to 0$), i.e. in a non-viscous solution.

But it is precisely in the case of free radicals that the influence of molecular mobility on the kinetics of elementary chemical reactions can be conveniently investigated from the EPR spectra where one can simultaneously follow the kinetics of chemical reactions and the molecular mobility. The frequency of the motions of the radical which entered into the chemical reaction has been measured for reactions (2) and (3), so one can assume that the parameters τ_c characterise the molecular dynamics of the kinetic cage responsible for the occurrence within it of the elementary reaction (reactants + surrounding molecules of the medium). Fig.1 shows that the variation of the rate constant for reaction (2) can be satisfactorily expressed in a linear form in terms of the variables $1/k$ and τ_c. A similar relation has been observed also for reaction (3), where $1/k_f \simeq 0$, so that the dependence of k on v_c is linear.

Evidently, the characteristics of the kinetics of the elementary chemical reactions examined above are due precisely to the specific features of the phase state of the polymer as a medium with limited molecular mobility. Such features are characteristic also of the elementary chemical reactions in solid matrices and viscous media.[19] It is therefore reasonable to find an analogous experimental approach to the study of the characteristic features of the kinetics of elementary biochemical processes, the most important of which is electron transfer.

The relation between the rate of a chemical reaction and rotational mobility has been investigated[20] for the model reaction

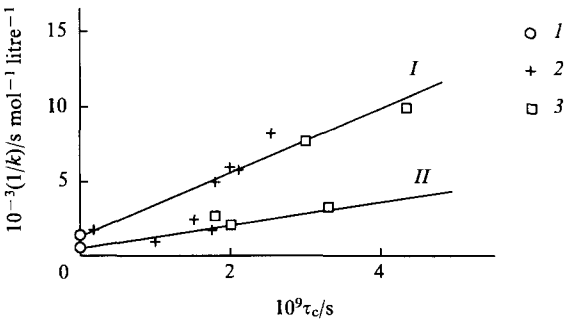
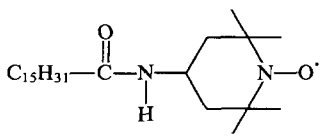


Figure 1. Experimental[7] dependence of the rate constants for the reaction of the nitroxyl radical with phenol on molecular mobility in terms of the variables of Eqn (4): (*1*) benzene; (*2*) polyethylene; (*3*) polypropylene; (*I*) 40 °C; (*II*) 50 °C.

involving the oxidation of the nitroxyl radical by tetranitromethane (TNM). The reaction was carried out in a homogeneous 3:1 water–*tert*-butyl alcohol mixture and in micellar systems based on non-ionogenic surfactants–Tritons X100 and WR1339, the viscous characteristics of which differ greatly. The micellar systems based on the Tritons involve a high degree of molecular organisation and can be regarded as simplified models of biological membranes. The nitroxyl radical



was used as the spin probe. The reaction kinetics were investigated simultaneously in terms of the intensity of the EPR spectrum of the radical.

The radical is used widely in the study of biological membranes and of liposomal and micellar systems. The long hydrophobic hydrocarbon chain of the radical enables it to be thoroughly incorporated in the micelles. In order to determine the location of the nitroxyl radical in the micellar solution, the dependence of the isotropic hyperfine interaction (HFI) constant for the nitrogen nucleus $2A_{iso}$ on the polarity of the medium was employed. It was found that the above quantity in micellar solutions is identical with the value in pure surfactants, which indicates that the radicals are located within the micelles.

The study of the rotational mobility of the nitroxyl radical showed that, on passing from aqueous alcoholic to micellar solutions of Tritons X100 and WR1339 at a constant temperature, the rotation correlation time τ_c increases sharply. It was found that the true rate constant, calculated taking into account the partition coefficient of tetranitromethane between the aqueous phase and the micelles, diminishes appreciably under these conditions. The reaction can be represented by the equations

$$\begin{aligned} R_2NO^{\cdot} + C(NO_2)_4 &\xrightarrow{k} R_2NO^+ + C(NO_2)_3^- + NO_2^{\cdot}, \\ R_2NO^{\cdot} + NO_2^{\cdot} &\xrightarrow{k'} R_2NO^+ + NO_2^-, \end{aligned} \qquad (5)$$

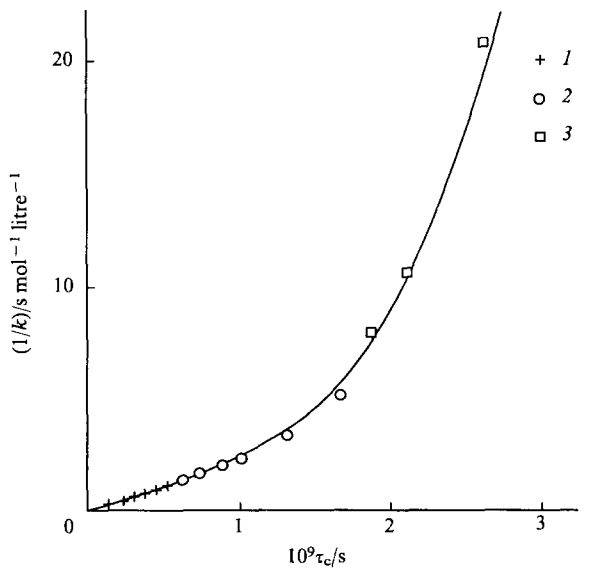


Figure 2. Dependence of the rate constant for reaction (5) on molecular mobility:[20] (*1*) 3:1 water–*tert*-butyl alcohol; (*2*) molecular solution of Triton X100; (*3*) WR1339.

where k is much smaller than k', so that the rate-limiting stage is electron transfer between the nitroxyl radical and the tetranitromethane molecule. Fig. 2 illustrates the dependence of $1/k$ on τ_c. Different values of τ_c at the same temperature are found for the aqueous alcoholic and micellar solutions. In the same medium, the quantity τ_c was varied by varying the temperature in the range 0–50 °C. The non-linearity of the plot in Fig. 2 can be attributed to the temperature dependence of the coefficient α in Eqn (4).

One should note specially that the transition from the homogeneous water–*tert*-butyl alcohol system to micellar systems with molecular organisation is manifested solely by a change in the reorientational mobility of the reactants. In other words, the reactivity is determined unambiguously by the molecular mobility, the measurement of which makes it possible to predict the rates of the elementary reactions even in complex systems such as micellar solutions.

III. The influence of the mobility of the medium on the kinetics of intramolecular radical substitution reactions

We examined above the correlation between the reaction kinetics and the molecular mobility of the reactants for bimolecular processes in which the characteristic reaction time exceeds by several orders of magnitude the characteristic time of rotation of the reactants. The influence of the mobility of the medium on the kinetics of slow bimolecular reactions appears comparatively evident in view of the high stereospecificity of these reactions and the need to assume a favourable mutual orientation of the reactants during the process. The kinetics of such reactions of free radicals have been investigated using the time variation of the intensity of the EPR spectra. The use under these conditions of stable nitroxyl radicals, for which a method of measurement of the rotational mobility correlation time has been well developed, makes it possible to find a relation between the reaction kinetics and the mobility of the medium. The effects associated with the modulation of anisotropic magnetic parameters (HFI constants and the g-factor), which lead to the broadening of the lines, are used to analyse the molecular mobility. In the region of rapid rotations of the radical ($\gamma b_{an}\tau_c \ll 1$, where b_{an} is the parameter of the anisotropy of the EPR spectrum and γ the gyromagnetic ratio for the electron), the line width, which depends on the molecular reorientations, is defined by the relation

$$\delta_m = d\gamma b_{an}^2 \tau_c , \qquad (6)$$

where $d \simeq 1$ is a coefficient. The parameter b_{an} includes the anisotropy of the g-factor and of the HFI constant:

$$b_{an} = H_0 \frac{\Delta g}{g} + \Delta B m , \qquad (7)$$

where H_0 is the external magnetic field, Δg the anisotropy of the g-factor, ΔB the anisotropy of the HFI constant, and m the overall projection of the nuclear spin. The components of the EPR spectrum of the radical with different values of m have different values of b_{an}, so that the degrees of broadening δ_m induced by the rotation of the radical differ for different components of the hyperfine structure.

In reality the observed line width Γ_m always includes also an intrinsic width δ_0 which is independent of molecular motions:

$$\Gamma_m = \delta_0 + \delta_m .$$

The contribution to line broadening due to rotation δ_m can be measured provided that $\delta_m > 0.1\delta_0$. The minimum measurable value of τ_c can then be defined thus:

$$\tau_c > 0.1 \frac{\delta}{\gamma d b_{an}^2} .$$

For stable nitroxyl radicals, the anisotropy parameters b_{an} are fairly large and can be measured in the usual 3 cm EPR range. This fact is apparently one of the main reasons for the widescale use of nitroxyl radicals in the study of molecular dynamics — in particular the relation between molecular dynamics and reactivity.

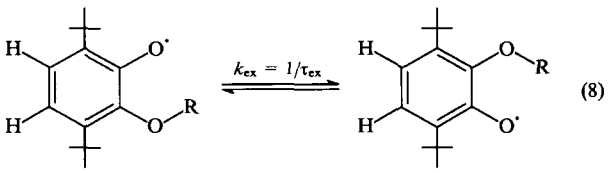
In order to discover this relation, it is essential to extend in experimental measurements the range of the measured rate constants for chemical reactions and to diversify the types of model objects. In particular, the elucidation of the reactivity of phenoxyl radicals in polymers is important in connection with the extensive application of substituted phenols as antioxidants.[21] For example, a purely qualitative correlation between the rate of reaction and the rotation frequency of the phenoxyl radicals in terms of the change in the line form of the EPR spectrum on passing from slow to fast motion has been observed[2] for reaction (1). For the PhO· radical, it is not possible to determine the quantity b_{an} from the EPR spectra in the 3 cm range and it is therefore not possible to obtain the values of τ_c and to compare them with the experimental rate constants, as has been done, for example, for reactions (2), (3), and (5) of nitroxyl radicals.

As 2 mm EPR spectroscopy developed, it became possible to measure the anisotropy parameters for a wide range of organic radicals, in particular, for radicals of the phenoxyl type.[22] This makes it possible to investigate the relation between molecular dynamics and the reactivity of such radicals. Furthermore, they constitute a unique class of free radicals entering into various chemical reactions, the elementary rate constants of which vary within a wide range as a function of the type of reaction and the structure of the radical.[23] In particular, rapid exchange processes, which, like rapid rotational motions of radicals, lead to dynamic effects in the EPR spectra, are characteristic of radicals of this type. However, in contrast to rotational processes, the effects of the chemical line broadening are based on the modulation of the isotropic magnetic parameters of the free radicals.[23] Such effects make it possible to obtain information about the kinetics and thermodynamics of rapid reversible chemical processes occurring with characteristic times $\tau = 1/k = 10^{-9}-10^{-6}$ s. The rotational mobility times τ_c in liquid viscous solutions fall within approximately the same range. This provides a unique possibility, where, by using simultaneously both types of dynamic effects in the EPR spectra of free radicals, one can obtain information under comparable conditions about the kinetics of the elementary chemical reaction and molecular mobility and the characteristic times τ and τ_c have comparable orders of magnitude.

The influence of the mobility of the medium on the kinetics of a series of intramolecular exchange reactions of phenoxyl or *o*-semiquinone radicals, which are intermolecular radical substitution reactions, was first demonstrated in a number of studies.[24-32] The methodological features associated with the corresponding EPR experiments will be examined in greater detail in relation to tin-containing substituted 2-R-oxyphenoxyl radicals. For other systems, we shall discuss only the kinetics of intramolecular reactions in viscous media.

1. EPR study of the molecular and chemical dynamics of free radicals in the 2 mm and 3 cm ranges

The 3,6-di-*tert*-butyl-2-R-oxyphenoxyl radicals were found to be convenient for the simultaneous investigation of the molecular and chemical dynamics of free radicals. A characteristic feature of these phenoxyl radicals is a degenerate tautomerism, which involves the reversible migration of the organoelement fragment R between two oxygen atoms and which constitutes an intramolecular radical substitution reaction.[33]



(8)

The rapid intramolecular migration of the fragment R at high temperatures leads to the equivalence of the two ring protons and a triplet EPR spectrum. At low temperatures, in the absence of chemical exchange the spectrum is represented by a doublet of doublets due to the two non-equivalent protons. In the intermediate temperature range, dynamic effects leading to the exchange broadening of the internal components of the quartet are observed. This makes it possible to find the rate constant or the characteristic time of the chemical exchange $k_{ex} = 1/\tau_{ex}$. We shall consider the possibilities of the EPR method for the simultaneous investigation of the molecular and chemical dynamics of radicals of the type indicated and shall analyse the relation between the quantities τ_{ex} and τ_c.

As noted above, for the calculation of the correlation times of the rotational mobility τ_c it is essential to know the parameters of the anisotropy of the radicals. In the original communications,[24-32] the measured values of τ_c for the radicals are quoted on the basis of rough estimates of the anisotropy parameters derived from poorly resolved 3 cm EPR spectra. The use of 2 mm spectroscopy for a more accurate measurement of the quantity τ_c is extremely important in the quantitative analysis of the influence of molecular mobility on chemical reactivity. The relation between τ_{ex} and τ_c has been investigated[34] with the aid of 2 mm EPR data for tin-containing 3,6-di-*tert*-butyl-2-R-oxyphenoxyl radicals, where R = $SnPh_3$ (**1**) or $SnClMe_2$ (**2**).

Fig. 3*a* presents the EPR spectra of frozen toluene solutions of radical **1** in the 3 cm and 2 mm ranges. Evidently in the former case it is impossible to obtain the anisotropy parameters, while in the latter the canonical components (g_x, g_y, g_z) of the *g*-tensor are manifested quite clearly. Furthermore, the corresponding component B_y of the HFI tensor is manifested in the *y*-orientation. Evidently, the doublet splitting is due to the interaction of the unpaired electron with the aromatic ring proton in the *para*-position relative to the non-coordinated oxygen atom, to which the highest spin density corresponds. The other two components of the HFI tensor (B_x and B_z) were estimated with the aid of computer modelling on the basis of the experimental line widths of the canonical components taking into account the fact that the isotropic HFI constant $a_H^{para} = (B_x + B_y + B_z)/3$ is known from the EPR spectra of the radical in solution. The anisotropy parameters found in this way for radical **1** are

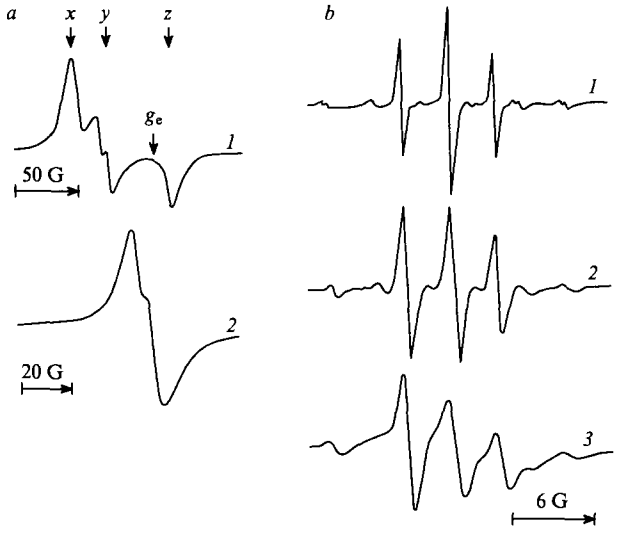


Figure 3. EPR spectra of radical **1**: (*a*) spectra of frozen toluene solutions of the radical in the 2 mm (curve *1*) and 3 cm (curve *2*) ranges; (*b*) spectra in the 3 cm range at 20 °C in the 1:2 (curve *1*) and 1:10 (curve *2*) hexane + liquid paraffin mixtures and in liquid paraffin (curve *3*); the satellite lines are due to the ^{117}Sn and ^{119}Sn isotopes.

as follows:

$$\Delta g_x = 1.88\times10^{-3},\ \Delta g_y = 0.44\times10^{-3},\ \Delta g_z = -2.32\times10^{-3},$$

$$\Delta B_x = 2.6,\ \Delta B_y = -2.6,\ \Delta B_z = 0.0\ \text{G}.$$

The contribution to the line width of the hyperfine structure component with an overall nuclear spin m can be represented in the form[35]

$$\delta_m = \frac{2}{15}\gamma\tau_c \sum_{i=x,y,z}\left(\frac{\Delta g_i H_0}{g} + \Delta B_i m\right)^2.$$

The overall line width for the hyperfine structure component is

$$\Gamma_m = \left(\frac{2}{3}\right)^{1/2}\left[\frac{2}{15}\gamma\tau_c \sum_{i=x,y,z}\left(\frac{\Delta g_i H_0}{g} + \Delta B_i m\right)^2\right] + \delta_0. \qquad (9)$$

It is assumed here that the lines of the hyperfine structure components have the Lorentzian shape and, since the line widths are measured between the points of maximum slope (the first derivative absorption line), it follows that $\Gamma_m = (2/3)^{1/2}(T_2)^{-1}$.

Fig. 3*b* illustrates the EPR spectra of radical **1** in media of different viscosity, which was varied with the aid of hexane–liquid paraffin mixtures having different component ratios. Under the conditions of rapid chemical exchange, the spectrum of this radical remains of the triplet type with a hyperfine structure constant $a = (1/2)\ (a_H^{para} + a_H^{meta})$, but an increase in the viscosity of the medium leads to a non-uniform broadening of the hyperfine structure components corresponding to the overall projection of the nuclear spin $m = -1, 0, +1$. We shall designate the widths of these components by Γ_{-1}, Γ_0, and Γ_{+1} respectively. Since the hyperfine structure constants for the protons in the *para*- and *meta*-positions in the aromatic ring of the radical are negative, the line width Γ_{-1} corresponds to the downfield component ($m = -1$). The following expressions for the line width of the hyperfine structure components can then be obtained from Eqn (9):

$$\Gamma_{-1} = \left(\frac{2}{3}\right)^{1/2}\left[\frac{2}{15}\gamma\tau_c \sum_{i=x,y,z}\left(\frac{\Delta g_i H}{g_0} - \Delta B_i\right)^2\right] + \delta_0,$$

$$\Gamma_0 = \left(\frac{2}{3}\right)^{1/2}\left[\frac{2}{15}\gamma\tau_c \sum_{i=x,y,z}\left(\frac{\Delta g_i H}{g_0}\right)^2\right] + \delta_0, \qquad (10)$$

$$\Gamma_{+1} = \left(\frac{2}{3}\right)^{1/2}\left[\frac{2}{15}\gamma\tau_c \sum_{i=x,y,z}\left(\frac{\Delta g_i H}{g_0} + \Delta B_i\right)^2\right] + \delta_0,$$

where δ_0 is the intrinsic line width and g_0 the isotropic g-factor of the radical.

Measurement of the line width showed that the central component with $m = 0$ is broadened to a much greater extent than predicted by Eqn (10). This is associated with the fact that the contribution to the broadening due to the inhibition of the intramolecular migration of the $SnPh_3$ group in radical **1** must be taken into account for this component. The contribution to the line broadening (only for the component with $m = 0$) due to chemical exchange is defined by the relation[35]

$$\delta_{ex} = \left(\frac{2}{3}\right)^{1/2}\gamma\tau_{ex}\left(\frac{\Delta a^2}{8}\right), \qquad (11)$$

where $\Delta a = a_H^{para} - a_H^{meta}$ is the difference between the hyperfine structure constants due to the protons in the *para*- and *meta*-positions, i.e.

$$\Gamma_0 = \left(\frac{2}{3}\right)^{1/2}\left[\frac{2}{15}\gamma\tau_c \sum_{i=x,y,z}\left(\frac{\Delta g_i H}{g_0}\right)^2\right] + \delta_0 + \delta_{ex}. \qquad (12)$$

The following expressions relating the line widths of the three components to τ_c and τ_{ex} can be obtained from Eqns (10)–(12) taking into account the anisotropies found for the magnetic parameters:

$$\Gamma_{+1} - \Gamma_{-1} = 1.47\gamma\tau_c,$$

$$\Gamma_0 - \Gamma_{-1} = 1.16\gamma\tau_c + 1.39\gamma\tau_{ex}. \qquad (13)$$

The numerical coefficients of τ_c and τ_{ex} have the dimensions G^2.

From the methodological point of view, the measurement of the line amplitude and not the line width is more convenient. The ratios of the integral intensities of the components with $m = -1, 0, +1$ are 1:2:1, i.e. $2I_{-1}\Gamma_{-1}^2 = I_0\Gamma_0^2 = 2I_{+1}\Gamma_{+1}^2$, where I_{-1}, I_0, and I_{+1} are the corresponding amplitudes. In this case, the line amplitudes I_{-1}, I_0, and I_{+1} and the widths of only the downfield component Γ_{-1} must be measured in order to calculate τ_c and τ_{ex}:

$$\left[\left(\frac{I_{-1}}{I_{+1}}\right)^{1/2} - 1\right]\Gamma_{-1} = 1.47\gamma\tau_c,$$

$$\left[\left(\frac{2I_{-1}}{I_0}\right)^{1/2} - 1\right]\Gamma_{-1} = 1.16\gamma\tau_c + 1.39\gamma\tau_{ex}. \qquad (14)$$

Fig. 4 presents the dependence of τ_{ex} on τ_c for radical **1**. The linear correlation $\tau_{ex} = \alpha\tau_c$ is retained, but the coefficient α, which is 3–4 according to the data of Rakhimov et al.,[28] is 0.5–1.0 according to more accurate estimates.[34]

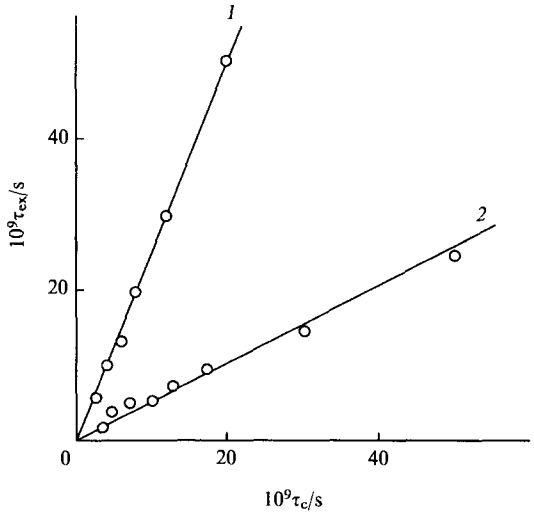


Figure 4. Dependence of τ_{ex} on τ_c for radical **1**: (*1*) according to data of Rakhimov et al.[28]; (*2*) calculation by Eqn (14) from EPR data in the 2 mm range[34] (τ_c was varied by raising the temperature from 0 to 50 °C in liquid paraffin).

The 2 mm EPR spectra of frozen solutions of radicals **1** and **2** are similar, but there is a somewhat different spectral pattern for radical **2**. Under comparable conditions (temperature, viscosity), the frequency of chemical exchange in radical **2** (intramolecular migration of the $SnClMe_2$ group) is smaller by 3–4 orders of magnitude than in radical **1**. As a result of this, the EPR spectra of radical **2** are quartets corresponding to slow and intermediate exchange conditions, where the two inner components of the quartet have undergone exchange broadening (Fig. 5*a*). An increase in the viscosity of the medium lowers the rate of chemical exchange (increases τ_{ex}). As for radical **1**, the extreme components of this spectrum are then non-uniformly broadened, which makes

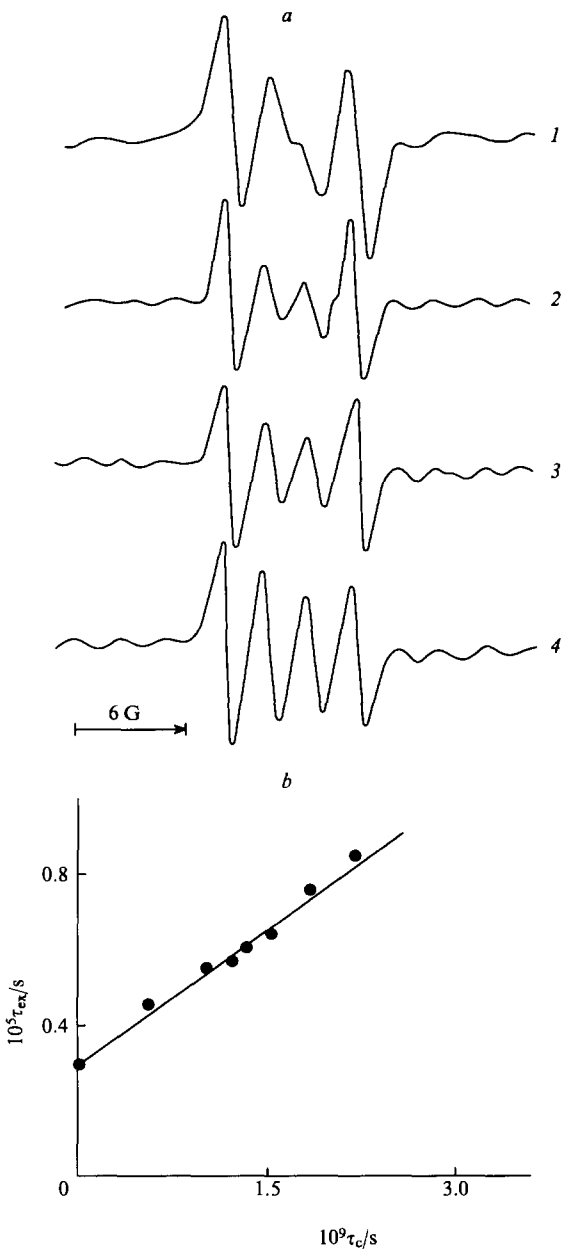


Figure 5. Spectroscopic characteristics of radical **2**: (*a*) EPR spectra in the 3 cm range at 30 °C in hexane (curve *1*), in the 1 : 1 hexane + liquid paraffin mixture (curve *2*), in the 1 : 10 hexane + liquid paraffin mixture (curve *3*), and in liquid paraffin (curve *4*); (*b*) dependence of τ_{ex} on τ_c obtained on varying the viscosity and temperature (from 20 to 30 °C).

it possible to estimate τ_c. The following experimental relation between τ_{ex} and τ_c has been obtained:[29]

$$\tau_{ex} = \tau_f + 8900\tau_c ,$$

where τ_f is the reaction time in a non-viscous medium ($\tau_c \to 0$). The times τ_{ex} and τ_c were found with the aid of the exact values of the anisotropy parameters for radical **2** (Fig. 5*b*). They are described by the relation

$$\tau_{ex} = \tau_f + 2400\tau_c .$$

The intramolecular radical substitution reaction (8) alters the directions of the magnetic axes in space (in particular the *y* axis of radicals **1** and **2** coincides with the axis passing through the C–O· bond involving the non-coordinated oxygen atom[22]). It is therefore impossible to rule out the possibility of the direct influence of chemical exchange on the effects of the modulation of the anisotropy parameters, leading to the broadening of the extreme components of the EPR spectra of radicals of the type considered (with $m = -1, +1$). In the case of radical **2**, the observed correlation between τ_{ex} and τ_c cannot be accounted for by the direct influence of chemical exchange on the measured τ_c, since the characteristic time of the exchange is three orders of magnitude greater than the characteristic time of molecular reorientations.

A completely different situation arises for radical **1**. As shown above, the characteristic times of the chemical exchange and the rotational motions for this radical are comparable ($\tau_{ex} \simeq \tau_c$), so that in the given instance it is necessary to consider the possibility of the direct influence of chemical exchange on the measured τ_c.

In order to elucidate the problem, a quantitative comparison was carried out[36] of the rotational mobilities of radical **1** and the corresponding isomeric radical 3,5-di-*tert*-butyl-2-triphenylstannyloxyphenoxyl **1A**.

Fig. 6 presents the EPR spectra of radicals **1** and **1A** under comparable conditions. In contrast to radical **1**, in radical **1A** there are no intramolecular migrations of the $SnPh_3$ group (because of the difference in the shielding of the oxygen atoms) and its EPR spectrum is a doublet due to the proton in the *meta*-position relative to the non-coordinated oxygen atoms. The non-uniform broadening of the components of the doublet is evidently caused solely by effects associated with the modulation of the anisotropic magnetic parameters of radical **1A** due to rotational motions. The anisotropic parameters of radical **1A** have been found[22] by 2 mm EPR. They make it possible to calculate the times τ_c for a radical in which there is no chemical exchange. The characteristic correlation time for the rotation of a radical without chemical exchange (i.e. radical **1A**) will be designated by τ_c'. Fig. 7 presents the rotation correlation times for radicals **1** (τ_c) and **1A** (τ_c') under comparable conditions. It is essential to note in the first place that the dependence of τ_c on τ_c' is linear: $\tau_c = b\tau_c'$. This means that the linear relation between the characteristic time of the chemical exchange τ_{ex} and the 'true' correlation time of the molecular motions is observed in all cases for radical **1**. In liquid paraffin, in the temperature range from 15 to 50 °C, we have $b = 0.4$, whereas in toluene at appreciably lower temperatures (−100 to −75 °C) we have $b = 0.75$.

Thus the correlation time of the rotational mobility τ_c' of a radical without chemical exchange is greater than that of a radical with chemical exchange. This can be explained by the direct influence of the latter on the measured time τ_c for radical **1**, i.e. if one assumes that τ_c' is the 'true' correlation time of the rotational mobility of the radical, then the measured τ_c for the radical with chemical exchange is reduced compared with τ_c'. Predictably, at high temperatures, where the contribution of chemical exchange increases, the difference between τ_c and τ_c' increases.

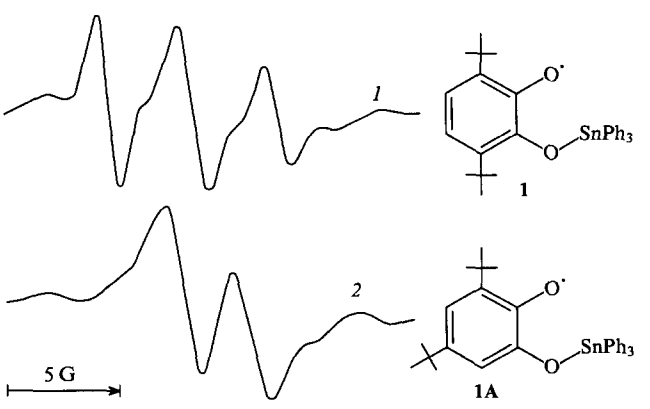


Figure 6. EPR spectra of radicals **1** (curve *1*) and **1A** (curve *2*) in liquid paraffin at 20 °C.

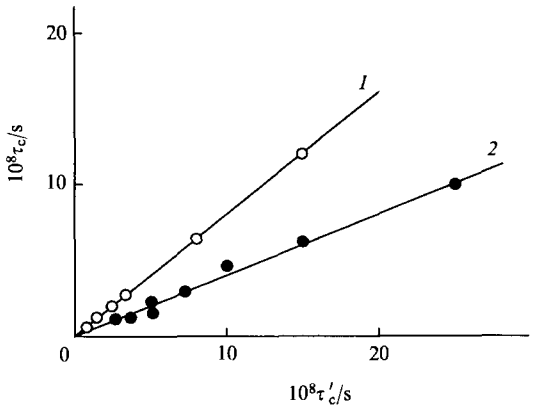
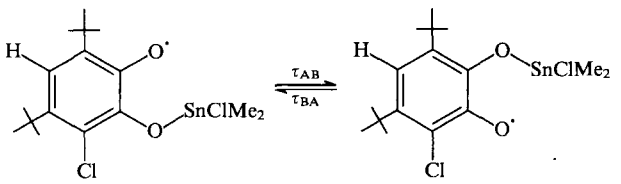


Figure 7. Correlation times of the rotational mobility for radicals **1** and **1A** in toluene for temperatures in the range −100 to −75 °C (line *1*) and in liquid paraffin for temperatures in the range 15 – 20 °C (line *2*).

The examples of the intramolecular reactions of radicals **1** and **2** examined represent chemical exchange between degenerate states (the forward and reverse reactions are identical). In substituted tin-containing oxyphenoxyl radicals with asymmetrically disposed substituents, one may observe reversible intramolecular processes which represent a non-degenerate tautomerism of the free radicals.[37] The influence of the mobility of the medium on the dynamics of the stannotropism of the 3,5-di-*tert*-butyl-2-chlorodimethylstannyloxyphenoxyl radical **3** has been investigated.[30] The chemical exchange process can be represented in this instance in the following form:



3A **3B**

The EPR spectrum of radical **3** in the absence of exchange at low temperatures constitutes a superposition of the spectra of two forms, **3A** and **3B**, differing in the constant for the hyperfine interaction with the aromatic ring proton. In the **A** form, the ring proton is in the *meta*-position relative to the non-coordinated oxygen atom with a_H^A = 2.3 G, whereas in the **B** form the ring proton is in the *para*-position with a_H^B = 4.9 G.[37] For high rates of exchange, an increase in temperature leads to the observation in the EPR spectra of dynamic effects due to transitions between the two forms of radical **3**. The equilibrium constant

$$K = \frac{I_B}{I_A} = \frac{k_{AB}}{k_{BA}} = \frac{\tau_{BA}}{\tau_{AB}}$$

can be determined from the ratio of the integral intensities, and analysis of the line broadening makes it possible to determine the chemical exchange frequency:

$$\nu_{ex} = k_{AB} + k_{BA} = \frac{\tau_{AB}\tau_{BA}}{\tau_{AB} + \tau_{BA}},$$

where $k_{AB} = 1/\tau_{AB}$ and $k_{BA} = 1/\tau_{BA}$ are the rate constants for the forward and reverse reactions respectively. Thus the rate constants for the forward and reverse reactions or the times τ_{AB} and τ_{BA} can be determined separately.

Similar dynamic effects are observed when the viscosity of the medium is varied: the exchange frequency diminishes on passing

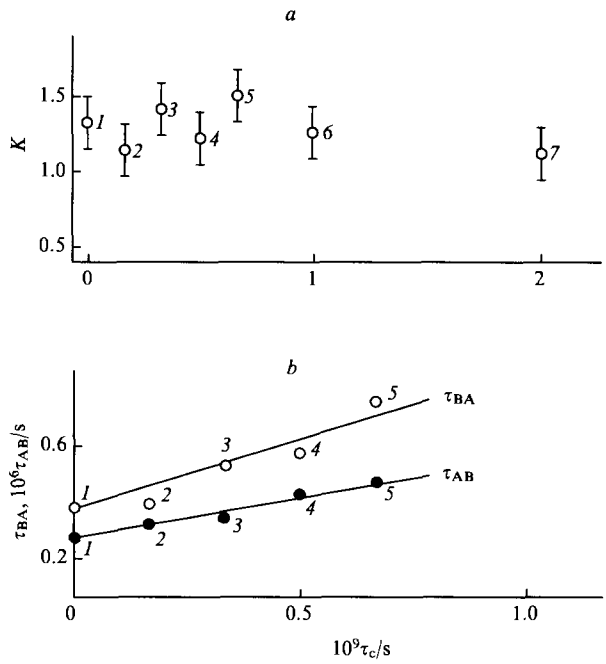


Figure 8. Dependence of the equilibrium constant (*a*) and the characteristic times for the forward (τ_{AB}) and reverse (τ_{BA}) reactions (*b*) on the correlation time of the rotational mobility τ_c at 15 °C: (*1*) hexane; (*2*)–(*6*) 1 : 1 (curve *2*), 1 : 3 (curve *3*), 1 : 5 (curve *4*), 1 : 7 (curve *5*), and 1 : 10 (curve *6*) hexane + liquid paraffin mixtures; (*7*) liquid paraffin; τ_{AB} and τ_{BA} were obtained under the conditions of intermediate exchange; since the spectrum at points *6* and *7* corresponded to slow exchange conditions, τ_{AB} and τ_{BA} were not calculated.

to more viscous media. The rotational mobility correlation time cannot be determined from the EPR spectra of radical **3** because the broadening induced by chemical exchange is much greater than the effects of the modulation of the anisotropic hyperfine interaction. For this reason, the values measured for radical **2** in the same media were adopted as the parameter τ_c. Fig. 8 presents the dependence of the equilibrium constant, τ_{AB}, and τ_{BA} on τ_c. Evidently, a nearly linear relation is observed between the chemical exchange times and the rotational mobility, while the equilibrium constant is independent of molecular mobility within the limits of the accuracy of the measurement.

2. Other intramolecular radical substitution reactions

The data presented above indicate a relation between molecular and chemical dynamics also for rapid reversible intramolecular reactions of free radicals. Eqn (4) also holds for such radicals and in the case of unimolecular reactions can be more conveniently expressed in the form

$$\tau = \tau_f + \alpha\tau_c, \qquad (15)$$

where $\tau = 1/k$ and $\tau_f = 1/k_f$.

The influence of molecular mobility on a series of intramolecular radical substitution reactions of type (8) involving other organoelement fragments R in 3,6-di-*tert*-butyl-2-R-oxyphenoxyl radicals, for example, R = ZnAcac (**4**), CdAcac (**5**), ZnS(S)CoBu (**6**), $PbPh_3$ (**7**), H (**8**) $\overset{+}{N}HBu^t_3$ (**9**), and $\overset{+}{N}H_2Bu_2$ (**10**), has been investigated in recent years. Since similar features of the EPR spectra in viscous media (under the conditions of rapid chemical exchange) are characteristic of radicals **4**–**10**, we shall discuss certain phenomenological characteristics of the relation between τ_{ex} and τ_c without going into the details of the EPR experiment.

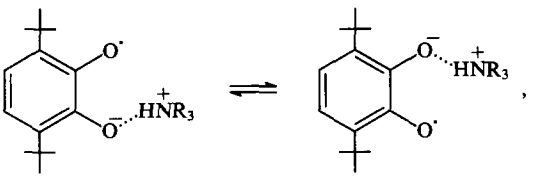
The study of the elementary reactions in condensed media can be usefully carried out within the framework of a formal-kinetic approach.[19] A characteristic feature of the temperature variations of the rate constants for reactions in condensed media, especially

reactions in the solid phase, is the deviation in certain cases from the Arrhenius relation

$$\ln k = \ln k_0 - \frac{E}{RT}. \quad (16)$$

Furthermore, this deviation is frequently 'masked', being manifested solely by anomalous values of the kinetic parameters—the pre-exponential factor k_0 and the activation energy E. The experimental values of $\ln k_0$ and E for isotypical reactions vary together under these conditions, i.e. the so called compensation effect is observed.[19]

The influence of the mobility of the medium on the kinetics of the intramolecular migration of a hydrogen atom in radical **8** and the kinetics of the migration of the hydrogen bond in the corresponding 3,6-di-*tert*-butyl-*o*-semiquinone radical-anion combined with alkylammonium cations,



where NR_3 = tri-*tert*-butylamine and di-*tert*-butylamine (radicals **9** and **10** respectively) has been investigated.[26]

The corresponding Arrhenius temperature dependences of the times τ_{ex} for media of different viscosity are represented by straight lines, i.e. the chemical reaction time τ_{ex} can be expressed in the form

$$\tau_{ex} = \tau_{ex}^0 \exp\left(\frac{E_{ex}}{RT}\right), \quad (17)$$

where $\tau_{ex}^0 = 1/k_0$ in conformity with Eqn (16) and E_{ex} is the activation energy for the reaction.

Table 1 presents the values of E_{ex} and τ_{ex}^0 for the migration of the hydrogen bond in radical **10** in media of different viscosity. Evidently, with increase in the viscosity of the medium, the quantity E_{ex} diminishes but τ_{ex}^0 increases. Furthermore, similar changes have been observed for a medium of the same composition when the temperature was reduced. Fig. 9 presents the dependence of $\ln \tau_{ex}^0$ on E_{ex}. The linearity of this relation indicates the existence of the compensation effect and the values of E_{ex} and τ_{ex}^0 have therefore no direct physical significance.

The observation of the compensation relation between E_{ex} and τ_{ex}^0 may indicate that the Arrhenius relation in the form of

Table 1. E_{ex} and τ_{ex}^0 for the migration of the hydrogen bond in radical **10** in different media.

Medium[a]	T/°C	E_{ex}/kcal mol^{-1}	τ_{ex}^0/s
LP	5–20	3.5	5.5×10^{-10}
H+LP (1:5)	−10–20	5.5	2.4×10^{-11}
H+LP (1:3)	−10–10	6.3	1.3×10^{-12}
H+LP (1:1)	−10–0	10.7	1.4×10^{-16}
H+LP (1:1)	−60 to −40	2.5	0.8×10^{-9}

[a] H = hexane, LP = liquid paraffin.

Eqn (16) or (17) does not in reality hold. This has been confirmed, in particular, by the temperature variation of τ_{ex} in terms of the Arrhenius variables (Fig. 10). Thus Eqn (17) cannot be used to estimate the elementary rate constants.

Evidently, the sharp change in the kinetic parameters of the reaction is associated with the sharp alteration of the state of the medium (phase or structural transition, etc.). Under these conditions, there is an abrupt change also in the nature of the motion of the radical, i.e. the parallel variation of τ_{ex} and τ_c with temperature is observed (Fig. 10). Consequently, the correlation between the molecular motions and reactivity exists both before and after the phase or structural transition. Despite the fact that the reaction considered is an extremely simple chemical process, occurring in a non-polar medium (hexane + liquid paraffin), the viscosity of the medium exerts a significant influence on its rate. Analysis of the relation between τ_{ex} and τ_c for radical **10** shows that τ_{ex} is approximately two orders of magnitude greater than τ_c. For the intramolecular hydrogen atom transfer reaction in radical **8**, a linear relation is also observed between τ_{ex} and τ_c, but these parameters are similar as regards order of magnitude, so that account must be taken of the possible direct influence of the migration of the hydrogen atom on the measured time τ_c.

A linear relation between τ_{ex} and τ_c for radical **10** is observed when both the temperature and the viscosity of the medium are varied, which can be accounted for by the weak temperature dependence of the coefficient α in Eqn (15). In certain cases, such a relation was observed for radicals of the type considered. As an example, we shall consider the data obtained for radical **7**.

Under conditions where $\tau_c = 0$ (the widths of the lines of the extreme components of the triplet EPR spectrum are identical), the ratios of the amplitudes of the components of the proton hyperfine structure are always 1 : 2 : 1. This means that $\tau_f = 0$, so that the coefficient represents the ratio of the chemical exchange time τ_{ex} and the rotational mobility correlation time τ_c.

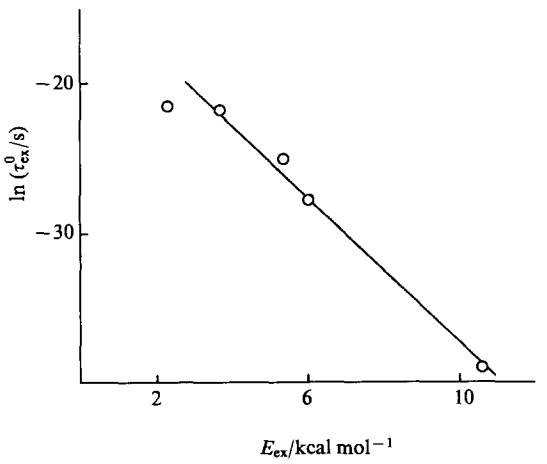


Figure 9. Dependence of $\ln \tau_{ex}^0$ on E_{ex} for radical **10**.

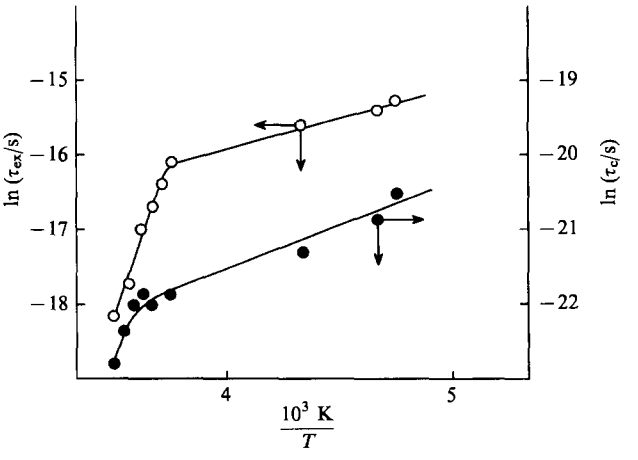


Figure 10. Temperature variation of τ_{ex} and τ_c in terms of the Arrhenius variables for radical **10** in the 1 : 1 hexane + liquid paraffin mixture.

Fig. 11 presents the EPR spectra of radical **7**. Evidently, a decrease in the rate of rotation of the radical leads to the inhibition of the chemical reaction both with increase in the viscosity of the medium and with decrease in temperature. However, comparison of spectra *4* and *5* shows that they correspond approximately to the same value of τ_c for the radical but at a low temperature (−134 °C, pentane) the central line is split, which corresponds to a slow chemical exchange. This means that, for the same value of τ_c, the inequality τ_{ex} (−134 °C) > τ_{ex} (20 °C) holds. This example indicates an increase in the coefficient α with decrease in temperature. Fig. 12 presents the relation between τ_{ex} and τ_c for radical **7**. The variation of τ_c with temperature and composition (viscosity) of the medium leads to a qualitatively different relation between τ_{ex} and τ_c. A satisfactory linear correlation between τ_{ex} and τ_c is observed only for the isothermal variation of the viscosity of the medium. If τ_c varies when the temperature is varied over a wide range, the relation between τ_{ex} and τ_c becomes non-linear and, as was to be expected, a decrease in temperature not only reduces the molecular mobility but also retards the chemical reaction proper, so that the relation between τ_{ex} and τ_c becomes steeper.

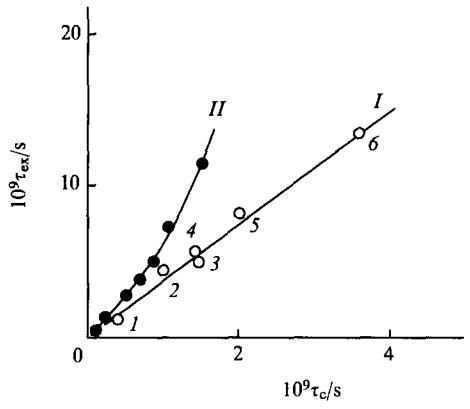


Figure 12. Dependence of τ_{ex} on τ_c for radical **7**: (*I*) variation of the composition of the medium at 20 °C with the aid of 1 : 1 (curve *1*), 1 : 3 (curve *2*), 1 : 5 (curve *3*), 1 : 7 (curve *4*), and 1 : 10 (curve *5*) heptane + liquid paraffin mixtures; (*6*) liquid paraffin; (*II*) variation of temperature in the range −85 to −20 °C in heptane.

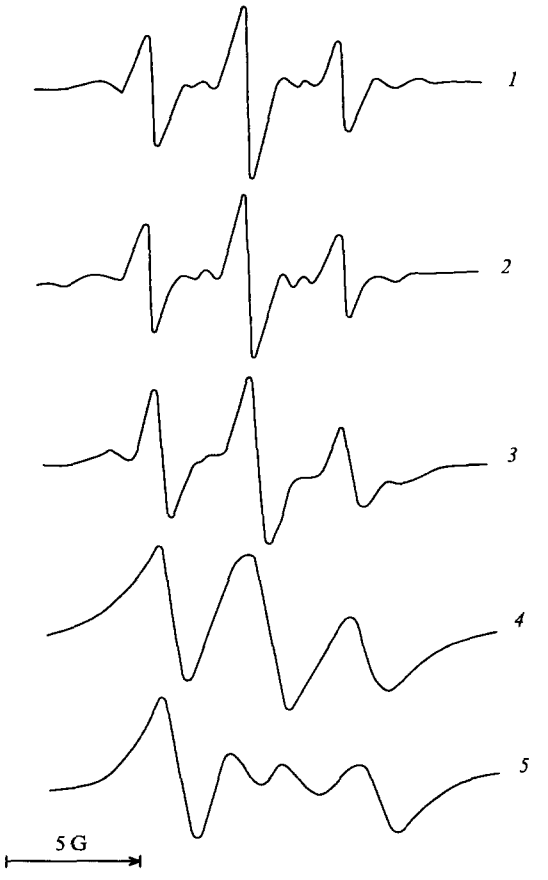
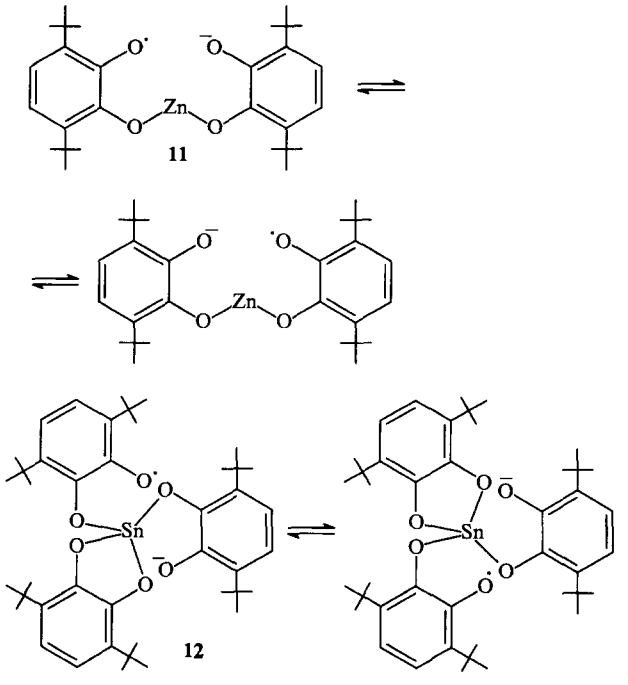


Figure 11. EPR spectra of radical **7** at 20 °C; heptane : liquid paraffin ratio in the heptane + liquid paraffin mixture: (*1*) 1 : 1; (*2*) 1 : 5; (*3*) 1 : 10; (*4*) liquid paraffin; (*5*) pentane at −134 °C; the satellite lines are due to the ^{207}Pb isotope.

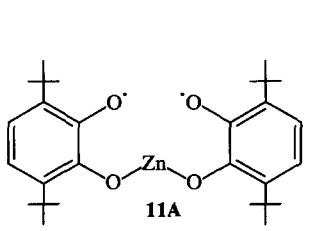
Hitherto we have considered the intramolecular radical substitution reactions in which the centre corresponding to the location of the unpaired electron changed as a result of the intramolecular transfer of an atom or group of atoms (exchange of the unpaired electron and of the bond within one ligand). Another type of intramolecular chemical exchange reactions may be observed for radical complexes of metals with two and three ligands between which the unpaired electron is exchanged (interligand exchange).

A similar interligand exchange of the unpaired electron (and charge) has been observed[38,39] by the EPR method in the radical-anion complexes of zinc and tin.

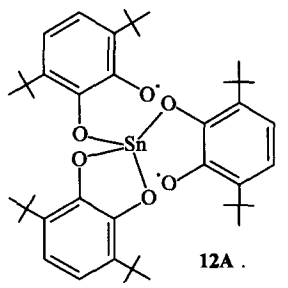


At low temperatures, the unpaired electron is located on one ligand, which leads to a triplet EPR spectrum determined by the hyperfine interaction with two equivalent protons (within one ligand, the unpaired electron either migrates rapidly between two oxygen atoms or is distributed symmetrically). At high temperatures, the unpaired electron migrates around all the ligands and the EPR spectra show splitting due to all the ligand protons (four protons in complex **11** and six protons in complex **12**). In the intermediate temperature range, the alternation of line widths is observed. Its analysis makes it possible to determine τ_{ex}. Specific line broadening, due to the effects of the modulation of the anisotropic magnetic parameters, has not been observed in the EPR spectra of the radical-anion complexes. This may be associated with the absence of an appreciable anisotropy of the

g-factor and the HFI constant. Therefore, the EPR spectra of the corresponding biradicals have been used[31] to determine τ_c:



11A



12A .

The EPR spectra of biradicals **11A** and **12A** in solution consist of broad singlet lines. In order to determine the rotation correlation time τ_c from the line width in the EPR spectra of the biradicals, the following formula must be used:[35]

$$T_2^{-1} = \frac{D^2}{20}\left(6\tau_c + \frac{10\tau_c}{1+\omega^2\tau_c^2} + \frac{4\tau_c}{1+\Delta\omega^2\tau_c^2}\right), \qquad (18)$$

where $D^2 = D_x^2 + D_y^2 + D_z^2$, D_x, D_y, and D_z being the principal values of the dipole–dipole interaction tensor in units of frequency. In our case, $\tau_c \simeq 10^{-9}$ s, so that $\omega\tau_c \gg 1$ and one need retain only the first term in Eqn (18). Having expressed D_x, D_y, and D_z in magnetic induction units, we obtain

$$\tau_c = \frac{5\delta H}{\sqrt{3}\gamma D^2},$$

where δH is the EPR line width of the biradical measured between points of maximum slope.

Fig. 13 presents the EPR spectra of the radical-anion complex **12** and the corresponding biradical **12A**. Evidently, with increase in rotational correlation time (with increase in the line width of the biradical in the EPR spectrum), the chemical exchange time τ_{ex} also increases (broadening of the components of the hyperfine structure with $m = \pm 2, \pm 1$). The relation between τ_{ex} and τ_c for the radical-anionic complexes **11** and **12** is described satisfactorily by Eqn (15). The times τ_{ex} and τ_c were measured in the temperature range -50 to 0 °C in solution in tetrahydrofuran (THF), the temperature variation of τ_{ex} and τ_c satisfying the Arrhenius relation. The kinetic parameters of the chemical exchange and of the rotational mobility for the radical-anionic complex **11** and biradical **11A** were found to be as follows: $E_{ex} = 4.5$ kcal mol^{-1}, $\tau_{ex}^0 = 3.9 \times 10^{-12}$ s, $E_c = 4.0$ kcal mol^{-1}, and $\tau_c^0 = 1.1 \times 10^{-13}$ s; for complexes **12** and **12A**, the corresponding parameters are $E_{ex} = 1.9$ kcal mol^{-1}, $\tau_{ex}^0 = 7.0 \times 10^{-10}$ s, $E_c = 4.6$ kcal mol^{-1}, and $\tau_c^0 = 2.5 \times 10^{-14}$ s (the accuracy of the determination of E_{ex} and E_c is to within 0.3 kcal mol^{-1}). We may note that the quantities E_c for biradicals **11A** and **12A** are actually identical, i.e. under comparable conditions τ_c (**11A**) = $b\tau_c$ (**12A**), where $b = 4$, which confirms the correlation between the rotation frequencies of probe radicals of different types in the same matrix. The quantities E_{ex} and E_c for radicals **11** and **11A** are similar and this is consistent with the observed relation between τ_{ex} and τ_c. For the radical-anionic complex **12**, the quantity E_{ex} is appreciably smaller than E_c, but τ_{ex}^0 is four orders of magnitude greater than τ_c^0. Here we are again dealing with the compensation effect, so that there is no point in discussing the absolute values of E and τ^0 but the correlation (15) nevertheless holds under these conditions.

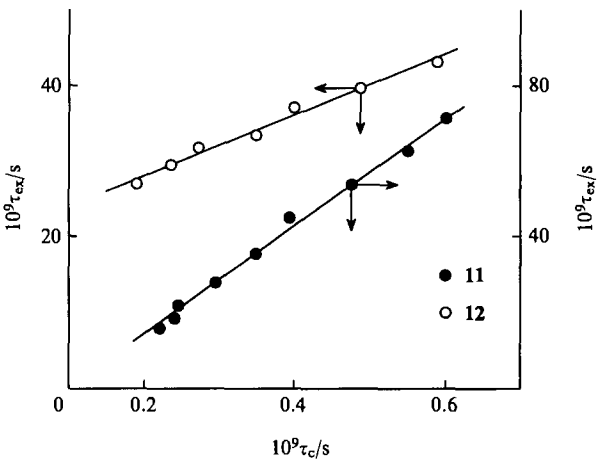
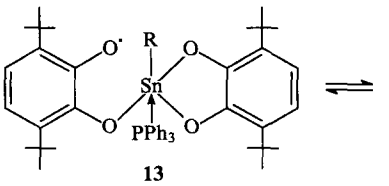
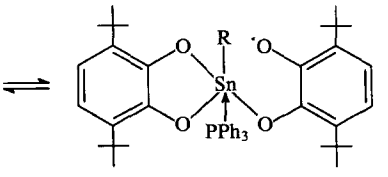


Figure 14. Correlation between τ_{ex} and τ_c for the radical-anionic complexes **11** and **12**.

Subsequently, it was possible to observe a relation between τ_{ex} and τ_c for interligand exchange under conditions where τ_c was varied by varying both the temperature and the viscosity of the medium. The correlation between the rotational mobility and the dynamics of the interligand exchange of the unpaired electron and the bond in radical **13** (R = 3,6-di-*tert*-butyl-2-R-oxyphenoxyl) has been investigated.[32]



13



It follows from the analysis of the EPR spectra of this radical that an increase in the viscosity of the medium leads to a broadening of the components with $m = -1$ and $+1$, i.e. the rate of the interligand exchange diminishes. This is also accompanied by a non-uniform broadening of the extreme

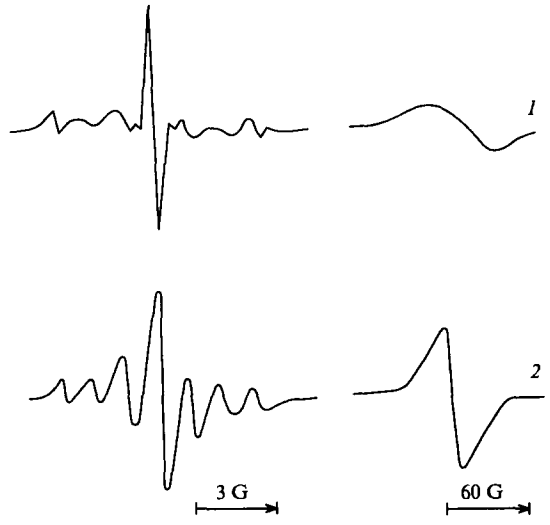


Figure 13. EPR spectra of complex **12** and the biradical **12A** in THF at different temperatures (°C): (*1*) -50; (*2*) 0.

components of the hyperfine structure, which made it possible to estimate also τ_c for radical **13** at the same time. When τ_c is varied by varying the composition of the medium over a comparatively narrow temperature range (0–20 °C), τ_f and α are respectively 0 and 8. When τ_c is varied over a wide temperature range (−90 to 0 °C), the coefficient α becomes 25. Extrapolation of the corresponding straight line to $\tau_c = 0$ yields a negative value of τ_f, which means that the function of τ_{ex} in terms of τ_c is in fact non-linear in this case owing to the temperature dependence of α.

3. Molecular mobility and chemical reactivity. Interpretation of the experimental results

Table 2 presents the parameters of the phenomenological equation (15) for radicals **1**–**13**. For radicals **4**–**10** and **13**, the times τ_c were calculated on the assumption that the EPR spectra of frozen solutions of the radicals are axially symmetrical and that the parameters of the anisotropy are ~1 G, so that the parameters α for these radicals may differ according to the revised data for radicals **1** and **2**, but these differences do not exceed one order of magnitude.

Table 2. Parameters of Eqn (15) for intramolecular radical substitution reactions.

Radical	$10^9\tau_f$/s	α	T/°C	Medium	Ref.
1	0	0.5–1	0–50	LP	34
2	3000	2400	20–30	H + LP	34
3A	400	600	15	H + LP	30
3B	300	300	15	H + LP	30
4, 5	0	7–8	−90 to −10	Toluene	24
6	0.03	0.6–1	0–20	H + LP	24
7	0	4	20	Heptane + LP	27
8	0.8	1	20	H + LP	26
9	0	240	−60–20	H + LP	26
10	0	230	−60–20	H + LP	26
11	0	160	−50–0	THF	31
12	20	40	−50–0	THF	31
13	0	8	0–20	Toluene + LP	29
13	<0	25	−90–0	Toluene	29

Evidently, the phenomenological relation (4), found for the bimolecular reactions (2), (3) and (5) of nitroxyl radicals, may lead to Eqn (15) if the characteristic time of bimolecular reactions $\tau_r \sim 1/k$ is used as the kinetic parameter. The kinetics of these reactions were investigated by measuring the decrease in the intensity of the EPR spectra of the reacting radicals as a function of time under conditions where the initial concentration of free radicals was much lower than the concentration [M] of the molecules with which the free radicals reacted, so that the reaction occurred in a pseudo-unimolecular regime and its characteristic time was $\tau_r = \{k[M]\}^{-1}$.

For the bimolecular reactions considered, the experimental rate constants k are in the range 10^{-4}–10 litre mol^{-1} s^{-1}, which is 10–15 orders of magnitude lower than the rate constants for diffusion-controlled reactions (10^{10}–10^{11} litre mol^{-1} s^{-1}). This actually means that the reaction proceeds in a radical–molecule contact pair R$^{\cdot}$...M surrounded by the molecules of the medium. The time τ_r can therefore be regarded as an analogue of τ_{ex} despite the fact that an electron or an atom is transferred between a radical and a molecule. A table of the parameters α and τ_f for bimolecular reactions was compiled on the basis of experimental data obtained for reactions (2), (3), and (5) (Table 3). The approximate relation[19]

$$\tau_{ex} = \frac{v^*}{k},$$

where v^* is the volume of the cage (usually ~5 litres mol^{-1}), was used.

Table 3. Parameters of Eqn (15) for bimolecular reactions.

Reaction	τ_f/s	α	T/°C	Medium	Ref.
(2)	10^3	10^{13}	40	Polypropylene (or polyethylene) + + benzene	7
(3)	$\ll 10^3$	10^5	28.5	Ditto	8
(5)	0	10^{10}	0–50	Water + *tert*-butyl alcohol (3 : 1)	20
(5)	0	$3\cdot10^{10}$	0–50	Triton X 100 (micellar solution)	20

Thus the EPR method is extremely effective in the study of the characteristic features of the kinetics of elementary reactions in viscous media. The results obtained hitherto have demonstrated convincingly the existence of a relation between molecular mobility (characterised by the time τ_c) and reactivity (characterised by the times τ_{ex} and τ_r) both for rapid intramolecular reversible reactions and for slow intermolecular irreversible chemical processes. In this connection, it becomes necessary to develop a general approach to an adequate explanation of Eqn (15) and an interpretation of experimental parameters of this relation.

Evidently, the classical theory of diffusion-controlled reactions as well as the transition state theory are unsuitable even for a qualitative explanation of the results. The existing models of the elementary chemical reactions in condensed media have been surveyed[19] and it was shown that some of them can be resorted to in order to account for the relation between the elementary rate constants for chemical reactions and the frequencies of molecular motions. One of such models is the Kramers model[14] in which the elementary chemical step is regarded as diffusional passage through the potential barrier in a viscous medium. The familiar expression for the chemical reaction rate constant, valid in a non-viscous medium, i.e.

$$\frac{1}{\tau_f} = \nu_0 \exp\left(-\frac{E}{RT}\right),$$

then assumes the following form for viscous solutions:

$$\frac{1}{\tau_r} = \frac{\beta}{\eta}\exp\left(-\frac{E}{RT}\right),$$

where η is the kinematic viscosity of the solvent and β is a parameter which depends on the frequency of the zero-point vibrations and the size of the reacting molecules.

Since $\tau_c \propto \eta$, the following expression can be obtained for the characteristic time of a chemical reaction:

$$\tau_r = b\tau_c \exp\left(\frac{E}{RT}\right).$$

Thus the Kramers model predicts qualitatively a linear correlation between τ_r (or τ_{ex}) and τ_c. The question arises to what extent this model is suitable for a quantitative (within the limits of an order of magnitude) interpretation of experimental results. Evidently, if $E = 0$, $\tau_r \simeq \tau_c$, and $b \simeq 1$ (in reality this coefficient can vary from 0.1 to 10), we have

$$\tau_r = \tau_c \exp\left(\frac{E}{RT}\right). \qquad (19)$$

In order to test this relation, use may be made of experimental results obtained, for example, for radical **2** (Fig. 5). The chemical line broadening effects for this radical are observed also in the limit of rapid molecular reorientations ($\tau_c \to 0$), so that $\tau_{ex} = \tau_f$ and it is possible to investigate the temperature variation of the chemical reaction time in the limit corresponding to the

unrestricted chemical mobility.[29] It was then found that the temperature variation of τ_f is described satisfactorily by the Arrhenius law:

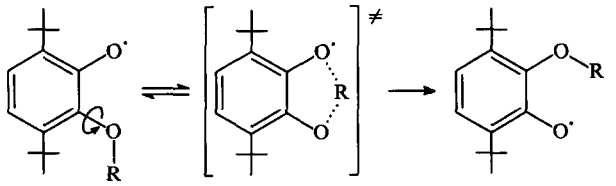
$$\tau_f = \tau_f^0 \exp\left(\frac{E_f}{RT}\right),$$

with $\tau_f^0 = 0.8 \times 10^{-13}$ s and $E_f^0 = E = 10.6$ kcal mol^{-1}. The normal value of the pre-exponential factor τ_f^0 permits the conclusion that the activation energy obtained is close to the true value.[19] Estimation of the ratio τ_{ex}/τ_c at 300 K by Eqn (19) yields $\sim 10^7$. However, it follows from the analysis of the spectroscopic characteristics that $\tau_{ex}/\tau_c \simeq 10^3 - 10^4$ (Fig. 5).

The Kramers model cannot explain also the insignificant difference between the rate constants for chemical reactions at different temperatures, which is reflected by the weak temperature dependence of the coefficient α (Table 2). This model also fails to explain the effect involving the levelling of reactivity observed for a series of bimolecular reactions in viscous media.[10]

A later theory of the electron transfer reactions in condensed media, developed by Marcus,[40] also includes the molecular mobility correlation time in the final expression for the rate constant, but this model deals only with electron transfer reactions in polar media, whereas the present review is concerned with purely homolytic processes in non-polar media. Nevertheless, one can adopt the principal idea of this theory, according to which a reorganisation of solvent molecules is essential for the occurrence of the elementary chemical step. This approach was used subsequently to devise a more general model of the indirect cage effect.[18] The principal idea underlying the model is that, even in the case of homolytic reactions in a non-polar medium, a change in the positions of the atoms and groups in the molecules surrounding the reactants is necessary for the formation of the transition state. Such molecular displacements can be characterised by the correlation time τ_c.

We shall assume that the elementary chemical reaction in a viscous medium proceeds via an intermediate metastable state which corresponds to the structure of the activated complex in a non-viscous medium (free space) but is attained via an additional energy barrier E_c associated with the necessity to reorganise the cages. For the intramolecular radical substitution reactions considered, this scheme can be represented in the form



$$A \underset{k_{-1}}{\overset{k_1}{\rightleftharpoons}} A^* \xrightarrow{k_2} A,$$

where A* corresponds to a symmetrical disposition of the organoelement fragment R between two oxygen atoms. This structure of the radical arises as a consequence of the internal rotation about the C–O bond characterised by the barrier E_c. Evidently, the activation energy for the chemical reaction proper E_f corresponds to the barrier to the displacement of the fragment R between two oxygen atoms in the symmetrical structure, which must be overcome regardless of whether the radical is in a dense environment comprising the solvent molecules or in free space. In terms of the approximation of the method of stationary concentrations of A*, the following expression can be obtained for the rate constant:

$$\frac{1}{\tau_r} = k = k_2 \frac{k_1}{k_{-1}(1 + k_2/k_{-1})}.$$

The barrier E_c can be estimated, by a procedure similar to that used by Marcus,[40] as the height of the point of intersection of two parabolic curves. Then

$$E_c = \frac{(E_r + E_f)^2}{4E_r},$$

where E_r is the cage reorganisation energy.[18] Usually $E_f < E_r$ and one can therefore assume that

$$E_c \simeq \frac{E_r}{4} + \frac{E_f}{2}.$$

If $E_f \to 0$, the rate constant corresponds to the frequency of rotational motions, so that

$$\frac{1}{\tau_c} = \nu_0 \exp\left(\frac{E_r}{4RT}\right).$$

The rate constant for the chemical reaction in free space is given by

$$k_f = \frac{1}{\tau_f} = \nu_0 \exp\left(-\frac{E_f}{RT}\right),$$

where ν_0 is the universal pre-exponential factor.

The quantity

$$\frac{1}{\tau_{ex}} = \frac{k_f}{1 + (\nu_0 k_f)^{1/2}\tau_c} \tag{20}$$

or

$$\tau_{ex} = \tau_f + (\nu_0 \tau_f)^{1/2}\tau_c \tag{21}$$

may be found from the equations obtained above.[18] Eqn (21) corresponds exactly to the phenomenological Eqn (15), where

$$\alpha = (\nu_0 \tau_f)^{1/2} = \exp\left(\frac{E_f}{2RT}\right).$$

The model considered predicts, like the Kramers model, a non-linear relation between τ_{ex} and τ_c, but in the case of highly viscous media [i.e. for $\tau_c \gg (\tau_f/\nu_0)^{1/2}$] we obtain, in contrast to Eqn (19), the expression

$$\tau_{ex} = \tau_c \exp\left(\frac{E_f}{2RT}\right), \tag{22}$$

i.e. the model of the indirect cage effect explains the experimental values of τ_{ex}/τ_c, the levelling of reactivity, and the weak temperature dependence of the coefficient α. The energies E_f may be found from the experimental relations between τ_{ex} and τ_c under conditions where the temperature is varied over a wide range.[27, 28]

Thus, despite its approximate nature, the model of the 'reorganisation of the cage' examined above is satisfactorily consistent with the phenomenological relation (15). The experimental relations therefore make it possible to estimate chemical reactivity from molecular mobility data.

IV. Conformational transitions in free radicals. Relation between intramolecular mobility and the mobility of the medium

The rotational mobility correlation time τ_c is not the only parameter characterising molecular mobility. The molecular motions of radicals, leading to the averaging of the magnetic anisotropy, can differ from the motions responsible for the occurrence of the elementary chemical step. The measured quantity τ_c is evidently averaged over different types of motions of the spin probe (the motions around different molecular axes,

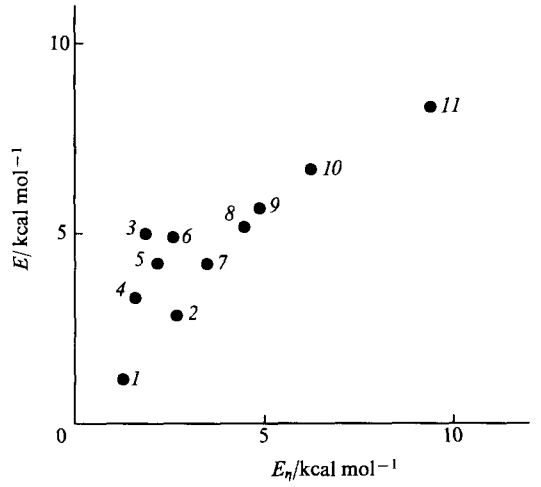


Figure 15. Relation between the activation energy for intramolecular rotations in radical **14** and the activation energy for the viscous flow of the solvent E_η (according to data of Jonkman and Kommandeur[42]): (*1*) carbon disulphide; (*2*) tetrachloroethylene; (*3*) mesitylene; (*4*) n-hexane; (*5*) n-octane; (*6*) n-decane; (*7*) ethanol; (*8*) 1-propanol; (*9*) 1-butanol; (*10*) 1-octanol; (*11*) cyclohexanol.

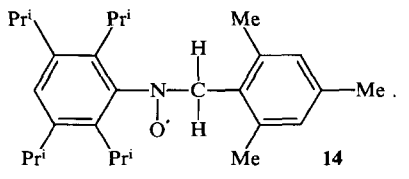
rotation of individual groups in the radical, molecular shifts responsible for the relaxation of the cage, etc.). A correction term must therefore be introduced into the expression for the coefficient α in Eqn (15):

$$\alpha = \alpha_0 \exp\left(\frac{E_f}{2RT}\right). \qquad (23)$$

The coefficient α_0 takes into account the correspondence between the molecular motions the average correlation time of which is measured experimentally and the motions leading to the occurrence of the reaction. For this reason, the parameter α_0 may be regarded as the ratio of the frequencies of the molecular motions along the reaction coordinate and the motions leading to the modulation of the anisotropic magnetic interactions of the probe radical. The necessity to take into account the coefficient α_0 in Eqns (4) and (15) makes it necessary to accumulate data on the molecular mobilities of the spin probes and on the relation between molecular motions of different types.

As a result of the development of 2 mm EPR spectroscopy, it has been possible to determine separately the characteristic frequencies of the rotation about different molecular axes for a series of nitroxyl radicals.[41] It was found that the ratio of the rotation correlation times depends only slightly on their absolute values, i.e. is independent of the viscosity of the medium.

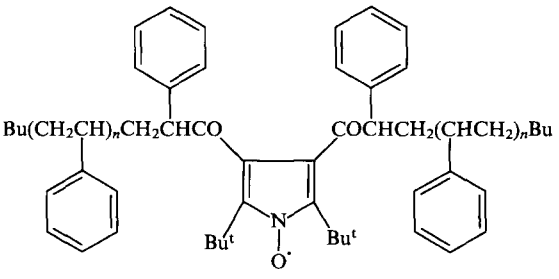
Analysis of the available literature data on intramolecular mobility or dynamics of conformational transitions has shown that these processes are also controlled by the molecular dynamics of the medium. As an example, one may consider a nitroxyl radical with the following structure:



14

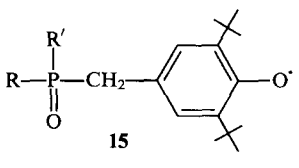
The EPR spectra of radical **14** indicate the intramolecular rotation of the benzyl group, which is manifested in the HFI modulation due to the two β-protons of this group.[42] Analysis of the line width led to the estimation of the kinetic parameters of the intramolecular rotation and it was shown that the activation energy for the intramolecular motion depends on the viscosity of the solvent. Fig. 15 presents the kinetic parameters of the intramolecular motions in radical **14** . Evidently, there exists a definite relation between the activation energies for the intramolecular motions and the solvent viscosity. The study of the dynamics of the reorientation motions of the spin probes in polymers has also shown that the activation energies for the rotation of radicals are close to the activation energy for segmental motions determined by the NMR method,[43, 44] but the rotation frequencies of the radicals are 2–3 orders of magnitude greater than the frequencies of the segmental motions. Thus a linear correlation of the type $\tau = \alpha\tau_c$, where $\alpha \sim 10^2 - 10^3$, also exists for these motions.

The dynamics of the conformational transitions in a spin-labelled molecule has been investigated[45] by the EPR method. It was found that the experimental results are described satisfactorily within the framework of the Kramers model.



In a study[46] of the relaxation-induced changes in the EPR spectra of a spin-labelled polyvinylpyridine, it was possible to characterise separately the motions of the macromolecule as a whole and the relative motions of the nitroxyl label, i.e. intramolecular motions. In the frequency range $10^8 - 10^9$ s^{-1}, these motions are characterised by the same activation energy, i.e. the mobility is determined in both cases by the solvent viscosity near the boundary of the macromolecule. In other words, the molecular mobility of the reactants (rotational, translational, conformational, etc.) is fully determined by the dynamic properties of the kinetic cage as a whole, including the molecules of the surrounding medium.

The examples considered above, indicating a relation between molecular motions of different types, were based on the parallel temperature variation of the frequencies of these motions. It has been shown[47] that the mobility of the medium exerts a direct influence on the dynamics of intramolecular rotational transitions in phosphorus-containing phenoxyl radicals having the following structure:



15

where R = R′ = Ph, R = Ph and R′ = EtO, or R = R′ = EtO.

The hyperfine interaction of the unpaired electron with the ^{31}P nucleus, the two equivalent protons of the CH_2 group in the *para*-substituent, and the two equivalent protons in the *meta*-positions in the aromatic ring is manifested in the EPR spectra of radicals **15** at high temperatures. As the temperature is reduced, the EPR spectra of radicals **15** exhibit a broadening of the central component of the triplet due to the protons of the CH_2 group of the *para*-substituent. At lower temperatures, these protons become non-equivalent. Such changes in the spectra are fully reversible as the temperature is varied, which indicates the occurrence of intramolecular processes in radical **15** owing to the

hindered rotation of the *para*-substituent around the C–C bond relative to the plane of the aromatic ring. In radicals of this type, the hyperfine interaction with the nuclei of the *para*-substituent takes place via a hyperconjugation mechanism[23] and the HFI constants are described by the relation

$$a = \rho_c^{\pi}(B_0 + B_2 \cos^2 \Theta) ,$$

where B_0 and B_2 are parameters which are respectively 0 and 43.5 G for the protons and 62 and 136 G for phosphorus,[48] $\rho_c^{\pi} = 0.4$ is the spin density in the *para*-position in the phenoxyl radical,[23] and Θ is the angle between the p orbital of the carbon atom in the *para*-position in the aromatic ring and the direction of the C–H or C–P bond. The difference between the HFI constants of the protons of the CH_2 group in the *para*-substituent at low temperatures is due to the difference between the angles Θ for these protons. Analysis of the line width makes it possible to find the characteristic time τ of the intramolecular transitions.

Fig. 16 presents the EPR spectra of radical **15** at the same temperature but in solutions of different viscosity (the viscosity was varied by adding liquid paraffin to toluene). Evidently, the increase in the viscosity of the medium entails a broadening of the central component of the triplets due to the protons of the CH_2 group, which indicates the inhibition of the intramolecular transitions. With increase in the viscosity of the medium, a non-uniform broadening of the components with a hyperfine structure, in particular the components due to the hyperfine interaction with the ^{31}P nucleus, also occurs. If one uses the anisotropic magnetic parameters of radical **15**, this makes it possible to determine the average rotational correlation time τ_c characterising the rotation of the radical as a whole.[47]

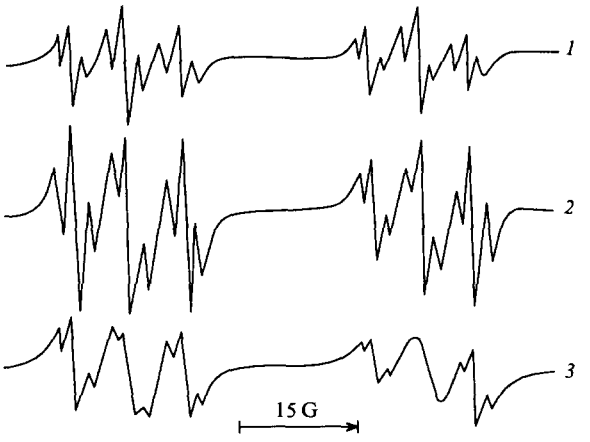


Figure 16. EPR spectra of radical **15** at 0 °C in different solvents: (*1*) toluene; (*2*) 1 : 3 toluene + liquid paraffin mixture; (*3*) 1 : 7 toluene + liquid paraffin mixture.

Fig. 17 presents the relation between τ and τ_c obtained on varying the composition of the medium and temperature. Evidently the experimental data are described satisfactorily by Eqn (15) for $\tau_f \ll \tau$. As the viscosity of the medium is varied, the coefficient $\alpha = 400$ remains constant under these conditions, while variation of the temperature over a wide range results in the variation of α in conformity with Eqn (23) ($\alpha_0 \simeq 30$, $E_f \simeq 2.8$ kcal mol^{-1}). The quantity α_0 is of the same order of magnitude as the parameters of the anisotropy of the rotational motions of nitroxyl radicals of complex shape obtained previously.

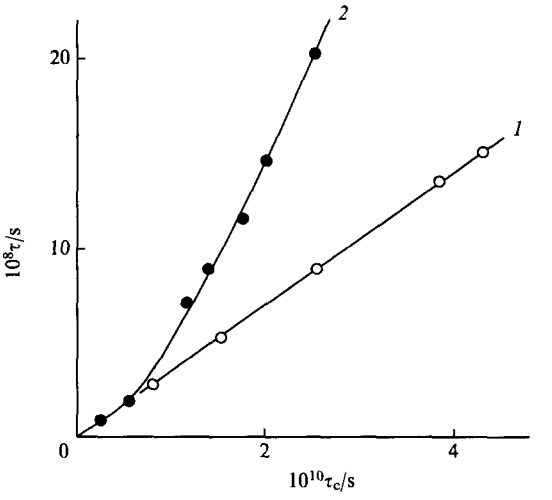
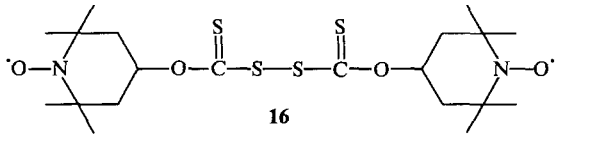


Figure 17. Dependence of τ on τ_c for radical **15**: (*1*) variation of the viscosity of the medium at 0 °C; (*2*) variation of temperature in toluene in the range from −70 to 20 °C.

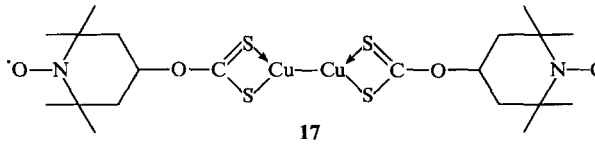
V. Relation between the rotational mobility and the dynamics of spin exchange in nitroxyl biradicals

Spin exchange can be regarded as a model of the electron transfer reaction, which is important in chemical and biochemical processes. The theory and methodological approaches to the study of spin exchange in nitroxyl biradicals have now been quite thoroughly developed.[49] Nitroxyl radicals and biradicals are the most convenient objects for the study of molecular mobility. We therefore regard it as evident that nitroxyl biradicals will also prove to be suitable objects whereby it will be possible to trace the relation between molecular and chemical dynamics — in the given instance the relation between molecular mobility and the dynamics of intramolecular spin exchange.

The influence of the mobility of the medium on the dynamics of spin exchange in biradicals based on a spin-labelled xanthate, having the structure

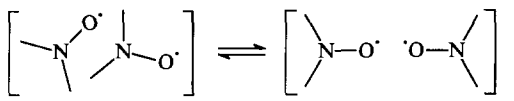


16



17

has been investigated.[50, 51] Biradicals **16** and **17** have quintet EPR spectra with alternately broadened biradical components.[52] They exist in solution in the form of at least three conformations: the 'extended conformation' with an exchange interaction constant $J = 0$ and two conformations with radical fragments in close proximity, for one of which $J = 0$ and for the other $J \gg a_N$, where a_N are HFI constants for the nitrogen nuclei. The mutual transitions between the conformations are described within the framework of the cage model.[49] According to the ideas of the 'cage' mechanism of exchange interactions in long-chain biradicals, the last two conformations are formed as a result of the mutual approach of the radical fragments, which enter a common 'cage' where they can interact. The elementary spin exchange step then occurs as a result of the direct collision of the radical fragments.



(24)

The alternation of the line widths of the biradical components of the EPR spectrum is caused by the changes in the conditions governing the modulation of the exchange integral within the cage.[49] Measurement of the line widths of the biradical components permits the calculation of the effective spin exchange time τ_{ex}:

$$\tau_{ex} = \frac{4(3)^{1/2}(\Delta H_2 - \Delta H_1)}{\gamma a_N^2}, \quad (25)$$

where ΔH_1 and ΔH_2 are the line widths of the first and second components of the EPR spectrum of the biradical measured between the points of maximum slope.

Since the EPR spectra of biradicals **16** and **17** constitute a superposition of the triplet and quintet spectra, the following formula must be used to determine τ_c for the radical fragments:[23]

$$\tau_c = 6.6 \times 10^{-10} \Delta H_1 \left[\left(\frac{I_1}{I_{1'}} \right)^{1/2} - 1 \right], \quad (26)$$

where I_1 and $I_{1'}$ are the amplitudes of the extreme components (downfield and upfield) of the EPR spectrum of the biradical. As will be shown below, $\tau_{ex} \gg \tau_c$ and the amplitudes of the biradical components and hence their widths remain unchanged. Therefore, in order to determine τ_{ex} one may use Eqn (25), neglecting at the same time the broadening of the biradical components associated with the effects due to the modulation of the anisotropic magnetic interactions by rotational motions.

Analysis of the EPR spectra of biradical **16** in media of different viscosity has shown (Fig. 18) that, with increase in τ_c, the biradical components become broadened and τ_{ex} also increases. The relation between τ_{ex} and τ_c for biradical **16** can be expressed in the form $\tau_{ex} = \alpha\tau_c$ and in the temperature range 0 to 60 °C the coefficient α remains unchanged. This permits the conclusion that the barrier to the activation of the spin exchange is low ($E_f < 2RT \simeq 1$ kcal mol^{-1}) and one can assume that $\alpha = \alpha_0$. For biradicals **16** and **17** in a hexane–liquid paraffin mixture, the parameter $\alpha_0 = 150-170$.[50] The comparatively high values of α_0 can be interpreted as follows: for 150–170 reorientation steps in the radical fragments there is only one spin exchange step, but the additional multiplier α_0 enters into the rate constant k_{ex} as a steric factor. In other words, the coefficient α_0 may be

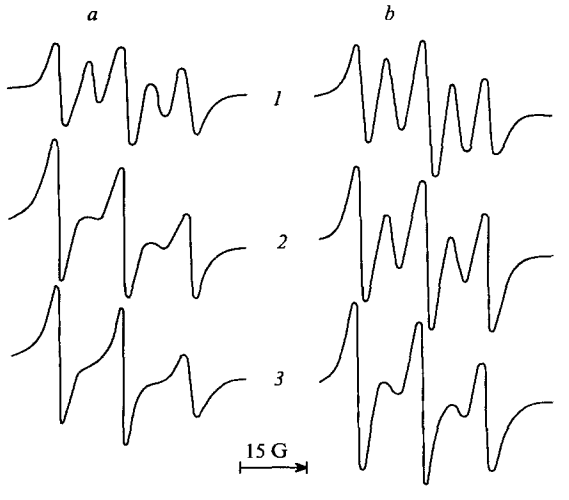


Figure 18. EPR spectra of biradical **16** at 20 °C (*a*) and 60 °C (*b*) in media with different viscosities: (*1*) 1 : 1 hexane + liquid paraffin mixture; (*2*) 1 : 10 hexane + liquid paraffin mixture; (*3*) liquid paraffin.

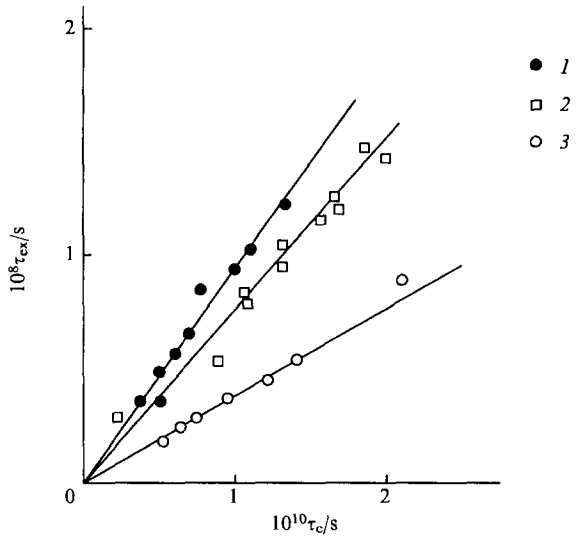


Figure 19. Dependence of τ_{ex} on τ_c for biradical **16** at variable temperatures in different solvents: (*1*) dimethyl sulfoxide; (*2*) 1-butanol; (*3*) THF.

interpreted as a parameter relating the frequencies of molecular motions of different types. For example, the rotation of radical fragments around the axis passing through the N–O bond does not lead to the collision of the radical fragments, as shown in Scheme (24).

The nature of the motion of the probe radicals may be influenced significantly by specific interactions with solvent molecules, so that, by analogy with the parameters of the anisotropy of the rotation of nitroxyl radicals,[41] one may expect changes in the parameters α_0 for biradicals **16** and **17** in different solvents. Fig. 19 illustrates the relation between τ_{ex} and τ_c for biradical **16** in different solvents (τ_c was varied by varying the temperature over a wide range). Evidently the linear correlation between τ_{ex} and τ_c holds satisfactorily, but the proportionality coefficient α_0 depends on the solvent. Table 4 presents the values of α_0 for different solvents together with the pre-exponential factors τ_c^0 and the activation energies E_c for the rotation of the radical fragment in the biradical. In all the solvents investigated, the temperature variation of τ_{ex} and τ_c is described satisfactorily by the Arrhenius relation. In conformity with the linear correlation obtained between τ_{ex} and τ_c, we find that

$$\tau_{ex}^0 = \alpha_0\tau_c^0 \quad \text{and} \quad E_{ex} = E_c .$$

Thus in a viscous medium the activation energy for intramolecular spin exchange in the biradical is identical with the barrier to the rotation of the radical fragment.

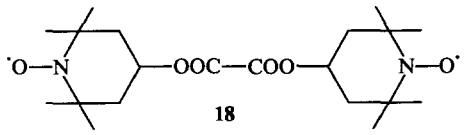
Evidently, the equality of the activation energies for different molecular processes frequently occurs in studies by the spin probe method. Some of these data were discussed above. Here one may

Table 4. The parameters α_0, E_c, and τ_c^0 for biradical **16** in different solvents.

Solvent	α_0	E_c/kcal mol^{-1}	τ_c^0/s	T/°C
Toluene	105±11	1.6±0.2	2.6×10^{-12}	−80 – 10
Acetone	100±10	2.2±0.4	7.7×10^{-13}	−60 to −5
DMF	85±8	4.5±1.0	3.4×10^{-14}	−30 – 60
DMSO	96±8	5.0±1.0	2.8×10^{-14}	10 – 80
Acetophenone	80±7	4.3±0.9	1.1×10^{-13}	30 – 90
Heptanol	75±15	7.9±1.0	1.1×10^{-15}	30 – 70
Butanol	78±9	3.3±0.5	6.8×10^{-13}	0 – 60
Methanol	50±7	3.7±0.5	1.1×10^{-13}	−50 – 10
THF	38±4	2.8±0.5	4.4×10^{-13}	−70 – 20

quote yet another example illustrating the relation between the dynamics of the intramolecular spin exchange and the rotational mobility.

The spin exchange in a biradical having the structure

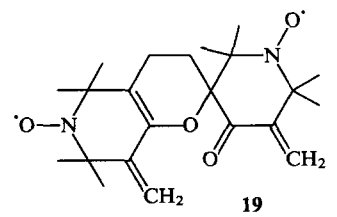


18

has been investigated[53, 54] by the double electron–electron resonance (DEER) method. The DEER method makes it possible to observe processes with lower frequencies than is possible when EPR is used. In the EPR spectra of biradical **18**, investigated in liquid paraffin at temperatures in the range −30 to +40 °C, hyperfine interaction with only one nitrogen nucleus is observed, i.e. intramolecular spin exchange is not observed on the EPR time scale. The DEER effect in biradical **18** is due to the intramolecular exchange interaction of the unpaired electron. The temperature variation of the frequency ν_{ex} of this interaction is described by the Arrhenius law with $\nu_{ex}^0 = 10^8\ s^{-1}$ and $E_{ex} = 3.5 \pm 0.7$ kcal mol^{-1}. The rotation frequency of the biradical ν_c, estimated from the EPR spectra as for the monoradical, is also described satisfactorily by the Arrhenius relation with $\nu_c^0 = 10^{11}\ s^{-1}$ and $E_c = 3.9 \pm 1.0$ kcal mol^{-1}. The values ν_{ex} measured for biradical **18** evidently correspond to the frequency of the rare collisions of radical fragments. The similarity of the activation energies for ν_{ex} and ν_c indicates a relation between the rotational and conformational motions of the biradical. Consequently, the relation $\tau_{ex} = \alpha_0\tau_c$, found previously for radicals **16** and **17**, also holds for biradical **18**. For biradical **18**, $\alpha_0 \simeq 1\,000$, which exceeds by an order of magnitude the corresponding values for radicals **16** and **17**.

As mentioned above, the spin exchange in flexible long-chain biradicals, to which biradicals **16**–**18** belong, takes place as a result of the collision between the nitroxyl fragments. Therefore the linear relation between the characteristic spin exchange time and the rotational mobility correlation time reflects the relation between the molecular motions of this type. The study of the relation between molecular mobility and the dynamics of spin exchange in nitroxyl biradicals, where the mutual approach and collision of the radical fragments is impossible and the spin exchange process takes place through the skeleton via an indirect mechanism, is of special interest. This type of spin exchange mechanism has been proposed for rigid nitroxyl biradicals.[49]

The influence of molecular mobility on the dynamics of spin exchange in a nitroxyl biradical having the structure



19

has been investigated.[55] The EPR spectra of biradical **19** have also been investigated.[56] In solutions with a low viscosity, the spectrum consists of a quintet with intensity ratios of 1 : 2 : 3 : 2 : 1 (if the spin had been localised on a single NO fragment, a 1 : 1 : 1 triplet would have been observed). The widths of the biradical components depended only slightly on temperature. This enabled the authors to conclude that an indirect mechanism of exchange via a chain of σ- and π-bonds operates.

The EPR spectra of biradical **19** in viscous solutions in liquid paraffin and in long-chain aliphatic alcohols have been investigated.[55] Fig. 20 shows that an isothermal increase in the viscosity of the medium entails an appreciable broadening of the biradical

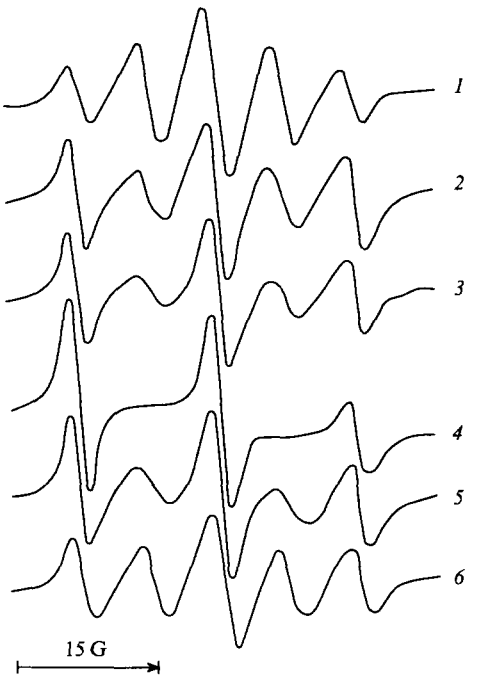


Figure 20. EPR spectra of biradical **19**: (*1*) in hexane at 20 °C; (*2*) in the 1 : 3 hexane + liquid paraffin mixture at 20 °C; (*3*) in the 1 : 5 hexane + liquid paraffin mixture at 20 °C; (*4*) in liquid paraffin at 20 °C; (*5*) in liquid paraffin at 40 °C; (*6*) in liquid paraffin at 60 °C.

components of the EPR spectra. A triplet is observed in the spectra in liquid paraffin, indicating the absence of intramolecular spin exchange on the EPR time scale. With increase in the temperature of the solution of biradical **19** in liquid paraffin, the appearance and subsequent narrowing of the biradical components are observed, which is clearly manifested by the increase in their relative amplitude. The ratios of the integral intensities of all the components of the spectrum always correspond to a binomial distribution. Similar changes are observed when the EPR spectra of biradical **19** in ethanol, butanol, octanol, and decanol are compared. The rate of intramolecular spin exchange falls in the series indicated.

Thus the inhibition of intramolecular spin exchange following a decrease in the mobility of the medium has also been observed for biradical **19**, although it is difficult to imagine what type of motion of the biradical may be responsible for the spin exchange process between the nitroxyl fragments. Despite the relatively rigid structure of biradical **19**, a definite rehybridisation of molecular orbitals, requiring relative shifts of the atoms in the molecule, is apparently necessary for the occurrence of the elementary spin exchange step. In this case, the relatively immobile species comprising the medium, forming 'the walls of the cage', hinder such displacements, which ultimately leads to the retardation of the intramolecular spin exchange. Thus a structural reorganisation of the cage (biradical + surrounding molecules of the medium) is necessary even for the occurrence of the very simple spin exchange step.

The relation between τ_{ex} and τ_c for biradical **19** is also linear (Fig. 21). In an inert medium, $\alpha_0 = 85$, whilst in an alcohol matrix $\alpha_0 = 200$. In solvents with a low viscosity (ethanol, hexane, toluene), the EPR spectrum of biradical **19** remains of the quintet type without appreciable broadening of the biradical components even at low temperatures (−60 to −80 °C), but the amplitudes of the extreme components of the spectrum also do not differ in this instance, which indicates a fairly rapid rotation of the biradical. This fact apparently reflects the characteristics of microscopic organisation of the cage around biradical **19**, since a monotonic decrease in the rotational mobility of nitroxyl fragments with

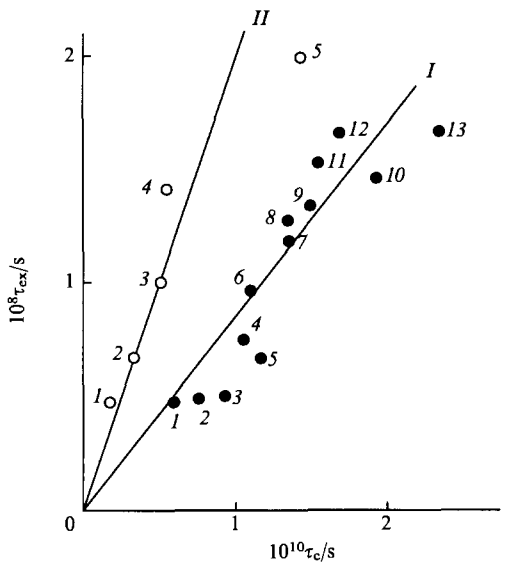


Figure 21. Dependence of τ_{ex} on τ_c for biradical **19**: (*I*) with variation of the composition of the medium (ratio of the concentrations of hexane and liquid paraffin) and temperature (°C): (*1*) 1 : 3, 60; (*2*) 1 : 3, 50; (*3*) 1 : 5, 60; (*4*) 1 : 3, 40; (*5*) 1 : 5, 50; (*6*) liquid paraffin, 60; (*7*) 1 : 5, 40; (*8*) 1 : 3, 30; (*9*) 1 : 5, 30; (*10*) liquid paraffin, 50; (*11*) 1 : 3, 20; (*12*) 1 : 5, 20; (*13*) liquid paraffin, 40. (*II*) In decanol at different temperatures (°C): (*1*) 60; (*2*) 50; (*3*) 40; (*4*) 30; (*5*) 20.

decrease in temperature is observed under these conditions for the 'usual' spin probes, for example, for biradicals **16** and **17**. By virtue of its structural characteristics in low-temperature solvents, biradical **19** can apparently ensure a molecular organisation of the immediate environment with a lower microscopic viscosity.

The data presented above indicate the need to consider the molecular dynamics of the kinetic cage as a whole, including the rotational mobility of the probe and the local motions of the medium. The stable perchlorotriphenylmethyl radical has been investigated[57] in the 2 mm EPR range. The absence of a hyperfine structure simplifies significantly the interpretation of the EPR spectra and the anisotropy of the *g*-factor is sufficient to obtain the necessary information both about the rotation of the spin probe and about the local motion of the medium. In this case, a linear relation was also observed between the characteristic time of the local displacements and the time of the reorientation of the probe molecule by large angles, which constitutes yet another example of the correlation between the frequencies of different processes in one matrix. One can imagine that the complex molecular motions in the condensed phase are effected as a result of the diffusional accumulation n of certain elementary 'quanta' of motion.[58] The frequencies of different types of motion then differ solely by the coefficient n^2 and are linearly correlated with one another. The local displacements of the medium, characterised by Grinberg et al.,[57] can play the role of such elementary motions, which constitutes the basis of the correlation between the frequencies of different molecular processes.

VI. Conclusion

The final aim of studies in the field of chemical physics is, in particular, the elucidation of the relation between the physical and chemical properties of molecules. In relation to chemical processes in condensed media, it is more correct to consider not the physical properties of individual molecules but the properties of the kinetic cage incorporating the reactants and the surrounding molecules of the medium which influence the reactivity. One of the main properties of such a cage is molecular mobility, the quantitative description of which permits the prediction of the difference between the reactivities in an ideal solution and in a real viscous medium of the type of glass, amorphous polymers, and biological structures.

The experimental results presented in this review give rise to the hope that the study of the molecular mobility of free radicals may provide a universal approach to the prediction of reactivity in viscous media and amorphous solids. The results of the investigation may be regarded as the starting point for the construction of microscopic models of chemical reactions in condensed media.

References

1. O E Yakimchenko, Ya S Lebedev, in *Kinetika i Mekhanizm Khimicheskikh Reaktsii v Tverdom Tele* (Kinetics and the Mechanism of Chemical Reactions in the Solid State) (Chernogolovka, 1981) p. 27
2. V A Roginskii, V B Miller *Dokl. Akad. Nauk SSSR* **213** 642 (1973)
3. V A Roginskii, V B Miller *Dokl. Akad. Nauk SSSR* **215** 1164 (1974)
4. E L Shanina, V A Roginskii, V B Miller *Vysokomol. Soedin. B* **19** 447 (1977)
5. A P Griva, L N Denisova, E T Denisov *Dokl. Akad. Nauk SSSR* **232** 1343 (1977)
6. A P Griva, E T Denisov *J. Polym. Sci., Polym. Chem. Ed.* **14** 1051 (1976)
7. A P Griva, L N Denisova, E T Denisov *Kinet. Katal.* **19** 309 (1978)
8. A P Griva, L N Denisova, E T Denisov *Vysokomol. Soedin. A* **21** 849 (1979)
9. A P Griva, L N Denisova, E T Denisov *Vysokomol. Soedin. A* **19** 219 (1977)
10. O N Karpukhin *Usp. Khim.* **47** 1119 (1978) [*Russ. Chem. Rev.* **47** 587 (1978)]
11. Ya S Lebedev, A I Burshtein *Chem. Phys.* **12** 259 (1976)
12. V S Gurman, V I Pergushov *Chem. Phys. Lett.* **1** 105 (1976)
13. V K Milinchuk, E R Klinshpont, S Ya Pshezhetskii *Makroradikaly* (Macroradicals) (Moscow: Khimiya, 1980)
14. A M Vasserman, A A Dadali, A L Kovarskii *Dokl. Akad. Nauk SSSR* **237** 130 (1977)
15. N M Emanuel', A L Buchachenko *Khimicheskaya Fizika Stareniya i Stabilizatsii Polimerov* (The Chemical Physics of the Ageing and Stabilisation of Polymers) (Moscow: Nauka, 1982)
16. A L Kovarskii, I I Aliev *Vysokomol. Soedin. A* **25** 2293 (1983)
17. N M Emanuel', A L Buchachenko *Khimicheskaya Fizika Molekulyarnogo Razrusheniya i Stabilizatsii Polimerov* (The Chemical Physics of the Molecular Decomposition and Stabilisation of Polymers) (Moscow: Nauka, 1988)
18. Ya S Lebedev *Dokl. Akad. Nauk SSSR* **281** 636 (1985)
19. Ya S Lebedev, in *Fizicheskaya Khimiya. Sovremennye Problemy* (Physical Chemistry. Current Problems) (Moscow: Khimiya, 1985) p. 220
20. Ya S Lebedev *Pure Appl. Chem.* **62** 261 (1990)
21. V A Roginskii *Fenoksil'nye Antioksidanty. Reaktsionnaya Sposobnost' i Effektivnost'* (Phenoxyl Antioxidants. Reactivity and Effectiveness) (Moscow: Nauka, 1988)
22. A Yu Brezgunov, A A Dubinskii, O G Poluektov *Zh. Strukt. Khim.* **33** 69 (1992)
23. A L Buchachenko, A M Vasserman *Stabil'nye Radikaly* (Stable Radicals) (Moscow: Khimiya, 1973)
24. R R Rakhimov, A I Prokof'ev, M I Kabachnik, Ya S Lebedev *Dokl. Akad. Nauk SSSR* **302** 889 (1988)
25. R R Rakhimov, A I Prokof'ev, M I Kabachnik, Ya S Lebedev *Dokl. Akad. Nauk SSSR* **306** 138 (1989)
26. R R Rakhimov, A I Prokof'ev, Ya S Lebedev *Khim. Fiz.* **8** 1377 (1989)
27. R R Rakhimov, P M Solozhenkin, R A Zhuliev *Zh. Fiz. Khim.* **64** 2281 (1990)
28. R R Rakhimov, A I Prokof'ev, Ya S Lebedev *Izv. Akad. Nauk SSSR, Ser. Khim.* 781 (1990)
29. R R Rakhimov, A I Prokof'ev, Ya S Lebedev *Izv. Akad. Nauk SSSR, Ser. Khim.* 1635 (1990)
30. R R Rakhimov, A I Prokof'ev, Ya S Lebedev *Izv. Akad. Nauk SSSR, Ser. Khim.* 368 (1991)
31. R R Rakhimov, A I Prokof'ev, Ya S Lebedev *Khim. Fiz.* **8** 1265 (1989)

32. R R Rakhimov, A I Prokof'ev, Ya S Lebedev *Izv. Akad. Nauk SSSR, Ser. Khim.* 1663 (1990)
33. N N Bubnov, S P Solodovnikov, A I Prokof'ev, M I Kabachnik *Usp. Khim.* **47** 1048 (1978) [*Russ. Chem. Rev.* **47** 549 (1978)]
34. Ya S Lebedev, R R Rakhimov, A I Prokof'ev, A Yu Bresgunov *Pure Appl. Chem.* **64** 873 (1992)
35. A Carrington, A D McLachlan *Introduction to Magnetic Resonance: with Applications to Chemistry and Chemical Physics* (Translated into Russian) (Moscow: Mir, 1970)
36. R R Rakhimov, A I Prokof'ev, Ya S Lebedev *Zh. Fiz. Khim.* **67** (1993)
37. Z K Kasymbekova, A I Prokof'ev, A A Khodak *Khim. Fiz.* **2** 401 (1983)
38. A I Prokof'ev, N A Malysheva, N N Bubnov *Dokl. Akad. Nauk SSSR* **252** 370 (1980)
39. A I Prokof'ev, T I Prokof'eva, N N Bubnov *Dokl. Akad. Nauk SSSR* **245** 1393 (1979)
40. R A Marcus *Ann. Rev. Phys. Chem.* **15** 641 (1972)
41. O Ya Grinberg, A A Dubinskii, Ya S Lebedev *Usp. Khim.* **52** 1490 (1983) [*Russ. Chem. Rev.* **52** 850 (1983)]
42. L Jonkman, J Kommandeur *Chem. Phys. Lett.* **5** 579 (1970)
43. V B Stryukov, G V Korolev *Vysokomol. Soedin. A* **11** 419 (1969)
44. A M Vasserman, A L Buchachenko, A L Kovarskii, M B Neiman *Vysokomol. Soedin. A* **10** 1930 (1968)
45. C Friedrich, F Laupretre, C Noel, L Monnerie *Macromolecules* **14** 1119 (1981)
46. O G Poluektov, A A Dubinskii, O Ya Grinberg, Ya S Lebedev *Khim. Fiz.* **2** 182 (1983)
47. R R Rakhimov, A I Prokof'ev, N A Kardanov *Khim. Fiz.* **8** 1619 (1989)
48. A I Prokof'ev, N P Provotorova, N A Kardanov *Izv. Akad. Nauk SSSR, Ser. Khim.* 1865 (1981)
49. V N Parmon, A I Kokorin, G M Zhidomirov *Stabil'nye Biradikaly* (Stable Biradicals) (Moscow: Nauka, 1980)
50. R R Rakhimov, P M Solozhenkin, Ya S Lebedev *Dokl. Akad. Nauk SSSR* **303** 1410 (1988)
51. R R Rakhimov, P M Solozhenkin, Ya S Lebedev *Zh. Fiz. Khim.* **64** 2057 (1990)
52. A V Ivanov, P M Solozhenkin, F A Shvengler *Dokl. Akad. Nauk SSSR* **289** 909 (1986)
53. V A Benderskii, P A Stunzhas, V A Sokolov *Opt. Spektrosk.* **28** 278 (1970)
54. V A Benderskii, V I Gol'danskii, A I Rakoed *Dokl. Akad. Nauk SSSR* **204** 1143 (1972)
55. R R Rakhimov, A I Semikopny, Ya S Lebedev *Mendeleev Commun.* 2 (1992)
56. A B Shapiro, V P Ivanov, O M Khvostach, E G Rozantsev *Izv. Akad. Nauk SSSR, Ser. Khim.* 1688 (1973)
57. O Ya Grinberg, A A Dubinskii, O G Poluektov, Ya S Lebedev *Zh. Fiz. Khim.* **64** 1568 (1990)
58. Ya S Lebedev, in *Soviet Scientifical Reviews Chemistry* (London: Harwood Academic, 1987) p. 67

Russian Chemical Reviews **62** (6) 527 – 538 (1993)
©1993 Russian Academy of Sciences and Turpion Ltd

UDC 539.19 + 547.117

The molecular spectra and structure of the oxides of boron and aluminium

A V Nemukhin, L V Serebrennikov

Contents

I. Introduction	527
II. General characteristics	527
III. Methods of study	528
IV. The structure and spectra of X_mO_n molecules	529
V. Summary	537

Abstract. The results of theoretical and experimental studies of the molecular structure of the oxides of boron and aluminium X_2O_3, X_2O_2, X_2O, and XO_2 (X = B, Al), carried out mainly by spectroscopic methods using matrix-isolation techniques, and also by quantum-mechanical calculations, have been reviewed. The bibliography contains 70 references.

I. Introduction

The present review gives the results of experimental and theoretical studies of the molecular structure of the oxides of boron and aluminium X_mO_n (X = B or Al, $m + n < 6$). The compounds X_mO_n are of both fundamental and applied interest. Thus in the published[1] 'league table' of the chemical elements (involving a comprehensive survey of the importance of the chemical elements in nature, industry, and chemical science), the elements O, B, and Al occupy leading positions.

The literature on the molecular structure of the oxides of boron and aluminium is fairly extensive, and covers a period of more than thirty years. Although it is too early to say that all problems have been resolved, our ideas about the structure of the molecules X_mO_n are fairly well developed. They are based primarily on the results of experimental spectroscopic studies and quantum-chemical calculations. One of the aims of the present review is to show the extent to which it is possible to accept the conclusions of both the experimental and the theoretical studies, which agree with one another in many respects, but not all.

The analysis of the structure of these chemical compounds must involve the question of the similarity and differences in the structure of the oxides of boron and aluminium, and possible explanations. We understand that any 'explanation of the regularities of chemical structure' is provisional, and depends primarily on the level of theory regarded as basic: whether it is sufficient to carry out the analysis using, say, the differences in the electronegativities, dimensions, and polarisabilities of the atoms, or some other parameters, or whether it is necessary to take account of completely different characteristics of the systems.

A V Nemukhin, L V Serebrennikov Chemistry Department, Lomonosov Moscow State University, Leninskie Gory, 119899 Moscow.
Fax (7-095) 939 01 26

Received 17th February 1973
Uspekhi Khimii **62** (6) 566–578; translated by D A Paterson

The theoretical analysis of this present review is based mainly on the molecular orbital model of the theory of electronic structure, with particular attention to the interpretation of the localised molecular orbitals and to such characteristics as the effective charges on the atoms. Analysis of the influence of effects of electron correlation on molecular structure will be regarded as especially important.

II. General characteristics

According to the canonical rules of chemistry, the principal oxide of an element X of group III is X_2O_3. The first studies of the composition of the vapour over solid B_2O_3 and Al_2O_3 showed, however, that oxide molecules with other stoichiometries exist: XO, X_2O, XO_2, and X_2O_2.[2] Later quantum-chemical calculations established that all these systems correspond to stable minima on the potential energy surfaces. Moreover, many of them have several equilibrium configurations of the nuclei. Correspondingly, the experimental spectra relate to different isomers of the molecules. The existence of the higher oxides B_3O_3, Al_3O_3, and Al_2O_4,[3,4] and even exotic species such as Al_3O and Al_4O,[5] has been predicted theoretically. The wide variety of compositions is one of the characteristics of the molecules X_mO_n.

Fig.1 compares the geometric configurations of the most stable isomers of the molecules X_2O, XO_2, X_2O_2, and X_2O_3. The characteristics of the geometric structure of each of the molecules will be discussed in detail later. Here we would only point out that the molecules X_mO_n show not only a variety of compositions but also a variety of geometric forms. It is not always easy to reach a definite conclusion about the geometry of a molecule; this is illustrated by the lively debate about the shape of B_2O_3.[6–9] It is still not completely clear which isomer of AlO_2, linear or cyclic, corresponds to the most stable configuration.[10] The compounds of this class provide a good illustration of one of the traditional problems of the structural chemistry of molecules with 3–5 atoms, namely the question of whether the linear or angular (or cyclic) configuration is preferred. In general, for the oxides X_mO_n we can expect a combination of ionic and covalent bonding, with ionic bonding predominating for the aluminium oxides. Thus linear structures, giving the minimum $O^- - O^-$ and $X^+ - X^+$ repulsion, are generally not unexpected. Angular configurations may be favoured, however, by the effects of sp^2 hybridisation of the boron and oxygen atoms.

Quantum-chemical calculations show that the difficulty of distinguishing between the linear and angular configurations of X_mO_n molecules is related to the flatness of the potential energy surfaces along the deformation coordinates.

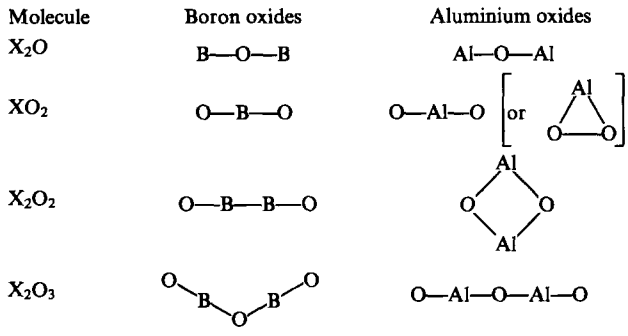


Figure 1. Geometric configurations of the ground-state isomers of the polyatomic molecules X_mO_n.

The structural formulae given in Fig. 1 indicate that the vibrational spectra of the molecules should contain characteristic bands which can be assigned to the groups X—O (in different positions), X—O—X, and O—X—O. The regularities observed in the vibrational spectra, particularly in the high-wavenumber stretching region, represent another characteristic of the molecules of this class.

III. Methods of study

As noted in the Introduction, the present review is based on the results of experimental spectroscopic studies and quantum-chemical calculations. In the present section we shall discuss briefly the possibilities provided by these approaches, mainly to understand how reliable they are for predicting the structure of the molecules B_mO_n and Al_mO_n.

1. Experimental methods

The difficulties in the study of the polyatomic oxides of boron and aluminium are related to the fact that in the equilibrium vapour above the corresponding condensed phases, only the molecules B_2O_3, B_2O_2, and Al_2O are present in quantities sufficient for study by non-resonance spectroscopic methods. Moreover, although resonance methods, for example laser-induced fluorescence (LIF), can be used to study products at low concentrations, with rare exceptions they do not give sufficient information for reaching reliable conclusions about the geometry and vibrational constants of poly-atomic molecules. Thus the data required for the interpretation of the spectra and structure of these materials have been obtained mainly using the methods of the spectroscopy of thermodynamically non-equilibrium systems—inert matrices in which chemical reactions are taking place, and beams obtained by the non-equilibrium (most frequently laser-pulse) volatilisation of appropriate targets. Here we shall discuss mainly data obtained by matrix studies, since almost all the fundamental experimental results on the oxides of boron and aluminium have been obtained from these studies.

The following experimental scheme is now generally accepted.

1. A non-equilibrium situation is created in a system containing boron (or aluminium) and oxygen. This may be a matrix of an inert gas or nitrogen, into which are introduced metal atoms and clusters, volatilised from a Knudsen cell or from the surface of a solid target by a laser, and molecules of an oxidant (oxygen, nitrous oxide, hydrogen peroxide, ozone, etc.). In another version, the products of the non-equilibrium volatilisation of an oxide target are deposited in the matrix.

2. The infrared or Raman spectra of the specimen obtained are recorded by the methods of low-temperature vibrational spectroscopy.

3. The matrix is subjected to external treatment—photolysis, controlled heating ('annealing'), or simple storage for a long time at a constant temperature—after which the changes in the spectra are recorded.

4. When the elements being studied have stable isotopes, the entire cycle of studies is repeated with isotope-enriched specimens.

5. Attempts are then made to obtain an internally consistent assignment of all the bands, or the strongest bands, in all the spectra, relating them to molecules with definite composition.

6. For those molecules whose existence has been established in the previous stage, the experimental wavenumbers and the measured isotope shifts are used to solve the vibrational problem in the harmonic approximation, to determine the symmetry of the equilibrium configuration and to estimate the missing vibrational wavenumbers.

Thus the reliability of the results of the experimental studies depends mainly on the quality of the interpretation of the observed spectra. The complexity of this problem is due to two factors. Firstly, the composition of the products of matrix chemical reactions depends significantly on temperature, the matrix material, and the concentration of the starting materials, and this leads to poor reproducibility of the results. Frequently, papers by different authors give quite different spectra for the same systems. Secondly, the optical properties of the matrices, particularly those containing metals, are very far from ideal, and this leads to various distortions of the spectra, such as displacement and splitting of the bands, and, which is most important, to a significantly non-linear dependence of the intensity of the bands on the concentration of the corresponding products.

We shall not discuss these problems (details can be found elsewhere[11]), and here we merely formulate the general position which we shall subsequently maintain: an individual specific result of an experimental study may prove to be incorrect when a more extensive study or a technically improved study is carried out, but for a sufficiently large number of molecules consisting of the same atoms, the general picture obtained in a systematic study with wide variation of the conditions and methods can apparently be taken as reliable. Thus in the examination of specific molecules we shall try to pick out not the differences between different authors, which naturally represent the principal topic for discussion in experimental and theoretical studies, but the results which can now be regarded as established.

2. Quantum-chemical calculations

According to the present-day ideas, structural data for molecules made up of a small number of atoms from the start of the periodic table should be obtained by non-empirical approaches with allowance for the effects of electron correlation. Calculations of this kind have been carried out for practically all the systems examined in the present review.[3,4,10] It is of course appropriate to discuss the results obtained by other approaches.

When carrying out quantum-chemical calculations, it is necessary to choose correctly the basis set of atomic orbitals (AO) and the method for taking account of electron correlation. It is then necessary, for the given version of the calculation to find the geometric configurations corresponding to stable minima on the potential energy surface (PES) of the molecule, to estimate the differences between the energies of the different minima (if several are found), and to calculate the wavenumbers and intensities for the normal vibrations, for example in the harmonic approximation. This calculation scheme can be simplified, by neglecting correlation effects, that is restricting the treatment to the self-consistent field (SCF) approximation, by introducing pseudo-potentials and excluding explicit consideration of the core electrons, and by using semi-empirical schemes.

In the discussion of theoretical results and their comparison with experimental data, it is not always easy to estimate the consequences of a given simplification. For example, in calculations of vibrational wavenumbers by the SCF method with scaling, that is in fact with semi-empirical corrections, in a number of cases it is possible to obtain better agreement with the line positions in the experimental spectrum than when various correlation approaches are used.

The structural characteristics of Al_mO_n and B_mO_n molecules have been calculated[3,4] using 6-31GF* basis sets (that is valence-split sets with the addition of polarisation AO) by SCF methods and second-order Moeller–Plesset perturbation theory (MP2). This procedure (MP2/6-31GF*) is now generally accepted, and should give an uncertainty of not more than 2% for the equilibrium geometric parameters and 5% for the vibrational frequencies. For the relative energies of the isomers and all other calculated energy differences, the situation is generally not so favourable, and the upper limit of the uncertainties in the worst cases may be appreciably higher.

The interpretation of the results of calculations of molecular properties in the MO LCAO approximation is facilitated considerably by analysing the electronic structure in terms of the so-called natural bond orbitals.[12] This involves the use of the methods of quantum chemistry to model familiar Lewis structures reflecting the structure of molecules by means of bonds and lone pairs. We shall make extensive use of this representation in the discussion of the properties of the molecules of the oxides of boron and aluminium.

IV. The structure and spectra of X_mO_n molecules

Specific molecular systems X_mO_n will be discussed in the following order. We shall examine first the geometric configuration of the ground-state isomer and its vibrational spectrum, and then other possible geometric configurations (for the boron and aluminium compounds separately). In each concluding section we shall formulate the common and distinguishing details of the structure of the oxides B_mO_n and Al_mO_n mainly on the basis of an analysis of the electronic structure.

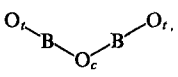
1. X_2O_3 molecules

We begin with the principal oxide of group III elements—X_2O_3. Fig. 1 shows that the ground-state isomers of the B_2O_3 and Al_2O_3 molecules have different geometric configurations—angular for B_2O_3 and linear for Al_2O_3. The simple explanation of this result is the more ionic character of the aluminium compounds, leading to the formation of linear structures. The path to this conclusion has been fairly complex, and other configurations, primarily trigonal bipyramidal, have been examined, but the accumulated experimental and theoretical data correspond to the structures given in Fig. 1.

The first studies of the infrared spectra of B_2O_3 vapour were published in the mid nineteen-fifties, when there was interest in the combustion products of boron compounds. Most progress in the study of the structure of the B_2O_3 molecule was made, however, using spectroscopic matrix and electron diffraction methods.[8,9,13–16] The first studies were carried out in the early nineteen-sixties,[13–15] and quantum-chemical calculations to establish the structure of B_2O_3 were carried out at the same time.[6,7,17–19] This was possibly one of the first examples of this complex approach to the solution of problems of molecular structure.

Boric oxide is a fairly convenient material for study by matrix-isolation infrared spectroscopy. The only problem in the assignment of the bands in the spectrum of this molecule was due to the presence of boric acids in the vapour above B_2O_3. This difficulty was overcome by systematic fractional volatilisation.[8] The complete infrared spectrum of natural boric oxide and all isotopic forms of the molecule with ^{10}B and ^{18}O have now been obtained.[8,13] For the molecules obtained by matrix reactions, the degree of reliability which has been achieved in the assignment of the frequencies in the infrared spectrum has not been obtained. Thus the B_2O_3 molecule provides an ideal 'calibration' system for determining the extent of the agreement that can now be obtained between the results of quantum-chemical calculations and the data obtained by infrared spectroscopy and electron diffraction.

The first quantum-chemical calculations for the B_2O_3 molecule by the non-empirical SCF method with a small basis set of AO[17] and by the semi-empirical INDO method[18] gave geometric configurations with C_{2v} symmetry. The results of several independent non-empirical calculations[6,7,19] in the SCF approximation with different AO basis sets, showing fairly good agreement with one another, were published in 1980 and 1981. The latest non-empirical studies of the B_2O_3 molecule were apparently carried out in 1992 (using the SCF method and MP2 perturbation theory with 6-31GF* basis sets),[4] and they did not lead to new qualitative changes in the earlier conclusions about the equilibrium geometry of the molecule



although the quantitative changes in the parameters were appreciable.

Table 1 compares the results of calculations of the equilibrium geometric parameters of the molecule with the C_{2v} configuration with data obtained by electron diffraction.[9] Comparison of the last two rows of Table 1 shows the very good quantitative agreement between the experimental and theoretical approaches. For this example we can estimate the uncertainties in the non-empirical calculations of the equilibrium internuclear distances in the MP2/6-31GF* approximation for the molecules being considered as 0.01 Å (that is about 1%).

It should nevertheless be remembered that the path to these consistent results was complex, and considerable work was required. Thus the electron diffraction data have been repeatedly refined as new measurements were made.[9,15,20,21] Difficulties were also encountered in the calculations; in particular, it has been emphasised that to to obtain a non-linear equilibrium structure it is necessary to include polarisation AO in the basis set.[7]

The vibrational wavenumbers of the B_2O_3 molecule for the principal isotopic form ($^{11}B_2{}^{16}O_3$) are given in Table 2, which compares the values calculated in the harmonic approximation (SCF or MP2 with different basis sets), the results of spectral studies in low-temperature matrices,[8,16] and the results of a combined treatment of data obtained by gas-phase electron diffraction and molecular spectroscopy by an original method which gives an estimate of the frequencies.[19]

The calculated intensities of the infrared bands and a qualitative description of the modes of the B_2O_3 molecule are given in Table 3. The position of the strongest ν_2 band in the infrared spectrum is known from spectroscopic studies of B_2O_3 in inert matrices [2061 cm^{-1} (Ref. 8) or 2062.3 cm^{-1} (Ref. 16)]. Isotope replacement $^{11}B \rightarrow {}^{10}B$ leads to a displacement [2061 → 2128 or 2062.3 → 2130.5 cm^{-1} with $R(10/11) = 1.033$], but the absence from the spectrum of the band corresponding to the mixed composition $^{10}B^{11}BO_3$ remains somewhat puzzling.

Table 1. Calculated and experimental (from gas-phase electron diffraction data) equilibrium geometric parameters of the B_2O_3 molecule (distances R in Å, angles Φ in °).

Method	R_{O_c-B}	R_{B-O_t}	$\Phi(B-O_c-B)$	$\Phi(O_t-B-O_c)$	Ref.
SCF/OST-3GF	1.363	1.237	137.5	176	6
SCF/4-21GF*	1.324	1.188	136.0	178.3	7
SCF/[4*s*2*p*1*d*]	1.330	1.191	137.1	178.8	7
SCF/6-31GF*	1.313	1.189	145.5	180	4
MP2/6-31GF*	1.334	1.221	136.1	177.6	4
Gas-phase electron diffraction	1.323	1.219	137.5	173.4	9

Note. The experimental uncertainties are: $\Delta R_{O_c-B} = \pm 0.008$, $\Delta R_{B-O_t} = \pm 0.007$ Å, $\Delta\Phi(B-O_c-B) = \pm 6.3°$, $\Delta\Phi(O_t-B-O_c) = \pm 4.4°$.

Table 2. Theoretical and experimental vibrational wavenumbers of the B_2O_3 molecule (cm^{-1}).

Vibration	Symmetry	Calculated data					Experiment	
		OST-3GF[6]	4-21GF*[4]	6-31GF*			Spectroscopy[8]	Electron diffraction[9]
				SCF	SCF(0.9)[a]	MP2		
ν_1	A_1	2201	2314	2272	2045	2100		2057
ν_2	B_1	2164	2293	2283	2055	2125	2061	2060
ν_3	B_1	1258	1308	1356	1220	1227		1099
ν_4	A_1	713	817	779	701	756		1050
ν_5	A_1	462	597	583	525	529	518	566
ν_6	A_2	429	462	508	457	466		288
ν_7	B_2	415	518	552	497	488	489	273
ν_8	B_1	378	491	501	451	456	462	512
ν_9	A_1	99	108	79	71	87	73	102

[a] Here and subsequently the column 'SGF(0.9)' gives wavenumbers obtained by the SCF/6-31GF* method by scaling with a factor 0.9.

From MP2/6-31GF* calculations,[4] the isotope shift $^{11}B_2O_3 \rightarrow {}^{10}B_2O_3$ [2125 $cm^{-1} \rightarrow$ 2197 cm^{-1}, $R(10/11) = 1.034$] shows good agreement with the experimental data. Estimates of the intensities with the calculated[4] force-constant matrix show that the band due to the mixed isotopic form $^{10}B^{11}BO_3$ should be fairly close to the $^{10}B_2O_3$ band, and this may make its identification difficult. However, this does not explain the absence of the band due to the mixed isotopic form from the spectrum despite the high intensity expected from the theoretical calculations. Oxygen isotope replacement $B_2^{16}O_3 \rightarrow B_2^{18}O_3$ for the ν_2 band gives a consistent picture for experiment [2062.3 $cm^{-1} \rightarrow$ 2024.1 cm^{-1}, $R(16/18) = 1.019$] and theory [MP2/6-31GF*, 2125 cm^{-1}, 2089 cm^{-1}, $R(16/18) = 1.017$].

For the ν_7 band, the measured[8] isotope shift $^{10}B_2O_3 \rightarrow {}^{11}B_2O_3$ is 489 $cm^{-1} \rightarrow$ 505 cm^{-1}, $R(10/11) = 1.033$; the theoretical (MP2/6-31GF*) shift is 488 $cm^{-1} \rightarrow$ 504 cm^{-1}, $R(10/11) = 1.033$. The experimental shift for oxygen $B_2{}^{16}O_3 \rightarrow B_2{}^{18}O_3$ [489 $cm^{-1} \rightarrow$ 480 cm^{-1}, $R(16/18) = 1.019$] also coincides with the calculated shift [488 $cm^{-1} \rightarrow$ 479 cm^{-1}, $R(16/18) = 1.019$].

Finally, for the ν_5 band the experimental shifts are:[8] for $^{11}B_2O_3 \rightarrow {}^{10}B_2O_3$, 518 $cm^{-1} \rightarrow$ 538 cm^{-1}, $R(10/11) = 1.039$; for $B_2{}^{16}O_3 \rightarrow B_2{}^{18}O_3$, 518 $cm^{-1} \rightarrow$ 510 cm^{-1}, $R(16/18) = 1.016$. The corresponding theoretical estimates are:[4] for $^{11}B_2O_3 \rightarrow {}^{10}B_2O_3$, 529 $cm^{-1} \rightarrow$ 548 cm^{-1}, $R(10/11) = 1.036$, and for $B_2{}^{18}O_3$, 529 $cm^{-1} \rightarrow$ 521 cm^{-1}, $R(16/18) = 1.015$.

The isotope shifts have not been obtained for the remaining two measured frequencies (ν_8 and ν_9).

Since the assignment of the known bands is fairly reliable, it is possible to discuss the accuracy of the theoretical calculations of the wavenumbers of the B_2O_3 molecule. It is appropriate to compare the values calculated by the 4-21GF* and 6-31GF* methods with the experimental spectroscopic data (Table 2). The calculations using the OST-3GF basis set are of considerable historical interest, but the frequencies estimated from experimental electron diffraction data are not all sufficiently reasonable, apparently because of the incorrect choice of reference spectral data.

Table 3. Intensities (km mol^{-1}) of the bands in the infrared spectra and the assignment of the vibrations of the B_2O_3 molecule (the symbols for the modes correspond to those in Table 2).

Mode	Intensities		Assignment
	SCF/4-21GF*	MP2/6-31GF*	
ν_1	68.5	38.0	B–O_t (symmetric stretch)
ν_2	1263.6	963.7	B–O_t (antisymmetric stretch)
ν_3	102.5	108.8	B–O_c (antisymmetric stretch)
ν_4	24.0	13.8	B–O_c (symmetric stretch)
ν_5	131.6	75.1	mixed deformation
ν_6	0	0	anti-phase out of plane
ν_7	16.7	100.6	in-phase out-of-plane
ν_8	21.2	11.6	O_c–B–O_t (deformation)
ν_9	14.0	8.5	B–O_c–B (deformation)

In the SCF approximation, the basis-set effects (the change from 4-21GF* to 6-31GF*) are fairly tyical—the frequencies differ by 10%. The change to the MP2 correlation method lowers the frequencies, and comparison of the data obtained by MP2 and SCF (0.9) methods shows that the use of the popular scaling factor 0.9 for the frequencies calculated in the SCF approximation, covering both correlation and anharmonic corrections,[22,23] in this case leads to values very close to those obtained by the MP2 method (see Table 2). At the very least, the SCF approximation with scaling shows no unique advantages over MP2 in this case, although the frequencies calculated in the SCF approximation with scaling are slightly closer to the experimental data for ν_2, ν_5, and ν_9.

Direct comparison of the calculated and measured wavenumbers is naturally made difficult by the fact that the theoretical values are obtained using the harmonic model and relate to the free molecule, while the experimental data correspond to the real vibrations of the molecule in a matrix environment. It is usually assumed that both the anharmonic and the matrix effects are small, so that the comparison of the frequencies obtained using the MP2 approximation with the experimental spectroscopic data (Table 2) is fully justified. The positions of the strong ν_2, ν_7, and ν_5 bands are effectively reproduced in the MP2/6-31GF* calculation; the differences between the results and the experimental wavenumbers do not exceed 3% (the published[6,9] assignment of the experimental[8] wavenumbers 518 cm^{-1} to B_1 and 462 cm^{-1} to A_1 is incorrect). The values of the ν_8 wavenumbers differ by the same amount. For the B–O_c–B deformation ν_9 with the lowest frequency, slightly greater differences between the experimental and theoretical results are observed, as expected.

The flatness of the PES along the given deformation coordinate (which gives grounds for regarding this molecule as quasi-linear) is responsible for the previously noted difficulties encountered in the quantum-chemical calculations[4,6,7] and for the difficulty in the interpretation of the electron diffraction data.[9,15,20,21] According to published calculations,[6,7] the barrier to inversion, that is the difference between the linear and equilibrium (C_{2v}) configuration, does not exceed 2.5 kcal mol^{-1}. Under these conditions it is fairly difficult to determine the equilibrium valence angle and the frequency of the deformation. Appreciable anharmonicity corrections can also be expected for the ν_9 vibration.

Even by increasing considerably the possible range of uncertainties for the wavenumbers calculated in the MP2/6-31GF* approximation, for example to 10%, it is not

possible to obtain from the calculated data a band in the Raman spectrum in the region of 1062 cm^{-1}, assigned[8] to the B_2O_3 molecule. The absence from the experimental infrared spectrum of the ν_3 band (theoretical wavenumber 1227 cm^{-1}), which should be fairly strong, and the strong ν_2 band due to the mixed isotopic form $^{10}B^{11}BO_3$ also remains unexplained.

An intensive search has been made[4] for other stationary points on the PES of the ground state of B_2O_3, but no structures other than the configuration with C_{2v} symmetry were found.

According to SCF and SCF-X_α SW calculations,[6] the excited states of B_2O_3 are fairly high; the estimated vertical excitation energies are 6–7 eV.

Thus calculation and experiment on the whole give similar pictures of the structure and infrared spectrum of the B_2O_3 molecule. Quantitative agreement is even obtained for the positions and intensities of a number of the spectroscopic bands. The differences noted above are also observed, however.

In contrast to B_2O_3, there are very few experimental data for the Al_2O_3 molecule. The vapour above solid aluminium oxide apparently does not contain free Al_2O_3 molecules.[2] A large number of products are formed in the reaction of atomic aluminium with oxygen in argon and nitrogen matrices.[24–30] Attempts have been made to assign various bands in the infrared and Raman spectra of these products to Al_2O_3. Characteristic features of the infrared spectra of the Al + O_2 system in published studies[26,27] are the 1101, 1095 cm^{-1} doublet in dilute nitrogen matrices, and the 1101, 1095, 1092 cm^{-1} triplet in concentrated matrices. The less intense 502, 492 cm^{-1} doublet is recorded under the same conditions. These two bands have been provisionally assigned to the vibrations of a linear Al_2O_3 molecule with $D_{\infty h}$ symmetry. The doublet band at 1031, 1024 cm^{-1} in the Raman spectrum has been assigned to the same linear molecule.

The band at 1211.2 cm^{-1} in the infrared spectrum of the products of the reaction of aluminium volatilised by a laser from solid Al_2O_3 with oxygen in an argon matrix was recently assigned[30] to the O–Al–O–Al–O molecule. The band at 1101 cm^{-1} was assigned to a molecule with the composition AlO_3 in which two oxygen atoms are joined to one another and the third is a terminal atom. The author cited previously assigned this band to an unsymmetrical aluminium dioxide molecule.

From semi-empirical MNDO quantum-chemical calculations, it was suggested[26] that there exist a number of molecular isomers with the composition Al_2O_3, and the band at 964 cm^{-1} in the infrared spectrum was assigned to one of these which was completely unsymmetrical.

According to non-empirical calculations,[3,31] the ground-state minimum on the PES of Al_2O_3 corresponds to the linear symmetrical $D_{\infty h}$ structure

$$O_t-Al-O_c-Al-O_t\,.$$

Table 4 gives the results of quantum-chemical calculations of the equilibrium internuclear Al–O distances by SCF and MP2 methods. From calculations for the B_2O_3 molecule and other similar molecular systems, the uncertainties in the calculated equilibrium distances in the MP2/6-31GF* approximation should be about 0.01 Å.

Table 4. Equilibrium internuclear distances (Å) in the linear molecule $O_t-Al-O_c-Al-O_t$.

Method of calculation	R_{O_c-Al}	R_{Al-O_t}	Ref.
SCF/(10*s*6*p*1*d*,7*s*3*p*)/[6*s*4*p*1*d*,4*s*2*p*]	1.641	1.561	31
SCF/(12*s*8*p*1*d*,9*s*5*p*1*d*)/[6*s*4*p*1*d*,4*s*2*p*1*d*]	1.657	1.565	31
SCF/6-31GF*	1.666	1.571	3
MP2/6-31GF*	1.691	1.626	3

The wavenumbers and intensities of the vibrations of the linear Al_2O_3 molecule are given in Table 5. The results of two independent calculations by the SCF method with basis sets of comparable quality[3,31] practically coincide. As with B_2O_3, scaling the wavenumbers gives values close to the results obtained in the MP2 approximation with the same basis set. The correlation of the calculated wavenumbers with the experimental spectra in this case, however, is not so successful as in the case of B_2O_3.

Table 6 gives the wavenumbers and the corresponding isotope ratios $R(16/18)$ of the isotopic forms of the Al_2O_3 molecule for those bands in the spectra to which the experimental data are assigned. The band recorded[30] at 1211.2 cm^{-1} apparently in fact corresponds to the $\nu_1(\Sigma_u)$ vibration of O–Al–O–Al–O. The agreement between the isotope ratios is almost quantitative, and the experimentally determined ν_1 wavenumber coincides with that calculated by the SCF method with scaling, and with the wavenumber obtained by the MP2/6-31GF* method to within 3%. The bands observed[26,27] at 1101, 502 (infrared), and 1031 cm^{-1} (Raman) possibly correspond to other compounds or to a molecule with a different structure.

The assignment of the bands is fairly obvious: the pairs ν_1, ν_2 and ν_3, ν_4 correspond to the vibrations of terminal $Al-O_t$ and central $Al-O_c$ groups respectively. All the deformations have fairly low wavenumbers, particularly the ν_7 vibration (40–50 cm^{-1}) describing the deformation about the central oxygen atom. The section of the PES along this coordinate is even flatter than that for B_2O_3.

The question of the isomers of the Al_2O_3 molecule has been examined.[3,26,31] According to quantum-chemical calculations, the at first sight attractive trigonal bipyramidal model must be rejected, since the energy of this configuration is too high compared with the linear form (more than 200 kcal mol^{-1} in the MP2/6-31GF* method); moreover, the D_{3h} structure does not correspond to a minimum on the PES. The configurations found by the semi-empirical MNDO method[26] were not confirmed by subsequent non-empirical calculations.[3]

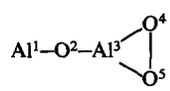
Of considerable interest is one of the equilibrium configurations of Al_2O_3 found by the SCF/6-31GF* and MP2/6-31GF* methods,[3] namely the planar structure with C_{2v} symmetry

Table 5. Calculated wavenumbers (cm^{-1}) and infrared intensities (in curly brackets, km mol^{-1}) of the vibrations of the linear molecule O–Al–O–Al–O.

Vibration	Symmetry	SCF [31]	SCF/6-31GF* [3]	SCF (0.9)	MP2/6-31GF* [3]
ν_1	Σ_u		1345	1211	1242 {387}
ν_2	Σ_g	1269	1263	1137	1130
ν_3	Σ_u		1016	914	924 {105}
ν_4	Σ_g	461	459	413	428
ν_5	Π_u	326	324	292	250 {116}
ν_6	Π_g	197	209	188	175
ν_7	Π_u	72	55	50	36 {20}

Table 6. Theoretical and experimental wavenumbers of the isotopic forms of the linear Al_2O_3 molecule and the corresponding isotope ratios $R(16/18)$ (given in brackets).

Positions of the bands and isotope ratios $R(16/18)$						Assignment	Ref.
$^{16}O_2$		$^{16}O_2+^{18}O_2$		$^{18}O_2$			
1211.2	1206.1	1200.0	1187.4	1183.1	1172.9	$\nu_1(\Sigma_u)$ (expt)	30
(1.000)	(1.004)	(1.009)	(1.020)	(1.025)	(1.033)		
1242		1230	1217		1202	$\nu_1(\Sigma_u)$ (theor)	3
(1.000)		(1.009)	(1.020)		(1.033)		
1101					1068	$\nu_1(\Sigma_u)$ (expt)	26
(1.000)					(1.031)		

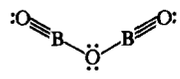


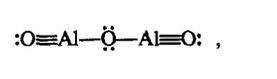
whose energy is higher than that of the linear form by only 11 kcal mol^{-1} in the SCF method, or 32 kcal mol^{-1} in the MP2 method. Experience suggests that the MP2 approximation should give a value for the energy difference which is too large, so that the C_{2v} structure being considered should correspond to an energy of $\sim$20 kcal mol^{-1}, which does not exclude its presence in Al + O_2 matrix reactions. The presence of a similar structure was suggested in the interpretation of electron diffraction data for B_2O_3, but was rejected.[9] According to MP2/6-31GF* data, the equilibrium geometric parameters of the C_{2v} Al_2O_3 molecule are: $R_{Al^1-O^2}$ 1.745, $R_{O^2-Al^3}$ 1.683, $R_{Al^3-O^4}$ and $R_{Al^3-O^5}$ 1.723 Å, $\Phi(O^4-Al^3-O^5)$ 59°.

One of the vibrations of the C_{2v} isomer, 1146 cm^{-1} (MP2/6-31GF*) or 1109 cm^{-1} (SCF/6-31GF* with a scaling of 0.9), should be extremely intense in the infrared spectrum.[3] The corresponding wavenumber might be observed in the experimental spectra.[26,27,30] The electronic structure of this compound is effectively described by the formula $Al^+(AlO_3)^-$.

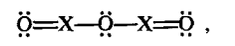
Thus with reference to the structure of the Al_2O_3 molecule there remain a fairly large number of unanswered questions, particularly regarding the experimental data.

Formally, the Lewis structures of the B_2O_3 and Al_2O_3 molecules coincide:[3,4]

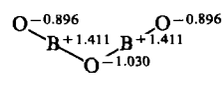


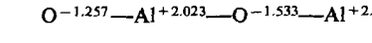


(it is of course possible to use the alternative description



since the boundary between the orbital of the lone pair of the terminal oxygen atom and one of the π-orbitals of the X–O_t bond is somewhat provisional). The pictures of the effective charges on the atoms, obtained by analysis of the populations of the natural orbitals,[3,4] however, differ significantly:





The Mulliken populations[7,31] for systems of this kind give effective charges which are much too low.[12] As expected, the contribution of ionic components to the interaction is greater for aluminium oxide. This also explains the differences in the equilibrium geometric configurations and the lower frequency of the deformation involving the central oxygen atom for Al_2O_3.

The greater contributions of the covalent components to the characteristics of the B–O bonds in B_2O_3 are reflected in the higher values of the force constants (MP2/6-31GF*):

f_{B-O_t} = 13.7 mdyn Å^{-1} $\quad f_{Al-O_t}$ = 6.68 mdyn Å^{-1}

f_{B-O_c} = 7.94 mdyn Å^{-1} $\quad f_{Al-O_c}$ = 4.95 mdyn Å^{-1}

In both molecules, B_2O_3 and Al_2O_3, the dominant correlation effects should be associated with excitations of the type $\pi(X-O_t)\rightarrow\pi^*(X-O_t)$,[3,4,32] leading finally to an increase in the equilibrium internuclear $X-O_t$ distances obtained in the correlation approaches, compared with the results obtained by the SCF method (see Tables 1 and 4). This effect is greater for Al_2O_3 [$\Delta R_{corr}(Al-O_t)$ = 0.06 Å, $\Delta R_{corr}(B-O_t)$ = 0.03 Å]; this can be related to the smaller difference between the energies of the orbitals $\pi(X-O_t)$ and $\pi^*(X-O_t)$ for the Al–O_t bonds, compared with B–O_t.

2. X_2O_2 molecules

Fig. 1 shows that the configurations of the ground-state isomers with the composition X_2O_2 for boron and aluminium are fundamentally different: a linear structure with a B–B bond for B_2O_2 and a cyclic structure for Al_2O_2. Both theoretical and experimental data indicate the existence of other X_2O_2 isomers with low energies. Future more accurate studies will possibly alter present conclusions about the configurations of the ground-state isomers. Nevertheless, it is clear that for oxides with this stoichiometry the differences between the structures of the molecules containing boron and aluminium are considerable.

The B_2O_2 molecule has been studied in parallel with B_2O_3, since mass-spectrometric studies[33] show that when elemental boron is added to solid boric oxide B_2O_3, B_2O_2 molecules predominate in the vapour above the mixture. Until recently, only one isomer had been characterised experimentally. For this isomer, two vibrational wavenumbers were obtained (1898 cm^{-1} and 213 cm^{-1}), and all possible isotope shifts measured. It was concluded that this isomer has a symmetrical linear structure, the force field was calculated, and the frequencies of forbidden transitions in the absorption spectrum were estimated.[34,35] These data were subsequently confirmed[36] in a study of the photoelectron spectra of B_2O_2 vapour. The two bands (at 2048 cm^{-1} and 1408 cm^{-1}) found in recent studies[16,37] of the reactions of atoms in boron clusters with oxygen and water in inert matrices were assigned to the unsymmetrical linear isomer B–O–B–O. In a study of the mass spectra[38] of the vapour above B_2O_3 it was concluded that the compound B_2O_2 corresponds to the unsymmetrical isomer B–O–B–O.

Semi-empirical and non-empirical SCF calculations with the minimum basis set OST-3GF predicted[39,40] that the ground-state

Table 7. Geometric parameters (Å) and relative energies ΔE/kcal mol^{-1} of the linear molecules O–B–B–O and B–O–B–O.

Method of calculation	O–B–B–O		B^1–O^2–B^3–O^4			ΔE	Ref.
	R_{B-O}	R_{B-B}	$R_{B^1-O^2}$	$R_{O^2-B^3}$	$R_{B^3-O^4}$		
SCF/4-31GF	1.196	1.631	1.337	1.314	1.202	16.8	36
SCF/6-31GF*	1.182	1.667	1.306	1.311	1.190	19.9	4,36
MP3/6-31GF*	1.201	1.647	–	–	–	29.5	36
MP2/6-31GF*	1.218	1.636	1.317	1.332	1.220	40.0	4

Semi-empirical and non-empirical SCF calculations with the minimum basis set OST-3GF predicted[39,40] that the ground-state isomer should have the linear symmetrical structure O–B–B–O.

The parameters of the equilibrium configurations of the linear systems O–B–B–O and B–O–B–O, calculated in a fairly good approximation (SCF and MP with generally accepted basis sets),[4,36] are given in Table 7. As with B_2O_3, we expect that the MP2/6-31GF* method makes it possible to predict internuclear distances with an uncertainty of about 0.01 Å. Comparison with the data in Table 1 shows that for all the molecules (B_2O_3, O–B–B–O, and B–O–B–O) the distances from boron to the terminal oxygen agree within this uncertainty and are equal to 1.22 Å.

The vibrational frequencies and infrared intensities for the two isomers are compared in Table 8. As in the previous examples, noteworthy features are the similarity in the frequencies calculated by the SCF(0.9) and MP2 methods, and the fact that the calculated harmonic frequencies of the MP2/6-31GF* approximation coincide with the measured values in the infrared spectrum (ν_2 and ν_5) for the ground-state isomer O–B–B–O. The published[16,34,35,37] $^{16}O \rightarrow {}^{18}O$ and $^{11}B \rightarrow {}^{10}B$ isotope shifts in different combinations for the ν_2 band are reproduced almost quantitatively by the calculations. The large differences for the ν_3 and ν_4 bands can be explained, since the wavenumbers forbidden in the infrared spectrum were predicted[35] with molecular force constants estimated from known bands. Comparison of the results of different calculations[4,36] shows the very large difference between the ν_1 and ν_2 vibrational wavenumbers obtained by the MP2 and MP3 methods with the same basis set 6-31GF* (in the SCF method, the corresponding values are identical).

The observation[16,37,38] of the unsymmetrical isomer B–O–B–O is also confirmed by non-empirical calculations. From the isotope shifts, the experimental[37] bands at 2048 cm^{-1} and 1408 cm^{-1} agree with the calculated values 2123 cm^{-1} and 1488 cm^{-1} for ν_1 and ν_2 respectively:

ν_1, $R(16/18) = 1.016$ and $R(10/11) = 1.034$ from experiment, and $R(16/18) = 1.017$ and $R(10/11) = 1.035$ from calculation; ν_2, $R(16/18) = 1.034$ and $R(10/11) = 1.019$ from experiment, and $R(16/18) = 1.035$ and $R(10/11) = 1.019$ from calculation (MP2/6-31GF*).

The differences between the theoretical and experimental wavenumbers are 4% for ν_1 and 6% for ν_2, which are slightly greater than those observed in the previous examples. The question of the magnitude of the energy of the isomer B–O–B–O relative to that of O–B–B–O remains unresolved, that it is not clear whether it is sufficiently low for it to be possible to obtain the isomer B–O–B–O experimentally.

As has been suggested,[40] the cyclic isomers of B_2O_2 also correspond to stationary points on the PES of the ground state,[4,36] but their energies differ from that of the ground-state configuration O–B–B–O by more than 60 kcal mol^{-1}.

The presence of the compound Al_2O_2 in the vapour above solid aluminium oxide has been confirmed by mass spectrometry.[2] The interpretations of the infrared spectra of the products of matrix reactions of aluminium with oxygen, assigned to Al_2O_2, are contradictory. For a long time, the band at 496 cm^{-1} (or 498 cm^{-1}) was assigned to an Al_2O_2 molecule with a rhomb-shaped configuration.[41,42] According to Serebrennikov and coworkers,[24,25] this band belongs to a cyclic isomer of Al_2O_2, and this was confirmed in recent experiments.[30] An infrared band at 691 cm^{-1} and (provisionally) a Raman band at 713/721 cm^{-1} have been assigned[26,28] to a vibration of the square isomer of Al_2O_2; the infrared bands at 640 cm^{-1} and 545 cm^{-1} and the Raman band at 563 cm^{-1} were assigned to the rhomb-shaped isomer. In the work cited,[30] the bands in the infrared spectrum were assigned only for the linear isomer Al–O–Al–O: 1176/1169/1167, 945/943/940 cm^{-1}. The band at about 943 cm^{-1} has been assigned[26] to this isomer.

A number of quantum-chemical calculations have been carried out for Al_2O_2.[3,43–45] SCF calculations using pseudopotentials[43] for the molecule gave three stationary points on the PES: the ground-state isomer corresponds to an almost square configuration with D_{2h} symmetry, the isomer with the rhomb-shaped configuration has an energy 37 kcal mol^{-1} higher, and the third isomer is the linear molecule Al–O–Al–O. From the calculated vibrational wavenumbers it was concluded that the experimental band at 496 cm^{-1} can be assigned to the ground-state square isomer of Al_2O_2. Calculations have been carried out[44] by non-empirical SCF (with different basis sets) and MP2/6-31GF* methods. It was confirmed that the ground-state equilibrium configuration is square, and that the linear Al–O–Al–O (10.2 kcal mol^{-1} higher) and rhomb-shaped (71.5 kcal mol^{-1}) configurations have higher energies. As before, one of the vibrational wavenumbers of the ground-state isomer, found only in the SCF approximation (476 cm^{-1} without scaling), was compared with the experimental data. Attention was drawn[45] to the fact that in the square configuration the energy of the triplet state is fairly close to that of the singlet state.

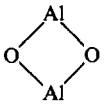
The equilibrium geometric parameters and the wavenumbers and intensities of the vibrations have been calculated[3] in the SCF and MP2 approximations with the basis set 6-31GF*. For the geometries and wavenumbers in the SCF approximation

Table 8. Wavenumbers (cm^{-1}) and intensities (in curly brackets, km mol^{-1}) of the vibrations of the molecules O–B–B–O and B–O–B–O

Method	O–B–B–O					B–O–B–O					Ref.
	$\nu_1(\Sigma_g)$	$\nu_2(\Sigma_u)$	$\nu_3(\Sigma_g)$	$\nu_4(\Pi_g)$	$\nu_5(\Pi_u)$	$\nu_1(\Sigma)$	$\nu_2(\Sigma)$	$\nu_3(\Sigma)$	$\nu_4(\Pi)$	$\nu_5(\Pi)$	
SCF/4-31GF	2253	2031	639	547	236	2206	1458	843	553	176	36
MP3/6-31GF*	2222	2052	628	432	216						36
SCF/6-31GF*	2314	2131	631	538	235						4
SCF(0.9)	2083	1918	568	484	212						4
MP2/6-31GF*	2073	1898 {40}	625	501	215 {41}	2123 {597}	1488 {516}	828	478 {53}	50	4
Experiment	2060[a]	1898	585[a]	410[a]	213						35
		1899				2048	1408				16,37

[a] Estimated from the force field.

Table 9. Equilibrium geometric parameters of the lower isomers of Al_2O_2

Molecule	Method of calculation	Parameter			Ref.
		R_{Al-O}/Å	Φ(Al−O−Al)/°	Φ(O−Al−O)/°	
 singlet	SCF	1.764	90.6	89.4	43
	SCF/6-31GF*	1.741	87.9	92.1	3,44
	MP2/6-31GF*	1.780	86.3	93.7	3,44
triplet	SCF2/6-31GF*	1.737	88.3	91.7	3
D_{2h}	MP2/6-31GF*	1.776	86.3	93.7	3
$Al_t-O_c-Al_c-O_t$	SCF	1.743 (Al_t-O_c); 1.670 (O_c-Al_c); 1.591 (Al_c-O_t)	–	–	43
$C_{\infty v}$	SCF/6-31GF*	1.718 (Al_t-O_c); 1.658 (O_c-Al_c); 1.574 (Al_c-O_t)	–	–	3,44
	MP2/6-31GF*	1.735 (Al_t-O_c); 1.692 (O_c-Al_c); 1.628 (Al_c-O_t)	–	–	3,44

and the geometries in the MP2 approximation, the values obtained for the two lower isomers agreed completely with published data.[44] The characteristics of the vibrations calculated in the MP2/6-31GF* approximation, however, make necessary a radical re-examination of the previous interpretation.

The geometric parameters of the Al_2O_2 isomers of lowest energy are given in Table 9. Table 9 does not give results for the second rhomb-shaped configuration, although it is of considerable interest from the viewpoint of structural theory, or results for the other linear isomers obtained, O−Al−Al−O, Al−O−O−Al, and Al−Al−O−O,[3] since the energies of all these configurations are too high compared with the energy of the ground-state isomer (more than 70 kcal mol^{-1}) for them to be observed experimentally.

For the cyclic (almost square) isomer, noteworthy features are, firstly, the small deviations of the valence angles from 90° at the aluminium and oxygen atoms, and, secondly, the similarity in the equilibrium configurations of the molecule in the singlet and triplet states. Comparison of the internuclear distances for the linear isomer $Al_t-O_c-Al_c-O_t$ with the distances in the linear molecule $O_t-Al_c-O_c-Al_c-O_t$ (see Table 4) shows (like the comparison of the data for O−B−B−O and B_2O_3) that the Al_c-O_t distances coincide to within 0.01 Å (1.63 Å, MP2/6-31GF*); the Al_c-O_c distances also coincide (1.69 Å). The Al_t-O_c distance in $Al_t-O_c-Al_c-O_t$ (1.74 Å) is greater than the distance within the fragment O−Al−O. The Al−O bond length in the ring is even longer (1.78 Å).

The relative energies of the lower isomers of Al_2O_2 calculated[3] by the SCF and MP2 methods with the 6-31GF* basis set are shown in Fig. 2. These results show the importance of allowing for the effects of electron correlation in the Al_2O_2 system; on going beyond the one-electron model, the qualitative conclusions about the structure of the molecule change. It is known that the MP2 approximation does not always give energy differences sufficiently accurately, and calculations at a higher level (for example by the MP4 method or the method of bound clusters) may in principle change the relative energies of the linear and cyclic structures. The results obtained, however, provide sufficient grounds for assigning the experimental data to both structures.

Table 10 gives the experimental vibrational wavenumbers for the cyclic Al_2O_2 molecule; the calculated wavenumbers, infrared intensities, and isotope ratios for the singlet and triplet states of the almost square isomer are indicated. As in other examples, the wavenumbers calculated in the SCF/6-31GF* approximation are systematically greater than the corresponding values calculated in the MP2/6-31GF* approximation with a factor close to 0.9. For the ν_3 vibration of the singlet isomer, however, an extremely unusual situation is observed; there is a dramatic change in both the wavenumber (476 →690 cm^{-1}) and intensity of the vibration when corrections for correlation effects are introduced. It is for this reason that earlier attempts to correlate the theoretical wavenumbers calculated in the SCF approximation[43,44] with the experimental data led to an erroneous assignment of the observed band at 496 cm^{-1} to the Al_2O_2 molecule. We shall return to the discussion of the role of correlation effects in the cyclic Al_2O_2 molecule. Meanwhile, we are justified in assigning to the almost square molecule the intense band in the infrared spectrum at 691 cm^{-1}, as previously proposed.[28] The situation is more complex for the other suggestions made in the work cited.[28] The most active vibration in the Raman spectrum is the ν_5 vibration with a wavenumber of about 516 cm^{-1} and an isotope ratio R(16/18) = 1.020. The possibility of assigning the experimental band at 563 cm^{-1} to this vibration[28] cannot be excluded. For the other bands in the infrared and Raman spectra,[28] appropriate assignments were not made.

Table 11 gives the vibrations of the linear Al−O−Al−O molecule. Comparison with experimental data[30] shows that there is practically no doubt about the assignment of the bands at 1176.3 cm^{-1} and 945.5 cm^{-1} (or the bands close to them for

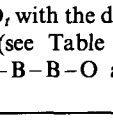
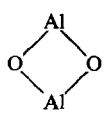
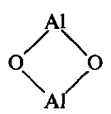
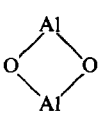
Molecule	Energy/cal mol^{-1}	Molecule	Energy/cal mol^{-1}
O—Al—Al—O	104		72
		O—Al—Al—O	70
 singlet	37.7		
Al—O—Al—O	21.4	Al—O—Al—O	10.4
 triplet	0.0	 triplet singlet	8.2 0.0

Figure 2. Relative energies of the lower isomers of Al_2O_2, calculated in the SCF/6-31GF* (on the left) and MP2/6-31GF* (on the right) approximations.

Table 10. Wavenumbers (cm^{-1}) and infrared intensities (in curly brackets, km mol^{-1}) of the cyclic isomer of Al_2O_2 [the isotope ratios $R(16/18)$ for complete replacement $^{16}O \rightarrow {}^{18}O$ are given in round brackets].

Vibration	Al_2O_2 (singlet)			Al_2O_2 (triplet)	
	SCF/6-31GF* [3,44]	MP2/6-31GF* [3]	experiment[28]	SCF/6-31GF* [3]	MP2/6-31GF* [3]
$\nu_1(A_g)$	861	782 (1.041)		868	784
$\nu_2(B_{2u})$	819 {198}	772 {110} (1.036)		827	759 {104}
$\nu_3(B_{1u})$	476 {828}	690 {193} (1.036)	691 (1.028)	811	738 {349}
$\nu_4(B_{3g})$	664	622 (1.035)		680	624
$\nu_5(A_g)$	553	516 (1.020)		565	524
$\nu_6(B_{3u})$	327 {45}	308 {51} (1.037)		322	276

(MP2/6-31GF*) frequencies differ by not more than 3%, although the difference between the intensities is much greater.

In contrast to the X_2O_3 systems, the structures of the B_2O_2 and Al_2O_2 molecules differ considerably. The two lowest isomers of B_2O_2 are the Lewis structures of the linear configuration:[4]

$$:O{\equiv}B-B{\equiv}O: \quad \text{and} \quad :B-\ddot{O}-B{\equiv}O: .$$

The contributions of ionic interactions are not so large, as follows, for example, from the effective natural charges of the ground-state isomer

$$O^{-0.824}-B^{+0.824}-B^{+0.824}-O^{-0.824} .$$

For Al_2O_2 the situation is more interesting. The Lewis structures of the linear isomer Al–O–Al–O obtained with Hartree–Fock and correlation (MP2) electron densities can be represented as follows:

$$:Al:\ddot{O}-Al{\equiv}O: \text{ (SCF)} \qquad :Al{\equiv}O-Al{\equiv}O: \text{ (MP2)},$$

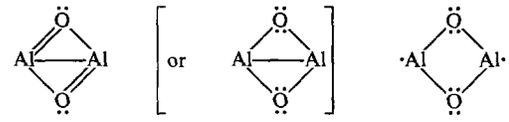
reflecting the general trend in the change in the electronic structure of aluminium oxides—correlation effects lead to an increase in the covalent character of the bond.[3]

Naturally, because of the appreciably higher effective natural charges

$$Al^{+0.867}-O^{-1.595}-Al^{+2.007}-O^{-1.278},$$

the structures with X–X contacts are less favourable for aluminium than for boron (the ground-state linear isomer is O–B–B–O for B_2O_2, and Al–O–Al–O for Al_2O_2). Allowance for correlation effects leads to a lowering of the energy of O–X–X–O relative to X–O–X–O (Table 7 and Fig. 2), but in the case of Al_2O_2 this lowering is insufficient for the O–Al–Al–O isomer to be regarded as sufficiently low-lying. In the limit of a completely ionic description, the linear molecule Al–O–Al–O can be represented as $Al^+[O-Al-O]^-$. The fragment $[O-Al-O]^-$ is identified in the Al_2O_2 and Al_2O_3 molecules both from the geometric parameters and from the vibrational frequencies.

The Lewis structures for the cyclic isomer of Al_2O_2 in the singlet and triplet states can be represented as follows:[3]



singlet triplet

In this picture, the highest occupied and lowest unoccupied MO for the singlet state are the orbitals $\sigma(Al-Al)$ and $\sigma^*(Al-Al)$ with an extremely small energy gap between them (0.1 a.u.). This leads to the marked changes in the energies and in the vibrational wavenumbers of the molecule observed on going beyond the SCF approximation.[3,32] The triplet state corresponds to a biradical structure with unpaired electrons on Al. The rigid framework of Al–O σ-bonds is responsible for the similarity in the geometries and vibrational frequencies of the cyclic Al_2O_2 molecule in the two spin states.

3. X_2O molecules

Of all the polyatomic oxides X_mO_n, the compounds with the composition X_2O are apparently the least puzzling. There is almost no doubt that the ground-state isomers correspond to the linear symmetrical configurations X–O–X. For quantum-chemical calculations, these triatomic systems are not very complex, and sufficiently reliable theoretical results can be expected. From the experimental viewpoint also, there is no doubt about the correctness of the understanding of the structure of the B_2O and Al_2O molecules.

There is only one published experimental study in which, in an investigation of the reaction of atomic boron with water, the bands in the infrared spectrum were assigned to the matrix-isolated B_2O molecule.[37] From the behaviour of the band at about 1420.5 cm^{-1} on isotope replacement it was concluded that the molecule in the matrix has a linear or almost linear symmetrical configuration.

Table 11. Wavenumbers (cm^{-1}) and infrared intensities (in curly brackets, km mol^{-1}) for the linear isomer of Al_2O_2 [the isotope ratios $R(16/18)$ for the replacement $^{16}O \rightarrow {}^{18}O$ are given in round brackets].

Vibration	SCF/6-31GF* [3,44]	MP2/6-31GF* [3]	Experiment [30,26]
$\nu_1(\Sigma)$	1301	1183 {276} (1.014; 1.015; 1.030)	1176.3 (1.013; 1.030)
$\nu_2(\Sigma)$	1020	946 {233} (1.018; 1.034; 1.051)	945.5; 943 (1.019; 1.034; 1.051)
$\nu_3(\Sigma)$	497	468	
$\nu_4(\Pi)$	281	225 {56}	
$\nu_5(\Pi)$	72	49	

Table 12. Vibrational wavenumbers (cm^{-1}) of the B–O–B molecule and the isotope ratios for the replacements $^{10}B \rightarrow {}^{11}B$ [$R(10/11)$] and $^{16}O \rightarrow {}^{18}O$ [$R(16/18)$] for the strong ν_1 band.

Method	Wavenumber/cm^{-1}			$R(10/11)$	$R(16/18)$	Ref.
	$\nu_1(\Sigma_u)$	$\nu_2(\Sigma_g)$	$\nu_3(\Pi_u)$			
SCF/6-31GF*	1585	1126	120			4
SCF(0.9)	1426.5	1013	108			4
MP2/6-31GF*	1496	1052	111	1.021	1.034	4
MP2/6-311GF**	1456	1043	24			4
Experiment	1420	–	–	1.020	1.033	37

In a study of the gas-phase oxidation of atomic boron by NO_2 and N_2O molecules, the authors[46] tried to assign the chemiluminescence spectrum to the B_2O molecule, supposedly in the form of the unsymmetrical isomer B–B–O (if the vibration with wavenumber 582 cm^{-1} can be associated with this molecule), although the assignment of the experimental spectrum to B_2O_2 is not excluded.

Quantum-mechanical calculations by the SCF method[39,47] predict a linear symmetrical equilibrium configuration, while the energy of the other linear isomer B–B–O should be appreciably higher. According to recent calculations for B_2O, carried out by SCF and MP2 methods,[4] the equilibrium internuclear distance in the linear symmetrical molecule B–O–B is 1.313 (SCF/6-31GF*), 1.333 (MP2/6-31GF*), or 1.329 Å (MP2/6-311GF**), demonstrating again that for these compounds the MP2/6-31GF* method predicts the bond lengths with an uncertainty of not more than 0.01 Å.

The vibrational wavenumbers of the B_2O molecule are compared in Table 12. The experimentally determined wavenumber of the ν_1 vibration is close to that calculated by the MP2/6-31GF* method (error ~5%). Comparison of the wavenumbers calculated by the MP2/6-31GF* and MP2/6-311GF** methods shows that they are fairly sensitive to the basis set, particularly for the ν_3 deformation. The low wavenumber of the deformation indicates a very flat section for the PES along this coordinate, confirming the arguments[37] about the possible quasi-linearity of B–O–B in the matrix. However, the proposed[37] assignment of the emission spectrum[46] to B–O–B is of course excluded. There is more justification for assigning the observed chemiluminescence[46] to the O–B–B–O molecule.

The strong band of the matrix-isolated Al_2O molecule at 992 cm^{-1} (992.8 cm^{-1} according to recent measurements[30] in an argon matrix) with an isotope ratio $R(16/18) = 1.045$, assigned to the antisymmetric stretch, is well known and reliably established.[25,29,30] The electronic spectrum of the gas phase has also been used to estimate the wavenumber of the symmetric stretch (471 cm^{-1}).[48] The bands at 472 cm^{-1} and 475 cm^{-1} in the Raman spectra of the argon and nitrogen matrices were assigned to this vibration.[27,49] In the earliest studies[49] it was pointed out that the wavenumber of the Al–O–Al deformation should be low (below 190 cm^{-1}).

Many non-empirical calculations have been carried out for the Al_2O molecule.[3,5,43,44,50–52] All the data agree in predicting a linear symmetrical equilibrium configuration Al–O–Al. Some of the calculation results are given in Table 13. The positions of the strong ν_1 band in the infrared spectrum and the corresponding isotope ratios $R(16/18)$ obtained by calculation (MP2/6-31GF* or the scaled SCF/6-31GF* wavenumber) and by experiment show very good agreement. The agreement between the calculated ν_2 frequency and that estimated from the electronic spectra is also satisfactory.

Electron diffraction studies of the Al_2O molecule in the gas-phase electron diffraction laboratory of the Chemistry Department of Moscow State University led to the conclusion that the molecule has an angular configuration with an Al–O–Al angle of about 140°. This conclusion is evidently a consequence of the extremely low deformation frequency of the molecule.

Table 13. Equilibrium distance R_{Al-O} (in Å) and vibrational wavenumbers of the Al–O–Al molecule.

Method	R_{A-O}	Wavenumber/cm^{-1}			$R(16/18)$	Ref.
		$\nu_1(\Sigma_u)$	$\nu_2(\Sigma_g)$	$\nu_3(\Pi_u)$		
SCF	1.691	1076	553	126	–	51
SCF	1.723	1012	531	129	–	43
SCF/6-31GF*	1.703	1043	549	112	–	3, 5, 44
GF2/6-31GF*	1.733	988	513	90	1.045	3, 5
Experiment	–	992.8	471; 472; 475	–	1.045	30, 47, 27, 69

The other possible isomer of the molecule, namely Al–Al–O, has a fairly high energy (more than 80 kcal mol^{-1}) relative to Al–O–Al.[3,5]

Comparison of the details of the electronic structures of the B–O–B and Al–O–Al molecules does not lead to any unexpected features.

The more ionic character of the bonding for Al, which can be seen by comparing the natural charges on the atoms,[3,4]

$$B^{+0.645}-O^{-1.290}-B^{+0.645} \qquad Al^{+0.830}-O^{-1.660}-Al^{+0.830},$$

is responsible for certain differences in the descriptions of the systems. The Lewis structures of aluminium oxide, obtained with the Hartree–Fock (SCF) and correlation (MP2) densities,[3] indicate an increase in the covalent contributions when allowance is made for electron correlation

$$:Al:\ddot{O}:\ Al: \text{ (SCF)} \qquad :Al-\ddot{O}-Al: \text{ (MP2)}.$$

For the boron oxide, the description at the level of the Lewis structures is fairly obvious:

$$B\equiv O-B: \quad \leftrightarrow \quad :B-O\equiv B: .$$

In both molecules, correlation effects are responsible for an increase in the equilibrium internuclear distance X–O (0.02 Å for X = B, 0.03 Å for X = Al), which is slightly smaller than for the other oxides.

4. XO_2 molecules

Species with the composition XO_2 are formed and play an extremely important role in the oxidation of boron and aluminium. A fairly large amount of experimental information on XO_2 molecules has been obtained, including spectral data for the matrix-isolated molecules. From the theoretical viewpoint, the analysis of the XO_2 systems is much more complex than that for the molecules of the other oxides examined above. This is due chiefly to the fact that these molecules have open electron levels; moreover, methods of calculation based on the single-configuration representation of electronic wave-functions are generally speaking inadequate in the present application.

The results of experimental and theoretical studies indicate that the equilibrium configuration of the BO_2 molecule is the linear symmetrical configuration.

The vibrational wavenumbers of the BO_2 molecule, obtained by different methods, are given in Table 14. In this case it is possible to compare the experimental results for the gas phase[53–57] and the matrix-isolated molecules.[14,16,58] Most information has been obtained for the ν_1 antisymmetric stretch. The vibration frequencies of the molecule in the gas phase has been measured extremely accurately, and the shifts observed in matrix-isolation experiments are estimated relative to this quantity. According to the latest measurements,[16] the shifts differ considerably, depending on the material of the matrix and (presumably) on the type of capture position. The maximum deviation from the gas-phase value for ν_1 is ~20 cm^{-1} (not more than 2%).

Thus the characteristic uncertainties in the vibrational wavenumbers calculated by present-day methods of quantum chemistry (MP2/6-31GF*) (about 3%) are close to the relative shifts in the wavenumbers as a result of the matrix environment. For the ν_3 deformation, the matrix shifts have even higher values. Since modelling the matrix shifts is extremely difficult,[60,61] the agreement between the experimental molecular spectra, obtained for these compounds primarily under matrix-isolation conditions, and the theoretically calculated spectra cannot have a higher accuracy than that already noted (3–5%).

There have been few non-empirical calculations of the properties of the BO_2 molecule. For the ground electronic state $X^2\pi_g$, Lomp and coworkers[59] calculated the equilibrium internuclear distance B–O in the linear molecule—1.34 Å (SCF/OST-3GF) and 1.26 Å {SCF/[9*s*5*p*]/(4*s*2*p*)} (experimental value 1.265 Å [53])—and also the harmonic frequencies of the ν_2

Table 14. Vibrational wavenumbers (cm^{-1}) for the BO_2 molecule (the oblique lines separate wavenumbers associated with different positions of capture of the molecule by the matrix).

Method	Wavenumber/cm^{-1}			Ref.
	ν_1 (Σ_u)	ν_2 (Σ_g)	ν_3 (Π_u)	
Experiment (gas phase)	1278.3	1070	464	53–57
Experiment (matrix isolation)	1276	–	–	14
	1299.3/1282.8/1274.6 (Ar)	–	398.2/446.6 (Ar)	16
	1285.5/1300.7 (Kr)	–	394.6 (Kr)	16
	1292.2 (Xe)	–	–	16
Calculation SCF/OST-3GF	–	1079	464	59

and ν_3 vibrations (Table 14). In the calculations, considerable difficulty was encountered in obtaining symmetrically stable solutions of the electronic equation.

The AlO_2 molecule has been detected among the products of the reaction of aluminium with oxygen in an argon matrix. For this molecule, a cyclic structure with an O–Al–O angle of 30–50° was proposed, as for all the dioxides of the group III elements.[24] Evidence in support of this interpretation is provided by the presence in the infrared spectrum of a band at 1096 cm^{-1}, close to the wavenumber of the O_2^- vibrations (1089 cm^{-1}). It has been suggested[24] that the molecule has an ionic structure $Al^+O_2^-$. The band at 496 cm^{-1} was assigned to this structure. The remaining wavenumber was estimated at 550 cm^{-1}. Subsequent studies[25,26] showed that in the matrix reactions of aluminium with oxygen, another isomer of the molecule is formed, namely the linear O–Al–O. The wavenumber of the antisymmetric stretch in the infrared spectrum (918 cm^{-1}) was assigned to this isomer, and the laser fluorescence spectra gave the wavenumbers of the symmetric stretch (635 cm^{-1}) and the deformation (70 cm^{-1}).[70]

In other studies of the matrix reactions of aluminium with oxygen,[29] the formation of an unsymmetrical isomer of AlO_2 with a C_s structure was assumed; later,[30] the wavenumber 496.3 cm^{-1} in the infrared spectrum was assigned to a cyclic configuration, and the wavenumber 1129.5 cm^{-1} to the linear O–Al–O isomer.

Nonempirical quantum-mechanical calculations for the AlO_2 molecule are difficult, due to the symmetry instability of the Hartree–Fock equations.[10,62,63] To construct the potential surfaces of this system it is necessary to use many-configuration approximations, and in the last case also considerable difficulties are encountered, particularly in the estimation of the vibrational frequencies. The many-configuration SCF method (MC SCF) combined with the pseudo-potential approximation has been used[62] to model the field of the core electrons. It was established that of the two molecular configurations examined—the cyclic configuration and the linear unsymmetrical Al–O–O—the cyclic form corresponds to the energy minimum. Its equilibrium geometric parameters and the wavenumbers of the harmonic vibrations were estimated (Tables 15 and 16). The methods of configuration interaction (CI) and many-particle perturbation theory (PT) with basis sets of restricted dimensions have been used[63] to examine both the cyclic and the linear symmetric isomers of the AlO_2 molecule. These calculations indicate only that these isomers have similar energies.

Table 15. Geometric parameters of the AlO_2 molecule (distances in Å, angles in °) and difference between the energies (kcal mol^{-1}) of the linear and cyclic isomers.

Method of calculation	Linear isomer R_{Al-O}	Cyclic isomer R_{Al-O}	Cyclic isomer Φ(O–Al–O)	Energy difference	Ref.
MC SCF	–	1.97	38	–	62
CI, PT	1.72	1.88	41	1.2	63
MC SCF	1.67	1.93	42	6.0	10

Table 16. Experimental and calculated vibrational wavenumbers of the AlO_2 molecule (cm^{-1}).

Molecule		Wavenumber/cm^{-1}			Ref.
		ν_1	ν_2	ν_3	
	calculation	1081	591	277	10
		1394	528	242	62
	experiment	1096	496	–	24
		–	496.2	–	30
O–Al–O	calculation	932	582	75	10
		978	659	92	63
	experiment	918	635	70	24

The MC SCF method (the version of the complete configurational space of the active orbitals) was also used by Nemukhin and Almlof,[10] but with allowance for all the electrons, in contrast to the work of Rubio and coworkers.[62] The orbitals were represented using basis sets specially designed for calculations with allowance for correlation effects, the so-called atomic natural orbitals of the type (20*s*13*p*5*d*)/[6*s*5*p*2*d*] for Al and (13*s*8*p*5*d*)/[5*s*4*p*1*d*] for O. It was concluded that on the potential surface of the ground state of the molecule ($^2A_2$) there are two minimum points separated by a high barrier (~60 kcal mol^{-1}), and that the energy of the linear symmetrical form is 6 kcal mol^{-1} lower than that of the cyclic configuration. More accurate estimates of the ratio of the energies of the linear and cyclic forms apparently require additional calculations with a more detailed allowance for correlation effects, but it can be taken as established that both isomers may be formed in matrix reactions of aluminium with oxygen. The linear and cyclic isomers of AlO_2 are described by appreciably different electron configurations, and are characterised by different distributions of the effective charges.[10]

The experimental and theoretical vibrational wavenumbers for the two isomers are compared in Table 16. Unfortunately, the non-empirical calculations for this system were carried out using a scheme different from that used for the other oxides examined (here, generally speaking, the single-configuration SCF and MP2 approximations are inapplicable), so that we cannot use the regularities noted above. Overall, the theoretical and experimental wavenumbers show agreement but the agreement is not yet quantitative.

In the comparison of the properties of BO_2 and AlO_2 in the linear configurations, the significant difference in the wavenumbers of the deformation is noteworthy: 464 cm^{-1} for O–B–O and 70 cm^{-1} for O–Al–O.

5. XO molecules

Information on the diatomic oxides BO and AlO at the level mainly developed in the present review (geometry, vibrational wavenumbers) is already given in reference works,[64] and therefore is not discussed here. In connection with the questions dealt with above, we would merely refer to new spectral studies of matrix-isolated BO and AlO molecules.[16,30,65] From these data it follows

that the experimental matrix shifts for BO and AlO have different signs. For example, in argon matrices the shift of the principal vibrational wavenumber of BO is -7 cm^{-1} (1854.7 cm^{-1} relative to the gas-phase value of 1862.1 cm^{-1}),[16] while that for AlO is 10 cm^{-1} (975 cm^{-1} compared with 965 cm^{-1} for the gas phase).[30,65]

One may also mention fairly detailed studies of the potential energy curves of diatomic oxides by non-empirical methods of quantum chemistry,[66–68] which show significant changes in the electronic structure with change in the internuclear distance.

V. Summary

One of the principal conclusions from the comparison of the results of studies of the oxides X_mO_n (X = B, Al) is that these compounds show a great variety of compositions and molecular geometries. For practically all the systems X_2O_3, X_2O_2, X_2O, and XO_2 we can now formulate definite conclusions about the structure, based on the experimental spectra of the molecules and the results of quantum-chemical calculations. For these compounds it may be concluded that the accuracies of the determination of the equilibrium geometric parameters and the vibrational frequencies from experiment and from calculation are comparable.

Most of the differences in the structures of the oxides of boron and aluminium can be attributed to the more ionic character of the Al–O bond in the compounds Al_mO_n; the balance of the ionic and covalent contributions depends considerably on allowance for correlation effects, which increase the covalent components. Aluminium oxides, to a greater extent than boron oxides, are characterised by the existence of low-lying isomers with the same stoichiometry.

Most of the unresolved theoretical questions remaining relate to the BO_2 and AlO_2 molecules. From the experimental viewpoint, the situation for the Al_2O_3 and Al_2O_2 molecules is least satisfactory.

For a more complete understanding of the processes accompanying the reactions of atoms and clusters of boron and aluminium with oxygen or other oxidants in the gas phase and under matrix-isolation conditions it is extremely important to study systems of the type $(XO)_n$ and $(XO_2)_n$ with $n > 2$.

References

1. P G Nelson *J. Chem. Educ.* **68** 732 (1991)
2. R D Srivastava, M Farber *Chem. Rev.* **78** 627 (1978)
3. A V Nemukhin, F Weinhold *J. Chem. Phys.* **97** 3420 (1992)
4. A V Nemukhin, F Weinhold *J. Chem. Phys.* **98** 1329 (1993)
5. A I Boldyrev, P v R Schleyer *J. Am. Chem. Soc.* **113**, 9045 (1991)
6. N G Rambidi, N F Stepanov, Yu G Abashkin, A I Berezin, A I Dement'ev, B I Zhilinskii, V K Mikhalko, V I Pupyshev, V Ya Simkin, I A Topol' *Zh. Strukt. Khim.* **22**, 29 (1981)
7. H Sellers, J Boggs, A V Nemukhin, J Almlof *J. Mol. Struct. (THEOCHEM)* **85** 195 (1981)
8. L V Serebrennikov, Yu N Sekachev, A A Maltsev *High Temp. Sci.* **16** 23 (1983)
9. V P Spiridonov, A G Gershikov, E Z Zasorin, A A Ivanov *High Temp. Sci.* **16** 325 (1983)
10. A V Nemukhin, J Almlof *J. Mol. Struct. (THEOCHEM)* **253** 101 (1992)
11. G V Chertikhin, I L Rozhanskii, L V Serebrennikov *Vestn. Mosk. Univ., Ser. 2: Khim.* **29**, 27 (1988)
12. A E Reed, R B Weinstock, F Weinhold *J. Chem. Phys.* **83** 735 (1985)
13. W Weltner, J R W Warn. *J. Chem. Phys.* **37** 292 (1962)
14. A Sommer, D White, M J Linevsky, D E Mann. *J. Chem. Phys.* **38** 87 (1963)
15. P A Akishin, V P Spiridonov *Dokl. Akad. Nauk SSSR* **131**, 557 (1960)
16. T R Burkholder, L Andrews *J. Chem. Phys.* **95** 8697 (1991)
17. J F Chiang, D R Witman *Theor. Chim. Acta* **17**, 155 (1970)
18. M A Ali, A J Shaikh *J. Mol. Struct.* **13** 179 (1972)
19. A I Dementjev, N G Rambidi, V Ya Simkin, I.A.Topol *J. Mol. Struct.* **68** 199 (1980)
20. Yu S Ezhov, S M Tolmachev, V P Spiridonov, N G Rambidi *Teplofiz. Vys. Temp.* **6** 68 (1968)
21. Yu S Ezhov, S M Tolmachev, V P Spiridonov, N G Rambidi *Zh. Strukt. Khim.* **11** 527 (1970)
22. G Fogarasi, P Pulay *Ann. Rev. Phys. Chem.* **35** 191 (1984)
23. B A Hess, L J Schaad, P Carsky, R Zahradnik *Chem. Rev.* **86** 709 (1986)
24. L V Serebrennikov, S B Osin, A A Maltsev *J. Mol. Struct.* **81** 25 (1982)
25. L V Serebrennikov, A A Mal'tsev *Vestn. Mosk. Univ., Ser. 2: Khim.* **26** 137 (1985)
26. I L Rozhanskii, G V Chertikhin, L V Serebrennikov, V F Shevel'kov *Zh. Fiz. Khim.* **62**, 2351 (1988)
27. I L Rozhanskii, L V Serebrennikov, V F Shevel'kov *Zh. Fiz. Khim.* **64** 521 (1990)
28. G V Chertikhin, L V Serebrennikov, V F Shevel'kov *Zh. Fiz. Khim.* **65** 1078 (1991)
29. S M Sonchik, L Andrews, K D Carlson *J. Phys. Chem.* **89** 2009 (1983)
30. L Andrews *J. Phys. Chem.* **96** 10182 (1992)
31. V G Solomonik, V V Sliznev *Zh. Neorg. Khim.* **32** 1301 (1987)
32. A V Nemukhin, F Weinhold *J. Chem. Phys.* **97** 1095 (1992)
33. M G Inghram, R F Porter, W A Chupka *J. Chem. Phys.* **25** 498 (1956)
34. Yu N Sekachev, L V Serebrennikov, V S Nikitin, A A Mal'tsev *Vestn. Mosk. Univ., Ser. 2: Khim.* **20** 589 (1979)
35. L V Serebrennikov *Vestn. Mosk. Univ., Ser.2: Khim.* **22** 606 (1981)
36. B M Ruscic, L A Curtiss, J Berkovitz *J. Chem. Phys.* **80** 3962 (1984)
37. L Andrews, T R Burkholder *J. Phys. Chem.* **95** 8554 (1991)
38. R J Doyle *J. Am. Chem. Soc.* **110** 4120 (1988)
39. R L DeKock, M R Barbachyn *Inorg. Nucl. Chem.* **43**, 2645 (1981)
40. A I Dement'ev, S S Kramarenko, N F Stepanov *Zh. Strukt. Khim.* **24** 99 (1983)
41. P A Finn, D M Gruen, D L Page *Adv. Chem. Ser.* **158** 30 (1976)
42. M A Douglas, R H Hauge, J L Margrave *High Temp. Sci.* **16** 35 (1983)
43. J Masip, A Clotet, J M Ricart, F Illas, J Rubio *Chem. Phys. Lett.* **144** 373 (1988)
44. L Bencivenni, M Pelino, M Ramondo *J. Mol. Struct. (THEOCHEM)* **253** 109 (1992)
45. A V Zaitsevskii, G V Chertikhin, L V Serebrennikov, N F Stepanov *J. Mol. Struct. (THEOCHEM)* in press
46. T C Devore, J R Woodward, J L Gole *J. Phys. Chem.* **92** 6919 (1998)
47. T S Zyubina, O P Charkin, A S Zyubin, V G Zakchevskii *Zh. Neorg. Khim.* **27** 558 (1982)
48. M A Douglas, R H Hauge, J L Margrave *High Temp. Sci.* **16** 35 (1983)
49. A Snelson *J. Chem. Phys.* **74** 2574 (1970)
50. E L Wagner *Theor. Chim. Acta*, **32** 295 (1974)
51. V G Solomonik, I G Sazonova *Zh. Neorg. Khim.* **30** 1939 (1985)
52. A M Mebel', T S Zyubina *Zh. Neorg. Khim.* **32** 1285 (1987)
53. J W C Johns *Can. J. Phys.* **39** 1738 (1961)
54. D K Russell, M Kroll, D A Dows, R A Beaudet *Chem. Phys. Lett.* **20** 153 (1973)
55. D K Russell, M Kroll, R A Beaudet *J. Chem. Phys.* **66** 1999 (1977)
56. K Kawaguchi, E Hirota, C Yamada *Mol. Phys.* **44** 509 (1981)
57. A Maki, J B Burkholder, A Sirha, C J Howard *J. Mol. Struct.* **130** 238 (1988)
58. L V Serebrennikov *Vestn. Mosk. Univ., Ser. 2: Khim.* **16** 363 (1975)
59. P E Lomp, V Ya Simkin, N F Stepanov *Izv. Akad. Nauk Est. SSR* **32** 286 (1983)
60. A I Krylova, A V Nemukhin, N F Stepanov *J. Mol. Struct. (THEOCHEM)* **262** 55 (1992)
61. L V Serebrennikov *Vestn. Mosk. Univ., Ser. 2: Khim.* (in the press)
62. J Rubio, J M Ricart, F Illas *J. Comput. Chem.* **9** 836 (1988)
63. A V Zaitsevskii, S A Bogdanova, A I Dement'ev, V Ya Simkin *Vestn. Mosk. Univ., Ser. 2: Khim.* **31** 604 (1990)
64. K P Huber, G Herzberg *Molecular Spectra and Molecular Structure* Vol. 4 *Constants of Diatomic Molecules* (Translated into Russian) (Moscow: Mir, 1984)
65. S J Bares, M Haak, J W Nibler *J. Chem. Phys.* **82** 670 (1985)
66. A V Nemukhin, J Almlof, A Heiberg *Chem. Phys.* **57** 197 (1981)
67. J Almlof, A V Nemukhin, A Heiberg *Int. J. Quantum Chem.* **20** 655 (1981)
68. B H Lengsfield, B Liu *J. Chem. Phys.* **77** 6083 (1982)
69. I V Ovchinnikov, L V Serebrennikov, A A Mal'tsev *Zh. Fiz. Khim.* **59** 1558 (1985)
70. I L Rozhanskii, L V Serebrennikov, V F Shevel'kov *Vestn. Mosk. Univ., Ser. 2: Khim.* **29** 560 (1988)

Russian Chemical Reviews **62** (6) 539 – 552 (1993)
© 1993 Russian Academy of Sciences and Turpion Ltd

UDC 543.42

Excimers of organic molecules

N N Barashkov, T V Sakhno, R N Nurmukhametov, O A Khakhel'

Contents

I.	Introduction	539
II.	Excimers in liquid solutions of monochromophoric molecules	540
III.	Excimer fluorescence of crystals	540
IV.	Excimers in polymers	542
V.	Excimer-forming molecular dimers	544
VI.	Excimer phosphorescence and slow excimer fluorescence	547
VII.	The structure of excimeric complexes	548
VIII.	Conclusion	550

Abstract. Studies devoted to excimers in organic systems are surveyed. Processes leading to the excitation of the excimer luminescence are examined. Examples of the excimer-like glow of dimers are described. The relation between the structure of the complexes and their fluorescence properties is demonstrated. The bibliography includes 218 references.

I. Introduction

Excimers are dimers a distinctive feature of which is instability in the ground state. Their formation is observed only on photoexcitation of the system. (Here and henceforth physical dimers are considered.) After deactivation of the dimers, the latter dissociate into individual molecules. The term 'excimer' was adopted on the suggestion of Stevens and Hutton[1] and was recommended by the International Symposium on Molecular Luminescence[2] instead of the term 'excited dimer' employed previously. Dimers comprising two different chemical compounds (in particular organic molecules and inorganic species[3,4]) have been called 'exciplexes'.[2] The state of the research into these species has been described in detail in a monograph.[3]

In inorganic systems, excimers were known long before their detection in organic molecules. The atoms of certain metals and noble gases are capable of forming excimers. The optical transitions in their excimers are used for the generation of laser radiation.[5] The excimers of organic compounds were first identified in 1954.[6,7] The class of excimer-forming molecules has not been clearly outlined but it embraces almost all aromatic hydrocarbons with a planar structure and certain compounds with heteroatoms. Certain coordination compounds with organic ligands can be included among them.[8,9]

A characteristic spectroscopic feature of excimers is a luminescence band with an anomalously large Stokes shift (5000 – 12000 cm^{-1}). Its identification is based primarily on the following features. Its intensity relative to that of the monomer (molecular) glow in solutions increases with increase in the concentration of the chromophore. In certain media, such variation may not be observed but a common feature is the absence of visible qualitative changes in the absorption spectra of the test systems, i.e. the absence of aggregation in the ground state. Since the radiative transitions in the excimer lead to an unstable state, the excimer component is represented by a broad structureless spectral band. The overlap of the monomer and excimer components of the luminescence is as a rule appreciable. For example, for pyrene — a typical excimer-forming compound — the short-wavelength emission edge in the spectra of excimers occurs at 375 nm, while the 0 – 0 transition of molecular pyrene occurs at 372 nm, i.e. the excimer component almost fully overlaps the region corresponding to the luminescence of the molecular form.[10]

One of the principal characteristics of excimer-forming systems is the ratio of the excimer luminescence intensity to the intensity of the molecular fluorescence band (I_d/I_m).

The formation of excimers is observed in liquid solutions of monochromophoric molecules, in condensed and gas phases, in polymer matrices, and other media over a wide range of physicochemical conditions. The increased interest in excimer systems is due to their use for the solution of applied problems. In particular, the methods for the structural studies on polymers[11–15] and the determination of the properties of biological systems[16,17] are based on the analysis of excimer fluorescence. The spectroscopic parameters of excimers have attracted the attention of investigators also in connection with the attempts to create effective devices for the concentration of radiation.[18]

There exist also dimers which are stable in the ground state, but exhibit the spectroscopic properties of excimers. Such formations have been designated in various studies as sandwich dimers[19–21] and associated dimers.[22–26] Strictly speaking, their luminescence cannot be identified as excimer luminescence in conformity with the definition adopted[2] and they constitute an example of other forms of aggregation of excimer-forming molecules. The formation of dimers is observed in various media but the number of communications on this topic is small.

N N Barashkov¶, R N Nurmukhametov. O A Khakhel' L Ya Karpov Physicochemical Institute (¶ also Chemical Scientific-Technological Association 'Chemprogress'), ul. Obukha 10, 103064 Moscow. Fax (7-095) 975 24 50
T V Sakhno Poltava Cooperative Institute, ul. Kovala 3, 314601 Poltava, Ukraine. Fax (7-05322) 79 160

Received 10 January 1993
Uspekhi Khimii **62** (6) 579 – 593 (1993); translated by A K Grzybowski

A specific analysis of the recorded excimer-like luminescence was not carried out in all investigations, which suggests that such objects are more common (for example, in the case of many polymers).

II. Excimers in liquid solutions of monochromophoric molecules

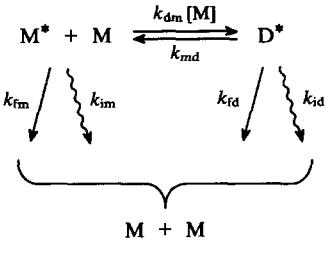
The study of processes involving the formation of the excimers of monochromophoric molecules in liquid solutions was carried out particularly vigorously in the 1960s.[27-30]

Eximer formation is determined by the mutual diffusion of molecules. The quenching of the luminescence of the monomer component obeys the Stern–Volmer relation, i.e. the ratio I_d/I_m increases linearly with increase in the dye concentration:

$$\frac{I_d}{I_m} = K[M],$$

where K is the constant of the equilibrium between the monomer and excimer centres and [M] the phosphor concentration. The equilibrium constant K is expressed in terms of the constants of the reactions presented in Scheme 1. This scheme was put forward by Forster[6,7] and was subsequently developed by Birks.[28]

Scheme 1



The constants k_{dm} and k_{md} in this scheme correspond to the rates of formation and decomposition of the excimers, k_{fm} and k_{fd} are the constants for the radiative deactivation of the monomers and excimers, and k_{im} and k_{id} are the internal conversion constants for both luminescence centres.

Analysis of the kinetics of the formation of excimers in accordance with Scheme 1 leads to the following definition of the quenching function for the luminescence of the monomer and excimer components after the exciting pulse:[28]

$$I_m(t) = A_1 \exp(-\lambda_1 t) + A_2 \exp(-\lambda_2 t),$$

$$I_d(t) = A_3[\exp(-\lambda_2 t) - \exp(-\lambda_1 t)].$$

The constants for the process taken into account in Scheme 1 are expressed in terms of the parameters A_1, A_2, A_3, λ_1, and λ_2 and can be determined by various procedures.[31]

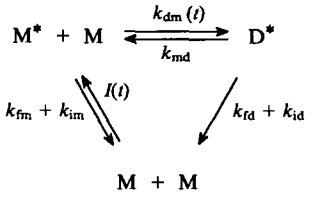
Scheme 1 has been hitherto resorted to for the interpretation of the results of experiments,[32-35] but it describes only approximately the excimer formation processes in liquid solutions. The fact that the rate of formation of excimers is assumed to be independent of time in Scheme 1 is most striking. This approximation is justified only for systems after a considerable time has elapsed since the excitation step. Since the rate of formation of excimers is controlled by the diffusion of chromophores, it follows that, in conformity with the theory of diffusion-controlled reactions,[36] it should be expressed in the form

$$k(t) = a(1 + bt^{-1/2}),$$

where $a = 4\pi D N_A R/1000$, $b = R/(\pi D)^{1/2}$, t is the time, N_A the Avogadro number, D the mutual diffusion coefficient of the chromophores, and R the effective reaction radius. The excimer kinetics in various systems have been analysed after adopting this approximation.[37-39] The time variation of the rate of formation of excimers has been called the 'transient effect'.

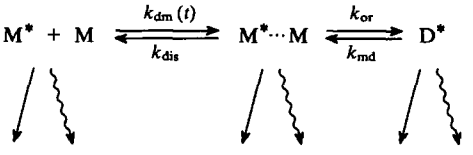
The development of experimental techniques has made it possible in recent years to obtain data for the construction of better models. In particular, a model has been proposed[40,41] (Scheme 2) in which account is taken of the possibility of the formation of excimers as a result of the reassociation of molecules [the parameter $I(t)$]. The results of calculations taking into account this parameter agree much better with experimental data than those of calculations in accordance with Scheme 1.

Scheme 2



Further improvement of Birks's scheme involved taking into account the orientation processes in the intermediate molecular complexes. Vogelsang and Hauser[42] investigated the kinetics of the quenching of the excimer and monomer luminescence using two approaches: with and without allowance for the time variation of the rate of formation of excimers. The agreement between the calculated and experimental data was better in the first case, but for the initial period both methods yielded results which differed appreciably from the experimental data. The discrepancies were explained by putting forward the following scheme (Scheme 3):[42,43] the excited and unexcited molecules approach one another, after which either excimers are formed as a consequence of the relaxation orientation (constant k_{or}) or the pre-excimer complexes dissociate (constant k_{dis}).

Scheme 3



As already mentioned, excimer formation processes lead to the appearance of physical dimers in which the electronic excitation is delocalised over both molecules.[30] However, a different approach has been developed.[44,45] According to the hypothesis put forward by the author, the appearance of the structureless emission band of the excimers (exciplexes) can be accounted for within the framework of the idea of a fractional energy transfer: as the two molecules approach one another, part of the electronic excitation energy of the first is transformed into the vibrational and rotational excitation of the second, which functions as a quenching agent. The remaining energy is emitted. In this process, the main role is attributed to the interaction of the vibrational states. It has been suggested that this theory possesses quantitative predictive power in relation to the Stokes shift of the excimer luminescence and provides criteria for the assessment of the ability of chromophores to form excimers.

III. Excimer fluorescence of crystals

Excimers are formed not only in liquid solutions but also in media with a greatly restricted mobility of the molecules. In such cases, one is dealing with the so-called excimer-forming centres and the migration of excitation energy towards them. In crystals of organic compounds, the appearance of such centres (predimer sites) is attributed to the presence of structural defects in the bulk phase,[46] the concentration of which can be raised by applying pressure (as a consequence of the sliding of dislocations, neighbouring molecules undergo a reorientation to a productive

geometry similar to the excimer geometry). The activation of these centres is usually explained by the localisation of singlet excitons on them.

The excimer fluorescence of crystals is determined by the temperature. At room temperature, the excimer state in anthracene has a higher energy than the free exciton state and at high temperatures (>400 K) the lattice stabilisation energy is reduced[47] and thermal equilibrium is established between the excimer and free exciton states with appearance of excimer fluorescence.

Typical crystals giving rise to excimer fluorescence under normal conditions are those of pyrene and the α-modification of perylene. In contrast to other polyacenes, the predimer sites in these compounds are not structural defects but regular elements of the crystal lattice—dimers arranged in parallel.[48] The excimer states in such crystals may be populated both by direct excitation and as a consequence of energy migration. The time of the transfer of excitation in pyrene is 5×10^{-5} s and the process activation energy is $\sim8.8\times10^{-21}$ J.[46] Three possible mechanisms of the migration of the excimer state have been proposed:[49] (1) dissociation of excimers into two monomers (in the ground and excited states) with subsequent energy transfer to a neighbouring pair; (2) nondissociative thermal activation of the excimers to a level having the same energy as the S_1 level of the monomer with subsequent energy transfer to a neighbouring pair; (3) the assumption of the pre-excimer geometry by the nonexcited dimeric pair as a result of thermal excitation with subsequent energy transfer from another excited pair.

In the crystals of pyrene and the α-modification of perylene, other excimer states also arise, such as the *B*-state[50] or the *V*-state[51] for pyrene and the *Y*-state[52] for perylene. Fluorescence in the frequency range between the free exciton and normal excimer bands is characteristic of these compounds. In the crystals of the α-form of perylene, normal emission is appreciably quenched below 70 K with the appearance of a new emission band of the excimer type. In the crystals of pyrene at ~120 K, there is a structural transition[48] and normal fluorescence is not quenched as the temperature is reduced. Until recently, the *V*-band was observed only in the time-resolved spectra.[50,53] Mizuno and Matsui[51] were able to obtain a metastable pyrene crystal with the structure of the high-temperature phase at temperatures below the critical temperature. The emission spectra of this and similar specimens are presented in Fig. 1. The *V*-fluorescence of the metastable crystal is recorded by the usual spectroscopic methods.

The dynamics of the excitation of the excimer luminescence in crystals with two excimer states has been investigated.[51,53] Fig. 2 presents the time-resolved spectra of a pyrene crystal in the picosecond range. The *V*-fluorescence is observed most distinctly in the early stage of the development of luminescence, which may indicate the initial relaxation of the excited dimeric pairs to the *V*-state with subsequent transition to the normal excimer state. All the transitions are activated. At high (room) temperatures, the *V*-state gives rise to a relatively indistinct potential minimum in the spectrum, so that the excited state in pyrene under the usual conditions is represented mainly by the free-exciton state and by traps of the normal type.

The situation in the crystals of α-perylene differs only by the rate of the relaxation processes. The relaxation of excitons from the free-exciton state takes place faster than in pyrene, possibly via a tunnel mechanism.[51,53] In the temperature range 4–160 K, the *Y*-state is metastable and lies above the normal excimer state.[54]

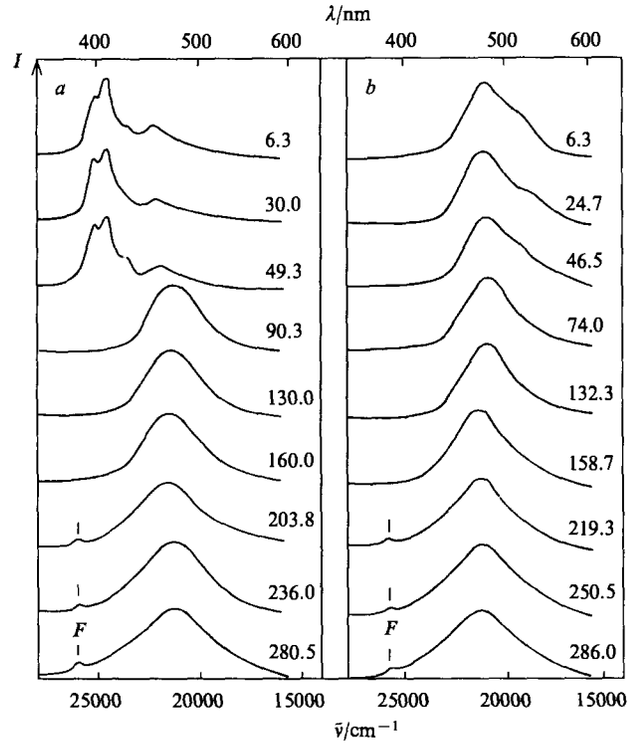


Figure 1. Temperature variation of the fluorescence spectra of crystalline pyrene:[51] (*a*) spectra of the metastable high-temperature phase; (*b*) spectra of the usual crystal; the numerals opposite the curves denote the temperature (K) at which the corresponding spectrum was obtained; *F* denotes the free exciton band.

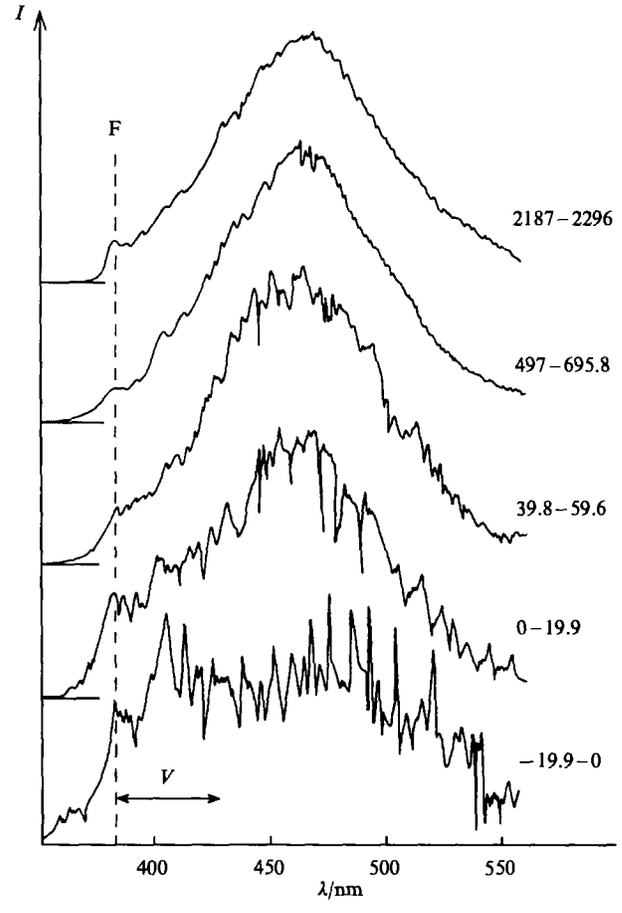


Figure 2. Time-resolved spectra of the pyrene crystal obtained at 293 K. The numbers to the right—time intervals (ps) over which the corresponding curves were integrated; the instant when the exciting laser pulse (λ = 316 nm) reaches maximum intensity is assumed to be the zero time; *F* denotes the free exciton band; *V* denotes the region corresponding to the luminescence of the *V*-centres.[51]

The energy barrier between them is[54] ~ 310 cm^{-1}. It increases following the application of pressure, so that *Y*-fluorescence can be observed also at room temperature.[55]

In melts of organic substances, the specific features of the corresponding crystalline structures are apparently retained. Thus the excimer emission band in the spectra of anthracene melts[47] in the range 460–470 nm is observed only ~ 100 ps after the exciting pulse, which is evidently associated with the necessity for orientation processes on formation of excimers. On the other hand, in the pyrene melt the molecules are evidently in a predimeric state, as in the crystal, because the excimer band is recorded directly after the excitation step.[47] Admittedly, in the temperature range 450–600 K the appearance of a new emission band (390–420 nm) is observed for pyrene. It is either due to the monomolecular form (on the assumption of the thermal dissociation of dimers) or is caused by the formation of yet another kind of excimer complexes.

IV. Excimers in polymers

Almost all the aromatic vinyl polymers, certain heterocyclic polymers, and their various copolymers belong to the excimer-forming class of polymers. Luminescence from both solid specimens and liquid solutions is observed. Similar properties are shown also by solid solutions of excimer-forming molecules in polymer matrices. The excimer luminescence of polymers is due to the presence in their bulk phase of two types of excimer-forming centres.

The excimer-forming centres in polymeric media can be represented both as conformations of sections of polymer chains favourable for the formation of excimers and as sections for which the energy barrier to the assumption of the excimer configuration is very small and which are capable of reorientation during the lifetime of the excited state.[11] The centres of the first type play a major role in solid polymers but they may be formed also in solutions. Neglecting the energy migration processes, the fraction of these centres can be expressed in terms of spectroscopic parameters:[31]

$$f_d = \varphi_{fd}\varphi_{fm} \Big/ \left(\frac{\varphi_{fd}}{\varphi_{fm}} + \frac{q_{fd}}{q_{fm}}\right),$$

where φ_{im} and φ_{id} are the quantum yields of the luminescence of the monomeric† and excimeric centres and $q_{fd}/q_{fm} = Q$ is the ratio of the number of quanta absorbed by the monomeric and excimeric centres. It is assumed here that $\varepsilon_d = 2\varepsilon_m$, ε_m and ε_d being the extinction coefficients of the monomeric and dimeric centres. In this case

$$\frac{I_d}{I_m} = \frac{1}{2}Q\left[(1 + 8[M]_0K)^{1/2} - 1\right],$$

where $[M]_0$ is the overall concentration of the chromophoric fragments and K is the constant of the equilibrium between the dimeric and monomeric forms.

The fraction of conformations favourable for excimer formation is defined by the expression[11]

$$f_d = \frac{W_d \exp(-\Delta E/kT)}{W_m + W_d \exp(-\Delta E/kT)},$$

where W_m and W_d are the multiplicities of the degeneracies of the monomeric and excimeric states and ΔE is the difference between their energies.

† In this section, the monomeric and dimeric centres are understood as isolated chromophores and excimer-forming pairs of chromophores respectively.

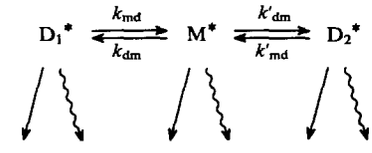
Calculations of the structures of poly-2-vinylnaphthalene, polyvinylcarbazole and polystyrene have shown that the fractions of the excimer-forming centres are of the order of 10^{-2}, 10^{-3} and 10^{-3} respectively.[11,56] In the solid polymers, the populations of the excimeric states are determined by the irradiation temperatures of the specimens.

The insignificant concentration of the excimer-forming centres in the polymers together with the observed intensity of the excimer fluorescence lead to the conclusion that the excitation energy is transferred to centres with the monomeric form of the phosphor.[11] The nonradiative migration of energy in solutions may lead to an even greater effect owing to the possibility of the rotational motions of the centres during the lifetime of the excited state of the monomer. Thus the formation of excimers in polymeric systems is a complex process involving the migration of energy and segmental rotation. Furthermore, in solutions there is also a possibility of the macroscopic diffusion of the chromophores, leading to an excimeric configuration, but in polymers these processes are less significant than in solutions of monochromic molecules. For aromatic polymers, the fluorescence of the monomers and excimers is described satisfactorily taking into account the energy migration along the chain[57–62] and in the bulk phase.[63–66] The overall schematic representation of the processes in the polymers taking into account the energy migration and the rotation of the chromophoric fragments has been examined.[59] However, the role of energy migration in polymers still has not been ultimately elucidated. There are experimental facts which cast doubt on its effectiveness. For example, polarisation measurements of the fluorescence of polystyrene films have shown[67,68] that the luminescence retains a high degree of polarisation. This agrees poorly with the hypothesis that energy transfer processes make a significant contribution.

The probability of the formation of excimers in polymeric systems is determined by the structure of the chain and its composition. Attempts have therefore been made in numerous investigations to establish the steric structure of the polymers.[69–82] The formalism of the dynamics of the rotational transitions has been developed[83] for copolymers of the type $A-B_n-A$, where A is the chromophore and B_n are neutral units. In order to establish the possible number of units in contact, computer modelling has been employed.[31,84–86] Studies have also been carried out for low-molecular-mass and bichromophoric analogues of polymers.[87–93]

Among the bichromophoric molecules, one may distinguish two types of compounds—compounds with a flexible linkage between the two chromophores and cyclophane compounds. For the former, the intramolecular excimer formation is preferred to the greatest extent if the chain between the chromophores consists of three carbon atoms.[94] However, this process takes place, albeit with a lower effectiveness, also without the maintenance of this stringent requirement.[95] The formation of intramolecular excimers in bichromophoric molecules is described by two kinetic schemes. In the first case, in the absence of the necessary degree of freedom the excimers are formed only in one steric configuration (see Scheme 1), while in the second (Scheme 4) there is a possibility of two types of complexes.[90] A similar situation is observed also for paracyclophanes,[11] anthracenophanes,[96] pyrenophanes,[97,98] etc.

Scheme 4



The effectiveness of the formation of the excimers of bichromophores in solutions is determined by the kinetics of the conformational changes in the chains linking the chromophores.[11] Depending on the method of formation of the crystals and also on the size and structure of the saturated chains, some of the cyclophanes can give rise to excimer fluorescence also in the solid state.[96]

In individual instances, excimer formation may be an intermediate stage in photochemical reactions. This applies particularly to systems incorporating anthracene chromophores.[31,99-104]

The influence of the composition of the polymer chain on the formation of excimers has been examined for vinylaryl polymers. Fig. 3 presents the dependence of I_d/I_m on the fraction of adjacent chromophores in the chain for solutions of copolymers of the two most typical representatives of this class. The nonzero value of I_d/I_m in the absence of diads in the copolymer chain indicates a finite probability of the formation of excimers between chromophores remote from one another along the chain or between chromophores of different chains. There are also polymers (for example polyacenaphthalene) in which excimers are formed between remote chromophores with a high probability.[31,74,106]

Yet another factor influencing the yield of the excimer luminescence is the molecular mass of the polymers. Typical dependences of I_d/I_m on the chain length for a solution of a copolymer with isolated chromophores and for a solution of a chromopolymer are presented in Fig. 4. Both curves tend to reach a plateau for high molecular masses. However, sometimes, as the length of the polymer chain increases, a decrease in the relative yield of the excimer luminescence is observed. Thus I_d/I_m for dilute solutions of polyindole decreased[86] with increase in chain length and tended to zero already for $N \approx 500$. This result agrees with the results of the calculation of the number of units in contact within the polymer.

Considerable interest in the kinetics of the formation of excimers and polymers has been shown in a large number of studies. The quenching of the luminescence of the monomeric and excimeric components in these media is frequently described by the sum of not two but three or more exponential functions. This shows that the processes in the system cannot be explained within the framework of Scheme 1. One (or several) of the following factors have apparently not been taken into account:[31] the different energy migration distances, the formation of excimeric states as a result of the rotation of segments, and the multiplicity

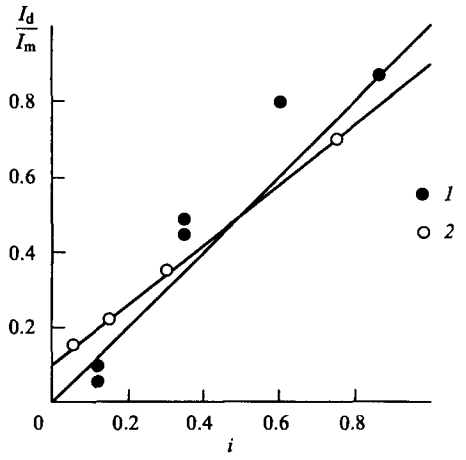


Figure 3. Dependence of I_d/I_m on the fraction of neighbouring chromophores in the chain (i): (*1*) solution of styrene-acrylonitrile in ethanol;[105] (*2*) 2-vinylnaphthalene-dimethyl-maleate in a 3:2 (by volume) tetrahydrofuran–diethyl ether mixture.[71]

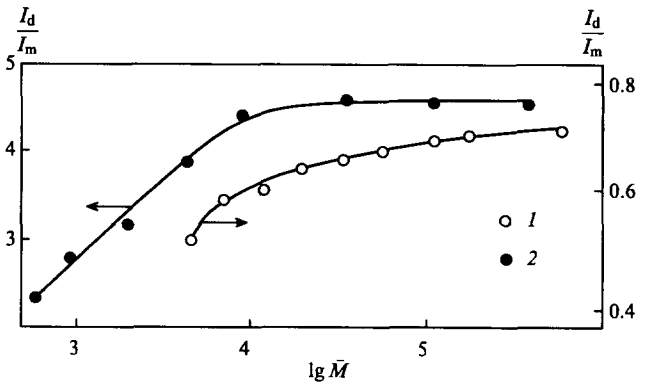
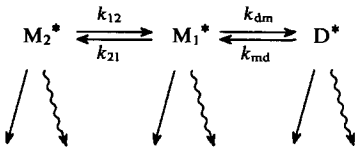


Figure 4. Dependence of I_d/I_m in solution on the molecular mass: (*1*) copolymer of the type $(A-B_n)_N$ (where A = chromophore, B_n = neutral unit, and n = 100) in tetrahydrofuran;[107] (*2*) styrene homopolymer in 1,2-dichloroethane.[11]

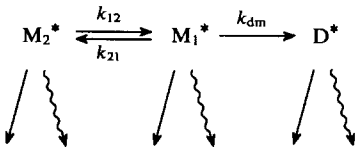
of types of excimeric and monomeric states. Thus models postulating the existence of two different monomeric states have been put forward (Schemes 5–8; M_1 and M_2 designate different conformers).[106,108,109]

In Schemes 5–7, excimers may be formed only from the conformers M_1 as a result of the mutual rotation of the segments. Scheme 8 presupposes their formation also from the conformers M_2 as a result of macroscopic chain motions.

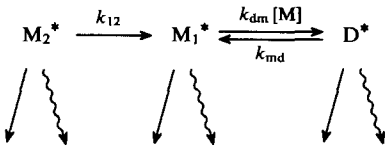
Scheme 5



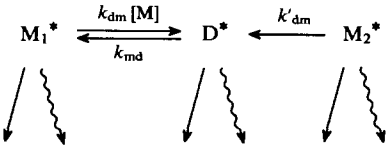
Scheme 6



Scheme 7

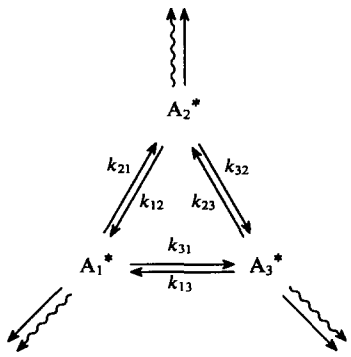


Scheme 8



The formation of several types of excimeric states has been postulated.[110,111] In order to account for the kinetics of the quenching of the luminescence in styrene copolymers, a model with three different monomeric and two excimeric centres, not taking into account the energy migration, was put forward.[112] The general Scheme 9, including three equivalent interconvertible spectral centres A_n, has been analysed.[108]

Scheme 9



However, the models presented in Schemes 5–9 are applicable only to the interpretation of experiments in which the quenching of the luminescence is described by a triexponential function.

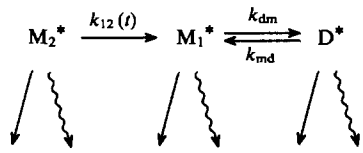
Systems in which the quenching of the fluorescence is described more aptly by a tetraexponential relation have been investigated.[111,113,114] The appearance of the fourth component in the expression for $I(t)$ can be attributed to the formation of the fourth luminescence centre, designated as a relaxing monomer or the third excimer. However, the approaches involving allowance for a larger number of luminescence centres for the description of multiexponentially decaying systems have not come to be used widely. Another approach is probably more productive. Thus it has been suggested[59] that the multiexponential decay of fluorescence be regarded as the sum of several dominant energy migration pathways, each of which is represented by the combination of all the possible versions of this process. In this case, the characteristic times of the dominant processes are not related directly to the times of specific physical transformations. Because of this, it has been stated that the excimer kinetics in aromatic polymers must not be described by any kind of phenomenological model on the basis of the number of allowed exponential functions. This approach agrees with the results of studies on the diffusion of energy in nonordered donor–acceptor systems, which indicate the nonexponential nature of the decay of their fluorescence.

A kinetic model based on the initial postulate that chromophores are not constant-energy centres as a consequence of the high dispersion of their relative positions has been developed[65,66] for polyvinylcarbazole films. The excitation energy of the high-energy chromophores migrates to low-lying states with the transfer frequency

$$v(T,t) = v_0 \exp\left[-\left(\frac{T_0}{T}\right)^2\right] + v_1^{\alpha} t^{\alpha-1},$$

where v_0 is the frequency of the transfer of excitation in a hypothetical regular constant-energy polymer, v_1 the discrete step in the variation of the excitation transfer frequency, α a dimensionless parameter assuming values from 0 to 1, T_0 the experimental temperature, and t the time. The dependence of I_d/I_m for the model on λ_{exc}, observed in the region of the long-wavelength edge of the absorption band of polyvinylcarbazole, constitutes experimental confirmation of the proposed model.[65] Scheme 10, which explains the tetraexponential decay of the excimer fluorescence in liquid solutions of polyvinylcarbazole, has also been examined in accordance with this model.[115] If $\alpha = 1/2$, the expression for the transfer frequency formally agrees with the expression for the excimer formation constant, which occurs in the kinetic equations for solutions of monochromic molecules. This approach has been extended to polymer systems.[59,116–120]

Scheme 10



The excimer kinetics have been studied in detail in polyvinylcarbazoles.[121] Studies on polymers of different tacticity by time-resolved spectroscopic methods have in the main confirmed the postulates put forward by Fredriekson and Frank.[59] The existence of two excimeric states has been demonstrated (the formation, together with the usual excimers, of excimeric complexes of yet another kind is observed fairly frequently).[73,76,116,122] The transformations of the high-energy excimeric complexes into normal complexes as a result of the excitation of fluorescence is of interest in this instance.

V. Excimer-forming molecular dimers

So far as we are aware, special studies on dimers of excimer-forming molecules which are stable already in the ground state have not been carried out with the exception of a series of early investigations.[19–21] The spectroscopic manifestations in absorption and emission attributed to such dimers are not subject to clear-cut rules as in the case of excimers. Furthermore, the same compounds have dissimilar optical characteristics under different conditions which can be explained by the nonuniformity of the aggregates formed.

The fact that excimer-forming molecules can be associated in the ground state is not unexpected because attraction forces between the molecules always exist.[123] For example, the interaction energy is $\sim 3.1 \times 10^4$ J mol^{-1} in naphthalene dimers[124] and $\sim 5.9 \times 10^4$ J mol^{-1} in pyrene dimers.[125] Calculations carried out also in other investigations[126] yielded a positive heat of formation of the unexcited excimer-forming dimers. However, quantum-chemical calculations for excited and unexcited dimers have yielded data for the interaction energies of only isolated pairs—a state which is remote from the real conditions. In organic solvents, the potential barrier stabilising the dimeric state vanishes owing to the interaction of the molecules with the solvent,[127] so that the interpretation of the ground and excited states of the pair of chromophores in the form presented in Fig. 5 is in general correct in a qualitative description of the potential energy levels of the excimer-forming system. Dimers stable in the ground state were not detected in special studies of solutions of pyrene in isooctane (10^{-3} M).[10] Presumably the dynamics of the processes in other organic solvents at moderate concentrations of the chromophore is also described satisfactorily by Schemes 1–3. However, even in good solvents one cannot neglect the interaction of the dissolved molecules. As an example, one may quote the result of a study[128] where an anomalously high yield of the excimer fluorescence of dilute solutions of pyrene (10^{-6} M) in ethylene liquefied under pressure and in other solvents was observed. This indicates the existence of a certain degree of long-range order between the chromophores in solution, although naturally one is not dealing in this instance with dimers.

Another picture has been observed in solvents such as water. In aqueous solutions of pyrene, the aggregation of the latter is attributed to its hydrophobic nature. In this case, the maximum of the structureless excimer fluorescence band undergoes a hypsochromic shift by 10–20 nm.[129] The luminescence excitation spectra of the dimeric and monomeric components differ considerably under these conditions. The hydrophobic nature of the chromophores leads to their aggregation in aqueous solutions also in the case of several water-soluble polymers, which is manifested in the absorption spectra.[130–134] The constant of the equilibrium between the monomeric and dimeric centres depends

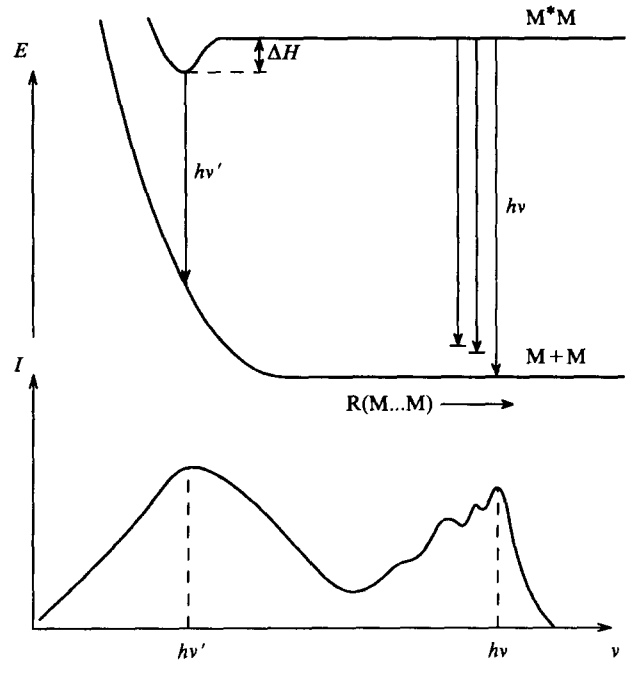


Figure 5. Potential energy (E) diagram for the monomer–excimer system: R(M ... M) = intermolecular distance; ν and ν' = frequencies of radiative transitions in the monomer and excimer respectively; ΔH = heat of formation of the excimers; the upper curve corresponds to the interaction of the molecules in the excimer and the lower to the interaction of the unexcited molecules; the Franck–Condon transitions in the excimer lead to a dissociative ground state which is responsible for the appreciable Stokes shift and the lack of structure in the luminescence.[1]

on temperature. The emission from the phenanthrene dimers has been recorded[135] in the slow fluorescence spectra of solutions in perfluorohexane only at 200 K. On raising the temperature to room temperature, the unexcited dimers dissociated.

There are data indicating the establishment of thermal equilibrium between the excimeric and dimeric centres. Perylene, added to films of the Langmuir–Blodgett type, has been investigated.[136] At room temperature, only the monomeric and dimeric components were recorded in the fluorescence spectra. As the temperature was reduced to 110 K, a new structureless fluorescence band appeared in the long-wavelength region of the spectrum and was attributed to the appearance of excimeric centres.

A pyrene crystal consists of pairs of molecules interacting in the ground state even at room temperature. With decrease in temperature to helium temperature, interaction in the dimers intensifies. Because of this, a new component appears in the absorption spectra of the pyrene crystal in the form of an inflection in the region of 395 nm, which has undergone a bathochromic shift of ~20 nm relative to the molecular absorption band.[49] The existence of pre-excimeric states of this type has been detected also in the absorption spectra of fused anthracene.[137]

Two types of dimers, formed as a result of different processes, have been identified on the basis of the absorption spectra of pyrene single crystals in Shpol'skii's matrices[138] at $T = 4.2-77$ K. The first process, with an activation energy of ~6 cm^{-1}, predominated in the temperature range 4.2–30 K. The formation of excited complexes from aggregates corresponding to the regular crystal structure was postulated in this instance. The second process, with an activation energy of ~70 cm^{-1} and manifested above 30 K, was explained by the presence of defects in the microcrystals, i.e. by the photoexcitation of the dimers, the structure of which differs from the regular crystal structure.

In the emission spectra, the luminescence of the dimers can sometimes be difficult to distinguish from the excimer fluorescence, so that studies on absorption spectra are more reliable for the identification of the dimers. The appearance of an absorption band in the long-wavelength section of the spectrum of the monomolecular form of the phosphor indicates the formation of dimers. As a rule, the new component is indistinct. Fig. 6 presents the absorption spectra of metastable dimers of anthracene and its derivatives obtained by the photochemical decomposition of the chemical dimers in a solid matrix at low temperatures. The luminescence of such species is fully excimer-like, while in the absorption spectrum only a slight bathochromic shift is recorded. Therefore, if both monomeric and dimeric centres absorb radiation in the system, then the fraction of dimers formed can be recorded from the intensity of the absorption band of the molecular S_1 transition.[24, 129, 134, 139] Fig. 7 shows how the optical density in the dimer–monomer system, induced by the displacement of the equilibrium, is redistributed as a function of the solvent composition.

The absorption spectra of the dimers (Fig. 6) demonstrate the general features characteristic of aggregates of this type:[19] the intensity maxima of all the bands due to the dimers have lower energies than the corresponding maxima in the spectra of the monomers (the intensity maximum is represented by the 0–1 transition in the spectra of the dimers and by the 0–0 transition in those of the monomers); an appreciable broadening of the bands in the spectra of the dimers relative to those of the molecules is observed; the total oscillator strength of the transition in the dimer is lower than twice the oscillator strength of the corresponding transition in the monomer.

The greatest number of communications refer to the formation of excimer-like molecular dimers in Langmuir–Blodgett films of different kinds[136, 140–144] or in films obtained by depositing the chromophore onto a solid base[139, 145, 146] and also in fluorescent polymers[130–134, 147, 148] and in solid solutions of the molecules in organic[149] and inorganic[150–152] glasses. Depending on the conditions in the formation of the specimens, the chromophores in such systems can apparently exist in the form of dimers, which may or may not be manifested spectroscopically. If they are not, the excitation of the excimer fluorescence is explained by the migration of energy to the excimer-forming centres.[153–159]

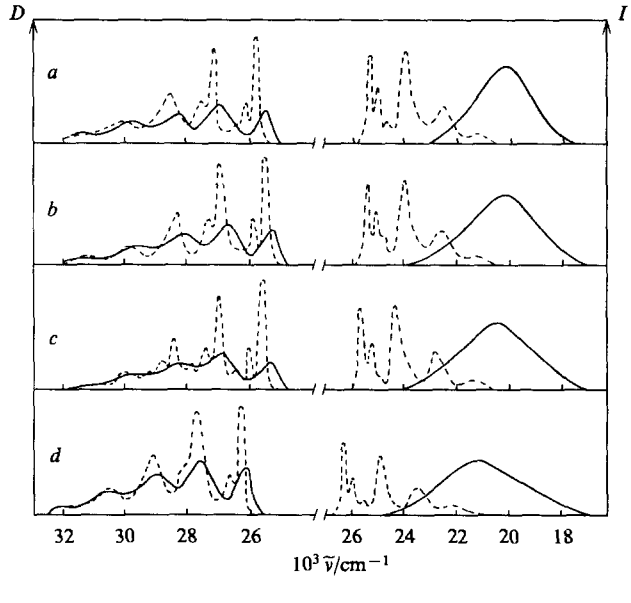


Figure 6. Absorption and emission spectra of the sandwich dimers in methylcyclohexane[19] at 77 K; the spectra of the monomer obtained after unfreezing and refreezing the specimens are indicated by dashed lines: (*a*) 9-methylanthracene; (*b*) 9-bromoanthracene; (*c*) 9-chloroanthracene; (*d*) anthracene.

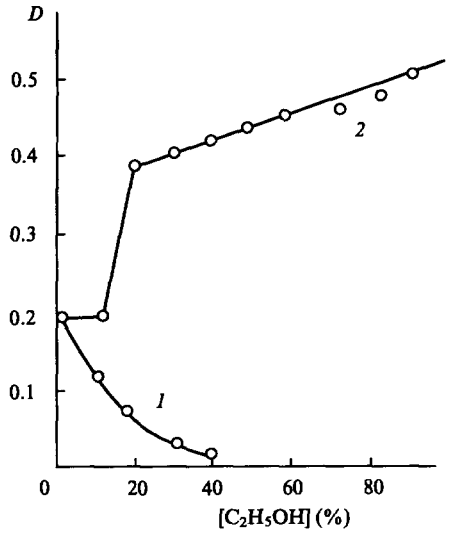
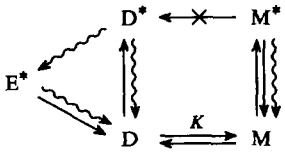


Figure 7. Optical densities of solutions of pyrene in a water–ethanol mixture[129] (phosphor concentration 14×10^{-6} M). Wavelength (nm): (*1*) 360 (S_1 transition in the monomer); (*2*) 319 (S_2 transition in the monomer).

The attempts at a systematic treatment of the observed wide variety of the fluorescence properties of the dimers have demonstrated the following features. Radiation is absorbed by dimers which differ in their interaction energies in the ground state in different systems. Energy transfer processes from isolated chromophores also play a definite role. The type of interaction between the molecules in the ground state of the dimer is close to the type in the excited state,[20] so that the transitions between the levels yield a spectrum which resembles that of molecular fluorescence. If during the excitation period the dimer can relax to the excimer geometry, its spectrum resembles that of the excimer. A structured spectrum of the luminescence due to the dimer has been published.[135] The case of strong interaction has been described for anthracene dimers,[96] the maximum of the excimer-like fluorescence showing a bathochromic shift by ~100 nm relative to the spectrum illustrated in Fig. 6.

Pyrene and naphthalene, adsorbed in the form of dimers (stable in the ground state) on the surface of silica gel, have been investigated.[139,145] Dimerisation was recorded on the basis of the luminescence excitation spectra. The proposed process dynamics is illustrated in Scheme 11.[139]

Scheme 11



It is suggested that the fluorescence arises in the excimeric state, although the dimeric centres absorb. The symbols M* and D* in the scheme denote the monomers and dimers excited respectively from the ground states M and D, E* is the excimer formed as a result of small steric relaxations of the excited dimer, and K is the constant of the equilibrium between the monomeric and dimeric centres in the ground state. It is suggested that, during the lifetime of the excited state of the monomer, there is no energy transfer to the dimeric form. In this case, the dependence of I_d/I_m on the concentration of the chromophores is expressed thus:

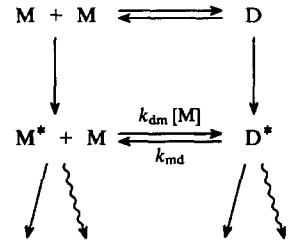
$$\frac{I_d}{I_m} = A\left[(1 + 8K[M_0])^{1/2} - 1\right],$$

where $A = \varepsilon_d \varphi_{ed} \varphi_e / 4K\varepsilon_m \varphi_m$ (φ_m and φ_e are the quantum yields of the fluorescence of the monomer and excimer respectively and φ_{ed} is the quantum efficiency of the formation of the excited dimers). The excited dimers relax to the excimeric state very rapidly[145] and the fluorescence arises after less than 1 ns.

These experiments may be compared with studies on the van der Waals fluorene dimers formed in molecular beams on expansion at an ultrasonic velocity.[160,161] The potential energy curves for such systems and the energy transitions are illustrated in Fig. 8. The radiative transitions lead to the dissociated state, although radiation is absorbed by the dimeric form. Similar data are available for benzene[162] and naphthalene derivatives.[163] Excimer-like fluorescence has been recorded under analogous conditions also on excitation of the trimers of 1-cyano-4-methylnaphthalene and its higher-order clusters. The excitation of the stable associated species of 1-cyanonaphthalene with triethylamine[164] and of fluorene with methyl-substituted dienes[165] also led to the appearance of an exciplex-like glow. Comparison of the spectroscopic parameter of the dimers and excimers has shown that the latter are characterised by a greater Stokes shift of the luminescence and a longer lifetime of the excited state (150 and 62 ns for the excimers and dimers of 1-cyano-4-methylnaphthalene respectively).[163]

The excimer-formation processes in liquid-crystal systems began to be studied comparatively recently.[166–168] The formation of excimers in such systems has been unambiguously confirmed by time-resolved spectroscopy.[167] At high chromophore concentrations, one cannot rule out the formation of excimers via the migration of energy to the excimer-forming centres.[168] Subsequent studies on these systems demonstrated the possibility of molecular association in the ground state. In order to explain the experimental results, Scheme 12, including the formation of dimers stable in the ground state, was put forward:[169]

Scheme 12



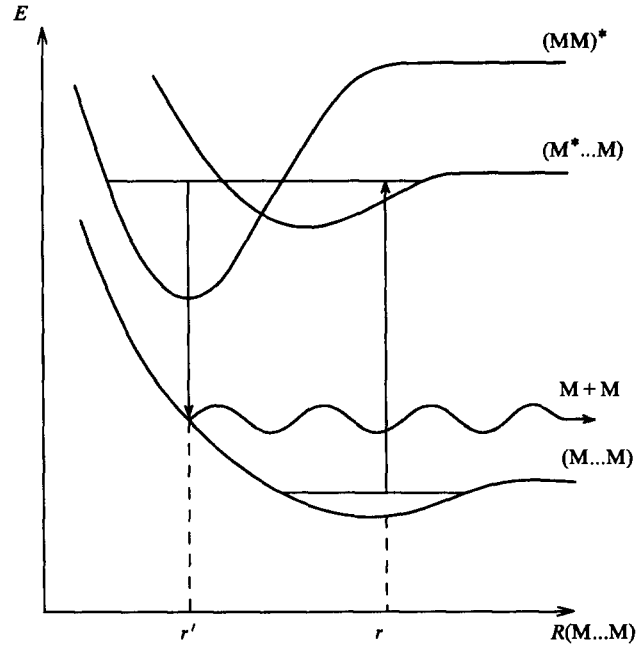


Figure 8. Potential energy curves for the interaction of fluorene molecules.[161]

According to this scheme, the decay of the fluorescence of the monomeric and dimeric components is described by a biexponential relation. In all probability, a more complex model of the excitation of the excimer-like luminescence is also possible in liquid-crystal mixtures. The fluorescence of the dimers stable in the ground state has been recorded[170] in time-resolved spectra. A triexponential function best described the decay of the luminescence of the excimer-like component.

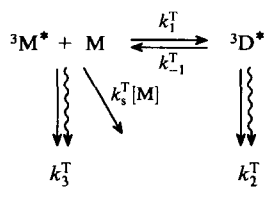
The fluorescence properties of the excimer-forming dimeric systems have been described most fully by Yamanaka et al.[152] Solid solutions of pyrene in an inorganic glass exhibit a structured band in the time-resolved spectra due to the fluorescence of the dimers (the *D* band in Fig. 9) with maxima at 381, 399, and 418 nm. At the same time the luminescence of the sandwich (E_2 band) and high-energy (E_1 band) excimers is observed in the spectrum. Isolated molecules emit the *M* band, which is manifested after the decay of the *D* fluorescence.

VI. Excimer phosphorescence and slow excimer fluorescence

The interaction of two excimer-forming molecules, one of which is in the excited triplet state, leads to the appearance of excited triplet dimers. Their phosphorescence was observed in almost all media where the singlet excimers were found to be formed: in liquid solutions, crystals, and polymers.

In liquid solutions, the existence of excimer phosphorescence was established on the basis of the following experimental facts:[171,172] the excitation spectrum of this type of phosphorescence is identical with the absorption spectrum of the corresponding monomer; the yield of the excimer phosphorescence increases with increasing solute concentrations; the excimer phosphorescence bands are observed only in liquid solutions and are absent from the spectra of frozen specimens; the phosphorescence of the excimers, like that of the monomers, is quenched by oxygen when the hermetic seal in the cell is broken. Analysis of the kinetics of the formation of the triplet complexes in conformity with Scheme 13 showed that the rate of the process is much lower than the rate of diffusion. It has been suggested that dimers are formed via a stage of intermediate complexes even before the acquisition of the excimer configuration.

Scheme 13



The constants k_1^T and k_{-1}^T in the scheme correspond to the rates of formation and dissociation of the complexes, the constants k_3^T and k_2^T correspond to the rates of the radiative and nonradiative deactivation of the monomers and dimers respectively, and k_s^T is the self-quenching rate constant.

The reliability of data concerning the existence of triplet excimers in liquid solutions has been questioned. Nickel and Prieto[124] reproduced the experiments from a large number of studies (see the list of references in their communication) where the breakdown of triplet phosphorescence had been reported. The reproduced experiments yielded a negative result and it was concluded that the observed luminescence is more likely to be the impurity glow of the solvents. The results lead to the conclusion that the triplet excimers of aromatic hydrocarbons are unstable, although the existence of weakly bound intramolecular triplet excimers in certain diarylalkanes has been admitted.

Such conclusions aroused the active opposition of a number of investigators, which has given rise to a controversy.[173] On the other hand, the presence of triplet excimers in crystals and

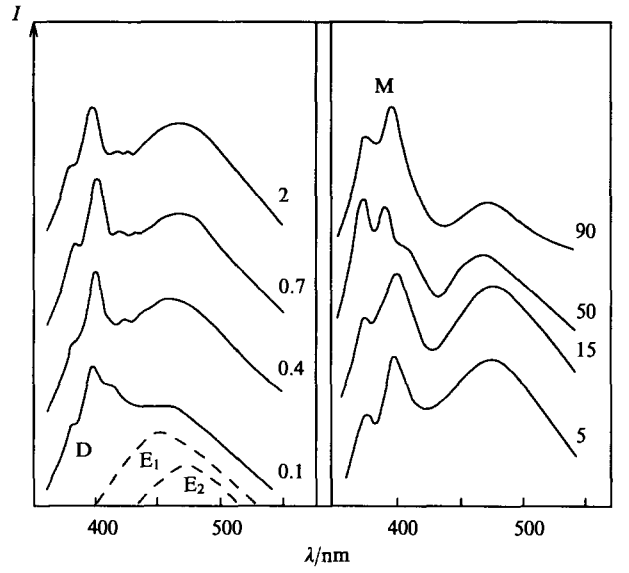
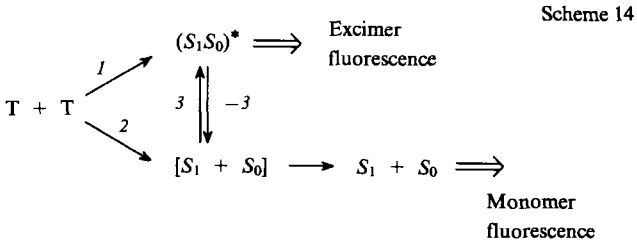


Figure 9. Time-resolved fluorescence spectra of solid solutions of pyrene in a silicate glass[152] (4×10^{-2} M); the numerals opposite the curves represent time (ns).

polymeric media is apparently not open to doubt. Two types of excimers have been detected in pyrene crystals[174-176] and excimer phosphorescence has been observed at low temperatures also in the crystals of halo-derivatives of benzene,[174,177,178] phenanthrene, and naphthalene.[179] Triplet excimers are formed in carbazole-containing[29,180-182] and naphthyl-containing[183-187] polymers.

Apart from the formation of triplet excimers, intersystem crossing processes initiate a slow excimer fluorescence. In the general case, its appearance is a consequence of processes leading to a slow *P* type fluorescence.[27] Different versions of the excimer formation processes on interaction of two triplet molecules in solutions are illustrated in Scheme 14.

Scheme 14



Three pathways leading to the excitation of excimer fluorescence of this type are possible: (1) simultaneous formation of singlet excimers and pairs of monomers (reactions *2* and *1*); (2) formation of singlet excimers with their subsequent dissociation to the monomeric form (reactions *1* and *3*); (3) exclusive formation of monomeric centres with subsequent formation of singlet excimers as a result of the reassociation of the molecules in the ground and excited singlet states (reactions *2* and *3*). Singlet excimers are formed after triplet–triplet annihilation via a stage involving intermediate complexes. The slow excimer fluorescence may be recorded if the rapid excimer fluorescence does not arise.[100,188,189]

The slow excimer fluorescence, induced by the migration of triplet excitons, is also observed both in liquid solutions of polymers and in solid polymer matrix at low temperatures. This confirms data indicating an increase in the intensity of the slow singlet fluorescence relative to phosphorescence with increase in the molecular mass of the homopolymer.[182,187]

VII. The structure of excimeric complexes

Excimers have a structure with a coplanar (sandwich) disposition of the molecular planes and an intermolecular distance of 3–3.5 Å. This conclusion was reached already at an early stage of the research into excimers, which agrees with data on the structures of crystals of the type of pyrene, α-perylene, 1,12-benzoperylene, etc.[19,48,96] The luminescence of such crystals is of the excimer type. This is also confirmed by the results of numerous experiments with flexible bichromophores in liquid solutions: the formation of intramolecular excimers is observed only when the molecule is capable of assuming the sandwich form. This type of structure has been confirmed also by the analyses of the polarised excimer fluorescence,[190] quantum-chemical calculations,[35,126,191–196] and the results of photochemical experiments.[3,11,19,20] However, the structure of the chromophores themselves or the influence of external factors frequently prevent the assumption of this geometry.

The introduction of bulky substituents, crystal structure defects, the morphological characteristics of chromophore-containing polymers, etc. frequently lead to the appearance of several types of excimeric configurations in real systems: in certain cases, it is possible to distinguish spectroscopically, together with excimers of the normal (sandwich) type, also one or several other types of excimers, which can be identified in terms of the polarisation characteristics of the glow, the position of the fluorescence band maximum, and the lifetime of the excited state of the complex. The wavelengths of the luminescence maxima of different types of excimers of certain compounds are listed in Table 1.

Excimers exhibiting luminescence in the region between the molecular band and the band due to normal excimers exist for virtually all classical excimer-forming chromophores (pyrene, naphthalene, anthracene, and carbazole). This type of luminescence is attributed to aggregates, which, in contrast to the normal ones, are characterised by an incomplete overlap of the orbitals of the aromatic nuclei. Such states are designated as high-energy states, second excimers, or dimer-like excimers. Nevertheless, their stabilisation requires a significant degree of overlap of the aromatic rings; for example, a degree of overlap of 25% is insufficient for naphthalene.[204] For more bulky chromophores, the degree of overlap of the electron shells may be smaller compared with compounds with a short conjugation chain.[11] An incomplete sandwich structure may arise also for a not fully parallel relative arrangement of the chromophores in the polymer chain.[86]

Spectroscopic data do not permit the determination of the details of the spatial disposition of the molecules in the excimeric complex, but in the case of polymeric systems the geometry of the excimeric centres may be found from conformational calculations for the chains.[72,78,101,199,203,205,206] The polarisation characteristics of the luminescence of excimers for different helicoidal configurations of the polymer chain have been obtained by computational methods and from the analysis of the fluorescence.[203,207–210] The different structures of the excimers in polymers have been attributed to the positions of the interacting molecules in the chain: the structures of the complexes are different when they are formed between neighbouring and remote sections of the polymer. If the polymer chain contains two types of nonequivalently linked chromophores, the formation of three types of excimeric complexes is noted.[199]

Isolated ('free') isomers are characterised by a finite number of relatively stable states, the population of which is determined by the influence of external factors. Calculations have shown that, for an intermolecular distance of ~3 Å, the excimers of naphthalene, anthracene, and pyrene can assume only two steric configurations. The interaction energy depends on the angle between the long molecular axes in the sandwich dimer and, together with the principal minimum (at 0°), has local minima at 55°[35] or 40°–50°[126] for pyrene, at 75° for naphthalene,[193,194] and at 65° for anthracene.[195]

The ability of molecules to form different excimeric configurations is associated with the contributions of different states to the wave function for the system. The stability of excimeric complexes is determined by the exciton-resonance interaction and the forces arising as a result of charge transfer.[30] In this sense, excimers are regarded as a special case of exciplexes. With increase in the length of conjugation in the benzene–naphthalene–anthracene–pyrene, etc. series, the energy gap between the molecular levels diminishes, which leads to an increase in the role of the exciton–resonance interaction. For example, the interaction due to charge transfer predominates in the benzene complexes,[162] whereas pyrene excimers are described almost entirely by the exciton-resonance component of the wave function.[35,211] Since the charge-resonance interaction is more isotropic, the benzene excimers may be formed in different configurations, although the sandwich configuration is nevertheless the most stable.[162]

In this connection, one should note that there are virtually no literature data on high-lying excited states of the excimers. As a rule, they do not play a significant role in the kinetic process examined in the previous sections. They aroused interest precisely in connection with the study of the two-photon ionisation of benzene. The stabilisation energy of its excimers in the second excited state exceeds by an order of magnitude this parameter for the S_1-excited complexes (1.8×10^4 and 5.9×10^2 J mol^{-1} respectively).[162]

For compounds with a pyrene fragment (i.e. with a long aromatic system), two configurations of excimers, differing by the displaced positions of the molecules in the sandwich complexes relative to one another (by half the length of the benzene ring along the long axes), can be clearly distinguished. Excimers of one of these type are formed in crystals, being retained also in liquid solutions.[28] The centrosymmetric structure of the excimer determines its zero ground state overall dipole moment and hence the forbidden optical transitions. This is reflected in the different fluorescence decay times: ~150 ns for the centrosymmetric model and 60–70 ns for the structure with incomplete overlap of the π-systems of the aromatic rings.[90] The same type of system occurs also in α-perylene crystals. Calculations have shown[191] that an isolated perylene excimer has an energy minimum for the complete overlap of the rings, but dimers of this type do not occur in crystals.

The short decay time of the V and Y components relative to the normal glow in pyrene and α-perylene makes it possible to attribute these types of fluorescence to the formation of weakly bound complexes. It is assumed that such states arise as a consequence of the incomplete relaxation of the molecules in the dimers.[50,54,191] According to Sumi,[52] the nature of these centres can be related to the association of pairs of molecules more remote from one another in the crystal than in the case of the dimeric pairs discussed above.

The relation between the thermodynamic parameters and structure of excimers has been examined.[90] It was shown that the entropy–enthalpy ($\Delta S-\Delta H$) relations are different for different excimeric configurations (Fig. 10). Another conclusion is that the entropy gain may be responsible for the formation of weakly bound complexes with a small or even positive value of ΔH. This accounts for the existence of weakly bound triplet excimers.

The structures of triplet excimers have been calculated, but contradictory results were obtained.[126,192,195,212] According to the data of Padma and coworkers,[126,192] the structure of the naphthalene and anthracene triplet excimers differs from the sandwich structure. For pyrene, the structures of the complexes of both multiplicities were obtained for virtually identical asymmetric configurations. The structure of the triplet state of all the molecules considered is virtually identical with the structure of the corresponding unexcited dimers. This has been explained by the fact that the stability of the triplet structure of excimers is determined by van der Waals forces, as in the unexcited dimers.

Table 1. The fluorescence maxima of the excimers

Chromophore	Experimental conditions	λ_{max}^{fl}/nm	Ref.
Benzene (phenyl)	Liquid state	320	197
	Solution of polystyrene–acrylonitrile copolymer in methanol	325	105
	Solution of polystyrene in 1,2-dichloroethane	332	82
	Solution of low-molecular-mass polystyrene analogues (2,4-diphenylpentane, 2,4,6-triphenylpentane, 2,4,6,8-tetraphenylnonane) in methylene chloride	330	198
	Solutions in dichloromethane		
	of hexaphenoxycyclotriphosphazene	~340	199
	hexacresoxytriphosphazene	~330	199
	polybisphenoxyphosphazene (T = 160–300 K)	305–310	199
	polybis-*p*-cresoxyphosphazene (T = 160–300 K)	320–330	199
Naphthalene (naphthyl)	Solution in cyclohexane	390	200
	Aqueous solution of the 2-vinylnaphthalene–maleic acid copolymer		
	normal excimer	400	71
	high-energy excimer	<400	71
	Adsorbed on SiO_2	390	145
	Solid solution in silicate glass (high-energy excimer)	375	150
Anthracene (anthryl)	Single crystal (T > 400 K)	~475	47
	Sandwich dimer in methylcyclohexane (T = 77 K)	475	19
	Poly-9-vinylanthracene film deposited electrochemically on a SnO_2 electrode	500	201
	Solution of anthracenophane in methanol in the presence of $NaClO_4$	510	96
	Anthracenophane in the crystal phase	570	96
	Solution of 9-methylanthracene in benzene	580	96
		~560	200
Pyrene (pyrenyl)	Aqueous solution	460	129
	Adsorbed on SiO_2	470	139
	Solution in cyclohexane	482	200
	Langmuir–Blodgett films		
	normal excimer	470	157
	high-energy excimer	420	157
	Single crystal	460	47
	Melt (T = 428–578 K)	460–450	47
	low-energy excimer (T = 448 K)	~500	47
	Solution in silicate glass		
	normal excimer	475	152
	high-energy excimer	450	152
	structured band due to dimers	380–420	152
	Solution of methyl 4-(1-pyrenyl)butyrate		
	in toluene	480	202
	in methyl benzoate	485	202
	in polystyrene	445	202
	in poly(methyl methacrylate)	440	202
	Solution of a pyrenyl-substituted polypeptide in tetrahydrofuran (T = 210–290 K)	440–480	203
Phenanthrene	Solution in perfluorohexane (T = 200 K) structured band due to dimers	330–450	135
	Adsorbed on Al_2O_3	400	153
Carbazolyl	Polyvinylcarbazole		
	normal excimer	420	121
	high-energy excimer	380	121
Perylene	Solution in benzene	588	200
	Single crystal	625	52
	Langmuir–Blodgett films		
	excimer	600	144
	band due to dimer	546	144

The differences between the singlet and the corresponding triplet complexes are determined largely by the different contributions of the exciton–resonance interaction.

The geometrical differences between excimers of different multiplicities have been demonstrated experimentally in relation to the following examples. Chandross and Dempster[20] obtained naphthalene sandwich dimers in a methylcyclohexane glass at 77 K. The fluorescence of such dimers was excimer-like whereas the phosphorescence was of the structural type corresponding to the naphthalene monomer. In another study,[213] where solutions of binaphthalene compounds were investigated, only the fluorescence due to the monomer and the triplet excimer glow were actually recorded; the association of the singlet complexes was hindered, whereas the triplet ones might have been formed with an asymmetric configuration.

Calculations of the geometries of the unexcited naphthalene, anthracene, and pyrene dimers showed that[126] the centrosymmetric sandwich conformation does not give rise to a stable ground state. The benzene dimers, which are stable in the ground state, are assumed to be capable of assuming the T-type, sandwich,[214,215] and V-type (house of cards)[216] forms. These states are separated by small potential barriers, so that the geometry of the benzene dimers is very sensitive to external influences.[217]

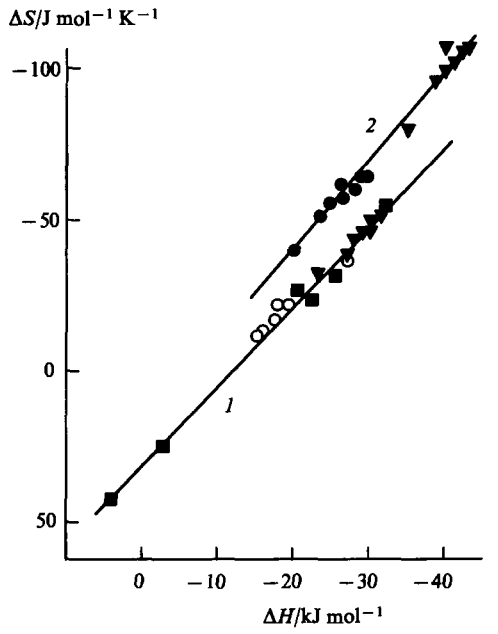


Figure 10. Dependence of ΔS on ΔH for intramolecular excimers of certain dipyrenylalkanes in various solvents.[90] The data plotted along straight line *1* correspond to centrosymmetric complexes with full overlap, while those plotted along line *2* correspond to complexes with displaced molecules (partial overlap).

VIII. Conclusion

In the present review we have attempted to concentrate attention on questions which arose during the last 10–15 years and which have not been adequately analysed in the scientific literature. This concerns primarily the conditions under which various excimer species arise. Unfortunately the available information does not permit a deeper elucidation of this problem. Without accurate calculations of the geometries of the complexes, it is impossible to achieve significant results in studies on the assignment of the spectroscopic manifestations of the excimeric centres to their structure. Such calculations have still not been carried out. Nevertheless steps taken in this direction would make it possible to obtain a more precise method in the field of studies, which have already become traditional (studies on the kinetics and the structure of the medium), using excimer-forming fluorescent probes.

Another problem which has become urgent is due to the unsuccessful definition of excimers adopted in the literature.[2] In particular, one may point to the lack of clear-cut criteria for the assignment of fluorescence to the excimeric or dimeric type. Nevertheless, this is not a fundamental problem. In the literature, there are examples of the study of dimers and excimers from a general standpoint (i.e. when no account is taken of the difference between them).[46,218] However, the simplified consideration of excimers from the standpoint of the somewhat idealised Scheme 1 frequently hinders the understanding of the essential features of the phenomenon. Attention was already drawn to this at an earlier stage. For example, two definitions of excimers have been formulated:[124] kinetic and spectroscopic. The former reflects the dynamic aspect of the formation of the excited complexes, while the latter definition postulates the similarity of the fluorescence characteristics of the excimeric and dimeric centres. The data presented in this review show that the second approach is also limited in character. For example, the low-temperature fluorescence of crystalline pyrene (Fig. 1) is excimeric despite the resolved vibrational structure if its consideration is based on the fact that the excitation is initially localised in a free-exciton state (i.e. in the monomer). In our view, the term excimers should be given to appropriately excited associated species stabilised by resonance interaction, regardless of the nature of the ground state.

References

1. B Stevens, E Hutton *Nature (London)* **186** 1045 (1960)
2. J B Birks *Mol. Photochem.* **1** 157 (1969)
3. E I Kapinus *Fotofizika Molekulyarnykh Kompleksov* (The Photophysics of Molecular Complexes) (Kiev: Naukova Dumka, 1988)
4. A G E Laufer, H Dreeskamp, K A Zachariasse *Chem. Phys. Lett.* **121** 523 (1985)
5. V M Smirnov *Usp. Fiz. Nauk* **139** 52 (1983)
6. T Forster, K Kasper *Z. Phys. Chem.* **1** 275 (1954)
7. T Forster, K Kasper *Z. Elektrochem.* **59** 976 (1955)
8. V M Miskowski, V M Houlding *Inorg. Chem.* **28** 1529 (1989)
9. H Kunkely, A Vogler *J. Am. Chem. Soc.* **112** 5625 (1990)
10. R Andriessen, N Boens, M Amelot, F C De Schryver *J. Phys. Chem.* **95** 2047 (1991)
11. J E Guillet *Photophysics and Photochemistry of Polymers. Introduction to the Study of Photoprocesses in Macromolecules* (Translated into Russian) (Moscow: Mir, 1988)
12. N N Barashkov, O A Gunder *Fluoreststsiruyushchie Polimery* (Fluorescent Polymers) (Moscow: Khimiya, 1987)
13. L L Kosbar, S W J Kuan, C W Frank, R F W Pease *ASC Symp.* **381** 95 (1989)
14. L Bokobza *Prog. Polym. Sci.* **15** 337 (1990)
15. S N Semerak, C W Frank *Adv. Polym. Sci.* **54** 31 (1983)
16. Yu A Vladimirov, G E Dobretsov *Fluoreststsiruyushchie Zondy v Issledovaniyakh Biologicheskikh Membran i Lipoproteinov* (Fluorescent Probes in Studies on Biological Membranes and Lipoproteins) (Moscow: Nauka, 1980).
17. G E Dobretsov *Fluoreststsiruyushchie Zondy v Issledovanii Kletok, Membran i Lipoproteinov* (Fluorescent Probes in the Study of Cells, Membranes and Lipoproteins) (Moscow: Nauka, 1989)
18. N N Barashkov, T V Sakhno *Opticheski Prozrachnye Polimery i Materialy na Ikh Osnove* (Optically Transparent Polymers and Materials Based on Them) (Moscow: Khimiya, 1992)
19. E A Chandross, J Ferguson *J. Chem. Phys.* **45** 3554 (1966)
20. E A Chandross, C J Dempster *J. Am. Chem. Soc.* **92** 704 (1970)
21. F Dupuy, M Martinnaud, G Nouchi, J-M Turlet *J. Chem. Phys.* **69** 614 (1972)
22. A Ueno, F Morivaki, T Osa, F Hamada, K Murai *J. Am. Chem. Soc.* **110** 4323 (1988)
23. A Ueno, I Suzuki, T Osa *J. Am. Chem. Soc.* **111** 6391 (1989)
24. A Ueno, I Suzuki, T Osa *J. Chem. Soc., Chem. Commun.* 1373 (1988)
25. A Ueno, I Suzuki, T Osa *Anal. Chem.* **62** 2461 (1990)
26. F Hamada, K Murai, A Ueno, I Suzuki, T Osa *Bull. Chem. Soc. Jpn.* **61** 3758 (1988)
27. C A Parker *Photoluminescence of Solutions* (Translated into Russian) (Moscow: Mir, 1972)
28. J B Birks *Photophysics of Aromatic Molecules* (New York: Willey, 1970)
29. W Klopffer, in *Organic Molecular Photochemistry* Vol. 1 (Ed. J B Birks) (London: Willey, 1973) p. 1
30. M Gordon, W R Ware (Eds) *The Exciplex* (New York: Academic Press, 1975)
31. D Phillips *Br. Polym. J.* **19** 135 (1987)
32. D I S Birh, R E Imhof, A Dutch *J. Lumin.* **31/32** 703 (1984)
33. M Okazaki, Y Tai, K Nunome, K Toriyama *Chem. Phys. Lett.* **171** 537 (1990)
34. F Lopes-Arbeloa, R Goedeweeck, F C De Schryver *J. Photochem. Photobiol. A: Chem.* **42** 133 (1988)
35. F Lopes-Arbeloa, R Andriessen, F C De Schryver *J. Photochem. Photobiol. A: Chem.* **45** 295 (1988)
36. J Keizer *Chem. Rev.* **87** 167 (1987)
37. J M G Martinho, M Campos, M A Winnik *Macromolecules* **22** 322 (1989)
38. K Sienicki, G Durocher *J. Chem. Phys.* **94** 6590 (1991)
39. R Xu, M A Winnik *J. Photochem. Photobiol. A: Chem.* **57** 351 (1991)
40. M N Berberan-Santos, J M G Martinho *Chem. Phys. Lett.* **178** 1 (1991)

41. M N Berberan-Santos, J P Pinheiro, J P Farinha, J M G Martinho *J. Lumin.* **48/49** 456 (1991)
42. J Vogelsang, M Hauser *Ber. Bunsenges. Phys. Chem.* **94** 1326 (1990)
43. M Okamoto, M Sasaki *J. Phys. Chem.* **95** 6548 (1991)
44. N L Vekshin *Perenos Vozbuzhdeniya v Makromolekulakh. Itogi Nauki i Tekhniki. Ser. Radiats. Khimiya. Fotokhimiya* (The Transfer of Excitation in Macromolecules. Advances in Science and Engineering. Radiation Chemistry and Photochemistry Series. Photochemistry) (Moscow: VINITI, 1989) Vol. 7
45. N L Vekshin *Drobnyi Perenos Energii v Eksimerakh i Eksipleksakh* (Fractional Energy Transfer in Excimers and Exciplexes) Preprint from NTsBI, USSR Academy of Sciences, Pushchino, 1989
46. M Pope, C Swenberg *Electronic Processes in Organic Crystals* (Translated into Russian) (Moscow: Mir, 1985) Vol. 1
47. R Hariguchi, N Iwasaki, Y Maruyama *J. Phys. Chem.* **91** 5135 (1987)
48. E Silins, M V Kurik, V Capek *Elektronnye Protsessy v Organicheskikh Molekulyarnykh Kristallakh* (Electronic Processes in Organic Molecular Crystals) (Riga: Zinatne, 1988)
49. D Fischer, G Haukdorf, W Klopffer *Z. Naturforsch. A* **28** 973 (1973)
50. H Port, R Seyfang, H C Wolf *J. Phys. (Paris)* **46** 391 (1985)
51. K Mizuno, A Matsui *J. Lumin.* **38** 323 (1987)
52. H Sumi *Chem. Phys.* **130** 433 (1989)
53. A Matsui, K Mizuno, N Tamai, T Yamasaki *Chem. Phys.* **113** 111 (1987)
54. B Walker, H Port, H C Wolf *Chem. Phys.* **92** 177 (1985)
55. A Matsui, T Ohno, K Mizuno, T Yokoyama, M Kobayashi *Chem. Phys.* **111** 121 (1987)
56. D Coulter, U Miskowski, A Gupta *Polym. Prepr.* **30** 372 (1990)
57. G H Fredriekson, H C Andersen, C W Frank *Macromolecules* **17** 54 (1984)
58. M D Ediger, M D Fayer *Macromolecules* **16** 1839 (1983)
59. G H Fredriekson, C W Frank *Macromolecules* **16** 572 (1983)
60. K Sienicki, W L Mattice *Macromolecules* **22** 2854 (1989)
61. K Sienicki *Macromolecules* **23** 5025 (1990)
62. K A Peterson, M D Fayer *J. Chem. Phys.* **85** 4702 (1986)
63. R Gelles, C W Frank *Macromolecules* **15** 547 (1982)
64. W C Tao, C W Frank *Macromolecules* **23** 3275 (1990)
65. K-D Rockwitz, H Bessler *Chem. Phys.* **70** 307 (1982)
66. G Peter, H Bessler, W Schrof, H Port *Macromolecules* **94** 445 (1985)
67. J R Mac Callum, L Rudkin *Nature (London)* **266** 338 (1977)
68. J R Mac Callum *Eur. Polym. J.* **17** 209 (1980)
69. M D Major, J M Torkelson *Macromolecules* **19** 2801 (1986)
70. H Itagaki, K Horie, I Mita, M Washio, S Tagawa, Y Tabata, H Sato, Y Tanaka *Macromolecules* **20** 2774 (1987)
71. I Morishima, H S Lim, S Nosakura, J L Sturtevant *Macromolecules* **22** 1148 (1989)
72. D K Chakraborty, K D Heitzhaus, F J Hamilton, H J Harwood, W L Mattice *Macromolecules* **24** 75 (1991)
73. S Ito, K Takami, Y Tsujii, M Yamamoto *Macromolecules* **23** 2666 (1990)
74. F Mendicuti, B Patel, R Kulkarni, W L Mattice *Macromolecules* **23** 2560 (1990)
75. F Evers, K Kobz, R Memming, D R Terrell *J. Am. Chem. Soc.* **105** 5988 (1983)
76. F C De Schryver, P Collart, J Vandendriessche, R Goedeweeck, A M Swinnen, M Van der Auweraer *Acc. Chem. Res.* **20** 159 (1987)
77. M A Winnik *Acc. Chem. Res.* **18** 73 (1985)
78. W L Mattice *Polym. Prepr.* **31** 706 (1990)
79. F Mendicuti, V N Viswanadhan, W L Mattice *Polymer* **29** 875 (1988)
80. F Mendicuti, B Patel, V N Viswanadhan, W L Mattice *Polymer* **29** 1669 (1988)
81. F Mendicuti, B Patel, D M Woldeck, W L Mattice *Polymer* **30** 1680 (1989)
82. D Sarazin, J Gan, J Francois *Polym. Bull.* **19** 311 (1988)
83. I Bahar, W L Mattice *J. Chem. Phys.* **90** 6775 (1989)
84. S Blonski, K Sienicki *Macromolecules* **19** 2936 (1986)
85. S Blonski, K Sienicki, A Herman *Macromolecules* **20** 329 (1987)
86. C S Reramayor, M R Gomes-Anton, B Colafote *Macromolecules* **24** 3328 (1991)
87. P Collart, S Toppet, Q F Zhou, N Boens, F C De Schryver *Macromolecules* **18** 1026 (1985)
88. C Salom, M R Gomes-Anton, A Horta, I Hernandez-Fuentes, I F Pierola *Macromolecules* **20** 1627 (1987)
89. D A Holden, A Safarzadeh-Amiri, C P Sloan, P Martin *Macromolecules* **22** 315 (1989)
90. K A Zachariasse, G Duveneck *J. Am. Chem. Soc.* **109** 3790 (1987)
91. F Mendicuti, B Patel, W L Mattice *Polymer* **31** 453 (1990)
92. F C De Schryver, P Goedeweeck, P Collart, J Vandendriessche *Polym. Prepr.* **30** 320 (1990)
93. K Hara, S Akimoto, H Suzuki *Chem. Phys. Lett.* **175** 493 (1990)
94. F Hirayama *J. Chem. Phys.* **42** 3163 (1965)
95. F C De Schryver, N Boens, J Put *Adv. Photochem.* **10** 359 (1977)
96. J Hinschberger, J-P Desvergne, H Bouas-Lourent, P Marsau *J. Chem. Soc., Perkin Trans. 2* 993 (1990)
97. K A Zachariasse, G Duveneck, W Kuhnle *Chem. Phys. Lett.* **113** 337 (1985)
98. H A Staab, N Riegler, F Diederich, C Krieger, D Schweitzer *Chem. Ber.* **117** 246 (1984)
99. G D Scholes, K P Ghiggino, G J Wilson *Chem. Phys.* **155** 127 (1991)
100. M A Fox, P F Britt *Macromolecules* **23** 4533 (1990)
101. M A Fox, P F Britt *J. Phys. Chem.* **94** 6351 (1990)
102. N N Barashkov *Usp. Khim.* **54** 1175 (1985) [*Russ. Chem. Rev.* **54** 690 (1985)]
103. K Kimura, H Ohno, K Marikawa, Y Hiramatsu, Y Odaira *Bull. Chem. Soc. Jpn.* **55** 2169 (1982)
104. A S Cherkasov *Trudy GOI* **52** 3 (1983)
105. L Alexandru, A S Somersall *J. Polym. Sci.* **15** 2013 (1977)
106. D Phillips, A J Roberts, J Soutar *Eur. Polym. J.* **17** 101 (1981)
107. C Cuniberti, A Perico *Eur. Polym. J.* **16** 887 (1980)
108. D Ng, J E Guillet *Macromolecules* **14** 405 (1980)
109. F C De Schryver, K Demayer, M Van der Auweraer, E Quanten *Ann. N.Y. Acad. Sci.* **366** 93 (1981)
110. S E Webber, P E Avots-Avotins, M Deumie *Macromolecules* **14** 105 (1981)
111. A J Roberts, C G Cureton, D Phillips *Chem. Phys. Lett.* **72** 554 (1980)
112. J R MacCallum *Eur. Polym. J.* **17** 797 (1981)
113. S Tagawa, M Washio, Y Tabata *Chem. Phys. Lett.* **68** 276 (1979)
114. A Itaya, K Okamoto, H Masuhara, N Ikeda, N Mataga, V Kusabayashi *Macromolecules* **15** 1213 (1982)
115. H F Kauffmann, W-D Weixelbaumer, J Burbaumer, B Mollay *Polym. Prepr.* **30** 364 (1990)
116. H Itagaki, K Horie, J Mita *Macromolecules* **16** 1395 (1983)
117. V B Biteman, O A Gunder, V G Senchishin *Zh. Prikl. Spektrosk.* **28** 823 (1978)
118. K Sienicki, M A Winnik *J. Chem. Phys.* **87** 3922 (1987)
119. M F Kauffman, B Mollay, W-D Weixelbaumer, J Burbaumer, M Riegler, E Meisterhofer, F R Aussenegg *J. Chem. Phys.* **85** 3566 (1986)
120. K Sienicki, C Bojarski *Macromolecules* **18** 2714 (1985)
121. A Itaya, M Sakai, H Masuhara *Chem. Phys. Lett.* **138** 231 (1987)
122. Y Utena, H Yajima, T Tadahiro, T Handa *Eur. Polym. J.* **23** 643 (1987)
123. Yu S Barash *Sily Van der Waalsa* (Van der Waals Forces) (Moscow: Nauka, 1988)
124. B Nickel, M F R Prieto *Z. Phys. Chem. N. F.* **150** 31 (1986)
125. A Warshel, E Huler *Chem. Phys.* **6** 463 (1974)
126. E J Padma Malar, A K Chandra *Indian J. Chem. A.* **19** 283 (1980)
127. A I Kitaigorodskii *Molekulyarnye Kristally* (Molecular Crystals) (Moscow: Nauka, 1971)
128. J F Brennecke, D L Tamasko *J. Phys. Chem.* **94** 7692 (1990)
129. N L Vekshin *Studia Biophysica* **106** 69 (1985)
130. F M Winnik *Macromolecules* **23** 233 (1990)
131. N J Turro, K S Arora *Polymer* **27** 783 (1986)
132. H T Oyama, W T Tang, C W Frank *Macromolecules* **20** 474 (1987)
133. W G Herkstroeter, P A Martic, S E Hartmant, J L R Williams, S Farid *J. Polym. Sci., Polym. Chem. Ed.* **21** 2473 (1983)
134. H T Oyama, W T Tang, C W Franc *Macromolecules* **20** 1839 (1987)
135. B Nickel, M F R Prieto *Ber. Bunsenges. Phys. Chem.* **92** 1493 (1988)
136. G Vitukhnovsky, M J Sluch, J G Warren, M C Petty *Chem. Phys. Lett.* **184** 235 (1991)
137. N Iwasaki, R Horiguchi, Y Maruyama *Bull. Chem. Soc. Jpn.* **58** 2409 (1985)
138. A I Ogloblina, Abstract of Candidate's Thesis in Physico-Mathematical Sciences, Moscow State Pedagogic Institute, Moscow, 1978
139. T Fujii, E Shimizu, S Suzuki *J. Chem. Soc., Faraday Trans. 1* **84** 4387 (1988)

140. W Mooney, P Brown, J Russell, S Costa, L Pedersen, D Whitten *J. Am. Chem. Soc.* **106** 5659 (1984)
141. W Mooney, D Whitten *J. Am. Chem. Soc.* **108** 5712 (1986)
142. G Biesmans, G Verbeek, B Verschuere, M Van der Auweraer, F C De Schryver *Thin Solid Films* **142** 127 (1989)
143. G Warren, J P Cresswell, M C Petty *Thin Solid Films* **179** 515 (1989)
144. A G Vitukhnovsky, M J Sluch, J G Warren, M C Petty *Chem. Phys. Lett.* **173** 425 (1990)
145. K Hara, P de Mayo, W R Ware, A S Weedon, G S Wong, K S Wu *Chem. Phys. Lett.* **69** 105 (1980)
146. C Francis, J Lin, L A Singer *Chem. Phys. Lett.* **94** 162 (1983)
147. O A Khakhel', R N Nurmukhametov, V V Nekrasov, T V Sakhno, N N Barashkov, T M Murav'eva *Zh. Prikl. Spektrosk.* **55** 503 (1991)
148. O A Khakhel', R N Nurmukhametov, T V Sakhno, S A Serov, N N Barashkov, T M Murav'eva *Zh. Fiz. Khim.* **66** 2639 (1992)
149. P Avis, G Porter *J. Chem. Soc., Faraday Trans. 2* **70** 1057 (1974)
150. T Yamanaka, Y Takahashi, K Uchida *Chem. Phys. Lett.* **172** 405 (1990)
151. T Matsui, N Usuki *Bull. Chem. Soc. Jpn.* **63** 3516 (1990)
152. T Yamanaka, Y Takahashi, T Kitamura, R Uchida *J. Lumin.* **48/49** 265 (1991)
153. D R Haynes, K R Helwig, N J Tro, S M George *J. Chem. Phys.* **93** 2836 (1990)
154. N J Tro, A M Nishimura, S M George *J. Chem. Phys.* **93** 3276 (1989)
155. T Yamazaki, N Tamai, I Ymazaki *Chem. Phys. Lett.* **124** 326 (1986)
156. T Yamazaki, N Tamai, I Ymazaki *J. Chem. Phys.* **91** 3572 (1987)
157. S Ohmori, S Ito, M Yamamoto *Macromolecules* **23** 4047 (1990)
158. R Subramanian, L K Patterson *J. Chem. Phys.* **109** 1202 (1985)
159. P K J Kinnunen, A P Tulkki, R C Ahuja, D Mobius *Thin Solid Films* **132** 193 (1985)
160. M Itoh, Y Morita *Chem. Phys.* **92** 5693 (1988)
161. H Saigusa, E C Lim *J. Phys. Chem.* **95** 2364 (1991)
162. H Shinohara, N Nishi *Chem. Phys.* **129** 149 (1989)
163. M Itoh, M Takamatsu *Chem. Phys. Lett.* **170** 396 (1990)
164. H Saigusa, M Itoh, M Baba, J Hanazaki *J. Chem. Phys.* **86** 2528 (1987)
165. M Itoh, A Hayashi *J. Phys. Chem.* **93** 7789 (1989)
166. V C Anderson, B B Craig, R G Weiss *J. Am. Chem. Soc.* **104** 2972 (1982)
167. N Tamai, I Yamazaki, H Masuhara, N Mataga *Chem. Phys. Lett.* **104** 485 (1984)
168. M Sisido, X-F Wang, K Kawaqushi, Y Yamanishi *J. Phys. Chem.* **92** 4797 (1988)
169. P Reyners, H Dreeskamp, W Kuhnle, A K Zachariasse *J. Phys. Chem.* **91** 3982 (1987)
170. T Ikeda, S Kurihara, S Tazuke *J. Phys. Chem.* **94** 6550 (1990)
171. T Takemura, M Aikawa, H Baba *J. Lumin.* **12/13** 819 (1976)
172. T Takemura, M Aikawa, H Baba, Y Shindo *J. Am. Chem. Soc.* **98** 2205 (1976)
173. E C Lim *Acc. Chem. Res.* **20** 8 (1987)
174. G Castro, R M Hochstrasser *J. Chem. Phys.* **45** 4352 (1966)
175. O L G.Gijzeman, J Langelaar, J D W Van Voorst *Chem. Phys. Lett.* **5** 269 (1970)
176. O L G Gijzeman, J Langelaar, J D W Van Voorst *Chem. Phys. Lett.* **11** 526 (1971)
177. E C Lim, S K Chakraborti *Mol. Phys.* **13** 293 (1967)
178. G A George, G C Morris *Mol. Cryst. Liq. Cryst.* **10** 187 (1970)
179. J Langelaar, R P H Rettschick, A M F Lambooy *Chem. Phys. Lett.* **1** 609 (1969)
180. R D Burkhart, N-I Ihon, S Boileau *Macromolecules* **24** 6310 (1991)
181. W Klopffer, D Fischer *J. Polym. Sci., Polym. Symp.* **40** 43 (1973)
182. W Klopffer, D Fischer, G Naundorf *Macromolecules* **10** 450 (1977)
183. C-H Tung, Y-M Wang *Chem. Soc., Chem. Commun.* 1891 (1989)
184. N Kim, S E Webber *Macromolecules* **13** 1233 (1980)
185. D K Chakraborty, R D Burkhart *J. Phys. Chem.* **93** 4797 (1989)
186. L Flamigui, N Camaioni, P Bortolus, F Minto, M Gleria *Macromolecules* **95** 971 (1991)
187. N F Pasch, S E Webber *Chem. Phys.* **16** 361 (1976)
188. J Hertzberg, B Nickel *Chem. Phys.* **132** 235 (1989)
189. C Bohne, E B Abuin, J C Scaiano *J. Am. Chem. Soc.* **112** 4226 (1990)
190. A S Ghosh, D Gupta, S Basu *J. Photochem.* 4 227 (1975)
191. M D Cohen, R Haberkorn, E Huler, Z Ludmer, M E Michel-Beyerle, D Rabinovich, R Sharon, A Warshel, V Yakhot *Chem. Phys.* **27** 211 (1978)
192. E I Padma Malar, A K Chandra *Theor. Chim. Acta* **55** 153 (1980)
193. T Azumi, H Azumi *Bull. Chem. Soc. Jpn.* **39** 1829 (1966)
194. T Azumi, H Azumi *Bull. Chem. Soc. Jpn.* **39** 2317 (1966)
195. B S Subhindra, A K Chandra *Mol. Phys.* **30** 319 (1975)
196. S G Semenov, Yu F Sigolaev, *Vestn. Leningr. Univ.* **2** 106 (1991)
197. T V Ivanova, G A Mokeeva, B Ya Cveshnikov *Opt. Spektrosk.* **2** 568 (1962)
198. L Bokobza, B Jasse, L Monnerie *Eur. Polym. J.* **13** 921 (1977)
199. A S Yeung, C W Frank, R E Singler *Polymer* **31** 1092 (1990)
200. J B Birks, L G Christophorou *Proc. R. Soc. London. A* **277** 571 (1963)
201. P V Kamat *Anal. Chem.* **59** 1636 (1987)
202. S Farid, P A Matric, R S Daly, D R Thompson, D P Specht, S E Hartman, J L R Williams *Pure Appl. Chem.* **51** 241 (1979)
203. J Inai, M Sisido, J Imanishi *J. Phys. Chem.* **94** 8365 (1990)
204. E A Chandross, C J Dempster *J. Am. Chem. Soc.* **92** 3586 (1970)
205. R Goedeweek, F C De Schryver *Photochem. Photobiol.* **39** 515 (1984)
206. R Goedeweek, M Van der Auweraer, F C De Schryver *J. Am. Chem. Soc.* **107** 2334 (1985)
207. J P Riehl, F S Richardson *Chem. Rev.* **86** 1 (1986)
208. M Sisido, S Egusa, A Okamoto, Y Ymanishi *J. Am. Chem. Soc.* **105** 3351 (1983)
209. Y Inai, M Sisido, Y Imanishi *J. Phys. Chem.* **94** 2734 (1990)
210. K Kano, H Matsumoto, Y Yoshimura, S Hoshimoto *J. Am. Chem. Soc.* **110** 204 (1988)
211. E M S Castanheira, J M G Martinho *Chem. Phys. Lett.* **185** 319 (1991)
212. A K Chandra, E C Lim *Chem. Phys. Lett.* **45** 79 (1977)
213. P C Subudhi, E C Lim *Chem. Phys. Lett.* **44** 479 (1976)
214. K H Fung, H L Seizie, E W Schlag *J. Phys. Chem.* **87** 5113 (1983)
215. K S Law, M Schauer, E R Bernstein *J. Chem. Phys.* **81** 4871 (1984)
216. K O Bornsen, H L Selzle, E W Schlag *J. Chem. Phys.* **85** 1726 (1986)
217. B W Van de Waal *Chem. Phys. Lett.* **123** 69 (1986)
218. V I Yuzhakov *Usp. Khim.* **48** 2007 (1979) [*Russ. Chem. Rev.* **48** 1076 (1979)]

Russian Chemical Reviews **62** (6) 553–578 (1993)
© 1993 Russian Academy of Sciences and Turpion Ltd

UDC 547.221:112

[3,3]-Sigmatropic rearrangements as a method of organofluorine synthesis

V G Andreev, A F Kolomiets

Contents

I.	Introduction	553
II.	Rearrangements of polyfluoroaryl ethers	554
III.	Rearrangements of polyfluorocycloalkenyl ethers	559
IV.	Rearrangements of polyfluorovinyl ethers	562
V.	Rearrangements of polyfluorocarboxylic acid esters	570
VI.	Rearrangements of polyfluoroallyl ethers	572
VII.	Conclusion	574

Abstract. Literature data on [3,3]-sigmatropic rearrangements of organofluorine compounds are surveyed and described systematically in terms of the type of substances and intermediates involved in the rearrangements. The characteristic features of these reactions are considered as a function of the structure of the isomerising molecules and the positions in the latter of fluorine atoms and fluorine-containing substituents. The possibilities arising from the use of the [3,3]-sigmatropic rearrangements for the specific synthesis of fluorine-containing compounds belonging to particular classes are assessed. The bibliography includes 180 references.

I. Introduction

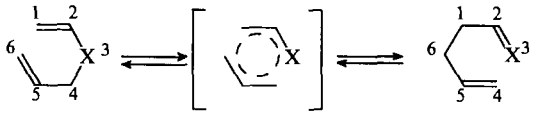
The [3,3]-sigmatropic rearrangements, which include the Claisen and Cope rearrangements, as well as their different modifications (Carroll, Ireland–Claisen, Johnson–Claisen, etc. rearrangements) and their numerous versions based on unsaturated compounds with hetero- and functional-group substituents constitute one of the most important synthetic methods in modern organic chemistry.

This type of intramolecular rearrangements was discovered by Claisen[1] in 1912 in relation to the thermal transformations of the allyl ethers of phenol and 2-naphthol into the corresponding *C*-allyl derivatives. Later similar reactions were investigated for a large number of substituted allyl (propargyl) aryl ethers, which made it possible to develop high-temperature synthesis of a wide variety of unsaturated aryl-substituted aliphatic substances (see the relevant reviews[2–4]).

The extension of the Claisen rearrangement to aliphatic and alicyclic systems (ethers, sulfides, and amines) as well as heteroaromatic compounds and the discovery of the Cope rearrangement[5] and its modifications converted the [3,3]-sigmatropic reactions into a universal method for the specific construction of the carbon skeletons of compounds containing multiple bonds in the 1,5-positions relative to one another. The principal advances in the last two decades of the study of the Claisen and Cope rearrangements have been described in a number of reviews[6–13] and numerous data on hetero-[3,3]-sigmatropic rearrangements are available in other reviews.[14–18]

The [3,3]-sigmatropic rearrangements are irreplaceable in the syntheses of many substances with a complex structure. For example, effective methods for the synthesis of polyenes have been developed on the basis of consecutive [3,3]-sigmatropic rearrangements,[13] while certain versions of the Cope aza-rearrangement have been used to synthesise the previously unavailable nitrogen-containing polycyclic systems.[17, 18] However, the importance of these reactions is mainly associated with the total synthesis of polyfunctional unsaturated compounds, the preparation of which by other methods usually involves several stages.

The extensive synthetic possibilities of the [3,3]-sigmatropic reactions are responsible for the continued interest in the theoretical aspects of these reactions. In accordance with the ideas of Woodward and Hoffman,[19] the [3,3]-sigmatropic rearrangements are assigned to the class of unimolecular pericyclic reactions. They take place as thermal concerted processes in accordance with the general **1** → **2** mechanism predominantly via a six-centre quasi-aromatic transition state of type **A***.



1 **A*** **2**

X = CH_2, O, S, Se, NH.

The most preferred pathway in these reactions involves a supra-suprafacial formation of the transition state **A*** in the chair form.[6, 13, 19] This is the reaction for the high effectiveness of the stereochemical control of the rearrangements, which frequently lead to the enantioselective formation of a C–C bond. By virtue of this, they are widely used in asymmetric synthesis,[20, 21] primarily for the preparation of biologically active natural products and their analogues.[22–26]

The formation of the transition state **A*** in the aliphatic Claisen rearrangement (in contrast to the purely carbon systems) is accompanied by an appreciable charge separation,[27] i.e. is a charge-controlled process, which leads to extensive possibilities for controlling it. Thus the rate of the [3,3]-sigmatropic reactions increases by 2–6 orders of magnitude in the presence of polar solvents or catalysts stabilising the zwitter-ionic or ionic states of the intermediates.[9, 10] The principal reagents generating anions

V G Andreev, A F Kolomiets A N Nesmeyanov Institute of Organoelement Compounds, Russian Academy of Sciences, ul. Vavilova 28, 117813 Moscow. Fax (7-095) 135 50 85

Received 26 February 1993
Uspekhi Khimii **62** (6) 594–620 (1993); translated by A K Grzybowski

derived from the initial substrates exert an even stronger influence. For example, the rate of the sigmatropic shift in the Cope oxy-rearrangement increases by a factor of $10^{10}-10^{17}$ if the reaction intermediate is the anion formed when the substrate is acted upon by metal hydrides.[28] A similar acceleration is observed in the carbanionic Claisen rearrangements[29-32] and in all these reactions the temperature of the rearrangement is reduced sharply. A similar but less marked effect may be produced by substituents at the multiple bonds of allyl vinyl ethers **1**, which enhance the π-donor properties of the 'vinyl' and/or the π-acceptor properties of the 'allyl' fragments.[29, 33-35] Thus the [3,3]-sigmatropic rearrangements, which had been previously considered as hard thermal processes, can be achieved as soft chemo-, regio-, and stereo-selective transformations of 1,5-diene systems.

The mild conditions and the high rate of the reactions are especially characteristic of the relatively little investigated [3,3]-sigmatropic rearrangements of fluorine-containing unsaturated compounds. The anomalous behaviour of aliphatic fluoro-compounds in reactions of this type was first described in 1967 by Krespan in the paper "Negative substituents in the Claisen rearrangements".[36] The unexpected results of this study, which has since become classical, have served as a powerful stimulus to the more extensive use of [3,3]-sigmatropic rearrangements of compounds of the organofluorine series. It was shown subsequently[37] that not only the specific features of the electronic effects of the fluorine atoms and the fluoroalkyl groups but also the special nature of the double bond in the fluorinated olefins, which tends to combine with fluorine and alkoxide ions to form carbanions, exerts a significant influence on the conditions and nature of the reactions of the fluorine-containing substrates.

The rearrangements of the allyl and propargol ethers of polyfluorophenols polyfluorocycloenols, and aliphatic polyfluorophenols as well as the esters of the polyfluorocarboxylic acids and polyfluoroallyl ethers have been investigated. However, until recently there were no surveys of data concerning the [3,3]-sigmatropic rearrangements as a method of organofluorine synthesis. In the reviews published recently,[37, 38] only individual aspects of the problem are considered which emphasises still further its timeliness.

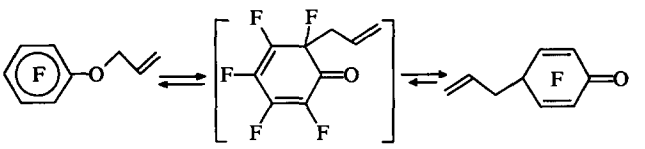
In the present review, an attempt is made for the first time to survey fully and to give systematic account of data on the [3,3]-sigmatropic reactions of fluorine-containing compounds and to assess the possibilities and prospects of their use for the specific synthesis of new organic derivatives of fluorine.

The review is not concerned with the Cope rearrangements (see the relevant communications[38-43]), because studies on the thermodynamic, kinetic, and stereochemical effects of fluorine and the trifluoromethyl group in these reactions are of no preparative value.

II. Rearrangements of polyfluoroaryl ethers

Allyl(propargyl) aryl and allyl heteroaryl ethers and sulfides fully or partly fluorinated in the aromatic ring as well as the corresponding phenyl trifluoromethyl ethers and phenyltrifluoromethylamines have now been involved in the Claisen rearrangement or its different versions. The most interesting results have been obtained in the study of the rearrangements of compounds with aromatic perfluoro-fragments in the gas phase and in solutions. The characteristic features of these reactions were elucidated in an excellent series of studies by Brooke[44-53, 56-60] in relation to perfluorinated phenyl, 2-naphthyl, 2-, 3-, and 4-pyridyl, quinolin-2(4)-yl, and pyrimidin-4-yl ethers.

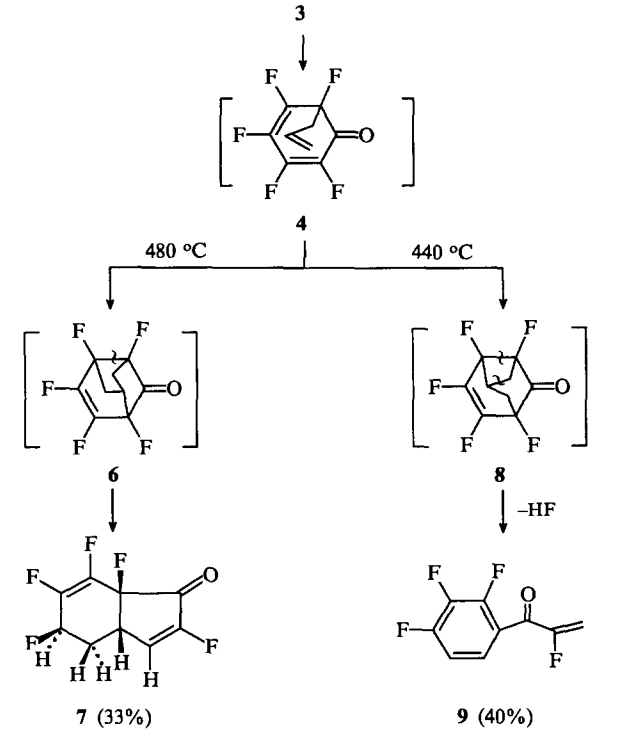
In contrast to allyl phenyl ether,[6, 54] heating of allyl pentafluorophenyl ether **3** in the gas phase at 137–141 °C (for 13 days) or at 365 °C leads to the *para*-rearrangement product 4-allylpentafluorocyclohexa-2,5-dien-1-one **5** and not to the expected *ortho*-rearrangement product the 2,4-dien-1-one **4**.[44, 45]



3 **4** **5**

The yield of compound **5** increases from 10% to 32% with increase in temperature. The absence of the dienone **4** among the reaction products is associated with its low thermodynamic stability, its ability to undergo reversible isomerisation to the ether **3**, and also its tendency to undergo side reactions.[45]

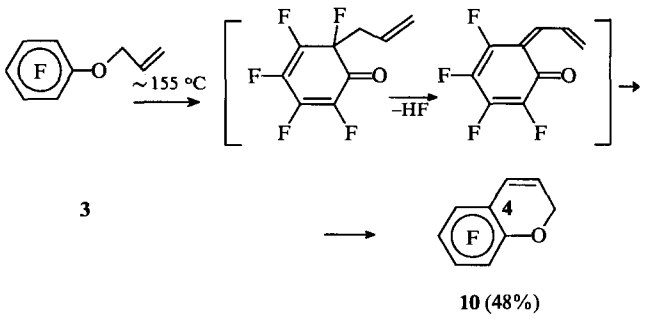
Indeed, the gas-phase pyrolysis of compound **3** at 440 °C–480 °C in a quartz tube filled with siloxane fibre affords either pentafluorotetrahydroinden-1-one **7**[46] or 1′-fluorovinyl 2,3,4-trifluorophenyl ketone **9** mixed with compound **7** as the main product.[47] Their appearance is explained by the alternative transformations of the dienone **4** into the intermediate tricycloketones **6** and **8**, which are formed as the stereoisomeric adducts as a result of the intramolecular Diels–Alder [4 + 2]-cycloaddition.[46, 47]



Under these conditions (480 °C), the dienone **5** is also converted into compound **7** in 28% yield, which demonstrates the reversibility of the rearrangements **4** ⇄ **5** under severe conditions.[46]

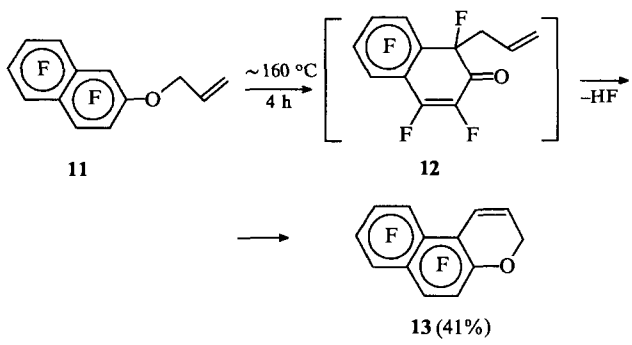
It was possible to isolate the tricyclic ketone **8** after the low-temperature (137–141 °C and 13 days) thermolysis of compound **3** in the gas phase.[48] This compound, which is the first carbocyclic Diels–Alder adduct obtained in the rearrangement of an allyl aryl ether, was characterised by spectroscopic methods and by conversion into a hemihydrate,[48] which was subsequently obtained also from compound **3** but without the intermediate isolation of compound **8**.[45]

Another type of reaction of the ether **3** take place in the liquid phase (DMF, refluxing, 4 h) in the presence of potassium fluoride.[49] In this case, the temperature of the rearrangement of the ether **3** is appreciably reduced compared with the temperature of the isomerisation of the allyl phenyl ether,[6, 54] while the primary *ortho*-rearrangement product **4** undergoes successive dehydrofluorination and intramolecular electrocyclisation to tetrafluoro-2*H*-1-benzopyran **10**.



3 10 (48%)

Allyl heptafluoro-2-naphthyl ether **11** is similarly converted into 5,6,7,8,9,10-hexafluoro-2*H*-napththopyran **13** in the KF/sulfolan system.[49]

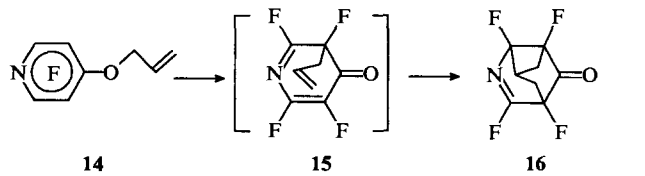


11 **12** **13** (41%)

However, at 135 °C in xylene the ether **11** isomerises smoothly, in 64% yield, to the *ortho*-rearrangement product 1-allylheptafluoronaphthalen-2-one **12**, which is stable, in contrast to compound **4**.[50]

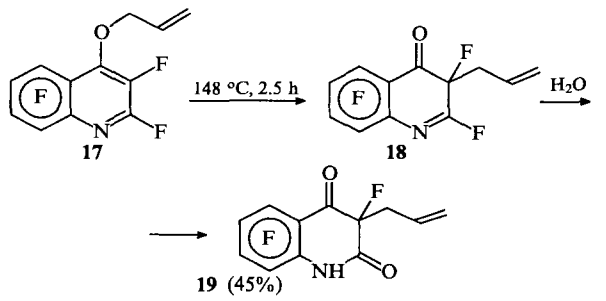
The structural rearrangements occurring in the [3,3]-sigmatropic rearrangements of allyl tretralfluoropyridyl and allyl hexafluoroquinolinyl ethers are in many respects similar to the reactions of allyl perfluoroallyl ethers examined above. The mode of these reactions is determined primarily by the position of the allyloxy-group relative to the nitrogen atom and they occur as a rule under milder conditions than the rearrangements of the non-fluorinated analogues.[6, 12]

Thus the low-temperature gas-phase thermolysis (138 °C, 10 h) of allyl tetrafluoro-4-pyridyl ether **14** leads to the tricyclic ketone **16** in a yield up to 25%. This compound is formed as a result of the stabilisation via the [4 + 2]-cycloaddition of the product **15** of the *ortho*-rearrangement.[51]



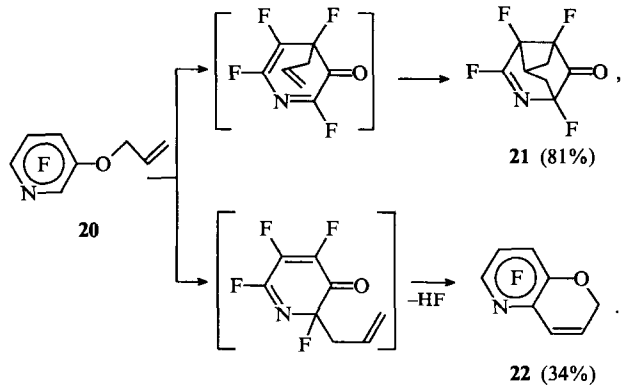
14 **15** **16**

On the other hand, when allyl hexafluoroquinolin-4-yl ether **17** is refluxed in *o*-xylene the stable product of the *ortho*-rearrangement is produced—the quinolinone **18**, which readily hydrolyses to the dione **19** during isolation.[52]



17 **18** **19** (45%)

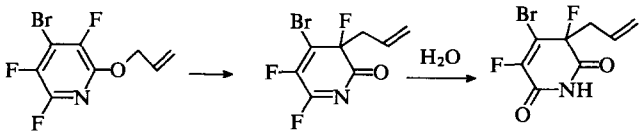
Allyl tetrafluoro-3-pyridyl ether **20** is converted under conditions more severe than for the ether **14** (gas phase, 185 °C, 113 h), into the tricyclic ketone **21**,[51] whilst heating in sulfolan in the presence of KF (nickel flask, 184 °C, 4 h) leads to its conversion into 6,7,8-trifluoro-2*H*-pyranopyridine **22**.[49]



20 **21** (81%) **22** (34%)

The opposite direction of migration of the allyl group in the [3,3]-sigmatropic shift in the second reaction is explained by the strong influence of the protophilic solvent.[49]

It is of interest to note that, in contrast to the ethers **14** and **20**, the rearrangement of allyl 4-bromo-3,5,6,-trifluoro-2-pyridyl ether **23** is completed, even after prolonged heating in the gas phase (160 °C, 139 h), by the formation of the stable product **24** of the *ortho*-C-migration of the allyl group, which is hydrolysed during isolation to 3,4-dehydropiperidinedione **25**. The degree of conversion of the ether **23** is 38%.[51]



23 **24** **25** (7%)

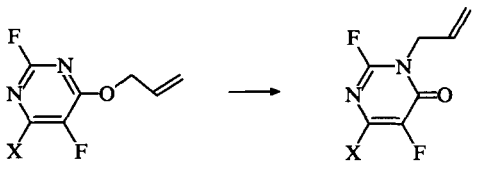
The formation of the *N*-allyl-substituted product was not detected in this reaction.

Nevertheless the migration of the allyl group exclusively to the nitrogen atom is characteristic of the thermal reactions of allyl hexafluoroquinolin-2-yl and allyl hexafluoroisoquinolin-1-yl ethers in tetralin (212 °C, 48 h). These rearrangements result in the formation of fluorine-containing *N*-allylquinolinone **26** and *N*-allylisoquinolinone **27** in satisfactory yields.[52]



26 (69%) **27** (45%)

The rearrangements of allyl polyfluoropyrimidin-4-yl ethers **28** take place with much more difficulty. The products **29** of the [3,3]-sigmatropic shifts were obtained from the ethers **28** in 53%–67% yields only at 440–475 °C under the conditions of gas-phase pulsed pyrolysis.[53]



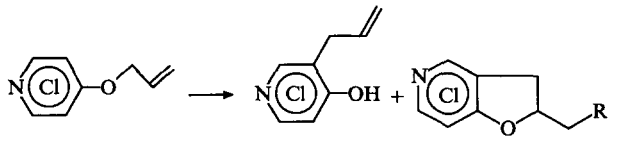
28 29

X = H, F, OMe.

The probability of the migration of the allyl group to the N(3) atom in this reaction proved significantly higher than that of the migration to the C(5) atom, which made it possible to develop on its basis a new approach to the preparative synthesis of derivatives of 5-fluorouracil and barbituric acid.[53]

Evidently the features of the [3,3]-sigmatropic rearrangement of allyl perfluoroaryl and allyl polyfluoroheteroaryl ethers noted above can be explained primarily by the high $+E$ contributions of the fluorine atoms to the aromatic and conjugated cyclohexa-2,4-diene systems and also by the reaction conditions. These factors are responsible, in the first place, for the enhancement of the π-donor properties of the aryl fragment and hence for the appreciably milder, compared with the non-fluorinated analogues, conditions in the Claisen rearrangement, which is completed (in aprotic solvents) by the formation of stable *ortho*-rearrangement products — bicyclic 2-aryl ketones incapable of isomerising to the corresponding *ortho*-hydroxyallyl derivatives. In the second place, they are responsible for the higher probability of the stabilisation of the intermediate 2,4-dienones either (in the gas phase) via the intramolecular [4 + 2]-cycloaddition or (in protophilic media) via dehydrofluorination, with subsequent electrocyclisation.

By virtue of the influence of the fluorine atoms, the Claisen rearrangements of aromatic polyfluoro-compounds and the subsequent reactions of the *ortho*-rearrangement products are unique. Even chlorine, which is very close to fluorine as regards the electromeric contribution, is incapable of altering quite so radically the traditional modes of these reactions. Thus allyl tetrachloro-4-pyridyl ether **30** isomerises under conditions more severe than in the case of compound **14** (sulfolan, 190 °C, 1.5 h).[55] The product of the *ortho*-rearrangement of the ether **30** does not exhibit a tendency to undergo any of the transformations examined above and is stabilised by a homolytic mechanism with formation of a mixture of allyl-2,5,6-trichloro-4-hydroxypyridine **31** and fluoropyridines **32**.

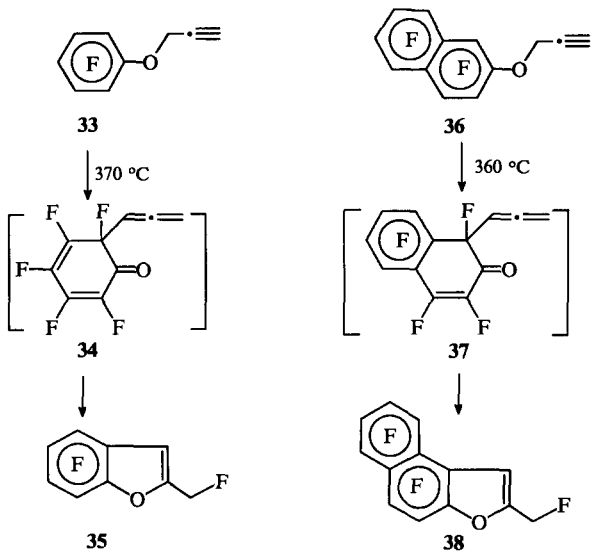


30 31 (26%) 32 (16.5%)

R = H, Cl.

The data obtained by Brooke and coworkers[56-60] in the study of the rearrangements of pentafluorophenyl propargyl ether **33** and heptafluoro-2-naphthyl propargyl ether **36** confirm the strong influence of the perfluoroallyl groups on the nature of the [3,3]-sigmatropic shift. The gas-phase pyrolysis of the ethers **33** and **36** at 360–370 °C leads to tetrafluorobenzofuran **35**[56] and hexafluoronaphthofuran **38**[57, 58] in 8% and 43% yields respectively. The polyfluorofuranes are formed as a result of the electrocyclisation of the intermediate *ortho*-rearrangement products **34** and **37** accompanied by the [1,4]-fluorotropic shift.

In solutions, these rearrangements occur already at 140 °C–150 °C, the structure of the final products being determined under these conditions by the nature of the solvents employed. The maximum selectivity in the formation of compounds **35** (yield 17%) and **38** (yield 81%) is observed in solution in Khladon 113 [Freon 113].[58] In solvents of the π-donor type (benzene, *p*-xylene),



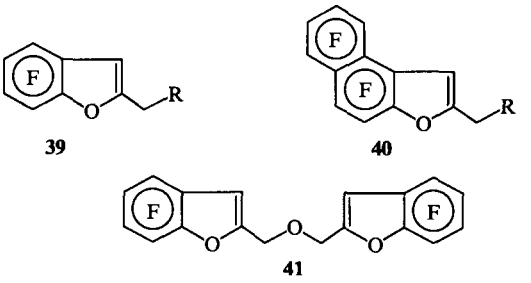
33 36

370 °C 360 °C

34 37

35 38

the products of the incorporation of the solvents into the molecules of the annelated furans **39** and **40** are formed together with compounds **35** and **38**.[56] In addition an appreciable amount (11%–18%) of the ether **41** is formed from the ether **33** in Khladon 113 and benzene.[58, 59]



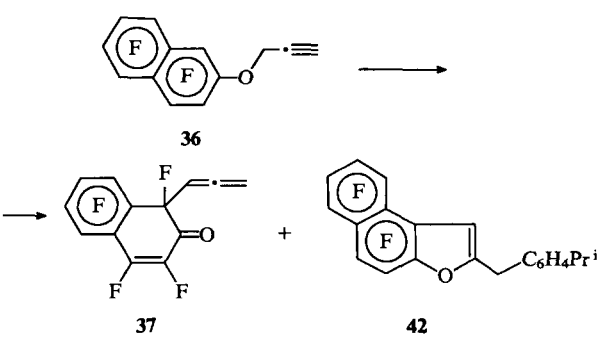
39 40

41

For **39**: R = Ph (28%), 2,5-$Me_2C_6H_3$ (21%);
For **40**: R = Ph (64%), 2,5-$Me_2C_6H_3$ (73%).

When the ether **33** is isomerised in *N*,*N*-diethylaniline (153 °C, 134 h), the latter solvent is also incorporated into the structure of the final furan, but numerous products of side reactions of the initial compound are mainly formed in the given reaction.[60] On the other hand, the rearrangement of the fluorine-free phenyl propargyl ether in boiling *N*,*N*-diethylaniline proceeds relatively smoothly and affords 2*H*-1-benzopyran (yield 2%) as the main product, formed on cyclisation of the intermediate products of the *ortho*-rearrangement.[6]

Interesting results have been obtained in the study of the rearrangement of the ether **36** in isopropylbenzene (155 °C, 24 h),[59] where the naphthalenone **37**, which is a stable compound, was isolated in 10% yield together with the naphthofuran **42**.



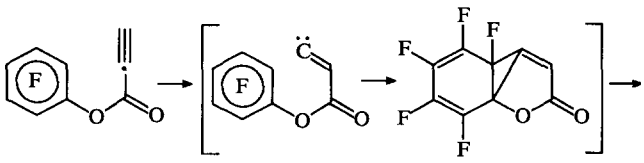
36

37 42

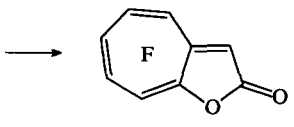
The appearance of the naphthalenone among the reaction products indicates that the [3,3]-sigmatropic shift is of the usual type in perfluoroaryl propargyl ethers and is accompanied by the inversion of the propargyl group and the acetylene–allene rearrangement. At the same time, the stability of compound **37** suggests that compound **35** and **38–42** would not necessarily be formed solely from the products of the *ortho*-rearrangement of compounds **34** and **37**.[56] Their synthesis is probably ensured also by another pathway — directly from the type **A*** transition state of the reaction. This mode of reaction is associated with the thermodynamically favourable homolytic cleavage of the C–F aromatic bond and a subsequent [1,4]-fluorotropic shift. At any rate, the involvement of arene solvents of the π-donor type (and apparently of traces of moisture) in the formation of the furans **39–42** can be explained solely by a free-radical mechanism of the reactions.

Pentafluorophenyl ethers containing fragments related to the allyl propargyl groups are also capable of undergoing rearrangements, being converted into exotic products under these conditions.

Under the conditions of vacuum pyrolysis (640 °C, 0.01 Torr), pentafluorophenyl propiolate **43** is transformed into 4,5,6,7,8-pentafluoro-2*H*-cycloheptatrieno[*b*]furan-2-one **46**.[61a] The formation of compound **46** is attributed[61a] not to [3,3]-sigmatropic shift[61b] but to the thermal acetylene–methylenecarbene rearrangement[61c] leading to the generation of the carbene **44** in the first stage. The subsequent intramolecular conversion of the pentafluorophenyl group into a cyclopropane derivative and rearrangement of the intermediate oxatricyclodecanone **45** with ring expansion afford the furanone **46** in 8% yield.



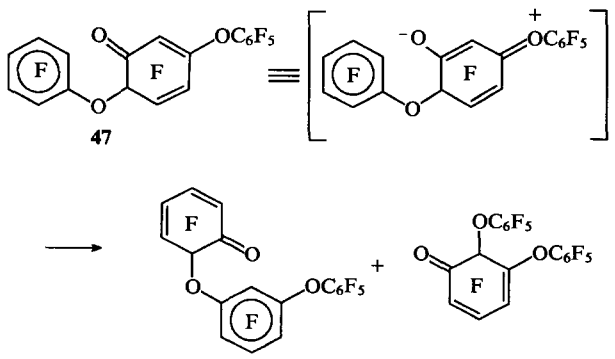
43 **44** **45**



46

When phenyl propiolate is used as the initial compound in this reaction, the yield of the corresponding furanone reaches 45%.[61b]

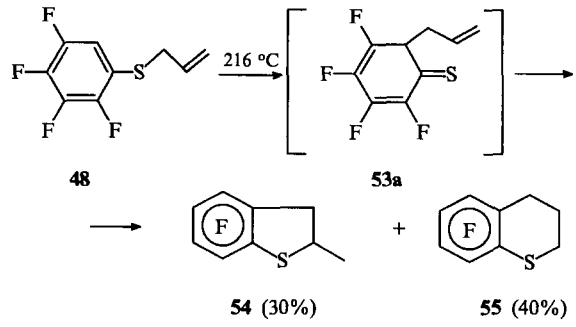
It is believed[62] that the O–O′ migration of the C_6F_5 group in the molecule of perfluoro-3,6-diphenoxycyclohexa-2,4-dien-1-one **47** takes place via a mechanism involving the [3,3]-sigmatropic rearrangement under exceptionally mild conditions (CCl_4, 50 °C, 3.5 h). The authors suggest[62] that this reaction is favoured by the appreciable charge separation in the initial compound **47** with the localisation of the excess electron density on the carbonyl oxygen.



47

The Claisen thio-rearrangement has been investigated by Brooke and coworkers[49, 63] in relation to allyl 2,3,4,5-tetrafluoro-phenyl sulfide **48**, allyl 2,3,5,6-tetrafluorophenyl sulfide **49**, allyl pentafluorophenyl sulfide **50**, pentafluorophenyl propargyl sulfide **51**, and heptafluoro-2-naphthyl propargyl sulfide **52**.[64]

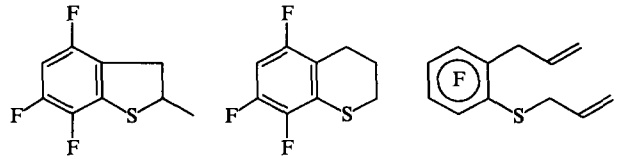
The rearrangement of the sulfide **48** proceeds smoothly in boiling *N*,*N*-diethylaniline with the intermediate formation of the 2,4-diene-1-thione **53a**, which cyclises, after a [1,3]-prototropic shift, to the dihydrobenzothiophene **54** and the dihydrobenzothiopyran **55**.[63]



48 **53a**

54 (30%) **55** (40%)

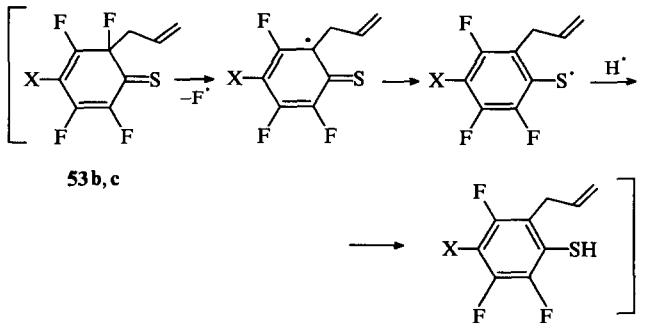
The thiophene **56** and the thiopyran **57** were obtained under the same conditions from the sulfide **49** in 5% and 12% respectively. The reaction of sulfide **50** in *N*, *N*-diethylaniline, which led to the isolation of compounds **54** and **55** in an overall yield of 7% and of the sulfide **58** (yield 8%) is just as ambiguous.[63]



56 **57** **58**

Furthermore, the rearrangements of the sulfides **49** and **50** result in the formation of appreciable amounts of ethyl polyfluorophenyl sulfides, which indicates the dominant role of *N*,*N*-diethylaniline in the side reactions.

In contrast to the thione **53a**, the *ortho*-rearrangement products **53b** and **53c**, formed initially from the sulfides **49** and **50** respectively, undergo subsequently reductive defluorination. The homolysis of the aliphatic C–F bond is favoured by the biradical nature of the thiocarbonyl group in compounds **53b** and **53c** and by the presence of a highly electron-donating solvent in the reaction sphere.[63]

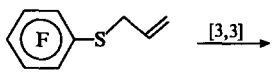


53b,c

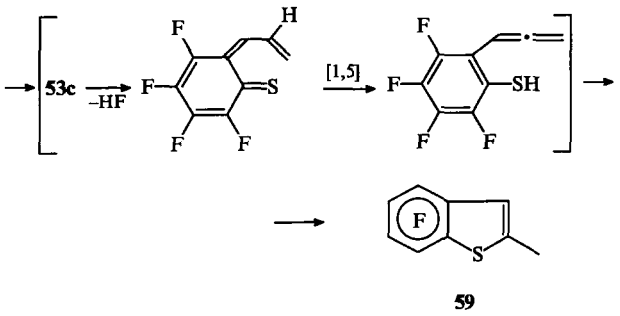
X = H (b), F (c).

On heat treatment of the sulfide **50** in the KF-sulfolan system (nickel flask, 192 °C, 22 h), the reaction proceeds via a different pathway.[49] In this case, only 4,5,6,7-tetrafluoro-2-methylbenzo-[*b*]thiophene **59** was isolated in 9% yield from a complex mixture of final products. According to Brooke,[49] the intermediate **53c** is

initially dehydrofluorinated, the process being accompanied by the [1,5]-migration of the vinyl hydrogen atom to the terminal heteroatom.

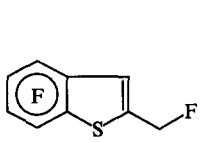


50

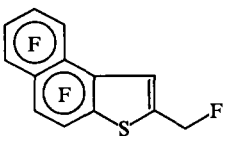


59

The rearrangements of the perfluoroaryl propargyl sulfides **51** and **52** in Khladon 113 at 160–180 °C lead to the thiophene **60** and **61** in 13% and 14% yields respectively.[64] Evidently, as in the case of perfluoroaryl propargyl ethers, these reactions are accompanied by a [1,4]-fluorotropic shift.



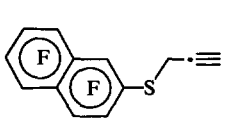
60



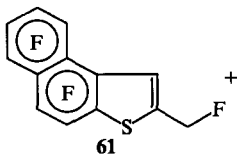
61

In the gas phase at 360 °C, the yield of the thiophene **61** reaches 81%.

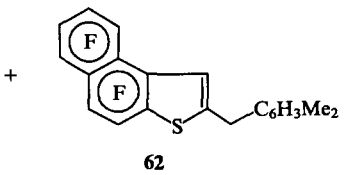
The thermal reactions of the sulfide **52** in *p*-xylene make it possible to obtain either mainly the thiophene **61** (nickel flask, yield 61%) or exclusively the product **62** of incorporation of *p*-xylene (glass bulb, yield up to 85%), depending on the material of the reactor.[64]



52



61



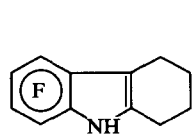
62

The mode of the rearrangement of the sulfide **52** probably depends on the ability of the reactor wall to sorb fluorine atoms, which determines the probability of the involvement of the arene in the transformation of the reaction intermediate.

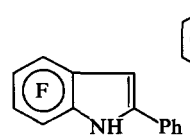
The Cope 3,4-diaza-rearrangement, which is a key stage in the Fischer synthesis of indoles,[17] has been investigated in relation to 2,3,4,5-tetrafluorophenyl-, pentafluorophenyl-, and heptafluoro-2-naphthylhydrazones.[65–67]

On refluxing in concentrated hydrochloric acid, cyclohexanone tetrafluorophenylhydrazone is converted smoothly into 5,6,7,8-tetrafluoro-1,2,3,4-tetrahydrocarbazole **63** (yield 50%), while acetophenone tetrafluorophenylhydrazone in converted on heating (215 °C) with $ZnCl_2$ into tetrafluoro-2-phenylindole **64** in 15% yield.[65]

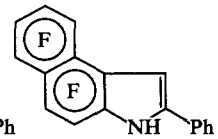
The indole **64** is the main product (yield 12%) also on refluxing acetophenone pentafluorophenylhydrazone in tetralin (208 °C) in the absence of any catalyst or condensing agents.[66] The non-catalysed thermolysis of acetophenone heptafluoro-2-naphthylhydrazone is more effective under the same conditions: the product of this reaction — hexafluoro-2-phenylbenzo[*e*]indole **65** — was isolated in 37% yield.[66] The corresponding fluorinated indoles were obtained by a similar procedure from the pentafluorophenyl- and heptafluoro-2-naphthyl-hydrazones of various aldehydes and ketones.[67] It has been noted[67] that the presence of a fluorine atom in the *ortho*-position relative to the nitrogen atom in the initial hydrazones accelerates their conversion into products of the Fischer reaction. The formation of polyfluoroindoles is apparently formally associated under these conditions with the reductive defluorination of the primary products of the *ortho*-rearrangement.



63

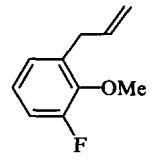


64

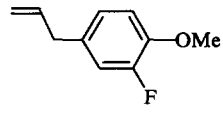


65

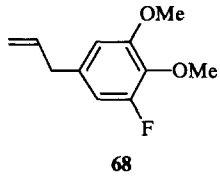
The [3,3]-sigmatropic rearrangements of the partly fluorinated allyl aryl ethers have been less investigated. It has been shown[68a] that allyl 2-fluorophenyl ether is converted in *N*-methylpyrrolidinone (195 °C, 3.5 h) preferentially into the *ortho*-rearrangement product **66** with an admixture of the *para*-rearrangement product **67**. On the other hand, heat treatment of allyl 2-fluoro-6-methoxyphenyl ether does not lead to its isomerisation, but in the presence of Lewis acids as the catalysts a mixture of the *para*-isomer **68** and the *meta*-isomer **69** is formed from this ether even at −20 °C, the latter compound being an unusual product of the Claisen rearrangement.[68b] All the compounds obtained in the above studies[68a, 68b] were isolated in the form of the corresponding methyl ethers.



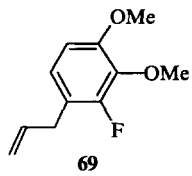
66



67



68

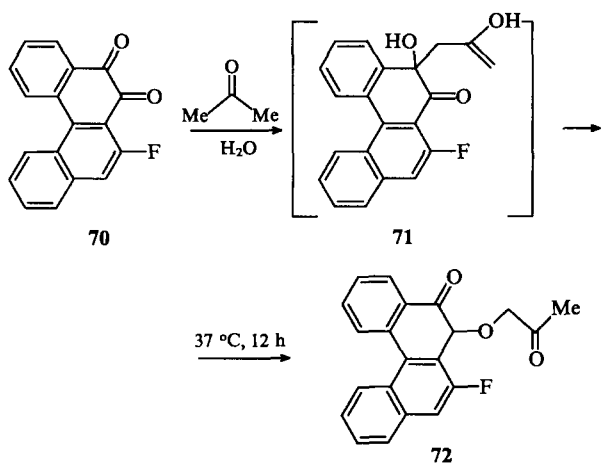


69

The rearrangement of 3-fluoro-substituted aryl penta-2′,4′-dienyl ethers takes place just as readily in the presence of $AlCl_3$ etherate.[69]

Interestingly, the presence of Lewis acids (which lower the reaction temperatures and accelerate not only the Claisen rearrangement[68b, 69] but also the Claisen retro-rearrangement[13]) is not required for the Claisen retro-rearrangement of the monofluroro-derivative of a quinone.[70] The aldol condensation of 7-fluoro-benzo[*c*]phenanthrene-5,6-quinone **70** with an excess of water-containing acetone leads to the primary formation of two regioisomeric intermediates **71** of the aldol type (one regioisomer is illustrated). The intermediate aldols **71** undergo the spontaneous

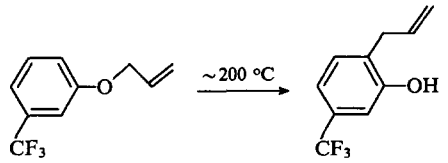
Claisen retro-rearrangement with formation of acetylmethyl ethers **72** (one regioisomer is shown).[70]



70 **71** **72**

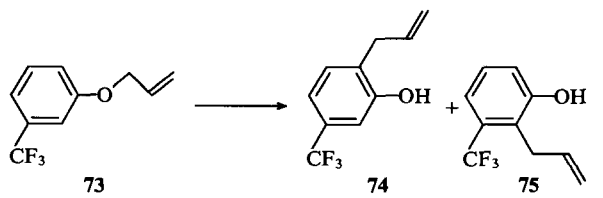
The interaction of the 7-fluoroquinone **70** with acetophenone in solution in $MeCN/H_2O$, reaching completion in the stage involving the formation of the corresponding aldol which is incapable of undergoing the Claisen retro-rearrangement, constitutes an indirect confirmation of the reaction mechanism proposed by the authors.[70]

The influence of the trifluoromethyl group in the *meta*-position relative to the allyl group in allyl phenyl and methylallyl phenyl ethers on the rate and conditions of the Claisen rearrangement has been investigated. On refluxing (without a solvent) under a CO_2 atmosphere, methylallyl 3-trifluoromethylphenyl ether does not rearrange, while allyl 3-trifluoromethylphenyl ether **73** gives rise to the *ortho*-rearrangement product **74** at a rate lower by a factor of 15 than the fluorine-free analogue.[71]



73 **74**

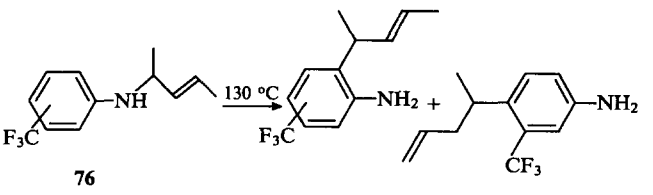
In dimethylformamide at 220 °C, the difference between the rates of rearrangement of the ether **73** and of its non-fluorinated analogue is abolished and, together with the phenol **74**, an equal amount of its regioisomer **75** is formed in an overall yield of the rearrangement products of 81%.[72a]



73 **74** **75**

A mixture of the same composition was obtained when the above reaction was catalysed by boron trichloride and under the conditions of an electric discharge, the induction of which increases, according to the authors' calculations,[73] the rate of the [3,3]-sigmatropic shift by tens of orders of magnitude.

The CF_3 group exerts a greater influence, compared with the rearrangement of the ether **73**, on the rate of the Claisen amino-rearrangement. Thus, in solution in nitrobenzene, the hydrochlorides of *N*-alkenyl-3(4)-trifluoromethyl-anilines **76** rearrange 100 times more slowly than the hydrochloride of *N*-(1-methyl-but-2-enyl)aniline.[74]



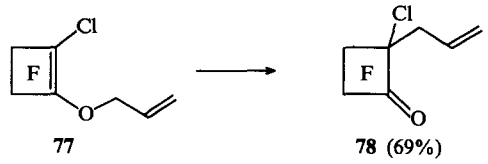
76

Thus the CF_3 group lowers the rate of isomerisation of compounds **73** and **76** similarly to other electron-accepting substituent in the *meta*-position[72a] or the *para*-position[72b] in the aromatic ring and has a negative influence on the rate of the Claisen rearrangement and on the conversion of the initial allyl aryl ethers (up to their decomposition).

III. Rearrangements of polyfluorocycloalkenyl ethers

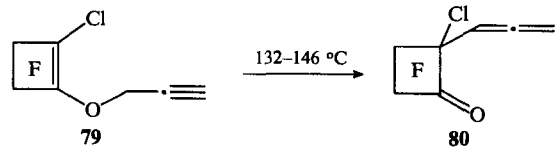
The [3,3]-sigmatropic rearrangements of compounds of this class have been investigated in relation to derivatives of polyfluorinated cyclobut-1-enols, cyclopent-1-enols, and cyclohex-1-enols as well as five-membered heterocycles with one or two heteroatoms. The sigmatropic shift in these systems takes place much more readily (at 25–150 °C) than in the case of allyl(propargyl) polyfluoroaryl ethers. The ring size, the effects of the substituents at the C(1) atom of the 'vinyl' fragment, the nature of the 'allyl' fragment of the molecule, and probably the degree of aromaticity of the ring in the initial compounds have a decisive influence on the conditions and rate of the rearrangement.

In the series of ally(propargyl) cycloalkenyl ethers, the polyfluorocyclobutenyl ethers enter into the Claisen rearrangement with the greatest difficulty. Thus allyl 2-chlorotetrafluorocyclobut-1-enyl ether **77**[75] is converted at an appreciable rate into chlorotetrafluorocyclobutanone **78** only at 120–130 °C.[36] The reaction is completed in 8 h.



77 **78** (69%)

The propargyl ether **79** isomerises with much greater difficulty. Under these conditions, the [3,3]-sigmatropic shift is accompanied by the acetylene–allene rearrangement and the formation of the cyclobutanone **80** in 55% yield.[36]



79 **80**

The presence of the fluorine atom and other electron-donating substituents at the C(1) atom apparently hardly lowers the thermodynamic stability of allyl polyfluorocyclobutenyl ethers. Thus allyl perfluorocyclobutenyl ether **81** and the 2X-substituted ether **82** synthesised from it distil without change at a reduced pressure and temperature up to 75 °C.[76]



81 **82**

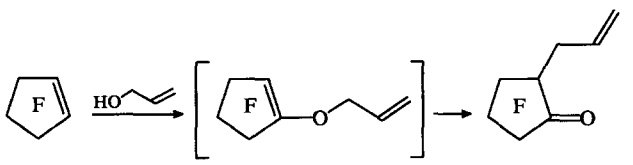
X = H, OMe, NEt_2 .

Ring expansion leads to appreciably milder conditions and acceleration of the Claisen rearrangement. Allyl 2-chlorohexafluorocyclopent-1-enyl ether **83** isomerises smoothly to the cyclopentanone **84** even at 95 °C.[77]



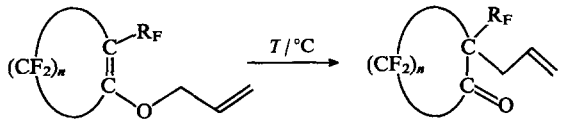
83 **84**

Allyl perfluorocyclopentenyl ether **86**, formed in the reaction of perfluorocyclopentene **85** with allyl alcohol in the presence of KOH, probably rearranges under similar conditions. After the reaction mass had been heated for a short time up to 106 °C, only the product of the rearrangement of the ether **86**—2-allylperfluorocyclopentanone **87**—was isolated from it.[36]



85 **86** **87** (35%)

The influence of ring size and of the perfluoroalkyl groups at the C(1) atom on the conditions and rate of the rearrangement of allyl ethers **88** has also been investigated.[78, 79] An appreciable increase in the rate and a decrease in the temperature of the reaction in parallel with a decrease in ring strain were noted. The yield of 2-allylperfluorocycloalkanones **89** is 90%–94%.[78, 79] The bulky perfluoroethyl group hinders the [3,3]-sigmatropic shift. The equal half-reaction times ($\tau_{1/2}$ = 1.0–1.5 h at 100 °C) for the cyclopentenyl ether **88b** and the cyclohexenyl ether **88c** have been attributed to the inhibiting effect of the C_2F_5 group, which compensates for the increase in the rate of the rearrangement on passing from the five-membered to the six-membered ring.[78, 79]

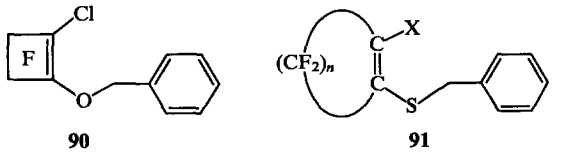


88 **89**

Compound	n	R_F	T/°C
a	2	C_2F_5	130
b	3	CF_3	100
c	4	C_2F_5	100

It is noteworthy that benzyl ethers (sulfides) derived from polyfluorocycloenols do not enter into the Claisen rearrangement, in contrast to allyl ethers. All the attempts to subject the rearrangement of the benzyl ether **90** to radical or anionic catalysis, including those under photolytic conditions, were unsuccessful.[36]

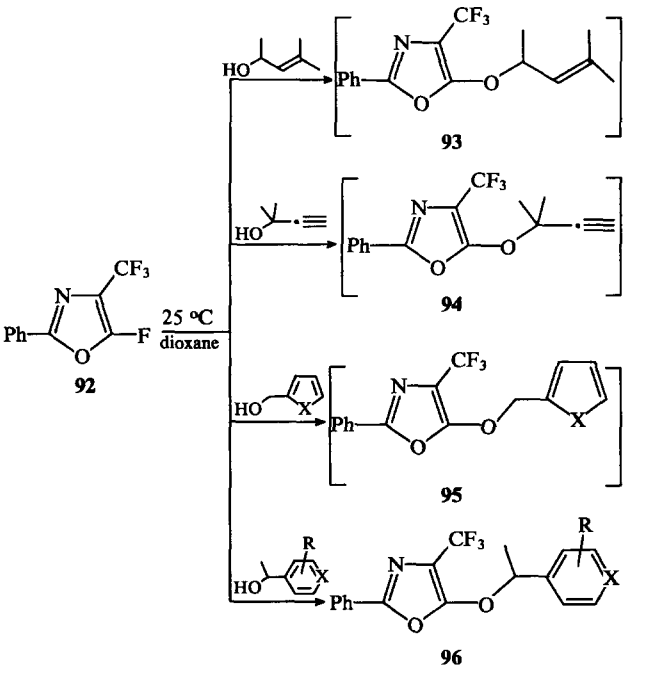
Benzyl polyfluorocycloalkenyl sulfides **91**, formed in the reactions of the corresponding cycloalkenes with toluene-α-thiol in the presence of triethyl-amine, are evidently just as stable.[80]



90 **91**

n = 2, X = F; n = 3, X = CF_3; n = 4, X = Cl.

Unexpected results were obtained by Burger and coworkers[81–86] in the study of the reactions of polyfluoroheterocycloallenes with 2,3-unsaturated alcohols. 5-Fluoro-2-phenyl-4-trifluoromethyl-1,3-oxazole **92**,[87] reacting exothermically in the presence of KOH with allyl type alcohols which involves the primary formation of the ethers **93**–**96**, proved to be a convenient model for the study of certain characteristics of the low-temperature [3,3]-sigmatropic rearrangement observed in these reactions and for the development of new approaches to the synthesis of trifluoromethyl substituted α-aminoacids.[81, 82, 84, 85]

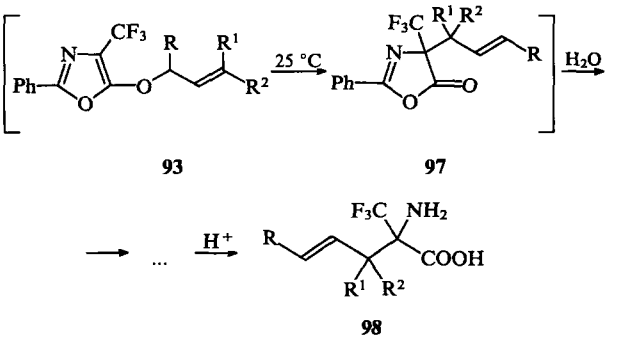


92 **93** **94** **95** **96**

5-Allyloxy-1,3-oxazoles, which do not have pronounced aromatic properties, are known[88] to enter more readily than allyl aryl ethers into the [3,3]-sigmatropic reaction (the oxazole–oxazolone rearrangement or the Steglich–Claisen rearrangement). The allyl group then migrate initially to the 4-position in the ring and then to the 2-position.

In contrast to the non-fluorinated analogues, 4-trifluoromethyl-1,3-oxazoles **93**–**95** undergo the spontaneous Steglich–Claisen rearrangement under the conditions of their synthesis even at 25 °C. The rearrangement is completed by the shift of the 'allyl' fragment of the molecule only to the 4-position.

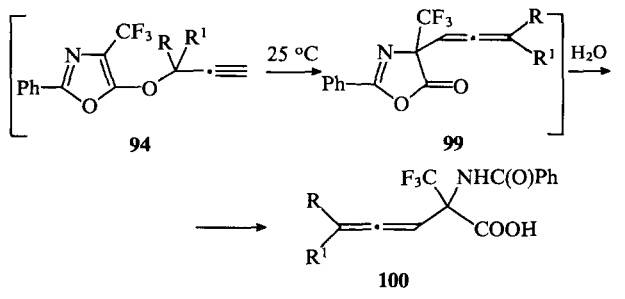
The conditions in the rearrangement of the allyl ethers **93** are almost independent of the numbers of substituents in the allyl group. The oxazolones **97** formed as a result of the rearrangement are hydrolysed without isolation (the reaction was followed by ^{19}F NMR spectroscopy) to give a satisfactory yield (up to 78%) of 2-alkenyl-3,3,3-trifluoroalanines **98**.[81]



93 **97** **98**

R, R^1, R^2 = H, Me, Et, Pr^n.

The propargyl ethers **94** isomerise just as smoothly to the oxazolones **99**, the hydrolysis of which leads to derivatives of 2-alkadienyl-3,3,3-trifluoroalanines **100** in yields up to 64%.[81]

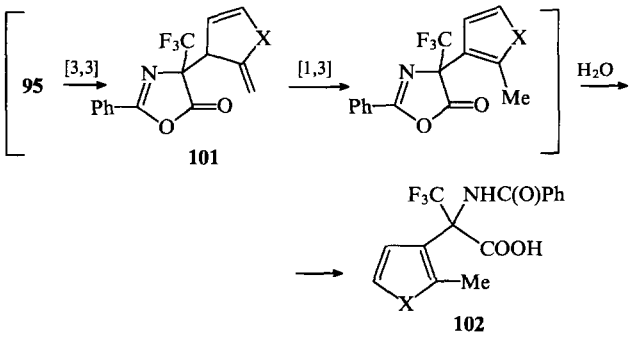


94 **99** **100**

R, R^1 = H, Me, Et.

The [3,3]-sigmatropic rearrangements of the furfuryl and thienyl ethers **95** are accompanied by a [1,3]-prototropic shift.[84]

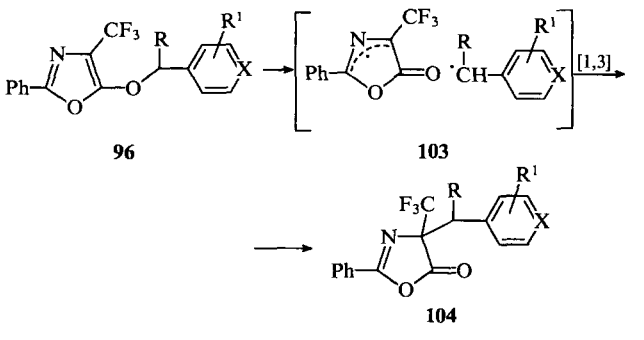
The high reactivity of the *exo*-methylene intermediates **101** is apparently the reason for the low-yield of the final products **102a** (47%) and **102b** (30%).



101 **102**

X = O(**a**), S(**b**).

The rearrangement of the benzyl ethers **96**, which is a key stage in a new method of synthesis of fluorine-containing derivatives of phenylalanine developed by Burger and coworkers,[82-85] constitutes a special case. In contrast to the oxazoles **93-95**, the benzyl derivatives **96** can be isolated in a free state although some of them are extremely thermolabile and isomerise to the corresponding oxazolones **104** at room temperature even in the crystalline state.[83, 84]

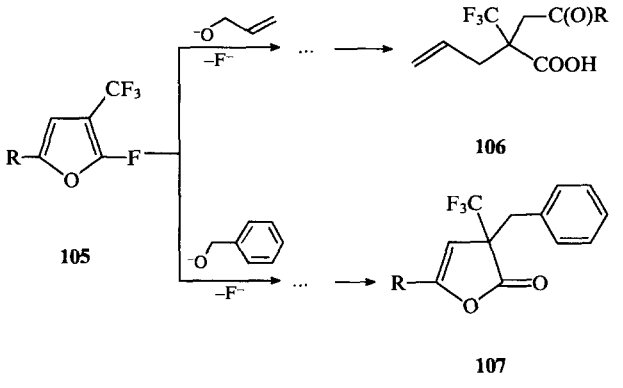


96 **103** **104**

X = CR^2, N; R = H, Me, COOH;
R^1 = H, OMe; R^2 = H, F, Cl, Br, NO_2, OMe, Ph.

The temperature range of this reaction is fairly wide (25 °C–120 °C). However, its main feature consists in the fact that, according to the authors,[84] it is not a concerted [3,3]-sigmatropic process and takes place as a result of the [1,3]-shift of the benzyl group, formed on thermal dissociation of the ethers **96** into the radical pair **103**. This mode of reaction has been demonstrated by the isolation of the mixed products in 'cross-experiments'.[84] The absence of the inversion of the benzyl fragment is also evidence in support of this mechanism.

The slight enhancement of the aromatic properties of the 'vinyl' component on replacement of the fluorine-containing oxazole fragment by the furan fragment apparently also exerts only a slight influence on the rearrangement conditions. The reactions of 2-fluoro-3-trifluoromethyl-5R-furans **105** with allyl and benzyl alcohols in the presence of HF acceptors leads either to the products of the low-temperature Claisen rearrangement (with subsequent ring opening), namely the ketoacids **106**, or to the products of the [1,3]-benzyl shift—the butenolides **107**.[86] The isolation of the intermediates in the nucleophilic substitution of the fluorine atom was not reported.

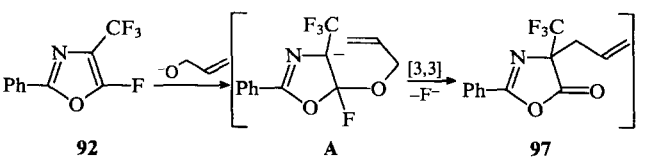


105 **106** **107**

One may postulate that the corresponding allyl and benzyl ethers obtained from 2-fluoro-3-trifluoromethylthiophene[86] can exhibit an increased thermal stability (which is characteristic of, for example, 5-benzyloxy- and 5-benzylthio-4-trifluoromethyl-1,3-thiazoles[87]) as a consequence of the much greater aromacity of the thiophene ring compared with the furan ring.

The [3,3]-sigmatropic rearrangements of derivatives of polyfluorinated cycloenols and heterocycloenols examined above made it possible to synthesise previously unavailable organofluorine compounds such as polyfluorocycloalkenones containing the allyl and 1,2-dienyl groups and CF_3-containing carboxylic 4-ketoacids, butenolides, and oxazolones. The last compounds proved to be promising precursors of a wide variety of trifluoromethylated α-aminoacids[81, 82, 84] (including derivatives of aspartic acid[89]), which were used in their turn for the modification of biologically active peptides.[85, 90]

The instances of the low-temperature Steglich–Claisen rearrangement in the reactions of the oxazole **92** with 2,3-unsaturated alcohols are of special theoretical interest. In our view, the spontaneous transformations of the intermediates are caused, in the first place, by the synchronous influence of the electron-accepting CF_3 group in the C(1) position and the electron-donating substituents (fluorine and oxygen) at the C(2) atom on the kinetic lability of the multiple bond of the oxazole **92**, as a result of which these reactions apparently occur via a carbanionic mechanism. The concerted effects of the substituents in the molecule of the oxazole **92** at the instant of attack by the alkoxide ion favour the stabilisation of the carbanionic intermediate A and the subsequent [3,3]-sigmatropic shift coupled with the elimination of the fluoride ion.



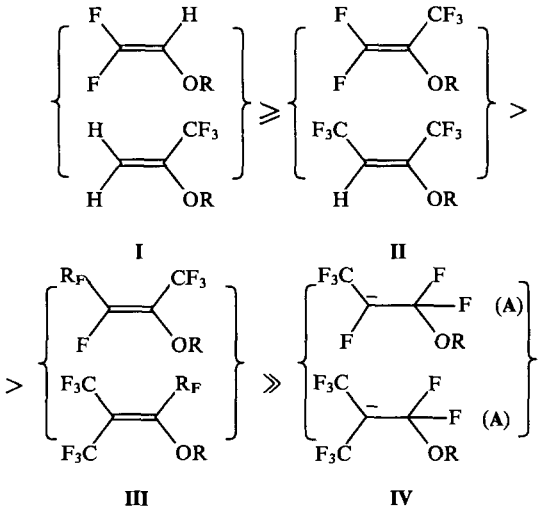
92 **A** **97**

IV. Rearrangements of polyfluorovinyl ethers

The allyl and propargyl ethers of acyclic polyfluoroenols enter into the Claisen rearrangement even more readily than the derivatives of polyfluorocycloenols, because in this case the fluorine atoms and the fluorine-containing substituents exert the maximum influence on the properties of the vinyl fragment.

According to Dolbier's data,[41, 91a] the conjugation of the geminal fluorine atoms with the sp^3 orbitals of carbon is thermodynamically more favourable (almost to the extent of 5 kcal mol^{-1}) than the conjugation with the sp^2 orbitals, which gives rise to, for example, the mild conditions in the rearrangement of allyl difluorovinyl ethers.[92] On the other hand, the trifluoromethyl group, which increases the thermodynamic stability of unsaturated compounds, the same time increases greatly the kinetic lability of the unsaturated bond.[91b] The combination of the effects of these substituents, which depends on their number and positions, leads to a sharp differentiation of polyfluorovinyl ethers (PFVE) in terms of their tendency to undergo the [3,3]-sigmatropic shift, which is manifested most clearly under the conditions of the rearrangement of these compounds.

In conformity with this finding, the PFVE can be divided into four groups (I–IV) in order of decreasing temperature and apparently in order of increasing rate of rearrangement of the compounds. The first two groups (I and II) contain relatively stable CFVE, which isomerise as a rule at 50–100 °C.



I II

III IV

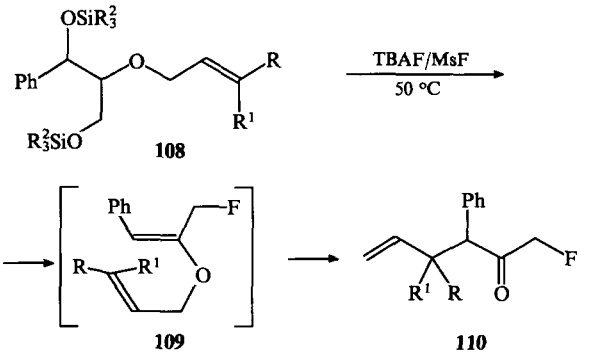
R_F = CF_3, C_2F_5; R = CH_2CH = CH_2.

As the CF_3 groups accumulate in the C(1) position, the rearrangement temperature falls to 20–40 °C (group III), whilst, following the appearance in the PFVE of the capacity to stabilise carbanionic states, the changes in the rate under the conditions of the reactions become dramatic: the fluorocarbanions A (group IV) undergo a spontaneous rearrangement in the instant of generation even on strong cooling.

1. Rearrangements of stable polyfluorovinyl ethers

The synthesis of stable PFVE has been determined only in recent years and for this reason there are few examples of rearrangements of compounds of this kind. The monofluoro- and difluoro-substituted vinyl ethers, capable of undergoing the Claisen rearrangement with formation of α-fluoroketones, are usually obtained by three methods.

In the first method, developed by Japanese workers[93, 94] and called 'fluoroolefin formation', the starting materials employed are alkyl allyl ethers, the alkyl fragment of which contains two readily removable groups (for example, trimethylsiloxy- or methanesulfonyloxy-groups), one of which is exchanged for fluorine. Thus treatment of alkenyl 2-phenyl-2,2'-bis(trimethylsiloxy)isopropyl ethers **108** with a mixture of tetrabutylammonium fluoride (TBAF) and methanesulfonyl fluoride (MsF) in tetrahydrofuran (THF) leads regiospecifically to alkenyl 1-fluoromethyl-2-phenylvinyl ethers **109** which are either transformed *in situ* in the fluoroolefin formation process (THF), 50 °C, 12–36 h) or are converted into monofluoromethyl ketones **110** under more severe conditions (toluene, refluxing, 2 h).[93]

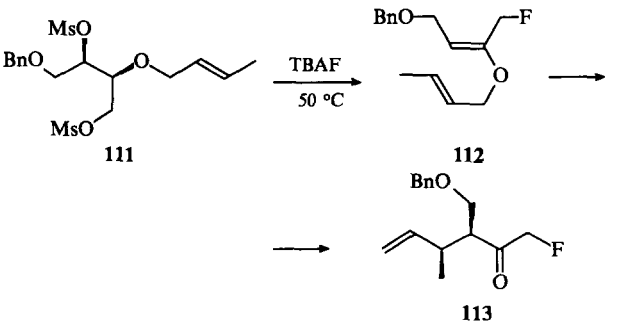


108 **109** **110**

R = R^1 = H (95%);
R = H, R^1 = Me (89%);
R = R^1 = Me (53%).

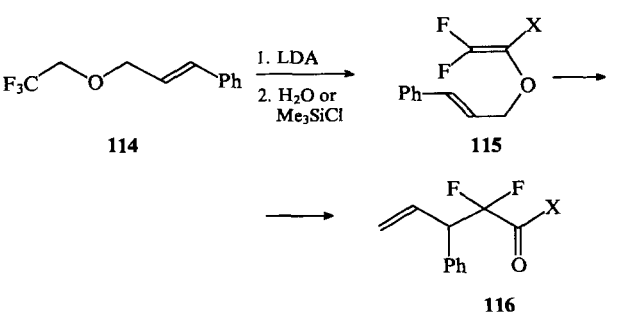
Benzyl 1-fluoromethyl-2-phenylvinyl ether synthesised in this way[93] proved to be a stable compound incapable of undergoing the Claisen rearrangement.

The monofluoromethyl ketone **113**, which is a key compound in the multistage stereospecific synthesis of (±)-fluorobotriodiplodin — a fluoride containing analogue of a natural micotoxin — was obtained by a procedure similar to that used for the ketones **110**.[94] The fluoroolefin formation reaction involving crotyl 2-2'-bis(methanesulfonyloxy)isobutyl ether **111** affords crotyl 1-fluoromethylvinyl ether **112** in 70% yield. Compound **112** rearranges in boiling xylene to compound **113** in 92% yield and with a high degree of stereoselectivity.



111 **112** **113**

The second method is based on the dehydrofluorination of allyl trifluoroethyl ethers, formed on alkenylation of 2,2,2-trifluoro-IR-ethanols.[92] For example, the trifluoroethyl ether **114**, synthesised by the reaction of sodium trifluoroethoxide with cinnamyl chloride, is readily (THF, −70 °C) dehydrofluorinated

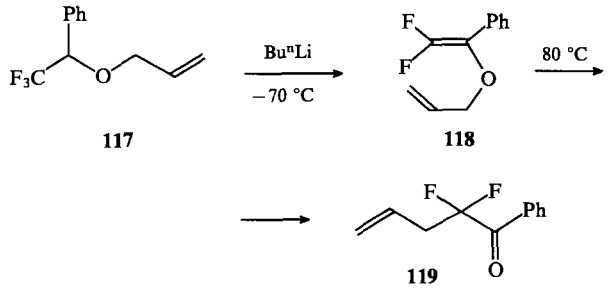


114 **115** **116**

X = H (**a**), AR (**b**).

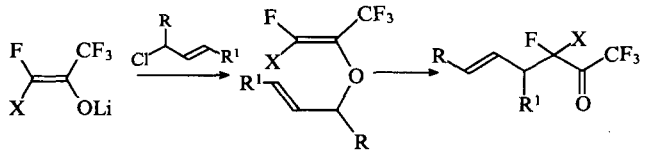
by lithium diisopropylamide (LDA). The resulting cinnamyl 2,2-di-fluorovinyl ethers **115** fully isomerise to the 2,2-difluoro-substituted aldehyde **116a** or the ketone **116b** on refluxing in CCl_4 (80 °C, 1 h).[92] It is remarkable that the cinnamyl vinyl ether rearranges only at 200 °C.[95]

Butyllithium is also a convenient dehydrofluorinating agent in these reactions. Treatment of allyl 1-phenyltrifluoroethyl ether **117** with this reagent affords the ether **118**, which is converted on subsequent heating into the difluoroketone **119** in 41% yield.[92]



117 **118** **119**

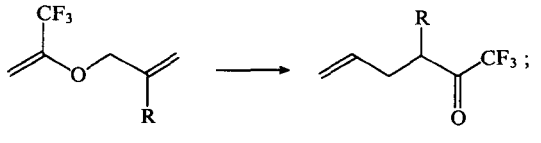
The third method of synthesis of stable PFVE is extremely promising and is applicable only in organofluorine synthesis. It consists in the *O*-alkenylation of the lithium salts of stable polyfluorophenols such as the enol of pentafluoroacetone and its analogues **120**. The alkenyl 2-fluoro-1-trifluoromethylvinyl ethers **121** obtained in this way undergo the Claisen rearrangement at 40–65 °C with formation of trifluoromethyl ketones **122**.[96]



120 **121** **122**

X = F, Bu, Ph .

Evidently the CF_3 group in the C(2) position does not prevent the [3,3]-sigmatropic shift. The influence of the trifluoromethyl group at the C(2) atom on the rate of the Claisen rearrangement has been studied in greater detail by Gajewski et al.[35] They established that allyl 1-trifluoromethylvinyl ether **123a** is converted into the trifluoromethyl ketone **124a** in cyclohexane (61–98.5 °C, $\tau_{1/2}$ = 7.5 h) 73 times faster than the non-fluorinated analogue in a similar reaction.



123 **124**

R = H(**a**), Ar(**b**).

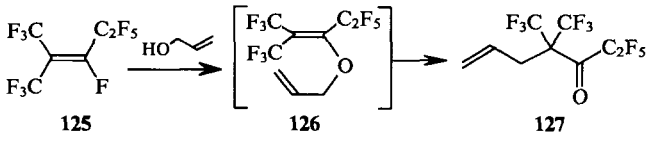
On the other hand, a similar effect is not observed in the Cope rearrangement of *cis*-2-trifluoromethylocta-1,5-diene. According to the authors,[35] the acceleration of the rearrangement of the ether **123a** is associated with the destabilisation of the ground state of the molecule under the influence of the CF_3 group and with the increase in the polarity of the transition state. Indeed the rate of the rearrangement of the ether **123a** in a polar solvent (DMSO, 80 °C, $\tau_{1/2} \simeq 2.4$ h) is higher almost by a factor of 3.[35]

For comparison, one may note that the methoxycarbonyl group in the C(2) position accelerates the Claisen rearrangement by a factor of 79,[97] while the CN group in the same position causes an acceleration by a factor of 111,[33] the gain in the free energy of activation for the C(2)-substituted substrate amounting to 2.0–2.5 kcal mol^{-1}.[35]

2. Rearrangements in the reactions of internal polyfluoroalkenes

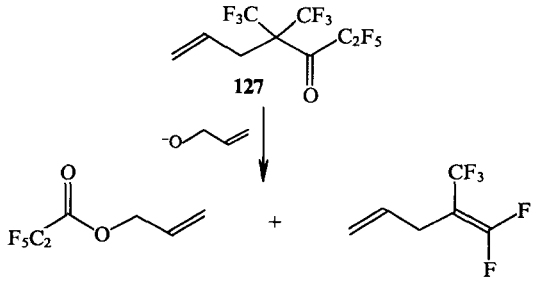
The interaction of 2,3-unsaturated alcohols with internal polyfluoroalkenes (PFA) and fluorinated alkynes and cumulenes leads to the ethers of poly(fluoroalkyl)enols, which isomerise more readily than monofluoro-, difluoro-, and monotrifluoromethyl-substituted vinyl ethers.

Thus the ether **126**, formed in a mixture with other products by the reaction of perfluoro-2-methylpent-2-ene **125** with allyl alcohol in the presence of NEt_3, rearranges to the ketone **127** already under the conditions of the synthesis (Et_2O, 20 °C, 2 h).[98]



125 **126** **127**

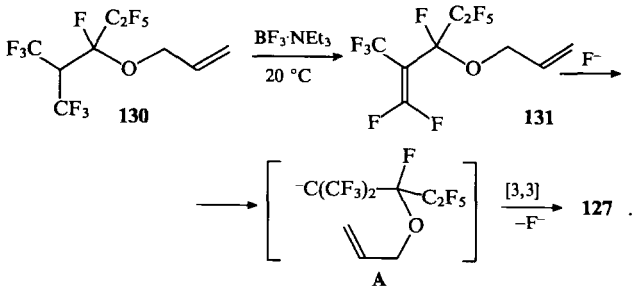
The half-conversion time for the ether **126** at 36 °C, established by ^{19}F NMR, is ~1 h. As the ketone **127** accumulates, it undergoes a partial 'haloform' cleavage under these conditions by the allylate anion to allyl perfluoropropionate **128** (yield 28%) and pentafluoropentadiene **129**.[98]



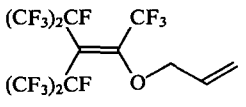
128 **129**

In a polar medium, the rate of conversion of the pentene **125** into the propionate **128** increases, so that, when the reaction of the pentene **125** with allyl alcohol is carried out in acetonitrile (NEt_3, 60 °C),[99] the propionate **128** is formed in 65% yield, while the ketone **127** is not isolated at all.

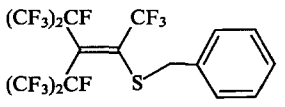
It is essential to emphasise that, under the conditions of the above study,[98] the rearrangement of the ether **126** takes place in the presence of fluoride ions, so that the smooth formation of the ketone **127** can be explained also by a carbanionic reaction mechanism. The latter probably operates in the reaction with the fluoride ion of the stable allyl pentafluoroalkenyl ether **130** — one of the products of the reaction of the pentene **125** with allyl alcohol.[98] However, one cannot rule out the possibility that the formation of the ketone **127** as a side product (yield 25%) in this reaction is altogether independent of the synthesis of the ether **131** and takes place in a reaction competing with the formation of the latter in the instant of the deprotonation of the initial adduct via the mechanism **130** → **A** → **127**.



The stability of tris(polyfluoroalkyl)vinyl ethers depends significantly on the steric effects of the fluoroalkyl groups and their position. For example, the allyl ether **132**[100] and the sulfide **133**,[101] substituted in the C(1) position by the bulky $(CF_3)_2CF$ groups, do not undergo the Claisen rearrangement.

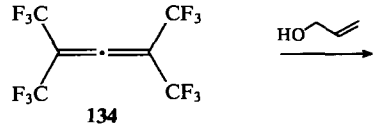


132

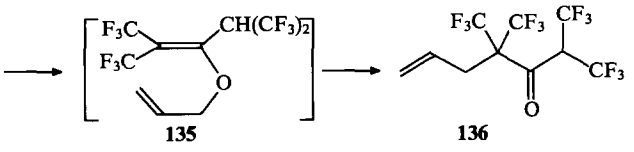


133

The steric effects of the substituents at the C(2) atom exert a much smaller influence on the tendency towards their rearrangement. Allyl 1-(α-*H*-hexafluoroisopropyl)-2,2-bis(trifluoromethyl)-vinyl ether **135**, obtained by the addition of allyl alcohol to tetrakis(trifluoromethyl)allene **134**, isomerises slowly to the ketone **136** even at 36 °C. At 65–72 °C, the ether **135** is fully converted after 1.5 h into the ketone **136**, the yield of which reaches 71%.[102]

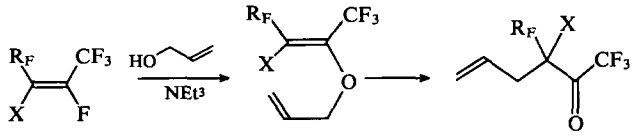


134



135 **136**

Vicinal bis(perfluoroalkyl)-substituted vinyl ethers proved to be, like the ethers **126** and **135**, thermodynamically unstable. The allyl ethers **138a** and **138b**, obtained from 2-chloroheptafluoro-but-2-ene **137a** and perfluoropent-2-ene **137b** can be isolated only by vacuum fractionation at 30–35 °C.[79] At 36 °C, they are slowly transformed into the ketones **139a** and **139b** with half conversion periods of 24 h (**a**) and 72 h (**b**).[79]

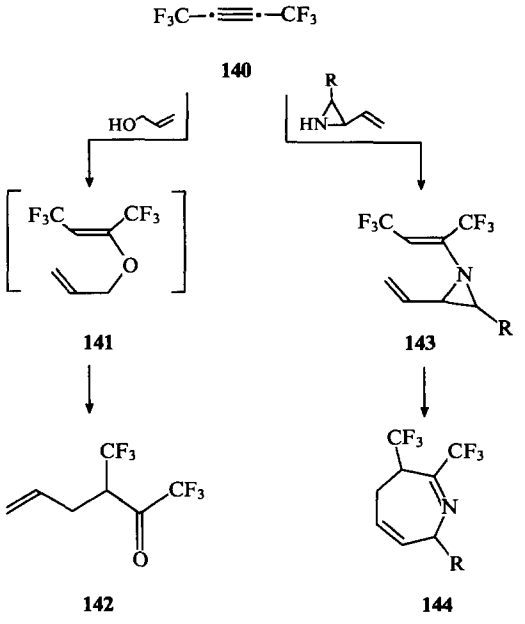


137 **138** **139**

$R_F = CF_3$, X = Cl(**a**) ;
$R_F = C_2F_5$, X = F(**b**) .

The mild conditions in the rearrangement of ethers **138** are appreciably influenced apparently by the halogen atom in the C(1) position, because allyl 1,2-bis(trifluoromethyl)vinyl ether **141**, formed in the reaction of perfluorobut-2-yne **140** with allyl alcohol (catalysed by NaOH), rearranges to the ketone **142** (yield 74%) on heating to 89 °C.[36]

The low-temperature Claisen amino-rearrangement is observed in the reaction of perfluorobutyne **140** with 2-vinyl-aziridines.[103] The adducts **143** isomerise at room temperature or on slight heating (50 °C) to CF_3-containing azepines **144**, which are rare products of the [3,3]-sigmatropic rearrangement, by virtue of the involvement of the aziridine ring in the latter.



140 **141** **142** **143** **144**

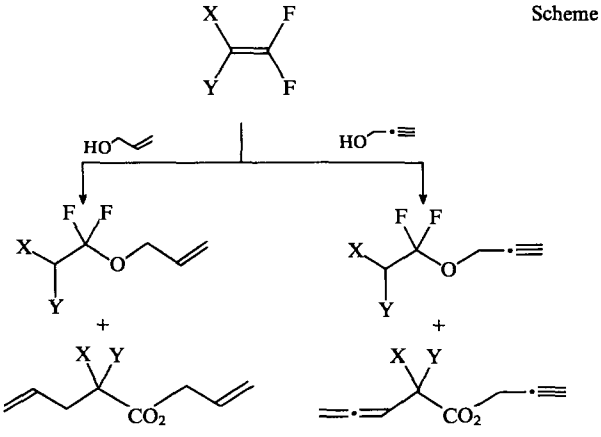
R = H, CH = CH_2.

3. Rearrangements in the reactions of terminal polyfluoroalkenes

The interaction of terminal PFA with unsaturated alcohols proceeds via intermediate fluorocarbanions and leads to either adducts of the initial reactants or to alkyl polyfluorovinyl ethers†.[104, 105a, 106] The latter pathway operates as a rule in the presence of favourable conditions for the transformation of the carbanionic intermediates via the elimination of the fluoride ion, for example, in the reactions of PFA with alkoxides in protophilic or aprotic solvents.

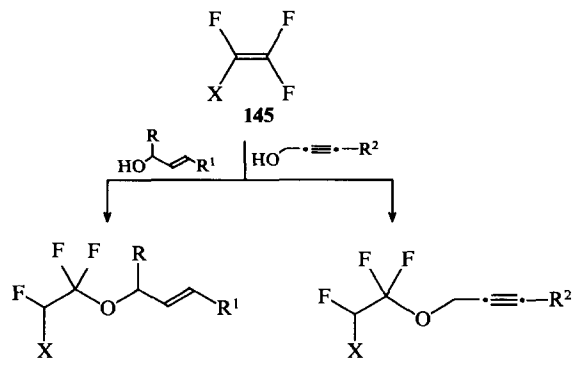
Accordingly, in the reactions of terminal PFA with 2,3-unsaturated alcohols one might have expected the generation in the first stage of the fluorocarbanions **A** (see p. 562, group IV) with the subsequent formation of allyl(propargyl) polyfluorovinyl ethers capable of undergoing the non-catalysed thermal Claisen rearrangement. However, in none of the reactions investigated was it possible to isolate the corresponding PFVE. The products of these reactions were found to be exclusively the adducts of the initial compounds and the rearrangement products — derivatives of fluorine-containing alk-4-ene(alka-3,4-diene)carboxylic acids (Scheme 1), the proportions of which depend on the structure of the PFA and the conditions of its interaction with the alcohol.

Scheme 1



† The products of the substitution of the allylic fluorine atom are sometimes formed.[104, 106]

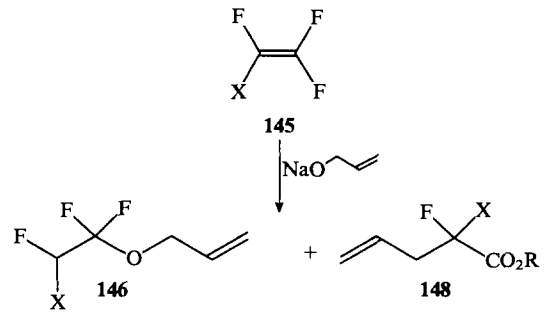
The tetrafluoroethylene **145a** and chlorotrifluoroethylene **145b** interact with allyl[107-112] and propargyl[113-116] alcohols‡ in the presence of KOH,[107, 108, 115, 116] catalytic amounts of metallic sodium,[110-113] or ion exchange resin[114] or at a low§ pressure[108] with formation of only adducts — allyl 2-*H*-polyfluoroethyl ether **146** and propargyl 2-*H*-polyfluoroethyl ether **147**.



145 **146** **147**

X = F(**a**), Cl(**b**); R = H, Me; R^1 = H, Me, Ph; R^2 = H, Cl, Br, I.

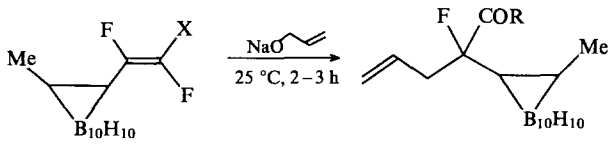
In the reactions of the polyflurorethylenes **145** with sodium allylate,[110, 117] which take place particularly readily (0 °C) in THF,[110] the products of the rearrangement — derivatives of 2-fluoropent-4-enoic acid **148** (yield 16%-34%) — were obtained together with the ethers **146** (yield 22%-25%).



145 **146** **148**

X = F(**a**), R = H; X = Cl(**b**), R = $CH_2CH=CH_2$.

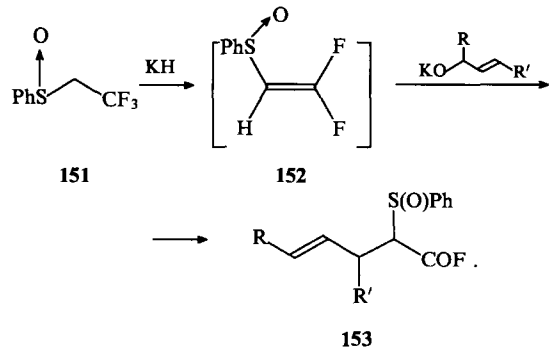
Fluoroethylenes with functional group-substituents interact unambiguously with allylates. Thus the reaction of 1-methyl-2-polyfluoroalkenyl-*o*-carbaboranes **149** with sodium allylate results in the formation of only the rearrangement products **150** in 40% (**a**) and 44% (**b**) yields.[118]



149 **150**

X = Cl, R = $OCH_2CH=CH_2$(**a**); X = R = CF_3 (**b**).

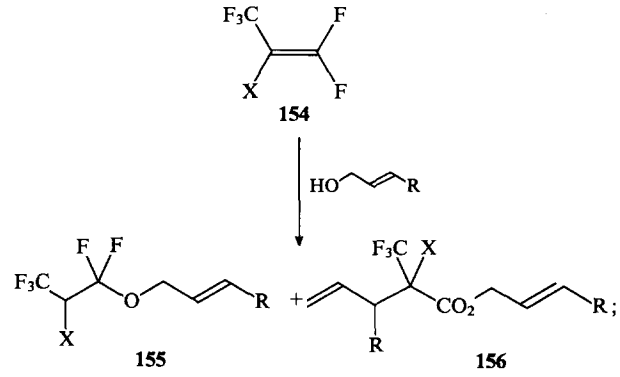
The reaction of allylates with *gem*-difluorovinyl phenyl sulfoxide **152**, generated *in situ* from trifluoroethyl phenyl sulfoxide **151** with the aid of potassium hydride, under mild



151 **152** **153**

conditions (THF, 0-5 °C, 0.5-2.0 h) also leads exclusively to the rearrangement products — the acid fluorides 153.[199]

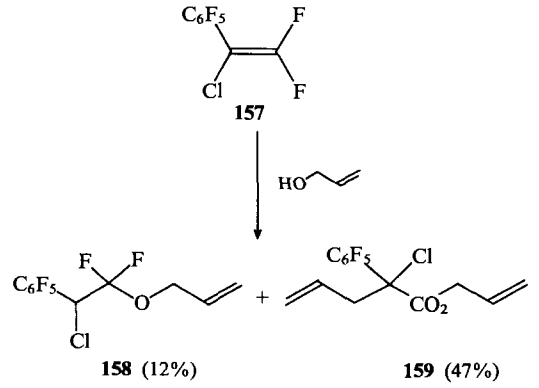
The terminal PFA **154**, which are more electrophilic than the perfluoroethylene **145a**, interact with 2,3-unsaturated alcohols to form a mixture of adducts and rearrangement products. In the reaction of hexafluoropropene **154a** with allyl alcohol (catalysed by KOH, 20-30 °C¶), allyl 2-fluoro-2-trifluoromethylpent-4-enoate **156a** was isolated in 5% yield together with allyl 2-*H*-hexafluoropropyl ether **155a**.[120]



154 **155** **156**

X = F, R = H(**a**); X = CF_3, R = H, Me(**b**), X = SMe, R = H(**c**).

α-Chloroperfluorostyrene **157** reacts under similar conditions (KOH, 20-45 °C, 0.5-1.0 h) with allyl alcohol to form preferentially the rearrangement product — allyl 2-chloro-2-pentafluorophenylpent-4-enoate **159**.[121] The adduct — allyl β-chloro-β-*H*-heptafluorophenylethyl ether **158** — is formed in an insignificant amount.



157 **158** (12%) **159** (47%)

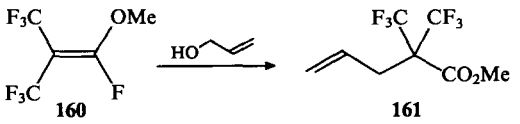
In the reaction of the perfluoroisobutene **154b** with allyl alcohol (0-50 °C)[36] even in the absence of bases, the yield of the rearrangement product — allyl 2,2-bis(trifluoromethyl)pent-4-

‡ The reaction of propargyl alcohols with *gem*-bromochlorodifluoroethylene, formed under the conditions of phase transfer catalysis from $CF_3CHBrCl$, has been investigated.[116]

§ The reaction of compound **145a** with allyl alcohol at a pressure of 500 atm affords a product of the cyclodimerisation of the initial

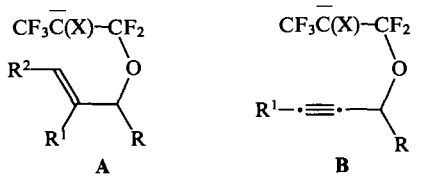
¶ In the absence of bases, the polyfluoroalkenes **154a** and **157** do not interact with allyl alcohol.

enoate **156b** (R = H)† — reaches 15%. 1-Methoxy heptafluoroisobutene **160** reacts with allyl alcohol just as smoothly in the presence of KOH, being converted into methyl 2,2-bis(trifluoromethyl)pent-4-enoate **161** in 39% yield.[36]



160 **161**

In the examples examined above, the yield of the rearrangement products is correlated with the ability of the internal PFA to generate stable fluorocarbanions‡, which are transformed into PFVE after the elimination of the fluoride ion. However, these intermediates could not be detected in the reaction medium by ^{19}F NMR even at −30 °C.[120] It was therefore natural to suppose[37, 120, 123] that the precursors of the rearrangement products in these reactions are the fluorocarbanions **A** or **B**, which at the instant of formation undergo, at a high rate, a spontaneous [3,3]-sigmatropic rearrangement coupled with the elimination of the fluoride ion.

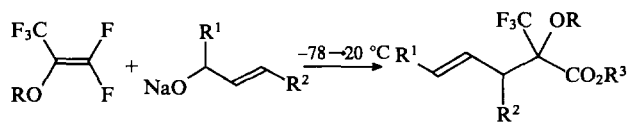


A **B**

The probability of the [3,3]-sigmatropic shift is determined by the structural features of the fluorocarbanions and their lifetime necessary for the formation of the transition state of type **A***.

Indeed in protophilic solvents [DMF, DMSO, hexamethylphosphoramide (HMPA)], which tend to stabilise carbanionic intermediates, and in the presence of 'mild' HF acceptors, for example potassium fluoride, the reactions of the perfluoroisobutene **154b** with allyl and crotyl alcohols proceed unusually easily (−30 to −10 °C), the formation of the rearrangement products **156b** being the main pathway§ (yield up to 70%).[37, 120, 123] Under similar conditions (KF/DMF, 5–20 °C), in the interaction of allyl alcohol with hexafluoropropene **154a**[120, 123] and 2-methylthiopentafluoropropene **154c**[124] the rearrangement products **156a** and **156c** were obtained in 15% and 32% yields respectively.

Another approach to the stabilisation of the intermediate fluorocarbanions is associated with the use of powerful nucleophiles such as alkoxides. Derivatives of 2-alkoxy-2-trifluoromethylalk-4-enoic acids **163** were obtained in this way from 2-alkoxy-pentafluoropropenes **162** in a yield up to 66%.[125, 126]



162 **163**

R = CH_2OMe,  ; R^1, R^2 = H, Me, Ph;

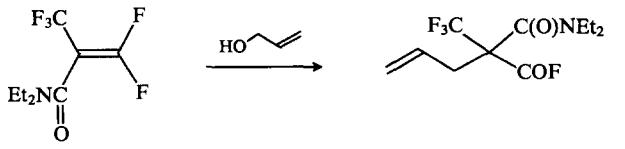
R^3 = H, $CH(R^1)CH = CHR^2$.

† It was believed previously[122] that the side product in this reaction is not the pentenoate **156b** but *O,O*-diallylbis(trifluoromethyl)ketenal.

‡ For the influence of fluorine atoms and CF_3 and CO_2R groups on the stability of the fluorocarbanions, see Refs 106 and 127a, b.

§ The corresponding adducts **115** and a fairly large amount of $(CF_3)_2CHX$ — the adducts of HF and the initial PFA — are also formed in these reactions.

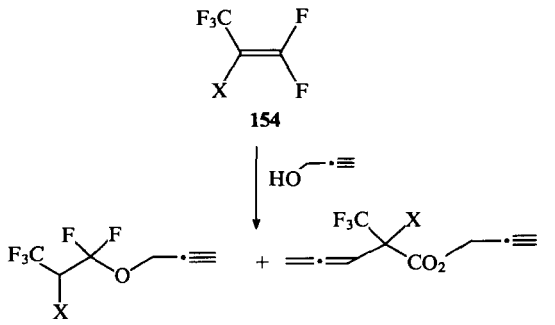
Under the conditions of effective intermolecular stabilisation of the carbanionic states, there is no need to use protophilic solvents, HF acceptors, or alkoxides. In the absence of any kind of reagents, the reaction of perfluoromethacrylic acid diethylamide **164**, the amide group of which stabilises the adjoining carbanionic centre,[127a] with allyl alcohol leads chemospecifically to the rearrangement product — the acid fluoride **165** (yield up to 90%).[128] The excess of the amide **164** serves as the HF acceptor in this reaction.



164 **165**

Terminal PFA reacts similarly with acetylenic alcohols.[120, 123, 129]

In a protophilic medium (KF/DMF), the reactions of perfluoroalkenes **154a** and **154b** with propargyl alcohol take place at −10 to 0 °C, while the [3,3]-sigmatropic shift in the intermediate **B** is accompanied by the acetylene–allyne rearrangement, which makes it possible to obtain CF_3-substituted penta-3,4-dienoates **167** in yields of 13% (**a**) and 59% (**b**) together with 2-*H*-polyfluoroalkyl propargyl ethers **166**.[120, 123]

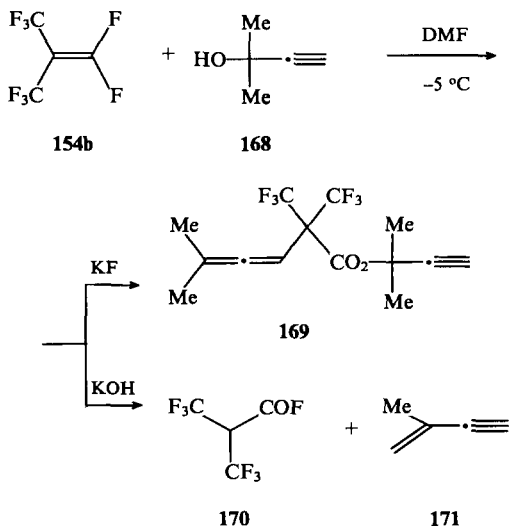


154

166 **167**

X = F (**a**), CF_3(**b**).

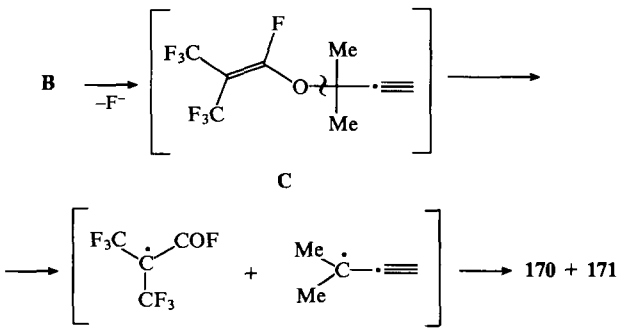
In a number of instances, the influence of the nature of the base employed on the mode of the reactions of PFA with homologues of propargyl alcohol has been noted. The reaction of the perfluoroisobutene **154b** with 1,1-dimethylprop-2-yn-1-ol **168**



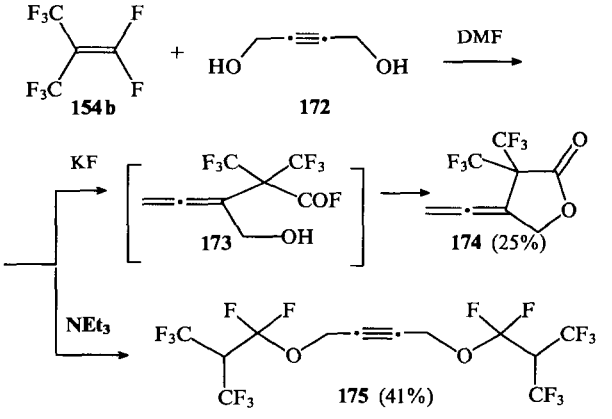
154b **168** **169** **170** **171**

under optimum conditions (KF/DMF) leads to the rearrangement product **169** (yield 48%), while the reaction catalysed by KOH affords a mixture of the acid fluoride **170** and isopropenylacetylene **171**.[129]

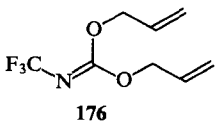
Apparently in the presence of a strong base the elimination of the fluoride ion from the intermediate **B** is faster that its rearrangement and the resulting polyfluorovinyl ether **C** undergoes homolytic decomposition owing to the steric hindrance to the [3,3]-sigmatropic shift.

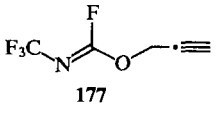


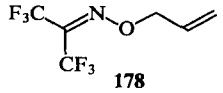
Two pathways operate also in the reaction of the perfluoroisobutene **154b** with but-2-yne-1,4-diol **172**.[129] In the presence of an excess of KF, the main product is 2,2-bis(trifluoromethyl)-3-vinylidene-4-butanolide **174**, formed on lactonisation of the intermediate **173** in the rearrangement, but, when this reaction was catalysed by triethylamine, only the adduct **175** was obtained.

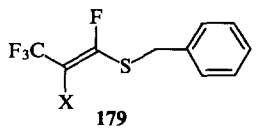


It is noteworthy that, in the reactions of a terminal azaalkene such as perfluoro-2-azapropene with allyl and propargyl alcohols, the products of the [3,3]-sigmatropic rearrangement are not formed at all and allyl polyfluoro-2-azapropenyl ether **176** and propargyl polyfluoro-2-azapropenyl ether **177** do not isomerise even at 150 °C.[130] The *O*-allyl ether of hexafluoroacetone oxime **178** is just as stable.[130]









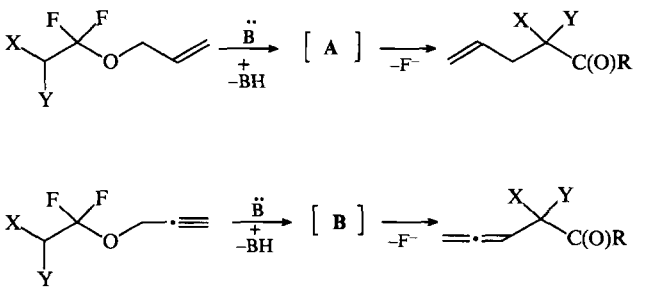
X= CF_3, $C(O)NMe_2$.

The benzyl sulfides **179**, obtained in the reactions of toluene-α-thiol with perfluoroisobutene[131] and perfluoromethacrylic acid dimethylamide,[132] also proved to be thermodynamically stable.

4. Rearrangements on deprotonation of 2-*H*-polyfluoroalkyl ethers

Another preparative method of synthesis of alkyl polyfluorovinyl ethers is based on the dehydrofluorination of the products of the addition of alcohols to terminal PFA, for example, to perfluoroisobutene.[133] On the other hand, the dehydrofluorination of the adducts of 2,3-unsaturated alcohols and terminal PFA—allyl(propargyl)2-*H*-polyfluoroalkyl ethers—leads not to the expected polyfluoroenols but to the rearrangement products—derivatives of fluorine-containing alk-4-enoic and alka-3,4-dienoic acids. The fluorocarbanions **A** or **B**, generated at the instant of the deprotonation of the initial CH acids, are probably the direct precursors of the rearrangement products in this case too (Scheme 2).

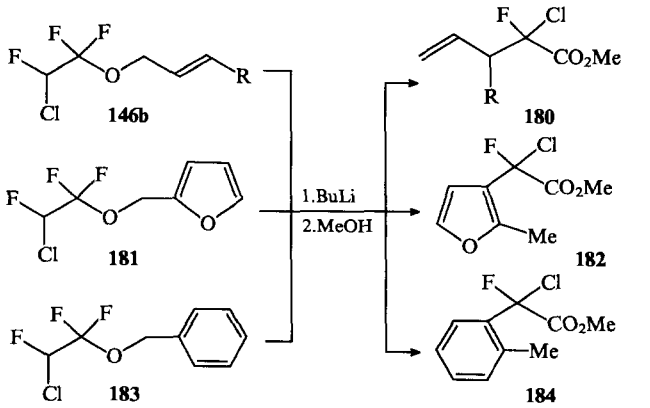
Scheme 2



R = F, OH, OMe.

This method of synthesis of unsaturated carboxylic fluoroacids and their derivatives was first used by Normant and coworkers[110, 111] in relation to the initial 2-*H*-chlorotrifluoroethyl ethers. The use of butyllithium as the deprotonating agent made it possible to obtain from the adducts of chlorotrifluoroethylene with allyl, crotyl, cinnamyl (compound **146b**; R = H, Me, Ph), furfuryl (compound **181**), and benzyl (compound **183**) alcohols at negative temperatures the corresponding products **180**, **182**, and **184** of the [3,3]-sigmatropic rearrangement in satisfactory yields.

The low-temperature preparative syntheses of derivatives of 2,2-difluoropent-4-enoic acid were subsequently developed on the basis of Normant's method.[112, 134]

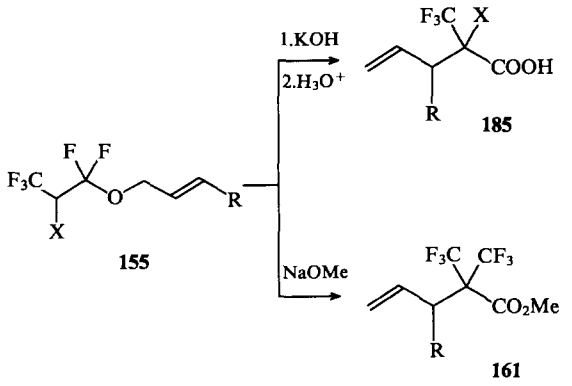


R = H, Me, Ph.

According to Normant and coworkers,[110, 111] the products of the rearrangement in the reactions described above are formed from the intermediate PFVE. However, it is difficult to explain from this standpoint the very high rate of the Claisen rearrangement of the above intermediates even at −70 °C,[111, 134] whereas cinnamyl 2,2-difluorovinyl ether **115a** is extremely stable.[92]

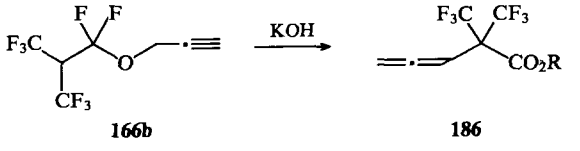
Even stronger CH acids, for example the 2-*H*-hexafluoropropyl ether **155a**, the 2-*H*-octafluoroisobutyl ether **155b**, and 2-methylthio-2-*H*-pentafluoropropyl ether **155c** are depronated by potassium hydroxide, being converted into 2-trifluoromethylpent-4-enoic acids **185** in yields of 32% (**a**), 60%–78% (**b**), and 67% (**c**).[123, 124, 135]

Methyl 2,2-bis(trifluoromethyl)pent-4-enoates **161** have been synthesised from the ether **155b** with the use of sodium methoxide or Claisen's alkali (a solution of KOH in dry methanol) as the deprotonating agents.[120]



X = F, R = H (**a**) (DMSO, 60–65 °C);
X = CF_3, R = H, Me (**b**) (Et_2O, 30–35 °C);
X = SMe, R = H (**c**) (THF, 60–65 °C).

The propargyl ether **166b** is converted into 2,2-bis(trifluoromethyl)pent-3,4-dieonoic acid **186** (R = H) on reaction with KOH in diethyl ether (35 °C, 2 h),[136] whilst in methanol the reaction affords the ethyl ester of the acid **186** (R = Me).[120]

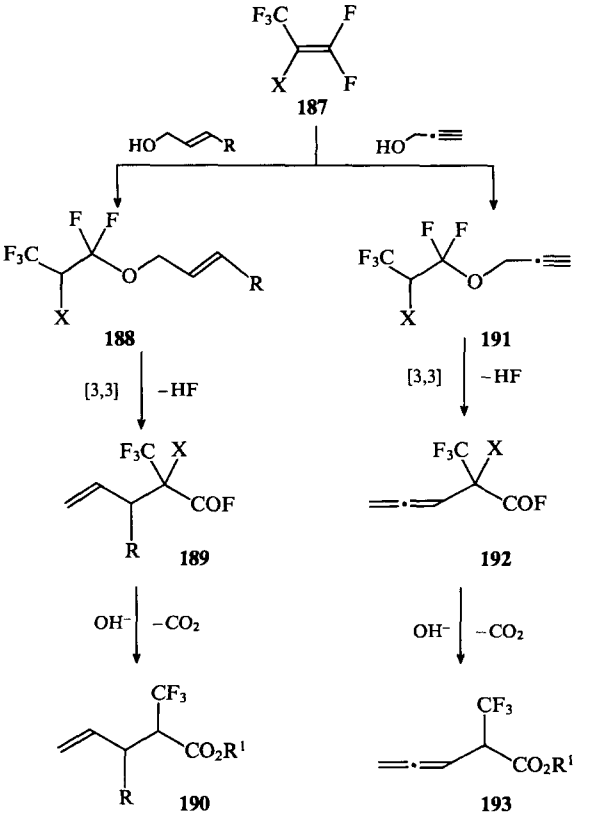


R = H (54%), Me (51%).

Allyl 2-*X*–2-*H*-pentafluoropropyl ether **188** and propargyl 2-*X*–2-*H*-pentafluoropropyl ether **191**, obtained by the addition of 2,3-unsaturated alcohols to highly electrophilic PFA with functional-group substituents in the 2-position, namely methyl perfluoromethacrylate **187a**, perfluoromethacryloyl fluoride **187b**, and 2-fluorosulfonylpentafluoropropene **187c**, are particularly readily deprotonated. Being strong CH acids, the adducts **188** and **191** interact smoothly with a weak base such as the complex $BF_3 \cdot NEt_3$. Depending on the strength of the initial CH acid, the deprotonation begins at 25–30 °C (**c**),[137, 138] 40–45 °C (**b**),[138] or 70–80 °C (**a**).[123, 128] The subsequent [3,3]-sigmatropic rearrangements of the fluorocarbanions **A** or **B** take place almost instantaneously and with evolution of much heat, leading to the selective formation of the acid fluorides **189** and **192** in 85%–90% at 65%–85% yields respectively.

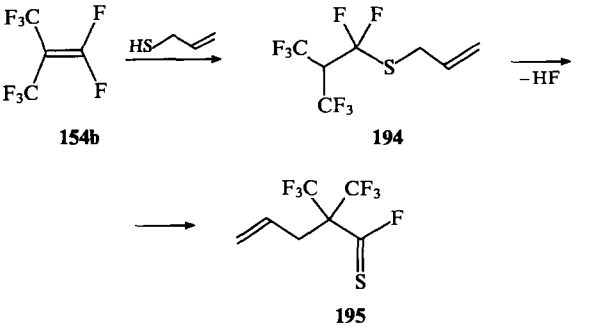
On alkaline hydrolysis, the acid fluorides **189a,b** and **192a,b** are readily decarboylated, being transformed into the 2-trifluoromethylpent-4-enoic acid **190** (R = R^1 = H) and 2-trifluoromethylpenta-3,4-dienoic acid **193** (R^1 = H) or their methyl esters.[139] The latter can be obtained under the conditions of phase transfer catalysis directly from 2-methoxycarbonyl-2-*H*-pentafluoropropyl ethers, namely from compound **191a**,[139] by-passing the stage involving the isolation of the corresponding acid fluorides.

The thio- and amino-[3,3]-sigmatropic rearrangements proceed with greater difficulty on deprotonation of the adducts of perfluoroisobutene with propene-3-thiol [allyl mercaptan] **194**



X = CO_2Me (**a**), COF (**b**), SO_2F (**c**); R = H, Ph; R^1 = H, Me.

and allylamine **196**¶. The sulfide **194** is converted into 2,2-bis(trifluoromethyl)pent-4-enethioyl fluoride **195** in 70% yield only on heating with the complex $BF_3 \cdot NEt_3$ to 100–110 °C.[140]

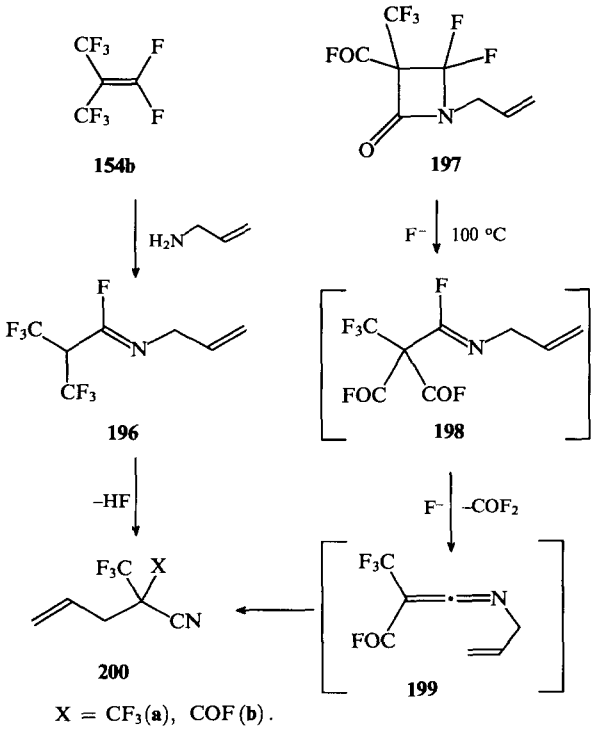


The thermolysis of the imidoyl fluoride **196** at 120 °C leads to the nitrile of 2,2-bis(trifluoromethyl)pent-4-enoic acid **200a** (yield 53%) in the absence of deprotonating agents.[141]

It is of interest that the reaction of the β-lactam **197** with caesium fluoride also involves the formation of the nitrile of 2-trifluoromethylpent-4-enoic acid **200b** in a low yield.[142] According to the authors, the ketene imine **199** — the product of the opening of the lactam ring and of the 'haloform' cleavage of the intermediate imidoyl fluoride **198** by the fluoride ion — is a precursor of compound **200b**.

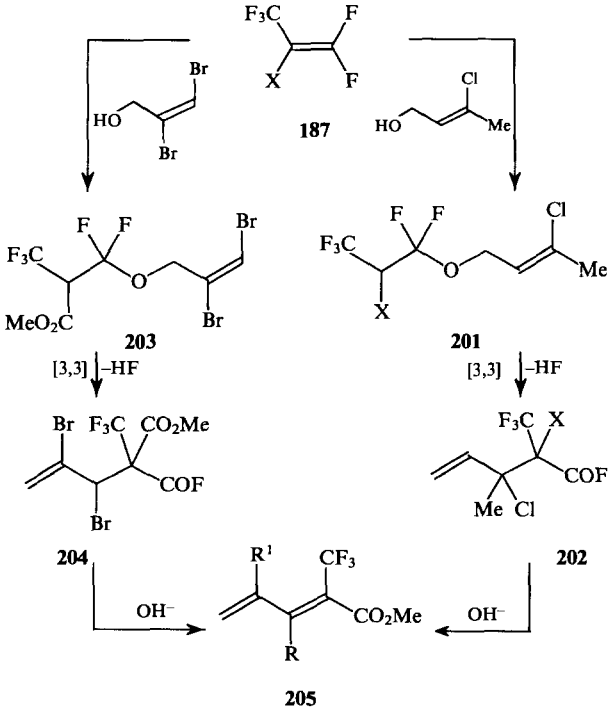
The deprotonation of 2-*H*-polyfluoroalkyl ethers proved to be a convenient method of synthesis of not only derivatives of fluorine-containing alk-4-ene- and alka-3,4-diene-carboxylic acids

¶ The rearrangement products are formed in extremely insignificant amounts in the reactions of perfluoroisobutene **154b** with propene-3-thiol and allylamine.[120]



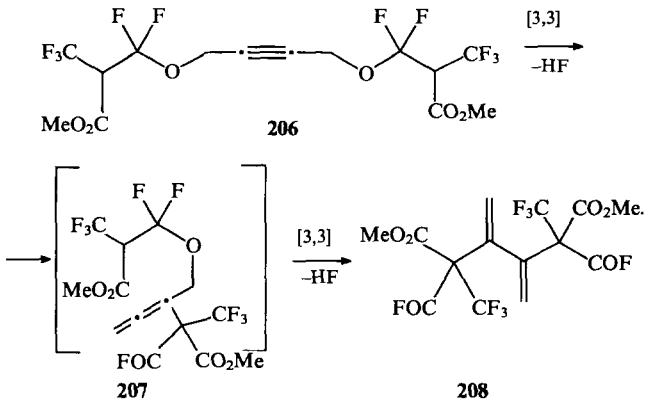
but also of the corresponding dienoates.[143, 144] Furthermore, the possibility of using this method for the synthesis of new[145] or the modification of the already available fluorinated heterocycles[146] has been demonstrated in individual instances. In all cases, the use of $BF_3 \cdot NEt_3$ as the deprotonating agent is most effective.

The adducts **201** and **203**, obtained by the addition of 3-chloro(bromo)allyl alcohols to the perfluoromethacrylates **187a,b** on heating with $BF_3 \cdot NEt_3$ to 85–110 °C, are converted into the acid fluorides **202** and **204** containing an allylic halogen atom.

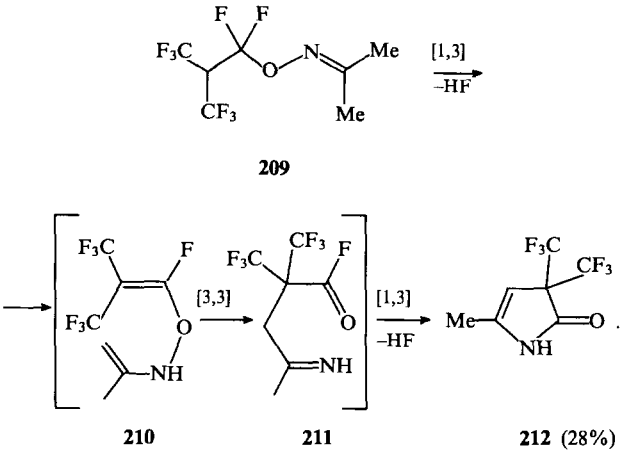


The formation of a vicinal (in relation to this atom) CH acid centre during the mild hydrolysis of the acid fluorides **202** and **204** is therefore accompanied by dehydrohalogenation with formation of methyl 2-trifluoromethylpenta-2,4-dienoates **205**† in yields up to 80%.[143]

When the 2:1 adduct of methyl perfluoromethacrylate and butynediol **206** is heated (85 °C) with the complex $BF_3 \cdot NEt_3$, the difluoride of 3,4-dimethylenehexane-1,6-dioic acid **208**—the product of the sequential [3,3]-sigmatropic reaction—is formed in 34% yield.[144] The relatively high selectivity of this reaction is achieved despite the significant steric hindrance to the [3,3]-sigmatropic shifts, especially in the deprotonation of the intermediate **207**.



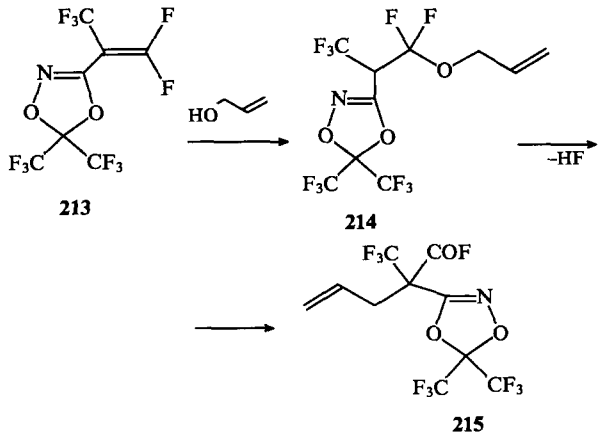
Sequential shifts in the intermediate structures occur also in the reaction of acetone *O*-(2-*H*-perfluoroisobutyl)oxime **209** with bases (KOH or $BF_3 \cdot NEt_3$). According to Zeifman et al.,[145] the dehydrofluorination of compound **209** is accompanied by a [1,3]-prototropic shift in the oxime part of the molecule with formation of the enamine **210**, which undergoes at 20 °C the Cope 3-oxa-4-aza-rearrangement to the imino-substituted acid fluoride **211**. The latter cyclises under the reaction conditions to the pyrrolinone **212**.[145]



The mild deprotonation conditions and the high rate of rearrangement, characteristic of strong fluorine-containing CH acids, have been used successfully for the modification of the pentafluoroisopropenyl-substituted 1,4,2-dioxazoline **213**.[146] The allyl ether **214** obtained from it is readily transformed on treatment with $BF_3 \cdot NEt_3$ into the acid fluoride **215**. There is no doubt that this method may prove to be extremely promising for the modification of other 2-heteroarylpentafluoropropenes.

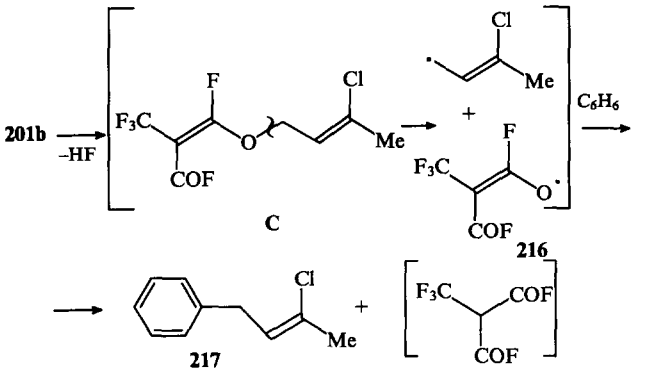
In a number of instances, the interaction of 2-*H*-polyfluoroalkyl ethers with bases is complicated by radical reactions. When 3-chlorocrotyl 2-fluorocarbonyl-2-*H*-pentafluoropropyl

† Derivatives of 2,4-dienecarboxylic acids have also been obtained in other studies[111, 119, 147, 148, 167, 169] as a result of the [3,3]-sigmatropic[111, 119, 147, 167, 169] or [2,3]-sigmatropic[148] rearrangements.



213 214 215

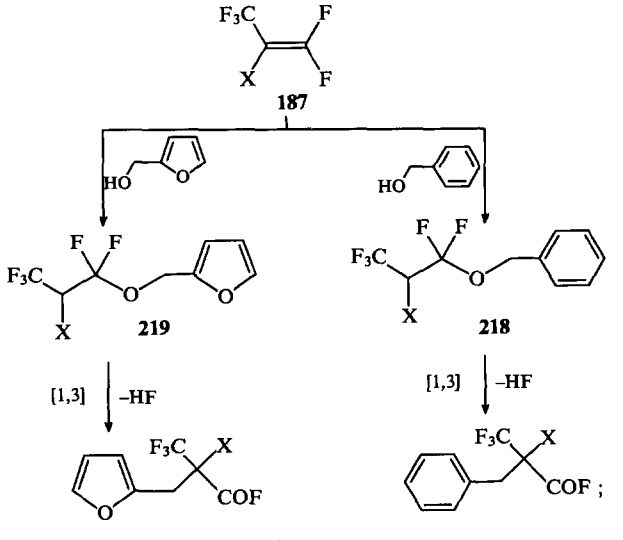
ether **201b** is heated with $BF_3 \cdot NEt_3$ in benzene, 3-chlorocrotylbenzene **217** is formed together with the rearrangement products **202b**.[143] Apparently, owing to the steric effect of the substituents at the double bond of the allyl group, stabilisation of the intermediate fluorocarbanion **A** is achieved in this instance not only via a [3,3]-sigmatropic shift but also via the elimination of a fluoride ion with subsequent homolytic cleavage of the tetrafluoropropenyl ether **C** to give the radical pair **216**.[143]



C **216** **217**

It must be emphasised that, on deprotonation of the ether **201a**, a similar reaction is not observed, evidently as a consequence of the greater stability of the corresponding carbanion.

The free radical reactions apparently occur also on dehydrofluorination of the very unstable adducts **218** and **219** formed in the reactions of the perfluoromethacrylates **187a,b** with benzyl and furfuryl alcohols.[37] [1,3] Shifts of benzyl (furfuryl) radical

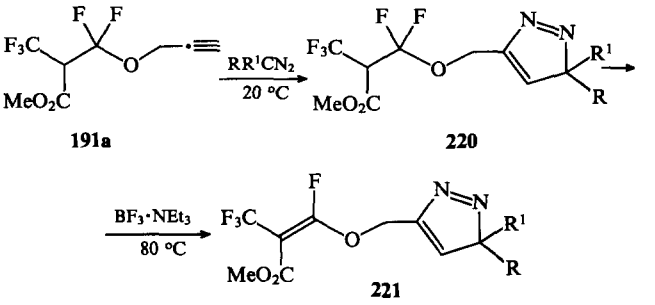


187 **219** **218**

X = CO_2Me (**a**), COF (**b**).

occur in these reactions, similar to those observed by Burger et al.[84] for benzyl ethers **96**.

On the other hand, the dehydrofluorination of the adduct **220**, obtained in the reaction of the propargyl ether **191a** with bis(trifluoromethyl)diazomethane or ethyl diazoacetate, afford the very stable 3'-pyrazolylmethyl tetrafluoropropenyl ethers **221**, the structure of which does not change even on heating to 150 °C.[149]



191a **220** **221**

R = R^1 = CF_3; R = H, R^1 = CO_2Et.

On the whole, it is essential to emphasise that the high rate and chemoselectivity, satisfactory yields, and the simplicity of the apparatus provide grounds for the claim that the deprotonation of the corresponding 2-*H*-polyfluoroalkyl ethers is the most convenient and most suitable for technological synthesis of a wide variety of aliphatic fluoro-products of the [3,3]-sigmatropic rearrangement —in the first place fluorine-containing alk-4-ene; and alka-3,4-dienecarboxylic acids and their derivatives. The choice of the deprotonating agent and of the conditions in the rearrangement are determined by the CH acid properties of the initial adducts.

The unsaturated carboxylic fluoroacids and their derivatives, which have become available as a result of the use of this method, are promising synthons for the synthesis of a large number of analogues of biologically active natural products of practical value, for example fluorine-containing 4-butanolides.[111, 136, 139, 150]

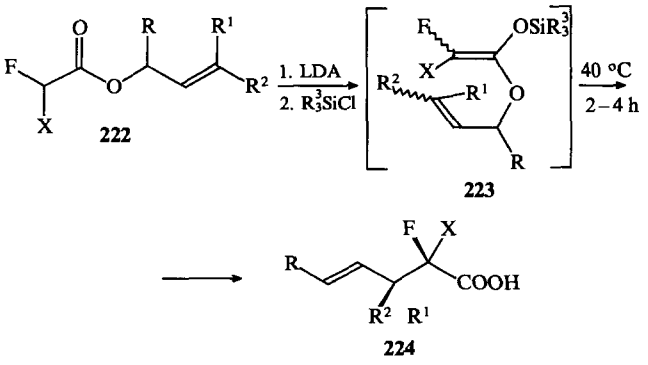
V. Rearrangements of polyfluorocarboxylic acid esters

The [3,3]-sigmatropic rearrangement of the alkenyl esters of 2-*H*-carboxylic acids, known as the Ireland–Claisen rearrangement,[151] usually occurs under mild conditions after the transformation of the alkenyl carboxylates under the influence of organolithium reagents into the corresponding lithium enolates or *O'*-alkenyl-*O*-trialkylsilylketenals. This method, characterised by an exceptionally high diastereoselectivity, is believed to be one of the best for the synthesis of alk-4-enecarboxylic acids.[152] In recent years, the Ireland–Claisen rearrangement has been successfully extended also to the allyl esters of 2-*H*-fluorocarboxylic acids as a result of the efforts of Welch and coworkers.[153–155]

The allyl esters of fluoroacetic acid **222a** and 1-fluoropropionic acid **222b** are stereoselectively deprotonated in THF (−100 to −78 °C) by lithium amides (the best of which is lithium diisopropylamide) with formation of 2-fluoropent-4-enoic acids **224**‡ in 15%–97% yield.[153, 154] The use of silylating agents as enolate traps in the second stage made it possible to establish that the (*E*)-form of the intermediate fluoroketenals **223** participates in the rearrangement.[153, 154]

The presence of fluorine atoms in the molecules of the fluoroketenals **223** apparently facilitates somewhat, and accelerates, their rearrangement. This is indicated by the half-reaction time ($\tau_{1/2}$ = 40 min at 40 °C) measured for compound **223a** (R = R^1 = H, R^2 = Me) and also by the fact that the ketenals **223** can be isolated in a free state,[153] in contrast to the non fluorinated analogues.[152]

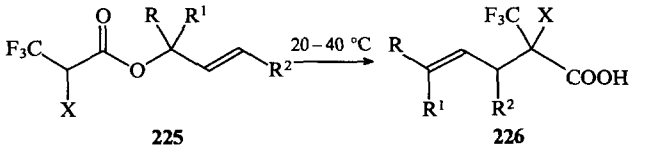
‡ 2-Fluoro-4-butanolides have also been obtained by converting the acids **224** into lactones.[153–155]



X = H(a), Me(b); R, R¹, R² = H, Me.

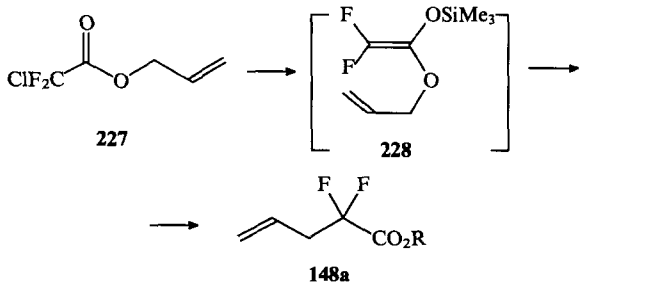
Equimolar mixtures of triethylamine and trialkylsilyl triflates (R_3SiOTf) are more convenient reagents for the generation of silylated fluoroketenals. In this case, the reactions do not require ultralow temperatures. The suitability of the Ireland–Claisen rearrangement for the synthesis in a satisfactory yield of not only the 2-monofluoro-substituted unsaturated acids[96, 155] but also of the polyfluorinated acids of this kind[96, 156, 157] must be regarded as its advantage.

Nakai and coworkers[156, 157] found that 2-trifluoromethylalk-4-ene carboxylic acid **226a** and 2-fluoro-2-trifluoromethylalk-4-enecarboxylic acid **226b** are formed smoothly when alkenyl polyfluoropropionates **225** are treated with a mixture of NEt_3 and Me_3SiOTf in methylene chloride with subsequent refluxing of the reaction solution for 5–12 h (**a**) or its stirring (at 20 °C) for 36 h (**b**).



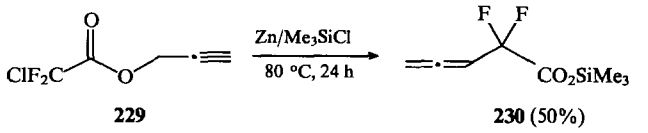
X = H (**a**), F (**b**); R, R¹, R² = H, Me.

Allyl chlorodifluoroacetate **227** undergoes the [3,3]-sigmatropic rearrangement only under the conditions of the Reformatskii reaction. When a mixture of compound **227**, freshly activated zinc, and chlorotrimethylsilane is heated in acetonitrile (100 °C, 20 h), derivatives of 2,2-difluoropent-4-enoic acid **148a** are formed after the rearrangement of the intermediate ketenal **228** and the appropriate treatment.[158]

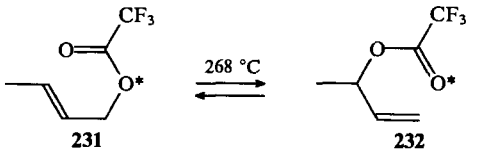


R = H (78 %), Et (60 %), $SiMe_3$ (95 %).

Other 2,2-difluoroalk-4-enecarboxylic acids, including some extremely difficult to obtain, are also formed under these conditions form the corresponding esters of chlorodifluoroacetic acid. In addition, the ester of 2,2-difluoropenta-3,4-dienoic acid **230** was obtained from propargyl chlorodifluoroacetate **229**.[158]

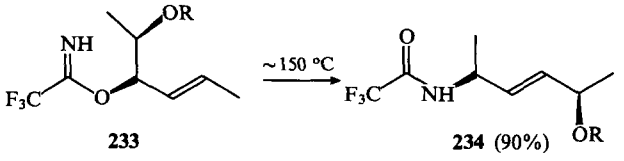


The allyl esters of trifluoroacetic acid are incapable of entering into a similar reaction. However, it has been shown with the oxygen-labelled crotyl trifluoroacetate **231**[159] that, when the latter compound is heated in the gas phase, a reversible [3,3]-sigmatropic rearrangement of this compound to the 1-methylallyl ester **232** takes place.

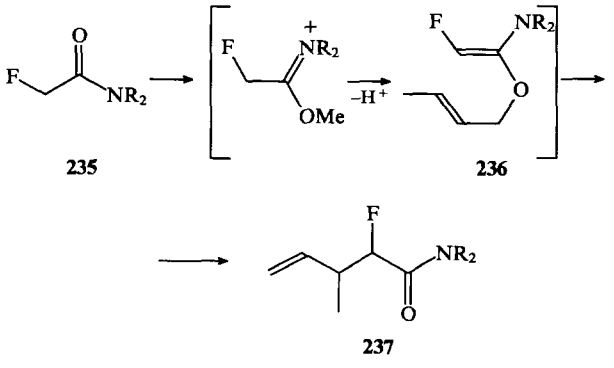


On the other hand, the trifluoroacetic acid iminoester **233** undergoes smoothly and stereoselectively the Cope 1-aza-3-oxa-rearrangement, on heating in xylene (20 h), to *N*-alkenyltrifluoroacetamide **234**, which is a precursor of an optically active polyoxamic acid.[160]

The analogous iminoester of trichloroacetic acid isomerises after more prolonged refluxing in xylene (48 h), but the yield of the final trichloroacetamide does not exceed 40%.[160]



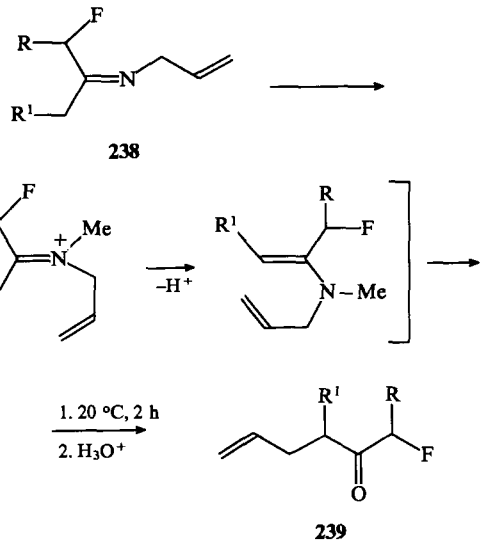
The optically active amides of monofluoro-substituted alk-4-enecarboxylic acids are obtained under milder conditions via intermediate aminoketenals, for example, compound **236**.[161a] The fluoroacetamides **235** are alkylated in the first stage with methyl triflate (MeOTf) or dimethyl sulfate, after which the product is treated with the lithium salt of the geometrically pure crotyl alcohol. The products of the rearrangement (the amides **237**) are isolated in 23%–78% yield (depending on the configuration of crotyl alcohol) after stirring the reaction solution (THF or methylene chloride, at 225 °C) for at least 14 h.



R = Me, $-(CH_2)_4-$, Pr^i.

The optically active *N*-(2′-fluoro-3′-methylpent-4′-enoyl)-2,5-dimethylpyrrolidine was obtained in the same way (at 20 °C, 24 h) in 61% yield.[161b]

The Claisen amino-rearrangement (the Cope 3-aza-rearrangement) of the α-halogenated and non-halogenated ketimines proceeds via a similar mechanism with participation of the quaternised nitrogen atom.[162] Successive treatment of *N*-fluoroalkylideneallylamines **238** with alkylating (MeOTf) and deprotonating [solution of 1,8-bis(dimethylamino)naphthalene in MeCN] agents under mild conditions leads to the monofluoroketones **239**.



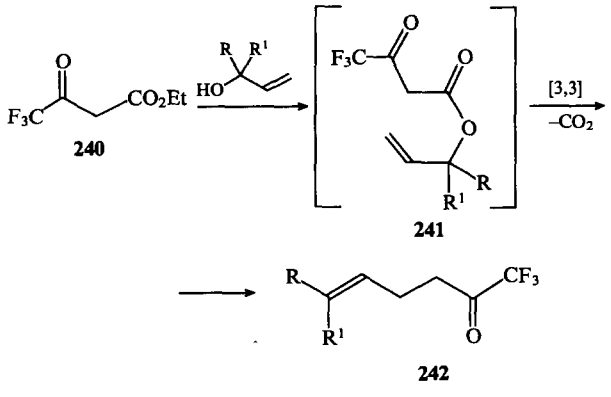
238

239

R = Me, R^1 = H (54%); R, R^1 = $-(CH_2)_3-$ (31%).

The high regioselectivity of these reactions[162] permits their use as a convenient method of synthesis of α-halogenated 4,5-unsaturated ketones.

Camps and coworkers[163, 164] investigated in relation to several examples the behaviour of the esters of fluorine-containing acids in the base-catalysed Carroll rearrangement. Ethyl 4,4,4-trifluoroacetoacetate **240** was used as the starting compound in this rearrangement. The transesterification of the acetate **240** with 1-substituted allyl alcohols is carried out in the presence of catalytic amounts of sodium acetate (150 °C, 15 h). The allyl ethers **241**, generated as a result of this reaction, undergo *in situ* a [3,3]-sigmatropic shift, coupled with decarboxylation and formation of CF_3-substituted 4,5-unsaturated ketones **242**.[163]



240

241

242

R = R^1 = Me (80%); R = Me, R^1 = $(CH_2)_2CH$ = CMe_2 (84%).

It has been noted[163] that the presence of the CF_3 group in the acetate **240** is responsible for the less severe reaction conditions compared with those which obtain in the Carroll rearrangement of ethyl acetoacetate.[165]

Although this method is not distinguished by a high stereoselectivity, it makes it possible to obtain in satisfactory yields certain compounds of practical value, for example geranyltrifluoroacetone,[164] which is a trifluoro-analogue of juvenile hormone.

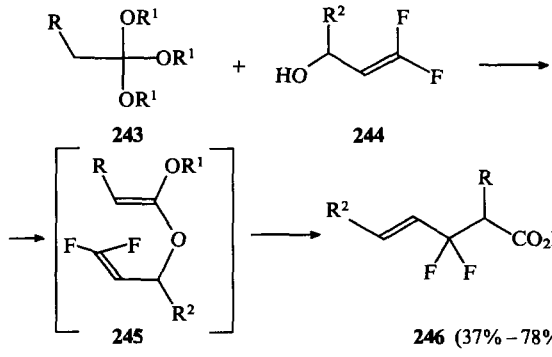
VI. Rearrangements of polyfluoroallyl ethers

Fluorine-containing 2,3-unsaturated alcohols are precursors of polyfluoroallyl vinyl ethers which undergo *in situ* [3,3]-sigmatropic transformations, involving Johnson–Claisen, Claisen, and Ireland–Claisen rearrangements. Preparative syntheses of fluorinated allyl and propargyl alcohols began to be actively developed only during the last decade and one can therefore postulate that there are good prospects for the development of methods of synthesis of unsaturated compounds based on the rearrangements of the corresponding polyfluoroallyl ethers.

The initial components in the Johnson–Claisen rearrangement[166] are trialkyl orthoacetates and allyl alcohols. The high stereoselectivity of the rearrangement requires the use of geometrically pure alcohols, whilst its fairly severe conditions (110 °C–150 °C, the presence of an acid catalyst generating the vinyl component) permit the involvement of highly substituted unsaturated alcohols in these reactions.

Among fluorinated alcohols, only the most readily available 3,3-difluoroallyl and trifluoromethylated allyl and propargyl alcohols have been made to undergo the Johnson–Claisen rearrangement.

The 3,3-difluoroallyl alcohols **244** react with the orthoesters **243** in boiling toluene in the presence of catalytic amounts of propionic acid. The resulting difluoroallyl vinyl ethers **245** isomerise under the reaction conditions (115 °C, 5 h) to the esters of 4,5-dialkyl-3,3-difluoroalk-4-enecarboxylic acids **246**.[167] Under the influence of alkali, the esters **246** are readily dehydrofluorinated, being converted into alkyl 3-fluoro-5R^2-penta-2,4-dienoates.[167]

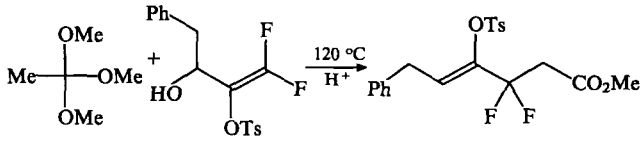


243 **244**

245 **246** (37%–78%)

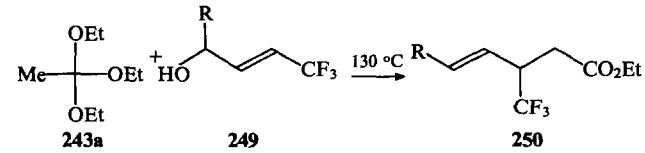
R = H (**a**), Me (**b**); R^1 = Me, Et; R^2 = H, CH_2CH_2Ph, C_5H_{11}.

The analogous reaction of the orthoester **243a** (R^1 = Me) with 1-benzyl-3,3-difluoro-2-tosyloxyallyl alcohol **247** is smoothly completed after 1.5 h by the formation of the ester **248** in 84% yield.[92]



243a **247** **248**

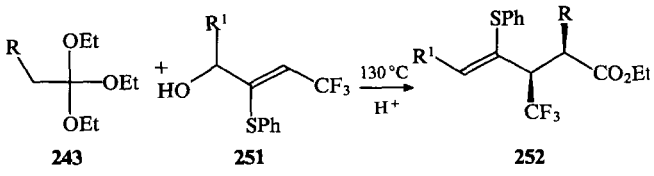
Trifluoromethyl-substituted unsaturated alcohols undergo the Johnson–Claisen rearrangements under virtually the same conditions. Japanese workers have shown[147, 168, 169] that these reactions constitute a convenient method for the stereoselective synthesis of the esters of 3- and 4-CF_3-substituted unsaturated acids. Thus, ethyl 3-trifluoromethyl-5R-pent-4-enoates **250** have been obtained by heating 1-alkyl-3-trifluoromethylallyl alcohols **249** in a large excess of the orthoester **243a** (R^1 = Et) in the presence of a catalyst (EtCOOH).[147]



243a **249** **250**

R = CH_2CH_2Ph (71%), CH_2OCH_2Ph (45%), n-C_6H_{13} (81%).

The reactions of 2-phenylthio-3-trifluoromethylallyl alcohols **251** with the orthoesters **243** lead stereoselectively to the esters of 4-phenylthio-3-trifluoromethylalk-4-ene carboxylic acids **252** in 55%–87% yield.[168]

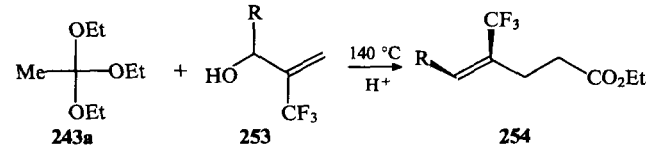


243 **251** **252**

R = H, Me; R¹ = Me, Et, Pr^i, Ph.

The presence of the phenylthio-group at the double bond in the alcohol **251** does not exert a significant influence on the conditions of the rearrangement.

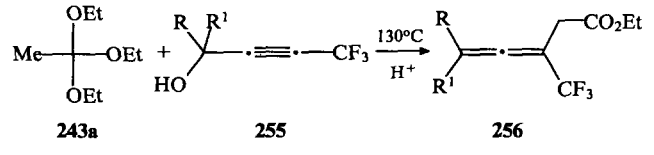
2-Trifluoromethylallyl alcohols **253** react with the orthoester **243a** under somewhat more severe conditions. The esters of 4-trifluoromethylalk-4-enecarboxylic acid **254** are formed stereoselectively as the final products in this instance.[169]



243a **253** **254**

R = CH_2CH_2Ph (86%), CH_2OCH_2Ph (73%).

Trifluoromethyl-substituted acetylenic alcohols also enter into a reaction of a similar type. Interaction of 1-R-3-trifluoromethylpropargyl alcohols **255** with the orthoester **243a** leads to derivatives of 3-trifluoromethylpenta-3,-4-dienoic acid **256** in 32%–55% yields.[147]

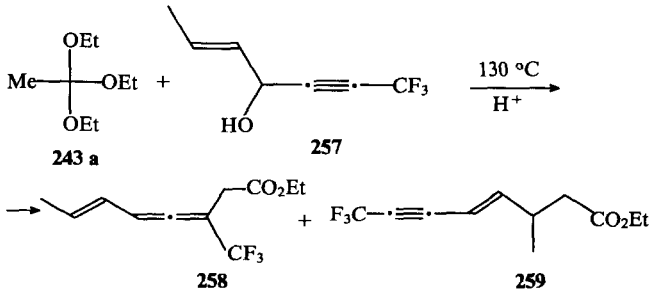


243a **255** **256**

R = CH_2CH_2Ph, CH_2OCH_2Ph, *n*-C_6H_{13}, R¹ = H; R = R¹ = $-(CH_2)_5-$.

The base-catalysed isomerisation of compound **256** affords 3-trifluoromethyl-5-R-penta-2,4-dienoate (R = CH_2OCH_2Ph).[147]

It is of interest that allyl and propargyl alcohols exhibit the same tendency to undergo the Johnson–Claisen rearrangement. The use of 1-propenyl-3-trifluoromethylpropargyl alcohol **257** in this reaction leads to a mixture of the esters of 3-trifluoromethylocta-3,4,6-trienoic acid **258** and 7-trifluoromethylhept-4-en-6-ynoic acid **259** in proportions of 1 : 1.[147]



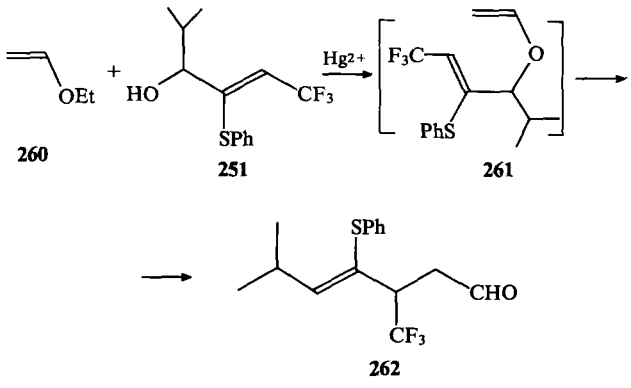
243 a **257**

258 **259**

At the same time, an attempt to involve 1-(4′-methoxyphenyl-2′,3′,6′-trimethyl)-3-trifluoromethylpropargyl alcohol in the Johnson–Claisen rearrangement was unsuccessful,[170] apparently owing to the powerful steric effect of the bulky substituent in the 1-position.

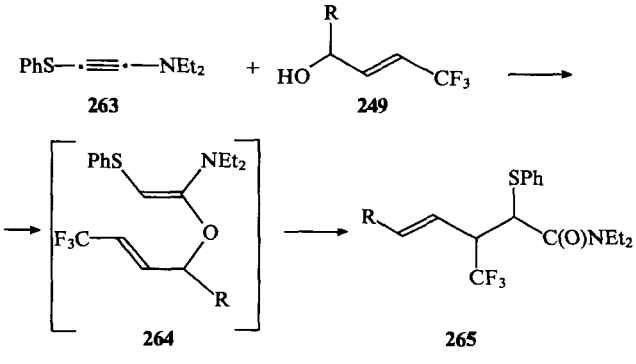
The ability of polyfluoroallyl ethers to enter into the Claisen and Ireland–Claisen rearrangements has also been investigated.

The thermal condensation (150 °C) of ethyl vinyl ether **260** and 3-trifluoromethylallyl alcohol **251** (R = Pr^i) catalysed by mercury acetate affords 3-trifluoromethylheptenal **262** in 50% yield.[168] At temperatures below 150 °C, the Claisen rearrangement of the initial 3-trifluoromethyl vinyl ether **261** does not occur.



260 **251** **261** **262**

Another method of generation of the intermediate Claisen substrate is involved in the reaction of phenylthioalkynamine **263** with trifluoromethylallyl alcohol **249**.[147] The adduct **264** of these reactants isomerises on refluxing in toluene to the amide **265**, which is subsequently oxidised to 3-trifluoromethylalk-2,4-dienoate. The use of (*Z*)-**249** instead of (*E*)-**249** lowers the yield of the amide **265** from 62% to 35%.

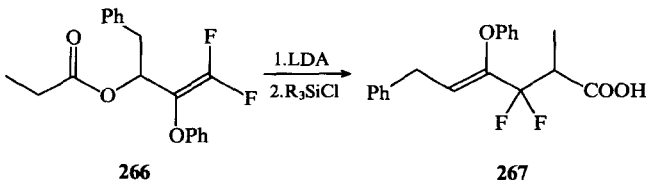


263 **249** **264** **265**

R = CH_2OCH_2Ph.

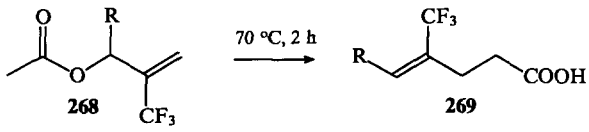
The polyfluoroallyl esters of carboxylic acids undergo the Ireland–Claisen rearrangement under standard conditions, although unsuccessful attempts to involve certain difluoroallyl carboxylates in this reaction have been noted.[167]

The difluoroallyl propionate **266** is readily transformed into 3,3-difluoro-2-methylalk-4-enecarboxylic acid **267** in 57% yield on successive treatment with lithium diisopropylamide and trialkylchlorosilane.[92]



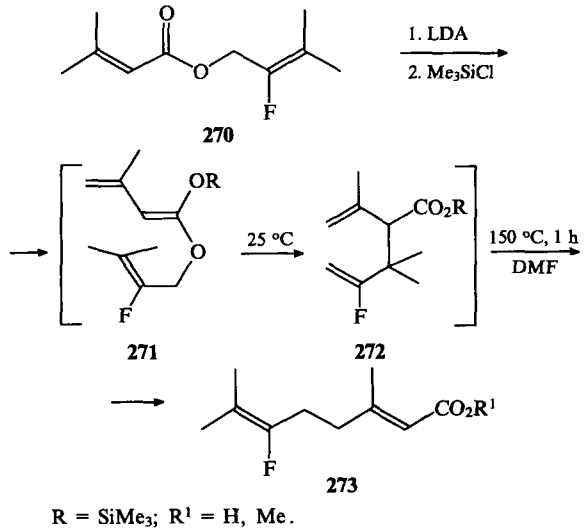
266 **267**

On treatment with lithium isopropylcyclohexylamide and *tert*-butylchlorodimethylsilane in hexamethylphosphoramide, 2-trifluoromethylallyl acetates **268** are similarly converted into 4-trifluoromethylalk-4-enecarboxylic acid **269** (in yields up to 86%).[169]



R = CH_2CH_2Ph, CH_2OCH_2Ph.

The tandem Ireland–Claisen/Cope rearrangement used by Camps et al.[171] is a key stage in the multistage synthesis of the monofluoro-analogues of one of the juvenile hormones from 2-fluoroallyl acrylate **270**.

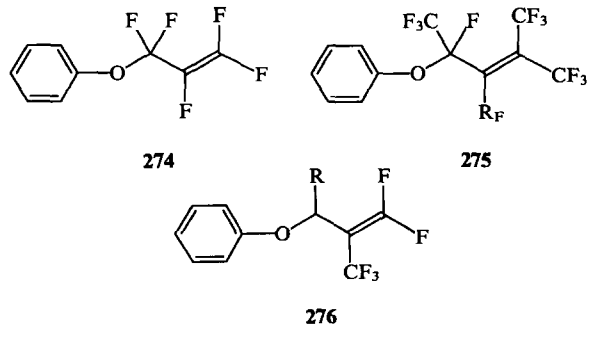


R = $SiMe_3$; R^1 = H, Me.

When these reactions are carried out in one stage without the isolation of the intermediates **271** and **272**, it is possible to obtain the ester of 6-fluoro-3,7-dimethyl-octa-2,6-dienoic acid **273** in 78% yield.[171]

Overall, one may note that the fluorine atoms and the trifluoromethyl group apparently do not exert a significant influence on the conditions and rate of the [3,3]-sigmatropic rearrangements of polyfluoroallyl ethers. This has been confirmed by the calculations of Gajewski et al.,[35] who determined the activation parameters for the Claisen rearrangement of 1-trifluoromethylallyl vinyl ether. According to the authors' data,[35] the CF_3 group at the C(4) atom does not have an appreciable influence on the rate of the rearrangement, in contrast to, for example, the CN group, which ensures a gain in activation free energy of 3.5 kcal mol^{-1} in this position.[33]

The thermodynamic stability of phenyl polyfluoroallyl ethers is evidently also close to that of the fluorine-free allyl ethers of phenols. Indeed, perfluoroallyl phenyl ether **274**[172] and phenyl polyfluoroalkenyl ethers **275**[100] and **276**[173] have fairly high thermal stabilities and do not isomerise after prolonged storage or on heating under the reaction conditions.



R_F = $CF(CF_3)_2$, R = $CF_2(CH_2CF_2)_nF$.

The absence of positive effects by the fluorine atoms on the CF_3 group in the [3,3]-sigmatropic rearrangements of polyfluoroallyl vinyl ethers in no way reduces the preparative value of these compounds. They make it possible to synthesise highly stereoselectively, and in a satisfactory yield, 3- and 4-fluoro(trifluoromethyl)-substituted unsaturated acids and their derivatives which are otherwise difficult to obtain.

VII. Conclusion

Whereas only two studies[35, 44] devoted to the Claisen rearrangement were mentioned in Hudlicky's fundamental monograph[105b] in 1976, towards the end of the 1980s the continuous growth in the number of studies on the [3,3]-sigmatropic rearrangements of organofluorine compounds already made it possible to recognise these reactions as one of the important methods of synthesis of fluorine-containing synthons.[174] Analysis of the data presented in this review permits an assessment at a deeper level of the applied and theoretical importance of the [3,3]-sigmatropic rearrangements of compounds of the organofluorine series.

In the first place, one should note their undoubted applied value. At the present time, this method is used to synthesise many organofluorine compounds of different classes. They include perfluorinated aromatic or heteroaromatic fragments of pyrans, furans, thiophens, and pyrroles condensed with a benzene ring, polyfluorinated 4,5-unsaturated ketones, derivatives of alk-4-ene, alka-3,4-diene-, and alka-2,4-diene-carboxylic acids, alkenylmalonic and carboxylic 4-ketoacids, furans, thiophens oxazolones, 4-butanolides, and compounds of other types. At the same time, the [3,3]-sigmatropic rearrangements have been used successfully in the preparative syntheses of fluorine-containing[81, 82, 84, 89] and non-fluorinated[160] α-aminoacids and fluorine- and trifluoromethyl-modified micotoxins,[94] phospholipids,[112] nucleosides,[155] juvenile hormones,[164, 171] and new medicinal[53, 157] and pesticidal[77, 157] preparations.

In addition, the considerable potential possibilities of the [3,3]-sigmatropic rearrangements as a universal method for the formation of the C–C bond can probably find applications in the solution of certain problems in the industrial chemistry of fluorine of current interest. For example, in the large-scale manufacture of hexafluoropropene, they can be used for the selective removal of a highly toxic impurity, namely perfluoroisobutene, from the main product with the simultaneous synthesis of the products of the rearrangement of the impurity. The same rearrangements can be used for the ecologically clean assimilation of the existing industrial manufacture of ozone-damaging Khladons (Freons), which are capable of being transformed into polyhaloalkenes under certain conditions.[175]

Theoretical studies on the [3,3]-sigmatropic rearrangements of organofluorine compounds have also proved extremely fruitful. By virtue of the unique effect of the fluorine atoms and the fluoroalkyl groups on the electronic system of the double bond of the 'vinyl' fragment in the series of 2,3-unsaturated ethers of polyfluoroalkenols and polyfluorocycloalkenols, compounds with a broad spectrum of reactivities were obtained (ranging from compounds thermodynamically stable at 150 °C to compounds which isomerise spontaneously under the conditions of their synthesis even on intense cooling). It has been shown that the probability and conditions of the rearrangement are determined primarily by the level of the population of the π-orbital of the vinyl bond, its capacity for polarisation from the C(2) to the C(1) atom, and the steric effect of the bulky fluorine-containing substituents in the C(1) position. The necessary preconditions for the prediction of the behaviour of the corresponding ethers of polyfluoroalkenols (polyfluorocycloalkenols) in the [3,3]-sigmatropic rearrangement and for the control of this process were thus created.

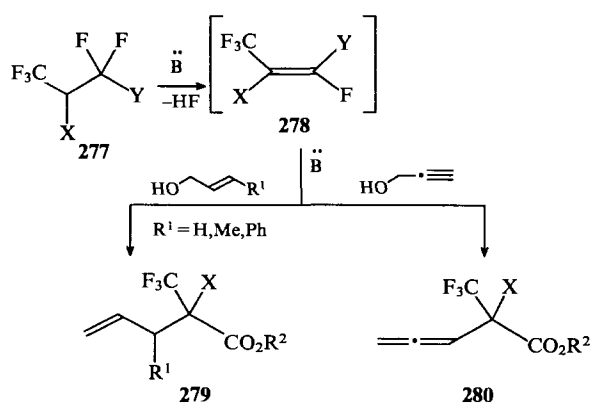
The phenomenon of the low-temperature anionic Claisen and Cope rearrangements, widely discussed in recent years,[9, 13, 28-32] has been manifested particularly clearly in the study of the [3,3]-sigmatropic rearrangements of fluorocarbanions.[37] The general features of an anionotropic [3,3]-sigmatropic process, the driving force of which is the highly effective symmetry-allowed charge-controlled pπ interactions, are characteristic of these rearrangements. However, instances of the easiest sigmatropic shifts have been noted precisely in the reactions of certain polyfluoroalkenes (perfluoroisobutene, perfluoromethacrylic acid diethylamide) with 2,3-unsaturated alcohols even in the absence of basic reagents.

The results in the study of the [3,3]-sigmatropic rearrangements of fluorine-containing compounds obtained hitherto indicate the appearance of a new modern method of organofluorine synthesis which reflects the unusual character of the fluorine chemistry as a whole. These results constitute a good practical and theoretical basis for further still more vigorous development of this field of chemistry.

* *
*

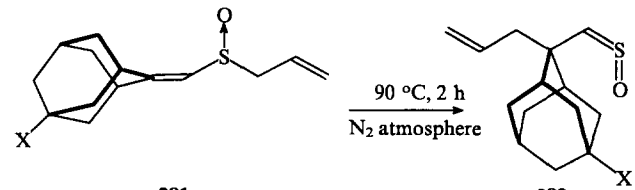
The studies published during the brief period of the preparation of the present review for the press confirm the steady interest of investigators in the problem considered. In one of the latest monographs devoted to fluorine chemistry, a review by Welch et al.[176] was published in which the Claisen rearrangements of the acetals of fluoroacetamides (fluorine-containing aminoketenals) are considered as an effective instrument for asymmetric synthesis.

A new convenient method of synthesis of derivatives of 2-trifluoromethyl-substituted unsaturated acids has been developed recently.[177] The fluorinated CH acids **277** interact in the presence of bases (B̈) with allyl and propargyl alcohols to form the products of the [3,3]-sigmatropic rearrangement — the esters of 2-trifluoromethylpent-4-enoic acid **279** and 2-trifluoromethylpenta-3,4-dienoic acid **280**. The reaction conditions and yields of the final products **279** and **280** are determined by the strength of the CH acids **277**, from which the polyfluoroalkenes **278** are generated initially. The latter undergo further reactions *in situ*. The new method[177] makes it possible to obtain in one stage the derivatives of unsaturated fluorocarboxylic acids, by-passing the laborious syntheses of polyfluroalkenes and their adducts with 2,3-unsaturated alcohols.



X = CF_3, CO_2R; Y = F, OR;
R = Me, Et; R^2 = R, $CH_2CH = CHR^1$, $CH_2C{\equiv}CH$.

American investigators[178] studied the thio-[3,3]-sigmatropic rearrangement of the unsubstituted and 5-fluoro-substituted adamantylidenemethyl allyl sulfoxides **281**, which leads to a mixture of the stereoisomeric sulfines **282** [the stable (*Z*)-form is illustrated]. The introduction of a fluorine atom in the 5-position does not alter the reaction conditions, but increases the number of diastereoisomers formed from 2 to 4.

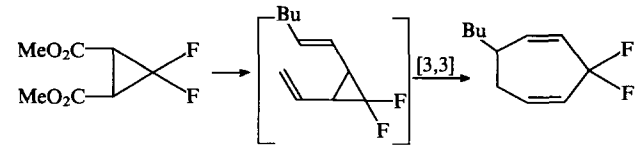


281 **282**

X = H, F.

It was established[178] that the steric and electronic effects of the substituents in compound **281** influence equally the stereochemistry of the process, in contrast to the Cope oxy-rearrangement,[43] investigated by the same workers, in which the influence of the steric factor predominated.

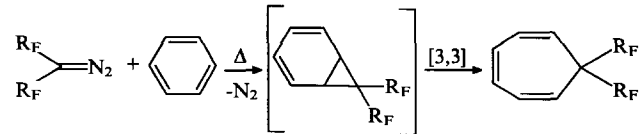
One of the few examples of the practical use of the Cope rearrangement has been described in a study[179] devoted to the preparative synthesis of fluorinated analogues of cycloheptadiene pheromones present in brown seaweed. The di(methoxycarbonyl)-substituted *gem*-difluorocyclopropane **283** was used as the synthon for the synthesis of the *trans*-dialkenyl-substituted *gem*-difluorocyclopropane **284**. The extreme instability of the cyclopropane **284**, which rearranges spontaneously at room temperature to 3,3-difluorocyclohepta-1,4-diene **285**, was unexpected.



283 **284** **285**

The kinetic parameters of the isomerisation of compound **284** to **285**, determined by the authors,[179] made it possible to discover the marked influence of the geminal fluorine atoms, weakening the opposite bond of the cyclopropane ring and leading to milder reaction conditions.

It is essential to note that a similar rearrangement had been observed earlier in relation to *gem*-perfluoroalkylnorcaradienes **287**. Krespan and coworkers[180] showed that the pyrolysis of the perflurodiazoalkanes **286** in an excess of benzene (150 °C–200 °C, 8 h) affords 7,7-bis(perfluoroalkyl)cyclohepta-1,3,5-trienes **288** as the main products in yields of 62% (**a**) and only 22% (**b**). Compounds **288** are formed as a result of the Cope rearrangement of the intermediate norcaradienes **287**.



286 **287** **288**

R_F = CF_3 (**a**), C_2F_5 (**b**).

The cycloheptatriene **288a** is formed as a side product in 11% yield on photolysis of bis(trifluoromethyl)diazomethane **286a** (benzene, 40 h).[180]

The preparative value of the Cope rearrangement of substrates of the type of compounds **284** and **287** increases sharply if this process is considered as a convenient approach to the synthesis of tropylidene structures containing fluorine and fluoroalkyl substituents, which are otherwise difficult to obtain.

References

1. L Claisen *Ber. Dtsch. Chem. Ges.* **45** 3157 (1912)
2. D S Tarbell *Org. React. (N.Y.)* **2** 1 (1944)
3. S J Rhoads, in *Molecular Rearrangements* Vol. 1 (Ed. P de Mayo) (New York: Interscience, 1963) p. 660
4. A Jefferson, F Scheinmann *Quart. Rev.* **22** 391 (1968)
5. A C Cope, E M Hardy *J. Am. Chem. Soc.* **62** 441 (1940)
6. S J Rhoads, N R Raulins *Org. React.* **22** 1 (1975)
7. T Hayashi *J. Synth. Org. Chem. Jpn.* **34** 396 (1976)
8. G B Bennett *Synthesis* 589 (1977)
9. R P Lutz *Chem. Rev.* **84** 205 (1984)
10. L E Overman *Angew. Chem., Int. Ed. Engl.* **23** 579 (1984)
11. A W Murray *Org. React. Mech.* 429 (1988); 457 (1989)
12. Ch J Moody *Adv. Heterocycl. Chem.* **42** 203 (1987)
13. F E Ziegler *Chem. Rev.* **88** 1423 (1988)
14. L E Overman *Acc. Chem. Res.* **13** (7) 218 (1980)
15. L Morin, J Lebaud, D Paquer, R Chaussin, B Daniel *Phosphorus Sulfur* **7** 69 (1979)
16. A V Anisimov, E A Viktorova *Khim. Geterotsikl. Soedin.* 435 (1980); A V Anisimov, E A Viktorova, T A Danilova *Molekulyarnye Peregruppirovki Seraorganicheskikh Soedinenii* (Molecular Rearrangements of Organosulfur Compounds) (Moscow: Izd. Moskov. Gos. Univ., 1989) p. 53
17. N M Przheval'skii, I I Grandberg *Usp. Khim.* **56** 814 (1987) [*Russ. Chem. Rev.* **56** 477 (1987)]
18. S Blechert *Synthesis* 71 (1989)
19. R B Woodward, R W Hoffmann *Angew. Chem., Int. Ed. Engl.* **8** 781 (1969)
20. T Nakai, K Mikami, N Sayo *J. Synth. Org. Chem. Jpn.* **41** 100 (1983)
21. R K Hill, in *Asymmetric Synthesis* Vol. 3 (Ed. J D Morrison) (Orlando: Academic Press, 1984) p. 503
22. F E Ziegler *Acc. Chem. Res.* **10** (6) 227 (1977)
23. P A Barlett *Tetrahedron* **36** 3 (1980)
24. T Nakai *Kagaku to Seibutsu* **23** 471 (1985); *Chem. Abstr.* **104** 19 192b (1986)
25. T Kametani, H Kasai, E Sato, T Suzuki *Proc. Indian Acad. Sci. Chem. Sci.* **100** (2–3) 91 (1988); *Chem. Abstr.* **110** 24 118k (1989)
26. T Suzuki, E Sato, K Unno *Akita Igaku* **15** 759 (1988); *Chem. Abstr.* **112** 56 391b (1990)
27. T I Temnikova, S N Semenova *Molekulyarnye Peregruppirovki v Organicheskoi Khimii* (Molecular Rearrangements in Organic Chemistry) (Leningrad: Khimiya, 1983) p. 36
28. D A Evans, A M Golob *J. Am. Chem. Soc.* **97** 4765 (1975)
29. S E Denmark, M A Harmata *J. Am. Chem. Soc.* **104** 4972 (1982)
30. S E Denmark, M A Harmata *J. Org. Chem.* **48** 3369 (1983)
31. G Buchi, D E Vogel *J. Org. Chem.* **50** 4664 (1985)
32. S E Denmark, M A Harmata, K S White *J. Am. Chem. Soc.* **111** 8878 (1989)
33. C J Burrows, B K Carpenter *J. Am. Chem. Soc.* **103** 6983 (1981)
34. M J S Dewar, E F Healy *J. Am. Chem. Soc.* **106** 7127 (1984)
35. J J Gajewski, K R Gee, J Jurayj *J. Org. Chem.* **55** 1813 (1990)
36. C G Krespan *Tetrahedron* **23** 4243 (1967)
37. V G Andreev, A F Kolomiets, A V Fokin *J. Fluorine Chem.* **56** 259 (1992)
38. S T Purrington, S C Weeks *J. Fluorine Chem.* **56** 165 (1992)
39. J F M Oth, R Merenyi, H Rottele, G Schroder *Tetrahedron Lett.* **9** 3941 (1968)
40. Y Kobayashi, A Ando, K Kawada, I Kumadaki *J. Am. Chem. Soc.* **103** 3958 (1981)
41. W R Dolbier, K S Medinger *Tetrahedron* **38** 2411 (1982)
42. W R Dolbier, A C Alty, O Phanstiel *J. Am. Chem. Soc.* **109** 3046 (1987)
43. M-h Lin, W J le Noble *J. Org. Chem.* **54** 997 (1989); M-h Lin, W H Watson, R P Kashyap, W J le Noble *J. Org. Chem.* **55** 3597 (1990)
44. G M Brooke *Tetrahedron Lett.* **12** 2377 (1971)
45. G M Brooke, D H Hall, H M M Shearer *J. Chem. Soc., Perkin Trans. 1* 780 (1978)
46. G M Brooke *J. Chem. Soc., Perkin Trans. 1* 233 (1974)
47. G M Brooke *J. Chem. Soc., Perkin Trans. 1* 1463 (1976)
48. G M Brooke, D H Hall *J. Fluorine Chem.* **20** 163 (1982)
49. G M Brooke *J. Fluorine Chem.* **22** 483 (1983)
50. G M Brooke, R S Matthews, N S Robson *J. Fluorine Chem.* **16** 461 (1980)
51. G M Brooke, R S Matthews, N S Robson *J. Chem. Soc., Perkin Trans. 1* 102 (1980)
52. G M Brooke, I M Eggleston, F A Hale *J. Fluorine Chem.* **38** 421 (1988)
53. G M Brooke, J A K J Ferguson *J. Chem. Soc., Perkin Trans.1* 515 (1986)
54. C K Ingold *Structure and Mechanism in Organic Chemistry* (Translated into Russian) (Moscow: Mir, 1973) p. 711
55. B Iddon, H Suschitzky, J A Taylor *J. Chem. Soc., Perkin Trans. 1* 2756 (1979)
56. G M Brooke, D I Wallis *J. Chem. Soc., Perkin Trans. 1* 1417 (1981)
57. G M Brooke, J R Cooperwaite, J A K J Ferguson, A G Morpeth *J. Fluorine Chem.* **29** 113 (1985)
58. G M Brooke, J R Cooperwaite, A G Morpeth *J. Chem. Soc., Perkin Trans. 1* 2637 (1985)
59. G M Brooke, D I Wallis *J. Fluorine Chem.* **20** 173 (1982)
60. G M Brooke *J. Chem. Soc., Perkin Trans. 1* 107 (1982)
61. (a) G M Brooke, R S Matthews, M E Harman, M B Hursthouse *J. Fluorine Chem.* **53** 339 (1991); (b) W S Trahanovsky, S L Emeis, A S Lee *J. Org. Chem.* **41** 4043 (1976); (c) R F C Brown, F W Eastwood *J. Org. Chem.* **46** 4588 (1981)
62. V N Kovtonyuk, L S Kobrina, G G Yakobson *Zh. Org. Khim.* **15** 1447 (1979)
63. G M Brooke, D I Wallis *J. Chem. Soc., Perkin Trans. 1* 1659 (1981)
64. G M Brooke, J R Cooperwaite *J. Chem. Soc., Perkin Trans. 1* 2643 (1985)
65. T D Petrova, V P Mamaev, G G Yakobson *Izv. Akad. Nauk SSSR, Ser. Khim.* 679 (1969)
66. G M Brooke *J. Chem. Soc., Perkin Trans. 1* 821 (1983)
67. F D Benke, G M Brooke *J. Fluorine Chem.* **26** 77 (1984)
68. (a) D L Ladd, D Gaitanopoulos, J Weinstock *Synth. Commun.* **15** 61 (1985); (b) M T Clark, D D Miller *Tetrahedron Lett.* **26** 4299 (1985)
69. K Maruyama, N Nagai, Y Naruta *J. Org. Chem.* **51** 5083 (1986)
70. M A Patrick, S K Sethi, S E Unger, S Mirsadegni, A A Ribeiro, D R Thakker *J. Org. Chem.* **56** 888 (1991)
71. E T McBee, E Rapkin *J. Am. Chem. Soc.* **73** 2375 (1951)
72. (a) J M Bruce, Y Roshan-Ali *J. Chem. Soc., Perkin Trans. 1* 2677 (1981); (b) T Hayashi, M Goto *Nippon Kagaku Kaishi* 1512 (1977)
73. J Borgulya, R Madeja, P Fahrni, H-J Hansen, H Schmid, R Barner *Helv. Chim. Acta* **56** 14 (1973)
74. A G Mustafin, R R Gatulin, Z N Saraeva, Z Kh Valitova, I B Abdrakhmanov, G A Tolstikov, in *Tezisy Dokladov VI Vsesoyuznoi Konferentsii po Khimii Ftororganicheskikh Soedinenii, Novosibirsk, 1990* (Abstracts of Reports at the VIth All-Union Conference on the Chemistry of Organofluorine Compounds, Novosibirsk, 1990) p. 76
75. R P Ruh US P. 2 613 228 (1952); *Chem. Abstr.* **47** 8 774i (1953)
76. R A Bekker, V Ya Popkova, I L Knunyants *Zh. Org. Khim.* **13** 2104 (1977)
77. S Gelfand US P. 3 655 765 (1972); *Chem. Abstr.* **77** 34 040t (1972)
78. V F Snegirev, K N Makarov *Izv. Akad. Nauk SSSR, Ser. Khim.* 1331 (1986)
79. V F Snegirev, Candidate's Thesis in Chemical Sciences, Institute of Organoelement Compounds, USSR Academy of Sciences, Moscow, 1989, p. 66
80. R A Bekker, V Ya Popkova, I L Knunyants *Izv. Akad. Nauk SSSR, Ser. Khim.* 2347 (1982)
81. K Burger, K Geith, K Gaa *Angew. Chem., Int. Ed. Engl.* **27** 848 (1988)
82. K Burger, K Gaa, K Geith, in *Abstracts of the IX European Symposium on Fluorine Chemistry, Leicester, UK*; *J. Fluorine Chem.* **45** 126 (1989)
83. Ch Schierlinger, K Gaa, K Geith, N Sewald, K Burger, in *Abstracts of the IX European Symposium on Fluorine Chemistry, Leicester, UK; J. Fluorine Chem.* **45** 146 (1989)
84. K Burger, K Gaa, K Geith, Ch Schierlinger *Synthesis* 850 (1989)
85. K Burger, K Gaa, E Hoss *J. Fluorine Chem.* **47** 89 (1990)
86. B Helmreich, O Jendrewski, K Burger, in *Abstracts of the X European Symposium on Fluorine Chemistry, Padua, Italy*; *J. Fluorine Chem.* **58** 380 (1992)
87. K Burger, R Ottlinger, H Goth, J Firl *Chem. Ber.* **115** 2494 (1982)

88. N Engel, B Kubel, W Steglich *Angew. Chem., Int. Ed. Engl.* **16** 394 (1977)
89. K Burger, K Gaa, K Geith *J. Fluorine Chem.* **41** 429 (1988)
90. K Mutze, W Hollweck, K Burger, in *Abstracts of the X European Symposium on Fluorine Chemistry, Padua, Italy*; *J. Fluorine Chem.* **58** 381 (1992)
91. (a) W R Dolbier *Acc. Chem. Res.* **14** (7) 195 (1981); (b) A Greenberg, J F Liebman, D Van Vechten *Tetrahedron* **36** 1161 (1980)
92. B W Metcalf, E T Jarvi, J P Burkhart *Tetrahedron Lett.* **26** 2861 (1985)
93. M Shimizu, Y Nakahara, S Kanemoto, H Yoshioka *Tetrahedron Lett.* **28** 1677 (1987)
94. Y Nakahara, M Shimizu, H Yoshioka *Tetrahedron Lett.* **29** 2325 (1988)
95. P Cresson *Bull. Soc. Chim. Fr.* 2618 (1964)
96. T Nakai, C-P Qian, M Kobayashi, T Hirasa, in *Abstracts of the XIII International Symposium on Fluorine Chemistry, Bochum, FRG*; *J. Fluorine Chem.* **54** 68 (1991)
97. J J Gajewski, J Jurayj, D R Kimbrough, M E Gande, B Ganem, B K Carpenter *J. Am. Chem. Soc.* **109** 1170 (1987)
98. V F Snegirev, K N Makarov *Izv. Akad. Nauk SSSR, Ser. Khim.* 106 (1986)
99. Y Katsuhara, M Ozawa, T Komatsu *Jpn. Kokai Tokkyo Koho* 78-144 525 (1978); *Chem. Abstr.* **90** 186 400s (1979)
100. K N Makarov, L L Gervits, Yu A Cheburkov, I L Knunyants, V P Sass *J. Fluorine Chem.* **10** 323 (1977)
101. V Ya Popkova, V F Snegirev, M Yu Antipin, Yu T Struchkov *Izv. Akad. Nauk SSSR, Ser. Khim.* 1123 (1989)
102. I L Knunyants, E G Abduganiev, S T Kocharyan, M V Urushadze, V A Lifshits, Yu E Aronov, E M Rokhlin *Izv. Akad. Nauk SSSR, Ser. Khim.* 110 (1971)
103. E L Stogryn, S J Brois *J. Am. Chem. Soc.* **89** 605 (1967)
104. O Paleta *Chem. Listy* **64** 31; 366 (1970)
105. (a) M Hudlicky *Chemistry of Organic Fluorine Compounds* (2nd Ed.) (Chichester: Ellis Horwood, 1976) p. 281; (b) p. 514
106. Yu V Zeifman, E G Ter-Gabrielyan, N B Gambaryan, I L Knunyants *Usp. Khim.* **53** 431 (1984) [*Russ. Chem. Rev.* **53** 256 (1984)]
107. J T Barr, K E Rapp, R L Pruett, C T Bahner, J D Gibson, R H Lafferty *J. Am. Chem. Soc.* **72** 4480 (1950)
108. A D Petrov, V A Ponomarenko, G V Odabashyan *Dokl. Akad. Nauk SSSR* **121** 307 (1958)
109. D R Baer *J. Org. Chem.* **23** 1560 (1958)
110. J F Normant, O Reboul, R Sauvetre, J Villieras *C.R. Acad. Sci. Ser. C* **274** 1954 (1972)
111. J F Normant, O Reboul, R Sauvetre, H Deshayes, D Masure, J Villieras *Bull. Soc. Chim. Fr.* 2072 (1974)
112. W Yuan, R J Berman, M H Gelb *J. Am. Chem. Soc.* **109** 8071 (1987)
113. D C England, L R Melby, M A Dietrich, R V Lindsey *J. Am. Chem. Soc.* **82** 5116 (1960)
114. Ch T Pumpelly, J J Pedjac, E R Larsen B. P. 1 208 010 (1970)
115. K von Werner *J. Fluorine Chem.* **20** 215 (1982)
116. O A Radchenko, A Ya Il'chenko, in *Abstracts of the X European Symposium on Fluorine Chemistry, Padua, Italy*; *J. Fluorine Chem.* **58** 154 (1992)
117. A T Monakhova, E L Zaitseva, A P Simonov, A Ya Yakubovich *Zh. Org. Khim.* **5** 1937 (1969)
118. L I Zakharkin, V N Lebedev *Zh. Obshch. Khim.* **41** 817 (1971)
119. T Nakai, K Tanaka, K Ogasawara, N Ishikawa *Chem. Lett.* 1289 (1981)
120. V G Andreev, Candidate's Thesis in Chemical Sciences, VAKhZ, Moscow, 1980
121. V G Andreev, A F Kolomiets, K V Dvornikova, V E Platonov *Izv. Akad. Nauk SSSR, Ser. Khim.* 1925 (1992)
122. R J Koshar, T C Simmons, F W Hoffman *J. Am. Chem. Soc.* **79** 1741 (1957)
123. V G Andreev, A F Kolomiets, G A Sokol'skii *Dokl. Akad. Nauk SSSR* **250** 1386 (1980)
124. V G Andreev, A Yu Sizov, A F Kolomiets, A V Fokin, in *Abstracts of the XIII International Symposium on Fluorine Chemistry, Bochum, FRG*; *J. Fluorine Chem.* **54** 263 (1991)
125. T Kubota, Y Kondoh, Y Suda, A Tanaka, S Katoh, T Ohyama, T Tanaka *Chem. Express* **2** 619 (1987)
126. T Kubota, Y Kondoh, T Ohyama, T Tanaka *Nippon Kagaku Kaishi* 1576 (1989)
127. (a) I L Knunyants, E M Rokhlin *Sov. Sci. Rev. B., Chem. Rev.* **5** 97 (1984); (b) A E Bayliff, M R Bryce, R D Chambers, R S Matthews *J. Chem. Soc., Chem. Commun.* 1018 (1985)
128. V G Andreev, A F Kolomiets, G A Sokol'skii *Zh. Org. Khim.* **15** 2417 (1979)
129. V G Andreev, Yu I Sorochkin, A F Kolomiets, G A Sokol'skii *Zh. Vses. Khim. O-va im. D I Mendeleeva* **24** 663 (1979)
130. V G Andreev, A F Kolomiets, G A Sokol'skii *Izv. Akad. Nauk SSSR, Ser. Khim.* 1643 (1990)
131. R A Bekker, V Ya Popkova, I L Knunyants *Izv. Akad. Nauk SSSR, Ser. Khim.* 1692 (1980)
132. U Utebaev, E M Rokhlin, E P Lur'e *Izv. Akad. Nauk SSSR, Ser. Khim.* 142 (1976)
133. I L Knunyants, L S German, B L Dyatkin *Izv. Akad. Nauk SSSR, Otd. Khim. Nauk* 1353 (1956)
134. M Kolb, F Gerhart, J-P Francois *Synthesis* 469 (1988)
135. V G Andreev, A F Kolomiets, G A Sokol'skii *Zh. Vses. Khim. O-va im. D I Mendeleeva* **25** 106 (1980)
136. V G Andreev, Yu I Sorochkin, A F Kolomiets, G A Sokol'skii *Zh. Org. Khim.* **15** 1999 (1979)
137. V G Andreev, A F Kolomiets, G A Sokol'skii *Izv. Akad. Nauk SSSR, Ser. Khim.* 2391 (1989)
138. V G Andreev, A F Kolomiets, A F Eleev, G A Sokol'skii *Izv. Akad. Nauk SSSR, Ser. Khim.* 1672 (1990)
139. V G Andreev, A F Kolomiets, A V Fokin *Izv. Akad. Nauk SSSR, Ser. Khim.* 2805 (1991)
140. V G Andreev, A F Kolomiets, G A Sokol'skii *Zh. Org. Khim.* **15** 2419 (1979)
141. V G Andreev, A F Kolomiets, G A Sokol'skii *Zh. Org. Khim.* **15** 2000 (1979)
142. D C England, C G Krespan *J. Fluorine Chem.* **3** 91 (1973/74)
143. V G Andreev, A F Kolomiets, A V Fokin *Dokl. Akad. Nauk SSSR* **323** 490 (1992)
144. V G Andreev, A F Kolomiets, G A Sokol'skii *Zh. Org. Khim.* **16** 1773 (1980)
145. Yu V Zeifman, G S Kaitmazova, E M Rokhlin, M B Gambaryan *Izv. Akad. Nauk SSSR, Ser. Khim.* 204 (1989)
146. N V Vasil'ev, A F Kolomiets, G A Sokol'skii, in *Tezisy Dokladov IV Vsesoyuznoi Konferentsii po Khimii Ftororganicheskikh Soedinenii, Tashkent, 1982* (Abstracts of Reports at the IVth All-Union Conference on the Chemistry of Organofluorine Compounds, Tashkent, 1982) p. 185
147. Y Hanzawa, K Kawagoe, A Yamada, Y Kobayashi *Tetrahedron Lett.* **26** 219 (1985)
148. G Shi, Y Xu, M Xu *Tetrahedron* **47** 1629 (1991)
149. V G Andreev, V V Linev, A F Kolomiets, A V Fokin, in *Abstracts of the X European Symposium on Fluorine Chemistry, Padua, Italy*; *J. Fluorine Chem.* **58** 344 (1992)
150. V G Andreev, A F Kolomiets, G A Sokol'skii *Izv. Akad. Nauk SSSR, Ser. Khim.* 516 (1991)
151. R E Ireland, R H Mueller, A K Willard *J. Am. Chem. Soc.* **98** 2868 (1976)
152. D Barton, W D Ollis, (Eds) *Comprehensive Organic Chemistry* (Oxford: Pergamon Press, 1979) Vol. 2
153. J T Welch, J S Samartino *J. Org. Chem.* **50** 3663 (1985)
154. J T Welch, J S Plummer, T-S Chou *J. Org. Chem.* **56** 353 (1991)
155. K Araki, J S Plummer, F Gyenes, J O'Toole, J T Welch, in *Abstracts of the XIII International Symposium on Fluorine Chemistry, Bochum, FRG*; *J. Fluorine Chem.* **54** 198 (1991)
156. T Yokozawa, T Nakai, N Ishikawa *Tetrahedron Lett.* **25** 3991 (1984)
157. T Nakai, O Takahashi, Eur. P. 350 334 (1990); *Chem. Abstr.* **113** 39 950m (1990)
158. H Greuter, R W Lang, A J Romann *Tetrahedron Lett.* **29** 3291 (1988).
159. E S Lewis, J T Hill *J. Am. Chem. Soc.* **91** 7458 (1969)
160. I Savage, E J Thomas *J. Chem. Soc., Chem. Commun.* 717 (1989)
161. (a) J T Welch, S Eswarakrishnan *J. Org. Chem.* **50** 5909 (1985); (b) T Yamazaki, J T Welch, J S Plummer, R H Gimi *Tetrahedron Lett.* **32** 4267 (1991)
162. J T Welch, B De Corte, N De Kimpe *J. Org. Chem.* **55** 4981 (1990)
163. F Camps, J Coll, A Messeguer, A Roca *Tetrahedron Lett.* 791 (1976)

164. F Camps, R Canela, J Coll, A Messeguer, A Roca *Tetrahedron* **34** 2179 (1978)
165. M F Carroll *J. Chem. Soc. Pt II* 1266 (1940)
166. W S Johnson, L Werthemann, W R Bartlett, T J Brocksom, T-t Li, D J Faulkner, M R Petersen *J. Am. Chem. Soc.* **92** 741 (1970)
167. T Taguchi, T Morikawa, O Kitagawa, T Mishima, Y Kobayashi *Chem. Pharm. Bull.* **33** 5137 (1985)
168. T Yamazaki, N Ishikawa *Bull. Soc. Chim. Fr.* 937 (1986)
169. Y Hanzawa, K Kawagoe, K Nobuyuki, Y Kobayashi *Chem. Pharm. Bull.* **34** 3953 (1986)
170. B A Pawson, K K Chan, J DeNoble, R-J Han, V Piermattie, A C Speciman, S Srisethnil, P W Trown, O Bohoslawec, L J Machlin, E Gabriel *J. Med. Chem.* **22** 1059 (1979)
171. F Camps, A Messeguer, F-J Sanchez *Tetrahedron* **44** 5161 (1988)
172. I L Knunyants, B L Dyatkin *Izv. Akad. Nauk SSSR, Otd. Khim. Nauk* 648 (1958)
173. G C Apsey, R D Chambers, M J Salisbury, G Moggi *J. Fluorine Chem.* **40** 261 (1988)
174. K Tanaka, in *Compounds of Fluorine, Synthesis and Applications* (Ed. N. Isikawa; Translated into Russian from Japanese) (Moscow: Mir, 1990) p. 265
175. *Promyshlennye Ftororganicheskie Produkty* (Industrial Organofluorine Products) Handbook (Leningrad: Khimiya, 1990) p. 464
176. J T Welch, T Yamazaki, R H Gimi, in *Synthetic Fluorine Chemistry* (Eds G A Olah, R D Chambers, G K S Prakash) (New York: Wiley, 1992) p. 329
177. V G Andreev, A F Kolomiets, in *Abstracts of International Symposium 'Fluorinated Monomers and Polymers' Prague, 1993* (Programme Booklet)
178. A Mukherjee, E M Schulman, W J le Noble *J. Org. Chem.* **57** 3120 (1992)
179. P Erbes, W Boland *Helv. Chim. Acta* **75** 766 (1992)
180. D M Gale, W J Middleton, C G Krespan *J. Am. Chem. Soc.* **88** 3617 (1966)

Russian Chemical Reviews **62** (6) 579 – 601 (1993)
© 1993 Russian Academy of Sciences and Turpion Ltd

UDC 542.91 + 547.455 + 547.458.2

Glycals in enantiospecific synthesis

A G Tolstikov, G A Tolstikov

Contents

I.	Introduction	579
II.	Synthesis of glycals	579
III.	A brief description of the reactions of glycals which have found applications in the synthesis of natural products	580
IV.	Glycals in the synthesis of natural products with a cyclic structure and their fragments	585
V.	Decyclisation of glycals as a basis for synthesis of natural products and their structural analogues	596

Abstract. The reactions of 1,2-unsaturated sugars (glycals) are considered in this review in relation to problems of the enantiospecific synthesis of natural products, their fragments, and their analogues. The reactions occurring both with retention of the heterocycle and those carried out with the aim of obtaining open chain chiral units are discussed. It is shown that the use of glycals as a stock of chiral substances which determine the configuration of the asymmetric centres in the target products of multistage synthesis is promising. Schemes for the synthesis of natural products of different types are considered: *O*- and *C*-glycosides, nucleosides, oligosaccharides, pheromones, antibiotics, toxins, glycosphingolipids, etc. The bibliography includes 161 references.

I. Introduction

Glycals — 1,2-unsaturated derivatives of pentoses and hexoses — were first obtained by Fischer and Zach.[1] The factual data on the chemistry of glycals accumulated during several decades have been surveyed in two reviews.[2, 3] Since a detailed description of the results of studies during the last twenty years would have exceeded the available space in the present review, it appears useful to concentrate attention on the most important and interesting aspects of the chemistry of glycals which are of value for fine organic synthesis.

The main principles of the enantiospecific synthesis of natural products using chiral building blocks obtained from carbohydrates were formulated at the beginning of the 1970s. The excellent book by Kochetkov et al.[4] and a number of reviews[5–7] are devoted to this question. On the other hand, a detailed study of the literature enabled us to note that, until the beginning of the 1980s, there were only a few isolated examples of the use of natural sugars such as glycals in the total synthesis of natural products. A notable feature of this decade has been an increasing interest in the chemistry of glycals in connection with problems of enantiospecific synthesis.

At the present time the glycal approach is regarded as one of the promising methods of synthesis of *O*- and *C*-glycosides and oligosaccharides. Reactions involving electrophilic addition to the double bond in glycals are important in this connection. Glycals are completely irreplaceable in the synthesis of natural metabolites incorporating in their structure oxygen-containing heterocycles (ionophoric antibiotics, sea toxins, etc.). The Ferrier reaction,[8] which proceeds as S_N2' substitution accompanied by the allyl rearrangement, has been noted among the reactions which are specially important for the specific modification of glycals. The reactions of alcohols and thiols under the influence of Lewis acids, *C*-glycosylation by cation-active alkenes, allylsilanes, and silyl ethers of enols, the coupling with arenes, malonates, and aryl halides in the presence of metal complex catalysts, and the synthesis of *N*-nucleosides proceed in precisely this way. The reactions of glycals based on the Claisen rearrangement are distinguished by a high enantiospecificity in the formation of new oxygen–carbon bonds. The [2+2]-, [3+2]-, and [4+2]-cycloaddition reactions, which make it possible to obtain cyclic systems and also to achieve the stereospecific introduction of heteroatomic functional groups, are finding applications to an increasing extent. A very promising approach, which has so far been little developed, involves the use of organometallic derivatives of glycals of vinyl type. The products of the oxidation reactions of glycals have acquired great synthetic value. The decyclisation reactions, which make it possible to obtain open chain chiral units, are widely used. Having restricted the present review to the discussion of the methods of synthesis of natural products, we intend at the same time to give a description, which is as detailed and systematic as possible, of the characteristic reactions of glycals and also to include a bibliography, which, although not necessarily referring to the synthesis of natural products and their molecular fragments, is nevertheless of interest to a wide range of readers.

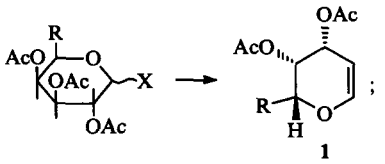
II. Synthesis of glycals

The characteristics of the classical method of synthesis of glycals, which involves treatment of the corresponding acylglycosyl bromides with zinc dust, are given in the paper of Fischer and Zach[1] and in the reviews by Ferrier.[2, 3] The method involves fairly mild conditions, since it makes it possible to obtain in satisfactory yields glycals from disaccharides, for example gentiobial,[9] and modified type **1** glycals from 6-deoxy-6-substituted galactopyranosides (Scheme 1).[10, 11]

A G Tolstikov, G A Tolstikov Institute of Organic Chemistry, Ufa Scientific Centre, Russian Academy of Sciences, prosp. Oktyabrya 69, 450054 Ufa. Fax (7-347-2) 35 60 66

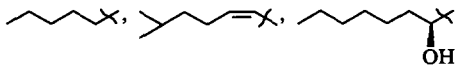
Received 2 November 1992
Uspekhi Khimii **62** (6) 621 – 643 (1993); translated by A K Grzybowski

Scheme 1



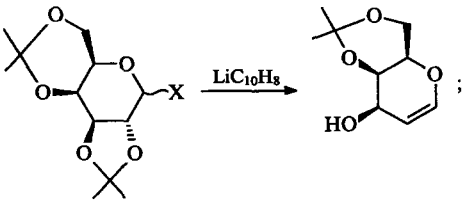
1

X = OAc, Br ;

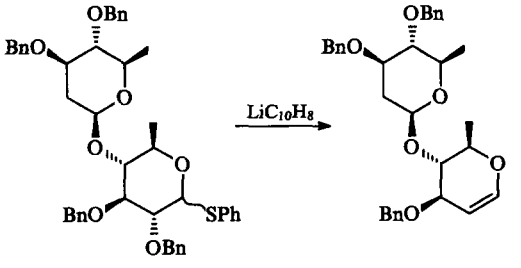
R = 

A number of studies have been devoted to the improvement of the method of synthesis of glycals.[12-14] The possibility of a significant increase in yields when the zinc–silver or the zinc–copper couple,[15, 16] aluminium amalgam,[17] a divalent chromium salt,[18] and lithium in liquid ammonia[19-21] are used was demonstrated. Lithium naphthalide was used successfully in the synthesis of glycals from *S*-glycosides and their oxidised derivatives (Scheme 2).[22, 23]

Scheme 2

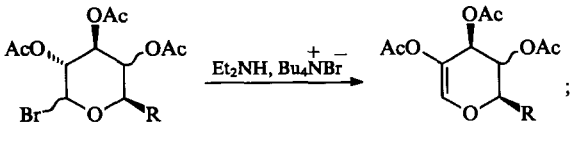


X = PhS, $PhSO_2$.



Derivatives of 2-deoxysugars, containing leaving groups of the type OMs, Cl, and SOPh at the C(1) atom are used in many instances.[24-26] 2-Acyloxyglycals, obtained by treating the corresponding acylglycosyl bromides with diethylamine in the presence of quaternary ammonium salts, have been acquiring increasing importance in the synthesis of natural products (Scheme 3).[27]

Scheme 3

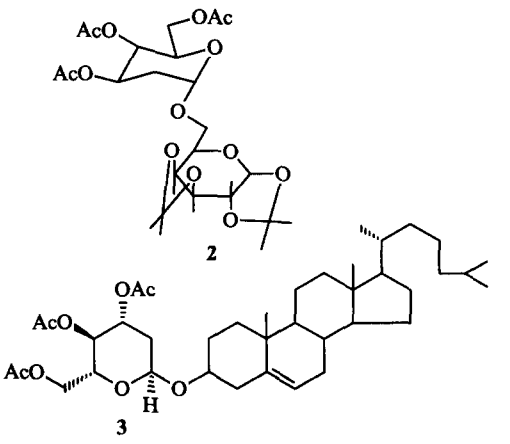


R = H, Me, CH_2OAc .

III. A brief description of the reactions of glycals which have found applications in the synthesis of natural products

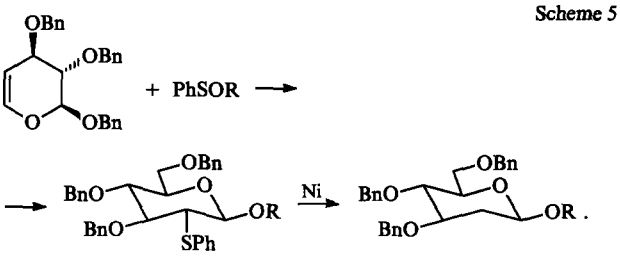
The addition of electrophiles to the double bond of glycals is used in the synthesis of *O*- and *C*-glycosides and oligosaccharides. According to Sabegam and Neira,[28] the very simple reaction involving the addition of water and alcohols is best catalysed by an acid cation exchanger and LiBr. The reactions in the presence of the complex $PPh_3 \cdot HBr$ take place with a high α-stereoselectivity.[29] The α-*O*-glycosides **2** and **3** were synthesised in this way from tri-*O*-acetyl-D-glucal, diisopropylgalactopyranose, and cholesterol (Scheme 4).[2, 3]

Scheme 4



The addition to glycals of benzenesulfenic acid esters, synthesised from PhSCl and the corresponding alcohols, is resorted to in order to obtain the β-*O*-glycosides of 2-deoxysugars (Scheme 5).[30]

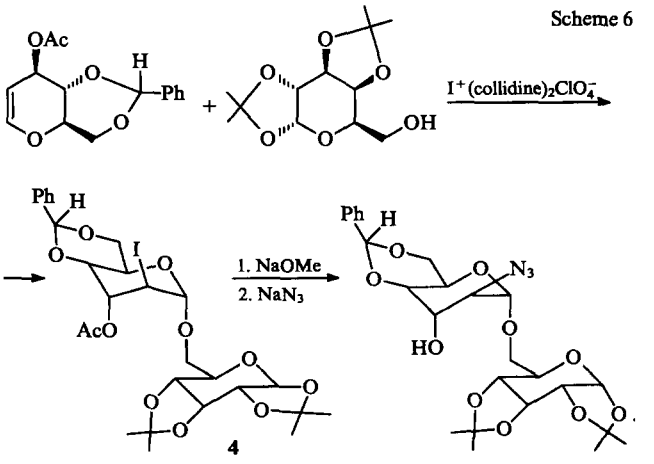
Scheme 5



Phenyl selenyl chloride[31, 32] and phosphorodithioic acid esters[33] can also be used for such purposes.

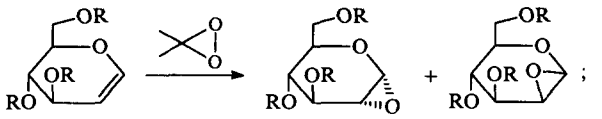
The method based on the addition of alcohols to glycals in the presence of donors of iodonium ions proved to be extremely promising. The complex $I^+(collidine)_2ClO_4^-$ or iodosuccinimide is used as a donor of this kind.[34, 35] The presence of the iodine atom in the adduct **4** makes it possible to introduce nucleophilic groups, in particular the azido-group (Scheme 6).[36]

Scheme 6



The use of 1,2-epoxysugars, obtained by epoxidising glycals with dimethyldioxiran (Scheme 7), has led to extensive prospects.[37, 38]

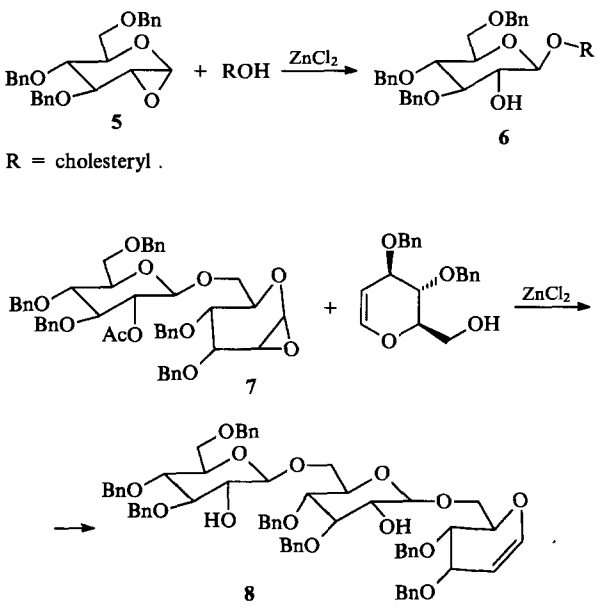
Scheme 7



R = Ac, Bn, Bu^{t}Me$_2$Si (TBS).

The great synthetic possibilities of this method are demonstrated in Scheme 8. Here the opening of the epoxide ring in compounds **5** and **7** by alcohols in the presence of $ZnCl_2$ proceeds regiospecifically with formation of the individual *O*-glycosides **6** and **8**. The configuration of the latter is determined by the stereochemistry of the initial epoxides.

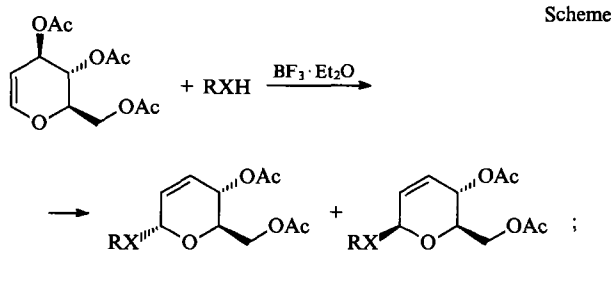
Scheme 8



R = cholesteryl.

The reactions of glycals accompanied by the allyl rearrangement have found wide scale application. The first of these, the so called Ferrier rearrangement, takes place with participation of alcohols and thiols in the presence of Lewis acids (Scheme 9).[2, 3, 8]

Scheme 9

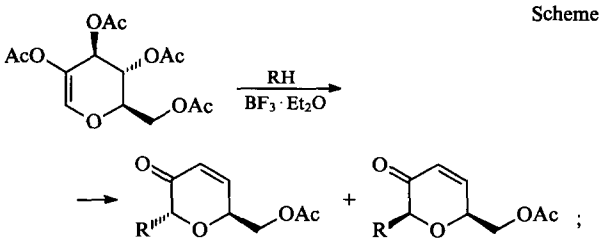


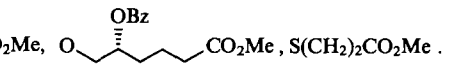
X = O, S.

This reaction is used to synthesise substituted 3-oxo-2*H*-pyrans from 2-acetoxyglycals (Scheme 10).[39, 40]

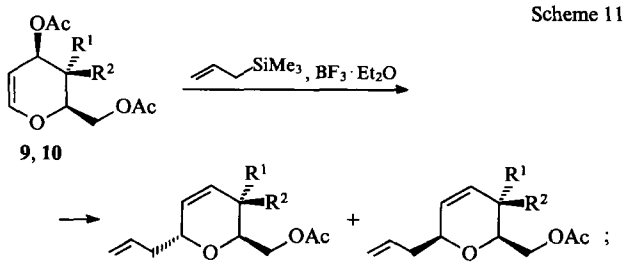
The synthesis of *C*-glycosides is of considerable interest because of the possibility of obtaining 2,6-disubstituted dihydropyrans — important building blocks in the total synthesis of many heterocyclic natural products. The reaction of allyltrimethylsilane with glycals is sensitive to steric factors, which follows from the greater α-stereoselectivity of the interaction of tri-*O*-acetyl-D-galactal **9** compared with tri-*O*-acetyl-D-glucal **10** (Scheme 11).[41]

Scheme 10



R = OCH_2CO_2Me,  , $S(CH_2)_2CO_2Me$.

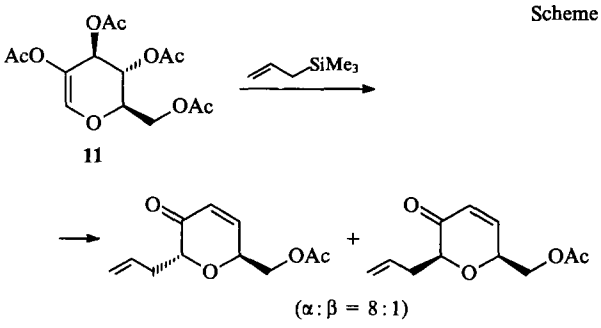
Scheme 11



R^1 = H, R^2 = OAc (**9**) (α:β = 30:1);
R^1 = OAc, R^2 = H (**10**) (α:β = 16:1).

It has been shown that the 2-acetoxyglucal **11** reacts with allyltrimethylsilane in the presence of $BF_2 \cdot OEt_2$ as the catalyst with formation of a mixture of anomeric 3-oxo-*C*-glycosides (Scheme 12).[39]

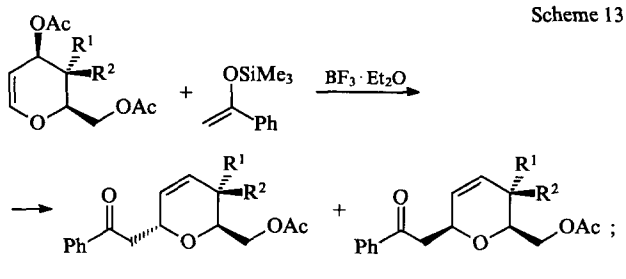
Scheme 12



(α:β = 8:1)

1-Trimethylsiloxystyrene interacts with glycal acetates in the presence of Lewis acids, affording a mixture of isomeric ketones (Scheme 13).[42]

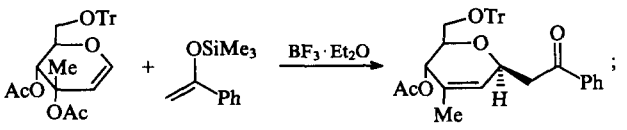
Scheme 13



R^1 = H, R^2 = OAc (α:β = 7:1);
R^1 = OAc, R^2 = H (α:β = 4:1).

This reaction can be carried out α-stereospecifically if a bulky substituent, screening the β-position, can be introduced into the molecule of the initial glycal at the C(6) atom (Scheme 14).[43]

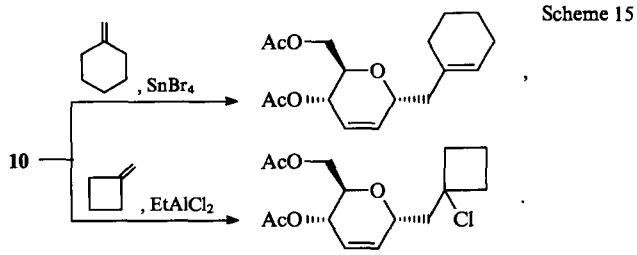
Scheme 14



Tr = Ph_3C .

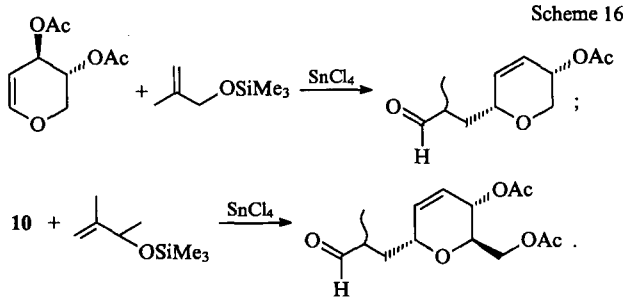
The reactions of cation-active alkenes with various glycals, which occur in the presence of $SnBr_4$ or $BF_3 \cdot OEt_2$, are surprisingly α-stereospecific. If they are carried out in the presence of $EtAlCl_2$ or $TiCl_4$ as catalysts, their products are chloro-substituted *C*-glycosides which also have exclusively the α-configuration (Scheme 15).[44]

Scheme 15



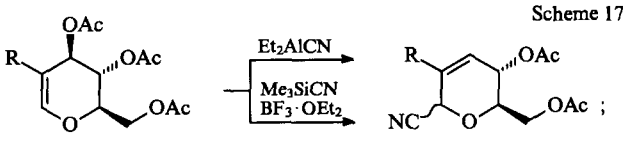
The reactions of glycal acetates with the silyl ethers of methylallyl alcohol and 2-methyl-3-siloxybut-1-ene lead with a high overall yield (77%–96%) to aldehydes in the form of a mixture of (*R*, *S*)-stereoisomers in relation to the side chain (Scheme 16).[45]

Scheme 16



The direct introduction of the cyano-group into glycal ethers by treatment with Et_2AlCN –[46] or $Me_3SiCN - BF_3 \cdot OEt_2$[47] also leads to the allyl rearrangement, affording the corresponding nitriles as a mixture of the α- and β-anomers (Scheme 17).

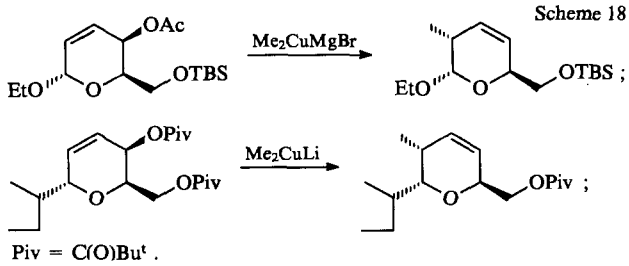
Scheme 17



R = H, OAc .

It is noteworthy that the application of organoelement reagents in the chemistry of glycals does not have particularly distinctive features. Nevertheless the cross-coupling of magnesium and lithium cuprate reagents with derivatives of glycals made it possible to obtain a series of important synthons (Scheme 18).[48, 49]

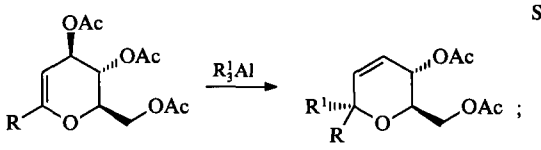
Scheme 18



Piv = C(O)Bu^t .

According to the data of Nicolaou et al.,[50] the $TiCl_4$-catalysed reaction of 1-substituted glycals with organoaluminium compounds proceeds stereospecifically (Scheme 19).

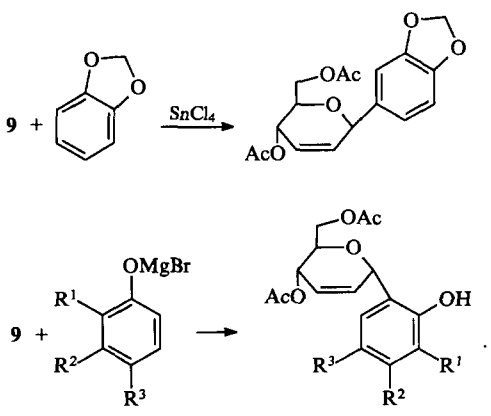
Scheme 19



R = Me, $CH_2CH{=}CH_2$;
R^1 = Me, Et .

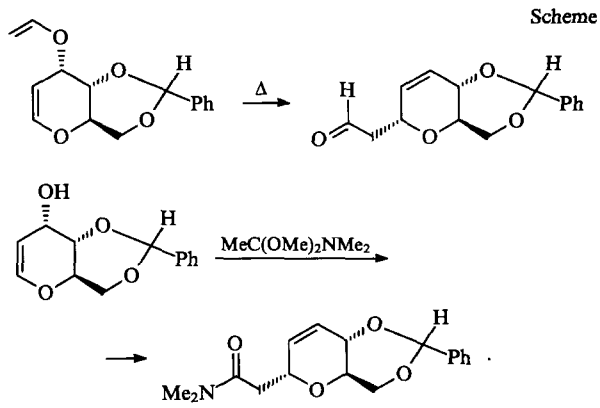
C-Arylglycosides of natural origin can be obtained from glycals. The reaction takes place with the Ferrier rearrangement and the stereochemistry of the product depends on the method selected for this purpose (Scheme 20).[51–56]

Scheme 20



The Claisen rearrangement with participation of glycal derivatives has been extended with the stereocontrolled formation of a new C–C bond. The thermal rearrangement involves the preliminary formation of the vinyl ethers of glycals or the direct reaction of the latter with the dimethyl acetal of *N*,*N*-dimethylacetamide (Scheme 21).[57]

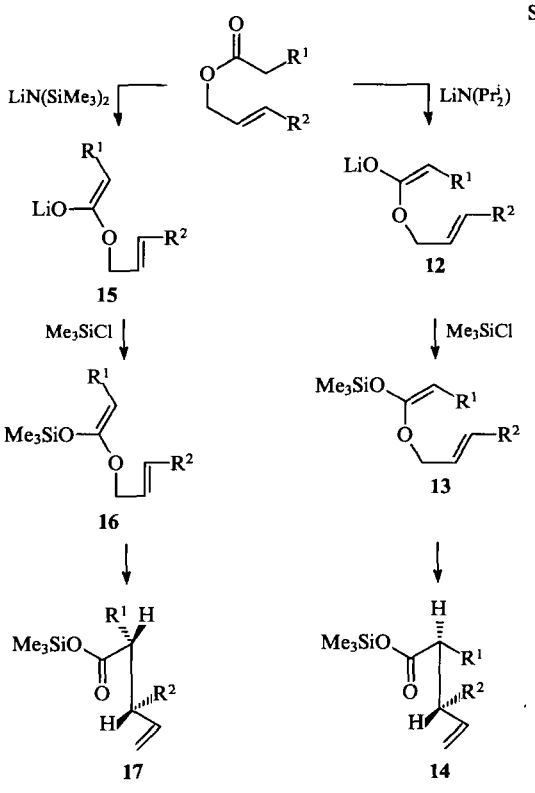
Scheme 21



However, this method is extremely restricted by the choice of the vinyl fragments and one cannot claim that it is widely used. Ireland and coworkers[58–60] found a general approach guaranteeing a high stereoselectivity of the reaction. It is striking that the stereochemistry of the target product can be regulated by altering the nature of the enolisable reagent. Thus the deprotonation of the ethers of allyl alcohols with lithium diisopropylamide in solution in tetrahydrofuran affords the (*Z*)-lithium enolate **12**, the treatment of which with Me_3SiCl leads to the (*E*)-ketene silyl acetal **13**. If the reaction is carried out in hexamethylphosphoramide or lithium bis-(trimethylsilyl)amide is used, then (*E*)-lithium enolate **15** and afterwards the (*Z*)-ketene silyl acetal **16** are formed.

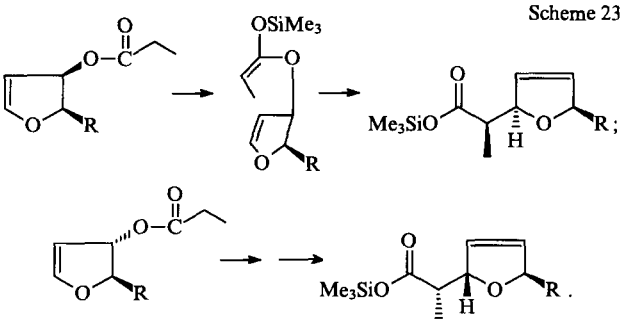
The [3,3]-sigmatropic rearrangement of silyl acetal takes place at −78 °C, the (*E*)-silyl acetal **13** and the (*Z*)-acetal **16** affording respectively the *erythro*-isomer **14** and the *threo*-isomer **17** (Scheme 22).

Scheme 22



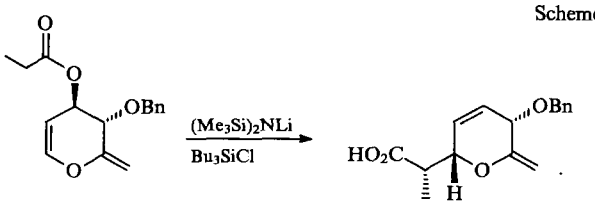
These principles have been clearly demonstrated in relation to the rearrangement of the silyl acetals prepared from the corresponding propionates of furanoglycals (Scheme 23).[60]

Scheme 23



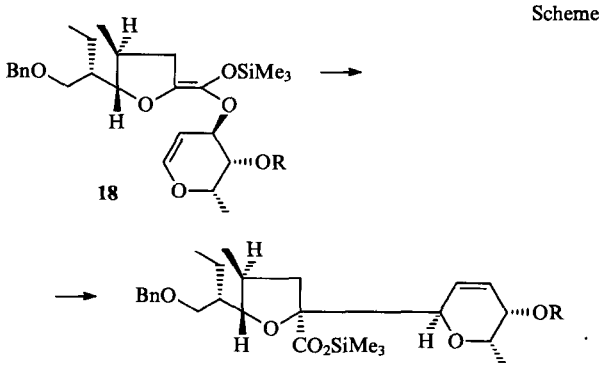
Unfortunately the stereospecificity of the formation of the chiral centre in the side chain breaks down for the propionates of pyranoglycals. For example, a mixture of *C*-glycosides enriched in the α-epimer (up to 86%) was obtained in one of the stages of the synthesis of streptolic acid (Scheme 24).[61]

Scheme 24



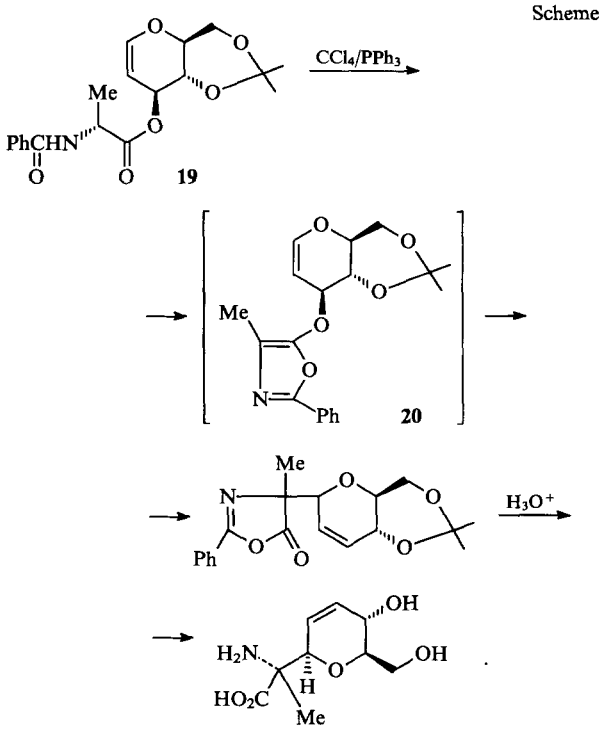
The synthetic possibilities of Ireland's method can be inferred in relation to the rearrangements of the silyl acetal **18**, which has a complex structure (Scheme 25).[62]

Scheme 25



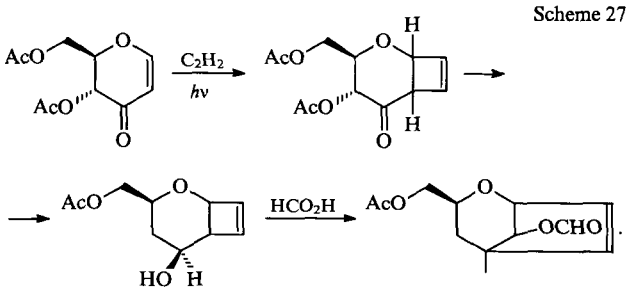
The enolisation of the esters of *N*-benzamidoacids of type **19** makes it possible to achieve an extremely interesting reaction via the oxazole intermediate **20** (Scheme 26).[63]

Scheme 26



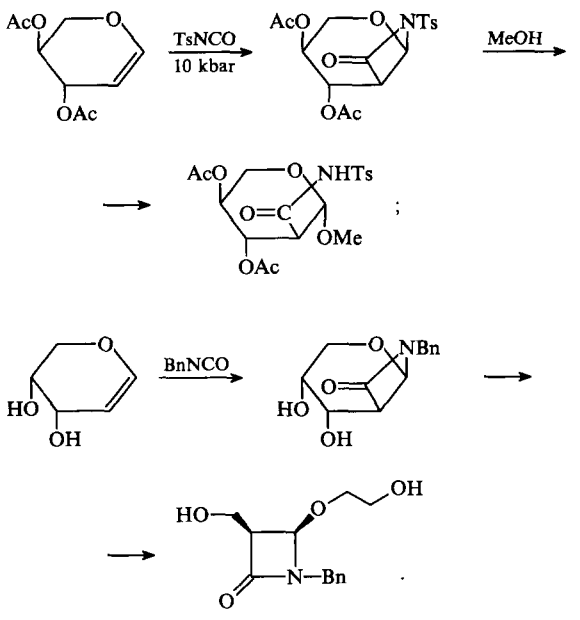
The cycloaddition reactions of glycals and their derivatives have found their place in the stereoselective synthesis of a series of useful bicyclic synthons. Thus the photocycloaddition of acetylene to glycal derivatives via the [2 + 2]-mechanism is regarded as a promising method of constructing the skeleton of trichothecene (Scheme 27).[64, 65]

Scheme 27



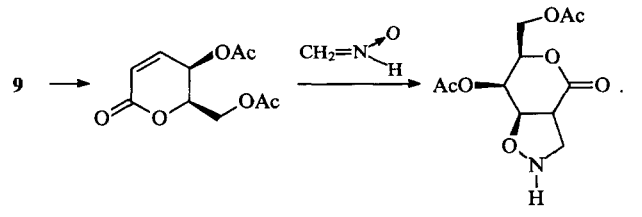
Acyl and sulfonyl isocyanates add to glycals at a pressure of several kilobars, affording [2 + 2]-adducts. The latter have been used in the synthesis of 2-carboxysugars[66, 67] and optically active β-lactams (Scheme 28).[68]

Scheme 28



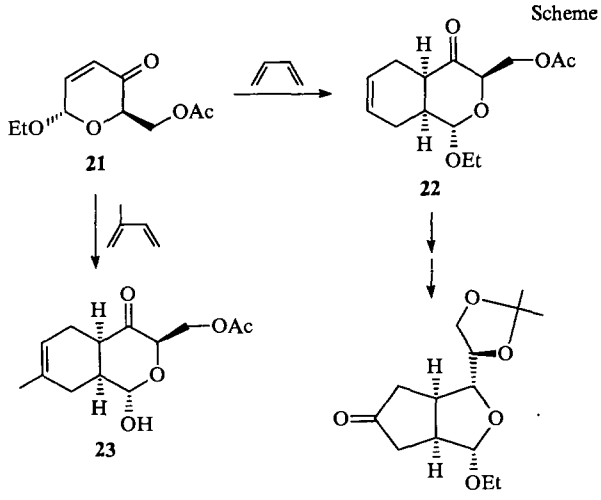
Glycals and their derivatives, which are active 1,3-dipolarophiles, combine with nitrile oxides,[69] nitrones,[70] and formaldoxime (Scheme 29).[71]

Scheme 29



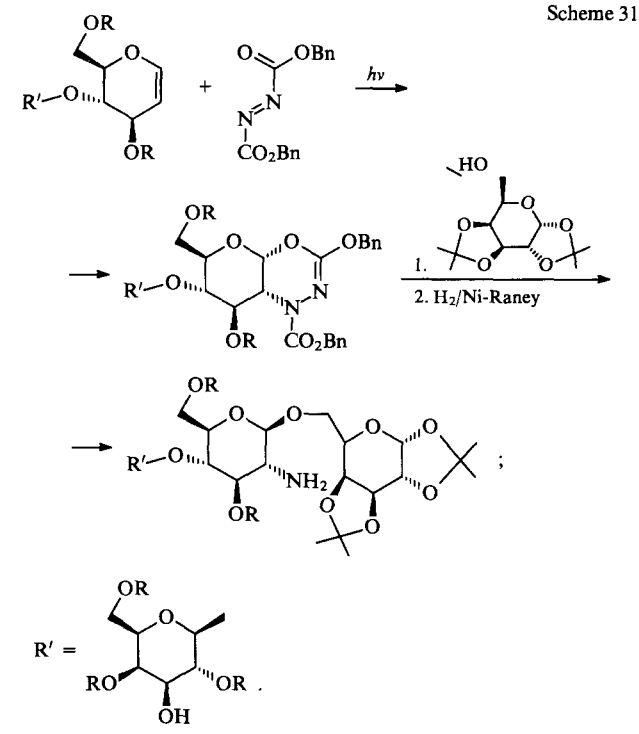
Chiral synthons have been obtained by the [4+2]-cycloaddition reactions of glycals and their derivatives with dienes. Thus the interaction of the enone **21** with butadiene results in the formation of the product **22**, which is used as the starting compound for the synthesis of cyclopentanoid compounds of the type of brefeldin.[72] The Lewis acid-controlled condensation of the enone **21** with isoprene makes it possible to obtain fairly readily compound **23** (Scheme 30).[73]

Scheme 30



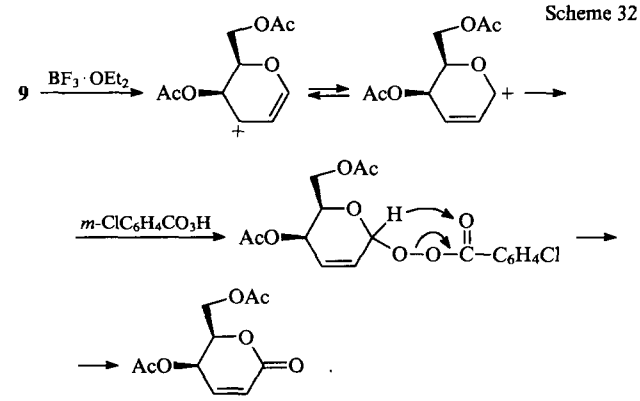
The approach to the synthesis of 2-amino-2-deoxysugars developed by Leblanc and Rokach is of great preparative value.[74-76] The photoinitiated reaction of glycals with dibenzyl azodicarboxylate proceeds as a [4+2]-addition. Treatment of the adducts with alcohols in the presence of toluene-*p*-sulfonic acid affords *O*-glycosides, which are converted after hydrogenolysis into 2-aminosugars (Scheme 31).

Scheme 31



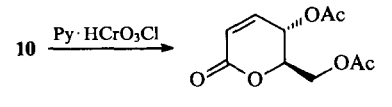
Among the oxidation reactions of glycals, their single-stage conversion into unsaturated lactones on treatment with *m*-chloroperbenzoic acid in the presence of $BF_3 \cdot OEt_2$ is striking.[77, 78] The proposed mechanism of the oxidation reaction is illustrated in Scheme 32.

Scheme 32



Glycals are oxidised similarly by the complex $Py \cdot HCrO_3Cl$. It has been pointed out[79, 80] that the yields of the lactones are higher than in oxidation with peracids (Scheme 33).

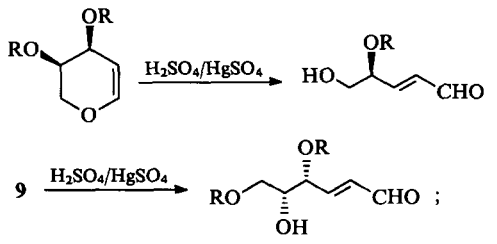
Scheme 33



The decyclisation reaction of glycals has been recently used with increasing frequency in enantiospecific synthesis. Several methods of synthesis of open chain synthons from glycals are known. One of these has been developed by Perlin and coworkers.[81, 82] On treatment with Hg^{2+} salts in an acid

medium, glycal acetates are converted into partial acetates of α,β-unsaturated hydroxyaldehydes. According to Tolstikov et al.[83] and Hirata et al.,[84] the ring is opened similarly to benzyl ethers of glycals based on pentoses and hexoses (Scheme 34).

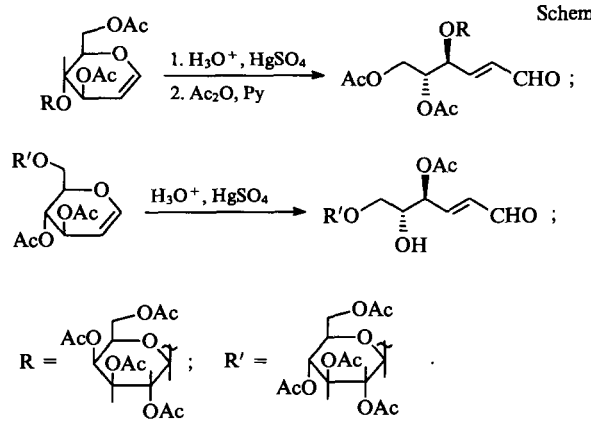
Scheme 34



R = Ac, Bn .

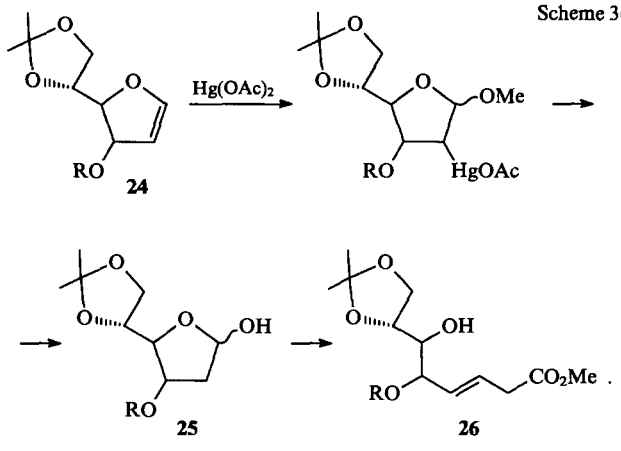
The acid $HgSO_4$-catalysed decyclisation of the full acetates of glycals derived from disaccharides leads to *O*-glycosylated α,β-unsaturated acetoxyaldehydes (Scheme 35).[85–88]

Scheme 35



A convenient method of decyclisation is based on the conversion of glycals into 2-deoxysugars with their subsequent conversion into olefins. Thus the 2-deoxysugar **25** was obtained from the furanoglycal **24** via a methoxymercuration stage, after which the unsaturated ester **26** was prepared (Scheme 36).[89]

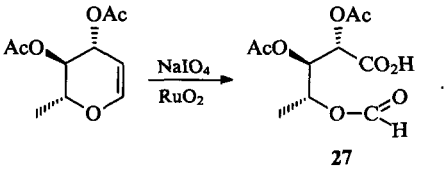
Scheme 36



This approach will probably be used in a specific synthesis, because the method proposed recently for the direct hydration of glycals[90] obviates the need for mercury salts.

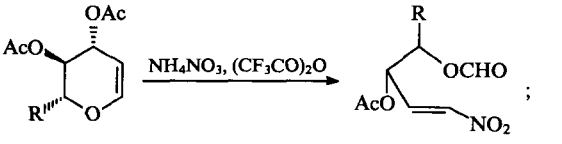
Oxidative degradation involving the double bond of glycals makes it possible to obtain nor-derivatives. For example, the RuO_2-catalysed oxidation of di-*O*-acetyl-D-rhamnal with $NaIO_4$ led to a 5-deoxyarabinonic acid ester **27** (Scheme 37).[91]

Scheme 37



An interesting oxidation reaction takes place when glycals are treated with ammonium nitrate in trifluoroacetic anhydride (Scheme 38).[92]

Scheme 38



R = CH_2OAc, Me .

As can be seen from the data presented, the reactions of glycals are distinguished by high stereoselectivity and in many cases conditions have been found for a stereospecific course of the reaction. Naturally, this characteristic of glycols cannot fail to draw attention to them in the selection of synthons used in the enantiospecific synthesis of natural products.

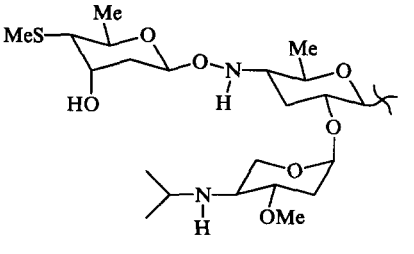
IV. Glycals in the synthesis of natural products with a cyclic structure and their fragments

1. Derivatives of monosaccharides. *O*- and *C*-glycosides

Glycals are being used to an increasing extent in the synthesis of rare mono-, di-, and oligo-saccharides and also *O*-glycosides with aglycones of different structural types. The examples described below convincingly demonstrate the extensive possibilities of the glycal approach.

The recently discovered carcinostatic enediyne antibiotics are distinguished by an abundance of functional groups and an unusual structure of the glycoside fragments. Thus esperamicin contains the trisaccharide fragment **28** incorporating thio- and amino-sugars (Scheme 39).

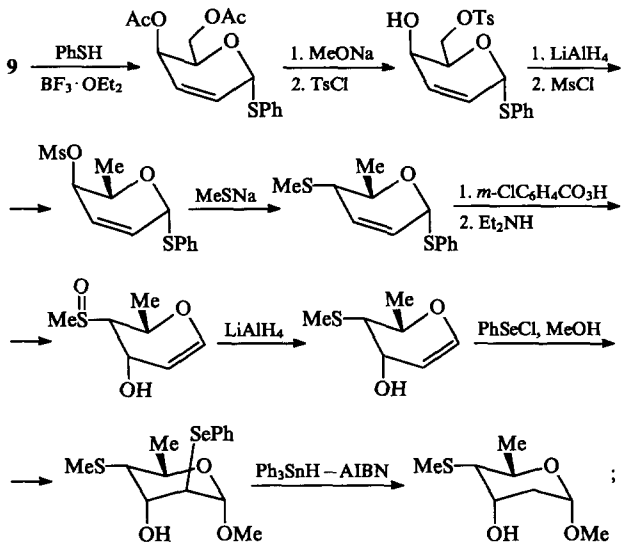
Scheme 39



The scheme for the synthesis of the thiosugar **29**, which forms part of the composition of the trisaccharide fragment of the antibiotic, based on the tri-*O*-acetyl-D-galactal **9**, is attractive because of the stereospecificity of all the stages and the twofold use of the reagent by virtue of the presence of a double bond of the glycal type (Scheme 40).[93]

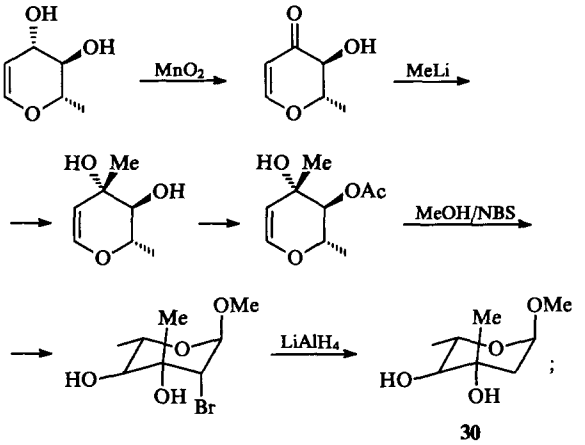
The antibiotics olivomycin and chromomycin contain L-olivomycose **30** as part of the composition of the trisaccharide fragment. Its synthesis from L-rhamnal consists of only a few stages (Scheme 41).[94]

Scheme 40



AIBN = azoisobutyronitrile.

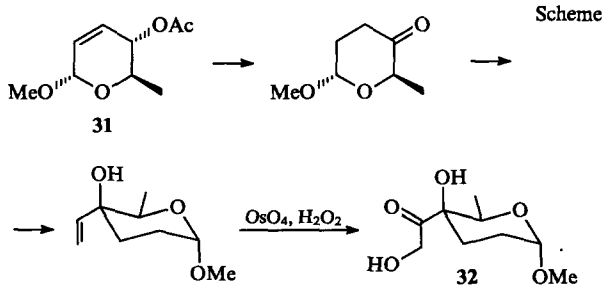
Scheme 41



NBS = *N*-bromosuccinimide.

Pillaromycin A—an antibiotic with anticancer activity—contains a deoxysugar—pillarose **32**, which has been synthesised from the Ferrier glycoside **31** (Scheme 42).[95]

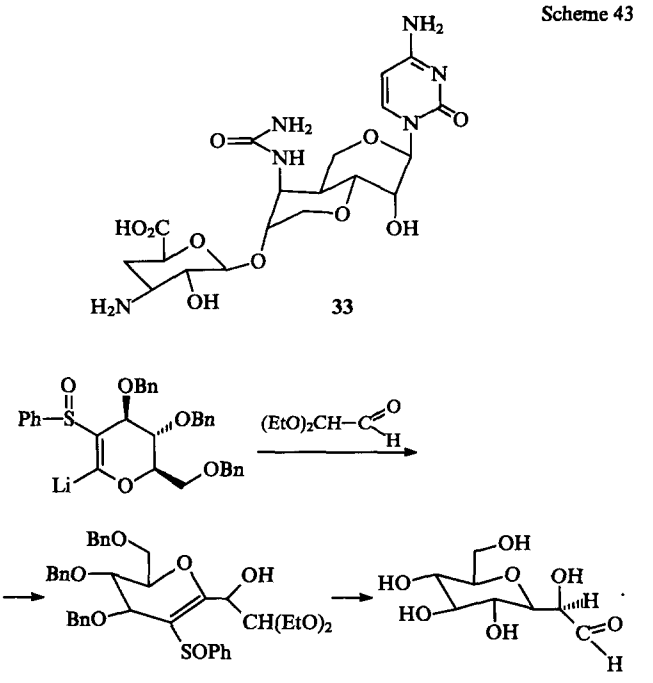
Scheme 42



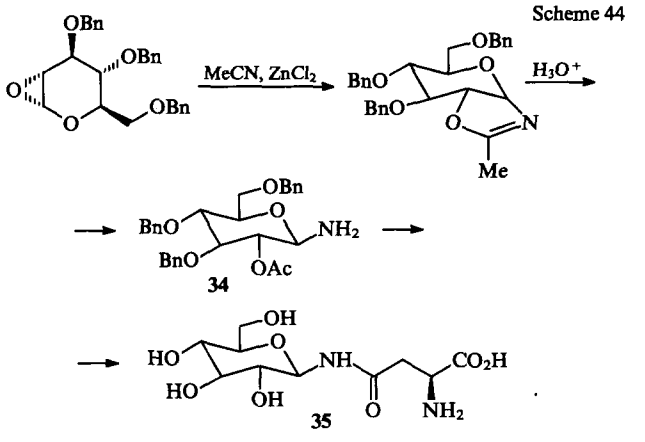
A derivative of vinyllithium, obtained by the direct introduction of lithium into tri-*O*-benzyl-2-benzenesulfoxygalactal, was used in the synthesis of the antibiotic ezomycin **33** from tri-*O*-benzyl-D-glycal. The reaction with the diethyl acetal of glyoxal took place smoothly with subsequent formation of the D-glucose *C*-glycoside as the key synthon (Scheme 43).[96]

Glucosylasparagine **35** was synthesised with the use of the epoxide of tri-*O*-benzyl-D-glucal (Scheme 44).[97] The formation of the indi-vidual β-glucosylamine **34** is striking.

Scheme 43

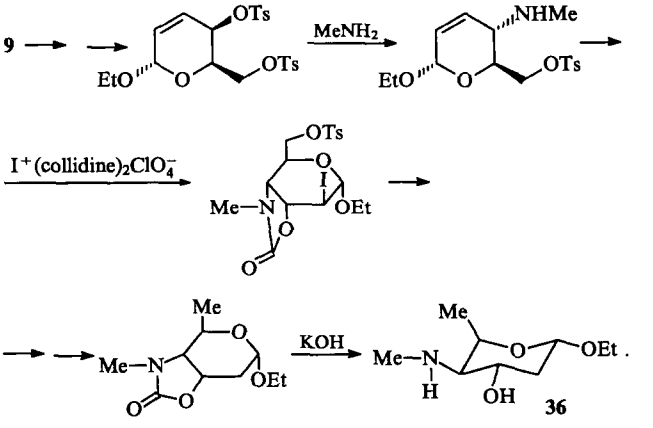


Scheme 44



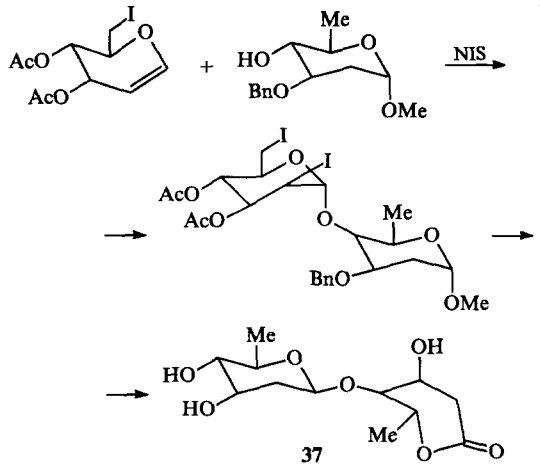
The aminosugar holacosamine **36**, which forms part of the composition of the steroid glycosides holacurtine and holarosine, has been synthesised from tri-*O*-acetyl-D-galactal **9** (Scheme 45).[98]

Scheme 45



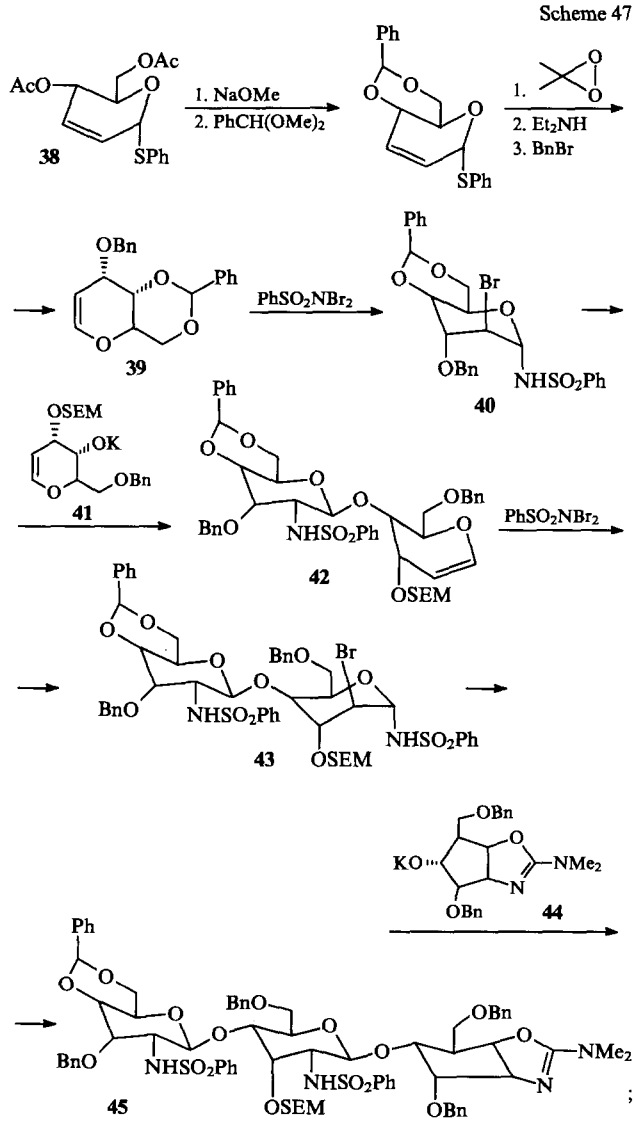
The formation of the glycosidic linkage with the aid of *N*-iodosuccinimide (NIS) has been used successfully in the synthesis of bamflalactone **37** (Scheme 46).[99]

Scheme 46



The glycoside allosamidin (compound **45** is its derivative), isolated the from *Streptomyces* mycelium, is a selective inhibitor of chitinase. Its synthesis represents a very characteristic example of the application of the varied reactivity of glycals. The phenylthioglycoside **38** was converted into the key synthon **39** via a stage involving oxidation to the sulfoxide and the subsequent sulfoxide rearrangement. The reaction of the synthon with *N*-dibromobenzenesulfonamide affords the bromosulfonamide **40**, which readily condenses with the potassium alkoxide derived from the glycal **41**.

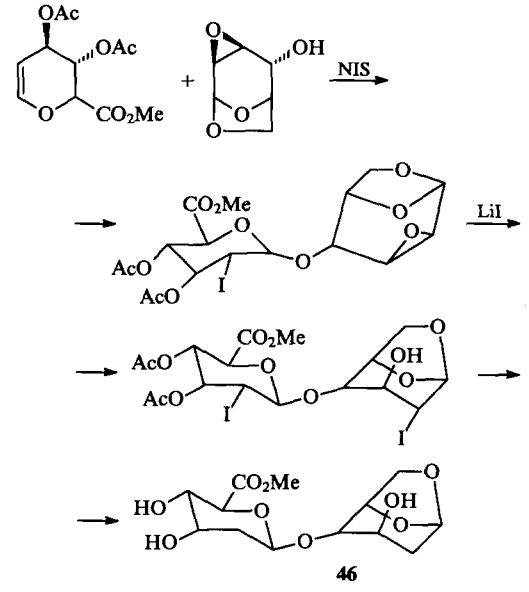
Scheme 47



The repeated reaction of compound **42** with the dibromosulfonamide and the condensation of the product **43** with the potassium alkoxide derived from the aglycone **44** made it possible to obtain the target glycoside **45** (Scheme 47).[100]

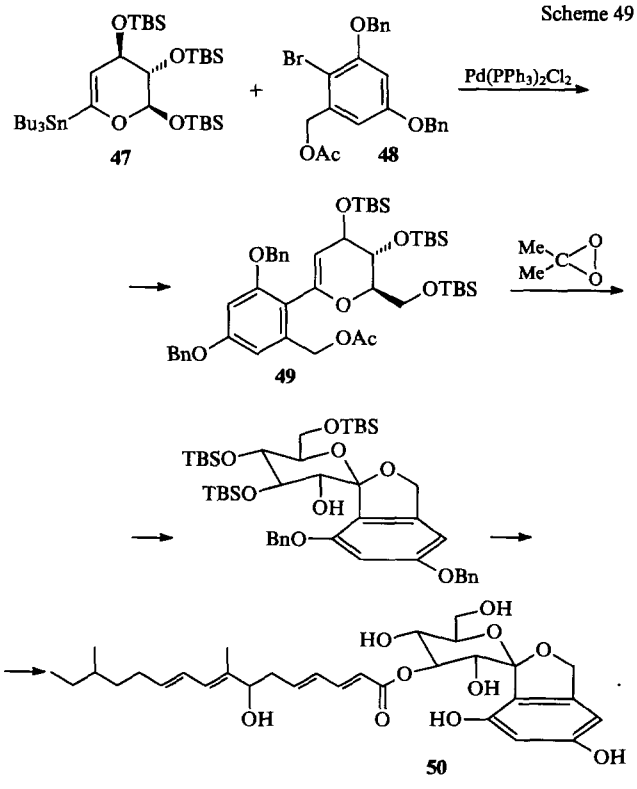
The disaccharide **46**, which forms part of the structure of the heptasaccharide orthosomycin, has been obtained from the glycal of glucuronic acid (Scheme 48).[101]

Scheme 48



Papulacandin **50** is one of the promising fungistatic agents. In the synthesis of the glycoside components of its molecule, the cross-coupling of the organotin glucal derivative **47** with the aryl bromide **48** and the oxidation of the *C*-arylglucal **49** by dimethyldioxiran constitute remarkable stages (Scheme 49).[102]

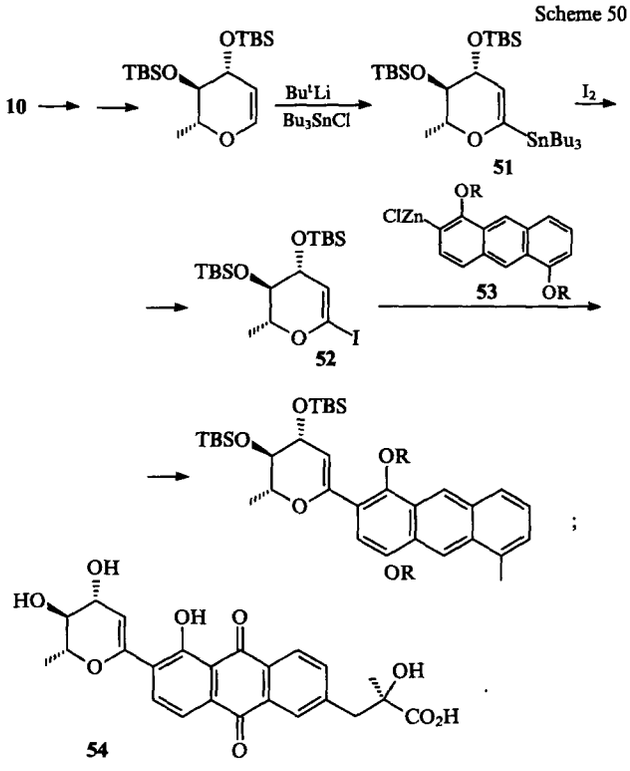
Scheme 49



SEM = β-(trimethylsilyl)ethoxymethyl .

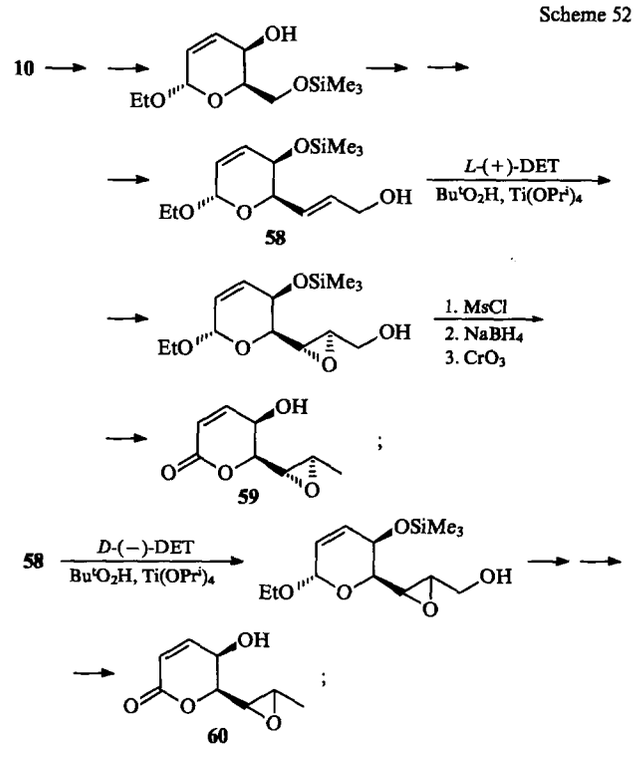
It has been suggested that tri-*O*-acetyl-D-glucal **10** be used for the synthesis of vineomycinone B_2 **54**. Compound **10** was converted in four stages into the organotin derivative **51** and then into the vinyl iodide **52**. The key stage—the coupling of compound **52** with the arylzinc **53**—is catalysed by a palladium complex (Scheme 50).[103]

Scheme 50



The weak point of this scheme is the stage involving the non-stereospecific epoxidation of the precursor **56**. Valverde et al.[104] were able to synthesise the isomers (6*R*, 7*S*)-**59** and (6*S*, 7*R*)-**60** of asperlin with a high optical purity by the asymmetric epoxidation of the allyl alcohol **58** obtained from tri-*O*-acetyl-D-glucal **10** (Scheme 52).

Scheme 52



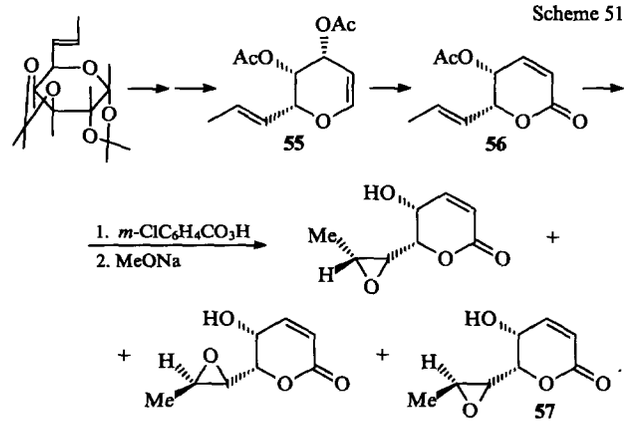
DET = diethyl tartrate .

2. Synthesis of natural products containing a hydropyran fragment

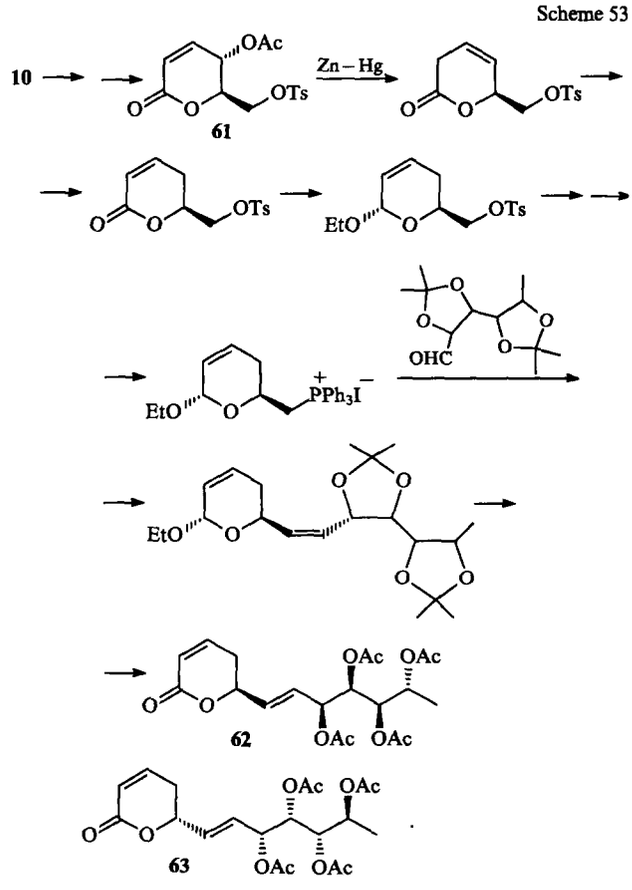
Compounds containing a hydropyran fragment are fairly common in nature. The total synthesis of many of them constitutes a fairly complex problem and is itself of interest as a stage in the development of the enantiospecific synthesis of compounds with a large number of chiral centres. The use of glycals makes it possible to obtain synthons containing up to five chiral centres with a specific configuration. It is noteworthy that compounds combining a high biological activity with a relative simplicity of structure, which renders their synthesis of practical interest, have been found with increasing frequency among natural hydropyrans.

Thus a series of studies have been devoted to the synthesis of the dihydropyran antibiotic asperlin, which exhibits carcinostatic activity. The D-enantiomer of asperlin **57** has been obtained from the modified galactal **55** (Scheme 51).[7]

Scheme 51



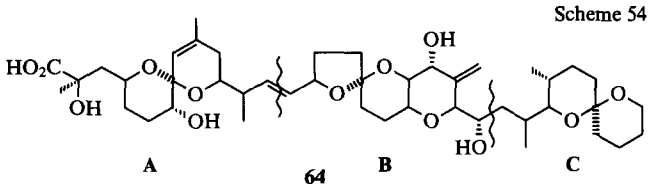
Scheme 53



Anamarin **63**, isolated from a plant of the genus *Hyptis*, has the (*R*)-configuration in the pyranoid ring and an unusual α-gluco-structure of the C(6)-side chain. The enantiomeric (−)-anamarin **62** was synthesised from the unsaturated lactone **61** obtained from tri-*O*-acetyl-D-glucal **10** (Scheme 53).[105]

Okadaic acid **64**, isolated from the sea sponge *Halichondria okadai*, is one of the specially complex compounds whose total synthesis has been undertaken (Scheme 54).

Scheme 54

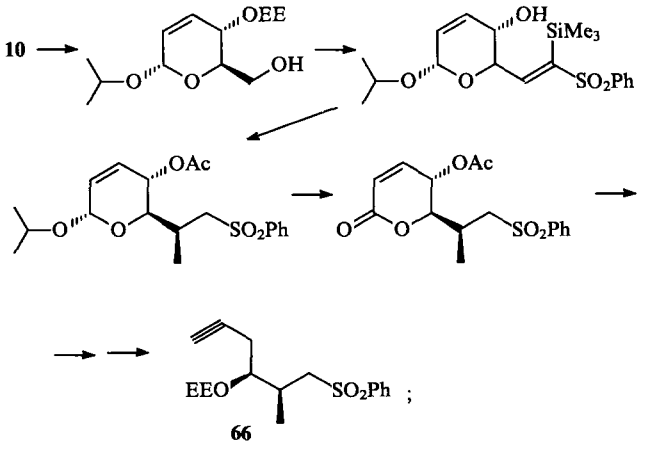


64

Isobe and coworkers described the synthesis of the **A**, **B**, and **C** fragments of the toxin molecule in a series of brilliant studies.[106–109]

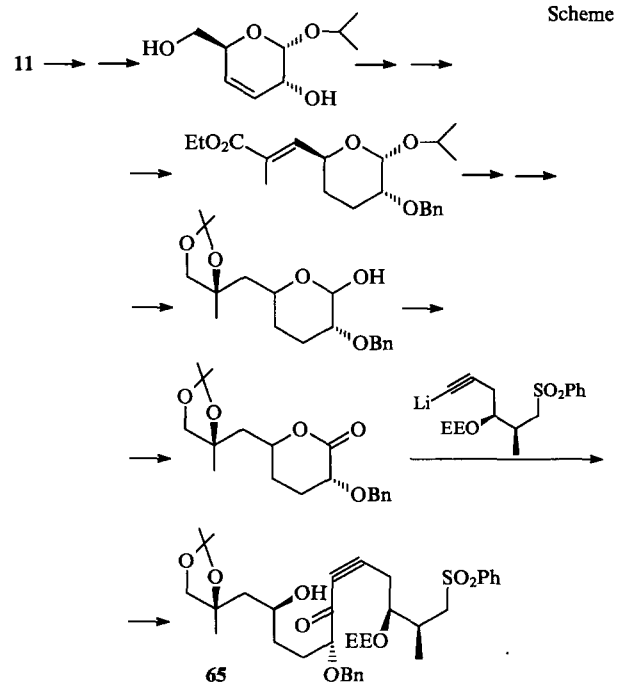
The synthesis of the fragment **A** (compound **65**) involves the preparation of two synthons based on tri-*O*-acetyl-D-glucal **10**

Scheme 55



EE = $EtOC_2H_4$.

Scheme 56

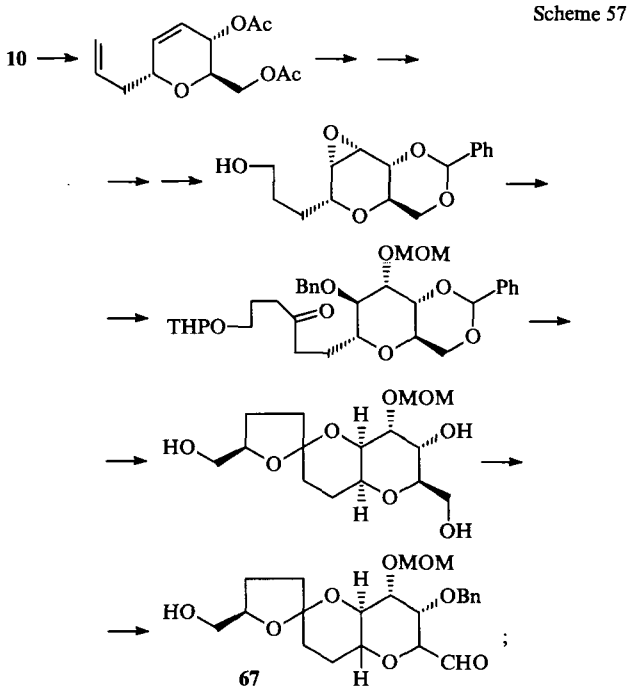


and tetra-*O*-acetyl-2-hydroxy-D-glucal **11**. As can be seen from Scheme 55, the configuration of the carbon atom to which a methyl group is attached in the molecule of the target acetylenic sulfone **66** is specified in conformity with the directing effect of the oxygen-containing functional groups in the 1,4-addition of lithium dimethylcuprate to the silicon-containing unsaturated sulfone.

The key stage in the synthesis of the fragment **A** is the reaction of the lithium derivative of the acetylenic sulfone with the lactone obtained from tetra-*O*-acetyl-2-hydroxy-D-glucal **11** (Scheme 56).[106]

The construction of the segment **B** (compound **67**) begins with the reaction of tri-*O*-acetyl-D-glucal **10** with allyltrimethylsilane. The key stages of this synthesis are presented in Scheme 57.[107]

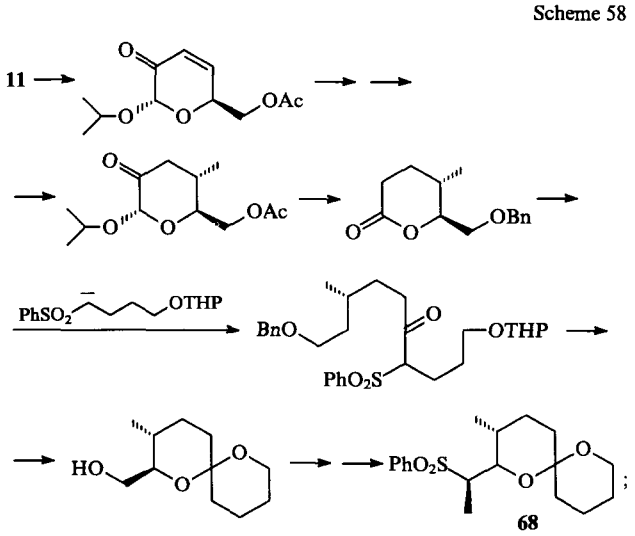
Scheme 57



MOM = $MeOCH_2^-$.

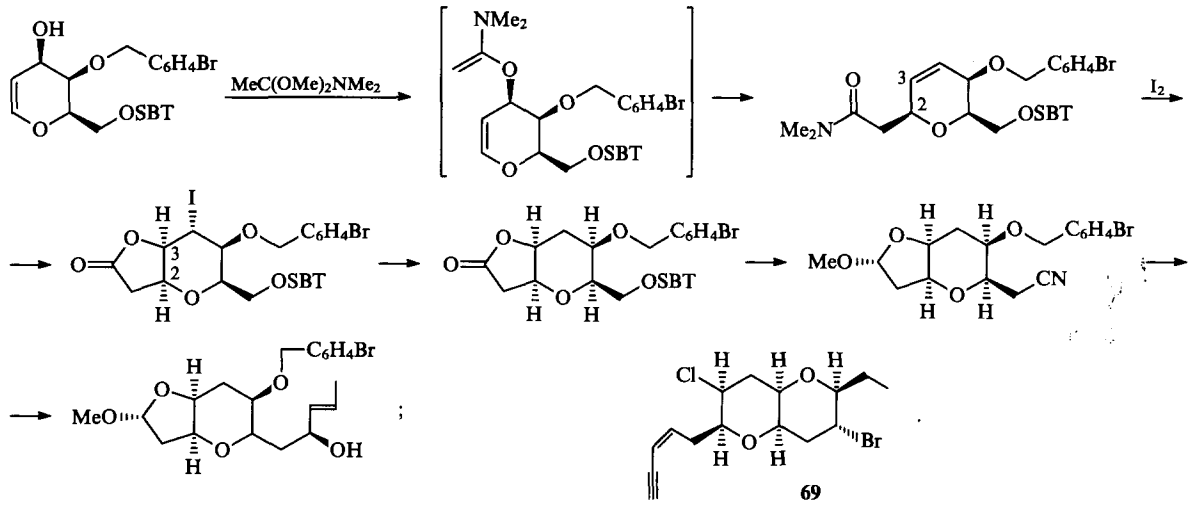
The synthesis of the comparatively simple segment **C** (compound **68**) is also based on the reactions of the 2-acetoxy-glucal **11** (Scheme 58).[108, 109]

Scheme 58



THP = tetrahydropyran-2-yl.

Scheme 59

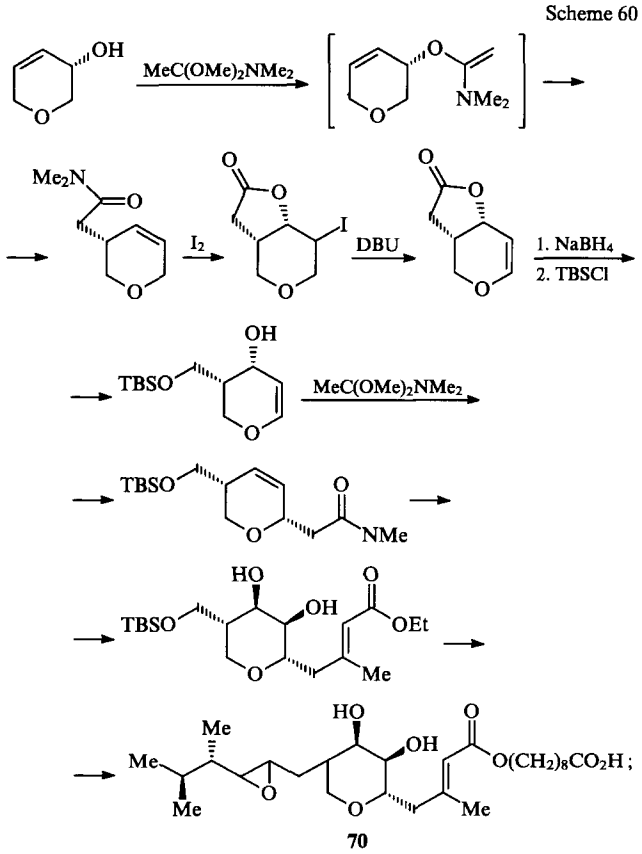


69

(3*E*)- and (3*Z*)-Dactomelynes **69**, pyranopyran derivatives isolated from the sea hare *Aplysia daktylomela*, exhibit a valuable biological activity. The chiral centres at C(2) and C(3) are formed by the enantiospecific stages of the Claisen rearrangement involving the dimethyl acetal of *N*,*N*-dimethylacetamide and conversion into an iodolactone. These steps have been incorporated into the synthesis of dactomelynes (Scheme 59).[110]

The Claisen rearrangement of natural glycals is used twice in the scheme for the synthesis of pseudomonic acid **70** (Scheme 60).[111]

Scheme 60

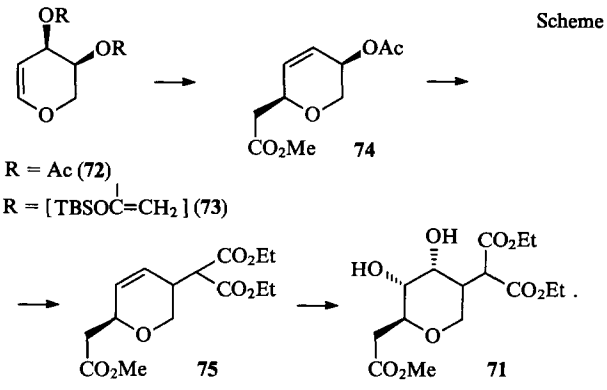


70

DBU = 1,5-diazabicyclo[5.4.0]undec-5-ene.

A short pathway to the key chiral intermediate **71**, essential for the synthesis of pseudomonic acid, has been proposed.[112] Di-*O*-acetyl-L-arabinal **72** was proposed as the initial chiral compound. It was converted via the rearrangement of the bisketene silyl acetal **73** into compound **74** and further into the ester **75** (Scheme 61).

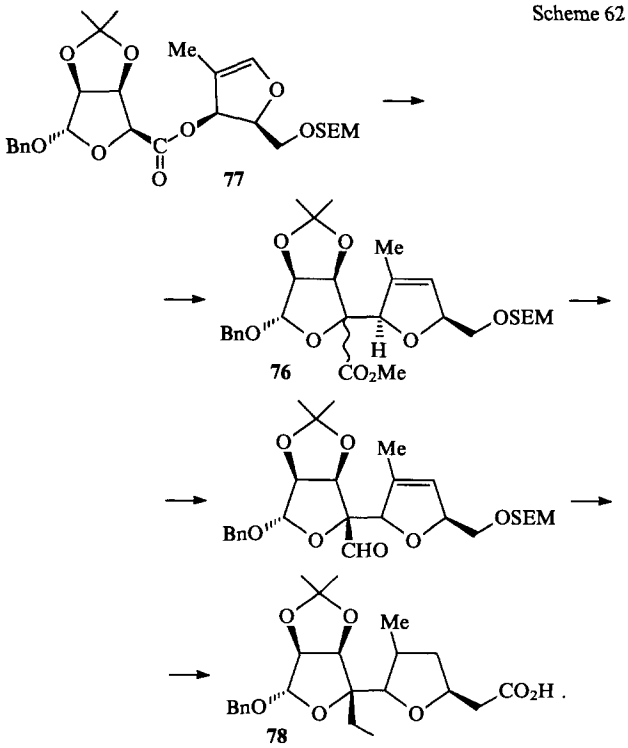
Scheme 61



R = Ac (**72**)

R = [TBSOC(=CH$_2$)] (**73**)

Scheme 62

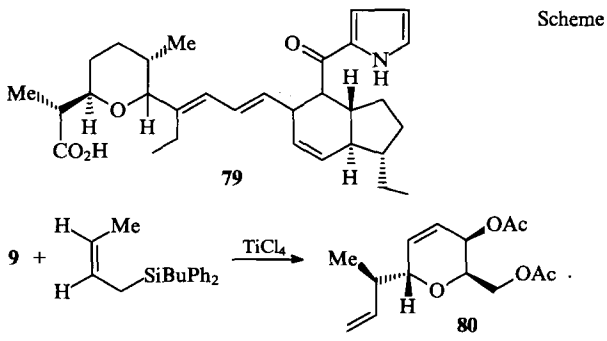


The use of the Claisen rearrangement in the synthesis of antibiotics of the hydropyran type, namely lasalocid, tirandamycin,[7] and monensin,[113] has been described. A strikingly high yield of compound **76** in the rearrangement of the ester **77**, constructed from two furanoid fragments, was noted in the synthesis of the last

compound.[114] One of the key units (compound **78**) necessary for the construction of the monensin molecule was obtained as a result of this reaction (Scheme 62).

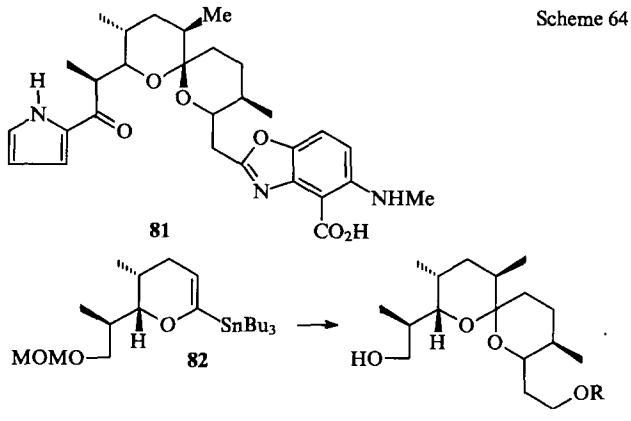
As mentioned above, the stereoselective reaction of glycal acetates with allylsilanes is one of the effective methods of synthesis of chiral building blocks.[41] In the synthesis of the antibiotic indanomycin **79**, the necessary dihydropyran synthon unit **80** was obtained by the reaction of tri-*O*-acetyl-D-galactal **9** with (*Z*)-crotylsilane (Scheme 63).[115]

Scheme 63

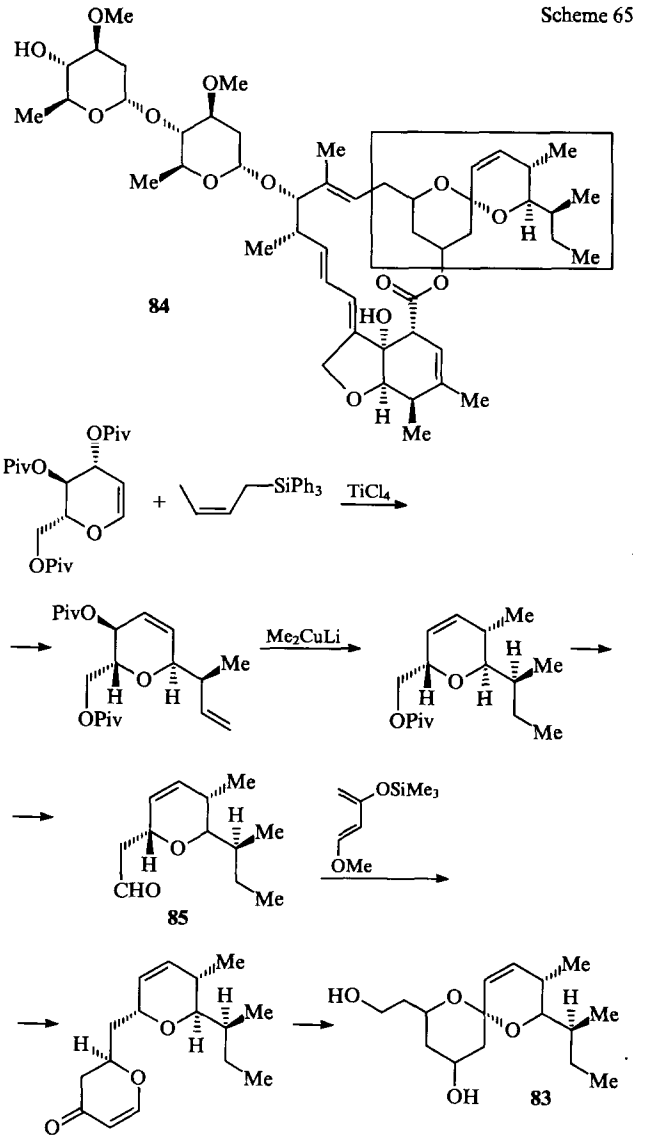


An organotin glycal derivative **82** has been used to synthesise the ionophor calcimycin **81** (Scheme 64).[24]

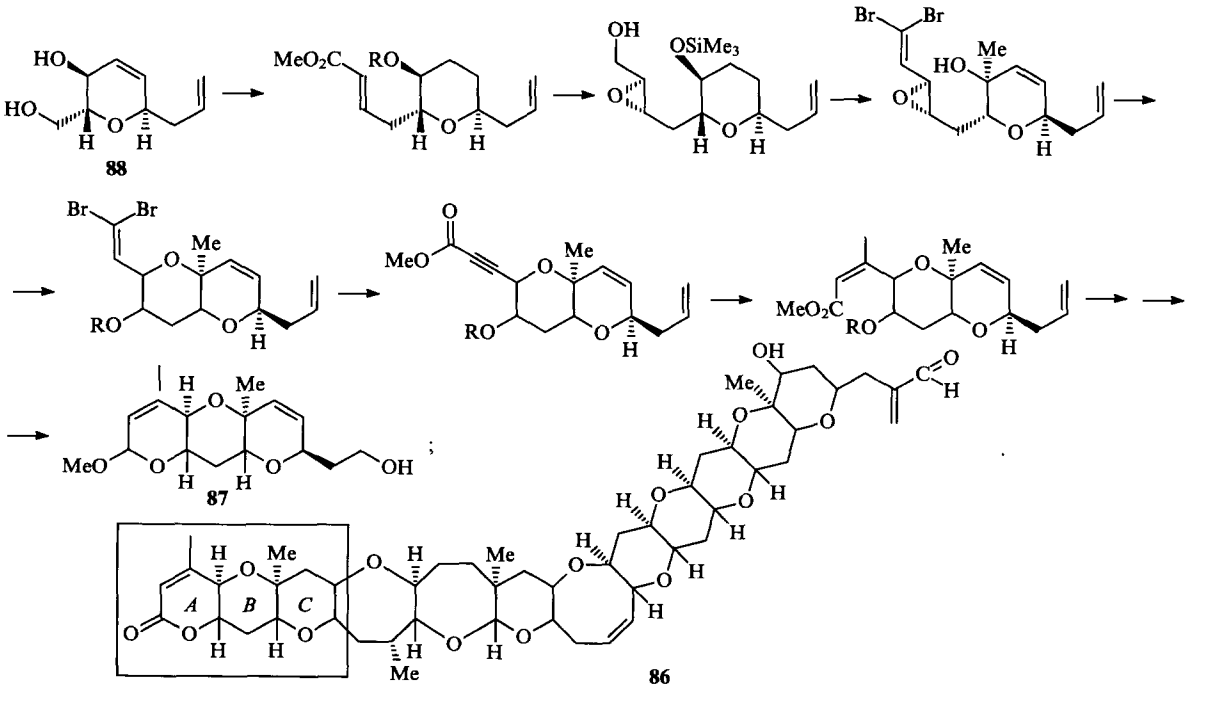
Scheme 64



Scheme 65



Scheme 66

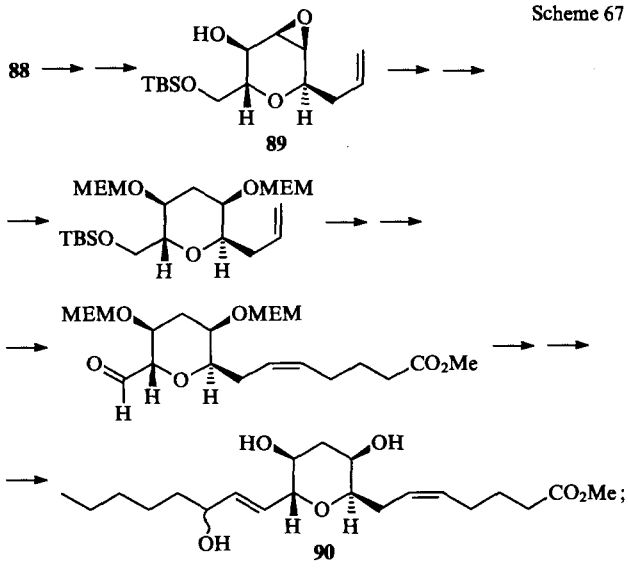


The strategy used in the synthesis of the spiroketal unit **83** of the insecticide avermectin **84** includes the reaction of tri-*O*-pivaloyl-D-glucal with (*Z*)-crotyltriphenylsilane and the [4+2]-addition of the so called Danishevskii's diene to the aldehyde **85** (Scheme 65).[116-118]

The total synthesis of one of the most powerful of the natural toxins — brevetoxin **86** — is extremely complex. The **ABC** fragment **87** of its structure was synthesised from (2*R*, 3*S*, 6*R*)-6-allyl-3,6-dihydro-3-hydroxy-2-hydroxymethyl-2*H*-pyran **88** — the product of the coupling of tri-*O*-acetyl-D-glucal **10** with allyltrimethylsilane (Scheme 66).[119, 120]

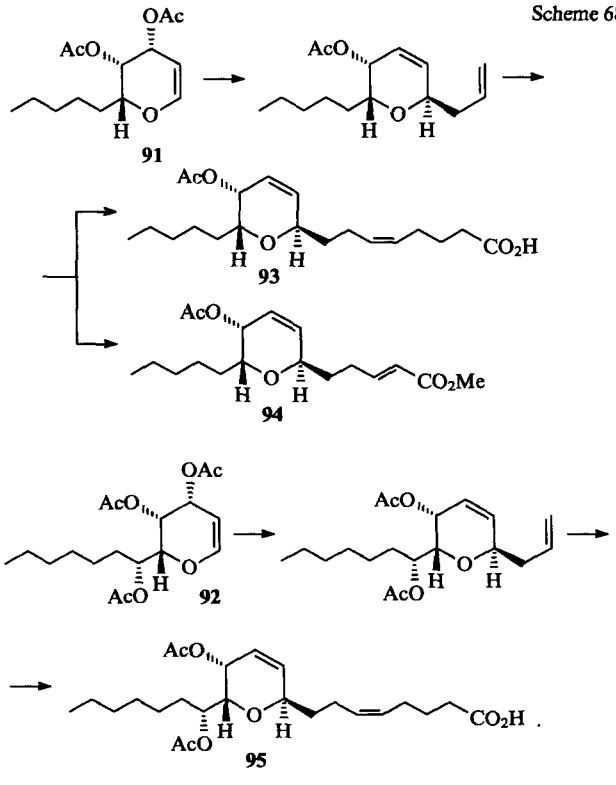
The substituted dihydroxy-2*H*-pyran **88** and its epoxide **89** have also been used as the starting compounds in the synthesis of (8*R*, 9*R*, 11*S*, 12*R*, 15*R*, *S*, 5*Z*, 13*E*)-9,11,15-trihydroxy-8,12-oxy-5,13-eicosadienoic acid **90** — a stereoisomer of the natural metabolite of arachidonic acid (Scheme 67).[121]

Scheme 67



MEM = $MeOC_2H_4OCH_2$.

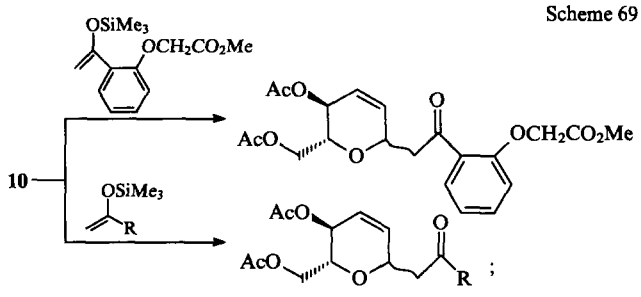
Scheme 68



The stereospecific reaction of the modified glycals **91** and **92** with allyltrimethylsilane served as the key reaction for the synthesis of unsaturated carboxylic hydroxyacids **93**–**95** — structural analogues of arachidonic acid (Scheme 68).[122, 123]

New chiral building blocks, which are promising for the synthesis of the oxo-analogues of the cyclic metabolites of arachidonic acid, have been obtained by coupling silyl ethers of enols with tri-*O*-acetyl-D-glucal **10** (Scheme 69).[124]

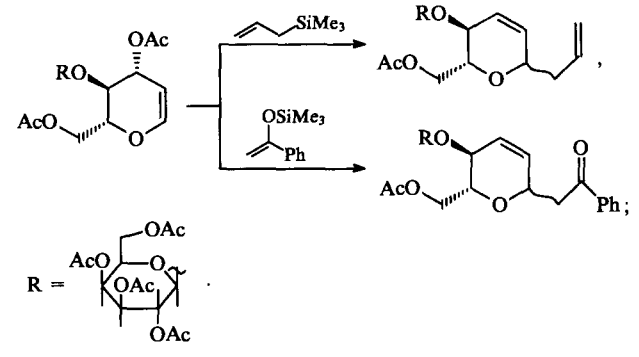
Scheme 69



R = $(CH_2)_nCO_2Me$.

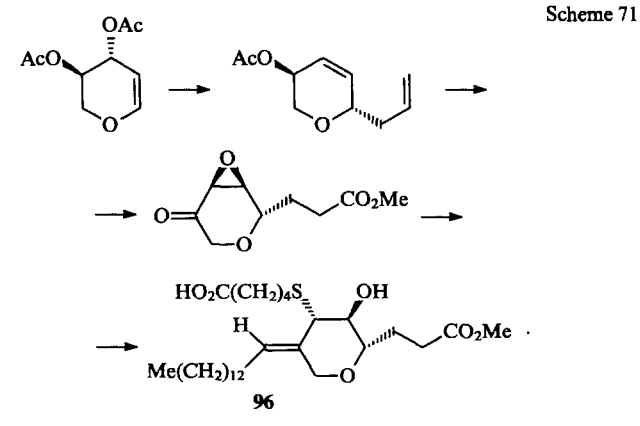
Hexa-*O*-acetyl-D-lactal reacts smoothly on treatment with $BF_3 \cdot OEt_2$ both with allylsilanes and with siloxyethers, affording units suitable for the synthesis of glycosylated derivatives of hydropyran (Scheme 70).[125]

Scheme 70



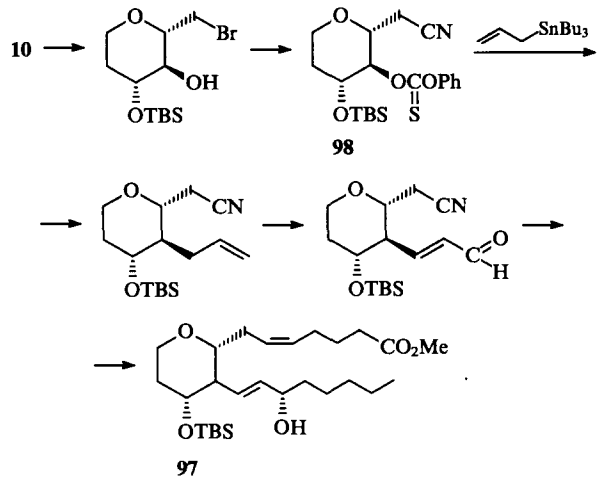
Compound **96**, the synthesis of which from xylal is fairly simple, is able to inhibit the biosynthesis of leucotriene D_4 (Scheme 71).[126]

Scheme 71



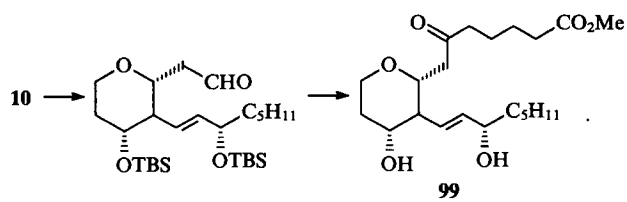
The key stage in the synthesis of the tetrahydropyran analogue of prostaglandin $F_{2\alpha}$ **97** from tri-*O*-acetyl-D-glucal **10** is the free-radical allylation of the intermediate phenyl thiocarbonate **98** by treatment with allyltributyltin (Scheme 72).[127]

Scheme 72



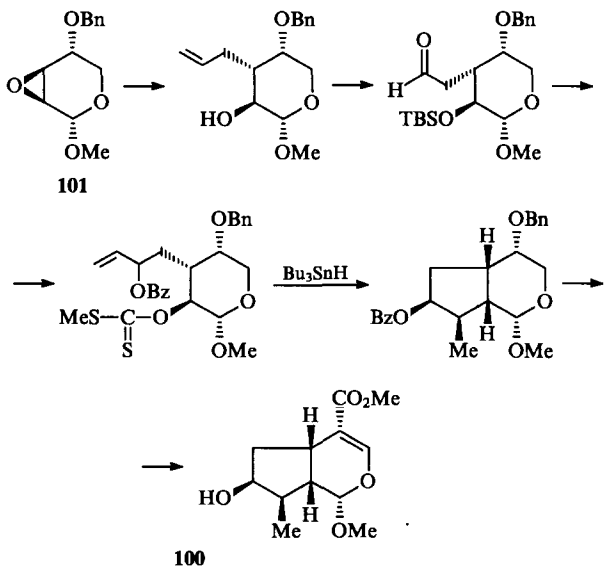
An analogous reaction of tri-*O*-acetyl-D-glucal **10** has been used to synthesise the 6-oxoprostanoid **99** (Scheme 73).[128]

Scheme 73



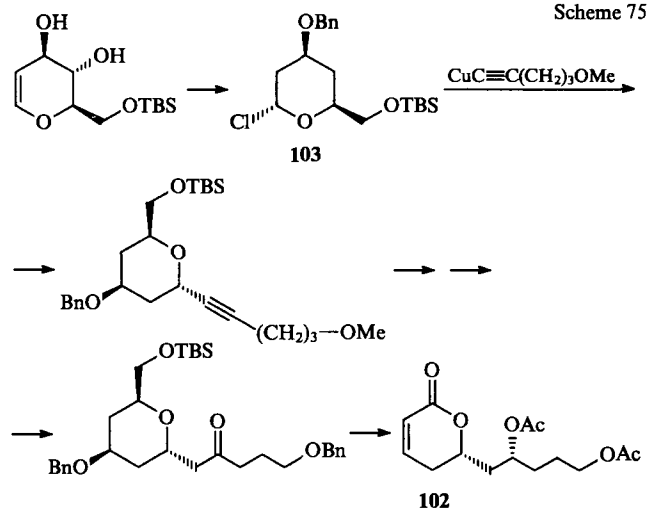
Various approaches have been used in applying the schemes for the synthesis of hydropyran fragments in a series of natural products. Thus in the scheme for the synthesis of α-*O*-methylloganin **100**, in which the starting material is compound **101**, the free-radical cyclisation stage is noteworthy. It affords a cyclopentane fragment with four chiral centres, each having a rigorously defined configuration (Scheme 74).[129]

Scheme 74



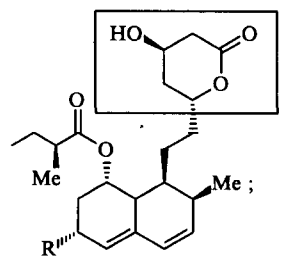
One of the fragments (compound **102**) of the antibiotic nystatin has been obtained by coupling copper acetylide with the chloro-derivative **103** obtained from the monosilyl ether of D-glucal (Scheme 75).[130]

Scheme 75



In the last decade, much attention has been devoted to the synthesis of mevinoids — substances which inhibit the biosynthesis of cholesterol. Analogues of commercial value as medicinal drugs reducing the cholesterol content in the blood have been described. An important element of the structure of compactin **104** and mevinolin **105** as well as their structural analogues is a pyranoid lactone fragment, the synthesis of which has aroused considerable interest (Scheme 76).

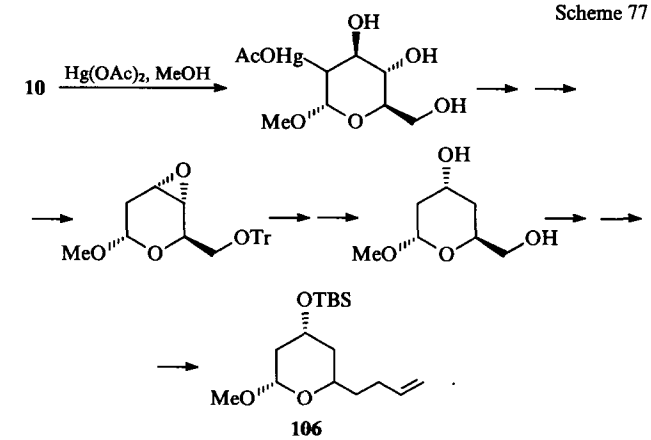
Scheme 76



R = H (**104**), R = Me (**105**).

One of the approaches to the synthesis of the lactone fragment **106** of the (+)-compactin molecule presupposes[131] the methoxymercuration of the initial tri-*O*-acetyl-D-glucal **10** with subsequent transformation of the intermediate epoxide in accordance with Scheme 77.

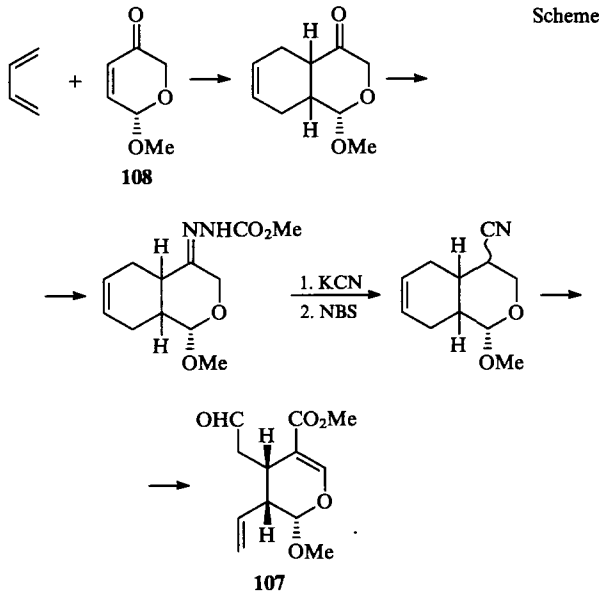
Scheme 77



The [4+2]- and [3+2]-cycloaddition reactions with participation of glycals and their derivatives have served as key reactions in the synthesis of a series of polycyclic natural products containing a hydropyran fragment. Thus the aglycone of the

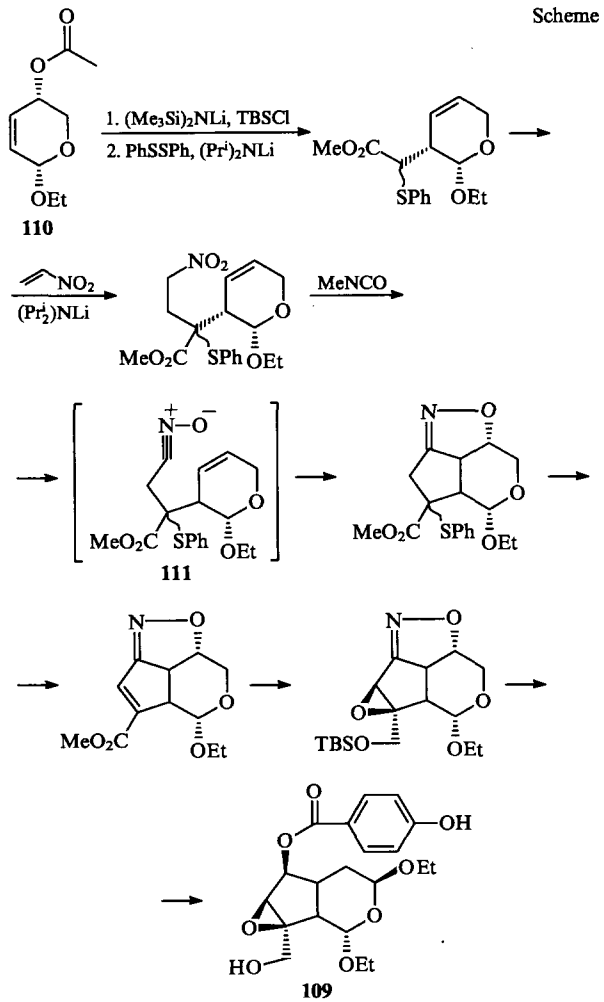
iridoid secologanin **107** has been obtained by the reaction of the methoxyenone **108** with butadiene (Scheme 78).[132]

Scheme 78



Bicyclic iridoids are a group of natural products of interest from the practical point of view. Substances with antileukemic and antimicrobial activities have been found among them. The characteristic cyclopentanopyran skeleton of iridoids determines the approaches to the synthesis based on the use of carbohydrates.

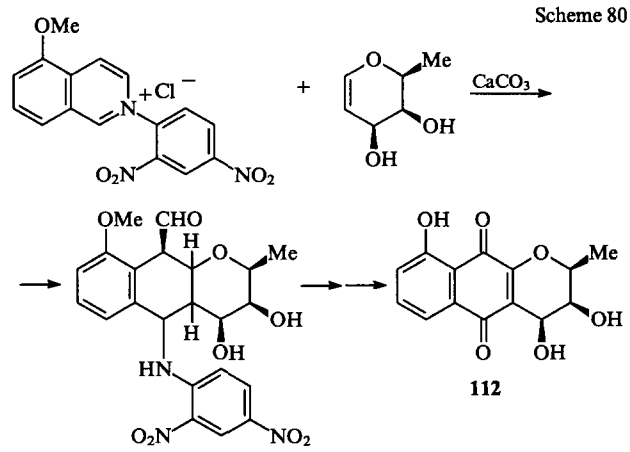
Scheme 79



Specionin **109** is regarded as a promising antifeedant. The multistage scheme for its synthesis includes reaction such as the Ireland–Claisen rearrangement of (*E*)-ketene silyl acetal derived from the D-xylal **110** and the dipolar [3 + 2]-addition of the nitrile oxide **111**, which ensures the stereospecific synthesis of the polyfunctional cyclopentane ring (Scheme 79).[133, 134]

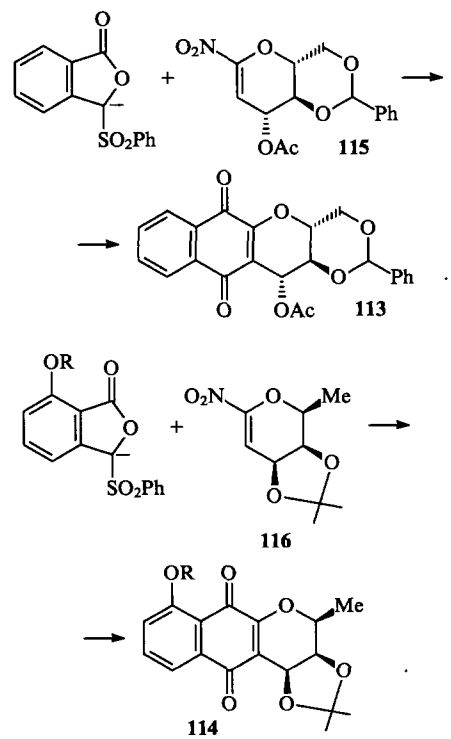
The generation of quinodimethanes from isoquinoline salts has led to extensive possibilities for the synthesis of polycyclic structures based on the [4 + 2]-cyclo-addition reaction. In Scheme 80 for the synthesis of the fungal metabolite cryptosporin **112**, which is active against gram-positive bacteria, the above reaction constitutes the key stage.[135]

Scheme 80



The reaction of glycals with the anions of arenesulfonyl- or cyano-phthalides, which formally constitutes [4 + 2]-addition, has found an application in the synthesis of natural metabolites of the quinone type. In particular, the derivatives **113** and **114** of the cryptosporin mentioned above have been obtained by reaction with the nitroglycals **115** and **116** (Scheme 81).[136]

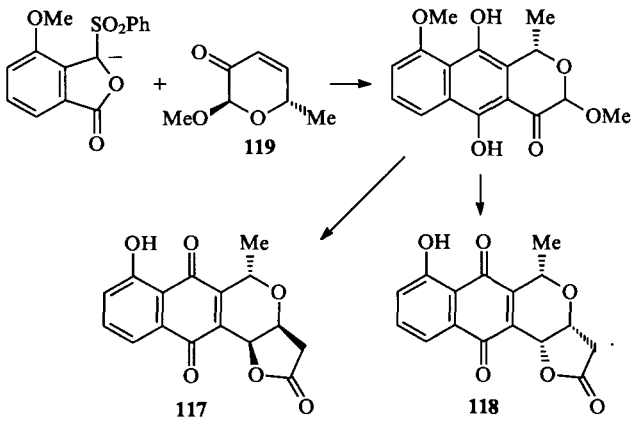
Scheme 81



Nanaomycine **117** and its natural stereoisomer kalafungin **118** have attracted attention by their high antimicrobial and anticancer activities. Japanese investigators developed a synthesis based

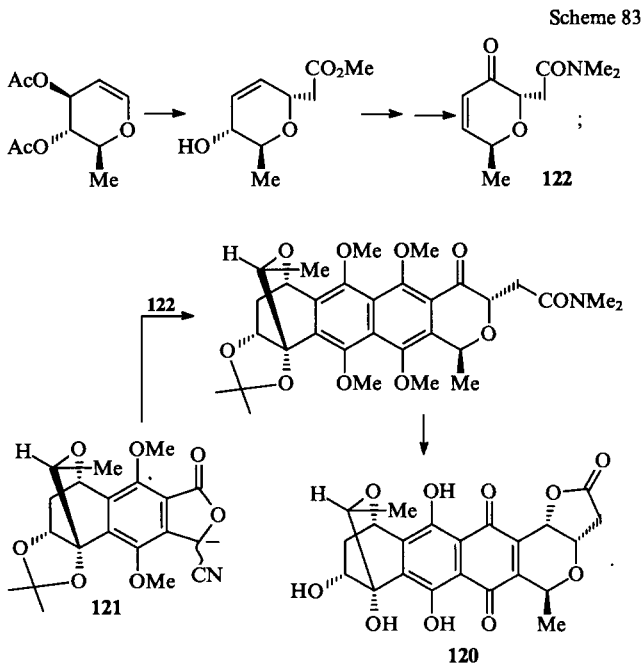
on the reaction of benzenesulfonylmethoxyphthalide with the methoxyenone **119** obtained from L-rhamnal (Scheme 82).[137]

Scheme 82



Scheme 83 for the synthesis of the antibiotic granaticin **120** includes a stage involving the condensation of the cyanophthalide **121** with the ketoamide **122** obtained from di-*O*-acetyl-D-rhamnal.[138]

Scheme 83



3. Synthesis of nitrogen-containing compounds

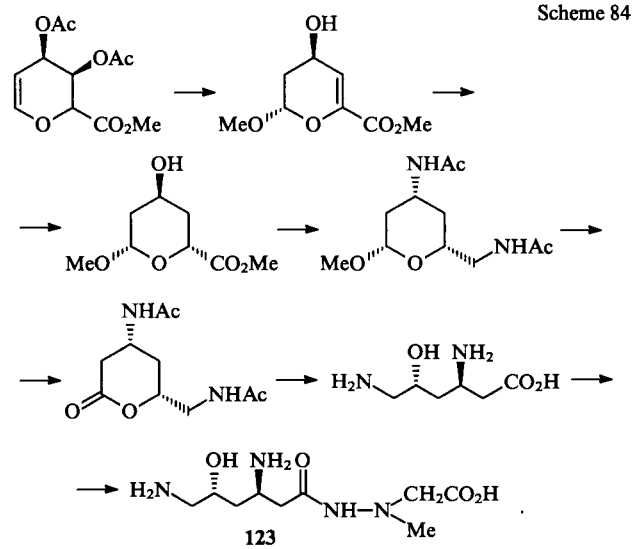
The use of glycals in the synthesis of nitrogen-containing natural products so far covers only a small number of examples. However, the schemes described in the literature are fairly interesting and demonstrate new possibilities in the chemistry of glycals.

The antibiotic negamycin **123** belongs to the class of hydrazine derivatives which are rarely encountered in nature. Its synthesis from the glycal of D-galacturonic acid includes more than ten stages,[139] some of which are presented in Scheme 84.

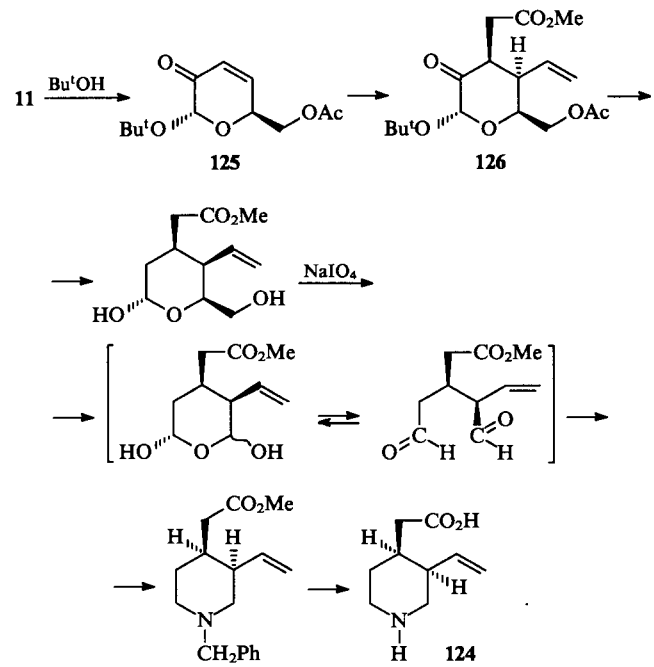
In Scheme 85 for the synthesis of meroquinene **124** from tetra-*O*-acetyl-2-hydroxy-D-glucal **11**, there is a stereospecific stage including the conversion of the enone **125** into the ketoester **126**, which involves the 1,4-addition of the vinylcuprate reagent and the alkylation of the enolate with methyl bromoacetate.[140]

The quinuclidine fragment enters into the structures of a whole series of important alkaloids. One of the approaches to the synthesis of optically active quinuclidines is based on the use of the natural D-glucal **127** (Scheme 86).

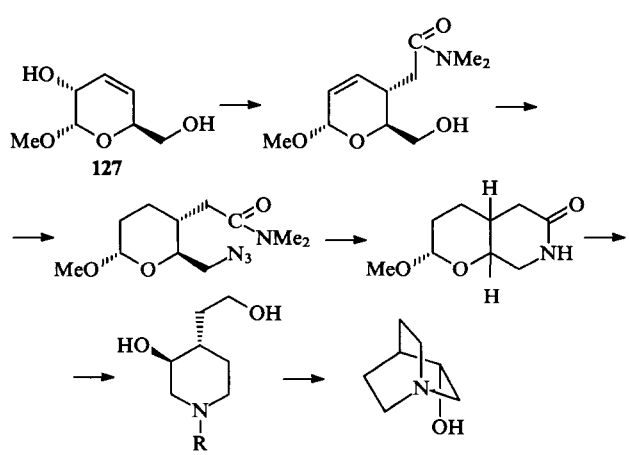
Scheme 84



Scheme 85

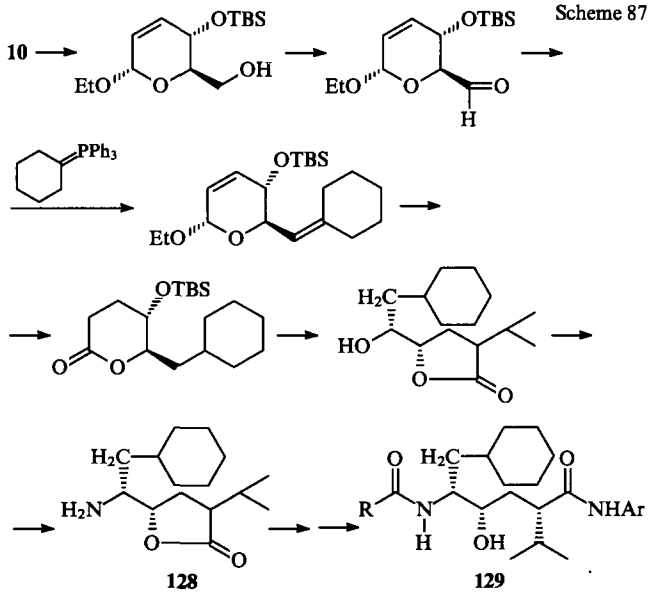


Scheme 86



The inhibitors of renin belonging to the group of low molecular mass peptides are regarded as highly effective antihypertensive agents. The aminolactone **128**, which is a key synthon unit for the construction of peptides of type **129**, was synthesised from tri-*O*-acetyl-D-glucal **10** (Scheme 87).[142]

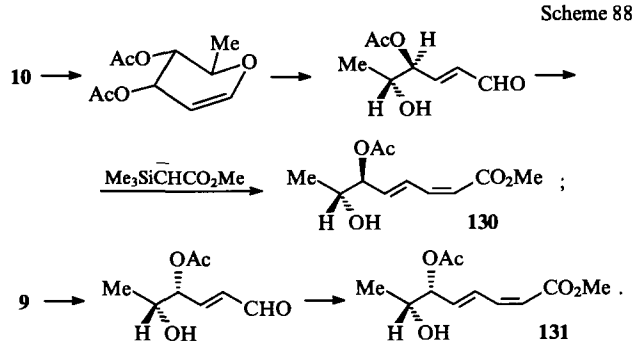
Scheme 87



V. Decyclisation of glycals as a basis for synthesis of natural products and their structural analogues

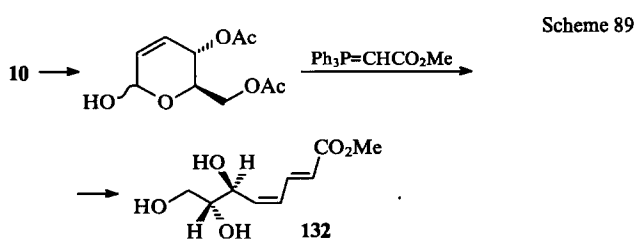
The products of the decyclisation of glycals were not considered for a long time as objects meriting attention in designing schemes for enantiospecific synthesis. The situation began to change after the publication of a study[143] devoted to the synthesis of 6,7-dihydroxyocta-2,4-dienoic acids, which form part of the structures of a series of toxins of the trichothecane series. Thus (6*R*, 7*R*)- and (6*S*, 7*R*)-dihydroxyacids **130** and **131** with the (2*Z*, 4*E*)-configuration of the double bonds have been synthesised from tri-*O*-acetyl-D-glucal **10** and tri-*O*-acetyl-D-galactal **9** (Scheme 88).[143, 144]

Scheme 88



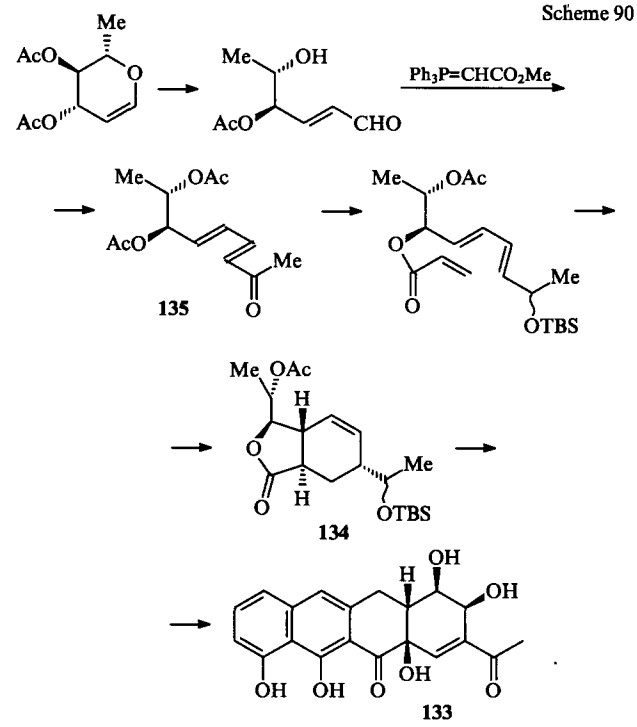
The method of synthesis of the (2*E*, 4*Z*)-isomer **132** is based on the two-stage conversion of tri-*O*-acetyl-D-glucal **10**. Derivatives of compound **132** have been used in the synthesis of trichoverrol B and trichoverrin B (Scheme 89).[144]

Scheme 89



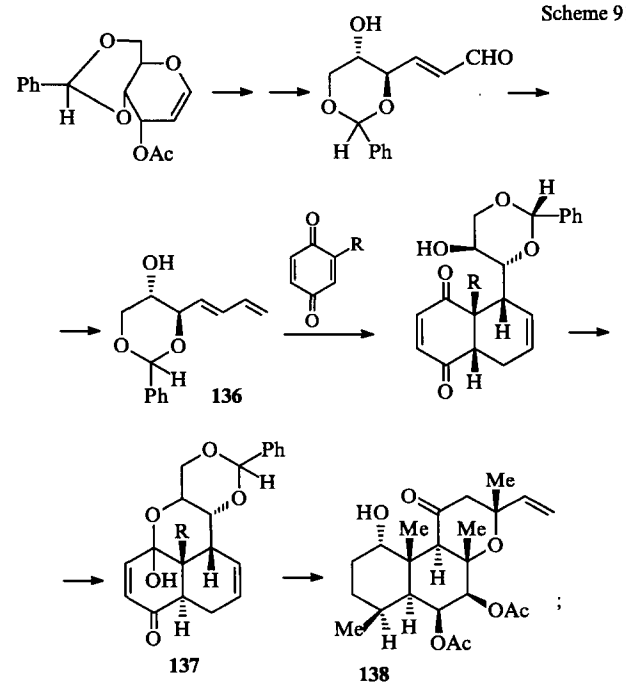
The synthesis of (+)-pillaromycinone **133** includes a stage involving the intramolecular Diels–Alder reaction, which leads to the key cyclic adduct **134**. The diene component **135** was obtained from di-*O*-acetyl-L-rhamnal (Scheme 90).[145]

Scheme 90



The reaction of 2-methoxycarbonylquinone with the diene **136**, synthesised from 3-*O*-acetyl-4,6-*O*-benzylidene-D-allal, has been proposed as a convenient method of synthesis of compound **137**—an intermediate for the construction of the molecule of the diterpenoid forskolin **138** with an exceptionally valuable biological activity (Scheme 91).[146]

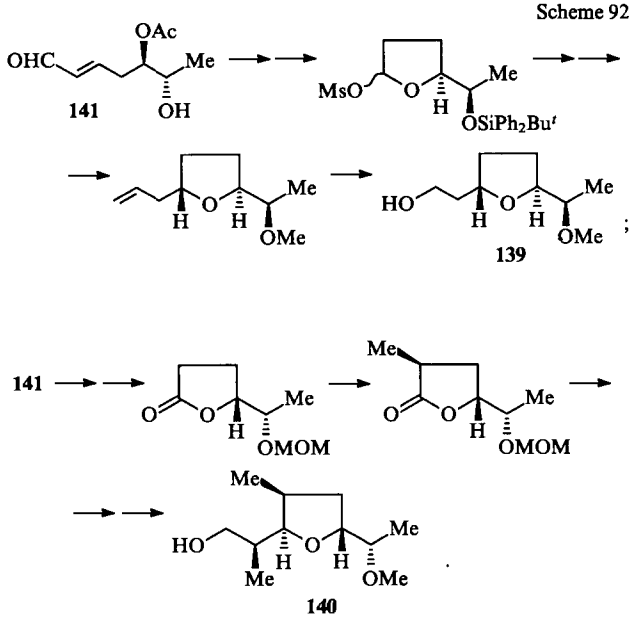
Scheme 91



R = CO_2Me.

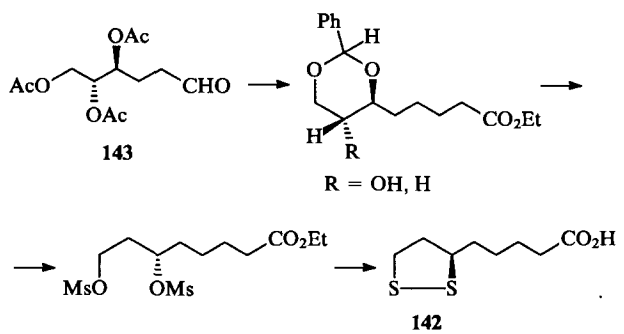
The tetrahydrofuran fragments **139** and **140** of the antibiotics tetronasin and tetronomycin have been synthesised from the heptenal **141**—a product of the decyclisation of di-*O*-acetyl-L-rhamnal (Scheme 92).[147]

Scheme 92



The syntheses of (*R*)-(+)-α-lipoic acid and its (*S*)-(−)-enantiomer from the products of the opening of the dihydropyran ring in glycals based on hexoses and pentoses have been described. The scheme for the synthesis of (*R*)-(+)-α-lipoic acid **142**, in which the triacetoxyhexenal **143**, obtained from tri-*O*-acetyl-D-glucal, was used, has been realised in practice (Scheme 93).[148]

Scheme 93



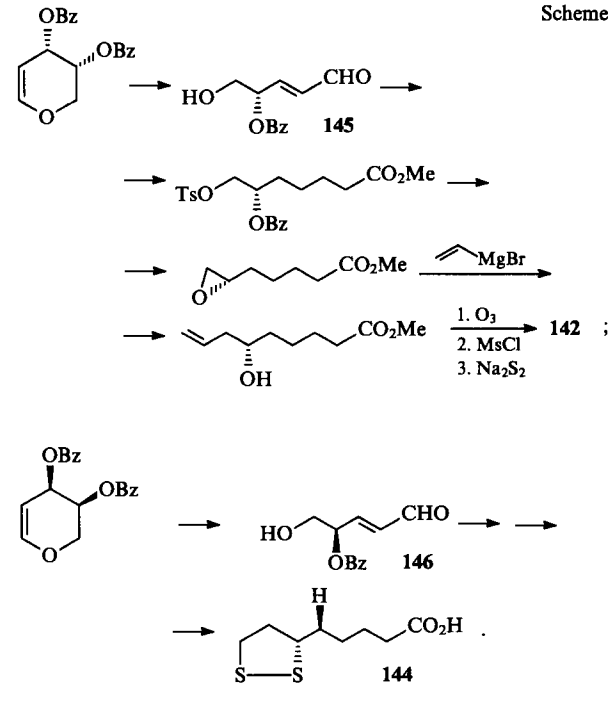
According to Tolstikov et al.,[149] (R)-(+)-α-lipoic acid and its (*S*)-(−)-enantiomer **144** can be obtained from the pentenals **145** and **146** synthesised from di-*O*-benzoyl-D-arabinal and di-*O*-benzoyl-L-arabinal (Scheme 94).

The products of the acid decyclisation of glycal esters proved to be convenient starting materials for the synthesis of open-chain insect pheromones. Thus the gypsy moth pheromone (+)-*cis*-disparlure **147** was synthesised from (4*R*, 5*R*)-4,5,6-triacetoxy-(2*E*)-hexenal **148**—a derivative of tri-*O*-acetyl-D-galactal (Scheme 95).[150, 151]

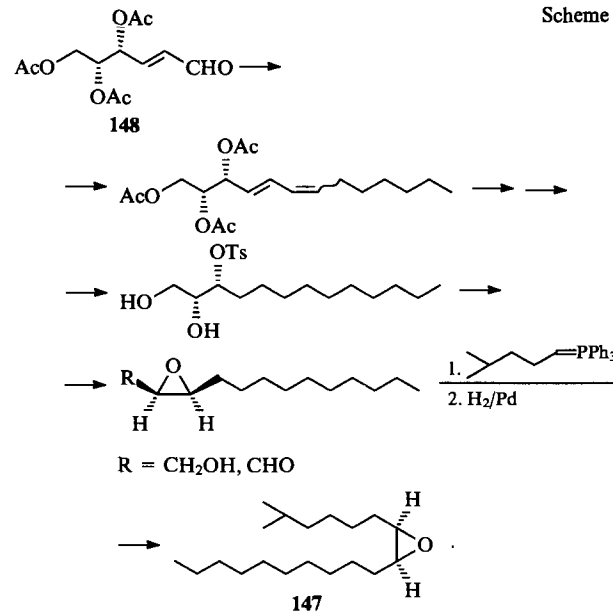
The key synthon **149** for (−)-*cis*-disparlure **150** has been obtained by decyclising a modified D-galactal **151** (Scheme 96).[10]

The α,β-unsaturated aldehyde **148** served as the initial compound in the synthesis of (3*Z*, 6*Z*, 9*S*, 10*R*)-*cis*-9,10-epoxyheneicosa-3,6-diene **152**—the principal component of the sex pheromone of the American white butterfly *Hyphantria cunea drury* (Scheme 97).[152]

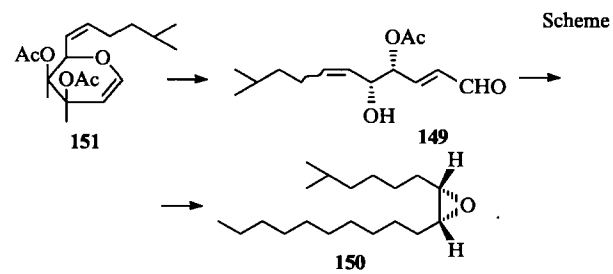
Scheme 94



Scheme 95

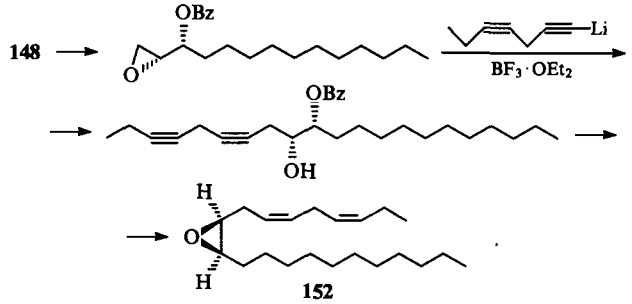


Scheme 96

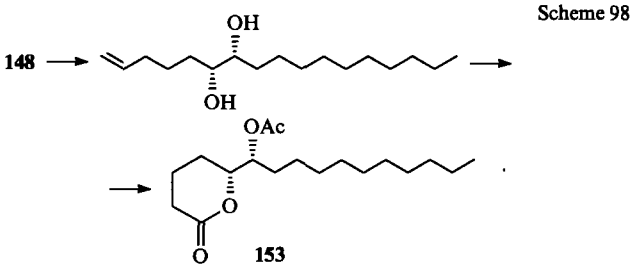


The hexenal **148** has also been used to synthesise (5*R*, 6*R*)-6-acetoxy-5-hexadecanolide **153**—the stereoisomer of the oviposition of pheromone of the gnat *Culexpipiens fatigans* (Scheme 98).[153]

Scheme 97

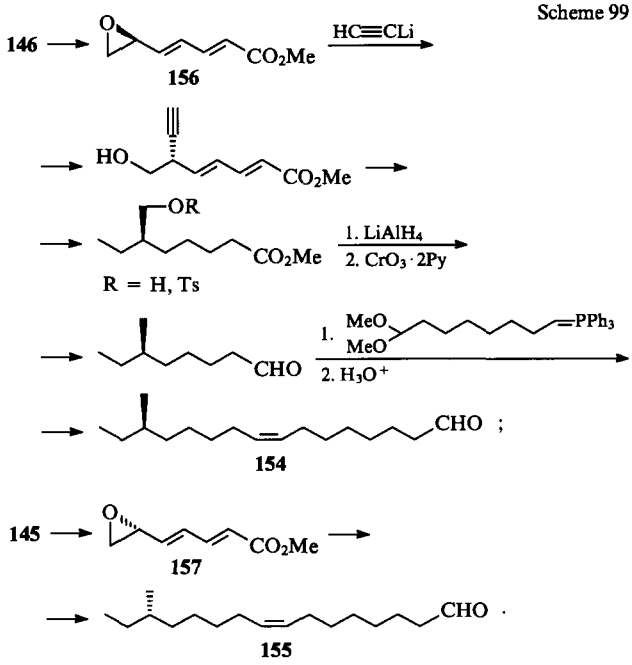


Scheme 98



The key stage in the synthesis of the aggregation pheromone of the leather eating beetles of the genus *Trogoderma*, namely (14*R*, 8*Z*)-trogodermal **154** and its (14*S*, 8*Z*)-enantiomer **155**, from the aldehydes **145** and **146** is the stereospecific reaction of their derivatives, i.e. (6*S*, 2*E*, 4*E*)- and (6*R*, 2*E*, 4*E*)-methyl-6,7-epoxyhepta-2,4-dienoates **156** and **157** respectively, with ethynyllithium. An approach to the synthesis of the enantiomerically pure methyl-branched synthons has been developed in relation to this reaction (Scheme 99).[154]

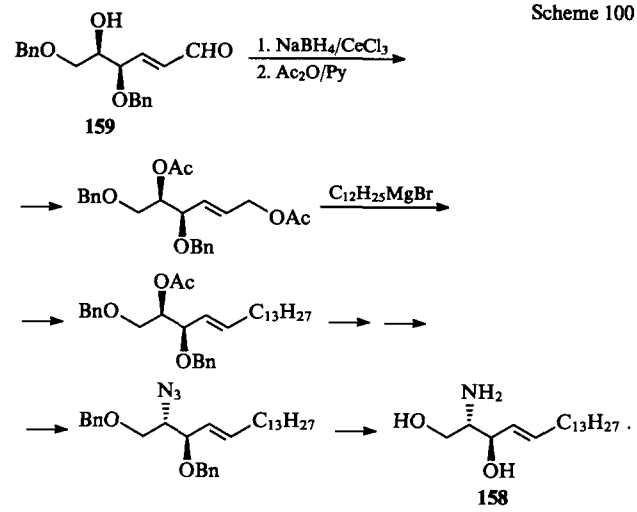
Scheme 99



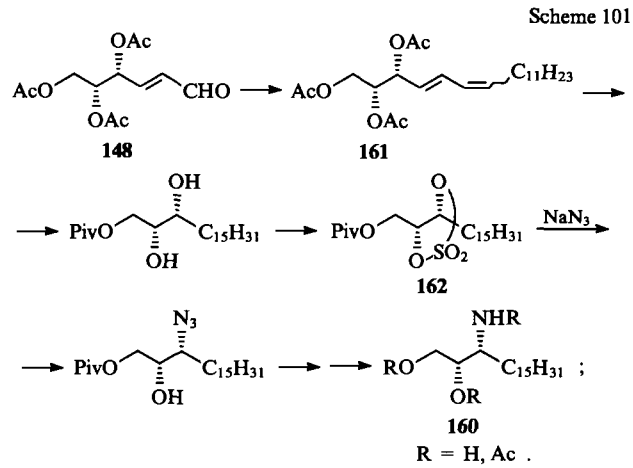
Six-carbon units with two chiral centres, obtained from glycals based on hexoses, have been used in the synthesis of sphingolipids. Thus a highly effective stereocontrolled synthesis of D-*erythro*-C_{18}-sphingosine **158**, based on the transformations of (4*R*, 5*R*, 2*E*)-4,6-di-*O*-benzyl-5-hydroxyhex-2-enal **159**, has been described (Scheme 100).[84]

The synthesis of the regioisomer of dihydrosphingosine **160** presupposes the use of the triacetoxydiene **161** obtained by converting the familiar hexenal **148** into an olefin (Scheme 101).[155]

Scheme 100



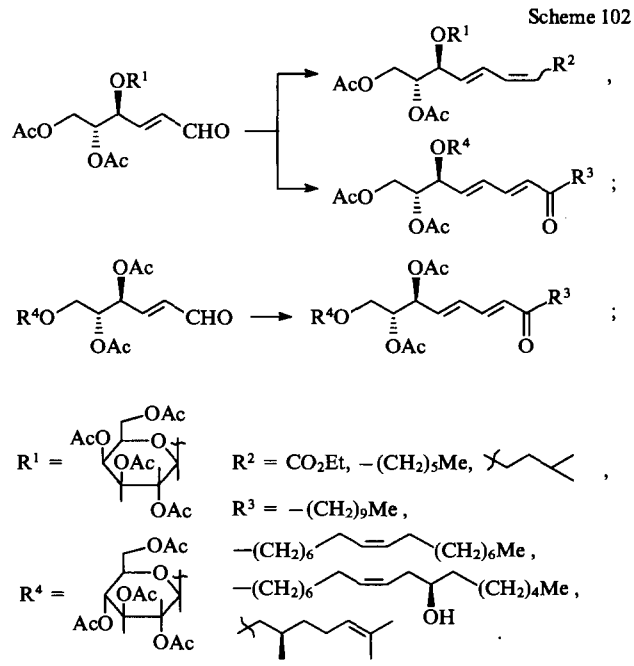
Scheme 101



The stage involving the regiospecific opening of the cyclic sulfate ester **162** on treatment with sodium azide is noteworthy.

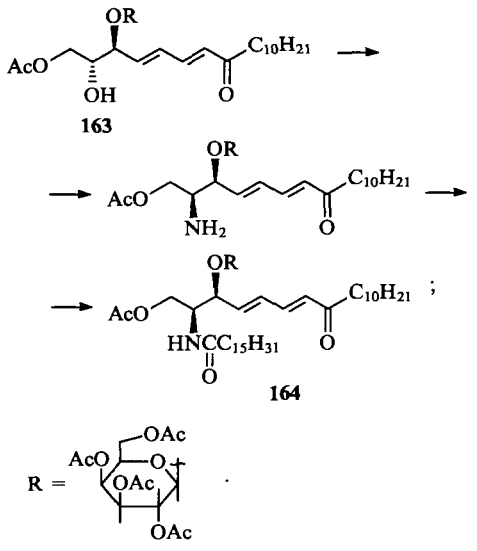
The *O*-glycosylated α,β-unsaturated aldehydes, synthesised by the decyclisation of glycals derived from disaccharides, enter fairly readily into the olefin formation reaction with various phosphoranes and 2-oxophosphonates (Scheme 102).[9, 85–88]

Scheme 102



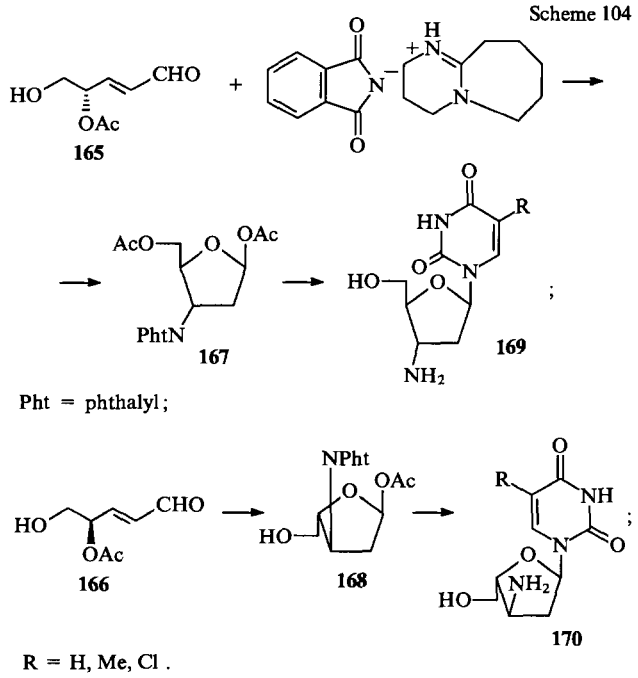
The glycoside **163**, obtained in this way, has been used in the synthesis of the pentaacetate of (2*S*, 3*S*, 4*E*, 6*E*)-3-*O*-(β-D-galactopyranosyl)-2-*N*-hexadecanoyl-8-oxosphinga-4,6-diene **164** — a structural analogue of the membrane galactocenebroside (Scheme 103).[156]

Scheme 103



The monoacetates of the α,β-unsaturated dihydroxypentenals **165** and **166**, obtained by the decyclisation of di-*O*-acetyl-D-xylal and di-*O*-acetyl-L-arabinal, react with phthalimide in the presence of 1,8-diazabicyclo[5.4.0]undec-7-ene via a recyclisation mechanism, affording the phthalimido-2',3'-dideoxypentoses **167** and **168**. The latter have been used in the synthesis of 3'-amino-3'-deoxythymidine **169**[157] and L-3'-amino-2',3'-dideoxyuridines **170** (Scheme 104).[158]

Scheme 104



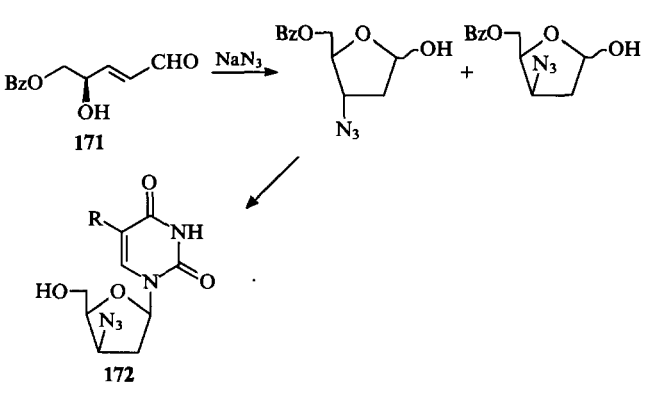
Pht = phthalyl;

R = H, Me, Cl .

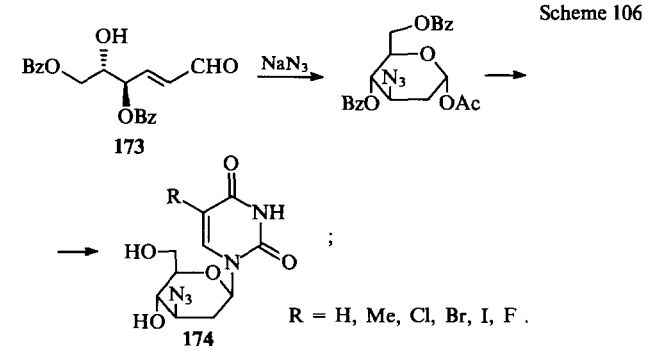
The cyclisation of the benzoyloxypentenal **171** on treatment with NaN_3 leads to stereoisomeric azidopentoses, one of which has been used to synthesise azidothymidine **172**, which possesses a high antiviral activity (Scheme 105).[159]

3'-Azido-2',3'-dideoxyhexosouridines **174** have been synthesised from the aldehyde **173** in accordance with a similar scheme (Scheme 106).[160]

Scheme 105



Scheme 106



R = H, Me, Cl, Br, I, F .

The syntheses of analogues of azidothymidine from the products of the decyclisation of glycal esters derived from hexoses have been described.[161]

As can be seen from the present review, the study of the reactions of glycals has outgrown the framework of the chemistry of carbohydrates proper and has made it possible to discover their extensive possibilities in relation to enantiospecific synthesis. One cannot fail to draw attention to the fact that synthon units of special preparative value by virtue of the enantiomeric purity of the natural and synthesised chiral centres and the presence of the reactive functional groups most suitable for subsequent transformations can be obtained precisely from the glycals. Judging from the rate of growth of the publications during the last five years, glycals are rapidly occupying an honourable place among the series of sources of chiral carbon which are of general importance for the synthesis of complex natural products, their analogues, and their derivatives.

References

1. E Fischer, K Zach *Sitz. Ber. Kgl. Preuss. Akad. Wiss.* **16** 311 (1913)
2. R J Ferrier *Adv. Carbohydr. Chem.* **20** 67 (1965)
3. R J Ferrier *Adv. Carbohydr. Chem. Biochem.* **24** 199 (1969)
4. N K Kochetkov, A F Sviridov, M S Ermolenko, D V Yashunskii, O S Chizhov *Uglevody v Sinteze Prirodnykh Soedinenii* (Carbohydrates in the Synthesis of Natural Products) (Moscow: Nauka, 1984)
5. T D Inch *Tetrahedron* **40** 3161 (1984)
6. K A Kochetkov, A F Sviridov *Bioorg. Khim.* **17** 293 (1991)
7. A G Tolstikov, V N Odinokov, G A Tolstikov *Zh. Vserossiisk. Khim. O-va im. D. I. Mendeleeva* **36** 400 (1992)
8. R J Ferrier, N Prasad *J. Chem. Soc. C* 570 (1969)
9. A G Tolstikov, O F Prokopenko, R Kh Yamilov, G A Tolstikov *Mendeleev Commun.* 64 (1991)
10. A G Tolstikov, O F Prokopenko, L M Khalilov, L V Spirikhin, G A Tolstikov *Mendeleev Commun.* 51 (1991)
11. A G Tolstikov, O F Prokopenko, A A Panasenko, L V Spirikhin, V N Odinokov, G A Tolstikov *Zh. Org. Khim.* **27** 798 (1991)
12. S J Eitelman, R H Hall, A Jordaan *J. Chem. Soc., Perkin Trans. 1* 595 (1978)
13. M Sharma, R K Brown *Can. J. Chem.* **44** 2825 (1966)

14. J Lancelin, L Morin-Allory, P Sinay *J. Chem. Soc., Chem. Commun.* 355 (1984)
15. A Furstner, H Weidmann *J. Org. Chem.* **54** 2307 (1989)
16. R Csuk, A Furstner, B J Glanser *J. Chem. Soc., Chem. Commun.* 1149 (1986)
17. J Sudha, S N Suryawanshi, D S Bhakuni *Indian J. Chem.* **26B** 866 (1987)
18. J Pollon, L Levellin, J Wilianes *Synthesis* 758 (1989)
19. Jane Chi-Ya Cheng, U Hacksell, G Doyle Daves *J. Org. Chem.* **50** 2778 (1985)
20. R E Ireland, D Norbeck *J. Am. Chem. Soc.* **107** 3279 (1985)
21. R E Ireland, C S Wilcox, S Thaisrivongs *J. Org. Chem.* **43** 786 (1978)
22. A Fernandez-Mayorales, A Marra, M Trumtel *Tetrahedron Lett.* **30** 2537 (1989)
23. V Pedretti, A Veyrieres, P Sinay *Tetrahedron* **46** 77 (1990)
24. R Boeckman, A B Charette, T Asberom, B Iohwson *J. Am. Chem. Soc.* **109** 7553 (1987)
25. F Acramone, A Bargiotti, G Casinelli, L Senpino *J. Med. Chem.* 733 (1976)
26. R Halcomb, M Wittman, A Olson, S Ardarlli, S Hanessian, A Di Marco, A Casarra, C Dasdia, A Necco, P Reggiani, S Danishefsky *J. Am. Chem. Soc.* **113** 5080 (1991)
27. R U Lemieux, D R Lenebach *Can. J. Chem.* **43** 94 (1965)
28. S Sabegam, S Neira *J. Org. Chem.* **56** 5468 (1991)
29. V Bolitt, Ch Nioskowski, S G Lee, G Falk *J. Org. Chem.* **55** 5812 (1990)
30. Y Ito, T Ogawa *Tetrahedron Lett.* **28** 2723 (1987)
31. M Perez, G-M Beau *Tetrahedron Lett.* **30** 75 (1989)
32. A Barrett, T Miller *Tetrahedron Lett.* **29** 1873 (1988)
33. I Borowiecka, P Lipka, M Michalska *Tetrahedron* **44** 2067 (1988)
34. R Ewans, J H Schauble *Synthesis* 551 (1987)
35. G Vite, R Alonso, B Fraser-Reid *J. Org. Chem.* **54** 2268 (1989)
36. R Friezen, S Danishefski *Tetrahedron* **46** 103 (1990)
37. R Halcomb, S Danishefski *J. Am. Chem. Soc.* **111** 6661 (1989)
38. J Gervag, S Danishefsky *J. Org. Chem.* **56** 5448 (1991)
39. A G Tolstikov, E E Savateeva, L V Spirikhin, G A Tolstikov *Mendeleev Commun.* 133 (1991)
40. A G Tolstikov, E E Savateeva, L V Spirikhin, V R Sultanmuratova, G A Tolstikov *Izv. Akad. Nauk SSSR, Ser. Khim.* **9** 2165 (1991)
41. S Danishefsky, G F Kerwin *J. Org. Chem.* **47** 3803 (1982)
42. R D Dawe, B Fraser-Reid *J. Chem. Soc., Chem. Commun.* 1180 (1981)
43. R D Dawe, B Fraser-Reid *J. Org. Chem.* **49** 522 (1984)
44. J Herscovici, K Mileka, L Boumaiza, K Antonakis *J. Chem. Soc., Perkin Trans. 1* 1995 (1990)
45. J Herscovici, S Delatre, K Antonakis *J. Org. Chem.* **52** 5691 (1987)
46. D Grierson, M Bouin, H P Husson *Tetrahedron Lett.* **25** 4645 (1984)
47. F D Heras, A S Felix, R P Fernandez *Tetrahedron* **39** 1617 (1983)
48. M B Yunker, D E Plaumann, B Fraser-Reid *Can. J. Chem.* **55** 4002 (1977)
49. S Valverde, M Bernabi, S Garcia-Ochoa, A Gomes *J. Org. Chem.* **55** 2294 (1990)
50. K C Nicolaou, C K Hwang, M E Duggan *J. Chem. Soc., Chem. Commun.* 925 (1986)
51. G Casiraghi, M Cornia, L Colombo, G Rossu, G Fava, M Belicchi, L Zetta *Tetrahedron Lett.* **29** 5549 (1988)
52. G Casiraghi, M Cornia, G Rossu, L Zetta, G Fava, M Belicchi *Tetrahedron Lett.* **29** 3323 (1988)
53. S Czernecki, V Dechavanne *Can. J. Chem.* **61** 533 (1983)
54. V Bellosta, S Czernecki, D Avenel, S E Bahig, H Giller-Pandrant *Can. J. Chem.* **68** 1364 (1990)
55. R A Outten, G S Doyle Daves *J. Org. Chem.* **54**, 29 (1989)
56. U Hacksell, G Doyle Daves *J. Org. Chem.* **48** 2870 (1983)
57. D B Tulshian, B Fraser-Reid *J. Org. Chem.* **49** 518 (1984)
58. R E Ireland, R H Mueller *J. Am. Chem. Soc.* **94** 5897 (1972)
59. R E.Ireland, R H Mueller, A R Willard *J. Am. Chem. Soc.* **98** 2868 (1976)
60. R E Ireland, S Thaisrivongs, N Vanier, C S Wilcox *J. Org. Chem.* **45** 48 (1980)
61. R E Ireland, M G Smith *J. Am. Chem. Soc.* **110** 854 (1988)
62. R E Ireland, G McGarvey, R C Anderson, R Badoud, B Fitzsimmons, S Thaisrivongs *J. Am. Chem. Soc.* **102** 6178 (1980)
63. L Colombo, J Casiraghi, A Pittalis, G Rossu *J. Org. Chem.* **56** 3897 (1991)
64. M Fetizon, Duc Do Khac, Nguyen Dinh Tho *Tetrahedron Lett.* **26** 1777 (1986)
65. T Matsui, T Morooka, M Nakayama *Bull. Chem. Soc. Jpn.* **60** 417 (1987)
66. M Chmielewski, Z Kaluza, C Belzecki, P Salanski, I Iwrczak, H Adamowich *Tetrahedron Lett.* **25** 2441 (1985)
67. M Chmielewski, Z Kaluza *J. Org. Chem.* **51** 2397 (1986)
68. M Chmielewski, Z Kaluza, W Adamek *Tetrahedron* **45** 227 (1989)
69. H Gnichtel, L Autenrieth-Ansorge *Liebigs Ann. Chem.* 2217 (1985)
70. J Panfil, M Chmielewski *Tetrahedron* **41** 4713 (1985)
71. J Panfil, C Belzecki, M Chmielewski *Tetrahedron* **45** 233 (1989)
72. J Primean, R Anderson, B Fraser-Reid *J. Am. Chem. Soc.* **105** 5874 (1983)
73. J Dyong, H-W Hagedorn, J Thiem *Liebigs Ann. Chem.* 551 (1986)
74. B J Fitzsimmons, Y Leblanc, J Rokach *J. Am. Chem. Soc.* **109** 285 (1987)
75. Y Leblanc, B J Fitzsimmons *Tetrahedron Lett.* **30** 2889 (1989)
76. Y Leblanc, B J Fitzsimmons, J Rokach *J. Am. Chem. Soc.* **111** 2995 (1989)
77. P Jarglis, F W Lichtenthaler *Tetrahedron Lett.* **23** 3781 (1982)
78. F W Lichtenthaler, P Jarglis, S Roniger *Liebigs Ann. Chem.* 1153 (1989)
79. P Rollin, A Sinay *Carbohydr. Res.* **98** 193 (1981)
80. B Roth, H Roak *Tetrahedron Lett.* **29** 1255 (1988)
81. F Gonzales, S Lesage, A Perlin *Carbohydr. Res.* **42** 267 (1975)
82. B Fraser-Reid *Acc. Chem. Res.* **18** 347 (1985)
83. A G Tolstikov, N V Khakhalina, L V Spirikhin *Synthesis* 221 (1988)
84. N Hirata, Y Yamagiwa, T Kamikawa *J. Chem. Soc., Perkin Trans. 1* 2279 (1991)
85. G A Tolstikov, A G Tolstikov, O F Prokopenko, L M Khalilov, V N Odinokov *Synthesis* 533 (1990)
86. A G Tolstikov, O F Prokopenko, L M Khalilov, V N Odinokov, G A Tolstikov *Zh. Org. Khim.* **24** 1341 (1988)
87. A G Tolstikov, O F Prokopenko, R Kh Yamilov, L V Spirikhin, G A Tolstikov *Izv. Akad. Nauk SSSR, Ser. Khim.* 1705 (1991)
88. A G Tolstikov ,O F Prokopenko, L M Khalilov, V N Odinokov, G A Tolstikov *Zh. Org. Khim.* 27 788 (1991)
89. E J Corey, G Gobo *Tetrahedron Lett.* **21** 3463 (1980)
90. S Sabesan, S Neira *J. Org. Chem.* **56** 5468 (1991)
91. S Torii, T Inokuchi, Y Masatsugu *Bull. Chem. Soc. Jpn.* **58** 3629 (1985)
92. W W Zajac, P J Dampawan, D Ditrow *J. Org. Chem.* **51** 2618 (1986)
93. M Wittman, R Halcomb, S Danishefsky *J. Org. Chem.* **55** 1979 (1990)
94. J Thiem, J Elvers *Chem. Ber.* **112** 818 (1979)
95. D Walker, B Fraser-Reid *J. Am. Chem. Soc.* **97** 6251 (1975)
96. S Maier, R Preuss, R Schmidt *Liebigs Ann. Chem.* 483 (1990)
97. D Gordon, S Danishefsky *J. Org. Chem.* **56** 3713 (1991)
98. M Georges, D Mackay, B Fraser-Reid *Can. J. Chem.* **62** 1539 (1984)
99. J Lundt, J Thiem, A Prahst *J. Org. Chem.* **49** 3063 (1984)
100. D Griffith, S Danishefsky *J. Am. Chem. Soc.* **113** 5863 (1991)
101. J Thiem, A Prahst, J Lundt *Liebigs Ann. Chem.* 1044 (1986)
102. P Friezen, C Sturino *J. Org. Chem.* **55** 5808 (1990)
103. M Tius, J Gomez-Galeno, Xue-gin Gu *J. Am. Chem. Soc.* **113** 5775 (1991)
104. S Valverde, B Herradon, R Rabanal, H Martin-Tomas *Can. J. Chem.* **65** 339 (1987)
105. F W Lichtenthaler, K Lorenz, Wei-yong Ma *Tetrahedron Lett.* **28** 47 (1987)
106. Y Ichikawa, M Isobe, Dong-Lu Bai, T Goto *Tetrahedron* **43** 4737 (1987)
107. Y Ichikawa, M Isobe, T Goto *Tetrahedron Lett.* **25** 5049 (1984)
108. M Isobe, Y Ichikawa, H Masaki *Tetrahedron Lett.* **25** 3607 (1984)
109. Y Ichikawa, M Isobe, H Masaki *Tetrahedron* **43** 4759 (1987)
110. A Kozikowski, J Lee *J. Org. Chem.* **55** 863 (1990)
111. G W Fleet, M J Gough, T K Shing *Tetrahedron Lett.* **24** 3661 (1983)
112. D P Gurran *Tetrahedron Lett.* **23** 4309 (1982)
113. R E Ireland, D Habich, D W Norbeck *J. Am. Chem. Soc.* **107** 3271 (1985)
114. R E Ireland, D W Norbeck *J. Am. Chem. Soc.* **107** 3279 (1985)
115. S J Danishefsky, S Deninno, P Lartey *J. Am. Chem. Soc.* **109** 2082 (1987)
116. F E Wincott, S J Danishefsky *Tetrahedron Lett.* **28** 4951 (1987)

117. S J Danishefsky, D M Armistead, F E Wincott *J. Am. Chem. Soc.* **109** 8117 (1987)
118. S J Danishefsky, D M Armistead, F E Wincott *J. Am. Chem. Soc.* **111** 2967 (1989)
119. K C Nicolaou, M E Duggan, C-K Hwang, P Somers *J. Chem. Soc., Chem. Commun.* 1359 (1985)
120. K C Nicolaou, M E Duggan, C-K Hwang *J. Am. Chem. Soc.* **111** 6666 (1989)
121. A G Tolstikov, O F Prokopenko, L V Spirikhin, G A Tolstikov *Bioorg. Khim.* **19** 262 (1993)
122. A G Tolstikov, O F Prokopenko, L V Spirikhin, V R Sultanmuratova, V T Odinokov, G A Tolstikov *Zh. Org. Khim.* **26** 879 (1991)
123. A G Tolstikov, O F Prokopenko, G A Tolstikov, L M Khalilov, L V Spirikhin, A A Berg, V R Sultanmuratova *Mendeleev Commun.* 52 (1991)
124. A G Tolstikov, E E Savateeva, G A Tolstikov, M V Khakhalina, L V Spirikhin *Izv. Akad. Nauk SSSR, Ser. Khim.* 1285 (1992)
125. A G Tolstikov, O F Prokopenko, G A Tolstikov, L V Spirikhin, V R Sultanmuratova, A A Berg *Izv. Akad. Nauk SSSR, Ser. Khim.* 1939 (1991)
126. J Sabol, R Cregge *Tetrahedron Lett.* **30** 6271 (1989)
127. M J Kelly, R Newton, S M Roberts, G Whitenhead *J. Chem. Soc., Perkin Trans. 1* 2352 (1990)
128. M J Kelly, S M Roberts *J. Chem. Soc., Perkin Trans. 1* 787 (1991)
129. H Hashimoto, K Furuichi, T Miwa *J. Chem. Soc., Chem. Commun.* 1002 (1987)
130. J Prandi, J-M Bean *Tetrahedron Lett.* **30** 4517 (1989)
131. G E Keck, D F Kachensky *J. Org. Chem.* **51** 2487 (1986)
132. K Mattess, Mong Hsia, R Hutchinson, S Sisk *Tetrahedron Lett.* **18** 3541 (1977)
133. D Curran, P Jacobs, R Elliott, B Kim *J. Am. Chem. Soc.* **109** 5280 (1987)
134. B H Kim, P B Jacobs, R L Elliott *Tetrahedron* **44** 3079 (1988)
135. R B Gupta, R W Franck *J. Am. Chem. Soc.* **111** 7668 (1989)
136. W Brade, A Vasella *Helv. Chim. Acta* **72** 1649 (1989)
137. K Tatsuta, R Akimoto, M Annaka *Bull. Chem. Soc. Jpn.* **58** 1699 (1985)
138. K Okazaki, K Nomura, E Yoshii *J. Chem. Soc., Chem. Commun.* 355 (1989)
139. S Shibahara, S Kondo, M Ohno, H Umezana, K Malda *J. Am. Chem. Soc.* **94** 4353 (1972)
140. S Hanessian, A-M Faucher, S Leger *Tetrahedron* **46** 231 (1990)
141. G M Fleet, K James, R J Lunn *Tetrahedron Lett.* **27** 3053 (1986)
142. M Shiozaki, T Hata, J Furukawa *Tetrahedron Lett.* **30** 3669 (1989)
143. Ch Tamm, N Jeker *Tetrahedron* **45** 2385 (1989)
144. D B Tulshian, B Fraser-Reid *J. Am. Chem. Soc.* **103** 474 (1981)
145. J D White, E G Nolen, G H Miller *J. Org. Chem.* **51** 1150 (1986)
146. A Mukhopadhyay, S M Ali, M Husain, S Suryawanshi *Tetrahedron Lett.* **30** 1853 (1989)
147. K Hori, K Nomura, H Kazuno, E Yoshii *Chem. Pharm. Bull.* **38** 1778 (1990)
148. A V Rama Rao, A V Purandare, E R Reddy, M Gugar *Synthetic Commun.* **17** 1095 (1987)
149. A G Tolstikov, E E Savateeva, G A Tolstikov, L V Spirikhin, L M Khalilov, V N Odinokov *Bioorg. Khim.* **16** 1670 (1990)
150. A G Tolstikov, N V Khakhalina, V N Odinokov, V M Khalilov, L V Spirikhin, G A Tolstikov *Zh. Org. Khim.* **25** 296 (1989)
151. A G Tolstikov, N V Khakhalina, V N Odinokov *Zh. Org. Khim.* **23** 2469 (1987)
152. A G Tolstikov, N V Khakhalina, G A Tolstikov, L V Spirikhin, L N Khalilov, A A Panasenko, V N Odinokov *Zh. Org. Khim.* **27** 792 (1991)
153. A G Tolstikov, N V Khakhalina, E E Savateeva, L V Spirikhin, V N Odinokov, G A Tolstikov *Bioorg. Khim.* **18** 733 (1992)
154. A G Tolstikov, N V Khakhalina, E E Savateeva, L V Spirikhin, V N Odinokov, G A Tolstikov *Khim. Prir. Soedin.* 707 (1991)
155. A G Tolstikov, R Kh Yamilov, G A Tolstikov, L V Spirikhin, L M Khalilov, V N Odinokov *Bioorg. Khim.* **17** 147 (1991)
156. A G Tolstikov, R Kh Yamilov, O F Prokopenko, G A Tolstikov *Mendeleev Commun.* 96 (1992)
157. M S Motawia, J Wengel, E B Pedersen, A Abdel-Megid *Synthesis* 384 (1989)
158. J Wengel, J Lau, E B Pedersen *Synthesis* 829 (1989)
159. J Wengel, J Lau, E B Pedersen *J. Org. Chem.* **56** 3591 (1991)
160. P Hansen, J Lau, E B Pedersen, C Nielsen *Liebigs Ann. Chem.* 1079 (1990)
161. J Lau, J Wengel, E B Pedersen *Synthesis* 1183 (1991)

Russian Chemical Reviews **62** (6) 603 – 623 (1993)
© 1993 Russian Academy of Sciences and Turpion Ltd

UDC 678.048

New aspects of the problem of the ageing and stabilisation of polymers

G E Zaikov, A Ya Polishchuk

Contents

I. Introduction 603
II. Thermodynamic and kinetic aspects of the photo- and radiation-induced ageing and photostabilisation of polymers 603
III. Stability of elastomers and water-soluble polymers. Their applications in medicine and petrochemistry 609
IV. New approaches to the fundamental investigation and practical application of polymer degradation and stabilisation processes 613

Abstract. The results of the most recent studies in the field of the ageing and stabilisation of polymers are presented. The review deals with the questions of the photo-ozone and radiation induced ageing of polymers, and thermo-oxidative degradation and stabilisation of elastomers, various aspects of the interaction of polymers with corrosive media, the problems of the synthesis and efficiency of natural and synthetic stabilisers, and various applications of polymers and polymer blends. New approaches and methods for the investigation of the degradation of polymers are described. The bibliography includes 78 references.

I. Introduction

The regulation of the lifetime of polymer articles is not only a chemical but also a social problem of current interest. On the one hand, prolongation of the duration of use and of storage life is equivalent to an increase in the output of polymeric articles and an improvement in their quality.[1] On the other hand, the accumulation of polymer waste brings to the fore problems of the protection of the environment and of the utilisation of polymeric products.[2] The search for a new method for the modification of polymeric articles in order to improve their operational characteristics (in the first place, in order to modify the properties of their surface) and for the synthesis of polymers with a controllable lifetime has not lost its interest.[3]

Studies on the diffusion, sorption, and desorption of low-molecular-mass compounds in a polymer phase are of interest. This is associated not only with the problem of the protection of polymeric materials against the loss of stabilisers but also with the use of polymers in medicine and the creation of new polymeric long-acting medicinal systems.

The present review deals with problems of regulating the duration of the use and storage and the ageing and stabilisation of polymers as well as the search for ways of prolonging and shortening the lifetime of polymeric articles within the framework of studies carried out in our country during recent years. The review includes also information concerning the prediction of a reliable operating lifetime, which will permit a fuller use of polymeric articles without risk of their premature breakdown.

G E Zaikov, A Ya Polishchuk N N Semenov Institute of Chemical Physics, Russian Academy of Sciences, ul. Kosygina 4, 117977 Moscow.
Fax (7-095) 938 21 56

Received 10 January 1993
Uspekhi Khimii **62** (6) 644 – 664 (1993); translated by A K Grzybowski

II. Thermodynamic and kinetic aspects of the photo- and radiation-induced ageing and photostabilisation of polymers

1. Photo-ozone ageing of polymers

The ageing of polymers under natural conditions takes place under the simultaneous influence of many factors (light, ozone, heat, etc.). Ivanov and Shlyapintokh[4] showed recently that synergism may be observed in photo-ozone ageing. Thus it was observed in a study of the ageing of rubbers based on polydieneurethanes that, under the simultaneous influence of ozone and light, cracks arise much faster than on exposure to ozone alone, while exposure to light alone does not lead to the formation of cracks during the period of observation (Fig. 1*a*).

The synergistic effect of light and ozone is also manifested on non-stabilised resins and resins containing antiozonants and photostabilisers. The mechanisms of the action of these influences are then different. Fig. 1*b* shows that an antiozonant of the class of *p*-phenylenediamine, which protects the polymer against ozone quite effectively, becomes inactivated when acted upon by light and ozone simultaneously. On the other hand, a photostabiliser of the class of azo-compounds actually accelerates the ozone-induced ageing process, which is apparently due to its catalytic properties. At the same time, when one uses a mixture of this photostabiliser with an antiozonant acting in accordance with a physical mechanism, a synergistic enhancement of the protective effect is observed. Thus, during the photoozone-induced ageing of a polymer, synergistic phenomena of two types are manifested: the synergistic effect of UV light and ozone; the mutual synergistic influence of antiozonants and photostabilisers.

2. A special type of kinetics in the photochemical oxidation of polyamides

A series of independent tests confirmed[5] the hypothesis, put forward by Postnikov, of the ketoimide mechanism of the oxidation of aliphatic polyamides (PA). An unusual type of kinetics, for which there are as yet no analogues in the photochemical oxidation of other polymers, of the variation of the concentrations of the principal intermediates, i.e. the ketoimide fragment of the macromolecule ($\sim CONHCOCOCH_2 \sim$) and the structurally similar unsaturated ketone, correspond to this new mechanism. Both products have dual functions: under the influence of light, they behave as photoinitiators of the oxidation chains and at the same time, regardless of the influence of light, they participate in kinetic chain transfer with dissociation of the macromolecule accompanied by the alternation of radicals of two types.

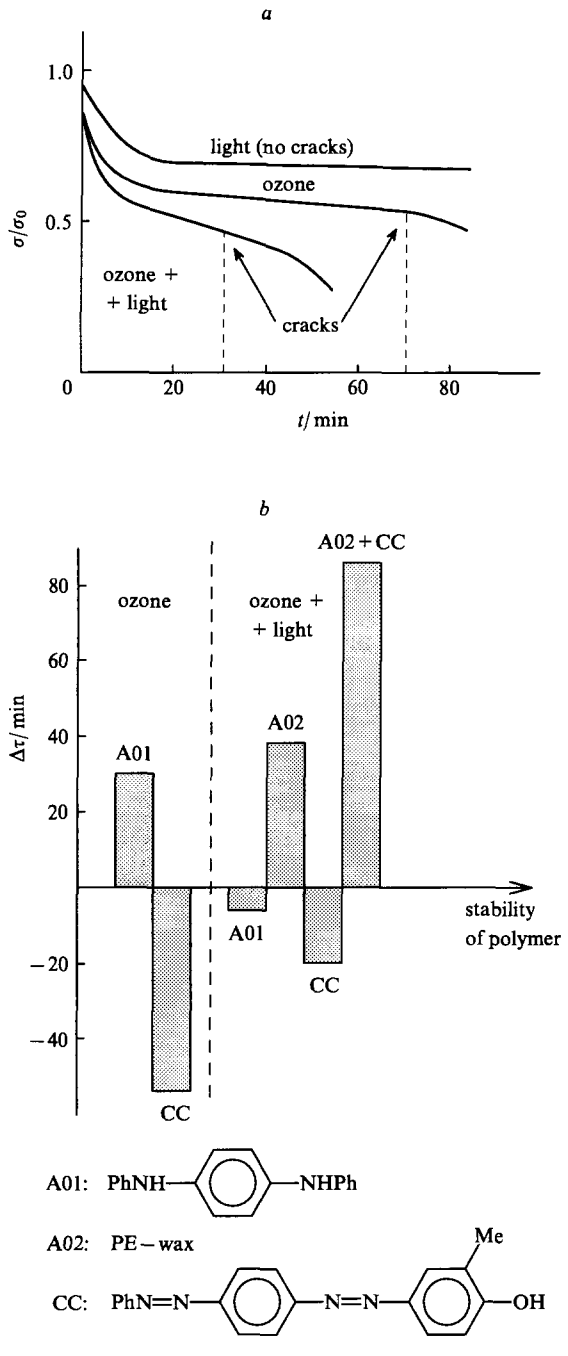


Figure 1. The synergistic effect of UV light and ozone in the ageing of polydieneurethanes: (*a*) kinetics of the relaxation of stresses; (*b*) kinetics of the formation of cracks.

Under any conditions of the photochemical oxidation of polyamides the stationary concentrations of these products are established after a time and for deliberate regulation of the process it is necessary to discover the quantitative parameters which determine both the stationary concentrations themselves and the kinetics of their attainment. The ketone mechanism explained for the first time the known kinetics of the photochemical oxidation of polyamides under all irradiation conditions of practical interest.

The kinetics of the approach to a stationary regime in the case where a polyamide is acted upon by the longest-wavelength light still capable of inducing photooxidative degradation may serve as a clear example of the importance of the above findings. Under such conditions, the kinetic chain is transferred by intermediates (K and K′), but the photoinitiator is only one of them (the ketoimide K). The kinetics of the variation of their concentrations from the initial (K_0 and K'_0) to the stationary (K_{st} and K'_{st}) values are then described by the following functions:

$$K = K_{st}\left[\coth\left(\frac{F+Gt}{2}\right)\right]^2,$$

$$K' = K_{st} - (K'_{st} - K'_0)\times$$

$$\times\left[\left(\sinh\left(\frac{F+Gt}{2}\right)\right)^{Ak'_5/G} \Big/ \sinh\left(\frac{F}{2}\right)\right],$$

where F, G, A, and k'_5 are familiar parameters with a known physical significance:

$$F = \ln\left|\frac{(K_0)^{1/2} - (K_{st})^{1/2}}{(K'_0)^{1/2} - (K'_{st})^{1/2}}\right|,$$

$$G = -\left[\frac{k_7}{k_5}I_0\left(\frac{k_7}{k_5}I_0 + 4\frac{k_2}{k_6}\right)\right]^{1/2}\frac{k_5}{2},$$

$$A = 2\frac{k_2}{k_3}\left(\frac{k_3k_7I_0}{k_6k_2}K_{st}\right)^{1/2},$$

$$PO_2 + PA \xrightarrow{+O_2} POOH + PO_2^{\cdot}, \quad (1)$$

$$PO_2^{\cdot} \longrightarrow A + r^{\cdot}, \quad (2)$$

$$PO_2^{\cdot} \longrightarrow B + r^{\cdot}, \quad (2')$$

$$r^{\cdot} + PA \xrightarrow{+O_2} rH + PO_2^{\cdot}, \quad (3)$$

$$A \xrightarrow{+2O_2} K, \quad (4)$$

$$A \xrightarrow{+2O_2} K', \quad (4')$$

$$K + r \longrightarrow PO_2 + S, \quad (5)$$

$$K' + r \longrightarrow PO_2 + S, \quad (5')$$

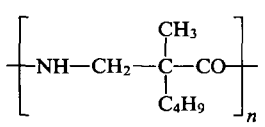
$$PO_2 + r \xrightarrow{-O_2} S, \quad (6)$$

$$K \xrightarrow{+I_0+2O_2} 2PO_2 + S. \quad (7)$$

Here k_i is the rate constant, the subscript i corresponding to the ordinal number of the reaction in the mechanism, I_0 is the light intensity, P is a polymer radical, PO_2 are the peroxide macroradicals $\sim CH_2CONHCH(OO^{\cdot})CH_2\sim$, r are low-molecular-mass radicals $HO_2^{\cdot}$ or O_2^{-}, A, K, and K′ are intermediate molecular products, B is the final product, and S denotes the dissociation of the macromolecule.

Functional relations of this type have not so far been considered in the kinetics of the photodegradation of polymers. Such relations help in the rational selection of photostabilisers. Previously stabilisers were selected without taking into account the actual mechanism of the photochemical oxidation of polyamides.

The observed mechanism is valid for different industrially manufactured aliphatic polyamides regardless of the number of CH_2 units. However, it ceases to operate in the absence of hydrogen atoms attached to the α- or β-carbon atom, for example, when they are substituted by alkyl groups, because the formation of the ketoimides

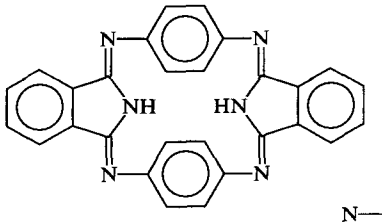


becomes impossible. As a result of this, the photochemical oxidation of poly(3-butyl-3-methylazetidine) follows completely different kinetics.

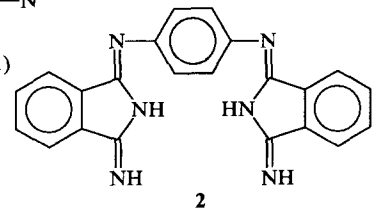
3. A new class of photostabiliser

Cellulose acetates (CA) are widely used nowadays in different branches of industry, but, owing to their inadequate photostability, the operating characteristics of articles made from this material become strongly impaired after a time. Therefore, despite the great variety of cellulose acetate stabilisers, the search for effective photostabilisers is still a timely problem.[6, 7]

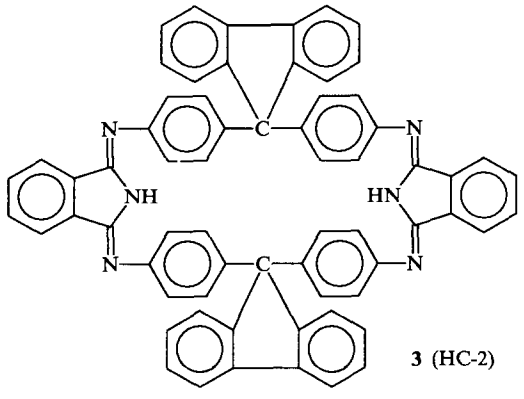
A new class of photostabilisers based on macroheterocyclic substances — hexaazacyclanes (HC) — has been developed.[8] Among different derivatives of hexaazacyclanes, phthalonitrile and its derivatives comprising *p*-phenylenediamine (a conjugated substance — compound **1** or HC-1) and 9,9-bis(4-dianilino)fluorene (a non-conjugated substance — compound **3** or HC-2) were selected for study. In order to determine the influence of the structure of the macrocyclic stabiliser on its properties, the product of the linear condensation of phthalonitrile and *p*-phenylenediamine (compound **2**) was also investigated. All the substances are powders with different colours (depending on the structure) ranging from yellow to brown. They are fairly compatible with cellulose acetate and do not impair the operating properties of the latter at concentrations in the range 5–7.5 mass%.



1 (HC-1)



2



3 (HC-2)

The proposed photostabiliser can act simultaneously via several mechanisms, among which the most important involve shielding from UV light, inhibition, and photosensitivity. The contribution of UV shielding to the overall effect of the stabiliser is calculated using the formula proposed by the present authors:[4]

$$i_p = \frac{D_{d+st}(1 - 10^{-D_d})}{D_d(1 - 10^{-D_{d+st}})},$$

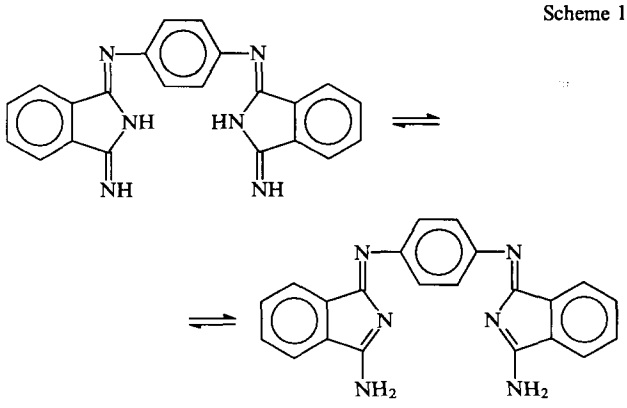
where D_d and D_{d+st} are the optical densities of the non-stabilised and stabilised films respectively. The coefficient i_p characterises the quantitative decrease in light absorption by the polymer owing to the presence of the stabiliser. Thus, if the effect of the stabiliser is limited to the absorption of UV light, then the rate of degradation falls by factor i_p relative to the amount of absorbed light.

The principal product of the degradation of cellulose acetate by UV radiation is acetic acid, the rate of formation of which characterises the photostability of the material. The overall effect of the increase in stability (A) is determined by the ratio of the rates of formation of acetic acid without stabiliser (W_0) and in its presence (W_{st}):

$$A = \frac{i_p W_0}{W_{st}}.$$

Data concerning the influence of the structure of the photostabiliser on the overall increase in the photostability of the composition are presented in Table 1. For all stabilisers, $A < 1$. Consequently these stabilisers not only provide a shield against UV light but they also operate as photosensitive elements.[9] The highest photosensitivity is shown by compound **2**. The point is that this substance has two resonance states (see Scheme 1 below), one of which contains amino-groups. Evidently these amino-groups act as photostabilisers in relation to the photodegradation of cellulose acetate, in agreement with the present authors data.[4]

Scheme 1



In terms of its photostabilising properties, HC-2 is superior to compound **2** but is inferior to HC-1. This is probably associated with the shorter length of the conjugated chain and the smaller number of aromatic groups in the structure of HC-2.

HC-1 is the most effective stabiliser. Its effective photostabilising properties could be accounted for by the simultaneous shielding and inhibiting activities. In order to estimate the possible contribution of the inhibition mechanism to the overall effect of HC-1, measurements were made of the kinetic parameters of the photochemical oxidation of unstabilised cellulose acetate and cellulose acetate stabilised by HC-1. These parameters are the chain oxidation parameters $k_p[PH]k_t^{-1/2}$ and the photoinitiation quantum yield P_i.

The results are presented in Table 2. The HC-1 stabiliser does not influence the cellulose acetate chain oxidation parameter or, in other words, it is not an inhibitor interacting with polymer radicals. On the other hand, the photoinitiation quantum yield P_i diminishes sharply in the presence of HC-1. This means that transition from the pure to the stabilised cellulose acetate alters the initiation mechanism, i.e. the stabiliser becomes the initiator instead of cellulose acetate. However, the significant decrease in P_i in the presence of HC-1 is also responsible for the overall protection against light. Thus HC-1 introduced into cellulose

Table 1. Dependence of the overall increase in photostability on the stabiliser structure.

Stabiliser[a]	A
1	0.40
2	0.21
3	0.31

[a] The stabiliser concentration in cellulose acetate was 5 mass%.

Table 2. Kinetic parameters of the photochemical oxidation of cellulose acetate at 25 °C in dry air.

Specimen	$10^{-4}k_p[PH]k_t^{-1/2}$/mol litre^{-1} s^{-1}	P_i
CA without stabiliser	2.2 ± 0.2	0.100
CA stabilised with HC-1 (concentration 5 mass%)	2.4	0.004

acetate acts both as a screen against UV light and as a photosensitive element.

The stabilising properties of HC-1 have been confirmed by comparative data, presented in Table 3, and the decrease in the viscosity of cellulose acetate solutions in acetone after the UV irradiation of films stabilised by HC-1 and one of the most effective stabilisers—carbazole-5,10,12-trisulfonamide (CTS). The stabilising properties of HC-1 are significantly more effective than those of CTS. The protective effect of HC-1 begins to be manifested at its relatively low concentrations (0.5 mass%), the maximum effect being attained at a concentration of 3 mass%. The high stabilising effect under the conditions of prolonged irradiation is also remarkable.

The photostabilising properties of polyhexaazacyclanes (PHC) have been investigated in cellulose acetate and polycaproamide (PA). The photostabilising activity of PHC was estimated from the change in the viscosity of a 5% solution of cellulose acetate in dimethylformamide (DMF) and a solution of polycaproamide in formic acid. Comparative data on the photostability of cellulose acetate and polycaproamide films stabilised by PHC over a period of 24 h are presented in Table 4. They show that PHC is a stabiliser in relation to the photooxidative degradation of both cellulose acetate and polycaproamide, its photostabilising properties in relation to cellulose acetate being more effective than those in relation to polycaproamide. Comparison of the data presented in Tables 3 and 4 demonstrates that the photostabilising properties of HC-1 are significantly more effective than the analogous properties of PHC.

A further search for new effective stabilisers for cellulose acetate and polycaproamide should be continued among macrocyclic aromatic substances with an extensive conjugated chain and a nearly planar structure. A characteristic feature of all macrocyclic stabilisers is their ability to colour textiles yellow, red, and brown depending on the nature and amount of the stabiliser.

Table 3. Changes in the viscosity of a 0.5% cellulose acetate solution after UV irradiation for different irradiation times t_r (%).

Stabiliser	Concentration (mass%)	t_r = 24 h	t_r = 48 h
Without stabiliser	0.0	13	7
TSC	0.5	25	–
	2.0	79	–
	5.0	70	–
HC-1	0.5	79	–
	2.0	92	–
	3.0	94	66
	5.0	93	–

Table 4. Changes in the viscosity of 0.5% solutions after irradiation (%).

Stabiliser	Solution of CA in DMF	Solution of PA in HCOOH
Without stabiliser	13	64
PHC-1	25	73
PHC-2	76	76
PGC-3	47	80

4. Certain problems of the photodegradation and photostabilisation of polymers

Mel'nikov et al.[10] showed in relation to the photooxidative ageing of polystyrene that the photochemical reactions of the peroxyl radicals formed from the central macroradicals

$$\sim CH_2\underset{\displaystyle C_6H_5}{\overset{|}{C}}(O\dot{O})CH_2\sim$$

lead to the disruption of the main polymer chain. The spectroscopic characteristics of this reaction are presented in Fig. 2. The quantum yield of the reaction, accompanied by the formation of low-molecular-weight transfer agents (OH· radicals), is 10^{-3} at 77 K. The photochemical reactions of radicals of other types—cyclohexadienyl radicals, central macroradicals, peroxyl radicals obtained from cyclohexadienyl radicals—have quantum yields ranging from 10^{-1} to 2×10^{-5}; they lead to the migration of the free valence and the formation of low-molecular-mass products without involving the main chain.

The photochemical reactions of radical-anions and polymers such as poly(vinyl acetate), polyacetals, and aliphatic polyurethanes do not exert any significant influence on the molecular mass distribution of the polymers indicated.[11]

In the study of the mechanisms of the photochemical reactions of peroxyl radicals of different types grafted to the surface of chemically activated silicon dioxide, it was possible to show[12] that the primary step in the photolysis involves dissociation at the O–O bond (Table 5).

$$R\dot{O}_2 \longrightarrow [R\dot{O} + O] .$$

The subsequent course of the process is determined by the behaviour of the [RO· + O] pair formed. In particular, the energy evolved in the reverse reaction (250 kJ mol^{-1}) exceeds the energy of the C–O bonds in the peroxyl radicals and hence the vibrationally excited radical may decompose:

$$[R\dot{O} + O] \longrightarrow [RO_2] \longrightarrow \dot{R} + O_2 .$$

The extent of the reaction should be correlated with the strength of the C–O bond in the peroxyl radicals. These results are important for the interpretation of many data on the photooxidative ageing of polymers.

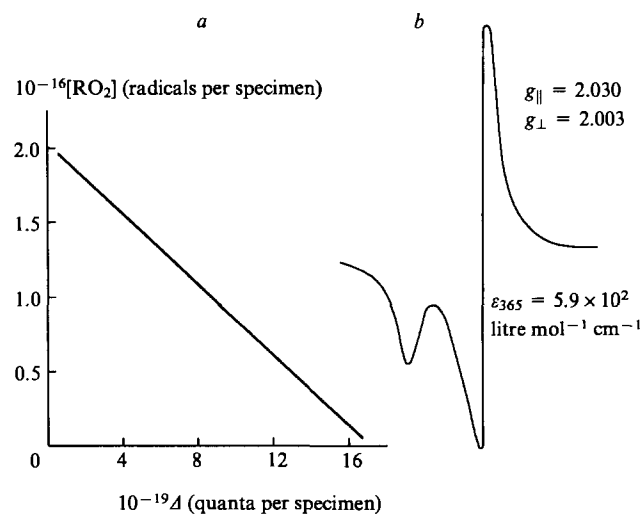


Figure 2. Dependence of the concentration of the RO_2 radicals on the irradiation dose (*a*) and the absorption spectrum at a wavelength of 365 nm (*b*).

Table 5. Photochemical reactions of peroxyl radicals stabilised on the RSi surface at 77 K.

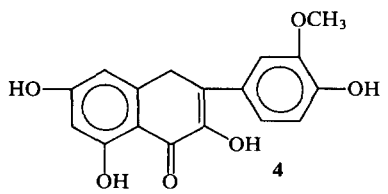
Radical	Detected paramagnetic products[a]	Suggested mode of reaction
$\geqslant SiO\dot{O}$	$\geqslant Si\dot{O}$ (0.8 ± 0.1)	$\geqslant SiO\dot{O} \xrightarrow{h\nu} \geqslant Si\dot{O} + O$
$\geqslant Si(OH)CH_2O\dot{O}$	$>Si(OH)O\dot{C}H_2$ (0.3 ± 0.1)	$>SiOHCH_2O\dot{O} \xrightarrow{h\nu} \geqslant SiOHCH_2\dot{O} + O$, $>SiOHCH_2\dot{O} \longrightarrow >SiOHO\dot{C}H_2$, $>SiOHCH_2\dot{O} \longrightarrow >Si\dot{O}H + CH_2O$
	$>Si\dot{O}H$ (0.6 ± 0.1)	
$\geqslant SiOCH_2O\dot{O}$	$>Si\dot{O}$ (0.5 ± 0.1)	$\geqslant SiOCH_2O\dot{O} \xrightarrow{h\nu} \geqslant SiOCH_2\dot{O} + O$, $\geqslant SiOCH_2\dot{O} \longrightarrow \geqslant Si\dot{O} + CH_2O$, $\geqslant SiOCH_2\dot{O} \longrightarrow \geqslant SiOCHO + H$, $>Si: + H \longrightarrow Si\dot{H}$
	$>Si\dot{H}$ (0.5 ± 0.1)	
$\geqslant SiCH=CHO\dot{O}$	$\geqslant Si\dot{C}HCHO$ (0.7 ± 0.1)	$\geqslant SiCHCHO\dot{O} \xrightarrow{h\nu} \geqslant SiCHCH\dot{O} + O$, $\geqslant SiCHCH\dot{O} \longrightarrow \geqslant Si\dot{C}HCHO$
$\geqslant SiCH_2CH_2C(=O)O\dot{O}$	$\geqslant SiCH_2\dot{C}H_2$ (0.7 ± 0.1)	$\geqslant SiCH_2CH_2CO(O\dot{O}) \xrightarrow{h\nu} \geqslant SiCH_2CH_2CO\dot{O} + \cdot O$, $\geqslant SiCH_2CH_2CO\dot{O} \longrightarrow \geqslant SiCH_2\dot{C}H_2 + CO_2$
$\geqslant SiOCH_2CH_2C(=O)O\dot{O}$	$\geqslant SiOCH_2\dot{C}H_2$ (0.5 ± 0.1)	$\geqslant SiOCH_2CH_2CO(O\dot{O}) \xrightarrow{h\nu} \geqslant SiOCH_2CH_2CO\dot{O} + O$, $\geqslant SiOCH_2CH_2CO\dot{O} \longrightarrow \geqslant SiOCH_2\dot{C}H_2 + CO_2$
$\geqslant SiCH_2CH_2O\dot{O}$	$\geqslant SiOCH_2\dot{C}H_2$ (0.8 ± 0.1)	$\geqslant SiCH_2CH_2O\dot{O} \xrightarrow{h\nu} \geqslant SiCH_2CH_2\dot{O} + O$, $\geqslant SiCH_2CH_2\dot{O} \longrightarrow \geqslant SiOCH_2\dot{C}H_2$
$\geqslant SiOCH_2CH_2O\dot{O}$	$\geqslant SiO\dot{C}H_2$ (0.7 ± 0.1)	$\geqslant SiOCH_2CH_2O\dot{O} \xrightarrow{h\nu} \geqslant SiOCH_2CH_2\dot{O} + O$, $\geqslant SiOCH_2CH_2\dot{O} \longrightarrow \geqslant SiO\dot{C}H_2 + CH_2O$
$\geqslant SiCH_2CH=CHCH_2O\dot{O}$	$\geqslant Si\dot{C}H_2$ (0.75 ± 0.1)	$\geqslant SiCH_2CHCHCH_2O\dot{O} \xrightarrow{h\nu} \geqslant SiCH_2CHCHCH_2\dot{O} + O$, $\geqslant SiCH_2CHCHCH_2\dot{O} \longrightarrow \geqslant SiCH_2CHCHCHO + H$, $>Si: + H \longrightarrow Si\dot{H}$
$\geqslant SiCH_2CH(O\dot{O})CH=CH_2$	$>Si\dot{H}$ (0.15 ± 0.1)	$\geqslant SiCH_2CH(O\dot{O})CHCH_2 \xrightarrow{h\nu} \geqslant SiCH_2CH(O^{\cdot})CHCH_2 + O$, $\geqslant SiCH_2CH(O^{\cdot})CHCH_2 \longrightarrow \geqslant Si\dot{C}H_2 + CH_2=CHCHO$
$\geqslant SiC_6H_4O\dot{O}$	$\geqslant Si\dot{}$ (0.3 ± 0.1)	$\geqslant SiC_6H_4O\dot{O} \xrightarrow{h\nu} \geqslant SiC_6H_4\dot{O} + O$, $\geqslant SiC_6H_4\dot{O} \longrightarrow \geqslant Si\dot{} + C_6H_4O$
	$>Si(OH)\dot{O}$ (0.5 ± 0.1)	
$\geqslant SiOC_6H_4O\dot{O}$	$>Si\dot{H}$ (0.5 ± 0.1)	$\geqslant SiOC_6H_4O\dot{O} \xrightarrow{h\nu} \geqslant SiOC_6H_4\dot{O} + O$, $>SiOC_6H_4\dot{O} \longrightarrow \geqslant Si\dot{O} + C_6H_4O$
	$\geqslant Si(OH)\dot{O}$ (0.5 ± 0.1)	

[a] The fraction of the corresponding paramagnetic products of the photolysis of the peroxyl radicals is indicated in brackets.

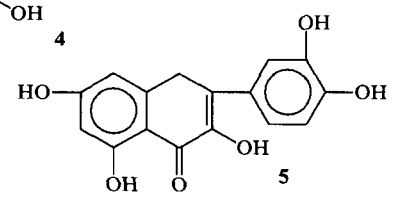
5. Photostabilisation of cellulose diacetate and cellulose paper by natural products

The problem of the photostabilisation of cellulose diacetate (CDA) and cellulose paper (CP) by compounds of natural origin has become of primary importance, since it is directly associated with the protection of the environment and the utilisation of waste.

Studies of the use as stabilisers of flavanoids (isorhamnetin **4** and quercetin **5**) as well as extracts of the walnut, henna, and the total dyes of the polypore (bracken fungus) (TDP) have been carried out by Kalontarov, Niyazi, and coworkers.[13] The walnut extracts contain 25% of juglone and the henna extracts contain 1.85% – 2.23% of lawsone.

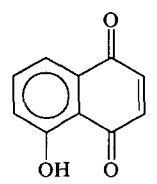


4

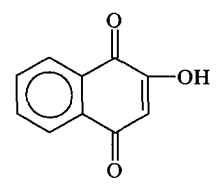


5

These natural products are coloured antioxidants. This permits their use as dyes and photostabilisers for cellulose and its acetates.



juglone



lawsone

It is known that, during the photoageing of cellulose materials, the degree of their polymerisation (DP) diminishes, the concentration of >C=O groups increases, and their physico-chemical properties are impaired.[14] The results of certain tests are presented in Table 6. The introduction of such additives retards the decrease in the degree of polymerisation and the formation of

Table 6. The influence of additives on the photostability of paper after UV irradiation for 20 h.

Dye[a]	Content of carboxy-groups (%)		Content of aldehyde groups (%)		Average DP	
	I	II	I	II	I	II
Without dye	0.048	0.123	0.061	0.028	970	390
Quercetin, 1:1000	0.096	0.167	0.012	0.230	990	415
Walnut, 1:10	0.051	0.118	0.065	0.230	990	420
Henna, 1:10	0.056	0.117	0.064	0.215	985	425
TPD, 1.5 mass%	0.049	0.119	0.063	0.226	995	420

[a] The concentration of the dye or its dilution is quoted.

Note. The following notation has been adopted here and in Table 7: (I) before irradiation; (II) after irradiation.

carboxy- and aldehyde groups. The stabilising effect of the additives is manifested to the greatest extent in the case of quercetin.

In order to investigate the mechanism of action of the additives, transparent films of cellulose diacetate into which these additives had been introduced were obtained. The results of tests on the retention of viscosity are presented in Table 7.

Table 7 shows that all the additives promote the retention of viscosity after irradiation for 24 h. The best result has been achieved with isorhamnetin (78%). After UV irradiation of cellulose diacetate films containing isorhamnetin, a change in is colour is observed — decolorisation as a consequence of the consumption of the dye. The rate constant for the consumption of isorhamnetin was determined from the initial portion of the kinetic optical density curve. Since this relation is linear in terms of logarithmic variables (Fig. 3), the rate constant was calculated from the equation for a first order reaction.[15]

Fig. 3 shows that the rate of consumption of isorhamnetin is inversely proportional to the concentration of the additive. Isorhamnetin is consumed at the lowest experimentally determined rate when its concentration is 3 mass%. These data agree with the literature.[13, 14] According to Kalontarov, at low concentrations the molecules of the additive are distributed in the polymer, forming a monolayer. With increase in the isorhamnetin concentration, the forces of the interaction between the additive and the polymer are overcome and ultimately the isorhamnetin molecules are converted into aggregates, which are decolorised more slowly as a consequence of the effect of the concentration-induced quenching.[16]

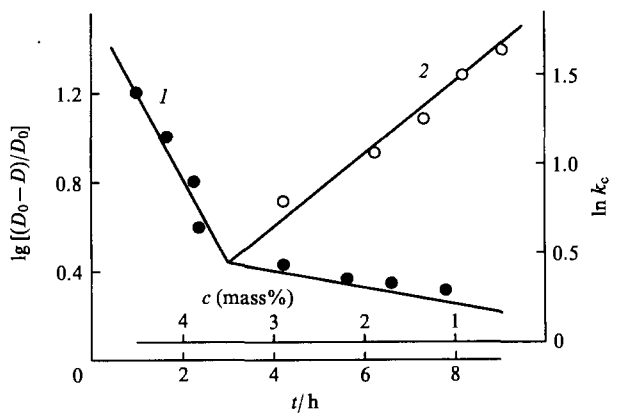


Figure 3. Kinetics of the consumption of isorhamnetin under UV irradiation: (*1*) $\lg[D_0-D)/D_0] = f(t)$; (*2*) $\ln k_c = f(c)$; k_c is the consumption rate constant, D_0 and D are the initial and current optical densities, and c is the concentration of the additive.

Table 7. Changes in the relative viscosity of CDA solutions during UV irradiation.

Additive	Concentration (mass%)	Relative viscosity		Degree of retention of viscosity (%)
		I	II	
Without additive	0	1.12	0.08	6.8
Isorhamnetin	3	1.30	1.02	78.0
Quercetin	3	1.04	0.74	71.5
Walnut	3	1.14	0.74	64.6
Henna	3	1.17	0.73	61.9
TPD	1	1.02	0.59	58.8

6. Laser-induced degradation of polymers

Kalontarov and Marupov investigated in recent years[17-21] the degradation of certain materials — poly(vinyl alcohol) (PVA), polyacrylonitrile (PAN), and polyimide (PI) — by the continuous radiation from an argon laser (514.5 nm). It was shown that the laser-induced degradation process is determined by the kinetics of the accumulation of the products of the thermal decomposition of the macromolecules. Typical dependences of the absorbances of the polymer films on the duration of the laser irradiation are illustrated in Fig. 4. The figure shows that the laser-induced degradation process has two stages: the activation stage (for the duration t_a) and the stage involving a sharp increase in absorption (for the duration t_b), which is completed by the breakdown of the film. The avalanche-like nature of the decomposition is due to the establishment of a positive feedback between the heating of the polymer and the absorption of radiation in the degradation zone. The phenomenon of the sharp increase in absorption and temperature on laser decomposition of polymers has been called photothermochemical instability (PTCI). The first and second stages of the laser-induced degradation (Fig. 4) are therefore called respectively the activation phase and the PTCI development phase. The duration of both phases (t_a and t_b) depends on the power of the absorbed radiation.

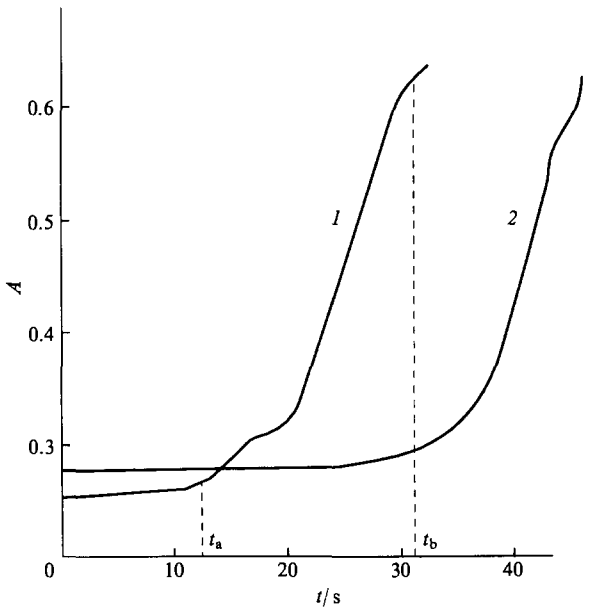


Figure 4. Kinetics of the variation of the absorbance of dyed PVA during laser irradiation for a solid solution of the dye (curve *1*) and for the dye bound chemically to the polymer (curve *2*).

A model of PTCI based on the non-stationary approximation has been constructed[17] and the temperature variation of t_a has been obtained:

$$t_a = \left(\frac{2T_0}{\alpha\gamma}\right)^{1/2} \exp\frac{\alpha}{2}, \quad (8)$$

where $T_0 = \mu P + T_a$ is the temperature of the specimen in the field of the irradiation before the development of the PTCI, P = the power of the incident radiation, T_a the ambient temperature, μ a coefficient, $\alpha = E/RT_0$, $\gamma = (P\varepsilon v)/(\rho C_p S)$, E and v are the activation energy and the pre-exponential factor for the rate of accumulation of the thermal degradation products, C_p is the heat capacity of the polymer film, and ε the extinction coefficient. It has been shown[17] that the activation times calculated by Eqn (8) agree with data for the laser-induced degradation of PVA (Fig. 5).

It has been observed[19, 20] that the duration of the second phase is determined by the rate of development of the PTCI and obeys the following empirical relation:

$$t_b = \tau_0 \exp(-\beta T_0), \quad (9)$$

where τ_0 and β are constants.

The difference between the $t_b(T_0)$ and $t_a(T_0)$ relations is of greatest interest. Eqn (8) was derived on the hypothesis that the Arrhenius equation holds for the chemical reaction rate constant. The fact that the experimental values of t_a are described satisfactorily by Eqn (8) confirms the validity of the Arrhenius equation for the initial stage of the laser-induced degradation when the changes in the temperature and concentration of the degradation products are still small. The qualitative PTCI model shows[20] that the process involving the development of instability is significantly non-stationary. Under these conditions, the Arrhenius kinetics break down, which is reflected in its turn in the dependence of the time of the development of the PTCI on the temperature T_0 [Eqn (9)].

The non-linear thermochemical processes in polymers under the conditions of the thermal effect of the laser radiation have been investigated.[21, 22] The effect involving the self-stabilisation of the laser-induced dehydration of PVA, the propagation of travelling degradation waves, and the vibrational and random dynamics of the evolution of volatile products during the laser-induced decomposition of polymers have been observed.

The effect of the radiation of a Nd : YAG continuous wave laser (1064 nm) on the colour of the PVA film has been investigated.[23, 24] It has been established by mass-spectrometric analysis[23] that the qualitative composition of the volatile products on thermal and laser decomposition is virtually the same, but the relative contributions of the individual components can differ significantly. It was concluded that the laser-induced decomposition of polymers takes place on the whole via a thermal mechanism, although the dynamics of the laser-induced processes differ from the dynamics of the usual thermal degradation. It has been shown[24] that the laser stability of the coloured PVA depends both on the type of the dye introduced and on the way in which the dye is bonded to the polymer. It has also been observed that the resonance effect of the radiation decomposes polymers much more effectively than the non-resonance effect.

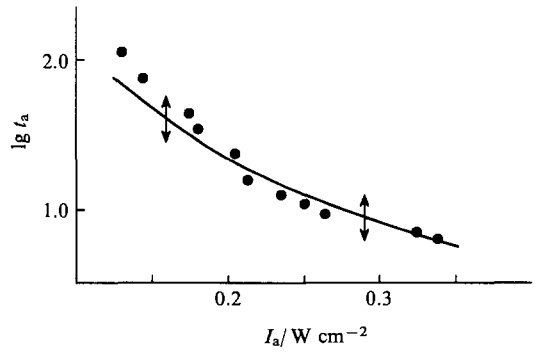


Figure 5. Dependence of the thermochemical instability activation time on the initial intensity of the absorbed radiation: circles — experimental data; continuous line — calculations; C_p = 2.0 kJ kg^{-1} K^{-1}; ρ = 1.2 g cm^{-3}.

III. Stability of elastomers and water-soluble polymers. Their applications in medicine and petrochemistry

1. A new method for estimating the thermal and radiation stabilities of elastomers

The existing methods for the determination of the lifetime (τ) of elastomers, widely used in practice and based on thermal ageing, take a long time, consume a large amount of materials, and are unsuitable for high temperatures. A new method, developed by Prokopchuk et al.,[25] is free from these disadvantages and makes it possible to estimate the contributions of different factors in the external medium to the decrease in the lifetime of rubbers. A distinctive feature of the new method involves the thermooxidative degradation of elastomers in a field of a tensile mechanical stress. The method is based on a single relation (Fig. 6) between the lifetime and the activation energy U_0, established on the basis of extensive experimental data obtained by the existing thermal ageing method. It includes also a high-speed method for the estimation of the values of U_0 from the temperature variation of the breaking stress when the thermooxidative degradation takes place with the specimen being acted upon simultaneously by heat, atmospheric oxygen, and a mechanical tensile stress, i.e. is accelerated by the applied field of mechanical forces.

The lifetimes of 20 types of rubbers, based on different polymers and having different compositions, have been determined by the above method.[25] The results agree with data obtained by the existing method in parallel experiments.

In order to estimate the contribution of ionising radiation to the decrease in the lifetime of rubbers based on butadienenitrile (SKN-18SM) and chloroprene (nairit M) raw rubbers,[26] their specimens were irradiated with ^{60}Co γ-rays. The radiation dose was 500 kGy (50 Mrad) and the dose rate was 4 Gy s^{-1} (400 rad s^{-1}). The results of the investigation are presented in Table 8.

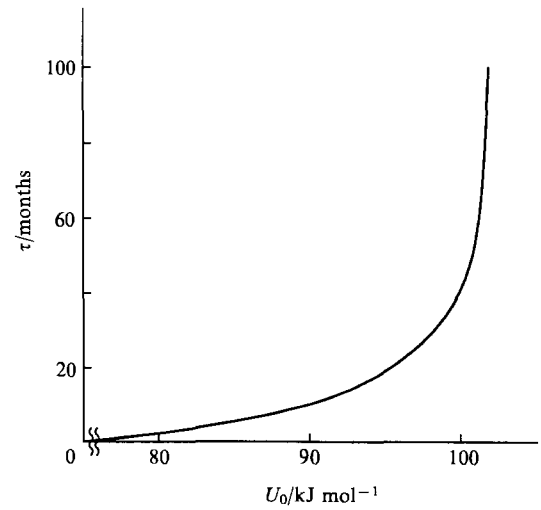


Figure 6. Dependence of the lifetime of rubbers in air at 25 °C on the activation energy for their thermal ageing.

Table 8. Changes in the properties of rubbers under the influence of ionising radiation.

Polymer	Initial specimen			Specimen after irradiation		
	$\sigma(1+\varepsilon)$/ MPA	U_0/ kJ mol^{-1}	τ^a/ months	$\sigma(1+\varepsilon)$/ MPA	U_0/ kJ mol^{-1}	τ^a/ months
SKN-18SM	30	109	190	14.2	102	68
Nairit M	75	121	1103	22.2	105	106

[a] Lifetime at 25 °C.

It follows from the above table that the breaking stress $\sigma(1 + \varepsilon)$ is reduced on irradiation by a factor of 2.1 for the SKN-18SM specimens and by a factor of 3.4 for the nairit M specimens, the activation energies for the thermooxidative degradation U_0 being reduced by 7 and 16 kJ mol^{-1} respectively. The quantity U_0 is a critical parameter for the determination of the lifetimes of rubbers.[25] The influence of γ-radiation on the lifetimes of rubbers with a different polymer base varies: the value of t for irradiated SKN-18SM specimens is 35% of the values for the initial specimens, while for nairit M it is only 9.6%. However, the lifetimes of both rubbers are fairly long after irradiation with a dose of 500 KGy and they meet fully the technical requirements for rubbers serving as components of different technological objects.[25]

2. Elastomers in medicine

Highly elastic materials employed in the manufacture of articles for medical purposes play an important role among polymers. In the first place, these are elastomers based on *cis*-1,4-polyisoprene and obtained mainly from natural rubber (NR) and natural latex (NL). Apart from their natural origin, one may include among their advantages a unique set of properties associated with strength and elasticity. The latex technology based on the natural latex ensures an ecologically safe manufacture of articles for mass consumption and makes it possible to obtain articles with a specified thickness and with a complex configuration.

However, owing to their low resistance to different types of ageing and the risk of toxic effects of different low-molecular-mass substances used for the vulcanisation of polyisoprene, the materials based on it have come to be regarded as undesirable or unsuitable for prolonged contact with living tissues. Nevertheless, because of the lack of systematic studies, existing ideas about the biocompatibility of these materials are fairly contradictory.

Khodzhaeva et al.[27] investigated in recent years the influence of prolonged contact between polyisoprene and a biologically active medium (blood serum). The structure and properties of the polyisoprene, vulcanised polyisoprenes, and latex materials were studied. The relative contributions of several factors influencing the above materials were estimated in parallel experiments: water, salt (isotonic) solution, proteins, at the temperature of living tissues (~40 °C).

The following results of the above study are of greatest interest and importance.

It was established that the biological medium does not exert a specific disruptive influence on natural rubber. Water and the protein components of the blood serum, adsorbed on the polymer surface, protect it against the thermooxidative degradation gradually developing at 40 °C. After being kept in blood serum for 2 years, polyisoprene retains a high molecular mass, while in air the latter diminishes (Fig. 7).

Biologically stable highly elastic materials can be obtained from natural rubbers. For this purpose, it is essential that the vulcanisation network should be resistant to thermooxidation at 40 °C and that the composition of the material should ensure a minimal level of sorption of the components of the medium. The cross-linking density of natural rubbers changed little in the course two years of contact with different media and they retained a high strength and elasticity (Table 9).

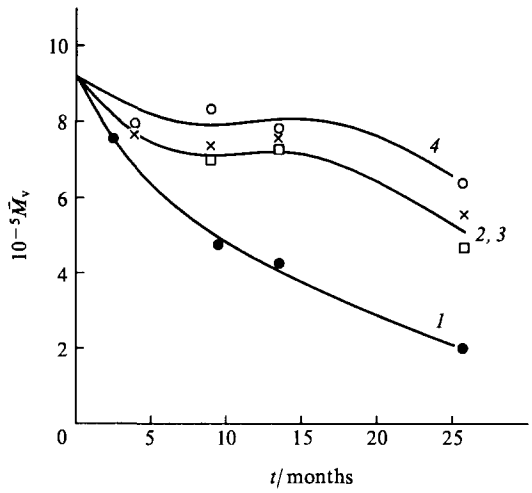


Figure 7. Variation of the molecular mass of *cis*-1,4-polyisoprene under conditions of prolonged contact at 40 °C with air (curve *1*), water (curve *2*), isotonic solution (curve *3*), and blood serum (curve *4*).

For latex materials, which are on the whole inferior to vulcanised block polyisoprene as regards resistance to thermooxidation, the most active disruptive factors during prolonged contact with a biological medium are the absorption of water and the effect of temperature. The negative effect of these factors can be to a large extent abolished by the specific regulation of the microstructure and composition of the material.[28] The application of these principles made it possible to obtain from natural latexes thin-walled film articles which retain highly effective properties during contact with aqueous and biological media in the course of a year.

Table 9. Changes in the properties of vulcanised natural rubbers on exposure to air, in isotonic solution, and in blood serum at 40 °C.

Time/months	$10^5(1/M_s)$/mol cm^{-3}	f_{700}/ MPa	f_r/ MPa	ε(%)
	Initial specimen			
0	12.9	17.5	32.8	880
	Specimen maintained in air			
12.0	16.1	24.6	35.0	820
22.2	12.5	24.2	29.8	750
	Specimen maintained in isotonic solution			
12.0	12.2	12.1	34.9	920
22.2	13.3	14.9	29.8	810
	Specimen maintained in blood serum			
12.0	14.8	13.8	30.7	850
22.2	15.6	13.4	29.8	890

Note. $1/M_s$ = density of cross-linking; f_{700} = modulus of elasticity; f_r = tensile strength; ε = relative elongation on rupture.

Materials and articles for medical purposes with thromboresistant properties have been developed on the basis of natural latexes; the characteristics of the structure of the latex gel and the presence in the latter of protein components served as a basis for the improvement of the method of ionic-covalent immobilisation of heparin.[29-31]

In order to increase the biological compatibility of latex articles and to impart to the latter new functional properties, procedures have been developed for the preparation of composite materials based on the combination of a natural latex with an aqueous dispersion of a high-molecular-mass polyorganosiloxane[32] and on the surface modification by coatings consisting of segmented polyesterurethanes.[33]

The present state of the problem of the biological compatibility of highly elastic materials based on *cis*-1,4-polyisoprene and also the advances in the field of their preparation and application have been surveyed in a review.[34]

3. Stabilisation of coatings in biochemically active media

The problem of the stabilisation of the protective properties of coatings used in biochemically active media is of great theoretical and practical importance.

The complexity of the solution of the problem arises from the fact that the protective properties of coatings depend on many physicochemical factors: the adhesion strength of the bond between the coating and the support; the magnitude and the kinetics of the growth of internal stresses, arising during their formation and use, which are comparable to the adhesion and cohesion strengths; the barrier properties of coatings; the ability of polymers to inhibit electrochemical processes at the interface; the resistance of polymers to the effect of the microflora in undertakings for the food industry.

In order to stabilise the structures and properties of protective coatings used in biochemically active media, Rozantsev[36] developed structure-forming additives for the industrially produced compositions based on organoelement and other compounds with an aromatic conjugation system, which promote the creation in the coatings of an ordered structure of the mesomorphic type. The influence of these additives on the specific features of the structure formation during the production of epoxide coatings as well as the internal stresses and the physicomechanical protective properties of the coatings have been investigated.

It has been shown by the NMR method and electron microscopy that the introduction of these additives in small amounts (1–2 mass%) promotes the formation of structures of the nematic type made up of uncoiled macromolecules with a coplanar orientation in the plane of the support. The mesomorphic level of order in the structure ensures a kinetically convenient order for the involvement of the functional groups in the adhesion and cohesion interactions.

Table 10 presents data concerning the influence of an organosilicon additive on the stability of the properties of epoxide coatings in corrosive media. Modifying agents based on derivatives of the piperidinoxyl (PPO) radical have been developed for the stabilisation of the properties of the coatings in acid media.[36] It was shown that they are capable of retarding strongly the rates of oxidation processes at the interface and in the bulk of the polymer.

Table 10. The mechanical and adhesive properties of polymeric coatings.

Properties	Without additive	With additive
Internal stress/ MPa	4.0	1.5
Adhesion scale points		
initial	1	1
after ageing		
in 3% lactic acid solution	4	2
in 1.5% NaOH solution	2	1
Impact strength/ N m		
initial	5	5
after ageing		
in 3% lactic acid solution	1	3.5
in 1.5% NaOH solution	1.5	4
Lifetime/days		
in 3% lactic acid solution	7	350
in 1.5% NaOH solution	34	400

The introduction of small amounts of the PPO into the corrosive medium increases the corrosion stability of the material as a result of the adsorption of the inhibitor molecules on the surface and a change in the kinetics of the electrochemical reactions (Table 11). The effectiveness of the inhibitor (W) is estimated from the formula

$$W = \frac{i_k - i_k''}{i_k},$$

where i_k and i_k'' are the corrosion currents without and with the inhibitor.

Table 11 shows that the introduction of PPO into electrolyte solutions in an amount of 0.5–2 mass% shifts the stationary potential in the positive direction by 100–120 mV, lowers the maximum dissolution currents by a factor of 8, and increases the degree of protection to 80%–85%.

Similar features have been observed after the introduction of PPO in an amount of 0.5–1 mass% into perphthalic, perchlorovinyl, and epoxide coatings. The modified coatings have already found practical applications for the protection of equipment in the food industry.

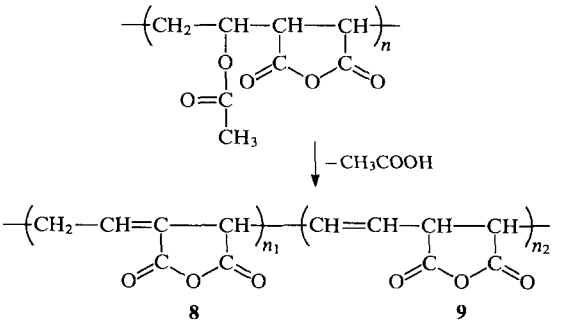
Table 11. The influence of piperidine oxide on the electrochemical characteristics of steel (ST-3).

PPO content (%)	Stationary potential/mV		Maximum dissolution current/mA cm^{-2}		Degree of protection (%)	
	I	II	I	II	I	II
0	−500	−600	16.7	80.0	0	0
0.5	500	−600	10.0	62.0	39	25
1.0	−450	−570	2.2	43.0	80	50
1.5	−450	−500	3.0	15.0	66	80
2.5	−450	−480	4.4	10.0	66	85
3.0	−550	−530	25.0	80.0	–	0

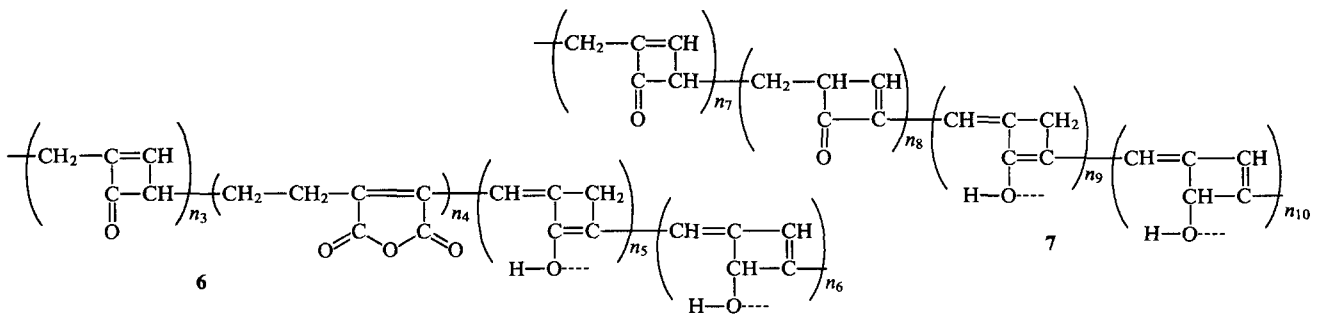
Note. Electrolyte: (I) 0.5 N Na_2SO_4; (II) 5% HCl.

4. Regulation of the liberation of medicinal preparations by the controlled degradation of polymers

Among various applications of the degradation of polymers, yet another has been discovered in the study of the copolymer of maleic anhydride and vinyl acetate (MA/VA). The present authors investigated the thermal degradation of this copolymer jointly with McNeill using his method for the thermal analysis of the volatile degradation products (TV/ATVA).[37, 38] The results showed that the first stage of the isothermal degradation at 205 °C can be represented in the form



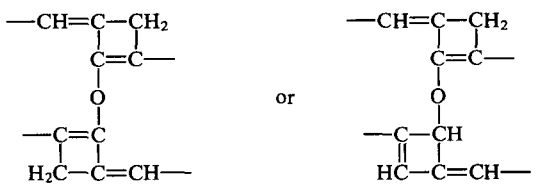
8 9



6 7

The next stage involves rearrangements of structures **8** and **9** without the evolution of carbon dioxide or as a result of such evolution, which leads to structure **6**†. The last stage of the isothermal degradation involves the decomposition of the anhydride ring, which leads to structure **7**.

The quantities n in the above structures can vary and we have no adequate grounds for attributing any definite values to them. The appearance of a cyclic structure in the side chain diminishes the mobility of the latter and is one of the causes of the decrease in solubility. Another cause may be the cross-linking of the polymer as a result of the dehydration of the hydroxy-groups. This explanation has been confirmed by the liberation of water as a consequence of isothermal degradation. This type of reaction may lead to the cross-linking of individual units.



Conclusions concerning the presence of the above structures were based on data obtained by UV, IR, and NMR spectroscopic and mass-spectrometric methods and also by gas chromatography.

Apart from thermal degradation, the behaviour of the polymer in the presence of water was also investigated. In the first place, the question to what extent the sorption of the polymer can be regulated by its controlled degradation was elucidated.

The first stage of the interaction of water vapour with the polymer involved reversible sorption up to an equilibrium value. The increase in the activity of water vapour induced its irreversible binding accompanied by the rupture of the chemical bonds in the copolymer chain with subsequent dissolution. The critical concentration for hydrolysis was attained only for an activity of water vapour close to unity (liquid phase). The general characteristics of the sorption of water by partly degraded polymers are the same as for the initial material and the observed differences are associated with the degree of structural rearrangement as a consequence of the equilibrium sorption. The specimens obtained after degradation for 10 and 20 min are insoluble in water, although their partial hydrolysis was observed. After degradation for 30 min, a swollen polymer was obtained for which the irreversible sorption stage was limited.

The change in the hydrophilicity of the copolymer as a result of the different degrees of its degradation has been used to create a system where it was necessary to regulate the hydrophilic-hydrophobic balance in the polymer matrix, namely a system for the controlled liberation of medicinal preparations.[39]

We investigated a multicomponent system incorporating polyamide coated by a mixture of the MA/VA copolymer with furacilin. The redistribution of the drug between the two polymers controls the multistage process involving is liberation, which includes desorption from the moderately hydrophilic polyamide and subsequent transfer in the swollen or dissolving copolymer.

The retardation of the liberation of the medicinal preparation as a result of the partial degradation of the polymer is illustrated in Fig. 8, which describes the kinetics of the liberation of furacilin from the above system containing the initial or degraded copolymer.

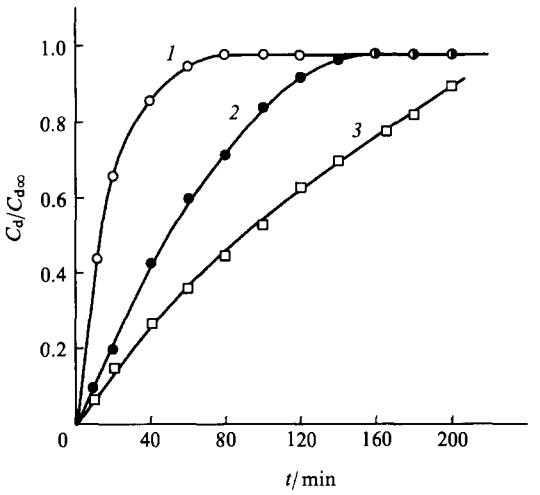


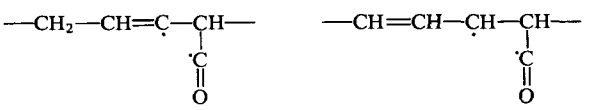
Figure 8. Kinetics of the liberation of furacilin from polyamide coated by the initial (curve *1*) and partially degraded copolymer of maleic anhydride and vinyl acetate. Thermodegradation time (min): (*2*) 10; (*3*) 20.

Following the appearance of the possibility of the simultaneous monitoring of the polymer structure and of its transport properties, good prospects have arisen for the development of new systems in which it will be possible to regulate the rate of liberation of medicinal drugs.

5. Regulation of the stability of water-soluble polymers

Studies by Golubev and coworkers[40, 41] on the regulation of the stability of water-soluble polymers have been published recently. These investigations were undertaken because of the expanding use of such substances in the petroleum industry to make good the non-uniformities in the productive stratum and to increase its coverage when it is flooded. Polymers based on acrylamide are used widely for this purpose. The employment of polyacrylamide

† In the last case, one can postulate the following intermediate states of the chain fragments:



The 1755 cm^{-1} absorption band in the IR spectrum of the partly degraded polymer as well as the appearance of signals at 3.0 and 23 ppm in its ^1H and ^{13}C NMR spectra respectively allow the assumption that the structure of a four-membered ring ketone is more probable than that of other ketones and aldehydes. On this hypothesis, we obtain structure **6**.

(PAA) to increase the extraction of petroleum from the strata has a number of advantages, but at the same time it suffers from a series of important disadvantages. The principal disadvantage is the degradation of PAA under the conditions of joint exposure to elevated temperatures and pressures, shear stresses, as well as metal salts, oxygen, and hydrogen sulfide dissolved in the water within the strata.

Studies on numerous commercial PAA specimens showed that, even when the polymer contains traditional stabilisers, a sharp impairment of the viscous characteristics of aqueous PAA solutions is observed in the presence of iron ions and hydrogen sulfide, especially at elevated temperatures.

The decrease in the viscosity of PAA solutions under the conditions in the strata is associated not only with the degradation of the polymer molecules as such, accompanied by a decrease in the molecular mass, but also with a series of more complex intramolecular and intermolecular processes, cross-links, and conformational changes, which diminish the volume of the macromolecular coil with retention and even an increase in the molecular mass. This has been confirmed by independent methods of measurement, such as viscometry, light scattering, and sedimentation (Table 12).

Table 12. The molecular mass characteristics of polyacrylamide.

Type of influence		Molecular mass/ 10^6 M			
T/ °C	$[Fe^{3+}]$/mg litre^{-1}	M_η	M_w	M_s	$M_{s\eta}$
20	–	8.5 (0)	7.4 (0)	8.3 (0)	8.5 (0)
45	–	1.1 (28)	8.84 (28)	0.91 (28)	0.96 (28)
20	10	3.2 (16)	8.92 (10)	10.8 (16)	8.65 (16)
45	10	3.6 (12)	5.43 (12)	8.52 (45)	10.14 (45)

Note. The molecular mass characteristics were determined for a zero degree of hydrolysis at a PAA concentration of 0.005 mass%; the subscripts to M correspond to the methods used: η = viscometry, w = light scattering; s = sedimentation; the numbers in brackets denote time in days.

Different classes of new PAA stabilisers and metal deactivators, the joint application of which makes it possible to improve significantly the viscous characteristics of aqueous PAA solutions under the conditions of the saturation of the polymer with water, have been investigated.[41]

The copolymers of acrylamide with cationic monomers (dialkyldiallylammonium halides, aminoesters) possess effective flocculating properties. This permits their use in the extraction of petroleum to restrict the inflow of water and also to solve ecological problems, for example, that of the purification of petroleum-containing waste waters. However, it has been established that, during processing in storage, these polymers can lose their solubility in water, probably as a consequence of structure formation in them or they can be degraded, which diminishes their molecular mass.

A study was therefore made of the influence of a series of additives on the stability of polymers in the course of their processing. It was found that mercaptobenz-imidazole and thiourea exhibit a high stabilising activity. Polymers containing 0.3 mass% of these additives do not lose their solubility in water during processing and storage. The intrinsic viscosity of solutions of these polymers is higher than that for polymers processed in the absence of stabilisers.

IV. New approaches to the fundamental investigation and practical application of polymer degradation and stabilisation processes

1. A new approach to the estimation of the physical and thermal parameters of polymers

Askadskii developed in recent years an approach to the estimation of the physical and thermal characteristics of polymers based on the chemical structure of the repeating unit.[42-46] According to this approach, the repeating unit of the polymer consists of a set of anharmonic oscillators each of which consists of a pair of interacting atoms. In order to estimate properties such as the glass and melting points and the coefficient of volume expansion, intermolecular interactions at different levels have been considered: weak (dispersion) and strong (dipole–dipole interaction, hydrogen bonds) due to the presence of polar groups. The temperature corresponding to the loss of stability of such an oscillator characterises the glass and melting points of the polymer.

In order to estimate the temperatures of the onset of the intense thermal degradation of the polymer, when the loss of stability by the set of anharmonic oscillators is due to the dissociation of chemical bonds, chemical reactions are considered. As a result, it is possible to calculate on the basis of the chemical structure of the repeating unit of the polymer, apart from the temperature of the onset of the intense thermal degradation, chemical characteristics such as the glass and melting points as well as a number of other properties—density, refractive index, dielectric constant, the coefficient of the optical sensitivity to stress, the Hildebrand solubility parameter, and the criterion of the solubility of polymers.

In the case of thermal degradation, there is a possibility of estimating by means of the proposed approach the influence of the end groups on the thermal stability of the polymer as well as the influence of other 'weak points' in the composition of the repeating unit.

The possibility, in principle, of synthesising polymers with glass points which are much higher than the temperature of the onset of the intense thermal degradation has been demonstrated.

Askadskii's ideas have been successfully applied to the prediction of the properties of polymer networks, particularly for highly cross-linked polymers, which constitute the basis of many polymeric building materials. In the case of a dense network, the thermal stability of the network nodes themselves and not only the internodal fragments begins to play a major role.

The application of this approach made it possible, in particular, to predict the possibility of obtaining highly cross-linked polymers with extremely unusual properties. Networks containing massive nodes and very short flexible linear fragments between them can have any prespecified modulus of elasticity in the range from 3 MPa to 3 GPa. Despite the fact that these values of the modulus of elasticity are in the intermediate range between those characterising the vitreous and viscoelastic states, such materials have elastic properties and not viscoelastic properties like the majority of polymers.

2. The influence of organic acids on the effectiveness of phenolic inhibitors of the oxidation of polymers

Higher organic acids may be present in the polymer for various reasons: they may be the products of the oxidation of the polymer and can also be present in mixtures of antioxidants. Unfortunately, the contribution of higher organic acids to the effectiveness of the inhibition of the oxidation of polymers has not yet been adequately described in the literature.

The studies of Shlyapnikov and coworkers[47, 48] were devoted to the influence of stearic acid on the effectiveness of antioxidants—2,2'-methylenebis(6-*tert*-butyl-4-methylphenol) (MBP) and the ester of 3,5-di-*tert*-butyl-4-hydroxyphenylpropyldiethyleneglycolic acid (fenozan 28)—in the oxidation of fused isotactic polypropylene (PP).

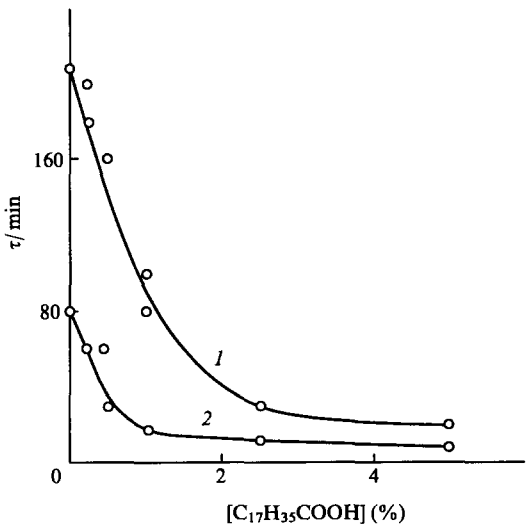


Figure 9. Dependence of the induction period in the oxidation of polypropylene on the concentration of stearic acid in the presence of 0.015 mol kg^{-1} MBP (curve *1*) and fenozan 28 (curve *2*); T = 200 °C; P = 300 torr.

At the same initial concentration of the antioxidant, the induction period in the oxidation of PP diminishes appreciably with increase in the concentration of the acid, the action of the latter on the oxidation process being opposed to that of the antioxidant (Fig. 9).

The dependence of the induction period on the initial concentration of MBP is characterised by the fact that in the initial stage at low concentrations of the antioxidant and MBP the latter slightly retards the oxidation reaction and, after the attainment of a definite critical MBP concentration, the induction period increases (Fig. 10). The critical MBP concentration depends on the amount of acid and increases from 0.0012 mol kg^{-1} (in the absence of the acid) to 0.0053 mol kg^{-1} (at a stearic acid concentration of 0.06 mol kg^{-1}). It is suggested that the acid binds the antioxidant into complexes which do not retard the oxidation process. This leads in its turn to an increase in the critical concentration.

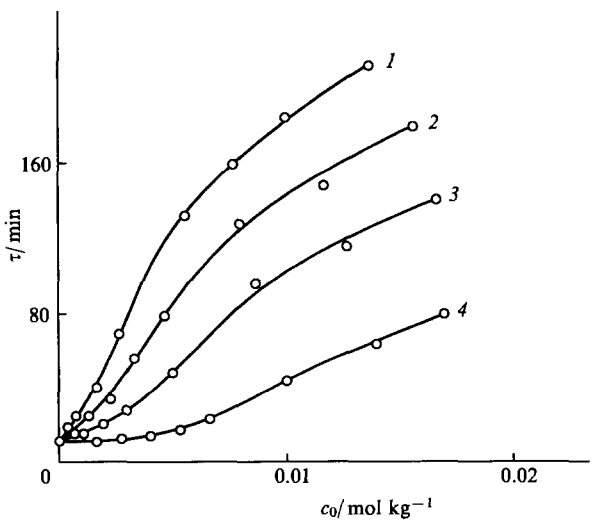


Figure 10. Dependence of the induction period in the oxidation of polypropylene on the MBP concentration in the absence (curve *1*) and in the presence of stearic acid at different concentrations (mol kg^{-1}): (*2*) 0.015; (*3*) 0.03; (*4*) 0.06.

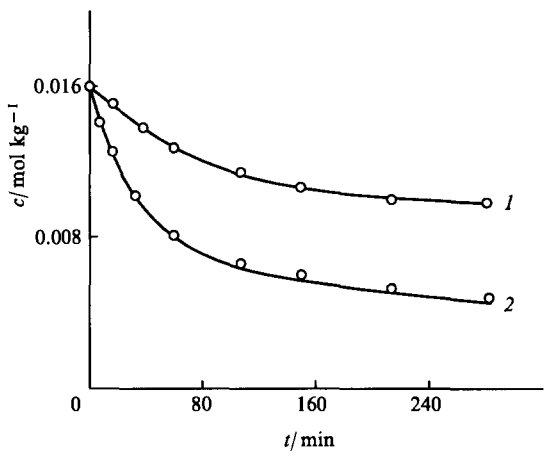


Figure 11. Kinetics of the consumption of MBP in the course of its reaction with stearic acid in polypropylene at 200 °C; initial stearic acid concentration (mol kg^{-1}): (*1*) 0.03; (*2*) 0.06.

Another cause of the observed effect may be the esterification of phenol by stearic acid. In order to confirm the latter hypothesis, specimens of PP containing phenol and stearic acid were heated under a nitrogen atmosphere to 200 °C. In the presence of stearic acid, a slight consumption of phenol was observed, its rate increasing with increase in the initial acid concentration (Fig. 11). A sharp decrease in the induction period and in the critical antioxidant concentration was not observed.

The above phenomena may be explained by the formation of complexes between phenol and the acid and also by the slow reaction between these substances. This leads to the synthesis of the ester, the contribution of which becomes significant only in later stages of the process.

The formation of phenol–acid complexes has been confirmed by the IR spectra of solutions of these substances in CCl_4. A mixture of MBP with stearic acid is characterised by absorption bands at 3840 cm^{-1} (isolated OH groups) and 3520 cm^{-1} (bound OH groups). The absorption of bound OH groups diminishes on complex formation, whilst the absorption band due to isolated hydroxy-groups shifts to (3540 cm^{-1}).

3. Estimation of the effectiveness of antioxidants

The estimation of the effectiveness of antioxidants in polymer systems is a problem the solution of which is of considerable interest from both theoretical and practical points of view. The attempts to find a unique parameter determining the activity of the antioxidant, such as, for example, the oxidation-reduction potential or the rate constant for the reaction of the inhibitor with the peroxyl radical derived from the substrate, have not yielded positive results. The reason for this is primarily the fact that the process involving the consumption of the antioxidant is complex and includes a whole series of reactions involving the antioxidant itself as well as radical and molecular products of its conversion.

According to Shanina,[49, 50] the effectiveness of the antioxidant can be estimated by studying the kinetics of its consumption. The kinetic curves reflect the entire wide variety of the processes occurring in the polymer containing the antioxidant. Comparison of the results obtained at different initial concentrations of the antioxidant makes it possible to estimate the contribution of side reactions, whilst comparison of the kinetic curves for its consumption in the polymer and in an inert medium permits the estimation of the contribution of the inhibitor oxidation process (apparently the main one among side processes which significantly reduce the effectiveness of the antioxidants).

We shall consider two examples of the kinetics of the consumption of phenolic antioxidants in polymer systems.

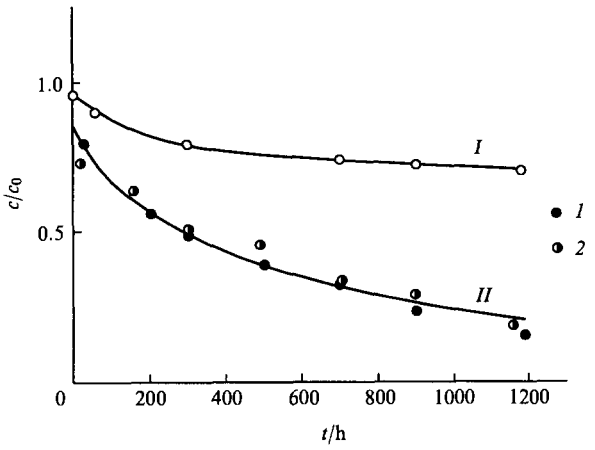


Figure 12. Kinetics of the consumption of antioxidants in isotactic polypropylene (I) Irganox 1076; (II) Topanol CA; concentration (mol kg^{-1}): (*1*) 10^{-2}; (*2*) 2×10^{-3}.

Fig. 12 presents kinetic curves for the consumption in isotactic polypropylene of two industrial antioxidants produced by the Himont Company. Evidently, under experimental conditions in air at 130 °C, the Irganox 1076 stabiliser is consumed much more slowly than Topanol CA. The lower effectiveness of the latter can apparently be accounted for by its slightly sterically hindered structure, which is known to facilitate the occurrence of side reactions. Experimental data confirm this hypothesis. Points corresponding to an initial concentration of 2×10^{-3} mol kg^{-1} were plotted on the curve for the consumption of Topanol CA, obtained at an initial stabiliser concentration of 10^{-2} mol kg^{-1} (relative concentrations of the stabilisers were plotted along the ordinate axis). Despite the fact that the initial concentrations differ by a factor of 5, these points fit satisfactorily on a single curve, i.e. the initial sections of the consumption curves virtually coincide. This shows that an appreciable proportion of the stabiliser is consumed in side processes.

Fig. 13 presents kinetic curves for the consumption of the Nonox WSP stabiliser in the polyethylene–polypropylene (PE/PP) composition at different temperatures. This composition is used in the cable industry for the insulation of optical cable. It is important to note that in the PE/PP blend the antioxidant is consumed at a higher rate than in each of its constituent polymers, which may indicate a higher rate of oxidation of the blend compared with its components.

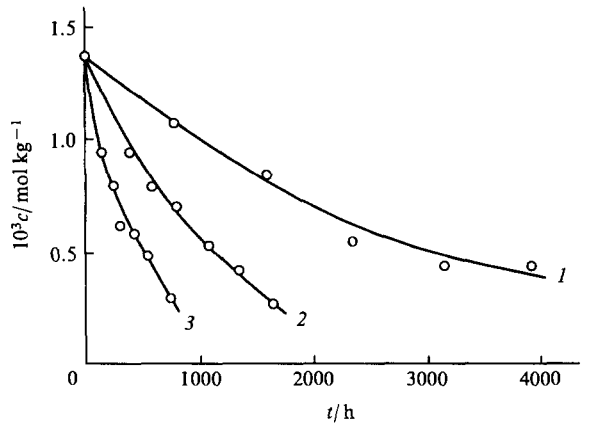


Figure 13. The influence of temperature on the kinetics of the consumption of the antioxidant Nonox WSP in the PE/PP blend; T (°C): (*1*) 60; (*2*) 80; (*3*) 105.

The results permit the estimation of the time required for the consumption of the antioxidant until the attainment of the critical concentration. The accuracy of such an estimate is not very high, but it can serve as a guide in determining the operating stability of the material. Furthermore, the knowledge of the temperature dependence of the rate of consumption makes it possible to extrapolate these rates to any temperatures corresponding to the real operating conditions.

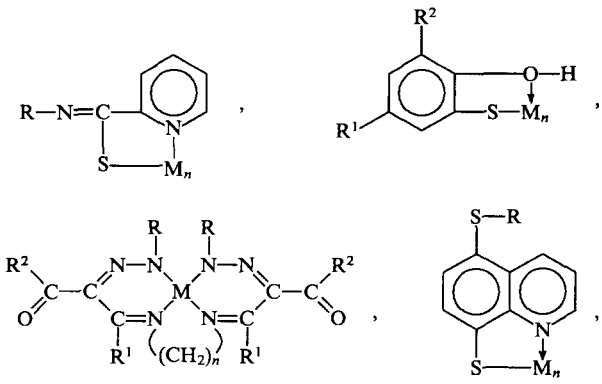
4. The inhibiting properties of heavy metal chelates

Studies on the inhibiting properties of heavy metal chelates have been prosecuted in the course of a number of years by Vinogradova and coworkers.[51–53]

A range of problems associated with the deactivation of alkyl and peroxyl radicals by metal chelate complexes of different classes have ben investigated. Chelates differing in the composition and structure of the chelate units as well as in the nature of the substituents in the ligands and their reactions of the type

$$RO_2^{\cdot} + ML_x \longrightarrow \text{termination},$$
$$R^{\cdot} + ML_x \longrightarrow \text{termination},$$

were investigated. The reactivities of both well known compounds (dithiocarbamates and salicylideneamine complexes) as well as new compounds with N,N-, S,N-, and S,O-containing chelate units, for example



were studied.

The influence of added chelates was investigated in two types of model autoxidation systems: in the oxidation of solutions of polyoxyethylene and its low-molecular-mass analogues, hydrocarbons, and ethers, and in the polymerisation of styrene in solution.

It was shown that the inhibiting activity of the chelates is determined by the composition and hence the properties of the radicals propagating the oxidation chain. The inhibiting activity is different for different oxidation substrates: in ethers and hydrocarbons, only chelates containing sulfur (or selenium) atoms in the chelate units are active, some of them (the copper and antimony chelates) being characterised by a high activity, which is independent of the nature of the substrate. In the oxidation of polyoxyethylenes having different molecular masses, a high inhibiting activity was shown, apart from the sulfur-containing chelates, by compounds with N,N-units. For sulfur-containing chelates in such systems, there is a sharp increase (by more than an order of magnitude) in the inhibiting activity of the chelates. Data have been obtained indicating the possibility of the repeated termination of the oxidation chains of polyoxyethylene involving copper and cobalt chelates and/or their reaction products.

The structure of the ligands of the majority of the chelates investigated contains no functional groups capable of the classical hydrogen atom transfer reaction, which deactivates the peroxyl radicals $RO_2^{\cdot}$ (the OH an NH atoms in phenols and amides). Inhibition is due to the redox mechanism of the interaction between the peroxyl radicals and the chelate units of the complexes.

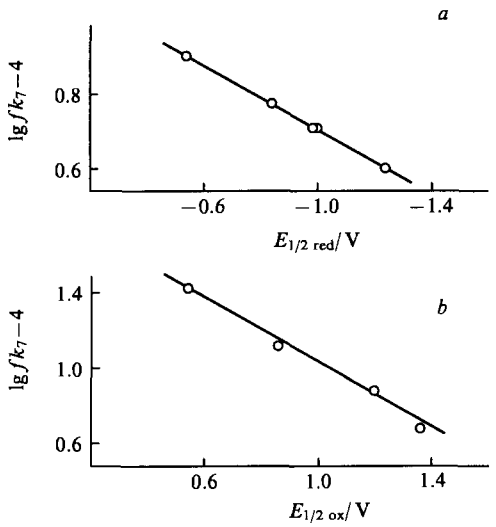


Figure 14. Dependence of the chain termination rate constant on the reduction potentials of copper complexes (*a*) and the oxidation potentials of cobalt complexes (*b*).

Comparison of the rate constants for the chain termination in the interaction of the $RO_2^{\bullet}$ radical derived from polyoxyethylene with chelates and of the half-wave potentials for the electrochemical oxidation and reduction of the chelates demonstrates the presence of a relation between the 'antiradical' activity of the chelates and the oxidation and reduction potentials of the metal complexes (Fig. 14). This correlation indicates that the peroxyl radicals responsible for the oxidation of polyoxyethylene have dual, i.e. oxidising and reducing, properties.

In the interaction with arylalkyl radical R$^{\bullet}$ (in the polymerisation of styrene), the highest reactivity is manifested by the sulfur-containing copper(II) and iron(III) chelates. The inhibiting properties are also characteristic of the cobalt analogues of the above chelate complexes. Copper chelates with nitrogen and oxygen atoms in the chelate unit exhibit catalytic properties.

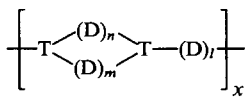
Comparison of the oxidation-reduction properties of chelates and their activities in the inhibition of the polymerisation of styrene showed that in this instance two mechanisms of the interaction of the chelates with the R$^{\bullet}$ radicals operate — a redox mechanism accompanied by the reduction of copper(II) to copper(I) and a mechanism involving the transfer of a hydrogen atom from the activated ligand in the chelate.

5. Stabilisation of polydimethylsiloxanes by the introduction of cyclic fragments into the linear chain

The stabilisation of linear polyorganosiloxanes by the introduction of cyclic fragments both into the chain and into the side groups has been the subject of the latest studies by Khananashvili and coworkers.

It is known that the introduction of various cyclic fragments into the linear dimethylsiloxane chain leads to the decomposition of the helical structure of the polymers and hence alters their physicochemical properties. The glass point can be varied within a wide range by merely altering the organic groups attached to the silicon atoms in the linear macromolecules. As a result of the extensive possibilities for the structural modification of polysiloxane chains by the introduction into the latter of polyfunctional branching centres, mono- and poly-cyclic fragments having a different structure [spirocycles and condensed rings (for example sections corresponding to a 'ladder' structure)], and others, polysiloxanes occupy an exceptional position as excellent model systems for the creation of polymeric materials with a set of physicochemical properties capable of being varied over a wide range.

The influence of the introduction into the dimethylsiloxane chain of organocyclotetrasiloxanes, organocyclopentasiloxanes, and organocyclohexasiloxane with a 1,5- and 1,7-disposition of the organocyclohexasiloxane fragments in a chain of the following composition has been demonstrated:



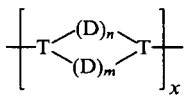
$n, m = 1, 2, 3; n \neq m,$
$l = 2-50$

where D are siloxane units and T are silsesquioxane units.

The principal process leading to the degradation of such copolymers begins at a temperature higher by 80–100 °C than for linear polydimethylsiloxanes.[54–56] A similar result was achieved by introducing cyclocarbosiloxanes and bissiloxaindan fragments into the dimethylsiloxane chain.[57, 58]

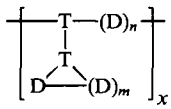
When cyclic fragments are introduced into the linear dimethylsiloxane chain, the copolymers are stabilised, since the cyclic fragments prevent, during depolymerisation, the chain transfer, which proceeds with formation of type D organocyclosiloxanes.

The synthesis of a new class of copolymers, occupying an intermediate position between linear and ladder polymers, has been described.[59, 60] The ratio of the D and T units can be varied in such copolymers. It was shown that, by varying the ratio of the D and T units in the atactic polymer, it is possible to vary the properties of copolymers having the following composition:



$n, m = 1, 2; n \neq m.$

Studies have also been carried out on the synthesis of new copolymers in which the branching segments are organocyclosiloxanes distributed regularly in the side chain.[61, 62]



$m = 1, 2, 3;$
$n = 2-30.$

It has been shown that, with increase in the bulk of the cyclic fragments, the thermooxidative stability of the copolymers diminishes. In addition it has been demonstrated that copolymers with cyclic fragments in a side chain behave in the same way as copolymers with cyclic fragments within the main chain.

6. The ageing of the ABS plastic under atmospheric conditions

In the latest studies by Seitablaev and Kalontarov[63, 64] the influence of climatic factors on the physicomechanical, electrical, and structural properties of acrylonitrilebutadienestyrene (ABS) plastic of type 2020 S were investigated under the conditions of prolonged exposure to the atmosphere in various regions of Tajikistan at different heights above sea level: in the mountain settlement Gissar, 800 m, non-industrial zone; in Dushanbe, 890 m, industrial zone; in the mountain gorge Varzob, 1 700 m; on the mountain pass Anzob, 3 372 m.

It was established experimentally that, during the initial period of the climatic tests on the ABS plastic specimens, the degradation processes predominate greatly over structure formation processes. During the first 1.5–2 months of atmospheric ageing, the decrease in the breaking stress (σ_r) is 28% – 30% and the relative deformation leading to rupture (ε_d) is reduced to 80%. This is followed over the three years by slow ageing processes, whilst towards the fourth year an increase in σ_d is observed. IR spectroscopic studies showed that, during the first 100–200 h of atmospheric ageing, the formation of C=O groups takes place most vigorously (the 1720 cm^{-1} band). After the saturation of

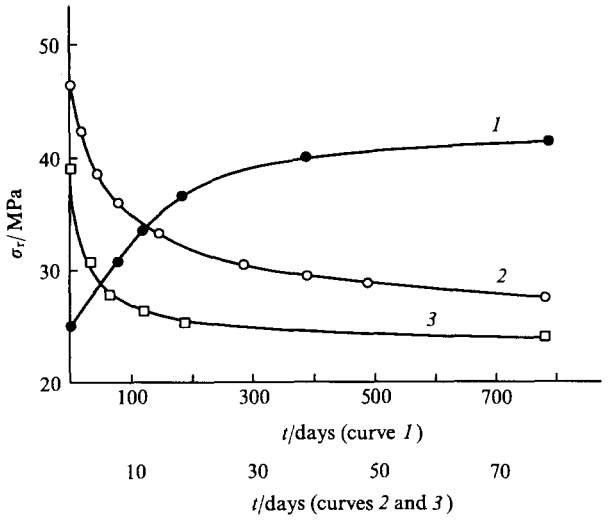


Figure 15. Dependence of the breaking stress (σ_r) for the ABS plastic on the exposure time in an enclosed space (curve *1*) and in open areas (curves *2* and *3*).

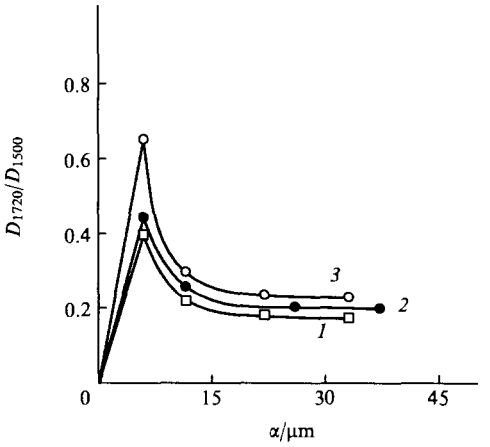


Figure 16. Dependence of the ratios of the optical densities on the thickness of the layer of the ABS plastic undergoing degradation in tests in the Dushanbe climatic area in the course of different periods (days): (*1*) 4; (*2*) 7; (*3*) 13.

surface layers by oxygen-containing products and the closure of the so called channels for the free access of oxygen into the deeper layers of the plastic, a monotonic decrease in σ_d is observed. Under the conditions of prolonged 'oxygen starvation', dark reactions begin to be manifested. Their occurrence is indicated by the increase in σ_d after ageing for 3 years on open areas exposed to the atmosphere. A similar situation has been observed also in specimens stored for a long time under laboratory conditions after climatic tests.

Thus under the conditions of natural ageing of the plastic, dark reactions are manifested towards the fourth year of exposure, whilst under conditions where the influence of atmospheric factors has ceased they become apparent towards the beginning of the 'rest' period. The tensile strength of the plastic after a year's 'rest' is restored to 87% of its initial value, i.e. an increase in σ_d by 34% is observed (Fig. 15).

A considerable accumulation of defects in the first stage of the ageing process is known to be associated with the intense degradation processes in the surface layers of the plastic. It has been established experimentally that, as the surface layer of specimens aged for a short time (2–3 months) is removed, both the strength and viscous properties are restored. On the other hand, in the specimens subjected to prolonged climatic influences (for a year and more), this is not observed and subsequently quasi-brittle decomposition takes place. This finding is explained by the predominance in the bulk of the plastic of cross-linking reactions over degradation processes, which has been confirmed by studies on gel formation. During the first 12 months of ageing, the content of the gel fraction diminishes by 10%–30%, while after an increase in the ageing period from 12 to 48 months, the content of the insoluble fraction rises by 30%–40%. Furthermore, in the specimens aged in the Dushanbe climatic area the degree of gel formation is higher than in the specimens aged in other areas. The high degree of contamination of the atmosphere and the increased temperature of the air probably have an effect here. IR spectroscopic studies on different layers of the plastics showed that the dependence of the ratio of the optical densities D_{1720}/D_{1500} on the thickness of the degraded layer is exponential and, furthermore, with increase in the duration of the exposure during the initial ageing period the degradation processes proceed most vigorously in a surface layer having a depth up to 10 μm, where the C=O groups mainly accumulate (Fig. 16).

Fractographic analysis of the specimens after natural climatic ageing showed that the structure of the surface of the plastic has undergone appreciable changes—microcracks appeared. This is characteristic of all the regions where the specimens were tested. With increase in the ageing period, the number of microcracks and their density also increase.

Thus it has been established that the nature of the decomposition of the ABS plastic under different climatic conditions is determined by processes leading to the degradation of the surface layers and structure formation in the bulk of the material.

7. Radical processes in filled polymers

In filled polymers, boundary layers, the properties of which differ appreciably from the polymer bulk phase, are formed near the surface of the filler particles. It has been shown that the structural features of the boundary layers affect the kinetics of the elementary radical reactions. Thus a dependence of the effectiveness of the thermal reaction of the radical-cations generated at 77 K by the photochemical reduction of iron(III) chloride in polyvinylpyrrolidinone (PVP) on the content of the aerosil filler has been observed.[65, 66]

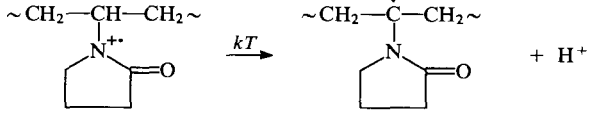
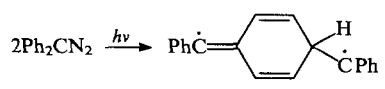


Fig. 17 presents the relative concentrations of macroradicals during the thermal reaction of the radical-cation in PVP without a filler and with 15 and 50 mass% of aerosil. The maximum relative amounts of the macroradicals characterise the fraction of their precursors stabilised at 77 K during the reduction of iron(III) chloride. It was found that in the highly filled specimens (~50% of aerosil) only 10% of the radical-cations are stabilised at 77 K, whereas in the unfilled specimens approximately 70% are stabilised.

In solid polymers [polycarbonate, poly(methyl methacrylate)], the dimerisation of diphenylcarbenes in the quasi-clusters of the added diphenyldiazomethane (DDM), accompanied by the formation of biradicals in which the distance between the unpaired electrons is $r \simeq 5$ Å, was observed.



The relative yield of the biradicals, recorded by the EPR method, serves as a quantitative characteristic of the non-uniformity of the distribution of the low-molecular-mass additive.

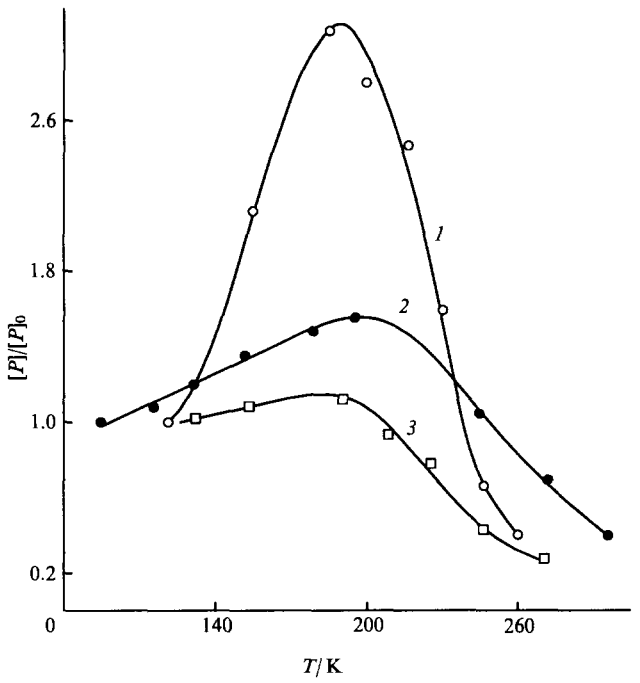


Figure 17. Variation of the concentration of macroradicals during the heating of PVP with $FeCl_3$ irradiated at 77 K: (*1*) without filler; (*2*) 15 mass% of aerosil; (*3*) 50 mass% of aerosil.

Fig. 18 presents the dependence of the yield of the biradicals in the polymer on the additive concentration. At fairly high concentrations (~0.1 M), biradicals with $r \simeq 10$ Å were detected. They are formed in larger quasi-clusters. The study of the dependence of the yield of the biradicals made it possible to estimate the non-uniformity of the distribution of various low-molecular-mass additives whose structures is similar to that of diphenyldiazomethane, for example, photostabilisers, antioxidants, and photosensitisers (salicylates, bisphenols, and benzophenones).

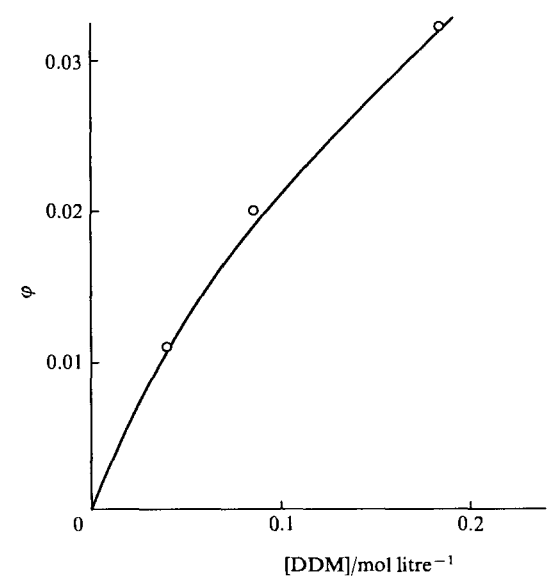


Figure 18. Dependence of the yield of biradicals on the concentration of diphenyldiazomethane in polycarbonate.

8. The inhibiting capacity of natural phenols in radical reactions

Askarov and Saidov[67] estimated the reactivities of a series of natural phenols such as vanillin, guaiacol, eugenol, and gossypol in the model cumene oxidation reaction. Their approach makes it possible to estimate rapidly and quantitatively the ability of various additives to inhibit radical reactions and to reach thereby a preliminary conclusion about the usefulness of the further employment of such substances as stabilisers for polymeric materials. These compounds are also interesting because they can be obtained from reproducible sources — plants and seeds.

In the initiated chain reaction involving the oxidation of cumene (isopropylbenzene), the inhibiting capacity of the additive is estimated in terms of the rate of constant k_7 in the classical oxidation mechanism. For this purpose, the induction period is determined in a preliminary step from the slope of the kinetic oxidation curve under the conditions of fairly long chains:

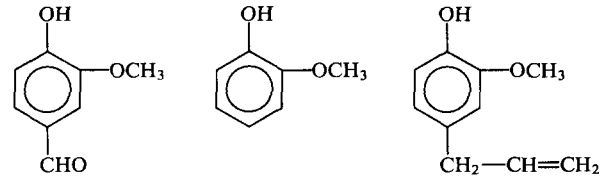
$$\tau = f_n \frac{[\mathrm{InH}]}{W_i},$$

where n is the number of inhibiting groups in the inhibitor molecule, f the inhibition coefficient for one group, [InH] the initial inhibitor concentration, and W_i the rate of initiation.

The inhibition rate constant k_7 is then determined from the relation

$$\frac{[\mathrm{O_2}]}{[\mathrm{RH}]} = -\frac{k_3}{k_7} \ln\left(1 - \frac{t}{\tau}\right),$$

where $[O_2]$ is the amount of absorbed oxygen (mol litre^{-1}), [RH] the amount of cumene taken for the reaction (mol litre^{-1}), and k_3 the chain propagation rate constant (for cumene at 60 °C, $k_3 = 1.75$ litre mol^{-1} s^{-1}).

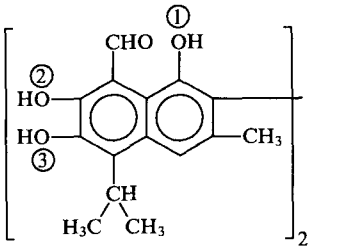


vanillin $k_7 = 3.6 \times 10^{-3}$, guaiacol $k_7 = 5 \times 10^{-3}$, eugenol $k_7 = 1 \times 10^{-4}$.

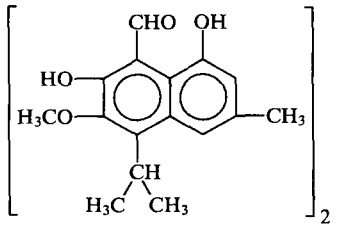
A typical initiated and inhibited cumene oxidation curve as well as its logarithmic form are presented in Fig. 19. The ratio k_3/k_7 is determined from the slope of the logarithmic plot and then k_7 is found. The corresponding calculations yielded the following inhibition rate constants (litre mol^{-1} s^{-1}):

These data make it possible to reach a conclusion about the nature of the influence of the substituent in the *para*-position (with the inevitable presence of a methoxy-group in the *ortho*-position). The transition from the electron-accepting aldehyde group to the electron-donating allyl group leads to a successive increase in k_7. This provides grounds for the assumption that the role of the substituents must always be taken into account in predicting the subsequent application of substances as inhibitors. The Hammett constant of the substituent permits a preliminary conclusion about the usefulness of the antioxidant for the inhibition of the oxidation of particular polymers.

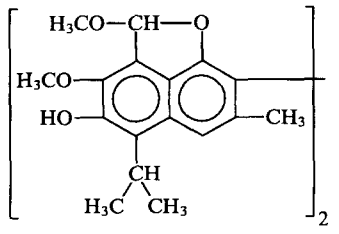
The study of gossypol and its derivatives concerned mainly the determination of their physiological properties. The use of gossypol as an antioxidant in the oxidation of various classes of substances, including polymers, appears promising. In the first place, this is associated with the enormous renewable raw materials base for its preparation. For a detailed estimation of the reactivity of each of the numbered hydroxy-groups, a series of derivatives of the methyl ethers of gossypol were obtained.



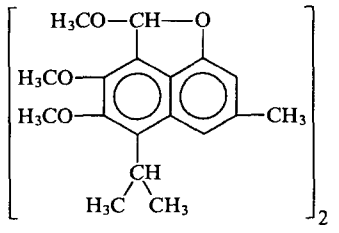
Gossypol
T_m = 282–284 °C ,



Dimethylgossypol
T_m = 168–170 °C ,



Tetramethylgossypol
T_m = 205–207 °C ,



Hexamethylgossypol
T_m = 210–215 °C .

It is noteworthy that hexamethylgossypol does not exhibit an inhibiting effect on the initiated oxidation of cumene.

The subsequent study of the role of the hydroxy-groups responsible for the inhibition of the oxidation reaction can be conveniently begun with tetramethylgossypol. Calculation based on the results presented in Fig. 19 yielded $k_7 = (0.83 \pm 0.03) \times 10^{-4}$ litre mol^{-1} s^{-1} for this compound. When cumene is oxidised in the presence of dimethylgossypol, we are apparently dealing with hydroxy-groups differing in their reactivity. This conclusion was reached on the grounds that a break point is clearly observed on the logarithmic form of the curve (Fig. 20). This shows that, after the consumption of the 'stronger' hydroxy-groups during the induction period, the 'weaker' groups begin to be consumed. From the slope of the logarithmic curve, we obtain respectively for the initial and final sections of the kinetic curve

$$k_7 = (5 \pm 0.04) \times 10^{-4} \text{ litre mol}^{-1} \text{ s}^{-1} ,$$

$$k_7 = (0.85 \pm 0.04) \times 10^{-4} \text{ litre mol}^{-1} \text{ s}^{-1} .$$

There is also only one point of inflection on the logarithmic form of the cumene oxidation curve in the presence of gossypol. This justifies the conclusion that one pair of hydroxy-groups have approximately the same reactivity. If all three types of hydroxy-groups had different reactivities, two points of inflections with three sections of the logarithmic plot would have appeared. Calculation of k_7 for gossypol yielded the following values:

$$(5.2 \pm 0.05) \times 10^{-4} \text{ and } (0.8 \pm 0.04) \times 10^{-4} \text{ litre mol}^{-1} \text{ s}^{-1} .$$

It appears logical to assume that the hydroxy-groups in the 2- and 3-positions have the same reactivities.

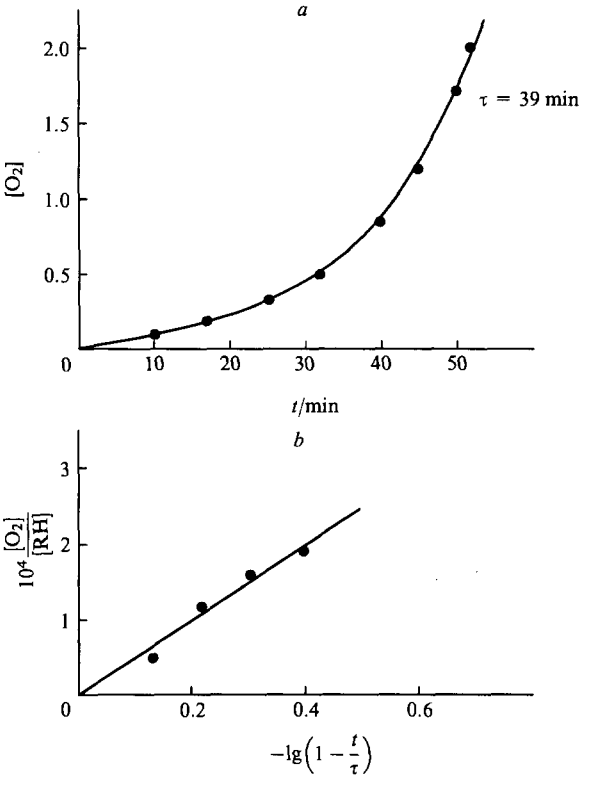


Figure 19. Curve for the initiated oxidation of cumene in the presence of tetramethylgossypol (*a*) and its logarithmic form (*b*); [InH] = 10^{-5} M; $W_i = 1.26 \times 10^{-8}$ mol litre^{-1} s^{-1}.

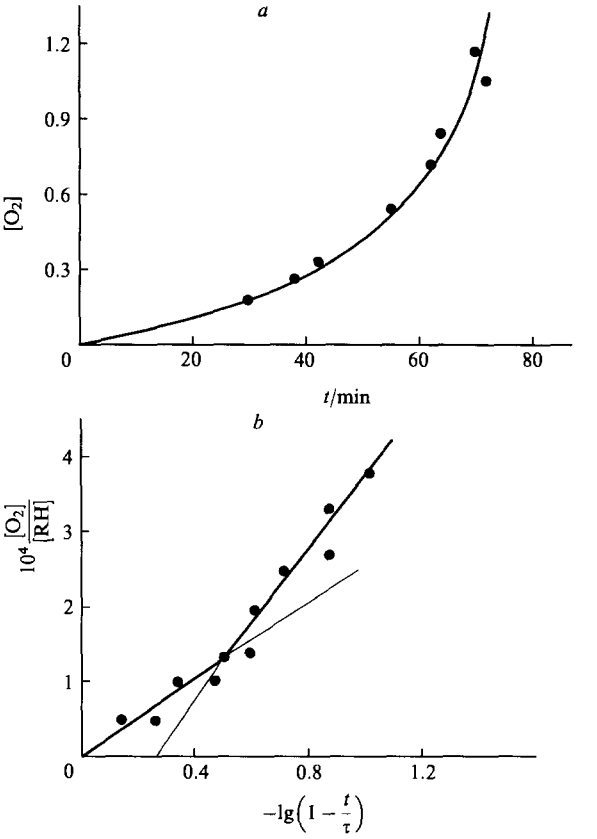


Figure 20. Curve for the initiated oxidation of cumene in the presence of dimethylgossypol (*a*) and its logarithmic form (*b*); [InH] = 1.2×10^{-1} M; $W_i = 5.44 \times 10^{-8}$ mol litre^{-1} s^{-1}.

Since $k_7 = (0.83 \pm 0.03) \times 10^{-4}$ litre mol^{-1} s^{-1} for the OH group in the 3-position (tetramethylgossypol), it is difficult to postulate that $k_7 = (5 \pm 0.04) \times 10^{-4}$ litre mol^{-1} s^{-1} can be assigned to the hydroxy-group in the 2-position. This becomes particularly evident if the constants k_7 for gossypol and its derivatives are compared with the corresponding values for vanillin, guaiacol, and eugenol taking into account the nature of the substituents in the corresponding positions relative to the hydroxy-group. Therefore $k_7 = (5.2 \pm 0.05) \times 10^{-4}$ litre mol^{-1} s^{-1} should be assigned to the hydroxy-group in the 1-position.

In contrast to synthetic sterically hindered phenols, for the majority of which the inhibition rate constant (of the order of 10^{-4} litre mol^{-1} s^{-1}) depends little on the nature of the substituents (provided that they are not highly polar), in the case of sterically unhindered phenols the role of substituents is more pronounced. If the chemical formula of a potential stabiliser (antioxidant) of radical processes is known, then, taking into account the nature and positions of the substituents, it is possible to predict the behaviour of the compound. It must be emphasised that the estimates are preliminary. The final conclusion about the usefulness of a particular compound as a stabiliser can be reached only taking into account the results of technological tests.

9. Structural model of the autoxidation of polypropylene

The autoxidation model proposed by Mikheev and coworkers[68-71] includes heterophase-coupled reaction chains distributed among non-uniform structural zones of the polymer being oxidised. The operation of the heterophase mechanism had been demonstrated previously in relation to the modification of polymers by benzoyl peroxide.

The autoxidation of PP has a number of characteristic features which cannot be explained within the framework of the traditional mechanism of the homogeneous oxidation of hydrocarbons. Some of these features have become the subject of acute controversy in the literature, whilst others remained unnoticed. The latter include the presence of kinetic macroscopic stages due to the change in the reaction order with respect to the hydroperoxide (HP). It is possible to distinguish three stages.[72]

In the first stage, which is of average duration (induction period), the oxidation proceeds via an unbranched chain reaction and the accumulating hydroperoxide does not catalyse the process. The hydroperoxide becomes a catalyst (branching agent) in the second stage. To date theoretical studies have been concentrated on the second stage. It is brief and the degree of oxidation during this period is small. This period is convenient for the conservative employment of the established oxidation mechanism for liquid hydrocarbons.

The third stage of the oxidation of PP is prolonged and is characterised by a zero reaction order with respect to the hydroperoxide. The latter is the principal process initiator in this stage. A similar situation had been observed earlier for the oxidation of poly(ethylene oxide) and was accounted for by a heterophase mechanism.[73, 74]

Furthermore, the oxidation of PP exhibits a specific dependence of the rate on the oxygen pressure P. The dependence is different for the initial and subsequent stages. Namely, during the induction period the rate of oxidation increases gradually over a very large range of values of P but it reaches saturation rapidly as a function of P in the subsequent stages. This property has not been explained.

The problem of the mechanism of the degradation of macromolecules in the oxidation process also remained unsolved. It was established that the rate of degradation in the initiated process is directly proportional to the rate of initiation (macroradicals are destroyed). A mechanism was proposed for the degradation of polymer chains in the oxidation chain with quadratic termination steps. However, this mechanism does not explain the effect of inhibitors. Degradation is known to occur even when the inhibitor fully suppresses the oxidation chains.

The above features agree with the heterophase mechanism based on the micellar-cellular model of the supermolecular structure of the non-crystalline polymer (the oxidation reaction involves primarily the non-crystalline PP phase).[75, 76]

The model is based on the consideration of two structural zones within the polymer globules made up a large number of macromolecules. The point is that the polymer chains encapsulated in the globule form a conglomerate of micropores. The surface forces operating in this conglomerate compress the internal micropores (the v-zone) but at the same time stretch and increase the size of other micropores adjoining the rigid envelope of the globules (the s-zone). This alters in its turn the reactivity of the reactants belonging to different micropores and is the cause of the kinetic polychromaticity. In particular, the narrow v-micropores suppress the reactivity as regards dissociation of the hydroperoxide and the impurity initiator. Dissociation takes place in the spacious s-micropores. Furthermore, elastic mechanical forces suppress the macroradical decomposition steps in the compressed v-zone but promote degradation in the extended sections of the chains of the s-zone.

The primary formation reactions of macroradicals as well as their degradation and destruction take place in the micropores of the s-zone. The s-mechanism should not include the hydroperoxide formation reaction. The latter occurs in another reaction chain, in the v-zone, by virtue of the interzonal s–v transfer of the free valence.

$$PH_s + O_{2s} \xrightarrow{k_{0s}} \delta_1 P_s^{\bullet}, \qquad P_s^{\bullet} \longrightarrow R_s^{\bullet}\text{(degradation)},$$

$$R_s^{\bullet} \xrightarrow{k_{1s}} R_{1s}^{\bullet}\text{(isomerisation)}, \qquad R_s^{\bullet} + R_{1s}^{\bullet} \longrightarrow \text{(products)}.$$

The mechanism of the s–v transfer includes steps (which occur with a low probability) involving the transfer to the thermal $R_s^{\bullet}$ radicals from the lattice structure of the s-micropore and conversely as well as the oxidation of $R_m^{\bullet}$ within the volume of the micropore and the ejection of HO$^{\bullet}$.

$$R_s^{\bullet} \underset{k_{-m}}{\overset{k_m}{\rightleftharpoons}} R_m^{\bullet},$$

$$R_m^{\bullet} + O_{2s} \xrightarrow{k_{tr}} RO_{2m}^{\bullet} \longrightarrow HO_m^{\bullet}.$$

The light hydroxyl penetrating into the v-zone initiates the oxidation chains

$$HO_m^{\bullet} \longrightarrow HO^{\bullet} \xrightarrow{PH} P^{\bullet}, \qquad P^{\bullet} + O_2 \xrightarrow{k_1} PO_2^{\bullet},$$

$$PO_2^{\bullet} + PH \xrightarrow{k_2} POOH + P^{\bullet}, \qquad 2PO_2^{\bullet} \xrightarrow{k_3} \text{termination}.$$

As it accumulates, the hydroperoxide begins to pass from the v-zone to the s-zone, i.e.

$$HP_v \xrightarrow{k_{vs}} HP_s,$$

as a consequence of which steps involving the generation of the radicals HP_5, i.e.

$$HP_s \xrightarrow{k_{0s}} \delta P_s^{\bullet},$$

and the heterogeneous non-radical bimolecular reaction

$$HP_v + HP_s \xrightarrow{k''} \text{molecular products},$$

are included in the process. The latter reaction limits the rate of generation of the radicals and ensures the attainment of a stationary rate of the oxidation process in a zero order reaction with respect to the hydroperoxide.

The above mechanism reproduces the principle of the heterophase conjugation of the s- and v-reaction chains and entails the non-equivalent involvement in the chains of the oxygen dissolved in the polymer. The O_2 molecules (like those of other low molecular mass compounds) are localised within the micropores under the influence of surface forces. This results in steric hindrance to the oxidation reaction, which promotes within the micropores of the s-zone the destructive pathway competing with the oxidation reaction and involving the conversion of alkyl macroradicals into $P_s^{\cdot}$. On the other hand, in the v-zone the destruction of the $P^{\cdot}$ radicals is suppressed by the change in structure and the radicals are oxidised.

In the initial stage of the heterophase reaction, oxygen participates twice in the stages determining the rate of the process: in the radical generation steps with participation of CH_2 groups and in the s–v free valence transfer steps. As a consequence of such 'double initiation', the rate of oxidation is initially

$$W^{(1)} = k_2[\mathrm{PH}][\mathrm{PO}_2^{\cdot}]_1 = \frac{aP}{\sqrt{b+P}} \simeq \tau_{\mathrm{ind}}^{-1},$$

where a and b are constants subject to the condition that the microporous structure does not change in the course of the oxidation reaction.

As a result of the migration of the hydroperoxide into the s-zone, the hydroperoxide becomes the main source of radicals and after a time increases the rate of reaction as a result of the increase in the rate of initiation:

$$W^{(2)} = \frac{\delta k_{0s} k_{vs} g}{(k_{0s} + k'' g)} \gg \delta_1 k'_{0s}[\mathrm{PH_s}][\mathrm{O_{2s}}],$$

where g is the hydroperoxide concentration, but after a short autoaccelerated stage, the maximum rate of initiation is established for a long period:

$$W_i^{(3)} = \frac{\delta k_{0s} k_{vs}}{k_{0s}}.$$

It is independent of the overall hydroperoxide content. In stages (2) and (3), the role of oxygen in the generation of radicals is negligible, but it retains its influence as a participant in the interzonal transfer of radicals.

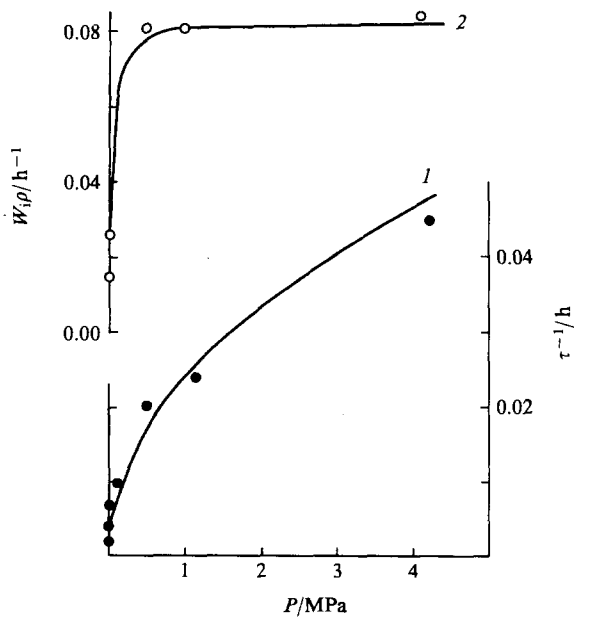


Figure 21. Dependence of the induction period (curve *1*) and of the maximum rate of oxidation of polypropylene (curve *2*) on the oxygen pressure; T = 90 °C.

The rate of oxidation is now described by the expressions

$$W^{(2)} \simeq \left(\frac{P_0}{b+P}\right)^{0.5} \left(\frac{\delta k_{0s} k_{vs}}{c+g}\right)^{0.5},$$

$$W^{(3)} \simeq \left(\frac{P}{b+P}\right)^{0.5},$$

where b and c are constants and $W^{(2)}$ and $W^{(3)}$ differ from $W^{(1)}$ by faster saturation as a function of P.

The calculated $W^{(1)}(P)$ and $W^{(3)}(P)$ curves for PP and polyethylene (PE) oxidation are presented in Figs 21 and 22. Experimental data have been obtained for PP films[77] and for a PE melt.[78] The unique mechanism of the oxidation in all stages of the process is confirmed by the finding that the expressions for $W^{(2)}$ and $W^{(3)}$ include the same value of b: 0.1 MPa for PP and 10, 50, and 200 torr for PE at 141 °C, 157 °C, and 165 °C respectively.

The observed correspondence between the calculated curves and the experimental points permits the conclusion that the heterophase mechanism predominates over the traditional homogeneous oxidation mechanism in relation to a hydrocarbon polymer, which differs fundamentally from a homogeneous liquid by its supermolecular organisation.

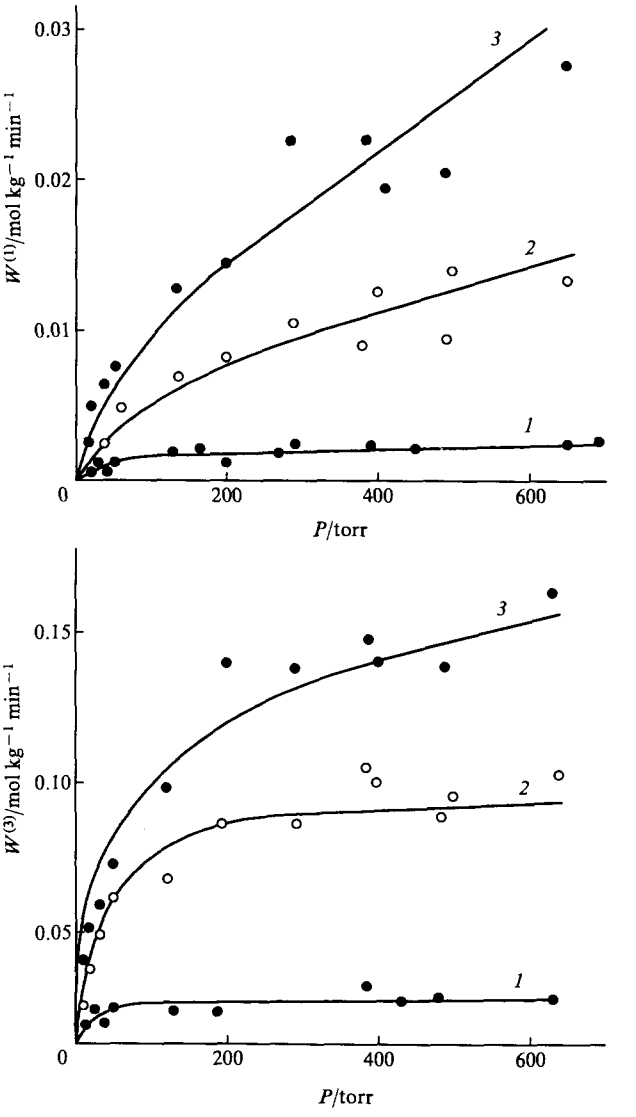


Figure 22. Dependence of the rate of oxidation of polyethylene on the oxygen pressure; T(°C): (*1*) 141; (*2*) 157; (*3*) 165.

References

1. G E Zaikov *Usp. Khim.* **60** 2220 (1991) [*Russ. Chem. Rev.* **60** 1145 (1991)]
2. K S Minsker, Al Al Berlin, G E Zaikov *Usp. Khim.* **60** 430 (1991) [*Russ. Chem. Rev.* **60** 225 (1991)]
3. G E Zaikov *Polym. Yearbook* **9** 362 (1992)
4. V B Ivanov, V Ya Shlyapintokh *Polymer Degradation and Stability* (28) 249 (1990)
5. L M Postnikov, A V Dubovitskii, in *Abstacts of International Conference on Regulation of Polymeric Materials Stability, Moscow, 1992* p. 38
6. I Ya Kalontarov, A A Stotskii, K M Makhkamov, N P Tkhcheva, V I Sobolev *Izv. Vyssh. Uchebn. Zaved., Khim.* **19** 1863 (1976)
7. L E Maksimova, V I Shishkina, I Ya Kalontarov, F F Niyazi, A Abdirazakova *Dokl. Akad. Nauk Tadzh. SSR* **13** 713 (1980)
8. S A Siling, A L Margolin, I Ya Kalontarov, S V Vinogradova, F F Niyazi, Yu V Chaiko, Sh S Dzhumayev *Acta Polym.* **42** 133 (1991)
9. Yu V Makedonov, A L Margolin, N Ya Rapoport, L S Shibryaeva *Vysokomol. Soedin. A* **28** 1380 (1986)
10. M Ya Mel'nikov, E N Seropegina, N I Osokina, V I Pergushov *Dokl. Akad. Nauk SSSR* **330** 77 (1993)
11. M Ya Mel'nikov, E N Seropegina *Radiat. Phys. Chem.* **33** 151 (1989)
12. E M Korol'kova, V A Radtsig, M Ya Mel'nikov *Khim. Fiz.* **10** 41 (1991)
13. F F Niyazi, O A In, I Ya Kalontarov, L E Elizarova, I M Potapova *Zh. Prikl. Khim.* **7** 1959 (1988)
14. A L Margolin in *Uspekhi Nauki i Tekniki. Khimiya i Tekhnologiya Vysokomolekulyarnykh Soedinenii* (Advances in Science and Engineering. The Chemistry and Technology of Macromolecular Compounds) (Moscow: VINITI, 1988) Vol. 24, p. 89
15. G E Krichevskii, J Gombkete, in *Svetostoikoist' Okrashennykh Tekstil'nykh Izdelii* (Photostability of Coloured Textiles) (Moscow: Legkaya Industriya, 1975) p. 17
16. I Ya Kalontarov, in *Ustoichivost' Okrasok Tekstil'nykh Materialov k Fizikokhimicheskim Vozdeistviyam* (Resistance of the Colours of Textile Materials to Physicochemical Influences) (Moscow: Legpromizdat, 1985) p. 118
17. L I Kalontarov, R Marupov, N S Abdullaev *Khim. Fiz.* **6** 1380 (1987)
18. L I Kalontarov, R Marupov, T Shukurov *Vysokomol. Soedin. B* **31** 33 (1989)
19. L I Kalontarov, R Marupov, T Shukurov *Khim. Fiz.* **9** 294 (1990)
20. L I Kalontarov, R Marupov *Chem. Phys. Lett.* **181** 27 (1991)
21. L I Kalontarov, R Marupov *J. Mater. Sci.* **26** 5770 (1991)
22. L I Kalontarov, R Marupov A T Bekmukhamedov *Macromol. Chem.* **193** 735 (1992)
23. L I Kalontarov, A T Bekmukhamedov *Vysokomol. Soedin. A* **33** 1986 (1991)
24. L I Kalontarov, R Marupov, A T Bekmukhamedov *Int. J. Polym. Mater.* **19** 45 (1993)
25. N R Prokopchuk, A G Alekseev, T V Starostina, L O Kisel' *Dokl. Akad. Nauk Beloruss. SSR* **34** 1026 (1990)
26. A G Alekseev, T V Starostina, L O Kisel', N R Prokopchuk *Vestsi Akad. Belarusi, Khim. Ser.* **8** 108 (1992)
27. I D Khodzhaeva, N V Kislinovskaya, E V Smurova, in *Tekhnologiya, Pererabotka i Primenenie Kauchukov* (Technology, Processing, and Applications of Raw Rubbers) (Moscow: TsNIITENeftekhim, 1989) p. 16
28. I D Khodzhaeva *Izv. Vyssh. Uchebn. Zaved., Khim.* **35** 3 (1992)
29. N V Kislinovskaya, I D Khodzhaeva, S P Novikova, G A Vakhtberg, in *Khimicheskaya Modifikatsiya Elastomerov i Lateksov* (Chemical Modification of Elastomers and Latexes) (Moscow: TsNIITENeftekhim, 1988) p. 104
30. N V Kislinovskaya, I D Khodzhaeva, S P Novikova, N B Dobrova *Int. J. Polym. Mater.* **18** 57 (1992)
31. N V Kislinovskaya, I D Khodzhaeva, S P Novikova, USSR P. 1 666 473; *Byull. Izobret.* **28** 85 (1991)
32. E P Torchilina, A A Kashina, I D Khodzhaeva, in *Tezisy Dokladov II Vsesoyuznoi Konferentsii 'Smesi Polimerov' Kazan, 1990* (Abstracts of Reports at the IInd All-Union Conference on 'Polymer Blends' Kazan, 1990) p. 94
33. N V Kislinovskaya, I D Khodzhaeva, I A Elkina, in *Tezisy Dokladov Nauchnotekhnicheskoi Konferentsii 'Modifikatsiya Polimernykh Materialov v Protsesse Ikh Pererabotkir', Izhevsk, 1988* (Abstracts of Reports at the Science and Engineering Conference on 'Modification of Polymeric Materials during Their Processing', Izhevsk, 1988, p. 29
34. I D Khodzhaeva, N V Kislinovskaya *Polym. Yearbook* **11** in press (1993)
35. L M Postnikov, A V Dubovitskii, in *Abstracts of International Conference on Regulation of Polymeric Materials Stability, Moscow, 1992* p. 10
36. E G Rozantsev, in *Nitroksil'nye Radikaly: Sintez, Khimiya, Primenenie* (Nitroxyl Radicals: Synthesis, Chemistry, and Applications) (Moscow: Khimiya, 1987) p. 267
37. I C McNeill *J. Polym. Sci., Polym. Chem. Ed.* **15** 2381 (1977)
38. I C McNeill, A Ya Polishchuk, G E Zaikov *Polymer Degradation and Stability* **37** 223 (1992)
39. A Ya Polishchuk, G E Zaikov, J H Petropoulos *Intern. J. Polym. Mater.* **19** 1 (1992)
40. I A Golubeva, L I Tolstych, E P Gallyamova, S S Zeldina *Int. J. Polym. Mater.* **16** 131 (1992)
41. I A Golubeva, V F Gromov, E V Buneau, O N Tkachenko, R N Almaev, in *Abstracts of International Conference on Regulation of Polymeric Materials Stability, Moscow, 1992* p. 28
42. A A Askadskii *Vysokomol. Soedin. A* **32** 1517 (1989)
43. A A Askadskii *Mekhanika Kompozitsionnykh Materialov* **6** 963 (1990)
44. A A Askadskii *Polym. Yearbook* **4** 93 (1987)
45. A A Askadskii, in *Encyclopedia of Fluid Mechanics* Vol. 9 (Houston, 1990) p. 103
46. A A Askadskii *Chem. Rev.* **16** 137 (1992)
47. A P Mar'in, Yu A Shlyapnikov *Vysokomol. Soedin. B* **31** 386 (1989)
48. A P Mar'in, Yu A Shlyapnikov *Polymer Degradation and Stability* (36) 1 (1992)
49. E L Shanina, V A Belyakov, G E Zaikov *Polymer Degradation and Stability* (27) 309 (1990)
50. E L Shanina, G E Zaikov *Plastmassy* in the press (1993)
51. A B Mazaletskii, V G Vinogradova, G V Panova *Neftekhimiya* **29** 414 (1989)
52. A B Mazaletskii, V G Vinogradova, G V Panova *Kinet. Katal.* **31** 1065 (1990)
53. V G Vinogradova, A N Zverev *Zh. Obshch. Khim.* in the press (1993)
54. K A Andrianov, A I Nogaideli, N M Makarova, O V Mukbaniani *Izv. Akad. Nauk SSSR, Ser. Khim.* **6** 1383 (1977)
55. S M Meladze, O V Mukbaniani, L M Khananashvili *Vysokomol. Soedin. A* **26** 250 (1984)
56. O V Mukbaniani, N A Koyava, L M Khananashvili *Vysokomol. Soedin. A* **27** 2261 (1985)
57. V A Achelashvili, O V Mukbaniani, V Yu Levin, S M Meladze, I A Inaridze, L M Khananashvili *Izv. Akad. Nauk Gruz. SSR, Ser. Khim.* **16** 20 (1990)
58. V A Achelashvili, O V Mukbaniani, L M Khananashvili, V Yu Levin, N G Komalenkova, E A Chernyshev *Vysokomol. Soedin. A* **32** 480 (1990)
59. V A Achelashvili, O V Mukbaniani, N A Koyava, L M Khananashvili, I Sturua *Soobshch. Akad. Nauk Gruz. SSR* **122** 537 (1986)
60. O V Mukbaniani, V A Achelashvili, L M Khananashvili, S M Meladze, N A Koyava, G I Sturua *Soobshch. Akad. Nauk Gruz. SSR* **122** 105 (1986)
61. I G Esartiya, O V Mukbaniani, N A Koyava, in *Tezisy Dokladov VII Vsesoyuznoi Konferentsii 'Khimiya, Tekhnologiya Proizvodstva i Prakticheskoe Primenenie Kremniiorganicheskikh Soedinenii', Moskva, 1990* (Abstracts of Reports at the VIIth All-Union Conference on 'The Chemistry, Technology of the Manufacture, and Practical Applications of Organosilicon Compounds' Moscow, 1990, Part 1, p. 217
62. I G Esartiya, O V Mukbaniani, L M Khananashvili *Soobshch. Akad. Nauk Gruz. SSR* **144** 277 (1991)
63. I E Seitablaev, Ya R Gun, L D Koltunova, V V Lavrent'ev, B Tsoi *Plastmassy* **11** 36 (1985)
64. I E Seitablaev, E Baimuratov, D S Saidov, I Ya Kalontarov *Dokl. Akad. Nauk Tadzh. SSR* **34** 371 (1991)

65. E Ya Davydov, V P Pustoshnyi, A P Vorotnikov, G B Pariiskii *Vysokomol. Soedin. B* **32** 370 (1991)
66. A P Vorotnikov, E Ya Davydov *Khim. Fiz.* **10** 1475 (1991)
67. M A Askarov, N A Abduvaliev, in *Abstracts of International Conference on Regulation of Polymeric Materials Stability, Moscow, 1992*, p. 28
68. Yu A Mikheev, L N Guseva, D Ya Toptygin *Khim. Fiz.* **6** 251 (1987)
69. Yu A Mikheev *Khim. Fiz.* **8** 1110 (1989)
70. Yu A Mikheev *Khim. Fiz.* **10** 715 (1991)
71. Yu A Mikheyev *Int. J. Polym. Mater.* **16** 237 (1992)
72. Yu A Mikheev, L N Guseva *Khim. Fiz.* **11** 964 (1992)
73. Yu A Mikheev *Khim. Fiz.* **8** 399 (1989)
74. Yu A Mikheev, L N Guseva, D Ya Toptygin *Vysokomol. Soedin. A* **31** 2544 (1989)
75. Yu A Mikheev, L N Guseva *Khim. Fiz.* **10** 724 (1991)
76. Yu A Mikheyev *Int. J. Polym. Mater.* **16** 221 (1992)
77. D L Faulkner *Polym. Eng. Sci.* **22** 466 (1982)
78. T Kelen, M Iring, F Tudos *Eur. Polym. J.* **12** 35 (1976)

Russian Chemical Reviews **62** (7) 625 – 636 1993
© 1993 Russian Academy of Sciences and Turpion Ltd

UDC 541.67 + 541.124

Influence of the polarity of the medium on the electronic structure and energetics of molecules in solutions

I P Gol'dshtein, E S Petrov

Contents

I.	Introduction	625
II.	Theoretical approaches to the problem	625
III.	Changes in the electronic structure, energetics, and physicochemical properties of molecules under the influence of a polar medium	627
IV.	Molecular and ionic forms of H complexes in media with different dielectric permittivities	631
V.	Electronic structure of salts in media with different polarities	633
VI.	Conclusions	635

Abstract. Recent data on the effect of the polarity of the medium on the state of solute molecules having different types of chemical bond are reviewed. The changes in electronic structure and in the energetics of the molecules are discussed, and their influence on the physicochemical properties and role of the molecules in various liquid-phase processes (tautomeric and con-formational transformations, nucleophilic substitution, proton transfer) is examined. Special attention is paid to the new concept of preferential stabilisation of molecular and of ionic forms of salts and of complexes with intermolecular hydrogen bonds in media of different polarity. The bibliography includes 98 references.

I. Introduction

The influence of the medium on the state and properties of substances in solution (a problem first formulated towards the end of the last century) continues to stimulate the interest of research workers, because the properties of the solvent play a substantial (and often a dominant) role in the thermodynamics and kinetics of many important liquid-phase processes. Various aspects of the effects of solvation on the energetics and dynamics of these processes, the role of structural changes in the solvent, and the influence of the solvent on the reaction kinetics and on the physicochemical characteristics of dissolved substances have been discussed in several reviews and monographs.[1-13] However, like many of the original papers, the review literature fails (in our view) to give due weight to the influence of solvation on the electronic and the geometrical structure of the solute molecules. Thus, recent studies have shown that the transfer of molecules from the gas phase to a strongly solvating medium can result in marked structural changes, due to electron donor–acceptor (EDA) interactions between the solvent and the solute molecules (specific solvation) or to the polarising effect of the medium (nonspecific solvation).

Both experimental and calculated results suggest that the role of nonspecific solvation in the structural change of dissolved molecules can be as important as the role of specific solvation. Thus, in a very polar solvent a substantial charge separation can take place in easily polarisable molecules, leading to a transition to the ionic state. Furthermore the interaction with the polar medium also affects the electronic structure of the molecular complexes produced by the EDA interaction. As has been reported,[14-21] an increase in the dielectric permittivity (ε) of the medium increases the intermolecular charge transfer in these complexes, which can lead to the creation of ionic forms in specifically solvating media with a high value of ε. Large changes in the relative acidity and basicity of compounds, in the rates of (electron or proton) charge transfer reactions, and shifts in the tautomeric and other equilibria are also possible.

The aim of the present review was to highlight the general features of changes in the electronic and the geometrical structure of molecules under the influence of a polar medium and to show how these changes are reflected in the physicochemical properties of the molecules (such as dipole moments, spectral characteristics, etc.), in their solvation energy, and in their ionisation in solutions, and also in processes which are controlled by these properties.

II. Theoretical approaches to the problem

The rapid developments in theoretical methods of studying solvation effects during the last two decades[1-4] created a much wider understanding of the nature of changes stimulated in various systems by the presence of a solvent. However, even the most recent theoretical studies[1, 2] have not allowed adequately for the polarising effect of the medium on the electronic structure of molecules and of molecular complexes in solution. Three basically different approaches can be identified among the computational methods used in studies of solvation processes: statistical calculations by the Monte Carlo method (MC) and by molecular dynamics (MD), quantum-chemical calculations on the molecule to be solvated and on its nearest-neighbour solvent molecules (treated as a single super-molecule), and lastly calculations in the continuum approximation, in which the solute molecule is treated as surrounded by a continuous medium with a known value of ε. The polarising effect of the medium is usually ignored in the MC and MD methods, which treat the solvated molecule as a geometrically rigid species with an invariant electronic structure, whereas in the super-molecule approach no allowance is made for the influence of the whole volume of the polar solvent on intermolecular charge transfer.

Simkin and Sheikhet have described the theoretical methods of calculating the solvation effects, and have compared their

I P Gol'dshtein, E S Petrov Complex Catalysis Laboratory, Ya Karpov Physicochemical Research Institute, ul. Obukha 10, 103064 Moscow. Fax (7-095) 975 24 50

Received 18 January 1993
Uspekhi Khimii **62** (7) 667 – 679 (1993); translated by J I Carasso

prospects when applied to various aspects of the problem, in a recently published monograph[2] as well as in earlier reviews.[3, 4] As they clearly state,[4] no one method can be classified as 'good' or 'bad': the most important consideration is that the method should be adequately matched to the problem of interest.

Since the structure of the solvent and the mobility of its molecules in the solvation shell can be analysed only by the MC and MD methods, whereas the supermolecular approach is better suited to studies of specific solvation, in the absence of specific solvation it is more rational to use quantum-chemical calculations (which allow for the effect of the medium in the continuum approximation) in studies of the effect of the polarity of the medium on the electronic structure of solute molecules.

The distribution of electron density and the energy of a molecule immersed in a dielectric continuum are calculated by the Schrödinger equation in one of its approximations, defining the Hamiltonian of the molecule immersed in the medium as

$$\hat{H} = \hat{H}_0 + \hat{U}; \tag{1}$$

$\hat{H}_0$ is the Hamiltonian of the molecule in a vacuum and $\hat{U}$ is an operator describing the interaction of the molecule with the medium.

Eqn (1) provides the foundations of a wide range of methods of calculation, described in the review literature[2-4, 22-24] as well as in the original papers.[25-46] Therefore we shall only dwell on the most significant differences between the methods adopted in these approaches to construct the operator $\hat{U}$, since our further discussion requires the differences to be explicitly stated. The operator $\hat{U}$ is usually expressed in terms of the classical Born, Onsager, and Kirkwood theories of the electrostatic interaction between charged or polar particles and the medium. The Born equation (2) (E_B) and the Onsager equation (3) (E_{Ons}) are the most frequently used:

$$E_B = \frac{\varepsilon - 1}{2\varepsilon} \frac{q_i q_j}{r_{ij}}, \tag{2}$$

where q_i, q_j, and r_{ij} are (respectively) the charges on the interacting particles and the distance between them, and

$$E_{Ons} = \frac{\varepsilon - 1}{2\varepsilon + 1} \frac{\mu^2}{a^3}, \tag{3}$$

where μ is the dipole moment of the solute molecule, and a is the radius of the cavity which this molecule produces in the solvent.

Eqn (2), derived by Born in order to calculate the interaction energy of ions in a solution, found an interesting application in Klopman's solvaton model,[25] which provided a new impetus for the development of quantum-chemical methods of calculation allowing for the effect of the medium. In this model each atom A of a molecule immersed in the medium is conjugated with a solvaton C, at a distance r_{AC} and having a charge q_C equal to the charge of the atom A (Z_A) but of opposite sign. It is assumed that the solvatons do not mutually interact, and that the energy of the interaction between the atom and the solvaton is described by Eqn (2) in the form

$$E = \frac{\varepsilon - 1}{2\varepsilon} \frac{q_C Z_A}{r_{AC}}. \tag{4}$$

In this case the operator $\hat{U}$ becomes

$$\hat{U} = \frac{\varepsilon - 1}{2\varepsilon} \left[\sum_{C=1}^{N} \sum_{i=1}^{M} \frac{q_C}{r_{C_i}} - \sum_{C=1}^{N} \sum_{A=1}^{M} \frac{q_C Z_A}{r_{AC}} \right], \tag{5}$$

where N and M are the numbers of atoms and of electrons in the molecule respectively. Various modifications of the solvaton model[26-29] converge towards the ideas underlying the models of molecular perturbation by point dipoles[36] and of 'virtual charges'.[37-39]

An essentially different approach to the construction of the operator $\hat{U}$ was used by Tapia and coworkers,[38-42] who developed the self-consistent reactive field (SCRF) theory by analogy with Onsager's reactive field model. This approach allows not only for the effect of the polar medium on the molecule immersed in it (resulting in a redistribution of the charges in the molecule and therefore also in a change in the dipole moment), but also for the polarising interaction of this dipole with the surrounding medium, which produces the so-called 'reactive' Onsager field (R) in the medium. The quantum-chemical analogue of the classical electrostatic interaction energy ($E = -\mu R$) in the SCRF model is the operator $\hat{U}$, in the form

$$\hat{U} = -\hat{\mu} g \langle \Psi | \hat{\mu} | \Psi \rangle, \tag{6}$$

where $\hat{\mu}$ is the operator of the dipole moment vector, Ψ is the wave function of the molecule in a medium with a dielectric constant ε, and g is a tensor which defines the susceptibility of the reaction field, expressed [by analogy with Eqn (3)] as

$$g = \frac{\varepsilon - 1}{2\varepsilon + 1} \frac{2}{a^3}. \tag{7}$$

It is assumed that the molecule occupies a spherical cavity of radius a, within which ε is equal to 1.

The assumption of a spherical cavity seriously restricts the application of the SCRF model when the molecules of interest are asymmetric. In this case an improved Onsager model is used, in which the cavity produced by the molecule in the surrounding dielectric continuum has the same shape as the molecule.[30, 43-46] The molecule in its cavity is treated as a system of charges, defined by the distribution of electron density $\rho(x)$, which induce in the boundary surface S of the cavity the charges $\sigma(S)$ responsible for the reactive field.[44-46] Under these conditions the perturbation operator takes the form

$$\hat{U} = \sum_i q_i \int \frac{\sigma(S)}{r_i - S} \mathrm{d}S, \tag{8}$$

where q_i and r_i are the charge and the position of the ith particle respectively. The density of the surface charges $\sigma(S)$ is determined by the polarisation of the inner (P_+) and of the outer (P_-) boundary surface of the cavity:

$$\sigma(S) = P_+ \boldsymbol{n} + P_- \boldsymbol{n}, \tag{9}$$

where $\boldsymbol{n}$ is a unit vector perpendicular to the boundary surface at the point S. The polarisation vector is related to the ε value for the medium by the Maxwell relation

$$P = \frac{1}{4\pi}(\varepsilon - 1)E. \tag{10}$$

The electric field E is determined by the electrostatic potential Φ generated by the distributions $\rho(x)$ and $\sigma(S)$:

$$\Phi(r) = \int \frac{\rho(x)}{r - x} \mathrm{d}x + \int \frac{\sigma(S)}{r - S} \mathrm{d}S. \tag{11}$$

Thus in the SCRF model proposed by Miertuš[30] and subsequently developed by Hochi[44-46] and by Bazilevskii[47] the reactive field is created by the charges induced by the molecule in the surrounding dielectric, and the interaction of the molecule with the dielectric is described by its interaction with these charges. This approach brings the SCRF model close to the solvaton or virtual charges model described above.

Eqns (1)-(11) show that the Hamiltonian (1), in which the perturbation operator allows for the electrostatic interaction with the medium, can be used to solve the Schrödinger equation for an arbitrary value of ε. This allows the quantum-chemical calculations to be used to determine the electronic structure and the geometry of the molecules, and their physicochemical parameters, as a function of the ε value for the medium. As in the case of isolated molecules, these calculations have been carried out in both nonempirical[30-35] and semiempirical variants.[27-29, 45-49] In spite of the great sensitivity of the calculated results to the method used in the approximate solution of the Schrödinger equation and to the model chosen for the effect of the medium this approach usually gives a correct description of the general trends seen in the changes in electronic structure and in the properties and the

Table 1. Quantum-chemical calculations of the changes in total energy (ΔE) and in free energy (ΔF/kJ mol^{-1}) and dipole moments (μ/D) of the molecules resulting from the transfer from a vacuum ($\varepsilon = 1$, μ_1) to a medium with $\varepsilon = 80$ (μ_{80}).[45]

Compound	Calculated parameter	SCRF method			Virtual charges method	
		CNDO/2	INDO	STO-3G	4-31G	CNDO/2
H_2O	$-\Delta E$	34.0	39.4	–	42.8	366.0
	$-\Delta F$	16.5	19.4	–	21.4	105.2
	μ_1	2.1	2.14	–	2.69	2.10
	μ_{80}	2.19	2.24	–	2.86	3.07
H_2CO	$-\Delta E$	30.3	28.6	51.5	36.4	565.5
	$-\Delta F$	14.2	8.8	22.4	21.2	123.2
	μ_1	1.95	2.15	1.52	3.06	1.95
	μ_{80}	2.24	2.46	2.09	3.48	4.95
H_2NCHO	$-\Delta E$	72.2	74.6	–	70.7	911.0
	$-\Delta F$	33.3	29.3	–	33.0	257.7
	μ_1	3.68	3.90	–	–	3.68
	μ_{80}	4.30	4.57	–	–	7.26
$H_3N^+CH_2COO^-$	$-\Delta E$	540.1	535.9	–	–	2745.8
	$-\Delta F$	254.3	244.0	245.5	233.4	939.1
	μ_1	13.16	12.82	11.97	13.13	13.16
	μ_{80}	14.68	14.58	13.72	15.48	17.94

energetics of the molecules under the influence of a polar medium, and (as will be shown below) they are acceptably consistent with experimental data. The good agreement between calculations by different methods is shown in Table 1, where changes in the total energy (ΔE) and in the Helmholtz free energy (ΔF) of various molecules when transferred from a vacuum or from a gas phase to a medium with $\varepsilon = 80$ are compared.

The difference between the total energies of a molecule calculated for a medium with a given value of ε (E) and for a vacuum (E_0) can be used as a measure of the stabilisation energy experienced by the molecule in the polar medium as a result of electrostatic interactions.

III. Changes in the electronic structure, energetics, and physicochemical properties of molecules under the influence of a polar medium

Quantum-chemical calculations followed by an analysis of the Mulliken populations of the orbitals show that when a molecule is transferred from the gas phase ($\varepsilon = 1$) to a solution ($\varepsilon > 1$) the charges on almost all its atoms change by an amount which is greater, the greater the ε value of the medium. The most substantial changes are seen in easily polarisable bonds. Thus, in the case of the C=O bond in some carbonyl compounds (Table 2) it was established that a change in ε from 1 to 80 markedly

Table 2. Charges on the atoms (q), bond populations (P), and dipole moments (μ/D) of molecules in media with different ε.

1. $H-\underset{\underset{O}{\|}}{C}-NH_2$ (INDO–solvatons[48])

Parameter	$\varepsilon=1$	$\varepsilon=4$	$\varepsilon=20$	$\varepsilon=80$
q(O)	−0.408	−0.425	−0.441	−0.446
q(C)	+0.504	+0.521	+0.536	+0.550
q(N)	−0.260	−0.270	−0.280	−0.283
μ	3.90	4.02	4.12	4.15

2. $H^1-\underset{\underset{O}{\|}}{C^1}-N\begin{matrix}C^2H_3\\C^3H_3\end{matrix}$ (CNDO/2–solvatons[28])

Parameter	$\varepsilon=1$	$\varepsilon=2$	$\varepsilon=5$	$\varepsilon=40$
q(O)	−0.282	−0.316	−0.344	−0.355
q(C^1)	+0.231	+0.297	+0.306	+0.324
q(N)	−0.323	−0.264	−0.129	+0.114
q(C^2)	−0.323	−0.531	−0.894	−1.443
q(C^3)	−0.317	−0.525	−0.887	−1.429
q(H^1)	+0.069	+0.022	−0.008	−0.009
P(O–C^1)	1.197	1.197	1.193	1.185
$P$$C^1$–N)	0.900	0.914	0.940	0.976
P(C^2–N)	0.745	0.742	0.736	0.729
P(C^3–N)	0.745	0.743	0.739	0.732
P(C^1–H^1)	0.670	0.668	0.655	0.648
μ	2.69	2.89	3.30	3.89

3. $H_3C^4-C^3H=C^2H-\underset{\underset{H}{|}}{C^1}=O$ (INDO–SCRF[46])

Parameter	$\varepsilon=1$	$\varepsilon=2$	$\varepsilon=80$
q(O)	−0.2950	−0.3226	−0.3606
q(C^1)	+0.3159	+0.3324	+0.3557
q(C^2)	−0.0921	−0.0963	−0.1021
q(C^3)	+0.0509	+0.0603	+0.0753
q(C^4)	+0.0040	+0.0041	+0.0050

4. $O=N^1-N^2\begin{matrix}C^1H_3\\C^2H_3\end{matrix}$ (CNDO/2–solvatons[28])

Parameter	$\varepsilon=1$	$\varepsilon=2$	$\varepsilon=5$	$\varepsilon=40$
q (O)	−0.139	−0.150	−0.161	−0.169
q (N^1)	−0.026	−0.039	−0.095	−0.190
q (N^2)	−0.139	−0.126	+0.178	+0.465
q (C^1)	−0.360	−0.638	−1.110	−1.731
q (C^2)	−0.369	−0.646	−1.115	−1.728
P (O–N^1)	1.016	1.013	1.005	0.992
P (N^1–N^2)	0.860	0.871	0.889	0.908
P (N^2–C^1)	0.735	0.735	0.727	0.711
P (N^2–C^2)	0.751	0.750	0.744	0.730
μ	2.97	3.08	3.48	4.06

Table 3. Effect of ε for the medium on the electronic characteristics and the geometrical parameters of benzophenone (CNDO/S–VC method).[50]

ε	$-q_O$	μ/D	$r_{C=O}$/Å	r_{C-C}/Å[a]
1	0.438	4.68	1.214	1.504
2	0.550	5.68	1.223	1.494
3	0.642	6.46	1.233	1.491
4	0.717	7.06	1.242	1.485
35	1.015	–	1.300	1.460

[a] The distances between the carbon atom of the CO group and the neighbouring C atoms of the benzene rings are quoted.

increases the electron density on the O atoms and lowers it on the C atoms. In particular, polarisation of the C=O bond in dimethylformamide lowers its population, whereas the population of the neighbouring C–N bond increases: the lengths of these bonds are altered,[50, 51] and the dipole moment of the molecule shows a large increase. In *N*-nitrosodimethylamine changes in electron density on the O, N^1, and N^2 atoms lower the population of the $N^1=O$ bond and increase that of the N^1-N^2 bond in proportion to the ε value of the medium. Similar results were obtained for benzophenone, showing that an increase in ε stretches the C=O bond and shortens the C–C bond between the carbon atoms of the carbonyl group and the benzene rings (Table 3). Thus the polarisation of the surrounding medium affects the geometry of the molecule by causing a redistribution of charge in the molecule.

The changes in the charges of the individual atoms of the molecule caused by an increase in ε are also reflected by the screening parameters (σ) of the nuclei, which are correlated with the chemical shifts (δ) in the NMR spectra. For example, the decrease in electron density (Δq) on the C^1, C^3, and C^4 carbon atoms of crotonaldehyde (see Table 2) caused by increasing ε for the medium from 1 to 80 results in a deshielding (Δσ) of the nuclei of these atoms, which is consistent with the shift of the corresponding ^{13}C NMR signals (Δδ) towards weak fields on going from pentane (ε = 1.8) to DMSO (ε = 49.6), whereas an increase in the negative charge on the C^2 atom corresponds to a shift of the ^{13}C NMR signal towards strong fields.[46]

An extensive experimental and theoretical study[52–54] of the effect of the polarity of the medium on the screening parameters and on the ^{14}N NMR chemical shifts in nitrogen compounds with chemical bonds of different types involving the N atom has been reported. It was shown, in particular, that the change from a nonpolar medium (ε < 2) to a polar medium increases the screening of the nitrogen nuclei in nitriles, whereas the opposite effect (deshielding) is found in compounds where the N atom is attached to an O atom or to a C=S group, in complete agreement with the changes in electron density on the nitrogen atoms in these compounds. Both effects increase with the ε value of the medium (Table 4).

The results of quantum-chemical calculations are satisfactorily consistent with experimental data on the ^{14}N NMR chemical shifts, which are described by the relation[52–54]

$$\delta = \delta_0 + S(\pi^* + d\delta) + a\alpha + b\beta , \quad (12)$$

where δ and δ_0 are the ^{14}N NMR chemical shifts (relative to nitromethane) of the experimental compound in this solvent and in the standard (ε ~ 2) respectively; *S*, *a*, and *b* are parameters which characterise the polarisability, the proton-donor, and the electron-donor strength of the compound, π^*, α, and β are parameters which characterise the polarising strength and the proton-donor and electron-donor strength of the medium respectively,[55] dδ is a correction for polychlorinated (δ = 0.5) and for aromatic solvents (δ = 1). Comparing the *S* values for the compounds shown in Table 4 shows that both theory and experiment suggest a large increase in the screening of the N nuclei as a result of the polarisation of the C=N bond in nitriles (compounds 1–4), whereas in *tert*-butyl nitrite (compound 5) the most marked effect is the deshielding of the nitrogen nuclei caused by the polarisation of the N=O bonds.

Good agreement between calculations by the CNDO/2–solvaton method and experiment (^{29}Si NMR) has been reported[56] for the chlorosilane series. The changes in the deshielding parameter (σ) and the shift of the ^{29}Si NMR signals towards weaker fields relative to TMS are described by the equation

$$\delta(-\sigma) = A\frac{\varepsilon - 1}{2\varepsilon} + B . \quad (13)$$

The agreement between calculated and experimental values of *A* in Eqn (13) is acceptably good.[56]

The observed deshielding of the nuclei as ε for the medium is increased can be attributed to the polarisation of the Si–Cl bonds, the effect decreasing in the following sequence: Me_3SiCl (μ = 2.09) > Me_2SiCl_2 (μ = 1.89) > $MeSiCl_3$ (μ = 1.87) > $SiCl_4$ (μ = 0); Me_2HSiCl (μ = 1.8) > $MeHSiCl_2$ (μ = 1.7) > $HSiCl_3$ (μ = 1.0) > $SiCl_4$ (μ = 0). Obviously, these effects are related to the decreases in the same sequence of the μ values for these compounds and to the consequent strengthening of the electrostatic interaction of the molecules with the polar medium.

The results of the quantum-chemical calculations show that the polarising effect of the medium and the associated redistribution of the charges in the molecule usually result in an increase in the dipole moments and therefore also in the ε values of the medium (Tables 1 and 2). Experimental data on the μ values of molecules in a series of solvents with different ε values point to the same conclusion. For example, in a molecule such as triphenylchloromethane (Ph_3CCl), which contains the covalent (in a nonpolar medium) but easily polarisable C–Cl bond the μ value increases from 1.9 to 12.2 D when ε for the solvent is increased from 2 to 65 (Table 5).

The change in electronic structure produced by the polarising effect of the solvent strongly influences the energy characteristics of the molecules. An analysis of the data in Tables 1, 2, 6, and 7 identifies the three most important types of change in the

Table 4. Changes in the screening parameters (Δσ) of the N nuclei produced by increasing the ε value of the medium from 2 to ε_i (INDO/S–solvatons method).[52–54]

Compound	Δσ					*S*
	$\varepsilon_i = 4$	$\varepsilon_i = 10$	$\varepsilon_i = 20$	$\varepsilon_i = 40$	$\varepsilon_i = 80$	
1. MeCN	1.68	2.46	2.57	2.63	–	8.81
2. EtCN	1.76	2.69	2.83	2.85	–	8.75
3. Pr^iCN	1.79	2.77	3.05	3.49	–	8.59
4. Bu^tCN	2.06	3.14	3.49	3.53	–	8.72
5. $Bu^tO-N=O$	−12.30	−15.89	−16.88	−17.34	−17.53	−9.88
6. $MeO-NO_2$	−3.18	−5.02	−5.65	−5.87	−6.14	−3.75
7. $MeN=C=S$	−2.2	−3.2	−3.3	−3.4	−3.7	−7.36
8. $Bu^tN=NBu^t$	−0.31	−0.49	−0.55	−0.58	−0.60	0

Table 5. Results of a dielectrometric and calorimetric study of triphenylchloromethane in solvents of different solvating power.[57]

Solvent	Solvent			Ph_3CCl			
	ε	DN	δ^2	μ	$-\Delta H_s$	ΔE_{cav}	$-\Delta E_{int}$
1. Tetrachloromethane	2.23	0	308.8	1.9	98.6	68.3	166.9
2. Chlorobenzene	5.62	1.2	370.4	2.54	98.0	82.0	180.0
3. Dichloromethane	8.93	1.6	403.2	3.79	93.0	89.2	182.2
4. 1,2-Dichloroethane	10.38	0.1	409.7	4.22	97.0	90.7	187.7
5. Isobutyl methyl ketone	14.6	–	306.7	5.27	105.7	67.9	173.6
6. Acetone	20.7	17.0	389.8	6.52	100.3	86.3	186.6
7. Hexamethylphosphorotriamide	29.6	38.8	334.1	8.42	124.7	73.9	198.6
8. Nitrobenzene	34.89	4.4	512.4	8.84	106.4	113.4	219.8
9. Acetonitrile	36.7	14.1	603.2	8.85	97.8	133.5	231.3
10. Nitromethane	36.7	2.7	664.6	9.0	88.7	147.1	235.8
11. Propene carbonate	65.1	15.1	555.5	12.2	104.5	122.9	227.4

Notes. DN is the Gutmann donor number of the solvent;[58] δ^2 is the cohesion energy density of the solvent;[59] μ/D is the dipole moment of Ph_3CCl; ΔH_s/kJ mol^{-1} is the solvation enthalpy of Ph_3CCl; ΔE_{cav}/kJ mol^{-1} is the energy of formation of a cavity; ΔE_{int}/kJ mol^{-1} is the energy of interaction of Ph_3CCl with the solvent.

energetics of molecules induced by an increase in the polarity of the medium:

1. A decrease in the energy of the molecule (E), and therefore in its stabilisation energy (E_{st}), resulting from the transfer of the molecule from the gas to the solution.

2. A change in the energy of the highest occupied (n, π) and the lowest unoccupied (π^*) MO, and therefore in the energies of the singlet $n-\pi^*$ and $\pi-\pi^*$ transitions.

3. An increase in the barriers to internal rotation round the bonds (C–N in amides, N^1-N^2 in nitrosamines), whose population increases.

These changes have a marked effect on the physicochemical characteristics of molecules and of processes involving those molecules in solutions.

The stabilisation energy of molecules in polar media (Table 1) is higher for molecules with a high intrinsic dipole moment. The parameter μ increases with the ε value of the medium, with a corresponding increase in the stabilisation energy of the molecule. This justifies the conclusion that the stabilisation energy in polar media is strongly dependent on the dipole–dipole interaction between the solute and the solvent molecules, and that this contribution increases with the polarities of both the participants. The same conclusion follows directly from Onsager's classical reactive field model in conjunction with Eqn (3), and is confirmed by Monte-Carlo modelling[60] of the dependence of the electrostatic interaction energy of solute molecules with the medium (ΔE_{int}) on their dipole moment.

Neither the lack of dependence of the enthalpy of solvation (ΔH_s) on μ for the solute molecules[61] nor the lack of a definite dependence of ΔH_s on μ and ε for the solvent (Table 5) can be interpreted as proof of the absence of a stabilising effect from dipole–dipole interaction. We must allow for the energy used to cut out the cavity (ΔE_{cav}), which makes a substantial endothermic contribution to ΔH_s. By introducing the correction $\Delta E_{cav} = \delta^2 V$ (where δ is Hildebrand's parameter and V is the molar volume of the solute) we can present the data in Table 5 as a linear dependence of ΔE_{int} on the μ value of the solute (Fig. 1). It is noteworthy that the solvents under study give two almost parallel straight lines, of which the lower corresponds to the solvents 5–7 and 11 (which according to their Gutmann donor numbers have the strongest specific solvation power). A possible explanation is the failure to allow for the contribution to ΔH_s from the reorganisation of the solvent associated with the creation of solvation shells in the calculation of ΔE_{int} from ΔH_s. In the case of specific solvation, which is accompanied by the formation of more rigid shells, this reorganisation requires a more substantial

Table 7. Energy (E_{MO}) of the molecular n, π, π^* orbitals and singlet transitions ($\Delta E_{n\to\pi^*}$ and $\Delta E_{\pi\to\pi^*}$) of *N,N*-dimethylformamide and *N*-nitrosodimethylamine in media with different ε values.[28]

ε	E_{MO}/a.u.			$\Delta E_{n\to\pi^*}$/eV	$\Delta E_{\pi\to\pi^*}$/eV
	n	π	π^*		
			A. $O=\overset{H}{\overset{|}{C}}-NMe_2$		
1	−0.4290	−0.4257	0.1744	5.892	10.616
2	−0.4140	−0.4077	0.1895	5.981	10.505
5	−0.3887	−0.3780	0.2103	5.916	10.260
40	−0.3504	−0.3354	0.2393	5.604	9.906
			B. $O=N-NMe_2$		
1	−0.4546	−0.4854	0.1613	3.535	10.714
2	−0.4314	−0.4655	0.1839	3.522	10.635
5	−0.4001	−0.4359	0.2123	3.507	10.397
40	−0.3647	−0.4016	0.2448	3.413	10.139

Table 6. Effect of the polarity of the medium (ε) on the physicochemical characteristics of *N,N*-dimethylformamide and *N*-nitrosodimethylamine in solution.[28]

ε	Me_2NCHO				Me_2NNO			
	$-E$	μ	ΔE_{C-N}	$\Delta\mu$	$-E$	μ	ΔE_{N-N}	$\Delta\mu$
1	53.22	2.69	33.0	−0.51	57.79	2.97	75.6	−0.45
2	53.31	2.89	32.9	−0.53	57.91	3.08	66.3	−0.51
5	53.40	3.30	55.5	−0.62	58.05	3.48	81.2	−0.66
40	53.53	3.89	94.4	−0.78	58.22	4.06	105.9	−0.88

Notes. E(a.u.) is the total energy of the molecule; ΔE/kJ mol^{-1} is the barrier to rotation round the C–N or N–N bond,; $\Delta\mu$/D is the change in dipole moment caused by the change from the planar to the nonplanar form (i.e. by a 90° rotation).

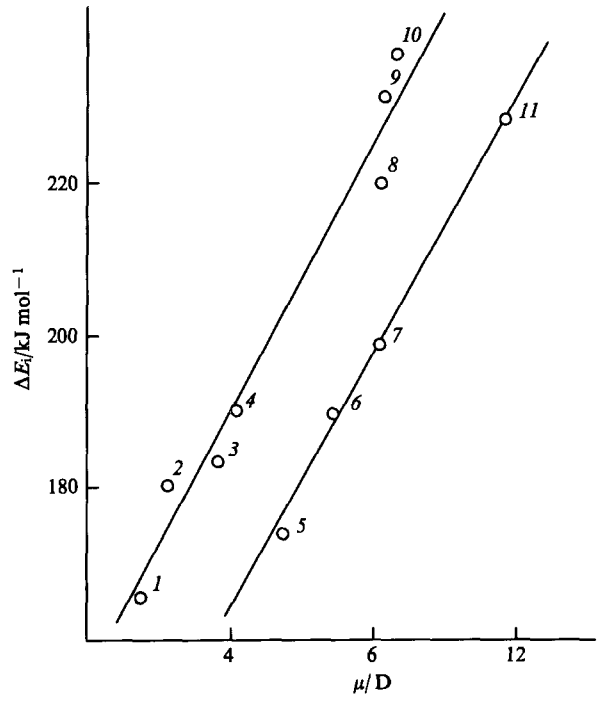


Figure 1. Plots of the interaction energy ΔE_{int} of triphenylchloromethane with the medium against its dipole moment for different ε values of the solvents (numbered as in Table 5).

consumption of energy than in nonspecific solvation. The important role of the formation of the cavity in solvation processes is also made clear by the reported[62] linear dependence

$$\ln \tau = a + b\Delta E_{cav} , \quad (14)$$

where τ is the dielectric relaxation time, which characterises the rotational mobility of the solute molecules.

Eqn (14) is consistent with the rotational diffusion model, in which the molecule can undergo discontinuous changes in its axis of rotation by overcoming a potential barrier equal to the cavity formation energy, i.e. by passing from one cavity into the next.

The dependence of the stabilisation energy of the molecules of the polar medium on their dipole moment is reflected by the nature of the dependence of ε for the solvent on the position of the absorption bands in the electronic spectra of the dissolved substances. Theoretical calculations[28, 48, 50] and experimental data[63-65] show that an increase in ε for the medium can either raise or lower the energy of the electronic transitions. CNDO/S calculations for benzophenone[50] have confirmed that the transition to the excited state can be accompanied by either an increase or a decrease in the dipole moment of the molecule (Table 8), as suggested by the experimental data.[65] Under these conditions the

Table 8. Dipole moments of benzophenone in the ground state (μ/D) and in excited states (μ^*/D) and energies (ΔE/eV) of the corresponding singlet transitions in media of different polarities.[50]

$f(\varepsilon)$[a]	μ	$\mu^*_{n\pi^*}$	$\mu^*_{\pi\pi^*}$	$\Delta E_{n\to\pi^*}$	$\Delta E_{\pi\to\pi^*}$
0	4.68	2.33	8.05	3.39	5.14
0.1	5.05	2.59	8.39	3.52	5.08
0.25	5.68	3.15	8.96	3.80	5.60
0.4	6.46	4.08	9.58	4.21	4.91
0.5	7.06	–	10.03	4.52	4.85

[a] $f(\varepsilon) = 1 - \varepsilon^{-1/2}$

energy of the $n-\pi^*$ transition increases, and that of the $\pi-\pi^*$ transition decreases, in keeping with data on the blue and the red shift of the corresponding spectral bands produced by an increase in ε for the solvent (Table 9). The increase in the $n-\pi^*$ transition energy calculated theoretically[43] agrees with the experimentally observed[64] blue shift of pyridine and of acetone: in the latter compound a decrease in the energy of the $\pi-\pi^*$ transition consistent with the red shift of the absorption band has also been reported.[48, 64] The change in the transition energy combined with a decrease in μ (shown schematically in Fig. 2) can be explained by postulating that when ε is increased the stabilisation of the ground state is more marked than that of the less polar excited state. The opposite state of affairs is observed when the transition involves an increase in μ during excitation.

The change in the electronic structure and in the energetics of molecules under the influence of a polar medium strongly affects the processes taking place in solutions, and in particular the tautomeric and conformational equilibria.[2, 48]

Low-barrier intramolecular proton transfer processes (prototropic tautomerism) have attracted wide interest because of their dominant role in many important processes such as the activity of living cells. An example of this type of tautomerism can be found in the keto–enol equilibria between 2-pyridone and 2-hydroxypyridine, or between uracil and 4-hydroxyuracil. The equilibrium constants of these processes, which determine the concentration ratio of the keto and the hydroxy form, can vary by several orders of magnitude when the system is transferred from the gas phase to a strongly polar solvent.[2, 48] This shift in the equilibrium is largely due to the preferential stabilisation by the polar medium of the tautomeric form having the higher dipole moment. For example, whereas in the pair of tautomers uracil and 4-hydroxyuracil, which have similar μ values in the gas phase, the uracil (keto form) is predominant, in aqueous solutions we find mainly 4-hydroxyuracil, which is not observed in the gas phase.[66] This is because the increase in μ, and therefore the decrease in E in media of high polarity is more marked for the hydroxy form than for uracil, and this form becomes the more stable when $\varepsilon > 8$ (see Table 10).

Table 9. Absorption bands (in nm) in the electronic spectra of benzophenone and energies (in eV) of the corresponding transitions in solvents of different polarities.[50]

Solvent	ε	$f(\varepsilon, n)$[a]	$n\to\pi$		$\pi\to\pi^*$	
			λ	ΔE	λ	ΔE
Hexane	–	0.0	364	3.57	259	5.01
Cyclohexane	1.87	0.002	363	3.58	260	4.99
Diethyl ether	3.89	0.317	360	3.60	261	4.98
Chloroform	4.55	0.289	352	3.68	–	–
Acetonitrile	36.6	0.711	355	3.66	262	4.95
Methanol	30.7	0.707	347	3.74	264	4.91
Water	76.6	0.775	337	3.85	270	4.81

[a] $f(\varepsilon, n) = (\varepsilon-1)/(\varepsilon-2) - (n^2-1)/(n^2+2)$.

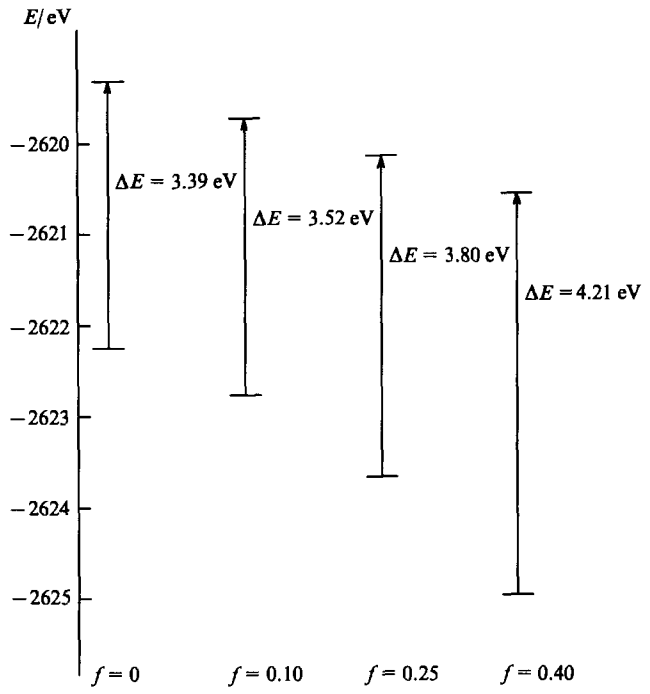


Figure 2. Changes in the energies of the ground and the excited states of benzophenone corresponding to the $n \rightarrow \pi^*$ transition, and energies of this transition as a function of the polarity of the solvent (f values, see Table 8).

The effect of a polar medium on the conformational equilibria is associated with a change in the energy of the barriers opposing the interconversion of the isomers. Thus, the conversion of *N,N*-dimethylformamide and *N*-nitrosodimethylamine from the planar to the nonplanar form (by a 90° rotation) requires surmounting barriers to internal rotation round the C–N and N^1–N^2 bonds whose height increases with the ε value of the medium. This may be due to two possible factors: the stabilisation of the more polar, planar conformer and the increased population (Table 2) of the bonds round which the rotation takes place. The difference between the dipole moments ($\Delta\mu$) of the planar and the nonplanar form increases with the ε value of the medium (see Table 6), and this effect should be accompanied by a relative stabilisation of the first form and a shift of the equilibrium towards it. An increase in the height of the barriers to internal rotation with increase in ε for the medium has been established also for formamide on the basis of INDO and CNDO/2 calculations, allowing for the effect of the medium in the solvaton formalism.[48, 67] The calculated results are acceptably consistent with the experimental determination of the barrier to internal rotation round the C–N bond in amides.[48, 68–70] For example, the barriers to rotation in formamide found by NMR increase from 70 to 80 kJ mol^{-1} when the compound is transferred from a nonpolar solvent (ε = 2) to water (ε = 80), whereas the calculated values increase from 87 to 90–100 kJ mol^{-1} when ε increases from 1 to 40 (see Ref. 48).

Table 10. Dipole moments and total energies (E/a.u.) of uracil and 4-hydroxyuracil in media of different polarities (INDO-solvatons method[48]).

ε	Uracil		4-Hydroxyuracil	
	μ	$-E$	μ	$-E$
1	4.26	86.45815	4.61	86.45140
8	4.46	86.48542	4.78	86.49878
80	4.55	86.49794	4.86	86.52064

IV. Molecular and ionic forms of H complexes in media with different dielectric permittivities

Compounds which are easily polarised in solutions include complexes with an intermolecular hydrogen bond, formed by acids AH and bases B and existing in a molecular (AH · B) or an ionic form (A^-HB^+). In the molecular form we observe intermolecular charge transfer from the B molecule to the AH molecule, acting as electron n-donor and σ-acceptor respectively,[71–74] whereas in the ionic form proton transfer from the AH to the B molecule takes place, with formation of an ion pair. Problems concerning the role of charge transfer in the stabilisation of the molecular forms of H complexes and the role of the effect of the polarity of the medium on the transfer of a proton and on the formation of ionic forms have been widely discussed in the literature on the nature of the hydrogen bond. The many theoretical and experimental approaches aimed at solving these problems have been examined in depth in a series of recently published monographs and reviews.[14, 16, 75–81]

There are two fundamentally different ways of describing the hydrogen bond. According to the first[14, 75, 76, 80] the molecular forms of H complexes are stabilised only through the electrostatic interaction of the component molecules, and the substantial increase in the dipole moment resulting from the formation of the H complexes is attributed to the equilibrium between the low-polarity molecular form and the high-polarity ionic form:

$$AH + B \rightleftarrows AH \cdot B \rightleftarrows A^-HB^+ . \qquad (15)$$

According to the second concept of the hydrogen bond,[71–74] based on the EDA interaction between the AH and the B molecule, the increase in μ accompanying the formation of the H complexes is due to the intermolecular charge transfer or to the shift of electron density from B to AH. Evidence in favour of this interpretation is provided by the experimentally[71, 72] and theoretically well established[73, 74] linear relationship between the energy (ΔE_c) or enthalpy (ΔH_c) of formation of the H complexes and the extent of the charge transfer (Δq_{ct}) in low-polarity media. However, as regards the equilibrium (15), the ionic forms have never been observed in the gas phase or in low polarity media.[17] The erroneous conclusions stipulating the presence of this equilibrium are often based on the observation of two minima on the potential curves. However, in amine–hydrogen halide systems in a vacuum it has been shown that two minima can be obtained on the potential curve even in very strict nonempirical calculations if no allowance is made for the electronic correlations or for the dispersion interaction of the component molecules.[82–84] Allowance for electron correlations results in the merging of the two minima into a single, wide minimum, corresponding to the molecular form of the H complex. Zundel and coworkers have shown[16, 85, 86] that the second minimum experimentally found on the potential curves of AH · B systems is due to the polarising effect of the solvent.

Quantum-chemical calculations on systems with H bonds, allowing for the solvent,[15, 19, 21, 87–89] have shown that changing from the gas phase to a polar medium has a marked effect on the shape of the potential curves, consistent with the change in electronic and geometrical structure resulting from complex formation. As shown by the increase in the μ value for the H complexes, and as in the case of individual molecules, the charge separation under the influence of the medium is greatest in media with the highest dielectric permittivity. For example, the dipole moment of the complex $Bu_3N \cdot HCl$ increases from 8 to 13 D as ε for the medium is increased from 2.3 to 35, the μ and ε values being related by the expression[19]

$$\mu = 13.6 - \frac{12.7}{\varepsilon} \quad (r = 0.985) . \qquad (16)$$

The intermolecular charge transfer (Δq_{ct}) calculated for μ = 8 D and the enthalpy of formation of the complex $Bu_3N \cdot HCl$ in benzene (ε = 2.3) satisfy the linear relation between ΔH_c^0 and Δq_{ct}

which characterises the EDA complexes.[72] The value 8 D agrees well with the μ value (7.2 D) calculated by the CNDO/2 method for the model complex $Me_3N \cdot HCl$ in the gas phase, which gives only one minimum on the potential curve (for $\varepsilon = 1$, Fig. 3*a*). In the same figure we show the potential curves calculated with allowance for the effect of the medium by the solvaton model. Under these conditions a second minimum appears on the potential curves: it corresponds to the ionic form, and its depth increases with the ε value for the medium. The calculations for the molecular and the ionic form of the complex indicate large differences between their geometric (and their charge) characteristics (Table 11). The N–Cl distance in the molecular form is much shorter than in the ionic form. Whereas the binding of the HCl molecule in the $Me_3N \cdot HCl$ complex lengthens the H–Cl bond by only 0.14 Å the H–Cl distance in the ionised complex reaches 2.3 Å. Essentially this implies the breaking of the H–Cl bond, as shown by the decrease in its population (P_{H-Cl}) almost to zero. The intermolecular distance N...H in the molecular complex is 0.2 Å longer than the corresponding distance in the ionic form, whose value is close to the length of the N–H bond in the Me_3NH^+ ion. The binding Me_3N and HCl molecules into a molecular complex lowers the population of the orbital of the unshared pair (P_{up}) on the N atom and increases P_{up} for the Cl atom (calculated as already described[90]) by an amount close to Δq_{ct}. This state of affairs is consistent with the normal behaviour of molecular H complexes with charge transfer from the unshared pair (UP) of the hetero-atom in the donor molecule to the electronegative atom attached to the proton in the acid. The transition to the ionic form increases P_{up} for the Cl atom to a value corresponding to the formation of a Cl^- ion. As could have been expected in this type of complex,[90] the population of the N...H bond is substantially less than unity, but in the ionic form it is very close to unity. The same is true of the charge on the Cl atom (q_{Cl}). However, the q_{Cl} value in $Me_3NH^+Cl^-$ is less than unity by approximately 0.15, and the μ value (13.03 D) is smaller than the value calculated for the contact ion pair with unit charges on the cation and the anion (16.3 D for $r_{N-Cl} = 3.4$ Å). This suggests the presence of interionic charge transfer from the Cl^- anion to the Me_3NH^+ cation.[91, 92] We note that μ for the ionic form is close to the value given by Eqn (16) for $Bu_3N \cdot HCl$ with $\varepsilon \to \infty$.

Table 11. Parameters of the molecular and the ionic forms of the $Me_3N \cdot HCl$ complex and of their components, calculated by the CNDO/2 method.[19]

Parameter	$Me_3N \cdot HCl$	$Me_3NH^+Cl^-$	Me_3N	HCl	Me_3NH^+
r_{N-Cl}/Å	2.75	3.40	–	–	–
r_{N-H}/Å	1.31	1.10	–	–	1.08
r_{H-Cl}/Å	1.44	2.30	–	1.30	–
q_{Cl}	−0.42	−0.86	–	−0.09	–
P_{N-H}	0.24	0.85	–	–	–
P_{H-Cl}	0.70	0.05	–	0.99	–
P_{up} (N)	1.72	1.39	1.94	–	–
P_{up} (Cl)	1.42	1.91	–	1.09	–
μ/D	7.17	13.04	1.43	2.48	0.48
Δq_{ct}	0.27	–	–	–	–
$-\Delta E_c$/ kJ mol^{-1}	115	–	–	–	–

The results in Table 12 shows that the μ values of both the molecular and the ionic form of the H complex increase with the ε value of the medium: this is due mainly to an increase in the level of intermolecular charge transfer, and also to an increase in the level of charge separation.[90, 91] An increase in Δq_{ct} (and therefore in ΔH_c) for the complexes with a Y...H–X intermolecular hydrogen bond (where Y is the heteroatom with an UP in the B molecule and X is the electronegative atom bound to the H atom in the acid molecule) shortens the Y...H distances and lengthens the X–H bond. These changes in the geometry of the H complexes are observed also when the increase in Δq_{ct} is due to an increase in the polarity of the medium, as shown in particular by *ab initio*

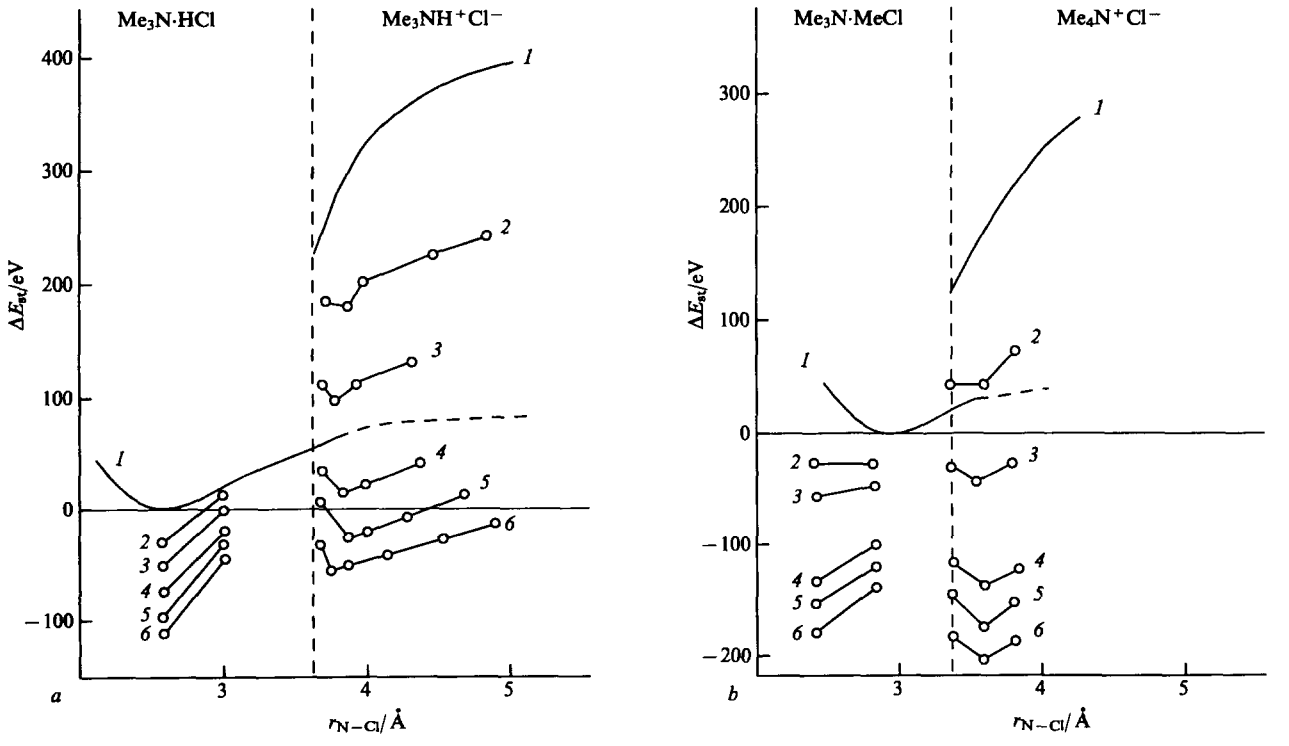


Figure 3. Plots of ΔE_{st} against r_{N-Cl} for Me_3NHCl (*a*) and Me_4NCl (*b*) in media with different ε: (*1*) 1; (*2*) 1.5; (*3*) 2.3; (*4*) 5.6; (*5*) 10; (*6*) 40.

Table 12. Dipole moments (μ/ D), charges on the Cl atoms (q_{Cl}), stabilisation energies (ΔE_{st}/ kJ mol^{-1}) of the molecular and the ionic forms of the complex of Me_3N with HCl contributed by the medium, and energies of interaction with the medium (ΔE_{int}) as a function of ε (CNDO/2 and CNDO/2–solvatons methods[19]).

ε	$Me_3N{\cdot}HCl$ (r_{N-Cl} = 2.75 Å)			$Me_3NH^+Cl^-$ (r_{N-Cl} = 3.4 Å)			
	μ	$-q_{Cl}$	$\Delta E_{st} - \Delta E_{int}$	μ	$-q_{Cl}$	ΔE_{st}	E_{int}
1	7.17	0.42	0	13.04	0.78	–	–
2.3	6.78	0.52	−40	14.25	0.90	118	−165
5.6	7.34	0.57	−74	14.68	0.93	24	−237
10	–	–	–	14.77	0.94	−3	−280
20	7.34	0.58	−97	14.83	0.94	−26	−309
40	7.39	0.59	−99	14.86	0.94	−36	−319

calculations[21] allowing for the effect of the medium in the SCRF formalism for the $Me_nH_{3-n}N{\cdot}HX$ series of model complexes, where X = F, Cl, or Br, and n = 0–3.[21] In the gas phase the energy of formation of these complexes (ΔE_c) increases with n in the series Br > Cl > F. The N–H distances decrease in the same sequence, and the H–X bonds become longer. However, even in the most stable complexes (n = 3, X = Br, Cl) the r_{N-H} lengths do not reach the very low values found in the $Me_nH_{4-n}N^+$ cations.

Allowing for the polarising effect of the medium shortens r_{N-H} and lengthens r_{H-X} in all the complexes by an amount which increases with ε for the medium. Conversion of the molecular complexes into the ionic form $Me_nH_{4-n}N^+X^-$ was observed only for X = Cl or Br and in media of relatively high polarity ($\varepsilon > 10$), the $Me_nH_{3-n}N{\cdot}HCl$ complexes giving the ionic form less readily than their HBr analogues. An analysis of the potential curves (Fig. 3) shows that the change from the gas phase to a polar medium stabilises the ionic form only when $\varepsilon > 10$. This effect is caused by the need to expend energy in rearranging the molecular structure into an ionic structure (mainly, in breaking the H–X bond). These energies are quite substantial: for example, 283 kJ mol^{-1} for $Me_3N{\cdot}HCl$.[19] The total stabilisation energy (ΔE_{st}) resulting from the change from the gas to a solution can be expressed as the sum of terms for the rearrangement (ΔE_r) and for the interaction with the medium (ΔE_{int}):

$$\Delta E_{st} = \Delta E_r + \Delta E_{int} . \quad (17)$$

The energy of the electrostatic interaction with the medium is higher for the more polar ionic form of the complex than for the molecular form, but in both forms $-\Delta E_{int}$ increases with the ε value of the medium as it does in the individual molecules (Table 12). The lack of stabilisation of the ionic forms in media with $\varepsilon < 10$ is due to the fact that in these cases $|\Delta E_r| > |\Delta E_{int}|$.

V. Electronic structure of salts in media with different polarities

Studies of the simplest members of this class of compounds, such as the alkali metal halides and the tetra-alkylammonium salts,[19, 90–93] have shown that in the gas phase and in nonpolar solvents their dipole moments are much lower and their interionic distances are much shorter than the values expected for ion pairs (Table 13). An attempt to explain these differences by the mutual polarisation of ions model[94] was unsuccessful, as can be seen by comparing the experimental values of the dipole moments observed in the gas phase (Table 13) with those calculated for the ion pairs (μ_{ip}) by the equation

$$\mu_{ip} = er^3\left[1 - \frac{r(\alpha_+ + \alpha_-) + 4\alpha_+\alpha_-}{r^6 - 4\alpha_+\alpha_-}\right] . \quad (18)$$

Mulliken's model, which treats the ion pairs as EDA complexes in which the anion acts as the electron donor and the cation as the electron acceptor,[95] proved more successful. This approach accounted for the decrease in μ for the ion pair in terms of the oppositely oriented dipole moment resulting from the interionic charge transfer, and the shortening of the bond between the ions was ascribed to the additional stabilisation of the pair.

Calculations on the LiCl and Me_4 NCl molecules by CNDO/2 method (in a vacuum) with full optimisation of the geometry showed[90] that in both compounds the charges on the Cl atoms (q_{Cl}) are close to 0.5 of a unit charge, and the dipole moments and interionic distances are much lower than those expected for ion pairs. Under these conditions the distance between the C and Cl atoms in Me_4NCl (Table 14) is almost equal to the sum of their covalent radii (0.99 Å for Cl and 0.77 Å for C), and the N–C distance exceeds the sum of the covalent radii of C and N (1.47 Å)

Table 13. Dipole moments (μ_r/ D) and interatomic distances (r_r/ Å) of the alkali metal halides measured in the gas phase, and values of these parameters expected for contact ion pairs (μ_{ip}, r_{ip}).[93]

Compound	μ_r/ D	r_r/ Å	$\mu_{ip} = er_r$	$r_{ip} = r_+ + r_-$	$\mu_{ip} = er_{ip}$	μ_{ip}[a]
1. LiF	6.30	1.56	7.49	2.01	9.65	7.97
2. LiCl	7.12	2.02	9.70	2.57	12.34	10.51
3. LiBr	7.27	2.17	10.42	2.75	13.20	11.38
4. LiI	7.43	2.39	11.48	3.02	14.50	12.62
5. NaF	8.16	1.93	9.27	2.31	11.09	9.70
6. NaCl	9.00	2.36	11.34	2.81	13.49	12.00
7. NaBr	9.12	2.50	12.01	2.98	14.30	12.77
8. NaI	9.24	2.71	13.02	3.23	15.50	13.87
9. KF	8.6	2.17	10.42	2.66	12.77	10.85
10. KCl	10.27	2.67	12.82	3.14	15.07	13.44
11. KBr	10.41	2.82	13.54	3.29	15.79	14.21
12. KI	8.5	3.05	14.65	3.53	16.94	14.16

[a] Calculated by Eqn (18).

Table 14. Parameters of the molecular and the ionic forms of the Me_4NCl complex, of the Me_3N and MeCl molecules, and of the Me_4N^+ cation (CNDO/2 method).[19]

Parameter	Me_4NCl	$Me_4N^+Cl^-$	Me_3N	MeCl	Me_4N^+
r_{N-Cl}/Å	3.40	3.80	–	–	–
r_{N-C}/Å	1.63	1.50	1.41	–	1.43
r_{C-Cl}/Å	1.77	2.30	–	1.68	–
HCH angle[a]/deg	120	107	–	110.9	107.3
q_{Cl}	−0.46	−0.91	–	−0.14	–
P_{N-C}	0.55	0.74	–	–	–
P_{C-Cl}	0.76	0.09	–	0.98	–
P_{up} (N)	1.66	1.36	1.94	–	–
P_{up} (Cl)	1.37	1.99	–	1.05	–
μ/D	8.64	15.2	1.43	3.06	–
q_{ct}	0.274	–	–	–	–
$-\Delta E_c$/kJ mol^{-1}	28	–	–	–	–
$-\Delta E_c$[b]/kJ mol^{-1}	141	–	–	–	–

[a] The quoted angle is for the C atom directly attached to the Cl atom.
[b] Energy of the rearrangement of MeCl during the formation of a complex with Me_3N.

by only 0.16 Å. All these observations indicate a molecular (rather than an ionic) structure for the compounds in the gas phase and in nonpolar solvents.

The R_4NX compounds are electronic analogues of the $R_3N \cdot HX$ H complexes. In particular, the potential curves for Me_3NHCl and Me_4NCl (Fig. 3) are identical. Both gas-phase curves show a single minimum which in the case of Me_4NCl can be assigned to the molecular $Me_3N \cdot MeCl$ $n\sigma$ complex, with the alkyl halide acting (like HCl) as a σ acceptor. The geometric and the charge characteristics of the N–C and C–Cl bonds, calculated by the CNDO/2 method in a vacuum with full optimisation of the geometry of Me_4NCl (Fig. 3*b*, minimum on curve *1*), are also consistent with the EDA interpretation of the N...C–Cl bond and with the assumed analogy of this bond with the N...H–Cl bond in $Me_3N \cdot HCl$. Comparing the data in Tables 11 and 14 shows that the C–Cl (or H–Cl) bonds in the σ-acceptor molecules MeCl (or HCl) are only slightly stretched by the formation of molecular complexes with Me_3N, and that their population, though decreased, remains close to 1, whereas the population of intermolecular N–C and N–H is substantially less than 1. In the ionic structures the geometric and the charge characteristics of the N–C, C–Cl, N–H, and H–Cl bonds are markedly different. The C–Cl and H–Cl bonds are effectively broken, as shown by their elongation to 2.3 Å and by the decrease of their population to practically zero. Under these conditions the N–C and N–H bonds are shortened to values close to the r_{N-C} or r_{N-H} distances in the cations Me_4N^+ or Me_3NH^+ respectively.

The binding of the MeCl molecule in a complex with Me_3N is accompanied by an increase in the HCH bond angle from 111° to 120°, while the N–C–Cl fragment ion in the molecular complex adopts a trigonal bipyramidal structure with a planar CH_3 group, corresponding to sp^2 hybridisation of the C atom. This rearrangement of the MeCl molecule requires an energy expenditure of ~113 kJ mol^{-1}, which explains the much lower energy of formation of the $Me_3N \cdot MeCl$ complex (as compared with $Me_3N \cdot HCl$) for similar Δq_{ct} values of the two complexes. Applying a correction for the rearrangement energy gives similar values of ΔE_c (Tables 11 and 14). The conversion of the $Me_3N \cdot MeCl$ complex into the ionic form decreases the HCH angle in the methyl group to 107°, corresponding to the Me_4N^+ cation with a Walden inversion of the carbon tetrahedron relative to the methyl group in the free MeCl molecule.

As in the case of the $Me_3N \cdot HCl$ complex (Table 14) the dipole moments of the molecular and of the ionic form of Me_4NCl increase with the polarity of the medium (Table 15) as a result of the increase in the intermolecular charge transfer in the former and of the decrease in the interionic charge transfer in the latter. Corresponding increases in the energy of the electrostatic interaction with the medium take place: these are substantially higher for the more polar ionic form than for the molecular form. The energy of the rearrangement of the molecular structure $Me_3N \cdot MeCl$ into the ionic structure (151 kJ mol^{-1}) is substantially lower than for $Me_3N \cdot HCl$ (283 kJ mol^{-1}), and therefore the stabilising effect of the polar medium is higher in the former than in the latter (see Fig. 3). Whereas in Me_4NCl the minimum for the ionic form is deeper than that of the molecular form when $\varepsilon > 5.6$, in Me_3NHCl the effect is not observed even for $\varepsilon = 40$.[19] The validity of the theoretical predictions has been confirmed by a dielectrometric and conductimetric study of R_4NX (X = Cl or Br) and $R_3N \cdot HCl$.[19, 90, 91]

Studies of several organic chlorides and hexachloroantimonates[90, 91, 96–98] by the dielectrometry of conducting media method[92] showed that as ε for the solvent is increased from 2 to 10 the dipole moments of the salts rapidly increase to values of the same order as μ_{ip} for $\varepsilon = 35$, the dependence of μ on $1/\varepsilon$ taking the linear form

$$\mu = \mu_{ip} - \frac{A}{\varepsilon}. \qquad (19)$$

The parameter A characterises the sensitivity of the electronic structure of the given salt to the polarising effect of the medium. In the light of the theoretical ideas discussed above this type of dependence [Eqn (19)] can be explained by a transition from a molecular $n\sigma$ or $n\nu$ complex (a halogen complex of a metal with an n donor in Mulliken's terminology) to a complex with interionic charge transfer, followed by charge separation up to the formation of contact ion pairs with unit charges on the cation and the anion. Whereas the quaternary ammonium halides in nonpolar solvents have an $n\sigma$ complex structure the molecular

Table 15. Dipole moments (μ/D), charges on the Cl atoms, stabilisation energies (ΔE_{st}/kJ mol^{-1}) of the molecular and the ionic forms of the complex of Me_3N with MeCl provided by the medium, and energies of the interaction with the medium (ΔE_{int}) as a function of ε (CNDO/2-solvatons method[19]).

No.	ε	$Me_3N \cdot MeCl$ (r_{N-Cl} = 3.4 Å)			$Me_4N^+Cl^-$ (r_{N-Cl} = 3.8 Å)			
		μ	$-q_{Cl}$	$\Delta E_{st} \approx \Delta E_{int}$	μ	$-q_{Cl}$	ΔE_{st}	ΔE_{int}
1	1[a]	8.69	0.46	0	15.24	0.91	–	–
2	1.5	8.93	0.52	−28	16.21	0.95	46	−105
3	2.3	9.44	0.56	−58	16.59	0.97	−39	−190
4	5.6	10.65	0.64	−101	16.93	0.98	−141	−292
5	10	10.22	0.63	−123	17.02	0.99	−173	−324
6	20	10.35	0.64	−136	17.08	0.99	−194	−345
7	40	10.42	0.65	−143	17.11	0.99	−205	−356
8	80	10.45	0.65	−146	–	–	–	–

[a] Gas phase

form of the hexachloroantimonates is an $n\nu$ complex in which the intermolecular bond is formed by the UP of the Cl atom, bound to the cation, and the unoccupied sp^3d^2 orbital of the $SbCl_5$ molecule, known as a very strong V electron acceptor.[17, 58] The similarity of the electronic structure and of its changes under the influence of a polar medium which we have established for the salts and the H complexes offers the possibility of a unified treatment of the mechanism of two types of reaction: the bimolecular nucleophilic substitution (S_N2) and the proton transfer reaction in solutions, by the interaction of bases B with alkyl halides X–C in the first case and with bases A–H in the second:

$$X-C + B = C-B^+ + X^- , \quad (20)$$

$$A-H + B = H-B^+ + A^- . \quad (21)$$

In both these reactions two types of complex behave as intermediates: molecular (X–C...B or A–H...B) and ionic ($X^-...C-B^+$ or $A^-...H-B^+$). The reactions (20) and (21) produce a transition from molecular to ionic complexes by surmounting an activation barrier as the system moves along the reaction coordinate.[2]

Molecular complexes stable in the gas phase and in low-polarity solvents are formed by intermolecular charge transfer from the electron donor B to the electron acceptor (alkyl halide or acid). The complete transfer of an electron from the molecule B to the alkyl halide or acid, accompanied by the breaking of the X–C or A–H bond and by the addition of an alkyl radical or of a proton to the B molecule, leads to ionic complexes, stabilised mainly by the contribution from the interionic charge transfer. The formation of an ionic complex is a necessary precursor of the appearance of free ions.[87]

The conversion of a molecular complex into the ionic form is accomplished by using the energy of the interaction of the molecular complex with the polar solvent (ΔE_{int}), which increases with the ε value of the medium.

When ΔE_{int} exceeds ΔE_r the ionic complex becomes more stable than the molecular, the dissociation into free ions becomes possible. The dielectric permittivity (ε) of the solvent for which dissociation is possible depends on the properties of the system, as can be seen from the results of the experimental and theoretical study of the tri- and tetra-alkylammonium halides discussed above.

The important role of the polarising effect of the medium in controlling reactions such as (20) is underlined by a study of the interaction of various azoles with alkyl halides.[98] The stable products of this reaction in low-polarity solvents are molecular $n\sigma$ complexes, and in more polar solvents they are quaternary azolium salts. The quaternisation of azoles (like that of tertiary amines) during their interaction with alkyl halides is accompanied by Walden inversion of the tetrahedron of carbon atoms, which contributes to the formation of N–C bonds in the azolium cation. This is preceded by the formation of a molecular complex having a structure close to trigonal bipyramidal. Evidence for the EDA nature of the interaction of azoles with alkyl halides comes from the fact that only one of the several N atoms in the azole heterocycles acts as a reaction centre: it has n-donor properties, whose theoretically calculated indices for a series of azoles of different structure are linearly correlated with the logarithms of the rate constants of their interaction with methyl iodide in acetonitrile.

VI. Conclusions

The above discussion demonstrates the importance of effects from the polar medium in determining the distribution of electron density and the energetics of the molecules dissolved in the medium. Obviously, the mechanisms of liquid-phase processes cannot be described correctly without allowing for this effect.

The charge separation in the solute molecules and the stabilisation of their more polar forms under the influence of polar media are reflected in the changes of their physicochemical characteristics, which play an important role in many processes taking place in solutions. The shift of tautomeric or conformational equilibria towards the more polar forms and the increase in the rate constant of S_N2 or proton transfer reactions in solvents with a high dielectric permittivity are largely the result of an increase in the charge separation and in the stabilisation energy of the reacting molecules, of the intermediates, or of the reaction products. Processes involving the conversion of various compounds from the molecular into the ionic form take place at a reasonably high rate only in highly polar solvents, which induce an effective charge separation in the relevant molecules up to the formation of ion pairs.

Obviously, liquid-phase processes cannot be correctly described without allowing for these factors. We must therefore take careful note of the results and conclusions of theoretical studies of the mechanisms and kinetics of reactions in solutions which allow for solvation effects only in the approximation of structurally rigid reactant molecules.

References

1. R R Dogonadze et al. (Eds) *The Chemical Physics of Solvation* Part A (Amsterdam: Elsevier, 1985)
2. B Ya Simkin, I I Sheikhet *Kvantovokhimicheskaya Statisticheskaya Teoriya Rastvorov* (Quantum-chemical Statistical Theory of Solutions) (Moscow: Khimiya, 1989)
3. B Ya Simkin, I I Sheikhet, in *Fizicheskaya Khimiya. Sovremennye Problemy* (Modern Problems in Physical Chemistry) (Ed. Y M Kolotyrkin) (Moscow: Khimiya, 1983) p. 148
4. B J Simkin, I I Sheikhet *J. Mol. Liquids* **27** 79 (1983)
5. N A Smirnova *Molekulyarnaya Teoriya Rastvorov* (Molecular Theory of Solutions) (Leningrad: Khimiya, 1987)
6. G A Krestov (Ed.) *Sovremennye Problemy Khimii Rastvorov* (Modern Problems in Solution Chemistry) (Moscow: Nauka, 1986)
7. G A Krestov (Ed.) *Rastvory Neelektrolitov v Zhidkostyakh* (Solutions of Nonelectrolytes in Liquids) (Moscow: Nauka, 1989)
8. G A Krestov (Ed.) *Kompleksoobrazovanie v Rastvorakh* (Complex Formation in Solutions) (Moscow: Nauka, 1989)
9. K Burger *Solvation, Ionic Reactions, and Complex Formation in Nonaqueous Solutions* (Translated into Russian) (Moscow: Mir, 1984)
10. B Bogchi *Adv. Rev. Phys. Chem.* **40** 115 (1989)
11. E M Kosower, E V Huppert *Ann. Rev. Phys. Chem.* **37** 127 (1986)
12. P F Barbara, W Jarerta *Acc. Chem. Res.* **21** 195 (1988)
13. E Arnett *J. Chem. Educ.* **62** 385 (1985)
14. H Ratajczak (Ed.) *Molecular Interactions* (New York: Wiley, 1980) Vol. 1
15. P Th Duijen, B T Thole, in *Quantum Theory of Chemical Reactions* (Eds R Daudel et al.) (Dordrecht: Reidel, 1983) Vol. 3, p. 85
16. R Daudel et al. (Eds) *Quantum Theory of Chemical Reactions* (Dordrecht: Reidel, 1983) Vol. 3
17. Z Powelka *Acta Univ. Wratisl.* **692** 5 (1986)
18. I P Gol'dshtein, I E Paleeva, S I Gryzlov, O V Braverman, T A Pestova, E N Gur'yanova *Zh. Fiz. Khim.* **62** 3333 (1988)
19. I P Gol'dshtein, O V Braverman, I A Abronin, A N Fedotov, E N Gur'yanova *Zh. Obshch. Khim.* **58** 138 (1988)
20. R Sahai, P C Paude, V Singh *Indian J. Chem. A* **18** 211 (1979)
21. J Y Kuring, S Scheiner *Int. J. Quantum Chem.* **14** 47 (1987)
22. I A Abronin, K Ya Burshtein, G M Zhidomirov *Zh. Strukt. Khim.* **21** 145 (1980)
23. L G Gorb, I A Abronin, N V Kharchevnikov, G M Zhidomirov *Zh. Fiz. Khim.* **58** 9 (1984)
24. K Vaiss, I A Abronin *Izv. Akad. Nauk SSSR, Ser. Khim.* 364 (1984)
25. G Klopman *Chem. Phys. Lett.* 1 200 (1967)
26. G Klopman, P Andreozzi *Theor. Chim. Acta* **55** 77 (1980)
27. H A Jermer Jr *Theor. Chim. Acta* **35** 273 (1974)
28. H A Jermer Jr *Theor. Chim. Acta* **34** 145 (1974)
29. S Miertuš, O Kysel *Chem. Phys.* **21** 27 (1977)
30. S Miertuš, E Scroccj, J Tomasi *Chem. Phys.* **55** 177 (1981)
31. S Miertuš, J Tomasi *Chem. Phys.* **65** 239 (1982)
32. A Y Duben, S Miertuš *Chem. Phys. Lett.* **88** 395 (1982)
33. R Cimiraglia, S Miertuš, J Tomasi *Chem. Phys. Lett.* **80** 286 (1981)

34. R Bonaccorsi, R Cimiraglia, J Tomasi *J. Comput. Chem.* **4** 567 (1983)
35. R Bonaccorsi, P Palla, J Tomasi *J. Am. Chem. Soc.* **106** 1945 (1984)
36. K Ya Burshtein *J. Mol. Struct.* **153** 195 (1987)
37. R Constancial *Theor. Chim. Acta* **54** 123 (1980); **69** 505 (1986)
38. O Tapia, O Josciuski *Mol. Phys.* **29** 1653 (1975)
39. R Constancial, O Tapia *Theor. Chim. Acta* **48** 75 (1978)
40. O Tapia, B Silvi *J. Phys. Chem.* **84** 2646 (1980)
41. O Tapia, G Johannin *J. Chem. Phys.* **75** 3624 (1981)
42. J E Sanhuesa, O Tapia *J. Mol. Struct.* **89** 131 (1982)
43. J Langlet, P Claveric, J Cailett, A Pulman *J. Phys. Chem.* **92** 1617 (1988)
44. H Hochi, S Sacurai *J. Chem. Phys.* **87** 1107 (1987)
45. H Hochi, M Sacurai, R Chujo *J. Mol. Struct.* **180** 267 (1988)
46. M Sacurai, H Hochi, J Inoul, R Chujo. *Bull. Chem. Soc. Jpn.* **63** 1335 (1990)
47. M V Bazilevskii, D V Napolov, G E Chudinov *Khim. Fiz.* **11** 691 (1992)
48. M Saunders, G A Webb *J. Mol. Struct.* **158** 69 (1987)
49. H A Jermer *J. Chem. Phys.* **58** 3524 (1973)
50. A Botrel, F Corre, A Le Benze *Chem. Phys.* **75** 383 (1983)
51. F Corre *J. Mol. Struct.* **86** 69 (1981)
52. M Witanowski, W Sicinska, G Webb *Magn. Reson. Chem.* **27** 380 (1989)
53. M Witanowski, J Sitkowski, S Biernat, B Kamienski, B Hangin, G Webb *Magn. Reson. Chem.* **25** 729 (1987)
54. M Witanowski, J Sitkowski, S Biernat, L V Sudha, G A Webb *Magn. Reson. Chem.* **23** 748 (1985)
55. M J Kamlet, J L Abond, R W Taft *Prog. Org. Chem.* **13** 485 (1980)
56. T Takajama, J Ando, T Asacura *Bull. Chem. Soc. Jpn.* **62** 1233 (1989)
57. S I Gryznov, I P Gol'dshtein *Zh. Fiz. Khim.* **63** 1637 (1989)
58. V Gutmann *Co-ordination Chemistry in Nonaqueous Solutions* (Translated into Russian) (Moscow: Mir, 1971)
59. J H Hildebrand, R L Scott *The Solubility of Nonelectrolytes* (New York: Dover, 1964)
60. V N Levchuk, I I Sheikhet, B Ya Simkin, I V Dorogan *Zh. Strukt. Khim.* **3** 75 (1990)
61. B N Solomonov, A N Konovalov *Zh. Obshch. Khim.* **55** 2529 (1985)
62. A N Fedotov, E S Isaeva, I P Gol'dshtein *Zh. Fiz. Khim.* **65** 2501 (1991)
63. W L Dilling *J. Org. Chem.* **31** 1045 (1966)
64. H Suzuki *Electronic Absorption, Spectra and Geometry of Organic Molecules* (New York: Academic Press, 1967)
65. O Exner *Dipole Moments in Organic Chemistry* (Stuttgart: Thieme, 1975)
66. D Shugar, K Szczepaniak *Int. J. Quantum Chem.* **20** 573 (1981)
67. A J Duben, S Miertuš *Theor. Chim. Acta* **60** 327 (1981)
68. A Calzolari, F Conti, C Franconi *J. Chem. Soc. B* 555 (1970)
69. W E Stewart, T H Siddal *Chem. Rev.* **70** 577 (1970)
70. W T Raynes, V A Raza *Mol. Phys.* **20** 334 (1971)
71. I P Gol'dshtein, E N Gur'yanova, T I Perepelkova *Zh. Obshch. Khim.* **42** 2091 (1972)
72. I P Gol'dshtein, T I Perepelkova, E H Gur'yanova *Dokl. Akad. Nauk SSSR* **226** 91 (1976)
73. I P Gol'dshtein, E S Shcherbakova, I A Misurkin, E N Gur'yanova *Fiz. Molekul* 51 (1980)
74. A E Read, F Weinhold, L A Curtiss, D J Pochatko *J. Chem. Phys.* **84** 5687 (1986)
75. H Ratajczak, W J Orville-Thomas (Eds) *Molecular Interactions* (Translated into Russian) (Moscow: Mir, 1984)
76. N D Sokolov (Ed.) *Vodorodnaya Svyaz'* (The Hydrogen Bond) (Moscow: Nauka, 1981)
77. B Pullman, P Schuster (Eds) *Molecular Interactions from Diatomics to Biopolymers* (Translated into Russian) (Moscow: Mir, 1981)
78. L M Epshtein, A V Iogansen *Usp. Khim.* **59** 229 (1990) [*Russ. Chem. Rev.* **59** 134 (1990)]
79. Z Sobczyc *J. Mol. Struct.*, **177** 111 (1988)
80. A C Legon, D J Millen *Acc. Chem. Res.* **20** 39 (1987)
81. J Zipinski *J. Mol. Struct.* **201** 87 (1989)
82. Z Latajka, S Sakai, K Morokuma, H Ratajczak *Chem. Phys. Lett.* **110** 464 (1984)
83. Z Latajka, S Scheiner, H Ratajczak *Chem. Phys. Lett.* **35** 5 (1987)
84. A Breiz, A Karpfen, H Lischka, P Schuster *J. Chem. Phys.* **89** 337 (1984)
85. U Bohner, G Zundel *J. Phys. Chem.* **90** 964 (1986)
86. G Zundel, Y Fritsch, in *Chemical Physics of Solvation* Part B (Eds R R Dogonadze et al.) (Amsterdam: Elsevier, 1986) Ch. 2
87. S Miertuš, Y Bartos *Collect. Czech. Chem. Commun.* **48** 2308 (1980)
88. O Tapia, F M Stamato, J G Smeyers *J. Mol. Struct.* **123** 67 (1985)
89. J E Sanhueza, O Tapia *J. Mol. Struct.* **131** 131 (1982)
90. I P Gol'dshtein, A N Fedotov, I A Misurkin *Zh. Obshch. Khim.* **56** 40 (1986)
91. I P Gol'dshtein, O V Braverman, I A Misurkin, E N Gur'yanova *Dokl. Akad. Nauk SSSR* **284** 150 (1985)
92. I P Gol'dshtein, O V Braverman, Yu V Podgornyi *Zh. Obshch. Khim.* **55** 2720 (1985)
93. G E Grunwald, S Higsneith, J Ting-Po, in *Organic Reactions* Vol. 2 (Ed. M Szwarc) (New York: Wiley Interscience, 1974) p. 448
94. C J F Böttcher *Theory of Electric Polarization* (Amsterdam: Elsevier, 1952)
95. R S Mulliken, W B Person *Molecular Complexes* (New York: Wiley Interscience, 1969)
96. I P Gol'dshtein, S I Gryzlov, O V Braverman *Dokl. Akad. Nauk SSSR* **305** 890
97. S I Gryzlov, I P Gol'dshtein, O V Braverman *Zh. Obshch. Khim.* **60** 2529 (1990)
98. I P Gol'dshtein, L D Khamaganova, A N Fedotov *Zh. Fiz. Khim.* **65** 959 (1991)

Russian Chemical Reviews **62** (7) 637–646 1993
© 1993 Russian Academy of Sciences and Turpion Ltd

UDC 546.725 + 546.94 + 546.95 + 547.3

Iron-subgroup metal carbonyls in reactions with olefins having functional group substituents

L V Rybin, M I Rybinskaya

Contents

I. Introduction 637
II. η^2-Olefin complexes of iron carbonyls. Synthesis and properties 637
III. Reactions of ruthenium and osmium carbonyl complexes with olefins having functional group substituents 644

Abstract. The review covers the results of studies on the reactions of iron, ruthenium, and osmium carbonyls with olefins having functional group substituents, the behaviour of which differs significantly from that of simple olefins. Such studies have made it possible to create a new aspect of the chemistry of olefin complexes. The development of this field has led to the synthesis of previously unknown mononuclear and polynuclear complexes and to the discovery of unusual rearrangements of the complex compounds. The reactions of iron carbonyls differ from those of ruthenium and osmium carbonyls. In the last case, the hapticity of the unsaturated ligands increases and the ligands are found to be capable of giving rise to extremely unexpected structures. The present review surveys mainly the results of studies by the authors, who made a significant contribution to the development of this field. The bibliography includes 73 references.

I. Introduction

η^2-Olefin complexes occupy a special position in the chemistry of organometallic compounds of transition metals as the simplest compounds with a metal–organic ligand π-bond. They have served as a model for the development of the theory of the π-complex linkage. Furthermore, they are key intermediates in the catalytic reactions of olefins in the presence of transition metal compounds. Studies on such complexes have promoted the development of ideas about the mechanisms of catalytic hydrogenation, isomerisation, carbonylation, oligomerisation, and polymerisation of olefins. The chemistry of olefin complexes has therefore attracted for many years the attention of investigators.[1, 2] However, attention has been concentrated on the study of the properties of the complexes with ethylene and its homologues and to a lesser extent the complexes with olefins containing functional group substituents.

In the course of a number of years, we have carried out systematic studies on the thermal reactions of iron carbonyls with olefins having functional group substituents XCH=CHY and showed that the electronic nature of the substituents influences significantly the course of the reactions and the formation of the complexes $Fe(CO)_4$ (η^2-olefin).

These investigations have also shown that the coordination of an olefin to the $Fe(CO)_4$ group increases the electron density at the double bonds and the functional group adjoining it. The chemical reactions of these groups in the complexes have been used successfully to achieve the transition from η^2-olefin compounds to η^3-allyl or η^3-elementaallyl compounds, which made it possible to develop methods of synthesis of previously unknown organoiron compounds and also to discover and investigate new types of haptotropic rearrangements.

In order to deduce the general pattern for all the iron-subgroup metals, we included in the reactions with olefins having functional group substituents also ruthenium and osmium carbonyls. It was found as a result that, in contrast to iron carbonyls, which readily form the mononuclear complexes $Fe(CO)_4$ (η^2-olefin), the less reactive ruthenium and osmium carbonyls react with α,β-unsaturated ketones and esters under severe thermal conditions to form polynuclear compounds. The reactions proceed non-selectively and frequently lead to multicomponent mixtures which are difficult to separate. The elucidation of the structures of the complexes formed proved to be extremely useful, because it throws light on the possibility of the coordination of a polymetallic fragment to the organic ligand. The ligand in the sphere of the polynuclear fragment not only undergoes an increase in its hapticity compared with the mononuclear complexes but also proves capable of giving rise to different and frequently unexpected structures.

The data obtained are of interest for the understanding of the mechanisms of catalysis on clusters and, what is particularly important, heterogeneous catalysis on metallic surfaces.

II. η^2-Olefin complexes of iron carbonyls. Synthesis and properties

1. Interaction of iron carbonyls with substituted olefins

β-Substituted unsaturated ketones, acids and their derivatives[3–17] as well as the vinyl compounds of transition metals, silicon, and germanium,[18–29] have been used in the reactions with iron carbonyls as mono- and di-substituted olefins: XCH=CHY, where X and (or) Y = COR, COOH, COOR, COCl, COF, CONRR′, C(=NR)OEt, $C^+(OEt)NR_2$, CONHNHR, CONRNR′CO, $CON^-N^+R_3$, Cl, I, SPh, SO_2R, NR_2, NO_2, CF_3, SiRR′R″, $GeRR'_2$, $CpFeC_5H_4$, $Fe(CO)_2Cp$, $W(CO)_3Cp$, $Re(CO)_5$, etc.

The majority of these mono- and disubstituted olefins form η^2-olefin complexes:

$$XCH{=}CHY + Fe_2(CO)_9 \longrightarrow Fe(CO)_4(\eta^2\text{-}CHX{=}CHY)\,.$$

In certain cases, the substituents at the double bond can influence significantly the mode of these reactions and the nature of the products formed. It has been established[8] that, depending on the electronic effects of the substituent X, the unsaturated

L V Rybin, M I Rybinskaya A N Nesmeyanov Institute of Organoelement Compounds, Russian Academy of Sciences, ul. Vavilova 28, 117813 Moscow. Fax (7-095) 135 50 85.

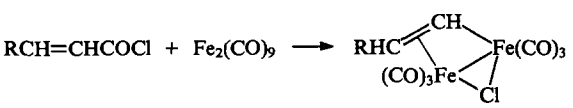
Received 15 April 1993
Uspekhi Khimii **62** (7) 680–689 (1993); translated by A K Grzybowski

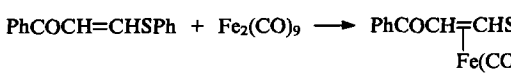
ketones RCOCH = CHX can give rise to qualitatively different results in reactions with iron carbonyls. When the substituent X is a strong electron-donating group, for example, the amino-group, a π-complex is not formed. When there are two strong electron-accepting groups at the double bond, as happens, for example, in β-nitrovinyl ketone, the reaction with iron carbonyls proceeds extremely vigorously but a polymeric product is formed. Vinyl ketones having substituents with stronger electron-donating or electron-accepting properties (X = Cl, H, COOR, etc.) form olefin complexes.

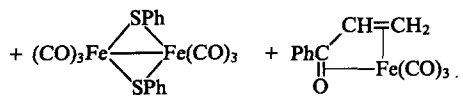
Such differences are determined by the difference between the energies of the lowest unoccupied π* orbital of the olefin and the 3*d* and 4*s* orbitals of iron. According to calculated data,[8] the unoccupied π* orbital is highest in amonovinyl ketone. For this reason, the formation of a π-complex by the latter is unlikely. The lowest orbital occurs in nitrovinyl ketone and in this instance there is a possibility of complete electron transfer from the metal to the ligand with subsequent polymerisation of the latter.

The energy of the π* orbitals in β-chlorovinyl ketone occupies an intermediate position, which ensures adequate reverse electron donation from the metal to the ligand and hence permits the formation of a stable π-bond.

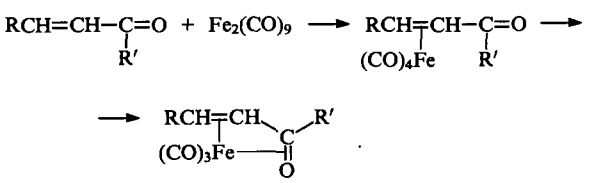
Certain substituents complicate the synthesis of η^2-olefin complexes by participating in reactions with iron carbonyls, for example:[14, 30]





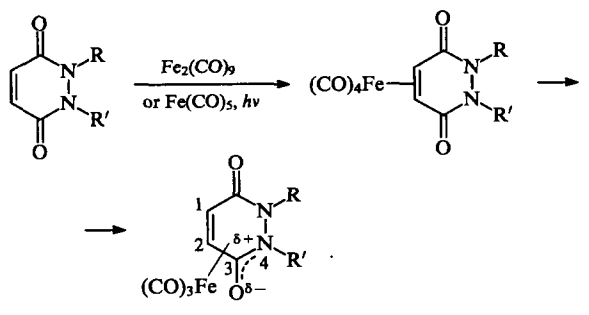


If the substituted olefins contain a heterodiene bond system, there is a possibility of the formation of heterodiene tricarbonyl complexes as a result of the $\eta^2 \rightarrow \eta^4$ transition in the initial η^2-olefin complexes:[5-9, 11, 31]



$\eta^2 \rightarrow \eta^4$ transition of this type have been observed also by other investigators.[32-34]

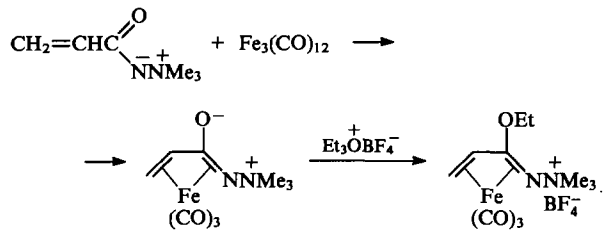
In the study of the reactions of unsaturated acid amides and related compounds with iron carbonyls, the possibility of the coordination of the metal to the amide fragment in the unsaturated ligand was demonstrated for the first time.[15] This was established unambiguously in the study of the reactions of cyclic maleic acid hydrazides with iron carbonyls.[17]



1

The structure of the η^4-complexes **1** was established by X-ray diffraction. The iron atom in complex **1** is linked to four neighbouring C(1), C(2), C(3), and N(4) ring atoms, i.e. the maleic acid hydrazide can be regarded as an azadiene ligand.

A stable η^4-complex of the azadiene type was also obtained for an open-chain compound, namely for the acrylic acid aminoimide.[15]



The interaction of the unsaturated acid amides themselves with iron carbonyls results in the formation, together with the complexes $Fe(CO)_4(\eta^2\text{-RCH}=\text{CHCONR'R''})$ as the main product of extremely unstable iron tricarbonyl compounds which can be characterised only with the aid of IR spectra. On the basis of the analogy between unsaturated amides, on the one hand, and maleic hydrazides and acrylic acid aminoimide on the other, one can postulate that the unstable $Fe(CO)_3$ complexes of unsaturated amides also have the η^4-azadiene structure. This hypothesis agrees with calculated data.[15]

2. The change in the properties of substituted olefins on π-coordination to zerovalent iron

Coordination to the iron carbonyl group entails significant changes in the electronic state, structural parameters, and reactivity of the η^2-olefin ligand with functional group substituents.

X-Ray diffraction study[35] of the complex $Fe(CO)_4$ (η^2-PhCOCH = CHCOPh) demonstrated a significant increase in the length of the coordinated double bond to 1.47 Å and a decrease in the bond angles of the olefinic carbon atoms by 5° – 6° (Fig. 1). These structural changes indicate a decrease in the order of the double bond and partial sp^2-sp^3-rehybridisation of the olefinic carbon atoms, which is probably a result of the significant back-donation of electrons from the metal to the ligand in such complexes. A similar conclusion can be arrived at by analysing the spectroscopic data for the complexes $Fe(CO)_4$ (η^2-XCH = CHY).

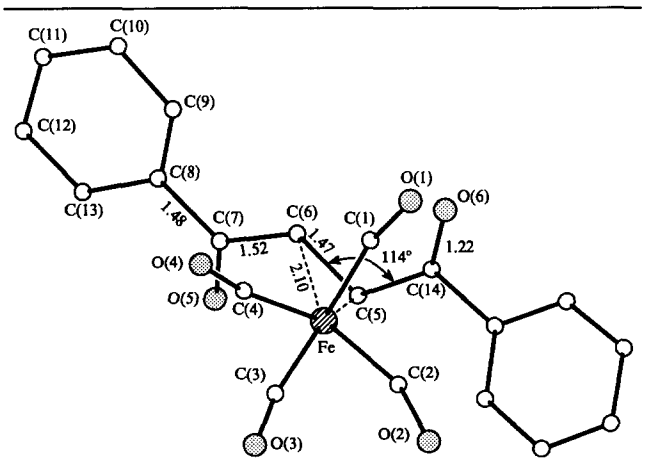
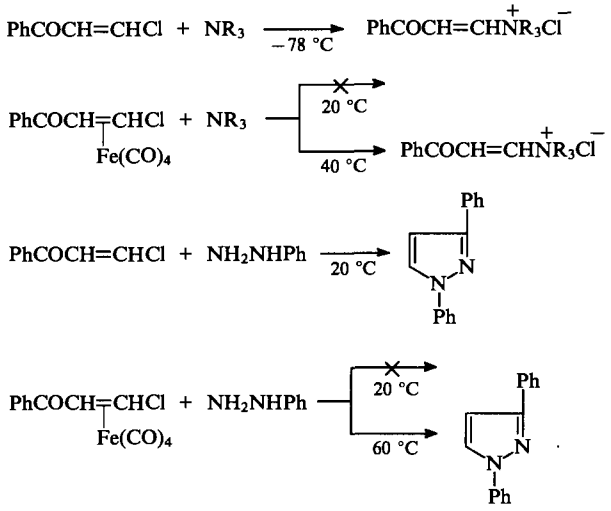


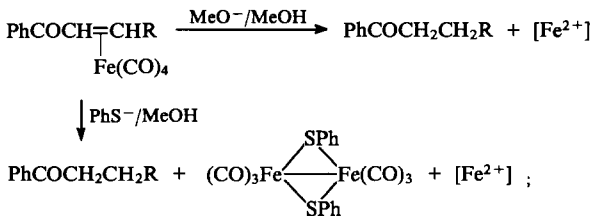
Figure 1. The structure of the $Fe(CO)_4(\eta^2\text{-PhCOCH}=\text{CHCOPh})$ molecule.

Such changes are reflected in the chemical properties of the olefin ligand and are manifested by a decrease in the electrophilicity of the double bond and of the functional groups in the ligand. For example, β-chlorovinyl ketones are known to react readily with nitrogen-containing bases,[36, 37] but their $Fe(CO)_4$ complexes are resistant under mild conditions to the action of these nucleophiles and the iron–olefin bond is ruptured only on heating.[16]



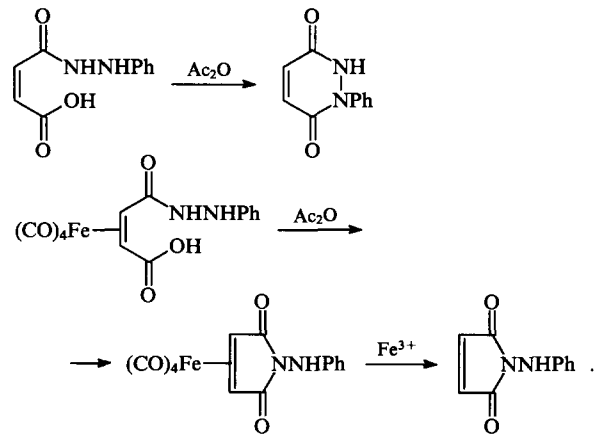
The cleavage of the π-bond accompanied by the reduction of the unsaturated ligand on treatment of stable olefin complexes with anionic nucleophiles has been observed.[30, 31]

Free β-substituted vinyl ketones combine with nucleophiles under these conditions.[38]



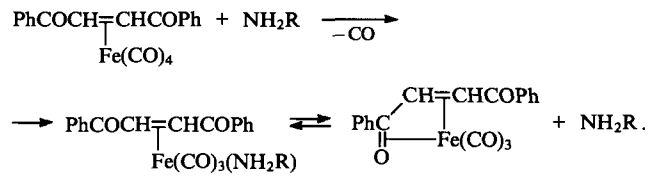
R = COPh, COOMe.

The change in the chemical properties of the unsaturated ligand on coordination to the $Fe(CO)_4$ group is manifested in the cyclisation of β-carboxyacryloylhydrazines: in the case of the substitution of the free olefin, six-membered rings are formed, whilst in the case of its $Fe(CO)_4$ complex the products are five-membered rings.[16]



This factor has been used for synthetic purposes in order to obtain substituted maleimides.

In addition, reactions due to the presence of iron carbonyl groups, for example, the reaction involving the substitution of CO ligands with retention of the metal–olefin bond, are characteristic of complexes of substituted olefins.[39]

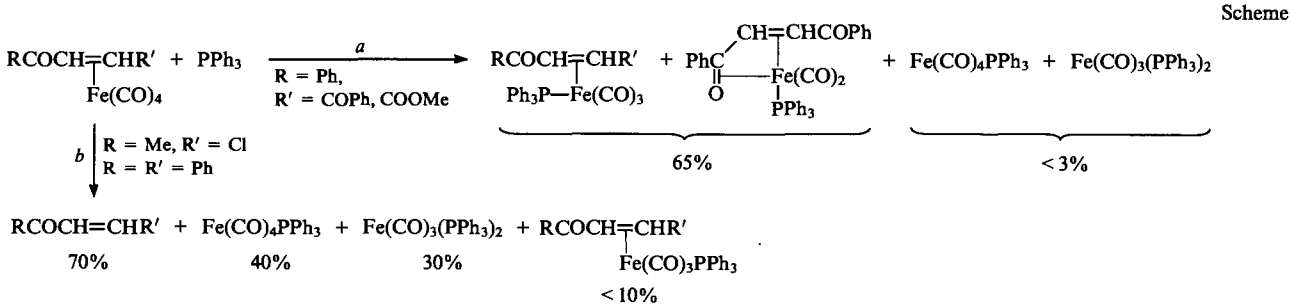


The reactions with triphenylphosphine may be used for the comparative characterisation of the strength of the Fe–CO and Fe–olefin bonds. It has been shown that the enhancement of the electron-accepting properties of the olefin and hence the increase in the strength of the π-bond alter the mode of the substitution reactions.[10] Thus the interaction of the complexes of α,β-dibenzoylethylene and methyl β-benzoylacrylate with PPh_3 results in the formation mainly of the products of the substitution of the CO ligand (Scheme 1, pathway *a*), whereas treatment of the less stable complexes of chalcone and methyl β-chlorovinyl ketone with phosphine leads to the preferential substitution of the unsaturated ligand (Scheme 1, pathway *b*).

3. The formation of the olefin, allyl, and elementaallyl structures in the iron carbonyl complexes. Haptotropic rearrangements.

The question of the interaction of the metal with the substituents is important in the study of complexes with substituted olefins. One can imagine two limiting cases: complexes of the η^2-olefin type **A** in which there is no such interaction and complexes **B** in which the metal is bound to the substituent.

Scheme 1





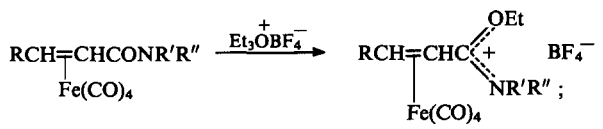
A B

In the general cases complexes **B** can be assigned to the η^3-allyl type if the metal is linked to X via a carbon atom, or to the η^3-elementaallyl type if the bond between the metal and the substituent X is formed via a non-carbon atom.

The question of the formation of the olefin and allyl structures has been investigated for complexes containing a positively charged substituent at the double bond. It was assumed that the degree of delocalisation of the charge can influence significantly the structure of such compounds.

a. Olefin complexes

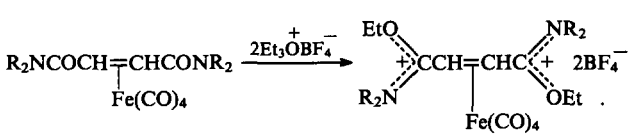
The olefin complexes with a positively charged substituent in the ligand can be synthesised by ethylating the amide group in the iron tetracarbonyl complexes of unsaturated acid amides.[40-42]



2

R = R′ = R″ = H; R = H, R′ = R″ = Me;
R = R′ = H, R″ = Me; R = Ph, R′ = R″ = H.

In the case of dibasic acid amides, dicationic complexes were obtained.



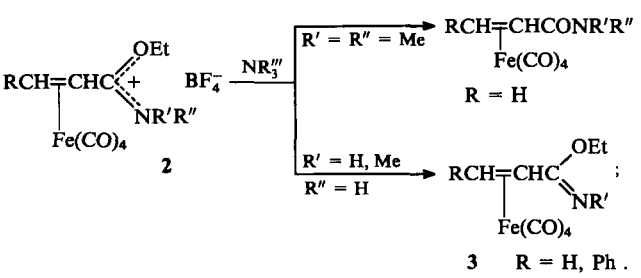
2a

Complexes **2** have the η^2-olefin structure. The signal of the α-carbon atom in the ^{13}C NMR spectra is significantly displaced downfield ($\delta \approx 180$ ppm) in comparison with the signals of olefinic carbon atoms (δ = 130–140 ppm), i.e. into the region characteristic of carbonium ions.

Complexes **2** were the first olefin complexes with a positively charged substituent.

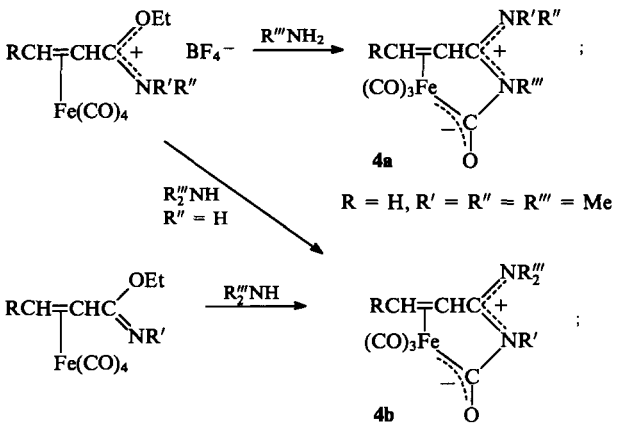
The reactions of complexes **2** with amines proceed with retention of the Fe–C(olefin) and Fe–C(carbonyl) bonds, which constitutes a fundamental difference between them and the reactions of the neutral olefin complexes of iron considered previously. Tertiary amines are dealkylating or deprotonating agents.

The deprotonation of the imidate group in the η^2-ligand in complexes **2** constitutes a method of synthesis of complexes of unsaturated acid iminoesters **3**. These complexes cannot be obtained directly from the iminoesters and iron carbonyls, whereas coordination to the $Fe(CO)_4$ group stabilises the unstable acrylic iminoesters.



2 **3** R = H, Ph.

The dipolar chelate olefincarbamylate complexes **4** are formed in the reactions of the complexes of the iminoesters and their salts with primary and secondary amines.[40, 41, 49]



4a **4b**

R = H, R′ = R″ = R‴ = Me

R = H, R′ = R‴ = Me, H; R′ = H, R‴ = Me;
R′ = Me, R_2''' = $(CH_2)_5$; R′ = H, R_2''' = $(CH_2)_5$;
R = Ph, R′ = H, R‴ = Me.

The structure of the chelate complexes **4** has been established by X-ray diffraction (Fig. 2).[40, 44]

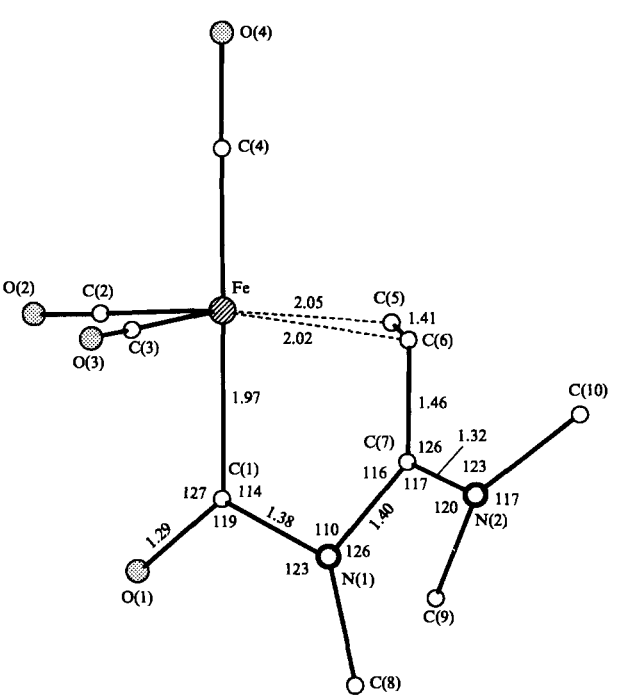
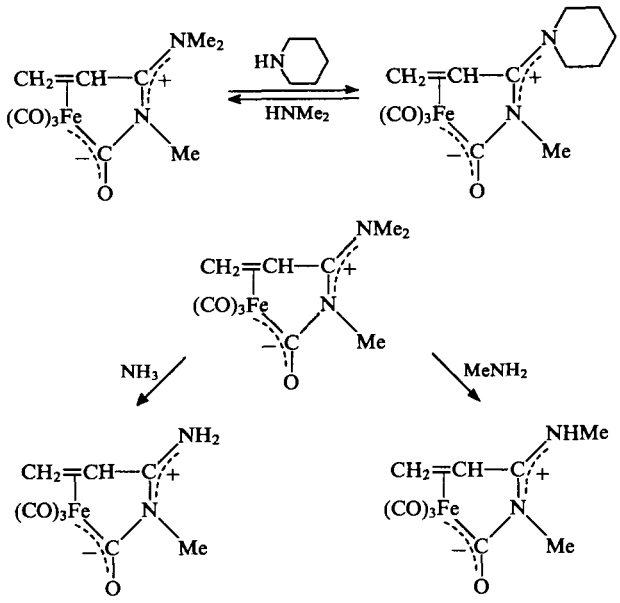
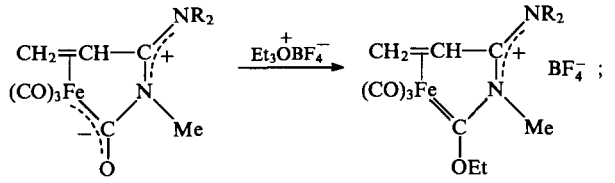


Figure 2. The structure of the molecule of complex **4** (R = H, R′ = R″ = R‴ = Me).

In conformity with the dipolar structure, complexes **4** react both with nucleophiles and electrophiles. The transamination reactions, which make it possible to convert a more readily available complex into others which are less easy to obtain, are important for synthetic purposes.[43]

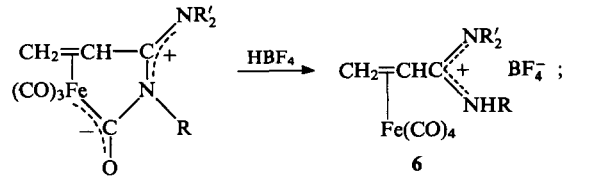


The reactions with electrophiles, for example, with the triethyloxonium cation and acids, lead to new olefin complexes with an α-cationic centre[40, 41, 43] — the vinylcarbene complex **5** and the acrylamidinium complex **6**.



R = Me, $R_2 = (CH_2)_5$.

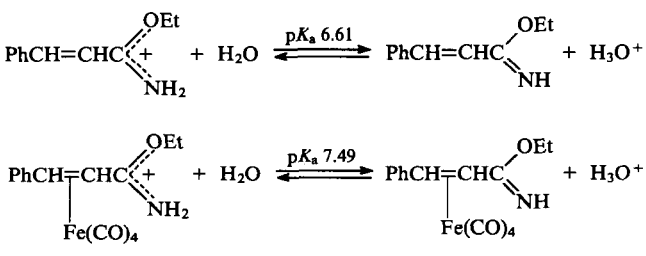
5



R = R′ = Me; R = Me, $R'_2 = (CH_2)_5$;
R = H, R′ = Me.

Examination of the characteristic features of the structures of complexes **2**–**6** permits the conclusion that the olefin structure with direct interaction between the metal and the cationic centre occurs in those cases where the charge is delocalised to a large extent owing to the presence of strong electron-donating substituents, for example, amino-groups.

The stabilising effect of the $Fe(CO)_4$ group in olefin complexes with a cationic centre has been estimated quantitatively by measuring and comparing the pK_a of ethyl cinnamidate and the corresponding iron tetracarbonyl complex.[45]

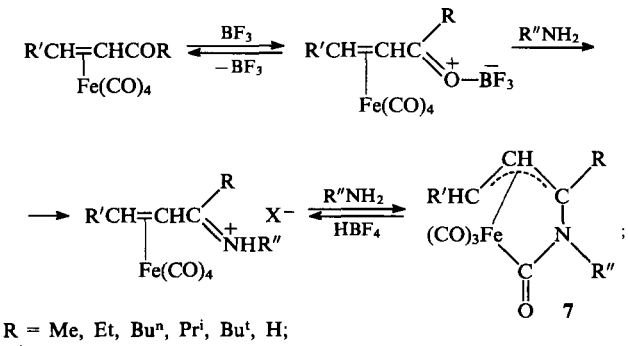


Comparison of the pK_a indicates a powerful electron-donating effect of the $Fe(CO)_4$ group, which more than compensates for the loss of conjugation as a result of the π-coordination.

b. Allyl complexes.

$\eta^3:\eta^1 \rightleftarrows \eta^2$-Tautomerism and the $\eta^2 \rightarrow \eta^1$(N) rearrangement.

The replacement of the strong electron-donating amino-group at the cationic centre in the olefincarbamylate complexes **4** by a weaker electron-donating group — an alkyl or aryl group — alters their structure, namely leads to a transition to compounds of the allyl type. Such compounds have been synthesised from the $Fe(CO)_4$ complexes of unsaturated ketones and cinnamaldehyde via their adducts with BF_3 and the subsequent reaction with amines.[39, 46, 47]



R = Me, Et, Bu^n, Pr^i, Bu^t, H;
R′ = Ph, PhCO, H;
R″ = H, Me, Et, Pr^i, Bu^n, Bu^t, n-C_6H_{13}, cyclo-C_6H_{11}, CH_2Ph .

The structure of the chelate $\eta^3:\eta^1$-allylcarbamoyl complexes **7** in the solid state has been established by X-ray diffraction (Fig. 3).[46, 48]

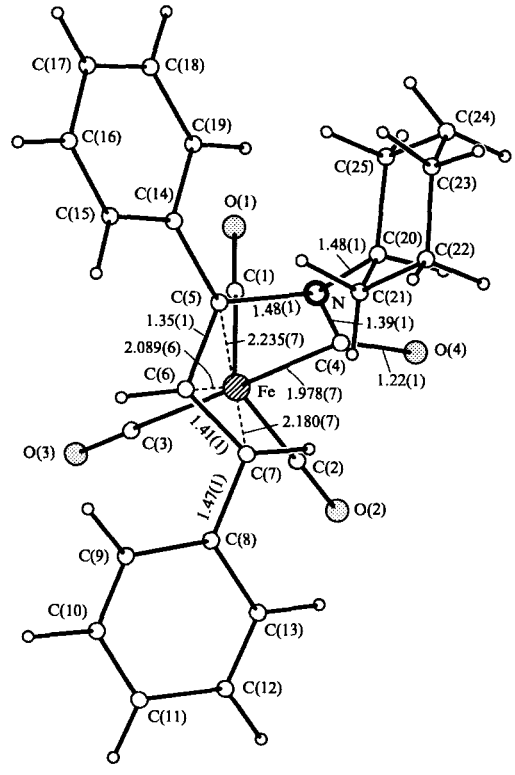
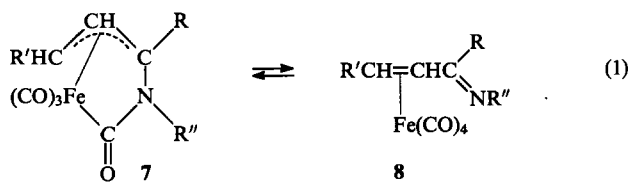


Figure 3. The structure of the molecule of complex **7** (R = R′ = Ph, R″ = cyclo-C_6H_{11}).

Table 1. Thermodynamic parameters of the equilibrium **7** ⇄ **8** (R = Me, R′ = Ph, R″ = cyclo-C_6H_{11}).

Solvent	ΔH/kJ mol^{-1}	ΔS/J mol^{-1} deg^{-1}	ΔG/kJ mol^{-1}		
			295 K	250 K	210 K
Hexane	11.8	49.5	−2.8	−0.6	1.4
Hexane-CH_2Cl_2 (96:4)	20.3	72.8	−1.2	2.1	–

In solutions, complexes **7** rearrange reversibly to the isomeric η^2-olefin complexes **8**.[12, 41, 47]



(1)

7 **8**

The IR spectra of complex **7** with R = Me or n-alkyl, R′ = Ph or H, R″ = Me, Et, Pr^i, Bu^n, cyclo-C_6H_{11}, or CH_2Ph in non-polar solvents, for example in hexane, are seen to contain not only the three $\nu(C\equiv O)$ bands referring to the allylcarbamoyl form (~2065, 2010, and 1990 cm^{-1}) but also additional bands (~2085, 2020, 2010, and 1985 cm^{-1}), the positions and relative intensities of which indicate the presence in the molecule of the complex of the $Fe(CO)_4$ group η^2-linked to the olefin ligand.

The formation in solution of the η^2-olefin complexes **8** has been confirmed also by NMR spectroscopic data. Thus equilibrium (1) with R = Me, R′ = H, and R″ = Pr^i is displaced to the right so much that the ^{13}C NMR spectrum shows only signals due to the olefin form [$\delta(C_{olef})$ = 148.97 and 140.06 ppm and $\delta(C_\alpha)$ = 146.06 ppm; cyclopentane; 10 °C]. The ^1H NMR spectra can also serve as a demonstration of the appearance in solutions of the η^2-olefin form **8**. However, complex **8** could not be isolated in a pure state.

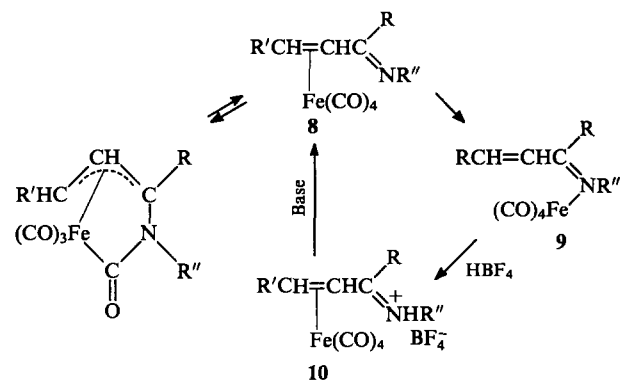
The dependence of the equilibrium position on the temperature, the solvent polarity, and the nature of the substituent in the ligand has been investigated quantitatively by IR spectroscopy.[12, 49]

The thermodynamic parameters of the reversible transition from the cyclic allyl form to the open-chain olefin form for the complex with R = Me, R′ = Ph, and R″ = cyclo-C_6H_{11} are presented in Table 1. With decrease in temperature, the equilibrium shifts towards the formation of the chelate form. The positive entropy change can probably be accounted for by the transition from the rigid chelate molecule to the more mobile molecule with an open chain. On passing to a more polar solvent, the relative stability of the more readily solvated chelate form also increases. The lower limit of the rate constant for the forward reaction ($k > 2.3 \times 10^{-3}$ s^{-1}) and the corresponding upper limit to the activation energy ($\Delta G^{\neq} < 90$ kJ mol^{-1}) were estimated.

The thermodynamic and kinetic parameters of the equilibrium isomerisation of the chelate alkylcarbamoyl complexes to the open-chain olefin complexes are within the limits of the corresponding scales for the tautomeric transformations.[50] Such isomerisation can be regarded as the first example of the ring–chain valence $\eta^3:\eta^1 \rightleftarrows \eta^2$-tautomerism. A characteristic feature of this process consists in the fact that, simultaneously with the opening and closure of the ring, the hapto-binding of the metal to the unsaturated ligand and the formal oxidation state of the metal change.

The steric requirements of the substituents R at the α-carbon atom and R″ at the nitrogen atom exert a significant influence on the equilibrium position.[12] An increase in the bulk of the substituent R leads to a sharp shift of the equilibrium towards the cyclic form. As a consequence of the increase in the bulk of the substituents R″ at the nitrogen atom, there is a smaller shift in the opposite direction.

The η^2-olefin complexes **8**, formed as a result of the tautomeric shift, are capable of rearranging further to the η^1(N)-complexes **9**.[51] Such $\eta^2 \rightarrow \eta^1$(N) rearrangement occurs when the substituents R and R″ are small alkyl groups or one of them is a hydrogen atom. The rate of the rearrangement is appreciably lower than the rate of the tautomeric transformations. Complexes with R = H rearrange faster. The reverse η^1(N) → η^2 rearrangement occurs on protonation of complexes **9**. The deprotonation of the η^2-complexes **10** formed again opens the way to the $\eta^3:\eta^1 \rightleftarrows \eta^2$ tautomerism and the η^1(N) → η^2 rearrangement.

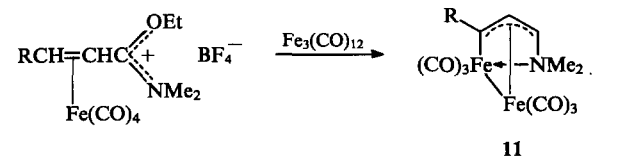


10

R = H, R″ = Me, cyclo-C_6H_{11}, Ph; R = Me, R″ = Me, Et; R = Et, Bu^n, R″ = Me, Et, Bu^n; R = Ph, Bu^t, R″ = H.

The tautomeric transformations and rearrangements investigated are characterised by the ease of the interconversions of various types of complexes containing unsaturated ligands with functional group substituents.

The conversion of the acrylimidate η^2-complexes **2** into the dinuclear η^3-aminoallyl† complexes **11** on heating with $Fe_3(CO)_{12}$ can also be formally classified as a hapto-transition.[42, 52]



11

The structure of these complexes was established by X-ray diffraction.[52]

c. Olefin and elementaallyl complexes

σ-Vinyl derivatives of elements of the type $RCH{=}CHER'_n$ occupy a special place among substituted olefins. The reactions of such compounds with iron carbonyls open the way to the synthesis of dinuclear and polynuclear complexes with a η^2-olefin or η^3-elementaallyl structure.

† Complexes **11** can also be regarded as compounds containing the azaferra-ring, which is η^4-coordinated to the other iron atom via its ferradiene system.

The structure of the complexes formed is influenced by the nature of the element. Thus the interaction of the σ-ketovinylrhenium compound with $Fe_2(CO)_9$ results in the formation of only the η^2-olefin complex without the Re–Fe bond.[26]

$$(CO)_5Re(\sigma\text{-}CH{=}CHCOMe) + Fe_2(CO)_9 \longrightarrow \longrightarrow MeCOCH{=}CHRe(CO)_5 \; . \quad | \; Fe(CO)_4$$

The σ-ketovinyltungsten derivative affords under the same conditions the tungstaallyl complex with an intermetallic bond together with the olefin and oxadiene complexes.[24]

$$Cp(CO)_3W(\sigma\text{-}CH{=}CHCOPh) + Fe_2(CO)_9 \longrightarrow \longrightarrow PhCOCH{=}CHW(CO)_3Cp + \; | \; Fe(CO)_4$$

$$+ \; PhC(O)CH{=}CHW(CO)_3Cp + PhCOCH{=}CHW(CO)_2Cp \; . \quad Fe(CO)_3 \qquad (CO)_3Fe{-}CO$$

On the other hand, in the case of the σ-vinyl derivatives of iron, the metallallyl complexes are the only reaction products.[23, 25, 26, 53]

$$Cp(CO)_2Fe(\sigma\text{-}CH{=}CHR) + Fe_2(CO)_9 \longrightarrow \longrightarrow RCH{=}CHFe(CO)Cp \; ; \quad (CO)_3Fe \; CO$$

R = H, Ph, COMe, COPh, CON⬡.

The structure of the ferraallyl complexes was established by X-ray diffraction.

The reactions of $Fe_2(CO)_9$ with various σ-vinyl derivatives of metals described above are the first examples of π-complex formation involving a σ-linked unsaturated ligand.

The nature of the complexes formed changes when the olefin contains two σ-linked iron carbonyl groups.[28]

In this case, a trinuclear complex with a bridging carbyne ligand, the formation of which requires an extensive rearrangement of the acryloyl ligand, was isolated together with the olefin and ferraallyl complexes. Its structure was demonstrated by X-ray diffraction (Fig. 4).[28]

$$Cp(CO)_2FeCOCH{=}CHFe(CO)_2Cp + Fe_2(CO)_9 \longrightarrow \longrightarrow Cp(CO)_2FeCOCH{=}CHFe(CO)_2Cp + \; | \; Fe(CO)_4$$

48%

$$+ Cp(CO)_2FeCOCH{=}CHFe(CO)Cp + MeC{\equiv}CFeCp \; . \quad (CO)_3Fe{-}CO \qquad Fe{-}CO \; (CO)_3$$

15% 2%

π-Complexes could not be obtained in the reactions of iron carbonyls with substituted σ-vinylpalladium(II) compounds.[29] At the same time it was found that, on heating in benzene, the σ-alkoxycarbonylvinylpalladium complexes undergo the $\eta^1 \rightarrow \eta^2$ rearrangement.

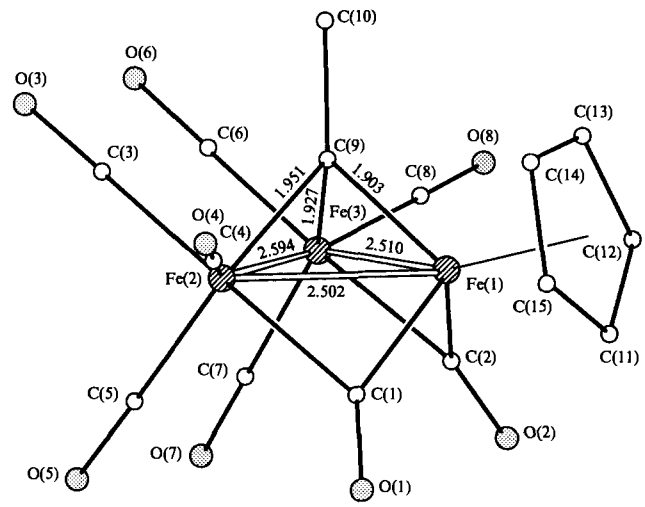


Figure 4. The structure of the molecule of the μ_3-ethylidyneoctacarbonyltriiron complex.

$$Ph_3P(X)Pd(CH{=}CHCOOR) \xrightarrow{80\ ^\circ C} X(Ph_3P)Pd^{-}(CH{-}PPh_3)^{+} \; ; \quad CH{-}COOR$$

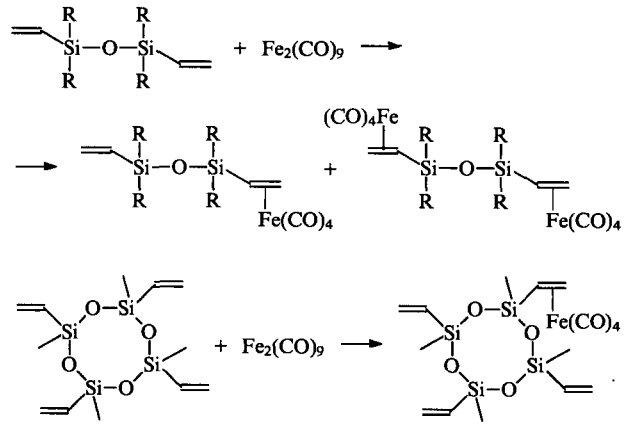
R = Me, Et; X = Cl, I.

Complexes in which the metal is coordinated only to the carbon–carbon double bonds have been obtained in the reactions of various vinyl compounds of silicon with iron carbonyls.[19, 20]

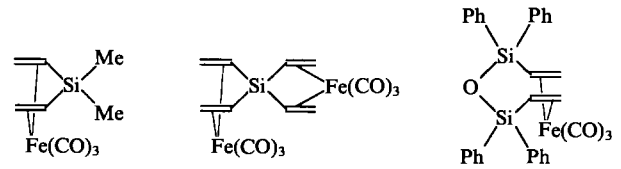
$$CH_2{=}CHSiRR'_2 + Fe_2(CO)_9 \longrightarrow CH_2{=}CHSiRR'_2 \; ; \quad | \; Fe(CO)_4$$

R = R′ = Me, OMe;

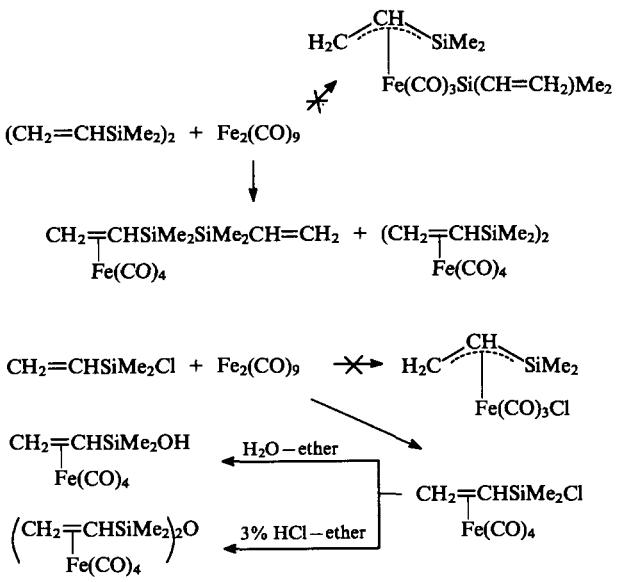
R = CH=CH$_2$, R′ = Me; R = R′ = CHCH$_2$;



η^4-Diene complexes have been obtained from dimethyldivinyl- and tetravinyl-silanes and also from 1,3-divinyltetraphenyldisiloxane and iron carbonyls.[20, 55]



η^3-Silaallyl complexes could not be obtained from divinyldisilanes or chlorovinylsilane.[18]



The absence of compounds of the silaallyl type among the reaction products can probably be explained by the fact that the stabilisation as a result of the formation of a π-complex with a metal is insufficient for the formation of stable structures with silicon–carbon multiple bonds.

The reactions of vinylgermanes and digermanes with $Fe_2(CO)_9$ also lead to complexes of the olefin type.[21]

$$CH_2{=}CHGeR_2R' + Fe_2(CO)_9 \xrightarrow{30-40\ ^\circ C} CH_2{=}\underset{\displaystyle Fe(CO)_4}{CH}{-}GeR_2R';$$

R = R′ = Et, $CH{=}CH_2$;

R = $CH{=}CH_2$, R′ = $Ge(CH{=}CH_2)_3$.

The interaction of iron carbonyls with germanes containing at least one vinyl group leads, under more severe conditions, to the elimination of all the organic groups from germanium and the formation of an iron-germanium cluster.[21, 22]

$$CH_2{=}CHGeR_2R' + \begin{matrix} Fe_2(CO)_9 \\ \text{or} \\ Fe_3(CO)_{12} \end{matrix} \xrightarrow{110\ ^\circ C} (CO)_4Fe\!-\!Ge\!-\!Fe(CO)_4$$

III. Reactions of ruthenium and osmium carbonyl complexes with olefins having functional group substituents

The reactions of ruthenium and osmium carbonyl compounds with substituted olefins have been less investigated than those of their iron analogues. The main cause of the slow development of this field is apparently not only the high cost of the compounds of the above metals but also the specific features of the behaviour of the most readily available carbonyls $M_3(CO)_{12}$, the chemical properties of which are determined by the greater strength of their M–M and M–CO bonds compared with iron carbonyls (Table 2).[56]

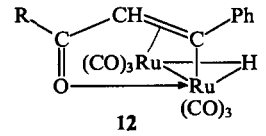
The products formed initially undergo further reactions under severe thermal conditions. This frequently results in the formation of mixtures of complexes which are difficult to separate. The metallic M_3 skeleton is either retained in these reactions or actually increases, whilst unsaturated hydrocarbons are dehydrogenated and undergo oxidative addition to the metal with formation of structures containing allyl, allenyl, alkyne, and vinylidene ligands.[57]

Table 2. The bond enthalpies in the carbonyls $M_3(CO)_{12}$ (in kJ mol^{-1}).

Bond	Fe	Ru	Os
M–M	80.37	117.2	130.2
M–CO	117.6	172.5	191.7

Trinuclear ruthenium and osmium carbanions react with olefins also under photochemical conditions. On UV irradiation, the M–M bonds are ruptured and mononuclear η^2-olefin complexes, similar to the η^2-olefiniron complexes already examined, are formed.[58–60]

The pattern becomes even more complicated after the introduction of functional groups into the olefin molecule. The study of the thermal reactions of $M_3(CO)_{12}$ (M = Ru, Os) with organic unsaturated carbonyl compounds showed that such systems can be coordinated in different ways to the polynuclear fragment. Thus, in the interaction of the unsaturated ketones $PhCH{=}CHCOR$ (R = Me, p-MeC_6H_4) with $Ru_3(CO)_{12}$ in boiling hydrocarbons (hexane, benzene, heptane), dinuclear complexes **12** are formed as the main products.[61]



12

12a: R = Me;
12b: R = p-MeC_6H_4.

The structure of complex **12a** was established by X-ray diffraction. Previously this complex had been obtained by the reaction of benzylideneacetone with mononuclear (η^4-cycloocta-1,5-diene)tricarbonylruthenium.[62] The ruthenium atoms in complex **12a** are linked by a metal–metal bond, a μ-hydride ligand, and an enone ligand which has lost one hydrogen atom. The last ligand chelates one Ru atom via the β-carbon atom (σ-bond) and the ketone oxygen atom (n-donor bond). The other ruthenium atom is η^2-coordinated to the same ligand.

Apart form complexes **12**, a series of other complexes are also formed in the reaction of $Ru_3(CO)_{12}$ with $PhCH{=}CHCOR$. The structure of one of them, namely complex **13**, was determined by X-ray diffraction (Fig. 5).[61]

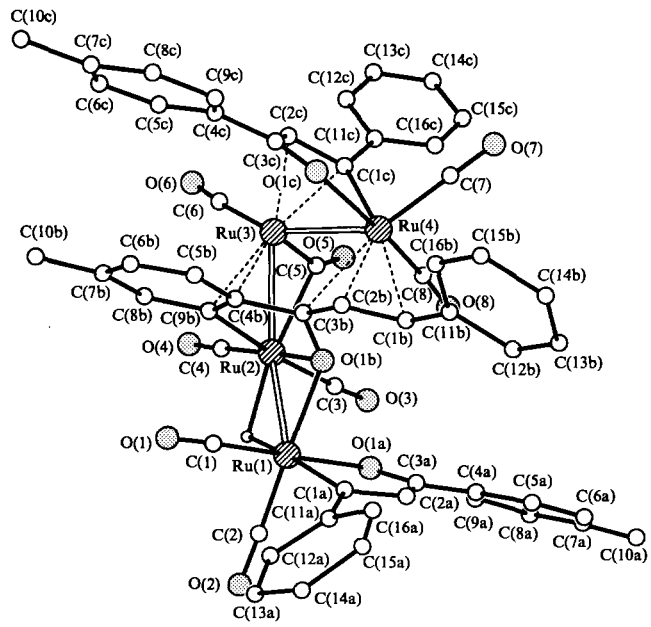
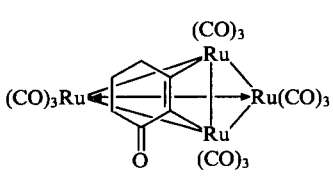


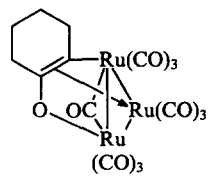
Figure 5. The structure of the molecule of complex **13**.

The molecule of complex **13** includes a chain made up of four ruthenium atoms and three organic ligands. One $PhC=CHCOC_6H_4Me$ ligand at the edge chelates the Ru(1) atom via the β-carbon atom (σ-bond) and the oxygen atom of the keto-group (n-donor bond), forming a five-membered metallocycle. Another similar ligand chelates the Ru(4) atom via the formation of σ-bonds with carbon and oxygen atoms and is also η^2-linked to Ru(3) via the C=C double bond.

The central ligand serves as a μ^4-bridge between all the ruthenium atoms and is linked to them in various ways. Its oxadiene fragment is converted into the hydroxyallyl fragment, which is η^3-linked to Ru(4) and is σ-O-linked to Ru(1) and Ru(2). In addition, Ru(2) forms a σ-bond with the *ortho*-carbon atom of the tolyl substituent and Ru(3) is involved in π-olefin coordination with the same substituent. Thus the ways in which the α,β-unsaturated ketones are coordinated in the ruthenium clusters are extremely varied. They depend primarily on the structure of the unsaturated ketone. When cyclohex-2-en-1-one was used in the thermal reaction with $Ru_3(CO)_{12}$, complexes **14** and **15** were obtained.[63, 64]



14



15

In complex **14**, the four ruthenium atoms form the 'butterfly' configuration. The metal atoms 'at the ends of the wings' are π-linked, while the axial metal atoms are σ-linked to the dehydrogenated cyclohexene.

Interesting examples of the wide variety of the ways in which bonding takes place in the ruthenium clusters are provided by the complexes formed in the reactions of unsaturated aldehyde imines (azadienes) with $Ru_3(CO)_{12}$.[65-69] Various types of bonds between the metal and the organic ligand are formed in these polynuclear compounds: σ-N, σ-C, η^2-C = C, η^2-C = N, η^3-allyl, and η^3-azaallyl.

Complex **16**, in which there is no intermetallic bond and the metal atoms are linked only to the common organic ligand, is formed in the reaction of $Ru_3(CO)_{12}$ with dimethylfumarate.[70] According to X-ray diffraction data (Fig. 6), the double bonds in the three dimethylfumarate ligands in complex **16** were opened [partly dissociated?] and two ligands dimerised with formation of three condensed metallacycles. One hydrogen atom was then transferred to the third ligand forming the fourth metallacycle.

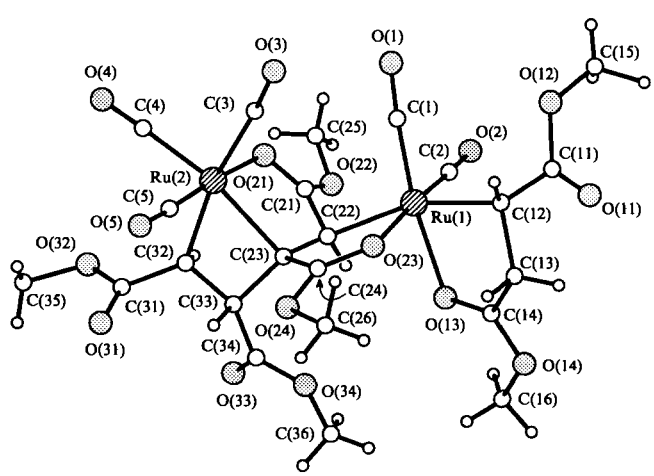
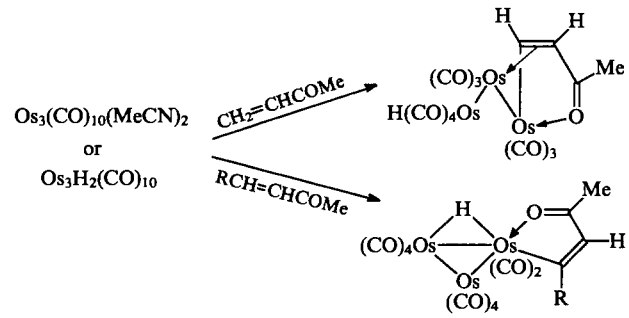


Figure 6. The structure of the molecule of complex **16**.

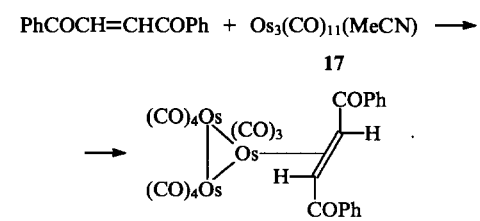
Several other complexes were obtained in this reaction, including the mononuclear complex $Ru(CO)_4(\eta_2$-MeOCOCH=CHCOOMe).

The examples examined above show that organic α,β-unsaturated carbonyl compounds in the ruthenium carbonyl complexes exhibit a tendency towards many-centre bonding, including the formation of σ-Ru–O and σ-Ru–C_β bonds.

The situation is similar also in the case of reactions of osmium carbonyl complexes with unsaturated ketones.[71]



For this reason, relatively few simple η^2-olefin complexes of transition metal clusters are known. In order to obtain a η^2-olefinosmium cluster complex, the monoacetonitrile derivative $Os_3(CO)_{11}(MeCN)$ **17** was used. The latter is normally employed for the synthesis of undecacarbonylosmium compounds.[72] When compound **17** was refluxed with *trans*-α,β-dibenzoylethylene in hexane, the η^2-olefin complex **18**, in which the Os_3 cluster skeleton is retained, was obtained.[73]



18

References

1. M I Rybinskaya, in *Metody Elementoorganicheskoi Khimii. Tipy Metalloorganicheskikh Soedinenii Perekhodnykh Metallov. Kniga Pervaya* (Methods in Organoelement Chemistry. Types of Organometallic Transition Metal Compounds. Book One) (Eds A N Nesmeyanov, K A Kocheshkov) (Moscow: Nauka, 1975) p. 217
2. M Herberhold *Metal Pi-Complexes. Complexes with Monoolefinic Ligands* (Translated into Russian) (Moscow: Mir, 1975), p. 449
3. E Weiss, K Stark, J E Landcaster, H D Murdoch *Helv. Chim. Acta* **46** 288 (1963)
4. A N Nesmeyanov, Ahmed Khalil, L V Rybin, M I Rybinskaya, Yu A Ustynyuk *J. Organomet. Chem.* **10** 121 (1967)
5. A N Nesmeyanov, L V Rybin, M I Rybinskaya, N T Gubenko, I F Leshcheva, Yu A Ustynyuk *Zh. Obshch. Khim.* **38** 1476 (1969)
6. A N Nesmeyanov, L V Rybin, M I Rybinskaya, N T Gubenko, I F Leshcheva, Yu A Ustynyuk *Izv. Akad. Nauk SSSR, Ser. Khim.* 1242 (1969)
7. A N Nesmeyanov, L V Rybin, M I Rybinskaya, N T Gubenko, I F Leshcheva, Yu A Ustynyuk *Zh. Obshch. Khim.* **39** 2091 (1969)
8. M I Rybinskaya, L V Rybin, N T Gubenko, A N Nesmeyanov *Zh. Obshch. Khim.* **41** 2020 (1971)
9. A N Nesmeyanov, L V Rybin, M I Rybinskaya, N T Gubenko, T V Petrovskii *Izv. Akad. Nauk SSSR, Ser. Khim.* 2739 (1971)
10. A N Nesmeyanov, L V Rybin, M I Rybinskaya, N T Gubenko, T V Petrovskii *Zh. Obshch. Khim.* **42** 2473 (1972)

11. A N Nesmeyanov, G B Shul'pin, L V Rybin, M I Rybinskaya, N T Gubenko, P V Petrovskii, V I Robas *Zh. Obshch. Khim.* **44** 2032 (1974)
12. L V Rybin, N A Stelzer, I A Garbusova, B V Lokshin, M I Rybinskaya *J. Organomet. Chem.* **265** 295 (1984)
13. A N Nesmeyanov, M I Rybinskaya, L V Rybin, E A Petrovskaya, A I Lutsenko *Izv. Akad. Nauk SSSR, Ser. Khim.* 904 (1977)
14. M I Rybinskaya, A A Pogrebnyak, L V Rybin *Izv. Akad. Nauk SSSR, Ser. Khim.* 2155 (1981)
15. L V Rybin, A A Pogrebnyak, M I Rybinskaya, D A Bochvar, E G Gal'pern, N P Gambaryan *Izv. Akad. Nauk SSSR, Ser. Khim.* 1596 (1976)
16. A N Nesmeyanov, M I Rybinskaya, L V Rybin, A V Arutyunyan *Zh. Obshch. Khim.* **44** 604 (1974)
17. A N Nesmeyanov, M I Rybinskaya, L V Rybin, A V Arutyunyan, L G Kus'mina, Yu T Struchkov *J. Organomet. Chem.* **73** 365 (1974)
18. G V Nurtdinova, L V Rybin, A A Pogrebnyak, M I Rybinskaya, V P Yur'ev *Izv. Akad. Nauk SSSR, Ser. Khim.* 2166 (1980)
19. M I Rybinskaya, L V Rybin, A A Pogrebnyak, G V Nurtdinova, V P Yur'ev *Izv. Akad. Nauk SSSR, Ser. Khim.* 2186 (1980)
20. M I Rybinskaya, L V Rybin, A A Pogrebnyak, G V Nurtdinova, V P Yur'ev *J. Organomet. Chem.* **217** 373 (1981)
21. I M Salimgareeva, N G Bogatova, O Zh Zhebarov, L V Rybin, A A Pogrebnyak, M I Rybinskaya, V P Yur'ev *Izv. Akad. Nauk SSSR, Ser. Khim.* 1161 (1982)
22. A S Batsanov, L V Rybin, M I Rybinskaya, Yu T Struchkov, I M Salimgareeva, N G Bogatova *J. Organomet. Chem.* **249** 319 (1983)
23. A N Nesmeyanov, L V Rybin, M I Rybinskaya, V S Kaganovich, Yu A Ustynyuk, I F Leshcheva *Zh. Obshch. Khim.* **38** 1471 (1968)
24. A N Nesmeyanov, L V Rybin, M I Rybinskaya, V S Kaganovich *Izv. Akad. Nauk SSSR, Ser. Khim.* 348 (1971)
25. A N Nesmeyanov, L V Rybin, M I Rybinskaya, V S Kaganovich, P V Petrovskii *Izv. Akad. Nauk SSSR, Ser. Khim.* 2733 (1971)
26. A N Nesmeyanov, M I Rybinskaya, L V Rybin, V S Kaganovich, P V Petrovskii *J. Organomet. Chem.* **31** 257 (1971)
27. L V Rybin, E A Petrovskaya, A S Batsanov, Yu T Struchkov, M I Rybinskaya *J. Organomet. Chem.* **212** 95 (1981)
28. L V Rybin, E A Petrovskaya, Yu T Struchkov, A S Batsanov, M I Rybinskaya *J. Organomet. Chem.* **226** 63 (1982)
29. L V Rybin, E A Petrovskaya, M I Rybinskaya, L G Kus'mina, Yu T Struchkov, V V Kaverin, N Yu Koneva *J. Organomet. Chem.* **288** 119 (1985)
30. N T Gubenko, Candidate's Thesis in Chemical Sciences, Institute of Organoelement Compounds, Russian Academy of Sciences, Moscow, 1975, p. 60
31. A N Nesmeyanov, M I Rybinskaya, L V Rybin, N T Gubenko, P V Petrovskii *J. Organomet. Chem.* **71** 271 (1974)
32. K Stark, J E Landcaster, H D Murdoch, E Weiss *Z. Naturforsch. B* **19** 284 (1964)
33. E Koerner von Gustorf, F W Grevels, G Krüger, G Olbrich, F Mark, D Schulz, R Wagner *Z. Naturforsch. B* **27** 392 (1972)
34. G Cardaci *J. Am. Chem. Soc.* **97** 1412 (1975)
35. V G Andrianov, Yu T Struchkov, M I Rybinskaya, L V Rybin, N T Gubenko *Zh. Strukt. Khim.* **13** 86 (1972)
36. A N Nesmeyanov, N K Kochetkov, M I Rybinskaya *Izv. Akad. Nauk SSSR, Otd. Khim. Nauk* 350 (1950)
37. M K Kochetkov, E D Khomutov, O B Mikhailova, A N Nesmeyanov *Izv. Akad. Nauk SSSR, Otd. Khim. Nauk* 1181 (1957)
38. T J Crowell, G C Helsley, R E Lutz, W L Scott *J. Am. Chem. Soc.* **85** 443 (1963)
39. A N Nesmeyanov, L V Rybin, N A Shtel'tser, M I Rybinskaya *Izv. Akad. Nauk SSSR, Ser. Khim.* 1607 (1981)
40. A N Nesmeyanov, T N Sal'nikova, Yu T Struchkov, V G Andrianov, A A Pogrebnyak, L V Rybin, M I Rybinskaya *J. Organomet. Chem.* **117** C16 (1976)
41. M I Rybinskaya, L V Rybin, A A Pogrebnyak, N A Shtel'tser *Koord. Khim.* **6** 1475 (1980)
42. A N Nesmeyanov, L V Rybin, A A Pogrebnyak, M I Rybinskaya *J. Organomet. Chem.* **116** 327 (1976)
43. A N Nesmeyanov, M I Rybinskaya, L V Rybin, A A Pogrebnyak *Izv. Akad. Nauk SSSR, Ser. Khim.* 2055 (1979)
44. T N Sal'nikova, V G Andrianov, Yu T Struchkov *Koord. Khim.* **3** 1607 (1977)
45. A N Nesmeyanov, A A Pogrebnyak, L V Rybin, M I Rybinskaya *Izv. Akad. Nauk SSSR, Ser. Khim.* 2824 (1979)
46. A N Nesmeyanov, M I Rybinskaya, L V Rybin, N T Gubenko, N G Bokii, A S Batsanov, Yu T Struchkov *J. Organomet. Chem.* **149** 177 (1978)
47. A N Nesmeyanov, L V Rybin, M A Stelzer, M I Rybinskaya *J. Organomet. Chem.* **182** 393 (1979)
48. A S Batsanov, Yu T Struchkov *J. Organomet. Chem.* **248** 101 (1983)
49. M I Rybinskaya, L V Rybin, N A Stelzer, I A Garbusova, B V Lokshin *J. Organomet. Chem.* **265** 291 (1984)
50. V I Minkin, L P Olekhnovich, Yu A Zhdanov, in *Molekulyarnyi Dizain Tautomernykh Sistem* (Molecular Design for Tautomeric Systems) (Rostov-on-Don: Izd. Rostov. Univ., 1977) p. 17
51. A N Nesmeyanov, L V Rybin, N A Stelzer, Yu T Struchkov, A S Batsanov, M I Rybinskaya *J. Organomet. Chem.* **182** 399 (1979)
52. L V Rybin, A A Pogrebnyak, M I Rybinskaya, T N Sal'nikova, V G Andrianov, Yu T Struchkov *Koord. Khim.* **2** 802 (1976)
53. M I Rybinskaya, L V Rybin, V P Yur'ev *Koord. Khim.* **10** 656 (1984)
54. V G Andrianov, Yu T Struchkov *Zh. Strukt. Khim.* **9** 845 (1968)
55. A S Batsanov, Yu T Struchkov, G V Murtdinova, A A Pogrebnyak, L V Rybin, V P Yur'ev, M I Rybinskaya *J. Organomet. Chem.* **212** 211 (1981)
56. J Lewis, B F G Johnson *Pure Appl. Chem.* **44** 43 (1975)
57. M J Bruce, in *Comprehensive Organometallic Chemistry* Vol. 4 (Ed. G Wilkinson) (Oxford: Pergamon Press, 1982) p. 847
58. F W Grevels, J G A Reuvers, J Takats *J. Am. Chem. Soc.* **103** 4069 (1981)
59. F W Grevels, J G A Reuvers, J Takats *Angew. Chem., Int. Ed. Engl.* **20** 452 (1981)
60. M R Burke, J Takats, F W Grevels, J G A Reuvers *J. Am. Chem. Soc.* **105** 4092 (1983)
61. L V Rybin, S V Osintseva, A S Batsanov, Yu T Struchkov, P V Petrovskii, M I Rybinskaya *Izv. Russ. Akad. Nauk, Ser. Khim.* (in the press) (1993)
62. A J P Domingos, B F G Johnson, J Lewis, G M Sheldrick *J. Chem. Soc., Chem. Commun.* 912 (1973)
63. A Basu, S Bhaduri, K Sharma, P C Jones *J. Organomet. Chem.* **328** C34 (1987)
64. S Bhaduri, N Sapre, K Sharma *J. Chem. Soc., Dalton Trans.* 1305 (1990)
65. W P Mul, C J Elsevier, K Vrieze, W J J Smeets, A L Spek *Rec. Trav. Chim.* **107** 297 (1988)
66. L H Polm, C J Elsevier, W P Mul, K Vrieze, M J N Christophersen, F Muller, C H Stam *Polyhedron* **7** 2521 (1988)
67. L N Polm, W P Mul, C J Elsevier, K Vrieze, M J N Christophersen, C H Stam *Organometallics* **7** 423 (1988)
68. W P Mul, C J Elsevier, M van Leijen, K Vrieze, A L Spek *Organometallics* **10** 533 (1991)
69. W P Mul, C J Elsevier, L H Polm, K Vrieze, M C Zoutberg, D Hejdenrijk, C H Stam *Organometallics* **10** 2247 (1991)
70. N A Shtel'tser, L V Rybin, E A Petrovskaya, A S Batsanov, M Kh Dzhafarov, Yu T Struchkov, M I Rybinskaya, P V Petrovskii *Metalloorg. Khim.* **5** 1009 1992)
71. A J Deeming, P J Manning, J P Rothwell, M B Hursthouse, N P C Walker *J. Chem. Soc., Dalton Trans.* 2039 (1984)
72. B F G Johnson, J Lewis, D A Pippard *J. Chem. Soc., Dalton Trans.* 407 (1981)
73. L V Rybin, E D Petrovskaya, M I Rybinskaya, M Kh Dzhafarov, A S Batsanov, Yu T Struchkov, N A Shtel'tser *Metalloorg. Khim.* **5** 684 (1992)

Russian Chemical Reviews **62** (7) 647 – 659 (1993)
© 1993 Russian Academy of Sciences and Turpion Ltd

UDC 547.241

Derivatives of diphosphonic acids: synthesis and biological activity

M M Zolotukhina, V I Krutikov, A N Lavrent'ev

Contents

I.	Introduction	647
II.	Biological activity and synthesis of compounds with geminal phosphonate groups	647
III.	Vicinal diphosphonic acids	654
IV.	Polyalkylpolyaminodiphosphonic acids	654
V.	Phosphonophosphinates and diphosphinates	655
VI.	Phosphonophosphates	656

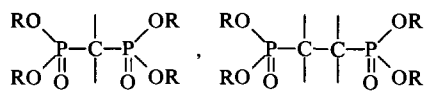
Abstract. The scientific-technical and patent literature on the synthesis of derivatives of diphosphonic acids is surveyed. Various methods of synthesis of diphosphonate, phosphonylphosphinyl, and phosphonophosphate compounds are described. The principal aspects of the use of the above compounds in medicine, biochemistry, and agriculture are examined. The bibliography includes 174 references.

I. Introduction

In recent years, many investigators have shown interest in the method of synthesis and the detection of biological activity of phosphonic acids and their derivatives, which can be regarded as analogues of natural phosphates. Pyrophosphates containing the P–O–P linkage are known to be natural regulators of the metabolism of calcium at the cellular level. Attempts have been made to use inorganic pyrophosphates in the treatment of diseases associated with the breakdown of the calcium metabolism, but the desired results were not achieved owing to the hydrolysis of the above compounds by pyro- and polyphosphatases. Synthetic analogues of pyrophosphates, namely diphosphonates, which are not metabolised because of the presence of P–C–P linkages, attracted the attention of investigators. There exists a series of monographs and reviews in which the methods of synthesis, properties, and the results of biochemical and clinical tests on diphosphonates are considered. However, these studies were devoted as a rule either only to the synthesis of these compounds[1,2] or only to the analysis of their pharmacological properties.[3–10] In a series of investigations attention was devoted merely to the narrow subclass of biphosphoryl substances.[11,12]

The biologically active derivatives of diphosphonic acids known at the present time, which contain two phosphorus atoms in the molecule, can be divided into the following main groups:

1. Compounds with geminal or vicinal phosphonate groups:



2. Polyalkylpolyaminodiphosphonic acids.

3. Phosphonylphosphinyl compounds containing the P–C–P–C linkages.

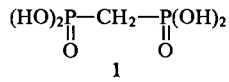
4. The phosphonophosphate compounds P–C–O–P.

The methods of synthesis and biological activities of such compounds are the subject of the present review.

II. Biological activity and synthesis of compounds with geminal phosphonate groups

1. Methylenediphosphonic acid and its halo-derivatives

The closest analogue of inorganic pyrophosphates is methylenediphosphonic acid **1** (MDP), which is capable of forming stable complexes with alkaline earth, transition, and heavy metals. This property of the above compound is used to prevent the deposition of calcium in living tissues.[2]



1

Methylenediphosphonic acid forms part of the composition of many disinfecting and radiopharmaceutical preparations.[13] The radioisotopes of certain metals, for example ^{99}Tc, capable of fulfilling the function of a radioactive probe, are used as the main components of such preparations. Chelation of the cations of the above isotopes by MDP makes it possible to increase their toxicological acceptability to the organism, to facilitate their transport, and to ensure the selectivity of their concentration in particular organs.

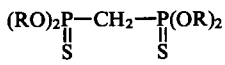
MDP can add to adenosine triphosphate and can also inhibit the incorporation of inorganic phosphate in nucleoside polyphosphates and phosphorolysis;[2,14] MDP acts on the immune system, inhibiting inorganic pyrophosphatase as a consequence of competition for the substrate and a decrease in the concentration of the activator (Mg^{2+}) and the substrate.[15] It has been observed that MDP exerts a mutagenic effect on plants.[16] A review has been devoted to the structure, properties,

M M Zolotukhina, V I Krutikov, A N Lavrent'ev
St. Petersburg Technological Institute, Moskovskii prosp. 26,
198013 St Petersburg. Tel. (7-812) 259 47 92, Fax (7-812) 110 62 85

Received 26th January 1993
Uspekhi Khimii **62** (7) 691 – 703 (1973); translated by A K Grzybowski

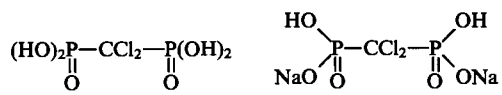
synthesis, and application of MDP and its full and mixed esters.[13] The main reaction leading to the synthesis of MDP and its derivatives is the Arbuzov reaction in its various versions. Another method incorporates the Michaelis–Bekker reaction of a dihaloalkane or a haloalkylphosphonate with a metal dialkyl phosphite in several modifications.[1,13,17] A consecutive method of synthesis using initially the Arbuzov reaction and then the Michaelis–Bekker reaction, which affords the products in an acceptable yield, has also been reported.[2] An exchange reaction between $CH_2(AlCl_2)_2$ and PCl_3, leading to $CH_2(PCl_2)_2$, has been proposed. The acid dichloride of MDP and methylenediphosphonite $CH_2[P(OR)_2]_2$, has been proposed. The acid dichloride of MDP and methylenediphosphonite $CH_2[P(OR)_2]_2$ have been synthesised from the latter and their oxidation in dimethyl sulfoxide (DMSO) afforded the corresponding MDP esters.[13] There exists a method of synthesis of MDP by the oxidation of the readily available methylenediphosphine $CH_2(PH_2)_2$ with nitric acid.[2]

A patent[18] describes a reaction in which the starting materials for the synthesis of MDP esters are white phosphorus, epoxyethane, and sodium alkoxide. MDP esters can also be obtained from tetraalkylmethylenebisphosphonites by a reaction with carbonyl compounds.[19,20] Any phosphonate can be converted into the acid by acid hydrolysis or via trimethylsilyl esters (by reaction with Me_3SiHal). The esters of methylenephosphonodithionic acid **2** are intermediates in the synthesis of biologically active substances. It has been suggested[21] that they can be obtained by the Michaelis–Bekker reaction induced by UV radiation at reduced temperatures in liquid ammonia.



2

Dichloromethylenediphosphonic acid **3** (DCMDP) and its disodium salt **4**, known as clodronic acid, are used to prevent the excess resorption of bone and the calcification of soft tissues, to regulate calcium metabolism at the cellular level, and to treat osteoporosis.[3,4,22]



3 **4**

It has been established that DCMDP prevents the spreading of the metastases of bone tumours.[23,24] By regulating the permeability of membranes, this compound also assists in the transport of antitumour drugs into the cell, preventing thereby the disintegration of bone tissue and suppressing the growth of tumours without manifesting toxic properties.[25]

In a study of the effect of dihalomethylenediphosphonates on the activity of alkaline phosphatase and the oxidation of aliphatic acids in cell cultures, it was shown that DCMDP is the most powerful stimulator of the above enzyme compared with the dibromo- and difluoro-derivatives of MDP. The monohalo-derivatives of MDP and the non-halogenated acids are less active in relation to phosphatase and are inactive or inhibit the oxidation of aliphatic acids.[26]

DCMDP can be obtained from trialkyl phosphite, bromotrichloromethane, and an excess of sodium hypochlorite[1] and also as a result of the radical reaction with carbon tetrachloride[27,28] or with $Cl_3CP(O)(OEt)_2$.[29,30]

Difluoromethylenediphosphonic acid (DFMDP) has been proposed as a therapeutic preparation for the treatment of diseases associated with increased desorption of bone. By virtue of the presence of fluorine, this compound can also be used as an experimental means for the investigation of the way in which all diphosphonates act.[31] It has been noted that monofluoro- and difluoro-methylenediphosphonic acids are isopolar analogues of pyrophosphoric acid.[32]

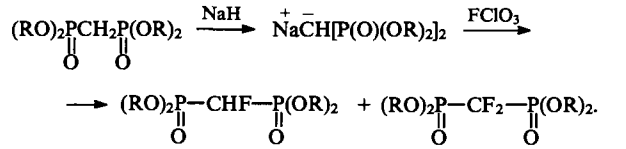
Both symmetrical and asymmetric difluoromethylene-diphosphonates can be obtained by the Michaelis–Bekker reaction[32,33]

$$(RO)_2P(O)M + CF_2XY \longrightarrow (RO)_2P(O)CF_2P(O)(OR)_2,$$

or by the reaction

$$(RO)_2P(O)M + XCF_2P(O)(OR^1)_2 \longrightarrow (RO)_2P(O)CF_2P(O)(OR^1)_2,$$

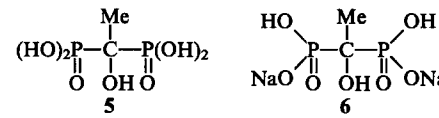
where X, Y = Cl, Br, or I; M = Na or K; and R, R^1 = alkyl. Another version of the synthesis of fluoromethylene-diphosphonates involves the use of methylenediphosphonic acid esters, which are treated with butyllithium, sodium hydride, or potassium *tert*-butoxide,[1,32,34,35] the carbanions $\bar{C}H(PO_3R_2)_2$ formed being subsequently fluorinated by perchloryl fluoride:[32,34,35]



The esters obtained can be hydrolysed to the corresponding acids.

2. Hydroxyethylidenediphosphonic acid

The best known compounds among diphosphonic acids used in medicine are hydroxyethylidenediphosphonic acid **5** (HEDP) and its disodium salt **6**, called etidronate.



5 **6**

The study of the complex-forming properties of HEDP showed that the combination in the molecule of this compound of two acid phosphono-groups and the hydroxy-group with its comparatively high basicity gives rise to the possibility of the formation by this ligand of stable complexes with alkaline earth, transition, and lanthanide metals. The stability constants of the HEDP complexes of certain metals[12] differ little from the corresponding constants of the MDP complexes. Therefore, by virtue of their ability to reduce the degree of resorption of bone and to diminish the liberation of hydroxyproline, HEDP and etidronate are used as regulators of calcium metabolism at the cellular level in the treatment of Paget's disease.[3,36] In minimal doses, HEDP increases the incorporation of calcium into bone tissue, prevents the development of various types of osteoporosis and myositis and prevents the destruction of the peridontal membrane and of the transplanted bone in animals.[12] HEDP inhibits the formation and growth of calcium oxalate stones in kidneys. The addition of HEDP to dental preparations and toothpastes is an excellent means whereby the formation of plaque and caries can be prevented.[3,11] The use of xydiphone — the potassium sodium salt of HEDP — for the treatment of urinary calculus as an anticalcifying and antiinflammatory agent has been permitted.[37] It has been suggested in the USA that HEDP be used as a pharmaceutical preparation for the treatment of persons suffering from metastatic bone cancer.[38]

The extremely high selectivity of the complex forming capacity of HEDP in relation to beryllium is notewothy.[12] Its introduction into the organism poisoned by Be^{2+} ions eliminates the inhibition of the activity of alkaline phosphates. As stabilisers of cell membranes, HEDP and its salts can be effective prophylactic

agents in diseases such as bronchial asthma and hyperglycemia. By virtue of its ability to reduce to the normal level the concentration of cholesterol and triglycerides in the plasma and also its ability to be incorporated in the phospholipids of cell membranes, HEDP prevents the accumulation of peroxide compounds in erythrocytes.[3,39]

HEDP is widely used for the treatment of rheumatoid diseases. It is particularly effective as an antiarthritic agent in combination with antiinflammatory agents. The antiatherosclerotic effect of HEDP has been described: it was found that it influences the immune system, the genetic apparatus of the cell, the biosynthesis of prostaglandins, the stimulation of the citric acid cycle,[16,40] the metabolism of vitamin D,[2,41] and the embryotropic effect of the latter.[42]

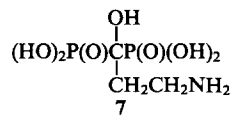
HEDP salts increase the bactericidal activity of phenolic compounds, which permits their use in disinfectants, shampoos, mouth washes, and other similar products. A series of publications have been devoted to the use of HEDP in cosmetics. HEDP esters are employed as pesticides.[11]

Thus comprehensive studies on the properties of HEDP and its salts have led to an extremely wide range of their applications, some of which have been successfully realised in practice.

The practical interest in HEDP is determined primarily also by the ready availability of the starting material and the comparative simplicity of its synthesis, which permitted the industrial manufacture of this product. The reaction of PCl_3 or H_3PO_3 (or their mixture) with acetic acid (or a mixture of acetic acid and acetic anhydride) as well as the reaction of H_3PO_3 with acetic anhydride or carboxylic acid chlorides have been used to synthesise HEDP. Numerous versions of the acylation of phosphorus(III) compounds differ in the reaction conditions, the reactant ratios, and the yields of the target product.[1,11,12,43-51] A method of synthesis of HEDP by the hydrolysis and acidolysis of dimethyl phosphite to H_3PO_3 followed by acetylation with acetic anhydride or acetyl chloride, affording a yield up to 96%, has been developed.[52] It has been suggested that the still residue remaining after the distillation of dimethyl phosphite, which is a waste product in the manufacture of chlorofos, be used as the starting material. An improved version of the synthesis of HEDP from dimethyl phosphite and acetic anhydride in solution in acetic acid has been described.[53] The methods of synthesis of HEDP introduced into industrial production have been considered in detail in a review.[54] A high yield of HEDP (97%) has been achieved in the synthesis based on the interaction of PCl_3 and acetic acid using a zinc catalyst.[55,56] A method has been proposed for the continuous synthesis of HEDP with a purity of 99.2% by the reaction of P_4O_6 with carboxylic acids[57] and also by the reaction of a mixture of phosphorus oxides, obtained as side products in the synthesis of P_4O_6, with acetic acid.[58] If the reaction of P_4O_6 with acetic acid is carried out in the presence of urea under a nitrogen atmosphere,[59] then the yield of HEDP increases to 97%. A procedure has been proposed for the synthesis of HEDP and its analogues by the nitrosation of aminodiphosphonic acid $H_2NC(R)(PO_3H_2)_2$ with nitrous acid or substances forming HNO_2 during the reaction (nitrogen oxides, nitrous fumes, NOCl, $NaNO_2$, and aqua regia).[60] The initial aminoalkylidenediphosphonic acid is obtained by the reaction of PCl_3 with acid amides in the presence of H_3PO_3 and subsequent hydrolysis; HEDP is isolated as the hydrate in yields up to 100%.

3. Aminohydroxyalkylidenediphosphonic acids

Compounds such as 3-amino-1-hydroxy-1,1-propylidenediphosphonic acid **7** (APD), 4-amino-1-hydroxy-1,1-butylidenediphosphonic acid (ABD), 6-amino-1-hydroxy-1,1-hexylidenediphosphonic acid, and 6-amino-1,1-hexylidenediphosphonic acid are used as regulators of the calcium metabolism for the prevention of the deposition of calcium in the soft tissues and the resorption of bone and for the treatment of poisoning by metal salts and alcohol.[3,4,12]



7

Their complexes with alkaline earth, transition, and lanthanide metals exhibit an enhanced solubility by virtue of the presence in the molecule, together with two acid phosphono-groups, of hydroxy- and amino-groups, which play the role of a basic centre in the molecule.[11] The use of the above compounds in the treatment of Paget's disease is based on this property. It has been established that APD has minimal side effects;[61] ABD is used in the treatment of urinary calculus.[62,63] It has been shown in experiments *in vivo* and *in vitro* that APD is 100–300 times more active than DCMDP as the inhibitor of the resorption of bone.[63] The acid **7** and other diphosphonates having a terminal amino-group are readily incorporated into the structure of cell membranes and into phospholipids. They also prevent the accumulation of peroxide compounds in erythrocytes.[39] APD and ABD participate in the metabolism of dihydroxyvitamin D. They effectively normalise the level of calcium in the blood in patients suffering from malignant hyperglycemia.[63,64] Synergistic compositions containing cytostatic or hormonal antitumour agents (melphalan, chlorambucil, methotrexate, etc.) and geminal diphosphonates such as ABD have been proposed for the treatment of metastatic bone cancer.[65]

Hydroxyalkylidenediphosphonic acids containing an amino-group have been synthesised from the corresponding carboxylic aminoacids by treatment with a mixture of H_3PO_4 and PCl_3 [3,66-71] or a mixture of H_3PO_3 and PCl_3 [63,72] and subsequent hydrolysis. If a sulfonic acid is added in the latter version,[73] then the yield of the product can be increased to 90%. It has also been suggested that P_4O_6,[74] a mixture of H_3PO_4 and P_4O_6,[75] and a mixture of H_3PO_3 and $POCl_3$ [62] be used as the phosphorus-containing reagents.

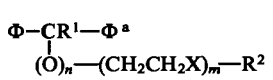
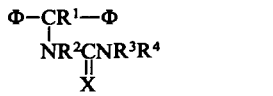
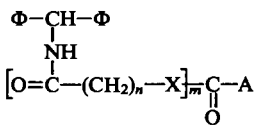
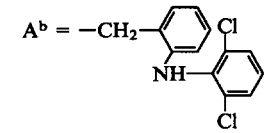
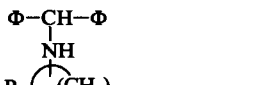
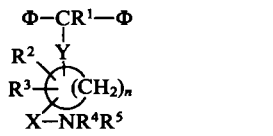
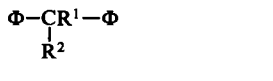
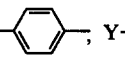
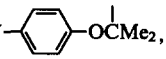
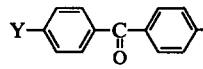
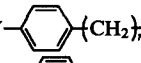
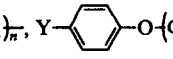
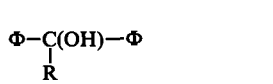
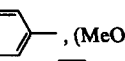
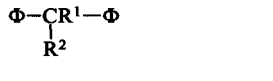
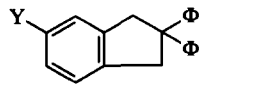
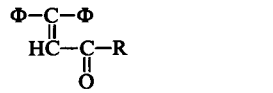
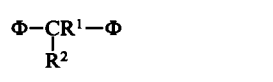
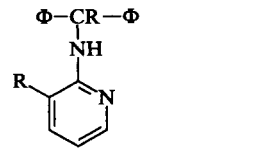
4. Inhibitors of the resorption of bone and antiinflammatory, antiarthritic, and antirheumatoid agents

Because of the ability of diphosphonic acids to form stable complexes with metal ions, they can be used in the treatment of diseases associated with the breakdown of calcium metabolism. A large number of new compounds of this class which can form part of pharmaceutical preparations for the treatment of the above diseases, have been synthesised in recent years. Furthermore, if the diphosphonic acid molecule includes a carboxylic acid residue with antiinflammatory and antipyretic activities, then the use of such a compound as an antiinflammatory agent is particularly effective.

Investigators followed the path leading to an increase in the complexity of the structures of compounds with known pharmacological activities (DCMDP, HEDP, APD, ABD) by introducing into the structure of the given substance all possible cyclic and acyclic hydrocarbon fragments and heterocycles. The synthesis of new compounds are based on the known phosphonylation methods (the Arbuzov and Michaelis–Bekker reactions, addition of di- and tri-alkyl phosphites to unsaturated bonds, phosphonylation of carboxylic acids and their derivatives)[1] in combination with various procedures for the further development of the structure which do not involve the phosphonate groups.

The principal representatives of the geminal diphosphonic acids and their salts and esters obtained during the last 20 years, which exhibit antiresorptive, antiinflammatory, and antiarthritic activities, are presented in Table 1.

Table 1. Geminal diphosphonic acids and their derivatives exhibiting antiresorptive, antiinflammatory, antiarthritic, and antirheumatoid activities.

Formula	Substituents	Ref.
	Compounds without heterocyclic fragments in the molecule	
	R^1 = H, OH, Alk, Hal, arylalkyl; R^2 = Alk, arylalkyl, hydroxyalkyl, alkenyl, arylalkenyl; n = 0, 1; X = CH_2, m = 1–9; O, m = 1, 2	76–79
	R^1, R^2 = H, Alk; R^3 = Alk, Ar, arylalkyl; R^4 = H, Ar; X = O, S	80
	A^b =  X = NH, O; m = 0, 1, n = 1–10	81, 82
	R = H, Alk(C_{1-5}); n = 3–10	83
	R^1 = H, OH, NH_2; R^2, R^3 = H, Alk, alkylene; R^4, R^5 = H, Alk, Ac, arylalkyl; X, Y = bond, alkylene; n = 5–7	84
	R^1 = H, OH, OAc, NH_2; R^2 = Bu^t, Y-  , Y-  , Y-  , Y-  , Y-  , (Y = H, Me, OMe, Hal; n = 1–6), Cl-, –CN, $-(CH_2)_2CN$, $-(CH_2)_3NH_2$, $-CH_2NMe_2$; R^1+R^2 =	85–88
	R = n-C_5H_{11}, Bu^t, n-$C_{15}H_{31}$, Ph, Y-  , $(MeO)_3C_6H_2$, Y = Me, Cl, F	89
	R^1 = H, Cl; R^2 = Cl-, n = 1–3	89
		90
	Compounds with a heterocycle in their structure[c]	
	R = $CR^1R^2R^3$, cyclo-Alk, Ar, cyclo-Het; R^1, R^2 = Alk(C_{1-3}); R^3 = Alk(C_{1-10})	91
	R^1 = H, Alk; R^2 = $C(X)NHR^3$, $NHC(O)R^3$, $NHSO_2R^3$; X = O, S; R^3 = Alk, Ar, Het {Het = pyridyl, 2-benzo[*b*]thienyl, 2-benzo[*b*]thiophenyl, imidazolyl, pyridyl, thienyl, quinolinyl}	92, 93
	R = H, Me	94

[a] $(CH_2CH_2X)_m$ = $(CH_2)_m$ or $(CH_2)_m$–X–$(CH_2)_m$.

[b] A =

[c] Het = pyridyl, 2-benzo[*b*]thienyl, 2-benzo[*b*]thiophenyl, imidazolyl, pyridyl, thienyl, quinolinyl.

Table 1 (continued)

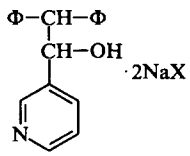
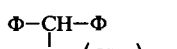
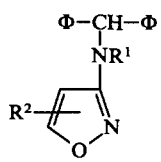
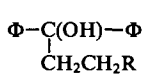
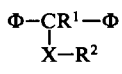
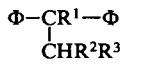
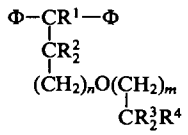
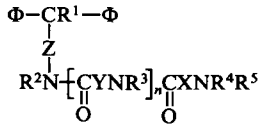
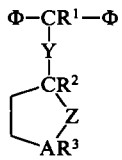
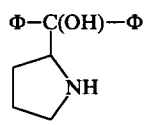
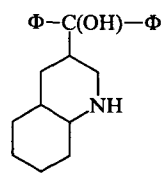
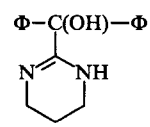
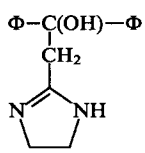
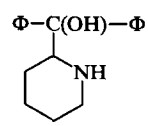
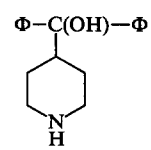
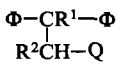
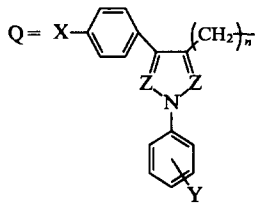
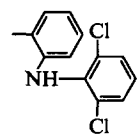
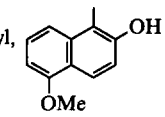
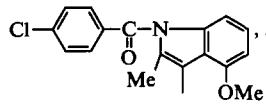
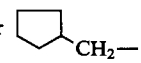
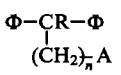
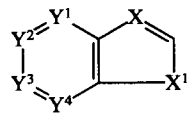
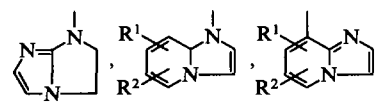
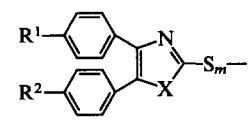
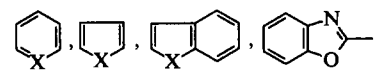
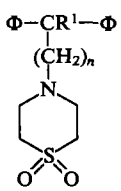
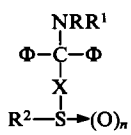
Formula	Substituents	Ref.
 (NE-58095)		95–97
	A = cycloalkyl (C_{5-8}), bicycloheptyl, bicycloheptenyl, saturated heterocycle (C_{4-7}) with O, S, SO, SO_2 groups; $m = 0-4$	98
	R^1 = H, Alk; R^2 = H, Alk, cyclo-Alk, Ph, alkenyl, phenylalkenyl, phenylalkyl, alkoxyphenylalkyl	99
	R = piperidinyl, morpholinyl	66
	X = alkylene (C_{2-8}); R^1 = H, OH, AcO, R^3N; R^2 = Het (Het = imidazole, oxazole, isoxazole, thiazole, pyridine, 1,2,3-triazole, 1,2,4-triazole, benzimidazole, alkyl-substituted), OAlk, Hal, OH, COOH, NH_2, NO_2, Ph, $PhCH_2$, CN, AlkOC(O), SAlk	100
	R^1 = H, OH, NH_2, R^4NH; R^2 = H, Alk; R^3 = Het	101
	R^1 = H, OH, NH_2; R^2, R^3 = H, Alk(C_{1-5}); R^4 = Het; m, n = 0–2	102
	R^1 = H, OH; R^2–R^5 = H, Alk; X, Y, Z = alkylene; n = 0–2 (R^2NZ, R^3NY, and R^4NX may be heterocycles)	103
	R^1 = H, OH, NH_2; R^2, R^3 = H, Alk; $R^2 + R^3$ = alkylene; Y = alkylene or bond; Z = heteroalkylene substituted or unsubstituted by an alkyl, benzyl, or cyclohexylmethyl group; A = N, CR^3; $Z + R^2$ = bond Examples:      	104

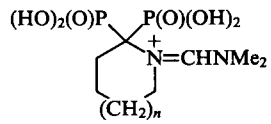
Table 1 (continued)

Formula	Substituents	Refs
	R^1 = H, Cl, OH, AcO, NH_2, $RCH_2C(O)O-$; R^2=H; R^1+R^2 = bond;	105, 106
	Q=  n = 0–2; X, Y = H, Cl, F; Z=CH, N, RC	
	For R^1 = OH: R^2 = H, Alk; Q^d = Ph (unsubstituted or substituted by Cl or F), biphenyl,	107–110
	1,2-naphthyl, 2-thienyl,  , $(CH_2)_n$Ar, 11-oxo-2-dibenzo[*b*,*f*]oxepinyl,  ,	
	 , 5-R^3,6-R^4-indan-1-yl, (R^3 =  or  ; R^4 = H, Cl);	
	R^5R^6CH, (R^5 = H, Me, Et; R^6 = phenoxyl, Ph, heteroaryl, etc.)	
	R = H, OH; n=0, 1;	111–113
	A =  X, X^1 = N, CH; X = X^1 ≠ CH; one of the Y^1-Y^4 = N, others are CH groups,	
	 R^1, R^2 = H, OH, Alk, Hal,	
	A = 	114
	R^1, R^2 = H, OH, OAlk, Hal; X = O, S, NH; m = 0, 1; n = 0–6	
	A = SR^3 (R^3=H, Alk, Ph, $-C(X)NZ^1Z^2$,  ; X = O, S; Z^1, Z^2 = H, Alk); n = 0–10	115
	R^1 = H, Me, Ph, OH; n = 0, 2, 5, 10	116, 117
	R = H, Alk(C_{1-5}), $CONH_2$; R^1 = H, Alk(C_{1-6}), CH_2Ph, Cl, MeC_6H_4, Ph; RR^1 = $(CH_2)_m$ (m = 4, 5); R^2 = Alk(C_{1-6}), cyclo-Alk(C_{5-7}), Ph, CF_3, 5-6-membered heterocycle with 1 or 2 heteroatoms (N, S); n = 0–2; X = $(CH_2)_{1-6}$	118, 119

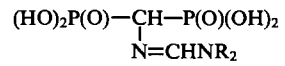
[a] Φ = $P(O)(OH)_2$.
[b] A = groups with antiinflammatory properties.
[c] Alkyl, aryl, and cycloalkyl groups can also be used instead of a heterocycle.
[d] Aromatic or heteroaromatic carboxylic acid residue with antiinflammatory and antipyretic properties.

5. Bactericidal, antiviral, and antitumour agents

Diphosphonic acids are capable of acting also upon bacteria. Thus the amidinodiphosphonic acids **8** and **9**, which possess bacteriostatic activity, have been patented.[120]



8, n = 0, 1;

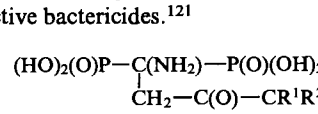


9, R = H, Me, Et.

They were obtained by the reaction of aminomethylenediphosphonates with formamides and $POCl_3$.

$$H_2NCH(PO_3H_2)_2 + HCONH_2 + POCl_3 \longrightarrow$$
$$\longrightarrow H_2N{-}CH{=}N{-}CH(PO_3H_2)_2$$

Compounds with the structure **10**, obtained by the phosphonylation of the 3-oxonitrile $R^1R^2R^3CC(O)CH_2CN$ with a mixture of H_3PO_3 and PBr_3 and subsequent hydrolysis, are effective bactericides.[121]

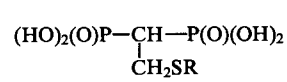


10

R^1 = Alk(C_{1-8}); R^2, R^3 = Me, Et.

The alkali metal salts of compound **10** exhibited an antimicrobial activity.[122]

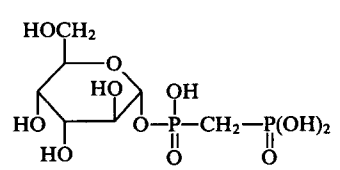
It is believed[123] that compounds with the structure **11** are potential inhibitors of the replication of the influenza A virus. They have been obtained by adding S-nucleophiles, such as thiophenol, 2-mercaptoethanol, ethanethiol, propane-1-thiol, and dodecane-1-thiol, to tetralkyl ethenylidenediphosphonates.



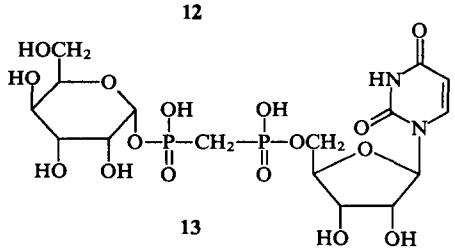
11

R = Et, Pr, Ph.

A series of geminal α-amino- and α-hydroxy-propylidene-α,α-diphosphonic acids derived from purines and pyrimidines (thymine, uracil, 6-methyluracil, and 5-fluorouracil) have been synthesised. They showed a low antiviral and a moderate antitumour activity on certain strains of tumours.[124] The synthesis and the results of biochemical studies on potential substrate inhibitors of glycosyltransferase on the surfaces of the membranes of cancer cells — the phosphonate analogues of nucleoside diphosphate sugars — have been described.[125] It was shown that, among all the intermediate and final products of synthesis, compound **12** exhibits a weak activity against the rhinovirus, while compound **13** inhibits competitively glycoproteingalactosyltransferase.

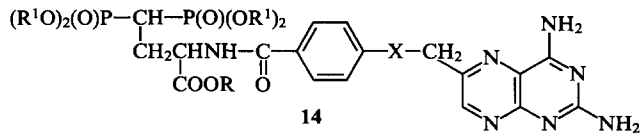


12



13

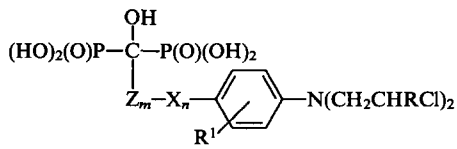
Geminal diphosphonic analogues of aminopterin (methotrexate) **14**, derivatives of 10*H*-deazamethopterin, and pharmaceutical compositions based on them have been proposed for the treatment of bone carcinomas, rheumatic psoriasis, different types of polymyositis, Reiter's disease, and rheumatic polyarthritis.[126]



14

X = NR or CHR^2; R, R^1 = Alk; R^2 = H, Alk.

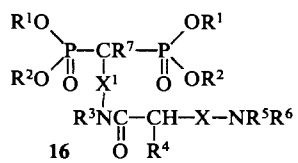
On the basis of the analysis of the structures of active diphosphonic acids, the authors of a patent application[127] proposed compounds **15**, containing two geminal phosphonate groups, a hydroxy-group, and a terminal amino-group in the hydrocarbon chain, as in ABD and APD [as antitumour agents? (Ed. of Translation)].



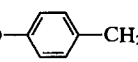
15

R = H, Me; R^1 = H, Hal, NH_2, OAlk, Alk;
Z = alkylene, aminoalkylene;
X = O, S, NH;
m, n = 0, 1.

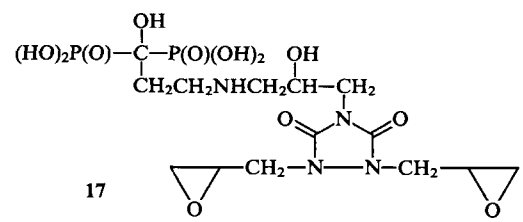
It was established that, as a result of their accumulation in bone tumours and metastases, compounds **15** induce a significant inhibition of the growth of tumours and increase the survival rate among rats. The rapid calcification of osteosarcoma and lung metastases was confirmed.[38] A patent has also been obtained for a method of synthesis of compounds **15** and pharmaceutical preparations based on them for the treatment of bone tumours.[128] It was shown that joint therapy using compounds **15**, APD, and melphalan yields the best results.[129] Compounds **16**, with an analogous structure, which are also inhibitors of malignant neoplasms, have been patented.[130]



16

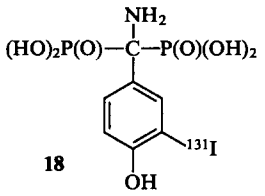
R^1, R^2 = H, Alk; R^3 = H, Alk, cyclo-Alk, Bn, Ph, MeO-  -CH_2;
R^4 = H, Alk, NH_2; R^5, R^6 = $HalCH_2CH_2$;
NR^5R^6 = aziridinyl; R^7 = H, Hal, OH, Alk;
X = alkylene, phenylene, arylalkylene;
X^1 = bond, alkylene, cycloalkylalkylene, arylalkylene.

It has been reported[131] that compound **17** also exhibits an appreciable antitumour activity and that the best results in the treatment of osteolytic metastases in rats were achieved by preliminary treatment with APD.



17

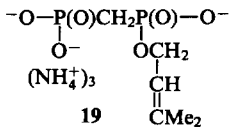
α-Amino-[3-^{131}I]-4-hydroxybenzylidenediphosphonate **18** was synthesised[132] in order to analgise and treat bone metastases. It proved to be the most effective among a series of analogues.[133,134] It has been noted that compound **18** accumulates in bone tissues and that its content is higher in diseased tissues than in healthy tissues. The β-emission from the compound has a smaller effect on bone marrow than the radiopharmaceutical preparations used previously.



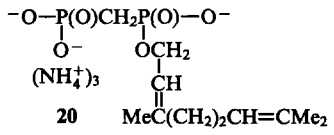
18

6. Artificial substrates and inhibitors of various enzymes

The search for synthetic substrates and inhibitors of various enzymes has continued. Thus the synthesis, properties, and the results of biochemical studies of dimethylallyl- and geranylmethylenediphosphonates **19** and **20**, which can serve as artificial substrates for prenyltransferase, have been described.[135]



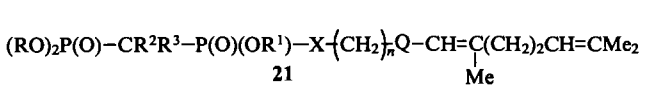
19



20

The ammonium salts of compounds **19** and **20** were synthesised by the reaction of $[HOPO_2CH_2PO_3]^{3-}(NBu_4^+)_3$ with $Me_2C{=}CHCH_2Br$ or geranyl chloride, which is obtained by treating geraniol with *N*-chlorosuccinamide and dimethyl sulfide. It has been established with the aid of compounds **19** and **20** that the presence of the high-energy O–P–O linkage is not important for enzymic reactions, but the structure containing two phosphorus atoms is topologically important for them. The behaviour of geranyl- and geranyldifluoro-methylenediphosphonates in reactions with various enzymes has been investigated.[136]

The synthesis of compounds **21**, used as inhibitors of squalene synthetase, has been described.[137]



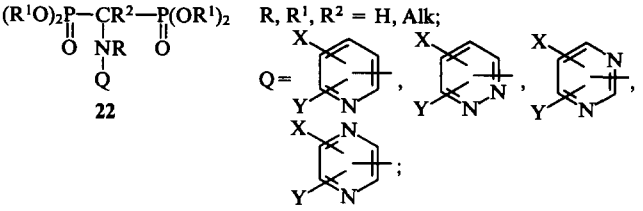
21

R, R^1 = M, H, Alk, alkenyl; R^2, R^3 = H, Hal; X = O, NH, NR^4; R^4 = Alk; Q = $-CH_2CH_2C(Me)=CH-$, bond; n = 1–4; when X = O, n = 2–4.

$(MeO)_2P(O)CH_2P(O)(OMe)OH$ in methylene chloride and ethyldiisopropylamine are treated with diphenylphosphoric acid chloride, after which farnesylamine is added and compounds **21** are obtained.

7. Herbicides

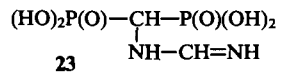
Diphosphonic acids exhibit also a herbicidal activity. Thus the syntheses and herbicidal properties of 46 compounds having the structure **22** have been described in patent applications.[138,139] The synthesis of compounds **22** is based on the reaction between the amino-derivatives of a N-containing heterocycle, $R^2C(OR^3)_3$, and dialkyl phosphite followed by the hydrolysis of the intermediates. (*N*-Pyridyl)aminomethylenediphosphonic acids **22** (R = R^1 = R^2 = H; Q = 3-X-2-pyridyl, X = H, alkyl, Hal; Y = H) and their salts are particularly effective in the fight against perennial weeds.[140]



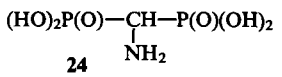
22

X, Y = H, Alk, Hal, NO_2, AcNH, CO_2H, CO_2Me, OH, OMe.

The formamidino- and aminomethylene-diphosphonic acids **23** and **24**, obtained from P_4O_6, anhydrous H_3PO_3, and $HCONH_2$ and by subsequent hydrolysis of the reaction mixture, are suitable as herbicides.[141]



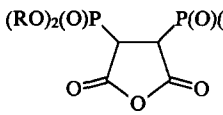
23



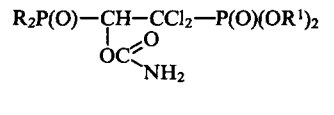
24

III. Vicinal diphosphonic acids

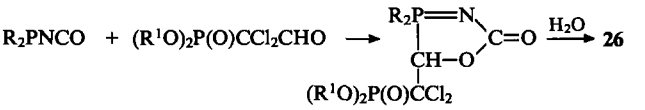
Among the biologically active diphosphonic acids, compounds with a vicinal structure occupy a modest place. Nevertheless, several representatives of substances of this class, which exhibit various types of activity, have been synthesised in recent years. Thus, 3,4-bis(dialkylphosphono)tetrahydrofuran-2,5-diones **25**, used as insecticides and acaricides, have been described in a patent.[142] The synthesis of compounds **26**, which, for R = BuO or Ph and R^1 = Et, exhibit weak pesticidal properties and affect the rate of plant growth, has been reported.[143] These compounds were synthesised by the reaction of phosphorus (III) acid isocyanates with phosphorylated acetaldehydes.



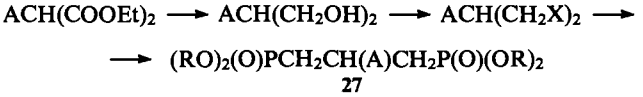
25



26



Specific inhibition of calcium metabolism at the celullar level is induced by the 1,3-diphosphonates **27**, synthesised in accordance with the following scheme;[144,145]

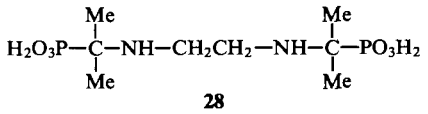


27

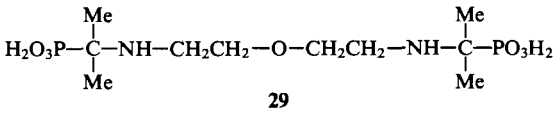
X = Hal, OTs; A = alkyl, arylalkyl, aryloxyalkyl; R = alkyl.

IV. Polyalkylpolyaminodiphosphonic acids

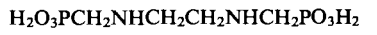
This group includes organophosphorus compounds containing a nitrogen atom in the alkylene chain adjoining the two PO_3H_2 groups. They are capable of activating certain enzymes. Nitrogen-containing diphosphonic acids such as ethylenediaminebisisopropylidenephosphonic acid **28** (phosphicine), 3-oxapentylenediamine-*N*,*N*′-bisisopropylidenephosphonic acid **29**, ethylenediamine-*N*,*N*′-bismethylenephosphonic acid **30**, ethylenediamine-*N*,*N*′-diacetic-*N*,*N*′-bismethylenephosphonic acid **31**, and 3-thiapentylenediamine-*N*,*N*′-bisisopropylidenephosphonic acid **32** possess this property.[12]



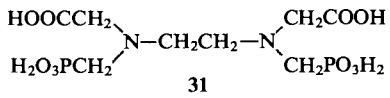
28



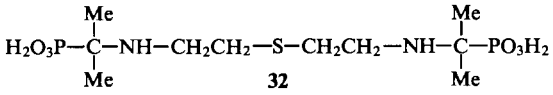
29



30



31

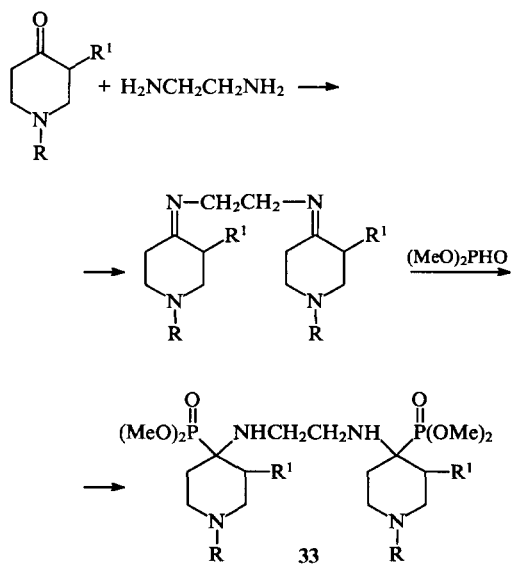


32

A systematic study of the biological properties of alkylenediaminebisalkylenephosphonic acids led to the discovery of the possibility of using substances of this type for the removal from the organism of incorporated toxic metals and also made it possible to discover the influence of these compounds on the removal of certain biologically important elements and on the state of metal complexes in the organism.

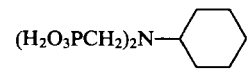
A characteristic feature of organophosphorus ligands containing a nitrogen atom in the alkylene chain linking the two PO_3H_2 groups is the preferential formation of complexes with cations having a small (Be, Fe) or large (lanthanides) radius but not with alkaline earth metals.[12] A unique property of substances of this group is the virtual absence of toxicity. By virtue of their ability to remove copper from the organism, they are used for the treatment of hepatocerebral dystrophy. Phosphicine is particularly effective for the removal of beryllium from the organism, without affecting calcium metabolism, and also for the removal of lead and uranium[11] and for the treatment of poisoning with alcohol.[4]

Phosphicine and its analogues have been synthesised by condensing the corresponding amine with the carbonyl group in aldehydes, ketones, piperidinones, etc. and with trivalent phosphorus compounds.[3] For example, treatment of alkylpiperidinones with ethylenediamine in benzene afforded[146] the corresponding bis-Schiff bases, which are made to react with dimethyl phosphite, whereby bis(phosphonylpiperidinyl)-ethylenediamines **33** are obtained.

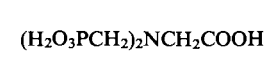


33

The syntheses of complexones **34** and **35** by the reaction of PCl_3 with glycine or cyclohexylamine in the presence of water followed by the interaction of the resulting intermediate with an aldehyde have been described.[147]

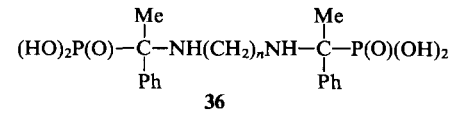


34

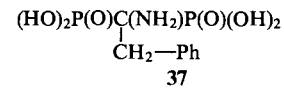


35

The alkylenediaminediphosphonic acids **36** (n = 2, 6), used to inhibit calcium salts, have been synthesised via the intermediate sodium ammonium salts.[148] It has been suggested[149] that 1-amino-2-phenylethylidenediphosphonic acid **37**, obtained by the reaction of $PhCH_2CN$ with PCl_3 and H_3PO_3, be used for the removal of toxic elements from the organism.

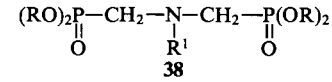


36



37

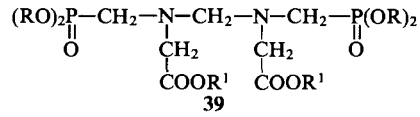
Phosphorus-containing complexones **38** have found extensive applications in medicine.[150-153]



38

R = H, M; R^1 = H, Alk, Ph, Bn, cyclo-C_6H_{11}.

Compounds **39**, which exhibit a herbicidal activity, have been patented.[154]

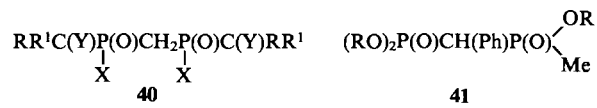


39

R = Ph; R^1 = Alk, arylalkyl.

V. Phosphonophosphinates and diphosphinates

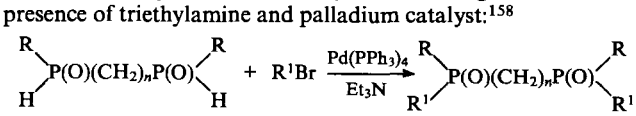
The reaction of esters of methylenediphosphonous acids with carbonyl compounds, which lead (after the hydrolysis) to the corresponding bis[α-hydroxyalkyl(aryl)]methylenediphosphinic acids **40**, has been investigated.[155,156] Compounds **40** are obtained also in the reaction of trialkylmethylenediphosphonite with benzaldehyde in the presence of a base. α-Phosphorus-substituted benzylphosphonate **41** is also formed in this reaction as an addition product.[155]



40 41

X = Cl, Alk, OAlk, OH; Y = Cl, OH; R = H, Me, Et;
R^1 = Alk(C_{2-6}), Ph.

Systematic study of the pesticidal activity of the derivatives of methylenediphosphorus acids showed that they can exhibit growth regulating, herbicidal, and fungicidal activities.[157] It has been suggested that diphosphonates with tetra- and hexamethylene bridges be obtained by the following reaction in the presence of triethylamine and palladium catalyst:[158]

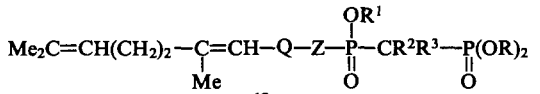


R = EtO, Ph; R_1 = Ph, 4-ClC_6H_4, 4-$Me_2NC_6H_4$, 4-$NO_2C_6H_4$, 4-AcC_6H_4, 2-naphthyl, etc.

Compounds **42**, which strengthen the bone tissue and can be used in stomatology, have been described.[159] They are synthesised by the reaction of $Ph_2P(O)CF_2Br$ with PCl_3 in the presence of zinc dust followed by hydrolysis and the oxidation of the intermediate with distilled water.

$$Ph_2P(O)-CF_2-P(O)(OH)_2$$
42

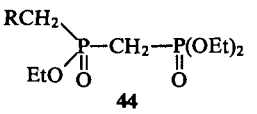
Alkenylphosphinylmethylphosphonates **43** are inhibitors of squalene synthetase, which are used as agents reducing the level of cholesterol.[160]



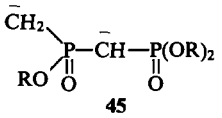
43

R, R^1 = H, Alk, M; R^2, R^3 = H, Hal; Z = $(CH_2)_n$, $(CH_2)_pCH=CH(CH_2)_m$; Q = $CH_2CH_2C(Me)=CH$, bond; n = 1–5, m,p = 0–2.

It has been suggested that the phosphinylphosphonyl compounds **44**, obtained by the Arbuzov reaction involving $(EtO)_2PCH_2P(O)(OEt)_2$ and the corresponding alkyl halides RCH_2Br [R = $CH_2CH_2C(Me)=CH_2$ or $Me_2C=CHCH_2$] be used as analogues of natural isoprenoids—isopentenyl and dimethylallyl diphosphates. The ammonium salts of both analogues are competitive inhibitors of the [1′,4]-condensation of isopentenyl diphosphate and geranyl diphosphate catalysed by diphosphate synthetase.[161] Furthermore, it has been reported[162] that the phosphinylphosphonyl dianion **45** is capable of undergoing the alkylation reaction with a multiplicity of electrophiles such as ethyl iodide, geranyl bromide, benzyl bromide, etc., which permits its use in the synthesis of analogues of natural diphosphates.

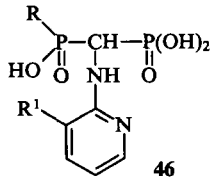


44



45

It has been established[94] that, in contrast to pyridylaminomethylenediphosphinates and the corresponding diphosphonates, pyridylaminomethylenephosphonoalkylphosphinates **46** exhibit a satisfactory antiresorptive activity.



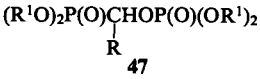
46

R = Me, Bu, $Ph(CH_2)_4$; R^1 = H, Me.

The synthesis of compounds **46** is based on the reaction of equimolar amounts of $(EtO)_2P(O)CH(OEt)_2$, EtO(R)P(O)H, and 2-aminopyridine (or 2-amino-3-methylpyridine) and subsequent hydrolysis.

VI. Phosphonophosphates

Nguyen Lan et al.[89] synthesised and investigated the medical and biological properties of geminal diphosphonates and phosphonophosphates **47**. It was established that, in relation to plasma lipids, these compounds exhibit the maximum pharmacological activity among all the substances of a similar type obtained and they are therefore potential antiatherosclerotic agents.



47

R^1 = H, Alk; R = Alk, Ph, $PhCMe_2$, $PhOCMe_2$, $PhCH_2CMe_2$, $ClC_6H_4C(O)C_6H_4$, cyclo-C_6H_{11}, 2-naphthyl, biphenylyl.

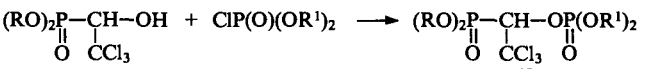
These compounds increase the concentration of the high density lipoprotein cholesterol, the amount of phospholipids, and the ratio of α-cholesterol to β-cholesterol. Compound **47** (R^1 = Me, R = 4-ClC_6H_4) was selected for further pharmacological and clinical studies.

Two methods were used to obtain these compounds, each of which begins with the formation of acylphosphonates $RC(O)P(O)(OR^1)_2$ via the reaction of RCOCl with trialkyl phosphite at 0 °C without a solvent.

The interaction of acylphosphonate with dialkyl phosphites in the presence of 80–100 mol% of dialkylamine at 0 °C in diethyl ether leads to geminal phosphonophosphates,[163] while in the presence of the catalytic amount (~5%) of an amine it affords geminal hydroxyldiphosphonates $RC(OH)[P(O)(OR^1)_2]_2$, which isomerise to phosphonophosphates on refluxing in alcohol.

The interaction of acylphosphonate with dialkyl phosphites at 80 °C without a solvent leads to geminal phosphonophosphates.[89]

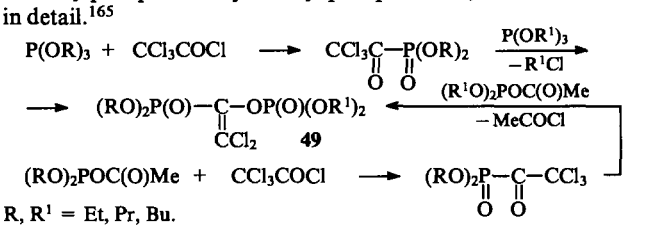
The synthesis of esters of α-(dialkylphosphono)-β,β,β-trichloroethylphosphoric acid **48** from the esters of α-hydroxy-β,β,β-trichloroethylphosphonic acid and the chlorides of dialkylphosphoric acids in the presence of triethylamine were described as early as 1958.[164]



48

R, R^1 = Alk(C_{1-4}).

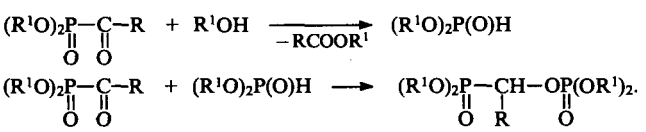
The esters showed strong insecticidal properties and also acted on certain species of stinging insects. The mechanism of the reactions of trialkyl phosphites and dialkyl acetyl phosphites with the chlorides of chloroacetic acids, leading to the formation of α-dialkylphosphonovinyl dialkyl phosphates **49**, has been studied in detail.[165]



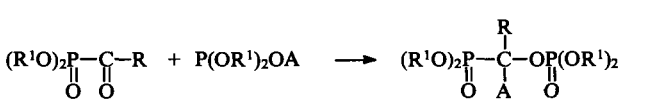
49

R, R^1 = Et, Pr, Bu.

It has been noted[166] that dialkyl α-dialkylphosphonoalkyl phosphates **47** are formed in the reaction of esters of α-ketophosphonic acids with alcohols and amines in 55% yield.

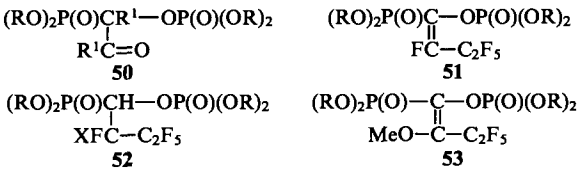


In a review devoted to esters of α-ketophosphonic acids,[167] the latter compounds are regarded as the most convenient initial reagents for the synthesis of phosphonophosphates in accordance with the following scheme:



A = Alk, C(O)Me.

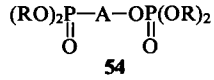
Yet another method of synthesis of phosphonophosphates in yields of above 50% from the esters of α-ketophosphonic acids involves the interaction of the latter with $LiN(CPr^i)_2$ or NaH in tetrahydrofuran.[168] A method of synthesis of phosphonophosphates by the reaction of trialkyl phosphite and R'C(O)X (X = Hal, Ac, NH_2, alkylamino-group, or alkoxy-group) below 45 °C, involving treatment of the intermediate with dialkyl phosphite in the presence of an organic base (NMe_3, NEt_3, Py) in a catalytic amount, has been patented.[169] The yield of the phosphonophosphates reaches 96% in this process. It has been suggested[170] that the reaction of tetraalkyl pyrophosphites $(RO)_2POP(OR)_2$ (R = Pr, Et) or dialkyl acyl phosphite with trifluoroacetic acid in acetonitrile be used for the synthesis of fluorinated phosphonophosphates. The synthesis of fluorine-containing phosphonophosphates **50** in yields in excess of 60% by the reaction of dialkyl phosphites with perfluorinated carboxylic acid anhydrides $(R^1CO)_2O$ ($R^1 = CF_3$, C_2F_5, C_3F_7) has been described.[171] The synthesis of the fluorinated phosphono-phosphates **51**, **52** (X = F, OMe), and **53** has also been investigated.[172]



50 **51**

52 **53**

The halogenated phosphonophosphates **54** have been obtained from PCl_3 and epoxyethane in the presence of $TiCl_4$ and by subsequent treatment of the intermediate with the chloride of monochloroacetic acid.[173]



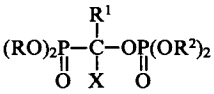
54

R = haloalkyl, for example CH_2CH_2Cl; A = CR^1R^2, $HC{=}CR^1$; R^1 = H, Hal, Alk; R^2 = H, Hal.

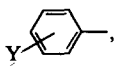
The phosphonates **55** have been obtained in yields of about 92% in two ways.

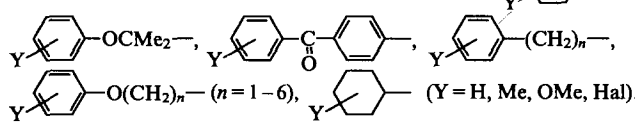
1. By the reaction of dialkyl phosphite with the corresponding acyl chloride in the presence of dialkylamine and the subsequent interaction of the resulting acylphosphonate with a phosphonite.

2. By the reaction of the corresponding aryl or aroyl halide with methylenediphosphonate and subsequent treatment of the resulting aryl or aroyl diphosphonate.



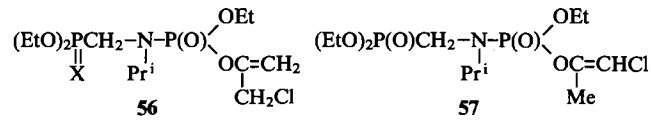
55

X = H, OH, OAc, NH_2; R, R^2 = H, Alk; R^1 = Bu^t,  ,



(Y = H, Me, OMe, Hal).

These compounds act on lipids and the lipid metabolism, lower the level of free aliphatic acids and triglycerides in the serum, increase the amount of phospholipids, and regulate the concentration of cholesterol. The acids **55** and their salts diminish the amount of calcium in the rat serum. Some of the derivatives are antiatherosclerotic and hypoglycemic agents.[85,86] The effect of compounds **56** and **57** on the enzymes of the Colorado beetle has been reported.[174]



56 **57**

X = O, S.

The above compounds inhibit arylesterase, carboxylesterase, acetylcholinesterase, and butyrylcholinesterase of insects, inducing 50% – 100%, mortality in 24 h.

* * *

Analysis of the scientific-technical and patent literature for the last two decades has shown that derivatives of phosphonic acids containing two phosphorus atoms (MDP, HEDP, diphosphonic analogues of amethopterin, phosphicine) have found extensive applications in medicine. These compounds are used as radiopharmaceutical preparations for the treatment of bone diseases and malignant tumours. The practical interest attaching to the physiological properties of compounds containing two phosphorus atoms has led to a vigorous search for ways of synthesising them. Although the syntheses of new preparations are usually based on known phosphonylation methods (the Arbuzov, Michaelis–Bekker, Kabachnik–Fields, Todd–Atherton, etc. methods), an expansion of the range of the initial reagents and the optimisation of the conditions in the above reactions are to be expected in the next few years. This is because the mechanisms and modes of many phosphonylation reactions depend to a considerable extent on the initial conditions. Furthermore, the use of organophosphorus compounds containing specific groups (formyl, amino-, epoxy-, etc.) is promising, which will permit a wider employment of 'non-phosphorus' reactions for the synthesis of diphosphonates and phosphonophosphates.

References

1. J D Curry, D A Nicholson, O T Quimby *Topics in Phosphorus Chemistry* 7 37 (1972)
2. R Engel *Chem. Rev.* 77 349 (1977)
3. Yu E Vel'tishchev, E A Yur'eva, A N Kudrin, A I Korytnyi, O G Arkhipova, N V Alekseeva, L V Krinitskaya, V K Shcherbakov, E A Varsanovich *Khim.-Farm. Zh.* 17 282 (1983)
4. V I Yudelevich, E V Komarov, B I Ionin *Khim.-Farm. Zh.* 19 668 (1985)
5. H Fleisch *Metab. Bone Dis. Relat. Res.* 3 279 (1981)
6. N M Gulaya, S V Komissarenko *Usp. Biol. Khim.* 22 195 (1982)
7. H Fleisch *Bone Miner. Res.* 1 319 (1983)
8. K Lindenhayn, H Haehnel, K Trzenschik, G Buehler, H H Haelmann *Dtsch. Gesundheitswes.* 39 1725 (1984)
9. D M Kramsch, in *Calcium Biol. Symp. 67th 1983* (1985) p. 685
10. O L M Bijvoet, S E Papapoulos, C W G M Loewik, H I T Harinck, *Excerpta Med. Int. Congr. Ser.* 735 93 (1987)
11. M I Kabachnik, T Ya Medved', N M Dyatlova, M V Rudomino *Usp. Khim.*, 43 1554 (1974) [*Russ. Chem. Rev.* 43 733 (1974)]
12. M I Kabachnik, N M Dyatlova *Fosforsoderzhashchie Kompleksony* (Phosphorus-containing Complexones) (Moscow: Znanie, 1989)
13. T Czekanski, S Witek, H Gross, B Costisella *Wiad. Chem.* 41 801 (1987)
14. S V Komissarenko, I N Kolesnikov, G Fomovskaya *Ukr. Biokhim. Zh.* 57 (2), 56 (1985)
15. K B Yatsimirskii, P A Manorik, G G Gaivoronskaya, E I Lopanina, N K Dovedenko, S V Komissarenko *Dokl. Akad. Nauk Ukr. SSR, Geol., Khim. Biol. Nauki* 11 55 (1983)
16. G G Gaivoronskaya, S I Strel'chuk, S V Komissarenko *Tsitologiya Genetika* 15 (5), 41 (1981)
17. E.O.Pajunen, O.E.O.Hormi, J.H.Näsman, in *VIII Int. IUPAC Conf. Org. Synth., Helsinki, 1990 (Abstr.)* p. 134
18. DDR P. 214610; *Chem. Abstr.* 103 196242 (1985)

19. I L Odinets, Z S Novikova, I F Lutsenko *Zh. Obshch. Khim.* **57** 525 (1987)
20. Z S Novikova, I L Odinets, I F Lutsenko *Zh. Obshch. Khim.* **55** 553 (1985)
21. Polish P. 136 622
22. R A Evans, C R Howlett, C R Dunstan, E Hills *Clin. Orthop. Relat. Res.* **165** 290 (1982)
23. A Jung, J Bornand, B Mermillod, C Edward, P J Meunier *Cancer Res.* **44** 3007 (1984)
24. M Pollard, P H Luckert *J. Natl. Cancer Inst.* **75** 949 (1985)
25. M Pollard, P H Luckert *Prostate (N.Y.)* **8** 81 (1986)
26. R Felix, H Fleisch, R Schenk *Experientia* **42** 302 (1986)
27. Czech P. 204 721; *Chem. Abstr.* **101** 23 716 (1984)
28. Czech P. 209 177; *Chem. Abstr.* **100** 6855 (1984)
29. Czech P. 209178; *Chem. Abstr.* **100** 6854 (1984)
30. Czech P. 204 722; *Chem. Abstr.* **101** 23 715 (1984)
31. D J Rowe, S J Hays *Metab. Bone Dis. Relat. Res.* **5** 13 (1983)
32. G M Blackburn, D A England, F Kolkmann *J. Chem. Soc., Chem. Commun.* 930 (1981)
33. US P. 4 478 761
34. E Fluck *Chem.-Ztg.* **105** 323 (1981)
35. US P. 4 478 763; *Chem. Abstr.* **102** 95 821 (1985)
36. O L M Bijvoet. *Pharm. Weekbl.* **119** 557 (1984)
37. V M Derzhavin, I V Kazanskaya, M M Zavurbegov, N V Alekseeva, N S Kozyreva, O A Troetskii, T M Balashova, in *Doklady II Vsesoyuznogo Rabochego Soveshchaniya po Primeneniyu Kompleksonov v Meditsine, 1989* (Reports at the IInd All-Union Working Conference on the Applications of Complexones in Medicine, 1989) (Eds Yu E Vel'tishchev, N M Dyatlova, E A Yur'eva) (Moscow, 1990) p. 51
38. F Wingen, H Sterz, H Blum, H Moeller, W Pittermann, B L Pool, H J Sinn, H Spring, D Schmaehl *J. Cancer Res. Clin. Oncology* **111** 209 (1986)
39. E A Yur'eva, O G Arkhipova, E K Balandina, N B Alekseeva, E S Vozdvizhenskaya, E A Varsanovich, L V Krinitskaya, T A Matkovskaya, in *Khimiya Kompleksonov i Ikh Primenenie* (The Chemistry of Complexones and Their Applications) (Ed. E A Ryabenko) (Moscow, 1985) p. 130
40. K Ohya, H Fleisch *Ensho* **4** 471 (1984)
41. J P Mallon, A Boris, G F Bryce, in *V Proc. Workshop Vitamin D* 809 (1982)
42. G N Krasovskii, L M Airapetova *Gigiena i Sanitariya* 88 (1983)
43. USSR P. 783 300; *Ref, Zh. Khim.* 9H83 (1981)
44. USSR P. 857 143; *Chem. Abstr.* **96** 69 208 (1982)
45. USSR P. 889 661; *Chem. Abstr.* **97** 39 139 (1982)
46. Spanish P. 493 010; *Chem. Abstr.* **96** 52 502 (1982)
47. Jpn. Appl. 82-88188; *Chem. Abstr.* **97** 182 660 (1982)
48. US P. 4 332 736; *Chem. Abstr.* **97** 163 254 (1982)
49. Polish P. 117 685; *Chem. Abstr.* **99** 140 167 (1983)
50. USSR P. 1 065 418; *Chem. Abstr.* **101** 38 650 (1984)
51. Belg. P. 1 000 075; *Chem. Abstr.* **109** 54 960 (1988)
52. L V Krinitskaya, E N Urinovich, T N Balashova, R P Lastovskii, in *Kompleksony i Khelatiruyushchie Sorbenty. Nauchnye Trudy VNII Khimicheskikh Reaktivov i Osobo Chistykh Khimicheskikh Veshchestv* (Complexones and Chelating Sorbents. Scientific Transactions of the All-Union Institute of Chemical Reagents and Specially Pure Chemicals) (Moscow: Izd. IREA, 1982) p. 93
53. L A Valitova, Sh N Ibragimov, N A Shibinskaya, B E Ivanov, G Ya Gordon, in *Khimiya i Tekhnologiya Elementoorganicheskikh Soedinenii i Polimerov. Mezhvuzovskii Sbornik Nauchnykh Trudov* (The Chemistry and Technology of Organoelement Compounds and Polymers. Intercollegiate Collection of Scientific Communications) (Ed. P A Kirpichnikov) (Kazan: Izd. Kazan. Khim.-Tekhnol. Inst., 1987) p. 12
54. L V Krinitskaya, E N Urinovich, T N Balashova, N P Nikonova, in *Kompleksony i Khelatiruyushchie Sorbenty. Nauchnye Trudy VNII Khimicheskikh Reaktivov i Osobo Chistykh Khimicheskikh Veshchestv* (Complexones and Chelating Sorbents. Scientific Transactions of the All-Union Institute of Chemical Reagents and Specially Pure Chemicals) (Moscow: Izd. IREA, 1982) p. 83
55. Hung. P. 34 759; *Chem. Abstr.* **103** 178 455 (1985)
56. Hung. P. 192 796
57. DDR P. 106 654
58. DDR P. 213 929; *Chem. Abstr.* **102** 221 018 (1985)
59. DDR P. 216 465
60. BRD Appl. 2 165 833; *Ref. Zh. Khim.*, 23H129 (1974)
61. C Nagant de Deuxchaisnes, C Rombouts-Lindemans, J P Huaux, in *Diphosphonates and Bone, IV Symp. CEMO, 1981* (Eds A Donath, B Courvoisier) (Geneva: Med. Hyg., 1982) p. 303; *Chem. Abstr.* **100** 96 683 (1984)
62. Belg. P. 896 453; *Chem. Abstr.* **100** 175 062 (1984)
63. US P. 4 621 077; *Chem. Abstr.* **111**, 187 624 (1989)
64. E B Mawer, P E Still, A R Morton, D C Anderson, in *VII Proc. Workshop Vitamin D* 1988, p. 869
65. BRD Appl. 3 804 686; *Chem. Abstr.* **113** 52 505 (1990)
66. USSR P. 1 002 300; *Chem. Abstr.* **99** 22 702 (1983)
67. BRD Appl. 3 151 038; *Ref. Zh. Khim.* 6H89 (1984)
68. Belg. P. 903 519; *Chem. Abstr.* **105** 191 395 (1986)
69. Eur. Appl. 320 455 ; *Chem. Abstr.* **112** 21 139 (1990)
70. Eur. Appl. 371 921; *Chem. Abstr.* **113** 172 349 (1990)
71. Eur. Appl. 387 194; *Chem. Abstr.* **114** 122 708 (1991)
72. BRD Appl. 3 623 397; *Chem. Abstr.* **108** 186 991 (1988)
73. US P. 4 922 007; *Chem. Abstr.* **113** 132 508 (1990)
74. DDR P. 222 030; *Chem. Abstr.* **106** 84 838 (1987)
75. DDR P. 235 068
76. BRD Appl. 3 334 211; *Chem. Abstr.* **103** 88 082 (1985)
77. PCT Int. Appl. WO 86-00902; *Chem. Abstr.* **105** 153 318 (1986)
78. Fr. Appl. 2 574 409; *Byull. Izobret.* **24** (1986)
79. Fr. Appl. 2 574 410; *Byull. Izobret.* **24** (1986)
80. Jpn. Appl. 88-88192; *Chem. Abstr.* **109** 129 298 (1988)
81. Jpn. Appl. 90-104 593; *Chem. Abstr.* **114** 82 119 (1991)
82. Jpn. Appl. 90-268 190; *Chem. Abstr.* **115** 49 974 (1991)
83. Eur. Appl. 325 482; *Chem. Abstr.* **112** 21 140 (1990)
84. BRD Appl. 3 540 150; *Chem. Abstr.* **107** 96 888 (1987)
85. US P. 4 416 877; *Chem. Abstr.* **100** 114 996 (1984)
86. Brit. Appl. 2 079 285; *Chem. Abstr.* **96** 218 031 (1982)
87. Fr. Appl. 2 629 716; *Ref. Zh. Khim.* 11O286 (1990)
88. BRD Appl. 3 225 469; *Chem. Abstr.* **100** 210 141 (1984)
89. M Nguyen Lan, E Niesor, C L Bentzen. *J. Med. Chem.* **30** 1426 (1987)
90. Eur. Appl. 189 662; *Chem. Abstr.* **106** 18 815 (1987)
91. BRD Appl. 3 724 653; *Chem. Abstr.* **111** 39 582 (1989)
92. Eur. Appl. 243 173; *Chem. Abstr.* **108** 94 778 (1988)
93. Jpn. Appl. 62-270 593; *Ref. Zh. Khim.* 5O26 (1989)
94. F H Ebetino, L A Jamieson *Phosphorus Sulfur Silicon Relat. Elem.* **51–52** 23 (1990)
95. T J Wronsky, L M Dann, K S Scott, L R Crooke *Endocrinology (Baltimore)* **125** 810 (1989)
96. W K Sietsema, F H Ebetino, A M Sabvagno, J A Bevan *Drugs Exp. Clin. Res.* **15** 389 (1989)
97. M D Francis, K Hovaneik, R W Boyce *Int. J. Tissue React.* **11** 239 (1989)
98. Eur. Appl. 337 706; *Chem. Abstr.* **112** 158 640 (1990)
99. Eur. Appl. 282 320; *Chem. Abstr.* **110** 128 650 (1989)
100. BRD Appl. 3 428 524; *Chem. Abstr.* **105** 134 140 (1986)
101. BRD Appl. 3 626 058; *Chem. Abstr.* **108** 186 996 (1988)
102. BRD Appl. 3 917 153; *Chem. Abstr.* **114** 164 505 (1991)
103. BRD Appl. 3 512 536; *Chem. Abstr.* **108** 187 281 (1988)
104. BRD Appl. 3 640 938; *Ref. Zh. Khim.* 12O135 (1989)
105. BRD Appl. 3 203 307; *Ref. Zh. Khim.* 6O69 (1984)
106. Israeli P. 67 762; *Chem. Abstr.* **109** 93 323 (1988)
107. BRD Appl. 3 203 308; *Chem. Abstr.* **99** 176 064 (1983)
108. Eur. Appl. 84 822; *Chem. Abstr.* **100** 6842 (1984)
109. Brit. Appl. 2 113 688; *Chem. Abstr.* **99** 176 071 (1983)
110. BRD Appl. 3 203 309; *Chem. Abstr.* **99** 195 220 (1983)
111. Jpn. Appl. 90-48 587; *Chem. Abstr.* **113** 78 695 (1990)
112. Jpn. Appl. 2 138 288; *Ref. Zh. Khim.* 16O133 (1991)
113. Eur. Appl. 354 806; *Chem. Abstr.* **113** 24 240 (1990)
114. Jpn. Appl. 63-66 190; *Ref. Zh. Khim.* 17O93 (1989)
115. Eur. Appl. 100 718; *Chem. Abstr.* **100** 192 078 (1984)
116. BRD Appl. 3 232 997; *Chem. Abstr.* **101** 91 221 (1984)
117. BRD Appl. 3 232 998; *Chem. Abstr.* **101** 72 946 (1984)
118. Eur. Appl. 151 072; *Chem. Abstr.* **103** 215 560 (1985)
119. Czech P. 247 198
120. BRD Appl. 3 208 600; *Chem. Abstr.* **100** 68 524 (1984)
121. BRD Appl. 3 611 522; *Chem. Abstr.* **108** 132 051 (1988)
122. H Blum *Z. Naturforsch.* **43** 75 (1988)

123. D W Hutchinson, D M Thornton *J. Organomet. Chem.* **346** 341 (1988)
124. G S Sakovich, V N Konyukhov, E V Larina, G M Anoshina, in *Komponenty Nukleinovykh Kislot. VIII Vsesoyuznyi Simpozium po Tselenapravlennomu Izyskaniyu Lekarstvennykh Veshchestv, Riga, 1989 (Tezisy Dokladov)* [Components of Nucleic Acids. The VIIth All-Union Symposium on the Specific Utilisation of Medicinal Drugs, Riga, 1989 (Abstracts of Reports)] p. 27
125. M M Vagnefi, P J Bernacki, W J Hennen, R K Robins *J. Med. Chem.* **30** 1391 (1987)
126. Fr. Appl. 2 611 203; *Ref. Zh. Khim.* 7O152 (1990)
127. BRD Appl. 3 425 812; *Chem. Abstr.* **105** 172 720 (1986)
128. Eur. Appl. 170 896; *Byull. Izobret.* 7 (1986)
129. F Wingen, B L Pool, P Klein, T Klenner, D Schmaehl *Invest. New Drugs* **6** 155 (1988)
130. PCT Int. Appl. WO 91-05 791; *Chem. Abstr.* **115** 71 885 (1991)
131. F Wingen, T Eichmann, C Manegold, B Krempien *J. Cancer Res. Clin. Oncol.* **111** 35 (1986)
132. M Eisenhut, B Kimmig, B Bubeck, D M Taylor, K Winkel *J. Labelled Comp. and Radiopharm.* **21** 1092 (1984)
133. BRD Appl. 3 425 746; *Chem. Abstr.* **105** 172 722 (1986)
134. M Eisenhut, J Barber, D M Taylor *Appl. Radiat. Isot.* **38** 535 (1987)
135. T Gotoh, T Koyama, K Ogura *Chem. Lett.* 1627 (1987)
136. K E Stremler, C D Poulter *J. Am. Chem. Soc.* **109** 5542 (1987)
137. Eur. Appl. 356 866; *Chem. Abstr.* **113** 115 623 (1990)
138. BRD Appl. 2 831 578; *Chem. Abstr.* **90** 187124 (1979)
139. Jpn. Appl. 79-144 383; *Chem. Abstr.* **93** 26 547 (1980)
140. US P. 4 447 256; *Chem. Abstr.* **101** 192 195 (1984)
141. DDR P. 249 482; *Ref. Zh. Khim.* 5H159 (1988)
142. DDR P. 246 023; *Chem. Abstr.* **108** 108 180 (1988)
143. R I Tarasova, T A Dvoinishnikova, N I Sinitsyna, F I Guseinov, V M Ismailov, V V Moskva *Zh. Obshch. Khim.* **59** 1031 (1989)
144. M Nguyen Lan, T Phan Hieu, S A Symphar, in *XI International Conference on Phosphorus Chemistry, Tallin, 1989* Vol. 2 (Abstr. Post.) p. 4
145. J R Rossier, J A Cox, E J Niesor, C L Bentzen *J. Biol. Chem.* **264** 16 598 (1989)
146. B Zh Dzhiembaev, B D Abiyurov, N I Zaporozhskaya, B U Minbaev *Zh. Obshch. Khim.* **59** 77 (1989)
147. Hung. P. 177 486
148. I V Shevchenko, Kh Sh Karimov, in *Organicheskie Kompleksoobrazuyushchie Soedineniya* (Sbornik Nauchnykh Trudov) [Organic Complex-forming Compounds (Collected Scientific Communications)] (Eds A B Alovitdinov, M S Mirkamilova) (Tashkent: Izd. Tashkent. Ped. Inst., 1987) p. 6
149. M M Grigorovich, T A Bandurina, I I Kalinchenko, V N Konyukhov, in *III Vsesoyuznoe Soveshchanie po Khimicheskim Reaktivam* (The IIIrd All-Union Conference on Chemical Reagents) (Ashkhabad, 1989) Part 2 (Abstracts of Reports) p. 30
150. Czech P. 190 240; *Chem. Abstr.* **96** 199 881 (1982)
151. F I Bel'skii, I B Goryunova, P B Petrovskii, T Ya Medved', M I Kabachnik *Izv. Akad. Nauk SSSR, Ser. Khim.*103 (1982)
152. USSR P. 1 011 650; *Byull. Izobret.* **14** 101 (1983)
153. B P Strumin, F F Khizbullin *Zh. Obshch. Khim.* **59** 537 (1989)
154. US P. 4 601 744; *Chem. Abstr.* **106** 5229 (1987)
155. I L Odinets *Vzaimodeistvie Proizvodnykh Metilen-difosforsoderzhashchikh Kislot s Karbonil'nymi Soedineniyami* (Interaction of Derivatives of Methylenediphosphorus Acids with Carbonyl Compounds) (Moscow, 1983); deposited at the All-Union Institute of Scientific and Technical Information (VINITI) 28.12.83, No. 7085-83
156. USSR P. 10 744 878; *Byull. Izobet.* **7** 89 (1984)
157. Z S Novikova, I L Odinets, I F Lutsenko, N G Rozhkova, G L Abramova, E I Andreeva *Vestn. Mosk. Univ., Ser. 2: Khim.* **27** 401 (1986)
158. Y Xu, H Wei, J Xia *Liebigs Ann. Chem.* 1139 (1988)
159. Jpn. Appl. 59-137 496; *Ref. Zh. Khim.* 19O42 (1985)
160. Eur. Appl. 324 421; *Chem. Abstr.* **112** 77 633 (1990)
161. R W McClard, T S Fujita, K E Stremler, C D Poulter *J. Am. Chem. Soc.* **109** 5544 (1987)
162. M H B Stowell, J F Witte, R W McClard *Tetrahedron Lett.* **30** 411 (1989)
163. USSR P. 1 207 397; *Byull. Izobret.* **3** (1986)
164. K V Nikonorov *Izv. Akad. Nauk SSSR, Otd. Khim. Nauk* 1340 (1958)
165. A N Pudovik, T Kh Gazizov *Zh. Obshch. Khim.* **39** 2225 (1969)
166. A P Pashinkin, T Kh Gazizov, A N Pudovik *Zh. Obshch. Khim.* **40** 28 (1970)
167. Yu A Zhdanov, L A Uzlova, Z I Glebova *Usp. Khim.* **49** 1730 (1980) [*Russ. Chem. Rev.* **49** 843 (1980)]
168. E Breuer, R Karaman, A Goldblum *Phosphorus Sulfur* **21** 119 (1984)
169. US P. 4 407 765; *Ref. Zh. Khim.* 17N146 (1984)
170. E N Ofitserov, V F Mironov, I V Konovalova, A N Pudovik *Zh. Obshch. Khim.* **53** 1941 (1983)
171. S F Aleinikov, V I Krutikov, A V Golovanov, A N Lavrent'ev *Zh. Obshch. Khim.* **55** 2792 (1985)
172. T Ishihara *Synthesis and Reactions of Fluorinated Enol Phosphates and Alkenephosphonates* (Tokyo, 1983); Article deposited at the All-Union Institute of Scientific and Technical Information (VINITI) 05.84, No. 68 238
173. BRD Appl. 3 643 684; *Chem. Abstr.* **110** 39 182 (1989)
174. V S Petrenko, G S Stepura, A A Lagun, E A Suvolova, Zh M Ivanova *Fiziologicheski Aktivnye Veshchestva* **13** 13 (1981)

Russian Chemical Reviews **62** (7) 661 – 682 (1993) © 1993 Russian Academy of Sciences and Turpion Ltd

UDC 542.91 : 541.63

Steroids with a side chain containing a heterocyclic fragment: synthesis and transformations

A V Baranovskii, R P Litvinovskaya, V A Khripach

Contents

I. Introduction	661
II. Synthesis of steroids containing a heterocycle in the C(17) position	661
III. Synthesis of steroids containing a heterocycle in the C(20) position	669
IV. Synthesis of steroids containing a heterocycle in the C(22) position	672
V. Syntheses of the side chains of steroids including the transformation of heterocyclic structures	674

Abstract. The latest data on the methods for the formation of the side chains of steroids containing a heterocyclic fragment are surveyed and described systematically. Attention is concentrated on the methods for the transformation of heterocycles in order to achieve the stereoselective formation of chiral centres in the side chain characteristic of a series of natural polyhydroxysteroids — ecdysones, brassinosteroids, vitamin D metabolites, etc. The bibliography includes 133 references.

I. Introduction

A series of steroids, characterised by a high physiological activity, contain a heterocyclic fragment or a polyfunctionalised side chain as a structural element. Cardenolides, withanolides, ecdysones, etc. can be included among steroids of this kind.

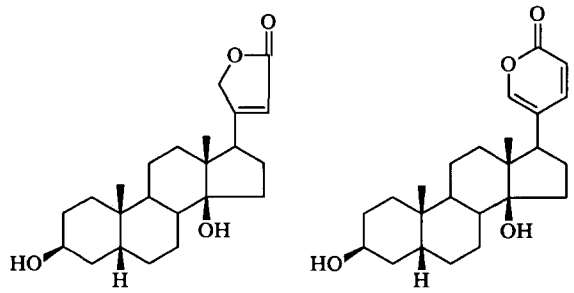
The present review is devoted to the formation and transformations of the steroid side chains containing a heterocyclic fragment and covers the literature for the last 15 years. Additional information on this problem can be found in other communications.[1-10]

The review includes problems concerning five-membered, six-membered, and the fairly rare four-membered heterocycles. The scope of the review precludes the consideration of steroid alkaloids and 17-spiroheterocycles. Dioxolans and acetonides, which actually constitute protective groups, are also excluded.

II. Synthesis of steroids containing a heterocycle in the C(17) position

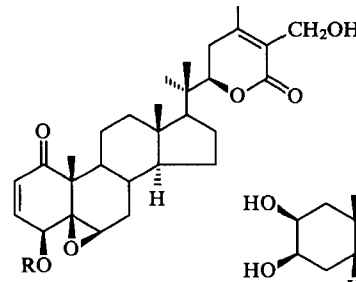
The synthesis of steroids having a heterocyclic substituent in the 17β-position involves mainly the development of convenient methods of construction of the side chain in cardenolides (five-membered lactones), bufadienolides (six-membered lactones), or their analogues, which are distinguished by a broad spectrum of biological activity.

The following most general approaches to their synthesis can be differentiated: (a) cyclisation of 21-derivatives of 20-keto-steroids involving a change in a functional group — primarily in the 21-position; (b) condensation of the reagent initially with the carbonyl group of the 21-derivatives of 20-ketosteroids followed by cyclisation; (c) addition of lithio-derivatives of heterocycles to the carbonyl group of 17-ketosteroids with subsequent transformation of the products.

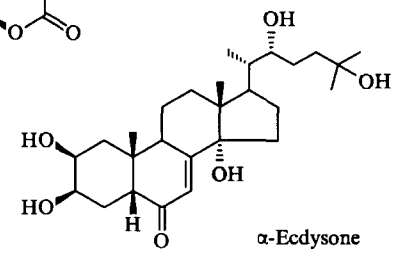


Digitoxigenin

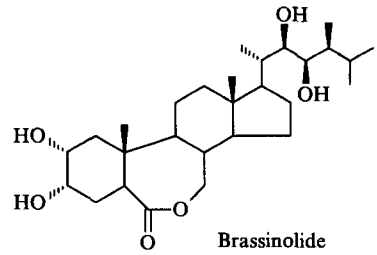
Bufalin



Withaferin A



α-Ecdysone



Brassinolide

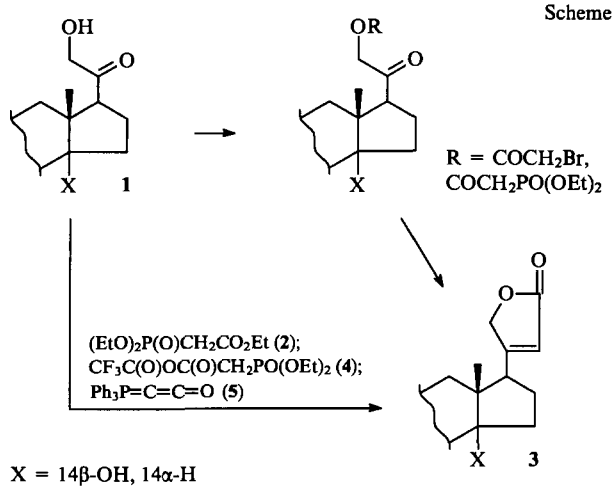
One of the main problems in the synthesis of cardiac aglycones is the formation of the butenolide side chain under mild conditions. The Horner–Emmons intermolecular condensation method is most attractive for this purpose. It includes either the esterification of the α-ketol **1** to the bromoacetate and the formation from the latter of a Wittig reagent and its cyclisation[3] or esterification[11-13] of the α-ketol with triethyl phosphonacetate **2** with simultaneous cyclisation to the lactone **3**. However, the

A V Baranovskii, R P Litvinovskaya, V A Khripach Institute of Bioorganic Chemistry, Academy of Sciences of Belarus, ul. Zhodinskaya 5/2, 220141 Minsk, Belarus

Received 20th April 1993
Uspekhi Khimii **62** (7) 704 – 725 (1993); translated by A K Grzybowski

large number of stages, which reduces the yield, in the first case and the poor reproducibility in the second hinder the use of this method. Attempts at improvement of the procedure by using new reagents have therefore not ceased. One of the versions involves the use of the mixed anhydride of trifluoroacetic and diethyl phosphonoacetic acids **4**.[14] Treatment of the ketol **1** with this reagent in the presence of potassium carbonate results in the formation of the lactone **3**. High yields of the lactone **3** have been obtained also using the ketene triphenylphosphoranylide **5**. Treatment of the ketol **1** with the latter results in the formation of the five-membered lactone **3** in one stage.[15] It is remarkable that this reaction does not involve the tertiary hydroxy-groups of the steroid (Scheme 1).

Scheme 1

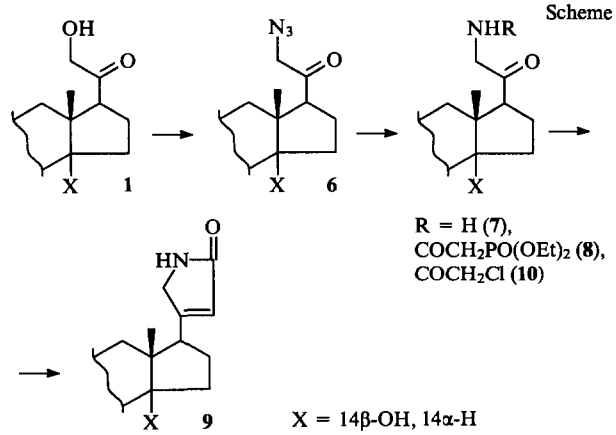


X = 14β-OH, 14α-H

The replacement of the hydroxy-group in the ketol **1** by the azide group or its conversion into the methanesulfonate or toluene-*p*-sulfonate, which undergo nucleophilic substitution, makes it possible to obtain a series of sulfur- and nitrogen-containing derivatives which afford heterocycles — analogues of digitoxigenin and bufalin — under mild conditions.

The reduction of the azide **6** to the amine **7** and acetylation of the latter with diethylphosphonacetic acid in the presence of dicyclohexylcarbodiimide lead[16] to the amide **8** and, after cyclisation, to the lactam **9**. This lactam is obtained by hydrogenating the azide **6** over $Pd/CaCO_3$ in the presence of chloroacetic anhydride.[17,18] The resulting chloroacetamide **10** is converted into a phosphonium salt and subjected to Wittig cyclisation (Scheme 2).

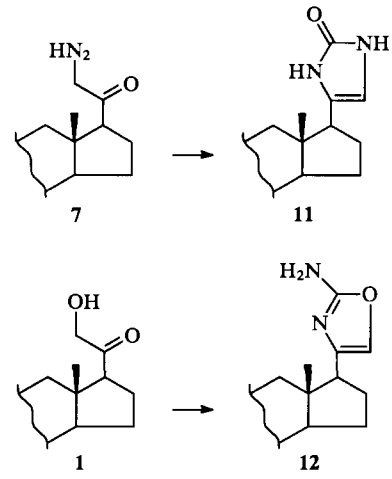
Scheme 2



X = 14β-OH, 14α-H

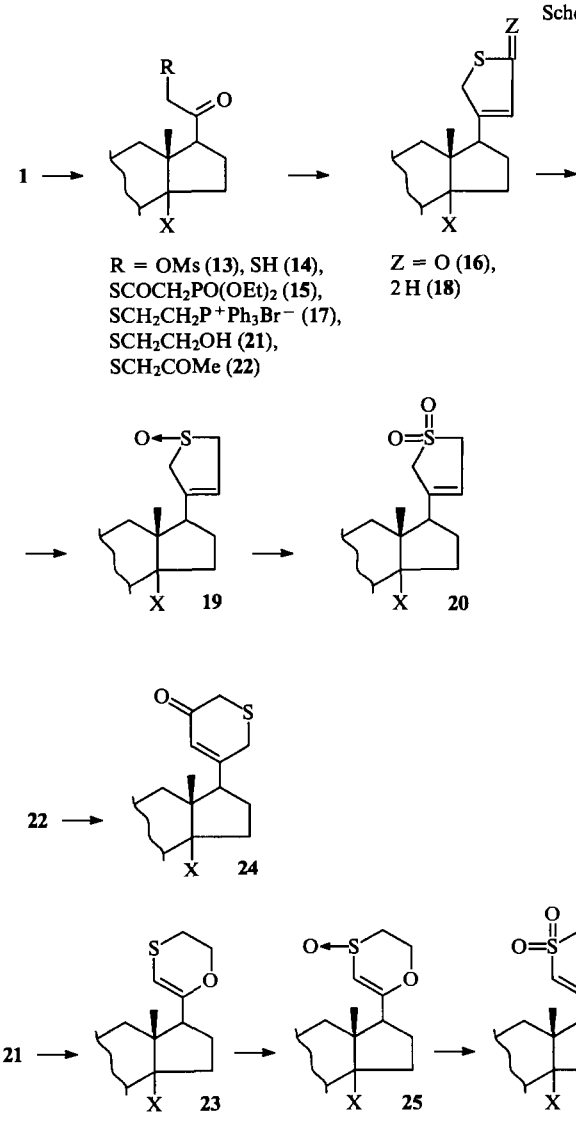
The imidazoline derivatives **11** were obtained from the amine **7** and were treated with carbamoyl chloride with subsequent cyclocondensation.[19] The aminooxazole **12** can be synthesised directly from the ketol **1** by treating the latter with cyanamide (Scheme 3).[20]

Scheme 3



The ease of the nucleophilic substitution of the methanesulfonate **13** makes it possible to form cyclic structures with the sulfur atom. The thiolactone **16** is formed via the phosphonate **15** from the thiol **14**, obtained by the reaction of the methanesulfonate **13** with sodium hydrogen sulfide. The 2,5-dihydrothiophene **18** is synthesised by substituting the methanesulfonate

Scheme 4

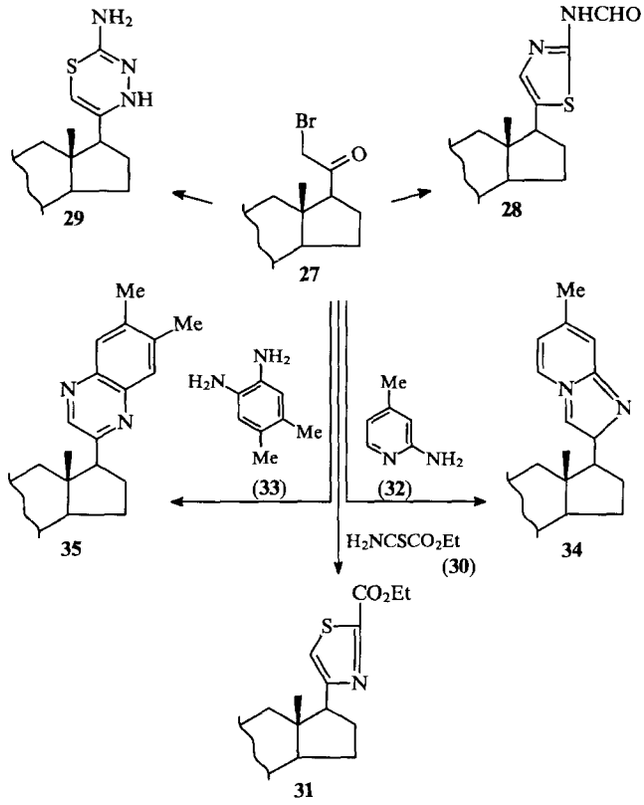


X = 14β-OH, 14α-H

group in compound **13** by the sodium salt of 2-mercaptoethyltriphenylphosphonium bromide and cyclisation of the intermediate **17**. The dihydrothiophene **18** is readily oxidised by sodium periodate to the sulfoxides **19** and the latter are oxidised in their turn to the sulfone **20** with *m*-chloroperbenzoic acid. Similar substitution of the methanesulfonate group in compound **13** by thiols can afford the derivatives **21** and **22**. The cyclisation of the former to the oxathiine **23** is achieved on treatment with acids, whilst cyclisation of the latter to the thiopyranone **24** is carried out in the presence of sodium methoxide. Similarly the oxathiine **23** can be oxidised[16,21] to the sulfoxides **25** and the sulfones **26** (Scheme 4).

The α-bromoketones **27** are used widely to synthesise steroids of different kinds with diaza- and thiaza-heterocycles in the side chain.[22-26] For example, their condensation with thiourea[22] in dimethylformamide (DMF) affords the thiazole **28**, the condensation with thiosemicarbazide[23] affords the thiadiazine **29**, the condensation with ethyl thioxamate[24] **30** gives rise to the thiazole **31**, while the condensation with aminopyridine[25] **32** or the diamine[26] **33** affords compounds **34** and **35** respectively (Scheme 5).

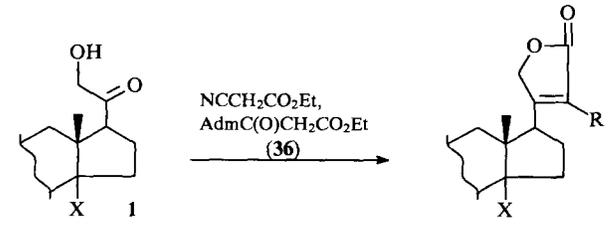
Scheme 5



In the cases considered, cyclisation to a heterocycle was preceded by reactions which did not involve the carbonyl group at C(20). Syntheses involving addition of various reagents to this centre and subsequent cyclisation are described below. They are mainly intended to produce the side chain in compounds related to digitoxigenin and its derivatives. Thus the condensation of the ketol **1** with cyanoacetic ester[27] or the acetoacetic ester derivative **36** affords the unsaturated cyanolactone **37** and the acyllactone **38** (Scheme 6).[28]

The lactone **3** ring was obtained from the ketosulfide **39** by reaction with bromoacetic ester in the presence of activated zinc.[29] The diastereoisomers **40** are converted, without separation, into the epoxyesters **41** via a methylsulfonium salt. The passage of the esters through a column with basic alumina led to cyclisation to the required lactone **3**. The Reformatskii reaction has been used successfully to synthesise the lactone **3** from the ketoacetate **42**.[30]

Scheme 6

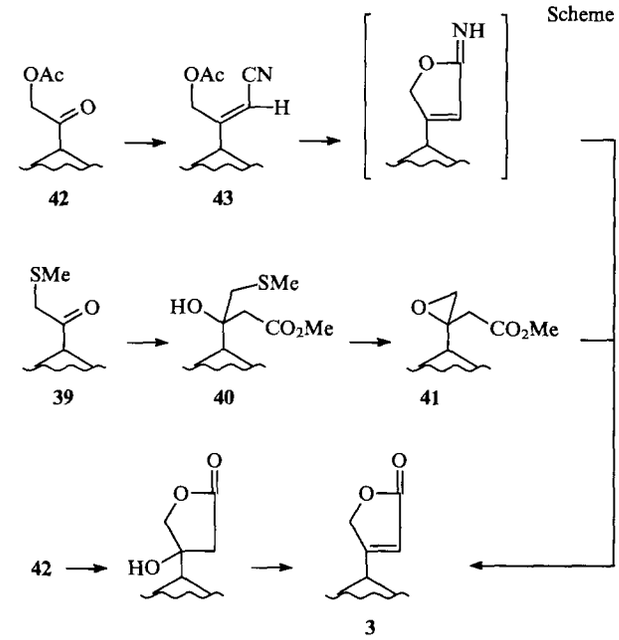


X = 14β-OH, 14α-H
Adm = Adamantine

R = CN (**37**),
C(O)Adm (**38**)

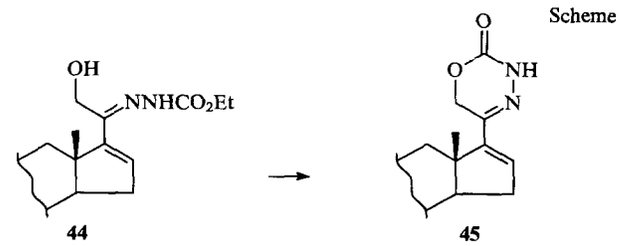
A more effective method, using the chemistry of phosphoranes, has been proposed.[31] The condensation of the ketoacetate **42** with diethyl cyanomethylphosphonate and subsequent treatment of the resulting nitrile **43** with toluene-*p*-sulfonic acid made it possible to isolate directly the lactone **3** (Scheme 7).

Scheme 7



An aza-analogue of cardiotonic steroids **45** of the type of bufalin has been obtained[32] by the alkaline treatment of the ethoxycarbonylhydrazone **44**. Evidently only the (*Z*)-isomers are capable of this kind of cyclisation (Scheme 8).

Scheme 8

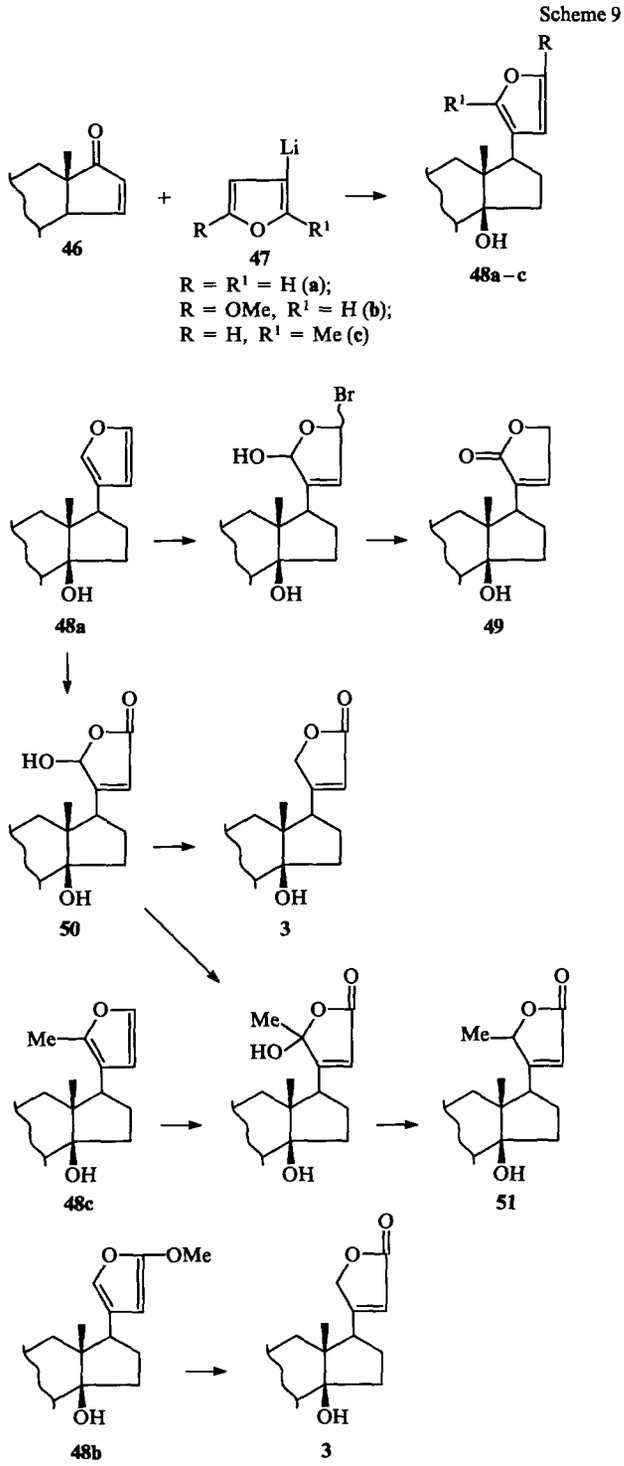


The chemistry of furan derivatives provides extensive possibilities for the synthesis of the lactone rings in cardenolides and bufadienolides. Thus the cardenolides **3**, the isocardenolide **49**, and the 21-hydroxy- and 21-methyl analogues **50** and **51** have been obtained by alkylating the 17-ketones with 3-lithiofurans and the transformation of the furylsteroids.[33-35]

These compounds were synthesised in the following way. As a result of the addition of 3-lithiofurans **47** to the ketone **46** and a series of transformations of the D ring of the steroid molecule, the

furyl steroids **48** were obtained. Oxidation of the furylsteroid **48a** with *m*-chloroperbenzoic acid and the reduction with $NaBH_4$ of the primary product—the hydroxylactone **50**—afforded the cardenolide **3**,[33] which can also be obtained as a result of the acid hydrolysis of the methoxy-group in the furyl steroid **48b**.[34] On the other hand, the oxidation of compound **48a** with *N*-bromosuccinimide leads to the lactone **49** which is isomeric with respect to compound **3** (Scheme 9).[33]

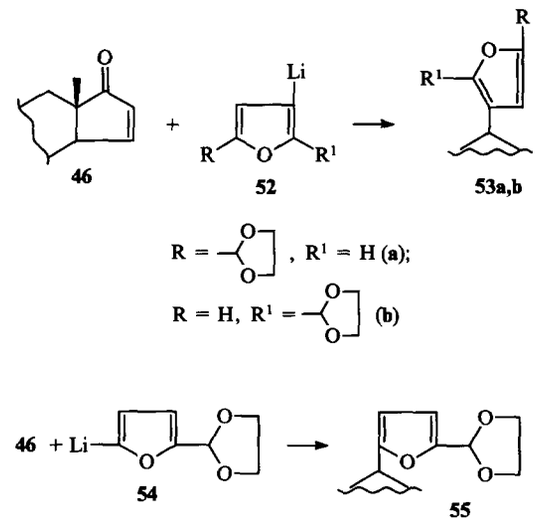
Scheme 9



Successive oxidation with *m*-chloroperbenzoic acid and reduction with $NaBH_4$ of the furylsteroid **48c** affords the 21-methyl derivative **51**. Another method of synthesis[35] of the cardenolide **51** involves the alkylation of the hydroxylactone **50** with methyllithium.

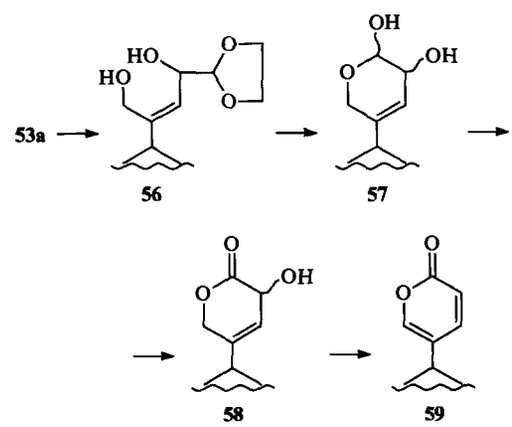
The method involving the alkylation of ketones by furans is suitable also for the synthesis of the lactone component of the bufalin and its α-, α′-, and β-isomers.[36–39] Thus alkylation of the ketone **46** by 3-lithiofurans **52a, b** or 2-lithiofuran **54** and subsequent transformations lead to the furylsteroids **53a, b** and **55** respectively (Scheme 10).

Scheme 10



The furylsteroid **53a** served as an intermediate in the synthesis of the pyrone fragment of bufalin[36,37] **59** and β-isobufalin[38,39] **63**. In the synthesis of bufalin, the furan **53a** was oxidised with oxygen in the presence of a sensitiser and the primary product—an endoperoxide—was cleaved with dimethyl sulfide to give an unstable ketoaldehyde. Without being isolated, the aldehyde was reduced with $NaBH_4$ to the hydroxyacetal **56**. Next the acetal was hydrolysed with hydrochloric acid, affording the six-membered lactol **57**, which was oxidised with silver carbonate on celite to the hydroxylactone **58**. The fragment **58** was converted into the lactone fragment of bufalin by refluxing its methanesulfonate with diazabicyclononene (Scheme 11).

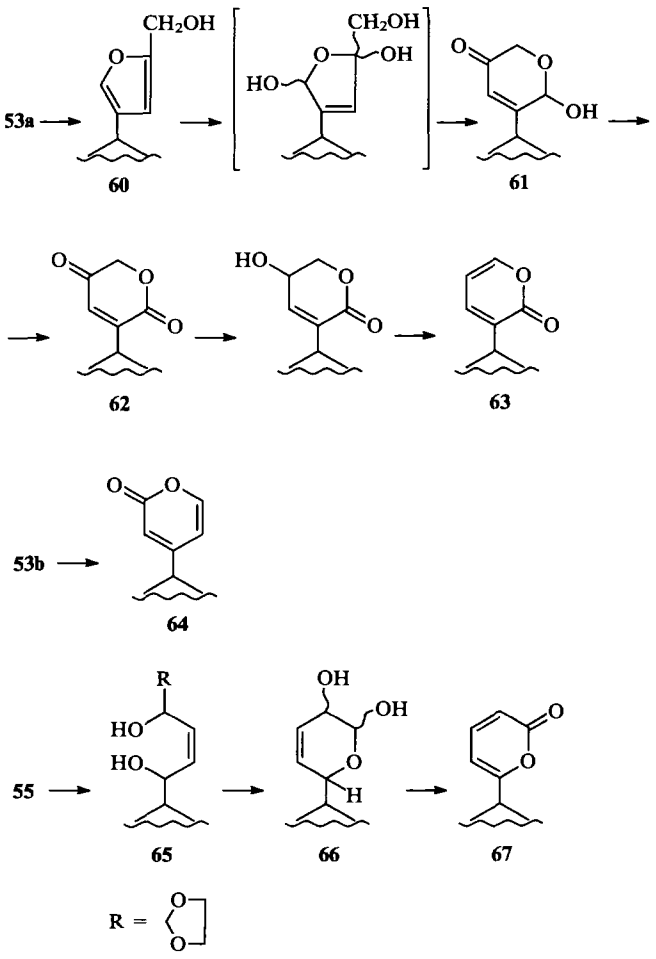
Scheme 11



In order to convert the furan ring of compound **53** into the lactone fragment of β-isobufalin, the acetal group was hydrolysed and the resulting aldehyde was reduced with $NaBH_4$ to the alcohol **60**. Oxidation of the alcohol **60** with *m*-chloroperbenzoic acid led to the ketolactol **61**, which was oxidised with chromic acid to the ketolactone **62** and the keto-group was then reduced selectively with zinc tetrahydroborate. The subsequent transformations into the pyrone ring of β-isobufalin were achieved via the methanesulfonate. A similar sequence of reactions in the case of the furan **53b** leads[38,39] to α-isobufalin **64**. In order to obtain α′-isobufalin

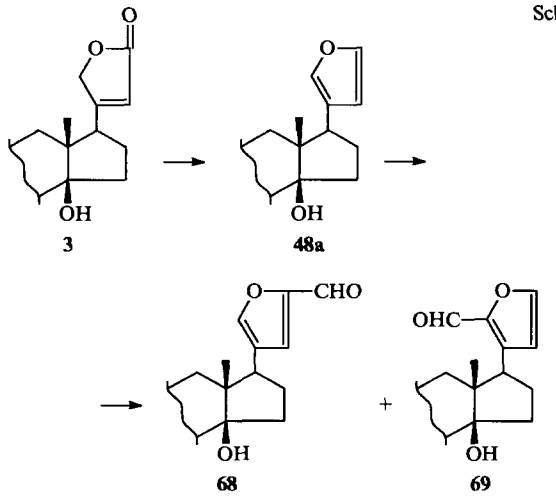
67, the furylsteroid **55** is oxidised with *N*-bromosuccinimide and the oxidation product is reduced with $NaBH_4$ to the diol **65**, the acetal group of which is hydrolysed to the lactol **66**, from which the lactone **67** is obtained in accordance with Scheme 12.

Scheme 12



Treatment of the lactone ring in compounds **3** with $LiAlH_4$ results in the formation[40] of the furan **48a**. This reaction has been used by Wiesner and coworkers[41,42] to synthesise bufalin and α- and β-isobufalins. Formylation of the furan **48a** gives rise to the aldehydes **68** and **69** (Scheme 13).

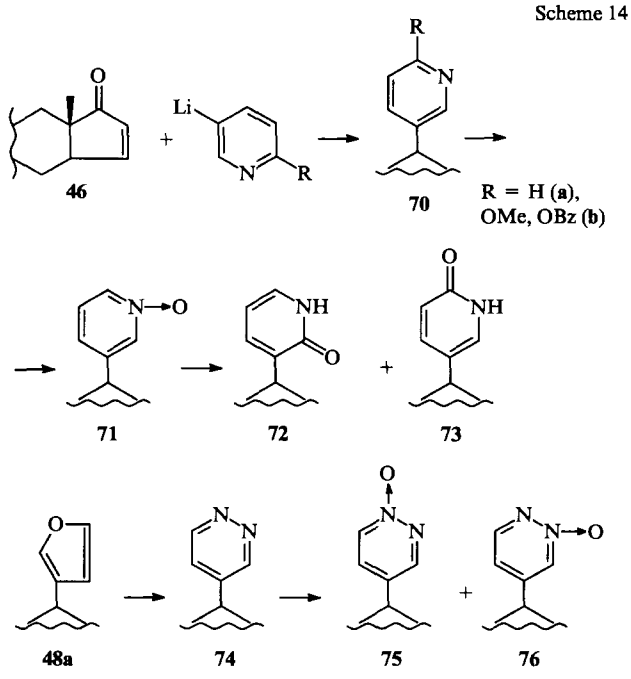
Scheme 13



The introduction of the acetal protective group into the aldehyde **68** leads to the furan **53a**, the subsequent transformations of which afford bufalin, while the reduction of the furans **68** and **69** with $NaBH_4$ affords the corresponding alcohols, from which α- and β-isobufalins were obtained.

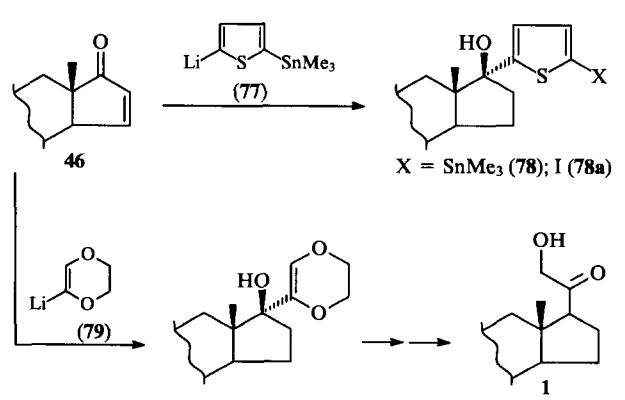
A series of aza-analogues of bufalin were obtained by alkylating the 17-ketosteroids **46** with 3-lithiopyridines. The transition from the pyridine to the pyridone ring was achieved by oxidising the pyridine **70a** with *m*-chloroperbenzoic acid to the *N*-oxide **71**, which afforded the pyridones **72** and **73** in equal proportions on refluxing in acetic anhydride and subsequent alkaline hydrolysis. In the case of compound **70b**, the pyridone **73** is formed as a result of the hydrogenolysis of the ether.[43-47] The reaction of the furan **48a** with *N*-bromosuccinimide and subsequent interaction of the oxidation product with hydrazine hydrate afford compound **74**, the treatment of which with *m*-chloroperbenzoic acid leads to a mixture of the *N*-oxides **75** and **76** in proportions of 3 : 2 (Scheme 14).[48,49]

Scheme 14



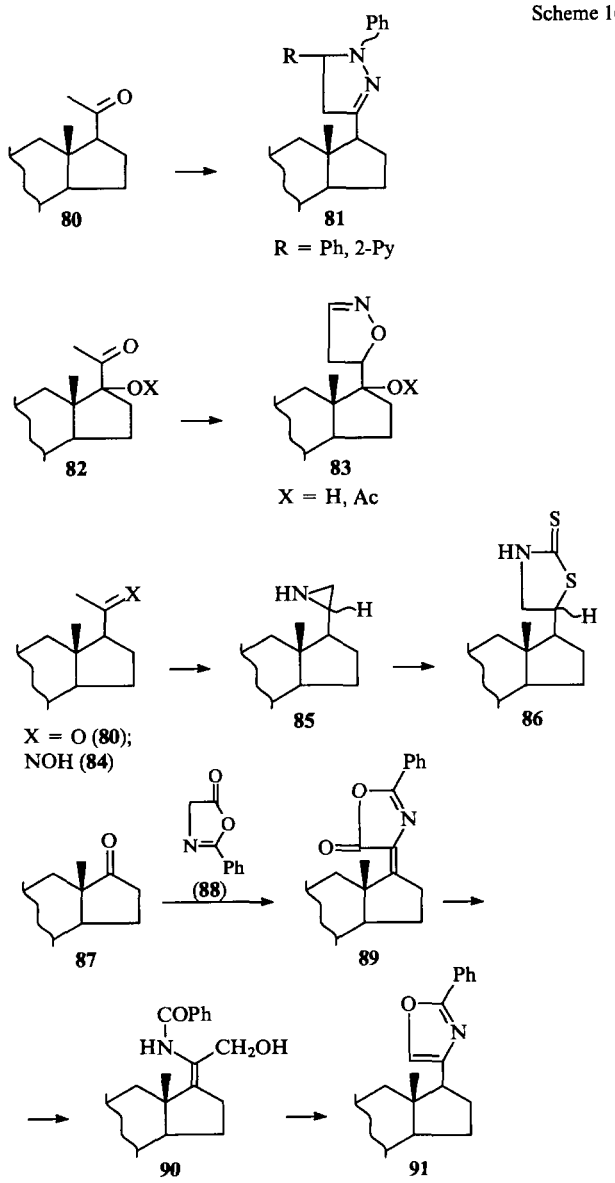
The alkylation of 17-ketosteroids by other heterocycles takes place just as readily. For example, the addition of the thiophene **77** gives rise to the product **78**, the ease of substitution of tin in which by iodine and other halogens makes it possible to obtain compounds with functional group substituents and to introduce radioactive isotopes.[50] Androstanes can be converted into pregnanes by reaction with the lithio-derivative **79** (Scheme 15)[51] (for a more detailed treatment, see Section V).

Scheme 15



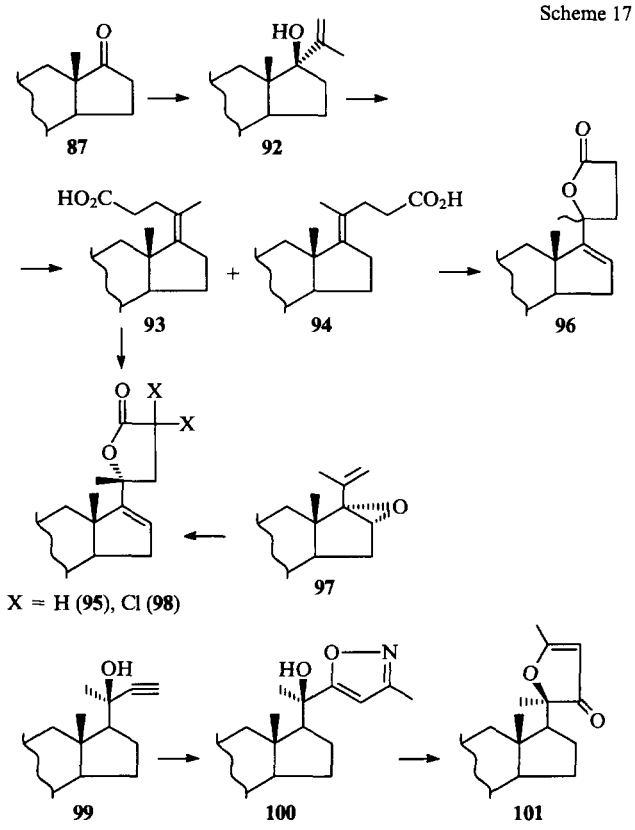
The synthetic possibilities of 20- and 17-ketosteroids for the construction of heterocycles containing nitrogen or sulfur are not limited to the examples described above. Thus the condensation of the ketosteroid **80** with benzaldehyde or 2-formylpyridine and subsequent treatment of the condensation product with phenylhydrazine afford the pyrazolines **81**.[52,53] When the ketol **82** or its acetate was refluxed in formamide in the presence of perchloric acid, the isoxazolines **83** were obtained.[54] The reduction of the oxime **84** with lithium tetrahydroaluminate afforded the aziridines **85**, the treatment of which with carbon disulfide leads to the thiazolidines **86**.[55] The condensation of the azalactone **88** with the ketone **87** affords the product **89** as a mixture of the (*Z*)- and (*E*)-isomers. The $TiCl_4$–pyridine system served as the catalyst in this reaction. Alkaline hydrolysis of compound **89** and subsequent reduction led to the synthesis of compound **90**, the hydrolysis of which with hydrochloric acid afforded the oxazole **91** (Scheme 16).[56]

Scheme 16



The application of a series of new reagents opens the way to the synthesis of rare compounds and compounds which are difficult to synthesise. Alkylation of the ketone **87** with isopropenyllithium gives rise to the allyl alcohol **92**, which, as a result of the Claisen rearrangement in the presence of ethyl orthoacetate, is converted into the acids **93** and **94** after separation and hydrolysis. Kosor and Bersz[57] carried out the lactonisation stage with chlorophenyl selenide in the presence of triethylamine, since the use of sulfuric acid led merely to the decomposition products of the steroid molecule. However, the lactone **95** was obtained from the acid **93** instead of the expected selenolactone (Scheme 17).

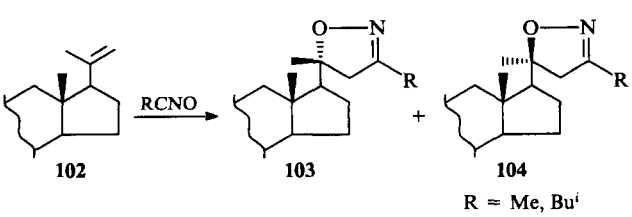
Scheme 17



A similar reaction occurs also with the acid **94**, which made it possible to obtain the isomeric lactone **96**. The dichloro-derivative **98** of the lactone **95** can be obtained stereoselectively[58] from the epoxyolefin **97** by the reaction of the latter with dichloroketene. The hydrogenation under acid conditions of the isoxazole **100**, obtained by the cycloaddition of the nitrile oxide to the acetylenic alcohol **99** led to high yields of the furanone **101**, which is otherwise difficult to obtain.[59]

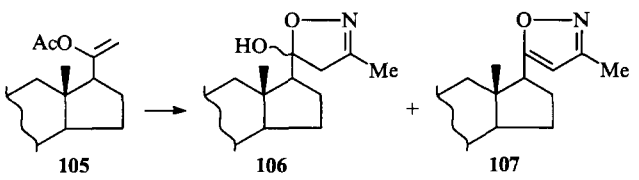
The previously unknown 17-isoxazolinylsteroids **103** and **104** have also been obtained[60] by the 1,3-dipolar cycloaddition of the corresponding nitrile oxides to the steroid 20(22)-olefins **102**. The addition of the nitrile oxides is regioselective and leads to the corresponding pairs of epimers at C(20) in proportions of 20*R*:20*S* = (2.5–3):1 (Scheme 18).

Scheme 18



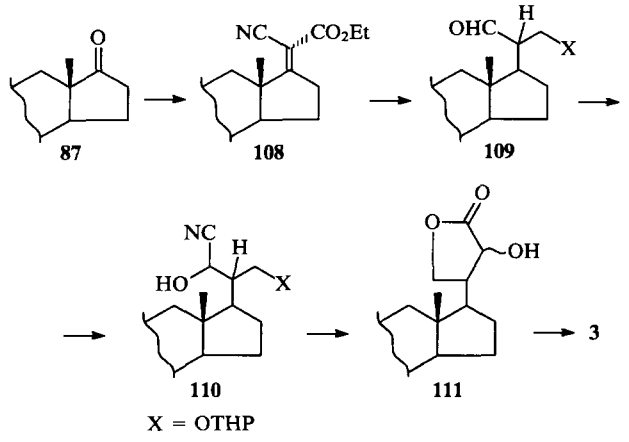
The use of the steroid enol ester **105** in the reaction with acetonitrile oxide leads to the formation of a mixture of a small amount of the isoxazoline **106** and its decomposition product—the isoxazole **107** (Scheme 19).[60]

Scheme 19



Other bifunctional compounds also serve, together with ketols, in the synthesis of cardiotonic steroids. Thus the product **108** of the condensation of the ketone **87** with cyanoacetic ester afforded the aldehyde **109** after the removal of the tetrahydropyranyl (THP) group (protecting the hydroxy-group) by treatment with $LiAlH_4$ in tetrahydrofuran (THF) and the reduction of the cyano-group with diisopropylaluminium hydride. This aldehyde is a common intermediate in the synthesis of the lactone ring in both cardenolides and bufadienolides. The γ-lactone was obtained from the cyanohydrin **110** by acid hydrolysis with simultaneous ring closure. The dehydration of the hydroxy-group in the resulting lactone **111** led to the required lactone **3** (Scheme 20).

Scheme 20

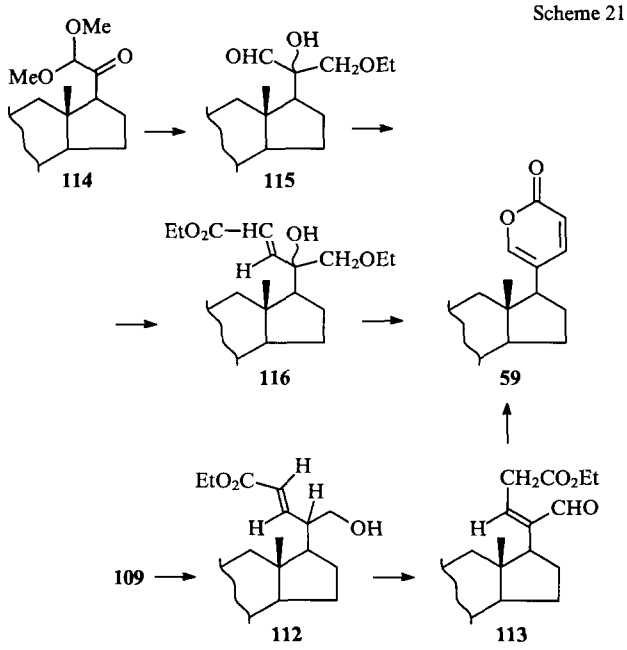


The δ-lactone **59** was formed by condensing the aldehyde **109** with the triethylphosphonoacetate ylide, the subsequent removal of the protective group, the oxidation of the alcohol **112** to the aldehyde **113** by pyridinium chlorochromate, and the cyclisation of the aldehyde to the lactone in the presence of toluene-*p*-sulfonic acid.[61,62] Engel and Dionne also used in an earlier study the aldehyde **113** in the synthesis of δ-pyrone **59**.[63]

The δ-lactone **59** can be obtained from the acetal of the ketoaldehyde **114**. The aldehyde **115** was synthesised by the reaction of the above acetal with the Grignard reagent, obtained from ethoxymagnesiochloromethane, and subsequent hydrolysis. The product **116** of its condensation with the triethylphosphonoacetate ylide afforded the required bufadienolide **59** after hydrolysis and lactonisation with iodine (Scheme 21).[64]

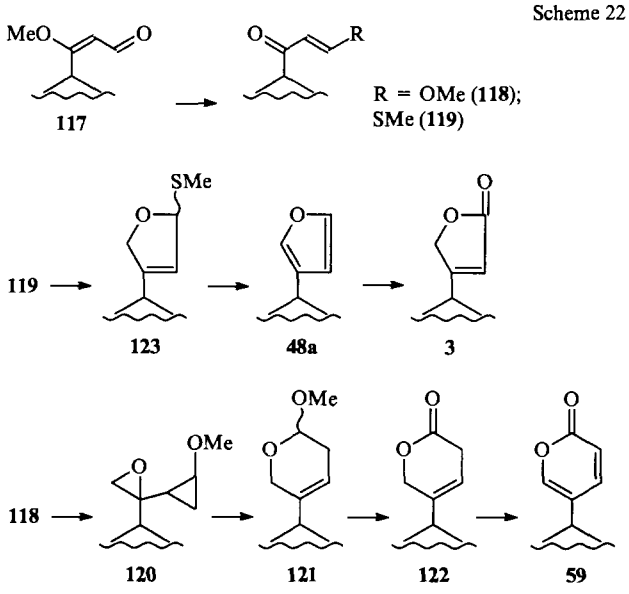
The enol ether **117** is a common intermediate (like compound **109**) in the synthesis of the γ- and δ-unsaturated lactones.[65,66] When it is heated in acidified methanol, compound **118** is obtained, while heating with methanethiol in benzene affords compound **119**. The reaction of the enol ether **118** with an excess of dimethylsulfonium methylide and subsequent treatment of the crude product with a methanol solution of HCl led to the dihydropyran **121**. After the hydrolysis of compound **121** and subsequent Jones oxidation, the lactone **122** was obtained. Its bromination and dehydrobromination by diazabicycloundecene led to the lactone **59**. The interaction of compound **119** with an equimolar amount of the methylide and subsequent desulfurisation led initially to the formation of the furan **48a** and then the lactone **3**. The formation of different compounds in the two fairly

Scheme 21



similar processes can be explained by the occurrence of different intermediates in these reactions. In the former case, the epoxide **120** is formed, its hydrolysis giving rise to the dihydropyran **121**, while in the latter case the intermediate is 2-methylthio-2,5-dihydrofuran **123** (Scheme 22).

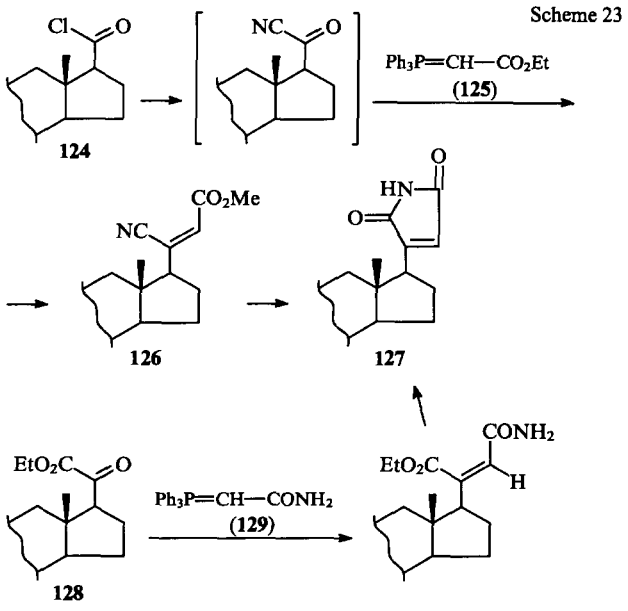
Scheme 22



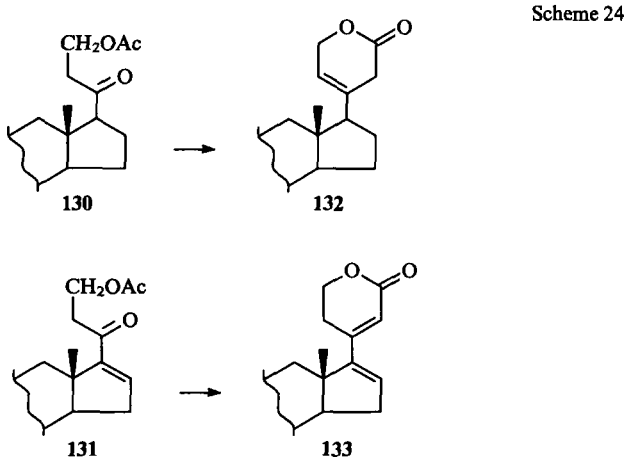
The cyanoacrylate **126**, obtained when the acid chloride **124** is treated with hydrogen cyanide in the presence of an excess of the ylide **125**, cyclises to the maleimide **127** on heating in a mixture of acetic acid, its anhydride, and sulfuric acid.[67] The maleimide **127** was synthesised in a higher yield from the ketoester **128** by condensing the latter with the ylide **129** and further cyclisation of the product (Scheme 23).[68]

An approach has been developed[69] to the synthesis of analogues of isobufadienolides from the ketoacetates **130** and **131**. Thus the lactone **132** has been obtained from the ketoacetate **130** under the conditions of the Reformatskii reaction with bromoacetic ester, while the ketoacetate **131** was converted under the same conditions into the conjugated lactone **133** (Scheme 24).

Scheme 23



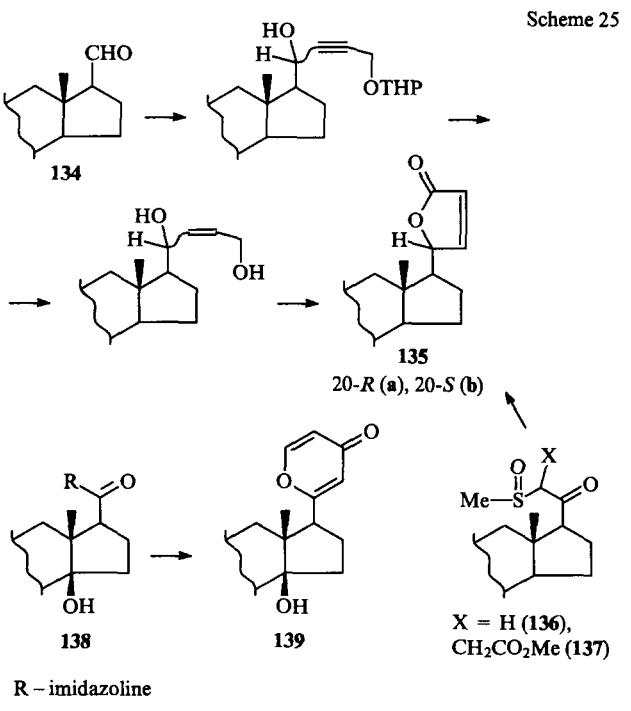
Scheme 24



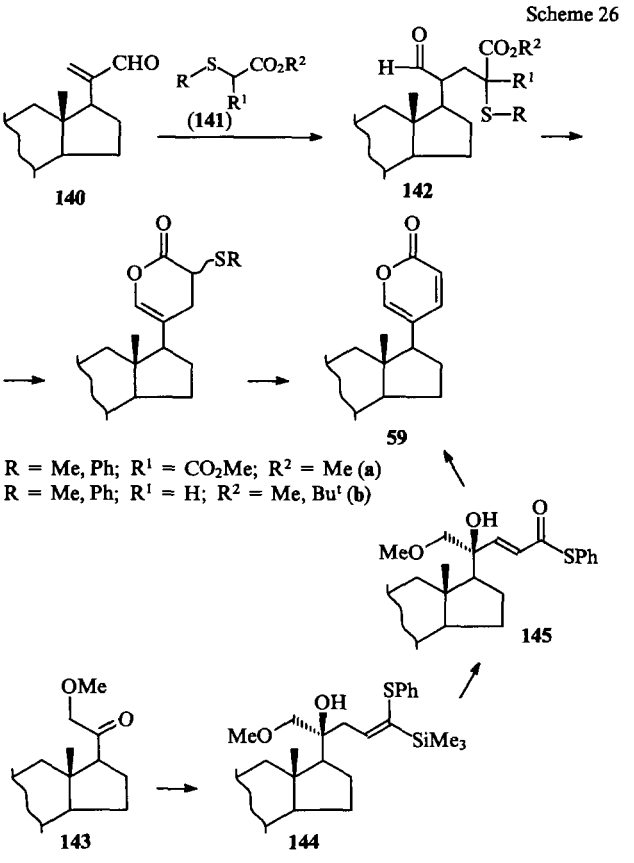
The isomeric lactones **135** have been obtained by alkylating the aldehyde **134** with acetylenes.[70] They had been synthesised previously[71] from bromoacetic ester and the ketosulfoxide **136** with subsequent reduction of compound **137** with $NaBH_4$. The addition of the potassium enolate derived from 4-methoxybut-3-en-2-one to the imidazoline derivative **138** led to the pyrone fragment of γ-isobufalin **139** (Scheme 25).[72]

The addition of sulfur-stabilised alkyl anions to carbonyl compounds proved to be effective for the synthesis of δ-unsaturated ketones.[73–76] Thus the Michael condensation of the aldehyde **140** with anions based on compounds **141** affords the 1,4-adducts **142**, the cyclisation and desulfurisation of which leads to the lactone fragment of bufalin **59**.[73–75] An interesting example of the formation of the δ-lactone from the ketoester **143** has been proposed.[76] The authors chose 1-phenylthio-1-trimethylsilyl-prop-2-ene as the equivalent of the homoenolate anion necessary for the introduction of three carbon atoms and capable of subsequent cyclisation to the pyrone ring. The addition of the propene to the ketoester **143** in the presence of butyllithium led to the formation of compound **144**. The oxidative desilylation reaction was achieved by treating the lithio-dianion of compound **144** with oxygen in solution in THF containing hexamethylphosphoramide. This resulted in the formation of the thioester **145** in 59% yield. Its cyclisation to the pyrone was achieved by treatment with hydrogen bromide in boiling acetonitrile (Scheme 26).[76]

Scheme 25



Scheme 26



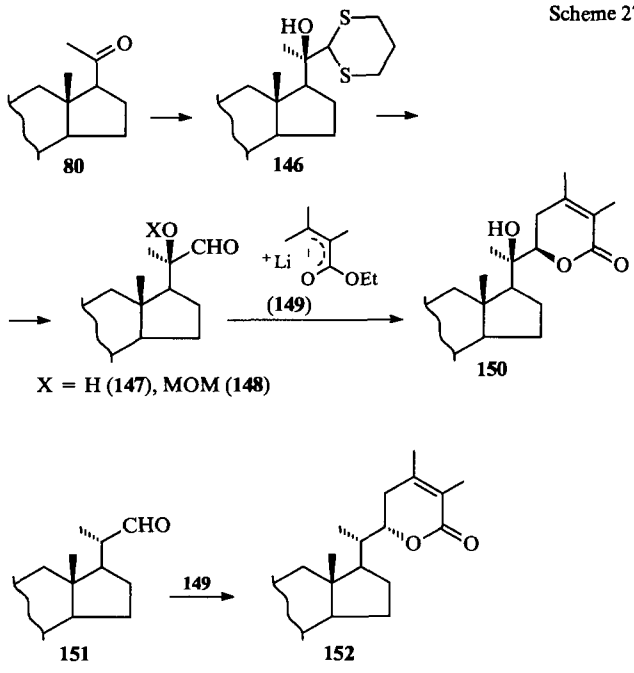
III. Synthesis of steroids containing a heterocycle in the C(20) position

This section is devoted to the methods of synthesis of the side chains of withanolides and jaborosalactones, which are homologues of cardenolides, i.e. compounds having a heterocycle in the C(20) position in the steroid molecule.

There are two main approaches to the synthesis of the lactone fragment of withanolides and jaborosalactones — via the addition of stabilised lithio-enolates or lithiodithianes and via the addition of lithiofurans and transformation of the latter.

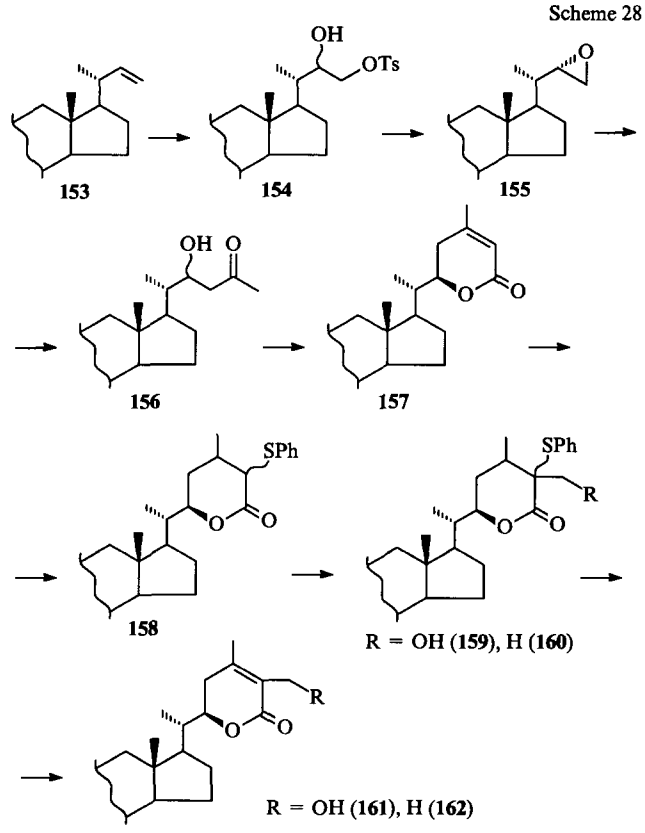
The aldehyde **147**, which is the starting material of the synthesis of the lactone fragment of the withanolide D, was synthesised by adding the anion of 1,3-dithiane to the ketone **80** with subsequent hydrolysis of the hydroxythioacetal **146**. After the protection of the hydroxy-group in the form of the methoxymethyl ester (MOM) **148** and the addition of the lithio-enolate **149**, formed from α,β-dimethylcrotonate and lithium diisopropylamide, the required lactone **150** was obtained.[77,78] It is of interest that the addition of the enolate **149** to the aldehyde **151** afforded the lactone **152** with the stereochemical configuration at C(22) opposite to that in 27-deoxywithaferin A, the attempts to invert the configuration proving unsuccessful (Scheme 27).[78]

Scheme 27



Since the addition of the enolate **149** to the aldehyde **151** does not ensure the required stereochemical configuration of the C(22) centre, another sequence of reactions, permitting the introduction of the hydroxy-group with the required configuration, was selected for the construction of the side chain in withaferin A, 27-deoxywithaferin A, and jaborosalactones. For this purpose, the olefin **153** was treated with OsO_4 and the reaction product was toluene-*p*-sulfonated, which led to a mixture of the isomeric toluene-*p*-sulfonates **154** in proportions of 5 : 1. The main isomer was converted quantitatively into the chiral epoxide **155**. The regiospecific alkylation of the epoxide with the 2-methyl-1,3 dithiane anion followed by the elimination of the thioketal ensured the necessary (22*R*)-configuration in the ketol **156**. Cyclisation to the lactone **157** was achieved by the McMorris method.[79] After the reduction of the double bond and treatment with diphenyldisulfide, the sulfide was obtained as a mixture of isomers with respect to C(24) (3 : 2). In order to obtain the side chain of jaborosalactone and withaferin A, the lithio-anion of the sulfide was treated[80,81] with monomeric formaldehyde, which afforded compound **159**, while for the synthesis of the side chain of 27-deoxywithaferin A the lithio-anion was treated with methyl iodide,[80–82] which afforded the methyl derivative **160**. Next, the sulfides were oxidised to the sulfoxides in both cases and after desulfurisation the required lactones **161** and **162** were obtained (Scheme 28).

Scheme 28



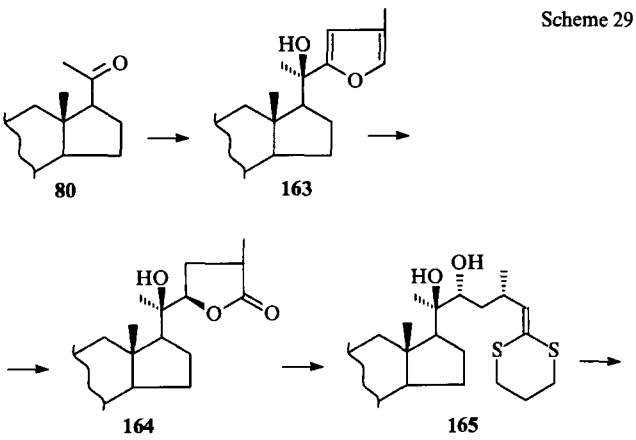
The synthesis of the side chain in withanolides by the addition of 2-lithio-4-methylfuran to the ketone **80** with formation of the furylsteroid **163** has been described.[83] After two-stage oxidation (with *m*-chloroperbenzoic acid and pyridinium chlorochromate) and hydrogenation over platinum dioxide, the lactone **164** was obtained. Its reduction with diisobutylaluminium hydride afforded a lactol, the treatment of which with 2-lithio-2-trimethylsilyldithiane resulted in the formation of the thioacetal **165**. The lactone **166**, obtained from the thioacetal after cyclisation in the presence of camphorsulfonic acid, was alkylated with methyl iodide in the presence of lithium isopropylcyclohexylamide. The lactone **167** was successfully converted into the sulfide, oxidised to the sulfoxide, and desulfurised. However, together with the required lactone **150**, the *exo*-product **168** was obtained in proportions of 1 : 4.2. The isomerisation of the *exo*-product to the *endo*-product was achieved on heating the lactone **168** in a sealed tube with rhodium trichloride in dry ethanol at 100 °C (Scheme 29).

The stereoselective epoxidation of the unsaturated ketones **169** with alkaline hydrogen peroxide proved to be an extremely useful reaction for the synthesis of 22,26-lactones.[79] Thus the ketol **171** was obtained by reducing the epoxide **170** with aluminium amalgam and was used as an intermediate in the synthesis of 23-deoxyantheridiol. The ketol **171** was converted into the bromoacetic ester **172** and the latter afforded the phosphonate **173** on heating with triethyl phosphite as a result of the Arbuzov reaction. The intermolecular Horner–Emmons condensation led to the required δ-lactone **174** (Scheme 30).

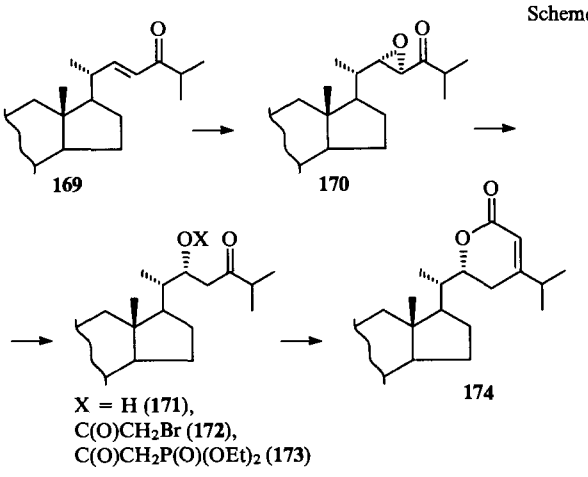
A compound with the side chain of withanolides was obtained from the ketone **175** by employing the sequence of reactions described above (Scheme 31).[84]

The isoxazoline **176** can serve as an intermediate in the formation of the side chain of 23-deoxyantheridiol.[85] Thus the 22-acetoxy-24-ketone **178**, formed after the acetylation of the β-ketol **177** (the product of the cleavage of the isoxazoline **176**) is converted by the Reformatskii reaction, followed by refluxing in acetic anhydride, into the δ-lactone **174** (Scheme 32).

Scheme 29

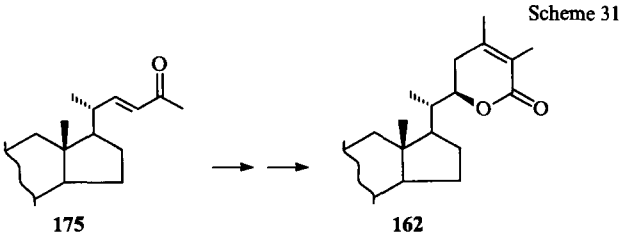


Scheme 30



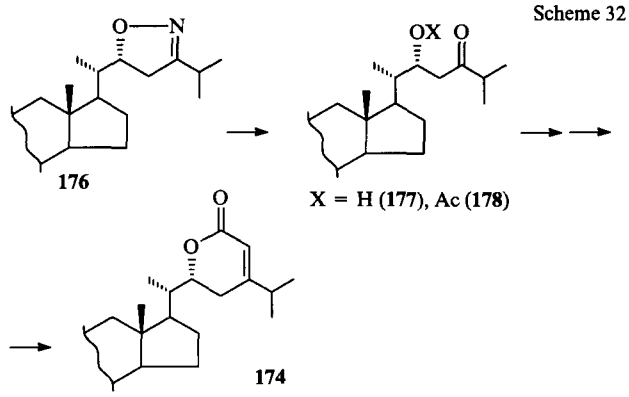
X = H (171),
C(O)CH$_2$Br (172),
C(O)CH$_2$P(O)(OEt)$_2$ (173)

Scheme 31



The synthesis of homologues of cardiotonic steroids was based on the approaches described in the previous section. The key feature of their synthesis is the stage in which the chain is lengthened by a CH_2 group. Thus the aldehyde **180**, obtained by reducing the ester **179**, was used[86] to synthesise the cardenolide homologue **185**. The lactone fragment was introduced by means

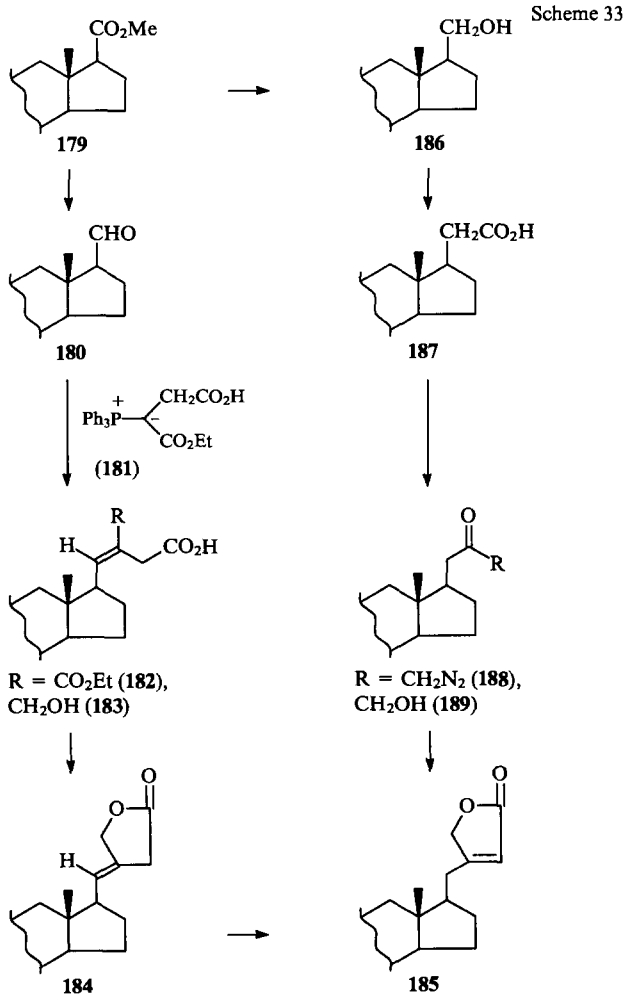
Scheme 32



X = H (177), Ac (178)

of the Witting reagent **181** obtained from triphenylphosphine and maleic anhydride. The product of the addition of this reagent to the aldehyde **180** — the half-ester **182** — was reduced with sodium diethylaluminium hydride to the alcohol **183**, which cyclised to the lactone **184** on heating in acetic anhydride. The shift of the double bond was achieved by treating the lactone **184** with alkali-activated alumina (Scheme 33).

Scheme 33



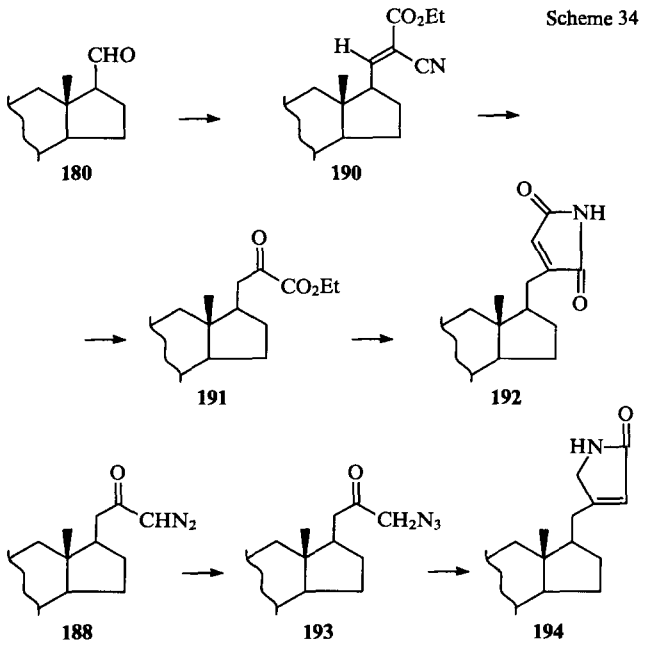
R = CO_2Et (182),
CH_2OH (183)

R = CH_2N_2 (188),
CH_2OH (189)

The unsaturated lactone **185** had been synthesised previously from the alcohol **186**, which was converted[87] via the toluene-*p*-sulfonate into a nitrile and, after hydrolysis, into the acid **187**. Treatment of the acid by the Arndt–Eistert method afforded the diazoketone **188**, which was converted into the hydroxyketone **189** and further into the lactone **185** using the method described by Fritsch et al.[11]

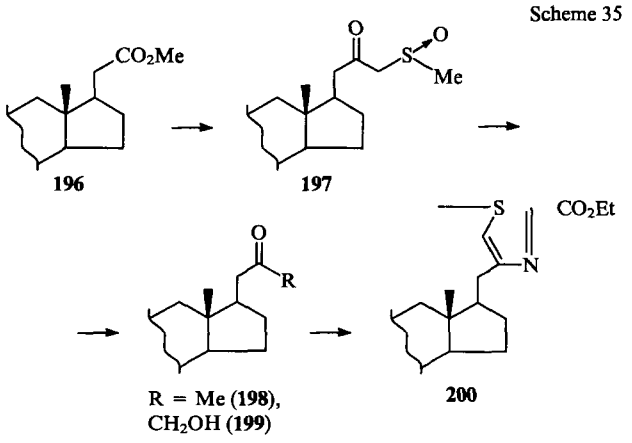
The approaches described have been applied in the synthesis of homologues of steroid compounds containing various heterocycles (maleimide, lactams, and thiazoles) in the side chain. Thus the ketoester **191** was obtained from the aldehyde **180** via the product of its condensation with the cyanoacetic ester **190**.[68] Compound **191** was transformed into the maleimide **192**. The lactam **194** was synthesised[88] from the diazoketone **188** by treatment with toluene-*p*-sulfonic acid, substitution of the toluene-*p*-sulfonate group by the azide group, and further transformation of the azide **193** (Scheme 34).[17,18]

Scheme 34



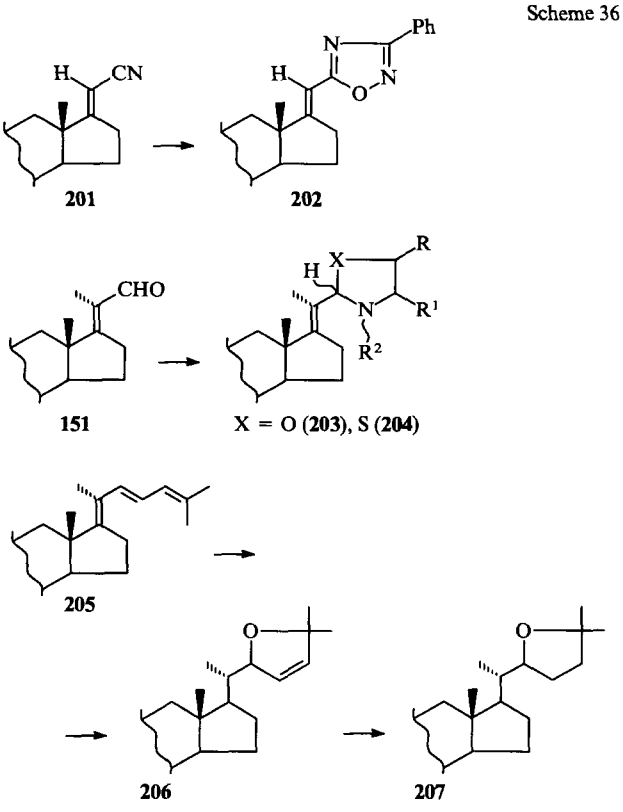
The methyl ester **196** served as the starting compound in the synthesis[89] of the thiazole **200**. It was converted into the ketone **198** by reducing with aluminium amalgam the ketosulfoxide **197** obtained from the ester **196** by treating the latter with dimsylsodium. Next the ketone **198** was oxidised via the silyl ether of the enol to the ketol **199**, which was converted in the usual way into an α-bromoketone. The addition of thioxamate to the latter by the Hantzch method afforded the thiazole **200** (Scheme 35).

Scheme 35



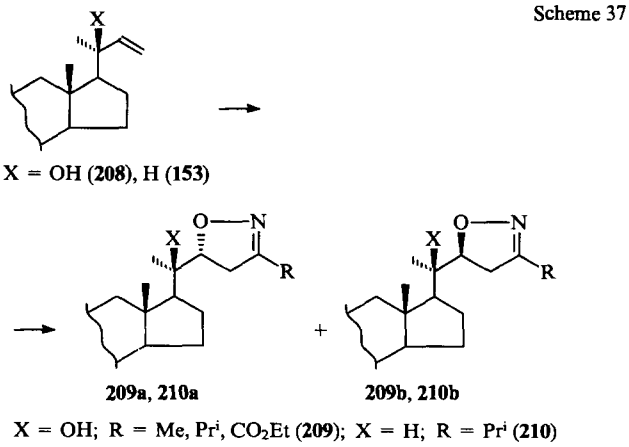
Apart from the approaches described above, steroids with a heterocycle in the C(20) position can be obtained by the dipolar cycloaddition of nitrile oxides, by the condensation of amino-alcohols, and by the hydroxymercuration of dienes. Thus the addition of benzonitrile oxide to the nitrile **201** led[90] to the formation of the oxadiazole **202**, while the condensation of amino-alcohols or aminothiols with the aldehyde **151** led to the formation of the oxazolidines **203** or the thiazolidines **204** respectively.[91] When an attempt was made to obtain the 22,25-dihydroxy-derivative from the diene **205** under hydroxymercuration conditions, the product **206** was isolated. Its reduction over $Pd/BaSO_4$ led to the formation[92] of the tetrahydrofuryl derivative **207** (Scheme 36).

Scheme 36



The synthesis of the new heterocyclic steroids **209** and **210** was achieved by the 1,3-dipolar cycloaddition of a series of nitrile oxides to the Δ^{22}-steroids **208** and **153** respectively.[85,93-97] The cycloaddition takes place stereoselectively[93] and in the case of allyl alcohols the epimer ratio 22*S*:22*R* reaches 6:1. The yield of the adducts depends on the nature of the substituents R in the nitrile oxide, diminishing when nitrile oxides with functional group substituents are used (Scheme 37).

Scheme 37

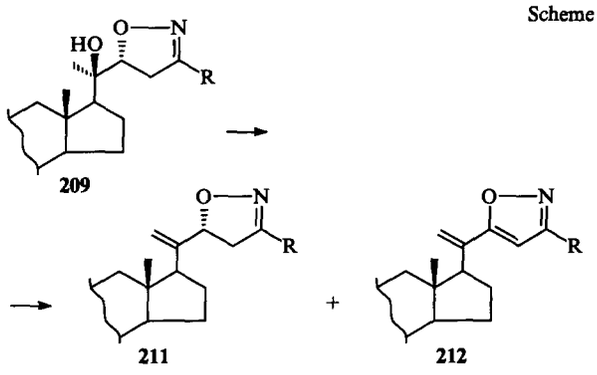


X = OH; R = Me, Pr^i, CO_2Et (**209**); X = H; R = Pr^i (**210**)

The observation[98] of the dehydrogenation of the steroid isoxazolines **209**, which makes it possible to achieve their transition to the corresponding isoxazoles **212**, is interesting. In the study of the dehydration reaction on treatment with thionyl chloride in chloroform, the formation of the isoxazole **212** as a side product together with the main product—the olefin **211**—was

established. The replacement of chloroform by pyridine or DMF led to the preferential formation of compounds **212** (Scheme 38).

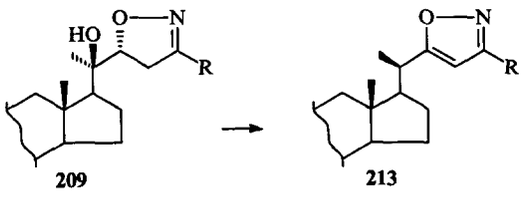
Scheme 38



R = Me, Pr^i, CO_2Et

A novel synthesis of 20-isosteroid isoxazoles has been proposed.[96] It consists in the transformation of the isoxazoline **209** into the isoxazole **213** with the simultaneous formation of a chiral centre at C(20). It was found that treatment of the isoxazoline **209** with trifluoroacetic acid in boiling nitromethane in the presence of lithium perchlorate affords only one C(20) isomer of compound **213** in a high yield (Scheme 39).

Scheme 39



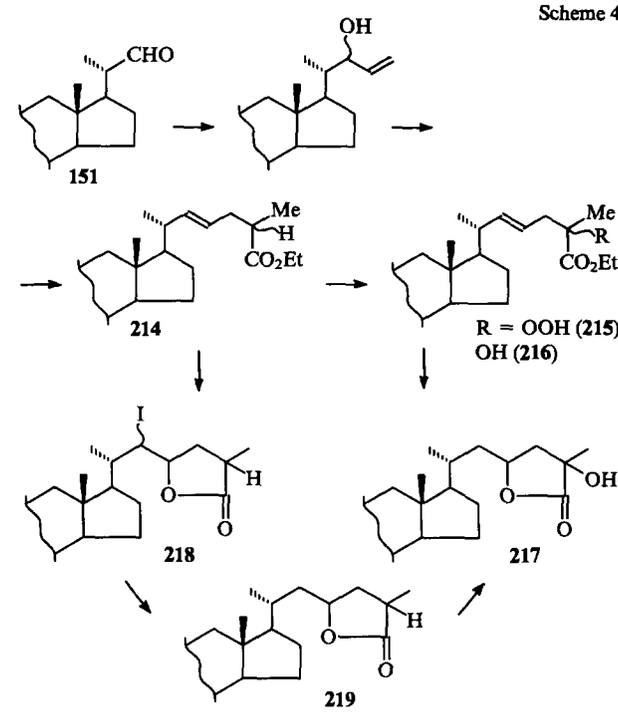
R = Me, Pr^i, CO_2Et

IV. Synthesis of steroids containing a heterocycle in the C(22) position

The approaches to the synthesis of the 25-hydroxycholecalciferol-26,23-lactone — the only known metabolite of vitamin D_3 having a lactone ring in the side chain — and several other compounds with the heterocycle in the C(22) position are considered in this section.

A new metabolite of vitamin D, having a 26,23-lactone ring, was isolated in 1979, but the stereochemical configuration of the C(23) and C(25) centres was not established. Synthetic chemists are therefore faced with the problem of not only obtaining this compound by chemical means but also of establishing the stereochemical configuration of the C(25) and C(23) centres. For this purpose, all four diastereoisomers were synthesised. One of the first syntheses of the side chain was achieved as follows. The aldehyde **151** was alkylated with vinylmagnesium bromide and the resulting mixture of isomers was used in the Claisen reaction with an excess of triethyl orthopropionate. This resulted in the formation of the ester **214**, which was converted into the enolate and oxidised at −78 °C with molecular oxygen. The hydroperoxide **215** formed in this reaction was reduced with triethyl phosphite, which afforded the α-hydroxyester **216**. After hydrolysis, the mixture of diastereoisomers was treated with iodine and potassium iodide under basic conditions, which led to the formation of a mixture of iodolactones. After their reduction with tributyltin hydride and separation, four diastereoisomers of compound **217** were obtained. However, the authors attributed[99] to the natural lactone the erroneous (23*R*,25*S*)-configuration (Scheme 40).

Scheme 40



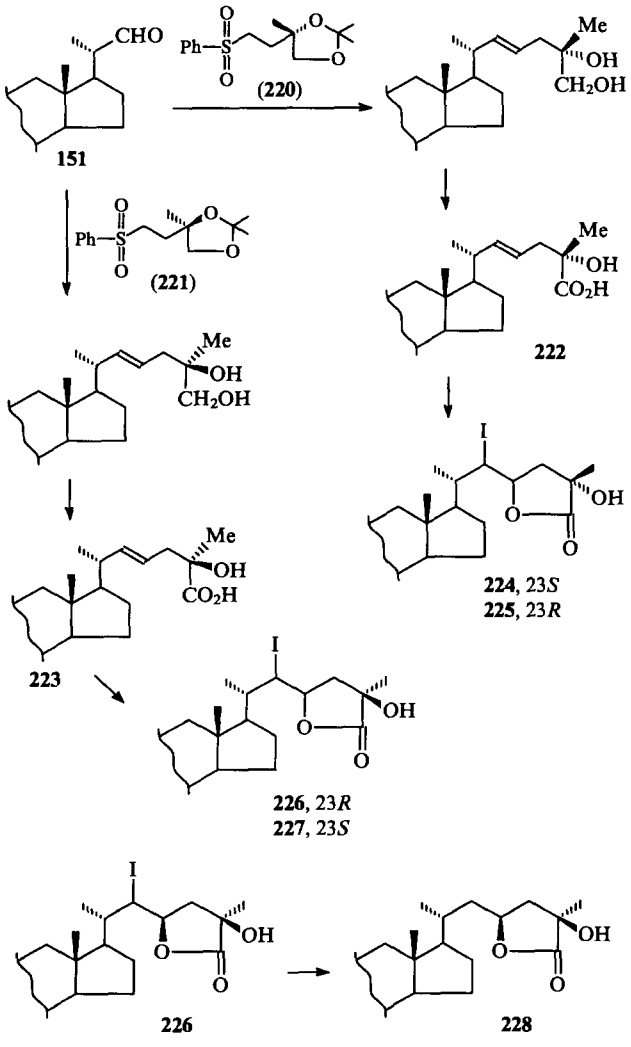
This procedure largely repeats the earlier synthesis,[100] in which the 25-hydroxy-group was introduced, in contrast to the method described above, in the last stage (after the reduction of the iodolactone **218** and the oxidation of the lactone enolate **219** by the MoO_3–pyridine–hexamethylphosphoramide complex). The authors determined the configuration of only the C(23) centre as 23*R*.

Several studies have been devoted to the determination of the structure of the above compound.[101–103] In order to avoid difficulties in the separation of the four diastereoisomers and to investigate in detail the iodolactonisation process, the stereoselective synthesis of the α-hydroxyacids **222** and **223** was carried out. The sulfones **220** and **221**, obtained respectively from (*S*)-(+)-citromalic acid (2-methylmalic acid)[101] and (*R*)-(−)-citromalic acid were used as the reagent with the required chirality.[102] The addition of these sulfones to the aldehyde **151** with subsequent desulfurisation, hydrolysis, and two-stage oxidation of the alcohol to the acid under mild conditions led to the hydroxyacids **222** and **223**. The iodolactonisation (iodine, MeCN) and reduction of the iodolactones led to the formation of two diastereoisomers of compounds **224**–**227** in each case (Scheme 41).

In their study of the iodolactonisation process[103] under various conditions, the authors observed that the selectivity of this reaction depends on stereochemical configurations at C(25) and the reaction conditions. The product **226** obtained by iodolactonisation under basic conditions afforded the lactone **228** in 56% yield relative to the acid **223** after reduction with tributyltin hydride. After the appropriate transformations of the cyclic component of this compound, its parameters proved to be identical with those of the natural metabolite. Thus the configuration of the C(23) and C(25) centres of the vitamin D metabolite was determined as 23*S*, 25*R*.

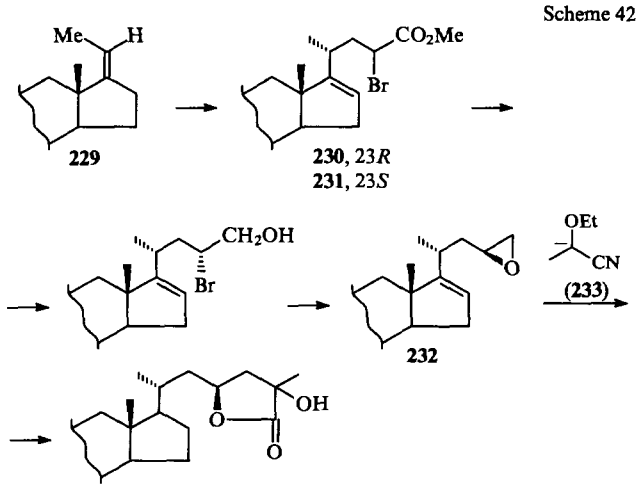
Yet another example of the synthesis of the side chain of the calciferol lactone, based on the introduction of chirality initially in the C(23) position, has been proposed.[104] Addition of α-bromo-acrylate to the olefin **229** in the presence of ethylaluminium dichloride afforded a mixture of bromo-derivatives in the proportions **230**:**231** = 13:87. The required diastereoisomer **230** was isolated from the mixture produced by reaction with lithium bromide in acetone. After four repetitions of this procedure, the bromo-derivative **230** was obtained from the

Scheme 41



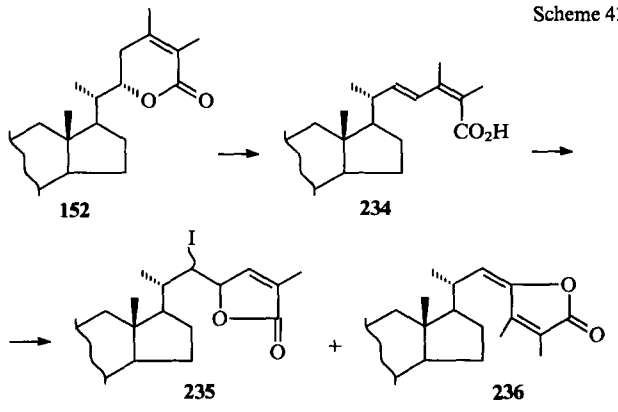
olefin in 63% yield. The ethoxycarbonyl group in compound **230** was reduced to the alcoholic group. The resulting bromohydrin afforded the epoxide **232** after treatment with a base. The missing three carbon atoms were introduced into the molecule by the addition of the anion **233** obtained from acetaldehyde cyanohydrin. After the hydrolysis of the intermediate, a 1 : 1 mixture of the lactones was isolated (Scheme 42).

Scheme 42



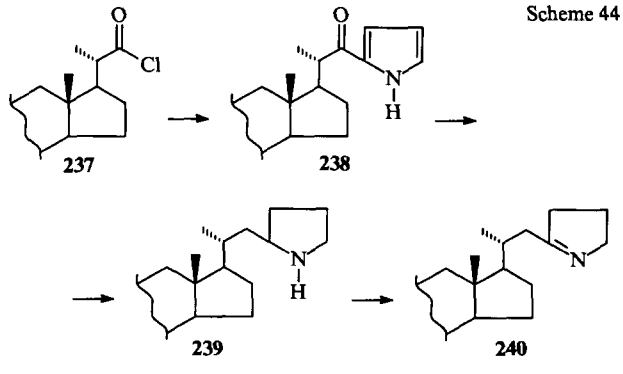
Steroids having a heterocyclic substituent in the C(22) position have not so far attracted much attention from organic chemists and syntheses of compounds of this kind are fairly rare. Thus the lactones **235** and **236**, which are structurally similar to calciferol lactone, have been isolated[78] after treating with iodine and selenium compounds the acid **234** obtained by hydrolysing compound **152** (Scheme 43).

Scheme 43



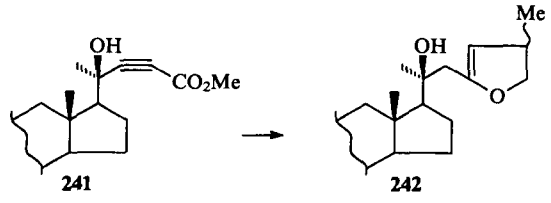
Compound **240**, which is related to steroid alkaloids, was synthesised in accordance with Scheme 44.[105] The acid chloride **237** was treated with pyrrolylmagnesium bromide and the adduct **238** was hydrogenated over Raney nickel, which led to the reduction of the pyrrole ring and the removal of the carbonyl group. The resulting stereoisomeric mixture of the pyrrolidines **239** was converted by reaction with *N*-bromosuccinimide into *N*-chloroamines, which afforded the pyrroline **240** after alkaline treatment.

Scheme 44



The dihydrofuran derivative **242**, the structure of the side chain of which is similar (according to the authors) to that in shidasterone, was obtained by the reaction of methyl acetylenecarboxylate **241** with methylmagnesium iodide (Scheme 45).[106]

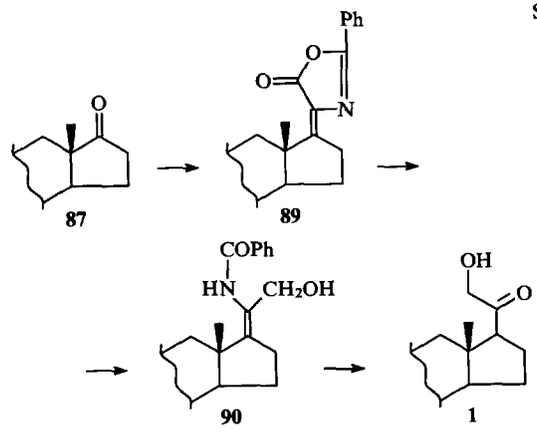
Scheme 45



V. Syntheses of the side chains of steroids including the transformation of heterocyclic structures

The synthetic possibilities of heterocycles for the construction of the side chains of steroids have not so far been employed in due measure. The only heterocycles which have found fairly extensive applications in the synthesis are probably furan derivatives. Nevertheless heterocyclic structures are attractive because of their fairly ready transformation into an open chain, which has stimulated interest in these compounds. This section deals with the syntheses of compounds with the side chains of the natural corticoids, ecdysones, brassinosteroids, vitamin D metabolites, etc. with participation of heterocyclic intermediates. The role of these intermediates is associated with the utilisation of the latent functionality of the heterocycle, which makes it possible to introduce the necessary substituents into definite positions, and also with the possibility of the stereocontrol of the products by virtue of the different accessibility of different sides of the heterocycle to the reagent. For example, the transformation of the heterocyclic derivatives **89** and **243**, obtained from the ketone **87**, makes it possible to form the side chain of corticosteroids.[51,56] Thus treatment of the product of alkaline hydrolysis with acetic acid and subsequent reduction of the heterocycle **89** via compound **90** lead to the formation of 21-hydroxyprogesterone **1** (Scheme 46).[56]

Scheme 46

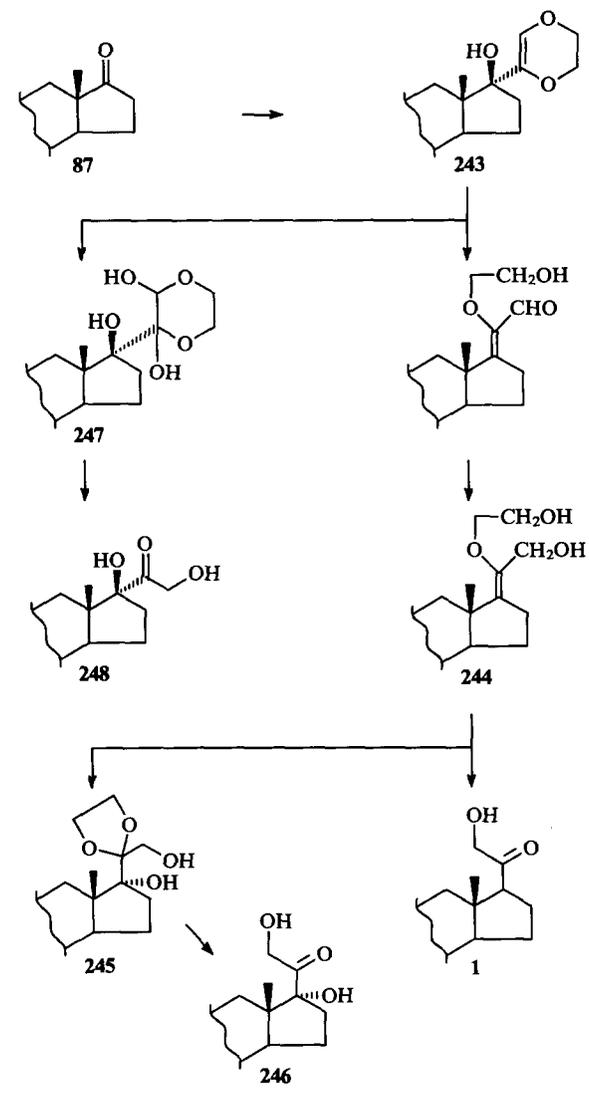


The cleavage of the heterocycle in compound **243** by various methods makes it possible to achieve the transition to a whole series of derivatives.[51] The acid-catalysed allyl rearrangement of compound **243** under very mild conditions (SiO_2, 5% oxalic acid) leads to the enol ether of an α-ketoaldehyde. Its reduction with $LiAlH_4$ and the subsequent hydrolysis of the ethyl ether afford the ketone **1**. Oxidation with *m*-chloroperbenzoic acid of the reduction product **244** led to the formation of the ketal **245** (via intramolecular cyclisation which followed the opening of the oxiran ring), the acid hydrolysis of which led to the ketodiol **246** with the natural orientation of the side chain. The authors also obtained the isomer of this compound with the 17α-configuration from the dioxene **243** (Scheme 47).

For this purpose, compound **243** was oxidised with *m*-chloroperbenzoic acid in methanol. The oxidation reaction occurred regioselectively at the electron-unsaturated C=C bond and led to the hemiacetals **247** in the form of a mixture of isomers with respect to C(20) and C(21). After their reduction with $NaBH_4$ and hydrolysis, the ketodiol **246** was obtained.

Barton and coworkers[107] developed a convenient and effective method for the conversion of cholic acids into pregnanes via oxazolines. The authors chose boric acid as the catalyst. Boric acid can react with cholic acid and the aminoalcohol, affording an intermediate of type **249** with an activated carbonyl group. Its subsequent reactions can lead to oxazolines. Using this method, the oxazoline **251** was obtained from the acid **250** in 95% yield.

Scheme 47

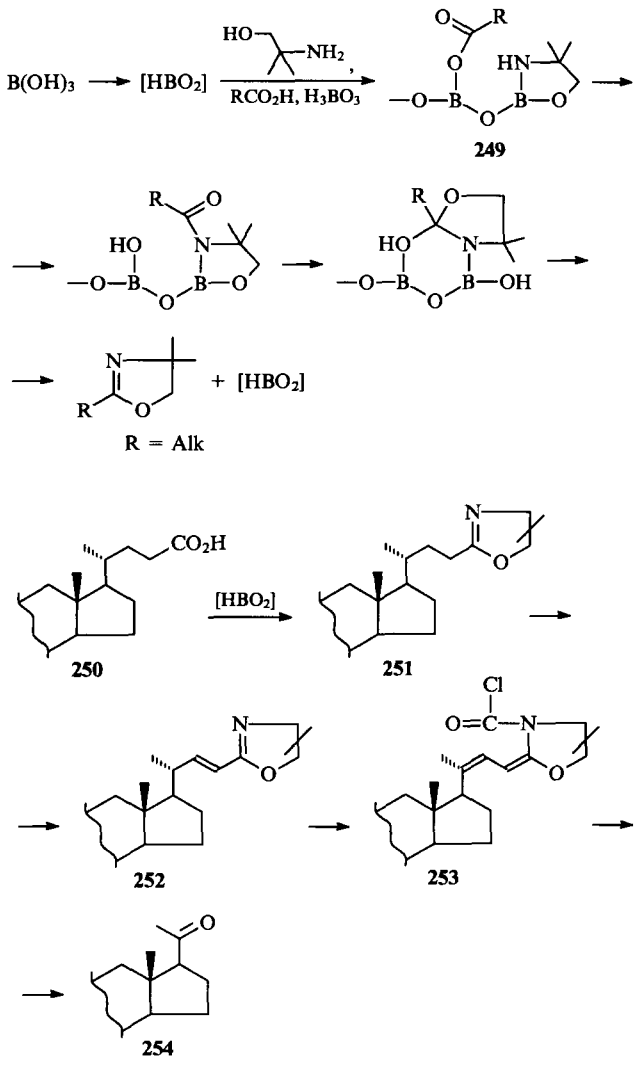


When it was heated with benzeneselenic acid in pyridine, the dehydrogenated compound **252** was obtained in a quantitative yield. In order to obtain the $\Delta^{20(22)}$-bond, the oxazoline **252** was acylated with phosgene at the nitrogen atom and the product **253** was ozonised, which led to the ketone **254** (Scheme 48).

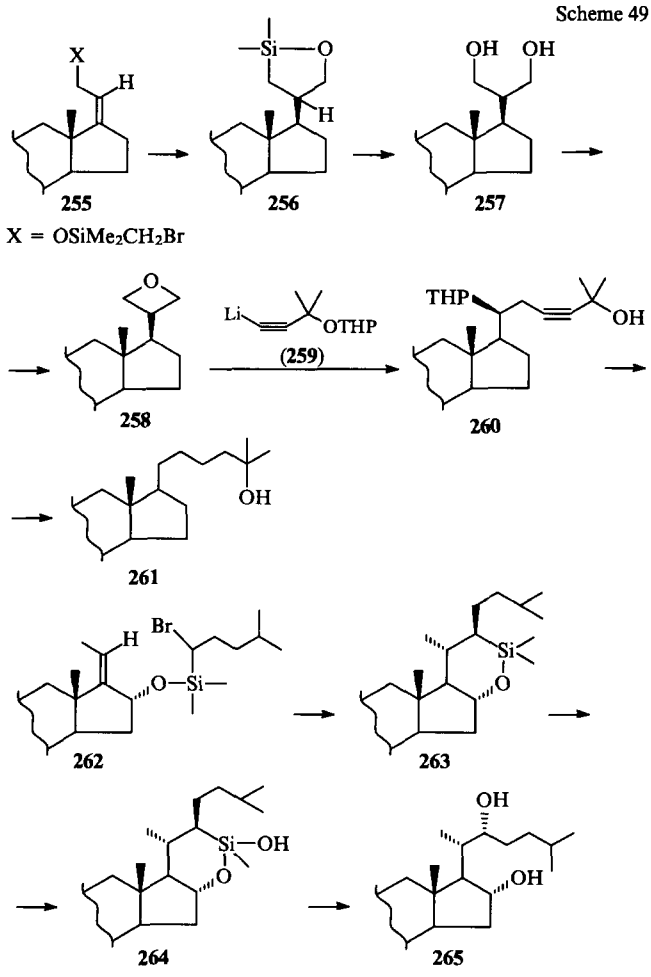
It has been observed recently[108,109] that the intramolecular cyclisation of α-silylsteroid groups to siloxanes proceeds with a high degree of selectivity, which makes it possible to employ the resulting siloxanes in the synthesis of the side chains. Thus the siloxanes **256** have been obtained[108] from the silyl ethers **255** by treatment with tributyltin hydride, while the siloxane **263** was obtained from the ether **262**.[109] Oxidation of the siloxanes **256** with hydrogen peroxide afforded the diol **257**. The latter was cyclised to the oxetan **258**, which was alkylated with lithium acetylide **259** in the presence of boron trifluoride etherate. This led to the isolation of the alcohol **260**. After removal of the 21-hydroxy-group via the methanesulfonate, hydrogenation of the triple bond, and hydrolysis, the tertiary alcohol **261** was obtained with the isosteroid (20*S*) side chain. The siloxane **263** proved to be resistant to the action of various oxidising agents, including concentrated (90%) hydrogen peroxide in DMF. Therefore, in order to open the heterocycle, the siloxane **263** was treated with KOH in dimethyl sulfoxide (DMSO), which led to a mixture of silanols **264**. The latter were readily oxidised with hydrogen peroxide to the diol **265** (Scheme 49).

Steroid γ-lactones have found applications as intermediates in the synthesis of the side chains of desmosterol[110] and (20*S*)-cholic acids.[111] The use of intermediates of this kind made it possible to

Scheme 48



Scheme 49



form stereoselectively the 20*R* or 20*S* centre in the steroid molecule via the controlled protonation of the lactone enolate. The nitrile **266** was obtained in two stages from the ketone **87**. Its condensation with (*S*)-benzyl 2,3-epoxypropyl ether **267** in the presence of lithium hexamethyldisilazide afforded a mixture of the corresponding cyanoalcohols **268**, which could not be separated. After the hydrolysis of the cyanoalcohols (KOH, EtOH), a mixture of the lactone **269** and its C(20) epimer was obtained. The mixture was treated with lithium hexamethyldisilazide in THF at −78 °C and then with a saturated solution of Na_2SO_4 at the same temperature, which led to the selective protonation of the enolate intermediate **270** at C(20) from the less hindered side (opposite to the benzyl group) and to the exclusive formation of the (20*S*)-lactone **269**. The latter was reduced with $LiAlH_4$ to the diol **271**, which was converted into the dimethanesulfonate and reduced selectively with lithium triethylboron hydride to the methanesulfonate **272**. Dehydration, reductive debenzylation, oxidation, and hydrogenation led to the formation[111] of compounds **273** and **274**, which had been isolated previously from marine organisms (Scheme 50).

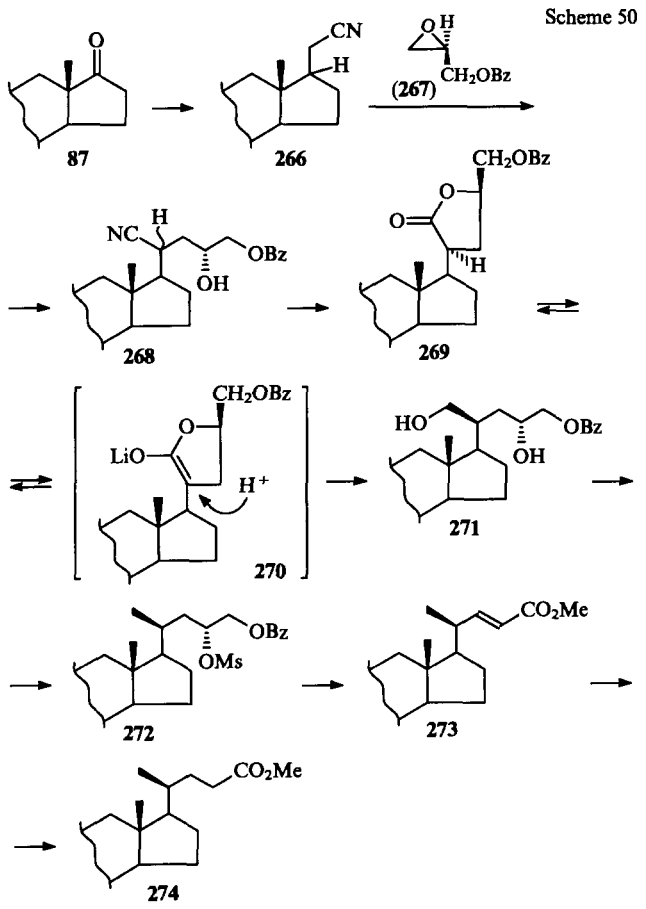
In the synthesis of desmosterol, the addition of the (*R*)-benzyl 2,3-epoxy propyl ether **275** to the nitrile **266** led, after cyclisation, to a 4 : 1 mixture of the lactone **276** and its C(20) epimer **277**. The protonation of this mixture under the conditions described above afforded exclusively the (20*R*)-lactone **277** (i.e. the minor component of the initial mixture). Like the lactone **269**, the lactone **277** was reduced and converted into the methanesulfonate **278** and the latter afforded the alcohol **279** as a result of reduction and debenzylation. The alcohol was oxidised to the aldehyde **280**, from which the product **282**, having the desmosterol side chain, was obtained on condensation with the ylide **281** (Scheme 51).[110]

The chemistry of furan derivatives has found an application also in the synthesis of side chains of ecdysones and brassinosteroids. The side chains of these compounds have from two (α-ecdysone) to four (brassinolide) chiral centres and several hydroxy-groups in different positions, which greatly complicates the synthesis of compounds of this kind. The use of heterocyclic intermediates in the synthesis in many respect helps in the solution of the problems of regio- and stereo-selectivity arising in this connection.

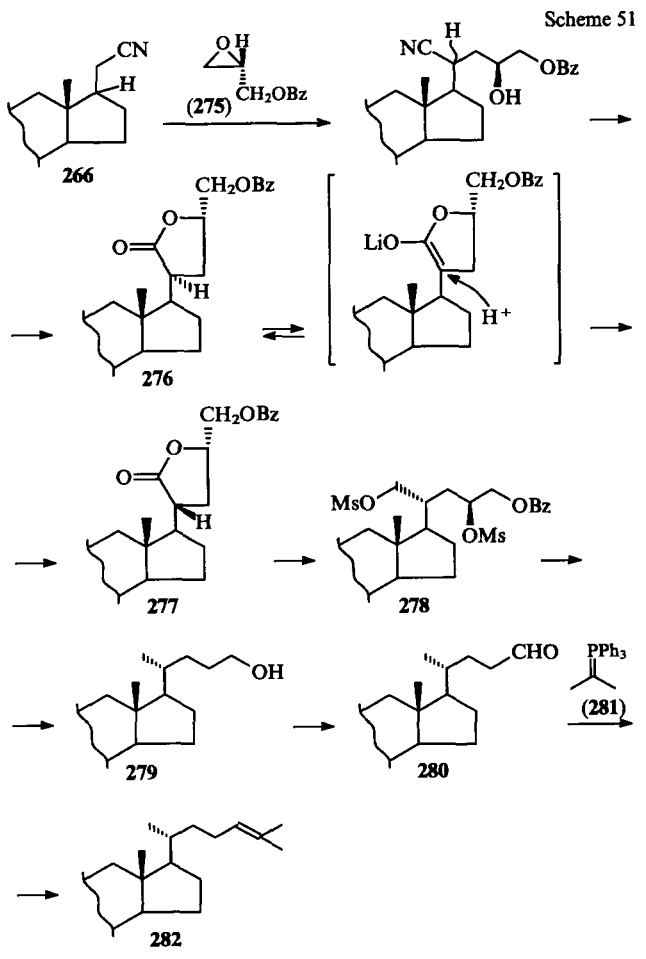
The dihydrofuran **283** was used to synthesise the side chain of 20-hydroxyecdysone.[112] The addition of its lithio-derivative to the ketone **80** led to a mixture of compounds **284** and **285** in 85% yield without any admixture of the (20*S*)-isomers. The dihydrofuran **284** was converted into compounds **285** by brief treatment with 0.1% HCl in THF. The reduction of the ketodiol **285** with Li selectride afforded, as expected, the (22*S*)-alcohol **286** (the ratio of the alcohol **286** to the isomer **287** was 16 : 1). Nevertheless, this product ratio as altered by protecting the hydroxygroup in the ketodiol **285** by forming the trimethylsilyl ether. The subsequent reduction with Li selectride at −78 °C and hydrolysis of the silyl ether led to the formation of the triol **287** in 58% yield (Scheme 52).

A more selective method was proposed by Kametani and coworkers.[113-115] After treatment of the furan **288** with *m*-chloroperbenzoic acid in sodium acetate and chloroform, the hemiacetal **289** was obtained and the oxidation of the latter with pyridinium chlorochromate afforded the lactone **290**. The stereoselective hydrogenation of the lactone **290** over PtO_2 proved to be the key stage. Hydrogen added from the less hindered side (opposite the bulky steroid skeleton) of the lactone afforded a mixture of the lactone **291** and its isomerisation

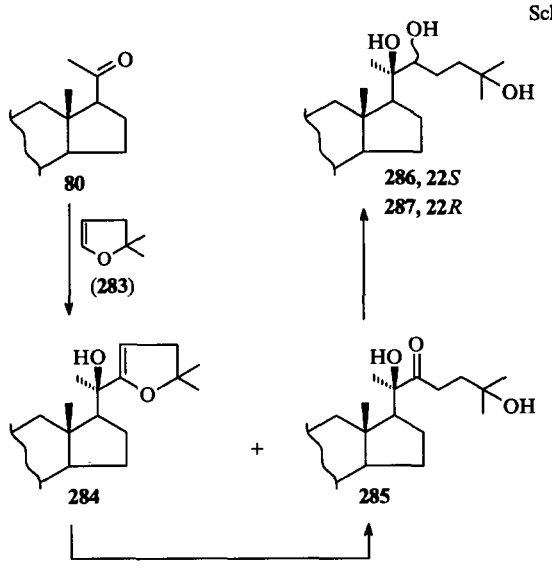
Scheme 50



Scheme 51

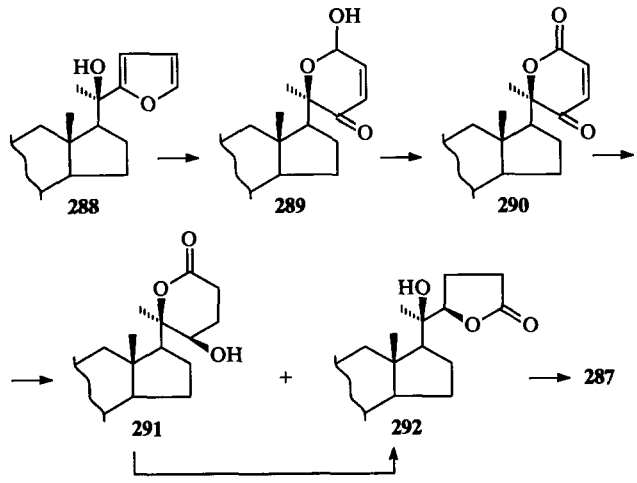


Scheme 52



product **292** (3 : 2) in an almost quantitative yield. The lactone **291** was converted by treatment with aqueous alkali into the thermodynamically more stable lactone **292**, which was alkylated with methyl magnesium bromide. Ultimately the (20*R*, 22*R*)-diol **287** was obtained in 88% yield. The stereoselective formation of the C(22) centre of ecdysones constitutes an appreciable advantage of the above investigation, because the reduction of 22-ketones by hydrides affords mainly the (22*S*)-hydroxy derivative (Scheme 53).[2]

Scheme 53

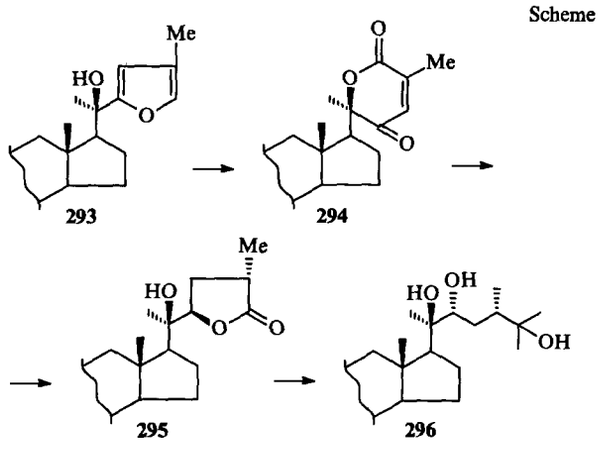


This approach was also applied to the synthesis of the side chain of makisterone A (three chiral centres in the side chain) and its 24-isomer.[115] The lactone **294** was obtained from the furan **293** and its stereoselective hydrogenation and recyclisation afforded the lactone **295** in a quantitative yield. The epimakisterone **296** was obtained by alkylating the latter with methylmagnesium bromide (Scheme 54).

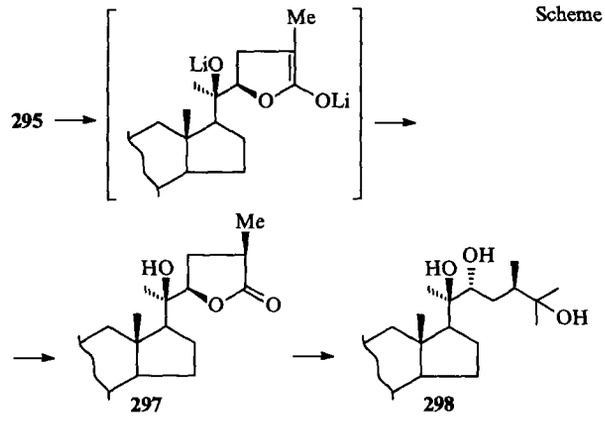
The side chain of makisterone was formed by inverting the C(24) centre in the lactone **295**, which is achieved by the kinetic protonation of γ-butyrolactone. For this purpose, the lactone **295** was enolised by treatment with lithium diisopropylamide and the enolate was treated at −78 °C with a Na_2SO_4 solution, which afforded the lactones **297** and **295** in proportions of 87 : 13 (Scheme 55).

Synthesis using furans has been applied also to the formation of the side chain of α-ecdysone.[116–118] After the dehydration on silica gel of the product of the addition of compound **299** to the ketone **80**, namely 2-lithio-5-methylfuran, the furan derivative **300**

Scheme 54



Scheme 55

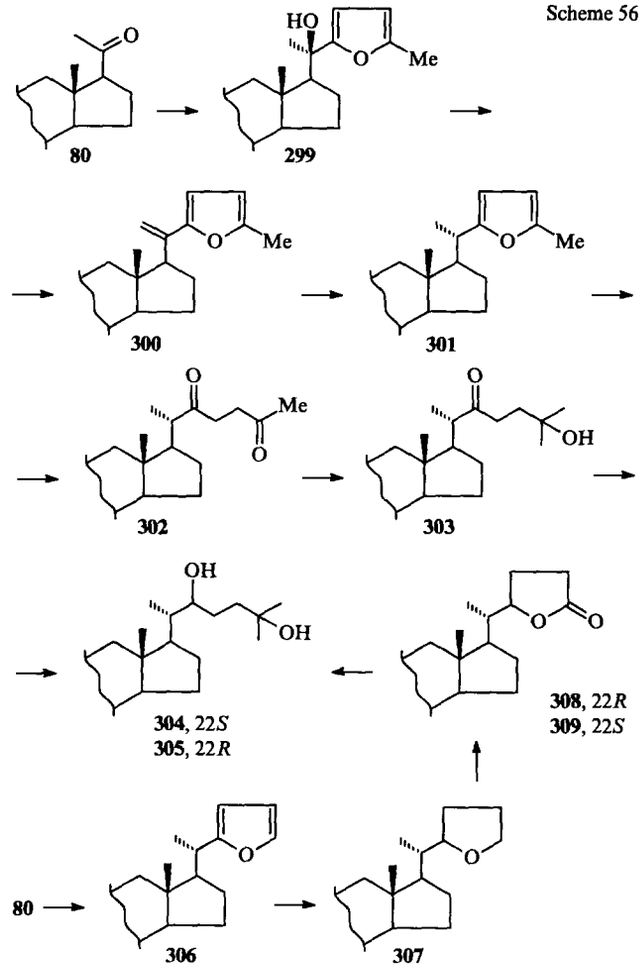


was obtained. The hydrogenation of its $\Delta^{20(21)}$-bond on Pd/C took place stereoselectively and afforded the product **301** without an admixture of the isomer. The furan ring in compound **301** was opened under acid conditions and the resulting diketone **302** was alkylated with methyllithium. The only product of this reaction was the ketol **303**, which was subjected to hydride reduction. As already pointed out, this process takes place with the preferential formation of the (22*S*)-isomer, which is uncharacteristic of the side chain of ecdysones. The best result was achieved using zinc tetrahydroborate in ether as the reductant.[116,117] The ratio of the (22*S*)- and (22*R*)-isomers was 2 : 1 (Scheme 56).

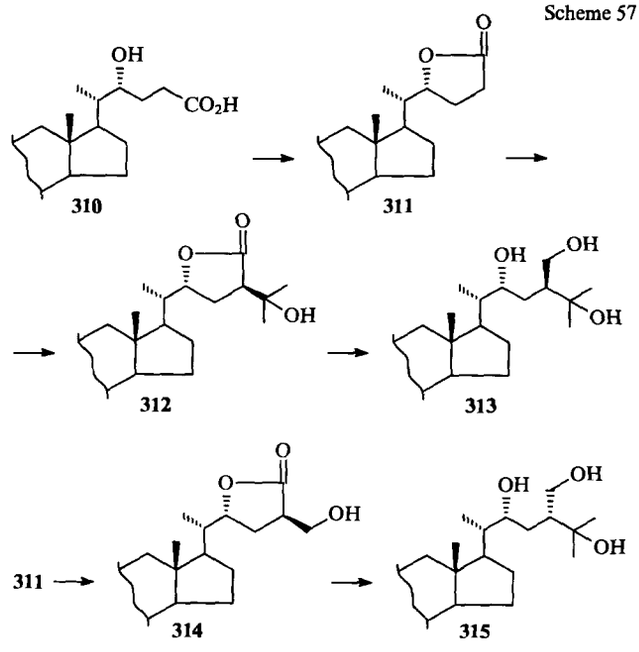
An increase in the yield of the (22*R*)-isomer was achieved by altering the strategy for establishing the chirality of C(22).[118] The furan **306**, obtained by the same mechanism as compounds **301**, was reduced over a rhodium-aluminium catalyst and the reduction product **307** was oxidised with ruthenium oxide. This resulted in the formation of a 1 : 1 mixture of the butenolides **308** and **309**. Grignard reaction with methylmagnesium bromide afforded the diols **304** and **305**.

An elegant method for the monitoring of the stereochemistry of the products formed via the steroid γ-lactones has been proposed[119] in order to establish the stereochemistry of depresosterol. The lactone **311**, obtained from the acid **310**, was enolised by treatment with lithium diisopropylamide and acetone was added, which led to the hydroxylactone **312**. This was converted, after reduction with $LiAlH_4$, into compound **313**, the latter proving to be the 24-stereoisomer of the natural steroid. Since the inversion of the C(24)-centre in the hydroxylactone **312** is impossible, the substituents were introduced at C(28) starting from the lactone **311**. The lactone enolate was treated with gaseous formaldehyde, which led to the hydroxylactone **314**, and the alkylation of the latter with methyllithium afforded the alcohol **315**, isomeric with respect to C(24), which is identical with the natural alcohol (Scheme 57).

Scheme 56



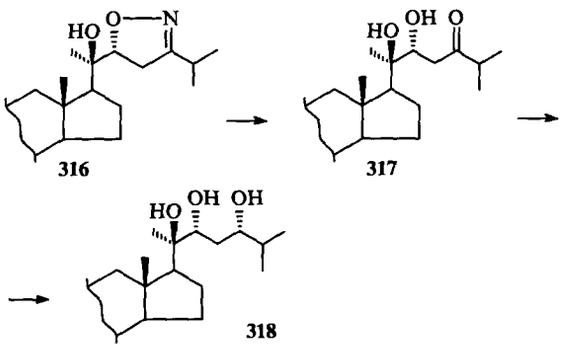
Scheme 57



A procedure using the synthetic possibilities of isoxazolines has been proposed recently for the construction of the side chain in ecdysteroids. Thus the reductive cleavage of the isoxazoline **316** on Raney nickel in the presence of an inorganic acid results in the formation of the β-ketol **317**. The reduction of its carbonyl group with sodium tetrahydroborate in alcohol led to the formation of two alcohols isomeric with respect to C(24). The side chain of the

(24*S*)-epimer **318** corresponds to that of the side chain of the phytoecdysones ponasterone C and pterosterone (Scheme 58).[120,121]

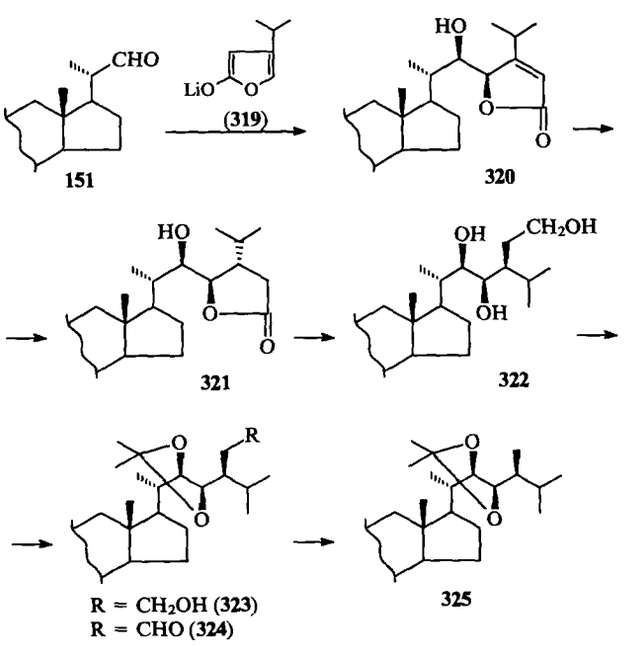
Scheme 58



The isolation in 1979 of brassinolide—the first phytohormone having a steroid structure—initiated a multiplicity of studies devoted to its partial chemical synthesis. Heterocyclic intermediates have been used[95,122–127] for the selective formation of the side chain in this compound. As in the case of ecdysones, syntheses involving furan derivatives have come to be most widely used.

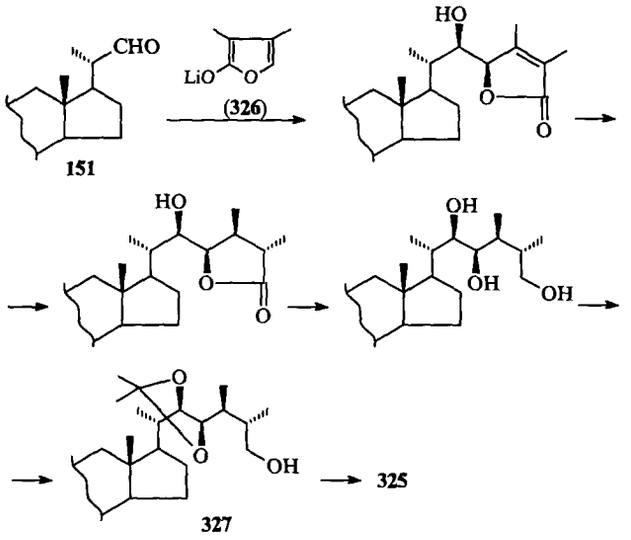
Having selected the aldehyde **151** as the starting material for the synthesis of side chains, it is necessary to form three chiral centres at C(22), C(23), and C(24). The use of furan derivatives[122–125] makes it possible to introduce the required functional groups in these positions, maintaining a high stereoselectivity. Thus the addition of the lithium enolate **319** at −78 °C to the aldehyde and treatment of the reaction mixture at this temperature (kinetic conditions) with dilute hydrochloric acid led to the formation of the butenolide **320** with the (22*R*, 23*R*)-configuration in 65% yield.[122] When the reaction mixture was treated at 0 °C, the main product was the (22*R*, 22*S*)-isomer, i.e. the thermodynamically more stable product is formed at a higher temperature (Scheme 59).

Scheme 59



Hydrogenation of the lactone **320** on platinum afforded a mixture of isomers with respect to C(24) in proportions of 78 : 22 in a quantitative yield. Since the constant for the spin–spin coupling of the protons of C(23) and C(24) in the main isomer **321** was smaller, the (24*S*)-configuration was attributed to the latter. After the reduction of the lactone **321** with $LiAlH_4$, the triol **322** was obtained and its refluxing with 2,2-dimethoxypropane in the presence of pyridinium toluene-*p*-sulfonate led to the formation of the acetonide **323** and the mixed acetal at C(29). The crude product was then refluxed in methanol, which afforded only the acetal **323** in 92% yield. The latter was oxidised with pyridinium chlorochromate and the resulting aldehyde **324** was decarbonylated with tris(triphenylphosphine)rhodium chloride. As a result of these transformations, the (24*S*)-methyl derivative **325** was obtained from the aldehyde **151** in an overall yield of 32%. A shorter synthesis of the side chain of brassinolide is possible when the lithium derivative **326** is used: a similar chain of transformations afforded the acetonide **327**, the treatment of which with methanesulfonyl chloride in pyridine and subsequent reduction of the methanesulfonate with $LiAlH_4$ lead to compound **325** (Scheme 60).[122]

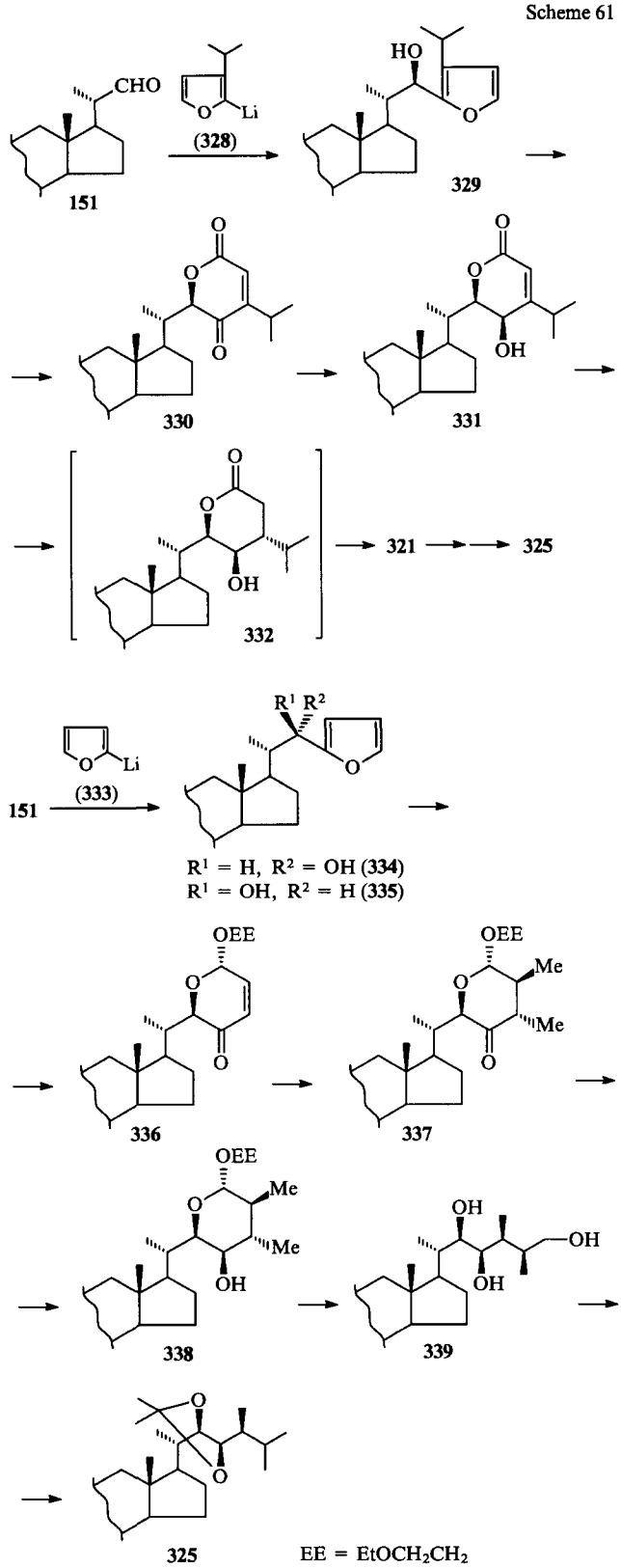
Scheme 60



The side chain of brassinolide was also formed by alkylating the aldehyde **151** with the lithiofurans **328** and **333**.[123,124] In the former cases, alkylation afforded 81% of the furylsteroid **329**, the successive oxidation of which the *m*-chloroperbenzoic acid and pyridinium chlorochromate led to the ketolactone **330**. The ketone functional group in compound **330** was reduced with sodium tetrahydroborate, which afforded exclusively the hydroxylactone **331**. Finally, its hydrogenation on PtO_2 and isomerisation (0.5 M NaOH) of the primary product **332** to the thermodynamically more stable γ-lactone led to the formation of 72% of the lactone **321** and 25% of its (24*R*)-isomer.[123] The addition of the furan **333** was less selective (**334** : **335** = 3 : 7), but the isomer **334** was converted into compound **335** by oxidising it with pyridinium chlorochromate and subsequently reducing the 22-ketone. As in the previous cases, the oxidation of the α-hydroxyfuran with *N*-bromosuccinimide led to a mixture of lactols, which were converted into ethoxyethyl ethers and separated. The ratio of the main product **336** to its 26-isomer was 3 : 1. Subsequently the ether **336** was subjected to coupled alkylation with lithium dimethylcuprate and methyl iodide. These reactions proceeded smoothly and it was assumed that the addition occurred on the opposite side of the plane of the ring in relation to the neighbouring group. The reduction of the carbonyl group of the dimethyl derivative **337** leads to the exclusive formation of the alcohol **338**. Hydrolysis of the ether group (10% HCl) and treatment with $LiAlH_4$ afforded the triol **339**, the subsequent transformations of which into compound **325** were described above (Scheme 61).[124]

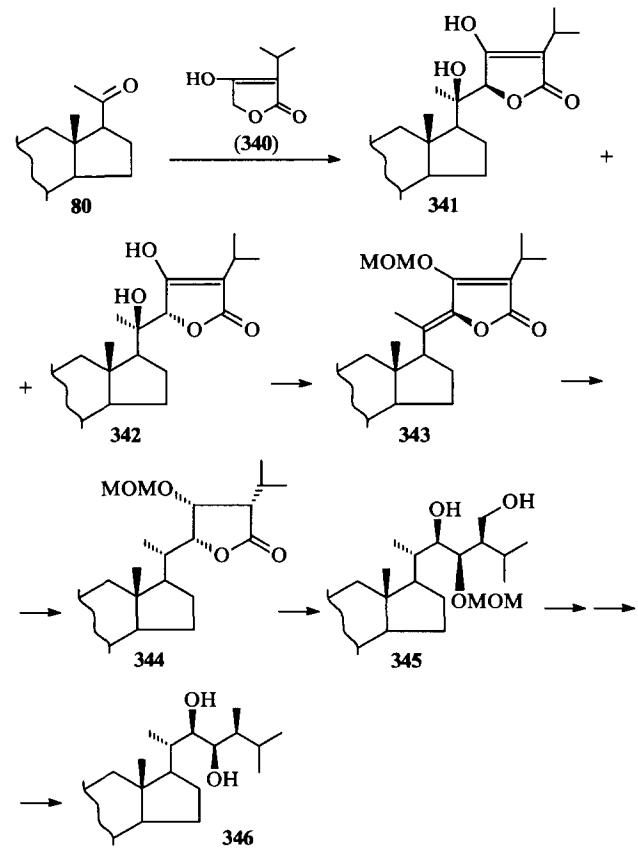
Kametani's group[125] were able to achieve the stereocontrolled formation of four chiral centres at once in the side chain of brassinolide. Alkylation of the ketone **80** with a fourfold excess

Scheme 61



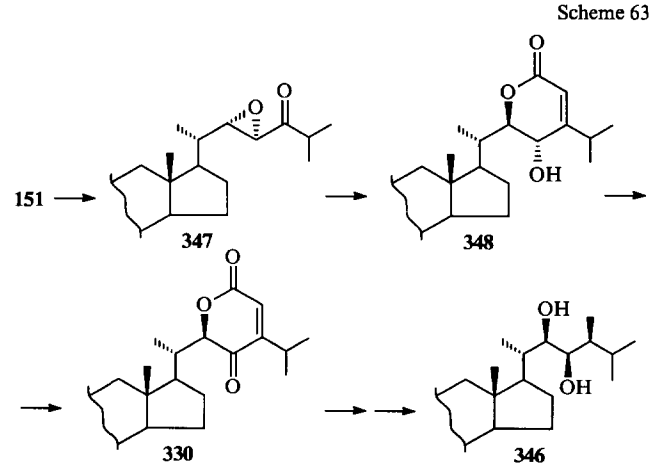
of the butenolide dianion **340** afforded a 9:91 mixture of the diastereoisomers **341** and **342** (84%), the enolic hydroxy-groups of which were protected by forming methoxymethyl ethers. The removal of the tertiary hydroxy-group of the MOM ether of the isomer **342** (via the formation of the trifluoroacetate) and hydrogenation over a rhodium catalyst of the (*Z*)-isomer **343** formed preferentially afforded the sole product **344** with the required stereochemical configuration of all four chiral centres in the side chain. After the reduction of the lactone **344** with $LiAlH_4$ to the alcohol **345**, the primary hydroxy-group of the latter was converted into the methanesulfonate and reduced, which led to the side chain of the brassinolide **346** (Scheme 62).

Scheme 62



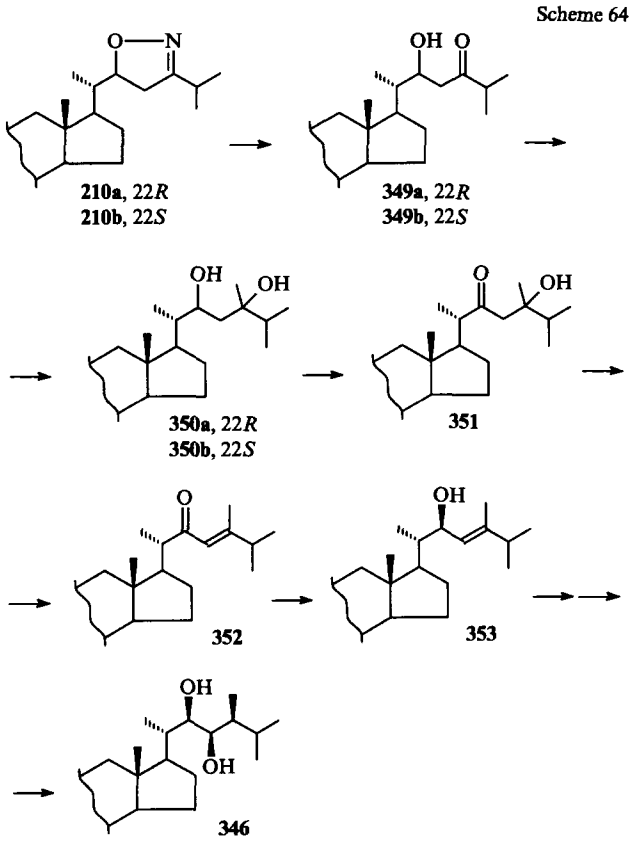
A somewhat different approach to increasing the length of the side chain of brassinolide, leading to common heterocyclic intermediates, has been developed by Chinese workers.[126] The aldehyde **151** was converted into the epoxyketone **347** by the method proposed in the synthesis of deoxyantheridiol.[79] The Wittig–Horner reaction of the epoxyketone with methoxycarbonylmethylphosphonate and subsequent lactonisation of the (*Z*)-isomer under acid conditions [occurring with inversion of the configuration at C(22)] ensured the formation of the hydroxylactone **348**. The oxidation of the hydroxy-group of this compound with pyridinium chlorochromate afforded the known intermediate **330**, the subsequent transformations of which lead to the side chain of brassinolide (Scheme 63).

Scheme 63



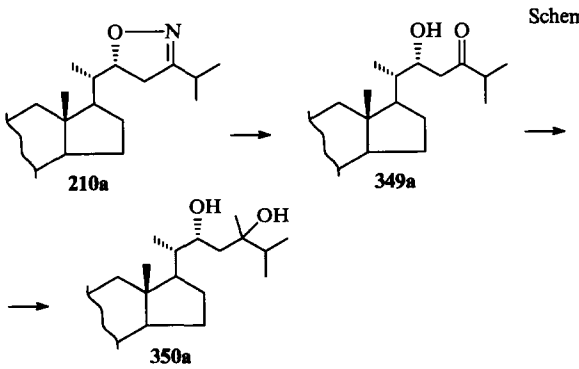
The growth of the side chain of brassinolide was achieved also by using isoxazoline intermediates.[95] Thus cleavage of the isoxazolines **210a, b** in the presence of acid on Raney nickel, the subsequent alkylation of the β-ketols **349** with methyllithium, oxidation of the resulting diols **350** by the Jones reagent, and finally dehydration of the tertiary alcohols **351** by thionyl chloride in pyridine led to the formation of the steroid 23-en-22-one **352**. Reduction of the eneketone **352** with diisobutylaluminium hydride leads[95] to the allyl alcohol **353** with a high stereoselectivity. The subsequent formation of the side chain of brassinolide can be readily achieved by Siddall's method (Scheme 64).[127]

Scheme 64



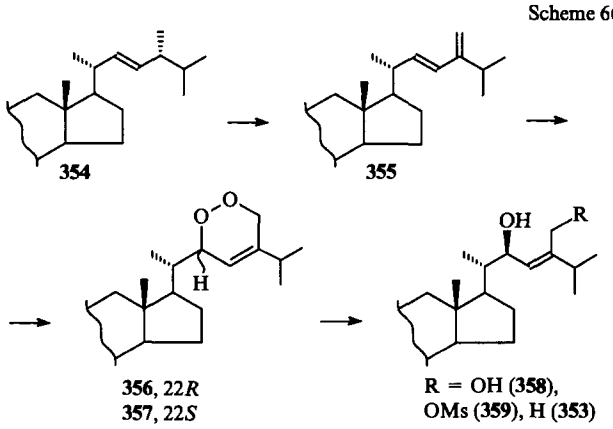
It is noteworthy that,using the (22*R*)-isoxazoline **210a**, it is possible to achieve, by means of a similar scheme, the formation of the side chain of the sapogenin isolated from the soft coral *Asterospicularia randalli* (Scheme 65).[128]

Scheme 65



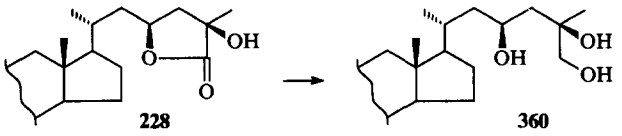
The use of heterocyclic derivatives[129] made it possible for the first time to transform the side chain ergosterol into the alcohol **353** (the intermediate in many syntheses of brassinolide and dolicholide[127]) without its cleavage. Thus the olefin **354** was converted via a bromination–dehydrobromination reaction into the diene **355**, the oxidation of which with molecular oxygen in pyridine under intense illumination in the presence of a sensitiser led to the chromatographically separatable mixture of the epidioxides **356** and **357** (in proportions of 7 : 3). The (22*R*)-isomer was reduced on the Lindlar catalyst to the diol **358**, the primary hydroxy-group of which was removed by reducing its methanesulfonate **359** with $LiAlH_4$. Analogous transformations of the epidioxide **357** led to the (22*S*)-isomer of the alcohol **353** (Scheme 66).

Scheme 66



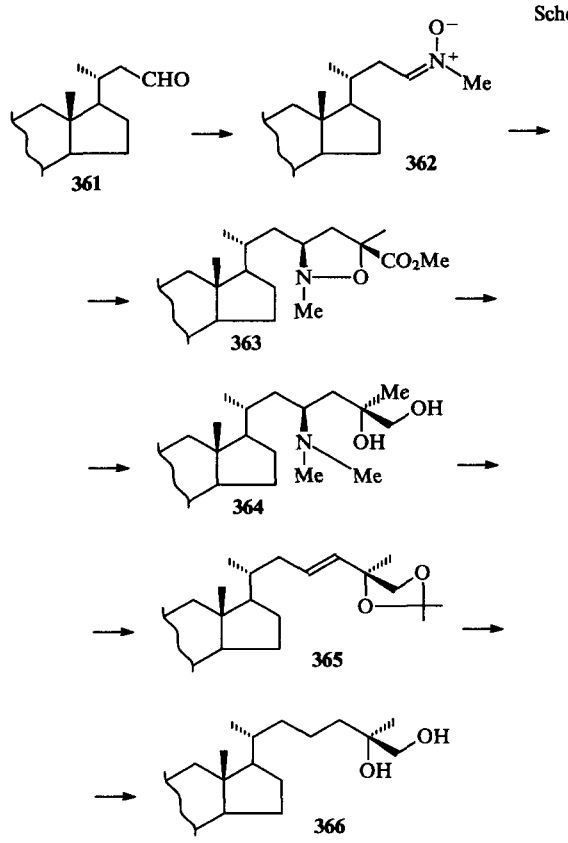
Heterocyclic intermediates have been used in a number of studies[103,130] of the vitamin D_3 metabolites, undertaken to achieve stereocontrol in the formation of the side chain. In particular, in the synthesis 23,25,26-trihydroxy-vitamin D_3 **360**, the intermediate of this kind was the lactone **228** (calciferol-lactone), the reduction of which with $LiAlH_4$ afforded the required product (Scheme 67).

Scheme 67



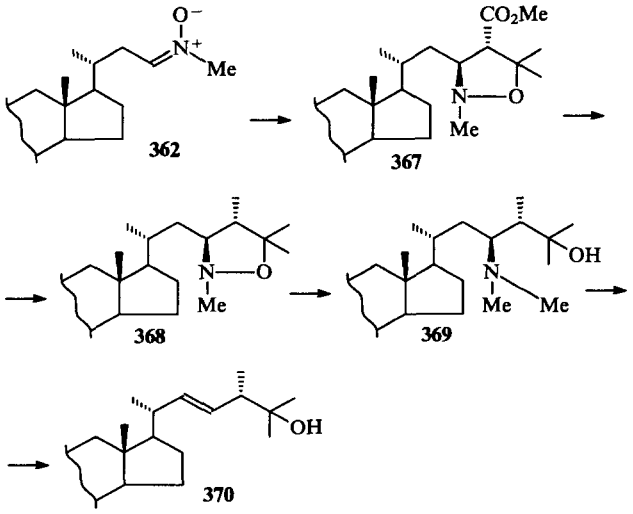
Uskokovic and coworkers[131–133] developed a fairly effective stereoselective method of synthesis of vitamin D_3[131] and D_2[132,133] metabolites via the cycloaddition of steroid nitrones to olefins. The synthesis of the side chain of 1α-(25*S*),26-trihydroxy-cholecalciferol **362**, a new vitamin D_3 metabolite isolated in 1981, has been described.[131] The nitrone **366** was obtained from the aldehyde **361** and *N*-methylhydroxylamine in the form of one (*Z*)-isomer, the structure of which was determined by X-ray diffraction. The cycloaddition of methylacrylate to this compound afforded a mixture of four isoxazolidines diastereoisomeric with respect to C(23) and C(25). The existence of thermal equilibrium between them makes it possible to monitor the stereochemical configuration of the product. For this purpose, after the separation of the required (*S,S*)-isomer, the other three were heated at 140 °C in xylene in the presence of an excess of methyl methacrylate. This again led to four isomers. By several repetitions of the process, the required isomer **363** was obtained from compound **362** in 71% yield. The isoxazolidine **363** was then treated with methyl iodide and the product was reduced with $LiAlH_4$, which afforded 86% of the aminodiol **364**. The aminodiol was converted into the acetonide and the amino-group was eliminated by the Hofmann method. This resulted in the formation of the olefin **365**, the hydrogenation of which over palladium on charcoal and hydrolysis led to the diol **366** (Scheme 68).

Scheme 68



The same approach has been used[132, 133] for the synthesis of a vitamin D_2 metabolite — 1α,25-dihydroxyergocalciferol **370**. The addition of 3,3-dimethylacrylate to the nitrone **362** in boiling xylene led to the formation (in contrast to the previous case) of only two of the four possible diastereoisomers (*RR* and *SS*) in proportions of 1 : 1. The enrichment in the required (*SS*)-isomer **367** was carried out by a procedure similar to that described above. Next the carboxymethyl group in compound **367** was reduced to the hydroxy-group and the latter was removed via the toluene-*p*-sulfonate, affording the isoxazolidine **368**. Its alkylation at the nitrogen atom and subsequent cleavage of the ring led to the aminoalcohol **369**. Its deamination ensured the formation of the *trans*-Δ^{22}-steroid **370** (Scheme 69).

Scheme 69



References

1. D M Piatak, J Wicha *Chem. Rev.* **78** 199 (1978)
2. J Redpath, F J Zeelen *Chem. Soc. Rev.* **12** 75 (1983)
3. J Boutagy, R Thomas *Chem. Rev.* **74** 87 (1974)
4. R Sondheimer *Chem. Brit.* **1** 454 (1965)
5. E Glotter, I Kirson, D Lavie, A Abraham *Bioorg. Chem.* **2** (Special Issue) 57 (1978)
6. A V Kamernitzky, A M Turuta *Heterocycles* **7** 547 (1977)
7. P Catsoulacos, C Camoutsis *J. Heterocycl. Chem.* **18** 1485 (1981)
8. T Kametani *Stud. Org. Chem. (Amsterdam)* **25** 143 (1986)
9. A V Kamernitskii, I G Reshetova, E I Chernoburova *Khim. Prir. Soedin.* 3 (1988)
10. A V Kamernitskii, I G Reshetova, V A Krivoruchko *Khim. Prir. Soedin.* 156 (1977)
11. W Fritsch, U Stache, U Ruschig *Liebigs Ann. Chem.* **699** 195 (1966)
12. P Kocovsky *Tetrahedron Lett.* **21** 555 (1980)
13. P Kocovsky *Collect. Czech. Chem. Commun.* **45** 2985 (1980)
14. S F Donovan, M A Avery, J E McMurry *Tetrahedron Lett.* **20** 3287 (1979)
15. K Nickisch, W Klouse, F Bholmann *Chem. Ber.* **113** 2038 (1980)
16. A Guzman, J M Muchowski, A M Strosberg *Can. J. Chem.* **59** 3241 (1981)
17. T W Guntert, H H Linde, M S Ragab, S Spengel *Helv. Chim. Acta* **60** 334 (1977)
18. T W Guntert, H H Linde, M S Ragab, S Spengel *Helv. Chim. Acta* **61** 977 (1978)
19. G Rapi, M Ginanneschi, M Chelli, S Chimichi *J. Chem. Res. (S)* 322 (1986)
20. G Rapi, M Ginanneschi, M Chelli *J. Chem. Soc., Chem. Commun.* 1999 (1975)
21. B R Samant, F Sweet *J. Org. Chem.* **41** 2292 (1976)
22. P Catsoulacos, D Kallias *J. Heterocycl. Chem.* **16** 763 (1979)
23. D Kallias, C I Stassinopoulou, P Catsoulacos *J. Heterocycl. Chem.* **17** 1045 (1980)
24. P Drasar, V Pouzar, I Cerny, J Smolikova, M Havel *Collect. Czech. Chem. Commun.* **49** 1039 (1984)
25. P Catsoulacos, E Souli *J. Heterocycl. Chem.* **11** 87 (1974)
26. P Catsoulacos *J. Heterocycl. Chem.* **10** 933 (1973)
27. US P. 3 944 541; *Chem. Abstr.* **85** 21728 (1976)
28. G Falcone, B Hundt *Arch. Pharm.* **318** 190 (1985)
29. E Yoshii, T Oribe, K Tumura, T Koizumi *J. Org. Chem.* **43** 3946 (1978)
30. E Yoshii, T Koizumi, H Ikeshima, K Ozaki, I Hayashi *Chem. Pharm. Bull.* **23** 2496 (1975)
31. G Lenz, J A Schulz *J. Org. Chem.* **43** 2334 (1978)
32. A V Kamernitskii, A M Turuta, Z I Istomina, A A Korobov *Izv. Akad. Nauk SSSR, Ser. Khim.* 194 (1987)
33. T Y Tsai, A Minta, K Wiesner *Heterocycles* **12** 1397 (1979)
34. R Marini-Bettolo, P Flecker, T Y Tsai, K Wiesner *Can. J. Chem.* **59** 1403 (1981)
35. K Wiesner, T Y Tsai, R Kumar, H A Sivaramakrishnan *Helv. Chim. Acta* **67** 1128 (1984)
36. A Sen, F J Jaggi, T Y Tsai, K Wiesner *J. Chem. Soc., Chem. Commun.* 1213 (1982)
37. K Wiesner, T Y Tsai, A Sen, R Kumar, M Tsubuki *Helv. Chim. Acta* **66** 2632 (1983)
38. K Wiesner, T Y Tsai, F J Jaggi, C S Tsai, G P Gray *Helv. Chim. Acta* **65** 2049 (1982)
39. Europ. P. 71 460; *Chem. Abstr.* **98** 88479w (1983)
40. H Minato, T Nagasaki *J. Chem. Soc. C* 377 (1966)
41. T Y Tsai, K Wiesner *Can. J. Chem.* **60** 2161 (1982)
42. F J Jaggi, T Y Tsai, K Wiesner *Heterocycles* **19** 647 (1982)
43. J Wicha, M Masnyk, H Duddeck *Bull. Pol. Acad. Sci., Chem.* **32** 75 (1984)
44. J Wicha, M Masnyk, H Duddeck *Bull. Pol. Acad. Sci., Chem.* **33** 29 (1985)
45. J Wicha, M Masnyk *Heterocycles* **16** 521 (1981)
46. M S Shiao, T Y Tsai, K Wiesner *Heterocycles* **16** 1879 (1981)
47. M S Shiao *J. Org. Chem.* **47** 5189 (1982)
48. D C Humber, P S Jones, G H Phillipps, M G Dodds, P G Dolamore *Steroids* **42** 3154 (1983)

49. D C Humber, G H Phillipps, M G Dodds, P G Dolamore, I Machin *Steroids* **42** 3155 (1983)
50. S-H Lee, R N Hanson, D E Seitz *Tetrahedron Lett.* **25** 1751 (1984)
51. M Fetizon, P Goulaouic, I Hanna *J. Chem. Soc., Perkin Trans. 1* 1107 (1990)
52. P Catsoulacos, C I Stassinopoulou *J. Heterocycl. Chem.* **15** 313 (1978)
53. C Camoutsis, S Nicolapoulos, P Catsoulacos *J. Chem. Eng. Data* **32** 478 (1987)
54. L N Volovel'skii, I B Skachek, I I Kuz'menko *Khim. Prir. Soedin.* 168 (1979)
55. A Tzikas, C Tamm, A Boller, A Furst *Helv. Chim. Acta* **59** 1850 (1976)
56. S Solyom, K Szilagyi, L Toldy *Liebigs Ann. Chem.* 153 (1987)
57. M Kosor, B Bersz *Tetrahedron* **41** 197 (1985)
58. U Ramesh, D Ward, W Reusch *J. Org. Chem.* **53** 3469 (1988)
59. A A Akhrem, V A Khripach, F A Lakhvich, M I Zavadskaya, O A Drachenova, I A Zorina *Dokl. Akad. Nauk SSSR* **297** 364 (1987)
60. A V Baranovskii, R P Litvinovskaya, V A Khripach *Zh. Org. Khim.* **26** 1274 (1990)
61. A Kurek, M Kabat, M Gumulka, J Wicha *Pol. J. Chem.* **55** 1369 (1981)
62. M Kabat, A Kurek, J Wicha *J. Org. Chem.* **48** 4248 (1983)
63. C R Engel, G Dionne *Can. J. Chem.* **56** 424 (1978)
64. BRD P. 2 361 059; *Chem. Abstr.* **83** 206484d (1975)
65. E Yoshii, T Koizumi, S Mizuno, E Kitatsuji *Chem. Pharm. Bull.* **24** 3216 (1976)
66. E Yoshii, T Oribe, T Koizumi, I Hayashi, K Tumura *Chem. Pharm. Bull.* **25** 2249 (1977)
67. P Drasar, M Havel *Collect. Czech. Chem. Commun.* **46** 1976 (1981)
68. P Drasar, V Pouzar, I Cerny, M Havel *Collect. Czech. Chem. Commun.* **48** 1224 (1983)
69. A V Kamernitskii, V A Krivoruchko, R P Litvinovskaya, I G Reshetova *Izv. Akad. Nauk SSSR, Ser. Khim.* 2073 (1975)
70. I Cerny, V Pouzar, P Drasar, M Havel *Collect. Czech. Chem. Commun.* **48** 2064 (1983)
71. P A Bartlett *J. Am. Chem. Soc.* **98** 3305 (1976)
72. S Lociuro, T Y Tsai, K Wiesner *Tetrahedron* **44** 35 (1988)
73. Y Takeuchi, Y Makino, K Maruyama *Heterocycles* **14** 163 (1980)
74. H W Hoppe, P Welzel *Tetrahedron Lett.* **27** 2459 (1986)
75. H W Hoppe, M Kaiser, D Muller, P Welzel *Tetrahedron* **43** 2045 (1987)
76. P E Bauer, K S Kyler, D S Watt *J. Org. Chem.* **48** 34 (1983)
77. K Gamoh, M Hirayama, N Ikekawa *J. Chem. Soc., Perkin Trans. 1* 449 (1984)
78. M Ishiguro, M Hirayama, H Saito, A Kajikawa, N Ikekawa *Heterocycles* **15** 823 (1981)
79. G R Weihe, T C McMorris *J. Org. Chem.* **43** 3942 (1978)
80. M Hirayama, K Gamoh, N Ikekawa *J. Am. Chem. Soc.* **104** 3735 (1982)
81. M Hirayama, K Gamoh, N Ikekawa *Tetrahedron Lett.* **23** 4725 (1982)
82. M Hirayama, K Gamoh, N Ikekawa *Chem. Lett.* 491 (1982)
83. T Kametani, M Tsubuki, T Honda *Heterocycles* **28** 59 (1989)
84. E Glotter, M Zviely, I Kirson *J. Chem. Res. (S)* 32 (1982)
85. R K Tkhaper, I G Reshetova, A V Kamernitskii, R P Litvinovskaya *Izv. Akad. Nauk SSSR, Ser. Khim.* 962 (1991)
86. C Lindig, K R Repke *J. Prakt. Chem.* **328** 695 (1986)
87. T W Guntert, H H Linde, M S Ragab, S Spengel *Helv. Chim. Acta* **59** 2125 (1976)
88. T W Guntert, H H Linde, M S Ragab, S Spengel *Helv. Chim. Acta* **59** 2138 (1976)
89. P Drasar, V Pouzar, I Cerny, J Smolicova *Collect. Czech. Chem. Commun.* **49** 1051 (1984)
90. G Ferrara, A Ius, C Parini, G Sportoletti, G Vecchio *Tetrahedron* **28** 2461 (1972)
91. Y Golander, E Breuer, S Sarel *Arch. Pharm.* **312** 192 (1979)
92. P Bisseck, G Charles *Tetrahedron Lett.* **24** 4223 (1983)
93. A A Akhrem, V A Khripach, R P Litvinovskaya, A V Baronovskii *Zh. Org. Khim.* **25** 1901 (1989)
94. V A Khripach, R P Litvinovskaya, A V Baronovskii, E A Ermolenko *Khim. Geterotsikl. Soedin.* 1389 (1990)
95. V A Khripach, R P Litvinovskaya, A V Baranovskii, A A Akhrem *Dokl. Akad. Nauk SSSR* **318** 597 (1991)
96. V Khripach, R Litvinovskaya, A Baranovsky, S Drach *Tetrahedron Lett.* **31** 7065 (1990)
97. A I Verenich, A A Govorova, N I Galitskii, A V Baranovskii *Zh. Strukt. Khim.* 542 (1992)
98. V A Khripach, R P Litvinovskaya, A V Baranovskii *Khim. Geterotsikl. Soedin.* 852 (1990)
99. D S Morris, D H Williams, A F Norris *J. Org. Chem.* **46** 3422 (1981)
100. N Ikekawa, Y Hirano, M Ishiguro, J Oshida, T Eguchi, S Miyasaka *Chem. Pharm. Bull.* **28** 2852 (1980)
101. S Yamada, K Nakayama, H Takayama *Tetrahedron. Lett.* **22** 2591 (1981)
102. S Yamada, K Nakayama, H Takayama *Chem. Pharm. Bull.* **29** 2393 (1981)
103. S Yamada, K Nakayama, H Takayama *J. Org. Chem.* **47** 4770 (1982)
104. P M Wovkulich, E G Baggilioni, B M Hennessy, M R Uskokovic *J. Org. Chem.* **48** 4433 (1983)
105. G Piancatelli, A Scettri *Tetrahedron* **32** 1745 (1976)
106. Zh S Sydykov, G M Segal' *Bioorg. Khim.* **2** 1531 (1976)
107. W B Motherwell, J Wozniak, D H Barton, S Z Zard *J. Chem. Soc., Perkin Trans. 1* 1865 (1985)
108. A Kurek-Tyrlik, J Wicha, G Snatzke *Tetrahedron Lett.* **29** 4001 (1988)
109. M Koreeda, I A George *Chem. Lett.* 83 (1990)
110. S Takano, S Yamada, H Numata, K Ogasawara *J. Chem. Soc., Chem. Commun.* 760 (1983)
111. S Takano, H Numata, S Yamada, S Hatakeyama, K Ogasawara *Heterocycles* **20** 2159 (1983)
112. U Hedtmann, P Welzel *Tetrahedron Lett.* **26** 2773 (1985)
113. T Kametani, M Tsubuki, H Furuyama, T Honda *J. Chem. Soc., Chem. Commun.* 375 (1984)
114. T Kametani, M Tsubuki, H Furuyama, T Honda *J. Chem. Soc., Perkin Trans. 1* 557 (1985)
115. T Kametani, M Tsubuki, K Higurashi, T Honda *J. Org. Chem.* **51** 2932 (1986)
116. T Kametani, M Tsubuki, H Nemoto *Tetrahedron Lett.* **22** 2373 (1981)
117. T Kametani, M Tsubuki, H Nemoto *J. Chem. Soc., Perkin Trans. 1* 3077 (1981)
118. T Kametani, T Katoh, M Tsubuki, T Honda *Chem. Lett.* 485 (1985)
119. E Nakamura, I Kuwajiama *J. Am. Chem. Soc.* **107** 2138 (1985)
120. V A Khripach, R P Litvinovskaya, A V Baranovskii *Bioorg. Khim.* **16** 1700 (1990)
121. V Khripach, R Litvinovskaya, A Baranovskii *Mendeleev Commun.* 117 (1992)
122. J R Donaybauer, A M Greaves, T C McMorris *J. Org. Chem.* **49** 2833 (1984)
123. T Kametani, M Kigawa, M Tsubuki, T Honda *J. Chem. Soc., Perkin Trans. 1* 1503 (1988)
124. T Kametani, K Keino, M Kigawa, M Tsubuki, T Honda *Tetrahedron Lett.* **30** 3141 (1989)
125. T Kametani, T Katoh, M Tsubuki, T Honda *J.Am. Chem. Soc.* **108** 7055 (1986)
126. Zhou Wei-Shan, Biao Jiang, Xin-fu Pan *J. Chem. Soc., Chem. Commun.* 612 (1989)
127. S Fung, J B Siddall *J. Am. Chem. Soc.* **102** 6580 (1980)
128. A V Khripach, R P Litvinovskaya, A V Baranovskii *Khim. Prir. Soedin.* 143 (1992)
129. M Anastasia, P Allevi, P Ciuffreda, A Fiecchi, A Scala *J. Org. Chem.* **49** 4297 (1984)
130. Jpn. P. 5 899 461; *Chem. Abstr.* **99** 158724t (1983)
131. P M Wovkulich, F Bacelos, A D Batcho, J F Sereno, E G Baggiolini, B M Hennessy, M R Uskokovic *Tetrahedron* **40** 2283 (1984)
132. T G Baggiolini, J A Iacobelli, B M Hennessy, A D Batcho, P M Wovkulich, M R Uskokovic *J. Org. Chem.* **51** 3098 (1986)
133. E G Baggiolini, B M Hennessy, A D Batcho, J F Sereno, P M Wovkulich, M R Uskokovic *Croat. Chem. Acta* **58** (Special Issue) 757 (1985)

Russian Chemical Reviews **62** (7) 683 – 691 (1993)
© 1993 Russian Academy of Sciences and Turpion Ltd

UDC 62.95.025:576.345

Mechanisms of interaction of pesticides with the lipid bilayer in cell membranes

V N Golubev

Contents

I.	Introduction	683
II.	Incorporation of pesticide molecules into the hydrocarbon region of the bilayer lipid membranes	684
III.	Adsorption of pesticide molecules in the region of polar groups	687
IV.	Interaction of amphiphilic pesticidal compounds with the lipid bilayer	688
V.	Conclusion	689

Abstract. The available information about the mechanisms of the interaction of pesticides having different chemical structures with the lipid bilayer in cell membranes is presented. It is shown that, depending on the degree of lipophilicity, the molecular dipole moment, and certain other characteristics of the pesticide compound, its interaction with the lipid bilayer generally takes place via one of the three main mechanisms involving the incorporation of the pesticide molecules in the hydrocarbon region within the bilayer, the adsorption of these molecules in the zone of the polar membrane phospholipids, or the incorporation of the amphiphilic pesticide compounds in both the non-polar and polar regions of the membrane. The bibliography includes 109 references.

I. Introduction

Various mechanisms of the action of pesticidal preparations on organisms are known at the present time. The principal site acted upon by pesticides is the cell membrane system. Pesticides can influence both the structure and the functions of membranes and are capable of damaging membrane systems directly (as a result of the physicochemical interaction with them) or indirectly (as a result of the physicochemical interaction with them) or indirectly (as a result of the blocking reactions involving the biosynthesis of specific membrane components).[1–5]

The direct interaction of pesticides with biological membranes is achieved as a result of the binding of the preparations to some type of component of the membranes, usually to the membrane proteins or lipids. The mechanisms of such interaction of pesticides with the lipid bilayer in cell membranes are considered in the present review.

The structural organisation and the principal functions of the lipid bilayer in cell membranes are fundamentally the same regardless of the purpose of the membranes. Therefore the nature of the direct interaction of pesticides with the lipid matrix of the membranes is as a rule independent of the particular membrane (plasma, chloroplast, mitochondrial, or some other membrane) with which the preparation interacts and is determined exclusively by the physicochemical properties as well as the overall types of organisation of lipids in the membranes.

Among the wide variety of the physicochemical properties of a pesticidal preparation, the nature of its interaction with the lipid bilayer is influenced decisively by its lipophilicity, which is usually characterised in terms of the partition coefficient of the pesticide between 1-octanol and water (K_{ow}). According to the value of K_{ow}, it is possible to differentiate three groups of pesticides — lipophilic, amphiphilic, and hydrophilic (Table 1).

The preparations of each group usually interact with the lipid bilayer via their own mechanism, which differs from the mechanisms of the interaction of the preparations of the other groups with the bilayer.

Table 1. The coefficients K_{ow} for certain pesticides.

Preparation	K_{ow}	Ref.
Lipophilic preparations		
Aldrin	7.5	6
Permethrin	7.44	7
Dieldrin	6.2	6
DDT	6.19	8
PCP† (undissociated form)	5.01	9
Methoxychlor	4.93	8
Parathion	3.761	10
Lindane	3.72	11
Dinoseb (undissociated form)	3.56	12
2,4-D (undissociated form)	2.90	13
Chlordime form	2.894	10
Malathion	2.838	10
Diurone	2.68	14
Metribuzin	1.70	14
Amphiphilic preparations		
Dodine	1.15	13
Benzyldimethyldecylammonium chloride	−0.08	13
Hydrophilic preparations		
2,4-D (dissociated form)	−0.24	13
Maleic hydrazide	−0.63	13

†Pentachlorophenol (translator).

V N Golubev Moscow State Correspondence Institute of the Food Industry, Zemlyanoi val 73, 109803 Moscow. Fax (7-095) 270 15 10

Received 3rd March 1993
Uspekhi Khimii **62** (7) 726 – 734 (1993); translated by A K Grzybowski

The nature of the interaction of the pesticide with the lipid matrix of the membranes depends not only on the lipophilicity of the preparation but also on its molecular properties, in particular on the molecular dipole moment, the size and shape of the molecule, and other steric factors.

II. Incorporation of pesticide molecules into the hydrocarbon region of bilayer lipid membranes

Most of the pesticide preparations are characterised by a high lipophilicity. Therefore the commonest way in which they interact with the lipids of cell membranes involves the incorporation of pesticide molecules into the hydrocarbon region of the lipid bilayer. It has been established that many organochlorine, organophosphorus, and pyrethroid insecticides, herbicides (derivatives of phenylureas), imidazole fungicides, and certain other compounds are incorporated into the non-polar region of the bilayer lipid membranes (BLM) (Table 2).

One of the most thoroughly investigated lipophilic pesticides is the organochlorine insecticide DDT [1,1,1-trichloro-2,2-bis-(*p*-chlorophenyl)ethane]. DDT is known to be capable of accumulating in living organisms for a long time. The principal objects in which insecticides accumulate are the lipid systems of the organism, in the first place the lipid-rich cell membranes.[42-44] This has been convincingly demonstrated by experiments both *in vivo* and *in vitro*. Studies on models of lipid systems have confirmed the hypothesis that DDT accumulates in the lipid matrix of cell membranes.[11, 15, 16, 45, 46]

Experimental determination of the localisation of DDT in biological membranes have shown that the preparation is present in the inner hydrophobic component of the lipid bilayer. Both DDT and its analogues DDE [1,1-dichloro-2,2-bis(*p*-chlorophenyl)ethylene] and DDA [bis(*p*-chlorophenyl)acetic acid] give rise to distinct proton magnetic resonance (^{1}H NMR) spectra in CCl_4. They also have a distinct ^{1}H NMR spectrum in a suspension of lecithin liposomes in D_2O. On the other hand, in the absence of liposomes, the peak corresponding to the protons of the aromatic ring of chlorohydrocarbons in an aqueous medium was not observed.[17] The most distinct spectrum has been observed for DDA. The appearance in the presence of liposomes of signals in the high-resolution spectra, which strongly resemble the spectrum in CCl_4, shows that DDT and its analogues are incorporated into the lipid bilayer in such a way that the aromatic rings of their molecules are in a medium resembling CCl_4. Such a medium is evidently the liquid crystal phase within the bilayer. On the other hand, some inconsistency between the chemical shifts of the ring protons in CCl_4 and in a suspension of liposomes is evidence of the non-identity of the local micro-environment of the aromatic ring of the DDT molecules in the lipid and in the organic solvent.

Table 2. Examples of the incorporation of pesticidal compounds into various regions of the lipid bilayer.

Region of bilayer	Preparation	Ref.
Hydrocarbon region	DDT	15, 16, 11, 17
	Methoxychlor	16, 11
	Lindane	18, 19, 20, 11
	Parathion	21
	Malathion	22
	Diurone	23
	Permethrin	24
Region of polar groups	2,4-D (undissociated form)	25
	PCP (dissociated form)	26
	Triforine	27, 28
	Phytone	29
Polar and non-polar regions	Dodine	30-32
	Glyodin	33, 34
	Benzylalkylammonium chlorides	35, 36, 37, 38, 39, 40, 41

The incorporation of DDT into phosphatidylcholine liposomes containing carbazole-labelled phospholipids — β-[11-(9-carbazolyl)undecanoyl]-L-α-phosphatidylcholine and β-[3-(9-carbazolyl)propionyl]-L-α-phosphatidylcholine — as fluorescent probes led to the intense quenching of the fluorescence of the probes.[11] DDT and certain other chlorinated hydrocarbons are known to quench effectively the fluorescence of *N*-ethylcarbazole in homogeneous solutions.[20] Therefore the quenching, observed in liposomes, of the fluorescence of phosphatidylcholines containing a fluorescent carbazole fragment in the aliphatic acid chain must be interpreted as the result of the incorporation of the molecules of the quenching agent into the region of the hydrocarbon chains of the membrane lipids. Methoxychlor and DDE interact similarly with the lipid bilayer.[11, 47]

Yet another indication of the localisation of DDT in the hydrophobic part of the lipid bilayer is the decrease in the polarisation of the fluorescence of 12-(9-anthroyloxy)palimitic acid incorporated into lecithin liposomes in the presence of the insecticide, because in this case too the fluorophor is in the region of the hydrocarbon chains.[48]

There exist different views concerning the possible location of DDT within the hydrocarbon chains. For example, the displacement of DDT by cholesterol from the membranes of liposomes is regarded as an argument in support of the disposition of the extended DDT molecules alongside the planar cholesterol molecules.[15] Experiments with lecithin monolayers without cholesterol have shown that, for a 1 : 1 DDT : lecithin molar ratio, the minimum area occupied by the lecithin molecule in the monolayer increases from 50.8 Å (in the absence of the insecticide) to 56.3 Å, which is exactly equal to the minimum cross-sectional area of the DDT molecule.[49] This result permits the conclusion that DDT may form 1 : 1 complexes with lecithin as a result of the deposition of DDT molecules layer by layer on the surface of the lipid monolayer. One cannot rule out the possibility that the DDT molecules in the bilayer membrane can also be arranged in the vicinity of the ends of the aliphatic acid chains of the membrane lipids and occupy the space within the centre of the bilayer.

Finally, experiments designed to investigate the interaction of DDT with lecithin in CCl_4 by ^{1}H NMR spectroscopy have shown that lecithin causes an appreciable shift and broadening of the signal corresponding to the proton of the diphenylmethyl group of DDT and the latter in its turn appreciably alters the positions of the proton resonances of the choline group of lecithin.[50] These data are interpreted as an indication of the binding of the proton of the diphenylmethyl group of DDT (the acidity of which is due to the presence in the insecticide molecule of five chlorine atoms) to the electronegative oxygen atom of the phosphate group of lecithin. The formation of similar complexes with lecithin has been observed also in the study of analogues of DDT such as methoxychlor, 1,1-dichloro-2,2-bis(*p*-chlorophenyl)ethane, and DDA.[51]

The possibility of the formation of complexes of this kind by DDT owing to the presence of the highly polar H-C-C-Cl group has been confirmed in experiments with a series of inorganic compounds,[52, 53] but the significance of these structures in biochemical processes remains controversial. Apparently, the formation of complexes in organic solvents is consistent with the ability of the DDT molecules to assume an arrangement in membranes such that the proton of the diphenylmethyl group is close to the phosphate group of the lecithin molecule, while the benzene rings of the insecticide molecule are 'immersed' in the hydrocarbon region of the bilayer. Such location of the insecticide molecules near the polar groups of the lipid molecules, while most of the insecticide molecule is still in the region of hydrocarbon chains, appears extremely likely for the more polar compounds of the DDT series, for example for dicofol.[54, 55]

A similar mechanism of the interaction with lecithin based on ^{1}H NMR data has been proposed also for the vinyl organophosphorus insecticides dichlorofos and azodrin.[56] It has been suggested tentatively that the insecticide–dipalmitoyllecithin complex is formed as a result of the interaction of the acid proton of the vinyl group of the insecticide molecule with the oxygen anion of the phospholipid molecule. However, as in the case of DDT, the toxicological importance of this interaction is not clear.

However, evidently the ability to form hydrophobic complexes with lecithin is characteristic also of imidazole antibiotics — miconazole and chlotrimazole, which are effective fungicides.[57] When unsaturated lecithins are added to a suspension of the fungi *Candida albicans*, which are sensitive to imidazole preparations, the fungicidal effect of both antibiotics virtually disappears. Saturated lecithins do not exhibit a similar protective action. Furthermore, it has been reported that these imidazole fungicides interact preferentially with liposomes consisting of unsaturated phospholipids.[58] These data as well as analysis of the UV spectra of the fungicides in the presence of lecithin indicate the possibility of the formation of miconazole and chlotrimazole complexes with unsaturated lecithin. The inter-action, responsible for the formation of complexes of this type probably leads to the incorporation of the molecules of the above antibiotics into the hydrophobic component of the lipid bilayer of the fungal membranes with a high content of unsaturated phospholipids.[57, 59]

The conclusion that molecules of imidazole fungicides are incorporated into the hydrocarbon component of the membrane has been confirmed by the results of conformational analysis.[60] It was observed that the molecules of the two dichlorophenyl groups of miconazole and the piperazine fragment of the molecule of kitaconazole are localised in the hydrophobic component of the lipid bilayer. On the other hand, part of the fungicide molecule (the imidazole ring of miconazole and the dichlorophenyl group of kitaconazole) are located in the region of the polar groups of the phospholipid molecules, which makes the pattern in the interaction of imidazoles with the lipid bilayer similar to the mechanism of incorporation of fungicidal surfactants into the lipid component of the membranes. The interaction of miconazole with the polar region of the cell membranes has been confirmed by the dependence of the effectiveness of its action on the permeability of lecithin liposomes and their surface charge[58] and also by the protective effect of magnesium ions when the plasma membranes of the fungi *Candida albicans* are damaged by high concentrations of miconazole. It may be that the protective effect is a consequence of the competition between Mg^{2+} and miconazole for common binding sites on the membrane.[61]

Various isomers of hexachlorocyclohexane (HCCH), namely the α-, β-, γ-, (lindane), and δ-isomers, are readily incorporated into the hydrocarbon component of cell membranes. They all effectively quench the fluorescence of carbazole-labelled phospholipids incorporated into the aliphatic acid chain liposomes.[11, 19, 20] Fluorescence data make it possible to estimate the diffusion coefficient of the quenching agent in the membranes of the liposomes, which, for example, in the case of lindane, is on average 10^{-6} cm^2 s^{-1}.[19] Comparison of this coefficient with the diffusion coefficients of other molecules in the hydrophobic part of the membranes (about 5×10^{-8} cm^2 s^{-1} for phospholipids, 10^{-7} cm^2 s^{-1} for pyrene, and 8×10^{-6} cm^2 s^{-1} for oxygen) confirms that lindane is localised in the hydrocarbon part of the lipid bilayer. The diffusion coefficient of the insecticide corresponds to an intermediate molecular size (between the molecular sizes of pyrene and oxygen). Experiments designed to investigate the incorporation of ^{14}C-labelled lindane into the lecithin liposomes have shown that the insecticide molecule is located within the lipid bilayer between the hydrocarbon chains of the phospholipids.[62]

Diurone, a well known inhibitor of the photosynthetic electron transport, is also localised in the hydrophobic component of the membranes of phospholipid liposomes.[23]

The study of the ^{1}H NMR spectra made it possible to determine the disposition of the phosphonothioate insecticide derived from bis(5-chloro-2-hydroxyphenyl)methane (GA-41).[63] The decrease in the spin–lattice relaxation time of the protons of the methyl group linked to the phosphorus atom of the insecticide molecule when the insecticide is transferred from an aqueous solution to a suspension of lecithin liposomes indicates the incorporation of GA-41 into the lipid bilayer. The absence of an effect by the insecticide on the spin–lattice relaxation time of the protons of the choline group of lecithin permits the conclusion that GA-41 is located in the region of the hydrocarbon chains of the membrane lipids. Certain insecticides (permethrin, cypermethrin, fenpropathrin, and fluvalinate) decrease the fluorescence and the lifetime of the excited state of 1,6-diphenylhexatriene incorporated into the liposomes comprising dipalmitoylphosphatidylcholine.[24] The 1,6-diphenylhexatriene molecule has an extended shape and is in all probability located within the bilayer parallel to the hydrocarbon chains of the lipids. The reason for the observed effects is evidently the disturbance of the packing of the membrane lipids in the presence of pyrethroids and also the quenching of the fluorescence of the probe as a result of the collisions with the insecticide molecules. One can therefore postulate that pyrethroids are localised in the hydrocarbon part of the membranes next to the molecules of 1,6-diphenylhexatriene. The molecules of certain herbicidal inhibitors — uncoupling agents, which also affect the anisotropy of the fluorescence of 1,6-diphenylhexatriene are probably also at least partly located in the same region of the membranes.[3, 64, 65]

Apart from the results of experiments specially carried out in order to elucidate the positions of the pesticide molecules in the lipid bilayer, there exist a series of experimental data indicating indirectly the incorporation of pesticides into the hydrophobic region of cell membranes. Thus the pronounced dependence of the partition coefficient of the pesticide between the membrane medium and water (K_{mw}) on the fluidity of the membranes, observed for parathion and malathion as well as DDT and various isomers of HCCH, indicates the incorporation of the preparations into the inner hydrophobic component of the cell membranes.[16, 18, 21, 22, 62]

The decrease in K_{mw} with decrease in the fluidity of the membrane lipids, observed in experiments with organophosphorus and organochlorine pesticides, is in all probability a reflection of the more general dependence of the degree of incorporation of lipophilic pesticidal preparations into the lipid bilayer on its fluidity. This is expressed, in particular, by the dependence of K_{mw} on parameters influencing the fluidity of membranes such as temperature, length and degree of unsaturation of aliphatic acid chains of the membrane phospholipids, and the concentration of cholesterol in the membrane. Table 3 presents typical values of K_{mw} for certain lipophilic pesticides.

A change in temperature has different effects on the incorporation of pesticides into membranes made up of phospholipids in the liquid crystal and gel states. In the liposomes comprising egg lecithin, which has largely unsaturated aliphatic acid chains and undergoes a phase transition in the range from −15 to −5 °C,[66, 67] an increase in temperature from 10 to 40 °C leads to a monotonic decrease in the partition coefficient of the ^{14}C-labelled DDT,[15] lindane,[62] parathion,[21] and malathion[22] between the membrane medium and water. Experiments involving the use of fluorescent probes have shown that, with increase in temperature in the same range, there is a significant decrease also in the partition coefficient of lindane[18,20] and one of its analogues (the α-isomer of HCCH[18]) between dioleoyl-phosphatidylcholine liposomes and water (the gel–liquid crystal phase transition temperature for dioleoylphosphatidylcholine is −22 °C).[68] A similar decrease in K_{mw} on

Table 3. The coefficients K_{mw} for certain lipophilic compounds and their analogues.

Preparation	Membrane lipid[a]	T/ °C	K_{mw}	Ref.
DDT	EL	40	260000	15
	DPPC	41	234000	15
DDE	PM	37	300000	47
Methoxychlor	PM	37	70000	47
	DPPC	25	28300	11
Lindane	EL	40	1300	62
	DPPC	41	2700	62
Malathion	EL	40	70	22
	DPPC	41	244	22

[a] The following abbreviations have been adopted: EL = egg lecithin, DPPC = dipalmitoylphosphatidylcholine, PM = plasma membranes of the mouse liver mitochondria.

raising the temperature has been observed for phospholipids with saturated aliphatic acid chains but only above their phase transition temperatures, where these lipids also exist in the liquid crystal state. Thus the incorporation of all the pesticides mentioned into dimyristoyl-, dipalmitoyl-, and distearoyl-phosphatidylcholine liposomes diminishes on raising the temperature in the region above the phase transition temperatures of the lipids.[15,21,22,62]

On the other hand, the incorporation of pesticidal preparations into the hydrocarbon component of membranes comprising phospholipids in the 'solid' state increases appreciably on raising the temperature. This effect has been observed in dimyristoyl-, dipalmitoyl-, and distearoyl-phosphatidylcholine liposomes for DDT, lindane, parathion, and malathion.[15, 18, 21, 22, 62]

The temperature variation of K_{mw} at temperatures both above and below the phase transition temperatures of the membrane lipids shows that the maximum value of K_{mw} should be observed directly in the phase transition. Experiments with synthetic phospholipid bilayers have clearly confirmed this conclusion.[15, 18, 21, 22, 62] The attainment of the maximum value of K_{mw} at the phase transition temperature of the membrane lipid is evidently associated with the fact that the incorporation of pesticides into the lipid bilayer takes place most effectively at the interface between the two phases coexisting in the membrane during the phase transition.

Comparison of the values of K_{mw} at temperatures equidistant from the phase transition temperature shows that pesticidal preparations are usually incorporated more readily into the more 'liquid' membranes. In other words, an increase in the fluidity of the membranes usually promotes the incorporation of pesticides into them. This effect has been clearly noted in experiments designed to investigate the incorporation of parathion, malathion, and lindane into dipalmitoyl- and distearoyl-phosphatidylcholine liposomes[21,22,62] and of DDT, 2-(2,4-dichlorophenyl)-1-chloro-2-(4-chlorophenyl)ethylene (DDE), and methoxychlor into dimyristoyl- and dipalmitoyl-phosphatidylcholine liposomes.[16] The preferential incorporation of pesticide molecules into bilayers with a higher fluidity makes it possible to explain the positive value of K_{mw} at temperatures below the phase transition temperature of the membrane lipid by the fact that, on raising the temperature in this region, there is an increase in the number of liquid crystal domains in the 'solid' phase, which promotes an enhanced incorporation of pesticides into the bilayer. On the other hand, the incorporation of certain insecticides into dimyristoyl-phosphatidylcholine liposomes takes place more effectively in the gel state of the membrane lipid. This serves as yet another confirmation of the fact that the incorporation of pesticides into lipid membranes is determined not only by the fluidity of the latter but also by other factors, in particular by the geometry of the molecules of the phospholipids and pesticides.

The facilitation of the incorporation of pesticides into membranes with increase in the fluidity of the membrane lipids is manifested also by the fact that, for example, DDA is hardly incorporated, according to ^{1}H NMR data, into dimerystoyl-lecithin liposomes below the phase transition temperature of this lipid,[17] while experiments with mouse liver mitochondria have shown that the inhibition, observed in the presence of DDT, of the valinomycin-induced absorption of potassium by the mitochondria is independent of temperature in the range up to 20 °C, but increases sharply on further heating of the suspension.[69] Furthermore, the insecticide increases the release of endogenic potassium from the mitochondria, although the effect is observed only at temperatures above 10 °C (the temperature corresponding to the phase transition of the mitochondrial lipids) and increases on raising the temperature.

Evidently this effect of DDT on the transport of potassium through the mitochondrial membranes is due to its incorporation into the membranes, which occurs much more effectively when the membranes are in the liquid crystal state. Finally, comparison of the ^{1}H NMR spectra of DDE obtained in D_2O in the presence of dipalmitoyl-lecithin at different temperatures permits the conclusion that DDE is also incorporated preferentially into the more 'liquid' part of the bilayer.[70]

Since the fluidity of the lipid membranes depends in many respects on the length of the hydrocarbon chains of the membrane lipids, it is natural to expect that the incorporation of pesticides into the lipid bilayer will also depend on this length. Indeed, experiments have shown that an increase in the length of the aliphatic chains of phosphatidylcholines in the range corresponding to 14–18 carbon atoms as a rule diminishes significantly the partition coefficients of insecticides between liposomes and an aqueous solution.[15,19,21,22,62] For example, in the case of DDT an increase in the length of the hydrocarbon chain by one methylene group is accompanied by a decrease in K_{mw} approximately by 50%.[15] The dependence of K_{mw} on the length of the hydrocarbon chain of phosphatidylcholines proves to be linear under these conditions.[15,22] As a result of such significant hindrance of the incorporation of pesticides into the membranes with increase in the length of the aliphatic acid chains of the membrane lipids, in mixtures of phospholipids having chains of different lengths the preparations may be distributed preferentially in the membrane domains consisting of lipids with shorter chains, as happens, for example, in the interaction of parathion with liposomes comprising a mixture of dimyristoyl- and distearoyl-phosphatidylcholines.[21]

The incorporation of pesticides into the hydrocarbon region in lipid membranes is greatly facilitated by the increase in the degree of unsaturation of the membrane phospholipids. Thus at 20 °C the transition from dipalmitoyllecithin to dioleoyllecithin liposomes increases K_{mw} for lindane by a factor of 2.7,[18] while K_{mw} for DDT increases by a factor of 6.3.[16] With increase in temperature, the promoting influence of the degree of unsaturation of the lipids on the incorporation of pesticides into the bilayer increases still further.[11] Furthermore, an increase in the degree of unsaturation of the membrane phospholipids of human erythrocytes, for example, by their preincubation with dioleoylphosphatidylcholine liposomes, greatly intensifies (by 60% after incubation for 4 h) the outflow of potassium from the erythrocytes induced by DDT.[71] This result can also serve as confirmation of the more effective incorporation of pesticides into membranes with an increased fluidity. Finally, the marked dependence of the fluidity of cell membranes on their cholesterol content is also reflected in the characteristic features of the incorporation of pesticides into the hydrocarbon component of the membrane. The increase in the cholesterol content from 0 to 50 mol% leads to almost complete elimination from the membranes of lecithin liposomes of lindane,[62] parathion,[21] and malathion[22] and appreciably reduces the content of DDT.[15]

The inclusion of cholesterol (20 mol%) in dipalmitoylphosphatidylcholine liposomes diminishes the partition coefficients of lindane in the membrane/water system from 3800 to 800.[59] Furthermore, the decrease in the cholesterol content in the erythrocyte membranes in the presence of DDT[71] is in all probability a consequence of the increased concentration of the insecticide in the membranes. Evidently, the cause of all the observed effects is that cholesterol displaces the insecticides from the membrane by occupying their place in the region of the aliphatic acid chains of the membrane lipids.

In the experiments designed to investigate the incorporation of pesticides into biological membranes, it has been observed that all the preparations investigated (parathion, lindane, malathion, DDT) are incorporated into cell membranes (and, incidentally, also into the liposomes comprising the total lipids of these membranes) much less effectively than into the membranes of the liposomes made up of the individual lipids.[15,21,22,62]

For all the preparations investigated, K_{mw} diminishes with increase in the content of cholesterol in membranes of different types (of the sarcoplasmic reticulum, mitochondria, microsomes, myelin, and erythrocytes). This confirms yet again the appreciable role of the fluidity of the lipid bilayer in the incorporation of pesticides into the membranes, but in this case this applies to biomembranes. However, when the dependence of K_{mw} on the cholesterol content in membranes is extrapolated, the total displacement of lindane, parathion, and malathion from the biomembranes occurs no longer for 50 mol% of cholesterol but at much higher concentrations of the latter. This result may indicate a definite role of the membrane proteins in the incorporation of insecticides into cell membranes, which consists in the facilitation of the entry of the molecules of the preparations into the membranes tentatively as a result of the formation of defects at the lipid/protein interfaces. On the other hand, the results of the determination of K_{mw} for certain organochlorine insecticides in various biological membranes with the aid of carbazole-labelled probes do not indicate any significant role of the membrane proteins in the incorporation of insecticides into the membranes,[47] so that the question of the influence of the proteins on this process still remains open.

III. Adsorption of pesticide molecules in the region of polar groups

The adsorption of pesticide molecules in the region of the polar groups of the membrane phospholipids is characteristic of the interaction of hydrophilic preparations and lipophilic compounds with the lipid bilayer.The molecules of hydrophilic substances are then distributed in the bilayer in a way designed to ensure the retention of the possibility of the interaction with the aqueous medium, while lipophilic molecules, which have a high dipole moment, are immersed in the lipid matrix somewhat deeper and much closer to the hydrocarbon chains of the phospholipids.

On the basis of a wide variety of experimental data, one may assume that individual phenoxyacetic and phenolic preparations as well as certain pesticides with different chemical structures are adsorbed in the region of the polar groups of membrane lipids (Table 2).

The commonest phenoxyacetic acid herbicide, namely 2,4-dichlorophenoxyacetic acid (the 2,4-D preparation) is effectively incorporated into the membranes only in the undissociated form, which is extremely lipophilic (Table 1). Experiments with lecithin BLM have shown that the undissociated form of the herbicide increases the rate of transport of lipophilic cations through the membrane and inhibits the transport of lipophilic anions, acting as a typical dipolar modifying agent.[25] Evidently the cause of the observed effect is that 2,4-D makes the potential within the bilayer more negative. In all probability, the herbicide molecules are adsorbed in the region of polar groups (closer to the hydrocarbon part of the membranes) in such a way that the vectors of their dipole moments are directed towards the aqueous medium, altering thereby the dipolar potential of the bilayer. The acid anions are probably adsorbed on the membrane surface itself.[72]

Such disposition of the 2,4-D molecules in the membranes is probably due to their interaction with the ammonium and/or phosphate groups of the polar part of the lecithin molecule. Evidence in support of such interaction comes from the sharp increase in the diffusion transport of 2,4-D from one aqueous phase to another via pentanol[73] and model lipid membranes formed on a millipore filter[74] in the presence of lecithin and also from the increase in the adsorption of 2,4-D by the parenchyma of the potato tubers under the influence of this lipid.[75] The influence of lecithin on the transport of the herbicide through lipid membranes increases with decrease in the pH of the medium, which may indicate a more effective interaction of the phospholipids with the undissociated form of 2,4-D.[74] Furthermore, the addition of lecithin to carbon tetrachloride in contact with an aqueous phase greatly diminishes the amount of 2,4-D present in the aqueous phase, which indicates a strong interaction of the latter with lecithin.[76,77] Tentatively, this interaction takes place via the formation of a hydrogen bond between the herbicide and the phosphate group of lecithin or, in the case of the dissociated form of 2,4-D, of an ionic bond with the ammonium group of the choline residue. Evidently, the carboxy-group of the 2,4-D molecule is located in the membrane close to the choline group of the lecithin molecule, while the benzene ring is immersed somewhat deeper in the bilayer.[74]

It may be that a similar mechanism of the binding to lecithin molecules operates in the incorporation of benzoic acid molecules into cell membranes, in particular those of 2,3,6-trichlorobenzoic acid when they are absorbed from solution by segments of the oat mesocotyls.[78] The carboxy-group of the acid molecule can interact with the nitrogen atom of the choline group of the phospholipid. One cannot rule out the possibility that these processes constitute the basis of the adsorption of 2-methyl-4-chloro-phenoxyacetic acid (the 2M-4C preparation) on plasma membranes observed in experiments with the leaves of various plants.[79]

Triforine and dinitro-*o*-cresol can be located, in all probability, like other lipophilic pesticidal compounds, in the region of the polar groups of the membrane phospholipids. Like 2,4-D, the systemic fungicide triforine increases the rate of transport through the lecithin BLM of lipophilic caitons, in the given instance the valinomycin-K^+ complexes, and diminishes the permeability of the membranes in the presence of the lipophilic tetraphenylborate anions.[80] Furthermore, the fungicide imparts to the BLM, formed in solution in KCl at physiological pH, a weak cationic selectivity.[28] The nature of the dependence of the cationic-anionic selectivity of the membranes on the pH permits the conclusion that, being a lipophilic compound, triforine is incorporated into the lipid matrix of the membranes and lowers the positive potential of the inner component, but is located in the vicinity of the polar groups of the lecithin molecules and not in the hydrocarbon region. Apparently the mechanism of the incorporation of triforine into the lipid membranes is in many respects similar to the mechanism of the inclusion of the undissociated form of 2,4-D in the lipid bilayer. Furthermore, measurements of the fluorescence of 1-anilino-naphthalene-8-sulphonate incorporated into erythrocyte membranes have shown that 2-methyl-4,6-dinitrophenol (the herbicide DNOC) is located in the polar component of the lipid bilayer.[81]

On the other hand, the herbicide dinoseb, a structural analogue of DNOC, partially penetrates into the hydrophobic region of the membrane by virtue of the intensified interaction with the hydrocarbon chains of the lipids resulting from the appearance of the alkyl side chain in the dinitrophenol molecule.[81] Evidently, when the dinitrophenol preparations are incorporated into the bilayer, their benzene ring is located between the polar groups of the phospholipid molecules, the hydroxy-group being apparently oriented in the direction of the

aqueous phase, while the alkyl chain, if present in the herbicide molecule, is directed towards the hydrocarbon component of the bilayer parallel to the aliphatic acid chains of the lipid molecules.[82] The results of ^{31}P and ^{13}C NMR studies permit the conclusion that the molecules of certain acylanilide (propanil, karsil) and phenylcarbamate (propham chlorpropham) herbicides, which also contain a benzene ring and a hydrocarbon side chain, are incorporated similarly into the lipid bilayer.[89]

Certain hydrophilic pesticidal preparations are likewise adsorbed in the region of the polar groups. Thus, when the readily water-soluble fungicide phytone is introduced into an aqueous solution on one side of a bilayer lipid membrane comprising brain phospholipids, it induces the appearance of a transmembrane potential difference on the membrane.[29] Since phytone is the complex between $CuCl_2$ and ε-caprolactam $[Cu(CLM)_2]^{2+}$ $[CuCl(CLM)_2]_2$ (CLM = caprolactam), a single crystal of which has an ionic structure, the generation of potentials on the membrane is evidently associated with the adsorption of the charged form of the fungicide on it. By virtue of the hydrophilicity of the preparation, it is probably adsorbed at the lipid/water interface.

Finally, according to the measurements of the electrophoretic mobility of lecithin liposomes, the ionised form of pentachlorophenol (PCP) may be adsorbed in the layer of lipid membranes adjoining the aqueous medium.[25,26] Apparently, the adsorbed PCP anion is capable of forming a hydrogen bond with a water molecule. On the other hand, the undissociated form of PCP is located in the hydrocarbon region of the membranes. The adsorption of the neutral and ionised forms of PCP in egg lecithin liposomes constitutes competitive processes. The adsorption centre consists of six lecithin molecules.[84] The undissociated form of the preparation is bound to the liposomes more effectively than the dissociated form (the corresponding association constants are 55000 litre mol^{-1} for the dissociated form and 279 litre mol^{-1} for the undissociated form).[85] It is of interest that the binding to the membrane alters the pK_a of PCP, increasing it from 4.75 in a homogeneous solution to 5.97 on a phosphatidylcholine membrane formed in 0.1 M KCl.[26]

The different nature of the interaction of the dissociated and undissociated forms of pesticides such as 2,4-D and PCP with the lipid membranes suggests a dependence of the effectiveness of their incorporation into the membranes on the pH of the medium. Indeed, the results of numerous studies have demonstrated an increase in the incorporation of 2,4-D and some of its analogues into various membrane systems with increase in the acidity of the solution employed.[13,74,86] This leads to an increase in the degree of adsorption of the herbicide,[73,75,87-90] the intensification of its influence on various processes associated with the membranes,[74,82,89-96] and an increase in its toxicity.[97] Thus 2,4-D and 2,4,5-triphenylacetic acid (the 2,4,5-T preparation) are adsorbed much more effectively by lecithin liposomes in a medium at pH 3 than in more alkaline solutions (pH 5.5 or 9.8).[86] On reduction of the pH from 6.5 to 4.5, the maximum concentration of the absorbed 2,4-D in the protoplasts isolated from the roots of the rye plant increases from 4.02 to 32.13 μM.[87] These data confirm yet again that 2,4-D is incorporated into the membranes mainly in the undissociated form. Indeed, it has been found, for example, that the permeability of the cell membranes of the roots of the barley plant to the dissociated form of the herbicide is smaller by a factor of 5.5×10^4 than to the undissociated form.[13]

A similar increase in incorporation into the cell membranes and the associated increase in the degree of absorption and toxicity with decrease in the pH has been observed for PCP,[98,99] and dinoseb.[12] On the other hand, the biological activity and the incorporation into the membranes of basic preparations, the molecules of which are protonated with decrease in pH, are appreciably reduced in acid solutions. The imidazole fungicide imasalil ($pK_a = 6.53$), the antifungal activity of which falls sharply as the pH is reduced from 0.7 to 5.2,[59] as well as the formamidine acaricide chlordimeform (its uncoupling activity increases with increase in the pH)[100] may serve as examples. The preferential incorporation into the lipid bilayer of the unionised compounds has been confirmed, in particular, by the appreciable weakening of the effect of chlorphenprop-methyl on the leakage of aminoacids from the tissues of *Avena fatua* when it is hydrolysed to chlorphenprop — the corresponding acid with the carboxy-group charged at physiological pH.[101]

The effectiveness of the adsorption of pesticidal preparations by cell membranes is also influenced by the molecular structure of the pesticides. This influence is clearly demonstrated, for example, by phenoxyacetic acids — when the latter are chlorinated, the effectiveness of their permeation into bean leaves increases.[102] As already mentioned, this is caused by the increase in the lipophilicity of compounds of the given series on chlorination.

The fluidity of the lipid bilayer also exerts a definite influence on the adsorption of pesticides in the polar component of the membrane. Thus, with increase in the cholesterol content in lecithin liposomes, the amount of uncharged 2,4-D in 2,4,5-T molecules bound to the membranes diminishes,[86] while the degree of adsorption of PCP on egg lecithin liposomes increases in the phase transition of the lipid from a gel to a liquid crystal.[84]

IV. Interaction of amphiphilic pesticidal compounds with the lipid bilayer

In the interaction of amphiphilic pesticidal compounds with the lipid bilayer, the polar component of the pesticide molecule is located in the region of the polar groups of the membrane lipids, while the non-polar component is incorporated into the hydrocarbon part of the membranes. This mechanism is characteristic of the interaction of various ionogenic surfactants with lipid membranes. Some of these substances (dodine, glyodin, quaternary ammonium salts) are effective fungicides (Table 2).

The cationic fungicides dodine and glyodin, which have long hydrocarbon chains and small polar components (the latter comprise the guanidine and imidazole basic groups in dodine and glyodine respectively), are readily incorporated into the cell membranes of different fungi. The fungicides then interact with the negatively charged sections of the membrane surfaces, neutralising their surface charge.[33] Thus dodine rapidly diminishes to zero the negative charge on the surfaces of intact conidia, cell walls, and protoplasts in the spores of *Neurospora crassa*. In the case of the protoplasts, this takes place at a fungicide concentration in solution of only 0.35 μM.[32] In other words, the process involving the incorporation of dodine into the cell membranes is extremely rapid and effective.[38] A further increase in the fungicide concentration in solution renders the surface charge on the membranes positive. Apparently dodine is bound to the membranes as a result of electrostatic interaction with the basic charge-generating components on the surfaces of fungal spores — the phosphate groups of the polar fragment of membrane lipids and the carboxy-groups of the aminoacid residues of the membrane proteins.

This hypothesis is consistent also with the decrease in the binding of the fungicide in the presence of divalent metal ions (apparently owing to competition for common binding sections) and also with suppression of the dissociation of the carboxy- and phosphate groups present on the surface of the membrane.[31] The van der Waals interaction of the fungicide hydrocarbon chains and the membrane phospholipids also plays a significant role in the retention of the dodine molecules in the lipid bilayer because these chains are evidently arranged parallel to one another in the bilayer.

Glyodin apparently also interacts in the same way with the cell membranes of microorganisms.[34] In the general case, the electrostatic interaction of virtually all the amphiphilic pesticidal compounds with the ionogenic groups of the membrane lipids and the van der Waals interaction with their non-polar components determine the detergent nature of the binding to the lipid bilayer.

A similar mechanism of the interaction with biomembranes has been proposed also for the morpholine fungicide tridemorph, which has a long alkyl chain.[103] The induction by the fungicide of the outflow of the electrolyte from the zoospores of *Plasmopora halstedii* and the *Corynebacterium* bacteria only a few minutes after treatment also supports this mechanism.[104,105] On the other hand, experiments on the determination of the electrophoretic mobility of the protoplasts of the micelia of *Neurospora crassa* and *Botrytis fabae* as well as the spores of *N. crassa* in the presence of this fungicide have not revealed any kind of influence on tridemorph on their surface charge.[106] In all probability, these results show that the long-chain molecules of tridemorph are incorporated into the lipid bilayer of the cell membranes in the same way as those of dodine and disturb the integrity of the bilayer but do not necessarily influence the surface charge of the membranes.

It may be that cationic imidazole fungicides — clotrimazole, miconazole, and econazole — are also capable of interacting with the lipid bilayer via the mechanism of the interaction of the amphiphilic detergents. These cationic fungicides are, on the one hand, lipophilic preparations, but they contain at the same time an imide nitrogen atom, which readily combines with a proton on acidification of the medium. This hypothesis is based on the increase in the effectiveness of the interaction of the above fungicides with lecithin liposomes when a negative charge is imparted to the surface of the latter (by incorporating diacetyl phosphate into their membranes) and also on the decrease in the effectiveness of the interaction when a positive charge is induced in the liposomes (with the aid of stearylamine).[58]

Quaternary ammonium salts with fungicidal activity constitute a large group of amphiphilic pesticides which interact effectively with the lipid bilayer. The disruptive effect of these cationic surfactants on the membranes, exerted via the usual detergent mechanism, has been known for a fairly long time,[107] but a systematic study of its characteristic features has been carried out comparatively recently. The detergent mechanism of the incorporation of the fungicidal ammonium salts into the lipid matrix of the membranes has been established in experiments with various compounds — benzylalkylammonium chlorides[108] and bromides[32] and nitro-vinylalkylammonium,[36,38,40] alkoxymethylenemorpholinium,[35] and nitrovinylbenzylmorpholinium[38,39] chlorides.

The experiments showed that the effectiveness of the incorporation of these preparations into the lipid bilayer depends significantly on the characteristics of the polar and non-polar fragments of their molecules. Thus, among the three benzylalkylammonium fungicides investigated, the preparation containing in the polar component of the molecule two electronegative groups at once — nitrovinyl and benzyl — exerts the greatest influence on the haemolysis of erythrocytes and the conductivity of bilayer lipid membranes.[39,40] The removal of one of these groups (nitrovinyl) from the molecule leads to some weakening of the effect of the fungicide on the membrane; an even greater effect is shown by the removal of both the electronegative fragments. Evidently the increased electronegativity of the polar component of the fungicide molecule intensifies its electrostatic interaction with the positively charged choline group in the polar component of the membrane lipids and ensures thereby a deeper penetration not only by the polar component but also by the entire molecule of the preparation into the lipid bilayer. The more effective incorporation of the hydrocarbon chain of the fungicide into the membrane inevitably leads in its turn to an increase in the degree of disorder in the internal part of the bilayer and hence to a stronger effect on the barrier properties of the membranes.

A similar dependence of the degree of incorporation into the lipid bilayer on the electronegativity of the polar component of the molecule has been observed also in the series of benzylalkylmorpholinium chlorides.[39] On the other hand, when the ammonium residue in the fungicide molecule is replaced by the morpholinium residue, the fungicidal activity of the preparations diminishes somewhat, which may be associated with the increase in the size of the polar part of the molecule.[38,39] It may be that the unduly large size of the polar components of the molecules of the quaternary ammonium salts weakens their interaction with the polar groups of the phospholipid molecules, which leads to a less deep incorporation of the fungicide molecules into the bilayer and hence to a weaker perturbation of the latter.

Furthermore, when quaternary ammonium salts are incorporated into the cell membranes, the membrane characteristics such as the surface charge of the lipid bilayer and the effectiveness of the interaction of the molecules of the membrane phospho-lipids with one another change in all probability.[36-39] These data also show that the positively charged polar part of the fungicide molecule is located at the membrane/water interaface, disturbing thereby the interaction of the polar groups of the membrane lipids.

Finally, the degree of interaction of benzylalkylammonium fungicides with the lipid matrix of cell membranes depends on the length of the hydrocarbon chain of the molecule of the preparation. In the series of alkoxymethylenetrimethylammonium chlorides, there is an optimum chain length, which influences the transport of Ca^{2+} and SO_4^{2-} through the liposome membranes. This length corresponds to 12-16 carbon atoms.[37] Approximately the same optimum length of the hydrocarbon chain (10-14 carbon atoms) is observed in the series of alkoxymethylenetrimethylammonium chlorides and also among alkylguanidine acetates — dodine analogues.[35] Evidently, the existence of an optimum hydrocarbon chain length is associated with the fact that compounds with chains much longer than those of the membrane phospholipids form fewer structural defects in the lipid bilayer than preparations with the optimum chain length. On the other hand, in the case of compounds with a much shorter chain length the hydrophobic interaction of the chain with the hydrocarbon tails of the membrane lipids may be too weak to affect the packing of the membranes.[37]

In conclusion, it is essential to note that, apart from amphiphilic pesticides, preparations such as metribuzin and D$_5$[*N*-butyl-*N*-(3,4-dichlorophenyl)-*N*-methylurea] — an analogue of the herbicide neburon — evidently possess the ability to form transbilayer structures. They apparently produce ionic channels in the lipid bilayer, resembling the dimeric channels of gramicidin A.[109]

Thus, depending on the degree of lipophilicity, the molecular dipole moment, and other characteirstics of the pesticide, its interaction with the lipid bilayer of cell membranes as a rule takes place via one of the three mechanisms described above. The type of the biological activity of the pesticide hardly affects the overall pattern of its interaction with the membrane lipids. Furthermore, it is usually impossible to observe correlations between the biological activity of the preparations and the effectiveness of their interaction with the lipid bilayer. These factors suggest that the membranotoxic activity of pesticides does not usually operate at the level of membrane lipids. On the other hand, the incorporation of pesticides into the lipid matrix of the membranes can frequently make a significant contribution to the usual toxicity of the pesticides as a result of the infringement of the barrier properties of the bilayer (for example, in the case of pesticide-protonophores) or of the allosteric effect on the operation of the membrane proteins when the properties of their lipid microenvironment are altered (for example, in the case of DDT and pyrethroids).

V. Conclusion

The studies carried out in recent years have made it possible to establish the mechanisms of the toxic activity of many organochlorine, organophosphorus, and carbamate insecticides, phenylurea, triazine, and phenolic herbicides, fungicidal azoles, pyrethroid compounds with insecticidal activity, and also a whole series of other pesticidal preparations.

The knowledge of the mechanisms of the action of pesticides makes it possible to increase appreciably their effectiveness, to modify specifically their structure and properties, and to synthesise new highly effective preparations. The increase in the effectiveness of pesticides resulting from the determination of the biochemical mechanisms of their action is achieved by improving the existing technologies for the treatment of harmful organisms. The specific synthesis of new pesticides is carried out taking into account the characteristic features of the interaction of the pesticide molecules with their molecular targets in sensitive organisms. Furthermore, the data obtained in the study of the mechanisms of the action of pesticides can be used to develop compounds with antidotal properties and compounds which diminish the toxicity of pesticides to warm-blooded organisms. Finally, studies of this kind are frequently of fundamental importance. The best known illustration of this is the determination of the mechanism of the action of the herbicide diurone, which has promoted the development of research into photosynthetic electron transport.

Various mechanisms of the toxic action of pesticides on the organisms sensitive to them are now known. However, in all cases the principal site where pesticides act is the system of cell membranes. Pesticides are capable of influencing both the structure and the functions of the membranes and can damage the membrane systems either directly or indirectly. The direct interaction of pesticides with biological membranes takes place via the binding of the preparations to certain components of the membranes, usually to the membrane proteins or lipids. An indirect effect of pesticides on membranes occurs when the biosynthesis of the proteins, lipids, or pigments of the cell membranes is affected and leads initially to changes in the protein-lipid or pigment composition of the membranes and then, as a consequence, to the breakdown of their structure and functioning.

References

1. B T Bowman, W W Sans *J. Environ. Sci. Health B* **18** 667 (1983)
2. H Miyoshi, T Nishioka, T Fujita *Bull. Chem. Soc. Jpn.* **59** 1099 (1986)
3. G Omann, J R Lakowicz *Pestic. Biochem. Physiol.* **16** 231 (1981)
4. D Chapman *Quart. Rev. Biophys.* **8** 185 (1975)
5. C M Rivera, D Penner *Residue Rev.* **70** 45 (1979)
6. W Chefurka, P Zahradka, S T Bajura *Biochim. Biophys. Acta* **601** 349 (1980)
7. S I Aksenov, Yu P Burt, A V Filatov *Nauchn. Dokl. Vyss. Shk., Biol. Nauki* **35** (1993)
8. J Sarapuk, H Kleszczynska, S Przestalski, S Witek *Stud. Biophys.* **113** 55 (1986)
9. J C Reinert, I J Tinsley *Pestic. Biochem. Physiol.* 7 578 (1977)
10. W Chefurka, R C Chtelier, W H Sawyer *Biochim. Biophys. Acta* **896** 181 (1987)
11. N K Wilson, W E Wilson *Sci. Total Environ.* 1 245 (1972)
12. J Weigl *Z. Naturforsch. B* **24** 367 (1969)
13. G Omann, J R Lakowicz. *Science* **197** 465 (1977)
14. M Bielska, J Ptaszkowska, R Heinrich *Tech. Ber. Akad. Landwirtsch.-Wiss. DDR* **253** 225 (1987)
15. A Leo, in *Pesticide Synthesis through Rational Approaches* (Eds P S Magee, G K Kohn, J J Menn) (Washington: Am. Chem. Soc., 1984) p. 213
16. M C Antunes-Madeira *Biochim. Biophys. Acta* **820** 165 (1985)
17. G E Blackman, R G Robertson-Cuningham *New Phytol.* **52** 71 (1953)
18. G Veerabhadraiah *Indian. J. Agr. Sci.* **50** 352 (1980)
19. I I Abdrashitova, T F Aripov, F G Kamaev *Biofizika* **32** 679 (1987)
20. E Somers, R Pring *J. Ann. Appl. Biol.* **58** 457 (1966)
21. D J Fisher *Pestic. Sci.* **4** 845 (1973)
22. M A Venis, G E Blackman *J. Exp. Bot.* **17** 771 (1966)
23. A M Omel'chenko, B A Bovykin, S S Kukalenko *Sel'skokhoz. Biol.* **5** 75 (1984)
24. J R Lakowicz, D Hogen *Chem. Phys. Lipids* **26** 1 (1980)
25. V N Golubev, S Kont *Biofizika* **34** 42 (1989)
26. P Ahnad, W Chefurka *Biochim. Biophys. Acta* **689** 135 (1980)
27. D E Moreland, in *Weed Physiology* Vol 2 (Ed. S O Duke) (Boca Raton, FL: CRC Press, 1985) p. 45
28. R D O'Brien, in *Environmental Dynamic of Pesticides* (Eds R Hadue, V N Freed) (New York : Academic Press, 1975) p. 331
29. B D Hilton, T A Bratkowski, M Yamada *Pestic. Biochem. Physiol.*, **3** 14 (1973)
30. M C Antunes-Madeira, V M C Madeira *Biochim. Biophys. Acta.* **904** 1201 (1990)
31. A Leo, C Hansch, D Elkins *Chem. Rev.* **71** 525 (1971)
32. P Smejtek, S Wang, A Barstad *Biochim. Biophys. Acta* **902** 213 (1987)
33. V N Golubev, A S Kont *Sel'skokhoz. Biol.* **3** 18 (1989)
34. J Weigl *Z. Naturforsch. B* **24** 1046 (1969)
35. J D Doherty, K Nishimura, N Kurihara, T Fujita *Pestic. Biochem. Physiol.* **29** 187 (1987)
36. W Ziegler, J Pokorny, D Remis *Biologia (Bratislava)* **39** 273 (1984)
37. R T Wedding, L C Erickson *Plant Physiol.* **32** 503 (1957)
38. D J Fisher *Pestic. Sci.* **15** 219 (1974)
39. D J Fisher, R W Wadleich *Exotoxicol. Environ. Safety* **11** 1 (1986)
40. A E Smith *Weed Sci.* **120** 46 (1972)
41. F Zsoldos, B Karvaly, I Toth, L Erdei *Physiol. Plant.* **44** 396 (1978)
42. F Zsoldos, E Haunold *Physiol. Plant.* **47** 77 (1979)
43. C Gauvri, S B Wilson *J. Exp. Bot.* **34** 367 (1983)
44. C D Kennedi *Pestic. Sci.* **2** 69 (1971)
45. T Ohyama, T Takahashi, H Ogama *Biochem. Pharmacol.* **31** 397 (1982)
46. M Kottke, H D Sisler *Phytopathology* **52** 959 (1962)
47. E Somers, D J Fisher *J. Microbiol.* **48** 1 (1967)
48. C D Kennedi, R A Stemart *J. Exp. Bot.* **31** 135 (1980)
49. B D Hilton, R D O'Brien *Pestic. Biochem. Physiol.* **3** 206 (1973)
50. W M Arnold, U Zimmerman, W Pauli *Biochim. Biophys. Acta* **903** 83 (1988)
51. G Omann, J R Lakowicz *Biochim. Biophys. Acta* **684** 83 (1982)
52. P Smejtek, A W Barstad, K Hsu *Biochim. Biophys. Acta* **902** 109 (1987)
53. J A Satgent, R G Powell, G E Blackman *J. Exp. Bot.* **20** 426 (1969)
54. S Stefann, J-P Joly, B Loubinoux, P Dizengremel *Pestic. Biochem. Physiol.* **32** 38 (1988)
55. J Gabrielska, D Grobelny, J Kuczera *Stud. Biophys.* **77** 193 (1979)
56. C Fedtke, R R Schmidt *Weed Res.* **17** 233 (1977)
57. J Gabrielska, J Kuczera, M Oswiecimska *Stud. Biophys.* **82** 149 (1981)
58. R S Morrod, in *Herbicides: Physiology, Biochemistry, Ecology* Vol. 1 (Ed. L J Audus) (London: Academic Press, 1976) p. 281
59. N Balke, in *Weed Physiology* (Ed. S O Duke) (Boca Raton, FL: CRC Press, 1985) p. 113
60. M C Bennet, E Rideal *Proc. Roy. Soc. B* **142** 483 (1954)
61. G P Naumov, A A Petunov in *I-ya Vsesoyuznaya Konferentsiya po Sel'skokhozyaistvennoi Radiologii. Tezisy Dokladov* (The 1st All-Union Conference on Agricultural Radiology. Abstracts of Reports) (Moscow: Izd. VNII S.-kh. Radiologii, 1979) p. 2
62. M C Antunes-Madeira, V M C Madeira *Biochim. Biophys. Acta* **778** 49 (1984)
63. N Abo-Khatya, R M Hollingworth *Pestic. Biochem. Physiol.* **3** 358 (1973)
64. D E Moreland, S C Huber, W P Novitzky, in *Biochemical Responses Induced by Herbicides. Symp. 181st ACS Nat. Meet. Washington, 1982* p. 79.
65. D E Moreland, W P Novitzky *Z. Naturforsch. C* **39** 329 (1984)
66. L N Vorob'ev, L Mamsadzianas *Fiziol. Rastenii* **31** 5 (1984)
67. V N Golubev, A S Kont *Sel'skokhoz. Biol.* **2** 64 (1987)
68. E P P Gnidec, W Chefurka *Pestic. Biochem. Physiol.* **24**, 1 (1985)
69. V D Luk'yanchuk, S E Mogilevich, B M Klebanov *Dokl. Akad. Nauk Ukr. SSR, Geol. Khim. Biol. Nauki* **4** 76 (1987)
70. H Kleszczynska, S Matyajasik, J Sarapuk *Stud. Biophys.* **84** 173 (1981)
71. R Hadue, I J Tinsiey, S E Randall *Biochemistry* **12** 2346 (1973)
72. R Hadue, I J Tinsiey, J K McCrady *Pestic. Biochem. Physiol.* **3** 73 (1973)
73. E Haunoid, F Zsoldos *Acta Biol. Nova Ser. (Szeged)* **30** 19 (1984)
74. A K Sijperstejn, in *Systemic Fungicides* (Translated into Russian) (Moscow: Mir, 1975) p. 142
75. H Yamaguchi *Antimicrob. Agents Chemother.* **13** 423 (1978)
76. H Yamaguchi *Antimicrob. Agents Chemother.* **15** 706 (1978)
77. M Murakami, J Fukami *Bull. Environ. Contam. Toxicol.* **21** 478 (1979)
78. R Hadue, I J Tinsiey, D Schmedding *Mol. Pharmacol.* **9** 17 (1973)

79. M C Antunes-Madeira, V M C Madeira *Biochim. Biophys. Acta* **901** 61 (1987)
80. V N Golubev, S Kontu, Yu S Sychev *Biofizika* **33** 541 (1988)
81. C Gaillardon, P Gauvril *Phytoma* **360** 12 (1984)
82. N K Wilson *J. Am. Chem. Soc.* **94** 2431 (1972)
83. J R Lakowicz, D Hogen, G Omann *Biochem. Biophys. Acta* **471** 401 (1977)
84. G G Briggs, R H Bromilow, R Edmondson, M Johnston, in *Herbicides and Fungicides M-Factors Affecting Their Activity. Proc. Symp. London, 1977* p. 129
85. P Smejtek, M Paulis-Illangasekare *Biophys. J.* **26** 441 (1979)
86. G G Briggs, L O Rigitano, R H Bromilow *Pestic. Sci.* **19** 101 (1987)
87. P Smejtek, S Wang, A Barstad *Biophys. J.* **51** 495 (1987)
88. G Omann, M Claser *Biochemistry* **23** 4962 (1981)
89. G Oros, S Sule *Abh. Akad. Wissen. DDR, Abt. Mathem.-Naturwissen.- Technik* **1** 417 (1982)
90. W Chefurka, H L McLeod, J E Steele *Pestic. Biochem. Physiol.* **28** 93 (1987)
91. J E Cope *J. Gen. Microbiol.* **119** 245 (1989)
92. G L Darmastadt, N E Balke, L E Schrander *Pestic. Biochem. Physiol.* **19** 172 (1983)
93. S B Wilson *J. Exp. Bot.* **34** 367 (1983)
94. R Brasseur, C Vandenbosch, H Van den Bossche, J M Ruysschaert *Biochem. Pharmacol.* **32** 2175 (1983)
95. M R Sigel, A Kerkenaars, A K Sijperstejn *J. Plant Path.* **83** 121 (1972)
96. O T Jones, A G *Biochim. Biophys. Acta* **812** 731 (1985)
97. J E Pormann *Proc. Roy. Soc. B* **189** 291 (1975)
98. A E Smith *Physiol. Plant.* **27** 338 (1972)
99. E Somers *Meded. Landbouwhogesch. Wageningen* **28** 580 (1963)
100. G Oros, F Viranyi *Acta Phytopathol. Entomol. Hung.* **21** 157 (1986)
101. M C Phillips, in *Progress in Surface and Membrane Science* Vol. 5 (New York: Academic Press, 1972) p.139
102. C D Kennedi *Pestic. Sci.* **3** 715 (1972)
103. C D Kennedi, R A Stemart, in *Herbicides and Fungicides M-Factors Affecting Their Activity. Proc. Symp. London, 1977* p. 99
104. J E A Kustera, J Gabrielska, R Zylka *Stud. Biophys.* **96** 203 (1983)
105. B D Ladbrooke, R M Williams, D Chapman *Biochim. Biophys. Acta* **150** 333 (1968)
106. F Zsoldos, E Hfunold *Physiol. Plant.* **54** 63 (1982)
107. K J Stelzer, M A Gordon *Biochim. Biophys. Acta* **812** 361 (1985)
108. M A Stidham, J N Siedow, D E Moreland *Biochim. Biophys. Acta* **812** 721 (1985)
109. F Zsoldos, E Haunold *Physiol. Plant.* **54** 6 (1982)

Russian Chemical Reviews **62** (7) 693 – 702 (1993) © 1993 Russian Academy of Sciences and Turpion Ltd

UDC 543.544

Gradient barochromatography

M S Vigdergauz

Contents

I.	Introduction	693
II.	Classification of gas-chromatographic methods	693
III.	Effect of the nature of the mobile phase on the retention of sorbates under the conditions of barochromatography	694
IV.	Contribution from pressure gradients to the retention and spreading of the bands	696
V.	Chromatography with programmed pressure and flow rate of the carrier gas	697
VI.	Retention of sorbates and the effectiveness of composite columns. Role of pressure gradients	697
VII.	Chromatography with discontinuous changes in the pressure and/or flow rate of the carrier gas between the sections of a composite column	698
VIII.	Modifications of the gradient barochromatography method	700

Abstract. We describe the gradient barochromatography method, in which the eluent plays an active as well as a transport role, and thus offers an increased resolving power. The effect of the nonideality of the mobile gas phase, determined by its nature and pressure, on the retention and spreading of the chromatographic bands is examined, together with the prospects of controlling the selectivity of the column and the degree of separation of the sorbates. Special attention is paid to the role of the pressure gradients and of the velocity of the gas, including discontinuous changes in work with composite columns. The prospects of the practical application of gradient barochromatography to the identification of the components of complex mixtures and to the control of the chemical composition of various types of sample are examined. The bibliography includes 81 references.

I. Introduction

The nature and the working conditions of the mobile phase play only a secondary role among the many variables which control the selectivity, the effectiveness, and the sorption capacity in gas chromatography. This is because many workers treat the carrier gas merely as a transporting agent, whose influence on the completeness of the separation of sorbates is confined to a relationship between the flow rate of the carrier and the spreading of the bands. However, by assigning active functions as well as transport functions to the gaseous eluent we can obtain some quite unexpected advantages. Furthermore this is a way of building a kind of bridge between gas and liquid chromatography. Supercritical fluid chromatography is one of the best examples of an intermediate variant of chromatography.[1–3]

The active functions of the eluent are determined by the following properties: the dissolving power of the eluent with respect to the sorbates, which depends on its nature and on its pressure; the solubility of the stationary liquid phase in the eluent, which determines the nonideality of the latter; the solubility of the eluent in the stationary liquid (or its condensation, in cases of low mutual solubility) and the formation of a binary stationary phase; the adsorption of the eluent on the gas–liquid and liquid–solid interfaces of the carrier, and the consequent change in the overall sorption characteristics for the sorbates to be analysed (in the partition chromatography regime); the adsorption of the eluent on the gas–liquid interface (in the adsorption chromatography regime) and in the gas–solid carrier interface (in the partition chromatography regime for incomplete coverage of the carrier surface with a layer of stationary liquid phase); the disequilibrium of the sorption process, which increases at high flow rates of the eluent (especially when the viscosity of the stationary liquid is high) with a corresponding change in the retention of the sorbates to be analysed.

When working with nonideal eluents in highly efficient columns we can exploit various factors which have little effect on the separation in the case of ordinary packed columns (i.e. which do not significantly alter the shape of the chromatogram).

At present the range of pressure used in gas chromatography extends from tens of millimetre mercury to thousands of atmospheres, in regimes varying from almost isobaric (in the case of low pressure drops) to gradient regimes, in which the pressure is programmed both over the length of the column and in time. In this respect the active (or pseudoactive) function of the gaseous eluent can also take the form of a change in the selectivity of the composite column, which is controlled by the ratio of the pressures in the sections packed with different sorbents.

The theoretical and the applied aspects of chromatography with nonideal eluents have been examined in various monographs and review articles.[2–5] The present review is aimed at recent work on the specific features of barochromatography.

II. Classification of gas-chromatographic methods

The following classification of gas-chromatographic methods[2] can be proposed in order to allow for the effect of the nature and pressure of the carrier gas on the chromatographic process.

1. Vacuum chromatography using conventional carrier gases or the vapours of low-boiling liquids under reduced pressure.[6–9]

2. The traditional gas chromatography, using carrier gases at ordinary pressures (near-atmospheric at the column outlet, and

M S Vigdergauz Department of General Chemistry and Chromatography, Samara State University, 443 011 Samara, ul. akad. Pavlova 1. Tel. (7-8462) 34 54 47

Received 17 May 1993
Uspekhi Khimii **62** (7) 735–744 (1993); translated by J I Carasso

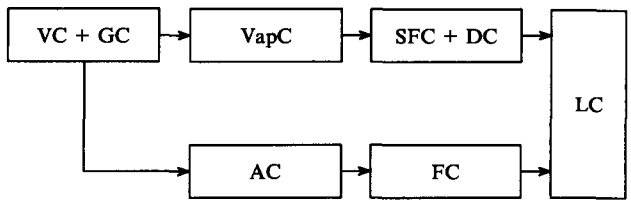


Figure 1. Variants of column molecular chromatography, classified according to the phase states of the mobile phase.
GC, traditional gas chromatography; VC, vacuum chromatography; VapC, vapour chromatography; DC, density chromatography; SFC, supercritical fluid chromatography; AC, aerosol chromatography; FC, foam chromatography; LC, liquid chromatography.

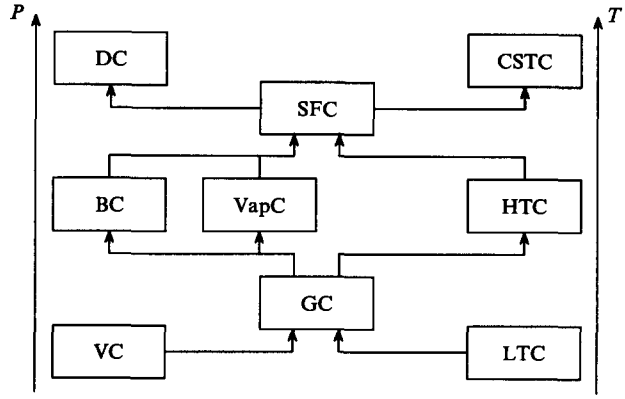


Figure 2. Chromatography methods and their intermediate variants, classified according to pressure and temperature levels (symbols as in Fig. 1); LTC, low-temperature chromatography; HTC, high-temperature chromatography; STC, super-high temperature chromatography; BC, barochromatography.

under an overpressure sufficient to give the required flow rate at the inlet).

3. Barochromatography, in which permanent-gas carriers at high pressures are used to embody some of the active functions listed above: of course, a pressure gradient along the column axis is unavoidable (unlike a temperature gradient) except in diffusion chromatography.[10]

3.1. Gradient barochromatography.

3.1.1. Gradient barochromatography with pressure and flow rate of the carrier gas programmed in time.

3.1.2. Gradient barochromatography with strong pressure gradients (pressure programmed along the column).

3.1.3. Gradient barochromatography with pressure programmed in time and strong pressure gradients.

3.2. Barochromatography with weak pressure gradients..

4. Vapour chromatography, in a flow of the vapour of low-boiling liquids (pure, or mixed with a gas) at ordinary or elevated (up to critical) pressures[11,12] including the addition of a ligand to the carrier gas in order to analyse chelates.[13] Vacancy chromatography, differential chromatography, and other forms of carrier-free chromatography can also be classified with this variant.[23,25,26]

5. Supercritical fluid chromatography, carried out in a flow of substances at a temperature and pressure just above their critical values.[3,4]

6. High-density chromatography, carried out in a flow of gases under pressures much higher than their critical values (up to thousands of atmospheres). Under these conditions the density and the solvent power can approach values typical of liquid solvents.[14]

Of course, this classification cannot claim to be complete, because it omits a number of possible methods, some of which have already been realised. The latter include, in particular, the programming of the parameters[15,16] and the establishment of conditions which favour turbulent flow,[17,18] whereas methods not yet realised include the use of heterogeneous eluents such as aerosols and foams†, and also the use of high vacua.

In the scheme shown in Fig. 1 the intermediate chromatographic methods are listed sequentially in the order of a change of the phase state of the eluent from gas to liquid. The upper branch of the diagram refers to homogeneous mobile phases, the lower branch to heterogeneous.

In order to establish a clear picture of the effect of the nature and of the operating conditions of the mobile phase on the chromatographic process it is useful to compare the above classification with the classification of the methods in which a temperature distribution is postulated. The same system of numbering is used for the variants (except variant 4).

†This method should not be confused with the well-known variant of foam chromatography in which the retention is determined by the formation of a foam between the sorbent and the stationary phase.[19]

1. Low-temperature chromatography, including cryogenic.[20-22]

2. Gas chromatography at ordinary temperatures (up to 200–250 °C).

3. Isothermal and gradient chromatography at elevated temperatures (up to 500–600 °C).

3.1. Programmed temperature chromatography.

3.1.1. Chromatography with time-programmed temperature.

3.1.2. Chromatography with time-programmed temperature and a constant temperature gradient along the column axis.

3.1.3. Chromathermography[23] and other variants of temperature programming in time and space. A variant[24] which stipulates the programmed transfer of the column from one part of the thermostat to another part (set for a different temperature) can also be classified in this section.

3.2. Isothermal chromatography.

5. Supercritical fluid chromatography.

6. 'Ultra-high temperature' chromatography (up to 1200–1350 °C).[27] Pyrolytic gas chromatography can be arbitrarily included in this section, since it features a large (though formal) increase in the mobility of the sorbate.[28]

The change from one methodology to another in terms of temperature and pressure is shown schematically in Fig. 2. In both cases an increase in the stated parameter tends to lower the sorption capacity of the stationary phase and hence to increase the mobility of the sorbates‡.

III. Effect of the nature of the mobile phase on the retention of sorbates under the conditions of barochromatography

Barochromatography covers the range from ordinary pressures to several tens of atmospheres when traditional carrier gases are used. Therefore in order to calculate the retention values we can use virial equations of state including the second and the third virial coefficients.[2] Obviously in most cases the solvent power of the eluent towards the sorbate and its dissolution in the stationary liquid are relatively small. However, they are usable for analytical purposes and for physicochemical measurements.

The first unambiguous example of the influence of the nature of the carrier gas on the retention was provided by the

‡Departures from this tendency in the right-hand loop of the scheme are due to phase transitions in the stationary phase (e.g., melting in the LC–GC stage). Little is known about the special problems of working with high vacua.

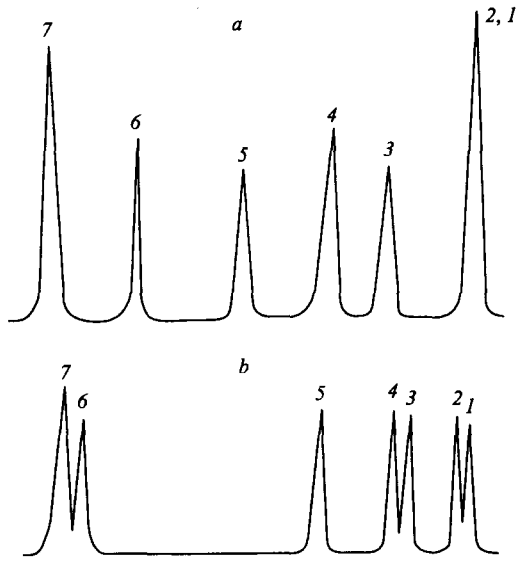


Figure 3. Chromatograms of a mixture of hydrocarbons obtained on a capillary column (270 m × 0.15 mm) with squalane and nitrogen (*a*) or hydrogen (*b*) as the carrier gas:[29] *1*, methylcyclopentane; *2*, 2,2-dimethylpentane; *3*, 2,4-dimethylpentane; *4*, benzene; *5*, 2,2,3-trimethylbutane; *6*, 3,3-dimethylpentane; *7*, cyclohexane.

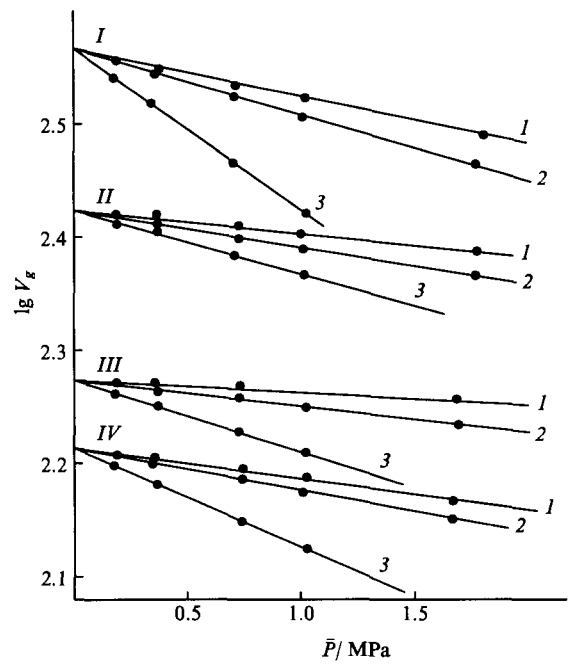


Figure 4. Plots of the logarithm of the absolute specific retention volume against the average pressure in the column at 80 °C in a nitrogen (*1*), argon (*2*), or carbon dioxide medium (*3*) for butyl acetate (*I*), toluene (*II*), n-octane (*III*), and dioxan (*IV*).[34]

chromatograms for hydrocarbons obtained on a capillary column 270 m long with a squalane stationary phase and using nitrogen and hydrogen as the carrier gases at an inlet pressure of 10.7 atm.[29] As can be seen from Fig. 3, replacing one carrier gas by the other affects both the retention and the selectivity of the separation of these sorbates. This effect is due to the well known relationship between the separation coefficient of the sorbate Γ and the second virial coefficient B_{12} in the gas-state equation for the mixture of sorbate and carrier gas:[30]

$$\Gamma = \Gamma_{(P\to 0)}\exp(\beta P)\,, \qquad (1)$$

where $\Gamma_{(P\to 0)}$ corresponds to zero pressure, $\beta = (2B_{12} - V_1^{\infty})/RT$ [V_1^{∞} is the partial molar volume of the sorbate at infinite dilution in the stationary liquid], and P is the pressure in the column.

At moderately high pressures, which satisfy the condition $\beta P \ll 1$, we can use the expression[31]

$$\Gamma = \Gamma_{(P\to 0)}(1 + \beta P)\,. \qquad (2)$$

Over a wider range of pressure we must include the third (mixed) virial coefficient C_{122} (See Ref. 32):

$$\ln\Gamma = \ln\Gamma_{(P\to 0)} + \beta P + \xi P^2\,, \qquad (3)$$

where

$$\xi = \frac{3C_{122} - 4B_{12}B_{22}}{2(RT)^2}\,. \qquad (4)$$

(B_{22} is the second virial coefficient in the equation of state of the carrier gas). A more complex equation was obtained when allowing for the solubility of the carrier gas in the stationary liquid.[33]

The effect of the nature of the carrier gas and of the pressure in the column on the retention of the sorbates is clearly shown by the plots in Fig. 4. Clearly, the commonly used carrier gases can be conveniently classified into three groups. The first includes hydrogen and helium, which are characterised by relatively small values of the second virial coefficient in the equation of state for the gas, and therefore in these gases the change in retention of the sorbates at higher pressures is very slight. In the case of nitrogen and argon (the second group) these changes become significant, and lastly to the third group we must assign carbon dioxide and some Freons, which produce an even larger shift in the phase equilibria of the sorbates. Furthermore the critical state of these eluents is reached at pressures as low as 30 atm.

A study of the dependence of the retention indices of the hydrocarbons in gasoline on the mean pressure of helium, argon, and carbon dioxide at pressures between atmospheric and 18 atm (using a capillary column 120 m long with octadec-1-ene) has been reported.[35] The results are consistent with the above argument (Fig. 5, see over). It was also established that the analysis time decreases when argon is replaced by carbon dioxide and the pressure is increased. The changes in the retention indices of aromatic hydrocarbons with increasing pressure in nitrogen and carbon dioxide have been discussed[36,37] by analogy with the corresponding changes in the retention index caused by an increase in temperature.

It has been pointed out[35] that carbon dioxide is sorbed by the wall of a copper capillary and blocks the active centres on the liquid–solid interface. This effect produces narrower and more symmetrical peaks for the aromatic hydrocarbons on the chromatograms: in a stream of CO_2 the height of the benzene peak is almost double that of the same peak in a stream of argon.

Of course, in gas adsorption chromatography the nature of the eluent produces even more marked effects, as shown by the possibility of separating gases by adsorption methods.[38,39]

Data on the role of the solubility of the eluent in the stationary phase and of the stationary phase in the eluent have been reviewed.[2] The most striking effects are seen in vapour chromatography. However, the effects can be substantial also when traditional carrier gases are used. For example, increasing the pressure of carbon dioxide in a column with a liquid-crystalline stationary phase suppresses the characteristic meta-para selectivity of the mesophase because of the disordering of the structure caused by the dissolution of the carbon dioxide.[40]

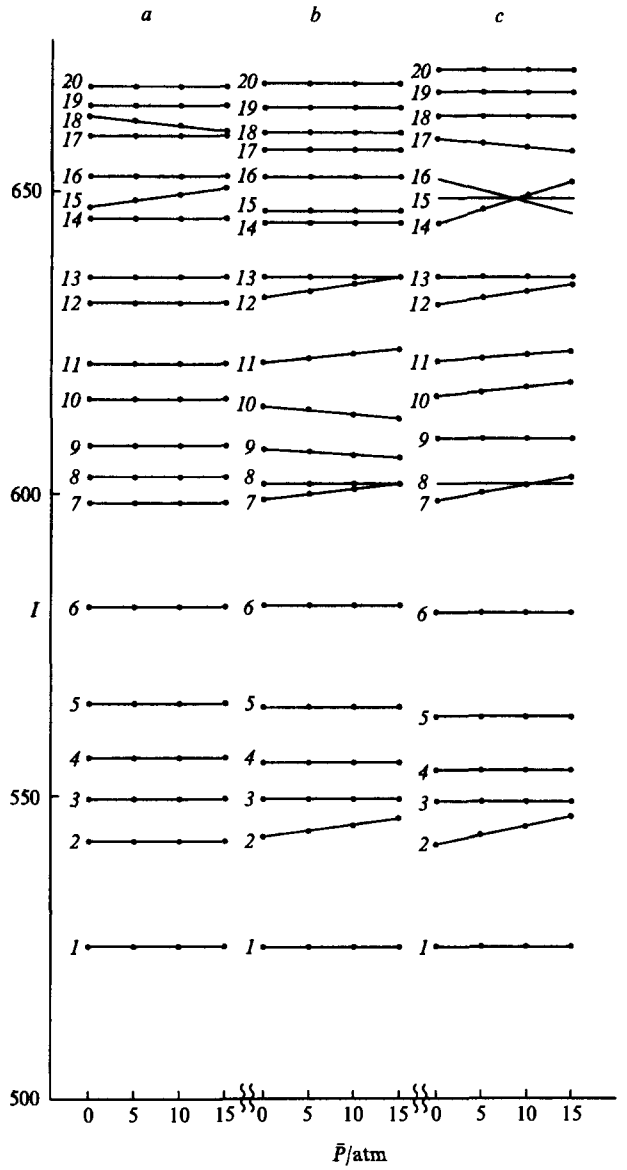


Figure 5. Dependence of the retention index of hydrocarbons at 25 °C on the average pressure in a column with octadec-1-ene with helium (*a*), argon (*b*), or carbon dioxide (*c*) as the carrier gas.[35] *1*, 2,2-dimethylbutane; *2*, cyclopentane; *3*, 2,3-dimethylbutane; *4*, 2-methylpentane; *5*, 3-methylpentane; *6*, n-hexane; *7*, methylcyclopentane; *8*, 2,2-dimethylpentane; *9*, 2,4-dimethylpentane; *10*, 2,2,3-trimethylbutane; *11*, benzene; *12*, cyclohexane; *13*, 3,3-dimethylpentane; *14*, 1,1-dimethylcyclopentane; *15*, 2-methylhexane; *16*, 2,3-dimethylpentane; *17*, 3-methylhexane; *18*, *cis*-1,3-dimethylcyclopentane; *19*, *trans*-1,3-dimethylcyclopentane; *20*, *trans*-1,2-dimethylcyclopentane.

IV. Contribution from pressure gradients to the retention and spreading of the bands

When discussing the role of the nonideality of the carrier gas and of its solubility (or adsorption) in the stationary liquid in the barochromatography regime it should not be forgotten that the contribution of these factors to the retention of sorbates in the presence of substantial pressure gradients can vary along the length of the column.

Since the specific retention volume V_g^T for a column temperature T is related to the distribution coefficient Γ (in gas – liquid chromatography) by the simple expression

$$V_g^T = \frac{\Gamma}{\rho_1} \tag{5}$$

(where ρ_1 is the density of the stationary liquid at the temperature T) we can use the expressions (1) – (4) given above to calculate the retentions.

According to van Swaay[41]

$$\ln V_g^T = \ln V_{g(P\to 0)}^T + \frac{\beta P_0}{J_3^2} . \tag{6}$$

Here $V_{g(P\to 0)}^T$ is related to the coefficient $\Gamma_{(P\to 0)}$, and J_3^2 is the pressure gradient factor,[42] equal to

$$J_3^2 = \frac{3(P_1/P_0)^2 - 1}{2(P_1/P_0)^3 - 1},$$

where P_1 and P_0 are the pressure at the inlet and at the outlet of the column respectively. The mean pressure over the length of the column is $\bar{P} = P_0/J_3^2$.

According to Everett,[30]

$$V_g^T = V_{g(P\to 0)}^T \left(1 + \frac{\beta P_0}{J_4^3}\right), \tag{7}$$

where the pressure $\bar{P} = P_0/J_4^3$ is averaged over the residence time of the sorbate in the column.

In general the pressure gradient factor can be expressed as

$$J_n^m = \frac{n}{m} \frac{(P_1/P_0)^m - 1}{(P_1/P_0)^n - 1} .$$

Equations of the following type are often used in published papers:[43,44]

$$\ln V_g^T = \ln V_{g(P\to 0)}^T + \beta P_0 J_3^4 \left[1 - aP_0(J_4^5 - J_3^4)\right], \tag{8}$$

where $a = cB_{22}/RT$ (and c is a constant).

Allowing for the dissolution of carrier gas in the stationary liquid Eqn. (6) becomes[37,45]

$$\ln V_g^T = \ln V_{g(P\to 0)}^T + \left[\beta + \lambda\left(1 - \frac{\delta \ln \gamma^\infty}{\delta X}\right)\right] \frac{P_0}{J_3^2}, \tag{9}$$

where λ is the molar solubility of the carrier gas in the stationary liquid, and $(\delta \ln \gamma^\infty)/\delta X$ is the change in activity coefficient of the sorbate as a function of its mole fraction in the stationary phase.

It follows that the slope of the straight lines in Fig. 4 is determined not by the virial coefficient B_{12} (which determines the factor β) but by its effective value[37]

$$B_{ef} = B_{12} + 0.5\lambda\left(1 - \frac{\delta \ln \gamma^\infty}{\delta X}\right) RT . \tag{10}$$

The effect of pressure and of the pressure gradients on the blurring of the bands has already been discussed in depth.[46] It was shown that the effectiveness of the column increases with pressure for the optimum flow rate of the carrier gas (the flow rate corresponding to the minimum on the curve, which defines the dependence of the height equivalent to a theoretical plate on the velocity of the gas). The latter decreases as the pressure increases. Theoretically, pressure gradients cannot lower the number of plates by more than 1/9, since

$$n^0 \geqslant n \geqslant \left(\frac{\varkappa}{J_3^2}\right)^2 n^0 , \tag{11}$$

where n^0 is the number of theoretical plates for the minimum gradient and

$$\varkappa = \sqrt{\frac{2}{(P_1/P_0)^2 + 1}}.$$

These conclusions are valid for a laminar flow of the eluent, to which Darcy's law applies. Changing to a turbulent regime by choosing an appropriate Reynolds number equalises the velocities over the cross-section and lowers the mass transport between the phases, increasing the effectiveness and the operating speed of the column.[17,18,47] Turbulence is produced not only by increasing the velocity of the mobile phase (i.e. by increasing the pressure at the column inlet) but also by increasing its density, since the Reynolds number is $d\alpha\rho/\eta$, where d is the diameter of the tube and α, ρ, and η are the linear velocity, the density, and the dynamic viscosity of the eluent respectively.

However, we should note that in addition to causing turbulence (which increases the effectiveness of the column) an increase in flow rate can disturb the thermodynamic equilibrium of the sorbate in the sorbent – carrier gas system. The equilibrium is usually shifted in the direction of a decrease in the distribution coefficient, and also it induces additional spreading of the bands.

Thus, it has been shown[48] that in a column with apiezon L (30% on hexasorb) an increase in the linear velocity of the carrier gas to 19.4 cm s^{-1} produces a relative change of 5% in the retention values. The problems resulting from the failure of the sorbate molecules to diffuse through the whole layer of liquid phase at high flow rates are even more serious when the viscosity is high. In a study[49] of polymers with a high molecular weight non-equilibrium was observed even at ordinary velocities of the carrier gas: this suggested a method of determining the retentions by extrapolating the experimental data to zero flow rate.

Kirsh et al.[50] have proposed the use of the equilibrium displacement effect to control the selectivity of chromatographic columns containing multilayer stationary phases. An experiment with columns 1.2 m long and an internal diameter of 3 mm with layers of apiezon L and 1,2,3,4,5,6-hexakis(β-cyanoethoxy)-hexane successively deposited on chromaton (from different solvents) showed that an increase from 5–8 to 500–550 cm^3 min^{-1} in the volume flow rate (at 60 °C) can lower the specific retention volumes of the sorbates by tens of per cent, the magnitude of the effect depending on the order in which the layers are deposited. The Kovats retention index can decrease by 4–13 units.

V. Chromatography with programmed pressure and flow rate of the carrier gas

Programmed flow rate of the carrier gas has been applied since 1959, usually by controlling the pressure at the column inlet.[51] It has been pointed out[16] that the use of this variant creates an alternative to temperature programming, since it makes possible the separation of mixtures of components boiling at very different temperatures as well as compressing the chromatographic bands, with a marked increase in sensitivity§. Also, since the analysis is carried out at relatively low temperatures, thermally unstable compounds can be separated, using more volatile and less thermally stable stationary phases if necessary. Both linear[52,53] and exponential[54,55] pressure programmes have been used, with or without a corresponding temperature programming. The relative advantages of packed and of capillary columns in pressure-programmed chromatography have been compared.[56,57]

There is no reference to the relationship between retention and changes in the nonideality of the eluent in papers on pressure-programmed measurements published so far, though it is evident from the above discussion that such a relationship exists.

§The height of the peak observed with a flow-type detector (for example, a flame ionisation detector) increases with the flow rate: this produces a convergence of the lower detection limits of light and of heavy sorbates.

VI. Retention of sorbates and the effectiveness of composite columns. Role of pressure gradients

Composite columns are widely used to achieve an intermediate separation of multicomponent mixtures. The selectivity is controlled by varying the ratio of the section lengths (or, more strictly speaking, the ratio of the amounts of individual sorbents). The classification of the binary sorbents and the fundamental relationships between the retention and the composition of the columns in each of the variants are discussed, in particular in our recent monograph.[46]

For low pressure gradients the retention volume on a composite column is determined by the sum of the retention volumes in the individual sections. For example, the specific retention volume in a two-section column is

$$V_g^T = \frac{g_1}{g} V_{g_1}^T + \frac{g_2}{g} V_{g_2}^T, \qquad (12)$$

where the subscripts 1 and 2 refer to the first and the second section respectively, and g is the total mass of the two stationary phases ($g = g_1 + g_2$).

However, in the presence of large pressure gradients we observe departures from this expression, which can be attributed to the difference in average pressure between the sections, and therefore to differences in the velocity of the carrier gas. The possibility of controlling the retention and the other chromatographic characteristics is determined mainly by the increased flow rate associated with the decrease in pressure along the column, so that the volume of substance entering the second section is greater than the volume corresponding to the average pressure in the first section. We can allow for this factor by using the expression

$$V_g^T = \frac{g_1}{g} V_{g_1}^T \frac{P_{0_1}}{P_0} \frac{J_3^2}{J_{3_{(1)}}^2} + \frac{g_2}{g} V_{g_2}^T \frac{J_3^2}{J_{3_{(2)}}^2} \cdot$$

$$= \frac{g_1}{g} V_{g_1}^T \frac{\bar{P}_1}{\bar{P}} + \frac{g_2}{g} V_{g_2}^T \frac{\bar{P}_2}{\bar{P}}, \qquad (13)$$

where $P_{0_{(1)}}$ is the pressure at the inlet of the first section; the pressure gradient factors J_3^2, $J_{3_{(1)}}^2$ and $J_{3_{(2)}}^2$ (and also the average pressures $\bar{P}$, $\bar{P}_1$, and $\bar{P}_2$) refer to the whole composite column and to its separate sections respectively.

Expressions for the effective values of the separation coefficients and for other quantities which characterise the retention (the coefficient Γ, associated with the volume composition, the molar retention volume, the molar composition, etc.) can be obtained in a similar way. The equation for the retention volume for unit length of the column V_L is

$$V_L = \frac{\bar{L}_1}{\bar{L}} V_{L_1} + \frac{\bar{L}_2}{\bar{L}} V_{L_2}, \qquad (14)$$

where the effective length $\bar{L}$ is equal to the product of the length of the column and of the average pressure (for each of the sections as well as for the whole column).

The linear retention index is calculated by the equation[46]

$$J = \frac{t_{R_i} - t_{R_z}}{t_{R_{(z+1)}} - t_{R_z}} + z,$$

where t_{R_i}, t_{R_z}, $t_{R_{(z+1)}}$ are the retention times of the experimental sorbate and of n-paraffins containing z and $z + 1$ carbon atoms. For a composite column

$$J = \frac{J_1 + mJ_2}{1 + m}, \qquad (15)$$

where $m = (\bar{L}_2/\bar{L}_1)(\Delta V_{L_2}/\Delta V_{L_1})$; ΔV_{L_1} and ΔV_{L_2} are the differences between the retention volumes of the standard n-paraffins (contains z and $z + 1$ carbon atoms) in the first and the second section.

From Eqn. (14) it follows, in particular, that inverting the order of the two sections in a given composite column affects the ratio of the average pressures in the sections, thus affecting also the total retention. This effect was first observed experimentally during the separation of a mixture of C_2-C_5 hydrocarbons using a composite column with mineral oil and β,β′-dicyanodiethyl ether.[23,58]

We have described[59] a method of determining propadiene and methylacetylene impurities in the propane–propene fraction in a composite column 7.1 m long consisting of two sections, one containing 20% n-heptadecane and the other 20% di-isodecyl phthalate on a diatomite carrier (2.4 and 4.7 m respectively). As can be seen from Fig. 6*a*, with the sections in the above sequence the impurities are detected as a single peak, which is convenient for operational production control. With the opposite arrangement of the sections (Fig. 6*b*) propadiene and methylacetylene give separate peaks, which allows a more detailed analysis of the chromatogram.

A 13-component mixture of naphthalene and its methyl and dimethyl derivatives was separated on a composite column with liquid-crystalline *p,p′*-azoxyphenetole and poly(ethylene glycol)-2000 on chromosorb.[60] The optimum value of $\bar{L}_2/\bar{L}$, which allows the separation of 12 peaks with a given effectiveness (broken line *A*), corresponds to the real column, consisting of a 4 m long poly(ethylene glycol)-2000 section and a 3 m long azoxyphenetole section (Fig. 7). In this case only the 2,6 and the 2,7 pair of dimethylnaphthalenes remains unresolved. Arranging the sections in the opposite order increases $\bar{L}_2/\bar{L}$ (broken line B) and allows even these isomers to be separated.

A study[61] of the spreading of sorbate bands in composite columns has shown that whereas at low pressure gradients the width ω of the peak (in units of the volume of carrier gas) is given by the formula

$$\omega^2 = \omega_1^2 + \omega_2^2 , \tag{16}$$

with large gradients the following expression should be used for the corrected peak width $\omega^0 = \omega J_3^2$:

$$(\omega^0)^2 = (\omega_1^0)^2\left(\frac{P_{0_{(1)}}}{P_0}\right)^2\left(\frac{J_3^2}{J_{3_{(1)}}^2}\right)^2 + (\omega_2^0)^2\left(\frac{J_3^2}{J_{3_{(2)}}^2}\right)^2 . \tag{17}$$

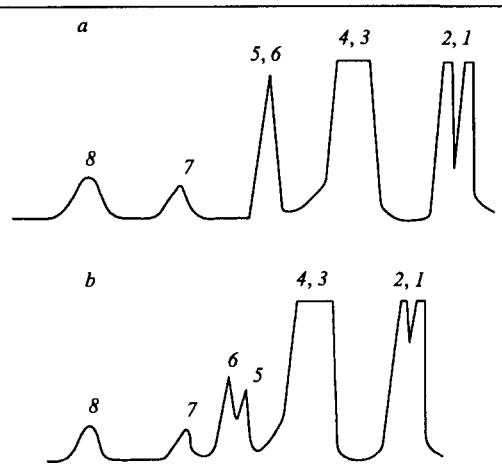


Figure 6. Chromatograms of a propane–propene fraction on a composite two-section column for different relative positions of the sections (see text).[59] *1*, ethylene; *2*, ethane; *3*, propene; *4*, propane; *5*, propadiene; *6*, methylacetylene; *7*, isobutane; *8*, n-butane.

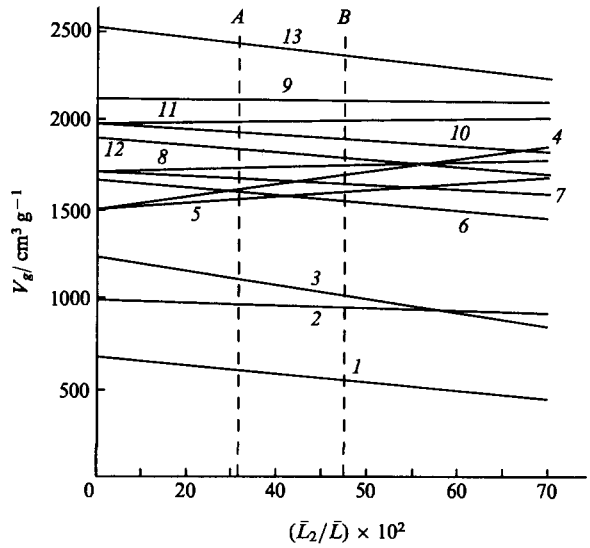


Figure 7. Plots of the retention volumes of alkylnaphthalenes against the ratio of the effective section lengths with *p,p′*-azoxyphenetole and poly(ethyleneglycol)-2000.[60] *1*, naphthalene; *2*, β-methylnaphthalene; *3*, α-methylnaphthalene; *4*, 2,6-dimethylnaphthalene; *5*, 2,7-dimethylnaphthalene; *6*, 1,7-dimethylnaphthalene; *7*, 1,3-dimethylnaphthalene; *8*, 1,6-dimethylnaphthalene; *9*, 1,2-dimethylnaphthalene; *10*, 1,5-dimethylnaphthalene; *11*, 2,3-dimethylnaphthalene; *12*, 1,4-dimethylnaphthalene; *13*, 1,8-dimethylnaphthalene.

Corresponding expressions have been obtained for the number of theoretical plates and for the degree of separation.[61]

VII. Chromatography with discontinuous changes in the pressure and/or flow rate of the carrier gas between the sections of a composite column

As was said above the retention of the sorbates (and therefore also the selectivity of the column) can be controlled by varying the ratio of the average pressures in the sections of a composite column, since this procedure varies the relative values of the volume flow rates in the sections and of the effective section lengths.

An analysis scheme[63] based on a system developed for multistage programmes includes introducing an additional flow between the sections (or extracting part of the flow emerging from the first section). By regulating the pressure of this additional flow we can control the pressure drop between the sections and thus determine the ratio of the average pressures and rates in the sections for constant inlet (P_1) and outlet pressures (P_0). A suitable assembly is shown diagrammatically in Fig. 8.

Deans and Scott[62] have shown that the relative retention of the sorbates A and B on a composite column, equal to the ratio of the reduced retention times

$$r = \frac{t'_{R(A)}}{t'_{R(B)}} \tag{18}$$

(where $t'_R = t_R - t_0 = t_0\Gamma/\beta'$, t_R is the retention time of the sorbate, t is the retention time of the non-sorbed gas, and $\beta' = \kappa/\kappa_1$ is the ratio of the volume fractions of the column occupied by the gas and the liquid phase respectively), can be expressed in terms of the ratio of the t_0 values for the two sections:

$$r = \left[\frac{\Gamma_{A_{(1)}}}{\beta'_1} + \frac{t_{0_{(2)}}}{t_{0_{(1)}}}\frac{\Gamma_{A_{(2)}}}{\beta'_2}\right] \Big/ \left[\frac{\Gamma_{B_{(1)}}}{\beta'_1} + \frac{t_{0_{(2)}}}{t_{0_{(1)}}}\frac{\Gamma_{B_{(2)}}}{\beta'_2}\right] . \tag{19}$$

The change in the pressure drop between the section produced by the insertion (or extraction) of an additional flow alters the velocities in the sections and thus affects the ratio $t_{0_{(1)}}/t_{0_{(2)}}$.

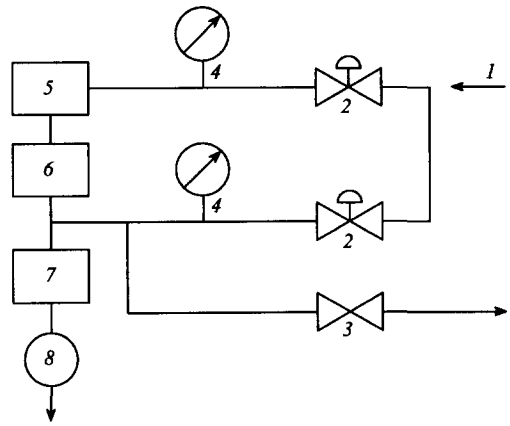


Figure 8. Two-section column with control of the flow and of the pressure drop between the sections.[68] *1*, gas flow; *2*, pressure regulator; *3*, needle valve; *4*, manometer; *5*, sample injection system; *6*, and *7*, sections of the composite column; *8*, detector.

Commercial equipment for assembling a similar scheme can be obtained from the German firms Gerstel and Siemens.

A group of papers[64,65] published in 1985 described a systematic study, with the scheme shown in Fig. 8, of the practical application of this method of analysis, called the multi-chromatographic method. In later work the technique was combined with liquid (column) chromatography and thin-layer chromatography. The method was used for 'tuning' the selectivity of capillary columns.[66,67]

Another suggested variant of barochromatography with composite columns uses an intermediate controllable throttle (Fig. 9) which allows the contribution of each section to the total retention to be varied precisely and between wide limits. Obviously, for a large enough ratio of the pressures in the sections the second section can be effectively 'switched off' (or the first, if the sections are connected in the opposite order). Thus by filling the sections with a suitable mixture of polar and of nonpolar sorbents the control range can be made to approach Rohrschneider's range of chromatographic polarities.[70]

Fig. 10 (see over) shows a series of chromatograms of a mixture of hydrocarbons and oxygen compounds recorded in a baro-chromatographic apparatus with different pressures in the sections, using poly(ethylene glycol adipate) and 1,2,3,4,5,6-hexakis-(β-cyanoethoxy)hexane on zeolite at 85°C in a stream of carbon dioxide.[68] Obviously the system offers adequate control over the selectivity of the separation: even the order in which the peaks appear in the chromatogram can be controlled.

The total effective sorption capacity is also controllable. Table 1 shows the absolute specific retention volumes $[V_g = V_g^T(273.15/T)]$ on a composite column which included sections with 1,2,3,4,5,6-tetrakis-(β-cyanoethoxy)hexane and almost com-pletely nonpolar silicon grease on chromosorb W at

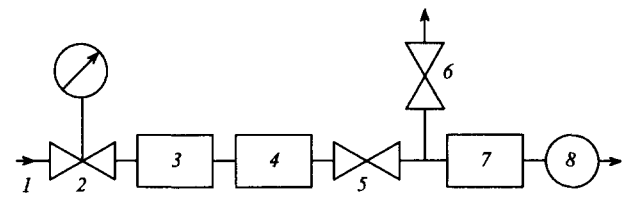


Figure 9. Barochromatography apparatus.[68,69] *1*, gas flow; *2*, pressure regulator; *3*, sample injection system; *4*, and *7*, column sections; *5*, intermediate throttle; *6*, vent to atmosphere; *8*, detector. In studies of the regime the pressure was measured also before and after the throttle *5* and after the section *7*.

353.15 K.[69] Of course in this case, since carbon dioxide was used as the eluent, the sorption capacity and the selectivity at high pressures are also affected by the nonideality of the mobile phase.

We have also examined[71] the possibility of using a universal equation for the *a priori* calculation of the retention of sorbates by binary sorbents[72] in a barochromatographic system. The equation takes the form

$$y = y_1 + \frac{X_{ef_2}}{1 - b(1 - X_{ef_2})}(y_2 - y_1)\,, \tag{20}$$

where y_1 and y_2 are the retentions of the sorbate by the binary and by the individual sorbents respectively, X_{ef_2} is the fraction of sorbent 2 in the total amount of binary sorbent (or the ratio of the length of section 2 or of its internal volume to the total length or volume of the composite column), and b is a coefficient which characterises the given system. It was shown, in particular, that whether or not the system included an intermediate throttle the average pressure in the composite column was

$$\bar{P} = \frac{L_1}{L}\frac{P_{0_{(1)}}}{J^2_{3_{(1)}}} + \frac{L_2}{L}\frac{P_{0_{(1)}}}{J^2_{3_{(2)}}}\,. \tag{21}$$

Since $\bar{P} = P_0/(J_3^2)_{ef}$, where $(J_3^2)_{ef}$ is the effective pressure gradient factor along the column, we have

$$\frac{1}{(J_3^2)_{ef}} = \frac{L_1}{L}\frac{P_{0_{(1)}}}{P_0}\frac{1}{J^2_{3_{(1)}}} + \frac{L_2}{L}\frac{1}{J^2_{3_{(2)}}}\,. \tag{22}$$

In general, if the intermediate throttle is used in conjunction with an additional gas flow (or with the partial extraction of the flow from the system) the equation for the relative retention becomes

$$r = \frac{(\Gamma_{A_{(1)}}/\beta'_1)\varkappa_{(1)} + K_V K_\alpha(\Gamma_{A_{(2)}}/\beta'_2)\varkappa_{(2)}}{(\Gamma_{B_{(1)}}/\beta'_1)\varkappa_{(1)} + K_V K_\alpha(\Gamma_{B_{(2)}}/\beta'_2)\varkappa_{(2)}} = \frac{\Gamma_{A_{(1)}}\varkappa_{l_{(1)}} + K_V K_\alpha \Gamma_{A_{(2)}}\varkappa_{l_{(2)}}}{\Gamma_{B_{(1)}}\varkappa_{l_{(1)}} + K_V K_\alpha \Gamma_{B_{(2)}}\varkappa_{l_{(2)}}}\,. \tag{23}$$

Table 1. Absolute specific retention volumes of the sorbates for different average pressures (in atm) in the sections.[69]

Sorbate	$\bar{P}_1 = 1.74$ $\bar{P}_2 = 1.36$	$\bar{P}_1 = 3.86$ $\bar{P}_2 = 1.66$	$\bar{P}_1 = 6.99$ $\bar{P}_2 = 1.65$	$\bar{P}_1 = 10.16$ $\bar{P}_2 = 1.68$	$\bar{P}_1 = 12.96$ $\bar{P}_2 = 1.68$	$\bar{P}_1 = 19.89$ $\bar{P}_2 = 2.18$
n-Hexane	13.3	11.6	6.9	5.6	5.0	4.5
Cyclohexane	24.1	19.9	12.2	10.3	9.3	8.6
Ethanol	24.7	29.8	29.0	29.7	29.2	29.6
Iso-octane	28.0	22.8	13.2	10.8	9.7	8.8
Ethyl methyl ketone	33.0	33.2	31.9	32.2	31.0	30.3
n-Heptane	29.7	23.8	14.0	11.5	10.3	9.6
Benzene	33.3	30.6	25.4	24.4	23.7	23.5
n-Octane	63.2	48.7	28.0	24.2	22.5	19.6
n-Nonane	–	–	–	51.0	47.2	42.9

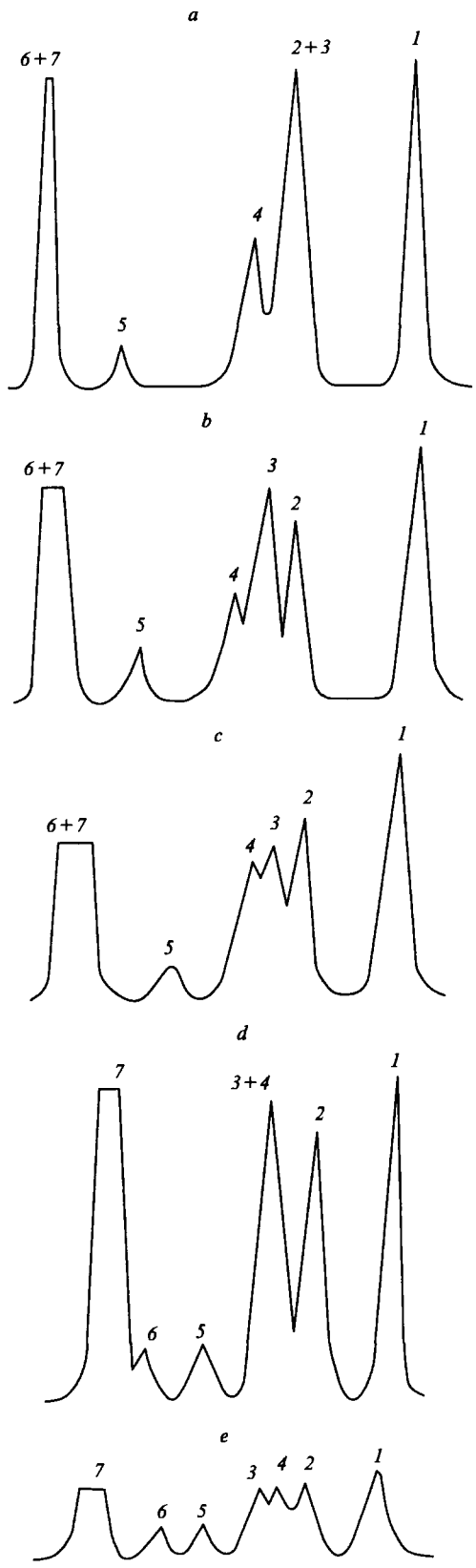


Figure 10. Chromatograms of a mixture of organic compounds obtained at different pressures in a barochromatographic column.[68] *1*, n-octane; *2*, propionaldehyde; *3*, n-nonane; *4*, acetone; *5*, butyraldehyde; *6*, ethyl methyl ketone; *7*, benzene. Average pressures in the first and the second section/atm:

	a	*b*	*c*	*d*	*e*
$\bar{P}_1$	2.24	3.79	6.67	9.69	19.72
$\bar{P}_2$	1.37	1.47	1.44	1.38	1.73

Here $K_V = [V_{\alpha_0} \pm (PV_\alpha)_{exc}]/V_{\alpha_0}$ is a coefficient which allows for the additional flow (the minus sign corresponds to the injection of an additional flow into the system, the plus sign to the extraction of part of the flow from the system). If the flow is injected (or extracted) at a point downstream from the intermediate throttle the pressure and the flow are P_2 and V_{α_2}; V_{α_0} is the flow of gas emerging from the second section (normalised to a pressure of 1 atm). If the fraction of the volume occupied by the phase $\varkappa_1$ is the same in both sections we can write

$$r = \frac{\Gamma_{A_{(1)}} + K_V K_\alpha \Gamma_{A_{(2)}}}{\Gamma_{B_{(1)}} + K_V K_\alpha G_{B_{(2)}}} . \qquad (24)$$

With sections of the same size $K_V = \bar{P}_2/\bar{P}_1$. In the absence of an additional flow (or extraction) we have $K_\alpha = 1$.

The above expressions do not allow for the nonideality of the gas or for the effect of pressure on its solvent power for the sorbate. A correction for the former effect can be inserted into K_α and K_V (by using the equation $PV = ZRT$), and a correction for the latter effect can be inserted into Γ [see Eqn. (1)].

VIII. Modifications of the gradient barochromatography method

The examples of the methods of controlling chromatographic processes discussed above can be used in practice to identify the optimum conditions of analysis of multicomponent mixtures while using the smallest possible number of stationary phases.[73] Since the use of composite columns with a controlled ratio of effective section lengths allows us to evaluate the chromatographic properties of sorbents of moderately high selectivity the presence of several sections with 6–10 sorbents undergoing different intermolecular interactions with the sorbates should enable us to solve a wide range of analytical problems by gas chromatography.

Furthermore in the chromatographic identification of substances from multiple retention spectra[74] an unambiguous correspondence between peaks obtained in columns with sorbents of different nature can be established by a series of measurements on columns with a gradually varying selectivity.[74–76] The barochromatographic method is a convenient way of obtaining the required series of chromatograms (see Fig. 10).

In a proposed variant of the design of the column, three sections are connected in a triangular arrangement. They contain sorbents of different types, and controllable flow resistances are mounted between the sections. The location of the points of insertion (or extraction) of the gas into or out of the system and the point at which the gas flow is led from the sections to the detector can be varied to produce the required sequence of sections.

Multielement spectra can be obtained in a cruciform barochromatographic column[77] (a modification of a column already described),[78] which includes sections with different sorbents, intermediate throttles, and detectors.

The range of possible applications of composite columns can be extended by the following methods: by operating both sections under vacuum conditions, which combine large values of $\bar{P}_1/\bar{P}_2$ with adequate resolution; by operating the first section under near-atmospheric pressure and the second in a vacuum,[79,80] which offers (as before) a wider range of selectivity control and a saving in eluent without introducing experimental complications or allowing nonideality to appear in the carrier gas; by assembling combined variants of chromatography,[81] in particular by operating the first section in the supercritical fluid chromatography regime and the second in the barochromatography or traditional gas chromatography regime; by programming the pressure in the course of the analysis in one or both of the sections (for example, by varying the pressure at the inlet to the first section, by varying the throttle setting, by varying the pressure of the gas flow inserted between the sections or by varying the flow of

gas vented to the atmosphere); by combining the partition and the adsorption regime; by programming the temperature in one or both sections; by using sections of different diameter, including narrow packed columns and capillary columns; by inserting samples and standards at intermediate points (between the sections); by using several parallel sections; by extracting from the system some components or fractions separated in the first section; by combining barochromatography with other multistage schemes (reverse, semireverse, parallel exhaust, etc.).

References

1. E Klesper, A H Corwin, D A Turner *J. Org. Chem.* **27** 700 (1962)
2. M S Vigdergauz, A V Garusov, V A Ezrets, V I Semkin *Gazovaya Khromatografiya s Neideal'nymi Eluentami* (Gas Chromatography with Nonideal Eluents) (Moscow: Nauka, 1980)
3. *Sverkhkriticheskaya Flyuidnaya Khromatografiya* (Supercritical Fluid Chromatography) (Ed. R Smith) (Moscow: Mir, 1991)
4. M S Vigdergauz, A L Lobachev, I V Lobacheva, I A Platonov *Usp. Khim.* **61** 497 (1992); [*Russ. Chem. Rev.* **61** 267 (1992)]
5. C L Young *Chromatogr. Rev.* **10** 129 (1968)
6. P F Komissarov, D A Vyakhirev *Trudy po Khimii i Khimicheskoi Tekhnologii* Vol. 4 (Research on Chemistry and Chemical Technology) (Gor'kii, 1961) p. 485
7. Haruki Tatsuro *Burseki Kagaku* **9** 865 (1960)
8. A F Shlyakhov, in *Sbornik Nauchnykh Trudov po Gazovoi Khromatografii, No. 19* (Collected Scientific Papers on Gas Chromatography, No. 19) (Karpov Physicochemical Research Institute, 1973) p. 4
9. N W Davies *Anal. Chem* **56** 2618 (1984)
10. M S Vigdergauz, V I Semkin *Usp. Khim.* **40** 1073 (1971) [*Russ. Chem. Rev.* **40** 533 1971]
11. M S Vigdergauz, Sh M Rakhmankulov *Usp. Khim.* **44** 377 (1975) [*Russ. Chem. Rev.* **44** 176 1975]
12. A V Garusov, M S Vigdergauz *Usp. Khim.* **46** 928 (1977) [*Russ. Chem. Rev.* **46** 492 1977]
13. Fujinaga Taitiro, Kuwamoto Toory, Sugiura Kenji *Bull. Inst. Chem. Res. Kyoto Univ.* **58** 201 (1980); *Anal. Chim. Acta* **136** 175 (1982)
14. J C Giddings, M N Myers, L McLaren, R A Keller *Science* **162** 67 (1968)
15. V Harris, G Habgood *Gas Chromatography with Temperature Programming* (Translated into Russian) (Moscow: Mir, 1968)
16. V A Ferapontov, D E Bodrina, in *Khromatografiya* (Itogi Nauki i Tekhniki, T. 2) [Chromatography (Advances in Science and Engineering, Vol. 2)] (Moscow: Izd. VINITI, 1978) p. 107
17. M Martin, G Guiochon *C R Acad. Sci., Ser. 2* **294** 899 (1982); *Anal. Chem.* **54** 1533 (1982)
18. A van Es, J Rijks, C Cramers *J. Chromatogr.* **477** 19 (1989)
19. F M Shemyakin, E S Mitselovskii, D V Romanov *Khromatograficheskii Analiz* (Chromatographic Analysis) (Moscow: Goskhimizdat, 1955)
20. E J Ledet *Ind. Res. Develop.* **20** 161 (1978)
21. T A Brettell, R L Grob *Int. Lab.* **18** 14 (1985)
22. C J Barinaga, S O Farwell *J. High Resolut. Chromatogr.* **9** 388 (1986)
23. A A Zhukhovitskii, N M Turkel'taub *Gazovaya Khromatografiya* (Gas Chromatography) (Moscow: Gostoptekhizdat, 1962)
24. Yu I Arutyunov, M S Vigdergauz, USSR P. 1 343 349; *Byull. Izobr.* **37** 192 (1987)
25. M L Sazonov, in *Khromatografiya* (Itogi Nauki i Tekhniki, T. 2) [Chromatography (Advances in Science and Engineering, Vol. 2)] (Moscow: Izd. VINITI, 1979) p. 80
26. A A Zhukhovitskii, S M Yanovskii, V P Shvartsman, in *Khromatografiya* (Itogi Nauki i Tekhniki) [Chromatography (Advances in Science and Engineering)] (Moscow: Izd. VINITI, 1978) p. 49
27. D N Sokolov, G N Nesterenko *Zh. Anal. Khim.* **30** 2377 (1975)
28. V G Berezkhin, V R Alishoev, N B Nemirovskaya *Gazovaya Khromatografiya v Khimii Polimerov* (Gas Chromatography in Polymer Chemistry) (Moscow: Nauka, 1972)
29. A Goldup, G R Luckhurst, W T Swanton *Nature (London)* **193** 333 (1962)
30. D H Everett *Trans. Faraday Soc.* **61** 1637 (1965)
31. S T Sie, W van Beersum, G W A Rijnders *Sep. Sci.* **1** 459 (1966)
32. A J B Cruickshank, M L Windsor, C L Young *Proc. R. Soc. A* **295** 259 (1966)
33. A J B Cruickshank, B W Gainey, C P Hick, T M Letcher, R W Moody, C L Young *Trans. Faraday. Soc.* **65** 1014 (1969)
34. M S Vigdergauz, V I Semkin *J. Chromatogr.* **58** 95 (1971)
35. M S Vigdergauz, V I Semkin *Neftekhimiya* **9** 470 (1969)
36. L Sojak, M S Vigdergauz *Plunova Chromatografie Uhlovodiku Universita, Pardubice,* 1993
37. M S Vigdergauz, V I Semkin *Zh. Fiz. Khim.* **46** 691 (1972)
38. A V Kiselev, Ya I Yashin *Adsorbtsionnaya Gazovaya i Zhidkostnaya Khromatografiya* (Gas and Liquid Adsorption Chromatography) (Moscow: Khimiya, 1979)
39. K I Sakodynskii, L I Panina *Polimernye Sorbenty dlya Molekulyarnoi Khromatografii* (Polymeric Sorbents for Molecular Chromatography) (Moscow: Nauka, 1977)
40. R Kh Mar'yakhin, V A Ezrets, R V Vigalok, M S Vigdergauz, in *Uspekhi Gazovoi Khromatografii* (Advances in Gas Chromatography) (Kazan': Izd. Kazansk. Filiala Akad. Nauk SSSR, 1973) No. 3, p. 43
41. D H Desty, A Goldup, G R Luckhurst, W T Swanton, in *Gas Chromatography* (Ed. M van Swaay) (London: Butterworths, 1962), p. 67
42. A T James, A J P Martin *Biochem. J.* **50** 679 (1952)
43. S Trestianu *Rev. Roum. Chim.* **13** 1307 (1968)
44. S Trestianu *Cercetari Chim. Stud.* **17** 463 (1969)
45. C L Young *Trans. Faraday Soc.* **64** 1537 (1968)
46. K A Gol'bert, M S Vigdergauz *Vvedenie v Gazovuyu Khromatografiyu* (Introduction to Gas Chromatography) (Moscow: Khimiya, 1990)
47. J C Giddings, W A Manwaring, M N Myers *Science* **154** 146 (1966)
48. S Wicar, J Novak, N Ruseva-Ranshieva *Anal. Chem.* **43** 1945 (1971)
49. S Dincer, D C Bonner *Macromolecules* **11** 102 (1978)
50. S I Kirsh, N T Karabanov, M S Vigdergauz, in *Uspekhi Gazovoi Khromatografii* (Advances in Gas Chromatography) (Kazan': Izd. Kazansk. Filiala Akad. Nauk SSSR, 1978) No. 5, p. 58
51. S R Lipsky, R A Landown, J E Lovelock *Anal. Chem.* **31** 852 (1959)
52. V V Ugrozov *Zh. Fiz. Khim.* **68** 2511 (1987)
53. R Collomb, B Devallez, J-M Vergnaud *C. R. Acad. Sci. C* **277** 1 (1973)
54. N V Sterkhov, S S Pavlov, V A Ferapontov, V P Chizhkov *Zh. Anal. Khim.* **37** 1521 (1982)
55. S Nygren *J. Chromatogr.* **366** 1 (1986)
56. Yu A Sultanovich, K I Sakodynskii, A P Nechaev *Dokl. Akad. Nauk SSSR* **271** 661 (1983)
57. B Devallez, J Guion, G Cognet *J. Chromatogr.* **463** 153 (1989)
58. A A Zhukhovitskii, M S Selenkina, N M Turkel'taub *Zh. Fiz. Khim.* **36** 993 (1962)
59. M S Vigdergauz, M I Afanas'ev *Zh. Anal. Khim.* **19** 1122 (1964)
60. M S Vigdergauz, R V Vigalokh *Neftekhimiya* **11** 141 (1971)
61. K A Gol'bert, M S Vigdergauz *Kurs Gazovoi Khromatografii* (Textbook of Gas Chromatography) (Moscow: Khimiya, 1967)
62. D R Deans, I Scott *Anal. Chem.* **45** 1137 (1973)
63. D R Deans *Chromatographia* **1** 18 (1968)
64. R E Kaiser, R I Reider *Labor. Praxis* **10** 1130 (1985); **10** 1133 (1986)
65. R E Kaiser, R I Reider, L Leming, L Blomberg, P Kusz *J. High Resolut. Chromatogr.* **8** 580 (1985)
66. L S Ettre, J V Hinshaw, in *Abstracts of Papers to the Pittsburgh Conference on Analytical Chemistry and Applied Spectroscopy* (Pittsburgh, PA, 1986) p. 1100
67. J V Hinshaw, L S Ettre, W Seferovic, in *Abstracts of Papers to the Pittsburgh Conference on Analytical Chemistry and Applied Spectrometry* (Pittsburgh, PA, 1987) p. 461
68. V A Ezrets, M S Vigdergauz *Zh. Anal. Khim.* **31** 2013 (1976)
69. V A Ezrets, M S Vigdergauz *Zavod. Lab.* **43** 277 (1977)
70. L Rohrschneider *Z. Anal. Chem.* **170** 256 (1959)
71. A V Bulanova, M S Vigdergauz, T A Garanina *Zh. Anal. Khim.* **45** 696 (1990)
72. M S Vigdergauz, A V Bulanova *Zh. Anal. Khim.* **43** (1) 102 (1988)
73. M S Vigdergauz *Zh. Anal. Khim.* **39** 151 (1984)
74. M S Vigdergauz, L V Semenchenko, V A Ezrets, Yu N Bogoslovskii *Kachestvennyi Gazokhromatograficheskii Analiz* (Qualitative Gas-chromatographic Analysis) (Moscow: Nauka, 1978)

75. M S Vigdergauz, M I Afanas'ev *Khim. Tekhnol. Topliv Masel* **12** 28 (1963)
76. M S Vigdergauz *Gazovaya Khromatografiya kak Method Issledovaniya Nefti* (Gas Chromatography as a Method of Studying Petroleum) (Moscow: Nauka, 1973)
77. M S Vigdergauz, P K Lange, A V Bulanova, S V Kurbatova, E A Kolosova, Fr. P 1 744 646; *Byull. Izobr.* **24** (1992)
78. Yu T Zvonareva, V M Obraztsov, M S Vigdergauz in *Gazovaya Khromatografiya, T. 7* (Gas Chromatography, Vol. 7) (Moscow: NIITEKHIM, 1967) p. 54
79. M S Vigdergauz, A V Bulanova, Fr. P 1 777 074; *Byull. Izobr.* **43** (1992)
80. A V Bulanova, M S Vigdergauz, T B Bashkinova *Zh. Fiz. Khim.* **67** 854 (1993)
81. M S Vigdergauz, in *8th Danube Symposium on Chromatography (Abstracts)* Warsaw, 1991 Paper Tu-0-4

Russian Chemical Reviews **62** (8) 703–727 (1993)
©1993 Russian Academy of Sciences and Turpion Ltd

UDC 541.18+532.6

Thermodynamics of free and of interacting curved interfaces in liquid films

V G Babak

Contents

I. Introduction	703
II. Thermodynamic description of free curved interfaces	704
III. Equilibrium of interfaces in the bulk meniscus region of a liquid film	713
IV. Thermodynamic description of interacting interfaces in the transition region of a liquid film	716
V. Conclusions	726

Abstract. Publications on the thermodynamics of free and of interacting curved interfaces in liquid films are reviewed. The approaches of Gibbs, Boruvka–Neumann, and others to the determination of the surface tension of free curved surfaces are compared. The dependences of differently defined interfacial tensions on the radius of curvature of the interface are obtained. The fundamental equilibrium equations for systems containing curved surfaces, including the transition region of the liquid film, are proposed. A generalised invariant of the profile of the liquid film is obtained, and used to derive all the known equilibrium equations for a liquid film with a bulk meniscus, including the equation for a liquid drop on a solid surface and precise analytical expressions describing the line tension for different thermodynamic models of the liquid film. The theory of the adhesion of fluid particles, which relates the adhesion force and the potential energy of the interaction between deformable particles to the parameters of the disjoining pressure isotherm, is discussed. The bibliography includes 88 references.

I. Introduction

Emulsion and foam films are formed at the contact between two liquid drops or gas bubbles (Fig. 1, phase β) in a liquid dispersion medium (Fig. 1, phase α).

The plane-parallel part of a liquid emulsion or foam film at the centre of the contact region is characterised by the equilibrium condition

$$\Pi = P_\beta - P_\alpha , \qquad (1)$$

where P_β and P_α are the hydrostatic pressures in the phases β and α respectively, and Π is the disjoining pressure in the film.

In the bulk meniscus region of the liquid film the interaction between the interfaces vanishes (i.e. $\Pi = 0$). Therefore the curvature of these surfaces is constant, and is determined exclusively by the difference between the hydrostatic pressures $P_\beta - P_\alpha$.

The profile of the liquid film $H(r)$ in the region of the meniscus [or the profile of the free curved surface $z(r)$] contains information on the contact force (compressive, f_p, or repulsive, f_a) applied to the fluid particles,[1–3] and on the integral characteristic of the surface forces [a large thermodynamic potential $\Delta\Omega(H_f)$]. Furthermore the experimental dependence of the contact angle θ_f on the radius of the film r_f contains information on the line tension in the liquid film, i.e. on the form of the profile of the disjoining pressure isotherm $\Pi(H)$ in the transition region.[4–6].

Unlike the region of the bulk meniscus the curvature of the interfaces in the transition region of a liquid film is not constant but shows a complicated dependence on the local thickness H of the film profile. Therefore the profile of the meniscus in the transition region of a liquid film contains information on the $\Pi(H)$ isotherm,[2, 3] which can be obtained from experimental plots of the contact angle against the thickness of the film in the transition region [$\phi(H)$]. Unfortunately the length of the transition region of the film is small, and therefore the disjoining pressure isotherm $\Pi(H)$ cannot be determined to within an acceptable precision from the $H(r)$ profile in this region, measured for example by the so-called topographic method.[7] In the region of the bulk meniscus this profile can be determined very accurately for small contact angles, and it is effectively the only meaningful source of information on surface forces.

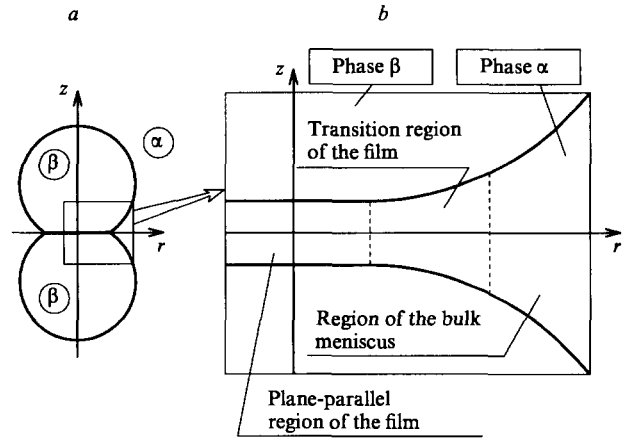


Figure 1. Thermodynamics of liquid films: (*a*) symmetrical microscopic liquid film (emulsion or foam) produced between two identical fluid particles (liquid or gaseous) of phase β in the liquid phase α; (*b*) central plane-parallel region, transition region, and region of the bulk meniscus (containing two non-interacting curved interfaces in the symmetrical liquid film).

V G Babak, Moscow State Correspondence Institute of Food Industry, Zemlyanoi val 73, 109803 Moscow. Fax (7-095) 292 65 11

Received 3 March 1993
Uspekhi Khimii **62** (8) 747–773 (1993); translated by J I Carasso

The thermodynamics of free curved surfaces in liquid films were established by Gibbs,[8] and further developed by Buff,[9] Ono and Kondo,[10] Rusanov,[11-13] Rowlinson and Widom,[14] Ivanov and Kralchevsky,[15] Markin et al.,[16, 17] Babak,[5, 18] and others.[19-21]

The next step forward in the development of the thermodynamics of free curved surfaces was its extension to the transition region of emulsion and foam films of variable thickness, in which a disjoining pressure is generated and which smoothly change into a plane-parallel film on one side and into a system of two free (non-interacting) curved interfaces in the region of the bulk meniscus.[1, 5, 18, 22] Clearly, the best thermodynamic model for this generalisation is the liquid film model, based on the assumption of two interfaces (in the Gibbs sense) defining a layer of finite thickness of a liquid reference phase (the Gibbs comparison phase). The thermodynamics of plane-parallel liquid films based on this model were developed by Rusanov,[11-13] and those of free curved interfaces in the region of the bulk meniscus by Gibbs.[8] However, neither of these models allows for the presence of a transition region characterised by a surface tension gradient.[1, 5, 18] As a result, the thermodynamics of plane-parallel liquid films and those of free curved surfaces are not mutually consistent.

The two approaches can be reconciled in terms of the thermodynamics of the transition region of the liquid film,[1, 5, 18] which naturally reduce to the thermodynamics of plane-parallel liquid films and to the thermodynamics of free curved interfaces in the appropriate regions of the system.

The aim of the present review is to discuss recent work on the thermodynamics of free and of interacting curved interfaces in emulsion and in foam films.

II. Thermodynamic description of free curved interfaces

The study of curved interfaces reveals a number of problems associated with the development of the thermodynamics of the transition region in thin liquid films.

First, the fundamental equation of the system containing a curved interface is no longer invariant with respect to the method of localisation of the curved interface. This is formally shown by the appearance in the fundamental equation of terms relating to the work of bending and twisting of the interface (whose magnitude depends on the mode of localisation of the interface).

Second, we find a problem in determining the interfacial tension, whose magnitude depends both on the position of the interface and on the method of selecting the reference system used to define the interfacial tension. The different possible choices of a reference system to determine the interfacial tension led to a discussion of the validity of the generalised Laplace equation.[15, 16, 19-21] We note that correct allowance for the bending and twisting moments in the generalised Laplace equation is essential also in the case of liquid particles with low and ultra-low interfacial tension, such as micelles, vesicles, and drops of a coacervate phase.

1. Cylindrical free interfaces

We shall begin our discussion of the thermodynamics of curved interfaces with the simplest case of cylindrical surfaces, i.e. surfaces having only one principal radius of curvature, thus avoiding mathematical difficulties due to the need to allow for the second radius of curvature without loss of generality.

Systems containing a free cylindrical interface. Let us consider a multicomponent system including two macroscopic phases α and β separated by a free cylindrical interface (Fig. 2). To simplify the discussion we shall ignore gravity, and we shall assume that the hydrostatic pressures P_α and P_β in the two phases are known. All the parts of the system in equilibrium have the same temperature T and the same chemical potential μ_i of the i-th component [$i = 1, 2, \ldots, N$; N is the number of components, of which the total number of moles (N_i) in the system is controlled by the material source ν_i].

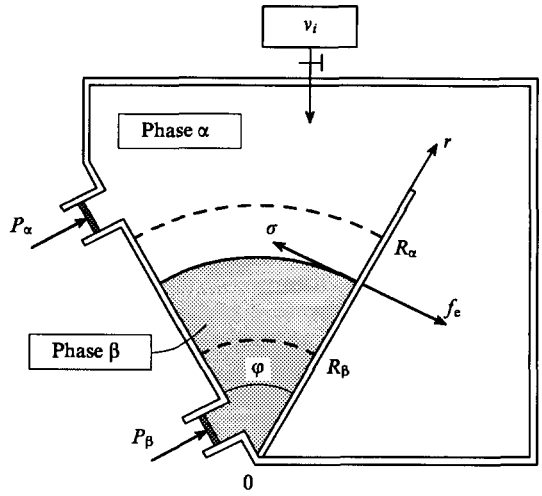


Figure 2. Thermodynamic system including a fluid (liquid or gaseous) phase β and a liquid phase α separated by a curved free cylindrical interface.

We shall also assume that the above system is in thermodynamic equilibrium with an open subsystem bounded on the right by a mobile side-wall (Fig. 2) forming a dihedral angle φ with the fixed left-hand wall, and by two arbitrarily located dividing surfaces having radii R_α and R_β (enclosing the interface) and two flat end faces forming a layer of thickness l_z. The moment of the external force f_e balances the moments of the interfacial tension σ and of the pressure force P_α and P_b acting on the system.

Hydrostatic description of the curved interface. The capillary properties of curved interfaces have been widely discussed in the framework of local thermodynamics.[9, 10-12, 16, 23, 24]

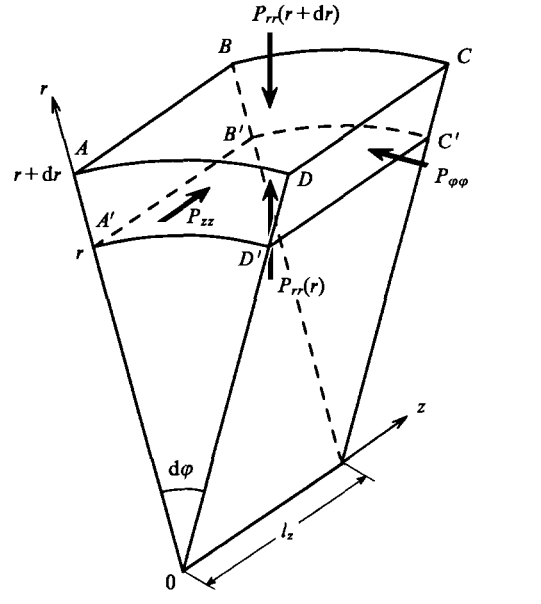


Figure 3. Element of volume of the thermodynamic system containing a cylindrical interface.

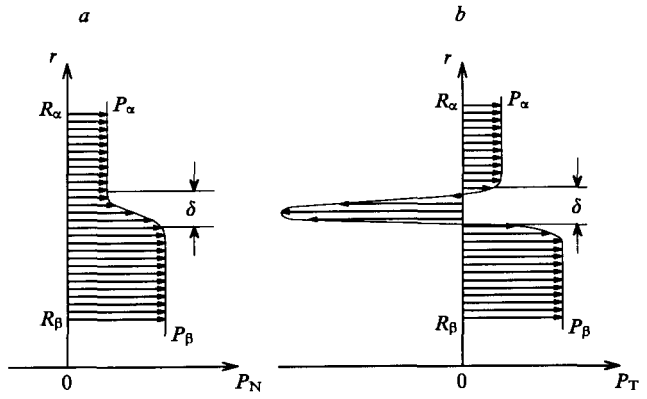


Figure 4. Distribution of the normal P_N (*a*) and of the tangential P_T component (*b*) of the hydrostatic pressure tensor in the transition region of a curved interface.

We shall use the following symbols for the non-zero components of the hydrostatic pressure $\hat{P}$ in cylindrical coordinates (Fig. 3):

$$P_N(r) = P_{rr}\,, \quad P_T(r) = P_{zz} = P_{\varphi\varphi}\,.$$

An idealised plot of the dependence of these components on the radius r is shown in Fig. 4. Unlike the planar interface[22] the normal component of the pressure tensor $P_N(r)$ (see Fig. 4*a*) varies sharply in a narrow region of the interfacial transition layer of thickness δ (see Fig. 4*b*). In the region of the bulk phases α and β the two components are equal to P_α and P_β respectively.

In cylindrical coordinates the hydrostatic equilibrium condition

$$\mathrm{div}\hat{P} = 0$$

becomes

$$\frac{dP_N}{dr} + \frac{P_N}{r} = \frac{P_T}{r} \tag{2}$$

and can be obtained from the mechanical equilibrium condition of the element of volume $ABCDA'B'C'D'$ (see Fig. 3) which experiences the pressure components $P_N = P_{rr}$ and $P_T = P_{\varphi\varphi} = P_{zz}$. Equating to zero the projection of the resulting force in the r direction and noting that

$$P_N(r + dr) = P_N(r) + \frac{dP_N}{dr}dr\,,$$

we find

$$-\left[P_{rr} + \frac{dP_{rr}}{dr}dr\right] l_z(r + dr)d\varphi + P_{rr}(r) l_z r\,d\varphi + P_{\varphi\varphi} l_z\,dr\,d\varphi = 0\,,$$

whence we obtain Eqn (2), which can also be rewritten

$$\frac{d(rP_N)}{dr} = P_T\,, \tag{3}$$

or

$$\frac{d(r^2P_N)}{dr} = r(P_N + P_T)\,.$$

The mechanical equilibrium condition (2) is sometimes used in the form[25]

$$\frac{dP_N}{dr} = (P_T - P_N)k_1(r)\,, \tag{4}$$

where $k_1(r) = 1/r$ is the curvature of the interface.

The integral form of the equilibrium Eqn (4) is

$$P_\alpha - P_\beta = \int_{R_\beta}^{R_\alpha} [P_T(r) - P_N(r)]k_1(r)\,dr\,, \tag{5}$$

with integration limits R_α and R_β in the region of the macroscopic phases where the difference $(P_T - P_N)$ is zero, since the pressures P_T and P_N are P_α and P_β in the phases α and β respectively. Eqn (5) can also be obtained by integrating Eqn (3):

$$P_\alpha R_\alpha - P_\beta R_\beta = \int_{R_\beta}^{R_\alpha} P_T(r)\,dr\,. \tag{6}$$

Interfacial tension. Using the method of Gibbs excesses[8] we shall replace the real open subsystem containing a cylindrical interface (Fig. 5*a*) by an idealised system (Fig. 5*b*) including two reference phases α and β and an interface (according to Gibbs) having an arbitrary radius R.

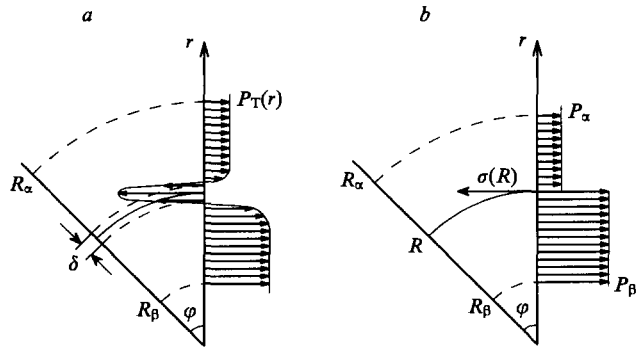


Figure 5. Definition of the interfacial tension of a cylindrical interface: (*a*) distribution of the pressure component $P_T(r)$ near the interface; (*b*) result of replacing the interface by a Gibbs cylindrical dividing surface.

The mechanical moment M applied by the real system to the right-hand (mobile) wall is

$$M = \int_{R_\beta}^{R_\alpha} P_T(r) r\,dr\,. \tag{7}$$

The mechanical moment is referred to unit length l_z of the cylindrical layer of the system (see Fig. 3).

The idealised system acts on a unit length of the mobile wall with a mechanical moment M^{id} equal to

$$M^{id} = \int_{R_\beta}^{R} P_\beta r\,dr + \int_{R}^{R_\alpha} P_\alpha r\,dr - \sigma(R)R\,, \tag{8}$$

where $\sigma(R)$ is the interfacial tension of the cylindrical surface of radius R. From the condition of mechanical equivalence between the idealised and the real system, i.e. for $M^{id} = M$, we obtain the following expression for the interfacial tension

$$\sigma(R) = \int_{R_\beta}^{R} [P_\beta - P_T(r)]\frac{r}{R}dr + \int_{R}^{R_\alpha} [P_\alpha - P_T(r)]\frac{r}{R}dr\,. \tag{9}$$

According to Kondo[26] the function $\sigma(R)$ has a single minimum σ_t at a radius R_t of the cylindrical surface, which Gibbs called the tension surface.[8]

The fundamental equation of the system containing a cylindrical interface. We shall derive the fundamental equation of a system containing a curved interface by considering the element of volume $ABCDA'B'C'D'$ shown in Fig. 3, of thickness $AA' = h$

and having a base area $A(r) = rl_z\,d\varphi$. The work done by the external forces in deforming this volume (at constant T and μ_i) is

$$\delta W = -P_N(r)A(r)\delta r - P_T(r)h\,\delta A(r)$$
$$= -P_N(r)\delta V + [P_N(r) - P_T(r)]h\,\delta A(r)\,, \qquad (10)$$

where $\delta V = A(r)\delta r + h\,\delta A(r)$ is the variation of the volume. Integrating (10) over the whole volume of the open subsystem gives

$$\Omega = \left\{-\int_{R_\beta}^{R_\alpha} P_N(r)r\,dr + \int_{R_\beta}^{R_\alpha}[P_N(r) - P_T(r)]r\,dr\right\}\varphi$$
$$= \left[\int_{R_\beta}^{R_\alpha} P_T(r)r\,dr\right]\varphi\,. \qquad (11)$$

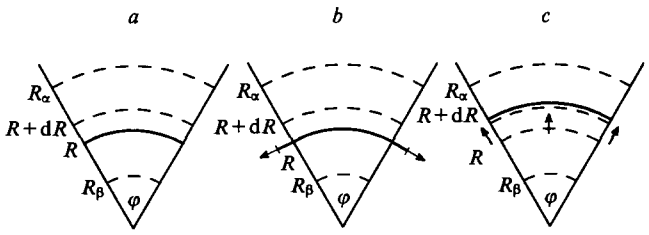


Figure 6. Derivation of the fundamental equation of a system containing a curved cylindrical surface of radius R. The deformation of the dividing surface produced by a change in the radius of curvature from R to $R + dR$ (*a*) includes the work of simple extension of the surface for constant R (*b*) and the work of simple bending of the surface for constant area (*c*).

Let us now consider an element of volume of the idealised system (Fig. 6) including a cylindrical interface of radius R, and let us calculate the work δW performed by the external forces in deforming this surface. It can be arbitrarily divided into four parts: the work of deformation of the phase α ($-P_\alpha\delta V_\alpha$, Fig. 6*a*), the work of deformation of the phase β ($-P_\beta\delta V_\beta$, Fig. 6*a*), the work of simple expansion of the interface with a constant radius of curvature $R[\sigma(R)\delta A(R)$, Fig. 6*b*], the work of simple bending of the interface with a constant area and a change in curvature of δk_1 ($C_1\delta k_1$, Fig. 6*c*).†

Thus the work of the external forces during the deformation of an element of volume of the idealised system (which includes the interface) can be written

$$\delta W = -P_\beta\,\delta V_\beta - P_\alpha\,\delta V_\alpha + \sigma(R)\delta A(R) + c_1A(R)\delta k_1\,. \qquad (12)$$

The fundamental equation for this system in the general case is

$$d\Omega^{id} = -S\,dT - \sum_i N_i\,d\mu_i - P_\beta dV_\beta - P_\alpha dV_\alpha$$
$$+\sigma(R)dA(R) + c_1A(R)dk_1\,, \qquad (13)$$

where S is the entropy of the open system.

By integrating this equation over the extensive parameters we obtain an expression for the grand thermodynamic potential of the idealised system:

$$\Omega^{id} = -P_\beta V_\beta - P_\alpha V_\alpha + \sigma(R)A(R)\,, \qquad (14)$$

† In the Gibbs terminology[8] the coefficient C_1 has the dimensions of J m^{-1}. Other workers refer this coefficient to unit surface area and express it as $C_1 = c_1A(R)$. In the case of a cylindrical surface the physical significance of the coefficient c_1 is that of a bending moment referred to unit width of the cylindrical surface.

which is easily converted into a form convenient for a comparison with Eqn (11):

$$\Omega^{id} = \left[-\int_{R_\beta}^{R} P_\beta r\,dr - \int_{R}^{R_\alpha} P_\alpha r\,dr + \sigma(R)R\right]\varphi\,. \qquad (15)$$

From the condition of energy equivalence of the real and the idealised system, $\Omega = \Omega^{id}$, we can obtain the expression (9) for the interfacial tension $\sigma(R)$.

Fundamental equation of a cylindrical separating surface. The separating surface method is based on the presentation of the extensive parameters Ω, S, V, N_i as sums of bulk parts, relating to the reference phases α and β, and excesses, relating to the separating surface. In this convention the fundamental equation (13) of the system can be written as follows for the reference phases:

$$d\Omega = d\Omega_\alpha + d\Omega_\beta + d\Omega_s\,, \qquad (16)$$

where

$$d\Omega_\alpha = -S_\alpha dT - \sum_i N_{i\alpha}d\mu_i - P_\alpha dV_\alpha\,, \qquad (17)$$

and

$$d\Omega_\beta = -S_\beta dT - \sum_i N_{i\beta}d\mu_i - P_\beta dV_\beta\,, \qquad (18)$$

where

$$d\Omega_s = -S_s dT - \sum_i N_{is}d\mu_i + \sigma(R)dA(R) + c_1A(R)dk_1 \qquad (19)$$

is the fundamental equation of the free curved (cylindrical) separating surface.

Eqn (19) differs from the corresponding equation for a planar separating surface[22] by the term $c_1A(R)dk_1$, equal to the work done by the external forces during the simple bending of the separating surface, and also by the dependence of the interfacial tension $\sigma(R)$ on the localisation of the curved separating surface. We note that the fundamental equation of the planar interface contains the interfacial tension σ_0, which is invariantly related to the position of the separating surface.[22]

The Gibbs–Duhem equation for a cylindrical separating surfaces. Integrating Eqn (19) over the parameter $A(R)$ for constant T, μ_i, and k_i gives

$$\Omega_s = \sigma(R)A(R)\,. \qquad (20)$$

By differentiating Eqn (20) and combining it with (18) we obtain the Gibbs–Duhem equation for this surface,

$$A(R)d\sigma(R) = -S_s dT - \sum_i N_{is}d\mu_i + c_1A(R)dk_1\,,$$

which can be written

$$d\sigma(R) = -s_s dT - \sum_i \Gamma_i\,d\mu_i + c_1dk_1\,, \qquad (21)$$

where $s_s = S_s/A(R)$ and $\Gamma_i = N_{is}/A(R)$ are the entropy excess and the excess in the number of moles of the ith component respectively referred to unit area of the separating surface.

Unlike the Gibbs–Duhem equation for a flat interface Eqn (21) is not invariant with respect to the position of the curved separating surface.[22]

Eqn (21) defines the relationship between the excesses of the thermodynamic quantities, but it contains no information on the condition of the equilibrium between this separating surface and the bulk reference phases α and β. This equilibrium condition can

be obtained only from the fundamental equation for the whole system containing the curved interface.

Fundamental equilibrium equation of a system containing a cylindrical interface. This equation can be obtained by minimising the grand thermodynamic potential of the system (13). The minimisation can be carried out by two methods: the imaginary displacement of the separating surface, i.e. a change in the radius R of this surface for a fixed physical state of the system, determined by the parameters T, μ_i, P_α, and P_β (Kondo's method[26]), or a real deformation of the separating surface with changes in the physical parameters P_β and P_α but constant T and μ_i (the method of Gibbs[8]).

Both methods lead to the same final equilibrium equation for a system containing a cylindrical interface.

By using Kondo's method,[26] i.e. by varying the grand thermodynamic potential of the system Ω^{id} in Eqn (14) over the radius R of the separating surface and equating the variation $\sigma\Omega^{id}$ to zero, we obtain

$$-P_\beta\left\{\frac{\partial V_\beta}{\partial R}\right\}\delta R - P_\alpha\left\{\frac{\partial V_\alpha}{\partial R}\right\}\delta R + \sigma R\left\{\frac{\partial A(R)}{\partial R}\right\}\delta R + A(R)\left\{\frac{\partial\sigma(R)}{\partial R}\right\}\delta R = 0\,,$$

where the braces denote a virtual differentiation. Allowing for the self-evident geometric relations

$$\frac{\partial V_\beta}{\partial R} = A(R)\,;\quad \frac{\partial V_\alpha}{\partial R} = -A(R)\,;\quad \frac{\partial A(R)}{\partial R} = \frac{A(R)}{R}\,; \tag{22}$$

we can convert the resulting equation into the fundamental equilibrium condition for a system containing a cylindrical separating surface:

$$\frac{\sigma(R)}{R} + \left\{\frac{\delta\sigma(R)}{\partial R}\right\} = P_\beta - P_\alpha\,. \tag{23}$$

For the tension surface, where $\partial\sigma(R)/\partial R = 0$, $R = R_t$, and $\sigma(R_t) = \sigma_t$ (the subscript t denoting quantities referred to the tension surface) we obtain from (23) the Laplace equation for a cylindrical tension surface:

$$\frac{\sigma_t}{R_t} = P_\beta - P_\alpha\,. \tag{24}$$

By minimising Eqn (13) with respect to δR (for a real deformation of the interface) with constant T and μ_i we arrive at

$$-P_\beta\frac{\partial V_\beta}{\partial R}\delta R - P_\alpha\frac{\partial V_\alpha}{\partial R}\delta R + \sigma R\frac{\partial A(R)}{\partial R}\delta R + c_1 A(R)\frac{\partial k_1}{\partial R}\delta R = 0\,.$$

Using the geometric relations (22) we can convert this equation into the fundamental equilibrium equation for a system containing a cylindrical separating surface:

$$\frac{\sigma(R)}{R} + c_1\frac{\partial k_1}{\partial R} = P_\beta - P_\alpha\,. \tag{25}$$

According to Gibbs[8] a separating surface having a zero bending moment is called a tension surface. On such a surface $c_1 = 0$, and Eqn (25) yields the Laplace equation (24).

Since according to the Gibbs–Duhem equation (21) we can write

$$c_1 = \left.\frac{\partial\sigma(R)}{\partial k_1}\right|_{T,\,\mu_i}\,, \tag{26}$$

Eqn (25) can be expressed as

$$\frac{\sigma(R)}{R} + \frac{\partial\sigma(R)}{\partial R} = P_\beta - P_\alpha\,. \tag{27}$$

Unlike Eqn (23) this equation contains the real derivative $\partial\sigma(R)/\partial R$.

By using the obvious relationship

$$\frac{\partial k_1}{\partial R} = -\frac{1}{R^2} = -k_1^2$$

we can convert (25) into

$$k_1\sigma(R) - c_1k_1^2 = P_\beta - P_\alpha\,, \tag{28}$$

which is known as the Gibbs–Kelvin equation for a system containing a cylindrical separating surface.[9, 25] For a tension surface ($c_1 = 0$) the Gibbs–Kelvin equation is converted into the simpler Laplace equation

$$k_1\sigma_t = P_\beta - P_\alpha\,. \tag{29}$$

We note that Boruvka and Neumann[19] have doubted the validity of Eqn (28). They suggest that in the case of cylindrical surfaces the Laplace equation (29) is satisfied for any position of the separating surface.

The problem of determining the interfacial tension of curved surfaces. During the last decade the work of Boruvka and Neumann[19] has been widely quoted and discussed in relation to proposed generalisations of the Laplace equation to include non-spherical surfaces.[15, 16, 20, 21] Let us examine the main topics of these discussions.

By using their fundamental equation for a system containing a non-spherical interface with two different principal radii of curvature Boruvka and Neumann[19] obtained a fundamental equilibrium equation for the system (of the Laplace equation type), which in the case of a cylindrical separating surface in any position (i.e. of a surface having only one principal radius of curvature) takes the form

$$k_1\sigma_{BN} = P_\beta - P_\alpha\,. \tag{30}$$

They called σ_{BN} the interfacial tension,[19] and did not consider the possibility of inconsistency between the definitions of interfacial tension given by Eqns (30) and (28). [We shall arbitrarily call the interfacial tension in formula (28) the Gibbs interfacial tension σ_G.] Eqn (28) in the form

$$k_1\sigma_G - c_1k_1^2 = P_\beta - P_\alpha \tag{31}$$

was criticised by Boruvka and Neumann, who believed it to be incorrect. The resulting controversy[20, 21] was widened by Markin et al.,[16] who pointed out that the interfacial tensions σ_G and σ_{BN} in the expressions (30) and (31) are defined in different ways, and therefore the two formulae for the generalised Laplace equation of non-spherical surfaces are both correct if allowance is made for the difference between σ_G and σ_{BN}. These workers[16] obtained expressions for σ_G and σ_{BN} within the scope of local thermodynamics and established a relationship between these quantities. For a cylindrical separating surface this relationship is

$$\sigma_G = \sigma_{BN} + c_1k_1\,. \tag{32}$$

We shall examine the physical meaning of the definitions of σ_G and σ_{BN} by considering a cylindrical separating surface.

From the fundamental Eqn (19) we obtain an expression for σ_G which is identically equal to $\sigma(R)$ for a cylindrical surface:

$$\sigma_G = \left.\frac{\partial\Omega_s}{\partial A}\right|_{T,\,\mu_i,\,k_1}\,. \tag{33}$$

A special feature of this definition is that the interfacial tension σ_G is interpreted as the increment of the specific excess of the grand thermodynamic potential resulting from an increase in the area $A(R)$ of a curved (rather than a planar) separating surface

having a constant curvature $k_1 = 1/R$. This means that σ_G includes both the intrinsic work of formation of a new separating surface and the work done in bending it. In fact, the interfacial tension σ_G is defined in terms of a reference system which includes the two phases β and α (with different hydrostatic pressures P_β and P_α: $P_\beta > P_\alpha$, see Fig. 2) and the curved separating surface.

Boruvka and Neumann used as a standard a hypothetical state of the system in which the interfacial surface has a zero curvature but the pressures in the phases α and β are different. In spite of the fact that this state of the system is not realisable in practice it allows an unambiguous definition of the interfacial tension, which we shall arbitrarily denote σ_{BN}:

$$\sigma_{BN} = \int_{R_\beta}^{R} [P_\beta - P_T(r)]dr + \int_{R}^{R_\alpha} [P_\alpha - P_T(r)]dr \,. \tag{34}$$

We note that an expression for σ_G [Eqn (9)] was obtained by using the principle of mechanical equivalence of the real and the idealised system, i.e. by equating the moments of the forces M and M^{id}, and that the expression for σ_{BN} follows formally from the condition of equality of the forces f and f^{id} which act on the side surface separating the real from the idealised system:

$$f = \int_{R_\beta}^{R_\alpha} P_T(r)dr \,;\; f^{id} = \int_{R_\beta}^{R} P_\beta dr + \int_{R}^{R_\alpha} P_\alpha dr - \sigma_{BN} \,. \tag{35}$$

According to the fundamental Eqn (19) the work done by external forces in increasing the area $A(R)$ of a cylindrical separating surface of radius R (with constant T, μ_i, and k_1) is $\sigma_G dA(R)$, as shown in Fig. 7*a*. According to Boruvka and Neumann[19] σ_{BN} is defined as the work which must be expended to create a unit area of planar interface by the deformation of the system illustrated in Fig. 7*b* (with constant T, μ_i, P_α, and P_β).

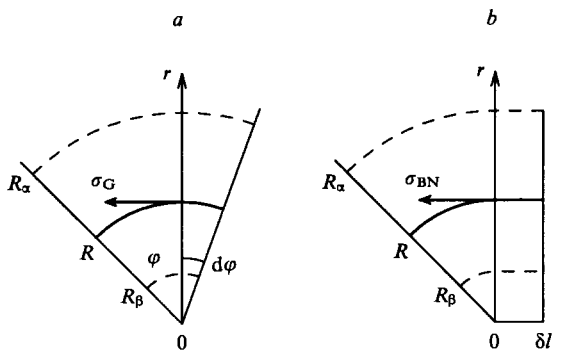


Figure 7. Illustration of the difference between the Gibbs (*a*) and the Boruvka–Neumann (*b*) definition of the interfacial tension.

The following expression has been proposed[19] for the fundamental equation in the case of the cylindrical separating surface:

$$d\Omega_s = -S_s dT - \sum_i N_{is} d\mu_i + \sigma_{BN} dA + c_1 d\tilde{K}_1 \,, \tag{36}$$

where

$$\tilde{K}_1 = \int_A k_1 dA \tag{37}$$

is the extensive parameter of the curvature, corresponding to the work needed to bend the separating surface.

It was also suggested[19, 21] that the free energy Ω_S is a uniform first-order function of the parameter $\tilde{K}_1$. Rowlinson rejected this suggestion,[20] and doubted the validity of the fundamental equation for the separating surface in the form of Eqn (36). The formal thermodynamic definition of σ_N follows from Eqn (36):

$$\sigma_{BN} = \left.\frac{\partial \Omega_s}{\partial A}\right|_{T, \mu_i, \tilde{K}_1} \,. \tag{38}$$

Since in the case of a cylindrical surface the right-hand side of Eqn (37) can be expressed as $k_1 A(R)$ we can apply Euler's theorem of uniform functions to Eqn (36) and write

$$\Omega_s = \sigma_{BN} A + c_1 \tilde{K}_1 \,. \tag{39}$$

By comparing (39) with the expression (20) previously obtained we obtain a relationship between σ_G and σ_{BN} [Eqn (32)]. Thus σ_{BN} is equal to the specific excess free energy at constant T and μ_i referred to unit area of a flat dividing surface, and σ_G includes also the excess free energy associated with the deformation (change in curvature) of the dividing surface.[16]

Dependence of the interfacial tensions on the radius of the dividing surface. The interfacial tensions σ_G and σ_{BN} depend on the method of localisation of the curved surfaces, i.e. on the subjective choice of a radius of curvature R for these surfaces. Analytical expressions for the functions $\sigma_G(R)$ and $\sigma_{BN}(R)$ in the case of cylindrical dividing surfaces can be obtained by using in the calculation an idealised function $P_T^0(r)$ in the form of a rectangular well with parameters Π_0 and Δ (Fig. 8*a*). The superscript '0' shows that the function $P_T^0(r)$ corresponds to a standard state, i.e. a flat dividing surface and pressures $P_\alpha = P_\beta$. Increasing the pressure P_β gives the function $P_T^0(r)$ a new form (Fig. 8*b*).

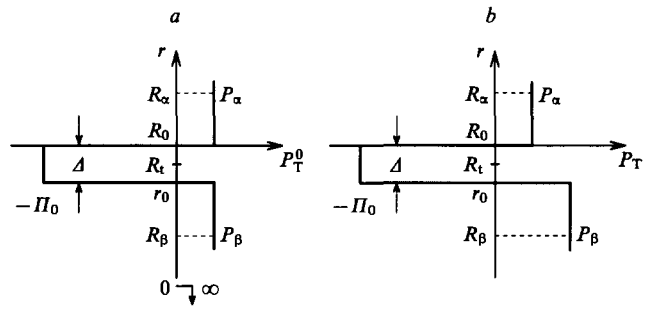


Figure 8. Representation of the function $P_T(r)$ as a rectangular well for a flat (*a*) and a curved interface (*b*).

One of the problems met when studying the bending of the interfacial surface is the ambiguous dependence of the parameters of the function $P_T(r)$ on the pressure P_β. In particular, it is not clear whether an increase in the pressure P_β affects the depth of the minimum (Π_0) in the $P_T(r)$ curve or the width Δ of the rectangular well, and we cannot describe the lower branch of the $P_T(r)$ curve (on the side of the phase β) analytically even when an analytical form of this curve is known for the $P_T^0(r)$ function when $P_\alpha = P_\beta$.

The interfacial tension σ_G and σ_{BN} can be calculated numerically when a complete and unambiguous description of the function $P_T(r)$ is available for any pressure P_β [i.e. when the function $P_T(r)$ is determined as a functional]. In the calculations shown below it is assumed that the parameters Π_0 and Δ of the function $P_T(r)$ are unaffected by an increase in the pressure P_β.

In particular, if the physical radius of the drop (in this case, a 'cylindrical' drop) is known, i.e. if we know the distance from the axis of curvature to some characteristic point of the $P_T(r)$ curve (which could be the radius r_0 or R_0 in the case of the rectangular well shown in Fig. 8*b*), we can use the hydrostatic equilibrium condition ($\operatorname{div} \hat{P} = 0$) to determine unambiguously the function

$P_N(r)$, and if the pressure P_α in the phase α is known the previously unknown pressure P_β in the phase β can be obtained from Eqn (6). Then, once P_β is known, the formulae (9) and (34) can be used to find the interfacial tensions σ_G and σ_{BN} for any radius R of the dividing surface.

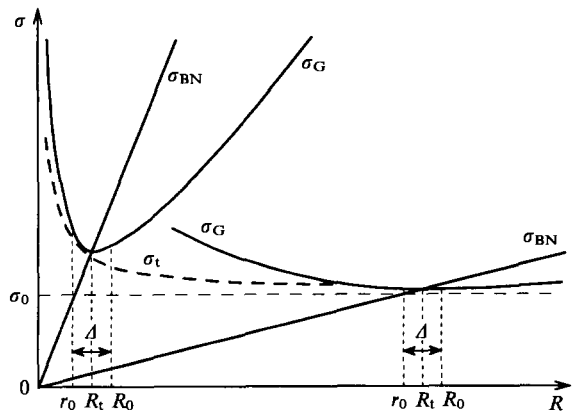


Figure 9. Dependence of the Gibbs and the Boruvka–Neumann interfacial tension on the radius of the cylindrical dividing surface for different values of the radius of the interfacial surface (see Fig. 7): σ_0 is the interfacial tension of the flat surface; R_t is the radius of curvature of the tension surface; $\sigma_t(r_0)$ is the interfacial tension of the Gibbs tension surface.

In Fig. 9 we show the dependence of σ_G and σ_{BN} on the radius of curvature R of the cylindrical dividing surface, calculated for the idealised form of the function $P_T^0(r)$ as a rectangular well with parameters Π_0 and Δ.

The $\sigma_G(R)$ functions calculated by Eqn (9) have a minimum (σ_t) at $R = R_t$ (the radius of the tension surface):

$$\frac{\sigma_G(R)}{R} + \frac{1}{2}\frac{\sigma_0}{r_0}\left(1 - \frac{R_t^2}{R^2}\right) = P_\beta - P_\alpha , \tag{40}$$

where

$$R_t = r_0(1+\alpha)^{1/2} , \tag{41}$$

$$\sigma_t = \sigma_0(1+\alpha)^{1/2} , \tag{42}$$

$$\sigma_0 = \int_{R_\beta}^{R_\alpha} [P_\alpha - P_T^0(r)]\mathrm{d}r = (\Pi_0 + P_\alpha)\Delta , \tag{43}$$

$$\alpha = \frac{\Delta}{r_0} .$$

We note an interesting property of the $\sigma_G(R)$ function. When the physical radius r_0 of the interface is decreased the radius of the tension surface R_t remains within the limits of the transitional interface layer, i.e. the system satisfies the condition

$$r_0 < R_t < R_0 = r_0 + \Delta ,$$

according to which the difference $\delta_t = R_t - r_0$ decreases from $\delta_t = \Delta/2$ for $r_0 \gg \Delta$ to zero for $r_0 \to 0$. Thus we may assume that the tension surface is almost indistinguishable from the Gibbs 'detachment surface', corresponding to a maximum density gradient in the inner phase. The interfacial tension σ_t increases as the radius r_0 decreases [see Eqn (42) and Fig. 9]. Eqn (40) is a generalised form of the Laplace equation, which in the case of the tension surface takes the simple form

$$\frac{\sigma_t}{R_t} = P_\beta - P_\alpha .$$

The interfacial tension σ_{BN} obtained from Eqn (34) is

$$\sigma_{BN} = \sigma_0 \frac{R}{r_0} . \tag{44}$$

The plots of the function $\sigma_{BN}(R)$ intersect those of $\sigma_G(R)$ at their minima (see Fig. 9). Under these conditions

$$\sigma_{BN}(R) = \sigma_t = \frac{\sigma_0 R_t}{r_0} .$$

Thus we may conclude that the Gibbs (σ_G) and the Boruvka–Neumann (σ_{BN}) interfacial tensions are indistinguishable for a tension surface of radius R_t.

With respect to this special property of the $\sigma_G(R)$ and $\sigma_{BN}(R)$ functions we note that some workers[10, 11, 14, 15] have calculated the radius of curvature R_t of the tension surface from the condition of simultaneous fulfilment of the equalities

$$f = f^{id} \quad \text{and} \quad M = M^{id} ,$$

but (as shown above) the condition $M = M^{id}$ leads to the Gibbs definition of the interfacial tension (σ_G) whereas the condition $f = f^{id}$ leads to the Boruvka–Neumann definition (σ_{BN}). Thus in that work the radius of curvature of the tension surface is obtained from the equality condition $\sigma_G(R_t) = \sigma_{BN}(R_t) = \sigma_t$.

For a cylindrical interfacial surface the generalised Laplace equation[19] is

$$\frac{\sigma_{BN}(R)}{R} = P_\beta - P_\alpha$$

for any radius of curvature R of the dividing surface (not only for the tension surface radius R_t) as function of $\sigma_G(R)$. The relationship between σ_G and σ_{BN} is obtained from Eqns (40) and (44):

$$\sigma_G = \frac{1}{2}\sigma_{BN}\left(1 + \frac{R_t^2}{R^2}\right) . \tag{45}$$

The choice of a standard state of the system in the determination of the interfacial tension. The difference between σ_G and σ_{BN} is significant (for all radii R of the dividing surface within the region $r_0 \leqslant R \leqslant r_0 + \Delta$) only when $r_0 \approx \Delta$ (a value typical of micelles and of nuclei of a new phase). A correct choice of the optimum reference system and of its standard state is very important for the thermodynamic description of these objects. The choice affects both the determination of the interfacial tension and the construction of the fundamental equation of the system and of the fundamental equilibrium equation in the most suitable form.

For example, in the Gibbs approach to the determination of σ_G [Eqn (9)] the fundamental equation for a cylindrical dividing surface (19) takes its simplest form for the tension surface of radius R_t:

$$\mathrm{d}\Omega_s = -S_s\mathrm{d}T - \sum_i N_{is}\mathrm{d}\mu_i + \sigma_t\,\mathrm{d}A_t ,$$

where $A_t = A(R_t)$ is the area of the tension surface, so that the excess in the grand thermodynamic potential is

$$\Omega_s = \sigma_t A_t ,$$

and the equilibrium equation of the system containing a cylindrical interfacial surface is the Laplace equation (24).

However, the interfacial tension σ_t and the radius of the tension surface are themselves dependent on the physical radius r_0 of the interfacial surface [see Fig. 9 and Eqns (41) and (42)], which complicates practical calculations of capillary effects.

Another method of determining the interfacial tension for a cylindrical surface relies on choosing as the standard state a state of the reference system for which $P_\beta^0 = P_\alpha^0$ and the interface is flat. The $P_T^0(r)$ function which corresponds to this interfacial surface is assumed to be known.

The deformation of a system containing a cylindrical interfacial surface can be arbitrarily divided into three stages: (1) the conversion of the curved surface into a flat surface by an imaginary change in the physical state of the system, i.e. by lowering the pressure from P_β to P_α^0; (2) stretching the flat interface to a new (larger) area; (3) bending the new surface to a new radius of curvature. Finally, by summing the amounts of work done in the three stages we obtain the fundamental equation for the excess in the grand thermodynamic potential (at constant T and μ_i) in the form

$$d\Omega_s = \sigma_0 dA_0 + dW_b(r_0) , \tag{46}$$

in which the dividing surface has a radius r_0, and the term $dW_b(r_0)$ is the work of bending the interface for an infinitesimally small change in curvature (the subscript b denotes a characteristic of the bending).

When the function $P_T^0(r)$ is modelled by a rectangular well (see Fig. 8) the work of bending $dW_b(r_0)$ for the cylindrical surface is zero. This follows from the fact that the interfacial tension σ_G calculated by Eqn (9) is independent of the pressure P_β and equal to σ_0. In this case Eqn (46) becomes

$$d\Omega_s = \sigma_0 dA_0 , \tag{47}$$

and the corresponding fundamental equation for the equilibrium of a system containing a cylindrical interface,

$$\frac{\sigma_0}{r_0} = P_\beta - P_\alpha^0 , \tag{48}$$

reduces to the Laplace equation (24), except that the pressure P_β is treated as arbitrary (not standard) and the interfacial tension σ_0 refers to a flat dividing surface with $P_\beta^0 = P_\alpha^0$.

We should stress the following advantages of the proposed thermodynamic description of a system containing a cylindrical interfacial surface which postulates a $P_T^0(r)$ function in the form of a rectangular well: (1) the dividing surface is identified with a physical surface of radius r_0 rather than with a tension surface of radius $R_t = r_0(1 + \Delta/r_0)^{\frac{1}{2}}$ (which depends on the radius of curvature r_0); (2) the interfacial tension σ_0 stays constant when the interface is bent, unlike the interfacial tension $\sigma_t = \sigma_0(1 + \Delta/r_0)^{\frac{1}{2}}$, which depends also on the radius of curvature r_0; (3) the Laplace equation is in its simplest form, and therefore makes the method very attractive for the thermodynamic description of systems in which the interfacial surface has a small radius of curvature.

When $P_T^0(r)$ is a function of arbitrary form the work of bending the dividing surface in (46) can be expressed as

$$dW_b(r_0) = c_1^0 A_0 dr_0 , \tag{49}$$

where

$$c_1^0 = \frac{1}{A_0}\frac{\partial \Omega_s}{\partial r_0}\bigg|_{T, \mu_i, A_0} .$$

The parameter r_0 must be chosen so as to make the interfacial tension $\sigma(R)$ equal to σ_0. We shall arbitrarily call this dividing surface a standard dividing surface.

2. Spherical free interfaces

Spherical free interfaces are characterised by two identical principal radii of curvature: $R_1 = R_2 = R$ (Fig. 10).

The work done by the tangential pressure $P_T(r)$ during changes in volume of a system containing a surface of this type (as a result of infinitesimally small changes $d\varphi_1$ and $d\varphi_2$ in the angles φ_1 and φ_2 at constant T and μ_i) can be expressed as

$$dW = \int_{R_\beta}^{R_\alpha} P_T(r) r\, d\varphi_1 r\, d\varphi_2 dr . \tag{50}$$

Replacing this real system by an idealised model formed by two reference phases α and β with a spherical dividing surface of

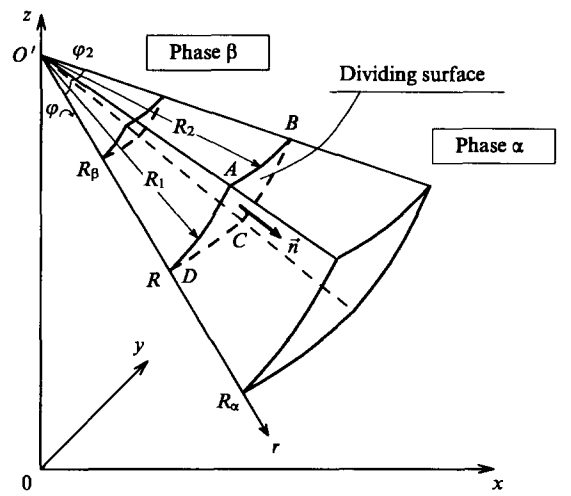


Figure 10. Element of volume of a system containing a spherical interface.

radius R gives an expression for the work dW^{id} in the form [see Eqn (15)]

$$dW^{id} = \left\{\int_{R_\beta}^{R} P_\beta r^2 dr + \int_{R}^{R_\alpha} P_\alpha r^2 dr - \sigma(R)R^2\right\} d\varphi_1 d\varphi_2 . \tag{51}$$

It follows from the condition of mechanical equivalence of the real system and of its idealised model.[11, 26] that

$$\sigma(R) = -\int_{R_\beta}^{R} [P_T(r) - P_\beta]\frac{r^2}{R^2} dr - \int_{R}^{R_\alpha} [P_T(r) - P_\alpha]\frac{r^2}{R^2} dr . \tag{52}$$

The fundamental equation of a system containing a spherical free interface is given as

$$d\Omega = -S dT - \sum_i N_i d\mu_i - P_\beta dV_\beta - P_\alpha dV_\alpha + \sigma(R) dA(R) + cA(R) dk , \tag{53}$$

where c is a coefficient for the differential of the average curvature k:

$$k = k_1 + k_2 = \frac{1}{R_1} + \frac{1}{R_2} = \frac{2}{R} . \tag{54}$$

Eqn (53) is the analogue of the fundamental equation for a cylindrical surface (13), but the coefficients c and c_1, and also the interfacial tensions, are differently defined in the two equations.

As in the case of the cylindrical surface we can obtain a fundamental equation for a spherical free dividing surface,

$$d\Omega_s = -S_s dT - \sum_i N_i d\mu_i + \sigma(R) dA(R) + cA(R) dk , \tag{55}$$

and the Gibbs–Duhem equation for this surface

$$d\sigma(R) = -s_s dT - \sum_i \Gamma_i d\mu_i + c\, dk . \tag{56}$$

By minimising the free energy in Eqn (53) through variations of the radius of curvature of the dividing surface we obtain the fundamental equilibrium equation of a system containing a spherical interface:

$$\frac{2\sigma(R)}{R} + c\frac{\partial k}{\partial R} = P_\beta - P_\alpha , \tag{57}$$

which reduces (allowing for the self-evident geometric relation $\partial k/\partial R = -k^2/2$) to an equation of the Gibbs–Kelvin type for a spherical surface,

$$k\sigma(R) - \tfrac{1}{2}ck^2 = P_\beta - P_\alpha . \tag{58}$$

For $c = 0$ (the condition for which the Gibbs tension surface is defined[8]) we obtain form (58) the familiar Laplace equation for a spherical surface

$$\frac{2\sigma_t}{R_t} = P_\beta - P_\alpha \,. \tag{59}$$

For the tension surface the fundamental equation of a system containing a spherical interface becomes[11]

$$d\Omega = -S\,dT - \sum_i N_i\,d\mu_i - P_\beta dV_\beta - P_\alpha dV_\alpha + \sigma_t dA_t \,. \tag{60}$$

Eqn (52) is the definition of the interfacial tension which may be called the Gibbs interfacial tension.[16] It is obtained from the condition of equality of the mechanical moments of the pressure forces $M = M^{id}$ acting in a plane drawn within an element of spherical volume (Fig. 10) of the real and of the idealised system respectively.

In the case of a spherical surface the Boruvka–Neumann interfacial tension,[19] defined by Eqn (34), does not follow from the condition of equality of the forces f and f^{id} acting on the side surface which limits the element of volume (see Fig. 10) of the real and the idealised system respectively, as it does in the case of a cylindrical interface.

On the other hand we obtain from the condition $f = f^{id}$ a new definition of the interfacial tension, denoted by the symbol σ_f:

$$\sigma_f(R) = \int_{R_\beta}^{R} [P_\beta - P_T(r)]\frac{r}{R}dr + \int_{R}^{R_\alpha} [P_\alpha - P_T(r)]\frac{r}{R}dr \,. \tag{61}$$

This parameter differs from the Gibbs and the Boruvka–Neumann interfacial tensions for spherical surfaces [Eqns (52) and (34), respectively], though its form is consistent with the expression (33) for σ_G in the case of a cylindrical surface.

Thus in the case of spherical dividing surfaces the interfacial tension can be defined in three ways: as σ_G, σ_f, or σ_{BN}. These quantities are different functions of the radius R of the spherical dividing surface. Some workers[10, 14, 19, 21] ignore this difference, or at least they fail to allow for it adequately: this accounts for the different version of the Gibbs–Kelvin equation which had been proposed.

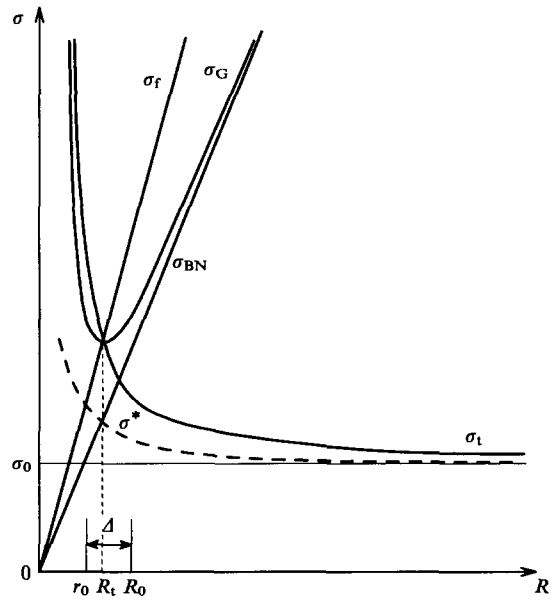


Figure 11. Dependence of the Gibbs and the Boruvka–Neumann interfacial tension and of σ_f [defined by Eqn (61)] on the radius of the spherical interface for $r_0 = \Delta$ (see Fig. 7): σ_0 is the interfacial tension of the flat surface; σ_t is the interfacial tension of the tension surface as a function of the radius of curvature r_0; σ^* is the interfacial tension defined by Eqn (37); R_t is the radius of curvature of the tension surface.

The dependences $\sigma_G(R)$, $\sigma_f(R)$, and $\sigma_{BN}(R)$, illustrated in Fig. 11, should be compared with Fig. 9, which shows similar plots of the functions $\sigma_G(R)$ and $\sigma_{BN}(R)$ for a cylindrical dividing surface.

The following relationships which follow from the condition of mechanical equilibrium $\operatorname{div}\hat{P} = 0$ for a spherical surface[10, 15] have also been used to calculate the hydrostatic pressure P_β and the interfacial tensions:

$$\frac{d(r^2 P_N)}{d(r^2)} = P_T \,, \tag{62}$$

$$\frac{dP_N}{dr} = \frac{2}{R}(P_T - P_N) \,, \tag{63}$$

$$\frac{d(r^3 P_N)}{dr} = r^2(P_N + 2P_T) \,. \tag{64}$$

Eqn (63) can also be written[25] as

$$\frac{dP_N}{dr} = k(r)(P_T - P_N) \,, \tag{65}$$

where $k(r) = 2/r$ is the curvature of a spherical dividing surface of radius r. In an integral form Eqn (65) becomes

$$P_\beta - P_\alpha = \int_{R_\beta}^{R_\alpha} [P_N(r) - P_T(r)]k(r)dr \,.$$

Integration of (62) leads to the equation[15]

$$\tfrac{1}{2}(P_\alpha R_\alpha^2 - P_\beta R_\beta^2) = \int_{R_\beta}^{R_\alpha} P_T(r) r\,dr \,.$$

We note that the plots of the functions $\sigma_G(R)$ and $\sigma_f(R)$ intersect at one point, corresponding to the values R_t and σ_t. As reported,[10, 11] the spherical tension surface is defined as the dividing surface which satisfies the condition

$$\sigma_G(R_t) = \sigma_f(R_t) \,, \tag{66}$$

where $\sigma_G(R)$ and $\sigma_f(R)$ are described by Eqns (52) and (61) respectively. Thus the values of R_t and σ_t given by the plots in Fig. 11 are respectively the radius and the interfacial tension of the tension surface. Fig. 11 also shows the $\sigma_t(R_t)$ dependence.

We also note that, in contrast to the cylindrical surface, in a spherical dividing surface the graphs of $\sigma_G(R)$ and $\sigma_{BN}(R)$ do not intersect anywhere.

As was pointed out above, in submicroscopic liquid drops (micelles, vesicles, coacervate drops), characterised by ultra-low interfacial tensions, a very important role is played by the form of the fundamental equation and of the generalised Laplace (or Gibbs–Kelvin) equation. Analytical equilibrium equations of the Gibbs–Kelvin type, obtained for the idealised profile of the $P_T(r)$ component of the hydrostatic pressure tensor shown in Fig. 8*a*, are given below for comparison.

The generalised Laplace equation for the tension surface is

$$\frac{2\sigma_t}{R_t} = P_\beta - P_\alpha \,. \tag{67}$$

Here

$$\sigma_t = \sigma_0\left[(1+\alpha)\left(1+\frac{\alpha}{2}\right)\right]^{2/3} \,,$$

$$R_t = r_0\left[\frac{(1+\alpha)^2}{1+\alpha/2}\right]^{1/3} \,, \tag{68}$$

where $\alpha = \Delta/r_0$, Δ is the width of the transition region, and σ_0 is the interfacial tension of the flat interfacial surface,

$$\sigma_0 = \int_{R_\beta}^{R_\alpha} [P_\alpha - P_T^0(r)]dr \,, \tag{69}$$

where the standard $P_T^0(r)$ function is a rectangular well (Fig. 8*a*), i.e. it corresponds to the condition $P_\alpha = P_\beta$.

For the Boruvka–Neumann interfacial tension[19, 21] the generalised Laplace equation is

$$\frac{2\sigma_{BN}}{R}\left(1+\frac{\alpha}{2}\right) = P_\beta - P_\alpha , \tag{70}$$

where

$$\sigma_{BN} = \sigma_0 \frac{R}{r_0} . \tag{71}$$

For the interfacial tension σ_0 defined by Eqn (69) we have

$$\frac{2\sigma_0}{r_0}\left(1+\frac{\alpha}{2}\right) = P_\beta - P_\alpha . \tag{72}$$

Lastly, for the interfacial tension σ^*, defined by the expression

$$\sigma^* = \int_{R_\beta}^{R_\alpha} [P_\alpha - P_T^0(r)]\frac{r}{r_0}dr = \sigma_0\left(1+\frac{\alpha}{\Delta}\right) , \tag{73}$$

the generalised Laplace equation takes the very simple form

$$\frac{2\sigma^*}{r_0} = P_\beta - P_\alpha . \tag{74}$$

By comparing the generalised Laplace equations for different definitions of the interfacial tension and different radii of the spherical separation surfaces we may conclude that the simplest thermodynamic description of these surfaces is offered by using the interfacial tension σ_0, defined for flat interfaces, and the physical radius of curvature of the surface r_0 [see Eqn (72)]. On the other hand, the advantage of using the interfacial tension σ^* [defined by Eqn (73)] and the radius r_0 [see Eqn (74)] is not clear. In practical calculations of the Gibbs interfacial tension (including calculations of the tension surface) and of the Boruvka–Neumann interfacial tension slight deviations of the radius of the dividing surface from the chosen value (for example, from the value R_t) produce changes in the functions $\sigma_G(R)$ and $\sigma_{BN}(R)$, i.e. they complicate the form of the Laplace equation. However, we should stress that all these remarks are of practical significance only for the interfacial surfaces of submicroscopic objects, having radii commensurate with the transition region of the interfacial surface. For higher values of the radius r_0, i.e. $\alpha \to 0$, all the interfacial tensions are effectively equal.

3. Non-spherical free interfaces with two principal radii of curvature

By analogy with the cylindrical and the spherical interfacial surfaces we shall write the fundamental equation for systems containing a non-spherical free interface with two principal radii of curvature R_1 and R_2 in the form

$$d\Omega = -S\,dT - \sum_i N_i\,d\mu_i - P_\alpha dV_\alpha - P_\beta dV_\beta + \sigma_G dA + c_1 A dk_1 + c_2 A dk_2 , \tag{75}$$

in which $k_1 = 1/R_1$ and $k_2 = 1/R_2$ are the principal values of the surface curvature, c_1 and c_2 are the coefficients of the curvature differentials, and R_1 and R_2 are the radii (i.e the distances along the z axis from the points O_1 and O_2 to the dividing surface, see Fig. 12). Integrating Eqn (75) with respect to the extensive parameters V_α, V_β, and A with constant intensive parameters T, μ_i, k_1, and k_2 yields an expression for the grand thermodynamic potential of the system:

$$\Omega = -P_\alpha V_\alpha - P_\beta V_\beta + \sigma_G A , \tag{76}$$

where A is the area of interfacial surface generated by stretching with constant values of k_1 and k_2, and σ_G has the meaning of a Gibbs interfacial tension.

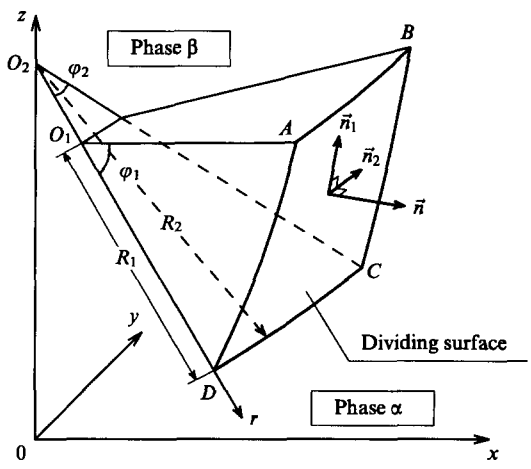


Figure 12. Element of volume of a system containing a non-spherical interface with two different principal radii.

By minimising the grand thermodynamic potential while varying the displacement of the separation surface in the direction of the normal $\vec{n}$ by δR and allowing for the obvious geometric relations

$$\frac{\partial V_\beta}{\partial R} = A ; \quad \frac{\partial V_\alpha}{\partial R} = -A ; \quad \frac{\partial A}{\partial R} = kA ;$$

$$k = k_1 + k_2 ; \quad c_1\frac{\partial k_1}{\partial R} + c_2\frac{\partial k_2}{\partial R} = \frac{\partial \sigma_G}{\partial R} ;$$

we obtain

$$k\sigma_G + \frac{\partial \sigma_G}{\partial R} = P_\beta - P_\alpha . \tag{77}$$

Eqn (77) is the fundamental equilibrium equation for a system containing a non-spherical separation surface.

The fundamental equation of the non-spherical separation surface itself is[8]

$$d\Omega_s = -S_s dT - \sum_i N_{is} d\mu_i + \sigma_G dA + c_1 A dk_1 + c_2 A dk_2 , \tag{78}$$

which should be compared with the equations (19) and (55) for cylindrical and for spherical surfaces respectively.

By applying Euler's theorem of homogeneous functions we find that, by analogy with (21) and (56), the Gibbs–Duhem equation for a non-spherical separation surface is

$$d\sigma_G = -s_s dT - \sum_i \Gamma_i\,d\mu_i + c_1 dk_1 + c_2 dk_2 . \tag{79}$$

We shall now briefly review various approaches to the description of non-spherical free interfaces.

The concepts of average curvature (H) and of differential curvature (D) were first proposed by Gibbs,[8] who defined them as

$$H = \tfrac{1}{2}(k_1 + k_2) \quad \text{and} \quad D = \tfrac{1}{2}(k_1 - k_2) . \tag{80}$$

In these symbols the fundamental equation of the system is

$$d\Omega = -S\,dT - \sum_i N_i\,d\mu_i - P_\alpha dV_\alpha - P_\beta dV_\beta + \sigma_G dA + AB\,dH + A\theta\,dD , \tag{81}$$

where B and θ are the specific bending and torsion moment respectively (referred to unit area of the separation surface):

$$B = c_1 + c_2 , \quad \text{and} \quad \theta = c_1 - c_2 . \tag{82}$$

In his derivation of the fundamental equilibrium equation of the system Gibbs[8] ignored the torsion moment θ (a second-order quantity as compared with the bending moment B: in the case of spherical surfaces the condition $\theta = 0$ applies exactly). By applying also the condition $B = 0$ to the tension surface Gibbs obtained the Laplace equation from the fundamental equation of the system (81) (by minimising the grand thermodynamic potential):

$$k_t\sigma_t = P_\beta - P_\alpha , \tag{83}$$

where

$$k_t = k_{1t} + k_{2t} , \tag{84}$$

and k_{1t} and k_{2t} are the principal curvatures of the tension interface.

Later work on the thermodynamics of non-spherical free interfaces dealt with the effect of the torsion moment θ on the generalised Laplace equation,[15, 16, 19, 21, 25]

Applying the minimisation procedure to Eqn (81) while allowing for the moment θ gives the following fundamental equilibrium equation:[25]

$$2H\sigma_G - B(H^2 + D^2) - 2\theta HD = P_\beta - P_\alpha . \tag{85}$$

Eqn (85) known as the Gibbs–Kelvin equation for non-spherical surfaces.[25] By comparing it with (77) we obtain

$$\frac{\partial\sigma_G}{\partial R} = -B(H^2 + D^2) - 2\theta BD . \tag{86}$$

The condition

$$\frac{\partial\sigma_G}{\partial R} = 0 , \tag{87}$$

corresponding to a minimum in the interfacial tension, takes the form

$$B(H^2 + D^2) + 2\theta BD = 0 . \tag{88}$$

The interface which satisfies the condition (88) is called the surface of minimum tension, in contrast to the Gibbs tension surface, obtained for the condition $B = 0$. Thus Gibbs ignored the term $2\theta HD$ in his definition of the tension surface. Obviously, the spherical surfaces of tension and of minimum tension coincide when $\theta = 0$.

Some workers[16, 19, 21] have suggested replacing H and D by the principal (first) curvature J and the Gaussian (second) curvature K of the surface:

$$J = k_1 + k_2 , \quad \text{and} \quad K = k_1k_2 . \tag{89}$$

In this case the fundamental equation of the system for a nonspherical surface becomes

$$d\Omega = -S\,dT - \sum_i N_i\,d\mu_i - P_\alpha dV_\alpha - P_\beta dV_\beta + \sigma_G dA + AC_1 dJ + AC_2 dK , \tag{90}$$

and the fundamental equilibrium equation of the system is[16]

$$J\sigma_G - C_1(J^2 - 2K) - C_2JK = P_\beta - P_\alpha , \tag{91}$$

where

$$C_1 = \frac{c_1k_1 - c_2k_2}{k_1 - k_2} ; \quad C_2 = \frac{c_1 - c_2}{k_1 - k_2} \tag{92}$$

[the coefficients c_1 and c_2 occur in Eqn (79)].

The condition which defines the interface of minimum tension (88) can be written[16]

$$C_1(J^2 - 2K) + C_2JK = 0 . \tag{93}$$

The Laplace equation is obtained by inserting the condition (93) into (91):

$$k_0\sigma_G^0 = P_\beta - P_\alpha , \tag{94}$$

where $k_0 = J_0 = k_{10} + k_{20}$, k_{10} and k_{20} are the principal curvatures of the minimum tension surface, and σ_G^0 is the minimum tension of the nonspherical surface.

III. Equilibrium of interfaces in the bulk meniscus region of a liquid film

If the separation surfaces in a liquid film are assumed to be surfaces of minimum tension, and allowance is made for the close similarity of σ_G^0 with σ_t for the tension surface with σ_0 for plane-parallel surfaces (when the radius of curvature is much greater than the thickness of the transitional interfacial layer, i.e. in practical terms for $r_0 > 10$ nm) the equilibrium equation (85) becomes

$$k_0\sigma_0 = P_\beta - P_\alpha = \Delta P , \tag{95}$$

where $k_0 = k_1 + k_2$, and k_1 and k_2 are the first and the second principal curvatures of the surface.

1. Invariants of the profile of a liquid film

Since the profile of liquid films is determined experimentally by the topographic method[7] (from interference pictures of the film in reflected monochromatic light) it is convenient to use Eqn (95) in $z(r)$ coordinates (Fig. 13). This gives invariants of the profile of liquid films related to differences in geometry.

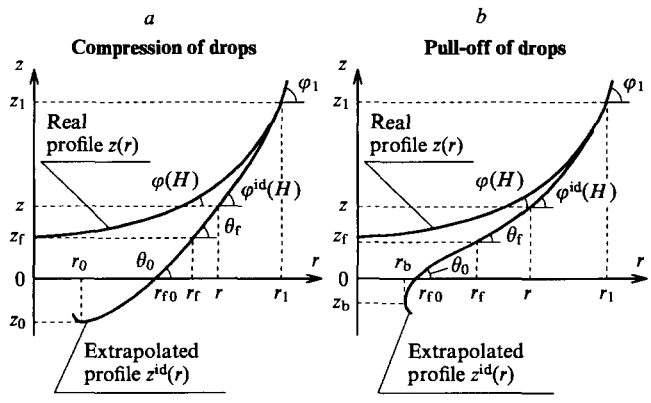


Figure 13. Form of the extrapolated profile of the surface of the liquid film between two liquid drops during compression by an external force (*a*) and pull-off (*b*).

It should be noted that because of the experimental difficulties in determining the real profile of a liquid film in the transition region a hypothetical profile (obtained by extrapolating the profile of the surface with a constant average curvature k_0 in the region of the bulk meniscus to the transition region) is often used in the thermodynamic description instead of the real profile, on the assumption that disjoining pressures are negligible (Fig. 13). This extrapolated (idealised) profile $z^{id}(r)$ differs from the real profile $z(r)$ in the transition region of the film, and coincides with the real profile in the region of the bulk meniscus.

The idealised profile can intersect the plane $z_f = H_f/2$ (where H_f is the thickness of the plane-parallel region of the film, and the subscript f denotes a quantity characteristic of the film) at a contact angle θ_f, or the plane $z = 0$ at a constant angle θ_0, whose values are used to calculate the specific free energy of the interaction in the flat part of the film.

For cylindrical interfaces, which have only one principal radius of curvature, Eqn (95) becomes

$$\sigma_0\frac{d\sin\varphi^{id}(r)}{dr} - \Delta P = 0 , \tag{96}$$

where $\varphi^{id}(r)$ is the local angle, formed by the surface of the idealised profile with the r axis. The equation

$$\frac{dz^{id}(r)}{dr} = \tan\varphi^{id}(r) \tag{97}$$

in conjunction with Eqn (96) forms a system which fully defines the profile of the film $H^{id}(r) = 2z^{id}(r)$ if the following boundary conditions are given: $\varphi^{id}(r) = \varphi_1$ and $z^{id}(r) = z_1$ for $r = r_1$, where r_1 is the radius of the film determined experimentally in the region of the bulk meniscus.

Integrating (96) over the idealised profile z^{id} from $z^{id}(r)$ to z_1 gives

$$\int_{z^{id}}^{z_1} \sigma_0 \frac{d\sin\varphi^{id}(r)}{dr} dz^{id} - \Delta P(z_1 - z^{id}) = 0 . \tag{98}$$

Since $[d\sin\varphi^{id}(r)/dr]dz^{id} = -\cos\varphi^{id}$ we obtain from (98) an invariant which is independent of the film thickness:

$$2\sigma_0\cos\varphi^{id}(r) + \Delta P H^{id}(r) = 2\sigma_0\cos\varphi_1 + \Delta P H_1 = \text{const} . \tag{99}$$

In the case of nonspherical interfaces characterised by two different radii of curvature the Laplace equation (95) becomes

$$\sigma_0 \frac{d\sin\varphi^{id}(r)}{dr} + \sigma_0 \frac{\sin\varphi^{id}(r)}{r} - \Delta P = 0 . \tag{100}$$

Integrating (100) as was done for the cylindrical surface gives an invariant independent of the local thickness of the idealised film profile $H^{id}(r)$:

$$2\sigma_0\cos\varphi^{id}(r) + \Delta P H^{id}(r) + 2\sigma_0 \int_{z^{id}}^{z_1} \frac{\sin\varphi^{id}(r)}{r} dz^{id}$$

$$= 2\sigma_0\cos\varphi_1 + \Delta P H_1 = \text{const} . \tag{101}$$

If the interfacial surface in the liquid film is spherical, i.e. if $k_1 = k_2$, the integral in Eqn (101) reduces to $\Delta P[H_1 - H(r)]/2$, and the invariant of the surface profile of the film takes the form

$$2\sigma\cos\varphi^{id}(r) + \tfrac{1}{2}\Delta P H^{id}(r)$$

$$= 2\sigma_0\cos\varphi_1 + \tfrac{1}{2}\Delta P H_1 = \text{const} . \tag{102}$$

2. Analytical expression for the idealised profile of the liquid film

Let us consider two fluid (liquid or gaseous) particles of the phase β forming a symmetrical liquid film in the phase α. To simplify the discussion we shall ignore the effect of gravity, and assume that the film is stable towards rupture and is not spontaneously thinned.

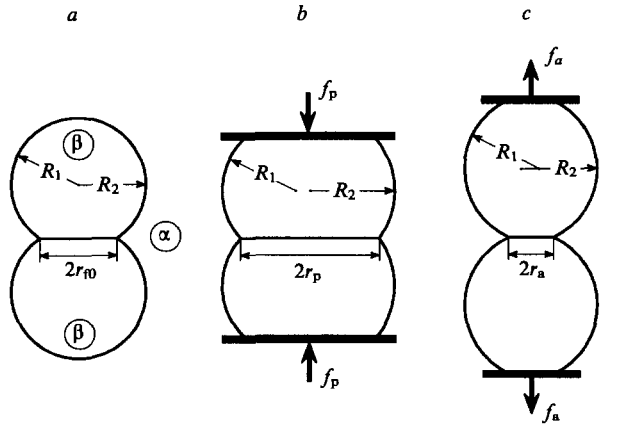


Figure 14. Shape of contacting drops in the absence of an external force (*a*), under compression (*b*), and during pull-off (*c*).

If the fluid particles do not experience an external force f_e (compressive, $f_p > 0$, or stretching, $f_a < 0$) the particles are spherical (Fig. 14*a*), and $k_1 = k_2 = k_0 = 2/R$, where R is the radius of the particles. In this case the profile of the surface of the particles, or the idealised profile of the film surface $z^{id}(r)$ [see Eqn (97)], is described by the equation

$$z^{id}(r) = z_1 - \int_{z^{id}}^{z_1} \tan\varphi^{id}(r) dr$$

$$= z_1 + R[\cos\varphi_1 - \cos\varphi^{id}(r)] . \tag{103}$$

If the particles are compressed by an external force f_p (Fig. 14*b*) the radius of the film increases to r_p, and the surface of the drops is no longer spherical, the radius R_2 increasing and R_1 decreasing. When a tensile force f_a is applied to the drops (Fig. 14*c*) R_2 decreases and R_1 increases.

By re-writing Eqn (100) as

$$\sigma_0 \frac{1}{r}\frac{d}{dr}[r\sin\varphi^{id}(r)] = \Delta P \tag{104}$$

and integrating it from r to r_1 we obtain the equation[1, 4]

$$\sin\varphi^{id}(r) = \frac{k_0}{2}r + \frac{B}{r} , \tag{105}$$

in which

$$k_0 = \frac{\Delta P}{\sigma_0} ,$$

$$B = r_1\sin\varphi_1 - \frac{k_0}{2}r_1^2 . \tag{106}$$

The physical significance of the parameter B can be understood by the following considerations. If the reference radius r_1 is taken to be R_2 (see Fig. 14*a*) we have $\varphi_1 = \pi/2$, and we arrive at the expression

$$B = \frac{k_{20} - k_{10}}{2k_{20}^2} = \frac{1}{k_{20}}\left(1 - \frac{k_0}{2k_{20}}\right) , \tag{107}$$

where k_{10} and k_{20} are the principal values of the curvature of the particle surfaces, corresponding to the 'equator', for which $\varphi_1 = \pi/2$. Obviously, the parameter B can be positive or negative, depending on the sign of the difference $(k_{20} - k_{10})$.

We shall now obtain expressions for the contact forces acting on fluid drops for the cases of mutual compression or pull-off.

In the case of a compressive force $f_e = f_p > 0$ the $z^{id}(r)$ profile has a maximum (see Fig. 13*a*) since, when $\varphi^{id}(r_0) = 0$, Eqn (105) has a real solution (allowing for the fact that $B < 0$):

$$r_0 = \sqrt{-\frac{2B}{k_0}} , \tag{108}$$

where k_0 is the average curvature.

From the condition of mechanical equilibrium of the drop we obtain the expression

$$f_p = \pi r_0^2 \Delta P = \pi r_0^2 \sigma_0 k_0 , \tag{109}$$

and in conjunction with (108) this gives

$$f_p = -2\pi\sigma_0 B . \tag{110}$$

The parameter B can be determined experimentally from the interference picture of the film.[27-29] The compressive force can also be determined[4] from Eqn (110). A mechanical interpretation of Eqn (109) is proposed in Fig. 15*a*. Evidently, the outer compressive force f_p is balanced by a pressure force of $\pi r_0^2\sigma_0 k_0$.

If a pull-off force $f_e = f_a < 0$ is applied to the drops (see Fig. 14*c*) it follows from (107) that $B > 0$, and Eqn (105) does not have a real solution for $\varphi^{id}(r) = 0$ [i.e. the profile $z^{id}(r)$ has no minimum].

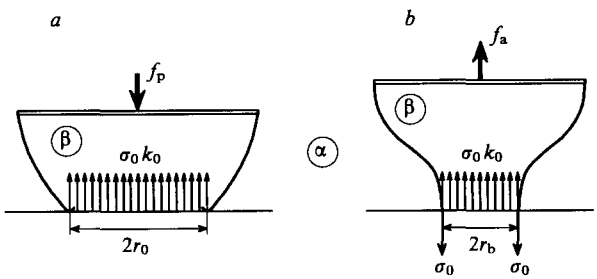


Figure 15. Equilibrium of a liquid drop under the influence of compression (*a*) and extension forces (*b*).

On the other hand for $\varphi^{id}(r) = \pi/2$, Eqn (105), written as

$$1 = \frac{k_0}{2} r + \frac{B}{r} , \tag{111}$$

has two real roots:

$$r_{(1)} = r_b = \frac{1 - \sqrt{1 - 2k_0 B}}{k_0} = \frac{1}{k_0}\left(1 - \frac{k_{10}}{k_{20}}\right) , \tag{112}$$

(see Fig. 13*b* for r_b), and

$$r_{(2)} = \frac{1}{k_{20}} = R_{20} . \tag{113}$$

The geometrical significance of the second root $r_{(2)} = R_{20}$ is illustrated in Fig. 13*b*. A positive value of the first root $r_{(1)} = r_b$ denotes the appearance of a 'neck' in the profile of the drop. Obviously, for $z^{id} = z_b$ (see Fig. 13*b*) the curvature $k_{20} = 1/r_b$ is positive, and $k_{10} = k_0 - k_{20}$ is negative for a positive average curvature k_0.

The relationship between r_b and f_a can be obtained by the following argument (Fig. 15*b*). Since the drop is assumed to be in equilibrium the resultant of all the forces acting on it must vanish. These forces are: the external pull-off force f_a; the interfacial tension force acting on the perimeter of the neck and equal to $-2\pi r_b \sigma_0$; and the hydrostatic pressure force, equal to $\pi r_b^2 \Delta P = \pi r_b^2 \sigma_0 k_0$. Equating their sum to zero gives

$$f_a - 2\pi r_b \sigma_0 + \pi r_b^2 \sigma_0 k_0 = 0 , \tag{114}$$

which becomes, when combined with (111),

$$f_a = 2\pi\sigma_0 \left[r_b - \tfrac{1}{2} k_0 r_b^2\right] = -2\pi\sigma_0 B . \tag{115}$$

Thus in the case of pull-off of the drops the parameter B is proportional to the applied negative force f_a.

Furthermore by using the sign convention for the force f_e, according to which $f_e = f_p > 0$ and $f_e = f_a < 0$, Eqn (110) and (115) can be re-written[4]

$$f_e = -2\pi\sigma_0 B , \tag{116}$$

while Eqn (105) becomes[4]

$$\sin\varphi^{id}(r) = \frac{k_0}{2} r - \frac{f_e}{2\pi\sigma_0} \frac{1}{r} . \tag{117}$$

Thus we may conclude that the extrapolated profile of the liquid film contains information on the external force f_e acting on the drop and on its sign: if $B > 0$ the drop is experiencing a pull-off force, whereas if $B < 0$ the applied force is compressive.

3. Various approximations to the idealised profile of the liquid film

The idealised profile of a curved liquid film (the profile of the film in the region of the bulk meniscus) contains information on the specific free energy of the interaction in the plane-parallel region of the film. Therefore measurements of the profile of these films are one of the main experimental methods of studying the energetics of thin liquid films.

Since the analytical expression for the function $z^{id}(r)$ usually contains elliptical integrals of the second kind various simplifications of the idealised profile have been suggested for practical use.[7, 28, 29] The approximating functions proposed by Kolarov et al.[7, 28] are among the most widely used:

$$z^{id}(r) = ar^2 + b , \tag{118}$$

$$z^{id}(r) = ar^2 + b' \ln r + c , \tag{119}$$

where a, b, b', and c are empirical coefficients, determined by measuring the profile of the film in the region of the bulk meniscus. The contact angles θ_f and θ_0 and the radii r_f and r_{f0} of the curved films (see Fig. 13) are found by extrapolating the approximating functions to the transition region of the film.

We should stress that the approximating functions (118) and (119) are obtained from the strict solution of the system of differential equations (97) and (117) for the following approximations: $\tan\varphi^{id} \simeq \sin\varphi^{id}$ and $f_e = 0$ for Eqn (118) and $\tan\varphi^{id} \simeq \sin\varphi^{id}$ for Eqn (119). For large enough values of the contact angle both these approximating functions are almost identical to the exact function. However, for the contact angles formed by the common black films or by the Newtonian black films, usually in the ranges $\lesssim 1°$ and $1° - 5°$ respectively, replacing the exact functions by the approximating functions can result in erroneous calculations of the contact angles.

In particular, an estimate of the precision of the approximated profile obtained by the functions (118) and (119) for a liquid film having an angle of contact of $\sim 1°$ has been reported.[30] It was shown that the function (119) satisfactorily describes the profile of these films. On the other hand, use of the parabola (118) introduces serious errors in the determination of the contact angles. It was also found[31] that the function (119) is convenient for describing the profiles of films which do not form contact angles θ_0 and θ_f (in the latter case the specific free energy of the interaction in the film is positive). On the other hand the use of the parabola to describe the profile of these films results in the formation of contact angles, i.e. it leads to the erroneous conclusion that the specific free energy is negative in these films.

4. Lens-like thickening in equilibrium with a thin liquid film

A lens-like thickening (or dimple) at the centre of a round liquid film is formed when two fluid drops (liquid or gaseous) are rapidly brought into contact in a liquid medium (Fig. 16*a*) or in the contact region between a drop and a solid surface (Fig. 16*b*).

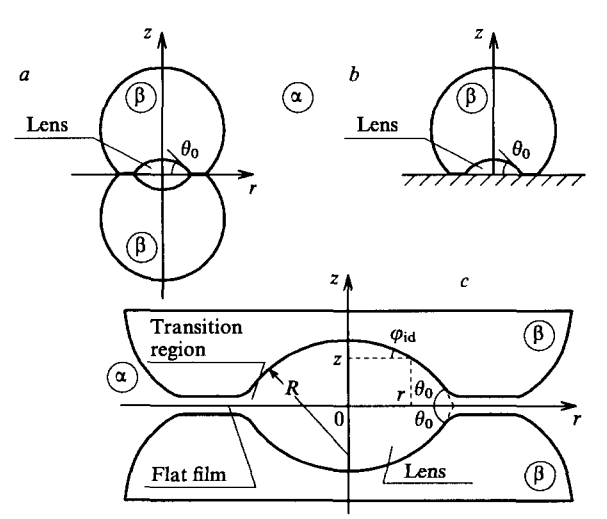


Figure 16. Lens-like thickening produced in the contact region between two fluid drops of phase β in the liquid phase α (*a*) and in the contact region between a fluid drop and a solid surface (*b*); geometric parameters of the liquid lens in equilibrium with the liquid film (*c*).

We shall obtain the equation for the profile of these lenses in the coordinates defined in Fig. 16c.

Since the first and the second principal curvature of the lens profile are given by the expressions

$$k_1 = -\frac{\mathrm{d}\sin\varphi^{\mathrm{id}}(r)}{\mathrm{d}r}\ ;\ k_2 = -\frac{\sin\varphi^{\mathrm{id}}(r)}{r}\ ,$$

the fundamental equilibrium equation (100) is[18]

$$\sigma_0\frac{\mathrm{d}\sin\varphi^{\mathrm{id}}(r)}{\mathrm{d}r} + \sigma_0\frac{\sin\varphi^{\mathrm{id}}(r)}{r} + \Delta P_\alpha = 0\ , \tag{120}$$

where $\Delta P = P_\alpha - P_\beta$ is the difference between the hydrostatic pressures in the lens and in the external medium (phase β).

Eqn (97) becomes

$$\frac{\mathrm{d}z^{\mathrm{id}}(r)}{\mathrm{d}r} = -\tan\varphi^{\mathrm{id}}(r)\ , \tag{121}$$

since $z^{\mathrm{id}}(r)$ decreases when r increases.

By integrating (120) with respect to r from zero to an arbitrary value of r corresponding to the bulk region of the meniscus (or to some point on the idealised profile coinciding with the real profile in the region of the bulk meniscus) we obtain

$$\sin\varphi^{\mathrm{id}}(r) = \tfrac{1}{2}k_0 r\ . \tag{122}$$

This expression is the equation for a region of radius $R = \frac{1}{2}k_0$, where $k_0 = \Delta P_{\mathrm{d}}/\sigma_0$. Extrapolating this profile to its intersection with the r axis gives the contact angle θ_0, which is used to calculate the specific free energy of the interaction in the plane-parallel region of the film.

This method of measuring the contact angle θ_0 is known as the floating lens method.[32] It has been used to measure the specific free energy of the interaction[33] in Newtonian black films of hydrocarbons (bilayer lipid membranes), within which microscopic lenses of liquid hydrocarbons had been formed.

We note that Eqns (120) and (121) are convenient for describing the profile of a liquid drop in contact with a flat solid surface under conditions of zero gravity, when the perturbing effect of the gravity forces on the profile of the drop can be neglected.

5. Vertical liquid films in a gravitational field

The effect of gravity on the form of the profile of liquid films will be examined by considering a vertical liquid film produced by drawing a flat plate (for example, a Wilhelmi plate) out of a liquid phase α into a fluid (liquid or gaseous) phase β (Fig. 17).[34]

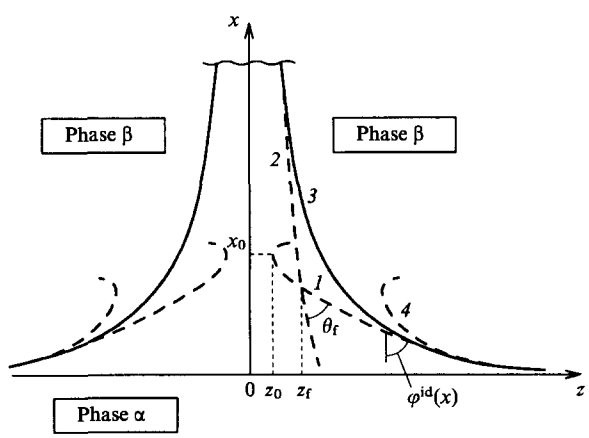


Figure 17. Vertical film in a gravitational force field: *1* and *4*, extrapolated profile of the cylindrical surface; *2*, extrapolated profile of the vertical film; *3*, real surfaces.

In this case the profile of the film in the region of the bulk meniscus is described by the system of equations

$$\sigma_0\frac{\mathrm{d}\sin\varphi^{\mathrm{id}}(x)}{\mathrm{d}x} = \Delta P\ ;\quad \frac{\mathrm{d}z^{\mathrm{id}}(x)}{\mathrm{d}x} = \tan\varphi^{\mathrm{id}}(x) \tag{123}$$

with the boundary conditions $x = 0$ and $\varphi^{\mathrm{id}}(x) = \pi/2$ for $z \to \infty$. Within the liquid film the difference in hydrostatic pressures is

$$\Delta P = P_\beta - P_\alpha = -\Delta\rho g x\ ,$$

i.e. ΔP is now no longer a constant, and Eqn (123), allowing for the chosen direction of the x axis and for the definition of the angle $\varphi^{\mathrm{id}}(x)$, takes the form

$$\frac{\mathrm{d}\sin\varphi^{\mathrm{id}}(x)}{\mathrm{d}x} = -\frac{\Delta\rho g x}{\sigma_0}\ , \tag{124}$$

where $\Delta\rho = \rho_\alpha - \rho_\beta$, and ρ_α and ρ_β are the densities of the phases α and β respectively. Since $\varphi^{\mathrm{id}}(0) = \pi/2$ for $x = 0$, the solution of (124) is

$$\sin\varphi^{\mathrm{id}}(x) = 1 - \frac{x^2}{a^2}\ , \tag{125}$$

where $a = \sqrt{2\sigma_0/\Delta\rho g}$ is the capillarity constant.

The idealised profile of the vertical liquid film in a field of gravity forces can be found by solving Eqn (123) with the boundary conditions $\varphi^{\mathrm{id}}(x) = 0$ and $z^{\mathrm{id}}(x) = z_0$ for $x = x_0$, where $x_0 = a$ [for which the idealised profile $z^{\mathrm{id}}(x)$ has a minimum].

Depending on the sign of the specific free energy of the interaction in the flat part of the film the idealised profile can pass either within the liquid film or outside it, i.e. in the phase β. The method of determining angles of contact in these films has already been discussed in depth.[18, 34]

IV. Thermodynamic description of interacting interfaces in the transition region of a liquid film

The main difficulty in constructing the thermodynamics of interacting interfaces in the transition region of liquid films is the absence of generally accepted views on the disjoining pressure. If the shear components of the generalised pressure tensor $\boldsymbol{P}$ are assumed to be zero in the plane-parallel region of the liquid film, and the tension γ is defined by the expression[22]

$$\gamma = \int_{-\infty}^{+\infty}[P_\beta - P_{\mathrm{T}}(z)]\mathrm{d}z\ , \tag{126}$$

in the transition region (and in particular in the symmetry plane for $z = 0$) the component P_{T} of the pressure tensor varies as a function of the coordinate r from a negative value at the centre of the circular thin liquid film (i.e. at $r = 0$) to a positive value for $r \to \infty$ (i.e. in the region of the bulk meniscus of the film). It is no longer convenient to use the tension γ to construct the fundamental thermodynamic equation of the system in the transition region of the film: firstly, because γ is now a function of the coordinate r, and secondly because shear components of the pressure tensor are now present in the transition region [due to the gradient $P_{\mathrm{T}}(z, r)$], and the relationship (126) ceases to be valid.

Thus we need to develop other approaches to the thermodynamics of the transition region in liquid films.

1. Various definitions of the disjoining pressure

An analysis of recent publications on this topic reveals two points of view on the physical nature of the disjoining pressure and on the mechanism of its action in the transition region of thin liquid films.

The disjoining pressure as a bulk force. According to this model[35–37] the disjoining pressure should be treated as a manifestation of 'forces of the second kind',[38] arising in the region of mutual overlapping of the 'surface forces of the first kind',

i.e. of the two phase separation surfaces (after Gibbs[8]). The disjoining pressure Π, defined by the expression[38]

$$\Pi = P_N - P_\alpha = P_\beta - P_\alpha , \quad (127)$$

is represented as a bulk pressure having tensor properties and existing independently of the separation surfaces of the film. According to this model the action of the disjoining pressure is normal to these surfaces in both the plane-parallel and the transition region of the film[37] (Fig. 18*a*). As a consequence of this model the separation surfaces in the film are treated as non-interacting, and therefore the interfacial tension is assumed to be constant over the whole of the transition region and equal to the interfacial tension σ_0 at the boundary of the bulk phases.[36, 37] The curved separation surfaces, characterised by a constant interfacial tension σ_0, are called 'surfaces of tension' by Eriksson and Toshev:[37] the fundamental equilibrium equation in the transition region of the film becomes[35, 37]

$$\sigma_0 k(H) + \Pi(H) - \Delta P = 0 , \quad (128)$$

where $\Pi(H)$ is the local value of the disjoining pressure (a function of the film thickness H); $\Delta P = P_\beta - P_\alpha$ is the difference between the hydrostatic pressures in the phases β and α; $k(H)$ is the local value of the curvature of the film surface in the transition region.

In the region of the bulk meniscus (Fig. 18*a*) $\Pi = 0$, and from Eqn (128) we obtain the Laplace equilibrium equation $\sigma_0 k_0 = \Delta P$, where k_0 is the constant average curvature of the free curved surface. Eriksson and Toshev[35, 39] define a reference pressure of the Gibbs type at the centre of the circular film, equal to the hydrostatic pressure in the phase β. This assumption formally leads to the creation of a hydrostatic pressure gradient in the transition region, since in the transition region of the bulk meniscus the hydrostatic pressure is P_α. Therefore Eriksson and Toshev[37] introduced into the model an additional force to balance the pressure gradient in the transition region. This expedient produced unnecessary complications in the thermodynamic description of this region of the film, including a number of inconsistencies. For example, the constancy of the interfacial tension σ_0, which follows from the assumption that the action of the disjoining pressure is in a direction normal to the dividing surfaces, is formally incompatible with the Gibbs–Duhem equation,[22] widely used (by Eriksson and Toshev,[37, 39, 40] among others, to describe plane-parallel films):

$$\Pi(H) = -2\frac{\partial\sigma}{\partial H}\bigg|_{T,\mu_i,A} . \quad (129)$$

This contradiction has been pointed out previously.[15]

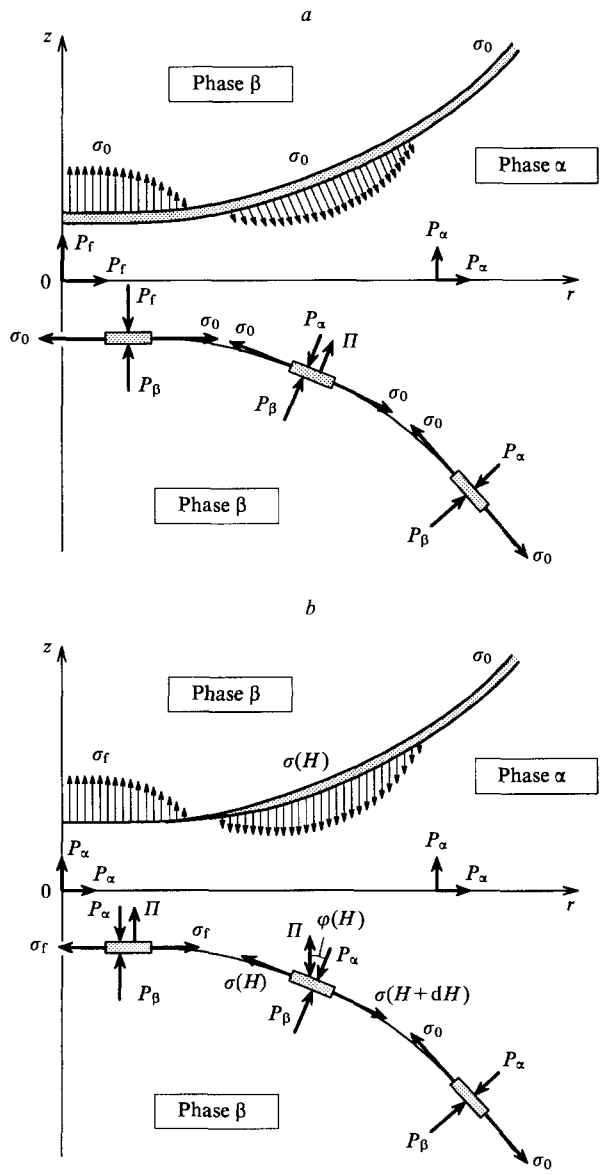


Figure 18. Representation of the disjoining pressure in a liquid film as a pressure tensor (*a*) and as a tensor of the specific interaction force between the dividing surfaces in the film (*b*).

The disjoining pressure as a specific interaction force between the dividing surfaces in the film has been discussed by the present writer[1–4] and by De Feijter et al.[41–43] The phase α and the pressure P_α are chosen as the reference phase and the reference pressure (in the Gibbs sense), and therefore no pressure gradient appears in the transition region in this model (Fig. 18*b*). An important assumption in this case is that the radial component of the disjoining pressure is zero: this leads to the following fundamental equilibrium equation for the film in the transition region:[1, 31, 44]

$$\sigma(H)k(H) + \Pi(H)\cos\varphi(H) - \Delta P = 0 , \quad (130)$$

where $\sigma(H)$ is the local value of the interfacial tension in the transition region; $\varphi(H)$ is the local contact angle of the real profile of the film surface.

Eqn (130) can be interpreted as the mechanical equilibrium condition of the dividing surface in a direction normal to this surface under conditions of an interfacial tension gradient $\sigma(H)$ in the transition region of the film. Diagrams illustrating the mechanical equilibrium of a dividing surface for a plane-parallel film in the transition region and in the region of the bulk meniscus are shown in Fig. 18*b*: here $\sigma_f = \sigma(H_f)$ is the interfacial tension in a plane-parallel film of thickness H_f. Thus the forces acting at right angles to the film surface in the transition region include the capillary pressure $\sigma(H)k(H)$, the hydrostatic pressures P_α and P_β, and also the projection of the disjoining pressure $\Pi(H)\cos\varphi(H)$, whose sum vanishes at equilibrium [see Eqn (130)].

Evidently, the equilibrium equation (130) reduces to the Eqns (127) and (95), which describe the equilibrium of the film in the plane-parallel region and in the region of the bulk meniscus respectively.

The fundamental equation (130) describes the equilibrium of the film surface in the transition region in a direction tangential to this surface, and allows it to be interpreted mechanically. The gradient of the interfacial tension $d\sigma(H) = \sigma(H + dH) - \sigma(H)$ in a direction tangential to the surface of the film is thus balanced by the force $-\Pi(H)\sin\varphi(H) \times dl$, which can be written

$$d\sigma(H) = \sigma(H + dH) - \sigma(H) = -\Pi(H)\sin\varphi(H) \times dl .$$

This equation is consistent with the Gibbs-Duhem equation (129), since the length of the element of surface dl under consideration is expressed in terms of dH and $\varphi(H)$ by the relation $dH = 2\sin\varphi(H) \times dl$.

2. The fundamental equation of a liquid film in the transition region

The writer has shown[22] that the fundamental equation of a system containing a plane-parallel film can be written in the form

$$d\Omega = -SdT - \sum_i N_i d\mu_i - \Delta P dV_\beta - \Pi(H) A dH + 2\sigma(H) dA . \quad (131)$$

We note that the layout of this equation does not require a subjective choice of the position of the dividing surfaces in the film, i.e. it is independent of H, even though $\sigma(H)$ and also V_α and V_β depend on the localisation of the dividing surfaces.

The fundamental equation of the system, including two curved non-interacting dividing surfaces of minimum tension in the region of the bulk meniscus, can be written in terms of the equation (90) and the condition (93) in the form[5]

$$d\Omega = -SdT - \sum_i N_i d\mu_i - \Delta P dV_\beta + 2\sigma_0 dA , \quad (132)$$

where $\sigma_0 \equiv \sigma_G^0$ [see Eqn (94) and discussion].

Eqn (131) has been used[1-5, 18, 44] as the fundamental equation for the transition region of a liquid film, the position of the dividing surfaces being chosen so as to satisfy the condition (94) over the whole of the transition region. In this case Eqn (131) is converted into Eqn (132) in the region of the bulk meniscus. Since the position of the dividing surfaces in the transition region is unambiguously fixed, the fundamental equation in the plane-parallel region of the film should be written[5]

$$d\Omega = -SdT - \sum_i N_i d\mu_i - \Delta P dV_\beta - \Pi(H_f) A dH + 2\sigma_f dA , \quad (133)$$

where $\sigma_f \equiv \sigma(H_f)$, since the minimum tension surfaces have now been chosen as the dividing surfaces in the plane-parallel film.

Minimising the functional (131) at constant T and μ_i in a direction normal ($\vec{n}$) to the surface of the film in the transition region leads to the expression

$$\delta\Omega = -\Delta P \frac{\partial V_\beta}{\partial \vec{n}_\beta}\delta\vec{n} - \Pi(H) A \frac{\partial H}{\partial \vec{n}}\delta\vec{n} + 2\sigma(H)\frac{\partial A}{\partial \vec{n}}\delta\vec{n} ,$$

which is converted, allowing for the self-evident geometric relations

$$\frac{A\partial H}{\partial \vec{n}} = -\cos\varphi(H)\left(\frac{\partial V_\beta}{\partial \vec{n}}\right) ; \quad \frac{2\partial A}{\partial \vec{n}} = k(H)\left(\frac{\partial V_\beta}{\partial \vec{n}}\right) ,$$

into the fundamental equilibrium equation for the surface of the film in the direction of the normal [Eqn (130)].[1, 5, 18, 44] Under these conditions the Gibbs–Duhem equation (129) defines the equilibrium of an element of surface in a direction tangential to the surface.

The fundamental equation for interacting curved dividing surfaces of minimum tension in the transition region of the film can be obtained from Eqn (131) by subtracting from it the 'bulk' part, corresponding to the macroscopic phases α and β:[5, 18]

$$d\tilde{\Omega}_s = -\tilde{S}_s dT - \sum_i \tilde{N}_{is} d\mu_i - \Pi(H) A dH + 2\sigma(H) dA , \quad (134)$$

where the tilde sign denotes Gibbs excesses of the corresponding quantity.

In the region of the bulk meniscus Eqn (134) becomes

$$d\tilde{\Omega}_s = -\tilde{S}_s dT - \sum_i \tilde{N}_{is} d\mu_i + 2\sigma_0 dA , \quad (135)$$

and the fundamental equation for interacting surfaces of minimum tension in a plane-parallel is

$$d\tilde{\Omega}_s = -\tilde{S}_s dT - \sum_i \tilde{N}_{is} d\mu_i - \Pi(H_f) A dH + 2\sigma_f(H) dA . \quad (136)$$

3. Shape of the profile of a liquid film in the transition region

The shape of the real profile $H(r) = 2z(r)$ of a symmetrical circular liquid film (see Fig. 1) is uniquely described by the system of Eqns (129) and (130), together with

$$\frac{dH(r)}{dr} = 2\tan\varphi(H) . \quad (137)$$

In the region of the bulk meniscus the real profile $H(r)$ coincides with the ideal profile $H^{id}(r) = 2z^{id}(r)$, which can be determined experimentally with adequate precision.[7] The position of the point (r_1, z_1) can be used as a boundary condition: it is the same for the real and the idealised profile in the region of the bulk meniscus, in which the two profiles have the same angle of contact φ_1 (see Fig. 13).

In cylindrical films, having only one principal radius of curvature, integration of the fundamental equilibrium equation of the film (130) over the thickness of the real profile from a value H in the transition region to a value H_1 in the region of the bulk meniscus yields an invariant, independent of the thickness of the profile:[1, 5, 6, 18]

$$2\sigma(H)\cos\varphi(H) + \Delta P H(r) = 2\sigma_0\cos\varphi_1 + \Delta P H_1 = \text{const} . \quad (138)$$

The invariant (138) is the analogue of (99), obtained for noninteracting cylindrical surfaces. Since the right-hand sides of the two invariants are equal the left-hand sides must also be equal. This produces a new generalised invariant:[1, 5]

$$2\sigma(H)\cos\varphi(H) + \Delta P H(r) = 2\sigma_0\cos\varphi^{id}(H) + \Delta P H^{id}(r) , \quad (139)$$

which establishes a mutual relationship between the parameters which characterise the real $[H(r)]$ and the idealised film profile $[H^{id}(r)]$.

From the generalised invariant (139) we obtain well known expressions, widely used in the thermodynamics of thin liquid films, which are usually based on mechanical models of the liquid films, for example[46, 47]

$$\sigma_f = \sigma_0\cos\theta_f , \quad (140)$$

or (see Sheludko et al.[48] and Fig. 13)

$$\sigma_f = \sigma_0\cos\theta_0 - \tfrac{1}{2}\Delta P H_f . \quad (141)$$

We shall illustrate these assertions with a number of examples.[1, 5, 6, 18]

Let us insert into the left-hand side of the generalised invariant (139) values corresponding to the real profile $H(r)$: $H = H_f$, $\varphi(H_f) = 0$, and $\sigma(H_f) = \sigma_f$. Into the right-hand side we insert the corresponding values for the idealised profile $H^{id}(r)$: $H^{id} = H_f$, and $\varphi^{id}(H_f) = \theta_f$. The result is

$$2\sigma_f + \Delta P H_f = 2\sigma_0\cos\theta_f + \Delta P H_f ,$$

from which we obtain Eqn (140).

On the other hand if the values $H_{id} = 0$ and $\varphi^{id}(0) = \theta_0$ are inserted into the right-hand side of the generalised invariant (139) they produce the equation

$$2\sigma_f + \Delta P H_f = 2\sigma_0\cos\theta_0 , \quad (142)$$

from which (141) is obtained. Since γ is related to the interfacial tension σ_f in a film of thickness H_f by the expression[22]

$$\gamma = 2\sigma_f + \Delta P H_f , \quad (143)$$

Eqn (142) leads to the well known relation[48]

$$\gamma = 2\sigma_0\cos\theta_0 . \quad (144)$$

By using the relationship [which follows from the Gibbs–Duhem equation (129)] between the specific free energy of

interaction (grand thermodynamic potential) in a plane-parallel film and the interfacial tension[34, 41, 45]

$$2\sigma_f - 2\sigma_0 = \Delta\Omega(H_f) = \int_{H_f}^{\infty} \Pi(H)\mathrm{d}H \,, \tag{145}$$

we obtain from Eqns (140) and (142) the familiar relations[46, 47]

$$\Delta\Omega(H_f) = 2\sigma_0(\cos\theta_f - 1) \tag{146}$$

or[48]

$$\Delta\Omega(H_f) = 2\sigma_0(\cos\theta_0 - 1) - \Delta P H_f \,. \tag{147}$$

Attention has been drawn[1, 5, 43] to the difference between the contact angles θ_f and θ_0 and to the need to allow for this difference when using the expressions (146) and (147) in order to avoid crude errors in the calculation of the specific energy of interaction in the film at low contact angles and relatively large thicknesses of the liquid films.

We shall now establish how the equilibrium equations of films with a bulk meniscus can be obtained from the universal invariant (139) when the contact angle θ_0 is not formed. For example, the common black films, also known as α-films, between drops in which the capillary pressure $P_c = \Delta P = P_\beta - P_\alpha$ is smaller than the height Π_2 of the coagulation barrier in the disjoining pressure isotherm. The profile of these films (curve *1* of Fig. 19*a*) is characterised by a relatively large thickness H_f^c of the central plane-parallel part: as a rule the idealised profile $H^{id}(r)$ does not form a contact angle θ_0 under these conditions.

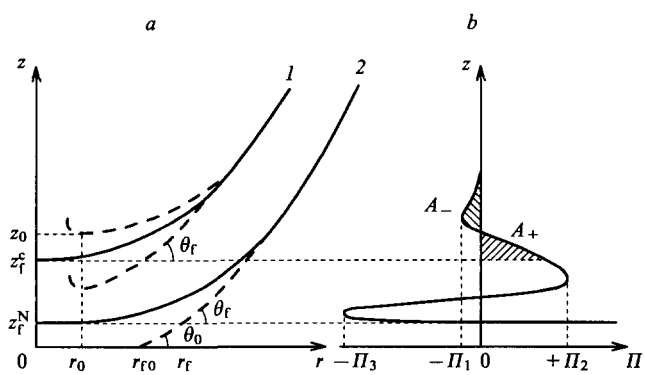


Figure 19. Creation of common and of Newtonian black films: (*a*) profiles of the common (*1*) and of the Newtonian black film (*2*); (*b*) profile of the disjoining pressure isotherm.

If $\Delta\Omega(H_f) < 0$, i.e. according to (145), the area of the cross-hatched negative region A^- (Fig. 19*b*) is greater than the area of the positive region A^+ (for example, for a high enough concentration of electrolyte in an aqueous dispersion medium, in which the coagulation barrier is low): the idealised profile $H^{id}(r)$ forms a contact angle θ_f and has a minimum $H_0 = 2z_0$, which is smaller than the film thickness $H_f^c = 2z_f^c$ (see Fig. 19*a*). On the other hand if $A^+ > A^-$ we have $\Delta\Omega(H_f) > 0$ and the idealised profile $H^{id}(r)$ lies above the real profile of the film $H(r)$, with $H_0 > H_f^c$.

Inserting into the right-hand side of the generalised invariant (139) the values $H^{id} = H_0$ and $\varphi^{id} = 0$, corresponding to a minimum on the $H^{id}(r)$ curve, we obtain the expression[18]

$$2\sigma_f + \Delta P H_f = 2\sigma_0 + \Delta P H_0 \,, \tag{148}$$

from which new relations are obtained:

$$\gamma = 2\sigma_0 + \Delta P H_0 \,, \tag{149}$$

$$\Delta\Omega(H_f) = \Delta P(H_0 - H_f) \,. \tag{150}$$

Thus, if $H_0 < H_f$ we have $\Sigma\Omega(H_f) < 0$. Eqn (150) for the case of $\Delta\Omega(H_f) > 0$ was obtained[45, 49, 50] for films with a cylindrical profile by applying the principle of detailed balancing developed by Deryagin for films.[51]

Newtonian black films, also known as β-films, are formed from the α-films when the height Π_2 of the coagulation barrier is lowered (for example, by increasing the concentration of electrolyte), or by increasing the capillary pressure P_c to a level higher than the coagulation barrier Π_2 (for example, by decreasing the radii of the liquid drops between which the liquid film is formed)[52] (see curve *2* of Fig. 19*a*).

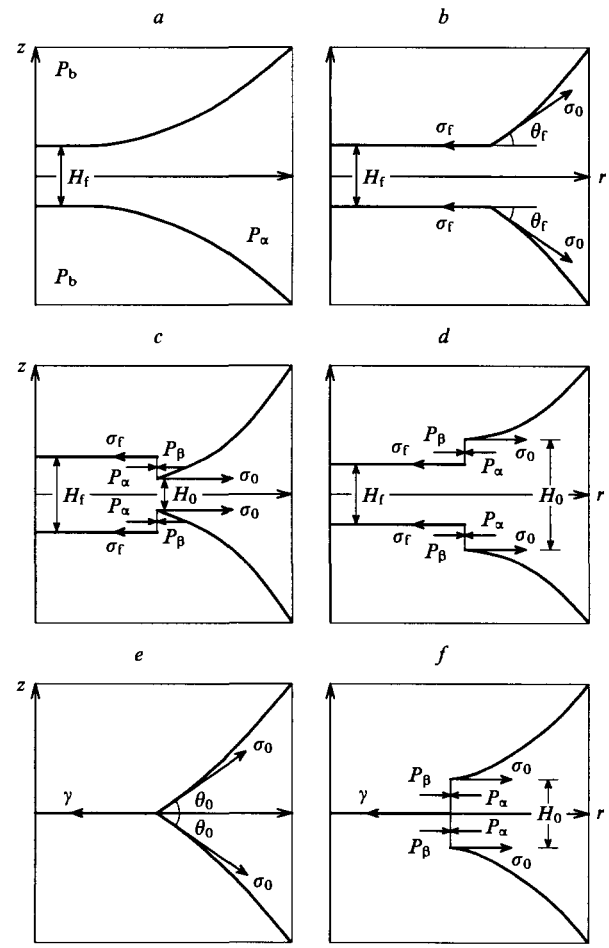


Figure 20. Equilibrium of a liquid film with a bulk meniscus (*a*) according to the thermodynamic model which stipulates two dividing surfaces (*b*–*d*) and according to the membrane model of the film (*e*, *f*).

The expressions (140), (144), (148), and (149) allow a clear mechanical interpretation of these effects (Fig. 20), which differs according to the thermodynamic model chosen to describe the thin liquid films.

If the model assumes two interacting dividing surfaces in the liquid film[53, 54] the equilibrium schemes illustrated in Fig. 20*b*–20*d* are usually adopted. Fig. 20*b* shows the equilibrium of the film with a meniscus, as in Eqn (140). When the contact angle θ_0 is not formed, and $H_0 < H_f$, Eqn (148) corresponds to the scheme shown in Fig. 20*c*. Under these conditions $\Delta\Omega(H_f) < 0$. If $\Delta\Omega(H_f) > 0$ we have $H_0 > H_f$, and the scheme shown in Fig. 20*d* corresponds to Eqn (148).

If the membrane model is chosen as a thermodynamic model of the film[55, 56] it is convenient to use the mechanical model shown in Fig. 20*e* [corresponding to Eqn (144)] for negative values of $\Delta\Omega(H_f)$, when the contact angle θ_0 is formed. On the other hand if the contact angle θ_0 is not formed we can use the mechanical model shown in Fig. 20*f*, corresponding to Eqn (149).

Under these conditions $\Delta\Omega(H_f)$ can take both negative and positive values.

The generalised invariant for circular liquid films can be obtained by integrating the fundamental equilibrium equation (130) over the thickness of the real profile [as was done for films with a cylindrical profile in the derivation of Eqn (138)], and combining the resulting expression with (101):

$$2\sigma(H)\cos\varphi(H)+\Delta PH(r)+\int_H^{H_1}\frac{\sigma(H)\sin\varphi(H)}{r}\,dH = 2\sigma_0\cos\varphi^{id}(H)+\Delta PH^{id}(r)+\int_{H^{id}}^{H_1}\frac{\sigma_0\sin\varphi^{id}(H)}{r}\,dH^{id}. \quad (151)$$

We shall show how accurate analytical expressions can be obtained from the generalised invariant (151) for circular films, allowing numerical estimates of the line tension.[1, 2, 5]

As was done for films with a cylindrical profile in the derivation of Eqns (140) and (146) we shall insert into the left-hand side of the invariant (151) the values $H = H_f$, $\varphi = 0$, and $\sigma = \sigma_f$, and into the right-hand side the values $H^{id} = H_f$ and $\varphi^{id} = \theta_f$, corresponding to the case of $\Delta\Omega(H_f) < 0$. The result is

$$2\sigma_f+\Delta PH_f+\int_{H_f}^{H_1}\frac{\sigma(H)\sin\varphi(H)}{r}\,dH = 2\sigma_0\cos\theta_f+\Delta PH_f+\int_{H_f}^{H_1}\frac{\sigma_0\sin\varphi^{id}(H)}{r}\,dH^{id},$$

which is usually written[41]

$$2\sigma_f+\frac{\tau}{r_f}=2\sigma_0\cos\theta_f, \quad (152)$$

or

$$\Delta\Omega(H_f)+\frac{\tau}{r_f}=2\sigma_0(\cos\theta_f-1), \quad (153)$$

where

$$\tau = r_f\left[\int_{H_f}^{\infty}\frac{\sigma(H)\sin\varphi(H)}{r}\,dH-\int_{H_f}^{\infty}\frac{\sigma_0\sin\varphi^{id}(H)}{r}\,dH^{id}\right]. \quad (154)$$

τ is the line tension in the film model based on the assumption of two dividing surfaces. Eqn (154) is the exact analytical expression[1, 18, 44] for the line tension τ, and differs substantially from the approximate expressions used by some workers.[36, 41] Detailed descriptions of the line tension theory and of results obtained in measurements of the line tension have already been published.[5, 6]

We shall now show how an expression for the line tension can be obtained in the membrane model of the film.[48, 57] To this end we shall insert into the right-hand side of the generalised invariant for a circular liquid film (151) the values $H^{id} = 0$ and $\varphi^{id} = \theta_0$ (postulating the formation of the contact angle θ_0). The result is

$$2\sigma_f+\frac{\varkappa}{r_{f0}}=2\sigma_0\cos\theta_0-\Delta PH_f, \quad (155)$$

or

$$\gamma+\frac{\varkappa}{r_{f0}}=2\sigma_0\cos\theta_0, \quad (156)$$

or

$$\Delta\Omega(H_f)+\frac{\varkappa}{r_{f0}}=2\sigma_0(\cos\theta_0-1)-\Delta PH_f, \quad (157)$$

where

$$\varkappa = r_{f0}\left[\int_{H_f}^{\infty}\frac{\sigma(H)\sin\varphi(H)}{r}\,dH-\int_0^{\infty}\frac{\sigma_0\sin\varphi^{id}(H)}{r}\,dH^{id}\right] \quad (158)$$

is the line tension in the membrane model of the liquid film.[6]

We note that the equilibrium equations for circular films (152) and (156) differ from the analogous equations for cylindrical films (140) and (144) by including the terms τ/r_f and $\varkappa/r_{f0}$ in the left-hand side: these can be interpreted as 'two-dimensional' capillary pressures, associated with an inflection in the contact line (or dividing line according to Gibbs), by analogy with the capillary pressure $2\sigma_0/R$ (in the case of a sphere of radius R) created by the bending of the dividing surface.

The equations (154) and (158) give the relationship between the two types of line tension in the various thermodynamic models of liquid films:[1, 6]

$$\frac{\varkappa}{r_{f0}}=\frac{\tau}{r_f}-\int_0^{H_f}\frac{\sigma_0\sin\varphi^{id}(H)}{r}\,dH^{id}.$$

Expressions for the equilibrium of circular films with a meniscus, analogous to (148)–(150) for cylindrical films, have also been given[1, 18] (see Fig. 19*a*):

$$2\sigma_f+\Delta PH_f+\int_{H_f}^{H_1}\frac{\sigma(H)\sin\varphi(H)}{r}\,dH = 2\sigma_0+\Delta PH_0+\int_{H_0}^{H_1}\frac{\sigma_0\sin\varphi^{id}(H)}{r}\,dH^{id}, \quad (159)$$

$$\gamma+\frac{\tau_B}{r_0}=2\sigma_0+\Delta PH_0, \quad (160)$$

$$\Delta\Omega(H_f)+\frac{\tau_B}{r_0}=\Delta P(H_0-H_f), \quad (161)$$

where

$$\tau_B = r_0\left[\int_{H_f}^{\infty}\frac{\sigma(H)\sin\varphi(H)}{r}\,dH-\int_{H_0}^{\infty}\frac{\sigma_0\sin\varphi^{id}(H)}{r}\,dH^{id}\right] \quad (162)$$

is the line tension.[1, 18, 44]

Profile of the lens-like thickening in equilibrium with a liquid film. In the transition region between the lens-like thickening and the plane-parallel liquid film (see Fig. 16) the first principal curvature changes sign from negative to positive, whereas the second principal curvature remains negative:

$$k_1=-\frac{d\sin\varphi(H)}{dr} \text{ and } k_2=-\frac{\sin\varphi(H)}{r}.$$

The average negative curvature of the surface in the transition region ($k = k_1 + k_2$) within the liquid lens decreases to zero in absolute value when r increases, then becomes positive, and finally decreases again to zero in the almost plane-parallel region of the liquid film surrounding the lens.

A characteristic feature of the lens–liquid system is its basic disequilibrium, due to the fact that the chemical potentials of the components μ_i within the lens exceed the corresponding values in the phase α. In particular, the hydrostatic pressure P_d within the lens is greater than the pressure P_α in the phase α, and therefore the material in the lens will tend to pass into the phase α by direct flow or as a result of bulk or surface diffusion. This tendency increases as the size of the lens decreases and as the pressure (i.e. the chemical potentials of the components) within the lens is increased.

If the rate of the hydrodynamic or diffusion processes is low the system can be treated as a quasi-equilibrium system. In a system of this type the energetics and the mechanical equilibrium can be described by the methods of equilibrium thermodynamics.

The main difficulty in the thermodynamic description of the lens–liquid film system is the lack of an unambiguous definition (in terms of the postulated presence of two dividing surfaces in the

film) of the reference system (in particular the Gibbs reference system) within the film itself, since a pressure gradient is formally present as a result of the obvious inequality $P_d > P_\alpha$. This gradient is increased by the flow of liquid from the lens.

Similar difficulties arise in the membrane approach to the description of the film, since the tension γ becomes a function of the coordinate r owing to the pressure gradient in the film in the direction of the r axis (see Fig. 16*c*).

A possible approach to the thermodynamic description of the transition region of the film at the boundary with the lens is described below.[18]

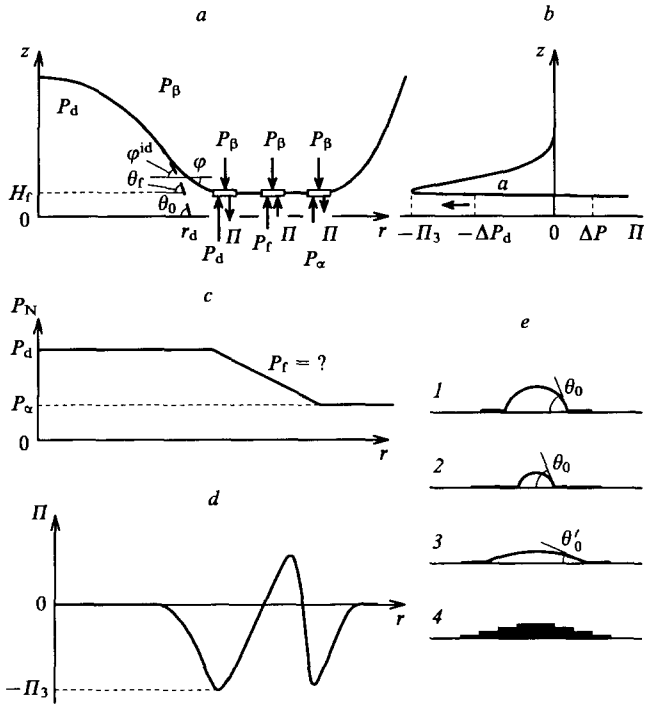


Figure 21. Equilibrium between the lens and the liquid film: (*a*) profile of the transition region between the liquid film and the lens; (*b*) profile of the disjoining pressure isotherm; (*c*) dependence of the normal component P_N of the reference pressure in the lens–liquid film system on the radius r; (*d*) distribution of the disjoining pressure in the lens–liquid film system; (*e*) evolution of the form of the liquid drop on a solid surface as a function of time.

The real profile of the film $z(r)$, including the profile of the lens itself (Fig. 21*a*), can be described by the Gibbs–Duhem equation or by the system of equations

$$\frac{dz(r)}{dr} = -\tan\varphi(H) , \tag{163}$$

$$\sigma(H)\frac{d\sin\varphi(H)}{dr} + \sigma(H)\frac{\sin\varphi(H)}{r} + \Pi(H)\cos\varphi(H) + \Delta P_f(r) = 0 , \tag{164}$$

where $\Delta P_f(r) = P_f(r) - P_\beta$, and $P_f(r)$ is the reference pressure in the film region. The form of the function $P_f(r)$ is not previously known, though it is obvious that $P_f(r) = P_d$ for $r < r_d$ (r_d is the radius of the lens) and $P_f(r) = P_\alpha$ in the bulk of the phase α. The form of the function $P_f(r)$ is shown schematically in Fig. 21*c*. The question mark in the symbol $P_f = ?$ denotes the ambiguity in the choice of the form of this function in the film region.

In spite of this ambiguity we can assume that the film will be accurately plane-parallel because of the low compressibility of the liquid. We can therefore write the equilibrium equation (164) in the film region as

$$\Pi(H) + \Delta P_f(r) \simeq 0 . \tag{165}$$

This means that in the transition region of the lens, where $P_f \simeq P_d$ (see Fig. 21*c*), the disjoining pressure is negative, since

$$\Pi + P_d - P_\beta = 0 \quad \text{and} \quad P_d > P_\beta$$

(see Fig. 21*a*). We should note that a negative sign for the disjoining pressure denotes mutual attraction of the dividing surfaces in the film

As we move away from the transition region of the film along the r axis the disjoining pressure becomes positive (Fig. 21*d*) because of the decrease in the reference pressure P_f caused by the repulsion of the dividing surfaces in the film. In considering the changes in sign of the disjoining pressure it should not be forgotten that within the model of two dividing surfaces in the film the disjoining pressure is defined as the excess of the specific interaction force (between the surfaces) over the effect of the arbitrarily chosen reference pressure. Therefore both the magnitude and the sign of the disjoining pressure are arbitrary. For example, if P_d is chosen as the reference pressure the disjoining pressure within the film will be negative everywhere.

Let us assume that the choice of reference pressure shown in Fig. 21*c* is an optimum. Then the disjoining pressure Π changes sign once again and becomes negative when r is increased within the transition region between the film and the phase α (see Fig. 21*a*) for the choice of disjoining pressure isotherm shown in Fig. 21*b*: this effect is due to the capillary pressure forces (see Fig. 18*b*).

By using the procedure described above for applying the generalised invariant of the film profile to the lens–liquid film system we obtain[18]

$$2\sigma(H)\cos\varphi(H) + \int_H^{H_1}\Delta P_f(r)dH - \int_H^{H_1}\frac{\sigma(H)\sin\varphi(H)}{r}dH = 2\sigma_0\cos\varphi^{id}(H) + \Delta P_d[H_1 - H^{id}(r)] - \int_{H^{id}}^{H_1}\frac{\sigma_0\sin\varphi^{id}(H)}{r}dH^{id} , \tag{166}$$

where H_1 is the thickness of the profile in the region of the bulk phase of the lens.

Inserting into the left-hand side of the invariant (166) the parameters corresponding to the real profile of the film ($H = H_f$, $\varphi = 0$, and $\sigma = \sigma_f$) and into the right-hand side the parameters corresponding to the idealised profile ($H^{id} = 0$, $r = r_d$, and $\varphi^{id} = \theta_0$) gives the following equilibrium equation:

$$2\sigma_f + \int_{H_f}^{H_1}\Delta P_f(r)dH - \frac{\varkappa}{r_d} = 2\sigma_0\cos\theta_0 + \Delta P_d H_1 , \tag{167}$$

where $\varkappa$ is the line tension, defined by the expression

$$\varkappa = r_d\left[\int_{H_f}^{\infty}\frac{\sigma(H)\sin\varphi(H)}{r}dH - \int_0^{\infty}\frac{\sigma_0\sin\varphi^{id}(H)}{r}dH^{id}\right] . \tag{168}$$

On the other hand inserting into the right-hand side of (166) the parameters $H^{id} = H_f$, $r \simeq r_d$, and $\varphi^{id} = \theta_f$ gives

$$2\sigma_f + \int_{H_f}^{H_1}\Delta P_f(r)dH - \frac{\tau}{r_d} = 2\sigma_0\cos\theta_f + \Delta P_d(H_1 - H_f) , \tag{169}$$

where the line tension τ is given by the expression[18]

$$\tau = r_d\left[\int_{H_f}^{\infty}\frac{\sigma(H)\sin\varphi(H)}{r}dH - \int_{H_f}^{\infty}\frac{\sigma_0\sin\varphi^{id}(H)}{r}dH^{id}\right] . \tag{170}$$

The equilibrium equations (167) and (168) can be simplified if $dP_f(r)/dr \ll 1$. Under these conditions the reference pressure P_f in

the transition region of the film can be treated as constant and equal to P_d, which allows the equilibrium equation to be written in the form[18, 33]

$$2\sigma_f - \frac{\varkappa}{r_d} = 2\sigma_0 \cos\theta_0 + \Delta P_d H_f \tag{171}$$

or

$$2\sigma_f - \frac{\tau}{r_d} = 2\sigma_0 \cos\theta_f . \tag{172}$$

Replacing the film by a membrane of zero thickness and using the definition (143) for the tension γ of the film converts Eqn (171) into

$$\gamma - \frac{\varkappa}{r_d} = 2\sigma_0 \cos\theta_0 . \tag{173}$$

For the equilibrium of a fluid (liquid or gaseous) drop in contact with a solid substrate (see Fig. 16*b*) the relationships (171)–(173) become[6, 36, 58]

$$\sigma_f - \frac{\varkappa}{r_d} = \sigma_0 \cos\theta_0 + \Delta P_d H_f , \tag{174}$$

$$\sigma_f - \frac{\tau}{r_d} = \sigma_0 \cos\theta_f , \tag{175}$$

$$\gamma - \frac{\varkappa}{r_d} = \sigma_0 \cos\theta_0 . \tag{176}$$

Eqn (176) has been used[59, 60] to determine the line tension $\varkappa$ from the experimental dependence of the contact angle θ_0 on the drop radius r_d on a solid or a liquid support. In these measurements it is usually assumed[6] that the tension γ of the film stays constant when the size of the drop or lens is changed, and Eqn (176) is used in the form[59, 60]

$$\cos\theta_0 = \cos\theta_0(\infty) - \frac{\varkappa}{\sigma_0 r_d} , \tag{177}$$

where $\theta_0(\infty)$ is the constant value of the contact angle corresponding to the condition $r_d \to \infty$.

The line tension $\varkappa$ is treated as positive if the contact line (or dividing line, according to Gibbs) has an excess of positive free energy, i.e. if it tends to shorten itself.[6] In particular, reported[59, 60] positive values of the line tension $\varkappa$ correspond to an increase in the contact angle with decreasing drop size. In this connection it has been pointed out[6, 18] that the dependence of the contact angle θ_0 on the drop radius r_d could be associated with the changes in the film tension γ rather than with changes in the line tension. In this case Eqn (177) should be replaced by the more general relation

$$\cos\theta_0 = \cos\theta_0(\infty) - \frac{\varkappa}{\sigma_0 r_d} + \Delta\gamma(r_d) , \tag{178}$$

where $\Delta\gamma(r_d) = \gamma(r_d) - \gamma(\infty)$, and allowance should be made for the $\gamma(r_d)$ dependence, which is not previously known.

We note that according to the generalised theory of the line tension[2, 3, 5, 18] $\varkappa$ can take only negative values for systems characterised by finite values of the angle of contact. Numerical estimates of the line tension as a function of the physicochemical parameters (shape of the profile of the disjoining pressure isotherm, size of the contact angle, capillary pressure, film size) have been recently reviewed.[6]

We shall discuss the causes and the character of the changes in the film tension γ in the lens–film (or drop–solid support) system.[18] A possible evolution of the liquid drop–solid substrate system induced by decreasing the radius r of the drop is illustrated in Fig. 21*e*. The existence condition of the finite contact angle θ_0 is the inequality

$$\Pi_3 > \Delta P_d = P_\alpha - P_\beta , \tag{179}$$

where Π_3 is the depth of the short-range coagulation minimum in the disjoining pressure isotherm $\Pi(H)$ shown in Fig. 21*b*. The representative point *a* on the $\Pi(H)$ isotherm corresponds to the state *1* of the system in Fig. 21*e*. Decreasing the size of the drop (state *2*) raises the pressure P_d in the drop, and the representative point on the $\Pi(H)$ isotherm moves to the left in the direction of the arrow. Under these conditions the angle of contact θ_0 remains finite, but changes in size under the influence of the line tension, and also of the change in the film tension γ.

By postulating that the thickness of the liquid layer H_f is not affected by the displacement of the representative point *a* to the left we can treat the interfacial tension σ as constant [see Eqn (145)]: this leads to a decrease in the film tension $\gamma = 2\sigma_f - \Delta P_d H_f$ with decreasing radius r_d of the drop.

When the size of the drop is decreased to the critical radius r_d^*, for which the capillary pressure ($2\sigma_0/R = 2\sigma_0 \sin\theta_0/r_d^*$) reaches the value Π_3, i.e.

$$r_d^* = \frac{2\sigma_0 \sin\theta_0}{\Pi_3} , \tag{180}$$

the finite contact angle θ_0 can no longer exist, and the drop discontinuously changes to the new state *3* (Fig. 21*e*) with a smaller contact angle θ_0' [if the $\Pi(H)$ isotherm has a long-range coagulation minimum Π_1, see Fig. 19*b*]. Under these conditions the new state is stable if the drop radius is greater than the critical value, defined by the relation (180), with Π_3 replaced by the new value Π_1.

If the Π_1 minimum does not exist, or the drop is smaller than the critical size, we observe spreading of the drop over the liquid layer, sometimes accompanied by the formation of several layers of molecular dimension[61–63] (state *4* in Fig. 21*e*).

This discussion of the equilibrium in the lens–liquid film system would not be complete without a mention of the possibility of spontaneous formation of lens-like thickening within initially plane-parallel films, accompanied by the thinning down of these initial formations. This effect can occur as a result of a local decrease in the interfacial tension σ_0: for example, during the mass transfer of SAS through a phase separation surface from the film to the boundary phase.[64]

The spontaneous thinning of plane-parallel liquid films stabilised by SAS at concentrations higher than the CMC often takes place by the stratification mechanism, i.e. a gradual layer-by-layer thinning to give increasingly thin layers.[65–67] The mechanism of this phenomenon is not clear.[67]

4. Interaction of interfacial surfaces in microscopic films

The microscopic liquid films (MLF) formed in the region of the contacts between emulsion drops and foam bubbles have an extremely small (almost zero) plane-parallel region, i.e. they consist almost entirely of a transition region, characterised by its profile $H(r)$ (Fig. 22*a*). This feature greatly complicates their thermodynamic description, since in order to determine the parameters of the interaction between fluid particles in a liquid medium we require information on the profile of the film, including the transition region.

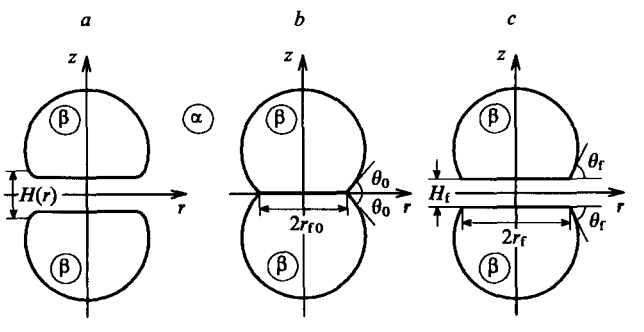


Figure 22. Representation of a microscopic liquid film (*a*) by the membrane model (*b*) and by a model which assumes two dividing surfaces in the film (*c*).

In particular this information is needed to calculate the grand thermodynamic potential Ω of the system which includes the volumes of the phases α and β, and also of the liquid film (for constant T and μ_i[5, 6, 14, 18]):

$$\Omega = -P_\alpha V_\alpha - P_\beta V_\beta + \int \sigma \, dA \,, \tag{181}$$

where the integration is carried out over the interfacial surface (the Gibbs dividing surface) allowing for the dependence of the interfacial tension σ on the position of the surface.

To simplify their thermodynamic description these systems are replaced by their analogues (reference or comparison systems), in which, for example, a circular membrane of zero thickness[55, 56] is used instead of the real microscopic liquid film (the membrane approach, Fig. 22*b*), or alternatively a circular plane-parallel film[12, 13] of thickness H_f (the approach based on the assumption of two dividing surfaces in the film, Fig. 22*c*). In this case the thermodynamic excess quantities are referred to the dividing (contact) lines. This creates the concept of linear thermodynamic excesses: for example, a line tension, representing the excess of the grand thermodynamic potential referred to unit length of the contact line.

In the membrane approach the expression for the grand thermodynamic potential of the idealised system is[5, 6, 14, 18]

$$\Omega^{id} = -P_\alpha V_\alpha^{id} - P_\beta V_\beta^{id} + \sigma_0 A^{id} + \pi r_0^2 \gamma + 2\pi r_{f0}^2 \varkappa \,, \tag{182}$$

where $\varkappa$ is the line tension of the film (or membrane) and the superscript id denotes quantities referred to the idealised system shown in Fig. 22*b* (in particular, A^{id} is the combined area of the two drops having a total volume V^{id} diminished by the two membrane areas πr_{f0}^2). The interfacial tension of this surface is arbitrarily taken to be equal to σ_0, even in the transition region, since it is assumed that no interaction exists between the drop surfaces (in keeping with stipulations of the method). By starting from the condition of energy equivalence of the real and the idealised system, i.e. $\Omega = \Omega^{id}$, we can define the line tension $\varkappa$ and calculate it. This approach has been fully discussed.[5, 6, 18]

When describing the interaction between drops in terms of the model of two dividing surfaces in the film the grand thermodynamic potential of the idealised system Ω^{id} is expressed[5, 6, 18] as (Fig. 22*c*)

$$\Omega^{id} = -P_\alpha V_\alpha^{id} - P_\beta V_\beta^{id} + \sigma_0 A^{id} + 2\pi r_f^2 \sigma_f + 2\pi r_f \tau \,, \tag{183}$$

where τ is the line tension, and the values V_α^{id}, V_β^{id}, and A^{id} differ from the corresponding quantities in Eqn (182), which relates to the membrane model of the film. Calculations of τ allowing for the condition $\Omega = \Omega^{id}$ have been reported.[5, 6, 18]

If the contact angles θ_0 and θ_f are not formed we can use idealised models (see Fig. 20*e*), relating to the membrane model and to the postulate of two dividing surfaces in the film respectively. The expressions for the grand thermodynamic potential corresponding to these models are

$$\Omega^{id} = -P_\alpha V_\alpha^{id} - P_\beta V_\beta^{id} + \sigma_0 A^{id} + \pi r_0^2 \gamma + 2\pi r_0 \varkappa_B \,, \tag{184}$$

$$\Omega^{id} = -P_\alpha V_\alpha^{id} - P_\beta V_\beta^{id} + \sigma_0 A^{id} + 2\pi r_0^2 \sigma_f + 2\pi r_0 \tau_B \,. \tag{185}$$

Calculations of the line tension τ_B have been reported.[5, 6]

5. Contact interactions in emulsions and foams

Theories of the adhesion of solid particles. The relationship between the adhesion force acting on solid (rigid) particles in liquid media and the parameters which characterise the interaction between phases in microscopic liquid films was established by Bradley[68] and Deryagin[69] during their development of the thermodynamic theory of solid particles. Their expression

$$f_a^* = \pi R \Delta F_a = \pi R \Delta \Omega(H_f) \,, \tag{186}$$

relates the force of adhesion f_a^* of solid non-deformable particles of radius R with the specific free energy of adhesion ΔF_a [equal to the specific grand thermodynamic potential of the interaction $\Delta\Omega(H_f)$ in a liquid film of thickness H_f for constant T and μ_i. In calculations of $\Delta\Omega(H_f)$ by formula (145) H_f is taken to be $\sim 0.2-0.5$ nm (see Refs 70 and 71), which corresponds to the short-range coagulation minimum on the $\Pi(H)$ isotherm.]

Eqn (186) can be used to calculate the influence of physicochemical factors (pH and ionic strength of the solution, surface charge, etc.) on the force of adhesion between the particles, since the effect of these factors on $\Delta\Omega(H_f)$ can be established on the basis of the Deryagin–Landau–Verwey–Overbeek theory[72, 73] or of the modern theories of the steric stabilisation of dispersions.[74–76]

The effect of the deformability of solid particles on the force of adhesion between them is allowed for in the Johnson–Kendall–Roberts theory,[77] according to which (in our symbols)

$$f_a^* = 0.75\pi R \Delta\Omega(H_f) \,. \tag{187}$$

The Muller–Yushchenko–Deryagin theory[78] led to the expression

$$f_a^* = \nu \pi R \Delta\Omega(H_f) \,, \tag{188}$$

in which the parameter ν takes values in the range $0.75-1$, depending on the size of the particles, their elastic properties, the thickness of the film, and the Hamaker constant (which characterises the energy of the molecular attraction between the surfaces).

The theory of adhesion of fluid particles was constructed and applied,[4, 18] and then further developed.[5, 6, 79] The proposed equation

$$f_a^* = \nu_a \pi R \Delta\Omega(H_f) \tag{189}$$

has the same form as the relationship of the previous theory, but the parameter ν_a, which lies in the range $0.5 \leqslant \nu_a \leqslant 1.0$, is more easily accessible for numerical calculations. For example, for the disjoining pressure $\Pi(H)$ isotherm, characterised by a single coagulation minimum (Fig. 23), the parameter ν_a is expressed as follows:[5]

$$\nu_a \approx \frac{1 + 0.5\alpha_a}{1 + \alpha_a} \tag{190}$$

where

$$\alpha_a = \frac{|\Delta\Omega(H_f)|}{\Delta_3 \sigma_0 k_0} = \frac{\Pi_3}{\sigma_0 k_0} = \frac{\Pi_3}{P_c} \,, \tag{191}$$

Δ_3 is the effective width of the short-range coagulation minimum, and P_c is the capillary pressure. If the particles are in the long-range coagulation minimum we must replace Π_3 by Π_1 according to Eqn (191) (see Fig. 20*b*).

The parameter α_a is characterised by the deformability of the particles: the lower the deformability, the greater is the similarity in properties between the fluid particles and the rigid solid particles during extension. For example, for $\Pi_3 \ll P_c$ we have $\alpha_a \simeq 0$, and therefore $\nu_a \simeq 1$, which corresponds to the Bradley–Deryagin adhesion theory. If $\Pi_3 \gg P_c$ we have $\alpha_a \gg 1$, and $\nu_a \approx 0.5$, and (189) becomes

$$f_a^* = 0.5\pi R \Delta\Omega(H_f) \,.$$

The dependence of the radius of the liquid film r_f between particles on the external force f_e has been obtained[4] by numerical modelling of the contact interactions between two identical liquid particles. This involved numerically solving the system of differential equations (97), (117), (129), (130), and (137) for fixed values of σ_0 and P_c, and also of the parameters which characterise the shape of the disjoining pressure isotherm $\Pi(H)$, but with a variable external force f_e [compressing ($f_e = f_p > 0$) or extending the particle ($f_e = f_a < 0$)]. The results of one series of

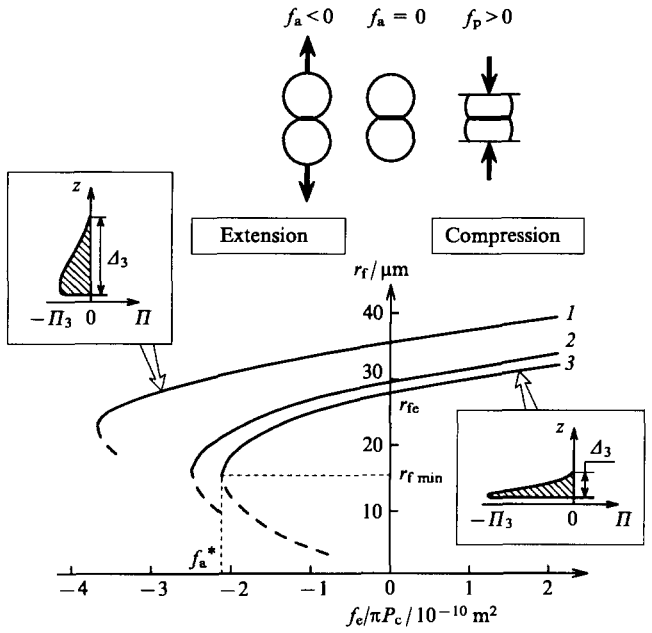


Figure 23. Dependence of the film radius on the reduced external force applied to a fluid particle of radius 1 mm ($\sigma_0 = 30$ mJ m^{-2}; $\Delta\Omega(H_f) = -60 \times 10^{-17}$ J m^{-2}) for different effective values of the parameter Δ_3, nm: (*1*) 10, (*2*) 10^2, (*3*) 10^3; $r_{f\,min}$ is the minimum stable radius of the film at the moment of detachment of the particle; r_{fe} is the equilibrium radius of the liquid film for $f_e = 0$.

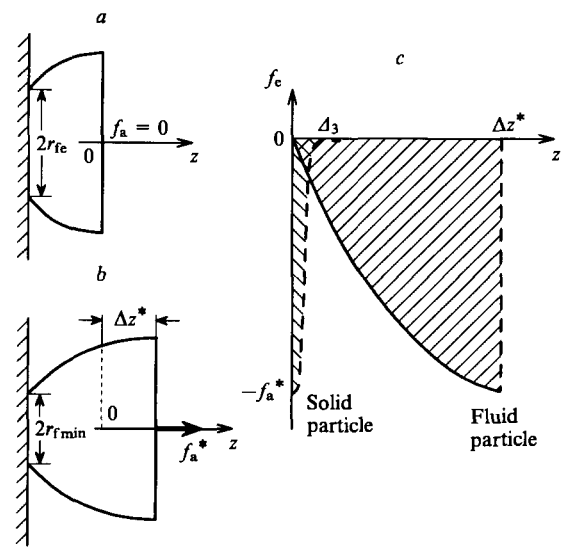


Figure 24. Illustration of the calculation of the work of removal of a fluid particle. Shape of the particle for $f_e = 0$ (*a*) and at the instant of removal f_a^* (*b*); dependence of the external force f_e on the displacement z for the removal of a solid or a liquid particle (*c*).

measurements of this type are shown in Fig. 23 as an illustration of the proposed method.[2, 4]

We should specially note that the shape of the $\Pi(H)$ isotherm (the width of the coagulation minimum Δ_3) for a given value of the free energy of interaction $\Delta\Omega(H_f)$ is strongly dependent on the force of adhesion f_a^* in the case of fluid particles, but in solid particles the dependence is negligibly small.

Work of separation of fluid particles. The strongest dependence on the shape of the disjoining pressure isotherm is seen in the work of separation of fluid particles W_a^f, which can exceed the work of separation of rigid solid particles W_a^s by more than a factor of 10^3 for equal values of $\Delta\Omega(H_f)$ and other parameters. The work W_a^f can be calculated by the relation (Fig. 24*c*)

$$W_a^f = \int_0^\infty f_e(H)\,dz \approx \tfrac{1}{2} f_a^* \Delta z^* , \tag{192}$$

where Δz^* is the displacement of the detachment force caused by the moment of the force which breaks the adhesion contact between the particles. The corresponding work W_a^s is

$$W_a^s = \int_0^\infty f_e(H)dz \approx \tfrac{1}{2} f_a^* \Delta_3 . \tag{193}$$

Obviously, the more deformable the particle, i.e. the greater the parameter α_a, the more markedly does the displacement Δz^* (Fig. 24*b*) exceed the radius of action of the molecular forces of attraction Δ_3, and the greater is W_a^f in comparison with W_a^s for a practically constant adhesive force f_a^*. In particular it has been shown[4, 5, 79] that

$$W_a^f \approx W_a^s\left(1 + \frac{\alpha_a}{2}\right) . \tag{194}$$

Eqn (194) provided the basis for the derivation of the criterion of the aggregation stability (stability towards coagulation) of emulsions,[5, 18] which for a disjoining pressure with one coagulation minimum takes the form

$$\nu_a \frac{R\Delta\Omega^2(H_f)}{\Pi_3}\left(1 + \frac{\alpha_a}{2}\right) \leqslant B , \tag{195}$$

where B is a parameter of the order of $10k_BT$, and k_B is Boltzmann's constant. If the emulsion is stable towards coalescence the relationship (195) is also the thermodynamic criterion for the spontaneous dispersing of the precipitate from such an emulsion.

In the cases of $\alpha_a = \Pi_3/P_c \to 0$ the liquid drops in the emulsion can be treated as completely rigid, and (195) is converted into the thermodynamic criterion of the aggregation stability of sols,[80, 81] i.e. (in our symbolism)

$$\frac{R\Delta\Omega^2(H_f)}{\Pi_3} \leqslant B . \tag{196}$$

For emulsions with a low value of the interfacial tension σ_0 and $\alpha_a \gg 1$ we obtain from (195) the corresponding criterion for the stability to aggregation and spontaneous dispersion of these emulsions:[5, 79]

$$\frac{R^2\Delta\Omega^2(H_f)}{\sigma_0} \leqslant B . \tag{197}$$

The expression (197) shows that if the isotherm $\Pi(H)$ has one coagulation minimum the coagulation tendency increases as σ_0 decreases, and that the tendency towards spontaneous dispersion of the precipitate from these emulsions decreases. The criterion (197) differs from the Lee and Tadros criterion for spontaneous emulsification,[82] given (in our symbols) by

$$\pi R^2\sigma_0 \leqslant B , \tag{198}$$

which describes the spontaneous formation of emulsions from macroscopic phases and predicts an increased propensity towards emulsification for lower values of σ_0.

Effect of the coagulation barrier on the adhesion of fluid particles. If the disjoining pressure isotherm $\Pi(H)$ has a coagulation barrier of height Π_2 (see Fig. 20*b*) the barrier can be surmounted in a fluid particle by applying the critical compressive force f_p^* (for a zero or negligibly small long-range coagulation minimum Π_1):[3, 5, 79, 83]

$$f_p^* = \nu_p \pi R\Delta\Omega(H_f^c) , \tag{199}$$

where $\Delta\Omega(H_f^c)$ is the specific free energy of the interaction for a thickness corresponding to the transition from a common black film to a Newtonian Black film or to coalescence, and $\nu_p = \Pi_2/P_c$ is a parameter which characterises the deformability of the particle in compression:

$$\nu_p \simeq \frac{1}{1-\alpha_p} \quad \text{for } P_c > \Pi_2 , \tag{200}$$

$$\nu_p = +\infty \quad \text{for } P_c \leqslant \Pi_2 .$$

Obviously, if the interfacial tension σ_0 is so low that the capillary tension P_c is smaller than Π_2 the coagulation barrier prevents the transition from α to β films (see Fig. 20*a*). At constant σ_0 the critical force f_p^* increases with the radius R of the particle. When $P_c > \Pi_2$ β-films are formed, and their adhesion force f_a^* is proportional to $\Delta\Omega(H_f^N)$ (see Fig. 20*a*). On the other hand if $P_c < \Pi_2$ α-films are formed, whose adhesion force f_a^* is proportional to $\Delta\Omega(H_f^c)$, i.e. it is $\sim 10^2 - 10^3$ times smaller than for β-films. During phase transitions (for example, during the melting of solid particles) we can expect a large decrease in the force of adhesion if the condition $P_c < \Pi_2$ applies to the liquid particles (assuming that compression of the solid particles invariably produces β-films).

These features of the contact interactions of liquid particles of emulsions and of the same particles with solid supports play an important role in technological processes (microencapsulation, filtration of emulsions, etc.), and also in biological processes.[27, 84–87]

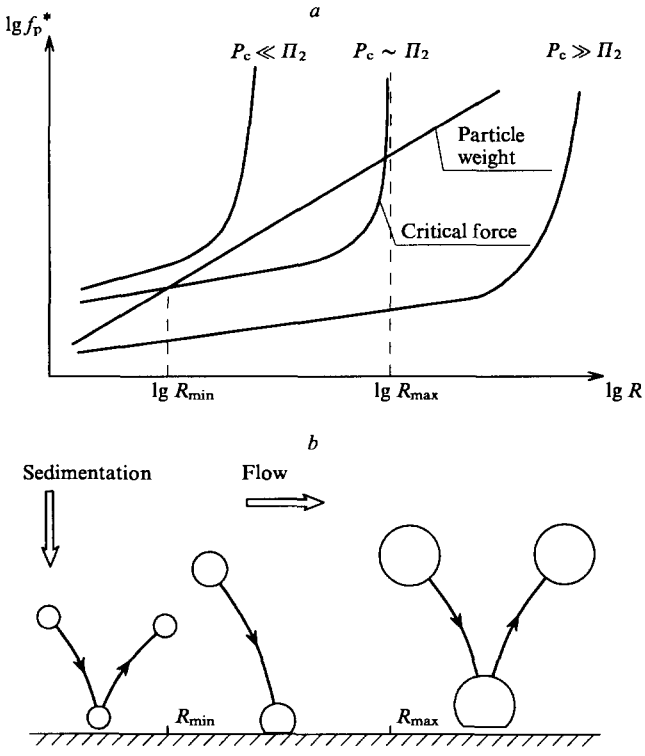


Figure 25. Effect of the radius of a liquid particle on its adhesion to a solid surface (idealised): (*a*) the dependence of the weight of a liquid particle and of the critical breaking force of the α-film for different relative values of the capillary pressure and of the height of the coagulation barrier in the disjoining pressure isotherm; (*b*) schematic illustration of the selective hetero-coagulation of the emulsion drops on the solid surface during sedimentation and flow.

The results of the theory of adhesion of solid particles are illustrated in Fig. 25*a*, which shows the dependence of the critical force f_p^* on the radius R, calculated by Eqn (199) for different heights of the coagulation barrier Π_2 in the disjoining pressure isotherm. For comparison we also show the dependence on R of the gravity force on the particles in the liquid.[3] In the case of the flow of a polydispersed emulsion with sedimentation of the liquid drops the drops accumulating at the bottom will experience the Stokes frictional force, and their weight will reflect the resultant of the force of gravity and of the repulsive force (Fig. 25*b*).

In the general case the plots of the critical force and of the weight against the radius of the particles intersect at two points, corresponding to R_{min} and R_{max}. In the region of $R < R_{min}$ the weight of the particle is insufficient to overcome the coagulation barrier Π_2, and the particles form α-films with a solid surface. They can be extracted by the flow because the force f_a^* is very small.

Similar effects are observed when $R > R_{max}$, i.e. for $P_c < \Pi_2$.

On the other hand if the condition $R_{min} < R < R_{max}$ applies the weight of the particles is insufficient to overcome the coagulation barrier and the drops form thin β-films with the surface. Under these conditions the force of adhesion may be sufficient to hold the drops on the surface during the flow of liquid. Thus we may achieve the selective heterocoagulation of fluid particles on a solid surface: only particles of a size within a fairly narrow range of radii become adsorbed.[3] The radius range corresponding to heterocoagulation can be varied by varying the physicochemical parameters of the system. For example, raising the coagulation barrier (by decreasing the concentration of electrolyte in solution) can make the $f_p^*(R)$ curve lie above the graph of the force of gravity experienced by the particles (Fig. 25*a*), and β-films will not be formed, whatever the radius of the particles. If the concentration of electrolyte is increased, i.e. if the coagulation barrier is lowered, the $f_p^*(R)$ curve will lie below the plot of the particle weight in a range of radii, and only β-films will be formed.

The radii R_{min} and R_{max} have been established experimentally[88] for a system in which gas bubbles are in contact with the phase boundary in gas–aqueous SAS solutions. The experimental values of R_{min} and R_{max} have been used[3] to calculate the parameters which characterise the coagulation barrier (Π_2 and Δ_2) of the disjoining pressure isotherm.

The work W_p^s needed to overcome the coagulation barrier at the contact of solid particles can be written as[18, 83]

$$W_p^s \simeq \pi R \frac{\Delta\Omega^2(H_f^s)}{\Pi_2}(1+\beta) , \tag{201}$$

where $\beta = \Pi_2/\Pi_3$. Under these conditions the corresponding work for liquid particles is[5, 18, 83]

$$W_p^f \simeq W_p^s \frac{1+\alpha_p}{1-\alpha_p} \quad \text{for } P_c > \Pi_2 . \tag{202}$$

The value of this work tends towards infinity for $P_c \leqslant \Pi_2$.

If the solid particle can overcome the coagulation barrier by expending an amount of work W_p^s it can be extracted (i.e. it can overcome the coagulation barrier in the reverse direction) by performing an amount of work[79]

$$W_a^s \simeq \pi R \frac{\Delta\Omega^2(H_f^N)}{\Pi_1} , \tag{203}$$

where

$$\Delta\Omega(H_f^N) \simeq \Pi_3 A_3(\alpha - 1) \quad \text{and} \quad \alpha = \frac{\Pi_2 A_2}{\Pi_3 A_3} .$$

The expression for the corresponding work in the case of a liquid particle is

$$W_a^f \simeq W_a^s(1 + \alpha_p + \alpha_a) , \tag{204}$$

where $\alpha_p = \Pi_2/P_c$ and $\alpha_a = \Pi_3/P_c$.

In conclusion we quote expressions for the aggregation stability criterion of the emulsion in the case of irreversible coagulation of the particles (for the condition $W_a^f \gg k_B T$),[83]

$$W_p^s \frac{1+\alpha_p}{1-\alpha_p} > B , \tag{205}$$

and for the spontaneous dispersion of the precipitates from the emulsion[83]

$$W_a^s(1 + \alpha_p + \alpha_a) < B . \quad (206)$$

The writer has discussed[18, 79, 83-87] the effect of σ_0 on the stability of emulsions and their propensity for spontaneous dispersion by allowing for the criteria (195), (196), (197), (205), and (206). In particular it was shown that whereas in a disjoining pressure isotherm without a coagulation barrier a decrease in the interfacial tension lowers the aggregation stability of the emulsion, in the presence of a coagulation barrier of sufficient height the effect of the surface tension on the stability of the emulsion is exactly the opposite. Therefore when examining the stability of emulsions and comparing the results of different studies of its dependence on σ_0 it is essential to allow for differences in the concentration of electrolytes and for other factors which influence the height of the coagulation barrier.

V. Conclusions

This review of studies of the thermodynamics of curved free interfacial surfaces in the region of the bulk meniscus of liquid films has identified different approaches to the determination of the interfacial tension of these surfaces.[8, 19, 21] We have shown that alternative methods of determining the interfacial tension of curved surfaces are possible, and that they lead to fundamental (Gibbs–Kelvin) equilibrium equations more convenient for practical applications in the case of objects of submicroscopic dimensions.

The thermodynamics of interacting curved interfaces (i.e. the thermodynamics of the transition region of a liquid film)[1-6, 18] are a self-consistent and closed system of concepts and of equations relating the disjoining pressure to other thermochemical parameters and functions. They reconcile the thermodynamics of free curved interfaces with those of the interacting interfaces in plane-parallel liquid films, and they reduce to the latter in the appropriate ranges.

The invariants obtained for the profiles of liquid films can be used to find all the known equations for the equilibrium of liquid films with a bulk meniscus, both in the membrane approach and in the approach based on the assumption of two dividing surfaces in the liquid film. These invariants can also be used to derive precise analytical expressions for the line tension.[3, 5, 6]

The theory of the adhesion of liquid particles developed by the writer[1, 4, 18] establishes the relationship between the adhesion forces and the parameters which characterise the disjoining pressure isotherm in the liquid film. The relationship between the force of adhesion and the specific free energy of adhesion obtained by this theory differs from the corresponding expression of the Johnson–Kendall–Roberts theory,[77] which is usually adopted to describe the adhesion of elastic solid particles and includes the Bradley–Deryagin theory[68, 69] as a limiting case (relating to liquid particles with a very large capillary pressure).

Our criterion[18, 79, 83] for the aggregation stability of emulsions can be used to explain the effect of the interfacial tension and of the shape of the disjoining pressure isotherm on the stability of emulsions towards coagulation. In particular we have shown that a decrease in σ_0 can both increase and decrease the aggregation stability of emulsions, depending on whether or not the $\Pi(H)$ isotherm includes a coagulation barrier. This large difference in the behaviour of emulsions as compared with sols under identical physicochemical conditions is attributed to the fact that in the interaction between liquid drops in emulsions the work associated with the deformation of the particle surfaces can exceed by a factor of $\sim 10^3$ the work of the disjoining pressure forces.[1, 4]

References

1. V G Babak *Colloids Surf.* **25** 1 (1987)
2. V G Babak *Colloids Surf.* **25** 25 (1987)
3. V G Babak *Colloids Surf.* **28** 123 (1987)
4. V G Babak *Colloids Surf.* **25** 205 (1987)
5. V G Babak *Voprosy Termodinamiki Geterogennykh Protsessov i Teorii Poverkhnostnykh Yavlenii* (Problems of the Thermodynamics of Heterogeneous Processes and of the Theory Surface Effects) (St Petersburg: Izd. Peterburgskogo Univ., 1992)
6. V G Babak *Usp. Khim.* **61** 1777 (1992) [*Russ. Chem. Rev.* **61** 975 (1992)]
7. T Kolarov, A Scheludko, D Exerova *Trans. Faraday Soc.* **64** 2864 (1968)
8. J W Gibbs *The Collected Works of J Willard Gibbs* (New York: Dover, 1971) Vol. 1
9. F P Buff, in *Handbuch der Physik.* (Berlin: Springer, 1960) Vol. 10, p. 281
10. S Ono, S Kondo, in *Handbuch der Physik* (Berlin: Springer, 1960) Vol. 10, p. 134
11. A I Rusanov *Fazovye Ravnovesiya i Poverkhnostnye Yavleniya* (Phase Equilibria and Surface Effects) (Leningrad: Khimiya, 1967)
12. A I Russanov *Phasengleichgewichte und Grenzflächenerscheinungen* (Berlin: Akademie-Verlag, 1978)
13. A I Rusanov, in *Sovremennaya Teoriya Kapillyarnosti* (Modern Theory of Capillarity) (Leningrad: Khimiya, 1980) p. 13
14. J S Rowlinson, B Widom *Molecular Theory of Capillarity* (Oxford: University Press, 1982)
15. I B Ivanov, P A Kralchevsky, in *Thin Liquid Films. Fundamentals and Applications* (New York: Marcel Dekker, 1988) p. 49
16. V S Markin, M M Kozlov, S L Leikin *J. Chem. Soc., Faraday Trans. 2* **84** 1149 (1988)
17. V S Markin, M M Kozlov *J. Colloid Interface Sci.* **135** 553 (1990)
18. V G Babak *Fizikokhimiya Mikroskopicheskikh Zhidkikh Plenok, Stabilizirovannykh Polimerami* Ch. 1 *Termodinamika Kontaktnykh Vzaimodeistvii v Zhidkikh Sredakh* (Physical Chemistry of Microscopic Liquid Films Stabilized by Polymers. Pt 1. Thermodynamics of Contact Interactions in Liquid Media) (Sverdlovsk: Izd. Ural. Univ., 1988)
19. L Boruvka, A W Neumann *J. Chem. Phys.* **66** 5464 (1977)
20. J S Rowlinson *J. Chem. Soc., Faraday Trans. 2* **79** 77 (1983)
21. L Boruvka, Y Rotenberg, A W Neumann *Langmuir* **1** 10 (1985)
22. V G Babak *Usp. Khim.* **62** 14 (1993) [*Russ. Chem. Rev.* **62** 11 (1993)]
23. A I Rusanov *Termodinamika Poverkhnostnykh Yavlenii* (Thermodynamics of Surface Effects) (Leningrad: Izd. Leningrad Univ., 1960)
24. F C Goodrich *Surface and Colloid Science* (Ed. E Matijevic) (New York: Wiley, 1969)
25. J C Melrose *Ind. Eng. Chem.* **60** 53 (1968)
26. S Kondo *J. Chem. Phys.* **25** 662 (1956)
27. V G Babak *Fizikokhimiya Mikroskopicheskikh Zhidkikh Plenok, Stabilizirovannykh Polimerami* Ch. 2 *Modelirovanie Kotaknykh Vzaimodeistvii v Polimersoderzhashchikh Dispersnykh Sistemakh* (Physical Chemistry of Microscopic Liquid Films Stabilized by Polymers. Pt 2. Modelling of Contact Interactions in Polymer-Containing Dispersed Systems) (Sverdlovsk: Izd. Ural. Univ., 1988) p. 168
28. T Kolarov, Z M Zorin *Colloid Polym. Sci.* **257** 1292 (1979)
29. Z M Zorin, D Platikanov, T Kolarov *Colloids Surf.* **22** 147 (1987)
30. B G Babak, VA Babaitsev *Khim. Khim. Tekhnol.* **29** 64 (1986)
31. V G Babak, R A Monissova *J. Disp. Sci. Technol.* **6** 539 (1985)
32. D A Haydon, J L Taylor *Nature* **217** 739 (1968)
33. P M Kruglyakov, Yu G Rovin, in *Fizikokhimiya Chernykh Uglevodorodnykh Plenok (Bisloinye Lipidnye Membrany)* [Physical Chemisty of Black Hydrocarbon Films (Bilayer Lipid Films)] (Moscow: Khimiya, 1978)
34. W G M Agterof *J. Colloid Interface Sci.* **86** 384 (1982)
35. B V Toshev *Colloids Surf.* **2** 243 (1981)
36. N V Churaev, V M Starov, B V Derjaguin *J. Colloid Interface Sci.* **89** 16 (1982)
37. J C Eriksson, B V Toshev *Colloid Polym. Sci.* **264** 807 (1986)
38. B V Deryagin, N V Churaev *Kolloidn. Zh.* **38** 438 (1976)
39. J C Eriksson, B V Toshev *Colloids Surf.* **5** 241 (1981)
40. B V Toshev *C.R. Acad. Bulg. Sci.* **39** 87 (1986)

41. J A De Feijter, A Vrij *J. Electroanal. Chem.* **37** 9 (1972)
42. J A De Feijter, J B Rijnbout, A Vrij *J. Colloid Interface Sci.* **64** 258 (1978)
43. J A De Feijter, in *Thin Liquids Films. Fundamentals and Applications* (New York: Marcel Dekker, 1983) p. 1
44. V G Babak *Specific Free Energy of Interaction, Contact Angle and Linear Tension in Microscopic Liquid Films* Manuscript desposited in TsNIITEIP, No. 1109, Moscow, 1985
45. W G M Agterof *Studies on Common Black Liquid Films* Ph.D. Thesis. University of Utrecht, Utrecht, The Netherlands
46. M M Princen, S G Mason *J. Colloid Sci.* **20** 156 (1965)
47. F Huisman, K J Mysels *J. Phys. Chem.* **73** 489 (1969)
48. A Scheludko, B Radoev, T Kolarov *Trans. Faraday Soc.* **64** 2213 (1968)
49. G A Martynov, I B Ivanov, B V Toshev *Kolloidn. Zh.* **38** 474 (1976)
50. I B Ivanov, B V Toshev, B P Radoev *Wetting, Spreading and Adhesion* (Ed. J F Padday) (London: Academic Press, 1978)
51. B V Deryagin *Kolloidn. Zh.* **17** 207 (1955)
52. D Platikanov, M Nedyalkov, A Scheludko *J. Colloid Interface Sci.* **75** 612 (1980)
53. B V Toshev, I B Ivanov *Colloid Polym. Sci.* **253** 558 (1975)
54. I B Ivanov, B V Toshev *Colloid Polym. Sci.* **253** 593 (1975)
55. B V Deryagin, G A Martunov, Yu V Gutop *Kolloidn. Zh.* **27** 367 (1965)
56. B V Derjaguin, G A Martunov, Yu V Gutop *Research in Surface Forces* (New York: Consultants Bureau, 1966) p. 9
57. A Scheludko, V Chakarov, B Toshev *J. Colloid Interface Sci.* **82** 83 (1981)
58. B V Toshev, D Platikanov, A Scheludko *Langmuir* **4** 489 (1988)
59. J Gaydos, A W Neumann *J. Colloid Interface Sci.* **120** 76 (1987)
60. J A Wallage, S Schürch *J. Colloid Interface Sci.* **124** 452 (1988)
61. F Heslot, A M Cazabat, P Levinson *Phys. Rev. Lett.* **62** 1286 (1989)
62. F Heslot, N Fraysse, A M Cazabat *Nature* **338** 640 (1989)
63. A M Cazabat *C. R. Acad. Sci.* **310** 107 (1990)
64. O D Velev, T D Gurkov, I B Ivanov *Abstracts of the 9th International Symposium on Surfactants in Solution, Varna, 1992* p. 170
65. E D Manev, S V Sazdanova, A A Rao, D T Wasan *J. Disp. Sci. Technol.* **3** 455 (1982)
66. E D Manev, S V Sazdanova, D T Wasan *J. Disp. Sci. Technol.* **5** 111 (1984)
67. P M Kruglyakov, in *Thin Liquid Films. Fundamentals and Applications* (Ed. I B Ivanov) (New York: Marcel Dekker, 1988) p. 767
68. R S Bradley *Philos. Mag.* **13** 583 (1932)
69. B V Deryagin *Kolloid. Zh.* **69** 155 (1934)
70. V V Yaminskii, V A Pchelkin, E A Amelina, E D Shchukina *Koagulyatsionnye Kontakty v Dispersionnykh Sistemakh* (Coagulation Contacts in Dispersion Systems) (Moscow: Khimiya, 1982)
71. B V Deryagin, N V Churaev, V M Muller *Poverkhnostnye Sily* (Surface Forces) (Moscow: Nauka, 1985)
72. B V Deryagin, L D Landau *Acta Physicochim. USSR* **14** 637 (1943)
73. G R Kruyt *Colloid Science* (Translated into Russian) (Moscow: Izd. Inostr. Lit., 1955)
74. P G De Gennes *Macromolecules* **15** 492 (1982)
75. J M H M Scheutjens, G J Fleer *Adv. Colloid Interface Sci.* **16** 361 (1982)
76. J Klein, P Pincus *Macromolecules* **15** 1129 (1982)
77. K L Johnson, K Kendall, A D Roberts *Proc. R. Soc. London, A Math. Phys. Sci.* **324** 301 (1971)
78. V M Muller, V S Jushcenko, B V Deryagin *J. Colloid Interface Sci.* **77** 91 (1980)
79. V G Babak *Colloids Interface Sci.* **30** 307 (1988)
80. E D Shchukin, E A Amelina, V V Yaminsky *Colloids Interface Sci.* **2** 221 (1981)
81. E D Shchukin, E A Amelina, V V Yaminsky *Colloids Interface Sci.* **90** 137 (1982)
82. G W J Lee, Th F Tadros *Colloids Surf.* **5** 105 (1982)
83. V G Babak, in *Proceedings of the 8th Conference on Surface and Colloid Chemistry, Liblice, CSSR, 1989*
84. V G Babak *Langmuir* **3** 612 (1987)
85. V G Babak *Kolloidnaya Khimiya v Tekhnologii Mikrokapsulirovaniya* (Colloids Chemistry in the Technology of Microcapsulation) (Sverdlovsk: Izd. Ural. Univ., 1991)
86. V G Babak *Food Hydrocolloids* **6** 45 (1992)
87. V G Babak *Trudy Vserossiiskogo Seminara po Kolloidnoi Khimii i Fiziko-Khimicheskoi Mekhanike Pishchevykh i Bioactivnykh Dispersnykh Sistem (1991–92)* [(Proceedings of All-Russian Seminar on Colloid Chemistry and Physicochemical Mechanics of Food and Bioactive Dispersed Systems (1991–92)] (Ed. V G Babak) (Moscow: Nauka, 1993) p. 265
88. D Platikanov, M Nedualkov, A Scheludko *J. Colloid Interface Sci.* **75** 612 (1980)

Russian Chemical Reviews **62** (8) 729–742 (1993) ©1993 Russian Academy of Sciences and Turpion Ltd

UDC 541.13

New trends in capillary isotachophoresis

O V Oshurkova, A I Gorshkov

Contents

I.	Introduction	729
II.	Modern ideas about electrical transport in electrolyte solutions	730
III.	Modifications of the isotachophoretic method	732
IV.	Classical capillary isotachophoresis	733
V.	The coulophoretic method	735
VI.	Steady-state concentration boundaries in isotachophoresis	738
VII.	Electrocrystallisation with the aid of isotachophoresis	739
VIII.	The isotachophoretic method for the determination of the electromigration transport of the solvent in electrolyte solutions	739
IX.	Conclusion	740

Abstract. Modern ideas concerning electrical transport in electrolyte solutions and capillary isotachophoresis—one of the microanalytical methods based on the different mobilities of ions in electrolyte solutions—are briefly considered. The isotachophoretic methods are classified in terms of the positions of the solutions and the directions of motion of the boundaries. The application of the coulophoretic method to the analysis of solutions, the measurement of the amount of electricity passed through the system, and the measurement of the internal cross-section of the capillaries are described. A description is also given of the electromigration method for crystallisation in capillaries and the isotachophoretic method for the determination of the electrical transport of the solvent in electrolyte solutions. The bibliography includes 96 references.

I. Introduction

The phenomena associated with the motion of ions in electrolyte solutions were discovered in the middle of the XIXth century. It was then observed that species migrate in an electrolyte solution when a constant electric field is applied to the latter,[1–3] the cations and anions of the same electrolyte moving at different rates in the electric field in the solution.[4] The concepts of the mobility and transport numbers of ions in solution were therefore introduced. The formation of a boundary between two electrolyte solutions with a common ion was later observed in a constant electric field.[5] The boundary between solutions having a common anion migrates to the cathode while that between solutions having a common cation migrates to the anode. Kohlrausch and Whethem formulated the stability conditions in their classical studies.[6,7] They showed that a boundary between solutions which are stable in time may be formed only when the mobility of the non-common ion of the electrolyte, present ahead of the boundary in the direction of its motion under the influence of the electric field, is greater than the mobility of the non-common ion of the electrolyte to the rear of the boundary. Kohlrausch also established that the concentration of the solution to the rear of the boundary in the steady state is constant under the given conditions and is determined by the concentration of the solution ahead of the boundary. He derived theoretically the so-called regulating function, one of the forms of which was later given his name:

$$\frac{c_1 z_1}{c_2 z_2} = \frac{u_{c1}}{u_{c1} + u_{a2}} \frac{u_{c2} + u_{a2}}{u_{c2}} = \frac{t_{c1}}{t_{c2}} . \qquad (1)$$

Here c_1 and c_2 are the concentrations of two solutions with a common anion separated by a steady-state boundary, the subscripts 1 and 2 denote that the given quantity refers respectively to the front and rear solutions, u_c and u_a are the mobilities, i.e. the velocities in a unit electric field, of the cations and anions respectively, z_1 and z_2 are the charges on the cations, and t_c are the transport numbers of the cations. The Kohlrausch function (1) was formulated for a boundary between two solutions with different cations and a common anion.

The electrode solution (catholyte or anolyte) ahead of the boundary is called the leading solution (leader), while that to the rear of the boundary is called the terminating solution (terminator). The concentration of the terminating solution changes during the adaptation process (the attainment of the stationary state) in such a way that after a certain time, determined by the strength of the electric field and the difference between the mobilities ($u_{c1} - u_{c2}$), it becomes comparable to the quantity required by the regulating function. The adaptation constitutes an important property of such boundaries.

The formation of boundaries between two solutions is used to determine the transport numbers and mobilities of ions. The widths of the boundaries have been estimated theoretically.[8–10] Towards the end of the 1920s, the first attempts were made to use ionic boundaries for the separation of certain chemical elements.[11] Considerable interest in electromigration methods arose again in the 1960s in connection with the use of capillaries and the development of instrumental methods for the detection of boundaries in them. Such is a brief history of the development of *isotachophoresis*—the term applied to this phenomenon at the present time. This term implies the motion of non-common ions

O V Oshurkova I M Sechenov Institute of Evolutionary Physiology and Biology, Russian Academy of Sciences, prosp. Morisa Toreza 44, 194223 St Petersburg, Fax (7-812) 85 23 012
A I Gorshkov A I Ioffe Physicotechnical Institute, Russian Academy of Sciences, ul. Politekhnicheskaya 26, 194021 St Petersburg, Fax (7-812) 247 10 17

Received 26 February 1993
Uspekhi Khimii **62**(8) 774–787; translated by A K Grzybowski

on either side of the boundary at the same rate (equal velocity motion).[12]

It is noteworthy that the study of the phenomenon of isotachophoresis involved mainly dilute solutions and certain fundamental problems of electrical transport in electrolyte solutions were not considered. Up to the 1960s, simplified ideas concerning the motion of species in electrolyte solutions predominated. It was assumed that, at least in strong electrolyte solutions, ions are rigidly bound to the nearest water molecules and migrate together with the latter under the influence of the field.[13] This led to the erroneous view that the water in the electrolyte solution is present in two states—'free' and 'bound'. The so-called free water was chosen as the reference system in the measurement of the mobilities and the corresponding transport numbers of ions. Hence appeared the widely used concepts of 'apparent' and 'true' transport numbers corresponding to the 'apparent' and 'true' mobilities, etc. The incorrect ideas about the kinetic phenomena in electrolyte solutions led to a whole series of errors, which entered into a familiar monograph on kinetic phenomena in electrolyte solutions[14] and electrochemical manuals.[15]

II. Modern ideas about electrical transport in electrolyte solutions

The initial concept in electrical transport phenomena is that of ionic mobility. The latter is considered, in particular, because it is assumed that the electrolyte under consideration dissociates in aqueous solution only into ions of known composition. According to modern ideas, this claim is valid only for a small number of strong electrolytes in an aqueous solution in the range of low and moderate concentrations. As regards the majority of ionogenic substances, one cannot assume that all the ions into which they dissociate in aqueous solutions are known over a wide range of concentrations. Therefore in the general case one introduces the concept of the mobility of an ionic component. This is the average mobility of all the ionic forms, which includes the ionic component under consideration.[16] For example, in a cadmium chloride solution, the ionic component (cadmium) forms part of the cations Cd^{2+} and $CdCl^{+}$ and the anions $CdCl_3^-$ and $CdCl_4^{2-}$, but at moderate concentrations it migrates to the cathode in an electric field. The experimentally measured quantity is in fact the transport number of the ionic component. It is equal to the number of equivalents of this component transported in the direction of the cathode (or anode) when one Farad (0.96×10^5 C) passes through the solution. Clearly, when the ion is identified with the ionic component, significant errors may arise in the interpretation of the experimental results for electrical transport.[16] Unfortunately, the necessary difference is not drawn between the ion and the ionic component in many monographs and textbooks.

The concept of mobility presupposes the existence of a reference system in the measurement of the rate of motion of the ionic component in a specified electric field. The reference systems may be various including stationary and mobile ones. The laboratory system linked to the measuring instrument is stationary. Mobile systems may be linked to any species migrating in the solution under the influence of the field, for example to solvent species. The reference system can move at a rate averaged over all the moving species constituting the solution (mass-average, molar-average, etc. rate).[17] Another characteristic of electrical transport is the transport numbers expressed in terms of the mobilities of the ionic components (J). According to IUPAC rules,[18] they should be referred to the ionic components and determined in the coordinate system in which the mobilities included in them have been measured. It is noteworthy that the majority of Russian textbooks on electrochemistry did not require, until very recently, the introduction of a reference system in the determination of mobilities and transport numbers (two textbooks are exceptions[19,20]). These problems have been considered in detail by the present authors.[21]

The question which transport numbers (and in what coordinate systems) are measured by the corresponding experimental methods is fundamental.

We shall begin its consideration with the isotopic boundary method,[22] since it made it possible to demonstrate experimentally the difference between the reference systems in the measurement of mobilities and transport numbers. The essential feature of the method is as follows. Conditions preventing the convective mixing of the solutions are established in the electrolytic cell. A boundary is formed in the cell between two solutions with the same electrolyte concentration but different concentrations of an isotope of one of the elements of the electrolyte and the solvent. The position of the isotopic boundary of the electrolyte and the solvent is fixed relative to the measuring tube. A definite amount of electricity is passed through the cell, after which a number of samples are taken and the isotopic concentrations of the ionic component and the solvent are measured in them. The positions of the isotopic boundaries of the solvent and the ionic component are found from these data after passing a current or, in other words, the migration of the ionic component in the solvent as a result of the passage of a definite amount of electricity is determined.

The isotopic boundary method can be applied using a specially developed apparatus.[23] In order to eliminate convective mixing, the working compartment is filled with finely dispersed quartz sand with a grain size of 20–40 μm. The introduction of a bypass tube with a tap precludes the possibility of hydrodynamic flow (and hence a displacement of the boundaries) by a process other than electromigration. The extent of electroosmotic flow (V_{osm}) and the displacement of the boundaries caused by it are calculated from preliminary measurements of the flow potential ΔV for a pressure drop ΔP from the thermodynamic relation

$$\frac{V_{osm}}{I} = \frac{\Delta V}{\Delta P},$$

where I is the electric current passed during the period of the experiment.

Special measures are taken in order to obtain results stable in relation to the flow potential. The isotopic solvent (water) boundary is established by adding deuterium-enriched water to the second solution. The concentration of deuterium does not then exceed several atomic per cent, which makes it possible to refer the measured characteristics of the electrical transport to aqueous solutions with the usual isotopic composition. The deuterium content in the water is determined by the highly sensitive temperature-flotation method from the temperature of the indifferent equilibrium of a quartz microfloat.[24] The isotopic analysis of the added components is carried out mass spectrometrically. The water and lithium isotopic boundaries in the lithium chloride solution under conditions where a 50 mA current is passed through the system for 5 h migrate in the tube towards the cathode without change in their initial form. The water isotopic boundary lags behind the lithium isotopic boundary. It should be noted specially that the migration of the boundary due to the electroosmotic flow of the entire solution is similar in terms of magnitude to the electromigration displacement even at the fairly high solution concentration of 2 M. Failure to take into account electroosmosis was apparently the principal cause of the considerable scatter in the experimental results in previous studies of electromigration in solutions.[25]

Thus it has been confirmed experimentally that water in the lithium chloride test solution migrates towards the cathode when the current is passed and the difference between the laboratory coordinate system and the 'solvent as a whole' system in the measurement of the mobilities and transport numbers was clearly demonstrated. This result agrees qualitatively with the idea that the frequency of exchange of the water molecules close to the surface of the strong electrolyte ion and the remaining water is close to the exchange frequency of the water molecules in water.[26] One may conclude that at the same time there are no grounds for

subdividing the solvent molecules into those which are bound and not bound to the electrolyte ion and for the selection of the free solvent as the reference system in measurements of mobilities and transport numbers. Naturally, all the above effects are manifested appreciably only at moderate and high concentrations of electrolyte solutions. When the solution concentration tends to zero, the differences between the reference systems disappear.

We shall consider, from the standpoint of modern ideas, the coordinate systems in which mobilities and transport numbers are measured by classical methods.

The *Hittorf method*–the first known method for the measurement of transport numbers—consists of the following steps. The change in the number of equivalents of the ionogenic substance is measured (the transport numbers of the ionic components are determined for this purpose) in the electrode compartment of the electrolytic cell after passing a definite amount of electricity. For this purpose, the cell is fitted with a tap, which makes it possible to remove part of the solution from the electrode compartment after electrolysis and to determine the concentration of the test substance in it. On the basis of the erroneous ideas concerning the water bound to ions, most workers assumed that the Hittorf method yields apparent transport numbers. This was explained by the presence of an unaccounted for amount of water transported into the electrode compartment, where the difference between the concentrations before and after electrolysis is determined.[13,15] However, the Hittorf method has one experimental feature which has not been noted by many investigators. The point is that the amount of solution in the section separated for analysis changes during electrolysis. Therefore one determines in this section not only the amount of the test substance but also that of the solvent. Since the volume of the corresponding section of the apparatus is known, the amount of the solvent in it before the start of the electrolysis is likewise known. The most important element of the calculation by the Hittorf method is the adjustment of the amount of the test substance after electrolysis to the amount of water which was present in the separated volume before the passage of current. Without such adjustment, the error in the interpretation of the results is negligible only for dilute solutions. It has been shown[27] that this computational procedure makes it possible to obtain transport numbers in a coordinate system linked to the solvent as a whole without determining the rate of migration of the solvent itself. The above study was carried out in a general form without resorting to any model ideas about electrical transport in electrolyte solutions.

There exist methods for the determination of transport numbers from measurements of the e.m.f.'s of concentration and galvanic cells in an external gravitational field. The accuracy of the determination of transport numbers by these methods is appreciably lower than that of the determination by other classical methods.[28]

The *isotachophoretic method* is based on the direct measurement of the rate of motion of ionic components (in the simplest case ions). In the past, this method was known under different names: ion migration, analysis based on ionic mobilities, and the moving boundary method. In its application, a steady-state boundary is created between two electrolyte solutions with a common ion. The theory of the method has been described most fully by Milios and Newman.[29] On the basis of the general postulates of the thermodynamics of irreversible processes, the authors showed that the isotachophoretic method makes it possible to obtain transport numbers rigorously in a 'solvent as a whole' coordinate system. A cell in the closed compartment around one of the electrodes, at which the electrode process is known exactly, is used for this purpose. This permits the calculation of all the changes in the volumes of the substances segregating and dissolving. A correction is also introduced for the volume change during diffusional mixing at the boundary between the saturated solution at the electrode and the working solution in the main volume. The hydrodynamic processes in the region of the isotachophoretic boundary have been considered in a theoretical study.[30] A general expression was obtained for the fluxes of all the components of the solutions on either side of the boundary:

$$\rho_i(v_i - w) = \text{const},$$

where ρ_i is the concentration of the ith component (g cm^{-3}) and v_i and w are respectively the velocities of the component and the boundary in the laboratory coordinate system (cm s^{-1}). This equation was quoted without derivation by Milios and Newman.[29] We recall that the ith component can be characterised by the subscript 1 or 2 depending on whether the given species belongs to the leading or terminating solutions respectively. For the solvent (water), we have

$$\rho_{01} = \rho_{01}(v_{01} - w) = \rho_{02}(v_{02} - w).$$

Hence it follows directly that, when a direct electric current is passed through the leading and terminating electrolyte solutions, component transfer of the solvent by electromigration should take place since the water concentrations in the two solutions are in general not equal ($\rho_{01} \neq \rho_{02}$). The occurrence of water transfer by electromigration in each of the solutions 1 and 2 considered separately for the electric fields which exist in them when they form an isotachophoretic boundary also follows from this relation. The attempts to measure the electromigration transport of the solvent were made a fairly long time ago, but the scatter of the experimental data was so great[25] that these studies can be regarded only as evidence for the occurrence of the effect itself. The modern method for the measurement of the electromigration transport of the solvent in electrolyte solutions, based on the isotachophoretic regulating function, will be considered below adducing some results obtained by the isotopic boundary method.

One of the versions of the isotachophoretic method is the *method involving the joint observation* of the motion of the ions and the solution.[31] It does not require the exact knowledge of the electrochemical process at the electrode and therefore expands the possibilities of the usual isotachophoretic method. Under certain conditions, the joint observation method also permits the determination of the transport number relative to the solvent.[32] This is confirmed by the agreement between the results of the measurements of the transport numbers by this method and by the Hittorf method.[28]

The regulating function (1) constitutes the basis of all the ideas about isotachophoresis. In principle, the boundary between two electrolyte solutions with a common ion can be created at any concentrations of these solutions, but, when a direct electric current is passed through this boundary, it will be stable as a function of time only when the concentrations of the solutions satisfy the regulating function. Otherwise the concentration of the terminating solution will vary continuously and spontaneously until it reaches the value determined by the regulating function. The regulating function can be written in the following forms:[33]

$$\frac{c_1 z_1}{c_2 z_2} = \frac{t_1}{t_2} \qquad \text{(Kohlrausch form)}, \qquad (2)$$

$$\frac{c_1^0 z_1}{c_2^0 z_2} = \frac{t_1^0}{t_2^0} \qquad \text{(Hartley form)}, \qquad (3)$$

where c_1 and c_2 are the molar concentrations of the solutions and c_1^0 and c_2^0 are the corresponding molal concentrations (mol/kg of water).

The transport numbers in Eqns (2) and (3) differ fundamentally from one another, since they are measured in different coordinate systems: in the first case, measurements are made in the laboratory coordinate system in the absence of the flow of the solutions as a single whole, i.e. in a coordinate system common to both solutions, while in the second case measurements are made relative to the solvent of each solution, i.e. in coordinate systems which are different for the two solutions, since the flow rates of the solvent in the leading and terminating solutions are different.

The discrepancy between the right-hand sides of Eqns (1) and (2) and the identity of the left-hand sides should be noted. The point is that in Kohlrausch's time it was assumed that the Hittorf method (the only one known at the time) yields transport numbers in the laboratory coordinate system which are suitable for the regulating function. It is now clear that only a small error was then introduced, since the experiments were carried out with fairly dilute solutions. The expression relating both forms of the regulating function was obtained for the first time by Gorshkov:[33]

$$\frac{t_1^0}{t_2^0} = \frac{\rho_{02} t_1}{\rho_{01} t_2} \quad (4)$$

We may note that the differences between the two forms of the regulating function vanish, like the differences between the reference systems for the measurement of transport numbers, when the concentrations of the solutions tend to zero. Eqns (2) – (4) have been used in the development of a method for the determination of the electromigration transport of the solvent (water) in electrolyte solutions over a wide concentration range.

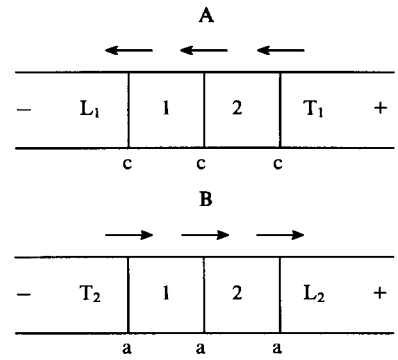
III. Modifications of the isotachophoretic method

Hitherto, in speaking of isotachophoresis, we considered only two solutions with a common ion. These solutions, placed in a electrolytic cell where their mixing is hindered, form after a time a moving steady-state isotachophoretic boundary when a current is passed. It is found that, when certain conditions are maintained in the electrolytic cell, several and not one boundary may exist. Depending on the type of these boundaries, on the direction of their motion in the electrolytic field, and on the disposition of the solutions in the column (electrolytic cell), it is possible to distinguish different varieties of isotachophoresis.[34]

1. Classical isotachophoresis

Classical isotachophoresis can be naturally subdivided into cationic and anionic. In the cationic version, the two electrolytes have a common anion and the boundary between the solutions with different cations accordingly migrates to the cathode. In anionic isotachophoresis, the electrolytes have a common cation and the boundary moves towards the anode in the electric field. The steady-state concentrations of the leading and terminating solutions are described by the regulating function. However, the terminating solution in the above pair can itself be the leading solution for a third solution if the mobility of the non-common ionic component of this third solution is lower than the mobility of the non-common ionic component of the given terminating solution. For the third solution, the former terminating solution becomes the leading solution. The concentration of the third solution is also determined by the regulating function, which includes the transport numbers of the non-common ionic components of the second and third solutions. Thus in cationic isotachophoresis it is possible to obtain a whole series of zones in the electrolytic cell, the boundaries between which correspond to the steady state. When the regulating function holds, they move to the cathode at the same rate. Similarly in anionic isotachophoresis it is likewise possible to obtain a series of zones of pure solutions, but this time with a common cation, which move at their constant rate towards the anode in the electric field. The disposition of the solutions in the direction of the movement of the boundaries in cationic (A) and anionic (B) isotachophoresis is illustrated in Scheme 1, which represents an electrolytic cell with solutions. The plus and minus signs in the scheme indicate the polarity of the applied potential, the numerals 1 and 2 denote the zones of the pure solutions, and L and T denote the leading and terminating solutions. The vertical lines indicate the boundaries of the solutions and the arrows show the direction of motion of the boundaries. The letters 'c' and 'a' denote the cationic and anionic boundaries.

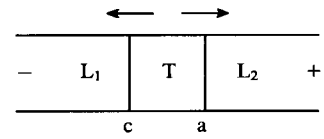
Scheme 1



2. Electrosynthesis at the ionic boundaries

The possibilities of isotachophoresis are greatly expanded when cationic and anionic boundaries are used simultaneously in the electrolytic cell. Electrosynthesis is the term given to the simultaneous formation and movement under the influence of the electric field of two diverging (cationic and anionic) isotachophoretic boundaries. The disposition of the solutions and the direction of the motion of the boundaries under the influence of the electric field are presented in Scheme 2.

Scheme 2

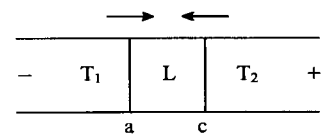


It is striking that one less electrically conducting solution can be synthesised from two more conducting solutions. During electrosynthesis, a third solution is formed from the leading solutions L_1 and L_2. It has a common cation with one leading solution and a common anion with the other. The amount of terminating solution synthesised increases continuously. The phenomenon of electrosynthesis frequently occurs in analytical capillary isotachophoresis and coulophoresis (see below). Electrosynthesis was first predicted by Kohlrausch.[6] Electrosynthesis at the ionic boundaries has nothing in common with the familiar synthesis of substances at electrodes. It makes it possible to obtain various electrolytic solutions — both inorganic and organic. Unfortunately, the method has not received a technological formulation and is not used in preparative let alone industrial practice.

3. Coulometric titration at ionic boundaries (coulophoretic method, coulophoresis)

In contrast to electrosynthesis, in coulophoresis the cationic and anionic isotachophoretic boundaries move towards one another under the influence of the electric field, as shown in Scheme 3.

Scheme 3



In this case, the leading solution is located between two terminating solutions and has a common cation with one of the terminating solutions and a common anion with the other. During electrolysis, the amount of the leading solution continuously diminishes up to its complete disappearance.

The coulophoretic method was proposed in 1974 as a new microanalytical method in capillaries based on the Faraday law.[35,36] The modifications of isotachophoresis (other than electrosynthesis) are considered below in the version performed

in capillaries, i.e. in the form of capillary isotachophoresis which is most widely used in practice.

IV. Classical capillary isotachophoresis

In order to carry out isotachophoretic processes, it is essential to ensure conditions under which convective stirring of the solutions in the column would be eliminated and instrumental methods for the detection of the boundaries must be available. The boundaries between coloured and colourless solutions can be detected visually at certain concentrations, but the region of applicability of isotachophoresis is then negligible. The conditions under which convective mixing is excluded in the electrolytic column have been examined.[37] The structure of the boundary between two solutions is influenced by the heat change. Heat is evolved in the column uniformly throughout its volume and is removed via the surface, as a result of which a temperature drop between the centre and the surface arises in the column cross-section. Since the mobility of ions depends on temperature, a convective mixing stream is superimposed on the rate of their translational motion. A second factor inducing the spreading of the boundary is the hydrodynamic and electroosmotic flow of the solutions in the column. All these factors can be described as purely diffusional mixing by introducing a quantity equivalent to the diffusion coefficient (D_{eq}). There exists an expression which makes it possible to estimate this quantity in columns with a circular cross-section.[37] Even for an electric field strength of 20–50 V cm^{-1}, the quantity D_{eq} differs little from the molecular diffusion coefficient provided that the column consists of a cylindrical capillary with an internal diameter of 0.2–0.5 mm. Even under the conditions of a hydrodynamic countercurrent the width of the majority of boundaries is then about 0.2 mm and the temperature drop between the centre and the periphery is about 1 °C. The countercurrent represents the hydrodynamic flow of both solutions against the motion of the boundary. If the velocity of the countercurrent is equal to the rate of mixing of the boundary in the electric field, then the boundary is stationary relative to the walls of the separating column.

The use of capillary columns makes it possible to eliminate the need for the maintenance of gravitional stability of the boundary. This means that in an electrolytic cell the boundary remains stable regardless of whether the denser solution is below it or above it. When columns with a large diameter are used, the mixing of the solutions due to the hydrodynamic flow, the operation of gravitational forces, and heating as a result of the evolution of heat are excluded by filling the column with an agar gel or finely disperse particles (sand, glass wool). The use of a gel is possible only in some cases, since it does not set at high concentrations of the solutions, decomposes in solutions of acids and alkalis, is sensitive to heating, and does not allow the use of a hydrodynamic countercurrent.

The choice of the geometrical parameters of the column and its operating conditions (the electric current, temperature, and the countercurrent) is made taking into account the proposed method for the detection of ionic boundaries. The optimum procedures for the detection of the boundaries are those which employ the common properties of the solutions. They include the thermometric method, the observation of the diffraction pattern when the capillary is illuminated with a narrow light beam, the measurement of the electrical conductivity of the solutions, and the measurement of the electric field in the solutions. These and other specific methods for the detection of boundaries in isotachophoresis have been briefly reviewed.[38] Yet another universal method for the detection of boundaries, based on detection with the aid of a thermoviewer of the IR radiation emitted from the surface of the column, was proposed in the same communication. For capillary columns with an internal diameter of 0.1–0.8 mm, it is most convenient to employ, depending on the tasks to be performed, the thermometric method and the methods involving the measurement of the electrical conductivity and the electric field, on the one hand, and the methods involving the observation of the diffraction pattern and the thermovisual observation, on the other. Such combination of a capillary electrolytic cell with instrumental methods for the detection of boundaries between the electrolyte solutions in them actually constitutes *capillary isotachophoresis*. It was proposed in 1962 in our country.[39,40] Studies on capillary isotachophoresis were subsequently published also abroad.[41]

Capillary isotachophoresis makes it possible to solve all analytical problems using microamounts of test substances and microvolumes of the solutions. At the present time, there are two versions of the instrumental formulation of the capillary isotachophoretic method. The first version, mainly developed abroad, presupposes the use of capillaries with an internal diameter up to 0.8 mm and the detection of the boundaries by means of a point detector on the basis of the temperature, the electrical conductivity, and the electric field strength frequently combined with additional detection based on the absorption of UV light. Such a detector makes it possible to determine the positions of all the boundaries only consecutively. One usually detects under these conditions boundaries moving past a stationary detector, although sometimes the detector is also moved (for example, a thermometric detector) relative to the capillary. In the second version, use is made of long detectors capable of detecting all the boundaries simultaneously. Such detectors are based on the observation of a diffraction pattern from a slit with sharp edges obtained when the capillary is illuminated with a narrow light beam. The capillary then acts as a cylindrical lens and the zones of solutions with various refractive indices appear on the screen as rectangles of different widths within which there are interference bands approaching one another towards the centre† (Fig. 1). The sensitivity of the method ensures the detection of boundaries for a difference between the refractive indices of the solutions forming them of 0.001–0.002.[42] A long detector based on measurements of the electrical conductivity of the solutions,[43] which consists of a horizontal section of a 9 cm long column with a rectangular cross-section (1 × 0.4 mm) on which 256 electrodes have been deposited at distances of 340 μm, has been described. A long detector in which the absorption of UV light is employed has also been proposed.[44] The detector in which the boundaries are detected with the aid of a thermoviewer also belongs to the class of long detectors.[38]

We shall now compare qualitatively the types of long detectors described. The diffraction detector makes it possible to detect relatively readily all the boundaries in a cylindrical transparent capillary over a section of any reasonable length. There are instruments in which the length of such a section reaches 240 mm.[45] This method of detection does not alter the natural width of the boundary. The detector has been used[43] in a column with a large cross-sectional area where the width of the boundary

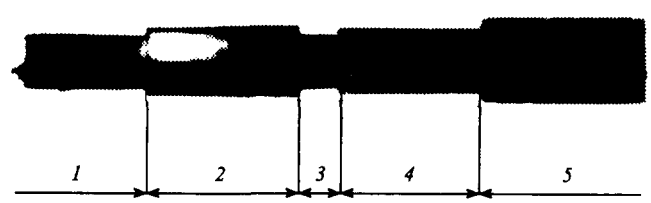


Figure 1. Photograph of the diffraction pattern obtained from a capillary after the separation of a mixture containing KCNS, K_2CO_3, and K_2TeO_3 solutions (a 0.5 mA current was passed for 2 h): *1*, terminating solution (4 M KCl solution); *2*, zone of KCNS solution; *3*, zone of K_2CO_3 solution; *4*, zone of K_2TeO_3 solution; *5*, leading solution (0.07 M KOH solution).

† These bands are visible only in the original and are lost on being rephotographed.

was therefore about 3 mm. The diffraction method is best used for highly concentrated solutions, although in the case of high-molecular-mass compounds the sensitivity indicated above (a difference between the refractive indices of 0.001–0.002) is attained at a concentration of about 0.01 M. A long thermal conductivity detector operates best in dilute solutions. Thus solutions with a concentration of about 0.01 M have been used.[43] The thermovisual method naturally has a higher sensitivity in the region of more dilute solutions. Industrial instruments in which this type of detection is employed have not so far been developed.

Evidently universal long detectors, effective over a wide concentration range (approximately from 0.001 M to saturated solutions) are most promising. Such detectors significantly facilitate the experiment, since they make it possible to observe the very process in which mixtures are separated into zones of pure solutions and one can make sure directly that it has reached completion when the lengths of the zones cease to change with time. The latter cannot be achieved when the zones move past a point detector and the completion of the separation process must be inferred in this case solely from indirect data.

Capillary isotachophoresis using the above methods for the detection of zone boundaries is a modern ultramicromethod for the qualitative and quantitative analysis of ionogenic substances in electrolyte solutions. The instruments used in capillary isotachophoresis in our country include the following: the single-channel AIP-1 apparatus,[37] the six-channel AIP-2 apparatus,[46] the four-channel IS-5501 apparatus,[45] and the single-channel ITFK-2-001 apparatus.[47] The electrolytic column and the optical part of the single-channel IS-5501 apparatus are illustrated schematically in Fig. 2.

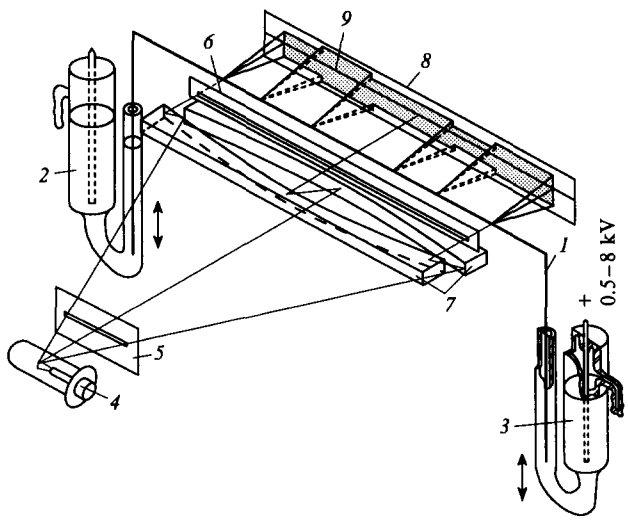


Figure 2. Schematic illustration of the optical component of one channel of the IS-5501 apparatus for capillary isotachophoresis: *1*, capillary with electrolyte solutions separated into zones; *2*, and *3*, electrode vessels with the leading and terminating solutions (the vessels can be lowered and raised in order to generate a hydrodynamic countercurrent); *4*, source of illumination; *5*, inlet diaphragm; *6*, outlet diaphragm; *7*, mirrors; *8*, screen; *9*, image of the capillary with the separated solutions.

1. Qualitative analysis

A method for qualitative analysis with the aid of capillary isotachophoresis, called the method of additives to standard mixtures, has been proposed recently.[48] Its essential feature is as follows. A preliminary study is carried out initially where the order in which the ionic components move to the electrode is investigated. For this purpose, one selects a series of compounds soluble in water (or another ionogenic solvent) with a common anion and another series with a common cation. The solutions are separated into zones with a single common anion by means of cationic capillary isotachophoresis and the sequence in which the zones move to the cathode is studied. This procedure includes the addition to the initial pure solution of a second solution with a common cation, the separation of the mixture into zones, the attainment of a steady state, and photography of the diffraction pattern. After this, the mixture is again separated changing the content of one of the components.

By comparing the photographs obtained, one can establish readily the order in which the two zones with a common anion follow one another. Next, a third pure solution is added with the same common anion, the mixture is again separated into zones and so on. It is thus possible to establish the order in which any number of zones with a common anion follow one another. For example, in solutions of formates the ammonium zone is followed by the sodium, barium, calcium, lithium, magnesium, cobalt, zinc, cadmium, and acetic acid zones.[49] At the same time conditions are selected under which the order in which the above zones follow one another is retained, i.e. the current, the concentration of the leading solution, and the concentration and pH of the terminating solution are selected.

The order in which the zones follow one another in solutions with other common anions and common cations are studied similarly. Examples of the separation of multicomponent solutions containing the cationic and anionic components of inorganic, organic, and amphoteric compounds have been published.[50–54] We may note that mixtures containing lanthanide ions and amino-acids, which are difficult to separate by the usual methods, were separated in the above investigations. The number of components in the mixtures separated sometimes reached 20. As already stated, the detection of the zone boundaries from the diffraction pattern is possible when the difference between the refractive indices of the solutions in the zones is not less than 0.001. For low-molecular-mass compounds, this difference is maintained when a solution with a concentration of about 0.5 M is used as the leading solution. For high-molecular-mass compounds, the lower limit of the concentration of the leading solution may be reduced by one or sometimes even two orders of magnitude.

The qualitative analysis of the mixture consists of the following steps. A standard solution with a known set of ionic components at approximately identical concentrations is separated under the chosen conditions with the aid of capillary isotachophoresis into zones of pure solutions. The zones obtained are then photographed. After this, part of the leading or terminating solution is removed from the capillary and the same volume of the test solution is introduced. An electric current is again passed through the column. Separation is carried out until the attainment of a steady state and the zones are photographed. The components of the test solution are then incorporated into the corresponding zones and increase their length [adaptation (Translator)]. The increase in the length of any one zone compared with the initial zone indicates the presence of the corresponding component in the test specimen.

The sensitivity of the qualitative analytical method described is determined by the width of the boundaries between the zones. The width is about 0.2 mm. The length of the zone for a specified amount of the substance in it is determined by the concentration and cross-sectional area of the column. If the initial length of the column of the test mixture placed in the capillary is 50 cm for a concentration of the leading solution of 0.5 M, then, in order that the length of the zone after adaptation should reach 0.2 mm (the width of the boundary), the concentration of the component in the solution should be not less than 10^{-4} M. There is in principle no upper limit to the concentration.

The analysis is carried out most readily when the concentrations of the components in the test solution differ by not more than two orders of magnitude for a length of the column

of solution of about 10 cm. In other cases, certain special procedures must be carried out in a preliminary step, which makes it possible to remove from the capillary the excess of the component present in an overwhelming amount. We may note that the qualitative analytical method considered requires the application of a universal long detector which detects simultaneously all the boundaries, for example a diffraction detector or a thermoviewer.

2. Quantitative analysis

Quantitative analysis with the aid of capillary isotachophoresis is based [40] on the regulating function. This is why so much attention was devoted above to the examination of its different forms. The quantitative analytical method may be absolute if the transport numbers of the ionic components of the leading and terminating solutions are known beforehand with the necessary accuracy (or, which is equivalent to the above, the concentration of the terminating electrolyte incorporated in the leading solution) over a wide range of concentrations of the solutions. Unfortunately, there are very few experimental data of this kind [28, 55–57] and the method is therefore used as a relative procedure requiring comparison with a standard. For this purpose, the length of the zone of the component to be determined (or the rate of movement of the zone past the detector, which is proportional to the above quantity) is measured in the standard and text mixtures under identical conditions. The methods for the quantitative analysis of dilute and concentrated solutions have been described in detail in numerous original communications and monographs [58–69] and we shall not be concerned with them here. We may note only that industrial products from different industries, natural waters and brines, aminoacids, as well as certain natural products were analysed.

Interesting features of the isotachophoretic separation of a two-component mixture have been noted.[70] It was found that the separation after adaptation is not accompanied by a change in the total volume of the solution. Therefore, by measuring during the separation process the lengths of the zones of the pure electrolyte solutions and the unseparated mixture, it is possible to determine, without waiting for the end of the separation process, the time required for the total separation and the contents of the components.

Thus the suitability of capillary isotachophoresis for both qualitative and quantitative analysis makes it an independent instrument in the laboratory identification and determination of ionogenic substances in electrolyte solutions.

3. Preparative possibilities of capillary isotachophoresis

A characteristic feature of capillary isotachophoresis is the use of ultrasmall amounts of substances and a virtually 100% separation of mixtures into pure solution zones, which leads to the possibility of its application as a preparative method. This concerns the isolation of a solution of the required substance from a mixture of electrolyte solutions and its separation in space for use in the solution of specific problems where pure substances in small amounts are required. Capillary isotachophoresis has been used, for example, for the separation of lithium salts from sodium salts.[71] The pure lithium chloride solution zone was cut off together with part of the capillary for subsequent isotopic analysis with the aid of a mass spectrometer.

The preparative possibilities of the method include also the concentration and dilution of solutions by adaptation with respect to the regulating function. A special case of such concentration is crystallisation with the aid of isotachophoresis.

Capillary isotachophoresis makes it possible to enrich a mixture of components present at low concentrations. The enrichment takes place as a result of the prolonged withdrawal of an element from a large volume into the capillary column. This preparative procedure has been used to determine small amounts of potassium chloride in an aqueous lithium chloride solution.[72]

The transfer of an ionic substance from one solvent to another can also be regarded as a preparative application of capillary isotachophoresis.[73] This procedure is based on the ability of the isotachophoretic boundary to transmit only the common ion and the solvent.

Thus capillary isotachophoresis may be used for preparative purposes. However, the use of large diameter columns will apparently become most promising in preparative isotachophoresis.

V. The coulophoretic method

1. Theoretical principles

Isotachophoresis was classified above in terms of the positions of the leading and terminating solutions in the column. One of its varieties is the coulophoretic method (coulometric analysis of the electrolyte solutions using ionic boundaries). A characteristic feature of the method is the presence in the electrolytic cell of cationic and anionic isotachophoretic boundaries moving towards one another (see Scheme 3). The formula for the rate of movement of a steady-state boundary between two solutions with a common anionic component is used in the theory of isotachophoresis.[29, 74, 75] It can include the characteristics of both the leading and terminating solutions. Thus the rate of movement of the cationic boundary v_c of the leading solution L_1 is

$$v_c = \frac{It_c}{zc_qS}.$$

where (in addition to the previous notation) I is the electric current (A), S the internal cross-sectional area of the electrolytic cell (dm^2), and c_q the concentration of the charges of the same sign per unit volume of the leading solution (C litre^{-1}). We recall that t_c is the transport number of the non-common cationic component in the laboratory coordinate system. A similar relation describes also the rate of movement of the second, anionic boundary between the above leading solution and the second terminating solution T_2:

$$v_a = \frac{It_a}{zc_qS}.$$

It includes the transport number of the anionic component of the leading solution in the same laboratory coordinate system. We transform the linear rates of movement of the boundaries into volume rates (v_cS and v_aS) and add together the last two expressions:

$$S(v_c + v_a) = \frac{I(t_c + t_a)}{zc_q},$$

where $S(v_c + v_a)$ is the volume traversed by the two (cationic and anionic) boundaries per unit time. We introduce yet another quantity – the time from the start of electrolysis until the instant t when the boundaries meet, and multiply both sides of the last equation by this time. Since $S(v_c + v_a)t = V$ is the volume of the leading solution before the start of electrolysis (as already mentioned, during the passage of current this volume continuously diminishes and becomes zero at the instant when the boundaries meet) and $t_c + t_a = 1$, it follows that

$$Vc_qz = VFcz = It, \qquad (5)$$

where F is the Faraday constant.

Eqn (5) constitutes the basis of the coulometric analysis of solutions using ionic boundaries. We shall consider it in greater detail. It relates the concentration of the leading solution investigated to the amount of electricity passed through the system and to the volume of the solution taken for analysis. Eqn (5) can be used to determine one of the three quantities mentioned above when the other two are known. The greatest interest attaches to the determination of the concentration of the solution from the amount of electricity passed through it and the volume traversed by the two boundaries. We have called this procedure the coulophoretic method of analysis of the solution or

coulometric analysis using ionic isotachophoretic boundaries. This analytical method will be examined in greater detail below. The second possibility presented by Eqn (5) consists in the determination of the amount of electricity passed in the circuit from the concentration of the solution and its volume. Such determination constitutes the basis of the new method, proposed by the authors, for the measurement of the amount of electricity by observing the motion of boundaries (see below). The determination of the volume traversed by the boundaries when the concentration of the solution and the amount of electricity passed through it are known constitutes the basis of the method for the determination of the internal cross-sectional area of the capillary and for the monitoring its constancy along the length.

The following characteristic features of the coulophoretic method may be noted. It is based on the Faraday law. However, the method differs fundamentally from the method of analysis of substances from their amounts produced at the electrode and the coulometric titration method, which is also associated with the reaction at the electrode. In the coulophoretic method, one compares the direct motion of the ions with the amount of electricity passed through the system, while the boundaries between the leading test solution and the two terminating solutions are actually set up in order to be able to follow the motion of the ions. Each boundary operates in a certain sense as an electrode with a 100% current yield;[76] only the common ionic component and the solvent pass through it. The rate of movement of the non-common ionic component constitutes the rate of movement of the boundary itself. The coulophoretic method is independent of the nature of the electrodes employed, the nature of the electrode reactions, and their current yield. This constitutes the fundamental difference between the electrodeposition and coulometric titration methods.

2. Analysis of electrolyte solutions

The theoretical aspects of the coulophoretic method were examined above. We shall now proceed to the description of its analytical application. The method may be used to solve three different problems: the determination of the concentration of the pure electrolyte solution; the analysis of a mixture of electrolyte solutions after its preliminary separation by capillary isotachophoresis into zones of pure solutions; the analysis of a two-component mixture without its complete separation into pure solutions.

Analysis of the pure solution. In order to determine the concentration of the test solution in conformity with Eqn (5), one should know the volume of the solution taken for analysis. For this purpose, a mercury column 20 – 30 cm long is introduced into a π-shaped capillary filament and narrow markers, 0.1 mm wide, are deposited on its ends with coloured sealing wax. The terminating electrolyte solutions are selected for the electrolyte test solution in accordance with the rules of isotachophoresis — one solution in terms of the cations and the other in terms of the anions; their chosen concentrations are close to that of the test solution. The exact concentration is unimportant, since the concentrations of the terminating solutions in the region of the boundaries automatically adapt to the concentration of the test solution in conformity with the regulating function when a current is passed. It is desirable that the concentrations of the terminating solutions should be below the equilibrium values, whereupon their adaptation is faster. In practice all these concentrations should not differ from the equilibrium concentrations by a factor greater than 10.

The capillary is filled with solutions with the aid of a water pump in the following way. Initially the entire capillary is filled with distilled water and then a tiny bubble (about 1 mm long) is formed at its end and beyond it one of the terminating solutions is introduced — up to the first marker. The bubble serves as an indicator of the movement of the solutions. The end of the capillary is then lowered into the test solution and the latter is introduced into the capillary until the indicator bubble moves to the second marker. Next, the end of the capillary is lowered into the second terminating solution and is filled until the bubble emerges from the capillary. As a result, the test solution is present in the middle part of the capillary between the markers and the terminating solutions are on either side of it. The ends of the capillary are lowered into approximately 5 cm^3 electrolytic vessels filled respectively with the solutions present at the two ends of the capillary. At the same time, the passage through the cell of a stabilised direct current is begun and a stopwatch, reckoning the time from the start of electrolysis to the instant when the boundaries meet, is started.

The cationic and anionic boundaries, moving towards one another, are formed between the test solution and the terminating solutions. The boundaries are observed with the aid of, for example, diffraction. At the instant when the boundaries meet, the stopwatch is arrested and the time from the start of electrolysis to the instant of the disappearance of the test solution is determined. The concentration of the test solution is calculated by Eqn (5). A universal long detector, for example a thermoviewer, is also suitable for the detection of the boundaries between the solutions. In certain cases the instant when the boundaries meet can be simply recorded visually.

The coulophoretic method has been used to determine the concentrations of solutions of various electrolytes: acids, alkalis, simple salts, and complexes with a low instability constant. The concentrations of an acid and alkali can be determined by this method with the aid of only one terminating solution, forming both the cationic and anionic boundaries, and salts can also be determined with the aid of another salt.[36]

Analysis of mixtures of electrolyte solutions. Mixtures are analysed after their preliminary separation into zones of pure solutions by isotachophoresis. The analytical method is as follows: as in the previous case, the volume of the marked section of the capillary is determined with the aid of mercury. Next, using the rules of isotachophoresis, the leading and terminating solutions are selected. The capillary column is filled with solutions in such a way that the test mixture is located in the capillary between the leading and terminating solutions. After this, the mixture is separated into pure solutions under the conditions of a hydrodynamic countercurrent. The separation is terminated when the number of zones becomes equal to the number of components to be determined and the lengths of the zones no longer vary with time. The leading solution is then replaced by a new solution (the second terminating solution prepared beforehand) in order to form a boundary moving through the solutions in opposition to the zones.

If the initial mixture was separated in terms of the cations, then the leading solution is the catholyte and is replaced by another solution, which serves as the terminating solution for the common anion of all the zones. Conversely, if the separation was carried out in terms of the anions, the leading solution is the anolyte and is replaced by another solution — the terminating solution for the common cation of the zones. In order to replace the leading solution by the second terminating solution, an electric current is switched on, the electrode vessel with the leading solution is lowered and is replaced by an electrode vessel with the new terminating solution prepared beforehand. This procedure should be carried out as fast as possible (about 3 s) in order to avoid the leakage of the solution, mixing, etc. After this, the current is switched on again and a boundary, moving through the leading solution in opposition to the zones, is formed at the end face of the capillary.

When this boundary meets the boundary of the first zone, the first stop-watch is started and the time up to the meeting of the given boundary with the boundary of the second zone is measured. At this instant, the first stopwatch is arrested and the second is started. The time reckoned by the first stopwatch is the initial quantity for the determination of the concentration of the

solution in the first zone. The time for the traversal of the second zone by the boundary is measured similarly, the stopwatch being stopped when this additional boundary encounters the beginning of the third zone. The first stopwatch, used for the preliminary reckoning of the time taken by the additional boundary to traverse the first zone, is started simultaneously. Thus one determines the time taken to traverse all the zones and hence also the concentrations of the solutions in these zones.[77] If a solid is analysed and all the components are determined by the coulophoretic method, it is not necessary to know the volume of the solution taken up into the capillary.

Analysis under conditions of incomplete separation of the mixture. In practice, one may encounter situations where a two-component mixture cannot be separated into zones of pure solutions by isotachophoresis. This happens, for example, if the mixture analysed includes a leading solution for which it is impossible to select a second leading solution with a greater mobility of the non-common ionic component. However it is found that the concentrations of the components of such a mixture can also be determined coulometrically by means of ionic boundaries, but this requires the use of standard specimens and a partial preliminary separation of the mixture analysed.[78]

We shall now estimate the error of the above coulophoretic method for the determination of the concentrations of solutions. It includes the contribution by the error of the determination of the volume of the capillary between the markers, the error of the measurement of the volume of the solution filling the capillary, the error of the determination of the time of traversal of the test solution by the boundaries, the error of the measurement of the current, and the errors of the stopwatches. The main contribution to the error of the method comes from that in the measurement of the volume of the section of the capillary between the markers ($\sim 0.5\%$) and also the error of the measurement of the volume of the solution taken up into the capillary (also $\sim 0.5\%$). The relative error of the measurement of the time of traversal of the zone by the additional boundary is equal to the ratio of the width of the boundary to the initial length of the zone. For a zone approximately 10 cm long and a width of the boundary of 0.2 mm, the error reaches 0.2%. Thus the overall error of the coulophoretic method for a zone length of 10 cm is not more than 1%.

The sensitivity of the method is determined by the potential of the chosen procedure for the detection of the boundaries. Thus when the diffraction pattern is used, the concentrations of the solutions should be not less than 0.1 M and for lower concentrations preliminary enrichment is necessary.

The following chemical compounds have been analysed hitherto by the coulophoretic method: HCl, KCl, NaCl, LiCl, NH_4Cl, $BaCl_2$, $CaCl_2$, $MgCl_2$, $CoCl_2$, $SmCl_3$, $NaNO_3$, NH_4NO_3, Na_2SO_4, $(NH_4)_2SO_4$, $(NH_4)_2HPO_4$, KCNS, $K_3Fe(CN)_6$, $K_4Fe(CN)_6$. Many of these were part of the composition of industrial products (fluxes, alloys, brines, melts, electrolytes), natural waters, and minerals.[36, 77, 79]

We may note the characteristic features of the coulometric analysis of solutions with the aid of ionic boundaries. The method is suitable for any ionogenic solutions of inorganic and organic substances and permits the analytical determination of the cationic and anionic components of electrolyte solutions. It is an ultramicromethod, which is fairly accurate, sensitive, and rapid. The method is absolute and does not require the use of standard specimens (with the exception of cases where a mixture with incomplete separation or with incomplete dissociation of ionogenic substances is analysed). In the analysis of a multi-component mixture where all the components are determined by the coulophoretic method, there is no necessity to know the weight of the initial mixture.[77] In practice, this method can be applied fairly simply: one can use commercial apparatus for capillary isotachophoresis with the detection of boundaries from the diffraction pattern; the capillary columns can be prepared under laboratory conditions; the capillaries need not necessarily have a constant internal cross section along the length; repeated use of the same capillary column is possible. Finally, a characteristic feature of all isotachophoretic methods, due to the adaptation of the terminating solution concentration, is the possibility of using terminating solutions at concentrations which have been determined only approximately.

The coulophoretic method has certain unique possibilities. It permits the analysis of a given solution with the aid of any terminating solution from the enormous set of those which are possible and conversely one can analyse many solutions using only one terminating electrolyte solution.[80] Terminating solutions containing mixed solvents can also be employed. Inert additives to a terminating solution do not affect the analyses. The coulophoretic method is perhaps the only one which makes it possible to determine the concentration of pure acids, alkalis, and salts with the aid of a solution of only one salt.[80] The method also permits the transfer of the ionogenic substance from one solvent to another simultaneously via two boundaries.[73]

However, the method described, which has important advantages, has not unfortunately found a sufficiently wide application consistent with its possibilities. This is probably associated with the rare use of the method of detection of the boundaries from the diffraction pattern.

3. Determination of the amount of electricity

The amount of electricity passed through the circuit is one of the fundamental quantities used in electrochemical studies. Therefore the new method for its measurement, proposed by Ansorg,[81] merits attention. The method is based on a familiar phenomenon — the transport of electricity by ions in the bulk of the electrolyte solution. The motion of the ions is followed by creating isotachophoretic boundaries between the solutions which can be readily detected experimentally. We recall that Eqn (5) relates the amount of electricity passed through the system to the number of charges of the same sign per unit volume of the solution and to the volume traversed by both boundaries (cationic and anionic) when a given amount of electricity is passed through the capillary.

The method of measurement of the amount of electricity depends on the electrolyte selected.

1. Suppose that a strong electrolyte solution, for which c_q is known and the degree of dissociation is unity, has been chosen. Then $c_q = czF$, where c is the molar concentration of the solution. In this case, the method of determining the amount of electricity passed through the circuit by Eqn (5) is absolute.

2. Suppose that an electrolyte solution for which c_q is not known beforehand, has been adopted. Then the proposed method is relative and requires preliminary calibration, i.e. the determination of c_q in the chosen solution at the concentration adopted by measuring, using some other procedure, the amount of electricity Q and the pathway traversed by both boundaries (cationic and anionic) ($l_c + l_a$) during the measurement. Clearly, such calibration constitutes simultaneously an independent method of determining the degree of dissociation of the electrolyte under the chosen conditions. These data could be of interest for the study of electrolyte solutions, particularly in the light of the attempts undertaken recently to consider certain strong electrolytes in solution as incompletely dissociated.[82]

The experimental formulation of the method for the measurement of the amount of electricity considered is in the main the same as that of the coulophoretic method for the determination of the concentration of a one-component solution, which was described above. The difference consists in the fact that in the given instance it is essential to have a capillary column with a constant cross-sectional area along its length. This makes it possible to determine the amount of electricity passed through the circuit during any time interval. The quantity measured directly as $l_c + l_a$. The maximum amount of electricity measured in an individual experiment is determined by the length

of the zone of the leading solution taken up into the capillary. The dependence of the amount of electricity passed on the path traversed by the cationic and anionic boundaries is linear, as can be seen from Eqn (5), which must be included among the advantages of the method. The range in which the amount of electricity can be measured depends on the concentration of the chosen solution, the cross-sectional area of the capillary, and the length of the column of the solution placed in the capillary. It can be readily varied. The optimum range is 0.15–3 C, the absolute sensitivity is 4 μC, and the accuracy of the determination for a column length of 200 mm is 0.1%. We may note that the method considered requires the use of high-voltage sources (1–10 kV).

4. Determination of the internal cross-sectional area of the capillary and the monitoring of its constancy along the length

Capillaries have been used widely in recent times in physicochemical practice—in capillary isotachophoresis, in high-pressure capillary chromatography, in ionic chromatography, and in capillary electrophoresis.[37,83–85] It is frequently necessary to measure the internal cross-sectional areas of transparent glass or quartz capillaries and to monitor their constancy along the length. The mercury method has been used traditionally for this purpose, but it suffers from evident disadvantages: it is laborious, it is difficult to automate, and it requires definite safety measures. The coulophoretic analytical method examined above can serve as a basis also for a novel method of measurement of the internal cross-sectional areas of transparent capillaries and for the monitoring of their constancy along the length.[86] In the horizontal part of the capillary the cross-sectional area of which is to be determined, one selects a column of the leading solution of a definite length between the two terminating solutions. By passing a stabilised direct current, one of the boundaries is made stationary relative to the walls of the capillary by means of a countercurrent. One then measures the distance Δl over which the secondary boundary moves during a time Δt. The average cross-sectional area of the capillary along the section Δl is found from the formula

$$S_{av} = \frac{I\Delta t}{Fcz\Delta l},$$

where z is the charge of the non-common ion of the leading solution forming the moving boundary. If the quantity $I\Delta t/F$, i.e. the amount of electricity passed through the column, is plotted against $cz\Delta l$, then the slope of the curve at a given point yields the internal cross-sectional area of the column at this point. The linearity of the relation indicates the constancy of the internal cross-sectional area of the capillary along its length. It has been suggested that a fully dissociated strong electrolyte solution be used as the leading solution. The accuracy of the determination of the internal cross-sectional area by this method for a width of the boundary of 0.2 mm is 2% along a section 1 cm long.

The method is suitable also for the determination of the free cross-sectional area of a column consisting of a transparent tube up to 10 mm in diameter with a filler (particle size 20–50 μm). The leading solution should then be coloured and the terminating solutions should be colourless or conversely. The positions of the boundaries at different times can be observed visually in this instance. Owing to the considerable width of the boundary, the accuracy of the determination of the free cross-sectional area of the tube with the filler is about 5% along a section 10 cm long.

The electrochemical procedure considered permits the measurement and the monitoring of the constancy of the internal cross-sectional areas of transparent capillaries with diameters of 0.05 to 0.8 mm without breaking them. This range is determined by the possibility of observing steady-state isotachophoretic boundaries in capillaries regardless of the ratio of the densities of the solutions employed. The method also permits the determination of free cross-sectional areas of columns with a diameter up to 10 mm and containing a finely dispersed filler.

VI. Steady-state concentration boundaries in isotachophoresis

The concentration boundaries are special types of boundaries in isotachophoresis. As a result of the passage of a direct current through the cell containing two electrolyte solutions with different concentrations of the same substance, it is possible to achieve a distribution of the concentrations of this substance in the intervening region which is stable as a function of time. The boundary between the solutions migrates to one of the electrodes at a constant rate. The conditions for the attainment of a steady distribution of concentrations or, in other words, the formation of a steady-state concentration boundary have been formulated by Stefanovskii:[87] (1) a stable boundary can exist only in solutions of electrolytes characterised by a non-linear dependence of the transport numbers of the ionic components on the concentration; (2) if the boundary is formed in such a way that $\partial c/\partial x > 0$ (the direction of the x axis coincides with the direction of motion of the cationic component in the electric field), then it will be stable for solutions of electrolytes where $\partial^2 t/\partial c^2 < 0$; (3) if the boundary is formed in such a way that $\partial c/\partial x < 0$, then it will be stable provided that $\partial^2 t/\partial c^2 > 0$ (here t is the transport number and c the concentration of the electrolyte solution). It has been shown in a study[88] where this process was examined most rigorously that the above conditions for the stability of concentration boundaries are valid only when the quantities t are understood as the transport numbers of non-common ionic components in the laboratory coordinate system and not relative to the solvent, as was implied in Stefanovskii's study.[87]

The criteria of the stability of concentration boundaries formulated above have been used to test the validity of the relations obtained by different workers between the transport numbers and the concentration of the electrolyte solution and for the prediction of the form of such relations if they have not yet been derived. For this purpose, the capillary column was filled with two solutions at different concentrations and a direct current was passed through it under the conditions of a hydrodynamic countercurrent. The migration of the concentration boundary was followed from the diffraction pattern. If the concentration boundary corresponding to the chosen direction of the current became stable after a time, the experiment was terminated. If the boundary remained unstable, the experiment was repeated having reversed the electric current. The direction of the current for which the concentration boundary is stable with time was found in this way.

The nature of the required relation was established from the results obtained, on the basis of conditions (1)–(3), i.e. it was found if this relation is convex or concave relative to the concentration axis in the chosen range. The instability of the boundary for any direction of the current implied that the concentration dependence of the transport number is linear in the selected range. The nature of the dependences of the transport numbers of the cationic and anionic components on the concentration in aqueous HCl, H_2SO_4, LiCl, NaCl, KCl, NH_4Cl, $BaCl_2$, $CuCl_2$, $NiCl_2$, Li_2SO_4, $LiNO_3$, $NaNO_3$, NaAc, KAc, $K_2Cr_2O_7$, $Na_2Cr_2O_7$, LiOH, NaOH, and KOH solutions was established by the method described.[89,90] The validity of the determination of the form of the relations (convex, concave) was confirmed by classical methods. At the same time, the conclusions concerning the form of the relations found by the method based on incorrect theoretical ideas concerning the motion of ions in electrolyte solutions were partly disproved. Certain concentration ranges were found in solutions of potassium and ammonium chlorides in which concentration boundaries are not formed whatever the direction of the current, which indicates a linear concentration dependence of the transport numbers.

Thus the apparatus for capillary isotachophoresis with detection of the boundaries from the diffraction pattern without any partitions can be used in experiments with concentration boundaries. Specially complex concentration boundaries,

considered, for example, by Stefanovskii,[91] require a comprehensive and systematic study.

VII. Electrocrystallisation with the aid of isotachophoresis

One of the most important features of isotachophoresis, namely the possibility of adaptation, i.e. a change in the concentrations of all the solutions following the leading solution when they differ from the steady-state concentrations, was examined in detail above. It was found that this feature can be used as a basis of a new electrochemical method for the crystallisation of ionogenic substances in a capillary.[92] The essential feature of the method is as follows. The transport numbers of any one ionic component of a saturated solution at room temperature are found directly from the literature or by extrapolating literature data. The leading solution having an ion in common with the solution to be crystallised, in which the mobility of the non-common ionic component is greater than that of the non-common ionic component of the solution crystallised, is selected on the basis of the accumulated data. The concentration of the leading solution, which as a result of adaptation determines the concentration of the saturated solution and the solution to be crystallised which follows it, is found from the regulating function (3). Next, the concentration of the leading solution calculated in this way is increased by 20% – 30% depending on the nature and properties of the solution to be crystallised. This is necessary for a number of reasons, including the possible inaccuracy of reference data, the tendency of the solution to be crystallised to become supersaturated in view of the small number of crystallisation centres, and the presence of a long latent period in which the onset of crystallisation is delayed when the degree of supersaturation is low. The crystallisation is carried out in a capillary employing the usual device for capillary isotachophoresis. The adaptation of the solution to be crystallised is followed from the diffraction pattern. The passage of current leads to the precipitation of crystals, which is manifested by a darkening of the diffraction pattern. The crystallisation of an aqueous potassium chloride solution with an initial concentration of 1 M using a hydrochloric acid solution at a concentration of 10 M as the leading solution and a cobalt chloride solution at a concentration of 1.5 M as the terminating solution has been described.[92] As a result of the passage of a direct current of 3 mA for 3 h, fine (approximately 0.1 mm) crystals were formed in the potassium chloride zone. As the potassium chloride solution zone migrated to the cathode under the influence of the electric field, the crystals migrated in the same direction.

The method considered makes it possible to carry out crystallisation under mild conditions, varying smoothly the degree of supersaturation. This variation can be made even smoother by altering the concentration of the leading solution during the experiment. The method is universal and permits the crystallisation of any inorganic, organic, and bioorganic ionogenic substances. One may add to this the advantages of the capillary isotachophoresis itself, the possibility of the preliminary purification of the solution itself and of the crystallisation of several zones simultaneously, as well as the possibility of using microgramme amounts of the substances and microlitre volumes of the solutions.

All the foregoing considerations make the proposed method promising, particularly in the study of the crystallisation process itself and for the practical preparation of small amounts of crystals of especially rare and expensive ionogenic substances.

VIII. The isotachophoretic method for the determination of the electromigration transport of the solvent in electrolyte solutions

The two forms of the regulating function and Eqns (2) – (4) relating them have been used to develop a relative method for the measurement of the electromigration transport of the solvent in electrolyte solutions.[93,94]

Electromigration transport of the solvent, constituting the migration of the solvent as component (not hydrodynamic) migration to the cathode or anode associated with its interaction with the ions, may occur in electrolyte solutions. This process, which takes place when a direct current passes through electrolyte solutions, has been the object of study since the 1930s, but hitherto the scatter of the experimental results has been considerable. This made it necessary to consider these data as only qualitative, indicating merely the occurrence of the effect itself.

The proposed method makes it apparently possible to solve this problem. One selects an electrolyte which forms aqueous solutions over a wide concentration range. It is necessary that the transport numbers of the cationic (or ionic) components of these solutions relative to the solvent are known. Suppose that the concentration of this solution is c_1 and the transport number relative to the solvent at the given concentration is $t_1^0(c_1)$. Next, one selects another, test electrolyte in solutions of which it is necessary to determine the electromigration mobility of the solvent (water). We shall assume for the sake of specificity that the transport numbers of the cationic component are smaller in the electrolyte solution investigated, which is the terminating solution, and that a steady-state isotachophoretic boundary may be formed between this solution and the first solution. For solutions of the test electrolyte, the transport numbers $t_2^0(c)$ of the cationic components relative to the solvent must also be known over a certain concentration range or must be specially measured. The relation

$$\frac{t_2^0}{c_2^0 z_2} = f(\lg c) \,. \tag{6}$$

is derived from these data.

According to the regulating function (2), a steady-state isotachophoretic boundary arises between the first and second solutions with concentrations (mol/kg of water) c_1^0 and c_2^0 respectively. Therefore, having calculated the quantity $t_1^0/c_1^0 z_1$ for the chosen concentration c_1 of the leading solution, the concentration c_2 of the terminating solution, forming with the former a steady-state isotachophoretic boundary, is found from the plot of Eqn (6). Next, the transport number $t_2^0(c_2)$ of the cationic component relative to the solvent is found for this concentration from reference data. After this, the quantity

$$t_2(c_2) = t_1(c_1)\frac{t_2^0(c_2)\rho_2^0}{t_1^0(c_1)\rho_1^0} \,, \tag{7}$$

i.e. the transport number of the same cationic component of the test solution at the concentration c_2 but this time in the laboratory coordinate system for a stationary solution, is found from Eqn (4). The electromigration mobility of water u_0 (the rate in a unit electric field) is calculated from these data:

$$u_0 = \frac{10^3 K}{czF}(t_2 - t_2^0) \,,$$

where K is the specific conductance of the test solution at the concentration c_2.

Eqn (7) includes one unknown quantity — $t_1(c_1)$, i.e. the transport number of the cationic component in the first (leading) solution at the concentration c_1 in the laboratory coordinate system, which must be measured independently.

A procedure for the determination of the electromigration mobility of the solvent in the chosen solution at a concentration c_2 was described above. The second, third, fourth, etc. concentrations of the initial solution are selected similarly and the corresponding second, third, fourth, etc. concentrations of the test solution are obtained, i.e. the concentration dependence is found. For each concentration of the two solutions, the transport numbers of the cationic components relative to the solvent must

be known. The transport numbers in the first solution at the chosen concentrations in the laboratory coordinate systems are unknown, which implies that their concentration dependence over a certain range or, what amounts to the same thing, the quantitative characteristic of the electromigration transport of water at the same concentrations, is unknown. A similar computational procedure can be applied to all electrolyte solutions where it is necessary to determine the electromigration transport of water. Using initial aqueous potassium chloride solutions at concentrations of 1 and 3 M, the absence of electromigration transport of water was noted by the isotopic boundary method. This means that $t_1(c_1)/t_1^0(c_1) = 1$ in Eqn (7).

The proposed method permits the calculation of the electromigration mobility of water in solutions of any electrolytes over a wide concentration range. The transport numbers relative to the solvent and the fact that there is no transport of the solvent in potassium chloride solutions at all concentrations are used in the calculations. The characteristics of the electromigration transport of water in solutions of a number of alkali metal halides and alkaline earth metal, zinc, cobalt, copper, and cadmium chlorides as well as a series of water-containing substances such as hydrochloric acid, ammonium chloride, and potassium hydroxide over a wide concentration range have been published.[94] The internal consistency of the method considered was confirmed by the results of measurements by the isotopic boundary method of the characteristics of the electrical transport of water in aqueous lithium chloride solutions at concentrations of 1 and 2 M and in rubidium chloride solutions at concentrations of 1 and 3 M and by comparing the results of these measurements with calculated data.

The characteristic features of the above method for the determination of the electromigration mobility of the solvent (water) are as follows.

1. The regulating function of isotachophoresis, constituting the basis of the method, is itself based on the law of conservation of matter and is therefore applicable without limitations as regards the types and concentrations of the solutions.

2. In proving the validity of the method, no model ideas and no mechanisms of the motion of the species in solutions were resorted to.

3. The method can be applied equally successfully to the determination of the electromigration mobility of any non-aqueous solvent.

4. Using a small number of experimental data, the method can be used to obtain the characteristics of the electrochemical transport of the solvent in all aqueous solutions of electrolytes for which the transport numbers relative to the solvent have been measured by the usual experimental methods.

IX. Conclusion

Progress in the development of new aspects of capillary isotachophoresis is linked directly to the establishment of modern ideas concerning the kinetic phenomena in electrolyte solutions and processes occurring near the isotachophoretic boundary. The aspects considered include those which are of purely theoretical importance as well as applied aspects. Thus the method for the determination of the electromigration transport of the solvent is important for the establishment of the physical picture of the passage of electric current through electrolyte solutions. Analytical capillary isotachophoresis has already become fairly common and in the present instance has been supplemented only by qualitative analysis. The coulophoretic analytical method constitutes a separate analytical electrochemical field. Methods for the measurement of the amount of electricity passed through the system, for the determination of the internal cross-sectional area of the capillary, for the monitoring of the constancy of the cross-sectional area of the capillary along its length, and for the determination of the free cross-sectional area of a tube with a filler have been developed on its basis. A property fundamental for isotachophoresis — the adaptation of the concentrations of all the solutions following the leading solution — has been used as the basis of a novel method for the electrocrystallisation of an ionogenic substance on passage of an electric current. In contrast to electrocrystallisation which occurs when a substance is segregated at electrodes, in this case crystallisation takes place in solution when opposed fluxes of cations and anions meet. The electrosynthesis of electrolyte solutions with the aid of ionic boundaries, which is one of the modifications of isotachophoresis for which this principle had already been nidicated by Kohlrausch, has expanded significantly the possibilities of capillary isotachophoresis as a preparative method.

All the modifications of isotachophoresis examined are characterised by a high resolving capacity, adequate sensitivity and accuracy, applicability over a wide concentration range (from dilute to saturated solutions), and satisfactory time parameters. The methods described make it possible to use microgramme amounts of test substances and microlitre volumes of the solutions and to work with aqueous and non-aqueous electrolyte solutions.

All the features listed above are possible exclusively owing to the availability of the universal diffraction method for the detection of electrolyte boundaries in capillaries. The ecological purity of all the processes examined, to which much attention has been devoted recently, is especially attractive.[95] The foregoing permits the assumption that capillary isotachophoresis and its modifications constitute a promising set of analytical and preparative methods.[96]

References

1. G Wiedemann *Pogg. Ann.* **99** 197 (1856)
2. G Wiedemann *Pogg. Ann.* **104** 166 (1858)
3. H Buff *Ann. Chem. Pharm.* **105** 168 (1858)
4. W Hittorf *Ann. Phys.* **89**, 177 (1853)
5. O Lodge *Br. Ass. Adv. Sci. Rep.* **56** 389 (1886)
6. F Kohlrausch *Ann. Phys. und Chem. (Leipzig)* **62** 209 (1897)
7. W C D Whethem *Philos. Trans. R. Soc. London, A* **184** 337 (1893)
8. D A Mak Innes, E R Smith *J. Am. Chem. Soc.* **45** 2246 (1923)
9. D A Mak Innes, T B Brighton *J. Am. Chem. Soc.* **47** 994 (1925)
10. H P Cady, L G Longsworth *J. Am. Chem. Soc.* **51** 1656 (1929)
11. J Kendall, W J West *J. Am. Chem. Soc.* **48** 2619 (1926)
12. H Haglund *Science Tools* **17** 1 (1970)
13. V V Skorchelletti *Teoreticheskaya Elektrokhimiya* (Theoretical Electrochemistry) (Leningrad: Khimiya, 1970)
14. T Erdey-Gruz *Transport Phenomena in Aqueous Solutions* (Translated into Russian) (Moscow: Mir, 1976)
15. K P Mischenko, G M Poltoratskii *Prakticheskie Raboty po Fizicheskoi Khimii* (Practical Physical Chemistry) (Leningrad: Khimiya, 1967)
16. M Spiro *J. Chem. Educ.* **33** 464 (1956)
17. J Newman *Electrochemical Systems* (Translated into Russian) (Moscow: Mir, 1977)
18. *Nomenclature for Transport Phenomena in Electrolyte Systems. Electrochim. Acta* **27** 631 (1982)
19. L I Antropov *Teoreticheskaya Elektrokhimiya* (Theoretical Electrochemistry) (Moscow: Vysshaya Shkola, 1984)
20. B B Damaskin, O A Petrii *Elektrokhimiya* (Electrochemistry) (Moscow: Vysshaya Shkola, 1987)
21. A I Gorshkov, O V Oshurkova *Elektrokhimiya* **26** 144 (1990)
22. USSR P. 737 823; *Byull. Izobret.* (20) 150 (1984)
23. USSR P.1 087 864; *Byull. Izobret.* (15) 150 (1984)
24. A I Shatenshtein, E A Yakovleva, E N Zvyagintseva *Isotopnyi Analiz Vody* (Isotopic Analysis of Water) (Moscow: Izd. Akad. Nauk SSSR, 1957)
25. A M Sukhotin, A F Kazankina *Elektrokhimiya* **6** 1323 (1970)
26. O Ya Samoilov *Struktura Vodnykh Rastvorov Elektrolitov i Gidratatsiya Ionov* (The Structure of Aqueous Electrolyte Solutions and the Hydration of Ions) (Moscow: Izd. Akad. Nauk SSSR, 1957)

27. A I Gorshkov, O V Oshurkova *O Sisteme Otscheta pri Izmerenii Chisel Perenosa Metodom Gittorfa* (The Reference System in the Measurement of Transport Numbers by the Hittorf Method) (Moscow, 1986); Article deposited at the All-Union Institute of Scientific and Technical Information (VINITI), No. 3077-V88 (1988)
28. E A Kaimakov, N L Varshavskaya *Usp. Khim.* **35** 201 (1966) [*Russ. Chem. Rev.* **35** 201 (1966)]
29. P Milios, J Newman *J. Phys. Chem.* **75** 298 (1969)
30. S I Rozov, A I Gorshkov *Elektrokhimiya* **15** 990 (1979)
31. E A Kaimakov, V B Fiks *Prib. i Tekh. Eksp.* **6** 95 (1957)
32. A I Gorshkov *Ob Odnom Vide Izotakhoforeticheskikh Izmerenii--Metody Sovmestnogo Nablyudeniya za Dvizheniem Ionov i Rastvora* (A Variant of Isotachophoretic Measurements—A Method for the Joint Observation of the Motion of Ions and the Solution) (Moscow, 1993); Article deposited at the All-Union Institute of Scientific and Technical Information (VINITI) (In the press)
33. A I Gorshkov *Zh. Fiz. Khim.* **59** 626 (1985)
34. O V Oshurkova, A I Gorshkov *Modifikatsii Izotakhoforeza. Elektrosintez Rastvorov Elektrolitov* (Modifications of Isotachophoresis. Electrosynthesis of Electrolyte Solutions) (Moscow, 1990); Article deposited at the All-Union Institute of Scientific and Technical Information (VINITI), No. 2665-V91 (1991)
35. USSR P. 410 302; *Byull. Izobret.* (1) 140 (1974)
36. O V Oshurkova, I A Ivanova *Dokl. Akad. Nauk SSSR* **227** 1371 (1976)
37. B P Konstantinov, O V Oshurkova *Zh. Tekh. Fiz.* **36** 942 (1966)
38. O V Oshurkova, A I Gorshkov *Elektrokhimiya* **26** 532 (1990)
39. B P Konstantinov, O V Oshurkova *Dokl. Akad. Nauk SSSR* **175** 1110 (1962)
40. USSR P. 150 294; *Byull. Izobret.* (4) 118 (1965)
41. J P Martin, F M Everaerts *Proc. R. Soc. London, A Math. Phys. Sci.* **316** 493 (1970)
42. B P Konstantinov, N S Lyadov, O V Oshurkova *Zh. Tekh. Fiz.* **38** 2117 (1968)
43. W Tormann, D Arn, E Schumacher *Electrophoresis* **5** 323 (1984)
44. T Hirokawa, K Nakahara, J Kiso *J. Chromatogr.* **463** 39 (1989)
45. P I Besler, I A Ivanova, O V Oshurkova *Zh. Anal. Khim.* **36** 593 (1981)
46. O V Oshurkova, in *Problemy Sovremennoi Fiziki* (Problems of Modern Physics) (Leningrad: Nauka, 1974) p. 46
47. *Khimiya i Zhizn'* **9** 109 (1989)
48. O V Oshurkova, A I Gorshov *Ukr. Khim. Zh.* **57** 187 (1992)
49. I A Kozhurkina, N S Lyadov, O V Oshurkova *Elektrokhimiya* **7** 1371 (1971)
50. O V Oshurkova, I A Ivanova, N V Chebotareva *Elektrokhimiya* **8** 1703 (1972)
51. B P Konstantinov, N S Lyadov, O V Oshurkova *Elektrokhimiya* **6** 584 (1970)
52. B P Konstantinov, N S Lyadov, O V Oshurkova *Zh. Prikl. Khim.* **45** 963 (1972)
53. O V Oshurkova, N S Lyadov, I A Kozhurkina *Zh. Prikl. Khim.* **46** 776 (1973)
54. O V Oshurkova, N V Chebotareva, N S Lyadov *Elektrokhimiya* **11** 1365 (1975)
55. B P Konstantinov, O V Oshurkova, N V Chebotareva *Zh. Prikl. Khim.* **43** 544 (1970)
56. O V Oshurkova, I A Kozhurkina, N V Chebotareva *Zh. Prikl. Khim.* **46** 1518 (1973)
57. O V Oshurkova *Parametry Reguliryushchego Sootnosheniya Izotakhoforeza i Ikh Eksperimental'noe Opredelenie* (Parameters of the Regulating Relation of Isotachophoresis and Their Experimental Determination) (Moscow, 1987); Article deposited at the All-Union Institute of Scientific and Technical Information (VINITI), No. 3093-V88 (1987)
58. B P Konstantinov, O V Oshurkova *Izv. Akad. Nauk SSSR, Ser. Khim.* 1648 (1967)
59. B P Konstantinov, O V Oshurkova *Agrokhimiya* **9** 99 (1967)
60. B P Konstantinov, O V Oshurkova *Dokl. Akad. Nauk SSSR* **175** 113 (1967)
61. V Ya Klyuchkin, B P Konstantinov, O V Oshurkova *Zavod. Lab.* **33** 556 (1967)
62. B P Konstantinov, O V Oshurkova, V Ya Klyuchkin *Zh. Prikl. Khim.* **40** 1265 (1967)
63. B P Konstantinov, O V Oshurkova, I Z Starobina *Zh. Prikl. Khim.* **40** 1260 (1967)
64. O V Oshurkova, S N Kholmogorov, L A Rzhevina *Zh. Anal. Khim.* **30** 1276 (1975)
65. M F Vodennikova, O V Oshurkova, V P Samusik *Zavod. Lab.* **44** 11 (1978)
66. O V Oshurkova, S N Kholmogorov, I A Ivnaova *Zavod. Lab.* **42** 388 (1976)
67. F M Everaerts, J L Beckers, Th P E M Verheggen *Isotachophoresis. Theory, Instrumentation and Applications* (Amsterdam: Elsevier, 1976)
68. Yu S Parilov, in *Fiziko-khimicheskie Parametry Mineraloobrazovaniya na Polimetallicheskikh Mestorozhdeniyakh Kazakhstana* (Physicochemical Parameters of Mineral Formation in the Polymetallic Deposits of Kazakhstan) (Alma Ata: Izd. Nauka Kaz. SSR, 1984) p. 41
69. O V Oshurkova, Yu S Parilov, in *XII Mezhdunarodnyi Mendeleevskii S'ezd. Sektsiya Analiticheskoi Khimii (Tezisy Dokladov)* [The XIIth International Mendeleev Congress. Analytical Chemistry Section (Abstracts of Reports)] (Baku, 1981) p. 299
70. O V Oshurkova *Zh. Fiz. Khim.* **59** 539 (1987)
71. A N Naumov, O V Oshurkova, G Ya Ryskin *Tr. Khim. Khim. Tekhnol. Gor'kovskii Khim.-Tekhnol. Inst.* **3** 24 (1969)
72. B P Konstantinov, O V Oshurkova *Elektrokhimiya* **3** 1409 (1967)
73. O V Oshurkova, A I Gorshkov *Izv. Vyssh. Uchebn. Zaved., Khim. Khim. Tekhnol.* **5** (1993) (In the press)
74. V G Babskii, M Yu Zhukov, V I Yudovich *Matematicheskaya Teoriya Elektroforeza* (Mathematical Theory of Electrophoresis) (Kiev: Naukova Dumka, 1983)
75. V G Babskii, M Yu Zhukov *Biofizicheskie Metody. Teoreticheskie Osnovy Elektroforeza. Uch. Metod. Posobie* (Biophysical Methods. Theoretical Foundations of Electrophoresis. Textbook of Scientific Methods) (Moscow: Izd. Moskov. Gos. Univ., 1990)
76. H G Hertz *Electrochemistry. New Outlooks* (Translated into Russian) (Moscow: Mir, 1983)
77. O V Oshurkova, I A Ivanova *Zh. Anal. Khim.* **32** 1707 (1977)
78. O V Oshurkova, A I Gorshkov *Osobennost' Kulonometrirovaniya po Ionnym Granitsam (Variant Izotakhoforeza) Smesi Vodnykh Rastvorov Solyanoi Kisloty i Khlorida Kobal'ta* [A Characteristic Feature of the Coulometric Analysis Based on Ionic Boundaries (A Version of Isotachophoresis) of a Mixture of Aqueous Solutions of Hydrochloric Acid and Cobalt Chloride] (Moscow, 1992); Article deposited at the All-Union Institute of Scientific and Technical Information (VINITI), No. 1682-V92 (1992)
79. O V Oshurkova, A I Gorshkov *Zavod Lab.* **55** 13 (1989)
80. O V Oshurkova, A I Gorshkov *Ukr. Khim. Zh.* **56** 618 (1990)
81. O V Oshurkova, A I Gorshkov *Elektrokhimiya* **26** 749 (1990)
82. R Heyrovska, in *Electrochemistry, Past and Present.* (Eds J T Stock, M V Orna) (Toronto, 1989); quoted after A M Skundin *Elektrokhimiya* **27** 1686 (1991)
83. V F Ruban, A B Belen'kii, A Ya Gurevich *Zh. Anal. Khim.* **43** 1502 (1988)
84. O A Shpigun, Yu A Zolotov *Zavod. Lab.* **48** 4 (1982)
85. H Huang, M Gordon, R Zare *Science* **239** 1377 (1988)
86. O V Oshurkova, A I Gorshkov *Zavod. Lab.* **56** 28 (1990)
87. A M Stefanovskii *Elektrokhimiya* **1** 446 (1965)
88. A I Gorshkov *O Stabil'nykh Kontsentratsionnykh Granitsakh Rastvorov Elektrolitov v Izotakhoforeze* (Stable Concentration Boundaries between Electrolyte Solutions in Isotachophoresis) (Moscow, 1984); Article deposited at the All-Union Institute of Scientific and Technical Information (VINITI), No. 8354-V (1985)
89. O V Oshurkova, N S Lyadov *Elektrokhimiya* **15** 1768 (1979)
90. O V Oshurkova *Ustanovlenie Kharaktera Zavisimosti Chisel Perenosa Ionov ot Kontsentratsii Rastvora po Stabil'nosti Kontsentratsionnykh Granits* (Determination of the Nature of the Dependence of the Ionic Transport Numbers on the Solution Concentration from the Stability of Concentration Boundaries) (Moscow, 1986); Article deposited at the All-Union Institute of Scientific and Technical Information (VINITI), No. 3607-V87 (1987)
91. A M Stefanovskii *Elektrokhimiya* **3** 71 (1967)
92. USSR P. 1 438 279; *Byull. Izobret.* (42) 263 (1988)
93. A I Gorshkov, O V Oshurkova *Elektrokhimiya* **26** 1225 (1990)
94. A I Gorshkov, O V Oshurkova *Elektrokhimiya* **26** 1230 (1990)
95. A I Lazarev *Zavod. Lab* **55** 1 (1989)
96. G A Pribylov, E K Korchemnaya, G A Goncharov *Zh. Anal. Khim.* **46** 2460 (1991)

Russian Chemical Reviews **62** (8) 743 – 749 (1993)
© 1993 Russian Academy of Sciences and Turpion Ltd

UDC 546.882 – 32:541.128

Niobic acid — a new heterogeneous catalyst for processes in petrochemical and organic syntheses

F A Chernyshkova

Contents

I. Introduction	743
II. The structure and properties of the surface of niobic acid	744
III. The use of niobic acid as a catalyst	745
IV. The use of niobium oxide as a carrier and promoting agent	748
V. Other niobium compounds used in catalysis	748

Abstract. Questions associated with the application of niobium compounds in catalysis are considered. Niobic acid $Nb_2O_5 \cdot nH_2O$ contains an appreciable amount of water, but its surface exhibits a high acidity — equivalent to the acidity of 70% sulfuric acid. This unusual solid acid manifests not only a high activity and sensitivity but also an appreciable stability as a catalyst in reactions in which water is present or is evolved (condensation, hydration, dehydration, and esterification). It may be used also as a catalyst in other reactions. The structure and properties of the surface of niobic acid are examined. The bibliography includes 54 references.

I. Introduction

Technologies which permit industrial production satisfying world standards, giving rise to a high output without contamination of the environment, have acquired prime importance at the present time. In this connection, the use of niobic acid, the term usually applied to hydrated niobium pentoxide $Nb_2O_5 \cdot nH_2O$, as a solid acid catalyst for a number of processes can undoubtedly be of practical interest. The most important property of niobic acid is that, after heat treatment at 100 – 300 °C, its surface acquires a high acidity, although an appreciable amount of water is present on it.[1] The activity of niobic acid is manifested already at a low temperature (100 – 120 °C) even in the presence of water vapour. The oxides of other metals do not possess similar properties: it is known that their acidity is lost or diminishes as a consequence of the adsorption of water. The use of niobic acid as a catalyst in reactions with participation or elimination of water — esterification, hydration, dehydration, Prins reaction, hydrolysis, and others — is especially effective. In these reactions, niobic acid exhibits a high activity, selectivity, and stability.[1 – 3] Even in the presence of components with a reducing capacity, the acidity of niobic acid does not diminish, since the oxide Nb_2O_5 is stable.

F A Chernyshkova Scientific – Industrial Association 'Lenneftekhim', Zheleznodorozhnyi proezd 40, 193148 St Petersburg.
Fax (7-812) 568 1498

Received 11 March 1993
Uspekhi Khimii **62** (8) 788 – 795 (1993); translated by A K Grzybowski

Until recently, niobium catalysts have not attracted special attention despite the fact that catalysts based on molybdenum and vanadium — elements adjoining niobium in the Periodic System — have been widely used in industry. However, during approximately the last five years, the attitude to niobium-based catalysts and especially to niobic acid changed significantly.[1 – 3] Niobic acid has begun to be used in Japan as an industrial catalyst of condensation, dehydration, hydration, and esterification reactions.[2]

H_2SO_4, H_3PO_4, HF, and sulfonic acid cation-exchange resins are frequently used in industrial processes as acid catalysts. A number of problems associated with the corrosion of equipment, the inadequate selectivity of the processes, the presence of a large amount of waste, and the need to utilise the spent catalysts and their toxicity then arise. The employment of niobic acid could help in many instances to solve these problems. Not only hydrated niobium oxide (niobic acid) but all composite systems based on niobium oxide are of interest for catalysis. There are prospects for their employment as both catalysts and carriers.

The world niobium resources (excluding the Union of Independent States) amount to 28 000 tonnes, which exceeds somewhat the resources of elements such as molybdenum, tungsten, and cobalt.[5] According to data concerning the state of the world market in niobium and its consumption,[6] the production of niobium in 1987 was 14 900 tonnes, of which 85% was produced by the CBMM Company (Brazil). According to these data, 87% of niobium is consumed as an additive to steel, 10% in the preparation of nickel – niobium alloys, and the rest in the manufacture of optical glasses, dielectric materials, and superconductors. According to a forecast,[5] the world production of niobium will increase by 8% – 10% annually.

Niobium is also extracted in our country.[5] An appreciable amount of niobium is present in the waste from tungsten ore in the processing plants (niobium is known to accompany tungsten). A low-waste technology has been proposed for the extraction of a niobium and tantalum concentrate from such waste.[7] Instances of occupational poisoning by niobium have not been described.[8]

The principal results achieved as a result of the use of niobic acid and other niobium-based materials in catalysis have been described in reviews [1 – 3] and in the proceedings of an international symposium on catalysis by niobium materials.[4]

The aim of the present review is to survey the latest advances in catalysis by niobic acid and other niobium-based compounds and also to draw the attention of investigators to this new problem, which is promising from the practical standpoint.

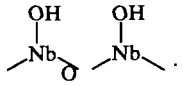
Data published during the last five years are mainly considered. References to earlier studies may be found in the papers of Tanabe[1,3] and Okazaki[2].

II. The structure and properties of the surface of niobic acid

Hydrated niobium pentoxide $Nb_2O_5 \cdot nH_2O$ is a white polymeric amorphous material. Its composition is variable owing to the inconstancy of its water content,[9] which varies depending on the method of preparation and drying. The nature and structure of niobic acid and of the products of its thermal decomposition have been examined in a number of publications.[9-11] It was established[9] that hydrated niobium pentoxide consists of the niobic isopolyacid having the composition $H_8Nb_6O_{19}$. On heating, the hydrated isopolyacid splits off water, forming stoichiometric hydrates, while above 1200 °C it also loses a certain amount of oxygen with formation of oxygen-deficient non-stoichiometric niobium oxides:[10]

$$H_8Nb_6O_{19} \cdot 18H_2O \longrightarrow H_8Nb_6O_{19} \cdot 12H_2O \longrightarrow$$
$$\longrightarrow H_8Nb_6O_{19} \cdot 6H_2O \longrightarrow H_8Nb_6O_{19} \cdot 3H_2O \longrightarrow$$
$$\longrightarrow H_8Nb_6O_{19} \longrightarrow [H_2Nb_6O_{16}]_n \xrightarrow{1200\ ^\circ C}$$
$$\longrightarrow [Nb_6O_{15}]_n \longrightarrow [NbO_{2.5-2.33}]_m .$$

The amorphous modification, called γ-niobic isopolyacid, exists up to 435 °C. On further heating, it passes to the low-temperature crystalline state and at 830 °C to the high-temperature crystalline state (α-Nb_2O_5). The steric structure of $H_8Nb_6O_{19}$, which will henceforth be referred to as niobic acid by tradition, is illustrated in Fig. 1. In this structure, the eight protons are located over the triangular faces of the octahedron formed by the six niobium atoms. Among the oxygen atoms, 12 bridging atoms, 6 terminal atoms, and one central atom are distinguished. Each hydrogen atom is coordinated to three bridging oxygen atoms, three terminal oxygen atoms, and one central oxygen atom. The protons in niobic acid form part of the composition of the hydroxy-groups linked to the niobium atoms:



The H...H distance is fairly long—more than 4 Å. Conductimetric and IR spectroscopic studies suggested the possibility of the migration of protons in the niobic acid matrix.[9] Water molecules are linked to $H_8Nb_6O_{19}$ by a hydrogen bond via the peripheral oxygen atoms.[10] Only 1.2% of the protons in $H_8Nb_6O_{19}$ can be substituted by sodium ions in a slow exchange process.[9]

When $Nb_2O_5 \cdot nH_2O$ is heated, the derivatogram shows[12] two endothermic peaks at 90 and 190 °C. The weight loss at these temperatures is associated with the dehydration of the gel-like niobic acid and its transition to the amorphous state. The surface of niobic acid then acquires strong acidic properties ($H_0 \leqslant -5.6$), corresponding to the acidity of 70% sulfuric acid. Strong acid centres arise even after mild heat treatment of niobic acid at 100 °C and the residual water can then cover the entire surface of the catalyst. The acidity of metal oxides is usually lost or reduced as a result of the adsorption of water. For example, strong acid centres appear on the surfaces of the $SiO_2-Al_2O_3$ and SiO_2-TiO_2 systems only after heat treatment at about 500 °C simultaneously with the removal of water from the surface. The dehydration of $Nb_2O_5 \cdot nH_2O$ terminates at 300 °C. Further heating from 300 to 700 °C is not accompanied by a change in the weight of the specimen. After heat treatment at 500 °C, niobic acid becomes almost inactive and does not exhibit any acid properties.[1,12] This occurs as a consequence of the phase transition of the amorphous $Nb_2O_5 \cdot nH_2O$ to a crystalline phase.[1]

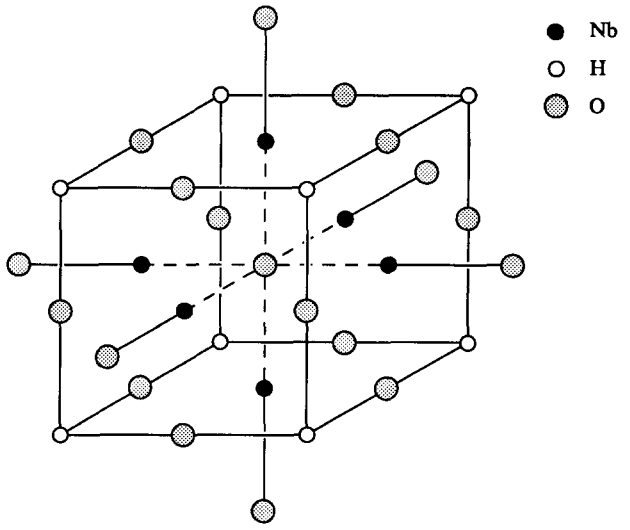


Figure 1. The structure of $H_8Nb_6O_{19}$.

According to Tanabe,[1] the specific surface of niobic acid is respectively 164, 126, and 42 $m^2\ g^{-1}$ after evacuation at 100, 300, and 500 °C. The number of OH groups on the surface of niobic acid depends on the heat treatment temperature:[1,12]

T/°C	120	200	300	400
[OH]/mmol g^{-1}	1.0	0.8	0.7	0.55

The acid properties of niobic acid, investigated by titration with *n*-butylamine in the presence of Hammett indicators, can be inferred from Fig. 2. The greatest number of strong acid centres ($H_0 = -5.6$) are present in niobic acid after its heat treatment at 120–300 °C.

Analysis of the IR spectra of pyridine adsorbed on niobic acid shows that the intensity of the absorption band (a. b.) corresponding to the Brønsted acid is a maximum when the temperature of the preliminary heat treatment of the specimen is 100 °C (Fig. 3*a*). It diminishes with increase in the heat treatment temperature.[12] On the other hand, the

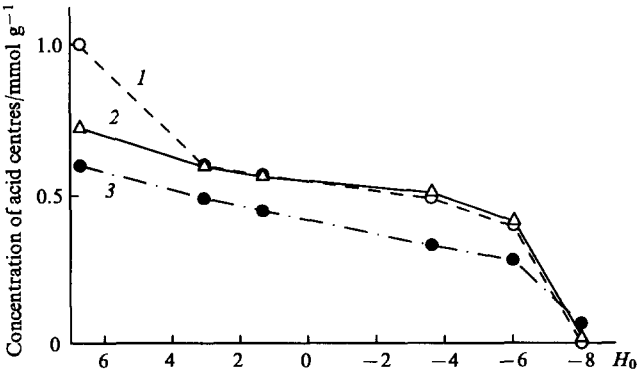


Figure 2. Distribution of the acid centres of niobic acid with respect to their strength as a function of the heat treatment temperature (°C): *1*, 120; *2*, 200; *3*, 300.[1]

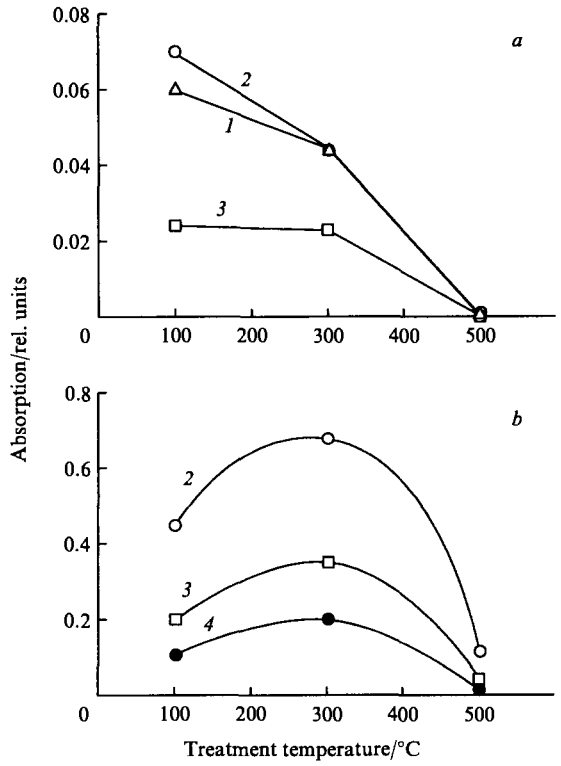


Figure 3. Variation of the Brønsted (*a*) and Lewis (*b*) acidities of niobic acid with the temperature of the preliminary treatment with the specimen evacuated after the adsorption of pyridine. Treatment temperature (°C): *1*, room temperature; *2*, 100; *3*, 200; *4*, 300.

intensity of the spectral band corresponding to the Lewis acid reaches a maximum at a preliminary heat treatment temperature of 300 °C (Fig. 3*b*).

The study of the IR spectra of adsorbed CO_2 showed that niobic acid has only weak basic properties.[12]

The data presented in Table 1 make it possible to compare the properties of the surfaces of different oxides.[2]

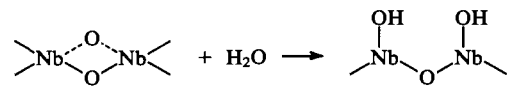
Table 1. The properties of the surfaces of different oxides treated with steam at 300 °C for 3 h.

Oxide	Specific surface/$m^2\ g^{-1}$	OH groups on the surface/mmol g^{-1}	OH groups on 100 Å^2
Nb_2O_5	124	0.84	4.2
Al_2O_3	218	2.29	6.3
TiO_2	177	1.14	3.9
ZrO_2	234	1.43	3.7

In terms of the density of OH groups, niobic acid does not differ from other oxides, but its specific surface is smaller.

The formation of highly acid centres on the surface of niobic acid cannot be explained solely by its structure. The elucidation of this problem would help in the development of new types of solid acid materials.[1]

It was of interest that the acidity of niobic acid evacuated at 300 and 400 °C virtually returns to the initial value after its treatment with water vapour for 3 h and subsequent evacuation at 100 °C, while the number of OH groups on the surface increases.[1,2] This finding is explained by the fact that, on heating to 400 °C, the process involving the removal of OH groups from the surface is almost completed and the acid passes to an unstable state in which crystallisation does not yet begin.



In this state, there is a possibility of hydration by water vapour.[2]

Even in the presence of components with a reducing capacity, the acidity of niobic acid does not fall,[1] since the oxide Nb_2O_5 is stable and is reduced with difficulty, in contrast to the related oxides V_2O_5 and MoO_3. Niobium pentoxide is reduced by hydrogen only at 800–1350 °C.

Niobic acid contains Fe, Cl, Na, and K as impurities. With decrease in their amount to several parts per million, very strong acid centres ($H_0 \leqslant -8.2$) are observed in niobic acid and are retained even in the presence of water vapour.[2] This phenomenon is of interest from the practical point of view.

It has also been noted[13] that, on promotion with 1 M phosphoric acid, the crystallisation of niobic acid begins at 570 °C and not at 435 °C, which is the temperature of the onset of crystallisation in the absence of the promoting agent. Under these conditions, there is also an increase in the number of strong acid centres ($H_0 \leqslant -5.6$).

The specific surface and hence the catalytic activity increase simultaneously. This effect has been explained by the formation of an amorphous layer of niobium phosphate on the surface of niobic acid.

Niobic acid is formed as an intermediate in the synthesis of niobium and its compounds. Very pure niobic acid is obtained on hydrolysis of the readily available and cheap chloride $NbCl_5$.[2] Different methods of preparation of niobic acid and of catalysts based on it have been described in greater detail in a review.[2]

III. The use of niobic acid as a catalyst

Niobic acid subjected to a preliminary vacuum heat treatment up to 200–220 °C exhibits a high activity in the hydration of ethylene to ethanol.[1,14] In the stationary state at 200–220 °C, it is 2–3 times more active than solid phosphoric acid, widely used as a catalyst in industry. The selectivity in the conversion of ethylene into ethanol exceeds 97%, acetaldehyde being formed as a side product. Niobic acid ($Nb_2O_5 \cdot nH_2O$, purity 99.8%), produced by the CBMM Company, was used in the reaction after being washed with distilled water, dried at 100 °C, and then evacuated at different temperatures for 2 h. The reaction was carried out in a reactor with a stationary catalyst bed and ethylene and water vapour pressures of 48 and 7.3 kPa. The unreacted ethylene was recycled. The activity of niobic acid gradually increased during the process and attained a constant value after 6 h. Deactivation of the catalyst was not observed. Best results were obtained at 200–220 °C. At 180 °C, the activity of niobic acid was lower. Ogasawara et al.[14] concluded that niobic acid is suitable for the industrial hydration of ethylene to ethanol. Niobic acid is active even in the hydration of isobutene and propene.[2]

A solid acid catalyst for the hydration of ethylene to ethanol and the conversion of methanol into dimethyl ether was obtained by treating niobic acid with phosphoric acid.[15,16] Niobic acid was kept without stirring in 0.5 M H_3PO_4 and was then dried in air. Such treatment increased its thermal stability: crystallisation occurred at ~600 °C (instead of 435 °C) and the specific surface and the concentration of strong acid centres with $H_0 \leqslant -5.6$ increased. Phosphoric acid was found to be dispersed on the surface of niobic acid.

Niobic acid exhibited a high activity also in the hydration of dicyclopentadiene.[17] At 170 °C and atmospheric pressure, the degree of conversion of dicyclopentadiene was 17%, which is 3–10 times higher than in the case where ion-exchange resins, SiO_2, TiO_2, Al_2O_3, TiO_2–SiO_2, and SiO_2–Al_2O_3 are used (Table 2). At 400 °C the activity of niobic acid fell sharply with a simultaneous decrease also in the acidity of its surface ($H_0 \leqslant 0.5$).[17]

Table 2. The activities of niobic acid and other catalysts in the hydration of dicyclopentadiene.[17]

Catalyst	Temperature of preliminary treatment/°C	Reaction temperature/°C	Conversion into alcohol (%)
Amberlist	–	100	2.0
Nafion H	–	150	0.3
Nafion H	–	170	0.4
SiO_2	400	170	2.0
TiO_2	400	170	5.2
Al_2O_3	400	170	3.1
$SiO_2-Al_2O_3$	500	170	4.0
TiO_2-SiO_2 {[Ti]/[Si] = 9}	500	170	4.3
Niobic acid	300	170	17.0

Niobic acid heat-treated at 100–600 °C is a highly active and selective catalyst of the isomerisation and hydration of phenyloxiran under mild conditions.[18] The isomerisation occurs on Lewis acid centres, while hydration occurs on Brønsted centres. In terms of its hydrophilic properties, niobic acid is more suitable for hydration than the $SiO_2-Al_2O_3$ system, H-ZSM, and H-silicalite, because it exhibits affinity both for water and the organic substrate. The hydrophilicity of the surface of niobic acid and the concentrations of the Brønsted and Lewis acid centres are regulated by the heat treatment temperature.[18] The monoamide $NC(CH_2)_nCONH_2$ has been obtained by hydrating the dinitrile $NC(CH_2)_nCN$ (n = 2–6) with niobic acid as the catalyst.[19]

Niobic acid is also an active and selective dehydration catalyst. $Nb_2O_5 \cdot nH_2O$ specimens evacuated at 100–200 °C showed a high activity, close to that of the $SiO-Al_2O_3$ system, in the dehydration of 2-butanol. The yield of but-2-ene was then higher than that of but-1-ene. Heat treatment of niobic acid at 300 °C induced a sharp decrease in its activity in the dehydration reaction, since this entailed a decrease in the number of Brønsted acid centres catalysing the dehydration reaction.[1] The high selectivity in the formation of olefins is due to the fact that Nb_2O_5 is a very stable oxide, which is hardly reduced under the reaction conditions. Niobic acid exhibited also a high activity and selectivity in the dehydration reactions of butane-1,4-diol and cyclopentanol.[2]

Niobic acid treated with 0.05–5 M H_3PO_4 solution exhibits a catalytic activity in the dehydration of cyclohexanol and in the alkylation of benzene by methanol.[13,20] The dehydration was carried out in a flow reactor at 180 °C, while benzene was alkylated in a pulse reactor at 400 °C using the ratio $[CH_3OH]/[C_6H_6]$ = 3. Best results were obtained when niobic acid was treated with 1 M H_3PO_4 solution (quantitative data are not quoted).[20] The addition of H_3PO_4 prevents the crystallisation of niobic acid and increases the acidity of its surface by virtue of the formation of an amorphous layer of niobium phosphate on the latter.[13]

Niobic acid is an effective catalyst of the esterification of acetic acid by ethanol at 120–160 °C (Table 3). When the reaction was carried out in the gas phase at 120 °C in the course of 1 h using the ratio $[C_2H_5OH]/[CH_3COOH]$ = 1, a rate of supply of 2.3 ml h^{-1}, and a niobic acid heat treatment temperature of 200 °C, the degree of conversion was 72% and the selectivity was 100%. The catalyst retained its activity throughout the period of 60 h during which the tests were carried out. In terms of its activity, it is superior to ion-exchange resins, $SiO_2-Al_2O_3$, and the solid superacids $ZrO_2-SO_4^{2-}$, $TiO_2-SO_4^{2-}$, and $Fe_2O_3-SO_4^{2-}$. A high and stable activity is also manifested by the zeolite H-ZSM-5 (the degree of conversion was 82%–99%, but the selectivity was lower, amounting to 72%–92%), diethyl ether and ethylene being formed as side products.

An increase in the heat treatment temperature of $Nb_2O_5 \cdot nH_2O$ from 120 to 300 °C leads to an increase in the number of acid centres with $H_0 = -8.2$. The active centres of the catalyst heat-treated at 120 °C are the numerous centres with H_0 up to -5.6. The likely usefulness of niobic acid as the catalyst of esterification reactions is due to its stability, activity, selectivity, and the ability to replace sulfuric acid, which is corrosive, leads to the appearance of a large amount of waste, and is difficult to regenerate. Cation-exchange resins are also inferior to niobic acid: they have a lower acidity and thermal stability, tend to swell, are fairly expensive, difficult to utilise in the spent state, etc.[1]

Esterification of methacrylic and acrylic acids by methanol occurred especially effectively on niobic acid with strong acid centres formed as a result of its heat treatment at 200 °C.[1]

Niobic acid subjected to preliminary heat treatment at 200–400 °C exhibits a high activity in the hydrolysis of acrylate in the presence of a large amount of water in the reaction medium.[1,21] The selectivity is 100%.

Table 3. The activities and selectivities of $Nb_2O_5 \cdot nH_2O$ and other solid acids in the esterification of ethanol by acetic acid.[1]

Catalyst	Heat treatment temperature/°C	Reaction temperature/°C	Conversion of ethanol (%)	Selectivity (%)	Side products
$Nb_2O_5 \cdot nH_2O$	200	120	72	100	–
		140	86	100	–
Sulfonic acid cation exchange resin	120	120	38	<99	–
		140	50	<98	–
$ZrO_2-SO_4^{2-}$	500	140	56	90	$(C_2H_5)_2O$
$Fe_2O_3-SO_4^{2-}$	500	140	13	93	$(C_2H_5)_2O$
$TiO_2-SO_4^{2-}$	500	120	95 (94)[a]	99 (98)[a]	
		140	100	95	C_2H_4
$SiO_2-Al_2O_3$	–	120	4	99	$(C_2H_5)_2O + C_2H_4$
		140	14	98	
H-ZSM-5	–	120	82	92	$(C_2H_5)_2O + C_2H_4$
		140	99	72	

Note. The mass of the catalyst was 1 g and the reaction time was 1 h.
[a] The reaction time was 2 h.

Niobic acid is an active and selective catalyst of condensation reactions.[2,3]

Isoprene can be obtained in 61% yield in one stage from isobutene and formaldehyde on $Nb_2O_5 \cdot nH_2O$ at 350 °C. After 50 h the yield falls to 54%.[22]

Condensation of butyraldehyde at 160 °C on $Nb_2O_5 \cdot nH_2O$ affords 2-ethylhexanol. The degree of conversion is 92% and the selectivity is 96%.[23]

2,5-Dimethylhexa-2,4-diene has been obtained[24] on condensing isobutene and isobutyraldehyde at 200 °C in the presence of niobic and sulfuric acids:

Catalyst	Conversion (%)	Selectivity (%)
$Nb_2O_5 \cdot nH_2O$	97	82
H_2SO_4 (16 mass%)	99	21

Evidently, niobic acid ensures a higher selectivity than sulfuric acid.

According to Japanese workers,[25] isobutyl methyl ketone can be obtained from acetone and H_2 in the presence of 0.1% $Pd/Nb_2O_5 \cdot nH_2O$. At 160 °C and a pressure of 2 mPa, the degree of conversion of acetone was 41.8% and the selectivity was 93.5%. Under the same conditions, the degree of conversion in the presence of the 0.1% Pd/Al_2O_3 catalyst did not exceed 3.8% and the selectivity did not exceed 62.3%.

Niobic acid catalyses also olefin isomerisation and polymerisation processes. $Nb_2O_5 \cdot nH_2O$ evacuated at 100 °C proved to be the most active catalyst in the isomerisation of but-1-ene.[1] After evacuation at 300 °C, the activity of the catalyst fell sharply, but it was almost completely restored after the introduction of water vapour and subsequent evacuation at 100 °C (Fig. 4). Hence it was concluded that the isomerisation reaction is activated mainly by the Brønsted acid centres, the number of which diminishes with increase in the evacuation temperature. After evacuation at 500 °C, treatment with water vapour does not restore the activity of the specimen. The phase transition, occurring at 500 °C and accompanied by a decrease in surface area, precludes the regeneration of the Brønsted acid centres.[1]

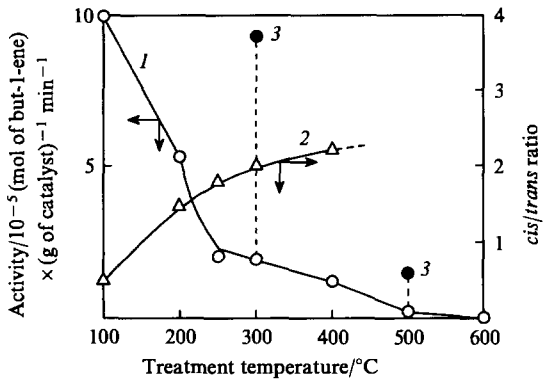


Figure 4. The activity (curve *1*), and selectivity (curve *2*) of niobic acid in the isomerisation of but-1-ene; the activity of the catalyst after its treatment with water and subsequent evacuation at 100 °C (curve *3*).

In the polymerisation of propene, niobic acid exhibits a high activity after being evacuated at 100 °C. Evacuation at 150–200 °C lowers the activity and after heat treatment at 250–300 °C the activity again increases (Fig. 5). After heat treatment at 500 °C, the activity vanishes.[1,12] Such a change in activity is explained by the fact that in the low-temperature heat treatment the polymerisation is catalysed by the Brønsted centres, but when the temperature of the heat treatment is 250–300 °C the catalysis is effected by the Lewis centres.[1]

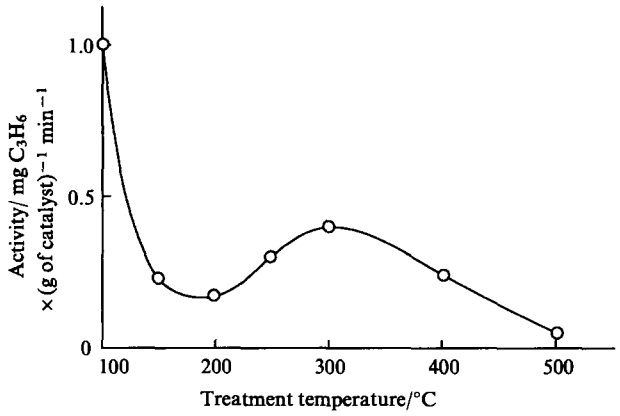


Figure 5. Dependence of the activity of $Nb_2O_5 \cdot nH_2O$ in the polymerisation of propene on the temperature of the heat treatment of the catalyst.

Much attention has been devoted to deposited catalysts based on niobic acid.[26–33] The stability of these catalysts is satisfactory and they crystallise and are reduced at higher temperatures than niobic acid. Catalysts obtained by depositing niobic acid on SiO_2 are especially effective. It has been suggested that the change in the properties of the deposited Nb_2O_5 is caused by the strong interaction at the $SiO_2-Nb_2O_5$ interface with formation of the Nb–O–Si linkage.

Amorphous Nb_2O_5, formed as a monolayer on SiO_2, has been tested[26] as a catalyst of the dehydration of ethanol to ethylene. The catalyst was prepared by depositing $Nb(OC_2H_5)_5$ on SiO_2 and subsequent treatment with H_2O and O_2. Its activity was manifested at 100–300 °C and exceeded by 1–2 orders of magnitude the activity of niobic acid without a carrier. The selectivity was 100%. The catalytic properties of mononuclear, dinuclear (0.1%–1% Nb_2O_5), and monolayer (2%–8% Nb_2O_5) niobium oxide catalysts, deposited on SiO_2 via the interaction of the OH groups with $Nb(\eta^3\text{-}C_3H_5)$, $[Nb(\eta^5\text{-}C_5H_5)H\text{-}\mu\text{-}(\eta^5,\eta'\text{-}C_5H_4)]_2$ and $Nb(OC_2H_5)_5$ respectively, have also been investigated.[27]

Analysis by the method of extended X-ray absorption fine structure (EXAFS) established that the niobium centres are fixed on the surface via the oxygen atoms (Nb–O–Si). The mononuclear niobium oxide centres are active in the dehydrogenation of ethanol at 250 °C, the selectivity in the formation of CH_3CHO reaching 96.1%. Dehydration with formation of 45% of ethylene and 52.7% of diethyl ether takes place on the dinuclear niobium centres at 250 °C.[27,28] The monolayer niobium catalyst 8% Nb_2O_5/SiO_2 is 20 times more active at 300 °C than niobic acid in the esterification of acetic acid by ethanol.[29] It has been suggested that its activity is determined by the Lewis acid centres. The catalyst is stable up to 600 °C. For a niobium content in the catalyst up to 8%, a thin homogeneous amorphous layer of niobic acid is formed on the SiO_2 surface.[29] The structure, acidity, and reactivity of Nb_2O_5 deposited on the MgO, Al_2O_3, TiO_2, ZrO_2, and SiO_2 surfaces have been investigated in the model methanol oxidation reaction.[30,31] Lewis acid centres are present on the surfaces of all the systems but, when niobic acid is deposited on the SiO_2 and Al_2O_3 surfaces, their activity is highest. On the SiO_2 surface, the Lewis acid centres exhibit oxidation-reduction properties, formaldehyde, and methyl formate being formed preferentially from methanol. On the other hand, on the Al_2O_3 surface they behave as acid centres, dimethyl ether being formed from methanol.[30] Brønsted acid centres are also present on the surfaces of the Nb_2O_5/SiO_2 and Nb_2O_5/Al_2O_3 catalysts.

The acidity of niobic acid and its capacity for crystallisation and reduction depend on the starting materials employed, the presence of impurities, and the method of deposition of niobic

acid on carriers.[32] Whereas pure amorphous Nb_2O_5 crystallises as the T-Nb_2O_5 phase after treatment at 500 and 600 °C and as the H-Nb_2O_5 phase at 1000 °C and begins to be reduced at temperatures above 600 °C, Nb_2O_5 present in catalysts obtained by impregnating SiO_2 with a solution of ethoxyniobium in hexane and sputtered onto the SiO_2 surface from the gas phase crystallises and is reduced at higher temperatures.[33] The catalyst obtained by impregnation is particularly effective. It has been suggested[33] that the change in the properties of the deposited Nb_2O_5 is caused by the strong interaction at the $SiO_2-Nb_2O_5$ interface, which influences not only the first monolayer but also the subsequent Nb_2O_5 layers as a consequence of the formation of Nb–O–Si linkages.

IV. The use of niobium oxide as a carrier and promoting agent

Hydrated niobium oxide is not the only niobium compound of interest for catalysis. Niobium oxides can also be used as promoting agents and carriers. For example, Nb_2O_5 used as a carrier in rhodium catalysts for the synthesis of higher hydrocarbons from CO and H_2 exerts a strong influence on the activity and selectivity.[3] The effectiveness of the carriers diminishes in the sequence $Nb_2O_5 > ZrO_2 > Al_2O_3 > SiO_2 > MgO$. At 220 °C the degree of conversion of CO on Rh/Nb_2O_5 reaches 76%,[3] whereas on Rh/Al_2O_3 it is only 1.4%.

The $Rh-Nb_2O_5$ interaction in the niobium pentoxide-promoted Rh/SiO_2 catalyst has been investigated by X-ray powder diffraction, X-ray photoelectron spectroscopy, IR spectroscopy, the EXAFS method, and the method based on the chemisorption of H_2 in relation to the test reaction involving the hydrogenolysis of ethane.[34,35] The degree of interaction of Rh with Nb_2O_5 depended on the heat treatment temperature. After heat treatment in air at 700 and 900 °C, strong interaction of rhodium with Nb_2O_5, involving the formation of the $RhNbO_4$ phase, was observed. Heat treatment at 500 °C did not give rise to this effect.

The strong metal–carrier interaction influences the hydroformylation of ethylene in the presence of palladium catalysts deposited on Nb_2O_5.[36] The influence of the temperature in the reduction with hydrogen on the chemisorption and catalytic properties of the 5% Pd/Nb_2O_5 and 5% Pd/SiO_2 catalysts has been investigated by X-ray powder diffraction and IR spectroscopy. The amounts of H_2 and CO chemisorbed on Pd/Nb_2O_5 reduced at 500 °C were respectively almost 4 and 2.5 times smaller than on Pd/Nb_2O_5 reduced at 200 °C. A strong metal–carrier interaction was observed in the catalyst reduced at 500 °C and the main product of the reaction of ethylene, CO, and H_2 at 64 °C was 2-methylpenten-2-al. Ethylene was hydrogenated to ethane on Pd/Nb_2O_5 reduced at 200 °C and on Pd/SiO_2.[36]

A strong promoting influence of Nb_2O_5 has been observed in a number of reactions.[3,37–39] For example, the $Pt/Nb_2O_5/SiO_2$ catalyst, in which the degree of coverage of Nb_2O_5 did not exceed the monolayer coverage, proved to be 40 times more active than Pt/SiO_2 and 1000 times more active than Pt/Nb_2O_5 in the hydrogenation of ethylene.[37]

The addition of Nb_2O_5 to V_2O_5/TiO_2 and to Fe_2O_3 appreciably improved the activity of the latter in the decomposition of NO using NH_3 as the reducing agent.[3]

$$4NO + 4NH_3 + 3O_2 \longrightarrow 4N_2 + 6H_2O.$$

On the catalyst having the composition (5% V_2O_5 + 2.7% Nb_2O_5)/TiO_2, the degree of conversion of NO at 200 °C was 100% whereas on the catalyst 7.5% V_2O_5/TiO_2 it was 40% at the same temperature and reached 100% only at 300 °C. The degrees of conversion of NO (expressed as percentages) on these catalysts varied as a function of the duration of the process in the following way:[3]

	Initial	After 15 h	After 30 h
$(V_2O_5-Nb_2O_5)/TiO_2$	99	94	89
V_2O_5/TiO_2	40	12	7

The use of the Rh/SiO_2 catalyst modified with Nb_2O_5 for the reduction of NO by ammonia has been examined.[38]

An active catalyst for the Fischer–Tropsch synthesis includes Ru/TiO_2 modified with 0.5%–25% of the oxide of a metal belonging to the Nb, V, and Ta group or their mixture in a non-crystalline form.[39]

V. Other niobium compounds used in catalysis

Other niobium compounds have also found applications in catalysis. Niobium sulfides, prepared by direct synthesis from the elements, are extremely active in the reactions involving the hydrogenation of biphenyl, toluene, and cyclohexene.[40] Their activity diminishes in the sequence $NbS_3 > NbS_2 > Nb_{1.12}S$. They exhibit the highest activity and selectivity (> 80%) in the cracking reaction.[40] Niobium sulfides are much more active than vanadium and ruthenium sulfides in the cracking and hydrodenitrogenation reactions.[41,42]

A series of niobium compounds exhibit a photocatalytic activity on irradiation with visible light.[43–45] Thus $K_4Nb_6O_{17}$ is extremely active in the photolysis of water.[44,45]

$$H_2O \longrightarrow H_2 + \tfrac{1}{2}O_2.$$

When 1% Ni is deposited on $K_4Nb_6O_{17}$, the activity of the latter increases.[45] A niobium-based catalyst for the metathesis of propene has been described.[46] A heterogeneous catalyst based on molybdenum or niobium chlorides deposited on SiO_2 is active in the reactions of unsaturated compounds—metathesis, cyclotrimerisation, and alkylation.[47] The catalytic and sorption properties of an aerosilogel modified with $NbCl_5$ in the ethanol decomposition reaction at 300 °C have been examined.[48]

The isomerisation and oligomerisation of olefins on the Nb_2O_5 and Nb_2O_5/SiO_2 catalysts reduced in a mixture of H_2 and H_2O at 600 °C have been investigated. The catalysts exhibited an activity in the isomerisation of *cis*-but-2-ene at 25 and 100 °C. It has been established by the EPR method[50] that the active catalytic centres are isolated coordinatively-unsaturated Nb^{4+} cations, which are more stable on the SiO_2 surface.

The high concentration of strong acid centres on the surface of crystalline β-Nb_2O_5, obtained by dissolving Nb_2O_5 in concentrated H_2SO_4 and subsequent crystallisation at 120 °C, is responsible for its activity in dehydration and esterification reactions.[51]

Amorphous and crystalline niobium phosphates,[52–54] which can be readily synthesised from niobium sulfate and phosphoric acid, may be of practical interest as acid catalysts.[52,53] The influence of the temperature of the preliminary treatment on the texture and acid and catalytic properties of niobium phosphate has been investigated by differential thermal analysis, thermogravimetric analysis, X-ray powder diffraction, the adsorption and indicator methods, the IR spectroscopy of adsorbed pyridine, and the test reactions involving the dehydration of 2-butanol, the isomerisation of but-1-ene, and the polymerisation of propene.[54] An increase in the heat treatment temperature diminishes the specific surface and the pore volume in the catalyst (Table 4). After heat treatment in the temperature range 100–500 °C, both Lewis and Brønsted acid centres with $H_0 = -8.2$ are present on the surface of the phosphate (Fig. 6). The catalyst treated at 150 °C is most active in the dehydration of 2-butanol, while the catalysts treated at 250 and 300 °C respectively are most active in the but-1-ene isomerisation and propene polymerisation reactions. Niobium phosphate is a more stable and active catalyst than niobic acid.

Table 4. The specific surfaces, pore volumes, and average pore diameters of niobium phosphate treated at different temperatures (niobium concentration in the specimen 43.44%).[54]

Treatment temperature/°C	Specific surface/$m^2\ g^{-1}$	Pore volume/$cm^3\ g^{-1}$	Average pore diameter/Å
150	277	0.352	34.8
300	230	0.310	39.0
500	182	0.287	39.0

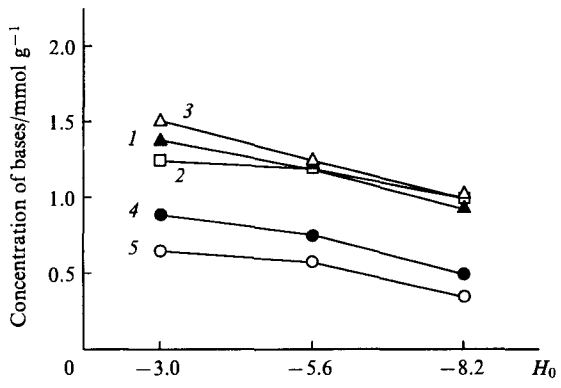


Figure 6. Distribution of the centres with respect to their acid strength in niobium phosphate heat-treated at different temperatures (°C): *1*, 100; *2*, 150; *3*, 300; *4*, 400; *5*, 500.

By adding phosphoric acid to a solution obtained when Nb_2O_5 is dissolved in concentrated H_2SO_4 in the presence of $(NH_4)_2SO_4$ and by subsequent addition of NH_4OH until the attainment of pH 1, the crystalline niobium(V) phosphate was isolated. It crystallises in a pseudocubic lattice with a_0 = 10.244 Å and has the rigid three-dimensional structure of a zeolite.[53] Its empirical formula was determined as $Nb_2O_5 \cdot 1.5P_2O_5 \cdot 7.5H_2O$, while its chemical formula was found to be $(NbO)_2(HPO_4)_3 \cdot 6H_2O$. The crystalline niobium phosphate was characterised by pH titration, IR and X-ray photoelectron spectroscopy, X-ray powder diffraction, thermogravimetric analysis, and differential scanning calorimetry. It was established that its chemical stability is higher than that of the amorphous phosphate and that it has a high exchange capacity, reaching 4.6 mmol g^{-1} for K^+ (the theoretical value is 4.8 mmol g^{-1}). According to Okazaki,[2] both the amorphous and crystalline niobium(V) phosphates can be used either as catalysts or as carriers in many processes.

References

1. K Tanabe *Mater. Chem. Phys.* **17** 217 (1987)
2. S Okazaki *Surface* **27** 112 (1989); *Ref. Zh. Khim.* 23B4591 (1989)
3. K Tanabe *Catal. Today* **8** 1 (1990)
4. "Catalytic Conversion with Niobium Materials" *Catal. Today* **8** (1990)
5. A N Zelikman, B G Korshunov, A V Elyutin, A M Zakharov *Niobii i Tantal* (Niobium and Tantalum) (Moscow: Metallurgiya, 1990)
6. *Niobii: Syr'e, Ferroniobat, Metall, Soedineniya* (Niobium: Raw Material, Ferroniobate, Metal, and Compounds); *Ref. Zh. Khim.* 4L119 (1989)
7. N A Borisova, A N Zelikman, N N Rakova, V A Totiev, in *Tezisy Dokladov VI Vsesoyuznogo Soveshchaniya po Khimii i Tekhnologii Molibdena i Vol'frama, Nal'chik, 1988* (Abstracts of Reports at the VIth All-Union Conference on the Chemistry and Technology of Molybdenum and Tungsten, Nal'chik, 1988) p. 174
8. V A Filov (Ed.) *Vrednye Khimicheskie Veshchestva: Neorganicheskie Soedineniya Elementov V-VIII Grupp. Spravochnik* (Handbook. Harmful Chemicals: Inorganic Compounds of Group V–VIII Elements) (Leningrad: Khimiya, 1989) p. 140
9. B K Sen, A V Saha, N Chatterjee *Mater. Res. Bull.* **16** 923 (1981)
10. B K Sen, A V Saha *Mater. Res. Bull.* **17** 161 (1982)
11. B K Sen, P Bandyopadhyay, A V Saha *Mater. Res. Bull.* **17** 611 (1982)
12. T Iizuka, K Ogasawara, K Tanabe *Bull. Chem. Soc. Jpn.* **56** 2927 (1983)
13. S Okazaki, A Kurosaki *Catal. Today* **8** 113 (1990)
14. K Ogasawara, T Iizuka, K Tanabe *Chem. Lett.* 645 (1984)
15. S Okazaki, M Kurimata, T Iizuka, K Tanabe *Bull. Chem. Soc. Jpn.* **60** 37 (1987)
16. US P. 4 652 544; *Ref. Zh. Khim.* 1L194 (1988)
17. S Okazaki, H Harada *Chem. Lett.* 1313 (1988)
18. T Hanaoka, K Takeuchi, T Matsuzaki, Y Sugi *Catal. Today* **8** 123 (1990)
19. Jpn. Appl. 63–14 760; *Ref. Zh. Khim.* 24N66 (1988)
20. A Kurosaki, T Okuyama, S Okazaki *Bull. Chem. Soc. Jpn.* **60** 3541 (1987)
21. T Iizuka, S Fujie, T Ushikubo, Z Chen, K Tanabe *Appl. Catal.* **28** 1 (1986)
22. Jpn. P. 62–174 032; quoted after K Tanabe *Catal. Today* **8** 1 (1990)
23. Jpn. P. 61–167 634; quoted after K Tanabe *Catal. Today* **8** 1 (1990)
24. Jpn. P. 62–42 939; quoted after K Tanabe *Catal. Today* **8** 1 (1990)
25. Jpn. Appl. 395 136; *Ref. Zh. Khim.* 13N13P (1992)
26. K Asakura, Y Iwasawa *Chem. Lett.* 859 (1986)
27. N Ichikuni, K Asakura, Y Iwasawa *J. Chem. Soc., Chem. Commun.* 112 (1991)
28. M Shirai, N Ishikuni, K Asakura, Y Iwasawa *Catal. Today* **8** 57 (1990)
29. M Shirai, K Asakura, Y Iwasawa *J. Phys. Chem.* **95** 9999 (1991)
30. J Jehng, I Wachs *Catal. Today* **8** 37 (1990)
31. J Jehng, I Wachs *J. Phys. Chem.* **95** 7373 (1991)
32. E I Ko, J C Weissman *Catal. Today* **8** 27 (1990)
33. P A Burke, J C Weissman, E I Ko, P Wynblatt, in *Catalyisis '87* (Proceedings of the 10th North American Catalysis Society Meeting, San Diego, CA, USA, 17–22 May 1987) Ed. J W Ward (Amsterdam: Elsevier, 1988) p. 457
34. K Kunimori, Z Hu, T Uchijima, K Asakura, Y Iwasawa, M Soma *Catal. Today* **8** 85 (1990)
35. Y G Yin, T Kagasugi, H Shindo, S Ita, K Kunimori, T Uchijima *Catal. Lett.* **9** 43 (1991)
36. A Maeda, F Yamakawa, K Kunimori, T Uchijima *Catal. Lett.* **4** 107 (1990)
37. K Asakura, Y Iwasawa *Chem. Lett.* 633 (1988)
38. P B Rasband, W C Hecker *Catal. Today* **8** 99 (1990)
39. US P. 4 711 871; *Ref. Zh. Khim.* 18L175 (1988)
40. M Vrinat, C Guilard, M Lacroix, M Breysse, M Kudri, M Danot *Bull. Soc. Chim. Belg.* **96** 1017 (1987)
41. M Danot, J Afonso, J Portefaix, M Breysse, T des Courieres *Catal. Today*, **10** 629 (1991)
42. M Breysse, J Afonso, M Lacroix, J L Portefaix, M Vrinat *Bull. Soc. Chim. Belg.* **100** 923 (1991)
43. Jpn. P. 63–107 815; *Ref. Zh. Khim.* 10L208 (1989)
44. A Kudo, K Sayama *J. Catal.* **120** 337 (1989)
45. K Domea, A Kudo, A Tanaka, T Onishi *Catal. Today* **8** 77 (1990)
46. K Asakura, M Nishimura, Y Iwasawa *J. Mol. Catal.* **55** 159 (1989)
47. USSR P. 1 666 177; *Ref. Zh. Khim.* 10L249 (1992)
48. M A Artemeva, Yu M Artem'ev, in *Tezisy Dokladov Shkoly-Seminara po Khimii Poverkhnosti Dispersnykh Tverdykh Tel, Slavsk, 1989* (Abstracts of Reports at the School-Seminar on the Chemistry of the Surfaces of Disperse Solids, Slavsk, 1989) p. 6
49. Y Murakami, Y Wada, A Morikawa *Bull. Chem. Soc. Jpn.* **61** 2747 (1988)
50. Y Wada, A Morikawa *Catal. Today* **8** 13 (1990)
51. C Guo, Z Sun, S Cui, L Wen, Z Qian *J. Catal.* **11** 313 (1990); *Ref. Zh. Khim.* 7B4240 (1991)
52. M Qureshi, A Ahmad, N Shakeel, A Gupta *Bull. Chem. Soc. Jpn.* **59** 3247 (1986)
53. M Qureshi, J Gupta, H Khan, A Ahmad *Bull. Chem. Soc. Jpn.* **61** 2191 (1988)
54. R L Martins, W I Schitine, F S Castro *Catal. Today* **5** 483 (1989)

Russian Chemical Reviews **62**(8) 751 – 767 (1993)
© 1993 Russian Academy of Sciences and Turpion Ltd

UDC 547.383

Methods of synthesis of acrolein and its α-substituted derivatives

N A Keiko, M G Voronkov

Contents

I. Introduction 751
II. Methods of synthesis of acrolein and α-alkylacroleins 751
III. Methods of synthesis of α,β-unsaturated aldehydes α-substituted by functional groups 758

Abstract. The methods of synthesis of acrolein and its α-alkyl-substituted derivatives are examined: (a) catalytic oxidation of propene, isobutene, propane, isobutane, propyl and *tert*-butyl alcohols, *tert*-butyl alkanoates, propionaldehyde isobutyraldehyde, and allyl alcohol and its ethers and esters; (b) condensation of formaldehyde with aliphatic aldehydes by the Mannich reactions and also in the vapour phase over heterogeneous catalysts. Both general methods (the Mannich reaction, *ipso*-substitution of a α-halogen in the acrylic system, and interaction of 1-bromo–2-ethoxycyclopropyl-lithium with electrophiles) and various special methods are used in the synthesis of α,β-unsaturated aldehydes with functional-group-substitutents. The bibliography includes 323 references.

I. Introduction

Acrolein and methoacrolein and industrial products produced on a large scale. The world production of the former compounds runs into hundreds of thousands of tonnes annually. The acrylic and methacrylic acids obtained from acrolein and methacrolein, as well as their esters have found extensive applications as monomers in the manufacture of various polymeric materials, synthetic fibres, emulsions, adhesives, etc. Industrial methods of synthesis of acrylonitrile, methionine, glycerol, allyl alcohol, glutaraldehyde, β-picoline, pheromones, pesticides, perfumes, and medicinal drugs from acrolein have been developed. The high reactivity of acrolein and its substituted derivatives has created extensive possibilities for its use in fine organic synthesis. During the last decade up to 300 articles and patents devoted to the methods of synthesis of acrolein and its derivatives and their involvement in various syntheses have been published annually. Acrolein itself is used as a herbicide and algicide and prevents the growth of biomass on technical water supply systems, as a slimicide which destroys slime in the manufacture of paper, as a binder in solutions for building purposes, as a component for the purification of waste water containing hydrogen sulfide and cyanide ions, as an ingredient in compositions for the protection of wood against water, as a stabiliser used in the finishing of textile materials, etc. It has been shown recently that latex microbeads based on polyacrolein can be used in immunoanalysis. All the expanding applications of acrolein and its derivatives have made it necessary to improve the known methods and to seek new ones for their synthesis using cheaper and more readily available raw materials.

The principal industrial method for the synthesis of acrolein and methacrolein available at present involves the incomplete selective vapour-phase oxidation of propene and isobutene respectively on heterogeneous catalysts. The last systematic review devoted to the oxidation of propene to acrolein covers the literature published up to 1981.[1] Review articles on other methods of synthesis of acrolein and its derivatives were published even earlier.[2–6] We therefore had to deal in the present review with studies published mainly during the last 15–20 years. In addition α,β-unsaturated aldehydes α-substituted by functional groups, the chemical reactions of which are extremely varied and frequently unexpected, have been scarcely represented in the review literature (with the exception of one publication by the authors of the present review[7]). As far as possible, they will be considered exhaustively in the text below.

N A Keiko, M G Voronkov Irkutsk Institute of Organic Chemistry, Russian Academy of Sciences, ul. Favorskogo 1, 664033 Irkutsk-33. Tel. (7-3952) 46 02 45

Received 21 March 1993
Uspekhi Khimii **62** (8) 796 – 812 (1993); translated by A K Grzybowski

II. Methods of synthesis of acrolein and α-alkylacroleins

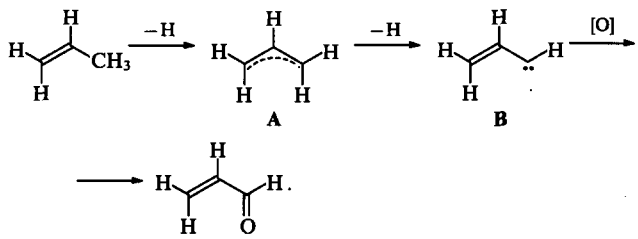
1. Oxidation of propene and isobutene

The partial vapour-phase oxidation of propene and isobutene on heterogeneous catalysts is at present the main industrial method of synthesis of acrolein and methacrolein respectively:

$$CH_2=CR-CH_3 + O_2 \longrightarrow CH_2=CR-CHO + H_2O;$$
$$R = H, Me.$$

This reaction constitutes the first stage of the large scale industrial production of acrylic and methacrylic acids from which acrylates and polyacrylates are obtained in their turn. Data on the improved methods of the oxidation of propene and isobutene available up to 1981 are surveyed in the existing reviews.[1,4–6,8–14]

The catalytic oxidation of propene is one of the most important allylic oxidation reactions.[12] In allylic oxidation, the alkene, for example propene, is activated as a result of the elimination of a hydrogen atom from the methyl group with formation of the allyl intermediate A. This stage determines the rate of the entire process.[12,15–18]



The intermediate B formed subsequently interacts with the oxygen of the catalyst lattice and is converted into acrolein. All the known selective oxidation catalysts have oxidation-reduction properties. They must be capable of not only being reduced during the formation of acrolein but also of being reoxidised with incorporation of oxygen from the gas phase into the catalyst lattice in the form of the O^{2-} ions, which results in the refilling of the free vacancies. A procedure in which the properties of various polyvalent oxides are combined has become one of the fruitful methods for the selection of catalysts of the process under consideration.[12] The participation of oxygen from the crystal lattice of bismuth molybdate or the three-component bismuth–vanadium–molybdenum oxide catalyst in the oxidation of propene has been confirmed experimentally using $^{18}O_2$ as the oxidant.[19,20]

Among the complex oxide catalysts for the selective oxidation of propene, molybdenum-containing catalysts have come to be most widely used during the last 20 years.[21–26] However, molybdenum catalysts are frequently used only for research purposes, for example, in the study of the dependence of the activity on the surface structure[27] or for the determination of the orientation of MoO_3 in the catalyst layers, which influences the selectivity of the reaction.[28,29] Bimetallic catalysts, which contain, apart from molybdenum oxide, also bismuth,[30] cobalt,[31] or vanadium[32] oxide, are much more active. The incorporation of bismuth in an amount of even several tenths per cent increases the conversion of butene and the reaction selectivity with respect to methacrolein by tens per cent.[33] The addition of bismuth increases the effectiveness of the oxidation of propene on $PbMoO_4$[34] or on the multicomponent molybdenum catalysts $Mo_{12}Bi_xFe_yTl_z$ and $Mo_{12}Bi_xFe_yTl_zNi_6Zn_3$.[35]

Systematic studies have been made on the oxidation of isobutene on Fe–Mo–Te and Fe–Mo–Sb oxide catalysts,[36–39] as well as on Co–Mo–Bi–Fe oxides.[40] On one of the specimens of the Fe–Mo–Te catalysts, it has been possible to attain the virtually complete conversion of the olefin in the oxidation of an isobutene–air mixture containing 1.8 vol.% of isobutene at 370 °C. The selectivity with respect to methacrolein was then 77% and the yield of the latter relative to the isobutene passed through the system was 75%–80%.

However, the multicomponent oxide catalysts containing added Co, Ni, Fe, K,[21] Ni, Co, Fe, K, P, Si,[41] and certain other elements,[42–43] apart from molybdenum and bismuth, are the most effective and selective. With the aid of such catalysts, it has been possible to achieve 93%–98% conversion of propene and a 79%–88% yield of acrolein.[41,44] Equally high parameters were obtained in the oxidation of butene, but the catalysts employed had a more complex composition:

$$Mo–Co–Fe–Bi–Tl–X–Y–Z–O,$$

where X = V and/or NB, Y = La and/or Ce, and Z = Cs and/or Te;[45]

$$Mo–Co–Fe–Ni–Pb–X–SmO,$$

where X represents two elements from the Rb, Cs, Tl triad:[46]

$$Mo–Bi–M^1–M^2–M^3–M^4–M^5–ZnO,$$

where M^1 = In, La, Ga or Al; M^2 = Fe or Fe and Cu; M^3 = Ni and/or Co; M^4 represents several elements from the P, W, Cr triad (usually W + P or W + Cr) and sometimes B, As, or V, and M^5 is one or several of the elements from the set Cd, Ta, Sm, Nb, Ag, Pb, Mn, Re, Sn, Ge, Mg, Ca, or Ba.[47] Each of the eight or nine elements is a necessary component for the attainment of a high productivity. For example, the last of the catalysts enumerated, with added zinc, is distinguished by an increase in selectivity and a higher stability.[47]

Since the catalysts are multicomponent systems, the choice of the composition ensuring the attainment of the optimum activity and selectivity is a task of enormous difficulty.

The stability and activity of the catalyst play an important role in the industrial manufacture of acrolein. For example, at the start of the catalyst bed, where the temperature has increased owing to the evolution of the heat of the reaction with the water present in the reacting gas, molybdic acid is formed and vaporises.[48] The vaporised molybdenum condenses in the colder part of the reactor. As a result of this, the yield of methacrolein is low at the beginning of the bed.

Apart from molybdates, metal anitmonates[49] and tellurates as well as multicomponent systems based on them[50,51] and phosphates of the type $2Bi_2O–P_2O_5$ [17] are active catalysts. The introduction of 0.2%–0.8% of Na_2O into the last catalyst increases the amount of basic surface centres and leads to the conversion of propene not into acrolein but into hexa-1,5-diene and benzene.[52]

Vanadium and titanium–vanadium oxide catalysts exhibit an increased selectivity, which depends on the presence of nonstoichiometric V–Na compounds.[53,54]

Iron–tin[16] and tin–antimony[27,55–58] catalysts constitute a separate group of effective catalysts of the oxidation of propene. The latter exhibit an especially high activity in the oxidation of isobutene to methacrolein.[59–64] Depending on the composition, the optimum temperature at which the highest activity of the catalyst is attained is in the range from 430 to 675 °C.[59] The activity and selectivity of the tin–antimony catalysts depend greatly on the method of their preparation. The dissolution of the metal in boiling nitric acid,[64] the coprecipitation of the corresponding Sn and Sb salts followed by heat treatment of the deposits,[49] the deposition of Sb oxides onto the SnO_2 matrix, mixing of SnO_2 and Sb_2O_4 or Sb_6O_3,[27] and spray drying of an aqueous suspension of the initial oxides with subsequent heat treatment at 800 °C [65] are most often used. The Sb–Sn oxide catalyst obtained in the last case exhibits a high mechanical strength and ensures a high yield of methacrolein (up to 85% relative to the initial isobutene). Highly active and selective tin–antimony catalysts of the gas-phase oxidation of isobutene to methacrolein (yield up to 72%) are obtained from a moist paste of tin(II) and antimony (preferentially Sb_2O_5) oxides by drying it and subsequent heat treatment.[61] The conditions in the preparation of the tin–antimony catalysts influence their structure and properties so significantly that the method of preparation of the catalyst is frequently more important than its chemical composition.[66]

It has been suggested that catalysts be compared in terms of their maximum selectivity attained for a specified conversion of isobutene and yield of methacrolein.[62] According to this criterion, the catalysts investigated can be arranged in the following series:

$$Sn–Sb > Bi–Mo–V–O > Bi–Mo–W–O.$$

The Sn–Sb–O mixed oxide catalyst is 1.5–2 times less active at 425 °C than the analogous Mo–Bi–O catalyst for the same initial selectivity with respect to methacrolein (80%).[67]

A series of the catalysts of the oxidation of propene to acrolein described in the literature have been compared using the thermal desorption method: $Co_6Mo_{12}Bi_{0.5}Fe_{0.75}O_x$, Bi_2MoO_6, 5 at.% Sb in SnO_2, USb_3O_3, $BiFeMoO_x$, $Bi_3FeMo_2O_x$, Cu_2O, $CoMoO_4$.[68]

It was established that the active intermediates arising from propene can be converted into acrolein via two pathways: they interact either with the oxygen of the catalyst lattice or with the adsorbed oxygen. The rate of the selective oxidation of propene on modified cobalt molybdate is determined by the acrolein desorption stage.

Overall, the idea that it is mainly the oxygen ions of the crystal lattice which participate in the selective oxidation of alkenes over the $MoO_3-Bi_2O_3$ or $Bi_{1-x/3}V_{1-x}Mo_xO_4$ catalysts while gaseous oxygen reoxidises the catalyst became firmly established towards the beginning of the 1990s.[19,20,34] The use of oxides with a scheelite structure of the type $Pb_{1-3x}Bi_{2x}\Phi_xMoO_4$ (Φ = cationic vacancy, x = 0 and 0.04) as the catalysts in the electrochemical oxidation of the alkenes made it possible to determine the mobility of the lattice oxygen ions, which is satisfactorily correlated with the catalytic activity.[20,34] The electrolyser cell incorporating the yttrium oxide-stabilised zirconium oxide (Y–s–Zr) as the solid electrolyte, namely $P(O_2)$, M/Y–s–Zr/M′, $P(O_2)'$, where M and M′ are electrodes, can perform the function of an oxygen pump, in which the oxygen stream passing through the electrolyte is regulated by the electric potential applied to the electrodes.[34,69] Under the conditions of the partial oxidation of alkenes in this system at 450–475 °C, the gaseous oxygen chemisorbed on the catalyst surface dissociates into ions, which diffuse into the bulk phase and are then incorporated in the allyl intermediate, forming oxidised compounds. On the other hand, the chemisorbed oxygen remaining on the surface accelerates only the more extensive oxidation of the alkenes to CO and CO_2. The ideas concerning the mechanisms of the oxidation of propene to acrolein current up to 1976 have been examined in detail in a monograph[13] (pp 81–102 and 120–132).

The copper catalyst for the oxidation of propene to acrolein, which was most effective in the 1940s, is little used. Nevertheless, the influence of reoxidation and of water vapour on the ion-exchange process catalysed by copper(II)-containing zeolites was studied recently.[70]

Apart from the composition of the catalysts and the method of mixing the components,[39,71] the valence state of the elements and hence the activity of the catalyst are influenced decisively by the heat treatment temperature,[33,50] the size and geometrical shape of the particles employed, and also their specific surface.[13,33,72]

The oxidation of olefins is usually carried out at 250–450 °C at a pressure close to atmospheric. A stationary catalyst bed is most often employed, but sometimes a fluidised bed is also used.[16,57] The effectiveness of reactants of different types in the oxidation process can be estimated by mathematical modelling methods.[60]

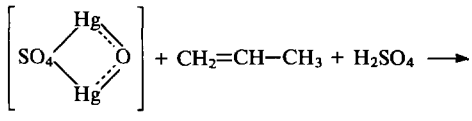
In order to make industrial processes more economical, it is essential to achieve in the latter a high conversion of the olefin and a greater selectivity with respect to the aldehyde in order to eliminate the cost of the recirculation of the unreacted initial alkene. An excess of oxygen 2–20 times greater than the concentration of the alkene is used for this purpose.[16,39,45,46,73] In order to prevent the overheating of the catalyst and to reduce the formation of the extensive oxidation product, the reacting gases are diluted with 10%–40% of water vapour,[23,24,36–39,45,46,74,75] nitrogen,[32,47,76] helium or argon,[46] or inert hydrocarbons — for example, but-1-ene.[73]

An increase in the conversion and selectivity during the oxidation of olefins to unsaturated aldehydes on a catalyst of the type $Mo_{12}BiCo_3NiFeK_{0.1}O_x$ is attained by introducing an inert material into the catalyst (up to 75% by volume). This promotes a more uniform distribution of the heat of reaction throughout the catalyst bed and the attainment of the optimum rate of the process.[74] The inert carriers employed are porcelain, quartz,[3,39,77] α-Al_2O_3,[37] SiO_2,[46,78] and 'inert' glass particles.[79] The Fe–Sb–O catalyst was diluted with silica gel containing 30% of SiO_2 (the SiO_2 content in the heat-treated catalyst was 2, 10, or 25 mass%).[16]

Acetone and acetaldehyde[53] and acetic and acrylic or methacrylic acids are encountered in small amounts, in addition to CO and CO_2,[46] among the side products of the oxidation of lower alkenes to acrolein and methacrolein respectively.[36,37,39,46,47] The side reactions involving the extensive oxidation of the initial alkenes and the unsaturated aldehydes formed can be suppressed by introducing promoting agents, for example thallium,[33,80] or by reducing the contact time.[39] The crystal structure,[27–30] phase composition,[75,81–83] and a number of other physicochemical properties of the catalysts of the vapour phase oxidation of lower alkenes[16,84,85] were investigated by IR, Raman,[51,86] UV, visible[87] and Mössbauer spectroscopy, electron microscopy,[88] and also X-ray diffraction.[61,88] The study of the kinetics of this process showed that the rate of formation of acrolein on a multicomponent molybdenum catalyst at 320 °C is independent of the partial oxygen and water vapour pressures, increasing with increase in the propene pressure.[89] The reaction involving the oxidation of propene to acrolein on a bismuth–molybdenum oxide catalyst with added Ni, Co, Fe, K, and P in the temperature range 300–390 °C is autocatalytic. Water vapour promotes the formation of acids as side products, but suppresses the extensive oxidation reactions of acrolein and acrylic acid.[64] Optimisation of the catalytic composition containing Mo, Co, Fe, Bi, and K oxides by Fabian's statistical method made it possible to attain the maximum selectivity with respect to acrolein.[90] The π-complexes of the allyl anion with transition metals have been investigated *ab initio* by the molecular orbital method.[91]

Technological schemes for the partial oxidation of propene on a multicomponent oxide catalyst have been developed with the aid of the mathematical modelling method.[21,60,89,90,92]

An effective laboratory liquid-phase method for the oxidation of propene to acrolein (in 85% yield) in an acid aqueous solution of mercury salts (preferentially the sulfate and perchlorate)[93] can be described schematically as follows:



$$\longrightarrow CH_2{=}CH{-}CHO + 2Hg_2SO_4 + 2HgSO_4 + 2H_2O.$$

An electrochemical process involving the allylic oxidation of propene to acrolein and acrylic acid has been patented.[94] When a palladium anode and 25% phosphoric acid as the electrolyte were used in this process, a high selectivity with respect to acrolein could not be attained.[95]

Acrolein and methacrolein are also formed in the oxidation of butadiene to isopropene by molecular oxygen in the presence of a rhodium catalyst (80 °C, 50 atm). However, the yield of the unsaturated aldehyde is only ~1%, so that this reaction is of no practical interest.[96]

2. Oxidation of propane and isobutane

Attempts were made in the 1980s to select a catalyst for the direct oxidation of propane by oxygen to the corresponding unsaturated aldehydes and acids.[97–99] The highest conversion (20%–30%) for a selectivity with respect to C_3 oxidation products of 13%–40% was attained on mixed oxide catalysts containing boron and phosphorus or molybdenum and tellurium at 500–550 °C. The selectivity with respect to acrolein of silver-doped bismuth vanadomolybdate exceeded 60%, but the conversion of propane was only 13%.[100]

Isobutane is oxidised by atmospheric oxygen to methacrolein at 250–450 °C over a reduced catalyst prepared from heteropolyacids, for example $H_3PMo_{12}O_{40} \cdot 30H_2O$.[101] The conversion of the alkane is 7%–8%, under these conditions, while the selectivity with respect to methacrolein and methacrylic acids is 12% and 48% respectively. Unsaturated aldehydes may be synthesised from the corresponding alkanes more conveniently in two stages without the isolation of intermediates.[102] The first stage involves the dehydrogenation of the mixture of alkanes (propane, isobutane, etc.) at 650 °C (approximately 45% conversion), while the second involves the oxidation of the products in another reactor at 340 °C (82% conversion).

3. Oxidation of propanol and *tert*-butyl alcohol

The vapour-phase oxidation of propanol by atmospheric oxygen to acrolein has been achieved using a two-bed catalyst.[103] Dehydration and oxidation occurred in the first and second catalyst beds respectively. BPO_4 coprecipitated with SiO_2 and Al_2O_3 and also WO_3 and Al_2O_3 were used as the dehydration catalyst. The second bed contained either the Fe–Co–Bi–P–Mo–K, Fe–Co–W–Bi–Mo–Mg, and Sb–U mixed oxides or a mixture of bismuth molybdate and phosphoromolybdate. The mixture of propanol and oxygen supplied to the reactor was diluted with an inert gas (N_2, He, CO_2) or water vapour and the process was carried out at 350–500 °C and pressures in the range 0.5–10 atm.

tert-Butyl alcohol is a side product of the processing of the butane–butene fraction and in many other industrial processes. A highly efficient process involving the direct oxidation of the alcohol to methacrolein without the preliminary dehydration to isobutene has been proposed for its utilisation.[104] The yield of methacrolein on the Fe–Te–Mo (1 : 0.85 : 1) oxide catalyst[36] is more than 80%. The reaction is carried out at 400–420 °C, a space velocity of 0.1–0.15 s^{-1}, and an alcohol concentration in the initial reaction mixture of 4–5 vol.%. The synthesis of methacrolein by the partial oxidation of *tert*-butyl alcohol is similar to the oxidation of isobutene examined above.[22,25,26,45,46,105,106] Both processes are carried out on the same incomplete oxidation catalyst. Comparison of the dependence of the selectivities of the processes (with respect to methacrolein and CO and CO_2) on the degree of conversion of the initial isobutene or *tert*-butyl alcohol showed that the oxidation reaction proceeds by a consecutive-parallel mechanism. *tert*-Butyl alcohol is initially dehydrated to isobutene, which is converted into methacrolein and extensive oxidation products.[105–107] The selectivity with respect to methacrolein in the oxidation of *tert*-butyl alcohol on the Co–Mo–Bi–Fe–Sb–K–O catalyst is somewhat higher than in the oxidation of isobutene.[105] As in the oxidation of isobutene, the initial mixture of the alcohol and oxygen is diluted with water vapour and nitrogen.[25,26,105,108–110] A yield of methacrolein of 80%–90% for a virtually complete conversion of *tert*-butyl alcohol can be achieved on modern multicomponent oxide catalysts based on Mo–Co–Bi.[45,46] The use of complex catalytic compositions of the type $Sm_aFe_bBi_cX_dNi_eZ_fQ_gMo_{12}O_h$, where X = K, Rb, Cs, or Tl, Z = B, Co, Si, Au, Ag, Cd, Hg, V, Ti, Zr, Nb, Ta, Cr, W, U, Tc, Re, Be, Mg, Ca, Sr, or Ba and Q = Gd, Sc, Tb, Ho, Hf, Lu, or Dy, and a selection of catalyst carriers (SiO_2, SiC_2, Al_2O_3) and partial pressures of $(CH_3)_3COH$, O_2, N_2 and H_2O make it possible to raise the conversion of the alcohol to 92% for a selectivity of 90%.[111] According to patent data, the modified Mo–Fe–Co catalyst to which other elements have been added exhibits a high resistance to compression and wear, has a high catalyst activity, and is long lived.[112] Silicon dioxide is the commonest carrier for multicomponent catalysts of the processes described[22,108,113] but granulated activated charcoal can be used instead.[114]

In contrast to the one-reactor method described, it has been suggested that, in order to obtain methacrolein from *tert*-butyl alcohol, the latter should be dehydrated to isobutene over the γ-Al_2O_3 (90%)–SiO_2 (10%) catalyst at 80 °C. The isobutene obtained in this way is oxidised further to methacrolein. This greatly increases the lifetime of the second catalyst bed prepared from the Mo–Bi–Fe–Co–Cs oxide composition.[115]

A method of synthesis of methacrolein involving the oxidation of *tert*-butyl alcohol and/or its isobutyl ether as well as isobutene by oxygen-containing gases at 100–300 °C with the Hg, Ba, Cr, Mo, V, Mn oxides and halides as catalysts has been described.[114]

Highly effective catalysts of the oxidation of methyl and butyl ethers of *tert*-butyl alcohol, having the composition $Mo_aW_bBi_cFe_dX_eY_fZ_gQ_hO_x$ (X = Ni and/or Co; Y is an alkali or alkaline earth metal and/or Tl; Z = P, Te, Sb, Sn, Ce, Pb, Nb, Mn, Zn, Ge, Ga, La, In, Cd, V, Cr, U and/or Ag; and Q = Si, Al, Ti, or Zr) have been proposed. The conversion of the ethers is 98% and the selectivity with respect to methacrolein is 82%.[116]

Acetic and methacrylic acids, but-1-ene or but-2-ene, buta-1,3-diene, CO, CO_2, and polymers are side products of the oxidation of *tert*-butyl alcohol.[117,118]

4. Oxidation of *tert*-butyl alkanoates

A continuous method of synthesis of methacrolein by the gas-phase oxidation of *tert*-butyl alkanoates with oxygen or air over the isobutene oxidation catalyst in the presence of water vapour has been proposed.[119]

$$RCOOC(CH_3)_3 \xrightarrow{[O]} CH_2{=}C(CH_3){-}CHO.$$

The Mo–Co, Mo–Bi, Mo–Fe, Mo–P, Mo–Bi–Fe–Co oxide mixtures, preferably with added Ni, Sb, W, Te, Cs, K, Cu, or their mixtures, are used as catalysts. The reaction is carried out at 200–600 °C with the molar ratio oxygen : ester = (0.5–10) : 1. Under optimum conditions, the conversion of the ester is 61% and the selectivity with respect to methacrolein is 88%.

5. Oxidative dehydrogenation of propionaldehyde and isobutyraldhyde

The vapour phase oxidative dehydrogenation of propionaldehyde and isobutyraldehyde to acrolein and methacrolein respectively can be carried out at 280–390 °C over catalysts containing Mo, P, and O as well as Zn, Cu, or Ag on Al_2O_3 or Si–C.[120]

$$CH_3CHRCHO + 0.5O_2 \longrightarrow CH_2{=}CRCHO + H_2O;$$

R = H, Me.

It is recommended that the initial aldehyde–air mixture be diluted with water vapour or nitrogen. When the mixture of isobutyraldehyde, air, steam, and nitrogen is used in proportions of 3.4 : 18.6 : 70 : 8.0, it is possible to obtain methacrolein in 61.5% yield. The corresponding unsaturated acid is a side product. There has been no demand for isobutyraldehyde, which is a waste product in the manufacture of 2-ethyl-hexanol[121] and a side product in oxo-synthesis,[122] but there arises now the prospect of using it to obtain polyacrylates via methacrolein and methacrylic acid. The competitiveness of the oxidative dehydrogenation process depends greatly on the efficiency of the catalyst. The most effective catalytic systems for the oxidative dehydrogenation of isobutyraldehyde are presented in Table 1.

Table 1. Conditions in the oxidative dehydrogenation of isobutyraldehyde (IBA) to methacrolein.

Catalytic system	Initial reactants	T/°C	Yield (%)	Conversion (%)	Selectivity (%)	Ref.
Bi–P–Mo–O	IBA + air	320	80 [a]			123
Mo–Co–O (W or W + Te)	IBA : O_2 : H_2O : N_2 = 5 : 10 : 30 : 55		21			124
Mg–Cr–Fe–O_4	IBA : O_2 = 1 : (1.5–3)	350		68	88	125
Zn–Cr–Fe–O_4	IBA : O_2 = 1 : (1.5–3)	350		65	87	125
$H_5Mo_{10}V_2PO_{40}$	IBA : O_2 : N_2 = 4.7 : 12.7 : 82.6	288	68			126
Bi_2O_3 + Group I and II metal oxides	IBA + lattice oxygen	450	47		65.5	127
Mo–P–Zr–V–X–X′–O (X = K, Pb, Cs or Tl; X′ = Li, Na, Mg or Ca)	IBA + air + water	260	76.5	100	65.5	128
		310	17			
	IBA : air : H_2O = 4 : 40 : 56	320	18.1			129
		280	65.3	10		
$A_aFe_bP_cO_x$ (A = Cs, Tb, Mn, U, Ag, Tl)	IBA : O_2 : H_2O = 1 : 3.7 : 26	250–600	80	100		130
$H_5Mo_{10}V_2PO_{40}$	IBA + air + nitrogen	205–210	100	>90		131
$H_5Mo_{10}V_2PO_{40}$	O_2 : IBA = 1.23–1.92					122
Sb_2O_5	IBA + air	325	81.5	20		134
Fe, Te, and Mo oxides (1 : 0.85 : 1)	IBA : air = 2.5 : 97.5	285		88	42	132
Fe, Te, Mo, and Mg oxides (1 : 0.85 : 1 : 0.1)	IBA : air = 2.5 : 97.5	340		100	39	132
$Mo_3Sb_2Te_{0.1}O_x$	IBA : air = 2.5 : 97.5	310		12	67	132
		420		53	40	132
$Mo_{12}Sb_2Te_{0.2}O_x$	IBA : air = 2.5 : 97.5	385		100	41	132
$Mo_{12}SbTe_2O_x$	IBA : air = 0.5 : 10	360		>90	60	133

[a] The overall yield of methacrolein and methyl methacrylate is quoted.

The table shows that catalysts based on heteropolyacids of the type $H_{3+x}Mo_{12-x}V_xPO_{40}$ ensure the highest conversion and selectivity of the process at a comparatively low temperature. However, for technological use, they must be deposited on inert supports. The problem of the long time stability of the catalyst, associated mainly with retention of molybdenum, must then be solved.[131]

The study of the kinetics and mechanism of the oxidative dehydrogenation of isobutyraldehyde[131,135,136] on the Sb_2O_3 and MoO_3 catalysts by a pulsed method showed that the aldehyde reacts with the catalyst oxygen, forming methacrolein. The catalyst surface is then reduced. The methacrolein molecule is also adsorbed and, when oxygen is passed over the system, the latter is oxidised by gaseous oxygen to side products. The catalyst surface is reoxidised.[135]

The influence of the alternate changes in the composition of the gases entering the reactor on the selectivity of the oxidative dehydrogenation of isobutyraldehyde (IBA) over the heteropolyacid catalyst $H_5Mo_{10}V_2PO_{40}$ has been investigated. The alternation of two gas streams—IBA/N_2 and O_2/N_2 (for the reoxidation of the catalyst)—ensures the conversion of isobutyraldehyde into methacrolein with a greater selectivity than for the continuous supply of oxygen under comparable conditions.[137]

6. Synthesis of acrolein from allyl alcohol and its ethers and esters

Acrolein and methacrolein can be readily obtained by the vapour-phase oxidation of allyl alcohol, allyl acetate, and methylallyl acetate over a heterogeneous catalyst containing Pd with added Cu or Ag and Au at 150–200 °C.[138–140]

$$CH_2{=}CH{-}CH_2OH + 0.5O_2 \longrightarrow CH_2{=}CH{-}CHO + H_2O.$$

Methacrolein, suitable for oxidation to the acid without further purification, has also been obtained in a high yield by oxidising 2-methylallyl alcohol in the presence of the $A_aFe_bBi_eX_dMo_eO_f$ catalyst, where A = Co and/or Ni and X = Li, Na, K, Rb, Cs, or Tl.[141] However, this reaction, to which numerous studies have been devoted, has not found extensive application.[142]

The mechanism of the oxidation of allyl alcohol on MoO_3, $Bi_2O_3 \cdot nMoO_3$ (n = 1, 3), and multicomponent molybdenum-bismuth oxide[15] and silver[142] catalysts has been investigated. In the last case, the π-allyl intermediate, of the kind observed in the case of the oxide catalyst, is not observed, and the process should be regarded as oxidative dehydrogenation.

Much more attention has been devoted to the liquid-phase oxidation of allyl alcohol with the aid of special oxidants. Thus, by oxidising it in an aqueous acid medium by divalent silver ions at 20 °C, it is possible to obtain acrolein in 70% yield.[143] Oxidation of allyl alcohol by palladium chloride in aqueous solution at 25 °C leads to the formation of acrolein and α-hydroxyacetone in 30% and 15% yields respectively.[144] The use of deuteriated derivatives in this reaction showed that the reaction mechanism includes a stage involving the transfer of a hydride ion from the carbon atom linked to the hydroxyl.

A convenient method of synthesis of acrolein (and some of its derivatives) is based on the oxidation of allyl alcohol (and its γ-substituted derivatives) with chromic acid adsorbed on silica gel.[145]

$$RR^1C{=}CHCH_2OH \xrightarrow{H_2CrO_4/SiO_2,\ CCl_4} RR^1C{=}CHCHO; \quad (70\%-80\%)$$

R = R^1 = H; R = H, R^1 = Me; R = H, R^1 = Cl.

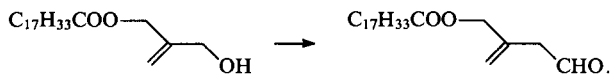
In the laboratory, acrolein can be obtained by oxidising alkyl allyl ethers with atmospheric oxygen in the presence of palladium chloride at 50–60 °C.[146] It has been demonstrated by the EPR method that an intermediate allyl radical is formed in this reaction.

$$CH_2{=}CH{-}CH_2{-}OR \xrightarrow[-RO^{\bullet}]{PdCl_2} CH_2{=}CH{-}CH_2^{\bullet} \xrightarrow{0.5\,O_2} CH_2{=}CH{-}CHO;$$

R = Me, Et, Bu^t, $C(C_2H_5)_3$.

The electrochemical oxidation of allyl alcohol to acrolein in a water–acetonitrile mixture is possible. By maintaining a potential difference of 2.3–2.6 V, it has been possible to attain a yield of acrolein of 30%.[147]

The oxidation of the α-substituted allyl alcohol **1** with manganese dioxide in hexane leads to the corresponding methacrolein **2** derivative in 60% yield.[148]



1 **2**

It has been found possible to obtain α-(4-methylcyclohexyl)acrolein in yields up to 50% by oxidising the corresponding α-substituted allyl alcohol **3** with lead tetraacetate in a non-polar solvent.[149]

$$CH_2{=}CR{-}CH_2OH \xrightarrow{80\,^{\circ}C} CH_2{=}CR{-}CHO;$$

3

R = 4-MeC_6H_{10}.

Highly effective oxidation of the allyl alcohols **4** to the corresponding aldehydes **5** has been achieved in the presence of the bis(η^5-cyclopentadienyl)zirconium(IV) complexes Cp_2ZrH and $Cp_2Zr(OPr^i)_2$ (the Oppenauer reaction).[150,151] The reaction is carried out in boiling toluene in the presence of 0.02 molar equivalent of the catalyst and an equimolar amount of benzaldehyde or benzophenone[15] as hydrogen acceptors (A). The yields of α,β-unsaturated products are 75%–95%.

$$R^1R^2C{=}CR^3CH_2OH + A \xrightarrow[\text{boiling toluene, 8 h}]{\text{Cat.}} R^1R^2C{=}CR^3CHO + AH_2$$

4 **5**

7. The aldol-crotonic condensation of formaldehyde with aliphatic aldehydes

The vapour-phase catalytic condensation of acetaldehyde with formaldehyde was the main industrial method of synthesis of acrolein in 1940–1960.[5,8]

$$H_2CO + CH_3CHO \xrightarrow{SiO_2} CH_2{=}CHCHO + H_2O.$$

In this process, formaldehyde (in the form of a 30% aqueous solution) and acetaldehyde, in proportions of 1 : 1 or 2 : 1, are passed over silica gel impregnated with NaOH,[152] Na_2SiO_3,[153] Li_2CO_3,[154] or KOH[155] at 260–320 °C. The yields of acrolein are 75%–90%.[8,156] Other catalysts have also been proposed: TiO_2,[155] Al_2O_3/SiO_2 mixtures in various proportions including catalysts impregnated with HF solution,[157,158] Ni, Mn, Fe, and V phosphates,[159] and a cation-containing diatomite.[160] CsOH proved to be the most active catalyst.[161]

Acetone, propionaldehyde, and ethyl methyl ketone are side products of the process considered.[157,162] The factorial experimental design method can be used to optimise the technological process involving the condensation of CH_2O with CH_3CHO.[163]

The study of the catalytic reactions of mixtures of formaldehyde with ethanol on metal phosphates and W, Zn, Ni, and Mg oxides deposited on silica gel at 240–320 °C[164] led to the conclusion that ethanol is dehydrogenated to acetaldehyde under these conditions.

Instead of acetaldehyde, its homologues can react with formaldehyde. This results in the formation of α-alkyl-substituted α,β-unsaturated aldehydes in 88%–94% yields.[165–167]

$$H_2CO + RCH_2CHO \xrightarrow{180-500\,^{\circ}C} CH_2{=}CRCHO + H_2O;$$

R = H, Me, Et.

The molar ratio H_2CO : RCH_2CHO ranges from 6.8 : 0.7 to 1 : 20. The catalysts may be phosphorus and vanadium pentoxides,[168] borosilicate molecular sieves on the Al_2O_3 carrier,[165] and even unmodified silica gel (its impregnation with KOH or alkali metal carbonates lowers the yield of α,β-unsaturated aldehydes).[166,169]

8. Condensation of formaldehyde with aldehydes in the presence of amines

Systematic study of the condensation of formaldehyde with aldehydes in an aqueous medium in the presence of an equimolar amount of an amine (preferably a secondary amine) salts made it possible to develop a method of synthesis of α,β-unsaturated aldehydes in nearly quantitative yields.[5] The hydrochloride of the Mannich base is an intermediate of this reaction:

$$RCH_2CHO + CH_2O + R'_2NH\cdot HCl \xrightarrow[-H_2O]{40-120\,^{\circ}C} [RCH(CHO)CH_2NR'_2\cdot HCl] \xrightarrow[90\%-99\%]{} RC(CHO){=}CH_2 + R'_2NH\cdot HCl;$$

R = Me, Et, Pr^i.

This process was developed up to the technical application stage.[170,171] Later this method was used to synthesise higher α-alkylacroleins.[172–179]

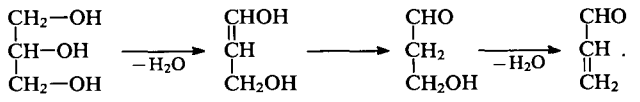
A convenient and economical version of the above procedure for the synthesis of α,β-unsaturated aldehydes involves the condensation of CH_2O with RCHO in the presence of only catalytic amounts of a secondary ammonium salt (10.3 and even 0.05 mol.%).[170,180–182]

Judging from patent data, the duration of the syntheses of α-alkylacroleins under the conditions of the Mannich reaction can be greatly reduced by carrying out the interaction between the reagents above 150 °C under pressure.[183]

9. Catalytic vapour-phase thermolysis of glycerol, 3-alkoxypropanal, and 3-acetoxypropanal

The method of synthesis of acrolein by the dehydration of glycerol, preferably in the presence of $KHSO_4$ or other acid catalysts, which was developed as early as the past century, is nowadays recognised as uneconomical. Furthermore, it proved cheaper to synthesise glycerol from acrolein.[10] However, the inevitable return to the renewable nature sources of organic raw materials in connection with the exhaustion of the resources of petroleum and gas will apparently again draw attention to the use of glycerol and then possibly also of biomass as sources of acrolein.[184,185] The replacement of $KHSO_4$ as the catalyst of the thermal dehydration of glycerol by phosphoric acid made it possible to obtain acrolein at 250 °C in 95% yield.[186]

The thermal conversion of glycerol into acrolein in 'supercritical' water, which has unusual properties, has been investigated recently.[184,185] At 360 °C under a pressure of 335 atm and in the presence of $NaHSO_4$, glycerol is converted into acrolein and acetaldehyde. The yield of acrolein reaches 70% and its formation is represented by the following scheme:



A method of synthesis of acrolein in yields up to 87% by the catalytic vapour-phase thermolysis of 3-alkoxypropanals, which are side products in the synthesis of acrylates, has been patented.[187,188] This reaction is catalysed by Al, Cu, Ca, Mn, Fe, Co, and Zn sulfates or their mixtures.

$$ROCH_2CH_2CHO \xrightarrow{250\,^\circ C} CH_2{=}CH{-}CHO + ROH.$$

Methacrolein has been obtained by the catalytic decomposition of 3-acetoxy-2-methylpropanol in the presence of tertiary amines, aluminosilicates, or zeolites.[189]

10. Thermolysis of unsaturated ethers, acetals, acylals, and other oxygen-containing compounds

The thermolysis of diallyl and allyl methylallyl ethers leads to the formation of the corresponding aldehydes together with other decomposition products.[190]

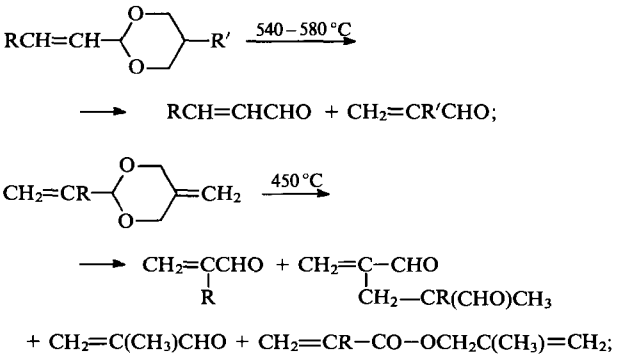
$$CH_2{=}CRCH_2OCH_2CH{=}CH_2 \xrightarrow{430-560\,^\circ C} CH_2{=}CRCHO + CH_3CH{=}CH_2.$$

When R = H, the yield is 88%, whereas for R = Me it is 28%. α,β-Unsaturated aldehydes are also obtained on thermal decomposition of diallyl acetals of alkenals.[191-193]

$$RCH{=}CR^1CH(OCH_2CR^2{=}CH_2)_2 \xrightarrow{360-420\,^\circ C} CH_2{=}CR^2CHO + RCH{=}CR^1CHO + CH_2{=}CR^2CH_2CR^1(CH_2R)CHO + RCH{=}CR^1{-}CO{-}OCH_2{-}CR^2{=}CH_2;$$

R = H, Me; R^1 = H, Me, $(CH_2)_2CN$; R^2 = H, Me.

The thermolysis of 2-(1-alkenyl)-5-alkyl-1,3-dioxanes[191] and 2-(2-alkenyl)-5-methylene-1,3-dioxanes leads to α,β-unsaturated aldehydes.[193,194]



R = H, Me.

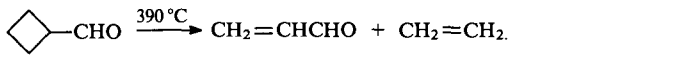
Acrolein is formed together with acetic anhydride in the catalytic thermolysis of 3,3-diacetoxypropene (and also 1,3-diacetoxypropane) in the presence of palladium or zinc halides.[195] The conversion and selectivity reach 98%.

$$CH_2{=}CHCH(OCOMe)_2 \xrightarrow{100-150\,^\circ C} CH_2{=}CHCHO + O(COMe)_2.$$

Acrolein and methacrolein can also be obtained in low yields (5%–30%) by the thermolysis of many oxygen-containing organic compounds. Thus, for example, dihydropyran decomposes preferentially to acrolein and ethylene over activated charcoal, platinised charcoal, or quartz.[196]



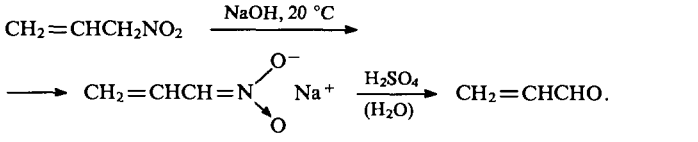
The thermal decomposition of formylcyclobutane also leads to the formation of acrolein and ethylene.[197]



Small amounts of acrolein and methacrolein (up to 10%) are produced on thermal decomposition of acrylates,[198] glucose,[199] allyl and methylallyl benzoates,[200] and diorganyl(2-propenyl)-*N*-oxides[201] and also on joint thermolysis of methanol with 1,2-dichloropropane.[202]

11. Other methods of synthesis

A novel method of synthesis of acrolein from 3-nitropropene is based on the Nef reaction.[203,204]

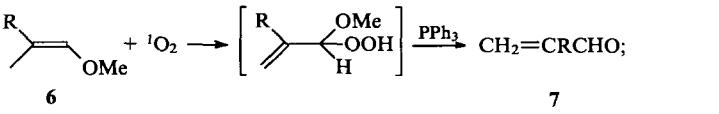


Acrolein is formed on photochemical oxidation of allyltrimethylsilane in the presence of palladium(II) salts.[205]

$$CH_2{=}CHCH_2SiMe_3 \xrightarrow{Pd^{2+},\ h\nu,\ O_2} CH_2{=}CHCHO.$$

The photochemical reaction of allene and ozone at 12 K leads to the formation of acrolein together with cyclopropane.[206]

The photochemical oxidation of the (*E*)-forms of the methyl ethers of corresponding enols **6** in the presence of triphenylphosphine made it possible to obtain α-cyclopropyl- and α-benzyl-acroleins **7** in 75%–90% yield. The addition of singlet oxygen in the (*Z*)-forms of the same ethers leads to a mixture of hydroperoxides, which are converted on treatment with PPh_3 not only into the α,β-unsaturated aldehydes mentioned above but also to their isomers cyclo-PrHC=CMeCHO and PhCH=CMeCHO.[207,208]



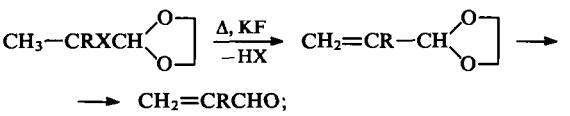
R = $(CH_2)_2CH-$, $PhCH_2-$.

The synthesis of α,β-unsaturated aldehydes by the dehydrohalogenation of the corresponding saturated aldehydes[209] was improved by using tetramethylammonium dimethyl phosphate as the hydrogen halide acceptor. The use of this reagent makes it possible to obtain methacrolein and its β-alkyl substituted derivatives.[210]

$$(CH_3)_2C(X)CHO \xrightarrow[-HX]{} CH_2=C(CH_3)CHO;$$

X = Br, Cl.

Acrolein and its α-organyl substituted derivatives can be obtained by dehalogenating 2-(1-haloorganyl)-1,3-dioxolans.[211]



$$\longrightarrow CH_2=CRCHO;$$

R = H, Me, Ph; X = Cl, Br.

Propargyl alcohol isomerises to acrolein over Mo, W, and Re oxides deposited on silica gel.[215-217] The yields of acrolein reach 70%–90%.

$$HC\equiv C-CH_2OH \xrightarrow[10-15\ mmHg]{300-400\ ^\circ C} CH_2=CHCHO.$$

The hydroformylation of acetylene catalysed by a mixture of $Co_2(CO)_8$ with polyvinylpyridine also leads to the formation of acrolein.[218]

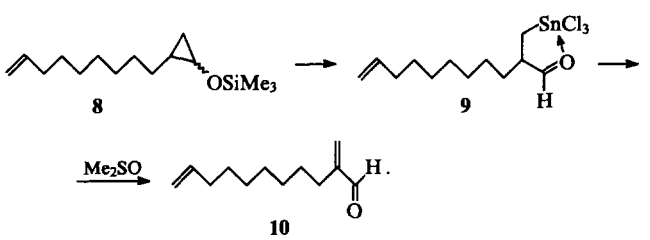
$$HC\equiv CH + CO + H_2 \longrightarrow CH_2=CHCHO.$$

Acrolein can be obtained in 81%–91% yield by the reaction of vinylacetic or crotonic anhydride with pyridine *N*-oxide.[219]

$$(H_2C=CHCH_2CO)_2O + 2C_5H_5N\rightarrow O \xrightarrow{140\ ^\circ C}$$

$$\longrightarrow CH_2=CHCHO + CH_2=CHCH_2COOH + 2C_5H_5N + CO_2.$$

The reaction of 1-(8-nonenyl)-2-(trimethylsiloxy)cyclopropane **8** with $SnCl_4$ in CH_2Cl_2 leads to 2-trichlorostannylmethylundecan-10-al **9**. Treatment with dimethyl sulfoxide in hexane converts it into α-(8-nonen-1-yl)acrolein **10**.[220]



8 **9**

10

It has been suggested that α-alkylacroleins be obtained by the reaction of substituted enamines **11** with phenylselenyl chloride and subsequent oxidative elimination of α-phenylselenoaldehyde **12** by treatment with *m*-chlorobenzoic acid or sodium periodate.[221]

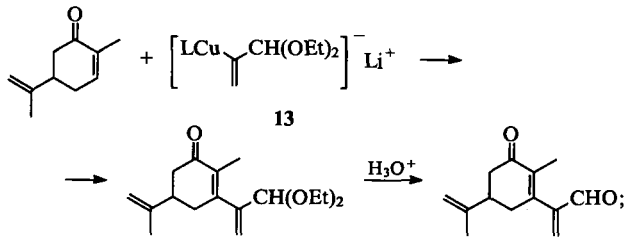
$$CH_3CR=CH-NC_5H_{10} \xrightarrow{PhSeCl} CH_3-CR(SePh)CHO \longrightarrow$$

11 **12**

$$\longrightarrow CH_2=CR-CHO;$$

R =  -Me.

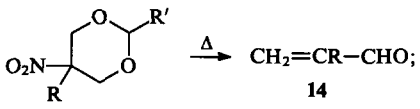
It is recommended that 3,3-diethoxyisopropenylcuprates **13**, which are carriers of the carbonyl functional group in a latent form, be used as synthons which make it possible to introduce the acrolein fragment into an organic molecule.[222,223] Their condensation with cycloalkenones and subsequent hydrolysis of the acetal formed permit the quantitative synthesis of acrolein derivatives containing a complex substituent in the α-position.



13

L = PhS–, $CH_2=\overset{|}{C}-CH(OEt)_2$.

Thermolysis[224] of 5-alkyl-5-nitro-1,3-dioxanes at 390 °C or their interaction with polyphosphoric acid at 160 °C in the presence of copper powder[225] leads to the formation of α-alkylacroleins **14.**



14

R = Me, Et; R′ = H, Pr^i.

It has been suggested that acrolein be stored and transported in the form of linear or cyclic acetals $CH_2=CHCH(OR')OR''$, where R′ and R″ are C_{1-6} alkyls or R′ + R″ are cycloalkyls $(CH_2)_{2-6}$. It can be regenerated quantitatively from these products by hydrolysis in the presence of perfluorinated ion-exchange resin.[226]

The synthesis of acrolein by the 'alcohol–aldehyde' exchange reaction catalysed by the microbial aldehyde dismutase from *Pseudomonas putida* has been described recently.[227] An equimolar mixture of allyl alcohol and isobutyraldehyde is converted into acrolein and isobutyl alcohol to the extent of 69% at 30 °C in 1 h:

$$CH_2=CHCH_2OH + Pr^iCHO \longrightarrow$$

$$\longrightarrow CH_2=CHCHO + Pr^iCH_2OH.$$

The microorganism *Coryne bacterium*, which transforms glycerol into acrolein, has been isolated from sugar cane.[228] It is suggested that the odour which sometimes appears in rum is due to the vital activity of this microorganism.

III. Methods of synthesis of α,β-unsaturated aldehydes α-substituted by functional groups

1. α-Haloacroleins

An effective method of synthesis of 2-chloropropenal is based on the dehydrochlorination of 2,3-dichloropropenal, which is obtained in its turn by chlorinating acrolein.

$$CH_2=CHCHO + Cl_2 \longrightarrow ClCH_2CHClCHO \longrightarrow$$

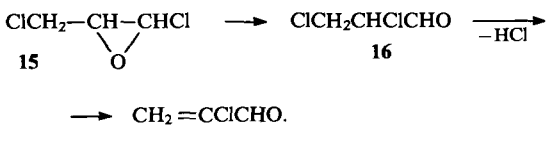
$$\longrightarrow CH_2=CClCHO.$$

Hydrogen chloride may be eliminated by a thermal method involving the passage of a mixture of acrolein vapour, chlorine, and nitrogen through a quartz tube at 75–200 °C. The maximum yield of α-chloroacrolein (91%) is obtained for the acrolein : chlorine ratio = 1 : 1.7 and for a contact time of 3 s.[229,230]

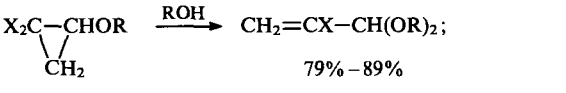
The liquid-phase dehydrochlorination of 2,3-dichloropropanal at 0–5 °C [231,232] or 20 °C [233,234] is more widely used. Diethylaniline is usually employed as the HCl acceptor. The yield of α-chloroacrolein reaches 80%.

α-Bromoacrolein is obtained by a similar procedure: by brominating acrolein and subsequent dehydrobromination of 2,3-dibromopropanal.[233,235,236] The yield of α-bromoacrolein is appreciably lower (45%–68%).

1,3-Dichloro-1,2-epoxypropane **15** is converted at 200 °C into α-chloroacrolein in 23% yield.[237] The isomerisation of 1,3-dichloro-1,2-epoxypropane to 2,3-dichloropropanal **16** and the subsequent dehydrochlorination of the latter to α-chloroacrolein in aqueous tetrahydrofuran in the presence of a phosphate buffer occur already at 37 °C.[238]

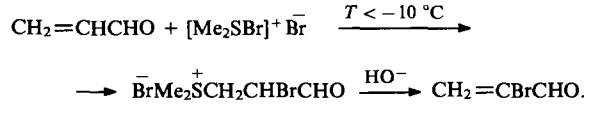


The ethanolysis of 2-alkoxy-1,1-dihalocyclopropanes in the presence of bases (K_2CO_3, NaOR) is widely used to obtain the acetals of 2-halopropenals.[239–241] The subsequent hydrolysis of the acetal makes it possible to obtain pure α-haloacrolein.[240]



X = Cl, Br, F; R = Et, Bu.

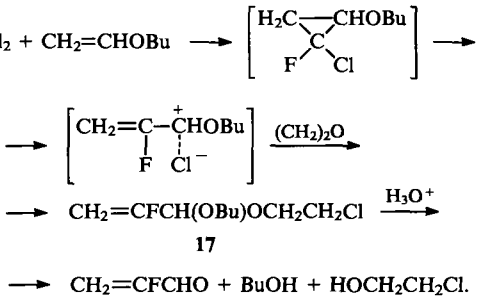
The interaction of bromodimethylsulfonium bromide with acrolein constitutes an elegant and simple method of synthesis of α-bromoacrolein in a satisfactory yield:[242]



Account must be taken of the fact that α-chloro- and α-bromo-acroleins are powerful direct-action mutagens.[243,244] The latter was identified in the organism as the metabolite of certain domestic preparations, for example the fumigant 1,2-dibromo-3-chloropropane and the fire extinguishing agent tris(2,3-dibromopropyl)phosphate.[243,245]

Traces of α-acrolein are formed on chlorination of humic acids.[246] It has been suggested that this induces a mutagenic activity in chlorinated drinking water. α-Chloroacrolein is also obtained by treating 2-chloroallyl alcohol with dehydrogenase.[247] It is also formed when the carcinogenic herbicide *S*-2,3-dichloroallyl diisopropylthiocarbamate (diallate) is treated with liver microsomal monoxygenase of *m*-chloroperbenzoic acid.[231,248,249] The photochemical decomposition of diallate also leads to α-acrolein.[250]

Like other α-haloacroleins, α-fluoroacrolein was first obtained by opening the ring in 2-alkoxy-1,1-difluorocyclopropanes.[239] A modified version of this method constitutes a continuous process proceeding in a single reactor (autoclave) and involves the formation of chlorofluorocarbene *in situ*.[251] For this purpose, a mixture of dichlorofluoromethane, butyl vinyl ether, epoxyethane, and tetraethylammonium bromide is heated at 150 °C.



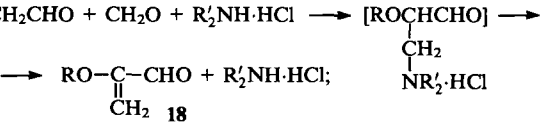
The resulting acetal **17** is hydrolysed with 5% H_2SO_4, which leads to the formation of α-fluoroacrolein (yield 41%). This lachrymatory substance polymerises rapidly during storage (in the absence of hydroquinone) and explodes during combustion when it is subjected to elemental analysis. When an attempt is made to synthesise more than one mole of α-fluoroacrolein, the pressure in the autoclave suddenly rises sharply from 20 to 300 atm, which makes this method too dangerous.[252] It has therefore been suggested that α-fluoroacrolein be synthesised in two stages using the mild phase transfer catalytic conditions.[252–255] The yield reaches 53% relative to the initial butyl vinyl ether. This method may be used on a large scale (for the synthesis of up to 200 moles of α-fluoroacrolein).

3-Alkyl-2-halo-2-alkenals can also be readily obtained by converting the corresponding enol ethers into cyclopropane derivatives under the conditions of phase transfer catalysis[256,257] or in the presence of potassium butoxide[258] with subsequent stereoselective opening of the ring in the cyclopropanes produced.

2. α-Organyloxy- and α-acetoxy-acroleins

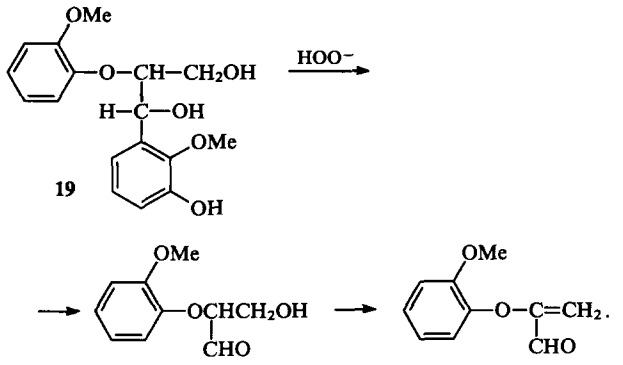
α-Alkoxy- and α-phenoxy-acroleins were first obtained by the aminomethylation of the corresponding organyloxyacetaldehydes followed by the decomposition of the hydrochloride of the Mannich base.[259–262]

Under optimum conditions (equivalent reactant proportions) at 60 °C, pH 7–7.1, 1.5–2 h), the yields of acroleins reach 66%–78%.



R = Me (**a**), Et (**b**), Pr (**c**), Bu (**d**), Ph (**e**), 2-$MeOC_6H_4$ (**f**), $PhCH_2$ (**g**).

This convenient method of synthesis of α-alkoxy-(phenoxy)acroleins using the Mannich reaction was subsequently used frequently.[263–267] For example α-guaiacoxyacrolein was obtained by this procedure from 2-(2′-methoxyphenoxy)-acetaldehyde and formaldehyde.[267] This acrolein derivative is also an intermediate in the oxidation of guaiacylglyceryl β-guaiacyl ether **19**—the most common structural fragment of lignin—in the technical peroxide bleaching process.[267,268]



Like aryloxyacroleins, α-benzyloxyacrolein **18g** can be obtained by the aminomethylation of benzyloxyethanal.[265]

2-Phenoxybutenal is formed from the diethyl acetal of 3-ethoxy-2-phenoxybutanal as a result of acid hydrolysis accompanied by the elimination of ethanol.[269]

$$MeCH(OEt)-CH(OPh)-CH(OEt)_2 \xrightarrow{H_3O^+} MeCH=C(OPh)-CHO.$$

However this procedure is unsuitable for the synthesis of α-ethoxycrotonaldehyde apparently owing to the hydrolytic instability of this compound in an acid medium.

2-Methoxypropenal was synthesised in 69% yield by the β-elimination of methanol from 2,3-dimethoxypropanal in an alkaline medium.[270,271]

$$MeOCH_2CH(OMe)CHO \xrightarrow{25\,^\circ C,\ pH\ 12} CH_2=C(OMe)CHO + MeOH.$$

69%

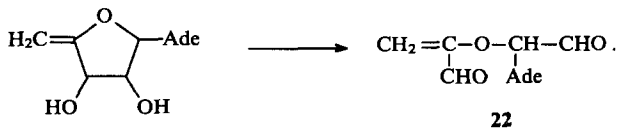
We shall now consider the kinetics and the proposed mechanism of this reaction.[272] α-Alkoxyacroleins **21** with functional group substituents are obtained from 2-alkoxy-3-vinylthiopropanols **20** by the mild Swern oxidation followed by the elimination of ethylenethiol.[273]

$$CH_2=CHSCH_2CH(OR)CH_2OH \xrightarrow[2.\ Et_3N\ (10\ equiv.)]{1.\ DMSO/ClCOCOCl/-78\,^\circ C} CH_2=C(OR)CHO$$

20 → **21**

R = $O(CH_2)_2OCH_3$, $CH=CH_2$, $\overline{CH_2OCH}$, $(CH_2)_3Br$, $(CH_2)_3N_3$.

Certain α-organyloxyacroleins containing an organic moiety with a functional group substituent play a definite role in biochemical reactions. They include the α-organyloxy-α,β-unsaturated aldehyde **22** – the first representative of the group of the so called nucleoside dialdehydes. It was obtained by the periodate oxidation of 9-(5-deoxy-*b*-D-*erythro*-pent-4-enofuranosyl)adenine.[274]

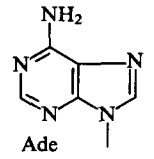
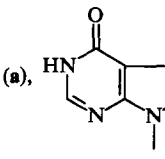


22

Purine-containing α-organyloxyacroleins **24a, b** are readily formed on heating the nucleoside dialdehydes **23a, b** to 100 °C.[275]

$$HOCH_2CH(CHO)OCHRCHO \xrightarrow[H_2O(EtOH)]{100\,^\circ C,\ 1\ h} CH_2=C(CHO)OCHRCHO;$$

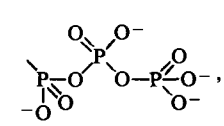
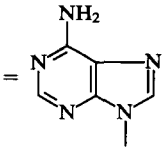
23 → **24**

R =  (a),  (b), —OMe (c).

This reaction was first observed in enzymic studies involving adenosinedeaminase. The purine ring does not play a significant role in the process described and elimination takes place readily also in the case of the aldehyde **23c**, which have been confirmed by UV spectroscopic data. The adenosine triphosphate oxidised by periodate (*o*-ATP) at 20 °C and pH 7 slowly gives rise to the adenosine-containing β,β-dihydroxyethoxyacrolein **25** as a result of the β-elimination of the triphosphate group.[276]

$$ROCH_2CH(CHO)OCH(CHO)-Ade \xrightarrow{Na_2B_2O_7} CH_2=C(CHO)O-CH(Ade)-CH(OH)_2;$$

ortho-ATP → **25**

R =  , Ade =  .

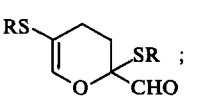
α-Acetoxyacrolein has been synthesised by acetylating the diethyl acetal of acetoxymercuriomethylglyoxal.[277] The reaction is accompanied by the formation of a number of side products, the principal of which is the hemiacylal of acetoxymethylglyoxal.

$$AcOHgCH_2COCH(OEt)_2 + CH_3COCl \longrightarrow [CH_2=C(OAc)CH(OEt)_2] \xrightarrow{Ac_2O} CH_2=C(OAc)CHO.$$

3. α-Organylthio- and α-organylseleno-acroleins

The attempts to obtain α-organylthioacroleins by the Mannich reaction (by analogy with α-alkoxyacroleins) led to the isolation of their cyclic dimers — 2,5-dialkylthio-2-formyl-2,3-dihydro-4*H*-pyrans (yield 31% – 61%).[278-280]

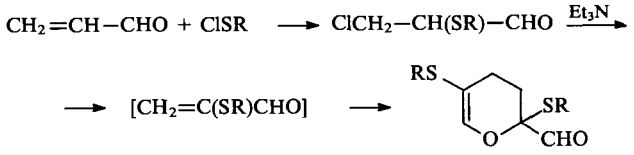
$$RSCH_2CHO + CH_2O + R^1_2NH\cdot HCl \longrightarrow RSCH(CHO)CH_2NR^1_2\cdot HCl \longrightarrow [CH_2=C(SR)CHO] \longrightarrow$$



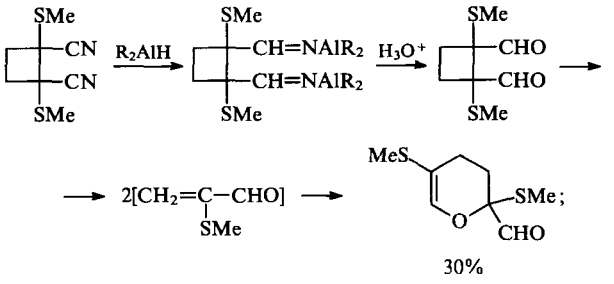
R = Me, Et, Pr, Bu, Bu^i, Pe^t, C_6H_{13}; R^1 = Et, Me.

The study of this process by the ^1H NMR method at 6 – 10 °C made it possible to observe the intermediate formation of the monomeric α-alkylthioacrolein.[281]

The extreme instability of α-alkylthioacroleins has been confirmed when an attempt was made to obtain them by the reaction of alkanesulfenyl chlorides with acrolein.[282] The labile alkylthiochloropropanals formed afford only the dimers of α-alkylthioacroleins in approximately 50% yield on dehydrochlorination with triethylamine at −15 °C.

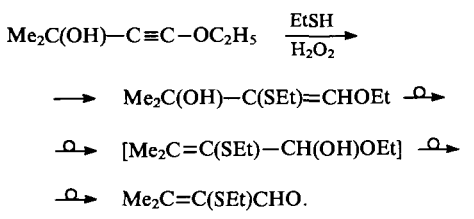


A cyclic dimer of α-methylthioacrolein has been obtained from 1,2-bis(methylthio)-1,2-dicyanocyclobutane.[283]

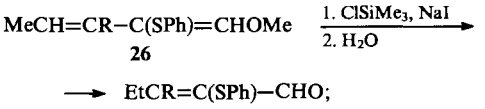


R = Bu^i.

In contrast to α-alkylthioacroleins, their β-alkyl derivatives exist in a monomeric form. Thus α-ethylthio-β,β-dimethylacrolein has been obtained from ethoxyethynyldimethylcarbinol by carrying out consecutive reactions involving thiylation, rearrangement, and elimination of the alcohol in accordance with the following scheme:[284]

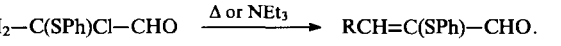


The specially synthesised dienes **26** have been used to synthesise β-alkyl-α-phenylthioacroleins.[285]

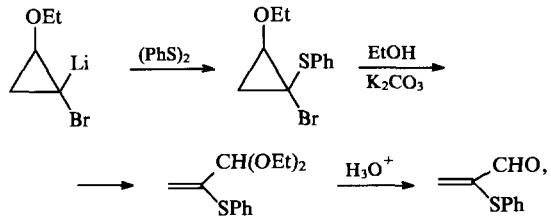


R = H, Me.

The synthesis of 2-phenylthio-2-alkenals in 65% yield by the dehydrochlorination of α-chloro-α-phenylthioaldehydes has also been described.[286]

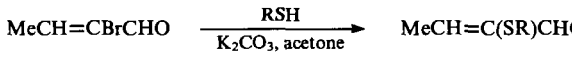


The possibility of obtaining α-phenylthioacrolein by treating 1-bromo-2-ethoxycyclopropyllithium with diphenyl disulfide with subsequent transformation of the reaction product via the scheme



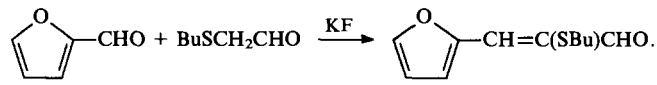
which is universal for the synthesis of 2-substituted alkenals, has been reported.[240]

The *ipso*-substitution of the halogen in vinyl halides activated by a geminal aldehyde group can also be used to synthesise β-alkyl-α-organylthioacroleins.[287,288]

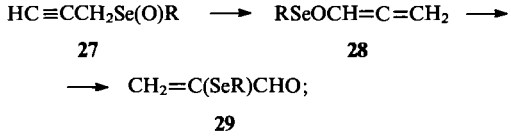


R = Bu, Ph.

The use of the aldol-crotonic condensation of butylthioacetaldehyde with furfural in the presence of KF with added tetraethoxysilane made it possible to obtain 2-butylthio-3-(2′-furyl)propenal in 60% yield.[289]

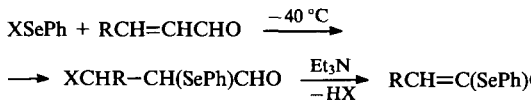


The formation of the α-phenylselenoacrolein **29a**, which is unstable at room temperature, was observed for the first time on isomerisation of phenylpropargyl selenoxide **27a** in methylene chloride at −31 °C.[290–292]



R = Ph (**a**), *m*-$F_3CC_6H_4$ (**b**), *o*-$O_2NC_6H_4$ (**c**).

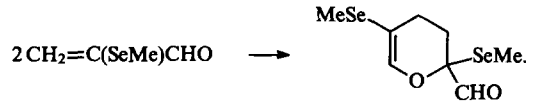
The trifluoromethyl analogue **27b** rearranges 1.6 times faster than the selenoxide **27a**. In both cases, the intermediate reaction product was not detected. The existence of the intermediate **28c** with the allenol structure, formed on isomerisation of 2-nitrophenylpropargyl selenoxide **27c**, has been demonstrated by ^{1}H NMR and IR spectroscopy and mass spectrometry. The allene **28c** was identified at −45 °C. Above −10 °C, it rearranges to the aldehyde **29c**.



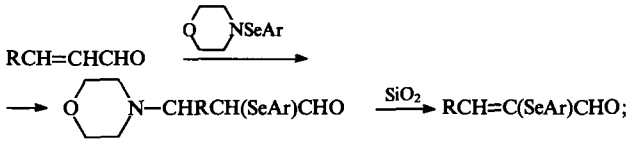
R = H (**a**), Me (**b**); X = Br, Cl.

Later α-phenylselenoalkenals were obtained in 68% yield by the haloselenation of the corresponding unsaturated aldehydes and subsequent elimination of hydrogen halides with triethylamine.[293,294]

In contrast to the unstable phenylselenoacrolein **29a**, its homologue **29b** can be vacuum-distilled. In order to obtain α-methylselenoacrolein in accordance with a scheme similar to that presented above, the dehydrohalogenation stage was carried out at −40 °C, but the expected aldehyde cyclodimerised fully and very rapidly (in 20 min at 20 °C). It was characterised only by the NMR method.[294,295]

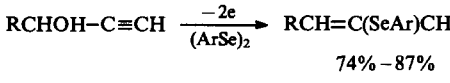


N-Arylselenomorpholines are effective α-selenating agents for α,β-unsaturated aldehydes.[296,297]



R = H, Me, Pr, MeCH=CH, Ph;
Ar = Ph, 4-ClC_6H_4.

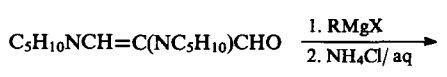
A single-stage method of synthesis of α-arylseleno-α,β-unsaturated aldehydes is based on the electrochemical oxidation of 3-hydroxyalkynes in the presence of diaryl diselenides.[298,299]



R = Me, Et, Pe, Ph.

4. α-Dialkylaminoacroleins and their homologues

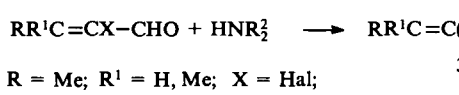
β-Alkyl-α-piperidinoacroleins were first synthesised by treating β-dialkylamino-α-piperidinoacroleins with Grignard reagents.[300]



R = Me, Et, Pr, Bu.

Although the yields of the final products are fairly high (60%−80%), the initial diaminoacroleins can be obtained in only 10%−30% yield by formylating the corresponding diaminoethylenes.

Subsequently the reaction involving the *ipso*-substitution of the halogen atom in 2-halo-2-alkenals was used to synthesise 2-dialkylamino-2-alkenals.[301-304] The interaction takes place even at room temperature and the substitution products **30** are formed as a mixture of (*E*)- and (*Z*)-isomers.



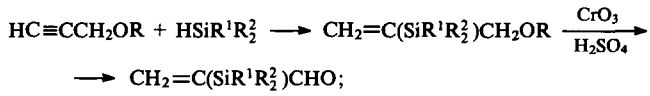
30

R = Me; R^1 = H, Me; X = Hal;

NR_2^2 = 

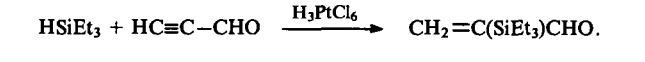
5. Organosilicon derivatives of acrolein

α-Trialkylsilylacroleins (in a mixture with the β-isomers) are formed when the product of the hydrosilylation of propargyl alcohol or its trimethylsilyl ether by trialkylsilanes is oxidised by chromium trioxide.[305,306]

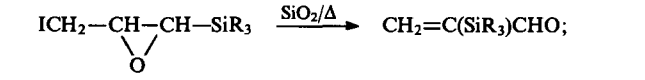


R = H, $SiMe_3$; R^1, R^2 = Me, Et.

A mixture of α- and β-triethylsilylacroleins is also formed on hydrosilylation of propynal,[307] the yields of the α- and β-adducts being 28% and 26% respectively.

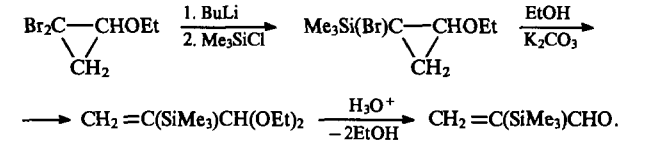


α-Triisopropylsilylacrolein is formed in a low yield from 2-iodomethyl-3-triisopropylsilyloxiran together with 3-iodo-2-triisopropylsilylpropanal.[308]

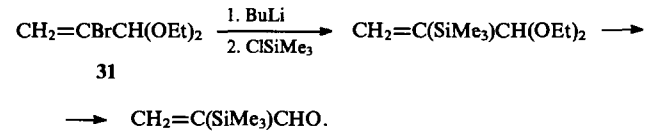


R = Pr^i.

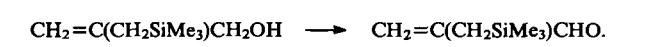
α-Trimethylsilylacrolein has been synthesised in 80% yield from 1,1-dibromo-2-ethoxycyclopropane in accordance with the following scheme: [240,309]



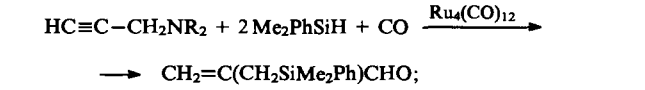
The most convenient method of synthesis of α-trimethylsilylacrolein is based on the reaction of 2-bromo-3,3-diethoxypropene **31** with butyllithium and subsequent interaction with chlorotrimethylsilane.[310] The removal of the acetal protecting group in an acid aqueous acetone solution leads to the formation of α-trimethylsilylacrolein from the initial acetal **31** in 73% yield.



α-Trimethylsilylmethacrolein has been obtained by oxidising α-trimethylsilyl methylallyl alcohol with oxalyl chloride in dimethyl sulfoxide (DMSO) [311] (cf. also Trost and Grese [312]).



2-Dimethylphenylsilylmethylpropen-2-al has been synthesised in a yield up to 94% by the reaction of diorganylpropargylamines with a twofold excess of dimethylphenylsilane and carbon monoxide in the presence of ruthenium carbonyl.[313]



R = Me, CH_2Ph.

α-(*tert*-Butyldimethylsiloxymethyl)acrolein **32** has been synthesised from acrolein, the latter part of the synthesis being[314]

$$CH_2{=}CBrCH(OEt)_2 \xrightarrow[2.\ H_2CO]{1.\ BuLi} CH_2{=}C(CH_2OH)CH(OEt)_2 \longrightarrow$$

72%

$$\xrightarrow[2.\ (COOH)_2]{1.\ ClSiMe_2(Bu^i)} CH_2{=}C(CH_2OSiMe_2Bu^i)CHO.$$

32 (87%)

The reaction of methylglyoxal with chlorotrimethylsilane in the presence of triethylamine leads to α-trimethylsiloxyacrolein.[315]

$$CH_3COCHO + Me_3SiCl \xrightarrow[-HCl]{Et_3N} CH_2{=}C(OSiMe_3)CHO.$$

6. Dialkylphosphonoacroleins

α-Dialkylphosphonoacroleins **36** have been synthesised by hydrolysing a mixture of the corresponding organophosphorus derivatives **33**–**35**, obtained in their turn by phosphorylating alkyl allyl ether with phosphorus pentachloride.[316] The unstable individual α-phosphorylated acroleins **36** were not isolated and were identified as products of the diene synthesis **37**.

$$(RO)_2P(O)C(=CHOR)CH_2OR + (RO)_2P(O)CH(CH_2OR)CH(OR)_2$$

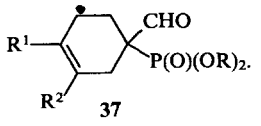
33 **34**

$$+ (RO)_2P(O)C(=CH_2)CH(OR)_2 \xrightarrow{H_3O^+}$$

35

$$\longrightarrow [(RO)_2P(O)C(=CH_2)CHO] \xrightarrow{CH_2=CR^1-CR^2=CH_2}$$

36

$$\longrightarrow$$ 

37

7. Oxygen and sulfur derivatives of α-alkylacroleins

Hydrolysis of the diethyl acetal of 3-hydroxy-2-hydroxymethylpropanal leads to the formation of the free aldehyde **38**, which is readily hydrated in the presence of bases to α-hydroxymethylacrolein **39**.[317]

$$(HOCH_2)_2CHCH(OEt)_2 \xrightarrow[-2\,EtOH]{H_3O^+} (HOCH_2)_2CHCHO \longrightarrow$$

38

$$\longrightarrow CH_2{=}C(CH_2OH)CHO.$$

39

An elegant method of synthesis of α-hydroxyalkylacroleins **42** is based on the condensation of the organolithium derivative of the diethylacetal of α-bromoacrolein **40** with various aldehydes at a low temperature. The subsequent cautious removal of the acetal protecting group in the acetals **41** leads to the formation of α-hydroxyalkylacroleins in 95% yield.[318]

$$CH_2{=}CLiCH(OEt)_2 + RCHO \longrightarrow$$

40

$$\longrightarrow CH_2{=}C[CH(R)OH]CH(OEt)_2 \xrightarrow[H_2O]{H_2SO_4} CH_2{=}C[CH(R)OH]CHO;$$

41 **42**

R = Me, Et, Pe, Ph.

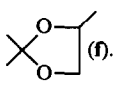
The single-stage alkylcarbonylation of 3,3-diethoxy-2-lithiopropene **40** with dimethylformamide or the dimethylamides of other carboxylic acids makes it possible to obtain α-diethoxymethylacrolein **43a** or the diethyl acetals of α-alkylcarbonylacroleins in 20%–70% yields.[319]

$$CH_2{=}CLiCH(OEt)_2 + RCONMe_2 \longrightarrow$$

40

$$\longrightarrow CH_2{=}C(COR){-}CH(OEt)_2;$$

43

R = H (**a**), Me (**b**), Bu^i (**c**), Pe (**d**), Ph (**e**),  (**f**).

Unfortunately the hydrolysis of the latter to the corresponding acroleins has not been achieved.

The reaction of 1-bromo-2-ethoxycyclopropyllithium **44** (the synthetic equivalent of 2-lithiopropenal) with heptanol leads to the intermediate **45**, the interaction of which with alcohol on heating in the presence of K_2CO_3 makes it possible to obtain the diethyl acetal of α-(1-hydroxy)heptylacrolein **46**. Hydrolysis of the latter leads to the corresponding aldehyde **47** (yield 77%).[240,309]

$$Li(Br)C{-}CHOEt + C_6H_{13}CH_2OH \longrightarrow X(Br)C{-}CHOEt \longrightarrow$$

44 **45**

$$\xrightarrow[K_2CO_3]{EtOH} CH_2{=}CX{-}CH(OEt)_2 \longrightarrow CH_2{=}C(X)CHO;$$

46 **47**

X = $-CH(OH)C_6H_{13}$.

The aldehyde **49** was synthesised by acetylating the acetal **46** with subsequent hydrolysis of the resulting acetal **48**.

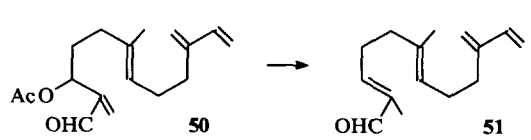
$$\mathbf{46} \xrightarrow[-AcOH]{Ac_2O} CH_2{=}C[CH(OAc)C_6H_{13}]CH(OEt)_2 \xrightarrow{H_3O^+}$$

48

$$\longrightarrow CH_2{=}C[CH(OAc)C_6H_{13}]CHO.$$

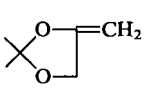
49

The method developed for the synthesis of α-substituted acroleins has been used to synthesise β-sinensal **51**, which determines the taste and smell of the oil of Chinese oranges.[309] The initial triene aldehyde **50** was obtained in the same way as the aldehyde **49**, from 4-methyl-8-methylenedecene-4,9-dienal:



50 **51**

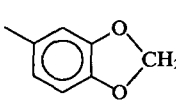
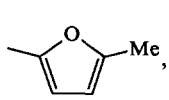
Various α-hydroxyalkylacroleins **54** can be synthesised in 65%–77% yield by adding to aldehydes a nucleophile such as allenoxylithium **53** (equivalent of 2-lithiopropenal), obtained from 2,2-dimethyl-4-methylene-1,3-dioxolan **52**.[320]

 $\xrightarrow{Bu^tLi,\ -78\,^\circ C}$ $CH_2{=}C{=}CHOLi$ $\xrightarrow{RCHO}$

52 **53**

$$\longrightarrow CH_2{=}C(CHO)CH(OH)R;$$

54

R = C_6H_{13}, Ph,  ,  ,

—CHMeOCH$_2$OMe.

The reaction of α-(methoxymetoxyethyl)acrylonitrile with diiso-propylaluminium hydride in toluene leads to the formation of the corresponding α-substituted acrolein in 73% yield.[321]

$$CH_2{=}CR{-}CN \xrightarrow{HAlR^1_2} CH_2{=}CR{-}CH{=}NAlR^1_2 \xrightarrow{5\%\ H_2SO_4} CH_2{=}CR{-}CHO;$$

R = $CH_2CH_2OCH_2OCH_3$; $R^1 = Pr^i$.

α-Carboxyacrolein has been obtained from the diethyl acetal of α-bromoacrolein by successive treatment with butyllithium, carbon dioxide, and water.[322]

$$CH_2{=}CBrCH(OEt)_2 \xrightarrow{BuLi} CH_2{=}CLiCH(OEt)_2 \xrightarrow[2.\ H_2O]{1.\ CO_2} CH_2{=}C(COOH)CHO.$$

The β-alkylthioacetals **55** are converted into the enals **56** on treatment with formalin and dimethylamine hydrochloride.[179, 323]

$$RSCH_2CH(OEt)_2 + CH_2O \xrightarrow[-H_2O]{Me_2NH\cdot HCl} CH_2{=}C(CH_2SR)CHO;$$

55 **56**

R = Et, Ph.

References

1. T G Alkhazov, K Yu Adzhamov, A K Khanmamedova *Usp. Khim.* **51** 950 (1982) [*Russ. Chem. Rev.* **51** 542 1982]
2. B P Geyer, in *Acrolein* (Ed. W Smith) (New York: Wiley, 1962) p. 4
3. H Rauch-Puntigam, T Volker *Acryl- und Metacrylverbindungen* (Berlin: Springer, 1967)
4. W M Weigert, H Haschke *Chem.-Ztg.* **98** 61 (1974)
5. G S Mironov, M I Farberov *Usp. Khim.* **33** 649 (1964) [*Russ. Chem. Rev.* **33** 311 (1964)]
6. W M Weigert, H Haschke *Encycl. Chem. Process. Des.* 382 (1976)
7. N A Keiko, M G Voronkov *Zh. Vses. Khim. O-va im. D I Mendeleeva* 468 (1991)
8. F Andreas, K Grebe, in *Khimiya i Tekhnologiya Propilena* (The Chemistry and Technology of Propene) (Leningrad: Khimiya, 1973) p. 61
9. K I Grobova, V A Selyakova *Zh. Vses. Khim. O-va im. D I Mendeleeva* **14** 281(1969)
10. M D Navalikhina, V Zinov'eva *Khim. Promst. (Moscow)* 249 (1976)
11. R K Grasselli, J D Burrington *Chem. Ind. (Dekker)* **5** 17 (1981) *Chem. Abstr.* **98** 162757t (1983)
12. R K Grasselli, J D Burrington *Adv. Catal.* **30** 133 (1981)
13. L Ya Margolis *Okislenie Uglevodorodov na Geterogennykh Katalizatorakh* (Oxidation of Hydrocarbons and Heterogeneous Catalysts) (Moscow: Khimiya, 1977)
14. H Arzoumanian, J Metzger *Synthesis* 527 (1971)
15. J D Burrington, C T Kartisek, R K Grasselli *J. Catal.* **63** 235 (1980)
16. U Illgen, J Scheve, R Feldhaus, K Anders *React. Kinet. Catal. Lett.* **20** 203 (1982)
17. Subagjo, M Blanchard, D Vanhove *J. Chem. Res. (S)* 252 (1982)
18. T Ono, M Kiryu, M Komiyama, R L Kuczkowski *J. Catal.* **127** 698 (1991); *Ref. Zh. Khim.* 12B4443 (1991)
19. G W Keulks *J. Catal.* **19** 232 (1970)
20. W Ueda, K Asakawa, Ch-L Chen, Y Moro-oka, T Ikawa *J. Catal.* **101** 360 (1986)
21. J Svachula, J Tichy, J Machek *Chem. Prum.* **35** 128 (1985)
22. Jpn. P. 59-31727; *Chem. Abstr.* **106** 50 772 (1987)
23. USSR P. 789 493; *Byull. Izobret.* **47** 96 (1980)
24. USSR P. 789 494; *Byull. Izobret.* **47** 97 (1980)
25. Jpn. P. 58-213726; *Chem. Abstr.* **100** 141 175 (1984)
26. Jpn. P. 58-213729; *Chem. Abstr.* **100** 141 174 (1984)
27. J C Volta, P Bussiere, G Coudurier, J M Herrmann, D S Veddrine *Appl. Catal.* **16** 315 (1985)
28. J C Volta, B Moraweck *J. Chem. Soc., Chem. Commun.* 338 (1980)
29. J C Volta *Synth. Mater.* **4** 319 (1982)
30. F Theobald, A Laarif, A W Hewat *Mater. Res. Bull.* **20** 653 (1985); *Chem. Abstr.* **103** 93551 (1985)
31. I I Zakharov, G Ya Popova, T V Andruschkevich *React. Kinet. Catal. Lett.* **19** 367 (1982)
32. Jpn. P. 89 157 930; *Chem. Abstr.* **111** 233 872 (1989)
33. S Nakamura, H Ichihashi *Stud. Surf. Sci. Catal.* 7 755 (1981)
34. T Hayakawa, T Tsunoda, H Orita, T Kameyama, M Ueda, K Fukuda, K Takehira *J. Chem. Soc., Chem. Commun.* 1593 (1988)
35. T Shiraishi, S Kishiwada, S Shimizu, H Ichihashi *Niihama Kogyo Koto Senmon Gakko Kiyo, Rikogaku-hen* **21** 33 (1985); *Chem. Abstr.* **103** 93 542 (1985)
36. V M Zhiznevskii, E V Fedevich, D K Tolopko *Zh. Prikl. Khim. (Leningrad)* **44** 846 (1971)
37. V M Zhiznevskii, E Dvonchova, V A Kozharskii *Zh. Prikl. Khim. (Leningrad)* **60** 1810 (1987)
38. V M Zhiznevskii, E Dvonchova, V A Kozharskii *Zh. Fiz. Khim.* **61** 2194 (1987)
39. E V Fedevich, V V Krylova, V M Zhiznevskii *Khim. Promst. (Moscow)* 335 (1980)
40. A A Firsova, M Yu Kutyrev, G A Vorob'eva, L Ya Margolis *Dokl. Akad. Nauk SSSR* **263** 147 (1982)
41. BRD P. 2 909 597; *Chem. Abstr.* **94** 102 833 (1981)
42. BRD P. 3 740 271; *Chem. Abstr.* **111** 174 820 (1989)
43. Jpn. Appl. 225 443; *Ref. Zh. Khim.* 6N25P (1991)
44. BRD P. 3 006 894 ; *Chem. Abstr.* **94** 47989 (1981)
45. US P. 4 250 339; *Ref. Zh. Khim.* 20N34P (1981)
46. US P. 4 258 217; *Ref. Zh. Khim.* 22N37P (1981)
47. BRD P. 2 338 111; *Ref. Zh. Khim.* 23N107 (1975)
48. J Buiten *J. Catal.* **10** 188 (1968)
49. Eur. P. 115 646; *Chem. Abstr.* **103** 28 031 (1985)
50. V M Zhiznevskii, L I Ivanyk, L F Yakubovskaya *Katal. Katal.* **23** 34 (1985)
51. P Forzatti, F Trifiro, P L Villa *J. Catal.* **55** 52 (1978)
52. D Vanhove, Subagjo, M Blanhard *J. Chem. Res. (S)* 176 (1980)
53. C Martiu, V Rives *J. Mol. Catal.* **48** 381 (1988)
54. T Tanaka, Y Nishimura, S Kavasaki *J. Catal.* **118** 327 (1989)
55. P L Silveston, M Forrisier *Ind. Eng. Chem. Proc. Res. Dev.* **24** 320 (1986); *Ref. Zh. Khim.* 20N43 (1985)
56. F Figueras, M Forissier, J P Lacharme, J L Portefaix *Appl. Catal.* **19** 21 (1986); *Chem. Abstr.* **104** 148 264 (1985)
57. R A Lemberanskii, O L Babasheva, B R Serebryakov, L V Arakelova *Azerb. Khim. Zh.* **4** 38 (1987)
58. P Ruiz, B Delmon *Catal. Today* **3** 199 (1988)
59. I B Annenkova, Z A Bakhshieva, E B Guseinova *Azerb. Khim. Zh.* **3**, 38 (1987)
60. R A Lemberanskii, O L Babasheva, B R Serebryakov, L V Arakelova *Azerb. Khim. Zh.* **3** 33 (1987)
61. R A Lemberanskii, I B Annenkova, O L Babasheva, B R Serebryakov *Izv. Vyssh. Uchebn. Zaved., Khim. Khim. Tekhnol.* **29** (9) 67 (1986)
62. R A Lemberanskii, M B Mazin, I I Pis'man, K M Mekhkiev, I B Annenkova *Azerb. Khim. Zh.* **3** 63 (1975)
63. M B Mazin, G F Vytnov, R A Lemberanskii *Azerb. Khim. Zh.* **2** 38 (1975)
64. R A Lemberanskii, E G Rostevanov, I B Annenkova, E S Liberman, K M Mekhkiev *Azerb. Khim. Zh.* **4** 24 (1974)
65. R A Lemberanskii, I B Annenkova, O L Babasheva *Izv. Vyssh. Uchebn. Zaved., Khim. Khim. Tekhnol.* **29** 52 (1986)
66. R A Lemberanskii, I B Annenkova, Z A Bakhshieva *Usp. Khim.* **61** 124 (1992) [*Russ. Chem. Rev.* **61** 67 (1992)]
67. A Perrard, J E Germain *Bull. Soc. Chim. Fr.* 55 (1978)
68. L D Krenzke, G W Keulks, A V Sklyarov, A A Firsova, V Yu Kutyrev, L Ya Margolis, O V Krylov *J. Catal.* **52** 418 (1978)
69. T Hayakawa, T Tsunoda, H Orita, T Kameyama, H Takahashi, K Takehira, K Fukuda *J. Chem. Soc., Chem. Commun.* 961 (1986)
70. J Yu, L Kevan *J. Phys. Chem.* **95** 6648 (1991)
71. USSR P. 1 003 886; *Byull. Izobret.* **10** 20 (1983)
72. H Batis, P Vergnon *Bull. Soc. Chim. Fr.* 334 (1989)
73. J Freiberg, J Herrmann, H Seeboth *J. Pract. Chem.* **324** 563 (1982)

74. Czech. P. 227 136; *Chem. Abstr.* **103** 89 314 (1985)
75. G K Boreskov, E M Erenburg, T V Andrushkevich, T V Zelenkova, V N Bibin, V D Meshcheryakov, N P Boronina, Yu N Tyurin *Kinet. Katal.* **23** 895 (1982)
76. Yu V Belokopytov, N D Konovalova *Ukr. Khim. Zh.* **44** 1255 (1978)
77. O M Vinogradova, G F Vytnov, L Ya Margolis *Kinet. Katal.* **18** 1595 (1977)
78. T G Vazhnova, V N Korchak, V I Timoshenko, O V Krylov, M G Slin'ko *Kinet. Katal.* **26** 1378 (1985)
79. A A Butakov, A G Merzhanov, V R Linde, N V Silyakova *Dokl. Akad. Nauk SSSR* **289** 920 (1986)
80. T Shiraishi, S Shimizu, H Ichihashi *Niihama Kogyo Koto Senmon Gakko Kiyo, Rikogaku-hen* **21** 62 (1985); *Chem. Abstr.* **103** 55 687 (1985)
81. I M Baryshevskaya, K M Kholyavenko *Katal. Katal.* **19** 36 (1981)
82. O V Krylov, Yu V Maksimov, L Ya Margolis *J. Catal.* **95** 289 (1985); *Chem. Abstr.* **103** 110 623 (1985)
83. Yu V Maksimov, A A Firsova, B Z Lubentsov, D P Shashkin, V R Linde, L Ya Margolis *Kinet. Katal.* **24** 460 (1983)
84. V R Linde, A V Sklyarov, B Z Lubentsov *Kinet. Katal.* **24** 505 (1983)
85. J L G Fierro, E Salazar, J A Legarreta *J. Chem. Tech. Biotechnol.* **36** 219 (1986)
86. A A Davydov *Zh. Fiz. Khim.* **765** 1803 (1991)
87. H Praliaud, M-V Mathieu *J. Chim. Phys. Phys.-chim. Biol.* **73** 509 (1976)
88. J C Volta, O Bertrand, N Floquet *J. Chem. Soc., Chem. Commun.* 1283 (1985)
89. J Svachula, A Tockstein, J Tichy *React. Kinet. Catal. Lett.* **31** 187 (1986)
90. J Svachula, J Tichy, J Machek *Chem. Prum.* **35** 354 (1988)
91. M Merchan, J Nebot-Gil, L R Gozalez, F Tomas *J. Mol. Struct.* **21** 479 (1985)
92. R Nakamura, M Shimoij, H Niijama *Catal. Today* **10** 119 (1991); *Ref. Zh. Khim.* 4B4173 (1992)
93. J C Strini, J Metzger *Bull. Soc. Chim. Fr.* 3145 (1966)
94. US P. 4 450 055; *Ref. Zh. Khim.* 7L423P (1985)
95. G R Stafford *Electrochim. Acta* **32** 1137 (1987)
96. H Bonnemann, W Nunez, D M M Rohe *Helv. Chim. Acta* **66** 177 (1983)
97. N Giordano, J C J Bart, P Vitarelli, S Cavallaro *Oxid. Commun.* **7** 99 (1984)
98. W Ueda *Kagaku To Kogyo* **43** 1296 (1991); *Ref. Zh. Khim.* 6N185 (1990)
99. T Komatsu, J Uragami, K Otsuka *Chem. Lett.* 1903 (1988)
100. Y C Kim, W Ueda, Y Morooka *Appl. Catal.* **70** 175 (1991)
101. Jpn. P. 88 145 249; *Chem. Abstr.* **110** 76 262 (1989)
102. BRD P. 3 313 573; *Chem. Abstr.* **100** 7 381 (1984)
103. US P. 4 137 271; *Ref. Zh. Khim.* 18N37P (1979)
104. V A Kozharskii, V M Zhiznevskii, D A Tolopko *Zh. Prikl. Khim. (Leningrad)* **57** 197 (1984)
105. E M Badebkina, Yu M Tyurin, B G Freidin *Zh. Prikl. Khim. (Leningrad)* **59** 1822 (1986)
106. S Zou, D Li *Shiyou Hoagong* **17** 554 (1989); *Chem. Abstr.* **110** 76 098 (1988)
107. M A Al'ziyud, V L Bagiev, K Yu Adzhamov *Azerb. Khim. Zh.* **1** 17 (1987)
108. V Macho, M Kavala, M Matuskova, M Polievka *Chem. Prum.* **33** 575 (1983)
109. US P. 4 219 670 (1980)
110. Jpn. P. 8 866 141; *Chem. Abstr.* **110** 58 259 (1989)
111. Jpn. P. 8 055 130; *Chem. Abstr.* **93** 185 763 (1980)
112. Eur. P. 58 046; *Chem. Abstr.* **98** 107 930 (1983)
113. Jpn. P. 8 019 227; *Chem. Abstr.* **93** 45 969 (1980)
114. Czech. P. 202 470; *Ref. Zh. Khim.* 24N38P (1983)
115. Jpn. P. 88 216 835; *Chem. Abstr.* **110** 76 275 (1989)
116. Eur. P. 304 867; *Chem. Abstr.* **110** 24 091 (1989)
117. V A Kozharskii, V M Zhiznevskii, E N Mokryi *Vestn. L'vov. Politekh. Inst.* **191** 118 (1985)
118. Jpn. P. 88-66141; *Chem. Abstr.* **110** 58259 (1989)
119. US P. 4 358 622; *Ref. Zh. Khim.* 16N88P (1983)
120. Jpn. P. 7 946 705; *Chem. Abstr.* **91** 40 091 (1979)
121. B Cornils, A Mullen *Hydrocarbon Process.* **59** 93 (1980)
122. L Uhlar, M Polievka *Popa Uhlie* **30** 659 (1989); *Chem. Abstr.* **110** 213 406 (1988)
123. C I Matthews, C F H Tipper *J. Appl. Chem.* **17** 81 (1967)
124. Jpn. P. 7 214 085; *Ref. Zh. Khim.* 14N65P (1973)
125. R I Rennard, R A Innes, H E Swift *J. Catal.* **30** 128 (1973)
126. Jpn. P. 7 378 112 ; *Chem. Abstr.* **80** 59 466 (1974)
127. M Akimoto, K Ichikawa, E Echigoya *Nippon Kagaku Kaishi* **3** 320 (1977)
128. Jpn. P. 78 124 211; *Chem. Abstr.* **90** 104 599 (1979)
129. Jpn. P. 78 124 210 ; *Chem. Abstr.* **90** 104 600 (1979)
130. US P. 4 381 411; *Chem. Abstr.* **99** 38 910 (1983)
131. K Kurzinger, G Emig, H Hofmann, in *Proceedings of the Eighth Congress on Catalysis, Berlin, 1984* Vol. 5, p. 499
132. V M Zhiznevskii, F M Gelevan, D K Tolopko *Neftepererab. Neftekhim.* 22 (1986)
133. V M Zhiznevskii, F M Gelevan, S Abdeddin *Izv. Vyssh. Uchebn. Zaved., Khim. Khim. Tekhnol.* **29** 27 (1986)
134. US P. 3 532 740; *Chem. Abstr.* **73** 120 089 (1970)
135. T Hattori, M Ii, Y Murakami *Sekiyu Gakkaishi* **23** 233 (1980)
136. E Muller, H Hofmann *Chem. Eng. Sci.* **42** 1705 (1987)
137. E Muller-Erlwein, J Guba *Chem.-Ind.-Tech.* **60** 1072 (1988)
138. US P. 4 051 181; *Chem. Abstr.* **87** 200 809 (1977)
139. US P. 4 107 204; *Chem. Abstr.* **90** 72 629 (1979)
140. US P. 4 144 398; *Chem. Abstr.* **90** 186 396 (1979)
141. Jpn. P. 61 137 833; *Chem. Abstr.* **106** 17 891 (1987)
142. M Imashi, N W Cant, R L Kuczkowski *J. Catal.* **75** 404 (1982)
143. L Super *Tetrahedron Lett.* **8** 4193 (1967)
144. K Zaw, M Lautens, P M Henry *Organometallics* **2** 197 (1983)
145. J D Lou, Y Y Wu *Chem. Ind. (London)* **15** 531 (1987)
146. S Paraskewas *Chem.-Ztg.* **99** 432 (1975)
147. F Sundholm, G Sundholm *Electrochim. Acta* **19** 565 (1974)
148. M Nishizawa, K Adachi, Y Hayashi *J. Chem. Soc., Chem. Commun.* 1637 (1984)
149. T J Brosksom, J T B Ferreira *J. Chem. Res. (S)* 412 (1980)
150. T Nakano, Y Ishii, M Ogawa *J. Org. Chem.* **52** 4855 (1987)
151. Y Ishii, T Nakano, A Inada, Y Kishigami, K Sakurai, M Ogawa *J. Org. Chem.* **51** 240 (1986)
152. S Malinowski, S Basinski *Bull. Acad. Polon. Sci., Ser. Chim.* **11** 55 (1963)
153. A P Khardin, V Z Sharf, A I Val'dman *Khim. Promst. (Moscow)* 460 (1980)
154. T Ishikawa, T Kamio *Tokyo Kogyo Shikensho Hokoku* **58** 40 (1963)
155. Polish P. 45 675; *Ref. Zh. Khim.* 2N25 (1963)
156. M Ai *Bull. Chem. Soc. Jpn.* **64** 1342 (1991) ; *Ref. Zh. Khim.* 20B4379 (1991)
157. W J Palion, S Malinowski *React. Kinet. Catal. Lett.* **1** 461 (1974)
158. S Malinowski, W J Palion *React. Kinet. Catal. Lett.* **1** 73 (1974)
159. M Ai *Bull. Chem. Soc. Jpn.* **64** 1346 (1991); *Ref. Zh. Khim.* 20B4380 (1991)
160. Polish P. 45 582; *Ref. Zh. Khim.* 12N34 (1963)
161. Y Ogata, A Kawasaki, K Yokoi *J. Chem. Soc. (B)* 1013 (1967)
162. N U Bykadorov, V K Rykov, A P Zheltonogov, S V Sukhanov, L A Chelyukanova, in *Funktsional'nye Organicheskie Soedineniya i Polimery* (Organic Compounds and Polymers with Functional Groups) (Volgograd, 1974) p. 156
163. A P Khardin, V K Rykov, L A Chelyukanova, A P Zheltonogov, N U Bykadorov, S V Sukhanov *Khim. Promst. (Moscow)* 258 (1974)
164. M Ai *Appl. Catal.* **77** 123 (1991); *Ref. Zh. Khim.* 2B4347 (1992)
165. US P. 4 433 174; *Chem. Abstr.* **100** 158 572 (1984)
166. BRD P. 1 804 469; *Chem. Abstr.* **71** 38 381 (1969)
167. J E Vik *Acta Chem. Scand.* **26** 3165 (1972)
168. A Mamoru *Appl. Catal.* **36** 221 (1988)
169. US P. 3 928 458; *Chem. Abstr.* **84** 135 070 (1976)
170. M I Farberov, G S Mironov, M A Korshunov *Zh. Prikl. Khim. (Leningrad)* **35** 2483 (1962)
171. M I Farberov, G S Mironov *Dokl. Akad. Nauk SSSR* **148** 1095 (1963)
172. L M Korobova, I A Livshits *Zh. Obshch. Khim.* **34** 3419 (1964)
173. Z G Pikh, M D Fedevich, I I Yatchishin, A I Klyuchkivs'kii *Vestn. L'vov. Politekh. Inst.* **96** 56 (1975)
174. V N Saprygina, S S Zlotskii, D L Rakhmankulov *Zh. Prikl. Khim. (Leningrad)* **60** 909 (1987)

175. Eur. P. 58 927; *Chem. Abstr.* **98** 71 487 (1983)
176. French P. 1 504 854; *Chem. Abstr.* **70** 37 191 (1969)
177. L Lardicci, R Menicagli *Chem. Ind.* **51** 1387 (1969)
178. L Lardicci, F Navari, R Rossi *Tetrahedron* **22** 1991 (1966)
179. R Menicagli, M L Wis *J. Chem. Res. (S)* 262 (1978)
180. BRD P. 3 740 293; *Chem. Abstr.* **111** 153 211 (1989)
181. BRD P. 2 855 504; *Ref. Zh. Khim.* 7N28 (1981)
182. US P. 4 560 499; *Ref. Zh. Khim.* 24R729P (1986)
183. BRD P. 3 213 681; *Chem. Abstr.* **100** 7382 (1984)
184. M J Antal, W S L Mok, J C Roy, A T Raissi *J. Anal. Appl. Pyrol.* **8** 291 (1985)
185. M J Antal, A Brittain, C De Almeida, S Ramayya *Prepr. Pap.-Am. Chem. Soc. Div. Fuel Chemistry* **30** 78 (1985)
186. D A Zhukov, N I Golovina, B A Golovin *Zh. Prikl. Khim. (Leningrad)* **53** 780 (1980)
187. Jpn. P. 7 648 603; *Chem. Abstr.* **85** 93 821 (1976)
188. Jpn. P. 49 121 257; *Ref. Zh. Khim.* 5N32P (1979)
189. US P. 3 943 166; *Chem. Abstr.* **84** 164 168 (1976)
190. R C Cookson, S R Wallis *J. Chem. Soc. B* 1245 (1966)
191. F Mutterer, J M Morgen, J M Biedermann, J P Fleury, F Weiss *Tetrahedron* **26** 477 (1970)
192. F Weiss, A Lantz, A Isard *Bull. Soc. Chim. Fr.* 3215 (1965)
193. J M Biedermann, J P Fleury, F Weiss *Bull. Soc. Chim. Fr.* 1187 (1970)
194. F Weiss, A Isard, R Bensa *Bull. Soc. Chim. Fr.* 1358 (1965)
195. BRD P. 2 061 240; *Chem. Abstr.* **77** 87 895 (1972)
196. N I Shuikin, R A Karakhanov, S N Khar'kov *Izv. Akad. Nauk SSSR, Ser. Khim.* 2044 (1966)
197. B C Roquitte, W D Walters *J Am. Chem. Soc.* **84** 4049 (1962)
198. R L Forman, H M Mackinnon, P D Ritchie *J. Chem. Soc. C* 2013 (1968)
199. V Prey, H Gruber *Starke* **29** 96 (1977)
200. F Weiss, A Isard, G Bonnard *Bull. Soc. Chim. Fr.* 2332 (1965)
201. G Hallstrom, B Lindeke, A H Khuthier, M A Al-Iraqi *Tetrahedron Lett.* **21** 667 (1980)
202. K Shinoda *Chem. Lett.* 883 (1978)
203. J D Lou, W X Lou *Synthesis* 179 (1987)
204. J D Lou, W X Lou *Kexue Tongbao* **30** 426 (1986); *Chem. Abstr.* **104** 167 953 (1985)
205. A Riahi, J Cossy, J Muzart, J P Pete *Tetrahedron Lett.* **26** 839 (1985)
206. K A Singmaster, G C Pimentel *J. Mol. Struct.* **194** 215 (1989)
207. G Rousseau, P Le Perchec, J M Conia *Tetrahedron* **34** 3483 (1978)
208. G Rousseau, P Le Perchec, J M Conia *Synthesis* 67 (1978)
209. A Kirrmann *Bull. Soc. Chim. Fr.* 657 (1961)
210. J L Kraus, G Sturtz *Bull. Soc. Chim. Fr.* 4012 (1971)
211. E Elkik *Bull. Soc. Chim. Fr.* 283 (1968)
212. M Dedieu, Y L Paskal *Bull. Soc. Chim. Fr.* 593 (1978)
213. BRD P. 1 945 530; *Chem. Abstr.* **74** 111 566 (1971)
214. BRD P. 2 054 988; *Chem. Abstr.* **77** 33 940 (1972)
215. A V Mushegyan, V Kh Ksipteridis, G A Chukhadzhyan *Arm. Khim. Zh.* **28** 674 (1975)
216. K A Torosyan, S G Babayan, A V Mushegyan, Zh G Martirosyan *Prom. Arm.* 68 (1977)
217. USSR P. 740 743; *Byull. Izobret.* **22** 139 (1980)
218. BRD P. 2 633 959; *Chem. Abstr.* **87** 173 430 (1977)
219. C Ruchardt, O Kratz, S Eichler *Chem. Ber.***102** 3922 (1969)
220. I Ryu, Sh.Murai, N Sonoda *J. Org. Chem.* **51** 2389 (1986)
221. D R Williams, K Nishitani *Tetrahedron Lett.* **21** 4417 (1980)
222. J P Marino, J S Farina *Tetrahedron Lett.* **16** 3901 (1975)
223. P A Grieco, C L Wang, G Majetich *J. Org. Chem.* **41** 726 (1976)
224. C S Rondestvedt, G J Mantell *J. Am. Chem. Soc.* **84** 3307 (1962)
225. L W Kissinger, T M Benziger, R K Rohwer, in *Nitro Compounds* (Proceedings of the International Symposium, Warsaw, 1963) p. 317 (pub. 1964)
226. US P. 4 851 583; *Ref. Zh. Khim.* 18N22P (1990)
227. Jpn. P. 6 037 992; *Chem. Abstr.* **103** 361 908 (1985)
228. P Lencrerot, A Parfait, C Jouret *Ind. Aliment. Agric.* **101** 763 (1984)
229. US P. 3 114 765; *Chem. Abstr.* **59** 7 377 (1963)
230. US P. 3 100 227; *Ref. Zh. Khim.* 10N39P (1965)
231. I Schuphan, J E Casida *J. Agric. Food Chem.* **27** 1060 (1979)
232. I V Andreeva, M M Koton, A N Akopova, N V Kukarkina *Zh. Org. Khim.* **11** 954 (1975)
233. USSR P. 186 421; *Ref. Zh. Khim.* 23N82P (1967)
234. M F Shostakovskii, V Z Annenkova, L G Ivanova, G S Ugryumova *Izv. Sib. Otd. Akad. Nauk SSSR, Ser. Khim. Nauk* **14** (6) 104 (1967)
235. J N Wells, M S Strahl *J. Pharm. Sci.* **60** 533 (1971)
236. E W Della, P E Pigou *Austr. J. Chem.* **36** 2261 (1983)
237. S A Kline, J J Solomon, B L Van Duuren *J. Org. Chem.* **43** 3596 (1978)
238. B Gold, T Leuschen *J. Org. Chem.* **46** 1372 (1981)
239. L Skattebol *J. Org. Chem.* **31** 1554 (1966)
240. T Hiyama, A Kanakura, H Yamamoto, H Nozaki *Tetrahedron Lett.* **19** 3047 (1978)
241. Yu P Savinykh, V S Aksenov *Izv. Sib. Otd. Akad. Nauk SSSR, Ser. Khim. Nauk* **2** (1) 125 (1978)
242. Y L Chow, B H Bakker *Can. J. Chem.* **60** 2268 (1982)
243. J G Omichinski, E J Soderlung, E Dybing, P J Pearson, S J Nelson *Toxicol. Appl. Pharmacol.* **92** 286 (1988)
244. Y Segall, E C Kimmel, D R Dohn, J E Casida *Mutat. Res.* **158** 61 (1985)
245. D R Dohn, M I Graziano, J E Casida *Biochem. Pharmacol.* **37** 3485 (1988)
246. K P Kringstad, P O Ljungquist, De F Sousa, L M Stromberg *Environ. Sci. Technol.* **17** 553 (1983)
247. E Eder, K Dornbusch *Drug Metab. Dispos.* **16** 60 (1988); *Chem. Abstr.* **108** 145 034 (1988)
248. I Schuphan, J D Rosen, J E Casida *Science* **205** 1013 (1979)
249. I Schuphan, J E Casida *Tetrahedron Lett.* **20** 841 (1979)
250. L O Ruzo, J E Casida *J. Agric. Food Chem.* **33** 272 (1985)
251. J Buddrus, F Nerdel, P Hentschel *Tetrahedron Lett.* **7** 5379 (1966)
252. C Wakselman, J P Lampin, H Molines, A Nonat, T Nguyen, G Vignal *Ann. Chim. Fr.* **9** 719 (1984)
253. H Molines, T Nguyen, C Wakselman *Synthesis* 754 (1985)
254. Fr. Appl. 2 560 595; *Ref. Zh. Khim.* 23N40P (1986)
255. Intern. P. 85 03 931; *Chem. Abstr.* **104** 206 718 (1986)
256. Y Bessiere, D N Savary, M Schlosser *Helv. Chim. Acta* **60** 1739 (1977)
257. F Camps, J Coll, G Fabrias, A Guerrero *Tetrahedron* **40** 2871 (1984)
258. P Amice, L Blaco, J M Conia *Synthesis* 196 (1976)
259. M F Shostakovskii, N A Keyko *Dokl. Akad. Nauk SSSR* **162** 362 (1965)
260. M F Shostakovskii, N A Keiko, A P Chichkarev, A Kh Filippova *Izv. Akad. Nauk SSSR, Ser. Khim.* 2351 (1967)
261. M F Shostakovskii, N A Keiko, A P Chichkarev, O N Vylegzhanin *Izv. Akad. Nauk SSSR, Ser. Khim.* 2715 (1971)
262. N A Keiko, A P Chichkarev, V V Keiko *Zh. Prikl. Khim. (Leningrad)* **46** 2691 (1973)
263. G A Russel, M Ballenegger *Synthesis* 104 (1973)
264. W C Agosta, W W Lowrance *J. Org. Chem.* **35** 3851 (1970)
265. C R Davies, J S Davies *J. Chem. Soc., Perkin Trans. 1* 2390 (1976)
266. T A Hase *Finn. Chem. Lett.* **6** 23 (1979)
267. S Omori, C W Dence *Wood. Sci. Technol.* **15** 113 (1981)
268. J Gierer, F Imsgard, I Noren *Acta Chem. Scand. (B)* **31** 561 (1977)
269. H Baganz, K Praefcke *Chem. Ber.* **96** 2661 (1963)
270. Czech. P. 220 295; *Ref. Zh. Khim.* 23N41P (1986)
271. M Petrusova, M Fedoronko *Chem. Zvesti* **36** 837 (1982)
272. M Fedoronko, M Petrusova, T Sticzay *Carbohydr. Res.* **115** 75 (1983)
273. D R Williams, R D Gaston, J F Hoover *Synthesis* 908 (1987)
274. A J Grant, L M Lerner *Biochemistry* **18** 2838 (1979)
275. A J Grant, L M Lerner *J. Med. Chem.* **23** 795 (1980)
276. P N Lowe, R B Beechey *Biochemistry* **21** 4073 (1982)
277. N A Keiko, T N Musorina, I D Kalikhman, M G Voronkov *Zh. Org. Khim.* **49** 170 (1979)
278. USSR P. 297 635; *Byull. Izobret.* **10** 81 (1971)
279. N A Keiko, L G Stepanova *Izv. Akad. Nauk SSSR, Ser. Khim.* 2516 (1972)
280. N A Keiko, L G Stepanova, I D Kalikhman, M G Voronkov *Izv. Akad. Nauk SSSR, Ser. Khim.* 1652 (1977)
281. N A Keiko, L G Stepanova, I D Kalikhman, M G Voronkov *Izv. Akad. Nauk SSSR, Ser. Khim.* 659 (1977)
282. K D Gunderman *Intra-Sci. Chem. Rep.* **6** 91 (1972)
283. K D Gunderman, P J Hnida *Angew. Chem.* **91** 930 (1979)
284. J H S Weiland *Recl. Trav. Chim. Pays-Bas* **75** 1358 (1956)

285. Z Kosarych, T Cohen *Tetrahedron Lett.* **21** 3959 (1980)
286. L Duhamel, J Chauvin *Tetrahedron Lett.* **21** 4171 (1980)
287. USSR P. 1 142 471; *Byull. Izobret.* **8** 96 (1985)
288. N A Keiko, L G Stepanova, I D Kalikhman, M G Voronkov *Izv. Akad. Nauk SSSR, Ser. Khim.* 1676 (1986)
289. N A Keiko, T N Mamashvili, L G Stepanova, E A Ivanova, M G Voronkov, in *Fourteenth International Symposium on the Organic Chemistry of Sulfur, Lodz, 1990 (Abstracts of Papers)*
290. H J Reich, S K Shah *J. Am. Chem. Soc.* **99** 263 (1977)
291. H J Reich, S K Shah, P M Gold, R E Olson *J. Am. Chem. Soc.* **103** 3112 (1981)
292. J A Latham, B P Branchaud, Y -C J Chen, Ch.Walsh *J. Chem. Soc., Chem. Commun.* 528 (1986)
293. Z Janousek, S Piettre, F Gorissen-Hervens, H G Viehe *J. Organomet. Chem.* **250** 197 (1983)
294. S Piettre, Z Janousek, R Merenyi, H G Viehe *Tetrahedron* **41** 2527 (1985)
295. Ch De Cock, S Piettre, F Lahousse, et al. *Tetrahedron* **41** 4183 (1985)
296. P Lerouge, C Paulmier *Bull. Soc. Chim. Fr.* 1219 (1985)
297. P Lerouge, C Paulmier *Tetrahedron Lett.* **25** 1987 (1984)
298. K Uneyama, K Takano, S Torii *Tetrahedron Lett.* **23** 1161 (1982)
299. K Uneyama, K Takato, S Torii *Bull. Chem. Soc. Jpn.* **56** 2867 (1983)
300. L Duhamel, G Ple, P Commare *C. R. Acad. Sci.* **278** 1113 (1974)
301. USSR P. 1 204 619; *Byull. Izobret.* **2** 102 (1986)
302. N A Keiko, A Yu Rulev, I D Kalikhman, M G Voronkov *Izv. Akad. Nauk SSSR, Ser. Khim.* 1801 (1987)
303. N A Keiko, A Yu Rulev, I D Kalikhman, M G Voronkov *Synthesis* 446 (1989)
304. A Yu Rulev, Candidate's Thesis in Chemical Sciences, Institute of Organic Chemistry of the Siberian Division of the USSR Academy of Sciences, Irkutsk, 1988
305. N V Komarov, S V Kirpichenko, E I Kositsyna, G A Kalabin *Zh. Org. Khim.* **38** 2102 (1968)
306. M G Voronkov, S V Kirpichenko, V V Keiko, L V Sherstyannikova *Izv. Akad. Nauk SSSR, Ser. Khim.* 2471 (1975)
307. N V Komarov, S V Kirpichenko *Izv. Akad. Nauk SSSR, Ser. Khim.* 2288 (1970)
308. J M Muchowski, R Naef, M L Maddox *Tetrahedron Lett.* **26** 5375 (1985)
309. Y Morizawa, A Kanakura, H Yamamoto, T Hiyama, H Nozaki *Bull. Chem. Soc. Jpn.* **57** 1935 (1984)
310. H Okumoto, J Tsuji *Synth. Commun.* **12** 1015 (1982)
311. B M Trost, T N Nanninga, T Satoh *J. Am. Chem. Soc.* **107** 721 (1985)
312. B M Trost, T A Grese *J. Org. Chem.* **57** 686 (1992)
313. I Matsuda, J Sakakibara, H Inoue, H Nagashima *Tetrahedron Lett.* **33** 5799 (1992)
314. A B Smith, III, P A Levenberg, P J Jerris, R M Scarborough Jnr, P M Wovkulich *J. Am. Chem. Soc.* **103** 1501 (1981)
315. T Sasaki, Y Ishibahi, M Ohno *Tetrahedron Lett.* **23** 1693 (1982)
316. V V Kormachev, Yu N Mitrasov, V S Tsivunin, in *Khimiya Nepredel'nykh Soedinenii (Tezisy Dokladov Vsesoyuznogo Simpoziuma, Kazan', 1986)* (Abstracts of Reports at the All-Union Symposium on the Chemistry of Unsaturated Compounds, Kazan, 1986) Part I, p. 78
317. J E Vik *Acta Chem. Scand.* **27** 239 (1973)
318. J C Depezay, Y Le Merrer *Tetrahedron Lett.* **15** 2751 (1974)
319. J C Depezay, Le Y Merrer, M Saniere, *Synthesis* 766 (1985)
320. M A Tius, D P Astrab, Gu Xue-gin *J. Org. Chem.* **52** 2625 (1987)
321. E Campi, N J Fitzmaurice, W R Jackson, P Perlmutter, A J Smallridge *Synthesis* 1032 (1987)
322. J Ficini, J C Depezay *Tetrahedron Lett.* **10** 4797 (1969)
323. T Mandai, K Osaka, M Kawagishi, M Kawada, J Otera *J. Org. Chem.* **49** 3595 (1984)

Russian Chemical Reviews **62** (8) 769 – 786 (1993)
© 1993 Russian Academy of Sciences and Turpion Ltd

UDC 547.541.521.07

Thiols as synthons

I V Koval'

Contents

I. Introduction	769
II. The structure and physicochemical properties of thiols	769
III. Methods for preparing thiols	770
IV. Preparations based on thiols	773

Abstract. The results of recent research in the field of thiol chemistry are arranged systematically and summarised. The structure and physicochemical properties of thiols and their methods of preparation are described and their use as synthons in the preparation of various sulfur-containing compounds is discussed. The bibliography comprises 419 references.

I. Introduction

Thiols play a very important part in living organisms and they are also used in many areas of science and technology. Glutathione and cysteine are known[1] to form part of proteins that are involved in biochemical reactions that take place by an oxidation-reduction scheme, and to bind free radicals. Dihydrolipoic acid takes part in the processes of photosynthesis[2] and metabolism in mitochondria[3] and also in other biochemical reactions.[4] A number of thiols have found applications as pharmaceutical preparations,[5] accelerants of the vulcanisation of rubber,[6,7] polymer stabilisers,[8] and additives to rocket fuels.[9,10] However the most important field of application of thiols is fine-organic synthesis. The lability of S–H and C–S bonds, their ability to undergo fission under the action of both nucleophilic and electrophilic reagents, and the presence of an active reaction centre with sulfur of variable valence all make thiols valuable synthons that are widely applicable in fine-organic synthesis.

The interest being shown in thiols by many investigators has in due course resulted in the appearance of a number of reviews,[4,11–19] which to some or other extent reflect particular aspects of the chemistry of thiols; however many experimental data have been accumulated since the publication of these reviews and these data need futher summarising.

II. The structure and physicochemical properties of thiols

The S–H and C–S bonds in thiols have fairly high dissociation energies but these bonds are not so strong as the O–H and C–O in the oxygen analogues of thiols, i.e. alcohols.

I V Koval' Department of the Chemical Technology of High-molecular-mass Compounds, Ukrainian Chemical-technology University, prosp. Gargarina 8, 320005 Dnepropetrovsk, Ukraine.
Tel. (7-0562) 47 24 91, Fax: (7-0562) 47 33 60

Received 4 January 1993
Uspekhi Khimii **62** (8) 813 – 830 (1993); translated by G J Bullen

The structure of the alkyl groups bonded to the sulfur atom in the alkanethiols has almost no effect on the strength of the S–H and C–S bonds; the strength of these bonds is greatly influenced by conjugation of the *p* electrons of the sulfur atom with the π electrons of the system (*p*,π-conjugation).[20,21]

As the electronegativity of the sulfur atom (2.6) is lower than that of the oxygen atom (3.5) thiols have a considerably smaller tendency than alcohols to form hydrogen bonds, as is confirmed by the IR and ^{1}H NMR spectroscopy.[22] This lower tendency to hydrogen-bond formation is responsible for the greater volatility of thiols as compared to alcohols (the boiling points of alkane thiols are 40 – 60 °C lower than the boiling points of the corresponding alcohols) and also the lower solubility of thiols in water. Thiols are stronger acids than alcohols,[23–27] the S–H bond being more polar than the O–H bond owing to the increased *s* character of the central atom.

Aromatic thiols have a higher acidity than aliphatic thiols owing to the increased polarity of the S–H bond due to *p*, π-conjugation.

The complexes of thiols with shift-reagents[28,29] are less stable than in the case of alcohols, as is shown by the much smaller values of the induced shifts of the resonance signals of the protons in the SH groups as compared to the corresponding values for the protons in OH groups.

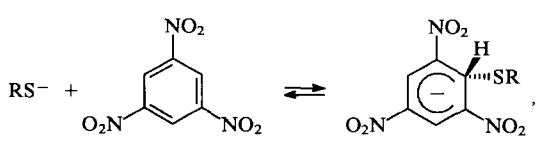
Thiols have a smaller proton affinity than alcohols. The rate of transfer of a proton to thiols in their reaction with trifluoromethanesulfonic acid is several orders of magnitude (10^4–10^5) smaller than the rate of the same reaction for alcohols,[30] as is consistent with the hard-soft-acid-base principle.[31]

$$RSH + CF_3SO_3H \rightleftharpoons \overset{+}{R}SH_2 + CF_3SO_3^-$$

Thiolate anions are weaker bases than alkoxide anions. If the basicity of thiolate anions is judged on the basis of the protonic scale of acidity, using the equilibria

$$RS^- + H^+ \rightleftharpoons RSH; \qquad RO^- + H^+ \rightleftharpoons ROH,$$

the following order of basicities is obtained: $MeO^- > EtS^- > PhO^- > PhS^-$.[4] However, with respect to CH-acids, on the basis of the equilibrium



the order obtained is: $EtS^- > MeO^- > PhS^- > PhO^-$.[32,33]

With respect to CH-acids the thiophenolate anion is a weaker base than the hydroxide anion by a factor of 10^3; this is due to the smaller degree of solvation of thiolate anions as compared to the hydroxide ion.[34] However, thiolate anions are more nucleophilic than either alkoxide anions or the hydroxide anion.

The greater the nucleophilicity of the less basic thiolate anion as compared to the corresponding alkoxide anion may be attributed to the greater polarisability of the sulfur atom as compared to the oxygen atom and also to the transition state in reactions involving a thiolate anion (in the stabilisation of which the *d* orbitals of the sulfur atom are involved) being energetically more favourable. However, one cannot discount the fact that in a protonic solvent oxygen will form a stable hydrogen bond, with the result that it becomes less nucleophilic.

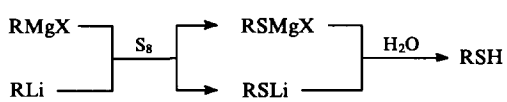
Photolysis, radiolysis, and thermolysis of thiols, and also the action of peroxides and diazo-compounds on them, lead to the production of thiyl radicals.[19] The nature and structure of the groups on the sulfur atom of the thiol have a considerable effect on the enthalpy of formation of the thiyl radicals. For example, arylthiyl radicals have higher enthalpies of formation than alkylthiyl radicals; for the phenylthiyl radical the value is 56.8 ± 2.0 kcal mol^{-1}.[35] The enthalpy of formation of alkylthiyl radicals decreases as the alkyl chain becomes longer and more branched: from 31 kcal mol^{-1} for the methylthiyl radical to 15 kcal mol^{-1} for the butylthiyl and 11 kcal mol^{-1} for the *tert*-butylthiyl radicals.[19] Thiyl radicals have higher electron affinities than oxyl radicals owing to the presence of vacant *d* orbitals on the sulfur atom. Their energy of stabilisation is significantly lower than that of oxyl radicals. For example, Macki[35] quoted 9.6 and 17.5 kcal mol^{-1} respectively for the energies of stabilisation of the phenylthiyl and phenoxyl radicals. The MNDO method has been used to calculate the molecular and electronic structures of the MeS$^{\bullet}$ and EtS$^{\bullet}$ radicals, which have C_s symmetry.[36]

S–H stretches occur in the IR spectra in the 2560 to 2592 cm^{-1} region for alkanethiols and in the 2538–2568 cm^{-1} region for thiols of the aromatic series.[37,38] In the NMR spectra of thiols the signal from the proton of the mercapto-group occurs as a singlet at 1.5–3.5 p.p.m. (δ scale).[39,40] In cyclohexanethiols the mercapto-group occupies an equatorial position preferentially.[41,42] For methanethiol and its carbanion the effective charges on the atoms and the bond orders have been calculated by the CNDO/2 method.[43,44]

III. Methods for preparing thiols

1. Syntheses using elemental sulfur and its inorganic derivatives

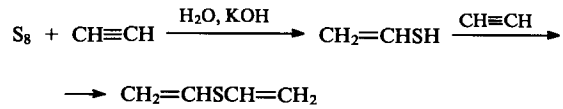
Reactions of elemental sulfur with aromatic hydrocarbons[12,45,46] and some heterocyclic compounds[47] have not been widely used in the synthesis of thiols. This is primarily due to the especially specific conditions for these reactions which are not always reasonable in practice in the laboratory. The reaction of elemental sulfur with organomagnesium and organolithium compounds[4,48,49] proved to be more promising in a preparative respect.



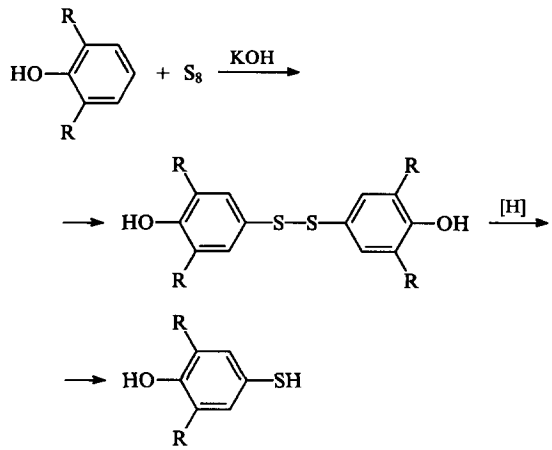
R = Alk, Ar, Het.

The relatively mild conditions for this reaction, and also the availability of the organomagnesium and organolithium compounds, enable a wide range of different thiols to be obtained.

In the reaction of elemental sulfur with acetylene, vinyl thiol is formed[50] and is then converted to divinyl sulfide.

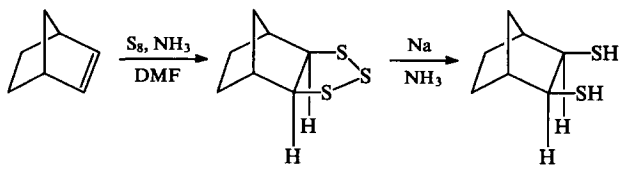


Some reactions of elemental sulfur with organic compounds lead to the formation of disulfides and polysulfides which are readily reduced to the corresponding thiols, e.g. the reaction with dialkylphenols.[51,52]

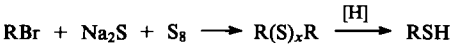


R = Me, Et, Bu^t.

The addition of elemental sulfur to the double bond in norbornene[53] gives the corresponding trisulfide which can be reduced to the dithiol using sodium metal in liquid ammonia.



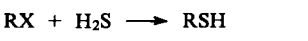
When mixed with sodium sulfide elemental sulfur also reacts with alkyl halides and highly reactive aryl halides to form polysulfides,[54] the reduction of which gives thiols.



R = Alk, Ar, Het; x = 2–4.

Because of the availability of a wide range of different halide derivatives and also the ease of reduction of the polysulfides, this method is fairly promising in a preparative respect.

Of the inorganic sulfur derivatives the most widely used in the preparation of thiols is hydrogen sulfide. Several variants of thiol preparations based on hydrogen sulfide have been developed. One of these is based on substitution reactions in which halogens, hydroxyl, arenesulfonyl, and other good leaving groups are replaced by a mercapto-group.[55–60]

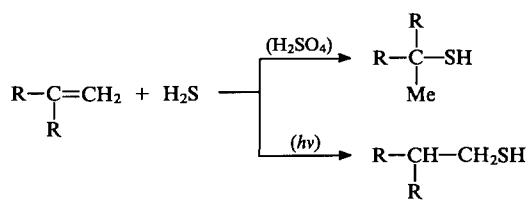


R = Alk, Ar, Het; X = Cl, Br, OTs, OH, NR_2.

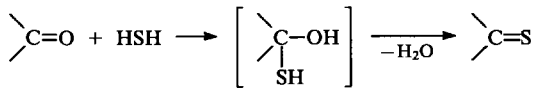
Replacement of a low-activity halogen atom by a mercapto-group in benzene[61-68] and thiophen[69] rings, and also in the vinyl chloride molecule,[70-72] will occur in the vapour phase under relatively severe conditions (400–700°C). In addition to the thiols, the corresponding sulfides and other products are formed, so hindering the isolation of the thiols. These methods therefore have no preparative importance.

The replacement of halogens by a mercapto-group can also be achieved by the action of alkali metal hydrosulfides[73-76] and other inorganic sulfur compounds[77-79] on the corresponding halogen derivatives. As a rule these reactions occur under relatively mild conditions and the wide range and availability of the initial reagents make these methods very valuable in a preparative respect. P_4S_{10} is sometimes used to replace a hydroxyl group by a mercapto-group (see Ref. 80).

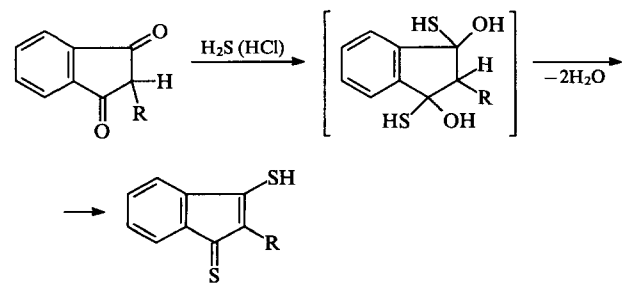
A second variant of thiol preparations based on hydrogen sulfide involves the addition of the latter to unsaturated C≡C, C=C, and C=O bonds. Using irradiation with X-rays, addition of hydrogen sulfide to substituted acetylenes takes place to form dithiols together with other products.[58] The addition of hydrogen sulfide to unsymmetrical ethylene hydrocarbons in the presence of catalysts (H_2SO_4, $AlCl_3$ etc.) takes place preferentially in accordance with Markovnikov's rule but under the action of UV-radiation or in the presence of peroxides the addition is anti-Markovnikov.[55,81-83]



Addition of hydrogen sulfide to the carbonyl group in aldehydes and ketones leads to the formation of 1-hydroxythiols[4] which are stable only if there are strong electron-acceptor groups on the carbonyl carbon atom.

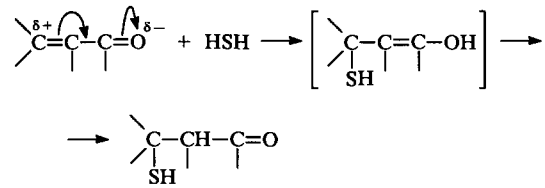


When the molecule of the carbonyl compound contains a labile α-H-atom that can participate in the dehydration process the addition of hydrogen sulfide to the carbonyl group can occur with preservation of a mercapto-group. An example is the preparation of 3-mercaptoindene-1-thiones which are formed in an 85%–90% yield by treating the corresponding diketones with hydrogen sulfide in the presence of hydrogen chloride.[84,85]

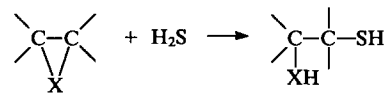


R = H, Et, Ph, 4-$MeOC_6H_4$, 4-ClC_6H_4.

In the presence of catalysts ($ZnCl_2$, HCl etc.) addition of hydrogen sulfide to α,β-unsaturated ketones takes place readily to form relatively stable 3-oxoalkanethiols.[86]



A third variant of the use of hydrogen sulfide in the preparation of thiols involves the opening of unstable rings in certain heterocyclic compounds by the action of hydrogen sulfide. Three-membered heterocyclic compounds, such as thiairans,[87] oxirans,[88] and aziridines[89-91] are used most frequently.



X = S, O, NH.

This method is very important for the preparation of multifunctional thiols containing such groups as NH_2, OH, SH, etc. in addition to the mercapto-group.

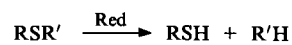
2. Alkylation (or arylation) of sulfur(II) compounds with subsequent breakdown of the products

This method of preparing thiols, which is widely used in practice in the laboratory, is based on forming a C–S bond and then converting the products to thiols. Formation of a C–S bond by means of nucleophilic substitution of a halogen can occur in the reaction of the corresponding alkyl and aryl halides with derivatives of thiocarbonic acid, thiourea, thiocarbamates, dithiocarbamates, xanthogenates, thiophosphonates, and thiosulfonates.[4,77,92,93] These methods are valuable in that the intermediate compounds are readily hydrolysed to thiols; this is very advantageous in a preparative respect and the method is often used in the laboratory to obtain very diverse thiols.

Alcohols in the presence of HBr and dialkyl sulfates are also used for the alkylation of thiourea.[77] Arylation of thiourea and xanthogenates can also be accomplished using diazonium salts.[77]

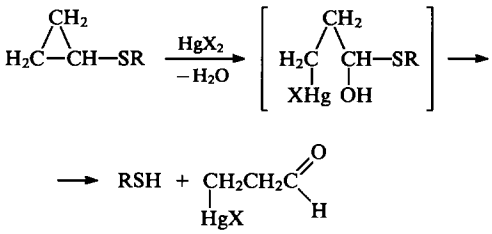
3. Cleavage of sulfides

Although cleavage of a C–S bond occurs more readily than that of a C–C bond or an unactivated C–H bond, the reductive cleavage of sulfides has not been widely used in the preparation of thiols with the exception of special cases. In these cases, as a rule, use is made of sulfides in which there is a distinct tendency to the preferential cleavage of only one of the two C–S bonds, i.e. unsymmetrical sulfides with groups such as allyl, benzyl, nitrile etc. on the sulfur atom.[4]



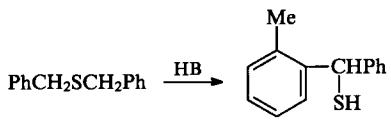
R′ = $ArCH_2$, $CH_2{=}CH{-}CH_2$, CN.

Reducing agents that have been used are lithium in ethylamine, sodium in liquid ammonia, Raney nickel in boiling ethanol, $NaBH_4$ in isopropanol, and also $LiAlH_4$.[94] Cleavage of cyclopropyl-alkyl or -aryl sulfides will take place in the presence of mercury halides or mercury acetate.[95]

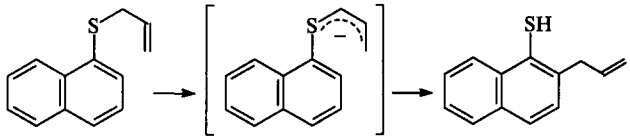


R = Alk, Ar; X = Cl, MeCOO.

Cleavage of alkyl trichloromethyl sulfides[96] is carried out in the presence of hydrochloric acid and that of trifluoromethyl silyl sulfides[97] in the presence of hydrogen iodide. In certain instances reductive cleavage is accompanied by various rearrangements. For example, the cleavage of dibenzyl sulfide in the presence of bases is accompanied by a Sommelet rearrangement.[98]

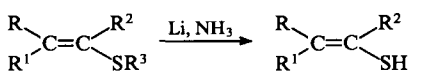


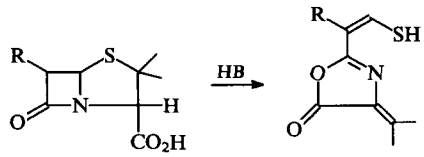
The cleavage of allyl naphthyl sulfides is accompanied by a (3,3)-sigmatropic rearrangement.[99]

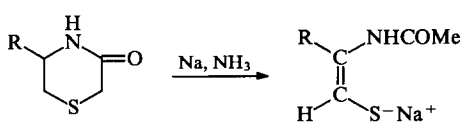


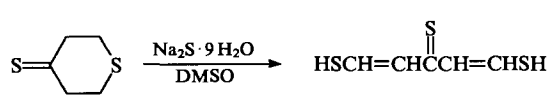
The cleavage of vinyl sulfides by lithium in liquid ammonia[100] provides a method for preparing enethiols, which are also formed by the cleavage of certain heterocyclic compounds.[101-106]

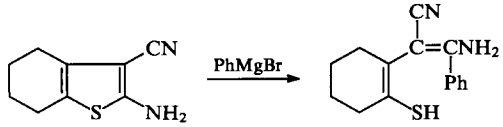
Other heterocyclic compounds, such as penicillin,[107] cyclic allyl sulfides,[108] and thiophene-2-carboxylic acids,[109] will also undergo reductive cleavage to form the corresponding thiols.

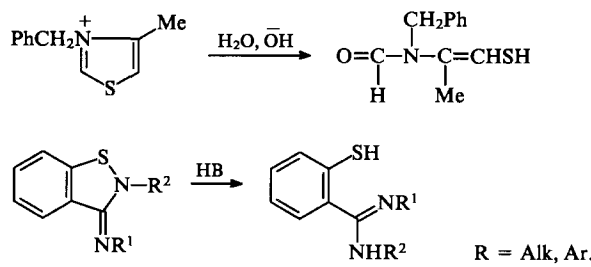








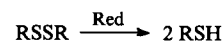




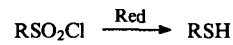
R = Alk, Ar.

4. Reduction of S-functions

The reduction of disulfides and sulfonyl chlorides is of primary importance in the preparation of thiols. The reduction of disulfides is used to prepare aliphatic, aromatic and heterocyclic thiols.



Reducing agents that have been used are zinc in acetic,[110] hydrochloric[111,112] and sulfuric[113] acids, sodium metal in xylene,[114] diethyl ether[115] and liquid ammonia,[116,117] lithium tetrahydroaluminate in ether or tetrahydrofuran,[118] sodium hydrosulfide in alcohol,[119,120] and formamidinesulfinic acid.[121] Triphenylphosphine and sodium hydroborate are also used for the reduction of some disulfides and polysulfides to thiols, and salicylic acid type reagents for the reduction of the disulfide grouping in proteins.[4]



The addition of sulfur monochloride to alkenes followed by reduction of the di-(2-chloroalkyl)disulfides is one of the methods of preparing 2-chloroalkanethiols.[121]

The reduction of sulfonyl chlorides is most often used to prepare aromatic[4,77] and heterocyclic[122] thiols but considerably less often for the preparation of aliphatic thiols.[77]

The reducing agents used are zinc dust in hydrochloric and sulfuric acids,[123-126] tin in hydrochloric acid,[127] tin dichloride,[128] iron powder,[129] aluminium amalgam,[130,131] alkali metal sulfides,[132] red phosphorus and iodine in acetic acid,[133] and lithium tetrahydroaluminate.[134] The last is sometimes used to reduce sulfonic acid to thiols.[135] In rare instances thiols have been prepared by the reduction of sulfinic acids with zinc in an acidic medium[136-138] and of dithiocarbamates with the complex $BH_3 \cdot SMe_2$ in toluene,[139] and also by the reductive cleavage of thiol sulfonates with zinc in an acidic medium.[4]

5. Preparation of thiols from thiones

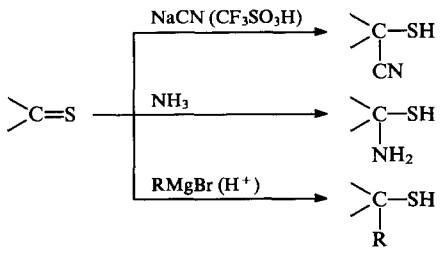
Several variants of thiol preparations based on thiones have been developed. One of these involves the conversion of the thiocarbonyl group to a mercapto-group by the reaction of thiones with butyllithium and also other organometallic compounds.[4,140]



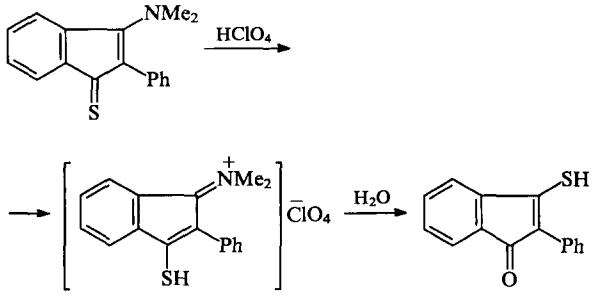
The reaction mixture contains other products as well as thiols, especially sulfides which are formed by the addition of the organometallic compounds at the C = S bond.

It is presumed[4] that the intermediate products in this reaction are dianions formed by the reaction of the thiones with the organometallic compounds. This hypothesis is confirmed to some extent by the fact that the dianion of thiobenzaldehyde is converted to the corresponding thiols and sulfides by reaction with electrophilic reagents.[141]

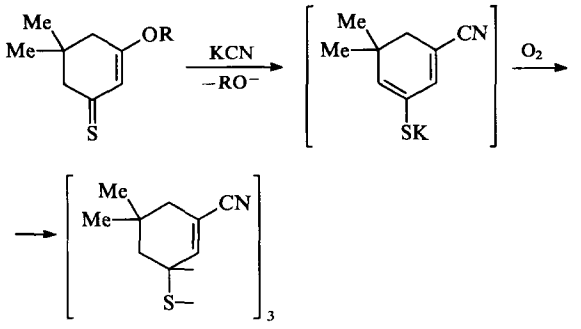
The corresponding thiols are also formed by the reaction of a thiocarbonyl group with hydrocyanic acid,[142,143] ammonia,[144] or Grignard reagents.[145]



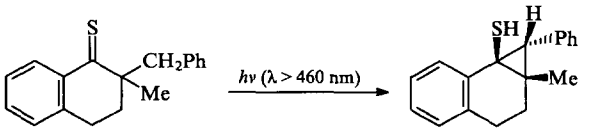
Participation of the thiocarbonyl group in a conjugated bond system facilitates its conversion to a mercapto-group. For example, 3-(*N*,*N*-dimethylamino)-2-phenylindene-1-thione is readily converted, in the presence of perchloric acid in acetone, to *N*,*N*-dimethyl-3-mercapto-2-phenylinden-1-iminium perchlorate which undergoes hydrolysis at the C=N bond to form 3-mercapto-2-phenylinden-1-one.[146]



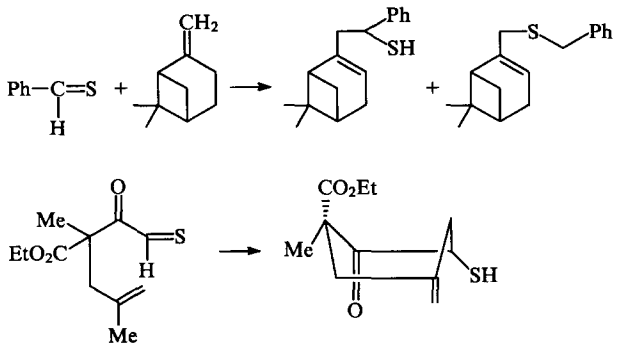
3-Alkoxy-5,5-dimethylcyclohex-2-ene-1-thiones are readily converted, by reaction with potassium cyanide in methanol, to potassium 3-cyano-5,5-dimethylcyclohexa-2,6-diene-1-thiolate, which trimerises to a 1,3,5-trithiane.[147]



2-Benzyl-2-methyltetralin-1-thione is readily converted to an isomeric thiol by UV-irradiation.[148]

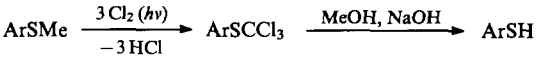


A thiocarbonyl group as a 2π-component can participate in an addition reaction to a C=C bond to form thiols.[149,150]

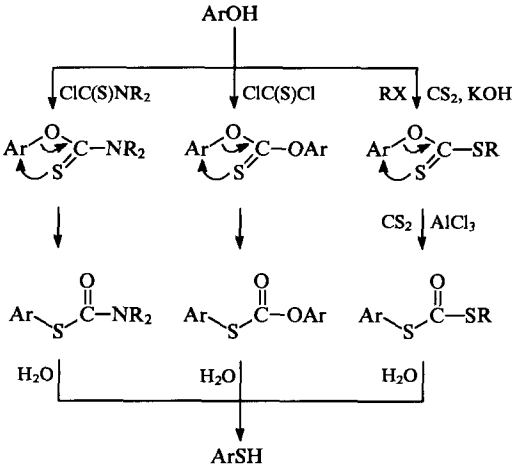


6. Other methods for preparing thiols

One of the methods for converting methyl aryl sulfides to thiophenols is exhaustive chlorination of the methyl group followed by methanolysis of the chlorination product.[151]



The Newman–Kwart rearrangement forms the basis of a method for converting phenols to thiophenols.[4]



The condensation of thiourea with various bifunctional compounds and also the reaction of carbon disulfide with amino- and hydroxyl-containing compounds are widely used in the preparation of heterocyclic thiols.[4,77,152–154]

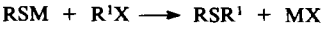
IV. Preparations based on thiols

1. Preparation of sulfur(II) compounds

a. Preparation of sulfides

Several methods have been developed for preparing sulfides from thiols.

Alkylation or arylation of thiols. Symmetrical and unsymmetrical sulfides are formed relatively easily by the reaction of thiols[77,155–159] and metal thiolates[160–171] with alkyl and aryl halides.

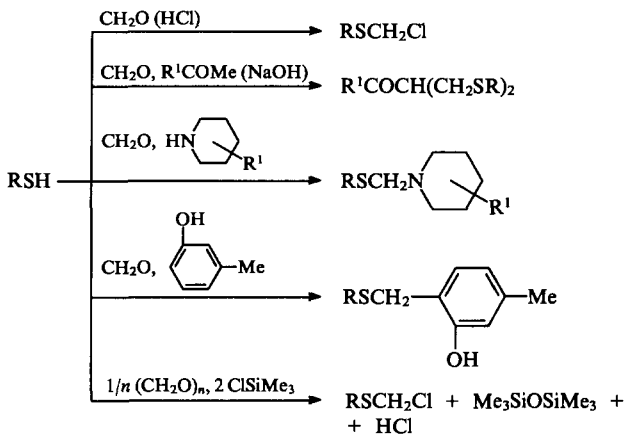


M = H, Na, K, Ag; X = Cl, Br, I;
R = Alk, Ar, Het; R^1 = Alk, Ar.

It is preferable to use alkyl bromides in these reactions because alkyl chlorides are not always sufficiently reactive and alkyl iodides may cause side reactions in which disulfides are formed.[4,77]

$$2RSH + R^1I \longrightarrow RSSR + R^1H + HI$$

The formation of disulfides is also observed when certain alkyl chlorides, especially diphenylchloromethane[172] and carbon tetrachloride,[173] are used. In certain instances the following can be used as alkylating agents: alcohols in the presence of mineral acids,[77,174,175] sodium alkoxides in the presence of phosphonium salts,[176] dialkyl sulfates,[4] dialkyl carbonates,[177,178] alkyl esters of phosphorus acid,[179] phosphoric acid,[180] nitric acid[181] and alkylsulfinic acids,[182] alkoxyformamidines,[183] methyl esters of phenols,[184] alkylamines[185] and diamines,[186] epoxy-[187,188] and thioepoxy-compounds,[4] ethyleneimines,[77] and pyridinium,[189] sulfonium,[190] iodonium[191] and diazonium[77] salts. For the preparation of sulfides containing a methylene group formaldehyde,[192-195] paraformaldehyde[196,197] and trioxane[198] are widely used in a variety of reactions.



The alkylation of thiols by alkyl halides with a normal structure usually takes place by an S_N2 mechanism in which the transition state is additionally stabilised by *d*-orbital resonance.[4]

The reaction of triphenylchloromethane with thiophenol in the presence of bronze filings takes place by a radical mechanism.[199]

$$Ph_3CCl \xrightarrow{\text{bronze}} Ph_3C^{\cdot} + Cl^{\cdot}$$

$$Ph_3C^{\cdot} + PhSH \longrightarrow Ph_3CH + PhS^{\cdot}$$

$$PhS^{\cdot} + Ph_3C^{\cdot} \longrightarrow PhSCPh_3$$

The reactions of perfluoroiodomethanes[200-208] and perfluorobromomethanes[209] with thiolates take place in ultraviolet light by an ion-radical mechanism $S_{RN}1$ (see Ref. 210).

$$RS^- + CF_3I \longrightarrow RS^{\cdot} + [CF_3I]^{\cdot -}$$

$$[CF_3I]^{\cdot -} \longrightarrow \dot{C}F_3 + I^-$$

$$RS^- + \dot{C}F_3 \longrightarrow [RS^{\cdot} + \bar{C}F_3] \longrightarrow [RSCF_3]^{\cdot -}$$

$$[RSCF_3]^{\cdot -} + CF_3I \longrightarrow RSCF_3 + [CF_3I]^{\cdot -}$$

It has been shown[211,212] that the ion-radical perfluoroalkylation reaction is of a general character and can be used with perfluoroalkyl iodides and bromides of any chain length and structure, and also with α,ω-di-iodoperfluoroalkanes.

The reaction of CF_2Br_2 with thiophenoxides takes place by a chain-type carbene mechanism.[213]

$$RS^- + BrCF_2Br \longrightarrow \bar{C}F_2Br + RSBr$$

$$\bar{C}F_2Br \longrightarrow :CF_2 + Br^-$$

$$:CF_2 + RS^- \longrightarrow RS\bar{C}F_2$$

$$RS\bar{C}F_2 + BrCF_2Br \longrightarrow RSCF_2Br + \bar{C}F_2Br$$

It has been shown[206,213] that in the reaction of CF_2BrCl and $PhSCF_2Br$ with thiolates two mechanisms, a carbene and an ion-radical mechanism, may coexist whereas the reaction of $ClCH_2CF_2Cl$, $BrCH_2CF_2Cl$, and $CHCl_2CF_2Cl$ with thiolates takes place via a stage in which hydrogen chloride is eliminated and addition of the thiolate anion to the difluoromethylene group of the halogeno-olefin occurs.[214] One cannot exclude the possibility that replacement of a halogen atom on an unsaturated carbon atom also takes place via a stage in which the hydrogen halide is eliminated.[215-218]

Thus the alkylation of thiols by alkyl halides may take place by different mechanisms, depending primarily on the structure of the initial alkyl halide and also the conditions under which the alkylation reaction is carried out; this has been discussed in detail in a monograph.[219]

The arylation of thiols (or thiolates) by aryl halides in which the halogen atom is activated by the presence of strong electron-acceptor groups in the *ortho* and *para* positions take place relatively easily by an S_N2ar mechanism, the *d* orbitals of the sulfur atom being involved in the stabilisation of the σ-complex.[4,77,220-222] Not only halogen atoms but also other atoms or groups (NO_2, H etc.) which are activated by strong electron-acceptor *ortho* and *para*-substituents can be replaced by an RS group.[34,223] Replacement of an unactivated halogen atom in an aromatic ring by an RS group will take place under relatively severe conditions,[224-232] presumably by an elimination-addition mechanism.[227] Arylation of the silver salt of trifluoromethanethiol can be accomplished using aryldiazonium salts.[228]

Thiylation of unsaturated compounds. Sulfides are formed relatively easily by the addition of thiols to unsaturated bonds (C=C, C=O, and C=N). The addition of thiols to compounds containing a C=C bond has been known for a long time and has been comparatively well studied.[4,11,12] Many of these reactions form the basis of methods for preparing sulfides.

Depending on the conditions, the addition of thiols to an ethylenic bond may occur by a nucleophilic, an electrophilic, or a radical mechanism. Nucleophilic addition of a thiol to an ethylenic bond usually takes place in an alkaline medium or in the presence of basic catalysts and the species attacking the sp^2-hybridised carbon atom are thiolate anions.

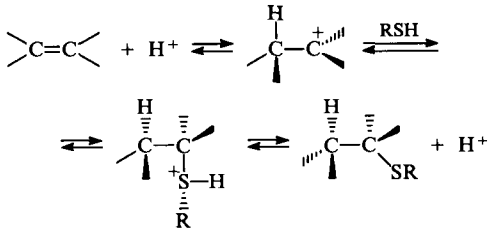
$$RSH + \bar{O}H \longrightarrow RS^- + HOH$$

$$RS^- + \rangle C{=}C\langle \longrightarrow RS{-}\overset{|}{C}{-}\overset{|}{\bar{C}}{-} \xrightarrow{HOH} RS{-}\overset{|}{C}{-}\overset{|}{C}H{-}$$

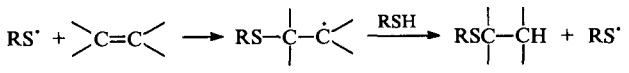
Nucleophilic addition of thiols to a polarised double bond will therefore take place readily if there are electronegative atoms or electron-acceptor groups present at the double bond. The thiyl fragment is attached to the electron-deficient carbon atom in the double bond which is usually in the β position (addition in accordance with Markovnikov's rule). There have been reports of the nucleophilic addition of thiols to acrolein,[77] vinylidene chloride[229,230] acrylonitrile,[231,232]

unsaturated carboxylic acids and their esters,[232–235] also other unsaturated carbonyl compounds,[235–239] unsaturated sulfones,[240,241] vinylpyridines,[242] vinylpyrroles,[243] and vinylpyrazoles.[244] The nucleophilic addition of thiols to maleinimides is used for the modification of thiol enzymes in studies of the interrelation of their structure and function.[4] For example, to determine the number of SH groups in proteins, and also to ascertain the reactivity of these groups, use is often made of the fluorescing agent *N*-(fluoranthen-3-yl)maleinimide, which combines with the protein by reacting with its SH groups.

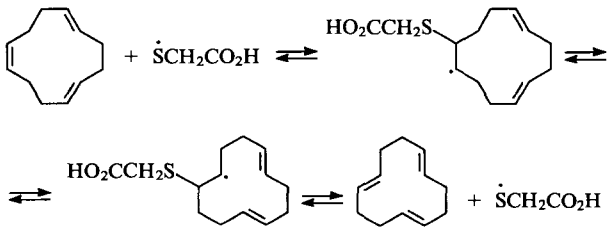
Electrophilic addition of thiols to a double bond[244,245] takes place in an acidic medium or in the presence of acidic catalysts (HCl, $AlCl_3$, SO_2Cl_2 etc.) via a stage in which a carbocation is formed.[12]



Anti-Markovnikov radical addition of thiols to a double bond takes place in the presence of peroxides or under the influence of ultraviolet light (photo-addition) and is often accompanied by isomerisation of the initial unsaturated compounds.[11,12,246]

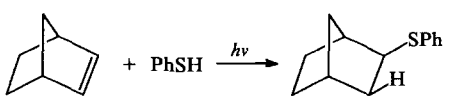


The involvement of thiyl radicals in the isomerisation of unsaturated compounds has been noted.[4] For example, in the presence of 1 equivalent of thioglycolic acid (*Z*, *E*, *E*)-cyclododeca-1,5,9-triene is readily converted to the corresponding (*E*, *E*, *E*)-isomer by an 'insertion–detachment' mechanism.[247]

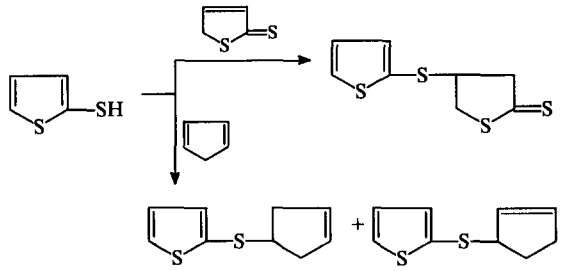


On account of the unusual tendency of thiyl radicals to react preferentially with the (*Z*)-alkene grouping, this method of isomerisation has been used in organic syntheses, especially for the conversion of oleic acid to (*E*)-octadec-9-enoic acid which will take place in the presence of ethanethiol.[248]

The photo-addition of thiols to a C=C bond usually gives products whose stereochemistry is dependent on the structure of the initial unsaturated compound. For example, in the photothiylation of norbornene an *exo-cis* adduct is formed.[4]



In view of the fact that thiyl radicals are easily obtained from thiols, e.g. by irradiation with light of wavelength 253.7 nm, it is likely that the autothiylation of thiophen-2-thiol[249,250] and the addition of the latter to cyclopentadiene[251] also take place by a radical addition mechanism.

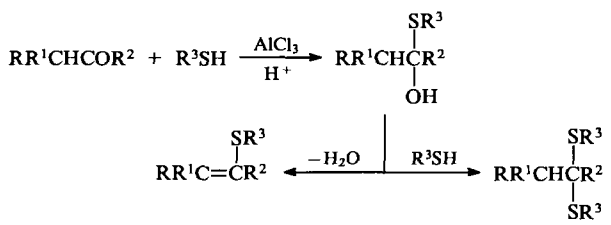


Unsaturated sulfides are also readily formed by the addition of thiols to acetylenic hydrocarbons.[4,11,12] The addition of thiols to a triple bond may take place by either a nucleophilic or a radical mechanism. Nucleophilic addition of thiols to an acetylenic bond takes place in an alkaline medium and, depending on the reaction conditions, the type of solvent, and also the structure of the reagents, it can give products with different steric structures. There have been reports of the nucleophilic addition of thiols to acetylene,[252,253] phenylacetylene,[254,255] alkoxyacetylenes,[256–258] acetylacetylenes,[259,269] acetylenecarboxylic acids and their derivatives,[261–263] diethoxyphosphonylacetylene,[264] alkylsulfonylacetylenes,[265] trialkylgermylacetylenes,[266] and diacetylenes.[267] The nucleophilic addition of thiols to alkylthioacetylenes,[12,268] occurs particularly easily due to the additional stabilisation of the intermediate carbanion involving the 3*d* orbitals on the sulfur atom.



Radical addition of thiols to a triple bond takes place on irradiation with ultraviolet light or in the presence of initiators of radical processes (peroxides, hydroperoxides, azo-compounds etc.) that facilitate the generation of thiyl radicals. The radical addition of thiols to acetylene[269,270] will occur under severe conditions but the addition of thiols to prop-2-yn-1-ol,[12] phenylacetylene,[12] ethoxyacetylene,[271] ethoxycarbonylacetylene,[271] acetylenecarboxylic acid,[271] 1-carboxy-2-ethylthioacetylene,[272] vinylacetylene,[273] trialkylsilylacetylene,[274,275] and 1-phenyl-2-trialkylsilylacetylene[276] takes place comparatively easily by a radical mechanism.

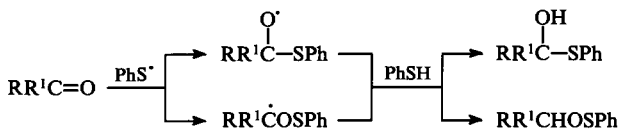
The addition of thiols to the C=O bond in carbonyl compounds in the presence of acidic catalysts produces unstable sulfides containing an α-hydroxyl group which can undergo dehydration to form unsaturated sulfides[277] or react with excess of the thiol to give thioacetals.[278,279] This method of obtaining thioacetals has been widely used in the laboratory for preparative purposes.



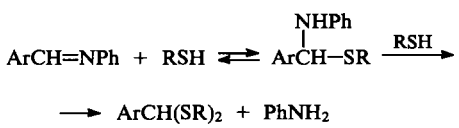
The addition of thiols to carbonyl compounds in the presence of trialkylchlorosilanes results in the formation of sulfides containing a trialkylsiloxy group in the α-position.[280]



In the radical addition of thiols to the C=O bond in carbonyl compounds the thiyl radical may be attached to either the carbon or the oxygen atom of the carbonyl group.[281,282]



The addition of thiols to the C=N bond in imines results in the formation of α-aminosulfides which, in the presence of excess of the thiol, can also be converted to thioacetals;[283-287] this method is of preparative importance and is widely used in the laboratory.



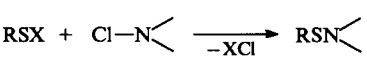
Condensation of thiols. The intermolecular condensation of thiols, which occurs at high temperatures or in the presence of catalysts, is sometimes used to obtain sulfides.



In the case of β-mercaptoanthraquinone condensation takes place with little heating[77] but with other aromatic thiols it occurs at higher temperatures.[224] By using such catalysts as cadmium or zinc sulfide, aluminium oxide[77] or aluminium trichloride[286,287] the temperature of this reaction can be reduced slightly.

b. Preparation of sulfenamides.

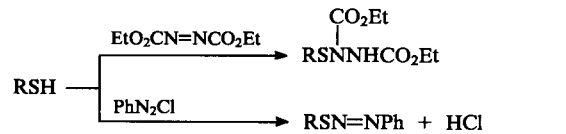
The amination of thiols by *N*-chloroamines,[288-290] *N*-chloroamides,[291] or *N*-chloroimides[292-294] is one of the methods of preparing sulfenamides that are either unsubstituted or substituted at the nitrogen atom.

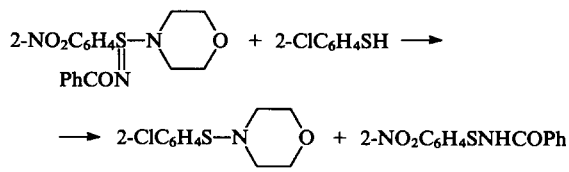


R = Alk, Ar, Het;

X = Na, H.

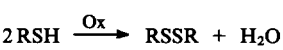
Rather more rarely aliphatic amines in the presence of oxidising agents,[290,295] the sodium salt of hydroxylaminosulfonic acid,[296] and derivatives of oxaziridine[297] have been used as aminating agents. Sulfenamides are also formed by the reaction of thiols with azo- and diazo-compounds[4] and with certain derivatives of iminosulfinic acids[298] but these methods have no preparative value.



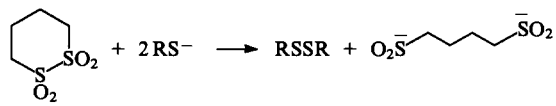


c. Preparation of disulfides

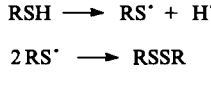
The oxidation of thiols using various oxidising agents is one of the most common methods of preparing disulfides.[4]



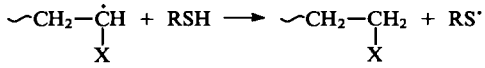
A wide range of reagents can be used as oxidants, including oxygen,[299] hydrogen peroxide,[300] halogens and halogenating agents,[4,301-304] *N*-halogenoamines and *N*-halogenoamides,[4,305] iron trichloride,[77] 1,3-di-iodopropyne,[306] carbon tetrachloride,[307] and other organic and inorganic reagents. On account of the possible further oxidation of the disulfides the choice of a suitable oxidant is of considerable importance and is conditional on the ease of oxidation, which increases from tertiary to secondary and primary mercaptans and even more for thiophenols.[77] The oxidation of a mercapto-group to a disulfide group plays an important role in the formation of the tertiary structure of proteins and also in other biochemical processes. Flavins will anaerobically oxidise an excess of a thiol to a disulfide and are reduced to dihydroflavins.[308] The tetraoxide of 1,2-dithiane oxidises thiolate ions to the disulfide quantitatively.[309]



This reaction is presumed to occur in biological systems.[4] In the presence of pyridine the dimethyl ester of dithiobis(thioformic acid) oxidises thiols to disulfides in a quantitative yield.[310] Photolysis or radiolysis of thiols and sulfides gives thiyl radicals which form disulfides by recombination or reaction with the solvent molecules.[4,311,312]



Owing to the ease with which thiyl radicals are formed, thiols are used as radical interceptors in various processes such as radiation protection,[4] the stabilisation of polymeric materials,[8] and the control of chain growth in radical-chain reactions.[313] For example, dodecyl mercaptan is widely used in industry as a regulator of molecular mass.[314] The basis of this process is the reaction:



A whole series of methods for preparing both symmetrical and unsymmetrical disulfides is based on nucleophilic substitution involving thiols or thiolate anions and various sulfenyl derivatives such as sulfenyl halides,[315-327] sulfenyl thiocyanates,[4,77,328] sulfenamides,[329-333] symmetrical disulfides[334-336] and tri-sulfides,[337] thiosulfonates,[4,77] and Bunte salts.[4,77]

$$RSX + R^1SY \longrightarrow RSSR^1$$

R = Alk, Ar, Het; R^1 = Alk, Ar; X = H, Na, Ag;
Y = Cl, Br, NR^2, NHAr, N-phthalimido,
SR^2, SSR^2, SO_2Ar, SO_2Na, SCN.

In view of the extensive possibilities for varying R and R^1, some of these methods, especially the reaction of thiols with sulfenyl halides, have become irreplaceable for the synthesis of unsymmetrical disulfides.

The esters $RSSCO_2Me$, which are obtained by the reaction of thiols with methoxycarbonylsulfenyl chloride, readily react with thiols to form disulfides.

$$RSH + MeO_2CSCl \longrightarrow RSSCO_2Me \xrightarrow{R^1SH} RSSR^1 + HO\overset{\overset{S}{\|}}{C}OMe$$

The so-called cyanogen bromide method for converting thiols to unsymmetrical disulfides[339] involves the reaction of the thiol with a sulfenyl bromide which is formed by the reaction of cyanogen bromide with a sodium thiolate.

$$RSNa + BrCN \xrightarrow[-NaCN]{} [RSBr] \xrightarrow[-HBr]{R^1SH} RSSR^1$$

A convenient method for obtaining unsymmetrical disulfides is the reaction of thiols with the diethyl ester of azodicarboxylic acid followed by cleavage of the resultant adduct.[4]

$$RSH + EtO_2CN{=}NCO_2Et \longrightarrow EtO_2CNH\overset{\overset{SR}{|}}{N}CO_2Et \xrightarrow{R^1SH} RSSR^1 + (EtO_2CNH)_2$$

d. Preparation of thiocyanates and sulfenyl thiocyanates.
The reaction of thiolate anions or heavy metal thiolates with cyanogen halides leads to the formation of thiocyanates.[4] This reaction has been used as a basis for developing the synthesis of labelled thiocyanates.[340]

$$RSH + BrCN \xrightarrow[-HBr]{} RSCN \xrightarrow{^{35}\bar{S}H} R^{35}SH \xrightarrow{BrCN} R^{35}SCN$$

4-Dimethylamino-1-cyanopyridinium perchlorate and fluoroborate[341] and 2-nitro-5-thiocyanatobenzoic acid[342] have also been used as cyanating agents.

The reaction of thiols with thiocyanogen gives sulfenyl thiocyanates and the further reaction of these products with the thiol can give a disulfide. This sequence of reactions has been proposed as a basis for synthesising cystine.[343]

$$XSH + (SCN)_2 \longrightarrow XSSCN \xrightarrow{HSY} XSSY$$

X = $HO_2C\overset{\overset{NH_2}{|}}{C}HCH_2$; Y = $HO_2C\overset{\overset{NH_2\cdot HCl}{|}}{C}HCH_2$

e. Preparation of thionitriles and thionitrates
Thiols react with nitrous acid in the cold to form *S*-nitroso-compounds or thionitrites; these are comparatively stable only in the case of tertiary thiols.[344]

$$RSH + HONO \xrightarrow{0\,^\circ C} RSNO + H_2O$$

R = Bu^t, MeCO.

Nitrosyl chloride and esters of nitrous acid are also used as nitrosating agents.[344] The reaction of thiols with an equivalent quantity of nitrogen(IV) oxide also results in the formation of thionitrites which, in the presence of excess of the oxide, are converted to thionitrates.[345]

$$RSH \xrightarrow{N_2O_4} RSNO \xrightarrow{N_2O_4} RSNO_2$$

R = Bu^t, MeCO.

f. Preparation of thiolic esters
The acylation of thiols with acyl chlorides is the main method of preparing thiolic esters of carboxylic acids.[77]

$$RSH + R^1COCl \xrightarrow[-HCl]{} RS\overset{\overset{O}{\|}}{C}R^1$$

This reaction often proceeds very smoothly even in the absence of bases but it is usually carried out by the Schotten–Baumann method[77] or in the presence of pyridine and triethylamine. Thiolates of alkali metals[346] and other metals[347] are sometimes used instead of thiols, and carboxylic acids[348,349] and their anhydrides[350] and acyl azides[346] are also used as acylating agents. The addition of thiols to ketene gives thiolic esters of acetic acid[4] but this method is hardly used in the laboratory because ketene is not readily available.

$$RSH + CH_2{=}C{=}O \longrightarrow RSCOMe$$

The preparation of thiolic esters of benzenesulfinic acid by the reaction of thiols with benzenesulfinyl azide has been reported.[351]

$$PhSON_3 + RSH \xrightarrow[-HN_3]{20\,^\circ C} PhS\overset{\overset{O}{\|}}{S}R$$

Thiolic esters of sulfonic acids are formed by the reaction of sodium thiolates with sulfonyl chlorides.[352]

$$RSNa + PhSO_2Cl \xrightarrow[-NaCl]{} PhSO_2SR$$

g. Preparation of compounds containing Si–S bonds
Alkali metal thiolates react with silicon tetrachloride comparatively easily to form tri(alkylthio)chlorosilanes or tetra(alkylthio)silanes, depending on the reagent ratio.[353,354]

$$SiCl_4 \xrightarrow[-3\,NaCl]{3\,RSNa} (RS)_3SiCl$$
$$SiCl_4 \xrightarrow[-4\,NaCl]{4\,RSNa} (RS)_4Si$$

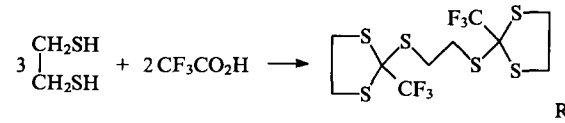
R = Me, Et, Pr.

Trihalogenoalkylsilanes,[355] trialkylchlorosilanes,[356,357] and alkylsilazanes[358,359] can also be used for the silylation of thiols.

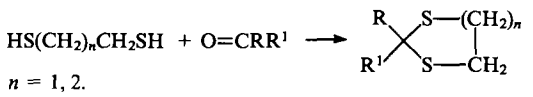
h. Preparation of heterocyclic compounds

A whole series of syntheses of various heterocyclic compounds have been developed on the basis of reactions characteristic of SH groups. These syntheses usually involve the use of thiols containing two SH groups or polyfunctional thiols.

Syntheses based on dithiols

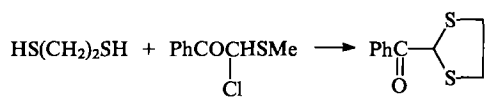


Ref. 360

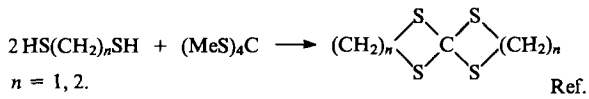


n = 1, 2.

Ref. 361

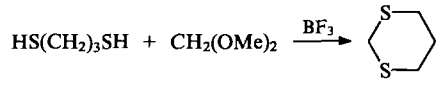


Ref. 362

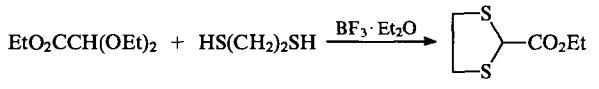


n = 1, 2.

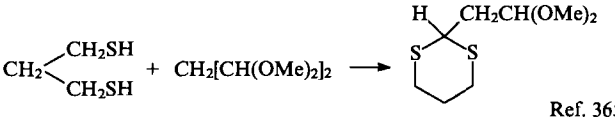
Ref. 363



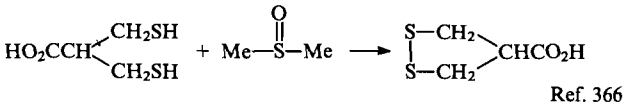
Ref. 363



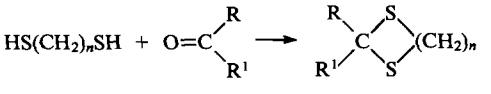
Ref. 364



Ref. 365

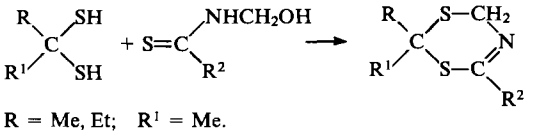


Ref. 366



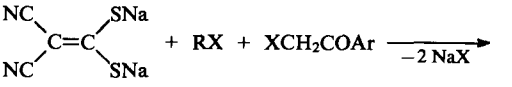
Ref. 367

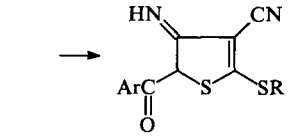
R = Me, Et; R^1 = Me.



R = Me, Et; R^1 = Me.

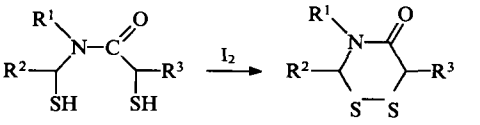
Ref. 367





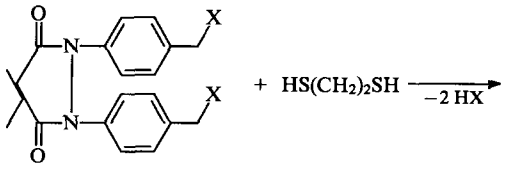
Ref. 368

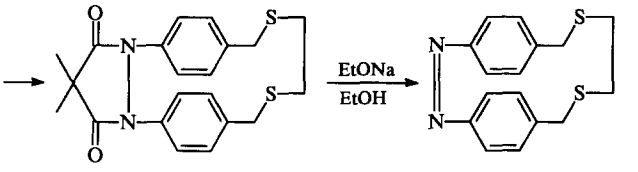
R = Me, Et; Ar = Ph, 4-ClC_6H_4, 4-MeC_6H_4, 4-$MeOC_6H_4$.



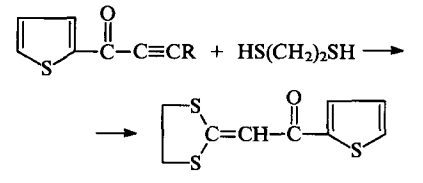
Ref. 369

R^1 = Alk; R^2 = CONHPh, CO_2Et.

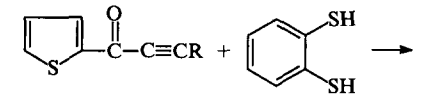




Ref. 370

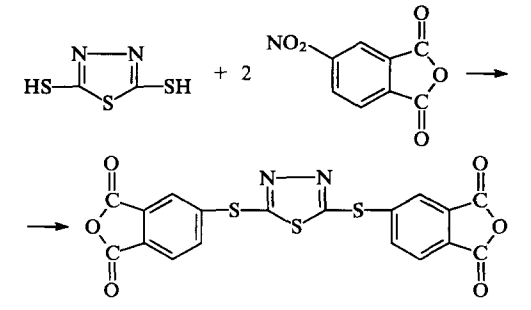


(371)



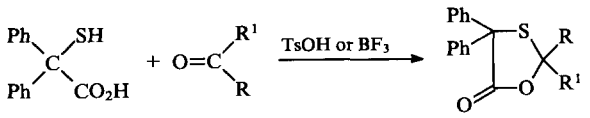
Ref. 371

R = H, Ph.

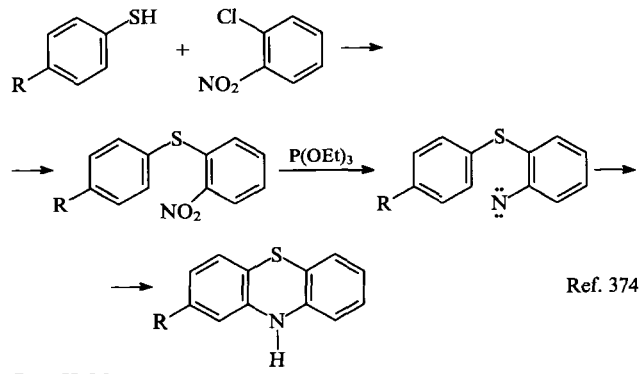


Ref. 372

Syntheses based on polyfunctional thiols

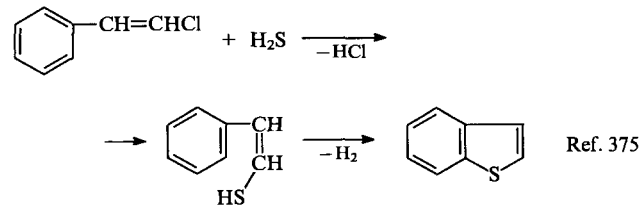


R = Me, Et; R^1 = Me. Ref. 373

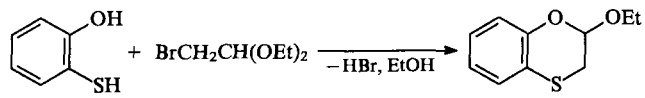


Ref. 374

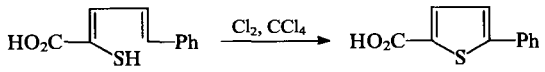
R = H, Me.



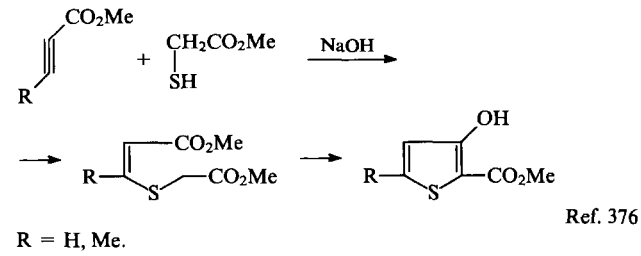
Ref. 375



Ref. 376

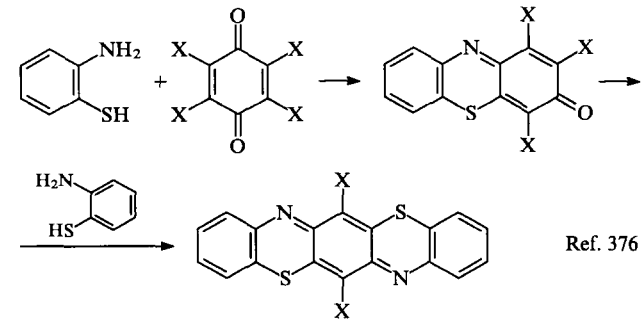


Ref. 376



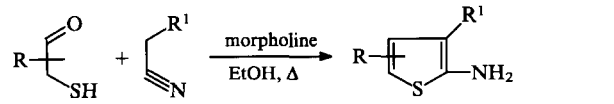
Ref. 376

R = H, Me.



Ref. 376

X = Cl, Br.



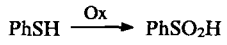
Ref. 376

R = Me, Et; R^1 = H, Me.

2. Preparation of sulfur(IV) compounds

a. Preparation of sulfinic acids and their derivatives

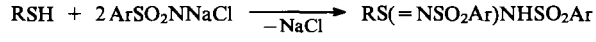
The oxidation of thiols in order to obtain sulfinic acids is only used in rare instances because the sulfinic acids formed can easily be oxidised to sulfonic acids. However in certain instances[4,377-379] oxidation is nevertheless used for the preparation of sulfinic acids.



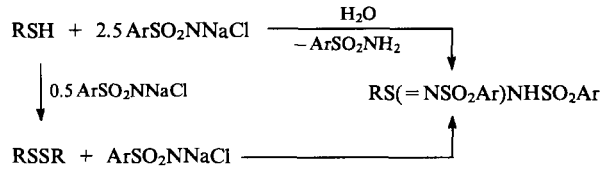
The oxidising agents used are chlorine, bromine, iodine, hydrogen peroxide, and *m*-chloroperbenzoic acid. Oxidative chlorination of thiols is sometimes used to prepare sulfinyl chlorides.[380,381] Esters of sulfinic acids are formed by oxidising thiols with lead tetra-acetate in the presence of alcohols.[4]

b. Preparation of amides of iminosulfinic acids

Oxidative imination of thiols with *N*-chloro-compounds. The first examples of amides of iminosulfinic acids, viz. *N*-(arenesulfonyl)amido-*N'*-(arenesulfonyl)-iminosulfinic acids or *N*,*N'*-bis(arenesulfonyl)sulfinamidines, were obtained by the reaction of thiols with sodium salts of chloroamides or sulfonic acids in aqueous solution.[382]



The yield of the sulfinamidine in this reaction is low because some of the sodium salt of the chloroamide is used to oxidise the thiol to a disulfide.



The formation of disulfides as intermediates has also been observed in the oxidative imination (using sodium salts of the chloroamides of sulfonic acids) of alkanethiols,[383] arylthiols,[384] 8-mercaptoquinoline,[385] and arylcarbamoyl-[386] and alkoxycarbonyl-methanethiols.[387] It follows that the imination of thiols and of disulfides by sodium salts of chloroamides of sulfonic acids are similar processes and the first stage of the imination of a thiol is its oxidation to a disulfide. This stage is not rate-determining because the rate of oxidation of the thiols to disulfides by various oxidising agents decrease in the order ArSH > $ROOCCH_2SH$ > AlkSH,[82] whereas the reactivity of thiols towards the sodium salts of chloroamides of sulfonic acids varies in the reverse order and is dependent on their acidic properties.[384] Thiols with $pK_a > 7$ undergo imination by the sodium salts of chloroamides comparatively readily. A reduction in the pK_a of the thiol to 5–6 leads to a reduction in the rate of imination and in the yield of the sulfinamidine. Thiols with $pK_a < 5$ do not undergo imination by the sodium salts of the chloroamides of sulfonic acids. Such thiols usually have strong electron-acceptor groups on the sulfur atoms, so making it less nucleophilic. Imination of thiols by *N*-chloroamides of carboxylic acids[388,389] and phosphoric acids[390] can be carried out in anhydrous organic solvents in the presence of pyridine.

$$2\,RSH + 5\,AcNHCl + 4\,C_5H_5N \longrightarrow$$
$$\longrightarrow 2\,RS(=NAc)NHAc + AcNH_2 + C_5H_5N\cdot Cl_2 + 3\,C_5H_5N\cdot HCl$$

R = Alk, Ar, Het; Ac = ArCO, $(PhO)_2PO$.

Oxidative imination of sodium thiolates with *N*-dichloro-compounds. The reaction of sodium thiolates with the dichloroamides of sulfonic acids in anhydrous organic solvents gives the sodium salts of *N,N'*-disubstituted amides of iminosulfinic acids.[391]

$$5\,RSNa + 2\,ArSO_2NCl_2 \xrightarrow[-4\,NaCl]{}$$
$$\longrightarrow RS(=NSO_2Ar)N(Na)SO_2Ar + 2\,RSSR$$

This reaction has been widely used for alkanethiols,[383,392] derivatives of thiourea,[393] 8-mercaptoquinoline,[394-397] and other heterocyclic thiols.[398-400] The dichloroamides of carboxylic acids[401-404] and phosphoric acids[405] and also *N,N*-dichlorodicyanoethylurea[406] have been used as iminating agents. The reactivity of the sodium thiolates towards the *N*-dichloroamides is dependent on the acidic properties of the thiol.[407] The sodium salts of thiols with $pK_a > 8$ undergo imination by *N*-dichloroamides comparatively readily but a reduction in the pK_a of the thiol to 5–7 lead to a reduction in the reactivity of the sodium thiolate towards *N*-dichloroamides. The sodium salts of thiols with $pK_a < 5$ do not undergo imination by *N*-dichloroamides. The intermediates in this reaction were found[408] to be *N*-(arylsulfenyl)-*N,N'*-bis(arenesulfonyl)arylsulfinamidines which are also formed in the reaction of sodium thiophenolates with dichloroamides of sulfonic acids in anhydrous carbon tetrachloride when the reagents are in a 4:2 ratio.[409]

$$4\,RSNa + 2\,ArSO_2NCl_2 \xrightarrow[-4\,NaCl]{}$$
$$\longrightarrow RS(=NSO_2Ar)N(SR)SO_2Ar + RSSR$$

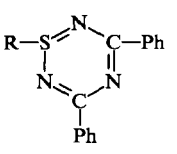
It is presumed[408] that these compounds are formed due to the following reactions:

$$2\,RSNa + 2\,ArSO_2NCl_2 \longrightarrow 2\,RSCl + 2\,ArSO_2NNaCl;$$
$$2\,RSCl + 2\,RSNa \longrightarrow 2\,RSSR + 2\,NaCl;$$
$$2\,ArSO_2NNaCl + RSSR \xrightarrow[-2\,NaCl]{} RS(=NSO_2Ar)N(SR)SO_2Ar.$$

In the presence of an additional mole of the sodium thiophenolate cleavage of the *N*-(arylsulfenyl)-*N,N'*-bis(arenesulfonyl)arylsulfinamidine takes place to form a disulfide and the sodium salt of the *N,N'*-bis(arenesulfonyl)arylsulfinamidine.[408]

$$RS(=NSO_2Ar)N(SR)SO_2Ar + RSNa \longrightarrow$$
$$\longrightarrow RS(=NSO_2Ar)N(Na)SO_2Ar + RSSR$$

The reaction of sodium thiolates with *N*-chloro- and *N*-bromobenzamidines gives cyclic amides of iminosulfinic acids.[410]

$$RSNa + 2\,PhC(=NH)NHX \longrightarrow$$
$$\longrightarrow$$  $$+ NH_4X + NaX$$

X = Cl, Br.

c. Preparation of iminosulfinyl chlorides

The formation of iminosulfinyl chlorides by the reaction of thiophenols with dichloroamides of sulfonic acids may take place via the following reactions, depending on the reagent ratio and the order in which the reagents are mixed[484] [incorrect reference (Ed. of Translation)]:

$$2\,ArSH + PhSO_2NCl_2 \longrightarrow 2\,ArSCl + PhSO_2NH_2;$$
$$2\,ArSCl + 2\,PhSO_2NCl_2 \longrightarrow 2\,ArS(=NSO_2Ph)Cl + Cl_2;$$
$$2\,ArSCl + 2\,ArSH \xrightarrow[-2\,HCl]{} 2\,ArSSAr;$$
$$ArSSAr + 2\,PhSO_2NCl_2 \longrightarrow 2\,ArS(=NSO_2Ph)Cl + Cl_2.$$

The formation of arenesulfonamides as by-products makes it difficult to isolate the iminosulfinyl chlorides. Consequently the preparation of iminosulfinyl chlorides from disulfides and *N*-dichloro-compounds is more convenient for preparative purposes.[411-417]

$$RSSR + 2\,R^1NCl_2 \xrightarrow[-Cl_2]{} 2\,RS(=NR^1)Cl$$

R = Alk, Ar; R^1 = $ArSO_2$, ArCO, Bu^t.

3. Preparation of sulfur(VI) compounds

a. Preparation of sulfonic acids

Thiols are readily converted to sulfonic acids by the action of strong oxidising agents.[77] A number of methods for preparing sulfonic acids have been developed on the basis of this reaction.

$$RSH \xrightarrow{Ox} RSO_3H$$

R = Alk, Ar, Het.

The oxidation of thiols to sulfonic acids takes place via a number of stages in which the intermediate compounds are disulfides, sulfinic and sulfonic acids. For example, the oxidation of thiols by the $Ti^{III}-H_2O_2$ system or Ce^{IV} salts leads to the successive generation of thiyl, sulfinyl and sulfonyl radicals, from which the final products are formed.[4] In biological systems inclusion of sulfur in the metabolism occurs starting with the oxidation of cysteine to alanine-3-sulfinic acid, which is subsequently converted to a β-sulfenylpyruvate, sulfite ions, and finally sulfate ions.

A method for preparing aliphatic sulfonic acids is based on the addition of thiols to alkenes followed by oxidation of the resultant thioethers by hydrogen peroxide in acetic acid.[4]

$$RCH{=}CH_2 + AcSH \xrightarrow{h\nu} RCH_2CH_2SAc \xrightarrow{H_2O_2}$$
$$\longrightarrow RCH_2CH_2SO_3H$$

b. Preparation of sulfonyl chlorides

Oxidative chlorination of aromatic and heterocyclic thiols with chlorine in glacial acetic acid gives the corresponding sulfonyl chlorides.[77]

$$RSH + Cl_2 \xrightarrow[-HCl,\,MeCOCl]{MeCOOH} RSO_2Cl$$

Oxidative chlorination of aliphatic thiols occurs in aqueous solution.[418]

$$RSH + 3\,Cl_2 + 2\,H_2O \longrightarrow RSO_2Cl + 5\,HCl$$

Oxidative chlorination of thioglycolic acid in concentrated hydrochloric acid gives dichloromethanesulfonyl chloride.[419]

$$HO_2CCH_2SH + Cl_2 \xrightarrow{HCl\,+\,H_2O} HO_2CCH_2SO_2Cl \xrightarrow[-2\,HCl]{Cl_2}$$
$$\longrightarrow [HO_2CCCl_2SO_2Cl] \xrightarrow[-CO_2]{} CHCl_2SO_2Cl$$

In this review an attempt has been made to demonstrate the great synthetic potentialities for fine-organic synthesis which lie hidden in a class of organosulfur compounds that is, on the face of it, just ordinary, viz. thiols. In the review thiols are discussed only as synthons although there are other reactions involving thiols which have no synthetic value but play an important role in various fields of human activity (e.g. the purification of petroleum from sulfur compounds etc.).

References

1. G Lowe *Tetrahedron* **32** 291 (1976)
2. L E Anderson, M Avron *Plant. Physiol.* **57** 209 (1976)
3. N Sabadie-Pialoux, S Abou-Khalil, D C Gautheron *J. Microsc. Biol. Cell.* **28** 19 (1976)
4. D Barton, W D Ollis (Eds) *Comprehensive Organic Chemistry* Vol. 5 (Translated into Russian; Moscow: Khimiya, 1983) Vol. 5, p. 134
5. G A Melent'eva, in *Farmatsevticheskaya Khimiya* (Pharmaceutical Chemistry) (Moscow: Meditsina, 1968) p. 414
6. G A Blokh, in *Organicheskie Uskoriteli Vulkanizatsii Kauchukov* (Organic Accelerants of the Vulcanisation of Rubber) (Leningrad: Khimiya, 1972) p. 241
7. G A Blokh, in *Organicheskie Uskoritseli Vulkanizatsii i Vulkaniziruyushchie Sistemy dlya Elastomerov* (Organic Accelerants of Vulcanisation and Vulcanising Systems of Elastomers) (Leningrad: Khimiya, 1973) p. 25
8. J Voigt *Stabilisation of Plastics against Light and Heat* Monographs on Chemistry, Physics, and Technology of Plastics, No. 10 (Berlin: Springer, 1966) (Translated into Russian; Leningrad: Khimiya, 1972)
9. G F Bol'shakov, A R Belous, E I Gulin, E A Glebovskaya, in *XII Nauchnaya Sessiya po Khimii i Tekhnologii Organicheskikh Soedinenii Sery i Sernistykh Neftei, Riga, 1971 (Tezisy Dokladov)* (Abstracts of Papers for the Twelfth Scientific Session on the Chemistry and Technology of Organic Sulfur Compounds and Sulfurous Petroleum, Riga, 1971) p. 388
10. A F Aksenov, Ya V Chertkov, V G Spirin, K S Chernova, A A Litvinov, S G Klimov, V I Terekhin, A A Shepel', in *XII Nauchnaya Sessiya po Khimii i Tekhnologii Organicheskikh Soedinenii Sery i Sernistykh Neftei, Riga, 1971 (Tezisy Dokladov)* (Abstracts of Papers for the Twelfth Scientific Session on the Chemistry and Technology of Organic Sulfur Compounds and Sulfurous Petroleum, Riga, 1971) p. 390
11. E N Prilezhaeva, M F Shostakovskii *Usp. Khim.* **32** 897 (1963) [*Russ. Chem. Rev.* **32** 399 (1963)]
12. S Oae, in *Organic Chemistry of Sulfur* (New York: Plenum) (Translated into Russian; Moscow: Khimiya, 1975) p.62
13. G C Barrett, in *Organic Compounds of Sulphur, Selenium and Tellurium* Vol.1, Chemical Society, London, 1970, p. 49
14. G C Barrett, in *Organic Compounds of Sulphur, Selenium and Tellurium* Vol. 3, Chemical Society, London, 1973, p. 1
15. G C Barrett, in *Organic Compounds of Sulphur, Selenium and Tellurium* Vol. 3, Chemical Society, London, 1975, p. 1
16. G C Barrett, in *Organic Compounds of Sulphur, Selenium and Tellurium* Vol. 4, Chemical Society, London, 1977, p. 1
17. M Toshiaki *J. Synth. Org. Chem. Jpn.* **43** 969 (1985)
18. G Richards, P G Urbem, P M Radley *Spec. Chem.* **7** 294 (1987)
19. M G Voronkov, E N Deryagina *Usp. Khim.* **59** 1338 (1990) [*Russ. Chem. Rev.* **59** 778 (1990)]
20. S M Benson *Chem. Rev.* **78** 23 (1978)
21. A J Colussi, S M Benson *Int. J. Chem. Kinet.* **9** 295 (1977)
22. S H Marcus, S I Miller *J. Am. Chem. Soc.* **88** 3719 (1966)
23. F G Bordwell, H M Andersen *J. Am. Chem. Soc.* **97** 3226 (1975)
24. M M Kreevoy, E T Harper, R E Duvall, H S Wilcus, L T Ditsch *J. Am. Chem. Soc.* **85** 4899 (1962)
25. D L Yabroff *Ind. Eng. Chem.* **33** 257 (1940)
26. Yu A Bankovskii *Khimiya Vnutrikompleksnykh Soedinenii Merkaptokhinolina i Ego Proizvodnykh* (The Chemistry of Inner-complex Compounds of Mercaptoquinoline and Its Derivatives) (Riga: Zinatne, 1978)
27. G P Sharnin, V V Nurgatin, V M Ginzburg *Zh. Org. Khim.* **15** 1635 (1979)
28. H Yanagawa, T Kato, Y Kitahara *Tetrahedron Lett.* **14** 2137 (1973)
29. H Duddeck, W Dietrich *Tetrahedron Lett.* **16** 2925 (1975)
30. J J Delpuech, D Nicole *J. Chem. Soc., Perkin Trans. 2* 1025 (1974)
31. S Hauptman, J Graefe, H Remane *Lehrbuch der organischen Chemie* (Translated into Russian; Moscow: Khimiya, 1979)
32. O A Reutov, I P Beletskaya, K P Butin *CH-Kisloty* (CH-Acids) (Moscow: Nauka, 1980)
33. M R Crampton *J. Chem. Soc. (B)*, 1208 (1968)
34. C A Bunton, S K Huang, C H Paik *Tetrahedron Lett.* **17** 2445 (1976)
35. H Macki *Tetrahedron* **19** 1159 (1963)
36. C Glidewell *J. Chem. Soc., Perkin Trans. 2* 407 (1984)
37. G F Bol'shakov in *IX Mezhdunarodnyi Simpozium po Khimii Organicheskikh Soedineni Sery, Riga, 1980 (Tezisy Dokladov)* (Abstracts of Papers for Ninth International Symposium on the Chemistry of Organic Sulfur Compounds, Riga, 1980) p. 247
38. L J Bellamy *Advances in Infrared Group Frequencies: Supplement to the Infra-red Spectra of Complex Molecules* (Translated into Russian; Moscow: Mir, 1971)
39. L A Kazitsina, N B Kupletskaya *Primenenie UF-, IK-, YaMR-Spektroskopii v Organicheskoi Khimii* (Applications of UV-, IR-, and NMR-Spectroscopy to Organic Chemistry) (Moscow: Vysshaya Shkola, 1971)
40. K Reid *Course of Physical Organic Chemistry* (Translated into Russian; Moscow: Mir, 1972)
41. I Hargittai *The Structure of Volatile Sulfur Compounds* (Translated into Russian; Moscow: Nauka, 1986) p. 18
42. J A Pappas *Chem. Phys.* **12** 397 (1976)
43. I V Koval', T G Panasenko, R M Minyaev, I S Panchenko *Zh. Org. Khim.* **23** 325 (1987)
44. I V Koval' *Usp. Khim.* **59** 1409 (1990) [*Russ. Chem. Rev.* **59** 819 (1990)
45. W Ando, K Sugimoto, S Oae *Bull. Chem. Soc. Jpn.* **37** 357 (1964)
46. W Ando, K Sugimoto, S Oae *Bull. Chem. Soc. Jpn.* **36** 893 (1963)
47. S Wawzonek, G H Hauser *J. Org. Chem.* **31** 3680 (1966)
48. E Block M Aslam *Tetrahedron* **44** 281 (1988)
49. K I Sadykov, S M Aliev, M M Seidov, in *XIII Nauchnaya Sessiya po Khimii i Tekhnologii Organicheskikh Soedinenii Sery i Sernistykh Neftei, Riga, 1974 (Tezisy Dokladov)* (Abstracts of Papers for the Thirteenth Scientific Session on the Chemistry and Technology of Organic Sulfur Compounds and Sulfurous Petroleum, Riga, 1974) p. 115
50. B A Trofimov, N K Gusarova, S V Amosova, M G Voronkov, in *XIII Nauchnaya Sessiya po Khimii i Tekhnologii Organicheskikh Soedinenii Sery i Sernistykh Neftei, Riga, 1974 (Tezisy Dokladov)* (Abstracts of Papers for the Thirteenth Scientific Session on the Chemistry and Technology of Organic Sulfur Compounds and Sulfurous Petroleum, Riga, 1974) p. 123
51. A I Medvedev, T S Romanenko, G B Zvyagintseva, L V Glushkova, L A Skripko, G I Levin, in *XIII Nauchnaya Sessiya po Khimii i Tekhnologii Organicheskikh Soedinenii Sery i Sernistykh Neftei, Riga, 1974 (Tezisy Dokladov)* (Abstracts of Papers for the Thirteenth Scientific Session on the Chemistry and Technology of Organic Sulfur Compounds and Sulfurous Petroleum, Riga, 1974) p. 124
52. T Fujisama, K Hata, T Kajima *Synthesis* 38 (1973)
53. T C Shields, A N Kurts *J. Am. Chem. Soc.* **51** 5415 (1969)
54. W E Parham, H Wynberg *Org. Synth.* **4** 295 (1963)
55. R Grossley, A C W Curran *J. Chem. Soc., Perkin Trans. 1* 2327 (1974)
56. M G Voronkov, L G Klochkova, G M Ivanova, E N Deryagina, in *XIII Nauchnaya Sessiya po Khimii i Tekhnologii Organicheskikh Soedinenii Sery i Sernistykh Neftei, Riga, 1974 (Tezisy Dokladov)* (Abstracts of Papers for the Thirteenth Scientific Session on the Chemistry and Technology of Organic Sulfur Compounds and Sulfurous Petroleum, Riga, 1974) p. 189
57. E N Deryagina, M Z Kuznetsova, M G Voronkov, in *IX Mezhdunarodnyi Simpozium po Khimii Organicheskikh Soedinenii Sery, Riga, 1974(Tezisy Dokladov)* (Abstracts of Papers for the Ninth International Symposium on the Chemistry of Organic Sulfur Compounds, Riga, 1980) p. 101
58. A R Procter, R H Wiekenkamp *Carbohydr. Res.* **10** 459 (1969)
59. K Buggle, D O'Sullivan, N D Ryan *Chem. Ind. (London)* 164 (1974)
60. V A Usov, L V Timokhina, M G Voronkov *Usp. Khim.* **55** 1786 (1986) [*Russ. Chem. Rev.* **55** 1003 (1986)]
61. G M Ivanova, L K Voronova, E N Deryagina, M G Voronkov *Zh. Prikl. Khim.* **50** 1297 (1977)
62. L G Klochkova, G M Ivanova, E N Deryagina *Khim. Geterotsikl. Soedin.* 131 (1977)

63. V I Perevalova, E N Deryagina, M G Voronkov *Zh. Org. Khim.* **14** 2626 (1978)
64. L G Shagun, E S Deriglazova, T V Kashik, E N Deryagina, M G Voronkov *Zh. Org. Khim.* **14** 187 (1978)
65. G M Ivanova, L K Voronova, E N Deryagina *Zh. Org. Khim.* **15** 1252 (1979)
66. M G Voronkov, E N Deryagina, G M Ivanova *Zh. Prikl. Khim.* **55** 2625 (1982)
67. M G Voronkov, E N Deryagina, G N Dolenko, G M Ivanova, V A Sukhomazova, V A Shagun, V F Sidorkin, L N Mazalov *Zh. Org. Khim.* **18** 2367 (1982)
68. M G Voronkov, E N Deryagina, V A Sukhomazova, G M Panova, N A Korchevin *Kinet. Katal.* **25** 265 (1984)
69. M G Voronkov, E N Deryagina, A S Nakhmanovich, L G Klochkova *Khim. Geterotsikl. Soedin.* 712 (1974)
70. M G Voronkov, E N Deryagina, M A Kuznetsov, I D Kalikhman *Zh. Org. Khim.* **14** 185 (1978)
71. V I Perevalova, O B Bannikova, E N Deryagina, M G Voronkov *Zh. Org. Khim.* **16** 399 (1980)
72. E N Deryagina, M A Kuznetsova, M G Voronkov *Zh. Org. Khim.* **24** 1781 (1988)
73. H Zinner *Chem. Ber.* **86** 825 (1953)
74. K A Petrov, G A Sokol'skii *Zh. Obshch. Khim.* **27** 2711 (1957)
75. S D Moshchitskii, A A Zeiken', L S Sologub, V P Kukhar', in *III Simpozium po Khimii i Tekhnologii Geterotsiklicheskikh Soedinenii Goryuchikh Iskopaemykh, Donetsk, 1978 (Tezisy Dokladov)* (Abstracts of Papers for the Third Symposium on the Chemistry and Technology of Heterocyclic Compounds in Combustible Minerals, Donetsk, 1978) p. 123
76. V A Usov, L V Timokhina, L I Lavlinskaya, M G Voronkov *Zh. Org. Khim.* **15** 2598 (1979)
77. C Weygand, G Hilgetag, in *Organisch-chemische Experimentierkunst* (Translated into Russian; Moscow: Khimiya, 1968) p. 944
78. P Wepplo *Synth. Commun.* **19** 1533 (1989)
79. J R Brindll, J L Liard *Can. J. Chem.* **53** 1480 (1975)
80. B. P. 917921; *Chem. Abstr.* **58** 13795 (1963)
81. W E Vaughan, F F Rust *J. Org. Chem.* 7 472 (1942)
82. M S Kharasch, W Nudenberg, G J Mantell *J. Org. Chem.* **16** 524 (1951)
83. V E Mazaev, M A Korshunov, in *XIII Nauchnaya Sessiya po Khimii i Tekhnologii Organicheskikh Soedinenii Sery i Sernistykh Neftei, Riga, 1974 (Tezisy Dokladov)* (Abstracts of Papers for the Thirteenth Scientific Session on the Chemistry and Technology of Organic Sulfur Compounds and Sulfurous Petroleum, Riga, 1974) p. 452
84. V A Usov, N A Korchevin, Ya S Tsetlin, M G Voronkov *Zh. Org. Khim.* **11** 410 (1975)
85. I A Dorofeev, N A Korchevin, V A Usov, M G Voronkov *Zh. Org. Khim.* **20** 1727 (1984)
86. T J P Pearce, J M Peacock, F Aylward, D R Haisman *Chem. Ind.* 1562 (1967)
87. J M Lalancette, M Laliberte *Tetrahedron Lett.* **14** 1401 (1973)
88. US P. 2 398 480; *Chem. Abstr.* **40** 3766 (1946)
89. R Luhowy, F Meneghini *J. Org. Chem.* **38** 2405 (1973)
90. J L Corbin, D E Work *J. Org. Chem.* **41** 489 (1976)
91. A A Potekhin, S M Shevchenko, in *XII Mezhdunarodnyi Simpozium po Khimii Organicheskikh Soedinenii Sery, Riga, 1980 (Tezisy Dokladov)* (Abstracts of Papers for the Twelfth International Symposium on the Chemistry of Organic Sulfur Compounds, Riga, 1980) p. 268
92. E Beretta, M Cinquini, S Colonna, R Fornasier *Synthesis* 425 (1974)
93. E Block, A Wall *Tetrahedron Lett.* **26** 1425 (1985)
94. P G Gassman, D P Gilbert, T J Van Bergen *J. Chem. Soc., Chem. Commun.* 201 (1974)
95. S M Shostakovskii, N S Nikol'skii, V G Kozyrev, L I Gubanova, M A Kuznetsova, in *XII Nauchnaya Sessiya po Khimii i Tekhnologii Organicheskikh Soedinenii Sery i Sernistykh Neftei, Riga, 1970 (Tezisy Dokladov)* (Abstracts of Papers for the Twelfth Scientific Session on the Chemistry and Technology of Organic Sulfur Compounds and Sulfurous Petroleum, Riga, 1970) p. 171
96. H Böhme, H J Gran *Ann.* **581** 133 (1953)
97. H Daecke, R Kranl *Z. Anal. Chem.* **178** 412 (1961)
98. C R Hauser, S W Kantor, W R Brasen *J. Am. Chem. Soc.* **75** 2660 (1953)
99. A V Anisimov, Z G Aukharieva, E A Viktorova, T A Danilova, in *XII Mezhdunarodnyi Simpozium po Khimii Organicheskikh Soedinenii Sery, Riga, 1980 (Tezisy Dokladov)* (Abstracts of Papers for the Twelfth International Symposium on the Chemistry of Organic Sulfur Compounds, Riga, 1980) p. 72
100. L Brandsma *Recl. Trav. Chim.* **89** 593 (1970)
101. S Hoff, A P Blok, B Zwanenburg *Recl. Trav. Chim.* **92** 890 (1973)
102. S Kukolij, R D G Cooper, B B Morin *Tetrahedron Lett.* **10** 3381 (1969)
103. J G Dingwall, D H Reid, J D Symon *J. Chem. Soc., Chem. Commun.* 466 (1969)
104. R Heckendorn, A R Gagneux *Tetrahedron Lett.* **14** 2279 (1973)
105. Y Gelernt, P Sykes *J. Chem. Soc., Perkin Trans. 1* 2610 (1974)
106. H Boeshagen, W Geiger, in *XII Mezhdunarodnyi Simpozium po Khimii Organicheskikh Soedinenii Sery, Riga, 1980 (Tezisy Dokladov)* (Abstracts of Papers for the Twelfth International Symposium on the Chemistry of Organic Sulfur Compounds, Riga, 1980) p. 124
107. R J Stoodley, N S Watson *J. Chem. Soc., Perkin Trans. 1* 1603 (1975)
108. J L Fourrey, P Jounin, J Moron *Tetrahedron Lett.* **14** 3229 (1973)
109. Ya L Gol'dfarb, E P Zakharov, F M Stoyanovich, in *XII Mezhdunarodnyi Simpozium po Khimii Organicheskikh Soedinenii Sery, Riga, 1980 (Tezisy Dokladov)* (Abstracts of Papers for the Twelfth International Symposium on the Chemistry of Organic Sulfur Compounds, Riga, 1980) p. 106
110. C F H Allen, D D McKay *Org. Synth.* **2** 586 (1955)
111. E Bourgeois, A Abraham *Recl. Trav. Chim.* **30** 407 (1911)
112. F N Mamedov, Sh R Aliev, M Movsun-zade, S M Gusein-zade, T Kh Achkurina, in *XIII Nauchnaya Sessiya po Khimii i Tekhnologii Organicheskikh Soedinenii Sery i Sernistykh Neftei, Riga, 1974 (Tezisy Dokladov)* (Abstracts of Papers for the Thirteenth Scientific Session on the Chemistry and Technology of Organic Sulfur Compounds and Sulfurous Petroleum, Riga, 1974) p. 113
113. E Fromm, H Jörg *Ber. Dtsch. Chem. Ges.* **58** 305 (1925)
114. R E Stutz, R L Shriner *J. Am. Chem. Soc.* **55** 1244 (1933)
115. C G Moses, E E Reid *J. Am. Chem. Soc.* **48** 776 (1926)
116. V Du Vigneaud, L E Audrieth, H.S.Loring *J. Am. Chem. Soc.* **52** 4500 (1930)
117. W E Parham, H Wynberg *Org. Synth.* **4** 295 (1963)
118. B C Arnold, A P Lian, R M Alm *Org. Synth.* **72** 731 (1950)
119. K Brand *Ber. Dtsch. Chem. Ges.* **42** 3465 (1909)
120. G Borgogno, S Colonna, R Fornasier *Synthesis* 529 (1975)
121. C A Groß, B Schmitz, A Sutter, A H Weber *Tetrahedron Lett.* **16** 3551 (1975)
122. M A Tsirule, Yu A Bankovskii *Izv. Akad.Nauk Latv. SSR, Ser. Khim. 502 (1968)*
123. E Bourgeois *Ber. Dtsch. Chem. Ges.* **28** 2319 (1895)
124. E Bourgeois *Recl. Trav. Chim.* **18** 432 (1899)
125. R Adams, C S Marvel *Org. Synth.* **1** 505 (1935)
126. A M Kuliev, A B Kuliev, G A Zainalova, M S Gasanov, L M Gyul'ikhmedov, in *XII Nauchnaya Sessiya po Khimii i Tekhnologii Organicheskikh Soedinenii Sery i Sernistykh Neftei, Riga, 1971 (Tezisy Dokladov)* (Abstracts of Papers for the Twelfth Scientific Session on the Chemistry and Technology of Organic Sulfur Compounds and Sulfurous Petroleum, Riga, 1971) p. 443
127. H J Backer, J Kramer *Recl. Trav. Chim.* **53** 1101 (1934)
128. C S Marvel, P D Caesar *J. Am. Chem. Soc.* **73** 1097 (1951)
129. E Profft *Chem. Tech.* **5** 239 (1953)
130. Wislicenus *J. Prakt. Chem.* **54** 18 (1896)
131. E Gebauer-Fülnegg *J. Am. Chem. Soc.* **49** 1386 (1927)
132. German P. 292457; *Chem. Abstr.* **11** 42 (1919)
133. F Voegtle, R G Lichtenfhaler, M Zuber *Chem Ber.* **106** 719 (1973)
134. C S Marvel, P D Caesar *J. Am. Chem. Soc.* **72** 1033 (1950)
135. H Alper *Angew. Chem., Int. Ed. Engl.* **8** 677 (1969)
136. K Fries, W Vogt *Ann.* **381** 331 (1911)
137. A Reißert *Ber. Dtsch. Chem. Ges.* **55** 858 (1922)
138. W B Price, S Smiles *J. Chem. Soc.* 2372 (1928)
139. I Jabre, M Saquet, A Thuillier *J. Chem. Res. (S)* 106 (1990)
140. J Masson, P Metzner, J Vialle *Tetrahedron* **33** 3089 (1977)
141. D Seebach, K H Geis *Angew. Chem.* **86** 202 (1974)

142. A Ohno, K Nakamura, S Oka *Chem. Lett.* 983 (1975)
143. A Ohno, K Nakamura, M Uohama, S Oka, T Vamabe, S Nagata *Bull. Chem. Soc. Jpn.* **48** 3718 (1975)
144. F Asinger, W Schüfer, K Halcour *Angew. Chem.* **75** 1050 (1963)
145. M Dagonneau, J Vialle *Tetrahedron* **30** 415 (1974)
146. L I Lavlinskaya, B A Pestunovich, Ya S Tsetlin, V A Usov, M G Voronkov *Izv. Akad. Nauk SSSR, Ser. Khim.* 2091 (1976)
147. V A Usov, L V Timokhina, T L Usova, M G Voronkov *Zh. Org. Khim.* **17** 1327 (1981)
148. A Couture, M Hoshino, P De Mayo *J. Chem. Soc., Chem. Commun.* 131 (1976)
149. J E Baldwin, R C G Loper *Tetrahedron* **39** 1487 (1983)
150. E Vedejs, T H Eberlein, R G Wilder *J. Org. Chem.* **53** 2220 (1988)
151. J M Lawanish *Tetrahedron Lett.* **14** 3847 (1973)
152. R C Elderfield (Ed.) *Heterocyclic Compounds* Vol. 6 (Translated into Russian; Moscow: Inostr. Lit., 1960) p. 611
153. J F Willems *Fortschr. Hochpolym.-Forsch.* 554 (1963)
154. M Yokoyama, T Imamoto *Synthesis* 791 (1984)
155. R J Cregge, J L Herrmann, J E Richman, R F Romanet, R H Schlessinger *Tetrahedron Lett.* **14** 2595 (1973)
156. M Raban, L J Chern *J. Org. Chem.* **45** 1688 (1980)
157. M K Gadzhiev, N M Nobeneridze, Kh I Areshidze, Z S Amiridze, M L Kantariya *Soobshch. Akad. Nauk Gruz. SSR* **114** 317 (1984)
158. K Wojcechowski *Org. Prep. Proced. Int.* **20** 493 (1988)
159. M K Gazhiev *Prepr. Akad. Nauk Gruz. SSR*; *Ref. Zh. Khim.* 2Zh138 (1991)
160. B C Pal, D G Schmidt *J. Am. Chem. Soc.* **94** 5943 (1974)
161. A W Herriott, D Picker *Synthesis* 447 (1974)
162. L N Markovskii, V V Vasil'ev, Yu G Shermolovich *Zh. Org. Khim.* **13** 843 (1977)]
163. W R Bowman, G D Richardson *J. Chem. Soc., Perkin Trans. 1* 1407 (1980)
164. L P Johnson, L B Holum, J A Montgomery *J. Am. Chem. Soc.* **80** 6265 (1958)
165. K E Rittle, C A Hunt, M B Freedman *J. Org. Chem.* **41** 1644 (1976)
166. V V Orda, L M Yagupol'skii, V F Bystrov, A U Stepanyants *Zh. Obshch. Khim.* **35** 1628 (1965)
167. L N Yagupolski, N V Kondratenko, V P Sambur *Synthesis* 721 (1975)
168. I G Oksengendler, N V Kondratenko, E A Luk'yanets, L M Yagupol'skii *Zh. Org. Khim.* **14** 1046 (1978)
169. N V Kondratenko, A A Kolomeytsev, V I Popov, L M Yagupolskii *Synthesis* 667 (1985)
170. A A Kolomeitsev, N V Kondratenko, V I Popov, L M Yagupol'skii *Zh. Org. Khim.* **19** 2631 (1983)
171. S V Pazenok, N V Kondratenko, V I Popov, V I Troitskaya, A Ya Il'chenko, M A Al'perovich, L M Yagupol'skii *Khim. Geterotsikl. Soedin.* 1493 (1983)
172. I V Koval, A I Tarasenko, I S Panchenko *Vopr. Khim. Khim. Tekhnol.* **84** 54 (1987)
173. M Heydenreich, I Kühn, R Runge, E Wenschuch *Sulfur Lett.* 65 (1989)
174. O Behaghel, E Schneider *Ber. Dtsch. Chem. Ges.* **68** 1588 (1935)
175. M P Balfe, J Kenyon, C E Searle *J. Chem. Soc.* 3309 (1950)
176. Y Tanigawa, H Kanamura, T Murahash *Tetrahedron Lett.* **16** 4655 (1975)
177. A Holy *Tetrahedron Lett.* **13** 585 (1972)
178. Y Tamura, T Saito, H Ishibashi, M Ikeda *Synthesis* 641 (1975)
179. Z Yoshida, T Kawase, S Yoneda *Tetrahedron Lett.* **16** 235 (1975)
180. P Savignac, P Controt *Synthesis* 282 (1974)
181. G W H Cheeseman *J. Chem. Soc.* 115 (1957)
182. J M Luteijn, H Dolman, H C Wals *Tetrahedron* **44** 5921 (1988)
183. E Vowinkel, C Wolff *Chem. Ber.* **107** 496 (1974)
184. M Shamma, N C Deno, J F Remar *Tetrahedron Lett.* **7** 2299 (1966)
185. L N Nikolenko, V A Koptyug *Zh. Obshch. Khim.* **25** 1757 (1955)
186. Y Le Floéh, A Briault, M Kerfanto *C. R. Acad. Sci., Ser. C* **268** 1718 (1969)
187. G I Zaitseva, V M Al'bitskaya *Zh. Org. Khim.* **5** 612 (1969)
188. Yu K Pikshilingaite, G K Krasil'nikov, O V Kil'dineva , in *XIII Nauchnaya Sessiya po Khimii i Tekhnologii Organicheskikh Soedinenii Sery i Sernistykh Neftei, Riga, 1974 (Tezisy Dokladov)* (Abstracts of Papers for the Thirteenth Scientific Session on the Chemistry and Technology of Organic Sulfur Compounds and Sulfurous Petroleum, Riga, 1974) p. 137
189. M Wakselman, E Guibé-Jampel, A Raoult, W D Busse *J. Chem. Soc., Chem. Commun.* 21 (1976)
190. L M Yagupolski, I I Maletina, N V Kondratenko, V V Orda *Synthesis* 835 (1978)
191. A A Mironova, I I Maletina, V V Orda, L M Yagupol'skii *Zh. Org. Khim.* **19** 1213 (1983)
192. V V Artemova, L A Palagushkina, T M Ishchuk, T A Mal'tseva, in *III Simpozium po Khimii i Tekhnologii Geterotsiklicheskikh Soedinenii Goryuchikh Iskopaemykh, Donetsk, 1978 (Tezisy Dokladov)* (Abstracts of Papers for the Third Symposium on the Chemistry and Technology of Heterocyclic Compounds in Combustible Minerals, Donetsk, 1978) p. 143
193. Zh G Saidaliev, A Kadyrov, A Safaev, M Mashranova, in *XIII Nauchnaya Sessiya po Khimii i Tekhnologii Organicheskikh Soedinenii Sery i Sernistykh Neftei, Riga, 1974 (Tezisy Dokladov)* (Abstracts of Papers for the Thirteenth Scientific Session on the Chemistry and Technology of Organic Sulfur Compounds and Sulfurous Petroleum, Riga, 1974) p. 138
194. O Tukhtasunov, in *Respublikanskaya Nauchno-prakticheskaya Konferentsiya Molodykh Uchenykh i Spetsialistov, Dushanbe, 1989 (Tezisy Dokladov)* (Abstracts of Papers for the Republican Scientific-practice Conference of Young Scientists and Experts, Dushanbe, 1989) p. 48
195. V I Dronov, I Kh Makhmutova, R F Nagmatullina, Yu E Nikitin *Zh. Org. Khim.* **21** 1847 (1985)
196. L P Turchaninova, N A Korchevin, A G Shipov, E N Deryagina, Yu I Baukov, M G Voronkov *Zh. Obshch. Khim.* **59** 722 (1989)
197. M V R Reddy, S Reddy, D B Reddy, V Padmavathi *Synth. Commun.* **19** 1101 (1989)
198. A Hosomi, Y Matsuyama, H Sakurai *J. Chem. Soc., Chem. Commun.* 1073 (1986)
199. A Schönberg, G Aziz *J. Org. Chem.* **22** 1697 (1957)
200. V I Boiko, G M Shchupak, L M Yagupol'skii *Zh. Org. Khim.* **13** 1057 (1977)
201. V N Boiko, G M Shchupak, N V Ignat'ev, L M Yagupol'skii *Zh. Org. Khim.* **15** 1245 (1979)
202. V I Boiko, T A Dashevskaya, G M Shchupak, L M Yagupol'skii *Zh. Org. Khim.* **15** 396 (1979)
203. V I Boiko, G M Shchupak, L M Yagupol'skii *Zh. Org. Khim.* **16** 995 (1980)
204. N V Kondratenko, L G Yurchenko, G I Matyushecheva *Ukr. Khim. Zh. (Russ. Ed.)* **47** 871 (1981)
205. N V Kondratenko, A A Kolomeitsev, V I Popov, L M Yagupol'skii *Zh. Obshch. Khim.* **53** 2500 (1983)
206. M Suda, C Hino *Tetrahedron Lett.* **22** 1997 (1981)
207. A A Kolomeitsev, N V Kondratenko, V I Popov, L M Yagupol'skii *Zh. Org. Khim.* **19** 2631 (1983)
208. C Wakselman, M Tordeux *J. Chem. Soc., Chem. Commun.* 793 (1984)
209. N V Ignat'ev, V N Boiko, L M Yagupol'skii *Zh. Org. Khim.* **21** 653 (1985)
210. J F Bannett, X Creary *J. Org. Chem.* **39** 3173 (1974)
211. V I Popov, V N Boiko, N V Kondratenko, V P Sambur, L M Yagupol'skii *Zh. Org. Khim.* **13** 2135 (1977)
212. V I Troitskaya, V I Popov, V I Rudykh, N V Kondratenko, L M Yagupol'skii *Ukr. Khim. Zh. (Russ. Ed.)* **46** 1181 (1980)
213. I Rico, D Cantacuzene, C Wakselman *J. Org. Chem.* **48** 1979 (1983)
214. V A Korin'ko, Yu A Serguchev, L M Yagupol'skii *Zh. Org. Khim.* **11** 1268 (1975)
215. L M Yagupol'skii, A M Aleksandrov *Zh. Org. Khim.* **4** 1503 (1968)
216. L M Yagupol'skii, A M Aleksandrov *Zh. Org. Khim.* **5** 765 (1969)
217. Yu V Samusenko, A M Aleksandrov, L M Yagupol'skii *Zh. Org. Khim.* **11** 626 (1975)
218. L M Yagupol'skii, Yu L Yagupol'skii *Zh. Org. Khim.* **13** 1996 (1977)
219. L M Yagupol'skii, in *Aromaticheskie i Geterotsiklicheskie Soedineniya s Ftorsoderzhashchimi Zamestitelyami* (Aromatic and Heterocyclic Compounds with Fluorine-containing Substituents) (Kiev: Naukova Dumka, 1988) p. 319

220. G Leandri, A Tundo *Boll. Sci. Fac. Chim. Ind. Bologna* **14** 31 (1956)
221. M E Peack, A M Smith *J. Fluorine Chem.* **4** 389 (1974)
222. V N Boiko, G M Shchupak, R K Orlova, L M Yagupol'skii *Zh. Org. Khim.* **21** 1477 (1985)
223. J B Baumann *J. Org. Chem.* **36** 396 (1971)
224. G M Ivanova, L G Klochkova, A S Nakhmanovich, E N Deryagina, M G Voronkov, in *XIII Nauchnaya Sessiya po Khimii i Tekhnologii Organicheskikh Soedinenii Sery i Sernistykh Neftei, Riga, 1974 (Tezisy Dokladov)* (Abstracts of Papers for the Thirteenth Scientific Session on the Chemistry and Technology of Organic Sulfur Compounds and Sulfurous Petroleum, Riga, 1974) p.190
225. P Caubere *Bull. Soc. Chim. Fr.* 3446 (1967)
226. F Gaspazzini, M Giovannoli, D Misiti, G Natile, G Palmieri *Tetrahedron* **39** 3181 (1983)
227. R T Morrison, R N Boyd *Organic Chemistry* (Translated into Russian; Moscow: Mir, 1974) p. 1132
228. N V Kondratenko, V P Sambur *Ukr. Khim. Zh. (Russ. Ed.)* **41** 516 (1975)
229. W E Truce, M M Boudakian *J. Am. Chem. Soc.* **78** 2748 (1956)
230. C F H Allen, W J Humphlett *Can. J. Chem.* **44** 2315 (1966)
231. K Z Guseinov, M A Mirzoeva, D N Mamedov, in *XIII Nauchnaya Sessiya po Khimii i Tekhnologii Organicheskikh Soedinenii Sery i Sernistykh Neftei, Riga, 1974 (Tezisy Dokladov)* (Abstracts of Papers for the Thirteenth Scientific Session on the Chemistry and Technology of Organic Sulfur Compounds and Sulfurous Petroleum, Riga, 1974) p. 133
232. E A I Haiba *J. Org. Chem.* **31** 776 (1966)
233. C D Hurd, L L Gershbein *J. Am. Chem. Soc.* **69** 2328 (1947)
234. A Schöberl, A Wagner *Chem. Ber.* **80** 379 (1949)
235. I I Kandror, I O Bragin, M A Galkin, B D Lavrukhin, Yu G Gololobov *Izv. Akad. Nauk SSSR, Ser. Khim.* 2798 (1990)
236. S Ruhemann *J. Chem. Soc.* **87** 17 (1905)
237. H Böhme, P Heller *Chem. Ber.* **86** 443 (1953)
238. G B Afanas'eva, E V Tsoi, O N Chupakhin, E O Sidorov, S V Konovalov *Zh. Org. Khim.* **21** 1921 (1985)
239. Sh S Kuliev, N S Kizimova, G A Zeinalova, in *XIII Nauchnaya Sessiya po Khimii i Tekhnologii Organicheskikh Soedinenii Sery i Sernistykh Neftei, Riga, 1974 (Tezisy Dokladov)* (Abstracts of Papers for the Thirteenth Scientific Session on the Chemistry and Technology of Organic Sulfur Compounds and Sulfurous Petroleum, Riga, 1974) p. 441
240. E N Prilezhaeva, N P Petukhova, N E Dontsova, in *IX Mezhdunarodnyi Simpozium po Khimii Organicheskikh Soedinenii Sery, Riga, 1980 (Tezisy Dokladov)* (Abstracts of Papers for the Ninth International Symposium on the Chemistry of Organic Sulfur Compounds, Riga, 1980) p.144
241. G A Tolstikov, N N Novitskaya, L E Zhuravleva, S I Lomakina, in *XII Nauchnaya Sessiya po Khimii i Tekhnologii Organicheskikh Soedinenii Sery i Sernistykh Neftei, Riga, 1974 (Tezisy Dokladov)* (Abstracts of Papers for the Twelfth Scientific Session on the Chemistry and Technology of Organic Sulfur Compounds and Sulfurous Petroleum, Riga, 1974) p. 124
242. A R Katritsky, in *VI Mezhdunarodnaya Konferentsiya po Organicheskomu Sintezu, Moskva, 1986 (Tezisy Dokladov)* (Abstracts of Papers for the Sixth International Conference on Organic Synthesis, Moscow, 1986) p. 30
243. I A Aliev, A I Mikhalev, B R Gasanov *Khim. Geterotsikl. Soedin.* 750 (1990)
244. K Geiss, B Seuring, R Pieter, D Seebach *Angew. Chem., Int. Ed. Engl.* **13** 479 (1974)
245. N K Lyapina, L A Mel'nikova, M A Parfenova, A D Ulendeeva, in *IX Mezhdunarodnyi Simpozium po Khimii Organicheskikh Soedinenii Sery, Riga, 1980 (Tezisy Dokladov)* (Abstracts of Papers for the Ninth International Symposium on the Chemistry of Organic Sulfur Compounds, Riga,1980) p. 328
246. F W Stacey, J F Harris Jnr *Organic Reactions* Vol. 13 (Translated into Russian; Moscow: Nauka, 1966) Vol. 13, p. 170
247. E W Duck, J M Locke *Chem. Ind. (London)* 507 (1965)
248. W G Niehaus *Bioorg. Chem.* **3** 302 (1974)
249. G S Ponticello, C N Habecker, S L Varga, S M Pitzenberger *J. Org. Chem.* **54** 3223 (1989)
250. V Yu Vvedenskii, S V Zinchenko, T A Shkarupa, N A Korchevin, E N Deryagina, M G Voronkov *Dokl. Akad. Nauk SSSR* **305** 624 (1989)
251. V Yu Vvedenskii, S V Zinchenko, T A Shkarupa, E N Deryagina, M G Voronkov, A R Zhnikin *Zh. Org. Khim.* **26** 2238 (1990)
252. E N Prilezhaeva, N P Petukhova, L I Shmonina, I A D'yakonova, V I Laba, in *XII Nauchnaya Sessiya po Khimii i Tekhnologii Organicheskikh Soedinenii Sery i Sernistykh Neftei, Riga, 1971* (Tezisy Dokladov) (Abstracts of Papers for the Twelfth Scientific Session on the Chemistry and Technology of Organic Sulfur Compounds and Sulfurous Petroleum, Riga, 1971) p. 173
253. E H Prilezhaeva, N P Petukhova, L I Shmonina, I A D'yakonova *Izv. Akad. Nauk SSSR, Ser. Khim.* 956 (1972)
254. V A Potapov, N K Gusarova, S V Amosova, L P Turchaninova, L M Sinegovskaya, L B Krivdin, B A Trofimov *Izv. Akad. Nauk SSSR, Ser. Khim.* 965 (1972)
255. W E Truce, J A Simms *J. Am. Chem. Soc.* **78** 2756 (1956)
256. W E Truce, D L Goldhamer *J. Am. Chem. Soc.* **82** 5798 (1960)
257. H J Alekman, J F Arens *Recl. Trav. Chem.* **79** 1257 (1960)
258. A M Borisova, A Kh Filippova, V K Voronov, M F Shostakovskii *Izv. Akad. Nauk SSSR, Ser. Khim.* 2498 (1969)
259. E N Prilezhaeva, G S Vasil'eva, I L Mikhelashvili, V S Bogdanova *Zh. Org. Khim.* **7** 1349 (1971)
260. E N Deryagina, V N Elokhina, L S Klochkova, in *XII Nauchnaya Sessiya po Khimii i Tekhnologii Organicheskikh Soedinenii Sery i Sernistykh Neftei, Riga, 1971 (Tezisy Dokladov)* (Abstracts of Papers for the Twelfth Scientific Session on the Chemistry and Technology of Organic Sulfur Compounds and Sulfurous Petroleum, Riga, 1971) p. 31
261. L P Rasteikene, V I Vidugirene, Z A Talaikite, N M Lukoshyavichyute *Zh. Org. Khim.* **20**, 713 (1984)
262. I Vidugirne, T P Pranskiene, Z A Talaikite, L P Rasteikene, in *VI Mezhdunarodnaya Konferentsiya po Organicheskomu Sintezu, Moskva, 1986 (Tezisy Dokladov)* (Abstracts of Reports for the Sixth International Conference on Organic Synthesis, Moscow, 1986) p. 201
263. K A Volkova, E P Levanova, A N Volkova *Zh. Org. Khim.* **24** 1379 (1988)
264. A F Peshkov, Yu G Trishin, V N Chistokletov *Zh. Org. Khim.* **19** 2797 (1983)
265. V I Laba, V I Snegotskii, E N Prilezhaeva, in *XII Nauchnaya Sessiya po Khimii i Tekhnologii Organicheskikh Soedinenii Sery i Sernistykh Neftei, Riga, 1971 (Tezisy Dokladov)* (Abstracts of Papers for the Twelfth Scientific Session on the Chemistry and Technology of Organic Sulfur Compounds and Sulfurous Petroleum, Riga, 1971) p. 170
266. V I Rakhlin, R G Mirskov, M G Voronkov, in *XIII Nauchnaya Sessiya po Khimii i Tekhnologii Organicheskikh Soedinenii Sery i Sernistykh Neftei, Riga, 1974 (Tezisy Dokladov)* (Abstracts of Papers for the Thirteenth Scientific Session on the Chemistry and Technology of Organic Sulfur Compounds and Sulfurous Petroleum, Riga, 1974) p. 151
267. W Schrath, F Billig, A Zschunke *Z. Chem.* **9** 184 (1969)
268. H J Boonstra, J F Arens *Recl. Trav. Chim.* **79** 867 (1960)
269. J C Sauear *J. Am. Chem. Soc.* **79** 5314 (1967)
270. N P Petukhova, E N Prilezhaeva *Zh. Org. Khim.* **2** 1947 (1966)
271. H J Alkema, J F Arens *Recl. Trav. Chim.* **79** 1257 (1960)
272. J Boonnema, J F Arens *Recl. Trav. Chim.* **79** 1137 (1960)
273. L G Sulimov, A A Petrov *Zh. Obshch. Khim.* **36** 767 (1966)
274. M G Voronkov, V I Rakhlin, R G Mirskov, S Kh Khangazheev *Zh. Obshch. Khim.* **49** 119 (1979)
275. M G Voronkov, V I Rakhlin, G V Kuznetsova, N K Yarosh, O G Yarosh, O S Stankevich, A I Albanov, V Yu Vitkovskii *Zh. Obshch. Khim.* **52** 1820 (1982)
276. M G Voronkov, R G Mirskov, V I Rakhlin *Izv. Akad. Nauk SSSR, Ser. Khim.* 610 (1975)
277. F Akiyama *J. Chem. Soc., Chem. Commun.* 208 (1976)
278. C S Marvel, E A Sienick, M Passer, C N Robinson *J. Am. Chem. Soc.* **76** 933 (1954)
279. C S Marvel, R C Farrar *J. Am. Chem. Soc.* **79** 986 (1957)
280. T H Chan, B S Ong *Tetrahedron Lett.* **17** 319 (1976)
281. S Cacchi, L Cuglioti, G Paolucci *Synthesis* 120 (1975)
282. R G Petrova, R G Gasanova, T D Churkina, in *IX Mezhdunarodnyi Simpozium po Khimii Organicheskikh*

Soedinenii Sery, Riga, 1980 (Tezisy Dokladov) (Abstracts of Papers for the Ninth International Symposium on Chemistry of Organic Sulfur Compounds, Riga, 1980) p. 199
283. T R Oakes, G W Stacy *J. Am. Chem. Soc.* **94** 1594 (1972)
284. Y Ogata, A Kawasaki *J. Chem. Soc., Perkin Trans. 2* 134 (1975)
285. H Bredereck, G Simchen, H Hoffmann *Chem. Ber.* **106** 3725 (1973)
286. Kh I Areshidze, M K Gadzhiev, in *XII Nauchnaya Sessiya po Khimii i Tekhnologii Organicheskikh Soedinenii Sery i Sernistykh Neftei, Riga, 1971 (Tezisy Dokladov)* (Abstracts of Papers for the Twelfth Scientific Session on the Chemistry and Technology of Organic Sulfur Compounds and Sulfurous Petroleum, Riga, 1971) p. 315
287. V E Mazaev, M A Korshunov, in *XII Nauchnaya Sessiya po Khimii i Tekhnologii Organicheskikh Soedinenii Sery i Sernistykh Neftei, Riga, 1971 (Tezisy Dokladov)* (Abstracts of Papers for the Twelfth Scientific Session on the Chemistry and Technology of Organic Sulfur Compounds and Sulfurous Petroleum, Riga, 1971) p. 454
288. S H Greenbaum *J. Am. Chem. Soc.* **76** 6052 (1954)
289. T J Hurley, M A Robinson *J. Med. Chem.* **8** 888 (1965)
290. G E P Smith, J G Alliger, E L Carr, K C Young *J. Org. Chem.* **14** 935 (1949)
291. A V Kharchenko, I V Koval', M M Kremlev *Zhur. Org. Khim.* **13** 2385 (1977)
292. L Graine, M Raban *Chem. Rev.* **89** 689 (1989)
293. O A Ermakov, T L Sorokina, T V Barinova *Zh. Org. Khim.* **12** 237 (1976)
294. A Yasuo, O Kunio, K Reiko, A Ryuichi, F Tsugio *Ann. Rep. Radio. Center Osaka Prefect.* **18** 77 (1977)
295. US P. 2 495 085; *Chem. Abstr.* **45** 177 (1950)
296. S Mayaard, Raasch *J. Org. Chem.* **37** 3820 (1972)
297. S Andreae, E Schmitz, in *VI Mezhdunarodnaya Konferentsiya po Organicheskomu Sintezu, Moskva, 1986 (Tezisy Dokladov)* (Abstracts of Papers for the Sixth International Conference on Organic Synthesis, Moscow, 1986) p. 189
298. N P Pel'kis, E S Levchenko *Zh. Org. Khim.* **22** 387 (1986)
299. S A Grachev, G A Bagiyan, I K Koroleva, in *XIII Nauchnaya Sessiya po Khimii i Tekhnologii Organicheskikh Soedinenii Sery i Sernistykh Neftei, Riga, 1974 (Tezisy Dokladov)* (Abstracts of Papers for the Thirteenth Scientific Session on the Chemistry and Technology of Organic Sulfur Compounds and Sulfurous Petroleum, Riga, 1974) p. 256
300. K Esses-Raiter, F Korentski, D Banfi, in *IX Mezhdunarodnyi Simpozium po Khimii Organicheskikh Soedinenii Sery, Riga, 1980 (Tezisy Dokladov)* (Abstracts of Papers for the Ninth International Symposium on Chemistry of Organic Sulfur Compounds, Riga, 1980) p. 59
301. SM Kolthoff, W E Harris *Anal. Chem.* **21** 963 (1940)
302. H Rheinboldt, E Motzkus *Ber. Dtsch. Chem. Ges.* **72** 657 (1939)
303. N N Vlasova, L N Kulikova, E O Tsetlina, M G Voronkov *Zh. Obshch. Khim.* **44** 27 (1974)
304. N N Vlasova, L N Neretina, F G Kletsko, E O Tsetlina, M G Voronkov *Izv. Akad. Nauk SSSR, Ser. Khim.* 2827 (1975)
305. H H Sisler, N K Kotia, R E Highsmith *J. Org. Chem.* **35** 1742 (1970)
306. F Kai, S Seki *Meiji Seika Kenku Nempo* **10** 32 (1968); *Chem. Abstr.* **72** 31696 (1970)
307. M Heydenreich, E Wenschun *Chemiedozententag (Leipzig)* 60 (1988)
308. M J Gibian, D V Winkelman *Tetrahedron Lett.* **10** 3901 (1969)
309. L Field, R B Barbee *J. Org. Chem.* **34** 1792 (1969)
310. E I Stout, B S Shasha, W M Doane *J. Org. Chem.* **39** 562 (1974)
311. M V Pachvidze, N Z Dalokishvili, in *XIII Nauchnaya Sessiya po Khimii i Tekhnologii Organicheskikh Soedinenii Sery i Sernistykh Neftei, Riga, 1974 (Tezisy Dokladov)* (Abstracts of Papers for the Thirteenth Scientific Session on the Chemistry and Technology of Organic Sulfur Compounds and Sulfurous Petroleum, Riga, 1974) p. 283
312. G G Chirakadze, E M Nanobishvili, D V Katsadze, in *IX Mezhdunarodnyi Simpozium po Khimii Organicheskikh Soedinenii Sery, Riga, 1980 (Tezisy Dokladov)* (Abstracts of Papers for the Ninth International Symposium on Chemistry of Organic Sulfur Compounds, Riga, 1980) p. 253
313. A M Shur *Vysokomolekulyarnye Soedineniya* (High-Molecular Compounds) (Moscow: Vysshaya Shkola, 1981)
314. V R Gawariker, N V Visvanathan, J Shridhar *Polimers* (Polymers) (Translated into Russian; Moscow, Nauka, 1990
315. F Runge, A Jumar, F Köhler *J. Prakt. Chem.* **21** 39 (1963)
316. I V Koval', T G Oleinik, M M Kremlev, in *Voprosy Khimii i Khimicheskoi Tekhnologii* Vol. 64 (Problems in Chemistry and Chemical Technology) (Kharkov: Vishcha Shkola, 1981) p. 17
317. F Fisher, R Gottfried *J. Prakt. Chem.* **30** 232 (1965)
318. L Almasi, A Hantz *J. Prakt. Chem.* **38** 113 (1968)
319. A J Parker, N Kharasch *J. Am. Chem. Soc.* **82** 3071 (1960)
320. G Zumach, E Kühle *Angew. Chem.* **82** 63 (1970)
321. D A R Happer, J W Mitchele, J W Wright *Austr. J. Chem.* **26** 121 (1973)
322. J Goerdeler, H Hohage, I Zeid *Chem. Ber.* **109** 3108 (1976)
323. R M De Marinic, W M Bryan *J. Org. Chem.* **42** 2024 (1977)
324. B I Stepanov, V Ya Rodionov, T A Chibisova, L N Yagodina, A D Stankevich *Zh. Org. Khim.* **13** 370 (1977)
325. C Hennart *Bull. Soc. Chim. Fr.* 4398 (1967)
326. N B Islam, H Kwart, S Khan *J. Chem. Eng. Data* **30** 509 (1985)
327. I V Koval' *Usp. Khim.* **60** 1645 (1991) [*Russ. Chem. Rev.* **60** 830 (1991)]
328. R G Hiskey, T Mizoguchi, E L Smithwick *J. Org. Chem.* **32** 97 (1967)
329. K S Boustany, A B Sullivan *Tetrahedron Lett.* **11** 3547 (1970)
330. D N Harpp, T G Back *J. Org. Chem.* **36** 3828 (1971)
331. M Masateru, K Tomonori, I Eikoh *Synthesis* 56 (1985)
332. L Benati, P C Montevecchi, P Spagnolo *Tetrahedron Lett.* **27** 1739 (1986)
333. I V Koval' *Usp. Khim.* **59** 681 (1990) [Russ. Chem. Rev. **59** 396 (1990)]
334. D T McAllan, T V Cullom, R A Dean, F A Fidler *J. Am. Chem. Soc.* **73** 3627 (1951)
335. L P Sevbo, O F Ginzburg, L N Zakharov, in *XII Nauchnaya Sessiya po Khimii i Tekhnologii Organicheskikh Soedinenii Sery i Sernistykh Neftei, Riga, 1971 (Tezisy Dokladov)* (Abstracts of Papers for the Twelfth Scientific Session on the Chemistry and Technology of Organic Sulfur Compounds and Sulfurous Petroleum, Riga, 1971) p. 176
336. Ya L Kostyukovskii, Yu A Bruk, N M Slavachevskaya, A V Kokushkina, L V Pavlova, in *XII Nauchnaya Sessiya po Khimii i Tekhnologii Organicheskikh Soedinenii Sery i Sernistykh Neftei, Riga, 1971 (Tezisy Dokladov)* (Abstracts of Papers for the Twelfth Scientific Session on the Chemistry and Technology of Organic Sulfur Compounds and Sulfurous Petroleum, Riga, 1971) p. 282
337. M Zbirovsky, V Ettel *Chem. Listy* **52** 105 (1958)
338. S J Brois, J F Pilot, H W Barmun *J. Am. Chem. Soc.* **92** 7629 (1970)
339. O Abe, M F Lukacovic, C Ressler *J. Org. Chem.* **39** 253 (1974)
340. B C Pal, D G Schmidt *J. Am. Chem. Soc.* **96** 5943 (1974)
341. M Wakselman, E Guibé-Jampel, A Raoult, W D Busse *J. Chem. Soc., Chem. Commun.* 21 (1976)
342. Y Degani, A Patchornick *J. Org. Chem.* **36** 2727 (1971)
343. R G Hiskey, T Mizoguchi, E L Smithwick *J. Org. Chem.* **32** 97 (1967)
344. D Williams, H Lyn *Chem. Soc. Rev.* **14** 171 (1985)
345. S Oae, K Shinkhama, J H Kim, in *IX Mezhdunarodnyi Simpozium po Khimii Organicheskikh Soedinenii Sery, Riga, 1980 (Tezisy Dokladov)* (Abstracts of Papers for the Ninth International Symposium on the Chemistry of Organic Sulfur Compounds, Riga, 1980) p. 55
346. I V Koval', in *Voprosy Khimii i Khimicheskoi Tekhnologii* Vol. 89 (Problems in Chemistry and Chemical Technology) (Kharkov: Vishcha Shkola, 1989) p. 73
347. S Masamune, S Kamata, W Schilling *J. Am. Chem. Soc.* **97** 3515 (1975)
348. S Yamada, Y Yokogama *J. Org. Chem.* **39** 3302 (1974)
349. S Masamune, S Kamata, J Diakur, Y Sugihara, G S Bates *Can. J. Chem.* **53** 3693 (1975)
350. A N Pudovik, E S Bat'eva, E N Ofitserov, O G Sinyashin, in *IX Mezhdunarodnyi Simpozium po Khimii Organicheskikh Soedinenii Sery, Riga, 1980 (Tezisy Dokladov)* (Abstracts of Papers for the Ninth International Symposium on the Chemistry of Organic Sulfur Compounds, Riga, 1980) p. 174
351. T J Maricich, C N Angeletakis *J. Org. Chem.* **49** 1931 (1984)

352. N N Vlasova, S A Bol'shakova, Yu G Skripnik, E O Tsetlina, M G Voronkov *Izv. Akad. Nauk SSSR, Ser. Khim.* 204 (1979)
353. K A Andrianov, L M Khananashvili *Tekhnologiya Elemento-organicheskikh Monomerov i Polimerov* (The Technology of Hetero-organic Monomers and Polymers) (Moscow: Khimiya, 1983)
354. D H Barton, W D Ollis (Eds) *Comprehensive Organic Chemistry* Vol. 6 (Translated into Russian; Moscow, Khimiya, 1984)
355. O M Trofimova, N F Chernov, A I Albanov, V A Pestunovich, M G Voronkov, in *IV Vsesoyuznaya Konferentsiya po Stroeniyu i Reaktsionnoi Sposobnosti Kremniiorganicheskikh Soedinenii, Irkutsk, 1989(Tezisy Dokladov)* (Abstracts of Papers for the Fourth All-Union Conference on the Structure and Reactivity of Organosilicon Compounds, Irkutsk, 1989) p. 63
356. M D Mizhiritskii, V O Reisfel'd *Usp. Khim.* **57** 803 (1988) [*Russ. Chem. Rev.* **57** 447 (1988)]
357. T Hayashi, H Baba *J. Am. Chem. Soc.* **97** 1608 (1975)
358. E Block, M Aslam *Tetrahedron Lett.* **26** 2259 (1985)
359. A Wright, D Long, P Boudjouk, R West *J. Am. Chem. Soc.* **94** 4784 (1972)
360. D L Coffen *J. Chem. Soc., Chem. Commun.* 1089 (1967)
361. G A Russell, L A Ochrymowycz *J. Org. Chem.* **34** 3618 (1969)
362. D L Coffen *J. Heterocycl. Chem.* **7** 201 (1970)
363. E J Corey, D Seebach *Org. Synth.* **50** 72 (1970)
364. E I Eliel, A A Hartmann *J. Org. Chem.* **37** 505 (1972)
365. F Sher, I L Isidor, H R Taneja, R M Carlson *Tetrahedron Lett.* **14** 577 (1973)
366. R H Cragg, A F Weston *Tetrahedron Lett.* **14** 635 (1973)
367. C Giordano, A Belli *Synthesis* 193 (1977)
368. L G Sharanina, Yu A Sharanin, A M Shestopalov, V K Promonenkov, V P Maritupa, in *III Simpozium po Khimii Geterotsiklicheskikh Soedinenii Goryuchikh Iskopaemykh, Donetsk, 1978 (Tezisy Dokladov)* (Abstracts of Papers for the Third Symposium on the Chemistry of Heterocyclic Compounds in Combustible Minerals, Donetsk, 1978), p.130
369. Z Lidert, S Gronowitz, in *IX Mezhdunarodnyi Simpozium po Khimii Organicheskikh Soedinenii Sery, Riga, 1980 (Tezisy Dokladov)* (Abstracts of Papers for the Ninth International Symposium on Chemistry of Organic Sulfur Compounds, Riga, 1980) p. 220
370. H F Gruetzmacher, U Funke, in *VI Mezhdunarodnaya Konferentsiya po Organicheskomu Sintezu, Moskva, 1986 (Tezisy Dokladov)* (Abstracts of Papers for the Sixth International Conference on Organic Synthesis, Moscow, 1986) p. 131
371. V N Elokhina, A S Nakhmanovich, M G Voronkov, in *III Simpozium po Khimii Geterotsiklicheskikh Soedinenii Goryuchikh Iskopaemykh, Donetsk, 1978 (Tezisy Dokladov)* (Abstracts of Papers for the Third Symposium on Chemistry of Heterocyclic Compounds in Combustible Minerals, Donetsk, 1978) p .125
372. I Batyrov, E A Startseva, I Ya Kalantarov, in *III Regional'noe Soveshchanie Respublik Srednei Azii i Kazakhstana po Khimicheskim Reaktivam, Tashkent, 1990 (Tezisy Dokladov)* Vol. 1 (Abstracts of Papers for the Third Regional Conference of the Republics of Central Asia and Kazakhstan on Chemical Reagents,Tashkent, 1990) p. 246
373. D H R Barton, B I Willis *J. Chem. Soc., Chem. Commun.* 1225 (1970)
374. J J G Cadogan, S Kulik, C Thomson, M J Todd *J. Chem. Soc. (C)* 2437 (1970)
375. E N Deryagina, M A Kuznetsova, in *VI Mezhdunarodnaya Konferentsiya po Organicheskomu Sintezu, Moskva, 1986 (Tezisy Dokladov)* (Abstracts of Papers for the Sixth International Conference on Organic Synthesis, Moscow, 1986) p. 102
376. D H Barton, W D Ollis (Eds) *Comprehensive Organic Chemistry* (Translated into Russian) (Moscow: Khimiya, 1985) Vol. 9
377. W W Truce, A M Murphy *Chem. Rev.* **48** 60 (1951)
378. C J M Stirling *Int. J. Sulfur Chem. (B)* **6** 277 (1971)
379. I Scheinfeld, J C Parham, S Murphy, G B Brown *J. Org. Chem.* **34** 2153 (1969)
380. I B Bougiass, B S Farsh, E G Thomas *J. Org. Chem.* **26** 1996 (1961)
381. M L Kee, I B Douglass *Org. Prep. Proced.* **2** 235 (1970)
382. S G Clarke, J Kenyon, H Phillips *J. Chem. Soc.* 1225 (1930)
383. M M Kremlev, I V Koval' *Zh. Org. Khim.* **5** 2014 (1969)
384. I V Koval', M M Kremlev, V A Alekseenko, in *Voprosy Khimii i Khimicheskoi Tekhnologii* Vol. 75 (Problems in Chemistry and Chemical Technology) (Kharkov: Vishcha Shkola, 1984) p. 111
385. I V Koval', A V Kharchenko, M M Kremlev, in *Voprosy Khimii i Khimicheskoi Tekhnologii* Vol. 54 (Problems in Chemistry and Chemical Technology) (Kharkov: Vishcha Shkola, 1979) p. 29
386. I V Koval', T G Oleinik, M M Kremlev, in *Voprosy Khimii i Khimicheskoi Tekhnologii* Vol. 54 (Problems in Chemistry and Chemical Technology) (Kharkov: Vishcha Shkola, 1979) p. 24
387. I V Koval', A I Tarasenko, T G Oleinik, M M Kremlev *Zh. Org. Khim.* **15** 1004 (1979)
388. I V Koval', A V Kharchenko, M M Kremlev, in *Voprosy Khimii i Khimicheskoi Tekhnologii* Vol. 57 (Problems in Chemistry and Chemical Technology) (Kharkov: Vishcha Shkola, 1979) p. 83
389. A V Kharchenko, I V Koval', M M Kremlev *Zh. Org. Khim.* **13** 2385 (1977)
390. A V Kharchenko, I V Koval', M M Kremlev *Zh. Org. Khim.* **16** 754 (1980)
391. M M Kremlev, G F Kodachenko, V F Baranovskaya *Zh. Org. Khim.* **5** 914 (1969)
392. USSR P. 249 377; *Byull. Izobret.* **10** (1969)
393. M M Kremlev, R P Naumenko *Zh. Org. Khim.* **6** 1042 (1970)
394. USSR P. 259 075; *Byull. Izobret.* **2** (1970)
395. M M Kremlev, I V Koval', A V Kharchenko, in *Voprosy Khimii i Khimicheskoi Tekhnologii* Vol. 30 (Problems in Chemistry and Chemical Technology) (Kharkov: Vishcha Shkola, 1972) p. 36
396. M M Kremlev, A V Kharchenko, I V Koval', in *Voprosy Khimii i Khimicheskoi Tekhnologii* Vol. 45 (Problems in Chemistry and Chemical Technology) (Kharkov: Vishcha Shkola, 1976) p. 24
397. I V Koval', A V Kharchenko, M M Kremlev, V F Voloshin, in *III Simpozium po Khimii i Tekhnologii Geterotsiklicheskikh Soedinenii Goryuchikh Iskopaemykh, Donetsk, 1978 (Tezisy Dokladov)* (Abstracts of Papers for the Third Symposium on Chemistry and Technology of Heterocyclic Compounds in Combustible Minerals, Donetsk, 1978, p. 7
398. USSR P. 238 551; *Byull. Izobret.* **10** (1969)
399. I V Koval', M M Kremlev, in *Khimicheskaya Tekhnologiya* Vol. 21 (Chemical Technology) (Kharkov: Vishcha Shkola, 1971) p. 15
400. USSR P. 384 823; *Byull. Izobret.* **25** (1974)
401. R P Naumenko, I V Koval', M M Kremlev, L I Bondar', S I Guseinov, in *Voprosy Khimii i Khimicheskoi Tekhnologii* Vol. 82 (Problems in Chemistry and Chemical Technology) (Kharkov: Vishcha Shkola, 1986) p.12
402. A V Kharchenko, M M Kremlev, I V Koval', in *Voprosy Khimii i Khimicheskoi Tekhnologii* Vol. 48 (Problems in Chemistry and Chemical Technology) (Kharkov: Vishcha Shkola, 1977) p. 6
403. I V Koval', in *Voprosy Khimii i Khimicheskoi Tekhnologii* Vol. 59 (Problems in Chemistry and Chemical Technology) (Kharkov: Vishcha Shkola, 1980) p. 58
404. A V Kharchenko, M M Kremlev, I V Koval' *Zh. Org. Khim.* **13** 459 (1977)
405. A V Kharchenko, I V Koval', M M Kremlev *Zh. Org. Khim.* **15** 443 (1979)
406. I V Koval', N D Borodavko *Zh. Org. Khim.* **17** 2022 (1981)
407. I V Koval', A I Tarasenko, M M Kremlev *Zh. Org. Khim.* **22** 410 (1986)
408. M M Kremlev, I V Koval' *Zh. Org. Khim.* **6** 1457 (1970)
409. USSR P. 2 454 771; *Byull. Izobret.* **20** (1969)
410. J Goerdeler, D Krause-Loevenich *Chem. Ber.* **87** 1079 (1954)
411. E S Levchenko, L V Seleznenko *Zh. Org. Khim.* **5** 492 (1970)
412. E S Levchenko, L N Markovskii, A V Kirsanov *Zh. Org. Khim.* **3** 1273 (1967)
413. M M Kremlev, I V Koval' *Zh. Org. Khim.* **6** 2559 (1970)
414. L N Markovskii, T N Dubinina, E S Levchenko, A V Kirsanov *Zh. Org. Khim.* **9** 1409 (1973)
415. E S Levchenko, L V Budnik *Zh. Org. Khim.* **9** 212 (1973)
416. E S Levchenko, T N Dubinina, L V Budnik *Zh. Org. Khim.* **12** 1846 (1976)
417. E S Levchenko, T N Dubinina, L V Budnik *Zh. Org. Khim.* **19** 2158 (1983)
418. A S Prochukhan, E M Baranovskaya, A S Lukmanova, in *XII Nauchnaya Sessiya po Khimii i Tekhnologii Organicheskikh Soedinenii Sery i Sernistykh Neftei, Riga, 1971 (Tezisy Dokladov)* (Abstracts of Papers for the Twelfth Scientific Session on the Chemistry and Technology of Organic Sulfur Compounds and Sulfurous Petroleum, Riga, 1971) p. 148
419. K Tomas, N Toyorn *Acta. Chem. Scand.* **27** 1451 (1973)

Russian Chemical Reviews **62** (8) 787 – 798 (1993)
©1993 Russian Academy of Sciences and Turpion Ltd

UDC 615.37 + 543.8 + 547.94

Immunoassay of alkaloids

S K Volkov

Contents

I.	Introduction	787
II.	Immune methods for the assay of low-molecular-mass compounds	788
III.	Immune methods for the assay of alkaloids	790
IV.	Conclusion	796

Abstract. A survey is presented of literature data concerning the development and application of the immunochemical methods for the assay of alkaloids — one of the classes of physiologically active compounds of plant origin most widely used in medical practice. The bibliography includes 141 references.

I. Introduction

Alkaloids are nitrogen-containing organic compounds which are encountered in plants and which as a rule exhibit physiological activity. Similar compounds have been detected also in certain animal organisms, in higher and lower fish, and in algae. More than 5000 different alkaloids have now been described and the chemical features of many of them have been fully established.

One of the most important branches of the modern science of medicinal plants involves the analytical determination of the content of biologically active substances in plant tissues. Not only the economic parameters of the manufacture of a number of medicinal preparations but also their quality depend on the content of physiologically active substances in the plant raw material.

Another important application of the analytical methods is the study of the biosynthesis of alkaloids in plant tissues.

Furthermore, analytical methods are widely used in the study of the metabolism and pharmacokinetics of the alkaloids used in medical practice.

A series of alkaloids possess narcotic properties, so that the rapid and reliable detection of these compounds in the human organism is very important from the medical point of view. Assay of narcotics is important also from the criminological standpoint.

The methods of synthesis of biologically active compounds in cell and plant tissue cultures have been vigorously developing in recent years. Theoretically this may make it possible to abandon the laborious operations involving the collection of plant material, especially wild species, and the use of large areas of fertile soil for the cultivation of such plants. The successful development of biotechnological methods is also associated with the analytical determination of the content of the target substances.

S K Volkov, The 'All-Russian Institute of Medicinal and Aromatic Plants' Scientific-Industrial Association, ul. Grina 7, 113628 Moscow.
Tel. (7-095) 388 45 22

Received 20 April 1993
Uspekhi Khimii **62** (8) 831 – 842 (1993); translated by A K Grzybowski

The necessity for a large number of analyses, especially in selection studies, has given rise to the need for the automation of analytical methods.

The methods for the quantitative assay of the substances present in plants can be divided into three groups: photometric, chromatographic, and protein-binding.

The photometric analytical methods have found the greatest application in the assay of biologically active substances of plant origin. These methods are relatively insensitive and non-specific, but, by virtue of their simplicity, they are still being used.

Chromatographic methods [thin-layer chromatography (TLC), gas – liquid chromatography (GLC), chromatography-linked mass spectrometry (GLC-MS), and high performance liquid chromatography (HPLC)] make it possible to determine fairly rapidly and accurately several substances being assayed in a single sample. However, these methods are fairly laborious. The most accurate and reliable of these is GLC-MS, but the application of this method is restricted by the high cost and complexity of the assay, which requires specially trained service personnel.

The protein-binding methods include the receptor and immune methods. The receptor assay method is based on the competitive inhibition by the compound assayed of the binding of a radioactively labelled ligand by membrane receptors specific to it.[1-3] This method is hardly used in the assay of substances present in plants. The reason for this is the difficulty in the identification and isolation of specific receptors.

The immunoassay methods are based on the specific interaction of the molecules of the substance assayed with the antibodies produced by the animal organism in response to the entry of foreign substances into the latter.

The protein-binding and in particular immune methods have a number of advantages over the photometric and chromatographic analytical methods: they do not require a large amount of work on the preparation of the specimen to be analysed, are highly sensitive, do not need complex and expensive equipment, and permit the simultaneous analysis of a large number of specimens.

The principal disadvantage of the immunoassay methods for low-molecular-mass substances is the necessity for preliminary work associated with the synthesis and purification of the antigen, the immunisation and maintenance of the animals, and the isolation, purification, and characterisation of the antibodies. Another significant disadvantage of the immunoassay methods is the possibility of the cross-interaction of the antibodies with a number of compounds having a structure similar to those of the antigen.

II. Immune methods for the assay of low-molecular-mass compounds

A fairly large number of reviews and monographs have been devoted to the immunoassay methods. They deal in detail with various procedures whereby the analyses are set up and carried out.[4-14]

There exist at present fairly numerous versions of immunoassay. The heterogeneous immunoassay methods used in the assay of low-molecular-mass compounds are as follows: radioimmunoassay, direct competitive enzyme immunoassay, and indirect enzyme immunoassay using secondary antibodies.

In radioimmunoassay (RIA), a standard amount of a radioactively labelled hapten is mixed with the specimen analysed. The radioactive hapten and the molecules of the specimen interact competitively with the antibodies, the degree of binding of the radioactive hapten to the antibodies being inversely proportional to the number of molecules assayed in the specimen. After equilibration, the hapten molecules bound to the antibodies are separated from the remaining free molecules either by the rapid adsorption of the haptens or by the precipitation of the proteins, after which the radioactivity of a particular phase is measured.

In the direct competitive enzyme immunoassay (EIA), an enzyme label and not a radioactive label is used. Antibodies present in a limited amount are bound to the solid phase, usually a polystyrene test tube or the walls of the microtitration tray. Competition between the substance assayed in the specimen and the enzyme-bound hapten leads to the immobilisation of a proportion of the enzyme on the solid phase. The free enzyme is removed and the amount of bound enzyme is determined, after adding the substrate, from the intensity of the colour of the solution caused by the substrate decomposition product.

In the analysis by the indirect immunoassay method using secondary antibodies [enzyme-linked immunosorbent assay (ELISA)], the hapten conjugated with the protein is sorbed on a solid phase — usually on the walls of the microtitration tray. The conjugate with which the animal was immunised is not used in this stage; instead one employs a conjugate with a protein unrelated to that of the immunogenic conjugate. Next the substance to be assayed, containing the free hapten and the antiserum, is added. The antibodies are distributed between the free hapten of the specimen and the immobilised hapten–protein conjugate. The liquid is decanted and an excess of secondary antibodies conjugated to the enzyme and specific to the immunoglobulins G (Ig G) of the immunised animal is added. The secondary antibodies are bound to the primary antibodies and are retained on the solid phase. The liquid phase is again decanted and the amount of secondary antibodies is determined after adding the substrate to the conjugated enzyme and the formation of the coloured product.

The homogeneous immunoassay methods most frequently used are those based on the measurement of the degree of polarisation of the fluorescence and the change in the activity of the enzyme.

In the immunoassay based on the measurement of the degree of polarisation of the fluorescence [fluorescence-polarisation immunoassay (FPIA)], a hapten conjugated to fluorescein or another molecule which fluoresces when irradiated with a beam of polarised light is employed. In the free state, the hapten–fluorescein conjugate in solution is mobile and the degree of polarisation of the light transmitted through the solution is low. In the form bound to the antibodies, the mobility of the hapten–fluorescein conjugate is restricted, which increases the degree of polarisation of the light. The amount of the hapten in the specimen is determined from the degree of substitution by the latter of the hapten–fluorescein conjugate in the interaction with the antibodies, which lowers the degree of polarisation of the light.

In the immunoassay based on the change in the activity of the enzyme [enzyme-multiplied immunoassay (EMIA)], one uses a hapten conjugated with the enzyme in such a way that the binding of the hapten to the antibodies lowers the activity of the enzyme owing to the blocking of its active centre. Thus the degree of recovery of the enzyme activity of the specimen analysed in the presence of the free hapten permits the determination of its amount.

Each of these methods has its advantages and disadvantages. Radioimmunoassay requires the synthesis of the radioactively labelled hapten. Fairly expensive equipment is also necessary — a centrifuge which permits the simultaneous centrifugation of up to 100–200 specimens and a liquid-scintillation (in the case of the ^{3}H isotope) or a γ-emission (in the case of the ^{125}I isotope) counter. The advantage of the ^{3}H isotope consists in the fact that the native structure of the molecule is retained.

The fluorescent and chemiluminescent labels, which make it possible to avoid the use of radioactive isotopes, appreciably alter the native structure of the hapten. These methods also require expensive equipment.

The use of enzyme labels in the stationary phase in the direct competitive enzyme immunoassay simplifies the analysis, since the phases can be separated very simply and only a colorimeter is required for the quantitative determination. However, this method requires the synthesis of the hapten–enzyme conjugate and the selection of the necessary hapten/enzyme ratio. Furthermore, owing to the incomplete adsorption of the enzyme, the antiserum — the most important component in the method — is not consumed in a rational manner. Another disadvantage of this method is that the enzyme and the specimen analysed, which frequently contains a multiplicity of components, are incubated together, which can lead to the inactivation of the enzyme. Furthermore the homogeneous methods are also less sensitive.

Direct immunoassay with the use of secondary antibodies is free from many of the above disadvantages. In this method, the antiserum is consumed fairly economically, since only dilute solutions are used. The high affinity and specificity of the antibodies make it possible to achieve a high sensitivity and specificity of the assay. Although in this method there is an additional stage involving incubation with the secondary antibodies, the employment of the latter makes it possible to increase the sensitivity of the assay and to extend the range of the measurable concentrations. The conjugates of enzymes with secondary antibodies to immunoglobulins from various sources are fairly readily commercially available. This method is the most popular and perhaps the best of all the immune methods which exist at the present time. The highest sensitivity of the method, attained in the analysis of the cholera toxin, amounts to 10^{-16} g, i.e. 600 molecules of this toxin is sufficient for the determination.[15]

The principal advantage of the homogeneous immunoassay methods is that, by performing the assay in one phase, it is possible to automate it and this makes them particularly attractive for routine assays of large numbers of specimens. It is more difficult to automate heterogeneous analytical methods, although here too the use of laboratory robots makes it possible to attain a productivity of up to 1000 specimens per day.

Analysis of the studies published during the period from 1959 to 1982 revealed a change in 1979–1981 from the radioimmunoassay to the enzyme immunoassay methods, which have virtually predominated since 1985.[14]

Analysis of chemical compounds by immune methods presupposes the employment of antibodies which recognise specifically the compounds to be analysed. However, substances with a molecular mass below 1000, including alkaloids, do not induce an immune response and formation of antibodies when they enter an animal organism. In order to stimulate an immune response, such substances must be bound covalently to large molecules (usually to a protein); the resulting conjugates are then used to immunise the animals. The antiserum produced after immunisation contains a mixture of antibodies, some of which may prove to be capable of recognising the hapten not only in the bound state but also in a free state.

A number of methods based on the use of various functional groups of the hapten have been proposed for the synthesis of immunogenic conjugates. The specificity of the antibodies thus obtained is determined by the sections of the molecule most remote from the conjugation point.[16] Careful study of the structure and properties of the hapten molecule and the correct selection of the conjugation point make it possible in many instances to obtain an antiserum with the required selectivity.[17] Many natural products contain several functional groups, which permits in many instances the variation of the way in which the conjugation is achieved. If there is no suitable group, it is possible to employ derivatives containing a functional group in the required site in the molecule.

Carboxy- or hydroxy-groups of the hapten frequently participate in the formation of the immunogenic conjugate. When the protein molecule is bound to the hapten via the carboxy-group, a two-stage synthesis takes place as a rule. In the first stage, a derivative of the hapten with a free carboxy-group is obtained with the aid of a bifunctional reagent. The mixed anhydride and carbodiimide methods are used for this purpose.

The mixed anhydride method,[18] widely known in organic chemistry, has been used to obtain ajmalicine conjugates as early as 1959,[19] while the carbodiimide method,[23] proposed for the synthesis of immunogenic conjugates in 1981, has been used to obtain the conjugates of serpentine,[19] cotinine,[20] vinblastine, vincristine,[21] and colchicine.[22]

Bifunctional reagents, for example succinic anhydride, are used in the synthesis of conjugates with participation of a hydroxy-group of the hapten. The anhydride has been used to obtain the conjugates of nicotine,[20] vindoline,[24] quinine,[25] and quinidine.[26] Glutaric anhydride has also been used to synthesise the vindoline conjugate.[27]

The presence of a phenolic hydroxyl in the hapten molecule permits the use of carboxymethylation in order to attach such a molecule to a protein; morphine conjugates have been obtained in this way.[28-30]

The presence of an amino-group in the hapten molecule makes it possible to obtain conjugates with the aid of the Mannich reaction or acrylic acid. The Mannich reaction has been used to synthesise the conjugates of vinblastine,[31, 32] while acrylic acid has been used to synthesise the conjugate of nor-(−)-scopolamine.[33]

The conjugation procedures described presuppose the insertion of a fairly short intervening chain (spacer) between the hapten and the protein molecule. However, in those cases where the spacer contains a chain of only 2–3 carbon atoms, it is not always possible to obtain an antiserum capable of recognising the hapten. In such cases, it is useful to increase the length of the spacer to 5–6 methylene units. An increase in the length of the spacer can be achieved, for example, by using 6-amino-n-hexanoic acid, the amino-group of which is attached to the hapten, while the carboxy-group is attached to the protein. A quinidine conjugate has been obtained in precisely this way.[26] The introduction of a spacer with a length corresponding to 4 or 5 carbon atoms is achieved using succinic or glutaric anhydride. A more rigid spacer is obtained when *trans*-cyclohexane-1,4-dicarboxylic dichloride is used, whilst a longer spacer can be secured with the aid of 4-aminohippuric acid.[34]

The nature of the spacer has a significant influence on the characteristics of the assay method. It has been established in relation to polarisation fluoroimmunoassay of methamphetamine by means of its conjugate with fluorescein that the best results are obtained when a spacer fully identical with that in the immunogenic conjugate used to obtain the antibodies is employed.[35]

The majority of conjugation methods are based on the interaction between the activated functional groups of the hapten and the amino-groups of the protein. Therefore one of the requirements which must be met by the protein is the accessibility of the ε-amino-groups of the lysine residues. Proteins such as bovine serum albumin (BSA), human serum albumin (HSA), and keyhole limpet hemocyanin (KLH) are most often used for conjugation. In certain cases, poly-L-lysin was employed for conjugation,[20, 29] but it was found that it has no appreciable advantages over the proteins listed above. It has been demonstrated empirically that it is preferable to conjugate the hapten with KLH rather than albumin in order to obtain antibodies to small compounds.[36]

In enzyme immunoassay methods, where there is conjugation with two proteins, it is important that these proteins should not be related and that the immunised animal should not have come into contact previously with these proteins.

The conjugate synthesised is usually purified by gel filtration on a column with Sephadex G-25 or by dialysis, which makes it possible to separate the unreacted low-molecular-mass components.

The molar ratio of the components of the conjugate — the hapten density — is determined in the purified conjugate. It has been established experimentally that one must avoid both very high and very low hapten densities. Thus the hapten : protein ratio for BSA should be in the range from 10 : 1 to 25 : 1, whereupon one usually obtains an antiserum of good quality. The hapten density can be frequently determined by UV or fluorescence spectroscopy, but in some cases it may be necessary to split off the hapten chemically and to determine its amount by other methods.[37]

Experiments with conjugates of low-molecular-mass compounds of plant origin hardly differ from the usual manipulations involving traditional (protein) antigens.

Since low-molecular-mass organic substances have a small and rigorously defined antigen determinant, highly specific polyclonal antibodies can be obtained successfully for them and can also be used successfully for routine assays of low-molecular-mass compounds. The monoclonal antibodies to haptens do not as a rule have special advantages and their preparation requires considerable effort and expense.

Immunochemical methods for the assay of a number of low-molecular-mass compounds (alkaloids, terpenes, vitamins, steroids, and regulators of the growth and development of plants) and biologically active compounds of plant origin such as phytohormones, cytokinins, phytoalexins, and enzymes have now been developed.

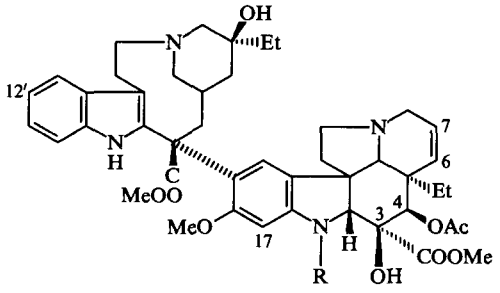
The therapeutic properties of medicinal plants are known to be largely determined precisely by low-molecular-mass compounds. The range of such compounds of plant origin, for which immunoassay methods have been developed, is being constantly expanded and these methods have now come to be fairly usual in clinical practice and are finding increasing application in plant cultivation and in the manufacture of medicinal preparations of plant origin. Immunochemical methods are used widely for the selection of the most productive plant species. Antisera to several of the low-molecular-mass biologically active substances isolated from plants and contaminating plant material are now produced industrially by a number of companies.[36, 38]

The high specificity of the antibodies makes it possible to determine individual substances in the presence of a multiplicity of other compounds or their metabolites by immunochemical methods, but in many instances it may be necessary to assay not just any one compound but a whole class of substances. The method employing mixtures of several highly specific antibodies is used for the simultaneous assay of several compounds. Thus a homogeneous polarisation fluoroimmunoassay using a mixture of antibodies to determine the majority of the classes of narcotics usually employed — amphetamines, barbiturates, and cannabinoids — has been described.[39]

III. Immune methods for the assay of alkaloids

1. Indole alkaloids of *Catharanthus roseus*

The extremely great pharmaceutical value of the alkaloids of *C. roseus*, especially vinblastine **1** and vincristine **2**, has aroused continuous interest by investigators of these alkaloids. The great demand for the alkaloids of *C. roseus*, and especially compounds **1** and **2**, has stimulated intense research designed to increase the manufacture of the alkaloids. The two main approaches to the solution of this problem—the selection of the most productive plants and the cultivation of *C. roseus* cells in fermenters—required the development of new rapid and accurate assay methods.



R = Me (**1**), CHO (**2**)

a. Vinblastine and vincristine

These bisindole alkaloids, which are minor components of the total alkaloid extract from *C. roseus*, are believed to be some of the most important biologically active substances of plant origin and are used widely in medical practice as antineoplastic agents. In view of their high activity and the presence of side effects such as neurotoxicity and myelosuppressivity, the clinical use of these alkaloids requires careful monitoring, for which immune methods are ideally suitable.

In terms of the site of the conjugation of the alkaloid molecule, the immunoassay methods for compounds **1** and **2** can be divided into several groups.[40]

Chronologically the first and most widely used procedure involves conjugation at the C(3) atom. A brief communication was published in 1975[41] concerning the development of a radioimmunoassay method for compounds **1** and **2**. Using the method for the conjugation of compound **1** to a protein, the Eli Lilly and Company Corporation (USA) began to manufacture an antiserum to the antigen obtained by converting compound **1** initially into the 3-hydrazide and then into the 3-carboxazide (4-desacetylvinblastine), which was conjugated to the protein.[42]

The antibodies to such conjugates, even monoclonal antibodies, exhibit as a rule a low specificity: cross reactions of the antibodies with derivatives of compound **1** (vindesine and its derivatives) and to compound **2** and its derivatives (leurosine and leurosidine) are observed. Polyclonal antibodies also participate in cross reactions with the monomeric alkaloids vindoline and catharanthine.

Polyclonal antibodies to the conjugates of compounds **1** and **2** via the C(3) atom have been used to develop radioimmunoassay[43] and enzyme immunoassay[32] methods for these compounds. In the radioimmunoassay method using [^{3}H]-**1** and [^{3}H]-**2**, the specimen analysed is incubated beforehand with the immune serum and is then treated with the radioactively labelled substance. This makes it possible to increase the sensitivity of the determination of the alkaloids: the concentration range in which compounds **1** and **2** can be determined is 0.2–30 ng. In the enzyme immunoassay method, compounds **1** and **2** are determined in microtitration trays the wells in which are coated by antibodies (dilution 1 : 10 000); the concentration range in which compounds **1** and **2** can be determined is 0.01–0.1 ng. However, none of these methods makes it possible to distinguish between the alkaloids **1** and **2**.

An RIA method[44] for the determination of compound **1**, also based on the use of the conjugate at the C(3) atom and used in the study of the pharmacokinetics and metabolism of compound **1** in humans, makes it possible to determine compound **1** in the concentration range 0.2–100 μg litre^{-1}. The monoclonal antibodies to the conjugates of compound **1** at the C(3) atom have been used in the development of solid-phase and liquid-phase RIA methods and an EIA method.[46] The latter permits the determination of compound **1** in the concentration range 1–100 μg litre^{-1}; the limit of the determination of compound **1** is 0.64 μg litre^{-1}. However, cross reactions with vindesine (3%), vinblastine (75%), leurosine (152%), and a number of other derivatives take place in this instance.

The conversion of compound **1** into an azide activated in the 3-position and its conjugation with the dipeptide Gly-Tyr made it possible to devise a radioimmunoassay method for vincristine and vindesine using a [^{125}I]-labelled conjugate.[47]

A conjugation method which makes it possible to determine both alkaloids and to distinguish reliably compound **1** from compound **2** was developed in 1979.[21] This method is based on the oxidation of the double bond between the C(6) and C(7) atoms with a mixture of potassium permanganate and sodium periodate.[48] Such oxidation leads to the formation of a dicarboxy-derivative, which affords a conjugate with the protein.

The antibodies formed in response to the introduction of such a conjugate into the organism are more specific: the antibodies to the conjugate of compound **1** interact with compound **2** five times more weakly than with compound **1**, whereas those to the conjugate of compound **2** interact with compound **1** 200 times more weakly than with compound **2**.

The two alkaloids **1** and **2** were converted in different ways into the 6,7-dicarboxy-derivatives, which were in their turn added to HSA. These conjugates were used to develop radioimmunoassay methods using [^{3}H]-**1** and [^{3}H]-**2**. The 'bound' and 'free' phases were separated with the aid of goat antibodies to the rabbit immunoglobulins G and the radioactivity of the 'bound' phase was measured. One of the antisera obtained proved to be specific to compound **2** and the contribution of the cross reaction with compound **1** was only 0.05%; compound **2** can be determined in the range 1–10 ng. Another antiserum was moderately selective to compound **1** and the contribution of the cross reaction with compound **2** was 25%; the range for the determination of compound **1** is 1–15 ng and the limit in its determination is 0.4 pg litre^{-1}.[21] These antisera can be used to select plants in terms of their content of compounds **1** and **2**.

A further increase in the sensitivity and selectivity of the determination of compounds **1** and **2** was achieved using an enzyme immunoassay method employing compound **1** attached by the Mannich reaction to BSA via the C(17) atom.[31, 32] The C(17) atom of the aromatic ring, which is close to the carbon atom carrying the methoxy-group, proves to be activated and is capable of interacting with formaldehyde.

The antibodies to the conjugate via the C(17) atom were used to develop a method for the radioimmunoassay of compound **1**. The method makes it possible to determine compound **1** in the plasma in the concentration range from 1 to 200 to 300 μg litre^{-1}.[31] An enzyme method for the immunoassay of compound **1** with the aid of monoclonal antibodies was developed later. This method made it possible to determine compound **1** in the concentration range 1–100 μg litre^{-1}; the limit in the determination of compound **1** is 0.54 μg ml^{-1}.[32]

The monoclonal antibodies to the conjugate via the C(17) atom are somewhat more specific than the antibodies to the conjugate via the C(3) atom, but appreciable contributions of the cross reactions with the derivatives of compound **1** (vindesine) compound **2** and its derivatives (leurosine, and leurosidine) have been noted for them also.[32]

Studies using the method involving the conjugation of compound **2** via the C(12′) atom of the aromatic ring of the molecule have been published in recent years.[49-51] The antibodies to the conjugate via the C(12′) atom are highly selective and there are virtually no cross reactions with compound **1**. For this purpose, *p*-aminobenzoic acid was added to the C(12′) atom [corresponding to the C(10) atom according to the biogenetic numbering] of compound **2** after nitration and the resulting derivative was attached to the protein via the amino-groups by the carbodiimide method.[49]

This conjugation procedure makes it possible to distinguish more reliably compounds **1** and **2**: the antibodies to the conjugate of compound **2** interact with compound **1** and vindoline 1500 times more weakly than with compound **2**.[50, 51]

The antiserum to this conjugate was used to develop a method for the radioimmunoassay of compound **2**.[51] The range of the determination of the latter is 0.1–100 ng; the contributions of the cross reactions with compound **1** and vindoline are 0.03% and 0.09% respectively. A method for the enzyme immunoassay of compound **2** was developed on the basis of the same conjugate;[50] the range of the determination is 5–500 pg.

A study in which compound **1** was attached to the protein with the aid of glutaraldehyde[53] was published in 1989.[52] The use of this conjugate leads to the formation of an antiserum, which recognises mainly compound **1**. This made it possible to develop a method for the radioimmunoassay of compound **1** in the range 0.5–10 ng ml^{-1}. The contributions of the cross reactions with compound **2** and leurosine are 30% and 0.23% respectively and that of the cross reactions with all the remaining alkaloids of *C. roseus* is less than 0.1%.

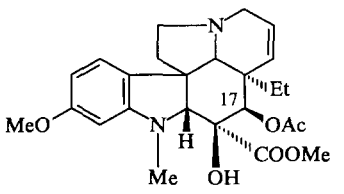
This conjugate was used in the development of a method for the radioimmunoassay of compound **1** in *C. roseus* tissue cultures.[52]

It is noteworthy that almost all the methods for the immunoassay of compounds **1** and **2** were developed and used to determine the content of these alkaloids in the blood sera of patients injected intraveneously with the preparations **1** and **2**[31, 43, 45, 50] and for the investigation of the pharmacokinetics and metabolism of these alkaloids.[32, 44, 54] Immunoassay methods have not so far found extensive application in the determination of the contents of compounds **1** and **2** in plants. Only radioimmunoassay[21] and enzyme immunoassay[50] methods have been used for the quantitative assay of the alkaloids in various parts of the *C. roseus* plant. It was established that the maximum concentration of the alkaloids is detected in the flowers, but, owing to the small absolute mass of the flowers, almost the total amount of the alkaloids is contained in the leaves.[21] The content of compound **2** in the extracts from the leaves of *C. roseus* was determined by an enzyme immunoassay method.[50] The total amount of the dimeric indole alkaloids in *C. roseus* was likewise determined by an enzyme immunoassay method.[46] The immuno methods are used somewhat more widely in the quantitative assay of compounds **1** and **2** in *C. roseus* cell cultures.[52, 55-57]

The high cost and pharmaceutical value of compounds **1** and **2** have led to the intensification of the development of methods for the immunoassay of these substances. This led to the appearance in the world market of primary antisera to compounds **1** and **2** manufactured by companies such as Bioanalysis Ltd and Guildhay Antisera (Great Britain) and Eli Lilly and Company.

b. Vindoline

Vindoline **3** is an indole alkaloid which is a biogenetic precursor of compounds **1** and **2** and can be used for the chemical synthesis of compound **1**.[58] In the development of a method for the immunoassay of compound **3**, 17-desacetylvindoline was initially activated by succinic anhydride and the resulting hemisuccinate was then attached to BSA by the carbodiimide method.[27] The antiserum obtained with the aid of this conjugate was used in the radioimmunoassay of compound **3**; the range of its determination is 0.2–45 ng. The conjugate of 17-desacetylvindoline with BSA was also synthesised with the aid of succinic anhydride.[24] This conjugate was used in the development of a method for the radioimmunoassay of compound **3**, but it proved to be less sensitive: the range of the determination of compound **3** is 10 to 1000 ng.



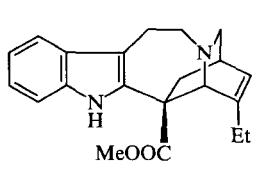
3

The use of the antiserum to the conjugate of compound **1** with BSA, obtained by reaction via the C(12′) atom, made it possible to develop methods for the enzyme immunoassay and radioimmunoassay of compound **3**.[59, 60] The range in which compound **3** can be determined by enzyme immunoassay is 5 to 500 pg.

These methods were used to determine the content of compound **3** in various parts of the *C. roseus* plant[27] and in *C. roseus* cell cultures.[27, 59, 61]

c. Catharanthine

Like compound **3**, catharanthine **4** is a biogenetic precursor of compounds **1** and **2** and constitutes, as it were, the 'upper' half of the molecules of the dimeric alkaloids and, like compound **3**, can be used for the chemical synthesis of the dimeric alkaloids. A method for the radioimmunoassay of compound **4** in the range 0.02–20 ng has been developed.[61] In order to obtain an antiserum, rabbits were immunised with a conjugate of catharanthic acid with HSA. [^{3}H]-**4** was used as the radioactive ligand. The limit in the radioimmunoassay of compound **4** is 66 pg. Cross reactions with catharanthic acid and the dihydro- and carboxy-derivatives of compound **4** have been noted.

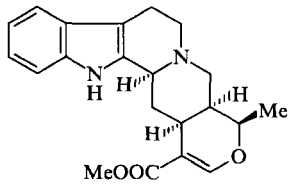


4

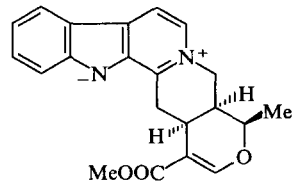
The radioimmunoassay has been used to determine compound **4** in *C. roseus*.[62]

d. Ajmalicine and serpentine

Ajmalicine **5** is one of the principal alkaloids isolated from plants of the *Catharanthus* and *Rauwolfia* species. It is used widely in the treatment of the blood circulation system — in particular in the pathology of the vessels in the brain. Serpentine **6**, which is an alkaloid related to ajmalicine, is not used as a medicinal drug but can serve as a source of compound **5**.



5



6

For the effective production of compound **5**, it is important to select plants in terms of the maximum contents of compounds **5** and **6**. Antisera to each of these alkaloids were therefore

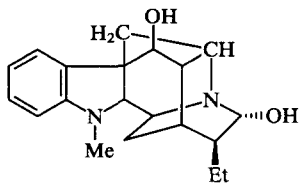
obtained.[19] For this purpose, ajmalinic acid was obtained by the alkaline hydrolysis of compound **5** and was attached to HSA by a modified mixed anhydride method. The resulting conjugate was used to produce an antiserum; the antiserum proved to be specific to compound **5** and was insensitive to compound **6**. The radioimmunoassay, developed using this antiserum makes it possible to determine compound **5** in the range 2–50 ng.[19]

Serpentinic acid, obtained by the alkaline hydrolysis of compound **6**, was conjugated with HSA via the *N*-hydroxysuccinimide ester modified by a carbodiimide method. The antiserum to this conjugate proved specific to compound **6** and insensitive to compound **5**. The radioimmunoassay makes it possible to detect compound **6** in the range 2–50 ng.[19]

Both these methods were used in the study of the distribution of compounds **5** and **6** in plant tissues. It was shown that, in contrast to compound **3**, the maximum concentration of both alkaloids is found in the plant roots immediately under the surface of the soil, the concentration of compound **6** being approximately five times higher than that of compound **5**. Radioimmunoassay was used in selection,[19] which made it possible to select a population of plants with an increased overall content of alkaloids and an increased **5/6** ratio, and also in the determination of these alkaloids in the cultivation of *C. roseus* cells by the suspension method.[62] The same methods have been used in the study of the biosynthesis of compound **5**.[63]

e. Ajmaline

In order to obtain an antiserum specific to the alkaloid ajmaline **7**, the hemisuccinate of compound **7** was conjugated with BSA and rabbits were immunised with this conjugate.[64] The resulting antiserum made it possible to develop a radioimmunoassay for compound **7**. [^{3}H]-**7** was used as the radioactive ligand. The range in which compound **7** can be determined is 0.05–20 ng. Appreciable cross reactions with 17-chloroacetylajmaline, sandwicine, and isoajmaline have been noted.



7

The method developed has been used to determine the content of compound **7** in the plants of the *Rauwolfia* family.[64]

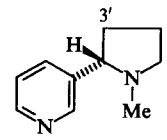
2. Tobacco alkaloids

One of the best known alkaloids of tobacco (*Nicotiana tabacum*, *Nicotiana rustica*, etc.) is nicotine **8**. At the present time compound **8** is isolated from plants mainly in order to oxidise it to nicotinic acid and to synthesise preparations based on it, while the alkaloid itself has found a limited application as an insecticide and an ectoparasitocide in veterinary practice.

In 1973 a radioimmunoassay was developed for compound **8** and its principal metabolite in the organism—cotinine **9**.[20]

a. Nicotine

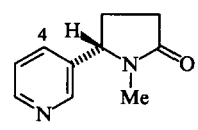
In order to synthesise an antigen for the assay of compound **8**, 3′-hydroxymethylnicotine, synthesised by the procedure described by Cushman and Castagnoli,[65] was activated with succinic anhydride and *trans*-3′-succinylmethyl niccotine was obtained and attached to HSA, KLH, and poly-L-lysine by the carbodiimide method. [^{3}H]-**8** was obtained by the catalytic ^{3}H exchange involving the pyridine ring. In the radioimmunoassay, the 'bound' and 'free' phases were separated by immunoprecipitation using goat antibodies to the rabbit Ig G and the radioactivity of the 'bound' phase was measured. The method makes it possible to determine compound **8** in the range 0.35 to 7 ng and an appreciable cross reaction has been observed only with *dl*-amino-**8** (2.4%). Cotinine is not detected if its content in the sample does not exceed 50 ng.[20]



8

b. Cotinine

In the synthesis of an immunogen for the assay of cotinine **9**, *trans*-4-carboxy-**9** was conjugated by the carbodiimides method with HSA, KLH, and poly-L-lysine. Radioactive ^{125}I was introduced into *N*-(4-hydroxyphenylethyl)-*trans*-carboxamide derived from compound **9**. The assay was carried out as for compound **8**. The sensitivity of the method corresponds to 0.01–1 ng. An appreciable cross reaction has been observed only for *dl*-desmethyl-**9** (0.9%); at a level below 70 ng, compound **8** is not detected.[20]

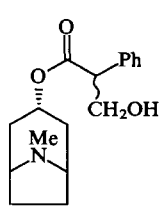


9

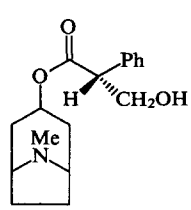
These methods have been used to investigate the conversion of compound **8** into compound **9** by extracts from rabbit liver. It was shown that compound **8** is not fully oxidised: after 10 h, only 37% of compound **8** is converted into compound **9**. These methods were also used to analyse the conversion of compound **8** into compound **9** *in vitro*, using extracts from cultivated liver cells, and for the determination of the content of these alkaloids in the biological liquids of smokers. It was established that the principal metabolite of compound **8** present in the blood serum and urine of smokers is compound **9**. Its content in the blood serum and urine falls after smoking has stopped. Compound **9** was not detected in the biological liquids of non-smokers.[20] The same method has been used to determine the content of nicotine and its metabolites in hair.[66] The method has not been used to determine compound **8** in plant tissues.

3. Tropane alkaloids

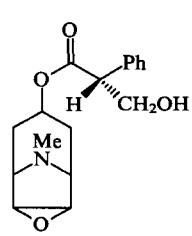
The structures of these alkaloids are based on the tropane skeleton. The most familiar of these are atropine **10**, hyoscyamine **11**, and scopolamine **12**. The alkaloids of the cocaine group, which will be examined below, can also be included with them. Antropine constitutes the racemic form of hyoscyamine formed when the alkaloids are isolated from plants.



10



11



12

Scopolamine, produced by plants of the *Datura* and *Duboisia* (*Solanaceae*) species, is used as a parasympatolytic, antiemetic, and anticholinergic agent. Being a typical agent blocking *m*-cholinoreceptors, it resembles compound **10** as regards its physiological activity, but its influence on the central nervous

system is much stronger and it is frequently used as a calming agent in psychiatry, in narcology, and in sea sickness. Together with the alkaloid **12**, plant tissues usually contain large amounts of compound **11** – the biogenetic precursor of compound **12**.

In the synthesis of the immunogenic conjugate, compound **12** was attached to HSA via the hydroxy-group with the aid of glutaric anhydride, but an active antiserum to this conjugate was not obtained.[33] A satisfactory antigen was synthesised by the reaction of nor-(−)-**12** with acrylic acid and subsequent attachment of the resulting derivative to HSA by the mixed anhydride method or the carbodiimide method. The antiserum to this conjugate, specific to compound **12** and nor-**12**, made it possible to develop a method for the radioimmunoassay of compound **12** in the range 0.5 – 50 ng. The contribution of the cross reaction with compound **12** is only 0.8%.

The method has been used to investigate the distribution of compound **12** in the tissues of *D. innoxia* and *D. sanguinea*. The maximum concentration of compound **12** was detected in unripe seeds, but, owing to the small absolute amount of the seeds, almost the entire alkaloid **12** is contained in the leaves. A similar method has been used to assay compound **12** in *Datura* tissue cultures.[67]

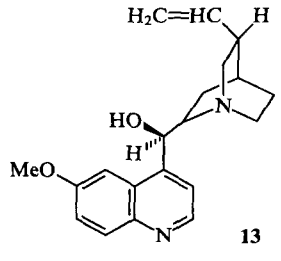
It was later reported[68] that an immunoassay had been developed using the rabbit antiserum to the conjugate of tropic acid with BSA. The method permits the simultaneous determination of the principal tropane alkaloids **10** – **12**. The detection limit of compound **10** is 0.1 ng. In the determination of compounds **11** and **12**, the latter are first racemised.

4. Quinoline alkaloids

Certain plant species of the genus *Cinchona* (*Rubiaceae*) produce the isomeric alkaloids quinine **13** and quinidine **14**. From the pharmacological point of view, compound **13** is an antibiotic. It is effective against the gametocytic forms of *Plasmodium vivax* and *Plasmodium malariae* in erythrocytes, the mechanism of its biological activity, which consists in the selective suppression of the replication of DNA and the transcription of RNA, being typical for antibiotics. Quinine is widely used as an antimalarial agent and as a bitter and has also found limited application in the treatment of certain cardiac affections and in midwifery. Quinidine, a stereoisomer of compound **13**, is a powerful antiarrhythmic agent.

a. Quinine

Activation of compound **13** with succinic anhydride and its attachment to BSA by the mixed anhydride method afford an immunogenic conjugate, which makes it possible to obtain an antiserum specific to compound **13**. A radioimmunoassay[25, 26] and an enzyme immunoassay[26] were developed on the basis of the antiserum and permitted the determination of compound **13** in the ranges 1 – 50 and 0.1 – 10 ng respectively. The detection limit of compound **13** is 10 pg for the enzyme immunoassay and 50 pg for the radioimmunoassay.[26]

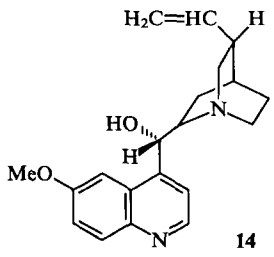


13

The enzyme immunoassay method was used to determine compound **13** in specimens of human biological liquids.[69]

b. Quinidine

There exist at present analytical sets for the immunoassay of compound **14**. The Beckman Company (USA) has developed an analytical set for nephelometric immunoassay, which makes it possible to determine compound **14** and a number of its physiologically active metabolites in mammalian organisms.[70] The Syva Corporation manufactures an analytical set for the immunoassay of compound **14**.[71] Both methods are designed to use special equipment, require a large amount of antiserum, and their sensitivity is fairly low (1 – 10 ng ml^{-1}). However, the complete automation of the assay process makes them very convenient for clinical application.



14

The immunoassay method developed by the Syva Corporation has been compared with the method using reversed-phase HPLC combined with detection by the fluorescence method.[72] It has been established that, in the determination of the content of compound **14** in the blood sera of patients receiving it, the enzyme immunoassay method yields values higher by a factor of 1.2 than the chromatographic method. An automatic system has been developed for the immunoassay with a fluorescence-labelled ligand, which makes it possible to determine compound **14** in the presence of other substances.[73]

Radioimmunoassay and enzyme immunoassay methods were developed in 1985 using the antiserum to the conjugate of 9-hemisucinylquinidine attached to BSA via 6-amino-n-hexanoic acid.[26] The ranges in which compound **14** can be determined by the radioimmunoassay and the enzyme immunoassay methods are 1 – 1000 ng and 0.1 – 10 ng. The radioimmunoassay method has been used for the screening of the clonal cultures of *C. ledgeriana* in analysis designed to determine compound **13**.[25]

The immune method based on the measurement of the degree of polarisation of fluorescence has been used to investigate the pharmacokinetics of compound **14**.[74] The rapid combined autofiltration – immunoenzyme and dialysis – immunoenzyme methods for the assay of compound **14** in the blood sera of patients yielded results which agreed well with those obtained by the autofiltration – liquid- chromatographic and dialysis – liquid-chromatographic methods.[75]

The immunoenzyme and immunofluorescence methods for the assay of compound **14** have come to be fairly widely used, principally in clinical practice.[76–78] An automatic system 'optimate', which makes it possible to assay compound **14** by the immunofluorescence method, has been developed and is being actively employed.[73]

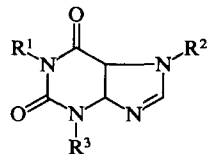
5. Purine alkaloids

This group includes derivatives of xanthine ($R^1 = R^2 = R^3 = H$): caffeine **15** ($R^1 = R^2 = R^3 = Me$), theophylline **16** ($R^1 = R^3 = Me$, $R^2 = H$), and theobromine **17** ($R^1 = H$, $R^2 = R^3 = Me$). Caffeine is present in tea leaves and coffee beans, theobromine was first detected in cocoa beans, and theophylline was detected in tea.

The mechanism of the physiological activity of these alkaloids involves the inhibition of phosphodiesterase and the accumulation of an intracellular mediator — cyclic adenosine-3′,5′-monophosphate (cAMP).

Two groups of methods are used for the quantitative assay of xanthine derivatives: the immune methods and methods based on HPLC.[79]

The presence in the molecules of these compounds of a large number of functional groups makes it possible to obtain fairly readily immunogenic conjugates of these alkaloids with proteins.



15–17

a. Caffeine

Caffeine is a typical psychostimulator. It also excites cardiac activity, dilates coronary blood vessels, and intensifies the respiratory activity and diuresis.

Immunoassay methods for the determination of compound **15** are used nowadays only in medical practice — in particular, the method for the enzyme immunoassay of compound **15** in the serum is used in pediatrics.[80]

Results of assays of compound **15** in serum and plasma by the immunoenzyme and HPLC methods have been compared and it has been shown that they are virtually identical.[80, 81]

b. Theophylline

Theophylline exhibits a physiological activity similar to that of compound **15**, but its broncholytic and diuretic activities predominate.

The fairly wide use of compound **16** as a medicinal drug has promoted the development of a large number of immunoassay methods for this alkaloid. The immunoenzyme,[82–86] immunofluorescence,[73, 87–90] immunochromatographic,[91] and immunoturbidimetric[92, 93] methods, the immunochromatographic methods using apoenzyme reagent strips,[94–98] and an immunoenzyme method employing an enzyme encapsulated in liposomes[99] are most widely used nowadays. The 'Optimate' system, based on the immunofluorescence method, is used for the automatic assay of compound **16**.[73]

These methods have been used in the study of the pharmacokinetics of compound **16**,[100–102] in the determination of the content of compound **16** in dry blood spots,[83, 84] in whole blood,[97] in urine,[103] in saliva,[88] in blood serum,[82, 83, 93–95, 104–106] and in the plasma.[89–91, 107–111]

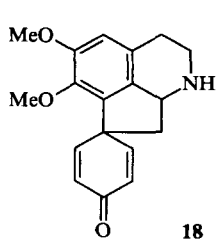
The influence of substances usually encountered in the specimens analysed on the results of the determination of compound **16** has been investigated.[108, 112–115]

Various immunoassay methods and the method based on the HPLC have been compared.[92, 98, 101, 104–107, 109–111] It has been established that the immunoenzyme method, the immune method based on the measurement of the degree of polarisation of fluorescence, and the method based on HPLC are best in terms of the accuracy and reproducibility of the results.[103, 109]

6. Proaporphine alkaloids

The structure of these alkaloids is based on that of aporphine.

Stepharine **18** is an alkaloid isolated from *Stephania glabra*. It exhibits a cholinesterase activity and is used in the treatment of diseases of the peripheral nervous system, myopathy, lateral amyotrophic sclerosis, and paresis of the facial nerve.

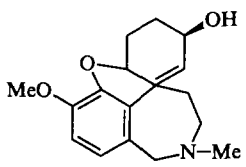


18

In order to obtain antibodies, compound **18** was treated with succinic anhydride and then with *N*-hydroxysuccinimide and *N,N'*-dicyclohexylcarbodiimide and was conjugated with BSA. The antibodies obtained with the aid of this conjugate were used in the development of a solid-phase enzyme immunoassay method with a sensitivity of 10 pg ml^{-1}. The method was used to assay compound **18** in a plant tissue culture and also for its determination in the blood of patients.[116]

7. Alkaloids of the physostigmine group

Galanthamine **19** is an alkaloid isolated from the tubers of the snowdrops *Galanthus woronowii* and *Galanthus nivalis*. The mechanism of its physiological activity is associated with the intensification of the influence of acetylcholine on the *n*-cholinergic synapses as a result of the inhibition of cholinesterase. It is used in medical practice to reduce the pressure within the eyeball and also for the treatment of certain nervous diseases and for the intensification of peristalsis on paresis of the intestine.

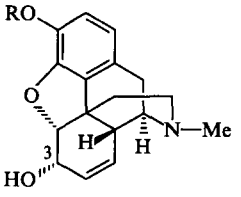


19

There exists a specific method for the radioimmunoassay of compound **19**. In order to obtain an immunogenic conjugate, the alkaloid **19** was treated with succinic anhydride and galanthamine 2-*O*-hemisuccinate was obtained and conjugated with BSA with the aid of 1-ethyl-3-(3-dimethylaminopropyl)carbodiimide. The method makes it possible to determine compound **19** in the range 0.5–100 ng.[117]

8. The poppy alkaloids

This group includes morphine **20**, codeine **21**, narcotine, papaverine **22**, thebaine, and about 20 other alkaloids.



R = H (**20**), Me (**21**)

a. Morphine

Morphine is the main alkaloid isolated together with 20 other alkaloids from the opium poppy (*Papaver somniferum*). Morphine belongs to the class of analgesic substances — narcotic analgesics. It also exhibits sedative and soporific activities, stimulates the smooth muscle, and at high concentrations induces vomiting and constipation, hinders diuresis, and inhibits the thermal regulation and respiration centres. It has been established that compound **20** influences specific receptors in the cortex of the cerebral hemispheres; it is widely used as an analgesic narcotic.

b. Codeine

Codeine also forms part of the composition of *P. somniferum*. It exhibits a weak narcotic activity and is widely used as an analgesic and also as an anti-cough preparation.

In view of the difficulties in the cross cultivation and selection of strains of *P. somniferum*, it was desirable to have a rapid method for the assay of compound **20**, which led at the beginning of the 1970s to the development of methods for the immunoassay of compound **20**.

Radioimmunoassay methods[28, 29, 118, 119] and methods based on the inhibition of haemagglutination[30, 120] were developed for the determination of compounds **20** and **21**. In all cases the immunogenic conjugate was obtained by the carboxymethylation of compound **20** at the hydroxy-group in the 3-position and by the attachment of the resulting derivative to the protein, as well as conjugation by the carbodiimide method. The antiserum to this conjugate was isolated from rabbit or guinea pig blood.

The most sensitive and specific method proved to be the radioimmunoassay employing the copolymer of L-Glu, L-Lys, L-Ala, and L-Tyr, to the ε-amino-groups of the lysine residues of which 3-*O*-carboxymethylmorphine had been attached and which had been [^{125}I]-labelled in the tyrosine residues, as well as the antiserum from the guinea pig blood. The range in which compound **20** can be determined is 0.05–5 ng. A disadvantage of this method[29] is the impossibility of distinguishing between compounds **20** and **21**. The method has been used to determine the lifetime of compound **20** in the blood[118] and also in the analysis of blood serum specimens taken in the case of the so called 'sudden death'. It has been shown that the results of the radioimmunoassay agree well with the results obtained by chromatographic methods.[29]

A homogeneous method for the enzyme immunoassay of compound **20**, based on the use a of conjugate of morphine with lysozyme and antiopiate antibodies, was developed at the beginning of the 1970s.[121, 122] This method makes it possible to determine compound **20** in the concentration range 0.5 to 3 μg ml^{-1}. Subsequently lysozyme was replaced by other enzymes (malate dehydrogenase and glucose-6-phosphate dehydrogenase), which made it possible to increase the sensitivity by a factor of 10.[123–125]

The antibodies to compound **20** were used to develop a method and a reagent set for the simultaneous automatic enzyme immunoassay of a number of narcotic preparations in urine microspecimens.[126] The concentration limit for the detection of compound **20** is 0.3 mg ml^{-1}.

The enzyme immunoassay method has been used for the determination of compound **20** in specimens of the blood of persons who died as a result of the consumption of heroin.[127]

A brief communication about the development of methods for the radioimmunoassay of (*S*)- and (*R*)-reticuline, salutaridine, thebaine, and compounds **20** and **21** appeared in 1984. All the antisera obtained were highly specific and made it possible to determine the above substances in the range 0.01–10 ng.[128] These methods make it possible to investigate the pathways leading to the biosynthesis of the above alkaloids and to select plants or cell cultures in terms of the productivity of the biosynthesis of these alkaloids.

Methods for the immunoassay of compound **20** are used mainly in clinical practice.[129] An immunoassay method involving the use of indicator strips has been used successfully to detect compound **20** in urine.[130]

A method based on latex agglutination has found extensive application in the screening assay of opiates.[131]

A heterogeneous enzyme immunoassay method is also used for the detection of opiates.[132] Competitive solid-phase enzyme immunoassay of opiates makes it possible to attain a high sensitivity — up to 0.25 ng ml^{-1}. When the method is used in its qualitative version without instrumental enhancement, the sensitivity of the determination is 300 ng ml^{-1}, which is comparable to the sensitivity of the homogeneous enzyme immunoassay.

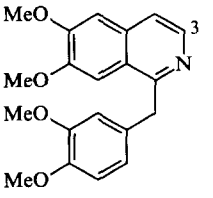
Information concerning the development of highly sensitive immunofluorescence methods for the assay of compound **20** in urine was published subsequently.[133, 134]

The Hofmann La Roche Company (Switzerland) produced a reagent set for a qualitative visual assay of opiates with a sensitivity of 300 ng ml^{-1}.[135]

Immunoassay methods are used for the determination of opiates in serum, urine, and saliva specimens as well as other human biological liquids.[135] There exists a highly sensitive method which makes it possible to determine compound **20** in hair;[136] the sensitivity reaches 0.2 ng ml^{-1} under these conditions.

c. Papaverine

Papaverine **22** is also one of the most valuable alkaloids isolated from the poppy plant. It exhibits spasmolytic and moderate vasodilating activities and increases the consumption of oxygen by the myocardium. Papaverine is administered in the hypertonic state, in stenocarditis, and in the treatment of the spasms of the coronary and brain blood vessels, the smooth muscle of the abdominal cavity, and other diseases.



22

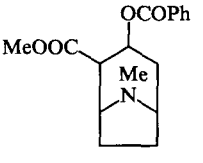
A conjugate of synthetic 3-aminopapaverine has been used to obtain antibodies to compound **22**.[137] For this purpose, 3-aminopapaverine was treated with glutaric anhydride and converted into 1-(3,4-dimethoxybenzyl)-3-*N*-(4-carboxybutyryl)-amino-6,7-dimethoxypapaverine, which was attached to BSA with the aid of *N*-hydroxysuccinimide and *NN'*-dicyclohexylcarbodiimide. A solid-phase enzyme method for the immunoassay of compound **22** was developed on the basis of the antibodies obtained.[138] Its sensitivity is 10^{-6} g ml^{-1}.

9. Alkaloids of the cocaine group

These alkaloids are present in the leaves of the coca plant (*Erythroxylon coca*). Their structure is based on the bicyclic tropane skeleton and in terms of this feature they can be included among tropane alkaloids.

As in the case of the purine alkaloids, the large number of functional groups in the molecules of these alkaloids makes it possible to obtain readily immunogenic conjugates with proteins.

Cocaine **23** exhibits a powerful local analgesic activity and is a local anaesthetic. It has a paralysing effect on the parasympathetic nervous system.



23

There exists at present a fluorescence-polarisation immunoassay method which makes it possible to determine compound **23** in urine at a concentration of 1 mg ml^{-1} and above.[40]

As for other narcotics, methods for the immunoassay of compound **23** and its metabolites are used virtually only in medical practice.[139]

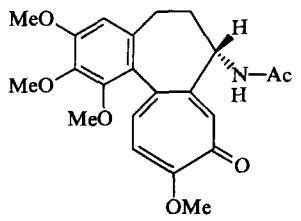
The attempts to simplify and accelerate the assay of narcotics have led to the appearance of methods involving the simultaneous assay of a broad spectrum of narcotics. Mixtures of antibodies to each substance or group of substances are used in these procedures. Among them, one may note the fluorescence-polarisation method which permits the simultaneous determination of the metabolites of compound **23**, amphetamine, and certain barbiturates in urine,[39] as well as an immunoenzyme method for the simultaneous assay of amphetamine, quinalbarbitone, oxazepam, benzoylecgonine, methadone, methaqualone, compound **20**, phencyclidine, phenytoin, propoxyphene, and nortriptyline in urine.[126]

Methods for the determination of narcotics proposed by the Syva Corporation and based on homogeneous immunoassay have come to be widely used in narcological practice.[98, 121, 124, 136, 140] Subsequently these methods have been automated.[140]

10. Alkaloids of the colchicine group

Colchicine **24** and colchamine are present together with other alkaloids in the pods of plants of the *Colchicum* and *Merendera* genera.

Colchicine is widely used in selection procedures as an agent which induces the doubling of the number of chromosomes and the formation of polyploid forms of plants and also in the study of the cytoskeleton of plants. Being a poison with a neuroparalytic activity, it is used at the same time for the treatment of the cancer of the gullet and skin and as an anticonvulsant and is in addition the best drug for the treatment of Mediterranean fever available at present.



24

A method for the radioimmunoassay of compound **24** was developed in 1975 using a conjugate of *N*-desacetylthiocolchicine, attached by the carbodiimide method to BSA, and [^{3}H]-**24**. The method makes it possible to determine compound **24** in the range 5–50 ng.[22] Cross reactions with *N*-desacetylthiocolchicine and *N*-desacetyl-*N*-colchicine (8%) have been noted. A method has been developed for the assay of compound **24** in human blood serum; it has not been used for the determination of compound **24** in plants.

A similar method, based on the use of monoclonal antibodies, which made it possible to increase appreciably the specificity of the assay, was developed subsequently.[141]

IV. Conclusion

Immunochemical methods for the assay of alkaloids are becoming increasingly popular. They are superior to chromatographic methods as regards sensitivity and speed of preparation of the analytical samples and are scarcely inferior to them as regards accuracy and reproducibility.

In the development of methods for the immunoassay of alkaloids, it is possible in most cases to obviate the difficulties associated with the preparation of immunogenic conjugates of the alkaloids with proteins and to obtain fairly specific antisera.

The methods for the radioimmunoassay of alkaloids, which were in the forefront in the 1960s–1970s, yielded the leading position in the 1980s to the enzyme immunoassay method; immunofluroescence methods are beginning to be used with increasing frequency.

The widest field in which immunoassay methods for alkaloids are used involves the measurement of their concentrations in the physiological fluids of patients receiving alkaloids preparations. This is associated both with the necessity for the rapid and accurate monitoring of the course of treatment and with the study of the pharmacokinetics and metabolism of alkaloids.

Rapid and accurate methods for the assay of alkaloids exhibiting narcotic properties are important from both medical and criminological points of view. Here too immunoassay methods are being employed to an increasing extent.

Since in many instances alkaloids are still being obtained from plant raw material, it is frequently necessary to know their content in such material. However, the lack in most countries of norms for the content of biologically active substances in plant raw material is an inhibiting factor in the development of immunoassay methods for plants. However, in a number of instances immunoassay methods have been used in studies on the biosynthesis of certain alkaloids in plants.

The deficiencies of the traditional procedure for the isolation of alkaloids from plant raw material—the dependence of the content of the alkaloids on the climatic and weather conditions, the difficulties in the collection of the plants (for plants growing under wild conditions), and the need for fertile soil (for cultivated plants)—have led to the active development at the present time of biotechnological methods for the synthesis of alkaloids in plant cell and tissue cultures. It is in the field of the monitoring of the content of alkaloids in such cultures that the immunoassay methods are being increasingly widely used and are replacing the chromatographic methods traditionally employed for such purposes.

References

1. V Marko *Farm. Obz.* **55** 37 (1986)
2. S D Varfolomeev, S V Zaitsev, A T Mevkh *Fiziko-khimicheskie Issledovaniya Molekulyarnykh Mekhanizmov Deistviya Fiziologicheski Aktivnykh Soedinenii. Itogi Nauki i Tekhniki. Ser. Bioorganicheskaya Khimiya* (Physicochemical Studies on the Molecular Mechanisms of the Activity of Physiologically Active Compounds. Advances in Science and Engineering. The Bioorganic Chemistry Series) (Moscow: Izd. VINITI, 1985) Vol. 3, p. 116
3. E L Manchester, E Geisbrecht, S J Soldin *Ther. Drug Monit.* **9** 61 (1987)
4. R V Petrov, I V Berezin *Zh. Vses. Khim. O-va im. D. I. Mendeleeva* **27** 362 (1982)
5. B B Dzantiev, A M Egorov *Zh. Vses. Khim. O-va im. D. I. Mendeleeva* **27** 442 (1982)
6. A M Egorov *Zh. Vses. Khim. O-va im. D. I. Mendeleeva* **33** 494 (1988)
7. S A Eremin *Zh. Vses. Khim. O-va im. D. I. Mendeleeva* **34** 46 (1989)
8. H Friemel (Ed.) *Immunological Methods* (Translated into Russian) (Moscow: Meditsina, 1987)
9. T T Ngo, H M Lenhoff (Eds) *Immunoenzymic Analysis* (Translated into Russian) (Moscow: Mir, 1988)
10. A M Egorov (Ed.) *Neizotopnye Metody Immunoanaliza. Itogi Nauki i Tekhniki. Ser. Biotekhnologiya* (Non-isotopic Immunoassay Methods. Advances in Science and Engineering. The Biotechnology Series) (Moscow: Izd. VINITI, 1987) Vol. 3
11. D M Kemeny, S J Challacombe (Eds) *ELISA and Other Solid Phase Immunoassays. Theoretical and Practical Aspects* (New York: Wiley, 1988)
12. B A Morris, M N Clifford (Eds) *Immunoassays in Food Analysis* (London: Elsevier, 1985)
13. H F Linskens, J F Jackson (Eds) *Immunology in Plant Sciences* (Berlin: Springer, 1986)
14. T Braun, A Klein, S Zsindely, W S Lyon *Trends Anal. Chem.* **11** 5 (1992)
15. C C Harris, R H Yolken, H Krokan, I C Hsu *Proc. Natl. Acad. Sci. USA* **76** 5336 (1979)
16. K Landsteiner *The Specificity of Serological Reactions* (Cambridge: Harvard University Press, 1946)
17. R J Robins, M R A Morgan, M J C Rhodes, J M Furze, in *Immunoassays in Food Analysis* (Eds B A Morris, M N Clifford) (London: Elsevier, 1985) p. 1977
18. B F Erlanger, O F Borek, S M Beiser, S Leiberman *J. Biol. Chem.* **234** 1090 (1959)
19. H Arens, J Stockigt, E W Weiler, M H Zenk *Planta Med.* **34** 37 (1978)
20. J J Langone, H B Gjika, H Van Vunakis *Biochemistry* **12** 5025 (1973)
21. J J Langone, M R D'Onofrio, H Van Vunakis *Anal. Biochem.* **95** 214 (1979)
22. C Boudene, F Duprey, C Bohuon *Biochem. J.* **151** 413 (1975)
23. H Meisner, P Meisner *Arch. Biochem. Biophys.* **208** 146 (1981)
24. J P Kutney, L S L Choi, B R Worth *Phytochemistry* **19** 2083 (1980)

25. R J Robins, A J Webb, M J C Rhodes, J M Furze *Planta Med.* **50** 235 (1984)
26. M R A Morgan, S Bramham, A J Webb, R J Robins, M J C Rhodes *Planta Med.* **51** 237 (1985)
27. P Westekemper, U Wieczorek, F Gueritte, N Langlois, Y Langlois, P Potier, M H Zenk *Planta Med.* **39** 24 (1980)
28. S Spector, C W Parker *Science* **168** 1347 (1970)
29. H Van Vunakis, E Wasserman, L Levine *J. Pharmacol. Exp. Ther.* **180** 514 (1972)
30. F L Adler, C-T Liu *J. Immunol.* **106** 1684 (1971)
31. J D Teale, J M Clough, V Marks *Br. J. Clin. Pharmacol.* **4** 169 (1977)
32. M P Hacker, J P Dank, W B Ershler *Cancer Res.* **44** 478 (1984)
33. E W Weiler, J Stockigt, M H Zenk *Phytochemistry* **20** 2009 (1981)
34. P S Jourdan, R L Mansell, E W Weiler *Planta Med.* **44** 82 (1982)
35. S A Eremin *Ther. Drug Monit.* **10** 400 (1988)
36. J Marrero *J. Med. Technol.* **1** 47 (1984)
37. M R A Morgan, R McNerney, J A Matthew, D T Coxon, H W-S Chan *J. Sci. Food Agric.* **34** 593 (1983)
38. L Fukal, J Kas *Trends Anal. Chem.* **8** 112 (1989)
39. D L Colbert, M Childerstone *Clin. Chem.* **33** 1921 (1987)
40. S K Volkov *Lekarstvennoe Rastenievodstvo. Obzornaya Informatsiya* (Medicinal Plant Cultivation. Review Information) (Moscow: Izd. VNIISENTI NPO "Medbioekonomika", 1990)
41. M A Root, K Gerzon, R W Dyke, in *Federation of Analytical Chemistry and Spectroscopy Societies, 2nd National Meeting, Indianapolis, IN, 1975* p. 125 (Abstr. 183)
42. C J Barnett, G J Cullinan, K Gerzon, R C Hoying, W E Jones, W M Newlon, G A Poore, R L Robison, M J Sweeney, G C Todd *J. Med. Chem.* **21** 88 (1978)
43. V S Sethi, S S Burton, D V Jackson *Cancer Chemother. Pharmacol.* **4** 183 (1980)
44. R J Owellen, C A Hartke, F O Hains *Cancer Res.* **37** 2597 (1977)
45. P A Ponarotti, R Rahmani, M Martin, J Barbet *Mol. Immunol.* **22** 277 (1985)
46. M C Cibotti, C Freier, J Andrieux, M Plant, L Cosson, C Bonuon *Phytochemistry* **29** 2109 (1990)
47. R Rahmani, J Barbet, J P Cano *Clin. Chim. Acta* **129** 57 (1983)
48. A S Perlin, in *Oxidation. Techniques and Applications in Organic Synthesis* Vol. 1 (Ed. R L Augustine) (New York: Marcel Dekker, 1969) p. 189
49. M Lounasmaa, R Jokela, A Huhtikangas, S Lapinjoki, J Heiskanen, T Lehtola, T Naaranlahti *Heterocycles* **24** 1355 (1986)
50. S P Lapinjoki, H M Verajankorva, A Huhtikangas, T J Lehtola, M Lounasmaa *J. Immunoassay* **7** 113 (1986)
51. A Huhtikangas, T Lehtola, S Lapinjoki, M Lounasmaa *Planta Med.* **53** 85 (1987)
52. K Hirata, M Kobayashi, K Miyamoto, T Hoshi, M Okazaki, Y Miura *Planta Med.* **55** 262 (1989)
53. M Reihlin, J J Schnurre, V K Vance *Proc. Soc. Exp. Biol. Med.* **128** 347 (1968)
54. R J Owellen, M A Root, F O Hains *Cancer Res.* **37** 2603 (1977)
55. M Tabata, in *Plant Tissue Culture and Its Bio-Technological Application* (Eds W Barz, E Reinhard, M H Zenk) (Berlin: Springer, 1977) p. 3
56. W G W Kurz, K B Chatson, F Constabel, J P Kutney, L S L Choi, P Kolodziejczyk, S K Sleigh, K L Stuart, B R Worth *Phytochemistry* **19** 2583 (1980)
57. J P Kutney, L S L Choi, P Kolodziejczyk, S K Sleigh, K L Stuart, B R Worth, W G W Kurz, K B Chatson, F Constabel *Helv. Chim. Acta* **64** 1837 (1981)
58. P Manganey, R Z Andriamialisoa, N Langlois, Y Langlois, P Potier *J. Am. Chem. Soc.* **101** 2243 (1979)
59. A Huhtikangas, J Heiskanen, V Kauppinen, S Lapinjoki, M Lounasmaa, H Verajankorva *Pharm. Weekblad – Sci. Ed.* **9** 236 (1987)
60. S Lapinjoki, H Verajankorva, J Heiskanen, M Niskanen, A Huhtikangas, M Lounasmaa *Planta Med.* **53** 565 (1987)
61. B Deus-Neumann, J Stockigt, M H Zenk *Planta Med.* **53** 184 (1987)
62. M H Zenk, H El-Shagi, H Arens, J Stockigt, E W Weiler, B Deus, in *Plant Tissue Culture and Its Bio-Technological Application* (Eds W Barz, E Reinhard, M H Zenk) (Berlin: Springer, 1977) p. 27.
63. J F Treimer, M H Zenk *Phytochemistry* **17** 227 (1978)
64. H Arens, B Deus-Neumann, M H Zenk *Planta Med.* **53** 179 (1987)
65. M Cushman, N Castagnoli Jr *J. Org. Chem.* **37** 1268 (1972)
66. S Balabanova, E Schneider, G Buhler *Dtsch. Apoth. – Ztg.* **130** 2200 (1990)
67. B J Savary, D K Dougall *Phytochemistry* **29** 1567 (1990)
68. M A Fliniaux, A Jacquin-Dubreuil *Planta Med.* **53** 87 (1987)
69. V Rowell, F J Rowell *Analyst* **112** 1437 (1987)
70. A J Quattrone, R Joseph, T Jones, S Sarmir, A Selvaggi, K Maloney, T Lockwood *J. Med. Technol.* **1** 381 (1984)
71. B E Pape *Ther. Drug Monit.* **3** 357 (1981)
72. C R Lehmann, K J Boran, W P Pierson, A P Melikian, G W Wright *Ther. Drug Monit.* **8** 336 (1986)
73. M Sheehan, G Caron *Ther. Drug Monit.* **7** 108 (1985)
74. M B Bottorff, R L Lalonde, A B Straughn *Biopharm. Drug Dispos.* **8** 213 (1987)
75. H R Ha, S Vozeh, F Follath *Ther. Drug Monit.* **8** 331 (1986)
76. D J Mazak, J Y Lee, J A Ferringer *ASHP Midyear Clinical Meeting* **25** 26E (1990)
77. M Tod, G Resplandy, R Farinotti, Y Provost, A Dauphin *J. Pharm. Biomed. Anal.* **8** 279 (1990)
78. Y W Lam, C Watkins *ASHP Midyear Clinical Meeting* **26** 348E (1991)
79. A Yamasaki, K Yamamoto, K Shinozaki, R Takao, Y Tanaka *J. Pract. Pharm.* **42** 191 (1991).
80. J V Aranda, K Beharry, J Rex, R J Johannes, L Charest-Boule *Ther. Drug Monit.* **9** 97 (1987)
81. K H Carpenter, M J Bennett *Ann. Clin. Biochem.* **24** (Suppl. 1) 61 (1987)
82. N P Danilova, N I Bekman, L V Shustova, R G Vasilov *Khim. – Farm. Zh.* **23** 871 (1989)
83. N P Danilova, N I Bekman, A S Ziganshin, R G Vasilov *Khim. – Farm. Zh.* **26** 92 (1992)
84. J M Rattenbury, T Taylor *Ann. Clin. Biochem.* **25** (1988)
85. P A Kyd, S J Evans *Ann. Clin. Biochem.* **24** (Suppl. 1) 60 (1987)
86. N Massoud, P Munzenberger, A Sarniak *Am. J. Hosp. Pharm.* **43** 1722 (1986)
87. J Babjuk, I Bilyk, J Kalousova, H Nekvasilova, B Rybakova *Cesk. Farm.* **36** 322 (1987)
88. A Neimann, M Oellerich, G Schumann, G W Sybrecht *J. Clin. Chem. Clin. Biochem.* **23** 725 (1985)
89. P W Thies, B Nalge *Hosp. Pharm.* **21** 230 (1986)
90. R Kino, R O Day, G A Pearce, G W Fulde *Aust. J. Hosp. Pharm.* **21** 292 (1991)
91. M J Otero, A Martin Suarez, M Barrueco, E Gomez, A Dominguez-Gil *Farm. Clin.* **4** 528 (1987)
92. G Gotelli, M Mitchell *Clin. Chem.* **31** 1085 (1985)
93. P Goebbels, J Boulander, P Ers, A Adam *Clin. Chem.* **33** 1077 (1987)
94. M Plebani, A Burlina *Ther. Drug Monit.* **7** 451 (1985)
95. D L Morris *Anal. Biochem.* **151** 235 (1985)
96. T Kuzuya, Y Ogura, M Hasegawa, T A Nakamura, S Katazama *Jpn. J. Hosp. Pharm.* **12** 362 (1986)
97. R Chen, T M Li, H Merrick, R F Parrish, V Bruno, A Kwong, C Stiso, D J Litman *Clin. Chem.* **33** 1521 (1986)
98. R H Drost, H U Schulz, R A Maes, J M Van Rossum *J. Toxicol. Clin. Toxicol.* **25** 231 (1987)
99. E F Ullman, T Tarnowski, P Felgner, I Gibbons *Clin. Chem.* **33** 1579 (1987)
100. P J Aznar, B M Toreda, A M Alos, B J Ezqner, O M D Fuentez *Farm. Clin.* **8** 139 (1991)
101. R L Lalonge, M B Bottorff, A B Staughn *Ther. Drug Monit.* **7** 442 (1985)
102. J H Jonkman *Ther. Drug Monit.* **10** 345 (1988)
103. M Pokrajac, D Agbaba, V M Varagic, L Glisovic *Acta Pharm. Jugosl.* **36** 445 (1986)
104. E Pietruszewska *Farm. Pol.* **41** 382 (1985)
105. H M Izquiero, F O Calatayud, G G Sangrador, A A Sanchez *Farm. Clin.* **4** 802 (1987)
106. H Wallinder, L L Gustafsson, K Angback, P Hoglung, L Arvanius *Ther. Drug Monit.* **13** 233 (1991)
107. M Mordelet-Dambrine, J Y Baglin, A Roux, D Dusser, G Huchon *Ther. Drug Monit.* **8** 106 (1986)
108. M M Canto Pascual, M Alos Alminana, J Magraner Gil, J Ezquer Borras, M D Fuentes Ortiz, M L Calduch Alvarez, M T Torrecilla Junyent *Farm. Clin.* **4** 38 (1987)
109. P-L C Lopez, M T Miranda-Leon, M A Agudo-Martinez, D Villalba-Bedoya *Farm. Clin.* **7** 485 (1990)

110. R J West, L N Sansom, A C Penna *Aust. J. Hosp. Pharm.* **20** 430 (1990)
111. A W Krings *Ziekenhuisfarmacie* **7** 7 (1991)
112. I S Kampa, J I Jarzabek *Ther. Drug Monit.* **7** 489 (1985)
113. I A Cohen, C E Johnson, L Wesolowicz, K Converse-Swastek *Clin. Pharm.* **4** 457 (1988)
114. J S Wei, C Y Tsai, H M Huang, M E Chai *Ther. Drug Monit.* **11** 84 (1989)
115. M Morton, R C Parish, W J Spruill *Ther. Drug Monit.* **11** 347 (1989)
116. N D Danilova, S N Lutskova, I I Fadeeva, R G Vasilov, A I Miroshnikov *Khim.–Farm. Zh.* **24** 56 (1990)
117. T Tanahashi, A Poulev, M H Zenk *Planta Med.* **56** 77 (1990)
118. S Spector *J. Pharmacol. Exp. Ther.* **178** 253 (1971)
119. D H Catlin, R Cleeland, E Grunbarg *Clin. Chem.* **19** 216 (1973)
120. F L Adler, C T Lin, D H Catlin *Clin. Immunol. Immunopathol.* **1** 53 (1972)
121. K E Rubenstein, R S Schneider, E F Ullman *Biochem. Biophys. Res. Commun.* **47** 846 (1972)
122. R S Schneider, P Lindqwist, E Tong-in-Wong, K E Rubenstein, E F Ullman *Clin. Chem.* **19** 821 (1973)
123. G L Rowley, K E Rubenstein, S T Weber, E F Ullman, in *Am. Chem. Soc. Meeting BIOL* (Washington, 1976) p. 151
124. G L Rowley, K E Rubenstein, J Huisjen, E F Ullman *J. Biol. Chem.* **250** 3759 (1975)
125. J W Lee, J E Pedersen, T L Moravetz, A M Dzerk, A D Mundt, K V Shepard *J. Pharm. Sci.* **80** 284 (1991)
126. D L Black, B A Goldberger, Y H Caplan *Clin. Chem.* **33** 367 (1987)
127. C Lora-Tamayo, T Tena, G Tena *J. Chromatogr.* **422** 267 (1987)
128. U Wieczorek, N Nagakura, M H Zenk *Phytochemical Society Symposium, London, 1984* (Abstr. 36)
129. P A Glare *Ther. Drug Monit.* **13** 1 (1990)
130. D J Litman, R H Lee, H J Jeong, H K Tom, S N Stiso, N C Sizto, E F Ullman *Clin. Chem.* **29** 1598 (1983)
131. R Ross, C A Horwitz, H Hager, M Usategui, M D Burke, P C J Ward *Clin. Chem.* **21** 139 (1975)
132. D Laurie, A J Manson, A Mounsey, F J Rowell, J Seviour *Analyst* **112** 687 (1987)
133. D L Colbert, G Gallacher, P Ayling, G L Turner *Clin. Chim. Acta* **171** 37 (1988)
134. D L Colbert, D S Smith, A M Sidki *Ann. Clin. Biochem.* **23** 37 1986
135. M A Myagkova, M V Lushnikova *Khim.–Farm. Zh.* **24** 76 (1990)
136. A Franceshin, L Morosine *Clin. Chem.* **33** 303 (1987)
137. A V Sereda, I E Sukhov, B M Zolotarev, I V Yartseva, O N Tolkachev *Tetrahedron Lett.* **33** 4205 (1992)
138. S N Eremenko, I E Sukhov, N P Danilova, O N Tolkachev, R G Vasilov, A I Miroshnikov *Khim.–Farm. Zh.* **26** 100 (1992)
139. M J Kogan, D J Pierson, M M Durkin, N J Willson *J. Chromatogr. Biomed. Appl.* **490** 236 (1989)
140. C R Hamlin *Clin Chem.* **34** 158 (1988)
141. S K Rouan, I G Otterness, D J Gans, C T Rhodes *Drug Dev. Ind. Pharm.* **17** 2391 (1991)

Russian Chemical Reviews **62** (9) 799–838 (1993)
©1993 Russian Academy of Sciences and Turpion Ltd

UDC 542.971.2; 547.235.421; 547.512

Catalytic decomposition of diazomethane as a general method for the methylenation of chemical compounds

Yu V Tomilov, V A Dokichev, U M Dzhemilev, O M Nefedov

Contents

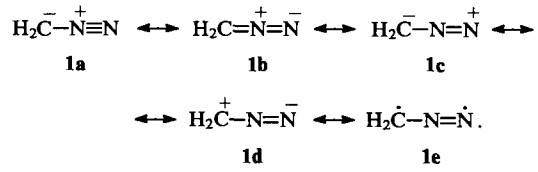
I.	Introduction	799
II.	Interaction of diazomethane with metal salts and complexes	800
III.	Catalytic conversion of unsaturated compounds into cyclopropane derivatives	802
IV.	Catalytic interaction of diazomethane with aromatic compounds	827
V.	Synthesis of ketones by converting carbonyl compounds into higher homologues	830
VI.	Catalytic methylation of alcohols and amines by diazomethane	832
VII.	Conclusion	835

Abstract. The principal advances and trends in the application of diazomethane as a methylenating agent in synthetic chemistry using transition and non-transition metal compounds as catalysts are surveyed and analysed. The catalytic reactions of diazomethane with olefins, acetylenes, aromatic compounds, ketones, alcohols, and amines are examined. A systematic account is given of data concerning the influence of the structure of the initial substrates and of the nature of the catalyst components on the regio- and stereo-selectivity of the reactions considered. The possibilities of the catalytic conversion by diazomethane (generated *in situ*) of unsaturated compounds into cyclopropane derivatives are considered. The bibliography includes 284 references.

I. Introduction

Diazomethane, which is the simplest representative of diazo-compounds, was first obtained by Pechmann[1] in 1894 and since then it has been firmly established as one of the popular reagents in synthetic organic chemistry, which are widely used to effect under mild conditions reactions involving the conversion of unsaturated compounds into cyclopropane derivatives, the conversion of carbonyl compounds into higher homologues, and the methylation of carboxylic acids, alcohols, and phenols. The present review is devoted mainly to the reactions of diazomethane with various organic compounds which occur as a rule in the presence of homogeneous metal complex catalysts.

Depending on the conditions, diazomethane can be regarded as an acid or base, as an electrophile or a nucleophile, and as a 1,3-dipole or a source of carbene (methylene). The linear structure of diazomethane has been established by electron diffraction[2] and by microwave spectroscopy.[3] It has a dipole moment of 1.4 D and carbon–nitrogen and nitrogen–nitrogen bond lengths of 0.132 and 0.112 nm respectively. These values are averages of the C–N and C=N bond lengths and the N=N and N≡N bond lengths respectively. Thus the structure of diazomethane can be represented by the following resonance structures, among which structures **1a** and **1b** make the greatest contribution:



1a **1b** **1c** **1d** **1e**

Other structural characteristics and spectroscopic data for diazomethane have been fairly fully presented in another review.[4]

The constant interest of investigators in diazomethane despite its high toxicity and explosive nature is due to the fact that it is a unique source of the simplest carbene — methylene, the high reactivity of which makes it possible to regard it as a promising one-carbon synthon for the creation of non-traditional chemical technologies. Furthermore, the development of the chemistry of diazomethane in relation to the problem of the synthesis and investigation of the reactivity of methylene has assisted in many respects in the understanding and determination of the mechanisms of important processes such as the metathesis of olefins, the Fischer–Tropsch reaction, the activation of alkanes, etc.[5–7] Finally, the majority of the methods of synthesis of diazomethane itself are based on the use of readily available compounds, in particular *N*-methyl-*N*-nitrosoamides, and extremely simple procedures for its generation.[4,8]

Diazo-compounds can be decomposed by three main methods — thermal, photochemical, and catalytic.[9,10] However, the first two are relatively unsuitable for preparative purposes, primarily because such processes are unsafe and there is an increased likelihood of side reactions, for example, those involving insertion in various C–H bonds. The progress in the chemistry of diazomethane during the last 10–15 years has been indissolubly linked with the application of metal complex

Yu V Tomilov, O M Nefedov Laboratory of the Chemistry of Carbenes and Small Rings, N D Zelinskii Institute of Organic Chemistry, Russian Academy of Sciences, Leninskii prosp. 47, 117913 Moscow, Tel. (7-095)13563 90. Fax (7-095)13553 28
V A Dokichev Institute of Organic Chemistry, Ufa Scientific Centre, Russian Academy of Sciences, prosp. Oktyabrya 69, 450054 Ufa, Russian Federation, Fax (347-2)35 60 66
U M Dzhemilev Institute of Petrochemistry and Catalysis, Academy of Sciences of the Republic of Bashkortostan, prosp. Oktyabrya 141, 450071 Ufa, Russian Federation

Received 17 June 1993
Uspekhi Khimii **62** (9) 847–886; translated by A K Grzybowskii

catalysts, which not only promote the formal generation of methylene under mild conditions but also make it possible to regulate its reactivity within wide limits. The results have made, in particular, a significant contribution to the development of modern highly efficient methods of synthesis of many cyclopropane derivatives from readily available olefins and the factual data accumulated make it possible to elucidate in greater depth the mechanistic aspects of the catalytic cyclomethylenation of various unsaturated compounds.

It is noteworthy that the use of diazomethane in catalytic reactions involving the conversion of various unsaturated compounds into cyclopropane and cyclopropene derivatives has developed virtually in parallel with the application for such purposes of well-known aliphatic diazo-compounds such as diazoacetic acid esters. Whereas in the 1950s–1960s, mainly copper compounds were used as the traditional catalysts for the decomposition of the above diazo-compounds, since the middle of the 1970s catalysts based on rhodium and palladium have begun to be vigorously introduced into laboratory practice. A series of monographs and reviews[10–22] devoted to the synthetic possibilities of the catalytic methods for the conversion of unsaturated substrates into cyclopropane derivatives with the aid of diazo-compounds and to the consideration of the probable mechanisms of these processes appeared during this period. However, the majority of the publications do not yield a complete picture concerning the use of metal complex catalysis in the chemistry of diazomethane and do not deal with the specific features of diazomethane itself which distinguish it from other aliphatic diazo-compounds.

On the basis of the factual data accumulated, an attempt is made in the present review to present as fully as possible the advances and prospects in the application of metal complex catalysis in the chemistry of diazomethane.

II. Interaction of diazomethane with metal salts and complexes

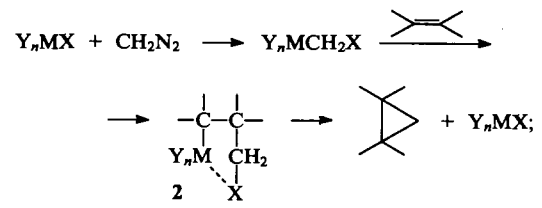
Diazomethane readily decomposes on treatment with many transition and non-transition metal compounds.[15,22–26] This includes its decomposition on the active surface centres of pure metals (Ni, Pd, Cu, Fe, Co, Ru, U),[27–28] heterogeneous catalysts, and various sorbents,[29,30] which by no means always involves the transfer of methylene to the double bonds of olefins or other substrates and this process is extremely sensitive to the nature of both the substrate and the catalyst. In most cases the decomposition of CH_2N_2 is accompanied by the liberation of ethylene and other volatile products, although it can also lead to the preferential formation of polymethylene.[31–33] For example, the dediazotisation of CH_2N_2 by nickelocene yields polymethylene almost quantitatively even in the presence of olefins.[31]

The interaction of CH_2N_2 with compounds of the majority of the elements in the Periodic Table with the properties of Lewis acids and primarily with their halides leads to the initial formation of organometallic (organoelement) compounds via the insertion of methylene in M–X bonds.

$$MX_n \xrightarrow{CH_2N_2} MX_{n-m}(CH_2X)_m \xrightarrow{CH_2N_2} M(CH_2X)_n.$$

According to data surveyed in a number of reviews[15–23], Zn, Cd, Hg, Al, In, Tl, Sn, Pb, Sb etc. interact via this mechanism and compounds of the Group IV and V elements in the highest oxidation states, for example Sn(IV), Pb(IV), and Sb(V), are initially reduced by diazomethane to the corresponding Sn(II), Pb(II), and Sb(III) compounds.

The conversion of olefins into cyclopropane derivatives by halomethylmetal compounds of this kind has been investigated most thoroughly for Zn and Al derivatives:[34–36] these compounds are relatively unstable and are in essence intermediates capable of adding to the double bond of olefins. Since the three-carbon ring is formed stereospecifically, the reaction mechanism implies the selectivity of the stages involving the addition of the halomethyl derivative and the γ-elimination of the metal halide, as well as the stability of the steric configuration of the organometallic intermediate **2**.



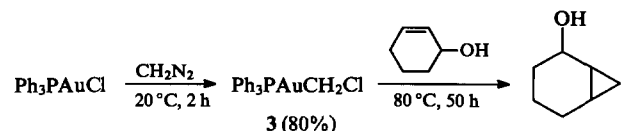
2

Y = Alk, Ar, Hal; X = Cl, I.

Thus, according to Hoberg's data,[36] diethylaluminium iodide reacts with CH_2N_2 in pentane at −80 °C with the evolution of nitrogen and the formation of crystalline Et_2AlCH_2I. By interacting with olefins, this compound affords the corresponding cyclopropane (for example, norcarane in the case of cyclohexene). Zinc compounds react via the same mechanism and the regeneration of the initial metal halide makes it possible to use it in catalytic amounts. The conversion of olefins into cyclopropane derivatives by CH_2N_2 in the presence of ZnX_2 is one of the versions of the Simmons–Smith method, various aspects of which have been considered in another review.[37]

It is noteworthy that virtually all the reactions involving the conversion of olefins into cyclopropane derivatives by diazomethane in the presence of zinc- or aluminium-containing catalysts are carried out under anhydrous conditions—mainly in ether. A disadvantage of the above catalysts is their high reactivity in relation to the initial olefins, which induces their oligomerisation or conversion into the corresponding halides.

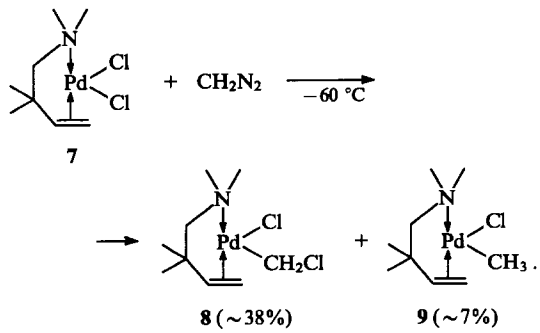
The insertion of methylene, generated from CH_2N_2, in the M–X bond occurs also when transition metal compounds are used. In certain cases, it was then possible not only to isolate the products of such insertion but also to demonstrate the possibility of converting olefins into cyclopropane derivatives by such products. Thus, according to Nesmeyanov et al.,[38] the interaction of Ph_3PAuCl with CH_2N_2 at 20 °C leads to the chloromethyl derivative **3**, which is capable of subsequently methylenating cyclohexenol to form 2-hydroxynorcarane **4**, albeit in low yield.



Halomethyl derivatives have also been obtained when complex palladium and platinum dihalides were used. The interaction of the platinum complex **5** with an excess of CH_2N_2 then affords a high yield of the bishalomethyl derivative **6**,[39] while the palladium complex **7** unexpectedly affords also the methyl complex **9** together with the chloromethyl derivative **8**.[40]

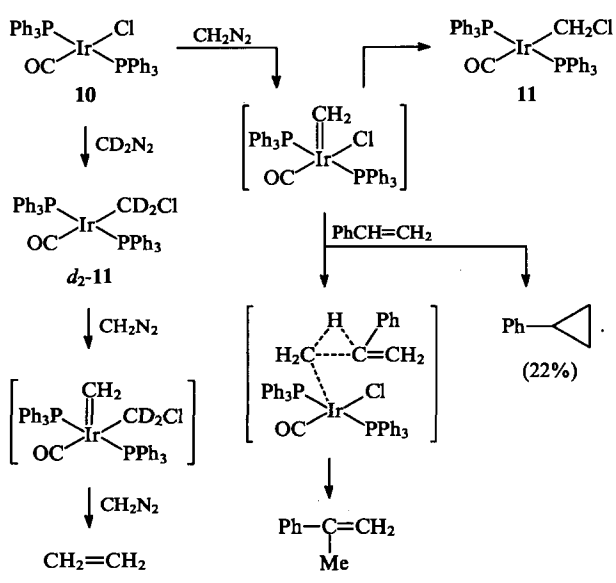
$$(COD)PtX_2 + CH_2N_2 \longrightarrow \underset{\mathbf{5}}{(COD)Pt(CH_2X)_2} \xrightarrow{PPh_3} \underset{\mathbf{6}}{(Ph_3P)_2Pt(CH_2X)_2};$$

COD =  ; X = Cl, I.



7 **8** (~38%) **9** (~7%)

It is noteworthy that, apart from the halomethyl derivatives of transition metals, products may be obtained in which the methylene fragment is coordinated to the metal atom. Thus the addition of CH_2N_2 to the iridium complex **10** at −30 °C leads to the adduct **11** (or d_2-**11**).[41] The formation of ethylene on subsequent addition of CH_2N_2 to the deuteriated complex d_2-**11** as well as the formation of phenylcyclopropane and α-methylstyrene on interaction of compound **11** with styrene have been attributed[41] in this instance to the involvement in the reaction of the methylene complexes of pentacoordinate iridium.



The complex chromium halides **12** interact with CH_2N_2, affording a high yield of the corresponding halomethyl derivatives **13**, which are converted in the presence of $AgBF_4$ into the cationic complexes **14**.[42] The attempt to convert cyclohexene into a cyclopropane derivative by compounds **14** proved successful only in the case of the pentamethylcyclopentadienyl ligand, the yield of norcarane not exceeding 5% under these conditions.

$$\underset{\mathbf{12}}{(C_5R_5)Cr(NO)_2X} \xrightarrow{CH_2N_2} \underset{\mathbf{13}}{(C_5R_5)Cr(NO)_2CH_2X} \xrightarrow{AgBF_4} \left[(C_5R_5)\overset{CH_2}{\overset{\|}{Cr}}(NO)_2\right]^+ BF_4^-;$$

14

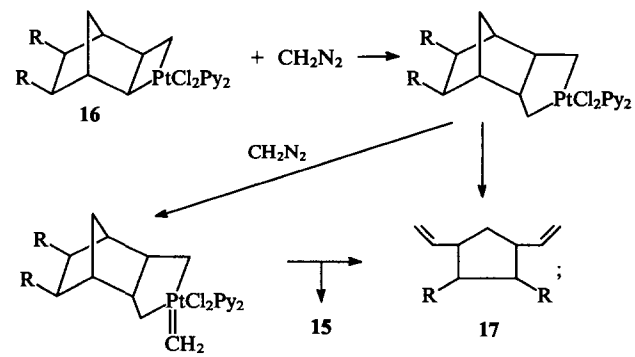
R = H, Me; X = Cl, Br.

The possible methods of the synthesis of cationic methylene complexes of transition metals not involving the use of CH_2N_2 as well as certain reactions with transfer of the methylene fragment from these complexes to the substrate, including the conversion of olefins into cyclopropane derivatives by such complexes, have been considered in a review.[43]

In contrast to complexes **5**, the pyridineplatinum complex, formed on controlled addition of pyridine to bis(ethyleneplatinum dichloride), interacts with a threefold excess of CH_2N_2, affording not the halomethyl derivatives of platinum but two enantiomeric forms of the ylide **15**.[44] The same compound is obtained also in the reaction of CH_2N_2 with the derivatives of platinacyclobutanes **16**, but in this case the main process reduces, according to Jennings et al.,[45] to the insertion of methylene into the Pt−C bond with subsequent conversion of the resulting platinacyclopentanes into *cis*-divinylcyclopentanes **17**.

$$[C_2H_4PtCl_2]_2 \xrightarrow{1\text{ eq. Py}} C_2H_4PtCl_2Py \xrightarrow[1\text{ eq. Py}]{3\text{ eq. }CH_2N_2} PyCl_2\overset{-}{P}t{-}CH_2{-}\overset{+}{P}y;$$

15 (95%)

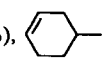


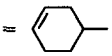
R = H, R−R is a chemical bond or CH_2.

The dediazotisation of CH_2N_2 by stable methoxycarbene complexes of chromium and tungsten is accompanied by the transfer of methylene to the carbene ligand, which results in the formation of the vinyl ethers **18** in satisfactory yields.[46,47]

$$(CO)_5M{=}C(OMe)R + CH_2N_2 \longrightarrow H_2C{=}C(OMe)R$$

18

M = W; R = Ph (97%), Me (93%),  (80%);

M = Cr; R =  (78%).

Copper and palladium compounds constitute another group of transition metal compounds catalysing the decomposition of CH_2N_2 and ensuring the successful transfer of methylene to the substrate (in particular, the conversion of

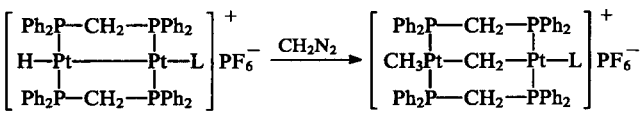
olefins into cyclopropane derivatives under mild conditions). The involvement of carbene complexes of metals in these reactions with the methylene generated from CH_2N_2 has so far been only postulated. However, despite the absence of direct experimental evidence for the formation of these complexes under the real conditions of the conversion of olefins into cyclopropane derivatives by CH_2N_2, their participation in the reactions is indicated by the existence of stable carbene complexes of other transition metals[6,43,48] as well as the detection of complexes of CH_2N_2 and methylene with atomic copper at 11 K in an argon matrix.[49]

Catalysts based on transition metals can be regarded as centres on which CH_2N_2 is coordinated and methylene is generated from it. The nature of the metal and the ligand environment of the central catalyst atom, which influence the strength of the bond linking the coordinated methylene, make it possible to vary its reactivity under these conditions, which leads in its turn to the possibility of regulating the regio- and stereoselectivity of the addition of methylene to various substrates.

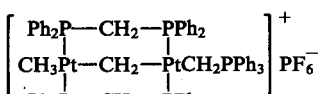
Finally, the reactions of CH_2N_2 with di- and poly-nuclear transition metal complexes, leading to the formation of μ-methylene complexes as a result of the addition of methylene to the metal–metal bond, are of independent interest:

Compound	Ref.
$(\mu\text{-}CH_2)[C_5H_5(NO)Fe]_2$	50
$(\mu\text{-}CH_2)[C_5Me_5(CO)Co]_2$	51
$(\mu\text{-}CH_2)[(C_5H_4Me)Mn(CO)_2]_2$	52, 53
$(\mu\text{-}CH_2)[C_5Me_5(CO)Rh]_2$	54, 55
$(\mu\text{-}CH_2)(\mu\text{-}CF_3C{\equiv}CCF_3)[ClRh(Ph_2PCH_2PPh_2)]_2$	56
$(\mu\text{-}CH_2)[ClPt(Ph_2PCH_2PPh_2)]_2$	57
$(\mu\text{-}CH_2)H_2Os_3(CO)_{10}$	58
$(\mu\text{-}CH_2)Os_3PtH_2(CO)_{10}\{P(C_6H_{11})_3\}$	59

The structural features of the μ-methylene complexes of transition metals have been analysed and the methods of their synthesis have been described in a review.[60] It is of interest to note that in the case of the hydridoplatinum complexes **19**, the insertion of CH_2 into the Pt–H bond with formation of complexes **20**, and into the Pt–P bond on interaction of compound **19c** with an excess of diazomethane, was observed simultaneously with its insertion in the Pt–Pt bond.[61]



19 **20a, b**



20c

L = CO (**a**), PMe_2Ph (**b**), PPh_3 (**c**).

The dinuclear complex $Mn_2(CO)_{10}N_2CH_2$, in which the Mn atoms are linked by a nitrogen bridge, while the methylene fragment is attached to one of the nitrogen atoms, was synthesised by the reaction of CH_2N_2 with $Mn(CO)_5H$ in tetrahydrofuran (THF) at −85 °C.[62]

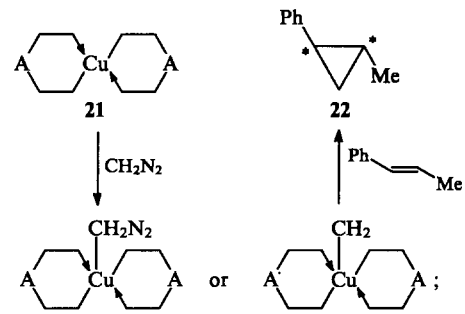
It is noteworthy that the interest in the stable μ-methylene complexes of transition metals has been mainly induced by the possibility of the involvement of such complexes as intermediates in the Fischer–Tropsch reaction. Unfortunately the reactions involving the transfer of the methylene fragment from these complexes to various substrates have been scarcely investigated.

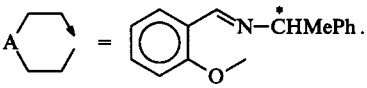
III. Catalytic conversion of unsaturated compounds into cyclopropane derivatives

1. The mechanism of the catalytic conversion of olefins into cyclopropane derivatives by diazomethane

Despite the abundance of compounds inducing the decomposition of diazomethane, copper and palladium compounds are the commonest and most effective agents for the catalytic conversion of olefins into cyclopropane derivatives by diazoalkanes. The experimental data accumulated hitherto have shown[63–66] that, among copper compounds, the salts of copper(I) are catalytically active in these reactions. The copper(II) salts, in particular $CuCl_2$ or $Cu(OSO_2CF_3)_2$, are initially reduced by diazomethane to the corresponding univalent copper compounds.[34,65]

According to Nefedov et al.,[66] when $Cu(acac)_2$ is used for the conversion of alkenes into cyclopropane derivatives, it is initially reduced by diazomethane to the relatively unstable Cu(acac), which is characterised primarily by the disappearance of the initial colour of the catalyst as a consequence of the conversion of Cu(II) into Cu(I). In view of this, one can assume that copper(I) compounds with one singly charged chelate anion are catalytically active in the case of other copper chelate compounds, in particular those with optically active ligands. Nevertheless, the pentacoordinate state of copper(II) has been considered[67] as an intermediate and the induction of the optical activity in the resulting cyclopropane **22** (yield 62%, optical yield 8%) is explained by the influence of the two optically active ligands in the initial complex **21**.

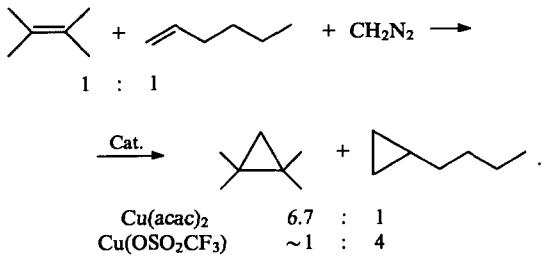




When palladium(II) compounds are used as the catalysts in the dediazotisation of CH_2N_2, a catalytically active species involving a change in the valence state of the palladium is also formed initially. Thus palladium halides or acetate are reduced to zerovalent palladium, which is either precipitated as a black deposit or is present in solution in the form of complexes stabilised by suitable ligands.[68] Under particular conditions, certain olefins, affording the corresponding π-olefin complexes, can also play the same role. However, the thermal stability of zerovalent palladium complexes is as a rule low[69] and depends significantly on the nature of the double bonds in the unsaturated compound. Inner complexes of palladium, for example $Pd(acac)_2$, apparently form more complex catalytically active structures with formally univalent palladium.[25]

There are two possible mechanisms of the catalytic conversion of olefins into cyclopropane derivatives by diazocompounds, in particular by diazomethane, in the presence of copper and palladium derivatives, the principal difference between which consists in the different sequences of the stages involving the interaction of the catalyst with the diazocompound and the olefin.[17,65,70,71]

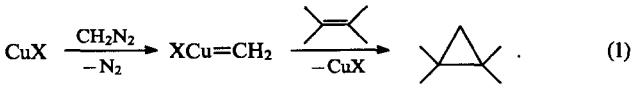
In relation to the conversion of mono- and tetra-substituted alkenes into cyclopropane derivatives, Salomon and Kochi[65] showed that regioselectivity in the conversion of various double bonds into cyclopropane groups differs depending on whether copper acetylacetonate or triflate is used as the catalyst. The more substituted double bond is converted into a cyclopropane group in the presence of $Cu(acac)_2$, whereas in the presence of $Cu(OSO_2CF_3)_2$ the terminal double bond undergoes such conversion.

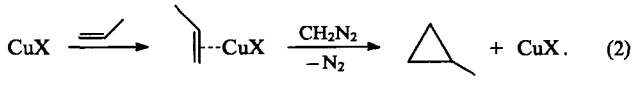


On these grounds, it was claimed that the change in the basicity of the anion affects the ability of the copper ion to form π-complexes with particular double bonds of olefins and is therefore capable of altering the sequence of the stages in the interaction of the catalyst with the diazo-compound and the olefin.

According to the first and commonest mechanism of the conversion of olefins into cyclopropane derivatives by diazoalkanes, a complex between the catalyst and the diazo-compound is formed initially. This is followed by the formation of a complex with the carbene, after which the double bond of the unsaturated compound is converted into a cyclopropane group by this complex.[17,65,70,71]

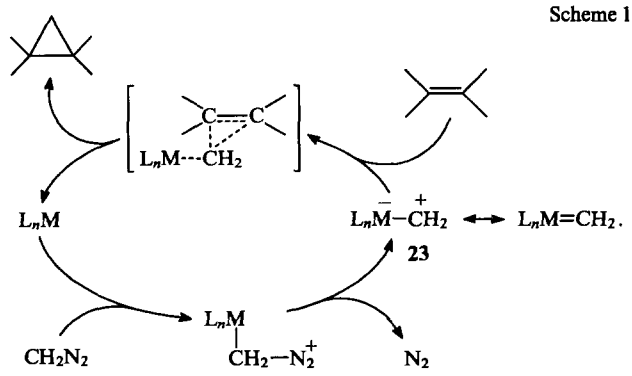
According to the other mechanism, a π-complex of the active form of the catalyst with the unsaturated compound is formed initially, interacting subsequently with the diazo-compound.[17,65,70]





In our view, the conversion of olefins into cyclopropane derivatives in the presence of copper compounds should be considered within the framework of one mechanism, because the key stage in both cases is the generation of the carbene complex (Scheme 1). The electrophilicity of the metal (Cu^+) induces, by analogy with the protonation of diazo-compounds, a shift of electron density towards the formation of an unstable diazonium cation, which readily eliminates a nitrogen molecule. The electrophilicity of the carbene species is in its turn largely determined by the contribution of the polarised structure **23**. Next, this complex reacts preferentially either with the more nucleophilic tetraalkyl-substituted double bonds, if the catalyst is incapable of effecting selectively the coordination of any one of the double bonds, or with monosubstituted double bonds. The latter reaction is less vigorous, but such bonds are present in excess in the coordination sphere of the metal as a consequence of complex formation. Here one should note that the regioselectivity of the conversion of double bonds into cyclopropane groups in the presence of copper catalysts is not high and the observed differences are of the same order of magnitude.

Scheme 1

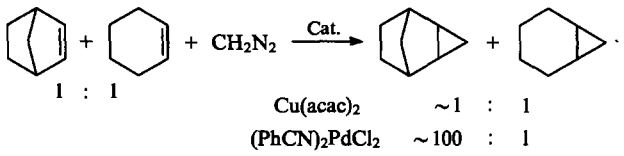


On the other hand, the effectiveness of the cyclopropane formation reaction is influenced very greatly in both cases by the competing side reaction between the methylene complex and yet another diazomethane molecule. This process involves the intermediate formation of organocopper compounds, which readily decompose with liberation of active metallic copper on which unsaturated compounds are scarcely converted into cyclopropane derivatives by diazomethane.[66] Obviously the ease of such reactions depends both on the nature of the olefin to be converted into a cyclopropane derivative and on the nature of the catalyst. The probability of the insertion of the methylene generated into the Cu−X bond of the catalyst is then found to be highest for nucleophilic anions. Thus, in the case of CuCN or CuI, this side reaction apparently plays a dominant role, which virtually rules out the possibility of the transfer of methylene to the olefin.[66] Furthermore, in order to reduce the probability of side reactions in catalysis by copper compounds, a very slow addition of CH_2N_2 to a mixture of the olefin and the catalyst is essential.

Within the framework of the mechanism considered, the possibility of the reverse polarisation of the carbene complex $L_nM{=}CH_2 \longleftrightarrow L_nM^+ - {}^-CH_2$ has been postulated in order to account for the preferential conversion of the electron-deficient double bond into a cyclopropane group.[72] Thus, in the interaction of CH_2N_2 with methyl acrylate, styrene, cyclohexene, and hex-1-ene, catalysed by zerovalent nickel complexes, the formation of a cyclopropane adduct was observed only for methyl acrylate. However, in such cases one must not apparently fail to take into account the active formation of complexes between the electron-deficient alkenes themselves and the central atom of the catalyst, which can influence significantly the nature of their interaction with CH_2N_2. The conversion of unsaturated compounds into cyclopropane derivatives by diazomethane in the presence of zerovalent nickel and especially zerovalent palladium complexes, which exhibit a series of significant and fundamental differences from the catalysis by copper compounds, should in fact be regarded as an alternative mechanism, in which the initial formation of π-olefin complexes is indeed an important stage of the entire process.

In contrast to the copper compounds, catalysts based on palladium compounds display an extremely high regio-selectivity in the conversion of individual double bonds into cyclopropane groups. This has no analogue among other methods for the conversion of unsaturated compounds into cyclopropane derivatives (without taking into account the influence of steric factors). The use of various palladium compounds as catalysts under these conditions hardly affects the regioselectivity of the cyclopropane formation reaction.

Instances of reactions exhibiting different stereoselectivities in the conversion of the same cycloolefins into cyclopropane derivatives under the influence of copper or palladium catalysts have also been observed (see Section III.3.b).



Finally, in contrast to copper catalysts, the conversion of double bonds into cyclopropane groups in the presence of palladium compounds proceeds without special complications up to the total conversion of the olefin into the corresponding cyclopropane even when the order in which the reactants are mixed is altered, for example when the catalyst is added to a mixture of the unsaturated compound and an excess of CH_2N_2.

Thus the results show that the mechanism of the action of palladium catalysts differs significantly from that of the catalysis of the cyclopropane formation reaction by copper compounds.

As mentioned above, the palladium compounds used as catalysts are initially reduced by diazomethane to low-valence palladium complexes stabilised in solution by suitable olefin ligands. In contrast to the olefin copper(I) complexes, where the coordinated ligand undergoes only slight changes compared with the initial olefin, in the π-olefin complexes of zerovalent palladium considerable changes occur in the coordinated ligand: the double bond is lengthened, the bond angles of the substituents are altered, and there is intense reverse donation of electrons from the metal to the olefin.

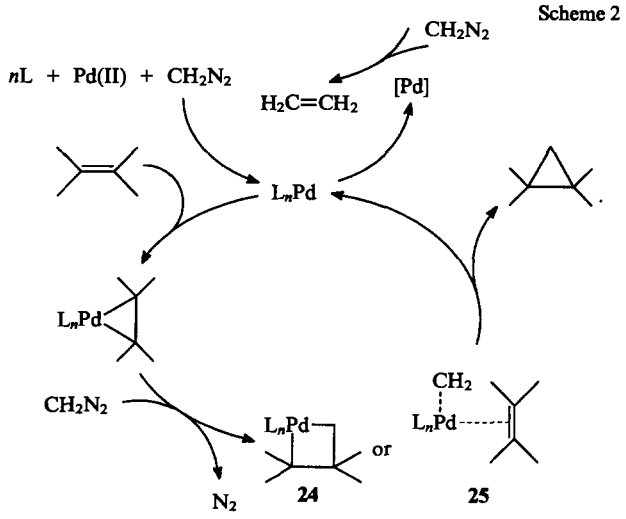
Thus the observed high selectivity in the conversion of various double bonds into cyclopropane groups by diazomethane in the presence of palladium compounds is undoubtedly due to their high selectivity in the formation and stabilisation of π-olefin complexes of zerovalent palladium.[68] According to Green et al.,[69] these complexes contain three equivalent olefin ligands. Furthermore, one can imagine two versions of the interaction of the π-olefinpalladium complexes with CH_2N_2.

In the first case, CH_2N_2 reacts directly with the polarised Pd–C bond of the π-olefin complex, affording the unstable palladiacyclobutane **24**, from which the cyclopropane adduct is eliminated and the initial π-olefin complex is regenerated under the influence of the next olefin molecule. Other complex-forming groups, for example the triphenyl phosphite or acetylacetonate groups, can also be present under these conditions as one or two ligands.

In the second version, CH_2N_2 substitutes one of the olefin ligands, eliminating the N_2 molecule and affording the metal–olefin–carbene complex **25**, from which the cyclopropane adduct is obtained either directly or via the palladiacyclobutane intermediate **24** (Scheme 2). The involvement of the latter in the reaction actually makes it possible to account for certain regio- and stereo-specific features of the conversion of olefins into cyclopropane derivatives by diazomethane in the presence of palladium catalysts. The existence of both metal–olefin–carbene complexes and metallacyclobutanes is now known.[73,74] However, the involvement of these intermediates in the conversion of olefins into cyclopropane derivatives, catalysed by copper and palladium compounds, is as yet tentative.

Unfortunately, under real experimental conditions, the yields of the cyclopropane adducts are determined not only by the contributions of the above mechanisms of the cyclopropane formation reaction but also by the possibility of the occurrence of side reactions associated primarily with the change in the active form of the catalyst. Thus the principal cause of the loss of catalytic activity by both copper and palladium compounds in the cyclopropane formation reaction is the liberation of the free metal and, as noted above, in the former case this is determined by the ease of the formation and α-decomposition of the organocopper intermediates, whilst in the latter it is due to the use of olefins with a low complex-forming capacity. The

Scheme 2



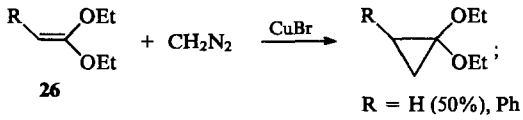
principal product of the decomposition of CH_2N_2 under these conditions is ethylene, which means that even the use of CH_2N_2 in manyfold excess does not lead to the complete conversion of olefins into the corresponding cyclopropane adducts.

2. Conversion of olefins into cyclopropane derivatives by diazomethane in the presence of copper catalysts

Copper compounds, in particular, CuCl and CuBr, were some of the first and commonest catalysts of the conversion of olefins into cyclopropane derivatives by diazomethane. Universality and the ability to catalyse the conversion of monosubstituted and polysubstituted olefins of different structure into cyclopropane derivatives are characteristic features of the above catalysts. In the copper salt-catalysed decomposition of CH_2N_2, the possibility of side reactions of the initial olefins and the resulting cyclopropanes is almost completely ruled out and there is also no insertion of the methylene fragment into the C–H bonds of these compounds.[11,12,71] However, the degree of conversion of olefins into cyclopropanes varies within wide limits even in the presence of an excess of the added diazomethane and depends significantly on the nature of the double bonds and the experimental conditions.

a. Conversion of unsaturated aliphatic compounds into cyclopropane derivatives

The conversion of unsaturated compounds into cyclopropane derivatives by diazomethane using copper catalysts was first achieved in 1959 by Dull and Abend,[75] who investigated the interaction of CH_2N_2 with ketene acetals **26** in the presence of CuBr in hexane.

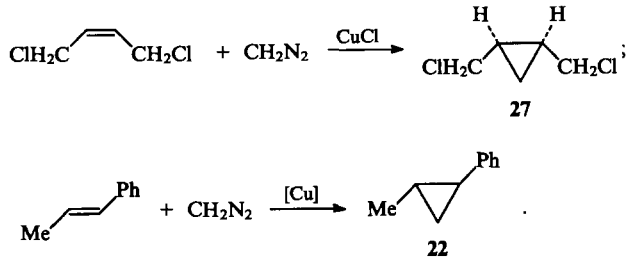


26

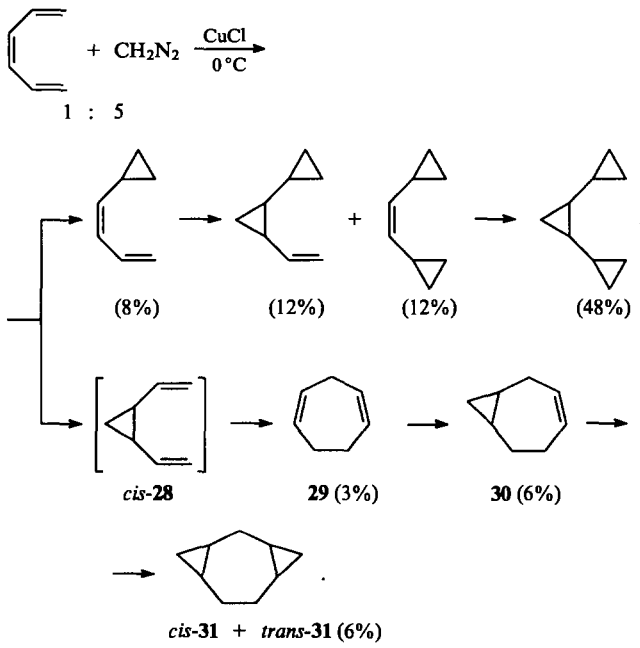
R = H (50%), Ph (12%).

Numerous studies, in which the method involving the catalytic conversion of multiple bonds into cyclopropane groups by diazomethane in the presence of copper compounds had been applied to a wide variety of unsaturated compounds containing both isolated and conjugated double bonds, were published in the 1960s. In order to eliminate or diminish the amount of solvent employed, particularly in the conversion of polyene compounds into polycyclopropane derivatives, which requires a large amount of CH_2N_2, the Gaspard–Roth method was frequently resorted to.[76] It consists in passing CH_2N_2 diluted with an inert gas into the olefin or its solution in a saturated hydrocarbon containing a catalytic amount of the copper salt at a temperature of about 0 °C.

The catalytic conversion of olefins into cyclopropane derivatives by diazomethane in the presence of various copper compounds proceeds stereospecifically with retention of the configuration of the initial unsaturated compound. Thus the interaction of CH_2N_2 with *cis*-1,4-dichlorobut-2-ene [77] in the presence of CuCl leads exclusively to *cis*-1,2-bis(chloromethyl)-cyclopropane **27**, while the conversion of *trans*-propenylbenzene into cyclopropane [67] in the presence of the copper complex **21** leads to *trans*-2-methyl-1-phenylcyclopropane **22**.

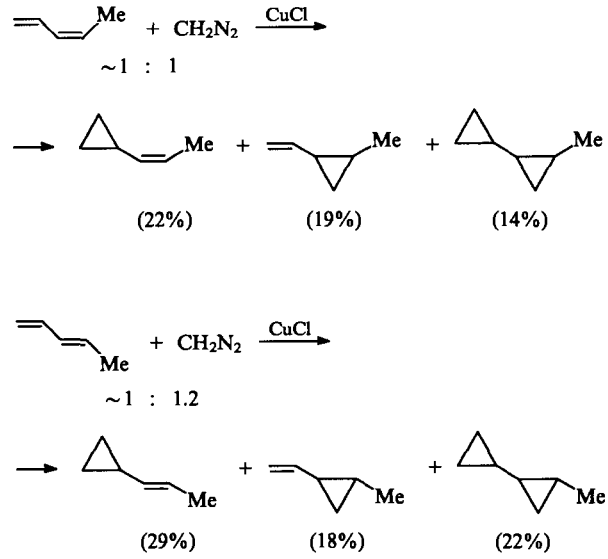


The regioselectivity of such reactions is as a rule low, which has been noted in relation to the conversion of a highly unsaturated hydrocarbon, namely hexa-1,3,5-triene, into a cyclopropane derivative.[76] Thus the interaction of *cis*-hexatriene with CH_2N_2 in the presence of CuCl leads to the formation of all the possible products of the addition of methylene to the double bonds in both the initial triene and in the mono- and di-adducts formed from it. The absence of *cis*-1,2-divinylcyclopropane **28** from the reaction mixture and the formation of the cyclic hydrocarbons **29–31** under these conditions has been explained[76] by the ready rearrangement of *cis*-**28** to the cyclodiene **29** and its subsequent conversion into cyclopropane derivatives.

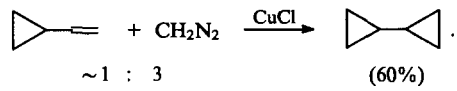


In contrast to the *cis*-isomer, *trans*-hexatriene affords only the expected linear cyclopropane formation reaction adducts, including also *trans*-1,2-divinylcyclopropane.[76] Despite the excess of CH_2N_2, the complete conversion of the hexatrienes is not then attained in both cases.

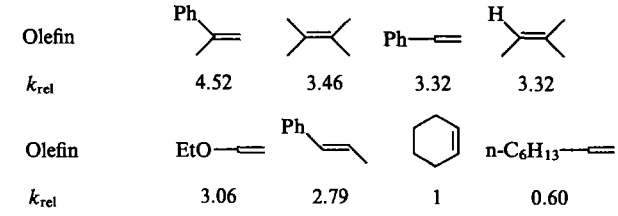
The interaction of *cis*- and *trans*-penta-1,3-dienes with CH_2N_2† in the presence of CuCl also takes place non-selectively[78] (but, as in the case of other olefins, with retention of the configuration of the double bond) and leads to a mixture of different products of the cyclopropane formation reaction. Despite the postulated electrophilic nature of the carbene intermediate, the conversion of the less substituted double bond into a cyclopropane group is somewhat preferred.



As was to be expected, the conversion of vinylcyclopropane itself by an excess of CH_2N_2 into bicyclopropyl proceeds fairly smoothly, which makes it possible to regard this method of synthesis of bicyclopropyl as preparative.[79]



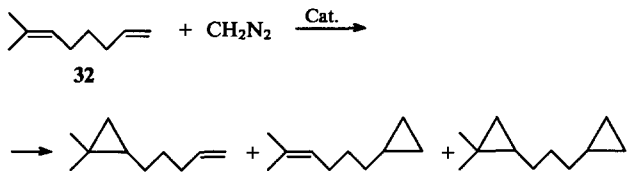
The constants of the relative reactivity of olefins of different structure in relation to CH_2N_2 have been published[67] (the reaction was carried out in the presence of copper salicylaldiminate **21**; the degree of conversion of the olefins was ~10%):



Interesting results as regards the relative reactivity of the double bonds have been obtained using copper catalysts containing anions with different basicities.[65] Thus passage of CH_2N_2 into a mixture of 2,3-dimethylbut-2-ene and hex-1-ene in proportions of 1 : 1 in the presence of a catalytic amount of $Cu(acac)_2$ leads to tetramethylcyclopropane and butylcyclopropane in proportions of 6.7 : 1. The same reaction in the presence of $Cu(OSO_2CF_3)_2$ leads to the formation of the above cyclopropanes in the reverse proportions (~1 : 4) (see Section III.1).

† Instead of the absolute amount of CH_2N_2, the amount of *N*-methyl-*N*-nitrosourea used to generate it has been stated in a number of communications. Therefore here and henceforth in specifying the olefin : CH_2N_2 molar ratio it is postulated that CH_2N_2 is formed in a yield of 55% – 60% on average.[66]

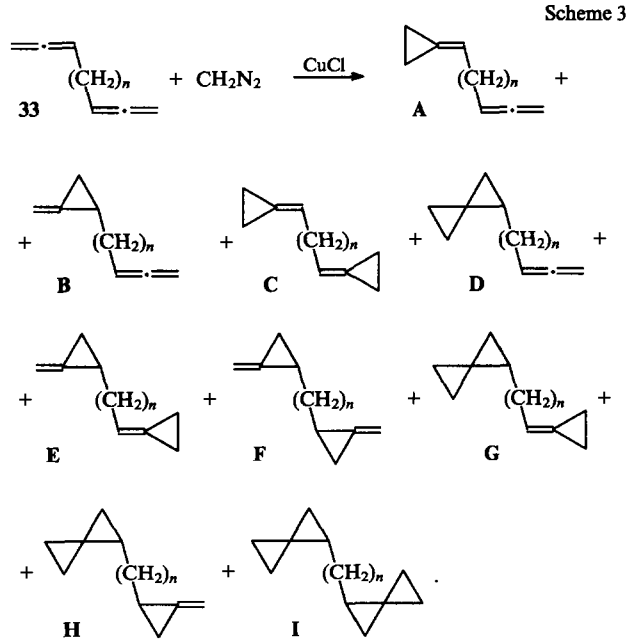
A similar dependence of the mode of the cyclopropane formation reaction on the degree of substitution of the double bond and the copper salt employed is manifested also in the conversion of 2-methylocta-2,7-diene **32** into a cyclopropane derivative.[65] In the presence of copper acetylacetonate, the more substituted double bond is converted into a cyclopropane group, while in the presence of copper triflate the terminal double bond is thus converted.



Cat.	Conversion of diene (%)	Adducts ratio
$Cu(acac)_2$	~10	6.1 : 1 : ~0.1
	90	10 : 1 : 6
$Cu(OSO_2CF_3)_2$	10	1 : 2 : ~0.1
	50	1 : 2.5 : 0.4

The results are probably associated with the unequal abilities of the catalyst to effect the coordination of different double bonds: copper ions coordinated to the acetylacetonate ligand are hardly involved in the formation of π-olefin complexes by reaction with the double bonds, whereas copper ions containing only the weak nucleophilic $CF_3O_2SO^-$ anion are capable of the selective formation of complexes by reacting with the less substituted (or strained) double bonds.[80,81] For this reason, the electrophilic methylene complex formed on decomposition of CH_2N_2 in the coordination sphere of copper reacts preferentially with the more nucleophilic (i.e. alkylated) C=C bonds in the former case, while in the latter case it reacts with the unsubstituted or strained double bonds, which, although less nucleophilic, show instead a greater tendency towards the formation of complexes with the metal atom and are therefore more accessible.

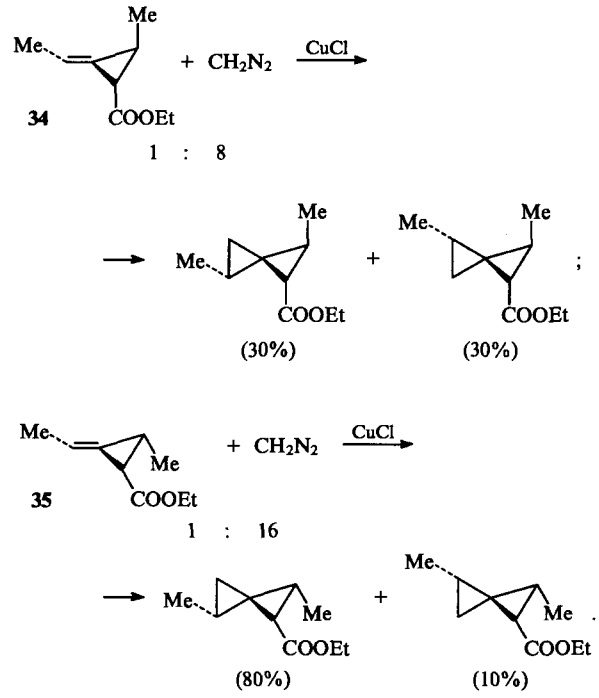
Scheme 3



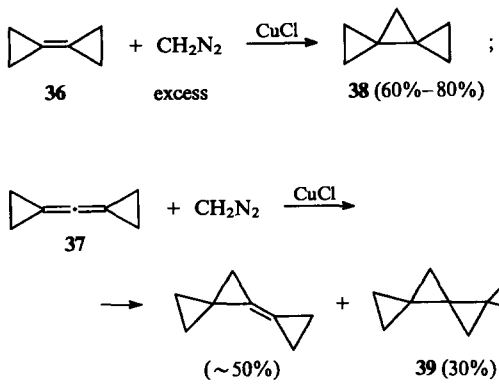
n	Reagents ratio	Yield of products (%)								
		A	B	C	D	E	F	G	H	I
0	1 : 5	8	13	3	15	9	8	13.5	17	11.5
2	1 : 8	8	9	4	10	7	6	14	14	14

The copper salt-catalysed interaction of CH_2N_2 with allenes and methylenecyclopropanes has been investigated in a number of studies.[82–88] Although this method is fairly general for the synthesis of spiropentanes which are difficult to obtain, it nevertheless frequently leads to the formation of a complex mixture of compounds in relatively low yields or requires the use of a large excess of CH_2N_2. Thus a more than tenfold excess of CH_2N_2 has been used to convert tetradeuterioallene into the corresponding spiropentane at −80° C,[82] while the conversion of hexa-1,2,4,5- or octa-1,2,6,7-tetraenes **33** with a fivefold to eightfold molar excess of CH_2N_2 in the presence of CuCl led to the formation of a complex mixture of hydrocarbons containing all the possible products of the conversion of the double bonds into cyclopropane groups (Scheme 3).[83,84]

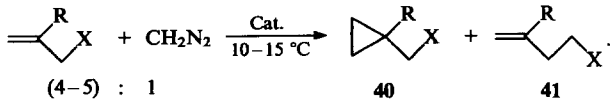
The conversion of methylenecyclopropanes into the corresponding spiropentane derivatives takes place significantly more smoothly under these conditions. Thus (in the presence of CuCl) the catalytic conversion of the esters of propylidenecyclopropanecarboxylic acid esters into cyclopropane derivatives by a large excess of CH_2N_2 was used as the basis of the synthesis of ethoxycarbonylspiropentanes.[85,86] Each individual isomer of the initial methylenecyclopropanes, for example compounds **34** and **35**, then forms two stereoisomeric spiropentanes. The steric disposition of the substituents can affect the degree of addition of the methylene attacking the double bond from different sides of the latter.



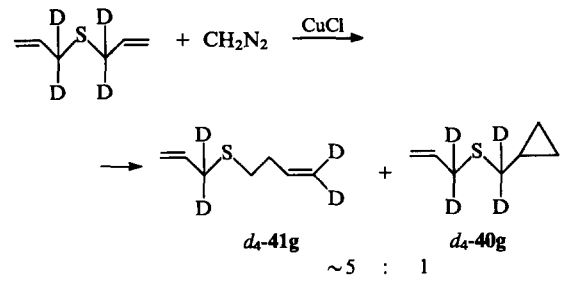
Fitjer and Conia[87,88] synthesised the polyspirane hydrocarbons **38** and **39**, consisting exclusively of cyclopropane fragments, from the bicyclopropylidene **36** and the allene **37** in 80% and 30% yields respectively. However, according to the data of Zefirov et al.,[89] who repeated the conversion of compound **36** into tercyclopropyl **38** in the presence of CuCl, the maximum yield of the latter was only 60%. As in all the previous cases, when copper compounds are used as catalysts, the target cyclopropane formation reaction proves to be extremely sensitive to the conditions under which it is carried out. One of the causes of the loss of catalytic activity of CuCl on transfer of methylene to the double bond of the olefin is probably its reduction to metallic copper.



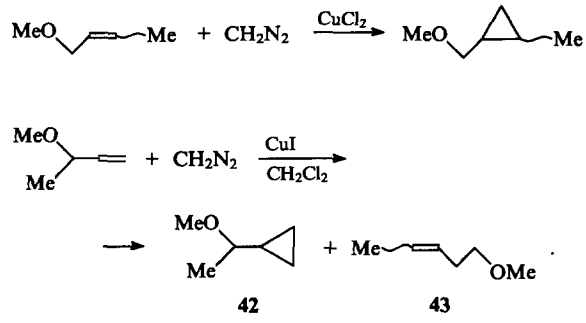
The catalytic interaction of CH_2N_2 with allyl derivatives in the presence of copper salts has been widely investigated by Kirmse and coworkers.[77,90–94] It was found that in the case of allyl halides as well as *O*- and *S*-allyl derivatives, the reaction leads to both the products of the conversion of the double bond into a cyclopropane group with formation of methylcyclopropanes **40** and to the products of formal insertion into the carbon–heteroatom bond with formation of 4-X-but-1-enes **41**, the yield and proportions of which depend significantly on the nature of the heteroatom and the reaction conditions (Table 1). Thus, when the reaction is carried out in pentane, allyl chloride affords predominantly chloromethylcyclopropane **40a**, whereas allyl bromide in CH_2Cl_2 gives rise to 4-bromobut-1-ene **41b**.



According to some data,[77,92] the formation of the homoallyl derivatives **41** proceeds via the stage involving the allyl rearrangement of the metastable ylide produced as a result of the addition of methylene to the heteroatom, which agrees well, in particular, with experimental data concerning the interaction of the deuteriated diallyl sulfide with CH_2N_2, as a result of which two deuterium atoms in compound d_4-**41g** formed are attached to the double bond.



It has also been noted[92] that the interaction of 1-methoxybut-2-ene with CH_2N_2 leads only to the conversion of the double bond into a cyclopropane group, whereas both the cyclopropane adduct **42** and a considerable proportion of the products of the allyl rearrangement—the isomeric 1-methoxypent-3-enes **43**—are formed from 2-methoxybut-3-ene.



The interaction of CH_2N_2 with allyl azide in the presence of CuCl affords 1,3,5-triallylhexahydro-*s*-triazine **44** together with cyclopropylmethyl azide.[93] This elegant synthesis of the *N*-allylaldimine trimer probably also proceeds via the intermediate formation of the ylide **45**.

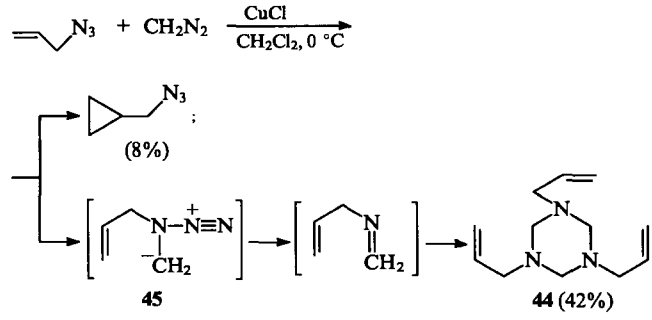
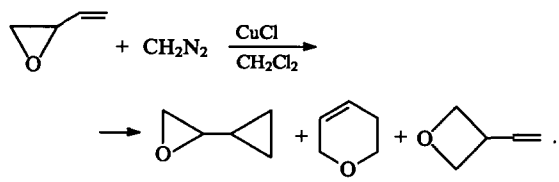


Table 1. Composition of the products of the interaction of CH_2N_2 with allyl derivatives ($H_2C=CRCH_2X : CH_2N_2 :$ Cat. ~5 : 1 : 0.6).

	$H_2C=CRCH_2X$		Catalyst (Cat.)	Solvent	Overall yield (%)	Content (%)		Ref.
	R	X				**40**	**41**	
a	H	Cl	CuCl	C_5H_{12}	30	83	14	77
			$CuCl_2$	C_5H_{12}	30	85	13	77
			$CuCl_2$	CH_2Cl_2	31	76	19	77
b	H	Br	$CuCl_2$	C_5H_{12}	17	21	79	77
			$CuCl_2$	CH_2Cl_2	29	6	90	77
			$(PhO)_3PCuCl$	CH_2Cl_2	79 [a]	2	98	95
c	Me	Cl	$CuCl_2$	CH_2Cl_2	30	34	59	77
d	Cl	Cl	$CuCl_2$	CH_2Cl_2	25	24	74	77
e	H	OMe	$CuCl_2$	C_5H_{12}	20	90	10	92
f	H	OC_3H_5	$CuCl_2$	C_5H_{12}	25	95	5	92
g	H	SC_3H_5	CuCl	C_5H_{12}	35	17	83	92
h	H	NMe_2	CuCl	CH_2Cl_2	26	100	–	93
i	H	$ONMe_2$	CuCl	Et_2O	7	100	–	93

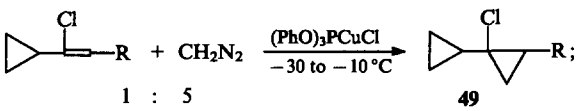
[a] Molar ratio $H_2C=CHCH_2Br : CH_2N_2 :$ Cat. ~1 : 3 : 0.01.

Under analogous conditions, vinyloxiran and CH_2N_2 give rise to the cyclopropane adduct **46**, the product of the allyl rearrangement—5,6-dihydropyran **47**, and also 3-vinyloxetan **48**, formed as a result of the formal insertion of methylene into the C–O bond of the initial epoxide.[94]



46 (64%) **47** (7%) **48** (29%)

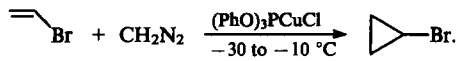
The catalytic interaction of CH_2N_2 with vinyl halides in the presence of CuCl or $(PhO)_3P \cdot CuCl$ leads to the corresponding cyclopropanes **49**, but, even in the presence of a fivefold molar excess of CH_2N_2, the degree of conversion of the vinyl halides into compounds **49** did not exceed 35%. An appreciable amount of CH_2N_2 then decomposed with formation of volatile products (mainly ethylene).[95]



1 : 5 **49**

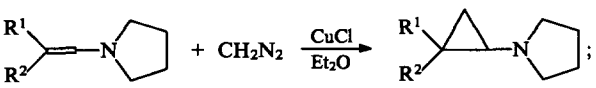
R = H (35%), CH(cyclo-C_3H_5)Me (24%), CH_2CH_2Cl (19%).

The conversion of vinyl bromide into a cyclopropane under the same conditions proceeds with a much lower degree of conversion.[95]



1 : 5 (13%)

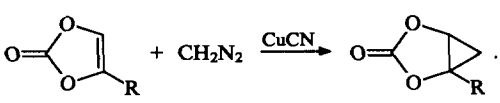
The conversion of vinylamines into cyclopropane derivatives occurred much more successfully. It was then noted[96] that the addition of CH_2N_2 to a mixture of the corresponding vinylamine **50** and 20 mol% of CuCl was accompanied by the appearance of a red colour, which vanished as CH_2N_2 was consumed. When a three–four-fold molar excess of CH_2N_2 was used, the yields of cyclopropylamines **51** were 69%–80% after isolation.



50 **51**

$R^1 = R^2 = H$ (73%), Me (69%);
$R^1 = H$, $R^2 = Et$ (80%);
$R^1 + R^2 = (CH_2)_4$ (70%).

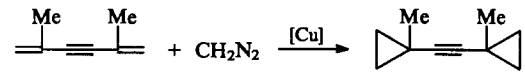
The conversion of ethylene carbonates **52** into cyclopropane derivatives was achieved under unusual conditions. In this case, the vapour of a mixture of CH_2N_2 with ether was passed into the unsaturated compounds **52** heated to 110–120 °C and containing CuCN as the catalyst.[98]



52

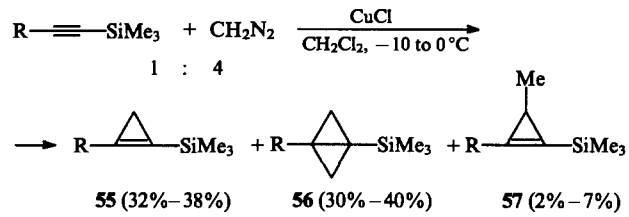
R	Reagents ratio	Yield of product (%)
H	4.2 : 1	28
Me	1.3 : 1	19

The simultaneous presence in the molecule of double and triple carbon–carbon bonds makes it possible under certain conditions to direct cyclopropane formation processes selectively to the double bonds. Thus a preparative method of synthesis of bis(1-methylcyclopropyl)acetylene **54** by the reaction of CH_2N_2 with the dienyne **53** in the presence of copper salicylaldiminate has been proposed.[99]. The triple bond in the product **54** is not involved despite the excess of diazomethane.



53 1 : 10 **54** (60%)

Nevertheless we were able to achieve for the first time the direct cyclomethylenation of the carbon–carbon triple bond with diazomethane in alkyl(trimethylsilyl)acetylenes using CuCl or $(PhO)_3P \cdot CuCl$ as the catalyst.[100,101] The reaction did not then stop with the formation of the cyclopropenes **55** but proceeded further, leading to the accumulation of the corresponding bicyclobutanes **56** in the mixture. Furthermore, the formation of methylcyclopropenes **57** as a result of the insertion of methylene in a C–H bond in the cyclopropenes **55** formed was an unexpected feature for the given reaction.

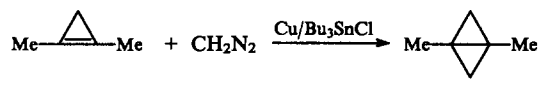


1 : 4

55 (32%–38%) **56** (30%–40%) **57** (2%–7%)

R = Me, Pr, cyclo-C_3H_5.

Before the above study, the only example of the catalytic cyclomethylenation of cyclopropenes by diazomethane was the interaction of 1,2-dimethylcyclopropene with CH_2N_2 in the presence of the modified bimetallic catalyst Cu/Bu_3SnCl.[102]

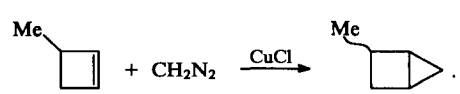


(13%)

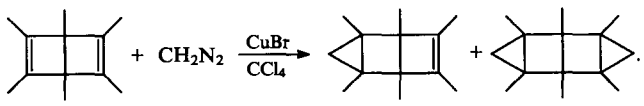
b. Conversion of cyclic unsaturated compounds into cyclopropane derivatives

The catalytic decomposition of CH_2N_2 on copper catalysts has been used widely for the conversion of cyclic and bicyclic hydrocarbons with one or several double bonds (conjugated and non-conjugated, endocyclic and exocyclic) into cyclopropane derivatives and also for the specific synthesis of compounds which are relatively unstable or difficult to obtain.

The possibility of the catalytic conversion of the C=C bond in cyclopropenes into a cyclopropane group was already mentioned above. Several examples of the conversion of the double bonds present in a four-membered ring into cyclopropane groups have been described.[103–105] Thus the interaction of CH_2N_2 with 3-methylcyclobutene leads to a mixture of *cis*- and *trans*-2-methylbicyclo[2.1.0]pentanes.[103]



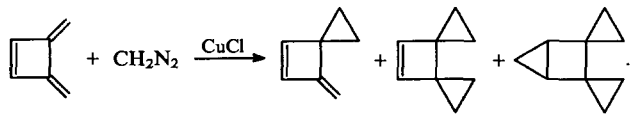
The tricyclic and tetracyclic hydrocarbons **58** and **59** have been synthesised by the reaction of hexamethylbicyclo[2.2.0]-hexa-2,5-diene with an excess of CH_2N_2 in the presence of CuBr.[104]



58 **59**

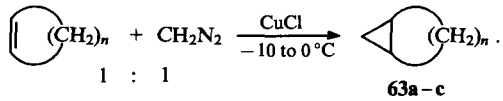
Reagents ratio	Yield of **58** (%)	Yield of **59** (%)
1:2	30	5
1:5	57	22

The spiro hydrocarbons **60–62** have been obtained by the reaction of 1,2-dimethylenecyclobut-3-ene with CH_2N_2 (in the proportions **60** : **61** : **62** = 5.8 : 1 : 1.7).[105] The absence of the mono- and di-adducts, produced by the conversion of the endocyclic double bond into a cyclopropane group, among the reaction products indicates the preferential conversion of the exocyclic bonds in the initial triene into cyclopropane groups.



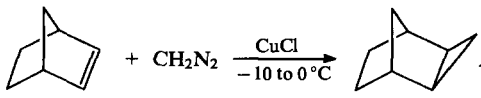
1 : 10 **60** **61** **62**

The interaction of C_6-C_8 cycloalkenes and norbornene with CH_2N_2 in the presence of CuCl leads to the corresponding bicyclo[*n*.1.0]alkanes **63** or the tricyclooctane **64**.[66] The yields of the cyclopropane derivatives under the same conditions increase on passing from cyclohexene to cyclooctene and norbornene, which is probably due to the ability of the strained cycloolefins to stabilise the catalyst in the form of π-olefin complexes.



1 : 1 **63a–c**

Product	*n*	Yield (%)
63a	4	20–25
63b	5	50–55
63c	6	75–80



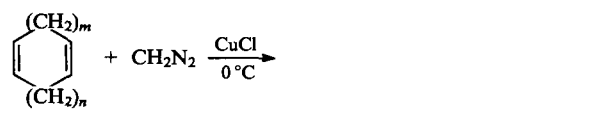
1 : 1 **64** (80%–85%)

This difference is manifested also in the competing reactions (CuCl, −5 °C) of norbornene and cyclohexene with CH_2N_2 (molar ratios 1 : 1 : 0.1)—the degree of conversion of the former into a cyclopropane derivative is greater by a factor of 2.7 than that of the latter. On the other hand, the conversion of the same mixture of cycloolefins into cyclopropanes in the presence of $Cu(acac)_2$ results in the formation of equal amounts of the cyclic adducts **64** and **63a** at any stage of the reaction, their yields amounting to 50%–55% for reactant ratios of ~1 : 1 : 2. In all cases, the cyclopropane formation reaction proceeds most effectively at the beginning of the addition of CH_2N_2, after which it is sharply retarded, particularly when the reaction mixture blackens.[66]

The conversion of cyclopentadiene,[106,107] cyclohexa-1,3-diene,[108] cycloheptа-1,3-diene, and cyclohepta-1,4-diene,[76] as well as cycloocta-1,5-diene [66] in the presence of CuCl into cyclopropane derivatives leads, as expected, to a mixture of mono- and di-adducts, namely to the bicycloalkenes **65** and the tricycloalkanes **66** (Table 2). The tricycloalkanes **66** are formed from the non-conjugated dienes in the form of a mixture of the *cis*- and *trans*-isomers (~1 : 1), whereas the *trans*-isomers predominate in the products of the reaction involving the double cyclopropane formation from conjugated dienes.

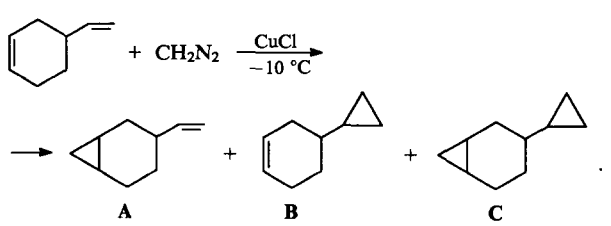
Table 2. Composition of the products of the conversion of cyclic dienes into cyclopropane derivatives by diazomethane in the presence of 5–6 mol% CuCl.

Cycloolefin		Molar ratio olefin : CH_2N_2	Yield of product (%)			Ref.
m	*n*		**65**	*trans*-**66**	*cis*-**66**	
0	1	1:3	40	45	11	106
0	2	1:3.5	7	54	32	108
0	3	1:5	45	35	10	76
1	2	1:3	45	20	20	76
2	2	1:2	35	24	27	66



65 *trans*-**66** *cis*-**66**

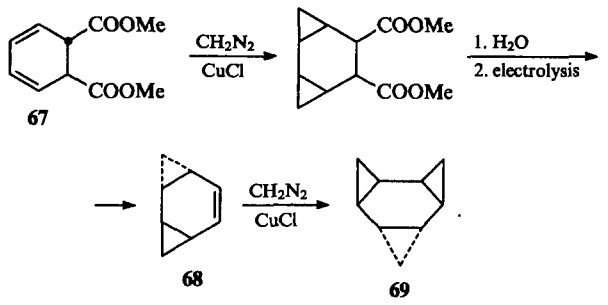
The catalytic conversion of 4-vinylcyclohexene into cyclopropane derivatives in the presence of CuCl proceeds via both the endocyclic and exocyclic double bonds, leading to mono- and di-adducts, the yields of which were found to be determined not only by the ratio of the olefin and CH_2N_2 but also by the amount of the catalyst employed.[66]



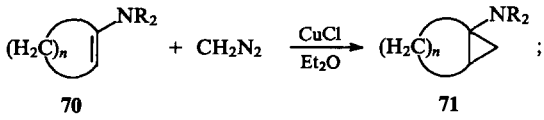
A **B** **C**

Olefin : CH_2N_2 : CuCl	Yield (%)		
	A	**B**	**C**
1:1:0.03	10	~8	2–3
1:2:0.03	13	10	3–4
1:2:0.40	17	21	~20

The diazomethane method for the catalytic conversion of cyclic double bonds into cyclopropane groups has been used successfully for the specific synthesis of trishomobenzene **69** from dimethyl *trans*-dihydrophthalate **67**, which cannot be obtained by the direct conversion of benzene into a cyclopropane derivative because of the ready isomerisation of the norcaradiene formed initially (see Section IV). For this purpose, the cyclodiene **67** was converted into the corresponding product of the double cyclopropane formation reaction by treatment with an excess of CH_2N_2 in the presence of CuCl, the ester groups were split off, and the resulting *trans*-tricyclooctene **68** was again subjected to the cyclopropane formation reaction by treatment with diazomethane and was converted into *trans*-**69**.[109]

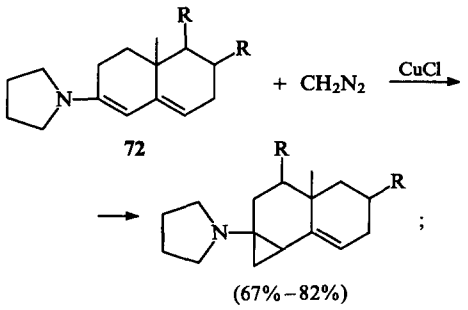


Like their aliphatic analogues **50**, the cyclic enamines **70** can also be fairly successfully converted into cyclopropane derivatives by treatment with an excess of CH_2N_2, which leads to high yields of the corresponding 1-aminobicyclo[*n*.1.0]alkanes **71**.[96,110]

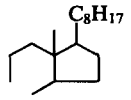


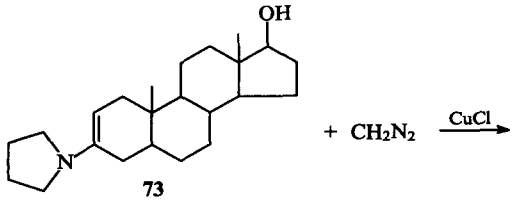
R = Me, Et; n = 3 (65%–72%);
R + R = $(CH_2)_4$; n = 3, 4 (72%–75%);
R + R = $CH_2CH_2OCH_2CH_2$; n = 3, 4 (86%–87%).

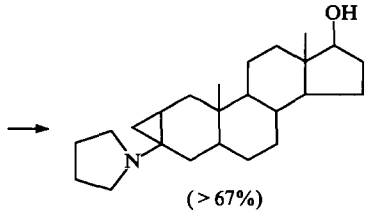
Under analogous conditions, the conversion of cyclic dienamines **72** into cyclopropane derivatives proceeds regioselectively despite the presence of an excess of CH_2N_2 and involves mainly the C=C bond conjugated with a nitrogen atom. As in the formation of a cyclopropane from the enamine **73**, one of the geometrical isomers is formed preferentially.[110]



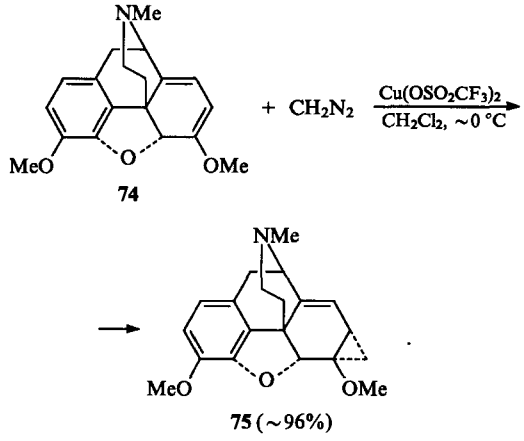
72 : CH_2N_2 = ~1 : (2.5–3);

R = H or R + R = 

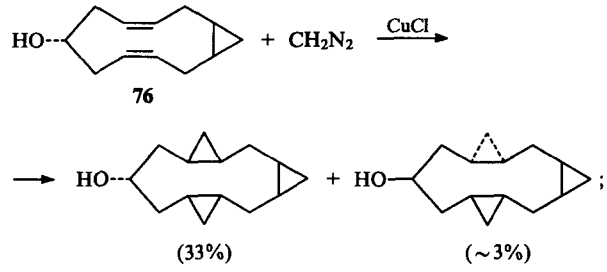


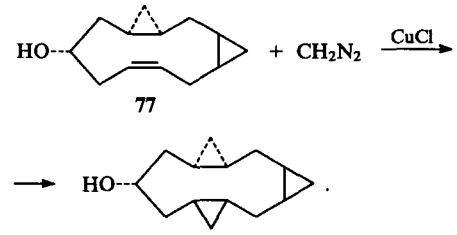


Generally speaking, the presence of bulky substituents and the configuration of the ring in the unsaturated compound can influence significantly the reactivity of the substrate and the stereochemical result of the addition of the methylene fragment to the double bond. Furthermore, the presence in the molecule of heteroatomic substituents capable of being coordinated to the catalyst also apparently affects the mode of addition of CH_2 to the double bond. Thus, in the reaction of thebaine **74** with an excess of CH_2N_2 in the presence of copper triflate, a high regio- and stereo-selectivity of the addition of the CH_2 fragment to the $C^6=C^7$ bond of thebaine **74** with formation of the previously unknown hydrophenanthrene alkaloid **75** was observed.[111]



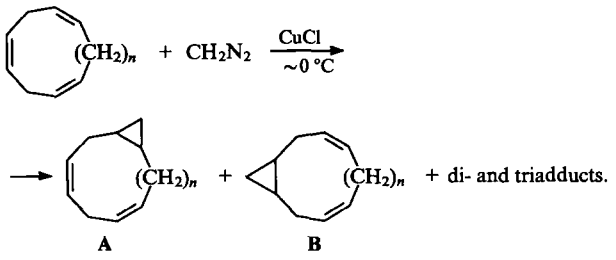
The high stereoselectivity of the conversion of endocyclic double bonds into cyclopropane groups has also been observed in the reaction of the unsaturated alcohols **76** and **77** with an excess of CH_2N_2 in the presence of CuCl.[112]





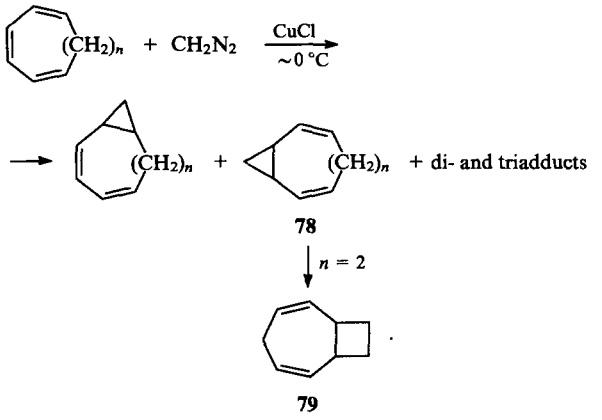
one isomer
(yield has not been given)

Cyclic trienes are converted into cyclopropane derivatives by treatment with diazomethane in the presence of CuCl similarly to cyclic dienes, the ratios and yields of the mono-, di-, and tricyclic adducts being determined mainly by the amount of the CH_2N_2 employed.[76,113]



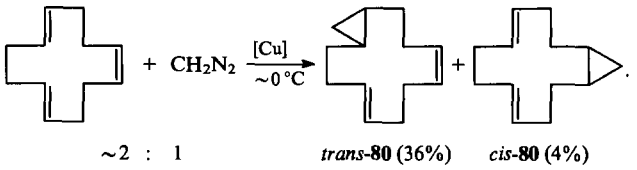
n	triene : CH_2N_2	Yield of adducts (%)		
		mono	di	tri
1	1 : 2.8	34	34	13

Furthermore, it has been shown[113] that the adduct **78** ($n = 2$), formed in 3% – 4% yield in the cyclopropane formation reaction from cycloocta-1,3,5-triene, isomerises to the bicyclic diene **79** (yield 8%) already during the course of the reaction.

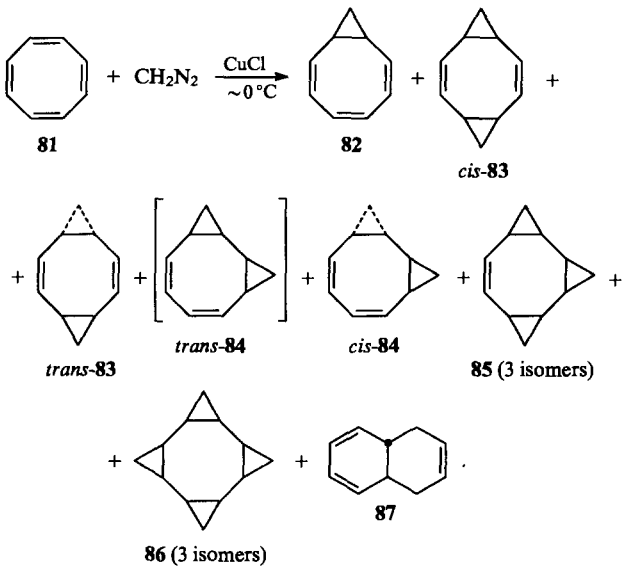


n	triene : CH_2N_2	Yield of adducts (%)		
		mono	di	tri
1	~1 : 4	18	45	28
2	1 : 2	34	31	8

In the cyclopropane formation reactions of unsaturated compounds with different configurations of the double bonds, the preferential conversion of the *trans*-C=C bond into a cyclopropane group has been noted. Thus the reaction of an excess of (*E*,*Z*,*Z*)-cyclododeca-1,5,9-triene with CH_2N_2 in the presence of the chelate copper complex **21** leads to the monocyclopropane derivatives **80** with a ratio *trans* : *cis* ≃ 9 : 1.[67]

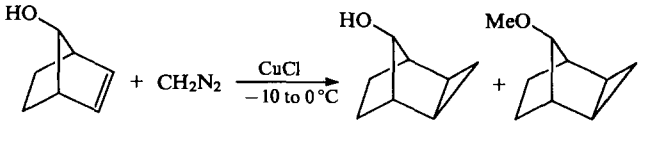


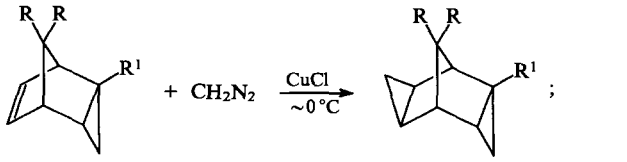
The catalytic conversion of cyclooctatetraene **81** into a cyclopropane derivative by treatment with diazomethane in the presence of CuCl was first achieved as early as the middle 1960s,[114,115] but only bicyclo[6.1.0]nona-2,4,6-triene **82** was isolated in ~30% yield and identified together with some products of the double cyclopropane formation reaction — *cis*-tricyclo[7.1.0.0^{4,6}]deca-2,7-diene (*cis*-**83**) and tricyclo[7.1.0.0^{2,4}]-deca-5,7-diene **84**, in which the configuration of the cyclopropane fragments was not established. Later the catalytic interaction of compound **81** with CH_2N_2 was investigated in detail by Nefedov and coworkers[116] and the stereochemistry of the cyclopropanes formed was established. In order to achieve a higher degree of conversion of compounds **81** and **82** into the tri- and tetra-cyclic adducts **85** and **86**, the reaction mixture was filtered twice under argon, as CH_2N_2 was added, and a fresh portion of CuCl (3–4 mol%) was introduced. It is of interest to note that the conjugated diene *trans*-**84** could not be detected in the double cyclopropane formation products **83** and **84** probably because of its ready isomerisation to the triene **87**, which was isolated in 2% – 3% yield.



81 : CH_2N_2	Yield of adducts (%)						
	82	*cis*-**83**	*trans*-**83**	*cis*-**84**	**85**	**86**	**87**
1 : 1	44	3–4	2–3	8	5	1–2	~2
1 : 3	13	~7	~5	14	36	15–17	~3

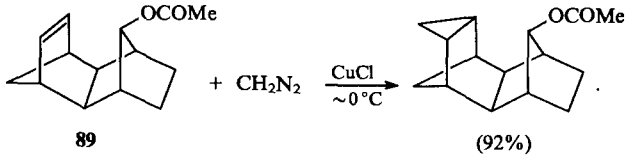
The fairly effective conversion of norbornene into a cyclopropane derivative by treatment with diazomethane in the presence of CuCl has already been mentioned.[66] It has been established recently[117] that, regardless of the nature of the catalyst [Cu(OTf)$_2$, CuCl, Cu(acac)$_2$], the main product is the *exo*-isomer **64**, while the fraction of the *endo*-isomer does not exceed 2%. The exclusive *exo*-addition of methylene to the norbornene double bond was observed also in the catalytic conversion into cyclopropanes of norbornene derivatives as well as other polycyclic compounds, for example compounds **88** and **89**, containing this fragment, on treatment with diazomethane.[118–122] It is striking that the *exo*-conversion of the





88

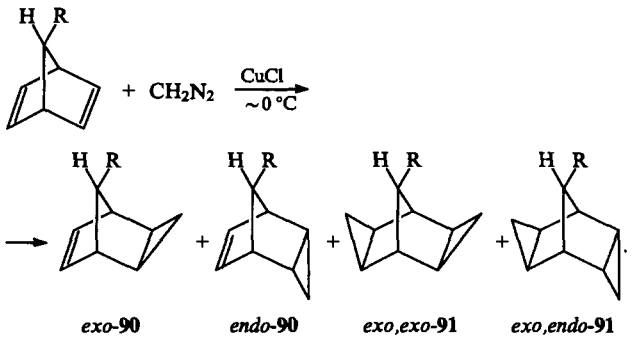
R = H, OMe; R^1 = H, Me (61% – 80%);
CR_2 = C=O; R^1 = H, Me (30% – 41%);
R + R = OCH_2CH_2O; R^1 = H (54%).



89 (92%)

double bond into a cyclopropane group occurs for both *anti*- and *syn*-orientations of the substituent in the 7-position of the bicyclo[2.2.1]heptene fragment and that the partial (~10%) formation of the corresponding methoxy-derivatives has been observed, together with conversion into a cyclopropane, for the hydroxy-derivatives.[119,121]

In contrast to norbornenes, the interaction of CH_2N_2 with norbornadiene and its derivatives in the presence of copper catalysts proceeds non-selectively and leads to a mixture of the mono- and di-adducts **90** and **91** containing both *exo* and *endo*-isomers.[117-119,123,124]

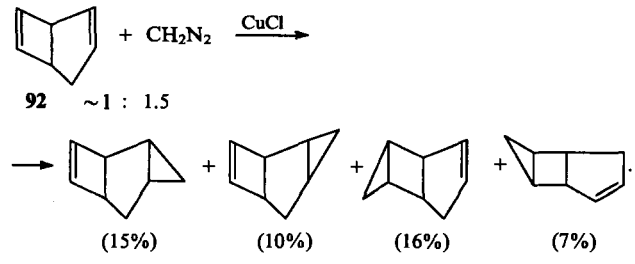


For a 1 : 1 norbornadiene (R = H) : CH_2N_2 ratio, the yields of the monoadducts (*exo*- and *endo*-) and triadducts (*exo,exo*- and *exo,endo*-) were respectively 33%, 15%, 8%, and ~4%. For R = OCOMe and OCOPh, the ratio *exo*-90 : *endo*-90 is ~5:1.

It was found that the partial formation of the *endo*-isomer is characteristic not only of norbornadienes but also of *exo*-tricyclo[3.2.1.$0^{2,4}$]octene (*exo*-**90**, R = H).[117] Whereas the subsequent conversion of *endo*-**90** (R = H) into a cyclopropane derivative in the presence of copper compounds leads exclusively to *exo,endo*-**91** (the *endo,endo*-isomer was not detected at all), the conversion of *exo*-**90** (R = H) into a cyclopropane derivative under the same conditions affords a mixture of the isomeric diadducts **91** in proportions of ~6:1.

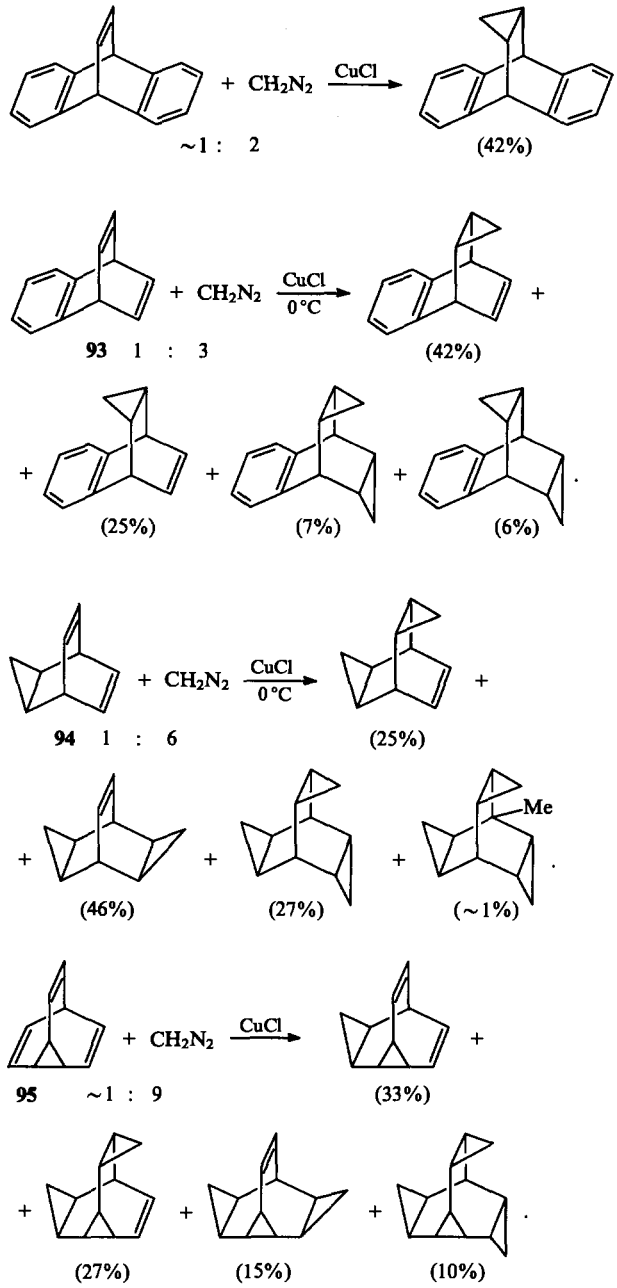
The increased content of the *endo*-isomer, compared with norbornenes, on conversion of norbornadiene into a cyclopropane derivative in the presence of copper catalysts is apparently associated with the characteristics of the geometry of the double bonds. Thus, according to calculations,[125] the angle of the *endo*-deformation of the vinyl C–H bonds in norbornadiene is smaller than in norbornene (2.3° and 4.9° respectively), so that the probability of the attack on the double bond by the carbene complex from the side of the *endo*-position is greater for the former compound. The detailed stereochemical aspects of the addition of methylene to the norbornene double bond in the presence of various catalysts will be examined in Section III.3.b (Table 5).

The conversion of the asymmetric bicyclo[3.2.0]hepta-2,6-diene **92** into a cyclopropane derivative in the presence of CuCl involves both double bonds and affords mixtures of the corresponding *syn*- and *anti*-isomers. The authors[126] observed the formation of four diadducts, in an overall yield of ~27%, together with the monoadducts.



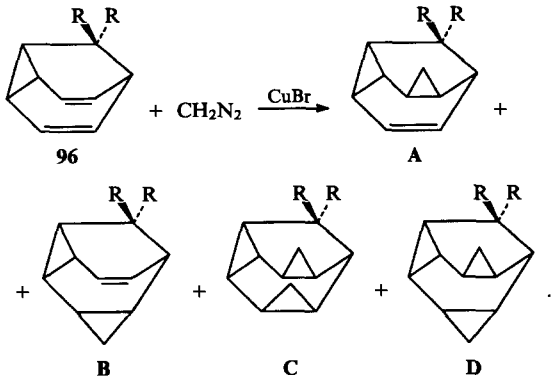
The mild conditions for the conversion of unsaturated compounds into cyclopropanes by diazomethane in the presence of copper compounds have been used widely for the synthesis and study of the chemical reactions of cyclopropane derivatives of bicyclo[2.2.2]octa-2,5,7-triene (barrelene),[127-130] tricyclo-[3.3.0.$0^{2,8}$]octa-3,6-diene (semibullvalene),[128] tricyclo[3.3.2.$0^{2,8}$]-deca-3,6,9-triene (bullvalene),[130] tricyclo[3.3.1.$0^{2,8}$]nona-3,6-diene (barbaralane),[131,132] and tricyclo[5.2.1.$0^{4,10}$]deca-2,5,8-triene (triquinacene).[133]

It is striking that, among the products of the conversion of benzobarrelene **93**, homobarrelene **94**, and also bullvalene **95** into cyclopropane derivatives, no *endo,endo*-isomers corresponding to the addition of methylene fragments oriented in opposition to one another were detected. However, in the case of the diene **94** deMeijere et al.[130] observed, in addition to the expected adduct, the appearance of a minor product corresponding to the formal insertion of methylene into the angular C–H bond.



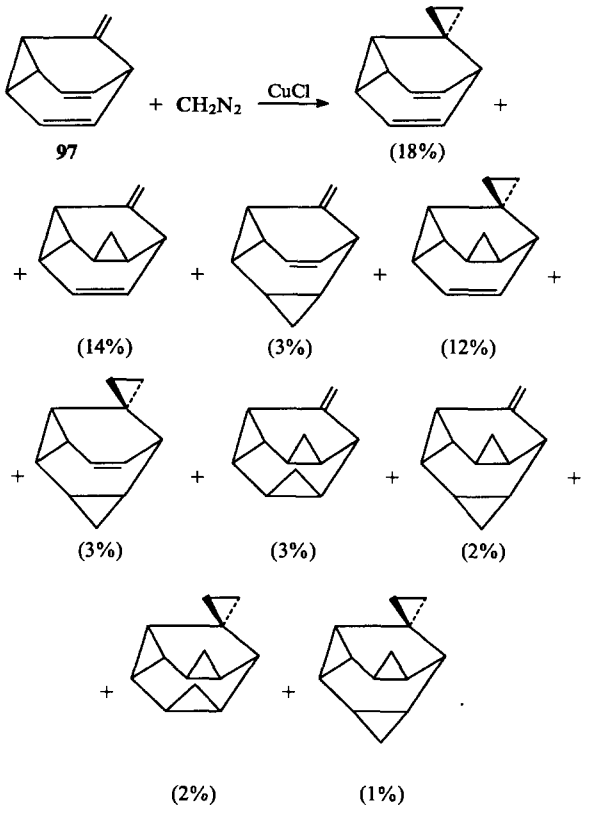
The high selectivity of the addition of methylene to the endocyclic double bonds is also characteristic of the structure of barbaralane, as for norbornene. Thus the interaction of the

tricyclodienes **96** with an excess of CH_2N_2 in the presence of CuBr leads to the mixture of the mono- and di-adducts with an appreciable predominance of the *exo*-isomers.[131]

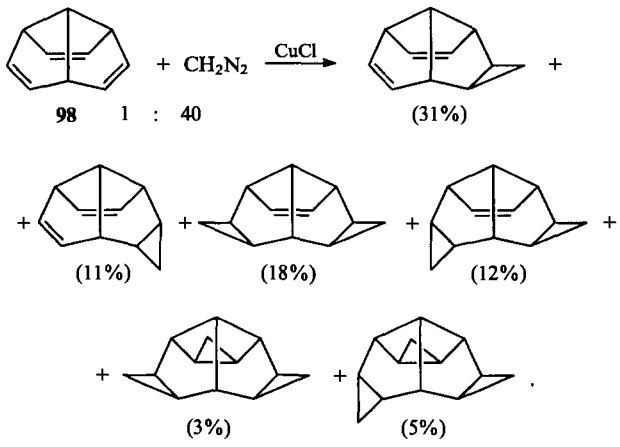


CR_2	Yield of adducts (%)			
	A	B	C	D
C=O	43.5	0.6	43.5	2.5
	~63	2.1	4.2	0.2

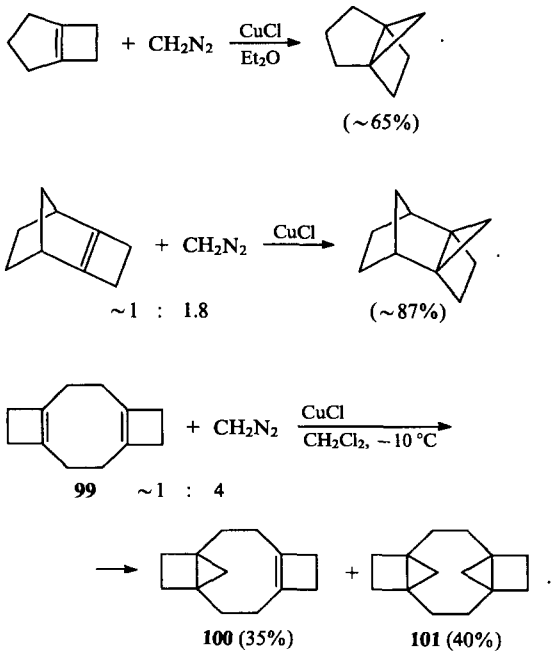
The conversion of 9-methylenebarbaralane **97** into a cyclopropane derivative proceeds in a more complex manner owing to the possibility of the conversion into cyclopropane groups of both endocyclic and exocyclic double bonds and leads to a mixture of nine cyclic adducts with different numbers and disposition of the cyclopropane fragments.[132] However, as in the case of norbornadiene, hydrocarbons with two *endo,endo*-oriented cyclopropane rings in the molecule were not detected in the products of the catalytic conversion of the polycyclenes **96**–**98** into cyclopropanes.



In many instances, the yields of cyclopropane adducts (particularly the products of the double and triple cyclopropane formation reactions) are significantly lower than might have been expected on the basis of the amount of CH_2N_2 employed and the structure of the unsaturated compounds. In particular, an unjustifiably large (40-fold) excess of CH_2N_2 was used in the formation of a cyclopropane derivative from triquinacene **98** [133] (cf the interaction of CH_2N_2 with cyclo-octatetraene[116]). The low degree of conversion of olefins into cyclopropanes is probably associated with the rapid change during the reaction of the nature of the catalyst, for example, with a gradual conversion of copper(I) salts by diazomethane into organometallic compounds or metallic copper, which, according to Nefedov et al.,[66] is reflected significantly in the target cyclopropane formation reaction.

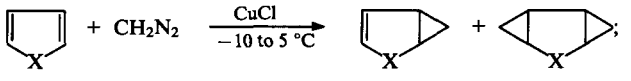


The ability of copper compounds to catalyse the formation of cyclopropanes on treating with diazomethane olefins with different degrees of substitution of double bonds, including tetrasubstituted olefins, proved useful for the synthesis of carbocyclic propellanes which are difficult to obtain and are highly strained.[134–136] In particular, isomeric polycyclic hydrocarbons **101**, containing two propellane fragments in the molecule (isomer ratio ~6 : 1), were synthesised, together with the monoadduct **100**, by the reaction of the diene **99** with CH_2N_2 in the presence of CuCl.[136]



c. Conversion of unsaturated heterocyclic compounds into cyclopropane derivatives

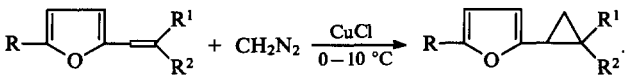
In the presence of copper salts, diazomethane is also capable of converting the double bonds in heterocyclic compounds into cyclopropane groups. Five-membered unsaturated heterocyclic compounds (furan, thiophene, pyrrole, and their derivatives) are then converted into the corresponding bicyclic and tricyclic compounds.[137-139] Thus the interaction of CH_2N_2 with an excess of furan in the presence of CuBr or CuCl leads to 2-oxabicyclohexene **102a** in 50%–65% yield; for the stoichiometric reactant ratio, the diadduct **103a** is formed in ~5% yield together with compound **102a**. The conversion of thiophene into a cyclopropane derivative proceeds less effectively probably owing to the lower stability of the adduct **102b**, the yield of which ranges from 6% to 22% according to different estimates.[137,138]



102 **103**

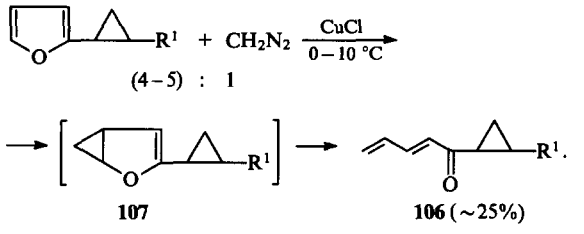
X = O (**a**), S (**b**).

The presence of substituents in the furan ring influences both the regioselectivity in the conversion of the double bonds into cyclopropane groups and the stability of the resulting adducts. Thus the interaction of CH_2N_2 with 2-alkenylfurans **104** leads in the first place to the conversion of the exocyclic double bonds into cyclopropane groups with formation of the corresponding 2-cyclopropylfurans **105**.[140] However, the subsequent interaction of compound **105** (R = H) with CH_2N_2 in the presence of CuCl affords 1-cyclopropylpenta-2,4-diene-1-ones **106**, apparently as a result of the addition of CH_2 to the unsubstituted double bond of the furan ring and the subsequent opening of the oxabicyclic adduct **107**.[140]



104 (3–4) : 1 **105** (21%–40%)

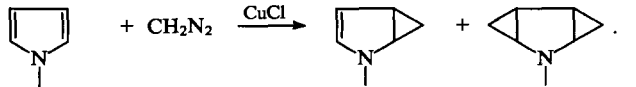
R, R^1, R^2 = H and/or Me.



107 **106** (~25%)

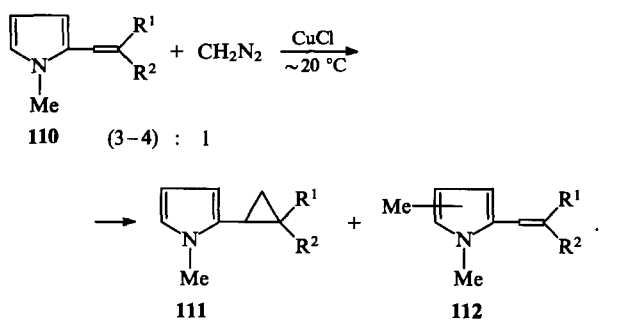
R^1 = Me, cyclo-C_3H_5.

In the catalytic reaction of CH_2N_2 with *N*-methylpyrrole in the presence of CuCl, the products of the formal insertion of methylene into the C–H bonds of the pyrrole ring were obtained instead of the cyclopropane adduct (see Section VI). On the other hand, *N*-methoxycarbonylpyrrole forms the bicyclic and tricyclic compounds **108** and **109** in moderate yields under similar conditions, the *trans*-isomer of the diadduct **109** predominating appreciably.[141,142]



~1 : 3 **108** (39%) **109** (12%)

In the reactions with 2-alkenylpyrroles **110**, diazomethane leads to the formation, in the presence of CuCl, of both the cyclopropane adducts **111** involving the exocyclic double bond and of the products **112** of the insertion of methylene into the C–H bonds of the pyrrole ring.[143] Together with the monoadducts **111** and **112**, a complex mixture of products of the addition (or insertion) of a second CH_2 fragment to the monoadducts formed was then obtained in an overall yield of 6%–10%.

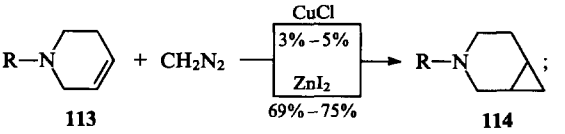


110 (3–4) : 1

111 **112**

R^1	R^2	Yield of **111** (%)	Yield of **112** (%)
H	H	18	6
H	Me	6	15
Me	Me	8	18

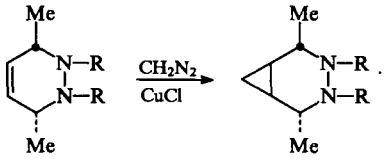
The interaction of CH_2N_2 with *N*-alkyldehydropiperidines **113** in the presence of 20 mol% of CuCl leads to the corresponding cyclopropanes **114** in a yield of only 3%–5%.[144] The reaction of compound **113** with an excess of an ethereal solution of the organozinc reagent obtained from CH_2N_2 and ZnI_2 makes it possible to synthesise the adduct **114** in preparative yields (69%–75%).[145]



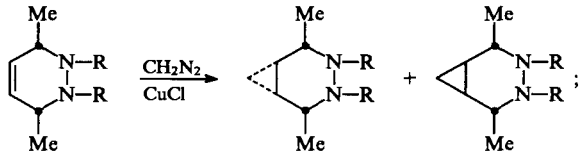
113 69%–75% **114**

R = Me, Et, Pr.

The conversion of the 1,2-diazacyclohexene **115**, containing electron-accepting substituents at the nitrogen atoms, into a cyclopropane derivative by treatment with diazomethane proceeds more successfully and leads in the case of *trans*-**115** to only the isomer **116a** and in the case of *cis*-**115** to the isomers **116b** and **116c** in proportions of ~8 : 1.[146]



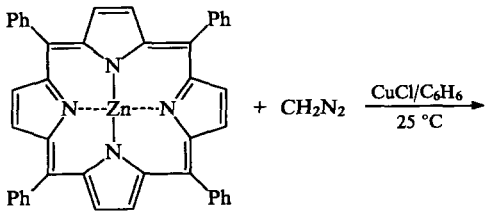
trans-**115** **116a**



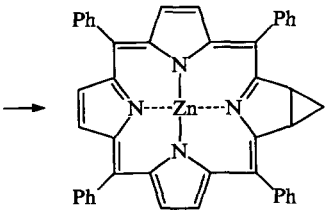
cis-**115** **116b** **116c**

R = COOMe.

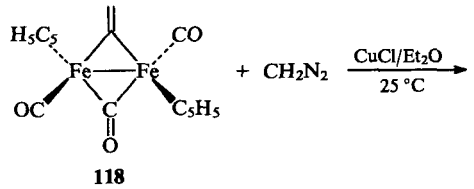
Finally one should note that, in the presence of CuCl, diazomethane is capable of converting into cyclopropane groups the double bonds in unsaturated ligands forming part of the composition of mononuclear or dinuclear metal complexes, for example compounds **117** and **118**.[147,148]



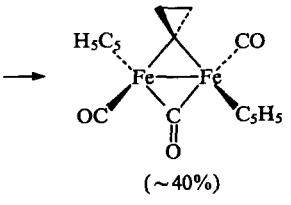
117



(~28%)



118



(~40%)

It follows from the results presented above that, in the presence of copper compounds, diazomethane is capable of converting into cyclopropane derivatives an extremely wide range of unsaturated compounds containing C=C bonds of different nature and with different degrees of substitution. However, the tendency of copper compounds to be readily 're-reduced' by diazomethane with the formation of highly active metallic copper, which leads to a vigorous side reaction involving the decomposition of CH_2N_2 and hence results in a low degree of conversion of the olefins into the corresponding cyclopropanes and limits the preparative use of this reaction.

3. Conversion of olefins into cyclopropane derivatives by diazomethane in the presence of palladium catalysts

One can say without exaggerating that the wide scale preparative use of diazomethane in the synthesis of cyclopropane derivatives from olefins has been recently associated with the employment of various palladium compounds as catalysts of the decomposition of CH_2N_2. The available literature data give grounds for the assertion that the nature of the cycloaddition of methylene to the double bonds is associated to a large extent with the ability of the initial olefins to be coordinated to the palladium atom, the regio- and stereo-selectivity in the conversion of various double bonds into cyclopropane groups differing significantly from those in their conversion into cyclopropane derivatives in the presence of copper compounds.[10,19,68,70] $Pd(OAc)_2$, $Pd(acac)_2$, and $(PhCN)_2PdCl_2$ are most often employed as palladium catalysts.

The catalytic activity of palladium compounds in the conversion of olefins into cyclopropanes was first noted in 1968 by Kirmse and Kapps,[92] who investigated the interaction of diallyl ether with CH_2N_2 in the presence of bis[η-allylpalladium chloride]. They then obtained the cyclopropane adduct **40f** in 38% yield without an admixture of the product **41f**, in contrast to catalysis by copper salts. In the next year, the same workers[94] reported the interaction of vinyloxiran with CH_2N_2, leading to the formation of the adducts **46** and **47** in proportions of ~6 : 1. However, at that time the above studies still failed to encourage investigators to employ palladium catalysts on a wider scale in the conversion of olefins into cyclopropanes.

Appreciable progress in the conversion of unsaturated compounds into cyclopropanes by treatment with diazomethane in the presence of palladium compounds and primarily in the presence of $Pd(OAc)_2$ is associated with the work of Teysie and coworkers,[149] who converted styrene into phenylcyclopropane in ~90% yield, and with the work of Vorbruggen and coworkers,[150,151] who demonstrated the possibility of the effective conversion into cyclopropanes of norbornene and norbornadiene as well as monosubstituted α,β-unsaturated carbonyl compounds by this method. Since then, the number of studies in this field began to increase sharply.

In the first place, it was established that the nature of the palladium catalyst {$PdCl_2$, $Pd(OAc)_2$, $[\eta\text{-}C_3H_5PdCl]_2$, $(PhCN)_2PdCl_2$} does not influence significantly the nature of the reaction of olefins when the latter is carried out in CH_2Cl_2, while the yields of the cyclopropane formation products are determined under identical conditions mainly by the nature of the C=C bonds.[68,152] Nevertheless, more detailed differences in the nature of the catalysts,[25] influencing the yield of the products of the cyclopropane formation reaction, in particular the formation of tricyclooctane **64** from norbornene, were discovered under conditions where the ethereal solution of CH_2N_2 was rapidly mixed with the olefin and the catalyst. Thus the introduction into $Pd(acac)_2$, which affords the highest yield of compound **64** under these conditions, of electron-donating ligands, for example NEt_3, Me_2S, PPh_3, etc., in the proportions $Pd(acac)_2$: L = 1 : 2 lowers the yield of the cyclopropane adducts from 72% to 23%.[25]

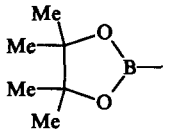
The observed dependence of the yields of compound **64** on the structure of the palladium compounds can be explained by the increasing hindrance by the ligands to the coordination of the olefin and also by the retardation of the formation of the catalytically more active low-valence palladium complexes when palladium(II) compounds are reduced by diazomethane (see Section III.1).

a. Conversion of aliphatic unsaturated compounds into cyclopropane derivatives

It has been established by numerous investigations that in the series of unsaturated aliphatic compounds those with terminal double bonds are most successfully converted into cyclopropane derivatives by diazomethane. The yields of the cyclopropane adducts are then determined by the amount of the added CH_2N_2 and in some cases are 88%–97% when a two–three-fold excess of CH_2N_2 is employed (Table 3).

It is noteworthy that the nature of the substituents at the C=C bond affects appreciably the nature of its conversion into a cyclopropane group. Thus the conversion of olefins with electron-donating substituents attached directly to the C=C bond, for example ethyl vinyl ether,[158] into cyclopropanes proceeds with an extremely low degree of conversion, whereas the conversion of oxygen- and nitrogen-containing allyl derivatives into cyclopropanes takes place fairly successfully. Furthermore, the results concerning the relative reactivities of various unsaturated compounds have demonstrated[159] that styrene and allyl alcohol are 15–20 times less reactive than alk-1-enes in their conversion into cyclopropanes by diazomethane.

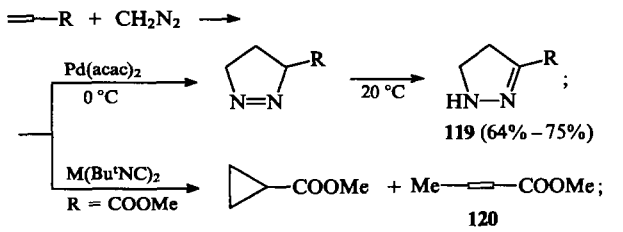
Table 3. Conversion of the monosubstituted olefins $CH_2=CHR$ into cyclopropane derivatives by treatment with diazomethane in the presence of 0.4–1.0 mol% of palladium compounds.

R	$CH_2=CHR : CH_2N_2$	Catalyst	Reaction conditions[a]	Yield of cyclo-C_3H_5R (%)	Ref.
n-C_4H_9–n-C_9H_{19}	1:1	$Pd(acac)_2$	A	44–60	25
n-C_8H_{17}	1:3	$Pd(OAc)_2$	A	89	153
cyclo-C_6H_{11}	1:1	$Pd(acac)_2$	A	41	25
Ph, CH_2Ph	1:1	$Pd(acac)_2$	A	43–46	25
CH_2CH_2COMe	1:1	$Pd(acac)_2$	A	60	25
$CH_2(CH_2)_7COOMe$	–	$Pd(OAc)_2$	B	>60	154
CMe_2CH_2COOEt	1:3	$Pd(OAc)_2$	A	89	153
CH_2OH, CH_2OMe	1:2	$(PhCN)_2PdCl_2$	B	72–74	155, 156
CH_2OPh, $CH_2OC_6H_4Br$-*m*	1:2	$(PhCN)_2PdCl_2$	B	88	155, 156
CH_2OPh	1:3	$Pd(OAc)_2$	A	97	153
CH_2OAc	1:2	$(PhCN)_2PdCl_2$	B	80	155, 156
CH_2NMe_2, CH_2NHPh	1:2	$(PhCN)_2PdCl_2$	B	62–68	155, 156
$CH(OEt)_2$	1:2	$(PhCN)_2PdCl_2$	B	77–80	155, 156
$CH_2NHCOMe$	1:1.9[b]	$(PhCN)_2PdCl_2$	C	73	157
OEt	1:3	$(PhCN)_2PdCl_2$	A	12–15	158
COOEt	~1:3	$Pd(OAc)_2$	B	82	160
	1:4	$Pd(OAc)_2$	B	98	161
	–	$Pd(OAc)_2$	B	92	162

[a] **Method A.** A solution of CH_2N_2 and the olefin was treated with 0.6–1.0 mol% of the catalyst at 10–0 °C. **Method B.** A mixture of the olefin and 0.4–0.8 mol% of the catalyst in ether or CH_2Cl_2 was treated with CH_2N_2. **Method C.** A mixture of the olefin, a 40%–50% solution of KOH, 0.2 mol% of the catalyst, ether, and CH_2Cl_2 was treated with *N*-methyl-*N*-nitrosourea.
[b] The ratio of the olefin to *N*-methyl-*N*-nitrosourea is indicated.

In contrast to allyl alcohol and its ethers, allyl halides (allyl chloride, allyl bromide, methylallyl chloride) are not converted into cyclopropanes by diazomethane in the presence of palladium compounds and do not afford the products of the formal insertion of methylene in the C–Hal bond, as happens when copper compounds are used as catalysts.

The interaction of CH_2N_2 with unsaturated compounds containing strong electron-accepting substituents (CN, COOR) at the double bond takes place in a more complex manner. In this case, there is competition between the possible formation of cyclopropanes and the readily occurring 1,3-dipolar cycloaddition of CH_2N_2. The nature of the palladium catalyst can then influence significantly the composition of the reaction products. Thus, in the presence of $Pd(OAc)_2$, ethyl acrylate and CH_2N_2 afford a high yield of ethyl cyclopropanecarboxylate,[160] whereas acrylonitrile and methyl acrylate react with CH_2N_2 in the presence of $Pd(acac)_2$ to form the pyrazolines **119**.[25]



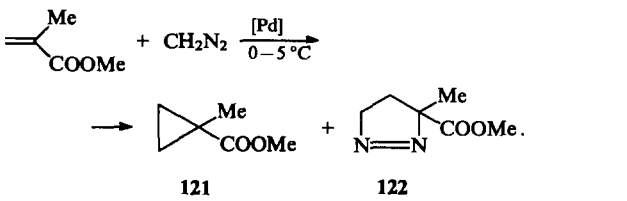
R = CN, COOMe.

M	Yield of C_3H_5COOMe (%)	Yield of **120** (%)
Pd	0.9	24.4
Ni	66.5	20.4

Finally, it has been noted[72] that methyl crotonate **120** is formed together with the cyclopropane adduct in the reaction of CH_2N_2 with methyl acrylate in the presence of $Pd(Bu^tNC)_2$.

It is noteworthy that a decrease in the polarity of the double bond in α,β-unsaturated ethers favours the formation of cyclopropane adducts.

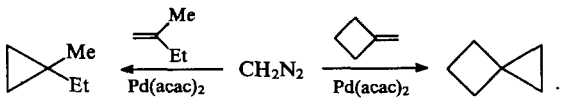
The interaction of CH_2N_2 with methyl methacrylate containing both electron-donating and electron-accepting substituents at the same carbon atom proceeds mainly with formation of the cyclopropane adduct **121** and even in the presence of $Pd(acac)_2$ its yield is fairly high compared with that of the 1-pyrazoline **122** formed simultaneously.[25,151]



121 **122**

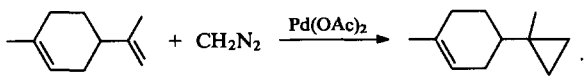
Reagents ratio	[Pd]	Yield of **121** (%)	Yield of **122** (%)
1:2.5	$Pd(OAc)_2$	88	–
1:1	$Pd(acac)_2$	76	15

The conversion of 1,1-disubstituted double bonds into cyclopropane groups occurs also in the case of *gem*-dialkylethylenes, but, in order to attain a high yield of cyclopropanes it is necessary to use a large excess of CH_2N_2 in virtually all cases.[25,89,151,153]



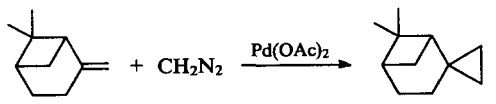
(18%) (48%)

Olefin : CH_2N_2 = 1 : 1



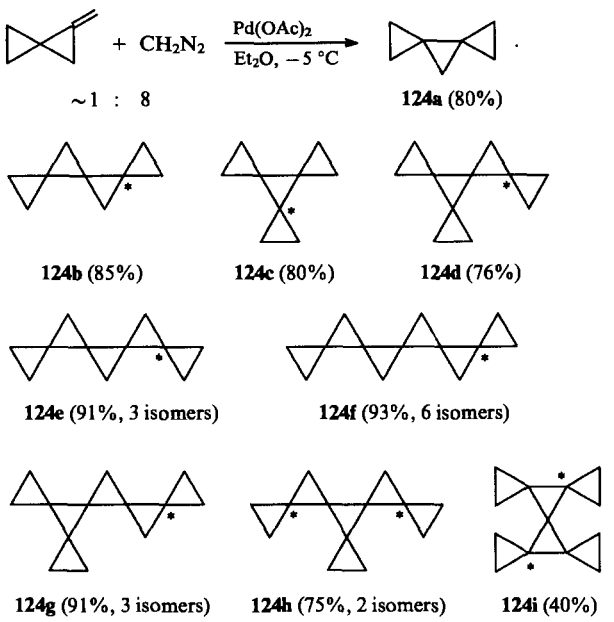
~1 : 3 (82%)

It is of interest to note that β-pinene **123** reacts with CH_2N_2, affording the cyclopropane adduct in 63% yield,[153] whereas derivatives of 2-methylenenorbornane are hardly converted into cyclopropanes even in the presence of a four–six-fold excess of CH_2N_2.[25, 163]



123 ~1 : 3 (63%)

The cyclomethylenation of methylenecyclopropanes by treatment with diazomethane in the presence of $Pd(OAc)_2$ is one of the stages in the general method of synthesis of linear and branched triangulanes **124**, made up of spiroannelated cyclopropane fragments. It was developed by Zefirov and coworkers.[89, 164–168]



~1 : 8 **124a** (80%)

124b (85%) **124c** (80%) **124d** (76%)

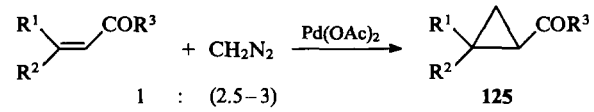
124e (91%, 3 isomers) **124f** (93%, 6 isomers)

124g (91%, 3 isomers) **124h** (75%, 2 isomers) **124i** (40%)

(The asterisks designate the carbon atoms constituting the methylene fragment in the initial methylenecyclopropanes.)

As a rule, the conversion of the corresponding olefins into cyclopropanes was then carried out under isotypical conditions using a large excess of an ethereal solution of CH_2N_2 and 4–5 mol% of $Pd(OAc)_2$ as the catalyst.

In the presence of palladium compounds, diazomethane is also capable of converting 1,2-disubstituted double bonds into cyclopropane groups, but in this case the reaction is even more sensitive to the nature of the substituents than in the case of terminal olefins. Thus hept-3-ene, *cis*- and *trans*-1,2-dichloroethylenes, as well as tri- and tetra-substituted alkenes (3-methylhept-3-ene, tetramethylethylene) do not give rise to cyclopropanes on reaction with CH_2N_2 in the presence of palladium compounds.[25] On the other hand, α,β-unsaturated carbonyl compounds afford satisfactory yields of the corresponding cyclopropanes **125** in the presence of $Pd(OAc)_2$.

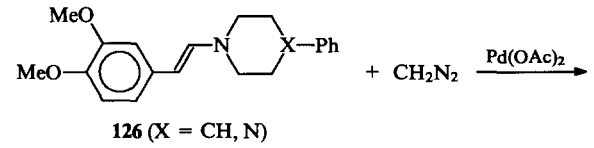


1 : (2.5–3) **125**

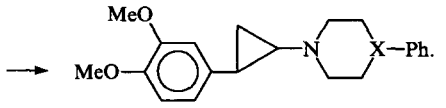
R^1	R^2	R^3	Yield of **125** (%)	Ref.
H	Ph	Ph (Me)	85–98	151
H	Ph (Me)	OEt (OMe)	89–90	151
Ph	H	OEt	85	151
H	$(CH_2)_3COOMe$	H	80	169
H	$(CH_2)_{18}Me$	OMe	99	154
H	$MeOC_6H_4$	OMe	84–99	170
H	$(RO)_2C_6H_3$	OMe	75–97	171
Me	Me	Me (OMe)	0	151

In contrast to internal alkenes, the esters of non-conjugated unsaturated carboxylic acids are also capable of being converted into cyclopropanes by treatment with diazomethane in the presence of palladium acetate and their reactivity depends on the configuration of the double bond. Thus methyl elaidate, containing a *trans*-C=C bond, is more reactive than methyl oleate containing a *cis*-C=C bond.[154]

In contrast to the esters of unsaturated carboxylic acids, the conversion of β-arylvinylamines into cyclopropane derivatives in the presence of palladium catalysts proceeds less successfully and in the case of the enamine **126** leads to the cyclopropane adduct **127** in only 10% yield.[172]



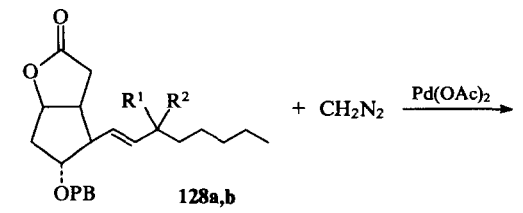
126 (X = CH, N)



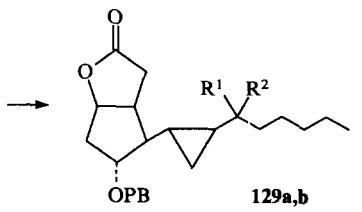
127 (~10%)

In this reaction, palladium compounds are apparently less effective than CuCl.[110]

The catalytic interaction of CH_2N_2 with unsaturated compounds makes it possible to synthesise certain prostaglandin preparations containing a cyclopropane ring.[173] Under these conditions, the reaction involving the formation of a cyclopropane from the hydroxy-derivative **128b**, containing, in contrast to allyl alcohol, a disubstituted double bond,[155] leads to the formation, together with the cyclopropane adduct **129b** (yield ~20%), of the methoxy-derivative **129** (R^1 = H, R^2 = OMe).

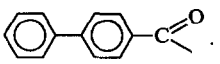


128a,b

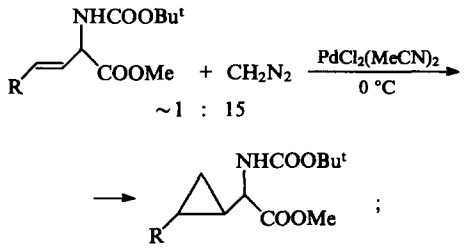


129a,b

CR^1R^2 = C=O (**a**) (92%);
R^1 = H, R^2 = OH (**b**) (20%);



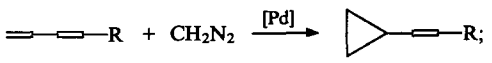
A method of synthesis of cyclopropyl-L-alanines and their derivatives—intermediates in the synthesis of food additives, medicinal drugs, and pesticides—has also been developed on the basis of the catalytic conversion of unsaturated compounds into cyclopropanes by diazomethane in the presence of palladium compounds.[174,175]



R = H (98%), CH_2OAc (68%).

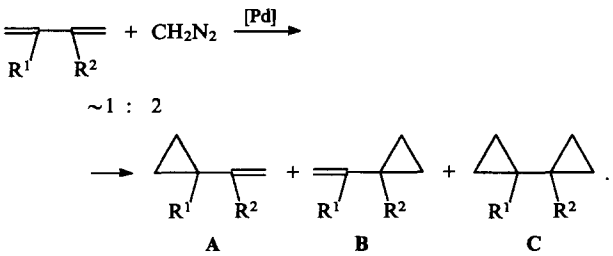
The regioselectivity of the conversion of various double bonds into cyclopropane groups and the possibility of obtaining polycyclopropane adducts are manifested most clearly in the interaction of CH_2N_2 with dienes and trienes.

The conversion of 1,3-dienes such as piperylene[25,68] as well as 1-cyclopropyl- and 1-alkoxy-butadienes[25,156,158] into cyclopropane derivatives in the presence of $Pd(acac)_2$ or $(PhCN)_2PdCl_2$ involves the terminal double bond and leads to the corresponding vinylcyclopropanes in high yields already in the presence of a (1.5–2)-fold excess of CH_2N_2.



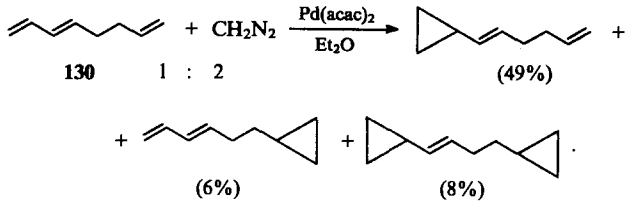
1 : 2 R = Me (90%), cyclo-C_3H_5 (91%), OMe, OEt, OAc, $OSiMe_3$ (80%–86%).

Under analogous conditions, the conversion of isoprene into a cyclopropane derivative proceeds less selectively, although a tendency towards the preferential formation of cyclopropanes from the less substituted C=C bond is retained.[68] In this case and also in the interaction of butadiene with 2,3-dimethylbutadiene[25] with an excess of diazomethane, the second double bond is converted into a cyclopropane group, which is accompanied by the partial formation of the corresponding bicyclopropyls, in agreement with the general tendency in the conversion of the terminal double bonds of alkenes into cyclopropyl groups.

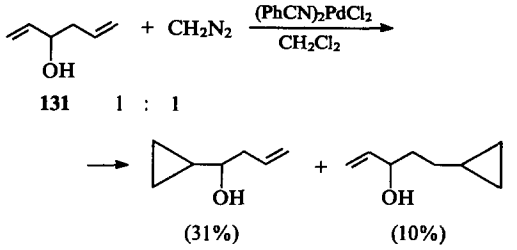


R^1	R^2	Yield of adducts (%)		
		A	B	C
H	H	67	–	29
H	Me	70	12	9
Me	Me	65	–	15

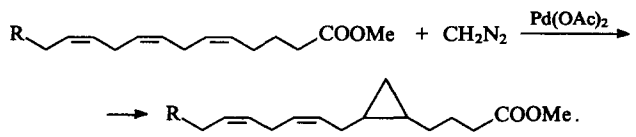
A terminal vinyl group conjugated with a double bond, as happens, for example, in octa-1,3,7-triene **130**, is approximately eight times more reactive than a terminal non-conjugated double bond.[25]



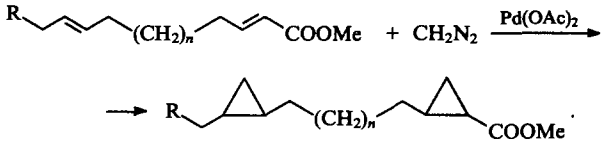
The catalytic reaction of CH_2N_2 with hexa-1,5-dien-3-ol **131**, containing different terminal double bonds, gives rise to the preferential conversion of the allyl C=C bond into a cyclopropyl group, in contrast to the homoallyl bond.[155]



The reactivity of vicinally substituted double bonds depends both on their position in the linear hydrocarbon chain and on their configuration. Thus the conversion of derivatives of arachidonic acid, containing *cis*-double bonds, into cyclopropanes involves only the C=C bond closest to the carboxy-group with formation of the cyclopropane adduct **132**, whereas the conversion into cyclopropanes of the esters of the *trans*-polyunsaturated acids affords satisfactory yields of the polycyclopropane adducts **133**.[176]

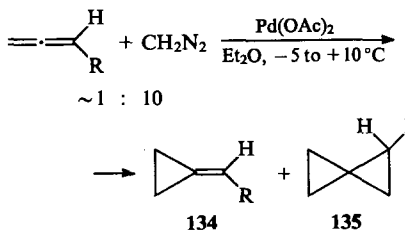


132 (~90%)



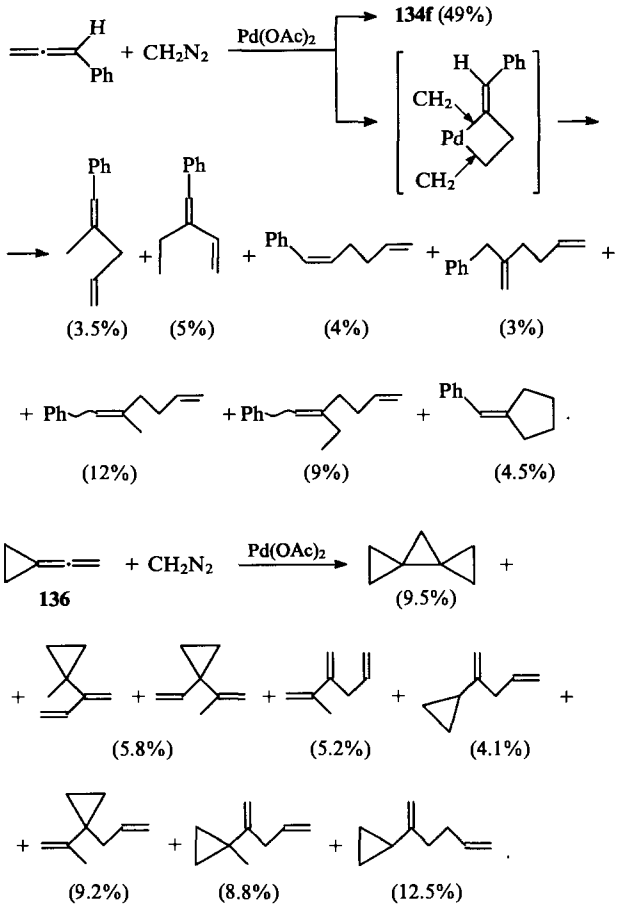
133 (80%–90%)

The conversion of allenes into cyclopropanes by treatment with diazomethane in the presence of $Pd(OAc)_2$ takes place most successfully when the catalyst is added to an ethereal solution of the allene and CH_2N_2, taken in a large excess.[177] The reaction then takes place fairly selectively with formation of adducts involving the least substituted double bond. However, in the conversion of alka-1,2-dienes into cyclopropanes, the corresponding spiropentanes **135** (yields up to 60%) are also formed together with the monoadducts **134**,[177,178] which indicates the possibility of the conversion into cyclopropyl groups of tri-substituted double bonds in the presence of palladium compounds.

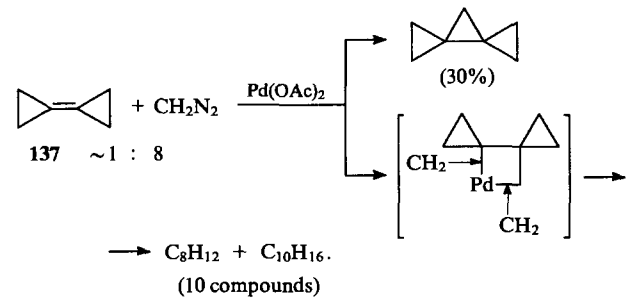


Compound	R	Yield of **134** (%)	Yield of **135**(%)
a	Bu	67	25
b	CH_2CH_2OH	~2	60
c	CH_2CH_2OAc	34	56
d	CH_2CH_2Br	63	27
e	CH_2CH_2OTs	78	–
f	Ph	49	–

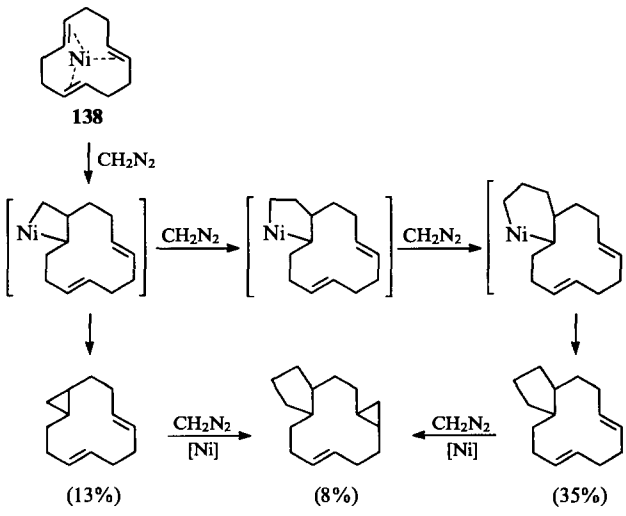
In a study of the interaction of CH_2N_2 with phenylallene (~10:1) and vinylidenecyclopropane **136** (~20:1) in the presence of $Pd(OAc)_2$, an unusual oligomethylenation reaction was discovered. It leads to the incorporation of several equivalents of methylene into the molecule with formation of a complex mixture of unsaturated hydrocarbons.[179,180] The use of a smaller relative amount of CH_2N_2 then affords the same mixture of products in approximately the same proportions as in the presence of an excess of CH_2N_2,[179] which is probably due to the possibility of their formation from the same intermediates.



A similar oligomethylenation reaction takes place also in the case of bicyclopropylidene **137**, which indicates, on the one hand, the possibility of the conversion of a tetrasubstituted double bond into a cyclopropyl group by diazomethane in the presence of palladium compounds,[181] and, on the other, the possibility of the existence of palladiacyclic intermediates stabilised by the spiro-linked cyclopropane ring and capable of reacting subsequently with several equivalents of methylene until their decomposition into the corresponding hydrocarbons, in which the bicyclopropyl fragment is largely retained.



The results agree with the non-trivial reaction of CH_2N_2 with *trans, trans, trans*-cyclododeca-1,5,9-trienenickel **138**, discovered previously, which resulted in the formation not only of cyclopropane derivatives but also of trimethylenation products, which are converted into compounds with a condensed five-membered ring.[182]



The formation of cyclopentane derivatives indicates that the reaction proceeds via a stage involving the formation of a metallacyclobutane fragment, the subsequent insertion of methylene in the Ni–C bond of which actually leads to the cyclopentane derivatives. The absence of a cyclobutane adduct is apparently due to the different stabilities of the four-, five-, and six-membered metallacycles and, in particular, the greater stability of nickelacyclopentanes (the reaction of which with CH_2N_2 goes to completion) compared with the other two metallacycles containing an odd number of carbon atoms in the ring, which they can readily eliminate in the form of the corresponding cycloalkane adducts.

b. Conversion of cyclic unsaturated compounds into cyclopropane derivatives

The possibility of the conversion of cyclic unsaturated compounds into cyclopropanes by treatment with diazomethane has led to extensive prospects for the synthesis of various cyclopropanes. The nature of the double bonds, determined primarily by the degree of strain in the cyclic system, exerts a significant influence on the nature of their conversion into cyclopropyl groups.

Thus, in the series of cycloolefins cyclohexene, cycloheptene, cyclooctene, and norbornene, the yields of cyclopropanes increase from 15% to 95% respectively under the same conditions (for example, when an equimolar amount of CH_2N_2 is passed at a uniform rate into the solution of the olefin in the

Table 4. Conversion of norbornene derivatives into cyclopropane derivatives by treatment with diazomethane in the presence of 0.3–1.2 mol% of palladium compounds in ether.

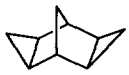
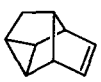
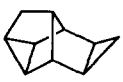
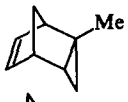
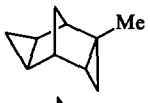
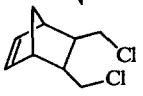
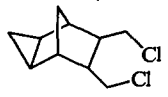
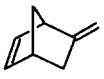
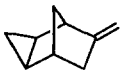
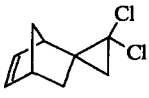
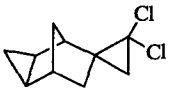
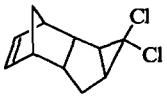
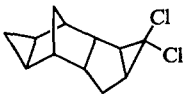
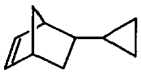
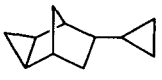
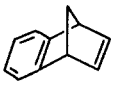
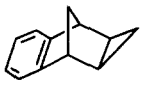
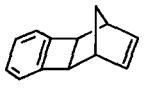
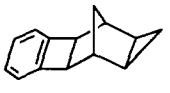
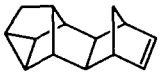
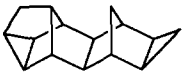
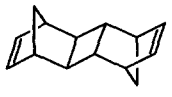
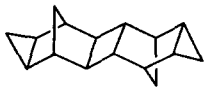
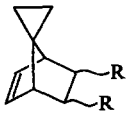
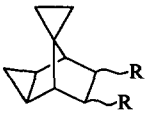
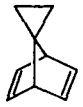
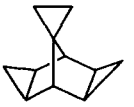
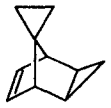
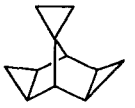
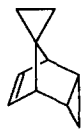
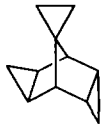
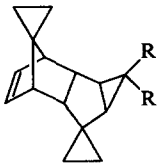
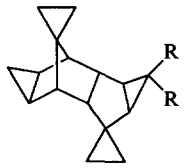
Unsaturated compounds	Olefin : CH_2N_2	Catalyst	Reaction product	Yield (%)	Ref.
	1:4.6[a]	$Pd(OAc)_2$		63	150
	1:1	$(PhCN)_2PdCl_2$[b]	*exo,exo*-**91a**	94	68
	1:7[a]	$Pd(OAc)_2$		~90	184
	1:1	$Pd(acac)_2$		54	25
	1:2	$Pd(acac)_2$[b]		~100	109
	~1:3[a]	$Pd(OAc)_2$		88	185
	~1:7[a]	$Pd(OAc)_2$		70	163
	1:2	$Pd(acac)_2$		88	25
	~1:7[a]	$Pd(OAc)_2$		80	163
	~1:9[a]	$Pd(OAc)_2$		85	186
	~1:6[a]	$Pd(OAc)_2$		90	187
	–	$[\eta\text{-}C_3H_5PdCl]_2$		~100	188
	1:10	$[\eta\text{-}C_3H_5PdCl]_2$		95	188
 (*exo,exo*-**139**)	1:3	$Pd(acac)_2$		78	189
endo,exo-**139**	1:3	$Pd(acac)_2$		93	189
exo,endo-**139**	1:3	$Pd(acac)_2$		82	189
endo,endo-**139**	1:3	$Pd(acac)_2$		60	189
 (*exo,exo*-**140**)	1:6	$Pd(acac)_2$		~65	189
exo,endo-**140**	1:6	$Pd(acac)_2$		80	189
endo,endo-**140**	1:6	$Pd(acac)_2$		87	189
					
R = H	1:1	$Pd(acac)_2$[b]	*exo*-**141** (R = H)	62	25
R = Cl	1:7[a]	$Pd(OAc)_2$		85	190
	1:7[a]	$Pd(OAc)_2$		65	190
	1:7[a]	$Pd(OAc)_2$		70	190

Table 4 (continued).

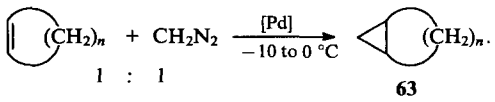
Unsaturated compounds	Olefin : CH_2N_2	Catalyst	Reaction product	Yield (%)	Ref.
	1 : 7[a]	$Pd(OAc)_2$		75	190
	1 : 7[a]	$Pd(OAc)_2$		80–85	191

R = H, Cl.

[a] The olefin : *N*-methyl-*N*-nitrosourea molar ratio is indicated.
[b] Solvent — CH_2Cl_2.

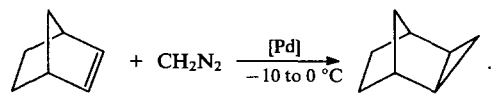
presence of 0.1–0.5 mol% of the palladium catalyst in CH_2Cl_2 at −10 to 0 °C).[68] As in the case of monosubstituted olefins, the use of $PdCl_2$, $Pd(OAc)_2$, $(PhCN)_2PdCl_2$, and $[\eta\text{-}C_3H_5PdCl]_2$ in these reactions hardly exerts a significant influence on the yields of the cyclic adducts.

The interaction of a mixture of cyclohexene and norbornene with CH_2N_2 in the presence of $(PhCN)_2PdCl_2$ proceeds, in contrast to copper compounds, regioselectively and leads to the almost complete conversion of norbornene into the adduct **64** without an appreciable conversion of cyclohexene into a cyclopropane derivative. Furthermore, a characteristic feature of palladium catalysts is their ability to propagate the reaction at a high CH_2N_2 concentration and to retain a high activity in the conversion of strained olefins into cyclopropanes virtually up to the completion of the reaction. These results undoubtedly indicate the preferential formation of π-olefin complexes in the conversion of unsaturated compounds into cyclopropanes with participation of palladium catalysts.[68]



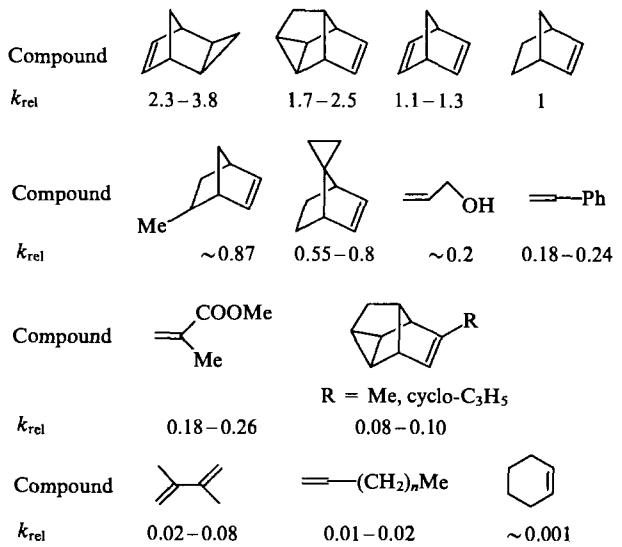
1 : 1 **63**

Product	*n*	Yield (%)
63a	4	10–15
63b	5	78–82
63c	6	90–92

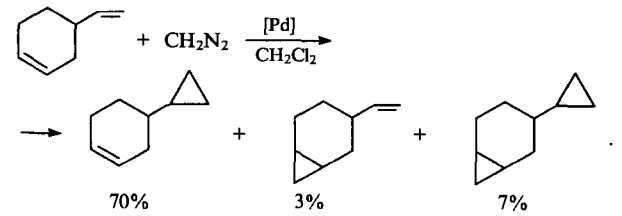


~1 : 1 **64** (93%)

One can now say without exaggeration that the conversion of polycyclenes into cyclopropanes by treatment with diazomethane, catalysed by palladium compounds, is one of the most promising methods of synthesis of polycyclic hydrocarbons of the norbornane series with a condensed cyclopropane fragment in the molecule (Table 4). The relative reactivities of certain unsaturated compounds in the reaction with CH_2N_2 in the presence of the palladium catalysts $Pd(OAc)_2$, $Pd(acac)_2$, and $(PhO)_3P \cdot PdCl_2$ have been investigated[159] and a significant difference between the rates of conversion of the norbornene and aliphatic mono- and di-substituted double bonds into cyclopropyl groups has been demonstrated.



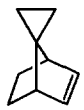
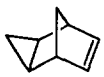
The substituted norbornene double bond proves to be more reactive than the terminal aliphatic double bond,[159, 183] which is in its turn an order of magnitude more reactive than cyclohexene. This is clearly illustrated by the catalytic conversion of 4-vinylcyclohexene into the cyclopropyl derivative.[68]



70% 3% 7%

The stereochemistry of the addition of methylene, generated by the catalytic decomposition of CH_2N_2, to certain norbornene hydrocarbons has been investigated;[117] comparative estimates of the degrees of *exo*- and *endo*-conversion of the double bonds into cyclopropyl groups are given in Table 5. The results combined with other data for the conversion of norbornene derivatives into cyclopropanes in the presence of various catalysts based on palladium compounds confirm the high stereoselectivity in the formation of the *exo*-adducts (the fraction of the *endo*-isomers does not exceed 1.5%). On the other hand, when copper compounds and especially $Rh_2(OCOCF_3)_4$ are used as catalysts, the formation of *endo*-isomers is observed. Their amount increases significantly on passing from norbornene to norbornadiene and reaches 36%–42%.[117]

Table 5. Stereochemistry of the conversion of norbornene hydrocarbons into cyclopropane derivatives by treatment with diazomethane in the presence of various catalysts (0.5 – 1.0 mol%).

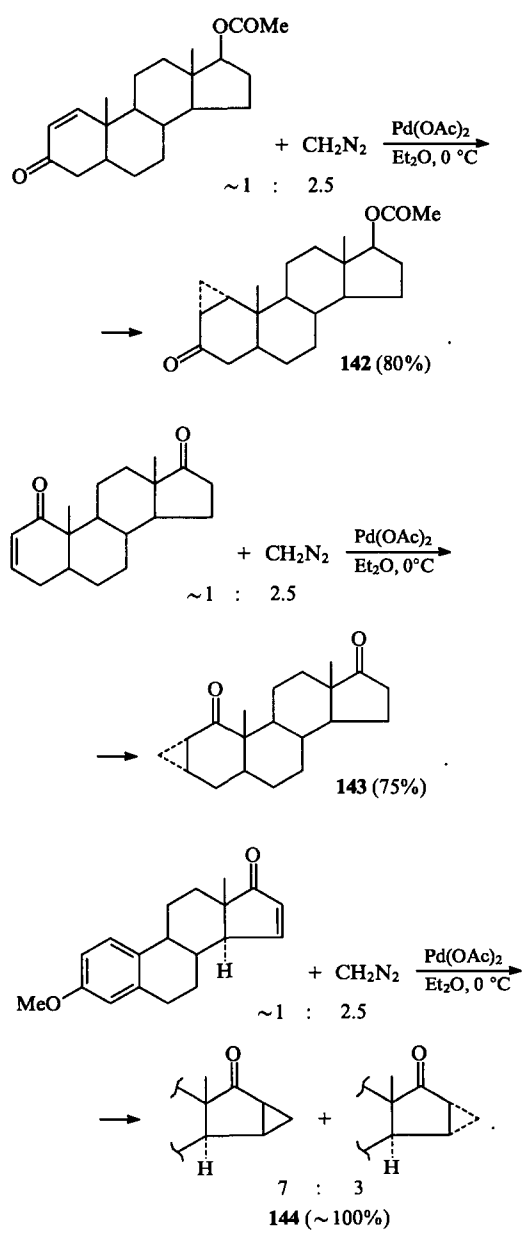
Original olefin	Reaction products	Ratio of *exo*- and *endo*-isomers [overall yield of isomers (%)]						
		$Pd(acac)_2$	$(PhCN)_2PdCl_2$	$Pd(OAc)_2$	$Cu(OTf)_2$	CuCl	$Cu(acac)_2$	$Rh_2(OCOCF_3)_4$
	*exo*- and *endo*-**64**	100:0 (87)	100:0 (81)	100:0 (78)	98:2 (73)	97:3 (58)	97:3 (38)	90:10 (18)
	*exo*- and *endo*-**141**	100:0 (32)	100:0 (36)	99:1 (18)	99:1 (23)	97:3 (38)	98:2 (18)	77:23 (20)
	*exo,exo*- and *exo,endo*-**91** (R = H)	99:1 (83)	100:0 (90)	99:1 (71)	95:5 (56)	86:14 (78)	96:4 (55)	74:26 (20)
	*exo*- and *endo*-**90** (R = H)	99:1 (52)	99:1 (54)	99:1 (48)	75:25 (34)	70:30 (48)	64:36 (36)	58:42 (19)
	exo,exo- and *exo,endo*-**91** (R = H)	98:2 (16)	99:1 (16)	98:2 (14)	72:28 (9)	65:35 (12)	62:38 (9)	53:47 (4)

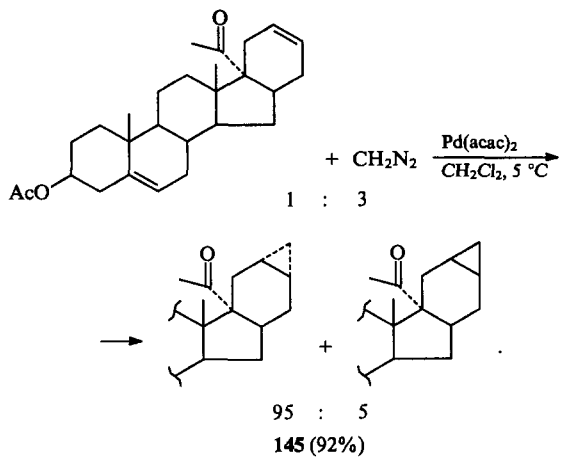
The *exo*-stereoselectivity in the conversion of norbornenes into cyclopropanes under the influence of palladium catalysts is probably associated with the ability of norbornenes to form initially coordinated π-complexes with the central metal atom, which react subsequently with CH_2N_2.[68,70] In view of the *endo*-deformation of the vinyl hydrogen atoms (the angle of deviation of the C–H bonds from the C–CH=CH–C plane of the norbornene fragment is 3°–5°),[125,192] this coordination is undoubtedly extremely sensitive to the electronic state of the double bond and takes place exclusively in the *exo*-position. In the case of copper and particularly rhodium catalysts, the double bond is attacked by metal–carbene complexes, as a result of which the interaction of the carbene centre with the double bond is less sensitive to the electronic state of the latter and takes place partially in the *endo*-position.

The increased content of the *endo*-isomers in the conversion of the norbornadiene into cyclopropane derivatives compared with norbornenes) in the presence of copper and rhodium catalysts is also apparently associated with the characteristic features of the geometry of the double bonds. Thus, according to calculations,[125] the angle of the *endo*-deformation of the vinyl C–H bonds in norbornadiene is smaller than in norbornene (2.3° and 4.9° respectively) and the probability of the attack on the double bond by the carbene complex from the direction of the *endo*-position is therefore increased for the former compound. This explanation is apparently valid also for many other cycloaddition reactions involving norbornadiene, accompanied by the formation of *exo*- and *endo*-isomers.

The conversion of an unsubstituted double bond in five-membered and six-membered rings into cyclopropyl groups, which is ineffective for the hydrocarbons themselves, is significantly activated by the presence of a conjugated carbonyl group. Thus the use of a comparatively small excess of CH_2N_2 led to the synthesis in high yields of the steroids **142**–**144** containing the cyclopropane ring in the molecule.[151]

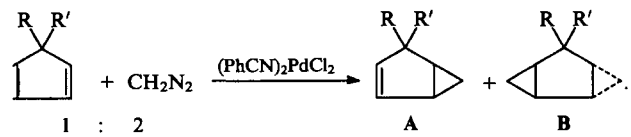
It has been established recently[176] that, when $Pd(acac)_2$ is used as the catalyst, it is possible to achieve the conversion into a cyclopropyl group, also of a non-conjugated endocyclic double bond in a six-membered ring, which is illustrated, in particular, by the formation of the isomeric adducts **145**. Trisubstituted double bonds in Δ^5-, Δ^7-, Δ^{11}-, and Δ^{14}-steroids do not give rise to cyclopropyl groups under the chosen conditions.



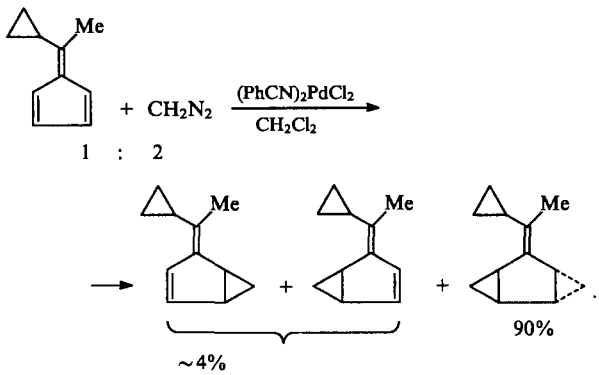


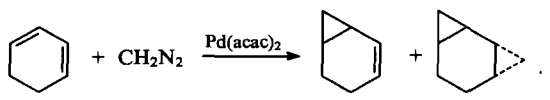
145 (92%)

The double bonds in cyclopentadiene,[68] spiro[2,4]heptadiene,[193] 6,6-disubstituted fulvenes,[68] cyclohexa-1,3-diene,[25,194] and cycloocta-1,5-diene[68,194] are fairly readily converted into cyclopropyl groups by diazomethane in the presence of palladium compounds and the formation of a cyclopropyl group from one of the double bonds sometimes accelerates the similar conversion of the second double bond, which is probably due to the increase in its strain as a result of the additional introduction of a cyclopropane fragment into the cyclic structure. The conversion of the second double bond in five- and six-membered cyclic dienes into a cyclopropyl group then occurs with formation of only the corresponding *trans*-isomers,[68,194] whereas in the case of cycloocta-1,5-diene, small amounts of the *cis*-isomer are also produced (*trans* : *cis* ≃ 7 : 1).



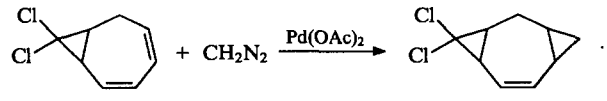
R	R′	Yield of A (%)	Yield of B (%)
H	H	15	75
$-CH_2CH_2-$		12	77

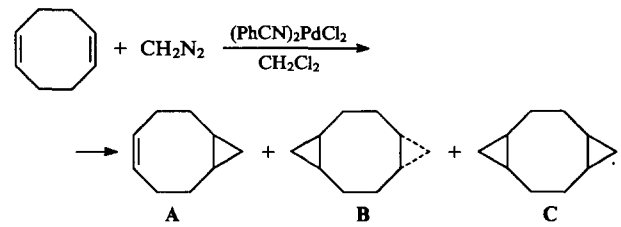




Reagents ratio	Yield of A (%)	Yield of B (%)
1:1	43	1
1:2	53	13

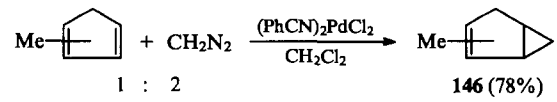
It is of interest to note that neither cyclohepta-1,3,5-triene[194] nor cycloocta-1,3,5,7-tetraene[116] are converted into cyclopropane derivatives by diazomethane in the presence of $Pd(OAc)_2$ despite the use of an excess of CH_2N_2.





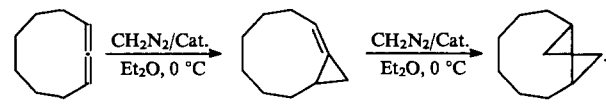
Reagents ratio	Yield of products (%)		
	A	B	C
1:1	5	38	5.5
1:2	6	72	10

The substituents in the cyclodienes exert the same influence on the regioselectivity of the addition of methylene as in alkenes. Thus the conversion of a mixture of methylcyclopentadienes into cyclopropane derivatives in the presence of palladium compounds involves only the unsubstituted double bond with formation of 2- and 3-methylbicyclohexenes **146**.[68]



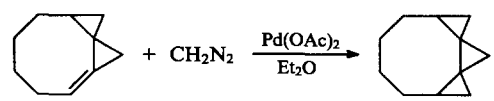
146 (78%)

The allene group in cyclonona-1,2-diene is converted into a cyclopropyl group by an excess of CH_2N_2 in the presence of the palladium catalysts $Pd(OAc)_2$ and $(PhCN)_2PdCl_2$, affording bicyclodecene **147** in a preparative yield (~60%). Repeated treatment of the reaction mixture with diazomethane leads to the partial formation of the spiran adduct **148**, the yield of which does not, however, exceed 10%.[177]

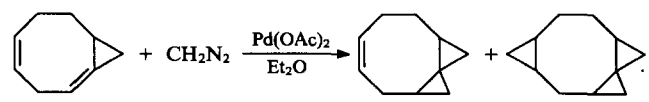


147 (~60%) **148** (~10%)

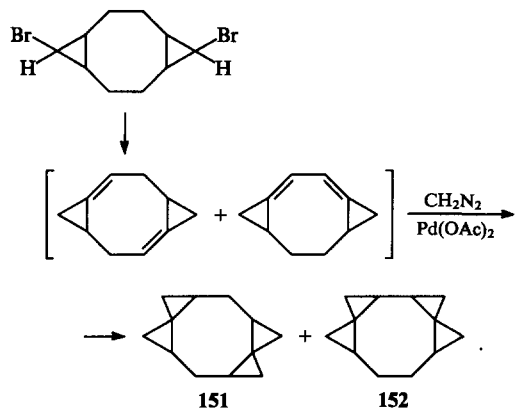
A similar approach, involving the catalytic introduction of an additional cyclopropyl group into alkylidenecyclopropanes, has been used recently to synthesise the polyspiran hydrocarbons **149–152** containing several three-membered rings in the molecule.[195]



149

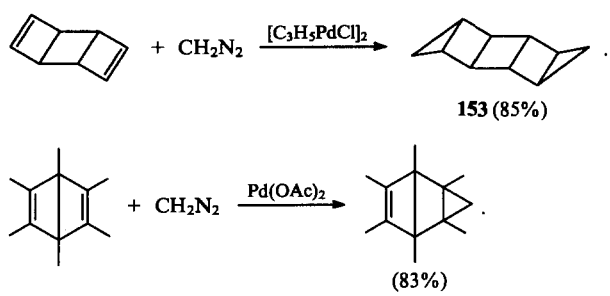


150



151 152

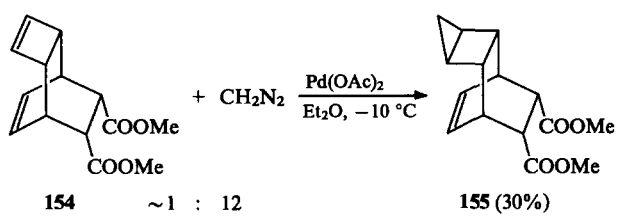
Polycyclic structures containing a C=C bond in a four-membered ring are also converted into cyclopropane derivatives by treatment with diazomethane in the presence of palladium compounds and the nature of the cyclopropane formation reaction involving such substances has a number of specific features. Thus, whereas the formation of the diadduct **153** in a high yield in the cyclopropane formation reaction involving tricyclo[4.2.0.0^{2,5}]octa-3,7-diene appears fairly evident,[188] the conversion of the tetrasubstituted double bond of the permethylated Dewar benzene into a cyclopropyl group using a palladium catalyst appears to be non-trivial.[150]



153 (85%)

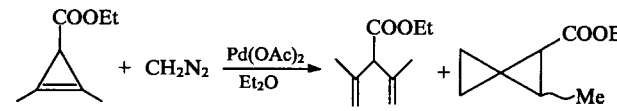
(83%)

The cyclobutene fragment in the polycyclic diene **154** is converted into a cyclopropyl group less effectively, which leads to the monoadduct **155** in a yield of ~30% even in the presence of a large excess of CH_2N_2.[196] The absence of the formation of a cyclopropane adduct from the second double bond is apparently associated with the steric hindrance generated by the four-membered ring and the methoxycarbonyl substituents. It is noteworthy that, according to Dzhemilev et al.,[25] bicyclo-[2.2.2]oct-2-ene itself affords the cyclopropane adduct in 64% yield.



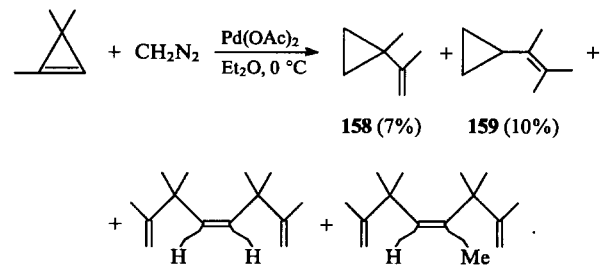
154 ~1 : 12 **155** (30%)

In contrast to the unsaturated compounds examined, the interaction of cyclopropenes with CH_2N_2 catalysed by palladium compounds proceeds in a more complex manner and is accompanied by the formation of appreciable amounts of oligomeric products. The nature of the compounds synthesised then depends to a large extent on the degree of substitution of the cyclopropenes, the electron-accepting properties of the substituents, and the reaction conditions.[197–199] Thus ethyl 1,2-dimethylcyclopropenecarboxylate reacts with an excess of CH_2N_2 to form the diene **156** and the spiropentane **157** in an overall yield of ~25%.[197,199] The appearance of the spiropentanes **157** (isomer ratio ~1 : 1.2) can be explained by the partial isomerisation of the initial cyclopropene ester to the corresponding ester of 2-methylene-3-methylcyclopropenoic acid and its subsequent conversion into a cyclopropane derivative.



156 (15%) **157** (10%)

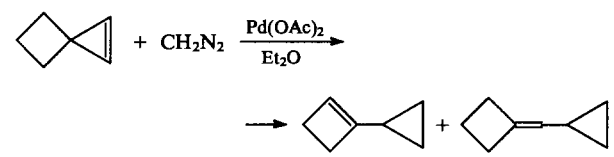
The addition of a catalytic amount of $Pd(OAc)_2$ to a mixture of an ethereal solution of CH_2N_2 and 1,3,3-trimethylcyclopropene leads to the vinylcyclopropanes **158** and **159** and the trienes **160** and **161** in an overall yield of ~40% (for the total conversion of the initial cyclopropene).[198,199]



158 (7%) **159** (10%)

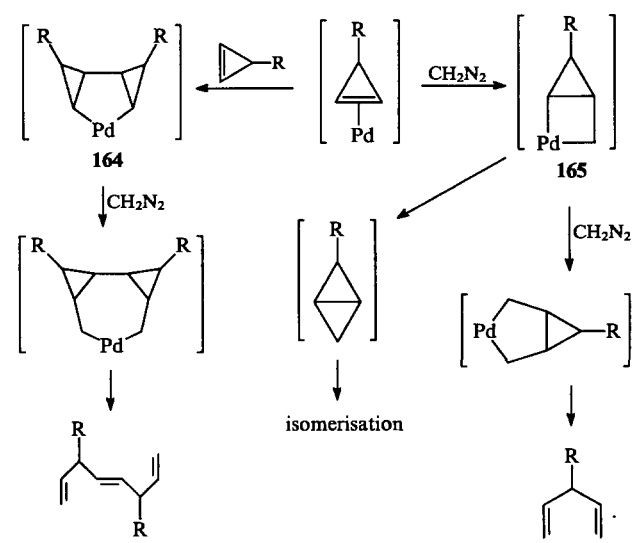
160 (8%) **161** (15%)

The monomeric products **162** and **163** are obtained in an even lower yield in the catalytic reaction of CH_2N_2 with spirohex-1-ene.[199]



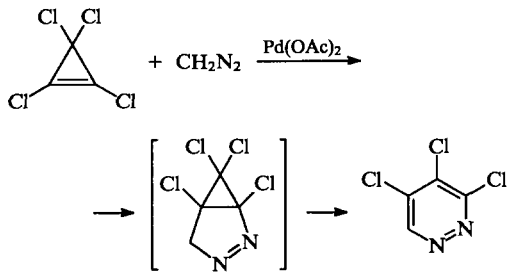
162 (3%) **163** (5%)

A probable mechanism of the observed reactions has been proposed.[197–199] It explains the formation of compounds **158–163** as a result of the catalytic conversion of the bicyclobutanes and/or metallacycles formed initially. The difference between the coordinating capacities of trimethylcyclopropene and the cyclopropenecarboxylate ester is then attributed to the possibility of the formation of two different intermediates—the metallacycles **164** and **165**. The subsequent



insertion of methylene in the Pd–C bonds leads to the expansion of the metallacycles and is completed by their decomposition with the opening of the cyclopropane fragment and the elimination of palladium.

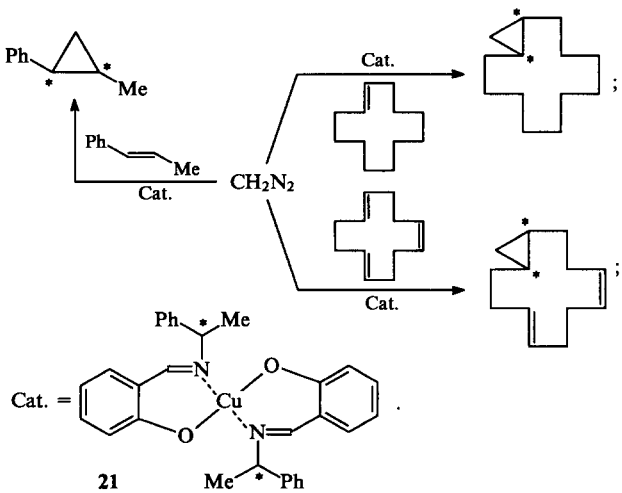
In contrast to the cyclopropenes mentioned above, the interaction of tetrachlorocyclopropene with CH_2N_2 leads to trichloropyridazine **166**. Owing to the combination of the low coordinating capacity of the tetrasubstituted cyclopropene with its high electron deficiency, the only reaction pathway in this instance is 1,3-dipolar addition with subsequent conversion of the resulting adduct **167** into the pyridazine **166**.[199]



167 **166** (75%)

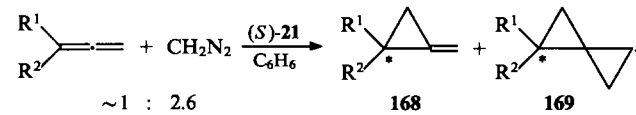
4. Asymmetric conversion of olefins into cyclopropane derivatives by diazomethane

The catalytic chiral [1 + 2]-cycloaddition of methylene, generated from CH_2N_2, to olefins with formation of optically active cyclopropanes was achieved for the first time in 1968 by Nozaki et al.,[67] who used salicylideneaminecopper complexes (*R*)- or (*S*)-**21**, obtained from chiral 1-phenylethylamines, as the catalyst. Thus (*E*)-propenylbenzene is converted on treatment with compound **21** into *trans*-2-methyl-1-phenylcyclopropane **22** in 62% yield with an enantiomeric excess of ~8%. Partial optical activity of the products formed in the presence of the optically active catalysts **21** has been observed also in the conversion of *trans*-cyclododecane and *Z*,*Z*,*E*-cyclododeca-1,5,9-triene into cyclopropane derivatives.[67]



21

Asymmetric induction has been observed also in the decomposition of CH_2N_2 on treatment with (*S*)-**21** as catalyst in the presence of phenyl-, 1-methyl-1-phenyl-, and hexylallenes.[200,201] Both the methylenecyclopropanes **168** and the corresponding spiropentanes **169** were then obtained in satisfactory yields. In the case of phenylallene,[201] the absolute configuration of the methylenecyclopropane **168a** was determined and the optical yield of compounds **168a** and **169a** was estimated as ~12%.

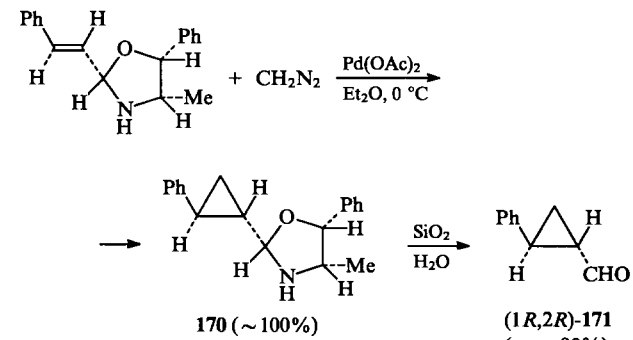


~1 : 2.6 **168** **169**

Compound	R^1	R^2	Yield of **168** (%)	Yield of **169** (%)
a	Ph	H	30	45
b	Ph	Me	43	52
c	C_6H_{13}	H	7	43

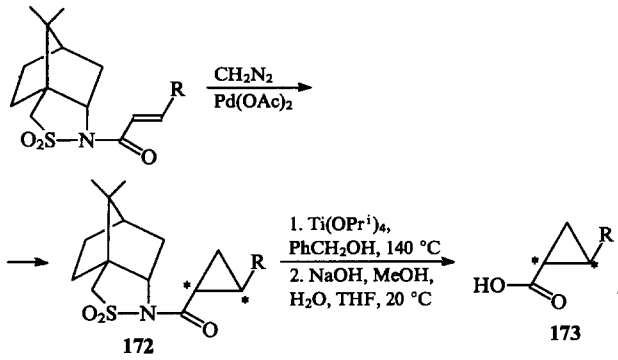
After the publication of these studies, which demonstrated only the possibility, in principle, of the induction of optical activity in the cyclopropanes produced, there were virtually no publications concerning the use of catalysts containing optically active ligands for the conversion of unsaturated compounds into cyclopropane derivatives by diazomethane. On the other hand, studies on the synthesis and use of chiral catalysts, in the first place rhodium compounds, for the decomposition of other diazo-compounds, especially alkyl diazoacetates, developed extensively.[202]

Nevertheless the interest in the synthesis of optically active compounds based on the catalytic conversion of olefins into cyclopropane derivatives by diazomethane has persisted in connection with the possibility of the effective conversion of suitable chiral substrates into cyclopropanes. The usual palladium catalysts, especially $Pd(OAc)_2$, are used in this instance and the optical activity is induced in the resulting *trans*-1,2-disubstituted cyclopropane by the presence in the initial olefin of an optically active substituent, which can be transformed, when necessary, into a suitable functional group. Thus a method of synthesis of (1*R*,2*R*)-phenylformylcyclopropane **171** with an optical purity not less than 90% from cinnamaldehyde and L-ephedrine has been proposed. The key stage of the reaction is the synthesis of the oxazolidine derivative **170**.[203]



170 (~100%) (1*R*,2*R*)-**171** (ee > 90%)

It has been shown recently[204] that *trans*-*N*-enoylsultams—derivatives of α,β-unsaturated carboxylic acids and bornane[10.2]sultam—undergo the stereoselective cyclopropane formation reaction on treatment with diazomethane in the presence of $Pd(OAc)_2$, forming the corresponding *trans*-disubstituted cyclopropanes **172** in high yields (the enantiomeric excess of the nonrecrystallised reaction products is 67%–91%). The subsequent hydrolysis of the cyclopropanes **172** in the presence of titanium tetraisopropoxide leads to the optically active cyclopropanecarboxylic acids **173**.[204]



R	Ph	2-MeOC$_6$H$_4$	3-MeOC$_6$H$_4$	Me	C$_{10}$H$_{21}$
Yield of **172** (%)	73	73	63	72	62

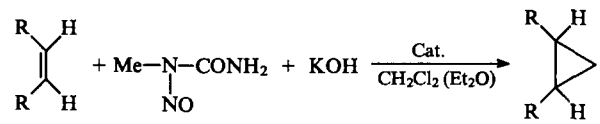
R	3,4,5-(MeO)$_3$C$_6$H$_2$		
Yield of **172** (%)	62	67	67

The authors [204] also noted that the diastereomeric excess of the cyclopropane products, for example **172** (R = Ph), increases from 53% to 87% when the reaction temperature is raised from −30 to 0 °C and remains almost unchanged on its further increase (from 0 to +30 °C).

5. Conversion of unsaturated compounds into cyclopropane derivatives by diazomethane generated *in situ*

The results presented above show that the catalytic reaction of diazomethane with unsaturated compounds constitutes a universal and fairly simple (from the standpoint of the initial reactants) method of synthesis of various cyclopropanes and that the use of palladium catalysts is especially promising. However, the standard procedure in the cyclopropane formation reaction suffers from a number of significant disadvantages and limitations, the main ones being the necessity for the preliminary preparation and transport of the toxic and explosive diazomethane, which renders it suitable only for laboratory purposes.

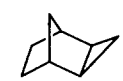
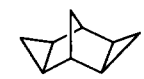
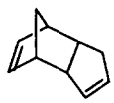
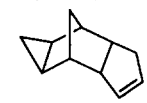
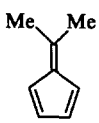
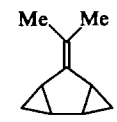
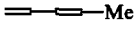
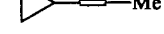
In 1987 we showed for the first time [205] that the conversion of allyl alcohol and allyl ethers into cyclopropane derivatives can be carried out successfully with the direct generation of CH_2N_2 by the alkaline hydrolysis of *N*-methyl-*N*-nitrosourea in the presence of the unsaturated compound and the palladium catalyst. In our subsequent studies [157,206] this method was developed further. In particular, it proved extremely effective for the conversion into cyclopropane derivatives of the majority of unsaturated compounds containing monosubstituted and strained endocyclic double bonds. In the method proposed, *N*-methyl-*N*-nitrosourea is added gradually at 10–20 °C to a mixture of the unsaturated compound, the palladium catalyst, an organic solvent, and 40%–50% KOH solution.



Cat. = $(PhCN)_2PdCl_2$, $Pd(OAc)_2$, $Pd(acac)_2$, $[(PhO)_3P]_2PdCl_2$, $[(PhO)_3P]_4Pd$.

The successful use of palladium catalysts in this method for conversion into cyclopropane derivatives, which involves the use of a concentrated solution of alkali, is apparently due to the involvement in the reaction of non-hydrolysable low-valence π-olefinpalladium complexes. The activity of the catalytic system hardly diminishes under these conditions and makes it possible to achieve conversion into cyclopropane in preparative yields,

Table 6. Catalytic conversion of unsaturated compounds into cyclopropane derivatives by the diazomethane generated *in situ* from *N*-methyl-*N*-nitrosourea (MNU) and KOH [catalyst : 0.2 mol% $(PhCN)_2PdCl_2$, temperature 12–15 °C].

Unsaturated compound	MNU : substrate	Solvent	Product	Yield (%)
	1.5 : 1	CH_2Cl_2		95
	2.9 : 1	CH_2Cl_2		92
	1.5 : 1	CH_2Cl_2–hexane		94
	3 : 1	CH_2Cl_2–Et_2O		84
	1.6 : 1	CH_2Cl_2		92
	1.9 : 1	Et_2O		92
	1.7 : 1	CH_2Cl_2		91
	1.8 : 1	CH_2Cl_2–Et_2O		88
	1.9 : 1	CH_2Cl_2–Et_2O		88

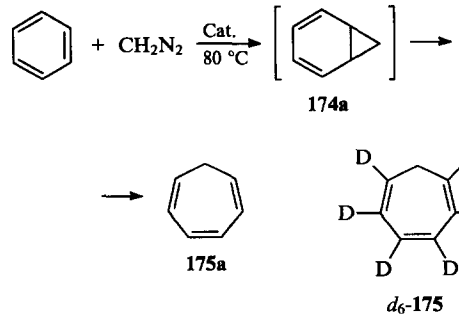
which are the same as in the *ex situ* procedure.[157] Table 6 presents the results of the conversion into cyclopropanes of certain unsaturated hydrocarbons and alkenes with functional group substituents under the conditions of the simultaneous generation and catalytic decomposition of diazomethane.

Thus the creation of a convenient and safe method for the conversion of unsaturated compounds into cyclopropane derivatives by diazomethane generated *in situ* has provided a powerful instrument in synthetic organic chemistry for the formation of cyclopropanes from the corresponding olefins (predominantly monosubstituted and disubstituted). Furthermore, the elimination of the need to employ large quantities of diazomethane to maintain the efficiency of the cyclopropane formation stage itself makes this method promising for application on an industrial scale.

IV. Catalytic interaction of diazomethane with aromatic compounds

The transition metal complex-catalysed interaction of diazomethane with aromatic compounds is accompanied by the dediazotisation of CH_2N_2 and the addition of the methylene fragment to the aromatic system. In the case of compounds of the benzene series, the main products of these reactions are cyclohepta-1,3,5-trienes.[207-213] The reaction involving the expansion of a six-membered ring to a seven-membered one is characteristic also of the catalytic decomposition of other diazo-compounds (for example, alkyl diazoacetates[214]) in different benzene derivatives. This leads to extensive possibilities in the synthesis of cyclohepta-1,3,5-trienes, which are otherwise difficult to obtain. Among the large number of metal salts and complexes tested as catalysts of the methylenation of aromatic compounds by diazomethane, those based on rhodium and copper are the most effective [$Rh_2(OCOCF_3)_4$, $Rh_2(OAc)_4$, Rh/C, $CuCl_2$, CuCl, CuBr].[207-210] On the other hand, the mononuclear rhodium complexes [$RhCl_3$, $Rh(acac)_3$, $Rh(PPh_3)_3Cl$] as well as palladium compounds and copper *N*-(1-phenylethyl)salicylaldiminate proved to be altogether inactive in this reaction.[210]

The catalytic interaction of CH_2N_2 with benzene was first achieved by Müller and coworkers.[207,208] Cycloheptatriene **175a** was obtained in this reaction in 85% yield (relative to CH_2N_2) by adding a benzene solution of CH_2N_2 to a suspension of CuCl or CuBr in benzene at 80 °C. The use of $Rh_2(OCOCF_3)_4$ instead of copper halides with the ratios C_6H_6 : CH_2N_2 : Cat. = 4000 : 200 : 1 makes it possible to increase the yield of compound **175a** to 95% and to carry out the process under milder conditions (~20 °C).



d_6-**175**

According to the data of Dzhemilev et al.,[210] the catalytic cycle in the formation of cycloheptatrienes by the reaction of CH_2N_2 with benzene in the presence of rhodium catalysts presupposes the involvement of dinuclear rhodium complexes,[215] which facilitate the multistage addition of CH_2 to the aromatic system via the formation of metallacyclic intermediates. The subsequent reductive elimination of the dinuclear rhodium complexes from complex **176** is accompanied by the formation of bicyclo[4.1.0]hepta-2,4-dienes (norcaradienes), which are converted into the corresponding cycloheptatrienes under the reaction conditions as a result of the synchronous electrocyclic opening of the cyclopropane ring (Scheme 4). This mechanism has been confirmed by the selective distribution of deuterium in the adduct d_6-**175**, obtained by the reaction of CH_2N_2 with perdeuteriobenzene in the presence of $Rh_2(OCOCF_3)_4$.[210]

Scheme 4

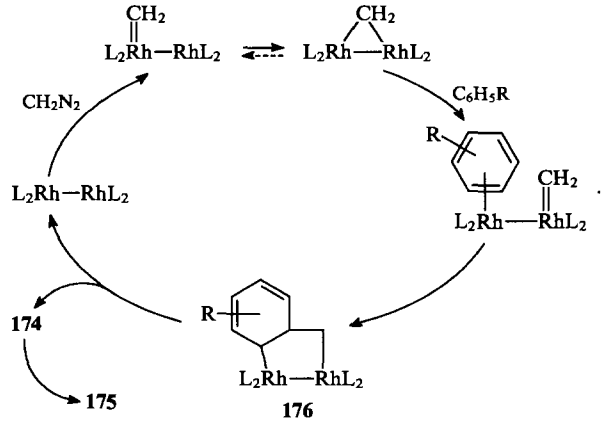
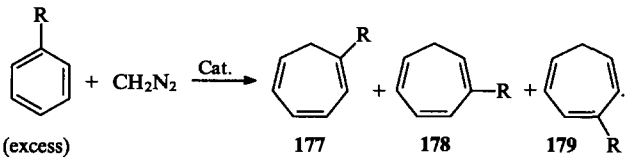


Table 7. The formation of substituted cyclohepta-1,3,5-trienes in the reaction of monosubstituted benzenes with CH_2N_2 in the presence of CuBr or $Rh(OCOCF_3)_4$.

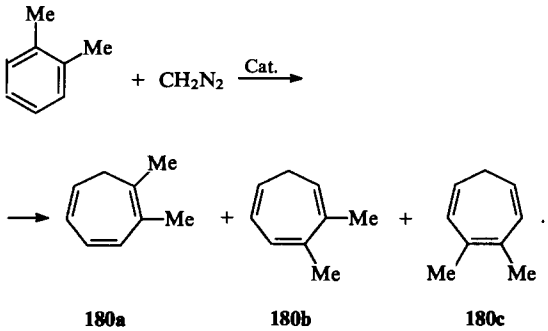
Catalyst (0.5-2 mol%)	Substituent R	Overall yield (%)	k_{rel} (PhR/PhH)	Proportions of isomeric products (%)		
				177	**178**	**179**
CuBr	Me	75	–	21	43	36
	Et	68	–	20	38	42
	Pr^i	64	–	17	37	46
	Bu^t	50	–	13	35	52
	F	41	–	23	25	52
	Cl	50	–	15	43	42
	Br	25	–	8	54	38
	OMe	75	–	30	25	45
$Rh_2(OCOCF_3)_4$	Me	98	1.02	24	26	50
	Ph	92	0.93	23	28	49
	Cl	20	0.16	25	11	64
	Br	8	0.06	19	27	54
	COOEt	7	0.07	12	33	55

Benzene derivatives react with CH_2N_2 similarly to benzene itself and in the presence of both copper and rhodium catalysts a mixture of isomeric 1-, 2-, and 3-substituted cycloheptatrienes **177–179** is then formed from monosubstituted benzenes (Table 7).[210–213]

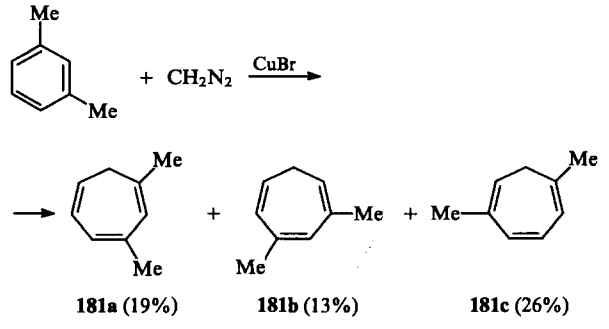


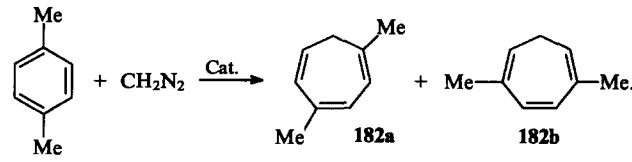
The introduction of bulky and electron-accepting substituents into the benzene ring lowers significantly the overall yield of the reaction products. Whereas in the case of halobenzenes the use of CuBr is preferred in this reaction, for benzene derivatives with electron-donating substituents a greater activity is shown by $Rh_2(OCOCF_3)_4$. It is striking that the preferential formation of 3-substituted cycloheptatrienes **179** is observed in virtually all instances. It has been suggested[210] that the cycloaddition of methylene to the six-electron π-system of substituted aromatic compounds largely involves the C(3)–C(4) bond of the benzene ring, where, according to Dewar,[216] the highest electron density is concentrated. Benzaldehyde, benzonitrile, nitrobenzene, and pyridine do not react with CH_2N_2 in the presence of $Rh_2(OCOCF_3)_4$; surprisingly, anisole behaves in the same way.[210]

Preparative methods of synthesis of isomeric dimethylcycloheptatrienes **180–182**, with a fixed relative disposition of the methyl groups, and of individual 1,3,5-trialkylcyclohepta-1,3,5-trienes **183** have been developed on the basis of the catalytic interaction of diazomethane with xylenes and 1,3,5-trialkylbenzene.[210–212] As was to be expected, the overall yield of cycloheptatrienes increases appreciably under these conditions when $Rh_2(OCOCF_3)_4$ is used as the catalyst.

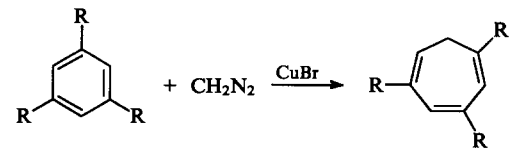


Cat.	Yield of **180** (%)		
	a	**b**	**c**
CuBr	8	31	12
$Rh_2(OCOCF_3)_4$	18	29	51





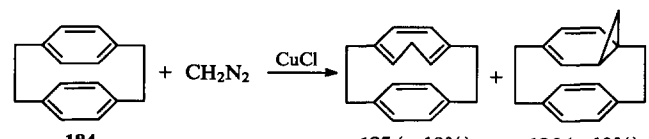
Cat.	Yield of **182** (%)	
	a	**b**
CuBr	25	37
$Rh_2(OCOCF_3)_4$	73	24



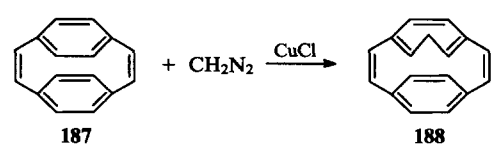
R = Me (75%), Et (59%), Pr^i (45%).

Like *p*-xylene, 1,4-dimethoxybenzene interacts with CH_2N_2, affording in the presence of CuCl two isomers — 1,4- and 2,5-dimethoxycyclohepta-1,3,5-trienes in an overall yield of ~65%.[213]

The catalytic methylenation of the aromatic ring by diazomethane occurs also in the case of cyclophanes.[217–220] Thus the interaction of CH_2N_2 with [2,2]paracyclophane **184** in the presence of CuCl leads to a mixture of different methylenation products, among which monoadducts are formed as a mixture of approximately equal amounts of compounds **185** and **186** containing both the cycloheptatriene and norcaradiene fragments.[217,218]

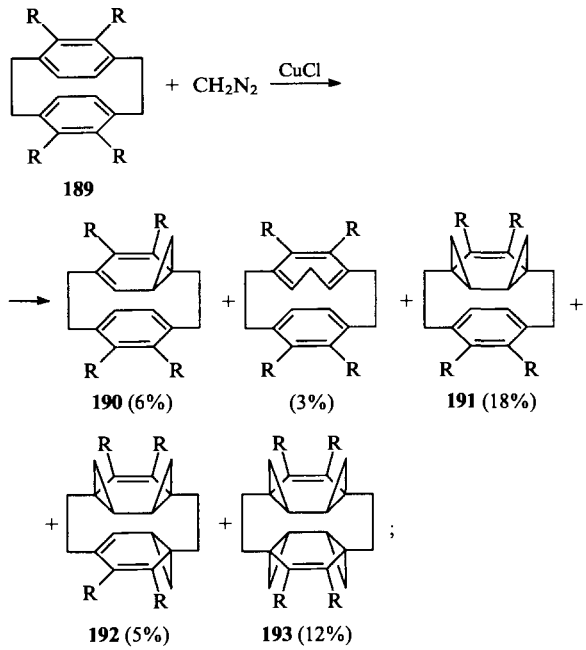


The methylenation of [2,2]paracyclophane-1,9-diene **187** takes place unexpectedly selectively under similar conditions; methylene then attacks benzene rings much faster than the double bond, adding preferentially to the unsubstituted bond with formation of the cycloheptatriene derivative **188**.[217]



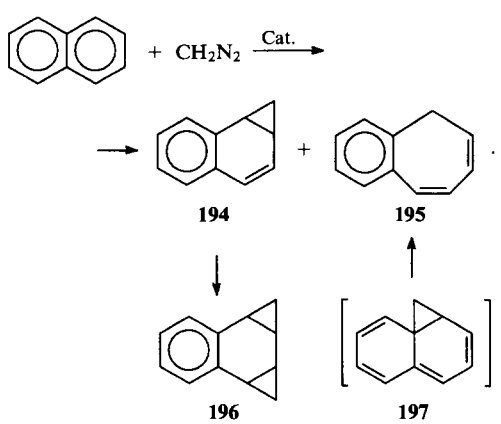
On the other hand, tetrakis(methoxycarbonyl)paracyclophane **189** reacts with a large excess of CH_2N_2 in the presence of CuCl and affords mainly the CH_2N_2 adducts **190–193** as a result of the addition of methylene to the monosubstituted bonds of the benzene ring.[219,220]

In contrast to benzene and its derivatives, the interaction of polynuclear aromatic compounds with CH_2N_2 in the presence of both copper and rhodium catalysts leads mainly to the formation of fairly stable cyclopropane adducts and in a number of instances the reaction proceeds with a high regioselectivity. Thus the interaction of CH_2N_2 with an excess of naphthalene at 80 °C in the presence of $Rh_2(OCOCF_3)_4$ affords 2,3-benzobicyclo[4.1.0]hepta-2,4-diene **194** in a yield of 98%, the relative reactivity of naphthalene in this reaction being higher by a factor

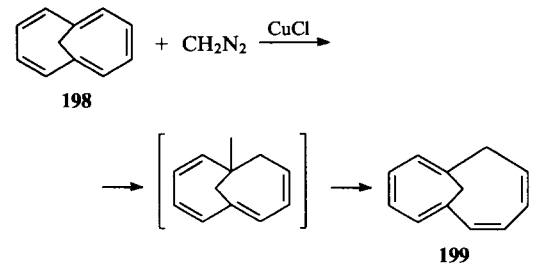


R = COOMe.

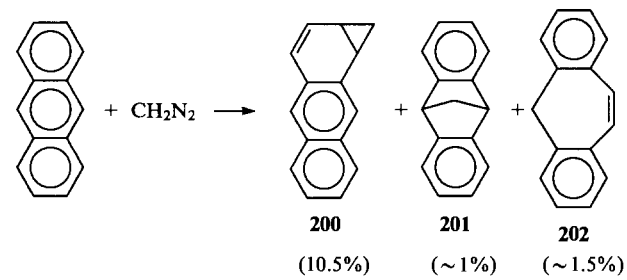
of 1.7 than that of benzene.[210] The same reaction in the presence of CuBr leads to an overall yield of about 30% of a mixture of the cyclopropane **194** and benzocycloheptatriene **195**, the ratio of which varies from 95 : 5 at 120–140 °C to 40 : 60 at 170–190 °C.[221] When a fourfold molar excess of CH_2N_2 was used, the product **196** of the double cyclopropane formation reaction was obtained with a yield of 18%. Since all attempts to isomerise compound **194** to compound **195** were unsuccessful,[210] one may assume that compound **195** is formed as a result of the isomerisation of another cyclic methylene–naphthalene adduct, for example compound **197**, formed at an elevated temperature as a consequence of the decrease in the regioselectivity of the reaction.



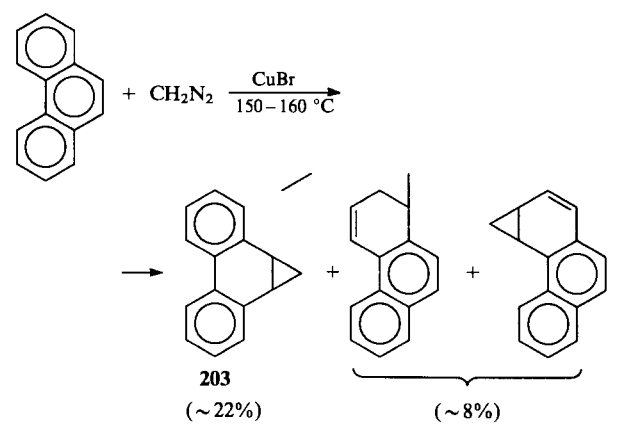
The catalytic interaction of diazomethane with another 10-electron aromatic system—bicyclo[4.4.1]-undeca-1,3,5,7,9-pentaene **198**[222,223]—apparently involves wholly the most substituted double bond, since, according to the data of Vogel et al.,[223] the reaction results in the formation of only bicyclo[5.4.1]dodeca-2,4,7,9,11-pentaene **199**.

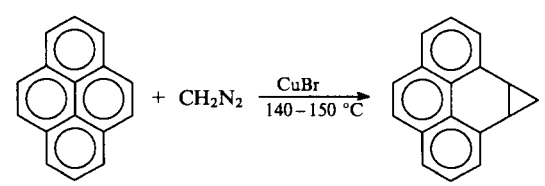


The interaction of CH_2N_2 with anthracene in the presence of CuBr has been carried out at 25 °C using CH_2Cl_2 as the solvent. A mixture of the products **200**–**202**, in which the cyclopropane adduct **200** predominated, was then obtained in an overall yield of 13%.[224]

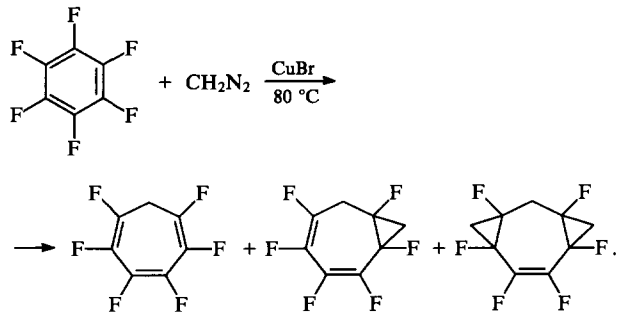


The catalytic addition of methylene to phenanthrene also leads to a mixture of compounds,[221,225] in which, according to the data of Müller et al.,[225] the dominant component is the cyclopropane adduct **203** formed as a result of the addition of methylene to the C(9)–C(10) bond. The higher reactivity of the bonds in the central rings of condensed aromatic systems compared with the bonds in the peripheral benzene rings is indicated also by the formation of only one isomer **204** in the catalytic conversion of pyrene into a cyclopropane derivative.[226]



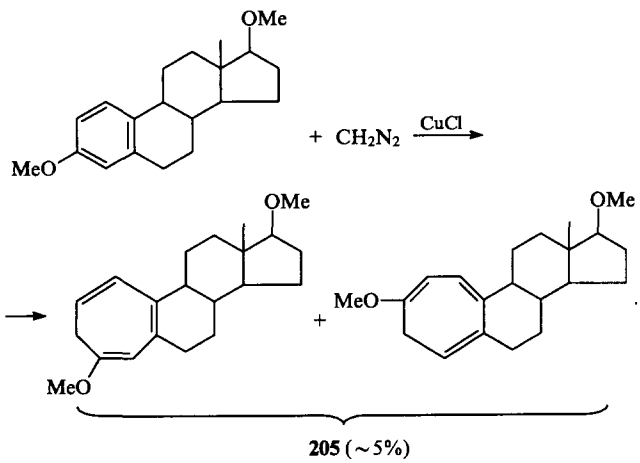


When diazomethane reacted with a boiling solution of hexafluorobenzene in the presence of CuBr, a complex mixture of compounds was obtained in which hexafluorocyclohepta-1,3,5-triene and the products of its further conversion into cyclopropane derivatives—hexafluorobicyclo[5.1.0]octa-2,4-diene and hexafluorotricyclo[6.1.0.$0^{3,5}$]-non-6-ene—were identified.[227]



The catalytic conversion of the benzene ring into the cycloheptatriene system in the series of steroids on treatment with CH_2N_2 has been achieved by Müller and coworkers[212,228] as early as 1963 in relation to the dimethyl ether of β-oestradiol.

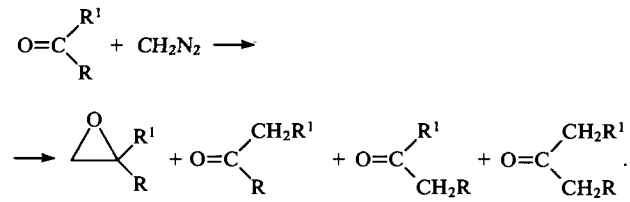
The low yield of the steroids **205** and the lack of other similar data did not promote further research on these lines. However, one may be optimistic about the possibility of converting complex aromatic compounds into higher homologues by varying the substituents in the aromatic ring and by using other catalytic systems, in particular rhodium compounds.



205 (~5%)

V. Synthesis of ketones by converting carbonyl compounds into higher homologues

The study of the reactions of diazomethane with aldehydes and ketones began with the discovery of diazomethane itself and embraced virtually all classes of organic compounds containing the carbonyl group—aliphatic, alicyclic, aromatic, and heterocyclic ketones, aldehydes,[229-234] ketosteroids,[235-238] and polycyclic ketones.[239] As a rule, the non-catalytic interaction of CH_2N_2 with aldehydes leads to ketones and epoxides, while its interaction with ketones leads to the higher homologues of the latter and/or the corresponding epoxides, ketones reacting with CH_2N_2 more slowly than aldehydes. The reaction is carried out predominantly in methanol and lasts from several hours to several days.



In this section, the results of catalytic reactions of diazomethane with carbonyl compounds will be briefly described. Interest in such reactions arose for the first time in the 1960s.

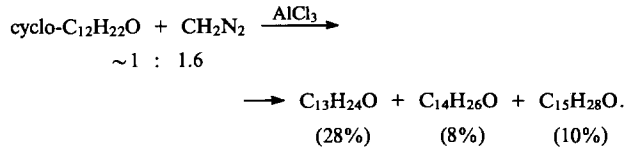
In 1960, two groups of investigators[240-242] established independently that boron trifluoride etherate increases appreciably the yield of higher homologues of ketones and the corresponding carbonyl compounds in the reactions of diazomethane with carbonyl compounds, suppressing at the same time the formation of epoxides. For example, the yield of cyclononanone, obtained from cyclooctanone and CH_2N_2 in the ring expansion reaction catalysed by $BF_3 \cdot OEt_2$, increases from 20% to 46% compared with the noncatalytic version.[243]

Together with boron trifluoride etherate, effective catalysts of the conversion of carbonyl compounds into higher homologues by diazomethane are also $ZnCl_2$, AlX_3 (X = Cl, Br, I), $GaCl_3$, $ZrCl_4$, HBF_4.[240-243] Table 8 presents examples of the catalytic conversion of cyclooctanone into its higher homologues on treatment with CH_2N_2.[243]

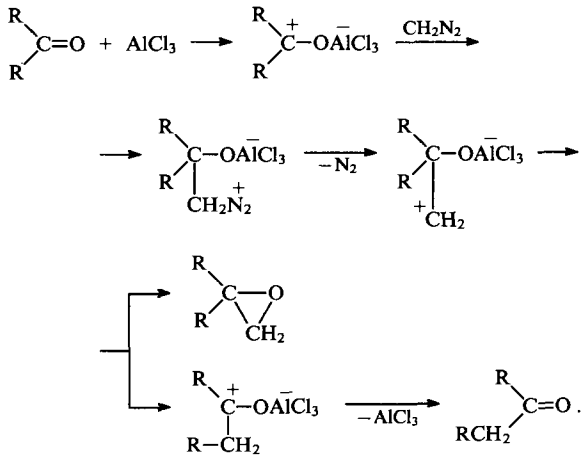
Table 8. Catalytic interaction of cyclooctanone with diazomethane.

Catalyst		Yield of cycloalkanones (%)	
(2–4 mol%)	Ketone : CH_2N_2	C_9	C_{10}
$ZnCl_2$	1 : 1.2	25	–
AlX_3 (X = Cl, Br, I)	1 : 1.3	48–49	11–14
$AlEt_3$	1 : 1.3	49	19
$GaCl_3$	1 : 1.4	42	5
$ZrCl_4$	1 : 1.3	49	13
HBF_4	1 : 1.2	33	–
$TiCl_4$	1 : 1.2	10	–

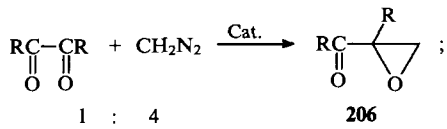
It has been noted[243] that the reactivity of cyclic ketones falls appreciably on passing from cyclohexanone to cycloundecanone. Starting with the latter, ketones with an odd number of carbon atoms in the ring are less reactive than ketones with an even number of carbon atoms. This rule is illustrated, in particular, by the reaction of CH_2N_2 with cyclododecanone, as a result of which cyclopentadecanone is actually formed in a somewhat higher yield than cyclotetradecanone.



The mechanism of the conversion of ketones into higher homologues presupposes the initial activation of the carbonyl group by Lewis acids and the addition of CH_2N_2 to the resulting complex with elimination of a nitrogen molecule and subsequent 1,2-migration of the alkyl group.[243]



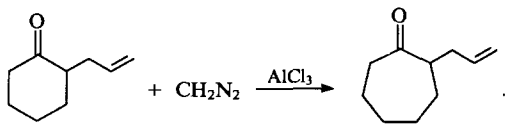
Depending on the nature of the carbonyl compound, the primary carbenium ion may be stabilised also by the carbonyl oxygen atom, which leads to the formation of the corresponding oxiran. In particular, the interaction of CH_2N_2 with α-diketones in the presence of both BF_3 and $AlCl_3$ leads mainly to the ketooxirans **206**.[242,243]



1 : 4 **206**

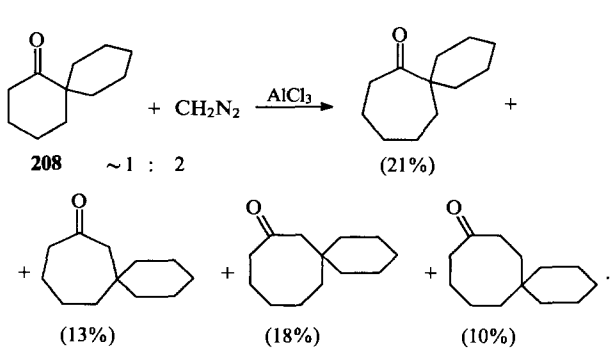
R = Ph, Me (54%, Cat. = $BF_3 \cdot OEt_2$).

The proposed mechanism has been confirmed also by the fact that the interaction of CH_2N_2 with 2-allylcyclohexanone in the presence of $AlCl_3$ involves predominantly the carbonyl group with formation of 2-allylcycloheptanone **207**, whereas the products of the conversion of the double bond into a cyclopropyl group were not detected.[243]



207 (~60%)

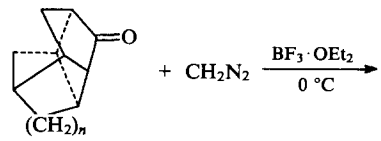
It is noteworthy that the insertion of methylene in the α-C–C bond takes place mainly from the side without substituents. However, in a number of instances such regioselectivity is not maintained. For example, the conversion of the spiran ketone **208** into a higher homologue leads to a mixture of cyclic ketones containing a carbonyl group in different positions relative to the spiran carbon atom.[244]



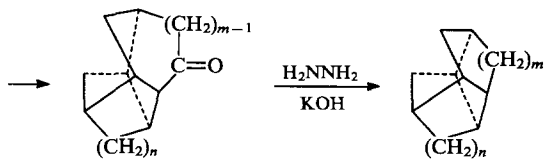
208 ~1 : 2 (21%)

(13%) (18%) (10%)

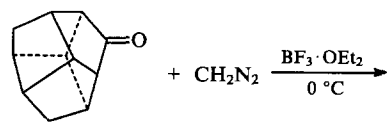
An example of the use of the ring expansion reaction on treatment with CH_2N_2 in the series of polycyclic ketones is provided by the synthesis of triblattanes—analogues of the D_3-twist-form of bicyclo-[2.2.2]octane, linked by different numbers of diagonal bridging groups. Thus the interaction of tetracyclo[4.3.0.$0^{2,5}$.$0^{3,8}$]nonan-9-one **209a** with an excess of CH_2N_2 in the presence of 1 equivalent of $BF_3 \cdot OEt_2$ and the subsequent Wolff–Kishner reduction of the resulting ketones leads to [*m*.0]-triblattanes **210a** (*m* = 2–4).[245] A mixture of [*m*.1]triblattanes **210b** (*m* = 2–7) and [*m*.1.1]-triblattanes **212** (*m* = 2–7) and [*m*.1.1]-triblattanes **212** (*m* = 2–6) has been obtained similarly from tetracyclodecanone **209b** and trishomocubanone **211** and it has been noted that in the absence of a catalyst the ketone **209b** does not react with diazomethane.[245,246]



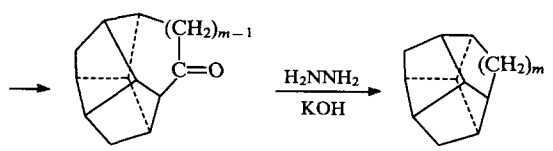
209 *n* = 0 (**a**), 1 (**b**)



210

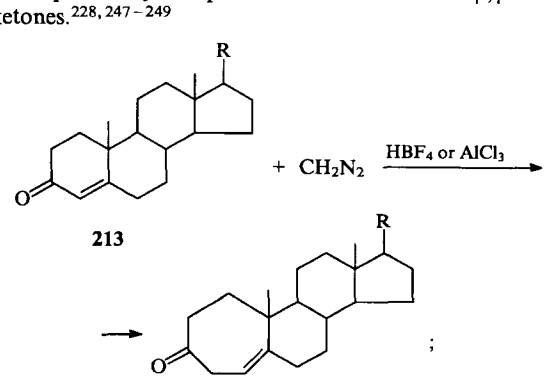


211



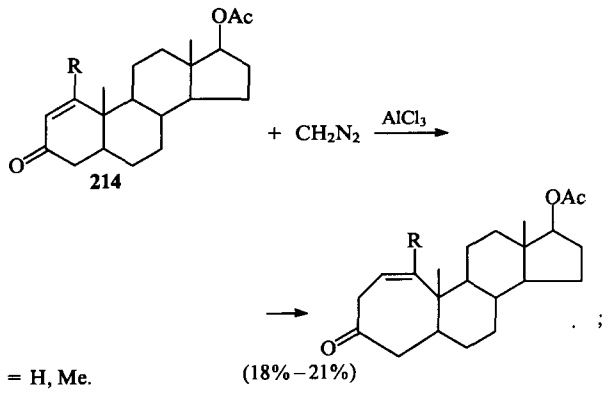
212

The non-catalysed reaction of diazomethane with α,β-unsaturated ketones usually proceeds as 1,3-dipole cycloaddition and leads to the formation of pyrazolines. On the other hand, the catalytic interaction of CH_2N_2 with conjugated ketones, carried out for the 3-ketosteroids **213** and **214**, proceeds as in the case of cycloalkanones—with ring expansion accompanied by the preferential formation of β,γ-unsaturated ketones.[228,247–249]



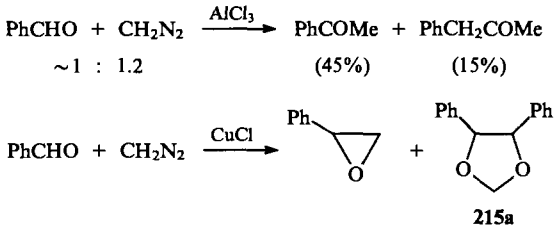
213

R = C_8H_{17} (40%); OAc (20%–30%); Ac (29%); $COCH_2OAc$ (31%).



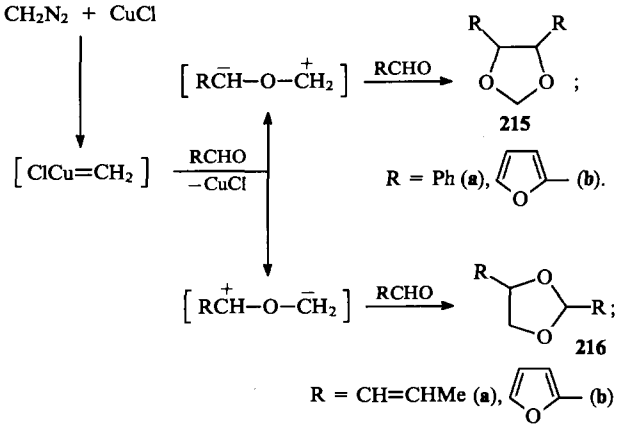
R = H, Me. (18%–21%)

In certain cases, the use of transition metal Lewis compounds instead of acids alters significantly the mode of reaction of carbonyl compounds with CH_2N_2. Thus the interaction of benzaldehyde with CH_2N_2 in the presence of $AlCl_3$ leads to acetophenone and phenylacetone,[250] whereas in the presence of CuCl diazomethane reacts with an excess of benzaldehyde to form phenyloxiran and a mixture of isomeric 4,5-diphenyl-1,3-dioxolans **215a**.[251]



215a

Crotonaldehyde and furfural react similarly with CH_2N_2 in the presence of CuCl, affording respectively the isomeric 2,4-dipropenyl-1,3-dioxolans **216a** in 18% yield, on the one hand, and 2,4-difuryl-1,3-dioxolans **216b** and 4,5-difuryl-1,3-dioxolans **215b** in an overall yield of 7%, on the other.

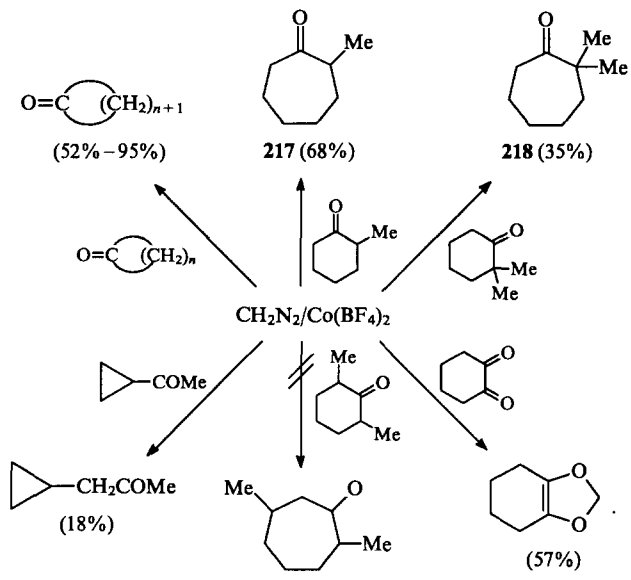


The formation of 1,3-dioxolans presupposes the addition of the methylene complex [ClCu=CH_2] to the carbonyl group of the aldehydes and then the addition of a second aldehyde molecule to the intermediate 1,3-dipoles.[251]

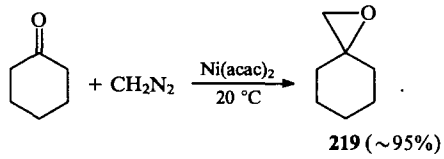
Cobalt tetrafluoroborate also behaves as an effective catalyst of the conversion of linear and cyclic carbonyl compounds into higher homologues by reaction with diazomethane. It makes it possible to obtain ketones with a specified number of carbon atoms in the chain under mild conditions, in one stage, with a high selectivity, and in high yields.[252] Thus the reaction of cyclohexanone with a threefold excess of CH_2N_2 in the presence of $Co(BF_4)_2$ at 0 °C leads to cycloheptanone in 81% yield. The formation of only an insignificant amount of polymethylene was noted under these conditions.

The catalytic activity of $Co(BF_4)_2$ depends extremely significantly on the structure of the initial cyclic ketone. The formal insertion of methylene, accompanied by ring expansion, involves the sterically least hindered C–C bond in the initial carbonyl compound. Thus α-methylcyclohexanones afford only α-methylcycloheptanones, for example compounds **217** and **218**, while α,α′-disubstituted cyclic ketones, for example 2,6-dimethylcyclohexanone, do not react at all under these conditions (Scheme 5).[252]

Scheme 5



The interaction of CH_2N_2 with cyclohexanone in the presence of $Ni(acac)_2$ takes place in a completely different manner. In this case, the only reaction product is oxiranylcyclohexane **219**, the yield of which reaches 95%.[252,253]



Thus the catalytic conversion of ketones into higher homologues with the aid of diazomethane is of preparative importance — especially in the synthesis of macrocyclic ketones.

VI. Catalytic methylation of alcohols and amines by diazomethane

In this section we do not claim to provide a complete description of the available data on the reactions of diazomethane with compounds containing a mobile hydrogen atom at the nitrogen and oxygen atoms. Only a general assessment of the catalytic interaction of CH_2N_2 with alcohols and amines is given.

Alcohols are as a rule inert to CH_2N_2, but in the presence of Lewis acids such as $BF_3 \cdot OEt_2$, HBF_4, $AlCl_3$, $SnCl_2$, etc. they form methyl ethers in fairly satisfactory yields (40%–92%).[254–272] The effectiveness of the methylation is then to a large extent determined by the nature of the hydrocarbon substituents. In particular, it has been shown in relation to the methylation of pentyl and butyl alcohols in the presence of HBF_4 and $BF_3 \cdot OEt_2$ that the yield of the corresponding methyl ethers falls on passing from primary to tertiary alcohols ($k_{rel} \simeq 2 : 1.5 : 1$).[255–258] The shielding influence of the substituents is manifested to an even greater extent in the

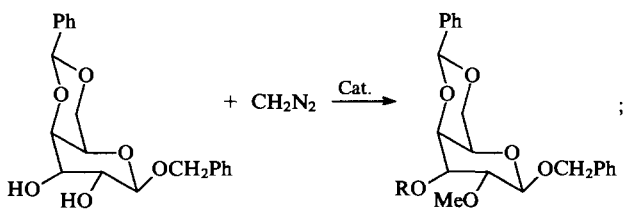
methylation of cyclic alcohols. Thus in the presence of BF_3 or $AlCl_3$, unhindered cycloalkanols afford the methyl ethers in 80%–84% yields,[259] while, for example, isoborneol is not methylated at all under these conditions.[258]

According to the data of Bawn and Ledwith,[260] the mechanism of the methylation of alcohols by diazomethane in the presence of boron compounds involves the formation of boron alkoxides and the insertion of methylene in the B–O bond with the subsequent cleavage of the boron–carbon bond by the alcohol.

$$BX_3 \xrightarrow{CH_2N_2} X_2BCH_2X \xrightarrow{ROH} X_2BOR \xrightarrow{CH_2N_2}$$

$$\longrightarrow X_2BCH_2OR \xrightarrow{ROH} X_2BOR + ROMe.$$

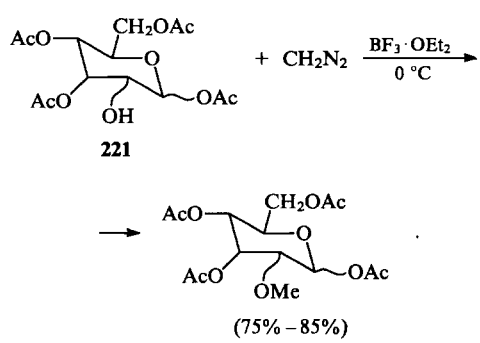
Diazomethane combined with boron trifluoride etherate or $SnCl_2 \cdot 2H_2O$ has been used in the carbohydrate chemistry for the complete or partial methylation of the hydroxy-groups.[261–265] For example, the methylation of the galacto-pyranoside **220** in the presence of $SnCl_2 \cdot 2H_2O$ involves preferentially one of the OH groups, whereas in the presence of $BF_3 \cdot OEt_2$ both hydroxy-groups are methylated.[261]



220

Cat. = $SnCl_2 \cdot 2H_2O$, R = H (91%);
Cat. = $BF_3 \cdot OEt_2$, R = Me (84%).

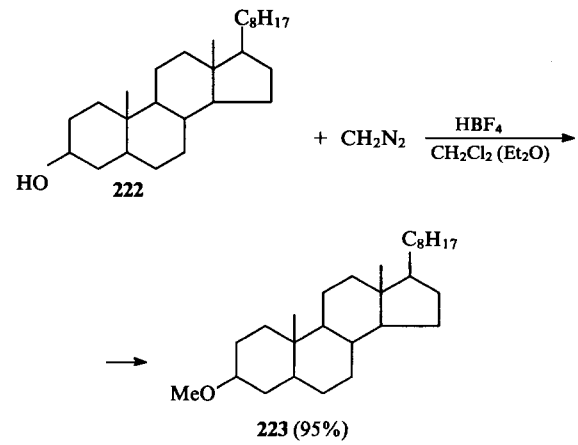
In the presence of $BF_3 \cdot OEt_2$, diazomethane proved to be an effective reagent also for the methylation of partially acylated carbohydrates, for example compound **221**, which in the case where the usual methylating agents (MeI, Me_2SO_4) are employed are readily hydrolysed by the bases used for this purpose.[263–265]



221

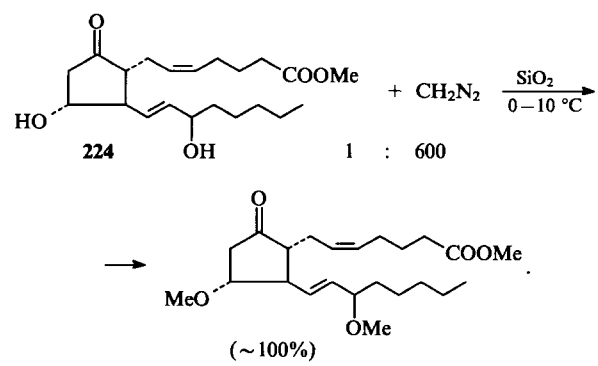
(75%–85%)

Catalytic methylation of steroid alcohols by diazomethane also takes place with high degrees of conversion.[258,266] Thus the interaction of cholestanol **222** with an excess of CH_2N_2 in the presence of HBF_4 leads to the formation of the methyl ether **223** in 95% yield.[266]



222 **223** (95%)

Alcohols, including prostaglandins, terpene alcohols, and carbohydrates, are fairly successfully methylated by an excess of CH_2N_2 when acted upon by silica gel suspended in ether.[267] Despite the large excess of CH_2N_2, methylene is inserted selectively in the O–H bonds of prostaglandin **224** without affecting the keto-group and the double bonds.



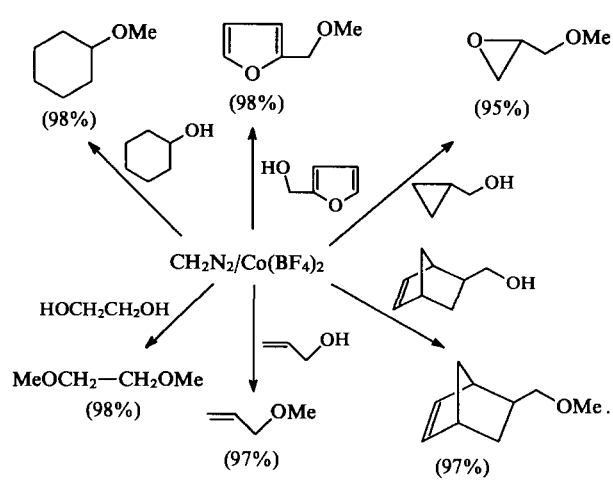
224 1 : 600

(~100%)

Later another method was proposed, according to which the alcohol adsorbed on silica gel was treated with gaseous diazomethane.[268] Even tertiary alcohols or sterically hindered phenols, such as 1-methylcyclohexanol or 2,6-di-isopropyl-phenol, afforded the corresponding methyl ethers in 99% and 79% yields on treatment with a large excess of CH_2N_2 (68 and 34 molar equivalents respectively) under these conditions.

Cobalt tetrafluoroborate also exhibits a high catalytic activity in the methylation of alcohols.[269,270] The use of 3–4 equivalents of CH_2N_2 then leads to *O*-methyl derivatives in high yields (Scheme 6). Reactivity of alcohols in the presence of

Scheme 6

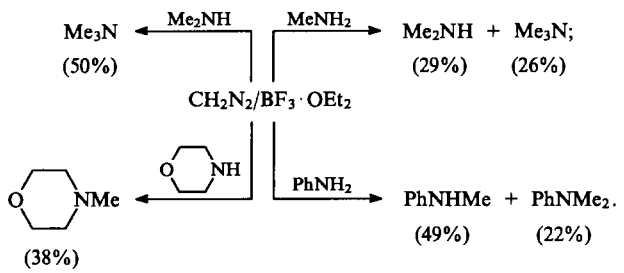


$Co(BF_4)_2$, can be arranged in the following sequence: secondary > primary > tertiary.[269] The double bonds of the unsaturated aliphatic or cyclic alcohols are then hardly involved, whereas under similar conditions palladium compounds catalyse mainly the conversion of double bonds into cyclopropyl groups.[155,156]

Like alcohols, primary and secondary amines are methylated by diazomethane in the presence of $BF_3 \cdot OEt_2$ or HBF_4, affording the corresponding methylamines in yields not exceeding 50%. The *N*-methylation of primary amines results in the formation as a rule of a mixture of the corresponding mono- and di-methylamines.[271-275]

Certain examples of the methylation of various amines by an excess of CH_2N_2 in the presence of $BF_3 \cdot OEt_2$ are presented in Scheme 7.

Scheme 7



Copper compounds (CuCN, CuCl) are also capable of catalysing the methylation of amines by diazomethane. The yields of the corresponding *N*-methylamines are then 32% and 25% respectively in the case of piperidine and morpholine.[276]

The use of $CF_3SO_3H-NEt_3$ as the catalyst of the methylation of secondary amines makes it possible to increase the yields of the methylamines to 68%–98%.[277,278]

$$R^1R^2NH + CH_2N_2 \xrightarrow[CH_2Cl_2]{CF_3SO_3H/Et_3N} R^1R^2NMe;$$

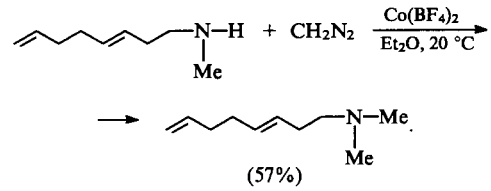
$R^1 = PhCH_2, Me_2CH, Me$; $R^2 = MeC_6H_4, PhCH_2, Ph$.

Cobalt compounds exhibit a high effectiveness in reactions of this kind. One of the best catalysts of the methylation of amines available at present is apparently $Co(BF_4)_2$, the use of which increases the yield of the methylated amines to 86%–98% even in the presence of a comparatively small excess of diazomethane.[269,279]

$$R^1R^2NH + CH_2N_2 \xrightarrow[Et_2O,\ 10-30\ ^\circ C]{Co(BF_4)_2} R^1R^2NMe;$$

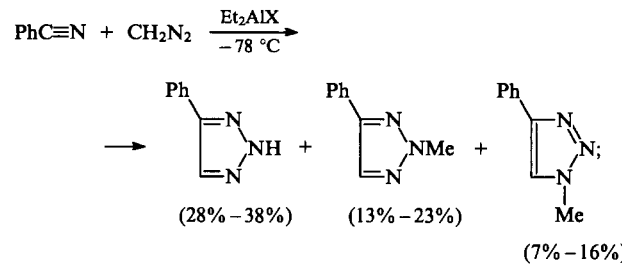
1 : (1–4)

$R^1 = R^2 = Et$ (89%), Pr^i (86%);
$R^1 = Me$, $R^2 = Ph$ (98%);
$R^1 + R^2 = (CH_2)_5$ (88%),
$(CH_2)_2O(CH_2)_2$ (97%).

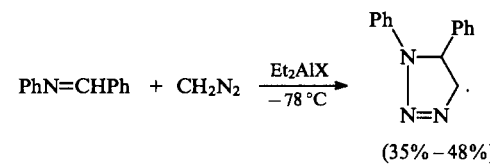


There are few data concerning other reactions of heteroatomic compounds with diazomethane, including those involving the use of catalysts, and they date back mainly to the 1950s–1960s.

For example, it has been noted that the interaction of CH_2N_2 with benzonitrile or benzylideneaniline in the presence of alkylalanes ($AlEt_3$, Et_2AlCl, etc.) is accompanied by the addition of CH_2N_2 to the C≡N and C=N bonds with formation of five-membered heterocycles — triazoles and triazolines.[280]



$PhC{\equiv}N : CH_2N_2 : Et_2AlX = 2 : 1 : 1$



According to the results of a number of studies,[281-284] diazomethane interacts with silanes, germanes, and stannanes in the presence of copper powder, affording the products of the insertion of methylene in Si–Cl, Ge–Cl, Si–H, and Sn–H bonds, the reactions with chlorogermanes and hydrostannanes being much more effective than those with the corresponding silanes.

$$MCl_4 + CH_2N_2 \xrightarrow[Et_2O,\ -60\ ^\circ C]{Cu} Cl_3MCH_2Cl;$$

1 : 1 M = Ge (93%); Si (45%–47%).

$$MeMCl_3 + CH_2N_2 \xrightarrow[Et_2O,\ -60\ ^\circ C]{Cu} MeCl_2MCH_2Cl;$$

1 : 1 M = Ge (78%); Si (13%).

$$Et_3MH + CH_2N_2 \xrightarrow[Et_2O,\ -0\ ^\circ C]{Cu} Et_3MMe;$$

M = Sn (75%);
Ge (9%); Si (~1%).

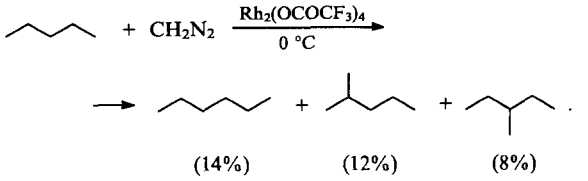
$$Cl_3Si{-}SiCl_3 + CH_2N_2 \xrightarrow[-30\ ^\circ C]{Cu} ClCH_2SiCl_2SiCl_2CH_2Cl.$$

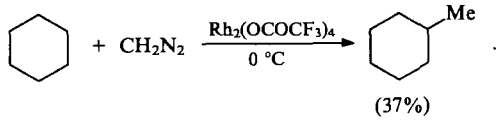
1 : 3 (28%)

$$Cl_3C{-}SiCl_3 + CH_2N_2 \xrightarrow[-60\ ^\circ C]{Cu} Cl_3C{-}SiCl_2CH_2Cl.$$

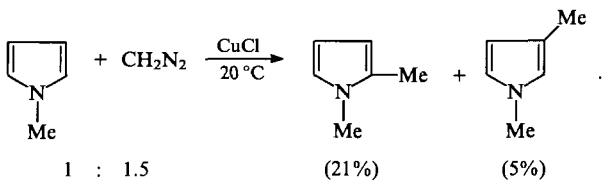
1 : 1 (22%)

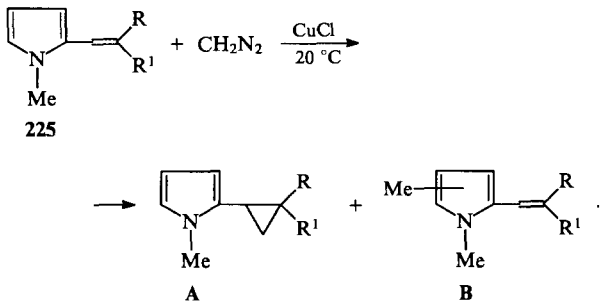
Despite the fact that the catalytic decomposition of CH_2N_2 does not generally yield the products of the insertion of methylene in the C–H bonds, nevertheless there is a possibility of the occurrence of such reactions. Thus the decomposition of CH_2N_2 in pentane or cyclohexane catalysed by $Rh_2(OCOCF_3)_4$, leads to the partial methylation of the latter.[252]





The formation of an appreciable amount of the products of the insertion of methylene in the C–H bonds in the CuCl-catalysed decomposition of CH_2N_2 has been observed also in the case of *N*-methylpyrroles.[143] Even when CH_2N_2 interacts with 2-alkenyl-*N*-methylpyrroles **225**, the products of the insertion of methylene into the vinyl C–H bonds of the pyrrole ring are formed together with the cyclopropane adducts.[143]





R	R¹	Yield of **A** (%)	Yield of **B** (%)
H	H	18	6
H	Me	6	15
Me	Me	8	18

VII. Conclusion

The data presented demonstrate the great potential possibilities of the use of diazomethane in laboratory practice for the modification of various classes of organic compounds. Furthermore, convincing evidence has been obtained recently for the possibility of the simultaneous generation and catalytic decomposition of diazomethane, which significantly enhances the prospect for its application in fine organic synthesis. In the first place, this applies to the reactions involving the direct conversion of unsaturated compounds into cyclopropane derivatives, which leads to the formation of cyclopropane synthons. Systematic study of these reactions in the presence of a number of catalytic systems made it possible not only to establish the characteristic features of the conversion of various double bonds into cyclopropyl groups, to estimate the effectiveness of the catalysts based on transition and non-transition metals, and to put forward the mechanisms of their reaction with diazomethane, but it has also been possible to develop a safe method for the conversion of many unsaturated compounds, including those with functional groups in the molecule, into cyclopropane derivatives.

Considerable advances in the attainment of this aim have been associated with the use of palladium compounds as process catalysts, which ensure a high degree of conversion of the initial olefins into cyclopropanes combined with a minimal consumption of diazomethane and hence of *N*-methyl-nitrosoamides used for its generation *in situ*.

The employment of metal complex catalysis in the chemistry of diazomethane has also made it possible to achieve the conversion of benzenes into cyclohepta-1,3,5-trienes and the selective conversion of ketones into higher homologues and the methylation of alcohols and amines. Apart from the copper compounds and Lewis acids put forward for these purposes as early as the end of the 1950s, other more effective catalysts are being used nowadays, for example $Rh_2(OCOCF_3)_4$ for the synthesis of cycloheptatrienes and $Co(BF_4)_2$ for the conversion of ketones into higher homologues and the methylation of alcohols and amines.

The successive development of studies on these lines will be determined by the further search for active and highly selective catalysts of the decomposition of diazomethane and of the transfer of the methylene fragment to the substrate molecule, including procedures involving the modification of the ligand sphere of transition metal compounds, and also by the advances in the elucidation of the mechanisms of the catalytic reactions with participation of diazomethane.

References

1. H von Pechmann *Chem. Ber.* **27** 1888 (1894)
2. H Boersch *Monatsh. Chem.* **65** 311 (1935)
3. A P Cox, L F Thomas, J Sheridan *Nature (London)* **181** 1000 (1958)
4. M Regitz, G Maas *Diazo Compounds. Properties and Synthesis* (New York: Academic Press, 1986)
5. E V Slivinskii, Yu P Voitsekhovskii *Usp. Khim.* **58** 94 (1989) [*Russ. Chem. Rev.* **58** 57 (1989)]
6. A J Gubert, in *Catalysis in C1 Chemistry* (Ed. W Keim) (Translated into Russian; Leningrad: Khimiya, 1987) p. 235
7. G Henrici-Olive, S Olive *The Chemistry of the Catalysed Hydrogenation of Carbon Monoxide* (Translated into Russian; Moscow: Mir, 1987) p. 155
8. L Fieser, M Fieser *Reagents for Organic Synthesis* (Translated into Russian; Moscow: Mir, 1970) p. 243
9. W Kirmse *Carbene Chemistry* (Translated into Russian; Moscow: Mir, 1966)
10. O M Nefedov, A I Ioffe, L G Menchikov *Khimiya Karbenov* (Carbene Chemistry) (Moscow: Khimiya, 1990) p. 158
11. *Methoden der Organischen Chemie (Houben Weyl) Vol. IV/III* (Stuttgart: Georg Thieme, 1971) p. 101
12. W Kirmse *Carbene Chemistry* (New York: Academic Press, 1971)
13. J S Pizey, in *Synthetic Reagents* (Chichester: Ellis Horwood, 1974) Vol. 2, p. 65
14. S Patai (Ed.) *The Chemistry of Double-Bonded Functional Groups* (London: Wiley, 1977) Part 1
15. D S Wulfman, R Poling, in *Reactive Intermediates* (Ed. R A Abramovitch) (New York: Plenum, 1980) Vol. 1, p. 321
16. B Bosnich *Asymmetric Catalysis* (Dordrecht: Martinus Nijhoff Publishers, 1986)
17. M P Doyle *Chem. Rev.* **86** 919 (1986)
18. P A Chaloner, in *Handbook of Coordination Catalysis in Organic Chemistry* (London: Butterworths, 1986) p. 337
19. G Maas, in *Topics in Current Chemistry* (Berlin: Springer-Verlag, 1987) Vol. 137, p. 78

20. A Demonceau, A F Noels, A J Hubert, in *Aspects of Homogenous Catalysis* (Dordrecht: D Reidel, 1988) Vol. 6, p. 199
21. I E Dolgy, E A Shapiro, O M Nefedov, in *Chemistry of Carbenes and Small-sized Cyclic Compounds* (Ed. O M Nefedov) (Moscow: Mir, 1989) p. 101
22. *Methoden der Organischen Chemie (Houben Weyl)* (Stuttgart: Georg Thieme, 1989) Vol. 19b, p. 278
23. D Seyferth *Chem. Rev.* **55** 1155 (1955)
24. G D Buckley, N H Ray *J. Chem. Soc.* 2714 (1950)
25. U M Dzhemilev, V A Dokichev, S Z Sultanov, R I Khusnutdinov, Yu V Tomilov, O M Nefedov, G A Tolstikov *Izv. Akad. Nauk SSSR, Ser. Khim.* 1861 (1989)
26. T V Mandel'shtam, in *Sovremennye Problemy Organicheskoi Khimii* (Modern Problems in Organic Chemistry) (Leningrad: Izd. Leningrad. Gos. Univ., 1976) Vol. 5, p. 87
27. E C Brady, E Pettit *J. Am. Chem. Soc.* **102** 6181 (1980)
28. C-C Chang *Inorg. Chim. Acta* **94** 259 (1984)
29. P P O'Neill, J J Rooney *J. Chem. Soc., Chem. Commun.* 104 (1972)
30. C S Lee, M M Wu *J. Chem. Soc., Chem. Commun.* 250 (1985)
31. H Werner, J H Richards *J. Am. Chem. Soc.* **90** 4976 (1968)
32. C E H Bawn, A Ledwith, in *Progress in Boron Chemistry* 1964, Vol. 1, p. 345
33. M Imoto, T Nakaya *J. Macromol. Sci., Rev. Macromol. Chem.* **8** 1 (1972)
34. G Wittig, K Schwarzenbach *Liebigs Ann. Chem.* **650** 1 (1961)
35. G Wittig, F Wingler *Liebigs Ann. Chem.* **656** 18 (1962)
36. H Hoberg *Liebigs Ann. Chem.* **656** 1 (1962)
37. H E Simmons, T L Cairns, S A Vladuchick, C M Hoiness, in *Organic Reactions* 1973, Vol. 20, p. 1
38. A N Nesmeyanov, E G Perevalova, E I Smyslova, V P Dyadchenko, K N Grandberg *Izv. Akad. Nauk SSSR, Ser. Khim.* 2610 (1977)
39. R McCrindle, G J Arsenault, R Farwaha *J. Organomet. Chem.* **296** 51 (1985)
40. R McCrindle, D W Sneddon *J. Organomet. Chem.* **282** 413 (1985)
41. J L Hubbard, W K McVicar *J. Am. Chem. Soc.* **108** 6422 (1986)
42. F D Mango, I Dvoretzky *J. Am. Chem. Soc.* **88** 1654 (1966)
43. M Brookhart, W B Studabaker *Chem. Rev.* **87** 411 (1987)
44. T W Hanks, R A Ekeland, K Emersen, R D Larsen, P W Jennings *Organometallics* **6** 28 (1987)
45. P W Jennings, R A Ekeland, M D Waddington, T W Hanks *J. Organomet. Chem.* **285** 429 (1985)
46. C P Casey, S H Bertz, T J Burkhardt *Tetrahedron Lett.* **14** 1421 (1973)
47. W D Wulff, W E Bauta, R W Kaesler, P J Lankford, R A Miller, C K Murray, D C Yang *J. Am. Chem. Soc.* **112** 3642 (1990)
48. K Weiss, in *Transition Metal Carbene Complexes* (Weinheim: Verlag Chemie, 1983) p. 227
49. S-C Chang, Z H Kafafi, R H Hauge, J L Margrave, W E Billups *Tetrahedron Lett.* **28** 1733 (1987)
50. W A Herrmann, C Bauer *Chem. Ber.* **115** 14 (1982)
51. W A Herrmann, J M Huggins, C Bauer, M Smischek, H Pfisterer, M L Ziegler *J. Organomet. Chem.* **226** C59 (1982)
52. W A Herrmann, B Reiter, H Biersack *J. Organomet. Chem.* **97** 245 (1975)
53. M Creswick, I Bernal, W A Herrmann *J. Organomet. Chem.* **172** C39 (1979)
54. N M Boag, M Green, R M Mills, G N Pain, F G A Stone, P Woodward *J. Chem. Soc., Chem. Commun* 1171 (1980)
55. W A Herrmann, C Bauer, J Plank, W Kalcher, D Speth, M L Ziegler *Angew. Chem.* **93** 212 (1981)
56. I R McKeer, S J Sherlock, M Cowie *J. Organomet. Chem.* **352** 205 (1988)
57. M P Brown, J R Fisher, S J Franklin, R J Puddephatt, K B Seddon *J. Chem. Soc., Chem. Commun.* 749 (1978)
58. R B Calvert, J R Shapley *J. Am. Chem. Soc.* **99** 5225 (1977)
59. M Green, D R Henkey, M Murrey, A G Orpon, F G A Stone *J. Chem. Soc., Chem. Commun.* 689 (1981)
60. W A Herrmann *J. Organomet. Chem.* **250** 319 (1983)
61. K A Azam, A A Frew, B R Lioyd, L Manojlović-Muir, K W Muir, R J Puddephatt *J. Chem. Soc., Chem. Commun.* 614 (1982)
62. W A Herrmann, M L Ziegler, K Weidenhummer, H Biersack, K K Mayer, R D Minard *Angew. Chem.* **88** 191 (1976)
63. I A D'yakonov, A G Vitenberg *Zh. Org. Khim.* **3** 1153 (1967)
64. T Saegusa, Y Ito, T Shimizu, S Kobayashi *Bull. Chem. Soc. Jpn.* **42** 3535 (1969)
65. R G Salomon, J K Kochi *J. Am. Chem. Soc.* **95** 3300 (1973)
66. O M Nefedov, I E Dolgii, Yu V Tomilov, V G Bordakov *Izv. Akad. Nauk SSSR, Ser. Khim.* 119 (1984)
67. H Nozaki, H Tokaya, S Moriuti, R Noyori *Tetrahedron* **24** 3655 (1968)
68. Yu V Tomilov, V G Bordakov, I E Dolgii, O M Nefedov *Izv. Akad. Nauk SSSR, Ser. Khim.* 582 (1984)
69. M Green, J A K Howard, J L Spencer, F G A Stone *J. Chem. Soc., Dalton Trans.* 271 (1977)
70. A J Anciaux, A J Hubert, A F Noels, N Petiniot, P Teyssie *J. Org. Chem.* **45** 695 (1980)
71. E Müller, H Kessler, B Zech *Fortschr. Chem. Forsch.* **7** 128 (1966)
72. A Nakamura, T Yoshida, M Cowie, S Otsuka, J A Ibers *J. Am. Chem. Soc.* **99** 2108 (1977)
73. C P Casey, in *Reactive Intermediates* (Eds M Jones, R A Moss) (New York: Wiley, 1985) Vol. 3, p.109
74. R H Grubbs, in *Comprehensive Organometallic Chemistry* (Oxford: Pergamon Press, 1982) p. 499
75. M F Dull, P G Abend *J. Am. Chem. Soc.* **81** 2588 (1959)
76. W E Doering, W R Roth *Tetrahedron* **19** 715 (1963)
77. W Kirmse, M Capps, R B Hager *Chem. Ber.* **99** 2855 (1966)
78. W R Roth, J Konig *Liebigs Ann. Chem.* **688** 28 (1965)
79. A deMeijere, W Lüttke, F Heinrich *Liebigs Ann. Chem.* 306 (1974)
80. R G Salomon, J K Kochi *J. Organomet. Chem.* **43** C7 (1972)
81. R G Salomon, J K Kochi *J. Am. Chem. Soc.* **95** 1889 (1973)
82. W E Doering, J C Gilbert *Tetrahedron Suppl.* **7** 397 (1966)
83. F Heinrich, W Lüttke *Angew. Chem.* **84** 263 (1972)
84. D Kaufmann, A deMeijere *Chem. Ber.* **117** 1128 (1984)
85. J J Gajewski, L T Burka *J. Org. Chem.* **35** 2190 (1970)
86. J J Gajewski, L T Burka *J. Am. Chem. Soc.* **94** 8860 (1972)
87. L Fitjer, J M Conia *Angew. Chem.* **85** 349 (1973)
88. L Fitjer, J M Conia *Angew. Chem.* **85** 832 (1973)
89. N S Zefirov, K A Lukin, S I Kozhushkov, T I Kuznetsova, A M Domarev, I M Sosonkin *Zh. Org. Khim.* **25** 312 (1989)
90. W Kirmse *Angew. Chem.* 77 1 (1965)
91. W Kirmse, M Kapps *Angew. Chem.* 77 679 (1965)
92. W Kirmse, M Kapps *Chem. Ber.* **101** 994 (1968)
93. W Kirmse, H Arold *Chem. Ber.* **101** 1008 (1968)
94. M Kapps, W Kirmse *Angew. Chem.* **81** 86 (1969)
95. I E Dolgii, K N Shavrin, O M Nefedov *Izv. Akad. Nauk SSSR, Ser. Khim.* 135 (1987)
96. D L Muck, E R Wilson *J. Org. Chem.* **33** 419 (1968)
97. E Wenkert, R A Mueller, E J Reardon, S S Sathe, D J Scharf, G Tosi *J. Am. Chem. Soc.* **92** 7428 (1970)
98. T W Breitbell, D T Deunerlein, A E Fiebig, R E Kuznicki *J. Org. Chem.* **33** 3389 (1968)
99. USSR P. 852849; *Ref. Zh. Khim.* 9N104P (1981)
100. Yu V Tomilov, A B Kostitsyn, O M Nefedov *Izv. Akad. Nauk SSSR, Ser. Khim.* 2156 (1989)
101. Yu V Tomilov, A B Kostitsyn, E V Shulishov, O M Nefedov *Izv. Akad. Nauk SSSR, Ser. Khim.* 1141 (1990)
102. W E Doering, J F Coburn *Tetrahedron* 991 (1965)
103. J Chesick *J. Am. Chem. Soc.* **84** 3250 (1962)
104. E Müller, H Kessler *Tetrahedron Lett.* **9** 3037 (1968)
105. P Blickle, H Hopf, M Bloch, T B Jones *Chem. Ber.* **112** 3691 (1979)
106. W Kirmse, K Pohlmann *Chem. Ber.* **100** 3564 (1967)
107. USSR P. 825475; *Ref. Zh. Khim.* 22N92P (1981)
108. S Braun, W Lüttke *Chem. Ber.* **109** 320 (1976)
109. M Engelhard, W Lüttke *Angew. Chem.* **84** 346 (1972)
110. M E Kuehne, J C King *J. Org. Chem.* **38** 304 (1973)
111. U M Dzhemilev, V A Dokichev, S Z Sultanov, E E Shul'ts, Yu V Tomilov, O M Nefedov, G A Tolstikov, in *Primenenie Metallokompleksnogo Kataliza v Organicheskom Sinteze (Tezisy Dokladov)* [Application of Metal Complex Catalysis in Organic Synthesis (Abstracts of Reports)] (Ufa: 1989) p. 82
112. R W Thies, M Gasic, D Whalen, J B Grutzner, M Sakai, B Johnson, S Winstein *J. Am. Chem. Soc.* **94** 2262 (1972)
113. W R Roth *Liebigs Ann. Chem.* **671** 10 (1964)
114. E Vogel, W Wiedemann, K Kiefer, W F Harrison *Tetrahedron Lett.* **4** 673 (1963)

115. W W Frey, Dissertation, Universität Köln, 1966 (see Ref. 11, p. 109)
116. Yu V Tomilov, T L Mitenina, A I Lutsenko, I E Dolgii, S P Kolesnikov, O M Nefedov *Izv. Akad. Nauk SSSR, Ser. Khim.* 77 (1986)
117. U M Dzhemilev, V A Dokichev, I O Maidanova, O M Nefedov, Yu V Tomilov *Izv. Akad Nauk, Ser. Khim.* 733 (1993)
118. R E Pincock, J I Wells *J. Org. Chem.* **29** 965 (1964)
119. J Haywood-Farmer, R E Pincock, J I Wells *Tetrahedron* **22** 2007 (1966)
120. M A Battiste, M E Brennan *Tetrahedron Lett.* **7** 5857 (1966)
121. R Bicker, H Kessler, A Steigel *Tetrahedron Lett.* **14** 2371 (1973)
122. J Haywood-Farmer, H Malkus, M A Battiste *J. Am. Chem. Soc.* **94** 2209 (1972)
123. S C Clarke, K J Frayne, B L Johnson *Tetrahedron* **25** 1265 (1969)
124. B Halton, M A Battiste, R Rehberg, C L Deyrup, M E Brennan *J. Am. Chem. Soc.* **89** 5964 (1967)
125. G Wipff, K Morokuma *Tetrahedron Lett.* **21** 7445 (1980)
126. W R Roth, B Peltzer *Liebigs Ann. Chem.* **685** 56 (1965)
127. H Hemetsberger, W Brauer, D Tartler *Chem. Ber.* **110** 1586 (1977)
128. H Hemetsberger, W Holstein *Tetrahedron* **38** 3309 (1982)
129. A deMeijere, C Weitemeyer *Angew. Chem.* **82** 359 (1970)
130. A deMeijere, C Weitemeyer, O Schallner *Chem. Ber.* **110** 1504 (1977)
131. H Prinzbach, C Rucker *Tetrahedron Lett.* **18** 4195 (1977)
132. D Bosse, A deMeijere *Tetrahedron Lett.* **19** 965 (1978)
133. D Bosse, A deMeijere *Tetrahedron Lett.* **16** 871 (1975)
134. P G Gassman, A Topp, J M Keller *Tetrahedron Lett.* **10** 1093 (1969)
135. D H Aue, R N Reynolds *J. Org. Chem.* **39** 2315 (1974)
136. Yu V Tomilov, A B Kostitsyn, O M Nefedov *Izv. Akad. Nauk SSSR, Ser. Khim.* 1707 (1989)
137. E Müller, H Kessler, H Fricke, H Shur *Tetrahedron Lett.* **4** 1047 (1963)
138. R Herges *Synthesis* 1059 (1986)
139. Y Noichi, I Moritani, N Obata, H Fujita, I Kawanichi *Koguo Kagaku Zasshi* **69** 1491 (1966); *Chem. Abstr.* **66** 94585g (1967)
140. A E Vasil'vitskii , Candidate's Thesis in Chemical Sciences, Institute of Organic Chemistry of the USSR Academy of Sciences, Moscow, 1979, p. 63
141. F W Fowler *Angew. Chem.* **83** 147 (1971)
142. S R Tanny, J Grossman, F W Fowler *J. Am. Chem. Soc.* **94** 6495 (1972)
143. V M Shostakovskii, A E Vasil'vitskii, A U Musaev, O M Nefedov *Azotsoderzhashchie Geterotsikly (Tezisy Dokladov IV Vsesoyuznoi Konferentsii po Khimii Azotsoderzhashchikh Geterotsiklicheskikh Soedinenii)* [Nitrogen-containing Heterocycles (Abstracts of Reports at the IVth All-Union Conference on the Chemistry of Nitrogen-containing Heterocyclic Compounds)] (Novosibirsk: 1987) p. 88
144. A Attia *J. Indian Chem. Soc.* **16B** 98 (1978)
145. M Ferles, A Attia *Z. Chem.* **11** 18 (1971)
146. J A Beron, S S Olin *J. Am. Chem. Soc.* **91** 777 (1969)
147. H J Callot *Tetrahedron Lett.* **13** 1011 (1972)
148. E L Hoel, G B Ansell, S Leta *Organometallics* **3** 1633 (1984)
149. R Paulissen, A J Hubert, P Teysie *Tetrahedron Lett.* **13** 1465 (1972)
150. J Kottwitz, H Vorbruggen *Synthesis* 636 (1975)
151. U Mende, B Raduchel, W Skuballa, H Vorbruggen *Tetrahedron Lett.* **16** 629 (1975)
152. Yu V Tomilov, V G Bordakov, I E Dolgii, in *XII Mendeleevskii S'ezd po Obshchei i Prikladnoi Khimii (Tezisy Dokladov)* [The XIIth Mendeleev Congress on General and Applied Chemistry (Abstracts of Reports)] (Moscow: Nauka, 1981) Vol. 2, p. 36
153. M Suda *Synthesis* 714 (1981)
154. A Gangadhar, R Subbarao, G Lakshminarayana *J. Am. Oil Chem. Soc.* **65** 601 (1988)
155. Yu V Tomilov, A B Kostitsyn, V A Dokichev, U M Dzhemilev, O M Nefedov *Izv. Akad. Nauk SSSR, Ser. Khim.* 2752 (1989)
156. Yu V Tomilov, A B Kostitsyn, E V Shulishov, O M Nefedov *Synthesis* 246 (1990)
157. O M Nefedov, Yu V Tomilov, A B Kostitsyn, U M Dzhemilev, V A Dokitchev *Mendeleev Commun.* 13 (1992)
158. Yu V Tomilov, A B Kostitsyn, E V Shulishov, A Kh Khusid, O M Nefedov *Izv. Akad. Nauk SSSR, Ser. Khim.* 2746 (1989)
159. U M Dzhemilev, V A Dokichev, S Z Sultanov, S L Khursan, O M Nefedov, Yu V Tomilov, A B Kostitsyn *Izv. Akad. Nauk, Ser. Khim.* 2353 (1992)
160. R A Periana, R G Berman *J. Am. Chem. Soc.* **108** 7346 (1986)
161. USSR P. 961 328; *Ref. Zh. Khim.* 19O57P (1986)
162. P Fontani, B Carboni, M Vaultier, R Carrie *Tetrahedron Lett.* **30** 4815 (1989)
163. I V Kazimirchik, K A Lukin, G F Bebikh, N S Zefirov *Zh. Org. Khim.* **19** 105 (1983)
164. N S Zefirov, S I Kozhushkov, T S Kuznetsova, O V Kokoreva, K A Lukin, B I Ugrak, S S Tratch *J. Am. Chem. Soc.* **112** 7702 (1990)
165. K A Lukin, A A Andrievskii, A Yu Masunova, N S Zefirov *Dokl. Akad. Nauk SSSR* **316** 379 (1991)
166. K A Lukin, S I Kozhushkov, A A Andrievski, B I Ugrak, N S Zefirov *J. Org. Chem.* **56** 6176 (1991)
167. K A Lukin, S I Kozhushkov, A A Andrievski, B I Ugrak, N S Zefirov *Mendeleev Commun.* 51 (1992)
168. N S Zefirov, S I Kozhushkov, B I Ugrak, K A Lukin, O V Kokoreva, D S Yufit, Yu T Struchkov, S Zoeliner, R Boese, A deMeijere *J. Org. Chem.* **57** 701 (1992)
169. B Spur, A Crea, W Peters *Z. Naturforsch.* **39B** 125 (1984)
170. L-E Arvidson, A M Johannson, U Hacksell, J L Nilsson, K Svensson, S Hjorth, T Magnusson, A Carlsson, P Lindberg, B Andersson, D Sanchez, H Wikstrom *J. Med. Chem.* **31** 92 (1988)
171. P W Erhardt, R J Gorczynski, W G Anderson *J. Med. Chem.* **22** 907 (1979)
172. K Rehse, S Behncke, U Siemann, W Kehr *Arch. Pharm. (Weinheim, Ger.)* **313** 221 (1980)
173. B Raduchel, U Mende, G Cleve, G -A Hoyer, H Vorbruggen *Tetrahedron Lett.* **16** 633 (1975)
174. N Kurokawa, Y Ohfune *Tetrahedron Lett.* **26** 83 (1985)
175. Jpn. P. 61-33149; *Ref. Zh. Khim.* 24O390P (1987)
176. V A Dokichev, I O Maidanova, U M Dzhemilev, O M Nefedov, Yu V Tomilov, I M Levina, A V Kamernitskii *Pyataya Konferentsiya po Khimii Karbenov (Tezisy Dokladov)* [The Fifth Conference on Carbene Chemistry (Abstracts of Reports)] (Moscow: 1992) p. 116
177. N S Zefirov, K A Lukin, A Yu Timofeeva *Zh. Org. Khim.* **23** 2545 (1987)
178. N S Zefirov, S I Kozhushkov, T S Kuznetsova, K A Lukin, I V Kazimirchik *Zh. Org. Khim.* **24** 673 (1988)
179. K A Lukin, N S Zefirov *Zh. Org. Khim.* **23** 2548 (1987)
180. K A Lukin, N S Zefirov *Zh. Org. Khim.* **25** 92 (1989)
181. K A Lukin, T S Kuznetsova, S I Kozhushkov, V A Piven', N S Zefirov *Zh. Org. Khim.* **24** 1644 (1988)
182. B Bogdanovich, M Kroner, G Wilke *Liebigs Ann. Chem.* **699** 1 (1966)
183. U M Dzhemilev, V A Dokichev, S Z Sultanov, S L Khursan, O M Nefedov, Yu V Tomilov *Pyataya Konferentsiya po Khimii Karbenov(Tezisy Dokladov)* [The Fifth Conference on Carbene Chemistry (Abstracts of Reports)] (Moscow: 1992) p. 114
184. I V Kazimirchik, K A Lukin, N S Zefirov *Zh. Org. Khim.* **22** 1554 (1986)
185. O Pilet, A Chollet, P Vogel *Helv. Chim. Acta* **62** 2341 (1979)
186. I V Kazimirchik, K A Lukin, A A Borisenko, G F Bebikh, S S Yarovoi, N S Zefirov *Zh. Org. Khim.* **18** 582 (1982)
187. I V Kazimirchik, K A Lukin, S K Rodkina, G F Bebikh, N S Zefirov *Zh. Org. Khim.* **20** 1221 (1984)
188. I Dinulescu, L N Enescu, A Ghencinlescu, M Avram *J. Chem. Res. (S)* 456 (1978)
189. U M Dzhemilev, R I Khusnutdinov, V A Dokichev, S Z Sultanov, G A Tolstikov *Izv. Akad. Nauk SSSR, Ser. Khim.* 1083 (1988)
190. I V Kazimirchik, K A Lukin, I L Taranyuk, G F Bebikh, N S Zefirov *Zh. Org. Khim.* **21** 313 (1985)
191. I V Kazimirchik, K A Lukin, G F Bebikh, N S Zefirov *Zh. Org. Khim.* **19** 253 (1983)
192. J Spanget-Larsen, R Gleiter *Tetrahedron Lett.* **23** 2435 (1982)
193. U M Dzhemilev, V A Dokichev, I O Maidanova, I R Kazyrgalin, O M Nefedov, Yu V Tomilov *Pyataya Konferentsiya po Khimii Karbenov (Tezisy Dokladov)* [The Fifth Conference on Carbene Chemistry (Abstracts of Reports)] (Moscow: 1992) p. 115

194. K A Lukin, N S Zefirov *Zh. Org. Khim.* **24** 1648 (1988)
195. N S Zefirov, T S Kuznetsova, O V Eremenko, O V Kokoreva *Mendeleev Commun.* 91 (1993)
196. I V Kazimirchik, K A Lukin, G F Bebikh, N S Zefirov *Zh. Org. Khim.* **20** 1691 (1984)
197. K A Lukin, N V Averina, N S Zefirov *Zh. Org. Khim.* **24** 1776 (1988)
198. K A Lukin, N S Zefirov *Zh. Org. Khim.* **25** 202 (1989)
199. K A Lukin, N S Zefirov *Zh. Org. Khim.* **26** 289 (1990)
200. R Noyori, H Takaya, Y Nakanisi, H Nozaki *Can. J. Chem.* **47** 1242 (1969)
201. T Aratani, Y Nakanisi, H Nozaki *Tetrahedron* **26** 1675 (1970)
202. M P Doyle *Recl. Trav. Chim. Pays-Bas* **110** 305 (1991)
203. H Abdallah, R Gree, R Carrie *Tetrahedron Lett.* **23** 503 (1982)
204. J Vallgarda, U Hacksell *Tetrahedron Lett.* **32** 5625 (1991)
205. Yu V Tomilov, A B Kostitsyn, O M Nefedov *Izv. Akad. Nauk SSSR, Ser. Khim.* 2878 (1987)
206. O M Nefedov, Yu V Tomilov, A B Kostitsyn, in *Organic Chemistry: Technological Perspectives* (Abstracts of 2nd International IUPAC Symposium) (Baden-Baden, 1991) p. 111
207. E Müller, H Fricke, W Rundel *Z. Naturforsch.* **15B** 753 (1960)
208. E Müller, H Fricke *Liebigs Ann. Chem.* **661** 38 (1963)
209. P Müller, J Rocek *J. Org. Chem.* **33** 3001 (1968)
210. U M Dzhemilev, V A Dokichev, S Z Sultanov, R A Sadykov, G A Tolstikov, O M Nefedov *Izv. Akad. Nauk SSSR, Ser. Khim.* 1063 (1991)
211. E Müller, H Kessler, H Fricke, W Kiedaisch *Liebigs Ann. Chem.* **675** 63 (1964)
212. E Müller, H Fricke, H Kessler *Tetrahedron Lett.* **4** 1501 (1963)
213. R W Hoffmann, K R Eicken, H J Luthardt, B Dittrich *Tetrahedron Lett.* **10** 3789 (1969)
214. A J Anciaux, A Demonceau, A F Noels, A J Hubert, R Warin, P Teyssie *J. Org. Chem.* **46** 873 (1981)
215. R P Hughes, in *Comprehensive Organometallic Chemistry* (Oxford: Pergamon Press, 1982) Vol. 5, p. 277
216. M J S Dewar *Theory of Molecular Orbitals in Organic Chemistry* (Translated into Russian; Moscow: Mir, 1977)
217. R Nader, A deMeijere *Angew. Chem.* **88** 153 (1976)
218. H Horita, T Otsubo, Y Sakata, S Misumi *Tetrahedron Lett.* **17** 3899 (1976)
219. K Menke, H Hopf *Angew. Chem.* **88** 152 (1976)
220. H Hopf, C Marquard, in *Strain and Its Implications in Organic Chemistry* (Eds A deMeijere, S Blechert) (Dordrecht: Kluwer Academic Publishers, 1989) p. 297
221. E Müller, H Fricke, H Kessler *Tetrahedron Lett.* **5** 1525 (1964)
222. W Grimme, H Hoffmann, E Vogel *Angew. Chem.* **77** 348 (1965)
223. E Vogel, R Feldmann, H Duwel *Tetrahedron Lett.* **11** 1941 (1970)
224. E Müller, H Kessler *Liebigs Ann. Chem.* **692** 58 (1966)
225. E Müller, H Kessler, H Suhr *Tetrahedron Lett.* **6** 423 (1965)
226. E Müller, H Kessler *Tetrahedron Lett.* **6** 2673 (1965)
227. L S Kobrina, G G Yakobson, N N Vorozhtsov *Zh. Vses. Khim. Ova im. D. I. Mendeleeva* **12** 597 (1967)
228. E Müller, B Zeeh, R Heischkeil, H Fricke, H Suhr *Liebigs Ann. Chem.* **662** 38 (1963)
229. B Eistert, in *New Methods of Preparative Organic Chemistry* (Translated into Russian; Moscow: Inostr. Lit., 1950) p. 91
230. C D Gutshe, in *Organic Reactions* (Translated into Russian; Moscow: Inostr. Lit., 1956) Vol. 8, p. 469
231. *Methoden der Organischen Chemie (Houben Weyl)* (Stuttgart: Georg Thieme, 1968) Vol. X/4, p. 712
232. *Methoden der Organischen Chemie (Houben Weyl)* (Stuttgart: Georg Thieme, 1976) Vol. VII/2b, Part 2, p. 1855
233. C D Gutsche, D Redmore *Carbocyclic Ring Expansion Reactions* (New York: Academic Press, 1968)
234. S Patai (Ed.) *The Chemistry of Diazonium and Diazo Groups* (New York: Wiley, 1978) p. 575
235. G D Meakins, D Morris *J. Chem. Soc. C* 394 (1967)
236. J B Jones, P Price *Can. J. Chem.* **44** 999 (1966)
237. J B Jones, J M Zander *Can. J. Chem.* **46** 1913 (1968)
238. J B Jones, P Price *J. Chem. Soc., Chem. Commun.* 1478 (1969)
239. G R Krow *Tetrahedron* **43** 3 (1987)
240. E Müller, M Bauer, W Rundel *Tetrahedron Lett.* **1** 30 (1960)
241. E Müller, M Bauer, W Rundel *Z. Naturforsch.* **15B** 268 (1960)
242. H O House, E J Grubbs, W F Gannon *J. Am. Chem. Soc.* **82** 4099 (1960)
243. E Müller, M Bauer *Liebigs Ann. Chem.* **654** 92 (1962)
244. E Müller, R Berele, M Bauer, W Kiedasch *Liebigs Ann. Chem.* **689** 65 (1965)
245. K Naemura, T Katon, R Fukunaga, H Chikamatsu, M Nakazaki *Bull. Chem. Soc. Jpn.* **58** 1407 (1985)
246. M Nakazaki, K Naemura, M Hashimoto *Bull. Chem. Soc. Jpn.* **56** 2543 (1983)
247. E Müller, B Zeeh, R Heischkeil *Liebigs Ann. Chem.* **677** 47 (1964)
248. W S Johnson, M Neeman, S P Birkeland, N A Fedoruk *J. Am. Chem. Soc.* **84** 989 (1962)
249. W S Johnson, M Neeman, S P Birkeland *Tetrahedron Lett.* 1 (1960)
250. E Müller, R Heischkeil *Tetrahedron Lett.* **5** 2809 (1964)
251. Y Noichi *Nippon Kagaku Zasshi* **88** 565 (1967); *Chem. Abstr.* **69** 10389x (1968)
252. V A Dokichev, R M Nasybullina, in *Primenenie Metallokompleksnogo Kataliza v Organicheskom Sinteze (Tezisy Dokladov)* [Application of Metal Complex Catalysis in Organic Synthesis (Abstracts of Reports)] (Ufa: 1989) p. 87
253. Russ. Fed. P. 1 657 502; *Ref. Zh. Khim.* 2N115P (1992)
254. H Meerwein, G Hinz *Liebigs Ann. Chem.* **484** 1 (1931)
255. E Müller, W Rundel *Angew. Chem.* **70** 105 (1958)
256. E Müller, M Bauer, W Rundel *Z. Naturforsch.* **14B** 209 (1959)
257. M C Caserio, J D Roberts, M Neeman, W S Johnson *J. Am. Chem. Soc.* **80** 2584 (1958)
258. M Neeman, M C Caserio, J D Roberts, W S Johnson *Tetrahedron* **6** 36 (1959)
259. E Müller, R Heischkeil, M Bauer *Liebigs Ann. Chem.* **677** 55 (1964)
260. C E H Bawn, A Ledwith *Chem. Ind. (London)* 1389 (1958)
261. G J P Chittenden *Carbohydr. Res.* **43** 366 (1975)
262. M Neeman, Y Hashimoto *J. Am. Chem. Soc.* **84** 2972 (1962)
263. E G Gross, S M Flematti *Chem. Ind. (London)* 1556 (1966)
264. I O Mastronardi, S M Flematti, J O Deferrari, E G Gross *Carbohydr. Res.* **3** 177 (1966)
265. J O Deferrari, E G Gross, I O Mastronardi *Carbohydr. Res.* **4** 432 (1967)
266. M Neeman, W S Johnson, in *Organic Synthesis* (New York: Wiley, 1961) Vol. 41, p. 9
267. K Ohno, H Nishiyama, H Nagase *Tetrahedron Lett.* **20** 4405 (1979)
268. H Ogawa, T Hagiwara, T Chinara, S Teratan, K Taya *Bull. Chem. Soc. Jpn.* **60** 627 (1987)
269. V A Dokichev, I O Maidanova, in *Primenenie Metallokompleksnogo Kataliza v Organicheskom Sinteze (Tezisy Dokladov)* [Application of Metal Complex Catalysis in Organic Synthesis (Abstracts of Reports)] (Ufa: 1989) p. 86
270. Russ. Fed. P. 1 699 992; *Ref. Zh. Khim.* 2N22P (1993)
271. E Müller, H Huber-Emden, W Rundel *Liebigs Ann. Chem.* **623** 34 (1959)
272. E Müller, W Rundel, H Huber-Emden *Angew. Chem.* **69** 614 (1957)
273. H Zinner, O Schmitt, W Schritt, G Rembarz *Chem. Ber.* **90** 2852 (1957)
274. J W Ralls *J. Org. Chem.* **26** 66 (1961)
275. W J Theuer, J A Moore *J. Org. Chem.* **32** 1602 (1967)
276. I Saegusa, Y Ito, S Kobayashi, K Hirita, T Shimuzu *Tetrahedron Lett.* 7 6131 (1966)
277. J Kang, S W Lee, W J Kim *Bull. Korean Chem. Soc.* **6** 379 (1985); *Chem. Abstr.* **105** 114657m (1986)
278. Jpn. P. 80-141418; *Chem. Abstr.* **94** 102 813 (1981)
279. Russ. Fed. P. 1 699 995; *Ref. Zh. Khim.* 2N37P (1993)
280. H Hoberg *Liebigs Ann. Chem.* **707** 147 (1967)
281. D Seyferth, E G Rochow *J. Am. Chem. Soc.* **77** 907 (1955)
282. M Weidenbruch, C Pierrard *Chem. Ber.* **110** 1545 (1977)
283. M Lesbre, R Buisson *Bull. Soc. Chim. Fr.* 1204 (1957)
284. K A W Kramer, A N Wright *J. Chem. Soc.* 3604 (1963)

Russian Chemical Reviews **62** (9) 839 – 850 (1993)
© 1993 Russian Academy of Sciences and Turpion Ltd

UDC 547.512'72 + 547.512'514

Activated cyclopropanes in the synthesis of five-membered carbocycles and heterocycles

O G Kulinkovich

Contents

I. Introduction 839
II. Synthesis of five-membered carbocyclic compounds 839
III. Synthesis of five-membered heterocycles 844

Abstract. The conversion of functionalised cyclopropane compounds to derivatives of cyclopentane and five-membered heterocycles is described. Topics discussed include reaction conditions, the regio- and stereo-selectivity of the reactions depending on the type of substituents in the three-membered ring, and also the main procedures for obtaining appropriate cyclopropane substrates. The bibliography comprises 174 references.

I. Introduction

Although the history of the chemistry of cyclopropane compounds stretches back more than a hundred years[1] the extensive use of this class of compounds as intermediates in organic synthesis began not much more than thirty years ago. Owing to the development of carbene methods for converting olefins to cyclopropane and to other effective approaches to the construction of a three-membered carbon ring,[2-8] various functional derivatives of cyclopropane have become accessible and in addition many synthetically useful reactions that involve opening of a three-membered ring have been found.[2,5-15]

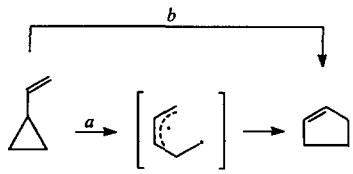
The main problem in using cyclopropane compounds in organic synthesis lies in securing high selectivity for two types of reaction: the formation and opening of a three-membered ring of carbon atoms. In many instances the nature of the substitution in the ring presupposes the possibility of both the straightforward production of the corresponding cyclopropane derivative and also chemo- and regio-selective cleavage of one of the three carbon–carbon bonds. A large amount of data has already been accumulated on the effect of substituents on the geometry of a three-membered carbon ring[16-21] and its energy characteristics.[16,20-24] Rules for predicting variations in the carbon–carbon bond lengths in a cyclopropane ring have been summarised:[20] π-electron-acceptor substituents, and also π- and σ-electron-donor substituents, that occur in a favourable conformation with respect to the cyclopropane ring cause lengthening of the adjacent bonds and shortening of the opposite bond whereas σ-electron-acceptor substituents have the opposite effect. Bearing in mind the normally observed direct correlation between the length of a carbon–carbon bond and its tendency to rupture, and also the predominant influence on this process of the π-electronic effects of substituents in a 'bisectrix' conformation for electron acceptors and a 'perpendicular' conformation for electron donors,[7,16,21] we may expect preferential rupture of the bonds in the ring that are adjacent to such substituents. Many experimental data are compatible with these conclusions,[7-12,15,16,25] so enabling us, in many instances, to make a reliable prediction of the results of possible conversions of 'activated cyclopropanes' and to design synthesis schemes involving them effectively. In the present review published data on the conversion of activated cyclopropanes to cyclopentane derivatives and five-membered heterocycles containing one hetero-atom (one of the best developed areas of the use of cyclopropanes in organic synthesis) are arranged systematically.

O G Kulinkovich Department of Organic Chemistry and the Chemistry of High-molecular-mass Compounds, Belarussian State University, prosp. F. Skoriny 4, 220050 Minsk, Belarus, Fax (7-017-2) 20 82 72

Received 28 May 1993
Uspekhi Khimii **62** (9) 887 – 899 (1993); translated by G J Bullen

II. Synthesis of five-membered carbocyclic compounds

The most important approach to the construction of five-membered carbocycles on the basis of cyclopropane precursors is the vinylcyclopropane–cyclopentene rearrangement.[26,27] The thermal version of this rearrangement[27] is usually effected at temperatures above 250 °C and can take place by a biradical mechanism (*a*)[28] or a concerted mechanism (*b*).[26-31]

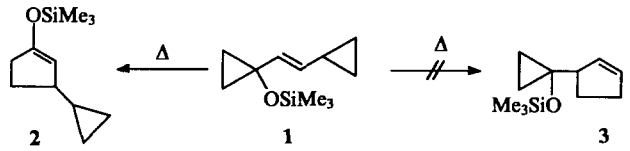


Considerable progress has also been achieved in the development of methods for synthesising cyclopentane systems using intra- and inter-molecular cyclisations, such as [3 + 2]-cycloaddition and intramolecular ring formation, with one or two carbon atoms from a cyclopropane ring incorporated in the newly generated cyclic system.[9-15,32-35]

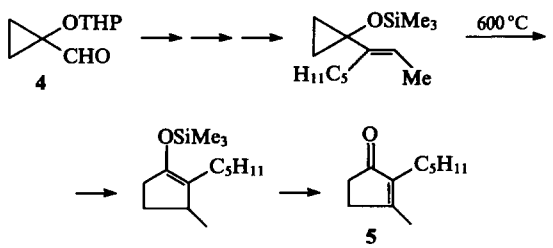
1. The vinylcyclopropane–cyclopentene rearrangement

Electron-donor substituents in the three-membered carbon ring, in either geminal or vicinal positions with respect to the vinyl group, considerably facilitate the occurrence of this rearrangement.[26] For example, the activating effect of a trimethylsiloxy group on the opening of a cyclopropane ring to which it is attached is clearly illustrated by the thermal

rearrangement of 1-(2-cyclopropylvinyl)-1-trimethylsiloxycyclopropane **1** which gives 3-cyclopropyl-1-trimethylsiloxycyclopent-1-ene **2** exclusively, but none of the isomeric compound **3**.[36]

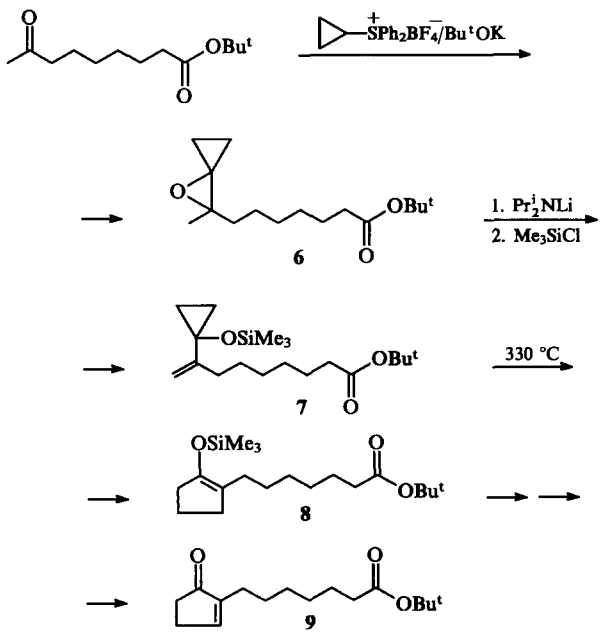


Several ways of obtaining substituted 1-trimethylsiloxyvinylcyclopropanes have currently been developed, starting from accessible hemiacetals of cyclopropanone,[12] oxaspiropentanes,[37] silyl ethers of enols,[38] 1-hydroxycyclopropylcarbonyl compounds[39] and certain other substrates.[40] This has enabled methods for synthesising different types of the cyclopentane system, including a number of natural compounds, to be proposed.[36,39,41-43] The methodology of the production of 2,3-disubstituted cyclopentenones starting from the available 1-tetrahydropyranyloxy-1-formylcyclopropane **4** can be followed using as an example the synthesis of dihydrojasmone **5** (with a total yield of 61%).

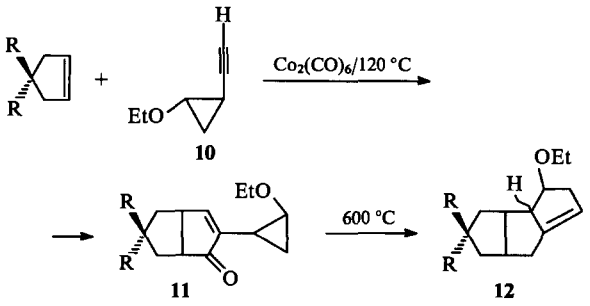


THP = tetrahydropyranyl.

The conversion of the keto-group in esters of 8-oxononanoic acid to a vinylcyclopropane group is accomplished via the intermediate formation of the corresponding oxaspiropentane **6**, isomerisation of the epoxide ring, and then silylation of the hydroxyl group. Thermal rearrangement of the resultant substituted trimethylsiloxycyclopropane **7** gives an ester of an enol **8** that is readily converted to the 2-substituted cyclopentenone **9**, which is used as a precursor of homoprostaglandins.[44] The use of cyclic ketones as the initial substrates enables the corresponding condensed systems to be synthesised.[33]

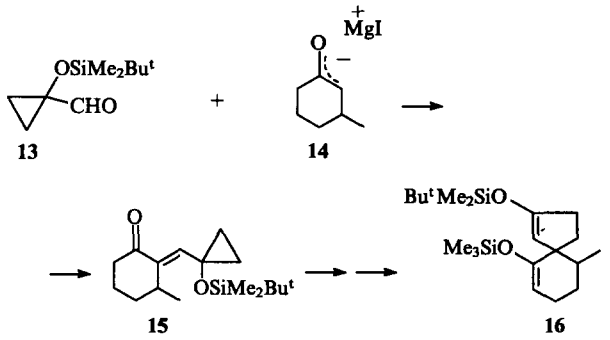


A combination of the cycloaddition of the dicobalt hexacarbonyl complex of the cyclopropylalkyne **10** to olefins and the vinylcyclopropane–cyclopentene isomerisation of the resultant cycloaddition products **11** makes it possible to carry out successive fusion of cycloalkenes to form tricyclic systems **12**.[45]

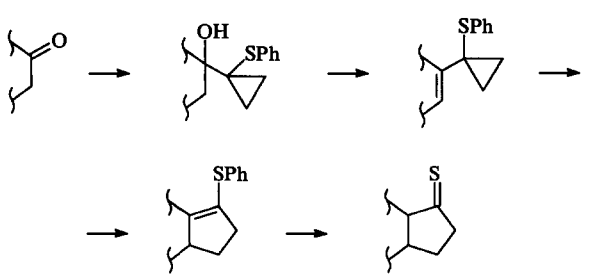


R = H, Me.

The *tert*-butyldimethylsilyl ether of 1-hydroxy-1-formylcycloproane **13** can be used for the synthesis of substituted vinylcyclopropane systems by a Wittig reaction or an aldol condensation.[47] For example, if the enolate anion **14**, which is obtained by the copper-iodide-catalysed addition of methylmagnesium iodide to cyclohex-2-enone, is captured by the aldehyde **13** the corresponding ketol is obtained and after its dehydration the siloxyvinylcyclopropane **15** can be isolated in a 73% yield (based on the aldehyde **13**). After a trimethylsilylation stage and vinylcyclopropane–cyclopentene rearrangement, **15** is converted to the spirocyclic derivative **16**.[47]

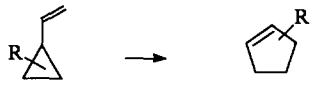


The main limitations of the methods described above for constructing cyclopentane systems on the basis of 1-oxo-substituted vinylcyclopropanes are usually due to difficulties in obtaining the latter. There is therefore considerable interest in the possible use of available 1-(phenylthio)cyclopropyllithium reagents for the introduction of a cyclopropane fragment into ketonic substrates.[48-50] For the formation of a cyclopentane ring the successive stages are indicated in a general form by the following scheme:[51,52]



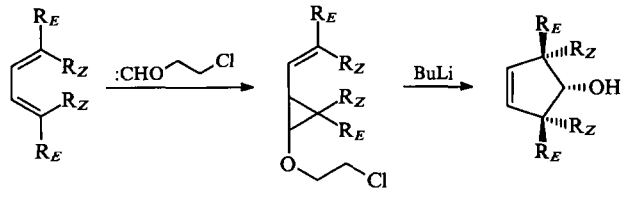
The yields are high at each of these stages and the vinylcyclopropane–cyclopentene rearrangement of 1-(phenylthio)-cyclopropyl derivatives takes place at even lower temperatures than in the case of the corresponding oxo-compounds.[27]

Electron-donor substituents in position 2 of the vinylcyclopropanes facilitate the thermal rearrangement of these compounds to a greater extent than the same substituents in position 1.[53–55]

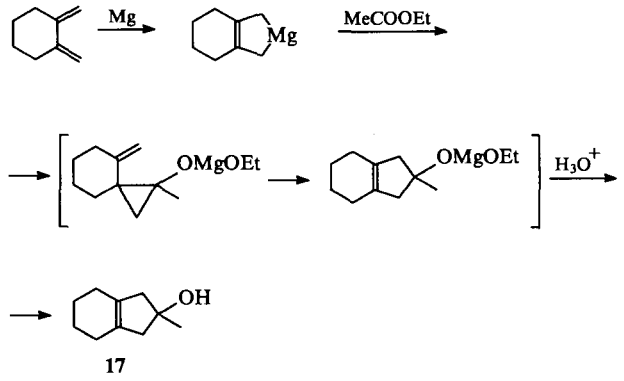


R	E_a/kcal mol^{-1}
H	49.7
1-OMe	44.7
2-OMe	38.7
2-NMe_2	31.1

When there are anionic substituents present in the ring the vinylcyclopropane–cyclopentene rearrangement takes place at room temperature or below.[56,57] In this case the reaction is by and large highly selective [4 + 1]-ring formation[57] whereas in the usual versions the rearrangement often takes place with only moderate stereoselectivity.[58]

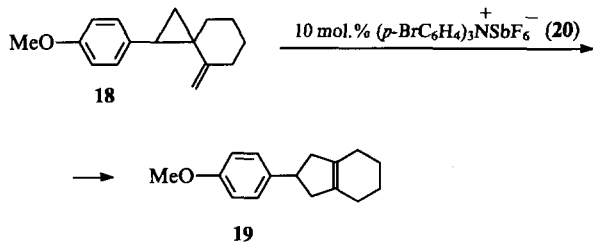


An alternative version involving the conversion of 1,3-dienes to the corresponding 3-cyclopentenols was proposed recently.[59] An example of this is the production of the bicyclic derivative **17** by treatment of the magnesium complex of 1,2-bis-(methylene)cyclohexane with esters followed by rearrangement of the resultant magnesium alkoxides of vinylcyclopropanols, which also occurs under exceptionally mild conditions.



17

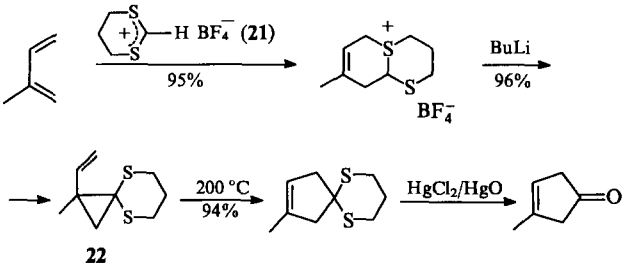
Ring expansion in vinylcyclopropane systems containing electron-donor substituents can also be expedited by the previous one-electron oxidation of the hetero-atom, an example being rearrangements of *p*-anisyl-substituted vinylcyclopropanes.[60] Thus in the presence of catalytic quantities of the one-electron oxidant **20**, rearrangement of **18** to the bicyclic derivative **19** will occur in 5 min at room temperature, with an 86% yield.



18

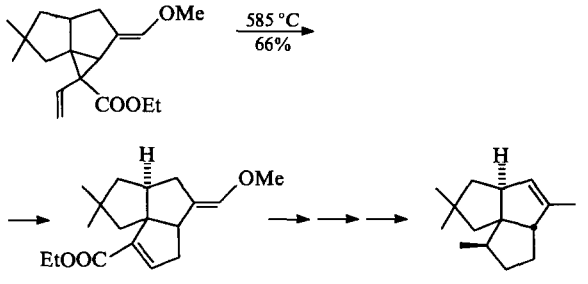
19

The 1,3-dithienium tetrafluoroborate **21** can also be used as a source of the single-carbon component in [4 + 1]-ring formation processes proceeding via a stage in which the corresponding activated vinylcyclopropane **22** is formed.[61]



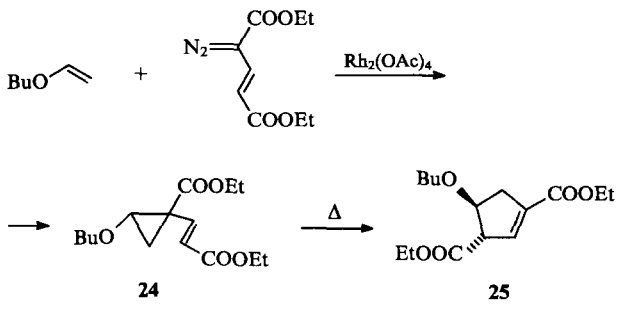
22

There are many examples of rearrangements of vinylcyclopropanes containing acceptor substituents in the ring; these usually occur under more mild conditions than the rearrangements of the corresponding unsubstituted compounds (see Refs 26 and 32). An example of the use of this type of rearrangement in the synthesis of natural compounds is the key stage in the construction of the non-linear tricyclic pentalene system **23**.[62]



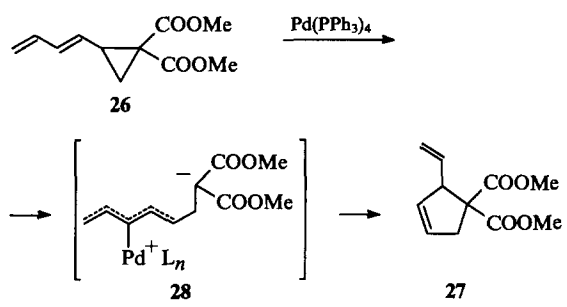
23

Compounds containing *p*-electron-donor and π-acceptor substituents in vicinal positions in the cyclopropane ring undergo the vinylcyclopropane–cyclopentene rearrangement particularly easily.[26,63] For example, the butoxyvinylcyclopropane **24**, unlike compounds with a similar structure that contain no alkoxy substituent, is unstable under chromatographic conditions and when its distillation is attempted it undergoes a smooth rearrangement to give the substituted cyclopentene **25** (total yield 61%).[63]

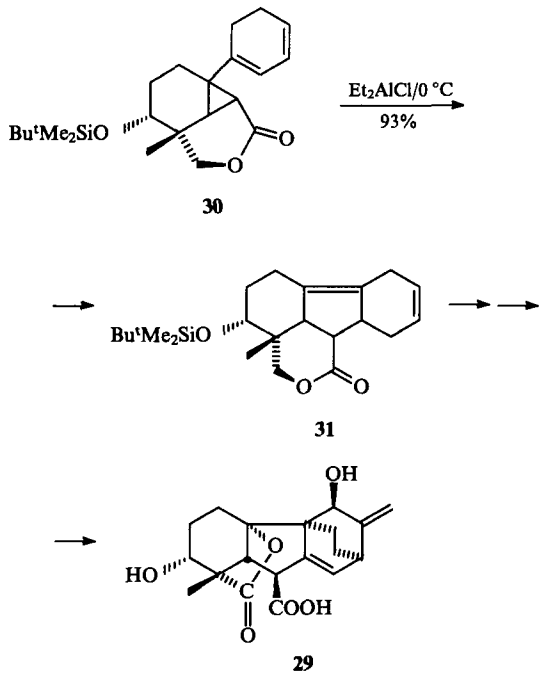


24 **25**

The presence of carbonyl substituents linked to the cyclopropane ring enables catalytic variants of the vinylcyclopropane–cyclopentene rearrangement to be carried out.[26,64–70] For example, the butadienylcyclopropane **26**, which contains two activating methoxycarbonyl groups, undergoes rearrangement to the corresponding vinylcyclopentene **27** at 50 °C (with an 87% yield) in the presence of catalytic quantities of $Pd(PPh_3)_4$. With other acceptor substituents the rearrangement can take place at even lower temperatures.[71] It is proposed[71] that the reaction occurs via nucleophilic attack by Pd^0 on the diene group to form the zwitter-ion **28**.

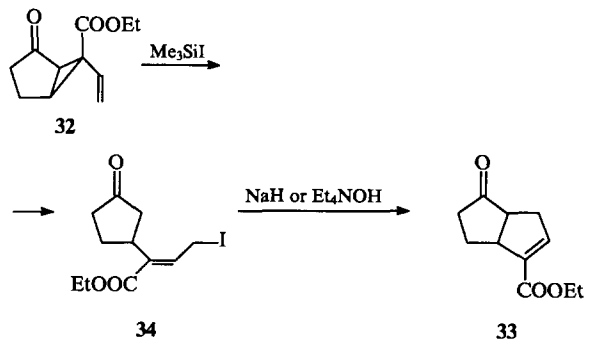


An extremely effective catalyst of the rearrangement of vinylcyclopropanes containing an ester function is diethylaluminium chloride.[66–88] It has been used to synthesise the tricyclic system of antheridic acid (**29**) (see Refs 67 and 68) via a stage in which the lactone **30** undergoes rearrangement to **31**, whereas an attempt to achieve this conversion by heating was unsuccessful.

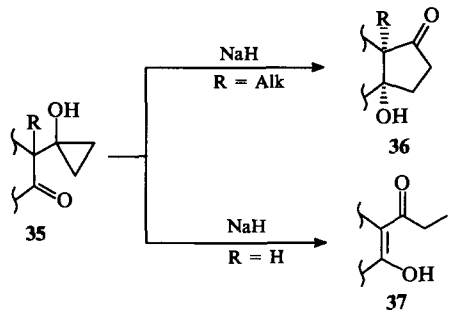


2. Other reactions that are accompanied by intramolecular cyclisation

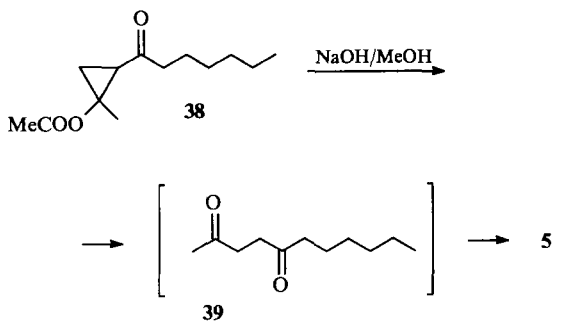
Complementary to the single-stage versions of the vinylcyclopropane–cyclopentene rearrangement considered above are procedures in which expansion of the ring in activated cyclopropanes to the corresponding cyclopentane derivatives is often accomplished by using consecutive heterocyclic ring opening and closure reactions, which are usually achievable in two or more stages. For example, conversion of the vinylcyclopropane derivative **32** to the bicyclanone **33** can be carried out under exceptionally mild conditions by opening the three-membered ring (which is activated by acceptor substituents) with trimethyliodosilane and then carrying out cyclisation of the iodoketone product **34** under the action of strong bases.[72,73]

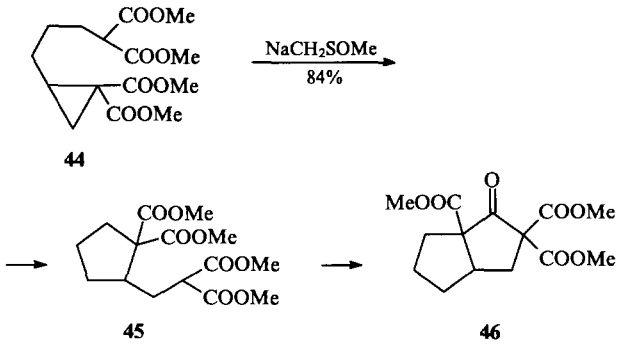


The ketone **32**, as well as a number of its analogues, are easily accessible and are readily formed by the reaction of the corresponding unsaturated cyclic ketones with the lithium dienolates of esters of α-bromocrotonic acid or its derivatives. In general, a sequence of conversions of cycloalkenones to the corresponding bicyclic derivatives is an effective method of [3 + 2]-ring formation which has been used successfully to synthesise a number of natural compounds.[72–74] A new variant of [3 + 2]-ring formation that has been developed recently for the synthesis of steroids[75] is based on intramolecular capture of the homoenolate anion that is generated when the cyclopropane ring in the 1-(2-ketoalkyl)cyclopropanols **35** is opened by the action of sodium hydride,[75–77] forming the corresponding cyclopentanols **36** or products obtained from them in further reactions. When a hydrogen atom is present in the position α to the carbonyl group and to the three-membered ring isomerisation to the ethyl ketones **37**, which is normal for substituted cyclopropanols, is observed.[76]

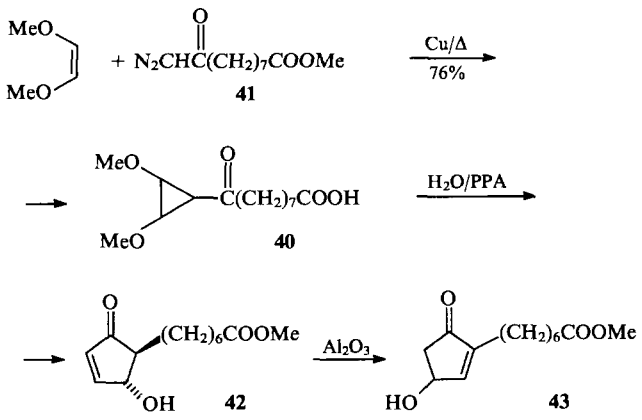


Carbonyl derivatives of cyclopropane with electron-donor substituents in a vicinal position will undergo solvolytic ring opening reactions under exceptionally mild conditions to give the corresponding 1,4-dicarbonyl derivatives or their latent forms.[7,11,25] These compounds are, as is well known, one of the most effective sources for obtaining substituted cyclopentenones by intramolecular cyclisation;[35] this provides a basis for using a sequence of such transformations in the development of effective methods for synthesising a number of cyclopentane derivatives.[78–81] For example, the reaction of the acetoxycyclopropyl ketone **38** with sodium hydroxide gives an 83% yield of dihydrojasmone **5** via the formation of the diketone **39** as an intermediate.[78]

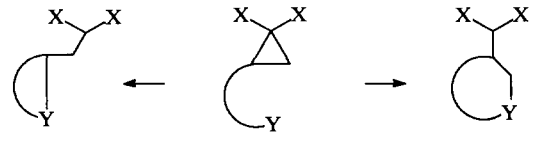




The dimethoxycyclopropyl ketone **40**, which is produced by the reaction of *cis*-1,2-dimethoxyethylene with the diazoketone **41**, will react with polyphosphoric acid in aqueous acetone in a single stage to give the hydroxycyclopentenone **42**, owing to the solvolytic opening of the cyclopropane ring, intramolecular aldolisation, and the elimination of methanol. Isomerisation of **42** on basic aluminium oxide gives the cyclopentanone **43** which is a well known key intermediate in the synthesis of PGF_1.[79]



Methods for synthesising cyclopentane structures with one or two carbon atoms from the initial cyclopropane incorporated into the five-membered ring have been developed to a considerably lesser extent than the reactions for expanding a three-membered carbon ring that have been discussed above (see Refs 9, 34, and 35). Of the two alternative versions of nucleophilic opening of an activated cyclopropane ring, called spirocyclisation and fused cyclisation respectively, spirocyclisation is kinetically preferred.[82]



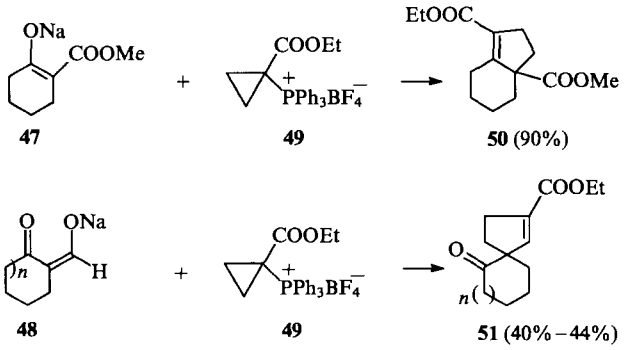
spirocyclisation fused cyclisation

For example, the reaction of the cyclopropane tetraester **44** with $NaCH_2 \cdot SO \cdot Me$ in dimethyl sulphoxide at room temperature gives the thermodynamically more stable cyclopentane tetraester **45** which undergoes smooth cyclisation to the bicyclo[3,3,0]octanone derivative **46** when the temperature is raised.[82]

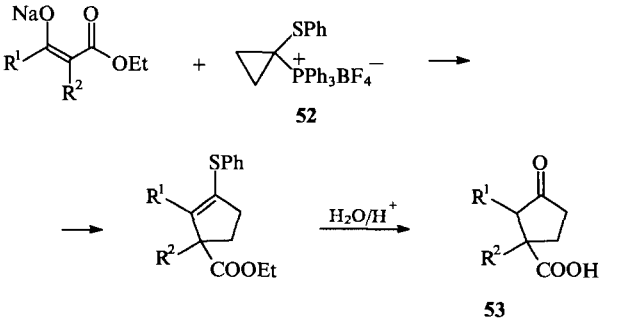
It was established in the same work that spirocyclisation is kinetically preferred in the formation of a four-membered ring but under conditions where there is thermodynamic control the corresponding cyclopentane derivatives can also be obtained.

3. Intermolecular ring formation reactions

The approaches to the synthesis of cyclopentane structures relying on intermolecular reactions of activated cyclopropanes that are known at the present time are based on the strategy of [3 + 2]-ring formation. For example, tetracyanoethylene forms the relevant cyclopentane adducts with donor or donor-acceptor cyclopropanes.[25] However this method has not achieved significant use in synthesis because it is not flexible enough. Another approach uses a series of homo-Michael addition reactions of enolate anions to cyclopropane derivatives doubly activated by acceptor substituents and intramolecular condensation.[83-91] For example, the sodium enolates of α-methoxycarbonylcyclohexanone **47** (data from Ref. 84) or the α-formylcycloalkanones **48** (data from Ref. 85) react with 1-(ethoxycarbonyl)cyclopropyltriphenylphosphonium tetrafluoroborate **49** to give condensed **50** or spiran **51** derivatives respectively. The latter approach has been used successfully in the synthesis of a number of natural sesquiterpenes.[85]

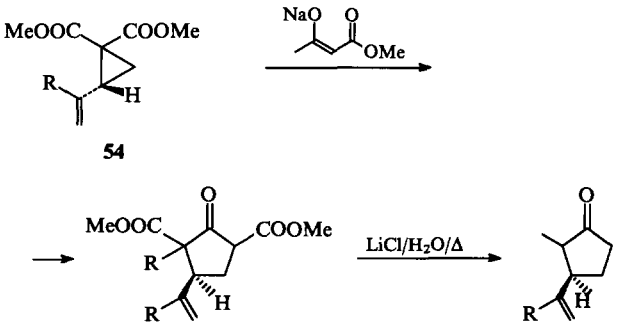


The use of [1-(phenylthio)cyclopropyl]triphenylphosphonium tetrafluoroborate **52** as the Michael acceptor opens up a simple route to substituted 2-carboxycyclopentanones **53**.[86,87]



R^1, R^2 = H, Me, Ph, CH_2Ph.

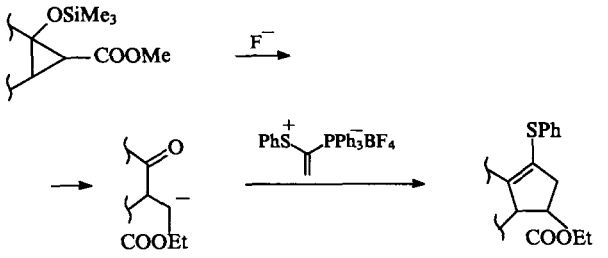
Similar transformations of the *R*-dimethyl-2-vinylcyclopropane-1,1-dicarboxylate **54** have been used as a basis for developing effective approaches to the complete asymmetric synthesis of certain steroids[88,89] and prostaglandins.[90] A key stage in the construction of a cyclopentane ring in these schemes is the stereospecific opening of the ring in **54** by enolates based on derivatives of malonic or acetoacetic ester as, for example, in the production of the enantiomerically pure vinylcyclopentanones **55**.[91]



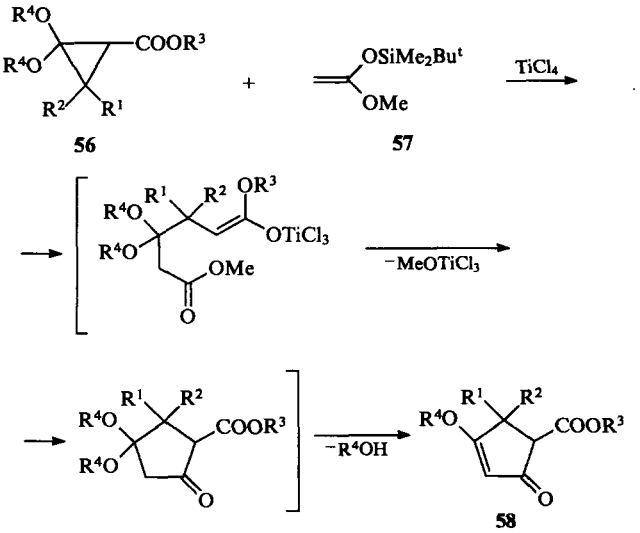
54

R = H, Me. **55**

The possible simultaneous generation of a carbanion centre and a carbonyl function by the action of fluoride ions on adducts of an ethoxycarbonylcarbene with silyl ethers of enols[25] provides a basis for developing an alternative strategy for [3 + 2]-ring formation.[92-94]



[3 + 2]-Cycloaddition of the donor-acceptor cyclopropanes **56** to the *tert*-butyldimethylsilylacetal of keten **57** is catalysed by titanium tetrachloride, resulting in the formation of derivatives of 3-alkoxycyclopentenones **58** with yields of 28%–75%.[95]



56 **57**

58

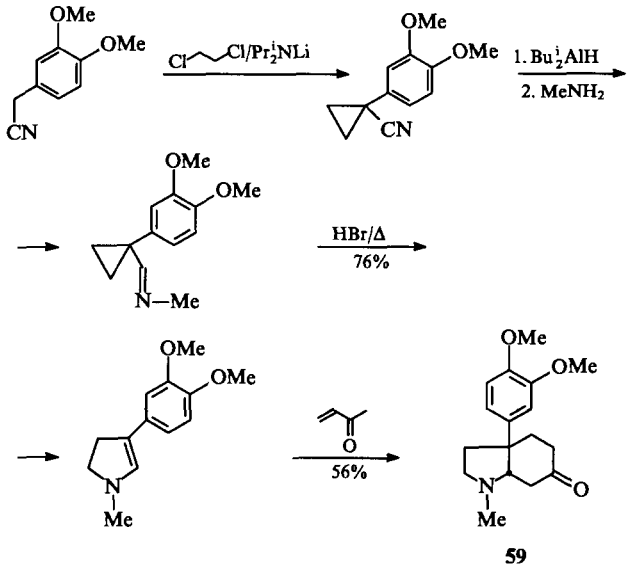
R^1–R^4 = Me, Et.

III. Synthesis of five-membered heterocycles

The number of publications devoted to the conversion of activated cyclopropane compounds to five-membered heterocycles is considerably greater than the number concerned with the production of cyclopentane derivatives from such compounds. However there are, to our knowledge, no papers in which data on the use of activated cyclopropanes in the synthesis of heterocycles are arranged especially systematically although there are a number of reviews devoted to particular aspects of this subject.[6,7,9,11,96]

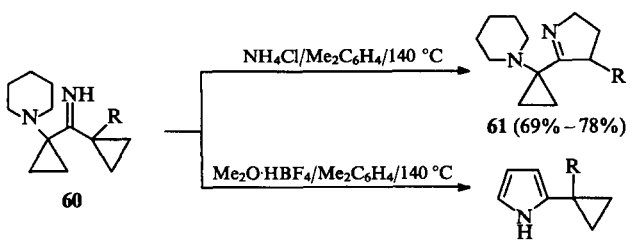
1. Ring expansion reactions in hetero-analogues of vinylcyclopropanes

The ring expansion reactions that have been studied most extensively are those in carbonyl and heterocarbonyl cyclopropane derivatives and a number of effective preparative methods for synthesising five-membered heterocycles have been developed on their basis. For example, the acid-catalysed rearrangement of cyclopropylketimines is one of the most flexible methods for obtaining 2-pyrrolines with various degrees of substitution (see Ref. 96). The use of this reaction for the synthesis of alkaloids is illustrated by the simple scheme for obtaining (±)-mesembrine **59**.[97-99]



59

The hetero-substituents in the cyclopropane ring have an appreciable effect on the course of the reaction but this effect is not always in accord with their effect on the thermal vinylcyclopropane–cyclopentene rearrangement.[100-103] For example, the thermolysis of the di(cyclopropyl)ketimines **60** in boiling xylene in the presence of ammonium chloride gives the pyrrolines **61** as a result of opening of the cyclopropane ring that has no piperidine substituent.[102]

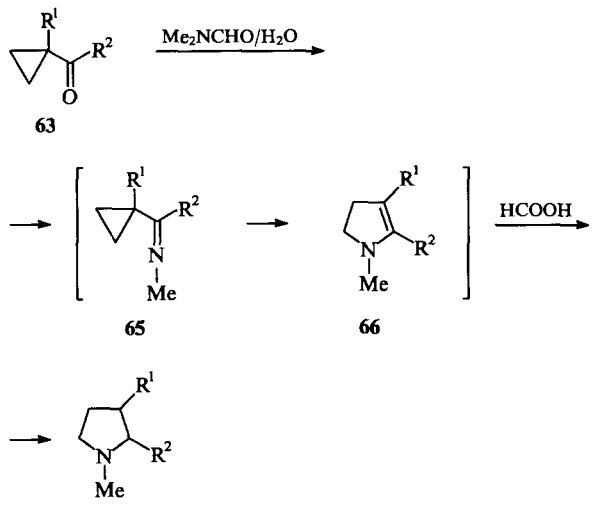


60

R = H, SPh. **61** (69%–78%) **62** (32%–42%)

The use of the dimethyl etherate of tetrafluoroboric acid as an acid catalyst gives the opposite result as regards selectivity of opening of the three-membered ring. The rearrangement of the di(cyclopropyl)ketimines **60** now gives the pyrrole derivatives **62** owing to opening of the three-membered carbon ring that has the electron-donating piperidyl substituent. These differences are attributed to the greater role of the nitrogen atom of the piperidyl radical in stabilisation of the positive charge in the transition state when an acid with a weakly nucleophilic tetrafluoroborate counter-ion is used as a catalyst.[103]

Cyclopropylimines often act as intermediates in the ring expansion reactions of cyclopropane carbonyl compounds with primary amines. For example, boiling the cyclopropyl ketones **63** in dimethylformamide in the presence of magnesium chloride gives the pyrrolidines **64**.[104] It is likely that the reaction proceeds via the formation of intermediate cyclopropylimines **65** and their rearrangement to substituted pyrrolines **66** which are reduced *in situ* by formic acid to give the final products.

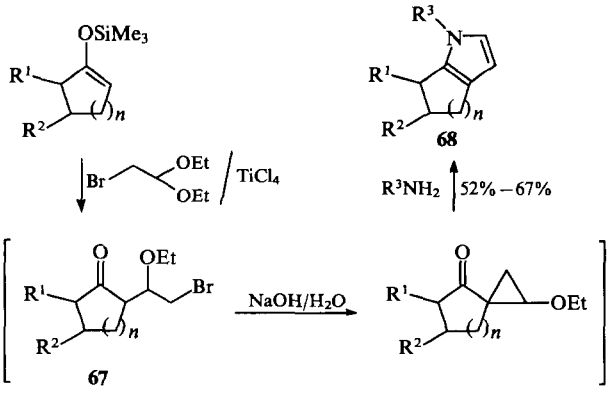


63 **65** **66**

64 (31%–72%)

R^1 = H, Ph; R^2 = Alk, cyclo-Alk, Ar.

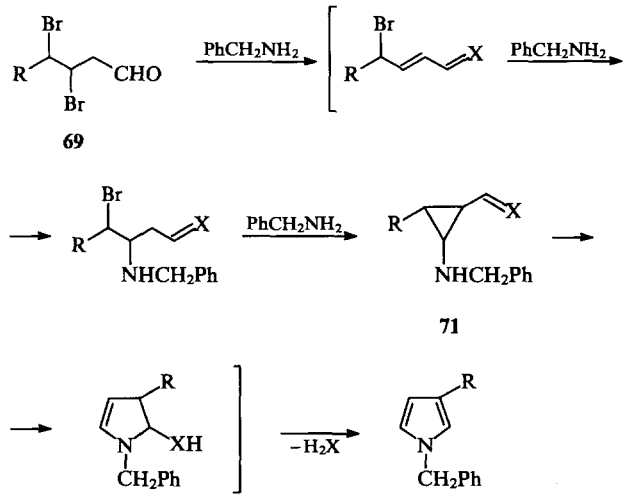
Cyclopropylcarbonyl compounds with electron-donor substituents in a β position to the carbonyl group will react with primary amines under mild conditions to give the corresponding pyrrole derivatives.[105–108] A convenient preparative method for obtaining this type of activated cyclopropane is 1,3-dehydrohalogenation of accessible 3-bromo-2-alkoxypropyl ketones.[105,106] The use of the cyclic ketones **67** as initial substrates in this reaction enables pyrrole derivatives condensed with cyclopentane and cyclohexane rings **68** to be synthesised.[106]



67 **68**

R^1, R^2 = H, Bu; R^3 = H, Me, CH_2Ph; n = 1, 2.

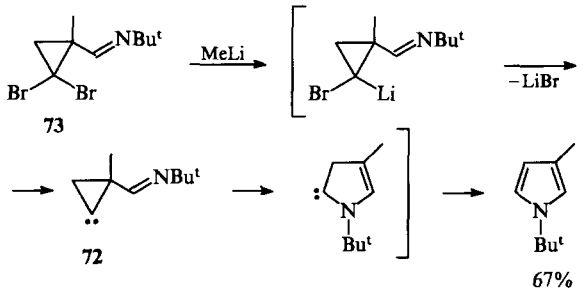
A similar approach was used in a convenient scheme for converting β,γ-dibromoaldehydes **69** to the inaccessible 3-alkyl-β-benzylpyrroles **70**.[108,109] The rearrangement of the linear carbon-carbon skeleton of the initial aldehyde **69** to give the branched structure of the 3-alkyl-pyrrole **70** is effected via the intermediate formation of the donor-acceptor cyclopropanes **71** by closure of the three-membered ring initiated by a Michael addition.



69 **71** **70**

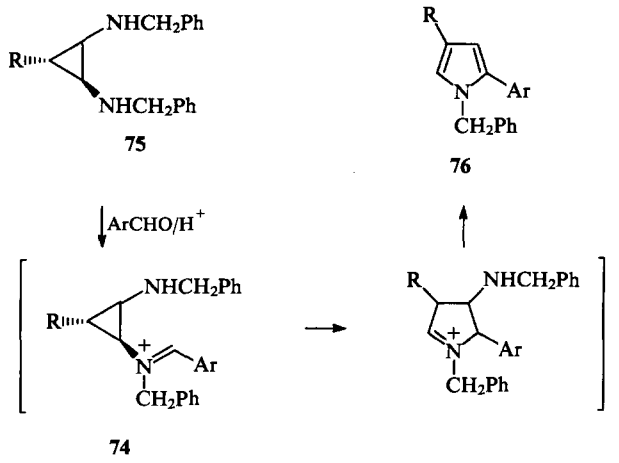
R = Alk; X = O, NCH_2Ph.

The role of the activating electron-donor substituent in the β position to the imine function can, at least formally, be performed by the lone pair of electrons of the carbene centre in the intermediate **72** which is formed when the dibromocyclopropylimine **73** is converted to 1-*tert*-butyl-3-methylpyrrole by the action of methyllithium.[110,111]



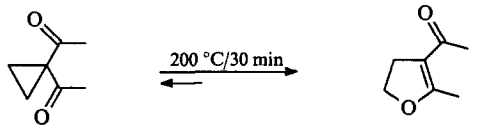
73 **72** 67%

Aza-analogues of vinylcyclopropanes in which the nitrogen atom is directly bonded to the three-membered ring are also able to undergo rearrangement to pyrrole derivatives.[112,113] In the case of the activated cyclopropanes **74**, which are intermediate products of the reaction of the 1,2-diaminocyclopropanes **75** with aromatic aldehydes, the rearrangement proceeds smoothly at room temperature to give the 2-arylpyrroles **76** as final products.[113]



R = H, Me.

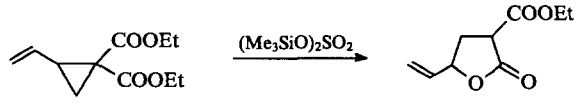
Rearrangements of cyclopropylcarbonyl compounds to give furan derivatives have been studied more thoroughly and there are many examples of their use in synthesis (see Refs 7, 11, 23, and 114). Formylcyclopropane[115] and acetylcyclopropane[116] undergo rearrangement reversibly in the gas phase at 400–500 °C to form 2,3-dihydrofuran and 2,3-dihydro-5-methylfuran respectively. The reaction is accompanied by the irreversible formation of a number of by-products and is of no preparative importance. On the other hand, 1,1-diacetylcyclopropane **77** will isomerise at 200 °C to give a high yield of the dihydrofuran **78**.[117,118]



77 **78** (92%)

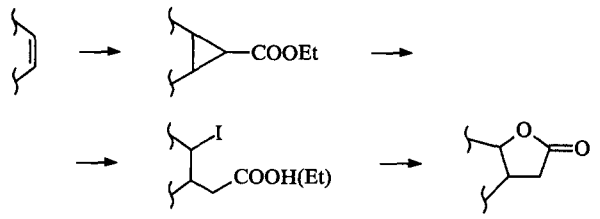
Other 1-acylcyclopropanes with electron-acceptor substituents in the α position to the acyl group undergo a similar isomerisation.[118,119]

Cyclopropanecarboxylic acid[120] and its derivatives[121–124] isomerise in the presence of various acid catalysts to give the corresponding γ-butyrolactones. The best yields of the final products are obtained by opening the three-membered ring in the carbonyl-substituted cyclopropanes using organosilicon reagents such as trimethyliodosilane or bis(trimethylsilyl) sulfate.[125] For example, treating 1,1-bis(ethoxycarbonyl)-2-vinylcyclopropane **79** with bis(trimethylsily) sulfate in 1,2-dichloroethane gives an excellent yield of the butyrolactone **80**.[126]

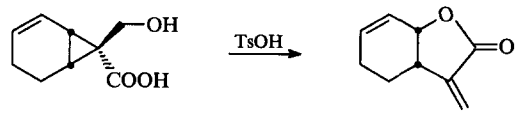


79 **80** (98%)

Other 1-carbonyl-substituted cyclopropanecarboxylates will also enter into reaction; the thermodynamically more stable butyrolactones with predominant inversion of the configuration of the reaction centre are formed.[126] A reaction in two stages, viz. opening the ring in the cyclopropanecarboxylic ester with trimethyliodosilane and closure of the lactone ring, is an effective method for converting olefins to γ-butyrolactones.[127]

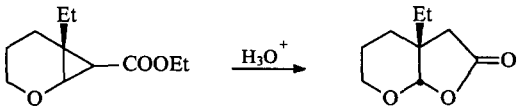


The use of 1-hydroxymethyl-,[128,129] 1-halogenomethyl-,[129] and 1-dialkylaminomethyl-substituted cyclopropanecarboxylate esters[130] enables α-methylene-γ-butyrolactones to be obtained. The regio-selectivity of the reaction is determined by the type of substituents in positions 2 and 3 of the three-membered ring.[128,129] For example, the rearrangement of the cyclopropylcarbinol substrate **81** to the lactone **82** takes place owing to rupture of the carbon–carbon bond in the cyclopropane ring that is adjacent to the double bond[128] whereas for the corresponding methoxyl analogue the reverse selectivity is observed.[129]



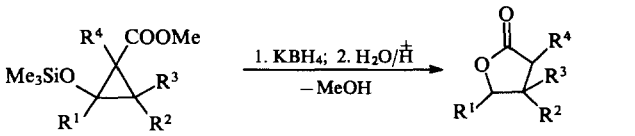
81 **82** (89%)

Cyclopropylcarbonyl compounds undergo rearrangement to furan derivatives especially easily when electron-donor substituents are present in the β position of the cyclopropane ring.[25] One of the most effective approaches to the synthesis of this type of substrate involves formation of the cyclopropane from esters of enols of diazocarbonyl compounds.[11,14,25,130] In certain instances not only the carbonylcyclopropanes are formed in these reactions but also the corresponding dihydrofurans. The latter may be obtained by 1,3-dipolar cycloaddition of ketocarbenes to olefins or isomerisation of the initially formed cyclopropane derivatives.[131–136] A typical example of this type of transformation is the synthesis of the bicyclic lactone **83** which is used as a key intermediate in the synthesis of certain indole alkaloids.[134] The cyclopropane precursor **84**, which is obtained from β-ethyldihydropyran, undergoes rearrangement to the lactone **83** smoothly when it is heated with dilute sulfuric acid.



84 **83** (93%)

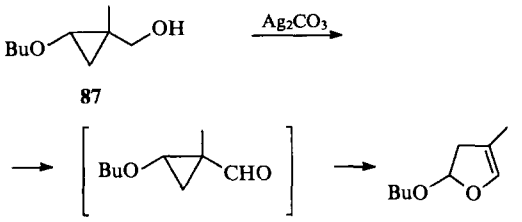
In certain instances, under the reaction conditions used, the hydroxylactones formed initially undergo dehydration to give the corresponding unsaturated lactones.[137] On the other hand, the reaction of the methyl 2-siloxycyclopropanecarboxylates **85** with potassium hydroborate in methanol enables the substituted saturated γ-butyrolactones **86** to be synthesised in a different way in a one-step procedure with a high yield. This multi-stage procedure evidently includes initial desilylation of **85** by potassium methoxide (generated *in situ* from potassium hydroborate and methanol), opening of the activated cyclopropane ring to form the corresponding 4-oxoalkanoates, their reduction and lactonisation.[138]



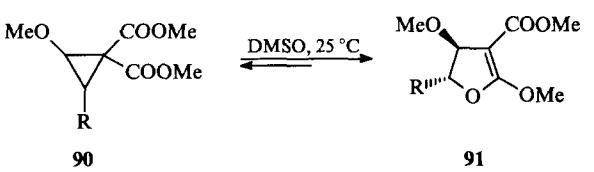
85 **86** (78%–95%)

R^1–R^4 = Alk, cyclo-Alk, Alkenyl.

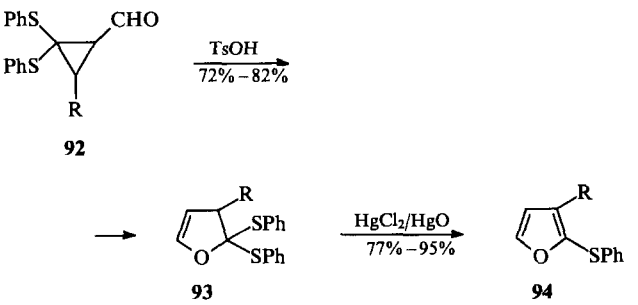
2-Oxy-substituted cyclopropyl ketones and aldehydes are considerably less stable and will undergo rearrangement to the corresponding dihydrofurans smoothly in the presence of acid catalysts or *in situ*.[131,133,139-141] For example, oxidation of the butoxycyclopropylcarbonyl **87** with silver carbonate on a zeolite gives a high yield of the dihydrofuran **88**, probably via the intermediate formation of the corresponding aldehyde **89**.[139,140] The reaction is of a general nature and in some instances the corresponding activated cyclopropanecarbaldehydes and cyclopropyl ketones can be identified.[139-141]



Cyclopropanes in which the three-membered ring has two geminal acceptor[132,135] or donor substituents and a substituent of the opposite type in a third position[142,143] will undergo rearrangement to dihydrofuran derivatives under very mild conditions. For example, in solutions of derivatives of 2-methoxycyclopropanecarboxylic acids **90** in dimethyl sulfoxide an equilibrium with the corresponding dihydrofurans **91** is established rapidly even at room temperature. The rearrangement typically takes place with retention of the stereochemical configuration at the reaction centre[132] (see also Ref. 136).

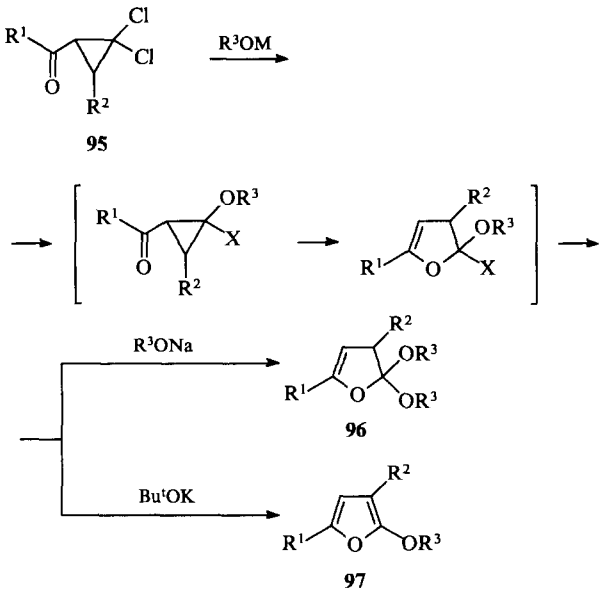


In the presence of catalytic quantities of *p*-toluenesulfonic acid the *gem*-di(phenylthio)cyclopropanecarbaldehydes **92** isomerise to the 3-substituted 2,2-di(phenylthio)-2,3-dihydrofurans **93** rapidly at room temperature and the latter can readily lose thiophenol to form the phenylthiofurans **94**.[144,145] Note that *gem*-di(phenylthio)cyclopropyl ketones with a similar structure isomerise smoothly under the same conditions to give acyclic products.[146]



R = Me, Ar.

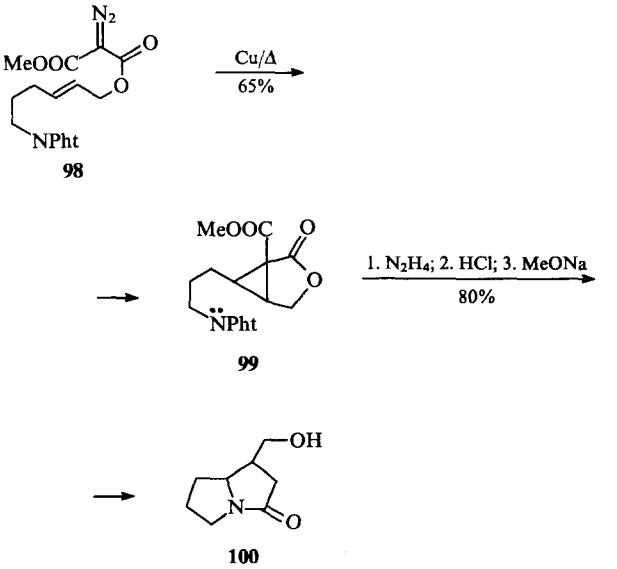
Nucleophilic substitution of the halogen atoms in 1-acyl-2,2-dichlorocyclopropanes **95** by reaction with alkali metal alkoxides leads directly to 2,2-dialkoxy-2,3-dihydrofurans **96**[147-150] or substituted 2-alkoxyfurans **97**,[151] depending on the type of alkoxide and the reaction conditions. 2-Dialkylaminofurans can be obtained by a similar scheme of reactions.[152]



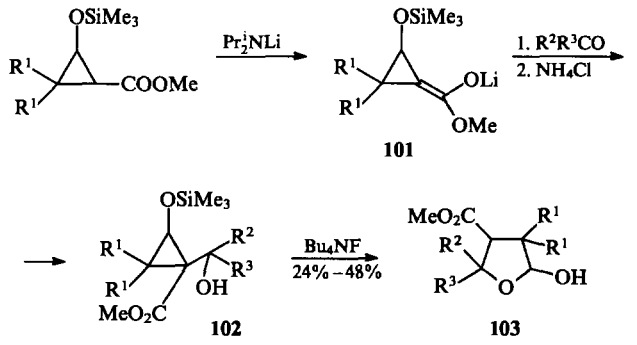
R[1], R[2] = Alk, Alkenyl, Ar; R[3] = Alk; M = Na, K; X = Cl, OR[3].

2. Other intramolecular cyclisation reactions

Intramolecular nucleophilic ring opening reactions in activated cyclopropanes also provide an effective approach to the production of five-membered heterocycles.[7,9,11,15,25] The intramolecularity factor has an additional activating effect on the opening of the three-membered ring[9] and the main problem in using this approach in directed synthesis is to obtain appropriate cyclopropane derivatives that contain suitable nucleophilic centres in the substituents. This approach has been used successfully in the synthesis of natural compounds,[9] particularly in the stereospecific synthesis of certain alkaloids where one of the stages involves intramolecular formation of cyclopropane from the multiple bond in **98**. The removal of the shielding phthalimide (NPht) group in the resultant cyclopropane derivative **99** using hydrazine hydrate leads to the formation of the key bicyclic product **100** due to spiro-opening of the cyclopropane ring with inversion of the configuration of the reaction centre.[153]

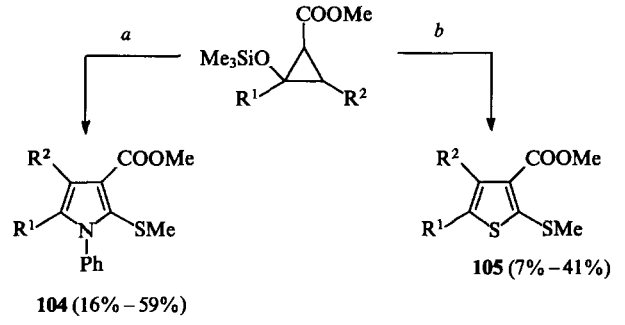


An alternative method of introducing nucleophilic substituents into activated cyclopropanes involves alkylation of deprotonated derivatives of a cyclopropanecarboxylic acid by using suitable substrates.[154-158] For example, the reaction of the ester enolates **101**, which are readily generated from methyl 2-siloxycyclopropanecarboxylates by the action of lithium diisopropylamide, with carbonyl compounds gives the trifunctional derivatives **102**. The latter are unstable and are converted, either spontaneously or by the action of desilylating agents, to the lactols **103** which are readily convertible to the corresponding tetrahydrofuran or γ-butyrolactone derivatives.[155]



R^1_2 = Me_2, $-(CH_2)_5-$; R^2, R^3, = H, Me, Ph, $-(CH_2)_5-$.

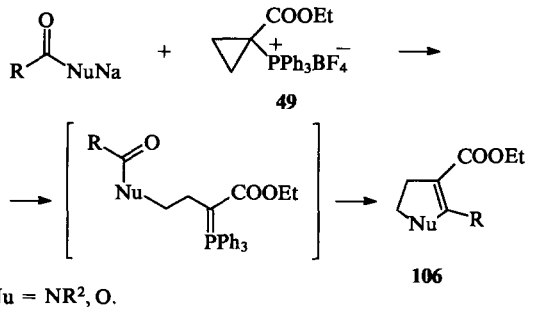
The use of hetero-analogues of carbonyl compounds, such as phenyl isothiocyanate and carbon disulfide, as electrophiles opens up a route to the corresponding derivatives of pyrrole **104** [158] and thiophen **105**.[156,157]



a — 1. Pr^i_2NLi, 2. PhNCS, 3. MeI, 4. CF_3COOH;
b — 1. Pr^i_2NLi, 2. CS_2, 3. MeI, 4. CF_3COOH
R^1, R^2 = Alk, cyclo-Alk.

3. Intermolecular hetero-ring formation reactions

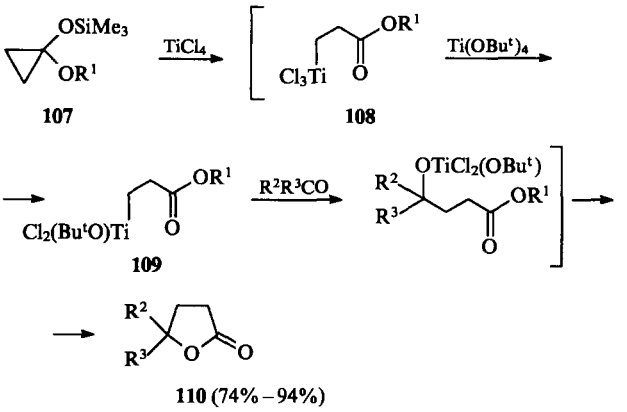
The synthesis of five-membered heterocycles by means of intermolecular hetero-ring formation, like that of cyclopentane derivatives (see above), is based on [3 + 2]-ring formation reactions. 1-Ethoxycarbonylcyclopropyltriphenylphosphonium tetrafluoroborate **49** will react with α-carbonyl-containing nucleophiles to give the corresponding five-membered heterocyclic compounds **106**. The stages in the reaction are nucleophilic opening of the three-membered carbon ring (which is doubly activated by the electron-acceptor substituents) and then olefination of the carbonyl group.[159-163]



Nu = NR^2, O.

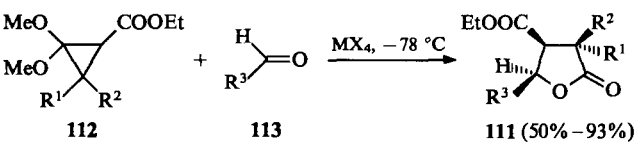
The reaction of anions of cyclic imides with the phosphonium salt **49** opens up a means of obtaining bicyclic lactams with a bridgehead nitrogen atom.[159,160,162]

The cyclopropanone acetals **107**, which are doubly activated by electron-donor substituents, are suitable precursors of homoenolate anions[40,164,165] which react with carbonyl compounds to give derivatives of γ-hydroxycarboxylic acids or γ-butyrolactones.[166,167] In the homoenolate anions an intramolecular back reaction with the carbonyl group is favoured to a considerable extent by the entropy factor and hence for the reaction with an external electrophile to take place a substantial gain in enthalpy is required. It is known that in reactions with carbonyl compounds titanium and zinc homoenolates of esters satisfy these conditions.[164,167] The addition of 0.5 equiv. of tetra(*tert*-butoxy)titanium to the trichlorotitanium homoenolate **108**, which is obtained by the reaction of the silylacetal of cyclopropanone **107** with titanium tetrachloride, gives an alkoxide derivative **109** that is more reactive than the initial enolate **108**. The reaction of **109** with ketones does not stop at the stage where the corresponding γ-oxyesters are formed but leads to their cyclisation *in situ* to give the γ-lactones **110**.[167-170]



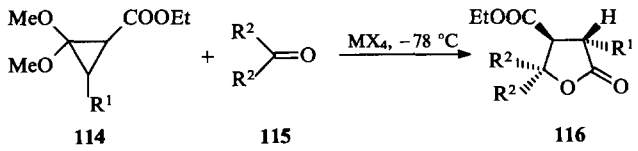
R^1 = Alk; R^2, R^3 = Alk, cyclo-Alk, Ar.

Cyclopropanes containing donor and acceptor substituents simultaneously are able to enter into a similar condensation with aldehydes and ketones in the presence of titanium tetrachloride, giving γ-hydroxyketones and dihydrofurans respectively.[168-170] There are also reports of the diastereoselective synthesis of *cis*-3,4-disubstituted γ-lactones **111**[171,172] and *cis*-3,4-disubstituted-γ-lactams[172] using the Lewis-acid-catalysed reaction of 2,2-dialkoxy-3,3-dialkylcyclopropanecarboxylic esters **112** with aldehydes **113** and *N*-toluenesulphonylaldimines respectively.[173]



R^1, R^2, R^3 = Alk; MX_4 = $TiCl_4$, $TiBr_4$, or $SnBr_4$.

The reaction of 2,2-dialkoxy-3-alkylcyclopropanecarboxylic esters **114** with symmetrical ketones **115** under the same conditions gives *cis*-2,3-disubstituted lactones **116**, also with high selectivity.[173]



114 **115** **116**

R^1, R^2, R^3 = Alk.

* * *

It is clear from the data presented in this review that the methods for synthesising five-membered carbocycles and heterocycles using activated cyclopropanes as intermediates are in many instances highly flexible and stereoselective. Since there are simple and effective methods for obtaining cyclopropane compounds of different structures, including individual optical isomers,[174] it is safe to say that these methods for synthesising cyclic compounds are undoubtedly of preparative importance. The majority of the publications are concerned with ring expansion reactions in vinylcyclopropanes and their oxa- and aza-analogues, and also other types of intramolecular cyclisation, as these have been used extensively to obtain five-membered rings. However the use of reactions that entail intermolecular [3 + 2]- and [4 + 1]-ring formation is no less promising.

References

1. W H Perkin *Chem. Ber.* **17** 54 (1884)
2. O M Nefedov, A I Ioffe, L G Menchikov *Khimiya Karbenov* (The Chemistry of Carbenes) (Moscow: Khimiya, 1990)
3. W Kirmse *Carbene Chemistry* (Translated into Russian; Moscow: Mir, 1966)
4. W Kirmse *Carbene Chemistry* (2nd Ed.) (New York: Academic Press, 1974)
5. N S Zefirov, I V Kazimirchik, K A Lukin *Tsikloprisoedinenie Dikhlorkarbena k Olefinam* (The Cycloaddition of Dichlorocarbene to Olefins) (Moscow: Nauka, 1985)
6. D Wendisch, in *Houben-Weyl Methoden der Organische Chemie* (Stuttgart: Georg Thieme, 1971) Vols IV/III
7. L A Yanovskaya, V A Dombrovskii, A Kh Khusid *Tsiklopropany s Funktsional'nymi Gruppami* (Cyclopropanes with Functional Groups) (Moscow: Nauka, 1980)
8. J-M Konia, L Blanko *Current Trends in Organic Synthesis* (Ed. H Nozaki) (Translated into Russian; Moscow: Mir, 1986)
9. S Danishefsky *Acc. Chem. Res.* **12** 66 (1979)
10. V S Aksenov, V A Terent'eva, Yu V Savinykh *Usp. Khim.* **49** 1039 (1980) [*Russ. Chem. Rev.* **49** 549 (1980)]
11. E Wenkert *Acc. Chem. Res.* **13** 27 (1980)
12. J Salaun *Chem. Rev.* **83** 619 (1983)
13. L A Paquette *Chem. Rev.* **86** 733 (1986)
14. O G Kulinkovich *Usp. Khim.* **58** 1233 (1989) [*Russ. Chem. Rev.* **58** 711 (1989)]
15. H N C Wong, M -Y Hon, C W Tse *Chem. Rev.* **89** 165 (1989)
16. A I Ioffe, V A Svyatkin, O M Nefedov *Stroenie Proizvodnykh Tsiklopropana* (The Structure of Cyclopropane Derivatives) (Moscow: Nauka, 1986)
17. F H Allen *Acta Crystallogr., Sect. B* **31** 81 (1980)
18. C A Deakyne, L C Allen, N C Craig *J. Am. Chem. Soc.* **99** 3895 (1977)
19. S Durmaz, H Kollmar *J. Am. Chem. Soc.* **102** 6942 (1980)
20. T Clark, C W Spitznagel, R Klose, P R Schleyer *J. Am. Chem. Soc.* **106** 4412 (1984)
21. A Meijere *Angew. Chem., Int. Ed. Engl.* **18** 809 (1979)
22. D J Dill, A Greenberg, J C Liebman *J. Am. Chem. Soc.* **101** 6814 (1979)
23. C J M Stirling *Chem. Rev.* **78** 517 (1978)
24. K B Wiberg *Angew. Chem., Int. Ed. Engl.* **25** 312 (1986)
25. H U Reissing, in *Topics in Current Chemistry* (Berlin: Springer, 1988) Vol. 144, p. 73
26. T Hudlicky, T M Kutchan, S M Naqvi *Org. React. (N.Y.)* **33** 247 (1985)
27. E M Mil'vitskaya, A V Tarakanova, A F Plate *Usp. Khim.* **45** 938 (1976) [*Russ. Chem. Rev.* **45** 469 (1976)]
28. H M Frey, R Walsh *Chem. Rev.* **69** 103 (1969)
29. P H Mazzochi, H J Tamburin *J. Am. Chem. Soc.* **92** 7220 (1970)
30. J J Quirante, F Enriguez, J M Hernando *J Mol. Struct.* **204** (*THEOCHEM* **63**) 193 (1990)
31. J J Gajewsky, M P Sguieciarini *J. Am. Chem. Soc.* **111** 6717 (1989)
32. B M Trost *Chem. Soc. Rev.* **11** 141 (1982)
33. B M Trost, in *Topics in Current Chemistry* (Berlin: Springer, 1986) Vol. 133, p. 3
34. M Ramaiah *Synthesis* 529 (1984)
35. T Hudlicky, J D Price *Chem. Rev.* **89** 1467 (1989)
36. J Salaun, J Ollivier *Nouv. J. Chem.* **5** 587 (1981)
37. S A Monti, F G Cowherd, McAninch *J. Org. Chem.* **40** 858 (1975)
38. C Girard, P Amice, J P Barnier, J M Gonia *Tetrahedron Lett.* **15** 3329 (1974)
39. J Salaun, Y Almirantis *Tetrahedron* **39** 2421 (1983)
40. J R Y Salaun, in *Topics in Current Chemistry* (Berlin: Springer, 1988) Vol. 144, p. 1
41. J Olliver, J Salaun *J. Chem. Soc., Chem. Commun.* 1269 (1985)
42. Y Nishimura, K Yamomoto, S S Me Elvain *J. Am. Chem. Soc.* **25** 1273 (1979)
43. J Salaun *Tetrahedron Lett.* **25** 1273 (1984)
44. B M Trost, S Kurozumi *Tetrahedron Lett.* **15** 1929 (1974)
45. A Maiere, in *Sovremennye Problemy Organicheskoi Khimii* (Current Problems in Organic Chemistry) (Ed. K A Ogloblin) (Leningrad: Izd. Leningrad. Univ., 1987) p. 5
46. S Keyaniyan, M Apel, P Richmond, A Meijere *Angew. Chem., Int. Ed. Engl.* **24** 770 (1985)
47. J P Barnier, J Salaun *Tetrahedron Lett.* **25** 1273 (1984)
48. B M Trost, D E Keeley, M J Bogdanowich *J. Am. Chem. Soc.* **95** 3058 (1973)
49. B M Trost, D E Keeley *J. Am. Chem. Soc.* **96** 1252 (1974)
50. J H Byers, T A Spencer *Tetrahedron Lett.* **26** 717 (1985)
51. B M Trost, D E Keeley *J. Am. Chem. Soc.* **98** 248 (1976)
52. R D Miller *J. Chem. Soc., Chem. Commun.* 277 (1976)
53. B M Trost, P H Sendder *J. Org. Chem.* **46** 506 (1981)
54. H G Richey, D M Shull *Tetrahedron Lett.* **17** 575 (1976)
55. D F Harvey, K P Lund *J. Am. Chem. Soc.* **113** 8916 (1991)
56. R J Anchus, J T Kadonaga *J. Am. Chem. Soc.* **103** 2443 (1981)
57. R L Danheiser, R L Bronson, J J Okano, K Okano *J. Am. Chem. Soc.* **107** 4579 (1985)
58. J E Baldwin, G D Andrews *J. Am. Chem. Soc.* **98** 6705 (1976)
59. H Xoing, R D Rieke *J. Am. Chem. Soc.* **114** 4415 (1992)
60. J P Dinnocenzo, D A Conlon *J. Am. Chem. Soc.* **110** 2324 (1988)
61. E J Corey, S W Walinsky *J. Am. Chem. Soc.* **94** 8932 (1972)
62. T Hudlicky, M S Natchus, G Sinai-Zingde *J. Org. Chem.* **52** 4641 (1987)
63. H M L Davies, T J Clark, L A Church *Tetrahedron Lett.* **30** 5057 (1989)
64. Y Morizava *Tetrahedron Lett.* **23** 2871 (1982)
65. T Hudlicky, F J Koszyd, T M Kutchan, J P Sheth *J. Org. Chem.* **45** 5020 (1980)
66. D F Harvey, M E Brown *Tetrahedron Lett.* **32** 2871 (1991)
67. E J Corey, A G Myers *J. Am. Chem. Soc.* **107** 5574 (1985)
68. E J Corey, H Kigoshi *Tetrahedron Lett.* **32** 5025 (1991)
69. M Doyle, D Vanheusen *J. Org. Chem.* **47** 5325 (1982)
70. K Muria, K Fugasi, K Oshima, K Utimoto *Tetrahedron Lett.* **29** 1543 (1988)
71. Y Morizava, K Oshima, H Nozaki *Tetrahedron Lett.* **23** 2871 (1982)
72. A Fleming, G Sinai-Zingde, M Natohus, T Hudlicky *Tetrahedron Lett.* **28** 167 (1987)
73. T Hudlichy, A Fleming, L Radesca *J. Am. Chem. Soc.* **111** 6691 (1989)
74. T Hudlicky, N E Heard, A Fleming *J. Org. Chem.* **55** 2570 (1990)
75. N S Narasimhan, N M Sunder *Tetrahedron Lett.* **29** 2985 (1988)
76. J T Carey, P Halguist *Tetrahedron Lett.* **29** 1243 (1988)
77. V Reydellet, P Helguist *Tetrahedron Lett.* **30** 6837 (1989)

78. E Wenkert, B L Buckwalter, A A Carverio *J. Am. Chem. Soc.* **100** 1267 (1978)
79. E Wenkert, R S Greenberg, M S Raju *J. Org. Chem.* **50** 4681 (1985)
80. Y Morizawa, A Kanakura, H Yamamoto T Hiyama, H Nozaki *Bull. Chem. Soc. Jpn.* **57** 1935 (1984)
81. S W Baldwin, H R Blomquist *Tetrahedron Lett.* **23** 3883 (1982)
82. S Danishefsky, J Dynak, E Hatch, M Yamamoto *J. Am. Chem. Soc.* **96** 1259 (1974)
83. N A Abraham *Tetrahedron Lett.* **14** 451 (1973)
84. P L Fuchs *J. Am. Chem. Soc.* **96** 1607 (1974)
85. W G Dauben, D J Hart *J. Am. Chem. Soc.* **99** 7307 (1977)
86. J P Marino, R C Ladnick *Tetrahedron Lett.* **16** 4531 (1975)
87. J P Marino, M P Ferro *J. Org. Chem.* **46** 1828 (1981)
88. G Quinkert, H Stark *Angew. Chem., Int. Ed. Engl.* **22** 637 (1983)
89. G Quinkert, U Schwartz, H Stark, W D Weber H F Adam, H Baier, G Frank, G Durner *Liebigs Ann. Chem.* 1999 (1982)
90. G Quinkert, F Adam, G Durner *Angew. Chem., Int. Ed. Engl.* **21** 856 (1982)
91. G Quinkert, H G Schmalz, E Walzer, S Gross, G Durner, J W Bats *Angew. Chem., Int. Ed. Engl.* **25** 732 (1986)
92. J P Marino, E Laborde *J. Org. Chem.* **52** 1 (1987)
93. J P Marino, E Laborde *J. Am. Chem. Soc.* **107** 734 (1985)
94. J P Marino, C Silveria, J Comasseto, N Petragnani *J. Org. Chem.* **52** 4139 (1987)
95. K Saigo, S Shimada, T Shibasaki, M Hasegawa *Chem. Lett.* 1093 (1990)
96. R V Stevens *Acc. Chem. Res.* **10** 193 (1977)
97. R V Stevens, P M Lesko, R Lapalme *J. Org. Chem.* **40** 3495 (1975)
98. R V Stevens, M P Wehtland *J. Am. Chem. Soc.* **90** 5580 (1968)
99. R V Stevens, J T Lai *J. Org. Chem.* **37** 2138 (1972)
100. H H Wasserman, R P Dion *Tetrahedron Lett.* **23** 1413 (1982)
101. H H Wasserman, R P Dion *Tetrahedron Lett.* **24** 3409 (1983)
102. H H Wasserman, R P Dion, J Fukuyama *Tetrahedron* **45** 3203 (1989)
103. H W Pinnick, Y H Chang *Tetrahedron Lett.* **20** 837 (1979)
104. K W Blake, I Gills, R C Denney *J. Chem. Soc., Perkin Trans. 2* 700 (1981)
105. V L Sorokin, A Azzuz, O G Kulinkovich *Khim. Geterotsikl. Soedin.* 334 (1991)
106. A Azzuz, V L Sorokin, O G Kulinkovich *Khim. Geterotsikl. Soedin.* 37 (1992)
107. A M Nadim, Yu N Romashin, O G Kulinkovich *Zh. Org. Khim.* **27** 1621 (1991)
108. O G Kulinkovich, V L Sorokin, A Azzuz, S V Sviridow, N V Masalov *Synthesis* (1993) (in press)
109. O G Kulinkovich, A Azzuz, V L Sorokin *Zh. Org. Khim.* **29** (1993) (in press)
110. J Arct, L Skattebol *Tetrahedron Lett.* **23** 113 (1982)
111. C Santelli *Tetrahedron Lett.* **21** 2893 (1980)
112. H Quast, J Stawitz *Tetrahedron Lett.* **17** 3803 (1976)
113. H Quast, W Saal, J Stawitz *Angew. Chem., Int. Ed. Engl.* **20** 5889 (1981)
114. D L Rakhmankulov, R T Akhmatdinov, E A Kantor *Usp. Khim.* **53** 1523 (1984) [*Russ. Chem. Rev.* **53** 888 (1984)]
115. C L Wilson *J. Am. Chem. Soc.* **69** 3002 (1947)
116. A T Cocks, K W Egger *J. Chem. Soc., Perkin Trans. 2* 197, 199 (1973)
117. N S Zefirov, S I Kozhushkov, T S Kuznetsova *Khim. Geterotsikl. Soedin.* 1285 (1981)
118. N S Zefirov, T S Kuznetsova, S I Kozhushkov, L S Surmina, Z A Rasshchupkina *Zh. Org. Khim.* **19** 541 (1983)
119. E G E Jahangen, D Phillips, R J Kobelsky, D M Demko *J. Org. Chem.* **48** 2472 (1983)
120. N C Deno, W E Billups, D La Vietes, F C Scholl, S Schneider *J. Am. Chem. Soc.* **92** 3700 (1970)
121. C S Handro, G L Humpherg *J. Org. Chem.* **44** 2146 (1979)
122. T V Mandel'shtam, S V Kolesova, T V Polina *Zh. Org. Khim.* **14** 1186 (1980)
123. B G Mahmulkar, G H Kulkarn, R B Mitra *Indian J. Chem.* **22B** 910 (1983)
124. L D Sychkova, O V Kharitonova, Yu S Shabarov *Zh. Org. Khim.* **19** 1445 (1983)
125. Y Morizawa, T Hiyama, H Nozaki *Tetrahedron Lett.* **22** 2297 (1981)
126. Y Morizawa, T Hiyama, K Oshima, H Nozaki *Bull. Chem. Soc. Jpn.* **57** 1123 (1984)
127. S P Brown, S B Balkrishna, H W Pinnick *Tetrahedron Lett.* **22** 4891 (1981)
128. P F Hudrlik, J M Takaes, D T W Chon, L R Rudnick *J. Org. Chem.* **44** 786 (1979)
129. P F Hudrlik, D T W Chon, M A Stephenson *J. Org. Chem.* **47** 2987 (1982)
130. T Hiyama, H Saimoto, K Nishio *Tetrahedron Lett.* **20** 2043 (1979)
131. E Wenkert, M E Alonso, B L Buckwalter, E L Sanchez *J. Am. Chem. Soc.* **105** 2021 (1983)
132. H Abdallah, R Gree, R Carric *Tetrahedron* **41** 4339 (1985)
133. E Wenkert, M E Alonso, B L Buckwalter, K J Chon *J. Am. Chem. Soc.* **99** 4778 (1977)
134. E Wenkert, T D J Halls, L D Kwart, G Magnusson, H D H Showalter *Tetrahedron* **37** 4017 (1981)
135. M E Alonso, A Morales *J. Org. Chem.* **45** 4530 (1980)
136. A P Marchand, N M Brockway *Chem. Rev.* **74** 431 (1974)
137. E Kunkel, I Reichelt, H U Reissig *Liebigs Ann. Chem.* 802 (1984)
138. E L Grimm, H U Reissig *J. Org. Chem.* **50** 242 (1985)
139. R Menicagli, C Malanga, L Lardicci *J. Chem. Res. (S)* 20 (1985)
140. M P Cooke *J. Org. Chem.* **44** 2461 (1979)
141. O G Kulinkovich, I G Tishchenko, S V Sviridov *Zh. Org. Khim.* **22** 1416 (1986)
142. A De Mesmacker, L Vertommen, R Merenyi, H C Viehe *Tetrahedron Lett.* **23** 69 (1982)
143. A De Mesmacker, H G Viehe *Tetrahedron Lett.* **24** 2765 (1983)
144. O G Kulinkovich, I G Tishchenko, N A Roslik *Khim. Geterotsikl. Soedin.* 132 (1984)
145. O G Kulinkovich, I G Tishchenko, N A Roslik *Zh. Org. Khim.* **20** 532 (1984)
146. O G Kulinkovich, I G Tishchenko, N A Roslik *Zh. Org. Khim.* **18** 1654 (1982)
147. O G Kulinkovich, I G Tischenko, N V Masalov *Synthesis* 886 (1984)
148. O G Kulinkovich, I G Tishchenko, Yu N Romashin *Khim. Geterotsikl. Soedin.* 163 (1988)
149. I G Tishchenko, O G Kulinkovich, Yu V Glazkov *Zh. Org. Khim.* **11** 587 (1975)
150. I G Tishchenko, O G Kulinkovich, Yu V Glazkov, M K Pirshtuk *Zh. Org. Khim.* **11** 576 (1975)
151. O G Kulinkovich, I G Tishchenko, N V Masalov *Khim. Geterotsikl. Soedin.* 1603 (1984)
152. O G Kulinkovich, I G Tishchenko, N V Masalov *Khim. Geterotsikl. Soedin.* 1028 (1983)
153. S Danishefsky, R Mekee, R K Singh *J. Am. Chem. Soc.* **99** 4783 (1977)
154. L A Paguette, C Blankenship, C J Wells *J. Am. Chem. Soc.* **106** 6442 (1984)
155. C Bruckner, H U Reissig *J. Chem. Soc., Chem. Commun.* 1512 (1985)
156. C Bruckner, H U Reissig *Angew. Chem., Int. Ed. Engl.* **24** 588 (1985)
157. C Bruckner, H U Reissig *Liebigs Ann. Chem.* 465 (1988)
158. C Bruckner, B Suchland, H U Reissig *Liebigs Ann. Chem.* 471 (1988)
159. W Flitsch, P Wernsmann *Tetrahedron Lett.* **22** 719 (1981)
160. W Flitsch, P Russkamp *Liebigs Ann. Chem.* 521 (1983)
161. W Flitsch, K Pandl, P Russkamp *Liebigs Ann. Chem.* 529 (1983)
162. J M Muchowski, P H Nelson *Tetrahedron Lett.* **21** 4585 (1980)
163. W G Dauben, D J Hart *Tetrahedron Lett.* **16** 4553 (1975)
164. I Kuwajima, E Nakamura, in *Topics in Current Chemistry* (Berlin: Springer, 1990) Vol.155, p. 3
165. N H Werstiuk *Tetrahedron* **39** 205 (1983)
166. E Nakamura, I Kumajima *J. Am. Chem. Soc.* **99** 3760 (1983)
167. E Nakamura, H Oshino, T Kumajima *J. Am. Chem. Soc.* **108** 3745 (1986)
168. H U Reissig *Tetrahedron Lett.* **22** 2981 (1981)
169. H U Reissig, I Reichelt, H Lorey *Liebigs Ann.Chem.* 1924 (1986)
170. H U Reissig, H Holzinger, G Glomsda *Tetrahedron* **45** 3439 (1989)
171. K Saigo, S Shimada, Y Hashimoto, M Nasegawa *Chem. Lett.* 1293 (1989)
172. K Saigo, S Shimada, M Hasegawa *Chem. Lett.* 905 (1990)
173. K Saigo, S Shimada, Y Hashimoto, T Nagashima, M Hasegawa *Chem. Lett.* 1101 (1990)
174. J Salaun *Chem. Rev.* **89** 1247 (1989)

Russian Chemical Reviews **62** (9) 851 – 876 (1994)
©1993 Russian Academy of Sciences and Turpion Ltd

UDC 537.228; 539

Electrical birefringence in solutions of rigid-chain polymers

V N Tsvetkov, N V Tsvetkov

Contents

I.	Introduction	851
II.	Theoretical aspects and experimental procedure	851
III.	Transient electrical birefringence in solutions of rigid-chain polymers. Experimental data	857
IV.	Steady electrical birefringence in solutions of rigid-chain polymers. Experimental data	862
V.	Effect of the structure of side groups and of the degree of substitution on the electro-optic properties of cellulose esters	868
VI.	Electro-optics of solutions of branched polymers with mesogenic groups in the side chains	870
VII.	Conclusions	873

Abstract. Experimental and theoretical aspects of the application of steady and transient electrical birefringence methods to dilute solutions of rigid-chain polymers are examined. The prospects of using the Kerr effect to study the conformational and the structural characteristics of macromolecular chains are analysed. The effect of the polarity of the medium on the electro-optical properties of polymeric molecules is discussed. The bibliography includes 117 references.

I. Introduction

The wide interest which studies of the molecular properties of rigid-chain polymers have attracted is due partly to the extensive industrial applications of materials based on these polymers and partly to the increasing need for general concepts concerning the structure and the physical properties of macromolecular compounds.

Latterly we have witnessed an increasing interest in studies of rigid-chain polymers able to undergo thermotropic and lyotropic mesomorphism, such as aromatic polyesters and polyamides, and also cellulose esters. This interest has been stimulated by the applications of substances of this type in various electronic devices and by improvements in the technology of polymer processing.

The structure and the conformation of the molecules of rigid-chain polymers, which are responsible for the unique properties of the materials prepared from these polymers, are determined by studying the behaviour of their macromolecules in very dilute solutions, in which the intermolecular interaction of the polymer chains is negligibly small. The measurement of electrical birefringence (EBR, the Kerr effect) is one of the most important methods of studying the conformational and the kinetic characteristics of rigid-chain polymers in dilute solutions, since it provides information on the structural and the dynamic properties of rigid-chain macromolecules which is needed in order to identify the interrelationship between the molecular structure and the physical properties of the polymers. This information is an essential first step in the creation of new materials having prescribed properties.

V N Tsvetkov Institute of Macromolecular Compounds, Russian Academy of Sciences, Bol'shoi prosp. 31, 199044 St Petersburg, Fax (7-812) 218 6869
N V Tsvetkov Physics Institute, St Petersburg State University ul. Ul'yanovskaya 1, 198904 St Petersburg, Fax (7-812) 428 7240

Received 5 May 1993
Uspekhi Khimii **62** (9) 900–926 (1993); translated by J I Carasso

II. Theoretical aspects and experimental procedure

1. Theory of the steady Kerr effect for rigid molecules

In 1875 Kerr established[1] that a transparent isotropic substance exposed to an electric field acquires the optical properties of a uniaxial crystal with its axis parallel to the field. In the case of weak DC fields the optical anisotropy generated in the substance is proportional to the square of the field intensity (Kerr's law):

$$\frac{\Delta n}{n} \equiv \frac{n_p - n_s}{n} = K_e E^2 . \quad (1)$$

Here $\Delta n = n_p - n_s$ is the difference between the refractive indices (extraordinary n_p and ordinary n_s) for two light rays with electric vectors oscillating in directions parallel and perpendicular to the electric field respectively; E is the intensity of the electric field, directed at right angles to the light rays; n is the average refractive index of the substance; K_e is the Kerr constant.

The electro-optical properties of substances are often described in terms of the specific Kerr constant K_ρ defined as

$$K_\rho = \frac{\Delta n}{\rho E^2} , \quad (2)$$

where ρ is the density of the liquid.

In the case of a solution the EBR caused by the presence of the solute can be characterised by the Kerr constant of the latter, defined by the expression

$$K = \lim_{E \to 0,\, c \to 0} \frac{\Delta n}{cE^2} , \quad (3)$$

where Δn is the excess difference in refractive indices, due to the solute, and c is the concentration of solute (g cm^{-3}).

The molar Kerr constant ${}_mK$, defined (according to Debye[2]) by the expression

$${}_mK = \frac{6K_\rho Mn}{[(n^2+2)(\varepsilon+2)]^2} , \quad (4)$$

is sometimes used to characterise the molecular properties of liquids. Here M is the molecular weight of the liquid and ε is its dielectric permittivity.

The molar Kerr constant ${}_mK_{12}$ of a two-component solution is an additive quantity, expressed in terms of the molar Kerr constants of the solvent ${}_mK_1$ and of the solute ${}_mK_2$ (see Stuart[3]):

$$ {}_mK_{12} = (1-f_2){}_mK_1 + f_2\,{}_mK_2 , \tag{5}$$

where f_2 is the mole fraction of the solute.

It follows from Eqns (3)–(5) that the molar constant of the solute extrapolated to zero concentration (${}_mK_{c\to 0}$) is given by

$$ ({}_mK)_{c\to 0} = \frac{6KnM}{[(n^2+2)(\varepsilon+2)]^2} . \tag{6}$$

Here n and ε are the refractive index and the dielectric permittivity of the solvent respectively.

The theories of Langevin[4] and Born,[5] developed for gases, relate the constant ${}_mK$ of a substance to the principal components of the tensor of the optical (γ_1, γ_2, γ_3) and the dielectric polarisabilities (δ_1, δ_2, δ_3) of the molecule and to the corresponding components (μ_1, μ_2, μ_3) of its dipole moment by the expression

$$ {}_mK = \frac{2\pi N_A}{405kT}\left[\sum_{i,j=1}^{3}(\gamma_i-\gamma_j)(\delta_i-\delta_j) + \frac{1}{kT}\sum_{i,j=1}^{3}(\gamma_i-\gamma_j)(\mu_i^2-\mu_j^2)\right] , \tag{7}$$

where N_A is Avogadro's number.

It should be noted that Eqn (7) does not contain terms explicitly dependent on the state of aggregation of the substance. This explains the many reported attempts to use the equation in descriptions of the electro-optic properties not only of gases but also of liquids and solutions. Experiments have shown[3] that Eqn (7) adequately describes those properties in the case of polar molecules and of nonpolar substances not only in the gas phase but also in their solutions in nonpolar solvents, but in the case of polar (conducting) liquids and of solutions in polar solvents the equation is unacceptable.

For substances in dilute solutions and consisting of molecules having axially symmetrical optical and dielectric properties the constant K in Eqns (6) and (7) is given by

$$ K = \frac{2\pi N_A}{135kTn}\left[\frac{(n^2+2)(\varepsilon+2)}{3}\right]^2 \frac{\gamma_1-\gamma_2}{M} \times\left[\delta_1-\delta_2+\frac{\mu^2}{kT}\,\frac{3\cos^2\theta-1}{2}\right] , \tag{8}$$

where θ is the angle defined by the dipole μ and the axis of symmetry of the optical and of the dielectric polarisability (γ_1 and δ_1).

Eqn (8) shows that the sign of K depends on the magnitude and direction (angle θ) of the dipole moment of the molecule. Thus for nonpolar molecules ($\mu = 0$) the Kerr constant is always positive, because the signs of $(\gamma_1-\gamma_2)$ and $(\delta_1-\delta_2)$ are the same. For strongly polar molecules, in which the term $\delta_1-\delta_2$ can be ignored, the Kerr effect is positive for $\theta < 54.72°$ and negative for $\theta > 54.72°$.

We should stress the fact that the Langevin–Born theory, which leads to Eqns (7) and (8), relies on the assumption that the potential energy of the molecules associated with their rotation in an electric field is small in comparison with the energy of the thermal motion, $\mu\epsilon/kT \ll 1$ and $(\delta_1-\delta_2)\epsilon^2/kT \ll 1$, where ϵ is the field acting on the molecule [according to Lorentz $\epsilon = E(e+2)/3$]. In the opposite case the dependence of Δn on E^2 reaches saturation (see Kuhn et al.[6] and O'Konski et al.[7]).

2. Transient electrical birefringence

The study of the electro-optical properties of molecules under the influence of electrical pulses of various forms yields valuable information on their rotational mobility and justifies a number of conclusions on the nature of the EBR under study (is it due mainly to the presence of a constant dipole moment in the molecule, or to the anisotropy of its dielectric polarisability, or even to a combination of these factors).

These possibilities arise because the reorientation of the molecules under the influence of the electric field is not instantaneous, but requires a certain time, depending both on the rotational diffusion coefficient of the particles D_r and on the nature of the observed effect. Experiments of this type are difficult when the samples under study are low-molecular substances, because the molecular reorientation times are very short in these materials (10^{-11}–10^{-9} s). However, in solutions containing supermolecular species or rigid macromolecules the reorientation times are significantly longer, and they can be measured electrooptically.

Rectangular-pulse and sinusoidal periodic fields are the types of field most often used in studies of the relaxation processes. The pulsed field method was proposed independently by Russian[8] and by French physicists.[9,10]

The disappearance of the EBR in a monodispersed system of rigid particles or molecules with an axial symmetry of form and of optical properties following the instantaneous switching off of the field is determined only by their spontaneous disorientation as a result of thermal rotation, is independent of the electrical properties of the species, and is described by the expression[9,10]

$$ \Delta n = \Delta n_0\, e^{-t/\tau_0} , \tag{9}$$

where Δn_0 is the initial EBR of the system in a steady field, t is the time, and τ_0 is the relaxation time,

$$ \tau_0 = \tfrac{1}{6}D_r . \tag{10}$$

Here D_r is the diffusion coefficient of the particles rotating round their short axis (normal to the axis of symmetry). The rate of the establishment of the EBR by switching on the electric field is determined not only by the thermal motion of the particles but also by the electrical properties of the molecules.

For axially symmetric particles, in which the vector or the dipole moment μ is parallel to the axis of symmetry, the dependence of Δn on t when the field has been switched on ($\mu\epsilon/kT \ll 1$) is described by the expression[9,10]

$$ \frac{\Delta n}{\Delta n_0} = 1 - 3\frac{\alpha^2}{\beta}\left(\frac{2\alpha^2}{\beta}+4\right)^{-1} e^{-t/\tau} + \left(\frac{2\alpha^2}{\beta}+4\right)^{-1}\left(\frac{\alpha^2}{\beta}-4\right)e^{-t/\tau_0} , \tag{11}$$

where

$$ \tau = \tfrac{1}{2}D_r ; \quad \alpha = \frac{\mu\epsilon}{kT} ; \quad \beta = \frac{(\delta_1-\delta_2)\epsilon^2}{2kT} . \tag{12}$$

If the particle has no dipole moment ($\alpha = 0$) and the EBR is determined exclusively by the anisotropy of its polarisability ($\delta_1-\delta_2$), Eqn (11) becomes

$$ \Delta n = \Delta n_0(1 - e^{-t/\tau_0}) . \tag{13}$$

In this case the growth of Δn on switching on the field (curve *1* of Fig. 1) corresponds exactly to its decay (curve *3*). If the molecules are oriented by the field E only because of the dipole moment μ we find from (11)

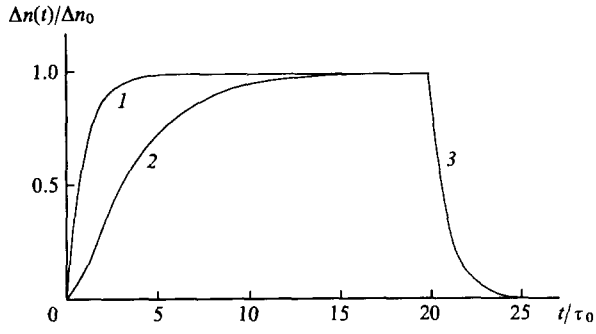


Figure 1. Dependence of the relative value of the EBR on the relative time for instantaneous switching the electric field on (*1*, *2*) and off (*3*): (*1*) and (*3*) nondipolar ($\alpha = 0$) and electrically anisotropic particles, (*2*) and (3) dipolar and electrically isotropic particles ($\beta = 0$).

$$\frac{\Delta n}{\Delta n_0} = 1 - \frac{3}{2}e^{-t/\tau} + \frac{1}{2}e^{-t/\tau_0} . \tag{14}$$

In this case Δn increases more slowly than in the case of inductive orientation, and the $\Delta n(t)$ dependence (curve *2* of Fig. 1) is tangential to the t axis for $t = 0$.

In the more general case, Δn increases more slowly when the steady dipole of the particles plays a dominant role in the EBR.

In a sinusoidal electric field of voltage $E = E_0 \cos\omega t$ the orientation distribution function of dielectrically anisotropic and polar particles should be time-dependent. Accordingly, the observed excess birefringence Δn stimulated by the dissolved substance is also time-dependent.

For dielectrically isotropic particles the instantaneous value of the excess EBR of the solution $[\Delta n(t)]$ and the corresponding instantaneous value of the Kerr constant $[K(t)]$ are defined by the expressions[11]

$$K(t) = \frac{2\Delta n(t)}{cE^2} = K\left\{1 + \left[\frac{\cos(2\omega\tau - \varphi)}{(1+\omega^2\tau_0^2)^{1/2}}\right]\right\} , \tag{15}$$

$$\tan\varphi = 2\omega\tau_0 ,$$

where ω and E_0 are the angular frequency and the amplitude of the electric field.

If follows from this expression that in a sinusoidal field $\Delta n(t)$ and $K(t)$ oscillate symmetrically with respect to the mean value of K with a doubled frequency, and that their sign at any instant is the same as that of K. The amplitude of these oscillations falls to zero as the frequency ω increases. When the time-average value of Δn is the monitored quantity the measured EBR is independent of the frequency of the field, and remains equal to its equilibrium value in a steady field of amplitude $E = E_0/\sqrt{2}$.

If particles having constant dipoles are exposed to a sinusoidal electric field the expression for their Kerr constant takes the form

$$K(t) = \frac{2\Delta n(t)}{cE^2}$$

$$= K\left[\frac{1}{1+\omega^2\tau^2} + \frac{\cos(2\omega t - \varphi)}{(1+4\omega^2\tau_0^2)^{1/2}(1-\omega^2\tau^2)^{1/2}}\right] , \tag{16}$$

$$\tan\varphi = \frac{5\omega\tau}{3 - 2\omega^2\tau^2} .$$

The first term in Eqn (16) is time-independent. It is a time-averaged value of the Kerr constant for a fixed field frequency ν:

$$K_\nu = \frac{K}{(1+\omega^2\tau^2)} . \tag{17}$$

This average value of K_ν decreases with increasing frequency of the field, and vanishes at high frequencies because of the relaxation of the rotational motion of the dipolar particles. According to Eqn (17) τ can be determined from the dispersion curve by using the condition

$$\tau = \frac{1}{\omega_m} , \tag{18}$$

where ω_m is the angular frequency for which $\Delta n_\nu = (\Delta n_0 + \Delta n_\infty)/2$ (Δn_0 and Δn_∞ are the values of Δn for $\omega = 0$ and $\omega = \infty$ respectively).

If a particle (or a rigid molecule) has both a steady dipole and dielectric anisotropy the time-dependent value of $K(t)$ is determined by the sum of the expressions (15) and (16) with appropriate weighting coefficients. If the quantity monitored in the experiment is the time-averaged value of the EBR as a function of the frequency of the external field the plot of K has the form shown in Fig. 2:

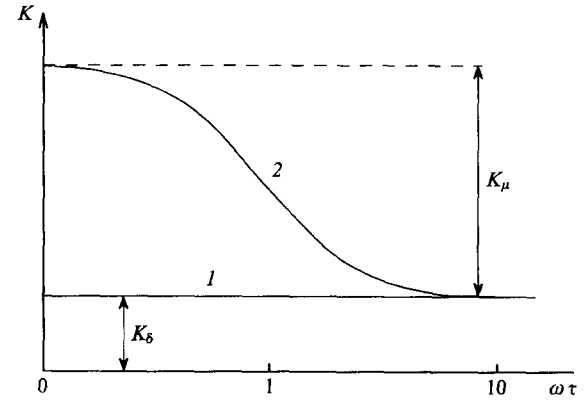


Figure 2. Frequency dependence of the mean Kerr constant for a solution of dielectrically anisotropic dipolar particles: (*1*) K_δ, the anisotropic part of the Kerr constant, (*2*) overall effect $K = K_\delta + K_\mu$ (K_μ is the dipolar part of the Kerr constant).

However, it should not be forgotten that the expressions (9)–(18) are valid only for monodispersed systems of particles or of rigid molecules. Substances studied experimentally are usually polydispersed in relaxation time. In this case the total value of $\Delta n(t)$ is a superposition of the $\Delta n_i(t)$ values (where i is the number of the group of molecules having identical relaxation times, allowing for their mass fractions in the sample). For rigid polar molecules Eqns (9) and (14) can be re-written

$$\frac{\Delta n(t)}{\Delta n_0} = \int_0^\infty \varphi(\tau) f(t,\tau)\, d\tau , \tag{19}$$

where $f(t,\tau) = e^{-3t/\tau}$ for the decay and $f(t,\tau) = 1 - (3/2)e^{-t/\tau} + (1/2)e^{-3t/\tau}$ for the growth of $\Delta n(t)$, and the function $\varphi(\tau)$ allows for the contribution to the EBR from molecules having relaxation times between τ and $\tau + d\tau$. The areas delinated by the growth and decay curves are, respectively,

$$Q_g = \int_0^\infty \left(1 - \frac{\Delta n(t)}{\Delta n_0}\right) dt \quad \text{and} \quad Q_d = \int_0^\infty \frac{\Delta n(t)}{\Delta n_0} dt .$$

Starting from Eqns (13) and (14) for monodispersed rigid particles or molecules we obtain

$$Q_d = \tfrac{1}{3}\tau = \tau_0 ,$$

for the decay curve and

$$Q_g = \tfrac{4}{3}\tau = 4Q_d$$

for the growth curve. In this case Q_d is the 'free relaxation' time.

In the presence of polydisperseness with respect to the molecular mass M or to the relaxation time τ the areas Q_g and Q_d are altered (in this case $Q_d = \langle\tau_0\rangle$ is the mean free relaxation time), but according to Eqn (19) their ratio stays the same: $Q_g/Q_d = 4$, irrespective of the form of the function $\varphi(\tau)$.

Often the experimental dispersion curves are wider than predicted by Eqn (17), suggesting polydisperseness of the ensemble of molecules with respect to the relaxation times. These dispersion curves can be described by replacing Eqn (17) by

$$\frac{\Delta n_\nu}{\Delta n_0} = \int_0^\infty \varphi(\tau)(1+\omega^2\tau^2)^{-1}\,d\tau. \tag{20}$$

3. Relationship between the relaxation times and the hydrodynamic and the structural properties of the molecules

Studies of the dynamics of the Kerr effect yield information on the rotational mobility of particles or of rigid molecules, and therefore on their size and shape, thus allowing meaningful conclusions on the nature of the observed EBR to be made. The same is true of studies of the time-dependent EBR in dilute solutions of polymers, but in this case the possibilities offered by the method are much wider: it can evaluate both the structural (equilibrium) and the kinetic rigidity of the macromolecules. The term kinetically rigid denotes a polymeric molecule whose orientation time (τ_{or}) under the stimulus of an external field is smaller than the time needed for its deformation (τ_{def}) in the same field. This definition suggests that a given macromolecule can behave both as kinetically rigid and kinetically flexible, depending on the nature of the forces acting on it. The length of the Kuhn segment (A)[12,13] can be used as a measure of the equilibrium rigidity ($\langle \boldsymbol{h}^2\rangle$). If the beginning and the end of a real polymeric molecule are super-imposed on the beginning and the end of a model, freely coupled Kuhn chain having the same contour line L the equilibrium rigidity can be evaluated by the equation[12-14]

$$\langle \boldsymbol{h}^2\rangle = LA\,; \quad L = NA\,, \tag{21}$$

where $\boldsymbol{h}$ is a vector connecting the end-points of the chain, and N is the number of Kuhn segments in the chain. The angle brackets in Eqn (21) denote averaging over all the conformations of the macromolecule.

Depending on their A value all polymers are usually classified into two groups: rigid-chain polymers (with a large A) and flexible-chain polymers (with a small A). Experimental data[13] show that macromolecules having a high equilibrium rigidity also show kinetic rigidity, and are oriented in externally applied fields by a mechanism involving the large-scale rotation of the molecule as a whole. Conversely, the molecules of flexible-chain polymers have a small kinetic rigidity,[13] and therefore their orientation in an electric field takes place by the deformation mechanism.

The study of the dependence of the relaxation time of the EBR on the molecular weight of the polymer is of fundamental importance for determining the character of the motion of the molecules in an electric field. This dependence can be described approximately by the following empirical expression, which is valid over a reasonably narrow range of molecular masses:

$$D = K_{D_r} M^{-b}\,, \tag{22}$$

where D is the rotational diffusion coefficient, K_{D_r} is a constant [$D_r = 1/2\tau$]; b lies between 3 (for infinitely thin kinetically rigid rods) and 1.5 (for kinetically rigid nonpercolating Gaussian tangles).

A more general expression relates the relaxation time τ of a kinetically rigid molecule to its molecular mass and to its characteristic viscosity $[\eta]$ in solution:[13]

$$\tau = \frac{M[\eta]\eta_0}{2FRT}\,, \tag{23}$$

where η_0 is the viscosity of the solvent and $R = kN_A$. The coefficient F depends on the hydrodynamic properties of the particles used as models of the molecules: its limiting values are 2/15 for thin rods and 5/12 for spherical tangles.

A quantitative description of the equilibrium conformational properties of polymeric molecules can be based on the theory of the rotational friction of kinetically rigid vermiform chains.

In the first variant, developed by Hearst[15] for the vermiform necklace model, the theoretical expressions were reduced to the form

$$\tau = \tau_r f(x)\,, \tag{24}$$

$$\tau_r = \frac{(6kT)^{-1}\pi\eta_0 L^3}{\ln(L/d) - 0.877 + 7[(1/\ln(2L/d)) - 0.28]^2}\,.$$

Here τ_r is the rotational relaxation time of the rod-like molecule[16] whose length L and diameter d are equal (respectively) to the contour line and to the hydrodynamic diameter of the molecule; $f(x)$ is a function which allows for the equilibrium flexibility of the chain, and $x = 2L/A$.

In Hearst's theory[15] the function $f(x)$ is a linear correction (with respect to x) applied to the τ_r value of a rod-like molecule and valid only for $x \ll 1$, which seriously limits the prospects of using this variant in conjunction with experimental data.

Hearst's theory was subsequently developed by Hagerman and Zimm,[17] who used it in conjunction with the Monte Carlo method to express the function $f(x)$ as a power series in x, thus markedly extending its region of validity to $0.1 \leqslant x \leqslant 5$:

$$f(x) = (1.0120 - 0.24813x + 0.033703x^2 - 0.0019177x^3) \times (1 - 0.06469x + 0.01153x^2 - 0.0009893x^3)\,. \tag{25}$$

By varying the parameters d and A we can construct a theoretical curve offering the best description of the experimental data [$\tau = \tau(M)$], and thus determine the equilibrium rigidity and the hydrodynamic diameter of the molecule. This calculation was carried out[18,19] for a group of DNA samples, and gave results satisfactorily consistent with data obtained by translational diffusion methods.

4. The Kerr effect in solutions of vermiform chains

As was pointed out above, macromolecules of rigid-chain polymers behave as kinetically rigid chains in an electric field. Furthermore, it was found that the EBR and the flow birefringence (FBR) had the same sign for solutions of this class of polymer in the Gaussian region. This shows that the character of the orientation of their molecules in electrical and in mechanical (shear) fields is the same, and involves a large-scale rotation mechanism. Therefore the use of data obtained by the FBR method for interpreting EBR results is fully justified. The equilibrium electro-optical properties of solutions of rigid-chain polymers can be described by starting from the theory of the Kerr effect for rigid dipolar particles with axially symmetrical optical and dielectric polarisabilities, using the $\boldsymbol{h}$ axis (which connects the ends of the chain) as a symmetry vector. The latter postulate is consistent with the basic conformational characteristics of polymer chains discussed in the original papers by Kuhn et al.[20-22]

Thus Eqn (8) becomes the starting expression for the Kerr constant of a rigid-chain polymer. However, in order to establish the quantitative dependence of K on the conformation and structure of the macromolecule we need a specific molecular model to describe its electro-optical properties. A large volume of experimental and theoretical information[13] confirms that the most universal model of the conformational, hydrodynamic, and dynamic-optical properties of rigid-chain polymeric molecules is the vermiform chain model, and that this model can reasonably be used also to describe the electro-optical properties of these molecules.

The theory of the equilibrium Kerr effect in dilute solutions of vermiform chains has been fully developed.[23,24] Since in the ensemble of unfolded vermiform polymer molecules the dipolar, the optical, and the dielectric terms which appear in Eqn (8) are statistical quantities, averaged over all the conformations of the macromolecules, a similar averaging is needed also for Eqn (8). In this case the difference between the two principal optical polarisabilities of the vermiform molecule (along the $\boldsymbol{h}$ axis and at right angles to it) is given by the expression[25]

$$\langle \gamma_1 - \gamma_2 \rangle = \frac{3}{5} \frac{\Delta a S x f_1(x)}{f_2(x)} , \tag{26}$$

where Δa is the optical anisotropy of the monomer unit of the chain, and S is the number of monomer units in the Kuhn segment. Throughout this review angle brackets will be used to denote quantities averaged over conformations. The functions $f_1(x)$ and $f_2(x)$ take the form

$$f_1(x) = x - 1 + e^{-x} ; \quad f_2(x) = x^2 - 0.8 f_1(x) . \tag{27}$$

The difference between the two principal dielectric polarisabilities $\langle \delta_1 - \delta_2 \rangle$ of a vermiform chain is also given by formula (26) when Δa is replaced by Δb (where Δb is the dielectric anisotropy of the monomer unit).

In addition to the geometric segment A, the electrical (dipolar) segment has been used to describe the properties of a freely coupled Kuhn chain: it consists of a rigid linear combination of uniformly oriented dipole moments μ_0 of the monomer units of the chain,[26] in which the 'dipolar' and the 'geometric' rigidities are assumed to be equal. However, allowance was made for the difference in the vector sum of the segment dipoles μ_s parallel to the axis of the geometric segment ($\mu_{s\parallel}$) and of the dipoles perpendicular to that axis ($\mu_{s\perp}$). In the former, the dipole moment of the molecule is parallel to the vector $\boldsymbol{h}$, and its mean square value is given by the expression

$$\langle \mu_\parallel^2 \rangle = N \mu_{s\parallel}^2 . \tag{28}$$

Eqn (28) reflects the 'accumulation' of the longitudinal components of the dipoles of the monomer units, resulting in an increase of the macromolecular dipole with increasing length of the polymer chain. In the latter case the overall dipole of the molecule is no longer parallel to $\boldsymbol{h}$, but has a longitudinal (parallel to $\boldsymbol{h}$) and a perpendicular component, whose mean square values are given by

$$\langle \mu_\parallel^2 \rangle = N \mu_{s\perp}^2 \left(\frac{h}{L}\right) \alpha^*\left(\frac{h}{L}\right) ;$$

$$\langle \mu_\perp^2 \rangle = N \mu_{s\perp}^2 \left[1 - \left(\frac{h}{L}\right) \Big/ \alpha^*\left(\frac{h}{L}\right)\right] , \tag{29}$$

where $\alpha^*(h/L)$ is the inverse Langevin function of the convolution parameter (h/L) of the chain.[22]

These ideas have been applied[23,24] to vermiform chains by considering the general case of the dipole moment μ_0 of the monomer unit at an angle ϑ to the tangent to the contour of the chain. It has also been pointed out[24] that the dipolar and the geometric rigidity of the chain can differ for reasons not allowed for in Kuhn's theory. The equality of the geometric and of the longitudinal (dipole) rigidity (characterised by the number $S_\parallel = S$ of longitudinal components $\mu_{0\parallel}$ of monomeric dipoles in the electrical segment) is beyond doubt. However, this hypothesis may not be applicable to many rigid-chain molecules met in practice: for example, *para* aromatic polyamides and polyethers. The high geometric rigidity of the chains of these polymers is due to their 'crankshaft' conformation,[27] one of whose features is a substantial freedom to undergo intramolecular rotations round the *para* aromatic axes. Allowance for the possible differences between the longitudinal and the transverse dipole rigidity can be made by introducing the parameter $\alpha \geqslant 1$;

$$S_\parallel = \alpha S_\perp = S ; \quad \mu_{s\parallel} = S_\parallel \mu_{0\parallel} = S_\parallel \mu_0 \cos\vartheta ; \tag{30}$$

$$\mu_{s\perp} = S_\perp \mu_{0\perp} = S_\perp \mu_0 \sin\vartheta .$$

Furthermore, noting that

$$\left\langle \mu^2 \frac{3\cos^2\vartheta - 1}{2} \right\rangle = \left\langle \mu_\parallel^2 - \frac{\mu_\perp^2}{2} \right\rangle , \tag{31}$$

using Eqn (30), and inserting into (29) $\langle h^2 \rangle / L$ for a vermiform chain, we obtain

$$\left\langle \mu^2 \frac{3\cos^2\vartheta - 1}{2} \right\rangle = \frac{M S \mu_0^2}{M_0} \frac{f_1(x)}{x} \left[\cos^2\vartheta \frac{3 f_1^2(\alpha x) \sin^2\vartheta}{5\alpha f_2(\alpha x) f_1(x)}\right] , \tag{32}$$

where M_0 is the molecular weight of the monomer unit in the polymer.

Inserting (26) and (32) into (8) gives an expression for the Kerr constant of the vermiform chain:

$$\frac{K}{K_\infty} = \frac{3\langle h^4 \rangle f_1^2(x)}{5\langle h^2 \rangle^2 f_2(x)} \times \left[1 - \frac{3 f_1^2(\alpha x)}{5\alpha^2 f_1(x) f_2(\alpha x)} \tan^2\vartheta + \frac{6 k T x \Delta b}{5\mu_{0\parallel}^2 S f_2(x) \cos^2\vartheta}\right] . \tag{33}$$

Here K_∞ is the limiting value of the Kerr constant in the region of $x \to \infty$:

$$K_\infty = \left(\frac{B \Delta a}{M_0 k T}\right) \mu_0^2 S^2 \cos^2\vartheta . \tag{34}$$

Using the Lorentz internal field multiplier gives the following expression for the coefficient B:

$$B = \left(\frac{2\pi N_A}{1215 k T n}\right) (n^2 + 2)^2 (\varepsilon + 2)^2 . \tag{35}$$

Eqn (33) contains the term

$$\frac{\langle h^4 \rangle}{\langle h^2 \rangle^2} = \frac{11}{3} x^2 - (2x + 8) f_1(x) + \frac{2}{27} \frac{f_1(3x)}{f_1^2(x)} , \tag{36}$$

introduced in order to allow for the polydisperseness with respect to conformations in the ensemble of vermiform chains; it varies from 1 to 5/3 as x is varied from 0 to ∞.

It follows from Eqn (34) that the sign of K_∞ is the same as the sign of Δa, since in a solution of kinetically rigid vermiform chains the signs of the EBR and of the FBR should coincide in the Gaussian region. We should stress that in order to achieve a quantitative characterisation of the dipole structure of macromolecules the parameter Δa must be known. For polymers Δa can be found by the FBR method, starting from the experimentally

determined value of the optical shift coefficient in the Gaussian region.

$$\left(\frac{\Delta n}{\Delta \tau}\right)_{\infty} = \frac{4\pi(n^2+2)^2}{45kTn}\Delta a S ,$$

where $\Delta\tau$ is the shear stress in the flow.

Fig. 3*a* shows plots of the relative Kerr constant $K/K_{\infty,\vartheta=0}$ against x for $\alpha = 1$ in the case of kinetically rigid vermiform chains. The curves differ not only in their asymptotic value (which is proportional to $\cos^2\vartheta$) but also in their shape. If the dipole is perpendicular to the direction of the chain ($\vartheta = 90°$) the Kerr effect is opposite in sign to Δa for all values of x, and decreases to zero (in absolute value) as x is increased. This is because the correlation in direction between the dipole moment of the chain molecule (obtained by summing all the perpendicular components of the dipole moments of the monomer units) and the direction of $\boldsymbol{h}$ decreases as x is increased, and disappears in the Gaussian region.

An entirely different situation is observed on summing the longitudinal components of the dipole moments of the monomer units, since in this case the dipole of the molecule is parallel to $\boldsymbol{h}$ and increases with x. These effects produce a sign inversion (at $90° > \vartheta > 54.74°$) in the plots of the relative Kerr constant against x (see Fig. 3*a*).

Possible effects of the difference between the longitudinal and the transverse dipole rigidity on the Kerr constant are illustrated in Fig. 3*b*, which shows plots of the ratio K/K_{∞} for fixed angles $\vartheta = 0°$ and 70° and different values of α.

The most widely used methods of measuring the EBR rely on monitoring changes in the light flow.[28-30] The methods therefore cannot be applied when the light flow undergoes time changes unrelated to the effect of interest. In these circumstances EBR measurements are possible only by the null method, in which an elliptical compensator is used to identify the effect due to birefringence.

Most of the rigid-chain polymers are soluble only in strongly polar, conducting solvents, and therefore their EBR can be studied only by using pulsed electric fields. The most widely used fields consist of rectangular pulses. However, in order to identify unambiguously the nature of the EBR we must use electric fields of varying sign: in this case sinusoidal-pulse fields are the most convenient.

The apparatus for measuring EBR in sinusoidal-pulse and in rectangular-pulse fields is shown diagrammatically in Fig. 4. The operating principle of its electrical part has

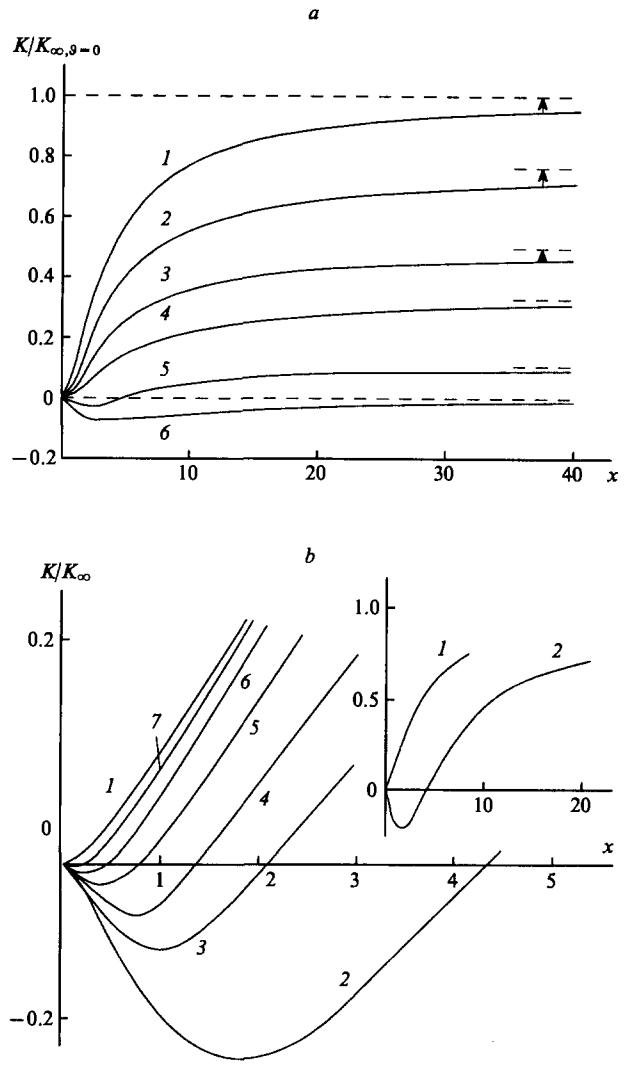


Figure 3. Plots of the relative Kerr constant against x for a kinetically rigid vermiform chain with $\alpha = 1$ (*a*) and different values of α (*b*): ϑ is the angle between the dipole of the monomer unit and the direction of the chain a: $\vartheta = 0°$ (*1*), 30° (*2*), 45° (*3*), 54.43° (*4*), 70° (*5*), 90° (*6*); *b*: $\vartheta = 0°$ (*1*), 70° (2–7); $\alpha = 0$ (*1*), 1.0 (*2*), 1.5 (*3*), 2.0 (*4*), 3.0 (*5*), 5.0 (*6*), 10.0 (*7*).

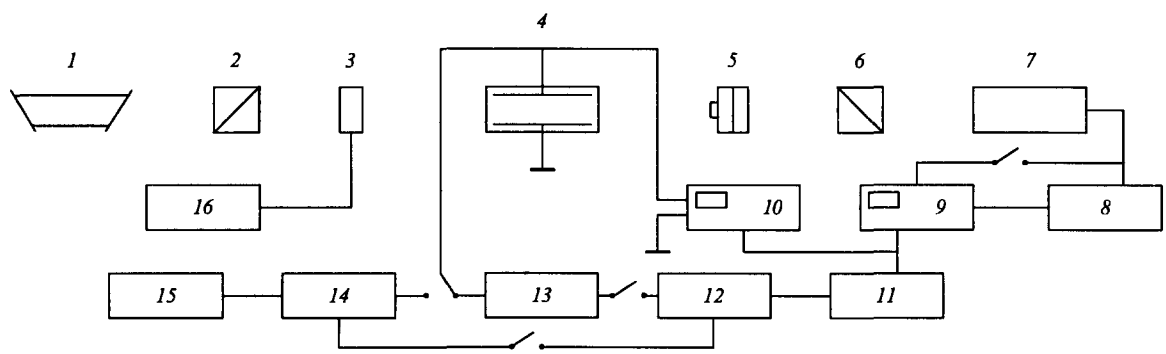


Figure 4. Apparatus for measuring the EBR by the compensation method in pulsed (sinusoidal and rectangular) electric fields: (*1*) helium–neon laser (λ = 632.8 nm); (*2*) and (*6*) polariser and analyser (Franck–Ritter prisms); (*3*) piezoceramic modulator of the ellipticity of the polarised light; (*4*) Kerr cell; (*5*) elliptical compensator with a path difference of 0.01 λ; (*7*) photodetector; (*8*) selective system; (*9*) and (*10*) oscillographs; (*11*) pulse delay generator; (*12*) rectangular pulse generator; (*13*) rectangular pulse former; (*14*) sinusoidal pulse former; (*15*) sinusoidal voltage generator; (*16*) generator for exciting the oscillations of the modulator.

already been described in detail.[31,32] The light flow Φ emerging from the analyser depends on the difference in phase between the mutually perpendicular oscillations of the two light waves created by the passage of light through the birefringent elements of the system. The azimuths of the optical axes of the birefringent layer and of the modulator form an angle of $\pi/4$ with the axis of the polariser. At low phase differences $\delta \ll 1$ we have the following expression for the light flux at the outlet to the photodetector:[31]

$$\Phi = \Phi_0 \frac{(\delta_E + \delta_m + \delta_0 \sin 2\varphi)^2}{4} . \quad (37)$$

Here Φ_0 is the amplitude of the light flux at the inlet to the system, δ_E is the phase difference generated by the solution ($\delta_E = 2\pi l \Delta n/\lambda$, where l is the optical length of the birefringent layer, and λ is the optical wave length), δ_0 and φ are the phase difference and the azimuth angle of the optical axis of the compensator, and $\delta_m = \delta_{m_0} \cos \Omega t$ is the phase difference introduced by the modulator ($\delta_{m_0} \ll 1$, $\Omega/2\pi = 5 \times 10^5$ Hz).

By using a selective system, tuned to the modulation frequency Ω, we can isolate the component of the light flux Φ',

$$\Phi' = \frac{\Phi_0}{2} (\delta_E + \delta_0 \sin 2\varphi) \delta_{m_0} \cos \Omega t , \quad (38)$$

which is linearly dependent on the azimuth angle φ of the rotation of the compensator. The compensation condition is defined by the expression

$$\delta_E = -\delta_0 \sin 2\varphi_c , \quad (39)$$

where φ_c is the azimuth angle for compensation.

In measurements of the growth and decay of the EBR the selective system is switched off, and the signal from the photodetector is taken directly to the input of the oscilloscope amplifier. However, the compensation condition (39) at the instant corresponding to the beginning of the pulse (determined by the time-delay of the master generator) stays unchanged. Under these conditions a signal at double the modulation frequency Ω is observed on the oscilloscope screen at the compensation instant.

Under the influence of an electric field of intensity $E = E_0 \cos \omega t$ the oscillations of the two light waves linearly polarised parallel and perpendicular to the voltage vector in the Kerr cell acquire a phase difference

$$\delta_E = \frac{\bar{\delta}_{E_0}}{2} + \left(\frac{\tilde{\delta}_{E_0}}{2}\right) \cos(2\omega\tau - \psi) , \quad (40)$$

where $\bar{\delta}_{E_0}$ is the phase difference characteristic of the constant component of the EBR, and $\tilde{\delta}_{E_0}$ is the amplitude of the oscillations in the EBR of frequency 2ω. These two values coincide under equilibrium conditions at low enough frequencies ω, and $\psi = 0$, but they differ in the frequency dispersion region corresponding to the Kerr effect.

The amplitude Φ of the oscillations in the flow of frequency Ω is linearly dependent on $\bar{\delta}_{E_0}$ and on $\sin 2\varphi$, and vanishes at the compensation point[31]

$$\bar{\delta}_{E_0} = -2\delta_0 \sin 2\varphi_k . \quad (41)$$

Eqn (41) is valid also when a sinusoidally pulsed field is applied.

The magnitude and the sign of the Kerr constant can be determined from Eqns (39) and (41). Various designs of the Kerr cell have been proposed.[28,29] In studies of the EBR in solutions of many rigid-chain polymers glass tubes fitted with titanium electrodes and with quartz side windows (held in position with springs or with adhesive) are most convenient. The length of the electrodes varies between 1 and 10 cm, and the interelectrode gap between 0.33 and 1.2 mm, depending on the chosen solvent.

The compensation method of measuring EBR by modulating the ellipticity of polarisation of the light gives the Kerr constants, the characteristic growth and decay times of the EBR, and also the dispersion relaxation times τ, with relative errors of 10%, 30%, and 20% respectively.

III. Transient electrical birefringence in solutions of rigid-chain polymers. Experimental data

1. Study of the dynamics of macromolecules in rectangular-pulse electric fields

Most of the recent studies of the rotational mobility of polymer molecules by the transient EBR method have used rectangular-pulse fields.[18,19,33-40] The free relaxation of the EBR following the removal of the field is usually monitored. The study of macromolecular dynamics by the free relaxation method offers information on the rotational mobility and on the conformational characteristics of polymer chains, and in this case, as was stated above, the nature of their orientation and of the observed EBR are unimportant. The combined study of the EBR growth and decay processes offers more information.

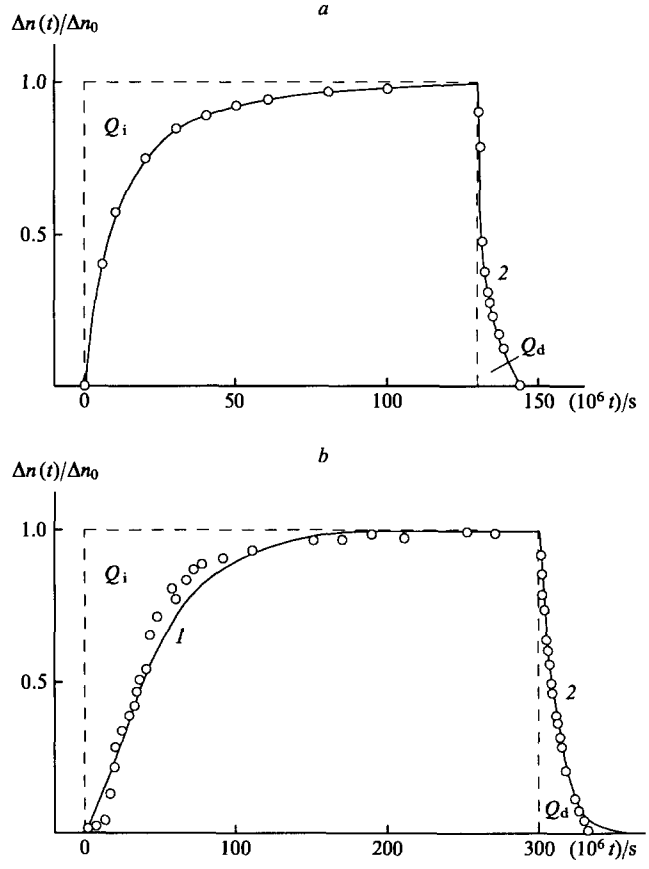


Figure 5. Time dependence of the relative EBR from the instant of switching on (*1*) and off (*2*) a rectangular electric pulse for a solution of the poly(butyl isocyanate) fraction with $M = 58 \times 10^3$ in tetrachloromethane[41] (*a*) and for a sample of polyamidohydrazide ($M = 26.6 \times 10^3$) in dimethyl sulfoxide[42] (*b*). Concentration of solution/g cm^{-3}: (*a*) 1×10^{-4}; (*b*) 0.11×10^{-2}.

Plots of the growth and decay of EBR following the instantaneous switching on and off of an electric field are shown in Fig. 5 for poly(butyl isocyanate) and poly(amido hydrazide). It can be seen that the growth of the EBR is markedly slower than its decay. This behaviour is characteristic of most of the rigid-chain polymers in which

Table 1. Dynamic characteristics of rigid-chain polymers in dilute solutions, obtained by the transient EBR method.

Fraction, polymer sample	Solvent	$10^{-2}[\eta]/cm^{-3}\,g^{-1}$	$10^{-3}M$	$10^{6}\tau_0/s$	$10^{6}Q_g/s$	$10^{6}\tau/s$	F	Ref.
Fractions								
cellulose nitrate	Cyclohexanone	2.6–16.5	130–822	13.5–270	–	–	0.38–0.76	38
cyanoethylcellulose	"	2.3–7.4	104–317	11–23	–	22–63	0.2–1.5	39
diphenyl substituted poly(phenylene terephthalate)	Dichloroacetic acid	1.7–6.45	14–86	3–68	–	–	0.3–0.4	40
poly(butyl isocyanate)	Tetrachloromethane	0.35–65	8.4–700	2–320	8–640	0.7–650	0.08–1.5	41
polyamidobenzimidazole	Dimethylacetamide	0.46–5.25	4–45	1–5	–	0.38–11	0.1–0.44	42
polyamidohydrazide	Dimethyl sulfoxide	0.85–5.7	8.6–46	0.7–7	4–20	2.4–17	0.14–0.7	42
cellulose acetobenzoate	Dioxan	0.16–1.75	13–198	–	–	1–22	0.03–0.37	43
cellulose acetocinnamate	"	0.1–6.5	7.7–878	–	–	0.63–200	0.04–0.91	44
cellulose carbanilate	"	0.09–0.78	14–107	–	–	0.3–4.5	0.18–0.43	45
cellulose carbanilate	"	0.1–2.1	10–195	–	–	0.22–19.6	0.12–0.53	[a]
Samples of cellulose carbanilate	"	1.6–11.5	340–4070	–	–	23–265	0.6–4.5	46
Samples of cellulose carbanilate	Dioxan	4.0	–	–	–	60	0.67	47
	Ethyl acetate	3.1	400	–	–	15	0.73	47
	Cyclohexanone	2.7	–	–	–	40	1.17	47
	Dimethylacetamide	2.6	–	–	–	18	1.06	47
Fractions								
cellulose nitrate	Dioxan	0.97–2.0	34–77	–	–	0.9–6.6	0.6–1.0	48
poly(chlorohexyl isocyanate)	Tetrachloromethane	0.4–3.8	8.8–159	–	–	0.8–227	0.23–0.54	49
Sample of poly(butyl isocyanate)	Tetrachloromethane – pentafluorophenol mixture (0%–10% mole fraction)	24–3.6	230	–	–	260–20	0.39–0.83	50
Samples of cellulose acetodiphenyl acetate	Dioxan	1.7–3.2	–	–	–	16–98	–	51
Sample								
ethylcellulose	"	2.5	80	–	–	14	0.29	52
benzylcelluose	"	0.6	30	–	–	1	0.38	52
cellulose diphenylphosphonocarbamate	"	4.9	1000	–	–	118	0.83	52
cellulose butyrate	"	6.5	780	–	–	236	0.43	52

[a] Data obtained in our laboratory.

the EBR is determined by the presence of a large steady dipole moment in the molecules.

The slight deviation of the experimental points in Fig. 5 from the theoretical curves for a monodispersed ensemble of rigid dipolar molecules indicates a relatively small polydisperseness of the sample in relaxation times. From the $\Delta n(t)/\Delta n_0$ curves obtained in this way we can determine the growth and decay times of the EBR whose values (extrapolated to infinite dilution) are listed in Table 1.

As can be seen from Table 1 the $\langle\tau_0\rangle$ values are strongly dependent on the molecular mass M, which is typical of rigid-chain polymers. The ratio $Q_g/\langle\tau_0\rangle$ is close to 4 for most of the fractions of poly(butyl isocyanate) and poly(amido hydrazide), as required by the theory for kinetically rigid dipolar molecules or particles. However, for the fractions of these polymers having the highest molecular mass we find $Q_g/\langle\tau_0\rangle < 4$. Two interpretations of this observation are possible. First, according to Eqns (11) and (12) the ratio $Q_g/\langle\tau_0\rangle$ should be less than 4. The development of kinetic flexibility in the macromolecules when M becomes very large can lead to the same result. An unambiguous choice between these two alternative explanations can be made by using only electric fields of variable sign, which immediately show whether or not the molecule has a substantial induced dipole. Studies based on sinusoidal-pulse electric fields[41,42] have indicated a preference for the second of these alternatives, which was shown to be responsible for a decrease in the ratio $Q_g/\langle\tau_0\rangle$.

2. Study of the dynamics of rigid-chain polymeric molecules in sinusoidal and in pulsed sinusoidal electric fields

As pointed out above, unambiguous conclusions on the nature of the EBR can be formulated by using electric fields of varying sign. Sinusoidal fields are the most convenient for this purpose. An additional advantage of a sinusoidal field as compared with a rectangular pulse field is that in studies of the dynamics of macromolecules of relatively low molecular weight in solutions the relaxation times can be so small as to be impossible to measure reliably by the free relaxation method. This shortcoming is almost totally eliminated in the method of determining τ in sinusoidal fields, which can be used at any frequency in the radio-frequency band: in other words, the sinusoidal field method can be used to determine τ over a much wider range of values.

The dynamics of macromolecules in electrically conducting polar solvents can be studied only in pulsed sinusoidal electric fields.

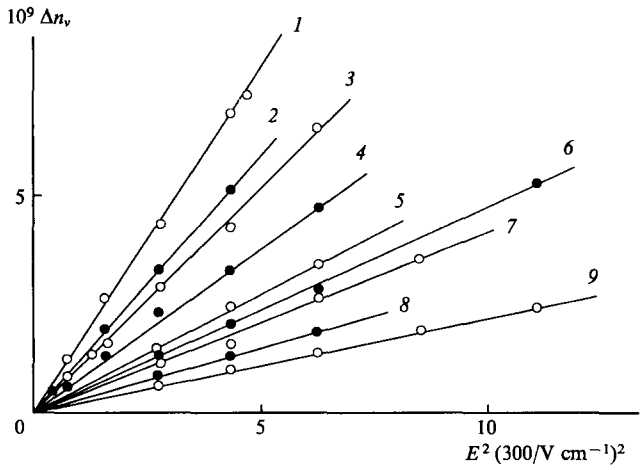


Figure 6. Dependence of the EBR on the effective intensity of a pulsed sinusoidal field for a solution of a sample of polyamidobenzimidazole ($M = 43 \times 10^3$) in dimethylacetamide ($c = 0.23 \times 10^{-2}$ g cm^{-3}) at different frequencies;[42] ν/kHz: (*1*) 0.5, 1, 3; (*2*) 7; (*3*) 10; (*4*) 20; (*5*) 50; (*6*) 70; (*7*) 100; (*8*) 200; (*9*) solvent at the same frequencies.

In Fig. 6 we show as an example the dependence of Δn on the square of the effective voltage of a pulsed sinusoidal field for a sample of polyamidobenzimidazole in dimethylacetamide. These plots can be used to determine the constant K_v of the polymer [Eqns (16) and (17)] for a fixed frequency ν of the pulsed field.

Figs 7 and 8 show dispersion plots of $\Delta n_v/\Delta n_0$ and of $K_v/K_{v\to 0}$ (where $K_{v\to 0}$ is the equilibrium value of the Kerr constant) against lg ν for several rigid-chain polymers. Similar data for other samples can be found in published reports.[13,53] It can be seen that all the plots in Figs 7 and 8 decay almost to zero as the frequency of the sinusoidal field is increased, and that they are strongly shifted towards lower frequencies by an increase in the molecular mass M of the polymers. These observations suggest that the mechanism mainly responsible for the observed EBR in solutions of rigid-chain polymers in both polar and non-polar solvents is a large-scale rotation of their dipolar molecules under the influence of the applied electric field. Furthermore, in the region of frequencies corresponding to the dispersion of the EBR dispersions of the dielectric increment $\Delta\varepsilon$ of the solutions have also been observed for cellulose poly(chlorohexyl isocyanate)[55] and carbanilate,[56] the dielectric dispersion curves almost coinciding with those of the Kerr effect. This indicates an identity of the molecular motion mechanisms and corresponds to the dispersion equation (17) for kinetically rigid molecules.

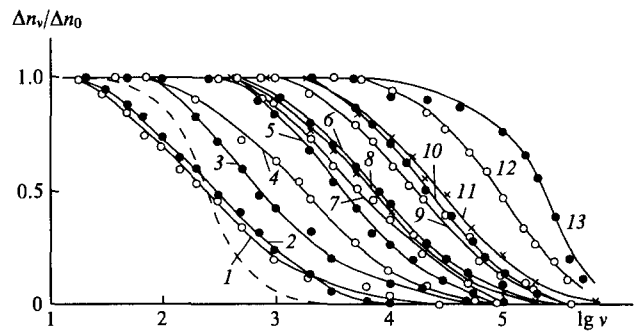


Figure 7. Dispersion plots of the EBR for the poly(butyl isocyanate) fractions in tetrachloromethane. The broken line is the Debye dispersion curve[41] with a relaxation time τ for the fraction *1*. 10^{-3} M: (*1*) 770; (*2*) 700; (*3*) 200; (*4*) 103; (*5*) 86; (*6*) 58.9; (*7*) 57.8; (*8*) 48.4; (*9*) 29.6; (*10*) 28.6; (*11*) 21.2; (*12*) 10.9; (*13*) 8.4; concentration of solutions 1×10^{-4} g cm^{-3}.

3. Kinetic and equilibrium rigidity of polymeric molecules

By using dispersion curves the 'mean' dispersion relaxation time τ can be calculated by Eqn (18). Typical concentration dependences of τ are shown in Fig. 9. Analogous data for several rigid-chain polymers have been published recently.[37] Values of τ for several rigid-chain polymers extrapolated to infinite dilution are shown in Table 1.

As can be seen from Table 1, the relaxation times τ increase rapidly as the molecular mass M of the polymers is increased. The model coefficient F can be calculated by using Eqn (23) in conjunction with the characteristic viscosities $[\eta]$.

An analysis of the dependence of F on the molecular mass for different classes of polymer is of interest. In a homologous series of fractions of a given polymer we note a tendency for F to increase with M in keeping with the accompanying change in the shape of the molecule from rod-shaped to tangle-shaped. Furthermore, it has been shown that in the fractions of these polymers having the highest molecular mass the F values exceed the maximum theoretical value for rigid particles. This is evidence of a weakening of the dependence of τ on M at high values of M. The weakening can be attributed to the general conditions of orientation and deformation of the chain molecule moving in an electric field.[57] Since τ_{or} increases with M in proportion to $M[\eta]$,

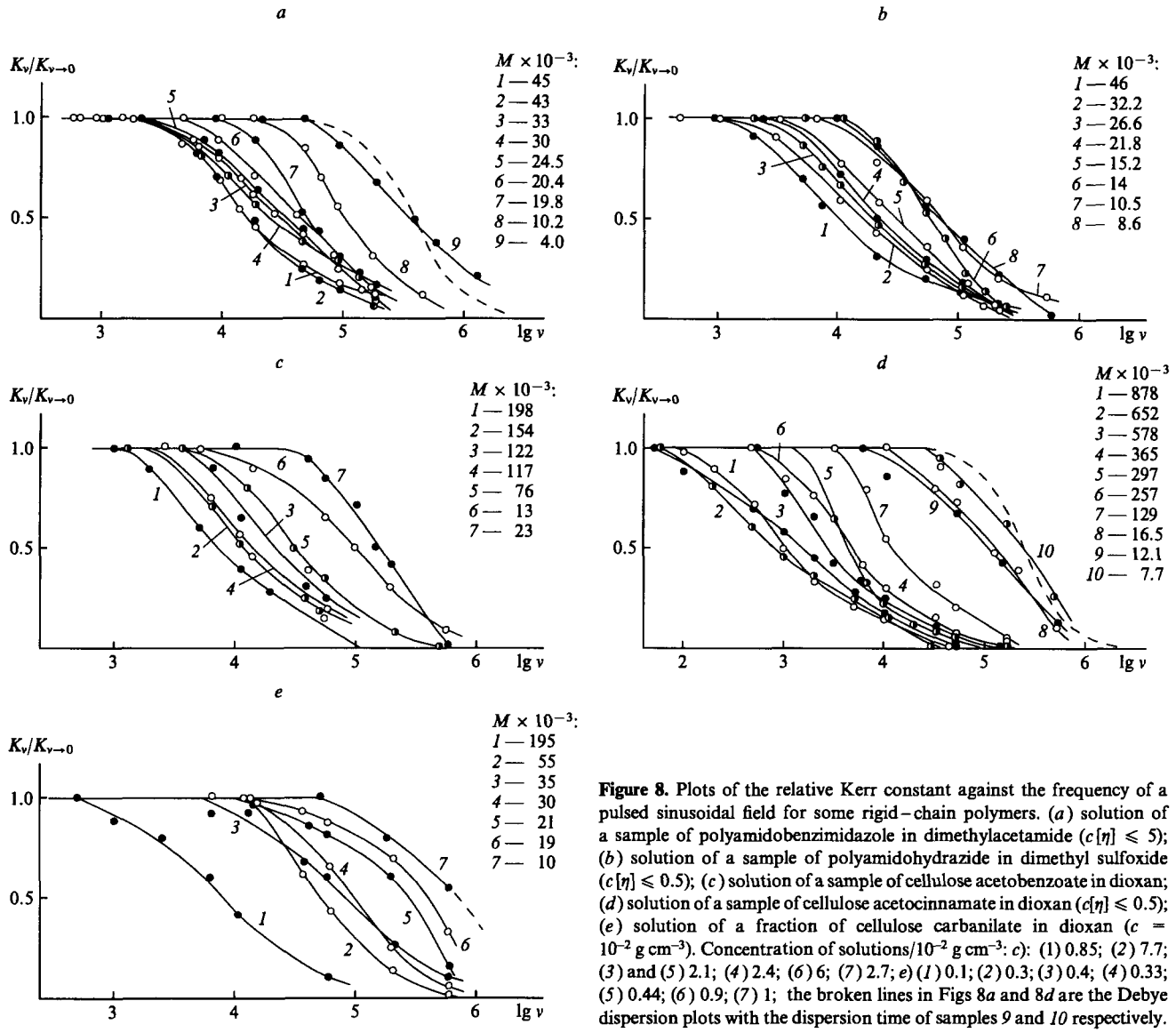


Figure 8. Plots of the relative Kerr constant against the frequency of a pulsed sinusoidal field for some rigid-chain polymers. (*a*) solution of a sample of polyamidobenzimidazole in dimethylacetamide ($c[\eta] \leqslant 5$); (*b*) solution of a sample of polyamidohydrazide in dimethyl sulfoxide ($c[\eta] \leqslant 0.5$); (*c*) solution of a sample of cellulose acetobenzoate in dioxan; (*d*) solution of a sample of cellulose acetocinnamate in dioxan ($c[\eta] \leqslant 0.5$); (*e*) solution of a fraction of cellulose carbanilate in dioxan ($c = 10^{-2}$ g cm^{-3}). Concentration of solutions/10^{-2} g cm^{-3}: *c*): (1) 0.85; (*2*) 7.7; (*3*) and (*5*) 2.1; (*4*) 2.4; (*6*) 6; (*7*) 2.7; *e*) (*1*) 0.1; (*2*) 0.3; (*3*) 0.4; (*4*) 0.33; (*5*) 0.44; (*6*) 0.9; (*7*) 1; the broken lines in Figs 8*a* and 8*d* are the Debye dispersion plots with the dispersion time of samples *9* and *10* respectively.

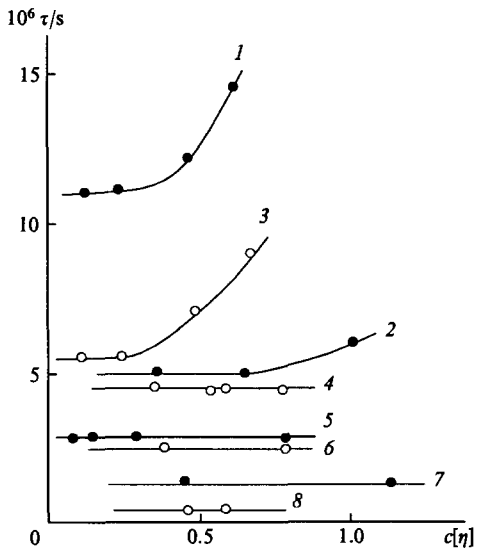


Figure 9. Plots of relaxation time against the volume fraction of the polymer in solutions of polyamidobenzimidazole in dimethylacetamide.[54] 10^{-3} *M*: (*1*) 45; (*2*) 33; (*3*) 30; (*4*) 24.5; (*5*) 20.4; (*6*) 19.8; (*7*) 10.2; (*8*) 4.

and τ_{def} is almost independent of *M*, we can expect to find $\tau_{or} > \tau_{def}$ for high enough values of *M*, and therefore the anisotropy of the solution in an electric field is produced by the deformation mechanism. The transition from an orientation to a deformation process as *M* is increased should result in an increase in *F*.

The results of Lewis, et al.[19] are of interest in this context. Starting from data on the free relaxation of the EBR in monodispersed samples of DNA of relatively high molecular mass these workers obtained the spectra of the times τ_0. The longest relaxation time in the spectrum corresponded to the large-scale motion of the DNA molecules, whereas the shortest times were determined by the small-scale motion and the corresponding deformation of the macromolecules. The largest relaxation time increased rapidly with the degree of polymerisation of the molecules, whereas the smallest was almost independent of *M*, though its contribution increased with *M*. These results are a clear illustration of the increased role of the deformation factor in the EBR of a polymer solution when *M* is increased.

A large increase in the *F* coefficient with *M* has been observed[46] in samples of cellulose carbanilate of high molecular mass ($M > 350 \times 10^3$). This effect was also treated as a manifestation of the intramolecular motion of the cellulose carbanilate molecules at large *M*, and it was described in terms of Zimm modes.[58,59]

An increase in the *F* coefficient upon changing the nature of the solvent has been reported[47,50] for cellulose carbanilate

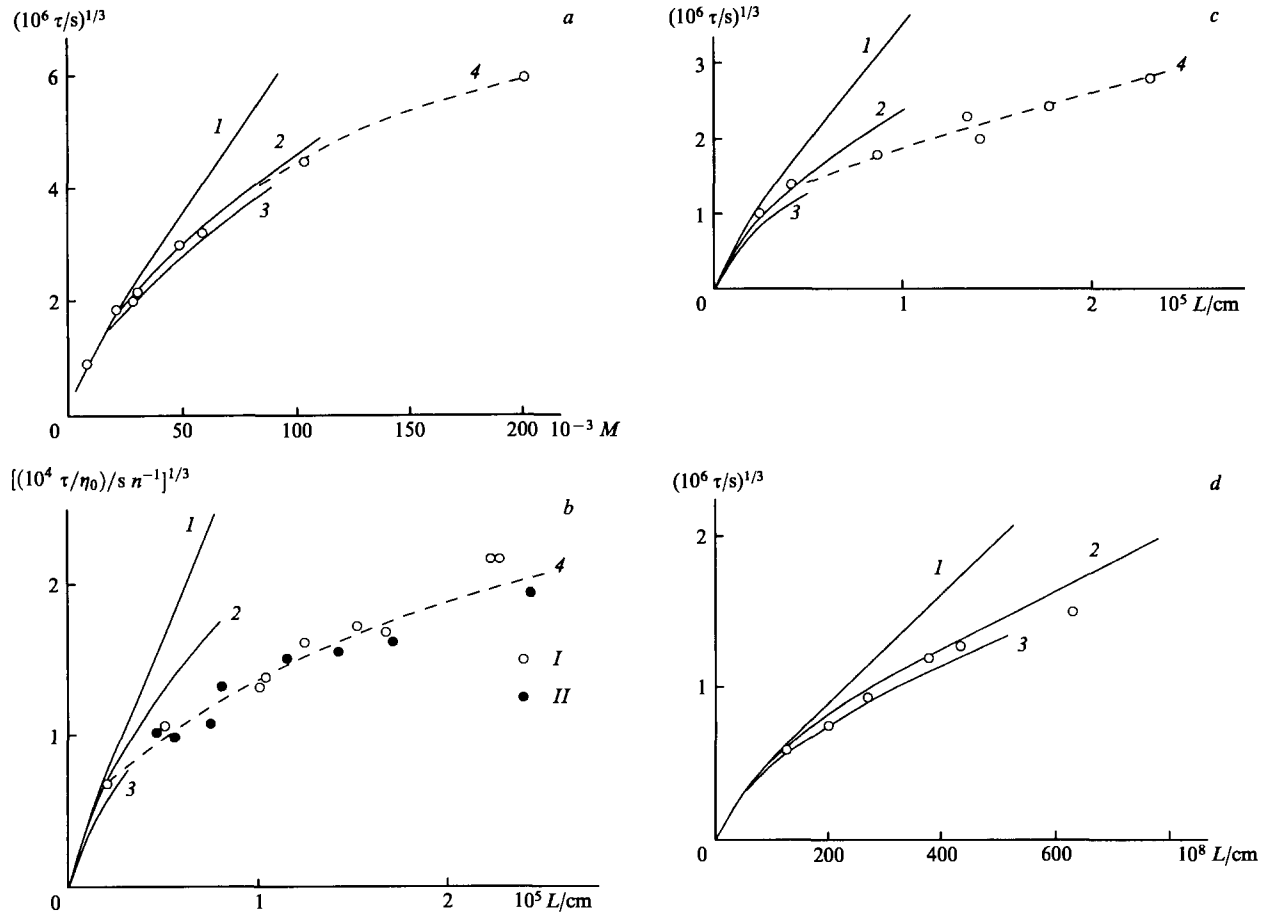


Figure 10. Dependence of the relaxation time for some rigid-chain polymers on the molecular mass (*a*) or on the chain length of the polymer (*b*–*d*). Polymers: poly(butyl isocyanate) (*a*); polyamidobenzimidazole (*b*, *I*); polyamidohydrazide (*b*, *II*); cellulose acetobenzoate (*c*) and carbanilate (*d*). Curves calculated: (*1*) for a cylindrical chain by Eqn (24), 10^8 *d*/cm: (*a*) 30; (*b*) 10; (*c*) 17; (*d*) 15; (*2*) and (*3*) for a vermiform chain in the region of $x \leqslant 5$ by Eqns (24) and (25) with 10^8 A/cm: (*a*) 900 (*2*), 700 (*3*); (*b*) 350 (*2*), 150 (*3*); (*c*) 400 (*2*), 200 (*3*); (*d*) 300 (*2*), 200 (*3*); (*4*) experimental data.

and poly(butyl isocyanate). This was treated as an increase in the kinetic flexibility of these polymers in a polar medium, resulting from the specific interactions of the macromolecules with the dipolar[47] or the aromatic[50] solvent molecules.

However, for the majority of rigid-chain polymers of not too high molecular mass the F coefficient lies between the limits predicted by the theory in the case of kinetically rigid molecules. This shows that the EBR in these solutions is due mainly to the large-scale motion of the macromolecules in an electric field.

This phenomenon allows us to use data on the transient EBR to determine the conformational characteristics (length A of the Kuhn segment) of polymers by using the theory of rotational friction in kinetically rigid vermiform chains.[17]

In Fig. 10 we show plots of the cube root of the dispersion relaxation time against the molecular mass M (or the chain length L) for several rigid-chain polymers. In addition to the experimental data we show theoretical dependences for a straight cylinder and for vermiform chains of the same diameter. The presence of experimental points in the region of $x < 1$ allows us to determine the hydrodynamic diameter of these macromolecules. These results can be obtained from measurements by molecular hydrodynamics methods (translational diffusion, viscometry).

Table 2. Conformational characteristics of some rigid-chain polymers in dilute solutions.

Polymer	Solvent	From transient EBR data			From hydrodynamic and diffraction data		
		10^8 *d*/cm	10^8 A/cm	Ref.	10^8 *d*/cm	10^8 A/cm	Ref.
Poly(butyl isocyanate)	Tetrachloromethane	30	800±100	41	28	840	60
Polyamidobenzimidazole	Dimethyl acetamide	–	250±100	42	5	130–260	61
Polyamidohydrazide	Dimethyl sulfoxide	–	250±100	42	9	160–190	62, 63
Cellulose acetobenzoate	Dioxan	–	300±100	43	17	210	64
Cellulose carbamate	"	15	250±50	[a]	11–16	240	65, 13

[a] Data obtained in the writers' laboratory.

These constructions can be used to determine the equilibrium rigidity (the length A of the Kuhn segment) in the polymers. The results are shown in Table 2, together with data obtained by molecular hydrodynamics and light scattering methods, included for comparison.

It is evident from Table 2 that the data obtained by the transient EBR method for rigid-chain polymers (in both polar and nonpolar solvents) agree reasonably well with the results of other methods, and can be used for a quantitative characterisation of the conformation properties of macromolecules.

IV. Steady electrical birefringence in solutions of rigid-chain polymers. Experimental data

1. The problem of choosing the internal field multiplier

As we know, many rigid-chain polymers are soluble only in strongly polar solvents, and therefore when discussing the electro-optical properties of macromolecules in these solvents we must allow for the difference between the electric field externally applied to the solution and the electric field experienced by the solvent molecules and by the macromolecules of the polymer dissolved in it. Formally this difference can lead to a definition of a suitable 'internal field' multiplier, which can be reasonably assumed to be the same for studies of dilute solutions of rigid-chain polymers in low-molecular polar solvents and for studies of the electro-optical properties of the solvents themselves.

In the expression for the molar Kerr constant ${}_mK$ defined by Eqn (4) allowance for this difference is made by introducing an internal field multiplier of the Lorenz type, $[(\varepsilon + 2)/3]^2$.[66] As was stated above, the results obtained from the expressions (4) and (7) agree well with the experimental data for substances studied in the gas phase,[3] and the agreement is reasonable for substances (both polar and nonpolar) dissolved in a nonpolar solvent.[67,68] However, attempts to apply these equations to concentrated polar liquids (while retaining the Lorenz multiplier) led to unacceptable results.[69,70,71]

An analogous situation was observed in studies of the dielectric properties of polar liquids. The widely used Debye theory,[72] which relates the dielectric permittivity ε of a liquid to the polarisability δ and dipole moment μ of its molecules, and which uses a Lorenz internal field multiplier, was found not to be applicable to undiluted polar liquids because it leads to physically unacceptable values of μ calculated from experimental values of ε. Much better results were obtained by using Onsager's theory,[73] which offers a more successful macroscopic model of the dielectric properties of a polar liquid by allowing for the long-range electrostatic interactions of the polar molecules, averaged over the volume of the liquid. The difference between the electric field applied to the sample and the electric field acting on an individual molecule was allowed for by using two multipliers: for the internal field P (the cavity field) and for the reactive field Q:

$$P = \frac{3\varepsilon}{2\varepsilon + 1}\ ; \qquad Q = \frac{(n^2 + 2)(2\varepsilon + 1)}{3(2\varepsilon + \varepsilon^2)}\ . \tag{42}$$

Onsager's theory can be used to calculate with acceptable precision the dipole moments of the molecules of polar liquids from the dielectric permittivity of the liquid.[74]

Further attempts to improve Onsager's model theory by introducing corrections for the non-sphericity of the molecules[75] or by allowing for the orientational correlations between nearest neighbours[76,77] proved to be ineffective because the final equations included unknown structural parameters of the liquid.

The successful application of the Onsager theory to describe the dielectric polarisation of polar liquids stimulated attempts to apply it also to the Kerr effect in the same systems. In some special cases these attempts were successful.[78]

According to currently held views[79-82] the EBR in polar liquids can be influenced by molecular 'hyperpolarisability'. It is assumed that in a polar liquid the field acting on a molecule from long-range and short-range neighbours is many orders of magnitude greater than the external field E (both electrical and optical) used in studies of the Kerr effect. Therefore the effective polarisability of the molecules γ_e in the electric field should be treated as a series in powers of E.

A two term expression for the specific Kerr constant has been obtained[80,81] by using this approach and allowing for the internal field by Onsager's theory in the special case of a molecule having a dipole moment μ parallel to its optical symmetry axis. The first (quadratic) term depends on μ and is proportional to the optical anisotropy of the molecule, whereas the second term is proportional to the first power of μ and provides a contribution for the hyperpolarisability in the Kerr effect. According to Buckingham[82] the first term plays a dominant role in the equation for K_ρ in the case of molecules in which $\mu \approx 1$ D, and the contribution from the second term is only $\sim 15\%$.

This allows us to ignore hyperpolarisability effects and to base the discussion of the EBR on the more general and more firmly established expressions (2), (4), and (7), replacing the Lorenz multiplier $(\varepsilon + 2)/3$ by the Onsager multiplier PQ:

$$K_\rho = \frac{\pi N_A}{135kTM}(PQ)^2\frac{(n^2+2)^2}{n} \times \left[\sum_{i,j=1}^{3}(\gamma_i - \gamma_j)(\delta_i - \delta_j) + \frac{1}{kT}\sum_{i,j=1}^{3}(\gamma_i - \gamma_j)(\mu_i^2 - \mu_j^2)\right]. \tag{43}$$

Eqn (43) is formally applicable to both polar and nonpolar liquids, since for the latter $\varepsilon = n^2$ and the multiplier PQ reduces to the Lorenz multiplier.

We have recently tested[83] Eqn (43) with a wide range of substances. Experimental values of K_ρ for polar and for nonpolar liquids were used in conjunction with (43) to calculate the optical anisotropies of the molecules. The results were compared with published data[3,68,84] or with data calculated by the valence-optical approach. This analysis led to the conclusion that the Onsager internal field multiplier can be used to describe the electro-optical properties of low-molecular liquids.

On the basis of these results[83] we obtained[85] an expression for the molar Kerr constant of polar liquids by using the Onsager internal field multiplier.

$${}_mK = K_\rho M\frac{2n}{3(n^2+2)^2(PQ)^2} \equiv \frac{2}{3}K_\rho Mn\left[\frac{2\varepsilon + n^2}{\varepsilon(n^2+2)^2}\right]^2. \tag{44}$$

Obviously, Eqn (44) is applicable also to non-polar liquids ($\varepsilon = n^2$), since under these conditions it reduces to Eqn (4). For an experimental demonstration of the validity of Eqn (44) we can examine the data in Table 3, which lists the ${}_mK$ values for several liquids calculated[85] from the K_ρ, ε, and n values by using the expressions (4) and (44). For comparison the table also gives the ${}_mK$ values obtained in dilute solutions in nonpolar tetrachloromethane or in the gas phase. It can be seen that the ${}_mK$ values calculated by using the Onsager internal field multiplier are reasonably well correlated with the values obtained in a dilute solution or in the gas phase, whereas the ${}_mK$ values calculated by Eqn (4) for polar substances are smaller (by a large factor) than the values for a solution or a gas.

We may therefore conclude that the Onsager internal field multiplier can justifiably be used to describe the electro-optical properties of low-molecular-mass polar or nonpolar liquids as well as those of rigid-chain polymers dissolved in these media.

2. Dependence of the Kerr constant on the molecular mass

According to the theory of the Kerr effect in solutions of vermiform chains the characteristic Kerr constant of rigid-chain polymers should be sensitively dependent on the molecular mass [Eqns (33), (34), and (36)]. The expected dependences have been observed in cellulose poly-γ-benzyl-L-glutamate,[87] poly-

Table 3. Calculated (I, II) and experimental values (III, IV) of ${}_mK$ for various substances.

Substance	ε	n	$10^{12}\,K_\rho/g^{-1}\,cm^5\,(300\,V)^{-2}$ (Ref.[85])	$10^{12}\,{}_mK/g^{-1}\,cm^5\,(300\,V)^{-2}$			
				in liquid [a]		in solution [68, 86]	in gas [3, 86]
				I	II	III	IV
Benzene	2.2	1.50	2.4	5.2	5.2	7	17
Chlorobenzene	5.6	1.53	66	64	125	137	190
o-Dichlorobenzene	11	1.55	170	70	334	362	–
m-Dichlorobenzene	5	1.55	37	53	89	74.7	–
p-Dichlorobenzene	2.4	1.53	10	36	36	38.9	–
o-Dibromobenzene	7.5	1.61	75	90	235	288	–
Nitrobenzene	35	1.56	1960	84	2780	1070	1330
Phenyl isothiocyanate	20	1.64	452	56	616	1230	–
1-Bromonaphthalene	4.8	1.66	33.6	66	100	213	–
Pyridine	12.3	1.51	123	24	139	150	–
Cyclohexanone	15.7	1.45	84	14	128	184	–
1,4-Dioxan	2.3	1.42	0.39	10	1.0	1.0	–
Nitromethane	36	1.38	55	1.3	56	89	55
Acetonitrile	37	1.35	353	5.3	256	239	–
Dimethyl sulfoxide	45	1.48	202	3.6	212	144	–
Dimethylacetamide	40	1.44	300	7.7	383	355	–
Acetone	21.5	1.36	90	5.2	94	107	99
Ethyl methyl ketone	18	1.38	85	8.3	107	88.2	–
Ethyl acetate	6.4	1.37	10.9	7.4	20.4	20.1	–
Chloroform	4.8	1.45	−12.7	−17	−30.8	−28.5	−26
Tetrachloroethane	8.2	1.45	−11.9	−9.8	−34.3	−15.2	–

[a] I, calculated by formula (4); II, calculated by formula (44).

(chlorohexyl isocyanate),[49] and nitrate,[38, 48, 88, 89] and in cyanoethylcellulose,[39] and cellulose carbanilate.[90]

Some interesting results were reported by Kolomiets, et al.[91] For the nitrates of flax cellulose in ethyl acetate and in cyclohexanone a change in sign of the Kerr constant with increasing molecular mass of the polymer was observed, as predicted by Eqn (33). This observation demonstrates the difference between the contributions to the EBR from the longitudinal and the transverse components of the dipole moments of the monomer units, and also reflects the accumulation of the longitudinal components of the molecular dipole $\mu_{0\parallel}$ when the chain length is increased.

In all the work discussed above the experimental points describing the homologous dependence of the Kerr constant for the polymer can be reconciled with the theoretical curve (33), which allows the A parameters of the equilibrium rigidity of the molecular chains to be determined. The values of A are shown in Table 4: they are reasonably well correlated with the lengths of the Kuhn segment, determined by hydrodynamic methods.

In Fig. 11 we show as an example plots of K against M for cellulose poly(butyl isocyanate) in tetrachloromethane,[92] for cellulose acetobenzoate,[43, 94] acetocinnamate,[44] and carbanilate in dioxan, and also the theoretical dependences (33) for the corresponding values of A and K_∞. The values of A for these polymers are given in Table 4.

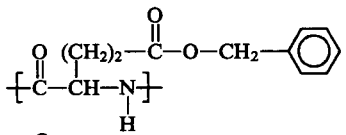
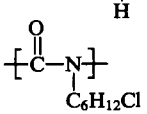
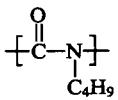
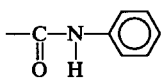
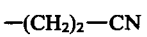
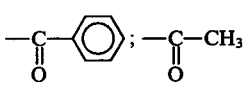
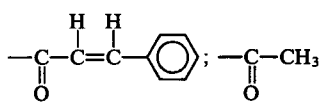
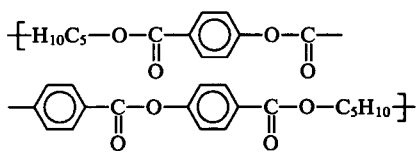
Interesting results have been reported[99, 101, 103, 105, 106] for various aromatic polyesters, mesogenic in the main chain. The mesogenic nuclei in these macromolecules are a sequence of ester groups separated by benzene rings introduced into the chain in the *para* position. Introducing into the same chain (as 'spacers') methylene groups which make the chain more flexible, as well as benzene rings in *meta* and *ortho* positions, markedly lowers the equilibrium rigidity of the chain. Furthermore an aromatic polyester containing an *ortho* benzene ring as a spacer[105] is known to orient itself in an electric field by the small-scale motion mechanism. At the same time an aromatic polyester with a decamethylene spacer,[99] in spite of its relatively low equilibrium rigidity, orients itself in an electric field by the large-scale motion mechanism (as a result of the accumulation of the longitudinal components of the dipoles of the monomer units as the chain length is increased).

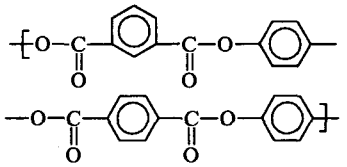
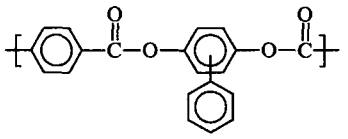
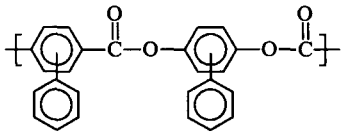
A large difference between the longitudinal-dipolar and the transverse-dipolar rigidity has been observed in mesogenic aromatic polyesters. This effect is illustrated by Eqn (33), which takes account of this difference by using the factor α. The difference is specially notable in the polyester 13 (Table 4), for which $\alpha \approx 3$. This finding is not unexpected, since the molecule of the polymer 13 is a good representation of the ideal *para*-aromatic polyester, i.e. it is structurally close to the ideal 'crankshaft' model. In Fig. 12 we show the molecular mass dependences of K for mesogenic polyesters.

We have studied[107] the equilibrium electro-optical properties of two aromatic polyamides: polyamidobenzimidazole and polyamidohydrazide, which are soluble only in strongly polar (conducting) solvents such as dimethylacetamide and dimethyl sulfoxide. A study of the kinetics of the orientation of these polymers by the transient EBR method showed that their molecules become oriented in an electric field by a large-scale mechanism. The Kerr constant for these substances shows a marked dependence on the molecular mass, characteristic of rigid-chain polymers. However, the experimental points cannot be fitted to the theoretical dependence (33) for any set of adjustable parameters. This is interpreted as a manifestation of an orientational correlation between the polar molecules and the dipolar bonds of the polymer chain.

We have calculated[107] the longitudinal component of the macromolecular dipole $\langle\mu_\parallel^2\rangle^{1/2}$ in these polymers. It was found to increase steeply as the chain length is increased (curve *1* of Fig. 13). Curve *2* of the same figure is the theoretical dependence for $\langle\mu_\parallel^2\rangle^{1/2}$, which can be calculated from the geometrical parameters of the macromolecules. It can be seen that curves *1* and *2* approach each other only in the region of small M, and that they are strongly divergent for large M. The large values of $\mu_\parallel^2$, for polyamidobenzimidazole and polyamidohydrazide cannot be attributed wholly to their dipole structure, and must be explained at least

Table 4. Length of the Kuhn segments of some rigid-chain polymers, determined by the equilibrium EBR method (A_1) and by hydrodynamic methods (A_2).

	Polymer	Structural formula	Solvent	$10^8 A_1$/cm	Ref.	$10^8 A_2$/cm	Ref.
1	Poly-γ-benzyl-L-glutamate		Dichloroethane	1600	87	2200	94
2	Poly(chlorohexyl isocyanate)		Tetrachloromethane	540	49	500	95
3	Poly(butyl isocyanate)		"	720	92	840	60
4	Cellulose carbanilate		Dioxan	210	90	240	13, 65
5	Cyanoethylcellulose		Cyclohexanone	260	39	290	96
6	Cellulose nitrate (10.7% N)		Dioxan Ethyl methyl ketone	155 –	48, 90 –	– 130	– 48
7	Cellulose nitrate (13.4% N)		Cyclohexanone Acetone Ethyl acetate	310 310 360	88 88 91	– – 300	– – 97
8	Cellulose nitrate (12.1% N)		Cyclohexanone	180	38	180	98
9	Cellulose acetobenzoate		Dioxan	210	93	210	64
10	Cellulose acetocinnamate		"	300	44	230	
11	Polydecamethylene terephthaloyl-dip-*p*-hydroxybenzoate		Trifluoroacetic acid	50	99	50	100

12	Aromatic polyester with *p*- and *m*-phenylene rings in the chain		Dichloroacetic acid	120	101	120	102
13	Monophenyl substituted poly-*p*-phenylene terephthalate		"	380	103	380	104
14	Diphenyl substituted poly-*p*-phenylene terephthalate		"	260	40	260	40
			Dioxan	–	–	260	40

[a]Data obtained in our laboratory

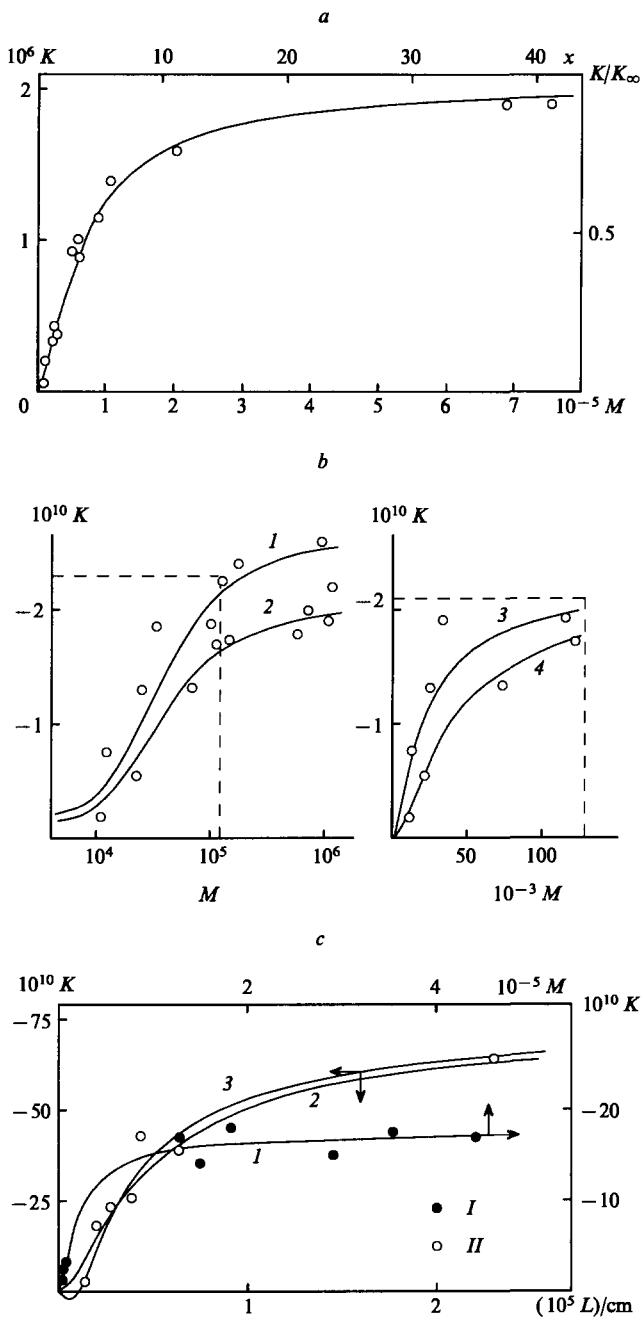


Figure 11. Plots of the Kerr constant for cellulose polybutylisocyanate in tetrachloromethane (*a*) and cellulose acetobenzoate (*b*) against the molecular mass, and also for cellulose acetocinnamate (*c*, *I*) and carbamate (*c*, *II*) in dioxan against the chain length. The points are experimental, the curves are calculated by formula (33). $10^{10} K/g^{-1}$ cm^5 (300 V)$^{-2}$: (*a*) 2.1 × 10^4; (*b*) −2.6 (*1*), −2.0 (*2*), −2.3 (*3*, *4*); (*c*) −18 (*1*); −7.5 (*2*, *3*); ϑ/deg: (*a*) 0; (*b*) 0 (*1*–*4*); (*c*) 0 (*1*–*2*), 70; α = 3 (*3*); $10^8 A$/cm: (*a*) 720; (*b*) 210 (*1*, *2*); 150 (*3*); 270 (*4*); (*c*) 300 (*1*); 250 (*2*); 200 (*3*).

partially by the influence of the strongly polar solvent on the electro-optical properties of the polymer chains.

Even more unexpected and instructive results have been obtained[40] for the diphenyl-substituted poly(*p*-phenylene terephthalate) (compound 14 in Table 4). This polymer differs from compound 13 by the presence of an additional benzene substituent in the self-repeating unit of the main chain. This additional benzene ring greatly improves the solubility of the polyester, which becomes soluble even in the nonpolar dioxan. Its

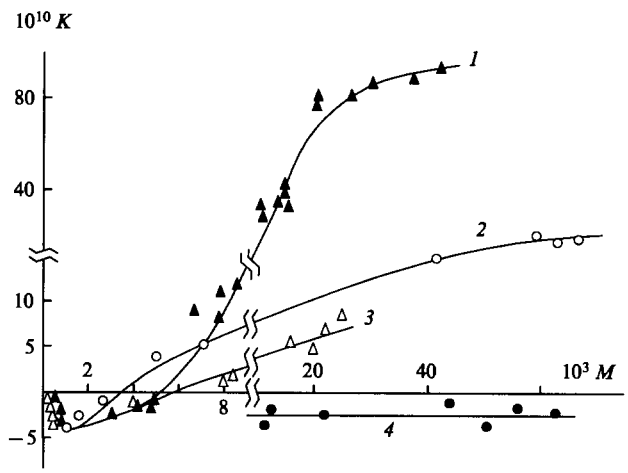


Figure 12. Dependence of the Kerr constant on the molecular mass for aromatic polyesters.[106] Polymer number (see Table 4); (*1*) 13; (*2*) 11; (*3*) 12; (*4*) analogue of 13, containing a benzene ring in the *ortho* position as a spacer; the points are experimental, the curves are calculated by Eqn (33) for α = 3 (*1*), 1 (*2*), 1.3 (*3*).

solubility is even higher in various polar solvents: for example, in dichloroacetic acid. In Fig. 14 we show the molecular-mass dependence of the Kerr constant for this polyester in dichloroacetic acid. It can be seen that K increases steeply with M, as expected for rigid-chain polymers oriented by a large-scale mechanism in an electric field. Furthermore K changes sign during the growth, suggesting an accumulation of the longitudinal components of the dipoles of the monomer units and a weakening of the correlation of the dipole formed by the normal components $\mu_{0\perp}$ with the direction of the vector $\boldsymbol{h}$ when M is increased. Lastly, the experimental points can be fitted to the theoretical curve with a reasonable choice of the parameters ϑ, A, and α.

However, in the nonpolar dioxan the Kerr constant of this polyester is almost unaffected by an increase in M, and remains close to the K value of the corresponding monomer. Furthermore

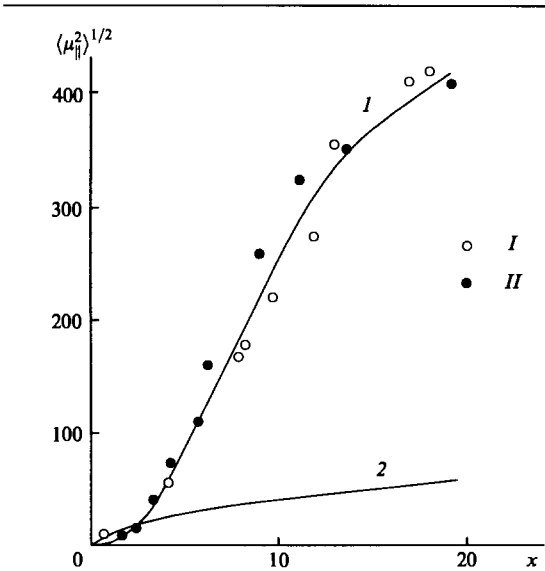


Figure 13. Dependence of the longitudinal component of the dipole moment of macromolecules $\langle\mu_\parallel^2\rangle^{0.5}$ in the direction of the vector $\boldsymbol{h}$ connecting the ends of the molecule upon the reduced chain length x = $2L/A$: (*1*) experimental dependence for polyamidobenzimidazole (*I*) and poly-amidohydrazide (*II*); (*2*) theoretical dependence for a vermiform chain with $\mu_{0\parallel}$ = 1.5 D.

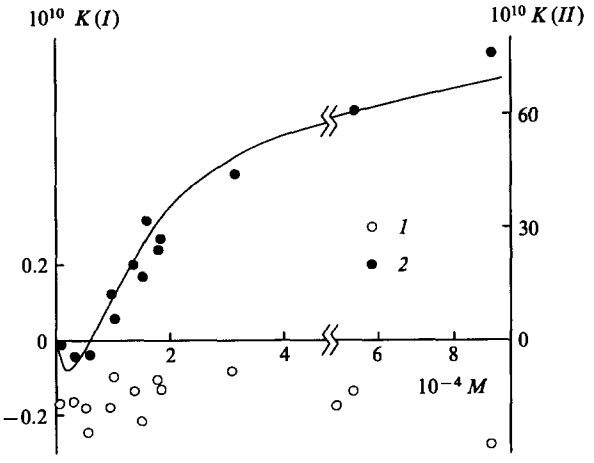


Figure 14. Dependence of the Kerr constant on the molecular mass for diphenyl-substituted poly(*p*-phenylene terephthalate) in dioxan (*1*) and in dichloroacetic acid (*2*). The points are experimental; the curve is the theoretical dependence according to Eqn (33) for $\alpha = 3$ and $K_\infty = 80 \times 10^{-10}$ g^{-1} cm^5 (300 V)$^{-2}$.

it is negative, i.e. its sign is the opposite of the sign of the flow birefringence of the same solution, and its magnitude is very small (see Fig. 14). All this suggests a small-scale orientation of the polyester (in its equilibrium state of rigidity) when exposed to an electric field in a nonpolar solvent. Noting the dipolar structure of the macromolecules of this polymer we can expect to find a substantial perpendicular component of the dipole of the monomer unit $\mu_{0\perp}$, with a negligibly small longitudinal component $\mu_{0\parallel}$. Data obtained by the steady EBR method for solutions of the *para-aromatic* polyester in dioxan point to the same conclusion, suggesting that in a solution of this polymer the EBR is due to the local reorientations of $\mu_{0\perp}$ accompanying the rotations round the *para*-aromatic axes.

The electrical birefringence in solutions of the same polymer in dichloroacetic acid is produced by the large-scale motion mechanism. This shows that a strongly polar solvent not only alters the dipole structure of the macromolecule, inducing the appearance of a substantial $\mu_{0\parallel}$ component, but also affects the process by which the EBR is created, replacing the small-scale by a large-scale mechanism. The latter effect may be due to an orientational correlation between the dipolar molecules of the solvent and the polar units of the polymer chain, leading to the formation in the polymer chain of an 'effective' electro-optical dipole which determines the mechanism, magnitude, and sign of the EBR in solutions of the polyester in a polar solvent.

3. Effect of polar solvents on the electro-optical properties of polymer chains

The results discussed in the previous section show that a polar solvent can strongly affect the electro-optical properties of rigid-chain polymers. This phenomenon has been examined in our laboratory[108] by studying the viscometric, dynamo-optical, and electro-optical characteristics of a cellulose carbanilate sample ($M = 4 \times 10^5$, degree of substitution 2.7), which is readily soluble in both the nonpolar dioxan and in various polar solvents such as ethyl acetate, cyclohexanone, and dimethylacetamide.

An analysis of these results suggests that the equilibrium rigidity of the polymer chain is decreased when a nonpolar solvent is replaced by a polar solvent. This is because the mechanism of formation of the equilibrium rigidity of the macromolecules of cellulose esters is strongly influenced by the interaction between side groups (substituents in neighbouring glucoside rings of the chain), which powerfully suppresses the intramolecular rotations. The bonds produced by the interaction of the side groups are weakened (and become easily broken) under the influence of the polar solvent molecules, capable of forming intermolecular bonds. A decrease in the optical anisotropy of the monomer unit of cellulose carbanilate in ethyl acetate has been noted and ascribed to microform effects.

The most interesting results were obtained in a study of the equilibrium electro-optical properties of cellulose carbanilate in various solvents. It was found that the Kerr constant of this polymer increases steeply with the polarity of the solvent (Table 5). The transient EBR data unambiguously show that the Kerr effect in solutions of this polymer is determined, in all the solvents examined, by the large-scale motion of its macromolecules under the influence of the electric field produced by the presence of a steady dipole moment in its chain.

In the calculation of the longitudinal component of the dipole moment of the monomer unit $\mu_{0\parallel}$ of cellulose carbanilate in various solvents allowance was made for two effects in addition to those mentioned above. Firstly, the molecular mass of the experimental sample is relatively high, and therefore its molecules are in a Gaussian tangle conformation and the EBR of its solutions is determined only by the longitudinal component of the dipole in the monomer unit $\mu_{0\parallel}$ [see Eqn (34)]. Secondly, we must note that in the description of the electro-optical properties of rigid-chain polymers in polar solvents it is reasonable to use the Onsager internal field multiplier. In these circumstances Eqn (34) can be re-written

$$K_\infty = (PQ)^2 2\pi N_A (n^2+2)^2 S^2 \Delta a \frac{\mu_{0\parallel}^2}{135 n (kT)^2 M_0} . \qquad (45)$$

Starting from (45) we calculated the $\mu_{0\parallel}$ values shown in Table 5. It can be seen that these values increase rapidly with the dipole moment of the solvent molecules. At the same time the $\mu_{0\parallel}$ value obtained for cellulose carbanilate in dioxan is reasonably well correlated with the dipole structure of the polymer chain. The large values of $\mu_{0\parallel}$ for cellulose carbanilate in polar solvents cannot be explained in terms of a single dipole structure of the macromolecule, and must be treated as effective quantities, denoting the presence of orientational correlations between the polar molecules of the solvent and the dipolar bonds in the polymer chain.

Table 5. Electro-optical characteristics of the solvents (ε, μ, K_ρ) and of the solutions (K,$\mu_{0\parallel}$) of cellulose carbanilate.

Solvent	ε	μ/D	$10^{12}K_\rho$/ g^{-1} cm^5 (300 V)$^{-2}$	$10^9 K$/ g^{-1} cm^5 (300 V)$^{-2}$	$\mu_{0\parallel}$/D
Dioxan	2.3	0	0.39	−7	0.95
Ethyl acetate	6.4	1.8	11.1	−10	1.4
Cyclo-hexanone	16	2.8	86.2	−45	2.8
Dimethyl-acetamide	40	3.8	351	−200	5.6

The present writers have recently carried out additional studies, aimed at explaining the effect of polar solvent molecules on the electro-optical properties of rigid-chain polymer molecules. The cellulose carbanilate sample ($M = 195 \times 10^3$, degree of substitution 2.3) was studied by viscometric, dynamo-optical, and electro-optical methods in mixed solvents (dioxan–ethyl acetate). The relative mole fraction of the components f was varied from 0 to 1. A dispersion of the EBR in the radio-frequency range was observed in all the solutions, the dispersion curves falling almost to zero whereas the relaxation times were reasonably well correlated with the size of the macromolecules. These observations suggested a large-scale motion in the orientation of the cellulose carbanilate macromolecules in an electric field for all the mixed solvents examined.

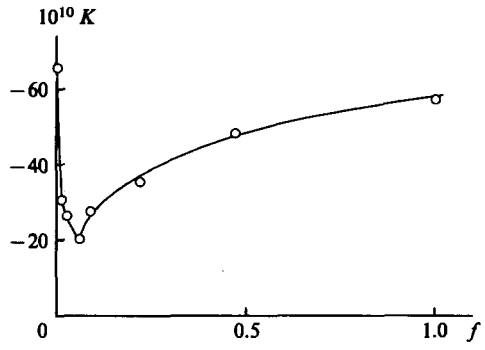


Figure 15. Plot of the Kerr constant of cellulose carbanilate (M = 195 × 10^3) against the mole fraction of ethyl acetate in the ethyl acetate–dioxan mixed solvent.

The dependence of the Kerr constant of the ester on the mole fraction f of ethyl acetate is shown in Fig. 15. The changes in K with f are strongly non-monotonic. In principle this behaviour could be due to changes in the dipole moment of the molecule, in its equilibrium rigidity, and in its optical anisotropy with changes in composition of the solvent. An analysis of these results led to the conclusion that all three parameters listed above are operating in the system. Noting that the molecular mass of the sample is relatively high, i.e. that the macromolecule is in the conformation of a Gaussian tangle, we can calculate $\mu_{0\parallel}$ from Eqn (45), allowing for changes in both S and Δa.

The dependence of $\mu_{0\parallel}$ for cellulose carbanilate on the mole fraction f of ethyl actate is shown in Fig. 16. The non-monotonicity of the changes in $\mu_{0\parallel}$ is evident. We specially note that for $f \geqslant 0.1$ $\mu_{0\parallel}$ value increases (within experimental error) almost linearly with f. This observation evidently suggests that the effective electro-optical dipole formed by the polar polymer chain with the dipole moments of the ethyl acetate molecules increases in direct proportion to the number of molecules of the polar component in the mixed solvent. The slight decrease in $\mu_{0\parallel}$ with increase of f at $f < 0.1$ can be ascribed to the partial screening of the dipole moment of the macromolecule by the polar solvent molecules.

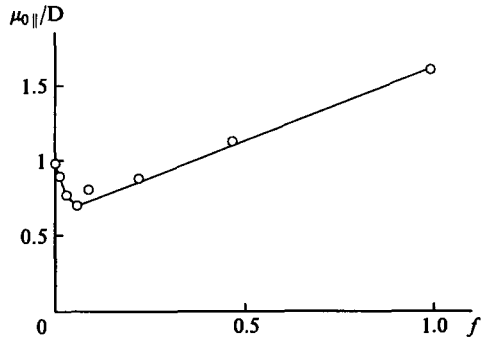


Figure 16. Plot of the longitudinal component of the dipole moment of the monomer unit of cellulose carbanilate against the mole fraction of ethyl acetate in a mixed ethyl acetate–dioxan solvent.

From the whole of this discussion we may conclude that the EBR in solutions of rigid-chain polymers is determined not only by the polar structure of their macromolecules but also (and to a large extent) by the dipole structure of the chosen solvents, the latter factor playing a dominant role in the case of strongly polar liquids. This can lead to a change in the dipole moment of the polymer chain, and also (as was pointed out above) to a change in the very nature of the observed EBR, depending on the choice of solvents. Therefore we can obtain quantitative information on the magnitude and direction of the dipole in the monomer unit of the macromolecules of rigid-chain polymers using only nonpolar solvents.

V. Effect of the structure of side groups and of the degree of substitution on the electro-optical properties of cellulose esters

Cellulose esters are an important class of polymers of the rigid-chain type. One property of these materials is particularly attractive to research workers: the possibility of changing the electro-optical characteristics of their molecules over a reasonably wide range by varying the chemical structure of the substituents and the extent of the esterification reaction (i.e. the average degree of substitution γ).

It has been firmly established [38, 49, 52, 88, 97, 98, 109] that both the optical shear coefficients $\Delta n/\Delta\tau$ in FBR effects and the Kerr constants for cellulose nitrates are sensitively dependent on the degree of substitution. Thus, for cellulose nitrate containing 10.7% of nitrogen the optical shear coefficients $(\Delta n/\Delta\tau)_\infty$ and the Kerr constant K_∞ in the Gaussian region are small and positive.[48, 109] At the same time in nitrates containing a larger percentage of nitrogen $(\Delta n/\Delta\tau)_\infty$ and K_∞ are negative, and K_∞ is greater by two orders of magnitude (in absolute value) than K_∞ for the less highly substituted nitrate.[38, 52, 88, 97, 98] The same papers point out a steep increase in the dipole moment of the monomer unit μ_0 of the cellulose nitrates with the nitrogen content of the side groups, but these results should be viewed with caution because they were obtained in a strongly polar, electrically conducting solvent, cyclohexanone, and this could introduce significant errors in the dipolar characteristics of the polymer chains.

We have reported [51] a study of the optical and the electrical properties of two substituted cellulose esters (the acetodiphenylacetate and the acetocinnamate) as a function of their degree of substitution. The measurements of EBR, FBR, and viscosity were carried out in a nonpolar, poorly conducting solvent (dioxan), and the molecular masses of the polymers corresponded to the Gaussian region. In both these cellulose esters we observed a steep increase in the optical shear coefficients $(\Delta n/\Delta\tau)_\infty$ and in the Kerr constant K_∞ upon increasing the degree of substitution γ (with respect to the benzene-containing radical). The results are shown in Fig. 17. The nonlinearity of the plot of $(\Delta n/\Delta\tau)_\infty$ against γ for cellulose acetodiphenylacetate may be related to a change in the rigidity of the polymer chain with changes in γ or to an incomplete equivalence of the contributions to the optical anisotropy from the large diphenylacetate radicals, attached to the second and to the third or sixth carbon atom in the glucoside ring.

A study of the transient Kerr effect of these two cellulose esters showed that the mechanism mainly responsible for the EBR observed in solutions of cellulose acetocinnamate and aceto-diphenylacetate at all degrees of substitution is the large-scale rotation of their macromolecules under the influence of the electric field, due to the presence of a steady dipole moment. However, as was stated above, the absolute value of K_∞ for these esters increases rapidly with γ. This dependence of the Kerr constant on the degree of substitution may be due to an increase in the optical anisotropy of the macromolecules (positive for the diphenylacetate and negative for the cinnamate) with increasing γ, as was also inferred from the dependence of $\Delta n/\Delta\tau$ on γ, or alternatively it may be due to changes in the dipole moment of the molecular chain.

By using Eqn (45) we have calculated [51] the $\mu_{0\|}$ values of the esters for different degrees of substitution γ. It can be seen from the results (Fig. 18) that in these esters $\mu_{0\|}$ increases with γ, especially in the acetocinnamate. This suggests that the dipole moment

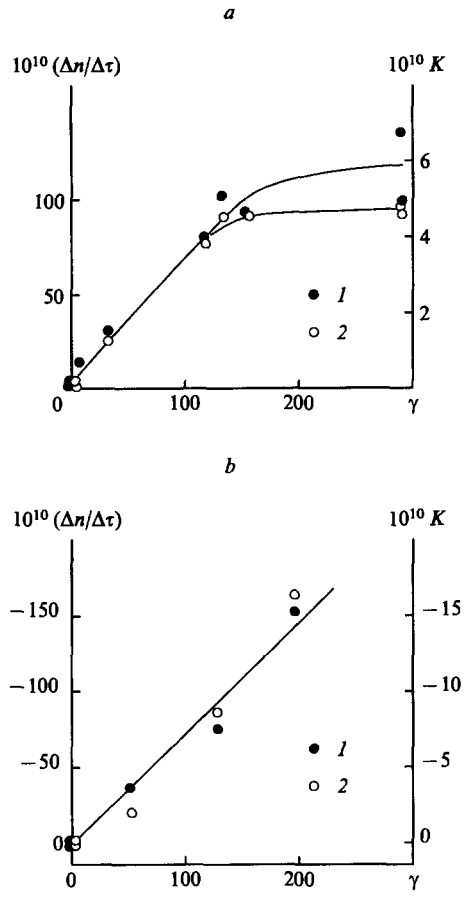


Figure 17. Plots of the optical shear coefficient (*1*) and of the Kerr constant (*2*) for cellulose acetodiphenylacetate (*a*) and acetocinnamate (*b*) against the degree of substitution.

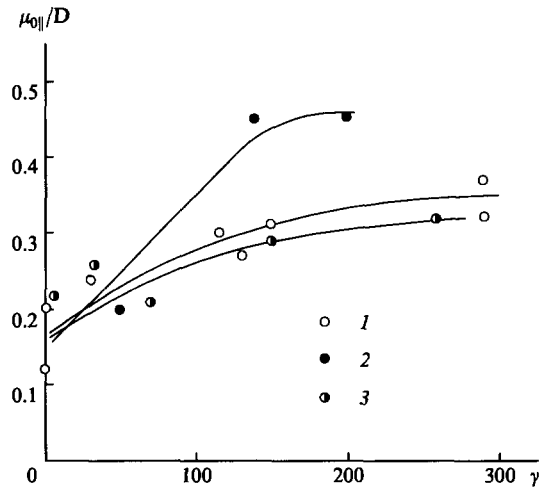


Figure 18. Dependence of the longitudinal component of the dipole moment of the monomer unit in cellulose acetodiphenylacetate (*1*), aceto-cinnamate (*2*), and acetophenylacetate (*3*) upon the degree of substitution.

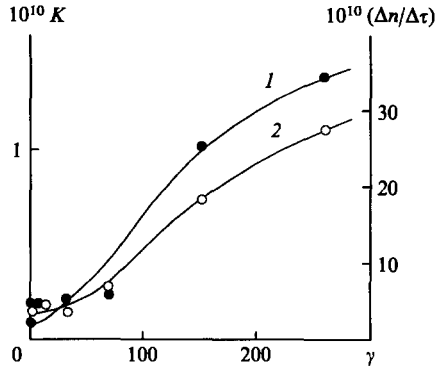


Figure 19. Plots of the Kerr constant (*1*) and of the optical shear coefficient (*2*) of cellulose acetophenylacetate against the degree of substituion.

contributed by the ester group in a side group of the glucose ring to the longitudinal component of the dipole moment of the monomer unit of the cellulose chain is strongly dependent on the structure of the side substituent. In fact, it follows from these results[51] that the presence of benzene groups in the substituent leads to an increase in the longitudinal component of the dipole of the monomer unit $\mu_{0\|}$ in the polymer chain as a result of the change in the contribution from the OCO group, whereas the presence of alkyl radicals lowers the $\mu_{0\|}$ value.

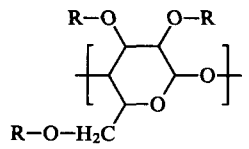
We have recently studied the effect of the degree of substitution on the electro-optical properties of cellulose acetophenylacetate in dioxan (Figs. 18, 19). The results were similar to those obtained previously.[51] The optical shear coefficients and the Kerr constants of these high-molecular samples were found to be strongly dependent on the degree of substitution γ with respect to the phenylacetate group. This dependence of $\Delta n/\Delta\tau$ upon γ is not unexpected, since the introduction of strongly anisotropic groups containing benzene rings should markedly increase the optical anisotropy of the whole molecule in comparison with that of cellulose acetate, which is not large. By using Eqn (45) we calculated the longitudinal component of the dipole moment of the monomer unit $\mu_{0\|}$ for the cellulose acetophenylacetates at different degrees of substitution (see Fig. 18). It can be seen from this figure that $\mu_{0\|}$ increases with γ. This effect should be interpreted in the same way as for the cellulose acetodiphenylacetate.

Thus we may conclude that the presence of conjugated bonds in the side chains increases the contribution from the ester group of the side chain to the overall $\mu_{0\|}$ value of the cellulose ester macromolecules.

Meaningful results were obtained for acetotritylcellulose (compound 29 in Table 6). It was found that changing the degree of substitution γ with respect to the trityl radical from 0 to 145 increases $(\Delta n/\Delta\tau)_\infty$ by an order of magnitude, whereas the Kerr constant increases by more than two orders of magnitude, corresponding to an increase in $\mu_{0\|}$ from 0.2 to 1.5 D. This large increase in $\mu_{0\|}$ suggests that the contribution to $\mu_{0\|}$ from the ether group is more substantial than the contribution from the ester group.

The other results in Table 6 also show that $\mu_{0\|}$ for compounds containing a simple ether group in a side group is usually higher than for compounds having an ester group in the side chains (exceptions to this rule are provided by the polymers 3 and 4, whose side substituents contain the strongly polar amide group). In a similar way, replacing the ester groups by hydroxyl groups increases $\mu_{0\|}$, as can be seen by comparing the data for cellulose acetobenzoate and cellulose benzoate (compounds 9 and 10). The strong effect of the structure of the side chain on the longitudinal component of monomeric dipole can be illustrated by comparing data for cellulose carbanilate and cellulose acetobenzhydroxamate (compounds 4 and 33). Passing from the structure of polymer 4 to that of polymer 33 decreases the negative value of $(\Delta n/\Delta\tau)_\infty$ and therefore also of the anisotropy Δa by a factor of two, whereas the modulus of K_∞ decreases 200-fold and $\mu_{0\|}$ decreases 10-fold.

Table 6. Electro-optical properties of some cellulose esters



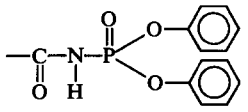
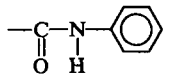
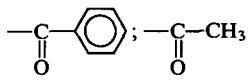
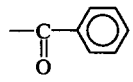
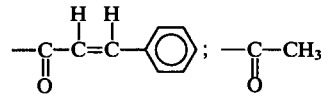
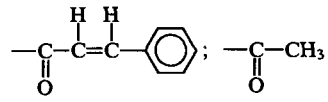
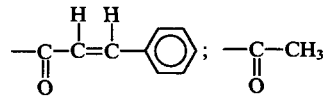
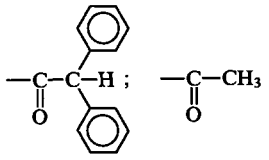
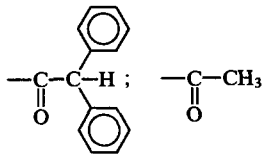
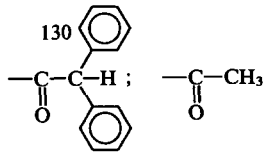
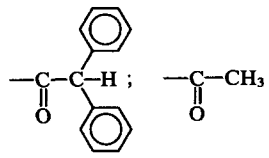
	Polymer	Structural formula of substituent radical	Degree of substitution [a]	$10^{25}\Delta a$/ cm^3	$10^{10}K_\infty$/ g^{-1} cm^5 (300 V)$^{-2}$	$\mu_{0\parallel}$/D	Ref.
1	Ethylcellulose	$-C_2H_5$	260	8	25	1	52
2	Benzylcellulose	$-CH_2-C_6H_5$	220	6	6	0.7	52
3	Cellulose diphenyl-phosphonocarbamate		200	12.5	25	1.4	52
4	Cellulose carbanilate		270	−40	−70	0.95	47
5	Cellulose nitrate	$-NO_2$	190	4.2	6	1	48, 90
6	Cellulose nitrate	$-NO_2$	230 [b]	−8.4	−550	–	38, 98
7	Cellulose nitrate	$-NO_2$	270 [b]	−9	−900	–	88, 97
8	Cyanoethylcellulose	$-(CH_2)_2-CN$	260 [b]	17.8	250	–	39, 96
9	Cellulose acetobenzoate		245 55	−26.6	−2.3	0.21	93, 110
10	Cellulose benzoate		216	−27	−7.7	0.38	[d]
11	Cellulose acetocinnamate		200 60	−38	−18	0.44	44
12	Cellulose acetocinnamate		140 160	−26	−9.4	0.44	51
13	Cellulose acetocinnamate		50 250	−9	−1.1	0.2	51
14	Cellulose acetodiphenylacetate		290 10	25.6	4.6	0.37	51
15	Cellulose acetodiphenylacetate		150 40	24	4.6	0.31	51
16	Cellulose acetodiphenylacetate		130 26.9 20	4.5	0.27	51	
17	Cellulose acetodiphenylacetate		115 130	20.4	3.9	0.3	51

Table 6 (continued).

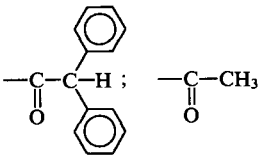
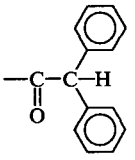
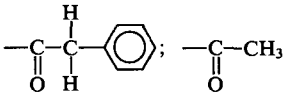
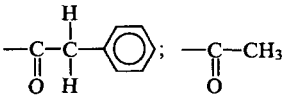
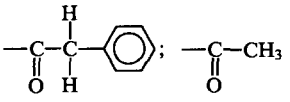
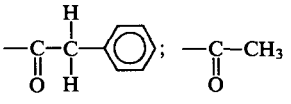
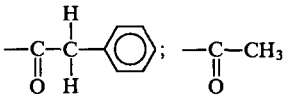
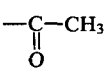
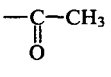
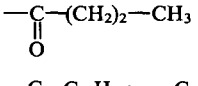
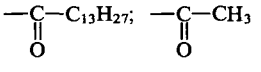
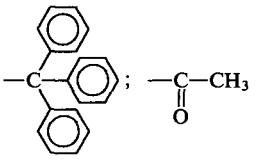
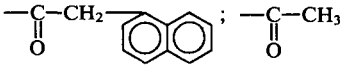
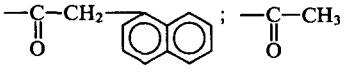
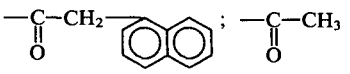
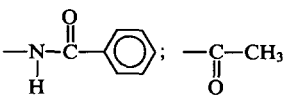
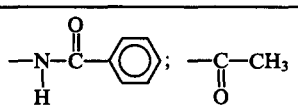
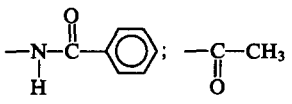
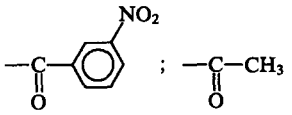
	Polymer	Structural formula of substituent radical	Degree of substitution[a]	$10^{25}\,\Delta a/cm^3$	$10^{10}\,K_\infty/g^{-1}\,cm^5\,(300\,V)^{-2}$	$\mu_{0\parallel}/D$	Ref.
18	Cellulose acetodiphenylacetate		30 270	8.1	1.3	0.24	51
19	Cellulose diphenylacetate		290	35.2	4.8	0.32	51
20	Cellulose acetophenylacetate		260 40	7.3	1.4	0.32	d
21	Cellulose acetophenylacetate		150 100	5	1.02	0.29	d
22	Cellulose acetophenylacetate		70 200	1.8	0.24	0.21	d
23	Cellulose acetophenylacetate		32 246	1.0	0.21	0.26	d
24	Cellulose acetophenylacetate		5 285	1.3	0.2	0.22	d
25	Cellulose diacetate		240	1	0.15	0.2	51
26	Cellulose triacetate		300	0.78	0.04	0.12	51
27	Cellulose butyrate		300	1.2	0.4	0.4	52
28	Cellulose acetomyristate		290[c] 10[c]	−2.2	−0.7	0.5	d
29	Cellulose acetotriphenylmethylate		145 110	22	87	1.53	d
30	Cellulose aceto-α-naphthylacetate		50 250	1.4	0.87	0.47	d
31	Cellulose aceto-α-naphthylacetate		25 275	1.4	0.18	0.2	d
32	Cellulose aceto-α-naphthylacetate		10 290	1.1	0.08	0.15	d
33	Cellulose acetobenzhydroxamate		285 15	−17.4	−0.3	0.1	d

Table 6 (continued).

Polymer	Structural formula of substituent radical	Degree of substitution[a]	$10^{25}\Delta a$/ cm^3	$10^{10}K_\infty$/ g^{-1} cm^5 (300 V)$^{-2}$	$\mu_{0\|\|}$/D	Ref.
34 Cellulose acetobenzhydroxamate		240 60	−11.5	−0.4	0.13	[d]
35 Cellulose acetobenzhydroxamate		170 90	−7	−0.15	0.1	[d]
36 Cellulose acetonitrobenzoate		25 275	−2.3	0.3	–	[d]

[a] If the degree of substitution is quoted in two lines the values in the second line refer to substitution by acetic acid.
[b] Solvent: cyclohexanone.
[c] Solvent: benzene.
[d] Data obtained in the writers' laboratory.

In various studies of the EBR of cellulose esters it has been assumed that the parameter $\mu_{0||}$ is determined by the dipoles of the polar O–C bonds of the glucopyranose ring in the main chain and is practically independent of the dipole structure of its side substituents.[52] The experimental information accumulated in more recent work (and discussed above) is not inconsistent with this assumption. As can be seen from the previous discussion the characteristics mainly responsible for the electro-optical properties of cellulose esters include not only the optical anisotropy but also the dipole structure of the side substituents in these molecules.

The parameter $\mu_{0||}$, which can be varied ten-fold by changes in the structure of the substituent groups and in the degree of substitution (see above), is determined by the sum of the dipole moments of all the polar bonds included in the monomer unit of the polyglucoside chain. Often the main part of this sum of moments is the contribution from the polar groups of the side substituents. Thus, in spite of the presence of some degree of rotational mobility of the polar groups in the side substituents, the dipolar contribution from these groups to the longitudinal component $\mu_{0||}$ of the dipole of the monomer unit is effectively 'fastened' in this unit and gives rise to the large-scale orientation of the polymer chain in an electric field.

Nevertheless the appearance of a freer 'small-scale' motion of the anisotropic polar groups in the side chains cannot be excluded in the EBR of solutions of cellulose esters. An obvious example is provided by the results (unexpected for rigid-chain polymers) obtained in solutions of celluiose acetonitrobenzoate (compound 36 in Table 6). The dynamic birefringence of this polymer is negative, whereas the EBR of its solutions is positive. Further-more in the radio-frequency band its EBR does not show dispersion, and K_∞ (allowing for the degree of substitution) is close to the value of the Kerr constant for a solution of nitrobenzene in dioxan at a corresponding concentration. All these observations suggest that the EBR in solutions of this polymer is produced by a large-scale orientation mechanism involving the polar nitrobenzene groups in the side substituents.

VI. Electro-optics of solutions of branched polymers with mesogenic groups in the side chains

Specific electro-optic properties are found in solutions of polymers of the branched type, whose molecular basis is a flexible polyacrylate or polymethacrylate chain with side groups also having a chain structure and containing mesogenic fragments of aromatic esters (Table 7).

Because of their dipole structure the monomer units of polyalkylacrylates and polyalkylmethacrylates (like those of other carbon-chain polymers) do not have a component of the dipole moment parallel to the polymer chain. Accordingly, the orientation of their chains in an electric field takes place by a mechanism involving local small-scale motions of the polar groups. The electrical birefringence observed in solutions of these polymers is quite small, and its sign is not correlated with that of the FBR.[13] The equilibrium rigidity of the molecules in these polymers also corresponds to the rigidity of ordinary polymers with flexible chains.

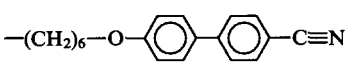
However, the physical properties of the polymethacrylate or polyacrylate chain are markedly affected if the alkyl part (R) of its side groups is replacd by the mesogenic chain of an aromatic ester (see Table 7). This leads to an increase in the equilibrium rigidity of the main chain of the resulting branched polymer to $A \simeq 50 \times 10^{-8}$ cm,[13] exceeding 2–4-fold the rigidity of typical flexible-chain polymers. This effect is related to the steric interactions of the large side groups (a phenomenon well known in other flexible-chain polymers[12]).

However, the strongest effect of mesogenic side radicals is observed in the electro-optical characteristics of branched molecules, many of which are soluble in nonpolar solvents. Thus, the study of the transient EBR in solutions of the polymers 1 and 2 (see Table 7) in a nonpolar solvent, using sinusoidal fields, showed a dispersion of the Kerr effect in the radio-frequency region ($\nu = 10^2 - 10^6$ Hz). As the frequency is increased in this band the Kerr constant falls almost to zero.[111,112] This result shows that the dominant contribution to the observed Kerr effect comes from the large-scale rotation of the dipolar macromolecules of these polymers in an electric field.

At the same time, though they show a tendency to increase with M, the F coefficients for polymer 2 exceed the theoretically maximum values for kinetically rigid molecules by a substantial factor.[112] Furthermore, for the high-molecular mass fractions of polymer 1 the relaxation time τ is independent of the molecular mass.[111] These observations show that (in addition to the rotation of the molecule as a whole) a deformation mechanism of molecular motion contributes to the development of the EBR in these polymers. Its role increases with the molecular mass of the fraction. The lack of dependence of τ on M for the polymer 1 is evidence that the condition $\tau_{or} > \tau_{def}$ applies to this polymer and that the motion of the molecular chain takes place by a

deformation mechanism, in which only part of the molecule acts as the 'kinetic unit', oriented in the electric field. However, under these conditions the rotational mobility of the kinetic unit is lower by 5 or 6 orders of magnitude than in ordinary flexible-chain polymers. Therefore this motion (though intramolecular) is similar in nature to a large-scale motion, since it is correlated through the chain.

A study of the equilibrium EBR in solutions of the polymers 1–3 (see Table 7) showed that the Kerr constant is strongly dependent on M: this behaviour is typical of monomers whose molecular chain



can accommodate an 'accumulation' of the longitudinal component μ of the monomeric dipoles. Further-more in these samples (as in compounds 4 and 5) the signs of K and of $\Delta n/\Delta\tau$ coincide in the region of high molecular masses (Table 7, see over), suggesting identical orientation mechanisms of their macromolecules in electrical and in hydrodynamic shear fields.

Thus both the transient and the steady-state electro-optical properties of branched polymers unambiguously show that the insertion of mesogenic side groups in the main methacrylate chain of polymers 1–5 (see Table 7) produces longitudinal components of the monomeric dipoles $\mu_{0||}$, uniformly oriented along the chain. The $\mu_{0||}$ values calculated by formula (45) from the Δa and K_∞ values in nonpolar solvents are shown in Table 7. They can account for only a small part of the total dipole moment μ_0 of the monomer unit of the branched macromolecule. However, these $\mu_{0||}$ components contributed by mesogenic side groups in the polymeric molecule can accumulate along its main chain and induce the orientational–polar ordering responsible for the Kerr effect in the polymer solution. The formation mechanism of the $\mu_{0||}$ dipoles uniformly oriented along the main chain of the branched polymer can be understood if one allows for the orientational interaction between the side chains, whose mesogenic nuclei contain dipolar components $\mu_\perp$ normal to these chains. In the presence of orientational order of the nematic type between the mesogenic side chains the $\mu_\perp$ components can contribute to the $\mu_{0||}$ component parallel to the main chain of the polymer.

The important role of the mesogenic structure of the side groups in the formation of the longitudinal components ($\mu_{0||}$) of the dipoles is clearly illustrated by the electro-optical properties of polymer 6 (Table 7), whose side chains are long, polar, and anisotropic, but not mesogenic. The equilibrium K values for this polymer are small and similar in order of magnitude to the K value for its monomer in tetrachloroethane, and also for low-molecular substances with a structure similar to that of its side groups. For sinusoidal fields at radio-frequencies no dispersion of the EBR has been detected [114] in solutions of the polymer. These results show that the branched molecules of polymer 6, whose side chains are not mesogenic in an electric field, behave as kinetically flexible and orient themselves by a deformation mechanism of the chain (relying on the local motion of the polar groups).

As the mesogenic nucleus of the side group in a branched polymer is moved further away from the main chain [by introducing a flexible segment (the spacer) between them] the correlation between the orientations of the main chain and of the side chains becomes less close. Therefore the large-scale motion of the macromolecule is replaced by a small-scale (local) motion, in which the orientation of the side chains in an electric field takes place as in a solution of the corresponding monomer: by the more or less independent rotation of the polar side groups. This conclusion is well illustrated by data [112] obtained for the polymer 7, whose solutions do not show radio-frequency dispersion of K: the equilibrium value of this constant is close to the K value for sample 6.

The weakening of the orientational correlation between the main chain and mesogenic side groups is of fundamental importance in demonstrating the mesomorphism of the branched polymer in a pure sample. As we know, branched polymers form a thermotropic nematic phase only if the orientation of the mesogenic side nucleus relative to the main chain is reasonably free, i.e. in the presence of a spacer. Thus, we have studied [115] the equilibrium and the transient EBR in the isotropic phase of a branched polymer containing mesogenic cyanobiphenyl groups in the side chains.

The relaxation time corresponding to a more or less independent (local) orientation of the mesogenic side groups has been obtained. Data on the equilibrium EBR confirmed these results: its magnitude and its positive sign corresponded to the magnitude and sign of the EBR in the isotropic phase (or in solution) of the mesogenic low-molecular analogue.

VII. Conclusions

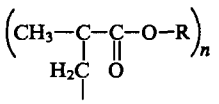
We have discussed the electro-optical properties of polymers whose macromolecules differ strongly in their equilibrium rigidity. The terms 'semirigid' and 'rigid-chain' polymers have been proposed for these materials. As we have pointed out, [116, 117] semirigid molecules cannot be treated as a class of polymers having a well defined structure. It is better to characterise them as a group of structures displaying a recognisable group of physicochemical properties. One of the most important of these properties is the large-scale orientation of the molecular chain in an electric field. The necessary condition for the appearance of this mechanism is the presence of a longitudinal component of the dipole moment of the monomer unit $\mu_{0||}$, correlated over the contour of the molecular chain.

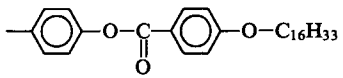
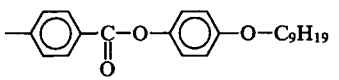
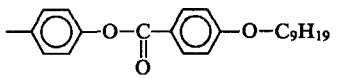
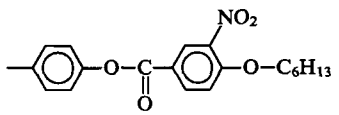
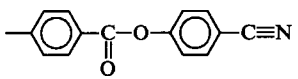
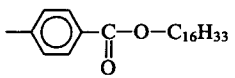
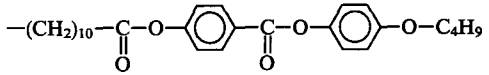
The maximum value of the Kerr effect for polymers (in the Gaussian region) is determined by the parameters Δa,, $\mu_{0||}^2$, and S^2. Depending on the possible values of these quantities the Kerr constant can vary over several orders of magnitude in absolute value, but the signs of K_∞ and $\Delta n/\Delta\tau$ are the same whenever $\mu_{0||}$ is orientationally correlated over the chain. For many flexible-chain polymers the fundamental condition for the formation of large-scale EBR is not fulfilled, and therefore in these cases K is small and is determined by the local orientation of the monomer units, and the signs of K and $\Delta n/\Delta\tau$ are not correlated. However, even in the presence of monomeric dipoles $\mu_{0||}$ uniformly oriented over the chain the Kerr effect can be difficult to observe because S^2 (and therefore also K) is small. In addition, the presence of anisotropic and of polar side groups interacting specifically in a flexible polymer chain can produce both a slight increase in S and Δa as well as some increase in the $\mu_{0||}$ parameters, and therefore it can lead to the development in these solutions of an EBR effect by the large-scale motion mechanism. A clear example of this behaviour is seen in the branched polymers with anisotropically interacting mesogenic side groups.

The nature of the development of a longitudinal component of the dipole of the monomer unit in a polymer can differ in different systems, but in nonpolar solvents $\mu_{0||}$ for the polymer is always determined by the dipolar structure of the macromolecules. Under these conditions $\mu_{0||}$ can be strongly dependent on the polar structure of the main chain [for example, in poly(alkyl isocyanates)] as well as on the dipolar properties of the side substituents, as is clearly seen in the cellulose esters.

When polar solvents are used the origin of the $\mu_{0||}$ component is not so well understood. Under these conditions $\mu_{0||}$ can be formed by the specific interactions between the polymer and the solvent, leading to the orientational correlation of the dipolar solvent molecules and of the polar bonds in the polymer chain, and resulting in the formation of an effective 'electro-optical' dipole in the macromolecule.

In studies of the transient EBR in dilute solutions of polymers the nature of the formation of $\mu_{0||}$ is unimportant in principle. Studies of the dependence of the relaxation times on the molecular

Table 7. Electro-optical properties of some branched polymers  mesogenic groups in the side chains.

	R	Solvent	$10^{10}\,K$/ $g^{-1}\ cm^5\ (300\ V)^{-2}$	$10^{10}\,(\Delta n/\Delta\tau)$/ $cm\ s^2\ g^{-1}$	$10^{25}\,\Delta a/cm^3$	$\mu_{0\parallel}/D$	Ref.
1		Tetrachloromethane	−4 to −20	−220	−110	0.7	111
2		"	−3.4 to −8.0	−220	−110	0.43	112
3		"	−3 to −7	−50	−40	0.8	111
4		Dioxan	−7	−95	−80	0.67	113
5		Dichloroacetic acid	−4.9	−22	−20	–	113
6		Tetrachloromethane	−0.5	−35	−18	–	114
7		Dioxan	−0.9	−8.5	−7	–	112

mass for rigid-chain polymers have yielded some quantitative conclusions on the equilibrium rigidity of macromolecules without introducing data obtained by other methods, and it also allowed their kinetic rigidity to be characterised qualitatively.

An analysis of the dependence of the Kerr constant on the molecular mass in rigid-chain polymers allows us to determine the equilibrium rigidity of the chain. Under these conditions the result is relatively unaffected by the choice of solvent. The problem is simplified when the contribution to the electro-optical effect from the normal component of the dipole of the monomer unit $\mu_{0\perp}$ is small, which corresponds either to a small value of ϑ or to a large value of α. Equilibrium EBR data can be used in studies of the dipole structure of a polymer chain (the magnitude of the dipole of the monomer unit μ_0 and its slope ϑ with respect to the contour of the macromolecule) only when nonpolar solvents are chosen. To determine the angle ϑ reliably it is important to include a change in sign of the dependence of K on M, which should be observed for $\vartheta > 54°$, since unless this is done the dependence of the Kerr constant on the molecular mass is an insensitive function of the angle ϑ and cannot be used to calculate it. Unfortunately, experimental data indicating a change in sign of K upon increasing M have not so far been obtained in nonpolar solvents.

References

1. J Kerr *Philos. Mag.* **50** 347 (1875)
2. P Debye, T Zakk *Theory of Electric Properties of Molecules* (Translated into Russian; Moscow, Leningrad: Glav. Red. Obshchetekhn. Lit-ry, 1936)
3. H A Stuart *Die Struktur des freien Molekuls* (Berlin: Springer, 1952)
4. M P Langevin *C. R. Acad. Sci.* **151** 457 (1910)
5. M Born *Ann. Phys.* **55** 177 (1918)
6. W Kuhn, H Dührkop, H Martin *Z. Phys. Chem., Abt.* **45** 121 (1939)
7. Ch O'Konski, K Yoshioka, W Orttung *J. Phys. Chem.* **63** 1558 (1959)
8. N A Tolstoi, P P Feofilov *Dokl. Akad. Nauk SSSR* **66** 617 (1949)
9. H Benoit *C. R. Acad. Sci.* **228** 1716 (1949)
10. H Benoit *C. R. Acad. Sci.* **229** 30 (1949)
11. A Peterlin, H Stuart, in *Hand- und Jahrbuch der Chemischen Physik* Vol. 8 (Eds A Eucken, K L Wolf) (Leipzig: Akadem. Verlag, 1943) p.1
12. V N Tsvetkov, V E Eskin, S Ya Frenkel' *Struktura Makromolekul v Rastvorakh* (Structure of Macromolecules in Solutions) (Moscow: Nauka, 1964)
13. V N Tsvetkov *Zhestkotsepnye Polimernye Molekuly* (Rigid-chain Polymer Molecules) (Leningrad: Nauka, 1986)
14. P Flory *Statistical Mechanics of Chain Molecules* (Translated into Russian; Moscow: Mir, 1971)
15. J E Hearst *J. Chem. Phys.* **38** 1062 (1963)
16. S Boersma *J. Chem. Phys.* **32** 1626 (1960)
17. P J Hagerman, B H Zimm *Biopolymers* **20** 1481 (1981)
18. P J Hagerman *Biopolymers* **20** 1503 (1981)
19. P Lewis, R Pecora, D Eden *Macromolecules* **19** 134 (1986)
20. H Kuhn *Experientia* **1** 1 (1945)
21. H Kuhn *Helv. Chim. Acta* **31** 1677 (1948)
22. W Kuhn, F Grün *Kolloid Z.* **101** 248 (1942)
23. V N Tsvetkov *Dokl. Akad. Nauk SSSR* **205** 328 (1972)
24. V N Tsvetkov *Vysokomol. Soedin., Ser. A* **29** 995 (1987)
25. V N Tsvetkov *Dokl. Akad. Nauk SSSR* **165** 360 (1965)
26. W Kuhn *Helv. Chim. Acta* **31** 1092 (1948)
27. V N Tsvetkov *Eur. Polym. J.* **12** 867 (1976)
28. E Fredericq, C Houssier *Electric Dichroism and Electric Birefringence* (Oxford: Clarendon Press, 1973)
29. C Houssier, C O'Konski *Molecular Electro-Optics* (Ed. S Krause) (New York: Plenum, 1980)
30. V Leute, T Smith *Macromolecules* **11** 707 (1978)
31. V N Tsvetkov, I P Kolomiets, A V Lezov, A S Stepchenkov *Vysokomol. Soedin., Ser. A* **25** 1327 (1985)
32. A V Lezov, N V Tsvetkov *Vysokomol. Soedin., Ser. A* **32** 162 (1990)
33. M S Beevers, D C Garrington, G Williams *Polymer* **18** 540 (1977)
34. M Matsumoto, H Watanabe, K Yoshioka *Biopolymers* **6** 929 (1968)
35. M Matsumoto, H Watanabe, K Yoshioka *Biopolymers* **12** 1729 (1973)
36. K Yamaoka, K Fukudome *Bull. Chem. Soc. Jpn.* **56** 60 (1983)
37. O P Nwammuo, G C Maitland *J. Chem. Soc., Faraday Trans.* **88** 1803 (1992)
38. I P Kolomiets, A V Lezov, G N Marchenko, V N Tsvetkov *Vysokomol. Soedin., Ser. A* **27** 2415 (1985)
39. I P Kolomiets, A V Lezov, A S Stepchenkov, L N Andreeva, A I Mashoshin, V N Tsvetkov *Vysokomol. Soedin., Ser. A* **28** 1040 (1986)
40. V N Tsvetkov, L N Andreeva, A P Filippov, E V Belyaeva, A Yu Bilibin, A S Stepanova *Vysokomol. Soedin., Ser. A* **33** 391 (1991)
41. A V Lezov, N V Tsvetkov, A A Trusov, V N Tsvetkov *Dokl. Akad. Nauk SSSR* **305** 659 (1989)
42. A V Lezov, N V Tsvetkov, A A Trusov *Vysokomol. Soedin., Ser. A* **32** 1887 (1990)
43. V N Tsetkov, G N Marchenko, N V Tsvetkov, A V Lezov, S A Didenko *Dokl. Akad. Nauk SSSR* **320** 672 (1991)
44. N V Tsvetkov, G N Marchenko, S A Didenko, A I Khripunov, A V Lezov, V N Tsvetkov *Vysokomol. Soedin.*, Ser. A **34** 98 (1992)
45. E I Ryumtsev, L N Andreeva, N V Pogodina, E U Urinov, L I Kutsenko, P N Lavrenko *Vysokomol. Soedin. Ser. A* **17** 61 (1975)
46. N V Pogodina, K S Pozhivilko, Kh. Dauttsenberg, K I Linov, B Filipp, E I Ryumtsev, V N Tsvetkov *Vysokomol. Soedin., Ser. B* **18** 851 (1976)
47. V N Tsvetkov, G N Marchenko, A V Lezov, N V Tsvetkov *Vysokomol. Soedin., Ser. A* **32** 2391 (1990)
48. N V Pogodina, K S Pozhivilko, N P Evlampieva, A B Mel'nikov, S V Bushin, S A Didenko, G N Marchenko, V N Tsvetkov *Vysokomol. Soedin., Ser. A* **23** 1252 (1981)
49. V N Tsvetkov, E I Ryumtsev, N V Pogodina, I N Shtennikova *Eur. Polym. J.* **11**, 37 (1975)
50. V N Tsvetkov, E I Ryumtsev, I N Shtennikova, N V Pogodina, T V Peker *Eur. Polym. J.* **11** 315 (1975)
51. N V Tsvetkov, G N Marchenko, M A Bezrukova, S A Didenko, V N Tsvetkov *Dokl. Akad. Nauk SSSR* **326** 678 (1992)
52. V N Tsvetkov, E I Ryumtsev, I N Shtennikova, T V Peker, N V Tsvetkov *Dokl. Akad. Nauk SSSR* **207** 1173 (1972)
53. V N Tsvetkov, E I Ryumtsev, N V Pogodina *Vysokomol. Soedin., Ser. B* **19** 2141 (1977)
54. V N Tsvetkov, A V Lezov, N V Tsvetkov, L N Andreeva *Eur. Polym. J.* **26** 575 (1990)
55. E I Ryumtsev, F M Aliev, V N Tsvetkov *Vysokomol. Soedin., Ser. A* **17** 1712 (1975)
56. E I Ryumtsev, L N Andreeva, F M Aliev, L I Kutsenko, V N Tsvetkov *Vysokomol. Soedin., Ser. A* **17** 1368 (1975)
57. A M North *Chem. Soc. Rev.* **1** 49 (1972)
58. B Zimm *J. Chem. Phys.* **24** 269 (1956)
59. B Zimm, G Roe, L Epstein *J. Chem. Phys.* **24** 279 (1956)
60. H Murukami, T Norishye *Macromolecules* **13** 345 (1980)
61. M G Vitovskaya, P N Lavrenko, O V Okatova, E P Astapenko, V B Novokovskii, S V Bushin, S A Didenko, L V Avrorova, G I Kudryavtsev, V N Tsvetkov *Vysokomol. Soedin., Ser. A* **23** 1959 (1981)
62. M G Vitovskaya, P N Lavrenko, E P Astapenko, O V Okatova, V N Tsvetkov *Vysokomol. Soedin., Ser. A* **20** 320 (1978)
63. V N Tsvetkov, S O Tsepelevich *Eur. Polym. J.* **19** 267 (1983)
64. S V Bushin, M A Bezrukova, E P Astapenko, S A Didenko, A K Khripunov, V N Tsvetkov *Vysokomol. Soedin., Ser. A* **32** 2054 (1990)
65. L N Andreeva, P N Larenko, E U Urinov, L I Kutsenko, V N Tsvetkov *Vysokomol. Soedin., Ser. B* **17** 326 (1975)
66. G A Lorentz *Theory of Electrons* (Translated into Russian; Leningrad, Moscow: ONTI, 1934)
67. C G Le Fevre, R J W Le Fevre *Pure Appl. Chem.* **5** 261 (1955)
68. R J W Le Fevre *Adv. Phys. Org. Chem.* **3** 1 (1965)
69. R S Amstrong, J J Aroney, C G Le Fevre *J. Chem. Soc.* **3** 1474 (1958)
70. R J W Le Fevre, A J Williams *J. Chem. Soc.* **3** 1671 (1961)
71. R J W Le Fevre, A J Williams *J. Chem. Soc.* **1** 562 (1964)
72. P Debye *Polar Molecules* (Translated into Russian; Moscow, Leningrad: GNTI, 1931)
73. L Onsager *J. Am. Chem. Soc.* **58** 1486 (1936)
74. O A Osipov, V I Minkin, A D Garnovskii *Spravochnik po Dipol'nym Momentam* (Handbook on Dipole Moments) (Moscow: Vysshaya Shkola, 1971)
75. J G Scholte *Physica* **15** 437 (1949)
76. J G Kirkwood *J. Chem. Phys.* **7** 911 (1939)

77. G Froelich *Theory of Dielectrics* (Translated into Russian; Moscow: Inostr. Lit., 1960)
78. V N Tsvetkov *Kolloidn. Zh.* **33** 154 (1971)
79. A D Buckingham, J A Pople *Proc. Phys. Soc.* **68** 905 (1955)
80. A D Buckingham, R E Raab *J. Chem. Soc.* **5** 2341 (1957)
81. J D Ramshaw, D W Schaefer, J S Wough, J M Dentch *J. Chem. Phys.* **54** 1239 (1971)
82. A D Buckingham *Molecular Electro-Optics* (Ed. C O'Konski) (New York: Marcel Dekker, 1976)
83. N V Tsvetkov *Vestn. Leningr. Univ., Ser. 4* **4** 22 (1990)
84. M J Aroney *Angew. Chem., Int. Ed. Engl.* **16** 663 (1977)
85. N V Tsvetkov, A A Trusov, V N Tsvetkov *Dokl. Akad. Nauk SSSR* **315** 664 (1990)
86. A N Vereshchagin *Kharakteristiki Anizotropii Polyarizuemosti Molekul* (Characteristics of the Anisotropy of the Polarization of Molecules) (Moscow: Nauka, 1982)
87. V N Tsvetkov, I N Shtennikova, E I Ryumtsev, V S Skazka *Vysokomol. Soedin., Ser. A* **7** 1111 (1965)
88. V N Tsvetkov, I P Kolomiets, A V Lezov, G N Marchenko *Dokl. Akad. Nauk SSSR* **265** 1202 (1982)
89. N V Pogodina, A B Mel'nikov, N P Evlampieva *Khim. Drevesiny* **6** 3 (1984)
90. N V Pogodina, Candidate's Thesis, Leningrad State University, Leningrad, 1975
91. I P Kolomiets, N V Pogodina, A V Lezov, N P Evlampieva, T A Stepchenkova, O T Shilina, G N Marchenko, V N Tsvetkov *Vysokomol. Soedin., Ser. A* **29** 2494 (1987)
92. V N Tsvetkov, A V lezov, L N Andreeva, N V Tsvetkov *Dokl. Akad. Nauk SSSR* **303** 672 (1988)
93. N V Tsvetkov, A V Lezov, G N Marchenko, S A Didenko, V N Tsvetkov *Vysokomol. Soedin., Ser. A* **34** 141 (1992)
94. V N Tsvetkov, Yu V Mitin, I N Shtennikova, V R Glushenkova, G V Tarasova, V S Skazka, N A Nikitin *Vysokomol. Sodin., Ser. A* **7** 1098 (1965)
95. M G Vitovskaya, V N Tsvetkov *Eur. Polym. J.* **12** 251 (1976)
96. V N Tsvetkov, P N Lavrenko, L N Andreeva, A I Mashoshin, O V Okatova, O I Mikriukova, L I Kutsenko *Eur. Polym. J.* **20** 823 (1984)
97. N V Pogodina, K S Pozhivilko, A B Mel'nikov, S A Didenko, G N Marchenko, V N Tsvetkov *Vysokomol. Soedin., Ser. A* **23** 2454 (1981)
98. N V Pogodina, P N Lavrenko, K S Pozhivilko, A B Mel'nikov, T A Kolobova, G N Marchenko, V N Tsvetkov *Vysokomol. Soedin., Ser. A* **24** 332 (1982)
99. V N Tsvetkov, I P Kolomiets, A V Lezov, L N Andreeva, AYu Bilibin, S S Skorokhodov *Eur. Polym. J.* **22** 543 (1986)
100. V N Tsvetkov, L N Andreeva, P N Lavrenko, E V Beliaeva, O V Okatova, A Yu Bilibin, S S Skorokhodov *Eur. Polym. J.* **20** 817 (1984)
101. V N Tsvetkov, I P Kolomiets, A V Lezov, L N Andreeva, A Yu Bilibin, S S Skorokhodov *Dokl. Akad. Nauk SSSR* **294** 850 (1987)
102. V N Tsvetkov, L N Andreeva, P N Lavrenko, E V Belyaeva, O V Okatova, A Yu Bilibin, S S Skorokhodov *Vysokomol. Soedin., Ser. A* **28** 2283 (1986)
103. V N Tsvetkov, I P Kolomiets, A V Lezov, A P Filippov, A Yu Bilibin, S S Skorokhodov *Dokl. Akad. Nauk SSSR* **296** 1167 (1987)
104. V N Tsvetkov, L N Andreeva, S V Bushin, E V Belyaeva, V A Cherkasov, A I Mashoshin, A Yu Bilibin, S S Skorokhodov *Vysokomol. Soedin., Ser. A* **30** 713 (1988)
105. V N Tsvetkov, I P Kolomiets, A V Lezov, A P Filippov *Dokl. Akad. Nauk SSSR* **307** 916 (1989)
106. V N Tsvetkov, L N Andreeva, A P Filippov *Eur. Polym. J.* **24** 565 (1988)
107. V N Tsvetkov, A V Lezov, N V Tsvetkov, L N Andreeva *Eur. Polym. J.* **26** 575 (1990)
108. V N Tsvetkov, A V Lezov, N V Tsvetkov, L N Andreeva *Eur. Polym. J.* **26** 1103 (1990)
109. N V Pogodina, E V Tarabukina, L V Starchenko, G N Marchenko, V N Tsvetkov *Vysokomol. Soedin., Ser. A* **22** 2219 (1980)
110. S V Bushin, M A Bezrukova, S A Didenko, A K Khripunov, V N Tsvetkov *Vysokomol. Soedin., Ser. A* **34** 107 (1992)
111. V N Tsvetkov, E I Ryumtsev, I N Shtennikova, I I Konstantinov, Yu B Amerik, B A Krentsel' *Vysokomol. Soedin., Ser. A* **15** 2270 (1973)
112. N V Pogodina, V N Tsvetkov *Vysokomol. Soedin., Ser. A* **24** 2275 (1982)
113. V N Tsvetkov, I P Kolomiets, N V Pogodina, A P Filippov *Dokl. Akad. Nauk SSSR* **287** 1172 (1986)
114. V N Tsvetkov, I N Shtennikova, E I Ryumtsev, N V Pogodina, G F Kolbina, E V Korneeva, P N Lavrenko, O V Okatova, Yu B Amerik, A A Baturin *Vysokomol. Soedin., Ser A* **18** 2016 (1976)
115. E I Ryumtsev, M A Agafonov, V N Tsvetkov *Vysokomol. Soedin., Ser. A* **29** 1091 (1987)
116. V N Tsvetkov *Usp. Khim.* **38** 1674 (1969) [*Russ. Chem. Rev.***38** 755 (1969)]
117. V N Tsvetkov *Eur. Polym. J.* **5** 237 (1969)

Russian Chemical Reviews **62** (9) 877–896 (1993) ©1993 Russian Academy of Sciences and Turpion Ltd

UDC 541.128.12:547.241

New reactions involving the oxidative *O*-, *N*-, and *C*-phosphorylation of organic compounds by phosphorus and phosphides in the presence of metal complexes

Ya A Dorfman, M M Aleshkova, G S Polimbetova, L V Levina, T V Petrova, R R Abdreimova, D M Doroshkevich

Contents

I.	Introduction	877
II.	Oxidative P–O coupling of tetraphosphorus to alcohols	877
III.	Oxidative P–N coupling of tetraphosphorus to amines	880
IV.	Oxidative P–O coupling of red phosphorus to alcohols	881
V.	Oxidative P–O coupling of phosphine to alcohols	883
VI.	Oxidative P–C coupling of phosphine to alcohols	886
VII.	Oxidative P–O coupling of phosphine to alcohols in the presence of chlorine	888
VIII.	Oxidative P–N coupling of phosphine to primary and secondary amines	889
IX.	P–C coupling of phosphine to aldehydes	890
X.	Oxidative P–C coupling of phosphine and tetraphosphorus to nitriles	891
XI.	Oxidative P–O coupling of zinc and copper phosphides to alcohols	892
XII.	Oxidative P–O coupling of zinc and copper phosphides to alcohols in the presence of chlorine	893

Abstract. The mechanisms of new catalytic reactions leading to the formation of di- and tri-alkyl phosphates, di- and tri-alkyl phosphites, phosphoramidites, phosphazenes, phosphines, and phosphine oxides from hydrogen, copper, and zinc phosphides and white and red phosphorus are analysed. The mechanisms of the activation of the reactants by metal complexes and of the reactions involving the oxidative P–O, P–N, and P–C coupling of organic compounds to phosphorus and phosphides are considered. The bibliography includes 124 references.

I. Introduction

The products of the P–C, P–N, and P–O coupling, namely di- and tri-alkyl phosphates, di- and tri-alkyl phosphites, phosphazenes, phosphorinanes, phosphines, and phosphine oxides, are stable organic compounds[1,2] and are widely used as extractants for the lanthanides, the actinides, and other heavy metals from mineral raw materials and the waste from atomic power plants,[3,4] as monomers for the synthesis of organophosphorus fire- and heat-resistant polymers,[5,6] as additives to fuels and lubricating materials, as corrosion inhibitors, etc.

The available methods for the synthesis of the above compounds are based on the P–C, P–N, and P–O coupling of organic substances to the high-valence phosphorus compounds $POCl_3$, and PCl_5, which are synthesised using the expensive and extremely toxic chlorine.[1–7] Dorfman et al[8] discovered the reactions involving the P–C, P–N, and P–O coupling of organic compounds to low-valence inorganic phosphorus compounds, which lead to the formation of some of the substances listed above. Low-valence phosphorus compounds, namely phosphine, transition metal phosphides, hypophosphite, tetraphosphorus, and polyphosphorus are highly toxic waste from modern phosphorus and hypophosphite manufacturing plants produced on a large scale.[9–11] White phosphorus is present in weak phosphorus sludge, which is not utilised nowadays and is stored in sludge accumulators.

Important advantages of the new reaction involving the oxidative P–C, P–N, and P–O phosphorylation of organic substances by low-valence inorganic compounds are mild conditions, a high rate, and a high selectivity, which facilitates the isolation technology of the pure product.[8] This makes it possible to use the waste from phosphorus undertakings in which phosphorus-containing compounds are present in small amounts.

The wide variety of the products formed in P–C, P–N, and P–O oxidative coupling to aliphatic and aromatic compounds (phosphine, transition metal phosphides, tetraphosphorus and polyphosphorus, and hypophosphite) and reaction conditions do not rule out the existence of a series of common features of interest in the organic chemistry of low-valence phosphorus compounds, which have been extremely little investigated, and in the metal complex catalysis of homogeneous and topochemical processes.

II. Oxidative P–O coupling of tetraphosphorus to alcohols

Despite the evident usefulness of tetraphosphorus in organic synthesis, there are as yet no data concerning the processes based on it.[12–40] Homolytic reactions are characteristic of tetraphosphorus, whereas heterolytic reactions proceed with

Ya A Dorfman, M M Aleshkova, G S Polimbetova, L V Levina, T V Petrova, R R Abdreimova, D M Doroshkevich Institute of Organic Catalysis and Electrochemistry, Academy of Sciences of the Republic of Kazakhstan, ul. Karla Marksa 142, 480100 Alma-Ata, Kazakhstan., Fax (7-327-2) 61 57 22

Received 24 May 1993
Uspekhi Khimii **62** (9) 928–948 (1993); translated by A K Grzybowski

difficulty.[10] It has been observed[41-43] that, when tetraphosphorus is placed in an arene–alcohol solution of divalent copper salts under a O_2 atmosphere at 50–150 °C, reactions involving the oxidative P–O coupling of P_4 to ROH proceed very rapidly and with a high selectivity.

Reactions (1) and (3) predominate in the arene–alcohol solutions of $CuHal_2$ (Hal = Cl, Br), while reaction (2) predominates in $CuSO_4$, and $Cu(CO_2R)_2$ solutions (R = CH_3, C_3H_7, $C_{17}H_{35}$; arene = benzene, toluene, xylene).[8] Copper(II) sulfate and carboxylate complexes stimulate also the formation of dialkyl phosphite, in contrast to the halide complexes. The product ratio $(RO)_3PO/(RO)_3P$ depends not only on the nature of the ligands but also on the ROH concentration. If the amount of ROH diminishes, the ratio $(RO)_3PO/(RO)_3P$ also falls. Dialkyl phosphate is obtained at elevated temperatures.

$$P_4 + 5O_2 + 12ROH \longrightarrow 4(RO)_3PO + 6H_2O; \quad (1)$$

$$P_4 + 3O_2 + 12ROH \longrightarrow 4(RO)_3P + 6H_2O; \quad (2)$$

R = CH_3, C_2H_5, C_3H_7, C_4H_9, *iso*-C_4H_9, C_5H_{11}, *iso*-C_5H_{11}, C_8H_{17}, C_6H_5.

$$P_4 + 3O_2 + 8R'OH \longrightarrow 4(R'O)_2HPO + 2H_2O; \quad (3)$$

R′ = *iso*-C_3H_7.

The catalytic activity of copper(II) complexes also depends on the nature of the anions and increases when the halides are replaced by the sulfates, acetates, and especially butyrates and stearates. Both the rate of reduction of copper(II) by tetraphosphorus and the rate of oxidation of copper(I) by oxygen increase in this series of ligands. In contrast to the sulfate and acetate complexes, the butyrate and stearate complexes are readily soluble in benzene–alcohol solutions and in their presence the oxidative P–O coupling of P_4 to ROH proceeds selectively and at a high rate. The acidopyridinecopper(II) complexes have a higher activity.[41] The addition of pyridine to arene–alcohol solutions of $CuHal_2$, $CuSO_4$, and $Cu(CO_2R)_2$ leads to a sharp increase in the rate of reaction and in the $(RO)_3PO/(RO)_3P$ ratio and to a decrease in the yield of $(RO)_2(HO)PO$.

$$P_4 + 5O_2 + 8ROH \longrightarrow 4(RO)_2(HO)PO + 4H_2O. \quad (4)$$

Under an argon atmosphere, tetraphosphorus reacts almost instantaneously with arene–alcohol solutions of copper(II) complexes.

Reactions (5)–(8) take place over a period of 30–50 s.[41-43] The univalent and metallic copper formed is readily reoxidised by air to the divalent state. During the regeneration period, the alkyl halides and sulfates are hydrolysed to the alcohol by the water formed in this process, while alkyl carboxylates accumulate in the system. In the presence of acids, trialkyl phosphites are dealkylated to dialkyl phosphites. The rate of dealkylation increases with increase in the acidity of the medium (on passing from the sulfate and carboxylates to the halides) and also with decrease in the molecular mass of the group R. The dealkylation of trialkyl phosphites ends in the stage involving the formation of dialkyl phosphites, which are dealkylated very slowly. The

$$P_4 + 16ROH + 20CuX_2 \longrightarrow 4(RO)_3PO + 20CuX + 4RX + 16HX; \quad (5)$$

$$P_4 + 16ROH + 20CuX_2 \longrightarrow 4(RO)_2(HO)PO + 20CuX + 8RX + 12HX; \quad (6)$$

X = Cl, Br.

$$P_4 + 12ROH + 6CuY_2 \longrightarrow 4(RO)_3P + 6Cu + 12HY; \quad (7)$$

$$P_4 + 12R'OH + 6CuY_2 \longrightarrow 4(R'O)_2HPO + 6Cu + 4R'Y + 8HY; \quad (8)$$

Y = SO_4^{2-}, RCO_2^-.

oxygen-containing acido-ions (OH^-, SO_4^{2-}, RCO_2^-) are relatively unreactive in these reactions. Trialkyl phosphites form[44] stable complexes with copper(I) halides of the type $CuX \cdot P(OR)_3$ and $CuX \cdot 2P(OR)_3$. Copper(I) trialkyl phosphite complexes are greasy substances with melting points from 90 to 180 °C depending on the nature of the alkoxy-group. They are soluble in ether, benzene, acetone, and alcohols, can be readily detected by ^{31}P NMR spectroscopy in the range −6 to −10 ppm,[44,45] and are readily decomposed by chlorine with formation of trialkyl phosphates and copper(II) complexes.

Reactions (3) and (4) have been investigated in detail by kinetic and potentiometric methods.[41-43] The introduction of an arene solution of P_4 into an alcoholic solution of CuX_2 or CuY_2 under a O_2–Ar atmosphere is accompanied by a sharp shift of the redox potential of the Cu(II)/Cu(I) couple in the cathodic direction. At the same time, the pressure falls in a closed system and the absorption of O_2 begins. As O_2 is absorbed, the redox potential gradually returns to the anodic region. Analysis of the reaction mixture during the experiment by gas chromatography and ^{31}P NMR spectroscopy showed that the sharp shift of the redox potential in the cathodic direction is caused by the rapid reduction of Cu(II) to Cu(0) by tetraphosphorus in conformity with reactions (5)–(8). At the end of the process, when P_4 has been consumed, the redox potential shifts in the anodic direction as a result of the oxidation of Cu(0) to Cu(I) by oxygen. The rate constant for the reduction of Cu(II) by tetraphosphorus to Cu(0) was calculated from the magnitude and time of the cathodic shift of the redox potential at the beginning of the experiment:

$$k_{red} = \frac{W}{[Cu(II)][P_4]} \text{ litre mol}^{-1} \text{ s}^{-1} \quad (9)$$

(in C_2H_5OH, k_{red} = 1–5 litre mol^{-1} s^{-1}), while the rate constant for the oxidation of CuX and CuY by oxygen was found from the magnitude and time of the anodic shift of the redox potential:

$$k_{ox} = \frac{W}{[Cu(I)][O_2]} \text{ litre mol}^{-1}\text{s}^{-1} \quad (10)$$

(in C_2H_5OH, k_{ox} = 0.1–0.9 litre mol^{-1} s^{-1}). Tetraphosphorus is sparingly soluble in polar solvents and readily soluble in weakly polar and non-polar solvents. Thus the solubility of P_4 is 10^4 g $litre^{-1}$ s^{-1} in carbon disulfide, 10^2 g $litre^{-1}$ in arenes, 50 g $litre^{-1}$ in alkanes, 40 g $litre^{-1}$ in carbon tetrachloride, 30 g $litre^{-1}$ in alcohol, and 10^{-3} g $litre^{-1}$ in water. Owing to the sparing solubility of P_4 in alcohol, benzene–alcohol and toluene–alcohol mixtures, which readily dissolve P_4 and copper(II) complexes, which only sparingly dissolve in H_2O, were used. Without the arene (in alcohol) and without alcohol (in the arene), the oxidation of P_4 by oxygen with formation of P_4O_{10} is slow.

The water formed by reactions (1)–(4) inhibits the reaction of P_4 with ROH and stimulates the P–O coupling to H_2O, affording phosphoric acid. Water is coordinated to copper(II) compounds more readily than ROH. According to UV spectroscopic data for water–alcohol solutions of copper(II) compounds, the alcohol complexes of copper(II) are formed at a H_2O concentration less than 10%.[46] In arene–alcohol solutions of copper(II) compounds, water exerts the least influence on the composition of the complexes. Owing to the presence of the arene, the water generated during reactions (1)–(4) does not affect the course of the oxidative *O*-phosphorylation of alcohols by tetraphosphorus. As a result of its sparing solubility in the arene–alcohol mixture (0.6 g $litre^{-1}$), water forms a separate phase. The arene can function as a phase transfer catalyst. It dissolves selectively ROH, P_4, and the copper(II) complexes, ensures the occurrence of the reaction between P_4 and ROH, and prevents the reaction between P_4 and H_2O.

An excess of acido-anions interferes with the coordination of P_4 to copper(II) complexes and has a negative influence on the rates of reactions (5)–(8). At a high concentration of

acido-ligands, P_4 does not reduce copper(II) complexes. In non-aqueous solvents, acido-ligands form stable complexes with copper(II) anions. On passing from aqueous to non-aqueous solutions, the stability constants of these acido-complexes increase by several orders of magnitude in opposition to the change in the dielectric constant [relative permittivity] and in the donor number (DN) of the solvent. Table 1 lists the formation constants (β_j) of the copper(II) chloride complexes in various solvents.

Table 1. The equilibrium constants (β_j) of the reaction $Cu^{2+}_{sol} + jCl^- \rightleftarrows CuCl_j^{2-j} + sol.$

Solvent (DN)	$CuCl^+_{sol}$	$CuCl_{2\,sol}$	$CuCl^-_{3\,sol}$	$CuCl^{2-}_{4\,sol}$
H_2O (18)	0.4	0.6	0.1	−0.8
DMF (24)	4.4	3.0	12.0	12.9
TMF (23)	7.3	12.4	16.8	19.4
$(CH_3)_2CO$ (17)	8.4	14.5	19.9	21.5
THF (20)	10.7	20.3	23.9	25.7
$(CH_3)_2SO$ (30)	3.4	5.2	7.3	7.9
PC (15)	12.0	22.7	29.0	34.0

Complexes saturated by acido-ligands are already obtained[47] at a ratio ligand/Cu(II) > 6. The maximum rates of reactions (1)–(4) are attained when coordinatively unsaturated copper(II) complexes predominate in the arene–alcohol solution. Coordinatively saturated copper(II) complexes do not react with tetraphosphorus.[41–43] The ligand effect observed is due to the fact that the η^1-tetraphosphorus complexes are characterised by a lower reactivity than the η^2-tetraphosphorus complexes. Since two free coordination sites in the equatorial plane are necessary for the η^2-coordination of P_4, an excess of acido-ligands interferes with the addition of P_4 to copper(II) ions. Only electron-donating ligands (Cl^-, Br^-, NH_3, SO_4^{2-}, RCO_2^-) interfere with the η^2-coordination of P_4, whilst electron-accepting ligands (CH_3CN, ROH, H_2O, Py) stimulate the incorporation of P_4 into the coordination sphere of Cu(II).[41–43] An important feature of reactions (1)–(4) is the fact that the O_2/P_4 ratio is equal to the stoichiometric coefficient and is independent of the O_2 concentration, temperature, and the composition of the system. Oxygen is consumed only in the oxidation of P_4 and does not participate in the alcohol oxidation reaction.[41–43]

The rate constants for the reduction of copper(II) salts by tetraphosphorus increase [k_{red} = 2.24 (CH_3OH) and 1.47 (C_4H_9OH) litre mol^{-1} s^{-1}], while the rate constants for the oxidation by oxygen change little [k_{ox} = 0.12 (CH_3OH) and 0.17 (C_4H_9OH) litre $mol^{-1}s^{-1}$], in parallel with increasing acidity of the alcohols. Such variation indicates the participation in the reaction of acidoalkoxophosphorus complexes of copper(II).

A decrease in the concentration of ROH in the system as a result of its replacement by $(C_4H_9O)_3PO$ leads to a fall in the yield of trialkyl phosphates [from 66% to 20% for tetrahydrofuran (THF)], to an increase in the yield of trialkyl phosphites, and to a slight change in the rate constants for reactions (5)–(7). After the addition of $(C_4H_9O)_3PO$ (c = 1.83 mol $litre^{-1}$), k_{red} changes from 2.35 to 2.63 litre mol^{-1} s^{-1} and k_{ox} changes from 0.1 to 0.09 litre mol^{-1} s^{-1}.

Acido-complexes of copper(II) not containing ROH react with P_4 to form acyl phosphates, which can be readily detected by ^{31}P NMR spectroscopy:[45] Cl_3PO (5 ppm), $(RCO_2)_3PO$ (−20 ppm), $(RCO_2)_2HPO$ (7 ppm), $(RCO_2)_2(OH)PO$ (−6 ppm), and $(RCO)_2(OH)_2PO$ (−3 ppm).

In an arene–acetic acid solution and other systems of the type arene–carboxylic acid, the previously unknown oxidative P–O coupling of P_4 to carboxylic acids takes place.

$$P_4 + 20Cu(RCO_2)_2 \longrightarrow 4(RCO_2)_3PO + 20Cu(RCO_2) + 4(RCO_2)O. \quad (11)$$

Triacyl phosphates partly decompose with formation of diacyl and monoacyl phosphates.

$$(RCO_2)_3PO + RCO_2H \longrightarrow (RCO_2)_2(HO)PO + (RCO_2)O; \quad (12)$$

$$(RCO_2)_2(HO)PO + RCO_2H \longrightarrow (RCO_2)(HO)_2PO + (RCO_2)O. \quad (13)$$

In the absence of copper(II) complexes, tetraphosphorus in an arene–alcohol solution is slowly oxidised by oxygen to the phosphorus oxide P_4O_{10}, the esterification of which proceeds extremely slowly and only as far as primary and secondary phosphoric acid esters.

$$P_4O_{10} + 6ROH \longrightarrow 2(RO)(HO)_2PO + 2(RO)_2(HO)PO. \quad (14)$$

The chain oxidation of P_4 by oxygen does not occur owing to the low O_2 and P_4 concentrations in the liquid phase.[48]

The influence of the acidity of the medium has been investigated by the method involving the addition of pyridine and by varying the HCl/LiCl ratio in the reaction system. With increase in the acidity of the medium, the rate of reactions (5)–(7) falls (k_{red} diminishes from 4.53 to 0 litre mol^{-1} s^{-1} in C_2H_5OH) and the yield of dialkyl phosphates increases (from 3.3% to 53.3% for diethyl phosphate). The addition of pyridine increases significantly the rates of reactions (5)–(7) and the yields of trialkyl phosphates.[41–43]

It follows from the data presented that P_4 reacts better with acidoalkoxocopper(II) complexes than with the acidoalcohol-copper(II) complexes. Iron(II) and iron(III) halides, sulfates, and carboxylates are an order of magnitude less reactive then the analogous copper(II) complexes.

The experimental data enumerated above indicate a coordination mechanism of the reduction of copper(II) complexes by tetraphosphorus.

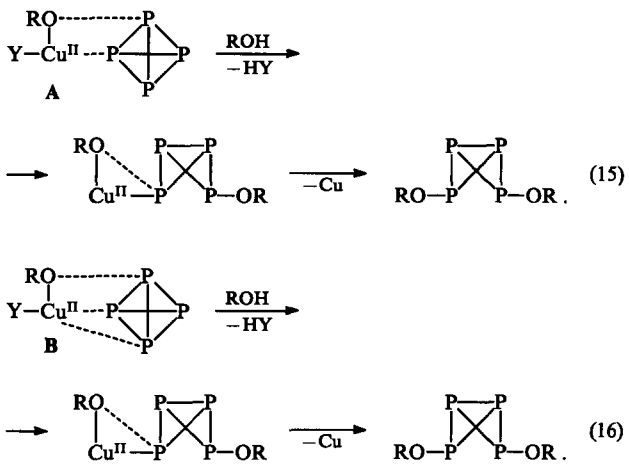
The reduction of acidoalkoxocopper(II) complexes by tetraphosphorus to Cu(0) consists of two stages: the insertion of P_4 in the Cu–OR bond with formation of the monoalkoxytetraphosphine anion $P_4(OR)^-$ and the reductive coupling of the RO^- and $P_4(OR)^-$ ligands with formation of dialkoxytetraphosphine.

The coordination mechanism is supported by the low activation energies (50–60 kJ mol^{-1}) compared with the dissociation energies of the bonds P–P (230 kJ mol^{-1}) and Cu–OR (260 kJ mol^{-1}) as well as the negative entropies of activation ($\Delta S^{\neq}_{red}$ = −82 J mol^{-1} K^{-1} and $\Delta S^{\neq}_{ox}$ = −80 J mol^{-1} K^{-1} in C_2H_5OH). The driving forces of the reaction involving the insertion of P_4 in the Cu–OR bond and the reductive dimerisation of the hydroxo- and polyalkoxyphosphine anions are the high energy of the P–O bond (340 kJ mol^{-1}) and the high redox potential of the Cu(II)/Cu(0) couple (0.34 V).

The subsequent stages of the oxidative alkoxylation of cyclic and linear dialkoxy- and tetraalkoxy-phosphides and dialkoxy- and tetraalkoxy-diphosphines by acidocopper(II) complexes are faster.

According to recent data,[29–33] P_4 can function both as a η^1- and η^2-ligand. On η^1-coordination (**A**) [(15)], the tetrahedral P_4 molecule is activated, being converted into a trigonal pyramid the vertex of which is directed towards the metal atom. The $P_{base}-P_{apex}$ distance (2.20 Å) is longer than the $P_{base}-P_{base}$ distance (2.09 Å). As a result of η^2-coordination (**B**), the edge linked to the metal is lengthened by 0.25 Å compared with the P–P bond in the free molecule (2.21 Å). Bidentate coordination of P_4 promotes a greater activation of the molecule than monodentate coordination. On bidentate binding of P_4, the P–P distance increases to an extent greater by 0.14 Å than on monodentate binding,[29–33] ensuring a greater loosening of P_4. The coordinatively saturated copper(II) complexes, incapable

of effecting the η^2-coordination of tetraphosphorus, are therefore characterised by a lower catalytic activity than the coordinatively unsaturated complexes, which are capable both of η^1- and η^2-coordination.[41-43]



(15)

(16)

The stages involving the insertion of P_4 in the Cu–OR bond and the reductive coupling of the OR^- and $P_4(OR)^-$ ligands have been investigated in detail by the CNDO method (complete neglect of differential overlap).[43] Calculations have been carried out for anionic acidoalkoxotetraphosphorus and acidomonoalkoxytetraphosphine complexes and cationic pyridinehydroxoaminoalkoxotetraphosphorus, aminoalkoxomonoalkoxytetraphosphine, aquoalkoxotetraphosphorus, and aquoalkoxomonoalkoxytetraphosphine complexes of copper(II).

The nature of the P_4 activation depends on the denticity of the ligands and the overall charge of the copper complex. The non-polar P_4 molecule is activated as a result of coordination: the energies of the P–P bonds diminish non-uniformly and effective charges appear on the P atoms, where they were absent before complex formation. In contrast to free P_4, the coordinated tetraphosphorus becomes an electron acceptor and interacts vigorously with ligands having an unshared electron pair (RO^-, HO^-, Hal^-). The HO^- ion models the behaviour of sulfate and carboxylate ligands. The ligands having no free unshared electron pair after coordination with copper(II) (H_2O, ROH, NH_3, Py) interact only weakly with P_4.[43]

The effective charges on the P atoms and the total, covalent, and ionic energies of the bonds between the ligands (between the chemically non-bonded atoms) were used to determine the composition of the many-centre transition state. The ligands in the copper(II) complex interact most strongly with the P atoms of the P_4 molecule which are not linked to the central copper atom. The energies of the bonds between the atoms and the ligands increase significantly with increase in the total positive charge on the complexes: in the anionic copper(II) complexes, the ligands interact much more weakly with P_4 than in the cationic complexes.[43]

The reductive coupling of the RO^- and $P_4(RO)^-$ ligands takes place with participation of the P atom bound covalently to the Cu(II) ion. If P_4 is inserted in the Cu–OR bond via a four-centre cyclic transition state (**A**) or (**B**), then the reductive elimination of the ligands RO^- and $P_4(RO)^-$ takes place via a three-membered cyclic intermediate. On the other hand, according to CNDO calculations, a covenient situation for the stage involving the reductive dimerisation of the alkoxo- and monoalkoxotetraphosphine ligands occurs in anionic complexes in the presence of electron-donating ligands. In such complexes the Cu–P bond, ruptured during the reductive coupling of the RO^- and $P_4(RO)^-$ ligands, is weakest.

$$P_4(OR)_2 \xrightarrow[-Cu]{Cu(OR)_2} P_4(OR)_4 \xrightarrow[-Cu]{2Cu(OR)_2} \longrightarrow 2P_2(OR)_4 \xrightarrow[-Cu]{2Cu(OR)_2} 4(RO)_3P. \quad (17)$$

Since cationic and anionic complexes are respectively more suitable for the stage involving the insertion of P_4 in the Cu–OR bond and the reductive coupling stage, optimum conditions are attained when uncharged copper(II) complexes are used. The rate of reaction therefore passes through a maximum when the number of acido-ligands is varied.[43]

III. Oxidative P–N coupling of tetraphosphorus to amines

Copper(II) complexes exhibit a high catalytic activity in oxidative P–N coupling of P_4 to primary and secondary amines.[49] Tetraphosphorus reacts with amines in the presence of oxygen with formation of phosphazo-compounds.

$$P_4 + 16RH_2N + 5O_2 \longrightarrow 4(RHN)_3P{=}NR + 10H_2O. \quad (18)$$

$$P_4 + 16R_2HN + 5O_2 \longrightarrow \longrightarrow 4(R_2N)_3P{=}NR + 6H_2O + 4ROH; \quad (19)$$

R = C_2H_5, C_6H_{11}, $C_6H_5CH_2$.

Under argon, tetraphosphorus reduces Cu(II) to Cu(0).

The zerovalent copper formed by reactions (20) and (21) is instantly regenerated by air. The new reactions (18)–(21) are very rapid. When primary ($C_6H_5CH_2NH_2$, $C_6H_{11}NH_2$) and secondary ($C_5H_{10}NH$) amines are used, we have the ratio $O_2/P_4 \simeq 5$. The formation of phosphazo-compounds by reactions (18)–(21) is of preparative value.[50,51] The new method of synthesis of triaminophosphazoalkyls is much simpler than that already available,[50] which is based on the P–N coupling of primary amines to trichlorophosphazohydrocarbons and the oxidative imination of phosphorus(III) compounds by *N*-chloroamines.[50-52]

$$P_4 + 10CuX_2 + 16RH_2N \longrightarrow \longrightarrow 4(RHN)_3P{=}NR + 10Cu + 20HX. \quad (20)$$

$$P_4 + 10CuX_2 + 16R_2HN \longrightarrow \longrightarrow 4(R_2N)_3P{=}NR + 10Cu + 4RX + 16HX. \quad (21)$$

Amines react with P_4 faster by one to two orders of magnitude than alcohols. In solutions in amines, the rate constants for the reduction of copper(II) by tetraphosphorus and for the oxidation of copper (I) by oxygen, calculated by Eqns (9) and (10), are higher than in alcoholic media. According to ^{31}P NMR spectroscopic data, reactions (18)–(21) proceed selectively. The ^{31}P NMR spectra contain only peaks characteristic of phosphazenes (10–20 ppm) and phosphorous triamide complexes of copper(I): $CuX[P(NR_2)_3]$ (10 ppm).[45]

The behaviour of amine systems under an oxygen atmosphere is similar to that of the alcohol systems. The kinetic ($W-\tau$) and conversion ($W-Q$) curves [τ is the time (s), W the rate of reaction (mol g^{-1} s^{-1}), and Q the degree of conversion of P_4] pass through an extremum for the ratio $Cu/P_4 < 10$ and have a descending form for $Cu/P_4 > 10$. When solutions of P_4 in an arene and of CuX_2 in an amine are mixed, the potential undergoes a sharp shift in the cathodic direction. As O_2 is absorbed, the redox potential of the Cu(II)/Cu(I) couple returns to the initial value. The rates of reactions (18)–(21) increase with increase in the concentrations of copper(II), NR_2H (or NRH_2), and O_2 and in temperature, whereas the addition of pyridine causes their increase by two orders of magnitude. It has been established by IR spectroscopy that the amine complexes of copper(II) in pyridine form acidoamino-complexes;[53] the reaction is accelerated in an excess of the amine and particularly after the addition of pyridine.[54]

The many-electron synthesis of phosphazo-compounds consists of stages involving the oxidative amination of tetraphosphorus and the oxidative imination of phosphorous triamide. In the rate-limiting stage, P_4 is inserted in the Cu–NRH or Cu–NR_2 bond. The diaminotetraphosphine is then rapidly oxidised by acidocopper(II) complexes in the presence of an amine to phosphorous triamide.

$$Cu(NRH)_2P_4 \longrightarrow Cu + P_4(NRH)_2. \quad (22)$$

$$P_4(NRH)_2 + 5CuX_2 + 10NRH_2 \longrightarrow$$
$$\longrightarrow 5Cu + 4P(NRH)_3 + 10HX. \quad (23)$$

In the presence of acids HX, phosphorous amides undergo acidolysis via a stage involving the formation of acyl phosphites, which acylate the amine produced. In order to prevent the acidolysis of phosphorous triamides, an excess of the amine was added to the reaction medium. The HX molecules generated as a result of reaction (23) are hydrolysed to the alcohol. The phosphorous triamides are oxidised further by the acidocopper(II) complexes to alkylaminophosphonium halides.

$$(R_2N)_3P + CuX_2 \longrightarrow Cu + (R_2N)_3PX_2. \quad (24)$$

The alkylaminophosphonium halides formed split off the alkyl halide by the Arbuzov reaction[55] with formation of dialkylaminohalophosphazoalkyl.

$$(R_2N)_3PX_2 \rightleftharpoons (R_2N)_2XP{=}NR + RX. \quad (25)$$

The dealkylation of alkylaminophosphonium halide takes place because of the considerable difference between the P–N (65–70 kcal mol^{-1}) and P=N (100–125 kcal mol^{-1}) bond energies. In contrast to the irreversible reactions of alkoxyphosphonium halides, leading to the conversion of P–O bonds into P=O, i.e. reaction (25) is reversible.

$$(RO)_3PX_2 \longrightarrow (RO)_2XP{=}O + RX.$$

The extent of reaction (25) depends on the reactivity of the reaction products—phosphazo-compounds and alkyl halides. Since dialkylaminohalophosphazoalkyls are highly basic,[51] the equilibrium constant of reaction (25) is small at the normal temperature. Aminophosphonium chlorides, containing only amino-groups, decompose fully at temperatures above 150 °.

In the catalytic process, the equilibrium in reaction (25) shifts to the right, since dialkylaminochlorophosphazoalkyl forms complexes with the copper(II) ion and reacts with the excess of dialkylamine, affording triaminophosphazoalkyl.

$$(R_2N)_2XP{=}NR + R_2HN \longrightarrow (R_2N)_3P{=}NR + HX. \quad (26)$$

Thus triaminophosphazoalkyls can be obtained from tetraphosphorus and primary and secondary amines in a high yield and at a high rate. Methods of synthesis of specific substances are being developed at the present time.

The phosphorus–nitrogen bond in triaminophosphazoalkyls is very stable and is not ruptured even after prolonged refluxing with water. According to ^{31}P NMR spectroscopic data,[51] triaminophosphazoalkyls react with water to form only phosphonium bases.

$$(R_2N)_3P{=}NR + H_2O \rightleftharpoons (R_2N)_3P(NHR)OH.$$

The hydrolytic stability of triaminophosphazo-compounds permits their extensive use for preparative purposes.[51]

IV. Oxidative P–O coupling of red phosphorus to alcohols

Despite the expansion in recent years of the scale of its manufacture, red phosphorus (P_n), is hardly used in organic synthesis because of its low reactivity.[12–40] It is inert in both homolytic and heterolytic reactions.[39,40]

In alcoholic solutions of CuX_2 and 80–200 °C, the topochemical oxidation of polyphosphorus by oxygen to trialkyl and dialkyl phosphates takes place at a high rate and with a high selectivity. This process was first described by Dorfman and coworkers.[56–59]

$$P_n + 3n\,ROH + 1.25n\,O_2 \longrightarrow n(RO)_3PO + 1.5n\,H_2O. \quad (27)$$

$$P_n + 2n\,ROH + 1.25n\,O_2 \longrightarrow$$
$$\longrightarrow n(RO)_2(HO)PO + 0.5n\,H_2O; \quad (28)$$

R = CH_3, C_2H_5, C_3H_7, C_4H_9, *iso*-C_4H_9, C_5H_{11}, *iso*-C_5H_{11}, C_8H_{17}.

In the absence of O_2 (and Ar), red phosphorus reacts with an alcoholic solution of CuX_2.

$$P_n + 5n\,CuX_2 + 4n\,ROH \longrightarrow$$
$$\longrightarrow n(RO)_3PO + 5n\,CuX + 4n\,HX + n\,RX. \quad (29)$$

$$P_n + 4n\,ROH + 5n\,CuX_2 \longrightarrow$$
$$\longrightarrow n(RO)_2(HO)PO + 5n\,CuX + 2n\,RX + 3n\,HX. \quad (30)$$

The ratio $(RO)_3PO/(RO)_2(HO)PO$ diminishes from 20.0 to 0.7 with decrease in the amount of ROH.

Oxygen and red phosphorus are consumed only in the formation of organic phosphates, the yields of which relative to P_n and O_2 are always equal and amount to ~100%. The reaction products—trialkyl and dialkyl phosphates—are good solvents for reactions (27) and (28), so that the organic phosphates can be synthesised virtually until the complete consumption of the alcohol. The organic phosphates are separated from the catalyst by extraction with heptane and subsequent vacuum distillation: at 4–5 Torr, trialkylphosphate is distilled away, whilst dialkyl phosphate remains in the still residue. The copper(I) ions formed by reactions (29) and (30) are rapidly oxidised by oxygen. During regeneration, copper(I) is oxidised to copper(II) and alkyl halides are hydrolysed by water to the alcohols.

The oxidative P–O coupling of P_n to glycols (glycerol, ethylene and diethylene glycols, butanediol) in dioxane leads to the formation of linear and cyclic alkyl phosphates.

In isopropyl alcohol, dialkyl phosphites are formed.

$$P_n + 0.75O_2 + 2n\,R'OH \longrightarrow n(R'O)_2HPO + 0.5n\,H_2O; \quad (31)$$

$$P_n + 3n\,CuX_2 + 3n\,R'OH \longrightarrow$$
$$\longrightarrow n(R'O)_2HPO + 3n\,CuX + 2n\,HX + n\,RX; \quad (32)$$

R' = *iso*-C_3H_7.

The organic phosphates obtained in reactions (27) and (28) were investigated by IR and ^{31}P NMR spectroscopy and gas chromatography. Their boiling points, densities, and refractive indices were also measured.

Red phosphorus purified with a hot NaOH solution was used for the investigations [according to spectroscopic emission analysis, the amount of the impurity (Si) did not exceed 0.1%–1.0%]. The existence of long-range order in P_n was established by X-ray powder diffraction, but the state of the substance is nearly amorphous.The surface of P_n is made up of chains of interlinked P_4 molecules.

The kinetic ($W-\tau$) and conversion ($W-\alpha$) curves (α is the degree of conversion of red phosphorus), having the shape typical of topochemical reactions,[60] pass through a maximum. With increase in temperature and the concentrations of CuX_2, O_2, ROH, and other reaction components, the maximum on the ($W-\tau$) curves becomes more distinct and is attained at lower values of τ. On the other hand, the position of the maximum on the ($W-\alpha$) curves, manifested at lower degrees of conversion (α = 0.01–0.1), changes little when the reaction temperature and the solution components are varied.

For alcohols ranging from CH_3OH to *iso*-C_5H_{11}, the activation energies for reactions (27) and (28) in the kinetic regime

(in the region of the maximum rate) are 50–140 kJ mol^{-1}, while the activation entropies are −145 to −75 J mol^{-1}K^{-1}. The kinetic and activation parameters depend on the composition of the solution. Studies with the aid of the Coulter counter and X-ray photoelectron spectroscopy showed that the specific surface and particle size of P_n do not change during the experiment and are 1200 cm^{3}g^{-1} and 24 μm respectively. During the reaction, the P_n surface is oxidised and is 90% covered by phosphorus(V) compounds. Intermediates in the phosphorus oxidation reaction were not detected.[56–59]

The maximum rate of reaction was used to calculate the specific surface by the formula

$$W_{sp} = \frac{2W_{max}}{\pi g S}, \text{ mol m}^{-2}\text{s}^{-1}, \quad (33)$$

where g is the sample weight, S is the specific surface of P_4, and W_{max} the maximum reaction rate.

The specific rates of reactions (27) and (28) are independent of the mass of P_n and increase with increase in the concentrations of O_2, ROH, and CuX_2 in the liquid phase. Furthermore, the rate of the reaction is influenced by the nature of the solvent. Thus reactions (27) and (28) are faster in benzonitrile than in $(RO)_3PO$, and the topochemical process is appreciably affected by pyridine, H_2O, HCl, LiCl, P_2O_5, H_2SO_4, and $C_6H_5CH_2N$ [$C_6H_5CH_2NH_2$?Ed. of Translation]. When the HCl concentration is varied, the specific rate curve passes through a sharp maximum (i.e. the promoting and inhibiting effects are manifested mainly by H^+ions), while variation of the LiCl concentration results in a broad maximum on the reaction rate curve. The amine inhibits reactions (27) and (28), whilst pyridine slightly reduces their rates. A small amount of added H_2SO_4 (up to a concentration of 1 mol litre^{-1}) leads to the formation of alkyl and dialkyl sulfates. However, large amounts of P_2O_5 (in excess of 1 mol litre^{-1}) induce the conversion of alcohols into olefins. The specific rates of reactions (27) and (28) and the yields of products change only slightly after the addition into an alcoholic solution of $CuCl_2$ of even large amounts of Br^- and I^- ions. However after the replacement of $CuHal_2$ by $CuSO_4$, $Cu(RCH_2CO_2)$, $MnCl_2$, $CoCl_2$, $Mn(AcO)_2$, $Co(AcO)_2$, $Fe(AcO)_3$, oxygen ceases to be absorbed.[56–59]

The data presented indicate the activation of the surface of red phosphorus by HX as a result of the rupture of the P–P bonds between the molecules of tetraphosphorus.

$$P_n + HX \rightleftharpoons P_n(HX). \quad (34)$$

Subsequently HX-activated red phosphorus adsorbs the heterovalent dimer $Cu_2X_3(ROH)$, which predominates, according to UV spectroscopic data,[47] in alcoholic solutions of the CuX_2–CuX mixture.

$$P_n(HX) + Cu_2X_3(ROH) \rightleftharpoons Cu_2X_3(ROH)P_n(HX). \quad (35)$$

The two-electron redox decomposition of the surface complex formed in stage (35) leads to the formation of polyphosphonite and metallic copper on the surface.

$$Cu_2X_3(ROH)P_n(HX) \longrightarrow$$
$$\longrightarrow Cu + CuX + P_n(OR)_2HX + 2HX. \quad (36)$$

In the presence of CuX_2, copper dissolves rapidly[49] and is oxidised by O_2 via reaction (37).

$$4CuCl + O_2 + 4HCl \longrightarrow 4CuCl_2 + 2H_2O. \quad (37)$$

According to ^{31}P NMR spectra,[45] reactions (27) and (28) proceed relatively selectively. Mainly trialkyl and dialkyl phosphates are obtained (chemical shifts of −1 and −2 ppm respectively), while in *iso*-C_3H_7OH peaks corresponding to derivatives of tetracoordinate phosphorus, i.e. $(RO)_2HPO$ (1 ppm), are observed. On the basis of these data, one can postulate that trialkyl phosphate is formed from dialkyl phosphite produced on dealkylation of trialkyl phosphite.

$$(RO)_3P + HCl \longrightarrow (RO)_2HPO + RCl. \quad (38)$$

According to the results of Okamoto et al.,[61,62] dialkyl phosphite is readily oxidised by $CuCl_2$ in alcohol to trialkyl phosphate.

$$(RO)_2HPO + 2CuCl_2 + ROH \longrightarrow$$
$$\longrightarrow (RO)_3PO + 2CuCl + 2HCl. \quad (39)$$

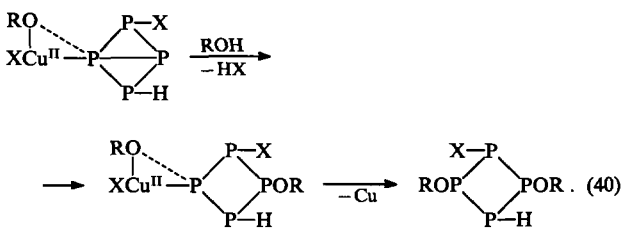
Thus reactions (29)–(37) include acid–base and oxidation-reduction stages. Copper(II) ions oxidise fairly rapidly the surface atoms of red phosphorus by virtue of the high potential of the two-electron Cu(II)/Cu(0) transition, which is 0.34 V. Iron(II), cobalt(II), and manganese(II) carboxylates, for which the potentials of such transitions are low (approximately −0.3 V), do not catalyse the reaction. Iron(III) ions, which tend to undergo only a one-electron transfer, do not exhibit an activity either. A distinctive characteristic of all the oxidants, under the influence of which the oxidative P–O and P–N coupling of low-valence phosphorus compounds to ROH, NRH_2, and H_2O,takes place, is the ability to transfer an even number of electrons.[63]

The acid–base stage is accelerated with increase in the acidity of the medium and of the alcohols (*iso*-$C_5H_{11}OH$ < *iso*-C_4H_9OH < C_4H_9OH ≪ C_3H_7OH < C_2H_5OH < CH_3OH), the pK values for which vary from 19 to 15. However, the oxidation-reduction stage is retarded with increase in the acidity of the medium, which hinders the formation of haloalkoxocopper(II) complexes. In the presence of an excess of Cl^- ions, the penta- and hexa-halo-complexes predominate. These are inactive in reactions (29) and (30) as a consequence of the absence of ROH in the coordination sphere.

On the one hand, water accelerates the acid–base stage owing to the increased acidity (pK_a = 14) and, on the other, it displaces the ROH molecules from the copper(II) complexes. Therefore, on raising the concentrations of HX, H_2O, and LiCl, the rate of formation of organic phosphates passes through a maximum.

The results obtained provide grounds for the assumption that the oxidation-reduction stage (36) takes place in two substages: the insertion of $P_n(HX)$ in the Cu–OR bond and the reductive coupling of the RO^- and $P_n(HX)(OR)^-$ ions with formation of the dialkoxypolyphosphine $P_n(HX)(OR)_2$ and metallic copper. The transition states in both substages have a cyclic structure. This is indicated by the low activation energies (~50 kJ mol^{-1}), negative activation entropies (~ −100 J mol^{-1} K^{-1}), and the nature of the dependence of the rates of reactions (29) and (30) and of the yields of products on the composition of the coordination sphere of copper(II). The subsequent stages in the oxidative alkoxylation of cyclic and linear di- and tetraalkoxypolyphosphines by haloalkoxocopper(II) complexes are fast.

The coordination mechanism (40) of reaction (41) has been investigated quantum-chemically by the CNDO method using the cluster model of adsorption.[59] The organic fragment of the solid (cluster) was used in the cluster models. The rupture of bonds in



(40)

$$P_4(OR)_2(HX) \xrightarrow[-Cu,\ HX]{Cu(OR)_2} P_4(OR)_4 \xrightarrow[-2Cu]{2Cu(OR)_2}$$
$$\longrightarrow 2P_2(OR)_4 \xrightarrow[-2Cu]{2Cu(OR)_2} 4(RO)_3P. \quad (41)$$

the tetraphosphorus clusters was compensated by the formation of bonds between the valence-unsaturated phosphorus atoms via a hydrogen atom (P_4H_2). This is the usual way of taking into account the boundary conditions in small clusters and of eliminating the influence of the bond dissociation between the atom clusters and the solid which is employed in cluster models.[64] It was assumed that the atoms of the tetraphosphorus clusters on the surface have the same structure as in the bulk phase.

In order to select the structure of the cyclic transition intermediate of the inner-sphere reaction (40), use was made of the method proposed by Dorfman et al.,[59] based on the comparison of the energies of the total, covalent, and ionic bonds between the ligands (between the chemically non-bonded atoms of the complex). Calculations were performed for both anionic and cationic clusters with different numbers of anions and molecules in the coordination sphere of copper(II).

The coordination of the tetraphosphorus cluster to the copper(II) ion results in a non-uniform weakening of the P–P bonds of the $P_4(H)_2$ cluster. The coordinated $P_4(H)_2$ cluster becomes an electron acceptor and forms bonds with the inner-sphere ligands (HO, RO, X) having an unshared electron pair after coordination. The ligands, which lose a free electron pair as a result of coordination to copper(II) (H_2O, ROH), react weakly with $P_4(H)_2$.[59] For this reason, the rate of the P–O coupling of P_n to alcohols passes through a maximum as the acidity of the medium is varied (as the HCl concentration in CH_3OH is varied from 0 to 5.6 mol litre^{-1}, the maximum rate is attained at c_{HCl} = 0.6 mol litre^{-1}) and increases with increase in the acidity of ROH. The ligands form the strongest bonds with the P atoms of $P_4(H)_2$ which are not linked to the central atom. In the cationic complexes, the bonds between $P_4(H)_2$ and the ligands are stronger than in the anionic complexes.[59] Therefore the catalytic activity of copper(II) halides passes through a maximum as the number of halide ions in the coordination sphere is varied.[56–59]

V. Oxidative P–O coupling of phosphine to alcohols

Since phosphine reacts poorly with organic substances,[9,10] a considerable amount of the highly toxic PH_3 in phosphorus and hypochlorite factories is burnt in order to achieve detoxification.[11]

As early as 1972, it was observed[46] that PH_3 is absorbed very rapidly by an alcoholic solution of copper(II) chloride. It was later established that PH_3 reacts with alcohol to form the products of oxidative phosphorylation, the nature of which depends on temperature and the nature of the ligand.[8,63,65–79] Under a O_2 atmosphere at 25–70 ° in halide systems ($CuHal_2$), the main reaction product is trialkyl phosphate (yield up to 100%).

$$PH_3 + 2O_2 + 3ROH \longrightarrow (RO)_3PO + 3H_2O; \quad (42)$$

R = CH_3, C_2H_5, C_3H_7, C_4H_9, *iso*-C_4H_9, C_5H_{11}, *iso*-C_5H_{11}, C_8H_{17}, $NH(C_2H_4OH)(C_2H_4)$.

Dialkyl phosphites are obtained from secondary alcohols—for example:

$$PH_3 + 1.5O_2 + 2iso\text{-}C_3H_7OH \longrightarrow (iso\text{-}C_3H_7O)_2HPO + 2H_2O. \quad (43)$$

In carboxylate and sulfate systems [alcoholic solutions of $Cu(RCO_2)_2$ and $CuSO_4$] at 25–70 °, trialkyl phosphites are formed preferentially:

$$PH_3 + 1.5O_2 + 3ROH \longrightarrow (RO)_3P + 3H_2O. \quad (44)$$

In contrast to tetraphosphorus, phosphine forms at 100–150 °C a considerable amount of dialkyl phosphate (up to 98%) in both halide and carboxylate systems.[8]

$$PH_3 + 2O_2 + 2ROH \longrightarrow (RO)_2(HO)PO + 2H_2O. \quad (45)$$

Reactions (42)–(45) can be achieved both by a continuous method involving the supply of a dilute PH_3–O_2–Ar mixture into the reactor and by a periodic method in which a mixture of PH_3 and Ar is initially introduced into the reactor and then O_2 is added.[8,63–70] Under an argon atmosphere at 25–75 ° in halide systems, the absorption of PH_3 is accompanied by the formation of univalent copper and trialkyl phosphate.

$$PH_3 + 8CuX_2 + 2ROH \longrightarrow (RO)_3PO + 8CuX + RX + 7HX; \quad (46)$$

X = Cl, Br.

In the carboxylate and sulfate systems at a low temperature (25–70 °C), trialkyl phosphite and metallic copper are obtained.

$$PH_3 + 2CuY_2 + 3ROH \longrightarrow (RO)_3P + 3Cu + 6HY; \quad (47)$$

Y = SO_4^{2-}, $R'CO_2^-$; R′ = CH_3, C_3H_7, $C_{17}H_{35}$.

At a high temperature (100–150 °C), dialkyl phosphate is formed in both cases.

$$PH_3 + 8CuX_2 + 4ROH \longrightarrow (RO)_2(HO)PO + 8CuX + 2RX + 6HX. \quad (48)$$

$$PH_3 + 4CuY_2 + 4ROH \longrightarrow (RO)_2(HO)PO + 4Cu + 2RY + 6HY; \quad (49)$$

X = Cl, Br; Y = RCO_2, $0.5\,SO_4$.

In the presence of H_2O, reactions involving the oxidative phosphorylation of the alcohol and water take place.

$$PH_3 + 8CuX_2 + ROH + 3H_2O \longrightarrow (RO)(HO)_2PO + 8CuX + 8HX. \quad (50)$$

$$PH_3 + 8CuY_2 + ROH + 3H_2O \longrightarrow (RO)(HO)_2PO + 4Cu + 8HY. \quad (51)$$

The addition of acid (HCl) stimulates the formation of dialkyl phosphate (up to 86%), while the addition of a base (pyridine) stimulates the formation of trialkyl phosphite (at 25–70 °C) and trialkyl phosphate (at 100–150 °C), the yield of the latter increasing to 88 %–100%.[8,63,65–70]

The univalent or metallic copper formed by reactions (46)–(51) is oxidised by oxygen or air via reactions (37) and (52).

$$2Cu + 4HY + O_2 \longrightarrow 2CuY_2 + 2H_2O. \quad (52)$$

Simultaneously with the regeneration of copper(II), alkyl halides and sulfates are hydrolysed to the initial alcohols.

$$RX + 2H_2O \longrightarrow ROH + HX. \quad (53)$$

Alkyl carboxylates do not decompose, accumulating in the system. In the presence of pyridine, the mode of reaction is independent of the nature of the acido-ligand but does depend on temperature. At low temperatures, a reaction of type (47) takes place, whilst at high temperatures the following reaction occurs;

$$PH_3 + 4CuY_2 + 4ROH \longrightarrow (RO)_3PO + 4Cu + RY + 7HY. \quad (54)$$

On dilution of the alcohol with another organic solvent, mainly a dialkyl phosphate is formed. Copper salts are separated from other reaction products by vacuum distillation and can be reused.[8,63–70]

The rate of the oxidative P–O coupling of PH_3 to alcohols also depends on temperature, the nature of the acido-ions, and the concentrations of ROH, CuX, H_2O, HX, and pyridine. Reactions (46)–(51) are autocatalytic and begin only after the accumulation of a certain amount of CuX or CuY. When the initial copper(I) concentration is appreciably lower than the copper(II) concentration, the initial rate is close to zero. With increase in the amount of the absorbed PH_3 and time, the rate of reaction also increases,

reaching a maximum and then falling to zero. The conversion ($W-Q$) and kinetic ($W-\tau$) curves pass through an extremum.[8,63-70] The maximum rate is attained when the current copper(II) and copper(I) concentrations are equal. The conversion curves are described by the equation

$$W = k_1[Cu(II)]^{0.5}[Cu(I)]^{0.5}[PH_3]^{0.5}[ROH]^{0.5}, \quad (55)$$

where k_1 is the rate constant (litre mol^{-1} s^{-1}); $k_1 = (0.2-2.7) \times 10^{-2}$ in the presence of $CuCl_2$, $Cu(C_3H_7CO_2)_2$, and $Cu(C_{17}H_{35}CO_2)_2$ and $k_1 = (0.2-20) \times 10^{-3}$ when the process is catalysed by $CuSO_4$. The rates of reactions (46)–(51) were determined from the consumption of PH_3, copper(II) and from the accumulation of $(RO)_3PO$, $(RO)_2HPO$, $(RO)_2(OH)PO$ and RY.

In a mixed aqueous alcoholic solution of acido-complexes of copper(II), reactions (50) and (51) take place. The rates of these reactions in the $ROH-H_2O-CuY_2-NH_4OH-HX$ system are minimal at pH 2–5. They increase with increase in the concentrations of both NH_4OH and HX.[49] A high yield of trialkyl phosphate (up to 100%) is achieved only in anhydrous systems.[8,63-70] According to UV spectroscopic data, copper(II) complexes of alcohols exist only for a H_2O content less than 10%. As in other organic solvents, in alcohol the stability constants of the copper(II) compounds increase.

On the basis of UV and EPR spectroscopic, magnetic susceptibility, and potentiometric data, one can assume that phosphine is oxidised by acidoalcoholcopper(II) complexes in the halide, sulfate, and carboxylate systems and by acidoammine- and acidopyridinecopper(II) complexes in the ammonia and pyridine systems.[63]

According to ^{31}P NMR spectroscopic data, the products of the incomplete substitution of the H atoms in PH_3 by alkoxy- or hydroxy-groups [the phosphinite $(RO)H_2P$ and the phosphonite $(RO)_2HP$], characterised by chemical shifts in the region of 100 and180 ppm, do not accumulate. Hence it follows that in the rate limiting stage one H atom of PH_3 is substituted by an alkoxy- or hydroxy-group as a result of the two-electron reduction of copper(II) to the zerovalent state.[8,63-70] The subsequent substitution of the remaining H atoms by an alkoxy- or hydroxy-group is rapid. The metallic copper formed is oxidised by copper(II) ions via a reaction of the type:

$$Cu + CuCl_2 \rightleftarrows 2CuCl; \qquad K_c = 8 \times 10^6.$$

Since the products of the incomplete substitution of the H atoms of PH_3 by a functional group, which are characterised by a higher oxidation–reduction potential and in which the ligand properties are more pronounced,[44] are oxidised faster then phosphine, a coordination mechanism of the rate-limiting stage must be postulated.[8,63-70] This is indicated by the low activation energy, the negative entropy, and fractional exponents in Eqn (55).

It follows from the UV spectra and kinetic data that copper(I) ions catalyse the reduction of copper(II) by phosphine as a result of the formation of the dimer Cu_2^{3+}.

Copper(II) and copper(I) ions form the dimeric complexes $Cu_2L_6Y_3$ by virtue of the presence in the coordination sphere of copper of the acido-ions (X^-, Y^-) having an unshared electron pair and capable of functioning as bridges between the two copper atoms. Such complexes, which increase the solubility of copper(I), are formed in both aqueous and non-aqueous media.[44,47] Phosphine, water, pyridine, and ammonia, which have no free unshared electron pair after coordination to copper, cannot serve as bridging ligands and cannot participate in the formation of dimers. Therefore the heteronuclear Cu_2^{3+} dimers predominate in mixed Cu(II)–Cu(I) solutions in the absence of PH_3.[47]

$$CuL_4Y_2 + CuL_2Y \rightleftarrows Cu_2L_6Y_3; \quad (56)$$

L = ROH, H_2O, NH_3, Py.

The catalytic effect of copper(I) is due to its unusual tendency to form complexes with phosphine.[44] Together with other low-valence ions of d^{10} metals [Ag(I), Hg(II), Au(I), Pd(II)], copper(I) ions form stable complexes with PH_3.[44,63] The ions of metals having a different electronic configuration, such as those of copper(II), do not form complexes with PH_3.[44] Apparently copper(II) oxidises the phosphine coordinated to copper(I) via the formation of a dimer.

The oxidative hydroxylation of PH_3 in acid aqueous alcoholic and alcoholic solutions of CuX_2 proceeds via the following key stages:

$$\left[\begin{array}{l} X \\ | \\ Cu_2X_2{-}PH_3 \end{array}\right]^{\neq} \longrightarrow Cu_2X_2(PH_3X) \xrightarrow[-HX]{}$$

$$\longrightarrow Cu + CuX + XPH_2. \quad (57)$$

$$XPH_2 + ROH \longrightarrow (RO)PH_2 + HX. \quad (58)$$

The low activation energy (10–40 kJ mol^{-1}) and the negative activation entropy (−140 to −300 J mol^{-1} K^{-1}) show that PH_3 reacts with the X^- ion in the coordination sphere of the copper atom, forming a three-membered transition state.

In the rate-limiting stage (57), PH_3 is inserted in the Cu–X bond with formation of a phosphorane (or a quasi-phosphonium salt), which decomposes with formation of a halophosphine (XPH_2), Cu(0), and HX. This mechanism agrees with the properties of derivatives of trivalent phosphorus.[48,71-73] A characteristic feature of the latter [PH_3, PR_3, $P(C_6H_6)_3$, $P(OR)_3$, $(RO)H_2P$, $(RO)_2HP$, etc.] is reactions involving the formation of pentacovalent products, in which the phosphorus atom forms with the substrate simultaneously either two σ-bonds or a σ- and a π-bond.[48] An analogous stage in which PR_3 undergoes inner-sphere insertion in the M–O bond is rate-limiting in the reaction where trialkylphosphines are oxidised by oxygen in the presence of platinum, ruthenium, cobalt, iron, rhenium, and copper complexes.[71]

In the synthesis of vinylarenes from alkenes and aryl halides in the presence of $Pd(CH_3CO_2)_2-P(C_6H_5)_3$, the reductive elimination of the aryltriphenyl phosphonium salt is a side reaction,[73] which is accelerated when the aryl halide contains strong electron-donating substituents (a hydroxy- or amino-group).

Since the stability of the phosphonium salt increases with decrease in the number of P–H bonds, the rate of the stage of type (57) increases as the H atoms of PH_3 are replaced by alkoxy- or hydroxy-groups. The alcoholysis of the halophosphine [reaction (58)] is rapid.[48]

In neutral alcoholic and aqueous alcoholic media, the reduction of copper(II) involves a different mechanism. In the key stage of reaction (59), phosphine is inserted in the Cu–OR bond, as a result of which the tricoordinate phosphorus atom is converted into a pentacoordinate atom. The resulting phosphorane decomposes with formation of a phosphinite, zerovalent copper, and HY.[8,63-70]

$$Y_3Cu(ROH)PH_3 \xrightarrow[-HY]{} \left[\begin{array}{l} OR \\ | \\ Y_2Cu_2{-}PH_3 \end{array}\right]^{\neq} \longrightarrow$$

$$\longrightarrow Y_2Cu_2(PH_3OR) \xrightarrow[-HY]{} Cu + CuY + (RO)PH_2. \quad (59)$$

The valence of copper ions does not change on formation of the intermediate phosphorane $Cu_2Y_2(ROPH_3)$. Since the acidity of the phosphorane is appreciably higher than that of PH_3, the redox decomposition is accompanied by the dissociation of a P–H bond. The subsequent oxidation of the phosphinite $ROPH_2$ to trialkyl phosphite is faster than for PH_3.

$$ROPH_2 + 2Cu_2Y_3 + 2ROH \longrightarrow$$

$$\longrightarrow (RO)_3P + 2Cu + 2CuY + 4HY. \quad (60)$$

In alkaline alcoholic media, the phosphine is oxidised by copper(II) ions in a different way. Whereas in neutral media

[reaction (59)] only the coordinated ROH molecule is deprotonated, in alkaline media not only ROH but also the phosphine is ionised [reaction (61)]. In the rate-limiting stage of reaction (61), the reductive elimination of the phosphinite takes place on interaction of the phosphide with the alkoxide ion.

$$Y_3Cu_2(ROH)PH_3 \xrightarrow[-2HY]{} \left[\begin{array}{c} RO \\ | \\ YCu_2 \cdots PH_2 \end{array}\right]^{\neq} \longrightarrow$$

$$\longrightarrow (RO)PH_2 + CuY + Cu. \qquad (61)$$

This mechanism also agrees with the coordination properties of metal phosphides.[71] The acidity of the HZ molecules [Z = OH, OR, NH_2, NR_2, Hal, RCO_2, SH, CN, SR, PH_2, PRH, PR_2, $PO(OR)_2$, $P(OR)_2$, PH(OR), OPH(OR), etc.] increases by several orders of magnitude on complex formation.[74] According to Kukushkina[71] and Dohle et al.,[72] the phosphide ligand bound to osmium, chromium, molybdenum, and tungsten ions and formed on deprotonation of secondary and primary phosphines is alkylated by methyl iodide (an electrophile) or is alkoxylated by an alkoxide ion (a nucleophile).

Pyridine promotes the formation of copper(II) alkoxide and phosphide complexes because it increases the acidity of the coordinated HZ molecules.[54] Pyridine not only influences the mechanism of the inner-sphere reactions of the phosphine–alcohol complexes of copper(II) but also the behaviour of the intermediate organophosphorus compounds. Together with the bands corresponding to the chemical shifts characteristic of trialkyl phosphates, dialkyl phosphates, and trialkyl phosphate complexes of copper(I) (−1, −2, and 15 ppm respectively), the ^{31}P NMR spectra of the reaction products always contain bands typical for dialkyl phosphites (8 ppm).[45] When a secondary alcohol is used, for example *iso*-C_3H_7OH, a dialkyl phosphite becomes the main product. The yield of dialkyl phosphite in the sulfate and carboxylate systems is always higher than in the halide systems.[8,63–70]

It follows from the data presented that trialkyl and dialkyl phosphates are obtained when dialkyl and monoalkyl phosphites, formed on the dealkylation of trialkyl phosphite, are oxidised by copper(II) complexes.

The derivatives of tricoordinate phosphorus $(RO)_3P$ are dealkylated much more readily than the derivatives of tetracoordinated phosphorus $(RO)_2HPO$, (RO)(HO)HPO, $(RO)_2(HO)PO$, and $(RO)_3PO$.[48] The rate of dealkylation falls with increase in the pH of the medium and the length of the hydrocarbon group and on transition from the halide to the carboxylate and sulfate systems. Pyridine and an excess of the alcohol bind HX and HY, forming oxonium and pyridinium salts, and reduce the degree of decarboxylation of trialkyl phosphates.[48]

$$(RO)_3P + HY \longrightarrow (RO)_2HPO + RY. \qquad (62)$$

$$(RO)_2HPO + CuY_2 + ROH \longrightarrow$$
$$\longrightarrow (RO)_3PO + Cu + 2HY. \qquad (63)$$

$$(RO)_2HPO + HY \longrightarrow (RO)(HO)HPO + RY. \qquad (64)$$

$$(RO)(HO)HPO + CuY_2 + ROH \longrightarrow$$
$$\longrightarrow (RO)_2(HO)PO + Cu + 2HY. \qquad (65)$$

It has been shown by kinetic and physicochemical methods that the mechanism of the P–O coupling of PH_3 to the alcohol in the coordination sphere of copper(II) depends on the pH of the medium. In neutral and acid media, phosphine is inserted in the Cu–ligand (X^-, RO^-) bond in the rate-limiting stage with formation of a phosphorane, which decomposes with formation of a phosphinite, acid, and zerovalent copper. In ammonia and pyridine media, which promote the deprotonation of phosphine and the alcohol, the phophinite undergoes reductive elimination in the key stage as a result of the coupling of the phosphide and the alkoxide. In an alkaline medium, the rate of reduction of copper(II) by phosphine increases with increase in the positive charge of the complex, i. e. with increase in the number of NH_3 or pyridine molecules in the inner sphere of copper(II). In acid and neutral media, the rate of reaction increases with increase in the number of acido-ligands, i. e. with increase in the negative charge of the copper(II) complex.[8,63–70]

In order to elucidate the causes of the dependence of the mechanism of the P–O coupling of PH_3 to ROH in the composition of the copper(II) complex, the hypothetical intermediates in reactions (46)–(51), formed in acid, neutral, and alkaline media, and the free PH_3 and ROH molecules were subjected to a detailed quantum-chemical study.

The complexes were investigated by the CNDO [65] and Mulliken–Wolfsberg–Helmholtz (MWH) [75–77] methods. The CNDO method yields a total energy of the complex, from which it is possible to estimate the probability of the formation of the postulated intermediate, the charges on all the atoms (permitting a comparison of the electrophilic and nucleophilic properties of the coordinated molecules), and the total, covalent, and ionic energies of the bonds between all the atoms of the adduct.[78] A program, employing a semiempirical version of the parametrisation of the CNDO method and modified for the investigation of the structures of transition metal complexes, was developed for the calculations.[78] The 3*d*, 4*s*, and 4*p* orbitals of copper(II) and the valence *s* and *p* orbitals of the coordinated molecules were employed as the basis set. A distorted octahedral structure of the copper(II) complexes, in which the reacting molecules (ROH, PH_3) and ions (RO^-, PH_2^-, X^-) are located in the equatorial plane in the *cis*-positions relative to one another, was adopted. The standard geometry of the ligands was assumed.[65]

Alcohols and phosphines are extremely weak OH and PH acids ($pK_a \simeq 15–32$). They are activated by very weak bases in anhydrous solvents[79] and by metal complexes.[71,74] High-valence and low-valence metal cations are required respectively for the activation of alcohols and phosphines. Under the influence of metal complexes, the acid dissociation constants of the PH and OH acids increase by several orders of magnitude.[74] In selecting the intermediates, account was taken of the fact that the composition of the coordination sphere of copper(II) changes as a function of the pH of the medium. Cationic and anionic complexes predominate in ammonia and halide solutions respectively.[54] With increase in the basicity of the medium, there is an increase in the probability of alkoxo- and phosphido-reactions, i. e. reactions that result in the formation of alkoxo- and phosphido-ligands.[54]

In order to investigate the behaviour of the intermediates, the energies of the bonds between the atoms within the coordinated molecules (P–H, O–H), and between the copper atoms and the electron-donating atoms of the ligands (Cu–P, Cu–O, Cu–X), which are ruptured in the reactions involving the oxidative P–O coupling of PH_3 to ROH, were calculated. In addition, the P–O, P–X, H_P–X, H_P–O, H_O–X, H_O–P, H_O–O bond energies in the initial reactants before the formation of chemical bonds in the reactions involving the oxidative P–O coupling of PH_3 to ROH were evaluated (H_O and H_P are hydrogen atoms linked to O and P atoms).[67]

The key stages in the reactions involving the inner-sphere P–O coupling of PH_3 to ROH — insertion and reductive elimination of ligands — proceed via the intermediate formation of a polar many-centre metallacycle in which bonds are dissociated and new ones are formed simultaneously [reactions (57), (59), (61)].

By comparing the energies of the bonds between atoms which are and are not linked chemically, it is possible to find the probable structure of the cyclic many-centre transition state and the direction of the concerted redox decomposition of the intermediate complex and to estimate the influence of the solvent. The energy of the bonds between atoms separated by a distance greater than the sum of the covalent radii is low and is much lower than the energies of chemical bonds.[65]

The behaviour of intermediates in an acid medium was investigated with the aid of copper(II) complexes containing

different numbers of alcohol, phosphine and water molecules and halide ions. The properties of the neutral medium were inferred from the results of calculations for hydroxo- and alkoxo-phosphinecopper(II) complexes. The hydroxo-ligands in these complexes were modelled by sulfate, phosphate, and carboxylate anions. The copper–ammonia and copper–pyridine systems were investigated by means of calculations for the hydroxo- and alkoxo-pyridinephosphinecopper(II) and hydroxo- and alkoxo-aminephosphinecopper(II) complexes. The number of neutral molecules (PH_3, NH_3, Py, H_2O) and anions (PH_2^-, Cl^-, HO^-, RO^-) was varied in such a way that the charge on the complexes changed from +2 to −4.[65]

In the coordination sphere, the weakly polar PH_3 molecule is activated and becomes polar. Whereas in the free PH_3 molecules the effective charges on the P and H atoms are zero, coordination results in the appearance on these atoms of charges which depend on the composition and the overall charge of the complex. In the anionic complexes, the charge on the phosphorus atom is positive, while in the cationic complexes it is negative. The ionic character of the P–H in the coordinated PH_3 molecule is enhanced. On complex formation, the alcohol molecule is activated to a much greater extent. The ionic character of the O–H bond increases significantly as a result of coordination, the effective negative charge on the oxygen atom increases, and there is also an increase in the positive charge on the H atom, which varies as a function of the composition and overall charge of the complex.[65]

The nature of the activation of PH_3 depends to a greater extent on the composition and charge of the complex than in the case of alcohols. Judging from the charge on the phosphorus atom, phosphine acquires nucleophilic and electrophilic reactivity in the cationic and anionic complexes respectively. Judging from the charges on the oxygen atom, the alcohol and water exhibit a nucleophilic activity in both positively and negatively charged complexes. Owing to the relatively weak ionic character of the P–H bond in phosphine compared with the O–H bond in the alcohol, the activity of phosphine depends more on the dielectric constant of the medium.[80] It follows from the comparison of the ionic characters of the P–H and O–H bonds and the charges on the P, O, and H atoms that the hydroxo-reaction is preferable to the alkoxo-reaction and especially the phosphide-reaction. The formation of hydroxide ions in the coordination sphere of copper(II) is more probable than the formation of alkoxide and phosphide ions. The Cu–P, Cu–O and Cu–X bond energies increase sharply on passing from the phosphine and alcohol complexes to the phosphide, alkoxide, and hydroxide complexes. As a result of the deprotonation of phosphine, there is a sharp increase in the ionic character of the Cu–P bonds. Since in polar media ionic bonds are more reactive than covalent bonds,[80] an increase in the amount of ionic character of the bond entails an increase in its reactivity.

In the haloaquophosphinealcohol complexes, which predominate in acid media, the Cu–X bond is most ionic. For this reason, oxidative halogenation of phosphine and alcoholysis of the halophosphine formed take place in acid media [reactions (57) and (58)].[46]

The coordination character of the reaction is stimulated by the bond arising between the ligands. According to quantum-chemical calculations,[65] the coordinated phosphine forms fairly strong bonds with the ligands in anionic copper(II) complexes. Presumably the redox decomposition of the haloaquophosphine-alcohol- and alkoxophosphine-copper(II) complexes takes place as a result of the insertion of PH_3 in the Cu–X and Cu–OR bonds [reactions (57)–(61)].[65]

Cationic copper(II) complexes predominate in ammoniacal and pyridine media.[54] According to the results of a quantum-chemical study,[65] phosphine does not form bonds with the ligands in such complexes. Furthermore in alkaline media, phosphide and alkoxide ligands are produced.[79] Ammine- and pyridine–copper complexes undergo redox decomposition as a result of the interaction between the phosphide and alkoxide ions. The phosphinite formed as a result of the reductive coupling of the phosphide and alkoxide ligands is more readily deprotonated ($pK_a = 15$) than PH_3 ($pK_a = -14$). Phosphinite and phosphonite are therefore more rapidly oxidised by copper(II) ions than phosphine.

The inner-sphere reactions (65) are also promoted by ligands which do not participate directly in the redox decomposition of the intermediate complex.[65] According to quantum-chemical calculations, these ligands form fairly strong bonds with the hydrogen atoms of PH_3 and ROH, offering nucleophilic support to the phosphido- and alkoxo-reactions leading to the formation of phosphide and alkoxide ions in the coordination sphere. Particularly strong bonds are formed between the H atoms of phosphine and the alcohol in the cationic copper complexes.

Thus the mechanism of the activation of phosphine and the alcohol in the coordination sphere of copper(II) has been investigated by the CNDO method. It was shown that the probability of the insertion of PH_3 in the metal–ligand bond and of the reductive coupling of the phosphide and alkoxide ligands can be estimated from the energy of the bond between the reacting ligands. In acid and neutral media, which promote the formation of anionic copper(II) complexes, phosphine is inserted in the metal–ligand bond in the key stage: in ammonia and pyridine solutions, which ensure the formation of cationic complexes, the reductive coupling of the phosphide and alkoxide ligands takes place in the rate-limiting stage.

VI. Oxidative P–C coupling of phosphine to alcohols

A whole series of new organic reactions with participation of platinum(II) and platinum(IV) halides, e.g. the oxidation of alkanes, arenes, olefins, alcohols, carbon monoxide, etc., have been observed in recent years.[81–86] The oxidising activity of platinum(II) and platinum(IV) halides as a rule varies in parallel with the kinetic constants for the exchange of ligands and the thermodynamic stability constants and antiparallel to the redox potentials and Pt–X bond energies.[81–87] Platinum(II) halides usually catalyse the reduction of platinum(IV) by various substrates via the formation of dimers containing platinum(II) and platinum(IV). New reactions involving the oxidative alkoxylation and hydroxyalkylation of phosphine have been described.[63,88–90]

$$PH_3 + 3Na_2PtCl_6 + 3ROH \longrightarrow \longrightarrow 3Na_2PtCl_4 + (RO)_3P + 6HCl; \quad (66)$$

R = CH_3, C_2H_5, C_3H_7, C_4H_9, *iso*-C_4H_9, C_5H_{11}, *iso*-C_5H_{11}, C_8H_{17}.

$$PH_3 + 3RCH_2OH + 1.5Na_2PtCl_6 \longrightarrow \longrightarrow (RCH_2)(RCHOH)_2PO + 1.5Pt + 3NaCl + 6HCl. \quad (67)$$

$$PH_3 + 4RCH_2OH + 2Na_2PtCl_6 \longrightarrow \longrightarrow (RCH_2O)_3PO + 2Pt + 4NaCl + RCH_2Cl + 7HCl; \quad (68)$$

R = C_3H_7, C_4H_9, *iso*-C_4H_9.

When a PH_3–Ar gas mixture, even one containing only traces of phosphine, is passed at 25–150 ° through an alcoholic solution of the Na_2PtCl_6 complex, known to be very inert and stable,[87] trialkyl phosphites (at 25–70 °) as well as trialkyl phosphates and tertiary phosphine oxides (at 90–150 °C) are formed.[88,89]

The new reactions are very rapid. Reaction (66) terminates after the reduction of platinum(IV) to platinum(II), whilst reactions (67) and (68) terminate after the reduction of platinum(IV) to zerovalent platinum, which is precipitated as a black fine-grained deposit on the bottom of the reactor. During the absorption of PH_3 by an alcoholic solution of Na_2PtCl_6, the redox potential (φ) of the Pt(IV)/Pt(II) couple shifts in the cathodic direction.[88,89]

The changes in the PH_3–Na_2PtCl_6–ROH system are analysed in terms of the nature of the conversion ($W-Q$), kinetic ($W-\tau$), and potentiometric ($\varphi-Q$, and $\varphi-\tau$) curves. The conversion and kinetic curves pass through a maximum in all cases.

The rate of reaction (66) is described by the equation

$$W = k_1[\text{Pt(IV)}]^{0.5}[\text{Pt(II)}]^{0.5}[\text{PH}_3]^{0.5}[\text{ROH}]^{0.5} \quad (69)$$

After the reduction of platinum(IV) to platinum(II), the spent solution is readily regenerated with a dilute Cl_2–Ar gas mixture.

$$NaPtCl_4 + Cl_2 \longrightarrow Na_2PtCl_6. \quad (70)$$

During the regeneration of platinum, trialkyl phosphites are oxidised to the phosphates.

$$(RO)_3P + Cl_2 + ROH \longrightarrow (RO)_3PO + RCl + HCl. \quad (71)$$

The kinetic parameters of reactions (67) and (68) are characterised by a more complex formula:

$$W = k_1[\text{PH}_3]^{0.5}[\text{ROH}]^{0.5}([\text{Pt(IV)}]^{0.5}[\text{Pt(II)}]^{0.5}) + k_2[\text{Pt(II)}], \quad (72)$$

where k_1 and k_2 are the rate constants (litre mol^{-1} s^{-1}).

It follows from Eqns (69) and (72) that reactions (66)–(68) proceed in the coordination spheres of dimeric and mixed haloalkoxophosphineplatinum(IV) and the corresponding platinum(II) complexes. As platinum(IV) is reduced to platinum(II), the colour of the solution changes from bright orange to dark brown, which indicates the formation of heterovalent platinum complexes.[80] The coordination mechanism of reactions (66)–(68) is indicated by the low activation energies ($E^{\neq}$ = 28–56 kJ mol^{-1}) and entropies ($\Delta S^{\neq}$ = −140 to −20 J mol^{-1} K^{-1}), the fractional order with respect to the reactants [Pt(IV), PH_3, ROH)], the negative influence of H_2O, HCl, and NaCl, and the positive influence of NaBr, NaI, and platinum(II). Platinum(II) iodides and bromides catalyse the insertion of PH_3 and ROH in the coordination spheres of platinum(IV) chlorides.[87]

At a low temperature, the products [$(RO)_3P$ and Pt(II)] form the stable complexes [$Pt(P(OR)_3]/PtCl_4$, which are insoluble in alcohols. The composition of the complexes was established by X-ray [powder? PCMA in Russian (Ed. of Translation)] diffraction and X-ray photoelectron and IR spectroscopic methods.[88,89] The intermediate organophosphorus compounds, formed at a high temperature, were investigated by ^{31}P NMR spectroscopy.[45] Analysis of the reaction medium during the experiment demonstrated the occurrence of chemical shifts characteristic of $(RCH_2O)_3P$ (95–100 ppm), $(RCHOH)_3P$ (−40 to −30 ppm), $(RCH_2)(RCHOH)_2PO$ (40–50 ppm),$(RCH_2O)_2HPO$ (4–8 ppm), and $(RCH_2O)_3PO$ (−3 ppm).[45] Hence it follows that trialkyl phosphates are formed in the following way:

$$Pt_2X_5(PH_3)(RO)^- \longrightarrow 2PtX_2 + (RO)PH_2 + HX. \quad (73)$$

$$Pt_2X_5(ROPH_2)(RO) \longrightarrow 2PtX_2 + (RO)PH + HX. \quad (74)$$

$$Pt_2X_5[(RO)_2PH](RO) \longrightarrow 2PtX_2 + (RO)_3P + HX. \quad (75)$$

$$PtX_2[(RO)_3P] + HX \longrightarrow PtX_2[(RO)_2HPO] + RX. \quad (76)$$

$$Pt_2X_5[(RO)_2HPO](RO) \longrightarrow 2PtX_2 + (RO)_3PO + HX. \quad (77)$$

According to Eqns (73)–(77), the alcohol is activated as a result of deprotonation and the formation of the covalent Pt–O bond.[91] Reactions (74)–(77) are faster than reaction (73), since, in contrast to phosphine, phosphinite, phosphonite, and phosphite readily form complexes with platinum(IV) and platinum(II).[92,93] Platinum(II) promotes not only the insertion of PH_3 and ROH into the coordination sphere of platinum(IV) [87] but also the dealkylation of trialkyl phosphites.[92,93] Thus the hydrolysis of $(CH_3O)_3P$ in water at 25 °C takes more than 40 h, whilst in the presence of K_2PtCl_6 it reaches completion instantaneously.[92] Whereas the conversion of trialkyl phosphite into dialkyl phosphite [reaction (76)] is rapid, the subsequent hydrolysis of dialkyl phosphite is slow even in the presence of platinum(II).[92]

Since the phosphine chlorination products (PCl_3 and PCl_5), characterised by chemical shifts of 220 and −80 ppm respectively,[45] were not detected, presumably trialkyl phosphites are formed under the influence of platinum(IV) via the successive substitution of the hydrogen atoms of phosphine by alkoxy-groups, dealkylation of trialkyl phosphite to dialkyl phosphite, and the substitution of the hydrogen atoms in dialkyl phosphites by alkoxy-groups. Phosphine, phosphinite phosphonite, and dialkyl phosphite are inserted in the Pt–O bond, forming a phosphorane.

Phosphine, phosphinite, phosphonite and dialkyl phosphite behave similarly to unsaturated compounds (olefins, carbon monoxide), which typically undergo insertion in the metal–ligand bond.[74,81,82,94,95] Since the stability of the phosphorane increases as the hydrogen atoms of phosphine are replaced by a functional group,[48] the reactions involving the oxidation of phosphinite, phosphonite, and dialkyl phosphite by platinum(IV) are faster than the oxidation of phosphine.[88,89] The driving forces of reactions (78) are the appreciable Pt(IV)/Pt(II) redox potential and the high P–O bond energy. Similarly, trialkyl phosphates are formed from phosphine on treatment with platinum(II), but the reaction is faster, since platinum(II) halides enter relatively easily into ligand exchange, in contrast to platinum (IV) halides.[87]

$$\left[\begin{array}{l} RO \\ X_5Pt_2{-}PH_3 \end{array}\right]^{\neq} \longrightarrow X_5Pt_2(PH_3OR) \longrightarrow$$

$$\longrightarrow 2PtX_2 + (RO)PH_2 + HX. \quad (78)$$

According to ^{31}P NMR spectroscopic data, alkyl(dihydroxyalkyl)phosphine oxide is obtained from tri(hydroxyalkyl)phosphine.

$$(RCHOH)_3P \longrightarrow (RCHOH)_2(RCH_2O)P \longrightarrow$$

$$\longrightarrow (RCHOH)_2(RCH_2)PO.$$

Tri(hydroxyalkyl)phosphines with electron-donating substituents isomerise to tertiary phosphine oxides, in contrast to tri(hydroxyalkyl)phosphines with electron-accepting substituents, which are converted into phosphites.[9]

Tri(hydroxyalkyl)phosphine can be obtained from phosphine and the alcohol on treatment with platinum(IV) and platinum(II) halides. In the rate-limiting stage, a hydrogen atom of phosphine is replaced by a hydroxyalkyl group. The subsequent substitution of the hydrogen atoms of primary and secondary phosphines by a hydroxyalkyl group proceeds similarly but faster, since, in contrast to phosphine, alkylphosphines are readily coordinated to platinum(IV).[93] There are no chemical shifts characteristic of primary (−60 ppm) and secondary (−140 ppm) phosphines in the ^{31}P NMR spectra.[45]

$$Pt_2X_6(PH_3)(RCH_2OH) \rightleftharpoons Pt_2X_4(PH_2)(RCHOH) + 2HX. \quad (79)$$

$$Pt_2X_4(PH_2)(RCHOH) \longrightarrow 2PtX_2 + PH_2(RCHOH). \quad (80)$$

$$Pt_2X_4(PH_2)(RCHOH) \rightleftharpoons Pt_2X_3(PH_2)(\eta^2\text{-RCHO}) + HX. \quad (81)$$

$$Pt_2X_3(PH_2)(\eta^2\text{-RCHO}) \xrightarrow[-PtX_2]{HX}$$

$$\longrightarrow PtX(PH_2)(RCHO) \longrightarrow PH_2(RCHOH). \quad (82)$$

The alcohol is activated by the β-elimination of hydrogen, the formation of a bidentate (η^2-type) aldehyde bound to the metal,[94,95] and the formation of the organometallic Pt–C bond.[81,82] The β-elimination reactions are typical for transition metal compounds.

The β-hydrogen atoms are eliminated on treatment with either the metal, or nucleophiles, or electrophiles. The stabilisation of the transition state by the π-bond formed renders the β-position extremely reactive.[95]

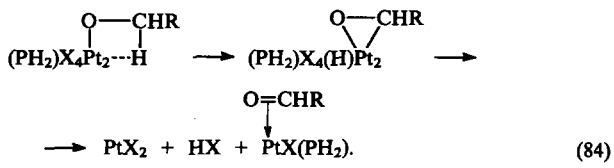
$$\begin{array}{l} HOHRC{-}H \\ (PH_2)X_5Pt_2 \end{array} \xrightarrow[-HX]{} X_4(PH_2)Pt_2(RCHOH) \longrightarrow$$

$$\longrightarrow PH_2(RCROH) + 2PtX_2. \quad (83)$$

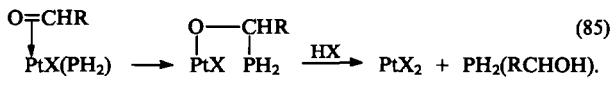
Mono(hydroxyalkyl)phosphine is formed as a result of the insertion of PH_3 in the Pt–C bond. Platinum(II) behaves similarly to platinum(IV), but all the stages involving platinum(II) are faster.[88,89]

The hydroxyalkylation of phopshine takes place as a result of the oxidation of the alcohol by platinum(IV) to the aldehyde and subsequent addition of phosphine to the carbonyl compound.

Studies have shown that reaction (84) without PH_3 proceeds very slowly,[85,86] whilst reaction (85) in the presence of platinum(IV) and platinum(II) occurs only when concentrated phosphine is employed.[9]



(84)



(85)

Reactions (66)–(68) take place not only in alcoholic but also in alcohol–pyridine solutions of Na_2PtCl_6. The pyridine complexes of platinum(IV) and platinum(II) activate PH_3 and ROH via deprotonation.

Phosphinite is formed as a result of the inner-sphere coupling of the ligands (the phosphide and alkoxide), the reaction being promoted by pyridine, which is a powerful π-acceptor.[54]

$$Pt_2X_4Py_2(PH_2)(RO) \longrightarrow 2PtX_2 + PH_2OR. \quad (86)$$

In a quantum-chemical study of the mechanism of the interaction of phosphine with the alcohol, the energies (total, covalent, and ionic) of the bonds between all the atoms of the platinum(IV) and platinum(II), containing different numbers of molecules (H_2O, ROH, NH_3, Py, PH_3) and ions (PH_2^-, RO^-, HO^-, X^-), were calculated by the CNDO method.[90] The total, covalent, and ionic bond energies were evaluated using the method described by Fischer and Kollmar.[78] Phosphine, the alcohol, and water in the coordination sphere of platinum(IV) and especially platinum(II) are appreciably activated as a result of the increase in the amount of ionic character of the P–H and O–H bonds, which increase the reactivity of molecules in polar media.[80] The energy of the bond between the alkoxide ion and phosphine increases on passing from platinum(IV) to platinum(II).[90] Platinum(II) activates the P–H dissociation process via the formation of the $Pt-H_P$ single bond. The deprotonation of the alcohol activates the halide ions, promoting the formation of the $X-H_O$.[90]

The mechanism of the reduction of platinum(IV) to platinum(II) by phosphine, including the stage in which PH_3 is inserted in the Pt–OR bond, operates only in alcoholic media, which promote the formation of ionic complexes distinguished by a high energy of the bond between the phosphorus atom of phosphine and the oxygen atom of the alkoxide ion. The mechanism of the oxidation of phosphine by platinum(IV) and platinum(II), including the stage in which the phosphide and alkoxide ions are coupled, operates only in alcohol–pyridine systems, where cationic complexes predominate. These are distinguished by the appreciable energy of the bond between the phosphorus and oxygen atoms of the phosphide and alkoxide ions.[90]

In order to elucidate the mechanism of the catalysis by platinum(II) complexes of the reduction of platinum(IV) by phosphine [reactions (66)–(68)], the quantum-chemical molecular orbital perturbation (MOP) method was used. The bond energy between atoms separated by a distance greater than the sum of the covalent radii was calculated by the MOP method, which had been first applied in the estimation of the reactivities of ligands.[75–77] The bond energy proved to be appreciably lower than the energies of chemical bonds.[96–98] By comparing the energies between the atoms of the intermediate complex which are not linked chemically, it was possible to find the probable structure of the multi-centre cyclic transition state.[96] The higher the bond energy between atoms not linked chemically (the more negative the stabilisation energy), the greater the probability of the chemical bond between them in the transition state.[97,98]

The stabilisation energies have been calculated by the MOP method for reactions in which the coordinated phosphine is the electron acceptor, while the alcohol (or the alkoxide ion) is the electron donor, and also for reactions where phosphine is the electron donor and the alcohol (alkoxide or chloride ion) is the electron acceptor.[67] On coordination to platinum(IV), phosphine is activated. The negative charge on the oxygen atom and the positive charge on the phosphorus atom increase. As a result of coordination, phosphine acquires electron-accepting properties, while the electron-donating properties of the alcohol are enhanced. In the case where PH_3 is the acceptor and the alcohol is the donor, the stabilisation energy is more negative than in the case where the above ligands act in the opposite directions. It becomes more negative when ROH is replaced by RO^- and Cl^- is replaced by Br^- and I^- ions.[67]

The stabilisation energies have been calculated by the MOP method for the reactions of phosphine coordinated to platinum(II) with the alcohol bound to platinum(IV) and of phosphine bound to platinum(IV) with the alcohol coordinated to platinum(II). It was found that the perturbation energies for the inner-sphere reactions are appreciably higher than for the outer-sphere reactions. Hence it follows that the reaction between phosphine and the alcohol occurs in the coordination sphere of platinum(IV), while platinum(II) catalyses the formation reactions of the platinum(IV) complexes of haloalkoxyphosphines by accelerating the ligand exchange processes.[87]

VII. Oxidative P–O coupling of phosphine to alcohols in the presence of chlorine

The reactions of chlorine with the halogens in aqueous media and in the gas phase have been investigated in fair detail.[99–102] It has been observed[49] that, on chlorination of PH_3 in an alcohol at 50–70 °C, trialkyl phosphate is formed rapidly and in a high yield.

$$PH_3 + 4Cl_2 + 4ROH \longrightarrow (RO)_3PO + RCl + 7HCl; \quad (87)$$

R = C_4H_9, *iso*-C_4H_9, C_5H_{11}, *iso*-C_5H_{11}.

At a low temperature (8–25 °C), reaction (87) takes place in the presence of pyridine.[49]

The development of the reaction via a branched-chain mechanism was suppressed by using dilute gaseous PH_3–Ar and Cl_2–Ar mixtures, which were mixed separately with the alcohol in a preliminary step. Phosphine and chlorine entered the reactor in a countercurrent, so that there was a high PH_3 concentration and a low Cl_2 concentration at the inlet to the reactor, while at the outlet the opposite situation obtained — a high Cl_2 concentration and a low PH_3 concentration. The rate of supply of Cl_2 and PH_3 was regulated by means of the Cl_2/Cl^- chlorine electrode potential.[103] For this purpose, the reactor was fitted with a potentiometric device consisting of platinum and calomel half-cells. The latter contained only Hg, Hg_2Cl_2, and a ground joint as the electrolytic bridge. Such a calomel electrode, without the traditional agar–agar bridge, did not break at high temperatures and did not affect the composition of the liquid phase.

The introduction of PH_3 into an alcoholic solution of Cl_2 is accompanied by a sharp shift of the potential in the cathodic direction up to a value which depends on the ratio Cl_2/PH_3 in the gas phase. On reducing the rate of supply of PH_3 or on increasing that of Cl_2, the potential shifted synchronously in the anodic direction, whilst on raising the rate of supply of PH_3 or reducing that of Cl_2 the shift was in the cathodic direction. Therefore the potentiometric method made it possible to follow continuously, during the experiment, the PH_3/Cl_2 ratio in the liquid phase and the reactivity of the system.[46]

The yield of alkyl phosphates in reactions involving different alcohols remained high up to high degrees of conversion of the alcohol. Chlorine reacted preferentially with phosphine and hardly reacted with the alcohol, since the rate constant for the chlorination of an alcohol is relatively low.[103]

The mechanism of reaction (87) was investigated by ^{31}P NMR spectroscopy.[45] Only trialkyl phosphate with a chemical shift of -2 ppm was formed in an excess of the alcohol. In the presence of a deficiency of the alcohol, small peaks due to the pentacoordinate phosphorus derivatives PCl_5, Cl_3PO, $(RO)_2ClPO$, $(RO)_4PCl$, $(RO)_3PCl_2$ (-40, 5, 4, -8, and -27 ppm respectively) appeared apart from the high $(RO)_3PO$ peak (-2 ppm). The tricoordinate phosphorus derivatives PCl_3, $(RO)_2PCl$, $(RO)_3P$ (219, 170, and 140 ppm) and pentaalkoxyphosphorus $(RO)_5P$ (-80 ppm) were not detected. Hence it follows that reaction (87) takes place with the rapid formation and subsequent reactions of phosphorus pentachloride.

The most important feature of the reactions of PCl_5 with alcohols as well as other hydroxylated compounds is the preliminary formation of phosphoryl chloride [reaction (89)]. The rate of the subsequent alcoholysis of Cl_3PO increases with increase in the pH of the medium.[48] This sequence of the reactions of PCl_5 with ROH and H_2O is caused by the formation of the stable phosphoryl group $P=O$.[48] The reactions of phosphoryl chlorides with H_2O and ROH take place as stepwise elimination of HCl [reactions (90) and (91)][104] and are accelerated in the presence of HCl binding agents (an excess of ROH and pyridine).[48] In the presence of a deficiency of the alcohol, reaction (92), leading to the formation of dialkyl phosphates, predominates.[104]

$$PH_3 + 4Cl_2 \longrightarrow PCl_5 + 3HCl. \quad (88)$$

$$PCl_5 + ROH \longrightarrow Cl_3PO + RCl + HCl. \quad (89)$$

$$Cl_3PO + 2ROH \longrightarrow (RO)_2ClPO + HCl. \quad (90)$$

$$(RO)_2ClPO + ROH \longrightarrow (RO)_3PO + HCl. \quad (91)$$

$$(RO)_2ClPO + ROH \longrightarrow (RO)_2(HO)PO + RCl. \quad (92)$$

By virtue of the very high rate and selectivity, reaction (87) can be applied to utilise even trace amounts of PH_3 and Cl_2.

VIII. Oxidative P–N coupling of phosphine to primary and secondary amines

The P–N coupling of primary and secondary phosphines to primary and secondary amines proceeds under severe conditions (only in the presence of formaldehyde) with formation of aminomethylation products.[9] The reaction involving oxidative P–N coupling of phosphine to primary and secondary amines, discovered by Dorfman et al.,[53] yields triaminophosphazoalkyls.

$$PH_3 + 4RH_2N + 4CuY_2 \longrightarrow (RHN)_3P{=}NR + 4Cu + 8HY. \quad (93)$$

$$PH_3 + 4R_2HN + 4CuY_2 \longrightarrow (R_2N)_3P{=}NR + 4Cu + 7HY + RY; \quad (94)$$

R = C_2H_5, $C_6H_5CH_2$, C_6H_{11}, .

A solution of CuY_2 in a primary or secondary amine at 15–30 °C rapidly absorbs even traces of PH_3 from the PH_3–Ar gas mixture.[53] When the reaction takes place in argon, phosphine is selectively converted into triaminophosphazoalkyl and copper(II) ions are reduced to zerovalent copper. The zerovalent copper formed by reactions (93) and (94) is almost instantaneously oxidiised by air. The following reactions take place in the presence of O_2:

$$PH_3 + 4RH_2N + 2O_2 \longrightarrow (RHN)_3P{=}NR + 4H_2O. \quad (95)$$

$$PH_3 + 4R_2HN + 2O_2 \longrightarrow (R_2N)_3P{=}NR + 3H_2O + ROH. \quad (96)$$

The rates of reactions (93) and (94) depend significantly on temperature and the concentrations of the reactants (CuY_2, RH_2N, R_2HN, PH_3) and reaction products [H_2O, CuX, $(RHN)_3P{=}NR$, $(R_2N)_3P{=}NR$]. The influence of the concentrations of the above substances on the reaction rate is described by the equation

$$W = k[Cu(II)]^{0.5}[Cu(I)]^{0.5}[PH_3]^{0.5}[RNH]^{0.5}, \quad (97)$$

where k is the rate constant (litre $mol^{-1}\,s^{-1}$). Pyridine is an effective solvent for reactions (93)–(96), which are two orders of magnitude faster in it.[53]

The fractional orders with respect to the reactants, the low activation energy ($E^{\neq}$ = 34 kJ mol^{-1}) and entropy ($\Delta S^{\neq} = -7160$ J $mol^{-1}\,K^{-1}$), and the negative influence of H_2O indicate a coordination mechanism for the rate-limiting stage. Only the products of the interaction of PH_3 with the components forming part of the composition of the coordination sphere of copper(II) are formed.

The composition of the copper(II) complexes in amines has been investigated by UV and IR spectroscopy.[80] The electronic spectra of solutions CuY_2 (Y = Cl, Br, OAc, RCO_2, etc.) in $C_6H_5CH_2NH_2$ contain an absorption band at 670 nm, indicating the identity of their structures regardless of the nature of the ligands. According to IR spectroscopic data, $Cu(OAc)_2$ induces a shift of the N–H absorption band from 1600 to 1550 cm^{-1} and the appearance in the stretching region of a new set of bands at 3210, 3290, 3320 and 3360 cm^{-1}. The decrease in the stretching vibration frequency of the carboxylate ion from 1405 to 1570 cm^{-1} indicates a decrease in the Cu–O bond order as a result of the formation of bridges in the dimeric copper(II) complexes. An additional absorption band at 660 cm^{-1}, due to the formation of the amide bond following the addition of benzylamine to the copper(II) ion, arises in the IR spectra of the complexes.

The nature of the intermediate organophosphorus compounds was investigated by ^{31}P NMR spectroscopy.[45] After the reduction of copper(II) with phosphine to copper(I), the regeneration of copper(II) with air, and the precipitation of copper ions with KI, the spectra of solutions of $Cu(OAc)_2$ and $CuCl_2$ in $C_6H_5CH_2NH_2$ and $C_2H_5NH_2$ contain only the bands at 30 and 20 ppm characteristic of phosphorous triamides. The products of the incomplete substitution of the hydrogen atoms of phosphine by amino-groups (phosphinamidite and phosphonamidite) do not accumulate. Characteristic narrow bands at 1000–1100 cm^{-1} (P–N); 1600, 1490, and 1450 cm^{-1} (C–H in C_6H_5); 3215, 3245 and 3230 cm^{-1} (N–H), and 695 and 740 cm^{-1} (H–C) were observed in the IR spectra of the product obtained in $C_6H_5CH_2NH_2$. The accumulation of HCl was inferred from the 2500–2700 cm^{-1} band and that of H_2O was inferred from the intense broad band at 3400, 1640 cm^{-1} (O–H). Hydrogen chloride appears as a result of reactions (93) and (94) and water is formed during the regeneration of the spent copper(II) solution with oxygen. According to IR spectroscopic data, amines are hardly oxidised by copper(II) chlorides and acetates. Amines are also not chlorinated by copper(II) chlorides.[53]

In solutions in primary and secondary amines, the reduction of copper(II) by phosphine includes the stage involving the deprotonation of the substrates.

Ammonia, amines, and phosphine are very weak NH and PH acids ($pK_a \simeq 31-35$) and are activated by strong bases in anhydrous solvents[79] and by metal complexes.[74] The activation of amines requires the high-valence Ti(IV), Pt(IV), Au(III), Rh(III), and Ir(III) metal cations,[74] while that of phosphines requires the low-valence Cu(I), Ag(I), Au(I), Hg(II), and Pd(II)metal cations.[63] The tendency of amines to enter into reactions involving the formation of amino- and phosphino-ligands on treatment with metal complexes becomes enhanced with increase in basicity on passing from ammonia to primary and secondary amines[54] and from phosphine to primary and secondary phosphines. Under the influence of metal complexes, the acid

dissociation constants of the PH and NH acids increase by several orders of magnitude.[74]

$$Cu_2X_3(R_2HN)_6PH_3 \longrightarrow Cu_2X(R_2HN)_5(PH_2)(R_2N) + 2HX. \quad (98)$$

The acid properties of coordinated amines and apparently phosphines increase by several orders of magnitude with increase in their number in the inner sphere or after the introduction of pyridine into the latter.[54] Pyridine therefore proved to be a convenient solvent for the oxidative P–N coupling of amines to phosphine.[53] The stepwise formation constants of the amine complexes of copper(II) and copper(I) are independent of the nature of the amines, but they are two orders of magnitude higher than the values of the constants of the pyridine complexes of copper(II) and copper(I) and for this reason the copper(II) and copper(I) ions contain the amine over a wide range of amine/pyridine ratios. This is indicated also by potentiometric data. The addition of amines to a pyridine solution of CuX_2 shifts the potential of the Cu(II)/Cu(I) couple in the cathodic direction. An amine does not inhibit reactions (93) and (94), whereas pyridine accelerates them, since it stimulates the amido- and phosphido[proton-loss]-reactions. The aminophosphino-copper(II) complexes undergo redox decomposition with formation of phosphinous amide.

Reaction (99), involving the reductive coupling of the phosphino- and amino-ligands, is consistent with the known tendency of the P–N bonds in organophosphorus compounds to dissociate under the influence of metal complexes with formation of oxidative addition products.[71] The mechanism of the reductive P–N coupling of phosphine to amine has been investigated by the CNDO method.[78]

$$Cu_2X(R_2HN)_5(PH_2)(R_2N) \longrightarrow$$
$$\longrightarrow Cu + CuX(R_2HN)_2 + 3R_2NH + R_2NPH_2. \quad (99)$$

The configurations of the PH_3 and NH_3 molecular orbitals are as follows: PH_3 $(a_1^2e^42a_1^22e^03a_1^0)$, NH_3 $(a_1^2e^42a_1^23a_1^02e^0)$.[98,105] In contrast to NH_3, the $2e$ orbital of PH_3 has a lower energy than $3a_1$, which indicates the inclusion of the $3d$ orbitals of phosphorus in the basis set, since the $2e$ molecular orbital has in the main $3d$ character. According to Pearson,[98] inversion in amines takes place readily, in contrast to phosphines, the barriers for NH_3 and PH_3 being respectively 5.2 and 37.2 kcal mol^{-1}. In the NH_3, PH_3, AsH_3, SbH_3 series, the ionisation potentials of the molecules change very little,[98] despite the fact that the energies of the atomic orbitals of the heteroatoms increase monotonically. In the above series of hydrides, the mixing of the s and p orbitals of the heteroatoms diminishes, which leads to an increase in the $2a_1 \rightarrow 3a_1$ energy difference, the stabilisation of the pyramidal form, the narrowing of the bond angle NH_3 (108°), PH_3 (93°)], a decrease in basicity [NH_3 (pK_a = 9.2), PH_3 (pK_a = −14)], and an increase in the total bond energy and in the positive charge on the heteroatom. For this reason, PH_3 differs from NH_3 by an appreciably lower reactivity.[63]

The weakly polar PH_3 molecule is activated in the coordination sphere and becomes polar. Whereas the effective charge on the phosphorus and hydrogen atoms in the free PH_3 molecule is zero, after coordination a charge, which depends on the composition and the total charge of the complex, arises on these atoms. In the anionic complexes, the charge on the phosphorus atom is positive, whilst in the cationic complexes it is negative. The ionic character of the P–H bond in the coordinated PH_3 molecule becomes more pronounced.

On complex formation, the amine molecule is activated to a much greater extent than the PH_3 molecule. As a result of coordination, there is a significant increase in the amount of ionic character of the N–H bond and negative and positive charges increase on the nitrogen and hydrogen atoms respectively, varying as a function of their composition and the overall charge of the complex.

The nature of the activation of PH_3 depends more on the composition and charge of the complexes than that of the activation of amines. Judging from the effective charge on the phosphorus atom, in the cationic and ionic complexes phosphine acquires nucleophilic and electrophilic reactivity respectively. Judging from the charges on the nitrogen atom, amines exhibit a nucleophilic reactivity in both positively and negatively charged complexes. Since the N–H bond is more polar than the P–H bond, the formation of amide ions in the coordination sphere of copper(II) is more realistic than the formation of phosphide ions.

The Cu–P and Cu–N bond energies increase sharply on passing from phosphine and amine complexes to phosphide and amide complexes. As a result of the deprotonation of the substrates, the amount of the ionic character of the metal–ligand bonds, especially the Cu–P bond, increases.

Since cationic copper(II) complexes, in which phosphine does not form bonds with the ligands, predominate in amine media, the mechanism which rules out the formation of phosphide and amide ions and their reductive coupling with formation of phosphinous amide predominates in the reactions. A three-centre transition state, characterised by a low activation energy and a negative activation entropy, is formed in the rate-limiting stage.

$$(R_2HN)_4Cu(R_2N)(PH_2) \longrightarrow \left[(R_2HN)_4Cu \begin{matrix} NR_2 \\ \diagdown\ \diagup \\ PH_2 \end{matrix} \right]^{\neq} \longrightarrow$$
$$\longrightarrow Cu + R_2NPH_2 + 4R_2HN. \quad (100)$$

Similarly phosphinous amide is oxidised by copper(II) ions to phosphonous diamide and the latter is oxidised to phosphorous triamide, but the reaction is faster since phosphinous amide and phosphonous diamide have a higher acidity ($pK_a \simeq 15$) than phosphine ($pK_a = -14$).[48]

Ligands which do not participate directly in the redox decomposition of the intermediate complex render considerable assistance in activating the substrates. According to CNDO data, these ligands form fairly strong bonds with the hydrogen atoms of PH_3, R_2HN, and RH_2N and are involved in nucleophilic cooperation with the amido- and phosphido-reactions, which lead to the appearance of amide and phosphide ions in the coordination sphere. Specially strong bonds are formed between the hydrogen atoms of phosphine and the amine in cationic complexes.

The driving forces of reactions (93)–(96), in which phosphine undergoes oxidative amination and oxidative imination, are the difference between the P–N and P=N bond energies as well as the high Cu(II)/Cu(0) redox potential, which increases after the addition of pyridine.[54] In contrast to trialkyl phosphites, phosphorous triamides are readily oxidised by oxygen and sulfur. They form stable pseudophosphonium salts because the P=N bond energy is appreciably lower than the P=O bond energy.[48] The state of the P=N bond depends on the electronegativity of the substituents at the nitrogen and phosphorus atoms. The multiplicity of the P=N bond increases with increase in the electronegativity of the substituents at the phosphorus atom and with decrease in the electronegativity of those at the nitrogen atom.[50,51]

IX. P–C coupling of phosphine to aldehydes

Reactions involving the P–C coupling of phosphine to carbonyl compounds lead to phosphines with functional group substituents.[9,106,107] It has been shown[108–110] that, when concentrated phosphine is passed through an aqueous solution of aldehydes and ethylenediaminenickel(II) complexes, reactions involving the hydroxymethylation of phosphine take place with a high selectivity and at a high rate. ($E^{\neq}$ = 10 kJ mol^{-1}, $\Delta S^{\neq} = -150$ J mol^{-1} K^{-1}).

$$PH_3 + 3CH_2O \longrightarrow P(CH_2OH)_3. \quad (101)$$

$$PH_3 + 4CH_2O + H_2O \longrightarrow (HO)P(CH_2OH)_4. \quad (102)$$

In $NiCl_2$ solution, the main product is tri(hydroxymethyl)-phosphine [reaction (101)], whilst in the presence of acidoamine-nickel complexes the main product is hydroxytetra(hydroxy-methyl)phosphine [reaction (102)]. Under optimum conditions, $(HO)P(CH_2OH)_4$ and $P(CH_2OH)_3$ are obtained in approximately 100% yields. The reaction products were isolated by distilling away the unreacted CH_2O and were analysed by ^{31}P, ^{13}C, and ^1H NMR and IR spectroscopic methods.

In the presence of $NiCl_2$, the rate of reaction (101) is given by the formula

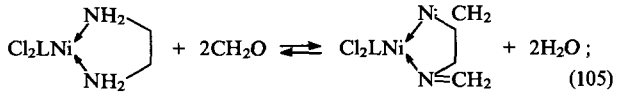
$$W = k[CH_2O]^{0.5}[NiCl_2]^{0.5}[PH_3]^{0.5}[P(CH_2OH)_3]^{0.5}. \quad (103)$$

The addition of primary and secondary amines to an aqueous formaldehyde solution of $NiCl_2$ leads to a significant increase in the rate of reaction (102), while the addition of tertiary amines inhibits this reaction.

In order to investigate the influence of the nature and concentration of the amine on the rate of reaction (102), primary monoamines (NH_2CH_3, $NH_2C_2H_5$) secondary monoamines [$NH(CH_3)_2$, $NH(C_2H_5)_2$], and tertiary monoamines [$N(CH_3)_3$, $N(C_2H_5)_3$] as well as the diamine $C_2H_4(NH_2)_2$ were used. The intermediate tri(hydroxymethyl)phosphine, aldehyde, amine, and mixed aminoaldehyde complexes of nickel(II) were investigated by ^{31}P NMR and UV spectroscopy. Ethylenediamine (En) complexes of nickel(II) showed the highest catalytic activity. The catalytic properties of this system are described by the formula

$$W = k[CH_2O]^{0.5}[NiCl_2]^{0.5}[PH_3]^{1.5}[En]^{0.5}[P(CH_2OH)_3]^{0.5}. \quad (104)$$

Investigations made it possible to put forward the following mechanism for the catalytic effects of ethylenediaminenickel(II) complexes in reaction (102):

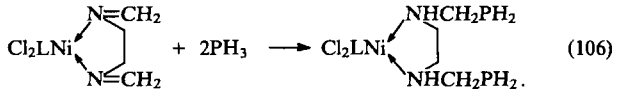


(105)

L = $P(CH_2OH)_3$.

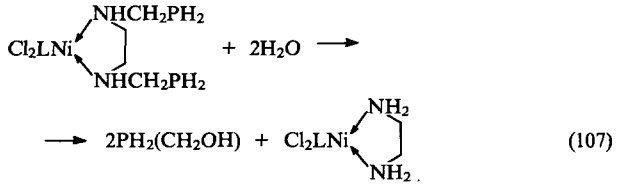
The outer-sphere condensation of coordinated ethylene-diamine with CH_2O [reaction (105)] leads to the formation of ethylenediaminenickel(II) complexes.[71]

Phosphine also reacts with the ethylenediamine complexes via an outer-sphere mechanism:



(106)

Ethylenebis(aminomethylphosphine) formed by reaction (106) decomposes subsequently with formation of the initial ethylenediaminenickel(II) complex and the reaction inter-mediate — mono(hydroxymethyl)phosphine.



(107)

Hydrolysis of ethylenebis(aminomethylphosphine) at the C–N bond occurs only in the presence of one methyl group. With increase in the number of these groups, the resistance of aminoalkylphosphines to hydrolysis at the C–N bond also increases.[9] The successive substitution of the hydrogen atoms in PH_3 by the hydroxymethyl group takes place in conformity with stages (105)–(107). The second and third hydrogen atoms are substituted faster since mono- and di-(hydroxymethyl)phosphines are appreciably more reactive than PH_3.

Tertiary amines deactivate nickel(II) complexes, since they do not contain a mobile hydrogen atom and do not form imines on interaction with CH_2O.

Thus the mechanism of the P–C coupling of phosphine to formaldehyde differs fundamentally from the mechanism of P–O and P–N coupling of phosphine to alcohols and amines. Whereas oxidative P–O and P–N coupling takes place via an inner-sphere mechanism, P–C coupling involves an outer-sphere mechanism. The catalytic cycle includes three key stages. In the first stage, ethylenediiminenickel(II) complexes are formed from the ethylenediamine complexes and formaldehyde, while in the second stage ethylenebis(aminomethylphosphine)nickel(II) complexes are produced from ethylenediiminenickel(II) complexes and PH_3. In the concluding stage, the ethylenebis(aminomethyl-phosphine)nickel(II) complexes are hydrolysed at the C–N bond with formation of mono(hydroxymethyl)phosphine and the regeneration of the initial ethylenediaminenickel(II) complex.

The effluent gas from hypophosphite factories, containing 70% of PH_3 and 30% of H_2, is an extremely suitable source of phosphine for reaction (102). The reaction product — hydroxy-tetra(hydroxymethyl)phosphine — is used as the monomer for the synthesis of fire-resistant and thermostable organophosphorus polymers. The reaction proceeds in aqueous media and the reaction product is a solid and can be readily separated from the reaction mixture after distilling away water.

X. Oxidative P–C coupling of phosphine and tetraphosphorus to nitriles

Copper(II) carboxylates and halides exhibit a high catalytic activity in the oxidative P–C coupling of phosphine and tetraphosphorus to acetonitrile.[49,63]

$$PH_3 + 3CuY_2 + 3CH_3CN \longrightarrow (CNCH_2)_3P + 4Cu + 6HY. \quad (108)$$

$$P_4 + 20CuX_2 + 16CH_3CN \longrightarrow 4(CNCH_2)_3P{=}NCX_2CH_3 + 20CuX + 12HX. \quad (109)$$

The Cu(0) and Cu(I) formed as a result of reactions (108) and (109) are oxidised by oxygen. Since acetonitrile coordinates more effectively to Cu(I) than to Cu(II), the redox potential of the copper couple in CH_3CN is much higher than in pyridine.[54] The rate of the Cu(II) → Cu(I) reduction stage therefore increases in CH_3CN but the Cu(I) → Cu(II) oxidation stage is retarded.

The nature of the products of the reaction of phosphine and tetraphosphorus with the nitrile depends on the nature of the ligand. Carboxylate ligands promote the formation of tri(cyano-methyl)phosphine, while halide ligands promote the formation of tri(cyanomethyl)phosphazoalkyl. In the former case, the ^{31}P NMR spectra contain only peaks in the region of −6 ppm, which are characteristic of phosphines, while in the latter case they contain peaks in the region of −6 and 14 ppm, which are typical for phosphines and phosphazo-compounds.[45]

Nitriles effectively activate transition[111] and non-transition[112] metal complexes. Complexes of the high-valence metals Ta(V), Nb(V), W(VI), U(IV), and Sn(IV), on the one hand, and the metals Pd, Pt, Rh, Cu, Ag, and Au,[74] on the other, induce respectively electrophilic and nucleophilic activities in the C≡N group. The low-valence metal complexes catalyse the dissociation of the C–C_α and C_α–H bonds in nitriles.[74] The α-cyano-carbanions (CH_2CN^-) formed under the influence of low-valence metal complexes are highly reactive and react rapidly with the coordinated electrophile.[71] When there are no hydrogen atoms in the α position and no coordinated electrophiles, low-valence metal complexes catalyse oxidative coupling of nitriles (C_6H_5CN) to phosphine with a break of the C–C_x bond.[74]

In the presence of high-valence non-transition metals, nitriles interact with a hydrogen halide and are converted into imines and amines.

$$RCN + HX \longrightarrow RCX{=}NH \xrightarrow{HX} RCX_2{-}NH_2. \quad (110)$$

The IR spectra of the products of the interaction of the nitrile with HX at 25 °C contain no bands due to the stretching vibrations of the C≡N bond of the nitrile, but the absorption bands due to the C–Cl, C=N and N–H bonds are observed.[112] Under the influence of high-valence metal ions, nitriles react at 70–90 °C with carboxylic acids to form primary and secondary amides.[112]

$$RCN + 2RCO_2H \longrightarrow RCONH_2 + (RCO)_2O. \quad (111)$$

$$RCN + RCO_2H \longrightarrow (RCO)_2NH. \quad (112)$$

Copper(I) ions effectively stimulate the hydration of nitriles.[113]

$$RCN + H_2O \longrightarrow RCONH_2. \quad (113)$$

In the presence of low-valence transition metals, reactions (111) and (112) are slow even at high temperatures (110–180 °C).[112]

The properties of the coordinated nitriles described above justified the assumption that copper(I) and copper(II) carboxylates stimulate the dissociation of the C_α–H bonds and the oxidative cyanoalkylation of phosphine, while copper(I) and copper(II) halides promote the dissociation of the C_α–H bonds, the oxidative cyanoalkylation of phosphine, and the oxidative imination of tri(cyanoalkyl)phosphine.

The new methods of synthesis of phosphines and phosphazo-compounds are simpler than the methods based on reactions of metallated alkyls with halophosphines or of alkali metal phosphides with alkyl halides.[1–6]

XI. Oxidative P–O coupling of zinc and copper phosphides to alcohols

The phosphides of *d* metals are not used in organophosphorus synthesis owing to their low reactivity.[114] Only alkali and alkaline earth metal phosphides are used in the chemistry of organophosphorus compounds because of their relatively high reactivity.[9] Bearing in mind that considerable amounts of waste containing transition metal phosphides (ferrophosphorus, copper and zinc phosphides, slags) are formed in the undertakings of the phosphorus industry, studies in the field of the organic chemistry of phosphides are of practical interest.

Dorfman and coworkers[115–122] established for the first time that zinc and copper phosphides can be used to obtain trialkyl and dialkyl phosphates. In an alcoholic solution of copper(II) chloride, Zn_3P_2 and Cu_3P are readily oxidised by oxygen to $(RO)_3PO$ and $(RO)_2(HO)PO$.

$$Zn_3P_2 + 6ROH + 4O_2 \longrightarrow 2(RO)_3PO + 3Zn(OH)_2. \quad (114)$$

$$Cu_3P + 3ROH + 2O_2 \longrightarrow (RO)_3PO + 3Cu(OH). \quad (115)$$

$$Zn_3P_2 + 8ROH + 4O_2 \longrightarrow 2(RO)_2(HO)PO + 3Zn(OH)_2 + 2R_2O. \quad (116)$$

$$Cu_3P + 4ROH + 2O_2 \longrightarrow (RO)_2(HO)PO + 3Cu(OH) + R_2O. \quad (117)$$

In the absence of O_2 (in argon) in alcoholic $CuCl_2$ solution, zinc and copper phosphides decompose rapidly with formation of $(RO)_3PO$ and $(RO)_2(HO)PO$.

Cyclic phosphates are formed from glycols, for example from butanediol. When a secondary alcohol (*iso*-C_3H_7OH) is used, dialkyl phosphites are obtained.

The copper(I) ions formed as a result of reactions (118)–(123) are oxidised by oxygen.

Alkyl halides, formed in reactions (118), (119), (122), and (123), hydrolyse [reaction (53)] during the regeneration of copper(II), while the alcohol is not oxidised by oxygen.

$$Zn_3P_2 + 16CuCl_2 + 8ROH \longrightarrow 2(RO)_3PO + 3ZnCl_2 + 16CuCl + 8HCl + 2RCl. \quad (118)$$

$$Cu_3P + 4ROH + 8CuCl_2 \longrightarrow (RO)_3PO + RCl + 11CuCl + 4HCl. \quad (119)$$

$$Zn_3P_2 + 16CuCl_2 + 12ROH \longrightarrow 2(RO)_2(HO)PO + 3ZnCl_2 + 4R_2O + 16CuCl + 10HCl. \quad (120)$$

$$Cu_3P + 8CuCl_2 + 6ROH \longrightarrow (RO)_2(HO)PO + 11CuCl + 2R_2O + 7HCl; \quad (121)$$

R = CH_3, C_2H_5, C_3H_7, *iso*-C_4H_9, C_4H_9, *iso*-C_5H_{11}, C_5H_{11}.

$$Zn_3P_2 + 6R'OH + 12CuCl_2 \longrightarrow 2(R'O)_2HPO + 2R'Cl + 12CuCl + 4HCl + 3ZnCl_2. \quad (122)$$

$$Cu_3P + 3R'OH + 6CuCl_2 \longrightarrow (R'O)_2HPO + R'Cl + 9CuCl + 2HCl. \quad (123)$$

$$Zn_3P_2 + 8R'OH + 3O_2 \longrightarrow 2(R'O)_2HPO + 3Zn(OH)_2 + 2R_2'O. \quad (124)$$

$$Cu_3P + 4R'OH + 1.5O_2 \longrightarrow (R'O)_2HPO + 3Cu(OH) + R_2O. \quad (125)$$

After regeneration, the solution can be reused to decompose Zn_3P_2 and Cu_3P. Trialkyl phosphates and dialkyl phosphonates can be extracted with heptane and separated by vacuum distillation.

Reactions (114)–(121) take place in the topochemical regime. The kinetic and conversion curves have the shape typical for topochemical reactions and pass through a sharp maximum at low conversions $\alpha = 0.1–0.3$.[60] The specific rate (W_{sp}, mol m^{-2} s^{-1}) of the topochemical reaction in the kinetic region was found from Eqn (33). The rate of the reaction was calculated having determined the consumption of O_2 and copper(II) and the accumulation of $(RO)_3P$, $(RO)_2(HO)PO$, Cu(I), $(R'O)_2HPO$, and RCl.

During the search for the optimum conditions and during the study of the mechanism of the oxidative P–O coupling of phosphides to alcohols, the influence of the concentrations of ROH, $CuCl_2$, CuCl, O_2, HCl, LiCl, H_2O, CH_3CN, $C_6H_5CH_2NH_2$, and $C_2H_5NH_2$ on this process was traced. According to atomic-absorption spectroscopic data and the results of laser microanalysis, the Zn_3P_2 and Cu_3P specimens contained less than 1% of impurities. The average Zn_3P_2 and Cu_3P particle sizes and the specific surfaces measured with the aid of a Coulter counter were 13–47 μm and 90–850 cm^2 g^{-1} respectively.

As the HCl and H_2O concentrations are varied, the rates of the topochemical reactions pass through a maximum at very low concentrations of the additives. Amines inhibit the topochemical process, while LiCl has only a weak influence on the latter. With increase in the concentrations of Cu(II), ROH, and O_2, as well as temperature, the rate of reaction also increases.[115–122]

$$Cu_3P + (3-n)HCl \rightleftharpoons Cu_nH_{3-n}P + (3-n)CuCl. \quad (126)$$

The state of the copper(II) complexes during the experiment was investigated by magnetic susceptibility (MS) and UV and EPR spectroscopic methods. According to MS and EPR spectroscopic data, copper chlorides exist predominantly in the monomeric state in alcoholic solutions. It follows from the UV spectra that water readily displaces alcohols from the coordination sphere of copper(II). Alcohol-containing copper(II) complexes exist only for the ratio $H_2O/Cu(II) < 20$. In the alcohol, the stability constants of copper(II) chlorides are higher than in water. The chloroalcoholcopper complexes predominate already for the ratio $Cl^-/Cu(II) \sim 2$.[47]

$$Cu_nH_{3-n}P + Cu_2Cl_3(ROH) \rightleftharpoons Cu_nH_{3-n}PCu_2Cl_3(ROH). \quad (127)$$

The ^{31}P NMR spectra contain an intense band corresponding to $(RO)_3PO$ (−1 ppm) and a weak band due to $(RO)_2(HO)PO$ (−0.5 ppm). Data taken from Nifant'ev and Vasyanina[45] were used in the analysis of the spectra.

The results presented above, obtained by physicochemical methods, suggest the following mechanism of the oxidative P−O coupling of alcohols to metal phosphides. The process begins with the stage involving the activation of the metal phosphide surface by the acid (however, the metal atoms are not fully substituted by hydrogen atoms and phosphine is not liberated). Subsequently the metal hydrogen phosphide adsorbs the heterovalent copper(II)–copper(I) chloride dimer, which is present, according to UV spectroscopic data,[47] in alcoholic solutions of $CuCl_2-CuCl$.

The two-electron redox decomposition of the surface complex, formed in stage (127), leads to the formation of a surface phosphinite and metallic copper.

In the presence of $CuCl_2$, copper dissolves rapidly.

$$Cu + CuCl_2 \rightleftarrows 2CuCl; \qquad K_c = 8 \times 10^6.$$

Thus the oxidative P−O coupling of the metal phosphide to an alcohol includes three main stages: acid hydrolysis of the metal phosphide to the metal hydrogen phosphide, reduction of the chloroalcoholcopper(II) complexes to copper(I) by the metal hydrogen phosphide, and regeneration of the copper(II) ions with oxygen. The acid–base stage (126) is accelerated with increase in the acidity of the medium and the alcohols. The oxidation–reduction stage (128) is retarded as the acidity of the medium increases, which hinders the formation of the alkoxy-ligand. When ROH is displaced from the coordination sphere of copper(II) by the addition of HCl, LiCl, and H_2O, the yield of organic phosphates is seen to fall from 100% to 20%.[115–122]
The oxidation–reduction decomposition reaction (128) takes place as follows:

$$Cu_nH_{3-n}PCu_2Cl_3(ROH) \longrightarrow \longrightarrow Cu + CuCl + Cu_nH_{2-n}P(OR) + 2HCl. \qquad (128)$$

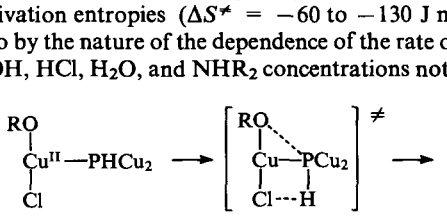
The subsequent stages of the oxidation of $(RO)PCu_2$ to $(RO)_2PCu$, $(RO)_3P$ and $(RO)_3PO$ are rapid.

The oxidation–reduction decomposition of (A) takes place with formation and subsequent reaction of a cyclic transition state.

$$Cu_2X_3(ROH)PCu_3 \underset{-CuX}{\overset{HX}{\rightleftarrows}} Cu_2X_3(ROH)PCu_2 \underset{-HX}{\rightleftarrows} \rightleftarrows Cu_2X_2(RO)PHCu_2 \longrightarrow Cu + CuX + (RO)PCu_2 + HX. \qquad (129)$$

A

The coordination mechanism of reaction (130) is indicated by the low activation energies ($E^{\neq}$ = 50–70 kJ mol^{-1}) and activation entropies ($\Delta S^{\neq}$ = −60 to −130 J mol^{-1} K^{-1}), and also by the nature of the dependence of the rate of reaction on the ROH, HCl, H_2O, and NHR_2 concentrations noted above.



$$\longrightarrow (RO)PCu_2 + Cu + HCl. \qquad (130)$$

The coordination mechanism of reaction (130) has been investigated by the CNDO method.[120] The molecular model of adsorption was used in the calculation.[64] For this purpose, calculations were made for the surface cluster complexes differing in the numbers of H and Cu atoms in the copper hydrogen phosphide and by the number of molecules (H_2O, ROH) and ions (RO^-, HO^-, Cl^-) in the coordination sphere of copper(II). The surface complexes chosen for the investigation modelled the influence of the number of halide, alkoxide, and hydroxide ions and water and alcohol molecules as well as the degree of substitution of copper atoms by hydrogen atoms in the copper phosphide on the nature of the bond between the atoms of the cluster.[120]

The quantum-chemical study established that the adsorption of chloroaquoalcoholcopper(II) complexes on the hydrogen phosphide is accompanied by the formation of bonds not only between the copper(II) ion and the phosphorus atom but also between the chlorine and copper (in the phosphide) atoms, between phosphorus and the alcohol, between phosphorus and water, and between phosphorus and chlorine. These bonds stimulate the oxidation of phosphorus and the reduction of copper(II).[120] The alkoxide ion forms a stronger bond with the phosphorus atom than do ROH, H_2, and the X^- ions. Hence it follows that the products of the oxidative P−O coupling are obtained as a result of the direct reaction of RO^- with the phosphorus atom. The strength of the bond between phosphorus and the alkoxide ion in the adsorption complex increases as the metal atoms are replaced by hydrogen atoms. The greater the number of hydrogen atoms in the hydrogen phosphide, the greater the tendency of the inner-sphere nucleophiles (X^-, HO^-, RO^-) to interact with the phosphorus atom. However, the complete replacement of the metal atoms in the phosphide by hydrogen atoms is not convenient, since the energy of the bonds between the coordinated bases and the metal atoms is much higher than that of the bonds between such bases and hydrogen atoms. Consequently hydrogen phosphides react with chloroalkoxocopper(II) complexes faster than do metal phosphides and phosphine.[120] Hence the cause of the positive influence of a small amount of added acid (up to 0.6 mol litre^{-1}), leading to only partial replacement of metal atoms by hydrogen atoms in the phosphide, on the rate of the topochemical process can be understood. However, when the ligands Cl^-, OH^-, and RO^- are replaced by O^{2-} ions, which form much stronger bonds with the metal atom of the phosphide, the oxidation process is accelerated. Thus the highest catalytic activity is shown by metal halides in weakly acid media and by metal oxides in alkaline media.[63]

XII. Oxidative P−O coupling of zinc and copper phosphides to alcohols in the presence of chlorine

Dorfman observed for the first time[49] that trialkyl and dialkyl phosphates can be obtained rapidly and in high yield (50%–90%) on chlorination of Zn_3P_2 and Cu_3P in alcoholic solutions.

The unreacted alcohol and the organophosphorus reaction products were separated from the inorganic substances by extraction with heptane and vacuum distillation.[115–122] A Cl_2-Ar gas mixture, supplied directly into the liquid phase, was used in the experiments. The rate of supply of the mixture was regulated in such a way that the potential of the Cl_2/Cl chlorine electrode remained constant during the study, while the Cl_2 concentration in the gas at the outlet from the reactor was close to zero. The rate of the reaction was inferred from the consumption of the phosphide, chlorine, and the alcohol and from the accumulation of the reaction products, which were analysed by gas chromatography and ^{31}P NMR spectroscopy.

The introduction of the phosphide into an alcoholic solution of chlorine at 10–80 ° is accompanied by a rapid cathodic shift of the reaction potential to a value which depends on the Cl_2 concentration in the Cl_2-Ar gas mixture. The potential shifts in the negative direction on lowering the Cl_2 concentration and with increase in the amount of the phosphide. On the other hand, it shifts in the anodic direction with increase in the Cl_2 content in argon and with decrease in the amount of the phosphide. The potentiometric method makes it possible to follow continuously during the experiment the chlorine/phosphide ratio in the reaction system.

$$Zn_3P_2 + 8Cl_2 + 8ROH \longrightarrow 2(RO)_3PO + 3ZnCl_2 + 8HCl + 2RCl. \quad (131)$$

$$2Cu_3P + 11Cl_2 + 8ROH \longrightarrow 2(RO)_3PO + 6CuCl_2 + 2RCl + 8HCl. \quad (132)$$

$$Zn_3P_2 + 8Cl_2 + 8ROH \longrightarrow 2(RO)_2(HO)PO + 3ZnCl_2 + 4RCl + 6HCl. \quad (133)$$

$$2Cu_3P + 11Cl_2 + 8ROH \longrightarrow 2(RO)_2(HO)PO + 6CuCl_2 + 4RCl + 6HCl; \quad (134)$$

R = C_4H_9, *iso*-C_4H_9, C_5H_{11}, *iso*-C_5H_{11}.

The sharp cathodic or anodic shift of the chlorine electrode potential depending on the chlorine/phosphide ratio indicates the high rate of the topochemical reaction of the phosphide with chlorine in the alcohol.

According to ^{31}P NMR data,[45] reactions (131)–(134) proceed relatively selectively. Mainly trialkyl and dialkyl phosphates are formed, their chemical shifts being −1 and −2 ppm respectively. The ^{31}P NMR spectra also contain small peaks due to the tetracoordinate phosphorus derivatives Cl_3PO (0.6 ppm), $(RO)_2ClPO$ (0.5 ppm), and $(RO)_2HPO$ (1 ppm). When phosphine is chlorinated in *iso*-C_3H_7OH the chemical shifts (ppm) are displaced upfield: (*iso*-$RO)_3PO$ (−4 ppm) and (*iso*-$RO)_2(HO)PO$ (−6 ppm). Hence it follows that reactions (131)–(134) proceed via the formation and subsequent reaction of phosphorus pentachloride.

The main feature of the reactions of PCl_5 with ROH and H_2O is the initial formation of phosphoryl chloride [reaction (136)], the rate of the subsequent alcoholysis of which increases with increase in the pH of the medium.[104] Such a sequence of reactions of phosphorus pentachloride with alcohols and water is due to the formation of the stable phosphoryl group P=O.[104] The reactions of phosphoryl chloride with ROH and H_2O proceed as stepwise elimination of HCl.[104] In the reactions of alcohols with phosphoryl chloride, phosphorodichloridates are generated initially. This is followed by the formation of phosphorochloridates and finally trialkyl phosphates. Reactions (136)–(138) are significantly accelerated in the presence of HCl binding agents. Without added pyridine, reaction (137) takes several hours, while in the presence of pyridine it reaches completion after several minutes. Therefore, in order to accelerate the reactions, the sample of the solution is treated with pyridine before chromatographic analysis.

$$Zn_3P_2 + 8Cl_2 \longrightarrow 2PCl_5 + 3ZnCl_2. \quad (135)$$

$$PCl_5 + ROH \longrightarrow Cl_3PO + RCl + HCl. \quad (136)$$

$$Cl_3PO + 2ROH \longrightarrow (RO)_2ClPO + 2HCl. \quad (137)$$

$$(RO)_2ClPO + ROH \longrightarrow (RO)_3PO + HCl. \quad (138)$$

$$(RO)_2ClPO + ROH \longrightarrow (RO)_2(HO)PO + RCl. \quad (139)$$

During the chlorination of Cu_3P, it was observed that the yield of trialkyl phosphate increases significantly when the Cl_2 concentration is reduced (to 10^{-3}–10^{-4} mol litre^{-1}) as fresh portions of Cu_3P are added. The autocatalysis is due to the fact that, following the appearance of $CuCl_2$ in the system as a result of the reaction

$$2Cu_3P + 11Cl_2 \longrightarrow 2PCl_5 + 6CuCl_2, \quad (140)$$

processes begin in which $CuCl_2$ becomes the catalyst and Cl_2 and Cu_3P are the reactants.

$$Cu_3P + 8CuCl_2 + 4ROH \longrightarrow 11CuCl + (RO)_3PO + RCl + 4HCl. \quad (141)$$

$$2CuCl + Cl_2 \longrightarrow 2CuCl_2. \quad (142)$$

Copper phosphide is oxidised to trialkyl phosphates by $CuCl_2$ in alcohols, while CuCl, a product of reaction (141), is reoxidised to $CuCl_2$. When there is a deficiency of Cl_2, copper phosphide reacts with $CuCl_2$ and not with Cl_2.

The catalytic pathway ensures a high selectivity of the reation, since the oxidative alcoholysis of Cu_3P proceeds without the preliminary formation of chloro-derivatives of phosphorus via the direct reaction of Cu_3P with ROH in the coordination sphere of copper(II). Tests showed that, in the absence of Cl_2, the stoichiometric reaction (141) taks place.[120,121]

It follows from the ^{31}P NMR spectra, indicating the presence of $(RO)_2HPO$ in the reaction mixture, that trialkyl phosphate is formed from the dialkyl phosphite produced on dealkylation of trialkyl phosphite.[61,62]

$$Cu_3P + 6CuCl_2 + ROH \longrightarrow (RO)_3P + 9CuCl + 3HCl. \quad (143)$$

$$(RO)_3P + HCl \longrightarrow (RO)_2HPO + RCl. \quad (144)$$

$$(RO)_2HPO + 2CuCl_2 + ROH \longrightarrow (RO)_3PO + 2CuCl + 2HCl. \quad (145)$$

According to Dorfman et al.[53] and Fridman et al.,[54] dialkyl phosphate is readily oxidised by $CuCl_2$ in the alcohol to trialkyl phosphate.

* * *

The studies described above were carried out in the little investigated field of the organic chemistry of phosphorus and phosphides, which, however, is of great practical importance. The principal features of the new reaction involving the oxidative phosphorylation of organic compounds by phosphorus and phosphides were described. Organophosphorus compounds can be obtained by this reaction much more simply than by the existing methods in which metallated organic substances and phosphorus halides or alkali metal phosphides and halo-derivatives of organic compounds are used.[1–6] By virtue of the high rates of the reactions considered, highly toxic waste from phosphorus factories with a low content of the phosphorylating agent (the effluent phosphine- and phosphorus-containing gases, dilute phosphorus sludge, transition metal phosphides, and red phosphorus) can be used as raw materials in these processes.[114,123]

It has been shown that the non-polar tetraphosphorus and the weakly polar phosphine, which tend to undergo homolytic reactions, enter vigorously into heterolytic organic reactions in the presence of metal complexes. The mechanism, rate, and mode of reaction depend on the nature of the ligands. The use of the ligand effect, described in 1972 [46] and applied successfully by Lupi and Chubar,[124] makes it possible to alter significantly the nature of the process by adding simple alkali metal salts.

The mechanisms of the activation of phosphorus and phosphides and of the reactions involving the oxidative O-, N-, and C-coupling of alcohols, amines, aldehydes, carboxylic acids, glycols, and nitriles to phosphine, white and red phosphorus, and transition metal phosphides, described above, can be used to discover new reactions of this type with participation of other organic compounds.

References

1. R S Edmundson (Ed.) *Dictionary of Organophosphorus Compounds* (London: Chapman and Hall, 1987)
2. U Aufl (Ed.) *Methoden der Organischen Chemie* (Houben-Weyl) (Stuttgart: Georg Thieme, 1963) Vol. 12
3. Ch Fest, K T Schmidt *The Chemistry of Organophosphorus Pesticides* (Berlin: Springer, 1982)
4. C Hanson (Ed.) *Recent Advances in Liquid–Liquid Extraction* (Translated into Russian; Moscow: Khimiya, 1974)

5. P A Kirpichnikov, L A Mukmenova, D G Pobedimskii *Usp. Khim.* **52** 1831 (1983) [*Russ. Chem. Rev.* **52** 1051 (1983)]
6. H R Allcock *Phosphorus–Nitrogen Compounds* (Translated into Russian; Moscow: Mir, 1976)
7. E E Nifant'ev, T S Kukhareva *Obzor Monografii i Obzorov po Khimii Fosfororganicheskikh Soedinenii* (A Survey of the Monographs and Reviews on the Chemistry of Organophosphorus Compounds) (Moscow: Mir, 1989)
8. Ya A Dorfman, L V Levina, T V Petrova, M M Aleshkova, G S Polimbetova, V S Emel'yanova *Zh. Obshch. Khim.* **60** 1275 (1990)
9. O A Erastov, G E Nikonov *Funktsional'no-Zameshchennye Fosfiny i Ikh Proizvodnye* (Phosphines with Functional Group Substituents and Their Derivatives) (Moscow: Nauka, 1986)
10. A I Rakhimov, S A Tungatarov, G S Polimbetova *Sintez Fosfororganicheskikh Soedinenii. Gomoliticheskie Reaktsii* (Synthesis of Organophosphorus Compounds. Homolytic Reactions) (Moscow: Nauka, 1986)
11. V M Koverya, V Ya Monin, V P Belyakov *Sposoby Ochistki Pechnogo Gaza ot Fosfora i Fosfina* (Methods for the Elimination of Phosphorus and Phosphine from Furnace Gas) (Moscow: Izd. NIITEKhIM, 1986)
12. N G Feshchenko, in *Uspekhi Khimii Fosfororganicheskikh i Seraorganicheskikh Soedinenii* (Advances in the Chemistry of Organophosphorus and Organosulfur Compounds) (Kiev: Naukova Dumka, 1970) p. 89
13. N G Feshchenko, L V Kirsanov, V G Kostin, L I Kudryavtseva, E A Mel'nichuk, Zh A Gorbatenko, I E Mitel'man, N D Gomelya, A G Matyusha, Yu P Makovetskii, T V Kovaleva, in *Khimiya i Primenenie Fosfororganicheskikh Soedinenii* (The Chemistry and Applications of Organophosphorus Compounds) (Leningrad: Nauka, 1987) p. 342
14. N G Feshchenko, E K Rutkovskii, Zh K Gorbatenko *Zh. Obshch. Khim.* **59** 1684 (1989)
15. A V Kirsanov, N G Feshchenko, in *Khimiya i Primenenie Fosfororganicheskikh Soedinenii. Trudy V Konferentsii* (The Chemistry and Applications of Organophosphorus Compounds. Proceedings of the Vth Conference) (Moscow: Nauka, 1974) p. 37
16. L Maier *Forts. Chem. Fortschr.* **19** 1 (1971)
17. A W Frank, C F Baranauckas *J. Org. Chem.* **31** 1644 (1971)
18. G A Leman, in *Khimiya i Primenenie Fosfororganicheskikh Soedinenii* (The Chemistry and Applications of Organophosphorus Compounds) (Kiev: Naukova Dumka, 1981) p. 194
19. H F Lehmann, G Grobmann *Pure Appl. Chem.* **53** 205 (1980)
20. L Riesel, M Kant, R Helbing *Z. Anorg. Allg. Chem.* **580** 217 (1990)
21. A S Romakhin, I M Zarinov, Yu G Budnikova, Yu A Ignat'ev, E V Nikitin, A P Tomilov, Yu M Kargin *Elektrokhimiya* **25** 780 (1989)
22. C Broun, R F Hudson, L A Wartew, H Coates *Phosphorus Sulfur* **6** 481 (1979)
23. A P Tomilov, Yu M Kargin, I N Chernykh *Elektrokhimiya Elementoorganicheskikh Soedinenii. Elementy IV, V, VI Grupp Periodicheskoi Sistemy* (Electrochemistry of Organoelement Compounds. Group IV, V, and VI Elements) (Moscow: Nauka, 1986)
24. L V Kaabak, N Ya Shandrikov, A P Tomilov *Zh. Obshch. Khim.* **40** 548 (1970)
25. I M Osadchenko, A P Tomilov *Zh. Obshch. Khim.* **40** 698 (1970)
26. L F Filimonova, L V Kaabak, A P Tomilov *Zh. Obshch. Khim.* **39** 2174 (1969)
27. M V Tsikalova, D N Lobanov, I Ya Levitin *Dokl. Akad. Nauk SSSR* **308** 386 (1989)
28. Yu P Makovetskii, N G Feshchenko, A N Chernega *Zh. Obshch. Khim.* **61** 1075 (1991)
29. R A Cherkasov *Metalloorg. Khim.* **2** 13 (1989)
30. M Di Vaira, P Stohhioni, M Peryzzini *Polyhedron* **6** 351 (1987)
31. W E Lindsell, K J McCullough *J. Am. Chem. Soc.* **105** 4487 (1983)
32. P Dapporto, L Sacconi *Inorg. Chem.* **20** 3834 (1981)
33. V Di Vaira, L Sacconi *Angew. Chem.* **94** 338 (1982)
34. R A Trofimov, N K Gusarova, S F Malysheva, T N Rakhmatullina, S I Shaikhuddinova, V I Dmitriev, in *Mekhanizmy Reaktsii Nukleofil'nogo Zameshcheniya i Prisoedineniya* (The Mechanisms of Nucleophilic and Electrophilic Addition and Substitution Reactions) (Donetsk, 1990) p. 272
35. N K Gusarova, S F Malysheva, T N Rakhmatullina *Zh. Obshch. Khim.* **60** 828 (1990)
36. B A Trofimov, N K Gusarov, S F Malysheva, V I Dmitriev, T N Rakhmatullina, M G Voronkov *Dokl. Akad. Nauk SSSR* **60**, 828 (1990)
37. B A Trofimov, N K Gusarova, S F Malysheva *Phosphorus Sulfur Silicon Relat. Elem.* **55** 271 (1991)
38. B A Trofimov, N K Gusarova, T N Rakhmatullina, V I Dmitriev, S I Shaikhuddinova *Zh. Obshch. Khim.* **61** 1310 (1991)
39. D E C Corbridge *Phosphorus. An Outline of Its Chemistry, Biochemistry, and Technology* [Amsterdam: Elsevier, 1978] (Translated into Russian; Moscow: Mir, 1982)
40. D Purdela, R Vilceanu *Chimiya Compusilor Organici al Fosforului* [Chemistry of Organophosphorus Compounds) (Translated into Russian; Moscow: Khimiya, 1972)
41. Ya A Dorfman, R R Abdreimova, L V Levina, T V Petrova *Kinet. Katal.* **30** 1484 (1989)
42. Ya A Dorfman, R R Abdreimova, L V Levina, T V Petrova *Zh. Obshch. Khim.* **59** 481 (1989)
43. Ya A Dorfman, R R Abdreimova, D M Doroshkevich *Teor. Eksp. Khim.* 659 (1991)
44. A E Arbuzov *Izbrannye Trudy po Khimii Fosfororganicheskikh Soedinenii* (Selected Works on the Chemistry of Organophosphorus Compounds) (Moscow: Nauka, 1977)
45. E E Nifant'ev, L K Vasyanina *Spektroskopiya YaMR ^{31}P* (^{31}P NMR Spectroscopy) (Moscow: Izd. MGPI im. V I Lenina, 1986)
46. Ya A Dorfman, D V Sokol'skii *Kataliz Ligandami v Vodnykh Rastvorakh* (Catalysis by Ligands in Aqueous Solutions) (Alma-Ata: Nauka, 1972)
47. E V Gusevskaya, V A Likholobov, E P Toyazi, Yu I Ermakov *Kinet. Katal.* **24** 53 (1983)
48. A J Kirby, S G Warren *The Organic Chemistry of Phosphorus* (Translated into Russian; Moscow: Mir, 1971)
49. Ya A Dorfman *Katalizatory Organicheskogo Sinteza* (Catalysts for Organic Synthesis) (Alma-Ata: Nauka, 1992) Vol. 2, p. 166
50. G I Dergach, I N Khmurova, A V Kirsanov, V I Shevchenko, A S Shtepanek *Fosfazosoedineniya* (Phosphazo-Compounds) (Kiev, 1965)
51. A P Marchenko, A M Pinchuk *Khimiya i Primenenie Fosfororganicheskikh Soedinenii* (The Chemistry and Applications of Organophosphorus Compounds) (Moscow: Nauka, 1987) p. 153
52. V P Kukhar, V F Gilyarov *Pure Appl. Chem.* **52** 891 (1980)
53. Ya A Dorfman, L V Levina, Shch M Pakhorukova *Kinet. Katal.* **32** 617 (1991)
54. Ya D Fridman, M G Levina, N V Dolgasheva, T V Danilova, R A Veresova, A Ya Fridman *Ustoichivost' Smeshannykh Kompleksnykh Soedinenii v Rastvorakh* (The Stability of Mixed Complexes in Solution) (Frunze: Ilim, 1971)
55. V A Gilyarov *Usp. Khim.* **47** 1628 (1978) [*Russ. Chem. Rev.* **47** 870 (1978)]
56. Ya A Dorfman, M M Aleshkova, M M Kebekbaeva, A S Karinskaya, A K Borangazieva *Zh. Obshch. Khim.* **61** 1101 (1991)
57. Ya A Dorfman, M M Aleshkova, A S Karinskaya *Kinet. Katal.* **32** 188 (1991)
58. Ya A Dorfman, M M Aleshkova, M M Kebekbaeva *Kinet. Katal.* **32** 1349 (1991)
59. Ya A Dorfman, D M Doroshkevich, M M Aleshkova *Kinet. Katal.* **32** 1357 (1991)
60. A Ya Rozovskii *Kinetika Topokhimicheskikh Reaktsii* (Kinetics of Topochemical Reactions) (Moscow: Khimiya, 1974)
61. J Okamoto, T Kusano, S Takamuku *Bull. Chem. Soc. Jpn.* **61** 3359 (1988)
62. J Okamoto, T Kusano, S Takamuku *Phosphorus Sulfur Silicon Relat. Elem.* **55** 195 (1991)
63. Ya A Dorfman, I M Yukht, L V Levina, G S Polimbetova, T V Petrova, V S Emel'yanova *Usp. Khim.* **60** 1190 (1991) [*Russ. Chem. Rev.* **60** 605 (1991)]
64. H H Dunken, V I Lygin *Quantum Chemistry of Adsorption on the Surfaces of Solids* (Translated into Russian; Moscow: Mir, 1980)
65. Ya A Dorfman, L V Levina, E Zh Aibasov, S A Tungatarov, G S Polimbetova *Zh. Obshch. Khim.* **60** 1987 (1991)
66. Ya A Dorfman, L V Levina, T V Petrova, V S Emel'yanova, I V Kel'man, A S Karinskaya *Zh. Obshch. Khim.* **60** 840 (1990)
67. Ya A Dorfman, L V Levina, G S Polimbetova *Koord. Khim.* **17** 280 (1991)

68. Ya A Dorfman, L V Levina, T V Petrova, V S Emel'yanova, G S Polimbetova *Kinet. Katal.* **30** 1483 (1989)
69. G D Zakumbaeva, Ya A Dorfman, N M Popova, in *Soviet-Japanese Seminar on Catalysis, Novosibirsk, 1990* p. 240
70. Ya A Dorfman, L V Levina, T V Petrova, R R Sagandykova, Zh U Ibraimova *Zh. Obshch. Khim.* **59** 1454 (1989)
71. Yu N Kukushkina *Reaktsionnaya Sposobnost' Koordinatsionnykh Soedinenii* (Reactivity of Coordination Compounds) (Leningrad: Nauka, 1987)
72. D S Dohle, T C Jones, C E A Richard, W R Poper *J. Chem. Soc., Chem. Commun.* 865 (1984)
73. C D Ziegler, R F Heck *J. Org. Chem.* **42** 2941 (1978)
74. Ya A Dorfman *Katalizatory i Mekhanizmy Gidrirovaniya i Okisleniya* (Catalysts and Mechanisms of Hydrogenation and Oxidation (Alma-Ata: Nauka, 1984)
75. I V Kel'man, Ya A Dorfman *Razvitie Rabot v Oblasti Kataliza v Kazakhstane* (Development of Studies in the Field of Catalysis in Kazakhstan) (Alma-Ata: Nauka, 1990)
76. Ya A Dorfman, I V Kel'man *Koord. Khim.* **15**, 1022 (1989)
77. Ya A Dorfman, I V Kel'man *Teor. Eksp. Khim.* 654 (1991)
78. N Fischer, N Kollmar *Theor. Chim. Acta* **6** 163 (1970)
79. B N Tsvetkov, N A Bondarenko, N G Malakhova, M I Kabachnik, in *Khimiya i Primenenie Fosfororganicheskikh Soedinenii* (The Chemistry and Applications of Organophosphorus Compounds) (Leningrad: Nauka, 1987)
80. N Beck, I Nadpal *Studies on Complex Formation by the Latest Methods* (Translated into Russian; Moscow: Mir, 1989)
81. G B Shul'pin *Kataliticheskie Reaktsii, Kataliziruemye Kompleksami Metallov* (Catalytic Reactions Catalysed by Metal Complexes) (Moscow, 1989)
82. A E Shilov, G B Shul'pin *Usp. Khim.* **56** 754 (1987) [*Russ. Chem. Rev.* **56** 442 (1987)]
83. A E Shilov, G B Shul'pin *Usp. Khim.* **59** 1468 (1990) [*Russ. Chem. Rev.* **59** 853 (1990)]
84. V I Spitsin, I V Fedoseev *Karbonil'nye Kompleksy Platinovykh Metallov* (Platinum Metal Carbonyl Complexes) (Moscow: Nauka, 1980)
85. V I Perevalova, N B Shitova, L Ya Alyi, V K Duplyakin *Zh. Obshch. Khim.* **58** 1715 (1988)
86. V I Perevalova, N B Shitova, L Ya Alyi *Zh. Obshch. Khim.* **58** 1994 (1988)
87. V I Peshchevitskii, A V Belyaev, R L Shchekochikhina, G D Mal'chikov *Kinetika Reaktsii Zameshcheniya Ligandov v Kompleksnykh Soedineniyakh Platinovykh Metallov i Zolota* (Kinetics of the Ligand Substitution Reactions in Platinum Metal and Gold Complexes) (Novosibirsk: Nauka, 1974)
88. Ya A Dorfman, L V Levina, G S Polimbetova, E Zh Aibasova, A O Kokpanbaeva, T D Ualieva, in *Khimicheskie Sintezy na Osnove Odnouglerodnykh Molekul* (Chemical Syntheses Based on One-Carbon Molecules) (Moscow, 1991) p. 154
89. Ya A Dorfman, L V Levina, E Zh Aibasova, S A Tungatarov, in *Primenenie Metallokompleksnogo Kataliza v Organicheskom Sinteze* (Application of Metal Complex Catalysis in Organic Synthesis (Ufa: Izd. BNTSUrO Akad. Nauk SSSR, 1989) p. 100
90. Ya A Dorfman, L V Levina, D M Doroshkevich *Koord. Khim.* **18** 109 (1992)
91. R C Mehrotra *Coord. Chem. Rev.* **68** 101 (1985)
92. A D Troitskaya, in *Problemy Koordinatsionnoi Khimii. Reaktsionnaya Sbosobnost' Koordinatsionnykh Soedinenii* (Problems of Coordination Chemistry. The Reactivity of Coordination Compounds) (Moscow: Nauka, 1976) p. 7
93. A D Troitskaya, Z L Shmakova *Zh. Neorg. Khim.* **16** 1650 (1971)
94. D E Berry, K A Reverige, J Browning *Can. J. Chem.* **64** 1903 (1986)
95. W Keim *Catalysis in C1 Chemistry* (Translated into Russian; Leningrad, 1987) p. 18
96. C Masters *Homogeneous Catalysis by Transition Metals* (Translated into Russian; Moscow: Mir, 1983)
97. G Klopman, in *Chemical Reactivity and Reaction Paths* (Translated into Russian; Moscow: Mir, 1977) p. 62
98. R G Pearson *Symmetry Rules for Chemical Reactions* (Translated into Russian; Moscow: Mir, 1979)
99. Ya A Dorfman, V I Zakharov, I V Kel'man *Zh. Neorg. Khim.* **36** 2699 (1991)
100. V V Azatyan, S G Gagarin, V I Zakhar'in *Kinet. Katal.* **26** 222 (1985)
101. N P Machara, B S Ault *J. Phys. Chem.* **92** 73 (1988)
102. Ya A Dorfman, G S Polimbetova, G N Nadyrova *Zh. Prikl. Khim.* **64** 1510 (1991)
103. T A Tumanova, I E Flis *Fiziko-khimicheskie Osnovy Otbelki Tsellyulozy* (Physicochemical Foundations of the Bleaching of Cellulose) (Moscow: Lesnaya Prom., 1972)
104. A I Klochkov, V V Malzurin, V P Savel'yanov *Zh. Obshch. Khim.* **60** 71 (1990)
105. L N Mazalov, V D Yumatov, G N Dolenko, in *Khimiya i Primenenie Fosfororganicheskikh Soedinenii* (The Chemistry and Applications of Organophosphorus Compounds) (Leningrad: Nauka, 1987) p. 105
106. K Kellner, A Izschach *Z. Chem.* **24** 365 (1984)
107. R F Hudson *Structure and Mechanism in Organophosphorus Chemistry* (Translated into Russian; Moscow: Mir, 1967)
108. Ya A Dorfman, L V Levina, L I Grekov, in *Mekhanizmy Reaktsii Nukleofil'nogo Zameshcheniya i Prisoedineniya* (The Mechanisms of Nucleophilic and Electrophilic Addition and Substitution Reactions) (Donetsk: 1991) p. 180
109. Ya A Dorfman, L V Levina, L I Grekov *Kinet. Katal.* **30** 662 (1989)
110. Ya A Dorfman, R K Valetdinov, I T Shaikhutdinova, A A Kutuev, in *Khimiya i Tekhnologiya Elementoorganicheskikh Soedinenii i Polimerov* (The Chemistry and Technology of Organoelement Compounds and Polymers) (Kazan: Izd. Kaz. KhTi, 1984) p. 22
111. M A Glushkova, N A Chumaevskii, M M Ershova *Koord. Khim.* **11** 193 (1985)
112. T A Sumarukova, in *Kataliticheskie Reaktsii v Zhidkoi Faze* (Catalytic Liquid-Phase Reactions) (Alma-Ata: Nauka, 1980) p. 154
113. E E Grigoryan, L G Bykova, R F Eremova *Poluchenie Akrilamida Kataliticheskoi Gidratatsiei Akrilonitrila* (The Synthesis of Acrylamide by the Catalytic Hydration of Acrylonitrile) (Moscow: Izd. NIITEKhIM, 1978)
114. V B Chernogorenko, in *Novoe v Poluchenii i Primenenii Fosfidov i Fosfosoderzhashchikh Splavov* (New Developments in the Synthesis and Application of Phosphides and Phosphorus-Containing Alloys) (Alma-Ata: Nauka, 1988) Vol. 1, p. 5
115. Ya A Dorfman, T V Petrova, M Maleshkova, R R Abdreimova, L D Savel'eva, G S Polimbetova, V S Emel'yanova, L V Levina, in *Primenenie Metallokompleksnogo Kataliza v Organicheskom Sinteze* (Application of Metal Complex Catalysis in Organic Synthesis) (Ufa: Izd. BNTS UrO Akad. Nauk SSSR, 1989) p. 98
116. Ya A Dorfman, T V Petrova, L D Savel'eva *Kinet. Katal.* **33** 304 (1992)
117. Ya A Dorfman, T V Petrova, R R Sagadykova *Zh. Obshch. Khim.* **59** 1452 (1989)
118. Ya A Dorfman, T V Petrova, R R Sagadykova *Zh. Obshch. Khim.* **62** 1077 (1992)
119. Ya A Dorfman, T V Petrova, L D Savel'eva, Zh U Ibragimova, R R Sagandykova *Kinet. Katal.* **31** 480 (1990)
120. Ya A Dorfman, T V Petrova, L D Savel'eva *Kinet. Katal.* **33** 304 (1992)
121. Ya A Dorfman, M M Aleshkova, T V Petrova, in *Khimicheskie Sintezy na Osnove Odnouglerodnykh Molekul* (Chemical Syntheses Based on One-Carbon Molecules) (Moscow: Khimiya, 1991) p. 156
122. Ya A Dorfman, T V Petrova, L D Savel'eva, R R Abdreimova, M M Kebekbaeva, R R Sagandykova, L D Savel'eva, D M Doroshkevich *Zh. Obshch. Khim.* **62** 2710 (1992)
123. E Ya Tarat, O G Vorob'ev, O S Balabekov *Ochistka Gazov v Proizvodstve Fosfora i Fosfornykh Udobrenii* (Purification of Gases in the Manufacture of Phosphorus and Phosphorus Fertilisers) (Moscow: Khimiya, 1979)
124. A Lupi, B Chubar *Salt Effects in Organic and Organometallic Chemistry* (Translated into Russian; Moscow: Mir, 1991)

Russian Chemical Reviews **62** (9) 897–906 (1993)
©1993 Russian Academy of Sciences and Turpion Ltd

UDC 547.513+547.466

Aminoacids of the cyclobutane series

F Avotins

Contents

I. Introduction 897
II. Aminocyclobutanecarboxylic acids 897
III. Aminocyclobutyl-substituted carboxylic acids 903

Abstract. The literature data on the methods of synthesis, the reactivities, and biological activities of aminoacids of the cyclobutane series and their derivatives are described systematically and discussed. The bibliography includes 112 references.

I. Introduction

Aminoacids of the cyclobutane series (AACB) are compounds which have been relatively little investigated. Until recently AACB were almost the only type of aminoacids (AA) which have not been detected in natural sources. It was not until 1980 that Bell et al.[1] isolated for the first time 1-aminocyclobutane-1,3-dicarboxylic (2,4-methanoglutamic) and 2,4-methanopyrrolidine-2-carboxylic (2,4-methanoproline) acids from the seeds of the plant *Atelia Herbert Smithii* (*Sophoreae*, *Leguminosae*). Austin et al.[2] isolated in 1987 from the same material yet another achiral non-protein aminoacid—*cis*-1-amino-3-hydroxymethylcyclobutane-1-carboxylic acid, while Adlington et al.[3] discovered in 1983 *trans*-2-amino-1-hydrocyclobutylacetic acid in a dipeptide—an antimetabolite of the unidentified microorganism *Streptomyces species X-1092*. Since biologically active substances with antiviral, neurotropic, analgesic, depressant, antimicrobial, and other activities have been found among AACB derivatives,[4–20] these compounds have attracted the attention of investigators during the recent decades.

In the present review, an attempt is made for the first time to give a systematic account of and to survey studies in which the methods of synthesis, reactivities, and biological activities of AACB and their derivatives are considered. In order to achieve an ordered arrangement of the literature data, we subdivided all the AACB into two groups: aminocyclobutanecarboxylic acids and aminocyclobutyl-substituted carboxylic acids. All the acids and their derivatives in which the carboxy-group is linked directly to the four-membered carbocycle were included in the present review among aminocyclobutanecarboxylic acids. Compounds in which the carboxy-group is separated from the carbocycle by one or several carbon atoms were assigned to the class of aminocyclobutyl-substituted carboxylic acids. In our view, this approach facilitates a systematic treatment of these compounds and also makes it possible to compare their properties and to survey the methods of their synthesis.

F Avotins Riga Technical University, Kalku Street 1, Riga, Latvia, Tel. (7-095) 62 62 21. Fax (7-095) 21 22 06

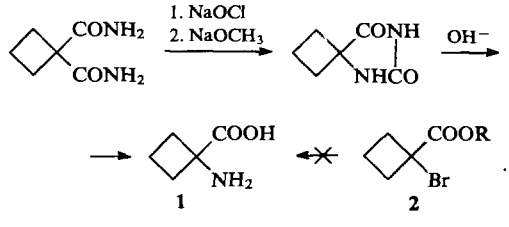
Received 14 May 1993
Uspekhi Khimii **62** (9) 949–958 (1993); translated by A K Grzybowski

II. Aminocyclobutanecarboxylic acids

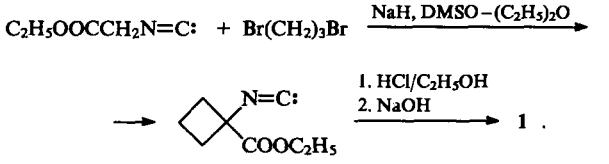
Various methods may be used for the synthesis of aminocyclobutanecarboxylic acids, including both the construction of molecules from individual units containing amino- and carboxy-groups as well as the introduction of the amino-group directly into the cyclobutanecarboxylic molecule.

1. 1-Aminocyclobutane-1-carboxylic acids

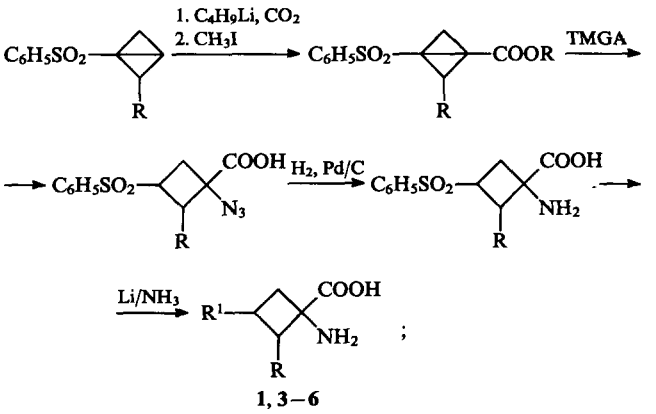
1-Aminocyclobutane-1-carboxylic acid **1** itself is of the greatest interest. Its toxicity is low and it is an inhibitor of the growth of tumours[10, 21] and a selective antagonist of *N*-methyl-D-aspartic acid in relation to the [^{2}H]-receptors of histamine and [^{3}H]-receptors of glycine,[22–25] while its 2-(3-methoxyphenyl) derivative inhibits aminooxidases in rat liver mitochondria.[6] The attempts to obtain compound **1** by the direct ammonolysis of 1-bromo-cyclobutane-1-carboxylic acid **2** (R = H) or its ester **2** (R = CH_3, C_2H_5) by ammonium hydroxide as well as by the reaction of compound **2** with potassium phthalimide (the Gabriel synthesis) or hexamethylenediamine did not yield satisfactory results. The synthesis of compound **1** by this procedure is complicated by the fact that dehydrobromination takes place in the ammonolysis stage, which, according to Connors and Ross[10] and Sudo and Ichihara,[26] leads to the formation of an unsaturated acid with the empirical formula $C_5H_{11}BrN_2O$, the structure of which has not been established. It has also not been possible to obtain compound **1** with the aid of the most often employed two-stage method of synthesis of aliphatic α-aminoacids—by the reaction of α-bromoacids or their esters with sodium azide and the subsequent reduction of the azido-group to the amino-group, since the replacement of the bromine atom in compound **2** by the azido-group was unsuccessful. A more successful preparative method of synthesis of compound **1** is the classical hydantoin synthesis of aminoacids.[10, 11, 27–31] Compound **1** was synthesised by this procedure for the first time as early as 1937,[27] and its yield reached 97%. The initial 5,5-trimethylenehydantoin was obtained by Ingold's method[32] from cyclobutane-1,1-dicarboxylic acid diamide.



The method of synthesis involving the use of ethyl isocyanoacetate and 1,3-dibromopropane has been developed recently for the preparative synthesis of compound **1** (in 95% yield). The reaction was carried out in the presence of sodium hydride in dimethyl sulfoxide/ether or acetone with subsequent stepwise hydrolysis of the intermediate cyclic α-isonitrile.[6, 33–35] Ethyl isocyanoacetate was obtained by dehydrating the ethyl ester of *N*-formylglycine with phosgene[36] or with trichloroacetic acid chloride in the presence of triethylamine.[33]

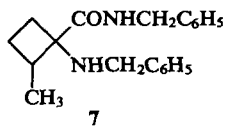


The aminoacid **1** as well as 1-aminocyclobutane-1-carboxylic acids of type **3–6** substituted in the carbocycle and their *N*-derivatives have been synthesised by the regiospecific addition of nitrogen-containing nucleophiles to 1-(arenesulfonyl)-bicyclo-[1.1.0]butane.[37] The synthesis was carried out in four stages: carboxylation of bicyclobutane, introduction of the azido-group by treatment with *N,N,N',N'*-tetramethylguanidinium azide or trimethylsilazide, reduction of the amide, and finally reductive elimination of the arenesulfo-group with lithium in liquid ammonia.

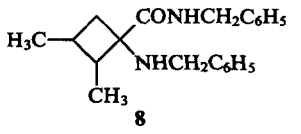


R = R^1 = H (**1**); R = H, R^1 = $C_6H_5SO_2$ (**3**);
R = CH_3, R^1 = $C_6H_5SO_2$ (**4**);
R = CH_3, R^1 = H (**5**); R = R^1 = CH_3 (**6**);
TMGA = *N,N,N',N'*-tetramethylguanidinium azide.

The carboxy-group was introduced into bicyclobutane at −78 °C in solution in hexane or tetrahydrofuran (THF), while the azido-group was introduced in *N*-methyl-2-pyrrolidinone or dimethylformamide (DMF) at 80–90 °C. Although the reaction of bicyclobutane with trimethylsilazide is ten times slower than that with *N,N,N',N'*-tetramethylguanidinium azide, the methoxycarbonyl groups are not solvolysed under these conditions and the corresponding esters are obtained in 92% yield. The aminoacids **1** and **3–6** were isolated on Dowex 50 × 8 ion-exchange resin mainly in the form of the *cis*-isomers. Amides substituted in the amino-group, for example, the benzamide of *N*-benzylmethanovaline **7** and the benzamide of *N*-benzylmethanoisoleucine **8**, were also synthesised in this way.

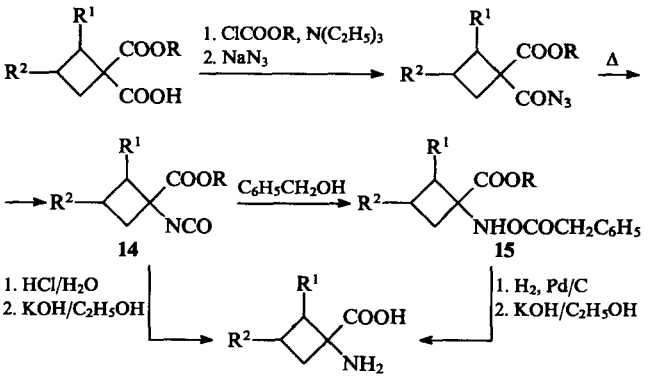


7



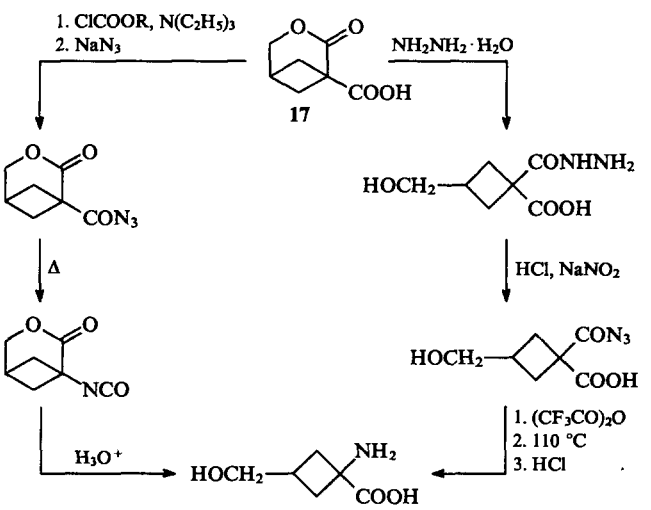
8

The conversion of the carboxy-group into the amino-group by the Curtius method has been used to obtain analogues of compound **1** aryl-substituted in the four-membered carbocycle.[9, 11, 38] A modified Curtius method has been proposed for the synthesis of 1-amino-2-arylcyclobutane-1-carboxylic acids **9** and **10** and 1-amino-3-arylcyclobutane-1-carboxylic acids **11–13**.[39] It is based on the conversion of 2- and 3-arylcyclobutane-1,1-dicarboxylic acids into the corresponding isocyanates of arylcyclobutane-1-carboxylic acids **14**. This was achieved by the successive treatment of the monoesters of cyclobutane-1,1-dicarboxylic acids initially with chlorocarbonic ester in the presence of triethylamine and then with sodium azide and by heating the resulting acyl azide in dry toluene.[38]

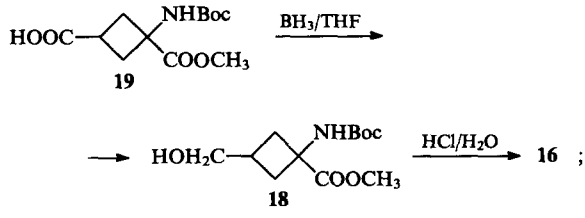


R = CH_3, C_2H_5; R^2 = H; R^1 = C_6H_5 (**9**), 3,4-$CH_2O_2C_6H_3$ (**10**);
R^1 = H; R^2 = C_6H_5 (**11**), 3,4-$(CH_3O)_2C_6H_3$ (**12**), 3,4-$CH_2O_2C_6H_3$ (**13**).

The reaction of the isocyanates **14** with benzyl alcohol made it possible to obtain the aminoacid esters **15** containing the *N*-benzyloxycarbonyl group. The catalytic elimination of the benzyloxycarbonyl group from compound **15** over Pd/C in ethyl acetate and alkaline hydrolysis of the ester group lead to the *trans*-aminoacids **9–13**. The *trans*-aminoacid **13** has been obtained[38] in this way in a yield exceeding 90%. The Curtius reaction has also been used as the key stage in the synthesis of the natural *cis*-1-amino-3-hydroxymethylcyclobutane-1-carboxylic acid(*cis*-**16**)[2] from oxabicyclo[3.1.1]-heptan-2-one-1-carboxylic acid **17**.[40, 41]

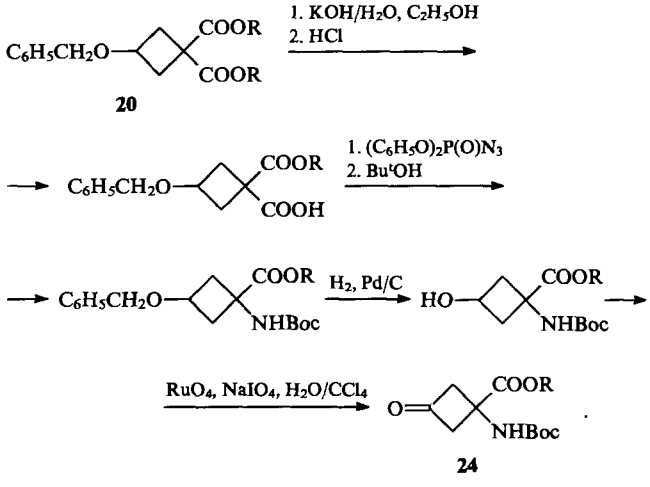


The lactone **17** is converted into the hydrazide, the reaction of which with nitrous acid affords the azide; the rearrangement of the latter in the presence of trifluoroacetic acid anhydride leads to compound *cis*-**16**. The rearrangement of the azide of 3-oxabicyclo[3.1.1]-heptan-2-one-1-carboxylic acid and the subsequent hydrolysis of the resulting isocyanate afforded compound *trans*-**16**, which Hughes and Clardy[42, 43] obtained by acid hydrolysis (yield ~97%) from the methyl ester of *cis*-1-[(*tert*-butoxycarbonyl)amino]-3-(hydroxymethyl)cyclobutanecarboxylic acid **18**, which was synthesised, in its turn, by the selective reduction of the methyl ester of *N*-(*tert*-butoxycarbonyl)-2,4-methanoglutamic acid **19** with borane in THF.



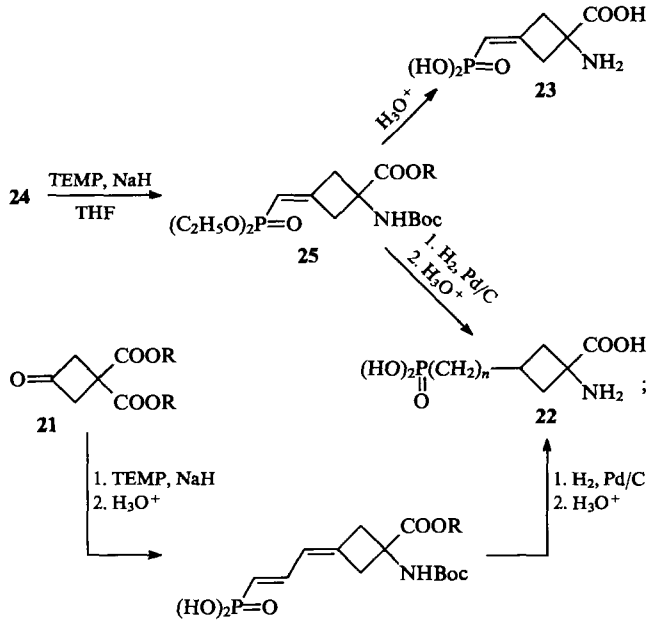
Boc = *tert*-butyloxycarbonyl.

cis- and *trans*-1-Amino-3-phosphonylmethylcyclobutane-1-carboxylic acids **22** (n = 1), 1-amino-3-(3-phosphonylpropyl)cyclobutane-1-carboxylic acid **22** (n = 3), 1-amino-3-phosphonylmethylenecyclobutane-1-carboxylic acid **23**, and their derivatives have been synthesised recently[44] from the esters of 3-benzyloxycyclobutane-1,1-dicarboxylic acid **20** and 3-oxocyclobutane-1,1-dicarboxylic acid **21** in order to investigate them as agonists and antagonists of neurotransmitter aminoacids, in particular *N*-methyl-D-aspartic acid (NMDA). The initial ester of 1-amino-3-oxocyclobutane-1-carboxylic acid **24** was obtained from 3-benzoyloxycyclobutane-1,1-dicarboxylic acid **20** in four stages.[44]



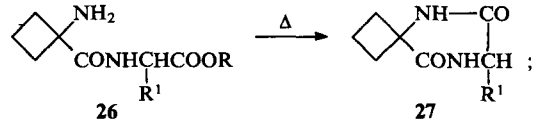
The interaction of the aminoester **24** with tetraethylmethylenebisphosphonate (TEMP) in the presence of sodium hydride leads to the ethyl ester of 1-[(*tert*-butoxycarbonyl)amino]-3-[(diethoxyphosphonyl)methylene]cyclobutane-1-carboxylic acid **25**, the acid hydrolysis of which affords the aminoacid **23** (yield 42%–74%), while the reduction and acid hydrolysis of the unsaturated intermediate ester give rise to a mixture of the *cis*- and *trans*-aminoacids **22** (n = 1) in 33% yield.

cis- and *trans*-1-Amino-3-(3-phosphonylpropyl)cyclobutane-1-carboxylic acids **22** (n = 3) were obtained by a similar procedure in an overall yield of 79% from *cis*- and *trans*-tetraethyl 2-propenylene-1,3-diphosphonate (TEPP) and diethyl 3-oxocyclobutane-1,1-dicarboxylate **21**.



R = C_2H_5; n = 1, 3 .

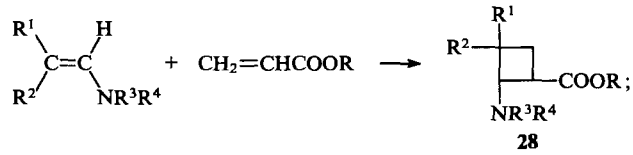
The stereoisomers were separated on Dowex AG50W ion-exchange resin.[44] L-Aspartyl and D-alanyl dipeptides[45, 46] and D-alanyl tripeptides,[45] the structure of which includes compound **1**, have been obtained. The cyclic dipeptides **27** have been synthesised by cyclising the dipeptides having the general formula **26**. They have been recommended for use in medicine and veterinary science.[46]



R = CH_3:
R^1 = H, CH_3, $CH_2CH(CH_3)_2$, $CH(CH_3)_2$, CH_2OH, $C_6H_5CH_2$.

2. 2-Aminocyclobutane-1-carboxylic acids

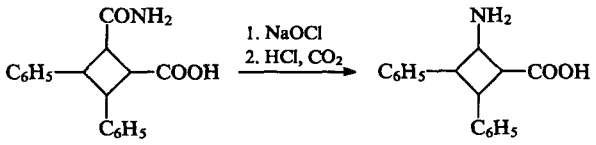
2-Aminocyclobutane-1-carboxylic acids **28** (R = H) are the most numerous among the AACB synthesised and are of interest as biologically active compounds,[7, 17–19, 46–48] antioxidants,[7, 46] and monomers for the synthesis of polyamide resins.[4] Substances with analgesic,[7, 17] anaesthetic,[18] and sedative[7] activities have been discovered among them.



R = CH_3, C_2H_5; R^1 = R^2 = CH_3, C_2H_5;
R^1+R^2 = $(CH_2)_5$; R^3 = R^4 = CH_3, C_2H_5, $CH_3(CH_2)_2CH_2$;
R^3+R^4 = $(CH_2)_5$, $CH_2CH_2OCH_2CH_2$; NR^3R^4 = CN .

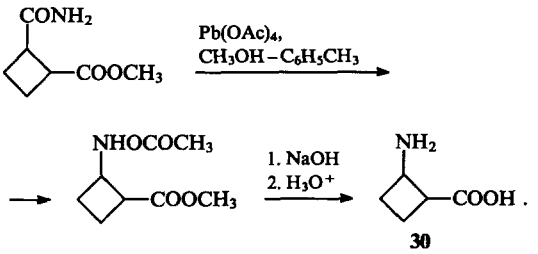
The principal method of synthesis of 2-aminocyclobutane-1-carboxylic acids is the cycloaddition of enamines to electrophilic olefins, for example acrylonitrile and acrylic acid esters.[7, 17, 18, 46, 50–56] Enamines without a hydrogen atom in the β-position, in particular enamines based on isobutenyl, have been mainly used. The reaction was carried out at ~85 °C in solution in acetonitrile (yield ~91%) or in an autoclave at 170–175 °C (yield 70%–75%). 2-(*N*,*N*-Dialkylamino)-3,3-dialkylcyclobutane-1-carboxylic acids **28** (R^1–R^4 = alkyl; R = H) and their esters

and amides have been obtained in this way. Shoemer and Schenk[57] used the Hofmann rearrangement for the synthesis of 2-amino-3,4-diphenylcyclobutane-1-carboxylic acid **29**. The target acid **29** was obtained from β-truxinic acid by treatment with sodium hypochlorite.



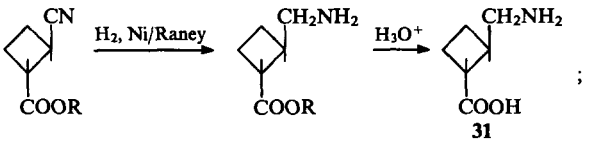
29

Unsubstituted *cis*- and *trans*-2-aminocyclobutane-1-carboxylic acids **30** have been synthesised from the esters of *cis* and *trans*-2-carbamoylcyclobutane-1-carboxylic acids. On treatment with lead tetraacetate, the ester amides were converted into the corresponding esters of *N*-(2-methoxycarbonylcyclobutyl)carbamates, the hydrolysis and decarboxylation of which led to a mixture of *cis*-**30** and *trans*-**30**.[58] The corresponding diastereoisomers were obtained in 56% and 66% yields by resolution on ion-exchange resins.[49]



30

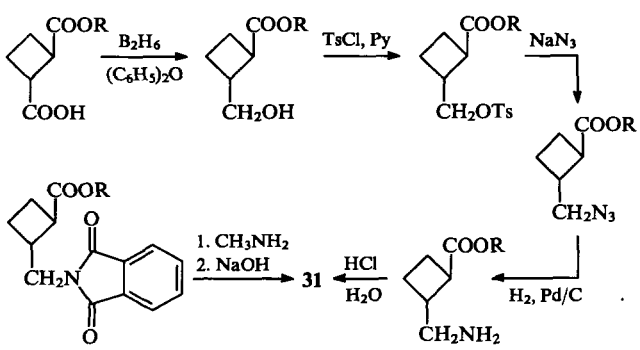
trans-2-Aminomethylcyclobutane-1-carboxylic acid **31** has been synthesised by the catalytic reduction of methyl 2-cyanocyclobutane-1-carboxylic acid and the subsequent acid hydrolysis of the ester. The reduction was carried out over Raney nickel at a pressure of ~14 MPa on heating to 130 °C.



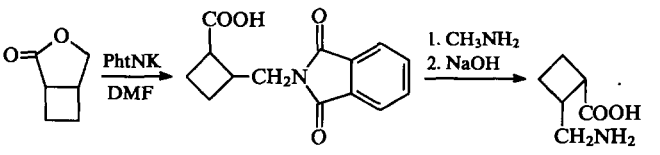
31

R = CH_3, C_2H_5, C_3H_7.

The aminoacid **31** was isolated in ~81% yield by chromatography on ion-exchange resins.[48] Methods in which *trans*-cyclobutane-1,2-dicarboxylic acid and its reaction products were used as the initial compounds have also been proposed for the preparative synthesis of compound **31**.[19, 49, 50] Thus compound **31** has been synthesised from the monoester of *trans*-cyclobutane-1,2-dicarboxylic acid by converting a carboxy-group into an alcoholic group. This was achieved by tosylation and the replacement of the tosyl group (Ts) by the azido-group. After the reduction of the azido-group, the ester of *trans*-2-methylamino-cyclobutane-1-carboxylic acid was obtained in 44% yield. Acid hydrolysis of the ester leads to compound **31** in 72% yield. The aminoacids **31** have also been synthesised by the Gabriel reaction,[50] but in this case the product was obtained in a lower yield (~47%).



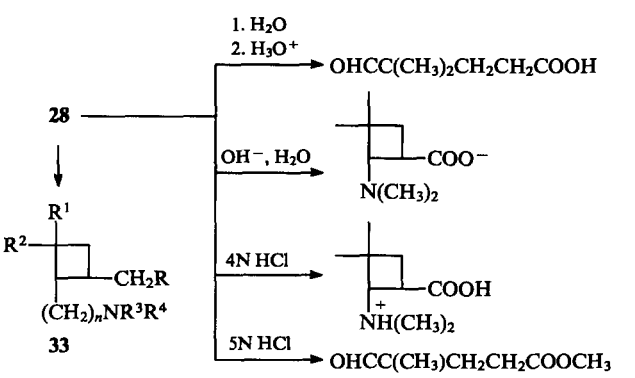
A convenient method of synthesis of *cis*-2-aminomethylcyclobutane-1-carboxylic acid **32** is based on the reaction involving the nucleophilic ring opening in *cis*-3-oxabicyclo[3.2.0]heptan-2-one with potassium phthalimide (PhtNK) and subsequent hydrolysis of the resulting phthalimide derivative with methylamine.[49]

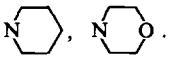


32

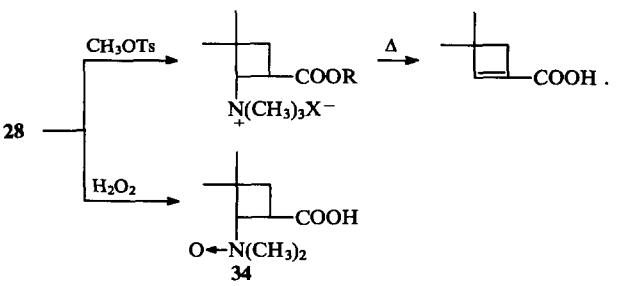
The aminoacid **32** was obtained in 67% yield.[50] Biological studies confirmed the hypothesis that the acids **31** and **32** exhibit a neurotropic activity.

The reduction of the esters **28** with metal hydrides leads to the aminoalcohols of the cyclobutane series **33**.[18, 50, 54–56] Substances with anaesthetic, analgesic, and anticholinergic activities have been discovered among the aminoalcohols **33**. They have been recommended also as intermediates for the synthesis of stabilisers of liquid fuels and for the modification of polymers.



n = 0; R = OH;
R^1 = H, CH_3, C_2H_5;
R^2 = H, C_6H_5, CH_3, C_2H_5;
R^3 = R^4 = CH_3, C_2H_5 or NR^3R^4 = 

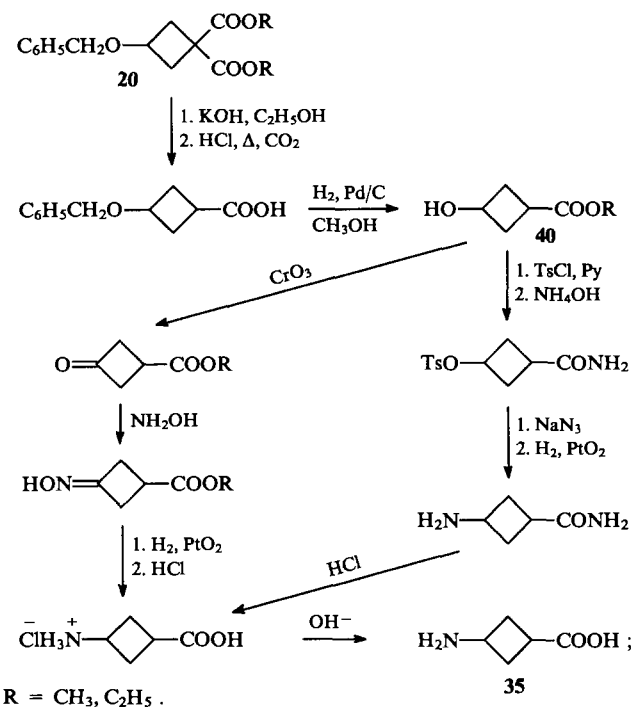
The hydrolysis of the esters **28** ($R-R^4 = CH_3$) in the presence of acids leads to the opening of the cyclobutane ring and the formation of dimethylglutaraldehyde and methyl dimethylglutarate.[52, 54] However, in an alkaline medium the hydrolysis involves only the ester group. The cyclobutane ring is also opened on treatment with Grignard reagents.[54] The quaternisation of the amino-group in compound **28** ($R-R^4 = CH_3$) by methyl tosylate and subsequent elimination of the quaternary amino-group by bases lead to 3,3-dimethylcyclobutene-1-carboxylic acid,[51, 52] whilst oxidation of compound **28** (R = H, $R^1-R^4 = CH_3$) with a H_2O_2 solution affords the *N*-oxide **34**.[52]



34

3. 3-Aminocyclobutane-1-carboxylic acid

Only the *cis*- and *trans*-3-aminocyclobutane-1-carboxylic acids **35**, *cis*-3-amino-2,2-dimethylcyclobutane-1-carboxylic acid **36**, *cis*-3-(α-aminoethyl)-2,2-dimethylcyclobutane-1-carboxylic acid **37**, 3-(β-aminoethyl)-2,2-dimethylcyclobutane-1-carboxylic acid **38**, and 3-amino-2,4-diphenylcyclobutane-1-carboxylic acid **39** have been synthesised in this group of AACB and described. The *cis*- and *trans*-aminoacids **35** and **36** are of interest as cyclobutyl analogues of γ-aminobutyric acid (GABA).[61] A multistage method has been proposed for the synthesis of compound **35**, in which the diester of 3-benzyloxycyclobutane-1,1-dicarboxylic acid **20** was used as the initial compound.[63] Alkaline hydrolysis and decarboxylation of compound **20** led to 3-benzyloxycyclobutane-1-carboxylic acid, which was converted in the presence of the Adams catalyst into the ester of 3-hydroxycyclobutane-1-carboxylic acid **40**. A mixture of the diastereoisomers of compound **35** was obtained from the latter in an overall yield of 25% (relative to the intial ester **40**).

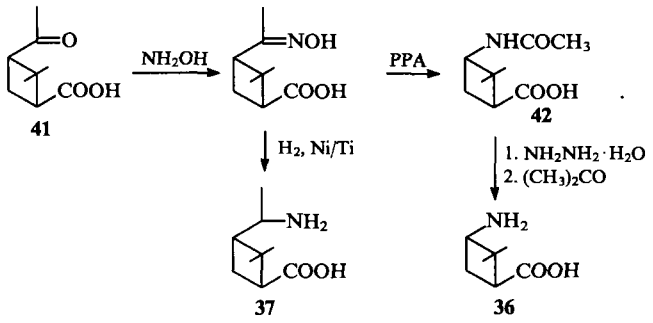


R = CH_3, C_2H_5 .

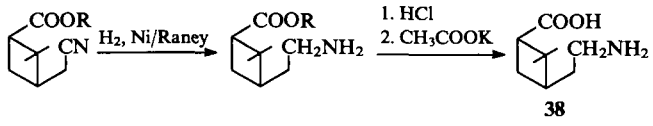
The *cis* : *trans* isomer ratio in the mixture was 1 : 1.8. The isomers were separated by crystallisation from *tert*-butyl alcohol or by chromatography on Dowex 50 × 8 ion-exchange resin. This method is distinguished by high yields at each stage of the process and by the relative availability of the initial compounds.

An alternative approach, involving the oxidation of the ester **40** with chromic acid, the conversion of the carbonyl group of 3-oxocyclobutane-1-carboxylic acid into an oxime group, and subsequent catalytic reduction of the oxime group, also affords a mixture of the diastereoisomers of compound **35** (yield ⩽20%), but the isomer ratio has not been established.[63] The aminoacid **35** exhibits a neurochemical activity, the *cis*-isomer proving to be much more active.[61]

cis-3-Amino-2,2-dimethylcyclobutane-1-carboxylic acid **36** has been synthesised from *cis*-3-acetyl-2,2-dimethylcyclobutane-1-carboxylic (pinononic) acid **41**.[64] 3-Acetamido-2,2-dimethylcyclobutane-1-carboxylic acid **42** was obtained from the ketoacid **41** in accordance with the usual scheme for the Beckmann reaction in polyphosphoric acid (PPA). Its hydrazinolysis with hydrazine hydrate leads to the aminoacid **36**. The catalytic hydrogenation of pinononic acid oxime in the presence of the Ni/Ti catalyst (Lyubarskii's catalyst) at atmospheric pressure afforded *cis*-3-(α-amino-ethyl)-2,2-dimethylcyclobutane-1-carboxylic acid **37** in 87.4% yield.[64]

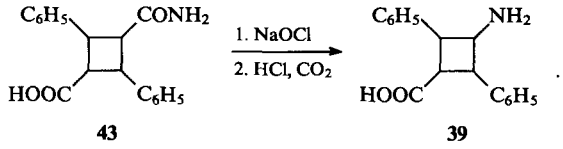


cis-3-(β-Aminoethyl)-2,2-dimethylcyclobutane-1-carboxylic acid **38** has been synthesised under similar conditions form *cis*-(3-ethoxycarbonyl-2,2-dimethyl-1-cyclobutyl)acetonitrile by reduction with hydrogen in the presence of Raney nickel.[65]



R = CH_3, C_2H_5 .

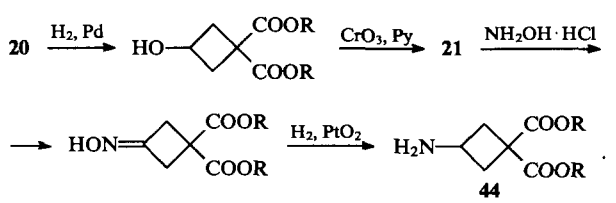
The monoamides of α-, β-, and ε-truxillic acids can be used as the key compounds in the synthesis of 3-amino-2,4-diphenylcyclobutane-1-carboxylic acid **39** by the Hofmann reaction. This was demonstrated in relation to the rearrangement of the monoamide of γ-truxillic acid **43**.[57] The rearrangement was carried out at 30–40 °C in an aqueous solution of sodium hypochlorite. The aminoacid was isolated by neutralising the reaction mixture with HCl and CO_2; the yield of compound **39** was 68% – 80%.



Biological tests showed that aminoacid **37** exerts a weak effect on the vesicular stomatitis virus and inhibits the multiplication of the group A_2 virus in chicken embryos. Among the hydrochlorides of its amides, substances were found with antistaphylococcal and antiviral activities.[64] The aminoacid **36** also exhibits a psychotropic activity, but there is no information concerning more detailed studies of this compound.

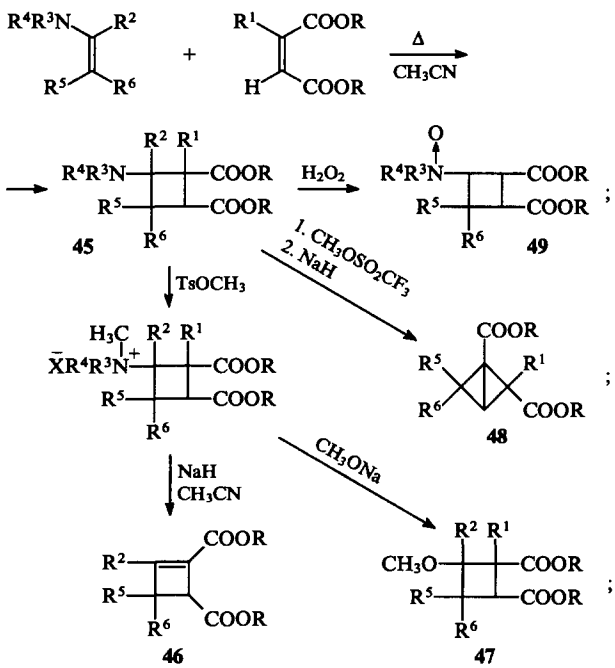
4. Aminocyclobutane-1,1-dicarboxylic and aminocyclobutane-1,2-dicarboxylic acids

Among aminocyclobutane-1,1-dicarboxylic acids, only 3-aminocyclobutane-1,1-dicarboxylic acid **44**, obtained solely as its diethyl ester, is known.[62] Compound **44** has been synthesised from diethyl 3-benzyloxycyclobutane-1,1-dicarboxylate **20** by a procedure similar to that used in the synthesis of compound **35**.[63]



The only examples of aminocyclobutane-1,2-dicarboxylic acids are 3-aminocyclobutane-1,2-dicarboxylic acids **45**, which, like the aminoacid **28**, have been obtained by the cycloaddition of

enamines to electrophilic olefins, in particular to the esters of maleic or fumaric acid.[17, 47, 51, 52, 55, 66] The reaction was carried out at 110–170 °C in solution in acetonitrile. The yields of compounds **45** are 70%–78%. It is noteworthy that the majority of the aminoacids **45** obtained were characterised as the methyl and ethyl esters. Systematic studies of their properties have not been carried out.



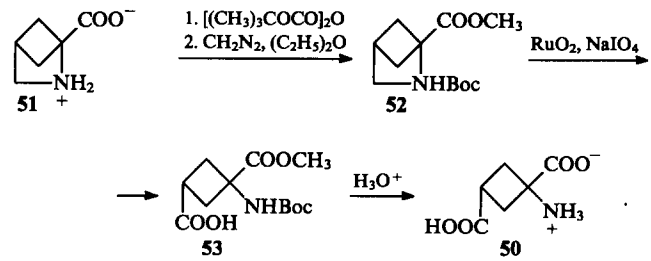
R = R^2 = H, CH_3; R^1 = H, CN, COOMe; R^3 = R^4 = CH_3, C_2H_5; R^5 = R^6 = H, CH_3, C_2H_5; R^6 = H, C_2H_5, $CH_2N(CH_3)_2$;

NR^3R^4 =  .

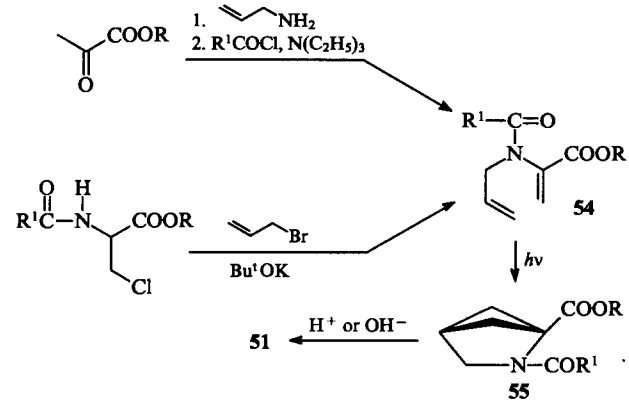
The reduction of the esters **45** (R = CH_3, C_2H_5) with $LiAlH_4$ or $NaBH_3$[55] leads to the corresponding 3-aminocyclobutane-1,2-glycols, which are of interest as intermediates for organic synthesis. As in compound **28**, the amino-group in the aminoacid **45** is quaternised with methyl iodide, methyl tosylate, and methyl trifluoromethane-sulfonate. However, in contrast to compound **28**, the elimination of the quaternary amino-group with sodium hydride, leading to the formation of cyclobutene-1,2-dicarboxylic acids **46**, proceeds only in aprotic solvents (for example, in CH_3CN).[51, 52] On the other hand, on treatment with sodium methoxide in methanol, the quaternary amino-group is replaced by the methoxy-group with formation of the corresponding 3-methoxycyclobutane-1,2-dicarboxylic acid **47**.[66] On quaternisation of 2-methoxycarbonyl-3-(*N*,*N*-dimethylamino)-4,4-dimethylcyclobutane-1,2-dicarboxylic acid **45** (R = CH_3, R^1 = $COOCH_3$, R^2 = H, R^3–R^6 = CH_3) with methyl trifluoromethanesulfonate and the elimination of the quaternary amino-group with sodium hydride, the methyl ester of 4,4-dimethylbicyclo[1.1.0]butane-1,2,2-tricarboxylic acid **48** (R = R^5 = R^6 = CH_3, R^1 = $COOCH_3$, R^2 = H) was obtained.[66] Oxidation of compound **45** with H_2O_2 solution is accompanied by partial hydrolysis and leads to the relatively stable *N*-oxides **49** (R = CH_3; R^1 = R^2 = H; R^3–R^6 = CH_3).

5. Aminocyclobutane-1,3-dicarboxylic acids

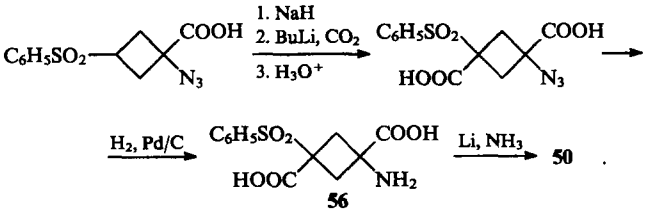
The only known aminocyclobutane-1,3-dicarboxylic acid is *trans*-1-aminocyclobutane-1,3-dicarboxylic(2,4-methanoglutamic) acid **50**, which was isolated form the seeds of *Atelia Herbert Smithii* (*Leguminosae*) together with 2,4-methanopyrrolidine-2-carboxylic acid (2,4-methanoproline) **51**.[1] The stereoisomers of compound **50** are of interest as potential antagonists of the NMDA [*N*-methyl-D-aspartic acid (Translator)] receptors,[44] as therapeutic agents for the treatment of the consequences of ischemia, and as anticonvulsants. They were synthesised by several methods. Hughes and Clardy[41, 42] obtained the achiral aminoacids **50** by oxidising the methyl ester of *N*-(*tert*-butoxycarbonyl)-2,4-methanoproline **52** with sodium metaperiodate and RuO_2 dihydrate in a solvent mixture (H_2O–CH_3CN–CCl_4). The removal of the protecting group by the acid hydrolysis of the intermediate ester of *N*-(*tert*-butoxycarbonyl)-2,4-methanoglutamic acid **53** leads to the aminoacid **50** in ~51% yield (relative to the initial compound **51**).



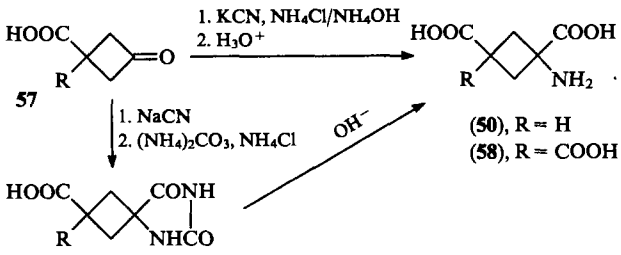
Pirrung[67] synthesised the initial aminoacid **51** from pyruvic acid and allylamine, but the yield of compound **51** proved unsatisfactory for preparative synthesis (~8.5% relative to the initial ester), since the ester of *N*-alkyl-2-acetamidopropenoic acid **54** (R = C_2H_5, R^1 = CH_3) is formed in a low yield and its photocyclisation is complicated by a side reaction and compound **55** was obtained in a yield of only 17%.



A method of synthesis of compound **51** from serine has been proposed.[42, 43] Serine was converted into 2-benzamido-3-chloropropionate, the condensation of which with allyl bromide under an inert atmosphere in the presence of potassium *tert*-butoxide at −78 °C in THF afforded the ester **54** (R = CH_3, R^1 = C_6H_5) and the photochemical cyclisation of the latter led to the ester of *N*-benzoyl-2-azabicyclo[2.1.1]hexane-1-carboxylic acid **55** in a higher yield (87%). Hydrolysis of compound **55** (R = CH_3, R^1 = C_6H_5) afforded compound **51** in 66.5% yield relative to the initial serine. Gaony[37] proposed a synthesis of a mixture of the stereoisomeric aminoacids **50** from 1-(arenesulfonyl)bicyclo[1.1.0]butane similar to the synthesis of the α-aminoacids **1** and **3**–**6**. 1-(Arenesulfonyl)bicyclo[1.1.0]-butane was converted by a standard method (see above) into the azide and then into 3-arenesulfonyl-1-azidocyclobutane-1,3-dicarboxylic acid. The reduction of the azido-group led to 1-amino-3-arenesulfonylcyclobutane-1,3-dicarboxylic acid **56**, from which the benzenesulfonyl group was removed by reductive elimination and a mixture of the stereoisomeric aminoacids **50** was obtained in 25%–30% yield.



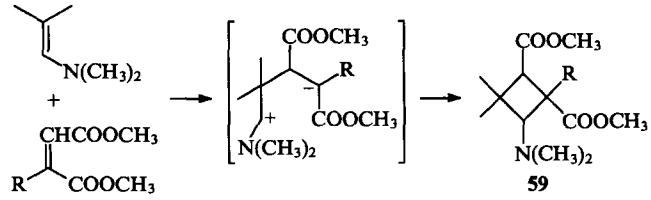
Allan et al.[44] proposed that the stereoisomeric aminoacids **50** be synthesised from 3-oxocyclobutane-1-carboxylic acid by the Strecker reaction. The yield of the aminoacids **50** was ~48% and the ratio of the *cis*- and *trans*-acids in the mixture was 3:2. An alternative synthesis of the aminoacid **50** was achieved by the Bucherer–Bergs reaction.[44] This method gives rise to a better result (overall yield 62%–66%) than the Strecker reaction, but the *cis*:*trans* isomer ratio is in this case 5:1. Pure *cis*- and *trans*-isomers of compound **50** were isolated by chromatography on Dowex AG50W resin in the H^+-form.



Biological tests showed that *trans*-**50** is 20 times more active as an agonist than NMDA; the *cis*-isomer of compound **50** is a third less active as an agonist, but it proved to be more selective.[44, 68]

6. Aminocyclobutanepolycarboxylic acids

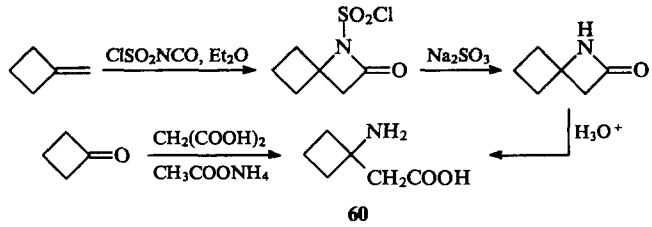
Aminocyclobutanepolycarboxylic acids are little known. 3-Aminocyclobutane-1,1,3-tricarboxylic acid **58** (R = COOH) has been obtained by the Bucherer–Bergs reaction from 3-oxocyclo-butane-1,1-dicarboxylic acid **57** (R = COOH) in solution in methanol.[44] By the cycloaddition of enamines to electron-accepting olefins, in particular by the addition of *N,N*-dimethylisobutenylamine to methyl ethylenetricarboxylate, Hall and Ykman[69] synthesised the trimethyl ester of 4-(*N,N*-dimethylamino)-3,3-dimethylcyclobutane-1,1,2-tricarboxylic acid **59** (R = $COOCH_3$), which was used for the synthesis of bicyclobutane derivatives.



III. Aminocyclobutyl-substituted carboxylic acids

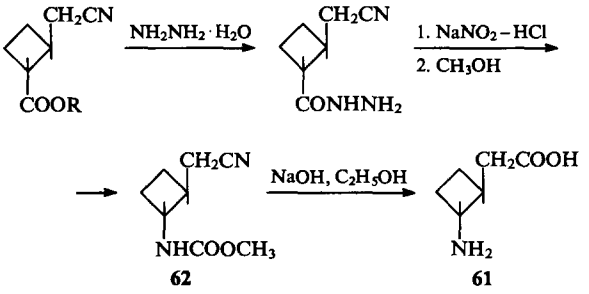
Aminocyclobutyl-substituted carboxylic acids are few in number and have been inadequately studied. Virtually all the known aminoacids of this group have been obtained by the reactions of carboxylic acids, amines, and carbonyl compounds of the cyclobutane series. The classical methods of synthesis of aminoacids have been mainly used to convert the initial compound into aminoacids.

The ability of olefins to form *N*-chlorosulfonyl-β-lactams in their reactions with chlorosulfonyl isocyanate has been used to synthesise the only known compound of this series — 1-amino-cyclobutylacetic acid **60**.[70, 75] The interaction of methylene-cyclobutane with chlorosulfonyl isocyanate led to the synthesis of *N*-chlorosulfonyl-1-azaspiro[3.3]heptan-2-one, the reduction of which with an aqueous solution of sodium sulfite[75] afforded 1-azaspiro[3.3]heptan-2-one.

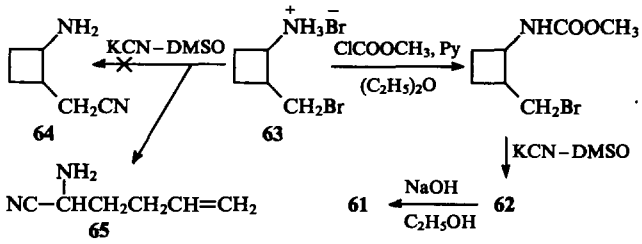


The opening of the β-lactam ring with the aid of hydrochloric acid leads to the aminoacid **60**. An alternative method of synthesis of compound **60**, from cyclobutanone, under the conditions of the Rodionov reaction has been proposed.[70] It was established that higher yields (60%–70%) of the aminoacid **60** were obtained when the monoammonium salt of malonic acid was used and on heating the reactants in solution in dimethyl sulfoxide (DMSO) or DMF. The acid **60** itself was isolated in the form of the neutral zwitter-ion on Dowex AG50W/H^+ and was used to obtain derivatives of 6-aminopenicillanic acid, which exhibit bactericidal activity.[70]

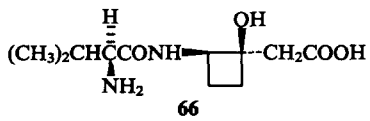
In order to investigate neurotropic activity, *cis*- and *trans*-2-aminocyclobutylacetic acids **61** were synthesised as analogues of GABA with a conformationally limited mobility.[49] *trans* **61** was obtained by a 7-stage synthesis from the diester of *trans*-cyclobutane-1,2-dicarboxylic acid.[19, 49] Using a scheme analogous to the synthesis of compound **31**,[50] the diester was converted into the ester of 2-cyano-methylcyclobutane-1-carboxylic acid.[49] The ester group was replaced by the hydrazide and further by the carbamide group, affording compound **62**. Alkaline hydrolysis of the cyanocarbamate **62** leads to *trans*-**61**.



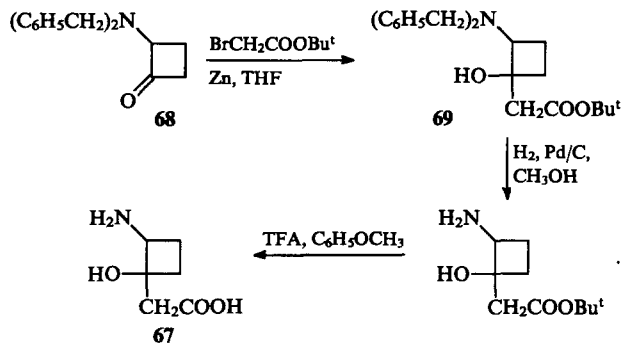
Compound *cis*-**61** was obtained by a similar procedure from the diester of *cis*-cyclobutane-1,2-dicarboxylic acid. The anhydride of *cis*-cyclobutane-1,2-dicarboxylic acid has also been used to synthesise *cis*-**61**.[49] An alternative method of synthesis of *cis*-**61** from the hydrobromide of 2-amino-1-bromomethyl-cyclobutane **63** has been proposed.[49] The conversion of the amino-group of compound **63** into the carbamide group and replacement of bromine by the cyano-group afforded the cyanocarbamate **62**, the hydrolysis of which gives rise to *cis*-**61**. It is noteworthy that the attempts to obtain the aminonitrile **64** by the direct replacement of bromine in compound **63** by the CN group as a result of treatment with potassium cyanide in DMSO at room temperature or on refluxing with sodium cyanide in ethanol led to the opening of the cyclobutane ring and the formation of the nitrile **65**. In the study of the possibility of the binding of *cis*- and *trans*-**61** to the GABA receptor, it was established that *cis*-**61** is a weak inhibitor and *trans*-**61** is a powerful inhibitor of the binding of [^{3}H]muscimol. On the other hand, *cis*- and *trans*-**61** proved to be ineffective as inhibitors of the absorption of [^{3}H]GABA.[49]



The antibiotic X-1092 was isolated from the culture medium of the unidentified microorganisms *Streptomyces species X-1092* under aerobic conditions. It proved to be a dipeptide—(1*S*, 2*S*)-1-hydroxy-2-[(*S*)-valylamino]cyclobutane-1-acetic acid **66**,[3, 72, 73] exhibiting antimicrobial activity on gram-positive and gram-negative microorganisms.



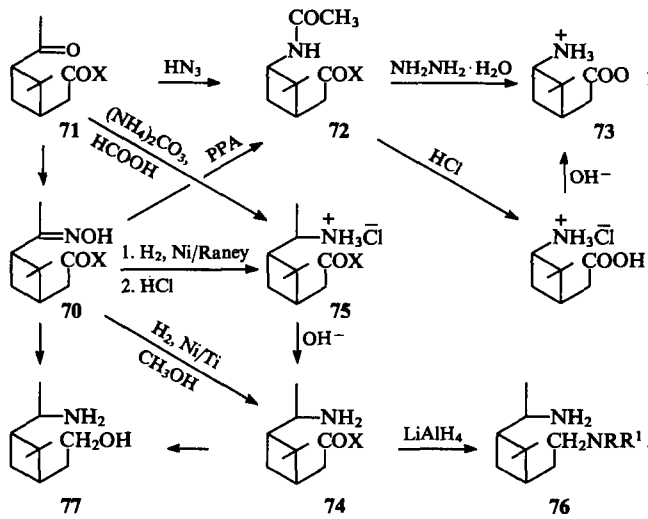
Acid hydrolysis of the dipeptide **66** yielded (1*S*, 2*S*)-2-amino-1-hydroxycyclobutylacetic acid **67**,[3, 72] which also possesses antibacterial activity against gram-positive bacteria. The aminoacid **67** and the dipeptide **66** were synthesised by Baldwin et al.[74], the initial 2-dibenzylaminocyclobutanone **68** being obtained in two stages from diethyl succinate.[76]



The *tert*-butyl acetate group was introduced into the cyclobutanone **68** by the Reformatskii reaction and the resulting mixture of racemic diastereoisomers of the dibenzylamino-alcohols (with a *cis*:*trans* isomer ratio of 8:1) was separated chromatographically on SiO_2, debenzylated, hydrolysed with trifluoroacetic acid (TFA) in anisole, and *cis*- and *trans*-**67** were obtained in 75% and 78% yields respectively (relative to *cis*- and *trans*-**69**) after purification on ion-exchange resins and subsequent high pressure liquid chromatography.

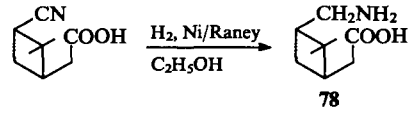
Certain aminocyclobutylacetic acids of the 2,2-dimethylcyclobutane series have been obtained from derivatives of the readily available 3-acetyl- and 3-hydroxycarbonyl-2,2-dimethylcyclobutylacetic (pinonic and pinic) acids.[8, 15, 65, 77–93] The Beckmann rearrangement of the pinonic acid oxime **70** (X = OH)[83, 84] or the interaction of pinonic acid and its esters **71** (X = OH, OR^2) with hydrogen azide (the Schmidt reaction)[15, 78, 81, 82] leads to 3-acetamido-2,2-dimethylcyclobutylacetic acid **72** (X = OH). Hydrazinolysis with hydrazine hydrate or acid hydrolysis of compound **72** affords 3-amino-2,2-dimethylcyclobutylacetic acid **73**.[15, 78, 81, 82, 84] It has been established that the best reagent for the Beckmann rearrangement of the oximes **70** (X = OH, OR^2) is polyphosphoric acid, where the optimum temperature of the rearrangement is 80 to 90 °C, and that the optimum deacylating agent is hydrazine hydrate.[84] The yield of the aminoacid **73** reaches 75.7%.

The amides of 3-acetamido-2,2-dimethylcyclobutylacetic acid **72** (X = NRR^1) have been synthesised under similar conditions from the oximes of pinonic acid amides **70** (X = NRR^1).[84] The amides **75** have been obtained by the reaction of the chloride of 3-amino-2,2-dimethylcyclobutylacetic acid with primary and secondary amines.[84] The aminoacid **73** has been recommended for the synthesis of polymeric materials forming transparent solid coatings.[5] Its esters and ureides are surfactants.[82] The reduction of compound **70** (X = OH) with sodium in isopentyl alcohol[77, 79] or catalytically over platinised nickel, Vavon platinum, Raney nickel,[79, 80, 86–89] and Lyubarskii's catalyst[90, 92, 94–98] leads to 3-(α-aminoethyl)-2,2-dimethylcyclobutylacetic (ε-aminopinanic) acid **74** (X = OH). An alternative method of synthesis of compound **74**—by the rearrangement of compound **71** (X = OH) and its esters **71** (X = OR) in the Leuckart reaction[91]—is less suitable for preparative purposes, since it requires relatively high temperatures (175–190 °C) and the yield of compound **74** (X = OH) does not exceed 33%–45%.

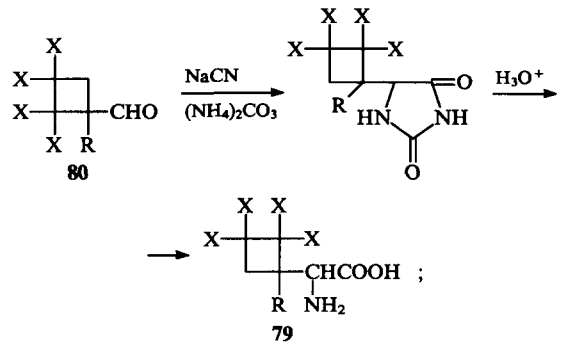


ε-Aminopinanic acid **74** and its esters[99] are of interest as starting materials for the synthesis of biologically active compounds[86–89] and polyamides[90, 91, 93, 100] The aminoacid **74** (X = OH) itself exhibits an antifibrinolytic activity.[8, 16] The hydrochlorides of the amides of ε-aminopinanic acid **75** (X = NRR^1)[95, 97] exhibit an antiviral activity.[101–103] The catalytic reduction or reduction with $LiAlH_4$ of the amides of ε-aminopinanic acid leads to the diamines **76**,[100, 104] while the reduction of the esters **74** (X = OR) leads to the aminoalcohols **77**, which are of interest as biologically active substances[12–14, 18] and as monomers for the synthesis of polymers.[104, 105]

3-Aminomethyl-2,2-dimethylcyclobutylacetic acid **78** has been obtained by the catalytic reduction of 3-cyano-2,2-dimethylcyclobutylacetic acid.[65, 85] The initial nitrile was synthesised in three stages from the monoester of pinanic acid.[65]



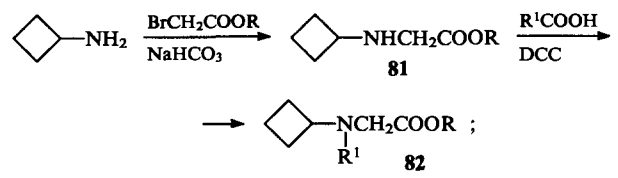
The Bucherer–Bergs method of synthesis of aminoacids has been employed to obtain the cyclobutyl analogue of glycine—α-aminocyclobutylacetic acid **79** (R = X = H) and its derivatives.[20, 106, 107] The unusual aminoacid **79** (R = CH_3, X = F) with the tetrafluorocyclobutyl substituent has also been obtained by this procedure from 2,2,3,3-tetrafluoro-1-methylcyclobutylaldehyde **80** (R = CH_3, X = F).[106]



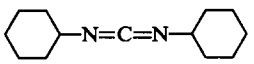
X = H, F;
R = H, CH_3 .

The amide **79** (R = X = H) exhibits a bactericidal activity[20] and certain esters of *N*-aryl-α-cyclobutylglycine exhibit an insecticidal activity.[108] α-Cyclobutylglycine **79** can be used successfully as an alternative substrate for valyl transport RNA-synthetase.[106]

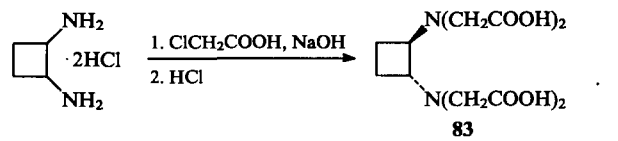
The esters of *N*-cyclobutylaminoacetic acid (*N*-cyclobutylglycine) **81** and the amido-derivatives of the esters **82**, which exhibit a hypotensive activity [antihypertensive (Translator)], have been synthesised by condensing cyclobutylamine with bromoacetic acid esters in the presence of alkaline agents.[109]



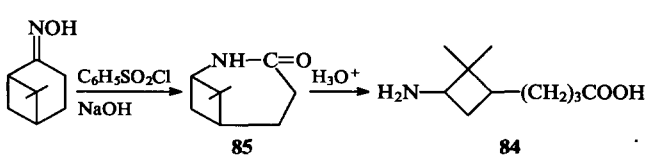
R = H, $C(CH_3)_3$;
R^1 = $COCH(CH_3)CH_2SH$, $COCH(CH_3)CH_2SCOCH_3$;

DCC =  .

trans-1,2-Diaminocyclobutane-*N*,*N*,*N*',*N*'-tetraacetic acid **83** has been obtained in the same way from the dihydrochloride of *trans*-1,2-diaminocyclobutane and monochloroacetic acid.[110] The dihydrochloride of *trans*-1,2-diaminocyclobutane was synthesised by the Curtius reaction from the dihydrazide of *trans*-cyclobutane-1,2-dicarboxylic acid.[111] The aminoacid **83** tends to form chelates with metal ions.



Of the higher AACB, only 3-amino-2,2-dimethylcyclobutylpropionic acid **84** has been described in the literature. It was obtained by the acid hydrolysis of 7,7-dimethyl-2-azabicyclo[4.1.1]octan-3-one **85**.[112] The lactam **85** was synthesised by the Beckmann rearrangement of nopinone oxime with benzenesulfonyl chloride.[112] The aminoacid **84** is also used for the synthesis of polyamides.



As can be seen from the literature data examined in this review, many AACB and their derivatives possess biological activity. They are of independent interest and are also of interest as intermediates in the synthesis of physiologically active and other compounds. On the other hand, their reactivity has been investigated relatively little. The majority of AACB can be obtained by the known methods of synthesis of aliphatic aminoacids. However, not all the methods quoted in this review are of preparative value. Therefore AACB still remain compounds which are difficult to obtain, particularly in the form of pure diastereoisomers and enantiomers. One may therefore expect that further studies on the synthesis of AACB will be directed towards the creation of new preparative methods of synthesis of these compounds from available starting materials and to a more detailed investigation of their reactivity, in particular the investigation of their C- and N-substituted analogues.

References

1. E A Bell, M Y Qureshi, R J Pryce, D H Janzen, P Lemke, J Clardy *J. Am. Chem. Soc.* **102** 1409 (1980)
2. G N Austin, P D Baird, H F Chow, L E Fellows, G W J Fleet, R J Nash, J M Peach, R J Pryce, Ch H Stirton *Tetrahedron* **43** 1857 (1987)
3. R M Adlington, J E Baldwin, R H Jones, J A Murphy, M F Parisi *J. Chem. Soc., Chem. Commun.* 1479 (1983)
4. Jpn. P. 7011315; *Chem. Abstr.* **73** 56624 (1970)
5. US P. 3143529; *Chem. Abstr.* **62** 4132 (1965)
6. Eur. P. 68373; *Chem. Abstr.* **98** 215224 (1983)
7. US P. 3133924; *Chem. Abstr.* **61** 2986 (1964)
8. Fr. P. 2283675; *Chem. Abstr.* **87** 5480 (1977)
9. A Burger, S T Zimmermann *Arznein.-Forsh.* **16** 1571 (1966)
10. T A Connors, W C Ross *J. Chem. Soc.* 2119 (1960)
11. A Burger, W E Cayne *J. Org. Chem.* **29** 3079 (1964)
12. P Schenone, L Mosti, C Bigardi *Farm. Sci. Ed.* **27** 200 (1972)
13. P Schenone, G Minardi, M Longobardi *Farm. Sci. Ed.* **25** 533 (1970)
14. P Schenone, M Longobardi *Bull. Chem. Farm.* **110** 380 (1971)
15. B A Parkin, G W Hendrick *J. Am. Chem. Soc.* **80** 2899 (1958)
16. P Mesnard, J Dupin, R Brasington *Eur. J. Med. Chem. – Chim. Theor.* **10** 315 (1975)
17. Ger. P. 1131207; *Chem. Abstr.* **57** 13642 (1962)
18. US P. 3029275; *Chem. Abstr.* **58** 10130 (1963)
19. J P O'Donnell, D A Johnson, A J Azzaro *J. Med. Chem.* **23** 1142 (1980)
20. BRD P. 2302184; *Chem. Abstr.* **79** 105246 (1973)
21. J B Longobardini, J R Sufrin *Biochem. Pharm.* **32** 489 (1983)
22. W F Hood, E T Sun, R P Compton *Eur. J. Pharm.* **161** 281 (1989)
23. P D Leeson, R Baker, W Robert, R W Carling, R N Curtis, W K Moore, B J Williams *J. Med. Chem.* **34** 1243 (1991)
24. G B Watson, M A Bolanonski, M P Baganoff, A C Foster, A E Donald, J A Kemp, G R Marshall *Eur. J. Pharm.* **167** 291 (1989)
25. N M Gray, M S Dappen, B K Cheng, A A Cordi, J P Biesterfeld, W F Hood, J B Monahan *J. Med. Chem.* **34** 1283 (1991)
26. R Sudo, S Ichihara *Bull. Chem. Soc. Jpn.* **36** 145 (1963)
27. N A Demyanov, S M Tel'nov *Izv. Akad. Nauk SSSR, Ser. Khim.* 529 (1937)
28. A W Coulter, C S Fenselau *Org. Mass. Spectrom.* **6** 105 (1972)
29. K K Chacko, R Zand *Cryst. Struct. Commun.* **4** 17 (1975)
30. J M Conia, J Gore *Bull. Soc. Chim. Fr.* 726 (1963)
31. W Dvonch, H Fletcher, H Alburn *J. Org. Chem.* **29** 2764 (1964)
32. C K Ingold, S Sako, J F Thorpe *J. Chem. Soc.* **121** 1177 (1922)
33. K Ramalingam, D Kalvin, R W Woodard *Label. Comp.* **21** 833 (1984)
34. D Kalvin, K Ramalingam, R W Woodard *Synth. Commun.* **15** 267 (1985)
35. M Jouda, M El Goumzili *Tetrahedron Lett.* **27** 1681 (1986)
36. I Ugi, F Fetzer, U Eholzer *Angew. Chem., Int. Ed. Engl.* **6** 472 (1967)
37. Y Gaony *Tetrahedron Lett.* **29** 1591 (1988)
38. US P. 3345405; *Chem. Abstr.* **68** 49173 (1968)

39. J Weinstock *J. Org. Chem.* **26** 3511 (1961)
40. G W J Fleet, J A Seijas, T M P Vazguez *Tetrahedron* **44** 2077 (1988)
41. H Musso, K Naumann, K Crychtol *Chem. Ber.* **100** 3614 (1967)
42. P Hughes, M Martin, J Clardy *Tetrahedron Lett.* **21** 4579 (1980)
43. P Hughes, J Clardy *J. Org. Chem.* **53** 4793 (1988)
44. R D Allan, J R Hanrahan, T W Hambley, G A R Johnson, K N Mewett, A D Mitrovic *J. Med. Chem.* **33** 2905 (1990)
45. M Rodrigez, J M Bland, J W Tsang, M Goodman *J. Med. Chem.* **28** 1527 (1985)
46. Czech P. 254 868; *Ref. Zh. Khim.* 15O158 (1989)
47. US P. 3 369 024; *Chem. Abstr.* **69** 52010 (1968)
48. Jpn. P. 7 727 154; *Chem. Abstr.* **87** 200907 (1977)
49. P D Kennewell, S S Matharu, J B Taylor, R Westwood *J. Chem. Soc., Perkin Trans.* 2553 (1982)
50. P D Kennewell, S S Matharu, J B Taylor, R Westwood *J. Chem. Soc., Perkin Trans.* 2563 (1982)
51. K C Brannock, A Bell, R D Burpitt, C A Kelly *J. Org. Chem.* **26** 625 (1961)
52. K C Brannock, A Bell, R D Burpitt, C A Kelly *J. Org. Chem.* **29** 801 (1964)
53. K C Brannock, R D Burpitt, J G Thweatt *J. Org. Chem.* **29** 940 (1964)
54. L Weintraub, A Wilson, D L Goldhamer, D P Hollis *J. Am. Chem. Soc.* **26** 4880 (1964)
55. B. P. 985 815; *Chem. Abstr.* **63** 512 (1965)
56. J Madsen, S Lawesson *Bull. Soc. Chim. Belg.* **85** 805 (1976)
57. R Shoemer, F Schenk *Chem. Ber.* **60** 2566 (1927)
58. L F Tieze, A Bergmann, K Brueggemann, in *Photochemical Cycloadditions of Enamine Carboxaldehydes. Mechanism Studies Using Carbon-13 Labelled Precursors* Vortragstag, Fachgruppe Photochem. (Ges. Dtsch. Chem.), 1983, p. 101; *Chem. Abstr.* **102** 5358 (1985)
59. J G Cannon, A B Rege, T L Gruen, J P Long *J. Med. Chem.* **15** 71 (1972)
60. US P. 3 365 451; *Chem. Abstr.* **68** 95384 (1968)
61. R D Allan, D R Curtis, P M Headley *Neurochem. Res.* **5** 393 (1980)
62. J Šafanda, P Sobotka *Collect. Czech. Chem. Commun.* **47** 2440 (1982)
63. M Avram, C D Nenitzescu, M Maxim *Chem. Ber.* **90** 1424 (1957)
64. F M Avotins, A S Gilis, E Gudriniece, B A Spince *Izv. Akad. Nauk Latv. SSR., Ser. Khim.* 339 (1984)
65. H Francois, Le Van Thoi *Bull. Soc. Chim. Fr.* 535 (1967)
66. K C Brannock, R D Burpitt, K W Goodlett, J G Thweatt *J. Org. Chem.* **29** 813 (1964)
67. M C Pirrung *Tetrahedron Lett.* **21** 4577 (1980)
68. T H Lathorn, W F Hood, G B Watson *Eur. J. Pharm.* **182** 397 (1990)
69. H K Hall, P Ykman *J. Chem. Soc., Chem. Commun.* 587 (1974)
70. B. P. 1 415 338; *Chem. Abstr.* **84** 106070 (1976)
71. B. P. 1 419 256; *Chem. Abstr.* **84** 121817 (1976)
72. D L Pruess, J P Scannell, J F Blomist *J. Antibiot.* **27** 754 (1974)
73. US P. 3 939 139; *Chem. Abstr.* **85** 3865 (1976)
74. J E Baldwin, R M Adlington, M F Parisi, Hong-Hoi Ting *Tetrahedron* **42** 2575 (1988)
75. T Durst, M J O'Sullivan *J. Org. Chem.* **35** 2043 (1970)
76. D D Muller, F L Hsu, K N Salman, P N Putil *J. Med. Chem.* **19** 180 (1976)
77. G Gallos, J Montaès *Ann. Quim.* **28** 1163 (1930)
78. US P. 3 031 499; *Chem. Abstr.* **57** 9693 (1962)
79. M Harispe, J Perkin *Bull. Soc. Chim. Fr.* **5** 660 (1950)
80. M Harispe, J Perkin *Bull. Soc. Chim. Fr.* **5** 662 (1950)
81. US P. 3 005 842; *Chem. Abstr.* **56** 2350 (1962)
82. US P. 2 943 110; *Chem. Abstr.* **55** 2521 (1961)
83. W D Lloyd, G W Hedrick *Ind. Eng. Chem., Prod. Res. Dev.* **2** 143 (1963)
84. USSR P. 2 943 110; *Byull. Izobret.* **27** (1973)
85. H Francois, Le Van Thoi *Bull. Soc. Chim. Fr.* 542 (1967)
86. I A Poplavskaya, M I Goryaev *Zh. Org. Khim.* **33** 1492 (1963)
87. M I Goryaev, I A Poplavskaya, in *Puti Sinteza i Izyskaniya Protivoopukholevykh Preparatov* (Methods of Synthesis and Use of Antitumour Preparations) (Moscow: Meditsina, 1967) No. 2, p. 37
88. I N Azerbaev, I A Poplavskaya *Izv. Akad. Nauk Kazakh. SSR, Ser. Khim.* **21** 77 (1971)
89. I A Poplavskaya *Zh. Org. Khim.* **38** 2677 (1968)
90. USSR P. 216 691; *Byull. Izobret.* **15** 28 (1968)
91. F Avotins, E Gudriniece, E Bizdena *Izv. Akad. Nauk Latv. SSR, Ser. Khim.* 484 (1969)
92. F Avotins, A Karklins, E Gudriniece *Izv. Akad. Nauk Latv. SSR, Ser. Khim.* 578 (1968)
93. I Pearl *Forest. Prod. J.* **8** 39 (1958)
94. F Avotins, E Gudriniece *Izv. Akad. Nauk Latv. SSR, Ser. Khim.* 191 (1970)
95. USSR P. 455 097; *Byull. Izobret.* **48** 46 (1974)
96. E Bizdena, E Gudriniece, F Avotins, L L Serebryanska *Izv. Akad. Nauk Latv. SSR, Ser. Khim.* 115 (1972)
97. F Avotins, E Bizdena, E Gudriniece, A Shtals *Izv. Akad. Nauk Latv. SSR, Ser. Khim.* 474 (1978)
98. F Avotins, Z Bore, E Gudriniece *Izv. Akad. Nauk Latv. SSR, Ser. Khim.* 588 (1978)
99. F Avotins, E Bizdena *Izv. Akad. Nauk Latv. SSR, Ser. Khim.* 191 (1970)
100. R W White, S W King, J L O'Braen *Tetrahedron Lett.* **12** 3591 (1971)
101. O T Andreeva, E A Izergina, E Gudriniece, in *Molekulyarnaya Biologiya Virusov, Khimoterapiya i Khimoprofilaktika Virusnykh Infektsii* (Molecular Biology of Viruses. Chemotherapy and Chemoprophylaxis of Viral Infections) (Minsk, 1974) p. 66
102. USSR P. 377 327; *Byull. Izobret.* **50** 43 (1973)
103. E Gudriniece, F Avotins *Izv. Latv. Akad. Nauk* 101 (1990)
104. Dutch P. 6 600 171; *Chem. Abstr.* **66** 11074 (1967)
105. US P. 3 387 021; *Chem. Abstr.* **69** 26858 (1968)
106. J W Anderson, L Fowden *Biochem. J.* **119** 691 (1970)
107. US P. 2 662 915; *Chem. Abstr.* **48** 12795 (1954)
108. Jpn. P. 58-116-442; *Ref. Zh. Khim.* 16O328 (1984)
109. US P. 4 256 761; *Ref. Zh. Khim.* 22O18 (1981)
110. V P Vashinskii, V T Yashunskii *Zh. Org. Khim.* **28** 1056 (1958)
111. E R Buchman, A O Reims, T Skei, M I Schlatter *J. Am. Chem. Soc.* **64** 2696 (1942)
112. H K Hall *J. Org. Chem.* **28** 3213 (1963)

Russian Chemical Reviews **62** (10) 907–918 (1993)
©1993 Russian Academy of Sciences and Turpion Ltd

UDC 541.138.3

Bifunctional electrochemical systems

N D Ivanova, S V Ivanov

Contents

I.	Introduction	907
II.	Formation of a film at the electrode–electrolyte interface	907
III.	Modelling of bifunctional electrochemical systems	911
IV.	Principles of the control of the electrochemical reduction of transition metals	915
V.	Conclusions	916

Abstract. The electrochemical reduction and oxidation of metal ions accompanied by the formation of a film at the electrode–electrolyte boundary is discussed. The formation of a film having a mixed conduction type and consisting of oxide–hydroxide compounds of the metal denotes the presence of a new system: the electrode–film–electrolyte system, called a bifunctional electrochemical system because it can act as an electrolyte and as an electrode simultaneously. The bibliography includes 112 references.

I. Introduction

Interest in the electrochemical reduction and oxidation of transition metals has increased continuously for many decades, in spite of the extensive fundamental studies which have already been reported. This can be attributed to the complexity of the relevant electrochemical reactions, especially in systems containing multivalent metal ions.

When the pH of the cathodic film on an electrode surface differs significantly from its value in the bulk of the electrolyte[3] the intermediate reduction products (compounds of a metal being deposited in lower states of oxidation or compounds of a metal being dissolved in higher states of oxidation) form a cathodic or anodic film whose composition includes compounds able to be discharged directly to the metal.

The formation of this film denotes the presence of a new electrode system (now called a bifunctional system because electrode processes can take place on both sides of the film). The film possesses both electronic and ionic conductivity: the ionic conductivity supports the electrolysis on the side of the electrode and the electronic conductivity supports it on the side of the electrolyte. Hence the film behaves as an electrode towards the electrolyte and as an electrolyte towards the electrode, thus fulfilling two functions simultaneously.

It is therefore of interest to examine electrochemical reduction and oxidation processes from the standpoint of assessing their degree of bifunctionality towards various systems.

N D Ivanova, S V Ivanov Institute of General and Inorganic Chemistry, Academy of Sciences of the Ukraine, prosp. Palladina 32/34, 252 680 Kiev, Ukraine, Tel. (7-044) 444 15 62

Received 12 January 1993
Uspekhi Khimii **62** (10) 963–974 (1993); translated by J I Carasso

II. Formation of a film at the electrode–electrolyte interface

1. Cathodic processes

The presence of a cathodic film was first suggested in the 1920s following a study of one of the most complex of these processes: the electrodeposition of chromium from solutions of chromic acid. The existence of such a film during the electrodeposition of chromium is now generally accepted, and has been confirmed by electrochemical[4–8] and optical methods, by microscopic observations with both still and ciné-film recording,[7–9] and also by an analysis of the zone adjacent to the electrode using special apparatus.[10, 11]

Two types of film (primary and secondary) have been defined, formed on the cathode in a solution of chromic acid in the absence of current and under polarisation respectively.[12, 13] They differ both in their composition and properties and in the mechanism of their formation.

The primary films, formed on the electrode surface before the current is applied, are very thin (~0.02 μm) and almost free from pores; they cover the cathode uniformly and they have an electronic conductivity.[5, 12] The metal atoms of the cathode contribute to their formation, and as a result the primary films formed on different cathodes have different compositions. This explains the effect of the cathode material and of the state of the surface on the nature and structure of the films.[11, 12, 14]

The secondary (truly cathodic) films are formed by the electrochemical reduction of the chromic acid. These films are porous and thicker than the primary films, and they can grow to macroscopic dimensions (~0.1 μm) (0.1 mm? Ed.).[10–12]

Obviously, the properties of the secondary films are independent of the initial state of the electrode surface. It has been suggested[5] that the secondary films have semiconducting properties.

Whereas the presence of a cathodic film is now no longer in doubt there is still a divergence of opinions concerning the influence of foreign ions on the film (and therefore also on the cathodic process). We know[12] that chromium is not deposited from solutions of chromic acid except in the presence of small quantities of H_2SO_4, H_2SiF_6, HF, or HCl. Interest in explaining the role of inorganic acids in the formation of the film was also stimulated by the widely held view[4, 5, 15–18] that chromium is reduced to the metal on the cathode from the film itself.

The direct study of the composition and of the behaviour of the cathodic film during *in situ* electrolysis is a complex problem. Consequently most judgements on the nature of the films have

been based on indirect experimental data.[4, 5] Thus it has been shown[19, 20] that irrespective of the $CrO_3 : H_2SO_4$ ratio in the bulk of the electrolyte this ratio is constant within the film, suggesting the formation of chemical compounds between CrO_3 and H_2SO_4 which are then discharged on the cathode. Possible explanations include the formation[21] of CrO_4^{2-} and Cr^{3+} compounds, complex particles $CrCrO_4^+$ and $CrCrO_4H$, and also the formation of complex compounds of chromium with chromium anions[22-24] and cations, connected through an oxygen bridge: Cr(III)–O–Cr(IV).[19, 22]

Studies of the composition of the cathodic film and of the reduction of chromic acid led many workers to conclude that the layer of liquid adjacent to the cathode may contain Cr^{2+}. This suggestion was first made[25] in the 1930s. In more recent work it has received both indirect and direct confirmation[10, 12]

The presence of bivalent chromium ions in solution denotes their interaction with the chromic acid, which should produce the dimer and hexa-aquo (tervalent) chromium ions (observed experimentally). These results led to the conclusion that the discharge as far as the metallic state is initiated by the bivalent chromium ions, and that the formation of tervalent chromium ions is the result of a secondary chemical reaction.[26]

Since the electrochemical reduction of chromic acid is accompanied by the reduction of H^+ the solution in the layer adjacent to the cathode becomes strongly alkaline, with formation[3, 12, 27] of chromium hydroxides [$Cr(OH)_3$] on the cathode surface by the reaction

$$Cr_2O_7^{2-} + 14H^+ + 6e \longrightarrow 2Cr^{3+} + 7H_2O ,$$

together with a small quantity of $Cr(OH)_2$. Thus the nature of the cathodic film is determined by the character of the interaction of the solid phase of the newly produced hydroxide $Cr(OH)_3$ with the divalent chromium ions and with the ions of the additives (SO_4^{2-}, SiF_6^{2-}, F^-, etc.).[12] The conversion of a finely divided sol into a solution with a molecular degree of dispersion, which has been called[12] a 'phase transformation', is accelerated by a factor of 6–94 in the presence of additive ions, depending on their concentration.

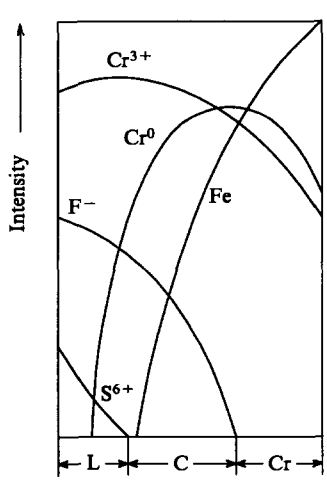


Figure 1. Distribution of the ions in the bulk of the film. Composition of the electrolyte/g dm^{-3}: CrO_3 180; H_2SO_4 0.54; Na_2SiF_6 54; T = 50 °C; i_c = 70 A dm^{-2}; τ = 2 s.

With the aid of recently developed apparatus[10] it was established that the cathodic film formed at the deposition potential of metallic chromium (−1.2 V) consists of two layers (Fig. 1): a dense, sparingly soluble internal layer (the C Layer) and a looser, more soluble external layer (the L layer). The ratio of the L and C layer thicknesses was found[10] to be 10 : 1. In spite of the small thickness of the dense C layer the largest potential drop occurs across this layer because this part of the film has the highest electrical resistance. Some interesting results on the distribution of the ions in the cathodic film have also been reported.[10] Since the electrolyte being studied contained mixed additive ions (SO_4^{2-} and SiF_6^{2-}) the film was found to contain sulfur and F^- ions, but the concentration of F^- decreased sharply on going from the looser to the denser layer, making the interface easily detectable.

A study of the reduction of the CrO_4^{2-} ions in the presence of CH_3COOH by the optical phase contrast method[15] additionally confirmed the presence of at least two layers in the vicinity of the electrode. It was found that if the thickness of the whole film is ~100 μm the main electrode process is confined to a small fraction (~0.01%–0.02%) of the total thickness.

The formation of bivalent chromium compounds which are reduced to the metal during the electrodeposition of chromium in the presence of H_3BO_3 has been established by Auger spectroscopy.[28] It was concluded[28] that the catalytic action of H_3BO_3 consists in the formation of a complex of tetrahydroxy $B(OH)_4^-$ ions with Cr^{3+}, which is then reduced to $Cr(OH)_2$. The latter is dehydrated, forming CrO, which then proceeds to form a complex with the $B(OH)_4^-$ ion, is adsorbed on the cathode surface, and is reduced to the metal. Thus the role of $B(OH)_4^-$ is similar to that of HSO_4^-, but since the hydrolysis constant of H_3BO_3 is small (pK = 9.00) the concentration of $B(OH)_4^-$ ions is also small. This explains the relatively low effect of $B(OH)_4^-$ as compared with that of HSO_4^-.

We may conclude from these observations that the cathodic film formed during the electrochemical reduction of the Cr^{6+} ions consists of lower-valency compounds of chromium formed by an intermediate reduction step.

The products of an intermediate reduction are observed in studies of many cathode processes. Especially interesting in this respect is the electrochemical reduction of the anionic forms of metals, whose deposition takes place with a current yield significantly lower than 100%.

These processes include the electrochemical reduction of the ReO_4^-, MoO_4^{2-}, WO_4^{2-}, and VO_4^{3-} ions. Detailed studies of these systems have established[29] the electrolysis conditions leading to the formation of products of the intermediate reduction of the transition metal ions (in the form of sparingly soluble, often powdery deposits), and also the composition and properties of these compounds. From the totality of the available information it was concluded that the composition of the compounds is described by the general formula $A_2O \cdot xMO_n \cdot yMO_{n-q} \cdot zH_2O$, where A is an alkali metal, ammonium, or hydrogen. The presence of water and of hydroxyl groups connected by hydrogen bonds of various strengths has been demonstrated.[29] The fraction of the current taken up by the formation of these oxygen compounds can be determined from the electrodeposition parameters.[30, 31] For the reduction of the ReO_4^- ions it was shown that the finely divided black deposits are rhenium compounds of various valencies. Since the average of the observed valencies of rhenium was close to 4 it was concluded that both more oxidised and more reduced forms must be present. In the electrochemical reduction of ReO_4^- ions from electrolytes with pH 1–2 the average valency of the rhenium is less than 4: this is attributed[29] to the presence of metallic rhenium in the cathodic deposit.

The formation of rhenium oxide from an aqueous electrolyte of pH ~1.65 has been reported.[32] Polarisation and X-ray diffraction studies have shown that the reduction process takes place in two steps. The first steps produces a film of partially reduced rhenium oxide, whereas in the second step the reduction proceeds to the metallic state. The composition of the oxide is determined by the cathode potential: shifting the potential towards more positive values produces black deposits of rhenium oxides in a higher state of oxidation. The deposition of metallic rhenium (with hydrogen evolution) takes place at potentials below −0.4 V.

Under ordinary conditions metals such as Mo, W, V, Zr and Nb are not deposited from aqueous electrolytes. The products of the incomplete reduction of molybdenum and tungsten have been studied in the greatest detail: the intermediates in the reduction of the MoO_4^{2-} ions are formed sequentially through a series of steps (giving quinque-, quadri-, and tervalent ions respectively), depending on the potential of the electrode, on the composition and temperature of the electrolyte, and on other factors.[33]

In the electrolysis of neutral and of weakly acid solutions of alkali metal molybdates or of ammonium molybdate a black deposit of composition $Mo_2O_3 \cdot 3H_2O$ is formed on the cathode.[29] The kinetics of the deposition and composition of the cathodic films formed in the reduction of MoO_4^{2-} ions have been studied in detail.[29, 34] The average valency of the molybdenum (4.96) was determined by chemical analysis, and the formula $xMoO_{2.4+z} \cdot yH_2O$ was assigned[29] to the compound deposited on the cathode (where $x:y = 1$ and $z = 0.1$). Similar results were obtained in studies of the reduction of molybdates from aqueous chloride solutions. Molybdenum blue, formed on a cathode, was given the formula[35] $MoO_{2.89} \cdot xH_2O$. This nonstoichiometric compound is a semiconductor,[36] and its conductivity is determined by the degree of dehydration.

The formation of a film of insoluble molybdenum oxides and hydroxides in a lower valency state on a cathode has been noted also in studies of the reduction in the presence of metals of the iron subgroup.[37] Experimental data lead to the conclusion that a film consisting of molybdenum compounds in a lower valency state [for example, Mo(III)] is permeable to Fe^{2+} and Ni^{2+} ions even if relatively thick. Introducing these into the film alters its structure and composition: the Mo–O bonds become weaker, bonds between the molybdenum, the iron, and the nickel are formed, and as a result the molybdenum is reduced to the metal with formation of an alloy. The reduction of the iron and of the nickel is also stepwise,[37] and increasing their concentration in the electrolyte increases the rate of reduction of the film.

Molybdenum oxides in a lower state of oxidation formed on a cathode are easily identified and can be used in practice. Thus molybdenum oxide prepared electrochemically has been used as a catalyst[38] and as a functional coating.[38, 39]

The reduction of the WO_4^{2-} ion from acid and from alkaline electrolytes takes place with deposition on the cathode of the lower oxides of tungsten or of a mixture of the oxide and the metal.[40] The composition $Na_2O \cdot nW_2O_5 \cdot mWO_3 \cdot qH_2O$ has been assigned[29] to the cathodic deposit obtained from a solution of Na_2WO_4.

The formation of intermediate reduction products takes place also in the electrochemical reduction of cationic forms of the metal. Thus, in the electrochemical reduction of copper from sulfate[41] and diphosphate[42] electrolytes† on a cathode, sparingly soluble copper compounds have been detected. In the sulfate electrolyte Cu_2O was detected on the cathode[41] in amounts increasing as the current density was decreased. In diphosphate electrolytes also a cathode film was detected:[42, 43] it was formed at all values of the electrode polarisation, and the film itself consisted entirely of univalent copper compounds. In these compounds copper can be reduced to the metallic state during cathodic polarisation in a supporting electrolyte not containing copper.

The presence of a film containing Cu_2O has been observed in a diphosphate electrolyte during a study of the interface by the electroreflectance method.[44] In this case the film was detected, as in a later patent,[45] only at relatively low polarisations (up to -0.1 V). At higher values of the cathodic polarisation the electroreflectance spectra had the characteristic shape of the spectra for metallic copper.

The formation of copper oxides has been established also in sulfate electrolytes at pH > 3 by measurements of the photoelectrochemical effect.[46, 47] It was assumed that the film with *n*-type conduction on the surface of a copper electrode consists of copper oxide. The change in the conductivity type at a well defined potential was attributed to the reduction of CuO to Cu_2O.

The formation of sparingly soluble compounds of the oxide-hydroxide type has been noted[48, 49] in studies of the fluorosilicate copper-plating electrolytes. The role of the concentration of hydrogen ions in the formation of these compounds has been studied by electrochemical reduction methods and by electron-diffraction studies of their composition. As a result it was established that Cu_2O, CuO, and $Cu(OH)_2$ are formed on the copper electrode surface. The relative amounts of these compounds are determined by the pH of the electrolyte: the content of $Cu(OH)_2$ increases with the pH of the solution, and in electrolytes with a low pH value no oxygen compounds are formed (as a rule) on the surface of the copper electrode.

At low current densities $Cu(OH)_2$ is formed in these electrolytes, but the fraction of the current used in this process is small.[48] The most significant process is the reduction of the Cu^{2+} ions. It has been suggested that the increase in the cathodic polarisation is caused by the blocking of the electrode surface by these compounds.[49]

The formation of sparingly soluble copper compounds on the cathode surface increases the cathodic polarisation also in fluoroborate electrolytes.[50]

A solid phase (black zinc) is formed in the electrochemical reduction zinc from a sulfate electrolyte under certain conditions.[51] X-ray diffraction analysis has shown that black zinc consists of finely divided metallic zinc, ZnO, and a small amount of inorganic salt absorbed from the electrolyte. The formation of oxides during the deposition of zinc has also been reported very recently.[52]

Studies of the mechanism of the cathodic deposition of nickel[53] and cadmium[54] have also led to the conclusion that a solid phase is formed on the cathode surface.

The electrolysis of solutions containing $FeCl_2$, $NiCl_2$, $CuCl_2$, $ZnCl_2$, and $PbCl_2$ has produced loose black deposits of composition α–FeOOH, $Ni(OH)_2$, Cu_2O, ZnO, and $PbO \cdot 0.5H_2O$ respectively on the cathode.[55]

The presence of a film of hydroxide on the electrode surface has been established also in the deposition of cobalt from diphosphate electrolytes.[56] In this case the reaction is not the discharge of the unstable diphosphate complex anions $[Co(P_2O_7)_2]^{6-}$ or $[Co(P_2O_7)]^{2-}$, but their dissociation in the cathode layer as a result of the increase in the pH, with formation of a substantial amount of $Co(OH)_2$. Thus, in the electrochemical reduction of cobalt ions the formation of a relatively thick film can be visually observed. The formation of a finely divided sol of composition $\{x[Co(OH)_2] \cdot z[Co(OH)^+]\}$ during the dissociation of the diphosphate cobalt complexes passivates the electrode surface and strongly influences the cathodic process even when the formation of a film cannot be detected visually.[57] A study of the electrocrystallisation of cobalt by the impedance method has shown[58] that the discharge process involves several steps, ultimately leading to the formation of partially reduced cobalt compounds of the $Co(OH)_{ads}$ type, as in the reduction of the Cu^{2+} and Ag^+ ions. This effect is responsible for the inductive component of the Faraday impedance in the low frequency region. On the other hand the composition of the film is determined by the electrolysis conditions.[59]

A study of the polarisation during the electrodeposition of antimony from fluoride electrolytes led to the conclusion[60] that a partially hydrolysed atom of the metal, not containing F^- ions, is contributing to the cathodic process. The retardation of the process at low current densities is attributed to passivation of the surface by oxides, which makes a multistage mechanism possible.[61]

† The term pyrophosphate for these compounds is now obsolete.

Black deposits containing oxides have been observed[62] in the deposition of manganese at potentials up to −0.88 V. The total metal content of these compounds is not more than 70%–80%.

A passivating layer has also been detected on the surface of a gold electrode in weakly acid or in alkaline solutions of $KAu(CN)_2$ by using ellipsometry, Auger spectroscopy, and spectroscopy in the UV and the visible region.[63, 64]

A cathodic film obtained during the deposition of gold from a weakly acid electrolyte consists of $Au(OH)_3$ or Au_2O_3, adsorbed $KAu(CN)_2$, and metallic gold. As reported,[64] the formation of compounds of tervalent gold is due to a disproportionation reaction, involving an unstable compound of univalent gold, induced by the development of alkalinity in the layer of solution adjacent to the cathode. The element composition of the surface layers formed at potentials of −0.33 and −0.88 V, which characterise the initial step of the chemical and the electrochemical gold-plating process respectively, has been determined by Auger spectroscopy. The surface layer formed at −0.88 V is richer in gold than the layer formed at −0.38 V. Under these conditions the total concentration of impurity elements cannot account for complete compound formation by the surface gold, thus showing that metallic gold must be present in the film. After the beginning of the electrolysis the pH of the layer of solution adjacent to the cathode increases from 5.5 to 9.0, thus producing conditions favourable to the formation of insoluble $Au(OH)_3$ on the cathode surface. The compound is initially formed by the oxidation of a univalent gold surface ion by adsorbed and by chemisorbed oxygen. These unstable compounds of univalent gold are subsequently disproportionated to give tervalent gold.

During the initial stage of the electrodeposition of gold from alkaline cyanide solutions the electrode reaction is retarded by the formation of a sparingly soluble film of overall composition $Au_x(OH)_y(CN)_z$ on the cathode. It has been shown by ellipsometric measurements[65] that the thickness of this film of poorly conducting material increases with the concentration of $KAu(CN)_2$. Under these conditions not only the concentration of CN^- ions but also the pH of the electrolyte can strongly influence the coverage of the electrode surface by a film. The maximum coverage is 0.9 monolayer, reached at pH 13.6 and a potential of −0.2 V.

The formation of oxides has been suggested also in the electrodeposition of uranium from an ammonium fluoride solution.[66, 67] The uranium oxide UO_2 is formed on the cathode as a result of the discharge and dissociation of the complex species $UO_2(L)^{n+}$ formed in solution, which migrate to the cathode

$$UO_2(L)^{n+} + ne \rightleftharpoons UO_2 + L ,$$

where L is the ligand of a complexing agent. Since hydrogen evolution takes place simultaneously with metal deposition it is reasonable to assume that the oxide can be reduced by atomic hydrogen:

$$H^+ + e \longrightarrow H^\cdot ,$$

$$UO_2 + 4H^\cdot = U + 2H_2O .$$

Under these conditions (and at low current densities) the metal is deposited together with oxygen-deficient oxides because of the low rate of discharge of H^+. Increasing the current density increases the rate of discharge of hydrogen and of reduction of UO_2 to the metal.

A study of the kinetics and mechanism of the passivation of the electrode during the electrodeposition of gallium from chloride electrolytes[68] has shown that the passivation is due mainly to the formation on the gallium surface of a film of sparingly soluble compounds, described by the general formula $Ga_x O_y H_z Cl_m$.

The cathodic reduction of the TcO_4^- ion has been shown[69–71] to be a multistage process leading to the formation of both compounds of technetium in a lower valence state and metallic technetium. The cathodic processes (deposition of technetium and formation of partial reduction products) take place in parallel, but there is no clear correspondence between changes in their rates.[71]

2. Anodic processes

Films are formed at the electrode–electrolyte interface also during the oxidation of metals, the preparation of oxides, anodic etching, electropolishing, and the chemical machining of metals. In these operations (as in cathodic processes) the film consists of products of variable composition of the oxide-hydroxide type.

A typical example is the oxidation of manganese in alkaline media. The compounds MnO, $Mn(OH)_2$, and MnOOH can be formed on the electrode surface, depending on the pH of the solution and on the polarisation of the electrode.[72] The oxidation process takes place in the solid phase through the interconversion of the different oxide phases:

$$MnO \longrightarrow Mn(OH)_2 \longrightarrow MnOOH \longrightarrow MnO_2 .$$

According to the results[73] of impedance measurements, of the analysis of chronoamperograms, and of measurements with a rotating disk electrode the mechanism of the electrochemical deposition of MnO_2 form solutions of bivalent manganese compounds consists in the formation of intermediate compounds such as MnOOH, Mn_2O_3, and $Mn(OH)_4$, and finally MnO_2. If the rate of conversion of these compounds into MnO_2 is smaller than their rate of formation a layer of intermediates is seen to grow on the outer surface. This layer hinders the transport of the Mn^{2+} ions from the bulk of the electrolyte to the electrode–electrolyte interface. As the thickness of the layer increases, the rate of diffusion of the Mn^{2+} ions changes towards a value comparable to the rate of transformation of the MnOOH and Mn_2O_3 intermediates into MnO_2. This creates a dynamic equilibrium in the electrode–film–electrolyte system.

Film formation takes place also during metal polishing. The electropolishing process depends on the ratio of the rates of formation of the oxide film (on the metal side) and of dissolution of the film (on the electrolyte side). The predominance of either reaction controls the character of the process, i.e. it determines whether etching or polishing is achieved. The highest surface brightness is obtained when he oxide film is as thin as possible (though thick enough to suppress the etching action of the electrolyte). This situation is found under conditions of dynamic equilibrium in the system, when the rates of the electrochemical formation of the film and of its chemical dissolution are equal.[74]

Studies of the capacitance and of the polarisation resistance at the metal–solution boundary during the polishing of steel have shown that under the optimum conditions a capacity minimum is obtained together with a large increase in resistance. This suggests the formation of an oxide film on the metal, since the presence of a salt film could not account for such large changes in the parameters of the electrode–electrolyte boundary.[74] The polishing process is usually carried out in relatively aggressive media, and therefore the ligand composition plays an important role in the dissolution of the film formed on the anode.

The electrochemical treatment of nickel also produces an oxide film (*p*-type) of nonstoichiometric composition on the metal surface. An analysis of the polarisation measurements and of activation energy data has indicated[75] anodic dissolution of the metal within the surface film, and therefore it is reasonable to interpret the role of the formation of films at the electrode–electrolyte boundary as rate-determining in the dissolution.

A similar picture of film formation applies to the polishing and electrochemical machining of metal surfaces. Thus, on the potentiostatic anodic dissolution curves of titanium in alkaline

solutions we observe a decrease in the rate of the process at potentials between −0.5 and −0.7 V, due to the saturation of the anodic layer by the reaction products and to the formation of a porous film of complex composition on the electrode surface.[76]

The oscillations in the electrode potential observed in various cathodic or anodic processes are a consequence of the formation and dissolution of the film. It should be noted that the best polishing results are obtained in the self-oscillatory regime.[77]

III. Modelling of bifunctional electrochemical systems

As was pointed out above, the first step in any electrochemical reduction involving aquo ions of metals (or their complexes with various ligands) or in the electrochemical oxidation of metals is the formation of a film at the electrode–electrolyte interface. The film is a dynamic multilayer system,[78] containing reducible or oxidisable substances in intermediate states of oxidation. The application of a range of research methods to the layer adjacent to the electrode has demonstrated the formation of a film at the phase boundary and its existence for finite times during electrode processes in aqueous and in molten media.

The fundamental property of the films formed at the electrode–electrolyte phase boundary is the presence of a well defined quantitative relationship between the amounts of ionic and of electronic conductivity, which determines the character and the features of the electron transfer process in the electrode–electrolyte system. On the external side of the film (towards the electrolyte) we observe parallel reactions of partial electrochemical reduction of the metal ions being discharged, or their oxidation to the highest oxidation state allowed in the given conditions, or the chemical dissolution of the film by interaction with the components of the solution. On the inner side of the film (towards the electrode) a topochemical process[79] takes place: the further electrochemical reduction to the metal or the electrochemical oxidation of the metal (Fig. 2).

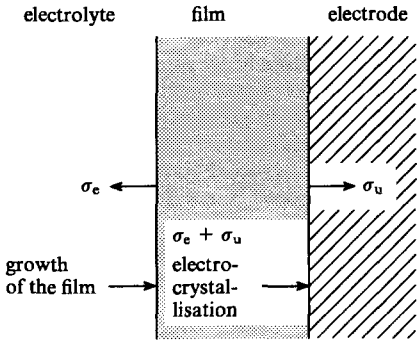


Figure 2. Model of the bifunctional electrochemical system.

The film formed on the electrode surface contributes directly to the electrochemical reactions, which are determined by the physicochemical properties of the film, including its chemical stability towards the reaction medium. A film is formed if the rate of its electrochemical production is greater than the rate of the heterogeneous chemical dissolution process.[80, 81]

The difficulties met in direct studies of the film during its formation and operation stimulated attempts to develop suitable models on the basis of the suggested similarity criteria.[82]

1. Phenomenological description of a model of the bifunctional electrochemical system

Along the normal to the electrode the film is characterised by the nonuniformity of its composition and of its physicochemical properties. We should stress that it is not easy to establish whether a given nonuniformity leads to the formation of discrete phases or whether it merely causes gradual changes in properties. In the former case the model should describe the formation of a sequence of bifunctional systems having a mixed conductivity type. Under these conditions each interface can be associated with one of the successive steps of the electrochemical reduction or oxidation process.

In general the electrochemical step of a cathodic process can be described by the reaction

$$M^{(z-q_{j-1})+} + p_j e \xrightarrow{k_j} M^{(z-q_{j-1}-p_j)+}, \quad (1)$$

where

$$q_{j-1} = \sum_{i=1}^{j-1} p_i$$

is the total number of electrons transferred to an ion during the previous $j-1$ steps of the process; p_j is the number of electrons taking part in the jth step; k_j is the rate constant of the electrochemical process. The reaction products formed under these conditions as a result of the chemical process dissolve on the side of the electrolyte at a constant rate k_j'.

Each of the intermediate phases (from $j = 1$ to $j = m-1$, Fig. 3) is characterised by the average concentration c_j of the partially reduced multivalent metal $M^{(z-q_j)+}$, which is included in the composition of the compounds forming this phase. The electrochemical process leading to the partial solid-phase reduction of the multivalent ions (and to their full reduction at

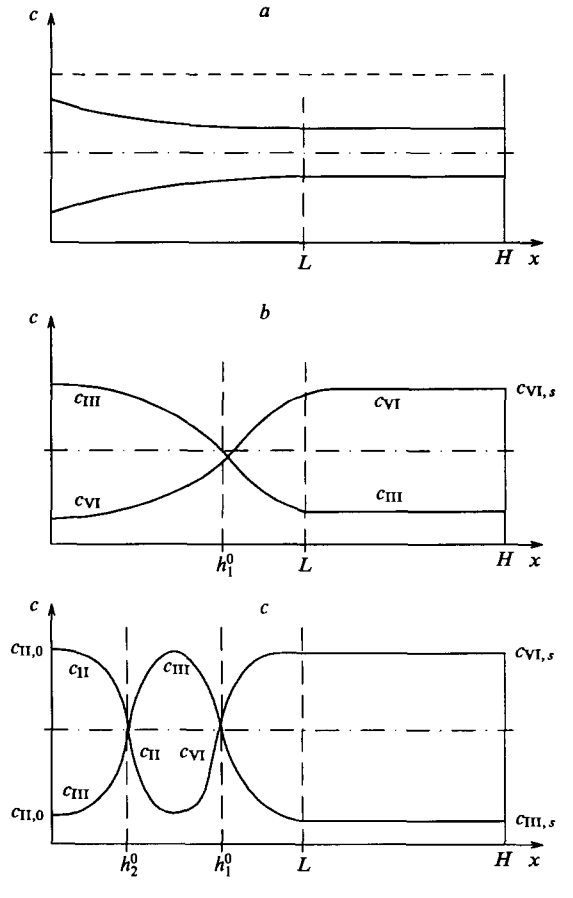


Figure 3. Concentration profile of the partial reduction products in a bifunctional electrochemical system. (*a*) smooth distribution; (*b*) with one boundary ($h_1^0 < L$); (*c*) with two boundaries ($h_2^0 < h_1^0 < L$).

the electrode–film boundary) takes place at increasingly negative potentials of each successive step in the process. The dynamical behaviour of this multilayer structure has recently been described.[78]

The reactions (1), which take place at the interfaces, can lead to changes in the volume of the intermediate phases. For a constant concentration of multivalent metal ions in each layer of thickness h_j the process can be described as follows:

$$c_j \frac{\partial h_j(t)}{\partial t} = Q_{j-1,j} - Q_{j,j+1}\,; \quad j = 1,2,\ldots,(m-1)\,. \tag{2}$$

Here

$$Q_{j,j'} = k_{j,j'} c_j n_{j,j'}^{p_j} - k'_{j,j'} c_j\,; \quad h_j(t)|_{t=0} = 0\,, \tag{3}$$

where $Q_{j,j'}$ is the flux, defined by the total number of multivalent $M^{(z-q_j)^+}$ ions formed in one second as a result of the electrochemical and the chemical processes per unit area of the boundary between phases j and j'; $n_{j,j'}$ is the concentration of conduction electrons in the jth phase near the boundary with phase j'. According to the Tafel equation the rate constant of the electrochemical reaction at the phase boundary is

$$k_{j,j'} = \tilde{k}_{j,j'} \exp(\alpha_{j,j'} e\beta\delta E_{j,j'})\,, \tag{4}$$

where $\alpha_{j,j'}$ is the transfer coefficient; $\beta^{-1} = k_B T$, where k_B is Boltzmann's constant; δ is the average distance between the charge localisation centres; $E_{j,j'}$ is the strength of the electric field at the phase boundary.

Increasing the current I_0 (in the galvanostatic regime) increases the field E_0 at the electrode–electrolyte boundary. When the potential reaches the value corresponding to the electrochemical reduction (1) (which is the first step of the discharge of the metal ions) the ions are reduced to the first intermediate state $M^{(z-p_1)^+}$.

A space charge layer is formed at the metal–semiconductor interface during the growth of the film: the presence of uncompensated charge affects the intensity of the electric field in a volume defined by the space charge region, whose size (in the case of semiconductors) is 10^{-5} to 10^{-4} cm.

The dependence of the electric field intensity on the distance to the cathode surface (where $x = 0$) produces a dependence on x of the rate constant of the electrochemical process, which determines the separation of the phases in space in the bifunctional system for the multistage discharge of multivalent metal ions. The space charge region at the metal–semiconductor interface (bifunctional films usually have semiconductor properties) has been described[80] in terms of the Schottky model on the assumption that the space charge is due mainly to the charge of uniformly distributed ionised donors with a concentration n_0. In this case when the film thickness H is greater than the thickness of the Schottky layer L the field strength in the space charge region ($x < L$) is given by the expression

$$E(x) = E_0 - \frac{en_0}{\varepsilon}(L-x)\,\mathrm{H}(L-x)\,, \tag{5}$$

where

$$L = \left(\frac{2\varepsilon\Delta\varphi}{e^2 n_0}\right)^{1/2}.$$

Here E_0 is the uniform field strength; H is the Heaviside function; ε is the permittivity of the semiconductor; $\Delta\varphi$ is the height of the barrier at the metal–semiconductor interface.

In the region of $0 < x < L$ the concentration of electrons $c_e(x)$ is also dependent on the x coordinate:[83]

$$c_e(x) = n_0 \exp[-\beta\varphi(x)]\,,$$

where

$$\varphi(x) = eE_0(x-L) + \frac{e^2 n_0}{2\varepsilon}(L-x)\,\mathrm{H}(L-x)\,. \tag{6}$$

The presence of a strong electric field $E(x)$ [Eqn (5)] allows the reduction of the multivalent metal ions to proceed in the bulk of the film. The steady state of the film corresponds to equality of the fluxes at the electrolyte–film and electrode–film phase boundaries ($Q_S = Q_0$). The intermediate reduction products are formed when $Q_0 > Q_S$ and the growth rate of the film is

$$V = Q_0 - Q_S\,. \tag{7}$$

When the chemical processes play a dominant role in comparison with the charge transfer process the film is not formed, and therefore the metal deposition is suppressed. This system can be dynamically unstable. The region giving a stable state is determined by the ratio of the rate of the electrochemical process (which depends on the current density) to the rate of the chemical dissolution process (which depends on concentration of the ligand, its nature, the electrolyte temperature, and other parameters).

The mechanism of formation of the bifunctional structure has been examined[80] for the case of the most widely studied of these processes: the electrochemical reduction of the CrO_4^{2-} ions. In this case the kinetic equations which describe processes of type (1) can be written as the following system of equations:

$$\begin{aligned} \frac{dc_{III}(x)}{dt} &= k_1(x)\,c_{VI}(x)\,c_e^3(x) - k'_1 c_{III}(x)\,,\\ \frac{dc_{II}(x)}{dt} &= k_2(x)\,c_{III}(x)\,c_e(x) - k'_2 c_{II}(x)\,,\\ c_{III}(x,t)|_{t=0} &= c_{II}(x,t)|_{t=0} = 0\,, \end{aligned} \tag{8}$$

where k_i, $k_{j'}$ are the rate constants of the reaction, describing the ith process in the discharge of the chromium ions; $k_i(x) = k_i \exp[\alpha_i\beta\delta E(x)]$; $c_{VI}(x,t)$, $c_{III}(x,t)$, $c_{II}(x,t)$ are the concentrations of the chromium ions with a valency of six, three, and two respectively.

The operating regime of the electrochemical system depends on the current flowing through the system. Depending on $E(x)$, i.e. on the current in the system, on the parameters of the Schottky layer, etc., and also on the concentration of the multivalent metal ions at the surface of the film (determined by the rate of the electrochemical processes at the electrolyte–film and the electrode–film boundary), the system of equations (8) can have two solutions, one solution, or no solution.

In the case of large currents, when the field E_0 created by the polarisation of the electrode exceeds the internal field of the Schottky layer, the ion distributions c_{III} and c_{VI} in the film are only slightly dependent on the distance to the electrode (Fig. 3*a*). Decreasing the current brings the field E_0 closer to the field of the electrical double layer, and the system of equations gives successively one solution (Fig. 3*b*) and two solutions (Fig. 3*c*), i.e. an internal multilayer structure is formed in the film under the influence of the field. A further decrease in the current lowers the rate of the electrochemical reaction on the outer surface of the film, and the dissolution of the film becomes the dominant process. The following are the existence criteria of a multilayer structure in the stationary state: for $\tilde{k}_1 c_e < k'$ and $k_2 c_e < k'_2$ the chemical process is dominant in comparison with the electrochemical reduction, and the film is not formed. When the system reaches the $V = 0$ state we observe periodic variations in the rates of growth and dissolution of the film,[84] which leads to oscillations in the potential with a frequency ω_{cr}. In this regime no metal is deposited, as has been observed[82] experimentally. The parameters h_1^0, h_2^0, ω_{cr}, and others, which determine the dynamical behaviour of the bifunctional system, are strongly dependent on the dissolution constants k'_1 and k'_2. In

its turn the parameter k_1' is determined by the nature and concentration c_L of the ligand in the electrolyte and in the bulk of the film, so that the operation of the system can be controlled fairly easily by varying c_L.

The most suitable model of a bifunctional electrochemical system, which allows as fully as possible for all its properties and special features, is provided by the compounds formed on the electrode when the charge transfer process is fixed at an intermediate stage during electrochemical reduction or oxidation. These compounds form a complex electrically conducting heterogeneous system containing the oxides and hydroxides of the appropriate metal in a lower or a higher state of oxidation than in the bulk of the electrolyte, and therefore able to undergo reduction or oxidation. Thus the following similarity criteria between the experimental model and the films actually present on the electrode can be adopted:[85] the presence of low-valency compounds of a mixed conductivity type, and the ability to undergo electrochemical reduction in the solid phase.

2. The presence of low-valency compounds

Let us examine fluorine-containing electrolytes. The rate of formation of partial reduction compounds is determined mainly by the concentration of the F^- ion in the electrolyte and also (to a much lesser degree) by the electrolysis parameters.[86-90] For chromium, nickel, and manganese, which are fairly easily deposited from aqueous solutions, we can define an optimum concentration of the ligand in the electrolyte, offering the maximum rate of formation of the solid phase on the cathode. For molybdenum and zirconium, whose electrode position from aqueous solutions is more difficult, we note a gradual decrease in the rate of deposition of the intermediate reduction products, depending on the concentration of the ligand.

The extent of reduction of the ion being discharged, quantitatively expressed as the total concentration of metal in the solid phase, depends on the concentration of ligand in the electrolyte. In the case of chromium and rhenium it has been shown[91] that this parameter is affected also by changes in the temperature of the electrolyte. An increase in the amount of metal in the deposit produces changes in its properties (colour, microhardness, corrosion resistance). In all the systems which have been examined, including molybdenum and zirconium, a ligand concentration which gives complete reduction to the metal can be identified.

Table 1. Formation conditions and composition of lower-valency oxides.

Metal being discharged	Content of F^- ions in the electrolyte (%)	Total concentration of metal in compound (%)	Phase composition (%)					
			M^0	M^+	M^{2+}	M^{3+}	OH^-	H_2O
Copper	5	92	28	28	–	–	trace	7
	10	95	54	40	–	–		4
	25	97	71	25	–	–		2
	50	99	79	19	–	–		1
Nickel	1	–	85	–	–	–	1.5	1.5
	2	–	90	–	–	–	1.5	1.0
	3	–	98	–	–	–	1.0	1.0
Zinc	2	79	29	–	–	–	8	2
	4	84	40	–	–	–	7	2
	6	87	47	–	–	–	7	1
	8	88	53	–	–	–	6	1
Rhenium	5	66	–	–	–	–	5	4
	10	72	–	–	–	–	4	3.5
	20	88	–	–	–	–	3	3.5
	25	98	–	–	–	–	1	1
Manganese	2	72	25	–	18	29[a]	5	2
	5	83	37	–	19	27[a]	4	2
	8	88	–	–	–	–	4	1
	12	95	–	–	–	–	4	1
Chromium(III)	0	39	7	–	3	29	6	5
	1	42	11	–	4	27	5	4
	2	42	12	–	4	24	4	4
	5	60	21	–	8	31	3	3
Chromium(VI)	0.2	70	30	–	18	22	6	5
	0.4	73	41	–	13	19	5	4.5
	0.6	75	49	–	11	15	5	4.5
	0.8	83	–	–	–	–	4	4
	1.2	90	–	–	–	–	3	4
	2.0	100	–	–	–	–	–	–
Molybdenum	5	56	–	–	–	–	14	9
	10	58	–	–	–	–	13	7
	25	61	–	–	–	–	12	6
Zirconium	5	25	–	–	–	–	–	–
	10	38	–	–	–	–	–	–
	15	58	–	–	–	–	–	–

[a] The total amounts of three- and four-valent manganese are quoted.

Table 2. Composition and rate of oxidation of chromium black.

Valency of chromium	Concentration of chromium in deposits (%)				Rate of deposition/ μm min^{-1}
	Cr_{tot}	Cr^{3+}	Cr^{2+}	Cr^{0}	
II	45–55	10–11	20–27	12–17	3–5
III	45–55	30–35	5–10	5–15	4–5
VI	65–80	7–25	10–20	20–60	0.5–1

The composition of the partial reduction products of various metals is shown in Table 1. We may conclude from these data that the concentration of ligand in the electrolyte determines the amount of metal in the deposit. Thus, for chromium the concentration of metal in the deposits obtained from an electrolyte containing six-valent chromium is higher than in the deposits from tervalent and bivalent chromium electrolytes (Table 2). This effect is produced by a change in the ratio of the rates of (1) the electrochemical formation of lower-valency metal compounds and (2) their further reduction to the metal. The higher the rate of formation of these compounds as compared with the rate of the electrochemical reaction leading to their further reduction, the lower must be the metal content of the deposit. Under these conditions we observe the electrochemical deposition of partially reduced compounds, as indicated by the data in Table 1. Thus the products of the partial reduction of rhenium and molybdenum ions are characterised by the presence of compounds in which the average valency of rhenium is 3 and that of molybdenum is 4.

The metal deposition takes place under conditions of dynamic equilibrium between the processes leading to the formation and to the further reduction of the substances in the cathode film. The presence of low-valency compounds in the solid phase suggests that these compounds exist in the layer adjacent to the cathode and act as a barrier between the bulk of the electrolyte and the reaction zone. At high concentrations of the ligand in solution the lower-valency compounds in the film are electrochemically reduced to the metal, and at low concentrations of the ligand some partial reduction products are formed. By varying the ligand concentration in the electrolyte we can easily control the cathodic process at the partial or the complete reduction stage.

The identical structures and compositions of the intermediate reduction compounds of the chromium, rhenium, manganese, molybdenum, zirconium, copper, nickel, and zinc ions suggest that their reduction processes from aqueous solutions have identical mechanisms irrespective of the form in which the ions exist in the bulk of the electrolyte.

3. Conductivity of the partial reduction products of the metal ions

According to our model of the bifunctional electrochemical system the film should have a mixed (ionic and electronic) conductivity. A quantitative assessment of the relative contributions from the ionic and the electronic conductivity has been made[92] by the pulse method (Table 3).

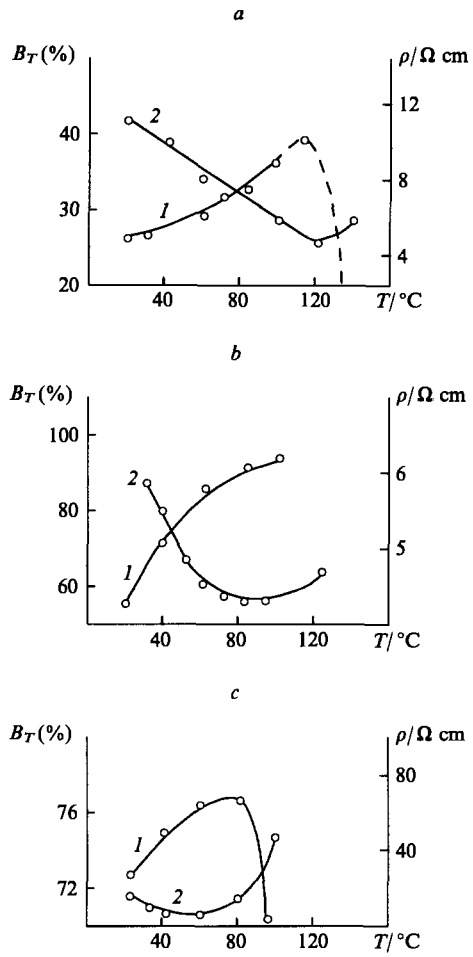


Figure 4. Temperature dependences of the current yield of metal (*1*) and of the resistivity (*2*) of the partial reduction products of chromium (*a*), nickel (*b*), and manganese (*c*).

The results of a study of the temperature dependence of the conductivity by alternating current methods are summarised in Fig. 4. The curves show either a maximum or a minimum, depending on the nature of the system. The systems in which the ionic component makes the larger contribution to the total conductivity (molybdenum, tungsten) show a minimum on the $\ln\sigma = f(T)$ curves, whereas systems in which the ionic conductivity plays a minor role have a maximum (manganese, chromium, nickel) or tend towards a maximum (copper).

A thermogravimetric analysis of these systems at 120 to 160 °C (the upper limit being set by the onset of substantial structural changes in these materials at higher temperatures) revealed the presence of an endothermic effect at 80–120 °C. These effects have only a small influence on the overall conductivity, since an extremum in one of the types of electrical

Table 3. Electrophysical parameters of the cathodic film.

Metal in the system	Temperature of change in slope of the $\ln\sigma-(1/T)$ dependence	Thermogravimetric analysis results: temperature of effects/°C	Total conductivity/Ω^{-1} cm^{-1}		Fraction of ionic conductivity (%)
			alternating current	direct current	
Copper	140	130–140	$2.9\cdot10^{-6}$	$2.6\cdot10^{-6}$	4
Nickel	80–90	80–90	0.22	0.18	8
Manganese	60	60–80	$0.9\cdot10^{-5}$	$0.2\cdot10^{-5}$	10
Chromium	120	120–130	0.25	0.80	11
Molybdenum	90–100	100–120	$1.3\cdot10^{-6}$	$2.4\cdot10^{-6}$	17
Tungsten	110–120	110–130	$0.3\cdot10^{-4}$	$1.5\cdot10^{-4}$	22

conductivity would have been produced if the influence had been large.

The temperature dependence of the conductivity is due to the structural changes associated with the removal of the water of crystallisation and of the OH^- groups, as shown by the correlation with the thermogravimetric analysis results (see Table 3).

Comparing the temperature dependences of the current yield of metal (B_T) deposited under normal conditions and of the resistivity (ρ) of the incompletely reduced compounds also showed a correlation[92] from which it is clear that the higher the electrical conductivity of the system, the higher is the current yield of the metal. This is evidence of a direct dependence of the technological parameters of the electrolysis (rate of deposition of the metals, and current yield) on the physicochemical properties of the cathode film.

4. Electrochemical reduction in the solid phase

An important contribution to the study of cathodic reduction was made by Gorbunova et al.,[93-97] who used a range of electrochemical and structural methods to establish the mechanism of the solid-phase reduction of sparingly soluble compounds (oxides and salts) in protic electrolytes. By applying the Avrami–Erofeev heterogeneous kinetics equation[98] they were able to characterise the process quantitatively. The same approach was used successfully by other workers.[99, 100]

Studies of solid-phase reduction processes have identified diffusional limitations in the solid phase, and also a dependence of the rate of the process on the concentration gradient of oxygen in the phase. Structural studies have established that the process begins at the solution interface and gradually spreads throughout the bulk of the oxide. Under these conditions the composition of the compounds deviates from stoichiometry.[97] Electric fields are formed in the region of the boundary[101, 102] as a result of the changes in concentration and structure.

The process leading to the formation of a metallic phase is localised in the bulk of the compounds of intermediate composition.[103-105]

The possibility of electrochemically reducing compounds of the partial reduction of metals in the anionic (chromium) and the cationic form (copper) in supporting electrolytes not containing ions in common with the solid phase has been demonstrated.[106-108]

The electrochemical reduction[106-108] and the chemical dissolution[109] of these compounds in a supporting electrolyte can be described by the Avrami–Erofeev heterogeneous kinetics equation. The kinetic parameters of these processes for various systems are summarised in Table 4. The rate constants of the electrochemical reduction and of the dissolution of all the compounds used to model the cathodic film are higher in hydrofluoric acid than in sulfuric acid. These data explain the formation of lower-valency compounds only at low concentrations in a hydrofluoric acid electrolyte[82] and the decrease in the rate of the process caused by increasing the concentration of ligand in the electrolyte.

Comparing the rate constants for the heterogeneous dissolution of the lower-valency oxides of chromium and copper in hydrofluoric and in sulfuric acid with the constants of the topochemical electro-reduction of these compounds in the same supporting electrolytes[109] allows us to calculate the role of the chemical processes in the control of bifunctional electrochemical systems.[110, 111]

In the electrodeposition of chromium the contribution of the chemical dissolution reactions of the cathodic film is small, as shown by the small value of the formal rate constant of this process. This accounts for the marked accumulation of film material on the electrode, which can be easily detected, even visually: not surprisingly, cathodic films were first detected in the electroplating of chromium. An entirely different situation is found in the electroplating of copper, because the rates of the chemical dissolution of the cathodic film and of the electrochemical reduction of the film material to the metal are comparable. Evidently, in this case the presence of a film can be detected only under conditions which make the rate of the formation reaction greater than the rates of both the above processes. It is clear that in the electrodeposition of copper film material is difficult to identify and to collect in all electrolytes except those containing fluorine,[112] since the required redistribution of the reaction rates can be achieved only in the latter electrolytes.

Thus the reduction mechanism is determined by the physicochemical properties of the compound: its electrical conductivity and its chemical stability towards the medium chosen for the process. The direct reduction of sparingly soluble compounds in the solid phase is achieved when the electrical conductivity of the substance is reasonably high. In cases of low electrical conductivity reduction takes place only at the points of direct contact between the compound to be reduced and the surface of the current lead. Whether a solid-phase or a liquid-phase mechanism is established depends on the rate of the chemical reaction in the chosen electrolyte: the higher the rate, the greater is the probability of controlling the process through a preliminary dissolution stage.

At a well defined ratio of the rates of the chemical and the electrochemical process the electrochemical reduction becomes possible by both mechanisms. Their relative contributions are determined by the properties of the substance itself and by the composition of the solution, and especially by the nature of the ligand.

IV. Principles of the control of the electrochemical reduction of transition metals

The concept of a bifunctional electrochemical system and the theoretical description of the special features of processes taking place in these systems have allowed us to formulate a set of principles for controlling the electrochemical reduction of transition metals.

Basically the control of electrochemical processes consists in regulating the composition (and therefore also the properties) of the bifunctional electrochemical system by controlled changes in the external factors such as the composition of the electrolyte, the nature and concentration of the ligand, the temperature of the electrolyte, and the current density. These parameters allow us to vary the rate of the electrochemical and of the chemical processes at the electrode–film and electrolyte–film interfaces, and the rates of deposition or of dissolution of the metals (as well as their current yield).

Table 4. Rates of the chemical and of the electrochemical processes in a bifunctional electrochemical system.

System	HF			H_2SO_4		
	K_{chem}/ cm s^{-1}	K_{ec}/ cm s^{-1}	$\lg\beta$	K_{chem}/ cm s^{-1}	K_{ec}/ cm s^{-1}	$\lg\beta$
Copper	$4.41 \cdot 10^{-2}$	$5.8 \cdot 10^{-2}$	0.85	$2.75 \cdot 10^{-2}$	$4.3 \cdot 10^{-2}$	0.50
Molybdenum	$5.07 \cdot 10^{-2}$	–	3.90	$5.01 \cdot 10^{-3}$	–	2.16
Manganese	$5.31 \cdot 10^{-2}$	–	5.48	$3.02 \cdot 10^{-2}$	–	2.30
Chromium	$8.10 \cdot 10^{-6}$	$3.22 \cdot 10^{-1}$	4.4	$1.20 \cdot 10^{-6}$	$9.1 \cdot 10^{-2}$	1.76

Nature and concentration of the ligand. The rates of the electrochemical and of the chemical reactions at the electrode–film and electrolyte–film interfaces are determined by the nature of the ligand and by its concentration, since the stability of the resulting complexes and the rate of dissolution of the partial reduction products are strongly dependent on these factors. We can define an optimum concentration of the ligand in the electrolyte ($c_{L,opt}$) which offers the appropriate ratio of the rates of the electrochemical and the chemical processes.

According to Eqn (7) at concentrations $c_L < c_{L,opt}$ the rate of the electrochemical processes exceeds the rate of the chemical processes. Partial reduction products are formed near the electrode, and are accumulated there. At concentrations $c_L \gg c_{L,opt}$ the rate of the chemical reactions becomes much greater than the rate of the electrochemical reactions, the film cannot be formed, and the new phase is not detected.

Electrodeposition of the metal is observed only for ligand concentrations close to the optimum, i.e. under conditions such that a dynamic equilibrium between the film formation processes and the further reduction of the film material to the metal can be established, i.e. when the equality $Q_S = Q_0$ is obeyed.

On the whole, however, and all other conditions being equal, departures (on either side) of the ligand concentration from the optimum value allow us to vary the composition of the compound formed on the electrode and to create conditions favouring either the electrodeposition or the dissolution of the metal or of its intermediate valency compounds. By varying the metal content of the partial reduction products we can control the ratio of the ionic and the electronic contributions to the electrical conductivity.

Current density. The rate of the electrochemical reactions at the electrode-film and at the electrolyte-film interfaces and within the film itself is determined by the current density. By varying this easily controllable parameter we can impose the required operating regime on the bifunctional electrochemical system. At any given concentration of the ligand we can identify an optimum value of the current density.

For $c_L < c_{L,opt}$ the rate of formation of a new phase on the electrode can be markedly increased by increasing the current density. Because of the relatively small rate of the chemical process at the electrolyte–film interface we can expect the formation of partial reduction products containing a higher proportion of low-valency compounds and a lower proportion of metallic phase. Under these conditions the contribution of the ionic component of the conductivity in the resulting oxides is increased.

For $c_L > c_{L,opt}$ the rate of the chemical process is high, and in order to suppress it (so as to obtain a new phase) we must increase the rate of the electrochemical process, i.e. we must increase the current density.

Electrolyte temperature. Other conditions being equal this factor affects the electrode process less markedly than does the concentration and nature of the ligand, or the current density.

For $c_L < c_{L,opt}$ the rate of the chemical reactions is usually small. Increasing the temperature of the electrolyte increases the rate of the electrochemical reduction processes. The result is an increase in the rate of formation of intermediate-valency compounds on the electrode, and an increase in their content of metallic phase.

For $c_L \gg c_{L,opt}$ increasing the temperature of the electrolyte usually produces predominance of the chemical processes over the electrochemical. As a result a large increase in the current density is needed to bring the bifunctional electrochemical system into dynamic equilibrium. Therefore the temperature dependence of the critical parameters of the process is qualitatively similar to their dependence on concentrations of the ligand.

V. Conclusions

It follows from our discussion that the necessary condition for the electrodeposition or the electrodissolution of the transition metals is the formation of a bifunctional electrochemical system consisting of compounds of the metal ion having a high or a low valency state and a mixed conductivity type. At the electrolyte–film interface the film is formed by the reduction of the metal ions being discharged or by the dissolution of the metal to an intermediate state of oxidation, and at the electrode–film interface the material of the film is consumed by being further reduced to the metal or oxidised to higher valency forms. As a result of the simultaneous occurrence of these processes the film remains continuously in a state of dynamic equilibrium.

Our ability to vary controllably the rate of the processes taking place at the two phase separation boundaries allows the bifunctional electrochemical system to be accurately controlled.

References

1. B G Ershov *Usp. Khim.* **50** 2137 (1981) [*Russ. Chem. Rev.* **50** 1119 (1981)]
2. Yu P Kitaev, T V Troepol'skaya, G K Budnikov *Promezhutochnye Produkty v Elektrokhimicheskikh Reaktsiyakh* (Intermediate Products in Electrochemical Reactions) (Moscow: Nauka, 1982)
3. V S Kublanovskii, A V Gorodynskii, V N Belinskii, T S Glushchak *Kontsentratsionnye Izmeneniya v Prielektrodnykh Sloyakh v Protsesse Elektroliza* (Changes in Concentration Transformations in Layers Adjacent to Electrodes during Electrolysis) (Kiev: Naukova Dumka, 1978)
4. Yu Yu Matulis *Tr. Akad. Nauk Lit. SSR, Ser. B* **3(154)** 3 (1986)
5. H Gerischer, M Käppel *Z. Phys. Chem.* **8** 258 (1956)
6. M Käppel, H Gerischer *Z. Elektrochem.* **72** 235 (1960)
7. Z Kolanko *Powl. Ochr.* **7** 16 (1979)
8. J P Hoare *Plat. Surf. Finish.* **67** 42 (1980)
9. J Chmiel, K Cieszczyk-Chmiel, J Matosik *J. Electroanal. Chem.* **99** 259 (1979)
10. K Yoshida, Y Tsuhahara, K Kuyama *J. Metal. Finish. Soc. Jpn.* **30** 457 (1979)
11. K Yoshida, A Susuki, K Doi, K Arai *J. Metal Finish. Soc. Jpn.* **30** 338 (1979)
12. *Blestyashchie Elektroliticheskie Pokrytiya* (Bright Electrodeposited Coatings) (Vilnius: Mintis, 1979)
13. Yu Yu Matulis, M A Mitskus *Tr. Akad. Nauk Lit. SSR, Ser. B* **1(36)** 57 (1964)
14. V T Stepanenko, A I Vitkin *Zh. Prikl. Khim.* **45** 1247 (1972)
15. F Zin-Cai, D Plecher *J. Appl. Electrochem.* **13** 245 (1983)
16. J P Hoare, M A Laboda, A N Holden *Plat. Surf. Finish.* **79** 101 (1982)
17. M N Shlepakov, A M Sukhotin, Yu P Kostikov, E G Kuz'mina *Elektrokhimiya* **22** 125 (1986)
18. L D Burke, M E Lyons *J. Electroanal. Chem.* **122** 403 (1981)
19. N E Ryan *Metal Finish.* **63** 1 (1965)
20. M A Shluger, E N Osobenkova *Elektrokhimiya* **5** 1070 (1969)
21. Yu Yu Matulis in *Voprosy Teorii Khromirovaniya* (Problems of the Theory of Chromium Plating) (Moscow: Gosizdat, 1959) p. 7
22. V Yu Skominas, B S Radzhyunene *Tr. Akad. Nauk Lit. SSR, Ser. B* **2(153)** 153 (1986)
23. M A Laboda, J P Hoare *Plat. Surf. Finish.* **72** 66 (1985)
24. J P Hoare, M A Laboda *J. Electrochem. Soc.* **132** 798 (1985)
25. N D Biryukov, S P Makarova *Vestn. Metalloprom.* **14** 118 (1934); **5/6** 103; **11** 145
26. J Levitan *J. Electrochem. Soc.* **111** 286 (1964)
27. S S Savel'ev *Elektrokhimiya* **11** 563 (1975)
28. J P Hoare *Plat. Surf. Finish.* **71** 50 (1984)
29. A S Goncharenko, Doctorate Thesis in Chemical Sciences, Alma-Atinsk. Univ., Alma-Ata, 1974
30. V M Gershov, B A Purin *Izv. Akad. Nauk Latv. SSR* **4** 404 (1972)
31. G S Sinyakova, D R Arsh *Izv. Akad. Nauk Latv. SSR* **4** 414, (1976)
32. K Higashi, H Fukushima, O Takamatsu, O Hidetsugu *J. Min. Met. Inst. Jpn.* **95** 467 (1979)

33. V E Mertsalova, E F Speranskaya, D B Malebeeva *Khim. Khim. Tekhnol. (Kaz. SSR)* **5** 72 (1966)
34. A G Samartsev, E I Levitina *Zh. Fiz. Khim.* **32** 1023 (1958)
35. L Sacconi, R Cini *Ann. Chim.* **42** 706 (1952)
36. L Sacconi, R Cini *J. Chem. Phys.* **18** 1124 (1950)
37. A A Golubkov, B P Yur'ev *Zh. Prikl. Khim.* **44** 2419 (1971)
38. USSR P. 336 377; *Byull. Izobret.* **14** 95 (1972)
39. "Le molybdene dans la protection de metaux, et sa protection" *Galvano* **41** 231 (1972)
40. T Inui *J. Met. Finish. Soc. Jpn.* **8** 224 (1957)
41. E I Otglene, I I Zhitkyavichyute, A A Steponavichyus, in *Materialy XII Resp. Konf. Elektrokhimikov Lit. SSR., Vil'nyus, 1973* (Proceedings of the XIIth Conference of Electrochemists of the Lithuanian SSR, Vilnius, 1973) Vol. 1, p. 61
42. R P Sokolov, N A Zotov *Izv. Vuz. Tsv. Metallurgiya* **1** 20 (1972)
43. B A Purin, in *Tez. Dokl. Vsesoyuz. Konf. po Elektrokhimii, Tbilisi, 1989* (Abstracts of Reports of All-Union Conference on Electrochemistry, Tbilisi, 1969) p. 543
44. A G Akimov, E Ya Minenko, M G Astaf'ev, V A Kazakov *Elektrokhimiya* **12** 1619 (1976)
45. V D Reipa, K K Leinartas, R M Vishomirskis *Ellipsometricheskoe Issledovanie Poverkhnosti Katoda v Protsesse Elektroosazhdeniya Medi iz Etilendiaminovykh Rastvorov* (Ellipsometric Investigation of the Surface of the Cathode during the Electrodeposition of Copper from Ethylenediamine Solutions) (Vilnius, 1986) Manuscript deposited in LitNIINTI 23 09 86, No 1725-LI
46. A I Folomeev, in *Issledovaniya v Oblasti Osazhdeniya Metallov* (Investigations in the Field of Metal Deposition) (Vilnius: Mintis, 1985) p. 10
47. N G Krapivnyi, G F Afanas'ev, V I Chernenko *Elektrokhimiya* **13** 315 (1977)
48. Yu Yu Matulis, S P Pilite, S B Yankauskas *Issledovanie Protsessa Elektroosazhdeniya Medi iz Kremneftoristykh Elektrolitov Medneniya* (Investigation of the Process of Copper Electrodeposition from Fluorosilicate Electrolytes used in Copper Plating) (Vilnius, 1980) Manuscript deposited in LitNIINTI 26 09 80, No 614-80
49. S B Yankauskas, S P Pilite, Yu Yu Matulis, in *VI Vsesoyuz. Konf. po Elektrokhimii, Moskva, 1982, Tez. Dokl.* (The VIth All-Union Conference on Electrochemistry, Moscow, 1982, Abstracts of Reports) p. 334
50. I R Shikshnene, S P Pilite, Yu Yu Matulis *Issledovanie Protsessa Elektroosazhdeniya Medi iz Ftoroboratnykh Elektrolitov. I. Vliyanie Sostava Elektrolita na Katodnuyu Polyarizatsiyu Medi* (Investigation of the Process of Copper Electrodeposition from Fluoroborate Electrolytes. I. The Effects of Electrolyte Composition on Cathodic Polarization of Copper) (Vilnius, 1981) Manuscript deposited in LitNIINTI 08 09 81, No 756-81
51. E D Kochman, A M Nagornyi, G G Krinari, in *Khimicheskie i Elektrokhimicheskie Metody Zashchity Metallov* (Chemical and Electrochemical Methods of Protection of Metals) (Saratov, 1977) p. 32
52. C Cathet, B Saidani, R Wiart *J. Electrochem. Soc.* **138** 678 (1991)
53. B Le Gorres, These Doct. Univ. Sci. et Med., Grenoble, 1972, p. 36
54. G Statulyavichyus, Yu Shivitskis *Chemija* **4** 66 (1992)
55. V P Chalyi, in *Tr. IV Soveshch. po Elektrokhimii Akad. Nauk SSSR* (Proceedings of the IVth Conference on Electrochemistry of the Academy of Sciences of USSR) (Moscow: Izd. Akad. Nauk SSSR, 1959) p. 517
56. B A Purin, O B Kiselev, G A Ozol'-Kalnin' *Izv. Akad. Nauk Latv. SSR* **2** 245 (1970)
57. N A Bugene, L V Orlovskaya, F P Frolova, V S Rachinskas *Tr. Akad. Nauk Lit. SSR, Ser. B* **6(127)** 39 (1981)
58. F Lenoir, R Wiart *Metaux* **47** 59 (1972)
59. S P Semashka, V V Kadzyauskene, A K Byarnotas *Elektroosazhdenie Kobal'ta iz Yablochnokislykh Elektrolitov* (Electrodeposition of Cobalt from Malic Acid Electrolytes) (Vilnius, 1986) Manuscript deposited in LitNIINTI 15 08 86, No 1695-LI
60. V M Bigelis, M N Takhirova *Dokl. Akad. Nauk Uzb. SSR* **2** 19 (1983)
61. V M Bigelis, M N Takhirova *Dokl. Akad. Nauk Uzb. SSR* **6** 23 (1983)
62. R I Agladze, S N Basmanova, Dzh A Metreveli *Soobshch. Akad. Nauk Gruz. SSR* **73** 621 (1974)
63. V D Reipa, R M Vishomirskis, in *Issledovaniya v Oblasti Osazhdeniya Metallov* (Investigations in the Field of Metal Deposition) (Vilnius, 1985) p. 62
64. G A Kurnoskin, A N Moskvichev, V N Flerov, V A Sidorov, A I Finkel'shtein *Izv. Vyssh. Uchebn. Zaved., Khim. Khim. Tekhnol.* **29** 77 (1986)
65. V D Reipa, R M Vishomirskis *Tr. Akad. Nauk Lit. SSR, Ser. B* **4(149)** 44 (1985)
66. M M Elsemongy, Y A Elewady, M M Gouda, A Elaskiany *J. Electroanal. Chem.* **84** 359 (1977)
67. Y A Elewady *J. Radioanal. Nucl. Chem.Lett.* **103** 359 (1986)
68. S P Survilene, R M Vishomirskis *Tr. Akad. Nauk Lit. SSR, Ser. B* **1(92)** 53 (1976)
69. T C Pinkerton, W R Heineman *J. Electroanal. Chem.* **158** 323 (1983)
70. C D Russell *Int. J. Appl. Radiat. Isot.* **33** 883 (1982)
71. E N Zakharov, S P Bagaev, V N Kudryavtsev, K S Pedan. *Elektrokhimiya* **26** 266 (1990)
72. A M Sukhotin, I G Osipenkova *Zh. Prikl. Khim.* **51** 830 (1978)
73. R L Paul, A Cartwright *J. Electroanal. Chem.* **201** 113 (1986)
74. S Ya Trilikhes *Elektrokhimicheskoe i Khimicheskoe Polirovanie* (Electrochemical and Chemical Polishing) (Leningrad: Mashinostroenie, 1987)
75. S A Lilin, E M Rumyantsev, G A Krestov, A D Bocharov, A V Balmasov *Dokl. Akad. Nauk SSSR* **289** 409 (1986)
76. B I Bairachnyi, F K Andryushchenko *Elektrokhimiya Ventil'nykh Metallov* (Electrochemistry Rectifying Metals) (Khar'kov: Vishcha Shkola, 1985)
77. R I Anisimov, N Ya Kovarskii *Zashch. Met.* **19** 325 (1983)
78. N D Ivanova, I N Karnaukhov, A I Karasevskii, E I Boldyrev *Ukr. Khim. Zh. (Russ. Ed.)* **54** 928 (1988)
79. N D Ivanova, S V Ivanov, A V Gorodyskii *Ukr. Khim. Zh. (Russ. Ed.)* **52** 1048 (1986)
80. I N Karnaukhov, A I Karasevskii, N D Ivanova, A V Gorodyskii, Y I Boldyrev *J. Electroanal. Chem.* **288** 35 (1990)
81. A V Gorodyskii, N D Ivanova, N I Taranenko *Ukr. Khim. Zh. (Russ. Ed.)* **44** 3 (1978)
82. N D Ivanova, S V Ivanov, E I Boldyrev *Gal'vanotekhnika. Ftorsoderzhashchie Elektrolity i Rastvory: Spravochnik* (Electroplating. Fluorine-containing Electrolytes and Solutions. Handbook) (Kiev: Naukova Dumka, 1993)
83. K Kao, V Huan *Electron Transfer in Solids. Electric Properties of Organic Semiconductors* (Translated into Russian; Moscow: Mir, 1984) Chapter 2
84. G Haken *Synergy* (Translated into Russian; Moscow: Mir, 1985)
85. A V Gorodyskii, N D Ivanova, S V Ivanov, Y I Boldyrev *Surf. Coat. Technol.* **29** 59 (1986)
86. A V Gorodyskii, N D Ivanova, A E Aleksenko *Ukr. Khim. Zh. (Russ. Ed.)* **48** 658 (1982)
87. N D Ivanova, G A Alfintsev *Elektrokhimiya* **8** 332 (1972)
88. N D Ivanova, K B Kladnitskaya *Ukr. Khim. Zh. (Russ. Ed.)* **47** 1199 (1981)
89. N D Ivanova, T S Psareva *Ukr. Khim. Zh. (Russ. Ed.)* **48** 948 (1982)
90. N D Ivanova, N I Taranenko, A V Gorodyskii *Tekhnol. Organ. Proizvod.* **12** 55 (1975)
91. N D Ivanova *Ukr. Khim. Zh. (Russ.Ed.)* **43** 252 (1978)
92. A V Gorodyskii, N D Ivanova *Elektrokhimiya* **18** 275 (1982)
93. L I Lyamina, K M Gorbunova *Elektrokhimiya* **1** 546 (1965)
94. L I Lyamina, N I Korol'kova, K M Gorbunova *Elektrokhimiya* **6** 394 (1970)
95. K M Gorbunova, L I Liamina, N I Korolkova *Electrochim. Acta* **15** 1597 (1987)
96. I V Gorbunova, L I Lyamina, K M Gorbunova *Elektrokhimiya* **23** 1083 (1987)
97. L I Lyamina, N I Tarasova, K M Gorbunova *Kinet. Katal.* **16** 1158 (1975)
98. B Delmon *Introduction a la Cinetique Heterogene* (Translated into Russian; Moscow: Mir, 1972)
99. E F Zavgorodnyaya, T Yu Inyutina, Yu P Rodak *Elektrokhimiya* **11** 1727 (1975)

100. I A Kurmashova, Author's Abstract of Candidate's Thesis in Chemical Sciences, Inst. Phys. Chem. Acad. Sci. USSR, Moscow, 1982
101. V V Boldyrev, E Yu Ivanov *Kinet. Katal.* **17** 1447 (1976)
102. L I Lyamina, N I Korol'kova, K M Gorbunova *Elektrokhimiya* **8** 651 (1972)
103. E F Zavgorodnyaya, V P Galushko, T P Dorosh *Ukr. Khim. Zh. (Russ. Ed.)* **27** 43 (1961)
104. V P Galushko, E F Zavgorodnyaya, N V Podol'skaya *Ukr. Khim. Zh. (Russ. Ed.)* **39** 1217 (1973)
105. V P Galushko, E K Oshe, T Yu Inyutina, Yu P Rodak, E F Zavgorodnyaya *Ukr. Khim. Zh. (Russ. Ed.)* **42** 594 (1976)
106. N D Ivanova, S V Ivanov *Elektrokhimiya* **18** 314 (1982)
107. N D Ivanova, S V Ivanov *Elektrokhimiya* **18** 1126 (1982)
108. A V Gorodyskii, N D Ivanova, E I Boldyrev, S V Ivanov *Elektrokhimiya* **19** 1155 (1983)
109. S V Ivanov, N D Ivanova *Dokl. Akad. Nauk Ukr.* **9** 129 (1992)
110. S V Ivanov *Dokl. Akad. Nauk Ukr.* **58** 864 (1992)
111. S V Ivanov *Dokl. Akad. Nauk Ukr.* **59** 292 (1993)
112. A V Gorodyskii, N D Ivanova, E I Boldyrev *Ukr. Khim. Zh. (Russ. Ed.)* **48** 1262 (1982)

Russian Chemical Reviews **62** (10) 919–933 (1993)
©1993 Russian Academy of Sciences and Turpion Ltd

UDC 541:6

Orbital interactions through space and through σ-bonds

E I Brodskaya, G V Ratovskii, M G Voronkov

Contents

I. Introduction	919
II. Interactions between equivalent substituents having lone electron pairs of π-electron systems	919
III. Interactions between nonequivalent substituents	927
IV. The influence of the interaction through σ-bonds on the reactivity of organic compounds	930

Abstract. The present state of one of the comparatively new theoretical concepts in organic chemistry—the interaction of two heteroatoms having a lone electron pair or of groups incorporating a π-bond through the system of σ-bonds separating them—is considered. Two mechanisms of such interactions are discussed—through space and through the σ-bonds. These interactions are assessed in terms of UV, photoelectron, and electronic transmission spectroscopic and quantum-chemical data. The influence of the above interactions on the reactivity of the molecules is illustrated. The bibliography includes 139 references.

I. Introduction

For a qualitative and quantitative assessment of the mutual influence of substituents in an organic or organoelement molecule, a wide range of various electronic effects are used: the α-effect—interaction of two directly linked heteroatoms having lone electron pairs (LEP);[1,2] geminal interaction (also referred to as the α-effect)—interaction of two substituents separated by one carbon atom or an atom of another element;[3] orbital interaction through space or through σ-bonds—interaction of substituents separated by σ-bonds; the anomeric effect;[4–7] the 'rabbit-ear' or 'hockey sticks' effect;[8,9] vicinal interaction (the β-effect)—interaction of substituents separated by two carbon atoms;[10–12] the alternation effect (the field effect);[13] the inductive effect;[14] hyperconjugation;[15–17] various types of conjugation[18,19] etc.

In 1968–1971, Hoffmann[20,21] examined the interaction between σ-bond-separated heteroatoms having lone pairs or [groups having?] π-electron systems. In relation to biradical systems, he analysed two types of orbital interactions—through space and through σ-bonds. The splitting of the energy levels (ΔE) serves as a measure of the orbital interactions: thus, in the presence of such inte.actions, the energy levels should be [non-?] degenerate, whilst in their absence they should have similar energies. The present state of this problem is considered below. Several reviews on this topic have been published abroad,[17,18,22–28] but these are largely based on the consideration of only individual classes of compounds and differ in the theoretical approach used. Unfortunately, this problem has not been duly considered in Russian literature.

E I Brodskaya, M G Voronkov Irkutsk Institute of Organic Chemistry, Siberian Division of Russian Academy of Sciences, ul. Favorskogo 1, 664033 Irkutsk, Russian Federation. Tel. (7-395) 246 02 45.
G V Ratovskii Institute of Petrochemical and Coal Chemical Synthesis at the Irkutsk State University, ul. Lermontova 126, 664033 Irkutsk, Russian Federation.

Received 18 March 1993
Uspekhi Khimii **62** (10) 975–990 (1993); translated by A K Grzybowski

II. Interactions between equivalent substituents having lone electron pairs or π-electron systems

1. Model ideas

According to perturbation theory, in the interaction of two degenerate electronic levels n_1 and n_2 of a molecule (n_1 and n_2 are the LEP orbitals of identical heteroatoms or the π orbitals of unsaturated groups) through space, two new electronic levels are generated—a low-energy level corresponding to the bonding combination ($n_1 + n_2$) and a high-energy level corresponding to the antibonding combination ($n_1 - n_2$). For a biradical system (for which the initial study was performed) with three separating σ-bonds, the $n_1 + n_2$ combination is symmetrical (S or n^+) while the $n_1 - n_2$ combination is antisymmetrical (A or n^-) relative to the symmetry axis perpendicular to the C(2)–C(3) bond (Fig. 1). The interaction through space reduces the energy of the level S relative to A ($E_S < E_A$). When interactions through σ-bonds are considered, it is assumed that the bonding σ orbital of the C(2)–C(3) bond is symmetrical, while the antibonding σ* orbital is antisymmetrical relative to the symmetry axis. When account is taken of the possibility of

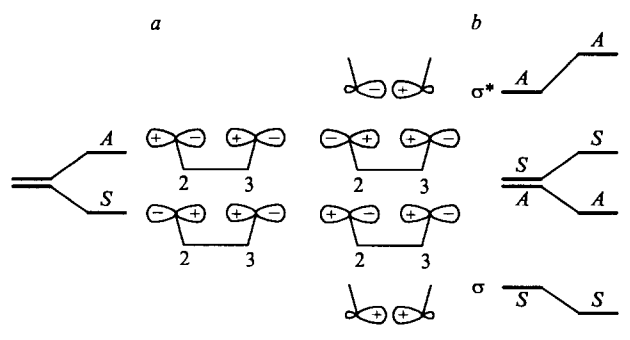


Figure 1. Schematic illustration of the interaction of the orbitals through space (*a*) and through σ-bonds (*b*).[20]

the mixing of only orbitals of similar symmetry, the $n_1 + n_2$ orbital interacts with the σ orbital, while the $n_1 - n_2$ orbital interacts with the σ* orbital. The energy of the level S then increases and that of the level A diminishes. 'Repulsion' of the levels leads to a lower energy of the level A compared with S ($E_S > E_A$). Their splitting ΔE is a function of the overlap of the above orbitals. The influence of the C(1)–C(2), C(3)–C(4), and C–H bonds on the relative positions of E_S and E_A is insignificant.[20,21]

In the general case, the interaction through σ-bonds depends only on the overlap of the LEP of the heteroatoms with the σ and σ* orbitals of the central C(2)–C(3) bond. The degree of overlap is independent of the rotation about this bond but does depend significantly on the rotation about the C–X bonds, since the symmetry is then infringed. On the basis of perturbation theory, displacements of the levels S and A (ΔE_S and ΔE_A) can be calculated by the formula[21]

$$\Delta E_i = \frac{|H_{ij}|^2}{E_i - E_j},$$

where $H_{ij} = \int \psi i_i^* H \psi_j \, d\tau$ is the perturbation matrix element and E_i and E_j are the energies of the interacting levels. Hoffmann did not discuss the influence of the energy difference $E_i - E_j$ on ΔE_S and ΔE_A. One can only note that, if E_j is the energy of an occupied σ orbital, then $|E_i - E_j| \approx 0.3$ eV and, if E_j is the energy of an unoccupied σ orbital, then $|E_i - E_j| \approx 10$ eV.[20] If the terminal substituents in the molecule are close to one another, the interaction through space predominates, but when they are separated by a distance greater than 3 Å the interaction through σ-bonds predominates.

Model calculations carried out by semiempirical methods led to certain important conclusions concerning the orbital interactions through a system of m intervening σ-bonds.[20,21,29–32]

1. The sequence of the energy levels generated on interaction through m intervening σ-bonds depends on their number: $E_S < E_A$ for even values of m and $E_S > E_A$ for odd values of m. It follows from this parity rule that the interactions through space and through m σ-bonds intensify one another in the case of even values of m and weaken one another for odd values of m (when these interactions are opposed).

2. For a given value of m, the orbital interactions through m σ-bonds depend on the geometry of the σ-skeleton and their extent is a maximum for the *trans*-structure of the σ-skeleton. Thus the manifestation of orbital interactions through four σ-bonds weakens in the following sequence of molecular conformations: *trans, trans* > *cis, trans* > *cis,cis*.

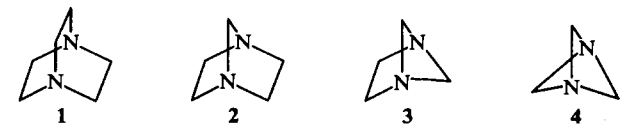
3. The interaction through σ-bonds on the whole stabilises the molecule, but the C–C σ-bond in the X–C–C–X fragment is then weakened.

The principal experimental methods for the investigation of orbital interactions through space or σ-bonds are photoelectron,[33] electronic transmission (electron capture),[34] and UV spectroscopy.

2. Diazabicycloalkanes

The interactions through space and through σ-bonds in diazabicyclic systems have been investigated by photoelectron spectroscopy and quantum chemically.[20,21,35–41] Quantum-chemical calculations by the extended Hückel[20] and MINDO/2 [36] methods for the 1,4-diazabicyclo[2.2.2]octane **1** molecule confirmed that the n^+ level is higher than the n^- level by 1.57 and 1.36 eV respectively. Photoelectron spectroscopy yields 2.13 eV.[35] Analysis of the vibrational structure of the bands in the photoelectron spectrum of compound **1** also confirms that $n^+ > n^-$.[37]

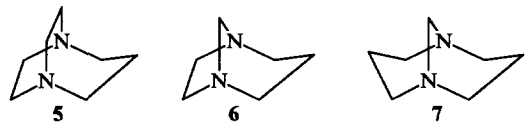
Quantum-chemical calculations for the diazabicycloalkanes **1–4** demonstrated the influence of the intervening σ-bonds on the relative disposition of the levels.[20]



1 **2** **3** **4**

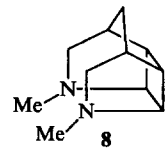
In the series of compounds **1–4**, the number of methylene bridges containing two intervening σ-bonds diminishes, which weakens the interaction through σ-bonds and intensifies those through space as a result of the mutual approach of the nitrogen atoms. The order of the levels S and A is then changed: for compound **1**, the $a_2''(A)$ level lies below $a_1'(S)$ ($\Delta E = 1.573$ eV); for compound **2**, $\Delta E = 0.371$ eV for the levels arranged in the same order; for compound **3**, the opposite order of the levels obtains, i.e. $S < A$ ($\Delta E = -0.605$ eV); for compound **4**, the level S is appreciably below the level A ($\Delta E = -2.878$ eV).

The photoelectron spectra of 1,5-diazabicyclo[3.2.2]nonane **5**, 1,5-diazabicyclo[3.2.1]octane **6**, 1,5-diazabicyclo[3.3.1]-nonane **7**, and various piperazine and hydroxypyrimidine derivatives show that the splitting ΔE for 1,3- and 1,4-diamines depends on the spatial orientation of the LEP of the nitrogen atoms[38] (Fig. 2). The influence of ring strain on the ionisation energies of the bicyclic diamines has been described.[39]



5 **6** **7**

The low ionisation potentials (7.29 and 8.24 eV) of *N,N*-dimethyl-2,7-diazatetracyclo[3.3.3.$0^{4,9}0^{8,11}$]undecane **8** and the appreciable splitting ΔE of the energy levels of the LEP of the nitrogen atoms (0.95 eV) were interpreted in terms of the interaction of the LEP of the nitrogen atoms through space ($n^- > n^+$) (the lone pairs are oriented at an angle of 70° within the undecane skeleton).[41]



8

Non-empirical calculations in terms of the STO-3G basis set for 1,4-diazabicyclooctane **1** and two model molecules containing respectively one and two C–C bonds between the two nitrogen atoms indicate that two types of interaction are mainly responsible for the splitting of the two LEP orbitals—the first

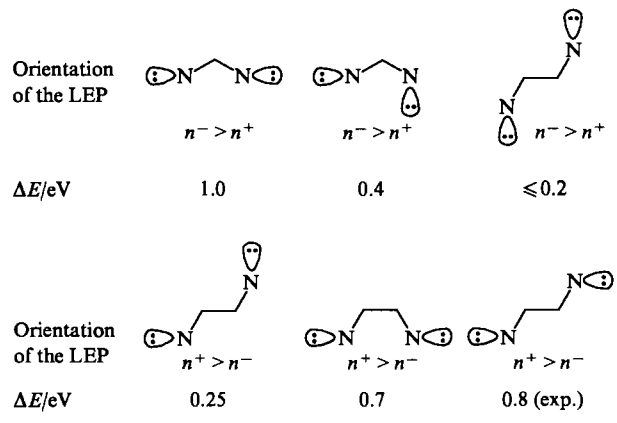


Figure 2. The splittings of the energy levels of the lone pairs in 1,3- and 1,4-diamines.[38]

type involves the interaction between the LEP nitrogen and the central C–C bond in the same N–C–C–N fragment, while the second involves the interaction between the neighbouring N–C bonds in different fragments.[40]

3. Oxygen- and sulfur-containing heterocycles

According to the symmetry of the immediate environment of the oxygen or sulfur atoms in saturated ethers and sulfides, their highest occupied nonbonding MO have a π-type symmetry (p_z-orbitals) (Table 1). A number of studies have been devoted to interaction through space and through σ-bonds in heterocyclic compounds containing at least two oxygen and sulfur atoms.[24,42–47]

Table 1. Vertical ionisation potentials of the LEP of oxygen- and sulfur-containing heterocycles.[42]

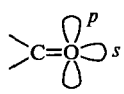
Compound	IP (*n*)/eV		ΔIP(*n*)/eV
1,3-Dioxolan **9**	10.10	10.65	0.55
2,2-Dimethyl-1,3-dioxolan **10**	9.71	10.20	0.49
Tetrahydropyran **11**	9.50		
1,3-Dioxane **12**	10.10	10.35	0.25
1,4-Dioxane **13**	9.43	10.65	1.22
Thiane **14**	8.45		
1,3-Dithiane **15**	8.54	8.95	0.41
1,4-Dithiane **16**	8.58	9.03	0.45
1,4-Thioxane **17**	8.67 (S)	10.0 (O)	

It follows from the analysis of the photoelectron spectra of 1,4-dioxane **13** and 1,4-dithiane **14** that the splitting of the highest occupied levels due to the interaction of the LEP of the oxygen and sulfur atoms is 1.22 and 0.45 eV respectively. The direct overlap of the p_z orbitals of the LEP in these molecules is impossible as they have the chair conformation, so that the interaction through σ-bonds is the main one. The greater splitting for 1,4-dioxane compared with 1,4-dithiane may be a consequence of the better energy correspondence between the LEP orbitals and the σ orbitals of the C–C bonds.

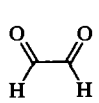
In 1,3-dioxane **12** and 1,3-dithiane **15**, which also have the chair conformation, there is a possibility of the direct overlap of the LEP of the heteroatoms, which is more effective in the case of 1,3-dithiane.[42] Calculations by the MNDO method confirmed that the interaction of the LEP of the sulfur atoms in the 1,3-dithiane is through space, whilst that in 1,4-dithiane is through σ-bonds.[47]

4. Dicarbonyl compounds

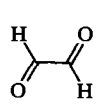
In dicarbonyl compounds, there is also a possibility of both types of interactions of the nonbonding *n* orbitals of the oxygen atoms.[17,33,48–60] In the description of the MO of the carbonyl group, taking into account its symmetry, two nonequivalent orbitals of the *p* and *s* types[48] or *p* and *sp* types[19,61] correspond to the LEP of oxygen (the energy of the *p*-type orbital is higher).



In the molecules containing two carbonyl groups, the interaction of the nonbonding *p*-type orbitals results in the splitting of the energy levels. Their order $n_A < n_S$ follows from quantum-chemical calculations for the *s-cis*- and *s-trans*-conformers of glyoxal on the assumption of ideal geometry.



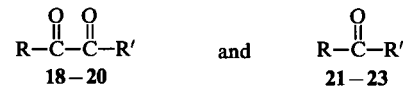
s-cis



s-trans

The splitting ΔE for *s-cis*-glyoxal is 1.46 eV (EHM) or 2.96 eV (CNDO), whilst for *s-trans*-glyoxal it is 1.46 eV (EHM) or 3.27 eV (CNDO).[48] The experimental splitting ΔE is 1.46 eV.[33] The interaction through space in *s-cis*-glyoxal is insignificant as a consequence of the low value of the overlap integral (0.011) of the two *p*-type orbitals (EHM calculations). However, with decrease in the CCO bond angle, binding through space increases. The energy of the level *A* then increases and that of the level *S* hardly changes.

Similar effects have been discovered[50] in the analysis of the photoelectron spectra of the 1,2-diketones **18–20** and the corresponding ketones **21–23**.



18–20 and **21–23**

18, 21: R = R′ = cyclo-C_3H_5;
19, 22: R = cyclo-C_3H_5, R′ = Me;
20, 23: R = R′ = Me.

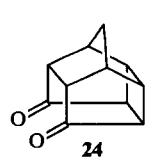
The intense low-energy peaks in the vibrational structure of the spectra of the three monocarbonyl compounds **21–23** are largely determined by the liberation of an electron from the localised *p* orbital of the oxygen LEP. Diffuse bands with higher energies are observed in the spectra of the 1,2-diketones **18–20**. The interaction of the nonbonding *n* orbitals of the oxygen atoms through σ-bonds leads to the splitting of the n_S and n_A levels amounting to ~2 eV (Table 2).

Table 2. Ionisation potentials of carbonyl compounds.[50]

Compound	IP/ eV		Assignment[a]
1,2-Dicyclopropylethane-1,2-dione **18**	9.09		n_S
	10.40	11–12	e_A, e_S and n_A
1-Cyclopropylpropane-1,2-dione **19**	9.33		n_S
	10.78	11.35	e_A, e_S and n_A
Diacetyl **20**	9.57		n_S
	11.41		n_A
Dicyclopropyl ketone **21**	9.28		n_O
	10.43	11.50	e_A, e_S
Cyclopropyl methyl ketone **22**	9.50		n_O
	10.62	11.40	e_A, e_S
Acetone **23**	9.71		n_O

[a] n_O is the nonbonding orbital of the oxygen LEP, e_S and e_A are the symmetrical and antisymmetrical orbitals of cyclopropane, and n_S and n_A are the symmetrical and antisymmetrical combinations of the nonbonding *p* orbitals of the oxygen atoms.

The photoelectron spectrum of pentacyclo-[5.4.0.$0^{2,6}$.$0^{3,10}$.$0^{5,9}$]undecane-8,11-dione **24** indicates an appreciable splitting of the *n* levels of the oxygen LEP (0.55 eV).[60] The contribution to this splitting by the interaction of the two oxygen atoms through space is very low, since they are quite far apart (4.05 Å).[62,63] The interaction of the *n* orbitals of the oxygen LEP with the σ orbitals of the skeleton becomes more intense if the C–C bonds separating the carbonyl groups form part of a strained system (a three- or four-membered ring).[55,57]



24

Analysis of the first two ionisation bands in the photoelectron spectra of cyclohexane-1,4-dione and its derivatives **25**–**32** indicates an increase in the splitting between the n^+ and n^- combinations of the orbitals from 0.2 eV in the spectra of compound **25** to 0.6 eV in those of compounds **29** and **30** and to 0.9 eV in those of compound **26** (Fig. 3). This can be explained by the intensification of the n^-,σ-interaction on passing from compound **25** to compounds **29** and **30** and further to compound **26**, whereas the n^+,σ-interaction in these molecules remains almost constant.[57]

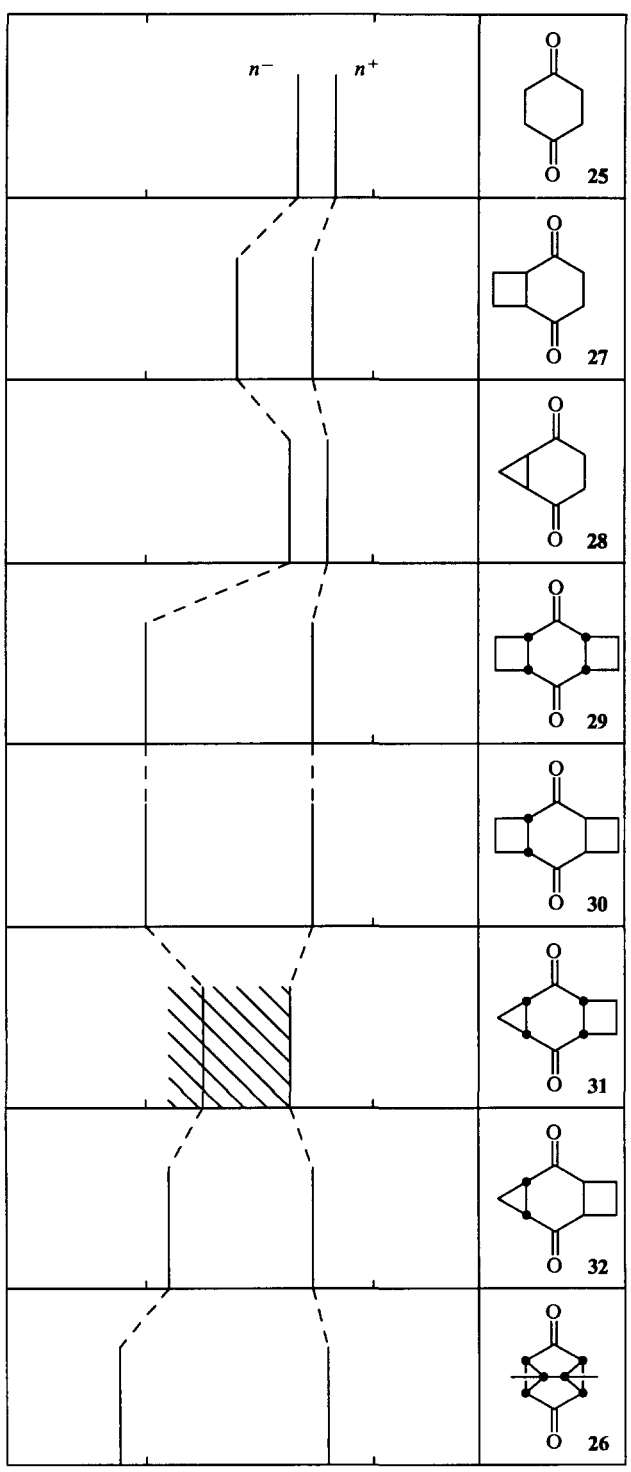


Figure 3. Diagram of the first two bands in the photoelectron spectra of compounds **25**–**32**.[57]

The study of the photoelectron spectra of a large series of α-, β-, γ-, and δ-dicarbonyl compounds demonstrated (the n^+ and n^- ionisation energies were calculated by the CNDO/S and CNDO/2 methods) that the most intense interaction through σ-bonds is observed in the α-dicarbonyl compounds ($\Delta IP = 1.5-3.1$ eV).[23] The extent of this interaction is independent of the dihedral angle between the planes of the carbonyl groups,[49] but diminishes rapidly with increase in the number of intervening CH_2 groups between the two carbonyl groups. The sequence of the energies of the nonbonding MO is determined by the assignment of the dicarbonyl compounds to two classes: compounds with coaxial carbonyl groups are assigned to the first class, whilst those with the noncoaxial groups are assigned to the second. Thus the parity rule, which holds for acyclic dicarbonyl compounds with noncoaxial carbonyl groups, breaks down for the cyclic compounds in which the carbonyl groups are coaxial (the C=O bonds are located on a single axis).[23] For example, the order of the levels is $n^+ > n^-$ for 2,2,4,4-tetramethylcyclobutane-1,3-dione **33** in which the LEP of the oxygen atoms interact through the four σ-bonds, whereas for tetramethyl-1,4-benzoquinone **34**, in which the LEP interaction is effected through five σ-bonds, the order of the levels is $n^- > n^+$, although, according to the parity rule, it should have been the opposite for these compounds. The opposite bond order, namely $n^- > n^+$, is also observed for derivatives of cyclohexane-1,4-dione. Since the carbonyl groups in all the symmetrical four- and six-membered cycloalkanediones are located in virtually one plane and are coaxial, their molecules have a centre of symmetry (Fig. 4).[57] In such compounds, the *p* orbital of the oxygen LEP interacts with the group σ orbital incorporating the two C–C bonds formed by the carbon atom of the carbonyl group. In contrast to the model proposed by Hoffmann,[20,21] in which the overlap of mainly the first lobe of the *p* orbital of the LEP of the heteroatom with one σ orbital of the C–C bond was considered, in this case the overlap of two lobes of the *p* orbital with the σ orbitals localised in two C–C bonds is postulated. Here the n^+ combination is antisymmetrical and the n^- combination is symmetrical relative to the centre of symmetry (in contrast to the plane of symmetry). Therefore the parity rule does not hold for compounds with coaxial carbonyl groups.

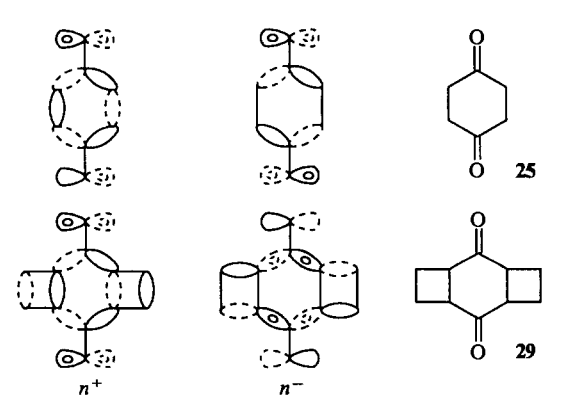


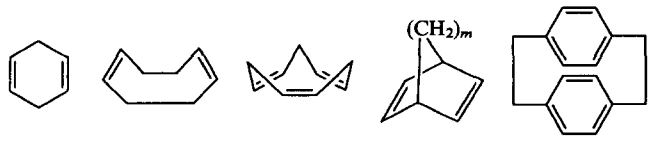
Figure 4. Schematic representation of the highest occupied MO (n^-, n^+) of compounds **25** and **29**. The double contour lines designate a higher electron density.[57]

Four singlet *n*, π* transitions are observed in the polarised UV spectrum of a single crystal of 2,2,4,4-tetramethylcyclobutane-1,3-dione **33** at a low temperature.[51,52] Theoretical analysis (EHM, CNDO/2, CNDO/S) confirmed that the interaction through σ-bonds is in fact the main cause of the greater splitting of the *n* orbitals of the oxygen LEP and of the occurrence of *n*, π* transitions.

5. Nonconjugated π-electron systems

In molecules containing π-electron systems (double or triple bonds, aromatic or heteroaromatic fragments) separated by a system of σ-bonds, both types of interactions considered are also manifested — through space and through σ-bonds.[22,25,27] The interactions through space in compounds of this type are divided into two types — homoconjugation[17,64] and spiroconjugation.[65]

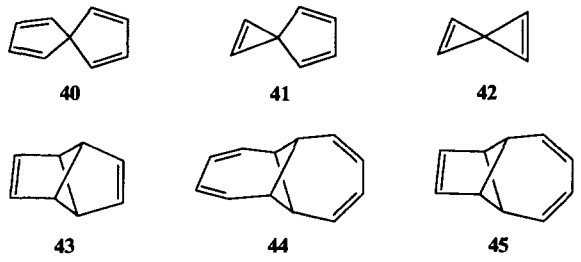
The homoconjugation effect can be demonstrated in relation to cyclohexa-1,4-diene **35**, cycloocta-1,5-diene **36**, cyclonona-1,4,7-triene **37**, [2.2.*m*]bicyclanes **38**, and [2.2]paracyclophane **39**.[22,27,66,67]



35 **36** **37** **38** **39**

The interaction through space predominates in norbornadiene **38** (*m* = 1).[66] In view of the presence of two symmetry planes (Fig. 5), the energy level corresponding to the symmetrical combination of the occupied π orbitals (*SS*) has a lower energy, while the energy level corresponding to the antisymmetrical combination (*SA*) has a higher energy. Similarly a level with a lower energy corresponds to the symmetrical combination of the unoccupied π* orbitals (*AS*) and one with a higher energy corresponds to the antisymmetrical combination (*AA*).

The spiroconjugation effect is manifested in molecules where the rings linked to one another contain unsaturated fragments located in mutually perpendicular planes (compounds **40–42**).[65,68–70]



40 **41** **42**

43 **44** **45**

Owing to the specific symmetry of these molecules, the interaction of the occupied (π) and unoccupied (π*) orbitals of the unsaturated fragments through space is mainly manifested. The group orbitals constituting a combination of the π(π*) orbitals of two unsaturated fragments have the a_2 and b_1 symmetries.[68] For compounds **40–42** having a spiro-centre, the interaction through σ-bonds is insignificant and the level b_1 lies below the level a_2. For compounds **43–45**, the interaction through the σ-bonds of the intervening four-membered ring is more significant and the opposite order of the energy levels obtains ($b_1 > a_2$).[68,70] These differences determine the characteristic features of the photoelectron and UV spectra of the spiro-compounds.[65,69,70] Thus the splitting of the above levels of the spiro[4.4]nonatetraene **40** is 1.23 eV according to photoelectron and UV spectroscopic data.[65]

In order to estimate the relative contributions of the interactions through space and through σ-bonds, Table 3 presents the experimental π-ionisation energies $IP_{v,1}$ and $IP_{v,2}$ of the bicyclic dienes **38** as a function of the number of methylene groups (*m*): Dewar benzene (*m* = 0), norbornadiene (*m* = 1), bicyclco[2.2.2]octadiene (*m* = 2), bicyclo[3.2.2]nona-6,8-diene (*m* = 3), bicyclo[4.2.2]deca-7,9-diene (*m* = 4), and the hypothetical hydrocarbon with *m* = ∞. The last system is modelled by the planar cyclohexa-1,4-diene **35**. The splitting ΔIP_v should decrease monotonically with increase in the dihedral angle between the planes of the double bonds. However, it passes through a minimum in the case of compound **38** (*m* = 3) and then again increases to 1.0 eV for the hypothetical hydrocarbon (*m* = ∞). This indicates the mutual cancelling of the interactions through space and through σ-bonds. In compounds with *m* = 1 and 2, the interaction through space between the π_a and π_b orbitals predominates, whereas in compounds with *m* = 3, 4, or ∞ the interaction through σ-bonds predominates.

The effective unit connecting the two π-electron systems in a structure of the type $\pi_1-CH_2-\pi_2$ is a single methylene group. For interaction to occur, it is approached by the π-symmetrical combinations of the σ and σ* orbitals (pseudo-π orbitals) localised on the C–H bonds. The interaction diagram[21] illustrates the result of the mixing of the σ and σ* orbitals with the two *p* orbitals of the trimethylene radical (Fig. 6). The antisymmetrical combination of the *p* orbitals cannot then become mixed with the pseudo-π orbitals of the CH_2 group for symmetry reasons. In four-membered cyclic systems, the interaction between the endocyclic n_0 or π orbitals also takes place via the pseudo-π orbitals.[26,71,72]

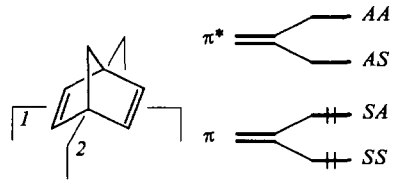


Figure 5. The electronic levels of norbornadiene **38** (*m* = 1) before and after interaction through space (the designations *S* and *A* refer to the mirror planes *1* and *2* shown on the left).[66]

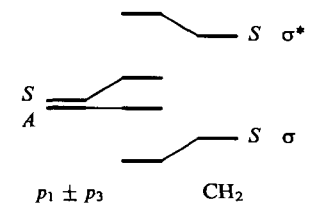


Figure 6. Diagram of the orbital interactions for the trimethylene radical.[21]

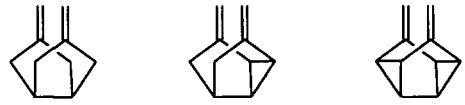
Table 3. Ionisation potentials (eV) of the bicyclic dienes **38** and cyclohexa-1,4-diene **35**.[22]

Ionisation band	Ionisation energy	*m*						**35**
		0	1	2	3	4	∞	
1	$IP_{v,1}$	9.4	8.7	8.8	9.0	8.9	8.6	8.8
2	$IP_{v,2}$	9.7	9.5	9.4	9.2	9.3	9.6	9.8
	ΔIP	0.3	0.8	0.6	0.2	0.3	1.0	1.0

The interaction through σ-bonds is manifested most strikingly in the planar cyclohexa-1,4-diene.[66] In this compound, the π orbitals of the two double bonds overlap with the group σ orbitals (incorporating the two C–H bonds of the methylene groups), which are suitable on symmetry grounds. As a result of the interaction of the π orbitals of the double bonds through the two methylene groups, the opposite order of the splitting of the *SS* and *SA* levels is observed (*SS* > *SA*) compared with that in norbornadiene, where there is interaction through space (*SS* < *SA*, Fig. 5). Quantum-chemical calculations (EHM) for the planar model of cyclohexa-1,4-diene confirmed this order of the levels with a splitting of 0.65 eV (the experimental value is 1.0 eV).[66]

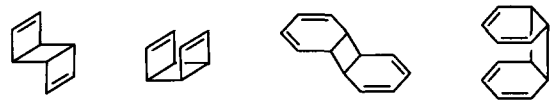
The dependence of the interaction through space and through σ-bonds on distance and the mutual orientation of the basis orbitals has been examined[22] for the model compound **35**. In the boat conformer of cycloocta-1,5-diene **36**, the interaction through space should be considerable. However, the experimental difference between the two π-bonds is only 0.2 eV;[66] on the other hand, the calculated splitting is 1.67 eV with the levels arranged in the order *SS* < *SA*. This is caused by the superposition on the interaction through space in compound **36** of a further interaction of the π orbitals with the *SS* combination of the C(3)–C(4) and C(7)–C(8) σ-bonds which are ideally oriented for the interaction of the two π-electron systems through σ-bonds. This destabilises the π-*SS* combination. When account is taken of this fact, the calculated splitting diminishes to 0.48 eV. In compound **36** in the chair conformation, there is no interaction through space and the interaction through σ-bonds predominates.

According to photoelectron and transmission electronic spectroscopic data, which have been confirmed by quantum-chemical calculations, the interaction of two double bonds separated by a σ-skeleton becomes more marked in the series of compounds **46**–**48**.[54,55] The splitting of the energies of the π^+ and π^- orbitals increases on passing from compound **46** to compounds **47** and **48** (0.2 < 0.4 < 1.26 eV respectively). The interaction through σ-bonds, which intensifies with increase in the rigidity of the σ-skeleton, predominates in these compounds[58,59] and leads to the inverted order of the π orbitals ($\pi^- < \pi^+$).



46 **47** **48**

In the series of cyclic hydrocarbons **49**–**52**, the splitting (0.6–1.0 eV) between the π-bonds is greater for the *anti*-isomers of compounds **49** and **51**, which indicates the predominance of the interaction through σ-bonds.[27]

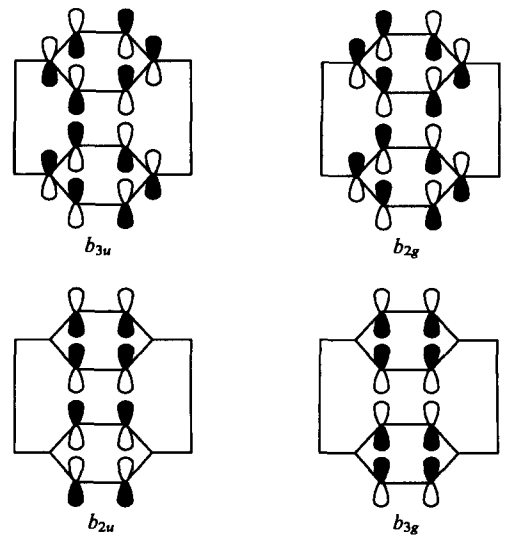


49 **50** **51** **52**

Compound	**49**	**50**	**51**	**52**
ΔIP/eV	1.0	0.3	0.67	0.46

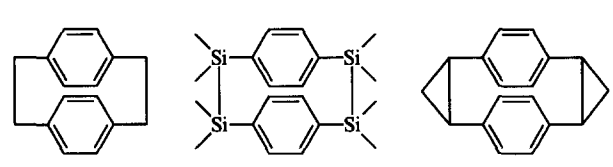
According to electronic, spectroscopic, and Penning ionisation data as well as the results of non-empirical calculations, the differences between the symmetrical and antisymmetrical π orbitals in the molecules of norbornadiene **38** (*m* = 1) and 1,4-diazabicyclo[2.2.2]octane **1** are due to the interaction through space or through σ-bonds.[73] In norbornadiene, where the interaction through space is manifested, the π_S MO is looser than π_A and is characterised by a greater probability of ionisation on electrophilic attack by helium atoms in the metastable excited state. On the other hand, in the case of 1,4-diazabicyclo[2.2.2]octane the n_A MO is looser than n_S owing to the strong interaction through σ-bonds and is distinguished by a greater probability of ionisation.

Orbital interactions have been examined in [2.2]paracyclophane **39** and its analogues, in which two parallel aromatic rings interact through space and through the system of σ-bonds.[67,74] The four $e_{1g}(\pi)$-orbitals of the two benzene rings in compound **39** form the four linear combinations b_{3u}, b_{2g}, b_{2u}, and b_{3g}.



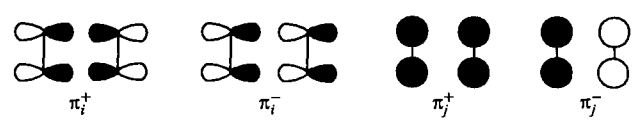
The b_{2g} and b_{3g} combinations, which are antisymmetrical relative to the plane separating the parallel rings, cannot interact with the σ orbitals of the bridging CH_2-CH_2 fragments. The overlap integral between the b_{2u} combinations and the σ orbitals is in fact zero. Their splitting (~1.5 eV) is caused by the interactions through space.[22] Only the linear b_{3u} combination can be effectively mixed with the above σ orbitals (interaction through σ-bonds). Its energy depends significantly on the nature of the bridging fragment.

On passing from the cyclophane **39** to its analogues **53** and **54**, the energy of the σ orbitals of the bridge connecting the benzene rings increases.[73,74] The b_{3u} ionisation energy therefore shifts towards lower values. The opposite shift is observed in *exo*-octafluoro[2.2]paracyclophane as a consequence of the decrease in the energy of the CF_2-CF_2 fragment.[22,27]



39 **53** **54**

As a consequence of the cylindrical symmetry of the π-system of the triple bond, in alka-α,ω-diynes and their analogues, the interaction through space can occur for different orientations of the ethynyl groups.[27] When the two triple bonds are in the same plane, two sets of bonding and antibonding linear combinations of the two in-plane (π_i) and the two out-of-plane (π_j) π orbitals are formed.



For distances between the C≡C bonds ranging from 2.5 to 3.5 Å, small and large splittings may be expected for linear combinations of π_j and π_i respectively. Photoelectron spectroscopic data for the cycloalkanediynes **55–59** indicate a strong dependence of the splitting of the energy levels corresponding to the π_i combinations (Fig. 7) on the distance between the triple bonds.[76]

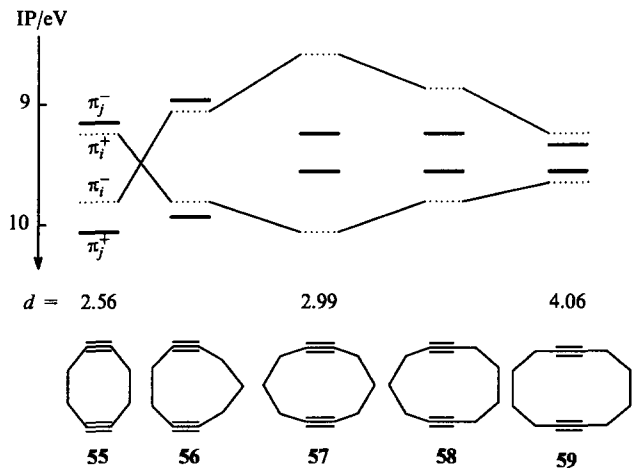


Figure 7. The ionisation potentials in the photoelectron spectra of compounds **55–59** as a function of the average distance (d) between the triple bonds. The continuous lines indicate the out-of-plane π_j MO and the dashed lines indicate the in-plane π_i MO.

In the case of the in-plane π MO of the two C≡C groups, separated by several σ-bonds, the interaction through space in compounds **55–59** stabilises the bonding (π_i^+) and destabilises the antibonding (π_i^-) linear combinations which have different symmetries relative to the xz planes (Fig. 8*b*). The interaction of the π-system of hexa-1,5-diyne **60** with the σ orbital of the CH_2-CH_2 fragment, symmetrical relative to the xz plane, destabilises the π_i^+ energy level but does not alter the energy of the π_i^- orbital (Fig. 8*a*). The splitting of the levels caused by the interaction through space diminishes correspondingly.

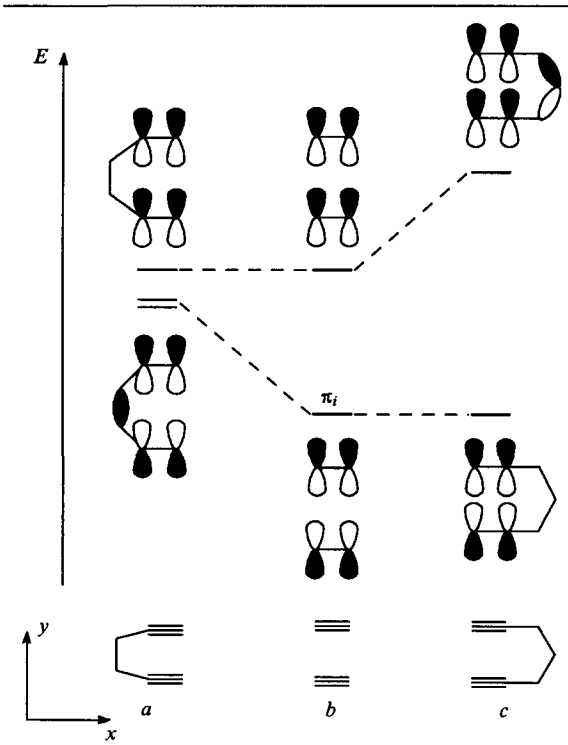
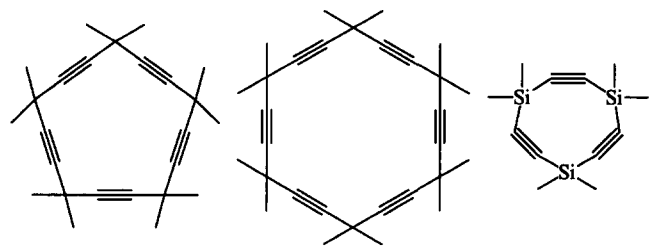


Figure 8. Interaction of the in-plane π MO of the two acetylene fragments in hexa-1,5-diyne **60** (*a*) and hepta-1,6-diyne **61** (*c*) with the σ-skeleton.[27]

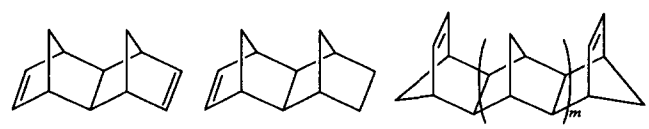
The antisymmetrical σ orbital of the trimethylene chain in hepta-1,6-diyne **61** interacts mainly with the π_i^- orbital, increasing its energy (Fig. 8*c*). In this case, the interactions through space and through σ-bonds increase the splitting of the levels. Thus the interaction of the π_i^+ and π_i^- combinations with the σ-skeleton of the methylene chain depends on the number of CH_2 groups: an even number diminishes the splitting caused by the interaction through space, while an odd number increases it.

The relative contributions of the interactions through space and through σ-bonds depend also on the energy of the σ-skeleton. Thus, in the study of the orbital interactions in compounds **62–64**, stronger interactions were observed for hexamethylcyclotrisilethyne **64**, which has higher [energy] σ orbitals than the carbon analogues **62** and **63**. In perfluorocycloalkadiynes with lower energy σ orbitals, the contribution of the π,σ interaction is not high.[27] Thus the homoconjugation of the triple bonds predominates in the pericyclynes **62–64**.[27,77] Photoelectron and transmission electroscopic data indicate a weak homoconjugation in compounds **62** and **63** in the cationic and anionic states. A similar effect has also been observed for compound **64**.[77]



62 **63** **64**

Hoffmann's model, considered above, has been applied mainly to the analysis of the electronic structures of compounds containing three or less intervening σ-bonds.[21,29] Paddon-Row[25,32,78–85] investigated in detail the dependence of the interaction of the π and n orbitals through m σ-bonds on the value of m for compounds with $m \geqslant 3$ and on the mutual orientation of the σ-bonds. In contrast to Hoffmann's model, in his initial approach, Paddon-Row examined the interactions of the π or n orbitals only with occupied σ orbitals. Here account was taken of the increase in the energies of both the $\pi^+(n^+)$ and $\pi^-(n^-)$ orbital combinations and the initial $\pi(n)$ orbitals relative to model compounds in interactions with σ orbitals. For an even number m, the energy of the $\pi^-(n^-)$ combination increases by a significantly greater amount than for $\pi^+(n^+)$.[25,32] The application of this model to the description of the orbital interactions through four σ-bonds is demonstrated in Fig. 9. An increase in the energy of the basis π orbital in the hex-1-ene molecule by an amount x takes place as a result of its mixing with the highest occupied σ MO (here there are no limitations as regards symmetry). Since the highest of the occupied σ orbitals in antisymmetrical, it interacts with the π^- combination, while the symmetrical σ orbital, having a lower energy, interacts with the π^+ combination.



65 **66** **67**

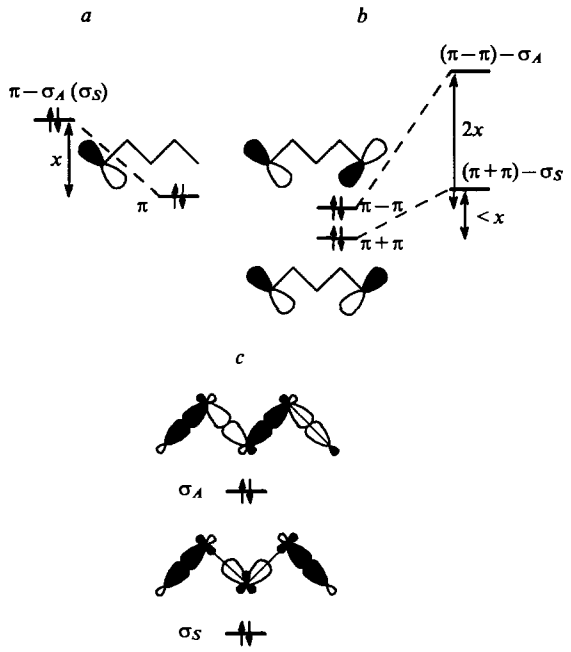


Figure 9. Schematic representation of the σ,π mixing in the molecules of compounds **65** and **66**:[32] (*a*) mixing of the π and highest σ MO: (*b*) mixing of the $\pi^+ - \pi$ combinations with the highest σ MO; (*c*) the π orbital and the two highest σ-type orbitals (*S* and *A*).

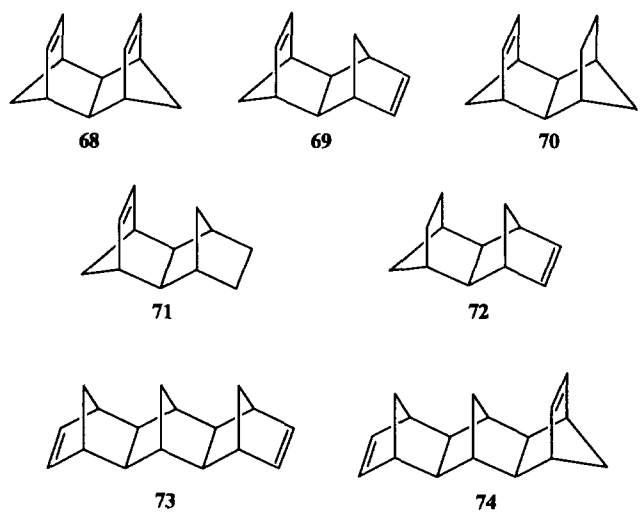
In compounds **67** (*m* = 1), the energy of the π^- combination increases by an amount 2*x* on mixing with the antisymmetrical highest occupied σ MO. In contrast to this, the energy of the π^+ combination increases only slightly ($\Delta E < x$) on mixing with the symmetrical occupied σ MO having a lower energy. This difference is due to two factors: the energies of the π^- and σ_A orbitals are closer and their overlap is greater than in the interaction of the π^+ and σ_S orbitals.

Analysis of the photoelectron spectrum of the hydrocarbon **67** (*m* = 1) confirmed the above scheme. The first ionisation π band is wide, which indicates σ,π-mixing. The fairly sharp second band indicates the ionisation of an electron from the more localised π MO.

The orbital interactions through space and through four and more σ-bonds have been examined in relation to the photoelectron spectra of the hydrocarbons **65**, **66**, and **68–72**, the ionisation potentials of which are presented in Table 4. The higher value of ΔIP(π) for compound **65** (0.87 eV) is a consequence of the interactions through four σ-bonds,[32] while the higher values of ΔIP for compound **68** (1.26 eV) is caused by the overall contribution of the interactions through space and through σ-bonds. The value of ΔIP(π) for compound **73** (0.32 eV) demonstrates the appreciable manifestation of the interactions through six σ-bonds.[25]

Table 4. Vertical ionisation potentials (eV) of dimethanonaphthalenes.[25]

Compound	IP(π)	ΔIP	Assignment
65	8.48	0.87	π^-
	9.35		π^+
66	8.85		π
68	8.08	1.26	π^-
	9.34		π^+
69	8.46	0.44	π^-
	8.90		π^+
70	8.60		π
71	8.65		π
72	8.78		π
73	8.58	0.32	π^-
	8.90		π^+



The decrease in the extent of the π-orbital interactions through four bonds in the series **65** (0.87 eV), **69** (0.44 eV) agrees with the rule governing the dependence of the orbital interactions on the geometry of the σ-skeleton: for the same values of *m*, the interaction in the molecule with a *trans*-orientation of the σ-bonds is a maximum (the *trans*-rule). Indeed the σ-bonds in compound **65** are in the *trans*, *trans*-positions, whilst in compound **69** they are in the *cis*, *trans*-positions. However, the *trans*-rule clearly breaks down on passing to compounds where there is interaction through six σ-bonds. ΔIP for compounds **73**, **74**, and **67** (*m* = 1) increases in the sequence 0.32 < 0.38 < 0.52 eV.[79] This trend has been confirmed by quantum-chemical calculations and indicates the occurrence of an additional orbital interaction, which is manifested to the maximum extent in compound **67**, to a lesser extent in compound **74**, and is virtually absent in compound **73**. In the presence of such additional interaction, called the laticyclic hyperconjugation, the π MO of the two vinyl groups are mixed with the group orbital of the central CH_2 bridge, which embraces the two C–H bonds.[81,83,86,87] In contrast to the pericyclic hyperconjugation of the planar cyclohexa-1,4-diene mentioned earlier, in these compounds the pseudo-π orbital indicated and the orbitals of the double bonds are located virtually in one plane (Fig. 9). (In the planar cyclohexa-1,4-diene, the pseudo-π orbital and the π orbitals of the vinyl groups are located at right angles to the molecular plane.[21]) A direct estimate of the extent of the π-interaction in compound **67** via the intervening CH_2 group has been obtained from the results of non-empirical calculations.[81]

In subsequent studies,[80,82] similar interactions were also examined taking into account the involvement of aromatic rings in them. Laticyclic hyperconjugation—interaction through the so called 'ribbons'—is also observed in the series of polycyclic hydrocarbons with increase in the number of intermediate cyclic units containing CH_2 groups with the orientation indicated (the orbital schemes are illustrated in Fig. 10).[81,86,87] This results in effective delocalisation of the positively charged 'holes' in the radical-cation of the nonconjugated diene containing two double bonds at a distance of 6 Å.[88]

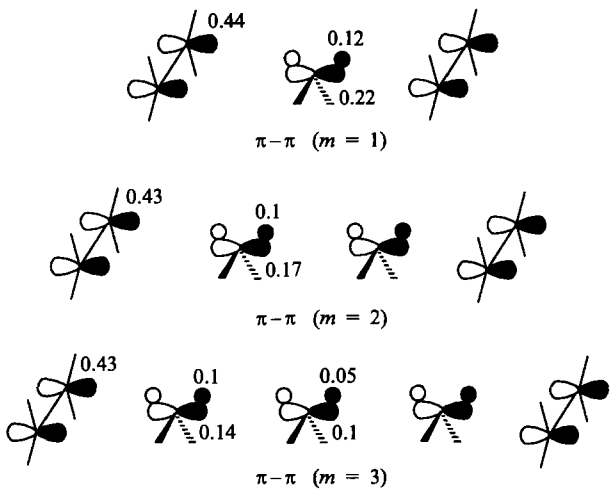
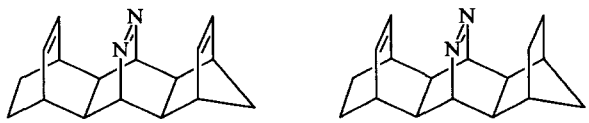


Figure 10. The forms of the orbitals and the coefficients of the π,π interaction calculated by the non-empirical STO-3G method for compound **67** (m = 1–3).[81]

In an experimental study of the electron affinities of compounds **75** and **76**, it was observed that laticyclic conjugation involving the π* orbitals takes place in compound **75**.[78] As the inductive effect and the interaction through σ-bonds in the norbornene fragments of compounds **75** and **76** are identical, the appreciable difference between the ionisation energies (9.02 and 8.40 eV in compounds **76** and **75** respectively) indicates the existence of laticyclic [2 + 2 + 2]-conjugation in compound **75**, which contains three parallel π-bonds.[89,90]



75 **76**

The mechanisms of the interactions under discussion have been analysed[30] on the basis of data derived from semiempirical quantum-chemical calculations in which localised MO were used. With the aid of nonempirical quantum-chemical calculations in terms of different basis sets, a study has been made of the dependence of the splitting of occupied (π^+,π^-) and unoccupied (π^{+*},π^{-*}) orbitals of the vinyl fragments (ΔE) on the number of intervening σ-bonds (m) and their mutual orientation.[91–93] The exponential dependence obtained of $(\Delta E)^2$ on m permits a quantitative prediction of the experimental splittings of the levels and of the rates of electron transfer. The contributions of individual fragments in the transmission of the interaction between π(π*) orbitals have been calculated for similar structures in the analysis of orbitals localised on individual bonds (nature bond orbitals). A more effective transmission of interaction through intervening C–Si bonds has been predicted.

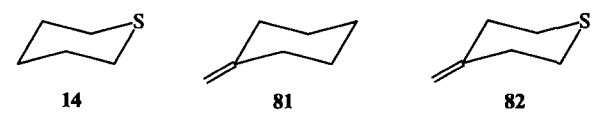
III. Interactions between nonequivalent substituents

Interactions through space and through σ-bonds between nonequivalent substituents are divided into two main types: interaction of occupied π(n) orbitals of two substituents and interaction of occupied n(π) orbitals of a donor (D) with the unoccupied π* or σ* orbitals of the acceptor (A). Interactions of the first type are most strikingly manifested in the analysis of the photoelectron spectra and those of the second type in the analysis of the electronic absorption and emission spectra. In the second case, there is a possibility not only of a change in the energies of the electronic transitions characteristic of the donor and acceptor but also of the manifestation of new transitions accompanied by a significant intramolecular charge transfer (ICT) from the donor to the acceptor.

1. Photoelectron spectra

In the photoelectron spectra of aza-, methyleneaza-, thia-, and methylenethia-cycloalkanones as well as oxygen derivatives, the interaction of the occupied π(n) orbitals of two substituents gives rise to changes in the ionisation potentials referring to the LEP of the heteroatoms (n_S, n_N, n_O) and the π orbitals of the unsaturated fragment. This leads to an increase in the distance between the corresponding energy levels.[94–101]

The increase in the energy splitting of the levels assigned to the n and π orbitals, relative to the difference between their energies in the corresponding monofunctional cyclic compounds (for example, 0.06, 0.29, and 0.35 eV for compounds **14**, **81**, and **82** respectively[96]) is a characteristic feature of the interactions indicated (Fig. 11).



14 **81** **82**

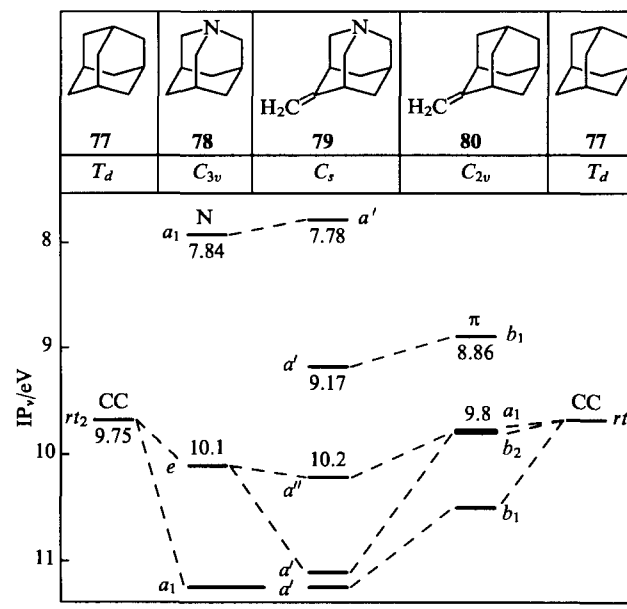
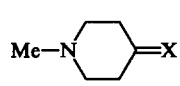


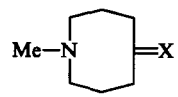
Figure 11. The highest occupied energy levels of compounds **77–80** according to photoelectron spectroscopic data.[95]

The energy splitting of the levels (ΔE = 0.47 eV) in the case of compound **79** is much smaller than in 1,4-diazabicyclooctane (ΔE = 2.1 eV [35]) as a consequence of the greater symmetry of the latter (D_{3h}). For adamantane **79** and thiacyclohexane **81** derivatives, containing an exocyclic double bond or a carbonyl group and having the chair conformation, the interaction through σ-bonds predominates.[94–96] For the analogous derivatives of thiaperhydronaphthalene, a weak interaction through σ-bonds takes place for the *trans,trans*-orientation of the five σ-bonds, such interaction being absent for the *trans,cis*-orientation,[96] which is consistent with Hoffmann's ideas.[20,21]

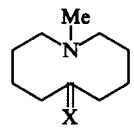
In the azacycloalkanones **83–86** or methyleneazacycloalkanones **87–90**, the increase in the splitting of the levels of the n_N nitrogen orbital and the π orbital of the carbonyl group or the double bond compared with that in the cyclic monofunctional compounds is due to the transannular interaction.[97]



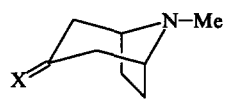
83, 87



84, 88



85, 89

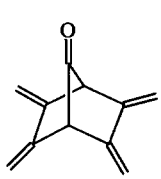


86, 90

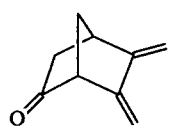
83–86: X = O;
87–90: X = CH_2.

The manifestation of the appreciable n,π interactions in the eight-membered rings of compounds **84** and **88** has been explained by the mutual approach in space of the corresponding structural groups. In 1-azacyclodecan-6-one **85**, n,π interaction also occurs, whereas in 6-methylene-1-azacyclodecane **89** it is not observed, which can be accounted for by the difference between the conformations of these molecules.[97] Furthermore, interactions of the n orbitals of the nitrogen atom and the oxygen atom of the carbonyl group have been observed for compounds **83–86**.[97]

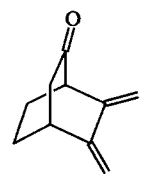
Comparison of the photoelectron spectroscopic data for 2,3,5,6-tetramethylidenebicyclo[2.2.1]heptan-7-one **91**, 5,6-dimethylidenebicyclo[2.2.1]heptan-2-one **92**, 5,6-dimethylidenebicyclo[2.2.2]octan-2-one **93**, and 5,6,7,8-tetramethylidenebicyclo-[2.2.2]octan-2-one **94** with the spectra of other β,γ-unsubstituted ketones and related alkenes as well as the results of nonempirical calculations (STO-3G) for compounds **91–94** confirmed that the appreciable interactions of the n_O orbital of the oxygen LEP and the π orbitals of the double bonds are largely effected through σ-bonds.[98]



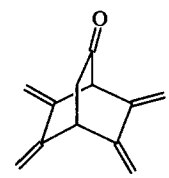
91



92

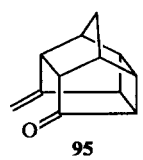


93

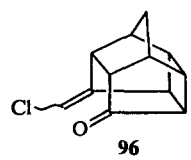


94

In the photoelectron spectra of paracyclophanes containing π-donor and π-acceptor substituents in the aromatic rings, the splitting of the first ionisation bands (~0.3 eV) as a consequence of the interaction of the π orbitals through space is observed.[98] In the study of the photoelectron spectra of 8,11-disubstituted pentacycloundecanes **95** and **96**, the splitting of the peaks (0.4–0.6 eV), caused by the interaction of the two unsaturated fragments through space, has also been observed.[56]



95



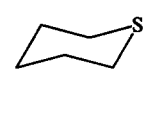
96

In the molecules of ethanolamine and its derivatives containing the O–C–C–N group, there is a possibility of interaction of the LEP of the nitrogen and oxygen atoms with the neighbouring σ-bonds of the skeleton or their interaction through σ-bonds is possible for certain conformations.[100,101] This entails the transfer of electron density from the less electronegative nitrogen atom to the more electronegative oxygen atom. The same effect has been observed in the study of acyclic and cyclic organosilicon compounds containing the Si–O–C–C–N fragment. In these compounds, the basicity of the nitrogen atom is appreciably reduced regardless of the presence or absence of the transannular Si ← N.[102]

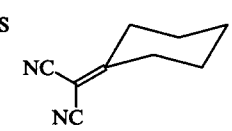
Similar phenomena have been observed also in other X–C–C–Y systems, for example in N–C–C–Cl and S–C–C–Cl, in which the chlorine atom is distinguished by a high mobility (in the O–C–C–Cl system, the chlorine atom is chemically inert), whereas in the X–C–Y systems (for example, in α-chloroethers) electron density is transferred from the more electronegative heteroatom (oxygen) to the less electronegative heteroatom (chlorine).

2. Absorption and emission spectra

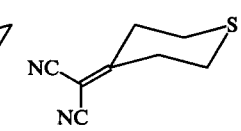
UV spectroscopy has been used widely in the study of interactions through space and through σ-bonds in molecules containing an explicit donor and acceptor separated by σ-bonds.[95,103–108] A new UV band (the ICT band) appears in the absorption spectra of bifunctional compounds with fixed geometries in which the donor and acceptor are separated by three or five σ-bonds. The band is due to charge transfer from an occupied orbital of the donor (nitrogen, sulfur, etc.) to the unoccupied π^* orbital of the acceptor [C=C, C=O, $C=C(CN)_2$, $C=CHCO_2R$, $C=C(CN)CO_2R$].[107]



14 (λ = 228 nm)



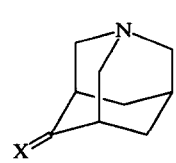
97 (λ = 235 nm)



98 (λ = 230 and 294 nm)

In our view, this transition can take place with a fairly high probability both on partial overlap of the above two orbitals in space and when they are mixed with the occupied (σ) and unoccupied (σ*) orbitals of the intervening system. The charge transfer between the structural groups (D and A) separated in space has been confirmed by the higher dipole moments of these molecules in the excited state (10.5–23.0 D).[104,108]

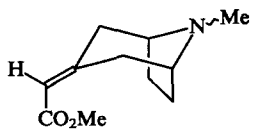
As a consequence of the large distance between the nitrogen atom and the electron-accepting substituent ($C=CH_2$, C=O) and also the unfavourable mutual orientation of the LEP of nitrogen and the π^* orbital of the acceptor, in rigid bicyclic systems (derivatives of azaadamantane) direct overlap (through space) is impossible.[94,95,104,106,108] An ICT band has been observed in the UV absorption and emission spectra of compounds **79** and **99** in solutions (at 220 and 241 nm for compounds **79** and **99** respectively); it has a very weak vibrational structure (even in the gas phase).[95,104] It was assigned to the transition from the orbital embracing mainly the nitrogen LEP to the antibonding π^* orbital of the $C=CH_2$ or C=O group. Similar ICT bands in the range 280–330 nm ($\varepsilon \simeq 4500$) have been observed for the derivatives of azaadamantane containing the electron-accepting groups $C=CHCO_2R$ (λ = 275 nm), $C=C(CN)CO_2R$ (λ = 316 nm), and $C=C(CN)_2$ (λ = 317 nm). Similar effects have been noted also in the analysis of the UV spectra of nitroazaadamantanes.[109]



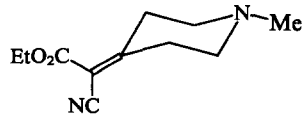
X = CH_2 (**79**), X = O (**99**)

The spectrum of compound **100**, in which the nitrogen atom is separated from the $MeO_2CCH=C$ group by three σ-bonds, also contains an ICT band (at 250 nm).[108] This molecule has a

geometry which is consistent with all the necessary conditions for the mutual orientation of the nitrogen LEP and the σ-bonds suitable for the occurrence of the interactions under consideration.[20,21,30,31] An ICT band is absent from the spectrum of compound **101**, the conformation of which is inconsistent with the above conditions.

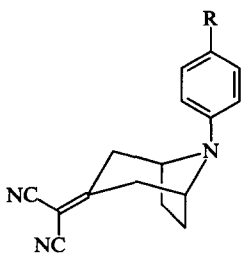


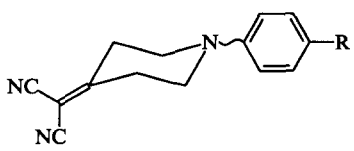
100



101

The influence of the conformation on the extent of the interaction through σ-bonds has been studied in relation to compounds **102**–**105** containing donor and acceptor centres.[110]





102 (R = H), **103** (R = OMe) **104** (R = H), **105** (R = OMe)

In compound **102**, the phenyl group occupies an axial position relative to the piperidine rings, which leads to an antiparallel orientation of the nitrogen LEP and of the central C–C bond. This conformation is retained also in solution in the solid phase (according to X-ray diffraction data). The spectrum of compound **102** contains an ICT band, the intensity of which hardly changes with decrease in temperature (Table 5).

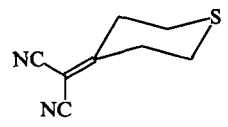
Table 5. The ICT bands in the spectra of compounds **102**–**105** (293 K, solvent — CH_2Cl_2).[110]

Compound	λ_{CT}/ nm	ε/litre mol^{-1} cm^{-1}
102	360	6100
103	378	5100
104	352	3065
105	368	2130

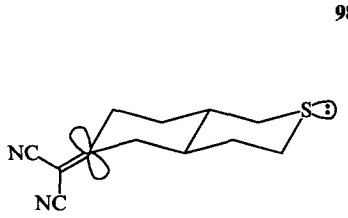
Similar results were also obtained in the study of the structural and spectroscopic characteristics of compound **103**. The spectrum of compound **104** likewise contains an ICT band, but its intensity is appreciably lower, increasing significantly with decrease in temperature. This feature of the compound can be explained by the existence in solution of an equilibrium between conformers with axial and equatorial disposition of the phenyl group, although in the solid phase compound **104** has only one (axial) conformation.[110] In the spectrum of compound **105**, the intensity of the ICT band is lowest and equilibrium between the conformers is observed, but the relative content of the axial conformer is low (in the crystalline state, this compound exists in the equatorial conformation). According to X-ray diffraction data, the length of the central C–C bond in compound **102** is much greater (1.559 Å) than in compound **105** (1.526–1.529 Å).

In compound **98**, having the chair conformation, the mutual orientation of the LEP of the sulfur atom and the C–C π-bonds is favourable for their interaction. An ICT band is observed in the spectrum of compound **98** at 294 nm (ε = 2860).[107]

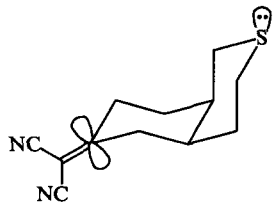
For the fixed *trans*-orientation of the bicyclic compound **106a**, an ICT band is also observed in the spectrum of the latter (at 270 nm), indicating the interaction of the sulfur LEP with the π-acceptor through five σ-bonds. For the *cis*-orientation in compound **106b**,[107,108] there is no such interaction, in conformity with Hoffmann's requirement that the σ-bonds must have the *trans,trans*-orientation.



98

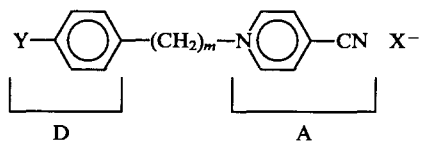


106a



106b

The band due to the intramolecular charge transfer between the aromatic fragment (the donor D) and the pyridinium cation (the acceptor A) is observed in the electronic spectra of compounds **107** having the general formula.[111–113]



107

m = 1–4, Y — electron-donor substituents.

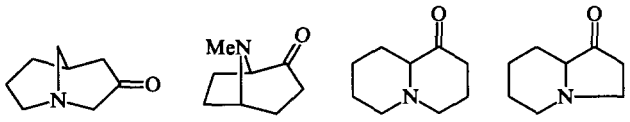
The transition energy is determined by the difference between the π and π* energy levels of the donor and acceptor. Accordingly the length of the methylene chain has little influence on the position of the band but does have a significant effect on its intensity.[111] For certain conformations of compound **107** (m = 1), there is a possibility of a direct overlap of the π orbitals of the donor and the acceptor.

The *trans*- and *gauche*-conformations are believed to be the main ones in compound **107** (m = 2). They are described by the angle φ (rotation about the central C–C bond). For $\varphi > 60°$, only the interaction through σ-bonds takes place, whilst for $\varphi < 60°$ there is in addition also direct π,π overlap due to the interaction through space. The interaction through σ-bonds depends on the overlap of the π orbitals of the donor and the π* orbitals of the acceptor with the σ and σ* orbitals of the intervening C–C bond. The intensity of the ICT band is then determined by their mutual orientation and varies from 225 litre mol^{-1} cm^{-1} ($\varphi \sim 60°$) to 1715 litre mol^{-1} cm^{-1} ($\varphi \sim 144°$).

Quantum-chemical calculations have made it possible to estimate the extent of the interaction of the LEP of the nitrogen atom and the carbonyl oxygen atom with the occupied and unoccupied σ and σ* orbitals of the intervening C–C bond and also with the π orbitals of the carbonyl group in α-aminoketones containing the N–CH_2–C=O group.[105,114,115] It was established at the same time that the interactions under consideration depend on the mutual orientation of the functional groups. The conformations of the molecules of these compounds are specified by the angles φ and θ ($\varphi = 0$, if the C–N bond eclipses C=O and $\theta = 0$ if the nitrogen LEP eclipses the C–C bond).[105]



The interaction through σ-bonds is a maximum in the (φ, 0) and (φ, 180) conformations, whereupon there is maximum overlap between the orbitals of the nitrogen and oxygen LEP and of the adjoining σ-bond. As a consequence of the manifestation of the above interactions, the band due to the $n \rightarrow \pi^*$ transition at 290 nm in the UV absorption spectra of unsaturated cyclic ketones shifts to the region 300–335 nm in the spectra of the cyclic α-aminocarbonyl compounds **108–111** (Table 6).[105]



108 **109** **110** **111**

Table 6. Spectroscopic parameters for certain α-aminoketones with a fixed conformation.[105]

Compound[a]	φ/deg	θ/deg	Solvent	λ/nm (ε)
108	160	165	Hexane	330 (55)
109	180	330	Ethanol	314 (68)
110	150	300	Isooctane	314 (48)
111	170	270	Isooctane	293 (29)

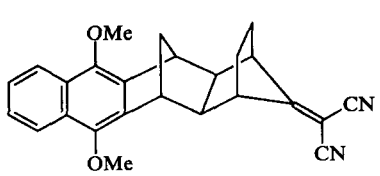
[a] The compounds are quoted in order of increasing deviation of n_O and n_N from coplanarity.

The angle φ for these compounds is close to 180° and the interaction through space is hardly manifested. The energy of the $n \rightarrow \pi^*$ transition depends mainly on the angle θ. When the orbital of the nitrogen LEP is oriented at right angles to the N–C–C=O plane (θ = 90°), the interaction through σ-bonds is ruled out and the energy of the $n \rightarrow \pi^*$ transition is the same as in saturated ketones.

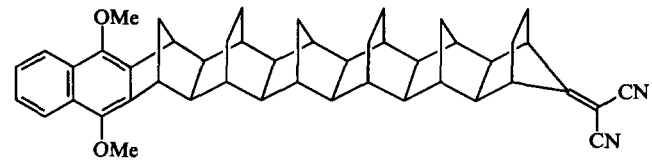
Appreciable changes are observed in the circular dichroism spectra of azacyclohexanones containing the $N-CH_2-C=O$ group when the nitrogen LEP is antiperiplanar relative to the $C_\alpha-C(O)$ bond. Such effects are absent when the nitrogen LEP is in the *gauche*-conformation relative to this bond.[114,115] This demonstrates the influence of the conformations on the interaction through σ-bonds and shows how the interaction with charge transfer differs in stereoisomers containing donor and acceptor fragments with different orientations.

The characteristics of the ICT bands are more sensitive to the interaction through the σ-bonds of nonequivalent groups than photoelectron spectroscopic data.[96]

Studies by pulse radiolysis and photoinduced electron transfer methods of the interactions between the donor and acceptor separated by saturated σ-bridges in rigidly fixed systems containing between 4 and 13 intervening σ-bonds (for example, in compounds **112** and **113**) confirmed the theoretical ideas concerning the mechanism of the interaction through σ-bonds.[28,116] The very rapid intramolecular electron transfer between the donor and the acceptor separated by distances ranging from 7 to 14.9 Å is due to the interaction of their π and π* orbitals with the σ and σ* orbitals of the hydrocarbon bridge.



112



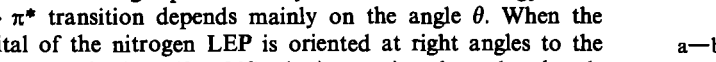
113

The experimental rate constant for the intramolecular electron transfer depends on the number of intervening σ-bonds (m). A similar dependence has been obtained with the aid of nonempirical calculations in the analysis of the interaction through σ-bonds in model compounds.[28] The intramolecular electron transfer rate constant is also determined by the geometry of the intervening bridge. It decreases by a factor of approximately five on passing from the *trans,trans*- to the *trans,cis*-conformation (m = 8) and diminishes from 10^{11} s^{-1} to 4×10^8 s^{-1} on passing from compound **112** to **113**. The high electron transfer rate constants have been explained by the interaction through σ-bonds, including the σ,π interaction.[28,116] Electron transfer processes between equivalent and nonequivalent groups joined by different hydrocarbon bridges have been investigated by the luminescence and EPR methods and by electronic spectroscopy.[117–121]

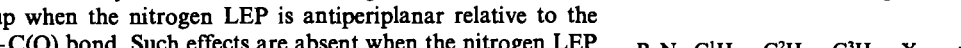
IV. The influence of the interaction through σ-bonds on the reactivity of organic compounds

Electronic interactions cannot fail to influence the reactivity of organic compounds. We shall consider this influence in relation to several examples.

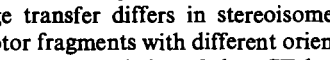
The heterolytic fragmentation



is a very common reaction in organic chemistry and has been studied in detail by Grob.[103,122] The fragmentation of 1-amino-3-halopropanes to ethylene and the corresponding iminium salt can also serve as an example.



Reaction may occur either via a concerted mechanism or as a two-stage process. In the former case, the C^1-C^2 and C^3-X bonds are ruptured simultaneously, while in the latter the cation

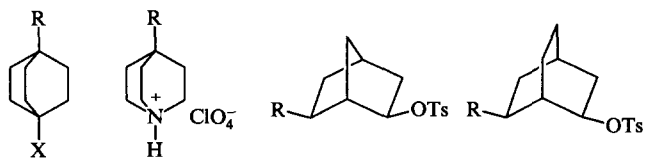


is formed initially. Analysis of the experimental and theoretical results led Grob to the conclusion that the concerted fragmentation occurs if the nitrogen LEP and the C^1-C^2 and C^3-X σ-bonds lie in the same plane and are oriented approximately parallel to one another. Such orientation of the fragments presupposes their interaction through σ-bonds. As a result, the C^1-C^2 bond is weakened, which leads to fragmentation.

For the antiperiplanar orientation of the nitrogen LEP, the C^1-C^2 σ-bond, and the free p orbital of the C^3 atom, the interaction in the cation through σ-bonds likewise induces a weakening of the C^1-C^2 bond; the following order in the arrangement of the levels has been established: A(HOMO) < S(LUMO). Thus both mechanisms presuppose a definite role of the interaction through σ-bonds in the fragmentation reaction.

It has been established that, in the solvolysis of 4-substituted bicyclo[2.2.2]oct-1-yl *p*-nitrobenzenesulfonates **114**, 4-substituted quinuclidinium perchlorates **115**, and the 2-substituted norbornyl tosylate **116** and bicyclo[2.2.2]octyl tosylate **117**, the

influence of the substituents R on the reaction centre X is largely determined by their inductive effect.[123-125] However, for R = $HOCH_2$, CH_3OCH_2, H_2NCH_2, $AcOCH_2$, $ClCH_2$, $TsOCH_2$, and H_2NCO, the rate of reaction increases by a factor of 2–8 compared with the rate calculated from the inductive constant of the substituent R. The increase in the rate of reaction has been explained by the interaction through σ-bonds. For the same reason, the solvolysis of compound **114** with R = $Sn(CH_3)_3$ is 3000 times faster than for R = Alk.[126]



114 **115** **116** **117**

X = p-$NO_2C_6H_4SO_3$

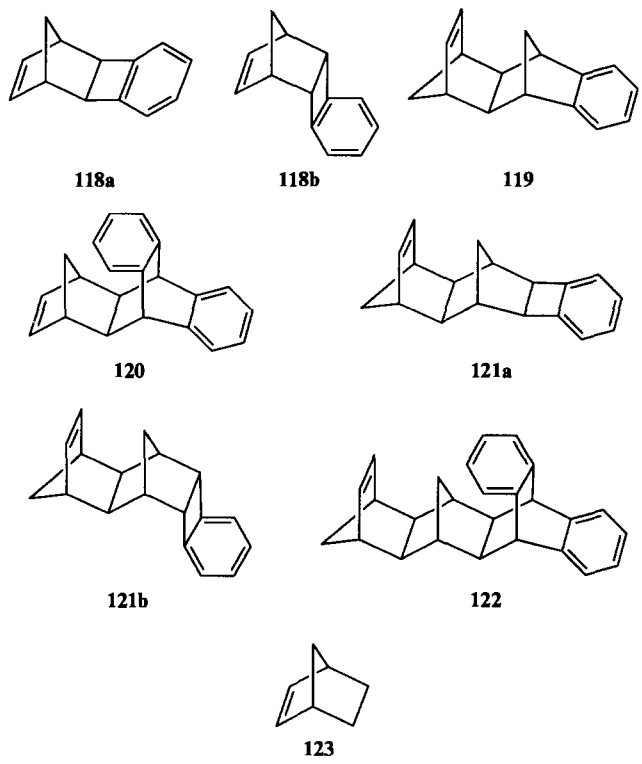
According to quantum-chemical calculations (EHM), the interaction through σ-bonds between the lowest unoccupied MO of aryl cations, localised on a positively charged centre, and the occupied $n(\pi)$ orbitals of the substituents leads to their stabilisation compared with the unsubstituted phenyl cation.[29,127] Similarly, electron-accepting substituents stabilise the aromatic carbanion $XC_6H_4^-$.[29] The photolysis of cyclobutanones entails ring expansion with formation of the corresponding tetrahydrofurans. This has been explained by the interaction through σ-bonds in the intermediate radical.[128]

The high stereospecificity of the cycloaddition of tetracyanoethylene to alkyl propenyl ethers with the intermediate formation of the 1,4-dipoles has also been explained by the predominance in the latter of the interaction through σ-bonds.[29,129]

A striking example of the influence of the interaction through σ-bonds on the reactivity of unsaturated organic compounds is provided by their Birch reduction with a solution of an alkali metal in liquid ammonia.[25,130,131] Isolated double bonds are usually not reduced by this method. However, when they approach one another or an aromatic ring, the rate of hydrogenation increases sharply, which is largely due to the interaction through space. Thus norbornadiene **38** (m = 1) and the related compounds **118–122** are reduced 10^5 times faster than norbornene **123** (Table 7).

Table 7. The coefficients (k_D^E) of the increase in the rate of the Birch reduction of double bonds[25] (*tert*-butyl alcohol served as the proton donor).

Substrate	Standard	Metal	k_D^E
38 (m = 1)	**123**	Li	10^5
118a	**123**	Li	140
	123	Na	169
	123	Na/cryptand[2.2.2]	206
118b	**123**	Li	78
69	**71**	Li	26
65	**66**	Li	18
119	**71**	Li	96
120	**66**	Li	2900
121a	**71**	Li	3
121b	**71**	Li	3.5
122	**71**	Li	5
71	**123**	Li	5.8
66	**123**	Li	0.6



118a **118b** **119**

120 **121a**

121b **122**

123

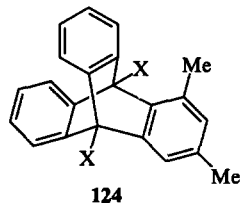
In the Birch reduction of the polycyclic unsaturated hydrocarbons **65**, **69**, and **118–122**, in which the unsaturated fragments are separated by three (compounds **118a, b**), four (compounds **65**, **69**, **119**, and **120**), five (**121a, b**), or six (compound **122**) σ-bonds, the rates of reduction of the double bonds (k_D^E) reflect the interaction of these fragments through σ-bonds (Table. 7).[25] Thus the double bond in the *exo*-compound **118a** is reduced 140 times faster than in norbornene **123**. The lower value of k_D^E for the *endo*-compound **118b** compared with the *exo*-compound **118a** can be explained very successfully by the competition in this system of the interaction of the π orbitals through space and through σ-bonds.[131] An example of the chemical manifestation of the interactions through four σ-bonds is provided by the Birch reduction of the hydrocarbons **119** and **120**, in which the rate constants k_D^E are 96 and 2900 respectively.[132] In terms of the mechanism adopted for this reaction, the interaction between the π* levels of the double bonds and the aromatic ring diminishes the energy of the lowest unoccupied MO and increases the probability of the formation of a radical-anion.[25,131] This has been confirmed by quantum-chemical calculations (EHM, INDO) for compound **118a**, indicating an appreciable mixing of the π* MO of the double bond and the aromatic ring.

The interaction through space and through σ-bonds of the vinyl groups in hexa-1,5-diene and hepta-1,6-diene determines their capacity for photochemical [2 + 2]-cyclisation.[133,134]

The change in reactivity in many intramolecular reactions proceeding with formation of intermediate radicals or biradicals can be explained by the effects of the interaction through space or through σ-bonds of two p orbitals with unpaired electrons (a biradical) or of p orbitals with an unpaired electron and an occupied π orbital (a radical).[135] The stability of the cyclic transition state depends on the number of intervening σ-bonds, the state incorporating ($4m$ + 2) σ-electrons being energetically more favourable. This concept of the 'σ-cooperation' indicates the preferential formation in the transition state of odd-membered rings on biradical cyclisation and of even-membered rings on intramolecular hydrogen or hydride migration.[136]

Analysis of the unoccupied π* orbitals and reactivities of triptycene derivatives **124** showed that the deprotonation of compound **124a** (X = H) takes place preferentially with

participation of the methyl group in the 1(C_α)-position, whereas the corresponding reaction of compound **124b** (X = Cl) takes place with participation of the methyl group in the 3(C_β)-position.[137]



124

X = H (**124a**), Cl (**124b**)

By virtue of the interaction of the π* orbitals of the benzene rings of triptycene through σ-bonds, the relative energies of the degenerate unoccupied levels are $e' < e''$. In interaction through space, this relation is reversed. On passing from X = H ($e' < e''$) to an electronegative substituent (X = Cl), the interaction through σ-bonds is weakened and the order in the arrangement of the levels changes ($e' > e''$). The reactivity agrees with the nature of the lowest unoccupied orbitals e' and e''.

Yet another example of the chemical effect of orbital reactions through σ-bonds and through space on the reactivity of molecules may be provided by the reactions of unsaturated cyclic sulfones with ethyl azidoformate and peracids, which is accompanied by the formation of the corresponding aziridine and oxiran derivatives.[138] There is a correlation between the reactivity of the double bond and its π-ionisation potential, which is higher in the compounds investigated compared with olefins. This increase is caused by the orbital interaction through σ-bonds and/or through space between the sulfone group and the double bond.[138] Similar effects have been noted in the interaction of a series of bicyclic olefins with nitrenes.[139]

References

1. A P Grekov, V Ya Veselov *Usp. Khim.* **47** 1200 (1978) [*Russ. Chem. Rev.* **47** 631 (1978)]
2. S Hoz, E Buncel *Isr. J. Chem.* **26** 313 (1985)
3. V P Feshin, L S Romanenko, M G Voronkov *Usp. Khim.* **50** 460 (1981) [*Russ. Chem. Rev.* **50** 248 (1981)]
4. N S Zefirov, N M Shekhtman *Usp. Khim.* **40** 594 (1971) [*Russ. Chem. Rev.* **40** 315 (1971)]
5. P Deslongchamps *Stereoelectronic Effects in Organic Chemistry* (Oxford: Pergamon Press, 1983) Vol. 1
6. J Tvaroska, T Bleha *Chem. Pap.* **39** 805 (1985)
7. A J Kirby *The Anomeric and Related Stereoelectronic Effects at Oxygen* [New York: Springer, 1983] (Translated into Russian; Moscow: Mir, 1985)
8. R O Hitchins, L D Kopp, F L Eliel *J. Am. Chem. Soc.* **90** 7174 (1968)
9. A J Hoog, H R Buys, C Altona, E Havinga *Tetrahedron* **25** 3365 (1969)
10. C Eaborn, R W Bott *Organometallic Compounds of the Group IV Elements* (Ed. A G MacDiarmid) (New York: Marcel Dekker, 1968) Vol. 1, p. 1
11. A W P Jarvie *Organomet. Chem. Rev., Sect. A* **6** 153 (1970)
12. T-H Chan *Acc. Chem. Res.* **10** 442 (1977)
13. M G Voronkov, V P Feshin, in *Determination of Organic Structures by Physical Methods* (New York: Academic Press, 1973) Vol. 1, p. 169
14. A N Vereshchagin *Induktivnyi Effekt* (The Inductive Effect) (Moscow: Nauka, 1987) p. 325
15. A A Korkin *Usp. Khim.* **61** 865 (1992) [*Russ. Chem. Rev.* **61** 473 (1992)]
16. M J S Dewar *Hyperconjugation* (New York: Ronald Press, 1962)
17. H D Martin, B Mayer *Angew. Chem., Int. Ed. Engl.* **22** 283 (1983)
18. N D Epiotis (Ed.) *Structural Theory of Organic Chemistry* (Berlin: Springer, 1977) Vol. 70, p. 245
19. V F Traven' *Elektronnaya Struktura i Svoistva Organicheskikh Molekul* (The Electronic Structure and Properties of Organic Molecules) (Moscow: Khimiya, 1989)
20. R Hoffmann, A Imamura, W J Hehre *J. Am. Chem. Soc.* **90** 1499 (1968)
21. R Hoffmann *Acc. Chem. Res.* **4** 1 (1971)
22. E Heilbronner, J P Maier *Electron Spectroscopy: Theory, Techniques and Applications* (London: Academic Press, 1977) p. 207
23. D Dougherty, P Brint, S P McGlynn *J. Am. Chem. Soc.* **100** 5597 (1978)
24. R Gleiter, J Spanget-Larsen, in *Topics in Current Chemistry* (Berlin: Springer, 1979) Vol. 86, p. 139
25. M N Paddon-Row *Acc. Chem. Res.* **15** 245 (1982)
26. D J Pasto, D M Chipman, J J Worman *J. Phys. Chem.* **86** 3981 (1982)
27. R Gleiter, W Schäfer *Acc. Chem. Res.* **23** 369 (1990)
28. M N Paddon-Row, J W Verhoeven *New J. Chem.* **15** 107 (1991)
29. R Gleiter *Angew. Chem.* **86** 770 (1974)
30. E Heilbronner, A Schmelzer *Helv. Chim. Acta* **58** 936 (1975)
31. T K Brunck, F Weinhold *J. Am. Chem. Soc.* **98** 4392 (1976)
32. M N Paddon-Row, H K Patney, R S Brown, K N Houk *J. Am. Chem. Soc.* **103** 5575 (1981)
33. D W Turner, C Baker, A D Baker, C R Brundle *Molecular Photoelectron Spectroscopy* (New York: Wiley, 1970) p. 252
34. K D Jordan, P D Burrow *Acc. Chem. Res.* **11** 341 (1978)
35. P Bischof, J A Hashmall, E Heilbronner, V Hornung *Tetrahedron Lett.* **10** 4025 (1969)
36. M J S Dewar, J S Wasson *J. Am. Chem. Soc.* **92** 3506 (1970)
37. E Heilbronner, K A Muszkat *J. Am. Chem. Soc.* **92** 3818 (1970)
38. S F Nelsen, J M Buschek *J. Am. Chem. Soc.* **96** 7930 (1974)
39. R W Alder, R J Arrowsmith, A Casson, R B Sessions, E Heilbronner, B Kovač, H Huber, M Toagepera *J. Am. Chem. Soc.* **103** 6137 (1981)
40. A Imamura, M Ohsaku, K Akagi *Tetrahedron* **39** 1291 (1983)
41. N H Werstiuk, D N Butler, S Datta *Can. J. Chem.* **64** 760 (1986)
42. D A Sweigart, D W Turner *J. Am. Chem. Soc.* **94** 5599 (1972)
43. H Bock, G Wagner *Angew. Chem., Int. Ed. Engl.* **11** 150 (1972)
44. C Guimon, M-F Guimon, G Pfister-Guillouzo *Tetrahedron Lett.* **16** 1413 (1975)
45. A D Baker, M A Brisk, T J Venanzi, Y S Kwon, S Sadka, D C Liotta *Tetrahedron Lett.* **17** 3415 (1976)
46. M Kobayashi, R Gleiter, D L Coffen, H Bock, W Schulz, V Stein *Tetrahedron* **33** 433 (1977)
47. T Vondrak, Z Bastl *J. Mol. Struct.* **160** 117 (1987)
48. J R Swenson, R Hoffmann *Helv. Chim. Acta* **53** 2331 (1970)
49. D O Cowan, R Gleiter, J A Hashmall *Angew. Chem.* **83** 405 (1971)
50. J Kelder, H Cerfontain, B R Higginson, D R Lloyd *Tetrahedron Lett.* **15** 739 (1974)
51. R Spafford, J Baiardo, J Wrobel, M Vala *J. Am. Chem. Soc.* **98** 5217 (1976)
52. R Spafford, J Baiardo, J Wrobel, M Vala *J. Am. Chem. Soc.* **98** 5225 (1976)
53. D C Frost, N P C Westwood, N H Werstiuk *Can. J. Chem.* **58** 1659 (1980)
54. R Gleiter, C Jähne *Tetrahedron Lett.* **24** 5063 (1983)
55. C Jähne, R Gleiter *Angew. Chem.* **95** 500 (1983)
56. A P Marchand, R Kaya, A D Baker *Tetrahedron Lett.* **25** 795 (1984)
57. R Gleiter, C Jähne, M Oda, M Iyoda *J. Org. Chem.* **50** 678 (1985)
58. V Balaji, K D Jordan, R Gleiter, C Jähne, C Müller *J. Am. Chem. Soc.* **107** 7321 (1985)
59. R Gleiter, C Jähne, C Müller *Helv. Chim. Acta* **69** 71 (1986)
60. A P Marchand, C Huang, R Kaya, A D Baker, E D Jemmis, D A Dixon *J. Am. Chem. Soc.* **109** 7095 (1987)
61. P R Bunker *Molecular Symmetry and Spectroscopy* (Translated into Russian; Moscow: Mir, 1981)
62. R Bartetzko, R Gleiter, J L Muthard, L A Paquette *J. Am. Chem. Soc.* **100** 5589 (1978)
63. D Dougherty, R L Blankespoor, S P McGlynn *J. Electron Spectrosc. Relat. Phenom.* **16** 245 (1979)
64. L A Paquette *Angew. Chem.* **90** 114 (1978)
65. H Dürr, R Gleiter *Angew. Chem.* **90** 591 (1978)
66. R Hoffmann, E Heilbronner, R Gleiter *J. Am. Chem. Soc.* **92** 706 (1970)
67. S Canuto, M C Zerner *J. Am. Chem. Soc.* **112** 2114 (1990)

68. K Kanda, T Koremoto, A Imamura *Tetrahedron* **42** 4169 (1986)
69. R Gleiter, J Uschmann *J. Org. Chem.* **51** 370 (1986)
70. R Gleiter, A Toyota, P Bischof, G Krennich, J Dressel, P D Pansegrau, L A Paquette *J. Am. Chem. Soc.* **110** 5490 (1988)
71. J J Worman, M Boerger *Proc. North Dakota Acad. Sci.* **33** 28 (1979)
72. P C Martino, P B Shelvin, S D Worley *Chem. Phys. Lett.* **68** 237 (1979)
73. K Ohno, T Ishida, Yu Naitoh, Y Izumi *J. Am. Chem. Soc.* **107** 8082 (1985)
74. R Gleiter, M Eckert-Maksic, W Schäfer, E A Truesdale *Chem. Ber.* **115** 2009 (1982)
75. R Gleiter, W Schäfer, G Krennrich, H Sakurai *J. Am. Chem. Soc.* **110** 4117 (1988)
76. R Gleiter, M Karcher, R Jahn, H Irngartinger *Chem. Ber.* **121** 735 (1988)
77. R Gleiter, W Schäfer, H Sakurai *J. Am. Chem. Soc.* **107** 3046 (1985)
78. V Balaji, K D Jordan, P D Burrow, M N Paddon-Row, H K Patney *J. Am. Chem. Soc.* **104** 6849 (1982)
79. F S Jorgensen, M N Paddon-Row, H K Patney *J. Chem. Soc., Chem. Commun.* 573 (1983)
80. M N Paddon-Row, H K Patney, J B Peel, G D Willett *J. Chem. Soc., Chem. Commun.* 564 (1984)
81. M N Paddon-Row *J. Chem. Soc., Perkin Trans. 2* 257 (1985)
82. N S Hush, G D Willett, M N Paddon-Row, H K Patney, J B Peel *J. Chem. Soc., Perkin Trans. 2* 827 (1986)
83. M N Paddon-Row, L M Englehardt, B W Skelton, A H White, F S Jorgensen, H K Patney *J. Chem. Soc., Perkin Trans. 2* 1835 (1987)
84. V Balaji, L Ng, K D Jordan, M N Paddon-Row, H K Patney *J. Am. Chem. Soc.* **109** 6957 (1987)
85. M F Falcetta, K D Jordan, J E McMurry, M N Paddon-Row *J. Am. Chem. Soc.* **112** 579 (1990)
86. M J Goldstein, R Hoffmann *J. Am. Chem. Soc.* **93** 6193 (1971)
87. F S Jorgensen, M N Paddon-Row *Tetrahedron Lett.* **24** 5415 (1983)
88. A M Oliver, M N Paddon-Row, M C R Symons *J. Am. Chem. Soc.* **111** 7259 (1989)
89. K Beck, S Hünig, G Kleefeld, H D Martin, K Peters, F Prokschy, H G von Schnering *Chem. Ber.* **119** 543 (1986)
90. S Hünig, H D Martin, B Mayer, K Peters, F Prokschy, M Schitt, H G von Schnering *Chem. Ber.* **120** 195 (1987)
91. K D Jordan, M N Paddon-Row *Chem. Rev.* **92** 395 (1992)
92. M N Paddon-Row, K D Jordan *J. Chem. Soc., Chem. Commun.* 1508 (1988)
93. M N Paddon-Row, S S Wong, K D Jordan *J. Am. Chem. Soc.* **112** 1710 (1990)
94. T Sasaki, S Eguchi, T Kiriyama, Y Sakito *J. Chem. Soc., Chem. Commun.* 725 (1974)
95. C Worrell, J W Verhoeven, W N Speckamp *Tetrahedron* **30** 3525 (1974)
96. R Sarneel, C W Worrell, P Pasman, J W Verhoeven, G F Mes *Tetrahedron* **36** 3241 (1980)
97. G Spanka, P Rademacher *J. Org. Chem.* **51** 592 (1986)
98. P-A Carrupt, R Gabioud, A Rubello *Helv. Chim. Acta* **70** 1540 (1987)
99. R Gleiter, W Schäfer, H A Staab *Chem. Ber.* **121** 1257 (1988)
100. S Leavell, J Steichen, J L Franklin *J. Chem. Phys.* **59** 4343 (1973)
101. C Alsenoy, K Siam, J D Ewbank, L Schäfer *J. Mol. Struct.* **136** 77 (1986)
102. E I Brodskaya, M G Voronkov, D D Toryashinova *J. Organomet. Chem.* **336** 49 (1987)
103. R Gleiter, W D Stohrer, R Hoffmann *Helv. Chim. Acta* **55** 893 (1972)
104. A W J D Dekkers, J W Verhoeven, W N Speckamp *Tetrahedron* **29** 1691 (1973)
105. C C Levin, R Hoffmann, W J Hehre, J Hudec *J. Chem. Soc., Perkin Trans. 2* 210 (1973)
106. P Pasman, J W Verhoeven, T J de Boer *Tetrahedron* **32** 2827 (1976)
107. P Pasman, J W Verhoeven, T J de Boer *Tetrahedron Lett.* **18** 207 (1977)
108. P Pasman, F Rob, J W Verhoeven *J. Am. Chem. Soc.* **104** 5127 (1982)
109. O V Agashkin, L M Shustova, V A Kosmakov, A I Kuznetsov, B V Unkovskii *Dokl. Akad Nauk SSSR* **303** 373 (1988)
110. B Krijnen, H B Beverloo, J W Verhoeven, C A Reiss, K Goubitz, D Heijdenrijk *J. Am. Chem. Soc.* **111** 4433 (1989)
111. J W Verhoeven, I P Dirks, T J de Boer *J. Mol. Spectrosc.* **42** 149 (1972)
112. A J de Gee, J W Verhoeven, W J Sep, T J de Boer *J. Chem. Soc. Perkin Trans. 2* 579 (1975)
113. M R De Filippis, M Faraggi, M H Klapper *J. Am. Chem. Soc.* **112** 5640 (1990)
114. J Hudec *J. Chem. Soc., Chem. Commun.* 829 (1970)
115. J Hudec *J. Chem. Soc., Perkin Trans. 1* 1020 (1975)
116. H Overing, M N Paddon-Row, M Heppener, A M Oliver, E Cotsaris, J W Verhoeven, N S Hush *J. Am. Chem. Soc.* **109** 3258 (1987)
117. M R Wasilewski, M P Niemczyk, D G Johnson, W A Svec, D W Minsek *Tetrahedron* **45** 4785 (1989)
118. G J Snyder, D A Dougherty *J. Am. Chem. Soc.* **111** 3927 (1989)
119. D A Dougherty *Acc. Chem. Res.* **24** 88 (1991)
120. J Pranata, V S Marudarajan, D A Dougherty *J. Am. Chem. Soc.* **111** 2026 (1989)
121. J A Novak, R Jain, D A Dougherty *J. Am. Chem. Soc.* **111** 7618 (1989)
122. C A Grob *Angew. Chem.* **81** 543 (1969)
123. C A Grob, R Rich *Tetrahedron Lett.* **19** 663 (1978)
124. C A Grob, R Rich *Helv. Chim. Acta* **62** 2793 (1979)
125. R Bielman, C A Grob, D Küry, G W Yao *Helv. Chim. Acta* **68** 2158 (1985)
126. W Adcock, A R Krstic, P J Duggan, V J Shiner Jnr, J Coope, M W Ensinger *J. Am. Chem. Soc.* **112** 3140 (1990)
127. R Gleiter, R Hoffmann, W-D Stohrer *Chem. Ber.* **105** 8 (1972)
128. C Quinkert, P Jacobs, W-D Stohrer *Angew. Chem.* **86** 197 (1974)
129. R Huisgen, R Schug, G Steiner *Angew. Chem.* **86** 48 (1974)
130. A J Birch, G S Rao *Adv. Org. Chem.* **8** 1 (1972)
131. M N Paddon-Row, R Hartcher *J. Am. Chem. Soc.* **102** 662 (1980)
132. M N Paddon-Row, R Hartcher *J. Am. Chem. Soc.* **102** 671 (1980)
133. R Gleiter, W Sander *Angew. Chem.* **97** 575 (1985)
134. E Fischer, R Gleiter *Angew. Chem.* **101** 925 (1989)
135. J W Verhoeven, P Pasman *Tetrahedron* **37** 943 (1981)
136. J W Verhoeven *Recl. Trav. Chim. Pays-Bas* **99** 369 (1980)
137. S Inagaki, T Okajima, K Tanaka *Chem. Lett.* 1219 (1988)
138. R A Aitken, J Gosney, H Farries, M N Palmer, I Simpson, J I G Cadogan, E J Tinley *Tetrahedron* **40** 2487 (1984)
139. R A Aitken, J Gosney, H Farries, M N Palmer, I Simpson, J I G Cadogan, E J Tinley *Tetrahedron* **41** 1329 (1985)

Russian Chemical Reviews **62** (10) 935–950 (1993)
©1993 Russian Academy of Sciences and Turpion Ltd

UDC 547.548 + 547.592.2 + 541.254.9 + 595.1

Reactions of cyclopropene derivatives with electrophiles

V R Kartashov, E V Skorobogatova, N S Zefirov

Contents

I. Introduction 935
II. The influence of the nature of the reagent on the reactions of cyclopropene derivatives 935
III. The mechanisms of the interaction of cyclopropene derivatives with electrophiles 947

Abstract. A systematic account is given of data on the reactions of cyclopropene derivatives with acids, halogen- and sulfur-containing electrophiles, and mercury salts. The influence of the nature of the electrophile and of the structure of the cyclopropenes on processes with retention and opening of the ring, on the stereochemistry of the addition of reactants to the cyclopropene bond, and on the stereochemistry of the formation of the ring opening products is examined. The reaction mechanisms are discussed. The bibliography includes 120 references.

I. Introduction

Cyclopropene derivatives as highly strained systems[1–11] have aroused much scientific interest. For a long time, the study of the physicochemical properties and reactivities of cyclopropene derivatives was held back by the difficulty of their synthesis. However, since the appearance in the 1960s of new methods of synthesis which have made these compounds entirely available, such studies have developed vigorously. The chemical properties of cyclopropenes in the diene synthesis,[3,4,12–15] dipolar addition,[3,4,16–20] and cyclodimerisation[21–23] reactions as well as reactions with electrophiles have been investigated systematically. Cyclopropene derivatives have proved convenient substances for the synthesis of a wide variety of heterocyclic and polycyclic systems.[3,4,12–23] Numerous studies have been devoted to the molecular and orbital structures of cyclopropenes, the main results of which may be found in the relevant publications[1,2,7–9,24–26] and in the literature quoted therein.

A large number of studies have led to the need for a systematic arrangement of the literature data. However, there have been very few review publications[3,4,27,28] and none whatever exist for reactions of cyclopropenes with electrophiles.

The aim of the present review is to survey the experimental data on the reactions of cyclopropene derivatives with electrophiles. Some information about these reactions has been published in review articles[3,4,27] and where necessary it is considered in the context of the data discussed in the present communication.

Although in the description of the literature data the probable reaction mechanisms are also considered, we thought it desirable to describe in a separate section of the review, on the basis of the data presented, the most general mechanisms of these reactions and also to consider in greater detail the publications devoted specifically to these problems. The review reflects the state of the problem at the end of 1992.

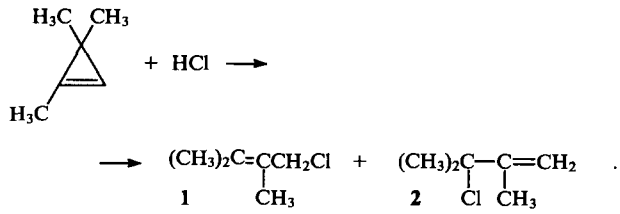
V R Kartashov, E V Skorobogatova Department of Physical and Colloid Chemistry at the Nizhny Novgorod State Technical University, ul. Minina 24, 603600 Nizhny Novgorod, Russian Federation.
Fax (7-831) 236 93 57
N S Zefirov Department of Organic Chemistry, Lomonosov Moscow State University, Leninskie Gory, 119899 Moscow.
Fax (7-095) 939 01 26

Received 25 June 1993
Uspekhi Khimii **62** (10) 991 – 1006 (1993); translated by A K Grzybowski

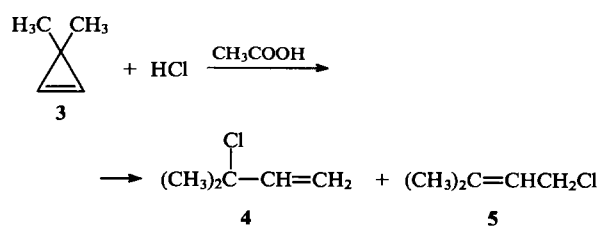
II. The influence of the nature of the reagent on the reactions of cyclopropene derivatives

1. Reactions of cyclopropenes with protic and Lewis acids

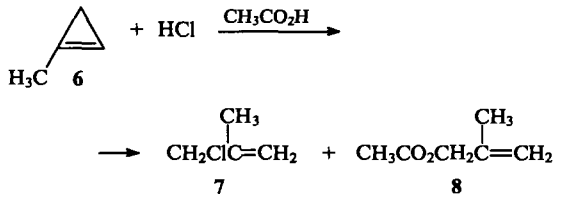
The reactions of propenes with protic acids usually lead to ring opening products. Thus the reaction of 1,3,3-trimethylcyclopropene with dry hydrogen chloride at –50 °C leads to the formation of 1-chloro-2,3-dimethylbut-2-ene **1** and 3-chloro-2,3-dimethylbut-1-ene **2** with compound **1** predominating.[3]



The reaction of 3,3-dimethylcyclopropene **3** with hydrogen chloride in acetic acid takes place similarly to the preceding reaction and involves the formation of 3-chloro-3-methylbut-1-ene **4** and 4-chloro-2-methylbut-2-ene **5**, the product ratio **4**:**5** varying during the course of reaction and amounting to 42 : 58 on extrapolation to zero time.[29]

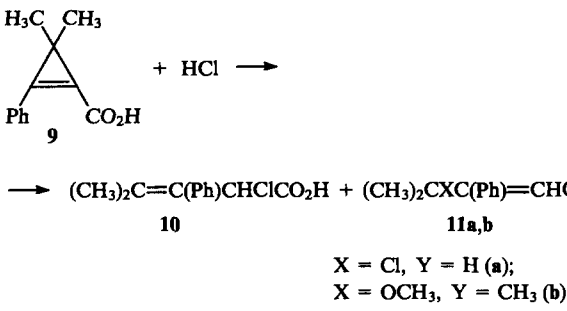


Under the same conditions, the interaction of 1-methylcyclopropene **6** with hydrogen chloride leads to a mixture of methylallyl chloride **7** and methylallyl acetate **8**.[29]



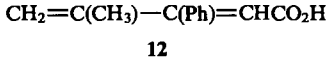
The formation of compound **8** with participation of the solvent indicates the cationoid nature of the intermediate, while the presence of the isomeric products of types **4** and **5** is evidence for its allylic structure.[29]

The reactions involving cyclopropene derivatives containing an electron-accepting substituent at the double bond, which hinders the formation of an allylic intermediate, proceed with formation of a cationoid intermediate. Thus 3,3-dimethyl-2-phenylcyclopropene-1-carboxylic acid **9** is converted into 2-chloro-4-methyl-3-phenylpent-3-enoic acid **10** and 4-chloro-4-methyl-3-phenylpent-2-enoic acid **11a** on treatment with hydrogen chloride.[30]

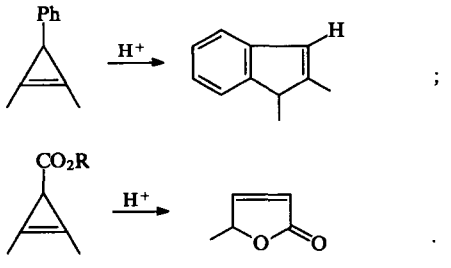


At 40–80 °C, compound **10** is formed preferentially (**10**:**11a** = 4:1, overall yield 60%), whilst at 20 °C the main product is compound **11a** (**10**:**11a** = 3:7).[30] The reaction of hydrogen chloride with the cyclopropene derivative **9** in methanol affords methyl 4-methoxy-4-methyl-3-phenylpropene-2-carboxylate **11b**.[31]

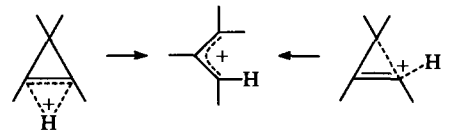
On treatment with toluene-4-sulfonic acid in boiling toluene, compound **9** is converted into 4-methyl-3-phenylpenta-2,4-dienoic acid **12**.[30]



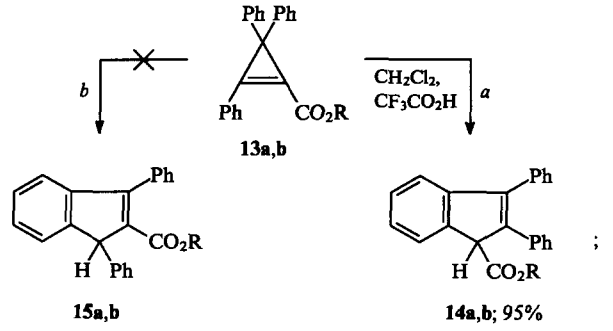
In the presence of a nucleophilic substituent at the methylene fragment of the cyclopropene derivative, treatment with acid leads to the isomerisation of the substrate.[3,27]



It has been suggested that this is a result of the protonation of the double bond or electrophilic attack on the C–C bond.[3,27]

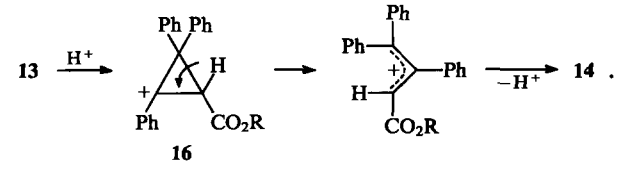


The occurrence of the reaction via the first mechanism is apparently more likely. This is indicated, for example, by the isomerisation of the esters of 2,3,3-triphenylcyclopropene-1-carboxylic acid **13**, which results in the exclusive formation of the indenes **14**.[32,33]

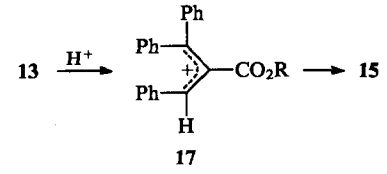


R = CH_3 (**a**), C_2H_5 (**b**).

The authors propose the following mechanism for the formation of the indenes **14**:



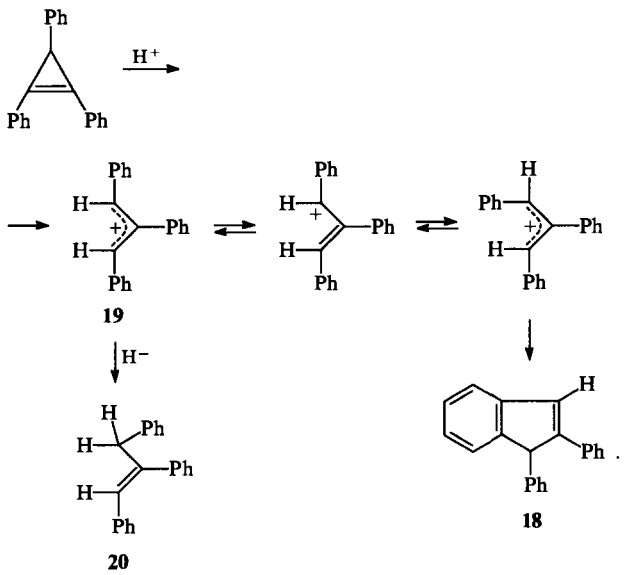
In the alternative version, one should expect the formation of the intermediate **17** and hence of the indenes **15**.



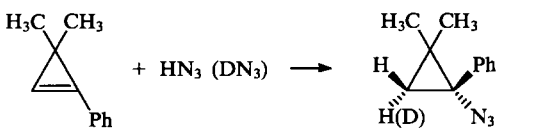
The question of the involvement in the reaction of the cyclopropyl type intermediate **16** is extremely controversial.[3] It is more probable that the allylic intermediate is formed directly as a result of the interaction of the electrophilic hydrogen with the double bond. This mechanism will be analysed in detail in the subsequent sections.

Kudryavtseva and Nesmeyanova[34] attempted to obtain data confirming the formation of the allylic intermediate in the reactions of cyclopropene derivatives with protic acids. For this purpose, a study was made of the isomerisation of 1,2,3-triphenylcyclopropene catalysed by trifluoroacetic acid in methylene chloride using triethylsilane as the donor of a hydride ion. Under the usual conditions, 1,2,3-triphenylcyclopropene is converted on

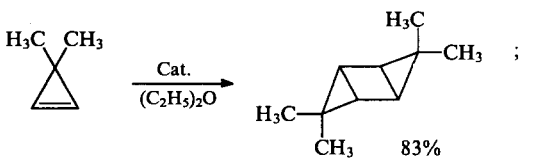
treatment with acid into 1,2-diphenylindene **18**. On the other hand, in the presence of triethylsilane, *cis*-1,2,3-triphenylpropene **20** is formed in a quantitative yield, which indicates the involvement of the allylic intermediate **19** in the reaction.



In the light of the data described above, the results of the reaction of 3,3-dimethyl-1-phenylcyclopropene with hydrazoic acid and deuterium azide were unexpected. Only adducts having the *cis*-configuration are formed in 60% and 38% yields respectively.[35]

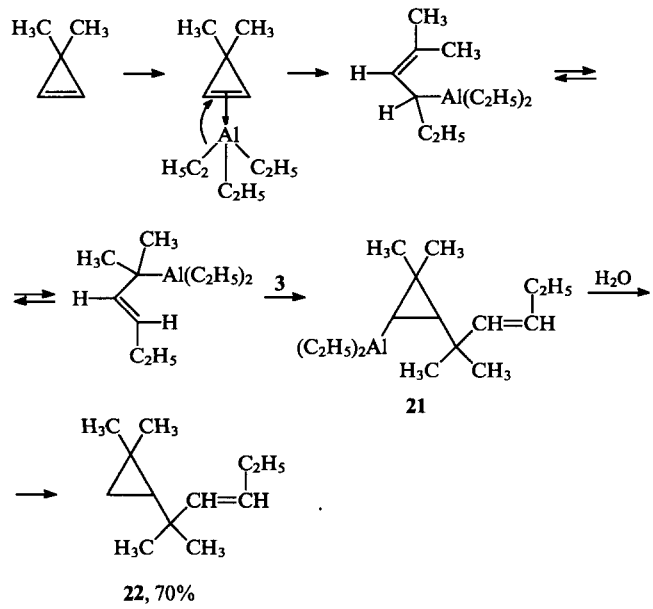


Extensive studies have been carried out on the reactions of cyclopropenes on treatment with Lewis acids. A characteristic feature of these processes is the wide variety of products and modes of reaction, which are determined mainly by the nature of the Lewis acid. For example, the cyclodimerisation of 3,3-dimethylcyclopropene[36] takes place smoothly on treatment with a number of Lewis acids and leads to the formation of *trans*-3,3,6,6-tetramethyltricyclo[3.1.0.$0^{2,4}$]hexane.

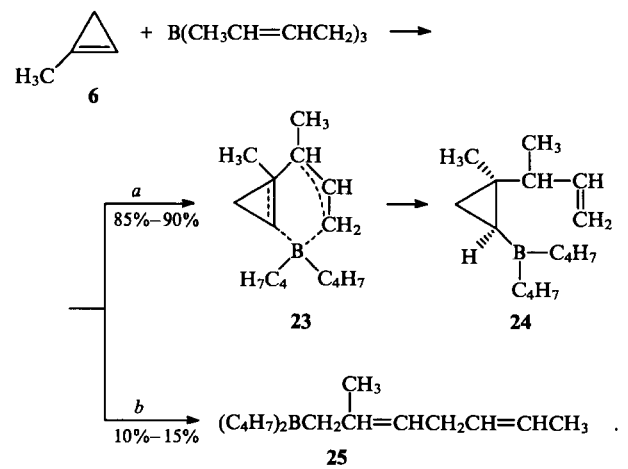


Cat. — $BF_3O(C_2H_5)_2$, $AlCl_3O(C_2H_5)_2$, $B(C_2H_5)_3$, $Al(C_2H_5)_3O(C_2H_5)_2$.

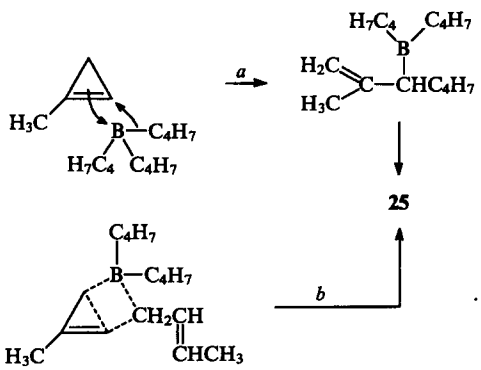
If the triethylaluminium dimer is used as the catalyst, then the process takes place differently and involves the formation of the product **21**, which affords *trans*-2-methyl-2-(2′,2′-dimethylcyclopropyl)hex-3-ene **22** after hydrolysis.



1-Methylcyclopropene **6** cyclodimerises in the reaction with boron trifluoride diethyl etherate,[36] but, when it is treated with triethylborane,[37] triallylborane,[38] and tricrotylborane,[39] the reagent adds to the cyclopropene with retention or opening of the ring. Thus, in the last case the products are *cis*-2-(but-3-en-2-yl)di(but-2-enyl)(2-methyl-1-cyclopropyl)borane **24** and di(but-2-enyl)(2-methylhepta-2,5-dien-1-yl)borane **25**.

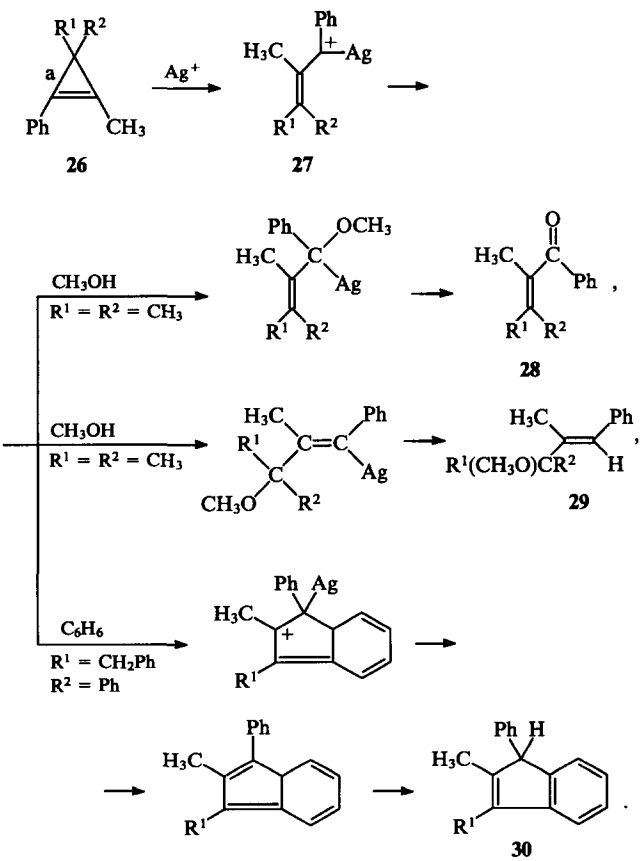


According to Bubnov et al.,[39] the formation of compound **24** shows that the addition of allylboranes to the double bond in cyclopropene derivatives is accompanied by the allyl rearrangement, apparently via the six-centred transition complex **23** with cyclic electron transfer. The formation of compound **25** can be represented by alternative schemes, according to which tricrotylborane attacks the double bond of the cyclopropene (pathway *a*) or the single C3 – C2 σ-bond (pathway *b*). The latter scheme appears less likely according to the authors,[39] as the location of the boron atom at the trigonal rather than the tetragonal carbon atom in the transition state is energetically more favourable.

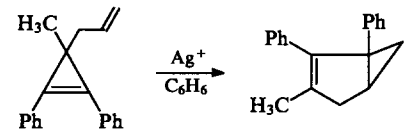


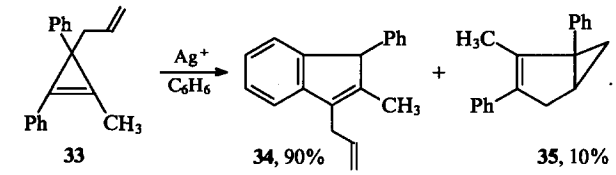
On treatment with silver perchlorate in benzene and methanol, the regio-selective opening of the ring compound **26** takes place with rupture of the single bond 'a'.[40] The structure of the product depends on the nature of the substituents. Thus 2,3,3-trimethyl-1-phenylcyclopropene **26** ($R^1 = R^2 = CH_3$) affords a mixture of 2,3-dimethyl-1-phenylbut-2-en-1-one **28** (65%) and 3-methoxy-2,3-dimethyl-1-phenylbut-1-ene **29** (45%). On the other hand, 3-benzyl-2-methyl-1,3-diphenylcyclopropene **26** ($R^1 = CH_2Ph$, R^2 = Ph) in benzene is converted into 3-benzyl-2-methyl-1-phenylindene **30** in a quantitative yield.

It is believed[40] that the silver ion, which is a strong Lewis acid, attacks the cyclopropene ring, forming the intermediate **27**, the stabilisation of which by the phenyl group determines the selectivity of the ring opening at the bond 'a'.

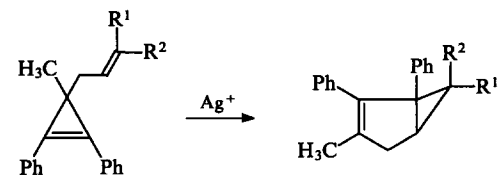


3-Allyl-3-methyl-1,2-diphenylcyclopropene **31** is converted into 3-methyl-1,2-diphenyl-bicyclo[3.1.0]hex-2-ene **32** in the presence of silver ions in benzene, while its analogue 3-allyl-2-methyl-1,3-diphenylcyclopropene **33** affords 3-allyl-2-methyl-1-phenylindene **34** and 2-methyl-1,3-diphenylbicyclo[3.1.0]hex-2-ene **35**.





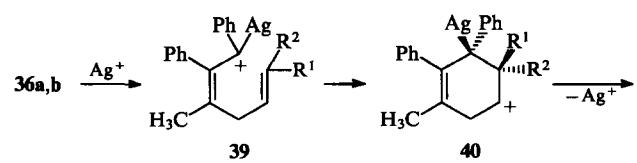
The isomerisation of (*E*)- and (*Z*)-1-(1-methyl-2,3-diphenyl-2-cyclopropen-1-yl)-but-2-enes **36a, b** takes place stereoselectively under these conditions with formation of *exo* and *endo*-3,6-dimethyl-1,2-diphenylbicyclo[3.1.0]hex-2-enes **37** and **38** respectively.[40]



$R^1 = CH_3$; R^2 = H (**a**)
R^1 = H; $R^2 = CH_3$ (**b**)

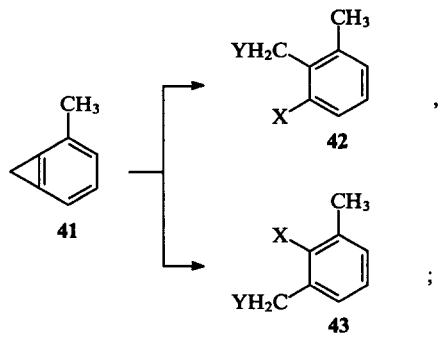
37: $R^1 = CH_3$; R^2 = H; 96%
38: R^1 = H; $R^2 = CH_3$; 97%

The authors[40] explain the stereoselectivity of the latter reaction within the framework of the mechanism of the formation of the argentocarbonium ion **39** and the subsequent interaction of the terminal double bond with the carbonium ion centre. The intermediate **40** formed under these conditions is converted into the products **37** and **38** after the elimination of silver.



The way in which the cyclopropene ring is opened in the reactions of methylbenzocyclopropenes depends on the nature of the electrophiles.[41] On reaction with silver nitrate in ethanol or

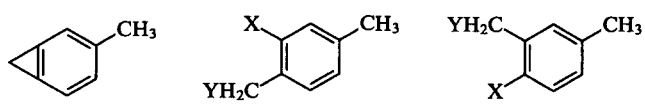
aniline, 2-methylbenzocyclopropene **41** affords compounds **42e, f** as the main products, whereas the reactions with bromine, iodine, and hydrogen chloride give rise to compounds **43a, c, d** as the main products. The overall yield of the products **42** and **43** in these reactions ranges from 54% to 70%.



41 **42** **43**

X = Y = Br (**a**); X = Br, Y = H (**b**); X = Y = I (**c**);
X = H, Y = Cl (**d**); X = H, Y = OC_2H_5 (**e**); X = H, Y = NHPh (**f**)

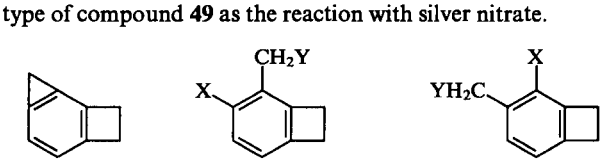
Similarly 3-methylbenzocyclopropene **44** reacts with silver nitrate to form mainly the *p*-xylenes **45**, while the reactions with the halogens and hydrogen chloride afford compounds **46**.



44 **45** **46**

X = H, Y = OC_2H_5, NHPh

Cyclopropa-3,4-benzocyclobutene **47** also affords various products on reaction with silver nitrate and the halogens, but in this case the reaction with hydrogen chloride leads to the same type of compound **49** as the reaction with silver nitrate.



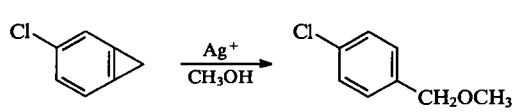
47 **48** **49**

X = Y = I (**a**)
X = Y = Br (**b**)
X = Y = H (**c**)

X = Y = I (**a**)
X = H, Y = Cl (**b**)
X = H, Y = OC_2H_5 (**c**)
X = Y = H (**d**)

The different behaviour of compounds **41**, **44**, and **47** in relation to two types of electrophiles has been explained[41] as due to the attack by silver ions (and the proton in the case of the reaction of compound **47**) on the σ-electrons of the cyclopropene ring, while other electrophiles attack the π-system of the benzene ring.

In the silver ion-catalysed reaction of 3-chlorobenzocyclopropene **50** with methanol, only one product is formed.[42]

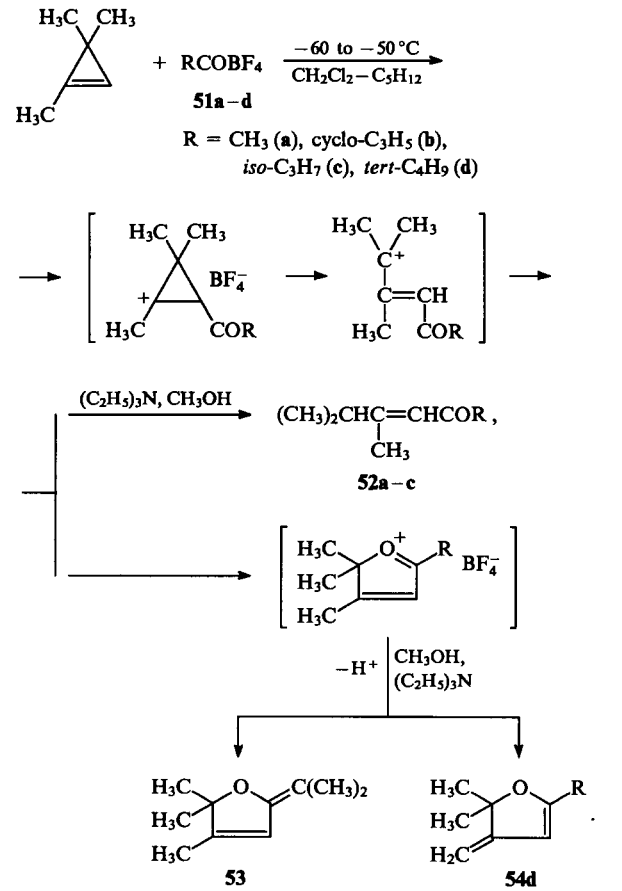


50

A reaction with ring opening is characteristic also of other electrophiles.

The acyl tetrafluoroborates **51a–d** react with 1,3,3-trimethylcyclopropene to form the acyclic ketones **52a–c** and the products **53** and **54** (Scheme 1).[43]

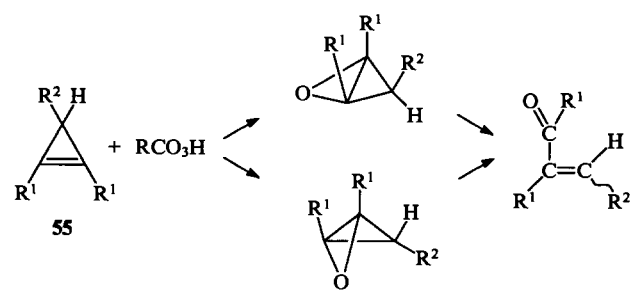
Scheme 1



R = CH_3 (**a**), cyclo-C_3H_5 (**b**), *iso*-C_3H_7 (**c**), *tert*-C_4H_9 (**d**)

52a–c **53** **54d**

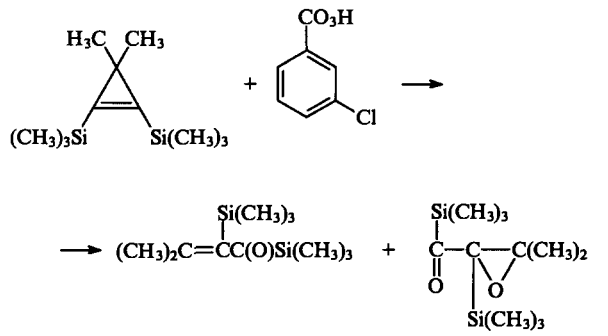
The opening of the cyclopropene ring has also been observed in the epoxidation reactions.[44–47] On treatment with peracids, compounds **55** are converted into acyclic ketones.[47]



55

R^1 = R^2 = Ph (Ref. 44); R^1 = Ph, R^2 = CH_2OH, CH_2OCH_3 (Ref.45);
R^1 = CH_2CH_3, R^2 = $CO_2C_2H_5$, CH_2OH (Ref. 46).

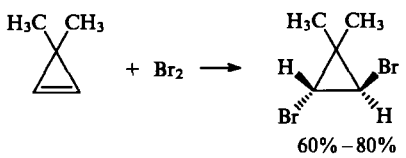
3,3-Dimethyl-1,2-bis(trimethylsilyl)-cyclopropene undergoes a similar reaction on treatment with *m*-chloroperbenzoic acid (reactant ratio 1 : 1, overall yield 65%).[47]



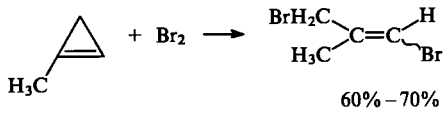
2. Reactions with the halogens and halogen-containing reagents

Cyclopropene combines with bromine and iodine in carbon tetrachloride with retention of the ring.[48] On bromination, a *trans*-adduct with a small admixture of the *cis*-isomer is formed in 57% yield.

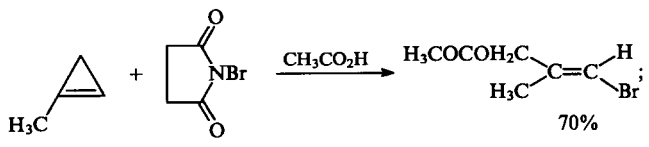
The bromination of 3,3-dimethylcyclopropene **3** in methylene chloride (−50 °C),[49] carbon tetrachloride, acetonitrile, and nitromethane[50] leads to *trans*-1,2-dibromo-3,3-dimethylcyclopropane.

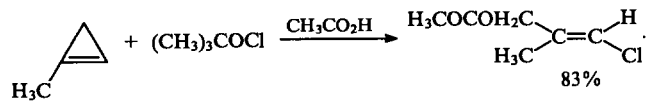


On passing from compound **3** to 1-methylcyclopropene **6**, the mode of addition changes. In this case, the reaction with bromine in carbon tetrachloride,[50] chloroform,[51] or methylene chloride[52] results in the formation of 1,3-dibromo-2-methyl-1-propenes as a mixture of the (*Z*) and (*E*)-isomers (*E* : *Z* = 1 : 2 in CCl_4 and 3 : 1 in $CHCl_3$ and CH_2Cl_2).

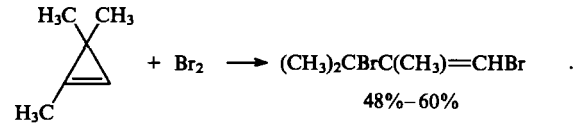


Complete ring opening is observed also in the reactions of 1-methylcyclopropene with *N*-bromosuccinimide (NBS)[51,52] and *tert*-butyl hypochlorite[52] in acetic acid, which results in the formation of the corresponding haloacetates with the (*E*)-configuration.

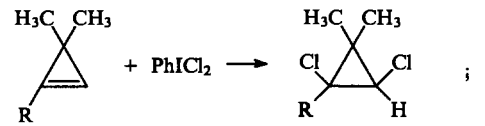




1,3,3-Trimethylcyclopropene reacts similarly with bromine (CCl_4, CH_2Cl_2, C_5H_{12}, T = 30 to −110 °C).[53]



In the reaction with chlorine under the same conditions, it affords a complex and a virtually unidentified mixture of acyclic products,[53] whereas treatment with dichlorophenyliodine resulted in the formation of 1,2-dichloro-1,3,3-trimethylcyclopropane **56a** in 50% − 70% yield. The reaction with 3,3-dimethylcyclopropene also takes place similarly (the yield of compound **56b** is 50%).

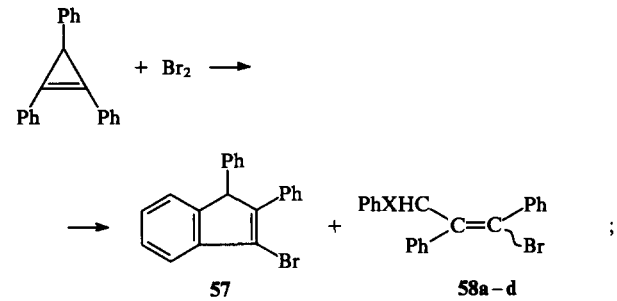


R = CH_3 (**a**), H (**b**). **56a,b**

It has been suggested[53] that the reaction of dichlorophenyliodine takes place in one stage, possibly via a concerted mechanism, whereas chlorination with free chlorine results in the formation of cationoid or radical intermediates.

The data presented show that the presence of a methyl substituent at the double bond of cyclopropene intensifies the tendency towards the formation of products with ring opening.

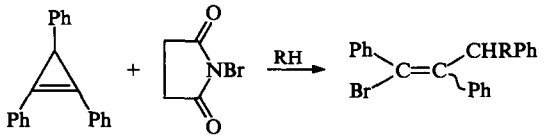
On interaction of 1,2,3-triphenylcyclopropene with bromine in acetic acid or nitromethane, virtually one product of intramolecular alkylation is formed — 3-bromo-1,2-diphenylindene **57**, whereas the reaction in methanol and aqueous acetic acid led to the isolation, together with compound **57**, of the acyclic solvatoadducts **58a − c** and that in acetonitrile led to the dibromo-derivative **58d**.[54]



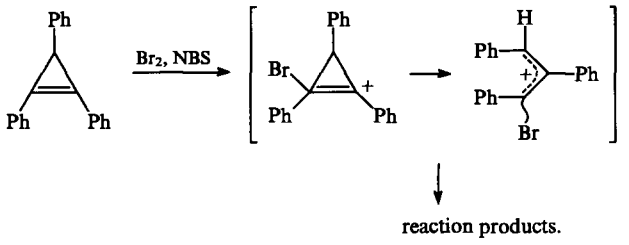
X = OCH_3 (**a**), $OCOCH_3$ (**b**), OH (**c**), Br (**d**).

Solvent	Yield of products (%)				
	57	**58a**	**58b**	**58c**	**58d**
CH_3OH	30	45	–	–	25
80% CH_3CO_2H	30	–	40	30	–
CH_3CO_2H	100	–	–	–	–
CH_3CN	90	–	–	–	10
CH_3NO_2	100	–	–	–	–

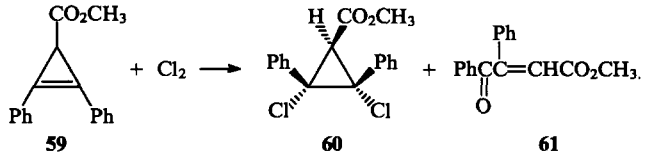
Bromination of 1,2,3-triphenylcyclopropene with *N*-bromosuccinimide in polar solvents affords a mixture of acyclic stereoisomeric products with the (*E*)-isomer predominating.[55]



The authors[54,55] proposed the following mechanism for the above reactions of triphenylcyclopropene with bromine and NBS. As will be shown below, this mechanism is consistent with the nonstereoselectivity of the process:



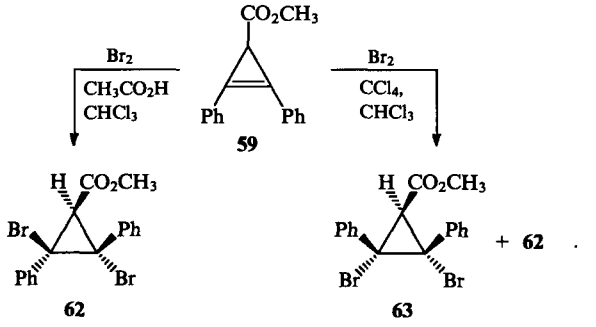
The tendency towards ring opening decreases sharply after the introduction of a carboxylate substituent into the cyclopropene ring. Thus the main pathway in the reaction of chlorine with methyl 2,3-diphenylcyclopropene-2-carboxylate **59** is its addition, which takes place stereoselectively in the *cis*-position regardless of the conditions (acetic acid or carbon tetrachloride in scattered light and under irradiation) with formation of methyl 2,3-dichloro-*cis*-*cis*-2,3-diphenylcyclopropanecarboxylate **60**.[56] Methyl 3,4-diphenylbut-2-en-4-oate **61** is formed at the same time, but the mechanism of its formation was not established.[56]



Reaction conditions	Yield of **60** (%)	Yield of **61** (%)
CCl_4, dispersed light, 0 °C	41	22
CH_3CO_2H, −12 to 13 °C	35	25
CCl_4, light irradiation (500 W electric lamp)	71	8

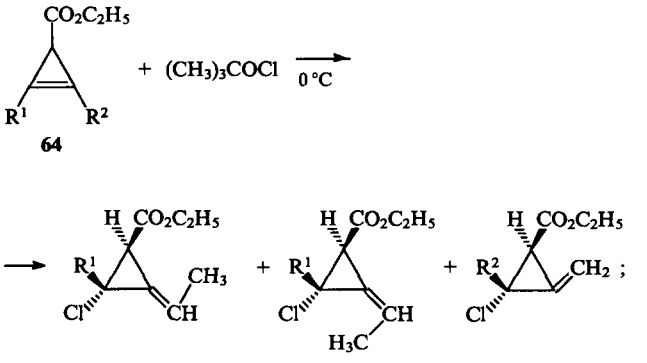
The following features are noteworthy: (a) the addition reaction proceeds not only stereoselectively but also regioselectively—the attack on the double bond takes place from the sterically less hindered side in the *anti*-position relative to the carboxylate group; (b) in acetic acid, where an electrophilic mechanism is most probable, the contribution of the pathway with retention of the ring diminishes compared with the reactions which probably proceed via a radical mechanism (CCl_4, irradiation). According to Grigorova and Komendantov,[56] this may be evidence for the greater stability of the intermediate cyclopropyl radical compared with the cationic species of the cyclopropyl type.

The stereochemistry of the bromination of the ester **59** depends on the reaction conditions.[57] In chloroform or acetic acid in the dark or in the light, bromine adds in accordance with a *trans*-mechanism to form methyl *cis*, *trans*-2,3-dibromo-2,3-diphenylcyclopropanecarboxylate **62** in 30%–39% yield. The rest of the mixture was not identified. On irradiation with light in carbon tetrachloride, bromine adds to the ester **59** mainly with formation of methyl 2,3-dibromo-*cis*,*cis*-2,3-diphenylcyclopropanecarboxylate **63**. The *trans*-adduct **62** is obtained under these conditions in insignificant amounts (5%). As in chlorination, the double bond is attacked from the sterically less hindered side.

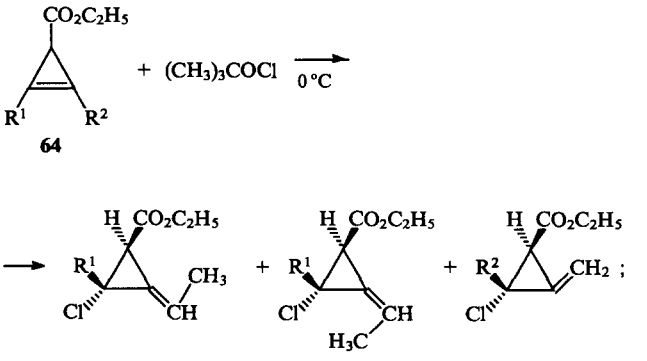


The halogenation of the esters of cyclopropene-2-carboxylic acid **64** by *tert*-butyl hypochlorite leads to isomerisation and the formation of a mixture of the products of the *cis*- and *trans*-addition of chlorine.[58,59]

At temperatures below 0 °C, the first pathway predominates (overall yield 50%), whereas at 60 °C the yield of the adducts increases (overall yield 85%).



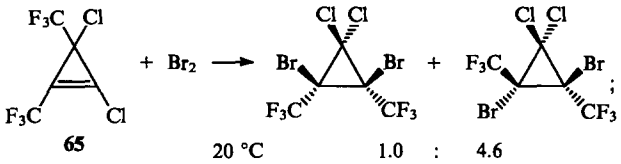
$R^1 = CH_3, C_2H_5$; $R^2 = C_2H_5$.



$R^1 = CH_3, C_2H_5$; $R^2 = C_2H_5$.

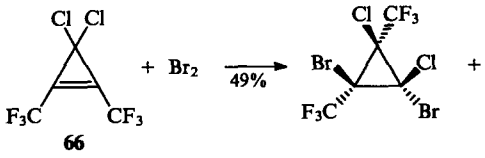
Choubani and coworkers[58,59] considered these results from the standpoint of a radical mechanism. There is no doubt that the cyclopropene derivatives **65** and **66** are brominated in the gas phase via a radical mechanism,[60] which results in the formation of

a mixture of *cis*- and *trans*-adducts. For compound **66**, the ratios of the reaction products are 4.0 : 2.2 : 1.1 : 1.0 with an overall yield of 49%.

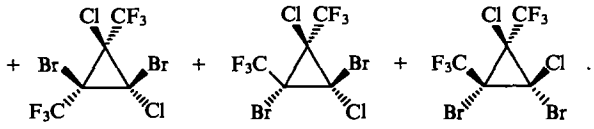


65

20 °C 1.0 : 4.6
70 °C 1.0 : 3.0

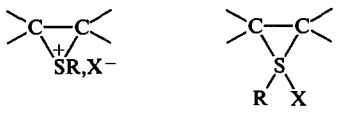


66



3. Reactions with sulfur-containing electrophiles

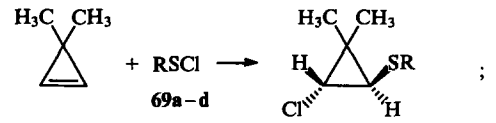
The reaction of sulfenyl halides with alkenes is one of the most thoroughly investigated reactions of the Ad_E type. It is characterised by a high *trans*-selectivity of the addition with a low tendency towards molecular rearrangement under the usual conditions. When the reaction is carried out in nucleophilic solvents, the products of the addition of the reagent are obtained as a rule as a mixture of regioisomers. The formation of mixed adducts with participation of the solvents, which is characteristic of the vast majority of electrophiles, is not observed in this case.[61-65] Salt additives exert an effective influence on this reaction (the phenomenon of the doping effect).[66-72] Under the conditions of the doping effect, there is a possibility of a series of unusual pathways in the reaction, which greatly extends its synthetic potential.[72] It has now been established that the above features are due to the formation in the sulfenyl halogenation of alkenes of a cyclic intermediate, the cationoid component of which is the highly symmetrical and relatively stable episulfonium ion **67**, which reacts selectively with the counterion. In weakly polar media, one cannot rule out the possibility of the formation of the species **68**, having the sulfurane structure, as intermediates.



67 **68**

A salt-like compound of type **67** was isolated in a stable form and its structure was determined by X-ray diffraction.[73] It is of interest to discover the extent to which the above rules hold for unusual systems such as cyclopropene derivatives.

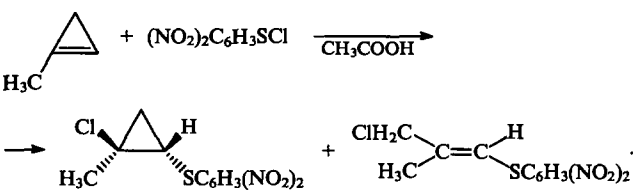
It has been established[74-76] that 3,3-dimethylcyclopropene reacts with benzene- and 2,4-dinitrobenzene-sulfenyl chlorides in acetic acid[74] and with sulfenyl halides **69a-d** in other solvents [$(C_2H_5)_2O$, CCl_4, $CHCl_3$],[75,76] forming *trans*-1-aryl(alkyl)thio-2-chloro-3,3-dimethylcyclopropanes in high yields (80% - 90%).



69a-d

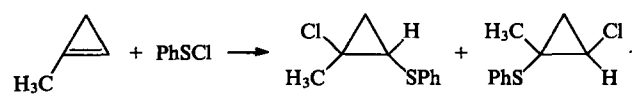
R = CH_3 (**a**), C_2H_5 (**b**), C_6H_5 (**c**), 2,4-$(NO_2)_2C_6H_3$ (**d**).

The same stereochemistry of the addition reaction has been observed in the reaction of 1-methylcyclopropene with 2,4-dinitrobenzenesulfenyl chloride. The structure of *trans*-1-chloro-2-(2′,4′-dinitrophenyl) thio-1-methylcyclopropane **70** was determined by X-ray diffraction.[52] It is noteworthy that the addition of the reagent takes place in accordance with the Markovnikov rule (overall yield 90%).[52]

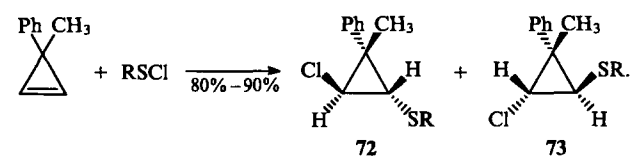


70 **71**

In contrast to this reaction, the addition of benzenesulfenyl chloride leads to a mixture of regioisomers in proportions which depend on the nature of the solvent.[29]



The reaction of 3-methyl-3-phenylcyclopropene with sulfenyl halides results in the formation of a mixture of isomers,[75,76] each of which was obtained from the *trans*-addition of the reagent.

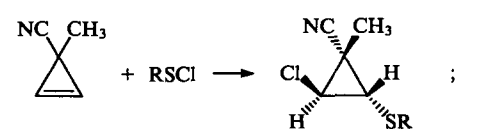


72 **73**

R	Solvent	72 : 73 Ratio
CH_3	$(C_2H_5)_2O$	1.0 : 1.5
	CH_3CN	2.5 : 1.0
C_2H_5	$(C_2H_5)_2O$	1.0 : 1.8
	CH_3CN	1.7 : 1.0
Ph	CCl_4	1.0 : 2.0
	CH_3CN	3.0 : 1.0

The product ratio depends on the polarity of the solvent: in weakly polar solvents (ether, CCl_4), the isomers **73** predominate, whereas in the appreciably more polar acetonitrile mainly the isomers **72** are formed.

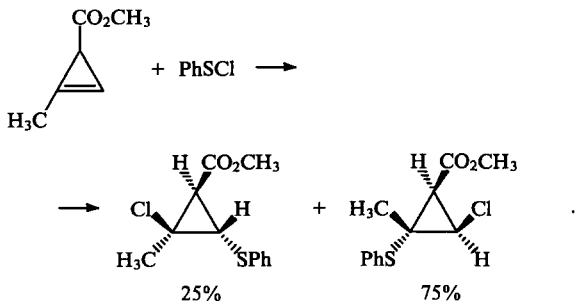
The data presented show that the general principle of *trans*-addition of the reagent holds in the sulfenyl halogenation of cyclopropenes. This postulate remains valid also for the substrates where there is a strongly electronegative group in the methylene unit. Thus 3-cyano-3-methylcyclopropene reacts smoothly with methane- and benzene-sulfenyl chlorides, forming *trans*-adducts, the nitrile and sulfide groups being in the *syn*-positions.[75,76]



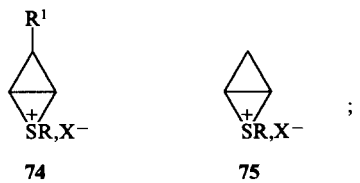
R = CH_3 (93%), Ph (94%).

The authors explain this mode of addition[75,76] by the attractive interaction in the transition state between the electrophile and the cyano-group.

The occurrence of *trans*-addition has also been established in the reaction of methyl 1-methylcyclopropene-3-carboxylate with benzenesulfenyl chloride, which results in the formation of a mixture of regioisomers in an overall yield of 85%–90%.[77] It is interesting to note that in this case the electrophile attacks the double bond from the *anti*-side relative to the ester group, in contrast to the preceding reaction.



The results demonstrate that, for the sulfenyl halogenation of cyclopropenes, the *trans*-addition principle is just as fundamental as for the unstrained systems. The introduction of highly negative groups undoubtedly renders the intermediate **74** less stable compared with its unsubstituted analogue **75**, but the sulfenyl halogenation of cyclopropenes, even when the latter contain electronegative substituents, is nevertheless exclusively *trans*-stereoselective.



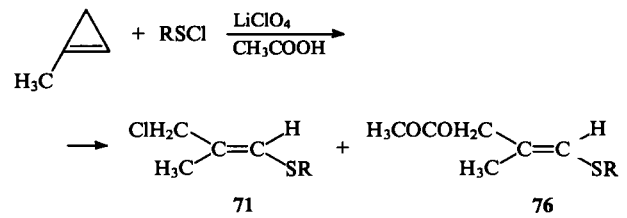
74 **75**

R^1 = electronegative group.

As can be seen from the data presented, the dominant pathway in the reaction of benzene- and alkane-sulfenyl halides with cyclopropenes involves the formation of cyclic adducts. However, the specific properties of the substrate can be manifested in this reaction too.

The introduction of electronegative substituents into the reagent and the presence of an electron-donating group at the cyclopropene double bond promote the occurrence of a reaction with ring opening. Thus the ring opening product (*E*)-3-chloro-1-(2,4-dinitrophenyl)thio-2-methyl-1-propene **71** is formed together with the cyclic adduct in the reaction of 1-methylcyclopropene with 2,4-dinitrobenzenesulfenyl chloride.[52] The amount of the acyclic compound **71** increases with increasing polarity of the medium and in solvents such as nitromethane and acetonitrile its yield reaches 50%. The (*E*)-configuration of compound **71** was established on the basis of ^{13}C and ^1H NMR spectroscopic data.[52]

The reaction of sulfenyl halides with cyclopropenes proved to be extremely sensitive to the addition of lithium perchlorate. In solution in acetic acid, the yield of compound **71** does not exceed 13%. If the reaction is carried out in the presence of a fivefold excess of $LiClO_4$ relative to RSCl, it takes place entirely with ring opening, which results in the formation of compound **71** and the product of the reaction with participation of the solvent—(*E*)-3-(2,4-dinitrophenyl)thio-2-methyl-propene-2-acetate **76**.[69]



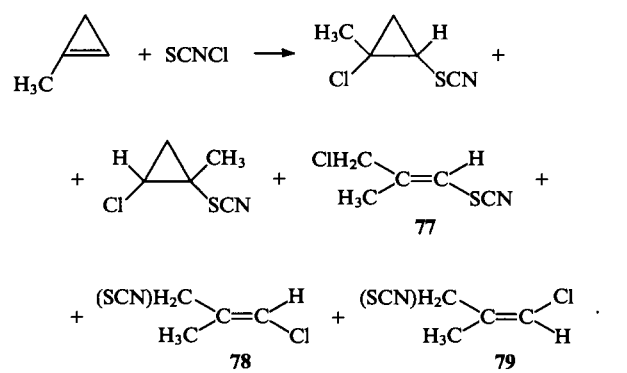
71 **76**

R = 2,4-$(NO_2)_2C_6H_3$.

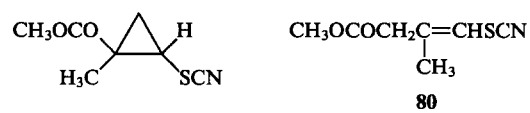
Thiocyanato-reagents interact with cyclopropenes in a more complex manner than sulfenyl halides, although both types of reagents have the same electrophilic centre. The main difference between these reactions consists in the fact that, in the substitution of thiocyanato-groups into cyclopropenes, the contribution of the pathway with ring opening is greater.

1-Methylcyclopropene reacts with thiocyanogen chloride in chloroform, affording up to 50% of acyclic products.[78,79]

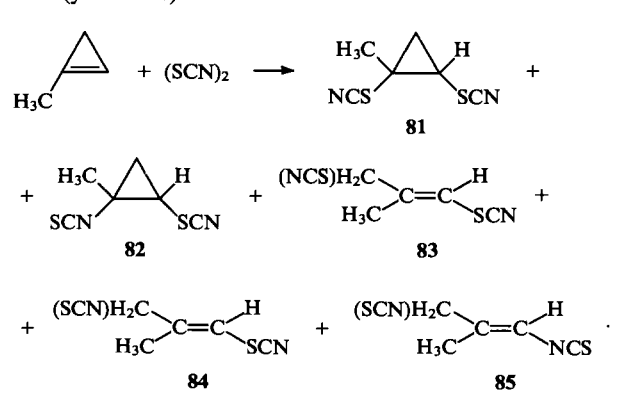
Chloro-2-methylpropen-1-yl thiocyanate **77** has the (*E*)-configuration, while 3-chloro-2-methylpropen-2-yl isothiocyanates **78** and **79** consist of a mixture of the isomers (*E*)-**78** and (*Z*)-**79** in proportions of 9 : 1.[79]



When the reaction is carried out in acetic acid, the products of solvo-addition are formed together with those indicated above:[79] 2-acetoxy-2-methyl-cyclopropyl thiocyanate and 3-acetoxy-2-methylpropen-1-yl thiocyanate **80** (overall yield 85%–90%).



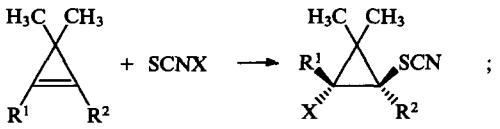
The reaction of 1-methylcyclopropene with thiocyanogen in chloroform and acetic acid results in the formation of the products **81**–**85** (yield 85%).[79,80]



The fraction of the acyclic products is in this case 42% – 43%. Ring opening takes place fully stereoselectively with formation of products having the (*E*)-configuration.[79]

It is striking that in the reactions indicated fundamentally different pathways leading to the synthesis of the acyclic products are observed. The formation of compounds **77** and **80**, (*E*)-2-methyl-1,3-dithiocyanato-1-propene **83**, and (*E*)-3-isothiocyanato-2-methylpropen-1-yl thiocyanate **84** is presumably induced by the electrophilic attack on the double bond in 1-methylcyclopropene by the sulfur atom, whereas compounds **78** and **79** are obtained in the reaction with thiocyanogen chloride as a result of the attack on this bond by the chlorine atom and (*E*)-1,3-diisothiocyanato-2-methyl-1-propene **85** is formed in the reaction with thiocyanogen as a result of the attack by the nitrogen atom on the double bond. One cannot rule out the possibility that thiocyanogen chloride and thiocyanogen exhibit the properties of an ambident electrophile in these reactions.[49,79]

As in the reactions with other electrophiles, substitution of the thiocyanato-group into 3,3-dimethylcyclopropene results in the formation of only the *trans*-adducts.[78]



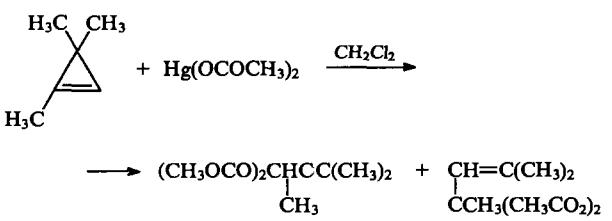
X = Cl, SCN;
$R^1 = R^2 = H$ (96%); $R^1 = H$, $R^2 = CH_3$ (81%);
$R^1 = R^2 = CH_3$ (100%); $R^1 = Ph$, $R^2 = CH_3$ (87%).

4. Reactions with mercury salts

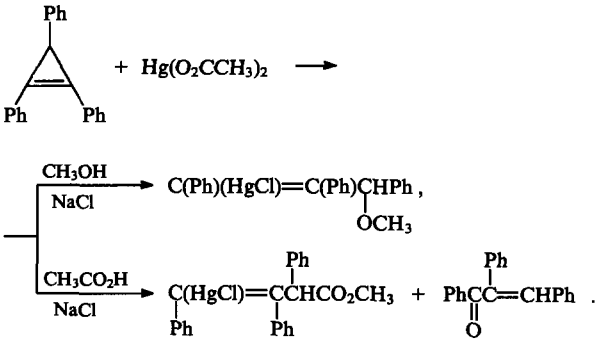
The reaction of mercury salts with cyclopropenes has aroused special interest for a long time. It follows from a large number of studies that a characteristic feature of the mercuration of unsaturated compounds, which distinguishes this reaction from others of the Ad_E type, is its high sensitivity to the structure of the substrate. Whereas mercury salts react with unstrained systems in accordance with the general *trans*-addition mechanism, the mercuration of strained unsaturated compounds, particularly those having a bridged structure, proceeds as a *cis*-process, frequently simultaneously with *trans*-addition.[81,82] Although the claim that the strain in the structure is the main cause of the 'anomalous' stereochemistry is not open to doubt, the specific mechanism of its influence on the *cis*-addition is very complex.[81,82] This is clearly manifested, for example, by the fact that in certain cases opposite stereochemical results are obtained for the same substrate depending on the reaction conditions.[81–85] However, it is noteworthy that quantum-chemical calculations have led to the conclusion that the *cis*-addition is determined not by the structural strain but by the unusual structure of the intermediate.[86]

Cyclopropene derivatives constitute a good model for testing the relationship between the process stereochemistry and the structure of the substrate because steric factors do not play a significant role in these systems, in contrast to bridged systems.

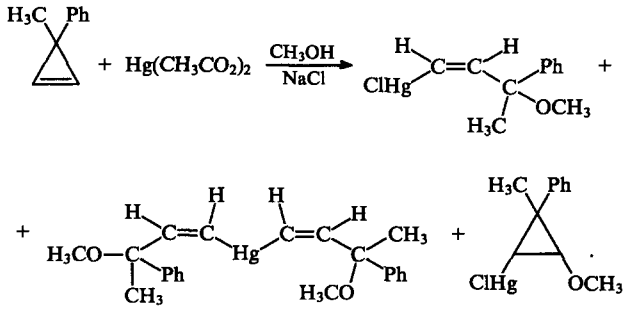
First attempts to elucidate the stereochemistry of the mercuration of cyclopropene derivatives were not successful, as mercury salts react with the simplest cyclopropenes to form acyclic compounds which do not contain mercury.[82,87,88] A characteristic example of reactions of this type is that between 1,3,3-trimethylcyclopropene and mercury acetate in methylene chloride.[87,88]



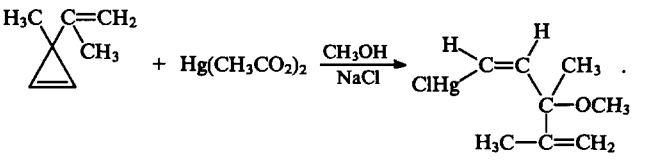
1,2,3-Triphenylcyclopropene interacts with mercury acetate in methanol and acetic acid with ring opening.[89]



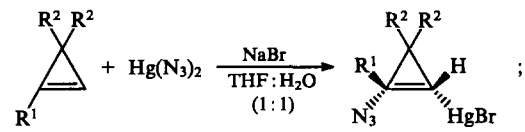
It has been shown in relation to the mercuration of 3-methyl-3-phenylcyclopropene that the acyclic products obtained in the reaction have the (*Z*)-configuration.[90]



A similar stereochemical result was obtained in the reaction with 3-isopropenyl-3-methylcyclopropene (yield of reaction product 10%).[90]



The results of the study of Galle and Hassner[35] constituted an important step in the investigation of the stereochemistry of the addition of mercury salts to cyclopropenes. It was established that mercury azide adds to a number of cyclopropenes with formation of *cis*-adducts.

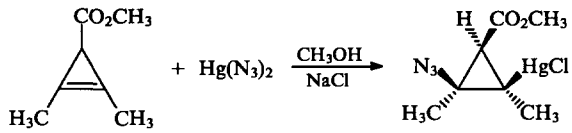


$R^1 = R^2 = H$; $R^1 = H$, $R^2 = CH_3$;
$R^1 = R^2 = CH_3$; $R^1 = Ph$, $R^2 = CH_3$.

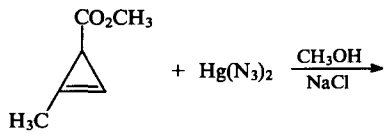
The esters of cyclopropene-2-carboxylic acids are a convenient model for the study of the stereochemistry of the mercuration of cyclopropenes as well as certain other aspects of this reaction. They react smoothly with mercury salts, affording products containing a three-membered ring, the nature of the reaction remaining unchanged on variation over a wide range of the electronic properties of the substituents at the double bond.

The azidomercuration of methyl 2,3-dimethylcyclopropene-2-carboxylate **86** and methyl 2-methylcyclopropene-2-carboxylate **87**, like that of cyclopropene hydrocarbons, proceeds in accordance with the *cis*-mechanism. In the reaction of

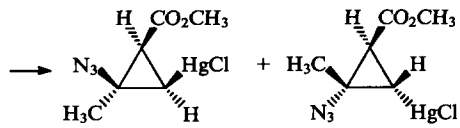
mercury azide with the ester **87**, a mixture of *cis*-2-azido-*cis*-3-chloromercurio-*trans*-2-methyl- and *trans*-2-azido-*trans*-3-chloromercurio-*cis*-2-methylcyclopropanecarboxylic acids was obtained after the exchange reaction with NaCl (**88**:**89** = 1:1).[91]



86 52%



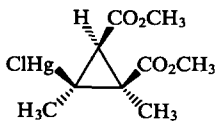
87



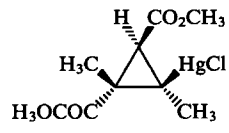
88 **89**

The use of mercury azide as the reagent made it possible to discover, in relation to monocyclic unsaturated compounds, a clear relationship between the strain in the substrate and the probability of the *cis*-addition. In contrast to the reactions with cyclopropenes, the azidomercuration of the less strained cyclobutene affords a mixture of the *cis*- and *trans*-azidomercurio-derivatives in proportions of 60:40,[92] while the reaction with cyclohexene results in the formation of only the *trans*-adduct.[85]

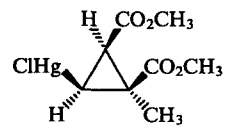
It follows from the data presented that mercury azide is a specific *cis*-azidomercurating agent for cyclopropene derivatives. The reactions with other mercury salts are nonstereoselective. The interaction of the esters **86** and **87** with mercury acetate in acetic acid results in the formation of mixtures of the methyl esters of *trans,trans*- and *trans,cis*-2,3-dimethyl-*cis*-3-chloromercurio-2-acetoxycyclopropanecarboxylic acids (compounds **90** and **91**) and the methyl esters of *trans*- and *cis*-2-methyl-*cis*-2-chloromercurio-2-acetoxycyclopropanecarboxylic acids (compounds **92** and **93**) in the proportions **90**:**91** = 31:46 and **92**:**93** = 4:1.[91]



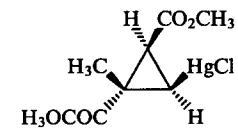
90



91

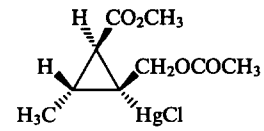


92



93

Furthermore, the methyl ester of *trans*-3-chloromercurio-*trans*-2-methyl-3-acetoxymethylcyclopropanecarboxylic acid **94** was isolated after the reaction with compound **87**. The mechanism of the formation of compound **94** has not been investigated (the overall yield of the products of the reactions indicated was 85%–90%).[91]

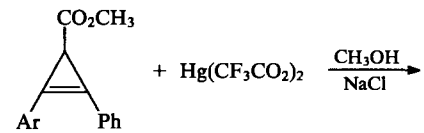


94

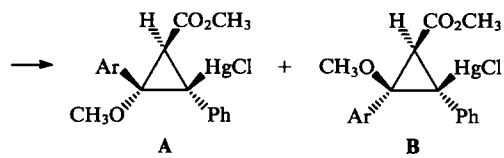
Although mercuration with mercury acetate takes place nonstereoselectively, nevertheless in this case too there is a tendency towards a decrease in the amount of *cis*-adducts with decrease in the substrate strain energy. For example, in the reaction of mercury acetate with cyclobutene in methanol, the amount of the *cis*-adduct does not exceed 7%, while in solution in acetic acid it is not formed at all.[92]

It follows from the data considered that the influence of strain on the degree of *cis*-addition of mercury salts depends radically on the nature of the reagent and the solvent. A convincing argument confirming this postulate is provided by the results of the mercuration of the methyl esters of 2-aryl-3-phenylcyclopropene-2-carboxylic acids. In this case, the influence of the reaction conditions on the process stereochemistry is so great that the strain factor is almost completely abolished.

Thus the interaction of the cyclopropenes **95a–c** with mercury trifluoroacetate in methanol affords a mixture of the *cis*- and *trans*-adducts.[93–96]



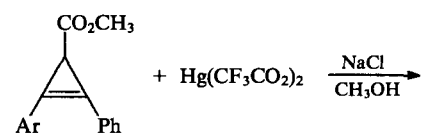
95a–c



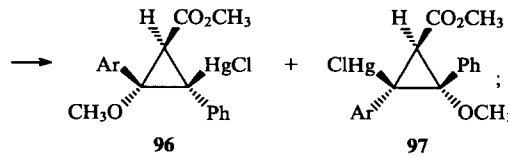
A **B**

Ar	Yield of A (%)	Yield of B (%)
4-$CH_3OC_6H_4$ (**a**)	42	16
4-$CH_3C_6H_4$ (**b**)	30	19
Ph (**c**)	54	4

The amount of the *trans*-adduct increases as the electron-donating properties of the aryl substituent in the substrate are weakened and the reaction of compound **95d** (Ar = 4-ClC_6H_4) proceeds mainly in accordance with the *trans*-mechanism with formation of two regioisomeric methyl esters of *cis*-2-chloromercurio-*trans*-3-methoxy-3-(4-chlorophenyl)-2-phenyl- and *cis*-2-chloromercurio-*trans*-3-methoxy-2-(4-chlorophenyl)-3-phenylcyclopropanecarboxylic acids (**96**:**97** = 33:67, overall yield 40%).[90]



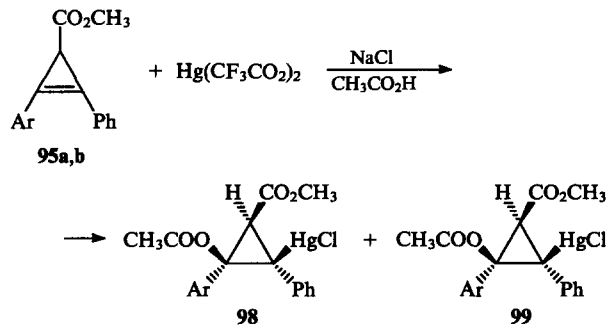
95d



96 **97**

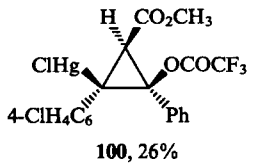
Ar = 4-ClC_6H_4.

The replacement of methanol by acetic acid makes the process *cis*-stereoselective[95-98] with formation of the adducts **98** and the solvatoadducts **99**.



Ar	Yield of **98** (%)	Yield of **99** (%)
4-$CH_3C_6H_4$ (**a**)	50	–
Ph (**b**)	30	8

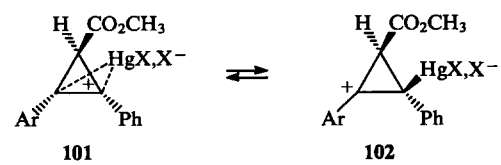
In the mercuration of compound **95d**, the change of solvent not only leads to the inversion of the stereochemistry of the process but also renders the reaction strictly regioselective with formation of methyl *cis*-2-chloromercurio-*cis*-3-trifluoroacetoxy-2-(4-chlorophenyl)-3-phenylcyclopropanecarboxylate **100**.[96]



100, 26%

As can be seen from the data presented above, in the mercuration of the esters of cyclopropene-2-carboxylic acids the carboxylate group exhibits a pronounced directing effect, as a consequence of which the substituent and the chloromercurio-group are in the *syn*-positions. The manifestation of the directing effect by functional groups in the mercuration of other unsaturated systems has been discussed.[99-102] Examination of the nature of the influence of the substituent on the course of solvatomercuration led to the conclusion that one of the causes of this phenomenon may be conformational effects.[102] Since these effects are absent for cyclopropene derivatives, the *syn*-regioselectivity indicates the interaction of the functional group and the mercury atom of the reagent.[103]

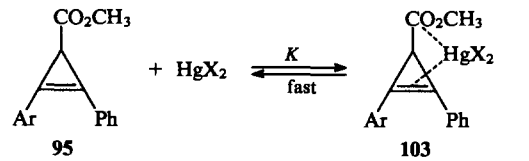
It is believed[96] that the reaction of the cyclopropene derivatives **95** with mercury trifluoroacetate in methanol leads to the formation of the mercurinium intermediate **101** (the *trans*-adduct), which is in equilibrium with the intermediate open-chain structure **102** (the *cis*-adduct).



In acetic acid, the reaction proceeds via a different mechanism. In this case, the close ion pair **102** is apparently formed as an intermediate species, which is converted into the reaction products as a result of the *cis*-addition of counterions from the solvent. The regioselectivity of the addition of the solvent to the ester **95d** is an argument in support of this hypothesis. Another no less important fact confirming the above hypothesis is that the solvatomercuration products **99** are formed as a result of the *cis*-addition of acetic acid from the sterically hindered side, i.e. the side from which the reagent attacks the double bond. This result is feasible if the solvent molecule completing the reaction is part of the solvation shell while the cation of the intermediate has an open-chain structure.

It was noted above that the regioselectivity of the mercuration of cyclopropenecarboxylic acid esters indicates the manifestation of the 'reagent–substrate' coordination. The occurrence of coordination of this type is indicated by the results of kinetic studies on the reactions of esters of cyclopropene-2-carboxylic acid **95** with mercury trifluoroacetate in methanol and acetic acid.[96]

The reaction in methanol is described by the kinetic scheme including the stage involving the formation of the pre-reaction complex **103**.



;

103 $\xrightarrow[k_1,\ \text{slow}]{CH_3OH}$ reaction products .

Under the conditions of a large excess of the mercury salt, the observed second-order rate constant depends on the initial reagent concentration $[HgX_2]_0$ in conformity with Eqn. (1), which made it possible to determine the equilibrium constant K from kinetic data.

$$\frac{1}{k_{II}} = \frac{1}{k_1}\left(\frac{1}{K} + [HgX_2]_0\right), \qquad (1)$$

where k_{II} is the observed second-order rate constant.

The equilibrium constant increases with enhancement of the electron-donating properties of the aryl substituent, which shows that not only the functional groups but also the cyclopropene double bond participates in the complex formation reaction.

The reaction in acetic acid proceeds in a more complex manner, but in this case too the kinetic data lead to the conclusion that there is a coordination interaction between the ester group and the reagent. The kinetic data are described by the equation

$$\frac{1}{k_{II}} = \frac{1}{k_1} + \frac{1}{k_1 K [HgX_2]_0}, \qquad (2)$$

which corresponds to the scheme

95 + HgX_2 $\underset{\text{fast}}{\overset{K}{\rightleftharpoons}}$ **103** ;

103 + HgX_2 $\xrightarrow[\text{slow}]{k_1}$ reaction product .

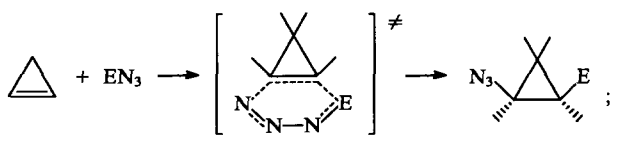
III. Mechanisms of the interaction of cyclopropene derivatives with electrophiles

It follows from the data presented that the main pathway in the reactions of cyclopropenes with electrophiles is the competitive formation of products with both retention of the ring and with its opening. The same data have shown that development of the competing pathways is influenced significantly by the substrate structure factors. Cyclopropenes with electron-donating substituents at the double bond tend more to form products with ring opening.[50-55] Conversely, electron-accepting substituents favour the formation of the products of addition to the double bond.[56,57]

Together with substrate structure factors, the nature of the electrophiles plays a major role in the development of the competing pathways. In terms of the increasing amount of acyclic products formed in the reaction, the reagents can be arranged in the sequence

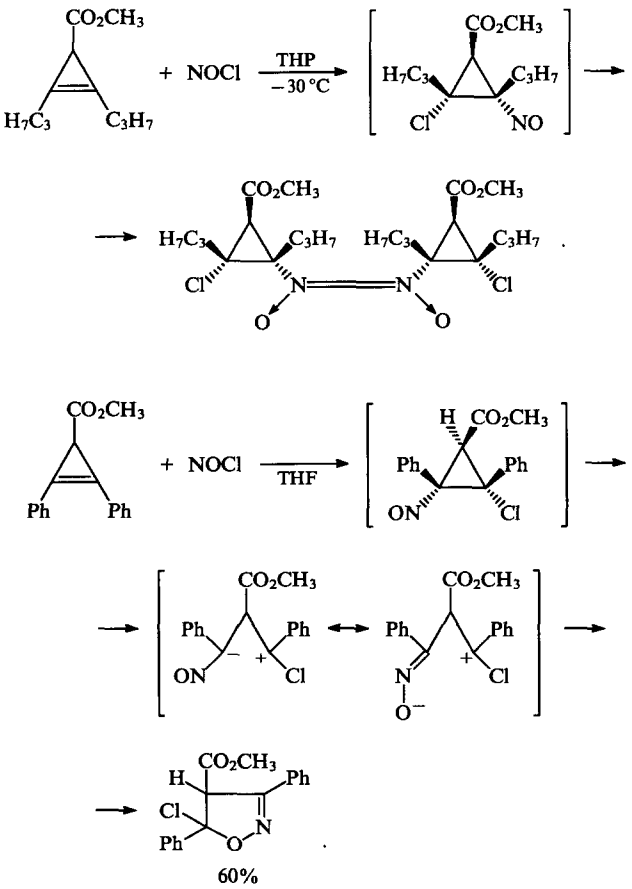
$$RS^+, I^- < SCN^+ < Br^+ \approx Cl^+ \ll H^+.$$

The view exists that the products of the addition to the double bond in cyclopropenes are formed in certain reactions via a concerted mechanism.[35,53] Indeed, a concerted mechanism is apparently most preferred for a series of reagents. Thus *cis*-adducts are probably formed via this mechanism in the reactions of cyclopropenes with hydrazoic acid[35] and mercury azide.[35,91] It may be that the high nucleophilicity of the azide group is in this case the decisive factor which determines the reaction pathway.



E = H, HgN_3 .

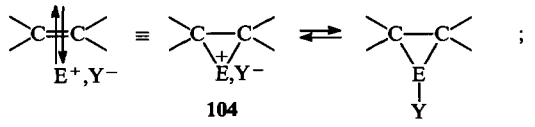
The interaction of the esters of cyclopropene-2-carboxylic acids with nitrosyl chloride, which results in the formation of either dimerisation or ring-opening products, is considered from these standpoints.[104,105]



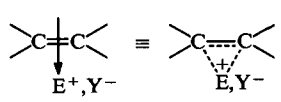
60%

It follows from stereochemical,[52,57,74-78] kinetic,[69,106] and other studies[29,52,69] that a stepwise mechanism operates for the remaining reagents of the series quoted above. As in the reactions with unstrained systems,[61,81,107] the structure of the intermediate species depends on the nature of the reagent. For reagents with a considerable tendency towards the reverse coordination, the formation of cyclic intermediates is most likely. According to Dewar's views,[109] the reverse coordination takes place as a result of the interaction of the occupied *p* or σ orbital of the electrophilic atom with the unoccupied antibonding π MO of the alkene. If the electronegativity of the electrophilic atom is comparable with that of the carbon atom, then the energies of the AO and MO are comparable and the interaction is strong. The linkage between the electrophilic atom E and the carbon atoms of the double bond is produced as a result of the formation of two usual two-electron bonds, while the intermediate has the structure of the onium species **104**.

For a highly electronegative electrophilic atom, the energy of the occupied AO is appreciably lower than that of the antibonding π MO and the reverse coordination is insignificant. For such electrophiles, the cyclic intermediate constitutes in essence the 'classical' Dewar π-complex **105** with a three-centre two-electron bond.[108,109]



104



105

Within the framework of this concept of the dependence of the reaction mechanism on the electronegativity of the electrophilic atom of the reagent, there should exist a continuum of cyclic species with different degrees of reverse coordination, the intermediates **104** and **105** being the extreme members of this series.

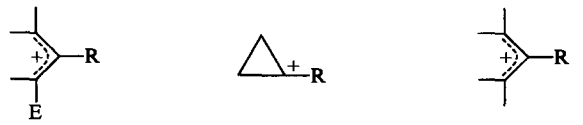
The stability of the cyclic species **104** and **105** and the reactions leading to their conversion into the final products are greatly influenced by the nature of the interaction of the electrophilic centre E^+ with the counterion Y^-. This problem has been recently investigated both experimentally and theoretically. The main results of these studies may be found in Refs 108–111.

Although the orbital structure of the cyclopropenes is more complex than that of the usual alkenes,[1,2,24-26,112] nevertheless they have an antibonding orbital similar to the π MO of the unstrained alkenes.[8] For this reason, the approach developed by Dewar is apparently valid also for the electrophilic reactions of cyclopropenes. In this case, the structures of the cyclic intermediates can be represented as **106** and **107**.

Considerations indicating that the reactions of cyclopropenes, especially with reagents having an electrophilic hydrogen atom, can proceed with participation of cyclopropyl ions **108** and the corresponding allyl ions **109** have been frequently proposed in the literature. Taking this into account, one may assume that in a multi-stage reaction of cyclopropene systems with electrophiles, the formation of the species **106**–**109** is most probable.[3,32,34,54,55]

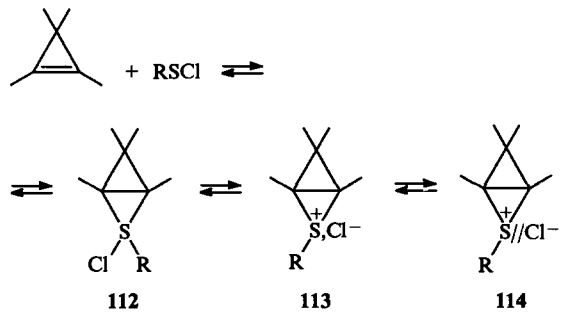


106 **107** **108**



109 **110** **111**

As mentioned above, a high *trans*-stereoselectivity of the addition to the double bond in cyclopropenes is character-istic of sulfenyl halides. Stereochemical as well as kinetic data[52,69,74,77,106] provide grounds for the assumption that, as in the sulfenyl halogenation of unstrained alkenes, this reaction results in the formation of either cyclic intermediates having the sulfurane structure **112** or the ion pairs **113** and **114** with the episulfonium cation.



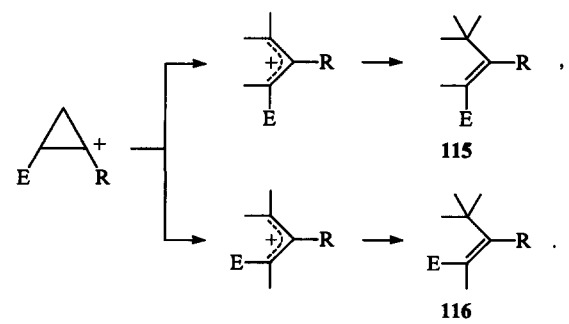
112 **113** **114**

In the reactions of cyclopropene derivatives with benzenesulfenyl chloride, only adducts are formed.[29,74-76] In contrast to this, in the interaction of 1-methylcyclopropene with 2,4-dinitrobenzenesulfenyl halides, the pathway leading to the formation of acyclic products may become the main one.[69] The electronegativity of the sulfur atom in 2,4-dinitrobenzenesulfenyl chloride is enhanced whilst the reverse coordination is diminished. This increases the electron deficiency on the carbon atoms of the three-membered skeleton in the intermediate **114**, which is in fact the reason for the occurrence of the reaction pathway involving the formation of acyclic adducts.

The sulfur atom in reagents containing the thiocyanato-group (thiocyanogen, thiocyanogen halides) is even more electronegative. For this reason, one may assume that the intermediates formed in the substitution of the thiocyanato-group into cyclopropenes have the character of π-complexes to an even greater extent and the reaction pathway involving the opening of the three-membered carbon ring becomes one of the main ones. An intermediate of type **107**, having a similar structure, is probably formed in the reactions of cyclopropenes with the halogens (Cl_2, Br_2) and their electrophilic analogues (*tert*-butyl hypochlorite, *N*-bromosuccinimide, etc.) in protic solvents.[52]

Quantum-chemical calculations have shown[113,114] that the total energy of the 1-R-cyclopropyl cations **110** is appreciably higher than the energy of the 2-R-allyl cations **111**. The relatively unstable high-energy intermediates are as a rule converted into the products or other intermediates with an insignificant activation energy. Consequently, if the formation of the ion **108** is possible in the electrophilic reactions of cyclopropenes, one should expect its conversion into the allyl cation **109** and further into acyclic products. There is also a possibility of another reaction pathway where the allyl cation **109** is obtained directly by electrophilic attack on the double bond of the cyclopropene,[3,52] by-passing the stage involving the formation of the cation **108**. However, if the substituents at the double bond are strong electron donors, the reaction can include only the stage involving the formation of a β-substituted cyclopropyl cation, which is subsequently converted into cyclic adducts. The most convincing data concerning the possibility of such a mechanism have been obtained in the reactions of esters of cyclopropene-2-carboxylic acids with mercury trifluoroacetate in acetic acid,[96,98] which were considered above.

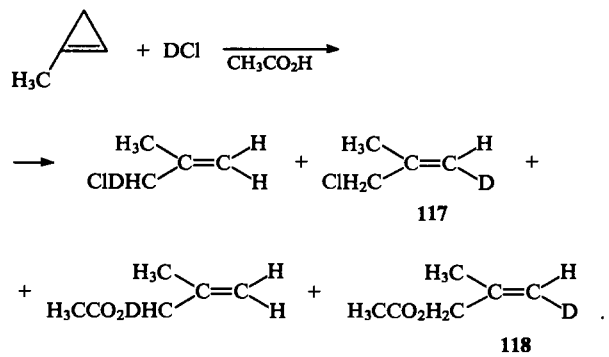
The stereochemistry of the opening of the cyclopropene ring is very important for the elucidation of the mechanism of the electrophilic reactions of cyclopropenes. In particular, it makes it possible to establish, in principle, whether the reaction proceeds via the stage involving the formation of the cyclopropyl cation **108**, which subsequently isomerises to the allyl cation **109**, or whether the latter is formed directly on electrophilic attack on the double bond of the cyclopropene. The Woodward–Hoffmann rules[115] and quantum-chemical calculations[116-119] predict a disrotatory reaction pathway **108**→**109**. There are two such procedures; if the electrophilic group E cannot make a decisive contribution to the stereochemistry of the ring opening for steric reasons, the isomeric products **115** and **116** will result. The formation reaction of the acyclic products is on the whole nonstereoselective.



115 **116**

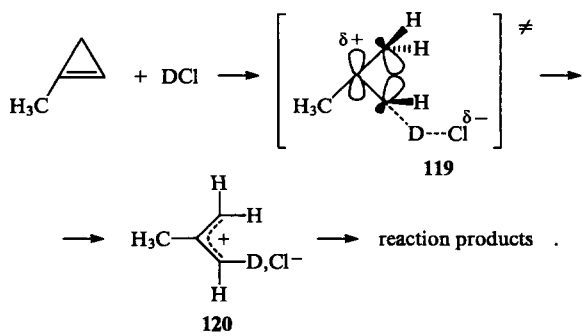
Stereoselective ring opening implies that the cyclopropyl cation of type **108** is not formed in the reaction.

It has been established[52] that the interaction of 1-methylcyclopropene with deuterium chloride entails the stereoselective opening of the cyclopropene ring and that the products of the reaction of 1-deuterio-3-chloro-2-methyl-1-propene **117** and 1-deuterio-3-acetoxy-2-methyl-1-propene **118** have the (*Z*)-configuration.



117 **118**

Within the limits of experimental error, a uniform distribution of the deuterium label is observed. This means that the reaction products are formed from the allylic intermediate **120**. The observed stereochemical result indicates a single-stage synchronous pathway leading to its formation. As the C–D bond is formed and a deficiency of electron density arises on the β-carbon atom disrotatory ring opening takes place in the transition state **119** in conformity with the stereoelectronic requirements, similarly to the behaviour manifested in the reactions involving the solvolysis of cyclopropane derivatives.[120]



119 **120**

The stereoselective formation of the product having the (*Z*)-configuration has also been observed in the isomerisation of 1,2,3-triphenylcyclopropene on treatment with trifluoroacetic acid.[34]

The reactions of 1-methylcyclopropene with 2,4-dinitrobenzenesulfenyl chloride, thiocyanogen, thiocyanogen chloride, and *tert*-butyl hypochlorite in acetic acid are likewise stereoselective, but the ring opening products have the (*E*)-configuration.[52] These data show that an intermediate with a fundamentally different structure is formed in the latter reactions. As mentioned above, it most probably has a cyclic structure.

One may conclude from the data presented that the (*Z*)-stereoselective ring opening is evidence for a single-stage formation of an allylic intermediate. If the reaction is (*E*)-stereoselective, the intermediate has a cyclic structure. More intensive stereochemical studies and theoretical calculations should show the extent to which this postulate is general and rigorous.

References

1. A Greenberg, T A Stevenson, in *Molecular Structure and Energetics* Vol. 2 (Eds J F Liebman, A Greenberg) (New York: VCH, 1986) p. 243
2. Kalvi Pihlaja, in *Molecular Structure and Energetics* Vol. 3 (Eds J F Liebman, A Greenberg) (New York: VCH, 1987) p. 173
3. G L Closs *Advances in Alicyclic Chemistry* Vol. 1 (Eds H Hart, G L Karabatos) (New York: Academic Press, 1966) p. 53
4. N S Zefirov, V I Sokolov *Usp. Khim.* **36** 243 (1967) [*Russ. Chem. Rev.* **36** 87 (1967)]
5. M P Kozina, V S Mastryukov, E M Mil'vitskaya *Usp. Khim.* **51** 1337 (1982) [*Russ. Chem. Rev.* **51** 765 (1982)]
6. V P Kolesov, M P Kozina *Usp. Khim.* **55** 1603 (1986) [*Russ. Chem. Rev.* **55** 912 (1986)]
7. J D Dill, A Greenberg, J F Liebman *J. Am. Chem. Soc.* **100** 6814 (1979)
8. M H Lien, A C Hopkinson *J. Mol. Struct.* **149** 139 (1987)
9. K B Wiberg, R Artis Dean, G Bonnevill *J. Am. Chem. Soc.* **113** 7969 (1991)
10. W E Billups, Gon-Ann Lee, E Arney Benny, K H Whitwire *J. Am. Chem. Soc.* **113** 7980 (1991)
11. A Padwa, M Wannamaker, S Wood *Tetrahedron* **47** 6139 (1991)
12. V V Plemenkov, L A Yanykina *Zh. Org. Khim.* **6** 2041 (1970)
13. L G Zaitseva, I V Avezov, V V Plemenkov, I G Bolesov *Zh. Org. Khim.* **10** 2227 (1974)
14. I G Bolesov, L G Zaitseva, V V Plemenkov *Zh. Org. Khim.* **14** 71 (1978)
15. V V Plemenkov, I G Bolesov *Dokl. Akad. Nauk SSSR* **248** 887 (1979)
16. D H Aue, G S Helwig *Tetrahedron Lett.* **15** 721 (1974)
17. L G Zaitseva, I V Avezov, O A Subbotin, I G Bolesov *Zh. Org. Khim.* **11** 1415 (1975)
18. I G Bolesov, A V Ignatchenko, N V Bovin, I A Prudchenko, L S Surmina, V V Plemenkov, P V Petrovskii, I V Romanov, I I Mel'nik *Zh. Org. Khim.* **26** 102 (1990)
19. K A Lukin, N V Averina, N S Zefirov *Zh. Org. Khim.* **24** 1776 (1988)
20. K A Lukin, N S Zefirov *Zh. Org. Khim.* **25** 202 (1989)
21. U Schuchardt, P Faria dos Santos Filho *Ciencia e Cultura* **30** 160 (1978)
22. A Padwa, W F Ricker *J. Am. Chem. Soc.* **103** 1859 (1981)
23. M S Baird, H H Hussain, W Clegg *J. Chem. Res.* 110 (1988)
24. A Skance *J. Mol. Struct.* **30** 95 (1976)
25. J Kao, L Radom *J. Am. Chem. Soc.* **100** 379 (1978)
26. F Allen *Tetrahedron* **38** 645 (1982)
27. M N Protopopova, E A Shapiro *Usp. Khim.* **58** 1145 (1989) [*Russ. Chem. Rev.* **58** 667 (1989)]
28. V N Plotkin, in *Sovremennye Problemy Organicheskoi Khimii* (Modern Problems of Organic Chemistry) (1991) p. 165
29. V R Kartashov, E V Skorobogatova, N F Akimkina, N S Zefirov *Zh. Org. Khim.* **18** 38 (1982)
30. R Schmitz, H Sonnenschein, R J Kuban *Tetrahedron Lett.* **26** 4911 (1985)
31. A Padwa, G D Kennedy *J. Org. Chem.* **49** 4344 (1984)
32. M I Komendantov, R R Bekmukhametov, I N Domnin *Zh. Org. Khim.* **14** 759 (1978)
33. M I Komendantov, R R Bekmukhametov, I N Domnin *Tetrahedron* **34** 2743 (1978)
34. G A Kudryavtseva, O A Nesmeyanova *Izv. Akad. Nauk SSSR, Ser. Khim.* 2357 (1974)
35. J E Galle, A Hassner *J. Am. Chem. Soc.* **94** 3930 (1972)
36. P Binger, H Schäfer *Tetrahedron Lett.* **16** 4673 (1975)
37. B M Mikhailov, Yu N Bubnov, O A Nesmeyanova, V G Kiselev, T Yu Rudashevskaja, B A Kazansky *Tetrahedron Lett.* **13** 4627 (1972)
38. Yu N Bubnov, O A Nesmeyanova, T Yu Rudashevskaya *Zh. Obshch. Khim.* **43** 127 (1973)
39. Yu N Bubnov, O A Nesmeyanova, T Yu Rudashevskaya, B M Mikhailov, B A Kazanskii *Zh. Obshch. Khim.* **43** 135 (1973)
40. A Padwa, T J Blackock, R Loza *J. Am. Chem. Soc.* **103** 2404 (1981)
41. L K Bee, P J Garratt, M M Mansuri *J. Am. Chem. Soc.* **102** 7076 (1980)
42. W E Billups, W I Chamberlain, M Y Asim *Tetrahedron Lett.* **18** 571 (1977)
43. E B Frolov, S N Anfilogova, I A Pomytkin, Yu A Luzikov, E S Balenkova *Zh. Org. Khim.* **16** 1839 (1980)
44. L E Fridrich, R A Cormier *J. Org. Chem.* **35** 450 (1970)
45. L E Fridrich, R A Cormier *Tetrahedron Lett.* **12** 4761 (1971)
46. J K Crandall, W W Conover *J. Org. Chem.* **43** 1323 (1978)
47. G D Maynard, L A Paquette *J. Org. Chem.* **56** 5480 (1991)
48. H B Wiberg, W J Bartley *J. Am. Chem. Soc.* **82** 6375 (1960)
49. E V Skorobogatova, Doctoral Thesis in Chemical Sciences, Gorky Polytechnic Institute, Gorky, 1990
50. O A Nesmeyanova, G A Kudryavtseva *Izv. Akad. Nauk SSSR, Ser. Khim.* 2629 (1982)
51. V R Kartashov, P S Afanas'ev, E V Skorobogatova, Yu K Grishin, N S Zefirov *Zh. Org. Khim.* **22** 452 (1986)
52. V R Kartashov, E V Skorobogatova, P S Afanas'ev, V A Chertkov, N M Sergeev, A N Chernov, N S Zefirov *Zh. Org. Khim.* **27** 1861 (1991)
53. L S Surmina, V A Novoselov, I G Bolesov *Zh. Org. Khim.* **12** 1594 (1976)
54. O A Nesmeyanova, G A Kudryavtseva *Izv. Akad. Nauk SSSR, Ser.Khim.* 2780 (1979)
55. O A Nesmeyanova, G A Kudryavtseva *Izv. Akad. Nauk SSSR, Ser. Khim.* 234 (1977)
56. T N Grigorova, M I Komendantov *Zh. Org. Khim.* **17** 317 (1981)
57. M I Komendantov, I N Domnin, R N Kentaeva, T N Grigorova *Zh. Org. Khim.* **9** 1420 (1973)
58. M Vincens, S Choubani, M Vidal *Tetrahedron Lett.* **22** 4695 (1981)
59. R Arnold, S Choubani, R Surba *Can. J. Chem.* **63** 2512 (1985)
60. J M Birchall, K Burger, R N Haszeidine, S N Nona *J. Chem. Soc., Perkin Trans. 1* 2080 (1981)
61. F Freeman *Chem. Rev.* **75** 438 (1975)
62. L Rasteikiene, D I Greiciute, M G Lin'kova, I L Knunyants *Usp. Khim.* **46** 1041 (1977) [*Russ. Chem. Rev.* **46** 548 (1977)]
63. W A Smit *Izv. Sib. Otd. Akad. Nauk SSSR, Ser. Khim. Nauk* 128 (1980)
64. W A Smit, N S Zefirov, I V Bodrikov, M Z Krimer *Acc. Chem. Res.* **12** 282 (1979)
65. W A Smit, N S Zefirov, I V Bodrikov *Organic Sulfur Chemistry* (Eds R R Freidline, A E Skorova) (Oxford: Pergamon Press, 1981) p. 159
66. I V Bodrikov, L G Gurvich, N S Zefirov, V R Kartashov, A L Kurts *Zh. Org. Khim.* **10** 1545 (1974)
67. V A Kartashov, I V Bodrikov, E V Skorobogatova, N S Zefirov *Zh. Org. Khim.* **12** 297 (1976)
68. V R Kartashov, I V Bodrikov, E V Skorobogatova, N S Zefirov *Phosphorus Sulfur* **3** 213 (1977)
69. V R Kartashov, E V Skorobogatova, E Yu Grudzinskaja, N F Akimkina, N S Zefirov, R Caple *Tetrahedron* **41** 5219 (1985)
70. N S Zefirov, A S Koz'min, V V Zhdankin *Tetrahedron* **38** 291 (1982)
71. N S Zefirov, A S Koz'min, V N Kirin, V V Zhdankin, R Caple *J. Org. Chem.* **46** 5264 (1981)
72. N S Zefirov, A S Koz'min *Sov. Sci. Rev B, Chem.* **7** 297 (1985)
73. G I Borodkin, Yu V Gatilov, E M Chernyak, V G Shubin *Izv. Akad. Nauk SSSR, Ser. Khim.* 2826 (1985)
74. V R Kartashov, N F Akimkina, E V Skorobogatova *Zh. Org. Khim.* **16** 889 (1980)

75. E I Gritsenko, G G Butenko, V V Plemenkov, A I Baluev, I G Bolesov *Zh. Org. Khim.* **22** 632 (1986)
76. E I Gritsenko, G G Butenko, V V Plemenkov, I G Bolesov *Dokl. Akad. Nauk SSSR* **289** 99 (1986)
77. V R Kartashov, E V Skorobogatova, O V Vasil'eva, N V Malisova, A M Chernov, A N Pushin, N S Zefirov *Zh. Org. Khim.* **28** 934 (1992)
78. V R Kartashov, E V Skorobogatova, P S Afanas'ev, N F Akimkina, E Yu Grudzinskaya, N S Zefirov *Zh. Org. Khim.* **22** 531 (1986)
79. V R Kartashov, E V Skorobogatova, P S Afanas'ev, V A Chertkov, N M Sergeev, N S Zefirov *Zh. Org. Khim.* **28** 2477 (1992)
80. E V Skorobogatova, N F Akimkina, V R Kartashov *Zh. Org. Khim.* **15** 753 (1979)
81. R C Faney, in *Topics in Stereochemistry* Vol. 3 (Eds N Allinger, E L Eliel) (New York: Wiley, 1968) p. 237
82. T G Traylor *Acc. Chem. Res.* **2** 152 (1969)
83. R D Bach, R F Richter *J. Am. Chem. Soc.* **94** 4747 (1972)
84. V R Kartashov, T N Sokolova, O V Vasil'eva, I V Timofeev, Yu N Grishin, D V Bazhenov, N S Zefirov *Zh. Org. Khim.* **26** 1800 (1990)
85. V R Kartashov, T N Sokolova, E V Skorobogatova, Yu N Grishin, D V Bazhenov, V A Roznyatovskii, A S Koz'min, N S Zefirov *Zh. Org. Khim.* **26** 1953 (1990)
86. M J S Dewar, K M Merz Jr *Organometallics* **4** 1967 (1985)
87. T Shirafuju, I Yamamoto, H Nazaki *Tetrahedron Lett.* **12** 4713 (1971)
88. T Shirafuju, H Nazaki *Tetrahedron* **29** 77 (1973)
89. Yu S Shabarov, L D Sychkova, S G Bandaev *Vestn. Mosk. Univ., Ser. 2: Khim.* 82 (1976)
90. V S Dombrovskii, N N Yakushina, I G Bolesov *Zh. Org. Khim.* **15** 1325 (1979)
91. V R Kartashov, E V Skorobogatova, T N Sokolova, O V Vasil'eva, N V Malisova, Yu N Grishin, D V Bazhenov, N S Zefirov *Zh. Org. Khim.* **27** 1240 (1991)
92. V R Kartashov, T N Sokolova, E V Skorobogatova, Yu N Grishin, D V Bazhenov, N S Zefirov *Zh. Org. Khim.* **27** 261 (1991)
93. V R Kartashov, N V Galyanova, E V Skorobogatova, A N Chernov, N S Zefirov *Zh. Org. Khim.* **20** 2623 (1984)
94. A N Chernov, N G Furmanov, V R Kartashov, E V Skorobogatova, N V Malisova, N S Zefirov *Dokl. Akad. Nauk SSSR* **289** 1391 (1986)
95. Yu K Grishin, D V Bazhenov, Yu A Ustynyuk, E V Skorobogatova, N V Malisova, V R Kartashov, N S Zefirov *Dokl. Akad. Nauk SSSR* **289** 620 (1986)
96. V R Kartashov, E V Skorobogatova, N V Malisova, Yu K Grishin, D V Bazhenov, N S Zefirov *Zh. Org. Khim.* **27** 2490 (1991)
97. L G Kuz'mina, Yu T Struchkov, A N Chernov, V R Kartashov, N V Malisova, E V Skorobogatova *Zh. Strukt. Khim.* **28** 109 (1987)
98. V R Kartashov, N V Malisova, E V Skorobogatova, Yu K Grishin, D V Bazhenov, N S Zefirova *Zh. Org. Khim.* **22** 867 (1986)
99. H B Henbest, B Nichols, *J. Organomet. Chem.* **56** 227 (1959)
100. N S Zefirov, L G Gurvich *J. Organomet. Chem.* **81** 309 (1974)
101. J Klein, R Levene *Tetrahedron Lett.* **10** 4833 (1969)
102. P Chamberlain, G H Whitham *J. Chem. Soc. (B)* 1382 (1970)
103. L G Kuz'mina, Yu T Struchkova, V R Kartashov, N V Galyanova, E V Skorobogatova, N S Zefirov *Zh. Strukt. Khim.* **27** 120 (1986)
104. T N Grigorova, K A Ogloblin, M I Komendantov *Zh. Org. Khim.* **8** 2197 (1972)
105. T N Grigorova, K A Ogloblin, M I Komendantov *Zh. Org. Khim.* **9** 711 (1973)
106. V R Kartashov, N F Akimkina, E V Skorobogatova, E P Trub *Kinet. Katal.* **21** 1330 (1980)
107. P B D De la Mare, R Bolton *Electrophilic Additions to Unsaturated Systems* (Translated into Russian; Moscow: Mir,1968)
108. M J S Dewar, G P Ford *J. Am. Chem. Soc.* **101** 783 (1979)
109. M J S Dewar, R C Dougherty *The PMO Theory of Organic Chemistry* (Translated into Russian; Moscow: Mir, 1977)
110. I V Bodrikov *Izv. Vyssh. Uchebn. Zaved., Khim. Khim. Tekhnol.* **29** 118 (1986)
111. S Yamabe, T Minato, S Inagaki *J. Chem. Soc., Chem. Commun.* 532 (1988)
112. H-L Hase, C Müller, A Schweig *Tetrahedron* **34** 283 (1978)
113. M H Lein, A C Hopkinson *J. Mol. Struct.* **121** 1 (1985)
114. S M Khalil *Z. Naturforsch. A, Phys. Sci.* **43** 801 (1988)
115. R B Woodward, R Hoffmann *Conservation of Orbital Symmetry* (Translated into Russian; Moscow: Mir, 1977)
116. H J S Dewar, S Kirschner *J. Am. Chem. Soc.* **93** 4290, 4291 (1971)
117. L Radom, P C Hariharau, J A Pople *J. Am. Chem. Soc.* **95** 6531 (1973)
118. D T Clark, G Smale *Tetrahedron* **25** 13 (1969)
119. A Jensen *Theor. Chim. Acta* **63** 269 (1983)
120. V S Aksenov, G A Terent'eva, Yu V Savinykh *Usp. Khim.* **49** 1039 (1980) [*Russ. Chem. Rev.* **49** 549 (1980)]

Russian Chemical Reviews **62** (10) 951 – 962 (1993) ©1993 Russian Academy of Sciences and Turpion Ltd

UDC 541.64:547.1'13:678.044

Coordination-radical (co)polymerisation of vinyl monomers in the presence of organic compounds of Group III – V elements

D F Grishin

Contents

I.	Introduction	951
II.	Characteristics of radical formation in organoelement compound – peroxide systems	951
III.	Accelerating influence of organoelement compounds on the homo- and copolymerisation of vinyl monomers	953
IV.	Specific effects of hydroquinone, benzoquinone, and other phenolic inhibitors on the (co)polymerisation of acrylates in the presence of organoelement compounds	954
V.	The influence of organoelement additives on the composition of the copolymer and on the kinetics of the copolymerisation of vinyl monomers	956
VI.	Copolymerisation of vinyl chloride with ethylene and α-olefins in the presence of organometallic compound – peroxide initiating systems	960
VII.	Conclusion	960

Abstract. The influence of catalytic amounts of organic compounds of Group III – V elements on the initiation stage and chain propagation in the (co)polymerisation of vinyl and certain other monomers is discussed. The question concerning the formation of complexes by the monomers and growth radicals with organoelement additives are examined. Examples of the practical application of the coordination-radical (co)polymerisation with participation of organic compounds of Group III – V elements, including peroxides, in the synthesis of high-molecular-mass substances, including the copolymers of vinyl monomers and olefins as well as alternating copolymers based on acrylates, are presented. The bibliography includes 105 references.

I. Introduction

The use of modifying additives, which alter the reactivity of monomers and macroradicals as well as the kinetic parameters of the process, and of novel initiators, ensuring the effective generation of radicals under energetically favourable conditions and the regulation of chain propagation and termination, leads to promising ways of solving the problem of the synthesis of polymers with specified properties. The first procedure (using protic and aprotic acids as additives) has already led to the creation of a new aspect of polymer chemistry — the complex-radical polymerisation.[1-3] The effectiveness of the second procedure depends on the use, together with azo-compounds and peroxides, of radical initiators based on organoelement compounds (OEC), subdivided into oxygen-reduction systems based on organic derivatives of non-transition metals and oxidants (oxygen, peroxide) and Ziegler-Natta catalysts.[4-7] The latter are used predominantly for the synthesis of the (co)polymers of olefins and dienes and are used for the polymerisation of vinyl monomers to a limited extent.

D F Grishin Department of Organic Chemistry, N I Lobachevskii Nizhny Novgorod State University, prosp. Gagarina 23, 603 600 Nizhny Novgorod, Fax (7-831) 235 64 80

Received 1 February 1993
Uspekhi Khimii **62** (10) 1007 – 1018 (1993); translated by A K Grzybowski

II. Characteristics of radical formation in organoelement compound – peroxide systems

The oxidation – reduction systems based on OEC and oxygen as well as OEC and hydroperoxides have been investigated in fair detail.[4, 5, 7-9]

The study of the products of the reactions of OEC with organic and then organoelement peroxides was begun as early as the 1960s. Such studies have been performed by a number of schools of organic chemists, including the school directed by Academician G A Razuvaev (see, for example, Refs 10 and 11).

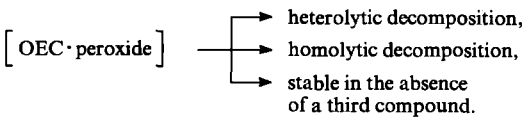
As a result of the vigorous application of physicochemical methods to the study of the above reactions, the use of kinetic approaches, and allowance for the influence of electron-donating and electron-accepting additives on the radical generation stage, a series of new data have appeared in recent years concerning the application of the systems in (co)polymerisation processes, which permitted certain generalisations.

It has now been reliably established that one of the initial stages in the interaction of organometallic compounds with peroxides is the formation of a complex of the donor – acceptor type:[12-14]

$$R_nM + R'OOR'' \rightleftharpoons \left[R_nM \cdot R'OOR''\right]. \qquad (1)$$

The majority of organoelement peroxides (OEP) of Group IV and V metals are fairly stable compounds, the thermal stability of which is likewise high and which undergo homolytic or heterolytic decomposition only at temperatures not below 80 – 100 °C.[5] As a result of the formation of the peroxide – OEC complex, the electron density in the peroxide molecule is redistributed, which leads to the loosening of the oxygen – oxygen bond and appreciably facilitates thereby its dissociation.

The OEC – peroxide complex can decompose both heterolytically with formation of ethers and homolytically with generation of radicals, or can dissociate reversibly into the initial components.



The complex formation constants in the OEC–peroxide system have been estimated in a series of studies[14–16] in relation to organoboron compounds (Table 1). Donor–acceptor complexes involving boron compounds have been investigated in greatest detail. The is because trialkylboranes are fairly convenient in practical use, are synthesised under industrial conditions, and are most promising as radical polymerisation coinitiators.

Table 1. The complex formation constants (litre mol^{-1}) in the OEC–peroxide system (T = 293 K).

OEC	Bu^tOOBu^t	$(C_6H_5)_3SiOOBu^t$	$(CH_3)_3SiOOBu^t$
$Bu^n_2BC_6H_5$	–	–	0.33
Bu^i_3B	–	–	0.64
Bu^n_3B	0.37	0.46	1.16
Bu^n_2BOBu	–	–	1.42
Bu^n_2BCl	–	–	2.78

The stability of the OEC–peroxide complex as well as the mode of its decomposition are determined by the structure of the peroxide and the OEC as well as the nature of the metal atom. Thus, whereas the complexes of organoboron compounds with *tert*-butyl peroxide (TBP) and its organosilicon and organogermanium analogues (*tert*-butylperoxytrimethylsilicon, *tert*-butylperoxytriethylgermanium) are stable in the temperature range up to 300 K and decompose reversibly to the initial components, the complexes involving *tert*-butylperoxytriethyltin, *tert*-butylperoxytetraphenylantimony, and di-*tert*-butylperoxytriphenylantimony undergo spontaneous homolytic decomposition at room temperature with formation of alkyl and alkoxyl radicals.[16]

$$R_3B + Bu^tOOER'_n \longrightarrow \left[R_3B \cdot Bu^tOOER'_n\right] \longrightarrow \begin{cases} \longrightarrow R^\cdot + R_2BOBu^t + {}^\cdot OER'_n , \\ \longrightarrow R^\cdot + R_2BOER'_n + Bu^tO^\cdot ; \end{cases} \quad (2)$$

E = Sn, Sb; n = 3, 4 .

The complexes of OEP with organic derivatives of aluminium, gallium, indium, and thallium undergo similar reactions. However, in this case there is both homolytic and heterolytic decomposition of the complexes.[17, 18]

$$\left[R_3Al \cdot R'OOR'\right] \begin{cases} \longrightarrow R_2AlOR' + R^\cdot + {}^\cdot OR' , \\ \longrightarrow R_2AlOR' + ROR' . \end{cases} \quad (3)$$

It has been shown in relation to the ethyl, butyl, and isobutyl derivatives of these metals with the aid of EPR[17, 18] and by analysing the reaction products that the ratio of the components in the complex is 1 : 1.

The methyl derivatives of Group III elements react with acyl peroxides, affording 1 : 2 complexes. The complex decomposes homolytically and the oxygen-centred radicals do not emerge into the solution under these conditions.

$$(CH_3)_3E + (C_6H_5COO)_2 \longrightarrow \left[\begin{array}{l} E(CH_3)_3 \\ \vdots \\ O \\ \| \\ C_6H_5C-O-O-CC_6H_5 \\ \| \\ O \\ \vdots \\ E(CH_3)_3 \end{array}\right] \longrightarrow 2C_6H_5COOE(CH_3)_2 + 2CH_3^\cdot . \quad (4)$$

The existence of the homolytic and heterolytic pathways in the decomposition of the OEC–peroxide complex makes it possible to postulate a one-electron transfer between the components of the complex as one of the probable stages of the process.

$$R_nE + R'OOR' \rightleftharpoons \left[R_nE \cdot R'OOR'\right], \quad (5)$$

$$\left[R_nE \overset{e}{\cdots} R'OOR'\right] \longleftrightarrow \left[R_nE^{\cdot+} \cdots {}^{\cdot-}R'OOR'\right], \quad (6)$$

$$\left[R_nE^{\cdot+} \cdots {}^{\cdot-}R'OOR'\right] \longrightarrow \left[\begin{array}{ll} R^\cdot & {}^+ER_{n-1} \\ R'O^\cdot & {}^-OR' \end{array}\right] \longrightarrow \begin{cases} \longrightarrow ROR' + R'OER_{n-1} \\ \longrightarrow R^\cdot + R'O^\cdot + R'OER_{n-1} . \end{cases} \quad (7)$$

The hypothesis of the one-electron transfer in the reactions of the OEC of nontransition elements with peroxides has been put forward in a number of studies[4, 19, 20] and has been demonstrated unambiguously by the EPR method in relation to organic compounds of iron and chromium and the peroxides of Group IV elements.[21]

$$Cr(C_6H_5C_2H_5)_2 + R'OOR' \longrightarrow \left[(C_6H_5C_2H_5)_2Cr^{\cdot+} \cdots {}^{\cdot-}R'OOR'\right] . \quad (8)$$

The complex formed decomposes via a radical mechanism and the alkoxyl radicals, obtained in the reaction, are not released into the surrounding volume but remain coordinated to the metal atom. This is followed by the abstraction of a hydrogen atom from the alkyl fragment of the OEC.

$$\left[(C_6H_5C_2H_5)_2Cr^{\cdot+} \cdots {}^{\cdot-}R'OOR'\right] \xrightarrow{-R'OH} \left[C_2H_5C_6H_5CrC_6H_5\dot{C}HCH_3\right]^+O\bar{R}' \longrightarrow Cr(OR')_4 + C_6H_5CH_2CH_3 + C_6H_5\dot{C}HCH_3 . \quad (9)$$

Organometallic compounds of Group V also react with OEP via a radical mechanism but without the liberation of alkoxyl radicals into the surrounding volume.[22]

$$R_3Bi + Bu^tOOER'_3 \longrightarrow \left[R_3Bi \cdot (Bu^tO)OER'_3\right] \longrightarrow 2R^\cdot + RBi(OBu^t)OER'_3 . \quad (10)$$

Oxygen-containing radicals remain in the coordination sphere of the metal atom. For example, evidence for the existence of radicals in the coordination sphere of the bismuth atom has been obtained in an EPR study of the interaction of triphenylbismuth with alcohols and alkoxides.[23]

A free-radical mechanism has been proposed for the interaction of TBP and acyl peroxides with organomercury and organotin compounds. It is believed[24] that the donor–acceptor complexes of the above OEC with peroxides are convenient sources of free radicals and that the addition of organomercury and organotin compounds greatly increases the initiating capacity of the organic peroxides.

Radicals (alkyl and alkoxyl) are formed in the reactions of virtually all the alkyl derivatives of Group II, III, and V elements with peroxides. Despite this, it is organoboron and organoaluminium compounds[12, 25] as well as alkyl derivatives of bismuth,[22] tin, and mercury[24] that have found the greatest application as initiators.

Initiating systems based on organoboron compounds occupy a special position. They make it possible to polymerise vinyl chloride and acrylates with a conversion close to 100% over a wide temperature range and to obtain polymers with effective physicochemical properties. Compositions based on trialkylboranes and peroxides are capable of glueing together Teflon, polyethylene, and a number of other 'nongluable' thermoplastic materials without a preliminary treatment of the surface.[10, 11, 25]

As stated above,[14, 15, 18] the complexes of trialkylboranes with TBP and its organosilicon and organogermanium analogues are stable at room temperature and dissociate reversibly into the initial components. The complexes decompose into radicals in the presence of a third compound — an electron-accepting additive, for example the polar vinyl monomer.[6, 26]

$$\left[R_3B\cdot(CH_3)_3SiOOBu^t\right] + M \longrightarrow \begin{cases} \longrightarrow R-M^{\cdot} + (CH_3)_3SiO^{\cdot} + R_2BOBu^t, \\ \longrightarrow R-M^{\cdot} + Bu^tO^{\cdot} + R_2BOSi(CH_3)_3; \end{cases} \quad (11)$$

(M = monomer).

Thus the monomer is directly involved in the radical generation stage.

The structure of the ternary OEC–OEP–monomer complex has not been established experimentally. It has been demonstrated by IR[27] and ^{1}H NMR[28] spectroscopy and by calorimetry[29] that the unsaturated compound may be coordinated both to the element in the peroxide and to the oxygen bridge.

$$R_nEOOR' + CH_2{=}CH{-}X \longrightarrow \begin{cases} \left[\begin{array}{c} CH_2{=}CH{-}X \\ \vdots \\ R_nEOOR' \end{array}\right], \\ \left[\begin{array}{c} CH_2{=}CH{-}X \\ \vdots \\ R_nE{-}O{-}OR' \end{array}\right]. \end{cases} \quad (12)$$

Like organoaluminium compounds,[30] trialkylborane can be bound to the monomer also via an unoccupied *p* orbital.

$$R_3B + CH_2{=}CH{-}X \rightleftharpoons \left[R_3B\cdots\begin{array}{c} CH_2 \\ \| \\ CH{-}X \end{array}\right]. \quad (13)$$

Ternary systems involving organoaluminium compounds have been investigated in detail by Milovskaya and coworkers.[12] According to Milovskaya,[12] an OEC–monomer complex is formed initially in the trialkylaluminium–peroxide–monomer complex and then reacts with the peroxide, affording radicals.

$$R_3Al + M \rightleftharpoons \left[R_3Al\cdot M\right], \quad (14)$$

$$\left[R_3Al\cdot M\right] + R'OOR' \rightleftharpoons \left[R_3Al\cdot M\cdot R'OOR'\right], \quad (15)$$

$$\left[R_3Al\cdot M\cdot R'OOR'\right] \longrightarrow R_2AlOR' + R^{\cdot} + R'OM^{\cdot}. \quad (16)$$

Aleksandrov and coworkers[31] put forward a general mechanism taking into account virtually all the principal coordination interactions in the three-component system:

$$MMA + A \rightleftharpoons \left[MMA\cdots A\right], \quad (17)$$

$$MMA + P \rightleftharpoons \left[MMA\cdots P\right], \quad (18)$$

$$P + A \rightleftharpoons \left[P\cdots A\right], \quad (19)$$

$$\left[MMA\cdots A\right] + P \rightleftharpoons \left[MMA\cdots A\cdots P\right], \quad (20)$$

$$MMA + \left[P\cdots A\right] \rightleftharpoons \left[MMA\cdots P\cdots A\right], \quad (21)$$

$$\left[P\cdots MMA\right] + A \rightleftharpoons \left[P\cdots MMA\cdots A\right], \quad (22)$$

where MMA = methyl methacrylate, P = peroxide, and A = Lewis acid.

The mechanism of the generation of radicals in such systems has not been established, but one can postulate that the monomer is capable of combining with the components of the complex [the organometallic compound (OMC) and the OEP]. Such interaction alters the reactivity of the monomers, which is characteristic of the so called complex-radical polymerisation.[3] The study of the characteristics of the (co)polymerisation of vinyl monomers and olefins has confirmed the above hypothesis.

III. Accelerating influence of organoelement compounds on the homo- and copolymerisation of vinyl monomers

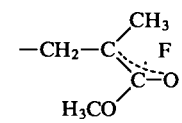
As stated above, organoelement initiating systems based on the OEC of Group III elements and OEP have a number of advantages compared with the traditional radical initiators,[10, 11, 25] in particular they are more effective than azo-compounds and percarbonates and make it possible to obtain a large amount of the polymer per unit time.[25, 32, 33]

The rapid chain propagation and certain features of the physicochemical properties suggest that the components of the organoelement initiator participate not only in the radical generation stage but also in the chain propagation and termination processes. As mentioned above, unsaturated compounds, including monomers, are capable of coordinating to the OEC of non-transition elements and OEP [Eqns (12) and (13)]. In these complexes, the monomers function as electron donors. On the one hand, such complex formation facilitates the decomposition of the peroxide into radicals and hence increases the rate of initiation[27] and, on the other, it promotes a redistribution of electron density to the π-bonds of the monomer and thereby alters its reactivity.

Complexes of vinyl monomers with Lewis acids (metal halides) have long been known and have been studied in detail by a number of investigators.[3] It has been established by IR[35–38] and NMR[39] spectroscopy that metal halides are coordinated to the carbonyl group of the monomer.[35] The constants for the complex formation reactions of organic compounds of Group III elements with MMA and acrylonitrile (AN) have been estimated in relation to organoaluminium compounds.[30]

Together with the formation of complexes with the monomers, organometallic compounds are capable of forming complexes with radicals,[40] including polymeric ones.[35]

It has been established by the EPR method that the components of the organoelement initiator trialkylborane(TAB)-di-*tert*-butylperoxytriphenylantimony (DPA), containing boron and antimony atoms with unoccupied *p* and *d* orbitals, are coordinated during the chain propagation process to the growing MMA macroradical.[41, 42]



F — fragment of the organoelement initiator

The formation of similar complexes of the macroradical with Group II and III metal halides as Lewis acids has been noted.[35]

Such interaction enhances the electron-accepting properties (electrophilicity) of the growing macroradical and increases its reactivity relative to the double bond of the monomer. This increases the propagation rate constant. Thus the rate of polymerisation of MMA in the presence of typical radical initiators — dicyclohexyl peroxydicarbonate (DCC) and azoisobutyronitrile (AIBN) — increases significantly after the introduction of triisobutylborane in amounts comparable to the initiator concentration.[43] Boron alkyls have no catalytic effects on the decomposition of the above initiators.

Rate of polymerisation/ 10^4 mol litre^{-1} s^{-1}	0.74	1.08	1.48
Triisobutylborane concentration (mol.%)	0	0.2	0.4

The polymerisation of acrylonitrile in the presence of AIBN is also accelerated by trialkylboranes. The rate of the process increases synchronously with increase in the content of the OEC in the mixture. Similar data have been obtained in studies of the copolymerisation of MMA with styrene[44] and allyl chloride[45] in

the presence of organoelement initiators. Other OEC of Group III elements, in particular dibutylbutoxyborane and triethylaluminium, also have an accelerating effect on the polymerisation of MMA (Table 2). Being a stronger Lewis acid than trialkylboranes, dibutylbutoxyborane exhibits an increased coordinating capacity and has an appreciably greater influence on the rate of polymerisation.

Table 2. The influence of certain OEC of Group III elements and phenolic inhibitors (1 mol.%) on the rate of polymerisation of MMA ($10^3 v$/mol litre^{-1} s^{-1}).

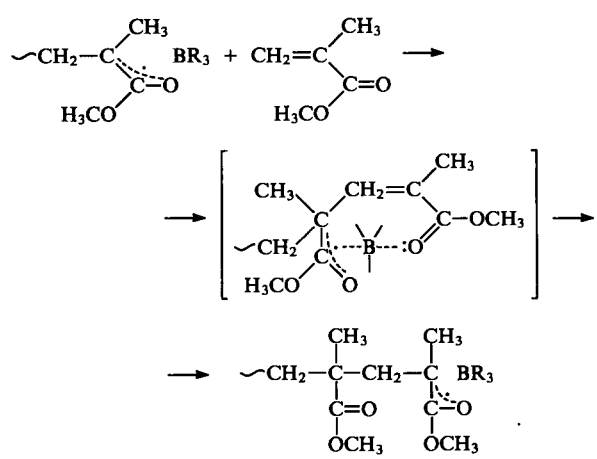
OEC	Without inhibitor	Hydroquinone	Di(hydroxyphenyl)propane	Ionol	Benzoquinone
–	0.08	0.01	–	–	–
Bu^i_3B	0.22	0.40	0.24	0.17	0.04
Bu^i_2BOBu	0.43	–	0.50	0.15	0.02
$(C_2H_5)_3Al$	0.11	0.16	0.20	0.12	0.01

Note. In all cases, the initiator was AIBN (0.1 mol.%). T = 313 K.

Certain metal halides have a similar activating effect on chain propagation in the polymerisation of acrylic monomers.[3] Thus, according to the data of Bamford et al.,[46] the propagation rate constant in the polymerisation of acrylonitrile in the presence of lithium chloride increases by a factor of two, while the termination rate constant remains unaltered. The accelerating effect is due to the formation of complexes between lithium ions and the acrylonitrile growth radical. It was shown subsequently in a series of studies[47–56] that the activating effect of the coordinatively unsaturated metal salts on the polymerisation of acrylic monomers is a common phenomenon, which has been discussed in detail in a monograph.[3]

In contrast to metal halides (Lewis acids), organometallic additives have a catalytic effect on chain propagation when they are introduced into the system in amounts comparable to the initiator concentration (0.01–0.1 mol.% relative to the monomers). This fact definitely shows that the formation of a complex between the OEC and the macroradical and not the monomer is responsible for the increase in the rate of (co)polymerisation in the presence of the Lewis acid indicator, particularly since the complex between the electron acceptor and the growth radical is somewhat more stable than the analogous complex with the monomer.[35]

Taking into account the foregoing, one may postulate that the same OEC molecule, functioning as a complex forming agent, can participate in several consecutive chain propagation stages, permanently retaining the growing macroradical in its coordination sphere. Chain propagation then occurs in a six-membered reaction complex, which includes the growing macroradical, the monomer, and the complex forming agent.



(23)

By retaining in its coordination sphere the growing macroradical, the atom of the element orients the monomer molecule and creates conditions for chain propagation which are most favourable from the energetic and steric standpoints.

A similar mechanism, except for the fact that it incorporates an eight-membered reaction complex, has been proposed by Kabanov[57] to explain the increase in the chain propagation rate constant in the polymerisation of MMA in the presence of metal halides and also by Semchikov and coworkers[58, 59] in studies of the copolymerisation of acrylic acid with vinyl acetate in the presence of germanium salts. However, the six-membered complex presented above, which includes a delocalised allylic macroradical, is thermodynamically most stable.[60]

The concept of the cyclic transition state has been frequently used in coordination chemistry to account for the characteristics of the chain propagation.[61] Precisely this analogy probably enabled Kabanov et al.[3] to introduce the term 'coordination-radical polymerisation' for polymer formation processes occurring in the presence of metal compounds as electron acceptors. However, the term 'complex-radical polymerisation' is used more frequently to describe the above reactions in both Russian and foreign literature. However, when organoelement compounds are used as chain propagation regulators the term 'coordination-radical polymerisation' appears more apt, since, firstly, it emphasises the interrelation and common features of the mechanisms in coordination and radical polymerisation with participation of OEC and, secondly, the coordination interaction between the monomer and the OEC and between the macroradical and the OEC is fairly weak, as stated above, and the formation of stable complexes should not be considered.

IV. Specific effects of hydroquinone, benzoquinone, and other phenolic inhibitors on the (co)polymerisation of acrylates in the presence of organoelement compounds

Hydroquinone, ionol, and certain other phenols are familiar inhibitors of the radical polymerisation of vinyl monomers and are used traditionally as stabilisers. The effectiveness of the inhibition increases significantly in the presence of oxygen, which, according to Dolgoplosk and Tinyakova,[62] is associated with the oxidation of phenols to quinones, which exert a stronger retarding effect on chain propagation.

According to the most common point of view,[62, 63] the inhibiting effect of hydroquinone is based on the ready abstraction by the radical of the mobile hydrogen atom from the phenol molecule with formation of a phenoxyl radical.

$$R^{\cdot} + ArOH \longrightarrow RH + ArO^{\cdot} . \qquad (24)$$

As a consequence of its low reactivity relative to the multiple bond in the monomer, the phenoxyl radical cannot initiate the radical process (polymerisation).

As early as the 1960s, it was noted[64–67] that the addition of certain OEC of Group III elements makes it possible to carry out the polymerisation of MMA with a high conversion in the presence of benzoyl peroxide (BP) or AIBN despite the presence of comparable amounts of hydroquinone.

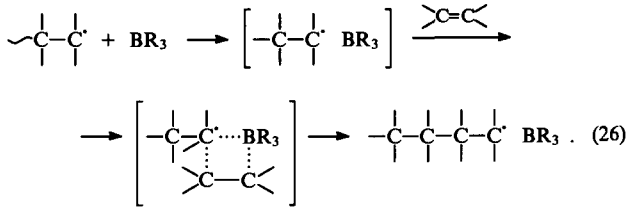
In the presence of OEC, the phenoxyl radicals probably enter into a S_N2 substitution reaction at a high rate.[68]

$$ArO^{\cdot} + R_3E \longrightarrow R^{\cdot} + ArOER_2 . \qquad (25)$$

The alkyl radicals formed in this reaction can again initiate the polymerisation. This means that organoboron compounds can function as chain transfer agents in the polymerisation of acrylates. The chain transfer rate constant in the polymerisation of MMA initiated by peroxides is 1.5×10^{-2} for tri-n-butylborane and 1.0×10^{-2} for triisobutylborane.[69]

A somewhat different point of view on the causes of the lack of the inhibiting effect of phenols in polymerisation in the

presence of organometallic compounds has been expressed by Arimoto,[65] who suggested that the OEC is coordinated to the growing macroradical via the unpaired electron of the latter.



(26)

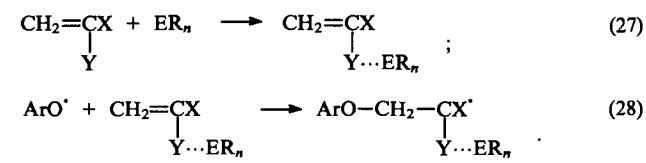
This results in the blocking of the reaction centre of the radical and its interaction with the phenol becomes impossible. It is essential to note that the experimental results obtained by Arimoto have been questioned.[64]

It has been shown in a number of studies published in the 1990s[43, 70–72] that hydroquinone and di(hydroxyphenyl)propane not only do not inhibit the radical polymerisation of acrylates but actually accelerate it (Table 3). Thus the rate of polymerisation of MMA and acrylonitrile increases significantly in the presence of the OEC of Group III elements and increases synchronously with increase in the content of the OEC and of the inhibitor. Such an unusual accelerating effect is associated with reactions involving chain transfer to the OEC [Eqn (25)]. However, the absence of the inhibiting effect in the polymerisation of MMA, acrylonitrile, and methyl acrylate in the presence of large amounts (an order of magnitude higher than the initiator concentration) of hydroquinone and di(hydroxyphenyl)propane as well as a significant weakening of the inhibiting effect when Lewis acids (metal halides) are introduced into the polymerising system cannot be accounted for solely by this factor.[73–75] Such nontraditional behaviour of phenols can be caused by the coordination-radical nature of the (co)polymerisation of acrylic monomers in the presence of organoelement initiators. In the presence of Lewis acids as electron acceptors, the macroradical and the monomer are coordinated (see above) to the components of the initiator. The formation of a complex between the OEC and the monomer activates the latter, as a result of which the initiation of the polymerisation by phenoxyl radicals becomes possible.

Table 3. The influence of hydroquinone, di(hydroxyphenyl)propane, and ionol on the rate of polymerisation of acrylic monomers.

Monomer	Inhibitor concentration (%)	Rate of polymerisation ($10^3 v$/ mol litre^{-1} s^{-1}) in the presence of different inhibitors		
		hydro-quinone	di(hydroxy-phenyl)propane	ionol
MMA	0	1.20	1.20	1.20
	0.5	1.40	1.31	0.78
	1.0	1.67	1.40	0.63
	5.0	–	1.59	0.28
AN	0	4.50	–	4.50
	0.5	6.10	–	1.31
	1.0	7.70	–	0.51
VA*	0	9.10	9.10	9.10
	0.1	4.30	–	–
	0.5	–	2.50	0.17
	1.0	0.05	0.75	0.04
	5.0	–	0.38	–

Note. In all cases, the initiator was triisobutylborane–di-*tert*-butylperoxytriphenylantimony (the content of triisobutylborane was 0.4 mol.%). T = 293 K.
* VA = vinyl acetate.



(27)

(28)

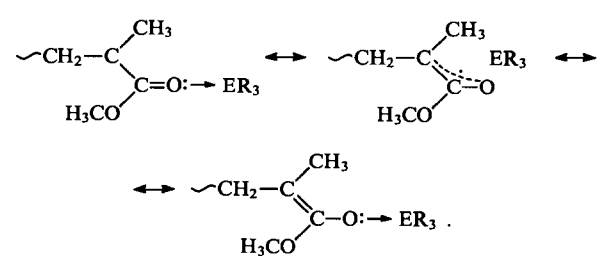
The hypothesis of the activation of the monomer by the complex-forming agent has been confirmed by the data of Bamford et al.,[53] who demonstrated a threefold increase (compared with the monomer) in the reactivity of the complex of MMA with zinc dichloride in the chain propagation stage. This permits the hypothesis that phenoxyl radicals can initiate the polymerisation of the monomer bound in a complex.

The occurrence of reaction (28) has been confirmed also by the detection of phenoxy-groups in poly(methyl methacrylate) by UV[70] and IR[72] spectroscopy. An indirect confirmation of the validity of the proposed approach to the consideration of the kinetic features of the polymerisation of acrylates in the presence of OEC and inhibitors is provided by the absence or weakening of the inhibiting effect in the polymerisation of MMA with added Group III metal halides. In this case, the occurrence of the S_R2 substitution reaction [Eqn (25)] is in principle impossible and an explanation of the observed effect can be found either in terms of Arimoto's mechanism [Eqn (26)] or in terms of the approach put forward above [Eqns (27) and (28)].

Reactions (25)–(28) lead to the observed increase in the rate of polymerisation of acrylates in the presence of OEC of Group III elements and phenols such as hydroquinone and di(hydroxyphenyl)propane. However, in the case of ionol—a sterically hindered phenol—some decrease in the rate of polymerisation of the monomers investigated has been observed.[70, 72] This is probably associated with the fact that, owing to steric factors, reactions (25) and (28) involving ionol proceed much less effectively than those involving hydroquinone and di(hydroxyphenyl)propane.

In contrast to acrylates, the polymerisation of vinyl acetate in the presence of OEC is effectively inhibited by phenols (Table 3) and, after the introduction of hydroquinone in amounts exceeding the concentration of trialkylborane, ceases completely.[71] The above inhibitors retard significantly also the polymerisation of vinyl chloride in the presence of organoelement initiators, but the process cannot be fully inhibited because of the low solubility of hydroquinone in vinyl chloride.

Trialkylborane is incapable of activating vinyl chloride and vinyl acetate owing to the characteristic features of their structure as electron-donating monomers.[76] As a consequence of the remoteness of the oxygen atom of the carbonyl group from the carbon–carbon double bond, in the coordination of the Lewis acid to vinyl acetate the activation of the π-bond of the latter is not quite so marked as in the case of acrylate and reaction (28) does not take place. Furthermore, whereas an appreciable delocalisation of the unpaired electron in the growing macroradical on coordination to the OEC (π-e conjugation[71]) is characteristic of acrylonitrile and (meth)acrylates, this is not possible in the poly(vinyl acetate) radical for steric reasons—as a consequence of a different disposition of the carboxy-group and the unpaired electron.[76]

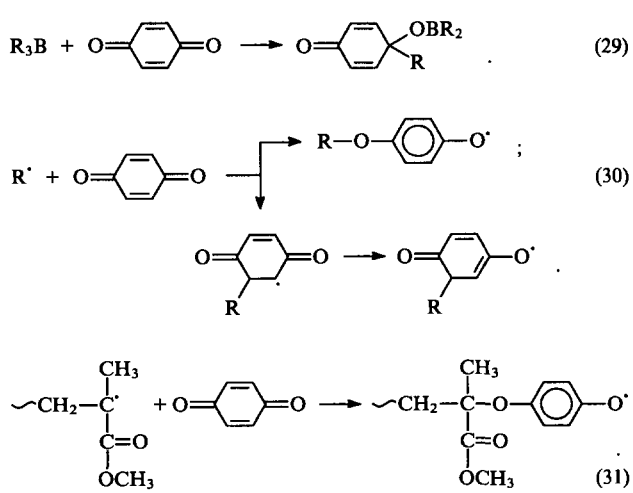


It is quite likely that, on transfer of electron density to the unoccupied orbitals of the trialkylborane as a result of coordination to the macroradical, the borane increases the electrophilicity of the coordinated poly(methyl methacrylate) radical or the polyacrylonitrile radical. This makes them inert to phenols [see Eqn (24)]. In this case, chain propagation takes place in a cyclic reaction complex incorporating the monomer, the growing macroradical, and the OEC, directly in the coordination sphere of the metal, which hinders the reaction of the macroradical with the mobile hydrogen atom of the phenol. Because of this, the polymerisation of MMA continues up to a high degree of conversion in the presence of a tenfold excess of the inhibitor relative to the OEC.[70]

Phenolic inhibitors exert a definite influence also on the molecular mass of the polymer:[70-72] thus the molecular mass of poly(methyl methacrylate) diminishes synchronously with increase in the content of the inhibitor in the monomer mixture. However, this change is insignificant compared with the analogous influence of the above inhibitors in the absence of OEC or when traditional chain transfer agents are introduced.

A significant role is attributed to oxygen in the mechanism of the inhibition of radical polymerisation by various phenols. According to Dolgoplosk, the influence of oxygen reduces to the oxidation of the phenol to the corresponding stable radicals or quinones. In the presence of organic compounds of boron and aluminium[64-67, 70] as well as benzoquinone (BQ), there is no induction period in the polymerisation of MMA. The inhibiting effect of benzoquinone in the presence of added trialkylborane depends on the molar ratio [TAB]:[BQ]. If the amount of benzoquinone is smaller than that of trialkylborane, the inhibiting effect hardly influences the polymerisation kinetics. The process proceeds up to a high degree of conversion and the molecular mass changes insignificantly.[72] Under similar conditions in the absence of trialkylborane, benzoquinone effectively inhibits the polymerisation of acrylates: the rate of polymerisation is initially close to zero and the limiting degree of conversion does not exceed 0.5%.[71, 72]

With increase in the concentration of benzoquinone, the rate of polymerisation diminishes. However, even in the presence of a twofold excess of benzoquinone relative to trialkylborane, it is significantly higher than in the absence of the latter. Analysis of the literature as well as data on the reactivities of organoboron compounds relative to benzoquinone indicates the effective involvement of trialkylborane and benzoquinone in the processes.[70-72, 77, 78]



The phenoxyl radicals formed by reactions (30) and (31) enter into the S_R2 substitution reaction with generation of alkyl radicals which are capable of again initiating the polymerisation [Eqn (25)]. The average chain length indicates that there are two chain transfers to the trialkylborane molecule.[66]

Organoaluminium compounds exert a no less effective influence on the polymerisation of acrylates in the presence of quinones.[67, 72] The rate of polymerisation increases with increase in the ratio [trialkylaluminium]:[BQ], reaches a maximum, and then falls again. Grotewold and Hirschler[67] explained this by the operation of two initiation mechanisms: the first is associated with the decomposition of the initiator into radicals and the second with the generation of radical centres as a result of the decomposition of the complex between triethylaluminium and the quinone. Analysis of the products of the reactions of organoaluminium compounds with quinones[79, 80] showed that the latter mechanism appears extremely controversial.

As in the case of trialkylboranes, a heterolytic reaction [Eqns (29)-(31)] and homolytic transfer of the reaction centre to the metal atom [Eqn (25)] probably take place in the given instance. Whereas the reaction involving trialkylborane can involve two alkyl groups, in the case of triethylaluminium only one such group is involved[67] (the chain transfer rate constant is 89 litre mol^{-1} s^{-1}; we may note for comparison that the chain propagation rate constant is 576 mol $litre^{-1}$ s^{-1}).[81]

V. The influence of organoelement additives on the composition of the copolymer and on the kinetics of the copolymerisation of vinyl monomers

Copolymerisation is at present the main method of synthesis of polymers with the required set of chemical and physical properties. This can be explained by the fact that in most cases it is difficult to regulate the properties of homopolymers while the need for such regulation in order to obtain polymers for different purposes does exist.[2, 3, 6]

Copolymerisation usually leads to the formation of statistical copolymers the composition and properties of which are determined both by the initial content of the monomers in the mixture and by the reactivity of the monomers and growth radicals. However, there exist monomer pairs in the copolymerisation of which a regular alternation of units in the monomer takes place. As a rule, a strict alternation of the monomer units is observed when one of the monomers is a distinct donor of electron density while the other is an electron acceptor. Since the number of monomers with pronounced electron-accepting properties is small (for example, maleic anhydride and its derivatives, sulfur dioxide), the number of monomer pairs forming alternating copolymers is likewise small.

For this reason, methods based on the introduction of special additives into the system, as a rule protic or aprotic acids, have been developed for the regulation of the composition of the copolymers.[2] As shown above, the acids are coordinated to the monomers or growth radicals, enhancing thereby their electron-accepting properties and permitting the synthesis of alternating copolymers.[1, 2] The main disadvantage of this procedure is the need for a large excess of the regulating additive (by 1-3 orders of magnitude) relative to the initiator. This leads to the contamination of the polymeric product and precludes the industrial application of this method for the regulation of the composition.

The use of initiators based on organometallic compounds of Group III elements and peroxides makes it possible to eliminate the above disadvantage because the regulating effect of these compounds on chain propagation is manifested, as stated above, when catalytic amounts of the initiator (0.1-1.0 mol.%) are used.

The effects of complex formation in radical copolymerisation in the presence of Lewis acids are determined to a large extent by the electronic structure of the monomer. The limiting systems are those in which only one of the monomers interacts with the complex-forming agent and also those in which both monomers interact with it. Both versions are analysed below.

It has been established unambiguously for the copolymerisation of acrylonitrile with a series of vinyl monomers[82, 83] that the organoelement initiator exerts a significant influence on the dependence of the composition of the copolymer on that of the monomer mixture.

Thus, in the case of the classical radical initiator—azoisobutyronitrile, the acrylonitrile–vinyl acetate (VA) copolymer is enriched in acrylonitrile as the more active monomer whatever the composition of the monomer mixture (the coefficients of the relative reactivities of the monomers are r_{AN} = 4.05 and r_{VA} = 0.06). When the trialkylborane–OEP organoelement initiator is used, the composition curve is S-shaped (Fig. 1). The section of the curve where the composition of the copolymer is virtually independent of that of the monomer mixture can be clearly seen, which suggests that there is a tendency towards the alternation of monomer units in the copolymer and indicates that the copolymerisation is of the complex-radical type. This is also indicated by the equalisation of the relative reactivities of the monomers [r_{AN} = 0.35 and r_{VA} = 0.42; for comparison, we may note that r_1 and r_2 calculated in accordance with the $Q-e$ scheme (the Alfrey–Price scheme)[6] are respectively 4.27 and 0.06] and by the deviation from linearity in the calculation of the copolymerisation constants by the Kelen–Tüdös method.

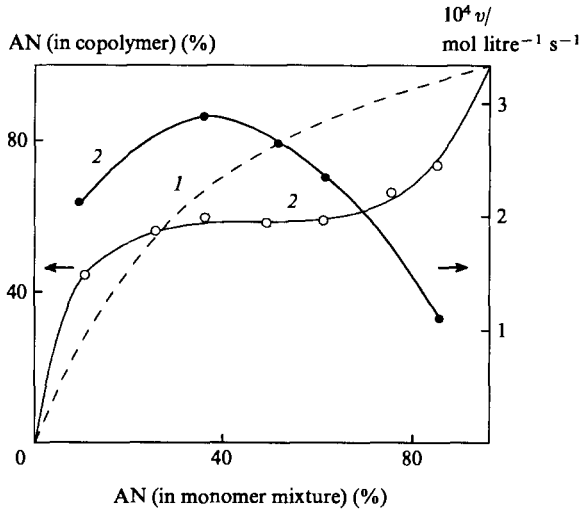


Figure 1. Dependence of the composition of the acrylonitrile–vinyl acetate copolymer and of the rate of copolymerisation on the composition of the monomer mixture. Initiator: (*1*) AIBN; (*2*) triisobutylborane–di-*tert*-butylperoxytriphenylantimony.

Table 4. Effective reactivities of the monomers.

Monomer		r_1	r_2	Initiator	Ref.	Monomer		r_1	r_2	Initiator	Ref.
1	2					1	2				
AN	VA	4.05	0.06	AIBN	63		VC	15.0	0.02	AIBN	63
		0.97	0.20	TBB–TBP	83			6.7	0.02	TBB–TBPA	42
		0.90	0.04	TBB–TBPT	83		AA	1.08	0.003	TBB–TBPS	42
		0.85	0.05	TBB–TBPG	83	VA	VDC	0.03	3.60	AIBN	88
		0.40	0.03	TBB–TBPA	83			0.12	0.20	TBB–DPA	88
		0.35	0.42	TBB–DPA	82		VC	0.23	1.68	AIBN	63
	MMA	0.15	1.20	AIBN	63			0.58	0.97	TBB–DPA	88
		0.04	3.53	TBB–TBP	42		VPD	0.20	3.02	AIBN	63
		0.15	0.75	TBB–TBPT	83			0.32	0.19	TBB–TBP	33
		0.26	0.67	TBB–TBPG	83			0.17	0.15	TBB–TBPG	33
		0.10	0.64	TBB–DPA	83			0.30	0.28	TBB–DPA	33
	VC	2.8	0.04	AIBN	63	VPD	ST	0.05	5.20	CPC	63
		0.86	0.05	TBB–DPA	99			0.05	0.96	TBB–DPA	33
		0.74	0.05	TBB–TBPT	99			0.29	0.94	TBB–TBPG	33
	AA	0.35	1.15	AIBN	63		VDC	0.40	0.35	CPC	63
		0.33	0.08	TBB–DPA	42			0.26	2.16	TBB–DPA	33
	VDC	0.91	0.37	AIBN	63	ST	AA	0.15	0.25	BP	63
		0.12	0.14	TBB–DPA	32			0.87	0.04	TBB–TBPA	41
	MAA	0.15	5.50	AIBN	63		MAA	0.15	0.70	BP	63
		0.15	0.43	TBB–DPA	83			0.27	0.03	TBB–TBPA	41
	ST	0.04	0.40	AIBN	63	Ethylene	VA	0.80	1.20	TBB–DPA	87
		0.04	0.27	TBB–DPA	83			0.95	1.10	TBB–TBPS	87
MMA	MAA	0.58	1.40	BP	44			1.0	1.30	AIBN	63
		0.95	0.99	AIBN–TBB	44		VC	0.22	0.50	TBB–DPA	94
		1.07	0.62	AIBN–DPA	44			0.24	3.60	AIBN	63
		0.45	0.28	TBB–DPA	44			0.20	2.0	Ziegler–Natta	89
		1.10	0.85	AIBN–DBPS	44	Propene	VC	0.28	0.39	TBB–DPA	94
	ST	0.46	0.52	CPC	63	Hex-1-ene	VC	0.05	0.65	TBB–DPA	94
		0.37	0.57	TBB–DPA	86			0.06	0.88	TBB–TBPA	94
		0.32	0.33	CPC–DPA	86			0.13	0.94	TBB–TBPS	94
	VDC	2.50	0.50	AIBN	63		AN	0.10	4.60	TBB–DPA	94
		1.04	0.06	TBB–DPA	32			0	12.2	AIBN	63

Note. The following abbreviations have been adopted: TBB = triisobutylborane, DPA = di-*tert*-butylperoxytriphenylantimony, TBPA = *tert*-butylperoxytetraphenylantimony, TBPS = *tert*-butylperoxytrimethylsilicon, TBPG = *tert*-butylperoxytriethylgermanium, TBPT = *tert*-butylperoxytriethyltin, VPD = *N*-vinylpyrrolidinone, VC = vinyl chloride, ST = styrene, VDC = vinylidene chloride, and CPC = dicyclohexylperoxy carbonate.

Such an appreciable influence of low concentrations of the initiator {[TAB] = $(2-8) \times 10^{-3}$ mol/mol of the monomer mixture, [OEP] = 10^{-3} mol/mol of the monomer mixture} is due to the coordination of the growing macroradical to the components of the initiating system. The trialkylborane, which has an unoccupied orbital in the boron atom, should then play the most active role. Its coordination to the growing acrylonitrile radical leads to a redistribution of electron density and enhances the electron-accepting properties of the polyacrylonitrile radical. The dependence of the rate of copolymerisation on the composition of the monomer mixture has a distinct maximum (Fig. 1). This suggests that the monomers form a reaction complex in the chain propagation stage.[1, 3]

Similar features have been observed also in the copolymerisation of acrylonitrile with acrylic and methacrylic acids and also with MMA.[83] Thus the composition curve for the acrylonitrile–vinyl acetate monomer pair contains a section where the composition of the copolymer is virtually independent of that of the monomer mixture. The relative reactivities (Table 4) in the case of an organoelement initiator differ appreciably from the values calculated in accordance with the $Q-e$ scheme and literature data.[63] The observed equalisation of the copolymerisation constants should lead to the synthesis of a polymer with a uniform composition.

Organoelement compounds exert a no less powerful influence on the dependence of the composition of the copolymer on that of the monomer mixture in the case of the methyl methacrylate–methacrylic acid pair as well.[41, 44] In the copolymerisation of the above monomers without the addition of organoelement compounds (with AIBN as the initiator, Table 4), the copolymer is enriched in methacrylic acid (MAA) whatever the composition of the monomer mixture. In the presence of the trialkylborane–OEP binary organoelement initiator, the composition curve is S-shaped and the relative reactivities of both monomers are significantly less than unity (Table 4). The product of the copolymerisation constants ($r_{MMA} \cdot r_{MAA}$) tends to zero, which indicates the alternation of the monomer units in the copolymer.[3]

The study of the separate influences of the components of the binary organoelement initiator on the chain propagation showed that the addition of 0.2 mol.% of triisobutylborane at a AIBN initiator concentration of 0.1% leads to an appreciable equalisation of the relative reactivities of the monomers. The introduction of an organoantimony peroxide together with AIBN also exerts a fairly strong influence on the reactivity of the monomers and growth radicals—the copolymer is enriched in MMA along all the sections of the composition curve. *tert*-Butylperoxytrimethylsilicon, which is used as a fairly effective coinitiator in relation to trialkylboranes, has a similar influence on the effective constants for the copolymerisation of MMA and methacrylic acid.[25, 32] Thus both components of the organoelement initiator (trialkylborane and OEP) have a regulating effect on the composition of the copolymer in the copolymerisation of acrylic monomers.

The rate of copolymerisation and the degree of conversion depend significantly on the nature of the heteroatom in the peroxide. Thus, in the copolymerisation of acrylonitrile with vinyl acetate, organoantimony and organotin peroxides are the most active as coinitiators in relation to trialkylborane (Table 5), while the composition with *tert*-butyl peroxide is least active: after 3 h, the degree of conversion does not exceed 5%. These data agree with the available information about the homopolymerisation of vinyl monomers in the presence of organoelement initiators[11, 25, 32, 33] and indicate a direct influence of the nature of the heteroatom in the peroxide on the rate of generation of radicals and on the chain propagation stage.

The last conclusion has been confirmed by a study of the dependence of the composition of the acrylonitrile–vinyl acetate copolymer on the composition of the monomer mixture when various OEP (Fig. 2) and *tert*-butyl peroxides are used. The form of the composition curves as well as the dependences

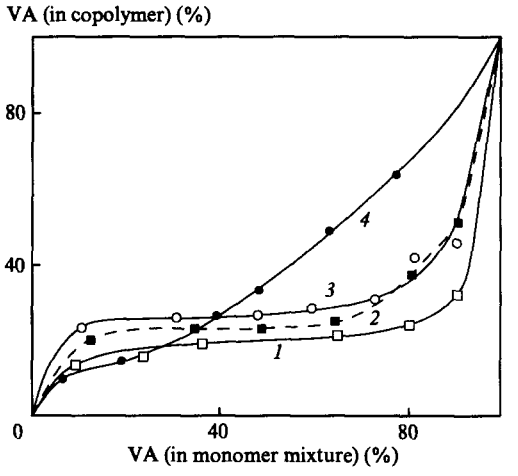


Figure 2. The influence of the nature of the heteroatom in the organoelement peroxide on the dependence of the composition of the vinyl acetate–acrylonitrile copolymer on the composition of the monomer mixture (T = 293 K) in the presence of the triisobutylborane–peroxide initiator; peroxide: (*1*) *tert*-butylperoxytriethylgermanium; (*2*) *tert*-butylperoxytriethyltin; (*3*) *tert*-butylperoxytetraphenylantimony; (*4*) *tert*-butyl peroxide.

of the rate of copolymerisation on the composition of the monomer mixture differ significantly in the case of *tert*-butyl peroxide and its organoelement analogues. When germanium, tin, and antimony OEP are used, a section is observed on the composition curve where the composition of the copolymer is virtually independent of the composition of the monomer mixture. For the composition involving *tert*-butyl peroxide, the composition curve is also S-shaped, but there is no linear section.

Similar relations have been observed also in the case of the acrylonitrile–MMA monomer pair.[83] When organoelement peroxides are used, the reactivities of the monomers are equalised, whereas in the presence of *tert*-butyl peroxide as the coinitiator, the composition curve is close to the analogous curve for AIBN as the initiator.[63] When OEP are used for the copolymerisation of MMA with acrylonitrile, the copolymerisation constants of the monomer are similar and less than unity in all cases (Table 4), differing from the analogous constants for *tert*-butyl peroxide and AIBN.

Organosilicon peroxides exert a regulating effect on the copolymerisation of acrylates in the presence of sulfuryl chloride and phosphorus trichloride,[84, 85] but it is not quite so explicit as in the case of organic compounds of Group III elements, which can be accounted for by the difference between the electron-accepting properties of the modifying agents.

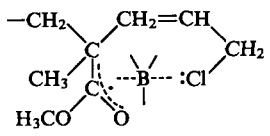
In the copolymerisation of two structurally related monomers, for example MMA–methacrylic acid, the differences between the coordination capacities of the heteroatoms in the peroxides do not exert a significant influence on the composition of the copolymer (Table 5),[41, 44] although on the whole a binary organoelement initiator exerts a regulating effect manifested by the equalisation of the relative reactivities of the monomer and by the S-shape of the composition curves. Similar features have

Table 5. Dependence of the rate of copolymerisation of acrylonitrile with vinyl acetate and methyl methacrylate in the presence of the triisobutylborane–peroxide binary initiator on the nature of the peroxide component (T = 293 K).

Comonomer (mol.%)	$10^4 v$ / mol litre^{-1} s^{-1}			
	TBP	TBPG	TBPT	DPA
VA, 49	0.05	0.86	1.40	2.02
MMA, 45	0.05	0.76	0.81	2.32

been observed also for the acrylonitrile–MMA, acrylonitrile–methacrylic acid, and acrylonitrile–acrylic acid monomer pairs.[41, 83] In all these pairs, two electron-accepting monomers are copolymerised, each of them being capable of coordination interaction with the OEC via its functional groups.

In the copolymerisation of electron-donating and electron-accepting monomers, for example MMA–styrene,[86] MMA–allyl chloride,[45] acrylonitrile–styrene,[83] and acrylonitrile–vinyl acetate, the regulating effect of the organoelement initiators is most explicit. The initiator influences not only the dependence of the composition of the copolymer on that of the monomer mixture but also the dependence of the rate of copolymerisation on the initial contents of the monomers in the mixture. For the monomer pairs indicated, the dependence of the rate of copolymerisation on composition passes through a maximum in the vicinity of a nearly equimolar monomer ratio (Fig. 1). This yet again constitutes evidence in support of the complex-radical nature of the copolymerisation and also suggests that the monomers and macroradicals can form a complex in the chain propagation stage.[45]



^{1}H NMR study of the MMA–styrene copolymer obtained in the presence of dicyclohexyl peroxydicarbonate (DCC) and an organoelement initiator has shown that the microstructures of the specimens differ significantly.[86] A satisfactory agreement between the calculated and experimental fractions of the triads has been observed for the copolymer synthesised using DCC. For the specimens obtained in the presence of organoelement compounds, the discrepancy between the experimental and calculated data is significant (Table 6), which demonstrates the inapplicability of the Mayo–Lewis scheme under these conditions. The triad ratio calculated from the relative reactivities in conformity with the penultimate unit model showed that the Mertz–Alfrey–Goldfinger equation describes the copolymerisation process much better. However, it is seen from the data presented that the influence of the penultimate unit is not the only factor which alters the composition of the copolymer. These data indicate yet again that the complex formation reaction between the monomer and the initiator and also between the initiator and the macroradical makes an appreciable contribution to the change in the relative reactivities of the monomers.

Table 6. The triad ratios (1–3) in the ^{1}H NMR spectra of the MMA–styrene copolymer (mole fraction of MMA in the copolymer 0.6)[86]

Triad*	DCC		Bu^i_3B–$Ph_4SbOOBu^t$		
	1	2	1	2	3
AAA	0.42	0.38	0.13	0.24	0.17
BAA	0.37	0.33	0.62	0.33	0.43
BAB	0.21	0.29	0.25	0.43	0.50

Note. 1–experimental fraction; 2–fraction calculated for the terminal model; 3–fraction calculated for the penultimate model.
* In the triads, A = MMA and B = styrene.

Data concerning the dependence of the instantaneous and overall compositions of the MMA–styrene copolymer on the degree of conversion show that, in copolymerisation in the presence of DCC, the copolymer is enriched in MMA at high degrees of conversion. This indicates the nonuniformity of the product. Initiation by the tetraalkylborane–OEP system leads to the formation of a copolymer with a narrower distribution of the fractions with respect to composition.[86]

In the copolymerisation of acrylates with alkenes, the regulating effect of organoelement compounds is not quite so explicit as in the examples examined above. The rate of copolymerisation of acrylonitrile with hex-1-ene and cyclohexene, of MMA with ethylene, and of vinyl acetate with ethylene diminishes linearly with increase in the content of the olefin in the mixture.[87] Although the relative reactivities of the monomers do differ somewhat from those for the classical radical initiators the difference is less than for the copolymerisation of two vinyl monomers (Table 4). This is associated with the fact that olefins and especially the growth radicals associated with them show a smaller tendency towards complex formation than the monomers containing functional groups or atoms with lone electron pairs.

An organoelement initiator exerts a modifying influence also on both copolymerising monomers or electron donors, for example *N*-vinylpyrrolidinone (VPD)–vinyl acetate.[33, 88] For this pair, the composition of the copolymer is constant within a certain range of monomer compositions, which indicates the alternation of the monomer units in the copolymer. This is also indicated by the equalisation of the relative reactivities of the monomers (Table 4) and also by the deviation from the linear variation of the calculated parameters in the determination of the copolymerisation constants by the Kelen–Tüdös method. The dependence of the rate of copolymerisation on the composition of the monomer mixture passes through an extremum in the region of the equimolar composition of the monomer mixture (Fig. 3). One cannot rule out the possibility that the monomers form a 1 : 1 reaction complex during chain propagation.[1]

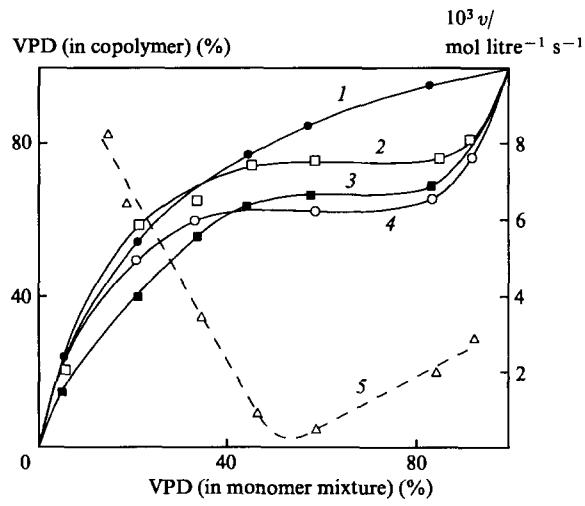


Figure 3. Composition curves (curves *1–4*) and the rates of copolymerisation (curve *5*) of *N*-vinylpyrrolidinone with vinyl acetate. Initiator: (*1*) AIBN; (*2*) triisobutylborane–*tert*-butyl peroxide; (*3*) and (*5*) triisobutylborane–di-*tert*-butylperoxytriphenylantimony; (*4*) triisobutylborane–*tert*-butylperoxytriethylgermanium.

The organoelement exerts a significant influence also on the copolymerisation of *N*-vinylpyrrolidinone with vinylidene chloride (*N*-vinylpyrrolidinone and vinylidene chloride are 'naturally alternating' comonomers).[33] The composition curve is S-shaped when DCC is used as the initiator. In the copolymerisation of the above pair of monomers in the presence of the trialkylborane–OEP initiator, a unilateral enrichment of the copolymer in vinylidene chloride is observed.

Thus catalytic amounts of organic compounds of Group III–V elements not only effectively initiate the low-temperature (co)polymerisation of vinyl monomers but also exhibit a regulating activity on the rate of (co)polymerisation and the composition of the copolymers.

VI. Copolymerisation of vinyl chloride with ethylene and α-olefins in the presence of organometallic compound–peroxide initiating systems

Vinyl chloride and α-olefins are known to polymerise effectively at a low pressure via different mechanisms: vinyl chloride via a radical mechanism and ethylene and its homologues via a coordination mechanism in the presence of Ziegler–Natta catalysts.[6, 7] The copolymers of vinyl chloride with olefins cannot be synthesised with a high degree of conversion under technologically convenient conditions in the presence of the usual radical initiators:[89] the maximum degree of conversion is 17% in the presence of AIBN,[90] 24% in the presence of Ziegler–Natta catalysts,[91] and 30% in the presence of electron-donating additives.[92] The lack of effective initiators has held back the industrial production in our country of the above copolymers, which are extremely promising as plastics: they can be easily worked, have a larger elongation on rupture than poly(vinyl chloride), have an enhanced impact strength, etc. Furthermore, the introduction of even 5%–10% of ethylene into poly(vinyl chloride) appreciably lowers the cost of the monomer.

The coordination-radical initiators based on organic compounds of Group III elements and organic peroxides of Group IV elements occupy an intermediate position between the traditional radical initiators and Ziegler–Natta catalysts by virtue of their structural characteristics. They make it possible to copolymerise vinyl chloride with ethylene and α-olefins at a high rate and with a high conversion under energetically convenient conditions.[93, 94]

After 5 h, the limiting conversion for the vinyl chloride–ethylene copolymer in the presence of the trialkylborane–OEP organoelement initiator reaches 90%. With increase in the length of the alkyl group in the olefin, the rate of polymerisation and the conversion fall and in the case of oct-1-ene the yield of the copolymer does not exceed 20%. The additional introduction of the initiator into the system leads merely to a slight increase in the yield of the copolymer. The reason for the decrease in conversion is probably associated with chain termination due to the mobile hydrogen atoms in the olefin in the α-position relative to the double bond.

The structure of the peroxide and the composition of the monomer mixture exert direct influence on the process kinetics. It has been shown in relation to hex-1-ene that, with increase in the content of vinyl chloride in the monomer mixture from 6% to 89%, the limiting conversion rises from 3% to 49%, which agrees well with the reactivity of the copolymerising monomers. It has been found that the olefins themselves are incapable of homopolymerisation in the presence of the systems indicated.[25, 94] Organoantimony peroxides are more active as coinitiators than their organogermanium and organosilicon analogues, which is probably associated with the characteristic features of the radical formation in the OEC–peroxide systems[27] and also agrees with data on the homopolymerisation of vinyl chloride in the presence of organoelement initiators.[95]

When traditional radical initiators as well as Ziegler–Natta catalysts are used for the copolymerisation of vinyl chloride with olefins, the possibilities for the variation of the composition of the copolymer are extremely limited. The form of the composition curves and the relative reactivities of the monomers (Table 4) show that the copolymer is enriched in one of the monomers. This is associated with the significant difference between the reactivities of vinyl chloride and olefins. The use of trialkylborane–OEP systems leads to an appreciable equalisation of the copolymerisation constants. For a series of systems, the composition of the copolymer is almost independent of the composition of the monomer mixture and is nearly equimolecular over a wide range of [mixture] compositions.[87, 94]

Calculations of the relative reactivities of the monomers by the Kelen–Tüdös and Fineman–Rossi methods reveal a deviation of the calculated parameters from the linear relation. This indicates the system does not obey the classical Mayo–Lewis equation and can be explained within the framework of the coordination-radical copolymerisation mechanism: the boron atom in trialkylborane and the element in the peroxide may be coordinated both to the monomers and to the growing macroradicals, altering their reactivity and hence the relative reactivities of the monomers.

Analysis of the physicochemical properties of the copolymers of vinyl chloride with olefins showed that, when olefin units are introduced, the Fikentscher constant is reduced. This facilitates the processing of the polymeric product and improves its plasticity.[96]

When oxidation-reduction systems based on triethylborane and organic oxidants (oxygen, *tert*-butyl hydroperoxide) are used, the regulating activity is manifested to a lesser extent[92, 97, 98] than in the case of the trialkylborane–OEP binary initiator. It is quite evident that the heteroatom in the OEP also participates in the propagation stage by virtue of its unoccupied *d* orbitals. The possibility of the formation of complexes between the peroxides of Group IV elements and the monomers, including olefins, has been demonstrated in a series of studies.[9, 28, 29]

The regulating activity of the OEC–peroxide initiator is manifested not only in the presence of organoboron compounds but also in the presence of alkyl derivatives of aluminium and bismuth.[99]

The trialkylborane–OEP binary initiator also made it possible to achieve the single-stage synthesis of terpolymers containing vinyl chloride, vinyl acetate, and olefin units.[100] The above terpolymers can be used as elastomers, effective adhesives, and constructional materials, including materials for the medical industry. A series of such copolymers, obtained in recent years by foreign companies, can be processed without the introduction of plasticisers. They have been called third generation polymers with internal plasticisation.

As for the ethylene–divinyl chloride copolymers, the main complication in the synthesis of the above terpolymers consists in the fact that under mild conditions (room temperature, low pressure) olefins and vinyl monomers in the presence of traditional radical initiators copolymerise ineffectively and as a rule graft polymerisation is used for their synthesis.[101, 102] The trialkylborane–OEP binary initiator makes it possible to obtain the above polymers with conversions up to 70% over a period of 5–6 h within a wide range of compositions. It is of interest that, along the initial sections, the copolymer is enriched in ethylene although its relative reactivity constant is somewhat lower than for vinyl acetate and vinyl chloride. On the other hand, for the limiting conversion the copolymer contains more vinyl chloride. The above features demonstrate yet again that the components of the initiator are capable of coordinating to the growing macroradicals and monomers and of altering their reactivity. In ter- and tetra-polymerisation in the presence of complex forming agents, the overall proportions of the monomer-donor and monomer-acceptor units which have entered into the polymer are known to be similar.[103–105]

VII. Conclusion

The set of data presented indicates the development of a promising aspect of the synthetic chemistry of polymers involving the application of catalytic amounts of organometallic compounds as modifying agents for the homo- and co-polymerisation of vinyl monomers and olefins. Small amounts of added organoelement compounds make it possible to influence the reactivity of the monomers and the macroradicals and to regulate thereby the kinetic process parameters in the initiation, chain propagation, and chain termination stages as well as the composition, structure, and properties of the (co)polymers.

The use of catalytic amounts of the modifying agent eliminates the problem of its removal from the final product and leads to the prospect of the industrial application of the above approach to the synthesis of (co)polymers with specified properties without the preliminary elimination of stabilisers.

References

1. J Furukawa *Vysokomol. Soedin. A* **21** 2591 (1979)
2. B A Krentsel', in *Novoe v Chereduyushcheisya Sopolimerizatsii* (New Advances in Alternating Copolymerisation) (Ed. B A Krentsel') (Moscow: Nauka, 1983) p. 4
3. V A Kabanov, V P Zubov, Yu D Semchikov *Kompleksno-Radikal'naya Polimerizatsiya* (Complex-Radical Polymerisation) (Moscow: Nauka, 1987)
4. B A Dolgoplosk, E I Tinyakova *Okislitel'no-Vosstanovitel'nye Sistemy kak Istochniki Svobodnykh Radikalov* (Oxidation-Reduction Systems as Sources of Free Radicals) (Moscow: Nauka, 1974)
5. Yu A Aleksandrov *Zhidkofaznoe Avtookislenie Elemento-organicheskikh Soedinenii* (Liquid Phase Autoxidation of Organoelement Compounds) (Moscow: Nauka, 1978)
6. S S Ivanchev *Radikal'naya Polimerizatsiya* (Radical Polymerisation) (Leningrad: Khimiya, 1985)
7. B A Dolgoplosk, E I Tinyakova *Metalloorganicheskii Kataliz v Protsessakh Polimerizatsii* (Organometallic Catalysis in Polymerisation Processes) (Moscow: Nauka, 1985)
8. V N Alyasov, V P Maslennikov, Yu A Aleksandrov, in *Radikal'nye Reaktsii Metalloorganicheskikh Soedinenii. Mezhvuzovskii Sbornik* (Radical Reactions of Organometallic Compounds. Intercollegiate Collection) (Gorky: Izd. Gor'kovsk. Gos. Univ., 1986) p. 64
9. N V Yablokova, Yu A Aleksandrov *Usp. Khim.* **58** 908 (1989) [*Russ. Chem. Rev.* **58** 534 (1989)]
10. V A Dodonov, I N Aksenova, in *Radikal'nye Reaktsii Metalloorganicheskikh Soedinenii. Mezhvuzovskii Sbornik* (Radical Reactions of Organometallic Compounds. Intercollegiate Collection) (Gorky: Izd. Gor'kovsk. Gos. Univ., 1986) p. 83
11. V A Dodonov, in *Metalloorganicheskie Soedineniya i Radikaly* (Organometallic Compounds and Radicals) (Ed. M I Kabachnik) (Moscow: Nauka, 1985) p. 40
12. E B Milovskaya *Usp. Khim.* **42** 881 (1973) [*Russ. Chem. Rev.* **42** 384 (1973)]
13. Yu N Baryshnikov, G I Vesnovskaya, S G Krinsburg *Kinet. Katal.* **17** 1603 (1976)
14. V A Dodonov, O S Morozov, D F Grishin, E G Lyutin, N N Vyshinskii *Dokl. Akad. Nauk SSSR* **225** 1123 (1980)
15. G A Razuvaev, M A Lopatin, V A Dodonov *Zh. Obshch. Khim.* **48** 2494 (1978)
16. V A Dodonov, D F Grishin, O S Morozov, V K Cherkasov *Zh. Obshch. Khim.* **52** 72 (1982)
17. V A Dodonov, D F Grishin, O P Stepovik, V K Cherkasov *Zh. Obshch. Khim.* **51** 2245 (1981)
18. V A Dodonov, D F Grishin, V K Cherkasov *Zh. Obshch. Khim.* **52** 868 (1982)
19. C G Scretas, J F Eastham *J. Am. Chem. Soc.* **87** 3276 (1965)
20. G I Vesnovskaya, Yu N Baryshnikov, in *Radikal'nye Reaktsii Metalloorganicheskikh Soedinenii. Mezhvuzovskii Sbornik* (Radical Reactions of Organometallic Compounds. Intercollegiate Collection) (Gorky: Izd. Gor'kovsk. Gos. Univ., 1986) p. 48
21. D F Grishin, V A Dodonov, in *Radikal'nye Reaktsii Metalloorganicheskikh Soedinenii. Mezhvuzovskii Sbornik* (Radical Reactions of Organometallic Compounds. Intercollegiate Collection) (Gorky: Izd. Gor'kovsk. Gos. Univ., 1986) p. 60
22. V A Dodonov, T I Starostina, D F Grishin, L A Zinina *Vysokomol. Soedin. B* **27** 783 (1985)
23. V A Dodonov, A V Gushchin, D F Grishin, T G Brilkina *Zh. Obshch. Khim.* **54** 100 (1984)
24. Yu D Semchikov, L M Mazanova, G A Voskoboinik, E B Soboleva, in *Fizikokhimiya Protsessov Sinteza i Svoistva Polimerov. Mezhvuzovskii Sbornik* (Physical Chemistry of the Synthetic Reactions and Properties of Polymers. Intercollegiate Collection) (Gorky: Izd. Gor'kovsk. Gos. Univ., 1988) p. 5
25. G A Razuvaev, V A Dodonov, Yu A Ivanova *Dokl. Akad. Nauk SSSR* **250** 119 (1980)
26. V A Dodonov, D F Grishin, V K Cherkasov, G A Razuvaev *Vysokomol. Soedin. A* **24** 451 (1982)
27. D F Grishin, Candidate's Thesis in Chemical Sciences, Gorky Polytechnic Institute, Gorky, 1981, p. 40
28. V V Gorbatov, Yu A Kurskii, Yu A Aleksandrov, N V Yablokova *Zh. Obshch. Khim.* **48** 365 (1978)
29. Yu A Aleksandrov, V V Gorbatov, V G Tsvetkov, N V Yablokova *Zh. Obshch. Khim.* **48** 933 (1978)
30. L M Dubinina, V V Amerik, B A Krentsel', E F Petrov, A F Kozhevnik *Izv. Akad. Nauk SSSR., Ser. Khim.* 2667 (1979)
31. Yu A Kurskii, E G Kabanova, N V Yablokova, Yu A Aleksandrov *Zh. Obshch. Khim.* **58** 1206 (1988)
32. D F Grishin, V A Dodonov, E V Bobina *Vysokomol. Soedin., Ser. B* **34** (4) 41 (1992)
33. D F Grishin, T V Zakharova *Vysokomol. Soedin., Ser. B* **34** (7) 18 (1992)
34. L N Nistratova, N A Kopylova, Yu D Semchikov *Vysokomol. Soedin., Ser. A* **27** 569 (1985)
35. V B Golubev, V P Zubov, L I Valuev, G S Naumov, V A Kabanov, V A Kargin *Vysokomol. Soedin., Ser. A* **11** 2689 (1969)
36. Yu D Semchikov, A N Egorochkin, A V Ryabov *Vysokomol. Soedin., Ser. A* **15** 893 (1973)
37. S Taruke, S Okamura *J. Polym. Sci. Part A, Polym. Chem.* **5** 1083 (1967)
38. Z A Tikhonova, Yu D Semchikov, A V Ryabov, T I Liogon'kaya, in *Trudy po Khimii i Khimicheskoi Teknologii. Mezhvuzovskii Sbornik* (Studies in Chemistry and Chemical Engineering. Intercollegiate Collection) (Gorky: Izd. Gor'kovsk. Gos. Univ., 1975) No. 3, p. 21
39. T Ikegami, J Hirai *J. Polym. Sci. Part A, Polym. Chem.* **8** 463 (1970)
40. G A Abakumov *Zh. Vses. Khim. O-va im. D. I. Mendeleeva* **24** 156 (1979)
41. D F Grishin, V A Dodonov, O V Zolotova, V K Cherkasov *Vysokomol. Soedin., Ser. A* **33** (7) 33 (1992)
42. D F Grishin, V K Cherkasov, P S Razmaev *Izv. Vyssh. Uchebn. Zaved., Khim. Khim. Tekhnol.* **35** (11 – 12) 63 (1992)
43. V A Dodonov, D F Grishin, I N Aksenova *Vysokomol. Soedin., Ser. B* **34** (1993)
44. D F Grishin, O Yu Chinyaeva *Vysokomol. Soedin., Ser. B* **34** 156 (1993)
45. D F Grishin, A B Radbil' *Vysokomol. Soedin., Ser. A* **34** 1425 (1993)
46. C H Bamford, A D Jenkins, R Jonson *Proc. R. Soc. London, A Math. Phys. Sci.* **241** 364 (1957)
47. V A Kargin, V A Kabanov, V P Zubov *Vysokomol. Soedin.* **2** 756 (1960)
48. M Imoto, T Otsu, S Shimizu *Makromol. Chem.* **65** 174 (1963)
49. S Taruke, N Sato, S Okamura *J. Polym. Sci. Part A, Polym. Chem.* **4** 2461 (1966)
50. S Taruke, K Shimadu, S Okamura *J. Polym. Sci. Part A, Polym. Chem.* **7** 879 (1969)
51. L M Novichkova, V I Pokrovskii, A G Koval'skaya, E I Rostovskii *Vysokomol. Soedin., Ser. B* **10** 813 (1968)
52. N I Loginova, R K Gavurina *Vysokomol. Soedin., Ser. B* **11** 355 (1969)
53. C H Bamford, S Brumby *Makromol. Chem.* **134** 159 (1970)
54. V P Zubov, M V Lachinov, L I Valuev, V A Kabanov, V A Kargin *Vysokomol. Soedin., Ser. B* **9** 667 (1967)
55. M B Lachinov, B M Abu el Khair, V P Zubov, V A Kabanov *Vysokomol. Soedin., Ser. A* **15** 504 (1973)
56. Yu D Semchikov, A V Ryabov, N L Morozova, N A Semina *Vysokomol. Soedin., Ser. B* **11** 656 (1969)
57. V A Kabanov, in *International Symposium on Macromolecular Chemistry: Preprints* (Budapest: IUPAC, 1969) p. 435
58. L A Smirnova, T E Knyazeva, Yu D Semchikov, Sh I Modeva *Vysokomol. Soedin., Ser. A* **22** 2137 (1980)
59. S A Bulgakova, L A Smirnova, Yu D Semchikov, T E Knyazeva, Sh I Modeva *Vysokomol. Soedin., Ser. B* **23** 691 (1981)
60. V M Potapov, in *Stereokhimiya* (Stereochemistry) (Moscow: Khimiya, 1988) p. 201
61. C H Bamford, in *Reactivity, Mechanism, and Structure in Polymer Chemistry* (Eds A D Jenkins, A Ledwith) (Translated into Russian; Moscow: Mir, 1977) p. 115
62. B A Dolgoplosk, E I Tinyakova *Generirovanie Svobodnykh Radikalov i Ikh Reaktsii* (Generation of Free Radicals and Their Reactions) (Moscow: Nauka, 1982)
63. *Entsiklopediya Polimerov* (Encylopaedia of Polymers) (Moscow: Sov. Entsiklopediya, 1976) Vol. 1, p. 836
64. J Grotewold, E A Lissi, A E Villa *J. Polym. Sci. Part A, Polym. Chem.* **6** 3157 (1968)
65. F S Arimoto *J. Polym. Sci. Part A, Polym. Chem.* **4** 275 (1966)
66. E Arancibia, J Grotewold, E Lissi, A Villa *J. Polym. Sci.* 7 3430 (1969)
67. J Grotewold, M Hirschler *J. Polym. Sci. Part A, Polym. Chem.* **15** 393 (1977)

68. K U Ingold, B P Roberts, in *Free-Radical Substitution Reactions* (Ed. B P Roberts) (Translated into Russian; Moscow: Mir, 1974) p. 68
69. G A Razuvaev, V A Dodonov, I N Aksenova *Vysokomol. Soedin., Ser. B* **28** 66 (1986)
70. V A Dodonov, I N Aksenova, S N Zaburdyaeva *Vysokomol. Soedin., Ser. B* **33** (8) 34 (1992)
71. V A Dodonov, D F Grishin *Vysokomol. Soedin., Ser. B* **34** 137 (1993)
72. D F Grishin, S A Vashurina *Vysokomol. Soedin., Ser. A* **34** 1236 (1993)
73. G Sattorf, R D Lundberg *J. Polym. Sci. Part B, Polym. Phys.* **10** 583 (1972)
74. M Hirooka *J. Polym. Sci. Part B, Polym. Phys.* **10** 171 (1972)
75. J Furukava, S Tsuruta, J Kiji *J. Polym. Sci. Part A, Polym. Chem.* **11** 1819 (1973)
76. Yu E Eizner, B L Erusalimskii *Elektronnyi Aspekt Reaktsii Polimerizatsii* (The Electronic Aspect of Polymerisation Reactions) (Leningrad: Khimiya, 1976)
77. G Kabalka *J. Organomet. Chem.* **33** 25 (1971)
78. B M Mikhailov, Yu N Bubnov *Bororganicheskie Soedineniya v Organicheskom Sinteze* (Organoboron Compounds in Organic Synthesis) (Moscow: Nauka, 1977)
79. Z Florjanczyk, W Kuran, S Pasynkewicz, I Kwas *J. Organomet. Chem.* **112** 21 (1976)
80. G A Tolstikov, V P Yur'ev *Alyuminiiorganicheskii Sintez* (Organoaluminium Synthesis) (Moscow: Nauka, 1976)
81. J Grotewold, M Hirschler *J. Polym. Sci. Part A, Polym. Chem.* **15** 383 (1977)
82. D F Grishin, V A Dodonov, O Yu Zolotova *Vysokomol. Soedin., Ser. B* **32** 643 (1991)
83. D F Grishin, V A Dodonov, O Yu Zolotova *Dokl. Akad. Nauk SSSR* **319** 395 (1991)
84. N A Kopylova, E G Kabanova, N V Yablokova, Yu D Semchikov, V A Puzankova *Vysokomol. Soedin., Ser. A* **31** 301 (1989)
85. N A Kopylova, N V Yablokova, T M Pisareva, E G Kabanova, Yu D Semchikov, Yu A Aleksandrov *Vysokomol. Soedin., Ser. B* **29** 506 (1987)
86. V A Dodonov, O Yu Chinyaeva, D F Grishin *Vysokomol. Soedin., Ser. B* **32** 470 (1991)
87. D F Grishin, B B Zhislina *Izv. Vyssh. Uchebn. Zaved., Khim. Khim. Tekhnol.* **35** (8) 47 (1992)
88. D F Grishin, V A Dodonov *Izv. Vyssh. Uchebn. Zaved., Khim. Khim. Tekhnol.* **35** (9) 107 (1992)
89. G P Belov *Plastmassy* **11** 29 (1980)
90. R D Burhalt, N L Zutty *J. Polym. Sci. Part A, Polym. Chem.* **2** 1137 (1963)
91. A Misono, Y Uchida, K Yamada *J. Polym. Sci. Part B, Polym. Phys.* **5** 401 (1967)
92. A Misono, Y Uchida, K Yamada, T Saeki *Bull. Chem. Soc. Jpn.* **41** 2995 (1968)
93. USSR P. 1 700 010; *Byull. Izobret.* **47** 97 (1991)
94. D F Grishin, V A Dodonov *Plastmassy* **2** 5 (1992)
95. V A Dodonov, L A Semenycheva, M A Gorshkova *Vysokomol. Soedin., Ser. B* **26** 101 (1984)
96. E N Zil'berman *Poluchenie i Svoistva Polivinilkhlorida* [The Synthesis and Properties of Poly(vinyl chloride)] (Leningrad: Khimiya, 1968)
97. A Misono, Y Uchida, K Yamada *Bull. Chem. Soc. Jpn.* **40** 2366 (1967)
98. J Ulbricht, Z Pirwit *Plaste Kautsch.* **21** 85 (1974)
99. D F Grishin, in *Vsesoyuznaya Konferentsiya "Polivinilkhlorid-91", Dzerzhinsk, 1991, Tezisy Dokladov* ['Poly(vinyl chloride)-91' All-Union Conference, Dzerzhinsk, 1991, Abstracts of Reports] p. 10
100. D F Grishin, V A Dodonov, M Yu Maleeva *Zh. Prikl. Khim.* **65** 1902 (1992)
101. D R Karamyan, D E Markorosyan, K L Belogorodskaya, A F Nikolaev *Poluchenie, Svoistva i Primenenie Sopolimerov Vinilatsetata* (The Synthesis, Properties, and Applications of Vinyl Acetate Copolymers) Article deposited at the ONIITEKhIM No. 675-KhN-D80, Leningrad, 1980
102. J Grerecke, F Zachans, R Wintzer *Plaste Kautsch.* **32** 332 (1985)
103. N G Gaylord, B K Patuaik *J. Polym. Sci. Part B, Polym. Phys.* **10** 6531 (1972)
104. M Hirooka, H Jabunchi, S Kawasuni, K Nakaguchi *J. Polym. Sci. Part A, Polym. Chem.* **11** 1281 (1973)
105. N G Gaylord, S S Dixit, S Maiti, B K Patuaik *J. Macromol. Sci., Chem.* **6** 1495 (1972)

Russian Chemical Reviews **62** (10) 963–979 (1993)
©1993 Russian Academy of Sciences and Turpion Ltd

UDC 54.07:547.567.2.655.741.577.3

Synthesis of molecular complexes based on porphyrins for the investigation of the energy transfer and primary charge separation in photosynthesis

S E Gribkova, R P Evstigneeva, V N Luzgina

Contents

I. Introduction 963
II. Methods of synthesis and photochemical properties of the model compounds 963
III. Conclusion 978

Abstract. Data on the synthesis, steric structures, and photochemical properties of molecular diad systems based on porphyrins as synthetic models of the reaction centre in photosynthesis are considered and treated systematically. The bibliography includes 102 references.

I. Introduction

The conversion of light energy into chemical energy has at present aroused much interest among investigators. Molecular photosynthetic systems, reproducing at a simpler level the individual stages of natural photosynthesis, are being created for the solution of this problem. The donor–acceptor systems based on porphyrin structures may serve as an example of such models.[1–3]

The most important stage in the transformation of light energy into chemical energy is the photochemical charge separation in the photosynthesis system. In nature, this problem has been solved by the creation during the evolutionary process of photosynthetic reaction centres in which charge separation takes place at a record speed. Studies in recent years have shown that synthetic molecular systems of the type D–P–Q, i.e. models containing a photosensitive pigment (P), an electron donor (D), and an electron acceptor (Q), are also capable of giving rise to the structure D^+-P-Q^- with separated charges simulating the primary charge separation in photosynthesis, where the singlet-excited porphyrin reduces the acceptor and is itself reduced by the donor. Such model systems make it possible to investigate in detail the dependence of the process itself on the distance between the donor and the acceptor, on their mutual orientation, on the free energy of the reaction, on the electronic interaction, and on the rates of electron transfer.[4–6]

All the compounds described, containing bound chromophores, are based on systems of two types: molecular diads and multicomponent structures—triads, tetrads, and pentads.

The synthetic methods for the creation of molecular assemblies[7] are discussed in the present review and the possibility of investigating the energy transfer and the primary charge separation in the photosynthesis on diad models is considered. Such models are the simplest systems for the photosynthetetic electron transfer, consisting of chromophores bound covalently to a donor or acceptor.

S E Gribkova, R P Evstigneeva, V N Luzgina Department of the Chemistry and Technology of Fine Organic Synthesis, M V Lomonosov Moscow Institute of Fine Organic Technology, prosp. Vernadskogo 86, 117571 Moscow, Fax (7-095) 430 79 83.

Received 3 May 1993
Uspekhi Khimii **62** (10) 1020–1036 (1993); translated by A K Grzybowski

II. Methods of synthesis and photochemical properties of the model compounds

1. Porphyrin dimers

Studies on the structure of the reaction centres in photosynthetic bacteria and of the mechanism of the electron transfer have shown that the reaction centre consists of six interacting tetrapyrrole pigments. It has also been established that the primary electron donor is a 'special pair' consisting of two aggregated chlorophyll molecules. The problem of current interest in the study of the primary photosynthetic process is therefore that of the creation of covalently bound conformationally-restricted structures containing two and more porphyrin units, i.e. molecular assemblies capable of participating very effectively in specific energy and electron transfer reactions.[4,8–10]

a. Methods of synthesis of porphyrin dimers

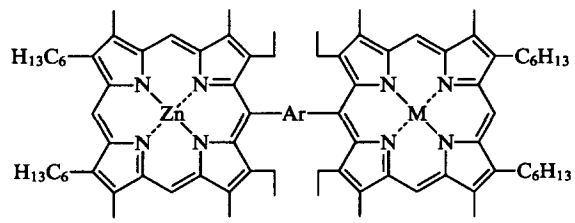
The synthesis of primary porphyrin dimers was described as early as the 1970s.[1] Since then, various multicomponent tetrapyrrole compounds have been obtained and investigated.[11–14]

It was shown that octaalkylporphyrin dimers **1a–q**,[8,9,15] **2a–o**,[16] **3a–i**,[17] and **4a–h**,[18] linked by aromatic spacers, are interesting models.

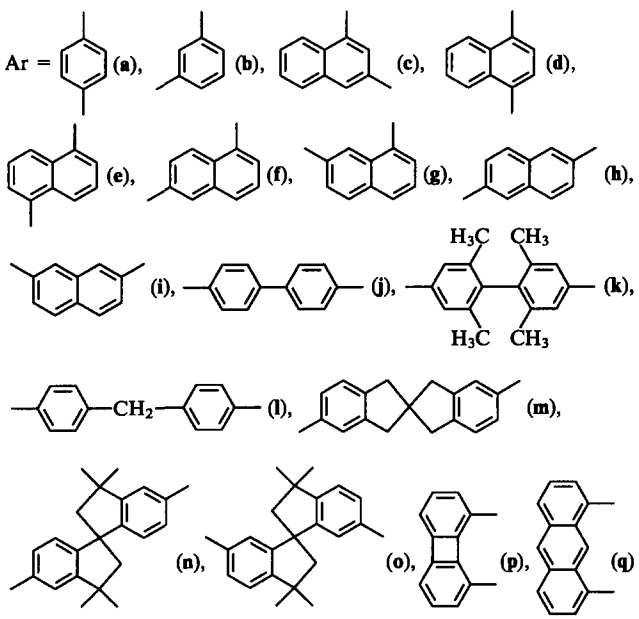
In these dimers, two porphyrin rings are held rigidly in a definite conformation as a result of steric hindrance. The aromatic spacer is perpendicular to the mean plane of the porphyrin, reducing to a minimum the direct $\pi-\pi$ interaction between the porphyrin and the connecting bridge.

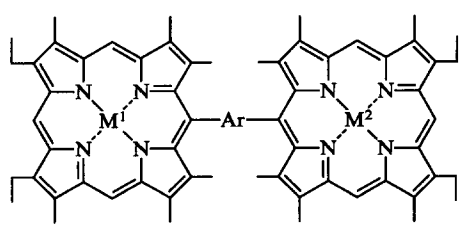
The spacer used in compounds **1m** and **1n** simulates the chromophores with a 'twist' type of conformation such as the haems and chlorophylls in natural systems, while compound **1o** serves as a model of the chromophore with the 'twist' conformation, which has partly the same geometry as the 'special pair' in the bacterial photosynthetic reaction centre. All these symmetrical porphyrins **1a–q**, **2a–o**, **3a–i**, and **4a–h** have been synthesised from the corresponding arenedialdehyde by Chang's method.[19,20]

An alternative approach has been used to synthesise the asymmetric dimer **5** (Scheme 1). Condensation of 1,19-dideoxybiladiene-ac dihydrobromide **6** with isophthalic aldehyde afforded the porphyrin **7a** with a formyl group, which was converted by the reaction with ethyl 4-ethyl-3-methyl-pyrrole-

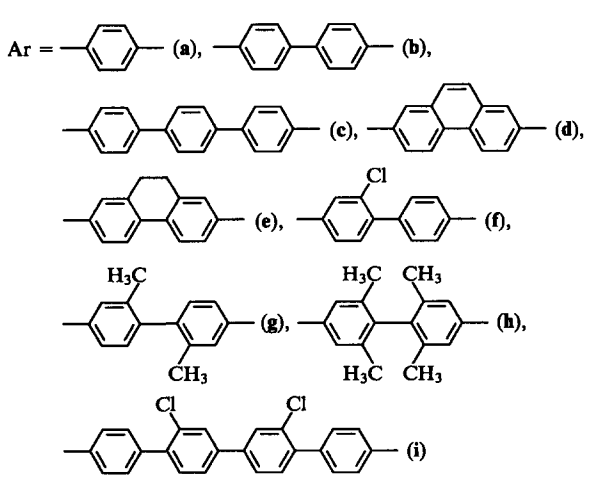


1a–q: M = 2H
2a–o: M = Fe^{III}





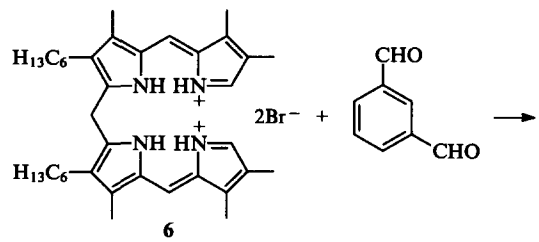
3a–i: $M^1 = M^2 = 2H$
4a–h: M^1 = Zn; $M^2 = Fe^{III}$



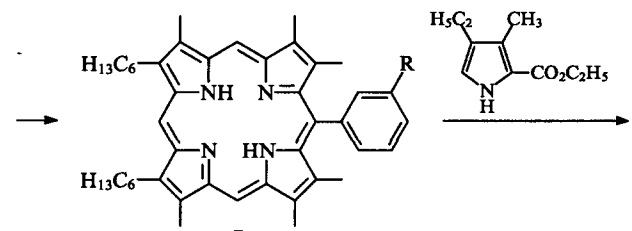
2-carboxylate into the porphyrin-dipyrrolylmethane **8a**. The latter was initially converted into the zinc complex **8b** and was then treated with $LiAlH_4$ in order to obtain the corresponding diol **9**, the interaction of which with 5,5′-unsubstituted dipyrrolmethane **10** afforded the dimer **5** in 9% yield.[9]

The principal task solved in relation to the given structures was the elucidation of the nature and degree of the interaction of the porphyrin components of these assemblies.

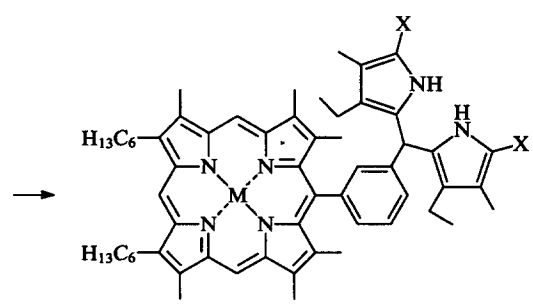
Scheme 1



6

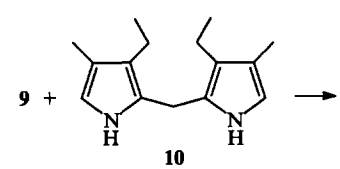


7
R = CHO (**a**), $CH(OCH_3)_2$ (**b**)

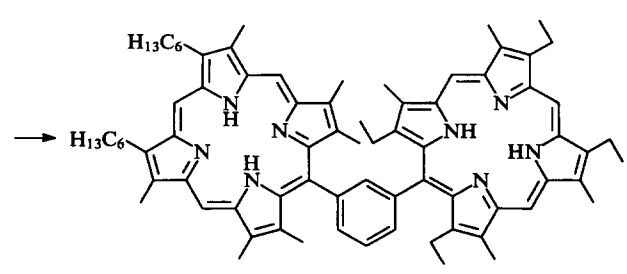


8, 9

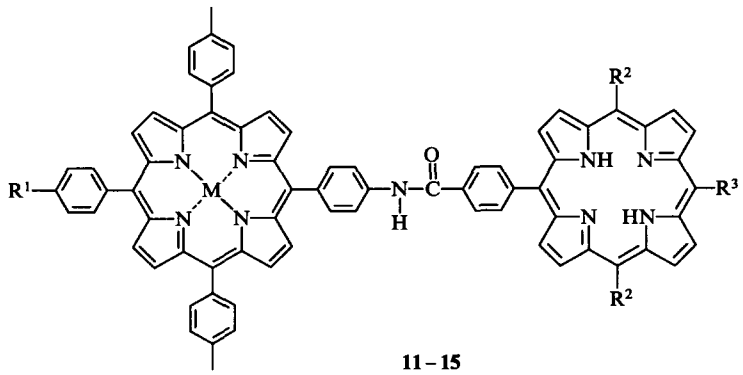
8: M = 2H, X = $CO_2C_2H_5$ (**a**); M = Zn, X = $CO_2C_2H_5$ (**b**)
9: M = Zn, X = CH_2OH



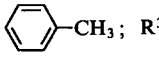
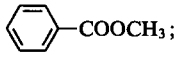
10

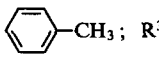
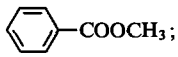


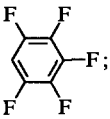
5

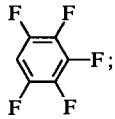


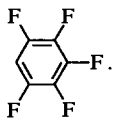
11-15

11: M = 2H; R^1 = $NHCOCH_3$;
R^2 =  ; R^3 =  ;

12: M = Zn; R^1 = $NHCOCH_3$;
R^2 =  ; R^3 =  ;

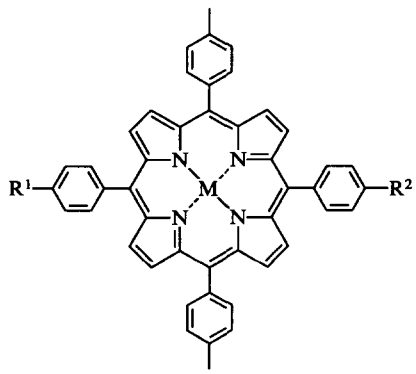
13: M = 2H; R^1 = $NHCOCH_3$; R^2 = R^3 =  ;

14: M = 2H; R^1 = CH_3; R^2 = R^3 =  ;

15: M = Zn; R^1 = CH_3; R^2 = R^3 =  .

The porphyrin dimers **11**–**15** were used to investigate the photoinduced electron transfer and the transfer of the energy of the excited state between the porphyrins.[21]

As an example, the synthesis of the porphyrin dimer **11** is described below. The diester **16** was hydrolysed to the corresponding monoester, from which the acid chloride was obtained by treatment with thionyl chloride. The condensation of the latter with 15-(4-acetamidophenyl)-5-(4-aminophenyl)-10,20-bis(4-methylphenyl)porphyrin, which had been obtained in its turn by the partial hydrolysis of compound **17**, leads to the amide **11** in 93% yield.



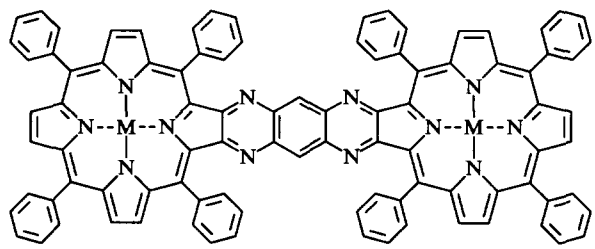
16, 17

16: R^1 = R^2 = $COOCH_3$; M = 2H;
17: R^1 = R^2 = $NHCOCH_3$; M = 2H.

The porphyrin dimer **12** was synthesised similarly in 63% yield. In this case, the acid chloride of the monocarboxyporphyrin was condensed with the zinc complex of 15-(4-acetamidophenyl)-5-(4-aminophenyl)-10,20-bis(4-methylphenyl)porphyrin.

5-(4-Methoxycarbonylphenyl)-10,15,20-tris(pentafluorophenyl)porphyrin was obtained by Lindsay's method involving the condensation of pyrrole, pentafluorobenzaldehyde, and methyl 4-formylbenzoate with trifluoroacetic acid and subsequent oxidation of the resulting product with 2,3-dichloro-5,6-dicyano-1,4-benzoquinone, after which the ester was hydrolysed and the acid made to react with thionyl chloride. Interaction of the resulting porphyrin acid chloride with an excess of 5,15-bis(4-aminophenyl)-10,20-bis(4-methylphenyl)-porphyrin led to the diad **13**. The dimers **14** and **15** were synthesised via the same mechanism in 95% and 54% yields respectively.[21]

The steric disposition of the porphyrins in the system **18** and the distance between them (7.5 Å) are very similar to those for the central haems in the cytochrome units of the photosynthetic reaction centre of the bacterium *Rhodopseudomonas viridis*,[22] where the tetrapyrrole macrocycles are almost coplanar and are linked in such a way that the distance between the porphyrins is 7.5–8.5 Å.



18a, b

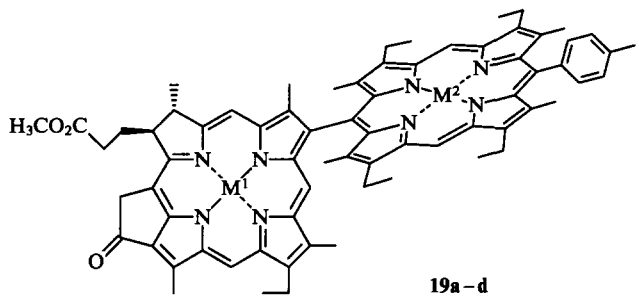
M = 2H (**a**), Zn (**b**)

The strategy used in the synthesis of such a rigidly linked bisporphyrin system involves the condensation of the α-dione (17,18-dioxo-5,10,15,20-tetraphenylchlorin) with the tetrahydrochloride of 1,2,4,5-benzotetraamine, taken in proportions of 2 : 1, in pyridine. The yield of the dimer **18** was 71%.

As already stated above, the electron donors and acceptors in the photosynthetic reaction centres are located at a fixed separation with a definite orientation relative to one another, which ensures an effective photoinduced separation of the charges and retards their recombination. However, it is believed that the intervening component located between the donor and acceptor exerts a major influence on the rate of electron transfer.

For example, in the bacterial photosynthetic reaction centre, the bacteriochlorophyll (BChl) molecule is located between the dimeric bacteriochlorophyll donor ($BChl_2$) and the bacteriopheophytin acceptor (BPh). It is believed that the 'super exchange' process, which involves the mixing of the low-energy ionic and virtual states of the intervening bacteriochlorophyll and of the selectivity excited donor, may lead to an appreciable increase in the rate of charge separation.[24]

For a better understanding of the influence of the low-energy states, formed during charge transfer, on the photophysical characteristics of the donor–acceptor systems, a series of chlorophyll-porphyrin molecules with a fixed distance between these two macrocycles were synthesised.[24]



19a–d

$M^1 = M^2 = 2H$(**a**);
$M^1 = M^2 = Zn$ (**b**);
$M^1 = Zn$; $M^2 = 2H$ (**c**);
$M^1 = 2H$; $M^2 = Zn$ (**d**).

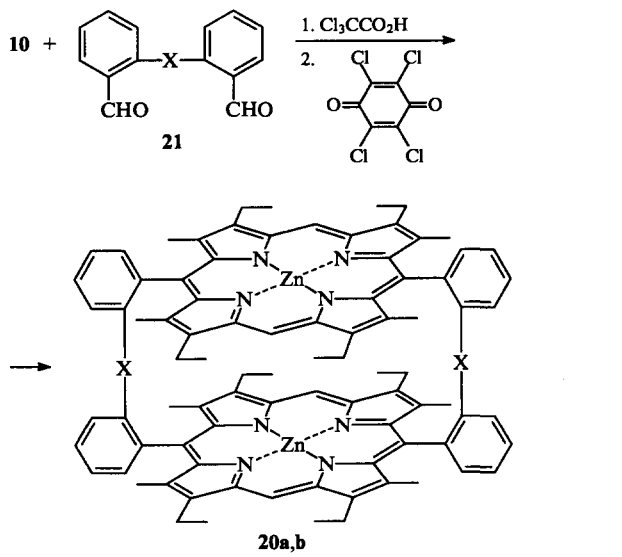
The dimer **19a** was obtained from methylpyropheophorbide *d* and *p*-toluic aldehyde by their condensation with the corresponding dipyrrolylmethane and subsequent oxidation of the resulting porphyrinogen with chloranil.

It was found that[24] the reaction of the dimer **19a** with zinc acetate at room temperature leads to the product **19d**, while compound **19b** is obtained on refluxing. After treatment of compound **19b** with a small amount of dichloroacetic acid, it loses the zinc atom more readily than the chlorin macrocycle, so that compound **19c** can be more effectively obtained from compound **19b**.

The structures of compounds **19a–d** contain a chlorophyll molecule bound rigidly to the porphyrin and the π-systems of the two macrocycles, restricted by steric interactions, are perpendicular to one another. Such orientation is preferred for the simulation of the geometrical relation between the bacteriochlorophyll donor and the spacer ($BChl_2$ and BChl) in the photosynthetic reaction centres.[23,24]

The porphyrin dimers, the macrocycles of which are in the 'face-to-face' configuration, are of interest. Compounds **20a,b** of this type have been synthesised from 3,3′-diethyl-4,4′-dimethyl-2,2′-dipyrrolylmethane **10** and the dialdehyde **21** (Scheme 2).[25,26]

Scheme 2



20a,b

X = $O(CH_2)_4O$ (**a**), $O(CH_2)_3O$ (**b**).

Although the yields of compounds **20a,b** are low (5% and 2% respectively), the reaction merits attention from the standpoint of its simplicity and the ease with which the starting materials can be obtained.[26]

The chemistry of porphyrin dimers and their metal complexes is at present in the stage of its establishment and a wide range of problems in this field still await solution. However, the accumulated experimental data indicate the importance of this field.[12]

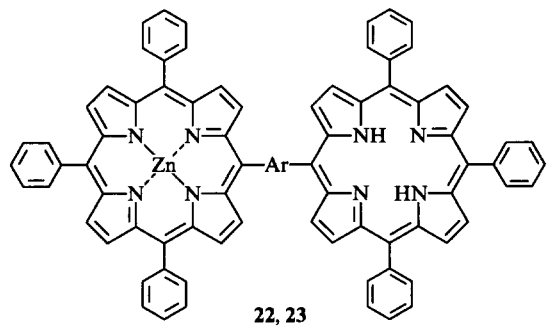
b. Photochemistry of porphyrin dimers

Considerable advances have been achieved hitherto in the study of the photochemical properties of the model compounds. Among the questions arising in the investigation of the photochemistry of such molecular structures, the most important involves the discovery of the characteristic features of the organisation of the photosynthetic apparatus ensuring a high efficiency of the charge separation.

In spectroscopic studies on the system **1a–q**, it was shown that the rates of the direct electron transfer diminish with increase in the 'centre-to-centre' distance between two porphyrins, whereas the rates of the reverse electron transfer remain almost constant [the rate constant is k = (4 to 6) × 10^8 s^{-1}] for a series of 'centre-to-centre' distances from 8 to 22 Å and are independent of the orientation and structure of the spacer.[15]

It has also been noted that the intensity of the fluorescence of the metal-containing porphyrin is appreciably weakened, whereas the intensity of the fluorescence of the second porphyrin component is intensified, which indicates an effective transfer of excitation energy from the singlet state.[27]

Results agreeing with the data described by Osuka et al.[27] have been obtained for the dimers **22** and **23**.[28] Although Rempel et al.[28] used other porphyrin subunits, the models which they presented are similar to compounds **1b** and **1l** in terms of geometrical parameters.



22, 23

22: Ar =

23: Ar =

The role of the intermediate linker in determining the electronic bonding between the electron donor and acceptor, which makes the electron transfer reaction possible, has attracted the attention of investigators in recent years. It has been found that, when the donor and acceptor are covalently bound via a rigid spacer, the rates of electron transfer increase. It has also been noted that, when aromatic spacers are employed, the rate constant depends on the distance between the chromophores to a much lesser extent than in the case where aliphatic linkers are used. Thus an increase in the length of the aromatic spacer by 4 Å leads to a decrease in the rate by a factor of 20, while in the case of an aliphatic bridge the rate falls by a factor of 100. Such an enormous difference can be explained by the fact that the electron transfer in the case of an aromatic linker proceeds via a 'super exchange' mechanism. Furthermore, it has been found that the rate constant for electron transfer depends on the electronic structure of the spacer.

All these data show that the electron transfer reactions between the spacer-bound chromophores are determined by the donor–acceptor interaction.[17]

Osuka et al.[16] described diporphyrins consisting of the hybrid metal complexes **2a–o** with different mutual orientations and a series of aromatic spacers including benzene, naphthalene, and spirobiindan fragments.

It has been demonstrated for these rigidly bound compounds that the reactions involving the separation and recombination of charges exhibit different dependences on distance. The rate constant for charge separation is related mainly to the distance and does not exhibit any dependence on orientation, whereas the rate constant for the recombination of charges is hardly influenced by either the distance or the mutual orientation.

In contrast to the well established dependence on distance, the data concerning the relation between the rate of electron transfer and the angle between the donor and acceptor are virtually lacking,[18] although Osuka et al.[16] believe that the recent studies have a bearing on precisely this problem.

The first results indicating the dependence on orientation were obtained using a series of bisporphyrins **4a–h**, in which the angle between the donor and acceptor varies systematically.

In these molecules the rate of intramolecular electron transfer changes by an order of magnitude when the angle between the porphyrin units is varied.[17,18]

In the dimers **4a–c**, the 'edge-to-edge' distances were measured and were found to be respectively 5.8, 10.1, and 14.4 Å. Studies showed that, with increase in the length of the spacer, the electron transfer rate constant diminishes: $(4 \pm 1) \times 10^{10}$, $(7 \pm 1) \times 10^{9}$, and $(1.1 \pm 1) \times 10^{9}$ s^{-1} for compounds **4a–c** respectively. However, Helms et al.[17] attribute this decrease in the rate not to the increase in the distance between the chromophores but to the break in the conjugation of the spacer owing to the biphenyl 'twist' angle (50°) for each junction between two benzene rings. The inadequate overlap of the chromophores for this value of the angle leads to an approximately sixfold decrease in the rate of electron transfer to the benzene ring, which is confirmed by the results.[17]

Much work has been done in the study of the photochemical characteristics of the dimers **11–15**.[21] The results clearly demonstrated the occurrence of the singlet–singlet energy transfer between the porphyrin components of the dimers **11–13** and **15**. The photoinduced electron transfer in compounds **13** and **15** was also observed, confirming the occurrence of electronic exchange interactions in these compounds, which probably lead to an increase in the rate constant for the singlet–singlet energy transfer. The fact that the quenching of the fluorescence is observed only in the diads where the charge-separated state is located at a lower energy level than the primary excited singlet state confirms the assignment of the fluorescence quenching process to electron transfer and not to other photophysical or photochemical processes.[21,24]

The photophysical properties of compounds **19b** and **19c** can be compared directly with the characteristics of the dimer $BChl_2$ in natural reaction centres. Spectroscopic studies of the natural reaction centre did not yield evidence for the formation of the ion pair $BChl^{+}-BChl^{-}$ in the bacteriochlorophyll dimer but made it possible to postulate that the low-energy state of the dimer with separated charges overlaps the singlet state of the dimer located at an even lower energy level. The results of the study of compound **19b** showed that the low-lying charge-separated state is located 0.1 eV above the excited singlet state and this influences strongly the rate of decomposition of compound **19b** without the formation of an ion pair. It may be that the dimer $BChl_2$ in the natural reaction centres also decomposes rapidly, like compound **19b**.

The considerable similarity of the photophysical characteristics of the dimers of the reaction centre and the heterodimers **19b,c** suggests that further studies should be carried out on these lines.[24]

2. Porphyrin-carotenoid compounds

Studies on the synthesis and properties of molecular diads consisting of a porphyrin or a chlorophyll derivative and a carotenoid polyene are of considerable interest.

Carotenoids (Car) simulate the functions of an antenna, absorbing light in the region of the solar spectrum where chlorophyll is ineffective, and transfer the energy of the excited singlet state to chlorophyll.[1,6,29–35]

$$\mathrm{Car} + h\nu \longrightarrow {}^{1}\mathrm{Car}^{*},$$

$${}^{1}\mathrm{Car}^{*} + \mathrm{Chl\,(BChl)} \longrightarrow \mathrm{Car} + {}^{1}\mathrm{Chl}^{*},$$

$${}^{1}\mathrm{Chl}^{*} \longrightarrow \mathrm{Chl} + h\nu\,\mathrm{(fluorescence)}.$$

Furthermore, they play the role of photoprotectors. On irradiation of chlorophylls, long-lived excited triplet states are generated. The chlorophyll triplets react with oxygen, forming singlet oxygen ($O_2^{*1}\Delta_g$), which is very reactive and is therefore dangerous to plant tissues.

$$\mathrm{Chl\,(BChl)} + h\nu \longrightarrow {}^{1}\mathrm{Chl}^{*},$$

$${}^{1}\mathrm{Chl}^{*} \longrightarrow {}^{3}\mathrm{Chl}^{*},$$

$${}^{3}\mathrm{Chl}^{*} + \mathrm{O_2} \longrightarrow \mathrm{Chl} + O_2^{*1}\Delta_g.$$

Carotenoid polyenes prevent the decomposition of plant tissues by singlet oxygen by 'extinguishing' the triplet state of chlorophyll before its interaction with oxygen. This energy transfer from the triplet state of chlorophyll leads to the triplet carotenoid (a harmless state) and the initial state of chlorophyll.

$$\mathrm{Chl\,(BChl)} + h\nu \longrightarrow {}^{1}\mathrm{Chl}^{*},$$

$${}^{1}\mathrm{Chl}^{*} \longrightarrow {}^{3}\mathrm{Chl}^{*},$$

$${}^{3}\mathrm{Chl}^{*} + \mathrm{Car} \longrightarrow \mathrm{Chl} + {}^{3}\mathrm{Car}^{*},$$

$${}^{3}\mathrm{Car}^{*} \longrightarrow \mathrm{Car} + Q.$$

Carotenoids can also fulfil the function of photoprotectors by 'extinguishing' singlet oxygen.

$$O_2^{*1}\Delta_g + \mathrm{Car} \longrightarrow {}^{3}\mathrm{Car}^{*} + {}^{3}\mathrm{O_2},$$

$${}^{3}\mathrm{Car}^{*} \longrightarrow \mathrm{Car} + Q.$$

It has been established that under certain conditions carotenoid polyenes can act as electron donors in photosynthetic systems, although their importance as electron donors is not known.[1,6,29–35]

In order to investigate the photochemical characteristics of carotenoids, namely their functions as photoprotectors and antennae, a series of porphyrin-polyene compounds **24–37** were synthesised.[36–41] (see over)

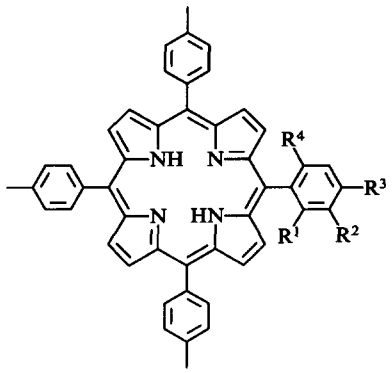
a. Methods of synthesis of porphyrin-carotenoid compounds

Compounds **24–36** have been obtained by condensing the corresponding 5-aminophenyl-10,15,20-tris(4-methylphenyl)porphyrins with the acid chloride of 7′-apo-7′-(4-carboxyphenyl)-β-carotene.

Compounds **27** and **28** were synthesised using 7′-apo-7′-(4-aminophenyl)-β-carotene and the acid chloride of the porphyrin obtained by treating 5-carboxyphenyl-10,15,20-tris(4-methylphenyl)porphyrin with oxalyl chloride.[36]

The reaction of 5-hydroxyphenyl-10,15,20-tris(4-methylphenyl)porphyrins with 7′-apo-7′-(4-iodomethylphenyl)-β-carotene leads to the model systems **29–31**.

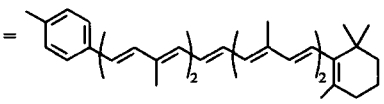
The porphyrin-carotenoid compounds **32** and **33** were obtained respectively by the interaction of dihydroxyphenyl derivatives of tetraphenylporphyrin with 7′-apo-7′-(4-iodomethylphenyl)-β-carotene.



24–37

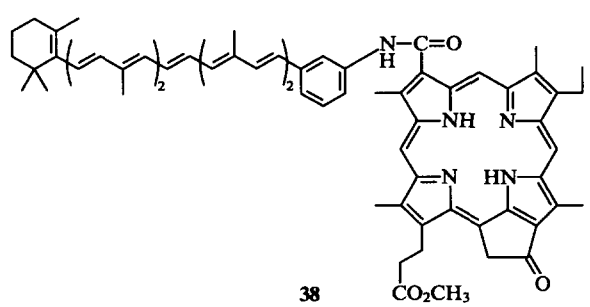
24: $R^1 = R^2 = R^4 = H$; $R^3 = NHCOX$;
25: $R^1 = R^3 = R^4 = H$; $R^2 = NHCOX$;
26: $R^2 = R^3 = R^4 = H$; $R^1 = NHCOX$;
27: $R^1 = R^2 = R^4 = H$; $R^3 = CONHX$;
28: $R^2 = R^3 = R^4 = H$; $R^1 = CONHX$;
29: $R^1 = R^2 = R^4 = H$; $R^3 = O\frown X$;
30: $R^1 = R^3 = R^4 = H$; $R^2 = O\frown X$;
31: $R^2 = R^3 = R^4 = H$; $R^1 = O\frown X$;
32: $R^2 = R^3 = H$; $R^1 = R^4 = O\frown X$;
33: $R^3 = R^4 = H$; $R^1 = R^2 = O\frown X$;
34: $R^1 = R^2 = R^4 = H$; $R^3 = O(CH_2)_3OCOX$;
35: $R^1 = R^2 = R^4 = H$; $R^3 = O(CH_2)_2OCOX$;
36: $R^1 = R^2 = R^4 = H$; $R^3 = COO\frown X$;
37: $R^2 = R^3 = R^4 = H$; $R^1 = COO\frown X$.

X =



Compound **34** was synthesised using the phosphonium salt of 5-[4-(3-hydroxypropoxy)phenyl]-10,15,20-tris(4-methylphenyl)-porphyrin and β-apo-8′-carotenal, while compound **35** was obtained in its turn by condensing 5-[5-(2-hydroxyethoxy)-phenyl]-10,15,20-tris(4-methylphenyl)porphyrin with 7′-apo-7′-(4-carboxyphenyl)-β-carotene in the presence of *N*,*N*-dicyclohexylcarbodiimide (DCC).[37–39]

Carotenal, which is necessary for the synthesis of compounds **36** and **37**, was itself synthesised from α-bromo-*p*-toluic aldehyde with the aid of the corresponding phosphonium salt. The aldehyde group was protected in the form of an acetal by means of ethylene glycol. The Wittig reaction of this salt and β-apo-8′-carotenal was accompanied by the hydrolysis of the protecting group with formation of an aromatic aldehyde, which was converted into an alcohol by reduction with KBH_4. Condensation of the polyene alcohol with the acid chloride of the corresponding porphyrin afforded the molecular systems **36** and **37**.

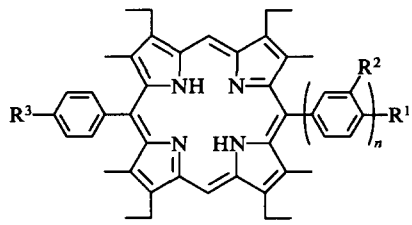


38

The synthesis of the diad **38**, in which the cartenoid is bound to a chlorophyll precursor—pyropheophorbide *a*, has been described.[42] Compound **38** was obtained from derivatives of the aminocarotenoid and pyropheophorbide *a* by the acid chloride method.

Compounds **24–38** described above are porphyrin-carotenoids with a flexible covalent bond. The appreciable conformational mobility of such systems gives rise to certain complications in photochemical studies and investigators have therefore endeavoured to create rigidly bound structures.

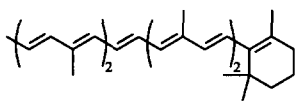
Model compounds in which the carotenoid is bound to the porphyrin by a rigid aromatic spacer have been described.[43,44]



39–42

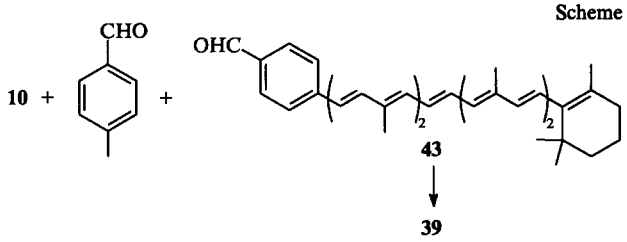
39: $R^1 = X$; $R^2 = R^3 = H$; $n = 1$;
40: $R^1 = X$; $R^2 = H$; $R^3 = CH_3$; $n = 2$;
41: $R^1 = H$; $R^2 = X$; $R^3 = CH_3$; $n = 1$;
42: $R^1 = R^3 = X$; $R^2 = H$; $n = 1$.

X =



Compounds **39–42** have been synthesised in accordance with Scheme 3. Condensation of 3,3′-diethyl-4,4′-dimethyl-2,2′-dipyrrolylmethane **10**, 7′-apo-7′-(4-formylphenyl)-β-carotene **43**, and 4-methylbenzaldehyde with dichloroacetic acid and subsequent oxidation of the reaction mass with *p*-chloranil led to the porphyrin-carotenoid **39** in 95% yield.

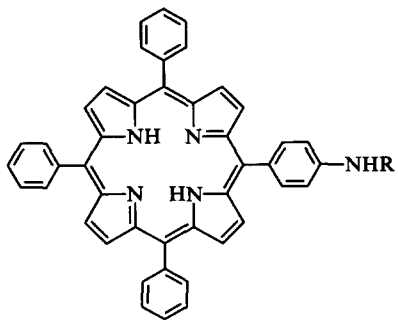
Scheme 3



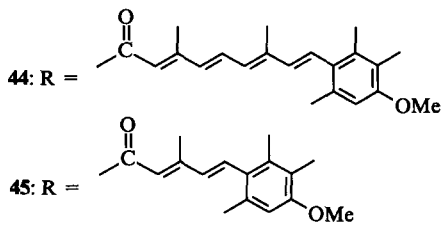
Compounds **40** and **41** were synthesised similarly in 50% and 15% yields respectively. The biscarotene-porphyrin **42** was obtained in 67% yield by condensing compounds **10** and **43**.[43]

The study of the properties of porphyrin-carotenoids has been continued[45] using the aromatic derivatives of retinoic acid, differing in the length of the conjugated bonds, as the polyenes.

The porphyrin-carotenoids **44** and **45** (see following page) were synthesised in 51% and 68% yields respectively from 5-(*p*-aminophenyl)-10,15,20-triphenylporphyrin and aromatic derivatives of retenoic acid by the mixed anhydride method using ethyl chloroformate as the activating agent.[45]



44, 45



b. Photochemical studies

Not only the porphyrin but also the carotenoid is excited by light. One of the functions of the carotenoid—that of an antenna—consists in the absorption of light and the singlet–singlet energy transfer to the porphyrin.

Such intramolecular energy transfer has been detected[43] for compounds **39** and **40** from fluorescence spectra. It was noted that in tetrahydrofuran (THF) ~30% of the excitation energy absorbed by the carotenoid is transferred to the porphyrin. In the porphyrin-carotenoid diad, the fluorescence lifetime (840 ps) is appreciably reduced compared with the porphyrin H_2P (10^4 ps), indicating the existence of an additional path to the decomposition of the singlet-excited state (^1P_e) in the carotenoid-containing system. A possible explanation of this effect may be electron transfer from the carotenoid to the excited state of the porphyrin with the appearance of a short-lived charge-separated state in the form $Car^{\cdot+}-P^{\cdot-}$. If this is so, then the charge-separated state should return very rapidly to the initial state, since the spectrum of the carotenoid radical-cation is not observed even over a time interval ranging from several picoseconds to several nanoseconds.[43,46,47]

A similar phenomenon has been noted in the covalently bound porphyrin-carotenoid compounds **24**–**37**. Thus the main manifestation of the decomposition of compound **24** accompanied by fluorescence is a decrease in the fluorescence lifetime to 3.4 ns. The study of compound **24** showed that the transfer of the energy of the singlet state takes place within the limits of 10%. This relatively small amount of energy is indeed quite appreciable, since the lifetime of the excited singlet state of the carotenoid is usually several picoseconds owing to the rapid internal conversion. The successful simulation of the function of the carotenoid antenna in compound **24** is due to the interaction between the chromophores as a result of the partial overlap of the π-electron systems of the carotenoid and the porphyrin through the amide bond and the aromatic ring. In other carotenoid-porphyrin systems, a high efficiency of the energy transfer was found. For example, in compound **37** the efficiency of the singlet–singlet energy transfer is about 25%. Such high efficiency is due to the disposition of the carotenoid chain over the porphyrin in such a way that the two π-electron systems can interact with one another (within the limits of ~4 Å).[6]

The reaction centre in the photosynthetic process may be protected against decomposition by singlet oxygen, which is generated by the triplet states of chlorophylls or porphyrins. The energy transfer from the triplet state may be investigated with the aid of laser flash spectroscopy: the maximum of the porphyrin triplet absorption is at ~440 nm, whereas the absorption maximum for the carotenoid is in the region of ~540 nm. The rapid and effective transfer of the energy of the triplet state from the porphyrin to the carotenoid requires an electron exchange mechanism. In the case of compound **24** the transfer is facilitated further by the partial conjugation between the chromophores. In the porphyrin-carotenoid systems, where there is a deficiency of such conjugations, a rapid triplet transfer can nevertheless occur through a series of conformations where the π-electron systems are in contact (compound **37**).[6]

There exist two different paths for the triplet–triplet energy transfer, which probably occurs via an electron exchange mechanism: a static transfer which does not require appreciable intramolecular motion, and dynamic transfer associated with intra-molecular changes. The relative importance of the triplet energy transfer via these pathways depends on the molecular structure. The photochemical and photophysical conditions for the protection of the reaction centre against damage by singlet oxygen both in photosynthetic systems and biological organisms are determined by them.[37]

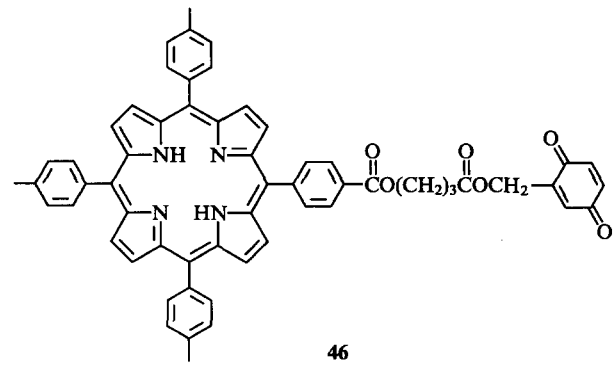
The energy transfer process has also been detected in the model compounds **44** and **45**. It was noted that the efficiency of the energy transfer increases with the length of the polyene chain from 33% to 55% on passing from system **45** to system **44**.[48,49]

Finally, most of the molecular diads obtained to simulate the photosynthesis electron transfer process are covalently bound porphyrin-quinone systems.

3. Porphyrin-quinone systems

a. Methods of synthesis

One of the first compounds of this type described was the porphyrin-quinone **46** obtained by condensing *meso*-(*p*-carboxylphenyl)tritolylporphyrin with substituted dimethoxybenzene and subsequent dimethylation and oxidation of the hydroquinone.[50]



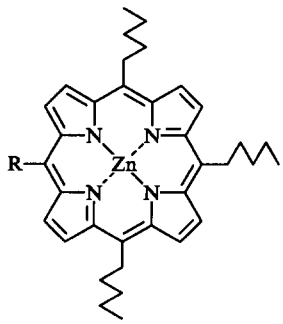
46

Data obtained by laser flash photolysis and EPR spectroscopy showed this compound can assume a conformation in which electron transfer from the porphyrin to the quinone occurs.[1,50]

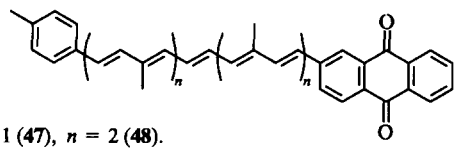
Data have been published[51] concerning two zinc complexes of the porphyrin-polyene-anthraquinone compounds **47** and **48** having five and nine double bonds between the donor and the acceptor (see over). The 'centre-to-centre' distance between the porphyrin and the quinone in these molecules is 25 Å for compound **47** and 35 Å for compound **48**.

Recent experiments have shown[6] that carotenoids usually act only as energy transfer agents in photosynthesis, although under unusual conditions there may be electron transfer from the carotenoids. However, it is believed[51] that the low electronic energy state of the polyenes can be used to create artificial photosynthetic systems which use the polyene as molecular 'conductors' to facilitate the electron transfer between the donor and the acceptor.

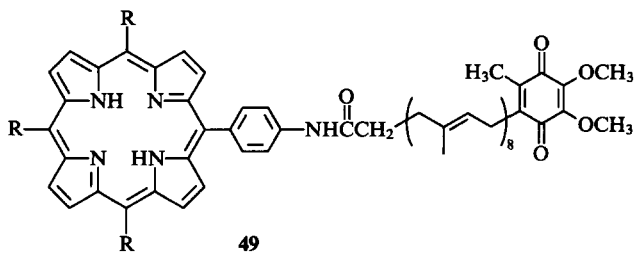
Compound **49**, containing a ubiquinone derivative, has been synthesised from 5-(*p*-aminophenyl)-10,15,20-triphenylporphyrin in order to study the photoinduced electron transfer.[52]



47, 48

R = 

n = 1 (47), n = 2 (48).



49

R = C_6H_5.

Ubiquinones — 2,3-dimethoxy-5-methyl-6-polyprenylbenzoquinones — are most important factors in cell metabolism; they play a significant role in the cell bioenergetics and also in the photosynthetic process.[4, 53, 54]

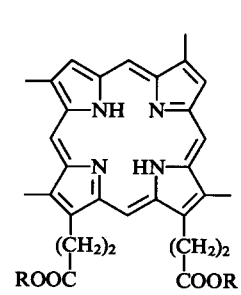
The addition of 5-(*p*-aminophenyl)-10,15,20-triphenylporphyrin to the ubiquinone acid Q_8 has been achieved by the mixed anhydride method using ethyl chloroformate (yield 5%).[52]

The natural porphyrins **50–52** — deuterioporphyrin IX, haematoporphyrin IX, and pheophorbide *a* linked to a quinone by an ester bond — have been used to synthesise porphyrin-quinone compounds.[55–57] An interesting feature of these systems consists in the fact that the quinone structure in them is linked directly to the heteroatom (nitrogen and sulfur). This is due to the strategy used in the synthesis. At the same time, there is a possibility of elucidating the influence of the heteroatom on the photochemical electron transfer reaction and the dark charge recombination.

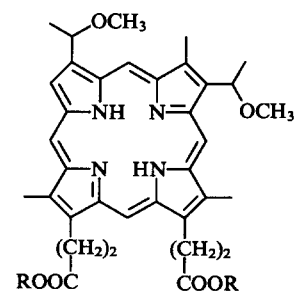
The length of the covalent chain between the quinone and porphyrin components corresponds to 5 or 7 atoms. The change in the distance between the chromophores makes it possible to determine the dependence of the degree of interaction between donor and acceptor and of the efficiency of the photoinduced charge separation on the distance: an increase in the length of the covalent chain under these conditions increases the lifetime of the separated charges, hindering their recombination.[6, 58]

Hydroxylated quinone derivatives have been obtained by adding 2-mercaptoethanol, 2-aminoethanol, and 3-aminopropanol to 2-methylnaphthoquinone and 2,3,5-trimethylbenzoquinone.

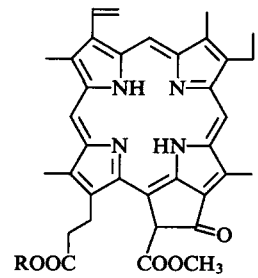
An advantage of this method of synthesis lies in the fact that the conditions in the modification of the quinone component and in its condensation with the porphyrin structure make it possible to employ unsubstituted quinones, reducing the total number of stages and simplifying the synthesis of the porphyrin-quinone derivatives.



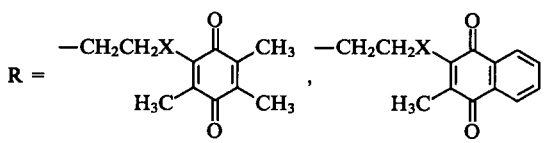
50



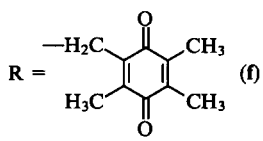
51



52

R = 

X = CH_2 (a), S (b), NH (c). X = S (d), NH (e).

R =  (f)

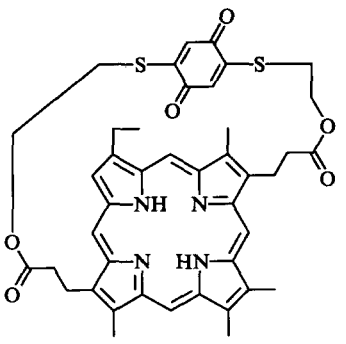
Condensation of hydroxylated quinones with porphyrins using di-*tert*-butyl pyrocarbonate (Boc_2O) and 4-dimethylaminopyridine (4-DMAP) leads to the formation of the diquinone derivatives **50–52** in satisfactory yields.[55–57]

However, the presence of a flexible covalent bridge in compounds **50–52** is responsible for their considerable conformational lability on exposure to external factors, which makes it difficult to explain the experimental data on electron phototransfer in such systems. The creation and study of model structures with a molecular geometry known beforehand therefore becomes important.[7, 59, 60]

One of the aspects of studies in this field involved the construction of models in which the quinone was strictly oriented over the centre of the porphyrin ring — the so called 'covered' porphyrins. The advantage of such model compounds arises from the possibility of monitoring during the synthetic process the relative oxidation-reduction potentials of the fragments, the distance between them, and their mutual orientation.[7]

Such a 'covered' porphyrin-quinone has been obtained from the symmetrical mesoporphyrin II and a quinone with two hydroxy-groups.[61]

In order to synthesise the 'covered' porphyrin-quinone **53**, a method was developed to obtain the bifunctional sulfur-containing electron-accepting component – 2,5-di-(2-hydroxyethylthio)-1,4-benzoquinone (DHEP). Condensation of the acid chloride formed when the mesoporphyrin II is treated with oxalyl chloride with DHEP affords the required compound **53**.

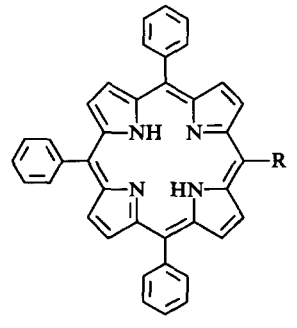


53

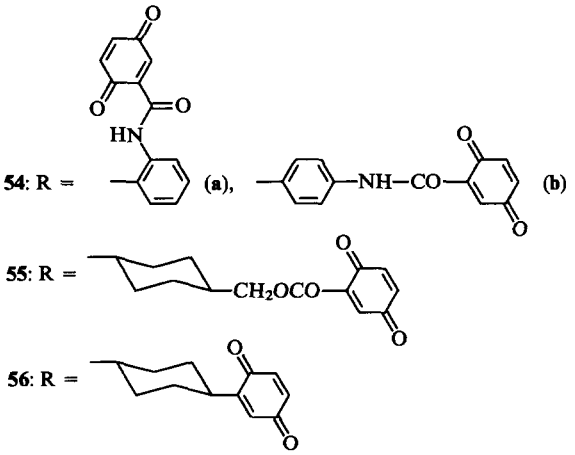
Compound **53** differs from the porphyrin-quinones known in the literature[7,59,60,62–65] by the presence of a sulfur atom linked directly to the quinone structure, which influences significantly the efficiency of the photoinduced transfer process.[61]

Another aspect ensuring the rigidity of the structure is the creation of models with a fixed distance between the porphyrin and the quinone. The synthesis of a compound meeting this requirement has been described.[66]

The mono-*o*-aminotetraphenylporphyrin, obtained by the Rothenmund reaction using pyrrole, benzaldehyde, and *o*-nitrobenzaldehyde with subsequent reduction of the nitro-group to the amino-group, was condensed with the chloride of 2,5-diethoxybenzoic acid. After selective hydrolysis and oxidation of the hydroquinone to the quinone with lead dioxide, the porphyrin-quinone **54a** was isolated.



54–56



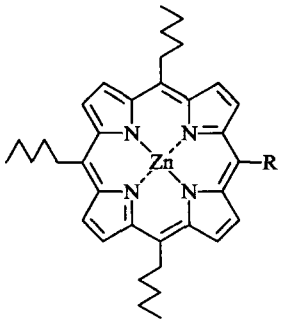
Another approach to the synthesis of a similar compound **54b** has been proposed.[67,68] Mono-*p*-aminotetraphenylporphyrin was made to react with acetylated gentisic acid in the presence of the ethyl ester of 2-ethoxy-1,2-dihydroxyquinoline. The protecting groups were then removed in a methanol solution of hydrochloric acid and the hydroquinone system was oxidised with lead dioxide to the quinone system (compound **54b**).

The porphyrin-quinone model compounds **55** and **56** have also been described.[67]

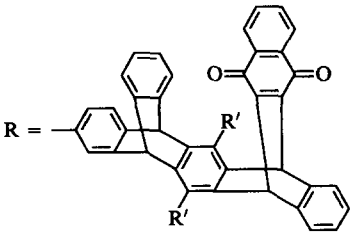
The Rothenmund condensation of pyrrole, benzaldehyde, and *trans*-4-(hydroxymethyl)cyclohexanaldehyde affords a hydroxylated porphyrin, the esterification of which with acetylated gentisyl chloride and subsequent removal of the protecting groups from the quinone component and oxidation of the hydroquinone system with lead dioxide lead to compound **55**.

In the synthesis of the porphyrin-quinone **56**, the monoester of cyclohexane-1,4-dicarboxylic acid was bound to *p*-benzoquinone by oxidative decarboxylation. After the substitution of the corresponding hydroquinone by treatment with sodium dithionite and reduction of the ester group with diisobutylaluminium hydride, the aldehyde was obtained. The latter reacts with pyrrole and benzaldehyde in the presence of atmospheric oxygen to form the required compound **56**, in which the porphyrin and quinone halves of the compound are connected by a rigid spacer.

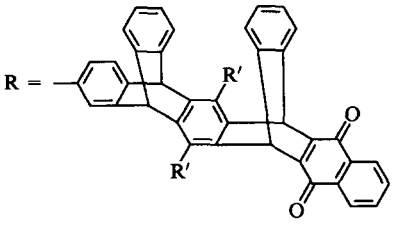
The four porphyrin-quinone compounds *syn*- and *anti*-**57** and *syn*- and *anti*-**58** with a fixed distance between the donor and the acceptor were synthesised to obtain information about the dependence of the electron transfer between the chromophores on the orientation of the quinone component.[69]



57, 58



R′ = H (*anti*-**57**), OCH_3 (*anti*-**58**).



R′ = H (*syn*-**57**), OCH_3 (*syn*-**58**).

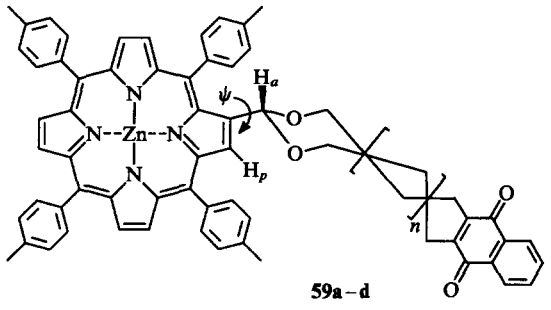
A hydrocarbon spacer—pentiptycene—was used to maintain a fixed distance and to restrict the spatial mobility between the porphyrin and the quinone in compounds **57** and **58**. The reasons for using this rigid system as a spacer are as follows: firstly, it is related to the thoroughly investigated triptycene spacer;[60,70,71] secondly, the presence of two

positional isomers, in which the porphyrin and the quinone are in the '*syn*'- or '*anti*'-positions relative to one another, makes it possible to investigate the dependence of the photoinduced electron transfer over a fixed distance on the orientation; thirdly, the presence of the central benzene ring, rigidly bound to two triptycene bridges, makes it possible to introduce substituents into the remaining free positions in this ring and to alter the influence of the ionic states of the spacer on the 'superexchange' electron transfer process.[69]

The Diels-Alder condensation of the reduced anthraquinone with the quinone and formylation of the naphthoquinone-pentiptycene derivative obtained afford a mixture of '*syn*'- and '*anti*'-aldehydes, which enter into the Lindsay reaction with 1-hexanal and pyrrole to form *syn*- and *anti*-**57** in an overall yield of 2.9%.

In order to obtain *syn*- and *anti*-**58**, anthracene was made to undergo the diene condensation with *p*-benzoquinone followed by hydrogenation of the diketone, the reaction of which with *o*-phthalaldehyde afforded 1,4-anthraquinone. The subsequent stages in the reduction of 1,4-anthraquinone to the hydroquinone and treatment with an excess of dimethyl sulfate led to the formation of the 1,4-dimethoxyanthracene derivative in 75% yield. Condensation of the latter with naphthoquinone and subsequent formylation gave rise to a mixture of the corresponding aldehydes required for the synthesis of *syn*- and *anti*-**58**. The yield of the isomers is 4.8%. The *syn*- and *anti*-isomers were separated as the corresponding zinc complexes by preparative thin-layer chromatography on silica gel.[69]

The rigid spirocyclic spacer[72] in the models **59a–d** controls the 'edge-to-edge' distance between the porphyrin and the quinone and reduces to a minimum the complications in the interpretation of the experimental data induced by the rotational degree of freedom of the porphyrin-acetal linkage (the angle ψ).

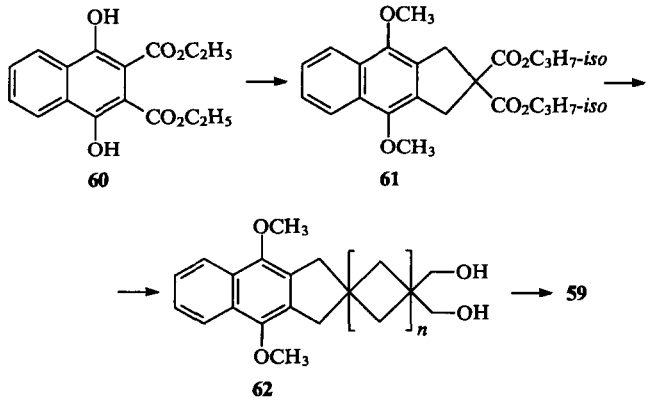


59a–d

n = 0 (**a**), 1 (**b**), 2 (**c**), 3 (**d**).

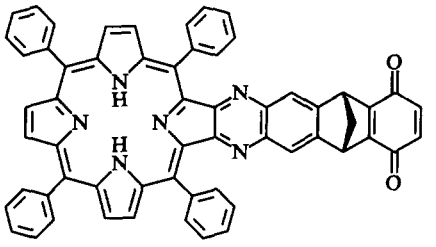
Compounds **59a–d** were synthesised in accordance with Scheme 4.

Scheme 4

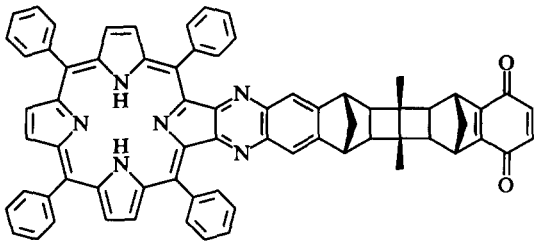


The diester **60** was treated with methyl iodide, reduced to the diol, and converted into the dichloro-derivative, which was cyclised and the resulting diisopropyl diester **61** was converted into compound **62**. The 1,4-dimethoxynaphthalene derivative **62** was oxidised to the corresponding naphthoquinone diol and condensation of the latter with 1-(dimethoxymethyl)tetra-tolylporphyrin afforded compound **59**.

The porphyrin-quinones **63** and **64**, in which the connecting bridge not only fixes rigidly the 'centre-to-centre' distance between the chromophores, amounting to 11.6 Å for compound **63** and 16.2 Å for compound **64**, but also, in contrast to other spacers, excludes the rotational degree of freedom of the quinone component, have been described.[73]



63



64

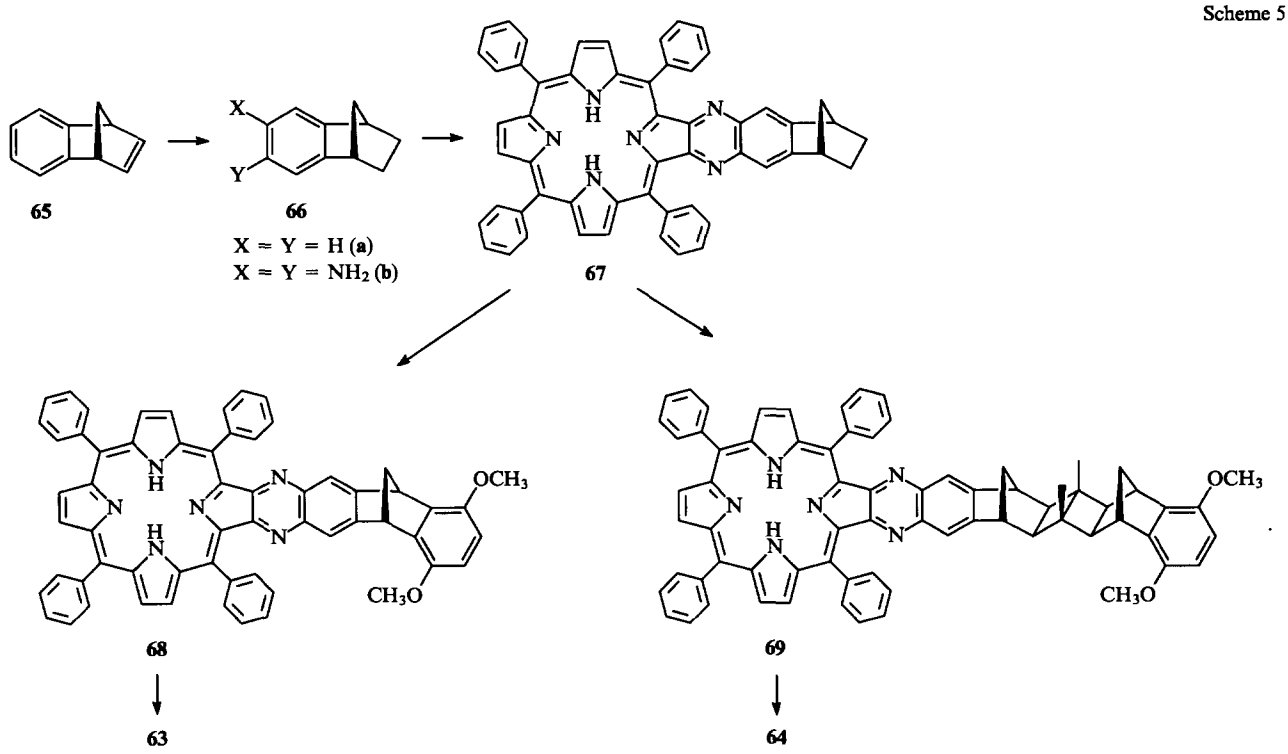
Two methods of synthesis of compounds **63** and **64**, differing in the sequence of operations, have been developed.[74]

The synthesis was begun with benzonorbornadiene **65** to which the porphyrin group was attached through the series of stages presented in Scheme 5.

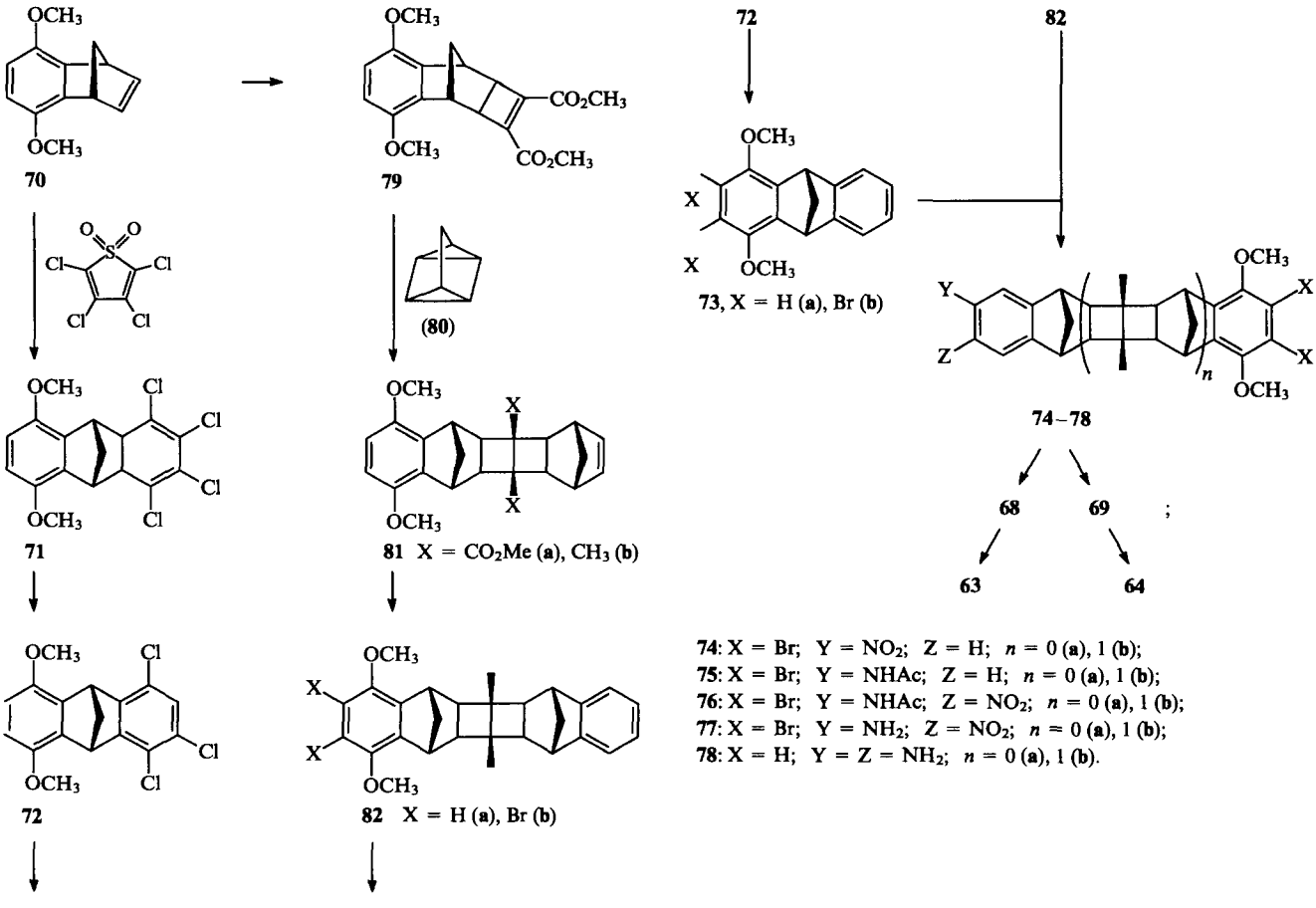
Compound **65** was initially reduced to compound **66a**, the nitration and subsequent reduction of which afforded the unstable diamino-compound **66b**. The latter was immediately treated with 17,18-dihydroxy-5,10,15,20-tetraphenylchlorin and compound **67** was obtained. The subsequent transformation of compound **67** led to the dimethoxybenzene derivatives **68** and **69**, from which the required porphyrin-quinones **63** and **64** were synthesised.

The other approach to the synthesis of such porphyrin-quinones is illustrated in Scheme 6. The key compound in this synthesis is 5,8-dimethoxybenzonorbornadiene **70**, the treatment of which with tetrachlorothiophene dioxide led to compound **71**. The dehydrohalogenation of the latter under standard conditions afforded compound **72**, the subsequent reductive dechlorination of which gave rise to the product **73a**. The protecting groups were introduced into the dimethoxybenzene ring of compound **73a** by bromination, which yielded compound **73b**. The subsequent synthetic stages presented no problems. Nitration of compound **73b** with copper nitrate led to compound **74a**, the reduction of which with zinc acetate afforded compound **75a**. The latter was subjected in its turn to nitration ($HNO_3-AcOH-Ac_2O$) with formation of compound **76a**, the treatment of which with hydrazine hydrate yielded compound **77a**. Compound **77a** was converted into compound **78a** in one stage using hydrazine hydrate and Pd/C in ethanol. The reaction of compound **78a** with the α-dione (17,18-dioxo-5,10,15,20-tetraphenylchlorin) led to compound **68** in 82% yield.

Scheme 5



Scheme 6



The following synthetic transformations were carried out in order to obtain compound **82a** from compound **70**. The ruthenium-catalysed cyclisation reaction between compound **70** and dimethyl acetylenedicarboxylate (DMAD) afforded the adduct **79**, which was subjected to a further cyclisation reaction with the quadricyclane **80**. The product **81a** was subsequently converted into compound **81b**. Further transformations were similar to those described above for the synthesis of compound **78a**. In the concluding stage, the dimethoxy-derivative **69**, synthesised from compound **78b**, was converted into the required porphyrin-quinone **64** in 62% yield.[74]

During the subsequent several years, it was shown that the rigidly bound polynorbornylenebicyclo[2.2.0]hexyl systems have a series of exceptional advantages over other hydrocarbon bridges usually employed. Firstly, the norbornyl spacer is extremely effective, which was demonstrated by numerous photoelectron and picosecond absorption spectroscopic studies. It was predicted that the intramolecular electron transfer in these systems should be especially rapid. This was subsequently confirmed. Secondly, the overall rigidity of the polynorbornylenebicyclo[2.2.0]hexyl spacers completely rules out any conformational uncertainties between the chromophores. Consequently, these spacers make it possible to achieve specific orientations and distances between the porphyrin and the quinone. Thirdly, and this is the most important advantage, there is a possibility of adding a series of chromophore rings, including benzenes, naphthalenes, anthracenes, pyrimidines, and pyrazoles, to both ends of the spacers.[73]

As already mentioned above, much attention is being devoted nowadays to the study of the role of the spacer connecting the donor and the acceptor.[23,24,69] It has been shown[73–75] that saturated hydrocarbon spacers effect electron transfer at a high rate between the oxidation-reduction sections similar to those found in the photosynthetic unit.

It has been suggested[69] that aromatic aminoacids, such as tyrosine, phenylalanine, and tryptophan, located between the electron donor and acceptor in proteins, can also accelerate the electron transfer reactions.

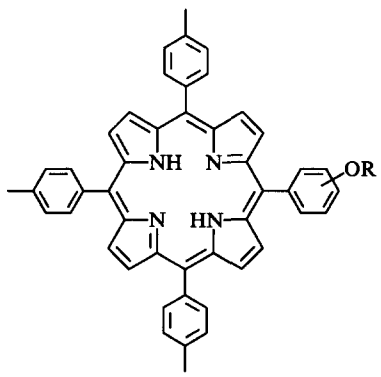
Osuka and Maruyama's study[76] is part of a research program designed to investigate the role of the aminoacid residues in biological electron transfer reactions in model compounds incorporating a porphyrin. Tyrosine was chosen among the aminoacids because it has been postulated that it performs the functions of both an electron and a proton donor.

The porphyrin-tyrosine **83** was obtained by condensing the acid chloride of the monomethyl ester of mesoporphyrin II with the ethyl ester of L-tyrosine (yield 96%). Irradiation of the porphyrin-tyrosine **83** in the presence of benzoquinone **84** in benzene by light at a wavelength > 590 nm under an argon atmosphere led to the formation of the adduct **85** in 75% yield (Scheme 7).[76]

Quinone-substituted porphyrins have been generally recognised recently as models of the primary electron transfer in the photosynthetic process. However, despite the vigorous investigation of the photoinduced electron transfer reactions between the porphyrin and the quinone, there have been only a few studies of synthetic interest.[77]

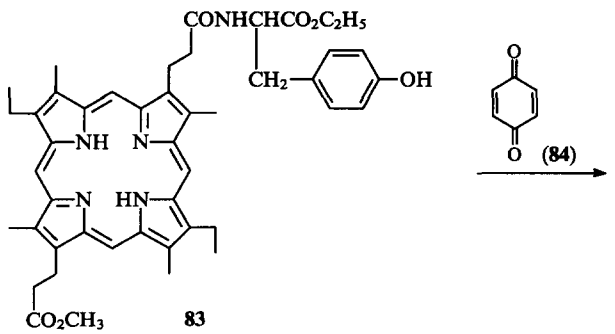
A highly effective synthesis of porphyrin-quinones, based on the self-photosensitisation of the porphyrin, has been reported.[64,76,77] The proposed method of synthesis has a number of advantages: firstly, it does not require the protection of the quinone groups and, secondly, different quinones, with a wide range of electrochemical and stereochemical properties, may be used.

Irradiation of hydroxyphenylporphyrin in the presence of benzoquinone or naphthoquinone (λ > 590 nm, Ar) in chloroform affords the quinone-substituted porphyrins **86a,b** or **87a,b** respectively.[77] The wavelength λ > 590 nm and the absence of air in the reaction solution are decisive factors for the high yield of the porphyrin-quinone compounds. Compounds **88a–c** and **89a–c** have been obtained similarly.[64]

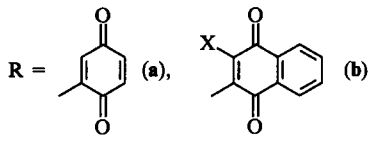


86 (*p*-OR)
87 (*o*-OR)

Scheme 7

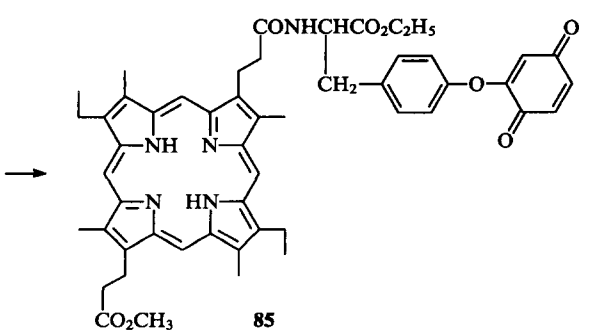


83

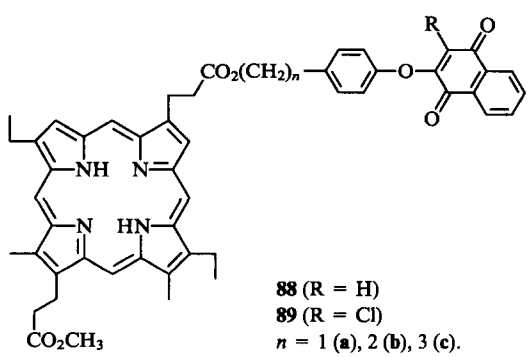


R = (a), (b)

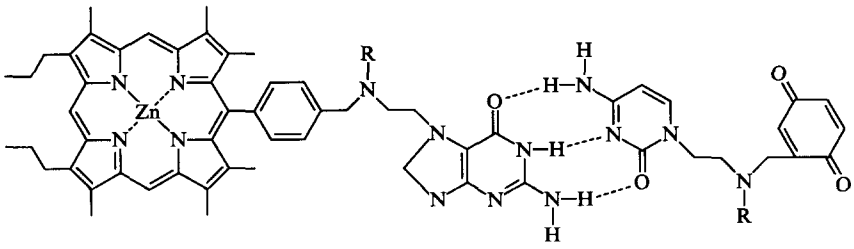
X = H, Cl, Br, CH_3



85



88 (R = H)
89 (R = Cl)
n = 1 (**a**), 2 (**b**), 3 (**c**).



90 91

R = $CH_2C_6H_4O(CH_2)_2O(CH_2)_2OCH_3$.

A multiplicity of covalently bound porphyrin-quinone derivatives have been synthesised to be used as models of the photoinduced electron transfer.

An alternative approach to the photosynthetic modelling includes the synthesis of supermolecular aggregates which are not covalently bound. The multichromophore structures of the photosynthetic reaction centres or light-absorbing antenna aggregates may serve as examples of such non-covalent binding in natural systems.

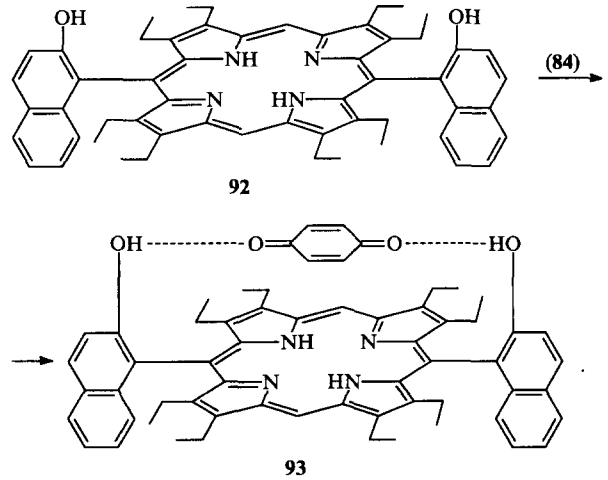
This new approach to the construction of photochemically active systems is simpler than that described above and based on the formation of covalent bonds between the chromophores.[78] The synthesis of the new noncovalently bound photosynthetic system **90**–**91** has been described recently.[79]

When the guanine and cytosine derivatives are mixed in methylene chloride, the formation of hydrogen bonds between the complementary bases is observed. The subunits of the assemblies formed in this way assume different conformations and the 'edge-to-edge' distance between them does not exceed 20 Å.

The rate constants for the binding of the guanine and cytosine derivatives in methylene chloride have been determined by ^{1}H NMR spectroscopy (k = 3100 ± 470 mol^{-1}). The 'coated' porphyrin-quinones, obtained as a result of the non-covalent binding, have been described by Aoyama et al.[80]

5,15-*cis*-Bis-(2-hydroxy-1-naphthyl)octaethylporphyrin **92** in chloroform binds selectively benzoquinone **84** with formation of the symmetrical adduct **93** of the 'face-to-face' type via hydrogen bonds (Scheme 8).

Scheme 8



92 93

The noncovalent binding used to construct porphyrin-quinones of the 'face-to-face' type is free from synthetic difficulties and the yield of complex **93** can reach 100% when a large excess of the quinone and a low temperature are used. It is noteworthy that the four free positions in the initial benzoquinone make it possible to obtain a whole series of derivatives with functional group substituents, which permits the modification of the electronic and steric structures of the quinones.[80]

Scheme 8 constitutes an extremely simple procedure for the synthesis of porphyrin-quinone compounds. On the basis of these results, one can postulate that the combination of the individual components into a single system via hydrogen bonds constitute a new and important strategy for the construction of biologically important structures[78] and in general of molecular aggregates with functional group substituents.[79,80]

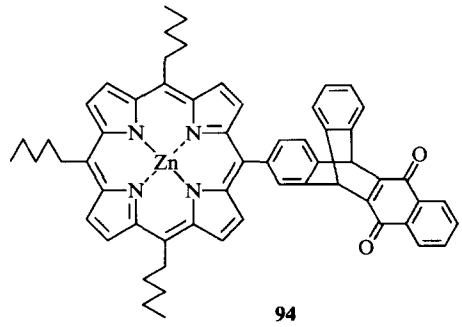
b. Photochemistry of the porphyrin-quinone compounds

In the first studies on the synthesis of porphyrin-quinone compounds, attempts were made to investigate their photochemical properties.

In the system **46** described, tetraphenylporphyrin plays the role of chlorophyll (an electron donor), while the quinone plays the role of the electron acceptor.

Important information about the photochemical processes occuring in porphyrin-quinone compounds can be obtained from the emission spectra. The fluorescence spectra of the derivatives **50a**–**f** and **51a**–**f** do not differ from the spectra of the initial porphyrins, but in their case an intense quenching of the fluorescence of the porphyrin is observed. The relative fluorescence quantum yield of the diquinone derivatives is 4%–5%. Such quenching of the fluorescence, which is characteristic of covalently bound porphyrin-quinone compounds, is a consequence of the photoinduced electron transfer from the porphyrin to the quinone.[55,56]

The introduction of the pentiptycene spacer between the porphyrin and the quinone in compounds **57** and **58** diminishes both the charge separation and charge recombination rate constants by a factor of ~10 compared with those observed for compound **94**.



94

The 'edge-to-edge' distance between the π-systems of the porphyrin and the naphthoquinone in compounds **57** and **58** is ~6 Å, while the corresponding distance in the porphyrin-quinone **94** is ~2.4 Å and, although the donor–acceptor distance has increased by 3.6 Å on passing from compounds **94** to compounds **57** and **58**, the presence of the benzene ring and of the unsaturated carbon atoms in the peptiptycene spacer in compounds **57** and **58** reduces the rate of electron transfer in these systems by more than an order of magnitude, which was in

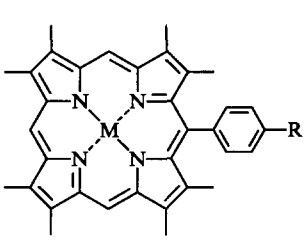
fact expected on passing from the spacer with one saturated carbon atom (compound **94**) to a spacer with two such atoms (compounds **57** and **58**).

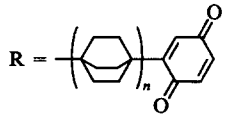
The electron transfer reactions involving the excited state and the recombination of the ion pair in the porphyrin-quinone compounds **57** and **58** exhibit an appreciable dependence on the orientation: the ion pair recombines twice as fast in the *anti*-isomers as in the *syn*-isomers. Such dependence on the orientation has also been observed for the fluorescence lifetimes of these compounds. Taking into account the nature of these dependences, one can postulate that the electron transfer is effected through the bonds of the rigid hydrocarbon spacer.[69]

A similar conclusion has also been reached by Antolovich et al.[73] The observed and theoretically predicted ability of the spacers to promote the electron transfer diminishes in the sequence spirocycles > bicyclo[2.2.2]octanes > alkanes. This result confirms the fact that the electron transfer over large distances in the porphyrin-quinone systems takes place through the hydrocarbon bonds of the spacer.[60,72]

As already stated above, the natural chromophores participating in the main stages of the photosynthetic electron transfer are represented by the special pair $BChl_2$, the excited electronic state of which transfers an electron to pheophytin in the first stage of the process at a rate of $\sim 3 \times 10^{11}$ s^{-1}, while in the second stage the charge is transferred from pheophytin to the quinone at a rate of $\sim 4 \times 10^9$ s^{-1}. It is assumed that this natural donor–acceptor pair is simulated in the second stage of the photosynthesis process by the porphyrin-quinone molecules connected by the spacer.[73] However, in only a few of the model compounds are the distance between the chromophores and the orientation of the latter similar to those in the natural photosynthetic unit.

One of the model compounds in which the spacer ensures a suitable 'centre-to-centre' distance is system **95**.[75]





95, 96

n = 1 (**95**), 2 (**96**)
M = 2H (**a**), Zn (**b**)

Compounds **95a,b** with a strong octaalkylporphyrin donor exhibit[73] high rates of charge separation in different solvents, reaching 1.25×10^{10} s^{-1}.

It is of interest to note that the rates of the photoinduced intramolecular electron transfer in the model system **95b** can exceed the rate of electron transfer from pheophytin to the quinone (4×10^9 s^{-1}) in the photosynthetic unit. Investigators attribute this to the fact that the spacer in compound **95** contains the *p*-phenylene π-system conjugated with the porphyrin. The degree of this conjugation is compensated by the marked rotation about the bond connecting these halves, which hinders the determination of the 'edge-to-edge' distance between the donor and the acceptor systems.[73] The increase in this distance and in the 'centre-to-centre' distance in compound **95** as a result of the introduction of a second bicyclooctane unit into the spacer[75] led to compound **96** in which the rate of electron transfer was found to be $< 10^7$ s^{-1}.

The results of a study of the porphyrin-quinone systems **63** and **64** have been reported.[73] This is yet another part of the studies of electron transfer over long distances. The distance (16.2 Å) between the chromophores attained in compound **64** and its zinc complex greatly exceeds the 'centre-to-centre' distances in compound **95** and **96** and in the photosynthetic BChl unit between the pheophytin and quinone halves (13–14 Å), whereas the angle between the normals to the chromophores is 40°–45° (established from extrapolated crystal structure data), which is comparable to the values for the natural systems (35° ± 6°). The rates of electron transfer in compound **95** are comparable with those obtained for compound **64** despite the greater number of saturated bonds and the greater distance in space between the chromophores, which is probably associated with the structures and configurations of the hydrocarbon spacers employed.[73] Thus the rate of charge separation in system **95** was found to be 3.7×10^7 s^{-1} in propionitrile,[75] which is comparable with the rate 3.6×10^7 s^{-1} for compound **64** in acetonitrile.[73]

The results obtained by Antolovich et al.[73], confirm and expand the data of Joran et al.,[75] who demonstrated the possibility of attaining high rates of charge separation ($> 10^9$ s^{-1}) between the porphyrin and quinone components with the aid of saturated bonds.

The system **90–91**, in which the effective specific electron transfer over long distances takes place through hydrogen bonds, has been considered.[79] In methylene chloride, the fluorescence of the porphyrin **90** is quenched following the addition of large amounts of compound **91**. The fluorescence quantum yield of compound **90** falls with increase in the concentration of compound **91** to 35%.

The binding constant for compounds **90** and **91** is 1290 ± 230 mol^{-1}, while the electron transfer rate constant is $k = (4.2 \pm 0.7) \times 10^8$ s^{-1}. These values correspond to electron transfer through bonds over a distance of 12 Å, which follows from the interpolation of data for porphyrin-quinone compounds bound covalently via a spacer.[74]

The porphyrin-quinone compound **93**, described by Harriman et al.,[79] has a 3 Å separation of the 'face-to-face' type and, as shown by UV spectroscopy, exhibits the porphyrin-quinone π–π-interaction. It was found that the fluorescence of the porphyrin-quinone **93** is fully quenched by effective electron transfer with the complex. The authors concluded that the ability of quinones to quench the fluorescence of the porphyrin **92** is determined not by their oxidation-reduction properties but by the degree of binding of the quinone to compound **92**.

4. Porphyrin compounds bound covalently to aminoacid residues — tyrosine and tryptophan

Much attention is being devoted nowadays to the study of the role of aromatic aminoacids, especially tyrosine (Tyr) and tryptophan (Trp), in the photosynthetic process. It was established previously that, together with other aromatic aminoacids, tyrosine influences the conformation of the protein component of the photosynthetic pigment,[81,82] but tyrosine began to be considered as an electron donor only in recent years.[34,82–86]

It has been shown that in the case of the photosystem II a further two cofactors, called Z* and D*, participate in the photosynthetic process in addition to chlorophyll. A series of studies[83,84,87,88] showed that the tyrosine radicals participating in electron transfer from the water-cleaving manganese-protein complex to the photochemically oxidised radical-cation P_{680}^+ are the Z* and D* cofactors. The spectroscopic characteristics of the tyrosine radicals Z* and D* of the photosystem II are being widely investigated at the present time.[89–94]

The study of the tyrosine radicals helped to discover the location of L-Tyr[162] in *Rhodopseudomonas viridis* and *Rhodobacter sphaeroides* — it was found to be located between the special pair and the nearest cytochrome subunit.[84,85,87,95]

As already mentioned above,[69,76] aromatic aminoacids such as Tyr and Trp accelerate the electron transfer reaction between the donor and the acceptor separated by a fairly long distance — via electron binding through the corresponding orbitals.[84]

The study of the mechanism of the photocatalytic decomposition of water made it possible to discover the

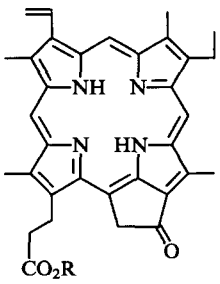
participation in this process of the manganese ion[96] located in the proteins of the photosystem II.

It is believed that tyrosine is an electron transfer agent between clusters made up of four manganese atoms in the oxygen complex formed and in the chlorophyll radical-cation P_{680}^{+} of the photosystem II of the green bacteria.[87,88,97,98] Furthermore, tyrosine-containing porphyrins exhibit a biological activity—they have a carcinostatic effect.[85,99]

The zinc complexes of pyrochlorophyllide *a* and bacteriochlorophyllide *a*, containing the methyl esters of the aminoacids Trp and Tyr in the side chain of the macrocycle and capable of being coordinated to the metal and of π–π interaction with the macrocycle, have been synthesised in order to investigate the chlorophyll–protein interactions. It was shown by ^{1}H NMR spectroscopy that, as a result of the above interactions, the aminoacid residues participate in the formation of the dimeric compounds in which the methoxycarbonyl group of the aminoacid is coordinated to the metal. The planes of the macrocycles are parallel and overlap in the rings IV.[82]

Such compounds can also serve as models of the reaction centre of the chlorophyll molecule.[82,100]

The condensation of the activated ester of pyropheophorbide *a* with a fivefold excess of the methyl esters of L-Tyr or L-Trp leads to the formation of the covalently bound complexes **97a** and **98** containing aminoacid residues (2-chloro-*N*-methylpyridinium iodide in a mixture of methylene chloride and triethylamine was used as the activating agent in the synthesis of the activated ester of pyropheophorbide *a*).[82]



97–99

97: R = NH–CH(CH$_2$–C$_6$H$_4$–OH)–CO$_2$X

X = CH_3 (**a**), C_2H_5 (**b**)

98: R = NH–CH(CH$_2$–3-indolyl)–CO$_2$CH$_3$

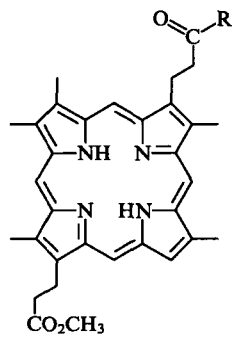
99: R = NH–CH(CH$_2$–C$_6$H$_4$–O–C$_6$H$_3$(=O)$_2$)–CO$_2$C$_2$H$_5$

Compounds **97b** and **98** were synthesised by the method described[83] (59% and 55% yields respectively) in order to carry out further investigations.[87,101]

Irradiation of compound **97b** in the benzene–acetonitrile solvent mixture in the presence of benzoquinone by light at a wavelength in excess of 590 nm under an inert gas atmosphere affords compound **99** in 56% yield, the yield depending on the quinone concentration. This concentration dependence clearly indicates that compound **99** is formed as a result of the quenching of the triplet state of pyropheophorbide-tyrosine **97b** by benzoquinone **84**. This reaction is similar to the photochemical reaction of tyrosine-mesoporphyrin II **83** with benzoquinone.[76,87,95]

Irradiation of compounds **98** and **84** under identical conditions did not yield a photochemical product.[87]

On the other hand, pulsed irradiation (0.3 s) of a solution of compounds **100a** and **84** in deuteriobenzene at 514 nm from an argon laser in the tube of a ^{1}H NMR spectrometer (400 MHz) under an inert gas atmosphere affords compound **100b** in 8% yield.[101]



100

R = NH–CH(CH$_2$–3-indolyl)–CO$_2$CH$_3$

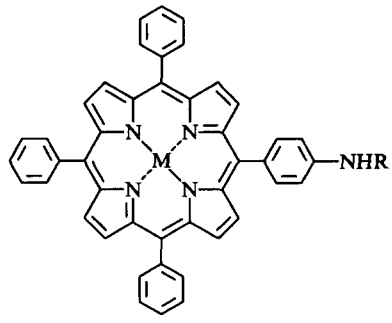
X = H (**a**), 1,4-benzoquinone (**b**)

Tyrosine-containing porphyrins have been synthesised from 5-(*p*-aminophenyl)-10,15,20-triphenylporphyrin and di-(*tert*-butoxycarbonyl)-protected tyrosine in order to create subsequently photosynthetic model systems and to investigate their biological activity.[102]

In this case tyrosine adds to the amino-group of the porphyrin and not to the carboxy-group, as described in other studies.[76,82,87,95,101]

Two methods were used to synthesise compound **101**. The mixed anhydride method using isobutyl chloroformate as the anhydride-forming agent (the yield of tyrosylporphyrin was 26.6%) and the *N,N'*-dicyclohexylcarbodiimide method (yield 80%).

Trifluoroacetic acid was used to remove the protecting groups from tyrosylporphyrin **101** and compound **102a** was obtained in 92.5% yield.



101, 102

101: R = NH–CH(CH$_2$–C$_6$H$_4$–OBoc)–CO–NH–Boc

M = 2H

102: R = NH$_2$–CH(CH$_2$–C$_6$H$_4$–OH)–CO–

M = 2H (**a**), Mn (**b**)

Manganese ions were introduced by heating the porphyrin **102a** with manganese acetate and the yield of compound **102b** was 42.8%.[102]

It follows from the foregoing that the porphyrins bound to tyrosine can serve as model compounds for the investigation of the photosynthetic process and, in particular, of the mechanism of the catalytic decomposition of water and also for the elucidation of the role of tyrosine in the natural photosynthetic process, which is at present the subject of scientific discussions.

III. Conclusion

The model compounds presented above have found extensive application in the study of the primary photosynthetic process. Furthermore, they are ideal models for the determination of the main principles of the photoinduced electron transfer.[1,4,7]

Only a small proportion of the enormous amount of work carried out on the study of the natural photosynthetic process is described in the present review. Such research has become possible as a result of the development of methods for the synthesis of complex molecules, for the determination of their structures, and for the investigation of their spectroscopic, photochemical, and photoelectric properties.

References

1. D Gust, T A Moore *Science* **244** 35 (1989)
2. D Gust, T A Moore *Top. Curr. Chem.* **159** 103 (1991)
3. M R Wasielewski *Chem. Rev.* **92** 435 (1992)
4. R K Clayton *Photosynthesis: Physical Mechanisms and Chemical Patterns* (Translated into Russian; Moscow: Mir, 1984)
5. T A Moore, D Gust, P Matkis, J-C Mialocq, C Chachaty, R V Bensasson, E J Land, D Doizi, P A Liddell, W R Lehman, G A Nemeth, A L Moore *J. Am. Chem. Soc.* **109** 846 (1987)
6. D Gust, T A Moore *J. Photochem.* **29** 173 (1985)
7. V V Borovkov, R P Evstigneeva, L N Strekova, E I Filippovich, R F Khairutdinov *Usp. Khim.* **58** 1032 (1989) [*Russ. Chem. Rev.* **58** 602 (1989)]
8. A Osuka, K Maruyama *J. Am. Chem. Soc.* **110** 4454 (1988)
9. K Maruyama, T Nagata, N Ono, A Osuka *Bull. Chem. Soc. Jpn.* **62** 3167 (1989)
10. J L Sessler, M R Johnson, S E Creager, J C Fettinger, J A Ibers *J. Am. Chem. Soc.* **112** 9310 (1990)
11. D Dolphin, J Hiom, J B Paine III *Heterocycles* **16** 417 (1981)
12. V A Makarov, E I Filippovich, R P Evstigneeva, V I Bol'shakov *Izv. Vyssh. Uchebn. Zaved., Khim. Khim. Tekhnol.* **29** 3 (1986)
13. V A Makarov, E I Filippovich, R P Evstigneeva *Khim. Geterosikl. Soedin.* 1190 (1987)
14. R Karaman, O Almarsson, T C Bruice *J. Org. Chem.* **57** 1555 (1992)
15. K Maruyama, A Osuka *Pure Appl. Chem.* **62** 1511 (1990)
16. A Osuka, K Maruyama, N Mataga, T Asahi, I Yamazaki, N Tamai *J. Am. Chem. Soc.* **112** 4958 (1990)
17. A Helms, D Heiler, G McLendon *J. Am. Chem. Soc.* **114** 6227 (1992)
18. A Helms, D Heiler, G McLendon *J. Am. Chem. Soc.* **113** 4325 (1991)
19. R Young, C K Chang *J. Am. Chem. Soc.* **107** 898 (1985)
20. C K Chang, I Abdalmuhdi *J. Org. Chem.* **48** 5388 (1983)
21. D Gust, T A Moore, A L Moore, F Gao, D Luttrull, J M De Graziano, X C Ma, L R Makings, S-J Lee, T T Trier, E Bittersmann, G R Seeley, M Rougee, F C De Schryver, M.Van der Auweraer *J. Am. Chem. Soc.* **113** 3638 (1991)
22. M J Crossley, P L Burn *J. Chem. Soc., Chem. Commun.* 39 (1987)
23. P Mathis *Pure Appl. Chem.* **62** 1521 (1990)
24. M R Wasielewski, D G Johnson, M P Niemczyk, G L Gaines III, M P O'Neil, W A Svec *J. Am. Chem. Soc.* **112** 6482 (1990)
25. A Osuka, F Kobayashi *Chem. Lett.* 1521 (1990)
26. A Osuka, F Kobayashi, T Nagata, K Maruyama *Chem. Lett.* 287 (1990)
27. A Osuka, K Maruyama, Y Yamazaki, N Tamai *Chem. Phys. Lett.* **165** 392 (1990)
28. U Rempel, B Von Maltzan, C Von Borczyckowski *J. Lumin.* **48** 415 (1991)
29. R J Cogdell, H A Frank *Biochim. Biophys. Acta* **895** 63 (1987)
30. D O Hall, K K Rao *Photosynthesis* (Translated into Russian; Moscow: Mir, 1983)
31. J Amesz *Prog. Bot.* **49** 87 (1987)
32. M Khaled, A Hadjipetrou, L D Kispert, R D Allendoerfer *J. Phys. Chem.* **95** 2438 (1991)
33. T Noguchi, H Hayashi, M Tasumi *Biochim. Biophys. Acta* **1017** 280 (1990)
34. B Demming-Adams *Biochim. Biophys. Acta.* **1020** 1 (1990)
35. H Hayashi, S V Kalaczkowski, T Noguchi, D Blanchard, G H Atkinson *J. Am. Chem. Soc.* **112** 4664 (1990)
36. D Gust, T A Moore, A L Moore, C Devadoss, P A Liddell, R Hermant, R A Nieman, L J Demanche, J M De Graziano, I Gouni *J. Am. Chem. Soc.* **114** 3590 (1992)
37. D Gust, T A Moore, R V Bensasson, P Mathis, E J Land, C Chachaty, A L Moore, P A Liddell, G A Nemeth *J. Am. Chem. Soc.* **107** 3631 (1985)
38. R V Bensasson, E J Land, A L Moore, R L Crouch, G Dirks, T A Moore, D Gust *Nature (London)* **290** 329 (1981)
39. A L Moore, A Joy, R Tom, D Gust, T A Moore, R V Bensasson, E J Land *Science* **216** 982 (1982)
40. G Dirks, A L Moore, T A Moore, D Gust *Photochem. Photobiol.* **32** 277 (1980)
41. A L Moore, G Dirks, D Gust, T A Moore *Photochem. Photobiol.* **32** 691 (1980)
42. P A Liddell, D Barrett, L R Makings, P J Pessiki, D Gust, T A Moore *J. Am. Chem. Soc.* **108** 5350 (1986)
43. A Osuka, H Yamada, K Maruyama *Chem. Lett.* 1905 (1990)
44. A Osuka, H Yamada, K Maruyama, N Mataga, T Asahi, I Yamazaki, Y Nishimura *Chem. Phys. Lett.* **181** 418 (1991)
45. E I Filippovich, R P Evstigneeva, V N Luzgina, T G Egorova, N R Kurdyumova, I E Mikerin, S M Makin *Zh. Obshch. Khim.* **60** 2511 (1990)
46. D Gust, T A Moore, P A Liddell, G A Nemeth, L R Makings, A L Moore, D Barrett, P J Pessiki, R V Bensasson, M Rougee, C Chachaty, F C De Schryver, M Van der Auweraer, A R Holzwarth, J S Connolly *J. Am. Chem. Soc.* **109** 846 (1987)
47. T A Moore, D Gust, G Dirks, G A Nemeth, A L Moore, P A Liddell, R V Bensasson *NATO ASI Ser. C, N 214 (Supramol. Photochem.)* 263
48. N A Sadovnikova, N D Gudkov, Yu M Stolovitskii, V N Luzgina, E I Filippovich, R P Evstigneeva *Dokl. Akad. Nauk SSSR* **312** 481 (1990)
49. V N Luzgina, S E Gribkova, R P Evstigneeva, N D Gudkov, N A Sadovnikova, G D Olovyanishnikova, Yu M Stolovitskii, N F Neznaiko, in *Tezisy Dokladov Mezhdunarodnoi Konferentsii po Fotosintezu i Fotobiologii, Pushchino, 1991* (Abstracts of Reports at the International Conference on Photosynthesis and Photobiology, Pushchino, 1991) p. 49
50. J L Y Kong, P A Loach *J. Heterocycl. Chem.* 17 737 (1980)
51. M R Wasielewski, D G Johnson, W A Svec, K M Kersey, D E Cragg, D W Minsek, in *Photochemical Energy Conversion* (Eds J R Norris, D Meisel) (Amsterdam: Elsevier, 1989) p. 135
52. R P Evstigneeva, V N Lusgina, E I Filippovich, S E Konanykhina, in *The 15th International Symposium on Macrocyclic Chemistry, Odessa, 1990 (Abstracts of Reports)* p. 68
53. T Heinis, S L Chowdhury, S L Scott, P Kebarle *J. Am. Chem. Soc.* **110** 400 (1988)
54. A I Kozhukhova, E A Obol'nikova, G I Samokhvalov *Zh. Org. Khim.* **24** 1778 (1988)
55. V V Borovkov, E I Filippovich, R P Evstigneeva *Khim. Geterosikl. Soedin.* 608 (1988)
56. V V Borovkov, A A Gribkov, R P Evstigneeva, I A Struganova, G V Ponomarev, G V Kirillova, B V Rozynov, P V Bondarenko, R A Zuborev, A N Knysh *Khim. Geterosikl. Soedin.* 1324 (1991)
57. V V Borovkov, A A Gribkov, A N Kozyrev, A S Brandis, A Ishida, Y Sakata *Bull. Chem. Soc. Jpn.* **65** 1533 (1992)
58. M Migita, T Okada, N Mataga, S Nishitani, N Kurata, Y Sakata, S Misumi *Chem. Phys. Lett.* **84** 263 (1981)
59. B Morgan, D Dolphyn, in *Metal Complexes with Tetrapyrrole Ligands* (Berlin: Springer, 1987) Vol. 1, p. 115
60. M R Wasielewski, in *Photoinduced Electron Transfer, Part A* (Eds M A Fox, M Chanon) (Amsterdam: Elsevier, 1988) p. 161
61. V V Borovkov, R P Evstigneeva, E I Filippovich, B V Rozynov *Dokl. Akad. Nauk SSSR* **308** 871 (1988)
62. J S Lindsey, J K Delaney, D C Mauzerall, H Linschitz *J. Am. Chem. Soc.* **110** 3610 (1989)
63. D Mauzerall, J Weiser, H Staab *Tetrahedron* **45** 4807 (1989)
64. A Osuka, K Maruyama *Tetrahedron* **45** 4815 (1989)
65. J K Delaney, D C Mauzerall, J S Lindsey *J. Am. Chem. Soc.* **112** 957 (1990)
66. I Tabushi, N Koga, M Yanagita *Tetrahedron Lett.* **20** 257 (1979)
67. J Von Gersdorff, M Huber, H Schubert, D Niethammer, B Kirste, M Plato, K Mobius, H Kurreck, R Eichberger, R Kietzmann, F Willing *Angew. Chem.* **102** 690 (1990)

68. F Von Lehdzian, J Schlupmann, J Von Gersdorff, K Mobius, H Kurreck *Angew. Chem.* **103** 1536 (1991)
69. M R Wasielewski, M Niemczyk, D Johnos, W A Svec, D Minsek *Tetrahedron* **45** 4785 (1989)
70. M R Wasielewski, M P Niemczyk *J. Am. Chem. Soc.* **105** 5043 (1984)
71. M R Wasielewski, M P Niemczyk, W A Svec, E B Pewitt *J. Am. Chem. Soc.* **107** 1080 (1985)
72. S Knapp, T G M Dhar, J Albaneze, S Gentemann, J A Potenza, D Holten, H J Schugar *J. Am. Chem. Soc.* **113** 4010 (1991)
73. M Antolovich, P Keyte, A Oliver, M Paddon-Row, J Kroon, J Verhoeven, S Jonker, J Warman *J. Phys. Chem.* **95** 1933 (1991)
74. M Antolovich, A M Oliver, M N Paddon-Row *J. Chem. Soc., Perkin Trans. 2* 783 (1989)
75. A R Joran, B A Leland, G G Geller, J J Hopfield, P B Dervan *J. Am. Chem. Soc.* **106** 6090 (1984)
76. A Osuka, K Maruyama *J. Chem. Res. (S)* 286 (1987)
77. A Osuka, S Morikawa, K Maruyama, S Hirayama, T Minami *J. Chem. Soc., Chem. Commun.* 359 (1987)
78. P Tecilla, R Dixon, G Slobodkin, D Alavi, D Waldeck, A Hamilton *J. Am. Chem. Soc.* **112** 9408 (1990)
79. A Harriman, Y Kubo, J Sessler *J. Am. Chem. Soc.* **114** 388 (1992)
80. Y Aoyama, M Asakawa, Y Matsui *J. Am. Chem. Soc.* **113** 6233 (1991)
81. M F Perutz *Br. Med. Bull.* **32** 195 (1976)
82. S G Boxer, R R Bucks *Isr. J. Chem.* **21** 259 (1981)
83. B A Barry, G T Babcok *Proc. Natl. Acad. Sci. USA* **84** 7099 (1987)
84. R Huber *The EMBO J.* **8** 2125 (1983)
85. Jpn. Appl. 62-33 180; *Ref. Zh. Khim.* 9O153P (1988)
86. P J Nixon, X-S Tang, J T Trast, D A Chisholm, B A Diner *Photosynth. Res.* **34** 87 (1992)
87. K Maruyama, H Yamada, A Osuka *Photochem. Photobiol.* **53** 617 (1991)
88. C B Buser, B A Diner, G W Brudvig *Photosynth. Res.* **34** 87 (1992)
89. D Le Nouen, J Marko, G Vermeersch, N Febvay-Garot, A Lablache Combiner, M Persce-Fauvet, A Gaudermer *J. Phys. Org. Chem.* **3** 69 (1990)
90. S Shochat, J Schutrups, S Otte, B Vrieze, R Bos, P Gast, A J Hoff *Photosynth. Res.* **34** 124 (1992)
91. B Svensson, L Davidsson, C Tommos, J Smith, W Vermaas, S Styring *Photosynth. Res.* **34** 140 (1992)
92. Y Kodera, K Takura, H Mino, A Kawamori *Photosynth. Res.* **34** 136 (1992)
93. H Mino, Y Kodera, A Kawamori *Photosynth. Res.* **34** 136 (1992)
94. C W Hoganson, G T Babcock *Photosynth. Res.* **34** 148 (1992)
95. K Maruyama, H Yamada, A Osuka *Chem. Lett.* 833 (1989)
96. M A Shafiev, S I Allakhverdiev, V V Klimov, in *Tezisy Dokladov Vsesoyuznoi Konferentsii po Preobrazovaniyu Svetovoi Energii v Fotosinteziruyushchikh Sistemakh i Ikh Modelyakh, Pushchino, 1989* (Abstracts of Reports at the All-Union Conference on the Transformation of Light Energy in Photosynthesising Systems and Their Models, Pushchino, 1989) p. 114
97. P J Van Leeuwen, M H Vos, H J Van Gorkom *Biochim. Biophys. Acta* 173 (1990)
98. C Jegerschold, H Agren, S Styring *Photosynth. Res.* **34** 150 (1992)
99. Jpn. Appl. 64-61 481; *Ref. Zh. Khim.* 19O155P (1990)
100. V N Luzgina, E I Filippovich, R P Evstigneeva *Izv. Vyssh. Uchebn. Zaved., Khim. Khim. Tekhnol.* **30** 3 (1987)
101. A Osuka, K Maruyama *Chem. Lett.* 1853 (1986)
102. S E Gribkova, V N Luzgina, R P Evstigneeva *Zh. Org. Khim.* **24** 758 (1993)

Russian Chemical Reviews **62** (10) 981–989 (1993) ©1993 Russian Academy of Sciences and Turpion Ltd

UDC 538.945:534.234

The chemistry of volatile β-diketonates and their application in the synthesis of high-temperature superconducting thin films

G V Bazuev, L D Kurbatova

Contents

I. Methods of preparing epitaxial high-temperature superconducting films 981
II. Volatile metal β-diketonates used in CVD technology 982
III. Structural changes of metal β-diketonates during their transfer to the gas phase 983
IV. Gas-phase thermal stability of yttrium, barium, copper, calcium, and bismuth β-diketonates, used in CVD technology 984
V. Use of CVD technology in the synthesis of high-temperature superconducting films 984

Abstract. We shall examine the fundamental aspects of the chemistry of volatile β-diketonates: the dependence of their volatility on the coordination unsaturation of the complexes, on the structure of the ligands, and on the nature of the metals. The gas-phase thermal stability of the β-diketonates and the structural changes which take place when these compounds are transferred to the gas phase are discussed. The most important results on the synthesis of Y–Ba–Cu–O, Bi–Sr–Ca–Cu–O, and Tl–Ba–Ca–Cu–O by chemical vapour deposition from the gas phase are reported. The bibliography contains 106 references.

I. Methods of preparing epitaxial high-temperature superconducting films

According to recent reports[1] high-temperature superconductors (HTSC) are finding practical applications in thin film form, mainly for the following reason. The best samples of high-temperature superconducting films now being produced have surprisingly high critical current densities. The use of HTSC in thin film form can solve several problems in cryoelectronics. In particular, in devices based on the Josephson effect the required current density (10^2–10^3 A cm^{-2}) can be obtained even with polycrystalline films. Many studies (in particular those based on tunnel spectroscopy, optical methods, etc.) aimed at establishing the physical characteristics of the material and the mechanism of the superconductivity in HTSC have had to be carried out with thin film samples.

The anisotropy of the physical characteristics of the materials is being studied with monocrystalline (epitaxial) HTSC films, of which the best samples have properties closer to those of an ideal crystal than is found in most of the monocrystals now being prepared.[2] Studies of the stability (ageing) of HTSC are also most conveniently carried out with films because chemical or physical instability effects are easily detected in film samples (for example, in studies of the effect of irradiation with high-energy particles on the properties of HTSC). Films are also widely used in the search for new superconductors: in particular, the high-temperature metastable phases NbGe and Nb_3Si have been prepared as thin films.

G V Bazuev, L D Kurbatova Institute of Solid State Chemistry, Urals Branch of the Russian Academy of Sciences, ul. Pervomaiskaya 91, 620219 Ekaterinburg, Russian Federation,
Fax (7-343-2) 44 49 43

Received 13 August 1993
Uspekhi Khimii **62** (10) 1037–1046 (1993); translated by J I Carasso

Various chemical (as well as physical) methods have been used to prepare HTSC films. According to Schieber[3] the most promising of these is the CVD method (chemical vapour deposition from the vapour phase). The basis of the method is to transport the components of the film to the substrate in the form of the vapours of volatile compounds: the vapours are decomposed on the substrate to give a film of the required composition. Halides, hydrides, or organometallic compounds are used as the volatile compounds; this variant of the method is called MOCVD. The CVD method offers a number of advantages over the PVD (physical vapour deposition) method.

1. The possibility of depositing films of uniform composition and thickness on component parts having a complex configuration. This feature is specially important for HTSC films because it makes possible the production of large current-carrying structures in film form, of magnetic screens, and of other 'nonplanar' components.

2. The possibility of achieving high rates of deposition (up to several micrometres per hour) while maintaining a high-quality product (i. e. while controlling its epitaxial character, density, and crystallinity). In contrast to the physical evaporation methods, in which the need for a high growth rate is met by providing a high-energy flux of particles of the substance to be evaporated, with the consequent danger of decomposing the substrate surface (or the already deposited film), in the CVD method a high production rate is achieved by using a high pressure of the transporting vapour or a high flow rate of the carrier gas.

3. A high reproducibility of the properties of the coatings prepared with constant process parameters.

4. Easy control of the process and flexibility in the choice of the technological regime (especially in changes of the chemical composition of the deposit).

5. The possibility of changing from high-vacuum apparatus to assemblies giving a vacuum of 10 Pa or to flow assemblies operating at pressures of 10^2–10^5 Pa.

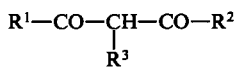
The development of the CVD technology has been fastest in Japan and in the USA. The best samples of HTSC film[4,5] prepared by CVD have been reported from those countries. It should be noted that this type of work is now being carried out, in preference to sustained studies of evaporation in a vacuum by physical methods, in the laboratories of the largest firms active in this field, such as Riken, Nissan Motors, Ori Electronics, Westinghouse, and others. This confirms the favourable prospects of the adoption of the CVD technology in the industrial production of HTSC films.

II. Volatile metal β-diketonates used in CVD technology

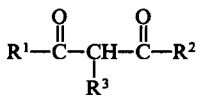
The first and most fundamental problem in the development of the CVD technology is the choice of volatile compounds which satisfy at least the following two requirements: they should have a technologically acceptable vapour pressure and they should pass into the vapour phase (by evaporation or by sublimation) without decomposition, since decomposition of the compound could affect its volatility and thus perturb the constancy of the rate of deposition and of the composition of the film.

In a study of the synthesis of $YBa_2Cu_3O_{7-x}$ the components were transferred through the gas phase as β-diketonates [organometallic chelated complexes having a high volatility at relatively low temperatures (100–300 °C)].

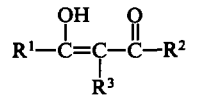
β-Diketones of the general formula



are liquid or solid colourless compounds which exist in two tautomeric forms:

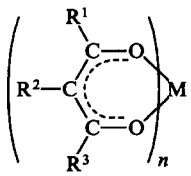


keto form



enol form

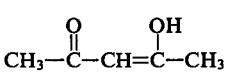
In aqueous solutions β-diketones have weakly acidic properties and react with many metals to give compounds of the chelate type:



where n is the charge on the metal ion. The double bond in the metal ring is delocalised, and the two O–M bonds are equivalent.

Extensive studies of the chemistry of β-diketonates have established quite unambiguously the fundamental principles which determine the relationship between the volatility of these compounds and their composition and structure.[6–8] Since the molecules must overcome the intermolecular interaction forces during evaporation or sublimation, the highest volatility is found in the coordinationally saturated complexes, which do not tend to form oligomers or hydrogen bonds.

Let us examine for example the metal acetylacetonates. When in the enol form



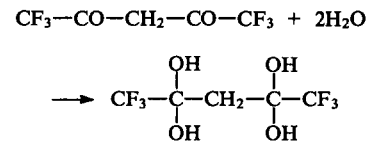
these compounds interact with many metals to give stable uncharged inner complexes (chelates) in which the bond between the metal and the ligands is often covalent. The complexes of acetylacetone with beryllium(II), aluminium(III), and chromium(III) are coordinationally saturated and have a high volatility. On the other hand the acetylacetonates of lithium, sodium, and magnesium are almost completely involatile, probably because of the ionic character of their bond, and also as a result of polymerisation in the condensed phase.

The complexes of the rare-earth elements (REE) with acetylacetone are coordinationally unsaturated, since their c.n. is 8–11, but the β-diketones occupy only six coordination sites in the inner coordination sphere of the metal. Therefore many REE β-diketonates are hydrated and usually contain two or three water molecules. The hydrated metal chelates undergo hydrolytic dissociation when heated, with formation of involatile hydroxy compounds. Furthermore the coordinationally unsaturated β-diketonates of many metals are often oligomerised or polymerised. These compounds have a low volatility and are thermally dissociated when heated.[9]

The replacement of the end methyl groups in acetylacetone by heavier unbranched hydrocarbon radicals (ethyl, n-propyl, n-butyl, phenyl, etc.) produces a change in the volatility of the corresponding complexes. This can be attributed to the increase in the molecular mass, and also to the strengthening of the intermolecular interaction. The latter factor plays a substantial role, because the volatility of the β-diketonates is strongly dependent on the degree of branching of the hydrocarbon end groups. These chelates are less readily hydrated or polymerised. In recent years a strong research effort has been aimed at the β-diketonato complexes of metals with the end methyl groups replaced by *tert*-butyl groups (dipivaloylmethane, DPM).[10–17]

Another indicator of the dependence of the volatility of chelates on the form of the molecule is the fact that the volatility of the REE β-diketonates increases rather than decreases in the series from lanthanum to lutetium, in spite of the increase in molecular mass. Sicre et al.[18] have attributed this effect to the decrease in the ionic radius of the metal (the lanthanide contraction). The result is either a decrease in the intramolecular local dipoles or a better screening from the neighbouring molecules, which weakens the intermolecular interaction forces.

Replacing the hydrogen in the end methyl groups of acetylacetone (AA) by fluorine greatly increases the volatility of the corresponding β-diketonates, evidently (again) as a result of the decrease in the intermolecular interaction forces and of the increased covalency of the metal–ligand bond.[19,20] The coordinationally saturated chelates of hexafluoroacetylacetone (HFA) $CF_3-CO-CH_2-CO-CF_3$ are the most volatile of all the known metal β-diketonates. However, hexafluoroacetylacetone has a serious disadvantage: it reacts with water to give a tetrahydroxy compound:[19]



Therefore the most 'popular' ligand is trifluoroacetylacetone (TFA) $CF_3-CO-CH_2-CO-CH_3$. The volatility of most of its chelates is slightly lower than that of the HFA chelates, but much higher than that of the corresponding acetylacetonates. However, it reacts with water at a negligible rate, and this allows the chelates to be synthesised by extraction of aqueous solutions of the metals with solutions of TFA in organic solvents. The trifluoroacetylacetonates do not tend to form adducts as readily as the hexafluoroacetylacetonates.[8]

Thus the replacement of hydrogen by fluorine increases the volatility of the β-diketonates, but it lowers the thermal stability of the complexes. Therefore some workers[8,21,22] concluded that the most effective complexes are those with β-diketones containing not only a fluorinated radical (which increases the volatility) but also a *tert*-butyl radical (which contributes additional thermal stability). These include pivaloyltrifluoroacetone (PTFA) and 2,2-dimethyl-6,6,7,7,8,8,8-heptafluoro-octan-3,5-dione (FOD), which contain the CF_3 and C_3F_7 radicals respectively. The rare-earth metals form monohydrates with FOD, which are readily dehydrated without decomposition when dried in a vacuum over P_2O_5. The chelates of REE with PTFA can react with uncharged donors with formation of thermally stable complexes.[23]

The volatility of the β-diketonates depends on the nature of the complex-forming metal. For example, films of HTSC can be produced by using complexes of copper with various ligands,

including the complex with acetylacetone, $Cu(AA)_2$, since they all have an adequate vapour pressure and thermal stability (see Table 1).[24–26]

Table 1. *Volatile chelated compounds used in the preparation of HTSC films from the vapour phase.*

Metal	Ligand		Designation of chelates
	R	R′	
Cu	CH_3	CH_3	$Cu(AA)_2$
Cu, Y, Ba, Sr, Ca	$(CH_3)_3C$	$(CH_3)_3C$	$M(DPM)_n$
Cu, Ba	CF_3	CF_3	$M(HFA)_2$
Ba, Y	C_3F_7	$(CH_3)_3C$	$M(FOD)_n$
Cu	$CH_3-C(=NH)-CH_2-CO-CH_3$		$Cu(Acim)_2$ [a]

[a] Acim is acetylacetoneimine.

The ions of the alkaline earth metals (the components of the HTSC, Sr^{2+} and especially Ba^{2+}) form involatile oligomeric complexes with β-diketones. The freshly prepared complexes of these metals are monomeric and contain between two (the magnesium, calcium, and barium β-diketonates) and four water molecules (the strontium β-diketonates). However, after dehydrating and heating the complexes additional lines are observed in the IR and Raman spectra[27] in the metal–ligand vibration region (400, 650 cm^{-1}) and in the bending region of the chelate ring (600–900 cm^{-1}). Under these conditions the chelates are characterised by a total involatility, and the mass spectra of the complexes indicate the formation of species with a molecular mass well in excess of the molecular mass of the monomeric compound. The appearance of new bands in the IR and Raman spectra after dehydration and heat treatment of the complexes may be associated with polymerisation during dehydration, which is the mechanism most likely to oppose the transfer of compounds to the gas phase. The degree of oligomerisation is strongly dependent on the nature of the central atom and increases with the atomic number of the metal. It has been established that the volatility of the alkaline-earth metal chelates is markedly affected by the method of dehydrating the prepared compounds, and also by the method of storage.[28] The sublimation characteristics of even the most suitable of these complexes for CVD technology (barium dipivaloylmethanate, $BaL_2 \cdot 2H_2O$) are markedly degraded during storage. The results of photoelectron spectroscopy in the gas phase and of thermal analysis have shown that barium dipivaloylmethanate is hydrolysed as follows during storage:

$$BaL_2 \cdot 2H_2O \longrightarrow Ba(OH)L + HL + H_2O .$$

The additional hydration of $BaL_2 \cdot 2H_2O$ during storage favours more extensive hydrolysis. It should be noted that storage over P_2O_5 is also undesirable because this drying agent appears to enhance the hydrolysis by shifting the equilibrium as a result of its interaction with the vapour of the acid (HL) evolved by the hydrolysis of $BaL_2 \cdot 2H_2O$. Large changes in the sublimation properties during the storage of the preparations over P_2O_5 are observed also in the β-diketonates of other metals (for example the REE).[29]

Thus the hydrolysis of $BaL_2 \cdot 2H_2O$ during the storage and subsequent sublimation processes is one of the main causes of instability of this compound. However, an equally important cause may be the slow oligomerisation of the anhydrous barium dipivaloylmethanate. It has been reported[28] that reproducible results on the sublimation of barium dipivaloylmethanate can be obtained by eliminating all the factors which favour polymerisation. One way of solving this problem is to add the BaL_2 in the form of compounds with additional uncharged ligands, $BaL_2 \cdot nQ$ whose inclusion in the composition of the complex suppresses the hydrolysis and favours the depolymerisation of $(BaL_2)_n$ by saturating the coordination sphere of the Ba^{2+} ion with the donor molecules of the additional ligand Q. The complex of the pivaloyltrifluoroacetonate of barium(II) with dimethylformamide has been discussed as an example.[27]

It would seem that the vapour pressure of the barium chelates could be increased by increasing the temperature. However, this method is limited by considerations of the thermal stability of the β-diketonates. The competition between the sublimation and the thermal decomposition of the barium complexes is one of the main problems in the CVD technology for the production of $Y(Ln)Ba_2Cu_3O_{7-x}$. As has already been pointed out[1] this problem can be solved by a careful choice of the sublimation regime and of the method of synthesis of the chelates, aimed at minimising the possibilities of oligomerisation.

III. Structural changes of metal β-diketonates during their transfer to the gas phase

The metal cation is usually attached to the β-diketonate anion through two oxygen atoms belonging to the hydroxyl and the carbonyl group, forming the chelate. However, recent physicochemical studies have shown that other methods of coordinating the β-diketone ligands are possible: in particular, the monodentate coordination of the metal by an oxygen atom. Compounds of this type include the complexes Cu(HFA)(MeNHCH$_3$NHMe), $Cu(AA)_2En_2 \cdot 2H_2O$, $(CH_3)Si(AA)$, and $(CH_3)_3Hg(AA)$, where Me is methylene and En is ethylenediamine.[30–34]

A similar method of coordination is possible also at temperatures close to the thermal dissociation temperature. ESR studies and studies by electronic and IR spectroscopy have shown that during the transfer to the gas phase at high temperatures the c. n. of the complex decreases as a result of the opening of the chelate ring. This effect is most clearly seen in compounds containing an additional electron donor molecule, for example $M(HFA)_2 \cdot 2TBPO$, where M = Co, Ni, Cu and TBPO is tributylphosphine oxide.[35,36] From the standpoint of thermodynamics this means that at least in the gaseous state the metal β-diketonates can exist as an equilibrium of two isomeric forms: a chelate and an open ring. The quantitative relationship between the bidentate and the monodentate form depends both on the temperature and on the energy of the M–O bond in the complex. Because of their structure the metal β-diketonates with a monodentate coordination should be chemically more active towards addition and exchange reactions.

It has been shown[37] that the vapour formation process is accompanied by exchange reactions induced by three

$$ML_n \rightleftharpoons ML_{n-1} + L^{\cdot} , \quad (1)$$

$$M'L'_n \rightleftharpoons ML'_{n-1} + L'^{\cdot} , \quad (2)$$

$$ML_n + L'^{\cdot} \rightleftharpoons ML_{n-1}L' + L^{\cdot} , \quad (3)$$

$$M'L'_n + L^{\cdot} \rightleftharpoons M'L'_{n-1}L + L'^{\cdot} \text{ etc.} \quad (4)$$

mechanisms. The first is the radical–chain mechanism:

The second mechanism is the formation of polymeric species in the condensed or the gaseous phase followed by dissociation

$$kML_n(\text{sol., gas}) + lM'L'_n(\text{sol., gas}) \rightleftharpoons (MM'L_nL'_n)_{k+l}(\text{sol., gas}), \quad (5)$$

$$(MM'L_nL'_n)_{k+l}(\text{sol., gas}) \begin{cases} \longrightarrow lML_{n-1}L'(\text{gas}) + kM'L'_{n-1}L(\text{gas}) \\ \longrightarrow lML'_n(\text{gas}) + kM'L_n(\text{gas}) . \end{cases} \quad (6)$$

into monomeric molecules during vapourization:
This mechanism probably applies to the exchange reactions between the β-diketonates which can either have an oligomeric structure in the condensed state or form dimeric molecules in the gas phase.

The third ligand exchange mechanism is possible when the β-diketonates exist in an open form. Under these conditions unstable polymeric molecules exist on the surface of the condensed phase, where they can subsequently dissociate into the initial complex and a mixed complex:

$$ML_n \rightleftharpoons ML_{n-1}L^* , \quad (7)$$

$$M'L'_n \rightleftharpoons M'L'_{n-1}L'^* , \quad (8)$$

$$ML_{n-1}L^* + M'L'_{n-1}L'^* \rightleftharpoons \{MM'L_nL'_n\} \rightleftharpoons ML_{n-1}L'^* + M'L'_{n-1}L , \quad (9)$$

where L* (L'*) is a ligand with monodentate coordination.

The possible occurrence of all the above mechanisms must be borne in mind when superconducting films are synthesised from the gas phase by the pyrolysis of organometallic compounds. Thus, it has been shown[38] by IR spectroscopy that when a mixture of gaseous $Cu(AA)_2$ and $Ba(DPM)_2$ is heated in an argon atmosphere at 200 °C a redistribution of the ligands is observed, leading to the formation of the involatile complexes $Ba(AA)_2$ and Ba(AA)L which perturb the stoichiometric relationship between Ba and Cu. In order to avoid uncontrolled changes in stoichiometry during the deposition of BaO and CuO/Cu_2O on an oriented Si(100) face the use of copper dipivaloylmethanate has been recommended as the source of the Cu phase.

IV. Gas-phase thermal stability of yttrium, barium, copper, calcium, and bismuth β-diketonates, used in CVD technology

The β-diketonates of elements such as yttrium, barium, copper, bismuth, etc. are used as the initial components for the synthesis of HTSC thin films by chemical deposition from the vapour phase. Data on the thermal stability of these compounds and on the effect of oxygen on the thermolysis process have been reported,[39-46] and the mutual effects of the β-diketonates during thermolysis have been discussed.

According to mass spectrometric results the main gaseous products of the thermal decomposition of the yttrium, copper, and barium acetylacetonates are acetone and ethylene. Passing from copper to barium increases the ethylene content of the thermolysis products from 22 to 87 mol%. By combining kinetic data with an analysis of the product we may conclude[39] that the thermolysis of $M(AA)_n$ takes place by an intramolecular process in the coordination sphere of the metal. The first step of this process is the opening of the chelate ring, followed by the breaking of the M–O and C=C bonds in the case of $Cu(AA)_2$ and of the C=C bond in the case of yttrium and barium chelates.

Changing to fluorine-substituted β-diketones gives thermolysis products with a more complex composition.[40] Thus the products of the thermal dissociation of the calcium, strontium, barium, and yttrium, trifluoroacetylacetonates are trifluoroacetone, trifluoromethanol, trifluoroethane, trifluoromethane, acetone, ethanol, carbon dioxide and monoxide, ethylene, hydrogen fluoride, and methane. The relative amounts of these products are determined by the nature of the metal. In the case of trifluoroacetylacetone (TFA) the main thermal decomposition product was trifluoroacetone, whereas for the derivatives of strontium, barium, and yttrium the main products were carbon dioxide and monoxide. Replacing the actylacetonato ligand by its fluorine-substituted analogue lowers the thermal stability of the calcium derivatives five-fold. The β-diketonates can be arranged in the following series of decreasing thermal stability:[41]

$$(AA)_2Ca > (TFA)_2Ca \approx (PTFA)_2Ca > (TFA)_2Sr.$$

In a study[42,43] of the sublimation of yttrium and barium dipivaloylmethanates it was established that $Y(DPM)_3$ sublimes in two steps at 130 and 160 °C. Evidently this effect is due to the formation of dimers. The ratio of dimers to monomers is 1 : 3. Barium dipivaloylmethanate sublimes at 300 °C. A mass spectrometric study has shown that the sublimed product is a trimer in the gas phase, and according to a thermal study of the vapour of the chelate complex the thermolysis is preceded by a depolymerisation process. A combination of mass spectrometric and DTA methods has been used[44] to study the thermal decomposition of the vapours and of the solid phase for bismuth chelates of general formula $Bi(R-CO-CH_2-CO-R')_3$, where $R = CF_3$, $R' = CH_3$, CF_3, $C(CH_3)_3$, $C(CH_3)_2OCH_3$. From an analysis of the mass spectra it was concluded that the vapour of these compounds consists of BiL_3 monomers. The volatility of the complexes with respect to the form of the substituent R' decreases in the sequence $C(CH_3)_2OCH_3 > C(CH_3)_3 > CH_3 > CF_3$. In the thermolysis of the chelate vapours the gaseous products are β-diketones and their fragments.

In a study of the thermal decomposition of the solid phase of the bismuth β-diketonates it was noted that in a flow of helium and oxygen the β-diketonates containing trifluoroacetylacetone and hexafluoroacetylacetone as ligands decompose at 100–150 °C. The thermal stability of the complexes containing *tert*-butyl groups rises to 300 °C, and these complexes are less likely to form oligomers because of the steric factors associated with the bulky substituents of the ligands in the octahedral bismuth complex. The increase in the steric factor produced by the replacement of the $C(CH_3)_3$ substituent by $C(CH_3)_2OCH_3$ suppresses the dimerisation of the molecules almost totally and thus allows the sample to be sublimed repeatedly with a yield of 90%–95%.

The thermal stability of the β-diketonates in the gas phase is strongly influenced by the presence of oxygen, which is added to the reaction volume, and of other volatile β-diketones (the initial complexes for the synthesis of the HTSC).[45,46] Thus the thermal stability threshold of the vapour of copper dipivaloylmethanate *in vacuo* is 330 ± 10 °C, whereas in the presence of oxygen it falls to 280 ± 10 °C. For the vapour of yttrium dipivaloylmethanate the stability threshold is 490 ± 10 °C. Oxygen lowers this threshold to 395 ± 5 °C. It was shown that the vapour of copper dipivaloylmethanate affects the thermolysis of yttrium dipivaloylmethanate in oxygen. Since the vapour of the $Cu(DPM)_2$ complex has a lower thermal stability than the vapour of $Y(DPM)_3$ a shortage of oxygen is produced in the reaction region during the thermolysis of the vapour of the yttrium complex. This raises the decomposition threshold to the temperature level observed in the absence of added oxygen.

A study of the thermal stability of the yttrium, barium, and copper β-diketonates with various ligands allowed Bykov et al.[46] to choose the optimum conditions for the deposition of layers at pressures of 1–5 torr on substrates of monocrystalline silicon and of sodium silicate glass in a reactor of the bell-jar type with heated walls, three heated evaporators, and an oxygen admission tube. The organometallic compound was introduced in a stream of argon.

The maximum growth rate of the copper, barium, and yttrium oxides obtained from the corresponding dipivaloylmethanates was found to occur at 530–550, 600–620, and 550–560 °C respectively. The rate of growth of the films of copper oxide from the acetylacetonate decreased at temperatures above 550 °C, probably as a result of the partial decomposition of the organometallic compound in the reactor volume. The optimum temperatures of the evaporators of the β-diketonates for the synthesis of films at suitable rates have been determined. For $Cu(AA)_2$, $Cu(DPM)_2$, $Y(DPM)_3$, $Ba(DPM)_2$ they are 110–140, 90–120, 60–120, and 210–260 °C respectively.

V. Use of CVD technology in the synthesis of high-temperature superconducting films

1. Y–Ba–Cu–O films

The volatility of β-diketonates under equilibrium conditions is determined by the temperature dependence of the saturated vapour pressure. The vapour pressures of the β-diketonates used in the synthesis of $YBa_2Cu_3O_{7-x}$ have been reported.[6,18,47,48] However, under real conditions these results are not always reproducible because non-equilibrium conditions tend to be established in flow-through reactors, which must be used because of the low volatility of the chelate compounds of barium and also because of the need to reconcile the sublimation and vapour transport conditions with the conditions for the oxidative thermal decomposition of the volatile compounds near the substrate surface.

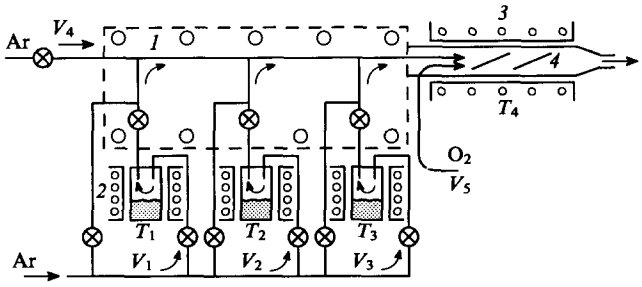


Figure 1. Apparatus for depositing coatings from the gas phase. T_1-T_3 are the temperatures of the evaporators (bubbler type); T_4, temperature of the substrate; V_1-V_3, flow rates of the inert gas (Ar) passing through the evaporators; V_4, flow rate of the inert gas (Ar) passing through the gas collector; V_5 flow rate of the oxygen; the arrows denote the directions of the gas flows; *1* gas collector, *2* evaporators, *3* heaters, *4* substrate.

A typical CVD apparatus[49,50] for the preparation of $YBa_2Cu_3O_{7-x}$ thin films is shown in Fig. 1. In these assemblies the independently variable parameters are the temperatures of the substrate and of three evaporators of the bubbler type, the rates of five gas flows (the flows of inert gas through the three bubblers and through the gas collector, and the flow of oxygen over the substrate), and the total pressure in the reactor. We know that the homogeneity region for the cations in the $YBa_2Cu_3O_{7-x}$ phase is very narrow, and therefore even small departures from stoichiometry induce the formation of a second phase. To avoid this danger a very precise control must be applied to the flow rates of the inert gas (~1%) and to the evaporator temperatures (~0.1 K).

Difficulties are also met in the construction of the 'hot' flow controllers at the outlet of the evaporators and of the hot collector, whose temperatures must not fall below the temperature of the evaporators (in order to avoid condensing the sublimed vapours). The vapours of the β-diketonates and of their thermal decomposition products can interact with the material of the reactor walls. Therefore the reactor must be constructed with an inert material or with materials coated with silver, which does not form stable β-diketonates. Quartz cannot be used because at high temperatures the hot quartz walls could absorb barium from the vapour (forming the stable barium silicate).

Let us examine the results of some studies of the synthesis of $YBa_2Cu_3O_{7-x}$ by the CVD technology,[51-56] using as the initial components the dipivaloylmethanates of yttrium, barium, and copper. The total flow of carrier gas in the three evaporators was 0.3 $dm^3\ min^{-1}$; the pressure in the horizontal quartz reactor was 660–1300 Pa. Depositing the condensate at a rate of 0.8–1.0 μm h^{-1} on a polycrystalline substrate of $ZrO_2(Y_2O_3)$ heated to 800 °C produced film with zero resistance at 45 K with inclusions of textureless[51,52] $BaCuO_2$ and CuO. Raising the temperature of the substrate to 900 °C improved the quality of the films: at a thickness of 0.8–1.0 μm they consisted of preferentially oriented crystallites (with the *c* axis perpendicular to the plane of the substrate, the so-called type 001 texture), and they began to enter the superconducting state at $T_c^H = 89$ K, $T_c(\rho = 0) = 80$ K. The best transition into the superconducting state was obtained by slowly cooling the films in a stream of oxygen ($p_{O_2} = 10^5$ Pa).[53,54] Textured films 2 μm thick with zero resistance at 84 K and a critical current density of 2×10^4 A cm^{-2} (at 77 K and the zero magnetic field *H*)[55] were obtained at 900 °C on a monocrystalline $SrTiO_3$ substrate cut in the (100) plane.

By lowering the substrate temperature to 850 °C (thus suppressing the chemical interaction at the film–substrate interface) Yamane [56] obtained the film with the best transport properties, having the following parameters at 77 K:

H/T	27	8	1	0
J/ A cm^{-2}	6×10^4	2.2×10^5	4.8×10^5	10^6.

In this case the total flow rate of the carrier gas (argon) was 0.45 $dm^3\ min^{-1}$, the flow rate of oxygen was 0.25 $dm^3\ min^{-1}$, and the pressure in the reactor was 130 Pa. The sublimation of $Cu(DPM)_2$, $Y(DPM)_3$, and $Ba(DPM)_2$ was carried out at 136, 145, and 253 °C respectively. The rate of growth of the film was 1–6 μm h^{-1}. By using masking techniques Muto[57] and Watanabe [58] obtained superconducting films 1 μm thick having $T_c = 92$ K and a high value of J_c ($10^5 - 10^6$ A cm^{-2} at 77 K in a magnetic field of up to 30 T).

Superconducting films have been obtained[5,59] on monocrystalline MgO by separating in time the condensation of the oxides and the solid-phase formation reaction of the superconducting phase. The dark brown condensate obtained at 400–600 °C was roasted in oxygen at 800–920 °C and was then slowly cooled. The $YBa_2Cu_3O_{7-x}$ films were converted into the superconducting state over a wide range of temperatures: 80–20 K (Berry[5]) and 76–60 K (Nakamori[59]).

Zhang et al.[60] have claimed slightly better characteristics for their superconducting films. The temperature of the onset of superconductivity was $T_c^H = 93$ K, and zero electrical resistance of the Y–Ba–Cu–O film was observed at 84 K. Good results have been obtained by using the two-stage technology.[61-63] Thus, Noh et al.[61] synthesised semitransparent films which had a resistance of >10 MΩ at a thickness of 1 μm on substrates of $SrTiO_3$ [oriented (100)] in a rotating high-speed disk reactor. After heat treatment at 860–980 °C the $YBa_2Cu_3O_{7-x}$ films became superconducting, some of the samples having $T_c = 90$ K and a transition width $\Delta T_c < 2$ K. Schmaderer et al.[62] used yttrium, barium, and copper 2,2,6,6-tetramethylheptan-3,5-dionates (TMHD), having evaporation temperatures of 112, 208, and 117 °C respectively, to prepare $YBa_2Cu_3O_{7-x}$ thin films on polycrystalline substrates of stabilised ZrO_2 and on monocrystalline $SrTiO_3$ (100) substrates, which were roasted at temperature ≥850°C. On these films the authors found $T_c > 90$ K, $\Delta T_c = 0.2-0.5$ K. The maximum critical current density J_c on a ZrO_2 substrate was 6×10^3 A cm^{-2} at 77 K, whereas on an $SrTiO_3$ substrate the films had $J_c \approx 10^6$ A cm^{-2} in a zero magnetic field and 10^5 A cm^{-2} in a field of 5.5 T. By using the same β-diketonates films of Y–Ba–Cu–O have been obtained[63] on substrates of stabilised $ZrO_2+Y_2O_3$ and BaF_2+ZrO_2/Y_2O_3. After being heat treated at high temperatures the best films on the BaF_2-ZrO_2/Y_2O_3 substrate had $T_c^H \approx 100$ K and $T_c(\rho = 0) = 80$ K.

The low volatility of the barium β-diketonates (including its dipivaloylmethanate) has been repeatedly pointed out.[5,21,50,59] Therefore even at high flow rates through the bubbler (0.5 $dm^3\ min^{-1}$ for a bubbler temperature of 253 °C) the growth rate of the films is unacceptably slow.[5] Raising the temperature of the bubbler to 300 °C does not usefully improve the growth rate

because it lowers the effectiveness of the barium source.[21,50] To increase the volatility some workers[21,22,49] have used fluorinated β-diketonates, but high rates of deposition of the films were not invariably achieved. Thus, when using barium hexafluoroacetylacetonate[49] with an evaporator temperature of 220 °C the rate of deposition was only 0.3 μm h^{-1}. The use of barium 1,1,1,2,2,3,3-heptafluoro-7,7-dimethyloctan-4,6-dionate increased the rate of deposition of the film to 1.6 μm h^{-1} in a stream of argon (0.3 dm^3 min^{-1}) for an evaporator temperature of 170 °C. For a rate of supply of argon of 1 dm^3 min^{-1} and an evaporator temperature of 350 °C the growth rate of the film rose[22] to 4.6 μm h^{-1}.

The use of fluorinated β-diketones introduces serious complications into the phase transition process during the synthesis of $YBa_2Cu_3O_{7-x}$ by the CVD method. Even in an oxygen atmosphere the decomposition of the fluoro-organic complexes of barium at 400–1000 °C leads to the formation of the thermally stable BaF_2. This is confirmed by a study[64] in which copper acetylacetonate and yttrium dipivaloylmethanate were mixed with barium hexafluoroacetylacetonate. After heat treatment in an oxygen atmosphere at 900 °C a mixture of Cu_2O, CuO, Y_2O_3, $Cu_2Y_2O_5$, and BaF_2 was formed.

To convert BaF_2 into an oxide phase some workers have used a mixture of oxygen and water vapour.[21,22,65] As has been pointed out,[65,66] in order to shift the equilibrium of the reaction

$$BaF_2 + H_2O \longrightarrow BaO + 2HF \qquad (10)$$

towards the right we need a large excess of water vapour in comparison with the HF. Thus, at 830 °C $\Delta G < 0$ if $p_{H_2O}/p_{HF} > 10^5$, and at 1200 °C $\Delta G < 0$ if $p_{H_2O}/p_{HF} > 10^3$.

In practice the process takes place under nonequilibrium conditions: the inert gas or the oxygen, saturated with water vapour, removes the HF from the reaction volume, which corresponds to conversion, and the resulting BaO reacts with the CuO and Y_2O_3. In a gas stream saturated with H_2O at 23 °C reaction (10) begins[22] at 550 °C. But BaF_2 can be incorporated in the film in substantial amounts even at high temperatures. The inclusion of the BaF_2 conversion stage into the kinetics of the solid-phase formation reaction of $YBa_2Cu_3O_{7-x}$ and the presence of water vapour (which assists the mass transfer in oxide systems) alter the morphology of the films as compared with those prepared from compounds not containing fluorine. The predominance of crystallites with their *a* axis oriented perpendicular to the substrate in these films has been pointed out.[22] However, it is also accepted[1] that the effect of residual fluorine on the properties of the film is still not understood.

Reaction (10) proceeds more smoothly if the evolved HF is trapped as SiF_4 by interacting with SiO_2. This requires the use of quartz reactor walls or alternatively the addition of a special charge of SiO_2. It has been shown[66] that films prepared in the presence of SiO_2 have a zero resistance at 89 K whereas in the absence of SiO_2 the superconducting state is reached only at 50 K. The best films of $YBa_2Cu_3O_{7-x}$, prepared by using fluorinated yttrium, barium, and copper β-diketonates, are characterised[22,67,68] by a temperature of transition to the superconducting state in the region of 70–90 K.

Some of the published work deals with the effect of various factors on the processes of deposition from the vapour phase and with the preparation of superconducting Y–Ba–Cu–O films of high quality (i.e. with high values of T_c and J_c). Thus, several workers[69–71] have determined the effect of the substrate material on the parameters of the superconducting film. The β-diketonates were deposited on different substrates, including MgO(100), $SrTiO_3$(100), ZrO_2(100), sapphire (1102), pure metals, and metals covered with a buffer layer of polycrystalline $SrTiO_3$. The best results (T_c = 90 K and ΔT_c = 2 K) were obtained[71] on $SrTiO_3$(100) substrates. These workers introduced the metal chelates into the reaction chamber in a stream of N_2 at temperatures above 100 °C. The residual pressure in the chamber was 1.01 × 10^4 Pa, and the oxygen partial pressure was 5.06 × 10^3 Pa. Singh et al.[72] tried to increase the stability of the film towards atmospheric degradation by depositing on the substrate a preliminary buffer layer of BaF_2. By chemically depositing $Y(TMHD)_3$, $Ba(TMHD)_2$, and $Cu(TMHD)_2$ from sources at temperatures of 150–250 °C on to a silicon substrate heated to 700 °C they obtained superconducting films with parameters T_c^H = 90 K and $T_c(\rho = 0)$ = 73 K.

Sugii et al.[73] studied the effect of the heat treatment temperature of the substrate on the properties of films prepared by the deposition of yttrium, barium, and copper 2,2,6,6-tetramethylheptan-3,5-dione complexes at temperatures in the range of 600–700 °C on monocrystalline $SrTiO_3$(100). It was established that the crystallinity, which was degraded by lowering the substrate temperature (T_c = 71 and 10 K for substrate heating temperatures of 650 and 600 °C respectively), could be restored by lowering the rate of addition of oxygen during the deposition process.

Attempts to lower the working temperature of the substrate by using a modified plasma method of chemical deposition from the vapour phase have been reported.[74–77] The presence of a plasma substantially alters the mechanism of film formation: the atomic mechanism is replaced by an atomic–ionic (or purely ionic) mechanism, which offers a large energy gain during compound formation. The Y–Ba–Cu–O films prepared at 580 °C had T_c = 82 K and $J_c = 10^6$ A cm^{-2} (at 50 K).[77] The effect of the vapour pressure of the organometallic compounds on the quality of the films has been studied.[78,79] It was found[78] that lowering the vapour pressure increases the $T_c(\rho = 0)$ temperature of the superconducting transition from 66 to 83 K. At the same time by lowering the pressure from 1.33 × 10^3 to 6.67 × 10^2 Pa the volatility of the yttrium and copper chelates was increased while that of the barium chelate remained unchanged, causing a depeltion of barium in the film. In order to obtain films of stoichiometric composition Kim et al.[79] increased the amount of the charge of barium 2,2,6,6-tetramethylheptan-3,5-dione in the reactor: this allowed them to prepare films of stoichiometric composition on an MgO substrate with T_c = 91 K (ΔT_c = 2 K), whereas on a substrate of $SrTiO_3$ they produced films with a critical current density of 10^5 A cm^{-2} in a zero magnetic field at 77 K.

The effect of the oxygen source (O_2, H_2O, O_2 + H_2O or N_2O) on the chemical deposition from the vapour phase of Y–Ba–Cu–O films by using metal β-diketonates containing (or not containing) fluorine atoms has been discussed.[80] The best conditions for the deposition of chelates without fluorine are found at low pressures and by using N_2O as the source of oxygen. With chelates containing fluorine better results are obtained by using O_2 and H_2O, but in this case the region of deposition of the required phase is narrowed. In a study[81] of the dependence of J_c and T_c on the thickness of $YBa_2Cu_3O_{7-x}$ films (0.2–2.4 μm), produced by coevaporation and heat treatment in O_2 and water vapour at 850 °C for 3.5 h on $SrTiO_3$(100) substrates it was found that J_c decreases exponentially from 1 × 10^6 to 4 × 10^3 A cm^{-2} as the film thickness is increased, whereas T_c falls from 90 to 85 K.

Khoroshun et al. [82] have proposed a new and apparently simpler aerosol method of chemical deposition of organometallic compounds from the gas phase. The main feature of this method is that predetermined amounts of the initial materials are introduced as aerosols into the reaction volume. Very thin monocrystalline $YBa_2Cu_3O_{7-x}$ films were prepared in this way. Films of thickness $d \geqslant 80$ nm had $T_c(\rho = 0)$ = 78–80 K and $\Delta T_c \approx 2$ K. The critical current density was 10^7 A cm^{-2} at 4.2 K in a magnetic field of 5 T. Thinner films (d = 10 nm) had $T_c(\rho = 0)$ = 50 K, $\Delta T_c \approx 13$ K.

2. Bi–Sr–Ca–Cu–O films

The preparation of Bi–Sr–Ca–Cu–O films is complicated by the existence of many cuprates of bismuth and of the alkaline

earths in this system, with similar thermodynamic characteristics.[83] The problem of the volatility of the initial components, which created the main difficulties in the synthesis of the Y–Ba–Cu–O films, is now of secondary importance because the β-diketonates of strontium and calcium are much more volatile than the corresponding barium compounds.[8] Bismuth is usually introduced as one of the volatile alcoholates or as a BiR_3 compound with various alkyl or aromatic radicals, because the β-diketonates of bismuth have not been adequately studied. A description of the synthesis and properties of the bismuth β-diketonates has been published very recently.[84]

Films of Bi–Sr–Ca–Cu–O have been synthesised[85,86] by using bismuth ethoxide and calcium, strontium, and copper dipivaloylmethanates. The deposits were produced on $ZrO_2(Y_2O_3)$ and MgO substrates at 800 and 900 °C respectively. Using a deposition rate of 8 μm h^{-1} gave superconducting films with T_c = 70–80 K and a tetragonal (or pseudotetragonal) lattice.

Several workers[87–93] used triphenylbismuth $Bi(C_6H_5)_3$ as the initial component for the deposition of Bi–Sr–Ca–Cu–O films. Some of these,[87,88] by combining this reactant with the β-diketonates of calcium, strontium, and copper, working at 550 °C, and heat treating the deposit in a stream of oxygen at 600–865 °C, obtained a superconducting film with T_c = 78.8 and ΔT_c = 7.7 K on an MgO(100) substrate (with some CuO phase as an impurity). An X-ray phase analysis of this system[88] detected the presence of a $Bi_2(Ca, Sr)_3Cu_2O_x$ phase with T_c = 85 K, and traces of phases with the lattice parameter c = 24.4 or 37 Å and T_c = 110 K. Bi–Sr–Ca–Cu–O films have been grown[89,90] on substrates of monocrystalline $SrTiO_3$(100) by using as the initial components triphenylbismuth, and also calcium, strontium, and copper 2,2,6,6-tetramethylheptan-3,5-dionates[89] and the fluorocarbon chelates of the same metals.[90] The use of lower pressures and a plasma gave[89] a single-phase film with its crystallographic c axis in a preferential orientation normal to the substrate surface. Nemoto and Yamana[90] used a horizontal quartz reactor with a residual pressure of ~1 Pa, and after heat treatment of the product they obtained films with T_c = 80 K and a zero resistance at 50 K.

Zhang et al.[91] described the synthesis of Bi–Sr–Ca–Cu–O films by the deposition of triphenylbismuth, copper acetylacetonate, and strontium and calcium dipivaloylmethanates on a polycrystalline silver substrate at 625–700 °C. Their films are a mixture of the $Bi_2(Sr, Ca)_2CuO_x$ and $Bi_2(Sr, Ca)_2Cu_3O_x$ phase, the proportion of the phase with T_c = 110 K increasing with the decomposition temperature. A study of these films by scanning electron microscopy showed that the deposition on polycrystalline silver greatly improves the texture and the morphology of the films as compared with those prepared on a magnesium oxide substrate. This effect was attributed to the nucleating properties of silver for films of the 2212 phase. The critical current density of these films was ~3.9×10^5 A cm^{-2} at 5.5 K.

The Bi-containing films were doped with lead in order to stabilise the high-temperature phase.[92] Bi–Pb–Sr–Ca–Cu–O films were prepared by two methods. In the first method the lead was introduced by depositing (alternately) Bi–Sr–Ca–Cu–O and PbO_x layers, using the volatile organometallic compounds $Cu[(CH_3)_2CHCOCOCH_3]_2$, $Sr[CH_2(COC(CH_3)_3)_2]_2$, $Ca[CH_2(COC(CH_3)_3)_2]_2$, $Bi(C_6H_5)_3$, and $Pb(C_6H_5)_4$. In the second method the lead was introduced in the initial deposition of the Bi–Sr–Ca–Cu–O film by using PbO as the source. The addition of lead greatly improves the crystal orientation and morphology of the films. On MgO(100) substrates films consisting mainly of the $Bi_2(Sr, Ca)_3Cu_2O_x$ phase were obtained, with T_c^H and $T_c(\rho = 0)$ equal to 110 and 80 K respectively. The formation of HTSC on MgO substrates at 850 °C has been monitored[93] by electron microscopy and X-ray phase analysis. It was established that the 2212 phase (with the lower critical temperature) is deposited during the early stages of the process. The 2223 phase is formed from the low-temperature phase after 30 min. Films 8 nm thick begin to be converted into the superconducting state at 110 K, and zero resistance is reached at 21 K.

Thus it follows from the results considered above that all the following modifications contribute to the stabilisation of the high-temperature $Bi_2SrCa_2Cu_3O_{10}$ with T_c = 110 °C: heating the substrate, plasma treatment during the growth of the film (followed by heat treatment), partial replacement (up to 30%) of the bismuth by lead, and a lengthy final heat treatment.

Volatile halides ($BiCl_3$, CuI_2, CaI_2, SrI_2), heated together in a single stream of inert gas, have been used[94–97] as the initial components for the synthesis of the films. In one method[94] the halides were placed in the tubular quartz reactor of a horizontal gradient furnace, each compound being located in a different temperature region: 150–250 °C for $BiCl_3$, 450–600 °C for CuI_2, 750–850 °C for CaI_2 and 800–850 °C for SrI_2. At the same time the substrate (heated to 800–850 °C) was placed in the region where the halide vapours came into contact with the water vapour entering the reactor with the external stream of inert gas, giving a pyrohydrolysis reaction. The film thus produced had the composition $BiSr_{0.8}CaCu_{3.7}O_x$, T_c = 70–80 K, and a critical current density of ~10^4 A cm^{-2} at 10 K. Films of a better quality were obtained[95] by omitting the additional heat treatment in oxygen. The films were deposited on an MgO(001) substrate at 700–850 °C from a gaseous mixture of halides which had reacted with oxidising agents (O_2 and H_2O). The films, of average thickness 0.1 μm, consisted of a mixture of phases with low or high critical temperatures (~80 and ~110 K). The films deposited at 850 °C had a zero resistance at 98 K. Their critical current density was ~1.7×10^4 A cm^{-2} at 4.2 K. The authors point out that the characteristics of the films depend both on the concentration of oxygen and on the deposition temperature. The structure of Bi–Sr–Ca–Cu–O, thin films deposited on MgO(001) from their chlorides or iodides with helium as the carrier gas and oxygen as the oxidising agent has been studied[97] by transmission electron microscopy. The best films, having a superconducting transition temperature of ~100 K, were oriented along their c axis, and consisted of large domains with an average size of 15–100 μm. Five types of layer were identified in the structure of the Bi–Sr–Ca–Cu–O films along the c axis, with crystal structures of the perovskite type and different thicknesses. It was pointed out that the phase with T_c = 80 K is predominant in these films, whereas the phase with T_c = 110 K is present in much smaller quantities.

3. Tl–Ca–Ba–Cu–O films

In the synthesis of films of high-temperature superconductors in the Tl–Ca–Ba–Cu–O system we again meet the problem of many possible phases. However, there are also other difficulties. Because of the high toxicity of thallium conventional evaporators cannot be used. To avoid contaminating the surface of the apparatus the toxic thallium compounds have to be kept in traps cooled in liquid nitrogen.[98] Because of the high volatility of the oxide Tl_2O_3 the heat treatment temperature of the thallium films must be very accurately controlled. However, the high volatility of thallium oxide can be exploited in the technological process for saturating the Ba–Ca–Cu–O film with the vapour of this compound.[99–102]

Lin and Wu[99] placed a Ba–Ca–Cu–O film prepared by magnetron evaporation in an Al_2O_3 boat at the centre of a tube furnace which also contained a crucible filled with powdered thallium oxide. After holding the charge for 15–60 min at 925 °C a film with $T_c^H \approx$ 120 K and zero resistance at 78 K was obtained. The main superconducting phase was the 2122 phase, which was found to contain large quantities of $BaCuO_2$, $CaCuO_2$, CuO, and other impurities. Other workers[100] used both pure thallium oxide and a mixture of powdered Tl_2O_3, BaO_2, CaO_2, and CuO heated at 895 °C to impregnate a film of Ba–Ca–Cu–O prepared by the pyrolysis of the salts of organic acids. This method gave thick films with T_c^H = 126 K and zero

resistance at 108 K, the high-temperature 2223 phase being dominant in the second case.

The use of massive ceramic samples as sources of thallium oxide allows films of stoichiometric composition to be synthesised, because the reaction takes place under thermodynamic equilibrium conditions.[83] The best film samples, containing mainly the highly oriented $Tl_2Ca_2Ba_2Cu_3O_{10+y}$ phase and traces of the $Tl_2CaBa_2Cu_2O_{8+y}$ phase were obtained[102] at 895–900 °C (in the region of the Ba–Ca–Cu–O film sample) and 810–805 °C (in the region of the Tl_2O_3 boat). These films had $T_c(\rho = 0) = 95-105$ K and a critical current density of 28 800 A cm^{-2} at 77 K in a zero magnetic field. It is pointed out that the films with the highest critical current densities have a highly textured structure consisting of platelet crystallites.

The preparation of high-temperature superconductor films in the Tl–Ba–Ca–Cu–O system by the direct CVD method has been reported.[103–106] Ba–Ca–Cu–O films were synthesised[103] on $ZrO_2(Y_2O_3)$ substrates using barium heptafluorodimethyloctandionate, calcium dipivaloyldimethanate, and copper acetylacetonate as the initial components. The thallium was introduced by two methods: as the gas phase from a solid source containing Tl, Ba, Ca, and Cu, and as the organometallic compound cyclopentadienylthallium. The films thus obtained consisted mainly of the $TlBa_2Ca_2Cu_3O_x$ phase with T_c = 100 K. Highly oriented epitaxial films of the 2122 phase with T_c > 105 K were synthesised[104] by decomposing organic compounds of thallium, calcium, barium, and copper on the surface of an MgO(100) crystal. By doubly annealing $Tl_2CaBa_2Cu_2O_y$ on sapphire substrates at 850 and 500 °C (the first anneal being in the presence of $Tl_2CaBa_2Cu_2O_y$ wafers for 40 min) Zhang et al.[105] increased $T_c(\rho = 0)$ from 87.5 to 94 K, but the films were contaminated by traces of the $BaCO_3$ and Ca_2Cu_3O phase. The best samples of thallium films were synthesised by Hamaguchi et al.,[106] who prepared oriented films of $Tl_2Ba_2Ca_{1.4}Cu_2O_x$ and $Tl_2Ba_2Ca_{2.3}Cu_3O_x$ by chemical deposition in the gas phase on monocrystalline MgO(100) substrates. The stoichiometry of the films was preserved by annealing them in dry oxygen in the presence of Tl_2O_3 vapour at 850–900 °C. These films had T_c^H and $T_c(\rho = 0)$ equal to 125 and 109 K respectively, and their critical current density was 10^4 A cm^{-2} at 90 K

* * *

This analysis of published results in the chemistry of volatile β-diketonates has shown that because of their high volatility at relatively low temperatures and of their thermal stability these materials have been widely applied in the synthesis of thin films of high-temperature superconductors containing yttrium, bismuth, and thallium.

The volatility of the β-diketonates is determined by their composition and structure, and depends on the nature of the complex-forming metal, on the coordinational saturation of the complexes, and on the degree of branching of the hydrocarbon end groups. The highest volatility is found in the coordinationally saturated complexes, which do not readily form oligomers or hydrogen bonds. Replacing the hydrogen in the end methyl groups by fluorine causes a large increase in the volatility. In order to improve the thermal stability we can use complexes containing a *tert*-butyl radical as well a a fluorinated radical.

In the gaseous state the metal β-diketonates exist as two isomeric forms in equilibrium: the chelate and the open ring. The quantitative relationship between the bidentate and the monodentate coordinated forms depends both on the temperature and on the energy of the M–O bond in the complex. The possible mechanisms of the exchange reactions in the vapour formation process discussed above should be allowed for when thin films are synthesised from the gas phase. The thermal stability of the β-diketonates in the gas phase is strongly influenced by oxygen, and also by the presence of other volatile β-diketonates, used as the initial components for the synthesis of the thin films. The high quality and the characteristics of the high-temperature superconducting films prepared in many laboratories by CVD confirm that this method offers very attractive prospects.

References

1. A R Kaul' *Zh. Vses. Khim. Ova im D.I.Mendeleeva* **34** 492 (1989)
2. A I Golovashkin *Zh. Vses. Khim. Ova im D.I.Mendeleeva* **34** 481 (1989)
3. M Schieber *J. Cryst. Growth* **109** 401 (1991)
4. H Yamane *Chem. Lett.* 939 (1988)
5. A D Berry *Appl. Phys. Lett.* **52** 1743 (1988)
6. I K Igumenov, Yu V Chumachenko, S V Zemskov, in *Problemy Khimii i Primeneniya β-Diketonatov Metallov* (Problems of the Chemistry and Application of Metal β-Diketones) (Moscow: Nauka, 1982) p. 10
7. V Yu Golubtsova, I A Murav'eva, L I Martynenko *Teoreticheskaya i Prikladnaya Khimiya β-Diketonatov Metallov* (Theoretical and Applied Chemistry of Metal β-Diketones) (Moscow: Nauka, 1985)
8. D N Sokolov *Gazovaya Khromatografiya Letuchikh Kompleksov Metallov* (Gas Chromatography of Light Complexes of Metals) (Moscow: Nauka, 1981)
9. L I Martynenko, V I Spitsyn, I A Murav'eva, in *β-Diketonaty Metallov* (β-Diketones of Metals) (Moscow: Nauka, 1978) p. 5
10. T Kuwamoto *Jpn. Anal.* **21** 445 (1972)
11. A Kito, Y Migake, Kabayashi *Jpn. Anal.* **20** 1363 (1971)
12. L M Moiseeva, N M Kuznetsova, G T Stepanova, in *β-Diketonaty Metallov* (β-Diketones of Metals) (Moscow: Nauka, 1978) p. 106
13. J E Schwarberg, R E Sievers, R W Moshier *Anal. Chem.* **42** 1828 (1970)
14. T Okubo, F Aoki *J. Chem. Soc. Jpn., Chem. Ind. Chem.* 1681 (1973)
15. T Okubo, F Aoki *J. Natl. Chem. Lab. Ind.* **69** 44 (1974)
16. A Kito, Y Mayake *Bull. Govt. Ind. Res. Inst., Osaka* **25** 93 (1974)
17. H A Swain, D G Karraker *Inorg. Chem.* **9** 1766 (1970)
18. J E Sicre, J T Dubois, K J Eisentraut *J. Am. Chem. Soc.* **91** 3476 (1969)
19. R W Moshier, R E Sievers *Gas Chromatography of Metal Chelates* (Translated into Russian; Moscow: Mir, 1967)
20. A G Goryushko, N K Davidenko, in *β-Diketonaty Metallov* (β-Diketones of Metals) (Moscow: Nauka, 1978) p. 24
21. J Zhao *Appl. Phys. Lett.* **53** 1750 (1988)
22. A J Panson *Appl. Phys. Lett.* **53** 1756 (1988)
23. K Utsunoniya, T Shigematsu *Bull. Chem. Soc. Jpn.* **45** 303 (1972)
24. I K Igumenov, Yu V Chumachenko, S V Zemskov *Zh. Koordinats. Khim.* **4** 163 (1978)
25. I K Igumenov, Yu V Chumachenko, S V Zemskov, in *Stroenie, Svoistva i Primenenie β-Diketonatov Metallov* (Structure, Properties and Application of Metal β-Diketones) (Moscow: Nauka, 1978) p. 105
26. I P Malkerova, A S Alikhanyan, I Yu Filatov *Zh.Neorg. Khim.* **36** 3112 (1991)
27. N B Morozova, G I Zhirnova, P A Stabnikov *Sintez i Fiziko-khimicheskoe Issledovanie β-Diketonatov Shchelochnozemel'nykh Metallov* (Synthesis and Physicochemical Investigation of β-Diketones of Alkaline-earth Metals) (Novosibirsk, 1989) Preprint Inst. Neorg. Khim. Sib. Otd. Akad. Nauk SSSR, No 89-06
28. N P Kuz'mina, I G Zaitseva, M V Chechernikova *Zh. Neorg. Khim.* **36** 2739 (1991)
29. L I Martynenko *Vysokochistye Veshchestva* 88 (1987)
30. D C Nonhebel *J. Chem. Soc.* 738 (1963)
31. J S Hommond, D C Nonhebel, C W Wu *Inorg. Chem.* **2** 73 (1963)
32. R West *J. Am. Chem. Soc.* **80** 3246 (1958)
33. J J Howe, T J Pinnavaia *J. Am. Chem. Soc.* **91** 5378 (1969)
34. L M Shkol'nikova, M A Porai-Koshits, in *Kristallokhimiya. (Itogi Nauki i Tekhniki T. 16)* [Crystal Chemistry (Advances in Science and Engineering, Vol.16)] (Moscow: Izd. VINITI, 1982) p. 117
35. P P Semyannikova, Candidate's Thesis in Chemical Sciences, Inst. Neorg. Khim. Sib. Otd. Akad. Nauk SSSR, Novosibirsk, 1989
36. E A Mazurenko *Zh. Koord. Khim.* **13** 1313 (1987)

37. A S Alikhanyan, I P Malkerova, I P Kazanskaya *Zh. Neorg. Khim.* **36** 3107 (1991)
38. C Sant, O Poncelet, M Laugt *Couches. Minces* **45** 205 (1990)
39. E I Tsyganova, G A Mazurenko, V V Drobotenko, in *Primenenie Metalloorganicheskikh Soedinenii dlya Polucheniya Neorganicheskikh Pokrytii i Materialov Ch. 1* (Application of Metalloorganic Compounds for Receiving Inorganic Cover and Materials Pt 1) (Nizhnii Novgorod, 1991) p. 166
40. E I Tsyganova, V I Faerman, L M Dyagileva, in *Primenenie Metalloorganicheskikh Soedinenii dlya Polucheniya Neorganicheskikh Pokrytii i Materialov Ch. 1* (Application of Metalloorganic Compounds for Receiving Inorganic Cover and Materials Pt 1) (Nizhnii Novgorod, 1991) p. 163
41. E I Tsyganova, O M Titova, L M Dyagileva, in *Primenenie Metalloorganicheskikh Soedinenii dlya Polucheniya Neorganicheskikh Pokrytii i Materialov Ch. 1* (Application of Metalloorganic Compounds for Receiving Inorganic Cover and Materials Pt 1) (Nizhnii Novgorod, 1991) p. 161
42. S A Gromilov, I A Baidina, S A Stabnikov, in *Primenenie Metalloorganicheskikh Soedinenii dlya Polucheniya Neorganicheskikh Pokrytii i Materialov Ch. 1* (Application of Metalloorganic Compounds for Receiving Inorganic Cover and Materials Pt 1) (Nizhnii Novgorod, 1991) p. 148
43. N E Fedotova, I K Igumenov, A F Bykov, in *Primenenie Metalloorganicheskikh Soedinenii dlya Polucheniya Neorganicheskikh Pokrytii i Materialov Ch. 1* (Application of Metalloorganic Compounds for Receiving Inorganic Cover and Materials Pt 1) (Nizhnii Novgorod, 1991) p. 158
44. P P Semyannikov, V M Grankin, G I Zharkova, in *Primenenie Metalloorganicheskikh Soedinenii dlya Polucheniya Neorganicheskikh Pokrytii i Materialov Ch. 1* (Application of Metalloorganic Compounds for Receiving Inorganic Cover and Materials Pt 1) (Nizhnii Novgorod, 1991) p. 127
45. A F Bykov, P P Semyannikov, I K Igumenov, in *Primenenie Metalloorganicheskikh Soedinenii dlya Polucheniya Neorganicheskikh Pokrytii i Materialov Ch. 1* (Application of Metalloorganic Compounds for Receiving Inorganic Cover and Materials Pt 1) (Nizhnii Novgorod, 1991) p. 157
46. A F Bykov, P P Semyannikov, I K Igumenov, in *Primenenie Metalloorganicheskikh Soedinenii dlya Polucheniya Neorganicheskikh Pokrytii i Materialov Ch. 1* (Application of Metalloorganic Compounds for Receiving Inorganic Cover and Materials Pt 1) (Nizhnii Novgorod, 1991) p. 160
47. S G Konstantinov, in *Teoreticheskaya i Prikladnaya Khimiya β-Diketonatov Metallov* (Theoretical and Applied Chemistry of Metal β-Diketones) (Moscow: Nauka, 1985) p. 148
48. W R Wolf, R E Sievers, G H Brown *Inorg. Chem.* **11** 1995 (1972)
49. H Abe *Jpn. J. Appl. Phys.* **27** L1473 (1988)
50. K Shinohara, F Manakata, M Yamanaka *Jpn. J. Appl. Phys.* **27** L1683 (1988)
51. H Yamane *Appl. Phys. Lett.* **52** 1743 (1988)
52. H Yamane *Jpn. J. Appl. Phys.* **27** L1275 (1988)
53. H Yamane *Seramikkusu Ronbunshi* **96** 799 (1988)
54. H Yamane *J. Ceram. Soc. Jpn. Int. Ed.* **96** 776 (1988)
55. H Yamane *Appl. Phys. Lett.* **53** 1548 (1988)
56. H Yamane *Superconductivity News* **21** 11 (1988)
57. Y Muto *Physica, C* **162–164** 105 (1989)
58. K Watanabe *Appl. Phys. Lett.* **56** 1490 (1990)
59. T Nakamori *Jpn. J. Appl. Phys.* **27** L1265 (1988)
60. K Zhang, B S Kwab, E P Boyd *Appl. Phys. Lett.* **54** 380 (1989)
61. D W Noh, B Gallois, C S Chern *J. Appl. Phys.* **66** 5099 (1989)
62. F Schmaderer, R Huber, H Oetzmann *Appl. Surface Sci.* **46** 53 (1990)
63. F Radpour, R Singh, S Singh *J. Electrochem. Soc.* **137** 2462 (1990)
64. O C Gonzalex, H Schachner, H Tippmann *Physica* 1042 (1988)
65. A Gupta *J. Am. Chem. Soc.* **110** 265 (1988)
66. S W Chan *Appl. Phys. Lett.* **53** 1443 (1988)
67. K Endo, S Misawa, S Hoshida *Showo Wire and Cable Rev.* **40** 66 (1990)
68. J Zhao, H O Mar Cy, L M Tonge *Physica, C* **159** 710 (1989)
69. R B Laibowitz *Thin Film Process and Charact. High-Temp. Supercond: Top. Conf.: Anaheim. Calif. Nov., 6, 1987* (New York, 1988) p. 2
70. T Yamagachi, S Aoki *Appl. Phys. Lett.* **55** 1581 (1989)
71. P A Zawadzki, G S Tompa, P E Norris *J. Electron. Mater.* **19** 357 (1990)
72. R Singh, S Sinha, N J Hsu *J. Appl. Phys.* **67** 3764 (1990)
73. N Sugii, K Kanehori, K Miyauchi *Solid State Ionics, Pt.2* 819 (1990)
74. H Suhr, Ch Ochr, H Holzschuh *Physica* 784 (1988)
75. G R Bai, W Tao, R Wang *Appl. Phys. Lett.* **55** 194 (1989)
76. J Zhao, D W Noh, C Chern *J. Electrochem. Soc.* **137** 226C (1990)
77. J Zhao, C S Chern, B Kear *J. Cryst. Growth* **107** 699 (1991)
78. K Kanehori, N Sughii, T Fakazawa *Thin Solid Films* **182** 265 (1989)
79. S H Kim, C H Cho, K S No *J. Mater. Res.* **6** 704 (1991)
80. A Harsta, J O Carlsson *J. Cryst. Growth* **110** 631 (1991)
81. A Mogro-Campero, L C Turner, E L Hall *Supercond. Sci. Technol.* **3** 62 (1990)
82. J V Khoroshun, E V Karyaev, V T Moshnyaga *Supercond. Sci. Technol.* **3** 493 (1990)
83. G Yu Grigor'ev *Sverkhprovodimost': Fizika, Khimiya, Tekhnika* **3** 1761 (1990)
84. A P Pisarevskii, L I Martynenko, N G Dzyubenko *Zh. Neorg. Khim.* **37** 72 (1992)
85. H Jamane, H Kurosawa, T Hirai *Chem. Lett.* **9** 1515 (1988)
86. H Jamane *Jpn. J. Appl. Phys.* **27** L1495 (1988)
87. A D Berry, D T Holm, E J Cukauskas *J. Cryst. Growth* **92** 344 (1988)
88. J Zhang, J Zhao, H O Marcy *Appl. Phys. Lett.* **54** 1166 (1989)
89. K Kabayashi, S Ichikawa, G Okada *Chem. Lett.* 1415 (1989)
90. M Nemoto, M Yamana *J. Mater. Res.* **5** 1 (1990)
91. J M Zhang, B W Wessels, D S Richeson *J. Cryst. Growth* **107** 705 (1991)
92. J M Zhang, H O Marcy, L M Tonge *Appl. Phys. Lett.* **55** 1906 (1989)
93. T Sugimoto, M Yoshida, K Yamaguchi *J. Cryst. Growth* **107** 692 (1991)
94. M Ihara, T Kimura, H Yamawaki *IEEE Trans. Magn.* **25** 2470 (1989)
95. T Kimura, M Ihara, H Yamawaki, in *Adv. Superconductivity: Proc. 1st. Int. Symp. Superconductivity, Nagoya, Aug. 28–31, 1988: ISS'88* (Tokyo, 1989) p. 495
96. A Harsta, J-O Carlsson *J. Cryst. Growth* **98** 561 (1989)
97. O Ueda, T Kimura, H Yamada *J. Cryst. Growth* **99** 958 (1990)
98. M Hong *Superconducting Thin Films in Tl–Ba–Ca–Cu–O System: AT & T Bell. Lab., Rep. Presented at Int. Conf.* (Hsinchu, Taiwan, 1989)
99. R J Lin, P T Wu *Jpn. J. Appl. Phys.* **28** L85 (1989)
100. R Sugise, M Hirabayashi, N Terada *Jpn. J. Appl. Phys.* **27** L2314 (1988)
101. D S Ginley, J F Kwak, R P Hellmer *Physica, C* **156** 592 (1988)
102. J A De Luca, M F Garbauskas, R B Bolon *J. Mater. Res.* **6** 1415 (1991)
103. S Richeson Darrin, M Tonge Lanen, Zhao Jing *Appl. Phys. Lett.* **54** 2154 (1989)
104. W L Olson, M M Eddy, T W James *Appl. Phys. Lett.* **55** 188 (1989)
105. K Zhang, E P Boyd, B S Kwab *Appl. Phys. Lett.* **55** 1258 (1989)
106. N Hamaguchi, R Gardiner, P S Kirlin *Appl. Surface Sci.* 411 (1991)

Russian Chemical Reviews **62** (11) 991 – 1003 (1993)
© 1993 Russian Academy of Sciences and Turpion Ltd

UDC 541.1;537.228;539.16

Electric charge in irradiated dielectrics, and their properties

V V Gromov

Contents

I.	Introduction	991
II.	Analysis of the space charging process. Microscopic approach. Irradiation with electrons	992
III.	Formation of an electric space charge. Total current model	993
IV.	Charging processes during the irradiation of dielectrics by γ quanta	993
V.	Electric charge of radioactive substances	995
VI.	The charging of radioactive samples	996
VII.	Charge and properties of solids	998
VIII.	Dissolution kinetics of charged crystalline substances	1000
IX.	Conclusions	1002

Abstract. The formation of a space charge in dielectrics under the influence of ionising radiation (one of the fundamental effects stimulated by the irradiation of solids) is discussed. An increasing interest in this problem has been generated by the wide use of powerful sources of ionising radiation in both science and technology. Radioactive dielectrics, i.e. highly resistive solids of various natures (glasses, crystalline compounds, ceramics, etc) containing a permanent source of ionising radiation (radionuclides) occupy a special place in this field of study. These materials are used, for example, for the treatment and consolidation of nuclear waste in atomic technology. It has been experimentally established that the properties of irradiated dielectrics are affected not only by the presence of space charge resulting from the permanent self-irradiation but also by the form of the charge distribution in the volume of the dielectric. Examples of the relationship between the volume charging of radioactive and of irradiated dielectrics and the characteristics of the materials such as their dissolution kinetics, mechanical and electrophysical properties, redistribution of the energy absorbed from the ionising radiation, etc, are discussed. The bibliography includes 42 references.

I. Introduction

The formation of substantial space charges in solids during their interaction with ionising radiation (radiation charging) was first recognised as an independent physical phenomenon during studies of radioactive salts. In 1900 Pierre and Marie Curie published the results of their study of the formation of space charge in radioactive preparations of $Ba(Ra)Cl_2$.[1] The chosen experimental method allowed them to establish the sign but not the magnitude of the stationary space charge†, since only the current of ionising species from the sample was monitored. Unfortunately, no other studies of the charging of radioactive samples were published at the time.

Almost the whole of the later work in this field was aimed at solving the fundamental technical problem of creating 'radioactive current sources' (atomic batteries). Some current sources of this type operate on the principle of collecting the charges on a collector separated from the radioactive preparation by an insulating layer.[2] Their operation is very closely associated with the accumulation and redistribution of charges in a heterogeneous medium consisting of a source of radiation, a dielectric interlayer, and a collector.

Similar effects have been noted in the interaction of accelerated electrons, γ quanta, and other ionising species with various solid materials. Even the irradiation with electrons having an energy of 50 – 100 keV, in an electron microscope, stimulates the explosive breakdown[3] of crystals such as $BaSO_4$ and KCl as a result of the accumulation of electric charges in the bulk of the crystals. Explosions due to the internal charging of the lead walls of protective chambers used in operations with a ^{60}Co γ source (several hundreds of curies) have had disastrous consequences.[4]

'Radiation charging' can also affect the properties of solids.[5] The catalytic activity of solids, their dissolution and vaporisation kinetics, and their electrochemical and other properties are all extremely sensitive to radiation charging. Thus, any solid having an electric resistivity greater than 10^{12} Ω m passes into the 'electret state' after lengthy irradiation.[6] For example, in ordinary window glass the space charge produced by electron irradiation decreases two-fold[7] after ~100 h.

In general the following changes take place in all dielectrics exposed to ionising radiation: the formation of primary and secondary radiation-induced defects (excited and ionised particles, localised holes and electrons, displaced atoms, etc); local disordering of the dielectric structure (thermal cracks, recrystallisation); radiation-chemical decomposition (degradation) of the material, characteristic of complex organic

V V Gromov Institute of Physical Chemistry, Russian Academy of Sciences, Leninskii prosp. 31, 117915 Moscow,
Fax (7-095) 335 17 89

Received 12 July 1993
Uspekhi Khimii **62** (11) 1064 – 1077; translated by J I Carasso

† The term stationary space charge denotes the maximum charge (in equilibrium under the stated conditions) found in the sample during irradiation.

molecules, followed by the evolution of volatile radiolysis products; strong local heat evolution (especially during irradiation with powerful beams of accelerated electrons), accompanied by the formation of large thermal stresses in a region of radius equal to one-third the penetration (range) of electrons in the substance, possibly leading to the evaporation of the substance by a microexplosion; the accumulation of electric space charge, often up to levels where spontaneous electric discharges can take place, leading to the breakdown of the material.

All these processes affect the properties of dielectrics, and in particular they degrade the radiation stability of electric insulators, enhance their electric conductivity, lower their mechanical strength, etc.

Irrespective of the formation conditions of the electric space charge (external irradiation, or self-irradiation in the case of radioactive materials) the formation mechanisms of the radiation-induced charge exploit the following basic processes: the retardation of the charged particles in the bulk of the irradiated uniform material (for example, in a heterogeneous system) and the appearance of electric charging as a result of the gradient (in space) of the flow density of ionising radiation.

In all these systems we observe a macroscopically nonuniform distribution of charge density over the volume of the solid, which in the case of radioactive dielectrics (ceramics, glasses, salts) is retained almost indefinitely as long as radionuclides remain in the sample. Because of the accumulation of space charge, conditions favourable to local electric discharges may be produced. This phenomenon, together with the formation of radiation-induced damage, should be interpreted as one of the fundamental effects associated with the action of ionising radiation on solid dielectrics. Under these conditions the energy needed to break down the material radiation-electrically is very much smaller than the energy needed for the purely radiation-mechanical degradation.

II. Analysis of the space charging process. Microscopic approach. Irradiation with electrons

The most thorough analysis of the models that have been proposed for the dynamics and the kinetics of the formation of space charge can be found in the work of Tyutnev et al.[8] and Evdokimov.[9] The following are the main propositions underlying the general approach to the solution of this problem: the dielectric contains both free and trapped charge carriers of different signs (electrons and holes); the action of the ionising radiation on the medium produces, in addition to excess (thermalised) electrons, also carriers of each sign, in equal amounts, as a result of the ionisation of the medium; a loss of carriers is produced by their recombination and drift towards the sample surface under the influence of the space-charge field; the irradiation acts on the trapping centres, i.e. the degree of filling of the traps by carriers may depend on the radiation dose; carriers of both signs contribute to the charge transfer; the diffusion component of the current of carriers is ignored; the charge transfer obeys Ohm's law. The polarisation of the dielectric under the influence of the space charge is indirectly allowed for in the analysis of the charge dynamics by postulating the presence of deep as well as of shallow traps. Furthermore it is assumed that the dielectric is isotropic in its properties, though this stipulation is valid only for amorphous materials. However, the assumption allows us to write the kinetic equations in a one-dimensional variant, which simplifies the solution:

$$\frac{\partial n}{\partial t} - \mu_n \frac{\partial (En_0)}{\partial x} = G + G_n - k_1 n_0 p - k_2 n p_0 , \tag{1}$$

$$\frac{\partial p}{\partial t} - \mu_p \frac{\partial (Ep_0)}{\partial x} = G - k_1 n_0 p - k_2 n p_0 , \tag{2}$$

$$\frac{\partial n_T}{\partial t} = k_{3,n} n_0 [M_n(\xi) - n_T] - \nu_{0,n} \exp\left(-\frac{\xi}{kT}\right) n_T - k_2 p_0 n_T , \tag{3}$$

$$\frac{\partial p_T}{\partial t} = k_{3,p} p_0 [M_p(\xi) - p_T] - \nu_{0,p} \exp\left(-\frac{\xi}{kT}\right) p_T - k_1 n_0 p_T , \tag{4}$$

$$n = n_0 + \int_0^\infty n_T \, d\xi ; \qquad p = p_0 + \int_0^\infty p_T \, d\xi ; \tag{5}$$

$$\frac{dE}{dx} = e \frac{p - n}{\varepsilon \varepsilon_0} , \tag{6}$$

where e is the electronic charge; n is the total concentration of electrons in the dielectric, equal to the concentration of holes; n_0 is the concentration of mobile quasi-free electrons having a mobility μ_n; G is the rate of injection of free electrons and holes into the volume during the irradiation of the dielectric; k_1 and k_2 are the rate constants of the bimolecular recombination of the carriers; k_3 is the rate constant for the capture of the quasi-free carriers; n_T and p_T are the densities of trapped (thermalised) electrons and holes respectively for the trap energy range $\xi \to (\xi + d\xi)$; ξ is the energy depth of the traps, measured from the bottom of the conduction band; $M_n(\xi)$ is the energy density of the distribution of electron traps; ν_0 is the frequency factor; G_n is the rate of the volume injection of electrons; the symbol p refers to holes (everywhere); E is the field generated by the space charge; k is Boltzmann's constant.

The functions of the carrier sources $G(x,t)$ and $G_n(x,t)$ depend on the irradiation conditions, on the type of radiation, on the thickness of the sample, and on the strength of the electric field produced by the space charge (i.e. they depend also on the local absorbed dose rate). The latter dependence makes the system of equations (1)–(6) strongly nonlinear. Therefore special cases of the solution are usually considered separately.

To make the discussion specific we shall examine only one variant, very often met in practice: the irradiation of a plate having end faces covered with a conducting layer, i.e. a short-circuited flat dielectric of thickness h. The system of equations (1)–(6) must now be supplemented by

$$\int_0^h E(x,t) dx = 0 . \tag{7}$$

The most difficult step in the solution of this problem is the evaluation of the source functions $G(x,t)$ and $G_n(x,t)$. It is often convenient to use the Monte Carlo method in the continuous retardation of the injected electrons approximation, to rely on semiempirical dependences, or to determine these functions by direct measurements.[8-11]

Case 1. The dielectric is irradiated with fast electrons whose depth of penetration exceeds the thickness of the sample. These conditions produce a uniform distribution of the absorbed dose and of the sources of thermalised electrons over the sample volume, i.e. they give a uniform primary distribution of space charge. Furthermore it is assumed that only the electrons behave as mobile charge carriers. Under these conditions the solution of the system of equations (1)–(7) takes the form

$$\bar{n}_0 = \left[\frac{(G + G_n) \sin \alpha\pi}{k_1 M_0 \alpha\pi}\right]^{\Delta} \left(\frac{\nu_0}{k_{3,n}}\right)^{\alpha/(1+\alpha)} , \tag{8}$$

where $\bar{n}_0$ is the stationary concentration of electrons; M_0 is the stationary distribution of the trap energy density; $\Delta = (1 + \alpha)^{-1}$; α is the dispersion parameter, equal to T/T_1 [where T is the temperature of the sample and T_1 is the distribution parameter of $M(\xi)$].

For the distribution of the electric field strength we can write

$$E(x) = -\frac{G_n}{\mu_n \bar{n}_0} x , \tag{9}$$

and the maximum value of the field is $G_0 h / 2\mu_n \bar{n}_0$. It follows from Eqn (9) that the field created by the space charge is proportional to the rate of injection of the carriers and inversely proportional to their loss rate. The conditions of space charge accumulation for

which $n \gg p$ are called the 'space charge current regime', whereas with $n \approx p$ we are in the 'plasma injection regime'. Thus, in this regime of space-charge accumulation the charge distribution is determined mainly by functions of the carrier sources in the bulk of the given sample, i.e. $G(x,t)$ and $G_n(x,t)$.

Case 2. The conditions specified above are supplemented by the assumption that both electrons and holes are mobile in the dielectric, and furthermore that $\mu_n = \mu_p$, $v_{0,n} = v_{0,p}$. For the stationary regime the space charge ($\bar{n}_0$) can be calculated by the equation

$$\bar{n} = \frac{\bar{n}_0}{(\bar{p} + \gamma_i \bar{n}_0)^{1-\alpha}} \left(\frac{k_3}{v_{0,n}}\right)^{\alpha} \frac{\alpha\pi}{\sin \alpha\pi} M_n \gamma_i^{1-\alpha}, \tag{10}$$

where γ_i is the radiation-induced electric conductivity of the dielectric. The stationary concentration of holes is

$$\bar{p}_0 = \left(\frac{G \sin \alpha\pi}{2M_p k_2 \alpha\pi}\right)^{A} \left(\frac{v_{0,p}}{k_3}\right)^{\alpha/(1+\alpha)} (1 + \gamma_i)^{(1-\alpha)/(1+\alpha)}. \tag{11}$$

An important aspect of this approach to the solution of the problem of space charge formation is that the final expressions contain microscopic characteristics of the dielectric such as $M(\xi)$, μ_n, μ_p, and α. Therefore it should be possible to find the microscopic parameters of the carrier migration from the experimentally determined macroscopic parameters which characterise the space charge.

III. Formation of an electric space charge. Total current model

In the present approach to the analysis of the formation of a space charge only the macroscopic (averaged) characteristics of the dielectric are taken into account: its electric conductivity (γ_0); its dielectric permittivity (ε), and the effective mobility of its carriers (μ), treated as a phenomenological quantity.[6-12] The most important component of the electric conductivity of a dielectric being irradiated (or previously irradiated) is its radiational component γ_i, which cannot be calculated by existing theoretical methods. Therefore it is usually determined either experimentally or from empirical relationships.

In the analysis of the formation of space charge in terms of the macroscopic approach an expression for the total current can be obtained in the one-dimensional variant. It is often called the total current integral:

$$J = \varepsilon\varepsilon_0 \frac{\partial E(x,t)}{\partial t} + \gamma_i(x,t)E(x,t) + j(x,t), \tag{12}$$

where all the currents are assumed to be calculated for unit area of the irradiated surface; ε_0 is the dielectric permittivity of a vacuum (equal to 8.85×10^{-14} F cm^{-1}); γ_i is the radiation-induced electric conductivity, depending on the local dose rate during irradiation (and in general on the density of the majority carriers, i.e. on the distribution of the space charge). Furthermore, in dielectrics $\gamma_i \gg \gamma_0$; $j(x,t)$ is the current density of the injected carriers. The first term in Eqn (12) corresponds to the displacement current, the second to the 'leakage' (or conduction) current; $E(x, t)$ is the field generated by the space charge. As before, the diffusion component of the conduction current is assumed to be negligibly small. Let us use Eqn (12) to examine different cases of the formation of space charge.

By adopting the total current model it is relatively simple to find the time dependence of the space charge density, i.e. $\rho(t)$. Thus by assuming that in the stationary regime (charge accumulation $\leftrightarrow$ leakage) discharge takes place mainly through the irradiated part of the dielectric we arrive at the following expression from Eqn (12)

$$\rho(x,t) = \frac{j(x,t)\varepsilon\varepsilon_0}{S\gamma_i}\left[1 - \exp\left(-\frac{t}{\tau_i}\right)\right], \tag{13}$$

where $\tau_i = \varepsilon\varepsilon_0/\gamma_i$; S is the surface area of the sample. This expression clearly shows the change in space charge with irradiation time for a material having purely electronic conduction. It was first obtained empirically.[6] It should not be forgotten that under our irradiation conditions the stationary space charge ρ_{st} (for $t \to \infty$) is given, according to (13), by

$$\rho_{st} = \frac{j_i(x)\tau_i}{S}, \tag{14}$$

i.e. it is limited only by the values of j_i and τ_i. With large injection currents j_i electric breakdowns can take place in the dielectric even before the formation of a space charge ρ_{st}. This suggests that the accumulation of space charge is limited by the dielectric strength of the material. Therefore electric breakdown occurs under the condition

$$j_i > j_l, \tag{15}$$

where j_l is the leakage current in the given sample during the irradiation, and the time changes of the space-charge field (at every point of the dielectric being irradiated) are described by an expression analogous to formula (13).

IV. Charging processes during the irradiation of dielectrics by γ quanta

In contrast to the widely investigated aspects of the formation of a stationary charge as a result of the action of fast electrons on dielectric materials the charging of highly insulating solid samples in a field of γ radiation has been poorly investigated, even though the first publications in both these fields appeared at about the same time. This state of affairs probably arose because the use of accelerated electrons to inject electric space charge into a dielectric is experimentally more convenient than the use of γ rays.

γ Quanta are not electric charge carriers, and in this case the charging is a secondary process induced by the ionisation of the irradiated material and by the redistribution of the resulting carriers (mainly Compton electrons) over the volume of the dielectric. From this standpoint there is a great deal in common between charging by the interaction of electrons with the material and charging by γ radiation.

Even the earliest experiments with γ-irradiated dielectric materials detected undeniable charge effects. Thus, it was shown that a substantial amount of electric charge can accumulate in borosilicate glasses under the influence of γ quanta.[13] The following experimental technique was used. After being irradiated in a cobalt source [absorbed dose 4×10^4 Gy (4 Mrad)] the glass samples in the form of disks fitted with pressure ohmic contacts were heated at 300 °C while maintaining a temperature difference of 30–50 K between the contacts. As a result of the heat treatment the injected charge leaked to the external circuit, producing a current of 10^{-12} A. The charge leaking to the contact which was held at the higher temperature was always negative, denoting a correlation between the direction of the thermal current through the irradiated glass and the direction of the temperature gradient. As the heating and discharge proceeded, the current in the external circuit gradually decreased, and the dark yellow colour produced by the irradiation disappeared. A small current could be detected even after the complete bleaching of the glasses.

In the qualitative experiments described above the accumulated charge could not be calculated even approximately. Nevertheless the presence of a space charge following γ irradiation was established beyond doubt.

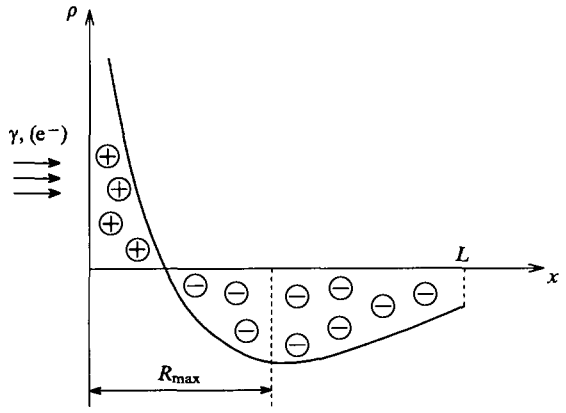


Figure 1. Charge distribution in a γ-irradiated dielectric with linear dimension L.[14] The ordinate axis coincides with the surface of the sample; ρ is the bulk density of the charge; the abscissa axis coincides with the direction of the γ quanta; the maximum penetration of the Compton electrons is R_{max}.

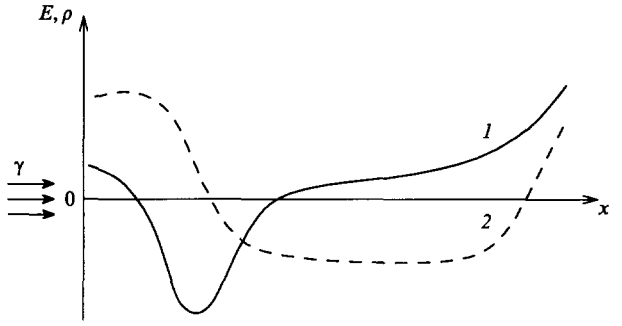


Figure 2. Distribution of space charge density (ρ) and of internal field (E) in a lead glass irradiated with γ quanta.[16] The abscissa axis coincides with the flow direction of the γ quanta: (*1*) charge; (*2*) field.

The magnitude, sign, and distribution of the charge are strongly affected by the irradiation conditions. For example, when the sample is not in electronic equilibrium and the Compton electrons leave the surface layer and move in the direction of the primary γ quanta the surface layer is positively charged, and the charge vanishes at a given depth (Fig. 1). If secondary electrons from the surroundings fall on the sample with the stream of γ quanta the charge can be negative as a whole and reside mainly near the irradiated surface. Experiments with irradiated paraffin wax[14] and Lucite‡[15] were satisfactorily consistent with these concepts.

The formation of large electric space charges by exposure to γ radiation leads to spontaneous internal discharges, as in the case of electron irradiation. The phenomenon was observed in experiments with large ^{60}Co sources in chambers shielded by thick lead walls,[7,16] the glasses being gradually broken down by spontaneous electric discharges. In some types of lead glass discharge formation was noted for doses of radiation higher than 5×10^5 Gy (5×10^7 rad).

It was established experimentally that a perturbation of the electronic equilibrium in the system is a necessary condition for the generation of radiation-induced charge by γ quanta. In other words, the number of electrons dislodged from the dielectric should be markedly different from the number of electrons arriving from the surroundings with the flux of γ quanta. If electronic equilibrium is established an excess of electric charge is not formed in the bulk of the dielectric during the irradiation: of course, this conclusion is valid only for isotropic solids.

The flux of γ quanta passing through the substance generates a flux of Compton electrons almost parallel to the γ flux. This is because the electrons are struck off mainly in the direction of motion of the γ quanta. For example, in Plexiglas exposed to a flow of γ radiation of 25 Jm^2s the average density of the accompanying electron flow was found[17] to be 1.37×10 A m^{-2}. A space charge is generated by the trapping of the Compton electrons as they travel through the material.

An empirical formula has been proposed[17] for the amount of charge accumulated in lead glass:

$$\rho = 4.4 \times 10^{-5} S\left[1 - \exp\left(-\frac{t}{\tau}\right)\right], \qquad (16)$$

where t is time (h), and τ is the relaxation time, equal to 64.1 h.

‡Lucite, Mylar, and Plexiglas are trade names of the same product: poly(methyl methacrylate) (PMMA).

If the dielectric experiences only the action of γ quanta, not accompanied by a flow of electrons from the surroundings, the charge distribution in the medium will be similar to that shown schematically in Fig. 2. If secondary electrons enter the medium simultaneously with the flow of γ quanta the distribution of charge in the depth of the sample can have an entirely different form. The absence of charge effects is certainly not guaranteed by the presence of an electronic equilibrium in the interaction of the γ quanta. Thus, even with an initially uniform distribution of positive and of negative carriers in the sample we can find a gradual separation of charges of opposite sign caused by the difference in their mobility in the solid matrix.

A simplified variant of the analysis of the accumulation of charge during the γ irradiation of dielectrics gives the following expression for the dependence of the total stored charge on the parameters of the sample and on the irradiation conditions:[6]

$$\bar{\rho} = S\frac{j_k(0)\varepsilon}{\mu_\gamma h\bar{\gamma}}\left[1 - (1 + \mu_\gamma h)\exp(-\mu_\gamma h)\right], \qquad (17)$$

where S is the surface area of the sample; h is its length; $\bar{\gamma}$ is the average electric conductivity; μ_γ is the linear absorption coefficient of the γ radiation; $j_k(0)$ is the current of Compton electrons near the sample surface. It is assumed that an equilibrium between the charge accumulation and the leakage currents was established during the γ irradiation.

To describe the charging process more correctly we need to allow for the appearance of a radiational component of the electric conductivity. A stricter derivation of formula (17) has been obtained[17] in the light of these considerations. In fact, the theory has been tested only for the region of linear charge accumulation, i.e. for the early stage of the irradiation. In lead glasses the charge accumulation in the initial stage has been shown to be satisfactorily described by these formulae.

In spite of this satisfactory agreement with experiment the above model of the charging of dielectrics in a field of γ radiation is not free from defects. In particular, many workers consider that the Compton electrons are trapped in the sample almost completely, and that their scattering can be ignored (thus ignoring the effect of the field from the charge on the path followed by the electrons and the spatial change in polarisation).

A commonly found case (the irradiation of an isotropic dielectric by a collimated monoenergetic beam of γ quanta) has been examined theoretically.[18] Under these conditions the charge becomes localised along the boundary between the irradiated and the nonirradiated part of the sample (Fig. 3). Charge formation is determined by the scattering of the Compton electrons. To simplify the treatment it was assumed (as in the work of Gross[17]) that the ratio of the dielectric permittivity to the conductivity is invariant during the exposure of the sample to γ quanta. It was

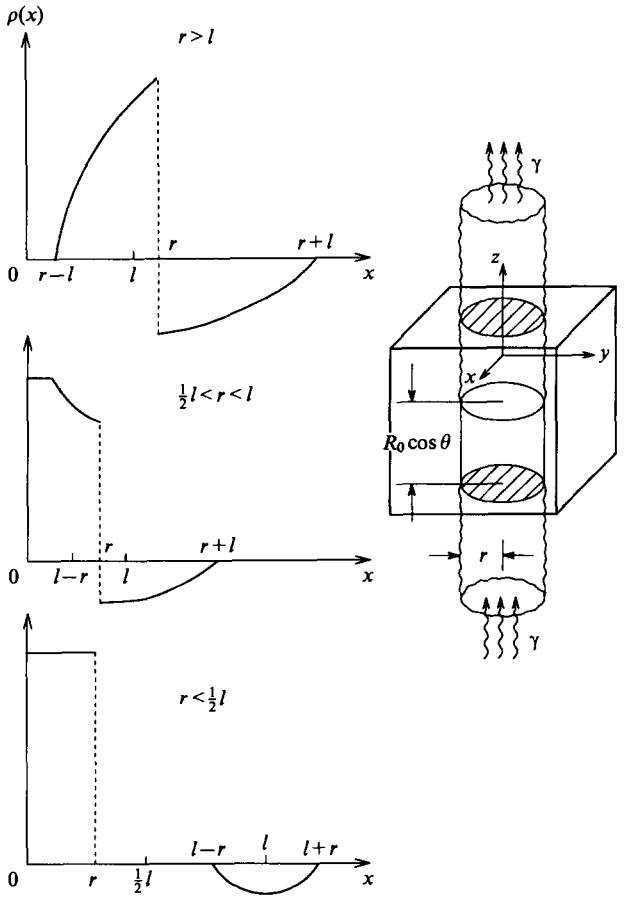


Figure 3. Distribution of charge density during the irradiation of a dielectric with a cylindrical stream of γ quanta for various ratios between the radius of the beam r and the deviation l of the Compton electrons from the direction of the γ quanta.[18] The orientation of the beam and of the sample relative to the chosen system of coordinates is shown on the right: θ is the average divergence angle, R_0 is the average path of the Compton electrons.

also assumed that the flux of particles incident on the surface consists only of γ radiation without any secondary Compton electrons from the surroundings, and that the suppression of the flux of electromagnetic radiation can be ignored.

If a cylindrical beam of γ quanta of radius r is used the charge distribution under stationary conditions is defined by the function f:

$$\rho(x) = ebf = ebj_\gamma \frac{1}{\pi} \arccos\left(\frac{x^2 - r^2 + l^2}{2lx - 1}\right), \qquad (18)$$

where l is the distance by which the Compton electron deviates from the direction of motion of the γ quanta; b is a coefficient which defines the link between the flux densities of the γ quanta (j_γ) and of the Compton electrons (with $r > l$). If $x > r$ the law for the dependence of $\rho(x)$ on x becomes

$$\rho(x) = ebj_\gamma \frac{1}{\pi} \arccos\left(\frac{x^2 - r^2 + l^2}{2lx}\right). \qquad (19)$$

The orientation of the sample and of the beam of γ quanta relative to the system of coordinates is shown in Fig. 3. The charge distribution is given for the xy plane.

A calculation shows that three special cases are possible.

1. $r > l$. In the region of $0 \leqslant x < r-l$ the sample does not become charged, since $f = 0$, and in the region of $r-l < x < r$ the charge density is proportional to f [see formula (18)]. Thus the centre of the irradiated cylindrical region is not charged. The density of positive charge to the left of the $x = r$ boundary is greater than the absolute density of negative charge outside the cylinder of radius r.

2. $\frac{1}{2}l < r < l$. Under these conditions the irradiated part of the sample is charged positively in the region of $0 < x < l-r$. For $l-r < x < r$ the charge is determined by the value of the function f according to formula (18), and for $x > r$ according to formula (19).

3. $r < \frac{1}{2}l$. In this case the whole of the dielectric enclosed in the cylinder of radius r is positively charged, and the charge density is proportional to $f = -ebj_\gamma$; the region between r and $l-r$ is uncharged, and in the region of $x > l-r$ the negative charge varies according to the expression (19).

We also note that on the side of the irradiated surface the region $r > l$ shown in Fig. 3 (a cylinder of radius r and height $R_0 \cos\theta$) becomes positively charged, as is also found in practice (compare with Fig. 2).

Under practical conditions the charge distribution is a superposition of all the cases which we have discussed. Therefore a discontinuity in the function f at the point $x = r$ should probably not be expected. However, the region outside the beam ($r < x < l-r$) should always be negatively charged.

In conclusion we should dwell briefly on the mechanism of the electrification of dielectrics by γ radiation. The effect is based on the difference between the rates of retardation and of generation of Compton electrons upon passing from one medium into the other, i.e. it can be realised in heterogeneous media in which the components have different absorption coefficients for the ionising radiation and different cross-sections for the formation of Compton electrons. A general discussion of this problem for systems composed of two media has been given by Lenchenko.[19]

V. Electric charge of radioactive substances

Radiation-induced charges were first observed, and then studied and used under practical conditions, in radioactive materials.[1,2,5] However, a reasonably complete theory of this phenomenon was developed only by abandoning to some extent the requirement of direct practical application and the existing theory of charging from external sources of ionising radiation. Unfortunately, even the present stage of development of the theoretical study of charge formation in radioactive materials cannot be taken as conclusive. Nevertheless, we now have some reasonably good theoretical models which can be used to establish an unambiguous relationship between the experimental results on the charging of radioactive materials and the properties of these materials.

One of the simplest and most effective methods of studying the electric properties of the surface of ionic crystals is to decorate the samples with charged particles of metallic sols.[20] The basis of the method is the fixing of the charged particles of the metallic sol on the appropriately charged regions when deposited on the surface. Experiments of this type have been carried out[5] with radioactive crystals of K_2SO_4* (containing ^{35}S, a β^- emitter).

It was established that individual sol particles are deposited, irrespectively of their charge, on elements of the surface topography (hillocks, growth steps, etc.). Thus, the negatively charged particles of a silver sol in methanol covered almost uniformly the whole surface of cleavage faces in radioactive crystals of potassium sulfate, which must obviously carry a positive charge. On the other hand, if the radioactive crystal was decorated with a nickel salt the metal particles were deposited only on surface nonuniformities. This is a direct proof that a stationary positive charge exists on the surface of β^- emitters.

One of the most characteristic features of radioactive dielectrics is the formation of a charged surface layer with a thickness equal to the maximum path length of the charged particles emitted by the radionuclide (if the linear dimensions of the sample are $L > R_{max}$), as was first reported by the present writer.[21]

In high-resistance radioactive materials the space charge can be so large that the electric field in the near-surface layer reaches the breakdown level. This assumption was tested by special experiments with a radioactive glass.[22]

The resistivity of the prepared glass blocks was $\sim 10^{22}$ Ω m. After solidification the samples began to darken and became opaque in a few minutes owing to the strong self-irradiation. According to tentative calculations the electric field intensity in the charged near-surface region of these glasses reached breakdown values ($\sim 10^8$ V m^{-1}). However, in order to stimulate electric discharges we need to create mechanical stresses by pressing a glass or a metallic rod on the surface of the radioactive glass block. A spark was seen in the charged layer beneath the pressure point. In most cases the discharges took place at the beginning of the experiment. The sparking then ceased, showing that the charge in the near-surface layer had become exhausted. After several days' storage of the blocks a new charge had accumulated, and the experiments on spark formation could easily be reproduced.

In contrast to irradiated materials a charge is always present in radioactive dielectrics: this is one of their most characteristic properties. The field generated by this charge can also extend beyond the dielectric, unless the charge is compensated by that of carriers drifting towards the surface of the radioactive sample from the surroundings. The charge accumulated in radioactive materials is most clearly detected in 'hot' aerosol particles, i.e. in solid formations whose specific radioactivity reaches ~ 10 Ci g^{-1} (3.7×10^{11} Bq g^{-1}) in particles of about micrometre size, so that the radioactivity of each aerosol particle is $\sim 10^{-8}$ Ci (or 200 Bq).[23]

VI. The charging of radioactive samples

The general theory of the formation of charge in radioactive solids has now been fully developed.[5,6,21,24] Two basic assumptions are made in the analysis of this phenomenon: Ohm's law is obeyed in the solid sample and the properties of the material are isotropic. In this case we can easily obtain a general expression which describes the dynamics of the charging both of radioactive materials (in which the radiation sources are located within the sample) and of materials irradiated from external radiation sources. Under these conditions the electrophysical properties of the system are characterised by macroscopic parameters such as γ (electric conductance) and ε (dielectric permittivity). It is also stipulated that charge neutralisation processes between charges of opposite sign can take place only on the surface. By allowing for these conditions we arrive at the following expression:

$$\rho(x,t) = \exp\left(-\frac{\gamma}{\varepsilon\varepsilon_0}t\right)\left[\int_0^t f(x,t)\exp\left(\frac{\gamma}{\varepsilon\varepsilon_0}t\right)\mathrm{d}t\right], \qquad (20)$$

where x is the coordinate of the reference point; $f(x,t)$ is the function of the charge sources (whose physical significance is to define the change in the charge density per unit time); γ is the electric conductance of the dielectric.

If the source of charged particles acts for a finite time (short-lived radionuclide) we can see from formula (20) that after the 'switching off' of the source the space charge density relaxes to zero with a time constant $\tau = \varepsilon\varepsilon_0/\gamma$. When the source of radiation acts for a long time with constant intensity (long-lived nuclide), i.e when f is independent of time, the solution of Eqn (20) takes the form

$$\rho(x,t) = \frac{\varepsilon\varepsilon_0}{\gamma}\left[1 - \exp\left(-\frac{\gamma}{\varepsilon\varepsilon_0}t\right)\right]f(x). \qquad (21)$$

Two special solutions of Eqn (21) are of interest.

1. Small electric conductance (dielectrics). By expanding the exponent into a Taylor series in powers of γ we obtain

$$\rho(x,t) = f(x)t.$$

Therefore, up to time t,

$$t \ll \frac{\varepsilon\varepsilon_0}{\gamma},$$

the charging will take place by a linear law, and at long times the charge ρ will tend towards the stationary value

$$\rho_{st} = \frac{\varepsilon\varepsilon_0}{\gamma}f(x). \qquad (22)$$

2. Large electric conductance (conductors), small relaxation time. Under these conditions the charge ρ immediately reaches the value ρ_{st} defined by Eqn (22), from which it follows that ρ depends only on the intensity of the sources of charged particles and on the electrophysical properties of the material.

At this stage of the solution the expressions obtained still retain their generality: they are valid also for an external source of radiation acting on the dielectric. The whole of the 'significance content', which allows ρ to be obtained in an explicit form for different particular conditions, is included in the 'source function' $f(x)$.

A strict derivation of the general form of the charge sources function for a uniform distribution of the radionuclide over the sample volume (when the specific radioactivity Q is independent of x) has been reported,[24] and also partial expressions for $f(x)$, which can be used to calculate the $\rho(x)$ values at various points in the radioactive sample. For example, for a radioactive preparation in the form of a sphere of radius r under stationary conditions we can write

$$\rho_{st} = b_n\int_0^x F_w(b_nR+1)\,\mathrm{d}R + \frac{b_n}{2}\int_x^{R_{max}} F_w\left(1+\frac{2Rx-x^2-R^2}{2R(r-x)}\right)\left(b_nR+1\right)\mathrm{d}R - 1, \qquad (23)$$

where ρ_{st} is expressed in relative units and is equal to

$$\rho_{st} = \frac{f(x)}{Q_0 e}$$

or

$$\rho_{st} = \rho\left(Q_0\frac{\varepsilon\varepsilon_0}{\gamma}\right)^{-1};$$

b_n is a constant, proportional to the concentration of electrons in the sample; Q_0 is the initial specific radioactivity; R is the range of β^- particles in the given material; x is the coordinate; F_w is a function which defines the form of the β^- spectrum. For a monoenergetic spectrum of β^- particles Eqn (23) simplifies to

$$\rho_{st} = 1 - \frac{1}{2}\left[1+\frac{2rx-x^2-R^2}{2R(r-x)}\right]. \qquad (24)$$

The results of a calculation of the charge distribution by using formula (23) for β-radioactive samples in the form of a plate or a sphere are shown in Fig. 4. As can be seen, in the radioactive samples the charge is accumulated in a near-surface layer of thickness R_{max}. Depending on the geometry of the sample the following cases are possible (for a sphere):

1. $r > R_{max}$; the central region of the sphere $(r-R)$ is uncharged.

2. $r < R_{max}$; the whole sphere is charged, but its near-surface layers have a charge density higher than in the central part.

3. $r \ll R_{max}$; the whole sphere is uniformly charged. This variant corresponds to hot aerosol particles.

Calculations by formula (24) give a qualitatively similar charge distribution, though some details of the changes in charge density over the volume of the radioactive sample are lost.

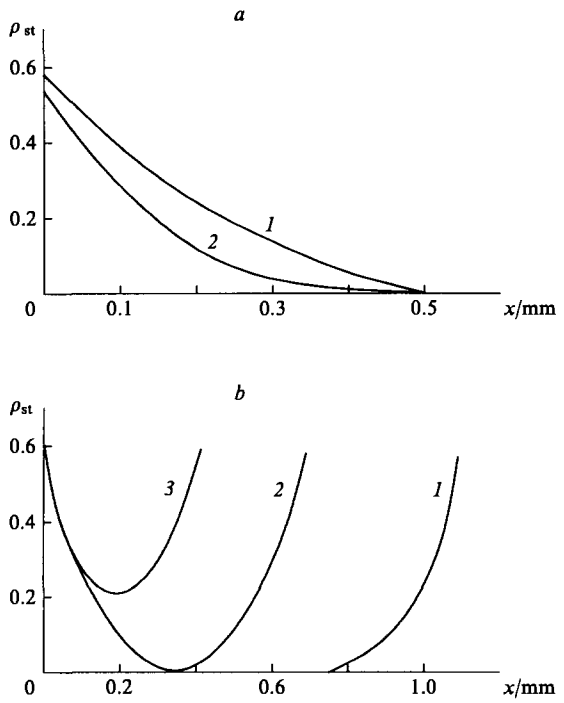


Figure 4. Changes in the charge density $\rho(+)$ of β^--radioactive samples of different size and shape. Maximum energy of β^- particles assumed to be 3 MeV, with a continuous emission spectrum; range R_{max} = 0.5 cm; (*a*) radioactive sphere, the ordinate axis coincides with the surface of the sphere, curves *1* and *2* correspond to sphere radii of 1 and 0.5 cm; (*b*) flat infinite layer, the ordinate axis coincides with the coordinate of one of its surfaces, layer thickness (cm): *1*, 1.1; *2*, 0.7; *3*, 0.4.

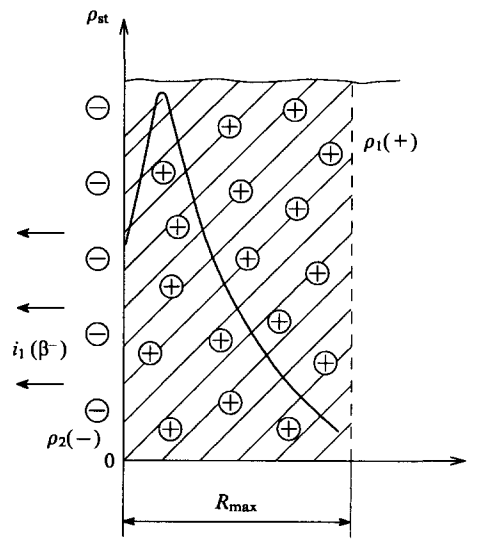


Figure 5. Charge distribution in a dielectric containing a β^- emitter and surrounded by a conducting medium (the ordinate axis coincides with the coordinate of the dielectric surface). i_1 is the flow of β^- particles emitted from the surface of the sample.

These calculations can account for the distribution of the charge expressed in relative units. To obtain the absolute values of ρ we must know the relationship between the change in γ and the dose rate of the ionising radiation, but at present only empirical formulae are available. This is one of the weaknesses of the theory in its present state of development.

Depending on the values and on the ratio of the conductivities of the radioactive material and of the surrounding medium, we may find different distributions of charge in the radioactive sample. For a β^- emitter in a conducting medium the distribution is shown in Fig. 5. The cross-hatched region corresponds to a positively charged near-surface region. Negative charge $\rho(-)$, created by ions from the surroundings, is localised on the surface. As can be seen from the figure, it is useful to distinguish between the total (positive) charge $\rho_1(+)$, distributed in a volume limited by a layer of thickness R_{max}, and the charge ρ_2, equal to the difference between $\rho_1(+)$ and the absolute value of $|\rho(-)|$.

The values of ρ_1 and ρ_2 can be calculated fairly accurately if the electrophysical parameters and the geometry of the radioactive sample and of the surrounding medium are known. By treating the formation of ρ_2 as a competition between the accumulation of charge ρ_1 (formed by the emission of β^- particles from the surface, which determines the current i_1) and the discharges in the surface layer resulting from the recombination with carriers of the opposite sign, i.e. by solving in a simplified variant the system of equations

$$\frac{d\rho}{dt} = i_1 - \frac{\rho_1}{\tau_{ef}}, \qquad \frac{di_1}{dt} = -\lambda t, \tag{25}$$

where λ is the disintegration constant and τ_{ef} is the effective relaxation time of the charge in the given system, we arrive at the expression

$$\rho_{t(2)} = \rho_{st\ (2)}\left[1 - \exp\left(\lambda t - \frac{t}{\tau_{ef}}\right)\right]\exp(-\lambda t)\,. \tag{26}$$

In the case of a time-invariant source intensity (i.e. for $\lambda = 0$) Eqn (26) simplifies to

$$\rho_{t(2)} = \rho_{st\ (2)}\left[1 - \exp\left(-\frac{t}{\tau_{ef}}\right)\right], \tag{27}$$

where $\rho_{st(2)} = i_1\tau_{ef}$. However, formula (27) gives no information on the distribution of charge in the bulk of the dielectric.

For practical purposes it is important to know not only the magnitude of the uncompensated (residual) charge of the radioactive sample ρ_2, but also the total charge ρ_1 distributed in the surface region. In the case of a spherical sample[5] these calculations can easily be made by using the following formula:

$$\rho_1 = \frac{b_1 emQ\varepsilon\varepsilon_0 f(\mu, r)}{4\pi r\gamma_1}, \tag{28}$$

where b_1 is a constant§; γ_1 is the electric conductivity of the sample (allowing for the radiational component). The function $f(\mu, r)$, which defines the fraction of the β^- particles leaving a sphere of radius r, is given in the form

$$f(\mu, r) = \frac{3}{4\mu r}\left[\frac{(2\mu r + 1)\exp(-2\mu r) - 1}{2\mu^2 r^2} + 1\right], \tag{29}$$

where μ is the linear absorption coefficient of the β^- particles in the given substance.

Thus, calculations for crystals of radioactive strontium sulfate containing ^{35}S ($\gamma \approx 10^{-16}$ S m^{-1}, r = 0.1 cm, ε = 5, μ = 840 cm^{-1}), showed that the charge averaged over the volume of a near-surface layer 8×10^{-3} cm thick for Q = 1 Ci g^{-1} (3.7×10^{10} Bq g^{-1}) is 3×10^{-3} C cm^{-1}, and the internal field in the charged layer is $10^3 - 10^4$ V cm^{-1}, $\tau \approx 5 \times 10^2$ s.

§ If the sample is an α emitter, the constant b_1 should include a factor for calculating the yield of δ electrons defining the magnitude and sign of the stationary charge.

These results agree tolerably well with experimental determinations, and they show convincingly that a fairly large charge with a corresponding electric field gradient exists in the near-surface layer of radioactive dielectrics, even if electrically neutral overall (the space charge is compensated though not neutralised).

A stationary distribution of electric charge should be established also at the boundary between two media (a radioactive and a nonradioactive solid dielectric).[25] Let us examine these cases.

Case 1. In a nonradioactive isotropic material we have a region containing a uniformly distributed β^- emitter. If this region is a sphere of radius r the volume density of electric charge at the point x can be found from the expression

$$\rho = \frac{eQ\varepsilon\varepsilon_0}{\gamma_0 - \varepsilon\varepsilon_0\lambda}\left(\frac{r^2 - R^2 - x^2}{4xR} \pm \frac{1}{2}\right)B(t)\,, \qquad (30)$$

where Q is the specific radioactivity; ε is the dielectric permittivity of the medium; λ is the disintegration constant; R is the range of the electrons emitted by the given radionuclide (it is assumed that all the β^- particles have the same energy, i.e. that the spectrum of the radiation is monoenergetic); γ_0 is the electric conductivity;

$$B(t) = \exp(-\lambda t) - \exp\left(-t\frac{\gamma_0}{\varepsilon\varepsilon_0}\right).$$

Eqn (30) defines the dependence of the bulk charge density upon the radioactivity of the dielectric, its electrical parameters, and the coordinate and time. In the region of $x \leqslant r$ (β^- emitting sphere) the term 1/2 of Eqn (30) takes the plus sign, and in the region of $x > r$ (nonradioactive dielectric) it takes the minus sign. Fig. 6 shows the 'coordinate part' of the dependence of the bulk charge density G:

$$G = \frac{r^2 - R^2 - x^2}{4xR} \pm \frac{1}{2}$$

for the case of $R < r$.

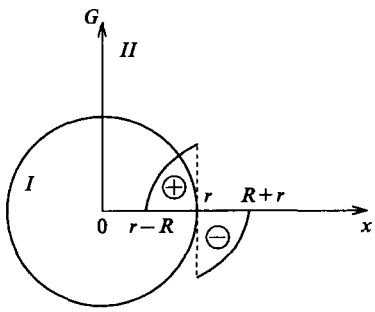


Figure 6. Plot of the 'coordinate part' of the charge density (G) for dielectric half-spaces with different radioactivities. R is the range of electrons in regions I and II; the plus and minus signs correspond to the sign of the space charge.

It should be noted that in every case the whole of the radioactive region (or part of it) becomes positively charged while the nonradioactive region is negatively charged; the $x = r$ boundary defines the charge separation zone. Furthermore 'radiative' electric charging does not take place at any point within the radioactive dielectric at a distance equal to or greater than R from the zone boundary (where $\rho = 0$).

A similar result is seen at the flat interface between the radioactive and the nonradioactive region of a dielectric: the near-surface region of the radioactive dielectric is charged positively, and that of the nonradioactive dielectric is charged negatively.

Case 2. In dielectric materials containing a uniformly distributed β^- emitter with a monoenergetic spectrum we can distinguish regions with different physical properties (i.e. two radioactive materials of different nature but with identical and uniformly distributed radionuclides, which produce an interface). Calculations have shown that the region with the higher electron density becomes negatively charged, and that with the lower electron density positively charged. For example, for a radioactivity of 10^{13} Bq m^{-3} and a conductivity of approximately 10^{-13} $(\Omega\,\mathrm{m})^{-1}$ the charge at the phase boundary is ~ 1 C m^{-3}, which corresponds to electric fields of flashover magnitude ($\sim 10^8$ V m^{-1}).

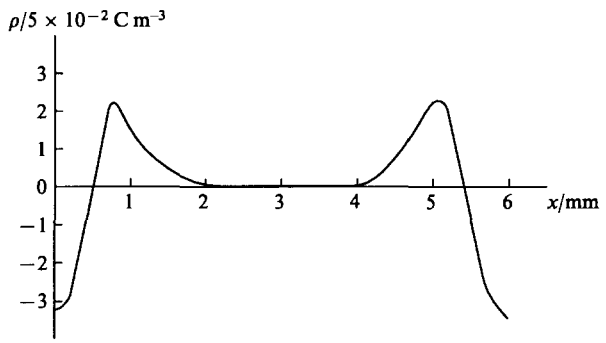


Figure 7. Distribution of electric charge in monocrystals of $Y_3Al_5O_{12}$ (yttrium-90 specific radioactivity 4×10^8 Bq g^{-1}).

The most correct experimental test of the theory of the distribution of space charge in the bulk of radioactive dielectrics was carried out by the acoustic probing method.[26] Thus, in the case of yttrium aluminium garnet ($Y_3Al_5O_{12}$) crystals irradiated with neutrons it was shown that the charge is not uniformly distributed on the surface of flat specimens (Fig. 7). Neutron irradiation of garnet crystals produces the β^- emitter yttrium-90.

It is clear from Fig. 7 that at the centre of the sample with $R < h$ (where h is the thickness of the sample and R the range of the β^- particles from yttrium-90) the charge is zero, whereas in the near-surface regions of thickness R we find an accumulation of positive charge. Narrow negatively charged layers are formed on the surface by the drift of carriers of opposite signs from the surroundings.[26,27]

VII. Charge and properties of solids

Many workers have noted the appearance of spontaneous electrical discharges during the irradiation of dielectrics, leading to the mechanical breakdown of the samples. For example, borosilicate glasses distintegrated when exposed to a flux of 10^{13} electrons cm^{-2} and a current density of $\sim 10^{11}$ electrons cm^{-2} s^{-1} (electron energy 1 – 2 MeV).[28] Discharges can occur in glasses even during lengthy storage (two weeks or more).

Some workers[29] associate the mechanical properties of irradiated glasses with the presence in those glasses of space charges, responsible for the production of internal mechanical stresses. It was pointed out[30] that the mechanical strength of a dielectric is decreased by charging. This effect can probably be attributed to an increase in the ponderomotive forces in a charged dielectric, since their bulk density increases linearly as charge is accumulated in the material.

The internal electric field of the space charge can also have a marked influence on the bleaching of the colour centres in transparent dielectric materials. For example, in glasses of composition $6B_2O_3.Na_2O$ the application of an external electric field of 7×10^7 V m^{-1} was found to break down the

radiation-induced colour centres. It was suggested that the internal 'cold' emission of trapped electrons into the conduction band is responsible for this process.[31]

According to both a theoretical analysis[32-35] and experimental determinations radiation-induced charging strongly decreases the penetration of electrons. The effect was observed visually[32] as a change in thickness of the luminescent layer in poly(methyl methacrylate) which had been irradiated with accelerated electrons with an energy of 1.3–1.7 MeV. This surface layer is a region of electron retardation and accumulation of space charge. The results of these studies are shown in Fig. 8.

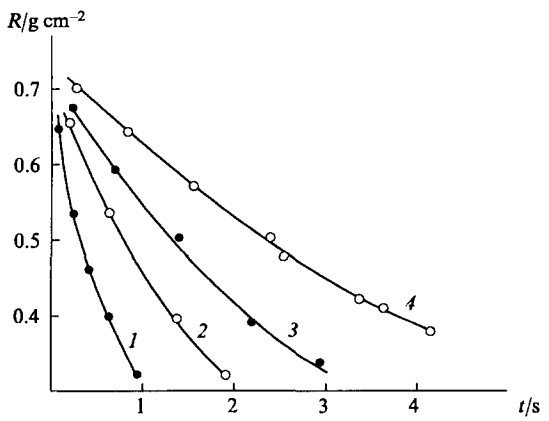


Figure 8. Plots of the range of electrons in poly(methyl methacrylate) against the time of irradiation.[32] Current density of electrons with an energy of 1.7 MeV in the beam (μA cm^{-2}): (*1*) 2.7; (*2*) 1.0; (*3*) 0.8; (*4*) 0.5.

It can be seen that the depth of penetration decreases with time (i.e. it decreases as space charge accumulates). Furthermore R tends towards a limiting value from which the maximum strength of the electric field generated by the space charge can be determined. According to the theory which has been proposed for this phenomenon the energy U_e of the electrons which reach the boundaries of the luminescence region is given by the nonlinear equation

$$\frac{dU_e}{dx} = -w(U_e) - eE(x), \tag{31}$$

where x is the coordinate of the motion of electrons in the materials; $w(U_e)$ is the stopping power of the material; $eE(x)$ is the force acting on an electron at a depth x from the field created by the space charge. Numerical solution of Eqn (31) for an initial electron energy of 1.3 MeV gives the maximum value of $eE(x)$ in poly(methyl methacrylate) as 3.4 MeV cm^{-1}.

Th existence of a relationship between the space charge field and the range of the electrons in irradiated dielectrics produces another interesting effect: the redistribution of absorbed energy.[36,37] In calculations of the profile of absorbed energy (which is very difficult to determine experimentally) it is assumed that some fixed distribution of electric field exists in the bulk of the dielectric. Therefore we need additional experimental definitions of the $E(x)$ or $\rho(x)$ dependences, which complicates the solution of the problem. However, at least when the thickness of the dielectric exceeds the range of the electrons, the required information on the distribution of absorbed dose can be obtained if a family of distributions calculated for a uniform electric field is available.[36] The method of calculation relies on a kinetic equation which describes the transport of electrons on the assumption of continuous retardation. The calculations were carried out for uniform dielectrics with $z_{ef} = 6$ and 14 (where z is the atomic number of the element). Some results of these calculations for a uniform field within the dielectric are shown in Fig. 9.

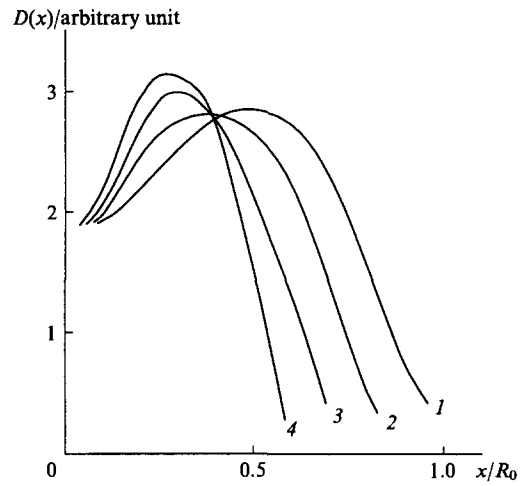


Figure 9. Distribution of the absorbed energy D for different values of the force $eE(x)$ acting on the electrons of energy 1 MeV injected into a dielectric ($z = 6$) from the side of the space charge field (MeV cm^2 g^{-1}): (1) 0; (*2*) 0.5; (*3*) 0.8; (*4*) 1.1.

The calculations show that as the interaction of the space-charge field with the electrons injected into the sample is increased the absorbed energy maximum moves towards the surface of the irradiated dielectric. This conclusion is of direct relevance to the study of the mechanical and optical properties of dielectrics exposed to a flux of charged particles. Allowance for this phenomenon should probably also be made in the measurement of radiation-chemical yield, which must also be varying over the thickness of the sample. Estimates[43] of the local values of the density of radiation-induced defects allowing for the space-charge field have confirmed this assumption.

The presence of large electric fields in irradiated dielectrics and semiconductors affects the yield of Compton electrons.[33] The change is characterised by the quantity δ, defined as the difference between the quantum yield in the electric field and without the field, and depending on the field intensity as follows:

$$\bar{\delta} = \int_0^R E(x) f(x) dx, \tag{32}$$

where $f(x)$ is the sensitivity function [$f(x) = \alpha x$], α is a constant, and R is the range. Integrating Eqn (32) by parts, and assuming that the electric potential is $V(x) = 0$ at $x = R$, we obtain

$$\bar{\delta} = 2\frac{\bar{\delta}_0}{ER}\int_0^R V(x)dx,$$

where $\bar{\delta}_0$ is the change in the quantum yield in a uniform electric field E. This result is strict in relatively weak fields. As the experiments show, $\bar{\delta}$ increases as E decreases. For example, in poly(methyl methacrylate) $\bar{\delta}$ increases almost 5-fold as the field strength is increased from 0.2 to 1.2 MV cm^{-1}.

Some published results[37] describe the formation of a powerful (explosive) emission from the free surface of dielectrics irradiated with strong beams of accelerated electrons in a pulsed regime. Unlike the previously known explosive emission from metallic samples this process is initiated by an internal (not by an external) electric field. It is observed in many dielectric materials —organic compounds, dielectric glasses, ionic crystals, and ceramic materials. It has been established that as soon as the intensity of the beam of bombarding electrons exceeds the threshold value characteristic of the particular material a powerful emission is produced, leading to a vacuum discharge [the experiments were carried out at a pressure of $10^{-6}-10^{-3}$ Torr, electron energy 0.35 MeV, pulse length $(2-30)\times 10^{-9}$ s, current density $(0.01-1.5)\times 10^3$ A cm^{-2}].

Threshold electron beam densities for various materials are shown below (10^{-5} cm^{-2} pulse^{-1}):

LiF	3
NaF	4
NaCl	6
KCl	7
Polyethylene	1
Teflon	3
Quartz glass	8

The strong explosive emission carries away from the dielectric, together with the ejected ion plasma, a charge ~100 times greater than the charge injected by the electron beam. This phenomenon could find practical applications in connection with the use of dielectrics excited by powerful electron beams as cut-off cathodes and commutators for high-current beams.

VIII. Dissolution kinetics of charged crystalline substances

The electrification of solids and the formation of electrical space charge in solids exposed to an ionising radiation have been studied reasonably widely, as has also the effect of the space charge on various physicochemical processes.[6]

We shall examine some examples in which the relationship between changes in the rates of dissolution and of electrification of the irradiated compounds can be monitored. We should point out first of all that the space charging of the dielectric is accompanied by its polarisation. Therefore when the substance is dissolved the transfer of ions (or of dipolar molecules) from the solid to the liquid phase takes place in an electric field.

In the dissolution of irradiated salts it is very difficult to separate the effects of one among several factors, such as charging, radiation-induced defects of the electronic type, displaced atoms, or structural surface changes. We shall discuss the changes in the dissolution rate constant k_v of irradiated crystals which may be attributed to radiation charging.

In crystals of $SrSO_4$ exposed to γ radiation or to accelerated electrons defects such as SO_4^- and SO_3^- ion radicals are produced, as well as e_{st}^- and others. At temperatures below −100 °C in the case of interaction with γ radiation (or at room temperature in the case of irradiation with electrons having energies of 1–3.5 MeV) only ion radicals and trapped electrons are formed. In Fig. 10 we show the changes in the rate of dissolution of crystals of natural celestine ($SrSO_4$) irradiated with fast electrons.

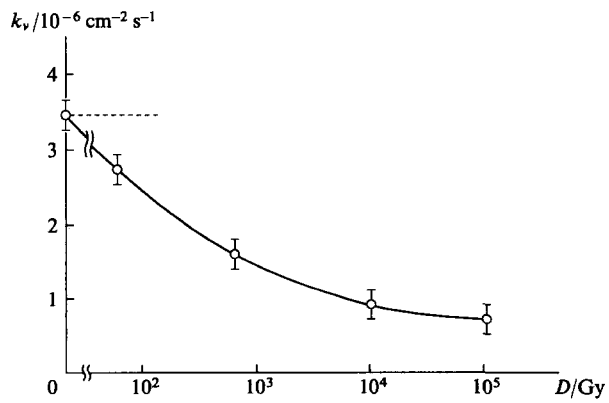


Figure 10. Dependence of the rate constant for the dissolution of a monocrystalline substance in water at 298 K on the dose of radiation. Crystals irradiated with accelerated electrons; energy 3.5 MeV; the broken line shows the value of k_v for nonirradiated crystals.

The experiments were carried out as follows. The crystals were irradiated at 20–30 °C (which produced only SO_4^- radicals and e_{st}^-) and immediately after the irradiation they were dissolved in distilled water at 20 °C. The outer layer of the crystals, damaged by the radiation, was removed by partial dissolution. Under these conditions a change in k_v could be attributed only to the radiation charging and to the formation of electronic defects. As can be seen from Fig. 10 the crystals of celestine freshly irradiated with 3.5 MeV electrons dissolve more slowly than the nonirradiated samples. In this effect the dominant role is played by the radiation charging, which nullifies the action of the radiation-induced defects.

When the crystals were stored (for several months) the charge produced by the irradiation decayed to some extent, and k_v increased, approaching the rate constant of the dissolution of the nonirradiated sample. We note that the concentration of SO_4^- fell slightly during storage, and SO_3^- ion radicals were formed instead. After heat treatment, which removed all the defects, the properties of irradiated and nonirradiated crystals became identical. This is confirmed by the results of experiments with polarised samples of $SrSO_4$ (Fig. 11). In this case the k_v value also gradually decreased as the polarisation field strength was increased.

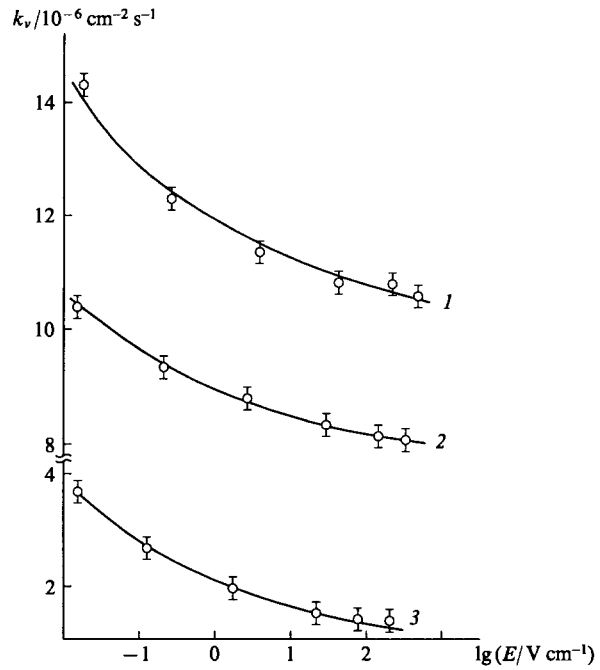


Figure 11. Changes in the rate constant for the dissolution in water for different values of the electric field strength (crystal polarisation). (*1*) NaF; (*2*) LiF; (*3*) $SrSO_4$.

In experiments on the action of fast electrons on LiF crystals[38] the thickness of the plates was chosen so that almost all the electrons with an energy of ~3.5 MeV were absorbed by the sample. After the irradiation the plates darkened, and a visual inspection showed that all the electrons had been absorbed near the irradiated surface. According to the experimental results the excess space charge was negative. Some of the irradiated crystals were placed in an electric field in a direction which increased the radiational polarisation, others were placed in a depolarising field (see Table 1). The lowest value of the dissolution rate constant was observed for the crystals in which the radiational polarisation was increased by the electric field. Decreasing the polarisation in the stimulated discharge of the irradiated LiF increases the rate of dissolution.

Table 1. Changes in the dissolution rate constant of LiF crystals irradiated with electrons and polarised in an external electric field[38] with a strength of 1500 V cm^{-1}.

Application conditions of electric field	$k_v/10^{-6}$ cm^{-2} s^{-1}	Notes
No field, crystal not irradiated	12.4	–
No field, crystal irradiated	11.2	Dose absorbed during irradiation 5×10^2 Gy
Field depolarisation used	10.4	Polarisation (depolarisation) time 48 h
Field polarisation used	9.4	–

The radiation-induced charging is often masked, and even counteracted, by the action of the radiation-induced defects. Obviously, opposing factors are developed simultaneously in the irradiated compounds: the dissolution is retarded by the radiational polarisation and the transfer of ions from the solid into the solution is accelerated by the formation of radiation defects. Similar effects are also seen in the dissolution of radioactive crystalline compounds, in which a stationary electric charge is permanently maintained during the disintegration of the radionuclides.[5, 38, 39]

A relationship between the charge in the crystals and their rate of dissolution was first established in studies of the dissolution of radioactive $SrSO_4$ crystals in water. It was then shown that NaCl, $SrSO_4$, and other salts dissolve more slowly than the nonpolarised compounds. The polarisation of the solvents also has an effect, and therefore the change in k_v is strongly dependent on the ratio of the dielectric constants of the solid and the liquid phase.[38, 39] Furthermore, the solubilities of the components of the system also play an important part.

Thus, according to the data in Fig. 11, the dependence of the change in the dissolution rate constant (in water) on the intensity of the electric field shows that as the field E is increased the k_v value decreases most markedly in $SrSO_4$, which has the lowest solubility. The decrease in k_v in a series of salts of the same type (NaCl, LiF, NaF) is strongest in the least soluble compound (LiF), which has the highest dielectric permittivity. The slower dissolution of ionic crystals after irradiation may to some extent be associated with their radiation-induced charging.

Let us examine the relationship between k_v and the strength of the field in the crystal. We shall express k_v in terms of two factors, one dependent and one independent of the polarisation of the crystal, and we shall discuss the elementary act of the dissolution of the crystal from the standpoint of the change in energy of the molecule during its transfer to the liquid phase. It will be assumed that the dissolution process obeys the Brønsted relation

$$\Delta Q_a = b\Delta Q_h , \tag{33}$$

where ΔQ_a is the activation energy of the dissolution; ΔQ_h is the heat of dissolution; b is an empirical constant ($0 \leqslant b \leqslant 1$). We can then write the following expression for the dissolution rate constant;

$$k_v = k_v^0 \exp\left(-\frac{b\Delta Q_h}{kT}\right) , \tag{34}$$

where k_v^0 is a temperature-independent quantity. Formula (34) can be rewritten

$$k_v = k_v^* \exp\left(-\frac{b\Delta F_{el}}{kT}\right) , \tag{35}$$

where ΔF_{el} is the change in the 'electric' component of the free energy (the Helmholtz free energy) of the molecules of the ionic crystal during the dissolution, and k_v^* includes both the entropy term and a term which characterises the free energy in terms of the strength of the electric field applied to the crystal. The parameter ΔF_{el} is $U_2 - U_1$ (the difference between the 'electric' free energies of the dissolution of the molecule in the solution and in the crystal respectively).

The dependence of the rate constant for the dissolution on the external electric field can be influenced only by that part of the free energy of the molecule in the crystal which is contributed to by the polarisability of the molecule. Therefore we can write the following expression for U_1:

$$U_1 = -\alpha|E|^2 , \tag{36}$$

where α is the total polarisation of one molecule; E is the strength of the electric field within the crystal. In the case of crystals with a uniform charge of anions and cations the energy U_2 (in the Gouy–Chapman approximation) is given as

$$U_2 = -16C_0K_D\pi r_0^2kT\sinh^2\frac{ez\phi}{4kT} , \tag{37}$$

where C_0 is the average equilibrium concentration of ions in the bulk of the solution; $K_D = (8\pi e^2z^2C_0/\varepsilon_2kT)^{1/2}$ is the reciprocal Debye length; z is the charge of the ions in the crystal; r_0 is the corresponding radius of the ion in solution; ϕ is the average potential of the outer Helmholtz plane (in which the centres of the ions in solution nearest to the crystal surface are localised); ε_2 is the average dielectric permittivity of the solution.

The total polarisability of the molecule in the solid phase α can be calculated by the Clausius–Mosotti relation

$$\alpha = 3M\frac{\varepsilon_1 - 1}{4\pi dN_A(\varepsilon_1 + 2)} , \tag{38}$$

where ε_1 is the static dielectric permittivity of the crystal; M is the molecular mass; d is the density; N_A is the Avogadro number.

In order to calculate E and ϕ we need to solve the problem of the distribution of potential in a system consisting of a polarised crystal with Helmholtz layers at its boundaries with the solution, and surrounded by the diffuse parts of the electrical double layer. If we adopt the Gouy–Chapman model to describe the distribution of charge in the diffuse part of the double layer the problem of the distribution of the ϕ potential (even only in the plane separating the crystal from the solution) reduces to the simultaneous solution of a system of two Poisson–Boltzmann equations (for the diffuse parts of the double layer) and three one-dimensional Laplace equations (for the Helmholtz part of the double layers and for the polarised crystal). The boundary conditions should ensure the continuity of the potential and of the electric induction at the interface between the crystal and the solution. After some algebra we arrive at the expressions

$$|E| = -\frac{4\pi}{\varepsilon_1}\left[|P| - \frac{4ezC_0}{K_D}\sinh\left(\frac{ez\phi}{2kT}\right)\right] , \tag{39}$$

$$\phi = \frac{4\pi e}{\varepsilon_1}\left[|P| - \frac{4ezC_0}{K_D}\sinh\left(\frac{ez\phi}{2kT}\right)\right] , \tag{40}$$

where $|P|$ is the polarisation of the crystal.

By combining the well known relationship between $|P|$ and the strength of the field applied to the crystal with Eqns (35)–(40) we obtain the dependence of the rate constant for the dissolution of the crystals upon their polarisation:

$$\ln\frac{k_v^*}{k_v} = 16b\left\{\sinh^2\left(\frac{ez\phi}{4kT}\right) - \frac{\alpha\pi^2}{\varepsilon_1^2kT}\left[|P| - \frac{4ezC_0}{K_D}\sinh\left(\frac{ez\phi}{2kT}\right)\right]^2\right\} . \tag{41}$$

The parameter P is related to the intensity E_1 of the electric field applied to the crystal by the expression

$$P = \frac{(\varepsilon_1 - 1)E_1}{4\pi\varepsilon_1}. \quad (42)$$

We may conclude from (39)–(42) that for sufficiently large values of α and not too small bulk concentrations of the solution k_v decreases with increase in E_1 (or P). However, it should not be forgotten that in strong fields ($ez|\phi| \gg kT$) the polarisability α is itself dependent on the field strength, decreasing as $|\phi|$ increases. Therefore an increase in the potential difference applied to the crystal should suppress the dependence of the rate constant of the dissolution on E_1, as is found in practice.

The theoretical prediction of an increase in the rate of dissolution of polarised crystals has been confirmed by observations of the dissolution of crystals of tartaric acid in solvents having different dielectric permittivities (Fig. 12).

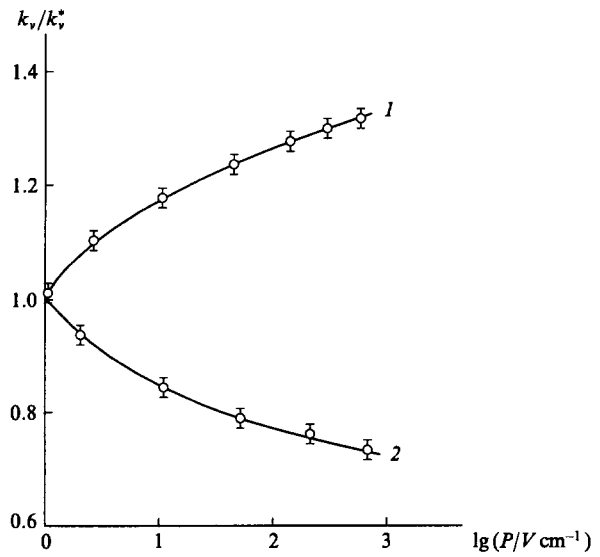


Figure 12. Changes in the rate of dissolution in water of crystals of tartaric acid as a function of the polarisation of the solid phase P ($\varepsilon_1 = 35.9$) in ethanol ($\varepsilon_2 = 20$) (*1*) and in water ($\varepsilon_2 = 80$) (*2*).

The physical significance of the slower dissolution of charged crystals is that the polarised dipole–molecule being transferred to the liquid phase must perform additional work against the force of the electric field. However, if the solvent also is polarised, it becomes more difficult for the dipole–molecule to return to the solid surface for $\varepsilon_{sol} \gg \varepsilon_{liq}$, i.e. the rate of dissolution increases and the molecule is 'pulled' into the liquid phase by the electric forces.

Similar effects have been observed[40] in a study of the rate of growth of etch pits at the emergence of dislocations on the surface of polarised LiF crystals.

Brief mention should be made of another possible way of suppressing the dissolution of crystalline dielectrics, in which the liquid phase is subjected to the orienting effect of an electric field. Thus, the polarisation of the solvent molecules in the boundary layer at the interface can stabilise the layer of liquid adjacent to the surface of the dissolving crystal.[41] In the present model the calculated strengths of the electric field produced by polarisation can vary between wide limits (from 0 to 10^3 V cm^{-1} or more). In actual systems the polarisation can strongly influence the viscosity and the perviousness of the surface layers. This is consistent with the views of a dependence of the viscosity of polar liquids on electric field effects. The dissolution of polarised crystals can also be retarded by the condensation (accumulation) of reaction products and other dissolved substances in the boundary layer under the influence of an electric field, and by the formation of crystal nuclei or polymer chains (for example, in P_2O_5 or SiO_2) able to interact with each other and with the molecules of the liquid medium. The new formations 'armour' the system and can induce the formation of a gel-like metastable state at the interface between the solid and the liquid phase. Therefore in some cases the polarisation of molecules on the surface of dissolving compounds can lead to the formation of protective gel-like films.

IX. Conclusions

The experimental work shows that the accumulation of electric charge in irradiated and in radioactive solid dielectrics is one of the most fundamental phenomena accompanying the action of ionising radiation on high-resistance materials. The developments in this field of study have been stimulated not only by their purely scientific interest but also by specific practical needs. Thus, the prediction of the service life of various electrical insulators and articles in fields of ionising radiation is impossible without a knowledge of the special features of the growth and relaxation processes which control the 'radiational' electric charging. This may ultimately determine the reliability of the operation of nuclear energy converters and apparatus used in cosmic flights when continuously exposed to ionising radiation, and other similar problems. Therefore further progress in this area is impossible without studies in depth of the mechanism of reversible and of irreversible processes initiated by ionising radiation in dielectrics.

At present the following promising fields of study in this area can be identified:

1. The development of a theory of the distribution of electric field in dielectric materials (or articles) in various configurations exposed to ionising radiation.

2. Improvements in the theory and methods of calculating the distribution of electric space charge (and its corresponding electric field) in heterogeneous structures (mixtures of solid substances, solid systems containing inclusions of various solid phases).

3. The acquisition of experimental information on the effect of external factors on the formation of an electric charge and on the 'freeing' of this charge from the given material (for example, in the form of electric discharges).

4. The study of the mechanism of radiation-chemical and radiation-physical processes in charged dielectrics: this should lead to the development of new methods of controlling the properties of these materials and of the physicochemical processes carried out by using them.

5. The modelling of actual operating conditions encountered by various materials in a field of ionising radiation, i.e. allowing for the combined effects on the dielectric of the charging, defect formation, temperature fields, mechanical interactions, and other factors.

The importance of this type of study arises because in many cases the formation of charge and the subsequent electric breakdown (which can even lead to the mechanical fracture of the dielectric) are the precursors of irreversible (and even, on occasions, reversible) radiation-chemical or radiation-physical changes in the material. For example, it has been shown[42] that at low temperatures (~77 K) the effectiveness of the charge accumulation in glasses irradiated by accelerated electrons increases, so that conditions conducive to electric discharges are produced even in a flow of 10^{12} electrons cm^{-2} (electron energy ~2 MeV). Heat treatment after irradiation merely accelerated this process. Similar effects are found in composite materials and polymers.

The solution of these problems should stimulate the development of reliable methods of increasing the radiation stability of various dielectric materials.

References

1. P Curie, M Curie *C.R. Acad. Sci.* **130** 647 (1900)
2. W Corliss, D Harvey *Energy Sources from Radioactive Isotopes* (Translated into Russian; Moscow: Mir, 1988)
3. V M Luk'yanovich, L V Radushkevich, in *Metody Issledovaniya Struktury Vysokodispersnykh i Poristykh Tel* (Methods of Studying the Structure of Highly Dispersed and Porous Solids) (Moscow: Izd. Akad. Nauk SSSR, 1953) p. 39
4. J Furuta, E Hirraoka, S Okamoto *J. Appl. Phys.* **37** 1873 (1969)
5. V I Spitsyn, V V Gromov *Fiziko-khimicheskie Svoistva Radioaktivnykh Tverdykh Tel* (Electric Properties of Radioactive Solids) (Moscow: Atomizdat, 1973)
6. V V Gromov *Elektricheskii Zaryad v Obluchennykh Materialakh* (Electric Charge in Irradiated Materials) (Moscow: Energoizdat, 1982)
7. R Kikuchi *J. Nucl. Energy (Tokyo)* **11** 11 (1965)
8. A P Tyutnev, A V Vannikov, G S Mingaleev, V S Saenko *Elektricheskie Yavleniya pri Obluchenii Polimerov* (Electric Phenomena in the Irradiation of Polymers) (Moscow: Energoatomizdat, 1985)
9. O B Evdokimov *Radiatsionnaya Stoikost' Organicheskikh Materialov* (Radiation Resistance of Organic Materials) (Moscow: NIITEKhIM, 1979)
10. A R Frederickson, S Woolf *IEEE Trans. Nucl. Sci.* **28** 4186 (1981)
11. A F Akkerman, Yu M Nikitenko, V A Botvin *Reshenie Metodom Monte-Karlo Zadach Perenosa Bystrykh Elektronov v Veshchestve* (Solution by the Monte Carlo Method of Problems in the Transport of Fast Electrons in Materials) (Alma-Ata: Nauka, 1972)
12. B Gross, in *Radiation-induced Charge Storage and Polarization. Electrets* (Berlin: Springer, 1980) p. 217
13. B Gross *J. Phys. Rev.* **107** 368 (1957)
14. G Asch, M C Felix, R Ongaro *J. Ind. Atom.* **10** 79 (1966)
15. V P Murphy, F E Hoecker *J. Appl. Phys.* **42** 4094 (1971)
16. T Asada, M Kawanishi, R Kikuchi *J. Mem. Inst. Sci. Industr. Res. (Osaka Univ.)* **24** 35 (1967)
17. B Gross *J. Appl. Phys.* **36** 1635 (1965)
18. A G Sakharov, V V Gromov *J. Radiat. Phys. Chem.* **23** 325 (1984)
19. V M Lenchenko *Atom. Energiya* **29** 53 (1970)
20. G I Distler, Yu M Gerasimov, N M Borisova *Dokl. Akad. Nauk SSSR* **165** 329 (1965)
21. V V Gromov *Atom. Energiya* **26** 250 (1969)
22. V V Gromov, V V Surikov *Atom. Energiya* **32** 172 (1972)
23. A V Bykhovskii, O M Zaraev *Goryachie Aerozol'nye Chastitsy pri Tekhnicheskom Ispol'zovanii Atomnoi Energii* (Hot Aerosol Particles in the Technical Exploitation of Atomic Energy) (Moscow: Atomizdat, 1974)
24. A G Sakharov, V V Gromov *Zh. Fiz. Khim.* **50** 1513 (1976)
25. A G Sakharov, V V Gromov *Zh. Fiz. Khim.* **59** 179 (1985)
26. A G Rozno, V V Gromov *J. Radiat. Phys. Chem.* **23** 295 (1984)
27. V V Gromov, A G Sakharov *J. Radiat. Phys. Chem.* **23** 307 (1984)
28. A G Kotov, V V Gromov *Radiatsionnaya Fizika i Khimiya Geterogennykh Sistem* (Radiation Physics and Chemistry of Heterogeneous Systems) (Moscow: Energoatomizdat, 1988)
29. E K Zavadovskaya, V A Starodubtsev *Izv. Tomsk. Politekh. Inst.* **170** 125 (1969)
30. A A Vorob'ev, E K Zavadovskaya, V A Starodubtsev, B V Fedorov *Izv. Vyssh. Uchebn. Zaved., Fizika* (2) 40 (1977)
31. V G Vakhromeev, S P Zinov'eva *Izv. Vyssh. Uchebn. Zaved., Fizika* (11) 146 (1974)
32. O B Evdokimov, N I Yagushkin *Fiz. Tverd. Tela* **16** 564 (1974)
33. O B Evdokimov, A P Yalovets, F V Shevelev *Fiz. Tverd. Tela* **16** 2398 (1974)
34. B Gross, S V Nablo *J. Appl. Phys.* **38** 2272 (1967)
35. B Gross, J Dow, S V Nablo *J. Appl. Phys.* **44** 2459 (1973)
36. O B Evdokimov, A P Yalovets *Khim. Vys. Energii* **7** 271 (1973)
37. I N Balychev, D I Vaisburd, G I Gering *Pis'ma Zh. Tekh. Fiz.* **2** 327 (1976)
38. I I Gromov *Vliyanie Ioniziruyushchego Izlucheniya na Kinetiku Rastvoreniya Tverdykh Tel* (Effect of Ionising Radiation on the Dissolution Kinetics of Solids) (Moscow: Atomizdat, 1976)
39. V V Gromov *Zh. Fiz. Khim.* **54** 2161 (1980)
40. L B Zuev, M G Tokmashev *Elektrokhimiya* **12** 106 (1976)
41. I F Efremov, O M Rozental *Zh. Fiz. Khim.* **47** 571 (1973)
42. A I Akishin, O E Aksenov, V E Aksenova, in *Radiatsionnaya Stoikost Elektroizolyatsionnykh Materialov Magnitnykh Sistem Termoyadernykh Reaktorov. Chetvertaya Mezhdunarodnaya Konferentsiya po Issledovaniyu i Razrabotke Konstruktsionnykh Materialov dlya Reaktorov Termoyadernogo Sinteza, Moskva 1990. Tezisy Dokladov* (Radiation Stability of Electric Insulators for the Magnetic Systems of Thermonuclear Reactors. Abstracts of Papers Presented to the Fourth International Conference on the Study and Development of Constructional Materials for Thermonuclear Synthesis Reactors, Moscow, 1990) p. 47

Russian Chemical Reviews **62** (11) 1005–1024 (1993)
©1993 Russian Academy of Sciences and Turpion Ltd

UDC 547.682+547.836

Naphthacenequinones: synthesis and properties

N T Sokolyuk, V V Romanov, L P Pisulina

Contents

I. Introduction	1005
II. Methods of synthesis of naphthacenequinones and their derivatives	1005
III. Chemical properties of naphthacenequinones	1012
IV. Spectroscopic properties	1015
V. Tautomerism of naphthacenequinone derivatives	1018
VI. Conclusion	1023

Abstract. The literature data on the methods of synthesis and the properties of naphthacenequinones and related compounds are surveyed. The tautomeric and photochromic transformations of naphthacenequinone derivatives are examined. The bibliography includes 158 references.

I. Introduction

The chemistry of polycyclic quinones is a promising and vigorously developing field of modern organic chemistry. This is associated with the fact that they have been finding increasingly wide application in many branches of science and engineering.

The first and so far the main application of quinones involves their use as organic dyes. In particular, naphthacenequinones—linear benzologues of anthraquinone—have been patented as dyes for synthetic fibres and polymeric resins.[1-10]

The study and synthesis of organic conducting materials based on certain naphthacenequinone derivatives has developed vigorously to the present time.[11-18]

Certain polycyclic quinones have found applications as pharmaceutical preparations. Thus anthracyclines, which are based on the naphthacenequinone carbon skeleton, constitute an important group of antibiotics.[19,20] Studies in the field of anthracyclines have developed vigorously in connection with the search for an alternative biochemical method of synthesis of compounds of this type in the preparation of new antitumour agents.[21-33]

It has been proposed that certain derivatives of naphthacenequinone be used in the manufacture of photochromic materials for the optical recording of information.[34]

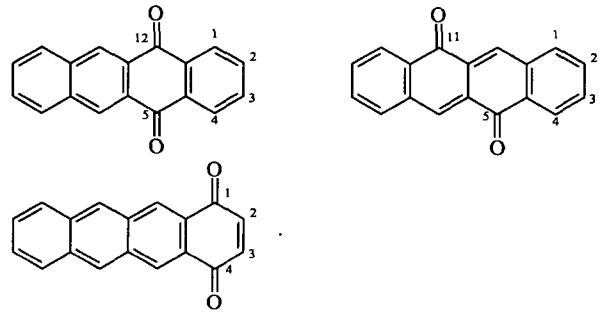
N P Sokolyuk Laboratory of Organic Synthesis, Institute of Fine Organic Synthesis of the 'TOS Industrial Association' Joint-Stock Company (AOPOTOS), Likhachevskii proezd 5, 141700 Dolgoprudnyi, Moscow Region, Russian Federation
V V Romanov Industrial-technical Division, 'Anilin' Stavropol Industrial Association, prosp. Kulakova 14, 355044 Stavropol, Russian Federation
L P Pisulina Laboratory of the Physical Chemistry of Solutions of Macrocyclic Compounds, Insitute of the Chemistry of Nonaqueous Solutions, Russian Academy of Sciences, ul. Akademicheskaya 1, 153045 Ivanovo, Russian Federation, Fax (7-093-2)37 85 09

Received 28 December 1992
Uspekhi Khimii **62** (11) 1078–1097 (1993); translated by A K Grzybowski

This review surveys the literature data on the methods of synthesis and the chemical and spectroscopic properties of naphthacenequinones and presents the results of studies on the tautomeric transformations of these compounds.

II. Methods of synthesis of naphthacenequinones and their derivatives

Depending on the position of the carbonyl groups in the naphthacene nucleus, naphthacenequinones are known to include three monoquinones—5,12-naphthacenequinone (*p*-naphthacenequinone), 5,11-naphthacenequinone (*ana*-naphthacenequinone), and 1,4-naphthacenequinone:



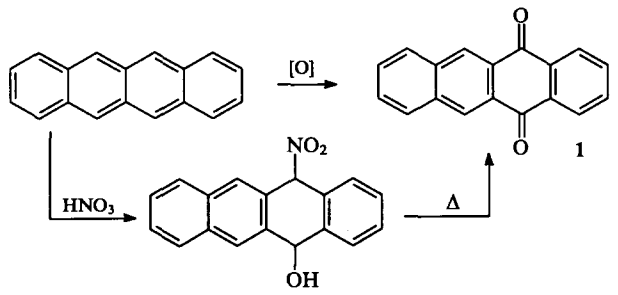
5,12-Naphthacenequinones have been most thoroughly investigated among these compounds.

1. Methods of synthesis of 5,12-naphthacenequinone and its derivatives

The existing methods of synthesis of 5,12-naphthacenequinones can be divided into two groups depending on whether they are based on the use of compounds already having the napthacene carbon skeleton or whether they involve its construction.

The first group includes the oxidation reactions of naphthacene and its derivatives. Chromium trioxide in acetic acid,[35-38] chromic acid,[39] ozone,[40] perbenzoic acid,[41] nitric acid,[42] etc. are used as oxidants.

The unsubstituted 5,12-naphthacenequinone **1** was first obtained by oxidising naphthacene with chromium trioxide in acetic acid.[43]



Substituted derivatives of 5,12-naphthacenequinone were synthesised by a similar procedure: 2-isopropyl-, 2,8-dimethyl-, and 2,9-dimethyl-naphthacenequinones.[35,36] When naphthacene is oxidised with nitric acid, an adduct is first formed, being converted on heating into 5,12-naphthacenequinone **1**.[42]

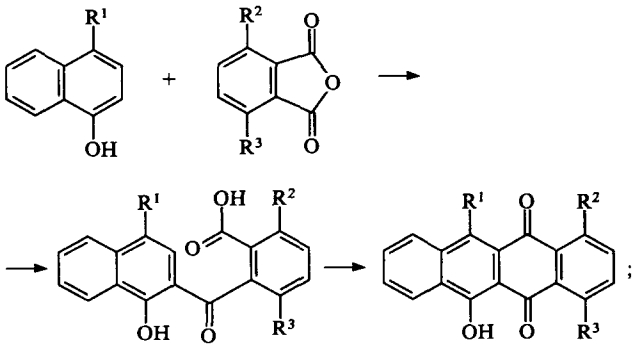
Compound **1** can also be obtained by oxidising naphthacen-5-one.[44,45]

The oxidation of 1,4-dichloronaphthacene leads to 7,10-dichloro-5,12-naphthacenequinone.[39] 6-Chloro- and 6-bromo-5,12-naphthacenequinones have been obtained from 5,11-dihalonaphthacenes.[38]

There exist data indicating the formation of 6,11-dihydroxy-5,12-naphthacenequinone in the vapour-phase oxidation of napthalene.[46,47] A method for the isolation of 6,11-dihydroxy-5,12-naphthacenequinone from the still residues remaining after the distillation of phthalic anhydride by codistillation with liquid paraffin has been proposed.[48]

The second group of methods of synthesis of 5,12-naphthacenequinone derivatives is based on cyclisation reactions, the main ones involving intramolecular acylation and diene synthesis.

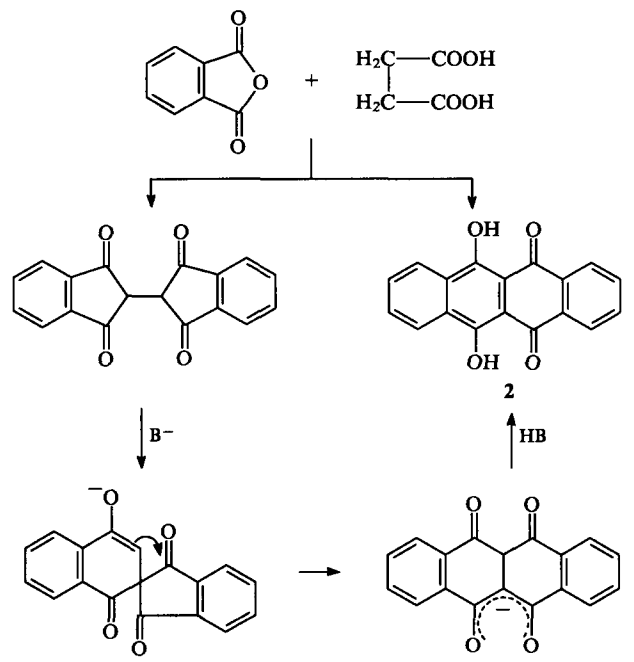
The intramolecular acylation reaction, widely used in the synthesis of anthraquinone derivatives, is also applicable to the synthesis of naphthacenequinones. Unsubstituted 5,12-naphthacenequinone **1** and many of its derivatives have been obtained by acylating naphthalene (or benzene) derivatives with phthalic anhydride (or the anhydride of naphthalene-2,3-dicarboxylic acid) by the Friedel–Crafts reaction in the presence of $AlCl_3$ or boron trioxide followed by the cyclisation of the resulting 2-(β-naphthoyl)benzoic (or 3-benzoyl-2-naphthoic) acid by a mixture of sulfuric and boric acids or in the $AlCl_3$–NaCl melt.[49,50]



R^1 = H, OH; R^2 = H, OH, NO_2, NH_2, NHAc, NMe_2, Cl; R^3 = H, OH, Cl.

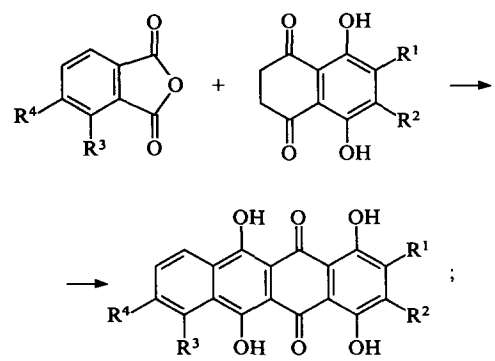
The synthesis of 6-chloro-5,12-naphthacenequinone by the cyclisation of the corresponding naphthoylbenzoic acid on treatment with P_2O_5 has been described.[57]

Condensation of phthalic anhydride with succinic acid leads[58] to diphthalideneethane, which can be readily converted into naphthacenequinone **2**, but 40% of bis-1,3-indandionyl **3** is then formed as a side product. Prolonged refluxing of compound **3** in aqueous ammonia or 10% sodium acetate solution leads to naphthacenequinone **2** in a low yield.[59] When compound **3** is fused with a mixture of sodium and potassium acetates, naphthacenequinone **2** is obtained in 50%–60% yield. A mechanism of this reaction has been proposed.[60]



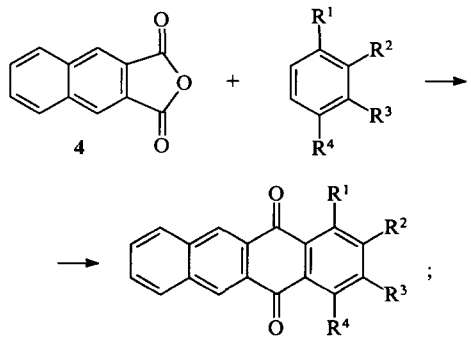
As in the case of the analogous anthraquinone derivatives, in the syntheses of a series of derivatives of 5,12-naphthacenequinone it is possible to carry out the acylation with phthalic anhydride and cyclisation of the resulting acids in a single stage in the presence of strong electron-donating substituents in the molecule to be acylated. The interaction of 1,4-dihydroxynaphthalene and 4,5-difluorophthalic anhydride with phthalic anhydride in the presence of boron trioxide afforded 6,11-dihydroxy-5,12-naphthacenequinone[52] and 2,3-difluoro-5,12-naphthacenequinone[61] respectively.

A whole series of 5,12-naphthacenequinones have been synthesised by the reactions of 3,4-disubstituted phthalic anhydride with derivatives of 2,3-dihydronaphthazarin in a melt of aluminium and sodium chlorides.[62,63]



R^1 = H, OH; R^2 = H; R^3 = OH; R^4 = Et.

A series of substituted 5,12-naphthacenequinones has been synthesised by the reaction of the anhydride of naphthalene-2,3-dicarboxylic acid **4** with substituted benzene derivatives in the presence of aluminium chloride.[49,64]

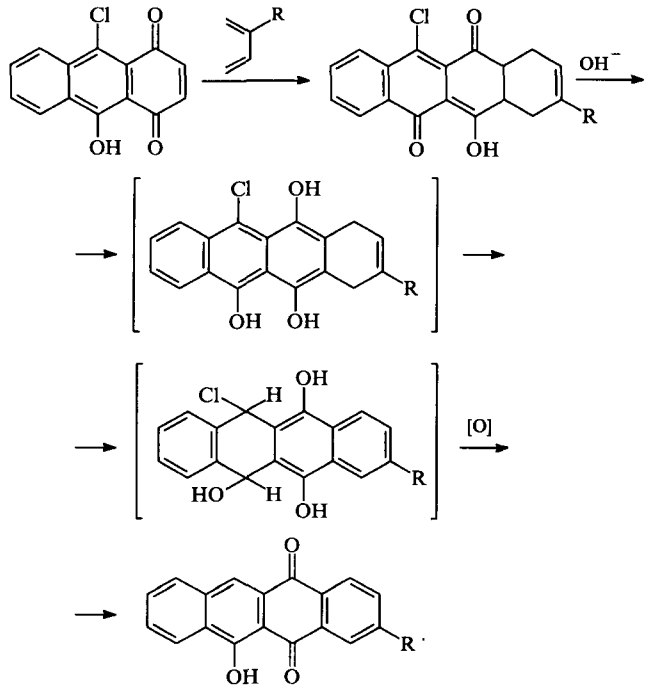


R^1 = Cl, NH_2, Me, OH; R^2 = H, Cl, Me, OH, OAlk, OPh; R^3 = OH; R^4 = H, Hal, OH, OAlk, SAlk, OPh, SPh, NH_2.

Condensation of compound **4** with substituted aminophenols in 80% – 100% sulfuric acid in the presence of boric acid at 100 – 200 °C afforded[65] disperse dyes which dye polyester fibres, giving rise to bright yellowish-red shades.

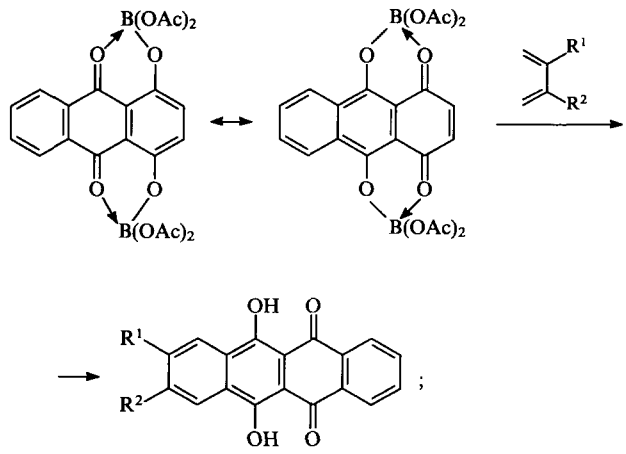
In the synthesis of 5,12-naphthacenequinones by the Diels – Alder reaction, anthraquinone derivatives, which combine with 1,3-dienes, are used as dienophiles. The adducts formed are then oxidised (Scheme 1).[66–70]

Scheme 1



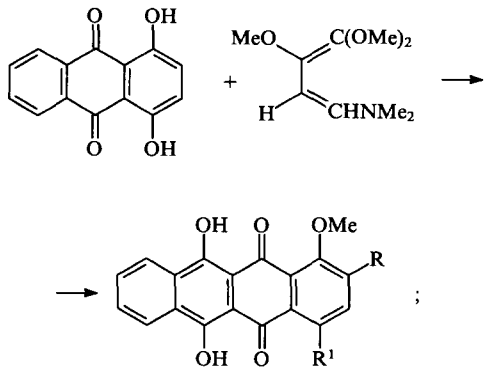
Analogues of natural antibiotics of the tetracycline series have been synthesised in this way.[71–73] There exists convincing evidence[74,75] that the dienophile enters into the reaction as a 1,4-anthraquinone.

The Diels – Alder reaction can be carried out also for the boron complexes of 1,4-dihydroxy- and 1,4-diamino-anthraquinones.[76]



R^1 = R^2 = H, Me.

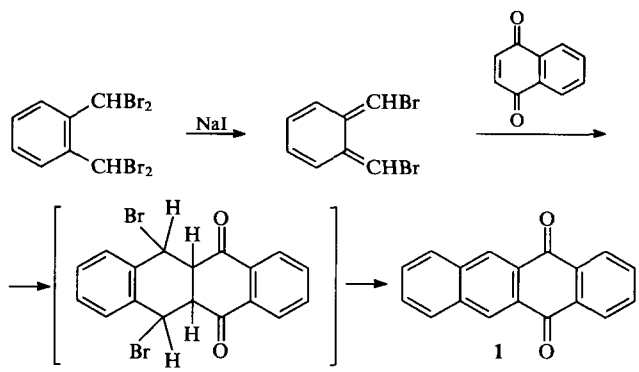
A mixture of naphthacenequinones **5a** and **5b** has been obtained from quinizarin and 4-dimethylamino-1,1,2-trimethoxybuta-1,3-diene.[77]



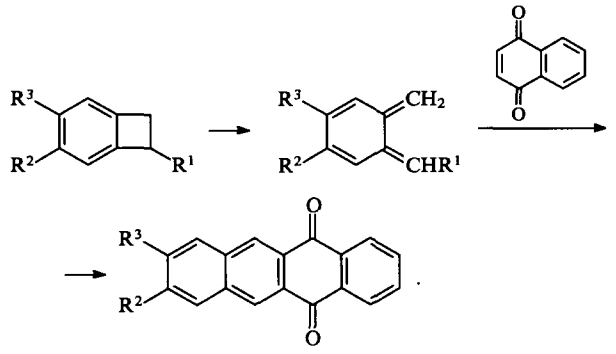
5a,b

5a: R = OMe, R^1 = H; **5b**: R = H, R^1 = NMe_2.

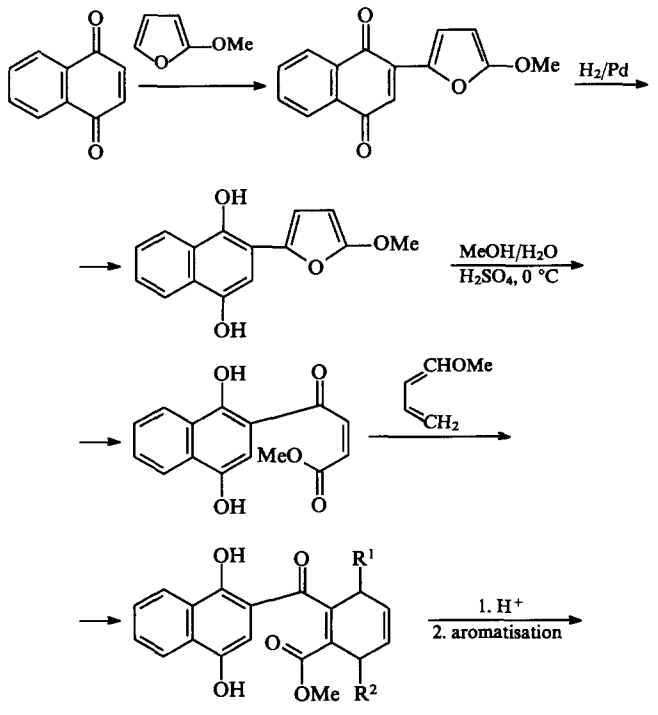
The addition of a dienophile such as dibromo-*o*-benzoquinodimethane to 1,4-naphthaquinone leads to 5,12-naphthacenequinone **1**. Dibromo-*o*-benzoquinodimethane is obtained by treating 1,2-bis(dibromomethyl)benzene with sodium iodide.[78]



The cycloaddition of benzocyclobutenes to 1,4-naphthaquinone apparently also involves the initial formation of the corresponding *o*-quinodimethanes.[79]



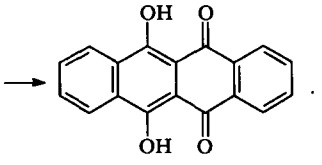
6,11-Dihydroxy-5,12-naphthacenequinone can be obtained in a low yield (13%) from 2-(5-methoxyfuryl)-1,4-naphthaquinone.[80]



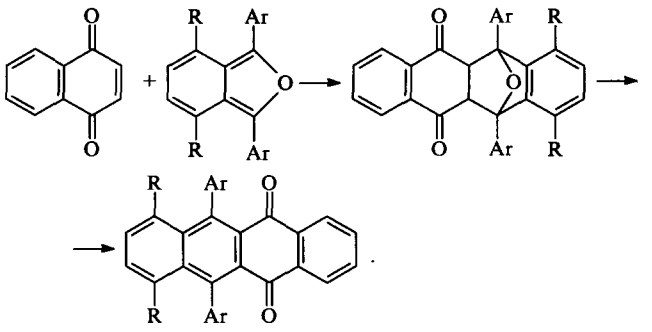
6a,b

6a: R^1 = H, R^2 = OMe; **6b**: R^1 = OMe, R^2 = H

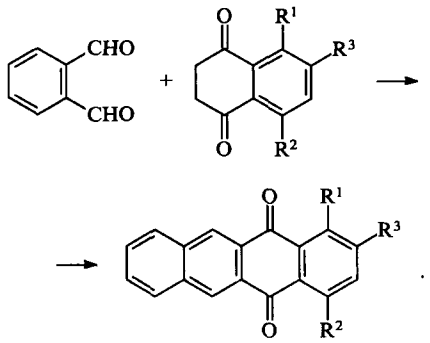
6a : **6b** = 2 : 3



The use of benzofurans in the reaction with 1,4-naphthaquinone permits the synthesis of 5,12-naphthacenequinone derivatives.[81-83]

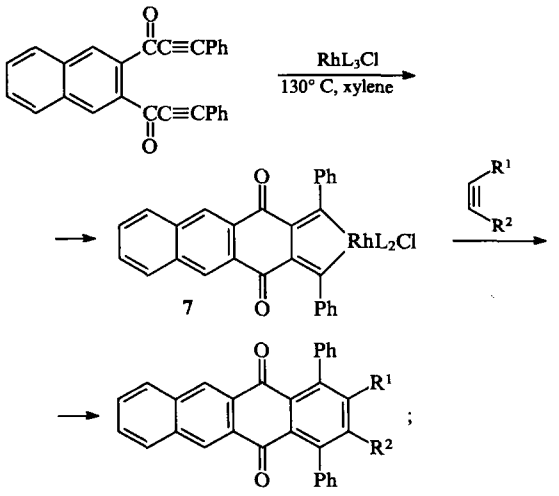


Derivatives of 5,12-naphthacenequinone have also been obtained by condensing aromatic *ortho*-dialdehydes with cyclic γ-diketones.[84-86]



1,4-Dihydroxy-5,12-naphthacenequinones can be obtained similarly from 1,2-diacylbenzenes and 2,3-dihydronaphthazarin in an acid medium.[87]

A method has been proposed for the synthesis of derivatives of 5,12-naphthacenequinone via the rhodium[88-91] and nickel[92] complexes obtained in the reaction of 1,2-bis(1-oxo-3-phenylprop-2-ynyl)naphthalene with ML_3Cl. Thus, when the rhodium complexes **7** are heated with disubstituted acetylenes, cycloaddition takes place with formation of tetrasubstituted naphthacenequinones:

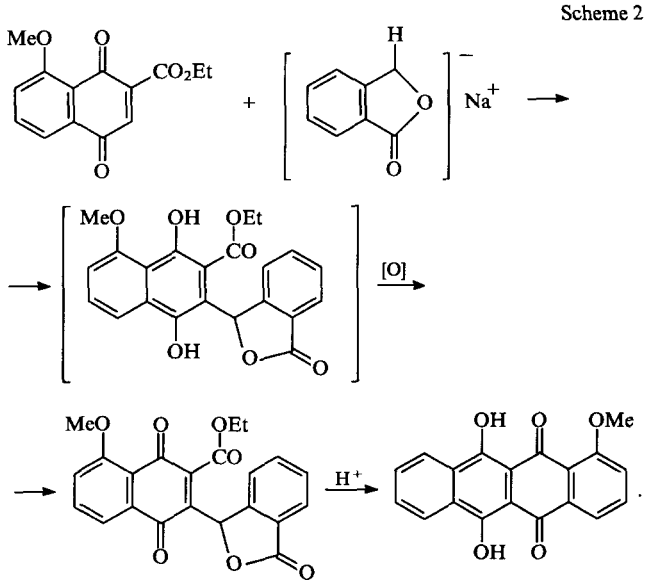


L = PPh_3; R^1 = Me, OEt, COOEt, NEt_2; R^2 = H, Me.

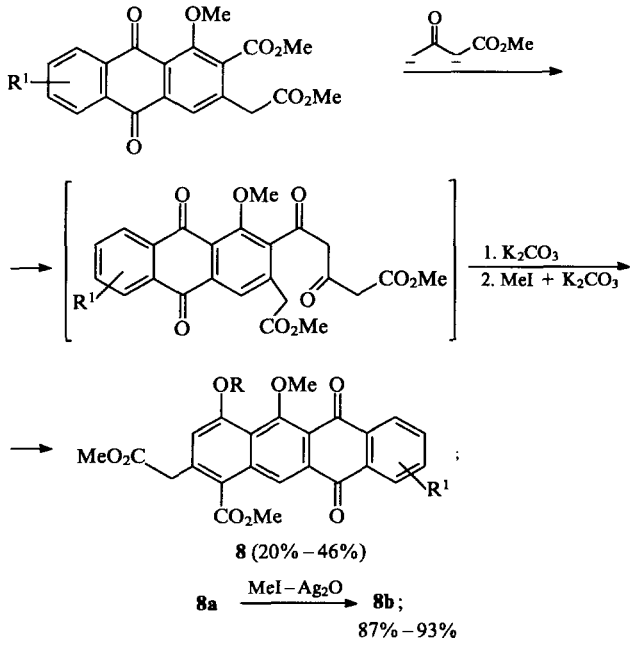
1,2-bis(1-oxo-3-phenylprop-2-ynyl)benzene isomerises to 6-phenyl-5,12-naphthacenequinone on heating or irradiation with UV light.[93]

The synthesis of 6,11-dihydroxy-1-methoxy-5,12-naphthacenequinone, the first stage of which is the addition of the phthalide ion to a substituted naphthaquinone, has been described. The adduct formed undergoes an acid-catalysed cyclisation with simultaneous decarboxylation, affording a substituted naphthacenequinone (Scheme 2).[94]

Scheme 2



Naphthacenequinone derivatives can be obtained by the Claisen condensation of substituted anthraquinones with the dianion of methyl acetoacetate and subsequent cyclisation on treatment with potassium carbonate.[95]

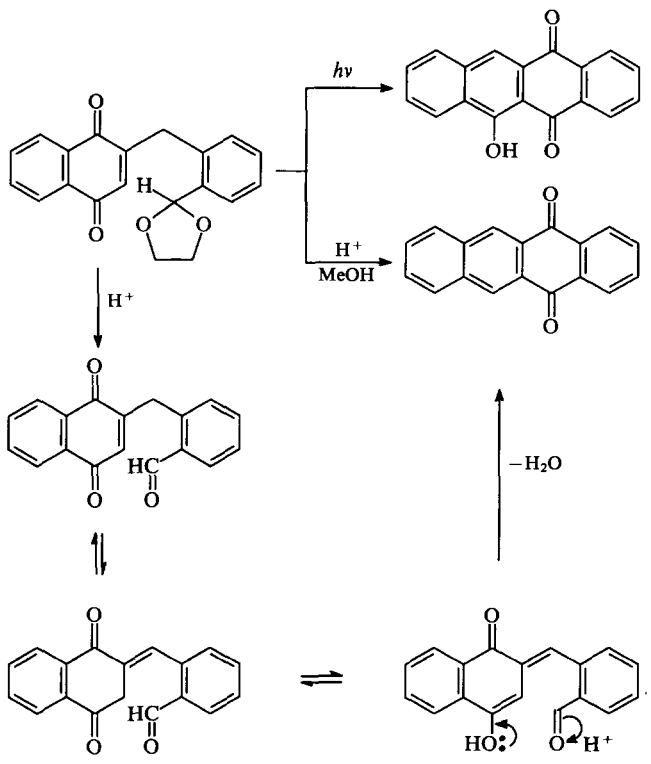


8 (20%–46%)

8a $\xrightarrow{MeI-Ag_2O}$ **8b**; 87%–93%

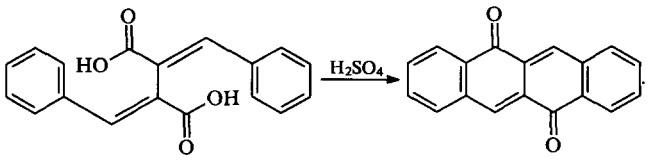
8a: R = H; **8b**: R = Me.

Irradiation of 2-[2-(1,3-dioxolan-2-yl)benzyl]-1,4-naphthaquinone in methanol (in a neutral, acid, or alkaline solution) affords a low yield of 6-hydroxy-5,12-naphthacenequinone. Hydrolysis of 1,4-naphthaquinone in sulfuric acid and methanol leads to naphthacenequinone (a mechanism is proposed for this reaction).[96]



2. Methods of synthesis of 5,11- and 1,4-naphthacenequinones

5,11-Naphthacenequinone (*ana*-naphthacenequinone), an isomer of 5,12-naphthacenequinone, was first obtained by cyclising 1,4-diphenylbuta-1,4-diene-2,3-dicarboxylic acid in concentrated sulfuric acid.[97]

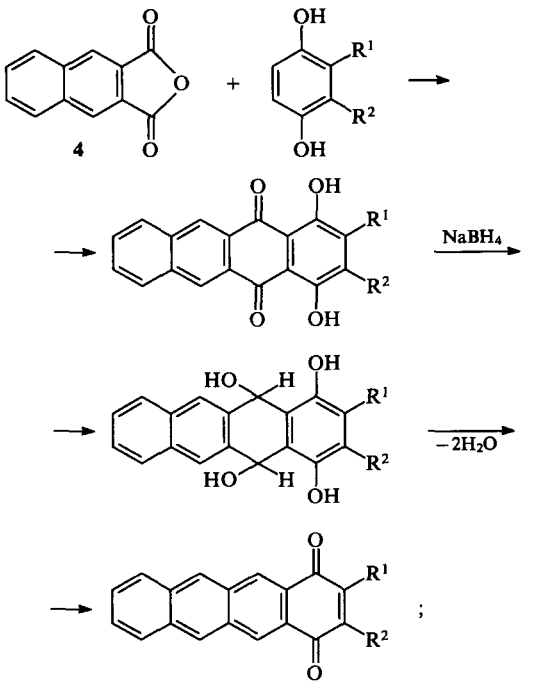


ana-Naphthacenequinone is also formed on hydrolysis of 5,11-dibromonaphthacene.[38] The synthesis of derivatives of 5,11-naphthacenequinone is described below in the section on the properties of 5,11-naphthacenequinone.

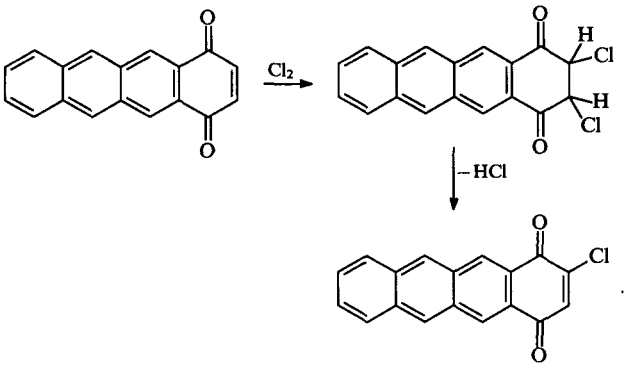
1,4-Naphthacenequinone and its derivatives have been obtained by condensing the anhydride of naphthalene-2,3-dicarboxylic acid **4** with derivatives of hydroquinones containing substituents in the 2- and 3-positions followed by the reduction of the resulting substituted 1,4-dihydroxy-5,12-naphthacenequinones with sodium tetrahydroborate and dehydration.[87,98,99]

1,4-Naphthacenequinone has many of the properties of the so called 'true' quinones having an isolated double bond, such as 1,4-naphthaquinone and 1,4-anthraquinone. Thus, 1,4-naphthacenequinone combines fairly readily with a chlorine molecule at the double bond, giving rise to 2,3-dichloro-2,3-dihydro-1,4-naphthacenequinone,[98,99] which readily splits off hydrogen chloride and is converted into the true monochloroquinone.[99]

The relatively unstable adduct was characterised in terms of the intense IR absorption band at 1721 cm^{-1} due to the carbonyl stretching vibration.



R^1 = H, Me, Cl, Br; R^2 = H, Cl, Me.



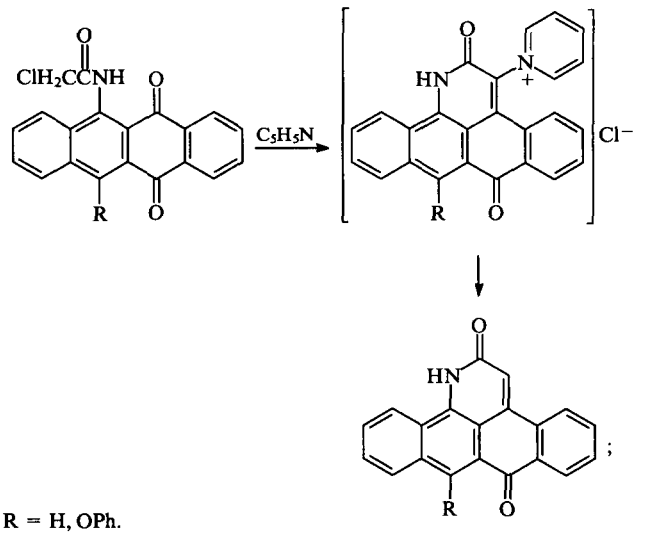
3. Methods of synthesis of heterocyclic *peri*-condensed derivatives of naphthacenequinone

In the series of naphthacenequinones, an important place is assumed by its heterocyclic *peri*-condensed derivatives. In terms of the site where the heterocycle has been added, 1,12- and 11,12-substituted derivatives are known.

As in the case of anthraquinone derivatives, the interaction of a heteroatom or functional group in the *peri*-position relative to one of the carbonyl groups of 5,12-naphthaquinone with this carbonyl group leads to the closure of a new ring beween these positions. The cyclisation reaction, leading to the formation of a new bond involving the carbon atom of the carbonyl group of naphthacenequinone, constitutes an intramolecular nucleophilic addition reaction with subsequent dehydration. The addition of a C-nucleophile and dehydration are accompanied by the replacement of a C=O bond by a C=C bond in 5,12-naphthacenequinone derivatives and the formation of a new ring.

Thus in 6-aminonaphthacenequinone the C-nucleophile bound to the nitrogen atom attacks the carbonyl group in the 5-position, which results in the closure of a six-membered nitrogen-containing ring with formation of a new heterocyclic derivative of naphthacenequinone—2*H*,8*H*-naphtho[1,2,3-*de*]-benzo[*h*]quinoline-2,8-dione (naphthacenopyridone).

Naphthacenopyridones are formed as a result of the cyclisation of 6-(*N*-chloroacetyl)amino-5,12-naphthacenequinones in pyridine to the corresponding naphthaceno(2-oxo-3-pyridyl)pyridinium chlorides[100,101] and subsequent reductive elimination of the pyridinium residue.

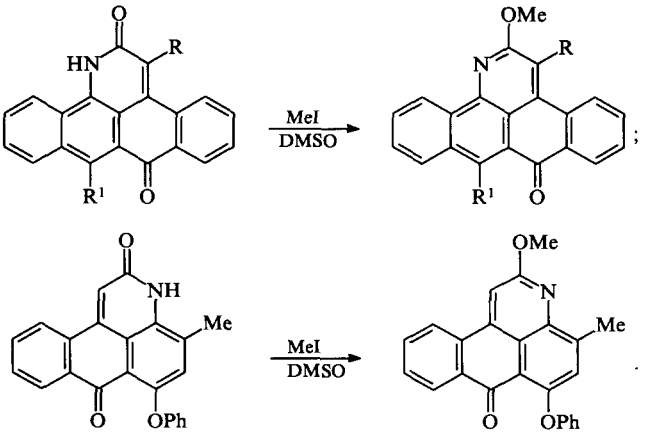


R = H, OPh.

When 6-acetamido-5,12-naphthacenequinone and its 11-chloro-derivative are heated in phenol in the presence of sodium carbonate, the elimination of the acetyl group results in the formation, together with naphthacenopyridone and its 9-phenoxy-derivative, of an appreciable amount of 6-amino- and 6-amino-11-phenoxy-5,12-naphthacenequinones.[101]

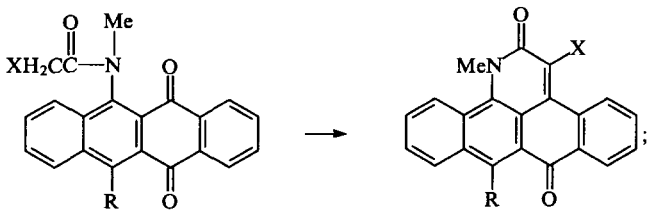
The 3-acetyl derivative of naphthacenopyridone has been obtained by the reaction of 6-amino-11-chloro-5,12-naphthacenequinone with acetoacetic ester in phenol in the presence of potassium carbonate.[101] The conditions in this reaction are the same as those used for the synthesis of anthrapyridones.[102]

Methylation of naphthacenopyridones with methyl iodide in dimethyl sulfoxide leads to 2-methoxynaphthacenopyridines (*O*-methyl derivatives), whereas methylation of anthrapyridone under the same conditions affords its *N*-methyl derivative.



This difference in the behaviour of similar structures under identical conditions is apparently associated with steric hindrance to alkylation at the nitrogen atom in the case of naphthacenopyridones. Indeed, the sterically hindered 4-methyl-6-phenoxyanthrapyridone forms on methylation 2-methoxy-4-methyl-6-phenoxyanthrapyridine (the *O*-methyl derivative), in contrast to 6-phenoxyanthrapyridone.[101]

2*H*,8*H*-Methylnaphtho[1,2,3-*de*]benzo[*h*]quinoline-2,8-diones (*N*-methylnaphthacenopyridones) are obtained by heating 6-(*N*-acetyl)methylamino-5,12-naphthacenequinone in 3% aqueous[104] or alcoholic[105] sodium hydroxide solution. 6-(*N*-Acetyl)methylamino-11-chloro- and 6-(*N*-acetyl)methylamino-11-phenoxy-5,12-naphthacenequinones are converted under these conditions into 9-hydroxy-*N*-methylnaphthacenopyridones. A convenient method of synthesis of *N*-methyl-9-phenoxynaphthacenopyridone involves heating 6-(*N*-acetylmethylamino-11-phenoxy-5,12-naphthacenequinone in phenol in the presence of potassium carbonate.[103]

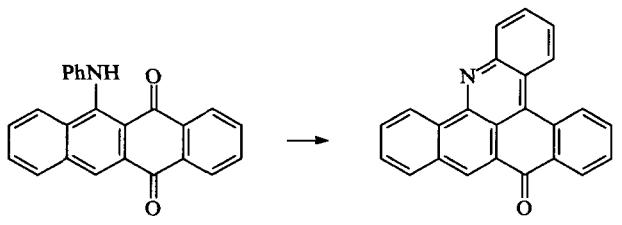


X = H: R = H, OPh, OH;
X = Cl: R = OPh.

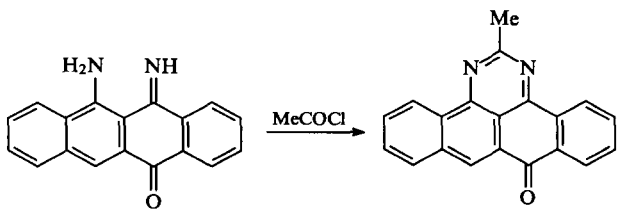
Heating of 6-(*N*-chloroacetyl)methylamino-11-phenoxy-5,12-naphthacenequinone in phenol leads to 3,9-diphenoxy-*N*-methylnaphthacenopyridone, i.e. cyclisation with simultaneous substitution in the resulting napthacenepyridone of the chlorine atom in the 3-position by a phenoxy-group takes place under these conditions.

A widely known method of synthesis of anthrapyridones, involving the cyclisation of chloroacetamidoanthraquinones in pyridine, proved to be applicable also to the synthesis of 3-chloro-*N*-methyl-9-phenoxynaphthacenopyridone.[100] 1-Methyl-9-phenoxynaphthaceno(2-oxo-3-pyridyl)pyridinium chloride, formed on heating the chloroacetamido-derivative of naphthacenequinone in pyridine, is converted into naphthacenopyridone on subsequent refluxing in nitrobenzene.[103]

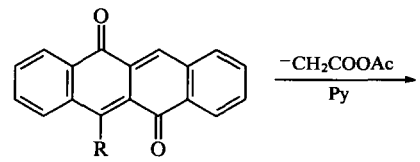
Cyclisation of 6-phenylamino-5,12-naphthacenequinone under the conditions used for the synthesis of ceramidonines, namely treatment with aluminium chloride or 75% sulfuric acid, leads to naphthacenoceramidonine[106] — 10*H*-naphtho-[*m*,*n*]benzo[*c*]-10-acridone.



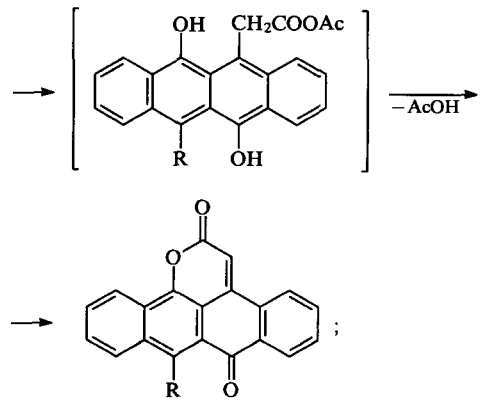
A naphthacenopyrimidine — 8*H*-dibenzo[*e*,*j*]pyrimidin-8-one — has been obtained by the reaction of 6-amino-5,12-naphthacenequinone imine with acetyl chloride in pyridine.[107]



Heterocyclic derivatives of naphthacenequinone with an oxygen-containing six-membered heterocycle — 2*H*,8*H*-naphtho[1,2,3-*de*]benzo[*h*]-1,2-chromene-2,8-diones (naphthacenopyrones) — are formed on reaction of 5,11-naphthacenequinones with acetic anhydride in pyridine or triethylamine.[108,109]



R = NAcPh (**9**), H, OPh.

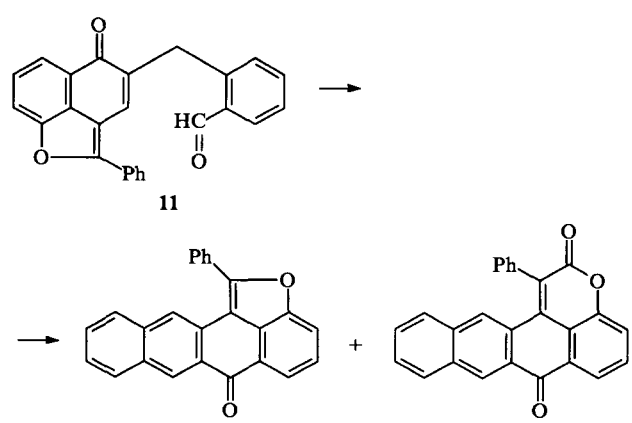


R = NAcPh, NHPh (**10**), H, OPh.

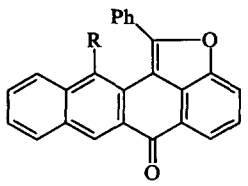
6-(*N*-Acetyl)phenylamino-5,11-naphthacenequinone interacts even more readily with malonic ester in pyridine to form 3-ethoxycarbonylnaphthacenopyrone.[108] In all the reactions enumerated above, the carbanion generated from acetic anhydride in the presence of pyridine apparently adds (via a Michael reaction) to the carbon atom in the 12-position with subsequent oxidation of the dihydro-derivative and the formation of the corresponding pyrone.

Refluxing of compound **9** (R = NAcPh) in a mixture of acetic and hydrochloric acids leads to the pyrone **10** (R = NHPh).[108]

Among the heterocyclic 1,12-*peri*-condensed derivatives of naphthacenequinone, compounds containing furan and pyrone rings are known. Treatment of the aldehyde **11** with sodium cyanide leads to a mixture of 1-phenylnaphtho[2,3-*e*]-benzo-[*h*,*i*]isobenzofuran-6-one (a naphthacenofuran) and 1-phenyl-7*H*,2*H*-benzo[*cd*]naphtho[2,3-*g*]-1,2-chromene-2,7-dione (a naphthacenopyrone). The naphthacenopyrone is formed on interaction of the naphthacenofuran with sodium cyanide.[110]



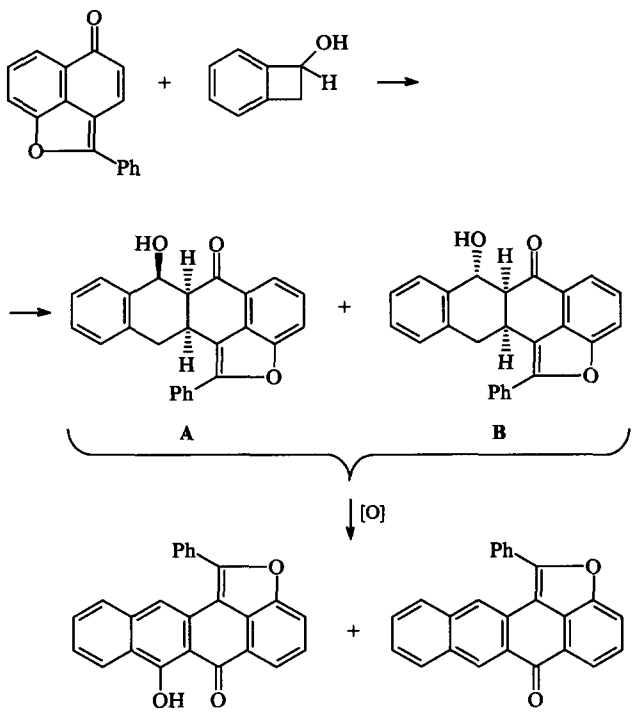
Treatment of the cyanohydrin of the aldehyde **11** with sodium hydride leads to cyano- and hydroxy-naphthacenofurans.[110]



R = OH, CN.

Thermal condensation of derivatives of naphthofuran with benzocyclobutenol in the dark results in the formation of a mixture of the stereoisomers **A** and **B**, the oxidation of which affords a mixture of naphthacenofurans (Scheme 3).[111]

Scheme 3



Treatment of the isomers **A** and **B** with a solution of alkali leads to a single naphthacenofuran.

III. Chemical properties of naphthacenequinones

1. Properties of 5,12-naphthacenequinone and its derivatives

On treatment with an alkaline solution of sodium hydrogen sulfite, 5,12-naphthacenequinone is converted into the unstable green 5,12-dihydroxynaphthacene. The latter is readily oxidised to 5,12-naphthacenequinone and also enters readily into disproportionation and ketone formation reactions.[113] The reduction potential of 5,12-naphthacenequinone has not been measured owing to the instability of the corresponding hydroquinone (the calculated value is −0.3146 V).[114] The reduction of 5,12-naphthacenequinone with tin in acetic acid leads to the stable naphthacene-5-one; refluxing with zinc dust in an alkaline alcoholic solution affords 5,12-dihydronaphthacene.[113]

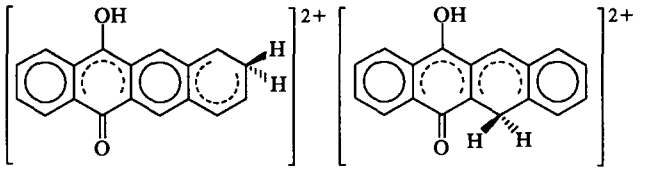
The reduction of alkylhydroxynaphthacenequinone with a cyclohexanol–aluminium cyclohexanolate mixture leads to alkylnaphthacenes.[115,116]

The polarographic behaviour of 5,12- and 5,11-naphthacenequinones in water–pyridine buffer mixtures of different composition has been investigated.[117] The reversible two-electron wave observed in acid solutions corresponds to the process[117]

$$Q + 2e^- + 2H^+ \rightleftharpoons QH_2,$$

where Q is the naphthacenequinone.

5,12-Naphthacenequinone is protonated twice in sulfuric acid. The pK_a for the first and second protonations have been determined[118] as −8.20 and −8.66 respectively. It has been suggested[118] that the second proton adds to the carbon atom of the terminal aromatic ring. Quantum-chemical calculation and ^1H NMR data indicate the formation of structures **A** and **B** on protonation.[119]

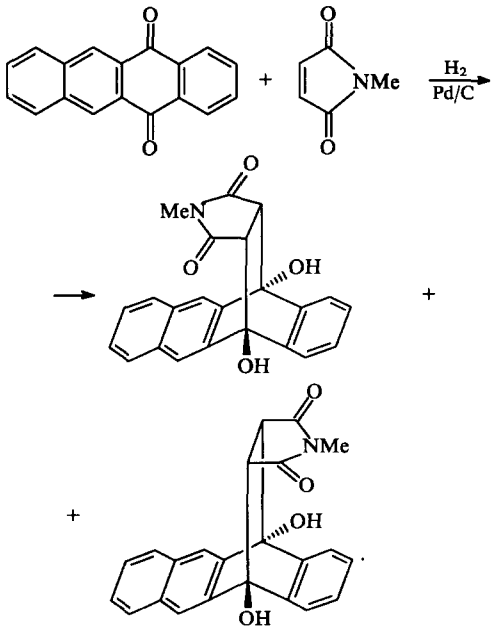


A **B**

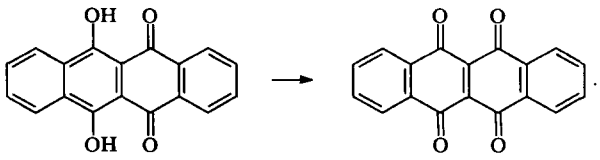
The mechanism of the electrochemical reduction in dimethylformamide of 6,11-dihydroxy-5,12-naphthacenequinone, which is reduced reversibly to 5,6,11,12-tetrahydroxynaphthacene, has been investigated by polarographic and cyclic voltammetric methods.[120]

The reduction half-wave potential of 5,12-naphthacenequinone in dimethylformamide in the presence of lithium perchlorate increases with increasing concentration of lithium ions, which has been explained by the formation of 1 : 1 and 1 : 2 ionic associated species.[121]

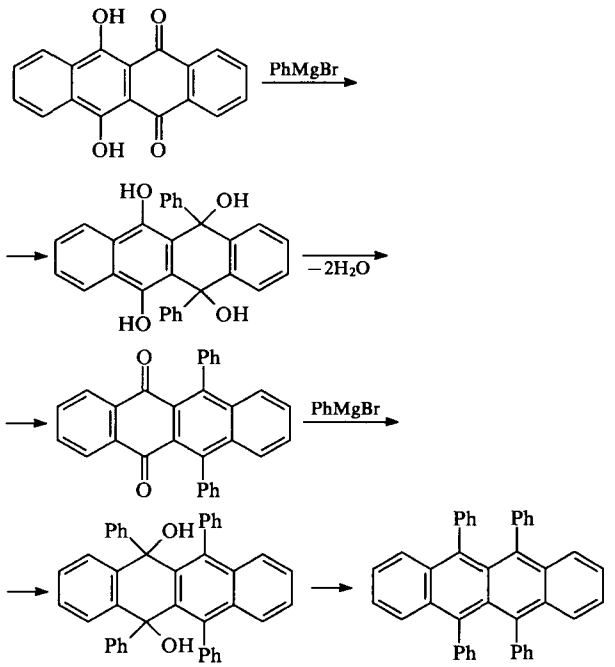
The catalytic reduction of a mixture of 5,12-naphthacenequinone and *N*-methylmaleimide in pyridine affords two products, which have been identified as the *endo*- and *exo*-adducts.[122]



Oxidation of 6,11-dihydroxy-5,12-naphthacenequinone with nitric acid leads to the formation of 5,12;6,11-naphthacenediquinone.[43]

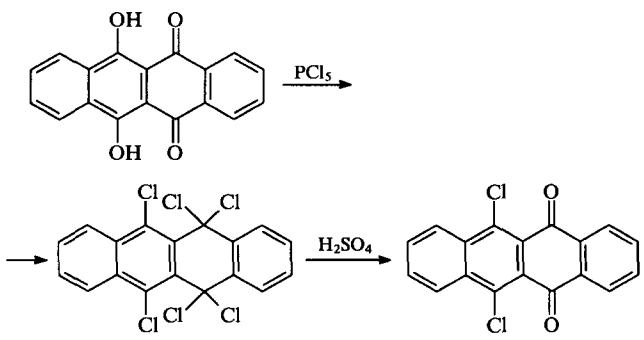


The interaction of naphthacenequinones with phenylmagnesium bromide leads to diols.



This reaction has been used in one of the syntheses demonstrating the structure of rubrene.[123]

The interaction of PCl_5 with 6-hydroxy-5,12-naphthacenequinone in nitrobenzene results in the formation of 6-chloro-5,12-naphthacenequinone,[38,57,124] while the reaction with 6,11-dihydroxy-5,12-naphthacenequinone affords 5,5,6,11,12,12-hexachlorodihydronaphthacene, the hydrolysis of which in sulfuric acid leads to 6,11-dichloro-5,12-naphthacenequinone.



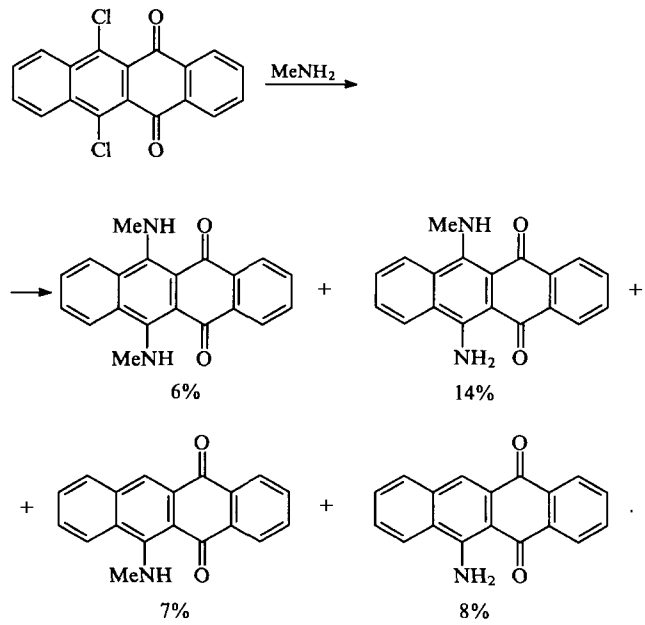
The reaction of 6,11-dihydroxy-5,12-naphthacenequinone with PCl_5 is carried out either in tetrachloroethane[125] or without a solvent in a sealed tube.[126] An improved method of synthesis of 6,11-dichloro-5,12-naphthacenequinone in a PCl_5—quinone melt has been proposed.[127]

6,11-Dichloro-5,12-naphthacenequinone is also formed on heating 5,12-naphthacenequinone with sulfuryl chloride in a sealed tube.[38,124] On reaction with thionyl chloride, 5,12-naphthacenequinone affords 11-chloro-6-hydroxy-5,12-naphthacenequinone.[128]

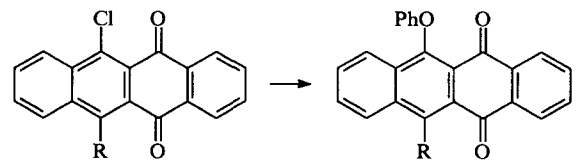
Like 1-halo- and 1,4-dihaloanthraquinones, 6-halo- and 6,11-dihalo-5,12-naphthacenequinones enter into nucleophilic substitution reactions. The mobilities of the halogen atoms in these compounds are similar.

6-Amino- and 6,11-amino-5,12-naphthacenequinones have been obtained by treating chloronaphthacenequinones with toluene-*p*-sulfonamide or benzamide in the presence of copper salts and subsequent hydrolysis of the resulting tosylamino-derivatives.[49,57] 6-Amino-5,12-naphthacenequinone can also be synthesised from 6-chloro-5,12-naphthacenequinone and ammonia under pressure.[129] The interaction of 6,11-dichloro-5,12-naphthacenequinone with one mole of toluene-*p*-sulfonamide in nitrobenzene in the presence of copper salts and subsequent hydrolysis in sulfuric acid lead to 6-amino-11-chloro-5,12-naphthacenequinone.[127]

Treatment of 6,11-dichloro-5,12-naphthacenequinone with methylamine led to the formation of a mixture of amines.[130]

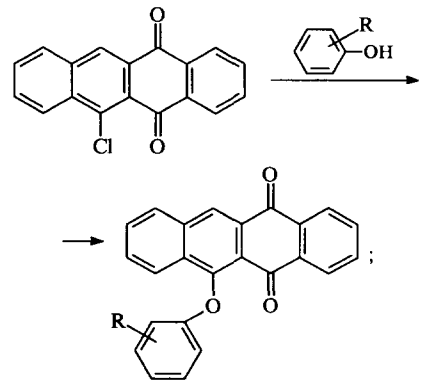


The interaction of halonaphthacenequinones with potassium phenoxide in phenol results in the formation of derivatives of 11-phenoxynaphthacenequinone.[127,129]



R = NH_2, H, NHTs, OPh.

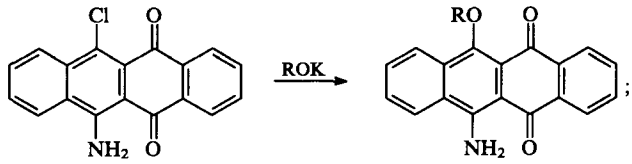
A series of 6-aryloxy-5,12-naphthacenequinones has been synthesised by the reactions of 6-chloro-5,12-naphthacenequinone with substituted phenols.



R = *p*-Br, *p*-OH, *p*-OMe, *p*-NHPh, 2,4,6-Me_3, *p*-MeCO, *p*-NO_2, *p*-NH_2.

6-(4-Aminophenoxy)-5,12-naphthacenequinone has been obtained by reducing 6-(4-nitrophenoxy)-5,12-naphthacenequinone on palladised charcoal in formic acid.[131]

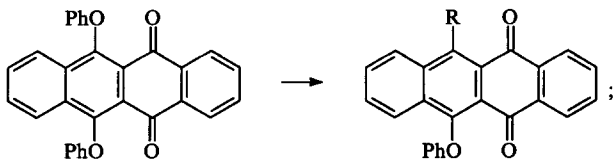
When 6-amino-11-chloro-5,12-naphthacenequinone and a substituted phenol were heated in an ArOH–ArO$^-$ melt in the presence of copper(I) chloride, 6-amino-11-aryloxy-5,12-naphthacenequinones were synthesised.[132]



R = *p*-MeC_6H_4, *p*-EtC_6H_4, *p*-$MeOC_6H_4$, *p*-$HPhNC_6H_4$, *p*-HOC_6H_4, *m*-ClC_6H_4, *p*-$O_2NC_6H_4$, α-$C_{10}H_7$.

The attempt to synthesise 6-amino-11-(4-hydroxyphenoxy)-5,12-naphthacenequinone by heating 6-amino-1-chloro-5,12-naphthacenequinone in an excess of the hydroquinone led only to the dehalogenation of the initial compound. 6-Amino-11-(4-hydroxyphenoxy)- and 6-amino-11-(4-phenylamino)-5,12-naphthacenequinones have been obtained by the reaction of 6-amino-11-chloro-5,12-naphthacenequinone with the corresponding substituted potassium phenoxide in dimethyl sulfoxide in the presence of copper(I) chloride.[132]

The interaction of 6,11-diphenoxy-5,12-naphthacenequinone with aliphatic and aromatic amines leads to 6-R-11-phenoxy-5,12-naphthacenequinone.[127]



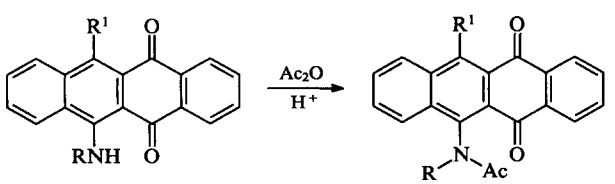
R = NHMe, NMe_2, NHPh.

6-Methoxy-11-phenoxy-5,12-naphthacenequinone has been obtained by the transesterification of diphenoxynaphthacenequinone with methanol in benzene.[127]

6-Acetoxy-11-phenoxy-5,12-naphthacenequinone has been synthesised from 6-hydroxy-11-phenoxy-5,12-naphthacenequinone and acetic anhydride in the presence of pyridine.[127]

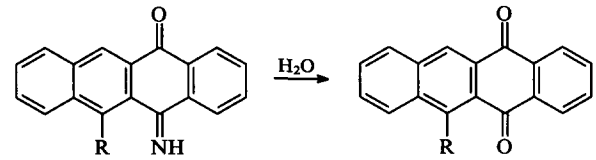
Acetoxy- and benzoyloxy-groups located in the *peri*-positions relative to the carbonyl group of naphthacenequinone are converted into hydroxy-groups on treatment with trifluoroacetic acid containing a small amount of water. With increase in the water content, the rate of the first-order reaction falls.[132]

Acetylation of aminonaphthacenequinones with acetic anhydride in the presence of sulfuric acid leads to *N*-acetyl derivatives.[127]



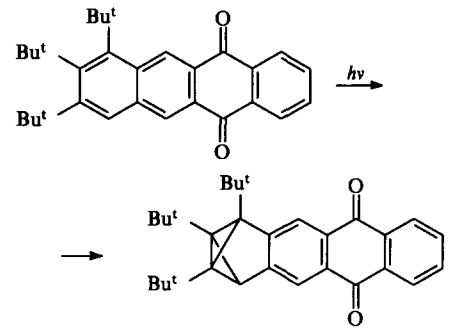
6-Nitro-11-phenoxy-5,12-naphthacenequinone has been synthesised by oxidising 6-amino-11-phenoxy-5,12-naphthacenequinone with peracetic acid.[127]

Hydrolysis of 5-iminonaphthacen-12-one leads to 5,12-naphthacenequinone.[44,45,107]



R = H, Ph, NH_2.

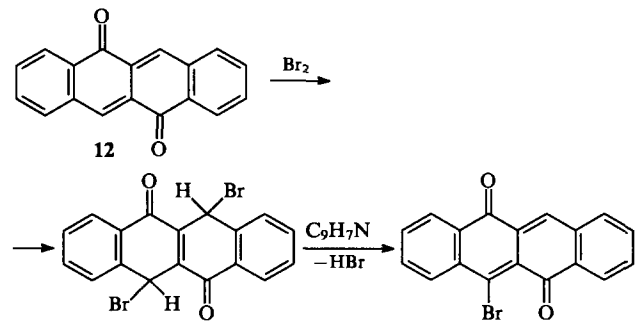
8,9,10-Tri(*tert*-butyl)naphthacenequinones have been synthesised. Under the influence of light, they undergo photovalent isomerisation with formation of a kinetically stable bicyclobutane derivative in a quantum yield of 0.09.[134]



2. Properties of 5,11-naphthacenequinones

The reduction of 5,11-naphthacenequinone **12** with zinc leads to the formation of naphthacene,[97] whilst its fusion with alkali in air gives rise to 6,11-dihydroxy-5,12-naphthacenequinone.[97]

5,11-Naphthacenequinone readily combines with bromine in the 6- and 12-positions with formation of a dibromodihydro-derivative, which on treatment with quinoline is converted into 6-bromo-5,11-naphthacenequinone.[39]



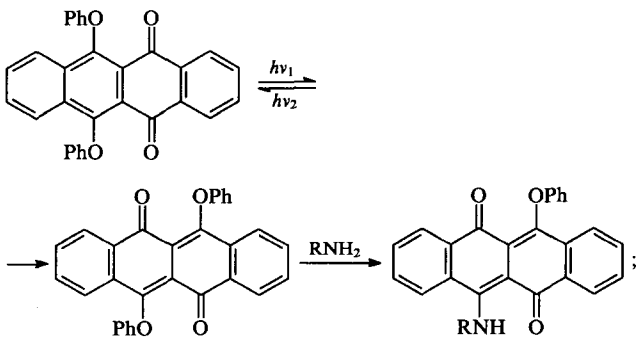
The reaction of 6-bromo-5,11-naphthacenequinone with aniline leads to 6-phenylamino-5,12-naphthacenequinone.[39]

When 5,11-naphthacenequinone is heated with sulfuryl chloride in nitrobenzene at 120–150 °C 6-chloro-5,12-naphthacenequinone is formed.[38,124] This reaction is an example of the conversion of an *ana*-quinonoid structure into a *p*-quinonoid structure. If the reaction is carried out with an excess of sulfuryl chloride in a sealed tube, 6,11-dichloro-5,12-naphthacenequinone is obtained.[38,124]

It follows from the foregoing that the 6- and 12-positions in the 5,11-naphthacenequinone molecule are reactive in relation to nucleophiles. Thus heating of 5,11-naphthacenequinone in aniline leads to 6-phenylamino-5,11-naphthacenequinone.[39]

Reactions involving the nucleophilic substitution of the halogen atom in 6-halo-5,11-naphthacenequinones proceed under much milder conditions[39] than the analogous reactions in the series of 5,12-naphthacenequinones and anthraquinones. 6-Bromo-5,11-naphthacenequinone interacts readily with primary amines at room temperature with formation of 6-amino-5,11-naphthacenequinones in quantitative yields.[39]

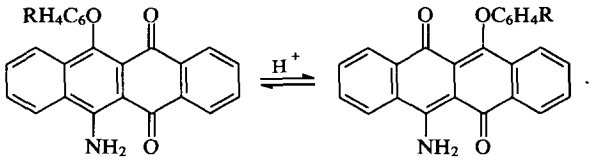
The phenoxy-group in 6-phenoxy-5,11-naphthacenequinones is extremely readily substituted by an amino-group.[135] 6-Amino-12-phenoxy-5,11-naphthacenequinones have been obtained by treating 6,12-diphenoxy-5,11-naphthacenequinone with an amine RNH_2; 6,12-diphenoxy-5,11-naphthacenequinone is formed as a result of a photorearrangement of the *p*-quinone.[127]



R = H, Me, Ph.

Treatment of 6-bromo- and 6-phenoxy-5,11-naphthacenequinones with secondary amines does not lead to tertiary amines but to 6-hydroxy-5,12-naphthacenequinone, which is probably associated with the impossibility of the existence of such tertiary amines in a stable *p*-quinone imine form.[108]

6-Amino-12-aryloxy-5,11-naphthacenequinones have been obtained by the acid rearrangement of the corresponding *p*-quinones.[132,136]



Acetylation of amino-derivatives of *ana*-naphthacenequinone with acetic anhydride leads to *N*-acetamido-5,11-naphthacenequinones.[108,127]

The interaction of 6-hydroxy- and 6,12-dihydroxy-5,11-naphthacenequinones with aniline in the presence of boric acid will be examined in the section devoted to the tautomeric transformations of naphthacenequinones.

IV. Spectroscopic properties

The IR spectra in the 1665–1678 cm^{-1} range of 5,12-naphthacenequinones contain absorption bands due to the C=O bond stretching vibrations characteristic of *p*-quinones with integral intensities $A_{C=O}$ of 2.0 for each C=O group. The presence of intramolecular hydrogen bonds lowers $\nu_{C=O}$ (the amino-group exerts a particularly strong influence). The intense absorption bands due to the stretching vibrations of the bonds of the quinonoid ring O=C–C=C–C=O in the region of 1280 cm^{-1}, which are typical of quinones, are observed in the range 1275–1290 cm^{-1} in the case of *p*-naphthacenequinones.

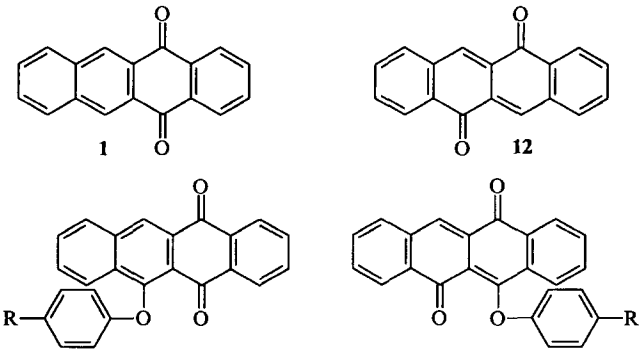
The IR spectra of 5,11-naphthacenequinones differ markedly[137] from those of 5,12-naphthacenequinones. The frequency of the stretching vibrations of the C=O bonds diminishes to 1650–1655 cm^{-1}, while the integral intensity $A_{C=O}$ falls to 1.3. In the absorption region of C=C bonds, there is only one absorption band at 1595 cm^{-1} with an enhanced intensity in the spectra of 5,11-naphthacenequinones, in contrast to 5,12-naphthacenequinones. The absorption bands due to the quinonoid ring bonds of the *ana*-isomers are displaced to 1320 cm^{-1} with retention of their intensity. The results indicate an increase in the degree of delocalisation of the π-electron density in the *ana*-isomers compared with the *para*-isomers, as suggested by Nurmukhametov et al.[138] This is confirmed both by the decrease in $\nu_{C=O}$ and $A_{C=O}$ (since the bond dipole moments, characterised by the integral intensities of the absorption bands, are reduced on delocalisation) and by the increase in the intensity of the absorption bands due to the C=C bonds in the region of 1595 cm^{-1}.

A two-dimensional electron-gas model has been used to calculate the π-electron density and spectral transition energies in naphthacenequinones; the transition energies obtained agree well with the experimental data.[139]

The localisation energies of different types have been calculated by the MO method for 5,12- and 5,11-naphthacenequinones.[140]

The main chromophore in the *p*-naphthacenequinone molecule is the naphthalene ring with two-carbonyl groups in the β-positions, while in the *ana*-naphthacenequinone molecule it is the diphenylbutadiene component with two carbonyl groups.[138,141]

The absorption spectrum of 5,12-naphthacenequinone **1** in hexane is characterised by the long-wavelength absorption band due to the $\pi \rightarrow \pi^*$ transition with vibrational structure and a relatively weak shoulder corresponding to the $n\pi^*$ absorption.[142] The validity of this interpretation is confirmed by the hypsochromic shift of the $n\pi^*$ absorption band with increase in the number of rings in the series benzoquinone → naphthaquinone → anthraquinone. On passing from anthraquinone to naphthaquinone, there are no further changes in the system of conjugated bonds, including the carbonyl group, and hence there are no reasons for a further hypsochromic displacement of the absorption band despite the increase in the number of rings in the molecule. Therefore the lowest singlet state in naphthacenequinone is the $n\pi^*$ state, as in the quinones with a smaller number of rings.[143]



R = H, NO_2, Ac.

The introduction of a phenoxy-group or of more complex substituents in the 6-position in the naphthacenequinone molecule does not induce any significant change in the position of the long-wavelength $\pi\pi^*$ band. The $n\pi^*$ band in the absorption spectra of these compounds is not observed explicitly, possibly owing to the electron-donor effect of the phenoxy-group which induces an increase in the energy of the $n\pi^*$ transition.

The bathochromic shift of the long-wavelength absorption band after the introduction of hydroxy- and amino-groups in the 6-position in naphthacenequinone can be readily accounted for

in terms of the molecular orbital theory concerning the influence of electron-donating substituents on the electronic spectra of aromatic molecules. When electron-donating substituents are introduced, a higher occupied π orbital appears, which induces a decrease in the $S_1 - S_0$ transition energy. In the case of a strong electron-donating substituent (the amino-group is of this kind), this orbital corresponds to a large extent to the heteroatom and can be designated as a π_{ED} orbital, whereas in the presence of a weaker substituent (the hydroxy-group) it is the perturbed highest occupied π_{Ar} orbital. In conformity with the foregoing, the long-wavelength absorption band of 6-aminonaphthacenequinone can be assigned to the $\pi_{ED} \rightarrow \pi^*_{EA}$ transition, while the band in the range 25 000–28 000 cm^{-1} can be assigned to the $\pi_{Ar} \rightarrow \pi^*_{EA}$ transition.[138]

The long-wavelength band of 5,11-naphthacenequinone **12** is of the $\pi\pi^*$ type. The introduction of substituents in the *para*-position of the phenoxy-group in 6-phenoxy-5,11-naphthacenequinone hardly affects the energy of the $^1\pi\pi^*$ transition, as in the corresponding *p*-naphthacenequinones.

The absorption of the $n\pi^*$ type is clearly not observed in the spectra of *ana*-naphthacenequinones. According to the results,[3] one may expect that the $n\pi^*$ absorption band in the spectra of *ana*-naphthacenequinones is in the immediate vicinity of the $n\pi^*$ levels of 1,4-naphthaquinone and benzylideneindandione. It is then found that the energy of the $n\pi^*$ level of the naphthacenequinone is very close to the energy of the $^1\pi\pi^*$ level, exceeding the latter somewhat.[143]

5,12-Naphthacenequinone does not fluoresce either at room temperature or at 77 K. At 77 K prolonged green phosphorescence of 5,12-naphthacenequinone in methylpentane has been noted.[145] In hexane, the phosphorescence spectrum has a well-resolved structure[147] with an intense peak at 1940 cm^{-1}. The appreciable gap between the absorption and phosphorescence bands (6000 cm^{-1}) and the long duration of the phosphorescence ($\tau_{ps} \simeq 0.3$ s) [145] make it possible to assign the phosphorescence to the $\pi\pi^*$ state. A similar picture has been observed also for substituted *p*-naphthacenequinone. 6-Phenoxy-5,12-naphthacenequinone does not exhibit an intrinsic fluoresence (Fig. 1).[143]

Solutions of 5,11-naphthacenequinone do not exhibit an intrinsic luminescence either at room temperature or at 77 K. A weak fluoresence, intensifying as a function of time, has been attributed to the appearance of 6-hydroxy-5,12-naphthacenequinone — the 5,11-naphthacenequinone conversion product.

In acetic acid, which quenches the fluorescence of 6-hydroxy-5,12-naphthacenequinone, the bright green fluorescence of 5,11-naphthacenequinone was observed at 77 K. The 'activation' of the fluorescence of 5,11-naphthacenequinone by a polar solvent shows that the $^3n\pi^*$ level, located below the $^1\pi\pi^*$ level in non-polar solvents, lies above the $^1\pi\pi^*$ level in the polar acetic acid and does not participate in the non-radiative deactivation of the latter.[143]

An intrinsic fluoresence has not been observed for 6-phenoxy-5,11-naphthacenequinone in acetic acid. The introduction of substituents in the phenoxy-group does not alter appreciably the luminescence properties of the molecule. This difference in the behaviour of 5,11-naphthacenequinone and that of its 6-phenoxy-substituted derivatives is probably associated with the occurrence of the competing photoisomerisation process in the phenoxy-derivative. Fig. 2 illustrates the energy state diagram and the most probable paths leading to the degradation of the excitation energy of 5,12- and 5,11-naphthacenequinones.[143]

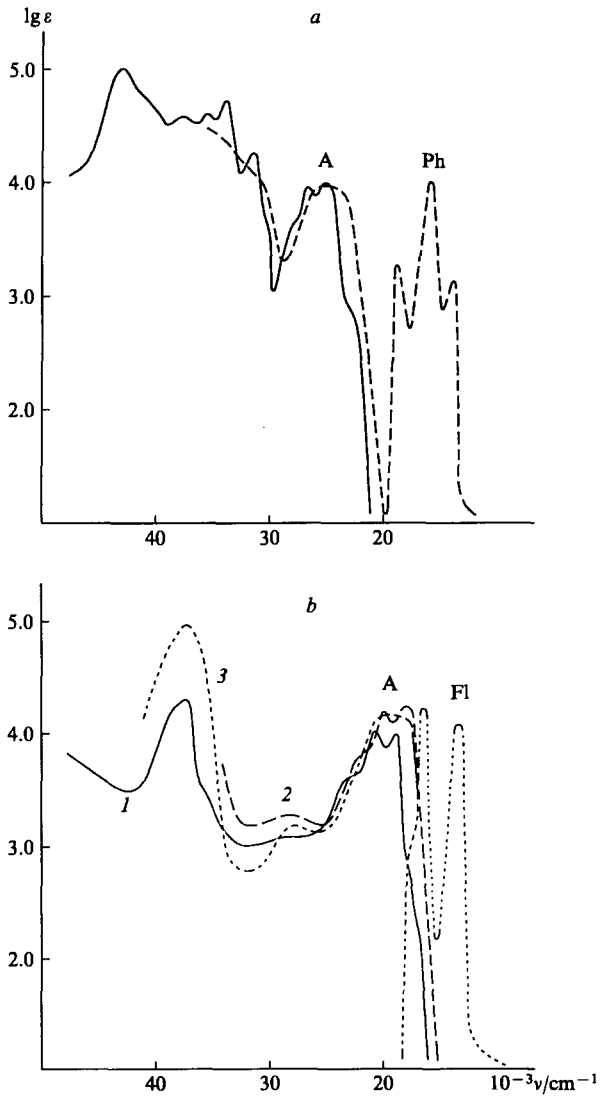


Figure 1. Absorption (A), phosphorescence (Ph), and fluorescence (Fl) spectra of the naphthacenequinones **1** (*a*) and **12** (*b*) in hexane (curve *1*), toluene (curve *2*), and acetic acid (curve *3*).[143]

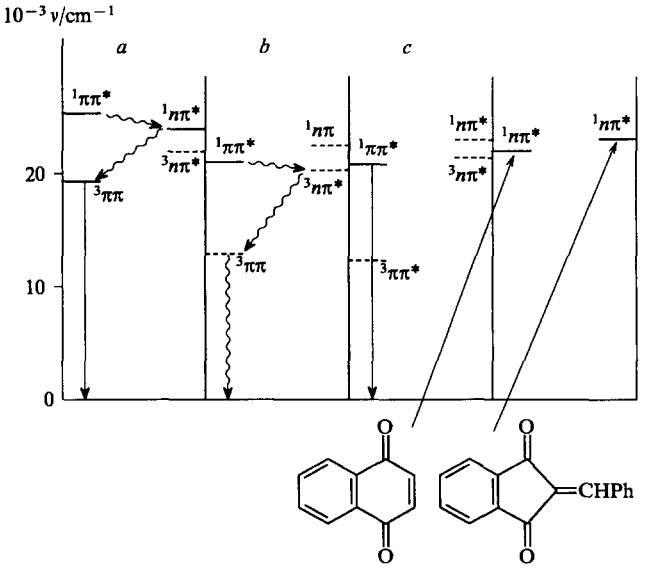
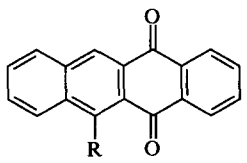
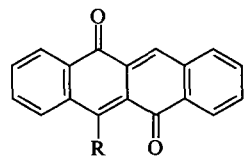
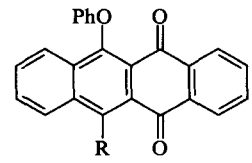
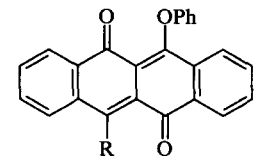


Figure 2. Electronic level diagram. The phosphorescence (Ph) (*a*, *b*) τ = 0.3 s and fluorescence (Fl) (*c*) of *p*-naphthacenequinone **1** and *ana*-naphthacenequinone **12** in hexane (*a*, *b*) and acetic acid (*c*); the dashed lines indicate the levels which are not manifested in the optical transitions.

Table 1. Electronic absorption spectra of 5,12- and 5,11-naphthacenequinones and the 6-derivatives of 11-phenoxy-5,12- and 12-phenoxy-5,11-naphthacenequinones in toluene.

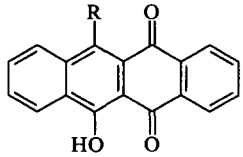
R	λ_{max}/nm (lg ε)			
				
Cl	402 (3.73)	451 (4.20)	398 (3.74) 479 (4.19)	444 (4.20) 472 (4.21)
TsNH	427 (3.77)	–	422 (3.77)	509
NH_2	382 (3.52) 474 (3.99)	490 (4.03) 513 (4.21) 522 (4.10)	389 (3.55) 468 (3.99)	474 (4.05) 503 (4.240 538 (4.17)
NHAc	436 (3.85)	509	429 (3.87)	504 (4.20)
NHCOPh	–	–	434 (3.88)	500 (4.21)
NO_2	–	–	394 (3.70)	453 (4.15) 479 (4.07)
NHMe	396 (3.52) 507 (4.09)	536 (4.11) 572 (4.01)	402 (3.73) 502 (4.09)	524 (4.15) 559 (4.07)
NMe_2	393 (3.69) 408 (3.68) 469 (3.57)	–	408 (3.78)	– 465 (3.60)
NHPh	401 (3.85) 504 (4.00)	472 (3.91) 536 (3.92) 572 (3.82)	404 (3.84) 496 (3.95)	525 (3.94) 558 (3.86)
OMe	401 (3.77)	–	400 (3.82)	447 (4.16) 469 (4.16)
NAcMe	397	455 (4.20) 485 (4.20)	396 (3.85)	448 (4.19) 476 (4.20)
OH	447 (3.98)	–	443 (4.00)	–
OCOMe	397 (3.86)	–	396 (3.89)	–

The electronic absorption spectra of 6-substituted naphthacenequinones[129] are very similar (as regards the position of λ_{max}) to the analogous spectra of the 6-derivatives of 11-phenoxynaphthacenequinone.[127] A definite analogy in the influence of the substituents in the 6-position in naphthacenequinone and in the 1-position in anthraquinone on the colour of these compounds can be traced.

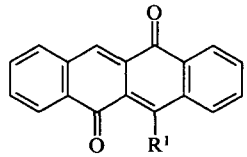
The nature of the substituents in the arene nucleus of 6-aryloxy-5,12-,[131] 6-amino-11-aryloxy-5,12-,[132] 6-aryloxy-5,11-naphthacenequinone[131] exerts little influence on the positions of the long-wavelength absorption maxima and the molar absorption coefficient (Table 1).

Comparison of the long-wavelength absorption band maxima of 6-R-11-phenoxy-5,12- and 6-R-11-phenoxy-5,11-naphthacenequinones by the proportional response method indicates the existence of a linear correlation (r = 0.992), which may apparently indicate that the nature of the bands is identical.[127]

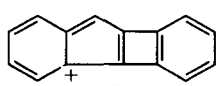
The study of the mass spectra of compounds **13–18** showed[146] that the main process involving the dissociative ionisation of compounds **13** and **16** is the consecutive removal of



13–15



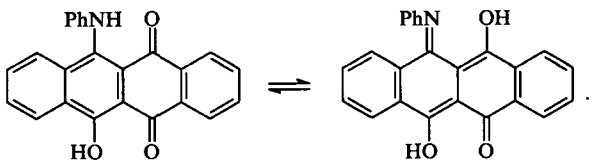
9, 16–18



19

R = H (**13**); NHPh (**14**); NAcMe (**15**); R^1 = NH_2 (**16**); NHPh (**17**); NAcPh (**9**); MeNCPh (**18**).
‖
O

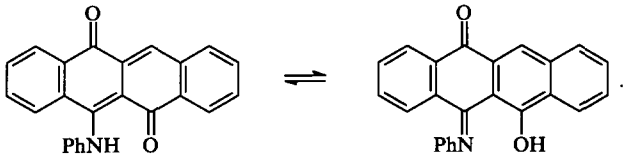
the two carbonyl groups, i.e. an anthraquinone type of decomposition leading to the formation of the stable structure **19**. The similar type of fragmentation of compounds **13** and **16** constitutes indirect evidence for the existence of 6-amino-5,11-naphthacenequinone **16** in an excited state following ionisation by electron impact in the *p*-quinonoid form. Together with the fragments characterising the *p*-quinonoid form **14a**, the mass spectrum of compound **14** contains a fairly large number of specific fragments corresponding to the *ana*-quinone imine form **14b**.



14a **14b**

The disporportionation of compound **15** after the removal of the acetyl group probably takes place in the *ana*-quinone imine form.

The successive elimination of the two carbonyl groups, characteristic of compounds with the *p*-quinonoid structure **13–15** is not observed in the dissociative ionisation of the *ana*-quinones **16–18**. The specific fragmentation processes are in all probability due to the fact that in the excited state, arising on ionisation by electron impact, 6-phenylamino-5,11-naphthacenequinone exists predominantly in the *p*-quinone imine form **17b**.



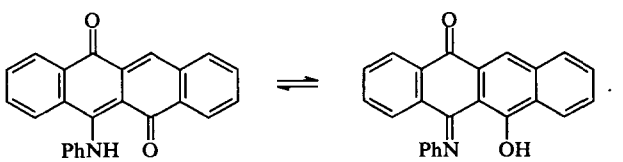
17a **17b**

Analysis of the mass spectra of compounds **17** and **18** also confirm this decomposition pathway for *ana*-phenylaminonaphthacenequinones.[147]

V. Tautomerism of naphthacenequinone derivatives

1. Prototropic and acylotropic rearrangements

The electronic absorption spectra of 6-phenylamino-5,11-naphthacenequinone **17** vary as a function of the polarity of the solvent employed. The family of spectral curves in CCl_4–EtOH mixtures of different composition is characterised by the presence of an isosbestic point, which indicates the presence of two coloured forms in solution (Fig. 3). The characteristic features of the spectroscopic properties of compound **17** can be explained[131] by the tautomerism due to the migration of a proton between the O and N atoms in the *peri*-positions.



17a **17b**

Bearing in mind the similarity of the absorption characteristics of the isoelectronic molecules, one might expect that the spectrum of the *p*-quinone imine tautomer would be similar to that of 6-hydroxy-5,12-naphthacenequinone and for this reason the shorter-wavelength absorption band, appearing in non-polar solvents, was assigned to 6-hydroxy-5-phenyliminonaphthacen-12-one **17b**, while the longer-wavelength band was assigned to the amino-derivative of *ana*-naphthacenequinone **17a**.

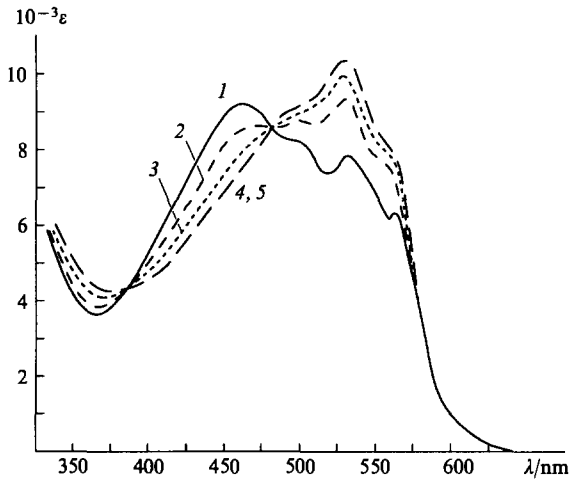
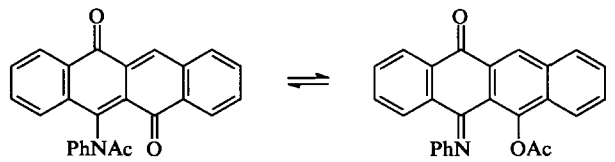


Figure 3. Electronic absorption spectra of 6-phenylamino-5,11-naphthacenequinone in CCl_4 (curve *1*), in C_2H_5OH (curve *5*), and in CCl_4–C_2H_5OH mixtures in different proportions: (*2*) 4 : 1; (*3*) 1 : 1; and (*4*) 1 : 4.

Similar prototropic transformations are characteristic also of 6-phenylamino-12-phenoxy-5,11-naphthacenequinone. 6-Amino- and 6-alkylamino-5,11-naphthacenequinones exist predominantly in the *ana*-quinonoid form in solvents of different polarity.[131]

A capacity for N,O-acylotropism has been observed for certain derivatives of 6-phenylamino-5,11-naphthacenequinone. Depending on the solvent used for recrystallisation, 6-(*N*-acetyl)-phenylamino-5,11-naphthacenequinone **9** can be isolated in two forms differing in the colour of the crystals. Analysis of the IR spectroscopic data led to the structure of the *ana*-quinone **9a** being attributed to the 'red' form, while the structure of the *p*-quinone imine **9b** was assigned to the 'yellow' form.

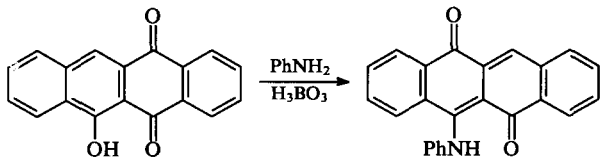


9a **9b**

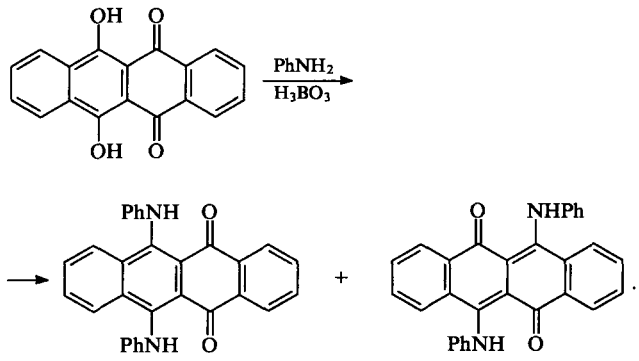
The electronic absorption spectra of compounds **9a** and **9b** in the same solvents are identical. The family of spectral curves of both compound **9a** and compound **9b** in decane–ethanol mixtures with different proportions of the individual solvents show isosbestic points, a consequence of the acylotropic equilibrium **9a** ⇄ **9b**. The tautomeric equilibrium constants were estimated approximately by the method of model compounds as 2.0 in ethanol and 0.4 in decane.[108]

6-Benzoylphenylamino-5,11-naphthacenequinone also exists in solution in two forms, but, in contrast to the acetyl derivative, the *p*-quinone imine form predominates in both polar and non-polar solvents.[108] 6-(*N*-Acetyl)methylamino-5,11-naphthacenequinone does not exhibit acylotropic properties.[108]

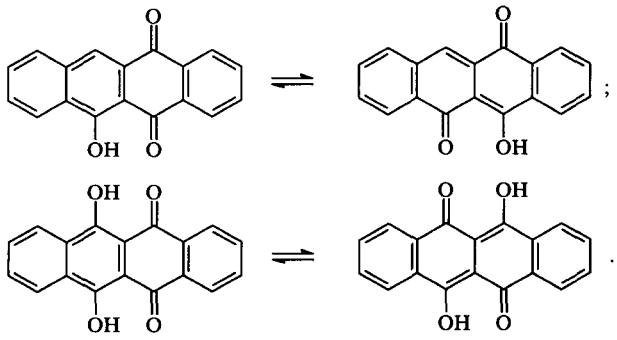
Instead of the expected 6-phenylamino-5,12-naphthacenequinone, its isomer 6-phenylamino-5,11-naphthacenequinone is formed on refluxing 6-hydroxy-5,12-naphthacenequinone with aniline in the presence of boric acid.[39]



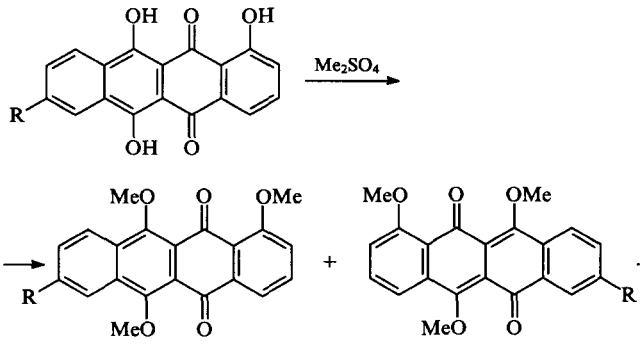
The analogous reaction of 6,11-dihydroxy-5,12-naphthacenequinone leads to a mixture of two isomers.[124,125]



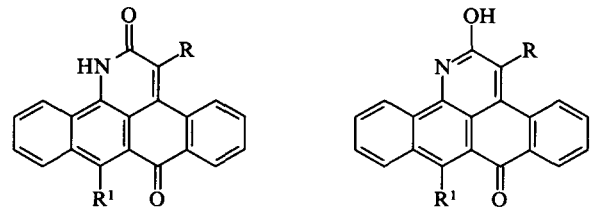
These facts suggested the existence of a tautomeric equilibrium.[39,124]



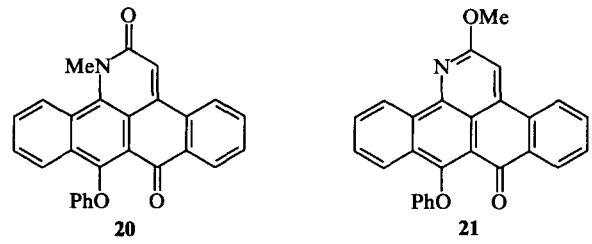
Methylation of derivatives of trihydroxynaphthacenequinone afforded isomeric compounds with *para*- and *ana*-quinonoid structures.[148]



Lactim–lactam tautomerism of naphthacenopyridones has been observed[101] for heterocyclic *peri*-condensed derivatives of naphthacenequinone, in contrast to the analogous derivatives of anthrapyridones which are incapable of this type of prototropism.



R = R¹ = H; R = H, R¹ = OPh; R = Ac, R¹ = OPh



20 **21**

It follows from the analysis of spectroscopic data for naphthacenopyridone and its fixed lactam (compound **20**) and lactim (compound **21**) forms that in polar solvents (*N*-methylpyrrolidone, hexamethylphosphoramide, dimethyl sulfoxide) pyridones exist mainly in the lactim form. The approximate constant of the lactam ⇄ lactim tautomerism for the unsubstituted naphthacenopyridone in *N*-methylpyrrolidinone is 0.4 at 25 °C.[101]

2. Arylotropic rearrangement of *peri*-aryloxynaphthacenequinones

One of the most interesting properties of derivatives of naphthacenequinone is the capacity of the *peri*-aryloxy-substituted 5,12-naphthacenequinones to undergo a reversible colour change in their solutions on exposure to light at different wavelengths, i.e. a capacity for photochromic transformations (Fig. 4).[135,149]

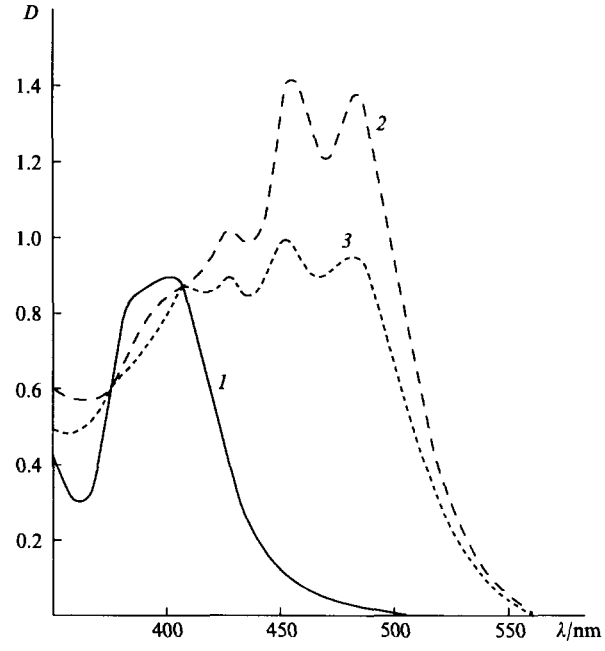
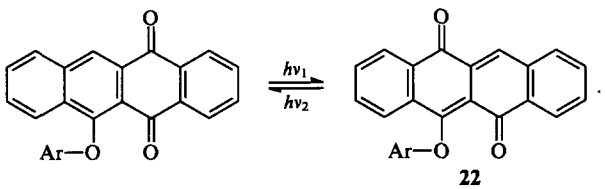


Figure 4. Electronic absorption spectra of 6-(β-naphthoxy)-5,12-naphthacenequinone in toluene ($c = 7.6 \times 10^{-5}$ M, $l = 2$ cm). (*1*) Initial solution prepared in the dark; (*2*) solution *1* irradiated for 2 min through a UFS-1 light filter; (*3*) solution *2* irradiated for 5 min through a ZhS-16 light filter. Source of radiation — DRK-120 mercury lamp.

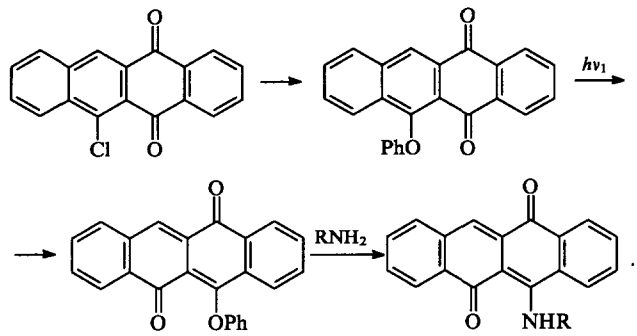
The photochromism of *peri*-aryloxynaphthacenequinones is due to the photoisomerisation of the *p*-quinonoid structure to the *ana*-quinonoid structure on exposure to light as a result of the migration of the arene nucleus to the oxygen atom of the carbonyl group in the *peri*-position relative to the ArO group.[149]



22

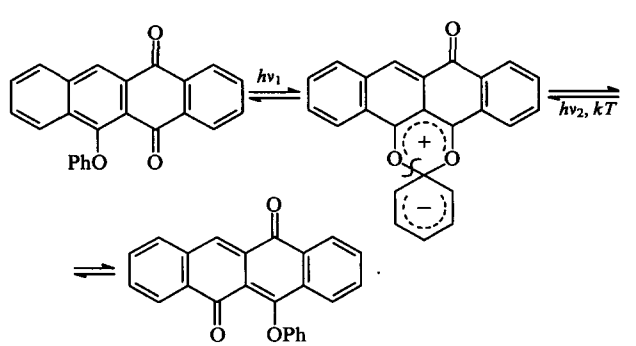
The formation of the *ana*-quinonoid structure as a result of the photorearrangement of 6-phenoxy-5,12-naphthacenequinone is confirmed by the similarity of the electronic absorption spectra of the photoinduced form **22** and those of 5,11-naphthacenequinone and 6-bromo-5,11-naphthacenequinone.[135] Furthermore, the intensities of the C=O stretching vibration bands (1685 and 1682 cm^{-1}) of 6-phenoxy-5,12-naphthacenequinone diminish after irradiation and new C=O absorption bands (1635 and 1660 cm^{-1}), characteristic of *ana*-naphthacenequinones, appear.[150]

The photoinduced form of 6-phenoxy-5,12-naphthacenequinone is stable under the usual conditions and is readily converted on treatment with ammonia and aniline into the nitrogen-containing derivatives **16** and **17** of *ana*-naphthacenequinone.[135]



16, 17

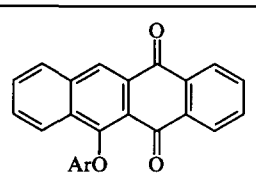
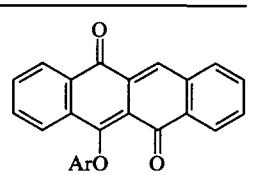
The unambiguous synthesis of compounds **16** and **17** from bromo-5,11-naphthacenequinone has been achieved.[39,97,151] It has been suggested that the intramolecular photoarylotropic rearrangement of naphthacenequinone most probably proceeds via an associative mechanism, although one cannot fully rule out the possibility of a dissociative mechanism with the intermediate formation of a contact ion or radical pair. The absence of radicals on irradiation of the *p*-quinone ⇄ *ana*-quinone system constitutes indirect evidence (obtained by the EPR method) for the heterolytic dissociation of the C=O bond. The dissociation of the C=O bond is preceded by the formation of a σ-complex, the stabilisation of which may lead to either the *p*- or *ana*-quinonoid structure.[149]



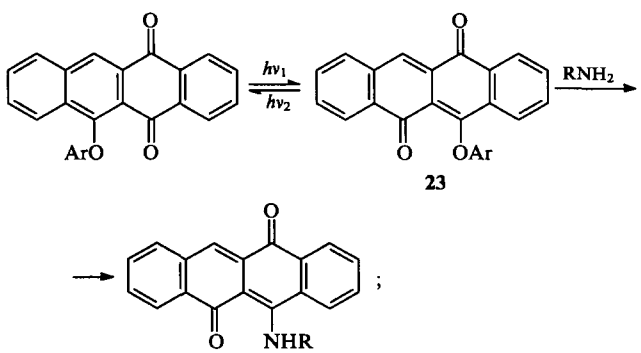
A mechanism of the isomerisation of 6-phenoxy-5,12-naphthacenequinone in solutions in organic solvents at room temperature has been proposed based on a comparative analysis of the spectral-kinetic behaviour of the intermediates and T-states of the nonphotochromic *p*- and *ana*-naphthacenequinones arising on laser photoexcitation. The photoexcitation of the initial form of 6-phenoxy-5,12-naphthacenequinone by radiation at a wavelength of 347 nm induces a transition of the molecule to a coloured form via an intermediate triplet photoproduct. The photoexcitation of the coloured form leads to the population of the T-state of this form, its deactivation not being accompanied by a transition of the molecule to the initial form.[152]

The nature of the substituent in the arene ring has little influence on the positions of the long-wavelength absorption maxima and the molar absorption coefficient but it does affect significantly the quantum yields of the forward and reverse reactions of aryloxynaphthacenequinones. However, a dependence of the quantum yields on the electronic structure of the substituent has not been observed (Table 2).[131]

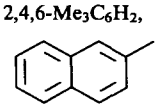
Table 2. Molar absorption coefficients and quantum yields of the forward (φ_B) and reverse (φ_A) photoisomerisation of 6-aryloxy-5,12- and 6-aryloxy-5,11-naphthacenequinones in toluene (λ_{act} = 366 nm).

Ar						
	λ_{max}/nm	$10^3\varepsilon$	φ_B	λ_{max}/nm	$10^3\varepsilon$	φ_B
C_6H_5	400	6.0	0.3	480	1.7	0.05
p-BrC_6H_4	397	5.9	0.36	480	1.8	0.10
p-OHC_6H_4	400	5.2	0.06	480	1.7	0.32
p-$OMeC_6H_4$	400	5.8	0.08	480	1.6	0.03
p-$PhNHC_6H_4$	396	6.4	0.02	476	1.8	0.01
2,4,6-$Me_3C_6H_2$	410	6.7	0.08	498	1.3	0.05
p-$MeCOC_6H_4$	400	6.0	0.27	480	1.8	0.10
p-$NO_2C_6H_4$	395	6.0	0.20	480	1.9	0.05
p-$NH_2C_6H_4$	395	5.5	0.13	480	1.7	0.07
β-$C_{10}H_7$	398	5.7	0.16	478	1.7	0.07
p-PhC_6H_4	398	5.4	0.20	478	1.8	0.10

The ability of the photoinduced form of aryloxynaphthacenequinones to react with amines at room temperature has been used to determine the molar absorption coefficients ε of *ana*-aryloxynaphthacenequinones **23** without their isolation in a pure form.[153]

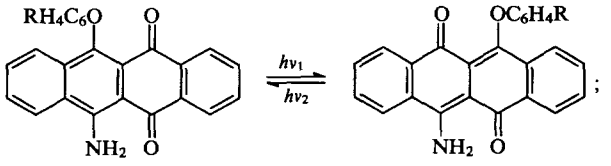


23

Ar = Ph, *p*-HOC_6H_4, *p*-$MeOC_6H_4$, *p*-$PhHNC_6H_4$, 2,4,6-$Me_3C_6H_2$, *p*-$MeCOC_6H_4$, *p*-$NO_2C_6H_4$, *p*-$NH_2C_6H_4$, *p*-PhC_6H_4,  .

Solutions of 11-phenoxy-5,12-naphthacenequinones containing substituents of different electronic nature (Cl, NO_2, OMe, NH_2, NHTs, NHAc, NAcMe), in the 6-position in the naphthalene nucleus exhibit photochromic properties in polar and non-polar solvents. 6-Dimethylamino-, 6-phenylamino-, 6-hydroxy-, and 6-acetoxy-11-phenoxynaphthacenequinones proved to be non-photochromic. In the series of 6-(*N*-acetyl)-methylamino-, 6-amino-, and 6-methylamino-11-phenoxy-5,12-naphthacenequinones, the photosensitivity of the compounds diminishes with enhancement of the electronic-donating properties of the substituent. 6-(*N*-Acetyl)methylamino-11-phenoxy-5,12-naphthacenequinone is photochromic, in contrast to the 6-methylamino-derivative, the photoinduced form of which is hardly observable spectroscopically after prolonged irradiation, while the reverse photochemical reaction does not occur. Substituents such as NO_2 and MeO, which exert very different electronic influences, also diminish the stability of the photoinduced form, which cannot be isolated in an analytically pure form owing to its degradation on contact with silica gel.[127]

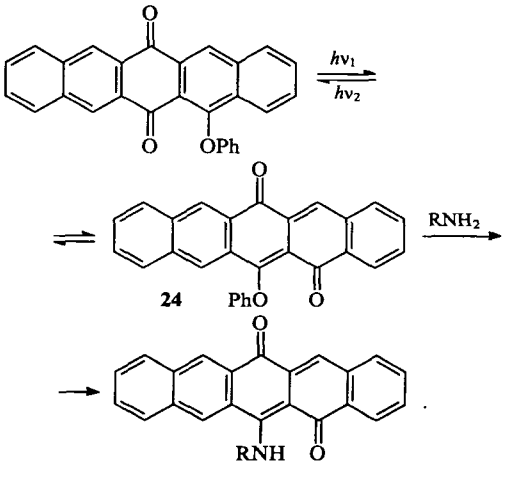
The presence of electron-donating substituents in the migrating group of 6-amino-11-aryloxy-5,12-naphthacenequinones promotes the occurrence of the photorearrangement in these compounds, in contrast to 6-amino-5,12-naphthacenequinone. 6-Amino-11-aryloxy-5,12-naphthacenequinones, containing electron-accepting substituents in the arene nucleus, isomerise under the influence of light less effectively than the unsubstituted 6-amino-11-phenoxy-5,12-naphthacenequinone.[132]



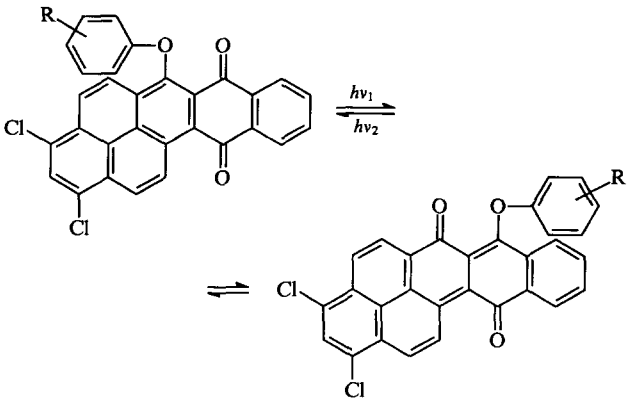
R = *p*-Me, *p*-Et, *p*-OMe, *p*-NHPh, *p*-OH, *p*-NO_2, *m*-Cl.

These data are consistent with experimental findings on substituent effects in photonucleophilic substitution and do not conflict with the hypothesis according to which the photoarylotropic rearrangement of *peri*-aryloxynaphthacenequinones is regarded as intramolecular photonucleophilic substitution.[149]

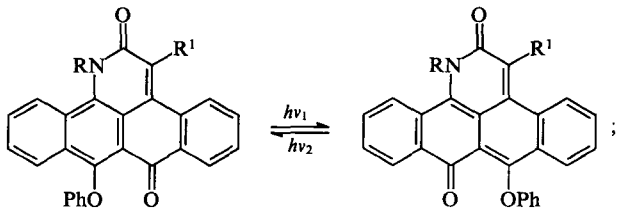
Derivatives of 5,12-naphthacenequinone with a linearly condensed benzene ring—5-phenoxy-6,13-pentacenequinone—isomerise reversibly under the influence of UV radiation to 6-phenoxy-5,13-pentacenequinone **24**. The photoinduced form was isolated in a pure form by virtue of the low rate of the dark isomerisation of the *ana*-quinone to the *p*-quinone. The high reactivity of the photoinduced form made it possible to obtain the first, previously unavailable, amino-derivatives of 5,13-pentacenequinone.[154]



Aryloxy-derivatives of a more complex polycyclic quinone—6,8-dichloro-2,3-phthaloylpyrene (structurally similar to 5,12-naphthacenequinone) are capable of arylotropism.[155,156]



peri-Phenoxy-substituted *N*-methylnaphthacenopyridones are photochromic, like their anthrone analogues—*N*-methylanthrapyridones.[103]

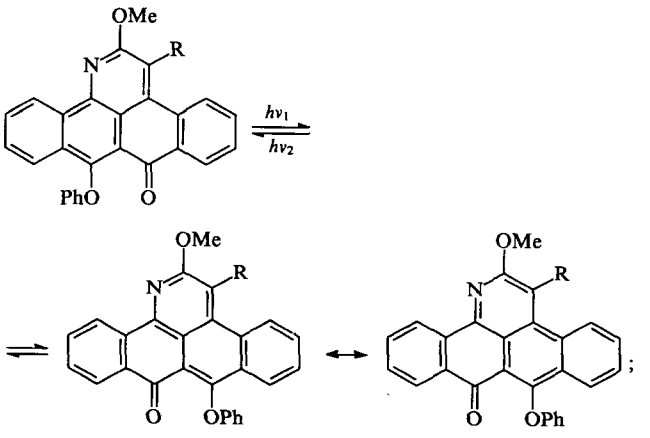


R = Me, R^1 = H, Cl, OPh,  ; R = H, R^1 = H, MeCO.

Naphthacenopyridones, which have no methyl group attached to the nitrogen atom of the heterocyclic fragment of the molecule, undergo in chloroform photochromic transformations similar to those of phenoxyanthrapyridones,[157] but, together with the photochromic transformations, the decomposition of the photoinduced form under the influence of light is also observed.[101]

In contrast to *N*-methylnaphthacenopyridones,[103] alcoholic solutions of *NH*-naphthacenopyridones are not photochromic, which may be associated with the occurrence in alcohol of the photoinduced prototropic transformation of the *NH*-naphthacenopyridone into the lactim form, which rapidly isomerises to the initial pyridone.[101]

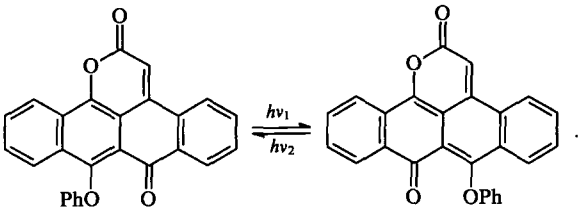
The ability to undergo the photophenyltropic rearrangement has been observed also in toluene solutions of naphthacenopyridones.[101]



R = H, COMe.

The photoinduced forms of naphthacenopyridines exist in solutions probably in the *p*-quinone imine forms, since the absorption band of the photoinduced form of naphthacenopyridines has undergone a hypsochromic shift relative to the band of the photoinduced form of naphthacenopyridones.[101]

9-Phenoxynaphthacenopyridone undergoes a reversible arylotropic rearrangement on exposure to light (Fig. 5).[109]



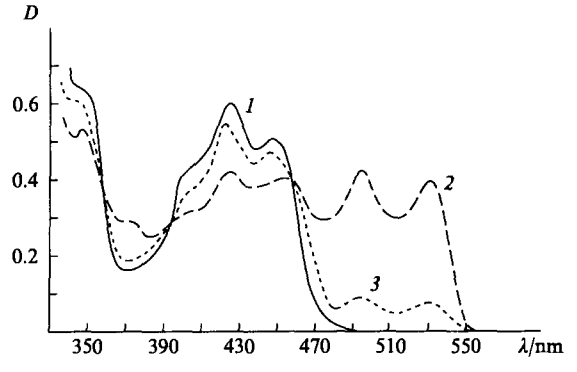
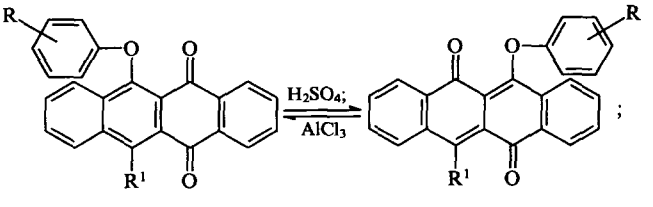


Figure 5. Electronic absorption spectra of 9-phenoxynaphthacenopyrone in toluene ($c = 6.97 \times 10^{-5}$ mol litre^{-1}). (*1*) Initial solution prepared in the dark; (*2*) solution *1* irradiated for 3 min through a SS-8 light filter; (*3*) solution *2* irradiated for 5 min through a ZhS-16 light filter. Source of radiation—DRK-120 mercury lamp.

The arylotropic rearrangement in the series of *peri*-phenoxynaphthacenequinones takes place not only under the influence of light but also in the dark. Treatment of *peri*-phenoxynaphthacenequinones with sulfuric acid or aluminium chloride leads to the corresponding *ana*-naphthacenequinones.[136]



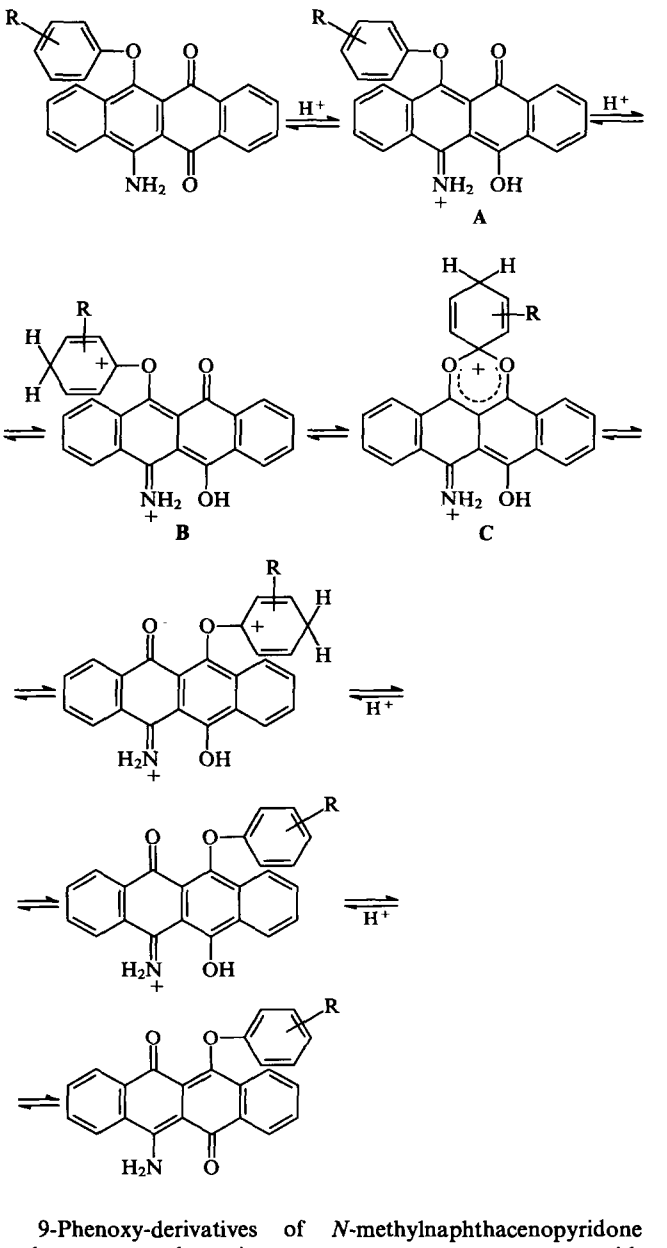
R^1 = NH_2, NHMe, NHPh, NHAc, H, OPh, OMe, Cl.

When naphthacenequinones containing an amino- or a substituted amino-group in the 6-position isomerise, the *ana*-isomer predominates in the equilibrium mixture; in the case of the remaining derivatives, the *p*-isomer predominates.[136]

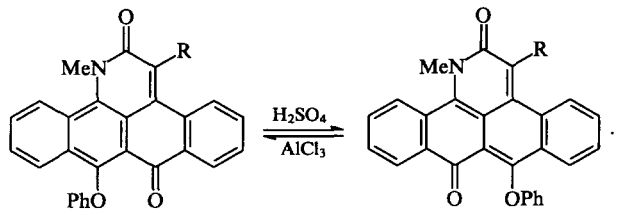
6-Amino-11-aryloxy-5,12-naphthacenequinones, containing electron-accepting substituents in the migrating group, isomerise in sulfuric acid with a higher yield than derivatives having electron-donating substituents.[132]

The *p*-quinone ⇄ *ana*-quinone rearrangement in sulfuric acid proceeds intramolecularly, which is indicated by the results of the cross-experiment: treatment of a mixture of 6-amino-11-(4′-ethylphenoxy)-5,12-naphthacenequinone and 6-phenylamino-11-phenoxy-5,12-naphthacenequinone with sulfuric acid at room temperature leads to the corresponding *ana*-isomers without admixture of intermolecular reaction products. The isomerisation of *peri*-aryloxynaphthacenequinones under the influence of sulfuric acid can apparently be represented as intramolecular nucleophilic substitution (Scheme 4). Protonation of the amino-group of *peri*-phenoxynaphthacenequinone and the appearance of the cation **A** with the *ana*-quinone imine structure in the equilibrium mixture apparently constitute an essential condition for the rearrangement. *peri*-Phenoxynaphthacenequinones, for which such protonation is impossible, for example 6-nitro-11-phenoxy-5,12-naphthacenequinone, do not isomerise under these conditions. In concentrated sulfuric acid, a second proton adds to the phenoxy-group of the monocation **A** with formation of the cation **B**. The latter is stabilised in the form of the spiro-complex **C**. Depending on which oxygen–carbon bond dissociation predominates in the spiro-complex **C**, both the *ana*-isomer and the initial quinone may be formed.[132]

Scheme 4

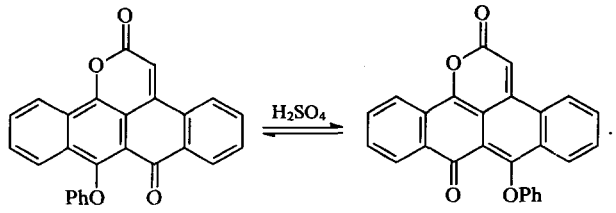


9-Phenoxy-derivatives of *N*-methylnaphthacenopyridone undergo an arylotropic rearrangement on treatment with sulfuric acid or aluminium chloride. The *para*-isomer predominates in the equilibrium mixture. The isomerisation is accompanied by degradation processes.



Phenoxynaphthacenopyridones without a methyl group at the nitrogen atom of the heterocyclic fragment as well as phenoxy-derivatives of *N*-methylanthrapyridones, anthrapyridines, and naphthacenopyridines do not isomerise under these conditions. 8-Phenoxy-derivatives of *N*-methylnaphthacenopyridones with the *ana*-quinonoid bond distribution have been obtained in a pure form by acid isomerisation.[158]

The acid arylotropic rearrangement is also characteristic of 9-phenoxynaphthacenopyrone.[109]



VI. Conclusion

The present review constitutes the first attempt to survey the literature data on the methods of synthesis and properties of naphthacenequinones and their derivatives. The observation of photochromism of a new type, involving the reversible photoarylotropic rearrangement of 6-phenoxy-5,12-naphthacenequinone to 6-phenoxy-5,11-naphthacenequinone, is especially interesting. The undoubted value of these data lies in the fact that the photochromism discovered for 6-phenoxy-5,12-naphthacenequinone proved to be general for the whole series of aryloxy-derivatives of polycyclic quinones (anthraquinone, pentacenequinone, and phthaloylpyrene) and also for heterocyclic derivatives based on them.

A high photostability and pronounced cyclic behaviour are characteristic of this class of photochromic materials. The photochromic materials obtained after the introduction of 6-phenoxy-5,12-naphthacenequinone into poly(methyl methacrylate) and other polymers can be used to record holograms with the aid of a helium-cadmium laser (λ = 441.6 nm) and for the non-disruptive recovery of the image from the holograms by means of the radiation from a helium-neon laser (λ = 632.8 nm).

Photochromism of this type can be used as a photochromic method of synthesis of compounds with the *ana*-quinoid structure, the synthesis of which by traditional methods is extremely difficult or impossible.

Data concerning the ability of 11-substituted derivatives of 6-phenoxy-5,12-naphthacenequinones to undergo the phenylotropic rearrangement under the influence of Lewis acids are extremely interesting.

It is noteworthy that the widely known reactions leading to the formation of heterocyclic derivatives based on 9,10-anthraquinone are also applicable to the synthesis of the analogous derivatives based on 5,12-naphthacenequinone, which makes it possible to synthesise a whole series of new heterocyclic derivatives with interesting properties.

Thus it may be hoped that the data presented in this review will attract the attention of investigators and that the chemistry of naphthacenequinones will undergo a new development.

References

1. Jpn. Appl. 74-81 440; *Chem. Abstr.* **83** 115 804w (1975)
2. Jpn. Appl. 75-53 684; *Chem. Abstr.* **83** 116 809p (1975)
3. Jpn. Appl. 75-53 685; *Chem. Abstr.* **83** 133 380j (1975)
4. Jpn. Appl. 75-65 539; *Chem. Abstr.* **84** 194 459p (1976)
5. Jpn. Appl. 75-121 580; *Chem. Abstr.* **84** 61 056d (1976)
6. Jpn. Appl. 77-40 684; *Chem. Abstr.* **87** 2 030 605u (1977)
7. Jpn. Appl. 77-94 326; *Chem. Abstr.* **88** 38 935t (1978)
8. Jpn. Appl. 49-14 892; *Ref. Zh. Khim.* 5N187P (1979)
9. Jpn. Appl. 54-17 877; *Ref. Zh. Khim.* 10N279P (1980)
10. German P. 138 325; *Frdl.* 241 (1905)
11. R Medne, V Kampar, O Neilands *Izv. Akad. Nauk Latv. SSR, Ser. Khim.* (4) 465 (1972)
12. R Medne, A Livdane, V Kampar, O Neilands *Izv. Akad. Nauk Latv. SSR, Ser. Khim.* (1) 83 (1975)
13. O Neilands, R Medne, A Okman, A Daneberg, V Kampar *Izv. Akad. Nauk Latv. SSR, Ser. Khim.* (1) 69 (1975)
14. R Medne, I Kraupsa, O Neilands *Izv. Akad. Nauk Latv. SSR, Ser. Khim.* (5) 633 (1989)
15. USSR P. 767 106; *Ref. Zh. Khim.* 11N122P (1981)
16. R P Shibaeva, V F Kaminskii *Cryst. Struct. Commun.* **10** 633 (1981)
17. Y Matsunaga, K Takayanagi *Bull. Chem. Soc. Jpn.* **53** 2796 (1980)
18. T Inabe, T Mitsuhashi, Y Maruyama *Chem. Lett.* **3** 129 (1988)
19. W A Remers *The Chemistry of Antitumor Antibiotics* (New York: Wiley, 1979) Vol. 1, p. 63
20. F Arcamone, in *Topics in Antibiotic Chemistry* Vol. 2 (Ed. P G Sammes) (Chichester: Ellis Horwood, 1978) p. 99
21. H Brokmann, I Hiemeyer *Naturwissenschaften* **48** 570 (1961)
22. H Brokmann, H Brokmann *Chem. Ber.* **94** 2681 (1961)
23. H Brokmann, P Boldt, J Niemeyer *Chem. Ber.* **96** 1356 (1963)
24. V M Bakshi, A B Kulkarni *Indian J. Chem.* **1** 215 (1963)
25. K Krohn *Tetrahedron* **46** 291 (1990)
26. N Gupta Dharmendra, P Hodge, N Khan *J. Chem. Soc., Perkin Trans. 1* 689 (1981)
27. Jpn. Appl. 63-188 674; *Ref. Zh. Khim.* 3O100P (1990)
28. T Antonsson, P Vogel *Tetrahedron Lett.* **31** 89 (1990)
29. G Sartori, G Casnati, F Bigi *Gazz. Chim. Ital.* **120** 13 (1990)
30. M H Frank, S Prasanna *J. Am. Chem. Soc.* **103** 6378 (1981)
31. Jpn. Appl. 63-188 694; *Ref. Zh. Khim.* 12O109P (1990)
32. H Fujioka, H Yamamoto, H Kondo, A Hirokazu, K Vasuyuki *J. Chem. Soc., Chem. Commun.* 1509 (1989)
33. Zheng Gihuang, Sui Leshu *Guo Gizxiamen Univ. Nat. Sci.* **28** 401 (1989); *Ref. Zh. Khim.* 11Zh193 (1990)
34. USSR P. 798 139 CCCP; *Ref. Zh. Khim.* 16N254P (1981)
35. E A Coulson *J. Chem. Soc.* 1406 (1934)
36. J W Cook *J. Chem. Soc.* 1412 (1934)
37. L F Fiser, E B Hershberg *J. Am. Chem. Soc.* **62** 49 (1940)
38. C Marschalk, C Stumm *Bull. Soc. Chim. Fr.* **15** 418 (1948)
39. C Marschalk *Bull. Soc. Chim. Fr.* **19** 155 (1952)
40. P G Copeland, R E Deen, L McNeil *J. Chem. Soc.* 3858 (1961)
41. J M Roitt, W A Waters *J. Chem. Soc.* 3060 (1949)
42. N P Bednyagina, G A Panfilov, I Ya Postovskii *Zh. Obshch. Khim.* **28** 365 (1958)
43. S Gabriel, E Leupold *Chem. Ber.* **31** 1272 (1898)
44. C Dufraisse, A Etienne, B Rütimeyer *C. R. Acad. Sci.* **236** 641 (1953)
45. C Dufraisse, A Etienne, B Rütimeyer *C. R. Acad. Sci.* **237** 1601 (1953)
46. H Oka *J. Jpn. Tar Ind. Assoc.* **3** 267 (1951); *Chem. Abstr.* **47** 3839c (1953)
47. V Kratochvil *Chem. Prum.* **23** 506 (1973)
48. USSR P. 505 623; *Ref. Zh. Khim.* 4N207P (1977)
49. H Waldmann, H Mathiowitz *Chem. Ber.* **64** 1713 (1931)
50. C Weizmann, E Bergmann, F Bergmann *J. Chem. Soc.* 1367 (1935)
51. C Deichler, C Weizmann *Chem. Ber.* **36** 547 (1903)
52. C Weizmann, L Haskelberg, T Berlin *J. Chem. Soc.* 398 (1939)
53. H Brokmann, W Müller *Chem. Ber.* **92** 1164 (1959)
54. J Finkelsteein, J A Romano *J. Med. Chem.* **13** 568 (1970)
55. D Harrop, R V Norris, C Weismann *J. Chem. Soc.* 279 (1909)
56. W H Bentley, A Fridl, F Tomas *J. Chem. Soc.* 411 (1907)
57. H Waldmann, G Polak *J. Prakt. Chem.* **150** 113 (1938)
58. S Gabriel, E Leupold *Chem. Ber.* **31** 1127 (1898)
59. G Wanag *Chem. Ber.* **10** 274 (1936)
60. R Medne, L Stradyns, O Neilands *Izv. Akad. Nauk Latv. SSR, Ser. Khim.* (6) 698 (1979)

61. Swiss P. 664963; *Ref. Zh. Khim.* 1N199P (1989)
62. K Zahn, P Ochwat *Liebigs Ann. Chem.* **462** 72 (1928)
63. H Brocmann, E Winner *Chem. Ber.* **96** 2399 (1963)
64. Jpn. Appl. 54-38 620; *Ref. Zh. Khim.* 23N213P (1980)
65. Jpn. Appl. 52-94 326; *Ref. Zh. Khim.* 15N209P (1978)
66. K Zahr *Chem. Ber.* **64** 2063 (1934)
67. Swiss P. 470 334; *Chem. Abstr.* 125 999c (1969)
68. Swiss P. 514 530; *Chem. Abstr.* 85 601p (1972)
69. R Winkler *Chimia* **20** 122 (1966)
70. R Winkler *Helv. Chim. Acta* **50** 2497 (1967)
71. K Yamamoto, E M Acton, D Henry *J. Med. Chem.* **15** 872 (1972)
72. A Di Marco, C Sjranco, A M Casazza *Cancer Chemother. Rep.* **53** 269 (1973)
73. W W Lee, A B Martinez, M T Smith, D W Henry *J. Org. Chem.* **41** 2296 (1976)
74. H Muxfeldt, V Koppe *Chem. Ber.* **91** 838 (1958)
75. M V Gorelik, S P Titova, V A Trdatyan *Zh. Org. Khim.* **15** 157 (1979)
76. A M Birch, A J M Mercer, A M Chippendale, C W Greenhalgh *J. Chem. Soc., Chem. Commun.* 745 (1977)
77. R Gompper, M Sramek *Synthesis (BRD)* 649 (1981)
78. M P Cava, A A Deana, K Muth *J. Am. Chem. Soc.* **81** 6458 (1959)
79. T Kametani, T Takanashi, M Kajiwara *Chem. Pharm. Bull.* **22** 2159 (1974)
80. J N Bridson, S M Bennet, G Butler *J. Chem. Soc., Chem. Commun.* 413 (1980)
81. W C Christopfel, L L Miller *Tetrahedron* **43** 3681 (1987)
82. J A Dodge, A R Chamberlin *Tetrahedron Lett.* **29** 1359 (1988)
83. J A Dodge, A R Chamberlin *J. Org. Chem.* **55** 4190 (1990)
84. Y Lepage, A Verine *C. R. Acad. Sci., Ser. C* **274** 1534 (1972)
85. A Verine, Y Lepage *Bull. Soc. Chim. Fr.* **3** 1154 (1973)
86. W Lange *Z. Naturforsch. B, Chem. Sci.* **31** 398 (1976)
87. M Peyrot, Y Lepage *Bull. Soc. Chim. Fr.* **9–10** 2856 (1973)
88. BRD P. 2 011 920; *Chem. Abstr.* **76** 14 189v (1972)
89. E Müller, E Langer. *Tetrahedron Lett.* **11** 989 (1970)
90. E Müller, H Muhm, E Langer *Chem.-Ztg.* **95** 525 (1971)
91. E Müller, G Odenigbo *Liebigs Ann. Chem.* 1435 (1975)
92. E Müller, A Scheller, R Winter *Chem.-Ztg.* **99** 155 (1975)
93. H A Staab, B Draeger *Chem. Ber.* **105** 2320 (1972)
94. W Trueb, E H Eugster *Helv. Chim. Acta* **55** 969 (1972)
95. M Yamaguchi, K Hasebe, H Higasi *J. Org. Chem.* **55** 1611 (1990)
96. D H R Barton, J H Bateson, S C Datta *J. Chem. Soc., Perkin Trans. 1* 503 (1976)
97. C Dufraisse, J Houpillart *C. R. Acad. Sci.* **206** 756 (1938)
98. J Deschamps, A Cohen, J Abbound *Bull. Soc. Chim. Fr.* **10** 2694 (1965)
99. A Cohen, J Deschamps *Tetrahedron* **42** 4409 (1968)
100. C Marschalk *Bull. Soc. Chim. Fr.* **1–2** 952 (1952)
101. Yu E Gerasimenko, N T Sokolyuk, L P Pisulina *Zh. Org. Khim.* **20** 1078 (1984)
102. Swiss P. 286 502; *Zbl.* **126** 2081 (1955)
103. Yu E Gerasimenko, N T Poteleshchenko *Zh. Org. Khim.* **18** 1039 (1982)
104. German P. 192 201; *Frdl.* **9** 732 (1908)
105. V P Shapkin, S I Popov *Zh. Org. Khim.* **16** 230 (1980)
106. H Waldmann, K G Hindenburg *J. Prakt. Chem.* **156** 157 (1940)
107. C Dufraisse, A Etienne, B Rutimeyer *C. R. Acad. Sci., Ser. C* **243** 878 (1956)
108. Yu E Gerasimenko, N T Poteleshchenko, V V Romanov *Zh. Org. Khim.* **16** 1933 (1980)
109. Yu E Gerasimenko, N T Sokolyuk, L P Pisulina *Zh. Org. Khim.* **21** 453 (1985)
110. E Aufderhaar, I E Baldwin, D H R Barton *J. Chem. Soc. C* 2175 (1971)
111. J A Barry, P G Sammes, T W Wallace *J. Chem. Soc., Perkin Trans. 1* 409 (1974)
112. D H R Barton, D L J Clive, P D Magnus *J. Chem. Soc. C* 2193 (1971)
113. L F Fiser *J. Am. Chem. Soc.* **53** 2329 (1931)
114. E Clar *Polycyclic Hydrocarbons* (Translated into Russian; Moscow: Khimiya, 1971) Vol. 1
115. USSR P. 406 821; *Byull. Izobret.* **46** 66 (1973)
116. R Medne, A Livdane, O Neilands *Zh. Org. Khim.* **13** 624 (1977)
117. J L Brisset *J. Electroanal. Chem.* **60** 217 (1975)
118. M Nepraš, V Kratochvil, M.Titz *Collect. Czech. Chem. Commun.* **38** 1003 (1973)
119. M Nepraš, M Titz, D Šnobl *Collect. Czech. Chem. Commun.* **38** 2397 (1973)
120. C Y Li, F M Whitehurst *Electrochim. Acta* **27** 601 (1982)
121. T Nagaoka, S Okaraki, T Fujinaga *Bull. Chem. Soc. Jpn.* **55** 1967 (1982)
122. M Roerner, B Rickborn *J. Org. Chem.* **56** 1373 (1991)
123. C Dufraisse, L Vellus *C. R. Acad. Sci., Ser. C* **201** 1394 (1945)
124. I Ya Postovskii, L N Goldyrev *Zh. Obshch. Khim.* **11** 429 (1941)
125. I Ya Postovskii, R G Beiles *Zh. Obshch. Khim.* **20** 522 (1950)
126. USSR P. 535 273; *Ref. Zh. Khim.* 14N204P (1978)
127. Yu E Gerasimenko, N T Poteleshchenko, V V Romanov *Zh. Org. Khim.* **16**, 1938 (1980)
128. H Waldmann, E Ulsperger *Chem. Ber.* **83** 178 (1950)
129. N T Poteleshchenko, Candidate's Thesis in Chemical Sciences, NIOPiK, Moscow, 1971
130. M Matsuoka, K Yoshida, M Kishimoto *Bull. Univ. Osaka Prefect.* **28** 33 (1979)
131. V V Romanov, Candidate's Thesis in Chemical Sciences, NIOPiK, Moscow, 1981
132. Yu E Gerasimenko, N T Sokolyuk, L P Pisulina *Zh. Org. Chem.* **26** 1100 (1990)
133. C R Harrison, P Hodge, N Khan *J. Chem. Soc., Perkin Trans. 1* 1592 (1980)
134. S Miki, H Kagawa, K Matsuo *Chem. Runct. Dyes* (First International Symposium, Osaka, June 5th–9th 1989) Tokyo, 1989, p. 299
135. Yu E Gerasimenko, N T Poteleshchenko *Zh. Org. Khim.* **7** 2413 (1971)
136. Yu E Gerasimenko, N T Poteleshchenko, V V Romanov *Zh. Org. Khim.* **16** 2014 (1980)
137. G N Rodionova, N I Karpova, V V Romanov, N T Sokolyuk, Yu E Gerasimenko *Zh. Fiz. Khim.* **58** 2323 (1984)
138. R N Nurmukhametov, G N Rodionova, V V Romanov, N T Poteleshchenko, Yu E Gerasimenko *Zh. Prikl. Spektrosk.* **30** 856 (1979)
139. L Navangu, V Himanskoo *Indian J. Chem.* **6** 85 (1968)
140. H Hopff, H R Schweirer *Helv. Chim. Acta* **45** 1044 (1962)
141. A Novak, M Titz, M Nepraš *Collect. Czech. Chem. Commun.* **39** 1532 (1974)
142. I L Belaits, N I Kunavin, R N Nurmukhametov, A E Podorol'skaya *Opt. Spektrosk.* **38** 908 (1975)
143. I L Belaits, N T Sokolyuk, A A Parshutkin, L P Samsonova, Yu E Gerasimenko *Zh. Fiz. Khim.* **50** 640 (1986)
144. M Nepraš, A Novak *Collect. Czech. Chem. Commun.* **42** 2343 (1977)
145. R N Nurmukhametov *Pogloshchenie i Lyuminestsentsiya Aromaticheskikh Soedinenii* (The Absorption and Luminescence of Aromatic Compounds) (Moscow: Khimiya, 1971)
146. A D Vasil'eva, N T Poteleshchenko, Yu E Gerasimenko *Zh. Org. Khim.* **19** 1529 (1983)
147. Z Horii, Y Osaki, S Yamamura *Chem. Pharm. Bull.* **22** 93 (1974)
148. Yu E Gerasimenko, N T Poteleshchenko *Zh. Vses. Khim. O-va im. D. I. Mendeleeva* **16** 105 (1971)
149. L V El'tsov (Ed.) *Organicheskie Fotokhromy* (Organic Photochromic Materials) (Leningrad: Khimiya,1982)
150. V N Kostylev, B E Zaitsev, V A Barachevskii, N T Poteleshchenko, Yu E Gerasimenko *Opt. Spektrosk.* **30** 86 (1971)
151. H Stobbe, P Haoum *Chem. Ber.* **37** 2240 (1904)
152. Yu P Strokach, B A Barachevskii, N T Sokolyuk *Khim. Fiz.* **6** 320 (1987)
153. Yu E Gerasimenko, A A Parshutkin, N T Poteleshchenko, V P Poteleshchenko, V V Romanov *Zh. Prikl. Spektrosk.* **30** 954 (1979)
154. Yu E Gerasimenko, N T Poteleshchenko *Zh. Org. Khim.* **15** 393 (1979)
155. Yu E Gerasimenko, N T Poteleshchenko *Zh. Org. Khim.* **4** 1473 (1968)
156. Yu E Gerasimenko, N T Poteleshchenko *Zh. Org. Khim.* **9** 2392 (1973)
157. Yu E Gerasimenko, N T Sokolyuk, L P Pisulina *Zh. Org. Khim.* **19** 1312 (1983)
158. Yu E Gerasimenko, N T Sokolyuk, L P Pisulina *Zh. Org. Khim.* **21** 2236 (1985)

Russian Chemical Reviews **62** (11)1025 – 1045 (1993) ©1993 Russian Academy of Sciences and Turpion Ltd

UDC 547.1'13

The chemistry of cymantrene

A G Ginzburg

Contents

I.	Introduction	1025
II.	The formation and cleavage of the cymantrene system	1026
III.	Reactions involving the substitution of hydrogen in the Cp ligand and the syntheses of compounds with the cymantrenyl substituent	1028
IV.	Chiral derivatives of cymantrene	1031
V.	Complexes with polycyclic ligands and polynuclear derivatives of cymantrene	1033
VI.	Compounds with organoelement substituents	1037
VII.	Cymantrene as an organometallic Lewis base	1039
VIII.	Stabilisation by the cymantrenyl group of the neighbouring cationic and radical centres	1040

Abstract. The advances in the synthesis and study of derivatives of cyclopentadienyltricarbonylmanganese (cymantrene) are considered. The bibliography includes 356 references.

I. Introduction

The cyclopentadienyl complexes of metals constitute one of the classes of organic transition metal complexes which have been studied in greatest detail. In terms of the number of experimental studies, cyclopentadienyltricarbonylmanganese (cymantrene, CTM) occupies the second place after ferrocene. Two stages may be distinguished in the studies on cymantrene. The synthetic aspect, based on the analogy with the electrophilic substitution reactions in benzene and ferrocene, was characteristic of the first stage in the chemistry of cymantrene. Other reactions involving the substitution of hydrogen in the Cp ring are known for cymantrene although their number is somewhat smaller than in the case of ferrocene. These are the acylation, alkylation, and phosphorylation reactions under Friedel – Crafts conditions, sulfonation, chloromethylation, metallation with butyllithium, mercuration with mercury(II) salts, and hydrogen isotope exchange with acids and bases. A multiplicity of cymantrene derivatives with a wide variety of substituents in the Cp ring have been obtained by means of the reactions listed above (for the literature data up to 1972, see the references in a review[1]).

On the other hand, reactions involving the substitution of CO by other ligands as well as processes occurring with a change in the ligand environment of the metal are extremely characteristic of cymantrene, as for all metal carbonyl complexes.

The second stage in the development of studies on cymantrene was associated with the synthesis of its derivatives both with 'classical' ligands, coordinated to manganese via the electron-donating atoms of Group IV – VI elements, and with ligands of a new type such as complexes with molecular hydrogen, free – radical complexes, complexes with 'indene' ligands, etc.

The combination of the reactions involving substitution of hydrogen in the Cp ligand and CO substitution reactions made it possible to obtain a large number of a wide variety of derivatives with C_5H_5Mn, C_5H_4RMn, C_5R_5Mn (R = alkyl, halogen, etc.) fragments. A unique feature of cymantrene is a combination of a varied reactivity with thermal and oxidative stabilities, which are unusually high for π-complexes.

On average, 30 – 40 studies devoted to the chemistry of cymantrene are published each year. However, despite very extensive experimental data, review information on the recent chemistry of cymantrene is virtually lacking. The reviews[1-3] and monographs[4] published previously are to a greater or lesser extent obsolete. A review[5] dealing with the structural aspects of manganese carbonyl complexes was published comparatively recently. The present review presents a compilation in one article of extremely extensive and comprehensive data for the last 10 – 12 years on the chemistry of compounds containing one or several cymantrene residues [the cymantrenyl radical $(CO)_3MnC_5H_4$ is designated below in the text by (**Mn**)]. The limited space available in the review precluded the consideration of data concerning the synthesis and properties of numerous complexes of the type $CpMn(CO)(LL')$, where L and L' are two-electron ligands. Studies in which the key role was assumed by various physicochemical and computational studies (optical and microwave spectroscopy, kinetic and electrochemical methods, gas-phase chemistry of cymantrene, mass-spectrometric studies, and quantum-chemical calculations) are also not considered.

Cymantrene, the isoelectronic cation $CpMn(NO)(CO)_2^+$, and their derivatives are diamagnetic 18-electron complexes which contain an Mn atom with the d^6 configuration and a formal +1 oxidation state. Cymantrene and its derivatives can be regarded as pseudooctahedral complexes in which the Cp ligand occupies three coordination sites. This follows from X-ray diffraction (XRD) data, according to which the OC – Mn – CO bond angles are 87° – 93° in virtually all structurally characterised cymantrene derivatives. However, in stereochemical studies it has become unusual to consider cymantrene and analogous molecules with the geometry of the 'piano stool with three legs' type as pseudotetrahedral assuming that the Cp ligand occupies one coordination site.

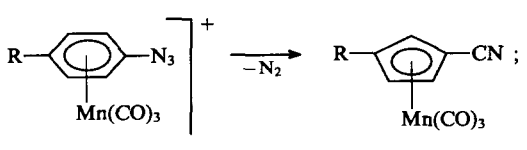
A G Ginzburg Laboratory of the Stereochemistry of Organometallic Compounds, A N Nesmeyanov Institute of Organoelement Compounds, Russian Academy of Sciences, ul. Vavilova 28, 117813 Moscow, Fax (7-095) 135 50 85, Tel. (7-095) 135 93 34.

Received 4 June 1993
Uspekhi Khimii **62** (11) 1098 – 1118 (1993); translated by A K Grzybowski

II. The formation and cleavage of the cymantrene system

Detailed X-ray diffraction data for cymantrene have been obtained by Fitzpatrick et al.[6] and Cowie et al.[7] A difference between the C–C bond lengths in the Cp ring was observed in the above investigations. They vary in the ranges 1.400–1.439 Å [6] and 1.399–1.426 Å.[7] The study of cymantrene by vibrational spectroscopic methods also indicated slight deviations from the C_{5v} symmetry for the Cp ligand, which may be induced by crystal packing effects.[6] The heat capacities of cymantrene and of its π-pyrrole analogue[8] as well as the heat of formation of cymantrene[9] have been measured.

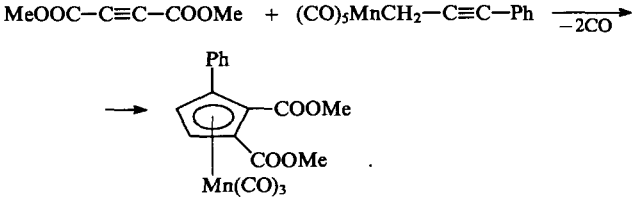
In addition to the procedures known earlier (see the relevant review[1]), a number of new methods of synthesis of cymantrene have been proposed. On reduction[10,11] of a mixture of anhydrous $MnCl_2$ and cyclopentadiene by metallic magnesium or manganese in the presence of $TiCl_4$ or $Ti(OBu)_3$ followed by carbonylation with CO (180 °C, 80 atm), the yield of cymantrene reaches 70%–75%. The interaction of anhydrous $MnCl_2$ and $Me_3SiC_5H_4^-Na^+$ and subsequent carbonylation afford $Me_3Si(\mathbf{Mn})$.[12] Cymantrene exhibits a high thermodynamic stability and its derivatives are formed as a result of thermal or photochemical reactions of manganese carbonyl complexes with olefins and dienes. Thus, in the thermal decomposition of solid cationic complexes of azidobenzene and azidotoluene with $Mn(CO)_3$, nitrogen is evolved even at 130 °C and an intermediate complex of phenylnitrene with $Mn(CO)_3$ is apparently formed. The ring contraction reaction takes place readily in the intermediate and leads to cyano- or 1-methyl-3-cyano-cymantrene.[13]



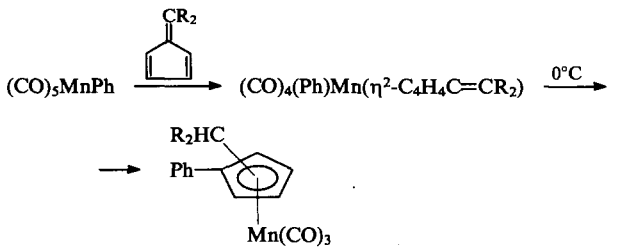
R = H, Me.

After the thermal decomposition of non-coordinated phenyl azide in solution, azobenzene (resulting from the dimerisation of phenylnitrene) and aniline (produced by the abstraction of hydrogen from the solvent) were detected among the reaction products. Thus coordination to $Mn(CO)_3$ alters sharply the mode of thermal decomposition of the coordinated azides.

The [3 + 2]-cycloaddition reaction takes place on interaction of $(CO)_5MnCH_2C{\equiv}CPh$ with dimethylacetylenedicarboxylate and affords a trisubstituted cymantrene derivative.[14]



One of the most general methods of synthesis of cymantrene derivatives is based on the reaction of the carbonyl halides $Mn(CO)_5X$ or $Mn(CO)_3L_2X$ (X = Cl, Br; L = a ligand, for example, amine, pyridine, etc., linked by labile bonds), $Mn(CO)_5Ph$, and $Mn_2(CO)_{10}$ with substituted cyclopentadienes or cyclopentadienylthallium derivatives. The reaction of $H_3Mn_3(CO)_{12}$ with 6-dimethylaminofulvene leads to the formation of dimethylaminomethylcymantrene $(\mathbf{Mn})CH_2NMe_2$.[15] Under the conditions of photchemical activation on irradiation with UV light of 6,6-dimethyl- or 6,6-diphenyl-fulvene in the presence of $Mn(CO)_5Ph$ in hexane at –20 °C, the displacement of CO and coordination of fulvene to one of the double bonds result in the formation of the intermediates $Mn(CO)_4LPh$ (L = η^2-fulvene), which rearrange on heating to 0 °C to disubstituted cymantrenes with insertion of the fulvene double bonds in the Mn–Ph bond.[16]



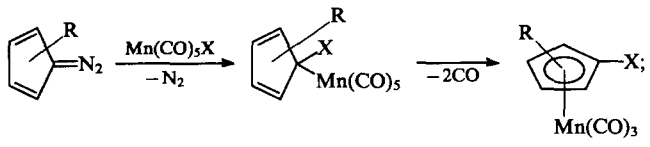
The phosphine oxide $Ph_2P(O)CH_2C_2H_5$ reacts with $Mn_2(CO)_{10}$ to form the complex $(\mathbf{Mn})CH_2P(O)Ph_2$.[17] Reaction of the bromide $Mn(CO)_5Br$ with the cyclopentadiene derivatives $Me_3SnC_5H_4CH_2CH_2PPh_2$ is accompanied by elimination of two CO molecules and Me_3SnBr and leads to the formation of the complex $(\mathbf{Mn})CH_2CH_2PPh_2$.[18] Phenylcymantrene is formed similarly from phenylcyclopentadiene and $Mn(CO)_5Br$.[19]

The reaction of $Mn(CO)_5Br$ with cyclopentadienylthallium derivatives containing functional group substituents constitutes a thoroughly developed method of synthesis of substituted cymantrenes.

$$RC_5H_4Tl + Mn(CO)_5Br \longrightarrow (\eta^5\text{-}RC_5H_4)Mn(CO)_3 + 2CO + TlBr\ .$$

Compounds with R = $-C(CN)=C(CN)_2$,[20,21] CF_3,[22] Ph, CH_2Ph,[23] Cl, Br,[24], *m*-, *p*-FC_6H_4,[25,26] CHO, C(O)Me, C(O)OMe, C(O)OEt [27] have been synthesised in this way. This reaction can be extended also to dinuclear complexes. Thus the corresponding biscymantrenyl derivative has been obtained from 1,4-bis(cyclopentadienylthallium)buta-1,4-dione by reaction with $Mn(CO)_5Br$.[28] The reaction of tricyano(ferrocenyl)ethylene $Fc-C(CN)=C(CN)_2$ with 1 equivalent of $Mn(CO)_5Br$ and C_5H_5Tl affords the dinuclear complex $Fc-C[=C(CN)_2](\mathbf{Mn})$.[21]

The simultaneous elimination of nitrogen and two CO molecules results in the ready formation of mono- and polyhalocymantrenes in the reactions of $Mn(CO)_5X$ with diazacyclopentadienes.[29]



X = Cl, Br, I.

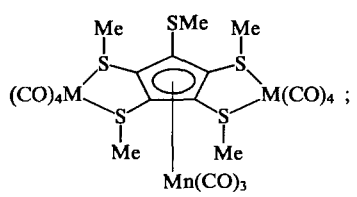
Chloro-, bromo-, and iodo-cymantrenes have been obtained in 60%–80% yields from unsubstituted diazacyclopentadiene $C_5H_4=N_2$ in one stage, while the reaction of $C_5Ph_4=N_2$ with $ClMn(CO)_5$ afforded chlorotetraphenylcymantrene.[30] The single-stage syntheses of halocymantrenes via CpTl or diazacyclopentadienes as well as the syntheses via the interaction of mercurio-derivatives of cymantrene with copper(II) salts[31] are much simpler than the previously proposed multistage method of synthesis via aminocymantrene (see the relevant review[1]). Halo-derivatives of indenylmanganese tricarbonyl have been obtained from diazaindene.[32]

The synthesis via diazacyclopentadienes constitutes a convenient path to polyhalocymantrenes. The reaction of tetrachlorodiazacyclopentadiene with $XMn(CO)_5$ leads to a mixture of the monohapto-complexes η^1-$C_5Cl_4XMn(CO)_5$ and to pentahalocymantrenes formed from them as a result of a σ → π

rearrangement and the elimination of CO. The proportions of the above products depend greatly on the reaction conditions. On heating to fusion, the η^1-complexes readily split off CO and are converted into the thermodynamically more stable pentahalocymantrenes in a quantitative yield.[33] The conversion of η^1-$C_5Cl_5Mn(CO)_5$ into η^5-$C_5Cl_5Mn(CO)_3$ can also take place photochemically via the intermediate η^3-$C_5Cl_5Mn(CO)_4$.[34] Pentabromo- and tetrabromoiodo-cymantrenes have been obtained from tetrabromodiazacyclopentadiene and $XMn(CO)_5$ (X = Br or I), while tri-iodocymantrene has been obtained from di-iododiazacyclopentadiene and $IMn(CO)_5$.[35] A preparative synthesis of mono- and poly-halocymantrenes by this procedure has been described.[36] When an attempt was made to obtain dibromocymantrene by the reaction of bis(bromomercurio)-cymantrene with $CuBr_2$ in acetone (by analogy with the synthesis of bromocymantrene[31]), a mixture containing cymantrene, bromocymantrene and all possible di-, tri-, tetra-, and penta-bromocymantrenes, which was separated into its components with the aid of preparative gas–liquid chromatography (GLC), was obtained instead of the expected dibromides.[37]

The chemistry of polychlorocymantrenes and their derivatives has developed vigorously in recent times. In the metallation of bromotetrachlorocymantrene with butyllithium (hexane, −60 °C), a key synthon—the lithio-derivative (η^5-$C_5Cl_4Li)Mn(CO)_3$—is formed as a result of the substitution of bromine by lithium. The reactions of the synthon with various electrophiles yielded a series of tetrachlorocymantrenes [(η^5-$C_5Cl_4R)Mn(CO)_3$, R = H, Me, $SiMe_3$, $SiPh_3$, COOH, COOMe, SMe, and SPh,[38] as well as $SnMe_3$, PPh_2, SePh, and CHO [39]]. The dicymantrenyl sulfide $S[(C_5Cl_4)Mn(CO)_3]_2$ has been obtained by the reaction of the lithio-derivative with SCl_2.[39] The corresponding acid chloride, azide, isocyanate, and amine have been synthesised from tetrachlorocymantrenecarboxylic acid. Haloferrocenes are known to form nitriles on reaction with CuCN. However, the reaction of $(C_5Cl_4Br)Mn(CO)_3$ and CuCN does not afford stable products in pyridine, and the usual procedure was therefore used to obtain the nitrile. The reaction of the acid chloride with ammonia afforded the amide [R = $C(O)NH_2$], while dehydration of the latter by $POCl_3$ afforded the nitrile (R = CN).[39]

A whole series of compounds having the general formula [η^5-$C_5Cl_{5-n}(SMe)_n$]$Mn(CO)_3$, where $n = 1-5$, have been obtained from (η^5-$C_5Cl_4SMe)Mn(CO)_3$ by successive metallation with BuLi and treatment with Me_2S_2.[40] The corresponding compounds containing two or three SPh groups and mixed complexes containing simultaneously the SPh and SBu groups have been obtained similarly from (η^5-$C_5Cl_4SPh)Mn(CO)_3$ by metallation and treatment with Ph_2S_2 or Bu_2S_2.[41] More than three SPh groups cannot be introduced in this way. The complexes $C_5(SMe)_5Mn(CO)_3$,[40] $C_5Cl_2(SPh)_3Mn(CO)_3$, etc.[41] have been characterised by XRD. Compounds containing two or four SMe or SPh groups in the Cp ring readily form a wide variety of dinuclear complexes as a result of the coordination of the metal-containing fragments to the sulfur atoms.[41,42] Trinuclear complexes with two chelate rings, whose structure has been established by the XRD method, are formed in the case of $C_5(SMe)_5Mn(CO)_3$.[42]



M = Cr, Mo, W.

The reaction of $(C_5Cl_4Li)Mn(CO)_3$ with sulfur leads to the monothiolate derivative $(C_5Cl_4SLi)Mn(CO)_3$, which does not afford the expected thiol on protonation, the disulfide $[(CO)_3MnC_5Cl_4S-]_2$ being formed instead. On the other hand, on repeated metallation of the monothiolate and treatment with sulfur, the dithiolate $C_5Cl_3(SLi)_2Mn(CO)_3$ was obtained. On protonation, the latter was smoothly converted into the dithiol $C_5Cl_3(SB)_2Mn(CO)_3$, which was characterised by XRD.[43]

Apart from the tetra- and penta-halocymantrenes, pentaalkylcymantrenes have also been obtained. Pentaethyl-cymantrene was synthesised as early as 1964 by the successive acylation of cymantrene with $MeC(O)Cl/AlCl_3$ and the reduction of the keto-group to CH_2 on treatment with $LiAlH_4/AlCl_3$ (ten stages altogether).[44] Pentamethylcymantrene is formed as a result of the reaction of pentamethylcyclopentadiene with $MeMn(CO)_5$ or $Mn_2(CO)_{10}$.[45,46] An improved version of this method, involving the interaction of C_5Me_5H with $Mn_2(CO)_{10}$ without a solvent at 180 °C, has been proposed,[47] but it was shown later that a mixture of pentamethyl- and tetramethyl-cymantrenes is formed under these conditions.[48] Pentabenzylcymantrene, the structure of which was confirmed by XRD, has been obtained by the reaction of pentabenzylcyclopentadiene with $Mn_2(CO)_{10}$.[49] A series of pentamethylderivatives of cymantrene have been investigated[50,51] by ^1H, ^{13}C, and ^{17}O NMR spectroscopic methods. The pentasubstituted complex $C_5(SiMe_2H)_5Mn(CO)_3$, characterised by XRD, as well as all the intermediates, each containing from one to four $SiMe_2H$ groups, have been synthesised from $C_5Br_5Mn(CO)_3$ by multistage metallation (2 equiv. of BuLi) and alkylation (2 equiv. of Me_2SiHCl).[52]

Penta(methoxycarbonyl)cymantrene $[C_5(COOMe)_5]Mn(CO)_3$ has been synthesised by the reaction of the anion $C_5(COOMe)_5^-$ with $BrMn(CO)_5$. It reacts with NH_3, affording a mixture of compounds containing simultaneously C(O)OMe and $C(O)NH_2$ groups in the ring. The reaction with butylamine leads to the monoamide derivative, while exhaustive reduction with $LiAlH_4$ results in the formation of $C_5Me_5Mn(CO)_3$.[53]

Apart from the reactions described above, in which the thermodynamically stable cymantrene system is formed, examples of reverse processes occurring with dissociation of the Mn–Cp bond are known. The reduction of cymantrene with sodium in hexamethylphosphoramide leads initially to $NaMn(CO)_5$ and then to $Na_3Mn(CO)_4$.[54]

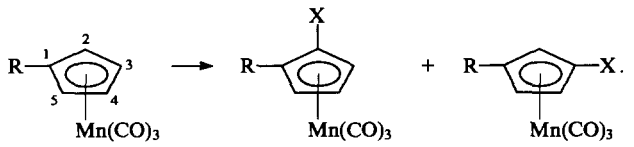
The thermal decomposition of cymantrene at 380–420 °C and a pressure of 10^{-2} Torr gives rise to the cyclopentadiene dimer, metallic manganese, and CO.[55,56] On catalytic hydrogenation in acetic acid in the presence of Pd/C, cymantrene and many of its derivatives are completely cleaved to cyclopentane and cyclopentene.[57] The reaction of ferrocene and cymantrene, adsorbed in the large cavities of zeolites, with phthalonitrile vapour at 100–150 °C *in vacuo* leads to cleavage, induced by the zeolite matrix, and to the formation of iron- and manganese-phthalocyanines. The latter are retained within the zeolite cavity, not as a consequence of chemical bonding with the skeleton, but as a result of the difference between their diameters and the dimensions of the inlet windows of the zeolite.[58]

The interaction of methylcymantrene with bis(1,3-diphenyl-propane-1,3-dionato)tin proceeds with complete cleavage of the molecule and the transfer of propanedionate ligands from tin to manganese. The complex bis(1,3-diphenylpropane-1,3-dionato)manganese$(THF)_2$, in which the manganese atom is surrounded octahedrally by six oxygen atoms, has been isolated from the reaction mixture and characterised by XRD.[59] Treatment of methylcymantrene with the potassium derivative of 18-crown-6 in THF resuts in two-electron reduction accompanied by a profound rearrangement of the molecule with dissociation of the Mn–Cp bond. In the presence of 1 equiv. of naphthalene, the reaction product is the anionic complex (η^4-$C_{10}H_8)Mn(CO)_3^-$, in which the naphthalene molecule is involved in η^4-type of coordination.[60] The Mn–Cp bond dissociates also when an attempt is made to achieve the photochemical substitution of CO by PPh_3 in the complex $Ph_2PC_5H_4Mn(CO)_3$.[61,62]

III. Reactions involving the substitution of hydrogen in the Cp ligand and the syntheses of compounds with the cymantrenyl substituent

Numerous cymantrene derivatives, examined in detail in a review,[1] have been synthesised by a set of substitution reactions. Yet another reaction involving the substitution of hydrogen atoms in the Cp ring was discovered subsequently: direct boryl-ation of the Cp ligand. It was shown that cymantrene, methyl-cymantrene, and ferrocene react with BI_3, BBr_3, $PhBI_2$, and $MeBI_2$ in carbon disulfide in cyclohexane or without a solvent at 80 to 100 °C with substitution of a hydrogen atom in the Cp ring by the BI_2, BBr_2, PhBI, or MeBI group. The resulting compounds enter into reactions with $SnMe_4$, Et_2O, Me_2S_2 and $NHMe_2$ involving the substitution of the halogen by the alkyl, OEt, SMe, and NMe_2 groups respectively.[63,64]

On passing from unsubstituted cymantrene to its mono-substituted derivative $RC_5H_4Mn(CO)_3$, the problem of the site of substitution arises, as in the case of the benzene derivatives RC_6H_5. The newly introduced substituent can replace hydrogen in the 2- and 3-positions. Substitution reactions in cymantrene as a rule proceed nonselectively and mixtures of 1,2- and 1,3-isomers are formed, the proportions of which depend significantly on the nature of the substituent and the type of reaction.



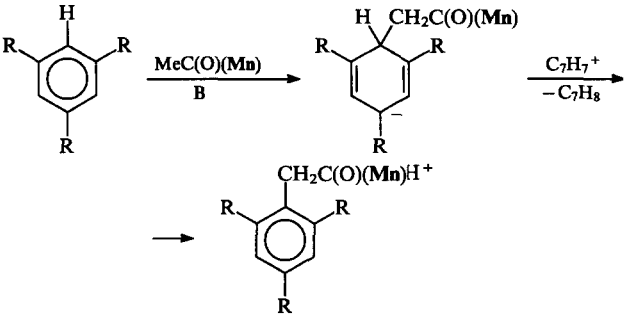
1,2- 1,3-

If the substituent R contains a chiral centre, then the CH groups in the 2,3- and 4,5-positions become nonequivalent (diastereotopic). In this case the substitution reaction may be stereoselective if the substitution proceeds exclusively or predominantly in one of the two nonequivalent positions. The instances of regio- and stereo-selectivity on substitution in cymantrene will be noted below.

A large group of ketones of the cymantrene series have been synthesised by the acylation and benzoylation of cymantrene, alkylcymantrenes, and other cymantrene derivatives (see the relevant review[1]). A series of substituted benzoylcymantrenes having the general formula $[\eta^5\text{-}C_5H_3(Y)C(O)C_6H_4X]Mn(CO)_3$ (X = *o*-, *m*-, and *p*-Me, MeO, Cl, Br, F, etc.; Y = H, 1- and 2-Me) have been obtained by benzoylating cymantrene and methylcymantrene with the acid chlorides $XC_6H_4C(O)Cl/AlCl_3$ in CH_2Cl_2.[19] β-Phenylethyl- and styryl-cymantrenes as well as the carbinol $PhCH_2CH(OH)(\mathbf{Mn})$ have been obtained from benzyl cymantrenyl ketone $PhCH_2C(O)(\mathbf{Mn})$.[19] Refluxing of substituted benzoylcymantrenes with $Cr(CO)_6$ in dibutyl ether leads to a series of benchrotrenyl cymantrenyl ketones having the general formula $(CO)_3Cr[\eta^6\text{-}XC_6H_4C(O)C_5H_3Y\text{-}\eta^5]Mn(CO)_3$ as a result of the coordination of the benzene ring to chromium.[65] On reduction with sodium, these ketones afford the corresponding Na ketyls, in which the radical centre is stabilised simultaneously by the cymantrenyl and benchrotrenyl substituents.[66]

The ω-chloroketones $Cl(CH_2)_nC(O)(\mathbf{Mn})$ have been synthesised by acylating cymantrene with the chlorides of ω-chlorocarboxylic acids. Clemmensen reduction of the ketones affords the ω-cymantrenyl chlorides $Cl(CH_2)_{n+1}(\mathbf{Mn})$, where n = 2 and 3.[67] The interaction of the chlorides with trimethyl-amine leads to the ammonium salts $Me_3N^+(CH_2)_n(\mathbf{Mn})Cl^-$,[68] while their reaction with $(EtO)_2PONa$ leads to the alkylphosphonic acid esters $(EtO)_2P(O)(CH_2)_n(\mathbf{Mn})$.[69] The ketoacid chlorides $PhC(O)(CH_2)_nC(O)Cl$, where n = 4 and 6, afford on acylation of cymantrene the asymmetric diketones $PhC(O)(CH_2)_nC(O)(\mathbf{Mn})$ in a high yield, but the acid chlorides with n = 2 and 3 do not interact with cymantrene under these conditions.[70]

Ketones of the cymantrene series form the corresponding derivatives with functional group substituents (oximes, hydrazones, etc.) and enter into reactions characteristic of ketones. Acetylcymantrene reacts with trinitrobenzene in the presence of bases (triethylamine) with abstraction of a proton and the formation of anionic cyclohexadienyl complexes, which react with the tropylium cation with transfer of a hydride ion, forming cymantrenyl trinitrobenzyl ketone and cycloheptatriene.[71]



R = NO_2.

Cymantrenecarbaldehyde and acetylcymantrene enter readily into the Wittig reaction with the ylide $Ph_3P=CH_2$ and its analogues with formation of the corresponding olefines — vinyl- and alk-2-enyl-cymantrenes.[72,73] Acetylcymantrene also enters into the Reformatskii reaction with ethyl bromoacetate in the presence of zinc dust.[73]

The acylation and benzoylation reactions constitute virtually the only method of synthesis of cymantrenyl ketones. The acyl-ation of cymantrene derivatives is a nonselective reaction. As early as 1970, it was shown that the acylation of alkyl-, halo-, acylamino-, and methoxy-cymantrenes always results in the formation of a mixture of two isomeric ketones.[74–76] The results of the study of the acetylation of methyl(methylthio)cymantrene agree with this finding. The acetylation of both the 1,2- and 1,3-isomers leads to the formation of a mixture of three isomeric ketones containing the Me, MeS, and C(O)Me substituents in different positions in the Cp ring.[77]

The alkylation of cymantrene with $Bu^tCl/AlCl_3$ results in the formation of a complex mixture of alkylation products containing one or two Bu^t and/or C(O)Bu groups in the Cp ring. Reactions involving the succinoylation of *tert*-butylcymantrene, leading to the synthesis of a series of compounds in which the substituted Cp ring has been condensed with the tetramethylene ring, were investigated in the same studies.[78,79]

The mononuclear ketones $(\mathbf{Mn})C(O)CH_2X$, the dinuclear ketones $(\mathbf{Mn})C(O)CH_2XCH_2C(O)(\mathbf{Mn})$, and their ferrocene analogues (X = residues with thiolan and thiolene 1,1-dioxide groups) have been obtained by acylating cymantrene and ferrocene with the acid chlorides $XCH_2C(O)Cl$ and the acid dichlorides $ClC(O)CH_2XCH_2C(O)Cl$.[80]

The reaction involving metallation with butyllithium,[81,82] which proceeds via two pathways depending on the conditions (temperature, solvent), is undoubtedly of greatest importance for the synthetic chemistry of cymantrene. In tetrahydrofuran (THF) or in THF–hexane mixtures at temperatures between −50 °C and −70 °C, the Cp ring is metallated with formation of only the monolithio-derivative.

$$C_5H_5Mn(CO)_3 + BuLi \longrightarrow LiC_5H_4Mn(CO)_3 + BuH.$$

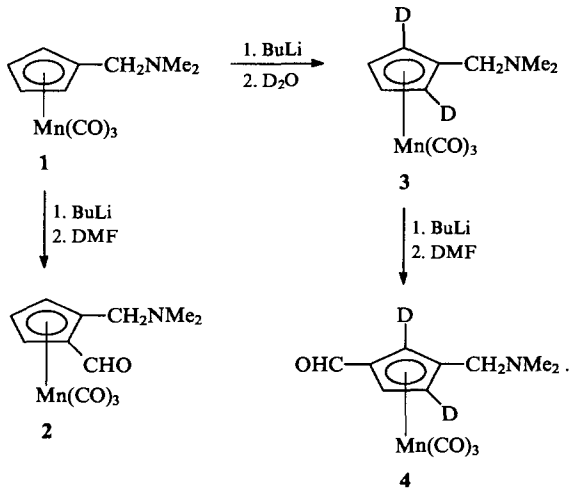
It has been established that, like phenyllithium, cymantrenyl-lithium is unstable in THF: the highest yield of the acid $(\mathbf{Mn})COOH$ (up to 70%–75%) is obtained only when the reaction with CO_2 is carried out 5–15 min after adding butyllithium. On the other hand, if the reaction mass is kept at −60 °C for 1–1.5 h and CO_2 is then added, the yield falls

appreciably.[83] A wide variety of complexes, which are difficult to obtain or are altogether unobtainable by other methods, including compounds with the (**Mn**)—M, (**Mn**)—B, etc. bonds, have been obtained via cymantrenyllithium.[1,83]

Under other conditions (ether, 20 °C), cymantrene reacts with various RLi (R = alkyl, Ph), in which the carbon atom of the carbonyl group is subjected to nucleophilic attack by R^- with formation of oxo-derivatives, the alkylation of which with trialkyloxonium salts leads to carbene complexes (classical Fischer synthesis of carbene complexes).[84]

$$C_5H_5Mn(CO)_3 \xrightarrow{RLi} C_5H_5Mn(CO)_2C(R)O^-Li^+ \xrightarrow{Me_3O^+\,BF_4^-} C_5H_5Mn(CO)_2{=}C(R)OMe\,.$$

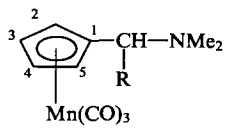
The reaction of cymantrenyllithium (**Mn**)Li with dimethylformamide leads to the formation of cymantrenecarbaldehyde (**Mn**)CHO.[85–87] The oxime (**Mn**)CH=N(OH) has been synthesised from the aldehyde and hydroxylamine in HCOOH. Its dehydration affords the nitrile (**Mn**)CN, which had been obtained previously by other methods.[1] The interaction of the aldehyde (**Mn**)CHO with dimethylformamide (DMF) on refluxing in HCOOH (the Leuckart—Wallach reaction) leads to the formation of dimethylaminomethylcymantrene **1**, the metallation of which with butyllithium takes place stereoselectively, the α-positions being metallated to the extent of 97%.[87]



After the decomposition of the lithio-derivative of the amine **1** with DMF, the 2-aldehyde **2** was obtained and after treatment with D_2O the product was 2,5-dideuteriodimethylaminomethylcymantrene **3**. However, if the amine **3**, where both α-positions contain C—D bonds, is metallated, then a mixture of aldehydes containing 30% of the 2-aldehyde and 70% of the 3-aldehyde **4** is obtained after treatment with DMF. Thus, when hydrogen is replaced by deuterium in the α-position in the amine **1**, the site of attack by butyllithium and the mode of substitution in the Cp ring are altered, i.e. the kinetic isotope effect in the metallation reaction (the ratio of the rates of reaction involving the C—H and C—D bonds) should be very large.[87] The fact that, when an attempt is made to metallate the 2,5-dideuterioamine **3** (with subsequent decomposition of the lithio-derivative with H_2O), deuterium is hardly removed from the α-position in the Cp ring agrees with the above finding.

The regioselectivity of the metallation of the amine **1** (the α-position is metallated exclusively) is apparently associated with the presence of the lone electron pair at the nitrogen atom to which lithium may coordinate. If this electron pair is blocked, as in the complex (**Mn**)$CH_2NMe_2W(CO)_5$, then metallation with butyllithium proceeds nonselectively and virtually to equal extents in the α- and β-positions.[88]

In the metallation of the chiral alkylamines **5** followed by decomposition with D_2O, the insertion of deuterium is also regioselective, and 2- and 5-positions being 75%—80% methylated.



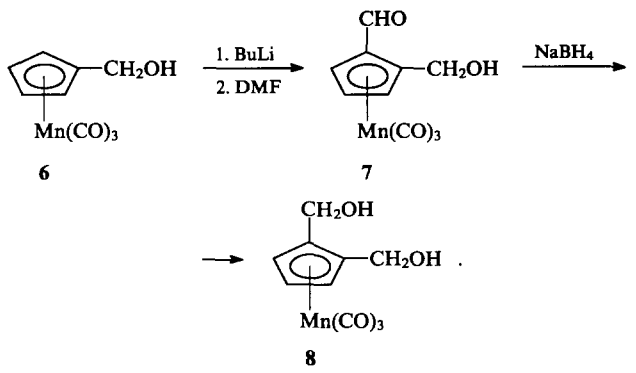
5

R = Me, Et.

Stereochemical induction takes place in the metallation of the amines **5**: substitution in the 2- and 5-positions is unequal, the ratio of the substitution products amounting to 65 : 35 (R = Me) and 95 : 5 (R = Et).[89] The protons and the carbon nuclei in the 2- and 5- (and also 3- and 4-) positions in the amines **5** are diastereotopic and give rise to four different signals in the ^1H and ^{13}C NMR spectra, as in those of the cymantrene derivatives containing a chiral centre in the side chain, which were investigated previously.[90,91]

The mode of substitution in the metallation of cymantrene derivatives has been investigated also for several substituents. In the case of R = Me, metallation takes place nonselectively—simultaneously in the α- and β-positions (the product ratio is 1 : 1.5).[92] However, the metallation of the carbinol (**Mn**)CH_2OH, obtained by reducing cymantrenecarbaldehyde with $NaBH_4$,[93] and also of the sulfonamide derivative (**Mn**)SO_2NMe_2 [94] proceeds regioselectively and only in the α-position. On the other hand, the metallation of diphenylphosphinocymantrene (**Mn**)PPh_2 as well as diphenylphosphinomethylcymantrene (**Mn**)CH_2PPh_2 also takes place stereoselectively but only in the β-position.[93,95] Apparently, in the metallation of the carbinol (**Mn**)CH_2OH **6**, the hydrogen atom in the OH group is initially replaced by lithium, and the lithium cation may remain bound to the oligomeric structure of butyllithium, which facilitates the abstraction of a proton, on treatment with a second molecule of butyllithium, and subsequent substitution in the nearest α-position. The directing influence of the amino-groups in the metallation of amines is most probably induced by the coordination of lithium via the nitrogen atom. The direction of the methylation reaction to the α-position in the case of the SO_2NMe_2 substituent may be associated both with the coordination of lithium to the nitrogen of the sulfonamide group and with the pronounced electron-accepting properties of this group, which are manifested more effectively precisely in the α-position adjoining the substituent. The direction of the substitution reaction to the more remote β-position in the case of the bulky substituents PPh_2 and CH_2PPh_2 is most probably associated with steric effects. Thus the metallation of monosubstituted derivatives constitutes a general method of synthesis of 1,2- and 1,3-disubstituted cymantrene derivatives, while methylation of diphenylphosphinocymantrenes represents the only method in the selective synthesis of 1,3-disubstituted compounds among metallocenes.[92–95]

The capacity of the carbinol **6** for selective metallation in the α-position made it possible to achieve the syntheses of a series of 1,2-disubstituted cymantrene derivatives. Carboxylation of the lithio-derivative of the carbinol **6** afforded 2-hydroxymethylcymantrenecarboxylic acid and reduction of the latter by the ionic hydrogenation method gave rise to 2-methylcymantrenecarboxylic acid.[92] Metallation of the carbinol **6** followed by decomposition with DMF affords the aldehydoalcohol **7**, the reduction of which with $NaBH_4$ leads to 1,2-dihydroxymethylcymantrene **8**.



Substitution of the hydroxy-groups in the diol **8** by Cl or Br on treatment with gaseous hydrogen halides leads to the corresponding 1,2-di(chloromethyl)- or 1,2-di(bromomethyl)-cymantrene. Oxidation of the diol **8** with manganese dioxide affords 1,2-diformylcymantrene, which is also obtained on oxidation of compound **7**.[96]

The interaction of (**Mn**)Li with benzopyridines and their *N*-acyl derivatives has been investigated.[97]

Other substitution reactions, apart from acylation and metallation with butyllithium, have been investigated in lesser detail. After the pioneering work by Cais on the sulfonation of cymantrene,[98] only two studies were published in which it was shown that the sulfonation of methylcymantrene proceeds nonselectively and leads to a mixture of 1,2- and 1,3-isomers.[77,99] Cymantrenesulfonic acids can be conveniently isolated in the form of readily crystallising salts with *p*-toluidine or *p*-chloroaniline. These salts serve as the starting materials for the synthesis of compounds with C_5H_4-S bonds. The sulfonyl chloride (**Mn**)SO_2Cl, obtained on treatment with PCl_5, is reduced with zinc dust to the thiol (**Mn**)SH, which can be extremely readily oxidised to the disulfide (**Mn**)SS(**Mn**).[76,100] Methylcymantrenesulfonic acids react similarly.[77,99] 1,2- and 1,3-Di(methylthiomethyl)cymantrenes were synthesised from 1,2- and 1,3-di(mercaptomethyl)derivatives by methylation with diazomethane.[99] The synthesis of the disulfide $[(CO)_3MnC_5Cl_4S]_2$ has been described.[43]

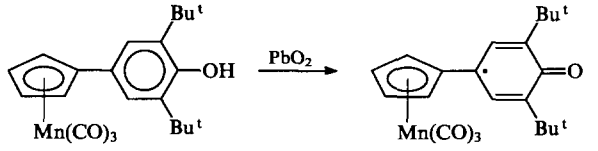
The mercuration of cymantrene with mercury acetate leads to the substitution of one and to a slight extent also two hydrogen atoms of the Cp ring. Early studies on the synthesis and properties of the mercurio-derivatives of cymantrenes were described in a review.[1] The interaction of cymantrene with mercury trifluoroacetate, a powerful mercurating agent, entails exhaustive mercuration with substitution of all five hydrogen atoms and the formation of $C_5(HgOCOCF_3)_5Mn(CO)_3$.[101] We may note that the reaction involving the cyclopalladation of amines, which has been thoroughly developed for ferrocene, has not been investigated in the cymantrene series.

A large series of studies on the hydrogen isotope exchange (HIE) reactions involving metallocenes (ferrocene, ruthenocene, cymantrene and its rhenium analogue, and benchrotrene) were carried out in the 1960s – 1970s. All these complexes enter into the HIE reactions with both acids and bases. Extensive experimental data on the HIE reactions involving cymantrene and its derivatives have been published in reviews.[102–104] A mechanism involving the protonation of the transition metal atom (Fe, Mn, Re, Cr) and subsequent migration of the proton to the π-linked ligand has been proposed for HIE reactions in the presence of acids.

Isotope exchange in the presence of bases, for example in the alcohol – sodium alkoxide and cyclohexylamine – lithium, sodium, potassium, etc. cyclohexylamide systems, as well as metallation with butyllithium are protophilic substitution reactions in which the rate-determining stage is the abstraction of a proton from the Cp ring by the base. For example, measurements of the kinetic isotope effects in the HIE reactions in basic media agree with this postulate. On the other hand, the mechanism of the isotope exchange with acids cannot be regarded as reliably established. For reactions with electrophiles, a special case of which is the hydrogen isotope exchange with acids, two mechanisms are possible. The first involves the attack by the reagent on the Cp ring, while the second involves the attack on the metal with subsequent migration of the electrophile to the Cp ring (the so called 'ricochet' substitution mechanism proposed at an early stage by A N Nesmeyanov). The hydrogen isotope exchange in the reactions of cymantrenylferrocene with acids has been investigated[105] and the acidity of the C – H bonds in the Cp ring of cymantrene and its derivatives in the HIE in alkaline media has been determined by a kinetic method.[106,107]

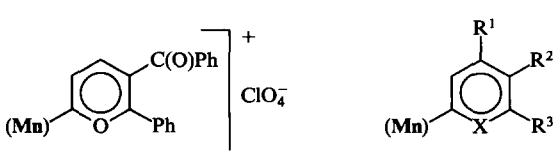
In addition to the early studies[1] concerned with the preparation of a wide variety of cymantrene derivatives, mention may be made of syntheses the majority of which have been carried out through cymantrenyllithium. In this connection, we may mention that, in contrast to benzene derivatives, for the syntheses of which both organolithium and organomagnesium compounds are equally widely employed, in the cymantrene chemistry the corresponding Grignard reagent, namely (**Mn**)MgI formed in a moderate yield from (**Mn**)I and magnesium,[76] is used extremely rarely.

The attack on the keto-group in the 4-position in the interaction of (**Mn**)Li with 2,5-di(*tert*-butyl)-1,4-quinone results in the formation of a carbinol, the Clemmensen reduction of which leads to the cymantrenylphenol **9**. The oxidation of the latter with PbO_2 affords the free-radical complex **10**, which has been characterised by EPR spectroscopy.[108]



9 **10**

A series of studies[109–113] have been devoted to the synthesis of pyryllium salts containing cymantrenyl substituents. The reaction of β-chloro-β-cymantrenylacrolein and dibenzoylmethane in $MeCOOH/HClO_4$ with acetic anhydride led to the formation of the cation **11**, the reactions of which with copper and cobalt acetates afford the bimetallic copper and cobalt β-keto-pyranolates.[109] The cyclisation of acetylcymantrene with α,β-unsaturated ketones $R^1CH=CR^2C(O)R^3$ in a mixture of acetic and perchloric acids gives rise to the tetrasubstituted pyryllium salts **12** with R^1-R^3 = Ph, $MeOC_6H_4$, etc. On treatment with ammonia and aniline, they are converted into the corresponding pyridines.[110]



11 **12**

X = O⁺, N.

Cymantrenyllithium (**Mn**)Li and 2,5-disubstituted pyryllium salts afford 4*H*-pyrans, the abstraction of a hydride ion from which on treatment with $Ph_3C^+ClO_4^-$ leads to the formation of pyryllium salts with the cymantrenyl substituent in the 4-position.[111] The reaction of acetylcymantrene with orthoformic ester in the presence of 70% $HClO_4$ affords 2,6-dicymantrenyl-pyryllium perchlorate, which, on refluxing in ethanol, reacts with $PdCl_2$ in the presence of Na_2CO_3 with cleavage of the pyryllium ring and the formation of the bis-η^3-allyl complex of palladium with perchlorate bridges. The reaction of the latter with CpTl in

acetonitrile leads to the rupture of the dimeric structure and the formation of the allyl complex (η^3-RCH···CH···CHR)PdCp, where R = $(CO)_3MnC_5H_4C(O)$.[112] The electrochemical properties of pyryllium salts with cymantrenyl substituents have been described.[113].

A series of studies have been devoted to the chemistry of thioketones of the cymantrene series. Benzoylcymantrene reacts with P_4S_{10} in CS_2 in the presence of the base $NaHCO_3$ to form the thioketone (**Mn**)C(S)Ph.[114] The latter is readily coordinated by the 16-electron fragments ML_n [ML_n = $W(CO)_5$, $Mn(CO)_2Cp$, etc.], forming dinuclear complexes of the type (**Mn**)(Ph)C=S →ML_n, in which the cymantrenyl thioketone is a two-electron ligand.[115] The structure of the dinuclear complex where ML_n = $Mn(CO)_2Cp$, was established by X-ray diffraction.[116] Reversible temperature variations have been noted in the ^1H and ^{13}C NMR spectra. It follows from them that in solution the complex exists as a mixture of (*E*)- and (*Z*)-isomers with different dispositions of the manganese-containing fragments relative to the C=S bond. The barriers to rotation about his bond, determined from the NMR data, amount to 12.4–13.0 kcal mol^{-1}.[116,117] The thioketone (**Mn**)(Ph)C=S reacts with the anions Cp^- or $CpFe(CO)_2^-$ to form initially phenyl(cymantrenyl)fulvene, which rapidly dimerises under the reaction conditions via a diene synthesis type of reaction or enters into a cycloaddition reaction via the C=S bond.[118] The formation of the dimer is reversible: on interaction of the dimer with $Cr(CO)_6$, it dissociates to the monomer, which affords the complex [η^6-C_4H_4C=C(Ph)(**Mn**)]$Cr(CO)_3$ in which the Cr atom is coordinated to the three C=C bonds of cymantrenylfulvene.[119]

Cymantrenylthioketones are reactive compounds. Thus, on being kept in air (at 25 °C, 20 days), the thioketone (**Mn**)C(S)Me is converted into a complex mixture of products, from which biscymantrenyl derivatives with trithiolan and dithietan rings, characterised by X-ray diffraction, were isolated.[120]

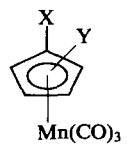
Among the numerous studies on the synthesis of various organic and heterocyclic compounds with a cymantrenyl substituent, one may distinguish the syntheses of cymantrenyl analogues of mandelic acid[121] and alanine[122] as well as cymantrenylthioglycolic acid.[100] Carbinols containing the $SiMe_3$ group have been obtained by the reactions of acetylcymantrene and benzoylcymantrene with the Grignard reagents Me_3SiCH_2MgCl and $Me_3SiC_6H_4MgBr$.[123] The syntheses and reactions of dihydric alcohols in the acetylene series of the type (**Mn**)C(OH)(R)C≡CC(OH)R^1R^2 have been studied.[124–126]

A series of cymantrenyl vinyl ketones (cymantrenyl analogues of chalcones) having the general formula (**Mn**)CH=CHC(O)R, where R = phenyl, cymantrenyl, ferrocenyl, and vinylcymantrene or vinylferrocene residues, have been obtained by condensing formylcymantrene with the ketones MeC(O)R.[127] These compounds readily enter into cyclisation reactions with hydrazine, forming relatively unstable pyrazolines, the acylation of which affords the more stable *N*-acetyl derivatives.[128] Condensation of the pyrazolines with benzaldehydes gives rise to 4-benzylidenepyrazolines.[129,130] Catalytic pyrolysis of cymantrenylpyrazolines results in the formation of cymantrenylcyclopropanes, including dicymantrenylcyclopropanes.[129–132] This reaction is nonselective and gives rise to mixtures of the *cis*- and *trans*-isomers of the substituted cyclopropanes.

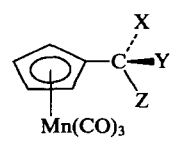
In reactions with $Fe_2(CO)_9$ or $Fe_3(CO)_{12}$, cymantrenyl vinyl ketones form mixtures of heterodiene complexes of iron tricarbonyl and olefin derivatives of iron tetracarbonyl in which the diene or olefin ligand contains the cymantrenyl substituent.[133,134] The reaction of ferrocenylideneacetylcymantrene with MeMgI affords a mixture of the substituted allyl alcohol FcCH=C(OH)Me(**Mn**) and the ketone FcCHMeCH$_2$C(O)(**Mn**).[135] Cymantrenyl vinyl ketones and their complexes with $Fe(CO)_3$ are protonated on treatment with CF_3COOH at the oxygen atom of the carbonyl group with formation of cations of the allyl type.[136,137] A reaction involving the addition of dimethyl malonate to cymantrenyl vinyl ketones has been described.[138]

IV. Chiral derivatives of cymantrene

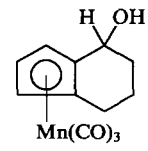
Two types of chiral derivatives of cymantrene are known. The structural characteristics of metallocenes as well as compounds containing one planar cyclic ligand (C_5H_5, C_6H_6, etc.), linked to a $M(CO)_3$ fragment, are such that, when the ring contains two different substituents, these molecules become chiral. Accordingly, disubstituted cymantrene derivatives are planarly chiral (type **A**) regardless of whether the two different substituents occupy the 1,2- or 1,3-positions. The second type of chiral derivatives consists of compounds containing a chiral centre in the α- or more remote position in the side chain (type **B**). Compounds containing simultaneously both elements of chirality, in particular the carbinol **13** and its analogues, have been obtained.



A



B

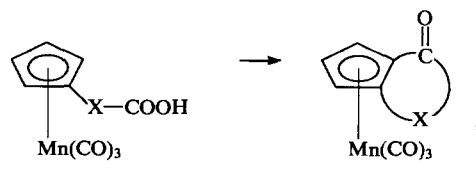


13

The first studies on the stereochemistry of cymantrene derivatives were carried out on compounds with planar chirality, mainly on a series of different derivatives of methylcymantrene. As early as 1961, 2- and 3-methylcymantrenecarboxylic acids, obtained by acylating methylcymantrene and then oxidising with iodine the mixture of ketones (2- and 3-methylacetylcymantrenes), were resolved into the enantiomers.[139] Systematic study of the stereochemistry of the cymantrene derivatives was begun in the middle of the 1960s. Schlögl and his group[140–143] synthesised, resolved into enantiomers, investigated the chirooptical properties, and established the absolute configurations of a series of derivatives of methylcymantrene [C_5H_3(R)Me]$Mn(CO)_3$, where R = COOH, C(O)Cl, $C(O)N_3$, Na_2, Cl, Br, I, NCO, etc.] and also cymantrenylbutyric acids and methylcymantrenylcyclohexa-1,2-dienes, obtained by succinoylating methylcymantrene with succinic anhydride and subsequent cyclisation (see also Schlögl[144,145]).

Studies on the synthesis, resolution into enantiomers, and the determination of the absolute configurations of 1-methyl-2-cymantrenyl- and 1-methyl-3-cymantrenylpropionic and 1-methyl-2-cymantrenyl- and 1-methyl-3-cymantrenyldimethylpropionic acids were carried out at the beginning of the 1970s.[146–149]

All the known planarly chiral derivatives of cymantrene have been obtained in one way — by introducing the second substituent into monosubstituted cymantrenes. Since the acylation reaction is nonselective, mixtures of the 1,2- and 1,3-isomers of different ketones of the cymantrene series are always formed (see the table in the relevant review[1]) with the sterically less hindered 1,3-isomers predominating. In order to separate the mixtures, laborious chromatographic separation procedures have to be resorted to.



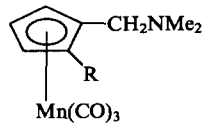
;

X = SCH_2,[76] CH_2CH_2,[150] $CH_2CH_2CH_2$ [151].

One of the methods of selective introduction of the second substituent in the 2-position involves the intramolecular acylation of monosubstituted acids and their chlorides, which leads to the 1,2-isomers of cymantrenyl ketones with a condensed polymethylene ring.[76,150,151]

When the keto-group is reduced to the CH(OH) fragment by $NaBH_4$ or $LiAlH_4$, a chiral centre arises in the α-position and diastereoisomers containing two elements of chirality — the plane and the centre — are formed.[152]

Metallation of monosubstituted derivatives of cymantrene has been used widely in recent times for the synthesis of planarly chiral cymantrene derivatives with substituents in the 1- and 2-positions. This reaction is based on the fact that, for certain substituents containing a heteroatom with a lone electron pair, such as CH_2NMe_2 and CH_2OH, metallation is regioselective and proceeds almost exclusively only in the position adjoining the substituent. Metallation of dimethylaminomethylcymantrene followed by treatment with electrophiles afforded the 1,2-disubstituted cymantrenes **14a–c**.[87,93]

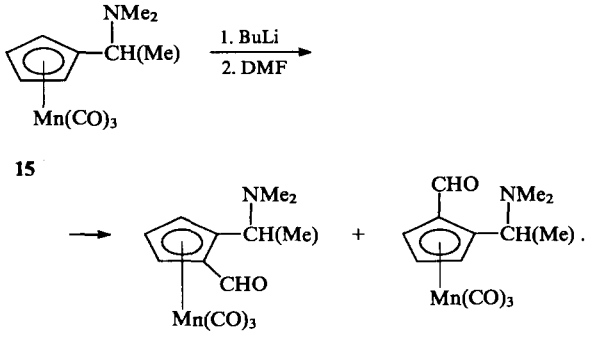


14a–c

R = D (**a**), CHO (**b**), PPh_2 (**c**).

Stable Cu^{2+} complexes with Schiff bases, obtained from the aminoaldehyde **14b** and chiral dipeptides, have been proposed for the resolution of the racemic aminoaldehyde **14b** into enantiomers. The copper complexes are mixtures of diastereoisomers, which were resolved by extraction and liquid chromatographic methods. Acid hydrolysis of the diastereoisomers affords the optically pure enantiomers of the aldehyde **14b**.[153–156] The absolution configuration of one of them as well as the structure of the copper complex of the dipeptide Ala–Ala have been established by X-ray diffraction.[155,157]

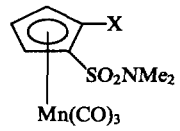
Metallation of α-(*N*,*N*-dimethylamino)ethylcymantrene **15**, containing a chiral centre in the α-position, followed by treatment with dimethylformamide produced a mixture of two diastereoisomers of the aminoaldehyde **16** in proportions of 7:2 (asymmetric induction). The Cu^{2+} complexes obtained from the Schiff bases formed from these aldehydes and a different dipeptide were resolved by liquid chromatography. The enantiomers of the aldehyde **16**, the absolute configuration of one of which was established by X-ray diffraction,[159] were obtained from them by acid hydrolysis.[158]



15

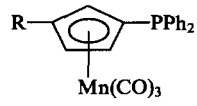
16

The regioselective metallation only in the α-position in cymantrene derivatives with the substituents R = CH_2OH [93] and SO_2NMe_2 [94] was noted above. A series of racemic 1,2-disubstituted complexes **17** [X = COOH, COOMe, CMe_2OH, CPh_2OH, CH(Ph)OH, etc.] have been obtained by the reactions of the lithio-derivative containing the sulfonamide group with electrophiles.[94]



17

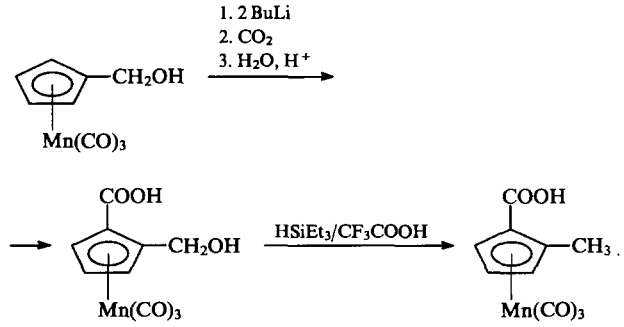
On the other hand, the metallation of the diphenylphosphino-derivative **(Mn)**PPh_2 also proceeds regioselectively but only in the β-position, which is evidently associated with steric factors. The reaction of the lithio-derivative of this phosphine with DMF and Ph_2PCl leads to the phosphinoaldehyde **18a** and 1,3-bis(diphenylphosphino)cymantrene **18b**. The dimethylaminomethyl derivative **18c** was obtained from the aldehyde in the reaction with DMF and HCOOH.[93]



18a–c

R = CHO (**a**), PPh_2 (**b**), CH_2NMe_2 (**c**).

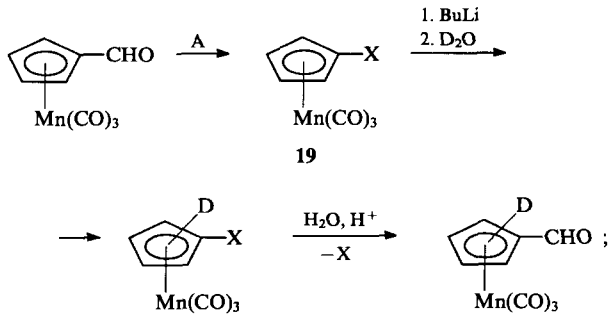
A method, based on the acylation of methylcymantrene with subsequent oxidation of the mixture of the resulting methylacetyl derivatives by iodine in pyridine and the separation by fractional recrystallisation and chromatography of the mixture of acids or their esters produced, was proposed previously for 2-methylcymantrene-1-carboxylic and 3-methylcymantrene-1-carboxylic acids.[141] As a result of the numerous stages in the synthesis, the yield of 2-methylcymantrene-1-carboxylic acid does not exceed 10%. An improved method of synthesis of 2-methylcymantrenecarboxylic acid, based on the stereoselective metallation of hydroxymethylcymantrene, obtained readily from cymantrenecarbaldehyde by reduction with $NaBH_4$ and EtOH,[93] has been developed recently.[92] The hydroxymethyl group was reduced to the methyl group by ionic hydrogenation in the Bu_2SiH_2/CF_3COOH system. The absolute configuration of 2-methylcymantrenecarboxylic acid was determined by chemical correlation with the aldehyde **14b**, the absolute configuration of which had been obtained earlier by X-ray diffraction.[155]



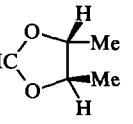
There are at present two methods of synthesis of optically active compounds of the cymantrene series with a planar chirality. The first of these is the classical resolution of racemates via the intermediate formation and separation of diastereoisomers.[141–143,155] The second method is based on the kinetically controlled enzymic reduction of disubstituted chiral and achiral compounds, one example of which has been described.[160] In each specific case, it is essential to select carefully the optimum reactants and resolution conditions.

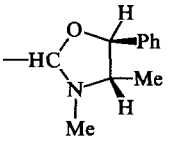
A new approach to the synthesis of optically active 1,2-disubstituted cymantrene derivatives with a planar chirality, based on the regioselective metallation of a series of new monosubstituted derivatives with butyllithium, has been

developed recently.[161-164] In this method, the initial achiral compound with a functional group substituent—cymantrenecarboxylic acid or cymantrenecarbaldehyde—is converted in a preliminary step into a chiral derivative with the aid of the optically active molecule of the inductor **A**. This is followed by the stage in which the second substituent is introduced—usually metallation with butyllithium and treatment with the appropriate reagents (D_2O, CO_2, etc.). In the third stage, the inductor molecule is removed from the diastereoisomeric product by acid hydrolysis.



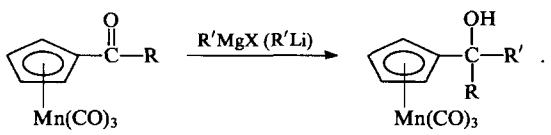
A = $CH(OEt)_3$; X =  ;

A = (2*R*,3*R*)-MeCH(OH)CH(OH)Me; X =  ;

A = (−)-ephedrine; X =  .

Metallation of compounds **19** by treatment with BuLi proceeded exclusively at the CH positions of the Cp ring, whereupon the regioselectivity of the process depends on the nature of the reagent **A**.[161,162] (−)-Norephedrine, (−)-2-aminobutanol, (*R*)-phenylethanediol, and (*S*)-prolinol may be used as the inductor molecules **A**.[162,163] This approach has been used to synthesise the enantiomers of 2-methylcymantrene-1-carboxylic and 3-methylcymantrene-1-carboxylic acids.[161] By virtue of the extensive possibilities of the metallation reaction, this method makes it possible to obtain directly the enantiomers of planarly chiral compounds with a wide set of substituents. Compounds containing two elements of chirality—the chiral centre at the metal atom and the chiral plane—have been obtained by substituting two CO groups in 3-methylcymantrenecarboxylic acid and its esters by various phosphine ligands.[165,166]

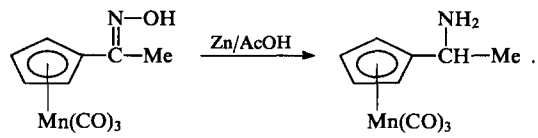
Cymantrene derivatives with a chiral centre in the side chain are usually obtained by forming this centre from a prochiral fragment already available. A typical example is provided by the synthesis of secondary and tertiary carbinols from ketones.[167,168]



In the case of cymantrenyl methyl ketones, it has been shown that the reduction of the 1,2-isomers proceeds with a high degree of stereoselectivity, whereas the selectivity for the 1,3-isomers is much lower.[169] The stereoselectivity in organomagnesium synthesis is fairly high, the proportions of the enantiomers depending significantly on the nature of the groups R and R'. Similar reactions for a ketone with a condensed polymethylene ring have been investigated.[152] Chiral carbinols of the cymantrene series can be converted into other chiral derivatives (esters, azides, nitriles, amines, etc.) by esterification and nucleophilic substitution reactions.

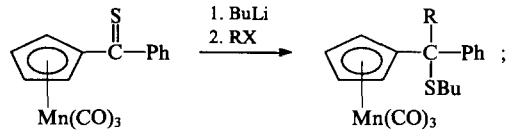
In certain cases, asymmetric synthesis has been used to obtain optically active cymantrene derivatives with a chiral centre. In the reduction of acetyl- and benzoyl-cymantrenes by a complex of lithium tetrahydroaluminate and quinine, the corresponding carbinols are formed, but their optical yield does not exceed 10%−15%.[169]

Yet another example of the formation of a chiral centre involves the reduction of ketone oximes to primary amines.[170]



The racemic α-aminoethylcymantrene synthesised in this way was resolved into enantiomers by crystallising the salts with (+)-*d*-tartaric acid. α-Dimethylaminoethylcymantrene (**Mn**)CH(Me)NMe_2, its methiodide (**Mn**)CH(Me)$^+NMe_3I^-$, and the acetamido-derivative (**Mn**)CH(Me)NHC(O)Me have been obtained from this amine. The absolute configuration of the acetamido-derivative was established by X-ray diffraction.[170] Subsequently 14 optically active derivatives of aminocymantrenes having the general formula (**Mn**)CH(Me)X [X = NH_2, NHCHO, NHMe, $NHCH_2Ph$, $NHCH_2$(**Mn**), N_3] as well as the Schiff bases (**Mn**)CH(Me)N=CHPh, (**Mn**)CH(Me)N=CH(**Mn**), etc. were synthesised and their chirooptical properties were investigated.[171] The reactions of the optically active (+)-α-phenylethylamine with (**Mn**)CH_2Cl, (**Mn**)C(O)Cl, and (**Mn**)CHO, which resulted in the synthesis of the corresponding compounds with a chiral centre in the β-position in the side chain, have been described.[172] As for compounds with the chiral centre in the α-position, the protons and carbon nuclei in the 2,5- and 3,4-positions are diastereotopic and give rise to different signals in the ^1H and ^{13}C NMR spectra.

The reaction of the thioketone (**Mn**)(Ph)C=S with butyllithium follows the so called 'thiophilic' path with metallation of the sulfur atom. Treatment of the reaction product with electrophiles afforded the previously unknown metallocenyl sulfides with the chiral centre in the α-position.[173]

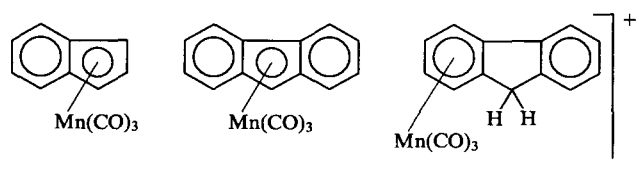


R = H, D, Me.

V. Complexes with polycyclic ligands and polynuclear derivatives of cymantrene

The synthesis and properties of the complexes of $Mn(CO)_3$ with indene, fluorene, and related compounds, in which the Cp ligand is part of a more complex cyclic system, are considered below.

If the ligand contains simultaneously five- and six-membered rings, there is a possibility of two types of coordination of the



20 **21** **22**

$Mn(CO)_3$ fragment. The η^5-type of coordination affords the neutral compounds **20** and **21**, containing the indenyl or fluorenyl ligands. The cationic complex **22**, in which the $Mn(CO)_3$ residue is η^6-linked to the cyclic ligand, is also known.

Metallotropic rearrangements, in which the $Mn(CO)_3$ fragment migrates from the five- to the six-membered ring and conversely, are characteristic of the indenyl and fluorenyl complexes.

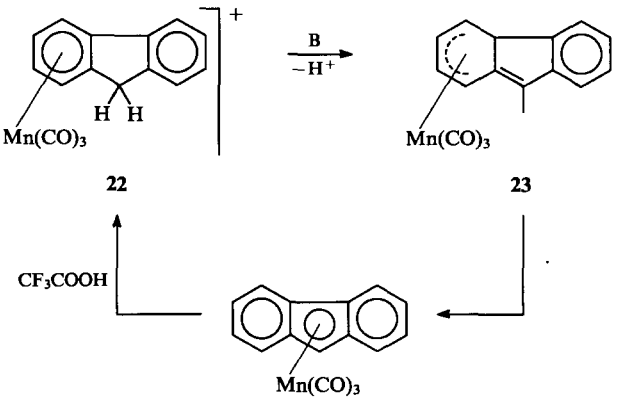
Complexes **20** and **21** were first obtained by the reaction of $Mn(CO)_5Br$ with indenyl- and fluorenyl-sodium (in 56% and 11% yields)[174] or with the $SnMe_3$ derivatives of indene and fluorene (in 62% and 20% yields).[175] An improved method of their synthesis by the reactions of $Mn(CO)_3(MeCN)_2$ with indenyl- or fluorenyl-potassium was developed subsequently.[176] The indenyl complexes of manganese and rhenium can also be obtained by direct synthesis in yields up to 90% on refluxing the decacarbonyls $M_2(CO)_{10}$ in an excess of indene as the solvent.[177]

The CO groups in complexes **20** and **21** undergo photochemical substitution by PPh_3, $AsPh_3$, and $SbPh_3$,[174] but, in contrast to cymantrene, in these compounds there is a possibility of not only photochemical but also of thermal substitution of CO by phosphines and phosphites. In the study of the kinetics of the thermal substitution of CO (decalin, 200 °C), an appreciable increase in the rate of reaction in the sequence $C_5H_5 < C_9H_7 < C_{13}H_9$ was noted.[178,179] These reactions are second order overall and first order with respect to the complex and the ligand; an associative mechanism has been proposed for them with the formation of an η^3-intermediate. In the photochemical substitution of CO by PPh_3, such an effect was not observed, which indicates a dissociative process mechanism.[180] A CO group in complex **20** can be substituted by NO with formation of the cation $(\eta^5\text{-}C_9H_7)Mn(CO)_2(NO)^+$.[176] The cationic complex $(\eta^5\text{-}C_9H_7)Mn(CO)(NO)(PPh_3)^+$, chiral with respect to the Mn atom, has also been obtained.[181] Its interaction with the anions $X^- = Br^-$, I^-, or CN^- involves the ready cleavage of the Mn—C(Cp) bond with the removal of the indenyl ligand and the formation of the complexes $Mn(NO)_2(PPh_3)_2X$.[181]

A series of studies on the hydrogen substitution reactions in the indenyl and fluorenyl ligands were carried out in the 1980s. In the reaction of $(\eta^5\text{-}C_9H_7)Mn(CO)_3$ with an excess of $MeC(O)Cl/AlCl_3$, acetylation takes place simultaneously both in the five- and six-membered rings, the ratio of the isomers depending significantly on the reaction conditions.[182] It has been shown by the competitive acylation method that the reactivity of the indenyl ligand is higher than that of the cyclopentadienyl ligand. In the case of $(\eta^5\text{-}C_{13}H_9)Mn(CO)_3$, acylation takes place only in the six-membered ring and is accompanied by the cleavage of the Mn—η^5-ligand bond.[183] Apart from the 2-acetyl derivative, 2-acetylfluorene and fluorenone were also isolated. The appreciably lower strength of the bond between the η^5-ligand and $Mn(CO)_3$ in $(\eta^5\text{-}C_{13}H_9)Mn(CO)_3$ compared with $(\eta^5\text{-}C_9H_7)Mn(CO)_3$ agrees with the mass-spectrometric data on the strength of the corresponding bonds in the gas phase.[184] The acylation of $(\eta^5\text{-}C_{13}H_9)Mn(CO)_3$ led to the isolation and characterisation by X-ray diffraction also of the products of the partial hydrogenation of one of the six-membered rings.[185]

In the isotope exchange of hydrogen in the $CF_3COOD/D_2SO_4/CH_2Cl_2$ system, H is substituted by D in both rings of the $\eta^5\text{-}C_9H_7$ ligand, although the substitution in the five-membered ring predominates.[183] The complex $(\eta^5\text{-}C_9H_7)Mn(CO)_3$ can be metallated by butyllithium in THF at −40 °C, but the reaction proceeds nonselectively and a mixture of the 1- and 2-isomers containing lithium in the five-membered ring is formed.[186] Competitive metallation of a mixture of $(C_9H_7)Mn(CO)_3$ and $(C_{13}H_9)Mn(CO)_3$ has shown that the indenyl ligand is more reactive.[187]

Metallotropic rearrangements are very characteristic of the indenyl and fluorenyl derivatives of manganese and rhenium. The reaction of fluorene with $Mn(CO)_5Br$ (refluxing in hexane) afforded the cationic complex **22**. Its deprotonation by bases (Bu^tOK, MeONa, NEt_3, etc.) gives rise to the neutral complex **23**, which on heating or storage in the solid state is converted into the thermodynamically more stable complex **21** as a result of the $\eta^6 \rightarrow \eta^5$ rearrangement.[188]



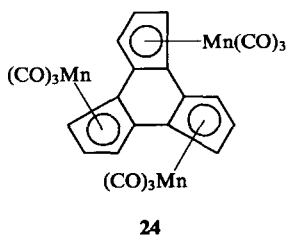
22 **23** **21**

It has been established by X-ray diffraction that complex **23** has a structure typical for cyclohexadineyl derivatives.[189] Quantum-chemical calculations for the $\eta^6 \rightarrow \eta^5$ rearrangement of fluorenyl complexes have shown[190] that the η^6-isomer is less stable (by ~7 kcal mol^{-1})† than the η^5-isomer, while the activation energy for the rearrangement via the η^3-intermediate is 25 kcal mol^{-1}. Kinetic studies on $\eta^6 \rightarrow \eta^5$ rearrangements for the fluorenyl complexes $(\eta^6\text{-}C_{13}H_9)Mn(CO)_2L$ (L = CO or PBu_3) confirmed the results of the calculations.[191]

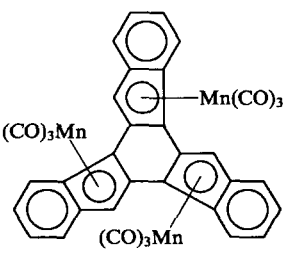
The reverse $\eta^5 \rightarrow \eta^6$ rearrangement has been observed in the study of the protonation of complex **21** in the presence of CF_3COOH.[192] It has been suggested that the acid proton adds directly to the fluorenyl ligand. In the η^5-indenyl complexes of manganese and rhenium, the analogous $\eta^5 \rightarrow \eta^6$ rearrangements take place (according to Ezernitskaya et al.[193]) only in the presence of stronger acids HSO_3F and $AlCl_3$ + HCl. In the complexes with phosphine ligands $(\eta^5\text{-}C_9H_7)Mn(CO)_2PPh_3$ and $(\eta^5\text{-}C_{13}H_9)Mn(CO)_2PPh_3$, the basicity of the central metal atom is greater than the basicity in the tricarbonyl complexes and in the presence of CF_3COOH only protonation at the Mn atom takes place and there is no metallotropic rearrangement..

The $\eta^5 \rightarrow \eta^1$ rearrangement of the fluorenyl ligand has been observed in the reaction of $(\eta^5\text{-}C_{13}H_9)Mn(CO)_3$ with an excess of PBu_3.[179] In a later study,[194] the complex $(\eta^1\text{-}C_{13}H_9)Mn(CO)_3(PEt_3)_2$ was isolated and characterised by a set of spectroscopic methods.

The properties of the indenyl and fluorenyl complexes of manganese and other transition metals have been examined in detail in a review.[195] Communications concerning the study of the metallotropic rearrangements of the manganese tricarbonyl complexes with other polycyclic hydrocarbons, such as fluoradene[196] and 9,10-dihydro-9-methylindeno[1,2-*a*]indene and its analogues,[197,198] have appeared recently. The structure of the dinuclear complex $(\eta^5,\eta^5\text{-}L)Mn_2(CO)_6$, where L = 3,5-dimethylazulene, has been established by X-ray diffraction.[199]



24



25

† 1 kcal = 4.18 kJ.

Bismanganese tricarbonyl complexes of *sym*- and *asym*- indacenes have been obtained[200,201] by the reaction of the corresponding biscyclopentadienyl anions with $Mn(CO)_5Br$ or $Mn(CO)_3Py_2Br$. The trismanganese tricarbonyl complex **24** has also been obtained recently[202] and complexes containing one and two $Mn(CO)_3$ residues as well as the triscomplex **25** have been synthesised from the hydrocarbon truxene.[203,204]

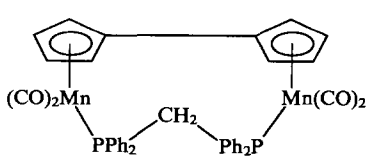
The simplest compound in which the two parts of the ligand are linked by a single C–C bond is the complex bicymantrenyl (**Mn**)–(**Mn**). It was synthesised in 1969 by three groups of investigators simultaneously.[76,205,206] A compilation of different methods of its synthesis is given in Table 1. These methods for the reactions involve the oxidative coupling of two $(CO)_3MnC_5H_4$ fragments, formed when the Grignard reagent (**Mn**)MgI or (**Mn**)Li is acted upon by metal salts, and radical dimerisation reactions in the course of the pyrolysis of cymantrene metallo-derivatives [(**Mn**)Cu, (**Mn**)Ag, $(\mathbf{Mn})_2$Hg]. The optimised yield of bicymantrenyl in the reaction of (**Mn**)Li with carefully dehydrated $CuCl_2$ reaches up to 90%.[212]

Table 1. Syntheses of bicymantrenyl.

Initial compounds	Yield of cymantrenyl, (%)	Other reaction products	Ref.
(**Mn**)$AuPPh_3$ + Cl_2	72	(**Mn**)Cl	205
(**Mn**)$AuPPh_3$ + Br_2	33	(**Mn**)Br	205
(**Mn**)MgI + $CoCl_2$	30	–	76
	15	–	206
(**Mn**)Li + $CoCl_2$	13	–	206
(**Mn**)I + Cu[a]	21	–	206
$(\mathbf{Mn})_2$Hg + Ag[a]	67	–	206, 207
(**Mn**)Cu + I_2	10	(**Mn**)I	208
(**Mn**)$B(OH)_2$ + $Cu(OAc)_2$	10	cymantrene	209
(**Mn**)Li + $CuBr_2$	52	–	210
(**Mn**)Li + $CuCl_2$	69	–	211
(**Mn**)Li + $CuCl_2$	90	–	212
(**Mn**)Cu + Br_2	50	–	211
(**Mn**)Ag + Br_2	23	–	211
$Mn(CO)_5Br$ + fulvalenedithallium	86	–	213

[a] Pyrolysis in the presence of metal powders.

Although bicymantrenyl has been known for more than 20 years, only one substitution reaction in the Cp ring has been described for this compound: acetylation with the MeC(O)Cl + $AlCl_3$ mixture, which proceeds in the 3-position.[207] Other substitution reactions, including metallation with BuLi, have not been investigated. As in cymantrene, the CO groups in one or simultaneously in two $Mn(CO)_3$ fragments can be substituted by n- and π-donor ligands (triphenylphosphine, ethylene, cyclooctene, dimethylacetylene, and pyridine) with formation of both mono- and di-substituted compounds. After the reaction of bicymantrenyl with the diphosphine $Ph_2PCH_2PPh_2$, complex **26** was isolated and characterised by X-ray diffraction. Because of the presence of the rigid chelate skeleton of the diphosphine, the coplanarity of the two Cp rings in complex **26** is significantly disturbed. Their planes form with one another a dihedral angle of 65°.[212]



26

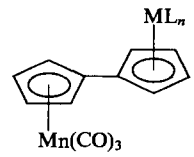
In the absence of steric hindrance, the similar bifulvalenyl system is known to be planar.

Cymantrenylferrocene[214] and a series of its derivatives[215–217] have been obtained by the thermal reaction of haloferrocenes with (**Mn**)Cu, (**Mn**)Ag, or $(\mathbf{Mn})_2$CuAg.

The properties of cymantrenylferrocene have been investigated in greater detail than those of bicymantrenyl.[217] Depending on the type of reagent, substitution takes place either in the ferrocene or in the cymantrenyl ring. Thus, on acetylation with acetic and anhydride in the presence of H_3PO_4, i.e. under mild conditions, the acetyl substituent enters the unsubstituted ferrocene ring. On the other hand, on treatment with BuLi the Cp ring in the cymantrene nucleus is metallated. The reaction of the lithio-derivative of cymantrenylferrocene with $B(OBu)_3$ affords after hydrolysis (3-ferrocenyl)cymantreneboronic acid, from which complexes with the Br or HgCl substituents in the cymantrenyl fragment were obtained after treatment with $CuBr_2$ or $HgCl_2$. The study of the hydrogen isotope exchange with acid showed that the introduction of the electron-accepting cymentrenyl substituent lowers the rate of exchange in the ferrocenyl nucleus approximately by an order of magnitude compared with the unsubstituted ferrocene.[105]

As a result of the coupling of the two metallocenyl fragments, the thermolysis of a mixture of the Ag derivative of dimethylaminomethylferrocene together with (**Mn**)Cu or (**Mn**)Ag at 120 °C afforded 2-(dimethylaminomethyl)-1-cymantrenylferrocene and a series of its derivatives.[218,219] The same complex is formed also by the oxidative coupling of a mixture of lithio-derivatives of dimethylaminomethylferrocene and cymantrene.[219]

A cymantrenylbenchrotrene complex has been obtained by the reaction of phenylcymantrene with $Cr(CO)_3(MeCN)_3$.[220] The interaction of $H_3Mn_3(CO)_{12}$ with azulene led to the isolation of a complex[221] in which two azulene nuclei are linked by a C–C bond in the 4–4′ positions; its structure was established by X-ray diffraction.[222] The heterodinuclear complexes **27** have been synthesised from the monometallic derivatives of difulvalene.[223]



27

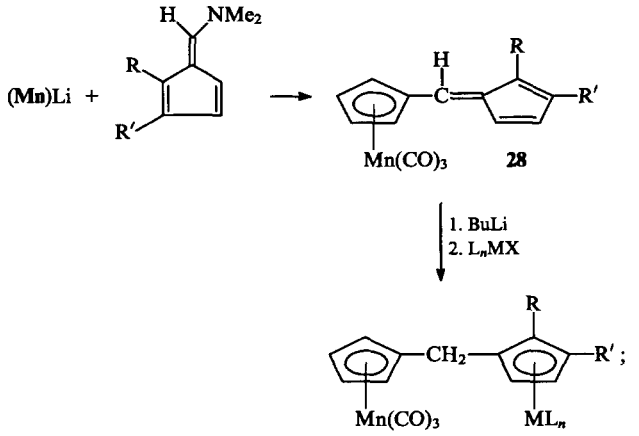
ML_n = $W(CO)_3$, $Mo(CO)(PMe_3)_2Me$.

In the compounds examined above, two identical or different metal-containing fragments are joined by a C–C bond. Together with these, a large number of compounds having the general formula (**Mn**)–X–ML_n, where the cymantrene residue is linked to another organometallic group ML_n via a carbon-containing fragment X [X = CO, CH_2, $C(O)CH_2$, etc.], have also been synthesised. The interaction of benzoylcymantrenes (**Mn**)$C(O)C_6H_4R$ or the ketone (**Mn**)$C(O)CH_2Ph$ and a series of its derivatives with $Cr(CO)_6$ on refluxing in diglyme led to the formation of the dinuclear complexes (**Mn**)–X–$C_6H_4RCr(CO)_3$, where X = CO, CH_2, CH_2CO, CHCH(OH), CH=CH, etc.[224] The dithallio-derivative of dicyclopentadienylmethane is a convenient precursor in the synthesis of various homo- and hetero-dinuclear complexes, including also dicymantrenyl-methane $(\mathbf{Mn})_2CH_2$.[225]

It has been suggested that 6-dimethylaminofulvene be used for the synthesis of heterodinuclear derivatives of cymantrene (Scheme 1).[226]

The comparatively ready availability of the intermediate **28**, the structure of which has been characterised by X-ray diffraction, opens a pathway to the synthesis of various dinuclear complexes

Scheme 1



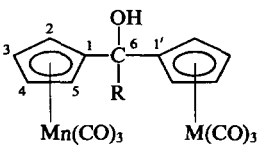
ML_n = $Co(CO)_2$, $Mo(CO)_3Br$.

with the $(Mn)CH_2$ fragment. The interaction of dimethylaminofulvene with indenyllithium and further with $(CO)_3Py_2Mn(Br)$ (Py = pyridine) led to the formation of cymantrenylbenzofulvene—an analogue of compound **28**, where RR′ = condensed benzene rings.[227] The auration of acetylcymantrene by treatment with the oxonium salt $(Ph_3PAu)_3O^+BF_4^-$ in the presence of NaH led to the formation[228] of the complex $(Mn)C(O)CH_2AuPPh_3$, in which the C—Au bond is readily cleaved on treatment with HCl. A series of dinuclear complexes having the general formula (Mn)—X—ML_n, where X = CH_2,[229] $C(O)CH_2$,[230] or C(O),[231–235] while ML_n = $Fe(CO)_2Cp$, $Mo(CO)_3Cp$, $W(CO)_3Cp$, $Mn(CO)_5$, or $Re(CO)_5$, have been obtained by the reactions of the chlorides $(Mn)CH_2Cl$ and $(Mn)C(O)CH_2Cl$ or the acid chloride (Mn)C(O)Cl with the carbonylate anions Na^+ML_n in THF. The compounds containing the $Fe(CO)_2Cp$ and $W(CO)_3Cp$ fragments were characterised by X-ray diffraction.[236, 237] The reactions involving the photochemical substitution of the CO ligands by PPh_3 at the Fe, Mo, and W atoms were carried out for some of the complexes of this type. A characteristic property of these compounds is the capacity for ready decarbonylation with formation of the corresponding compounds having the C_5H_4—M bonds (see below).

Tungsten hexacarbonyl $W(CO)_6$ reacts in the usual way with (Mn)Li, affording after alkylation with $Et_3O^+BF_4^-$, the carbene complex $(CO)_5W=C(OEt)(Mn)$ with the cymantrenyl substituent at the carbene carbon atom. On treatment with $AlBr_3$, it is readily converted[238] into the carbyne complex $[(CO)_4W\equiv C(Mn)]^+$. Dinuclear complexes of the type $(C_6H_6)Cr(CO)_2(Mn)L$, where L = PPh_2 or CH_2PPh_2, have been obtained by the reactions of $(C_6H_6)Cr(CO)_3$ with cymantrenylphosphines.[239]

Compounds containing two or three cymantrenyl fragments in one molecule have been synthesised in a series of studies. The vast majority of these syntheses were carried out via cymantrenyllithium. The reaction of (Mn)Li with cyanoferrocene in the presence of MeOH gives rise to the ketimine (Mn)—C(NH)—Fc (Fc = ferrocenyl).[240] Hydrolysis of the ketimine leads to the ketone (Mn)C(O)Fc, which is identical with the one obtained previously[241] by acylating ferrocene with the acid chloride $(Mn)C(O)Cl/AlCl_3$. Metallation of methylcymantrene and subsequent treatment with DMF result in the formation of a mixture of isomers of 2- and 3-methylformylcymantrenes,the reduction of which with $NaBH_3(CN)$ in the presence of NH_4OAc in MeOH leads to secondary amines of the type $[(CO)_3MnC_5H_3(Me)CH_2]_2NH$. Layered materials based on acid zirconium phosphate were obtained from the latter compounds.[242] The reaction of the Grignard reagent (Mn)MgI (obtained from iodocymantrene and magnesium in THF) with $N(CH_2Cl)_3$ leads to the tertiary amine $[(Mn)CH_2]_3N$.[243]

A series of studies have been devoted to the synthesis and the properties of polynuclear carbinols of the cymantrene series. The dinuclear carbinols $(Mn)_2C(R)OH$, where R = Me or Ph, have been synthesised by the reactions of (Mn)Li with acetyl- and benzoyl-cymantrenes,[83] while the carbinol $(Mn)_3C(OH)$ has been obtained in the reaction with dicymantrenyl ketones.[244] On treatment with acids, these carbinols are converted into the corresponding stable carbenium ions (see below). The dinuclear carbinols $(Mn)_2C(R)OH$ can be obtained also in one stage as a result of the interaction of 2 equiv. of (Mn)Li with the acid chloride RC(O)Cl. With M = Mn, the plane passing through the O(hydroxy-groups) and C(6) atoms and the neighbouring atom H or C of the group R in the carbinols **29** cannot be a plane of symmetry, because, as shown below, both $(CO)_3MnC_5H_4$ residues occupy different positions relative to it. Therefore, in each C_5H_4 fragment the CH groups in the 2,5- and 3,4-positions are diastereotopic (symmetry elements are absent). This is clearly manifested in the ^1H NMR spectra, where the four protons of the C_5H_4 ligand form the *ABCD* spin system and give rise to four individual signals,[245] and also in the ^{13}C NMR spectra. The study of the reactivities of the carbinols with R = H or Me showed that metallation with BuLi proceeds with a high regio- and stereoselectivity, while in the case where R = CF_3 or Ph the carbinols decompose. When the lithio-derivatives are quenched[245] with D_2O, deuterium is ~90% incorporated in only one of the two α-positions in each C_5H_4 ring. The study of the structures of these carbinols in the crystal by X-ray diffraction and by the method of molecular mechanics (calculation of conformations) showed that the molecules have a chiral conformation with different orientations of the two cymantrenyl residues and that the structure of the carbinols with R = Me differs from that of the carbinols with R = CF_3 or Ph, which makes it possible to explain the observed differences between their reactivities.[246] The structures of the carbinol with R = Me and related compounds have been established by X-ray diffraction.[247, 248]



29

M = Mn, Re; R = H, Me, CF_3, Ph.

A series of communications[249–252] have been devoted to the application of the palladium-catalysed cross-coupling of the organometallic fragments (Mn) in order to synthesise dinuclear complexes. The interaction of iodocymantrene [obtained from (Mn)Li and 1,2-diiodoethane or I_2] with $Bu_3SnC\equiv CSnBu_3$ in the presence of $(MeCN)_2PdCl_2$ in DMF results in the formation of the disubstituted acetylene $(Mn)C\equiv C(Mn)$, the reaction of which with $Co_2(CO)_8$ leads[249] to the tetrahedral cluster $(Mn)C\equiv C(Mn)Co_2(CO)_6$ with the Co_2C_2 skeleton. The initially monosubstituted acetylene $(Mn)C\equiv CH$ was obtained similarly from (Mn)I and $Bu_3SnC\equiv CH$ and its interaction with Et_2NSnR_3 afforded the complex $(Mn)C\equiv CSnR_3$ (R = Me or Bu). The cross-coupling of this acetylene with the iodo-derivatives $IC_5H_4ML_n$ led to the synthesis of the heterodinuclear complexes $(Mn)C\equiv CC_5H_4ML_n$, where ML_n = $Fe(CO)_2Me$, $W(CO)_3Me$, or $Re(CO)_3$.[250] The dinuclear complex $(Mn)C\equiv CC_5H_4Fe(CO)_2CH_2Ph$ was obtained from $(Mn)C\equiv CSnMe_3$ and $IC_5H_4Fe(CO)_2CH_2Ph$, while the reaction with $Co_2(CO)_8$ afforded a cobalt-containing cluster [as a result of the coordination of $Co_2(CO)_6$ to the triple bond]. The structure of the latter complex was demonstrated by X-ray diffraction.[251] Treatment of the acetylene complex $(Mn)C\equiv CH$ with the base KOH in MeOH at 0 °C in the presence of a source of iodine (*N*-iodosuccinimide or 1,2-diiodoethane) afforded the iodo-substituted acetylene $(Mn)C\equiv CI$, which is converted into the

β-vinyl iodide (**Mn**)CH = CHI by the reaction with an excess of the diimide NH = NH as a result of the reduction of the triple bond to a double bond. The cross-coupling of this vinyl iodide with $Me_3SnC{\equiv}CC_5H_4ML_n$ led to the formation of complexes of the type (**Mn**)CH = CH − C = $CC_5H_4ML_n$, where ML_n = $Re(CO)_3$, $W(CO)_3Me$, or $Fe(CO)_2Me$.[252]

The formation of the intermediate $CpMn(CO)_2$ and small amounts of a new dinuclear complex $Cp_2Mn_2(CO)_5$ was noted in a study of the photochemistry of cymantrene in liquid paraffin at 77 K. The new dinuclear compound is formed as a result of the addition of $CpMn(CO)_2$ to cymantrene.[253] The photochemical reactions of dinuclear complexes of manganese and chromium, including (**Mn**) − (**Mn**) and (**Mn**)CH_2(**Mn**), have been investigated in argon matrices at 12 K.[254].

A new organometallic porphyrin — *meso*-tetracymantrenylporphyrin — has been obtained by the reaction of cymantrenecarbaldehyde with pyrrole on refluxing in MeCOOH in the presence of a stream of air.

VI. Compounds with organoelement substituents

A multiplicity of compounds with the $(CO)_3MnC_5H_4$ − E bonds, where E = Group I − VIII elements (Li, Cu, Ag, Au, Mg, Cd, Hg, B, Tl, La, Y, Sm, Sr, Ge, Sn, Pb, P, Sb, Bi,Ti, Mo, W, Mn, Re, Fe, Ni, and Pt) have now been obtained. Their syntheses and properties are considered below.

1. Compounds with Group I − V elements

Syntheses of cymantrene derivatives via (**Mn**)Li have been described in a review[1] and in Sections III − V of the present review. Much attention has been devoted also to the synthesis of cymantrene derivatives containing copper, silver, and gold. The compounds (**Mn**)Cu and (**Mn**)Ag have been obtained by the reaction of cymantreneboronic acid (**Mn**)$B(OH)_2$ or its anhydride with $Cu(OAc)_2$ [208] and $AgNO_3$ [256] respectively. Two types of reactions are characteristic of these compounds: cleavage of the C − Cu and C − Ag σ-bonds on treatment with electrophiles and their use in syntheses as sources of the (**Mn**) fragment. The compounds (**Mn**)Cu and (**Mn**)Ag successfully supplement (**Mn**)Li, the coupling of the cymantrenyl radicals with formation of bicymantrenyl being characteristic of the reactions involving them.[208, 211]

Treatment of (**Mn**)Li with copper(I) halides (in proportions of 1 : 2) in THF at −50 °C leads to the dissolution of CuHal with formation of solutions of cymantrenyl cuprates, $(Mn)_2CuLi$, etc. In contrast to (**Mn**)Li, these solutions are stable both at room and elevated temperatures, which makes it possible to use the compounds for the introduction of the cymantrenyl residue over a wide range of temperatures.[257]

The polymeric or oligomeric derivative $(Mn)_2AgCu$ has been obtained by treating CuI with (**Mn**)Ag.[216] Its structure has not been established, whilst its properties are similar to those of the monometallic derivatives. In particular, the reactions with iodobenzene and bromoferrocene lead to the formation of phenylcymantrene and cymantrenylferrocene respectively.[216]

The complex (**Mn**)$AuPPh_3$, in which one carbonyl group can be replaced photochemically by PPh_3 without dissociation of the C − Au bond, has been obtained by the reaction of (**Mn**)Li with $ClAuPPh_3$.[205] The reaction of (**Mn**)$AuPPh_3$ and its phosphine derivative with HBF_4 or $Ph_3PAu^+BF_4^-$ affords the complex salts $[(CO)_2LMnC_5H_4(AuPPh_3)_2]^+BF_4^-$.[258] Later the same salts were obtained by the reaction of $(Mn)_2Hg$ with $MeAuPPh_3$ in the presence of HBF_4.[259] The C − Au bond in the cymantrenyl derivatives of gold is readily cleaved by electrophiles.[205, 256]

The properties of the mercury derivatives of cymantrene — (**Mn**)HgX (X = Cl, Br, I) and $(Mn)_2Hg$ — were investigated in detail in the 1960s (see the relevant review[1]). The use of $(Mn)_2Hg$ in the synthesis of bicymantrenyl was examined above.[207] Treatment of CdI_2 with (**Mn**)Li gave rise to a mixture of (**Mn**)CdI and $(Mn)_2Cd$.[260] The 1,2-disubstituted cymantrenes $(CO)_3MnC_5H_3(HgR)CH_2NMe_2$ were obtained by metallating the amine (**Mn**)CH_2NMe_2 and treating its lithio-derivative with the mercury compounds RHgX, where R = $Mn(CO)_5$, $Re(CO)_5$, or phenylcarbaboranyl. Depending on the reactant ratio, treatment of $(CO)_3MnC_5H_3(Li)CH_2NMe_2$ with mercury halides HgX_2 (X = Cl, Br, I) led to the isolation of the mercurio-derivatives $(CO)_3MnC_5H_3(HgX)CH_2NMe_2$ (1 : 1) and $[(CO)_3MnC_5H_3CH_2NMe_2]_2Hg$ (2 : 1); the latter was characterised by X-ray diffraction.[261] A weak intramolecular coordination of mercury to the two nitrogen atoms of the dimethylamino-groups was observed in this complex.

The synthesis of cymantreneboronic acid and of its anhydride was first described as early as 1969.[262] The acid (**Mn**)$B(OH)_2$ was used to obtain the copper and silver derivatives of cymantrene.[208, 256] Its reactions with the copper salts $CuCl_2$ and $CuBr_2$ constitute a convenient method of synthesis of chloro- and bromo-cymantrenes (in yields greater than 85%).[209] The synthesis and reactions of ferrocenylcymantrenelboronic acid have been described.[217]

Cymantrenyl derivatives of the lanthanides (Yb, Sm, Eu) have been obtained by treating the iodides $LnI_2.nTHF$ or metallic lanthanide powders with (**Mn**)Li or $(Mn)_2Hg$.[263−266]

$$(Mn)_2Hg + YbI_2{\cdot}nTHF \longrightarrow (Mn)YbI_2{\cdot}nTHF + Hg,$$

$$(Mn)Li + YbI_2{\cdot}nTHF \longrightarrow (Mn)_2Yb{\cdot}nTHF + LiI,$$

$$(Mn)I + Ln \longrightarrow (Mn)LnI{\cdot}nTHF,$$

$$(Mn)_2Hg + Ln \longrightarrow (Mn)_2Ln{\cdot}nTHF.$$

Like (**Mn**)Li, the complex (**Mn**)YbI reacts readily with Me_3SiCl and Ph_3SnCl, forming compounds with the (**Mn**) − Si and (**Mn**) − Sn bonds.[266] Dicymantrenylthallium chloride $(Mn)_2TlCl$ was obtained by the reaction of (**Mn**)Li with $TlCl_3$ (THF, −50 °C). The same compound has been synthesised from $(Mn)_2Hg$ and $TlCl_3$ in ether or in $CHCl_3$ at 25 °C.[267]

The reactions of (**Mn**)Li with the corresponding halides have been used to synthesise compounds with the (**Mn**) − E bonds, where E is a Group IV element (Si, Ge, Sn, Pb). Cymantrenylsilanes (**Mn**)SiR_3, where SiR_3 = $SiPh_3$ [268] or SiRR′R″,[269, 270] have been obtained from chlorosilanes R_3SiCl. The reaction of (**Mn**)SiMePhCl with $LiC{\equiv}CFc$ afforded cymantrenylsilylacetylene (**Mn**)SiMePh − C ≡ CFc.[271] Reactions involving the hydrosilylation of the acetylenes RC ≡ CH (where R = $SiEt_3$, $SiPh_3$, Ph, Fc) with the silane (**Mn**)SiMePhH in the presence of the Speier catalyst based on H_2PtCl_6 proceed nonselectively and give rise to mixtures of products of two types,[272−275] which have been characterised by X-ray diffraction.[276, 277] Tricymantrenylsilane $(Mn)_3SiMe$ has been synthesised by the reaction of (**Mn**)Li with $MeSiCl_3$.[278] The addition of a solution of (**Mn**)Li to the silane Me_2SiHCl (THF, −80 °C) affords (**Mn**)$SiMe_2H$, but when the reactants were introduced in the reverse order, the disubstituted complex $(Mn)_2SiMe_2$ was obtained. The reactions of (**Mn**)$SiMe_2H$ with $Co_2(CO)_8$ or $Ir(CO)(PPh_3)_3H$ are accompanied by the cleavage of the Si − H bond and lead to the synthesis of complexes of the type (**Mn**)$SiMe_2-ML_n$, where ML_n = $Co(CO)_4$ or $Ir(CO)(PPh_3)_2H_2$.[279]

The reactions of (**Mn**)Li with the chlorides Ph_3ECl led to the formation of the corresponding compounds (**Mn**)EPh_3, where E = Ge, Sn, or Pb.[268] For E = Sn, treatment with HCl results in the simultaneous cleavage of the C − Sn σ-bond (yield of cymantrene approximately 10%) and the substitution of Ph by Cl with formation of (**Mn**)$SnPhCl_2$, which reacts with $NaMn(CO)_5$ to form the trinuclear complex (**Mn**)$SnPh[Mn(CO)_5]_2$.[268] The syntheses of cymantrenylstannanes $(Mn)_2SnR_2$, where R = Cl, Ph, or Fc,[280] and also of $(Mn)_4Sn$ [280] as well as a series of their derivatives[281] have been described. The structures of the chlorostannanes $(Mn)_2SnCl_2$ and $(Mn)_3SnCl$ have been characterised by X-ray diffraction.[282, 283]

The cymantrenylphosphonic acids (Mn)P(O)(OH)H [cymantrenylphosphonous acid? (translator)] and $(Mn)_2P(O)OH$ [cymantrenylphosphinic acid? (translator)] have been obtained by direct phosphorylation under the conditions of the Friedel–Crafts reaction between cymantrene and PCl_3,[100] while the reaction of cymantrene with $Et_2NPCl_2/AlCl_3$ gave rise to the phosphine $(Mn)_3P$.[284] The phosphine $(Mn)PPh_2$ has been synthesised by treating Ph_2PCl with the Grignard reagent (Mn)MgI (obtained from iodocymantrene and magnesium in the presence of 1,2-dibromoethane) and its quaternisation by reaction with $PhCH_2Br$ afforded the quaternary phosphonium salt $(Mn)P^+Ph_2CH_2Ph\ Br^-$. Its decomposition with alkali gives rise to cymantrene (92.3%) and toluene (6.3%), which indicates the high stability of the anion $(Mn)^-$.[285] The phosphines $(Mn)PPh_2$ and $(Mn)CH_2PPh_2$ have also been obtained with the aid of (Mn)Li.[95] The phosphine $(Mn)PPh_2$ is formed in the reaction of the phosphine sulfide $C_5H_5P(S)Ph_2$ with $Mn_2(CO)_{10}$.[286] Dichlorophosphine $(Mn)PCl_2$ and $(Mn)PR_2$, where R = OEt or NEt_2, have been synthesised by the reactions of (Mn)Li with PCl_3 or chlorophosphines.[287] The interaction of $(Mn)P(OEt)_2$ with 1,3-dichloroacetone leads[288] to the cymantrenylphosphonate $(Mn)P(O)(OEt)OC(CH_2Cl)=CH_2$. Treatment of (Mn)Li with $PhPCl_2$ afforded dicymantrenylphenylphosphine $(Mn)_2PPh$.[289] It has been shown that cymantrenylphosphines exhibit all the usual properties of tertiary phosphines, in particular, they are oxidised to phosphine oxides, combine with sulfur, and enter into the Staudinger, Perkow, and other reactions.[284–287] Metallation of $(Mn)PPh_2$ followed by the reaction with Ph_2PCl led to the formation of 1,3-bis(diphenylphosphino)cymantrene — the only compound containing two phosphine substituents in the Cp ligand.[93]

Compounds with (Mn)–As bonds have not been described. The reaction of $BiCl_3$ with (Mn)Ag affords $(Mn)_3Bi$,[256] which has, according to X-ray diffraction data, a trigonal-pyramidal structure.[290] $(Mn)_3Sb$ and $(Mn)_3Bi$ have been obtained by the reaction of (Mn)Li with $SbCl_3$ and $BiCl_3$. Their thermolysis at 330 °C leads to the formation of the following products: cymantrene, CO, a cyclopentadiene polymer, and metallic manganese and antimony for the antimony compound and metallic bismuth and bicymantrenyl for the bismuth compound.[291] The lithio-derivative (Mn)Li reacts with $PhBiCl_2$, whereupon the product is $(Mn)_2BiPh$, which reacts with $CuCl_2$ to form chlorocymantrene, chlorobenzene, bicymantrenyl, and biphenyl.[292]

The sulfonation reaction has been used to obtain compounds with (Mn)–S bonds. Sulfonation of methylcymantrene results in the formation of a mixture of the 1,2- and 1,3-isomers of methylcymantrenesulfonic acid. Sulfonyl chlorides and other derivatives have been synthesised from them by reaction with PCl_5 in accordance with the following scheme:[76,77,99]

$$(Mn)SO_3 \xrightarrow{PCl_5} (Mn)SO_2Cl \xrightarrow{Zn} (Mn)SH \xrightarrow{CH_2N_2} (Mn)SMe.$$

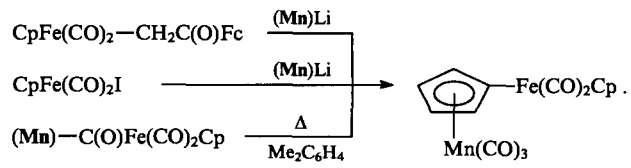
Acylation of the MeS derivatives gives rise to mixtures of ketones.[77,99] The synthesis of cymantrenes with MeS and PhS substituents has been described by Sunkel and coworkers,[39–42] while the preparation of the disulfides has been described in other communications.[43,76,100] Physiologically active derivatives of barbituric acid containing the $(Mn)SO_2CH_2$ fragments have been described.[293] The synthesis of the 1,2-disubstituted derivatives $(CO)_3MnC_5H_3(R)SO_2NMe_2$ was already mentioned above.[94]

The interaction of $Mn(CO)_3(MeCN)_3^+$ with the ylides $C_5H_5ER_3$ leads to the formation of new cationic complexes $(CO)_3MnC_5H_4-ER_n^+\ X^-$, where ER_n = PPh_3 or SMe_2.[294] The complex with the SMe_2 group was characterised by X-ray diffraction.[295] The interaction of (Mn)Li and also of its Re analogue with free chalcogens affords the relatively unstable intermediates (Mn)ELi as a result of the insertion of the chalcogen in the C–Li bond. On oxidation with atmospheric oxygen, the intermediates are converted into dimetallo-dichalcogenides with the general formula (M)–E–E–(M) [here (M) = $(CO)_3MnC_5H_4$ or $(CO)_3ReC_5H_4$ with E = S, Se, or Te]. The reactions of 2 equiv. of (M)Li with SCl_2, $SeCl_4$, or $TeCl_4$ led to the formation of complexes having the general formula (M)–E–(M).[289]

2. Compounds with transition metals

The reaction of (Mn)Li with Cp_2TiCl_2 affords the complex $Cp_2Ti(Mn)_2$ in which the titanium atom has a tetrahedral environment according to X-ray diffraction data.[296]

A series of studies by Nesmeyanov and coworkers[297–331] on the synthesis and the chemistry of complexes of the type (Mn)–ML_n, where M = Mo, W, Mn, Re, Fe, or Ni, were published in 1974–1984. The properties of the complex (Mn)–$Fe(CO)_2Cp$ **30** were investigated most fully. It is formed either on treatment of $CpFe(CO)_2I$ or $CpFe(CO)_2-CH_2C(O)Fc$ with (Mn)Li [297] or on thermal decarbonylation of $(Mn)C(O)Fe(CO)_2Cp$.[231]



30

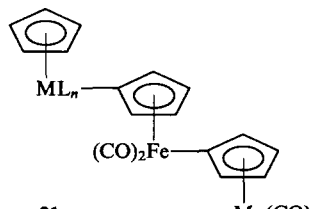
The analogous complexes (Mn)–ML_n, where ML_n = $Mo(CO)_3Cp$, $W(CO)_3Cp$,[232–234] $Mn(CO)_5$, or $Re(CO)_5$,[235] are also formed on thermal decarbonylation in accordance with the mechanism

$$(Mn)-C(O)ML_n \longrightarrow (Mn)-ML_n + CO.$$

The complex (Mn)–$Ni(PPh)_3Cp$ with the (Mn)–Ni bond is formed in the reaction of (Mn)Li with $CpNi(PPh_3)Cl$ or with nickelocene.[298] The ready cleavage of the C_5H_4-M bonds by electrophiles [acids, mercury salts, iodine, MeC(O)Cl, etc.] with formation of cymantrene, mercury halides, (Mn)HgX, and iodocymantrene respectively, is characteristic of all compounds of the type (Mn)–ML_n.[235,298] Under the conditions of the thermal or photochemical reaction, there is a possibility of the substitution of CO by PPh_3 at the Fe, Mo, and W atoms[231–234] or of CO at the Mn atom by PPh_3 and tolane in the complex (Mn)–$Ni(PPh_3)Cp$.[299] Thermal decarbonylation has also been used to synthesise the complex $(CO)_2PPh_3MnC_5H_4-Fe(CO)_2Cp$,[300] in which the CO group at the Fe atom is substituted by PPh_3 on UV irradiation.[301] The structure of the complexes (Mn)–Fe(CO)(L)Cp, where L = CO or PPh_3, has been established by X-ray diffraction.[302]

The chemistry of complex **30** and its derivatives has been studied in greater detail. The C–Fe bond is readily cleaved on treatment with I_2 in CH_3Cl or with $MeCO^+BF_4^-$, but it proved resistant to the action of $HgCl_2$ in benzene.[303] Under the conditions of the mercuration of cymantrene, complex **30** reacts with mercury acetate and mercuration takes place in the C_5H_4 ring at the Mn atom. After treatment with $CaCl_2$, the chloromercurio-derivative was obtained, forming readily a symmetrical compound.[304] It was found that the C–H bonds in the Cp ring attached to the Fe atom exhibit a high CH acidity and are capable of participating in the protophilic substitution reaction. Complex **30** enters into hydrogen isotope exchange with EtOD–EtONa (benzene, 100 °C) and is metallated on treatment with BuLi.[305] Carboxylation of the Li derivative of complex **30** affords the acid (Mn)–$Fe(CO)_2C_5H_4COOH$ (pK_a = 5.09 in 50% EtOH), which is three–four times stronger than benzoic acid (pK_a = 5.7 under the same conditions).[305] The capacity of complex **30** to be metallated made it possible to obtain a series of polynuclear complexes based on it. The trinuclear complexes **31**, where ML_n = $Fe(CO)_2$,[306] $Mo(CO)_3$, and $W(CO)_3$,[307] have been synthesised by the reaction of the lithio-derivative with the

organometallic halides $CpFe(CO)_2I$, $CpMo(CO)_3Cl$, or $CpW(CO)_3Cl$.



31

Compounds containing a sequence of metals, Fe–Fe–Mn and Mo–Fe–Mn, have been characterised by X-ray diffraction.[306, 307] Treatment of complex **30** with BuLi and then with C_3F_7I led to the formation of the iodo-derivative **(Mn)**–$Fe(CO)_2C_5H_4I$, which on reaction with the lithio-derivative **(Mn)**–$Fe(CO)_2C_5H_4Li$ affords the analogous tetranuclear complex of the 'ladder' type with the Mn–Fe–Fe–Mn metal sequence.[308] The synthesis of the tetranuclear complex with the sequence Fe–Fe–Fe–Mn, characterised by X-ray diffraction, has been described.[309]

The thermolysis of the complexes **(Mn)**–$M(CO)_3Cp$, where M = Mo [234] or W,[310] results in the formation of complex mixtures of dinuclear and trinuclear complexes containing the products of the migration of the **(Mn)** fragments to the Cp rings attached to Mo and of the $(CO)_3WC_5H_4$ fragment to the Cp ring at Mn. The interaction of **(Mn)**–$Ni(PPh_3)Cp$ with *p*-isocyanotoluene leads to the dissociation of the Ni–C bond.[311]

In the reaction of **(Mn)**Li with *cis*-L_2PtCl_2 at −50 °C, one Cl atom is readily substituted with formation of the complex **(Mn)**–PtL_2Cl (L = PPh_3).[312] The mercury halides **(Mn)**HgX readily react with the zerovalent platinum complex PtL_3 with insertion of the carbenoid fragment PtL_2 in the Hg–Cl or Hg–Br bonds.[313, 314] The structure of the reaction products depends on the conditions: at −20 °C in toluene, compounds with a Pt–Hg bond of the type **(Mn)**–Hg–PtL_2Cl are formed, readily splitting off mercury on heating to 20 °C and forming the complexes **(Mn)**–PtL_2Cl. The two PPh_3 ligands at the mercury atom are readily substituted by the chelating diphosphine $Ph_2PCH_2CH_2PPh_2$. Photolysis of platinum–mercury complexes involves protodemercuration with liberation of mercury and the formation of cymantrene.[314] Dicymantrenylmercury $(Mn)_2Hg$ readily reacts with PtL_3 at −20 °C, forming the compound **(Mn)**–Hg–PtL_2–**(Mn)**, which on heating to 20 °C is converted, as a result of the elimination of mercury, into the complex $(Mn)_2PtL_2$, where the Pt atom is linked simultaneously to two cymantrene residues.[315]

VII. Cymantrene as an organometallic Lewis base

Low-valence transition metal complexes constitute a new class of organometallic Lewis bases. Their basicity is associated with the presence in the metal of fully or partially occupied *d* orbitals,[316–318] which is characteristic mainly of complexes of Group V–VIII metals with the configuration d^6–d^9. Organometallic bases have several potential basicity centres. Depending on the structure of the complex, the ligand environment of the metal, and the nature of the electrophile and the solvent, the attack by the electrophile can be directed to one or several centres. Cymantrene and its phosphine derivatives exhibit all the properties of Lewis bases: they are capable of combining with a proton, aprotic acids, the halogens, etc.

1. Reactions with protic acids

It has been shown by IR and ^1H, ^{13}C, and ^{31}P NMR spectroscopic methods that cymantrene, pentaethylcymantrene, and mono- and di-phosphine derivatives of cymantrene are protonated at the manganese atom on treatment with protic acids.[319–324] Unsubstituted cymantrene is a very weak base: protonation of the metal takes place only in the presence of the strong acid HSO_3F in CH_2Cl_2 at low temperatures. Even at −100 °C, the exchange between the proton in Mn–H and the medium is rapid on the NMR time scale. Pentaethylcymantrene, in which the basicity of the metal is appreciably higher owing to the electron-donating effect of the five ethyl substituents, is wholly protonated under the same conditions with formation of the Mn–H bond. At −105 °C, there is a slow exchange of the proton in Mn–H with the medium.[324] On substitution of one and especially two CO groups by phosphine ligands, the basicity of the metal increases greatly: the mono- and di-phosphine complexes are capable of being protonated at the Mn atom even in the presence of CF_3COOH.[321–325] The proton affinity of $MeC_5H_4Mn(CO)_3$ was determined as 203 kcal mol^{-1} in a study of the gas-phase protonation.[326]

A new type of hydrogen bond in the η-complexes of transition metals has been discovered in cymantrene and benchrotrene derivatives. In a study of the interaction of cymantrene and its phosphine derivatives with weaker proton donors such as $(CF_3)_3COH$ and anhydrous HCl (in solution in liquid xenon at 160–240 K and also in CCl_4 at 293 K), it was possible to detect the formation of hydrogen bonds with the oxygen of the CO ligand. The formation of such bonds is accompanied by a shift of the ν(CO) frequencies and also of the ν(OH) frequency of the proton donor. The frequency shifts $\Delta\nu$(OH) depend greatly on the basicity of the metal and on the number of phosphine ligands, ranging from ~75 cm^{-1} for cymantrene to 240 cm^{-1} and more for the diphosphine complexes. There is a possibility of hydrogen bond formation with both one and two CO groups simultaneously.[327–330]

The formation of intramolecular and intermolecular hydrogen bonds as well as the preferred conformations in carbinols containing one **(Mn)** fragment, having the general formula **(Mn)**C(OH)RR', and also in their rhenium analogues have been investigated by IR spectroscopic and molecular mechanics methods.[331]

2. Reactions with aprotic acids

Cymantrene and its phosphine derivatives react as bases not only with a proton but also with aprotic acids — their Hg, Al, Ga, and Sn salts. Unsubstituted cymantrene does not react with $HgCl_2$, while in the case of mercury acetate or trifluoroacetate the final result of the reaction is mercuration with substitution of one or all five hydrogen atoms.[101] It may be that the initial attack by Hg is directed to the metal atom with subsequent migration to the Cp ring. Cymantrene does not react with $SnCl_4$, but pentaethylcymantrene affords an adduct via the Mn atom even on reaction with $SnCl_4$.

Coordination to the oxygen atoms of the CO groups occurs only on interaction of unsubstituted cymantrene with $AlCl_3$ or $AlBr_3$ in benzene.[332, 333] The site of attack by AlX_3 (the centre in the cymantrene molecule with the highest basicity) depends on the nature of the solvent. On passing from the nonpolar C_6H_6 to the polar CH_2Cl_2 or $ClCH_2CH_2Cl$, the site of attack changes: in benzene, AlX_3 affords adducts via the oxygen atoms of the CO groups, while in polar solvents the adducts are formed via the metal atom.[333] The site of attack and of the addition of AlX_3 follows unambiguously from the direction and magnitude of the ν(CO) frequency shifts in the IR spectra. The mono- and di-phosphine complexes react with AlX_3 and $GaCl_3$ only via the Mn atom.

The energetics of the interaction of cymantrene and pentaethylcymantrene with $AlBr_3$ has been studied by calorimetric titration:[334, 335] the enthalpy of formation of the adduct ($-\Delta H$) via oxygen, i.e. $Cp(CO)_2MnCO \cdots AlBr_3$, is 18.9 kcal mol^{-1}, while that of the adduct $(Et_5C_5)(CO)_3Mn \cdots AlBr_3$, formed as a result of coordination to the metal atom, is 22.0 kcal mol^{-1}.

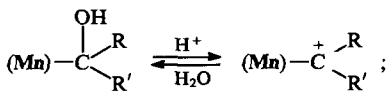
The halogens Cl_2 and Br_2 cleave cymantrene at 20 °C with dissociation of the Mn–ring bond.[1] However, on treatment of cymantrene in solution in CH_2Cl_2 at −50 °C with 1 equiv. of the

halogen in CCl_4, the latter adds to the metal with formation of the ionic complex $[CpMn(CO)_3Cl]^+Cl^-$ or $[CpMn(CO)_3Br]^+Br_3^-$.[336]

Thus the centre with the highest basicity in the cymantrene molecule may be either the Mn atom (H^+, halogens) or the oxygen atom of the CO group (only $AlCl_3$ and $AlBr_3$ in benzene) depending on the type of reagent. On passing to azacymantrene $(\eta^5\text{-}C_4H_4N)Mn(CO)_3$, the situation changes sharply: in this case, the attack by aprotic acids is directed to the nitrogen atom.[337]

VIII. Stabilisation by the cymantrenyl group of the neighbouring cationic and radical centres

Treatment of carbinols of the cymantrene series with acids (for example, with CF_3COOH) leads to the formation, as a result of the elimination of water, of very stable carbonium ions, which are stabilised by 1–3 (**Mn**) residues.[338–343]



R, R′ = H, Me, Et, Ph, Fc.

Treatment of the carbinol $(\mathbf{Mn})_3COH$ with acid afforded the tricymantrenyl carbenium cation $(\mathbf{Mn})_3C^+$, while the corresponding phosphine-containing carbonium ions, the stability of which is appreciably increased by the electron-donating phosphine ligands, were obtained from carbinols containing one or two phosphine ligands.[244] The conversion of the cymantrene carbinols into carbonium ions is accompanied by an increase in the frequency ν(CO) and a displacement of all the signals in the ^1H and ^{13}C NMR spectra, which is associated with the marked delocalisation of the positive charge with participation of the Cp ring and the metal carbonyl fragment. The kinetic stability of the carbonium ions with cymantrene residues has been characterised by measuring the rates of solvolysis of the acetates.[344] Treatment of the carbonium ions with HBF_4 led to the isolation of solid cymantrenylcarbenium tetrafluoroborate salts.[345] The ease of the reactions involving the ionic hydrogenation of cymantrenyl ketones is associated with the high stability of the cymantrenylcarbenium ions and the ability of the cymantrenyl group to stabilise greatly the neighbouring cationic centre.[346] The electrochemical properties of cymantrenylcarbenium salts have been investigated.[347]

In connection with the ability of the cymantrenyl group to stabilise effectively the neigbouring cationic centre mentioned above, it is of interest to estimate the electronic effects of the cymantrenyl group as a substituent. The inductive (σ_I) and resonance (σ_R) components of the overall electronic influence, amounting to 0.172 and −0.02 according to Gubin et al.[348] and 0.141 and −0.024 according to Bitterwolf,[26] have been estimated by the ^{19}F NMR method for the *meta*- and *para*-substituted fluorophenylcymantrenes. The cymantrenyl group is a weak acceptor in terms of its inductive influence and a weak donor in terms of the conjugation mechanism. On substitution of CO by phosphines, its electron-accepting properties are weakened, while its electron-donating properties are enhanced.[26]

The cymantrenyl group can also stabilise the neighbouring radical centre. The reduction with sodium of benzoylcymantrene[349] or dinuclear ketones[66] of the type $(CO)_3MnC_5H_3R-C(O)-C_6H_5RCr(CO)_3$ results in the formation of the corresponding radical-anions (ketyls), in which the radical centre is stabilised by a cymantrenyl, phenyl, or benchrotrenyl substituent. Their structure and th delocalisation of the unpaired electron have been investigated by the EPR method.

In describing the properties of compounds with the (**Mn**)–P bond above (see Section VI), it was noted that the alkaline decomposition of the phosphonium salt $(\mathbf{Mn})P^+Ph_2CH_2PhBr^-$ results in the formation of mainly cymantrene and of an insignificant amount of toluene. This led to the conclusion that the cymantrenyl group is capable of stabilising effectively the neighbouring anionic centre.[285]

* * *

In conclusion, we shall consider several studies which were published during the preparation of the manuscript for printing. The complex $(\eta^5\text{-}PhN{=}NC_5H_4)Mn(CO)_3$ has been obtained in 45% yield from the lithium salt of the phenylazocyclopentadienyl anion by reaction with $Mn(CO)_3(CH_3CN)_2Br$.[350] The preparation of new substituted cyclopentadienylthallium derivatives and the syntheses based on them have been described. The anion of $MeC_5H_4^-Na^+$ reacts with ethyl acetate to form a mixture of 1-acetyl-2-methyl- and 1-acetyl-3-methyl-cyclopentadienyl anions (in proportions of 1 : 1), which on treatment with EtOTl are converted into a mixture of the corresponding thallium derivatives. The latter were separated by recrystallisation from ethanol. The planarly chiral complex 1-acetyl-2-methylcymantrene has been obtained by the reaction of the 1,2-derivative with $Mn(CO)_5Br$.[351] Benzoylcyclopentadienylsodium has been obtained from the anion in Cp^-Na^+ by reaction with ethyl benzoate. On treatment with EtOTl, it gives rise to $TlC_5H_4C(O)Ph$. On reaction with $Mn(CO)_5Br$, the latter affords benzoylcymantrene.[352] Dinuclear complexes having the general formula (**Mn**)–X–(**Mn**), where X = S or $SiPh_2$, have been obtained by the reactions of cymantrenyllithium with SCl_2 and Ph_2SiCl_2. The reduction of 1-acetyl-2-methylcymantrene by $LiAlH_4/TiCl_3$ leads to mixtures of diastereoisomeric complexes of the type $(CO)_3MnC_5H_3Me-C_5H_3MeMn(CO)_3$. Under mild conditions, the products are the pinacols [X = C(OH)Me–C(OH)Me], which are converted into the olefins [X = C(Me)=C(Me)] under more severe conditions as a result of dehydration. The reduction of acetylcymantrene by the $KC_8/TiCl_3$ system results in the formation of a mixture of the analogous dinuclear olefins.[353] Further development of the study by Herberhold and Biersack[289] demonstrated that the lithio-derivatives of cymantrene and $C_5H_5Re(CO)_3$ readily react with the chalcogens, affording (**Mn**)ELi (E = S, Se, Te) and their rhenium analogues. These lithio-derivatives are protonated with formation of the chalcogenols (**Mn**)EH, which are readily oxidised to the disulfides; the reactions of (**Mn**)ELi with CH_2I_2, PhC(O)Cl, and other acid chlorides have been investigated.[354] The interaction of cymantrenyllithium with *C*-carbaboranyl derivatives of mercury or *B*-carbaboranyl derivatives of thallium leads to the synthesis of new dinuclear complexes with (**Mn**)–Hg and (**Mn**)–Tl bonds.[355] The reaction of $(CO)_3MnC_5Cl_4Li$ with the halide $Mn(CO)_5Br$ or $Au(PPh_3)Cl$ affords the complexes $(CO)_3MnC_5Cl_4X$, where X = $Mn(CO)_5$ or $AuPPh_3$.[356]

References

1. *Metody Elementoorganicheskoi Khimii. Podgruppy Medi, Skandiya, Titana, Vanadiya, Khroma, Margantsa* (Methods of Organoelement Chemistry. The Copper, Scandium, Titanium, Vanadium, Chromium and Manganese Subgroups) Book 2 (Moscow: Nauka, 1974), p. 781
2. G Wilkinson, F G Stone, E W Abel (Eds) *Comprehensive Organometallic Chemistry* Vol. 4 (New York: Pergamon Press, 1982), p. 113
3. K G Caulton *Coord. Chem. Rev.* **38** 1 (1981)
4. A G Ginzburg *Khimiya π-Tsiklopentadienilnykh Kompleksov Margantsa. T. 2. (Itogi Nauki i Tekhniki. Seriya Koordinatsionnaya Khimiya. Metalloorganicheskaya Khimiya)* [The Chemistry of π-Cyclopentadienyl Complexes of Manganese. Vol. 2 (Advances in Science and Engineering. The Coordination Chemistry Series. Organometallic Chemistry)] (Moscow: Izd. VINITI, 1990)
5. C E Holloway, M Melnik *J. Organomet. Chem.* **396** 129 (1990)
6. P J Fitzpatrick, Y Le Page, J Sedman, I S Butler *Inorg. Chem.* **20** 2852 (1981)

7. J Cowie, E J M Hamilton, J C V Laurie, A J Welch *J. Organomet. Chem.* **394** 1 (1990)
8. K Chor, C Pommer, M Diot *Mol. Cryst. Liq. Cryst.* **100** 193 (1983)
9. J R Chipperfield, J C R Sneyd, D E Webster *J. Organomet. Chem.* **178** 177 (1979)
10. USSR P. 647 303 CCCP; *Byull. Izobret.* **6** 84 (1979)
11. E A Chernyshev, M D Reshetova, A D Volynskikh *Zh. Obshch. Khim.* **50** 952 (1980)
12. E A Chernyshev, A S Dmitriev, N M Zharkova, Yu N Molokanov, O N Fursa *Khim. Prom.* 498 (1977)
13. G A M Munro, P L Pauson *J. Organomet. Chem.* **160** 177 (1978)
14. J P Williams, A Wojcicki *Inorg. Chem.* **16** 3116 (1977)
15. R B King, N N Ackermann *Inorg. Chem.* **13** 637 (1974)
16. C G Kreiter, W Lipps *J. Organomet. Chem.* **253** 339 (1983)
17. C Charrier, F Mathey *Tetrahedron Lett.* **19** 2407 (1978)
18. C Charrier, F Mathey *J. Organomet. Chem.* **170** C41 (1979)
19. N J Gogan, C K Chu *J. Organomet. Chem.* **93** 363 (1975)
20. M B Freeman, L G Sneddon, J C Huffman *J. Am. Chem. Soc.* **99** 5194 (1977)
21. M B Freeman, L G Sneddon *Inorg. Chem.* **19** 1125 (1980)
22. P G Gassman, C H Winter *J. Am. Chem. Soc.* **108** 4228 (1986)
23. P Singh, M D Rausch, T E Bitterwolf *J. Organomet. Chem.* **352** 273 (1988)
24. M D Rausch, B G Conway *Organometallics* **4** 688 (1985)
25. S P Gubin, A A Koridze, N A Ogorodnikova, B A Kvasov *Dokl. Akad. Nauk SSSR* **205** 346 (1972)
26. T E Bitterwolf *J. Organomet. Chem.* **7** 409 (1968)
27. S S Jones, M D Rausch, T E Bitterwolf *J. Organomet. Chem.* **396** 279 (1990)
28. T E Bitterwolf *J. Organomet. Chem.* **386** 9 (1990)
29. D W Macomber, W P Hart, M D Rausch *Adv. Organomet. Chem.* **21** 20 (1982)
30. K J Reimer, A Shaver *J. Organomet. Chem.* **93** 239 (1975)
31. V A Nefedov *Zh. Obshch. Khim.* **39** 665 (1969)
32. B Quinn, A Shaver *Inorg. Chim. Acta* **50** 141 (1981)
33. K J Reimer, A Shaver *Inorg. Chem.* **112** 157 (1990)
34. K M Young, M S Wrighton *J. Am. Chem. Soc.* **14** 2707 (1990)
35. W A Herrman, M Huber *J. Organomet. Chem.* **140** 55 (1977)
36. K J Reimer, A Shaver *Inorg. Synth.* **20** 190 (1980)
37. V A Nefedov *Zh. Org. Khim.* **9** 719 (1973)
38. K Sünkel, D Motz *Chem. Ber.* **121** 799 (1988)
39. K Sünkel, D Steiner *J. Organomet. Chem.* **368** 67 (1989)
40. K Sünkel, D Motz *Angew. Chem., Int. Ed. Engl.* **27** 939 (1988)
41. K Sünkel, D Steiner *Chem. Ber.* **122** 609 (1989)
42. K Sünkel, A Blum, K Polborn, E Lippmann *Chem. Ber.* **123** 1227 (1990)
43. K Sünkel, A Blum *Chem. Ber.* **125** 1605 (1992)
44. A N Nesmeyanov, K N Anisimov, N E Kolobova, I B Zlotina *Izv. Akad. Nauk SSSR, Ser. Khim.* 1326 (1964)
45. R B King, A Efraty *J. Am. Chem. Soc.* **94** 3773 (1972)
46. R B King, M Z Iqbal, A D King *J. Organomet. Chem.* **171** 53 (1979)
47. I Bernal, I D Korp, W A Herrmann, R Serrano *Chem. Ber.* **117** 434 (1984)
48. R C Hemond, R P Hughes, H B Locker *Organometallics* **5** 2391 (1986)
49. M Rausch, Tsai Woei-Min, J W Chambers, R D Rogers, H G Alt *Organometallics* **8** 816 (1989)
50. I R Lyatifov, P V Petrovskii, R B Materikova, V N Babin *Metalloorg. Khim.* **2** 789 (1989)
51. I R Lyatifov, G I Gulieva, V N Babin, P V Petrovskii *Metalloorg. Khim.* **2** 793 (1989)
52. K Sünkel, J Hoffmann *Organometallics* **11** 3923 (1992)
53. C Arsenault, P Bougeard, B G Sayer, S Yeroushalmi, M J McGlinchey *J. Organomet. Chem.* **265** 283 (1984)
54. J E Ellis, RA Faltynek, S G Hentges *J. Organomet. Chem.* **120** 389 (1976)
55. A A Barkatin, A K Baev *Izv. Akad. Nauk Beloruss. SSSR, Ser. Khim.* 64 (1984)
56. USSR P. 891 613; *Byull. Izobret.* **47** 101 (1981)
57. N S Khrushcheva, A G Ginzburg, N I Pyshnograeva, V N Setkina, V I Sokolov *Izv. Akad. Nauk SSSR, Ser. Khim.* 1200 (1986)
58. A N Zakharov, B V Romanovskii, D Luka, V I Sokolov *Metalloorg. Khim.* **1** 119 (1988)
59. A B Cornwell, P G Harrison *Acta Crystallogr., Sect. B* **35** 1694 (1979)
60. S Lee, N J Cooper *J. Am. Chem. Soc.* **113** 716 (1991)
61. M N Barsegova, N M Loim, N K Baranetskaya, V N Setkina *Izv. Akad. Nauk SSSR, Ser. Khim.* 2634 (1986)
62. N M Loim, M N Barsegova, V A Piven', E V Stepanova, I S Lakoba *Metalloorg. Khim.* **2** 1049 (1989)
63. W Ruf, T Renk, W Siebert *Z. Naturforsch., B. Chem. Sci.* **31** 1028 (1976)
64. T Renk, W Ruf, W Siebert *J. Organomet. Chem.* **120** 1 (1976)
65. N I Gogan, C K Chu *J. Organomet. Chem.* **132** 103 (1977)
66. N I Gogan, C K Chu, P A Narayana *J. Organomet. Chem.* **144** 125 (1978)
67. A N Nesmeyanov, L M Korneva, M I Rybinskaya *Koord. Khim.* **3** 1394 (1977)
68. G Sonnek, K Haage, H Reinheckel, L M Korneva, M I Rybinskaya *Z. Chem.* **21** 331 (1981)
69. L M Korneva, N I Rybinskaya, G Sonnek, K Haage, H Reinheckel, V S Kaganovich *Izv. Akad. Nauk SSSR, Ser. Khim.* 2159 (1980)
70. M Salisova, S Toma. *Chem. Pap.* **40** 619 (1986)
71. M I Kalinkin, G D Kolomnikova, V E Puzanova, M M Gol'din, Z N Parnev, D N Kursanov *Izv. Akad. Nauk SSSR, Ser. Khim.* 1852 (1977)
72. E J Miller, C A Weigelt, J A Serth, R Rusyid, J Brenner, L A Luck, M Godlewski *J. Organomet. Chem.* **440** 91 (1992)
73. T E Bitterwolf, X Dai *J. Organomet. Chem.* **440** 103 (1992)
74. H Egger, A Nikiforov *Monatsch. Chem.* **99** 2296 (1968)
75. H Egger, A Nikiforov *Monatsch. Chem.* **99** 2311 (1968)
76. H Egger, A Nikiforov *Monatsch. Chem.* **100** 1069 (1969)
77. C Sergheraert, P Marcinal, E Cuignet *J. Organomet. Chem.* **139** 283 (1977)
78. M P Balem, M Le Plouzennec, M Louer *Nouv. J. Chim.* **5** 283 (1981)
79. M P Balem, M Le Plouzennec, M Louer *Inorg. Chem.* **21** 2573 (1982)
80. N K Baranetskaya, M A Kondratenko, S M Lukashov, V N Setkina *Metalloorg. Khim.* **3** 83 (1990)
81. A N Nesmeyanov, K N Anisimov, N E Kolobova, Yu V Makarov *Izv. Akad. Nauk SSSR, Ser. Khim.* 686 (1968)
82. A N Nesmeyanov, K N Anisimov, N E Kolobova, Yu V Makarov *Dokl. Akad. Nauk SSSR* **178** 1335 (1968)
83. N E Kolobova, Z P Valueva, K N Anisimov, G Z Suleimanov *Izv. Akad. Nauk SSSR, Ser. Khim.* 910 (1978)
84. E O Fischer, A Maasböl *Chem. Ber.* **100** 2445 (1967)
85. N E Kolobova, M Ya Solodova, Z P Valueva *Izv. Akad. Nauk SSSR, Ser. Khim.* 735 (1978)
86. N E Kolobova, Z P Valueva, M Ya Solodova *Izv. Akad. Nauk SSSR, Ser. Khim.* 2387 (1980)
87. N M Loim, N A Abramova, Z N Parnes, D N Kursanov. *J. Organomet. Chem.* **168** C33 (1979)
88. A I Khatami, I A Mamed'yarova, I R Lyatifov, M N Nefedova *Metalloorg. Khim.* **3** 110 (1990)
89. N M Loim, Z N Parnes, D N Kursanov, in *Proceedings of VIII International Conference on Organometallic Chemistry, Sept. 1977 Kyoto, Japan,* p. 65
90. D N Kursanov, Z N Parnes, N M Loim, N E Kolobova, I B Zlotina, P V Petrovskii, E I Fedin *J. Organomet. Chem.* **44** C15 (1972)
91. N M Loim, D N Kursanov, Z N Parnes, N N Sul'dina, E I Fedin *J. Organomet. Chem.* **52** C33 (1973)
92. D N Kursanov, N M Loim, M V Laryukova, Z F Mullakhmetova, Z N Parnes *Dokl. Akad. Nauk SSSR* **277** 878 (1984)
93. N M Loim, P V Kondrat'ev, N P Solov'eva, V A Antonovich, P V Petrovskii, Z N Parnes, D N Kursanov *J. Organomet. Chem.* **209** 233 (1981)
94. R G Sutherland, A K V Unni *J. Chem. Soc., Perkin Trans. 2* 703 (1977)
95. K V Kondrat'ev, Candidate's Thesis in Chemical Sciences, Institute of Organoelement Compounds, USSR Academy of Sciences, Moscow, 1984
96. N M Loim, M A Kondratenko, V I Sokolov *Metalloorg. Khim.* **4** 813 (1991)
97. N M Loim, E V Fedash, A K Sheinkman *Metalloorg. Khim.* **2** 411 (1991)
98. M Cais, J Kozikowski *J. Am. Chem. Soc.* **82** 5667 (1960)
99. C Sergheraert, P Marcinal, E Guingnet *J. Organomet. Chem.* **120** 329 (1976)

100. L M C Shen, G G Long, C G Moreland *J. Organomet. Chem.* **4** 362 (1966)
101. L G Kuzmina, A G Ginzburg, Yu T Struchkov, D N Kursanov *J. Organomet. Chem.* **253** 329 (1983)
102. V N Setkina, D N Kursanov *Usp. Khim.* **37** 1729 (1968) [*Russ. Chem. Rev.* **37** 737 (1968)]
103. V N Setkina, N K Baranetskaya, A G Ginzburg, V I Zdanovich, M N Nefedova, D N Kursanov *J. Organomet. Chem.* **61** 287 (1973)
104. A G Ginzburg, Candidate's Thesis in Chemical Sciences, Institute of Organoelement Compounds, USSR Academy of Sciences, Moscow, 1983
105. A N Nesmeyanov, D N Kursanov, V N Setkina, V A Sazonova, E I Fedin, N N Sedova, Yu V Volgin *Dokl. Akad. Nauk SSSR* **221** 854 (1975)
106. E V Bykova, D N Kursanov, V N Setkina *Dokl. Akad. Nauk SSSR* **208** 1091 (1973)
107. M V Antonova, I O Shapiro *Metalloorg. Khim.* **4** 674 (1991)
108. A G Milaev, V B Panov, O Yu Okhlobystin *Dokl. Akad. Nauk SSSR* **257** 1144 (1981)
109. L Yu Ukhin, A I Pyshchev, V V Krasnikov, Zh I Orlova, G N Dorofeenko *Dokl. Akad. Nauk SSSR* **234** 1351 (1977)
110. V V Krasnikov, G N Dorofeenko *Khim. Geterotsikl. Soedin.* 21 (1979)
111. A G Milaev, O Yu Okhlobystin *Khim. Geterotsikl. Soedin.* 593 (1985)
112. L Yu Ukhin, V V Krasnikov, G N Dorofeenko *Koord. Khim.* **4** 455 (1978)
113. A A Bumber, A G Milaev, O Yu Okhlobystin *Zh. Obshch. Khim.* **53** 606 (1983)
114. D N Kursanov, V N Setkina, S P Dolgova *Izv. Akad. Nauk SSSR, Ser. Khim.* 869 (1979)
115. D N Kursanov, V N Setkina, S P Dolgova *Izv. Akad. Nauk SSSR, Ser. Khim.* 1886 (1980)
116. V G Andrianov, Yu T Struchkov, P V Petrovskii, E I Fedin, D N Kursanov, S P Dolgova, V N Setkina *J. Organomet. Chem.* **221** 183 (1981)
117. V I Bakhmutov, P V Petrovskii, S P Dolgova, V N Setkina, E I Fedin, D N Kursanov *J. Organomet. Chem.* **245** 177 (1983)
118. A S Batsanov, S P Dolgova, V I Bakhmutov, V N Setkina, D N Kursanov *J. Organomet. Chem.* **291** 341 (1985)
119. S P Dolgova, V N Setkina, D N Kursanov *J. Organomet. Chem.* **292** 229 (1985)
120. A S Batsanov, Yu T Struchkov, S P Dolgova, V N Setkina, M V Galakhov, S V Yakushin, Yu S Nekrasov *Metalloorg. Khim.* **5** 985 (1992)
121. V I Sokolov, G Z Suleimanov *Izv. Akad. Nauk SSSR, Ser. Khim.* 1647 (1981)
122. J C Brunet, E.Cuingnet, H Gras, P Marcinal, A Molz, C Sergheraert, A Tartar *J. Organomet. Chem.* **216** 73 (1981)
123. E A Chernyshev, A S Dmitriev, Yu V Makarov *Khim. Prom.* 276 (1982)
124. I M Gverdtsiteli, L P Asatiani, A A Tskvaradze *Soobshch. Akad. Nauk Gruz. SSR* **81** 353 (1976); *Ref. Zh. Khim.* 16Zh466 (1976)
125. L P Asatiani *Soobshch. Akad. Nauk Gruz. SSR* **87** 369 (1977); *Ref. Zh. Khim.* 9Zh338 (1981)
126. L P Asatiani *Soobshch. Akad. Nauk Gruz. SSR* **98** 89 (1980); *Ref. Zh. Khim.* 11Zh406 (1981)
127. A N Nesmeyanov, V A Sazonvoa, V N Postnov, A N Baran *Izv. Akad. Nauk SSSR, Ser. Khim.* 902 (1979)
128. A N Nesmeyanov, V A Sazonova, V N Postnov, A N Baran *Dokl. Akad. Nauk SSSR* **241** 1099 (1978)
129. A N Nesmeyanov, A M Baran, L Eggert, V N Postnov, V A Sazonova *Izv. Akad. Nauk SSSR, Ser. Khim.* 1402 (1979)
130. A N Nesmeyanov, V N Postnov, A M Baran, V A Sazonova *Dokl. Akad. Nauk SSSR* **258** 124 (1981)
131. A N Nesmeyanov, V N Postnov, A M Baran, V A Sazonova *Izv. Akad. Nauk SSSR, Ser. Khim.* 2829 (1980)
132. V N Postnov, E I Klimova, V A Sazonova *Dokl. Akad. Nauk SSSR* **262** 1398 (1982)
133. A N Nesmeyanov, A M Baran, V N Postnov, V A Sazonova, V A Chertkov, Yu N Polivin *Izv. Akad. Nauk SSSR, Ser. Khim.* 2828 (1979)
134. A N Nesmeyanov, A M Baran, V N Postnov, V A Sazonova *Dokl. Akad. Nauk SSSR* **250** 371 (1980)
135. A N Nesmeyanov, V N Postnov, V A Sazonova, T N Galakhova, A A Kuznetsov *Izv. Akad. Nauk SSSR, Ser. Khim.* 2172 (1978)
136. V N Postnov, V A Sazonova, Yu N Polivin, V A Chertkov *Dokl. Akad. Nauk SSSR* **264** 96 (1982)
137. V N Postnov, Yu N Polivin, D V Bazhenov, V A Sazonova *Dokl. Akad. Nauk SSSR* **276** 373 (1984)
138. J Frederic, S Toma *Coll. Czech. Chem. Commun.* **52** 174 (1987)
139. R Riemschneider, W Herrmann *Liebigs Ann. Chem.* **648** 68 (1961)
140. S G Gottis, H Falk, K Schlögl *Tetrahedron Lett.* **6** 2857 (1965)
141. H Gowal, K Schlögl *Monatsch. Chem.* **98** 2302 (1967)
142. H Gowal, K Schlögl *Monatsch. Chem.* **99** 267 (1968)
143. H Gowal, K Schlögl *Monatsch. Chem.* **99** 972 (1968)
144. K Schlögl *Pure Appl. Chem.* **23** (4) (1970)
145. K Schlögl, in *Izbrannye Problemy Stereokhimii* (Selected Problems in Stereochemistry) (Translated into Russian; Moscow: Mir, 1970) p. 48
146. R Dabard, M Le Plouzennec *Bull. Soc. Chim. Fr.* 3594 (1972)
147. R Dabard, M Le Plouzennec *Bull. Soc. Chim. Fr.* 3600 (1972)
148. M Le Plouzennec, R Dabard *J. Organomet. Chem.* **29** C33 (1971)
149. M Le Plouzennec, R Dabard *J. Organomet. Chem.* **112** 333 (1976)
150. A Modiano, M Cais *Tetrahedron Lett.* **1** 31 (1960)
151. J Tirouflet, B Gauteon, R Dabard *Bull. Soc. Chim. Fr.* 96 (1965)
152. M Le Plouzennec, R Dabard *J. Organomet. Chem.* **133** 359 (1977)
153. V A Tsiryapkin, N M Loim, L V Nedospasova, Z N Parnes, D N Kursanov *J. Organomet. Chem.* **182** 441 (1979)
154. V A Tsyryapkin, I E Zel'tser, N M Loim, L V Nedospasova, Z N Parnes, D N Kursanov *Izv. Akad. Nauk SSSR, Ser. Khim.* 872 (1979)
155. Yu N Belokon, I E Zel'tser, N M Loim, V A Tsiryapkin, G G Alexandrov, D N Kursanov, Z N Parnes, Yu T Struchkov, V M Belikov *Tetrahedron* **36** 1089 (1980)
156. Yu N Belokon, I E Zel'tser, N M Loim, V A Tsiryapkin, Z N Parnes, D N Kursanov, V M Belikov *J. Chem. Soc., Chem. Commun.* 789 (1979)
157. Yu T Struchkov, Yu N Belokon, V M Belikov, I E Zel'tser, G G Alexandrov *J. Organomet. Chem.* **210** 411 (1981)
158. V A Tsiryapkin, N M Loim, L V Nedospasova, Z N Parnes, D N Kursanov *J. Organomet. Chem.* **190** 83 (1980)
159. N M Loim, M V Larukova, V G Andrianov, V A Tsiryapkin, Z N Parnes, Yu T Struchkov *J. Organomet. Chem.* **248** 73 (1983)
160. Y Yamazaki, K Hosono *Tetrahedron Lett.* **30** 5313 (1989)
161. N M Loim, M A Kondratenko, V A Sokolov *Dokl. Akad. Nauk SSSR* **320** 1123 (1991)
162. N M Loin, M A Kondratenko, V M Sokolov, K M Turdybekov, Yu T Struchkov *Metalloorg. Khim.* **5** 1176 (1992)
163. N M Loim, M A Kondratenko, V I Sokolov *Izv. Russ. Akad. Nauk, Ser. Khim.* 182 (1993)
164. M A Kondratenko, Candidate's Thesis in Chemical Sciences, Institute of Organoelement Compounds, Russian Academy of Sciences, Moscow, 1992
165. F Le Moigne, R Dabard, M Le Plouzennec *J. Organomet. Chem.* **122** 365 (1976)
166. M Le Plouzennec, F Le Moigne, R Dabard *J. Organomet. Chem.* **132** 409 (1977)
167. A N Nesmeyanov, K N Anisimov, N E Kolobova, I B Zlotina *Izv. Akad. Nauk SSSR, Ser. Khim.* 1362 (1967)
168. A N Nesmeyanov, K N Anisimov, N E Kolobova, I B Zlotina *Izv. Akad. Nauk SSSR, Ser. Khim.* 901 (1968)
169. M Le Plouzennec, F Le Moigne, R Dabard *J. Organomet. Chem.* **111** C38 (1976)
170. N M Loim, Z N Parnes, V G Andrianov, Yu T Struchkov, D N Kursanov *J. Organomet. Chem.* **201** 301 (1980)
171. N M Loim, M A Laryukova, P V Kondrat'ev, Z N Parnes. *J. Organomet. Chem.* **301** 173 (1986)
172. M V Laryukova, Candidate's Thesis in Chemical Sciences, Institute of Organoelement Compounds, USSR Academy of Sciences, Moscow, 1988
173. S P Dolgova, B L Tumanskii, S P Solodovnikov, D V Zagorevskii, V N Setkina *Metalloorg. Khim.* **2** 781 (1989)
174. R B King, A Efraty *J. Organomet. Chem.* **23** 257 (1970)
175. E W Abel, S Moorhouse *Angew. Chem., Int. Ed. Engl.* **10** 339 (1971)
176. N E Kolobova, I A Lobanova, V I Zdanovich *Izv. Akad. Nauk SSSR, Ser. Khim.* 1651 (1980)
177. V I Zdanovich, I A Lobanova, N E Kolobova *Izv. Akad. Nauk SSSR, Ser. Khim.* 2149 (1984)

178. M E Rerek, L N Ji, F Basolo *J. Chem. Soc., Chem. Commun.* 1208 (1983)
179. L N Ji, M E Rerek, F Basolo *Organometallics* **3** 740 (1984)
180. V I Zdanovich, M G Ezernitskaya *Izv. Akad. Nauk SSSR, Ser. Khim.* 685 (1981)
181. N E Kolobova, I A Lobanova, V I Zdanovich, P V Perovskii *Izv. Akad. Nauk SSSR, Ser. Khim.* 935 (1981)
182. I A Lobanova, V I Zdanovich, N E Kolobova *Izv. Akad. Nauk SSSR, Ser. Khim.* 2606 (1982)
183. I A Lobanova, V I Zdanovich, P V Petrovskii, N I Vasyukova, N E Kolobova *Izv. Akad. Nauk SSSR, Ser. Khim.* 1384 (1987)
184. V F Sizoi, V A Semenov, V I Zdanovich, I A Lobanova, N E Kolobova *Izv. Akad. Nauk SSSR, Ser. Khim.* 2153 (1985)
185. I A Lobanova, A S Batsanov, V I Zdanovich, Yu T Struchkov, N E Kolobova *Izv. Akad. Nauk SSSR, Ser. Khim.* 682 (1988)
186. I A Lobanova, V I Zdanovich, N E Kolobova, P V Petrovskii *Izv. Akad. Nauk SSSR, Ser. Khim.* 684 (1983)
187. I A Lobanova, V I Zdanovich, P V Petrovskii, N E Kolobova *J. Organomet. Chem.* **292** 395 (1985)
188. P M Treichel, J W Johnson *Inorg. Chem.* **16** 749 (1977)
189. P M Treichel, K P Fivizzani, K J Haller *Organometallics* **1** 931 (1982)
190. T A Aibright, P Hoffmann, R Hoffmann, C P Lillya, P A Dobosh *J. Am. Chem. Soc.* **105** 3396 (1983)
191. M E Rerek, F Basolo *Organometallics* **3** 329 (1982)
192. M G Ezernitskaya, B V Lokshin, V I Zdanovich, I A Lobanova, N E Kolobova *J. Organomet. Chem.* **234** 329 (1982)
193. M G Ezernitskaya, B V Lokshin, V I Zdanovich, I A Lobanova, N E Kolobova *J.Organomet. Chem.* **282** 363 (1985)
194. R Biagioni, I M Lorkovic, J Skelton, J B Hartung *Organometallics* **9** 547 (1990)
195. I A Lobanova, V I Zdanovich *Usp. Khim.* **57** 1688 (1988) [*Russ. Chem. Rev.* **57** 967 (1988)]
196. O I Trifonova, Yu A Ustynyuk, N A Ustynyuk, Yu F Oprunenko, A S Batsanov, Yu T Struchkov *Metalloorg. Khim.* **2** 581 (1989)
197. O I Trifonova, R A Galiullin, N B Kazennova, Yu A Ustynyuk, N A Ustynyuk, D N Kravtsov, V A Piven' *Metalloorg. Khim.* **1** 1300 (1988)
198. O I Trifonova, R A Galiullin, N B Kazennova, D N Kravtsov, Yu A Ustynyuk, N A Ustynyuk *Izv. Akad. Nauk SSSR, Ser. Khim.* 1908 (1987)
199. M R Churchill, S A Julis *Inorg. Chem.* **17** 2951 (1978)
200. W L Bell, C J Curtis, C W Eigenbrot, C G Pierpont, J L Robbins, J C Smart *Organometallics* **6** 266 (1987)
201. W L Bell, C J Curtis, A Miedaner, C W Eigenbrot, R C Haltiwanger, C G Pierpont, J C Smart *Organometallics* **7** 691 (1988)
202. T J Lynch, M C Helvenston, A L Rheingold, D L Staley *Organometallics* **8** 1959 (1989)
203. M C Helvenston, T J Lynch *J. Organomet. Chem.* **359** C50 (1989)
204. T L Tisch, T J Lynch, R Dominguez *J. Organomet. Chem.* **377** 265 (1989)
205. A N Nesmeyanov, K I Grandberg, T V Baukova, A N Kosina, E G Perevalova *Izv. Akad. Nauk SSSR, Ser. Khim.* 2032 (1969)
206. M D Rausch, R F Kovar, C S Kraihanzel *J. Am. Chem. Soc.* **91** 1259 (1969)
207. R F Kovar, M D Rausch *J. Org. Chem.* **38** 1918 (1973)
208. A N Nesmeyanov, V A Sazonova, N N Sedova *Dokl. Akad. Nauk SSSR* **202** 362 (1972)
209. A N Nesmeyanov, V A Sazonova, N N Sedova *Dokl. Akad. Nauk SSSR* **194** 825 (1970)
210. USSR P. 484 222; *Byull. Izobret.* **34** 58 (1975)
211. A N Nesmeyanov, N N Sedova, Yu V Volgin, V A Sazonova *Izv. Akad. Nauk SSSR, Ser. Khim.* 2353 (1977)
212. W A Herrmann, D Andreiewski, E Herdtweck *J. Organomet. Chem.* **319** 183 (1987)
213. M D Rausch, W C Spink, B G Conway, R D Rogers, J L Atwood *J. Organomet. Chem.* **383** 227 (1990)
214. A N Nesmeyanov, V A Sazonova, N N Sedova, L S Klimenko *Izv. Akad. Nauk SSSR, Ser. Khim.* 735 (1972)
215. A N Nesmeyanov, N N Sedova, V A Sazonova, L S Borodina *Dokl. Akad. Nauk SSSR* **207** 617 (1972)
216. A N Nesmeyanov, V A Sazonova, N N Sedova, L S Borodina, Yu V Volgin *Dokl. Akad. Nauk SSSR* **213** 1099 (1973)
217. A N Nesmeyanov, N N Sedova, V A Sazonova, I F Leshcheva, I S Rogozhin *Dokl. Akad. Nauk SSSR* **218** 356 (1974)
218. A N Nesmeyanov, N N Sedova, Yu T Struchkov, V G Andrianov, E N Stakheeva, V A Sazonova *J. Organomet. Chem.* **153** 115 (1978)
219. A N Nesmeyanov, N N Sedova, S K Moiseev, V A Sazonova *Izv. Akad. Nauk SSSR, Ser. Khim.* 1171 (1980)
220. T E Bitterwolf *Polym. Mater. Sci. Eng.* **49** 368 (1983)
221. R B King, M N Ackermann *Inorg. Chem.* **13** 637 (1974)
222. M R Churchill, R A Lashewycz, F J Rotella *Inorg. Chem.* **16** 265 (1977)
223. M A Huffman, D A Newman, M Tilset, W B Tolman, P C Vollhardt *Organometallics* **5** 1926 (1986)
224. N I Gogan, C K Chu *J. Organomet. Chem.* **132** 103 (1977)
225. T E Bitterwolf *J. Organomet. Chem.* **312** 197 (1986)
226. P Härter, G Boguth, E Herdtweck, J Riede *Angew. Chem. Int. Ed. Engl.* **28** 1008 (1989)
227. P Härter, J Behm, K J Burkert *J. Organomet. Chem.* **438** 297 (1992)
228. E G Perevalova, M D Reshetova, G M Kokhanyuk *Zh. Obshch. Khim.* **54** 2711 (1984)
229. A N Nesmeyanov, N E Kolobova, Z P Valueva, M Ya Solodova, K N Anisimov *Izv. Akad. Nauk SSSR, Ser. Khim.* 1138 (1977)
230. A N Nesmeyanov, E G Perevalova, L I Leont'eva, S A Eremin *Dokl. Akad. Nauk SSSR* **243** 1208 (1978)
231. A N Nesmeyanov, E G Perevalova, L I Leont'eva, E V Shumilina *Izv. Akad. Nauk SSSR, Ser. Khim.* 1142 (1977)
232. A N Nesmeyanov, E G Perevalova, L I Leont'eva, E V Shumilina *Izv. Akad. Nauk SSSR, Ser. Khim.* 2328 (1977)
233. A N Nesmeyanov, E G Perevalova, L I Leont'eva, E V Shumilina *Izv. Akad. Nauk SSSR, Ser. Khim.* 683 (1979)
234. L I Leont'eva, E G Perevalova *Izv. Akad. Nauk SSSR, Ser. Khim.* 2352 (1984)
235. N E Kolobova, V N Khandozhko, V F Sizoi, Shch Guseinov, O S Zhvanko, Yu S Nekrasov *Izv. Akad. Nauk SSSR, Ser. Khim.* 619 (1979)
236. V B Rybakov, A I Tursina, L A Aslanov, S A Yeremin, H Schrauber, L Kutschabsky *Z. Anorg. Allg. Chem.* **487** 217 (1982)
237. V B Rybakov, L A Aslanova, V M Ionov, S A Eremin *Zh. Strukt. Khim.* **24** 74 (1983)
238. E O Fischer, V N Postnov, F R Kreissl *J. Organomet. Chem.* **127** C19 (1977)
239. M N Estekhina, V I Losilkina, N M Loim, M K Baranetskaya, V N Setkina *Izv. Akad. Nauk SSSR, Ser. Khim.* 2371 (1986)
240. E G Perevalova, M D Reshetova, E A Yankovskii *Zh. Obshch. Khim.* **55** 2093 (1985)
241. M Cais, M Feldkimel *Tetrahedron Lett.* **2** 440 (1961)
242. C F Lee, M E Thompson *Inorg. Chem.* **30** 4 (1991)
243. T J Lynch, R Dominguez, M C Helvenston *Organometallics* **7** 2566 (1988)
244. A G Ginzburg, V N Setkina, D N Kursanov, Sh G Kasumov *Izv. Akad. Nauk SSSR, Ser. Khim.* 2398 (1976)
245. N M Loim, A G Ginzburg, M V Galakhov *Metalloorg. Khim.* **4** 969 (1991)
246. A S Batsanov, T V Timofeeva, M Kh Dzhafarov, Yu T Struchkov, M N Loim, A G Ginzburg, M V Galakhov *Metalloorg. Khim.* **4** 976 (1991)
247. A W Cordes, B Durham, E Askew *Acta Crystallogr. Sect. C* **45** 1229 (1989)
248. A W Cordes, B Durham, E Askew *Acta Crystallogr. Sect. C* **45** 1231 (1989)
249. C Lo Sterzo, M M Miller, J K Stille *Organometallics* **8** 2331 (1989)
250. C Lo Sterzo, J K Stille *Organometallics* **9** 687 (1990)
251. C Lo Sterzo, G Bocelli *J. Chem. Soc., Dalton Trans.* 1881 (1991)
252. C Lo Sterzo *Organometallics* **9** 3185 (1990)
253. T E Bitterwolf, K A Lott, A J Rest, J Mascetti *J. Organomet. Chem.* **419** 113 (1991)
254. P E Bloyce, R H Hooker, A J.Rest, T E Bitterwolf, N J Fitzpatrick, J E Shade *J. Chem. Soc., Dalton Trans.* 833 (1990)
255. N I Pyshnograeva, N M Loim, V I Sokolov *Dokl. Akad. Nauk SSSR* **318** 345 (1991)
256. A N Nesmeyanov, V A Sazonova, N M Sedova *Dokl. Akad. Nauk SSSR* **198** 590 (1971)
257. V N Postnov, N N Meleshonkova, E I Klimova *Metalloorg. Khim.* **3** 710 (1990)

258. A N Nesmeyanov, E G Perevalova, T V Baukova, K I Grandberg *Izv. Akad. Nauk SSSR, Ser. Khim.* 866 (1974)
259. A N Nesmeyanov, E G Perevalova, O B Afanasova, M V Tolstaya, K I Grandberg *Izv. Akad. Nauk SSSR, Ser. Khim.* 1118 (1978)
260. G Z Suleimanov, R M Agaeva, S G Mamedova, T Kh Kurbanov *Azerb. Khim. Zh.* 62 (1983)
261. G Z Suleimanova, A Ya Usyatinskii, E A Zul'fugarly, L G Kuz'mina, E I Kazimirchuk, V N Khandozhko, P V Petrovskii, V I Bregadze, Sh M Makhmudov, I P Beletskaya *Metalloorg. Khim.* **5** 973 (1992)
262. A N Nesmeyanov, N E Kolobova, Yu V Makarov, K N Anisimov *Izv. Akad. Nauk SSSR, Ser. Khim.* 1992 (1969)
263. G Z Suleimanov, P V Petrovskii, Yu S Bogachev, I L Zhuravleva, E I Fedin, I P Beletskaya *J. Organomet. Chem.* **262** C35 (1984)
264. G Z Suleimanov, Yu S Bogachev, L T Abdullaeva, I L Zhuravleva, Kh S Khalilov, L F Rybakova, N N Shapet'ko, I P Beletskaya *Dokl. Akad. Nauk SSSR* **276** 378 (1984)
265. G Suleimanov, Yu S Bogachev, L T Abdullaeva, I L Zhuravleva, K S Khalilov, L F Rybakova, I P Beletskaya *Polyhedron* **4** 29 (1985)
266. G Z Suleimanov, T A Adamskii, Yu S Bogachev, L I Zhuravleva, Z M Umudova, R Yu Mekhdiev, P V Petrovskii, I P Beletskaya *Zh. Obshch. Khim.* **56** 1205 (1986)
267. A Ya Usyatinskii, T G Gashinova, V I Bregadze *Metalloorg. Khim.* **5** 971 (1992)
268. A N Nesmeyanov, K N Anisimov, N E Kolobova, Yu V Makarov *Izv. Akad. Nauk SSSR, Ser. Khim.* 2815 (1973)
269. USSR P. 370 210 ; *Byull. Izobret.* **11** 75 (1973)
270. I M Gverdtsiteli, L P Asatiani, S Kh Kiladze *Zh. Obshch. Khim.* **45** 1648 (1975)
271. L P Asatiani, D S Zurabishvili, I M Gverdtsiteli *Zh. Obshch. Khim.* **48** 2386 (1978)
272. L P Asatiani, A A El'-Agami, I M Gverdtsiteli *Dokl. Akad. Nauk Gruz. SSR* **90** 61 (1978)
273. L P Asatiani, A A El'-Agami, I M Gverdtsiteli *Dokl. Akad. Nauk Gruz. SSR* **90** 589 (1978)
274. L P Asatiani, S Kh Kiladze *Soobshch. Akad. Nauk Gruz. SSR* **99** 97 (1980)
275. L P Asatiani, A A El'-Agami *Zh. Obshch. Khim.* **50** 1584 (1980)
276. G V Gridunova, V E Shklover, Yu T Struchkov, L P Asatiani *Zh. Strukt. Khim.* **24** 693 (1983)
277. G V Gridunova, V E Shklover, Yu T Struchkov, L P Asatiani *Zh. Strukt. Khim.* **28** 111 (1987)
278. M E Wright, V W Day *J. Organomet. Chem.* **329** 43 (1987)
279. E Colomer, R J P Corriu, R Pleixats *J. Organomet. Chem.* **381** C1 (1990)
280. A N Nesmeyanov, T P Tolstaya, A A Korol'kov, A P Yarkevich *Dokl. Akad. Nauk SSSR* **221** 1337 (1975)
281. A N Nesmeyanov, T P Tolstaya, A A Korol'kov *Dokl. Akad. Nauk SSSR* **241** 1103 (1978)
282. N G Bokii, Yu T Struchkov *Koord. Khim.* **4** 134 (1978)
283. L N Zakharov, V G Andrianov, Yu T Struchkov, Yu T Sharugin, O N Suvorova *Koord. Khim.* **6** 1104 (1980)
284. A N Nesmeyanov, K N Anisimov, Z P Valueva *Dokl. Akad. Nauk SSSR* **216** 106 (1974)
285. G J Reilly, W E McEwen *Tetrahedron Lett.* **9** 1231 (1968)
286. F Mathey, J P Lampin *J. Organomet. Chem.* **128** 297 (1977)
287. G D Kolomnikova, S A Goloshchapova, Yu G Gololobov *Metalloorg. Khim.* **1** 921 (1988)
288. G D Kolomnikova, S A Kuznetsova, P V Petrovskii, Yu G Gololobov *Metalloorg. Khim.* **3** 1303 (1990)
289. M Herberhold, M Biersack *J. Organomet. Chem.* **381** 379 (1990)
290. L N Zakharov, Yu T Struchkov, V V Sharugin, O N Suvorova *Koord. Khim.* **6** 805 (1980)
291. G A Razuvaev, G A Domrachev, V V Sharugin, O N Suvorova *Dokl. Akad. Nauk SSSR* **237** 852 (1977)
292. V V Sharvgin, A E Ermoshkin *Izv. Akad. Nauk SSSR, Ser. Khim.* 187 (1987)
293. M Cais, N Tirosh *Bull. Soc. Chim. Belg.* **90** 27 (1981)
294. A N Nesmeyanov, N E Kolobova, V I Zdanovitch, A Zh Zhakaeva *J. Organomet. Chem.* **107** 319 (1976)
295. V G Andrianov, Yu T Struchkov, B I Zdanovich, N E Kolobova *Koord. Khim.* **7** 1699 (1981)
296. R J Daroda, G Wilkinson, M B Hursthouse, M Tornton-Pett *J. Chem. Soc., Dalton Trans.* 2315 (1980)
297. A N Nesmeyanov, E G Perevalova, L I Leont'eva, S A Eremin, O V Grigor'eva *Izv. Akad. Nauk SSSR, Ser. Khim.* 2645 (1974)
298. A N Nesmeyanov, E G Perevalova, L I Khomik, L I Leont'eva *Dokl. Akad. Nauk SSSR* **209** 869 (1973)
299. A N Nesmeyanov, E G Perevalova, L I Leont'eva, L I Khomik *Izv. Akad. Nauk SSSR, Ser. Khim.* 938 (1974)
300. A N Nesmeyanov, E G Perevalova, L I Leont'eva, E V Shumilina *Izv. Akad. Nauk SSSR, Ser. Khim.* 1156 (1977)
301. A N Nesmeyanov, E G Perevalova, L I Leont'eva, E V Shumilina *Izv. Akad. Nauk SSSR, Ser. Khim.* 2813 (1977)
302. A S Batsanov, Yu T Struchkov *J. Organomet. Chem.* **266** 295 (1984)
303. E V Shumilina *Vestn. Mosk. Univ., Ser. 2: Khim.* **18** 476 (1977)
304. E G Perevalova, L I Leont'eva, E V Shumilina *Izv. Akad. Nauk SSSR, Ser. Khim.* 1438 (1978)
305. T Yu Orlova, V N Setkina, D N Kursanov *J. Organomet. Chem.* **267** 309 (1984)
306. T Yu Orlova, V N Setkina, P V Petrovskii, A I Yanovskii, A S Batsanov, Yu T Struchkov *Metalloorg. Khim.* **1** 1327 (1988)
307. T Yu Orlova, V N Setkina, A S Batsanov, M Kh Dzhafarov, Yu T Struchkov, P V Petrovskii *Metalloorg. Khim.* **5** 1102 (1992)
308. T Yu Orlova, V N Setkina, P V Petrovskii, D V Zagorevskii *Metalloorg. Khim.* **5** 1098 (1992)
309. T Yu Orlova, V N Setkina, A S Batsanov, Yu T Struchkov, P V Petrovskii *Metalloorg. Khim.* **4** 559 (1991)
310. A N Nesmeyanov, E G Perevalova, L I Leont'eva, E V Shumilina *Dokl. Akad. Nauk SSSR* **238** 588 (1978)
311. A N Nesmeyanov, L I Leont'eva, L I Khomik *Izv. Akad. Nauk SSSR, Ser. Khim.* 1656 (1976)
312. G Z Suleimanov, T Kh Kurbanov, O A Reutov, M N Mamedov *Izv.Akad. Nauk SSSR, Ser. Khim.* 967 (1977)
313. V I Sokolov, G Z Suleimanov, V V Bashilov, T Kh Kurbanov, I A Amiraslanov, O A Reutov *Izv. Akad. Nauk SSSR, Ser. Khim.* 1894 (1977)
314. O A Reutov, G Z Suleimanov, I A Amiraslanov, V V Bashilov, V I Sokolov *Zh. Org. Khim.* **4** 1802 (1978)
315. G Z Suleimanov, V V Bashilov, V I Sokolov, O A Reutov *Izv. Akad. Nauk SSSR, Ser. Khim.* 1670 (1978)
316. B V Lokshin, A G Ginzburg, E B Nazarova *Usp. Khim.* **49** 223 (1980) [*Russ. Chem. Rev.* **49** 115 (1980)]
317. H Werner *Pure Appl. Chem.* **54** 177 (1982)
318. H Werner *Angew. Chem.* **95** 932 (1983)
319. B V Lokshin, A G Ginzburg, V N Setkina, D N Kursanov, I B Nemirovskaya *J.Organomet. Chem.* **37** 347 (1972)
320. B V Lokshin, M G Ezernitskaya *J. Organomet. Chem.* **256** 89 (1983)
321. A G Ginzburg, P O Okulevich, V N Setkina, G A Panosyan, D N Kursanov *J. Organomet. Chem.* **81** 201 (1974)
322. T C Flood, E Rosenberg, A Sarhangi *J. Am. Chem. Soc.* **103** 190 (1981)
323. A G Ginzburg, L A Fedorov, P V Petrovskii, E I Fedin, V N Setkina, D N Kursanov *J. Organomet. Chem.* **73** 77 (1974)
324. A G Ginzburg, P V Petrovskii, V N Setkina, D N Kursanov *Izv. Akad. Nauk SSSR, Ser. Khim.* 185 (1985)
325. A G Ginzburg, P V Petrovskii *Izv. Akad. Nauk SSSR, Ser. Khim.* 1389 (1987)
326. A E Stevens, J L Beauchamp *J. Am. Chem. Soc.* **103** 190 (1981)
327. B V Lokshin, S G Kazaryan, A G Ginzburg *Izv. Akad. Nauk SSSR, Ser. Khim.* 2605 (1986)
328. B V Lokshin, S G Kazaryan, A G Ginzburg *Izv. Akad. Nauk SSSR, Ser. Khim.* 333 (1988)
329. B V Lokshin, S G Kazaryan, A G Ginzburg *Izv. Akad. Nauk SSSR, Ser. Khim.* 561 (1988)
330. B V Lokshin, S G Kazaryan, A G Ginzburg *J. Mol. Struct.* **174** 29 (1988)
331. E S Shubina, A N Krylov, T V Timofeeva, Yu T Struchkov, A G Ginzburg, N M Loim, L M Epstein *J. Organomet. Chem.* **434** 329 (1992)
332. B V Lokshin, E B Rusach, Z P Valueva, A G Ginzburg, N E Kolobova *J. Organomet. Chem.* **102** 535 (1975)
333. A G Ginzburg, V N Setkina, D N Kursanov *Izv. Akad. Nauk SSSR, Ser. Khim.* 447 (1985)
334. E N Gur'yanova, A G Ginzburg, E S Isaeva, V N Setkina, D N Kursanov *Dokl. Akad. Nauk SSSR* **262** 1389 (1982)
335. E N Guryanova, A G Ginzburg, E S Isaeva *Koord. Khim.* **12** 23 (1987)

336. V V Korol'kov, L M Epshtein, E V Shumilina, T P Tolstaya *Vestn. Mosk. Univ. Ser. 2: Khim.* **18** 98 (1977)
337. N I Pyshnograeva, A S Batsanov, Yu T Struchkov, A G Ginzburg, V N Setkina *J. Organomet. Chem.* **297** 69 (1985)
338. N M Loim, L A Malutschenko, Z N Parnes, P V Petrovskii, D N Kursanov *J. Organomet. Chem.* **108** 363 (1976)
339. A G Ginzburg, V N Setkina, D N Kursanov *J. Organomet. Chem.* **77** C27 (1974)
340. N M Loim, P V Petrovskii, V I Robas, Z N Parnes, D N Kursanov *J. Organomet. Chem.* **117** 265 (1976)
341. A G Ginzburg, V N Setkina, P V Petrovskii, Sh G Kasumov, G A Panosyan, D N Kursanov *J. Organomet. Chem.* **121** 381 (1976)
342. A G Ginzburg, V N Setkina, Sh G Kasumov, G A Panosyan, P V Petrovskii, D N Kursanov *Dokl. Akad. Nauk SSSR* **228** 1368 (1976)
343. D N Kursanov, A G Ginzburg, V N Setkina, Sh G Kasumov *Dokl. Akad. Nauk SSSR* **240** 1368 (1978)
344. A G Ginzburg, Sh G Kazumov, V N Setkina, D N Kursanov *Izv. Akad. Nauk SSSR, Ser. Khim.* 884 (1981)
345. A G Ginzburg, Sh G Kasumov, V N Setkina, D N Kursanov *Izv. Akad. Nauk SSSR, Ser. Khim.* 431 (1982)
346. D N Kursanov, Z N Parnes, K N Anisimov, N M Loim, I B Zlotina, Z P Valueva *Izv. Akad. Nauk SSSR, Ser. Khim.* 713 (1972)
347. A A Arutyunyants, A A Bumber, A G Ginzburg, O Yu Okhlobystin *Zh. Obshch. Khim.* **56** 2728 (1986)
348. S P Gubin, A A Koridze, N A Ogorodnikova *Izv. Akad. Nauk SSSR, Ser. Khim.* 1170 (1981)
349. N J Gogan, C K Chu, G W Gray *J. Organomet. Chem.* **51** 323 (1973)
350. G N Knox, P L Pauson, D Willison *J. Organomet. Chem.* **450** 177 (1993)
351. T E Bitterwolf, T L Hubler, A L Rheingold *J. Organomet. Chem.* **431** 199 (1992)
352. S E Jones, M D Rausch, T E Bitterwolf *J. Organomet. Chem.* **450** 27 (1993)
353. S Pitter, G Huttner, O Walter, L Zsolnai *J. Organomet. Chem.* **454** 183 (1993)
354. M Herberhold, M Biersack *J. Organomet. Chem,* **443** 1 (1993)
355. A Ya Usyatinskii, G Z Suleimanov, E A Zul'fugarly, Sh M Makhmudov, V I Bregadze, I P Beletskaya *Izv. Ross. Akad. Nauk, Ser. Khim.* **3** 586 (1993)
356. K Sünkel, V Birk *J. Organomet. Chem.* **458** 181 (1993)

Russian Chemical Reviews **62** (11) 1047 – 1071 (1993)
©1993 Russian Academy of Sciences and Turpion Ltd

UDC 547.458:577.1

Oligosaccharins — a new class of signalling molecules in plants

A I Usov

Contents

I. Introduction	1047
II. Oligosaccharins in the reactions of plants with phytopathogenic fungi and bacteria	1047
III. Oligosaccharins as regulators of plant growth and morphogenesis	1061
IV. Interaction of plants with bacterial symbionts	1067
V. Conclusion	1068

Abstract. The review deals with oligosaccharins — biologically active oligosaccharides of the following structural types: the (1 → 6, 1 → 3)-β-D-glucan fragments of the fungal cell wall; the chitin and chitosan fragments; polygalacturonic acid fragments; the xyloglucan fragments of the plant cell wall; lipooligosaccharides synthesised by bacteria — symbionts of leguminous plants. The isolation, determination of the structure, and total syntheses of these complex compounds as well as the results of the study of their biological role as inductors of the immunity of plants to attack by pathogenic fungi and bacteria and as regulators of the morphogenesis in the development processes in plants and of the interaction of the latter with symbiont bacteria are described. The bibliography includes 197 references.

I. Introduction

Biologically active oligosaccharides, fulfilling signalling functions in plants, were discovered about 15 years ago.[1] Several years later, it was suggested that these oligosaccharide bio-regulators be called 'oligosaccharins', the suffix of which was chosen by analogy with the names of the most important phytohormones — auxins, gibberellins, and cytokinins.[2] Oligosaccharins are formed as a result of the partial cleavage of carbohydrate-containing biopolymers of the cell walls of plants or phytopathogenic fungi, act at extremely low concentrations, and participate in biological processes of the greatest importance for plants such as protection against attack by pathogenic fungi or bacteria, regulation of growth and morphogenesis, and interaction with bacterial symbionts.[3] The number of studies devoted to oligosaccharins has been growing at an increasing rate. The interest in these substances is associated not only with the possibility of investigating with the aid of oligosaccharins the detailed mechanisms of intercellular interaction and the regulation of plant metabolism but also with the very attractive prospect of the practical employment of this new class of regulators in the biotechnology of plants in agriculture.[4]

The low availability of oligosaccharins required considerable efforts on the part of carbohydrate chemists to improve the methodological procedures used in the isolation and the determination of the structure of oligosaccharins and the development of new effective approaches to the synthesis of these complex oligosaccharides. Without exaggerating, one may say that the high current level of the analytical and synthetic research in the field of complex oligomeric carbohydrates is in many respects determined by the brilliant studies on the chemistry of oligosaccharins.

There exist in the literature several excellent reviews devoted principally to the biological properties of oligosaccharins,[5–10] but there are no reviews on the chemical synthesis of these substances. There exists only one review in Russian,[11] the authors of which are the founders of this field — Albersheim and Darvill at the Complex Carbohydrate Research Center (Athens, Georgia, USA); it is devoted to the problems and advances in the early stages of the studies on oligosaccharins. The aim of the present review is to give an account of the present state of research into oligosaccharins not so much from the standpoint of the plant physiology as from the standpoint of carbohydrate chemistry in order to draw the attention of Russian investigators to this extremely interesting and practically important problem.

II. Oligosaccharins in the reactions of plants with phytopathogenic fungi and bacteria

1. The oligosaccharide fragment of the fungal cell wall β-glucan

One of the most thoroughly investigated mechanisms of the self-protection of plants against fungal infection is that of the formation of phytoalexins,[12–14] which serve as a kind of plant antibiotic. As a rule, they are hydrophobic, have low molecular masses, and are toxic to a wide range of microorganisms. Several hundreds of phytoalexins have already been isolated from plants. From the chemical standpoint, they belong to different classes of secondary metabolites — flavonoids, terpenoids, polyunsaturated compounds, etc.[15] It is essential to emphasise that there are virtually no phytoalexins in a healthy plant and their appearance in the infected plant is a response to a fully defined signal. Such signals are called elicitors of phytoalexins and they can be of abiotic or biotic origin. Abiotic factors frequently damage the plant cell wall, while biological elicitors are either enzymes which hydrolyse the cell wall biopolymers or fragments of these biopolymers; sometimes the nature of these substances is that of lipids. The accumulation of phytoalexins in plants is a result of the *de novo* formation of enzymes ensuring their synthesis and of RNA coding for these enzymes. Thus the phytoalexin elicitors regulate the metabolism at the level of the

A I Usov Laboratory of Plant Polysaccharides, N D Zelinskii Institute of Organic Chemistry, Russian Academy of Sciences, Leninskii prosp. 47, 117913 Moscow, Fax (7-095)135 53 28; Tel. (7-095) 137 67 91.

Received 7 June 1993
Uspekhi Khimii **62** (11) 1119–1144 (1993); translated by A K Grzybowski

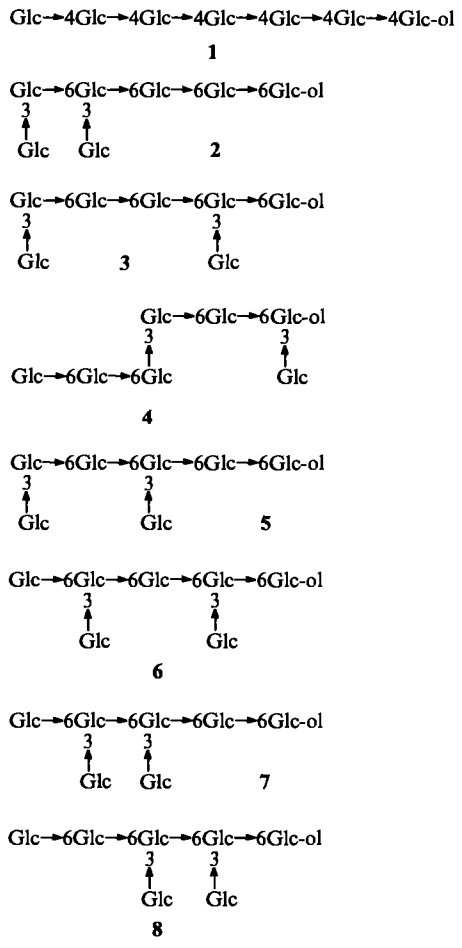
transcription of DNA. For many phytoalexins, there exist sensitive specific detection and quantitative determination methods, so that the elicitor—phytoalexin system can serve as an extremely reliable criterion for the estimation of the elicitor activity of a wide variety of chemical compounds.

The first oligosaccharin was discovered in the study of the responses of plants to attack by phytopathogenic fungi. When soya bean is infected by the pathogenic fungus *Phytophthora megasperma f. sp. glycinea*, the plant begins to produce phytoalexins (glyceollin and glycinol), which are derivatives of pterocarpan, the cell walls of the fungus, consisting mainly of carbohydrates, exhibiting a powerful elicitor activity.[16] The main component of these cell walls is a β-glucan, a sparingly soluble high-molecular-mass polysaccharide, having a branched structure with 1→6 and 1→3 bonds between β-D-glucopyranose residues.[17,18] In order to isolate a specific chemical substance, produced as a result of the elicitor activity, the fungal cell walls were subjected to partial acid hydrolysis, which led to the dissolution of ~50% of the initial material.[19] A mixture of oligosaccharides with degrees of polymerisation of 5–9, in which an appreciable elicitor activity persisted, was obtained with the aid of low-resolution gel chromatography of the hydrolysate in P-2 biogel. The testing technique involved the spectrophotometric determination of carbohydrates by reaction with anthrone, while that of pterocarpan derivatives—based on their intrinsic absorption at 285 nm[20]—enabled the authors to determine the content and activity of the elicitors in all the chromatographic fractions. Next the mixture was separated in terms of degree of polymerisation with the aid of high performance liquid chromatography (HPLC) on P-2 biogel and the heptasaccharide fraction was reduced with sodium tetrahydroborate to polyols (this did not affect the biological activity but facilitated significantly the subsequent separation) and was again separated with the aid of HPLC on a Whatman PAC column. Unfortunately such treatment led to the irreversible loss of about 50% of the oligosaccharides. The active fraction was then separated by reversed-phase chromatography on a Supelco Spherisorb ODS column, eluting with water, which again led to the loss of half the material but made it possible to concentrate the activity in a single peak. The final separation of the components of this peak on an Altex Ultrasphere ODS column (elution with a 2% solution of acetonitrile in water) made it possible to obtain seven components, six of which represented individual reduced heptasaccharides, while the seventh was shown by subsequent studies to be a mixture of such compounds. Only compound **6** (Scheme 1) exhibited elicitor activity.

Thus, in the course of the isolation of the elicitor **6**, the authors[19] were able to solve a problem of truly unique complexity: the only active oligosaccharide was isolated from a mixture of hundreds of closely related compounds. Although the authors of the above investigation had an unlimited supply of the initial cell wall material, the immensely laborious isolation procedure provided the final heptasaccharides in amounts of the order of 50 μg only. In order to establish the structures of these substances, it was necessary to develop a special strategy and methods for structural analysis (see, for example, Darvill and coworkers[21,22]), which made it possible to limit the requirements for the test substances to very small amounts.

The degree of polymerisation of both unsubstituted and methylated oligosaccharides was determined by mass spectrometry (MS) with bombardment by fast atoms. The monosaccharide composition (and at the same time the absolute configuration) was analysed with the aid of the GLC of the trimethylsilyl derivatives of (+)-2-butylglycosides of the hydrolysate[23] (only D-glucose and sorbitol were found in all cases). The pyranose forms of the monosaccharide residues and the β-configurations of all the glycosidic centres were demonstrated with the aid of ^{1}H NMR spectra of the methylated oligosaccharides. Despite the extremely small amounts of the

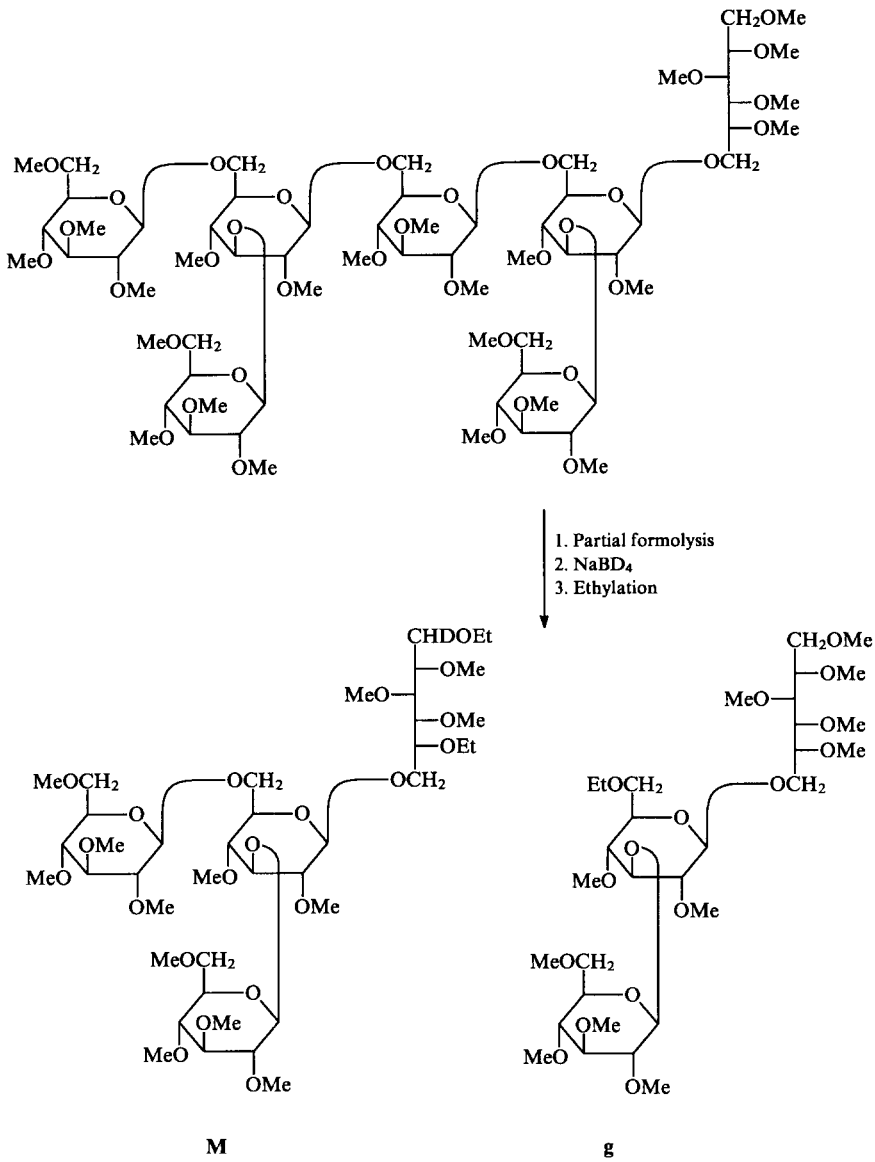
Scheme 1



test compounds, it was possible to obtain clear signals due to the anomeric protons and to make sure that the spectral range 5.0–5.5 ppm, in which the signals of the H(1) protons of the α-glucopyranose residues are observed, is unoccupied; furthermore, the H(1) signals observed in the spectrum had spin–spin coupling constants (SSCC) greater than 7.2 Hz, which is characteristic of *trans*-diaxial protons. A four-proton signal at 4.37 ppm, assigned to the anomeric protons of the glucose residues attached to O(6), and a two-proton signal at 4.73 ppm, characteristic of the anomeric protons of the residues bound to O(3) in a neighbouring unit, were observed in the spectra of the methylated compounds **2**–**8**. These signals were assigned by analogy with the methylated gentiobioside and laminaribioside respectively.[24]

The most complex problem, namely the elucidation of the disposition of the intermonomer bonds and the sequence of monosaccharide residues in the oligosaccharides, was solved by means of a mass-spectrometric study of the methylation products. The methylation stage itself was carried out by Hakamori's method modified for microamounts of the test substance,[21,22] while the methylated oligosaccharides were isolated from the reaction mixture with the aid of Sep-Pak C-18 cartridges.[25] The analysis of the derivatives obtained included partial formolysis, the reduction of the formolysis products with $NaBD_4$, ethylation of the reduced fragments at the liberated hydroxy-groups, and the determination of their structure with the aid of GLC-MS. As a result of the application of the method of derivative formation based on the incorporation of a deuterium atom, it was possible to distinguish all the fragments the reducing properties of which are due to elimination from the initial molecule on formolysis; the hydroxyls liberated in this process were marked by ethyl groups (Scheme 2).[26]

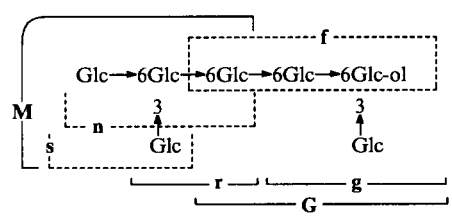
Scheme 2



M g

Naturally partial formolyis results in the formation, apart from the fragments **M** and **g** indicated in Scheme 2, also of many other substances. Overall, in the case of the oligosaccharide **6**, for example, trisaccharide (**f**, **g**, **n**, **r**, and **s**) and tetrasaccharide (**G** and **M**) cleavage products, shown in Scheme 3, were identified.

Scheme 3

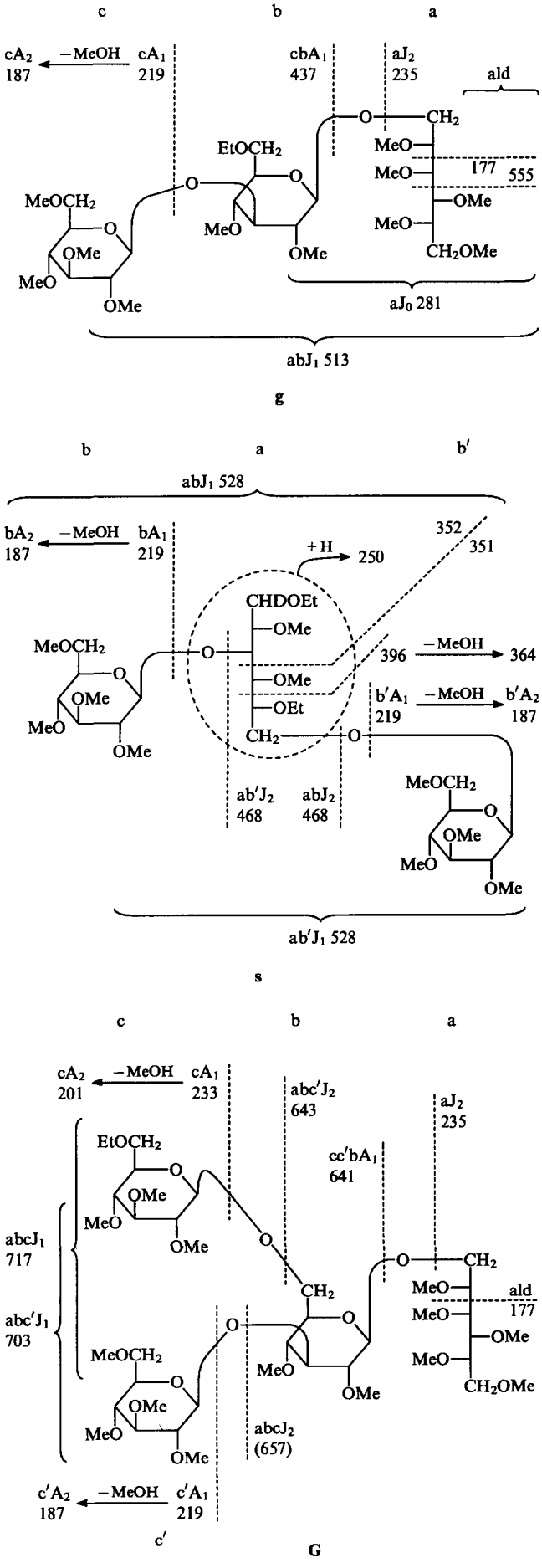


Analogous fragments are formed also from other methylated heptasaccharides. They can all be divided into three structural types: linear oligosaccharides, fragments branched at the polyol group, and substances with a branch at an inner glucose residue. The structures of the entire set of fragments, characteristic of each oligosaccharide, can be established with the aid of GLC-MS. Scheme 4 (see over) presents the most probable paths leading to the mass-spectrometric fragmentation and the diagnostic ions for representatives of each of the three structural types mentioned above (**g**, **s**, and **G**). The diagnostic ions in the mass spectrum belong to the A, J, and ald series. The nomenclature used for the fragments is the same as in the communication of Chizhov and Kochetkov[27] and in Aspinall's book.[28]

By applying the methods listed above in succession to the compounds isolated, Sharp et al.[26] were able to establish for them the structures shown in Scheme 1 (compounds **3** and **4** were not separated and their structures were determined by analysing the mixture).

The first of the heptasaccharides isolated is a fragment of the cellulose molecule and therefore differs by its origin from all the other heptasaccharides which are fragments of the β-glucan molecules in the fungal cell wall. Despite the evident similarity between the structures of these heptasaccharides, it was found that only one of them exhibits an elicitor activity and that this activity is observed clearly when 1 pmol of compound **6** per millilitre of the plant tissue is used (the highest of the known elicitor activities) and does not change in the presence of a twentyfold excess of the isomeric oligosaccharides. This surprising result demonstrated for the first time that the signalling molecules, in response to the appearance of which the protecting systems of the host plant are mobilised following attack by pathogenic fungi, may consist of purely carbohydrate fragments of the biopolymers in the fungal cell wall, while the

Scheme 4



system receiving the signal is capable of distinguishing clearly even between oligosaccharides which are structurally very similar.

The method of preparation of the heptasaccharide **6** from a natural source entailed, in principle, the possibility that the carrier of biological activity is some other substance, the chromatographic properties of which are only fortuitously identical with those of the heptasaccharide. In order to rule out this hypothesis, an unambiguous synthesis[29] of the heptasaccharide fragment of the fungal β-glucan was undertaken. Its successful completion coincided with the final determination of the structure of the natural product **6**.[26] Communications concerning the isolation,[19] determination of the structure,[26] and the synthesis[29] of this oligosaccharin and the comparative study of the biological activities of the natural and synthetic oligosaccharins[30] were published simultaneously in 1984.

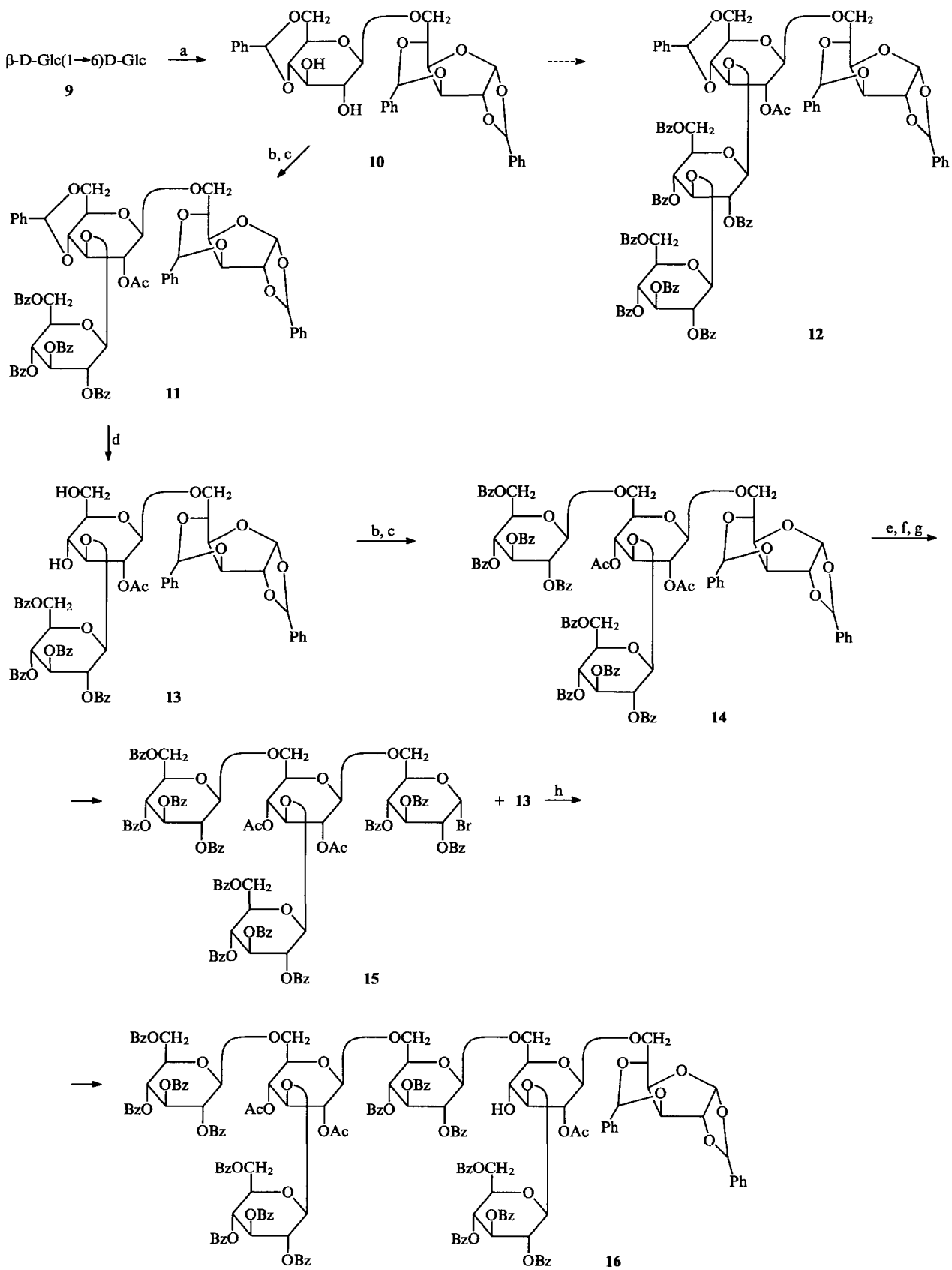
An elegant and extremely rational scheme (Scheme 5) has been developed for the synthesis of compound **6**. Its starting material was gentiobiose **9**. The condensation of this disaccharide with benzaldehyde led to the tri-*O*-benzylidene derivative **10**, containing two free hydroxy-groups. Partial acetylation of this substance afforded a mixture of the 2-*O*- and 3-*O*-acetyl derivatives, but glycosylation by treatment with 2,3,4,6-tetra-*O*-benzoyl-α-D-glucopyranosyl bromide in the presence of silver triflate occurred regiospecifically in the 3-position. Subsequent acetylation afforded the protected trisaccharide **11**. The tetrasaccharide analogue **12** was synthesised similarly, but the glycosylating agent was hepta-*O*-benzoyl-α-laminaribiosyl bromide.

Hydrolysis of compound **11** under fairly unusual conditions—on treatment with a solution of dichloroacetic acid in aqueous acetic acid—led to the selective removal of one of the three benzylidene groups occupying the 4- and 6-positions. This resulted in the formation of a derivative of the trisaccharide **13**—the key compound in the entire synthesis. Indeed, on the one hand, compound **13** served as a precursor of the reducing end of the future heptasaccharide, and, on the other, its glucosylation, occurring selectively at the primary alcoholic group, and subsequent acetylation afford the tetrasaccharide precursor **14** for the nonreducing end of the target heptasaccharide.

The removal of the benzylidene groups from compound **14** was probably accompanied by the partial hydrolytic cleavage of the 1→6 bonds, because the halogenose **15** was obtained in only 24% yield. However, other methods of synthesis of this compound were ineffective. Condensation of the glycosyl halide **15** with the partially protected trisaccharide **13** under glycosylation conditions, which had already been frequently used previously in this synthesis, led to a protected derivative of the required heptasaccharide **16**. The unblocking of the latter afforded the heptasaccharide **17**, which was reduced to a polyol indistinguishable in terms of its chemical properties and biological activity from the substance isolated as a result of the hydrolysis of the cell wall of the fungus *Phytophthora megasperma*.[30] The use of compound **12** instead of compound **11** in the same sequence of synthetic operations led to the octasaccharide **18**; the biological activity of the corresponding polyol was one-third of that of the heptasaccharide elicitor.

The synthesis of the biologically active oligosaccharide removed all doubt concerning the chemical nature of the new class of signalling compounds. Next, it was of great interest to elucidate the mechanism of its signalling activity and the structural elements of the oligosaccharin necessary for the manifestation of biological properties. The first data concerning the variation of their structure and biological activity, obtained on comparing compound **6** with its analogues **2**–**5**, **7**, and **8**, were extremely approximate, since the authors did not have the oligosaccharides in amounts sufficient for a detailed study. After the successful synthesis of compound **6**, it became possible to hope that analogues of this compound could be synthesised.

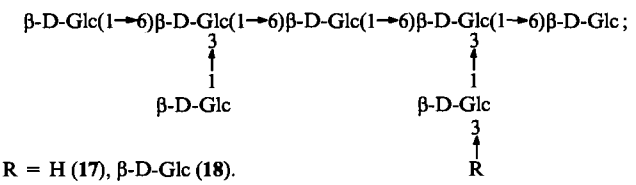
Scheme 5



(a) PhCHO, $ZnCl_2$; (b) tetra-*O*-benzoyl-α-D-glucopyranosyl bromide, CF_3SO_2OAg, 4 Å sieve, CH_2Cl_2;
(c) Ac_2O, Py; (d) $CHCl_2COOH - AcOH - H_2O$; (e) 90% AcOH; (f) BzCl, Py; (g) HBr, $AcOH - CH_2Cl_2$;
(h) CF_3SO_2OAg, 4 Å sieve, CH_2Cl_2

Scheme 5 continued over.

Scheme 5 (continued)



R = H (**17**), β-D-Glc (**18**).

Admittedly, it was necessary to develop for this purpose new synthetic procedures, because the elegant specific method of synthesis of the oligosaccharin **6** was rather unsuitable for the synthesis of its structural analogues.

Çhree years later, a communication concerning new methods of synthesis of the oligosaccharide **17** appeared[31] in which the authors used extremely effectively the latest advances in glycoside synthesis.[32] In the first stages of the construction of this complex molecule, as in the first synthesis, use was made of benzoylated glycosyl halides, which ensured the maximum yields and the stereospecificity of the glycosylation as a result of the simultaneous involvement of the benzoyl group at C(2) [33] and of silver triflate as the promoting agent.[34] In the last stages of the block synthesis of the heptasaccharide, the glycosylating agents were thioglycosides in the presence of methyl triflate.[35,36] As regards protecting groups, mention should be made of the extremely successful employment in this synthesis of the regiospecific opening of the 4,6-*O*-benzylidene acetals by reductive cleavage on treatment with the borane—trimethylamine complex and aluminium chloride[37] and also of the chloroacetyl groups attached to the primary hydroxyls, which are selectively removed in the presence of other ester groups on treatment with hydrazine dithiocarbonate[38] or thiourea.[39] The sequence of synthetic operations is clear from Scheme 6.

The starting material for the synthesis of the trisaccharide glycoside donor **22** was the 4,6-*O*-benzylidene derivative of methylthio-β-glycopyranoside **19**. Its glycosylation with 2,3,4,6-tetra-*O*-benzoyl-α-D-glycopyranosyl bromide and subsequent benzoylation led to the protected disaccharide **20**. The subsequent reductive cleavage of the acetal group and the repeated glycosylation by the same reagent afforded the required derivative of the branched trisaccharide **22**. In the synthesis of the tetrasaccharide glycosyl acceptor **26**, compound **20** was used as the glycosylating agent. Its condensation with benzyl-2,3,4-tri-*O*-benzoyl-β-D-glucopyranosyl bromide **23**, the subsequent reductive cleavage of the acetal group, and the glycosylation of the liberated primary hydroxyl with 2,3,4-tri-*O*-benzoyl-6-*O*-chloroacetyl-α-D-glucopyranosyl bromide **24** afforded the tetrasaccharide derivative **25**. The selective removal of the chloroacetyl group led to the acceptor **26**, the glycosylation of which with the thioglycoside donor **22** and subsequent removal of the protecting groups made it possible to obtain the synthetic heptasaccharide **17**, which was identical with the substance synthesised previously in terms of all the parameters.[29]

In order to produce the heptasaccharide in gramme amounts, the method of synthesis was modified (Scheme 7). Compound **21** was glycosylated with the chloroacetylated bromide **24** and the resulting chloroacetylated thioglycoside **27** was used both for the synthesis of the tetrasaccharide glycosyl acceptor **28** and as the glycosyl donor for the glycosylation of compound **28**.

Compared with the first synthesis of the heptasaccharide **17**,[29] the new approach provided incomparably greater possibilities for the preparation of analogues and derivatives of the compound. It is therefore not surprising that the communication of Fugedi et al.[31] was soon followed by new papers in which this approach was developed. The first of these[40] was devoted to the synthesis of the heptasaccharide **30**—an analogue of the oligosaccharin **17** differing from the latter by the position of the branching points. All the intermediates **20** and **22**–**24**, the glycosylation methods, and the combination of protecting groups described above were used in this synthesis (Scheme 8).

However, the use of the chloroacetylated thioglycosides **27** for the successive introduction of branched trisaccharide units with the required structure into the molecules being synthesised proved to be the most fruitful. In the next study,[41] this approach was employed to obtain two very interesting compounds. One of these is the glycoside of the biologically active heptasaccharide, where the aglycone is the methyl ω-hydroxynonanoate residue (Scheme 9). Evidently, this aglycone can be used as the spacer in the synthesis of affine sorbents designed for the isolation of cell components which exhibit a specific affinity for structure **6** or **17**, i.e. potential receptors which receive the chemical signal.

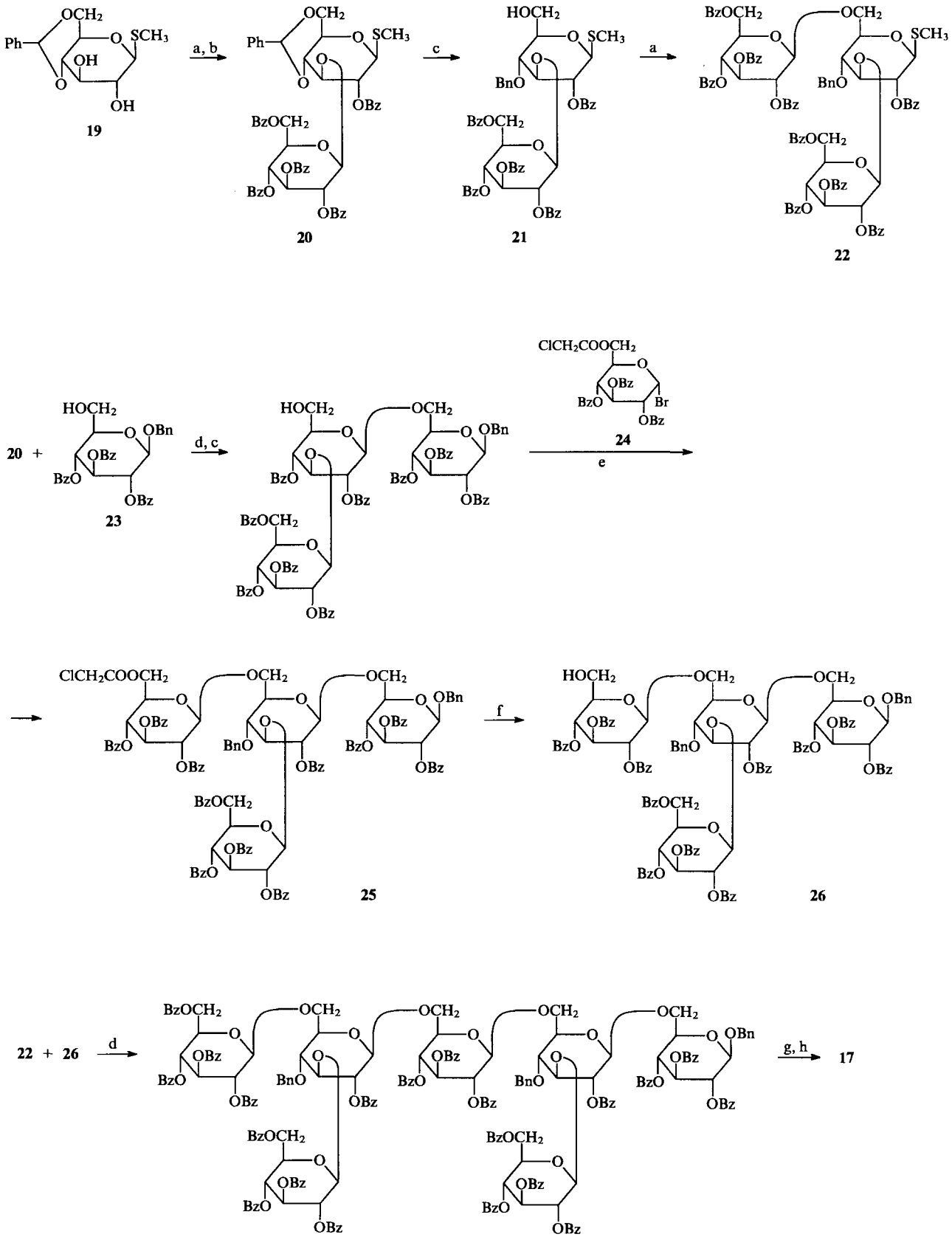
The second compound synthesised by Birberg et al.[41] is the decasaccharide **31** in which the trisaccharide structural element of compound **17** is repeated yet again. The problem involving the construction of such a complex molecule was solved by the threefold glycosylation of the corresponding precursors of the derivative of the branched trisaccharide **27** (Scheme 10).

A similar approach, in which use was made of the trisaccharide block **32** where the chloroacetyl group is attached to the primary hydroxyl of the glucose residue joined in the 6-position of a neighbouring unit and the other protecting groups are combined with the other hydroxyls, with another method (the trichloroacetimidate method) employed for the construction of the glycosidic linkage,[42] enabled Japanese investigators to obtain allyl α-glycosides of the hexasaccharide **33** and the nonasaccharide **34**, the carbohydrate chains of which are constructed in accordance with the same plan as in compound **6** (Scheme 11).[43] The same workers obtained analogues of the hexasaccharide **33**, containing the residues of β-D-xylose, *N*-acetyl-β-D-glucosamine, or β-D-glucosamine as one of the terminal nonreducing units.[44]

The first observations of the influence of structural modifications on the elicitor activity of the fungal β-glucan fragments date back to the period of the isolation of the heptasaccharide fractions[17] when it was established that the reduction of the heptasaccharides to the corresponding polyols does not affect the activity. This implied that the reducing end of the active heptasaccharide can apparently be subjected to appreciable changes without weakening the elicitor properties. This feature of the heptasaccharide **17** was used by two groups of investigators[44,45] to synthesise its conjugates with tyramine **35** and 2-(4-aminophenyl)ethylamine **37** via the reductive amination reaction. Iodination of these conjugates with radioactive iodine made it possible to obtain the labelled iodo-derivatives **36** and **38**, which are very essential for the investigation of the mechanism of the action of the oligosaccharin in the plant cell and of its fate (Scheme 12).

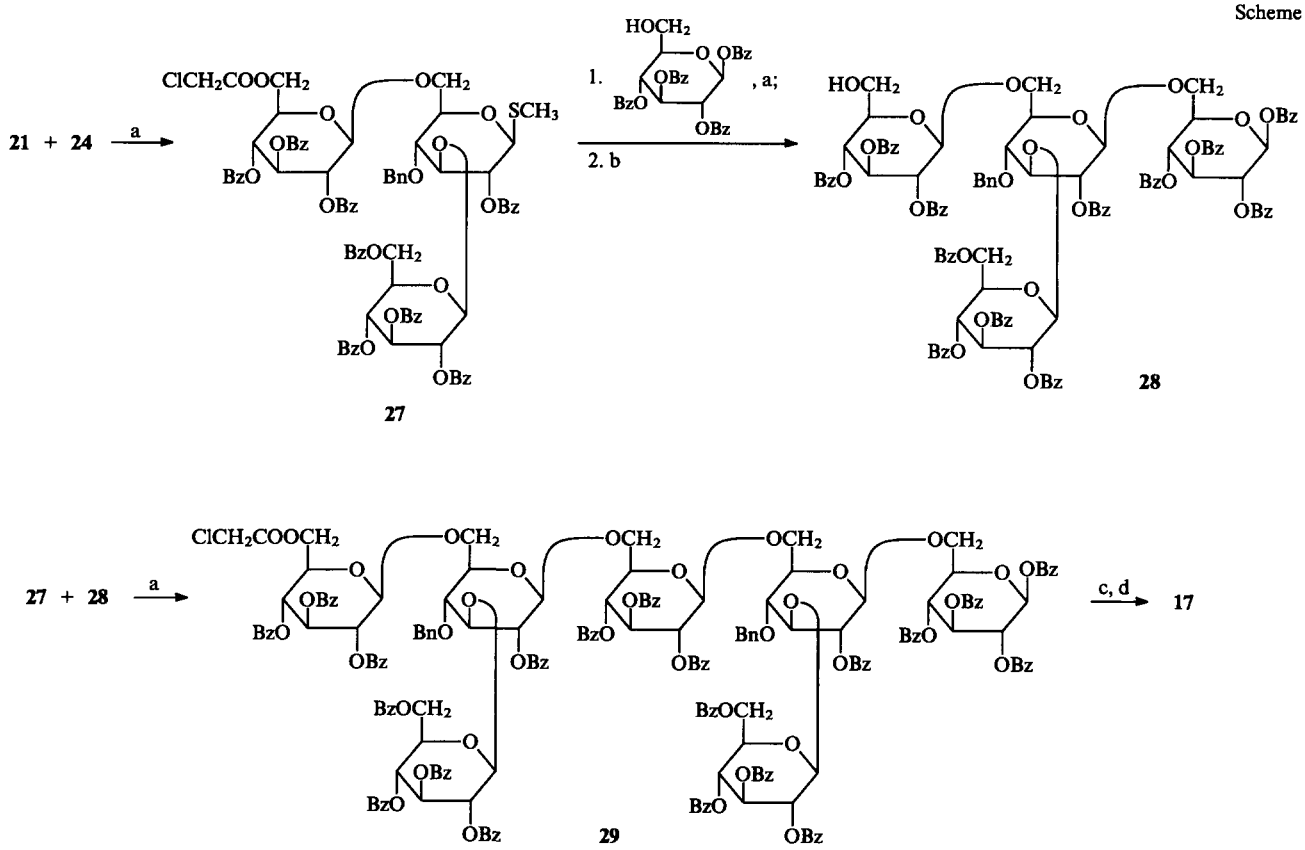
A comparative study of the elicitor activities of the majority of the synthetic analogues of the natural oligosaccharin mentioned above has been described.[44] As a result of quantitative measurements, it was established that the hexasaccharide allyl glycoside **33** is the smallest active molecule; virtually the same activity is exhibited by the heptasaccharide **17** and the higher oligosaccharides **31** and **34**. The branched trisaccharide fragment of the non-reducing end in these molecules is extremely important for the manifestation of the elicitor activity. Its modification, for example substitution of one of the terminal glucose residues by glucosamine or *N*-acetylglucosamine residues, lowers the activity by a factor of 10–1000. The activity also falls by a factor of 1000 if the glucose side residues are arranged next to one another, as in compound **30**, and are not separated by one unit, as in the natural elicitor. On the other hand, a wide variety of modifications of the reducing end of the heptasaccharide are permissible. Thus the activity is retained in the allyl α-glycosides of the hexasaccharide **33**; the conjugation of the heptasaccharide **17** with tyramine and subsequent iodination also have virtually no effect on the activity.

Scheme 6



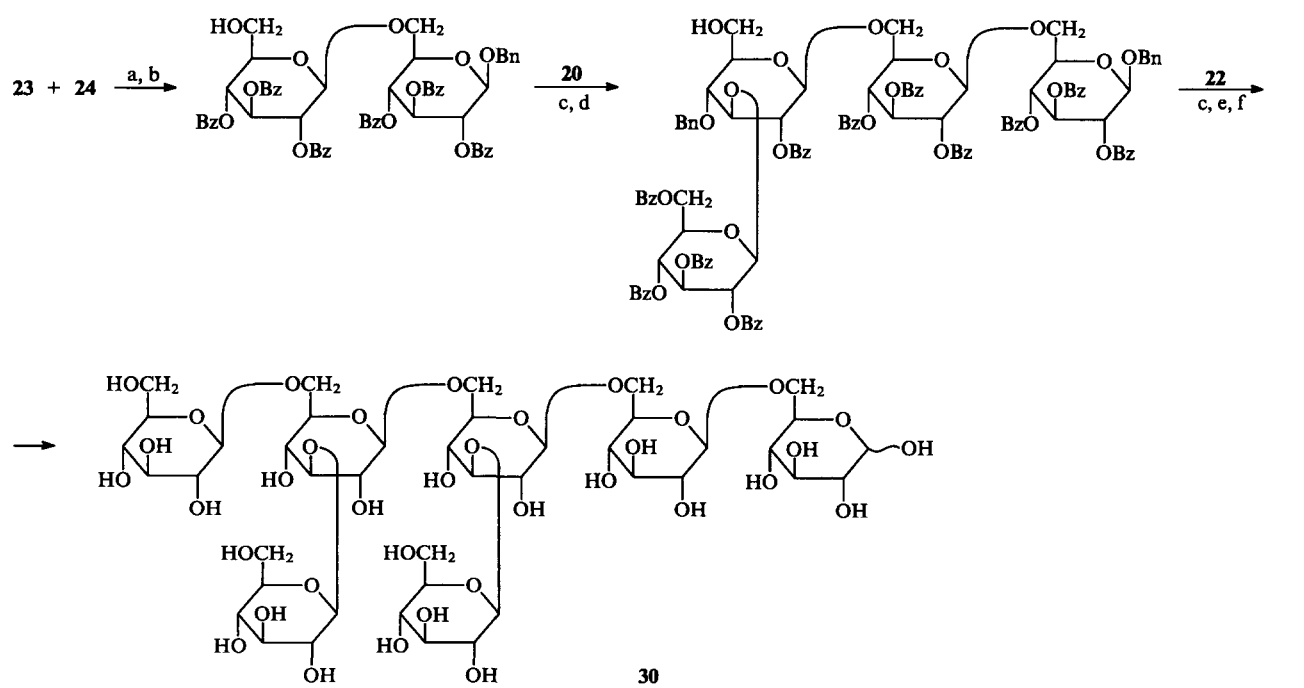
(a) tetra-*O*-benzoyl-α-D-glucopyranosyl bromide, CF_3SO_2OAg; (b) BzCl, Py; (c) $BH_3 \cdot Me_3N$, $AlCl_3$; (d) CF_3SO_2OMe, 4 Å sieve, CH_2Cl_2; (e) CF_3SO_2OAg; (f) $H_2NNH_2 \cdot H_2COS_2$; (g) MeONa, MeOH; (h) H_2/Pd – C.

Scheme 7



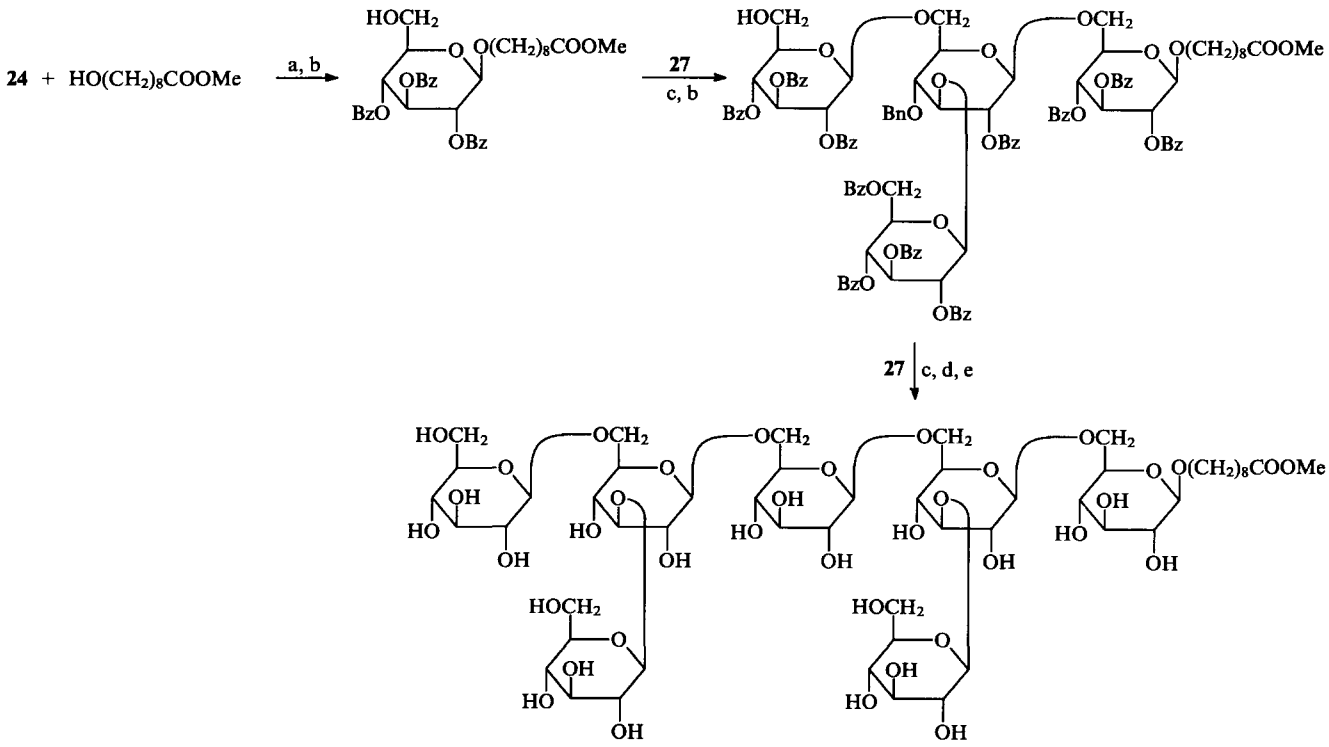
(a) CF_3SO_2OMe, 4 Å sieve, CH_2Cl_2; (b) $H_2NNH_2 \cdot H_2COS_2$; (c) MeONa, MeOH; (d) H_2/Pd – C.

Scheme 8



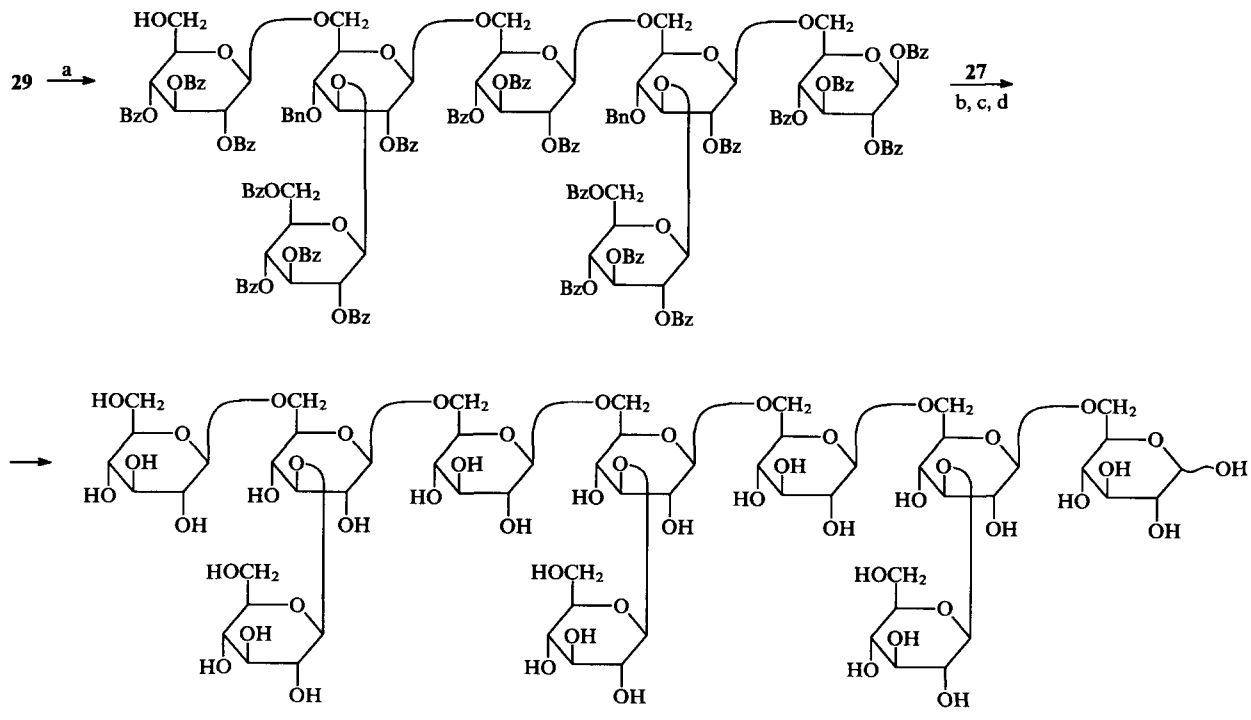
(a) CF_3SO_2OAg, 4 Å sieve, CH_2Cl_2; (b) $H_2NNH_2 \cdot H_2COS_2$; (c) CF_3SO_2OMe, 4 Å sieve, CH_2Cl_2; (d) $BH_3 \cdot Me_3N$, $AlCl_3$; (e) MeONa, MeOH; (f) H_2/Pd – C.

Scheme 9



(a) CF_3SO_2OAg ; (b) $H_2NNH_2 \cdot H_2COS_2$; (c) CF_3SO_2OMe ; (d) MeONa, MeOH ; (e) $H_2/Pd-C$.

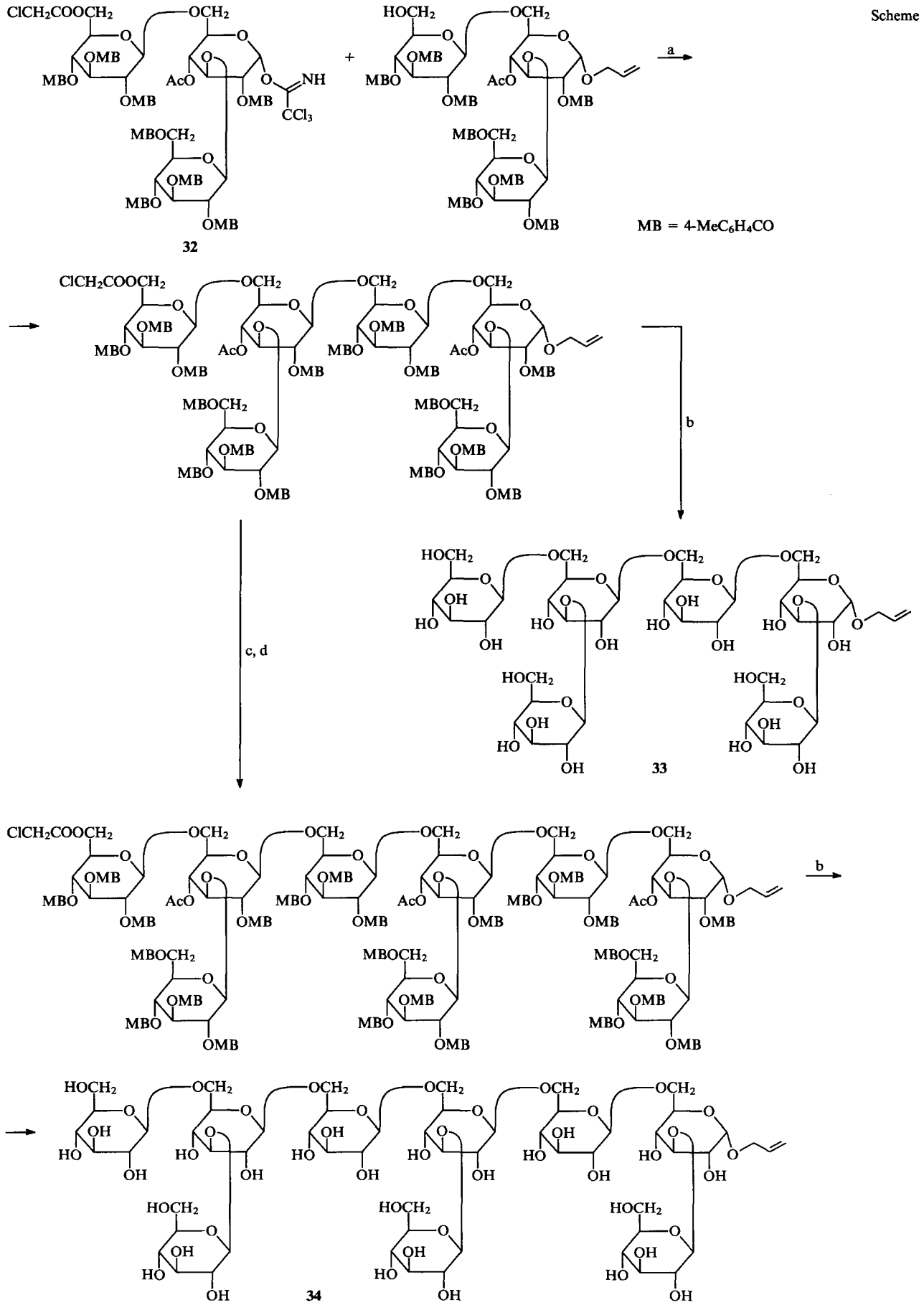
Scheme 10



31

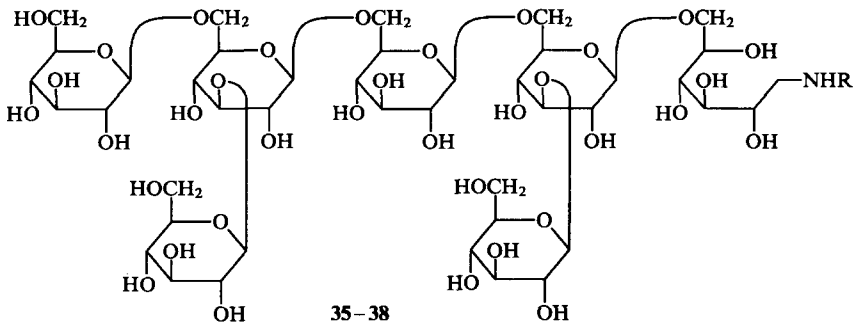
(a) $H_2NNH_2 \cdot H_2COS_2$; (b) CF_3SO_2OMe, 4 Å sieve, CH_2Cl_2 ; (c) MeONa, MeOH + THF; (d) $H_2/Pd-C$.

Scheme 11

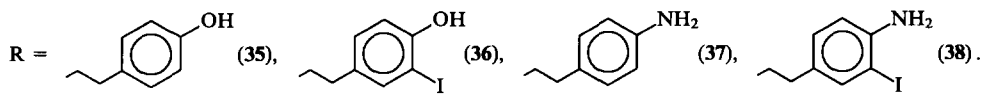


(a) $BF_3 \cdot Et_2O$, AW-300 sieve, $(CH_2Cl)_2$; (b) MeONa, MeOH; (c) H_2NCSNH_2, EtOH; (d) **32**, a.

Scheme 12



35–38



The first attempts to investigate the mechanism of the action of the oligosaccharide fragments of the fungal β-glucan on plant cells were made using a complex heterogeneous mixture of certain fragments,[46–49] but more reliable data were obtained with the aid of synthetic oligosaccharides.[45,50] In the latter studies, ^{125}I-labelled conjugates of the oligosaccharin with tyramine or 2-(4-aminophenyl)ethylamine were used. It was shown[51] that centres with a specific binding of oligosaccharins exist in the membranes of plant cells and that their binding process is characterised by saturation, reversibility, and an affinity ($K_\alpha = 7.5 \times 10^{-10}$ mol dm^{-3}) comparable to the concentration of compound **6** necessary for the manifestation of elicitor activity. All the binding centres are of the same type and are inactivated on proteolysis or on heat treatment, which is evidence in support of their protein (or glycoprotein) nature. The competitive inhibition of the binding process by numerous analogues demonstrates a direct relation between the affinity for the active centre and the elicitor activity. All these data confirm the hypothesis that the membranes of plant cells contain specific receptors for oligosaccharins. The high level of the specificity and of the discriminating capacity of the recognition system can be explained by the fact that the cells must recognise low concentrations of fragments of the foreign polysaccharide against the background of extremely large amounts of the 1 → 4-, 1 → 3-, and 1 → 3, 1 → 4-β-D-glucans present in the healthy plant under normal conditions.

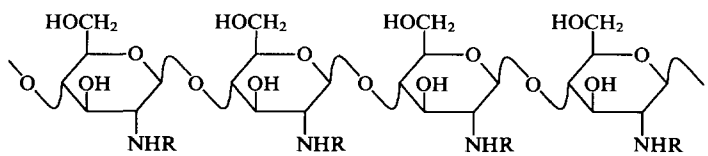
The initiation of the synthesis of phytoalexins is not the only biological effect of the oligosaccharide **17**. Other plant protecting mechanisms are also mobilised simultaneously (for a more detailed description of a multiplicity of the activities of oligosaccharins, see below in the subsequent sections of the review), in particular the synthesis of β-glucanase — the enzyme present also in healthy plant cells which is capable of cleaving the β-glucan of the fungal cell wall with formation of signalling oligomers — is induced. Whereas the protecting function of enzymes of this type had been treated previously as a direct effect of the phytopathogen on the cell wall, limiting its growth, after the discovery of oligosaccharins the role of β-glucanase appears to be more probably that of generating signalling molecules, which stimulate a multiplicity of mechanisms protecting the host plant.

In conclusion of this section, one may note that, as a result of extremely intensive chemical researches, the heptasaccharide **17** and its analogues have become fairly readily available. An excellent practical manual of the methods of synthesis and of the characteristics of these compounds, including the synthesis of conjugates with tyramine and the introduction of the ^{125}I isotope into the latter, has been published.[52] Therefore, new discoveries in the field of the mechanism of the action of substances of the type considered on plant cells are to be expected in the immediate future.

2. Oligosaccharide fragments of chitin and chitosan

Together with β-glucan, the cell walls of phytopathogenic fungi contain chitin — an insoluble high-molecular-mass homopolymer the linear molecules of which are made up of 1 → 4-linked residues of *N*-acetyl-β-D-glucosamine — and chitosan — the product of the deacetylation of chitin (Scheme 13).[53,54] In higher plants, these polymers are absent but fragments capable of cleaving the carbohydrate chains of chitin and chitosan (chitinases and chitosanases) occur very widely.[55,56] Since it is evident that these enzymes do not participate in the primary metabolism of the plants themselves, it has been suggested that their purpose is to protect the plants against pathogenic fungi. Indeed, by disturbing the finely balanced processes in the biosynthesis and lysis of the components of the growing cell walls of the fungus, the chitino-lytic enzymes of the plants can limit its growth.[57] On the other hand, the oligosaccharide fragments formed in the enzymic hydrolysis of chitin and chitosan serve as signalling molecules, in response to the appearance of which the mechanisms for the synthesis of phytoalexins and other protecting responses of the plant are switched on. This phenomenon should play a no less important role in the interaction of plants with pathogenic fungi.

Scheme 13



R = Ac, H.

In contrast to the branched β-glucan, the linear chitin and chitosan, which contain a single type of linkage, afford on fragmentation a comparatively less complex set of oligosaccharides, which can differ from one another only by the degree of polymerisation, the degree of acetylation, and (for incomplete acetylation) by the distribution of the acetyl groups. The oligosaccharide products of the fragmentation of the chitin and chitosan molecules can be obtained from these polysaccharides by chemical methods[58-61] or by enzymic hydrolysis.[62] However, the technical difficulties in the isolation of the individual oligomers are fairly considerable, so that the majority of studies on the biological activities have been carried out using either the whole cell walls of the phytopathogenic fungi or the polymeric chitin and chitosan as elicitors; oligosaccharide fractions containing 2–3 oligomer-homologues are frequently used.

The formation of phytoalexins on treatment with chitosan and its fragments has been observed both in the tissues of the whole plant[63] and in plant cell suspension culture.[64,65] Other protecting systems of the plants are switched on simultaneously—such as the formation of the inhibitors of proteinases[66,67] or the synthesis of the protecting (1 → 3)-β-D-glucan of callose;[65,68] the oligosaccharide fragments of chitin also stimulate the lignification of cell walls.[69-71] The induction of the formation of chitinases[72,73] and chitosanases,[74] which, together with the inhibitors of proteinases and 1,3-β-glucanases, belong to the group of proteins associated with the pathogenesis, is particularly clearly expressed.[75,76] It has been shown that the protecting action of the chitinases does indeed consist both in the direct inhibition of the growth of the fungus[77,78] and in the formation of the elicitors of numerous systems protecting the host plant by cleaving the biopolymers in the cell wall of the phytopathogen.[79] It is of interest to note that the transgenic tobacco plants, carrying the gene of the leguminous plant chitinase, exhibit an increased stability to attack by soil fungi.[80]

As a rule plant chitinases constitute a complex made up of several exo- and endo-enzymes. In the study of the induction of chitinases by individual chitin oligosaccharides, it was established[81] that the hexasaccharide is the best stimulator of the exo-chitinase activity, whereas the endo-chitinase activity is stimulated most effectively by the heptasaccharide; the octa- and nonasaccharides also exhibit an appreciable elicitor activity. The lower oligosaccharides (including the tetramer) and the fraction of higher oligosaccharides with a degree of polymerisation of 13–20 proved to be almost inactive. The response of the plant to the introduction of elicitors was fairly rapid: the maximum activity of the induced chitinases was observed after 12–24 h, the enzymes being detected not only at the site where the oligosaccharides had been introduced (the cotyledons of pumpkin seedlings) but also the remote parts of the plant (leaves). It has been shown that the biosynthesis of chitinases is associated with the activation of the corresponding genes and the formation of mRNA,[82,83] but it has not so far been established whether this phenomenon is due to the permeation of the chitin oligomers into the cell nucleus; the mechanism of the propagation of the signals through the plant tissues is likewise unknown.

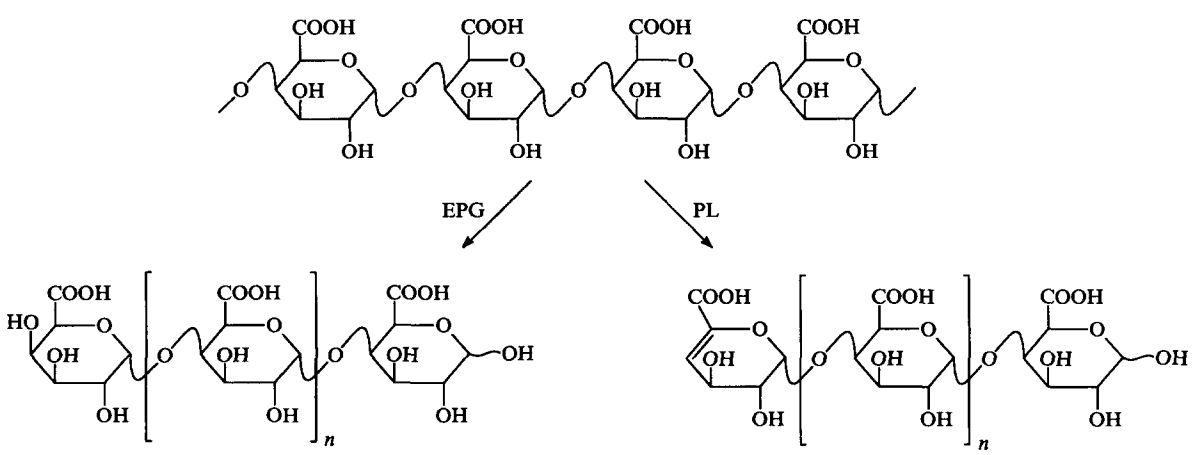
In the manifestation of other types of biological activity, a relation has also been observed beween the effect and the degree of polymerisation or structure of the oligosaccharide, although this problem has not been studied in detail. Thus the lignification of damaged wheat leaves is induced by chitooligosaccharides with a degree of polymerisation in excess of 4 but not by the corresponding fragments of chitosan.[70] However, oligomers of chitosan (degree of polymerisation in excess of 7) and not those of chitin serve as the elicitors of the formation of the phytoalexin pisatin in pea pods.[79,84] However, the deacetylated and partially acetylated oligosaccharides containing more than four monosaccharide residues stimulate equally effectively the formation of the inhibitors of proteinases in tomato and potato leaves.[66,67]

3. Oligogalacturonides

Pectin substances are important structural components of the primary plant cell wall.[5,85] The simplest representative of pectins is homogalacturonan or polygalacturonic acid—a linear polymer consisting of 1 → 4-linked α-D-galacturonic acid residues in the molecules of which some of the carboxy-groups may be present as the methyl ethers. Many microbial phytopathogens (both fungi and bacteria) produce enzymes capable of cleaving homogalacturonan either via a hydrolytic reaction [endopolygalacturonases (EPG)] or via an elimination reaction [pectate lyases (PL)]. The oligosaccharides formed possess the activity of phytoalexin elicitors,[86] the maximum of which corresponds to oligomers with a degree of polymerisation of 12 (Scheme 14).[87-90] Plants contain specific EPG inhibitors,[91] which regulate the activity of the enzymes produced by the phytopathogens, preventing an unduly far reaching cleavage of the polygalacturonic acid and thereby promoting the accumulation of higher oligosaccharides possessing the elicitor activity.[92]

Together with the formation of phytoalexins, other plant protecting mechanisms are switched on under the influence of oligogalacturonides, e.g. endo-(1 → 3)-β-gluconases, chitanases, and lysozyme are induced. They cleave the cell walls of phytopathogenic fungi and bacteria,[93,94] liberating the elicitors of the protecting reactions described in the previous sections. The lignification of protected tissues is also enhanced in the presence of oligogalacturonides.[95,96] It is important to note that the activities of the oligosaccharide elicitors, originating from the fungal or bacterial cell wall, on the one hand, and from the host plant, on the other, exhibit a synergism, i.e. the plant protecting reactions are switched on at lower concentrations of the oligosaccharides of different structure when these act together.[93,97]

Scheme 14



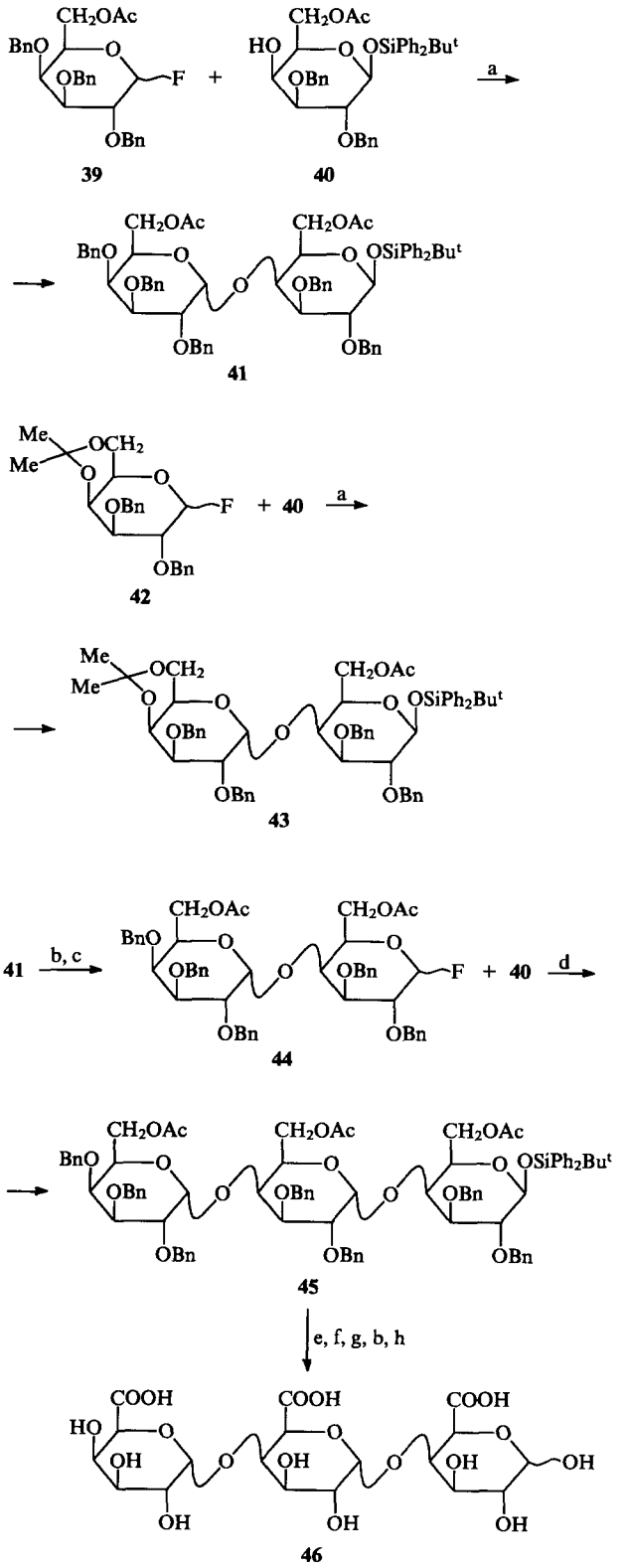
Several other types of biological activity of oligogalacturonides have been described. Compounds with a degree of polymerisation of 2–20 induce the formation of proteins inhibiting insect proteinases; it is believed that the plant is protected in this way against damage inflicted by plant eating insects.[98] In the presence of oligogalacturonides, cell suspension cultures produce endocellular isoperoxidases[96] and hydrogen peroxide.[99] Low concentrations of oligogalacturonides with a degree of polymerisation of 12–15 induce sharp changes in the permeability to K^+ and Ca^{2+} of the cell plasma membrane and its depolarisation.[100] Oligosaccharides with a degree of polymerisation of 14–15 induce the phosphorylation of the 34 kDa protein isolated from the plasma membrane.[101] It still remains to be elucidated to what extent these effects on the cell surface are associated with the elicitor activity of the oligogalacturonides described above.

The structural requirements imposed on the biologically active oligogalacturonides differ significantly from those for the heptasaccharide fragment of the fungal β-glucan described above. Thus the presence of the 'normal' α-D-galacturonic acid residue or even of the Δ^4-unsaturated uronic acid at the nonreducing end of the oligogalacturonide (Scheme 14) hardly affects the activity. On the other hand, reduction with sodium tetrahydroborate to alditol diminishes the activity.[102] The latter may be associated with the general decrease in the charge of the molecule as a result of the lactonisation of the reducing end.[8] The activity also falls on esterification[89] or reduction of the carboxy-groups.[90] A critical degree of polymerisation is apparently necessary for the acquisition by the oligogalacturonide of a stable conformation ensuring a fully defined spatial disposition of the charged groups, because acid oligosaccharides of a different chemical nature (fragments of chondroitin sulphate, hyaluronate) or acid polypeptides (polyglutamate) lack of elicitor properties.[102]

Oligogalacturonides, which are essential for the study of their activity on plant cells, can be obtained in preparative amounts from commercial pectin or polygalacturonic acid preparations in two ways: by partial acid hydrolysis or by enzymic cleavage.[52,103] An advantage of the first method is simplicity and low cost, while that of the second is high yields of the oligosaccharides and the absence of severe influences, which may induce undesirable structural changes in the native molecules. The most difficult task is the separation of the mixture of oligosaccharides with a degree of polymerisation of 10–15 into individual components, which is carried out at the limit of the resolving capacity of the modern chromatographic technique. It has been shown that even in the case of a successful isolation of the homopolymer fractions, the principal target components can contain up to 15% of impurities, which, whilst having the same degree of polymerisation, differ in the structure at the reducing end and also in certain unknown structural elements.[9,10] All this renders the chemical synthesis of oligogalacturonides extremely attractive.

The synthesis of oligomer-homologues of α-D-galacturonic acid appears at first sight to be a completely hopeless task for two reasons: in general, owing to the lack of convenient synthetic methods for the construction of α-glycosidic linkages and, in particular, because the methods for glycosylation by galacturonic acid derivatives have been little investigated. Nevertheless the problem was solved successfully when Nakahara and Ogawa proposed an extremely novel strategy for the synthesis.[104,105] They used data showing that benzylated glycopyranosyl fluorides react with alcohols in the presence of $SnCl_2$ and $AgClO_4$, affording predominantly 1,2-*cis*-glycosides.[106] It was established for galactose derivatives that the protected fluoride **39** interacts under these conditions with the partially protected derivative **40** to form a mixture of α- and β-disaccharides from which the α-isomer **41** was isolated in a satisfactory yield (Scheme 15). The fluoride **42** reacted even more selectively, giving rise almost exclusively to the α-linked

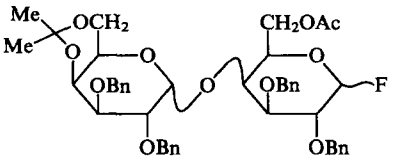
Scheme 15



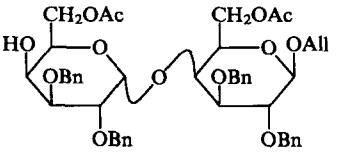
(a) $Sn(OTf)_2$ or Bu^n_3SnOTf; (b) Bu^n_4NF–AcOH, THF; (c) Et_2NSF_3, THF; (d) $SnCl_2$, $AgClO_4$, Et_2O; (e) MeONa, MeOH; (f) CH_3SOCH_3, $(COCl)_2$; (g) $NaClO_2$; (h) H_2/Pd–C.

protected disaccharide **43**. It proved easy to convert compound **41** into the disaccharide fluoride **44**, the repeated condensation of which with compound **40** led to the α-linked trisaccharide **45**. On deacetylation of this substance with subsequent two-stage oxidation of the three primary alcohol groups, initially to the

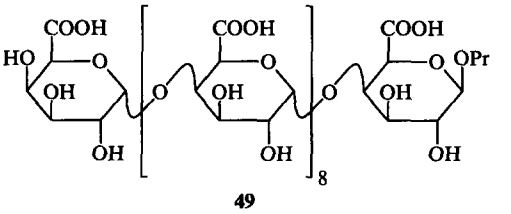
Scheme 16



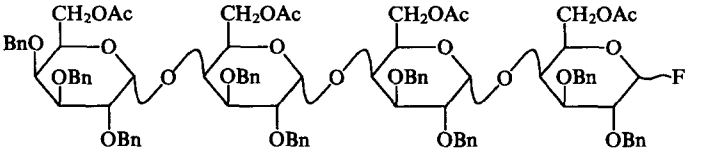
47

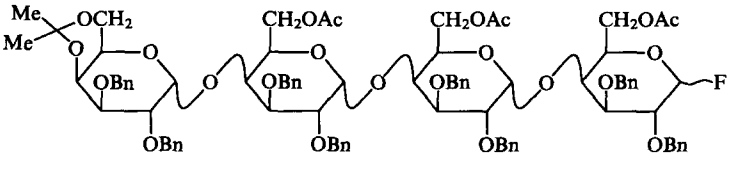


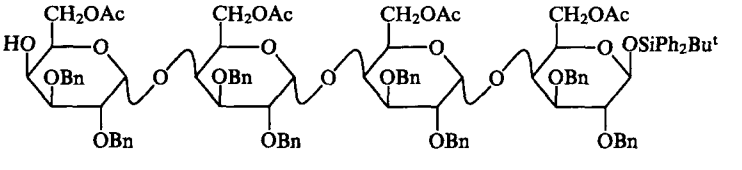
48

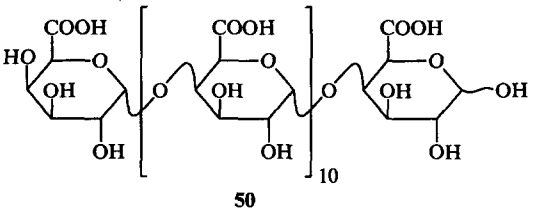


49









50

aldehyde groups by treatment with dimethyl sulfoxide and oxalyl chloride,[107,108] and then to carboxy-groups by treatment with sodium chlorite in the presence of hydrogen peroxide[109] yielded the trigalacturonide **46**. Using the same procedures, the authors synthesised subsequently a model disaccharide, which, however, was not obtained in a free form but only in the form of the n-propyl glycoside **49** (Scheme 16). The molecule of this compound was constructed using the disaccharide units **44**, **47**, and **48**.[110,111] Compounds **48** and **44** served as the precursors of the reducing and nonreducing ends of the future decasaccharide. The central part of the molecule was constructed by the threefold employment of compound **47** as the glycoside donor: first in the reaction with compound **48** and then, after each glycosylation, the new glycoside acceptor was prepared by removing the isopropylidene group from the terminal non-reducing galactose residue and by partial acetylation at the primary alcohol group. The final stage of the synthesis was the simultaneous oxidation of all ten primary alcohol groups.

The total synthesis of the dodecasaccharide elicitor **50** may be regarded as the completion of this series of studies. In this case, the molecule was assembled from tetrasaccharide units (Scheme 16).[112,113] However, the amount of the oligosaccharin synthesised in this way was small and data concerning the detailed study and the biological activity of the synthetic specimen have still not been published.

Derivatives containing a radioactive label are necessary for the investigation of the mechanism of the activity of oligogalacturonides. The reductive amination method using tyramine and subsequent introduction of radioactive iodine, used for the heptaglucoside **17** (see above), are unsuitable for oligogalacturonides; instead it has been suggested that hydrazones be obtained by reaction with tyrosine hydrazide and then iodinated.[52,114] It was shown in at least one of the biological tests that the conversion of the dodecagalacturonide into the hydrazone does not affect the biological activity.[114]

* * *

Summarising the above section, we may note that, in the interaction of the plant with phytopathogens, there is a possibility of the enzymic cleavage of the biopolymers in the cell walls of both partners. Some of the oligosaccharides thus liberated possess a specific biological activity and act as the elicitors of the protecting reactions of the host plant, oligosaccharides of different origin manifesting a distinct synergism in their activity. Although only one of the types of the plant protecting reactions is analysed in many experimental studies, it appears that in all cases there is a complex response to the appearance of oligosaccharins, whereupon, together with the synthesis of phytoalexins, enzyme systems cleaving the phytopathogen cell wall are activated and the tissue lignification process is intensified, which creates a barrier to further penetration by the phytopathogen, etc. By virtue of their multiple (pleiotropic) action on plants, oligosaccharins thus resemble the 'classical' phytohormones — auxins, gibberellins, cytokinins, abscisic acid, and ethylene. However, it must be emphasised that oligosaccharins are active at significantly lower concentrations. Another analogy with phytohormones involves the lack of species specificity: a similar activity of oligosaccharins has been demonstrated in many representatives of the plant kingdom, the relationship between which is extremely remote. Although the mechanism of the activity of oligosaccharins has still not been established, it is likely that in most cases a highly specific binding of the oligosaccharin to the membrane receptor protein takes place, which in fact constitutes the 'signal of fear' ['give away signal' in Ref. 8 (Ed. of Translation)] for the switching on of the plant protecting mechanisms.[8-10]

III. Oligosaccharins as regulators of plant growth and morphogenesis

1. Oligogalacturonides

The ability of plant cells to be differentiated and converted into specialised plant organs is controlled by many factors, among which hormones, light, and temperature are of primary importance.[115,116] The influence of various chemical compounds on organogenesis can be followed on explants of tobacco peduncles which, during cultivation on an artificial medium, produce, in the course of 24 days, flowers, vegetative shoots, or roots depending on the auxin and cytokinin concentrations and on the pH.[117] A sensational report stating that the oligosaccharide fragments of plant cell walls (tentatively the fragments of the pectin polysaccharides) alter the specificity of the action of phytohormones in relation to organogenesis appeared in 1985.[118] However, several years elapsed before it was possible to characterise more thoroughly the chemical structure of the active oligosaccharides and to achieve reproducible results in this fairly capricious biological test.[119,120]

It was believed for some time that fairly complex fragments of pectin substances containing, apart from D-galacturonic acid, the residues of neutral monosaccharides serve as regulators of organogenesis. However, it was shown subsequently that the active principle nevertheless comprises the simple linear oligogalacturonides, which have already been considered as elicitors of phytoalexins. It is now known [119-121] that oligogalacturonides with a degree of polymerisation of 10–14 induce the formation of flowers and inhibit the formation of roots under conditions where without the addition of oligosaccharins tobacco explants form only roots or altogether fail to produce new organs. Oligogalacturonides act at concentrations of the order of 10^{-7} M, the highest activity being shown by compounds with a degree of polymerisation of 12–14. The existence of two types of activity in these oligosaccharins is probably associated with the fact that the same groups of genes are activated both in organogenesis in a healthy plant and in the biosynthesis of proteins associated with pathogenesis.[122]

Several other examples of the influence of oligogalacturonides on plant development processes are known. Thus a mixture of these oligosaccharides retards the auxin-induced growth of segments of pea plant stems, acting at a fairly high concentration (10^{-4} M).[123] This type of activity has been investigated in greater detail for xyloglucan fragments (see below). Oligogalacturonides induce the formation of ethylene in tomatoes (tomato fruits)[124,125] and in a pear cell culture suspension.[126] Hence they can participate in the complex process involving the hormonal regulation of the ripening of fruits.[127]

2. Oligosaccharide fragments of xyloglucan

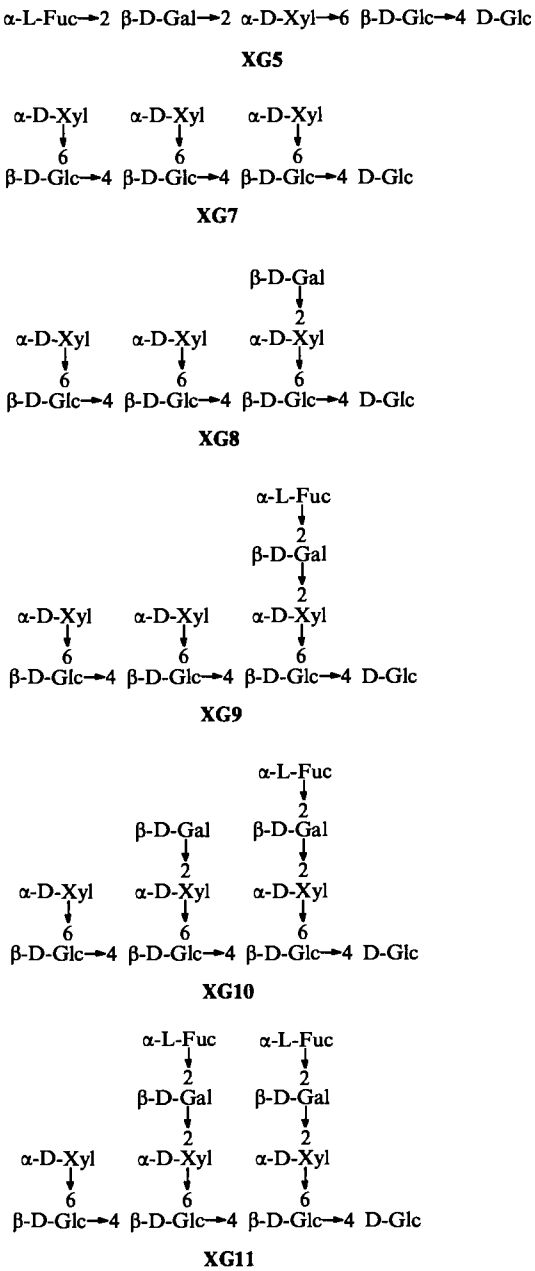
Xyloglucan is a universal component of the hemicelluloses in higher plants.[5,128-130] Its content in the primary cell walls of dicotyledonous plants is usually 20%–25%, while in the *Gramineae* its content may be significantly lower (2%–5%). Xyloglucan is deposited in large amounts in the seeds of certain plants, where it serves as a reserve of nutrient material used during growth. Apart from glucose and xylose, xyloglucans have been found to contain galactose, fucose, and arabinose. Whilst having a common regular design, xyloglucans of different origin can differ in the proportions of monosaccharides. In particular, storage xyloglucans usually virtually lack fucose residues. We shall consider below the structures of typical xyloglucans in dicotyledonous plants, which have been isolated from the cell walls or from the medium cell in suspension cultures.[131]

The basis of the xyloglucan molecule is a linear chain made up of 1 → 4-linked β-D-glucopyranose residues, which have the same structure as cellulose. About 75% of the glucose residues in this chain have been substituted in the 6-position by α-D-xylopyranose residues (a small proportion of these substituted glucose residues carry in addition α-L-arabinofuranose, β-D-xylopyranose, or 3-*O*-α-L-arabinofuranosyl-β-D-xylopyranose residues in the 2-position). From one-third to half of the xylose residues are substituted in their turn in the 2-position by β-D-galactopyranose residues. Finally, many lactose residues have in the 2-position a substituent in the form of a α-L-fucopyranose residue. In those cases where it was possible to isolate the polysaccharide without using alkaline extraction, it was demonstrated that certain galactose residues may carry one or two acetyl groups in the 6-, 3-, or 4-positions.[132,133]

In the structural analysis of xyloglucan, enzymic cleavage has played a most important role. The effect of a mixture of fungal enzymes, known under the commercial name 'Driselase' (Sigma), which results in the formation of 6-*O*-α-D-xylopyranosyl-D-glucose (isoprimeverose), is a diagnostic feature for the polysaccharide.[134] Other carbohydrate components of the plant cell wall do not contain such a structural fragment. Since the above disaccharide can be readily distinguished in terms of its chromatographic behaviour from other disaccharide products of enzyme treatment, the detection of isoprimeverose in the hydrolysate can serve as convenient and reliable evidence for the presence of xyloglucan in the raw material or in the mixture of polysaccharides analysed.

Fungal cellulases cleave xyloglucan at the glycosidic linkages connecting the unsubstituted β-D-glucopyranose in the main chain. The main products of such cleavage are a heptasaccharide and a nonasaccharide [designated in the literature by XG7 and XG9 (Scheme 17)], which demonstrates the considerable regularity of the distribution of substituents in the main chain, where each fourth glucose residue is free. Together with the XG7 and XG9 oligosaccharides, it is possible to detect in the hydrolysate the XG5, XG8, XG10, XG11, and higher oligosaccharides containing the L-arabinose residues, although their amounts are smaller.[21,131,134-138]

Scheme 17



Paper chromatography,[139,140] chromatography in a thin silica gel layer,[141] gel chromatography on P-2 biogel,[131,142] and high performance liquid chromatography (HPLC)[143] have been proposed for the separation of the products of the enzymic hydrolysis of xyloglucan. This includes the separation of the products in the form of pyridylamino-derivatives obtained by reductive ammination using 2-aminopyridine.[144] The determination of the structures of these complex oligosaccharides is due to several groups of investigators. We may note that in this field too the leading place is occupied by the team headed by Prof. Albersheim, who developed the most effective physicochemical methods for the characterisation of the structures of xyloglucan fragments—^{1}H NMR spectroscopy and mass spectrometry with bombardment by fast atoms.[137,138] In order to obtain well resolved NMR spectra, it has been suggested that the oligosaccharides be reduced with sodium tetrahydroborate to the corresponding alditols (this procedure also helps to improve the separation and purification of oligosaccharides with the aid of HPLC). The observed rules governing the positions and forms of the signals due to the anomeric protons[137,145] make it possible to establish the structures of the majority of oligosaccharides from one-dimensional ^{1}H NMR spectra.

Reduced oligosaccharides are also used for mass spectrometry with bombardment by fast atoms. The spectra of the negative ions of compounds which have not been converted into their derivatives then indicate the presence of intense pseudomolecular ions $[M - H]^-$, while the fragment ions formed as a result of the dissociation of the intermonomer bonds originate from the reduced end of the molecule. On the other hand, for acetylated oligosaccharide alditols most information is yielded by the spectrum of the positive ions, which contains the intense pseudomolecular ion $[M + NH_4]^+$, while the fragment ions originate from the nonreducing end of the molecule. The combination of two such mass spectra makes it possible to determine the sequence of the monosaccharide residues in the test compounds.[136,145,146] The effectiveness of these methods has been demonstrated particularly strikingly in the latest studies by the group of investigators mentioned above, which were devoted to the establishment of the structures of the higher oligosaccharide fragments of xyloglucan containing between 17 and 20 monosaccharide residues.[145,146]

The primary wall of a plant cell constitutes an extremely involved complex of biopolymers of several types: celluloses, xyloglucan, polysaccharides of the pectin group, and structural protein.[147,148] In all probability the xyloglucan molecules in the cell wall are bound covalently to the pectins and the latter are bound to the structural protein, whereas the cellulose microfibrils form stable noncovalent complexes with xyloglucan molecules via hydrogen bonds. It has been suggested that cell growth is ensured by the partial cleavage of the xyloglucan molecules, which enables the cellulose microfibrils to be displaced relative to one another. Indeed, it is well known that auxins stimulating cell growth activate cell cellulases and, as stated above, these enzymes are capable of cleaving xyloglucan.[149-151]

In this connection, the discovery of a specific biological activity of the XG9 nonasaccharide proved to be extremely interesting: at a very low concentration of the order of 10^{-8} M, this compound inhibited the auxin-induced growth of segments of pea plant stems.[152] Surprisingly, this effect diminished not only at low but also at high XG9 concentrations; the latter observation implied, incidentally, that the inhibition of growth is not a consequence of the cytotoxic activity of the preparation. The closely related XG7 oligosaccharide completely lacked the antiauxin activity. The hypothesis arose that the biologically active XG9 fragment of the xyloglucan participates in the regulation of cell growth, acting in accordance with the negative feedback principle: an increase in the amount of auxin should induce the appearance of the inhibitor which prevents unrestricted growth.[152]

The test for the antiauxin activity is not unduly reliable and is not very convenient in practice, but the existence of the antiauxin activity of XG9 described above has been confirmed in two other laboratories—both in similar experiments on the inhibition of the lengthening of stem segments[153,154] and in experiments on the regeneration of the cell walls of protoplasts.[155] It has also been possible to observe the formation of the nonasaccharide fragment of xyloglucan *in vivo*.[134] The set of oligosaccharides obtained by the enzymic hydrolysis of xyloglucan made it possible to carry out interesting observations on the relation between structure and biological activity.[142,156]

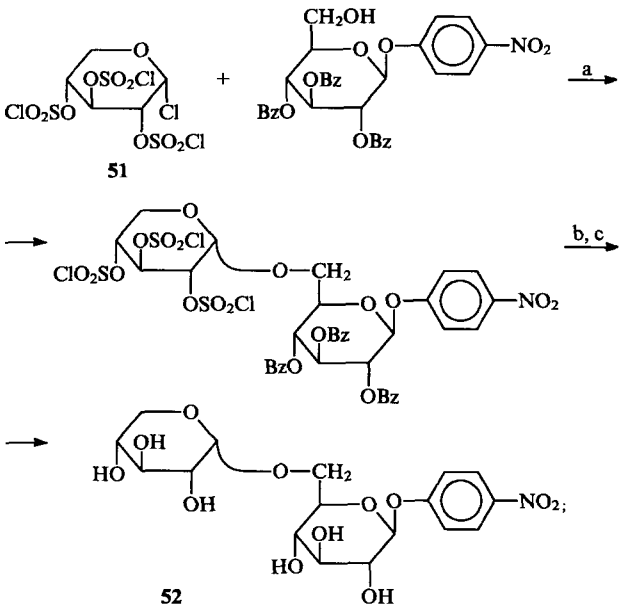
It was shown that the presence of the α-L-fucose residue is a necessary condition for the manifestation of the antiauxin activity, because all oligosaccharides lacking fucose proved to be inactive. However, the XG10 oligosaccharide, containing the fucose residue but having also an additional galactose residue in the neighbouring chain likewise failed to exhibit an antiauxin activity; on the other hand, XG11 with two fucose residues in the molecule had an activity higher than that of XG9.[157]

Other structural elements were less important: the activity of the reduced XG9 did not differ from that of the initial oligosaccharide; the activity did not fall even after the enzymic elimination of the α-D-xylo-pyranose residue most remote from the reducing end of XG9.[157] A biological activity was also shown by the fucose-containing XG5 and 2-*O*-α-L-fucopyranosyl-lactose—a trisaccharide which is not a xyloglucan fragment but has been isolated from human milk; admittedly, these oligosaccharides were active at higher concentrations. In the case of XG5, an optimum in the concentration dependence of the antiauxin activity, so characteristic of XG9, was also not observed.[142,146]

At significantly higher concentrations (1—200 μM), the XG9 oligosaccharide activates cellulase;[158] a similar effect is shown to a smaller extent by XG5 and XG7. This second activity of XG9 helps one to understand why the oligosaccharide loses its antiauxin activity at relatively high concentrations.[159] At extremely low concentrations (of the order of 1 nM), XG9 and XG10 inhibit the lengthening of segments of the pea plant stems induced by acidification,[160] from which it follows that the antiauxin activity of XG9 is not associated with the suppression of the entry of hydrogen ions into the cell wall under the influence of auxin[161] but involves some hitherto unknown common stages in the influence of auxin and the pH on cell growth.

The biological activity of the xyloglucan fragments aroused an increased interest by chemists engaged in synthetic chemistry in the problem of the synthesis of these oligosaccharides. As early as 1986, a communication was published concerning the synthesis of *p*-nitrophenyl β-isoprimaveroside **52** (Scheme 18).[162]

Scheme 18



(a) Ag_2CO_3, $AgClO_4$, $CHCl_3$; (b) NaI, MeOH—H_2O; (c) MeONa, MeOH.

The method used by the authors to form the α-xyloside bond is noteworthy: the glycoside donor employed is a tris(chlorosulfate) of α-xylopyranosyl chloride—a compound containing at the C(2) atom a group incapable of participating in the glycosylation process. It is obtained in one stage from xylose on treatment with sulfuryl chloride. Compound **52** was subsequently used to synthesise an artificial antigen (by reduction to *p*-aminophenyl glycoside, diazotisation, and azo-coupling to bovine serum albumin), with the aid of which antibodies specific to the β-isoprimeverose residue were obtained.[163] Analogous artificial antigens were also prepared using the XG7, XG8, and XG9 oligosaccharides isolated from the enzymic hydrolysates of the natural xyloglucan.[164] The corresponding antibodies can find applications in the study of the location of xyloglucan in plant cell walls, as had been done earlier with the antibiodies to native xyloglucan,[165] and for the quantitative determination of the polysaccharide by the immunosorbent method (ELISA).[166] It is of interest to note that the antibodies specific to XG7 and XG8 (as well as lectins, which bind fucose residues)[167] inhibit the auxin-induced lengthening of segments of the epicotyls of the beans of *Vigna angularis* but do not affect the growth of the segments of the oat coleoptiles[168] despite the fact that in both plants the antibodies prevent the decrease in the molecular mass of xyloglucan under the influence of auxin. These data confirm that the cleavage of xyloglucan in dicotyledonous plants is an important stage in cell growth, but in monocotyledonous plants the cleavage of hemicelluloses of another type can play a more significant role.

A communication concerning the synthesis of the tri- and penta-saccharide fragments of xyloglucan, containing L-fucose residues, appeared in 1990.[169] The benzylated 1,2-orthoacetates **53** and **55** were used to liberate the hydroxy-groups at C(2) in D-xylose and D-galactose derivatives. The trisaccharide **59** was synthesised by the stepwise addition of monosaccharide residues, starting with the reducing end of the molecule (Scheme 19).

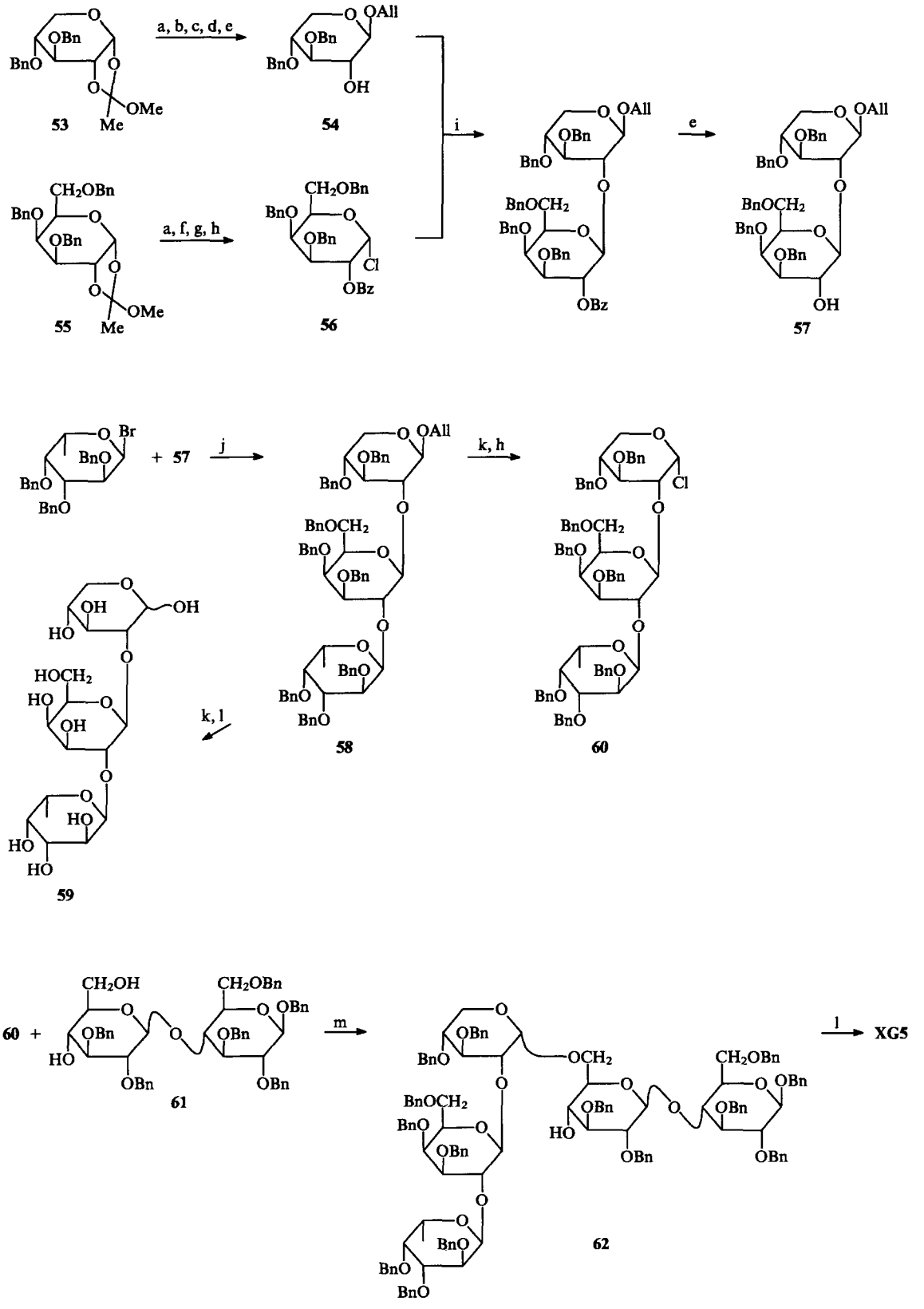
The interaction of the protected allyl xyloside **54** with the galactose derivative **56** and subsequent removal of the benzoyl group afforded the partly protected disaccharide **57**, the fucosylation of which under the conditions of the preferential formation of the α-glycosidic linkage led to the protected disaccharide **58**.[170] As a result of the removal of the protecting groups, this compound gave rise to the free trisaccharide **59** and in addition it was converted into the protected glycosyl chloride **60**, the reaction of which with the partly benzylated benzyl β-cellobioside **61** led to the protected pentasaccharide **62**. The deblocking of the compound afforded XG5.

Biological studies on the synthetic pentasaccharide led to the discovery of new types of activity of this compound.[171] It was found that the oligosaccharin at a concentration of the order of 10^{-8} M inhibits the growth of the fusicoccin (a hormone, the activity of which is close to that of auxins)-stimulated growth of pumpkin cotyledons but does not affect their growth if 6-benzylaminopurine (a hormone belonging to the group of cytokinins) is used as the stimulator. When a tissue culture of wheat germ was acted upon simultaneously by the auxin and the pentasaccharide, the formation of callus tissue was accelerated together with its faster growth, whereas in the absence of the auxin the pentasaccharide induced the vigorous formation of roots instead of the callus. The biological activity of the oligosaccharide fragments of xyloglucan was thereby confirmed on the synthetic specimen and the involvement of these compounds not only in growth processes but also in the processes associated with the morphogenesis of plants was observed.

Whilst developing approaches to the synthesis of XG9, the group of investigators[172] who described this synthesis also reported the synthesis of the second part of the XG9 molecule—6,6′-bis(*O*-α-D-xylopyranosyl)cellobiose. However, at the same time the total syntheses of XG7 and XG9 were achieved by another team of investigators (Scheme 20).[173]

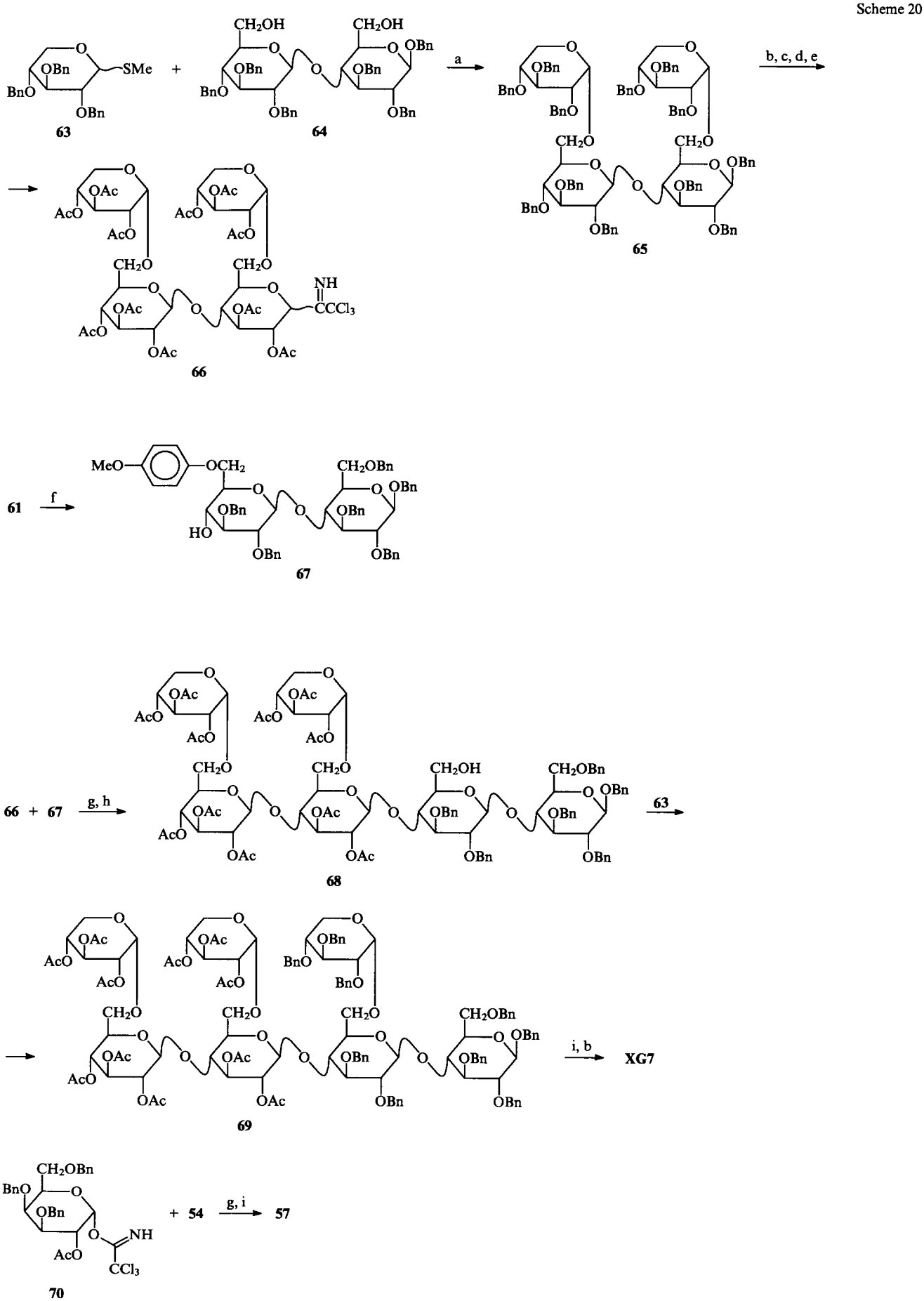
The key compound for the synthesis of both XG7 and XG9 was the hexasaccharide precursor **68**. In order to synthesise it, the derivative **64** of benzyl β-cellobioside with two free primary alcohol groups was glycosylated with the protected methyl thioxyloside **63** under the conditions of the preferential formation of α-glycosidic bonds,[174] which led to the tetrasaccharide derivative **65**. This compound was converted in several stages into the acetylated trichloroacetimidate **66**, which was used for the specific glycosylation of the protected benzyl β-cellobioside **67** obtained from compound **61** (Scheme 19) and *p*-methoxyphenol by Mitsunobu's reaction.[175] The removal of the *p*-methoxyphenyl group from this glycosylation product by

Scheme 19



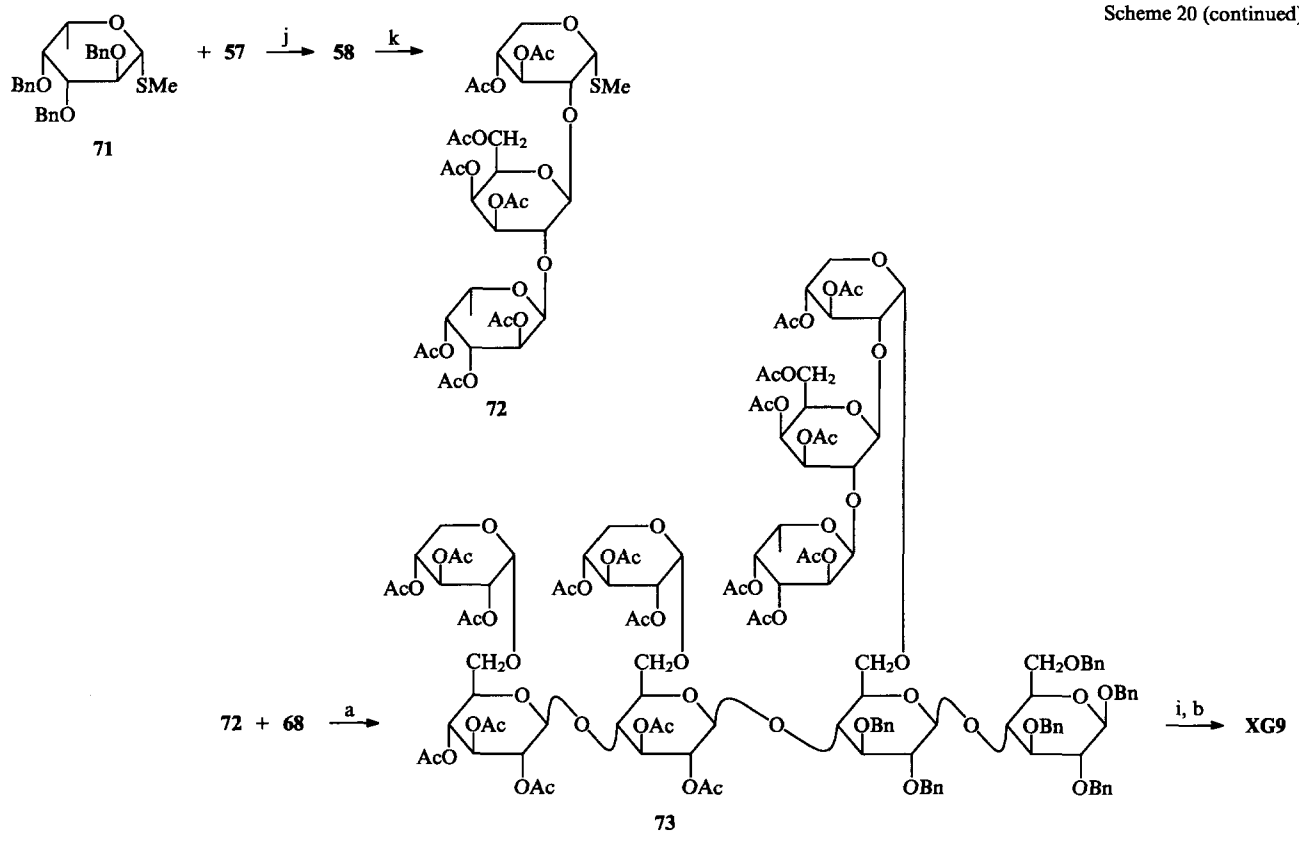
(a) 90% AcOH; (b) Ac_2O, Py; (c) HBr, CH_2Cl_2; (d) $CH_2{=}CHCH_2OH$, $Hg(CN)_2$, CH_3CN; (e) MeONa, MeOH; (f) BzCl, Py; (g) Et_3N, MeOH, 4 °C; (h) DMF–$(COCl)_2$; (i) $Hg(CN)_2$, CH_3CN; (j) Et_4NBr, 4 Å sieve, DMF–CH_2Cl_2; (k) Bu^tOK, DMSO, and then $Hg(OAc)_2$; (l) H_2/Pd–C; (m) CF_3SO_2OAg, 3 Å sieve, *sym*-collidine, −60 °C.

Scheme 20



Scheme 20 continued over.

Scheme 20 (continued)



(a) $CuBr_2$, Bu_4NBr, $HgBr_2$, 4 Å sieve; (b) $H_2/Pd-C$; (c) Ac_2O, Py; (d) $H_2NNH_2 \cdot AcOH$, DMF; (e) CCl_3CN, DBU, CH_2Cl_2; (f) 4-$MeOC_6H_4OH$, $(EtOCON)_2$, PPh_3, $(CH_2Cl)_2$; (g) $BF_3 \cdot Et_2O$; (h) $CeNH_4(NO_3)_4$, CH_3CN-H_2O (4 : 1); (i) MeONa, MeOH; (j) CF_3SO_2OMe, 4 Å sieve; (k) 7 stages, overall yield 31%.

treatment with cerium ammonium nitrate[176] led to the derivative **68**. Unfortunately, its xylosylation with methyl thioxyloside **63** under the conditions described above afforded a mixture of the α- and β-anomers in proportions of 4 : 3. Nevertheless, the mixture was separated, after which the deblocking of the derivative **69** led to the target heptasaccharide XG7.

The trisaccharide glycosyl donor, necessary for the conversion of compound **68** into the XG9 derivative, was synthesised in the following way. Allyl xyloside **54** and the galactose derivative **70** with the selectively protected O(2) atom were obtained, using the 1,2-orthoesters of the corresponding sugars, by procedures similar to that used by Torgov et al.[169] The disaccharide derivative **57** was glycosylated with the benzylated methyl thio-β-L-fucopyranoside **71**. The α-glycosidic bonds were formed preferentially in this stage (the ratio of the α- and β-anomers was 81 : 7). The trisaccharide derivative **58**, obtained by a fairly long although sufficiently effective method, was converted into the protected methyl thioglycoside **72**. Glycosylation of the hexasaccharide derivate **68** by this thioglycoside again led to a mixture of the α- and β-anomers in proportions of 3 : 1, but the required α-anomer **73** was isolated in a pure state and was converted into XG9 after the removal of the protecting groups.

The biological properties of the synthetic XG7 and XG9 were investigated with the aid of the classical test—inhibition of the auxin-induced growth of segments of the pea plant stems. The results agreed fully with data obtained in the study of fragments of the natural xyloglucan: XG7 was inactive, while the activity of XG9 did not differ from that of the natural specimen.[157]

* * *

In conclusion of this section, one should note that cell growth and the differentiation of plant tissues are accompanied by the partial cleavage of the carbohydrate polymers in the cell walls. Some of the oligosaccharide fragments thus formed play the role of signalling molecules: they control the hormonal influence on growth or include different groups of genes in morphogenesis. The antiauxin activity of the XG9 nonasaccharide fragment of the xyloglucan is the most thoroughly investigated example of such biological activity. The mechanism of this phenomenon is so far unknown, but fairly rigid structural requirements, the fulfillment of which is necessary for the manifestation of biological activity by the substances, have been established. The oligosaccharin XG9 acts at extremely low concentrations. As in the case of auxin,[177] in all probability the specific binding of the oligosaccharide to the membrane cell proteins serves as the signal. Presumably the influence of the xyloglucan fragments on cell growth is fairly universal and depends little on the plant species; only the cells of plants deficient in xyloglucan, the growth of which is evidently ensured by the partial cleavage of hemicelluloses of another type, constitute an exception. The discovery of morphogenetic activity in xyloglucan fragments is of great interest,[171] but these studies are still in the very initial stage.

IV. Interaction of plants with bacterial symbionts

A classical example of symbiosis is the interaction of leguminous plants with bacteria of the *Rhizobium* genus, which leads to the formation of new plant organs ('nodules') and the transformation of bacteria into bacteroids, which affords overall a biological system capable of fixing atmospheric nitrogen.[178,179] This interaction is specific: individual bacterial biovars can settle only on quite definite species of the leguminosae. The formation of nodules (nodulation) requires an extensive and concerted rearrangement of the activity of the gene apparatus of both partners, which is achieved as a result of the exchange of chemical signals. The cells of the root cortex are known to synthesise flavones or isoflavones, in response to the presence of which the bacteria begin to produce the 'nodulation factor'.[179,180] The host plant possesses a full genetic programme for the organogenesis of nodules, which is switched on in response to the appearance of this factor. The chemical structure of the first representative of the nodulation factors was established in 1990. The substance proved to be an extremely unusual lipooligosaccharide.[181,182]

The preparative isolation of this compound required much preliminary work. A reliable test was found, which made it possible to determine the activity of the nodulation factor from the deformation of the root hairs of the host plant.[183] In order to facilitate the processing of the culture liquid, a mutant strain *Rhizobium meliloti*, incapable of producing exocellular polysaccharides, was chosen for cultivation. The production of the nodulation factor by the cells of this strain was increased approximately by a factor of 100 by genetic engineering methods. The extraction of the culture liquid with butanol and subsequent purification of the extract by preparative chromatography on the C(18) reversed phase, on Sephadex LH-20, on DEAE-trisacryl and again with the aid of reversed phase HPLC led to the formation of a substance (about 4 mg from 10 litres of the culture) exerting a specific activity on the alfalfa root hairs. The preparation isolated was designated as NodRm-1.[181,182]

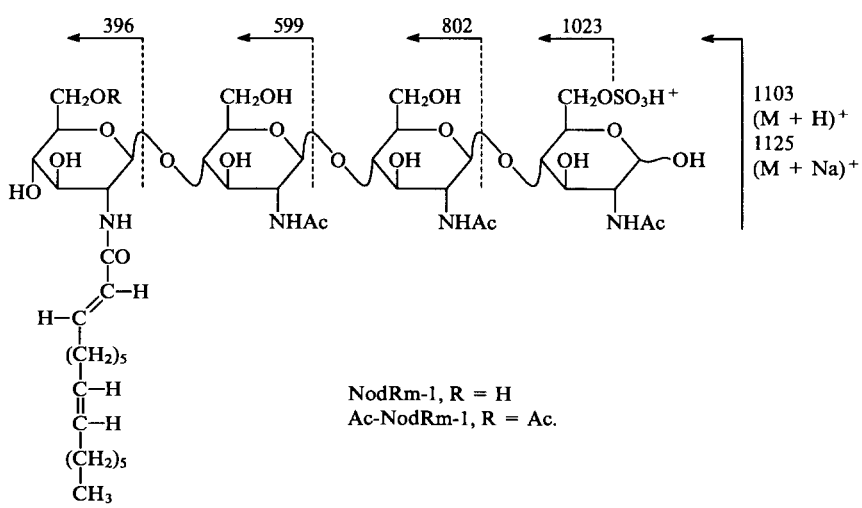
The structure of this substance is illustrated in Scheme 21. It was established using several chemical cleavages as well as mass-spectrometric and NMR spectroscopic data. The presence of the sulfate group was confirmed by the incorporation of the ^{35}S-labelled sulfate in the biosynthesis of the oligosaccharide. Glucosamine, the D-configuration of which was demonstrated with the aid of gas–liquid chromatography (GLC) of (−)-2-butyl glycosides, was identified in the products of the total acid hydrolysis. The nature of the intermonomer bonds was established by the methylation method and the configurations of the glycosidic centres and of the double bonds in the aliphatic acid residue were determined with the aid of the NMR spectra. Mass spectrometry with bombardment by fast atoms made it possible to determine the positions of the double bonds in the aliphatic acid and to find the locations of the substituents in the native oligosaccharides (the mass numbers of the most informative ions for NodRm-1 are indicated in Scheme 21). An admixture of a minor component, the tetrasaccharide Ac-NodRm-1 containing in addition the *O*-acetyl group in the 6-position in the terminal nonreducing glucosamine residue, was detected in the preparation by the same method.

Thus it was found that the signalling function was assumed by a compound having an extremely unusual structure for bacterial metabolites. Its carbohydrate chain is a tetrasaccharide whose structure is identical with that of the corresponding fragment of the molecule of chitin (which is absent from bacteria) and carries the lipophilic substituent in the form of a doubly unsaturated higher aliphatic acid residue at the non-reducing end and a highly polar substituent consisting of the sulfate group at the reducing end. The substance induces the deformation of the root hairs in alfalfa (the host plant for the chosen strain) but not in the closely related vetch, acts at very low concentrations (10^{-8}–10^{-11} Ũ), and is capable of inducing the organogenesis of nodules in the absence of bacteria.[184] The reduction of the double bonds in the aliphatic acid residue or the elimination of the sulfate group fully deprive NodRm-1 of its specific activity.[185] Admittedly, the tetrasaccharide from which the sulfate group has been removed is capable of inducing the deformation of the root hairs and nodulation at relatively high concentrations but only in leguminous plants other than the normal host plant (alfalfa).[184,185]

A more thorough analysis of the signalling oligosaccharide produced by *Rhizobium meliloti* demonstrated the presence of a further three minor components. One of them differed from the compounds described above solely by the structure of the higher aliphatic acid ($C_{16:3}\Delta^{2,4,9}$), containing an additional double bond in the 4-position. Two others differed from one another by the higher aliphatic acids ($C_{16:2}\Delta^{2,9}$ or $C_{16:3}\Delta^{2,4,9}$) and from the three preceding compounds by the fact that the carbohydrate basis of their molecules comprised a pentasaccharide and not a tetrasaccharide fragment of the chitin molecule.[186]

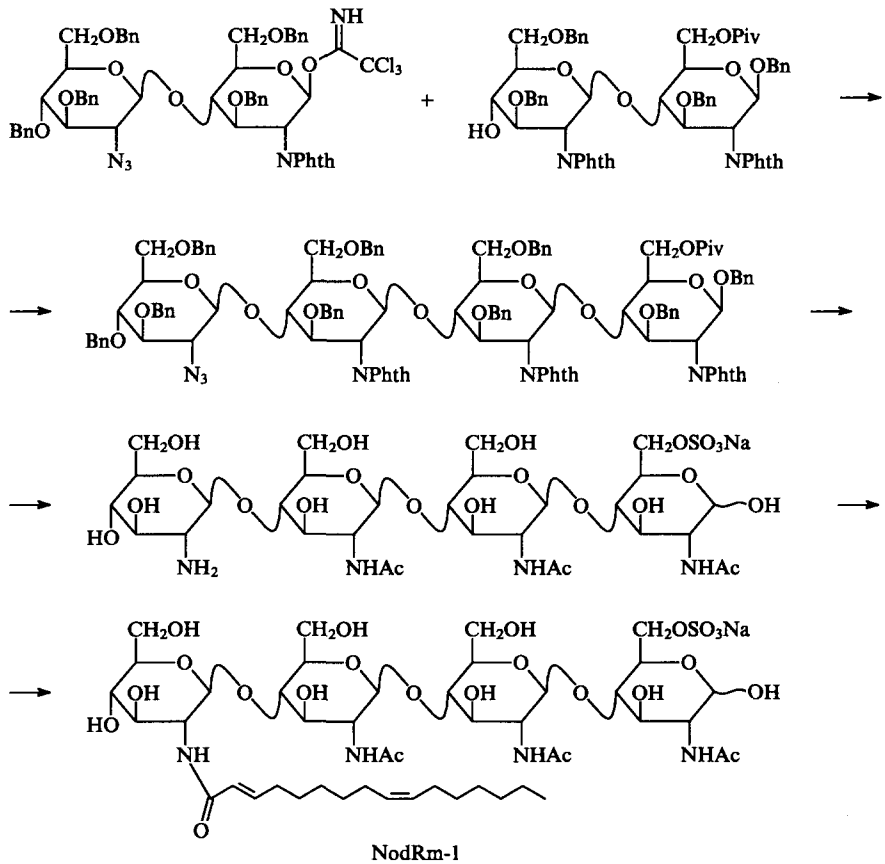
Lipooligosaccharides with a similar molecular structure have been found also in other bacterial species. Thus *R. leguminosarum var. viciae*, a symbiont of the pea plant, produces derivatives of chitotetraose and chitopentaose, lacking sulfate groups, in which the amino-group of the terminal nonreducing glucosamine residue has been acetylated by the $C_{18:4}\Delta^{2,4,6,11}$ or $C_{18:1}\Delta^{11}$ aliphatic acid, while the 6-position in this residue and all other amino-groups are acetylated.[187] The oligosaccharins of *Bradyrhizobium japonicum*, a symbiont of the soya bean plant and certain other leguminous plants, are derivatives of chitopentaose in which there are 2-*O*-methylfucose

Scheme 21



NodRm-1, R = H
Ac-NodRm-1, R = Ac.

Scheme 22



NodRm-1

derivatives in the 6-position at the reducing end instead of sulfate groups; the substances differ in the nature of the higher aliphatic acid residues ($C_{18:1}\Delta^9$, $C_{16:1}$ or $^{*}_{16:0}$) and by the presence or absence of the acetyl group in the 6-position at the nonreducing end.[188-190]

Despite the limited amount of the available information, an impression has thus been created that the symbiotic bacteria are capable of synthesising a chitotetraose or a chitopentaose as a common basis of the future signalling molecules, while the necessary specificity of the structure of oligosaccharin is achieved by the addition of definite substituents to the nonreducing and reducing terminal residues of these oligosaccharides.[191] Since the isolation of the individual signalling compounds produced by bacteria remains a complex task, there is so far no information about the mechanism of the reaction of these substances. The synthesis of these oligosaccharides is also fairly complex. Despite the relative availability of chitotetraose or chitopentaose, which can be obtained by the fragmentation of chitin or chitosan (see above), it has not so far been possible to put forward a satisfactory synthetic scheme which would permit the introduction of specific substituents into the complete chitooligosaccharide molecule. Two total syntheses of the nodulation factors have been published[192,193] (in the form of reports delivered at the XVI International Symposium on Carbohydrates without experimental details). In one of them (Scheme 22) the NodRm-1 molecule is assembled from two disaccharide derivatives substituted in different ways. The successive removal of the protecting groups and reduction of the azide group of the terminal nonreducing residue of the tetrasaccharide molecule permit the introduction of the sulfate group and the higher aliphatic acid residue in the required positions.[192]

In another synthesis (Scheme 23),[193] the molecule is assembled from derivatives of monosaccharides, the necessary **A**–**D** units being obtained from 2-azido-2-deoxy-3,4-di-*O*-benzyllaevoglucosan **75**. This substance was synthesised in only three stages from the D-glucal **74** using oxidative 1,6-iodocyclisation[194] and was converted into the monobenzyl ether **76** by a standard method.[195] Subsequent synthesis of the tetrasaccharide derivative **77** made it possible to place in the required positions not only the sulfate group and the higher aliphatic acid residue but also the acetyl group, so that the final result of the synthesis was the compound Ac-NodRm-1.

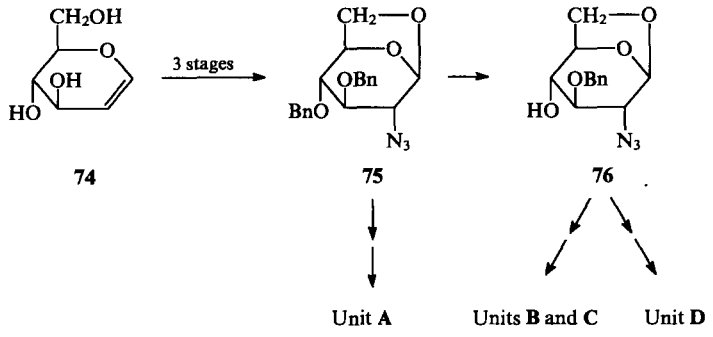
* * *

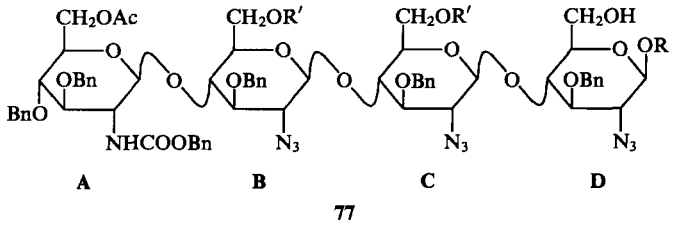
The oligosaccharins described in this section differ significantly from the substances examined in the previous sections of the review. They are not fragments of carbohydrate-containing biopolymers in the cell walls but represent the product of specific biosynthesis: the set of genes controlling this process in the bacterial cell is well known.[181,185,196] The nodulation factors are also characterised by a higher specificity, since their biological activity is manifested only in relation to a very limited number of plant species. It is extremely probable that the part of the plant receptor complex receiving the nodulation signals comprises lectins located on the surface of the cytoplasmic membrane of the cells in the root hairs and capable of the specific binding of oligosaccharins. The transfer of the pea lectin gene to the seedlings of white clover led to the transfer of susceptibility to the infection and nodulation by the *Rhizobium* strain specific to the pea plant.[197]

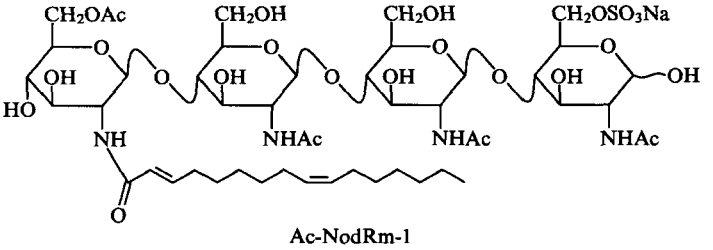
V. Conclusion

In the present review, we have examined five types of oligosaccharins which are used by plants to regulate most important physiological processes, such as growth and morphogenesis, and the relation with phytopathogens and symbiotic bacteria. Impressive results have already been

Scheme 23







achieved in this field of study, although many processes associated with the role of oligosaccharins *in vivo* and with the mechanism of their action still remain to be elucidated. The interest in oligosaccharins can be explained not only by the new possibilities of investigating with their aid the physiology of the plant cell but also with the extremely promising prospects for the creation on their basis of ecologically harmless growth regulators and plant protecting agents. However, oligosaccharins continue to remain difficult to obtain. Further progress in this field will depend in many respects on the development of new economical procedures for the preparation of oligosaccharins from natural sources and methods for the synthesis of both the oligosaccharins themselves and their analogues necessary for the elucidation of the dependence of the biological activity on the chemical structure of these compounds.

References

1. P Albersheim, B S Valent *J. Cell Biol.* **78** 627 (1978)
2. P Albersheim, A G Darvill, M McNeil, B S Valent, J K Sharp, E A Nothnagel, K R Davis, N Yamazaki, D J Gollin, W S York, W F Dudman, J E Darvill, A Dell, in *Structure and Function of Plant Genomes* (Eds O Ciferri, L Dure) (New York: Plenum Press, 1983) p. 293
3. P Albersheim, A G Darvill *Scientific American* **253** 58 (1985)
4. P Albersheim, A G Darvill *Comm. Eur. Communities (Rep.) EUR 1990, Eur. 12757* (Towards Carbohydrate-Based Chemistry) p. 175
5. M McNeil, A G Darvill, S C Fry, P Albersheim *Ann. Rev. Biochem.* **53** 625 (1984)
6. C A Ryan *Biochemistry* **27** 8879 (1988)
7. C A Ryan, E E Farmer *Ann. Rev. Plant. Physiol. Plant Mol. Biol.* **42** 651 (1991)
8. S Aldington, G J McDougall, S C Fry *Plant Cell Environ.* **14** 625 (1991)
9. P Albersheim, A Darvill, C Augur, J-J Cheong, S Eberhard, M G Hahn, V Marfa, D Mohnen, M A O'Neill, M D Spiro, W S York *Acc. Chem. Res.* **25** 77 (1992)
10. A Darvill, C Augur, C Bergmann, R W Carlson, J-J Cheong, S Eberhard, M G Hahn, V-M Lo, V Marfa, B Meyer, D Mohnen, M A O'Neill, M D Spiro, H van Halbeek, W S York, P Albersheim *Glycobiology* **2** 181 (1992)
11. P Albersheim, A G Darvill *V Mire Nauki* (11) 16 (1985)
12. A G Darvill, P Albersheim *Ann. Rev. Plant Physiol.* **35** 243 (1984)
13. R A Dixon *Biol. Rev.* **61** 239 (1986)
14. J Ebel *Ann. Rev. Phytopathol.* **24** 235 (1986)
15. J A Bailey, J W Mansfield (Eds) *Phytoalexins* (Translated into Russian; Kiev: Naukova Dumka, 1985)
16. R Cline, P Albersheim *Plant Physiol.* **68** 221 (1981)
17. A R Ayers, J Ebel, B Valent, P Albersheim *Plant Physiol.* **57** 760 (1976)
18. A R Ayers, B Valent, J Ebel, P Albersheim *Plant Physiol.* **57** 766 (1976)
19. J K Sharp, B Valent, P Albersheim *J. Biol. Chem.* **259** 11 312 (1984)
20. A R Ayers, J Ebel, F Finelli, N Berger, P Albersheim *Plant Physiol.* **57** 751 (1976)
21. B S Valent, A G Darvill, M McNeil, B K Robertsen, P Albersheim *Carbohydr. Res.* **79** 165 (1980)
22. M McNeil, A G Darvill, P Aman, L-E Franzen, P Albersheim *Methods Enzymol.* **83** 3 (1982)
23. G J Gervig, J P Kamerling, J F G Vliegenthart *Carbohydr. Res.* **62** 349 (1978)
24. J Haverkamp, M J A de Bie, J F G Vliegenthart *Carbohydr. Res.* **37** 111 (1974)
25. T J Waeghe, A G Darvill, M McNeil, P Albersheim *Carbohydr. Res.* **123** 281 (1983)

26. J K Sharp, M McNeil, P Albersheim *J. Biol. Chem.* **259** 11 321 (1984)
27. O S Chizhov, N K Kochetkov *Adv. Carbohydr. Chem.* **21** 39 (1966)
28. G O Aspinall, in *The Polysaccharides*. Vol. 1 (Ed. G O Aspinall) (New York: Academic Press, 1982) p. 35
29. P Ossowski, A Pilotti, P J Garegg, B Lindberg *J. Biol. Chem.* **259** 11 337 (1984)
30. J K Sharp, P Albersheim, P Ossowski, A Pilotti, P Garegg, B Lindberg *J. Biol. Chem.* **259** 11 341 (1984)
31. P Fugedi, W Birberg, P J Garegg, A Pilotti *Carbohydr. Res.* **164** 297 (1987)
32. H Paulsen *Angew. Chem., Int. Ed. Engl.* **21** 155 (1982); *Chem. Soc. Rev.* **13** 15 (1984)
33. P J Garegg, P Konradsson, I Kvarnstrom, T Norberg, S C T Svensson, B Wigilius *Acta Chem. Scand., Ser. B* **39** 569 (1985)
34. S Hanessian, J Banoub *Carbohydr. Res.* **53** C13 (1977)
35. H Lonn *Carbohydr. Res.* **139** 105, 115 (1985)
36. P Fugedi, P J Garegg *Carbohydr. Res.* **149** C9 (1986)
37. M Ek, P J Garegg, H Hultberg, S Oscarson *J. Carbohydr. Chem.* **2** 305 (1983)
38. C A A van Boeckel, T Beetz *Tetrahedron Lett.* **24** 3775 (1983)
39. C P J Glaudemans, M J Bertolini *Methods Carbohydr. Chem.* **8** 271 (1980)
40. P Fugedi, P J Garegg *J. Carbohydr. Chem.* **7** 389 (1988)
41. W Birberg, P Fugedi, P J Garegg, A Pilotti *J. Carbohydr. Chem.* **8** 47 (1989)
42. R R Schmidt *Angew. Chem., Int. Ed. Engl.* **25** 212 (1986)
43. N Hong, T Ogawa *Tetrahedron Lett.* **31** 3179 (1990)
44. J-J Cheong, W Birberg, P Fugedi, A Pilotti, P J Garegg, N Hong, T Ogawa, M G Hahn *Plant Cell* **3** 127 (1991)
45. E G Cosio, T Frey, R Verduyn, J Van Boom, J Ebel *FEBS Lett.* **271** 223 (1990)
46. B M Peters, D H Cribbs D A Stelzig *Science* **201** 364 (1978)
47. M Yoshikawa, N T Keen, M-C Wang *Plant Physiol.* **73** 497 (1983)
48. W E Schmidt, J Ebel *Proc. Natl. Acad. Sci. USA* **84** 4117 (1987)
49. E G Cosio, H Popperl, W E Schmidt, J Ebel *Eur. J. Biochem.* **175** 309 (1988)
50. J-J Cheong, M G Hahn *Plant Cell* **3** 137 (1991)
51. M G Hahn, J-J Cheong *Curr. Plant Sci. Biotechnol. Agric.* **10** 403 (1991)
52. M G Hahn, A Darvill, P Albersheim, C Bergmann, J-J Cheong, A Koller, V-M Lo, in *Molecular Plant Pathology: A Practical Approach* (Eds D J Bowles, S Gurr, M McPherson) (New York: IRL Press, 1991)
53. R A A Muzzarelli *Chitin* (New York: Pergamon Press, 1987)
54. E P Feofilova *Biol. Nauki* (6) 5; (11) 5 (1981)
55. J P Zikakis *ACS Symp. Ser.* **389** 116 (1989)
56. G W Gooday *ACS Symp. Ser.* **460** 478 (1991)
57. W K Roberts, C P Selitrennikoff *J. Gen. Microbiol.* **134** 169 (1988)
58. J J Distler, S Roseman, in *Methods of Carbohydrate Chemistry* (Translation from English edited by N K Kochetkov; Moscow: Mir, 1967) p. 240
59. B Capon, R L Foster *J. Chem. Soc. C* 1654 (1970)
60. C Bosso, J Defaye, A Domard, A Gadelle, C Pedersen *Carbohydr. Res.* **156** 57 (1986)
61. A Domard, N Cartier *Int. J. Biol. Macromol.* **11** 297 (1989)
62. M Izume, A Ohtakara *Agric. Biol. Chem.* **51** 1189 (1987)
63. L A Hadwiger, J M Beckman *Plant Physiol.* **66** 205 (1980)
64. H Kohle, D H Young, H Kauss *Plant Sci. Lett.* **33** 221 (1984)
65. U Conrath, A Domard, H Kauss *Plant Cell. Rep.* **8** 152 (1989)
66. M Walker-Simmons, L A Hadwiger, C A Ryan *Biochem. Biophys. Res. Commun.* **110** 194 (1983)
67. M Walker-Simmons, D Jin, C A West, L Hadwiger, C A Ryan *Plant Physiol.* **76** 833 (1984)
68. H Kauss, W Jeblick, A Domard *Planta* **178** 385 (1989)
69. F Kurosaki, N Tashiro, A Nishi *Plant Cell Physiol.* **29** 527 (1988)
70. M S Barber, R E Bertram, J P Ride *Physiol. Mol. Plant Pathol.* **34** 3 (1989)
71. M S Lesney *Plant Cell Tissue Organ Cult.* **19** 23 (1989)
72. E J Nichols, J L Beckman, L A Hadwiger *Plant Physiol.* **66** 199 (1980)
73. T Boller, in *Second Messengers in Plant Growth and Development* (Eds W F Boss, D J Morre) (New York: Alan R Liss, 1987) p. 227
74. J Grenier, A Asselin *Mol. Plant–Microbe Interact.* **3** 401 (1990)
75. T Boller, in *Plant–Microbe Interactions: Molecular and Genetic Perspectives*, Vol. 2 (Eds T Kosuge, E W Nester) (New York: Macmillan, 1987) p. 385
76. E Kombrink, M Schroder, K Hahlbrock *Proc. Natl. Acad. Sci. USA* **85** 782 (1988)
77. L A Hadwiger, R F Line *Physiol. Plant. Pathol.* **19** 249 (1981)
78. F Mauch, B Mauch-Mani, T Boller *Plant Physiol.* **88** 936 (1988)
79. D F Kendra, D Christian, L A Hadwiger *Physiol. Mol. Plant Pathol.* **35** 215 (1989)
80. K Broglie, I Chet, M Holliday, R Cressman, P Biddle, S Knowlton, C J Mauvais, R Broglie *Science* **254** 1194 (1991)
81. D Roby, A Gadelle, A Toppan *Biochem. Biophys. Res. Commun.* **143** 885 (1987)
82. D Roby, M T Esquerre-Tugaye *Plant Sci.* **52** 175 (1987)
83. S A Hedrick, J N Bell, T Boller, C J Lamb *Plant Physiol.* **86** 182 (1988)
84. D F Kendra, L A Hadwiger *Exp. Mycol.* **8** 276 (1984)
85. M O'Neill, P Albersheim, A Darvill, in *Methods in Plant Biochemistry*. Vol. 2. (Ed. P M Dey) (London: Academic Press, 1990) p. 415
86. F Cervone, G De Lorenzo, G Salvi, C Bergmann, M G Hahn, Y Ito, A Darvill, P Albersheim *NATO ASI Ser.* **H36** 85 (1989)
87. M G Hahn, A G Darvill, P Albersheim *Plant Physiol.* **68** 1161 (1981)
88. E A Nothnagel, M McNeil, P Albersheim, A Dell *Plant Physiol.* **71** 916 (1983)
89. D F Jin, C A West *Plant Physiol.* **74** 989 (1984)
90. K R Davis, A G Darvill, P Albersheim, A Dell *Plant Physiol.* **80** 568 (1986)
91. F Cervone, G De Lorenzo, R Pressey, A G Darvill, P Albersheim *Phytochemistry* **29** 447 (1990)
92. F Cervone, M G Hahn, G De Lorenzo, A G Darvill, P Albersheim *Plant Physiol.* **90** 542 (1989)
93. K R Davis, K Hahlbrock *Plant Physiol.* **85** 1286 (1987)
94. W F Broekaert, W J Peumans *Physiol Plant* **74** 740 (1988)
95. B Robertsen *Physiol. Mol. Plant Pathol.* **28** 137 (1986)
96. R J Bruce, C A West *Plant Physiol.* **91** 889 (1989)
97. K R Davis, A G Darvill, P Albersheim *Plant Mol. Biol.* **6** 23 (1986)
98. P D Bishop, G Pearce, J E Bryant, C A Ryan *J. Biol. Chem.* **259** 13 172 (1984)
99. I Apostol, P F Heinstein, P S Low *Plant Physiol.* **90** 106 (1989)
100. Y Mathieu, A Kurkdjian, H Xia, J Guern, A Koller, M D Spiro, M A O'Neill, P Albersheim, A Darvill *Plant J. Cell Mol. Biol.* **1** 333 (1991)
101. E E Farmer, T D Moloshok, M J Saxton, C A Ryan *J. Biol. Chem.* **266** 3140 (1991)
102. C A West, R J Bruce, D F Jin, in *Structure, Function and Biosynthesis of Plant Cell Walls* (Eds W M Dugger, S Bartnicki-Garcia) (Baltimore: Waverley Press, 1984) p. 359
103. P D Bishop, C A Ryan *Methods Enzymol.* **138** 715 (1987)
104. Y Nakahara, T Ogawa *Tetrahedron Lett.* **28** 2731 (1987)
105. Y Nakahara, T Ogawa *Carbohydr. Res.* **200** 363 (1990)
106. T Mukayama, Y Murai, S Shoda *Chem. Lett.* 431 (1981)
107. K Omura, D Swern *Tetrahedron* **34** 1651 (1978)
108. R E Ireland, D W Norbeck *J. Org. Chem.* **50** 2198 (1985)
109. E Dalcanale, F Montanari *J. Org. Chem.* **51** 567 (1986)
110. Y Nakahara, T Ogawa *Carbohydr. Res.* **167** C1 (1987)
111. Y Nakahara, T Ogawa *Carbohydr. Res.* **194** 95 (1989)
112. Y Nakahara, T Ogawa *Tetrahedron Lett.* **30** 87 (1989)
113. Y Nakahara, T Ogawa *Carbohydr. Res.* **205** 147 (1990)
114. M A Horn, P F Heinstein, P S Low *Plant Cell* **1** 1003 (1989)
115. M B Wilkins (Ed.) *Physiology of Plant Growth and Development* (London: McGraw-Hill, 1969)
116. T A Steeves, I M Sussex *Patterns in Plant Development* (Cambridge: Cambridge Univ. Press, 1989)
117. K Tran Thanh Van, N Thi Den, A Chlyah *Planta* **119** 149 (1974)
118. K Tran Thanh Van, P Toubart, A Cousson, A G Darvill, D J Gollin, P Chelf, P Albersheim *Nature (London)* **314** 615 (1985)
119. S Eberhard, N Doubrava, V Marfa, D Mohnen, A Southwick, A Darvill, P Albersheim *Plant Cell* **1** 747 (1989)
120. D Mohnen, S Eberhard, V Marfa, N Doubrava, P Toubart, D J Gollin, T A Gruber, W Nuri, P Albersheim, A Darvill *Development* **108** 191 (1990)
121. V Marfa, D J Gollin, S Eberhard, D Mohnen, A Darvill, P Albersheim *Plant J. Cell Mol. Biol.* **1** 217 (1991)

122. A D Neale, J A Wahleithner, M Lund, H T Bonnett, A Kelly, D R Meeks-Wagner, W J Peacock, E S Dennis *Plant Cell* **2** 673 (1990)
123. C Branca, G De Lorenzo, F Cervone *Physiol. Plant* **72** 499 (1988)
124. J K Brecht, D J Huber *Plant Physiol.* **88** 1037 (1988)
125. A D Campbell, J M Labavitch *Plant Physiol.* **97** 706 (1991)
126. A D Campbell, J M Labavitch *Plant Physiol.* **97** 699 (1991)
127. A W Galston, P Davies, R Setter *The Life of the Green Plant* (Translation from English edited by N P Voskresenskaya; Moscow: Mir, 1983)
128. S C Fry *J. Exp. Bot.* **40** 1 (1989)
129. D A Brummell, G A Maclachlan *ASC Symp. Ser.* **399** 18 (1989)
130. T Hayashi *Ann. Rev. Plant Physiol. Plant Mol. Biol.* **40** 139 (1989)
131. W D Bauer, K W Talmadge, K Keegstra, P Albersheim *Plant Physiol.* **51** 174 (1973)
132. W S York, J E Oates, H van Halbeek, A G Darvill, P Albersheim, P R Tiller, A Dell *Carbohydr. Res.* **173** 113 (1988)
133. L L Kiefer, W S York, A G Darvill, P Albersheim *Phytochemistry* **28** 2105 (1989)
134. S C Fry *Planta* **169** 443 (1986)
135. Y Kato, K Matsuda *Agric. Biol. Chem.* **44** 1759 (1980)
136. T Hayashi, G Maclachlan *Plant Physiol.* **75** 596 (1984)
137. W S York, H van Halbeek, A G Darvill, P Albersheim *Carbohydr. Res.* **200** 9 (1990)
138. M Hisamatsu, G Impallomeni, W S York, P Albersheim, A G Darvill *Carbohydr. Res.* **211** 117 (1991)
139. P Kooiman *Rec. Trav. Chim. Pays-Bas Belg.* **80** 849 (1961)
140. H G Edelmann, S C Fry *J. Exp. Bot.* **43** 463 (1992)
141. C Fanutti, M J Gidley, J S G Reid *Planta* **184** 137 (1991)
142. G J McDougall, S C Fry *Plant Physiol.* **89** 883 (1989)
143. G J McDougall, S C Fry *Carbohydr. Res.* **219** 123 (1991)
144. Z El Rassi, D Tedford, J An, A Mort *Carbohydr. Res.* **215** 25 (1991)
145. M Hisamatsu, W S York, A G Darvill, P Albersheim *Carbohydr. Res.* **227** 45 (1992)
146. L L Kiefer, W S York, P Albersheim, A G Darvill *Carbohydr. Res.* **197** 139 (1990)
147. K Keegstra, K W Talmadge, W D Bauer, P Albersheim *Plant Physiol.* **51** 188 (1973)
148. S C Fry *The Growing Plant Cell Wall: Chemical and Metabolic Analysis* (London: Longman, 1988)
149. S C Fry *Physiol. Plant.* **75** 532 (1989)
150. S C Fry *Trends Glycosci. Glycotechnol.* **4** 279 (1992)
151. Y Masuda *Bot. Mag. Tokyo* **103** 345 (1990)
152. W S York, A G Darvill, P Albersheim *Plant Physiol.* **75** 295 (1984)
153. G J McDougall, S C Fry *Food Hydrocolloids* **1** 505 (1987)
154. G J McDougall, S C Fry *Planta* **175** 412 (1988)
155. M Emmerling, H U Seitz *Planta* **182** 174 (1990)
156. G J McDougall, S C Fry *J. Exp. Bot.* **40** 233 (1989)
157. C Augur, L Yu, K Sakai, T Ogawa, P Sinay, A G Darvill, P Albersheim *Plant Physiol.* **99** 180 (1992)
158. V Farkas, G Maclachlan *Carbohydr. Res.* **184** 213 (1988)
159. G J McDougall, S C Fry *Plant Physiol.* **93** 1042 (1990)
160. E P Lorences, G J McDougall, S C Fry *Physiol. Plant* **80** 109 (1990)
161. R E Cleland, in *Encyclopedia of Plant Physiology. New Series.* Vol. 13B (Eds W Tanner, F A Loewus) (Berlin: Springer-Verlag, 1981) p. 255
162. Y Sone, A Misaki *J. Carbohydr. Chem.* **5** 671 (1986)
163. Y Sone, A Misaki *Carbohydr. Res.* **191** 79 (1989)
164. Y Sone, J Kuramae, S Shibata, A Misaki *Agric. Biol. Chem.* **53** 2821 (1989)
165. P J Moore, A G Darvill, P Albersheim, L A Staehelin *Plant Physiol.* **82** 787 (1986)
166. Y Sone, K Sato, A Misaki *Agric. Biol. Chem.* **55** 2155 (1991)
167. T Hoson, Y Masuda *Physiol. Plant* **82** 41 (1991)
168. T Hoson, Y Masuda, Y Sone, A Misaki *Plant Physiol.* **96** 551 (1991)
169. V I Torgov, O A Nechaev, A I Usov, V N Shibaev *Bioorg. Khim.* **16** 854 (1990)
170. M A Nashed, L Anderson *Carbohydr. Res.* **114** 53 (1983)
171. Z N Pavlova, O A Ash, V A Vnuchkova, A V Babakov, V I Torgov, O A Nechaev, A I Usov, V N Shibaev *Plant Sci.* **85** 131 (1992)
172. O A Nechaev, V I Torgov, A I Usov, V N Shibaev *Bioorg. Khim.* **17** 424 (1991)
173. K Sakai, Y Nakahara, T Ogawa *Tetrahedron Lett.* **31** 3035 (1990)
174. S Sato, M Mori, Y Ito, T Ogawa *Carbohydr. Res.* **155** C6 (1986)
175. O Mitsunobu *Synthesis* 1 (1981)
176. T Fukuyama, A A Laird, L M Hotchkiss *Tetrahedron Lett.* **26** 6291 (1985)
177. A M Jones *Physiol. Plant.* **80** 154 (1990)
178. P Raven, R Evert, S Eichhorn *Modern Botany* (Translation from English edited by A L Takhtadzhyan; Moscow: Mir, 1990) p. 146
179. N J Brewin *Ann. Rev. Cell Biol.* 7 191 (1991)
180. J W Redmond, M Batley, M A Djordjevic, R W Innes, P L Kuempel, B G Rolfe *Nature (London)* **323** 632 (1986)
181. P Lerouge, P Roche, C Faucher, F Maillet, G Truchet, J-C Prome, J Denarie *Nature (London)* **344** 781 (1990)
182. P Roche, P Lerouge, C Ponthus, J-C Prome *J. Biol. Chem.* **266** 10933 (1991)
183. C Faucher, S Camut, J Denarie, G Truchet *Mol. Plant–Microbe Interact.* **2** 291 (1989)
184. P Roche, P Lerouge, J-C Prome, C Faucher, J Vasse, F Maillet, S Camut, F De Billy, J Denarie, G Truchet *Curr. Plant Sci., Biotechnol. Agric.* **10** 119 (1991)
185. G Truchet, P Roche, P Lerouge, J Vasse, S Camut, F De Billy, J-C Prome, J Denarie *Nature (London)* **351** 670 (1991)
186. M Schultze, B Quiclet-Sire, E Kondorosi, H Virelizier, J N Glushka, G Endre, S D Gero, A Kondorosi *Proc. Natl. Acad. Sci. USA* **89** 192 (1992)
187. H P Spaink, D M Sheeley, A A N van Brussel, J Glushka, W S York, T Tak, O Geiger, E P Kennedy, V N Reinhold, B J J Lugtenberg *Nature (London)* **354** 125 (1991)
188. H P Spaink, A Aarts, G Stacey, G V Bloemberg, B J J Lugtenberg, E P Kennedy *Mol. Plant–Microbe Interact.* **5** 72 (1992)
189. J Sanjuan, R W Carlson, H P Spaink, U R Bhat, W M Barbour, J Glushka, G Stacey *Proc. Natl. Acad. Sci. USA* **89** 8789 (1992)
190. G Stacey, in *Plant Biotechnology Developments* (Ed. P M Gresshoff) (Boca Raton, FL: CRC, 1992) p. 45
191. H P Spaink *Plant Mol. Biol.* **20** 977 (1992)
192. Y-Z Hui, L-X Wang *XVI International Carbohydrate Symposium, Paris, France, 1992; Abstracts* p. 238
193. D Tailler, J-C Jacquinet, A-M Noirot, J-M Beau *XVI International Carbohydrate Symposium, Paris, France, 1992; Abstracts* p. 333
194. S Czernecki, C Leteux, A Veyrieres *Tetrahedron Lett.* **33** 221 (1992)
195. H Hori, Y Nishida, H Ohrui, H Meguro *J. Org. Chem.* **54** 1346 (1989)
196. P Roche, F Debelle, F Maillet, P Lerouge, C Faucher, G Truchet, J Denarie, J-C Prome *Cell* **67** 1131 (1991)
197. C L Diaz, L S Melchers, P J J Hooykaas, B J J Lugtenberg, J W Kijne *Nature (London)* **338** 579 (1989)

Russian Chemical Reviews **62** (12) 1073 – 1082 (1993)
©1993 Russian Academy of Sciences and Turpion Ltd

UDC 541.139

Second generation of magnetic effects in chemical reactions

A L Buchachenko

Contents

I.	Two scenarios of chemical reaction	1073
II.	Spin dynamics of the radical pair	1074
III.	First generation of magnetic effects	1074
IV.	Principles of chemical reception of microwaves	1075
V.	Reaction yield detected magnetic resonance	1077
VI.	Radio induced magnetic isotope effect	1079
VII.	Microwave stimulated nuclear polarisation	1080
VIII.	Conclusion	1082

Abstract. Spin selective chemical reactions must also be magnetically sensitive. The susceptibility of chemical reactions to magnetic interactions produces two generations of magnetic effects: the first includes the magnetic field effect, the magnetic isotope effect, and the chemical polarisation of nuclei, all induced by external or internal magnetic fields. The second generation effects are stimulated by external electromagnetic fields interacting with the chemically active spin systems. The bibliography includes 31 references.

I. Two scenarios of chemical reaction

Any chemical event, including its feasibility and its result, is traditionally rationalised according to its energy scenario: how much energy is required, how to pump this energy into the reacting species, and how efficiently is this energy exploited in the chemical system.

However, another physical property besides energy is of paramount importance in chemistry: the angular momentum (spin) of the electrons and nuclei of the reagents. The fundamental ruling principle of chemical reactions is that both the spins and their projections remains unchanged in elementary chemical events. The conservation of the total spin has important consequences: the chemical reactions are spin selective, they are allowed only for spin states of the products whose total spin is identical to that of reagents, and they are strictly forbidden if they require spin change. For example, the transformation of the radical pair into the molecule (through recombination or disproportionation) is allowed only from the singlet spin state of the pair, and forbidden from the triplet one. The reaction $H + O_2 \rightarrow HO_2$ takes place in the doublet spin state of the reagent ($H\cdots O_2$) since the total spin of the pair in this state is identical to that of the reaction product, but it is forbidden in the quartet spin state of the pair. Of the nine possible spin states of the pair of triplet carbenes Ph_2C:, each having spin $S = 1$, only one can undergo a spin allowed reaction and produce the recombination product tetraphenylethylene. The spin of the other eight states ($S = 1$ and 2) is not equal to that of the reaction product ($S = 0$), and therefore these states are chemically nonreactive.

In general the spin selectivity of chemical events implies that chemically identical but spin different intermediates (the reaction product precursors) have different, spin dependent chemical reactivities. The only interactions which can alter the spin of reaction precursors and transform nonreactive, spin forbidden into the reactive, spin allowed states are magnetic interactions. Their contribution to the total energy is insignificant, but they control the spin behaviour of the chemical species, they modify their chemical reactivity, and they establish a new, magnetic scenario of chemical reactions.[1–4]

Spin selectivity (and therefore also the magnetic sensitivity of chemical reactions) gives rise to two generations of magnetic effects, illustrated in Fig. 1 for the particular but widely met case of a radical pair (RP). The nonreactive, triplet spin state RP can be transformed into the reactive, singlet spin state pair either by magnetic interactions, characteristic of the reaction itself, or by external radiofrequency or microwave (mw) magnetic fields. The triplet-singlet spin conversion induced by 'native' magnetic interactions is responsible for the magnetic effects of the first generation, or native magnetic effects, while the triplet–singlet conversion stimulated by rf or mw magnetic fields induces the magnetic effects of the second generation. The former includes Magnetic Field Effect (MFE), Magnetic Isotope Effect (MIE) and Chemically Induced Dynamic Nuclear Polarisation (CIDNP) — three effects originating from the dependence of the reaction probability P in RP on the magnetic field H, hyperfine (Fermi) electron-nuclear interaction, and nuclear spin orientation I_z. The latter are the basis of Reaction Yield Detected Magnetic Resonance (RYDMR), Radio Induced Magnetic Isotope Effect (RIMIE) and Stimulated Nuclear Polarisation (SNP). The relation between these two generations of magnetic effects is schematically shown in Fig. 1*b*.

A L Buchachenko Institute of Chemical Physics, Russian Academy of Sciences, ul. Kosygina 4, 117334, Moscow,
Fax (7-095) 938 21 56.

Received 8 September 1993
Uspekhi Khimii **62** (12) 1139 – 1149 (1993); translated by J I Carasso

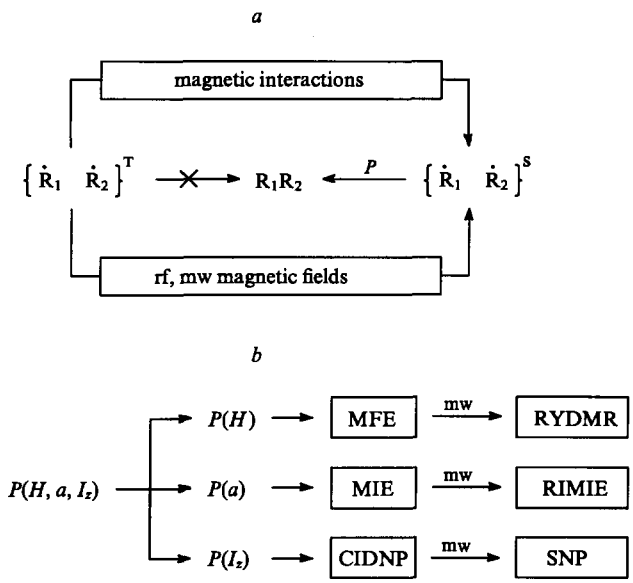


Figure 1. (*a*) Transformation of an unreactive triplet radical pair into a chemically active singlet pair under the influence of magnetic interactions and electromagnetic fields (radio-frequency or microwave); (*b*) relationship between first and second generation magnetic effects.

II. Spin dynamics of the radical pair

A radical pair is a dynamic intermediate or chemical microreactor from which the partners can diffuse without reacting, travel randomly in space and time, and then return and reencounter. The time between partner contacts, or repeated encounters, is used by the pair for its own spin conversion which is driven by magnetic interactions in the radicals resulting either in triplet–singlet transformation of the pair (if its starting spin state is triplet) or in singlet-triplet conversion (for pairs with singlet starting state).

To transform the triplet RP into a molecule at least four simultaneous events are required.

Firstly, the radicals leaving the RP at time $t = 0$ should return and reencounter at some time t. This process of regeneration of the contacts between RP partners is described by molecular dynamics. Secondly, at the same instance t the pair must have completed its triplet–singlet conversion and be ready to form a molecule. This process is controlled by spin dynamics. Thirdly, during their diffusional travels the radicals must not undergo chemical transformations: for the primary molecule to be reformed the initial pair must survive to time t. The probability of this event is determined by the chemical dynamics. Fourthly, the RP now ready to react (i.e. having survived to time t and being in a singlet state with the partners in contact) will recombine into a molecule only if a favourable orientation of the partners is achieved by rotational dynamics. Thus, the birth of a molecule from the RP is a result of the collective and coordinated efforts of three dynamics: spin, molecular and chemical.

The key act of the chemical interaction is spin conversion, controlled by the magnetic interactions, among which Zeeman and electron–nuclear (Fermi) hyperfine interaction (HFI) are the most important. Spin dynamics are modulated by molecular dynamics, which produce random variations of the distance between radicals and therefore of the exchange interaction potential. This, in its turn, influences the rate of spin conversion and ultimately the spin dynamics of the RP. The chemical reactions of RP partners destroy the pair, so that the spin dynamics are controlled by chemical dynamics.

The extended spin dynamics of the RP are the combination of all three dynamics considered cooperatively. The rate of triplet–singlet conversion is directly related to the matrix element Q of the RP spin Hamiltonian evaluated with the spin wave functions of triplet (T) and singlet (S) states.

For the multinuclear RP these Q_{ab} values are

$$Q_{ab}(T_0 - S) = \tfrac{1}{2}\left[\Delta g\mu_B H + \sum_i i m_i^a - \sum_j j m_j^b\right], \quad (1)$$

$$Q_{ab}(T_+ - S) = -\left(\tfrac{1}{8}\right)^{1/2} a_i\left[I_i(I_i+1) - m_i(m_i-1)\right], \quad (2)$$

$$Q_{ab}(T_- - S) = \left(\tfrac{1}{8}\right)^{1/2} a_i\left[I_i(I_i+1) - m_i(m_i+1)\right], \quad (3)$$

where the first describes the contribution of the T_0-S transition to the total rate of T–S conversion, the other two give the contributions of T_+-S and T_--S transitions; T_0, $T_\pm$ are the substates of the triplet spin state, with different electron spin projections: 0 for T_0 and ±1 for $T_\pm$ respectively. The term $\Delta g\mu_B H$ is the difference of Zeeman energies of the radical partners; Δg is the difference of their g-factors, $\Delta g = g_1 - g_2$; μ_B is the Bohr magneton; H is the strength of magnetic field; a_i and a_j are the HFI constants for the i-th and j-th kind of nuclei, with spins I_i and I_j: m_i^a are the quantum numbers of the projections of the nuclear spins I_i in the first radical of the pair and m_j^b are those for its partner.

It follows from Eqns (1)–(3) that the rate of triplet–singlet conversion (and consequently the probability of chemical reaction in the RP) depends firstly on the magnetic field strength H through the difference in electron Zeeman energies $\Delta g\mu_B H$; secondly on the nuclear magnetic moments through the HFI constant a, since $a = (8\pi/3)\mu_e\mu_n|\psi(0)|^2$, where μ_e and μ_n are the magnetic moments of the electron and nucleus, $|\psi(0)|^2$ is the electron spin density at the nucleus; thirdly on the nuclear spin orientation I_z through the quantum numbers m_i^a and m_j^b.

The reaction probability of the RP may be represented in the closed form as $P = F(H, a, I_z)$. This compact formula embodies the three main magnetic effects of the first generation (see Fig. 1*b*).

III. First generation of magnetic effects

1. Magnetic field effect

The modern theory of the MFE, based on the extended spin dynamics, identifies two main MFE sources.

1. In zero and in very low magnetic fields the S and T spin states are almost degenerate and the spin conversion involves all four states (S, T_0, $T_\pm$). In high fields the degeneracy of triplet substates is lifted and the $T_\pm$ levels are separated from the S state by Zeeman interaction and excluded from the spin conversion, so that the rate of the triplet–singlet RP transformation is reduced to approximately one third of the rate in zero field.

If the starting spin state of the pair is singlet the magnetic field closes the $S-T_\pm$ channels and partly locks the pair, increasing its chance to react. Conversely, if the starting state is triplet the magnetic field switches off the T–S conversion and partially suppresses (by about 60%) intra-pair chemical reactions.

The $T_\pm-S$ spin conversion is induced by HFI (usually in the 1–150 G range),† and therefore even these low magnetic fields ($H \approx a$) are sufficient to decouple electron–nuclear spin subsystems and produce marked and even multiple changes in reaction rates.

† 1 G = 10^{-4} T.

2. The rate of spin conversion by the T_0-S channel is magnetic field dependent according to Eqn (1). As in the previous case, the sign of the MFE is a function of the starting spin state: the magnetic field enhances the leakage of the reactive singlet pairs into nonreactive triplet pairs, and has the opposite effect on triplet pairs. As a result the magnetic field accelerates the reactions starting from triplet pairs (and triplet RP precursors) and hinders the reactions in singlets and in their precursors.

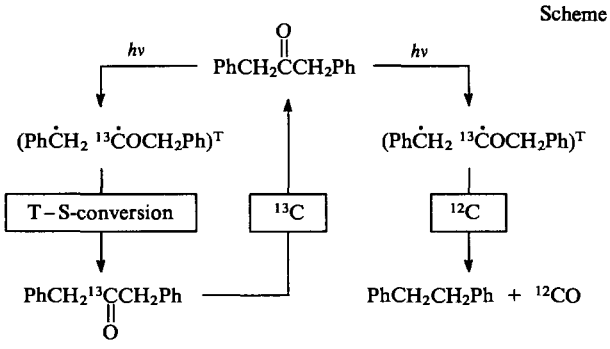
These two sources of MFE are easily distinguished because of the difference in their response to changes in the magnetic field: the field dependence for the MFEs originating from $T_{\pm}-S$ spin conversion channels reaches saturation at $H \gtrsim a$, while the magnitude of MFEs induced by T_0-S conversion varies monotonically with the magnetic field. For the RP with short-lived radicals (life-time $\tau \ll |Q_{ab}|^{-1}$) the effect is proportional to $(\Delta g \mu_B H)^2$, whereas for long-lived RPs ($\tau \gg |Q_{ab}|^{-1}$) the effect is proportional to $(\Delta g \mu_B H)^{1/2}$.[5] Furthermore it is evident that the signs of MFEs arising from these two sources are opposite; this provides an important criterion for identifying the spin states of the RPs and their precursors through the sign of the MFE.

2. Magnetic isotope effect

The coupling between chemical species or spin carriers (between radicals, in particular), being electron spin selective, must also be nuclear spin selective, since the two spin subsystems (electronic and nuclear) are coupled by Fermi HFI interaction. The nuclear spin system affects the magnetic behaviour of the electron spin system, thus influencing the chemical reactivity. The nuclear spin selectivity of chemical reactions produces a difference between the reaction rates of radicals (or, in general, of any other spin bearing chemical species) having magnetic or nonmagnetic nuclei. The name magnetic isotope effect (MIE) has been suggested by the present writer for this phenomenon, in contrast to the well known classical isotope effect (CIE) which follows from the nuclear mass selectivity of chemical reactions.[4,7]

A striking result of the MIE is the chemically induced separation of magnetic from nonmagnetic isotopes. MIE-induced isotope selectivity may be clearly exemplified by the photolysis of dibenzylketone (DBK), which is known to occur via the fragmentation of the excited triplet molecule and generation of a triplet RP (Scheme 1). The triplet RP can either undergo triplet–single spin conversion (driven by HFI) and recombine, recreating the starting ketone, or it can dissociate into the separate radicals $Ph\dot{C}H_2$ and $PhCH_2\dot{C}O$; the latter decomposes into $Ph\dot{C}H_2$ and CO. The main reaction products are dibenzyl $(PhCH_2)_2$ and carbon monoxide (Scheme 1).

Scheme 1



The rate of triplet–singlet conversion for magnetic RPs (i.e. the pairs with magnetic ^{13}C nuclei in benzoyl or benzyl radicals) is higher than that for nonmagnetic pairs (with nonmagnetic ^{12}C nuclei). Therefore the magnetic RPs will preferentially recombine and regenerate the starting ketone molecules, while the time lag of the triplet–singlet conversion in nonmagnetic RPs makes dissociation more likely for these pairs. As a result ^{13}C magnetic nuclei are accumulated in the ketone molecules, while carbon monoxide and dibenzyl are enriched in the ^{12}C nonmagnetic isotope. Thus, because of the difference in the rates of triplet–singlet spin conversion, the RPs can separate the nuclei according to their magnetic moments: they dispatch the magnetic and the nonmagnetic nuclei into the different chemical products.

MIE is a phenomenon of fundamental importance. It establishes a new chemical principle of isotope separation, it provides a new method of detection and identification of paramagnetic intermediates in chemical and biochemical processes, and it offers new ideas and approaches to problems in geochemistry, space chemistry, and molecular biology.[4,6,7]

3. Chemical polarisation of nuclei

Chemically induced dynamic nuclear polarisation (CIDNP) is the result of the nuclear spin selectivity of chemical reaction. The rate of T–S spin conversion according to Eqn (1) is a function of nuclear spin orientation, and therefore RPs which differ in nuclear spin orientation have different chemical reactivities. Hence the RP as a chemical reactor can not only separate magnetic from nonmagnetic nuclei (as it does in the MIE), but it can also assign differently oriented magnetic nuclei to different reaction products.

This is the first mechanism of CIDNP, which operates in high magnetic fields where the T_0-S channel of spin conversion is predominant. It selects the magnetic nuclei with respect to their orientations according to Eqn (1), and therefore the CIDNP is directly related to Δg and to a_i and to a_j.

The second CIDNP mechanism operates in low fields ($H < a$), where the $T_{\pm}-S$ channels also contribute to the RP spin evolution. The $T_{\pm}-S$ spin transitions are accompanied by reorientation of the nuclear spins, unlike the T_0-S transition which selects only the oriented nuclei without changing their alignment.

An excess of nuclear spins oriented with or against the field in the product molecules corresponds to overpopulation of the lower or the upper Zeeman nuclear levels respectively (for ^1H, ^{13}C, and ^{31}P nuclei with a positive magnetic moment). This non-equilibrium population manifests itself in the NMR spectra of the molecules as an anomalously strong absorption or emission, the latter corresponding to population inversion of Zeeman levels.

CIDNP is a well-known phenomenon, widely used as an efficient method of identifying reaction mechanisms and of detecting radicals and radical intermediates. CIDNP is a powerful means of defining the spin multiplicity of the radical pairs and of their molecular precursors, it can be used to separate radical from nonradical reaction pathways and to identify unstable intermediate products and reversible radical stages which cannot be detected by other methods. From the CIDNP kinetics we can determine the reaction rate constants, including those of fast reactions (10^8-10^9 s^{-1}). CIDNP can determine the signals of HFI constants in radicals in radicals and the spin-spin coupling constants in molecules, and it can also detect the hot, energy-rich radicals. The mechanisms of many types of chemical reaction have been studied by CIDNP and much valuable information has been collected.[8,9]

IV. Principles of chemical reception of microwaves

We should stress that the magnetic interactions do not influence the chemical reaction itself, i.e. that they do not affect the motion of chemically reacting atomic systems along the potential energy surface. Their effect is to switch the reaction from the spin-forbidden channels into spin-allowed ones, controlling the spin behaviour of the reactants (or vice versa, depending on whether the starting spin state of the reactants is spin-forbidden or spin-allowed). This statement applies to both the magnetic interactions (Zeeman, Fermi, dipolar, spin-orbital), specific to the reaction itself, and to the external electromagnetic fields and their influence on the spin-carrying reaction precursors (radical pairs in particular).

The principles of chemical reception of microwaves will be demonstrated by considering the RP example. The scheme of Zeeman energy levels of the RP is shown in Fig. 2. Let the pair be produced in a singlet spin state strongly coupled (for example, by HFI) with the triplet T_0 substate, so that the population of the mixed, ready-to-react ST_0 state is much higher than that of the T_+ or T_- substates. Resonant transitions between the T_0 and $T_\pm$ levels stimulated by an electromagnetic field (EMF) depopulate the reactive ST_0 mixed state and suppress the intrapair reactions, lowering the yield of reaction product from the singlet reaction channel. Conversely, if the starting spin state of the pair is triplet the reaction along the singlet channel depletes the population of the mixed ST_0 state: however, the $T_\pm - T_0$ pumping induced by the EMF additionally populates the reactive ST_0 state and increases the yield of reaction products. In general the EMF rearranges the spin system, switching the reaction between channels of different spin multiplicity and modifying the chemical reactivity of the RP as is found with other magnetic interactions.

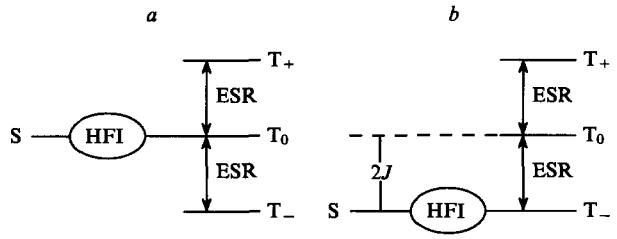


Figure 2. Microwave pumping of the Zeeman levels of a radical pair: (*a*) without exchange interaction ($J = 0$) the $T_\pm - T_0$ transitions stimulated by the EMF populate or depopulate (by hyperfine interaction) the ST_0 state; (*b*) in the presence of exchange interaction ($2J \approx g\mu_B H$) microwave pumping populates or depopulates the reactive mixed ST_- state. Possible ESR transitions are shown by arrows.

The exchange interaction J which appears at small inter-radical distances splits the S and T_0 levels, so that the T–S mixing now occurs only in the level crossing region (Fig. 2*b*), where $g\mu_B H \approx 2J$. However, in the spin evolution of the RP with distant partners the exchange interaction can be ignored. This situation is often met because the RP spends most of its lifetime in the state with remote partners.

Microwave pumping of the spin transitions modifies the rate of spin evolution of the RPs and therefore also their chemistry, providing a new principle of resonant, frequency-tuned chemical reception of microwaves. The change of the yield of products is the true chemical response to the perturbation of the reacting spin system by the EMF. (The frequency spectrum of the response is equivalent to the microwave absorption spectrum of the RP, and is therefore identical to its ESR spectrum.) Varying the external magnetic field H_0 allows us to detect the ESR spectrum of the RP by monitoring the yield of any product related to the reaction in the RP. Frankevich, who discovered the phenomenon, suggested the name Reaction Yield Detected Magnetic Resonance (RYDMR) for it.[10]

In order to visualise the spin transition induced by the EMF we shall consider the vector representation of spin dynamics in the radical pair.[2] To extract magnetic energy from the electromagnetic wave a particular polarisation is required: the magnetic vector $\vec{H}_1$ of the wave should lie in a plane normal to the permanent external magnetic field $\vec{H}_0$ (Fig. 3). The magnetic moment $\vec{M}_1$ of the spin carrier [assumed to have a spin $S = (1/2)\hbar$, so that $M_1 = (1/2)g_1\mu_B$] precesses with a Larmor frequency $\omega = \gamma H_0$ round the $\vec{H}_0$ magnetic field directed along the Z axis; $\gamma = g_1\mu_B/\hbar$ is the gyromagnetic ratio. The $\vec{H}_1$ vector of the EMF is directed along the Y axis: its value is $2\vec{H}_1 = 2H_1 \cos \omega t$. The total motion of the vector $2\vec{H}_1$ can be

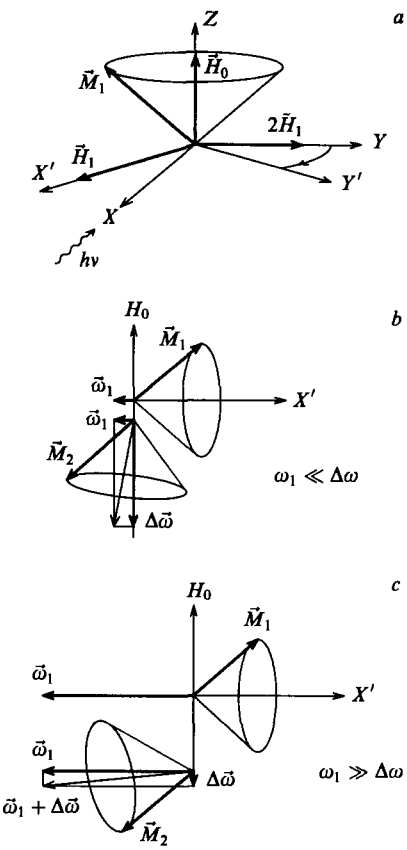


Figure 3. Vector diagram of the spin dynamics of a radical pair developed under the influence of the microwave field $\vec{H}_1$ (symbols defined in the text).

resolved into two circularly polarised vectors $\vec{H}_1$ rotating with a frequency ω in the XY plane in mutually opposite directions (Fig. 3*a*). One of these vectors, $\vec{H}_1$, rotating in phase with the Larmor precession appears to be motionless in a new frame of coordinates X', Y', Z chosen to rotate with the magnetic moment $\vec{M}_1$.

In this new, rotating frame the vector $\vec{M}_1$ experiences only the magnetic field $\vec{H}_1$ which is now permanent, and rotates round its direction with a frequency $\omega_1 = \gamma H_1$. This motion is equivalent to a periodic reorientation of the $\vec{M}_1$ vector with respect to the Z axis and therefore to $\vec{H}_0$. The magnetic moment $\vec{M}_2$ of the partner behaves similarly if the Larmor frequency of its precession is also equal to ω. These orientations are easily seen to correspond to $T_\pm - T_0$ spin transition.

We shall now assume that the magnetic moments $\vec{M}_1$ and $\vec{M}_2$ are not equivalent, owing to the difference Δg between their g-factors or to the hyperfine coupling a_2. Then the difference in the precession frequencies of the $\vec{M}_1$ and $\vec{M}_2$ vectors, $\Delta\omega$, is equal to $\Delta g\mu_B H_0/\hbar$ or $g_2\mu_B a_2/\hbar$ respectively. In the X', Y', Z frame rotating with the Larmor frequency of M_1 this vector is again motionless. However, the vector $\vec{M}_2$ now precesses with respect to $\vec{M}_1$ with a frequency $\Delta\omega$. This motion is equivalent to a $T_0 \rightleftarrows S$ spin evolution (Fig. 3*c*).

Switching on an EMF small enough (H_1) to satisfy the condition $\omega_1 \ll \Delta\omega$ stimulates the $T_0 \rightleftarrows T_\pm$ transitions responsible for the RYDMR phenomenon. At higher values of H_1, when $\omega_1 \geqslant \Delta\omega$, the vector $\vec{M}_1$ precesses round the vector $\vec{H}_1$ (or $\vec{\omega}_1$) as before, but the magnetic moment $\vec{M}_2$ now precesses round a total vector $(\vec{\omega}_1 + \Delta\vec{\omega})$ with a frequency $(\omega_1^2 + \Delta\omega^2)^{1/2}$ (see Fig. 3*c*). This means that the singlet–triplet spin mixing now takes place with new difference frequency

$$\Omega = (\omega_1^2 + \Delta\omega^2)^{1/2} - \omega_1 \approx \frac{\Delta\omega^2}{2\omega_1},$$

which is less than $\Delta\omega$ itself. This implies that at high enough EMF amplitudes the mw irradiation alters the spin behaviour of the radical pair: instead of stimulating triplet–singlet transitions it begins to suppress them. The spin state of the pair at high EMF amplitudes when $\omega_1 \gg \Delta\omega$ (see Fig. 3*c*) appears to be locked, so that the phenomenon is called spin locking. It manifests itself in distortion and ultimately in phase inversion of the RYDMR spectra.[11]

The jump of the $S-T_0$ mixing frequency from $\Delta\omega$ to $\Delta\omega^2/\omega_1$ can influence the properties of the mixed ST_0 state only under conditions such that the lifetime of the pair τ satisfies the relation $\tau < \omega_1/\Delta\omega^2$. Conversely, for $\tau \gg \omega_1/\Delta\omega^2$ the ST_0 mixing as well as the chemical properties of the pair will not depend on ω_1 and, therefore, on H_1 (spin scrambling). By varying ω_1 over wide limits and studying the dependence of the RYDMR spectra on ω_1 (or H_1) we may determine both $\Delta\omega$ and the lifetime τ of the radical pairs.[2]

V. Reaction yield detected magnetic resonance

The frequency spectrum of the chemical response to mw pumping is essentially the RYDMR spectrum, which may be recorded by monitoring any parameter of the chemical system under investigation providing that it is kinetically related to the RP reaction (and therefore to the population of spin substates of the pair). Among the most easily and precisely measurable parameters used to detect RYDMR spectra are the luminescence intensity, optical absorption, electric conductivity and radical concentration.

Electronically excited molecules able to emit from their singlet or triplet states (fluorescence or phosphorescence respectively) are usually produced by the recombination of ion-radical pairs (or, more precisely, by electron transfer reactions between partners). For example, the reaction between the ion radicals $D^{\cdot+}$ and $A^{\cdot-}$ may occur along singlet or triplet channels:

$$D^{\cdot+} + A^{\cdot-} \longrightarrow {}^1(D^{\cdot+}\,A^{\cdot-}) \longrightarrow {}^1D + A_0 \longrightarrow$$
$$\longrightarrow D_0 + A_0 + h\nu \qquad \text{(fluorescence)}$$

$$D^{\cdot+} + A^{\cdot-} \longrightarrow {}^3(D^{\cdot+}\,A^{\cdot-}) \longrightarrow {}^3D + A_0 \longrightarrow$$
$$\longrightarrow D_0 + A_0 + h\nu \qquad \text{(phosphorescence)}$$

The mw pumping of the singlet pairs stimulates their singlet–triplet conversion, thus suppressing the fluorescence in favour of the phosphorescence. Conversely, the mw pumping of triplet pairs induces the opposite effect. However, the intensity of fluorescence is usually small, and therefore fluorescence is seldom used to detect RYDMR spectra. Most of the RYDMR experiments are based on fluorescence intensity measurements.

Fig. 4 shows the RYDMR spectrum for the ion-radical pair $(M^{\cdot+}\ M^{\cdot-})$ generated by positron irradiation of a solution of naphthalene in squalane.[12] The reactions resulting in the formation and recombination of aromatic ion-radical pairs are:

$$S \longrightarrow S^{\cdot+} + e,$$
$$M + e \longrightarrow M^{\cdot-},$$
$$M + S^{\cdot+} \longrightarrow M^{\cdot+} + S,$$
$$M^{\cdot+} + M^{\cdot-} \longrightarrow M^* + M,$$

where S and M are solvent and aromatic molecules, respectively, $M^{\cdot+}$, $M^{\cdot-}$, $S^{\cdot+}$ are their cation and anion radicals, and M^* is the excited aromatic molecule (the fluorescence emitter). The pairs $(M^{\cdot+}\ M^{\cdot-})$ are mostly formed in the Onsager sphere and in the singlet spin state, so that their reaction product along the spin-allowed channel is an excited M^* molecule in the singlet spin state.

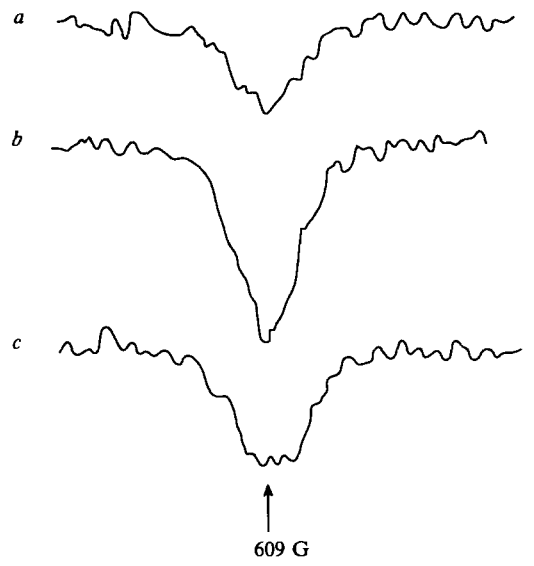


Figure 4. RYDMR spectra of an ion-radical pair [(naphthalene)$^+$/(naphthalene)$^-$] for a microwave pumping power of 1.3 (*a*), 3.8 (*b*), and 7.6 W (*c*).[12]

In order that the mw pumping may influence the spin evolution of the pair, two dynamic requirements must be satisfied:

$$\tau_{S-T_0} \lesssim (\gamma H_1)^{-1} \quad \text{and} \quad \tau_{RP} \approx (\gamma H_1)^{-1},$$

where H_1 is the amplitude of the mw field, $(\gamma H_1)^{-1}$ is the characteristic time of the mw-stimulated $T_0-T_\pm$ transitions, τ_{S-T_0} and τ_{RP} are the characteristic time of the $S-T_0$ spin evolution and of the lifetime of the ion-radical pair respectively.

The first relation ensures the fast $S-T_0$ transition and efficient chemical leakage of ion-radical pairs along the singlet channel, the second ensures that the pair undergoes mw-stimulated $T_0-T_\pm$ transitions before its disappearance.

The RYDMR signals (Fig. 4) are a single line with a halfwidth of 14 G, evidently due to the unresolved hyperfine structure of positive and negative naphthalene ion radicals, since the total HFI splitting is comparable to the width of the line. The centre of the RYDMR spectrum lies at 609 G, which corresponds to the *g*-factor of aromatic ion radicals at an operating frequency of 1704.6 MHz.

The optically detected RYDMR spectrum with resolved HFI splitting shown in Fig. 5 belongs to the ion-radical pair $(M^{\cdot+}\ M^{\cdot-})$, where M is biphenyl, generated under conditions similar to those used to generate the naphthalene ion-radical pair.[13]

As well as the radical–radical interactions, the chemical and physical processes in triplet–triplet and triplet–doublet pairs can be studied by the RYDMR technique in liquids and in molecular solids. The dynamics and mechanism of the triplet exciton annihilation and the quenching of triplet molecules by radicals and other spin carriers can also be elucidated by this technique. The mw pumping changes the population of the Zeeman spin levels in T–T or T–D pairs (as it does in D–D pairs) and thus controls the intensity of the prompt or the delayed fluorescence.[14]

The scheme of spin levels and mw-stimulated interlevel transitions in a pair of triplet excitons is shown in Fig. 6 as an example. In a strong magnetic field H two of the nine spin states of the pair (SQ_1 and SQ_2) include singlet components with amplitudes equal to $\frac{1}{2}$ and $\frac{2}{3}$ respectively. The singlet components of these states are mixed with the components of the quintet state, but the other states of the two-triplet pair ($Q_{\pm1}$ and $Q_{\pm2}$) are pure triplets and quintets.

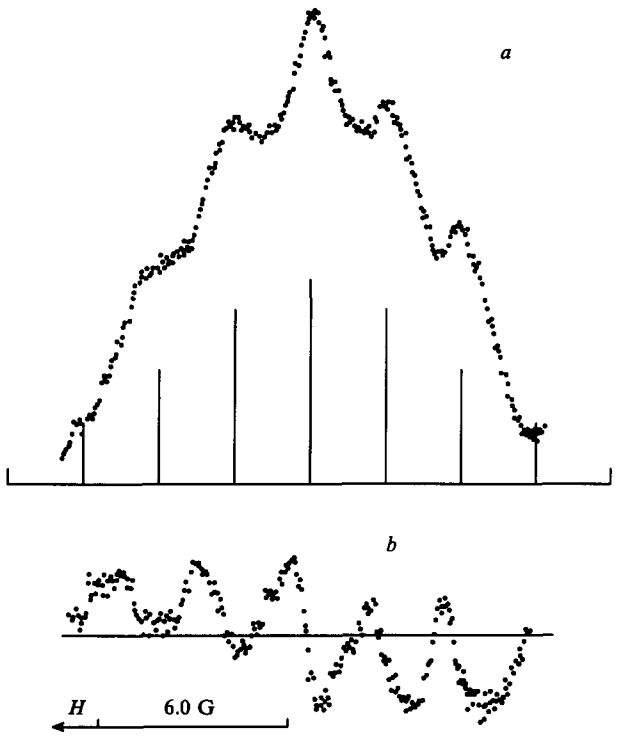


Figure 5. RYDMR spectrum of the (biphenyl)$^+$ – (biphenyl)$^-$ radical pair (*a*) and its first derivative (*b*).[13]

Upon exposure to a resonant mw field, transitions involving a change in the projection of the magnetic quantum number m by $\Delta m = \pm 1$, with the total spin S preserved ($\Delta S = 0$) are allowed. These transitions, shown by arrows in Fig. 6, increase the population—the SQ_1 and SQ_2 states which generate the annihilation product: the excited molecule which emits the fluorescence.

The mw-stimulated spectrum of the triplet exciton pair detected by the prompt fluorescence of the tetracene molecule in a tetracene single crystal is shown in Fig. 7 for

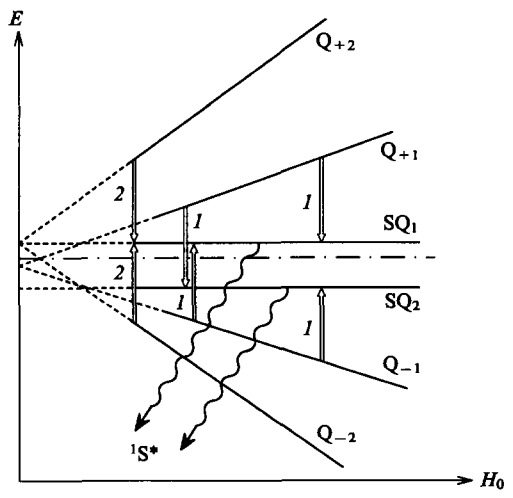


Figure 6. Energy level diagram of a triplet molecule pair: the Q levels are pure quintet states, SQ_1 and SQ_2 are levels of mixed quintet – singlet states. Triplet-levels do not contribute to the spin transitions and are not shown in the diagram. The arrows indicate transitions which populate the mixed SQ states and the formation of a source of fluorescence (the $^1S^*$ molecules).

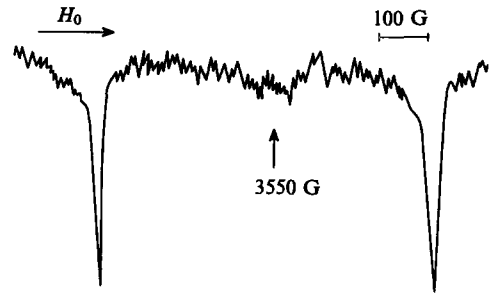


Figure 7. RYDMR spectrum of a pair of triplet excitons in a tetracene single crystal, detected by the prompt fluorescence.[15]

one particular orientation of the crystal with respect to the magnetic field.[15]

RYDMR spectra have been observed in studies of excitons and of charge-transfer complexes in liquids and in solids, F-centres in alkali halide crystals, electron-hole pairs in amorphous semiconductors, the reaction centres in photosynthetic systems, etc.[2,5]

The sensitivity of the RYDMR technique can be estimated. The relative variation $\Delta\gamma$ in the yield of the reaction in pairs produced by resonant mw-induced transitions is determined by the product of the probability P of the transition under the action of mw magnetic field H and of the lifetime τ of the pair:

$$\frac{\Delta\gamma}{\gamma} = \varkappa P\tau \,. \tag{4}$$

For a radical as a particle with a spin of $\frac{1}{2}$

$$P = \frac{1}{2}\left(\frac{g\mu_B}{\hbar}\right)^2 \frac{H_1^2\tau}{1 + (g\mu_B/\hbar)(H_0 - H_{res})} \,. \tag{5}$$

The coefficient $\alpha \leqslant 1$ determines the relative variation in the yield γ if the multiplicity of the pair is completely changed. At resonance ($H_0 = H_{res}$)

$$\frac{\Delta\gamma}{\gamma} = \alpha\omega_1^2\tau^2 \,, \tag{6}$$

where $\omega_1 = (g\mu_B H_1/\hbar)$. It is easily seen that for pairs with a lifetime $\tau = 5 \times 10^{-9}$ s a value of $\Delta\gamma/\gamma$ of about 1% is achieved for $H_1 = 1$ G at $\alpha = 1$. The very high sensitivity of the RYDMR technique is strikingly illustrated for the aromatic ion-radical pairs in liquids. They are generated at the rate of 2×10^8 s^{-1}, and have a lifetime of 10^{-7} s,[12] and hence the average concentration of the radical pairs available for detection by fluorescence intensity measurements is about 20 per sample, i.e. well below the sensitivity limit of modern ESR spectroscopy ($\sim 10^{11}$ spins per sample).[12]

The RYDMR spectra can be detected also by the optical absorption of triplet molecules produced by the pair-wise coupling of ion-radicals along the triplet channel. These molecules are usually sufficiently long-lived to be accumulated in measurable amounts and monitored by the triplet–triplet absorption of the probing light (in pulse excitation experiments, in particular).

The dissociation of ion-radical or electron-hole pairs produces free charge carriers in concentrations which are susceptible to the mw pumping of the pairs. Therefore RYDMR spectra can be also recorded by monitoring the electric conductivity both in crystals and in liquids.[2] Similarly, the dissociation of pairs of neutral radicals in solutions generates free radicals. This process is spin-independent, but it competes with the spin-selective intrapair coupling, and therefore the yield of free radicals which have escaped recombination should be as

sensitive to the mw pumping as the recombination itself (but, of course, in anti-phase).

RYDMR spectra detected by counting free radicals were first reported by Okazaki et al.,[16] who studied the photoreduction of menadione (MD, 2-methylnaphthoquinone) in sodium dodecyl sulfate (SDS) micelles. The reaction includes the removal of a hydrogen atom from the SDS molecule by the excited MD in triplet state:

$$^3MD + SDSC \longrightarrow (\dot{M}DH\ \dot{S}DS) \begin{cases} \longrightarrow \text{coupling products} \\ \longrightarrow M\dot{D}H + \dot{S}DS \end{cases}$$

Only $\dot{S}DS$ radicals are trapped by the added water-soluble nitroso spin trap TNO (perdeuterodimethylnitrosobenzene sulfonate) because the chemical reactivity of the spin trap towards the semiquinone radical $M\dot{D}H$ is negligibly low. The yield of the stable spin adduct [the nitroxyl radical T(SDS)NO] measured by ESR was shown to decrease under mw-pumping (in keeping with the reaction scheme). Indeed, stimulating the triplet-singlet conversion of the RP by resonant mw irradiation induces chemical annihilation of the pair. As a result, the leakage of free radical out of the pair (and consequently the yield of spin adduct) decreases quite noticeably, as shown by Fig. 8. The largest reduction in the yield reaches 8% for the photolysis of protonated SDS micelles and about 14% if the photolysis is carried out in deuterated micelles. The magnetic field dependences of the mw-stimulated chemical response are in fact RYDMR spectra detected by radical escape measurements. The difference in their hyperfine structure confirms the difference in isotopic composition of one of the RP partners: the SDS radical, in which hydrogen nuclei are replaced by deuterons.

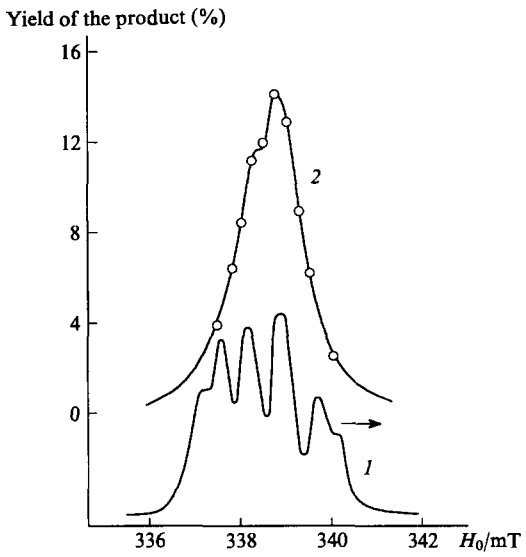


Figure 8. Dependence of the yield of the spin adduct under microwave pumping on the strength of the magnetic field H (or RYDMR spectra) for the photolysis of menadione in SDS (*1*) and deutero-SDS micelles (*2*).[16]

VI. Radio induced magnetic isotope effect

As a means of resonant chemical reception of microwaves RYDMR is nonselective because all the RPs are subjected to the mw perturbation. If the mw pumping is selective with respect to magnetic nuclei it induces a new, Radio Induced Magnetic Isotope Effect (RIMIE). The microwave irradiation of magnetic RPs should accelerate their spin conversion and stimulate their pair-wise reactions (usually recombination), enhancing the nuclear isotope selectivity induced by MIE of the first generation.

The concept of the RIMIE was clearly formulated[17] in 1981 and experimentally embodied[18] in 1991 in the photolysis of dibenzyl ketone (DBK) in SDS micelles. The photolysing laser pulses were synchronised with the mw pulses, and their lengths were chosen so that the RP generated by short laser pulses were exposed to the mw pulse throughout their life time. The frequency of the mw irradiation was chosen to pump selectively only the magnetic RPs [$Ph\dot{C}H_2$ $^{13}\dot{C}(O)CH_2Ph$], while the non-magnetic RPs [$Ph\dot{C}H_2$ $^{12}\dot{C}(O)CH_2Ph$] remained unperturbed by the microwaves (see Scheme 1).

The isotope enrichment S of dibenzyl ketone as a function of chemical conversion is described by the expression

$$\ln S = (1-\alpha)\ln(1-f^*), \qquad (7)$$

where $S = \delta/\delta_0$, δ_0 and δ are respectively the ^{13}C content in the starting ketone and in its residue after the chemical conversion of the 'magnetic' ketone $PhCH_2{}^{13}C(O)CH_2Ph$ has reached the value f^*.[4] The coefficient α is the efficiency of the isotope separation (a one-step enrichment coefficient similar to that introduced by Bernstein[19] for the classical, mass-dependent isotope effect).

The experimentally measured isotope enrichment S of DBK as a function of $1-f^*$ in the parameters of Eqn (7) is shown in Fig. 9. As can be seen the one-step enrichment coefficients are different: for the photolysis in the presence of mw $\alpha_{mw} = 1.25 \pm 0.01$, while without mw pumping we have $\alpha_0 = 1.21 \pm 0.01$. Thus the mw irradiation is found to increase the isotope selectivity in the RP and the isotope enrichment of the recovered ketone.

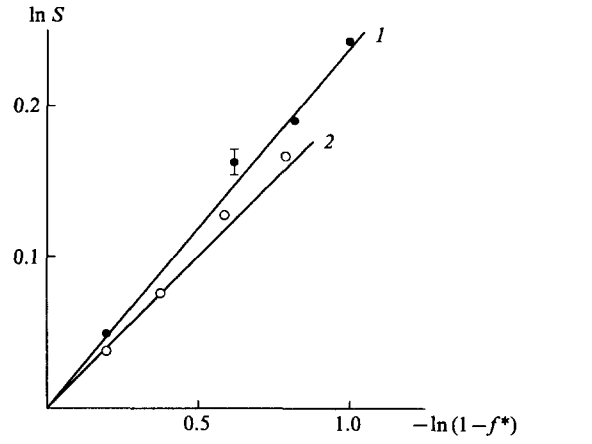


Figure 9. Isotope enrichment S as a function of the chemical conversion f^* of ^{13}C dibenzyl ketone in the coordinates of Eqn. (7):[18] (*1*) with microwave pumping (H_1 = 4.5 G); (*2*) without pumping.

The net contribution of the mw pumping to the recombination probability of the magnetic radical pair is about 6%. This value seems too small at first sight, but allowance should be made for the unfavourable experimental conditions. Firstly, the pumping of only one RP was carried out, which reduces the efficiency of mw irradiation at least two-fold. Secondly, the low amplitude of the mw pumping (H_1 = 0.3 mT) corresponds to the characteristic time of the mw-induced electron spin flip (the time of equilibrating the populations of $T_\pm - T_0$ spin levels) $\tau_{mw} = (\gamma H_1)^{-1} = 120$ ns. It is much larger than the time interval between radical reencounters in the radical pair (τ_{enc} = 136 ns), so that the pair has not enough time between reencounters to complete the mw-induced spin reorientation, and therefore the $T_\pm - T_0$ transition. This unfavourable relation ($\tau_{mw} > \tau_{enc}$) is probably the main reason for the relatively low efficiency of the mw pumping in the isotope selection. High amplitude microwave pumping would be desirable to bring τ_{mw} closer to τ_{enc} in order to equilibrate the

populations of the $T_{\pm}$ and T_0 states of the radical pair before the moment when the probing contact of the partners takes place.

From this viewpoint the spin locking regime for the nonmagnetic pairs ($PhCH_2$ $^{13}C(O)CH_2Ph$) is thought to be favourable to the separation of isotopes, since it prevents their recombination and thus increases the efficiency of isotope selection. A combination of the two regimes (spin locking for the nonmagnetic pairs and stimulating microwave pumping for the magnetic pairs) would be most efficient.

In these experiments the ideal selectivity of mw pumping is achieved, because the ESR transitions of 'magnetic' and 'nonmagnetic' RP do not overlap and are separately accessible to the pumping action. The radio induced magnetic isotope effect with partially selective pumping was observed by Okazaki et al.[20] even earlier (in 1988) in the photolysis of menadione in SDS micelles consisting of a mixture of protonated and of deuterated sulfonate molecules in a 1 : 1 ratio. The RYDMR spectra of this system were detected from the yield of SDS radicals (see Section V), taken up by the spin trap and measured as nitroxyl radicals. The spectra are shown in Fig. 8: their overlap prevents the separate pumping of the isotopic forms of the radical pairs, but even with joint, nonselective pumping the yields of protonated and of deuterated SDS are markedly different.[20]

VII. Microwave stimulated nuclear polarisation

Stimulated Nuclear Polarisation (SNP) is the result of mw pumping of ensembles of RPs with selected orientations of the nuclear spins. It is similar to CIDNP, the only difference being that in CIDNP the nuclear spin selection in the RPs via triplet-singlet conversion is accomplished by existing magnetic interactions characteristic of the radicals, whereas in SNP the selection is produced by the resonant microwave field. Again, the radical pair acts as a selective chemical microwave receiver, but now the indicator of the reception is the nuclear polarisation in reaction products.[21]

In chemical reaction subjected to resonant (and therefore nuclear spin selective) mw pumping these two phenomena, CIDNP and SNP, can coexist, so that the experimentally measured NMR spectrum of the product molecules displays both contributions. The experimental technique which can distinguish between them by performing the pumping and the detection separately in time and space was developed by Sagdeev and his coworkers,[26] the pioneers and leaders of SNP studies.[22–25] This technique eliminates the CIDNP contribution and measures the net nuclear polarisation, induced by mw pumping.

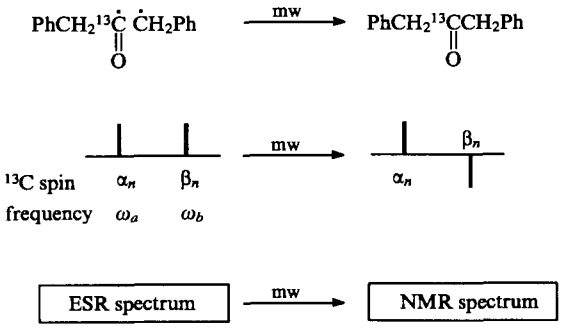


Figure 10. Development of SNP. The selective pumping of the ensemble of radical pairs with α_n and β_n orientations of the spins of ^{13}C nuclei at frequencies ω_a and ω_b accelerates their triplet-singlet conversion and transforms the ESR spectrum of the pair into the NMR spectrum of the molecule produced by its recombination (the molecule inherits the nuclear orientations of its precursor: the radical pair).[2]

The fundamental physics of the SNP phenomenon can again be clearly exemplified by the spin processes in the triplet radical pair [$PhCH_2{}^{13}C(O)CH_2Ph$], generated by the photolysis of DBK (Fig. 10). The ESR spectrum of the pair consists of a central group of lines (not shown in Fig. 10) which belong to the $PhCH_2$ radical, and of a doublet from the $PhCH_2{}^{13}CO$ radical with hyperfine splitting $a(^{13}C)$. Since $a(^{13}C)$ is known to be positive, the low-field line of the doublet is attributed to the ensemble of RPs with ^{13}C nuclei oriented with the field (α_n, spins on the lower Zeeman level), whereas the high-field line belongs to the ensemble with ^{13}C nuclei oriented against the field (β_n, spins on the upper Zeeman level). The fast intersystem T_0-S conversion induced by the HFI equalises the populations of these two spin levels. The mw pumping of the ESR transitions in the first ensemble of pairs at a frequency ω_a stimulates the $T_{\pm}-T_0$ spin conversion and additionally populates the T_0 states of the pairs with nuclear spins α_n causing acceleration of their recombination and the dominant formation of the DBK molecules with α_n spins (the positive SNP). The mw pumping of the second RP ensemble with β_n nuclear spins at frequency ω_b selectively produces DBK molecules with ^{13}C nuclei having β_n spins (the negative SNP). As a result the mw pumping transforms the ESR spectrum of the radical pair into NMR spectrum of a molecule with polarised nuclei, or an SNP spectrum of the absorption-emission, A/E type (Fig. 10, absorption in the high-field component and emission in the low-field component).

As a physical phenomenon SNP offers a powerful method of investigating the chemical reaction mechanisms and of detecting their radical intermediates. This is clearly illustrated by the SNP in the photolysis of deoxybenzoin $PhCOCH_2Ph$ in SDS micelles.[22] The quantum yield of its photolysis is very low: the products are formed in undetectable amounts. In the ^{13}C CIDNP spectra no lines are produced by photolysis with the exception of a single line belonging to the carbonyl ^{13}C nuclei of the starting ketone. It shows strong emission and indicates reversible photochemical processes accompanied by the almost complete regeneration of the starting ketone, so that the reaction scheme is:

$$PhCOCH_2Ph \rightleftharpoons X,$$

where X is the unknown intermediate responsible for the CIDNP of this ketone.

Tarasov and Bagryanskaya[25] have studied the ^{13}C SNP in this system and interpreted the strong SNP spectra (Fig. 11) as a superposition of two doublets. The first (A/E, with a splitting of 120 G) has been attributed to the acyl radical $Ph^{13}CO$, whereas the second, a poorly resolved A/E doublet with a smaller splitting (30 G), was attributed to the radical

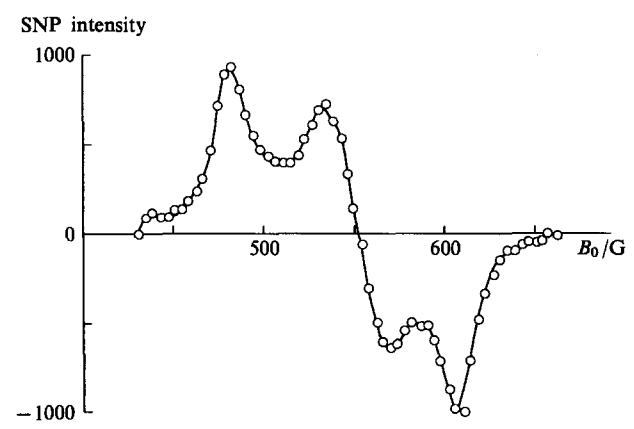


Figure 11. SNP spectrum detected during the photolysis of deoxybenzoin in SDS micelles.[25]

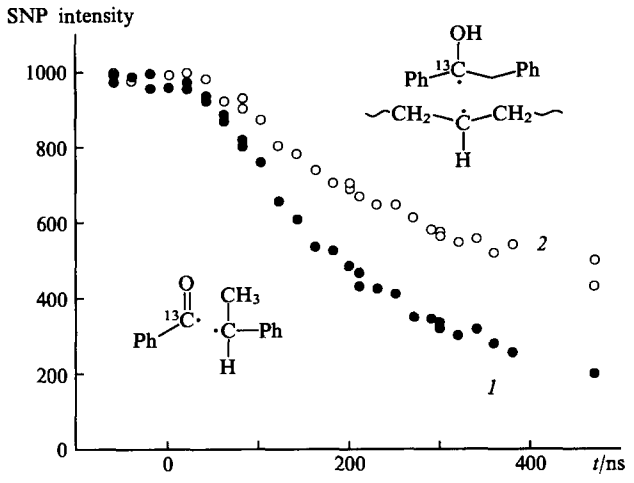


Figure 12. Kinetic behaviour of radical pairs generated by the photodissociation (*1*) and photoreduction (*2*) of deoxybenzoin in SDS micelles.[25]

$Ph^{13}C(OH)CH_2Ph$, the primary product of the photoreduction of the excited triplet ketone by the SDS molecule (RH). These SNP spectra suggest two competing paths for the photochemical transformation of deoxybenzoin: photodissociation and photoreduction via two different intermediates X {the radical pairs $(PhCOCH_2Ph)^T$ and $[PhC(OH)CH_2Ph\ R]^T$ respectively}. Both are highly reactive with respect to the ketone regeneration reaction, though their kinetic behaviour (Fig. 12) is different: the recombination is faster in the former than the disproportionation is in the latter.[25]

In stationary SNP detection the radical pairs are exposed to mw pumping throughout their lifetime. In time-resolved (TR) SNP experiments the laser and mw pulses are separated by the time delay τ_d, and therefore TR SNP offers a new possibility of influencing the ensembles of RPs with lifetimes in selected time domains but not shorter than the time resolution (about 30 ns in the best experiments by Sagdeev and coworkers[26–28]).

The study of the photolysis of benzoyl peroxide in CD_3OD [26] is a good illustration of the application of TR SNP. The reaction is known to involve a sequence of singlet RPs, including the pair $(PhCO_2Ph)$ which contains a phenyl radical not accessible by conventional ESR technique under standard conditions. The SNP spectra recorded at $\tau_d = 0$ (Fig. 13) show SNP of opposite signs for the cage (phenyl benzoate) and the escape (benzene) products, in excellent agreement with the reaction scheme and the SNP mechanism. However the TR SNP spectra taken with $\tau_d > 50$ ns are found to be completely inverted for both products. This is because, in the time domain of 50–200 ns, in which the inverted TR SNP spectra have been observed, the SNP is generated in the diffusional RPs such as $(PhPh)$ or $(PhCD_2OD)$. The sign of the SNP in these pairs is the same as in triplet RP. At times $\tau_d < 50$ ns the SNP is completely attributed to the geminal RP $(PhCO_2Ph)$ in the singlet state. The phase inversion as a function of τ_d is shown in Fig. 13*b*: two time domains corresponding to SNP in geminal and in diffusional radical pair ensembles are clearly shown.

A micelle (a microreactor with a boundary surface) confines the RP in a restricted volume. Hence the interradical exchange energy J in micellised RP should be a function of the micelle size, so that the SNP spectra, being sensitive to J, are in fact probes which monitor the exchange energy in RP.

A convincing confirmation of this statement was given by Tarasov et al.,[29] who studied the photolysis of methyldeoxybenzoin (99% ^{13}C abundance in the carbonyl group) in micelles of varying size controlled by the number n of carbon atoms in the detergent molecule $CH_3(CH_2)_{n-1}SO_4Na$. As expected the SNP spectra were strongly dependent on n and therefore on the micelle size (Fig. 14). Both the line broadening and the decrease in doublet splitting are evidence of an increase in J in the

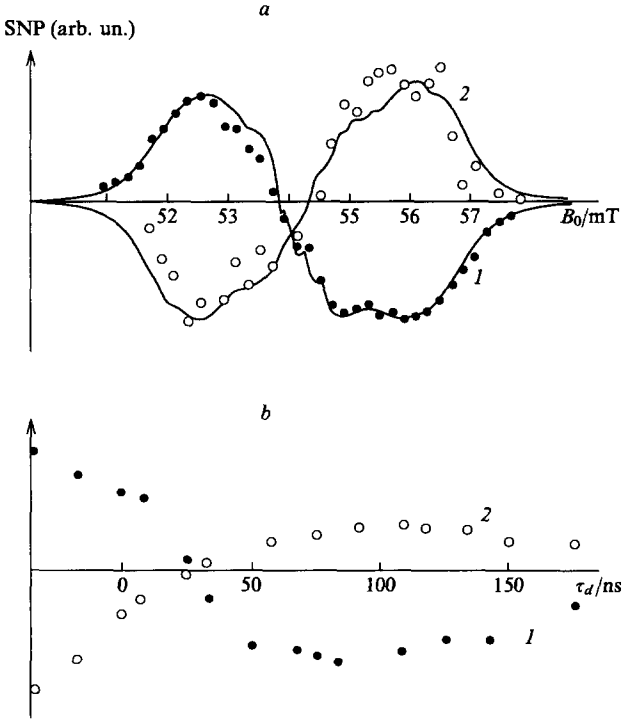


Figure 13. TR SNP spectra of phenyl benzoate (*1*) and benzene (*2*), detected by ^{13}C NMR during the photolysis of benzoyl peroxide (*a*), and their phase inversion as a function of τ_d (*b*).[26]

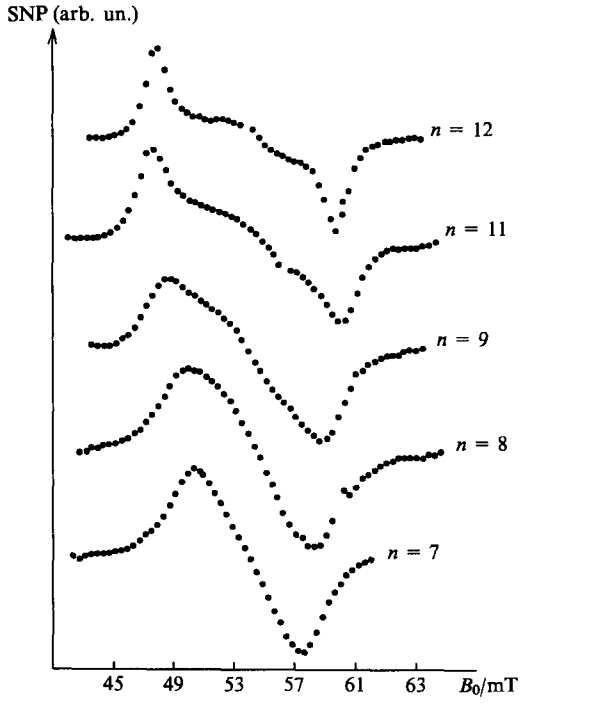


Figure 14. ^{13}C SNP spectra of the radical pair generated by photodissociation of deoxybenzoin in micelles of different size (n is the number of carbon atoms in the detergent molecule).[25]

[Ph^{13}ĊO ĊHMePh] RP as the micelles become smaller. Only in SDS micelles (n = 12) J is negligibly small and the doublet splitting corresponds to the hyperfine coupling constant $a(^{13}C)$ in the PhĊO radical (124 G). The doublet splitting and the J values are given below:[29]

n	$a(^{13}C)$/mT	J/mT
12	12.4	<0.1
11	12.0	0.5
9	10.0	3.4
8	8.4	8.0
7	7.6	14.0

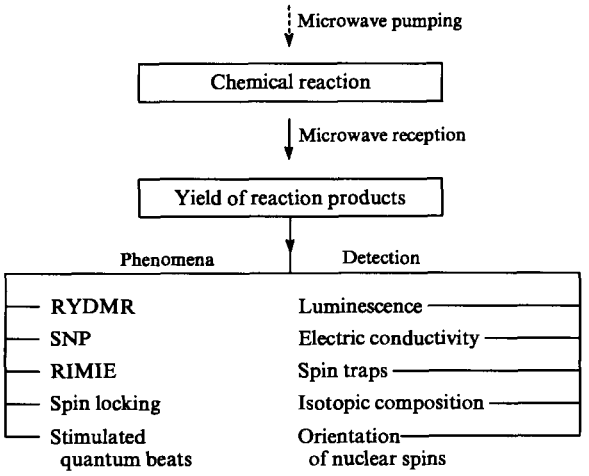
This information is of value for constructing the potential energy surfaces of the interradical reactions and for calculating the spin dynamics and the magnetic effects more exactly.

The strategy of magnetically probing the exchange potential (by SNP spectroscopy, in particular) along the reaction coordinate of chemical bond formation or dissociation is an important supplement to the transition state spectroscopy based on the femtosecond time-resolved optical spectroscopy developed by Zewail.[30] The difference is that femtosecond spectroscopy probes the transition state at short interatomic distances, where $J \gg kT$, whereas magnetic probing deals with the long-distance exchange potential ($J \ll kT$). From this point of view microwave magnetic probing can be treated as the radio spectroscopy of the transition state (the analogue of Zewail's transition state optical spectroscopy).[31]

VIII. Conclusion

Magnetic interactions (as a principal factor in the magnetic scenario of chemical reactions) regulate the spin dynamics and control the spin multiplicity of the radical pairs (as well as the pairs of other spin bearers), and therefore they also control their chemical reactivity. Electromagnetic fields influence the spin dynamics as a new factor which plays new scenes and initiates new phenomena: RYDMR, SNP, RIMIE, spin locking, quantum beats (the latter is beyond the scope of this paper). These remarkable magnetic effects of the second generation are schematically summarised in Scheme 2 as indicators of the chemical reception of radiowaves and microwaves.

Scheme 2



The author is grateful to the readers of this review and hopes that it will inspire them to use the achievements of electromagnetic spin chemistry. Financial support from the Russian Fund for Fundamental Research (grant 93-03-5227) is gratefully acknowledged.

References

1. K M Salikhov, Yu N Molin, R Z Sagdeev, A L Buchachenko *Spin Polarisation and Magnetic Effects in Radical Reactions* (Amsterdam: Elsevier, 1984)
2. A L Buchachenko, E L Frankevich *Chemical Generation and Reception of Electromagnetic Waves* (New York: VCH Publ., 1993)
3. U E Steiner, T Ulrich *Chem. Rev.* **89** 51 (1989)
4. A L Buchachenko *Progress in Reaction Kinetics* **13** 163 (1984)
5. Ya B Zel'dovich, A L Buchachenko, E L Frankevich *Usp. Fiz. Nauk* **155** 3 (1988)
6. A L Buchachenko, V F Tarasov *Acc. Chem. Res.* in press (1993)
7. I R Gould, N J Turro, M B Zimmt *Adv. Phys. Org. Chem.* **20** 1 (1984)
8. *Chemically Induced Magnetic Polarization* (Eds A R Lepley, G L Closs) (London: Wiley, 1978)
9. A L Buchachenko *Khimicheskaya Polyarizatsiya Elektronov i Yader* (Chemical Polarisation of Electrons and Nuclei) (Moscow: Nauka, 1974)
10. E L Frankevich, A I Pristupa, V I Lesin *Chem. Phys. Lett.* (47) 304 (1977)
11. S I Kubarev, S V Sheberstov, A S Shustov *Chem. Phys. Lett.* (73) 370 (1980)
12. O A Anisimov, V M Grigoryants, V K Molchanov, Yu N Molin *Chem. Phys. Lett.* (66) 265 (1979)
13. O A Anisimov, V M Grigoryants, Yu N Molin *Pis'ma Zh. Eksp. Teor. Fiz.* **30** 589 (1979)
14. E L Frankevich, S I Kubarev *Triplet State ODMR Spectroscopy* (Ed. R H Clarke) (New York: Wiley-Interscience, 1982) p. 138
15. E L Frankevich, A I Pristupa, V I Lesin *Chem. Phys. Lett.* (47) 304 (1977)
16. M Okazaki, S Sakata, R Konaka, T Shida *J. Chem. Phys.* **86** 6792 (1987)
17. A L Buchachenko, V F Tarasov *Zh. Fiz. Khim.* **55** 1921 (1981)
18. V F Tarasov, E G Bagryanskaya, Yu A Grishin, R Z Sagdeev, A L Buchachenko *Mendeleev Commun.* 85 (1991)
19. R Bernstein *J. Phys. Chem.* **56** 893 (1952)
20. M Okazaki, T Sakata, T Shida, R Konaka, K Toriyama *J. Phys. Chem.* **92** 1402 (1988)
21. R Z Sagdeev, Yu N Molin, K M Salikhov, Yu A Grishin, A V Dushkin, A Z Gogolev *Bull. Magn. Res.* **2** 66 (1980)
22. E G Bagryanskaya, Yu A Grishin, R Z Sagdeev, T V Leshina, N I Polyakov *Chem. Phys. Lett.* (117) 220 (1985)
23. E G Bagryanskaya, Yu A Grishin, N A Avdievich, R Z Sagdeev, Yu N Molin *Chem. Phys. Lett.* (128) 162 (1986)
24. R Z Sagdeev, E G Bagryanskaya *Pure Appl. Chem.* **62** 1547 (1990)
25. E G Bagryanskaya, R Z Sagdeev *Progr. React. Kinetics* **18** 63 (1993)
26. N A Avdievich, E G Bagryanskaya, Yu A Grishin, R Z Sagdeev *Chem. Phys. Lett.* (155) 141 (1989)
27. I V Koptyug, E G Bagryanskaya, Yu A Grishin, R Z Sagdeev *J. Chem. Phys.* **145** 375 (1990)
28. E G Bagryanskaya, Yu A Grishin, R Z Sagdeev *Chem. Phys. Lett.* (128) 417 (1986)
29. V Tarasov, N Ghatlia, N Avdievich, I Shkrob, A Buchachenko, N Turro *J. Am. Chem. Soc.* in press (1993)
30. A H Zewail *Science* **242** 1645 (1988)
31. A L Buchachenko, V F Tarasov, N G Ghatlia, N J Turro *Chem. Phys. Lett.* (192) 139 (1992)

Russian Chemical Reviews **62** (12) 1083 – 1095 (1994)
© 1993 Russian Academy of Sciences and Turpion Ltd

UDC 543.542:546.212

Relaxation of the surface properties of aqueous solutions of surfactants and the mechanism of adsorption

N N Kochurova, A I Rusanov

Contents

I.	Introduction	1083
II.	Experimental study of dynamic surface tension	1083
III.	Experimental study of the nonequilibrium surface electric potential	1087
IV.	Thermodynamic relation between surface tension and the surface electric potential under nonequilibrium conditions	1090
V.	Methods of studying the adsorption mechanism	1092

Abstract. The results of experimental studies of the dynamic surface tension and of the nonequilibrium surface electric potential of aqueous solutions of surfactants at various concentrations and temperatures are reviewed. Special aspects of the changes in these quantities as a function of the surface area are analysed. An equation of the thermodynamics of irreversible processes which relates the nonequilibrium properties of the surface to the adsorption and a correlation expression which relates the changes in surface tension to those in the surface potential are discussed. Methods of determining the adsorption mechanism are described. The bibliography includes 65 references.

I. Introduction

Many processes associated with the adsorption of surface-active substances (SAS), including separation, foaming, dispersion, wetting, etc., take place under conditions in which the surface layer and the bulk of the solution are not mutually in equilibrium. Therefore information on the nonequilibrium properties of the surface and on the kinetics of adsorption is needed in order to understand the mechanism of action of the SAS in natural and in technological processes.

Many studies of the kinetics of formation of adsorption layers have been published: this work is aimed mainly at the diffusion of the SAS from the bulk solution in the presence of complicating surface processes such as the electric interaction of the ions, the reorientation of the SAS molecules or ions, adsorption processes in the surface layer, etc. These results have already been extensively reviewed,[1-5] but more recent work aimed specifically at the measurement of the surface tension and the surface electric potential is not included. It should be stressed that the complexity of the nonequilibrium processes taking place on the surface make it impossible to allow for all the factors which affect the measurements. The lack of precision of the hydrodynamic models used to describe the kinetics of the adsorption adds to the unreliability of the results. Lastly, the difficulty met in the purification of the materials and the great sensitivity of the kinetics to a number of trace impurities should not be forgotten.

N N Kochurova, A I Rusanov St Petersburg State University, Universitetskii prosp. 2, 198904 St Petersburg, Staryi Petergof, Fax (7-812) 428 69 39

Received 21 January 1993
Uspekhi Khimii **62** (12) 1150 – 1162 (1993); translated by J I Carasso

All these factors point to an urgent need for improving the existing methods of studying the surface properties of solutions and for discovering entirely new methods. The aim of the present review was to examine the results of the experimental and the theoretical studies of the relaxation of the two most important surface properties of solutions of SAS: their surface tension and their surface potential, and to analyse the methods of determining the adsorption mechanism of the SAS.

II. Experimental study of dynamic surface tension

The first experimental study of the dynamic surface tension of soap solutions was reported by Dupré.[6] In a study of the stability of soap films Rayleigh[7] measured the dynamic surface tension in a jet of soap solution, and showed that in a surface 'aged' for less than 0.01 s the surface tension has a value equal to that of pure water. Different methods of measuring the dynamic surface tension were developed in later work. The oscillating jet, the funnel, the falling meniscus, and other methods were used[4,8-12] to study the fast relaxation of the surface ($10^{-1}-10^{-2}$ s). Slower relaxations (seconds, minutes, hours) were studied successfully by using the maximum bubble pressure, the capillary wave, and some other methods.[4,11-13] The oscillating jet and the maximum bubble pressure method were used most widely.

The relaxation of the surface tension can usually be studied over a reasonably wide range of time by monitoring the maximum pressure in a gas bubble. However, it has been reported[2,12] that in the range of $10^{-3}-10^{-2}$ s the results become less reliable and need additional corrections. The oscillating jet method also requires corrections, both traditional (though often ignored) and recently identified. Let us examine this problem in greater detail.

1. Corrections in the oscillating jet method

The oscillating jet method[14] is one of the most fully developed and accurate dynamic methods. It was proposed by Rayleigh in 1879 as a method of measuring the surface tension of an 'almost ideally pure and continuously regenerated surface'.[7] The changes in shape of a jet emerging under pressure from a noncircular orifice had previously been studied by Bidon and by Magnus and Buff. When the jet emerges from a circular orifice its cross-section remains circular but decreases in area. The cross-section of a jet emerging from an elliptical orifice oscillates about the equilibrium circle because the capillary forces are tending to produce a cylindrical jet. Rayleigh showed how the surface tension is related to the wavelength λ of the oscillations and to other parameters of the jet.

Substantial developments in the theory of the oscillating jet method were introduced by Niels Bohr,[14,15] who allowed for the effects of the viscosity, of the finite amplitude of the jet oscillations, of the density of the surrounding medium, and of the hydrodynamic profile of the velocity within the jet. Eqn (1) shows the modern form of the Bohr formula for the surface tension γ:

$$\gamma = \frac{4G^2(\rho+\rho_1)[1+(37/24)b^2/a^2]}{6a\lambda^2+10\pi^2a^3}K, \qquad (1)$$

where G is the volume flow of liquid, ρ is the density of the liquid, ρ_1 is the density of air, a is the mean radius of the jet, b is the amplitude of the jet oscillations, λ is the wavelength of the oscillations, and K is a coefficient which allows for the effect of the velocity profile in the jet.

The theory of the oscillating jet method requires as precise a description as possible of the form of the flow in the jet issuing from an elliptical orifice, i.e. we must define the velocity profile in the cross-section in order to calculate the correction K. The velocity is substantially greater at the axis of the jet than at its surface, especially near the origin of the jet. Rideal and Sutherland[16,17] pointed out that near the orifice the velocity of an element of the jet is 10% lower than the average velocity calculated from the flow of liquid. As a result of the viscosity of the liquid the scatter of the velocities gradually decreases along the jet.

While attempting to explain the effect of the flow hydrodynamics of the jet on the measured parameters, various workers[8-20] studied the dependence of the wavelength of the oscillations on the wave number, on the average velocity of the jet, and on the dimensions of the elliptical orifice. Semiempirical corrections have been introduced[21-25] to allow for the effect of the velocity profile on the dynamic surface tension. Thus, Hansen et al.[24] used the factor $V_s^{0.64}$ to correct for the wavelength of the fourth and subsequent waves, where $V_s = v_s/v_0$ is the ratio of the velocities of an element of the jet near the surface to the average velocity of the jet. A corresponding general expression for the first three wavelengths could not be obtained. However, Bohr[15] formulated the problem of the oscillations of a jet with a nonuniform velocity profile and proposed the following expression for the correction coefficient:

$$K \equiv \left[4\int_0^1 V(y,Z)y^3\,dy\right]^2, \qquad (2)$$

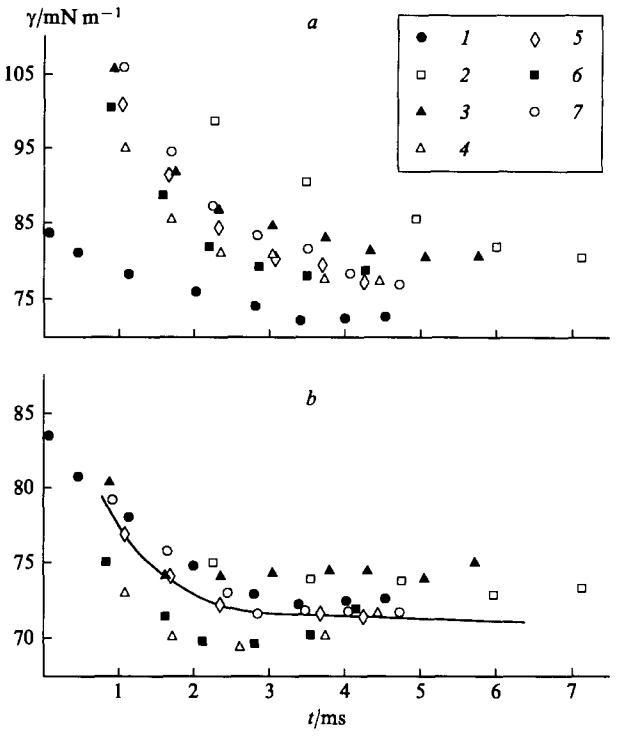
where

$$V(y,Z) = \frac{v_s}{v_0}, \quad y = \frac{r}{a}, \quad Z = \frac{\mu z}{\rho v_0 a^2}.$$

Here v_s is the axial velocity of the element of jet; $v_0 = G/\pi a^2$ is the average velocity of the jet; r is the radial coordinate; z is the axial coordinate (measured from the orifice where the jet is generated).

The present writers have calculated[26] the coefficient K. The theoretical velocity profile $V(y, Z)$ can be described by a Bessel function.[14] In calculations by formula (1) we used the initial velocity profile $V(y, 0)$ obtained experimentally[24] for a tube with a circular cross-section. Data on the velocity profile in a jet of liquid issuing from a capillary orifice have recently been published. A comparison of calculations of the K coefficient from the Bohr velocity profile[14] and from an experimental profile obtained by laser anemometry[27] gave adequately consistent results, tabulated in Ref. 26. The greater the distance z from the orifice, the closer to unity are the K values.

Special experiments[28] in which the dynamic surface tension was measured by using elliptical capillaries having different lengths and radii and different jet velocities showed that introducing the correction coefficient greatly lowers the scatter of the experimental data obtained in experiments carried out under different hydrodynamic conditions. Good agreement with the dynamic surface tension values determined by another method



Point	Length of capillary/cm	Radius of capillary/cm		v_0/cm s^{-1}
		r_{min}	r_{max}	
2	0.702	0.0211	0.0342	242.05
3	0.489	0.0297	0.0322	462.69
4	0.415	0.0160	0.0280	441.36
5	0.415	0.0160	0.0280	400.14
6	0.415	0.0160	0.0280	412
7	0.415	0.0160	0.0280	371

Figure 1. Dependence of the surface tension of water on time at 25 °C (*a*) without and (*b*) with allowance for the velocity profile in the jet. (*1*) from Ref. 29; (*2–7*) from Ref. 28.

(the falling meniscus method) is obtained (Fig. 1).[29] Applying the K coefficient to measurements[30] of the dynamic surface tension of carbon tetrachloride showed that in a simple liquid the dynamic and the static surface tension are identical, whereas in water and in aqueous solutions the two surface tensions are markedly different.

An additional correction is needed if the dynamic surface tension is determined by the oscillating jet method with an SAS solution rather than with a pure liquid.

The adsorption of the SAS at the liquid–gas interface can induce a marked elasticity of the surface, which influences the nature of the flow and of the oscillations of the jet of liquid in a way for which no allowance is made in the Bohr formula (1). In this case the difference between the true surface tension γ' and the value calculated by Eqn (1) is given by the formula[31]

$$\frac{\gamma'-\gamma}{\gamma'} = -\frac{2E(\pi g a v_0\mu/\lambda - E)}{g[E^2+(\pi g a v_0\mu/\lambda - E)^2]}, \qquad (3)$$

where $E = -(\Gamma\,d\gamma/d\Gamma)$ is the surface elastic modulus, Γ is the adsorption, $g \equiv (\pi a^2\mu_0\rho/\lambda\mu)^{1/2}$, and μ is the viscosity.

As E is increased (and therefore as Γ is increased and γ is decreased) the correction changes from zero to $-1/g$, after which it again approaches zero and changes sign at $E = gka\,v_0\mu/2$, then continues to increase, reaching $1/g$ as $E\to\infty$. According to our calculations[31] adding a correction to the experimental data for an aqueous solution of heptanol gives a satisfactory agreement between measurements of the surface tension by the oscillating

jet method and the adsorption potential jump method (in which the hydrodynamics of the liquid jet can be legitimately ignored).

Each measured value of the dynamic surface tension should be related to the age of the surface to which the measurement applies, whose accurate determination presents a separate problem.

The age of an element of fresh surface formed when the jet emerges from its orifice is defined by the expression

$$t = \frac{z}{v_s(z)}, \tag{4}$$

where z is the distance to the orifice and $v_s(z)$ is the velocity of the element of surface of the jet.

The quantity $v_s(z)$ can be determined, allowing for the velocity profile in the jet, by using Hansen's tabulations.[24,32] The error in the determination of the surface tension by formula (1) and of the age of the surface by formula (4) varies with the distance from the orifice. Near the orifice we usually find $\gamma \simeq \pm 2.5\%$, $t \simeq \pm 1\%$, and far from the orifice $\gamma \simeq \pm 1.5\%$ and $t \simeq \pm 0.1\%$.[26]

Let us examine some special features of the relaxation of the surface tension. The magnitude and the form of the change in the dynamic surface tension depend on the age of the surface, the composition of the solution, and the temperature. In different time intervals their rates of change can increase or decrease. The latter behaviour indicates the presence of an adsorption barrier.

On a young surface we also observe phenomena such as temperature and concentration inversion. The relaxation of the surface properties is also strongly influenced by the presence of inorganic salts in the SAS solutions.

2. Temperature inversion of the dynamic surface tension

For short growth times (1–3 ms) of water[29,33] and of binary solution surfaces[34,35] the surface tension increases with temperature (Figs 2–4), whereas on older surfaces it decreases with temperature, i.e. we see an inversion of the temperature dependence of the surface tension. However, in ternary water–SAS–salt systems the inversion is not always observed (see Figs 5 and 6). By comparing this behaviour with equilibrium data we conclude that an inversion of the temperature dependence of the surface tension is seen only rarely and only in solutions, where it can be attributed to differences in the temperature dependence of the adsorption (which affects the surface tension) and of the surface tension. On the other hand in pure liquids thermodynamic considerations allow only one type of dependence: a decrease in surface tension with increase of temperature. This is evident from the expression

$$\frac{d\gamma}{dT} = \tau\rho_s(s_\alpha - s_s), \tag{5}$$

where γ is the thickness, ρ_s is the molar density, s_α is the molar entropy of the bulk phase, and s_s is the molar entropy of the surface layer.[37] Under equilibrium conditions the entropy in the surface is higher than in the bulk, and therefore $d\gamma/dT < 0$.

It can be assumed that in surfaces departing only slightly from equilibrium, as in our measurements, the thermodynamic relationship (5) is valid (even if only qualitatively). In this case a positive value of $d\gamma/dT$ shows that the molar entropy of the layer is lower than the corresponding value for the bulk phase. However, we know[38] that under nonequilibrium conditions the dependence of γ on T is not the only reason for the difference between s_s and s_α.

A temperature inversion is observed in young surfaces, on which the adsorption is still far from equilibrium, and the dynamic surface tension of the solution of SAS is close to the dynamic surface tension of water and largely determined by the character of the relaxation of the surface structure of the water.

Special experiments with a jet of water showed[39] that heating the jet to 40–50 °C restores the equilibrium value in 3 ms. In water a temperature of 40 °C is known as the Mendeleev temperature, at which the network structure of the water is loosened, the activation energy of the electrical conductivity decreases, and the extent of dissociation increases. These processes also strongly increase the rate at which the equilibrium structure of the water surface is established upon increasing the temperature. For $T_1 > T_2$ we have

$$\left|\frac{d\gamma}{dt}\right|_{T_1} > \left|\frac{d\gamma}{dt}\right|_{T_2}.$$

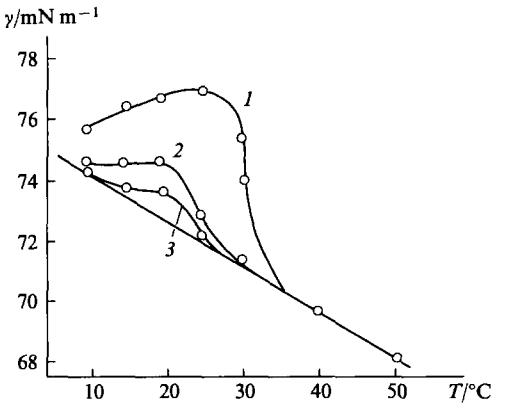


Figure 2. Temperature dependence of the dynamic surface tension of water. t/ms: (*1*) 1.4; (*2*) 2.2; (*3*) 3.0; the straight line corresponds to the equilibrium tension.

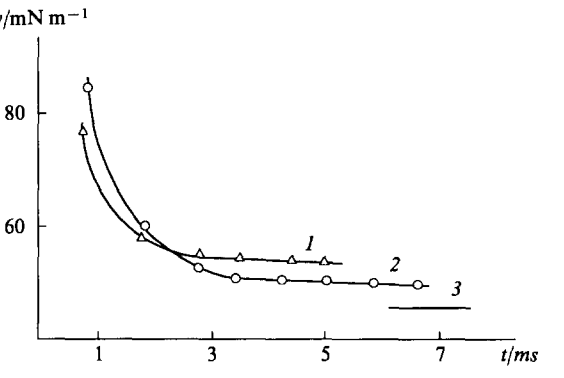


Figure 3. Dynamic surface tension in the water–sodium monobutylnaphthalenesulfonate system. c/mol dm^{-3} = 2.8 × 10^{-4}; T/°C: (*1*) 15; (*2*) 25; (*3*) $\gamma = \gamma_\infty$.

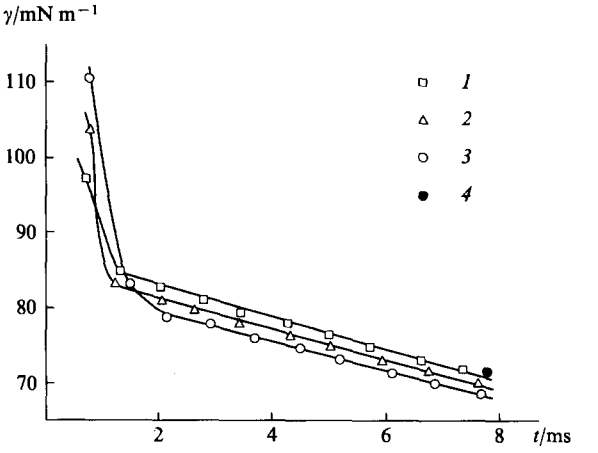


Figure 4. Dynamic surface tension in the water–cetyltrimethylammonium bromide (CTAB) system.[35] $c/10^{-4}$ mol dm^{-3} = 5.6; T/°C: (*1*) 15, (*2*) 20, (*3*) 25, (*4*) from Ref. 36.

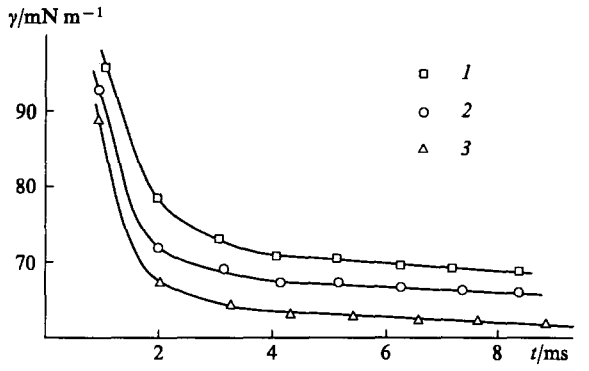


Figure 5. Dynamic surface tension in the water–potassium chloride–CTAB system.[35] $c_{KCl}/10^{-4}$ mol dm^{-3} = 5.6, c_{CTAB}/mol dm^{-3} = 0.56; T/ C°: (*1*) 15, (*2*) 20, (*3*) 25.

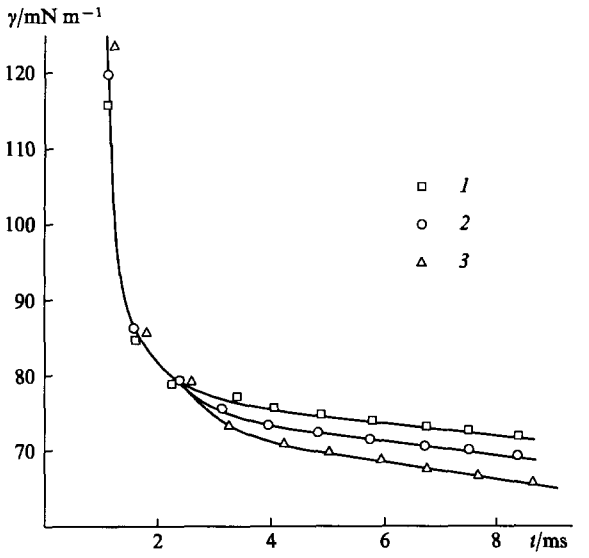


Figure 6. Dynamic surface tension in the water–potassium iodide–CTAB system.[35] c_{KI}/mol dm^{-3} = 0.56, $c_{CTAB}/10^{-4}$ mol dm^{-3} = 1.4. T/°C: (*1*) 15, (*2*) 20, (*3*) 25.

3. Conversion inversion of the dynamic surface tension

Fig. 7 shows the time dependence of the dynamic surface tension for water and aqueous solutions of cetyltrimethylammonium bromide (CTAB) at 25 °C. For t < 1.5 ms the rate of decrease of the surface tension is high and almost independent of the concentration of SAS. For $t \simeq 2$ ms the process becomes slower and the curves for different concentrations diverge (but intersect again at longer times). As a result the dynamic surface tension of SAS solutions at times between 1.5 and 6 ms is higher than that of water, and the effect is magnified as the concentration is increased. Under equilibrium conditions the surface tension of the solution of SAS decreases as the concentration is increased.

Thus under dynamic conditions we observe an inversion of the concentration dependence of the surface tension. A similar anomalous effect, in which the surface tension of the SAS exceeded that of the pure solvent during the initial period of adsorption, was observed by Thomas and Hall,[36] who attributed it to orientation effects involving the SAS molecules. As suggested, at high surface concentrations the SAS molecules 'inhibit' the orientation of their neighbours, and the higher the concentration, the slower is the molecular reorientation on the surface, with a corresponding decrease in the surface

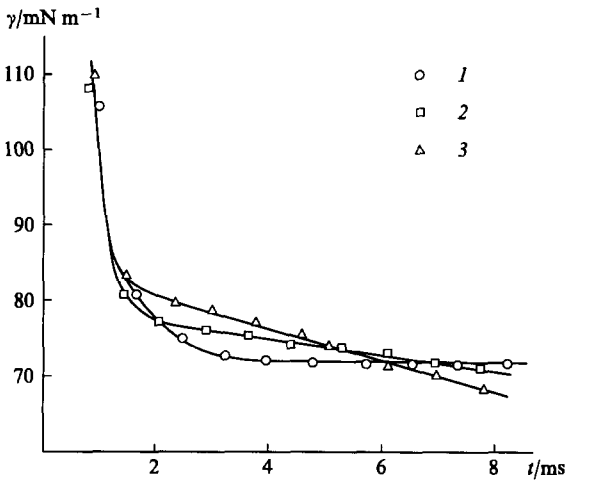


Figure 7. Dynamic surface tension in the water–CTBA system at 25 °C.[35] $c/10^{-4}$ mol dm^{-3}: (1) 0, (*2*) 2.8, (*3*) 5.6.

tension. Therefore as long as the structure of the surface layer differs substantially from the equilibrium structure the surface tension for high concentrations in solution remains higher than at low concentrations.

4. Effect of salts on the change in the surface tension of SAS solutions

In water–SAS–salt systems the ageing of a freshly created surface is accompanied by adsorption of the SAS, desorption of the salt, and relaxation of the properties of the solvent (water). The combined effects of these changes complicate the relaxation of the surface properties of the solutions.

Experiments[22,35] with water–salt solutions of SAS have shown that the addition of a salt accelerates the decrease in surface tension (Fig. 8).

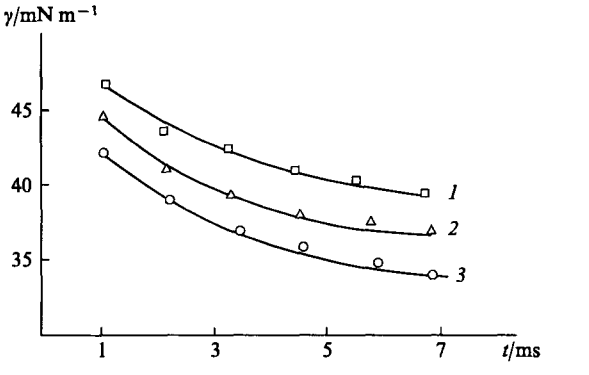


Figure 8. Effect of a salt on the dynamic surface tension of an aqueous solution of sodium dodecyl sulfate (c/mol dm^{-3} = 0.03) at 52 °C.[22] (*1*) no electrolyte; (*2*) c_{NaCl}/mol dm^{-3} = 0.03; (*3*) c_{MgCl_2}/mol dm^{-3} = 0.03.

The faster adsorption of the SAS produced by the desorption of the salt is explained by the salting-out effect of the salt itself, which increases with its concentration. This phenomenon is most clearly seen when the composition of the salt includes a structure-forming ion. It is evident from the results[35] reproduced in Fig. 9 that the addition of KI (a salt containing the strongly structure-forming iodide ion) accelerates the decrease in surface tension of a CTAB solution more markedly than the addition of KCl.

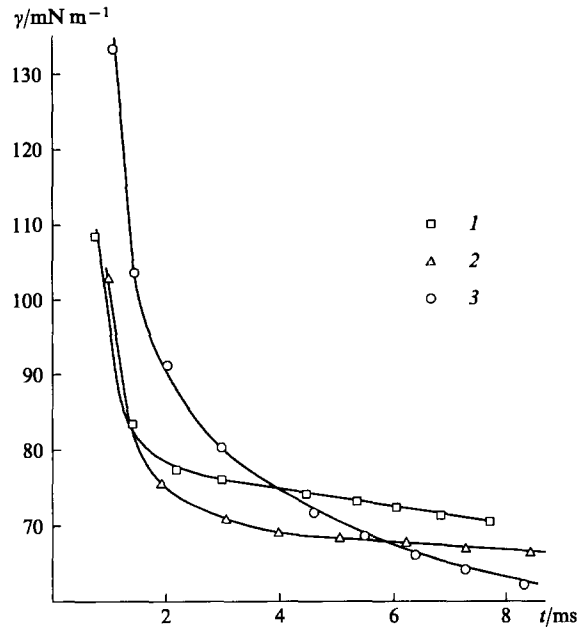


Figure 9. Effect of KCl and KI on the dynamic surface tension of an aqueous solution of CTAB at 25 °C.[35] (*1*) H_2O–CTAB; (*2*) H_2O–KCl–CTAB; (*3*) H_2O–KI–CTAB; $c_{CTAB}/10^{-4}$ mol dm^{-3} = 2.8, c_{KCl}/mol dm^{-3} = 0.56, c_{KI}/mol dm^{-3} = 0.56.

III. Experimental study of the nonequilibrium surface electric potential

The measurement of the electric potential of the surface is an independent method of studying the nonequilibrium properties of solution surfaces. The theory of the oscillating jet method is based on observing the flow and the vibrations of the jet emerging from an elliptical orifice, and relies on a number of assumptions. Unlike the surface tension, the surface potential is determined directly during the experiment (as opposed to being calculated from hydrodynamic equations). This offers some definite advantages in studies of the adsorption kinetics of SAS. The surface potential χ is the difference between the electric potentials at the boundary of two phases. In particular, at the solution–air interface χ is equal to the change in the electric potential between the air and the solution (treated as positive if the potential is increased, and negative if it is decreased on passing from the air to the solution). Being a Galvani potential the surface potential is not directly measurable. We can only determine changes in surface potential $\Delta\chi$ (for example, the time-changes caused by the ageing of a fresh surface or by changing the concentration of the solution). The change in surface potential seen on going from a standard to an experimental solution (containing additions of an adsorbable substance) is called the adsorption electric potential φ.

The methods most commonly used to measure $\Delta\chi$ or φ include the vertical jet method (Thomson–Kenrick), the radioactive probe method (Frumkin–Guyot), and the vibrating condenser method (Thomson–Zisman). The relaxation of a fresh surface is most conveniently studied by using a jet of liquid. In this case the age of the surface is easily calculable (as in the oscillating jet method), and the time-changes of the surface potential or of the adsorption potential can be determined without difficulty.

The adsorption potential of SAS is usually measured in solutions containing electrolytes as additives. Our measurements[40] on a liquid jet were aimed at monitoring the changes of the surface potential in aqueous solutions without added electrolytes. Furthermore the measurement method automatically excluded changes in the potentials of the measuring electrodes in air and in the solution during the experiment.[40] This was achieved by making measurements for a reference point at a fixed distance (in our experiments,[40] ~0.6 cm) from the orifice of the capillary which produced the jet. At this distance the surface potential has reached its equilibrium value and does not show any further changes along the jet. Thus we obtain from the experiment

$$\Delta\chi_t = \chi_t - \chi_0 , \qquad (6)$$

where χ_t is the surface potential for an element of surface of age t, [see formula (4)], and χ_0 is the surface potential at the reference point.

The adsorption potential φ_t for a surface of age t is determined from the difference $\Delta\chi_t$ between the experimental and the standard solution. Let us examine the results obtained in studies of the adsorption potential of various substances.

1. Alcohols

Several studies of aqueous solutions of normal primary alcohols (from propanol to decanol) have been reported.[41–46] The time interval needed to establish the equilibrium value of the potential is determined by the concentration of the solution and by the length of the hydrocarbon chain of the alcohol. As the molecular mass of the alcohol is increased, the concentration range in which a change in potential takes place at times between 2 and 20 ms is shifted towards lower values. An increase in the age of the surface makes the potential more positive (Fig. 10). The potential is relatively insensitive to changes in temperature: $d\varphi/dT \approx -0.0002$ V K^{-1}. A similar dependence was obtained[46] for the equilibrium potential.

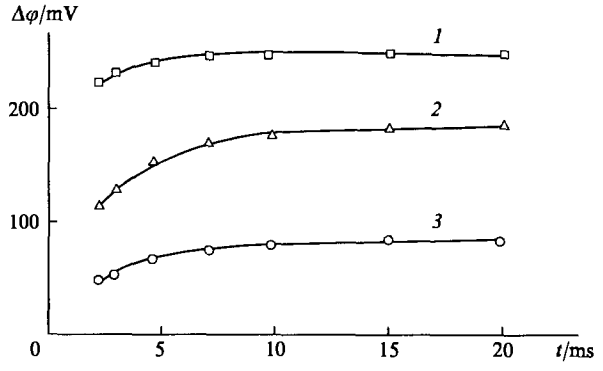


Figure 10. Adsorption potential step of solutions of hexanol in HCl (0.01 mol dm^{-3}) at 20 °C.[45] c/mmol dm^{-3}: (*1*) 10, (*2*) 4, (*3*) 2.

2. Aliphatic acids

Normal aliphatic acids are anion-active SAS. These electrolytes are weaker than the corresponding saturated alcohols: their surface activity is suppressed by the presence of the more polar carboxyl group.

Aqueous solutions of pentanoic, heptanoic, and octanoic acids have been studied in our laboratory.[47] In the lower homologues adsorption equilibrium is reached in less than 10^{-3} s, and the time dependence of the adsorption has not yet been established for these materials. On the other hand acids with a longer hydrocarbon chain (beginning with nonanoic acid) are very sparingly soluble in water, and meaningful measurements are not possible at the very low concentrations which are experimentally accessible. It is found that the adsorption of pentanoic acid is completed in 2×10^{-3} s, and that the equilibrium adsorption potential is ~100 mV at a concentration of 7.5×10^{-3} mol dm^{-3} and ~140 mV at 1.25×10^{-2} mol dm^{-3}. Within the error limits of ±5 mV the φ values are consistent with the equilibrium values given by Frumkin.[48]

Results for hexanoic, heptanoic, and octanoic acid are shown in Figs 11–13. The potential changes towards more positive values during the measurements. The largest change in the potential is observed for octanoic acid: in the other two acids the initial region (up to 7 ms) shows an initially fast change in potential followed by a slower change.

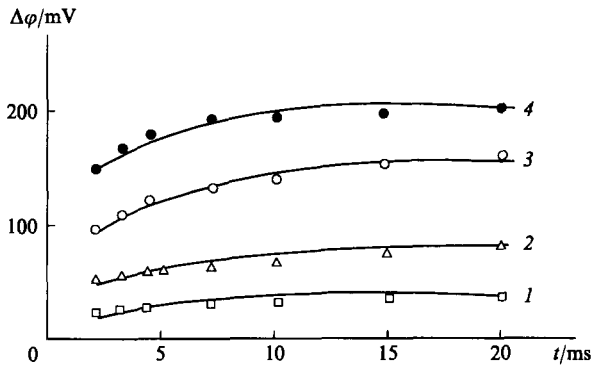


Figure 11. Electric adsorption potential of solutions of hexanoic acid.[47] $c/10^{-3}$ mol dm^{-3}: (*1*) 1, (*2*) 2, (*3*) 4, (*4*) 6.

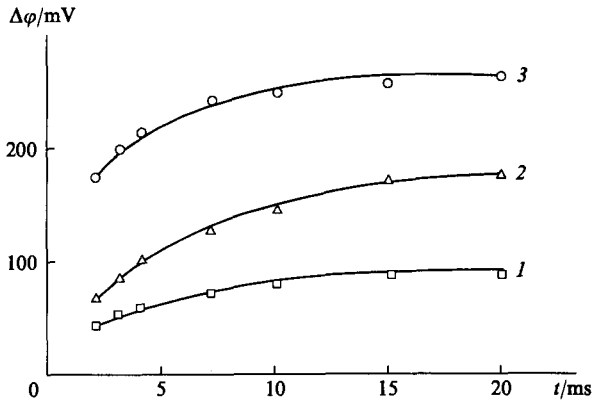


Figure 12. Electric adsorption potential of solutions of heptanoic acid.[47] $c/10^{-3}$ mol dm^{-3}: (*1*) 1, (*2*) 2, (*3*) 4.

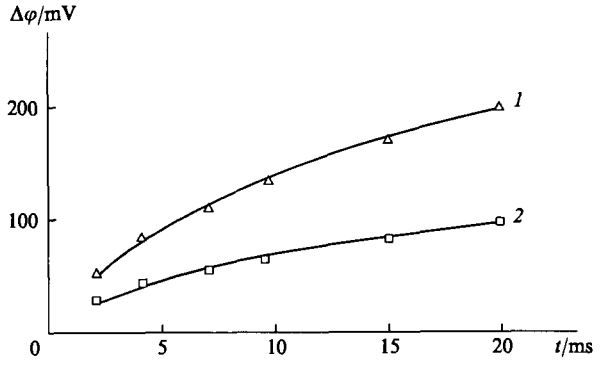


Figure 13. Electric adsorption potential of solutions of octanoic acid.[47] $c/10^{-3}$ mol dm^{-3}: (*1*) 0.75, (*2*) 1.5.

3. Cation-active SAS

Published measurements[41,49] show that in the case of cation-active SAS the potential usually changes (over times between 1 and 2 ms) towards more negative values, corresponding to the location of the cations closer to the air interface than the anions (Figs 14–17). For a given concentration the rate of the process decreases as the lifetime of the surface increases, and for a given lifetime it increases with the concentration. The absolute value of $\Delta\chi$ increases with the age of the surface, and with increasing concentration, indicating an increase in the adsorption of the SAS. At very low concentrations of the SAS, corresponding to low adsorptions, we observe a time dependence of the surface potential similar to that seen in water: $\Delta\chi$ moves towards more positive values (Fig. 17).

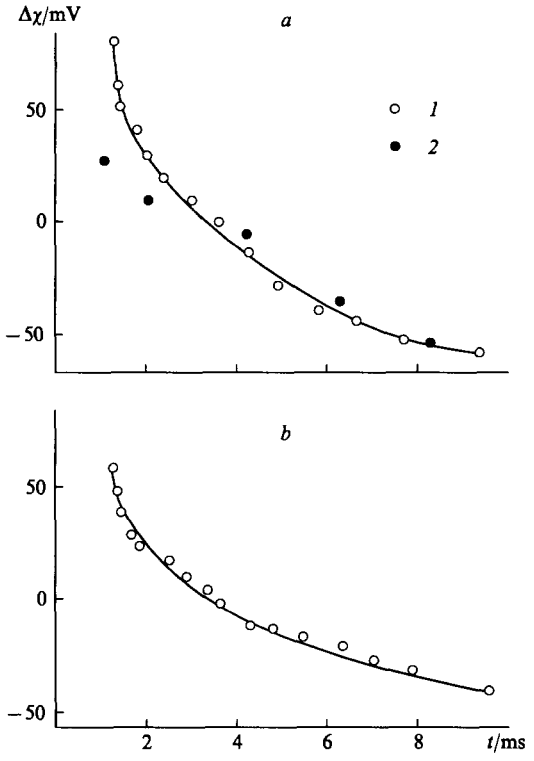


Figure 14. Time changes of the surface electric potential in the water–CTAB system. (*a*) c/mol^{-4} mol dm^{-3} = 5.6; (*1*) from Ref. 49, (*2*) from Ref. 41; (*b*) $c/10^{-4}$ mol dm^{-3} = 2.8.

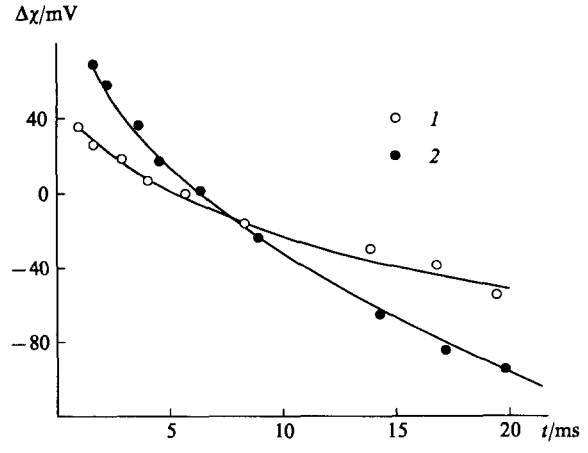


Figure 15. Time changes of the surface electric potential in the water–cetyltrimethylammonium chloride (CTAC) system. $c/10^{-4}$ mol dm^{-3}: (*1*) 2.8, (*2*) 5.6.

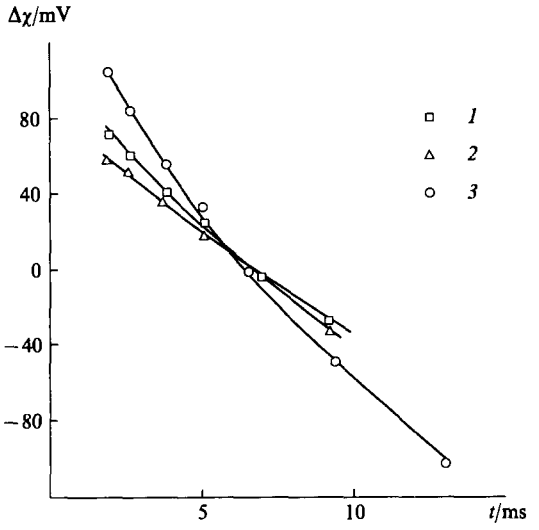


Figure 16. Time changes in the electric potential of hexadecylpyridinium bromide. $c/10^{-4}$ mol dm^{-3}: (*1*) 1, (*2*) 5, (*3*) 10.

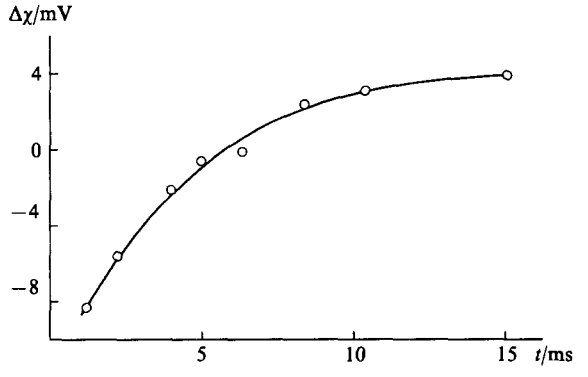


Figure 17. Changes in the surface electric potential of a solution of dodecylammonium chloride. $c/10^{-3}$ mol dm^{-3} ≈ 2.6.

4. Cation-active SAS with added inorganic salts

The time-dependences of the surface potentials for aqueous solutions of cetyltrimethylammonium bromide and chloride with additions of KCl and KI are shown in Figs 18–21. By comparing the $\Delta\chi$ values in solutions of the SAS with and without salt additions we conclude that in young surfaces (up to 6–8 ms) the change in potential is almost independent of the salt concentration. On the other hand, data on the dynamic surface tension indicate a salting-out effect associated with the additions of salt. Evidently, this behaviour is due to the differences in the polarity and in the relative electric potentials of the SAS and inorganic salt double layers, which make the relationship between the adsorption of the SAS and the surface potential less unambiguous than in the binary SAS–water system.

As the age of the surface is increased we observe a shift in the potential towards more positive values (most clearly seen in the solution with KCl additions, but relatively weak in the solution with KI). The effect becomes more marked as the salt concentration is increased, though it is relatively insensitive to the concentration of the SAS. These effects were explained by assuming micelle formation under dynamic conditions:[49] as the flow of adsorbed SAS ions meets the flow of desorbed salt in the near-surface layer the critical concentration may be exceeded, inducing micelle formation. Being surface-inactive the micelles should migrate towards the bulk of the solution, removing some of the SAS from the surface layer and as a result lowering the charge on the surface double layer and producing a positive shift of the potential.

Unfortunately there are no published data on the non-equilibrium surface potential for other SAS.

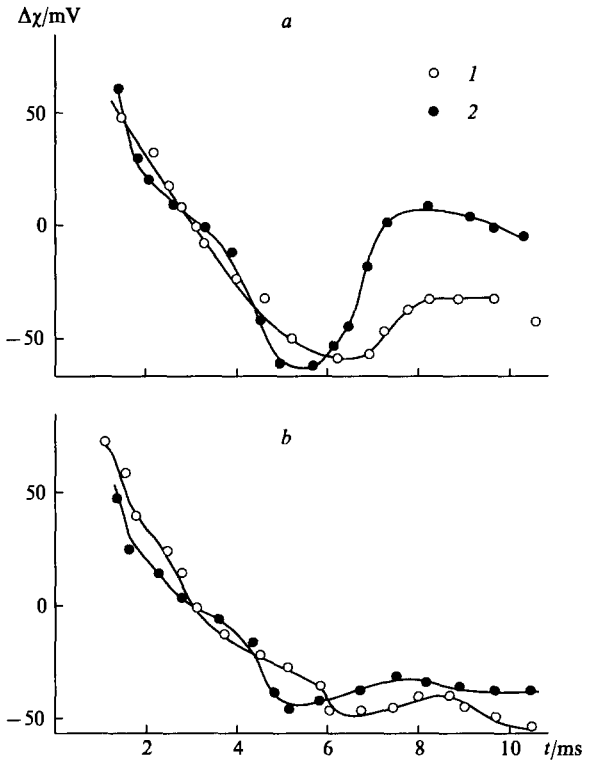


Figure 18. Time changes in the surface electric potential in the water–potassium chloride–CTAB system.[49] $c_{CTAB}/10^{-4}$ mol dm^{-3}: 5.6 (*a*), 2.8 (*b*); c_{KCl}/mol dm^{-3}: 0.12 (*1*), 0.56 (*2*).

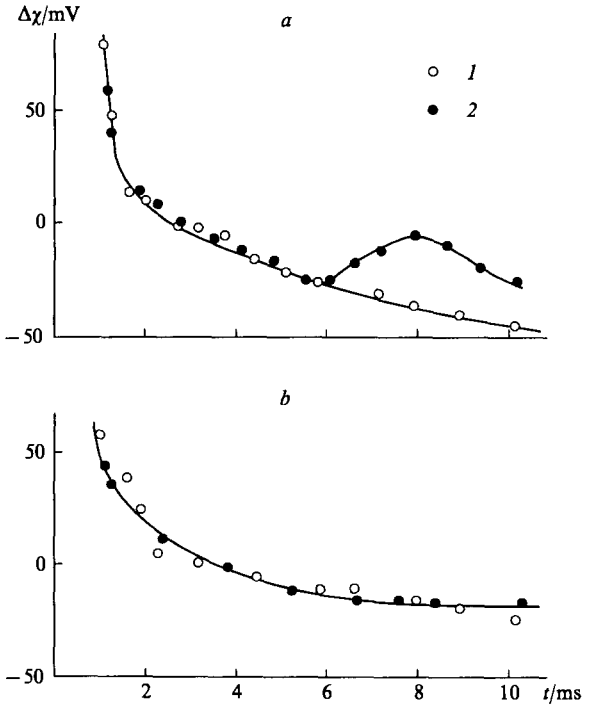


Figure 19. Time changes in the surface electric potential in the water–potassium iodide–CTAB system.[49] $c_{CTAB}/10^{-4}$ dm^{-3}: 2.8 (*a*), 1.4 (*b*); c_{KI}/mol dm^{-3}: 0.12 (*1*), 0.56 (*2*).

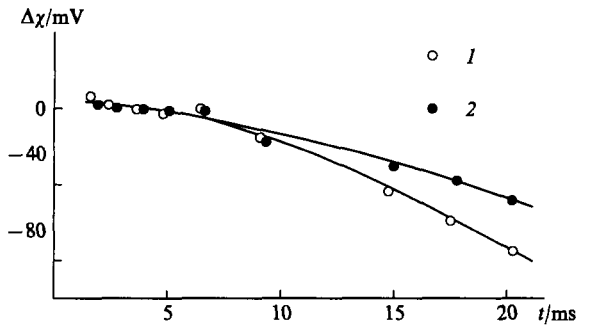


Figure 20. Time changes in the surface electric potential in the water–potassium chloride–CTAC system.[49] c_{KCl}/mol dm^{-3}: 0.12 (*1*), 0.56 (*2*); $c_{CTAC}/10^{-4}$ mol dm^{-3} = 2.8.

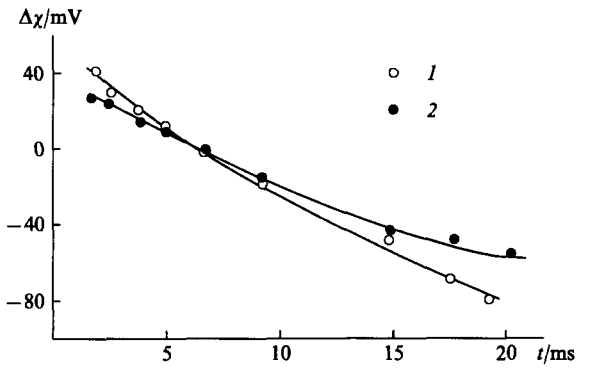


Figure 21. Time changes in the surface electric potential in the water–potassium chloride–CTAC system.[49] c_{KCl}/mol dm^{-3}: 0.12 (*1*), 0.56 (*2*); $c_{CTAC}/10^{-4}$ mol dm^{-3} = 5.6.

IV. Thermodynamic relation between surface tension and the surface electric potential under nonequilibrium conditions

1. Adsorption equation for a nonequilibrium surface

The most general and commonly met case of adsorption with polarisation of a fresh solution surface as a result of the orientation of polar molecules and of the formation of a double layer has been studied during the development of the thermodynamics of irreversible processes.[38, 50, 51] Whereas the double layer is formed naturally during the adsorption of the ions, and can be described without introducing additional variables, the orientation of the polar molecules creates a new specific problem which complicates the thermodynamics of the surface phenomena.

As was shown by Sanfeld,[50] six variables are sufficient to describe the orientation of dipoles: for example, the average components of the dipole moment $\langle m_x \rangle$ and of its square $\langle m_x^2 \rangle$, or of the modulus $\langle |m_x| \rangle$ ($x = x, y, z$). In Defay's multilayer model the multicomponent two-phase liquid–gas system with a flat surface layer is divided into elementary layers (within which the electrochemical or chemical potentials are assumed to be constant), and the generalised adsorption equation for the nonequilibrium surface becomes

$$d\gamma = -\bar{s}\,dT - \sum_i \Gamma_i\, d\tilde{\mu}_i^{\alpha} - \sum_{i,k} \frac{N_i^k}{A} d(\tilde{\mu}_i^k - \tilde{\mu}_i^{\alpha}) - \frac{1}{A}\sum_{i,k,x}\left(A_{ix}^k\, d\langle m_{ix}^k \rangle + B_{ix}^k\, d\langle m_{ix}^{k\,2} \rangle\right), \quad (7)$$

where $\bar{s}$ is the entropy excess per unit surface area, T is the temperature, A is the area of the surface, Γ_i and $\tilde{\mu}_i$ are the adsorption and the electrochemical potential of the particles of species i, N_i^k is the number of particles of species i in the sublayer k of the surface layer, $\langle m_{ix} \rangle$ and A_{ix}^k are the average component of the dipole moment of the molecules of species i in the direction ($x = x, y, z$) and the corresponding affinity; $\langle m_{ix}^2 \rangle$ and B_{ix} are the mean-square component of the dipole moment of the molecules of species i and the corresponding affinity. The difference $\tilde{\mu}_i^k - \tilde{\mu}_i^{\alpha}$ plays the role of the adsorption affinity for the k-th elementary layer in the region between the phases. The superscript α refers to the bulk phase α (the liquid solution). In the right-hand side of Eqn (7) the last two sums allow for the presence of nonequilibrium processes. At equilibrium these processes disappear, and Eqn (7) reduces to the Gibbs adsorption equation. This equation can be used as the relaxation equation for the fresh surface, and also as an equation describing the dependence of the surface tension on the parameters of state (and in particular on the concentration of the SAS).

2. Relaxation equation for the fresh surface

Eqn (7) can be simplified when applied to the relaxation of a surface for a given composition and state of the bulk phase α. The first two terms in the right-hand side vanish because the temperature and the chemical potentials of the phase α are fixed. In a single relaxation process $\langle m_{ix}^k \rangle^2$ values can be assumed to be proportional to m_{ix}^k (in practice we have only one component of $\langle m_{ix}^k \rangle$ in the direction of the normal z to the surface, since both $\langle m_{ix}^k \rangle$ and $\langle m_{iy}^k \rangle$ are equal to zero according to the symmetry conditions).[50] Noting also that each orientational affinity is proportional to the rate of change of the corresponding variable the relaxation equation which follows from (7) can be written in the form[52]

$$\frac{d\gamma}{dt} = -\sum_{i,k} N_i^k \frac{d(\tilde{\mu}_i^k - \tilde{\mu}_i^{\alpha})}{dt} - \sum_{i,k} C_i^k \left(\frac{d\langle m_{iz}^k \rangle}{dt}\right)^2, \quad (8)$$

where t is the time and C_i^k are constants.

The right-hand side of the relaxation equation (8) consists of two terms: a diffusion term and an orientation term. The quantity $\langle m_{iz}^k \rangle$ is related to the dipole component χ_d of the surface potential χ by the electrostatic equation

$$\chi_d = 4\pi \sum_{i,k} \langle m_{i,z}^k \rangle \frac{N_i^k}{A}. \quad (9)$$

Since the orientation is established mainly in the surface monolayer we can put $k = 1$. To simplify the problem we shall assume that only one component undergoes orientation, i.e. that $i = 1$. In this way we obtain from Eqn (9)

$$\langle m_z \rangle = \frac{\chi_d A}{4\pi N^{\sigma}}, \quad (10)$$

where N^{σ} is the number of molecules in the monolayer. In this model we obtain the following expression from Eqn (8):

$$A\frac{d\gamma}{dt} = -\sum_{i,k} N_i^k \frac{d(\tilde{\mu}_i^k - \tilde{\mu}_i^{\alpha})}{dt} - C\frac{d\langle m_z \rangle}{dt}. \quad (11)$$

Here C is equal to the C_i^k value for the monolayer model with one component. Obviously, $C > 0$, since the surface tension decreases as more molecules become oriented. It is clear from Eqn (11) that the decrease in surface tension is independent of the signs of $\langle m_z \rangle$ and χ_d.

Eqn (11) can be used to establish the relation between the dynamic surface tension and the nonequilibrium surface potential. We shall examine the two extreme cases in which only the orientation or only the diffusion relaxation mechanism (respectively) is operating.

a. Orientational relaxation mechanism

We shall assume initially that the orientation process is much slower than the diffusion of ions or molecules, so that in practice the process takes place under the condition of diffusion equilibrium ($\mu_i^k = \mu_i^\alpha$). Obviously, the electrochemical potentials in the surface layer is held constant by a change in the number of adsorbed ions and molecules during the orientation process. However, if we are considering a relaxation state close to equilibrium (as is found experimentally) in which the adsorption layer remains relatively dense we can assume that $N^\sigma = \text{const}$, and $d\chi = d\chi_d \approx d(m_z)$. Allowing for (10), Eqn (11) can then be rewritten

$$\frac{d\gamma}{dt} = -\frac{CA}{(4\pi N^\sigma)^2}\left(\frac{d\chi}{dt}\right)^2. \tag{12}$$

Hence we arrive at the expression

$$\frac{d\gamma}{d\chi} = -\frac{CA}{(4\pi N^\sigma)^2}\frac{d\chi}{dt}, \tag{13}$$

which shows that $d\gamma/d\chi \to 0$ for $t \to \infty$, since $d\chi/dt \to 0$.

b. Ion-diffusion relaxation mechanism

We shall now assume that the diffusion and the orientation of polar molecules are very fast processes and that the rate-limiting step of the relaxation is the formation of an ionic double layer.

In this case Eqn (11) gives

$$d\gamma = -\sum_{i,k}\left(\frac{N_i^k}{A}\right)d(\tilde{\mu}_i^k - \tilde{\mu}_i^\alpha), \tag{14}$$

where the summation with respect to i refers to the ions. Using the standard expressions for the electrochemical potentials,

$$\tilde{\mu}_i = \mu_i + q_i\varphi, \tag{15}$$

where μ_i is the chemical potential, q_i is the charge on the ion, and φ is the electric potential at the place where the ion is sited. Inserting (15) into (14) and dividing by $d\chi$ gives

$$\frac{d\gamma}{d\chi} = -\sum_{i,k}\frac{N_i^k}{A}\frac{d(\tilde{\mu}_i^k - \tilde{\mu}_i^\alpha)}{d\chi} - \sum_k q^k\frac{d(\varphi^k - \varphi^2)}{d\chi}, \tag{16}$$

where q^k is the charge on the elementary layer k per unit area,

$$q^k \equiv \sum_i \frac{q_i N_i^k}{A}.$$

The right-hand side of Eqn (16) contains two terms. The first describes the effect of the adsorption of ions (accompanied by the formation of the surface potential χ) on the distribution of chemical potentials in the double layer. The derivative $d\mu_i^k/d\chi$ should be large in the case of massive surface-active ions at the formation stage of the adsorption monolayer. If this stage dominates the formation of the equilibrium diffusion layer of counterions the derivative is small during the final stage of the relaxation. Obviously, the same derivative is small for the counter-ions, which usually have a small mass, if their concentration is small.

The second term of Eqn (16) is purely electrostatic. We note that it differs from zero even in an electrically neutral surface layer, and it lowers the surface tension irrespectively of the sign of the surface potential. For the last elementary layer we can write $d(\varphi^k - \varphi^\alpha)/d\chi = -1$ (By definition of χ); it follows immediately that the right-hand side of Eqn (16) remains finite at $t \to \infty$. This means that, in contrast to the orientational relaxation, a linear term appears in the dependence of $(\gamma - \gamma_\infty)$ upon $(\chi - \chi_\infty)$.

Thus the presence or absence of a linear term in the asymptotic dependence of $(\gamma - \gamma_\infty)$ upon $(\chi - \chi_\infty)$ allows us to identify the relaxation mechanism. If it is found experimentally that the dependence does not contain a term in which $(\chi - \chi_\infty)$ appears in the first power we may conclude that the surface potential is formed by the reorientation of the polar molecules. If a first-power term is detected the surface potential is the result of the formation of an ionic double layer.

3. Concentration dependence of the surface tension

When considering the concentration dependence of the surface tension (at constant temperature) we must allow for the second term in the right-hand side of the adsorption equation (7) as well as for the effects discussed above. Using once again the expression (15) we can write

$$\sum_i \Gamma_i\, d\tilde{\mu}_i^\alpha = \sum_i \Gamma_i\, d\mu_i^\alpha + \sum_i \Gamma_i q_i\, d\varphi^\alpha$$
$$= \sum_i \Gamma_i\, d\mu_i^\alpha + q\, d\chi,$$
$$q \equiv \sum_i \Gamma_i q_i, \tag{17}$$

where q is the overall charge on the surface. The electroneutrality condition ($q = 0$) is usually assumed for systems in equilibrium (which may, however, be charged), but in dynamic processes electroneutrality is not, of course, a necessary condition.

It has been reported [52-55] that the formation of a fresh surface may involve local breakdown of the electroneutrality of the electric double layer. According to Lopatenko and Kontush [54] the charging of a liquid surface takes place in a particular time interval during the formation of the surface because of the presence of a nonequilibrium electric potential which varies along the surface. The formation conditions of the fresh surface have a strong influence on the resulting surface charge. Thus, in the formation of an air bubble in an aqueous solution of NaCl the surface charge [52] is 4×10^{-5} to 4×10^{-7} C cm^{-2}, whereas in the formation of a drop of the same solution in air the charge [54] is $\sim 1.5 \times 10^{-12}$ C cm^{-2}. The formation of surface charge is most likely at low concentrations of electrolyte, when the electric double layer is relatively stretched and easily deformed. The Jones–Ray effect (the appearance of a minimum on the surface tension isotherm at low concentrations of electrolyte, of the order of 10^{-3} mol dm^{-3}) has been attributed [56] to the formation of surface charge.

The charging of droplets of electrolyte solutions has been observed not only with inorganic electrolytes but also with solutions of SAS. As an example we show in Fig. 22 the dependence of the charge on drops of an aqueous solution of cetylpyridinium chloride on the concentration of the solution.[57]

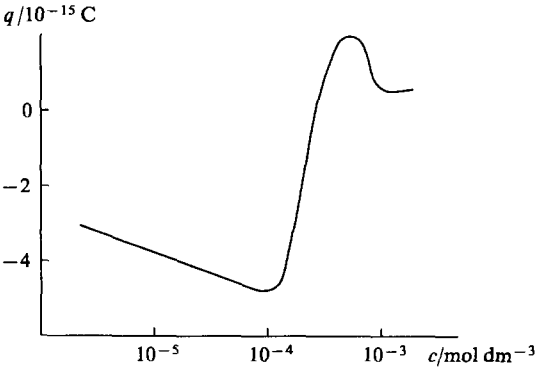


Figure 22. Dependence of the charge of drops on the concentration of a solution of cetylpyridinium chloride.[57]

We shall now rewrite Eqn (7) for the case of constant temperature in the system and on the assumption that the orientation and diffusion processes are significantly faster than the re-establishment of the electroneutrality of the surface:

$$d\gamma = -\sum_i \Gamma_i \, d\mu_i^{\alpha} - q \, d\chi . \tag{18}$$

In particular, for a dilute solution of a 1-1 electrolyte Eqn (8) simplifies to

$$d\gamma = \frac{-2RT\Gamma}{c} dc - q \, d\chi , \tag{19}$$

where c is the conconcentration of electrolyte in the bulk phase. This equation can be used, for example, to determine the dependence of the surface tension on the concentration.[56] In the case of an SAS on a fairly well aged surface, when the adsorption is substantial, the first term in the right-hand side of Eqn (19) can play the dominant role. The second term can make a significant contribution when the surface is still relatively fresh.

V. Methods of studying the adsorption mechanism

We know that the kinetics of the adsorption of SAS can be diffusion-controlled (in which case the relaxation time is determined by the diffusion of the SAS to the surface), adsorption-controlled (with an energy barrier on the surface), or under mixed control (when both the diffusion and the rate of establishing equilibrium in the surface and the subsurface layers must be allowed for). Even for one given substance different types of kinetics may be observed, depending on the concentration and temperature of the solution and on the duration of the process:[4, 58, 59] this must be allowed for when experimental data are analysed. Let us now examine the methods of studying the mechanism of adsorption of the SAS.

1. Calculations from experimental data by the diffusion theory

The relaxation of the surface properties of aqueous solutions of SAS characterises their adsorption kinetics. The time dependence of the adsorption can be obtained from experimental values of the surface tension $\gamma(t)$, of the surface electric potential $\Delta\chi(t)$, or of the adsorption potential $\varphi(t)$ by using the equilibrium isotherms of the surface tension $\gamma(c)$, of the adsorption potential $\varphi(c)$, and of the adsorption $\Gamma(c)$. Identical dependences of the dynamic surface tension or of the adsorption potential on the adsorption for equilibrium and for nonequilibrium conditions are assumed. In other words it is assumed that the molecules become oriented relatively rapidly and that the process is controlled exclusively by the rate of arrival of the adsorbate at the surface.

In the case of purely diffusion-controlled kinetics the dependence of the adsorption Γ on the time t can be calculated using the Ward–Tordai equation[60]

$$\Gamma(t) = 2c_0\left(\frac{Dt}{\pi}\right)^{1/2} - \left(\frac{D}{\pi}\right)^{1/2} \int_0^t \frac{\bar{c}(t')}{(t-t')^{1/2}} dt' , \tag{20}$$

where c_0 is the bulk concentration of the SAS, D is the diffusion coefficient, and $\bar{c}(t)$ is the concentration of SAS in the part of the bulk solution directly adjacent to the surface layer (known as the subsurface concentration). Because of the difficulty of determining this quantity experimentally the parameter c is often obtained by using one of the conventional adsorption isotherms. Thus, by adopting the linear adsorption isotherm

$$\Gamma = \varepsilon c , \tag{21}$$

Sutherland[61] converted Eqn (21) into:

$$\Gamma(t) = \varepsilon c_0\left[1 - \exp\left(\frac{Dt}{\varepsilon^2}\right) \operatorname{erfc}\left(\frac{\sqrt{Dt}}{\varepsilon}\right)\right]. \tag{22}$$

The adsorption kinetics are often studied in a jet of liquid. A study[61] of the effect of the velocity profile in the jet on the adsorption gave the following expression for $\Gamma(t)$:

$$\Gamma(t) = 2c_0\left(\frac{Dt}{\pi}\right)^{1/2} - \left(\frac{D}{\pi}\right)^{1/2} \int_0^t \frac{c(t')}{(t-t')^{1/2}} dt'$$

$$+ \frac{1}{(2\pi D)^{1/2}} \int_0^t \int_0^{t'} \int_0^{\infty} \frac{y'}{(t'-t'')^{3/2}} \exp\left[-\frac{(y')^2}{4D(t'-t'')}\right]$$

$$\times v_r(y', t') \, F(y', t'') \, dy' dt' dt'' \tag{23}$$

Here $v(r)$ is the radial component of the velocity, and $y' = a - r$ (where a is the radius of the jet and r is the radial coordinate); also,

$$F(y', t'') = \left(\frac{\partial c}{\partial y'}\right)_{t''} .$$

The first two terms of Eqn (23) are identical to the right-hand side of the Ward–Tordai equation, and therefore they allow for the transport of matter by molecular diffusion. The third term is a small correction for the effect of a nonuniform velocity profile.

Experimental dependences of the adsorption on time can be compared with dependences calculated by the diffusion theory [Eqns. (20)–(22)]. Good agreement between experimental and calculated values of $\Gamma(t)$ denotes diffusion-controlled adsorption kinetics. This is found, for example, for aqueous solutions of alcohols with moderately long hydrocarbon chains.[44] Data for an aqueous solution of heptanol are shown in Fig. 23 as an example. The curve was calculated by the Ward–Tordai equation. The points give the $\Gamma(t)$ values obtained from measurements of the adsorption potential.[45] The agreement between the experimental results and those calculated by the theory of diffusion is satisfactory.

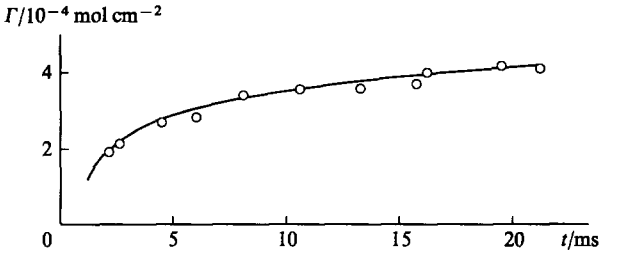


Figure 23. Time dependence of the adsorption of heptanol.[45] $c/10^{-3}$ mol dm^{-3} = 2.5.

In some cases the association of the dissolved substance is one of the main factors responsible for slow adsorption, as was shown by measurements of the adsorption potential of solutions of aliphatic acids.[47] The most significant difference between acids and alcohols is the presence of the polar carboxylic acid group –C(O)OH, which balances the hydroxyl and the hydrophobic parts of the acid molecule. For this reason the normal aliphatic acids can form associations, unlike the corresponding alcohols. The carboxylic acid group also enables the aliphatic acids to form relatively strong hydrogen bonds (as compared with the alcohols). Experimental results (Figs 24 and 25) show that the rate of adsorption is suppressed (as compared with the diffusion-controlled kinetics by increasing the concentration of the solution and by shortening the hydrocarbon chain. The adsorption barrier is lowered by the transition from C_6 to C_7, but it is raised by an increase in concentration. These results justify the conclusion that the adsorption is hindered by the formation of associations of the aliphatic acids.

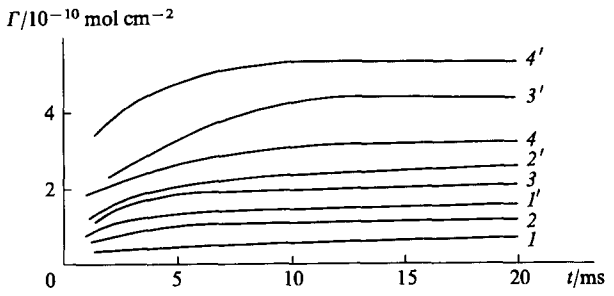


Figure 24. Time dependence of the adsorption of hexanoic acid.[47] $c/10^{-3}$ mol dm^{-3}: (*1*,*1'*) 1, (*2*,*2'*) 2, (*3*,*3'*) 4, (*4*,*4'*) 6; (*1*–*4*) calculated from experimental adsorption potential data, (*1'*–*4'*) calculated by the Ward–Tordai equation.

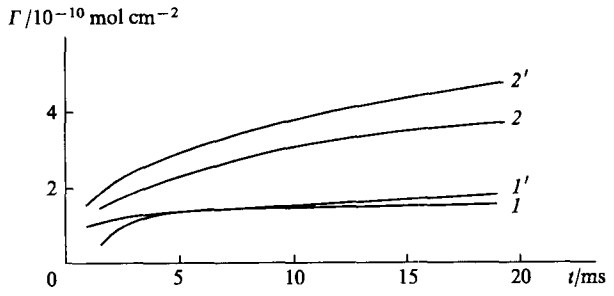


Figure 25. Temperature dependence of the adsorption of heptanoic acid.[47] $c/10^{-3}$ mol dm^{-3}: (*1*,*1'*) 1; (*2*,*2'*) 2; (*1*) and (*2*) calculated from experimental adsorption potential data, (*1'*) and (*2'*) calculated by the Ward–Tordai equation.

In the case of a purely diffusional adsorption mechanism we can replace the calculation of $\Gamma(t)$ by a calculation of the surface tension followed by a comparison with the experimental value. The surface tension is determined from the surface pressure $\pi(t)$:

$$\gamma(t) = \gamma_{H_2O}(t) - \pi(t) = \gamma_{H_2O}(t) - RT\Gamma(t), \qquad (24)$$

where $\gamma_{H_2O}(t)$ is the experimental value of the dynamic surface tension of water, and $\Gamma(t)$ is defined for a purely diffusional mechanism [for example, by formula (22)]. This approach does not require the traditional stipulation of local equilibrium between the surface and the subsurface layers, which is legitimate only for a purely diffusional adsorption mechanism.

Fig. 26 shows the experimental time dependence of the surface tension of a solution of CTAB and the same dependence calculated by formula (24). For surfaces aged up to 1.5 ms the two dependences are indistinguishable, but the curves show a significant deviation for $t > 1.5$ ms, probably associated with the appearance of an adsorption barrier. In this case the barrier is probably of the electrostatic type, since it has been shown [35] that in the adsorption of CTAB the absolute value of the surface electric potential increases, with a corresponding increase in the mutual repulsion of the adsorbed active cations and of those approaching the surface. The concept of an activation barrier was first proposed by Doss.[62]

An alternative method of revealing the presence of an adsorption barrier was discussed by Owens.[22] The rate of diffusion is markedly temperature-dependent. It follows that a lack of a temperature dependence of the rate of decrease of the surface tension (i.e. the rate of increase of adsorption) indicates the appearance of an adsorption barrier. Let us consider the above example of a solution of CTAB (see Fig. 26), in which an adsorption barrier appears to be formed for $t > 1.5$ ms (see also Fig. 4).

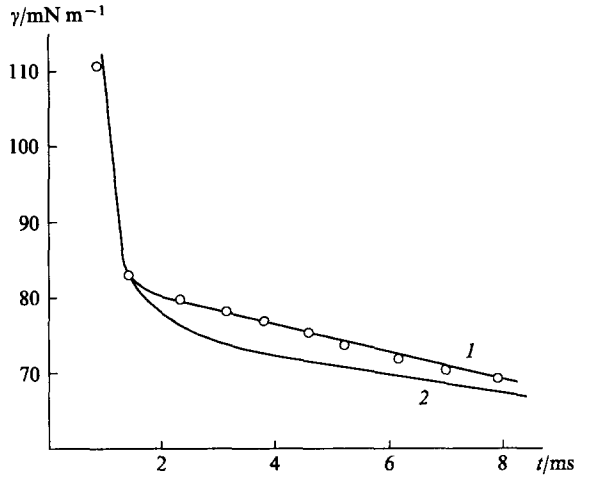


Figure 26. Experimental (*1*) and calculated time dependences (*2*) of the surface tension in the water–CTAB system at 25 °C with $c/10^{-4}$ mol dm^{-3} = 5.6 (see Rakhimov et al.[35]).

At $t > 1.5$ ms the rate of decrease of the dynamic surface tension becomes independent of temperature: this is interpreted by Owens as evidence for the formation of an adsorption barrier.

Thus we conclude from the behaviour of the CTAB solution that the different methods of identifying the mechanism of adsorption by studying the relaxation of the surface properties of the solution give adequately consistent results.

2. Analysis of the experimental dependence of the surface tension on the surface potential

Under equilibrium conditions the contribution to the surface tension from the orientation of the dipoles is proportional to the square of the discontinuity in the electric potential created at the surface.[63,64] As was said above, when the ionic double layer is formed under nonequilibrium conditions we find a term proportional to the first power of $\Delta\chi$.

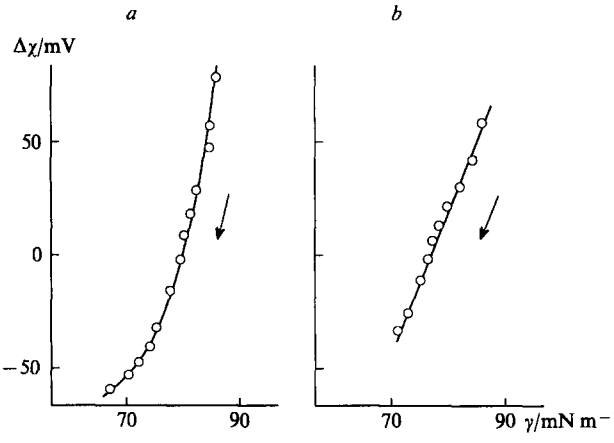


Figure 27. Dependence of $\Delta\chi$ on γ in the water–CTAB system with $c/10^{-4}$ mol dm^{-3} = 5.6 (*a*) and 2.8 (*b*).

Fig. 27 shows the $\gamma(t)-\Delta\chi(t)$ dependence for solutions of CTAB of two concentrations. At the lower concentration the $\gamma-\Delta\chi$ correlation is linear, but at the higher concentration we find a deviation from linearity. This means that in the former case the adsorption mechanism is diffusion-controlled, whereas in the latter case an adsorption barrier may be present.

3. Analysis of the experimental dependence of the adsorption on the surface potential

It has been shown[65] that under equilibrium conditions the adsorption potential increases linearly with the adsorption. This is explained by assuming that the molecular orientation is retained when the adsorption is increased. For a purely diffusional mechanism the calculation of adsorption by the Ward–Tordai equation assumes the presence of local equilibrium between the surface and the subsurface. It may be thought that for a diffusion-limited adsorption mechanism the parameter $\Delta\chi$ should be linearly dependent on Γ ($\Delta\chi$ and Γ are compared at the same instant). Therefore if Γ is calculated by the Ward–Tordai equation and φ(or $\Delta\chi$) is taken from experimental results a linear dependence of $\Delta\chi$ on Γ suggests a diffusion-controlled mechanism whereas deviations from linearity suggest the presence of a barrier.

The correctness of these views is confirmed by experiments with aqueous solutions of CTAB.[35] In the time region for which other methods had detected an adsorption barrier the dependence of $\Delta\chi$ on Γ was nonlinear. A similar analysis for aqueous solutions of hexadecylpyridinium bromide and dodecylammonium and cetyltrimethylammonium chlorides showed that in every case (except the cetyltrimethylammonium chloride of concentration 5.6×10^{-4} mol dm^{-3}) a linear relation between $\Delta\chi$ and Γ was obtained, indicating diffusion-controlled adsorption. In the exceptional case an adsorption barrier appears to be rate-limiting at short times (Fig. 28).

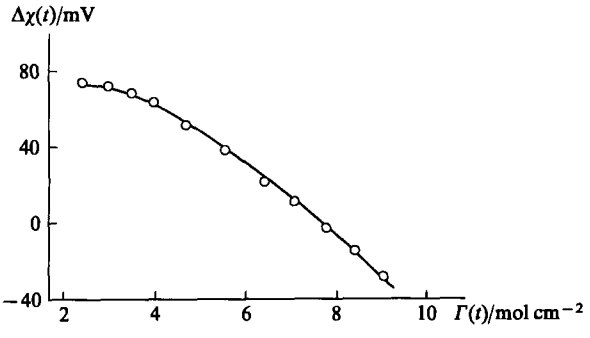


Figure 28. Dependence of $\Delta\chi$ on Γ calculated from experimental data for a solution of CTAC with $c/10^{-4}$ mol dm^{-3} = 5.8.

* * *

Thus the study of the properties of freshly created surfaces such as dynamic surface tension and surface electric potential allows us to compare different views on the structure of SAS solution surfaces.

The thermodynamic description of the relaxation of the surface layer offers practiclally useful conclusions on the mechanism of adsorption.

References

1. F T Davis, E K Rideal *Interfacial Phenomena* (New York: Academic Press, 1963)
2. M Van den Tempel, E H Lucassen-Reynders *Adv. Colloid Interface Sci.* **18** 281 (1983)
3. R Miller, S S Dukhin, A Kretzschmar *Colloid Polym. Sci.* **263** 420 (1985)
4. V B Fainerman *Usp. Khim.* **54** 1613 (1985) [*Russ Chem. Rev.* **54** 948 (1985)]
5. R P Borwankar, D T Wasan *Chem. Eng. Sci.* **43** 1323 (1988)
6. A Dupré *Théorie Méchanique de la Chaleur* (Paris: Gauthier-Villars, 1869)
7. Lord Rayleigh *Proc. R. Soc. London* **29** 71 (1879)
8. R E Defay, G Petre *Surf. Colloid Sci.* **3** 27 (1970)
9. A A Abramzon *Poverkhnostno-aktivnye Veshchestva* (Surfactants) (Leningrad: Khimiya, 1981)
10. A W Adamson *Physical Chemistry of Surfaces* (Translated into Russian; Moscow: Mir, 1979)
11. R Miller *Tenside* **16** 312 (1979)
12. P R Garett, D R Ward *J. Colloid Interface Sci.* **132** 475 (1990)
13. B A Noskov, N N Kochurova, in *Voprosy Termodinamiki Geterogennykh Sistem i Teorii Poverkhnostnykh Yavlenii.* Vyp. 7 (Problems in the Thermodynamics of Heterogeneous Systems and Theory of Surface Effects) No. 7 (Leningrad: Izd. Leningr. Univ., 1985) p. 178
14. N Bohr *Philos. Trans. R. Soc. London, A* **209** 281 (1909)
15. N Bohr *Proc. R. Soc. London, A Math. Phys. Sci.* **84** 395 (1910)
16. K L Sutherland *Aust. J. Chem.* **7** 319 (1954)
17. E K Rideal, K L Sutherland *Trans. Faraday Soc.* **18** 1109 (1952)
18. C C Addison *Philos. Mag.* **36** 73 (1945)
19. H Stocker *Z. Phys. Chem.* **94** 149 (1920)
20. R Defay, C Petre *J. Colloid Interface Sci.* **17** 565 (1962)
21. D Netzel, G Hogh, T Marz *J. Colloid Sci.* **19** 774 (1964)
22. D Owens *J.Colloid Sci.* **29** 496 (1926)
23. R Defay, J Hommelen *J. Colloid Sci.* **13** 553 (1958)
24. R S Hansen, M E Purchase, T C Wallace, R W Woody *J. Phys. Chem.* **62** 210 (1958)
25. W Thomas, L Potter *Proceedings of the Third International Congress on Surface Activity* (New York: Gordon and Breach, 1960)
26. N N Kochurova, B A Noskov, A I Rusanov *Kolloidn. Zh.* **36** 559 (1974)
27. F T Davis, R W Makepeace *AIChE J.* **24** 524 (1978)
28. N N Kochurova, Yu A Shevchenkov, A I Rusanov *Kolloidn. Zh.* **36** 785 (1974)
29. F Schmidt, H Steyer *Ann. Phys.* **79** 442 (1926)
30. A E Vandergrift *J. Colloid Interface Sci.* **23** 43 (1967)
31. B A Noskov, N N Kochurova *Kolloidn. Zh.* **41** 77 (1979)
32. R S Hansen *J. Phys. Chem.* **68** 2021 (1964)
33. N N Kochurova, A I Rusanov *J. Colloid Interface Sci.* **81** 297 (1981)
34. N N Kochurova, in *Voprosy Termodinamiki Geterogennykh Sistem i Teorii Poverkhnostnykh Yavlenii.* Vyp. 5 (Problems in the Thermodynamics of Heterogeneous Systems and Theory of Surface Effects) No. 5 (Leningrad: Izd. Leningr. Univ., 1979) p. 204
35. V I Rakhimov, N N Kochurova, A I Rusanov *Vestn. Leningr. Univ.* **22** 101 (1983)
36. W D Thomas, D J Hall *J. Colloid Interface Sci.* **51** 328 1975
37. A I Rusanov *Fazovye Ravnovesiya i Poverkhnostnye Yavleniya* (Phase Equilibriums and Surface Effects) (Leningrad: Khimiya, 1967)
38. N N Kochurova, A I Rusanov, in *Voprosy Termodinamiki Geterogennykh Sistem i Teorii Poverkhnostnykh Yavlenii.* Vyp. 8 (Problems in the Thermodynamics of Heterogeneous Systems and Theory of Surface Effects) No. 8 (Leningrad: Izd. Leningr. Univ., 1988) p. 109
39. N N Kochurova, A I Rusanov *Kolloidn. Zh.* **43** 36 (1981)
40. N N Kochurova, B A Noskov, A I Rusanov *Dokl. Akad. Nauk SSSR* **227** 1386 (1976)
41. A M Posner, A E Alexander *J. Colloid Sci.* **8** 575 (1953)
42. H L Jarvis, M A Scheiman *J. Phys. Chem.* **72** 74 (1968)
43. B A Noskov, N N Kochurova, A I Rusanov *Kolloidn. Zh.* **41** 579 (1979)
44. B A Noskov, N N Kochurova, A I Rusanov *Kolloidn. Zh.* **41** 804 (1979)
45. N N Kochurova, B A Noskov *Dokl. Akad. Nauk SSSR* **238** 1381 (1978)
46. J E Randles, D J Schiffrin *J. Electroanal. Chem.* **10** 480 (1965)
47. A E Shavrov, N N Kochurova *Vestn. Leningr. Univ., Ser. 4* **3** 101 (1989)
48. A N Frumkin, in *Sbornik Rabot po Chistoi i Prikladnoi Khimii (Trudy Khim. Instituta im L Ya Karpova* Vyp. 3) [Collected Reports on Pure and Applied Chemistry Proceedings of the Karpov Chemical Institute No. 3] (Moscow: Nauchno-tekhn. Otd. VSNKh SSSR, 1924) p. 3

49. V I Rakhimov, N N Kochurova *Issledovanie Zavisimosti Elektricheskogo Poverkhnostnogo Potentsiala ot Vremeni v Vodnykh Sistemakh* [(Study of the Dependence of Electric Surface Potential on Time in Aqueous Systems) Editorial Board of Journal *Vestn. Leningr. Univ. Fiz. Khim.* (Leningrad, 1983)] Article deposited at the All-Union Institute of Scientific and Technical Information (VINITI) No. 6194 (1983)
50. A Sanfeld *Introduction to the Thermodynamics of Charged and Polar Layers* (London, 1968)
51. N N Kochurova, A I Rusanov *Kolloidn. Zh.* **46** 9 (1984)
52. L Leb *Staticheskaya Elektrizatsiya* (Static Electrification) (Moscow; Leningrad: Gosenergoizdat, 1963)
53. T L Natanson *Dokl. Akad. Nauk SSSR* **73** 975 (1950)
54. S V Lopatenko, S M Kontush *Izv. Akad. Nauk SSSR, Energetika i Transport* 151 (1984)
55. S S Dukhin, D Liklema *Kolloidn. Zh.* **51** 244 (1989)
56. N N Kochurova, N O Myrzakhmetova, A I Rusanov *Dokl. Akad. Nauk SSSR* **316** 1425 (1991)
57. S V Lopatenko *Kolloidn. Zh.* **49** 162 (1987)
58. E Rillaerts, P Joos *J. Phys. Chem.* **86** 3471 (1982)
59. N M Zadymova, N N Tsikurina, Z N Markina *Vestn. Mosk. Univ., Ser. 2: Khim.* **23** 243 (1982)
60. A F H Ward, L Tordai *Recl. Trav. Chim. Pays-Bas* **71** 572 (1952)
61. K L Sutherland *J. Sci. Ind. Res., Sect. A, Gen.* **5** 683 (1952)
62. K S C Doss *Kolloidn. Zh.* **84** 138 (1938)
63. Ya I Frenkel' *Kineticheskaya Teoriya Zhidkostei* (Kinetic Theory of Liquids) (Moscow: Izd. AN SSSR, 1945)
64. A I Rusanov, V L Kuz'min, in *Materialy 11 Vsesoyuznoi Konferentsii po Poverkhnostnym Yavleniyam v Zhidkostyakh* (Proceedings of the XIth All-Union Conference on Surface Effects in Liquids) (Leningrad: Izd. Leningr. Univ., 1978) p. 146
65. B B Damaskin, O A Petrii *Vvedenie v Elektrokhimicheskuyu Kinetiku* (Introduction to Electrochemical Kinetics) (Moscow: Vysshaya Shkola, 1983)

Russian Chemical Reviews **62** (12) 1097 – 1105 (1993) ©1993 Russian Academy of Sciences and Turpion Ltd

UDC 547.239 + 547.793

Cycloaddition of nitrile oxides to multiple bonds containing a heteroatom

A A Esipenko, L I Samarai

Contents

I. Introduction	1097
II. General characteristics of the cycloaddition reactions of nitrile oxides	1097
III. Reactions involving the addition of nitrile oxides to multiple bonds	1098

Abstract. The review presents a compilation and a systematic account of the reactions involving the cycloaddition of nitrile oxides to multiple bonds containing noncarbon atoms. An attempt is made to trace the rules governing these processes on the basis of the available experimental data. The bibliography includes 219 references.

I. Introduction

The oxides of carboxylic acid nitriles occupy and important place among the 1,3-dipoles used widely in organic synthesis. These readily available compounds interact fairly easily with various dipolarophiles. They are therefore frequently used to obtain heterocyclic products and also in the synthesis of biologically active compounds with definite stereochemical parameters and of analogues of natural products. Nitrile oxides have recently found applications as modifying additives to polymeric materials. Their use as model compounds in theoretical studies on 1,3-cycloaddition reactions is no less important.

A monograph[1] and a series of reviews[2–5] on the chemistry of nitrile oxides are available at the present time. They cover the literature up to 1989. Attention is concentrated in these publications on the most thoroughly investigated reactions involving the cycloaddition of the dipoles to C=C and C≡C bonds. On the other hand, studies on the reactions of nitrile oxides with multiple bonds containing noncarbon atoms are adequately dealt with in the above monograph[1] but only up to 1970. In the subsequent reviews, only slight attention was devoted to such interactions. Furthermore, the reactions of nitrile oxides with certain multiple bonds (for example, C=As, C=P^{V}, C≡P, and Ge=S) began to be investigated comparatively recently and these are not mentioned in the above reviews.

The present review presents a systematic account of the literature (up to 1992 inclusive) on the reactions involving the addition of nitrile oxides to multiple bonds and an attempt is also made to trace certain rules governing these processes on the basis of the above experimental data.

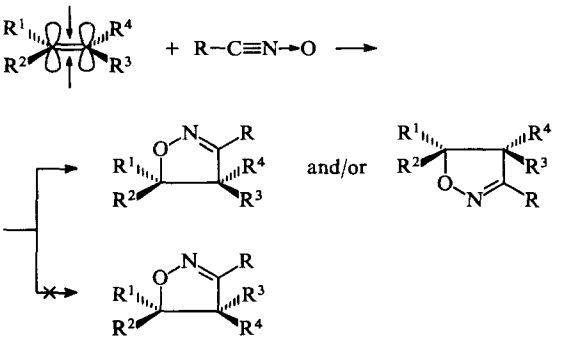
A A Esipenko, L I Samarai Department of the Chemistry of Heterocumulenes, Institute of Organic Chemistry, Academy of Sciences of Ukraine, Murmanskaya ul. 5, 252660 Kiev. Tel. (7-044) 551 06 74, Fax (7-044) 552 83 08

Received 1 October 1993
Uspekhi Khimii **62** (12) 1164 – 1172 (1993); translated by A K Grzybowski

II. General characteristics of the cycloaddition reactions of nitrile oxides

Before proceeding to the consideration of the reactions of nitrile oxides with particular multiple bonds, one should note certain features characteristic of all the cycloaddition reactions of nitrile oxides associated with their general mechanism.[2,6–9]

1. The high stereospecificity of the cycloaddition. The dipole adds in the *cis*-position relative to the multiple bond. The configuration, for example that of *cis*- and *trans*-olefins, is not then affected.



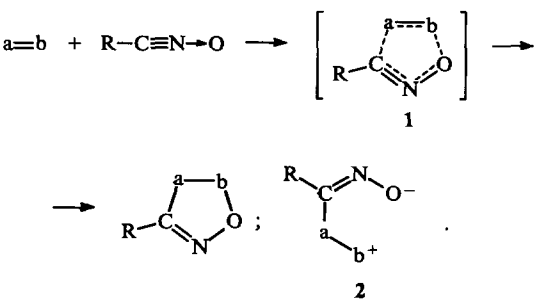
This property has found extensive application in the synthesis of analogues of natural products and biologically active compounds with specific stereochemical parameters.

2. Moderate enthalpies of activation (E_a = 9 – 16 kcal mol^{-1}) and high negative entropies of activation ($\Delta S_a^{\neq}$ = from −18 to −30 cal mol^{-1} K^{-1}), which are characteristic of a highly ordered transition state (TS).

3. A weak dependence of the rate of reaction on solvent polarity, indicating an insignificant charge separation in the transition state. This finding is also confirmed by the weak dependence of the rate of reaction on the nature of the substituents in the dipole and the dipolarophile. The values of the parameter ρ in the Hammett equation are in the range from 0.3 to 1.3.

Such experimental data indicate a concerted asynchronous mechanism of the cycloaddition reactions of nitrile oxides via the four-centre cyclic transition state **1** and rule out a stepwise mechanism via the formation of the highly charged zwitter-ions **2**.

The concerted mechanism of the cycloaddition presupposes the simultaneous dissociation of two π-bonds in the initial compounds and the formation of two new C–a and O–b σ-bonds. However, the new σ-bonds are formed at different rates and this is the reason why the cycloaddition reactions of nitrile oxides are somewhat asynchronous, which leads to a slight separation of the charges on the atoms of the transition state.



The structure of this transition state and the magnitude and signs of the charges depend both on the nature of the atoms a and b and on the nature of the substituents R in the dipole and the dipolarophile. The rate of reaction and the selectivity of the addition depend in their turn on the extent to which the formation of the transition state is favoured by energy factors.

In the description of the reactions under consideration, quantum-mechanical methods have been used recently to estimate the direction and relative rate of the addition. It is also possible to explain the influence of the nature of the substituents in the initial reactants on the course of the process.[2,9-13]

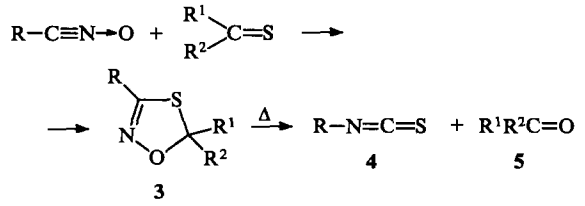
The lack of sufficient experimental data precludes at the present time a quantitative estimation of the reactivities of multiple bonds with different heteroatoms in the reactions with nitrile oxides. In purely qualitative terms, these bonds can be arranged in the following sequence based on decreasing reactivities: C=S, N=N, P^{V}=C > C=P^{III}, C=As (As=C), C=C, C=N, C=Se, B=N > C≡P, C≡C, Ge=S > P^{V}=N, C≡N > C=O. The atoms in each bond are arranged in an order such that the first adds to the oxygen atom at the end of the nitrile oxide group C≡N → O and the second adds to carbon atoms.

Next we shall consider the reactions of nitrile oxides with compounds containing all the bonds listed above (with the exception of C=C and C≡C which have been described in detail in other reviews[2-5]) in order of their decreasing reactivities.

III. Reactions involving the addition of nitrile oxides to multiple bonds

1. Addition to the C=S bond

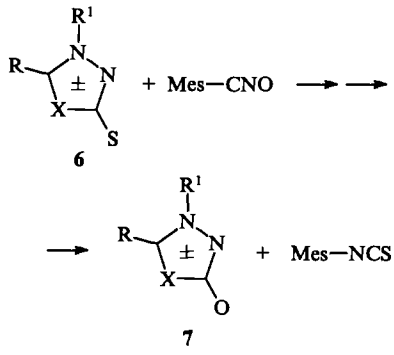
The C=S bond is the most reactive multiple bond in the series considered. At room temperature, the reactions involving the addition of nitrile oxides to C=S bonds take place over a period lasting from several minutes to several hours and lead to the formation of 3,5-disubstituted 1,4,2-oxathiazolines **3** in a satisfactory yield.[1,14-17]



Even in the case of sterically hindered aromatic nitrile oxides, the reaction with diphenyl thioketone at room temperature terminates after 30 min and leads to the cyclic product **3** in 80% yield.[18] In those cases where the dipolarophile molecule contains, apart from the C=S bond, also other reactive bonds, for example C=C [19,20] or C=N,[21,22] the nitrile oxides undergo cycloaddition primarily to the C=S bond.

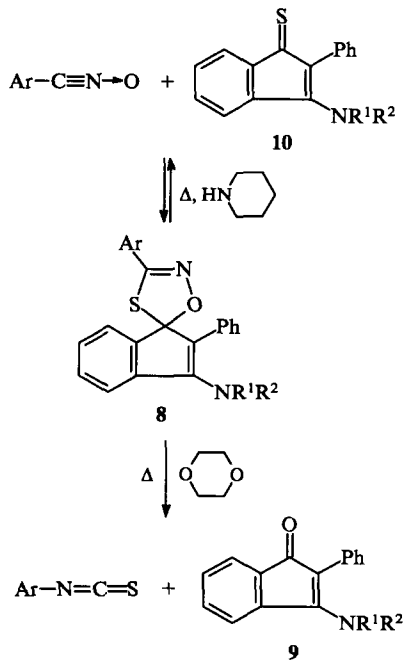
In most cases, compounds **3** are stable crystalline substances. On heating to 100-180 °C, they are cleaved to form the isothiocyanates **4** and the corresponding carbonyl compounds **5**.[14,23,2] Oxathiazoles containing an amino-group (NMe_2, NHR^3)[16,23,25,26] or the *p*-$Me_2NC_6H_4$ group[7] as the substituent R^1 (or R^2) are cleaved already at the instant of the reaction in the absence of heating. The influence of such substituents on the stability of the heterocycle is transmitted even through the C=C bond.[19,22]

In certain cases, the reactions of nitrile oxides with thiocarbonyl compounds are used to replace the sulfur atom by oxygen.[22,27,28] This method is particularly convenient for the synthesis of cyclic ketones from the more readily available thioketones.[21,28-32] A method for the conversion of the *meso*-ion of azolium thiolate **6** into the *meso*-ion of azolium olate **7** with the aid of the cycloaddition of mesityl cyanide has also been described.[33]

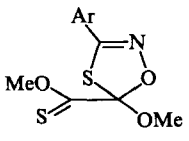


The fact that the cycloaddition reactions may be reversible under certain conditions is of interest. It has been shown[20] that, when the oxathiazole **8** is heated in dioxane, benzene, and dimethylformamide (DMF), its decomposition takes place with formation of the carbonyl compound **9**. The thermolysis of this compound in piperidine leads to the initial thioketone **10** (Scheme 1).

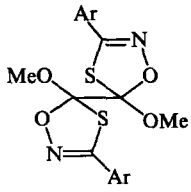
Scheme 1



O,O-Dimethyl dithiooxalate forms stable products of the cycloaddition of one (compound **11**) or two (compound **12**) molecules of a nitrile oxide.[34] Compound **12** exists in two diastereoisomeric forms, which have been separated. Dimethyl tetrathiooxalate reacts similarly with nitrile oxides, but the adducts proved to be unstable in this case.[34]



11

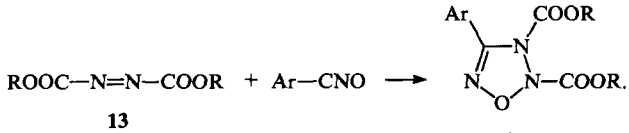


12

Kinetic studies on the reactions of nitrile oxides with 4,4'-disubstituted diphenyl thioketones have been carried out.[7] The regioselectivity of the addition of benzonitrile oxide to 2- thionoadamantane has been discussed[11] from the standpoint of the molecular orbital theory.

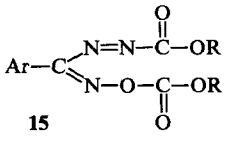
2. Addition to the N=N bond

Nitrile oxides readily react with the azodicarboxylates **13**.[35]

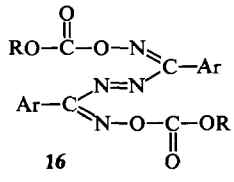


13 14

The process proceeds so vigorously that it is carried out at temperatures from −20 °C to −15 °C in order to prevent the formation of side products.[36, 37] The cycloaddition products—1,2,3,5-oxatriazolines **14**—were isolated only for the methyl esters of azodicarboxylic acid **13** (R=Me). At room temperature, they isomerise in solution to the linear products **15**. The latter can combine with yet another molecule of the nitrile oxide at the N=N bond, affording compound **16**.



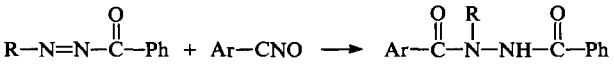
15



16

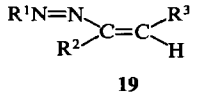
Only the isomerisation products **15** and **16**, the ratio of which depends on the nature of the group Ar, were isolated in the case of the ethyl esters **13** (R=Et). It has been suggested that the azo-compounds **15** and **16** obtained as a result of this reaction be used in the manufacture of dyes.[38]

Only the linear product **18** was isolated in the reactions of nitrile oxides with *N*-substituted *N*-benzoyl compounds **17**. The mechanism of its formation has not been established.[37]

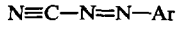


17 18

Despite the high reactivity of the N=N bond, the cycloaddition of nitrile oxides to the conjugated azoolefins **19** and azonitriles **20** takes place regioselectively at the C=C [39] or C≡N [40] bond.



19



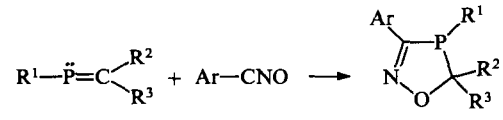
20

3. Addition to the C=P bond

In this group of dipolarophiles, it is necessary to distinguish compounds with trivalent and pentavalent phosphorus atoms. Their behaviour in reactions with nitrile oxides differs appreciably.

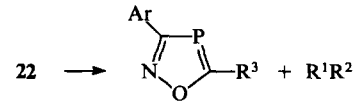
a. Addition to the C=P^{III} bond

Compounds of trivalent phosphorus are known to reduce nitrile oxides to nitriles.[1] However, in those cases where the reactivity of the phosphorus in the phosphaalkenes **21** is lowered due to steric factors, nitrile oxides undergo cycloaddition to the multiple bond with formation of 1,2,4-oxazaphospholines **22**.[41–45]



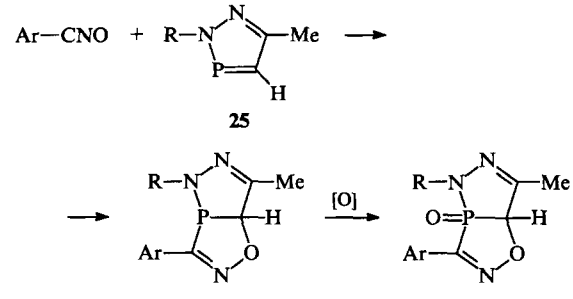
21 22

Compounds **22** are unstable in most cases. They either split off the R^1R^2 molecule and are converted into 1,2,4-oxazaphospholes **23** or are oxidised to compounds **24** with pentavalent phosphorus.[13]



23

$R^1 = Me_3Si$; $R^2 = Me_3SiO$ [39,40];
$R^1 = Cl$; $R^2 = Me_3Si$ [40,44,45].

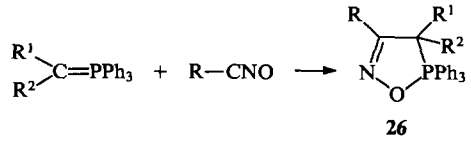


25 24

It has been shown[13] that the selectivity of the cycloaddition of nitrile oxides to compound **25** agrees well with quantum-mechanical calculations.

b. Addition to the C=P^{V} bond

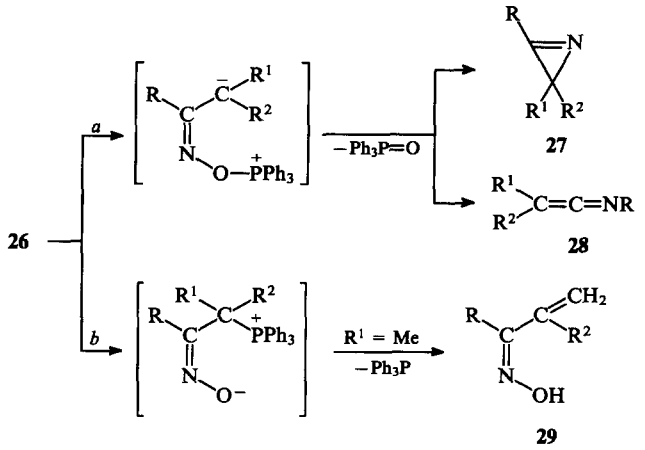
In the case of phosphinomethylenes, the cycloaddition of nitrile oxides proceeds with the opposite orientation of the atoms and leads to the formation of the P–O bond.[48–52]



26

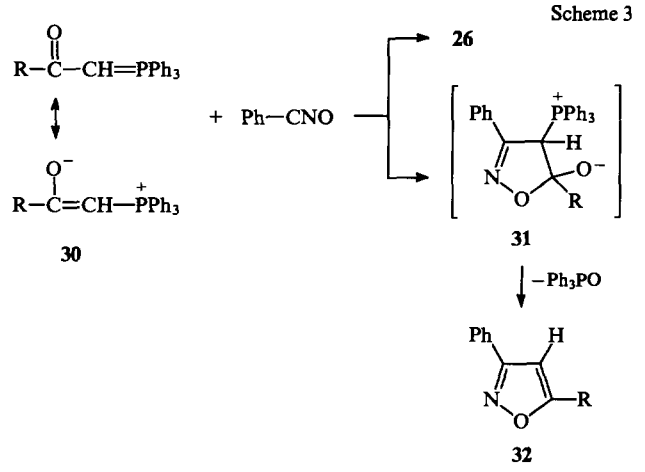
The resulting 1,2,5-oxazaphospholines **26** are unstable and in most cases are cleaved spontaneously. It has been noted in the literature that the cleavage usually begins with the dissociation of the C–P bond in the heterocycle (pathway *a*) and leads to the substituted azirines **27** or ketene imines **28**.[48, 50, 53–55] However, there are instances of the cleavage of the P–O bond (pathway *b*) with formation of the corresponding ketoximes **29**.[49] The mode of decomposition and the ratio of the final products depend on the nature of the substituents R, R^1, and R^2 (Scheme 2).

Scheme 2



The cycloaddition of nitrile oxides to phosphorus ketoylides **30** takes place at both C=P and C=C bonds. In the second case, the unstable cyclic adducts **31** are formed. They split off triphenylphosphine oxide and are converted into the oxazoles **32** (Scheme 3).[51,53]

Scheme 3



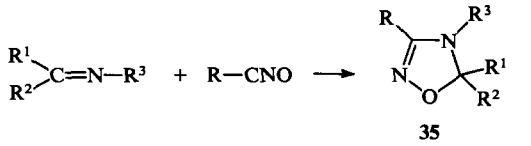
4. Addition to the C=As bond

The cycloaddition of nitrile oxides to the C=As bond began to be investigated comparatively recently, the first communication having appeared in 1981.[44] So far, this reaction is the only example where, depending on the conditions, one obtains either the product of the 'direct' (compound **33**—an As–C bond is formed) or 'reverse' (compound **34**—an As–O bond is formed) mode of addition (Scheme 4).[13,44,56]

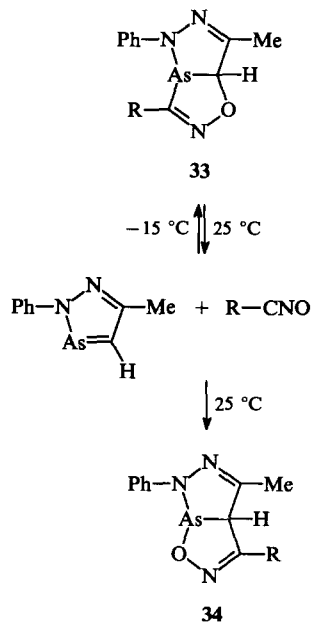
Compound **33** is obtained at a reduced temperature (−15 °C). At room temperature, it is spontaneously converted after 2 h into the isomer **34**. It has been shown that the change in the mode of addition takes place with cleavage of the oxazarsenoline ring of compound **33** to give the initial compounds. It is believed[44] that compounds **33** and **34** are formed via kinetic and thermodynamic mechanisms respectively.

5. Addition to the C=N bond

Among the reactions involving cycloaddition to multiple carbon–heteroatom bonds, those involving compounds containing the C=N bond have been studied most widely.

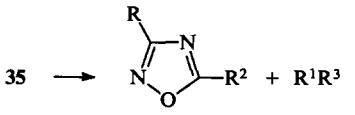


Scheme 4



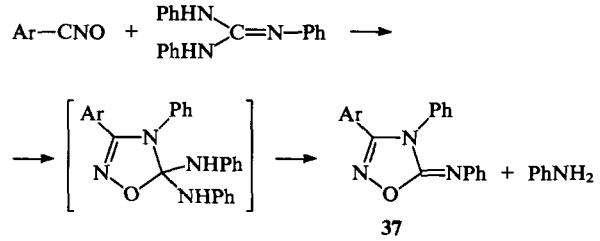
Nitrile oxides add fairly readily to this bond, forming substituted 1,2,4-oxadiazolines **35**.[1,57]

Compounds **35** are in most cases stable and can be readily isolated. At the same time, for a certain combination of the substituents R^1 and R^3, the R^1R^3 molecule is split off spontaneously and 1,2,4-oxadiazoles **36** are formed.



$R^1 = NH_2$; $R^3 = H$;[58,61]
$R^1 = OAlk$; $R^3 = H$;[58,59,62–64]
$R^1 = H$; $R^3 = OH$;[65–71]
$R^1 = CH_2C{\equiv}N$; $R^3 = H$;[72,73]
$R^1 = SMe$; $R^3 = H$.[58]

The product of the reaction of a nitrile oxide with *N,N',N''*-triphenylguanidine is stabilised somewhat differently. In this case, the aniline molecule is split off and 1,2,4-oxadiazoline **37** with an exocyclic C=N bond is formed.[74]



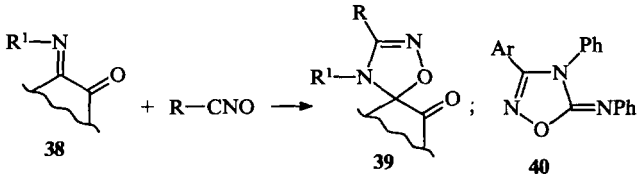
Studies have now been carried out on the interaction of nitrile oxides with virtually all classes of compounds containing the C=N bond: imines,[8,26,66,72,73,75–91] oximes,[56,65–71,92–94] derivatives of hydroxamic acid,[95] iminoesters,[58,59,62,64,96] iminothioesters,[58] amidines,[58,59,61] guanidine derivatives,[60,74,97] hydrazones,[98–101] azines,[99] and *O*(*S*)-alkyl-substituted ureas (thioureas).[58] However, despite extensive experimental data and the constantly growing interest in reactions involving the cycloaddition of nitrile oxides to the C=N bond, any kind of quantitative studies on this interaction are so far lacking. It is therefore at present impossible to determine unambiguously the dependence of the reactivity on the nature of the reactants and also to compare

the reactivity of the C=N bond with the reactivities of other multiple bonds in this reaction.

Analysis of the experimental data permits the hypothesis that electronic factors exert an insignificant influence on the reactivity of the C=N bond. As regards nitrile oxides, electron-accepting substituents in the *para*-position of the aromatic ring facilitate the reaction, shortening the time and increasing the yield of the cyclic product.[58,76]

The steric characteristics of the reactants have a much greater influence on the rate of cycloaddition. Benzonitrile oxide and its derivatives with substituents in the *meta*- or *para*-position react readily (frequently over a period of several minutes or hours at room temperature) with the C=N bond of the dipolarophile. On the other hand, in the case of sterically hindered nitrile oxides containing substituents in the *ortho*-position, the reaction does not take place at all[81] or leads to the formation of cyclic products in a low yield. In order to increase the yield, it is necessary to increase the reaction time,[102] to use more severe conditions, or to employ a catalyst.[71,94] With increase in the number and bulk of the substituents, the reactivity of the imino-group also diminishes somewhat. However, even in the case of trisubstituted imines the yield of the target product remains comparatively high: from 30% [77] to 60%–70% (provided that at least two substituents are methyl groups)[66] and up to 90% in the reaction with the reactive *p*-nitrobenzonitrile oxide.[76]

The above rules are obeyed also by the reactions involving the cycloaddition of nitrile oxides to exocyclic C=N bonds. Interaction with compounds of type **38** takes place at room temperature over a period of several hours and does not require the use of catalysts. The corresponding spirans **39** are then formed.[92,103,104]



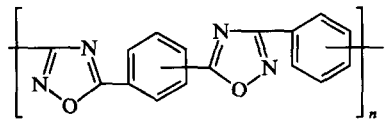
38 **39** **40**

On the other hand, more severe conditions are essential for the reactions of nitrile oxides involving the C=N bond of compound **40**; the reaction mixture is heated for several days in DMF at 75 °C with $BF_3 \cdot Et_2O$ as the catalyst.[74] The yield of the spiro-products is between 50% and 90% in all cases.

As in the case of linear azomethines, endocyclic C=N bonds in the ring readily combine with nitrile oxides, forming the corresponding bicyclic products. However, these reactions have certain unusual features. Together with the influence of steric characteristics of the substituents on the reactivity of the endocyclic C=N bond, in cyclic dipolarophiles there is an increased importance of electronic factors and a new important factor appears—that of ring strain. With increase in ring strain, there is an increase in reactivity of the imino-group, but the stability of the bicyclic compounds formed diminishes. It is noteworthy that it is stabilised in all cases with retention of the oxadiazoline ring formed.[96,105,106]

Reactions involving the cycloaddition of nitrile oxides to the C=N bonds in three-membered,[107] four-membered,[108,109] five-membered,[13,44,96,105,106,110–121] six-membered,[37,59,66,110,119,121–129] and seven-membered[102,123,130,131] rings have been investigated.

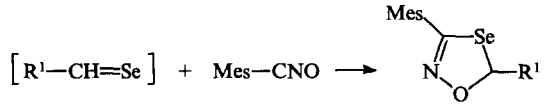
In conclusion of this Section, one should note that the reactions of nitrile oxides with imines can be used to obtain polymers or to modify them. Unfortunately, hitherto there has been only one study on this subject.[70] It was reported that the polycondensation of the bisoxides of the nitriles of terephthalic and isophthalic acids with the bisoximes of *para*- and *meta*-substituted benzaldehydes leads to polymers having the general structure **41**.



41

6. Addition to the C=Se bond

It has been reported recently that the oxide of mesityl cyanide adds even at 25 °C to the C=Se bond of selenoaldehydes, generated *in situ*, with formation of 1,4,2-oxaselenazolines **42**.[132]

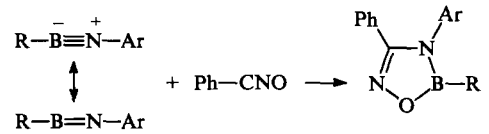


42

R^1 = H, Ph.

7. Addition to the N=B bond

There have been only two studies in which the reactions of nitrile oxides with borimides were described.[133,134] Cycloaddition products were obtained in both cases—2-bora-1,3,5-oxadiazolines **43**. It was noted that the reaction does not occur for R = C_6F_5 and Ar = mesityl.[134]

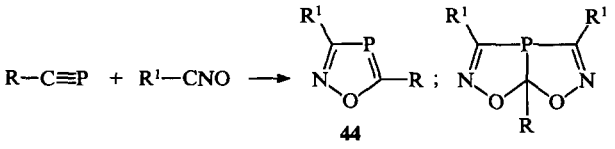


43

Ar = Ph; R = Ph;
Ar = Ph; R = 4-$MeOC_6H_4$.

8. Addition to the C≡P bond

As in the case of phosphaalkenes, the cycloaddition of nitrile oxides to phosphaalkynes is preferred to the oxidation-reduction process. The interaction even with a sterically hindered nitrile oxide terminates at room temperature in the course of 24 h and leads to the formation of stable 1,2,4-oxazaphospholes **44**. Compounds **44** combine fairly readily with a second nitrile oxide molecule via the endocyclic C=P bond, forming the bicyclic product **45** (R^1 = Ph, 4-ClC_6H_4).[45,136,137]

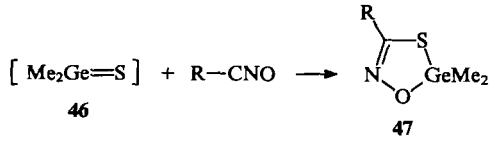


44 **45**

R = 1-Ad,[41] Bu^t.[135,136]

9. Addition to the Ge=S bond

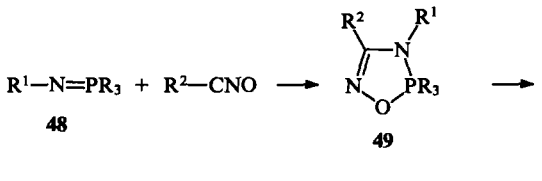
It has been reported[138] that the reaction of dimethyl germathione **46**, generated *in situ*, and nitrile oxides leads to the cyclic products **47**—2-germa-1,3,5-oxathiazolines—in 70% – 80%99 yield. Triethylamine is used as the catalyst.



46 **47**

10. Addition to the N=P^V bond

Nitrile oxides react readily with iminophosphoranes **48**. As in the case of phosphinomethylenes, cycloaddition leads to the formation of products with the 'reverse' orientation—1,2,4,5-oxadiazophospholines **49**.[139-141] The rings formed are as a rule unstable and are cleaved during the reaction to the carbodiimides **50**.[140]

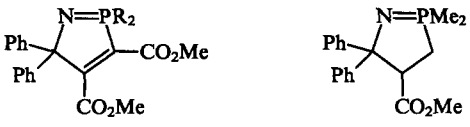


48 **49**

$\longrightarrow$ $R^2-N=C=N-R^1 + R_3P=O$

50

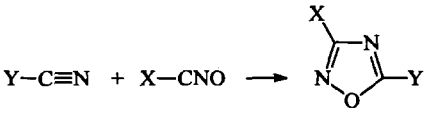
A product of type **49** can be isolated only in those cases where the N=P^{V}group is part of the composition of the ring (for example, in the azaphosphole **51** and the azaphospholine **52**) [141] or contains sufficiently powerful electron-accepting substituents ($R^1 = ArSO_2$, R = Cl).[142]



51 **52**

11. Addition to the C≡N bond

The interaction of nitrile oxides with nitriles has been investigated fairly widely. In all cases, the products are stable 3,5-disubstituted 1,2,4-oxadiazoles **53**.[1]



53

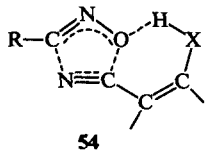
In the study of this reaction, use was made of nitriles containing a wide variety of substituents Y: Ar,[6,64,65,69,89,143-151] RC(O),[66,145,151] C_nH_m,[68,145,147,152-156] $C_nH_mHal_k$,[66,144,147,151,157-159] $R_2C(C\equiv N)$,[66,151,161-163] $R_2C=CH$,[164-173] $R_2C=C(C\equiv N)$,[162,172,174,175] $RN=N$,[40,66] $R(NR^1_2)C=CH$,[9,72,73,176] $RN=CR^1$,[177]), $R_nE^+-N^-$ (where E = S, P, N),[179] $R_2N-C(NH)-NH$,[97,139,180-182] ArO,[183,184] ArS,[185] $ArSO_2$,[186] $(AlkO)_2P(O)$ and $(AlkO)_2P(S)$,[187] $(NO_2)_3C$,[188] R_2N,[178] and Het.[66,134,136,139-141,151,189-192]

Kinetic studies have been carried out on the reaction under consideration.[6,138,154] The influence of the substituents in the reactants on the rate of cycloaddition can be determined unambiguously from the results of these studies and also from other experimental data. It was found that the reactivity of nitriles increases on passing from aliphatic to aromatic substituents and also following the introduction of electron-accepting groups and diminishes after the introduction of electron-donating groups.[66,72,150,160,190] As regards nitrile oxides, electron acceptors and donors increase somewhat the reactivity of benzonitrile oxides[72,154,187] but do not affect the reactivity of the oxides of benzoyl cyanides [$X-C_6H_4-C(O)-CNO$].[161]

Steric factors exert a much greater influence on the reactivity of the reactants. In the case of aromatic nitriles[148,150] and nitrile oxides,[187,189] it falls sharply after the introduction of substituents in the *ortho*-position. In many instances, such nitrile oxides fail altogether to enter into the reaction considered.[189]

The reactivity of unreactive nitriles and also the yield of cycloaddition products can be increased appreciably by employing catalysts (for example, $BF_3 \cdot Et_2O$).[137,152,163]

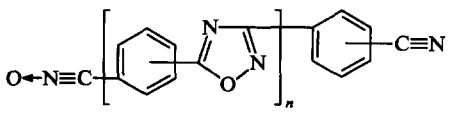
Despite the low reactivity of the C≡N bond in reactions with nitrile oxides, the cycloaddition of the dipole to unsaturated nitriles can be achieved in many instances exclusively or predominantly at the nitrile group.[9,40,66,72,97,162,164,171,174-176,182,189,191] Such increase in the reactivity of the C≡N bond has been explained[72,150,177,191] by the stabilisation of the transition state **54** and of the final product as a result of the formation of the O···H hydrogen bond.



54

X = NR^1, O.

On the other hand, in other cases the lower reactivity of the C=C bond has been explained by the influence of electronic or steric factors.[9,162]

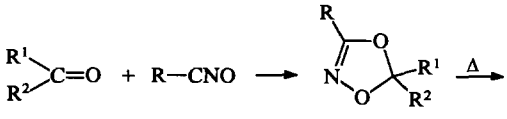


55

The possibility of using the above reaction for the synthesis of polymers has been investigated. The copolymers of the bisoxides of the nitriles of terephthalic and isophthalic acids with the bisnitriles of these acids. **41**,[70,193,194] as well as the polymer **55**, formed from *p*-cyanobenzonitrile oxide,[194,195] have been obtained. It was noted that these substances exhibit an increased stability. Their decomposition begins only at 400 °C.

12. Addition to the C=O bond

The cycloaddition of nitrile oxides to the C=O bond has been little investigated despite the fact that the first publication on this topic appeared as early as 1961.[196] In all cases, the occurrence of this interaction leads to the formation of stable 1,4,2-dioxazolines **56**.[1]



56

$\longrightarrow$ $R^1R^2C=O + R-N=C=O$

57

On heating above 150 °C, the dioxazoline ring **56** is cleaved with formation of the initial carbonyl compound and the corresponding isocyanate **57**.[57,197,198]

The interaction of compounds containing the C=O group, such as aliphatic[152,199] and aromatic[26,133,143,196,197,200] aldehydes, ketones,[75,87,196,201] vinyl ketones,[202,203] amides,[204] acid chlorides,[92,169,205] and trichlorocarbonyl isocyanate,[206] with nitrile oxides has been investigated. A series of studies have been devoted to the cycloaddition to exocyclic C=O bonds, which leads to the formation of the corresponding spiro-compounds.[91,103,129,152,199,207-210]

Merely the fact that the reactivity of the C=O bond decreases appreciably after the introduction of electron-accepting groups in the α-position relative to C=O has been firmly established for the reactions of nitrile oxides with carbonyl compounds. Thus carbonyl compounds which do not contain such substituents can interact with nitrile oxides only in the presence of catalysts

($BF_3 \cdot Et_2O$,[57,145,152,204,211] NEt_3 [203]). On the other hand, the reactions with aldehyde and ketones in which there are electron-accepting groups [CCl_3,[196,197,206] CF_3,[87,200,201] C(O)R, C(O)OR [196,197]] proceed without catalysts over a period of several hours and the yield of the cyclic adduct is 50%–90%. Aromatic aldehydes also exhibit an increased reactivity.[89,145,197,200] The behaviour of aromatic ketones in reactions with nitrile oxides has not been investigated.

The reactions of nitrile oxides with quinones have been investigated in fair detail. It was shown that *ortho*-quinones (*o*-benzoquinone, *o*-naphthoquinone, phenanthrenenequinone, and chrysenequinone) are active dipolarophiles and readily combine with2.9 nitrile oxides via the C=O (one or two) or C=C bonds depending on the nature of the substituents and the solvent.[92,103,210]

In contrast to *ortho*-quinones, the reactivity of *para*-quinones is very low. For example, the yield of the products of the cycloaddition of nitrile oxides to *p*-benzoquinone does not exceed 15%,[70,212–214] but increases appreciably when the $BF_3 \cdot Et_2O$ catalyst is used.[145,211]The reactions of nitrile oxides with substituted *p*-benzoquinones have been studied systematically since 1977.[12,198,215–218]

The dependence of the rate and mode (via the C=C or C=O bonds) of the addition on the number and nature of the substituents in the quinone has been demonstrated. The experimental data have been explained by the influence of steric and electronic factors[215,218] and have been compared with quantum-mechanical calculations.[12,217]

* * *

It is seen from the data described above that the cycloaddition reactions of nitrile oxides can be used successfully for the construction of five-membered heterocyclic structures. The latter can be both the final and intermediate products in the synthesis of various cyclic or acyclic compounds.

We hope that this review and also the recently published review of the reactions of nitrile oxides with heterocumulenes[219] will expand the range of applications of these readily available and fairly stable 1,3-dipoles.

References

1. G Grundmann, P Grünanger *The Nitrile Oxides* (Berlin: Springer 1971)
2. P Caramella, P Grünanger *1,3-Dipolar Cycloaddition Chemistry* (New York: VCH Publ., 1984) p. 291
3. G Bianchi, R Gandolfi, P Grünanger, in *The Chemistry of Triple-bonded Functional Groups* (New York: Interscience, 1983) p. 737
4. K B G Torssell *Nitrile Oxides, Nitrones and Nitronates in Organic Synthesis* (New York: VCH Publ., 1988)
5. S Kanemasa, O Tsuge *Heterocycles* **30** 719 (1990)
6. A Dondoni, G Barbaro *Gazz. Chim. Ital.* **105** 701 (1975)
7. A Battaglia, A Dondoni, G Maccagnani, G Mazzanti *J. Chem. Soc. (B)* 2096 (1971)
8. E Cadoni, G Gelli, P Beltrame *Gazz. Chim. Ital.* **120** 679 (1990)
9. G Gelli, E Cadoni, A Deriu, P Beltrame *J. Chem. Soc., Perkin Trans. 2* 245 (1990)
10. K N Houk, J Sins, C R Watts, L J Luskus *J. Am. Chem. Soc.* **95** 7301 (1973)
11. T Katada, S Eguchi, T Sasaki *J. Chem. Soc., Perkin Trans. 1* 2641 (1984)
12. T Hayakawa, K Araki, S Shiraishi *Bull. Chem. Soc. Jpn.* **57** 1643 (1984)
13. L Ko, Y Y C Yeung, F Tonnard, R Carrié *Tetrahedron* **39** 1507 (1983)
14. A Dondoni *J. Org. Chem.* **37** 3196 (1972)
15. E Vedejs, R G Wilde *J. Org. Chem.* **51** 117 (1986)
16. R Huisgen, W Mack *Chem. Ber.* **105** 2815 (1972)
17. B F Bonini, G Maccagnani, G Mazzanti, C Abdel-Lateef, A Atwa, P Zani, G Barbaro *Heterocycles* **31** 47 (1990)
18. A Battaglia, A Dondoni *Synthesis* 378 (1971)
19. N A Korchevin, V A Usov, M G Voronkov, N M Borodina *Zh. Org. Khim.* **22** 1276 (1986)
20. N A Korchevin, V A Usov, A F Tokareva, M G Voronkov *Khim. Geterotsikl. Soedin.* 278 (1975)
21. M Stavaux, N Lozac'h *Bull. Soc. Chim. Fr.* 4423 (1971)
22. K Métayer, M G Duguay *C. R. Acad. Sci.* **273** 1457 (1971)
23. K Friedrich, M Zamkanei *Chem. Ber.* **112** 1873 (1979)
24. V R Grashey, M Weidner *Chem.-Ztg.* **97** 623 (1973)
25. R Huisgen, W Mack, E Anneser *Angew. Chem.* **73** 656 (1961)
26. R Huisgen *Angew. Chem.* **75** 604 (1963)
27. S Holm, J A Boerma, N H Nilsson, A Senning *Chem. Ber.* **109** 1069 (1976)
28. A K Baruah, D Prajapati, J S Sandhu *Tetrahedron* **44** 6137 (1988)
29. V R Grashey, G Schroll, M Weidner *Chem.-Ztg.* **100** 496 (1976)
30. V R Grashey, M Weidner, C Knorn, H Bauer *Chem.-Ztg.* **100** 496 (1976)
31. F Boberg, J Knoop *Liebigs Ann. Chem.* **708** 148 (1967)
32. D Noël, J Vialle *Bull. Soc. Chim. Fr.* 2239 (1967)
33. V R Grashey, M Weidner, G Schroll *Chem.-Ztg.* **100** 497 (1976)
34. K Hartke, T Gillmann *Chem.-Ztg.* **110** 338 (1986)
35. P Rajagopalan *Tetrahedron Lett.* **15** 887 (1974)
36. R Huisgen, H Blaschke, E Brunn *Tetrahedron Lett.* **7** 405 (1966)
37. H Blaschke, E Brunn, R Huisgen, W Mack *Chem. Ber.* **105** 2841 (1972)
38. US P. 4 268 674; *Ref. Zh. Khim.* 1N193P (1982)
39. L P Vasil'eva, G S Akimova, V N Chistokletov, K N Zelenin *Zh. Org. Khim.* **18** 1853 (1982)
40. W Ried, M Fulde *Helv. Chim. Acta* **71** 1681 (1988)
41. T Alespach, M Regitz, G Becker, W Becker *Synthesis* 31 (1986)
42. F Zurmuehlen, W Roesch, M Regitz *Z. Naturforsch. B, Chem. Sci.* **40** 1077 (1985)
43. G Märkl, H-J Beckh *Tetrahedron Lett.* **28** 3475 (1987)
44. R Carrié, L Ko, Y Y C Yeung *J. Chem. Soc., Chem. Commun.* 1131 (1981)
45. L Ko, Y Y C Yeung, R Carrié, A Muench, G Becker *J. Chem. Soc., Chem. Commun.* 1634 (1984)
46. L Ko, Y Y C Yeung, R Carrié *J. Chem. Soc., Chem. Commun.* 1640 (1984)
47. G Markl, I Troetsch-Schaller, W Hölzl *Tetrahedron Lett.* **29** 785 (1988)
48. R Huisgen, J Wulff *Tetrahedron Lett.* 917 (1967)
49. H J Bestmann, R Kunstmann *Chem. Ber.* **102** 1816 (1969)
50. R Huisgen, J Wulff *Chem. Ber.* **102** 1833 (1969)
51. M I Shevchuk, S T Shpak, A V Dombrovskii *Zh. Obshch. Khim.* **45** 2609 (1975)
52. G Gaudiano, R Mondelli, P P Ponti, C Ticozzi, A Umani-Ronchi *J. Org. Chem.* **33** 4431 (1968)
53. G L'Abbe, J-M Borsus, R Ykman, G Smets *Chem. Ind. (London)* 1491 (1971)
54. H J Bestmann, R Kunstmann *Angew. Chem.* **78** 1059 (1966)
55. H J Bestmann, T Denzel, R Kunstmann *Tetrahedron Lett.* **9** 2895 (1968)
56. G Märkl, H Seitz *Tetrahedron Lett.* **27** 2957 (1986)
57. C Grundmann *Synthesis* 344 (1970)
58. T Sasaki, T Yoshioka, Y Suzuki *Bull. Chem. Soc. Jpn.* **42** 3335 (1969)
59. M Kurabayashi, C Grundmann *Bull. Chem. Soc. Jpn.* **51** 1484 (1978)
60. F Eloy, R Lenaers *Helv. Chim. Acta* **49** 1430 (1966)
61. G Musante *Gazz. Chim. Ital.* **68** 331 (1938)
62. P Rajagopalan *Tetrahedron Lett.* **10** 311 (1969)
63. F Eloy, R Lenaers *Bull. Soc. Chim. Belg.* **72** 719 (1963)
64. R K Howe, F M Schleppnik *J. Heterocycl. Chem.* **19** 721 (1982)
65. W M Williams, W R Dolbier *J. Org. Chem.* **34** 155 (1969)
66. K Bast, M Chistl, W Mack *Chem. Ber.* **105** 2825 (1972)
67. G Just, K Dahl *Tetrahedron* **24** 5251 (1968)
68. M Fetizon, M Golfier, R Milcent, I Papadakis *Tetrahedron* **31** 165 (1975)
69. T Sasaki, T Yoshioka, Y Suzuki *Bull. Chem. Soc. Jpn.* **44** 185 (1971)
70. S-J Hong *Daehan Hwakak Hwoejee* **15** 121 (1971)
71. T Sasaki, Y Suzuki, T Yoshioka *Yuki Gosei Kagaku Kyokaishi* **28** 742 (1970)
72. A Corsaro, U Chiacchio, G Purrello *J. Chem. Soc., Perkin Trans. 1* 2154 (1977)

73. A Corsaro, U Chiacchio, A Compagnini, G Purrello *J. Chem. Soc., Perkin Trans. 1* 1635 (1980)
74. C Grundmann, R Richter *Tetrahedron Lett.* **9** 963 (1968)
75. L A Simonyan, Yu V Zeifman, N P Gambaryan *Izv. Akad Nauk SSSR, Ser. Khim.* 1916 (1968)
76. F Lauria, V Vecchietti, G Tosolini *Gazz. Chim. Ital.* **94** 478 (1964)
77. F M Hershenson *J. Heterocycl. Chem.* **9** 739 (1972)
78. G Srimannarayana, R M Srivastava, B C Leallyn *J. Heterocycl. Chem.* **7** 151 (1970)
79. M Rai, K Krishan, A Singh *Indian J. Chem.* **15** 848 (1977)
80. A Singh, J S Sandhu, S Mohan *Tetrahedron Lett.* **9** 4453 (1968)
81. E Rajanarendar, C Rao, A K Murthy *Indian J. Chem.* **20** 839 (1981)
82. German P. 1 170 958; *Chem. Abstr.* **61** 8317f (1965)
83. S Morrocchi, A Ricca, L Velo *Chim. Ind. (Milan)* **49** 168 (1967)
84. R M Srivastava, L B Clapp *J. Heterocycl. Chem.* **5** 61 (1968)
85. L Fabbrini, F De Sarlo *Chim. Ind. (Milan)* **45** 242 (1963)
86. A K Baruah, D Prajapati, J S Sandhu *Tetrahedron* **44** 1241 (1988)
87. V A Soloshonok, V P Kukhar' *Zh. Org. Khim.* **26** 419 (1990)
88. L M A Santiago, R Perez-Ossorio, J Plumet *An. Quim., Ser. C* **77** 71 (1981)
89. G A Lee *Synthesis* 508 (1982)
90. V I Kelarev, G A Shvekhgeimer *Khim. Geterotsikl. Soedin.* 147 (1986)
91. T Yoshioka, K Yamamoto, Y Shimauchi, Y Fukagawa, T Ishikure *J. Chem. Soc., Chem. Commun.* 1513 (1984)
92. W J Awad, M Sobhy *Can. J. Chem.* **47** 1473 (1969)
93. H G Aurich, K Stork *Chem. Ber.* **108** 2764 (1975)
94. S Morrocchi, A Ricca *Chim. Ind. (Milan)* **47** 629 (1967)
95. P Caramella, E Cerede *Synthesis* 433 (1971)
96. J-P Gibert, R Jacquier, C Petrus *Bull. Soc. Chim. Fr.* **2** 281 (1979)
97. G Rembarz, E Fischer, F Tittelbach *J. Prakt. Chem.* **313** 1065 (1971)
98. M M El-Abadelah, A Q Hussein, A M Awadallah *Heterocycles* **29** 1957 (1989)
99. V G Andrianov, E N Rozhkov, A V Eremeev *Khim. Geterotsikl. Soedin.* 262 (1991)
100. V G Andrianov, E N Rozhkov, A V Eremeev *Zh. Org. Khim.* **25** 2028 (1989)
101. F Risitano, G Grassi, F Foti *J. Chem. Res. (S)* 65 (1981)
102. J Streith, G Wolff, H Fritz *Tetrahedron* **33** 1349 (1977)
103. W J Awad, S M Abdel, R Omran, M Sobhy *J. Org. Chem.* **31** 331 (1966)
104. A Franke *Liebigs Ann. Chem.* 717 (1978)
105. J-P Gibert, C Petrus, F Petrus *J. Heterocycl. Chem.* **16** 311 (1979)
106. J-P Gibert, R Jacquier, C Petrus, F Petrus *Tetrahedron Lett.* **15** 755 (1974)
107. V Nair *Tetrahedron Lett.* **12** 4831 (1971)
108. A-B N Luheski, R K Smalley, P D Dennewell, R Westwood *Tetrahedron Lett.* **31** 123 (1990)
109. C W Rees, R Somanathan, R C Storz, A D Woolhouse *J. Chem. Soc., Chem. Commun.* 740 (1975)
110. K-H Magosch, R Feinauer *Angew. Chem.* **83** 882 (1971)
111. P Caramella, G Cellerino, A C Coda, A G Invernizzi *J. Org. Chem.* **41** 3349 (1976)
112. P Caramella, P Frattini, P Grünanger *Tetrahedron Lett.* **12** 3817 (1971)
113. P Caramella, G Cellerino, P Grünanger, F V Albini, M R Re Cellerino *Tetrahedron* **34** 3545 (1978)
114. C Parini, S Colombi, A Ius, R Longhi, G Vecchio *Gazz. Chim. Ital.* **107** 559 (1977)
115. G Bailo, P Caramella, G Cellerino, A G Invernizzi, P Grünanger *Gazz. Chim. Ital.* **103** 47 (1973)
116. G F Bettinetti, A Gamba *Gazz. Chim. Ital.* **100** 1144 (1970)
117. G-A Hoyer, G Boroschewski *Arch. Pharm. (Weinheim, Ger.)* **310** 255 (1977)
118. G Bianchi, C De Micheli, R Gandolfi *J. Chem. Soc., Perkin Trans. 1* 1711 (1972)
119. G Stájer, A E Szabó, G Bernáth *Tetrahedron* **43** 1931 (1987)
120. E Coutouli-Argyropoulou, E Malamidou-Xenikaki, D Mentzafos, A Terzis *J. Heterocycl. Chem.* **27** 1185 (1990)
121. F M Albini, R De Franco, T Bandiera, P Grünanger, P Caramella *Gazz. Chim. Ital.* **120** 1 (1990)
122. P Sohár, G Stájer, G Bernáth *Magn. Reson. Chem.* **25** 635 (1987)
123. H Bartsch, T Erker *Heterocycles* **27** 1461 (1988)
124. G Stájer, A E Szábo, G Bernáth, P Sohár *Magy. Kem. Foly.* **94** 491 (1988)
125. A Corsaro, G Perrini, P Caramella, F M Albini, T Bandiera *Tetrahedron Lett.* **27** 1517 (1986)
126. P Caramella, T Bandiera, F M Albini, A Gamba, A Corsaro, G Perrini *Tetrahedron* **44** 4917 (1988)
127. F M Albini, R De Franco, T Bandiera, P Caramella, A Corsaro, G Perrini *J. Heterocycl. Chem.* **26** 757 (1989)
128. P Caramella, V Bertolasi, S Forte, R De Franco, T Bandiera, F M Albini *J. Chem. Res. (S)* 308 (1989)
129. N G Argyropoulos, E Corobili, A Terzis, D Mentzafos *J. Heterocycl. Chem.* **27** 1425 (1990)
130. T Sasaki, S Eguchi, N Toi *J. Org. Chem.* **44** 3711 (1979)
131. M C Abersa, P Bondcorsi, P Giannetto, D A Leigh *J. Heterocycl. Chem.* **26** 1619 (1989)
132. P T Meinke, G A Krafft *Tetrahedron Lett.* **28** 5121 (1987)
133. P I Paetzold *Angew. Chem.* **79** 583 (1967)
134. P I Paetzold, G Stohr *Chem. Ber.* **101** 2874 (1968)
135. W Rösch, M Regitz *Angew. Chem.* **96** 898 (1984)
136. W Rösch, M Regitz *Synthesis* 689 (1987)
137. E P O Fuchs, M Hermesdorf, W Schnurr, W Rösch, H Heydt, M Regitz, P Binger *J. Organomet. Chem.* **338** 329 (1988)
138. H Lavayssiere, J Satge, J Barrau, M Traore *J. Organomet. Chem.* **240** 335 (1982)
139. R Huisgen, J Wulff *Tetrahedron Lett.* **8** 921 (1967)
140. R Huisgen, J Wulff *Chem Ber.* **102** 1848 (1969)
141. A Schmidpeter, Th Criegern *Chem. Ber.* **112** 3472 (1979)
142. V N Fetyukhin, V E Shkarin, A M Pinchuk *Synlett.* in press
143. T Shimizu, J Hayashi, K Teremura *Bull. Chem. Soc. Jpn.* **58** 2519 (1985)
144. F Eloy *Bull. Soc. Chim. Belg.* **73** 793 (1964)
145. T Sasaki, T Yoshioka *Bull. Chem. Soc. Jpn.* **41** 2206 (1968)
146. R Huisgen *Angew. Chem.* **75** 742 (1963)
147. R Lenaers, F Eloy *Helv. Chim. Acta* **46** 1067 (1963)
148. C Laandri, M Pallotti *Ann. Chim. (Rome)* **47** 376 (1957)
149. G Leandri *Boll. Sei. Fac. Chim. Ind. Bologna* **14** 80 (1956)
150. A Corsaro, U Chiacchio, P Caramella, G Purrello *J. Heterocycl. Chem.* **21** 949 (1984)
151. R Huisgen, W Mack, E Anneser *Tetrahedron Lett.* **2** 587 (1961)
152. S Morrocchi, A Ricca, L Velo *Tetrahedron Lett.* **8** 331 (1967)
153. G Bianchi, C D Micheli, R Gandolfi, P Grünanger, P V Finzi, O V De Pava *J. Chem. Soc., Perkin Trans. 2* 1148 (1973)
154. P Beltrame, G Gélli, A Loi *J. Heterocycl. Chem.* **20** 1609 (1983)
155. P Beltrame, A Dondoni, G Barbaro, G Gélli, A Loi, S Steffe. *J. Chem. Soc., Perkin Trans. 2* 607 (1978)
156. G Bianchi, C De Micheli, A Gamba, R Gandolfi *J. Chem. Soc., Perkin Trans. 1* 137 (1974)
157. D P Del'tsova, E S Ananyan, N P Gambaryan *Izv. Akad. Nauk SSSR, Ser. Khim.* 362 (1971)
158. V Yu Rumyantsev, G A Shvekhgeimer, in *Tezisy Dokladov V Vsesoyuznoi Konferentsii po Khimii Azotsoderzhashchikh Geterotsiklicheskikh Soedinenii, Chernogolovka* (Abstracts of Reports at the Vth All-Union Conference on Chemistry of Nitrogen-containing Heterocyclic Compounds, Chernogolovka) 1991, p. 157
159. N G Popandopulo, O S Kartseva, in *Tezisy Dokladov V Vsesoyuznoi Konferentsii po Khimii Azotsoderzhashchikh Geterotsiklicheskikh Soedinenii, Chernogolovka* (Abstracts of Reports at the Vth All-Union Conference on Chemistry of Nitrogen-containing Heterocyclic Compounds, Chernogolovka) 1991, p. 158
160. N V Vasil'ev, A F Kolomiets, G A Sokol'skii *Zh. Org. Khim.* **16** 2233 (1980)
161. J J Tegeler, C J Diamond *J. Heterocycl. Chem.* **24** 697 (1987)
162. P S Lianis, N A Rodios, N E Alexandrou *J. Heterocycl. Chem.* **26** 1683 (1989)
163. R Neidlein, Z Sui *Helv. Chim. Acta* **74** 501 (1991)
164. T Sasaki, S Eguchi, T Esaki, T Suzuki *Tetrahedron* **35** 1073 (1979)
165. A K Baruah, D Parajapati, J S Sandhu *Heterocycles* **27** 1127 (1988)
166. H Dahn, B Favre, J-P Leresche *Helv. Chim. Acta* **56** 457 (1973)
167. T Sasaki, T Yoshioka *Bull. Chem. Soc. Jpn.* **41** 2212 (1968)
168. G S D'Alcontres, P Grünanger *Gazz. Chim. Ital.* **80** 741 (1950)
169. Y Otsuji, Y Tsujii, A Yoshido, E Imoto *Bull. Chem. Soc. Jpn.* **44** 223 (1971)
170. B H Kim *Synth. Commun.* **17** 1199 (1978)
171. C Antonino, C Ugo, P Giancarlo, C Pierluigi, P Giavanni *J. Chem. Res. (S)* 402 (1984)

172. P S Lianis, N A Rodios, N E Alexandrou *J. Heterocycl. Chem* **25** 1099 (1988)
173. J J Tegeler, C J Diamond *J. Heterocycl. Chem.* **24** 701 (1987)
174. J E Franz, R K Hows, H K Pearl *J. Org. Chem.* **41** 620 (1976)
175. K Gewald, U Hain *Z. Chem.* **26** 434 (1986)
176. A Corsaro, U Chiacchio, G Perrini, P Caramella, G Purrello. *J. Heterocycl. Chem.* **22** 797 (1985)
177. T O Stevens *J. Org. Chem.* **33** 2660 (1968)
178. V W Ried, M Fulde *Chem.-Ztg.* **113** 315 (1989)
179. V A Ogurtsov, O A Rakitin, N V Obruchnikova, L F Chertanova, A A Gazikasheva, L I Khmel'nitskii *Izv. Akad. Nauk SSSR, Ser. Khim.* 2084 (1990)
180. G Rembarz, H Brandner, E-M Bebenzoth *J. Prakt. Chem.* **31** 221 (1978)
181. T Sasaki, T Yoshioka *Bull. Chem. Soc. Jpn.* **40** 2608 (1967)
182. J Plenkiewicz, Z Eckstein *Bull. Acad. Pol. Sci., Ser. Sci. Chem.* **15** 99 (1967)
183. D Martin, A Weise *Chem. Ber.* **99** 317 (1966)
184. D Martin, H-J Herrmann, S Rackow, K Nadolski *Angew. Chem.* **77** 96 (1965)
185. R M Paton, D G Hamilton *Tetrahedron Lett.* **24** 5141 (1983)
186. A M V Leusen, J C Jagt *Tetrahedron Lett.* **11** 971 (1970)
187. S K Das, S N Balasubrahmanyan *J. Org. Chem.* **48** 4232 (1983)
188. T D Ladyzhnikova, K V Altukhov, N A Solov'ev *Zh. Org. Khim.* **22** 2618 (1986)
189. M S Chang, J U Lowe *J. Org. Chem.* **32** 1577 (1967)
190. G A Shvekhgeimer, V I Kelarev, L A Dyankova *Khim. Geterotsikl. Soedin.* 1609 (1984)
191. G Ferrara, A J C Parini, G Sportoletti, G Wicchio *Tetrahedron* **28** 2461 (1972)
192. A Corsaro, G Perrini, G Pugtisl, G Purrello *J. Chem. Res. (S)* 246 (1989)
193. C G Overberger, S Fujimoto *J. Polym. Sci. Pt B* **3** 735 (1965)
194. D A Klein, R A Fouty *Macromolecules* **1** 318 (1968)
195. M Akiyama, Y Iwakura, S Shiraishi, Y Imai *J. Polym. Sci. Pt B* **4** 305 (1966)
196. R Huisgen, W Mack *Tetrahedron Lett.* **2** 583 (1961)
197. R Huisgen, W Mack *Chem. Ber.* **105** 2805 (1972)
198. S Shiraishi, S Ikeuchi, M Seno, T Asahara *Bull. Chem. Soc. Jpn.* **50** 910 (1977)
199. V G Andrianov, A V Eremeev *Khim. Geterotsikl. Soedin.* 1426 (1989)
200. N A Genco, R A Partis, H Alper *J. Org. Chem.* **38** 4365 (1973)
201. D R Brittelli, G A Boswell *J. Org. Chem.* **46** 316 (1981)
202. G L'ablé, G Mathys *J. Org. Chem.* **39** 1221 (1974)
203. E Coutouli-Argyropoulou, E Thessalonikeos *J. Heterocycl. Chem.* **28** 429 (1991)
204. S Morrocchi, A Ricca, A Zanarotti *Chim. Ind. (Milan)* **50** 352 (1968)
205. T Shimizu, Y Hayashi, H Shibafuchi, K Teremura *Bull. Chem. Soc. Jpn.* **59** 2827 (1986)
206. V N Fetyukhin, A A Esipenko, L I Samarai *Zh. Org. Khim.* **21** 910 (1985)
207. N G Argyropoulos, N E Alexandrou, D N Nicolaides *Tetrahedron Lett.* **17** 83 (1976)
208. C De Micheli, R Gandolfi, P Grünanger *Tetrahedron* **30** 3765 (1974)
209. H Matsukubo, H Kato *J. Chem. Soc., Chem. Commun.* 412 (1974)
210. S Morrocchi, A Ricca, A Selva, A Zanarotti *Gazz. Chim. Ital.* **99** 565 (1969)
211. S Morrocchi, A Quilico, A Ricca, A Selva *Gazz. Chim. Ital.* **98** 891 (1968)
212. A Quilico, G S D'Alcontres *Gazz. Chim. Ital.* **80** 140 (1950)
213. E Pinter, M Müller, R Ott *Sci. Pharm.* **54** 244 (1986)
214. E A Titov, V I Prikhod'ko, in *Voprosy Khimii i Khimicheskoi Tekhnologii* (Problems of Chemistry and Chemical Engineering) No. 28 (All-Republic Interdepartmental Collection) (Kiev: Naukova Dumka, 1973) p. 6
215. S Shiraishi, S Ikeuchi, M Seno, T Asahara *Bull. Chem. Soc. Jpn.* **51** 921 (1978)
216. S Shiraishi, B S Holla, K Jmamura *Bull. Chem. Soc. Jpn.* **56** 3457 (1983)
217. T Hayakawa, K Araki, S Shiraishi *Bull. Chem. Soc. Jpn.* **57** 2216 (1984)
218. S Shiraishi, S Ikeuchi, M Seno *Nippon Kagaku Kaishi* 1127 (1978)
219. A A Esipenko, V N Fetyukhin, L I Samarai *Ukr. Khim. Zh.* 630 (1993)

Russian Chemical Reviews **62** (12) 1107–1117 (1993)
©1993 Russian Academy of Sciences and Turpion Ltd

UDC 547.735

Selenium- and tellurium-centred radicals

E N Deryagina, M G Voronkov, N A Korchevin

Contents

I. Introduction	1107
II. Selenyl and telluryl radicals	1107
III. Perselenyl and selenuranyl radicals	1114
IV. Seleninyl and selenonyl radicals	1116

Abstract. The principal types of radicals formed in various types of initiation of the reactions of organic compounds of selenium and tellurium, the methods for their detection, and their properties and reactivities are examined. The bibliography includes 98 references.

I. Introduction

During recent years the chemistry of selenium and tellurium has begun to develop vigorously, promoted to a considerable extent by their extensive application in medicine, the electronics industry, etc. Selenium plays an important role as a trace element in living organisms.

Selenium- and tellurium-centred radicals are short lived intermediates in many photolytic thermal reactions of organoselenium and organotellurium compounds. The first information about them appeared in the literature little more than twenty years ago and their study began to develop vigorously only in recent years. This was promoted primarily by the discovery of the important role of selenium as a trace element in living organisms, in food products for animals and man, and in biochemical processes,[1] as well as its employment in microelectronics.[2,3] In the second half of the present century, eight natural selenoproteins were discovered. It was observed that the deficiency of selenium in food and in soil can induce certain diseases in animals and anomalies in the growth and development of a number of plant species.[1]

Organoselenium and organotellurium compounds are used in the electronics industry, in xerography, in photoelectronics and in the glass, ceramics, and pigments industries. Selenium-containing polymers with semiconducting properties and photosensitivity have been obtained.[2,3] Neurotropic and psychotropic medicinal preparations, with much lower toxicity than their sulfur analogues, have been developed based on selenophene.[4,5]

Homolytic processes, which include the formation of free selenium- and tellurium-centred radicals, play an important role in the reactions of organoselenium compounds and to a lesser extent of their tellurium analogues. This is due to the low energies of the C–Se, Se–Se, and Se–E (E = heteroatom) as well as C–Te and Te–Te bonds, which are responsible for their ready homolytic dissociation.[4,7]

This review deals with the main types of radical formed in various types of initiation of reactions of organic compounds of selenium and tellurium, the methods for their detection, and their properties and reactivities. A comparison is made with the analogous data for sulfur-centred radicals.

Whereas radical reactions of the organic compounds of sulfur have been investigated quite fully,[7–10] information about the fairly similar free-radical reactions of organoselenium compounds, mainly photochemical reactions, has been surveyed only in brief reviews.[11,12] Data on the radical reactions of organotellurium compounds are scattered among various communications and the aim of the present review is to survey the existing literature on this question.

The following types of selenium- and tellurium-centred radicals are known: for selenium, these are the selenyl (RSė), perselenyl (RSeSė), selenuranyl [$R_2S\dot{e}-SeR$ and $R_2S\dot{e}-X$; X = Cl, Br, $OSiMe_3$, C(Me)OMe, SC(O)R′], seleninyl (RSėO), and selenonyl ($RS\dot{e}O_2$) radicals and for tellurium only the telluryl radicals (RTė).

II. Selenyl and telluryl radicals

1. Detection and physical properties

The simplest selenium-centred radicals—the selenyl radicals RSė—were first detected in the photolysis of diorganyl diselenides.[13]

Selenyl (HSė) and telluryl (HTė) radicals are generated by passing hydrogen through a microwave absorption cell, the walls of which are coated with selenium or tellurium respectively, in a silent electric discharge (the HṠ radicals are generated similarly). Certain physicochemical characteristics of the radicals HĖ (E = Se, Te, S) are presented in Table 1.

Table 1. Physicochemical characteristics of the radicals.[14]

Parameter	HSė	HTė	HṠ
I	60	3	240
P/Torr	5	1	10
$10^{-8}D$/electrostatic units	0.2	0.1	0.3
A_0/cm^{-1}	1600 ± 50	2250 ± 200	–

Note. I is the intensity of the microwave radiation, P the partial pressure, D the dipole moment, and A_0 the spin–orbit coupling constant of the ground state of the radical measured by the EPR method.

E N Deryagina, M G Voronkov, N A Korchevin Agricultural Chemicals Laboratory, Irkutsk Institute of Organic Chemistry, Siberian Division of the Russian Academy of Sciences, ul. Favorskogo 1, 664033 Irkutsk, Russian Federation. Tel. (7-395-2) 46 02 45.

Received 7 September 1993
Uspekhi Khimii **62** (12) 1173–1183 (1993); translated by A K Grzybowski

The adiabatic ionisation potential of the radical HSe (9.845 ± 0.003 eV) and the bond dissociation energies D_0(HSe–H) = 78.99 and D_0(H–Se) = 74.27 kcal mol^{-1} were determined on photoionisation of the radical HSe generated in the spectrometer cell during the interaction of atomic hydrogen with hydrogen selenide.

$$\dot{H} + H_2Se \longrightarrow H\dot{S}e + H_2$$

Organoselenyl radicals RSe are formed on photolysis of diorganyl diselenides.[13] Their direct detection by the EPR method is difficult (particularly in the liquid phase) owing to the high degree of spin–orbit coupling and in certain cases the occurrence of specific interactions,[16] which lead to orbitally degenerate (or almost degenerate) ground states and to a greater anisotropy of the *g*-factor.[17] As a result of this, the radicals RSe have short relaxation times and give rise to extremely broad lines in the EPR spectra.[9,16,17] Nevertheless, the selenyl radicals formed on photolysis of toluene-ω-selenol, and didodecyl, dioctadecyl, and diphenyl selenides have been detected by the EPR method. Because of anisotropy of the *g*-factor, selenyl radicals have (like thiyl radicals[11]) asymmetric spectra, the *g*-factor differing significantly from the values characteristic of the free electron and carbon-centred radicals.[18,19]

Radical	$g_\perp$	$g_\parallel$
PhSe	2.003	2.016
$PhCH_2Se$	2.091	2.124
$Me(CH_2)_{11}Se$	2.088	2.122
$Me(CH_2)_{17}Se$	2.083	2.115

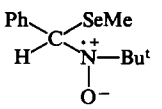
The methylselenyl radical MeSe could not be detected directly by the EPR method[18] and the available information concerning the measurement of the EPR spectrum of the PhSe radical is fairly contradictory.[18,20] The detection of the RTe radicals by the EPR method has not been reported at all.

Arylselenyl radicals can be detected by UV spectroscopy.[21,22] The absorption band of the radical PhSe is in the region of 490 nm (like that of PhS), while that of the radical 4-$MeOC_6H_4Se$ is in the region of 535 nm (in methanol). The corresponding absorption bands of the radicals 4-$MeOC_6H_4S$ and 4-$MeOC_6H_4Te$ are in the region of 525 and 508 nm.[22,23]

Like thiyl radicals,[9] selenyl radicals RSe can be readily identified by the EPR method as adducts with nitroso-compound spin-trapping agents.[24]

Methylselenyl radicals, formed on photolysis of dimethyl diselenide, do not interact with 2-methyl-2-nitrosopropane but are effectively bound by *tert*-butyl phenyl nitrone.[17] The adduct **1** is characterised by a high value of the *g*-factor (2.0097), the hyperfine structure (hfs) constants confirming its structure: a_N = 13.5 G, a_H(1H) = 2.06 G, and a_H(3H) = 0.85 G.[17]

$$Me_2Se_2 \xrightarrow{h\nu} 2MeSe \xrightarrow{PhCH=N(O)Bu^t}$$



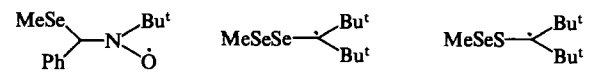
1

The arylselenyl radicals PhSe and 4-$O_2NC_6H_4Se$ have been detected as adducts with nitrosodurene.[17,25]

The radical complexes RSe·MX_3 (X = Cl, Br), formed from selenides and diselenides on their interaction with aluminium and gallium halides, can also be detected by EPR spectroscopy. The EPR spectra of the Ar_2Se_2–$AlBr_3$–C_6H_6 system consists of three singlet signals ($g \sim 2.07$, $g \sim 2.03$, and $g \sim 2.0025$). They have been assigned to the radicals Ar, ArSe, and ArSeSe bound in the complex.[26]

2. The formation reactions of organic compounds of selenium and tellurium on photolysis and radiolysis

The selenyl radicals generated by the photolysis of diorganyl selenides readily add to the C=C, C=S, C=Se, etc. multiple bonds. The methylselenyl radicals formed on photolysis of dimethyl diselenide add to the multiple bonds of the corresponding spin-trapping agents, affording adducts of the following type:[17]



The photolysis of dibenzyl diselenide takes place differently, beginning with the dissociation of the Se–C bond and the formation of dibenzyl selenide and selenium. The benzylselenyl radical is then generated in the stage involving the decomposition of the benzylperselenyl radical formed initially and then interacts rapidly with the benzyl radical.[27]

$$PhCH_2SeSeCH_2Ph \xrightarrow{h\nu} \begin{cases} 2\,PhCH_2Se \\ PhCH_2SeSe + \dot{C}H_2Ph \end{cases}$$

$$PhCH_2SeSe \longrightarrow PhCH_2Se + Se$$

$$Ph\dot{C}H_2 + PhCH_2SeSeCH_2Ph \longrightarrow PhCH_2Se + PhCH_2SeCH_2Ph$$

$$PhCH_2Se + \dot{C}H_2Ph \longrightarrow PhCH_2SeCH_2Ph$$

$$2\,PhCH_2Se \longrightarrow PhCH_2SeSeCH_2Ph$$

When dibenzyl diselenide in solution in benzene is irradiated in air or in acetonitrile, benzaldehyde, benzyl alcohol, and elemental selenium are formed,[28] whereas in carbon tetrachloride the product is benzyl chloride.[29] This confirms the preferential dissociation of the C–Se bond on photolysis of dibenzyl diselenide. Photolysis of diphenyl diselenide leads to the formation of phenylselenyl radicals PhSe, which are distinguished by a low reactivity in their reactions with hydrogen, oxygen, or halogen donors but add readily to activated olefins.[23,30,31]

$$PhSeSePh \overset{h\nu}{\rightleftharpoons} 2\,PhSe$$

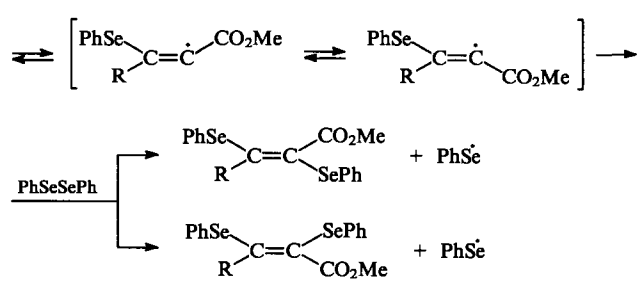
$$PhSe + CH_2{=}CHR \rightleftharpoons PhSeCH_2{-}\dot{C}HR$$

The rate constant for the addition reaction ranges from 2.0×10^6 mol^{-1} s^{-1} for α-methylstyrene to $\sim 10^3$ mol^{-1} s^{-1} for vinyl acetate. These values are lower by a factor of 10–50 than in the case of the radical PhS, which indicates a greater stability of the phenylselenyl radical.

The phenylselenyl radicals generated on UV irradiation add effectively to activated acetylenes, but their addition to non-activated acetylenes, for example to dec-1-yne, is very slow.[32]

$$PhSeSePh \overset{h\nu}{\rightleftharpoons} 2\,PhSe$$

$$PhSe + RC{\equiv}CCOOMe \rightleftharpoons$$



The (*E*)-isomers predominate in the mixture of the di(phenylseleno)ethylenes formed. Owing to steric hindrance, dimesityl diselenide reacts with activated acetylenes only slowly.

Phenylselenyl radicals are also generated on photolysis of phenylareneselenosulfonates, inducing the chain decomposition of the latter with formation of diphenyl diselenide and arenesulfonic anhydride.[33]

$$PhSeSO_2Ar \xrightarrow{h\nu} PhSe^{\cdot} + {}^{\cdot}SO_2Ar$$

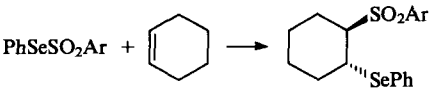
$$PhSe^{\cdot} + PhSeSO_2Ar \longrightarrow PhSeSePh + {}^{\cdot}SO_2Ar$$

$$2\,ArSO_2^{\cdot} \longrightarrow \left[ArS(=O)(=O)-O-S(=O)(=O)Ar \right] \longrightarrow \longrightarrow$$

$$\longrightarrow ArS(=O)(=O)-O-S(=O)(=O)Ar + \text{other products}$$

$$2\,PhSe^{\cdot} \longrightarrow PhSeSePh$$

The photolysis of phenylareneselenosulfonates in the presence of alkenes leads to aryl β-phenylselenoalkyl sulfones. The reaction is strictly stereoselective and involves the formation of *trans*-adducts.[34]



The photolytic addition of selenosulfonates to alkenes is faster than the thermal addition (in boiling chloroform or benzene). In both cases, the reaction proceeds via a free-radical chain mechanism. It is accelerated on initiation with azobisisobutyronitrile (AIBN) and is inhibited by 2,6-di-*tert*-butyl-*p*-cresol.[35]

$$ArSO_2SePh \xrightarrow{h\nu \text{ or } \Delta} ArSO_2^{\cdot} + Se^{\cdot}Ph$$

$$ArSO_2^{\cdot} + \underset{R^2}{\overset{R^1}{}}\!\!=\!\!\underset{R^4}{\overset{R^3}{}} \longrightarrow \underset{ArSO_2}{\overset{R^1}{}}\!\!-\!\!\underset{R^4}{\overset{R^2}{}}\!\!-\!\!\overset{R^3}{\cdot} \xrightarrow{ArSO_2SePh}$$

$$\longrightarrow \underset{ArSO_2}{\overset{R^1}{}}\!\!-\!\!\underset{R^4}{\overset{R^2}{}}\!\!-\!\!\underset{R^3}{\overset{SePh}{}} + ArSO_2^{\cdot}$$

The aryl β-phenylselenoalkyl sulfones formed eliminate spontaneously benzeneselenol in the presence of *m*-chloroperbenzoic acid or hydrogen peroxide and are converted into the corresponding vinyl sulfones.

The photolysis of diorganyl diselenides is accelerated by tertiary phosphines, whereupon the Se–Se bond dissociates preferentially both in diphenyl diselenide and in dibenzyl diselenide.[36–38]

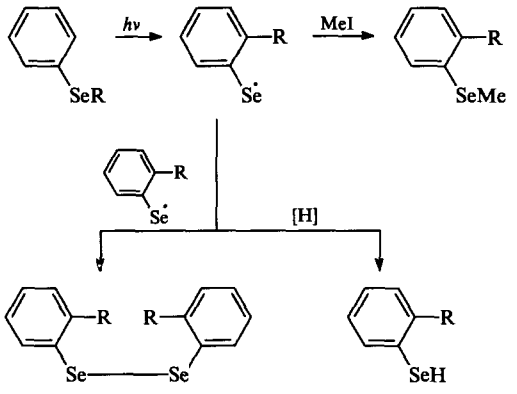
$$RSeSeR \overset{h\nu}{\rightleftharpoons} 2\,RSe^{\cdot}$$

$$RSe^{\cdot} + R'_3P \longrightarrow RSe{-}\dot{P}R'_3$$

$$RSe{-}\dot{P}R'_3 \longrightarrow \dot{R} + Se{=}PR'_3$$

$$\dot{R} + RSeSeR \longrightarrow RSeR + Se^{\cdot}R$$

Arylselenyl radicals are generated[39] also in the photorearrangements of aryl benzyl selenides containing a weakened Se–C bond.



R = CH_2Ph.

The photoinduced reaction of organocobaloximes with diphenyl diselenides involves the intermediate formation of phenylselenyl radicals.[40]

$$RCo(dmgH)_2Py \longrightarrow \dot{R} + Co(dmgH)_2Py$$

$$\dot{R} + PhSeSePh \longrightarrow RSePh + Se^{\cdot}Ph$$

$$Co(dmgH)_2Py + PhSeSePh \longrightarrow PhSeCo(dmgH)_2Py + Se^{\cdot}Ph$$

$$\dot{R} + Se^{\cdot}Ph \longrightarrow RSePh$$

$$Co(dmgH)_2Py + Se^{\cdot}Ph \longrightarrow PhSeCo(dmgH)_2Py$$

$dmgH_2$ = dimethylglyoxime

Diphenyl diselenide reacts via a similar mechanism with organic complexes of zirconium,[11] metal carbonyls,[42,43] and the adamantyl radical.[44,45]

The photolytic reaction of diphenyl diselenide with diazomethane proceeds via a free-radical chain mechanism.[45]

$$PhSeSePh \xrightarrow{h\nu} 2\,PhSe^{\cdot}$$

$$PhSe^{\cdot} + CH_2N_2 \longrightarrow PhSeCH_2N{=}\dot{N}$$

$$PhSeCH_2N{=}\dot{N} \longrightarrow PhSe\dot{C}H_2 + N_2$$

$$PhSe\dot{C}H_2 + PhSeSePh \longrightarrow PhSeCH_2SePh + Se^{\cdot}Ph$$

The photochemical reaction of diphenyl diselenide or benzeneselenosulfonate with alkylmercury halides is also initiated by the generation of selenyl radicals.[46]

$$PhSeY \xrightarrow{h\nu} PhSe^{\cdot} + \dot{Y}$$

$$\dot{Y} + RHgCl \longrightarrow \dot{R} + YHgCl$$

$$\dot{R} + PhSeY \longrightarrow RSePh + \dot{Y}$$

$$PhSe^{\cdot} + \dot{R} \longrightarrow PhSeR$$

Y = SePh or SO_2Ar.

Vinyl selenides are formed similarly from vinylmercury halides.[47] The reaction mechanism includes a stage where the phenylselenyl radical adds to the double bond.

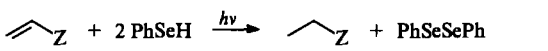
$$PhSe^{\cdot} + \underset{HgCl}{\overset{R}{}}\!\!=\!\!\!\!\diagup \xrightarrow{h\nu}$$

$$\longrightarrow \underset{H}{\overset{R}{}}\!\!-\!\!\underset{HgCl}{\overset{SePh}{}} \longrightarrow \underset{SePh}{\overset{R}{}}\!\!=\!\!\!\!\diagup + Hg^{\cdot}Cl$$

$$Hg^{\cdot}Cl + PhSeSePh \longrightarrow PhSeHgCl + Se^{\cdot}Ph$$

Pulse radiolysis of bis(4-methoxyphenyl) diselenide in methanol generates[48] two types of radicals, $ArS\dot{e}$ and $ArSeS\dot{e}$, whereas only the radicals $ArT\dot{e}$ are formed from the ditellurides under similar conditions.

On irradiation, benzeneselenol reduces via a radical mechanism α,β-unsaturated carbonyl compounds, activated olefins, and β-phenylseleno-substituted ketones to the corresponding saturated ketones and alkanes, while hydrazones, oximes, and anilides are reduced to hydrazines, hydroxylamines, and anilines.[49]



Benzyl phenyl selenide generates a benzyl radical under analogous conditions, the radical reacting with benzeneselenol to form toluene.[50]

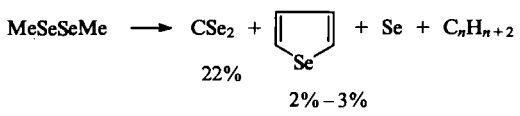
$$PhCH_2SePh + PhSeH \xrightarrow{h\nu} PhMe + PhSeSePh$$

3. The generation in thermal reactions of organic compounds of selenium and tellurium and their reactions

Diorganyl selenides and diorganyl diselenides decompose at 450–600 °C with formation of elemental selenium, hydrogen selenide, and a mixture of hydrocarbons. Pulse thermolysis of dimethyl diselenide *in vacuo* (0.1 Torr) at 550 °C leads to dimethyl selenide, methaneselenol, methane, and selenium as well as selenoformaldehyde.[51]

$$MeSeSeMe \longrightarrow MeSeMe + MeSeH + CH_4 + Se$$

On the other hand, the main product of the thermolysis of Me_2Se_2 at 430–500 °C under atmospheric pressure is carbon diselenide.[52] Selenophene and a mixture of gaseous hydrocarbons and selenium are formed together with carbon diselenide.



The corresponding alkaneselenol and dialkyl selenide predominate among the liquid products of the thermolysis of dialkyl diselenides $(C_nH_{2n+1})_2Se_2$ ($n = 2-4$) at 300–500 °C. Their formation is accompanied by the liberation of solid selenium and gaseous hydrogen selenide and alkenes as well as traces of selenophene.[51]

$$Pr^iSeSePr^i \longrightarrow CH_2{=}CHMe + Pr^iSeH + H_2Se + Se$$

Pulse thermolysis *in vacuo* (20 Torr) at 600 °C of dihexyl, didodecyl, and bis(2-phenylethyl) diselenides leads merely to the corresponding alkenes and selenium.[53]

$$RCH_2CH_2SeSeCH_2CH_2R \longrightarrow RCH{=}CH_2 + Se$$

90%–95%

R = Ph, Bu, C_6H_{13}.

Dibenzyl selenide and dibenzyl diselenide are converted on pulse pyrolysis *in vacuo* primarily into bibenzyl and selenium.[54,55] Their substituted derivatives react similarly.

$$ArCH_2SeCH_2Ar \xrightarrow{600\,^\circ C} ArCH_2CH_2Ar + Se$$

63%–89%

$$PhCH_2SeCH_2Ar \xrightarrow{600\,^\circ C} PhCH_2CH_2Ph + PhCH_2CH_2Ar + ArCH_2CH_2Ar + Se$$

13% 24% 8%

$$PhCH_2SeSeCH_2Ph \xrightarrow{210\,^\circ C} PhCH_2CH_2Ph + Se$$

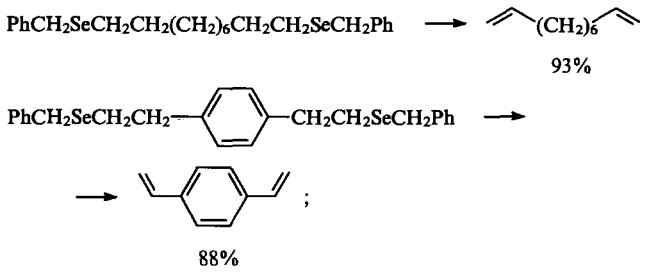
99.4%

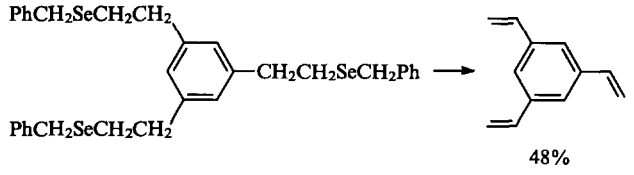
Pulse pyrolysis *in vacuo* of alkyl benzyl selenides is accompanied by the formation of the corresponding alkenes and methane together with bibenzyl and selenium.[53]

$$PhCH_2SeCH_2CH_2Ph \xrightarrow{600\,^\circ C} (Ph\dot{C}H_2 + S\dot{e}CH_2CH_2Ph) \longrightarrow PhMe + PhCH_2CH_2Ph + PhCH{=}CH_2 + Se$$

49% 37% 96%

The following alkenes have been similarly obtained from bis- and tris-(benzyl selenides) respectively:[53]





At comparatively low temperatures (150–170 °C), the thermolysis of dibenzyl diselenide leads to a mixture of dibenzyl polyselenides and the liberation of selenium.[56]

$$PhCH_2SeSeCH_2Ph \longrightarrow PhCH_2Se_nCH_2Ph + Se$$

$$PhCH_2Se_nCH_2Ph + m\,Se \longrightarrow PhCH_2Se_{n+m}CH_2Ph$$

$n = 1-3$.

Bis(diphenylmethyl) selenide reacts similarly.[55]

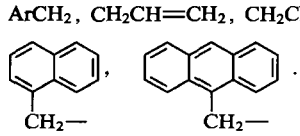
$$Ph_2CHSeCHPh_2 \xrightarrow{140\,^\circ C} Ph_2CHSe_nCHPh_2 + Se$$

Organyl phenyl selenides RSePh, where R represents a relatively stable radical, dissociate on thermolysis with rupture of the R–Se bond. The phenylselenyl radical is then generated.[53,57] Both radicals then dimerise.

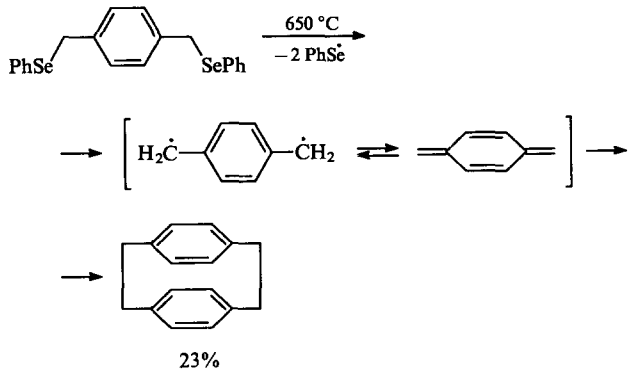
$$RSePh \xrightarrow{600\,^\circ C} \dot{R} + S\dot{e}Ph \longrightarrow R{-}R + PhSeSePh$$

50%–90% 80%–90%

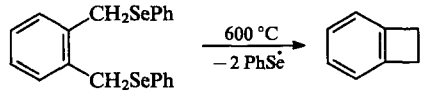
R = $ArCH_2$, $CH_2CH{=}CH_2$, CH_2CN, CH_2COMe,



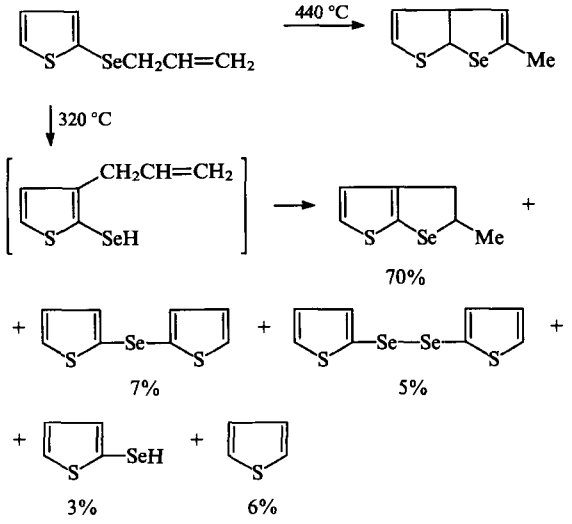
This mode of thermal decomposition of phenyl selenides makes it possible to employ the thermolysis of 1,4-bis(phenylselenomethyl)benzene in order to obtain [2,2]paracyclophane.[53,57]



The strained benzocyclobutene is formed similarly from 1,2-bis(phenylselenomethyl)benzene.[53,57]



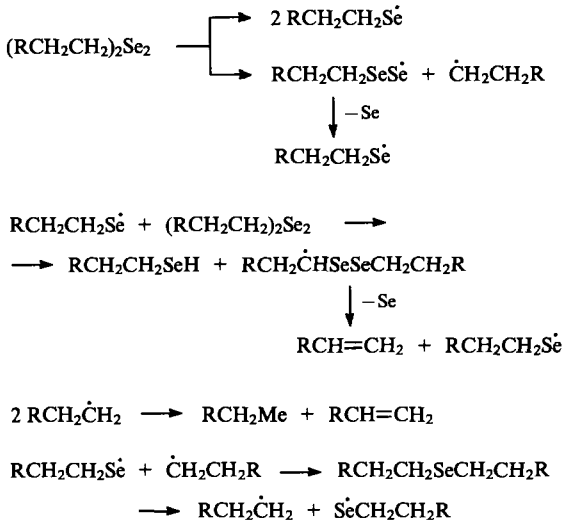
Allyl 2-thienyl selenide readily cyclises at 320 °C, this being preceded by the seleno-Claisen rearrangement.[58]



The reaction side products indicate the generation of thienylselenyl radicals. On vacuum distillation, allyl thienyl selenide cyclises quantitatively and at 440 °C is converted into 2-methylselenopheno[2,3-*b*]thiophene.

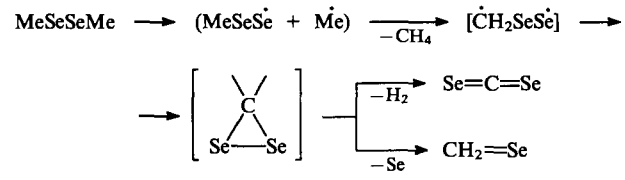
The mode of the thermal decomposition of diorganyl selenides and diorganyl diselenides is determined by the generation of selenyl, perselenyl, and carbon-centred radicals, the reactions of which are determined by their relative stabilities.

Free-radical chain mechanisms have been proposed for the thermal decomposition of diorganyl selenides and diorganyl diselenides.[52]

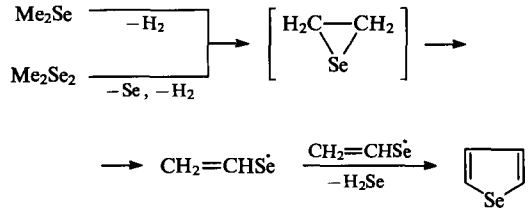


R = H, Me, Et, Ph.

The thermolysis of dimethyl diselenide proceeds via a different mechanism.[52]



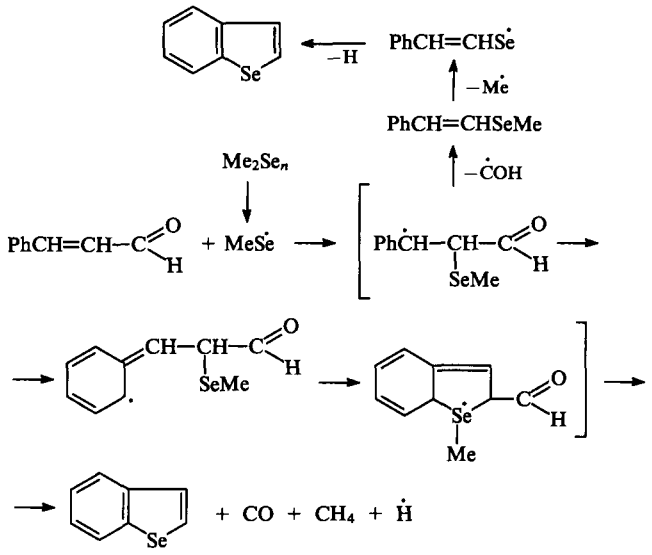
The formation of selenophene as a side product in the thermolysis of dimethyl selenide and dimethyl diselenide is due to the generation of vinylselenyl radicals.



The thermolysis of benzyl organyl selenides always involves the generation of stable benzyl radicals, which recombine to form bibenzyl. Organyl phenyl selenides eliminate phenylselenyl radicals, which also tend to recombine.

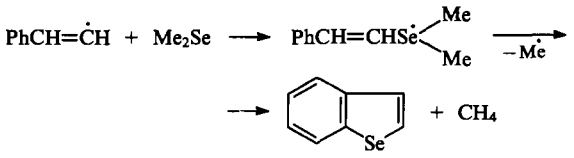
The selenyl and telluryl radicals generated on thermolysis of organic compounds of selenium and tellurium react in the gas and liquid phases with various unsaturated compounds.

A number of chemical trapping agents have been proposed for the alkylselenyl radicals formed as a result of the thermolysis. Thus the reaction of cinnamaldehyde with dimethyl selenide or dimethyl diselenide at 600–650 °C leads to benzoselenophene, the yield of which reaches 53%.[59] The reaction mechanism involves a stage where the methylselenyl radical adds to the double bond of cinnamaldehyde.

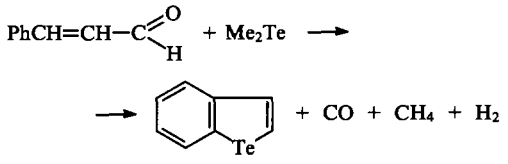


$n = 1, 2.$

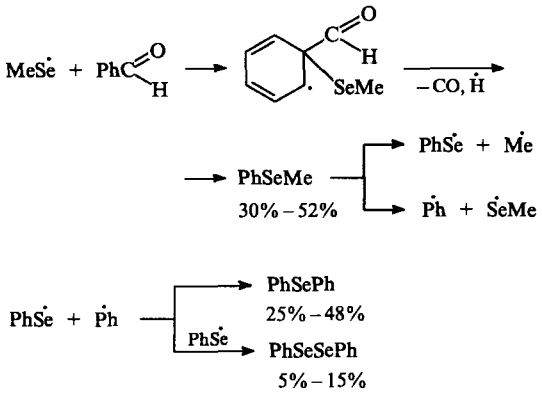
The possibility of the occurrence of the following reaction cannot be ruled out either:



Dimethyl telluride reacts with cinnamaldehyde at a lower temperature (500–550 °C) with formation of benzotellurophene, but its yield does not exceed 12%–17%.



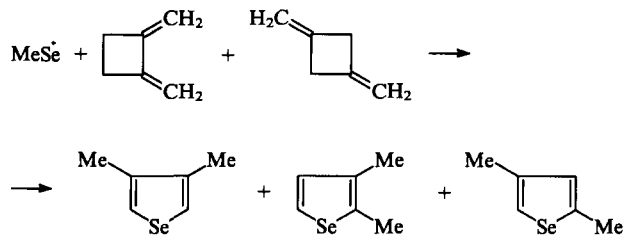
The reaction of Me_2Se or Me_2Se_2 with benzaldehyde takes place already at 400–500 °C with formation of mainly methyl phenyl selenide and diphenyl selenide.[60] Here too methylselenyl radicals attack the carbon atom of the benzene ring bound to the aldehyde group, which is followed by its substitution.



The reaction of ethylselenyl radicals with benzaldehyde is much more difficult (the yield of PhSeEt is 6%–9%).

Dimethyl telluride reacts with benzaldehyde similarly to dimethyl selenide, affording PhTeMe (40%) and PhTePh (3%–6%) at 350–400 °C.

The thermal reaction of dimethyl selenide with 1,2- and 1,3-dimethylenecyclobutanes (a mixture of isomers in proportions of 3:1)[61] leads to a mixture of 3,4-, 2,3-, and 2,4-dimethylselenophenes in proportions of 3:1:1.5. Their overall yield is 58%.

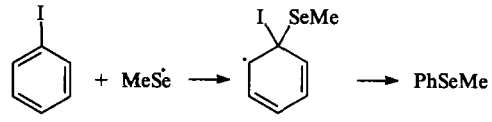


The predominance of the 1,2-isomer in the mixture of the isomeric dimethylenecyclobutanes and the easier, from the electronic and steric standpoints, attack by the radical $MeSe^{\cdot}$ on the ring bond remote from the methylene groups are responsible for the preferential formation of 3,4-dimethylseleneophene.

Alkylthiyl radicals react similarly with dimethylenecyclobutanes, but the yields of dimethylthiophenes do not then exceed 42%.

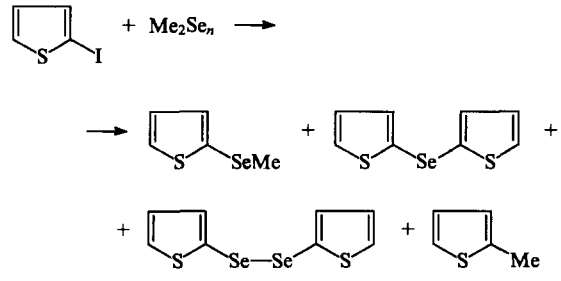
Alkylselenyl radicals react effectively with iodobenzene and iodothiophene in the gas phase.

The cothermolysis of Me_2Se or Me_2Se_2 with iodobenzene at 430 °C leads to selenoanisole (in 33% yield).[62]



The simultaneous formation of selenophenol, diphenyl selenide, and diphenyl diselenide indicates the successive thermal decompositon of selenoanisole accompanied by the formation of the $PhSe^{\cdot}$ radicals.

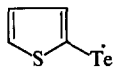
The main product of the reaction of 2-iodothiophene with Me_2Se_2 at 400 °C is methyl 2-thienyl selenide, the yield of which reaches 64%. The latter decomposes to di(2-thienyl) selenide (16%–28%), di(2-thienyl) diselenide (7%–8%), and 2-methylthiophene (2%–4%).[63]



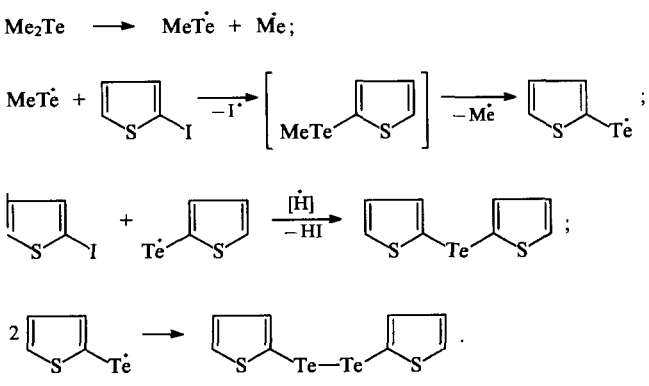
$n = 1, 2.$

Chloro- and bromo-derivatives of benzene and thiophene do not react with selenyl radicals (in contrast to thiyl radicals[7]).

The reaction of 2-iodothiophene with Me_2Te is accompanied by appreciable decomposition of the latter to metallic tellurium and hydrocarbons. Nevertheless the formation under these conditions of thiophene (30%), di(2-thienyl) telluride (8%), and di(2-thienyl) ditelluride (15%) indicates the initial trapping of methyltelluryl radicals by iodothiophene. The unstable methyl thienyl telluride subsequently generates the radical:



in accordance with the following scheme:



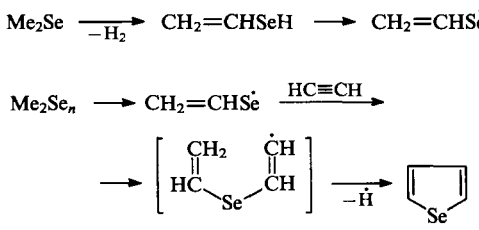
The mobile halogen atom in allyl bromide and benzyl chloride is substituted by radicals under fairly mild conditions already at 90–180 °C in the liquid phase.[64] Alkylselenyl radicals are then generated from dialkyl diselenides.

$$2\,PhCH_2Cl + R_2Se_2 \longrightarrow 2\,PhCH_2SeR + Cl_2$$

$$2\,CH_2{=}CHCH_2Br + R_2Se_2 \longrightarrow 2\,CH_2{=}CHCH_2SeR + Br_2$$

R = Me, Et.

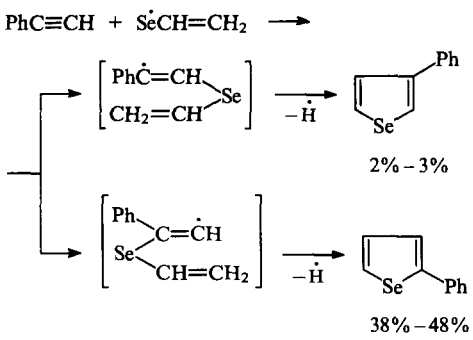
The gas-phase reactions of alkylselenyl radicals with acetylene do not lead to adducts—alkyl vinyl selenides. This may be due to either the low stability of the radical-adduct of acetylene and akylselenyl radicals or the low reactivity of the latter in the given reaction. However, the cothermolysis of dimethyl selenide and dimethyl diselenide with acetylene at 420–470 °C results in the formation of selenophene,[65] the yield of which reaches 80%–94%. The reaction mechanism involves the generation of vinylselenyl radicals from Me_2Se and Me_2Se_2. The vinylselenyl radicals subsequently add to acetylene and the resulting radical-adduct cyclises.



n = 1, 2.

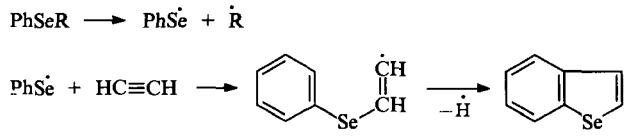
The use of other dialkyl selenides R_2Se (R = Et, Pr, Bu) in the reaction also leads to selenophene, the yield of which depends on R in the following way: Me > Et ≫ Pr > Bu.

The mechanism of the thermal decomposition of dialkyl selenide, including the stage involving the generation of vinylselenyl radicals, has been confirmed by the reaction of dimethyl selenide or dimethyl diselenide with phenylacetylene. The main product of this reaction at 490–500 °C is 2-phenylselenophene, the yield of which reaches 38% in its formation from Me_2Se and 48% in its formation from Me_2Se_2. The formation of phenylselenophene has been represented by a mechanism which involves the addition of vinylselenyl radicals to the triple bond of phenylacetylene predominantly in the α-position.

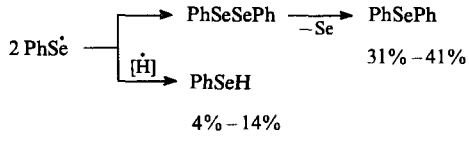


Selenophene, 3-phenylselenophene, and aromatic hydrocarbons are formed as side products.

The cothermolysis of methyl phenyl or allyl phenyl selenide with acetylene at 480–500 °C leads to benzoselenophene—the product of the addition of the phenylselenyl radical to the triple bond.[66]



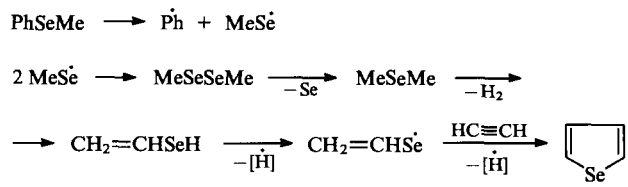
The radical PhSe rccombines simultaneously to diphenyl diselenide. The latter readily eliminates a selenium atom and is converted into diphenyl selenide.



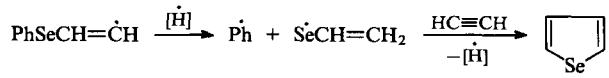
The PhSe radical is partly stabilised as a result of the abstraction of a hydrogen atom from the substrate, affording selenophenol.

The cothermolysis of PhSeR (R = Me, $CH_2{=}CHCH_2$) with acetylene also results in the formation of selenophene, the yield of which reaches 32% in the case of selenoanisole (R = Me).

It has been suggested that the thermolysis of selenoanisole is accompanied by the generation of methylselenyl radicals, the subsequent reactions of which lead to the vinylselenyl radical.



For allyl phenyl selenide, this pathway to selenophene is impossible and therefore the possibility cannot be ruled out that the vinylselenyl radicals, from which the selenophene molecule is formed, are generated on degradation of the radical-adduct.



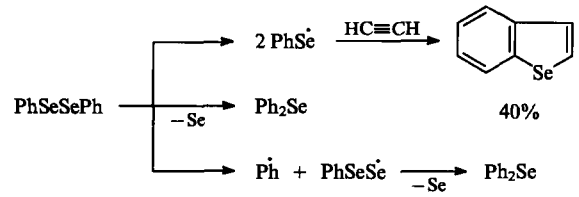
The cothermolysis of alkyl phenyl selenides with acetylene demonstrates the difference between the reactivities of radicals such as PhSe and $CH_2{=}CHSe$. The latter reacts more readily with acetylene. On the other hand, in the case of the isostructural radicals PhS and $CH_2{=}CHS$ the opposite relation is observed.

Allyl phenyl telluride does not react with acetylene at 440 °C but decomposes fully to diphenyl telluride and diphenyl ditelluride. However, at 500 °C the reaction takes place with formation of benzotellurophene and tellurophene in an overall yield not exceeding 3%–4%. This indicates the low reactivity of the PhTe· radicals in the interaction with acetylene. The radicals CH_2=CHTe·, generated in the thermolysis of divinyl telluride, add even at 420–450 °C to the acetylene triple bond with formation of tellurophene (yield 40%).[67]

$$CH_2{=}CHTeCH{=}CH_2 \xrightarrow[-(CH_2{=}\dot{C}H)]{} \rightarrow CH_2{=}CH\dot{T}e \xrightarrow[-\dot{H}]{HC{\equiv}CH}$$



The reaction of diphenyl diselenide with acetylene at 500–580 °C leads to benzoselenophene, selenophene, and diphenyl selenide as a result of the generation of the radical PhSe· and the elimination of a selenium atom.

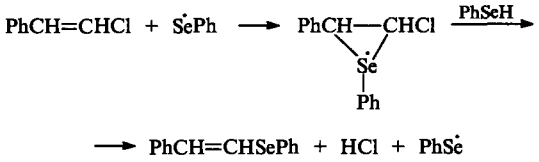


Only traces of benzotellurophene were detected in the reaction of diphenyl ditelluride with acetylene.

Benzeneselenol adds to styrene at 80–140 °C with formation of 1-phenyl-2-phenylselenoethane (i.e. the anti-Markovnikov adduct), which indicates a radical reaction mechanism.

$$PhCH{=}CH_2 + \dot{S}ePh \rightarrow Ph\dot{C}HCH_2SePh \xrightarrow{PhSeH} \rightarrow PhCH_2CH_2SePh + Ph\dot{S}e.$$

In the interaction of β-chlorostyrene with benzeneselenol in the liquid phase (80–140 °C), the chlorine atom is substituted by the PhSe· radical; the reaction takes place strictly stereospecifically.



At the same time, β-chlorostyrene is partly reduced to styrene, which subsequently reacts with PhSe· in accordance with the mechanism presented above; the phenylselenyl radicals recombine at the same time.

4. Generation of radicals and the reactions involved in chemical initiation

A series of reactions involving reduction by selenols proceed via a radical mechanism which includes a chemical initiation stage. Thus arenediazonium fluoroborates are converted into a mixture of aryl phenyl selenides and arenes in their reaction with PhSeH.[68]

$$ArN_2^+BF_4^- + HSePh \rightarrow ArSePh + N_2 + HBF_4$$

$$ArN_2^+ + PhSeH \rightarrow Ar\cdot + Ph\dot{S}e + N_2 + H^+$$

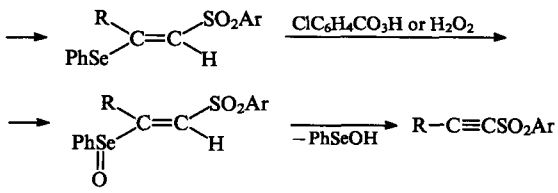
$$Ar\cdot + PhSeH \rightarrow ArH + Ph\dot{S}e$$

$$2\,Ph\dot{S}e \rightarrow PhSeSePh$$

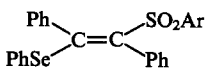
$$Ar\cdot + PhSeSePh\ (or\ PhSe)\cdot \rightarrow ArSePh$$

Selenosulfonates react with activated acetylene even on slight heating and chemical initiation with formation of anti-Markovnikov adducts. The latter are readily oxidised by H_2O_2 to selenoxides, which spontaneously eliminate selenophenol and are converted into acetylenic sulfones.[69–71]

$$R{-}CH{\equiv}CH + ArSO_2SePh \xrightarrow{\Delta\ (AIBN)}$$

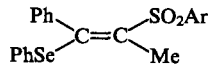


$$PhC{\equiv}CPh + ArSO_2SePh \xrightarrow[C_6H_6,\,\Delta]{AIBN}$$



52%

$$PhC{\equiv}CMe + ArSO_2SePh \xrightarrow[C_6H_6,\,\Delta]{AIBN}$$



97%

The mechanism of the reaction of selenosulfonates with monosubstituted acetylenes is the standard mechanism adopted for free-radical chain reactions (see above).

III. Perselenyl and selenuranyl radicals

The perselenyl radicals RSeSe· are formed together with selenyl radicals RSe· in the photolysis and thermolysis of diorganyl diselenides. They are less stable than the perthiyl radicals RSS·, but are more stable than the pertelluryl radicals RTeTe·.

$$RSeSeR \rightarrow RSeSe\cdot \rightarrow RSe\cdot + Se$$

The radicals RSeSe· are more readily detected by the EPR method[30] than the radicals RSe· owing to the delocalisation of the unpaired electron over the neighbouring selenium atom, which leads to the removal of the degeneracy of the levels.[16,72]

The anisotropies of the *g*-factor for the selenyl and perselenyl radicals are significantly different,[30] for example:

Radical	$g_\perp$	$g_\parallel$
PhSe·	2.003	2.016
PhSeSe·	2.026	2.043

λ_{max} = 600 nm corresponds to the radical 4-$MeOC_6H_4SeSe$· in the UV spectra.[21]

Like their sulfur and tellurium analogues, the selenuranyl radicals $R_2Se{-}X$ are intermediates in the S_N2 homolytic substitution reactions at the selenium atom occurring on treatment of organoselenium compounds with free radicals.[73,74]

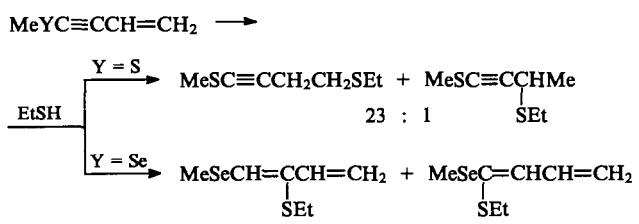
$$\dot{X} + R_2Se \rightarrow [R_2Se{-}X] \rightarrow RSeX + \dot{R}$$

X = $OSiMe_3$, SCF_3, SCOEt, $SCOBu^t$.

The radicals $Ph_2Se{-}X$ are formed on X-irradiation of triphenylselenium halides Ph_3SeX and can be detected by the EPR method. Their unpaired electron is localised predominantly on the orbital connecting the selenium and halogen atoms and oriented at right angles to the CSeC plane (the σ* orbital). The spin density is ~80% localised on the selenium atom and ~20% on the halogen atom.[75]

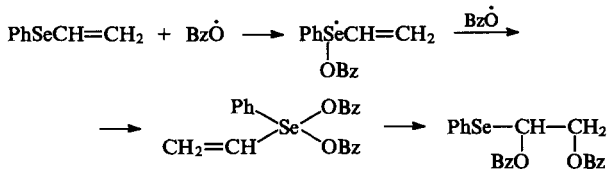
The structure of the σ*-type radical has also been confirmed by the EPR method for other selenuranyl radicals $R_2\dot{S}e-X$ [R = Me, Et, Ph, Ad (1-adamantyl)] and for their asymmetric derivatives with X = EtC(O)S, *tert*-BuC(O)S, CF_3, *tert*-BuO, and Me_3SiO.[76] For example, $a(^{77}Se)$ = 162.6 G for 1-$(Ad)_2\dot{S}e-SC(O)Bu^t$ which corresponds to 3% spin population of the 4*s* orbital of the selenium atom. The spin population of the 4*p* orbital of selenium (38%–71%), which determines the shift of the spin density in $Me_2\dot{S}e-X$, is consistent with the nature of the σ* orbital of the Se–X bond, which depends in its turn on the electronegativity of the atom X.[76]

The geometrical structure of the selenuranyl radical is identical with that of the radical-cations $(Me_2Se-SeMe_2)^{\cdot+}$, formed on γ-irradiation of dimethyl diselenide.[77] The different regiospecificities of certain reactions have been explained by the generation of selenuranyl radicals.[78]

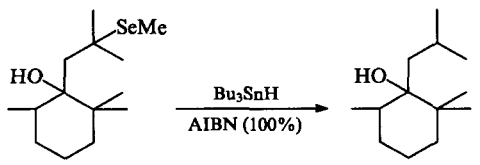


Evidently, when Y = Se, the thiyl radicals $\dot{S}Et$ attack the Se atom with formation of the selenuranyl radical, which subsequently rearranges with migration of the EtSe group to the neighbouring triple bond. Under these conditions, thiuranyl radicals are apparently not formed.

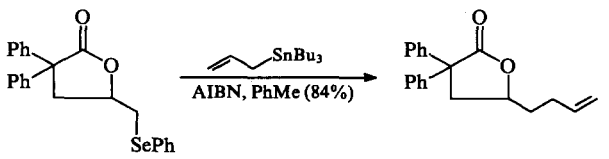
The interaction of phenyl vinyl selenide with benzoyl peroxide, which leads to the product resulting from the dibenzoyloxylation of the double bond, evidently proceeds via selenuranyl radicals.[79,80]



On initiation with AIBN, tributylstannane causes the reductive cleavage of the C–Se bond in hydroxyalkyl selenides.[81]



On chemical (AIBN) and radiation-induced initiation, allyltributylstannane reacts with phenyl selenides to form a new carbon–carbon bond (reductive allylation).[81]



The trialkylstannyl radicals, generated on photolysis of hexaalkylstannanes, cleave the alkyl–selenium bond in dialkyl selenides as well as the analogous bonds in dialkyl sulfides and dialkyl tellurides. The rate of reaction decreases in the sequence $R_2Te > R_2Se > R_2S$.[82]

$$RYR + \dot{S}nBu_3 \longrightarrow RYSnBu_3$$

Y = S, Se, Te.

Triphenylstannane reacts in accordance with a similar scheme with alkyl phenyl selenides in boiling toluene. It has been suggested that these reactions proceed by a free-radical mechanism via the intermediate formation of selenuranyl radicals.[83–88]

$$Ph_3SnH \longrightarrow Ph_3\dot{S}n + \dot{H}$$

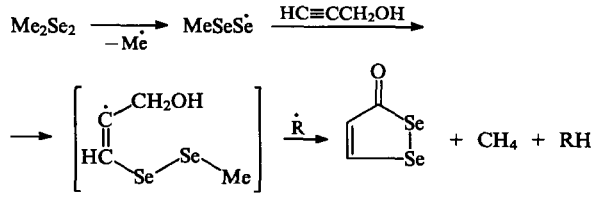
$$Ph_3\dot{S}n + RSePh \longrightarrow PhSe(SnPh_3)R \longrightarrow \dot{R} + Ph_3SnSePh$$

$$\dot{R} + Ph_3SnH \longrightarrow RH + Ph_3\dot{S}n$$

The reduction of organyl phenyl tellurides by tributylstannane apparently proceeds via similar radical states.

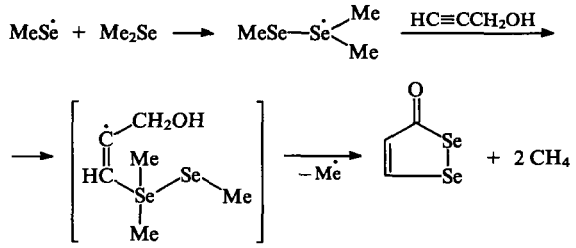
$$PhTeR + HSnBu_3 \longrightarrow PhTeSnBu_3 + RH$$

The cothermolysis of propargyl alcohol with Me_2Se at 460 °C or with Me_2Se_2 at 400–430 °C leads to 1,2-diselenol-3-one in 16%–25% and 73% yields respectively.[89] The reaction mechanism includes a stage in which propargyl alcohol binds perselenyl or selenuranyl radicals generated on thermolysis of dimethyl selenide and dimethyl diselenide.



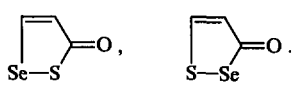
$$Me_2Se \longrightarrow MeSe\cdot + Me\cdot$$

$$2\,MeSe\cdot \longrightarrow Me_2Se_2 \xrightarrow[-Me\cdot]{} MeSeSe\cdot$$

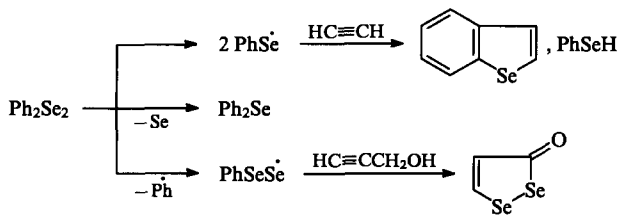


Other dialkyl diselenides, i.e. Et_2Se_2 and $Pr^i_2Se_2$, react similarly with propargyl alcohol. Propargyl alcohol traps perthiyl (sulfuranyl) radicals much less effectively and their tellurium analogues are not trapped at all

The thermolysis of a mixture of Me_2S_2 and Me_2Se_2 also results in the generation of mixed perchalcogenyl radicals, which form two mixed thiaselenolones on interaction with propargyl alcohol:



The gas-phase reaction of diphenyl diselenide with propargyl alcohol and the product of its thermolysis (acetylene) at 500–550 °C also leads to 1,2-diselenol-3-one (in 14%–16% yield). Diphenyl selenide (26%–31%), benzoselenophene (8%–12%), selenophene (2%–14%), and selenophenol (3%) are formed together with 1,2-diselenol-3-one.



Ph_2Te_2 hardly reacts with propargyl alcohol even at high temperatures.

IV. Seleninyl and selenonyl radicals

Seleninyl radicals PhSeȮ and selenonyl radicals $PhSe\dot{O}_2$ are generated on X-radiolysis of diphenyl selenoxide[25] and on ^{60}Co γ-radiolysis of diphenyl selenone[90] respectively. They have been detected by the EPR method in the solid phase and the distribution of the spin density on the selenium, sulfur, and oxygen atoms has been determined (Table 2). In chalcogeninyl radicals, the spin density is concentrated to a greater extent on the chalcogen atoms than in chalcogenonyl radicals. In the sulfur analogues of these radicals, the spin density is localised on the sulfur atom to a greater extent than on the selenium atom in the selenium analogues.

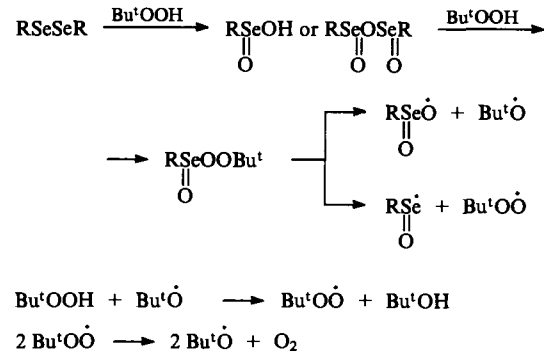
Table 2. Distribution of the spin density.

Radical	Spin density (%)		Ref.
	S, Se	O	
MeSO	87	13	92
$PhSO_2$	42 (38)	29 (31)	90 (91)
$PhSO_2$	46	27	90
PhSeO	78	22	25
$PhSeO_2$	40	30	90

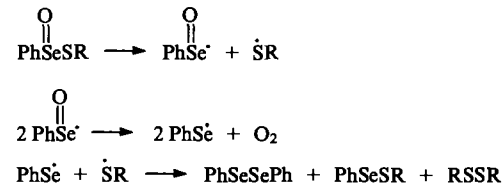
The seleninyl radicals PhSeȮ, in which the selenium atom is in a positive oxidation state, are generated as a result of the radical attack on the anhydride of the corresponding seleninic acid or on *S-tert*-butyl benzenethioseleninate [PhSe(O)SBu^t].[93]

The catalytic decomposition of *tert*-butyl hydroperoxide by diselenides, seleninic acids, or their anhydrides apparently involves the formation of peroxyseleninates as intermediates. Their subsequent homolysis with dissociation of the O–O or Se–O bond leads to the radicals $RSe\dot{O}_2$, RSeȮ, Bu^{t}Ȯ, and Bu^{t}OȮ.

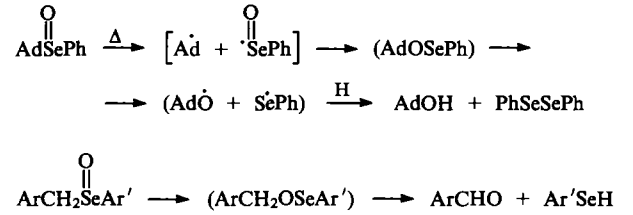
Selenium-containing radicals are subsequently converted into selenium acids or their anhydrides via a hitherto unknown mechanism.[94,95]



It has been suggested that thioselenates are formed as intermediates on oxidation of thiols by benzeneseleninic acid. They are subsequently destroyed via a radical mechanism.[96]



The thermolysis of aryl selenoxides includes stages involving the generation of the radicals ArSeȮ.[97,98]



References

1. J G Odom, in *Selenium Biochemistry. Chemical and Physical Studies. Structure and Bonding* Vol. 54 (Berlin, 1983) p. 3
2. Y Okamoto, in *The Chemistry of Organic Selenium Compounds* Vol. 1 (Eds S Patai, Z Rappoport) (New York, 1986) Ch. 10, p. 331
3. US P. 3 905 958; *Ref. Zh. Khim.* 13N415 (1976)
4. V N Kondrat'ev (Ed.) *Energii Razryva Khimicheskikh Svyazei. Potentsial Ionizatsii i Srodstvo k Elektronu* (Chemical Bond Dissociation Energies, Ionisation Potentials, and Electron Affinities) (Novosibirsk: Nauka, 1974)
5. V I Tel'noi, I B Rabinovich *Usp. Khim.* **49** 1137 (1980) [*Russ. Chem. Rev.* **49** 603 (1980)]
6. M G Voronkov, V A Klyuchnikov, S N Kolbin, G N Shvets, P I Varushin, E N Deryagina, N A Korchevin, S I Tsvetnitskaya *Dokl. Akad. Nauk SSSR* **305** 1139 (1989)
7. M G Voronkov, E N Deryagina *Usp. Khim.* **59** 1338 (1990) [*Russ. Chem. Rev.* **59** 778 (1990)]
8. L I Belen'kii (Ed.) *Khimiya Organicheskikh Soedinenii Sery* (The Chemistry of Organic Compounds of Sulfur) (Moscow: Khimiya, 1988) p. 23
9. M G Voronkov, E N Deryagina *Phosphorus Sulfur Silicon Relat. Elem.* **58** 151 (1991)
10. C Walling *Free Radicals in Solution* (Translated into Russian; Moscow: Inostr. Lit., 1960) p. 256
11. T G Back, in *Organoselenium Chemistry* (Ed. D Liotta) (New York: Interscience, 1987) p. 325
12. J Martens, K Praefcke *Organomet. Chem.* **198** 321 (1980)
13. A R Forrester, J M Hay, R H Thomson *Organic Chemistry of Stable Free Radicals* (London: Academic Press, 1968)
14. H E Radford *J. Chem. Phys.* **40** 2732 (1964)
15. S T Gibson, J P Greene, J Berkowitz *J. Chem. Phys.* **85** 4815 (1986)

16. J E Bennett, G Brunton *J. Chem. Soc., Chem. Commun.* 62 (1979)
17. J C Scaiano, K U Ingold *J. Am. Chem. Soc.* **99** 2079 (1977)
18. J J Windle, A K Wiersema, A L Tappel *J. Chem. Phys.* **41** 1996 (1964)
19. H C Box, E E Budzinski *J. Chem. Soc., Perkin Trans. 2* 553 (1976)
20. U Schmidt, A Müller, K Markau *Tetrahedron Lett.* 1091 (1963)
21. J Bergman, N Eklund, T E Eriksen, J Lind *Acta Chem. Scand., Ser. A* **32** 455 (1978)
22. M Nakamura, O Ito, M Matsuda *J. Am. Chem. Soc.* **102** 698 (1980)
23. O Ito *J. Am. Chem. Soc.* **105** 850 (1983)
24. H Nishimura, J Mizutani *J. Org. Chem.* **40** 1567 (1975)
25. R Franzi, M Geoffroy, M Leray *J. Organomet. Chem.* (193) 315 (1980)
26. E N Gur'yanova *Usp. Khim.* **57** 778 (1988) [*Russ. Chem. Rev.* **57** 433 (1988)]
27. W T House, M Orchin *J. Am. Chem. Soc.* **82** 639 (1960)
28. W Stanley, M R Van De Mark, P L Kumler *J. Chem. Soc., Chem. Commun.* 700 (1974)
29. J I C Chu, D G Marsh, W H Günter *J. Am. Chem. Soc.* **97** 4905 (1975)
30. U Schmidt, A Müller, K Markau *Chem. Ber.* **97** 404 (1964)
31. R Franzi, M Geoffroy *J. Organomet. Chem.* (218) 321 (1981)
32. T G Back, M V Krishna *J. Org. Chem.* **53** 2533 (1988)
33. R A Gancarz, J L Kice *Tetrahedron Lett.* **21** 4155 (1980)
34. R A Gancarz, J L Kice *J. Organomet. Chem.* **41** 4899 (1981)
35. T G Back, S Collins *J. Org. Chem.* **46** 3249 (1981)
36. R J Gross, D Millington *J. Chem. Soc., Chem. Commun.* 455 (1975)
37. J Y C Chu, D G Marsh *J. Org. Chem.* **41** 3204 (1976)
38. D H Brown, R J Gross, D Millington *J. Chem. Soc., Dalton Trans.* 159 (1977)
39. J-L Fourrey, G Henry, P Jouin *Tetrahedron Lett.* **21** 455 (1980)
40. J Deniau, N N V Doung, A Gaudemer, P Bougeard, M D Johnson *J. Chem. Soc., Perkin Trans. 2* 393 (1981)
41. S Pouly, G Tainturier, B Gautheron *J. Organomet. Chem.* (232) C65 (1982)
42. M K Chaudhuri, A Haas, A Wensky *J. Organomet. Chem.* (116) 323 (1976)
43. P Jaitner *J. Organomet. Chem.* (210) 353 (1981)
44. M J Perkins, E S Turner *J. Chem. Soc., Chem. Commun.* 139 (1981)
45. N Petragnani, G Schill *Chem. Ber.* **103** 2271 (1970)
46. G A Russell, H Tashtoush *J. Am. Chem. Soc.* **105** 1398 (1983)
47. G A Russell, J Hershberger *J. Am. Chem. Soc.* **102** 7603 (1980)
48. J Bergman, N Eklund, T E Eriksen, J Lind *Acta Chem. Scand., Ser. A* **32** 455 (1978)
49. W P Jackson, S V Ley, J A Morton *J. Chem. Soc., Chem. Commun.* 1028 (1980)
50. W P Jackson, S V Ley, A J Whittle *J. Chem. Soc., Chem. Commun.* 1173 (1980)
51. T Hirabayashi, S Mohmand, H Bock *Chem. Ber.* **115** 483 (1982)
52. L A Ostroukhova, N A Korchevin, E N Deryagina, M G Voronkov *Zh. Obshch. Khim.* **58** 2171 (1988)
53. H Higuchi, T Otsubo, F Ogura, H Yamaguchi, Y Sakata, S Misumi *Bull. Chem. Soc. Jpn.* **55** 182 (1982)
54. T Otsubo, F Ogura, H Yamaguchi, H Higuchi, S Misumi *Synth. Commun.* **10** 595 (1980)
55. J Y C Chu, J W Lewicki *J. Org. Chem.* **42** 2491 (1977)
56. M A Lardon *Ann. N. Y. Acad. Sci.* **192** 132 (1972)
57. H Higuchi, Y Sakata, S Misumi, T Otsubo, F Ogura, H Yamaguchi *Chem. Lett.* 627 (1981)
58. N A Korchevin, E N Sukhomazova, N V Russavskaya, E N Deryagina, M G Voronkov *Khim. Geterotsikl. Soedin.* **28** 1312 (1991)
59. A D Zorin, E N Karataev, R V Pakhomov, M Yu Gatilov, I A Feshchenko, M G Voronkov, E N Deryagina, N A Korchevin, M S Sheiman, in *V Vsesoyuznoe Soveshchanie 'Primenenie Metalloorganicheskikh Soedinenii dlya Polucheniya Neorganicheskikh Pokrytii i Materialov', Gorkii, 1987. Tezisy Dokladov* (The Vth All-Union Conference: 'The Use of Organometallic Compounds for the Preparation of Inorganic Coatings and Materials', Gorky, 1987. Abstracts of Reports) p. 103
60. P A Podkuiko, V K Stankevich, N A Korchevin, E N Deryagina, in *V Vsesoyuznyi Simpozium 'Novye Metody i Reagenty v Tonkom Organicheskom Sinteze', Moskva, 1988. Tezisy Dokladov* (The Vth All-Union Symposium: 'New Methods and Reagents in Fine Organic Synthesis', Moscow, 1988. Abstracts of Reports) p. 99
61. S P Chernykh, A I Rudenkov, I V Kalechits, V A Men'shikov, N L Apel'baum, A M Taber *Khim. Prom. (Moscow)* 335 (1982)
62. N A Korchevin, L A Ostroukhova, N D Ivanova, E N Deryagina, M G Voronkov *Zh. Obshch. Khim.* **60** 1675 (1990)
63. N D Ivanova, N A Korchevin, L A Ostroukhova, L V Klyba, E N Deryagina, M G Voronkov *Metalloorg. Khim.* **4** 128 (1991)
64. USSR P. 1 502 565; *Byull. Izobret.* (1989)
65. N A Korchevin, L A Ostroukhova, E N Sukhomazova, A R Zhnikin, E N Deryagina, M G Voronkov *Khim. Geterotsikl. Soedin.* 279 (1988)
66. N V Russavskaya, N A Korchevin, E N Sukhomazova, L P Turchaninova, E N Deryagina, M G Voronkov *Zh. Org. Khim.* **27** 359 (1991)
67. N A Korchevin, A R Zhnikin, N D Ivanova, E N Sukhomazova, A A Tatarinova, B A Trofimov, E N Deryagina, M G Voronkov *Metalloorg. Khim.* **3** 1201 (1990)
68. F C James, M J Perkins, O Porta, B V Smith *J. Chem. Soc., Chem. Commun.* 137 (1977)
69. T G Back, S Collins *Tetrahedron Lett.* **22** 5111 (1981)
70. T G Back, S Collins, R G Kerr *J. Org. Chem.* **48** 3077 (1983)
71. T G Back, S Collins, U Gokhale, K W Law *J. Org. Chem.* **48** 4776 (1983)
72. J R M Giles, B P Roberts *J. Chem. Soc., Chem. Commun.* 62 (1980)
73. A L J Beckwith, P E Pigou *Aust. J. Chem.* **39** 1151 (1986)
74. K U Ingold, B P Roberts *Free-Radical Substitution Reactions* (Translated into Russian; Moscow: Mir, 1974)
75. R Franzi, M Geoffroy, K Ginet, N Leray *J. Phys. Chem.* **83** 2898 (1979)
76. J R M Giles, B P Roberts *J. Chem. Soc., Chem. Commun.* 504 (1980)
77. K Nishikida, F Williams *Chem. Phys. Lett.* **34** 302 (1975)
78. S I Radchenko, I G Sulimov, A A Petrov *Zh. Org. Khim.* **10** 2456 (1974)
79. Y Okamoto, R Homsany, T Yano *Tetrahedron Lett.* **3** 529 (1972)
80. Y Okamoto, K L Chellappa, R Homsany *J. Org. Chem.* **38** 3172 (1973)
81. S K Konstantinovich, M L J Mihailovich *J. Serb. Chem. Soc.* **57** 468 (1992)
82. J C Scaiano, P Schmid, K U Ingold *J. Organomet. Chem.* **121** C4 (1976)
83. D L J Clive, C K Wong *J. Chem. Soc., Chem. Commun.* 441 (1978)
84. D L J Clive, G J Chittattu, V Farina, W A Kiel, S M Menchen, C G Russell, A Singh, C K Wong, N J Curtis *J. Am. Chem. Soc.* **102** 4438 (1980)
85. E J Corey, H L Pearce, I Szekely, M Ishiguro *Tetrahedron Lett.* **19** 1023 (1978)
86. K C Nicolaou, S P Seitz, W J Sipio, J F Blount *J. Am. Chem. Soc.* **101** 3884 (1979)
87. K C Nicolaou, R L Magolda, W J Sipio, W E Barnette, Z Lysenko, M M Joullie *J. Am. Chem. Soc.* **102** 3784 (1980)
88. K C Nicolaou, W E Barnette, R L Magolda *J. Am. Chem. Soc.* **103** 3480 (1981)
89. M G Voronkov, E N Deryagina, L A Ostroukhova, N A Korchevin *Khim. Geterotsikl. Soedin.* 855 (1987)
90. M Geoffroy, N Leray *J. Chem. Phys.* **72** 775 (1980)
91. R S Andersen *J. Chem. Phys.* **66** 5610 (1977)
92. K Nishikida, F Williams *J. Am. Chem. Soc.* **96** 4781 (1974)
93. J L Kice, D W Purkiss *J. Org. Chem.* **52** 3448 (1987)
94. K Fujimori, H Yoshimoto, S Oae *Tetrahedron Lett.* **20** 4397 (1979)
95. N Kambe, K Kondo, S Murai, N Sonoda *Angew. Chem., Int. Ed. Engl.* **19** 1008 (1980)
96. J L Kice, T W S Lee *J. Am. Chem. Soc.* **100** 5094 (1978)
97. I D Entwistle, R A W Jonstone, J U Varlay *J. Chem. Soc., Chem. Commun.* 61 (1976)
98. B E Norcross, J M Lansinger, R L Martin *J. Org. Chem.* **42** 369 (1977)

Russian Chemical Reviews **62** (12) 1119–1138 (1993)
©1993 Russian Academy of Sciences and Turpion Ltd

UDC 541.64: 536.7: 542.952

Polycarbodiimides

V A Pankratov

Contents

I. Introduction	1119
II. Synthesis of organic and organoelement polycarbodiimides	1119
III. The structure and certain physical properties of polycarbodiimides	1123
IV. Chemical properties of polycarbodiimides	1124
V. Practical use of polycarbodiimides	1134

Abstract. The literature data on the synthesis, structure, and properties of a promising class of polyfunctional polymers — polycarbodiimides — are surveyed. The polymerisation reactions of the carbodiimide groups of the polymers and the reactions involving polyaddition to various functional groups with formation of linear and network polymers are described. Certain aspects of the practical use of polycarbodiimides are considered. The bibliography includes 320 references.

I. Introduction

The most promising aspect of the synthesis of heat resistant and thermostable composite polymeric materials is believed at the present time to be their formation from thermoreactive polymers and oligomers capable of being converted into network structures without evolving volatile products.[1–17] Polycarbodiimides, polymers containing the N=C=N groups in the macrochain, are of undoubted interest in this connection.

Carbodiimides can be regarded as alkyl(aryl) derivatives of their simplest representative HN=C=NH, which exists mainly in the tautomeric form $NH_2-C\equiv N$. These compounds belong to the group of heterocumulenes, which comprise a large class of unsaturated compounds based on the allene structure.

Whereas 20 years ago carbodiimides were used solely for preparative purposes, nowadays they are widely employed in various branches of industry, particularly in polymer chemistry. This has been promoted by the discovery of selective catalysts for the decarboxylation of isocyanates, which make it possible to synthesise under mild conditions carbodiimides in virtually quantitative yields.

The preparation of low-molecular-mass carbodiimides and their physical and chemical properties have been described in a series of review articles.[1,18–25] However, to date there have been no surveys of polycarbodiimides and their properties. This review deals with the methods of synthesis of both low-molecular-mass and high-molecular-mass carbodiimides, attention being concentrated on the most promising and technological methods of synthesis, referring precisely to polycarbodiimides, which have been developed in recent years. The structures and properties of polycarbodiimides and of the products of their structure formation reactions are also dealt with in the review as regards the understanding of the principal aspects of their practical applications.

V A **Pankratov** Laboratory of Thermoreactive Polymers,
A N Nesmeyanov Institute of Organoelement Compounds,
Russian Academy of Sciences, ul. Vavilova 28, 117813 Moscow,
Fax (7-095) 135 50 85

Received 30 March 1993
Uspekhi Khimii **62** (12) 1185–1204 (1994); translated by A K Grzybowski

II. Synthesis of organic and organoelement polycarbodiimides

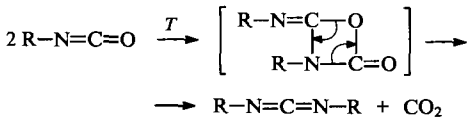
A large number of different methods of synthesis of carbodiimides have now been described in the literature. The principal of these are the desulfurisation of thioureas, the dehydration of urea, and the decarboxylation of isocyanates.[1,18–25]

The commonest method involves the decarboxylation of isocyanates.

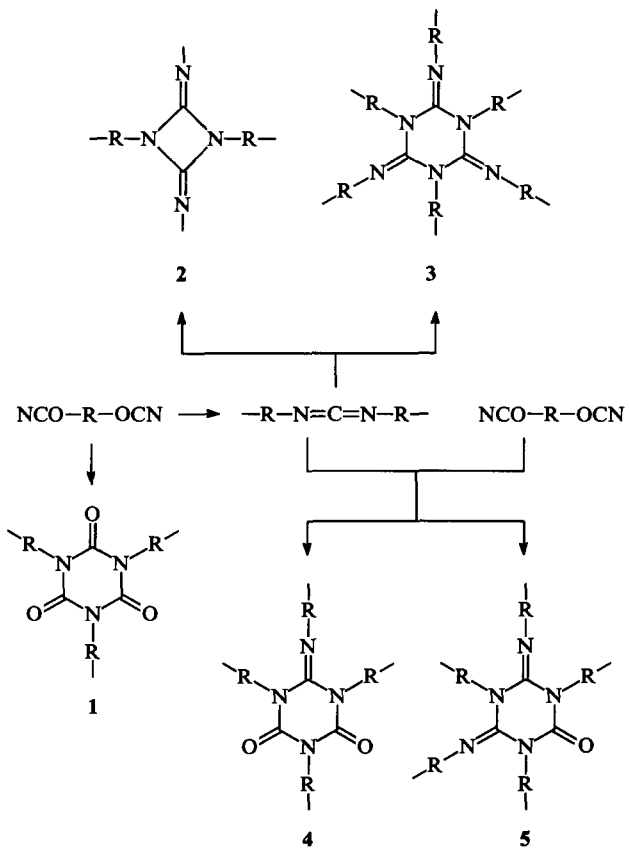
$$2\,R-N=C=O \longrightarrow R-N=C=N-R + CO_2 .$$

At elevated temperatures, this reaction can proceed vigorously even in the absence of catalysts.[26] Certain aromatic carbodiimides, for example, diphenylcarbodiimide (heating of phenyl isocyanate for 24 h at 180 °C), were in fact obtained for the first time in this way.[26] After prolonged heating, diisocyanates afford polycarbodiimides.

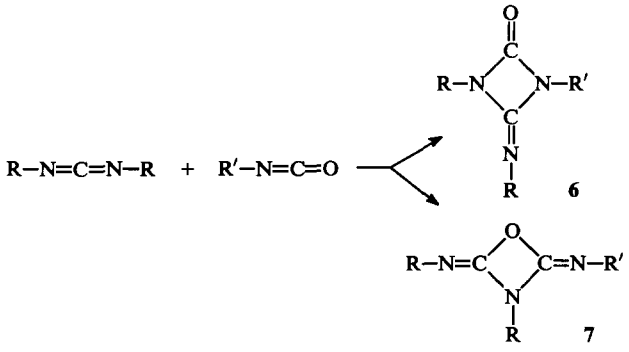
Neuman and Fischer[27] established that the thermal conversion of isocyanates into carbodiimides is autocatalytic and suggested that it proceeds via the formation of intermediate unsymmetric cyclic dimers.



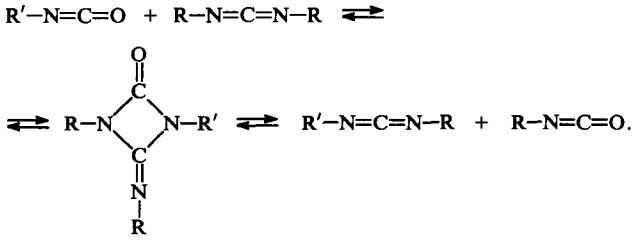
Unfortunately, the purely thermal decarboxylation of isocyanates is accompanied by numerous side reactions, for example the cyclotrimerisation of isocyanates (adduct **1**), the cyclodimerisation and cyclotrimerisation of carbodiimides (adducts **2** and **3**), and the interaction of isocyanates with carbodiimides (adducts **4** and **5**).



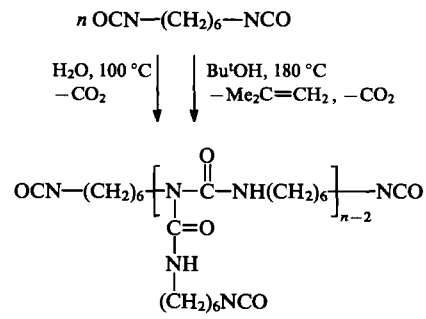
In the study of the reaction of carbodiimides with isocyanates in the absence of oxygen and moisture at 100–160 °C, Neuman and Fischer[27] isolated the unstable cyclic adducts **6** and **7**.



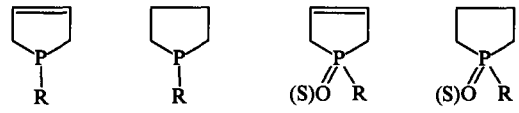
It was shown in the same study that adducts of type **6** (uretone imines) decompose on heating to an isocyanate and a carbodiimide with exchange of substituents in accordance with the following scheme:



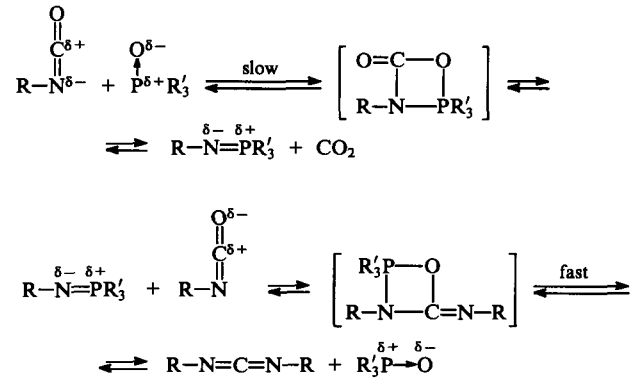
Acceleration of the decarboxylation reaction can be achieved by adding small amounts of water, *tert*-butyl alcohol, and mono- and di-amines to the reaction mixture. Polyisocyanates **8**, with a biuret main chain, have been obtained.[28] They function as catalysts of the carbodiimide formation reaction.



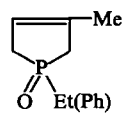
Numerous compounds have been proposed as catalysts, but the highest catalytic activity was found for P-substituted phosphacyclopentenes (phospholenes) **9** and phosphacyclopentanes (phospholans) **10**[29] as well as the *P*-oxides or sulfides **11** and **12**.[30–32]



The mechanism of the catalytic conversion into a carbodiimide has been investigated[33–36] and a two-stage mechanism has been proposed for the process.



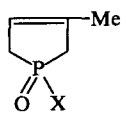
By comparing the catalytic activities of various phosphorus compounds in the carbodiimide formation reactions, Monagle et al.[36] established the following activity series: phosphine oxides > phosphinates > phosphonates > phosphates. Tertiary phosphine oxides, containing the phospholene ring, proved to be the most active.[29,34–38] The use of these catalysts ensured the formation of pure carbodiimides under mild conditions (60–100 °C) in high yields. 1-Ethyl-1-oxo- and 1-oxo-1-phenyl-3-methylphospholenes have been used most frequently as catalysts.



The ethyl derivative proved to be the most active but the phenyl derivative is most readily available.

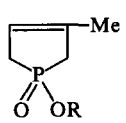
Much work has been done by Arbuzov and co-workers in the study of the influence of the structures of various phospholene derivatives on the catalytic activity in the carbodiimide formation reaction.[39] The catalytic activity in the series of phospholene-phosphinic acids was estimated from the rate constants for the conversion of phenyl isocyanate into diphenylcarbodiimide in solution in toluene at 20 °C.

It was shown that the conversion of the esters **14** (X = OR) into the amides (X = NR_2), the replacement of the alkyl group R in the esters by an aryl or alkylaryl group, the migration of the double bond in the ring, as well as the presence or absence of substituents at the carbon atoms of the phospholene ring induce only slight changes in the reaction rate constant [$k = (0.8-3.0) \times 10^4\ s^{-1}$]. On the other hand, all the compounds investigated are significantly inferior as regards catalytic activity to phospholene oxide (X = Ph) ($k = 68.6 \times 10^4\ s^{-1}$). On the basis of the results obtained, the authors[39] propose the following catalytic activity series: phospholene oxides > phospholenephosphinates > acyclic phosphine oxides > phosphinates.

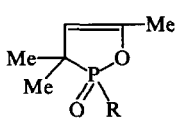


14

Subsequently Arbuzov and coworkers[40] investigated the influence of the environment of the phosphorus atom in organophosphorus compounds on their catalytic activity in carbodiimide formation reactions. The conversion of phenyl isocyanate into diphenylcarbodiimide at 242 °C in the presence of derivatives of phospholene **15** and oxaphospholene **16**, containing the same numbers of P–C and P–O bonds, was chosen as the model reaction.



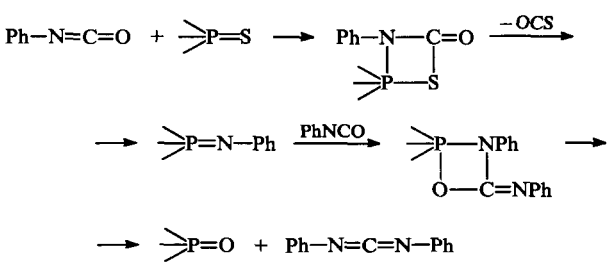
15



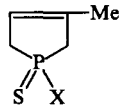
16

The replacement of the phospholene isomer by the oxaphospholene isomer led to a significant decrease in the catalytic reaction rate constant (from 17×10^4 to $3.8 \times 10^4\ s^{-1}$ for R = Et and from 14×10^4 to $0.8 \times 10^4\ s^{-1}$ for R = Ph). The conversion of exocyclic esters into amides (–NR_2 instead of –OR) caused by a further decrease in the carbodiimide formation reaction rate constant—approximately by a factor of two. The specific properties of phospholene derivatives, ensuring the maximum catalytic activity, were thereby confirmed.

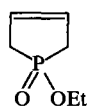
The replacement of the oxygen atom by a sulfur atom in phospholene oxides also diminished greatly the catalytic activity of these compounds. Kinetic experiments carried out on phosphoryl and thiophosphoryl compounds revealed a significant difference in the mechanisms of the reactions involving these compounds.[40] In the case of thiophosphoryl compounds, the plot of the relation $\ln(1-P)^{-1} = f(\tau)$ (P is the degree of conversion and τ the time) showed an inflection, which indicated an increase in the activity of the catalyst during the process. The following reaction mechanism was proposed:



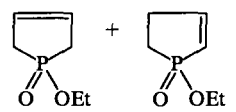
The phosphoryl catalyst accumulated during the reaction, increasing the overall reaction rate constant. The authors therefore determined two reaction rate constants: k_1 at the beginning (when the content of the phosphoryl compound was low) and k_2 at the end of the reaction (when virtually the entire thiophosphoryl catalyst was converted into the phosphoryl catalyst). For initial catalysts of the type



the ratio of the rate constants for the condensation of phenyl isocyanate at 442 K changed from ~1.5 (X = OEt) to ~6.5 (X = SEt). Guberman et al.[41] investigated the influence of the structure of the phosphospholene catalysts **13**, **17**, and **18** and of substituted initial phenyl isocyanates $X-C_6H_4-N=C=O$ on the kinetics of the conversion of the latter into carbodiimides.



17



18

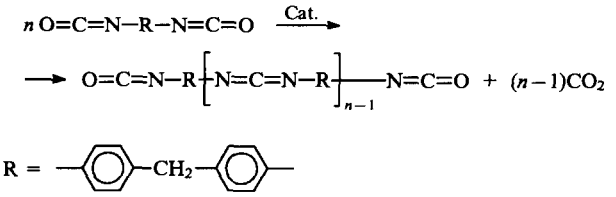
The reactions were carried out in benzene or toluene at concentrations of the isocyanates and the catalysts of 1 kmol m^{-3} and 0.04 kmol m^{-3} respectively. The catalyst **13** proved to be significantly more active than the catalysts **14** and **15**, which agrees well with the results of previous studies. The influence of the substituents (X) on the reactivities of substituted phenyl isocyanates was determined from the results.

$$o\text{-Cl} < H < p\text{-Cl} < m\text{-Cl} < m\text{-}CF_3 < m\text{-}NO_2 .$$

The relation obtained agrees well with the reaction mechanism proposed previously[33–36] (electron-accepting substituents, with the exception of those giving rise to steric hindrance, facilitate the nucleophilic attack of the phosphoryl group on the carbonyl carbon atom of the isocyanate).

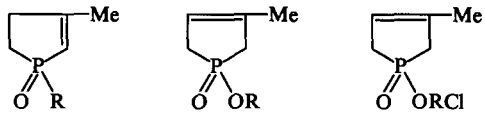
Aliphatic carbodiimides have also been obtained[33] in reactions catalysed by oxaphospholenes but at higher temperatures and in lower yields. Thus n-butyl isocyanate was converted into di-n-butylcarbodiimide to the extent of only 17% on refluxing for 20 h with 1.4 mol.% of 1-ethyl-3-methyl-1-oxo-3-phospholene. The yield was increased to 60% by carrying out the reaction in high-boiling solvents. The reaction was faster for high-boiling aliphatic isocyanates. For example, 2-octyl isocyanate was converted after 2 h at 413–433 K into the corresponding carbodiimides to the extent of 89%.

The influence of the chemical structures of a series of phospholene oxides on the rate of formation of polycarbodiimide



from bis(4-isocyanatophenyl)methane has been estimated.[42]

Derivatives of 3-methyl-1-oxophospholene of three types were used as catalysts: tertiary phosphine oxides **19**, phosphinates with unsubstituted ester groups **20**, and phosphinates with haloester groups **21**.

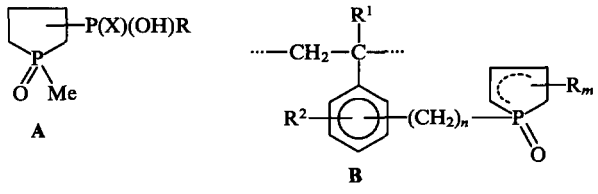


19 20 21

In all cases, the reaction was carried out in benzene at 353 K and diisocyanate and catalyst concentrations of 1 and 0.02 kmol m^{-3} respectively.

It was found that the catalytic activities of the phospholene derivatives investigated depend significantly on the catalyst structure, primarily on the nature of the exocyclic substituent at the phosphorus atom. Compounds **19** exhibited the highest catalytic activity. When the phosphinates **20** were used, the reaction rate constant fell by a factor of approximately 50. The haloesters **21** were found to be even less active. Thus the dependence of the rate constants for the carbodiimide formation reaction on the electronegativity of the substituents at the phosphorus atoms was also observed for the series of compounds investigated, as had been found for monoisocyanates.[39-41]

Insoluble polymeric catalysts for the condensation of isocyanates have found extensive application. They were synthesised in two ways. The first is based on the addition of soluble derivatives of phospholene oxides **A** (R = OH, Me; X = O, S) to an ion-exchange matrix with formation of insoluble high-molecular-mass carbodiimide formation catalysts.[43-46] The second procedure is based on the chloromethylation of the styrene–divinylbenzene copolymer (molar ratio 98:2).[47] The product thus obtained was treated, for example, with 1-chloro-3-methyl-3-phospholene, catalysts containing the repeating unit **B** (where R = Hal, Alk, AlkO, PhO, HalAlk; R^1 = H, Me; R^2 = radical not containing substituents interacting with isocyanate groups; m = 1–3; n = 0, 1) being obtained after oxidation with hydrogen peroxide.



A B

Since the polymeric catalysts are less active than the soluble phospholene derivatives, the condensation of isocyanates in their presence was carried out at higher temperatures (413–423 K). The advantages of the polymeric catalysts include the possibility of repeated use and the possibility of obtaining stable polycarbodiimides not containing an admixture of the catalyst.[43-50]

Apart from the phospholene derivatives, it has been suggested that acyclic trialkyl phosphine oxides,[51-53] phosphates,[51-54] alkoxyphosphines,[55] and triphenyl-n-butylphosphonitrobromide [bromo(n-butyl)triphenylphosphorane (Translator)],[56] as well as the product of the interaction of a bicyclic terpene (camphene) with dichlorophenylphosphine[57] be used as carbodiimide formation catalysts.

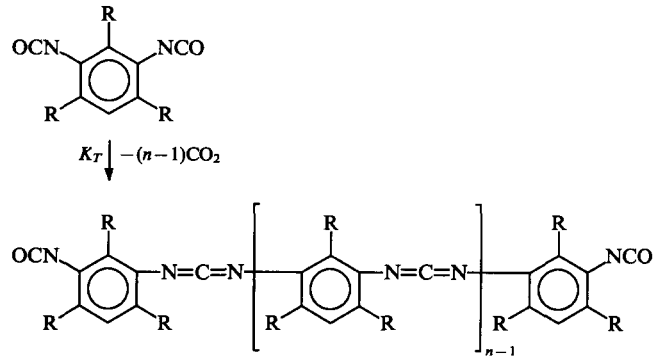
Certain organic compounds of arsenic, containing the highly polarised As–O bond, for example triphenylarsine oxides, also exhibit a fairly high catalytic activity.[51]

In order to obtain insoluble arsenic-containing catalysts, brominated or chlorinated polystyrene was treated with diphenylarsonium chloride and then oxidised with hydrogen peroxide. The polymers obtained contained the $AsO(C_6H_5)_2$ and $CH_2AsO(C_6H_5)_2$ groups. These catalysts were used to obtain low-molecular-mass carbodiimides from bis(4-isocyanatophenyl)-methane.[58-60]

It has been suggested that derivatives of *s*-triazine[61-65] or their mixtures with derivatives of hexahydro-*s*-triazine[66] as well as dialkyl sulfates, sulfites, or sulfoxides[67] be used as catalysts for the condensation of diisocyanates in industry, especially in the manufacture of polyurethane foams containing a controllable amount of carbodiimide groups.

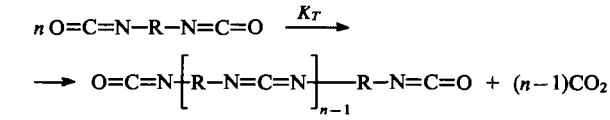
Despite the fact that the chemistry of carbodiimides has developed over a period of over 100 years, these compounds have found practical applications only recently. There is no doubt that this is to a large extent associated with the discovery of the possibility of obtaining polymeric carbodiimides from the corresponding industrial diisocyanates. The interest shown in polycarbodiimides is due to their high thermal stability and heat resistance and satisfactory physicomechanical parameters.

Neuman and Fischer[27] obtained by the catalytic condensation of isocyanates in the presence of phospholene oxides oligomeric ($M \leqslant 2000$) α,ω-diisocyanatopolycarbodiimides with aliphatic substituents in aromatic nuclei, which prevented the formation of cross-linked structures.



R = Me, Et, Pr^i.

Campbell and Smeltz[68] synthesised polycarbodiimides by the polycondensation of aromatic diisocyanates in hydrocarbon solvents in the presence of 1-ethyl-3-methyl-1-oxo-3-phospholene.[68]



R = Ar.

Polycarbodiimides have been synthesised by the polycondensation of a series of aromatic and aliphatic diisocyanates in hydrocarbon solvents or in mixtures with dimethyl sulfoxide (metastable solutions were formed in the latter case) in the presence of 3-methyl-1-oxo-1-phenyl-3-phospholene.[69] The polymers had high softening temperatures (200–350 °C) and were converted into pale-yellow films by pressing under pressure. Aliphatic polycarbodiimides formed weak and brittle films, whereas films based on aromatic polycarbodiimides were strong and rigid.

In order to reduce the softening temperatures of the polycarbodiimides and to obtain soluble polymers, it has been suggested that the polycondensation of diisocyanates be terminated at the stage involving the formation of low-molecular-mass oligomers. The reaction was carried out after a definite degree of conversion (3%–60%) of isocyanate groups into carbodiimide groups with subsequent cooling of the reaction mixture.[46,53,59,60,70-74] Liquid diisocyanatooligocarbodiimides based on bis(4-isocyanatophenyl)methane were synthesised in this way. They are stable during storage for 3–6 months.[60,70,75-78]

Studies on the synthesis of carbodiimide-containing polymers with a specified molecular mass by the introduction of monofunctional isocyanates into the reaction system are of considerable interest.[1,78-82] It was shown that the thermal characteristics of the polymers, synthesised from a mixture of di- and

mono-functional isocyanates, are close to the characteristics of high-molecular-mass carbodiimides based on diisocyanates alone. The polymers obtained for the molar ratios of the di- and mono-functional isocyanates ranging from 6:1 to 20:1 have a mechanical strength close to that of the high-molecular-mass polymer. The softening temperatures of such polymers were in the range 230–260 °C and the decrease in mass on heating in air at 300 °C was ~2% (at a heating rate of 15 K min $^{-1}$).[79]

Polycarbodiimides with an exceptionally high thermal stability have been obtained by the joint condensation of various aromatic diisocyanates.[24] For example, the copolymers of *p*-phenylene diisocyanate and 1,5-naphthylene diisocyanate had a softening temperature of about 300 °C. The average molecular masses of these α,ω-diisocyanatopolycarbodiimides were low, since limiting solubilities in inert solvents are reached with increase in the molecular mass of the polymers and the latter precipitate from the solution. After this, the increase in molecular mass ceases. Ternary mixed polycarbodiimides, consisting of 2,4-tolylene diisocyanate and the aromatic diisocyanates indicated above in proportions of 1:1:1, had average molecular masses of about 3500.

It has been established[24] that oligomeric α,ω-diisocyanatocarbodiimides are formed from 2,4-tolylene diisocyanate at room temperature in the presence of phospholene oxides as catalysts. Wagner et al.[24] synthesised a homologous series of carbodiimide oligomers based on 2,4-tolylene diisocyanate by fractionation in cyclohexanone or in a petroleum ether–hexane mixture. The oligocarbodiimides obtained in this way are of interest for use in polymer-analogue reactions.

The synthesis of organoelement polycarbodiimides $[-E-N=C=N-]_n$, the N=C=N groups of which are linked directly to the atom of the [inorganic] element, differs fundamentally from the synthesis of organic polycarbodiimides.

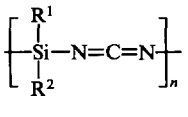
Thus polymeric silicon-containing carbodiimides are formed from silver cyanamide and dialkyl- or diaryl-dichlorosilanes.[83] The tetramer of dibutylbis(carbodiimido)stannane has been obtained similarly from $Bu^n_2SnCl_2$.[84]

$$n\,Ag_2NC{\equiv}N + n\,RR'MCl_2 \longrightarrow \longrightarrow \left[MRR'-N=C=N\right]_n + 2n\,AgCl$$

M = Si; R = Me, Ph, EtO; R′ = Me, Ph, Vinyl, EtO;
M = Sn; R = R′ = Bu; n = 4.

The corresponding polysilylcarbodiimides have been synthesised from dicyanodiamide and polysilazanes.[85]

Oligomeric silicon carbodiimides have been obtained by heating $Me_3SiN=C=NSiMe_3$ with dihalosilanes, trihalosilanes, or haloorganosiloxanes with simultaneous distillation of the Me_3SiCl evolved.[86,87]



R^1 = Me, Ph; R^2 = Ph.

A distinctive feature of polysilylcarbodiimides is the direct linkage between the carbodiimide group and the silicon atom, which alters significantly the reactivity of the former. In contrast to organic analogues, such compounds can react not only via the carbodiimide group but also via the silicon–nitrogen bond.

The oligomers obtained are highly viscous liquids or solids at room temperature. Their molecular mass, determined by the ebullioscopic method, is in the range 3000–5000, which corresponds to a polarisation coefficient in the range 15–25. Polysilylcarbodiimides exhibit a high thermal stability and do not undergo structure formation on heat treatment in contrast to their aromatic analogues. They do not lose mass on heating to 400 °C and retain their solubility in organic solvents under these conditions. The IR spectra of the initial polydiphenylsilylcarbodiimides and those heated at 350 °C for 2 h hardly differ. The temperature of the onset of the decrease in mass is 450 °C for these polymers. Oligomeric polysilylcarbodiimides contain a fairly high percentage of coke (up to 30% at 900 °C).[86,87]

In order to investigate the influence of the relative content of rigid aromatic and flexible siloxane units on the properties of oligocarbodiimides, the copolymers of aromatic diisocyanates—4,4′-bis(isocyanatophenyl)methane and 2,4-tolylene diisocyanate—with organosilicon macrodiisocyanates were obtained.[88] The molar ratio of the aromatic and organosilicon macrodiisocyanates varied from 0–1 to 50–1 (moles). Thermal and physicomechanical studies on these polymers showed that their properties depend significantly on the ratio of the starting materials taken for the reaction (Table 1).

Table 1. The properties of the linear copolymers obtained by the polycondensation of di(4-isocyanatophenyl)methane (**A**) and an organosilicon macrodiisocyanate (n = 14) (**B**) for different proportions of the starting materials.[88]

Molar ratio **A**:**B**	η_{int}/dl g^{-1}	Yield (%)	T_{soft}/°C	σ_t/kgf cm^{-2}	ε (%)
0:1	0.63	92	−84	72	118
10:1	–	93	140	190	95
20:1	0.84	89	160	240	70
30:1	–	95	170	300	45
40:1	0.89	96	180	350	20
50:1	–	94	190	420	10
C[a]	0.9	–	280	500	5

[a] The thermal and physico-mechanical parameters of the linear aromatic polycarbodiimide based on di(4-isocyanatophenyl)methane (**C**) are included for comparison.

The data presented show that the carbodiimides can be obtained by easy and varied procedures, in many instances in high yields. The practical value of polycarbodiimides consists in their high reactivity in relation to many organic compounds, which makes it possible to obtain from them a wide variety of polymeric materials, including those with high thermal stabilities and heat resistances. Therefore we shall consider below their structural features and also their physical and chemical properties.

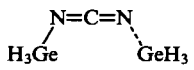
III. The structure and certain physical properties of polycarbodiimides

According to X-ray diffraction data, the carbodiimide group is not linear, the N=C=N angle varying in the range from 166° to 170° for both aliphatic and aromatic carbodiimides.[89–93] The dihedral angle between the substituents at the nitrogen atom is approximately 90°, but the C=N–Ar angle exceeds the expected value of 120° and varies in the range 123°–180°.

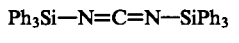
The anomalous value of the N=C=N angle has been explained[89] by the influence of the packing factors in the crystals. However, the fact that all the carbodiimides investigated[89–93] exhibit such anomaly casts doubt on the validity of this explanation. It has been shown that in other heterocumulenes the X=Y=Z triatomic group has a not entirely linear structure. Thus a microwave spectroscopic study of chlorine azide (ClN_3) yielded a N=N=N angle of ~172°.[94] According to microwave spectroscopic data and quantum-chemical calculations, the isocyanate group is also non-linear, the O=C=N angle amounting to 171°–175° depending on the nature of the group at the nitrogen atom.[95–97]

These data indicate that the bent structure of the carbodiimide group can arise also as a result of electronic effects and not only due to crystal packing effects.[22]

The results of both electron diffraction[98] and X-ray diffraction[99] studies on organoelement carbodiimides indicate the existence of nonlinear and linear structures of digermylcarbodiimide **22** and bis(triphenylsilyl)carbodiimide **23** respectively.



22



23

An electron diffraction study has also indicated a linear configuration of the NCNSi group in disilylcarbodiimide.[100]

The electronic structures and stereochemistry of aliphatic and organoelement low-molecular mass carbodiimides as well as nuclear magnetic resonance, IR, photoelectron, and UV spectroscopic, and mass-spectrometric data for these compounds have been examined in detail in a series of reviews,[18-25] so we need not dwell on their discussions in the present review. However, the physicochemical characteristics of high-molecular-mass carbodiimides merit a more detailed description.

Linear high-molecular-mass carbodiimides, obtained under mild conditions, exhibit film- and fibre-forming capacities, possess high thermal characteristics and effective strength parameters, and are resistant to the action of corrosive liquids.[68,69]

The effective physico-mechanical and dielectric properties of polycarbodiimides may be illustrated in relation to the film of poly(3,3'-dimethoxy-4,4'-diphenyl)carbodiimide obtained by pressing at 300 °C and oriented at 115 °C.

Initial modulus of elasticity/kgf cm^{-2} †	86200
Tensile strength/kgf cm^{-2}	2900
Elongation (%)	6.2
ε ($10^2 - 10^5$ Hz)	3.8 (170 °C)
tan δ ($10^2 - 10^5$ Hz)	0.006–0.02 (170 °C)

The study of the thermal properties of polycarbodiimides with blocked terminal groups established that oligocarbodiimides are characterised by a satisfactory fluidity in the temperature range 240 –270 °C, their fusion being accompanied by an increase in the viscosity of the melt and the transition of the specimen to the highly elastic state.[80] An increase in the viscosity of the melt with increase in the molecular mass of the initial oligocarbodiimide has been noted. Polycarbodiimides based on di(4-isocyanatophenyl)-methane have a glass point of 220 °C and pass to the highly elastic state at 250 °C, a further increase in temperature leading to an increase in the modulus of elasticity.

The preparation of polycarbodiimides and layered plastics based on them, containing reinforcing fibrous fillers, has been discussed.[101] The polycarbodiimides were obtained by heating di(4-isocyanatophenyl)methane at 20–150 °C in solution, for example in benzene, in the presence of 3-methyl-1-phenyl-2-phospholene 1-oxide with subsequent addition of monoisocyanates. The decrease in the mass of the resulting polymers in air (thermogravimetric analysis, heating rate 10 K min^{-1}) at 250 °C and 300 °C was 0.7% and 1.7% respectively. The polymer specimens, obtained by pressing in preheated moulds at 180–200 °C, had a tensile strength of 680 kgf cm^{-2}, a modulus of elasticity on extension of 10 100 kgf cm^{-2}, an elongation of 7%, and a glass point of 208 °C.

Polymeric organosilicon carbodiimides of the type $[-SiRR'N=C=N-]_n$, where R,R' = Me, Ph, or vinyl, obtained by the reaction of polychlorosilanes, or chlorosilanes with $Me_3SiN=C=NSiMe_3$, are colourless or pale-brown products, which on heating above 100 °C are gradually converted into viscous oils. Their thermal stability is apparently determined by the presence of a certain number of siloxane units in the macromolecular chain,[83] because the onset of the loss of mass by these products is observed already at 200 °C. The IR spectra of the specimens hardly change even on heating up to 350 °C for 2 h *in vacuo*, which indicates a higher thermal stability of the silylcarbodiimide groups.

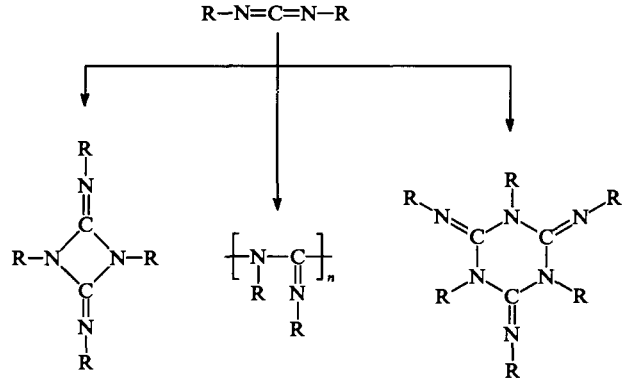
Organoelement carbodiimides possess N=C=N groups which are much more stable as regards polymerisation than in their organic analogues; silicon-, germanium-, tin-, and lead-containing monocarbodiimides can be stored virtually without change for many months.[102] Under these conditions, an increase in viscosity as a consequence of polymerisation, which is so characteristic of organic carbodiimides, is not observed. Organosilicon monocarbodiimides can be as a rule vacuum-distilled without decomposition at 250–260 °C.[102] This can be explained by the increased strength of their Si–N bond as a result of the $d_\pi - p_\pi$ interaction of the silicon and nitrogen atoms.[103]

Organosilicon polycarbodiimides are stable when irradiated, which makes it possible to use them under the conditions of intense irradiation. For example, mass loss is not observed for the polysilylcarbodiimide $[-Ph_2SiN=C=N-]_n$ with a molecular weight of 4285 on heating to 400 °C under a nitrogen atmosphere and it retains its elasticity on irradiation with a dose of 2000 Mrad.[86]

IV. Chemical properties of polycarbodiimides

The chemical properties of carbodiimides are determined primarily by the highly unsaturated nature of these compounds and hence by their tendency to undergo polymerisation and addition reactions.

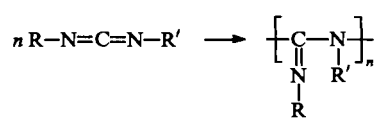
Like isocyanates, carbodiimides are capable of polymerising via the nitrogen–carbon bond with formation of linear polymers, and also of cyclodimerisation and cyclotrimerisation.[1,18-25]



Unfortunately, these interesting reactions have been inadequately investigated and there exist only a limited number of communications on this topic in the literature.[79-82,104-110]

1. Linear polymerisation of carbodiimides

The anionic polymerisation of carbodiimides, analogous to the polymerisation of isocyanates,[111] was first reported by Robinson.[112]



R, R' = Et, Bu, Hex, All, Ph.

† 1 kgf cm^{-2} = 0.9807 × 10^5 Pa.

The reaction was carried out in hydrocarbon solvents in the presence of n-butyllithium at 0–25 °C. Table 2 presents certain data on the polymerisation of carbodiimides and on the properties of the resulting polymers.

Table 2. The properties of the polymers obtained by the anionic polymerisation of carbodiimides.[112]

R	Solvent	Molar ratio monomer: catalyst	η_{int}[a]/dl g^{-1}	Yield of polymer (%)
Et	toluene	270	0.41	37[b]
	"	33	0.20	62
	[c]	–	0.22	–
Ph	toluene	17	0.11	60
$CH_2-CH=CH_2$	"	37	0.13	92
Bu^n	n-heptane	15	0.15	96
n-C_6H_{13}	"	15	0.12	90
Me	"	38	0.14	95

[a] Intrinsic viscosity in formic acid at 30 °C.
[b] Onset of polymerisation at 25 °C and then at 0 °C.
[c] Thermal polymerisation in the absence of a solvent.

The polymers are white powders insoluble in organic solvents. On heating, they partly decomposed to the initial monomers, the greatest thermal stability being shown by the polymers based on diphenylcarbodiimide. It has also been observed[112] that cationic catalysts do not polymerise carbodiimides but form ionic compounds with the latter.

$$p\text{-BrC}_6\text{H}_4\text{SO}_2\text{Cl} + \text{R–N=C=N–R}' \longrightarrow \longrightarrow \left[p\text{-BrC}_6\text{H}_4\text{SO}_2\text{–}\overset{\text{R}}{\underset{|}{\text{N}}}\text{–}\overset{+}{\text{C}}\text{=N–R}'\right]\text{Cl}^-$$

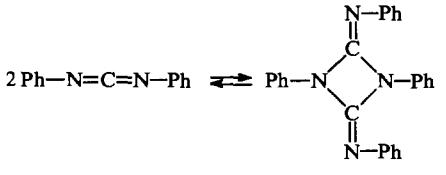
The characteristic features of the linear polymerisation of monocarbodiimides suggest that polycarbodiimides can react similarly, but such data are not available in the literature.

2. Polymerisation of mono- and poly-carbodiimides with formation of cyclic structures

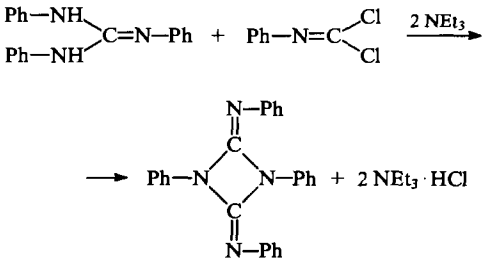
Since the study of the structures of network polymers, formed on polymerisation of polycarbodiimides, presents considerable difficulties, at the beginning of this section we shall consider studies devoted to the cyclodimerisation and cyclotrimerisation reactions of monocarbodiimides as well as studies on the low-molecular-mass structures of the resulting individual products. Investigation of such systems, modelling the corresponding processes in polymers, helps to interpret the more complex structures of the network polymers obtained from polycarbodiimides.

a. Cyclodimerisation and cyclotrimerisation of monocarbodiimides

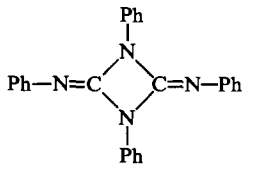
The cyclodimerisation of carbodiimides based on diphenylcarbodiimide has been investigated by Richter.[113] It was found that it occurred on heating even in the absence of a catalyst.



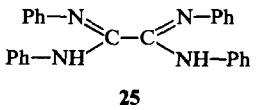
With increase in the reaction temperature, the yield of the dimer also rose, reaching a maximum at 165–175 °C (43% after 16 h). A further increase in temperature reduced the yield to 30% at 200 °C and 13.5% at 230–235 °C. On the basis of these results, Richter suggested that the thermal dimerisation of diphenylcarbodiimide is reversible. Tertiary phosphines proved to be its active catalysts. By adding, for example, tri-n-butylphosphine, it proved possible to attain a yield of the dimer of 75% at a reaction temperature of only 90 °C. In order to demonstrate the cyclic structure of the diphenylcarbodiimide dimer, Richter carried out its unambiguous synthesis[113] by the reaction of triphenylguanidine with phenyl isocyanide dichloride [*N*-phenylcarbonimidic dichloride (Translator)].



Tsuzuki and Iwakura[114] investigated the reactions of diphenylcarbodiimide in the presence of sodium naphthenate in an aprotic solvent, leading to the formation of both cyclic and linear structures. The cyclic dimer **24**, with a characteristic band due to the stretching vibrations of the ring C=N bond at 1690 cm^{-1}, as well as the linear dimer **25**, the structure of which was characterised on the basis of the IR absorption band near 1637 cm^{-1}, were obtained, isolated, and identified.



24

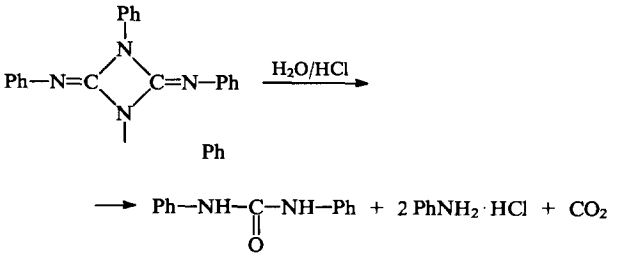


25

The authors[114] showed that the structure of compound **25** is formed in the presence of considerable amounts of sodium naphthenate and of protons in the reaction mixture. The formation of the diphenylcarbodiimide trimer was not observed under the conditions investigated.

There are also other examples of the study of the dimerisation of carbodiimides.[115–117]

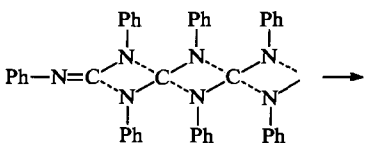
Pankratov et al.[118] synthesised the diphenylcarbodiimide dimer by prolonged heating of diphenylcarbodiimide at 160–170 °C in the absence of a catalyst. The product recrystallised from a 1 : 1 (by volume) benzene–ethanol mixture consisted of a white powder with a melting point of 162.5–163 °C. It was readily soluble in benzene, chloroform, and acetone. The diphenylcarbodiimide dimer was identified[118] by mass spectrometry and IR spectroscopy (the C=N bond absorption band at 1690 ± 10 cm^{-1}) and also on the basis of the composition of the hydrolysis products.

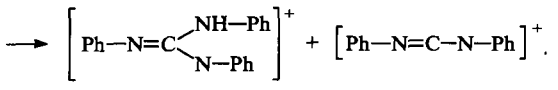


As early as the last century, it was known[119] that diphenylcarbodiimide polymerises slowly at room temperature with formation of the so called 'β-diphenylcarbodiimide', to which a trimeric structure was attributed.[120] The structure of this compound has not been established up to the present time apparently owing to its sparing solubility in organic solvents and instability on heating. Richter[113] obtained 'β-diphenylcarbodiimide' in a high yield by heating diphenylcarbodiimide in the presence of catalytic amounts of tris(diethylaminomethyl)-phosphine.

An attempt has been made[118] to identify 'β-diphenylcarbodiimide'. According to the authors,[118] their structure of 'β-diphenylcarbodiimide' agrees with IR spectroscopic data and the results of hydrolysis in the presence of hydrochloric acid and explains the sparing solubility of this compound in organic solvents in the cold as well as its low stability on heating.

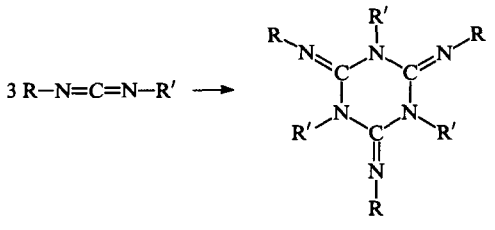
The peaks due to ions with m/e = 286 (intensity ~1%) and with m/e = 194 (intensity ~100%) were observed in the mass spectrum of 'β-diphenylcarbodiimide'. Taking into account the structure of this compound proposed in the above study, the mechanism of its decomposition by electron impact has been represented as follows:[118]





However, the above structure of 'β-diphenylcarbodiimide' still remains only tentative.

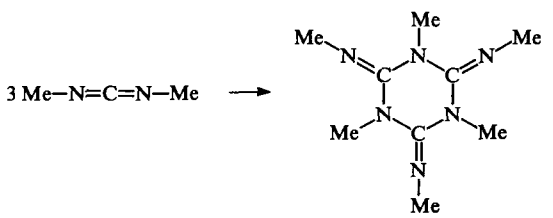
The cyclotrimerisation of carbodiimides with formation of derivatives of 1,3,5-hexahydro-2,4,6-triazine **26** is one of some comparatively little investigated reactions.[104,105,110,117,118,121–124]



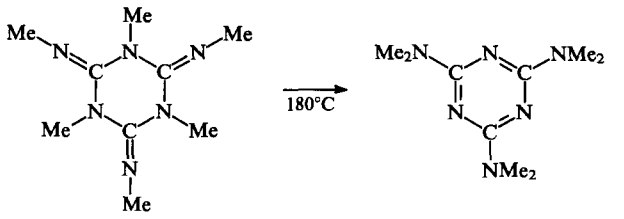
26

According to Busch and coworkers,[121,122] the cyclotrimerisation of diphenylcarbodiimide with formation of a cyclic trimer (hexaphenylisomelamine) takes place when dry hydrogen chloride is passed into a benzene solution of diphenylcarbodiimide containing a small amount of phenol.

The cyclotrimerisation of dimethylcarbodiimide has been reported.[106]

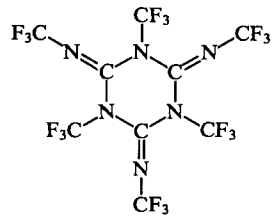


On heating to 180 °C, the isomelamine form **27** of the trimer is converted into the more stable melamine form **28**.



27 **28**

In the course of their synthesis of fluorinated carbodiimides by the reaction of $F_3C-N=CF_2$ with equimolecular amounts of amines RNH_2, Flowers et al.[117] isolated compound **29** as a side product.

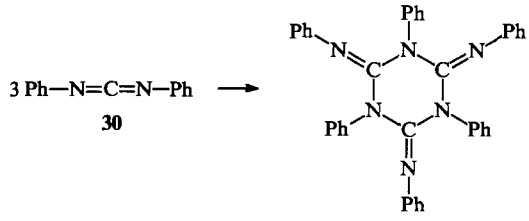


29

Hexaphenylisomelamine has also been isolated after heating phenyl isocyanate with *N*-methylhexamethyldisilazane.[125]

The literature contains a series of communications describing the cyclotrimerisation of carbodiimides with azomethines,[126,127] isocyanates,[128,132] acyl isocyanates,[133] chlorosulfonyl isocyanates,[134] and isothiocyanates,[135] which leads to the formation of *s*-triazine derivatives.

Pankratov et al.[118] obtained hexaphenylisomelamine **31** with a melting point of 196–196.5 °C by the cyclotrimerisation of diphenylcarbodiimide **30**.



30 **31**

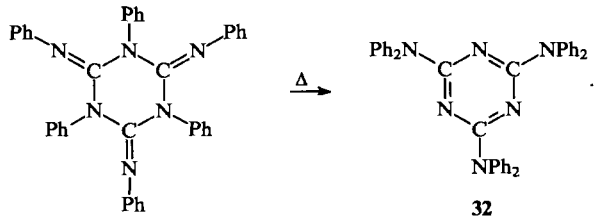
Comparison of the thermal stabilities of derivatives of diphenylcarbodiimide enabled Pankratov et al.[118] to arrange them in a series in terms of increasing thermal stability: 'β-diphenylcarbodiimide' < dimer < hexaphenylisomelamine.

'β-Diphenylcarbodiimide' decomposed on heating above 100 °C in the presence of high-boiling organic solvents, for example 1,1,2,2-tetrachloroethane. Its only decomposition product was diphenylcarbodiimide.[118]

The dimer melted without decomposition at 162.5–163 °C and decomposed vigorously only on heating above 200 °C. Diphenylcarbodiimide was obtained in 80% yield on thermal decomposition of the dimer at 250 °C.

Hexaphenylisomelamine underwent no changes whatever even on prolonged (40 h) boiling in high-boiling liquids, for example in *N*-methyl-2-pyrrolidinone, decalin, and benzyl alcohol. In contrast to triphenylisomelamine,[136] it does not

isomerise to the melamine derivative on heating in benzyl alcohol in the presence of alkali metal alkoxides. On heating in the absence of solvents, hexaphenylisomelamine is stable up to 300–320 °C. However, on heating at a higher temperature for 12 h under an inert atmosphere, hexaphenylmelamine was nevertheless obtained in 80% yield.[118]



32

In order to elucidate the causes responsible for the thermal isomerisation of the iso-form of hexaphenylmelamine to the normal form and to explain the greater thermal stability of the latter, the structures of the isomeric hexaphenylmelamines were investigated by X-ray diffraction.[104] It was established that the central heterocycle of the iso-form (Fig. 1) is nonplanar and has the configuration of a skewed flattened boat. In contrast to the planar configuration of the heterocycles in analogous compounds (cyanuric acid[139,140] and triphenyl isocyanurate[141]), such nonplanar configuration is probably a consequence of intramolecular steric strain. Distortions of the plane of the exocyclic bond angles and also distortions of the plane of the exocyclic C=N double bonds, the torsional angles of which reach 20°, indicate the phenyl–phenyl steric interactions. Such twisting is usual in the presence of bulky substituents at a double bond.[142] The steric repulsion in pairs of phenyl substituents proved to be so great that the C(21), C(41), and C(61) atoms were displaced from the average plane of the neighbouring atoms to the extent of approximately 0.06 Å, but the configuration of the C(11), C(31), and C(51) atoms remained virtually planar.[104]

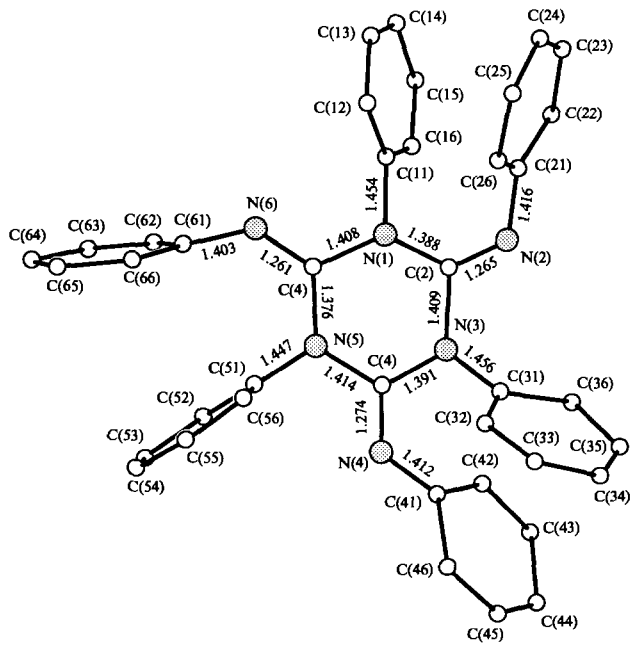
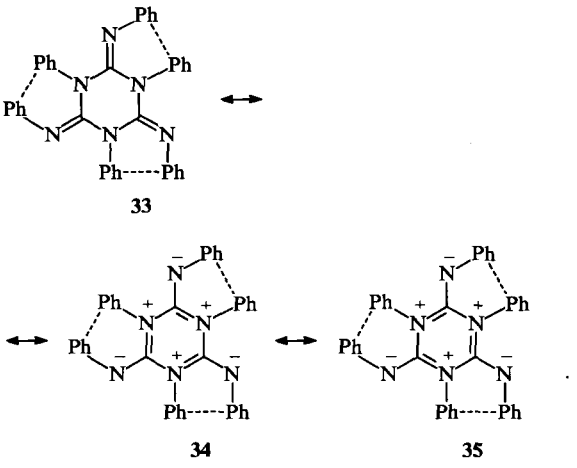


Figure 1. Projection of the hexaphenylisomelamine molecule onto the average plane of the heterocycle.

The lengths of the endocyclic C–N bonds in the hexaphenylisomelamine molecule (d_{av} = 1.398 Å) are intermediate between the lengths of single (1.47 Å) and double (1.23 Å) carbon–nitrogen bonds. This fact is partly due to the contribution to the molecular structure of hexaphenylisomelamine, apart from that of the main form **33**, also by the resonance forms **34** and **35** with alternation of double and single bonds in the heterocycle (the intramolecular contacts between the phenyl substituents are indicated by dashed lines in the formulae below).



33 34 35

The lengthening of the C–N exocyclic bonds on average to 1.267 Å is also associated with the contribution of the resonance forms **34** and **35**.[104]

In hexaphenylmelamine **31**, the atoms of the heterocycle as well as the exocyclic nitrogen atoms are located in a single plane (Fig. 2). The structure of this compound is of the usual type for n-melamine derivatives. The greater rotation of the benzene rings relative to one another than relative to the triazine ring leads to a weaker intramolecular interaction of the 'phenyl–phenyl' type compared with the 'phenyl–triazine ring' interaction. On this basis, the greater stability of the normal form of hexaphenylmelamine has been explained[104] by the significantly smallest steric strain in its molecule.

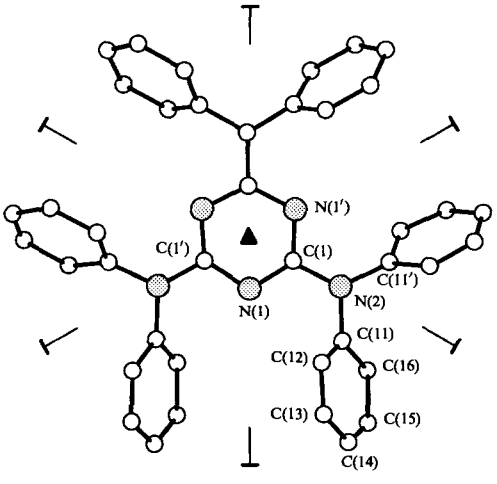


Figure 2. Projection of the hexaphenylmelamine molecule onto the plane perpendicular to the vertical symmetry axis.

Lebedev et al.[110] investigated the thermodynamic characteristics of a series of reactions modelling the processes occurring in the synthesis of oligocarbodiimides and structure formation in the latter.

The temperature dependence of the heat capacities of crystalline hexaphenylmelamine, hexaphenylisomelamine, as well as phenyl isocyanate and diphenylcarbodiimide in the crystalline, vitreous, supercooled liquid, and ordinary liquid states has been investigated in an adiabatic vacuum calorimeter in the temperature range 13.8–330 K with an accuracy to within ~0.3%; the enthalpies of combustion of the test substances at 298.15 K and a pressure of 101.325 kPa were investigated in an isothermal bomb calorimeter.

The functions $H^0(T)-H^0(0)$, $S^0(T)-S^0(0)$, and $G^0(T)-G^0(0)$ were calculated from the results in the temperature range 0–330 K; the zero point entropy and the difference between the zero point enthalpies of the vitreous and crystalline diphenylcarbodiimides and the thermochemical parameters of formation (ΔH_f^0, ΔS_f^0, ΔG_f^0) of the test substances were calculated at the standard temperature and pressure.

It was found that the enthalpy of the decarboxylation of phenyl isocyanate is comparatively small: $\Delta H_r = -(40.6 \pm 2.9)$ kJ mol^{-1}.

The enthalpies, entropies, and Gibbs free energies of the direct conversion of diphenylcarbodiimides into hexaphenylisomelamine and hexaphenylmelamine and of the isomerisation of hexaphenylisomelamine to the normal form are presented in Table 3.

Table 3. Thermodynamic parameters of the cyclotrimerisation of diphenylcarbodiimide to hexaphenylisomelamine and hexaphenylmelamine.[110]

T/K	Physical state of reactants	$-\Delta H^0$/ kJ mol^{-1}	$-\Delta S^0$/ J mol^{-1} K^{-1}	$-\Delta G^0$/ kJ mol^{-1}
	Cyclotrimerisation of compound **27** to **28**			
0	c, c	168.4	0	168.4
100	c, c	170.5	38.85	166.6
200	c, c	174.2	64.80	161.3
298.15	l, c	236.4	283.6	151.8
	Cyclotrimerisation of compound **27** to **29**			
0	c, c	326.6	0	326.6
100	c, c	329.7	61.76	323.5
200	c, c	334.5	94.42	315.6
298.15	l, c	397.4	316.3	303.1
	Isomerisation of compound **28** to **29**			
0	c, c	158.3	0	158.3
100	c, c	159.4	22.91	157.1
200	c, c	160.3	29.63	154.4
298.15	c, c	161.1	32.73	151.3

Note. The following designation of the states of the reactants has been adopted: l = liquid state, c = crystalline state.

In the temperature range 0–298 K, the cyclotrimerisation of the imide **30** and the isomerisation of compound **31** to **32** are thermodynamically allowed ($\Delta G < 0$). The upper limiting temperatures of these processes, found by extrapolation, exceed appreciably the temperatures of the onset of the thermal degradation of the reactants. The free energies of formation of compounds **31** and **32**, 1232.9 ± 7.4 and 1081.1 ± 13.1 kJ mol^{-1} respectively, indicate a greater thermodynamic stability of the latter compound, which confirms the conclusion that compound **31** may isomerise to compound **32** under kinetic conditions.[110]

Pankratov et al.[105] investigated in the temperature range 250–550 °C the thermal, thermooxidative, and thermohydrolytic stabilities of diphenylcarbodiimide **30**, the cyclic diphenylcarbodiimide dimer **24**, hexaphenylisomelamine **31**, and hexaphenylmelamine **32** — compounds which model the principal fragments of the network polymers based on oligo- and polycarbodiimides.

It was shown that, on thermolysis *in vacuo*, the stabilities of these compounds are approximately the same (the formation of the solid and liquid degradation products is observed at temperatures above 400 °C), but the thermooxidative stability of the products of the cyclotrimerisation of diphenylcarbodiimide, namely hexaphenylisomelamine and hexaphenylmelamine, is appreciably higher than that of the initial monomer. On the other hand, under the conditions of thermohydrolysis, the trimer **32** begins to decompose at 400 °C, which is 150 °C higher than the temperature of the decomposition of the N=C=N group in carbodiimide and the isomelamine ring.[105]

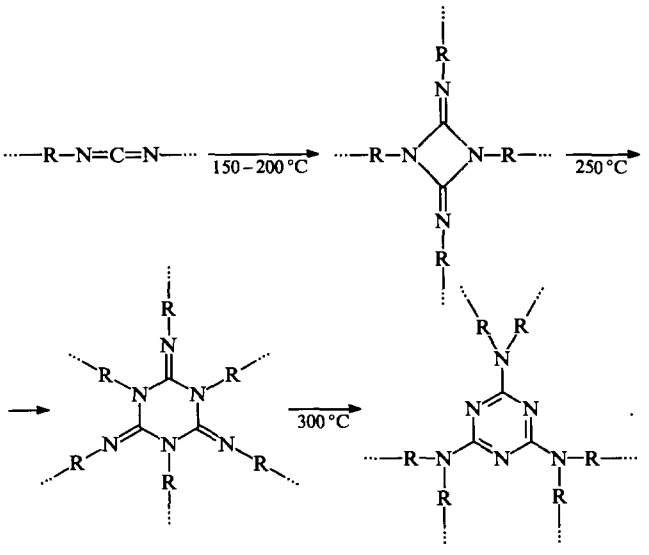
Taking into account the entire set of data concerning the chemical reactions of diphenylcarbodiimide under the influence of temperature, one may postulate that the reaction involving the formation of network polymers from oligocarbodiimides may involve, depending on the hardening conditions, the formation of three types of nodal fragments: uretediimine, isomelamine, and melamine fragments. Under these conditions, an increased number of melamine fragments in the structure of the cross-linked polymer should increase its thermal stability.

b. Polycyclisation of oligo- and poly-carbodiimides

There are literature data on the polycyclisation of polycarbodiimides. It has been stated in a number of studies[79,80,143,144] that the N=C=N groups of linear oligo- and poly-carbodiimides may polycyclise at elevated temperatures, but the structures formed have not been analysed.

In a number of studies[12,15,81,87,104,105,107–110,118,136,145–156] it was shown that, when aromatic oligocarbodiimides were heated, polymerisation took place with participation of the reactive N=C=N group and was accompanied by the loss of solubility and an increase in hardness and mechanical strength. At the same time, a weakening of the absorption band due to the carbodiimide groups in the range 2115–2145 cm^{-1} and the appearance of absorption bands in the range 1500–1700 cm^{-1}, corresponding to the vibrations of cyclic and dimeric (1690 cm^{-1}), isomelamine (1640 cm^{-1}), and n-melamine fragments (1530 cm^{-1}), were observed.

The influence of temperature and of process time on the degree and mode of isomerisation of oligocarbodiimides has been investigated by IR spectroscopy. A study was made of the dependence of the degree of conversion of the carbodiimide groups of the oligomers based on di(4-isocyanatophenyl)-methane and phenyl isocyanate (n = 25) on the duration of isothermal polymerisation at 150, 200, 250, and 300 °C. An increase in temperature from 150 to 300 °C induced an increase in the degree of conversion from 25%–30% to 70%–80%. The polymerisation temperature influenced significantly also the structure of the network polymers formed. Thus at 150–200 °C the principal reaction was cyclodimerisation, whilst on raising the temperature to 250 °C cyclotrimerisation of the carbodiimide groups predominated. At 300 °C and above, the appearance of an absorption band in the region of 1530 cm^{-1}, assigned to the vibrations of *sym*-triazine rings, was noted. Thus it is believed[81,105,107–109,118] that the following processes take place in the polymerisation of aromatic polycarbodiimides at different temperatures:



With increase in the temperature of the polymerisation of oligocarbodiimides, the degree of structure formation in the latter also increases. As a consequence of the preferential formation of the thermally more stable cyclotrimeric network nodes, the temperatures of the onset of mass loss and of the onset of deformation of the polymerisation products increase and there is also an increase in their hardness and mechanical strength (Table 4).

Table 4. Physicomechanical properties of the cross-linked polymers obtained by pressing the oligocarbodiimide (n = 25) based on di(4-isocyanatophenyl)methane and phenyl isocyanate (specific pressure 600 kgf cm^{-2}, material maintained for 1–3 min mm^{-1} at 25 °C).

Temperature/°C	Degree of structure formation (%)	Bending strength/ kgf mm^{-2}	Specific impact strength/ kJ m^{-2}	Brinell hardness/ kgf mm^{-2}
120	22–25	4.0–5.0	4–5	12.0–12.5
150	60–65	8.5–9.0	9–12	16.0–17.0
180	71–74	10.0–10.5	22–25	18.0–19.0
200	76–78	12.0–12.5	13–16	22.0–23.0
250	80–85	8.0–9.0	8–10	25.5–26.0
300	85–88	7.0–8.0	3–5	27.0–27.5

Analysis of the variation of the bending strength, specific impact strength, and Brinell hardness of the polymer specimens obtained by the compression pressing of the given oligomer under different conditions showed that an increase in the pressing temperature from 150 to 300 °C induces an increase in the Brinell hardness from 12–12.5 to 27–27.5 kgf mm^{-2}, while its specific impact strength and bending strength rise to a maximum for specimens structured at 180–200 °C and then fall again.

It has been shown [118] that the addition of 0.5 mass per cent of a cyclotrimerisation catalyst to oligocarbodiimides induced not only a 5%–10% increase in the degree of conversion of the carbodiimide group but also promoted the formation of isomelamine rings already at 150 °C. In the presence of catalysts, cyclotrimerisation becomes the dominant process at 220–250 °C. A further increase in the polymerisation temperature to 300 °C led to the formation of *sym*-triazine rings. Comparison of the IR spectra of the products of the purely thermal (at 300 °C) and catalytic polymerisation (at 250 °C) demonstrated a great similarity of their structures. In both cases, the polymer networks were constructed mainly from six-membered nitrogen-containing heterocycles.

A systematic survey has been made [107] of the thermal, thermooxidative, and thermohydrolytic stability of the structures of polycarbodiimides containing isomelamine and melamine fragments. A comparative study has also been made of linear polycarbodiimides based on 1,3-phenylene diisocyanate, 2,4-tolylene diisocyanate, and di(4-isocyanatophenyl)methane.

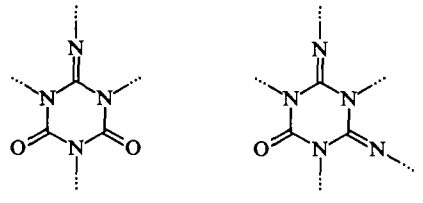
The kinetics of the degradation of these polymers have been investigated. [105, 107, 109] It was shown that the decomposition takes place as a first order reaction and obeys the Arrhenius equation. The rate constants and effective activation energies for the formation of gaseous degradation products as well as the effective activation energies for the decomposition reaction of the polymers were calculated.

Comparative study of the degradation reactions of polycarbodiimides *in vacuo* and in saturated water vapour demonstrated [107, 109] that the rate of decomposition of polycarbodiimides increases appreciably in a moist atmosphere. It was shown that the preliminary structure formation in the carbodiimide polymers *in vacuo* increases their resistance to thermal hydrolysis.

The principal types of oxidation reactions of polycarbodiimides have been established. They consist of the oxidation of the aliphatic and aromatic fragments of the macrochain and thermal structure formation involving the N=C=N groups.

Compounds containing melamine structures exhibit the highest thermo-oxidative stability. [105, 107, 109] The structure formation temperatures and times, ensuring an appreciable increase in the thermo-oxidative stability of network polymers relative to linear polycarbodiimides, have been determined. [107, 109]

There are literature data [144, 156] on the copolymerisation of diisocyanates with carbodiimides, which may result in the cocyclotrimerisation of the isocyanate and carbodiimide groups with formation of mixed cyclic trimers of the type



apart from the isocyanate and melamine rings.

3. Interaction of polycarbodiimides with various compounds

The existing numerous literature data concerning the interaction of polycarbodiimides with various compounds can be divided arbitrarily into two types.

1. Polymer-analogue reactions of polycarbodiimides based on the polymer chain of the polycarbodiimide, the reactive carbodiimide groups of which usually interact with monofunctional compounds of different nature.

2. Modification of various polymers by polycarbodiimides and monocarbodiimides. These reactions are no longer based on polycarbodiimides but on other polymers with other functional groups. In many cases, small amounts of added carbodiimides play the role of cross-linking agents, stabilisers, strengthening components, and agents imparting hydrophobic properties, i.e. substances which impart particularly valuable properties to the polymers.

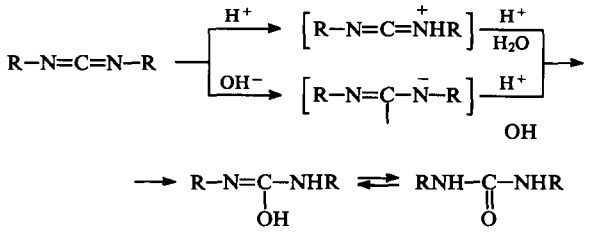
The chemical reactions of polycarbodiimides will be examined in this order in the present part of the review, resorting to examples of reactions of low-molecular-mass carbodiimides for a better understanding of the course of the reactions and of the structures of the products. There exist also other types of reactions of the carbodiimides. They have all been examined in detail in a series of thorough reviews on the chemistry of low-molecular-mass

carbodiimides.[18–25] However, they have not yet found applications in the chemistry of polycarbodiimides and we shall therefore not consider them.

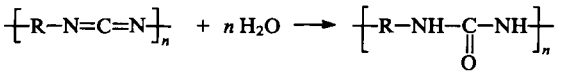
a. Polymer-analogue reactions of polycarbodiimides

The central carbon atom in the carbodiimide molecule exhibits striking electrophilic properties, so that nucleophilic addition reactions are the main type of reactions characteristic of carbodiimides.[18–25]

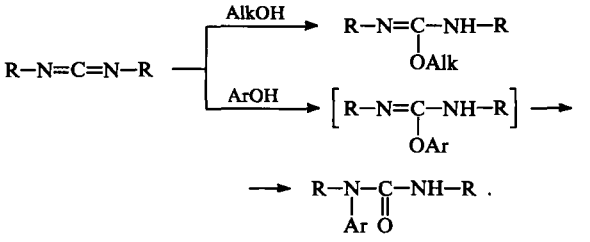
Hydrolysis of carbodiimides is a comparatively slow reaction catalysed by H^+ and OH^- ions.[157,158]



This reaction has been used to obtain polyureas.[69]



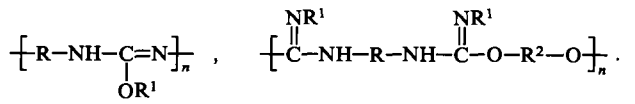
The interaction of carbodiimides with alcohols[159–162] results in the formation of *O*-alkylisoureas, whilst their interaction with phenols[163–165] affords *N*-phenylureas, which are formed via a stage involving the formation of *O*-arylisoureas.



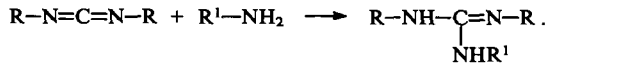
Reactions with certain acid phenols lead to the formation of *O*-phenylisourea derivatives.[166–171] They were obtained from pentachlorophenol[168,169] and 2,6-dichloronitrophenol.[172] It was postulated that the bulky *o*-chloro-substituents block the usual O→N shift in these compounds.[172]

However, picric acid reacts with carbodiimide to form *N*-arylurea, although the mechanism of this reaction apparently involves the formation of *O*-arylisourea as an intermediate.[173]

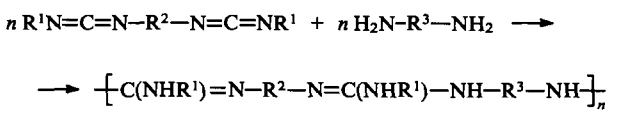
The application of this reaction to polymers[69,174] led to the formation of polyisoureas having the following structure:



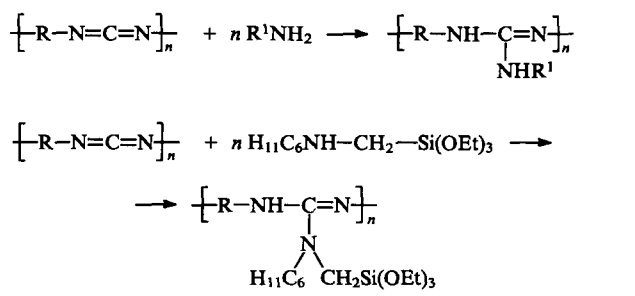
The study of the interaction of carbodiimides with amines showed that the products of this reaction are various guanidines.[175–177]



Polyguanidines were obtained as a result of the addition of biscarbodiimides to diamines.[178,179]

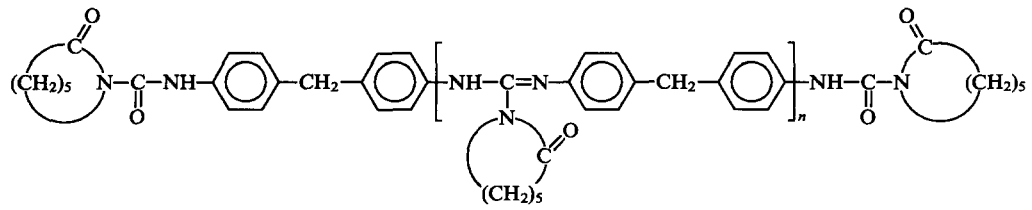


The synthesis of polyguanidines via the addition of primary and secondary amines to polycarbodiimides has also been described.[69,179]

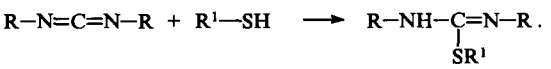


Interesting data have been obtained in a study of the interaction of ε-caprolactam with polycarbodiimides.[24] ε-Caprolactam is not only an excellent solvent for the sparingly soluble high-molecular-mass carbodiimides but it also adds quantitatively to polycarbodiimides on heating to 120 °C without the opening of the lactam ring (see the structure at the bottom of the page).

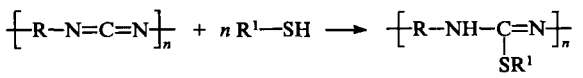
The adduct (n = 30) melted at 210–214 °C, i.e. at a temperature 70 °C lower than the melting point of the initial polycarbodiimide, and dissolved in dimethylformamide and *N*-methylpyrrolidinone. The polymers treated with ε-caprolactam had a wide molecular mass distribution with an average molecular mass of 11 000.

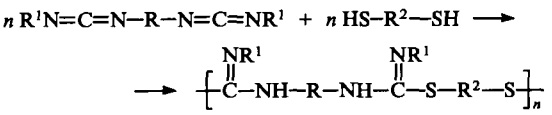


Mercaptans and thiophenols[180] interact with carbodiimide to form symmetrical alkyl(aryl)isothioureas.

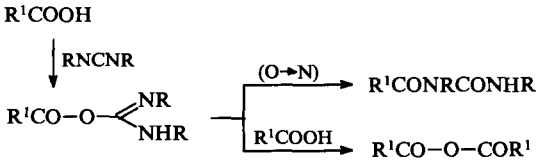


A similar reaction with polycarbodiimides[174,179] leads to the formation of polyisothioureas.

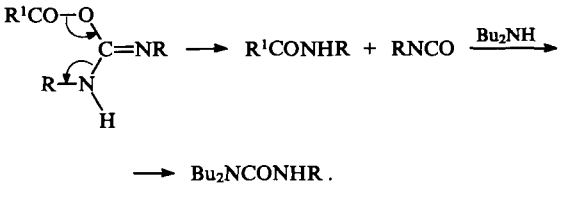




The interaction of carboxylic acids with carbodiimides has been investigated (together with the kinetics of such interaction) in fair detail.[181-190] The reactivity of the acids increases with their strength.[187] The reaction mechanism includes a stage involving the formation of anhydride via *O*-acylisourea and is complicated by the O→N shift.

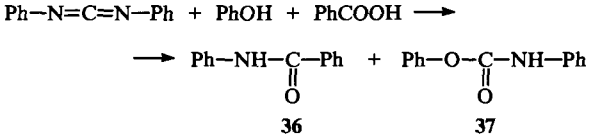


Another complication is the formation of the isocyanate (R—NCO) on decomposition of *O*-arylurea.[191]



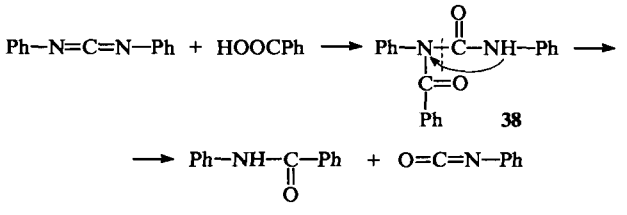
Di-n-butylamine was used as a 'trapping agent' for this isocyanate.[192]

The formation of isocyanates in the reactions of carbodiimides with carboxylic acids has been observed also in a study of the reaction of diphenylcarbodiimide with a mixture of benzoic acid and phenol.[193] Benzanilide **36** and phenylcarbamylate **37** were obtained as the products of this reaction.

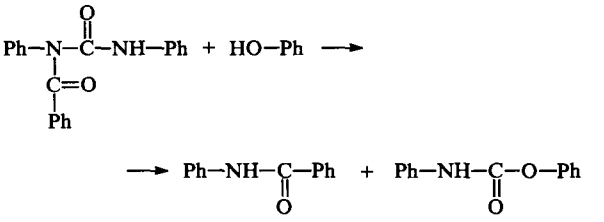


36 **37**

It was suggested that the anilide **36** is a product of the decomposition of *N*-benzoyl-*N,N'*-diphenylurea **38** formed in the first stage of the interaction of diphenylcarbodiimide with benzoic acid.

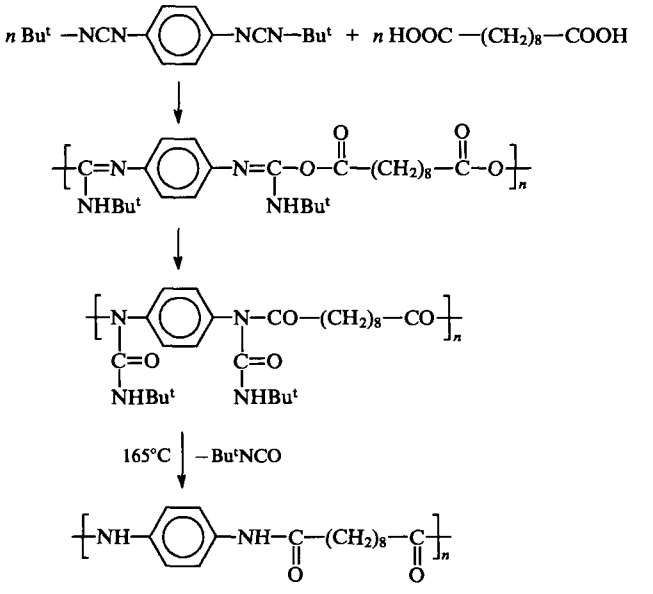


In order to test this hypothesis, compound **38** was allowed to react with phenol under the same conditions. This afforded benzanilide **36** in a satisfactory yield (80%).

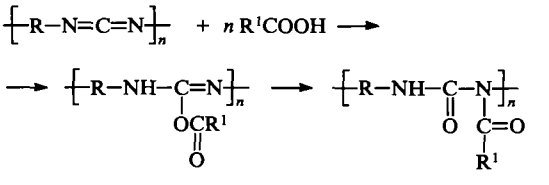


In addition, benzanilide **36** was isolated in 72% yield together with phenyl isocyanate from compound **38** itself on heating under the reaction conditions.

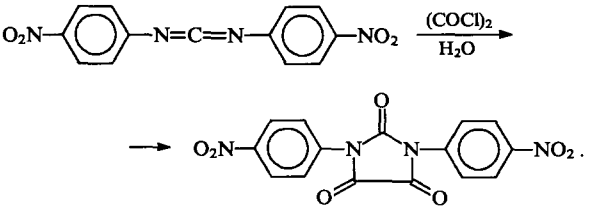
An interesting synthesis of the polymer has been achieved by the reaction of biscarbodiimide with dicarboxylic acids.[194] This synthesis was based on the use of the O→N shift of the acyl group.



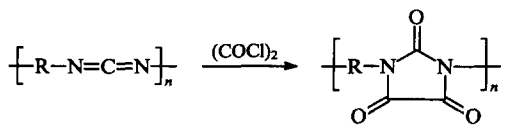
The interaction of monocarboxylic acids with polycarbodiimides leads to the formation of poly-*N*-acylurea, possibly via a stage involving the formation of poly-*O*-acylisourea.[195]



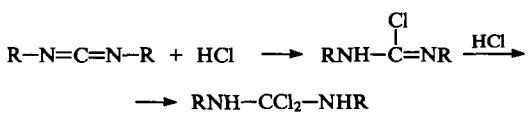
When arylcarbodiimides react with oxalyl chloride in the presence of water, the derivatives of parabanic acid are formed.[196]



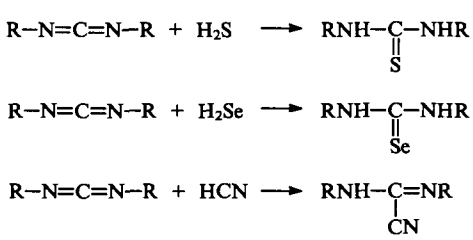
This reaction has been used [197] to obtain the highly thermally stable polyparabanic film by treating the polycarbodiimide film with oxalyl chloride.



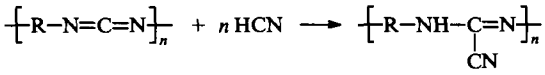
Dry hydrogen chloride reacts vigorously with carbodiimides with evolution of heat. Depending on the reactant ratio, one or two HCl molecules are added. [18]



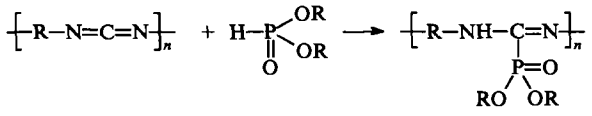
Carbodiimides react with weak acids, such as hydrogen sulfide [198] and hydrogen selenide, [199] to form the corresponding thio- and seleno-ureas, while the addition of hydrocyanic acid [200] leads to the formation of *N,N'*-dialkyl(aryl)-α-cyano-formamidines.



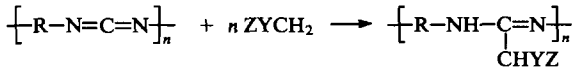
Among the reactions described above, that with hydrocyanic acid has been applied to polycarbodiimides, which resulted in the formation of polycyanoformamidines. [24]



Polymer-analogue reactions of polycarbodiimides involving the addition to the latter of dialkyl phosphites have also been carried out. [24]



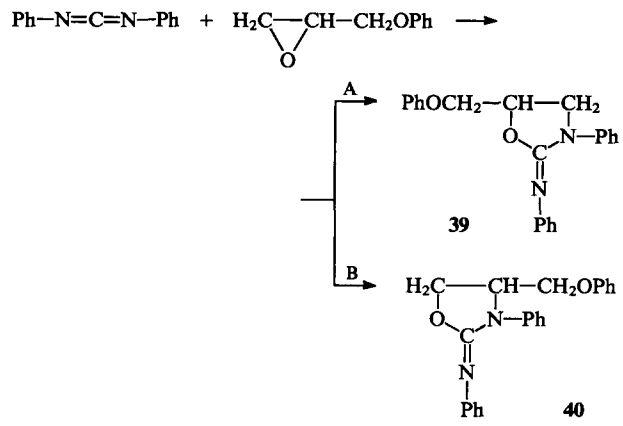
Polymers with formamidine fragments in the chain have been obtained by the addition of CH acids, for example malonic ester, to polycarbodiimides. [24]



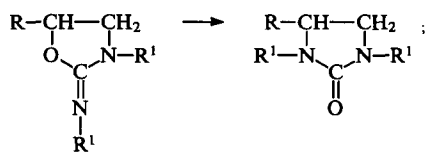
Z = COOEt, COMe;
Y = COOEt.

The interaction of the epoxide ring with the N=C=N groups of carbodiimides has been studied in detail on model and polymeric systems. [145–152] The model compounds employed were glycidyl phenyl ether and diphenylcarbodiimide. [145–147, 150–152]

Depending on the mode of opening of the epoxide ring, [12] there is a possibility of the formation of two isomeric structures: 5-phenoxymethyl-3-phenyl-2-*N*-phenyliminooxazolidine **39** and 4-phenoxymethyl-3-phenyl-2-*N*-phenylimidooxazolidine **40**.



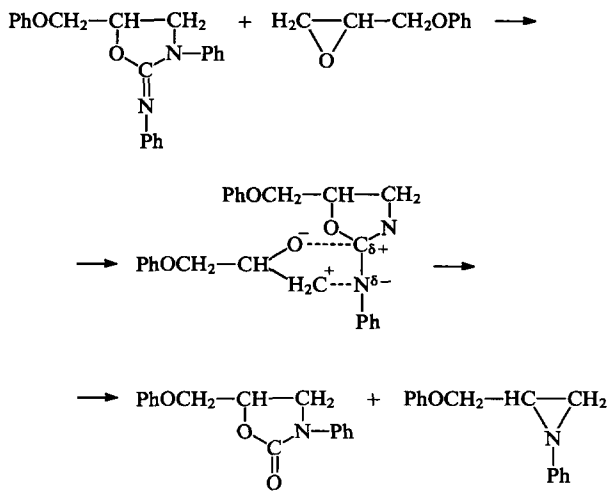
Analysis of the hydrolysis products as well as X-ray diffraction demonstrated [145, 147] that this reaction results in the formation of structure **39**. The X-ray diffraction data [147] made it possible to account for the absence of the isomerisation of compound **39** to the corresponding imidazolidinone, which is characteristic of iminooxazolidines with other substituents. [201, 202]



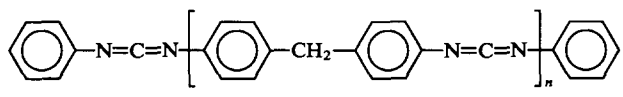
R = H, Ph; R^1 = Alk, Ph.

This is apparently associated with the fact that the phenoxymethyl substituent in structure **39** shields the ring oxygen atom, creating steric hindrance to the isomerisation process. [147]

It has been shown [150] that compound **39** interacts with an excess of glycidyl phenyl ether to form oxazolidinone.

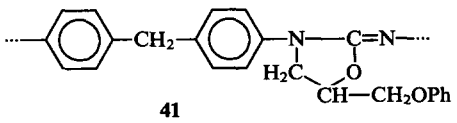


The interaction of oligocarbodiimides, synthesised from di(4-isocyanatophenyl)methane and phenyl isocyanate, i.e.

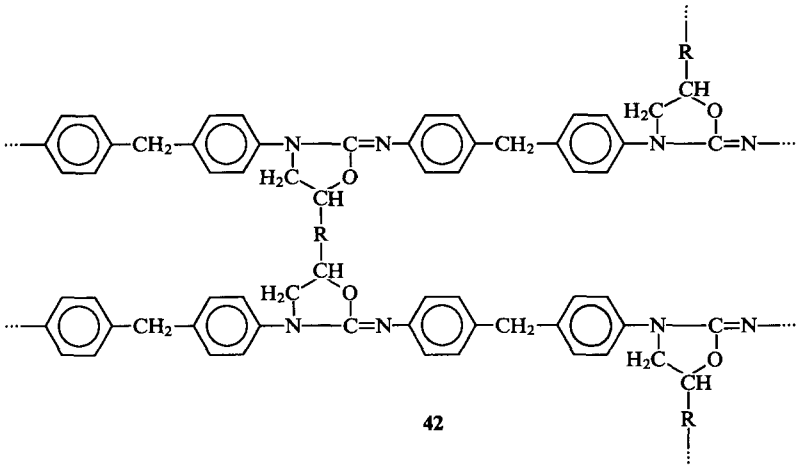


n = 30.

with glycidyl phenyl ether and the diglycidyl ether of di(hydroxyphenyl)propane has been investigated. The resulting polymeric structures are based on the fragments **41** and **42**. [146, 149]

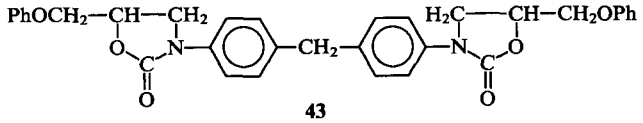


41



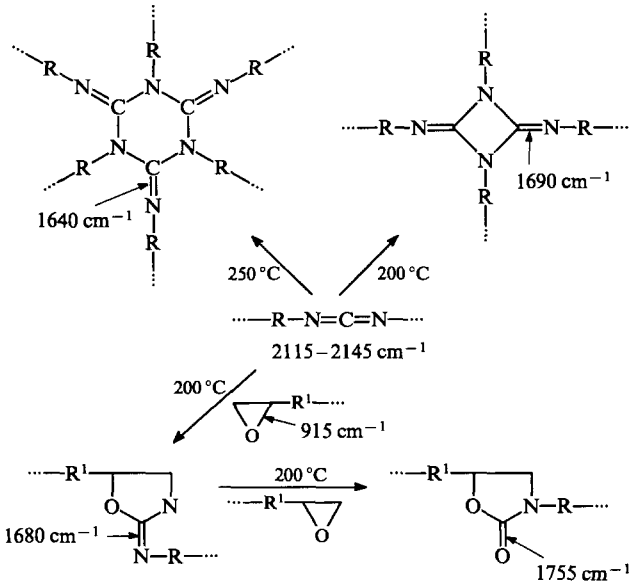
42

When an excess of glycidyl phenyl ether was used in the reaction with oligocarbodiimide,[146,149] bisoxazolidinone **43** was isolated, since iminooxazolidines decompose in an excess of the epoxide, which has been demonstrated in model reactions.[150]



43

The study[12,146,149] of the structures of network polymers obtained from oligocarbodiimides and oligoepoxides of different structure demonstrated the presence, together with imino-oxazolidine and other heterocyclic fragments, also of fragments obtained as a result of side reactions.

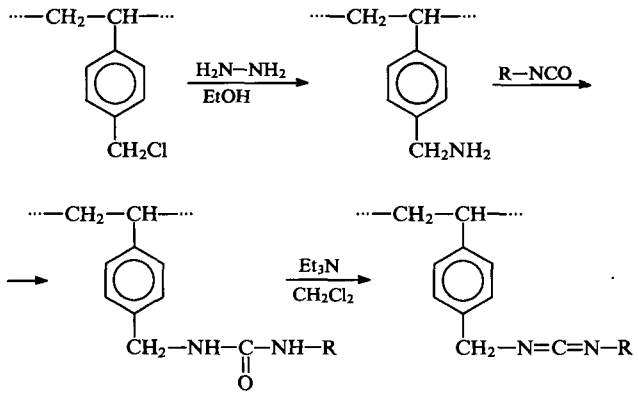


By altering the ratio of the carbodiimide and epoxide groups in the initial mixture of oligomers, the authors[12,146,149] regulated the content of heterocyclic fragments in the final product. In the presence of an excess of the oligocarbodiimide, urete diimine rings predominate in the structure, while at higher hardening temperatures (250 °C) the isomelamine groups predominate; in the presence of an excess of the epoxide component, the reaction involving the formation of iminooxazolidine and oxazolidine rings takes place preferentially.[12,146,149]

b. Modification of various polymers by mono- and polycarbodiimides

The development of new catalytic methods of synthesis of carbodiimides from available industrial isocyanates promoted the wide scale employment of mono- and poly-carbodiimides for the modification of various polymers.

Polystyrenes with carbodiimide side groups were obtained in this way. They were used subsequently as dehydrating agents.[203,204]

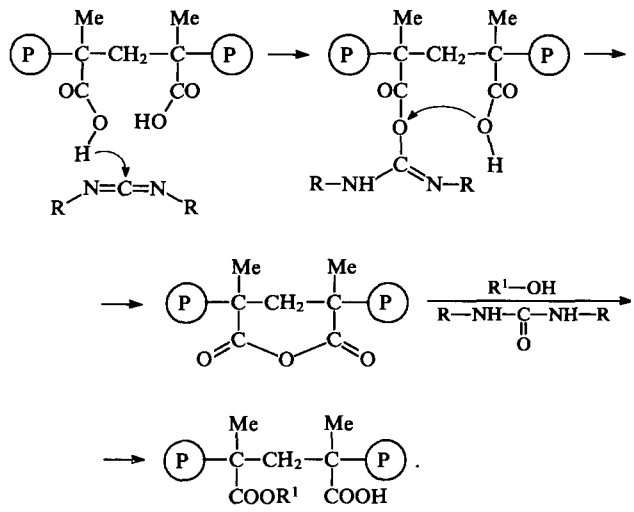


The cross-linking of butadiene–acrylonitrile copolymers, containing 0.09% of carboxy-groups, has been achieved.[205] The cross-linking agents were the bifunctional carbodiimides Ph–N=C=N–$(CH_2)_6$–N=C=N–Ph.

It has been shown in a patent[206] that hydroxyethylcellulose can be modified by means of dicyclohexylcarbodiimide in the presence of tetrafluoroboric acid with formation of a hydrophobic polymer containing *O*-alkylisourea units. Guanidine groups can also be introduced into the polymer under the conditions of such modification.[207]

When polyacrylic acids and polystyrenes with side carboxy-groups are treated with carbodiimides, polymers containing anhydride groups are formed.[208,209]

Syndiotactic polymeric methacrylic acid has been esterified by alcohols in the presence of carbodiimides and compounds with ester linkages have been obtained.[210–212] It has been suggested[210] that the formation of anhydride groups in accordance with the following scheme is an intermediate stage of the reaction:



Water-soluble carbodiimides have been used to bind ethyl glycinate to polyacrylic acid. It is suggested the reaction proceeds via the intermediate formation of a carboxylic acid anhydride.[208]

Scott et al.[209] investigated by IR spectroscopy the interaction between the carboxy-groups in cross-linked polystyrene in the presence of dicyclohexylcarbodiimide. It was postulated that *N*-acylurea groups are formed initially (absorption bands in the region of 1660 cm^{-1}) after which anhydride fragments appear, indicated by the presence of absorption bands at 1785 cm^{-1}.

Polymers containing amino- and carboxy-groups have been hardened with the aid of ditolylcarbodiimide.[213] The polymer films thus obtained are distinguished by improved physico-mechanical parameters.

Dicyclohexylcarbodiimide induces the formation of a sticky fire-resistant polyphosphoramide from diamines and inorganic phosphate.[214]

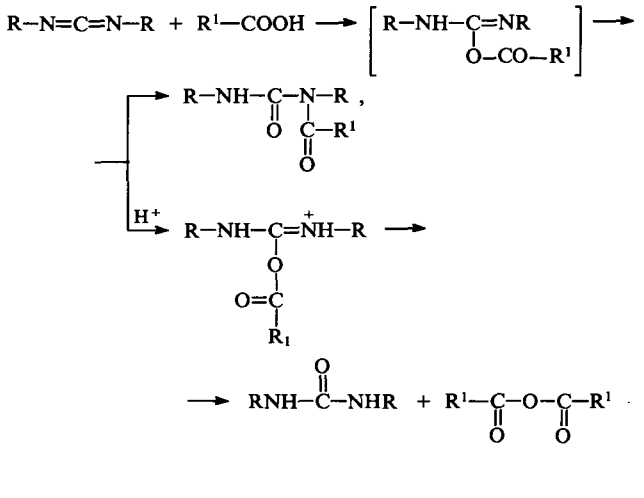
Carbodiimides have found extensive applications as hardening agents for gelatine.[215–227] The effect of carbodiimide consists in the binding of carboxy- and amino-groups in the gelatine chains, which leads to the cross-linking of the polymer.[227]

Polycarbodiimides have been used as dehydrating agents in the binding of peptides. Both linear polycarbodiimides and polymers containing carbodiimide groups in the side chain have been used for this purpose.[228–231]

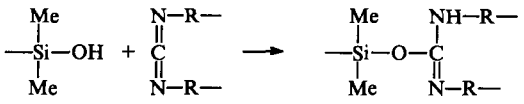
The storage time of liquid polyisocyanates can be increased by adding carbodiimides, which apparently remove water.[232–237]

Mono- and poly-carbodiimides are widely employed to prevent the hydrolysis of the ester bonds in polyesters[81,190,193,238–254] and as stabilising additives to polysiloxanes.[255,256]

It is believed[238] that the stabilising effect of carbodiimides is due to their interaction with the carboxy-groups of polymers.



It has been shown[255] that the siloxane linkages in polydimethylsiloxane are cleaved with formation of silanols at a temperature above 200–220 °C in the presence of water as well as alcohols and phenols. Such degradation leads to a decrease in the molecular mass of polydimethylsiloxane and hence to the loss of the initial physicomechanical parameters of the articles based on it. Piotrovskii and Metkin[255] state that the presence of polycarbodiimides during the hydrolysis of polydimethylsiloxanes may retard the decrease in the molecular mass of the latter as a consequence of the reaction of the silanol end groups with the polycarbodiimide.



V. Practical use of polycarbodiimides

The data presented above permit the conclusion that polycarbodiimides are promising polyfunctional thermoreactive compounds, which have found practical applications in various branches of technology, including the formation of highly heat-resistant and thermostable materials.

Polycarbodiimides are synthesised from available raw material in accordance with a technologically simple scheme. The high reactivity of carbodiimide groups permits both the thermal hardening of the polymers and different types of chemical modification of the latter. These positive qualities of polycarbodiimides promote their varied practical employment.

An important aspect of the practical use of polycarbodiimides is the formation on their basis of thermostable foams, the industrial manufacture of which has been initiated in recent years. They do not require the introduction of foam-forming agents (the role of which is assumed by the carbon dioxide evolved in the conversion of di- and poly-isocyanates into carbodiimides), their thermal stability is high, and they have effective physico-mechanical properties.[257–278]

It has been shown[259] that the modification of a polycarbodiimide composition by polyfunctional hydroxylated compounds makes it possible to economise on the carbodiimide formation catalyst, eliminates the differences between the technologies used for the preparation of foam polycarbodiimide and foam polyurethane, and increases the apparent density of the material. Under these conditions, 50% of the initial isocyanate groups of the polyisocyanate can be consumed on the formation of urethane fragments. The strength parameters of the resulting foam plastic are retained over a wide temperature range. For example, on raising the temperature to 127 °C, the relative elongation on rupture changes by only 50%.

It has been established[259] that foam polycarbodiimides, modified by urethane, exhibit a high fire resistance, have effective thermophysical parameters, and their water absorption capacity is low. This set of properties makes it possible to recommend them as insulating and constructional materials to be used at temperatures up to 200–250 °C.

Another possibility of modifying the polycarbodiimide structure arises from the simultaneous occurrence of the cyclotrimerisation of isocyanate groups with formation of isocyanurate fragments together with the polycarbodiimide.[259,269] They are highly fire-resistant: the mass loss does not exceed 15%–20% and the oxygen index is 29–32 in tests by the 'fire tube' method.[259]

A review has been devoted to fire-resistant carbodiimide foam plastics based on polyols derived from trichlorobutene oxides or epichlorohydrin.[279]

Organic[238,239,245–253,255,280–299] and organo-element[240,300–302] low-molecular-mass polycarbodiimides are used widely

as hydro- and thermo-stabilisers of polyesters,[238-254,280-284,290,291,295-298,300,301] polyurethanes,[299,300,301] polyamides,[280,292,298] polysiloxanes,[255,293] poly(vinyl chloride),[298,302] and other polymers.[46,53,59,70,72,215-237,285-288,294]

Aliphatic fluorocarbodiimides have been used to impart oil- and water-repelling properties to articles made from nylon and polyester [77] and also to impart these properties to leather. [77,303]

The addition of carbodiimides has made it possible to improve the adhesion of photographic emulsion to poly(ethylene terephthalate) carriers. The mechanism of the effect of carbodiimides apparently involves the formation of ester bonds. [304]

Mono- and poly-carbodiimides are used widely in the microencapsulation involved in the manufacture of pressure-sensitive copying paper. [305-307]

Organosilicon polycarbodiimides are stable in relation to irradiation, which makes it possible to employ them in various kinds of seals to be used under the conditions of intense irradiation. [25,86] Organotin carbodiimides are effective catalysts of the urethane formation reaction. [308,309] Thus $Bu_3N=C=NBu_3$ has been used as the catalyst for the preparation of film-forming polyurethane coatings based on organosilicon polyols and aliphatic isocyanates with the biurethane structure. [308]

Polycarbodiimides have been employed as nylon and polyester fibre and film strengthening agents. [310,311]

Polycarbodiimides have been used as composite binding materials: adhesives,[312-314] reinforced plastics,[15,82,197,315-317] compound materials,[12,79,146,149,156,232-237] electrically insulating materials,[153,155,318,319] and others. [77,320] This made it possible to obtain polymers with improved thermal and physicomechanical characteristics.

There is no doubt that further study of this promising class of polymers — organic and organoelement polycarbodiimides — will expand the scale of their practical applications‡.

References

1. G M Pogosyan, V A Pankratov, V N Zaplishnyi, S G Matnishyan *Politriaziny* (Polytriazines) (Erevan: Izd. AN Arm. SSR, 1987)
2. V A Pankratov, S V Vinogradova *Usp. Khim.* **41** 117 (1972) [*Russ. Chem. Rev.* **41** 66 (1972)]
3. F W Harris, S M Padaki, S Varaprath *Am. Chem. Soc. Polym. Prepr.* **21** 3 (1980)
4. V A Pankratov, A E Chesnokova *Usp. Khim.* **58** 1528 (1989) [*Russ. Chem. Rev.* **58** 879 (1989)]
5. J P Droske, J K Stille *Macromolecules* **17** 1 (1984)
6. V A Pankratov, S V Vinogradova, V V Korshak *Usp. Khim.* **46** 530 (1977) [*Russ. Chem. Rev.* **46** 278 (1977)]
7. K S J Lau, W J Kellghan, R H Boshan, N Bilou *J. Polym. Sci., Polym. Chem. Ed.* **21** 3009 (1983)
8. N A Sergeev, V K Shitikov, V A Pankratov *Usp. Khim.* **48** 148 (1979) [*Russ. Chem. Rev.* **48** 79 (1979)]
9. R B Seymour *Rev. Plast. Mod.* **36** 565 (1985)
10. V A Sergeev, Yu A Chernomordik, A S Kurapov *Usp. Khim.* **53** 518 (1984) [*Russ. Chem. Rev.* **53** 307 (1984)]
11. J K Stille *Am. Chem. Soc. Polym. Prepr.* **23** 1 (1982)
12. V A Pankratov, Ts M Frenkel', A M Fainleib *Usp. Khim.* **52** 1018 (1983) [*Russ. Chem. Rev.* **52** 576 (1983)]
13. P M Hergenrother *Polym. J.* **19** 73 (1987)
14. A K Zhitinkina, N A Shibanova, O G Tarakanov *Usp. Khim.* **54** 1866 (1985) [*Russ. Chem. Rev.* **54** 1104 (1985)]
15. V A Pankratov, D F Kutepov, G I Shukurov *Plastmassy* **2** 12 (1983)
16. D Martin, M Bauer, V A Pankratov *Usp. Khim.* **47** 1814 (1978) [*Russ. Chem. Rev.* **47** 975 (1978)]
17. Ya S Vygodskii, V A Pankratov *Usp. Khim.* **61** 1864 (1992) [*Russ. Chem. Rev.* **61** 1022 (1992)]
18. H G Khorana *Chem. Rev.* **53** 145 (1953)
19. B V Bocharov *Usp. Khim.* **34** 488 (1965) [*Russ. Chem. Rev.* **34** 212 (1965)]
20. F Kurzer, K Douraghi-Zadeh *Chem. Rev.* **67** 107 (1967)
21. Y Wolman *The Chemistry of Ketenes, Allenes and Related Compounds* (New York: Interscience, 1980)
22. A Williams, I T Ibrahim *Chem. Rev.* **81** 989 (1981)
23. M Mikolajczyk, P Kielbasinski *Tetrahedron* **37** 233 (1981)
24. K Wagner, K Findeisen, W Schifer, D Werner *Angew. Chem.* **93** 855 (1981)
25. A S Gordetsov, V P Kozyukov, I A Vostokov *Usp. Khim.* **51** 848 (1982) [*Russ. Chem. Rev.* **51** 485 (1982)]
26. R Stolle *Ber. Dtsch. Chem. Ges.* 1125 (1908)
27. W Neuman, P Fischer *Angew. Chem.* **74** 801 (1962)
28. K Wagner *Angew. Chem.* **74** 799 (1962)
29. US P. 2 663 736; *Chem. Abstr.* **49** 7 602 (1955)
30. US P. 2 663 737; *Chem. Abstr.* **49** 7 601 (1955)
31. US P. 2 663 738; *Chem. Abstr.* **49** 7 602 (1955)
32. US P. 2 663 739; *Chem. Abstr.* **49** 7 602 (1955)
33. T Campbell, J Monagle, V Foldi *J. Am. Chem. Soc.* **84** 3673 (1962)
34. T Campbell *Angew. Chem.* **74** 127 (1962)
35. T Campbell, J Monagle, V Foldi *J. Am. Chem. Soc.* **84** 1493 (1962)
36. J Monagle, J Mengenhauzer, V Foldi *J. Org. Chem.* **31** 2321 (1966)
37. K Hunger *Tetrahedron Lett.* **47** 5929 (1966)
38. BRD P. 2 614 323; *Chem. Abstr.* **86** 30 284 (1977)
39. B A Arbuzov, A O Vizel', K M Ivanovskaya *Dokl. Akad. Nauk SSSR* **170** 585 (1966)
40. B A Arbuzov, K M Ivanovskaya, A O Vizel' *Izv. Akad. Nauk SSSR, Ser. Khim.* 2079 (1973)
41. F S Guberman, M I Bakhitov, E V Kuznetsov *Zh. Obshch. Khim.* **44** 754 (1974)
42. B A Arbuzov, A K Zhitinkina, A O Vizel' *Vysokomol. Soedin., Ser. A* **17** 2748 (1975)
43. BRD P. 2 504 334; *Chem. Abstr.* **85** 178 460 (1976)
44. BRD P. 2 504 400; *Chem. Abstr.* **85** 161 253 (1976)
45. BRD P. 2 552 340; *Chem. Abstr.* **87** 58 978 (1977)
46. BRD P. 2 552 350; *Chem. Abstr.* **87** 40 290 (1977)
47. US P. 4 068 055; *Chem. Abstr.* **88** 121 930 (1978)
48. US P. 4 105 642; *Ref. Zh. Khim.* 11S 248P (1979)
49. US P. 4 068 065; *Chem. Abstr.* **88** 137 181 (1978)
50. BRD P. 2 504 331; *Chem. Abstr.* **85** 42 115 (1976)
51. J Monagle *J. Org. Chem.* **27** 3851 (1962)
52. T Campbell, J Monagle *J. Am. Chem. Soc.* **84** 4288 (1962)
53. US P. 4 177 205; *Chem. Abstr.* **92** 111 654 (1980)
54. BRD P. 2 543 704; *Chem. Abstr.* **85** 6 785 (1976)
55. Br. P. 1 510 424; *Chem. Abstr.* **89** 198 554 (1978)
56. US P. 4 066 629; *Chem. Abstr.* **90** 88 061 (1979)
57. US P. 3 960 950; *Chem. Abstr.* **85** 125 737 (1976)
58. BRD P. 2 802 521; *Chem. Abstr.* **89** 147 380 (1978)
59. BRD P. 2 802 525; *Chem. Abstr.* **89** 130 334 (1978)
60. US P. 4 143 065; *Chem. Abstr.* **90** 169 549 (1979)
61. US P. 3 922 238; *Chem. Abstr.* **84** 90 954 (1976)
62. BRD P. 2 754 011; *Chem. Abstr.* **89** 111 249 (1978)
63. BRD P. 2 247 500; *Chem. Abstr.* **79** 19 897 (1973)
64. US P. 4 029 611; *Chem. Abstr.* **87** 69 190 (1977)
65. US P. 3 933 699; *Chem. Abstr.* **84** 151 437 (1976)
66. BRD P. 2 545 312; *Chem. Abstr.* **85** 47 668 (1976)
67. DDR P. 121 461; *Chem. Abstr.* **86** 172 424 (1977)
68. T W Campbell, K C Smeltz *J. Org. Chem.* **28** 2069 (1963)
69. D J Lyman, N Sadri *Macromol. Chem.* **67** 1 (1963)
70. BRD P. 2 606 419; *Chem. Abstr.* **87** 168 843 (1977)
71. BRD P. 2 714 293; *Chem. Abstr.* **90** 7 042 (1979)
72. BRD P. 2 837 770; *Chem. Abstr.* **92** 199 247 (1980)
73. Br. P. 1 115 260; *Chem. Abstr.* **69** 28 119 (1968)
74. BRD P. 2 239 645; *Chem. Abstr.* **78** 148 446 (1973)
75. US P. 3 755 242; *Chem. Abstr.* **79** 147 012 (1973)
76. US P. 4 986 929; *Ref. Zh. Khim.* 15T 129P (1992)
77. US P. 4 024 178; *Chem. Abstr.* **87** 6 969 (1977)
78. Eur. P. 120 305; *Chem. Abstr.* **102** 167 712 (1985)
79. L M Alberino, W J Farrissey, A A R Sayigh *J. Am. Chem. Soc., Polym. Prepr.* **15** 77 (1974)
80. L M Alberino, W J Farrissey, A A R Sayigh *J. Appl. Polym. Sci.* **21** 1999 (1977)
81. V A Pankratov, I P Antonova-Antipova, A E Shvorak, A Sh Feofanova *Int. Polym. Sci. and Techn.* **15** 27 (1988)

‡This review was written in the course of research carried out with the financial support of the Russian Fundamental Research Fund (code 93-03-5259).

82. V A Pankratov *Zh. Vses. Khim. O-va im. D.I. Mendeleeva* **34** 459 (1989)
83. J Pump, E G Rochow *Z. Anorg. Allg. Chem.* **330** 101 (1964)
84. H Kohler, U Lange *Z. Chem.* **12** 146 (1972)
85. I A Vostokov, Yu I Dergunov *Khim. Elementoorg. Soedin.* 7 53 (1979)
86. US P. 3 352 799; *Chem. Abstr.* **68** 14164 (1968)
87. V A Pankratov, Yu V Vasil'ev, in *Tez. Dokl. III Vsesoyuznoi Konferentsii "Khimiya i Fizikokhimiya Oligomerov"* (Abstracts of Reports at the IIIrd All-Union Conference "Chemistry and Physical Chemistry of Oligomers") (Chernogolovka: Branch of the Inst. Khim. Fiz., 1986) p. 222
88. A A Askadskii, G V Surov, V A Pankratov *Vysokomol. Soedin., Ser. A* **32** 1528 (1990)
89. A T Vincent, P J Wheatley *J. Chem. Soc., Perkin Trans. 2* 687 (1972)
90. A T Vincent, P J Wheatley *J. Chem. Soc., Perkin Trans. 2* 1567 (1972)
91. H Irngartinger, H U Jeager *Acta Crystallogr., Sect. B, Struct. Crystallogr.* **34** 3262 (1978)
92. Nguen Minh-Tho, Ma Tac-Kyn *J. Chem. Soc., Perkin Trans. 2* 1297 (1983)
93. S T Malinovskii, Yu A Simonov, N G Luk'yanenko *Dokl. Akad. Nauk SSSR* **288** 887 (1986)
94. W H Hocking, M C L Gerry *J. Mol. Spectrosc.* **42** 547 (1972)
95. D Poppinger, L Rangom *J. Am. Chem. Soc.* **100** 3674 (1978)
96. T Sakaizumi, O Yamada, K Ushida *Bull. Chem. Soc. Jpn.* **49** 2908 (1976)
97. S P Bondarenko, R P Tiger, A A Bagatur'yants *Zh. Fiz. Khim.* **54** 1370 (1980)
98. J D Murdoch, D W H Rankin, B Beagley *J. Mol. Struct.* **31** 291 (1976)
99. G M Sheldrick, R Taylor *J. Organomet. Chem.* **101** 19 (1975)
100. C Glidewell, A G Robiette *Chem. Phys. Lett.* **28** 290 (1974)
101. US P. 3 929 733; *Chem. Abstr.* **84** 90 999 (1976)
102. J Pump, E G Rochow, U Wannagat *Monatsh. Chem.* **94** 588 (1976)
103. J E Drake, R T Hemmings, H E Henderson *J. Chem. Soc., Dalton Trans.* (3) 366 (1976)
104. S V Lindeman, V E Shklover, Yu T Struchkov *Kristallografiya* **27** 65 (1982)
105. V A Pankratov, V M Laktionov, A I Akhmedov *Vysokomol. Soedin., Ser. A* **26** 79 (1984)
106. Yu I Dergunov, I A Vostokov, A S Gordetsov *Zh. Obshch. Khim.* **46** 1573 (1976)
107. V A Pankratov, P N Gribkova, V M Laktionov *Vysokomol. Soedin., Ser. A* **26** 129 (1984)
108. L Z Rogovina, A Sh Feofanova, V A Pankratov *Vysokomol. Soedin., Ser. A* **30** 528 (1988)
109. V A Pankratov, V M Laktionov, A I Akhmedov *Acta Polymer.* **37** 39 (1986)
110. B V Lebedev, T A Bykova, V A Pankratov *Zh. Obshch. Khim.* **54** 417 (1984)
111. V E Shashova, W Sweeny, R F Tietz *J. Am. Chem. Soc.* **82** 866 (1960)
112. G Robinson *J. Polym. Sci.* **9** 3901 (1964)
113. R Richter *Chem. Ber.* **101** 174 (1968)
114. R Tsuzuki, Y Iwakura *J. Org. Chem.* **30** 2665 (1965)
115. F Zetsche, A Fredrich *Ber. Dtsch. Chem. Ges.* **73** 1114 (1940)
116. H Jakubke, C Klesson *J. Prakt. Chem.* **319** 159 (1977)
117. W Flowers, R Franklin, R H Haszeldin *J. Chem. Soc., Chem. Commun.* **14** 567 (1976)
118. V A Pankratov, S V Vinogradova, V V Korshak *Issledovanie Tsiklotrimerizatsii Difenilkarbodiimida* (Study of the Cyclotrimerization of Diphenylcarbodiimide) Article deposited at the All-Union Institute of Scientific and Technical Information (VINITI) (Moscow, 1981) N 5844-81
119. W Weith *Ber. Dtsch. Chem. Ges.* **7** 10 (1874)
120. W Miller *Ber. Dtsch. Chem. Ges.* **28** 1004 (1895)
121. M Busch, G Blume, E Pungs *J. Prakt. Chem.* **79** 519 (1909)
122. M Busch, J Ulmer *Ber. Dtsch. Chem. Ges.* **35** 172 (1902)
123. J H Saunders, R J Slocombe *Chem. Rev.* **43** 203 (1948)
124. D Rapi, G Sbrana *J. Chem. Soc.* 3827 (1971)
125. Jpn. P. 7 115 501; *Chem. Abstr.* **75** 152 313 (1971)
126. J Bldeker, K Courault *Tetrahedron* **34** 101 (1978)
127. H Hoberg, J Korff *Liebigs Ann. Chem.* 1111 (1978)
128. H Ulrich, B Tucker, A A R Sayigh *J. Am. Chem. Soc.* **90** 528 (1968)
129. H Ulrich, B Tucker, F A Stuber *J. Org. Chem.* **34** 2250 (1969)
130. Yu I Dergunov, A S Gordetsov, I A Vostokov *Zh. Obshch. Khim.* **44** 2166 (1974)
131. Yu I Dergunov, A S Gordetsov, I A Vostokov *Zh. Obshch. Khim.* **45** 2234 (1975)
132. Yu I Dergunov, A S Gordetsov, I A Vostokov *Zh. Obshch. Khim.* **44** 1523 (1974)
133. V I Gorbatenko, L I Gerchuk, L I Samarai *Zh. Org. Khim.* **13** 899 (1977)
134. H Suschitzky, W E Walrond, R Hull *J. Chem. Soc., Perkin Trans. 1* 47 (1977)
135. E Schaumann, E Kausch, W Walter *Chem. Ber.* **110** 820 (1977)
136. V V Korshak, V A Pankratov, D F Kutepov *Izv. Akad. Nauk SSSR, Ser. Khim.* 1408 (1973)
137. M Rosens *Bull. Soc. Chim. Belg.* **66** 109 (1957)
138. A Hoffman *Ber. Dtsch. Chem. Ges.* **18** 3217 (1885)
139. G C Verschoor, E Keulen *Acta Crystallogr.* **27** 134 (1971)
140. P Coppens, A Vos *Acta Crystallogr.* **27** 146 (1971)
141. A Usanmaz *Acta Crystallogr.* **35** 1117 (1979)
142. D Lenoir, H Dauner, R M Frank *Chem. Ber.* **113** 2636 (1980)
143. J Penfold, P Carter *Poliplasti Plast. Rinf.* **26** 51 (1978)
144. D Joel, G Behrendt *Plaste Kautsch.* **23** 162 (1976)
145. V A Pankratov, Ts M Frenkel', A M Fainleib *Izv. Akad. Nauk SSSR, Ser. Khim.* 474 (1983)
146. V A Pankratov, Ts M Frenkel, A M Fainleib *Acta Polym.* **36** 550 (1985)
147. G V Gridunova, V E Shklover, Yu T Struchkov *Khim. Geterotsikl. Soedin.* 1026 (1984)
148. Ts M Frenkel', V A Pankratov, L I Komarova *Vysokomol. Soedin., Ser. A* **28** 176 (1985)
149. V A Pankratov, Ts M Frenkel, A M Fainleib, V V Korshak, in *Cross-linked Epoxides* (Eds B Sedlacek, J Kohovec) (Berlin; New York, 1986) p. 41
150. V A Pankratov, Ts M Frenkel', A M Fainleib *Izv. Akad. Nauk SSSR, Ser. Khim.* 2152 (1983)
151. T A Bykova, E G Kiparisova, E N Tarasov *Izv. Akad. Nauk SSSR, Ser. Khim.* 1252 (1987)
152. B V Lebedev, T A Bykova, E G Kiparisova *Izv. Akad. Nauk SSSR, Ser. Khim.* 1232 (1988)
153. G I Shukurov, V A Pankratov, D F Kutepov *Elektrotekh. Prom., Ser. Elektrotekh. Mater.* **6** 6 (1984)
154. V V Korshak, V A Pankratov, A K Bonetskaya *Plastmassy* **1** 4 (1987)
155. G I Shukurov, V A Pankratov, D F Kutepov *Plastmassy* **7** 5 (1984)
156. DDR P. 121 460; *Ref. Zh. Khim.* 22S 358P (1977)
157. D G Knorre, V A Kurbanov, G S Mushinskaya *Izv. Sib. Otd. Akad. Nauk SSSR, Ser. Khim.* **3** 137 (1967)
158. I K Korobeinicheva, E D Krivonosova, O A Mirgorodskaya *Izv. Sib. Otd. Akad. Nauk SSSR, Ser. Khim.* **1** 115 (1969)
159. R T Markiw, E S Canellakis *J. Org. Chem.* **34** 3707 (1969)
160. H Tsutsumi, Y Kawai, Y Ishido *Chem. Lett.* **6** 629 (1978)
161. Jpn. P. 74108070; *Chem. Abstr.* **82** 112 066 (1975)
162. BRD P. 2 423 482; *Chem. Abstr.* **82** 162 978 (1975)
163. US P. 3 793 297; *Chem. Abstr.* **81** 24 532 (1974)
164. A D Hawtrey *Tetrahedron Lett.* 7 6103 (1966)
165. P H Batelaan, W Heerma, G Tadema *Proc. K. Ned. Akad. Wet., Ser. B* **72** 132 (1969)
166. F H C Stewart *Aust. J. Chem.* **21** 477 (1968)
167. E Vowinkel, C Wolff *Chem. Ber.* **107** 907 (1974)
168. K L Carraway, D E Koshland *Biochim. Biophys. Acta* **160** 272 (1968)
169. J Knovacs, L Kisfaludy, M Q Caprini *Tetrahedron* **25** 2555 (1969)
170. J Knovacs, L Kisfaludy, M Q Caprini *J. Am. Chem. Soc.* **89** 183 (1967)
171. M Allan, R Y Moir *Can. J. Chem.* **41** 252 (1963)
172. P A Colombo, M Moreno-Manas *J. Chem. Soc., Chem. Commun.* 229 (1967)
173. M Moreno-Manas *An. Quim.* **56** 175 (1969)
174. Y Iwakura, R Tsuzuki, K Noguchi *Makromol. Chem.* **98** 21 (1966)
175. M Komatsu, J Ohshiro, H Hotta *J. Org. Chem.* **39** 948 (1974)
176. BRD P. 2 551 499; *Chem. Abstr.* **87** 103 307 (1977)
177. BRD P. 2 545 648; *Chem. Abstr.* **87** 68 158 (1977)
178. Y Iwakura, K Noguchi *J. Polym. Sci., Polym. Lett.* **5** 821 (1967)

179. Y Iwakura, K Noguchi *J. Polym. Sci., Part. A* 7 801 (1969)
180. E Vowinkel, G Claussen *Chem. Ber.* **107** 898 (1974)
181. I T Ibrahim, A Williams *J. Am. Chem. Soc.* **100** 7420 (1978)
182. D F Mironova, G F Dvorko *Ukr. Khim. Zh.* **33** 602 (1967)
183. D F Mironova, G F Dvorko, T N Skuratovskaya *Ukr. Khim. Zh.* **35** 726 (1969)
184. D F Mironova, G F Dvorko, T N Skuratovskaya *Ukr. Khim. Zh.* **36** 190 (1970)
185. D G Knorre, O A Mirgorodskaya *Dokl. Akad. Nauk SSSR* **186** 340 (1969)
186. T A Budashanova, D G Knorre, O A Mirgorodskaya *Izv. Sib. Otd. Akad. Nauk SSSR* **5** 73 (1967)
187. D F Mironova, G F Dvorko *Ukr. Khim. Zh.* **41** 840 (1975)
188. B O Bohannon *Diss. Abstr.* **32B** 2062 (1971)
189. I T Ibrahim, A Williams *J. Chem. Soc., Chem. Commun.* 25 (1980)
190. V A Pankratov, in *Proizvodstvo i Primenenie Izotsianatov* (Production and Application of Isocyanates) (Ed. S Daranova) (Dzerzhinsk: Vses. Khim. O-vo im. D. I. Mendeleeva, 1989) p. 23
191. C Alexandre, F Rouessac *Tetrahedron Lett.* **11** 1011 (1970)
192. D B Guldener, D J Sikkema *Chem. Ind. (London)* 628 (1980)
193. V V Korshak, V A Pankratov, L I Komarova *O Reaktsiyakh, Protekayushchikh pri Vzaimodeistvii Slozhnykh Aromaticheskikh Poliefirov s Polifunktsional'nymi Karbodiimidami* (Moscow, 1986) (Reactions between Aromatic Polyesters and Polyfunctional Carbodiimides) Article deposited at the All-Union Institute of Scientific and Technical Information (VINITI) N 673-V86
194. Y Iwakura, K Noguchi, T Utsunomija *J. Polym. Sci., Part B* **6** 517 (1968)
195. Jpn. P. 205 518; *Chem. Abstr.* **99** 72 034 (1963)
196. C Bennett, W Heitz *Makromol. Chem.* **188** 475 (1987)
197. Y Imaki *Polym. Appl.* **40** 198 (1991)
198. A Huhn *Ber. Dtsch. Chem. Ges.* **19** 2404 (1886)
199. F Zetzsche, H Pinske *Ber. Dtsch. Chem. Ges.* **74** 1022 (1941)
200. S Hunig, H Lehmann, G Grimmer *Ann. Chim.* **579** 77 (1953)
201. K Gulbiks, K Hamann *Chem. Ber.* **94** 3287 (1961)
202. E Vowinkel, P Gleichenhagen *Tetrahedron Lett.* **15** 143 (1974)
203. N M Weinshenker, C M Shen *Tetrahedron Lett.* **13** 3281 (1972)
204. K Kondo, Y Ohbe, Y Imaki *Technol. Rep. Osaka Univ.* **25** 487 (1975)
205. Br. P. 1 056 202; *Chem. Abstr.* **66** 76 542 (1967)
206. Czech. P. 174 425; *Chem. Abstr.* **90** 123 404 (1979)
207. BRD P. 2 714 292; *Chem. Abstr.* **90** 7 043 (1979)
208. D G Knorre, L P Naumova, L S Sandakshiev *Izv. Sib. Otd. Akad. Nauk SSSR, Ser. Khim.* **2** 119 (1966)
209. L T Scott, J Rebek, L Ovsyanko *J. Am. Chem. Soc.* **99** 625 (1977)
210. E Klesper, D Strasilla *J. Polym. Sci., Polym. Lett.* **15** 23 (1977)
211. E Klesper, D Strasilla, M C Berg *Eur. Polym. J.* **15** 587 (1979)
212. E Klesper, D Strasilla, M C Berg *Eur. Polym. J.* **15** 593 (1979)
213. Jpn. P. 7 918 896; *Chem. Abstr.* **91** 6 346 (1979)
214. V G Shestakov, E M Kiseleva *Tr. Ural. Lesotekhn. Inst.* **28** 63 (1972)
215. I D Robinson *J. Photogr.* **16** 41 (1968)
216. Fr. P. 2 032 350; *Chem. Abstr.* **75** 28 259 (1971)
217. US P. 878 013; *Chem. Abstr.* **73** 125 716 (1970)
218. Jpn. P. 7 138 715; *Chem. Abstr.* **77** 82 172 (1972)
219. BRD P. 2 439 553; *Chem. Abstr.* **85** 12 299 (1976)
220. Jpn. P. 75 109 251; *Chem. Abstr.* **84** 114 163 (1976)
221. BRD P. 2 417 779; *Chem. Abstr.* **84** 67 815 (1976)
222. BRD P. 2 505 746; *Chem. Abstr.* **84** 67 802 (1976)
223. BRD P. 2 602 150; *Chem. Abstr.* **85** 151 772 (1976)
224. BRD P. 2 625 026; *Chem. Abstr.* **88** 129 015 (1978)
225. BRD P. 2 545 755; *Chem. Abstr.* **87** 31 930 (1977)
226. US P. 4 087 283; *Chem. Abstr.* **89** 120 841 (1978)
227. A Gardi, H Nitschamann *Helv. Chim. Acta* **55** 2468 (1972)
228. Y Wolman, S Kivity, M Frankel *J. Chem. Soc., Chem. Commun.* 629 (1967)
229. H Kamogawa, M Nanosawa, S Uehara *Bull. Chem. Soc. Jpn.* **52** 533 (1979)
230. H Ito, N Takematsu, I Ichinizaki *Chem. Lett.* 577 (1975)
231. US P. 4 102 877; *Chem. Abstr.* **90** 39 283 (1979)
232. US P. 4 199 524; *Chem. Abstr.* **93** 47 805 (1980)
233. US P. 4 284 730; *Chem. Abstr.* **95** 188 349 (1981)
234. Eur. P. 57 862; *Chem. Abstr.* **98** 17 483 (1983)
235. US P. 4 105 643; *Ref. Zh. Khim.* 11S 280P (1979)
236. US P. 3 771 502; *Ref. Zh. Khim.* 17S 474P (1974)
237. Belg. P. 851 491; *Chem. Abstr.* **88** 153 284 (1978)
238. US P. 3 527 800; *Chem. Abstr.* **73** 98 995 (1970)
239. Br. P. 1 137 869; *Chem. Abstr.* **70** 48 278 (1969)
240. US P. 4 857 603; *Ref. Zh. Khim.* 3S 614P (1991)
241. V A Pankratov, I P Antipova-Antonova, A E Shvorak *Izv. Vyssh. Uchebn. Zaved., Khim. Khim. Tekhnol.* **31** 96 (1988)
242. V V Korshak, V A Pankratov, T P Zalukaeva, in *Tez. Dokl. Nauchno-Tekhnicheskoi Konferentsii "Strukturnaya Modifikatsiya Polimernykh Materialov"* (Abstracts of Reports at the Scientific and Technical Conference "Structural Modification of Polymeric Materials") (Chernogolovka: Branch of Inst. Khim. Fiz., 1986) p. 29
243. US P. 4 113 676; *Chem. Abstr.* **90** 88 892 (1979)
244. BDR P. 132 969; *Chem. Abstr.* **91** 58 110 (1979)
245. US P. 3 450 669; *Chem. Abstr.* **71** 62 001 (1969)
246. BRD P. 2 528 589; *Chem. Abstr.* **84** 165 673 (1976)
247. BRD P. 2 334 828; *Chem. Abstr.* **81** 106 674 (1974)
248. Jpn. P. 7 500 044; *Chem. Abstr.* **82** 172 327 (1975)
249. US P. 3 852 101; *Chem. Abstr.* **82** 126 393 (1975)
250. BRD P. 2 020 330; *Chem. Abstr.* **76** 114 172 (1972)
251. R M Lum, *J. Polym. Sci., Polym. Chem. Ed.* **17** 3017 (1979)
252. BRD P. 1 285 747; *Chem. Abstr.* **70** 116 100 (1969)
253. BRD P. 2 545 647; *Chem. Abstr.* **87** 24 205 (1977)
254. C Papaspyrides, A W Birley *Polymer* **19** 1474 (1978)
255. K V Piotrovskii, I A Metkin *Zh. Prikl. Khim.* **51** 1673 (1978)
256. BRD P. 2 730 747; *Chem. Abstr.* **90** 138 867 (1979)
257. BRD P. 2 754 579; *Chem. Abstr.* **89** 75 939 (1978)
258. Br. P. 1 356 851; *Ref. Zh. Khim.* 24S 348P (1976)
259. A K Zhitinkina, T V Artamonova, L V Turetskii *Plastmassy* **4** 32 (1984)
260. US P. 4 051 082; *Chem. Abstr.* **88** 7 895 (1978)
261. US P. 4 151 334; *Chem. Abstr.* **91** 21 447 (1979)
262. Belg. P. 848 330; *Chem. Abstr.* **88** 38 673 (1978)
263. Br. P. 1 524 359; *Chem. Abstr.* **90** 152 999 (1979)
264. Br. P. 2 008 594; *Chem. Abstr.* **92** 23 781 (1980)
265. BRD P. 2 742 275; *Chem. Abstr.* **88** 171 058 (1978)
266. V M Kolobova, A A Gurov, S A Goryachenkov *Plastmassy* **10** 34 (1991)
267. BRD P. 2 161 475; *Chem. Abstr.* **105** 61 070 (1986)
268. BRD P. 2 114 976; *Chem. Abstr.* **100** 23 211 (1984)
269. USSR P. 1 134 572; *Chem. Abstr.* **102** 186 136 (1985)
270. K Morimoto, Y Imashiro *J. Soc. Mater. Sci. Jpn.* **41** 798 (1992)
271. N I Mysin, N A Bazin, Yu I Dergunov *Khim. Promst. (Moscow)* **6** 331 (1991)
272. N I Mysin, V T Sharafanov, Yu I Dergunov, in *Tez. Dokl. I Mezhdunarodnoi Konferentsii po Polimernym Materialam Ponizhennoi Goryuchesti, Alma-Ata, 1990* (Abstracts of Reports at the Ist International Conference on Polymer Materials with Reduced Combustibility, Alma-Ata, 1990) p. 120
273. H Ulrich, in *UTECH'90: Int. Polyurethane Exhib. and Conf.* (London, 1990) p. 274
274. A K Zhitinkina, V D Alpern, M Y Tsarfin, in *UTECH'90: Int. Polyurethane Exhib. and Conf.* (London, 1990) p. 212
275. DDR P. 219 030; *Ref. Zh. Khim.* 20S 559P (1985)
276. US P. 4 283 500; *Ref. Zh. Khim.* 9S 482P (1982)
277. Yu I Yamanov, A A Zhitinkina, P A Zinger, in *Tez. Dokl. Nauchno-Tekhnicheskoi Konferentsii "Strukturnaya Modifikatsiya Polimernykh Materialov"* (Abstracts of Reports at the Scientific and Technical Conference "Structural Modification of Polymeric Materials") (Chernogolovka: Branch of Inst. Khim. Fiz., 1985) p. 101
278. US P. 4 424 288; *Ref. Zh. Khim.* 3S 662P (1985)
279. B Hurd *Dev. Polyurethane* **1** 175 (1975)
280. US P. 4 128 599; *Chem. Abstr.* **90** 125 505 (1979)
281. US P. 4 113 676; *Chem. Abstr.* **90** 88 892 (1979)
282. Jpn. P. 57 205 518; *Chem. Abstr.* **99** 72 034 (1983)
283. Jpn. P. 81 161 452; *Chem. Abstr.* **96** 123 992 (1982)
284. Fr. P. 74 337; *Chem. Abstr.* **99** 6 538 (1983)
285. DDR P. 132 969; *Chem. Abstr.* **91** 58 110 (1979)
286. Eur. P. 274 402; *Chem. Abstr.* **110** 115 951 (1989)
287. BRD P. 2 941 253; *Chem. Abstr.* **95** 42 712 (1981)
288. BRD P. 3 512 918; *Chem. Abstr.* **106** 20 061 (1987)
289. US P. 4 612 054; *Chem. Abstr.* **106** 6 507 (1987)
290. Eur. P. 357 193; *Chem. Abstr.* **113** 99 182 (1990)

291. Eur. P. 294 179; *Chem. Abstr.* **110** 136 772 (1989)
292. S M Andreev, N A Samoilova, Yu A Davidovich *Usp. Khim.* **56** 629 (1987) [*Russ. Chem. Rev.* **56** 366 (1987)]
293. BRD P. 2 730 743; *Ref. Zh. Khim.* 23S 442P (1979)
294. Y K Noren, C E Lin, E Ecaridge *J. Coat. Technol.* **57** 61 (1985)
295. O Panaiotov, V Belcheva *Macromol. Chem.* **188** 2821 (1987)
296. Jpn. P. 6 160 723; *Ref. Zh. Khim.* 9S 550P (1987)
297. BRD P. 4 018 184; *Ref. Zh. Khim.* 17T 65P (1992)
298. Jpn. P. 2 175 757; *Ref. Zh. Khim.* 21T 43P (1991)
299. I M Kochnov *Plastmassy* **2** 19 (1977)
300. Yu I Dergunov, Doctoral Thesis in Chemical Sciences, Inst. of Organoelement Compounds, Academy of Sciences of the USSR, Moscow, 1979
301. BRD P. 1 190 176; *Chem. Abstr.* **63** 753 (1965)
302. A S Gordetsov, I A Vostokov, V I Zyuzina, in *Fiziko-Khimicheskie Osnovy Sinteza i Pererabotki Polimerov* (Physicochemical Bases of the Synthesis and Processing of Polymers) (Gorky, 1980) p. 71
303. US P. 3 922 143; *Chem. Abstr.* **84** 137 245 (1976)
304. Fr. P. 2 024 138; *Chem. Abstr.* **74** 133 010 (1971)
305. BRD P. 2 617 747; *Chem. Abstr.* **88** 30 404 (1978)
306. BRD P. 2 619 524; *Chem. Abstr.* **88** 51 675 (1978)
307. BRD P. 2 523 586; *Chem. Abstr.* **86** 44 538 (1977)
308. V N Kuznetsova, K V Zapunnaya, S I Omel'chenko, in *Sintez i Fizikokhimiya Polimerov* Vyp. 18 (The Synthesis and Physical Chemistry of Polymers) No. 18 (Kiev, 1976) p. 3
309. N M Noskov, A S Gordetsov, N K Gavrilova *Zh. Prikl. Khim. (Leningrad)* **52** 2083 (1979)
310. US P. 4 110 302; *Chem. Abstr.* **90** 125 505 (1979)
311. G L Berestneva, E A Goncharova, V A Pankratov, in *The 25th Europhysics Conference on Macromol. Physics, Orientational Phenomena in Polymers, St. Petersburg, 1992* p. 77
312. BRD P. 2 655 836; *Chem. Abstr.* **87** 69 352 (1977)
313. US P. 4 118 536; *Chem. Abstr.* **90** 24 918 (1979)
314. BRD P. 2 745 228; *Chem. Abstr.* **89** 25 427 (1978)
315. BRD P. 2 422 795; *Chem. Abstr.* **82** 87 173 (1975)
316. BRD P. 2 642 577; *Chem. Abstr.* **86** 172 547 (1977)
317. US P. 4 487 964; *Ref. Zh. Khim.* 20S 538P (1985)
318. US P. 3 247 350; *Ref. Zh. Khim.* 3S 569P (1985)
319. Jpn. P. 78 144 938; *Chem. Abstr.* **90** 153 177 (1979)
320. Russ. P. 1 694 594; *Ref. Zh.Khim.* 5T 49P (1993)